Astro
TL
501
S42
Index
11
Subject

Room use
ONLY

SPECIAL NOTICE INSIDE

# Scientific and Technical Aerospace Reports

The University of Michigan
Astronomy
Library

## ANNUAL INDEXES JANUARY–DECEMBER 1973

## SECTION I

### SUBJECT INDEX

Astronomy

FEB 25 1974

DECEMBER 31, 1973

VOLUME 11 • NUMBERS 1-24

N73-10001—N73-33931

NATIONAL AERONAUTICS AND SPACE ADMINISTRATION

## PURCHASE OF *STAR*

The semimonthly issues and the cumulative index issues are available postpaid on subscription and in single copy from the Superintendent of Documents, United States Government Printing Office, Washington, D.C. 20402, United States of America.

*Semimonthly issues. . .*

Annual subscription rates: $76.50 domestic; $95.65 foreign. Price per single copy: $3.25 domestic; $4.10 foreign.

*Cumulative index issues. . .*

Annual subscription rates: $25.55 domestic; $31.95 foreign. Price per single copy varies according to the number of pages.

*Domestic subscription rates. . .*

Apply to the United States, Canada, Mexico, and all Central and South American countries, except as noted below.

*Foreign subscription rates. . .*

Apply to Argentina, Brazil, French Guiana, Guyana, Surinam, British Honduras, and all other countries throughout the world.

Payment should be by check, money order, or document coupons, and must accompany order. Remittances from foreign countries should be made by international money order or draft on an American bank, payable to the Superintendent of Documents, or by UNESCO book coupons.

PUBLISHED BY:
**UNITED STATES GOVERNMENT**
**NATIONAL AERONAUTICS AND SPACE ADMINISTRATION**
SCIENTIFIC AND TECHNICAL INFORMATION OFFICE
*Scientific and Technical Aerospace Reports,* Volume 11, is prepared by the NASA Scientific and Technical Information Facility operated for the National Aeronautics and Space Administration by Informatics Tisco, Inc.

The Administrator of the National Aeronautics and Space Administration has determined that the publication of this periodical is necessary in the transaction of the public business required by law of this Agency. Use of funds for printing this periodical has been approved by the Director of the Office of Management and Budget through April 1, 1974.

# SPECIAL NOTICE

The abstract sections of the semimonthly *STAR* journals can be bound separately. Individual abstracts can be located readily by means of the page numbers given at each index entry, e.g. 12 p 1419. To assist the user in binding *STAR* Volume 11, four (4) title pages are included in the back of Section I of the Annual Indexes.

VOLUM

VOLUME 11 NUMBERS 1–24

# Scientific and Technical Aerospace Reports

Annual Indexes (Section I) January-December 1973

## TABLE OF CONTENTS

*Page*

SECTION I

Introduction . . . . . iii
Subject Index . . . . . A-1

SECTION II

Personal Author Index . . . . . B-1
Corporate Source Index . . . . . C-1
Contract Number Index . . . . . D-1
Report/Accession Number Index . . . . . E-1

# Introduction

## WHAT *STAR* ANNUAL INDEXES ARE

These Annual Indexes are edited consolidations of the indexes to the individual issues of *Scientific and Technical Aerospace Reports (STAR)* for the calendar year 1973 (Volume 11 Numbers 1 through 24). For the convenience of the user, they are divided into two sections, each bound separately. Section I contains the Subject Index. Section II contains the Personal Author Index, Corporate Source Index, Contract Number Index, and Report/Accession Number Index. The Annual Indexes supersede the semimonthly and semiannual indexes previously issued during 1973.

Each entry in these indexes includes a group of identifying numbers in the following form: **06 p0663 N73-15379**. The first two digits (06) identify the issue in which the document was announced. The "p" and the four digits that follow (0663) refer to the page number, in the designated issue, on which the abstract of the document appears. The next group of numbers (N73-15379) is the NASA Accession Number, a unique identification number assigned by NASA to each document that was acquired, indexed, and announced in *STAR* during the year.

In addition to these identifying numbers, each entry in the Subject Index contains a Notation of Content (a brief description of the contents of the document); each entry in the Personal Author and Corporate Source Indexes contains the exact title of the document.

At the beginning of each index in this cumulation, a typical listing is illustrated with each of its elements identified to assist the reader in using the different types of index entries.

## HOW TO USE THE SUBJECT INDEX

Subject terms in this cumulative index are arranged alphabetically, and are supplemented with cross-references which are intended to serve as directions that will enable the user to modify, enlarge, or narrow his search in accordance with his specific interests. Two types of cross-references are used:

1. Use (U) references indicate that the subject term is not "postable", i.e., not a valid term, and that the following term or terms are used instead. For example.

   COLUMBIUM
   U NIOBIUM
   ANNULAR JETS
   U ANNULAR FLOW
   U JET FLOW

2. Narrower Term (NT) references refer the user to more specific headings in the same subject area, under which additional material on the subject may be found. For example:

   EMISSION
   NT ELECTRON EMISSION
   NT NEUTRON EMISSION
   NT THERMAL EMISSION

Finally, a searcher should use the notations of content in the index to narrow further his quest for particular items. This is because subject terms can readily refer to more than one class of document. For example:

CATHODES
Cesium plasma cathodes as sources of high intensity electron beams.
Cathode material testing in electrochemical half cells.

illustrates a case where two references on different topics are listed under the same subject term.

## HOW TO USE THE CORPORATE SOURCE INDEX

The corporate source index entries are abridged versions of the corporate sources used in the abstract-section citations in the individual issue supplements. The corporate source supplementary (organizational component) does not appear in the index. For example:

NEW MEXICO STATE UNIV. LAS CRUCES. DEPARTMENT OF BIOLOGY.
(Corporate source at citation)
NEW MEXICO STATE UNIV. LAS CRUCES.
(Corporate source index entry)

## HOW TO USE THE PERSONAL AUTHOR INDEX

All personal authors identified in the abstract-section citations in the individual *STAR* issues appear in this index. Differences in transliteration schemes may require multiple searching of the index for variants of an author's name. For example:

EMELIANOV, M. D.
YEMELYANOV, M. D.

## HOW TO USE THE CONTRACT NUMBER INDEX

All contract numbers that are identified in the abstract-section citations in the individual *STAR* issues appear in this index. Changes by agencies in the style in which contract numbers are presented may require multiple searching for variants. For example:

AF 33(615)-67-C-1758
F33615-67-C-1758

## A COMPREHENSIVE INFORMATION SERVICE

The National Aeronautics and Space Administration makes the results of worldwide research and development activities in aeronautics, space, and supporting disciplines promptly available to participants in its programs. NASA's scientific and technical information system now contains nearly a million documents, which are abstracted, indexed, and obtainable through retrieval and dissemination services. These services, which include the abstract journal, *Scientific and Technical Aerospace Reports (STAR)*, are described fully in a bulletin, *The NASA Scientific and Technical Information System . . . and How to Use It*, available at no charge from the NASA Scientific and Technical Information Facility, P.O. Box 33, College Park, Maryland 20740.

## AVAILABILITY OF DOCUMENTS

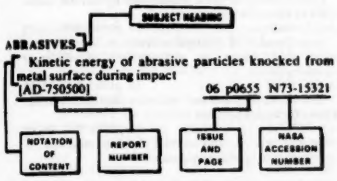
Information concerning the availability of documents announced in the *STAR* issues covered in this index is found in the Introduction to the most currently issued semimonthly issue.

# SUBJECT INDEX





## TYPICAL SUBJECT INDEX LISTING




The subject heading is a key to the subject content of the document. The Notation of Content (NOC), rather than the title of the document, is used to provide a more exact description of the subject matter. The report number helps to indicate the type of document cited (e.g., NASA report, translation, NASA contractor report). The issue and page identify the *STAR* issue in which the document was announced and the page number on which the citation appears. The NASA accession number denotes the number by which the citation is identified on that page. The NOC's are arranged under each subject heading in ascending accession number order.

## A

**A STARS**
Far ultraviolet photometry of peculiar B and A stars by OAO 2
22 p2734 N73-31883

**A-11 SATELLITE**
U ECHO 1 SATELLITE

**A-4 AIRCRAFT**
Static and vibration tests of graphite-epoxy stabilizer system for A-4 Skyhawk aircraft
[AD-750778] 06 p0689 N73-15610
Air cushion landing system effect on aerodynamic characteristics of A-4 aircraft
[AD-761621] 19 p2221 N73-27917

**A-6 AIRCRAFT**
Design and performance tests of solid state A-6 aircraft engine instruments
[AD-760351] 17 p2035 N73-26469

**A-7 AIRCRAFT**
Performance evaluation of airborne audio-video recording system as training device in A-7D tactical fighter
[AD-744041] 01 p0021 N73-10161
Method for predicting flight characteristics of F-5 and A-7 aircraft during atmospheric turbulence using large amplitude flight simulator
[AD-749480] 05 p0495 N73-14030
A-7 aircraft airborne, ground, and shipboard inertial navigator alignment methodology
11 p1319 N73-20710
Solid cadmium embrittlement in A-7 aircraft failure of six shaft and one horn fracture surfaces
[AD-756906] 13 p1545 N73-22525
Comparative evaluation of conventional and solid state simulators for A-7 aircraft electrical system
[AD-762295] 19 p2250 N73-28142
Design of automatic throttle control for Navy carrier based A-7 E aircraft
[AD-761764] 19 p2329 N73-28740
Redesign concept for A-7E approach power compensator system, including longitudinal feedback
[AD-761458] 19 p2330 N73-28742
Logistics performance data book on bombing and navigation system for A-7D aircraft to show reliability, maintainability, cost, and problems
[AD-762215] 19 p2357 N73-28960
Design, development, and evaluation of automatic departure prevention system and stall inhibitor for A-7 aircraft
[AD-764767] 23 p2745 N73-31972

**A-37 AIRCRAFT**
Development of boron composite materials for construction of aircraft landing gear for A-37 aircraft - Vol. 1
[AD-756922] 14 p1603 N73-22996
Design, fabrication, and test of boron composite material landing gear for use as main landing gear on A-37 aircraft - Vol. 2
[AD-756923] 14 p1603 N73-22997
Data analysis from A-37 aircraft flights to evaluate electronic strain-level counter as fatigue damage monitor
[AD-757210] 14 p1668 N73-23540

**ABBREVIATIONS**
U SYMBOLS

**ABEL FUNCTION**
Reliability analysis of Abel transformation algorithm applied to mass measurement in hypersonic wakes
[ISL-21/70] 01 p0041 N73-10324
Abel integral transform and ray tracing methods for radio occultation data inversion to obtain refractive index profiles of planetary atmospheres
02 p0197 N73-11596
Derivations of straight line, Abel transform and seismological Herglotz-Wiechert transform for reconstruction of refractivity profiles from radio wave phase data
[NASA-TN-D-7098] 02 p0230 N73-11868
MIMIC programming language for solving Abel integral equations
[AD-754003] 11 p1311 N73-20642
Operator theory of n-th order modular forms
[NASA-TT-F-15006] 19 p2313 N73-28605

**ABERRATION**
Aberration due to high velocity satellites for laser telemetry
05 p0557 N73-14526
Stomach shielding effects on chromosomal aberration frequency in guinea pig and rat marrow cells after gamma radiation at doses of 50 to 200 r
11 p1241 N73-20074
Optimum holographic mounting for maximal ultrahigh speed microparticle volume restitution
[ISL-32/72] 16 p1924 N73-25565
Machine assisted human chromosome karyotyping and aberration for radiation damage
[ANL-7960-PT-2] 17 p1988 N73-26068
Wing anomalies as result of weightlessness simulation for flour beetle Tribolium confusum
19 p2226 N73-27952
Aberrations and imaging properties of holographic optical elements
[NASA-CR-124334] 19 p2307 N73-28555
Correction of aberrations in long wavelength holography by direct injection in formation process and computer generation
22 p2680 N73-31466

**ABILITIES**
Overview of literature concerning retention of learned skills with emphasis on space flight skill retention
[NASA-CR-128611] 01 p0020 N73-10152
Relations between sociometric variables and criteria of ability and behavior of student pilots
19 p2226 N73-27954

**ABIOGENESIS**
Medical and biological problems of manned space flight
[NASA-TT-F-719] 10 p1114 N73-19077
Abiogenic syntheses of aliphatic and aromatic amino acids by ultraviolet radiation
10 p1119 N73-19119

**ABLATION**
Computation of thermochemical ablation rates of pyrolytic graphite surfaces using FORTRAN 4 computer code - Vol. 1
[AD-745440] 01 p0071 N73-10579
FORTRAN 4 program to compute thermochemical ablation rates of pyrolytic graphite surfaces as function of surface temperature and pressure including flow charts and program listings
[AD-744854] 01 p0117 N73-10969
Fortran program for axisymmetric, transient heating and material ablation
[AD-745441] 01 p0118 N73-10975
Differential equations for transient response of one dimensional, ablative thermal protection system, including thermal nonequilibrium, mass transfer, and chemical kinetics
[NASA-TM-X-68853] 02 p0137 N73-11108
Assessing laminar flow on conical vehicles during hyperbolic entry by studying boundary layer transition on ablating cones
[NASA-TM-X-68867] 03 p0283 N73-12293
Ablation of graphite surfaces heated in turbulent flow of air or carbon dioxide and development of method for calculating ablation rate
[AD-747727] 03 p0365 N73-12973
Theoretical analysis of ablation effects on dynamic stability of reentry vehicles
04 p0477 N73-13899
Development of proton-activated sensors to measure graphite nosetip recession due to ablation during nose cone reentry
[AD-748289] 05 p0548 N73-14456
Effect of ablation on aerodynamic characteristics of blunted slender cone during free flight ablating conditions
[NASA-TN-D-7196] 09 p0979 N73-18002
User manual for computer program to solve equations of fully coupled viscous, radiating flow at stagnation point of blunt body which may be ablating or nonablating
[NASA-CR-2237] 11 p1347 N73-20933
Radiative coupled viscous flow past ablating blunt body at hyperbolic entry conditions
[NASA-CR-2236] 11 p1347 N73-20934
Stationary hyperacoustic overflow of leading point of graphite blunt body by heat conducting stream of air
[AD-755784] 12 p1466 N73-21875
Mathematical models for surface ablation of silica-reinforced composites
15 p1801 N73-24596
Combustion phenomena in reinforced plastics ablation under simulated atmospheric reentry using plasma arc jets
[ONERA-NT-195] 15 p1844 N73-24939
Theory of dynamic viscous pressure interaction applied to surface ablation by sublimation
[AD-759186] 16 p1967 N73-25915
Interactions of radiation with conductive and convective heat transfer in ablation and boundary layer flow determined by normal mode expansion technique
18 p2128 N73-27200
Analysis of stagnation point on blunt body in massive ablation condition to show effects of absorption coefficient enhancement on mass loss rate
19 p2351 N73-28912
Effect of ablation modes and flow field distribution on cross hatching phenomenon at supersonic speeds
[TN-85] 20 p2485 N73-29963

**ABLATIVE MATERIALS**
Effect of heat transfer level on mechanical properties of elastomeric ablative material used on spherically blunted cones
[NASA-TM-X-2612] 02 p0191 N73-11548
Analysis of production method for manufacturing ablative heat shield panels using press filling and curing of ablation material
[NASA-CR-112124] 02 p0243 N73-11975
Measurement of surface recession of ablative materials in rocket nozzles by spectroscopic analysis
[AD-749968] 06 p0714 N73-15829
High temperature reactions of COF2 with CO and H2 in excess argon behind reflected shock waves
[AD-751270] 07 p0753 N73-16118
Material composition effects on ablation performance of low density elastomer ablators, such as nylon and hollow silica and phenolic spheres
[NASA-TN-D-7246] 14 p1719 N73-23945
Vacuum effects on mechanical properties of composite heat ablator and solid problem material
15 p1801 N73-24594
Carrier liquid system containing bodies of ablative material
[NASA-CASE-LEW-10359-2] 16 p1972 N73-25932
Differential equations for charring ablator with thermal nonequilibrium, chemical kinetics, and mass transfer
[NASA-TN-D-7180] 16 p1974 N73-25961
Ablation article and surface for analyzing flow transition on ablative surface
[NASA-CASE-LAR-10439-1] 18 p2205 N73-27796
Reusable ablative heat shielding for space shuttle orbiters
[NASA-CR-132282] 21 p2605 N73-30880

Thermal and mechanical properties of low density elastomeric ablation material
[NASA-CR-132281] 23 p2809 N73-32463
ABNORMALITIES
NT MAGNETIC ANOMALIES
Macroscale fluctuations in atmospheric and oceanic variables
[AD-744976] 01 p0075 N73-10621
Aerospace medicine for treating abnormal conditions caused by space flight
[NASA-TT-F-735] 09 p0994 N73-18116
Standardization of tests and classification of color perception abnormalities in military personnel
10 p1113 N73-19071
Postflight analysis of abnormalities in Apollo 17 flight
[NASA-TM-X-69122] 10 p1211 N73-19850
Calculation of expected anomaly criteria for some meteorological fields using statistical analysis methods
[NLL-M-22804-[5828.4F]] 12 p1420 N73-21507
Failure analysis of telemetry anomalies during Apollo 17 flight
[NASA-TM-X-69367] 18 p2117 N73-27118
Abnormalities of liquid He-3 measured below 5 m K
24 p2967 N73-33713
ABORT APPARATUS
Results of tug turnaround cost study and space transportation system abort modes and effects study
[NASA-CR-135765] 24 p2983 N73-33833
ABORT TRAJECTORIES
Trisonic wind tunnel tests to determine force and moment characteristics of space shuttle orbiter and modified external tank and solid rocket booster
[NASA-CR-120089] 12 p1460 N73-21831
ABRASION
Relative wear resistance and patterns of metals under hydroabrasive wear
[AD-747668] 03 p0318 N73-12595
ABRASION RESISTANCE
Abrasive wear resistance of vapor plated chrome coatings
[AD-749769] 05 p0567 N73-14605
Wear process and colloidal particle production test on sliding metal surfaces using magnetic measurements
[AD-753251] 09 p1040 N73-18481
ABRASIVES
Kinetic energy of abrasive particles knocked from metal surface during impact
[AD-750500] 06 p0655 N73-15321
Relationship between temperature and surface layer quality of two row roller bearings polished with abrasive cloth
[AD-754678] 11 p1301 N73-20559
Rheological properties of abrasive powder solutions considering particle dispersion
[AD-756082] 13 p1488 N73-22065
Quality control and composition of grinding wheels discussing microstructure and chemistry
[CRIF-MC-45] 13 p1530 N73-22399
ABSCISSAS
U COORDINATES
ABSORBENTS
Protein sterilization of firefly luciferase without denaturation
[NASA-CASE-GSC-10225-1] 18 p2113 N73-27086
Development of design information for molecular sieve sorbants regenerative CO2-removal systems for manned spacecraft
[NASA-CR-2277] 19 p2225 N73-27948
ABSORBERS [MATERIALS]
NT NEUTRON ABSORBERS
Performance tests on cryogenic insulation materials for nuclear radiation shielding
[NASA-CR-2162] 05 p0578 N73-14707
Radiation damage of electrically insulating polymeric materials used in electrotechnology
[AD-753367] 09 p1001 N73-18169
NO2 and UDMH absorbing properties of rocket propellant gas mask canisters
[AD-752538] 10 p1203 N73-19791
Solid amine filter material for humidity control and carbon dioxide removal in space shuttle
[NASA-CR-133963] 18 p2113 N73-27087
Analysis of errors in measurement of absorbances of liquid filters caused by instrumental and chemical uncertainties using three types of liquid filters
[PAPER-76A5-733] 21 p2545 N73-30402
Electromagnetic absorber reflectance and anechoic chamber design for microwave antenna measurements
[FTZ-A-454-TBR-13] 22 p2642 N73-31176
ABSORPTANCE
Reflectance, transmittance and absorbance spectra of normal and six types of maize leaves
[NASA-CR-130032] 07 p0745 N73-16065
ABSORPTION
Electrochemical analysis of cathodic hydrogen absorption by iron and steel
[BARC-585] 05 p0506 N73-14116
Influence of absorption magnetic thermal RF breakdown in superconducting cavities
[KFK-EXT-3/72-2] 06 p0708 N73-15780
Matrix solution for one dimensional model of radiation field arising from multiple scattered photons in planetary atmosphere
[NASA-CR-130755] 08 p0943 N73-17722
Absorption of bile acids and cholesterol by polymers
10 p1227 N73-19976
Design technique to reduce absorption in multilayer dielectric mirrors using optical interference coatings
15 p1812 N73-24688
IR laser study of absorption and saturation properties of molecular gases
[NASA-CR-132769] 19 p2307 N73-28554
ABSORPTION BANDS
U ABSORPTION SPECTRA
ABSORPTION COEFFICIENT
U ABSORPTIVITY
ABSORPTION CROSS SECTIONS
Relation between momentum transfer and capture, and total scattering cross sections for ion-dipole collisions
[NASA-TM-X-68151] 01 p0083 N73-10685
Absorption cross sections of Schumann-Runge bands of molecular oxygen
[A-107-1972] 04 p0385 N73-13127
Tables on molecular oxygen absorption in schumann-runge band
[AERONOMICA-ACTA-A-107-PT-2]
05 p0506 N73-14114
Tables of O2 absorption cross sections in Schumann-Runge band
[A-N-107-1972] 07 p0752 N73-16108
Tables of absorption cross sections of molecular oxygen in Schumann-Runge bands
[AERONOMICA-ACTA-A-107-1972-V-1]
12 p1375 N73-21157
Tables of absorption cross sections of molecular oxygen in Schumann-Runge bands
[AERONOMICA-ACTA-A-107-1972-V-2]
12 p1375 N73-21158
ABSORPTION SPECTRA
NT FRAUNHOFER LINES
NT TELLURIC LINES
Method for studying absorption spectra of colloidal solutions
[NASA-TT-F-14497] 01 p0023 N73-10177
Spectrophotometric analysis of Orion nebula emission spectra with dust lanes in hydrogen region
[AD-745314] 01 p0104 N73-10863
Absorption spectroscopic determination of nickel, chromium, and cobalt in airborne particulates
[NASA-TM-X-2672] 02 p0137 N73-11111
Infrared absorption spectra of stratospheric nitrogen dioxide
02 p0164 N73-11330
Absorption of 4 to 6 mm wavelength band in atmosphere from zenith attenuation measurements
[AD-745951] 02 p0168 N73-11363
Absorptive losses in carbon monoxide laser emission lines
[AD-746170] 02 p0182 N73-11479
Emission and absorption spectra for mixtures of liquid uranium and uranium oxide using carbon tube furnace facility
[AD-746687] 02 p0194 N73-11571
Spectral absorption coefficients of argon and silicon and spectral reflectivity of aluminum as function of pressure, temperature, and wave number
[NASA-CR-129300] 03 p0335 N73-12727
Iron absorption band analysis for discrimination of iron-rich zones in California and Nevada
[E72-10294] 04 p0410 N73-13344
Atmospheric water vapor absorption at CO, HF, and DF laser frequencies using 1-km white absorption cell and laser sources
[AD-748437] 04 p0430 N73-13501
Microphotometer analysis of absorption spectra, physical and chemical properties of NO2 system in Martian atmosphere
07 p0752 N73-16107
He-Xe tunable laser measurement of infrared line shape and CO2 absorption spectra
[AD-751230] 07 p0808 N73-16556
Distribution of charged particles in magnetic field for determining superhigh frequency wave absorption by palsma
[AEC-TR-7321] 08 p0949 N73-17768
Medium and high resolution radiometer measurements of water vapor absorption regions from Nimbus satellites
08 p0972 N73-17942
Observations of neutral hydrogen absorption spectrum of Cygnus X-3
[AD-752497] 09 p1085 N73-18856
Free bound, relative continuum-absorption cross sections for first 90 excited S, P, and D states of neutral argon
[AD-754007] 11 p1253 N73-20164
Spectra of prompt gamma rays following nuclear pion absorption
[NASA-CR-131398] 11 p1326 N73-20762
Search for Lambda 21 cm absorption in QSS and other sources near to spiral galaxies
[AD-754120] 11 p1339 N73-20871
Measurements of Mossbauer absorption spectra to investigate diffusion mechanism of iron in beta-titanium
12 p1413 N73-21449
Using transition from Ni-61 to obtain Mossbauer absorption spectra with Ni-Pd alloy
[TID-26197] 12 p1414 N73-21461
Intensity relations and spectral satellite studies of alkali/foreign gas interactions
13 p1528 N73-22385
Multiphonon infrared absorption by crystal inclusions of optical window materials
[AD-756080] 13 p1537 N73-22453
Measurement of absorption cross section values of nitric acid vapor in stratosphere at different wavelengths
[A-117-1973] 16 p1905 N73-25408
Spectral absorption and emission coefficient calculations for argon plasmas
[AD-759571] 17 p2070 N73-26748
Optical spectra and crystal field parameters of neodymium in lanthanum aluminate
17 p2071 N73-26757
Iron-absorption band analysis for discrimination of iron rich zones using ERTS-1 imagery
[E73-10789] 18 p2137 N73-27265
Ni-61 transition for obtaining Mossbauer absorption spectra with Ni-Pd alloys
18 p2185 N73-27641
Development of numerical method for computing transmission functions of atmospheric gases based on exact frequency integration using structure of absorption spectrum
20 p2401 N73-29296
Single orthoferrite crystal growth by crucibleless zone melting, including optical absorption spectra
20 p2461 N73-29777
Atmospheric absorption line parameters for infrared-active molecules occurring naturally in terrestrial atmosphere
[AD-762904] 21 p2542 N73-30382
Absorption spectra of laser excited Ba2NaNb5O15 crystal
21 p2585 N73-30714
CO2 laser and spectrophone for CO2 and water vapor absorption measurements
22 p2679 N73-31462
Water vapor absorption by highly attenuated CO laser lines
[AD-764376] 22 p2682 N73-31485
Collision frequency and velocity effects on ion cyclotron resonance line shape
[NASA-CR-135724] 23 p2821 N73-32552
Photon energy and polarization effects on optical absorption spectra of GMO at varying temperatures
23 p2824 N73-32574
Mossbauer absorption spectra of iron 57 in single crystal of potassium iron fluoride
[AD-764635] 23 p2827 N73-32597
Monte Carlo method for fitting iron 57 Mossbauer spectra
[AD-764634] 23 p2828 N73-32602
Pressure dependent absorption of CO2 laser in BCB at 10.6 micron
[DREV-TN-2086/73] 24 p2930 N73-33403
Spectrographic study of rare earth crystal absorption spectra in magnetic fields at liquid helium temperature
[NASA-TT-F-14732] 24 p2958 N73-33640
Absorption spectra of infrared window matrials
[AD-764904] 24 p2969 N73-33730
ABSORPTION SPECTROSCOPY
Absorption and emission spectra for trace element analyses on biological sample solutions
03 p0258 N73-12093
Analysis of errors in measurement of absorbances of liquid filters caused by instrumental and chemical uncertainties using three types of liquid filters
[PAPER-76A5-733] 21 p2545 N73-30402
Procedures for accurate measurement of molar absorptivities to show sources of determinant error and methods for elimination of errors
[PAPER-76A5-734] 21 p2545 N73-30403
Wavelength modulation spectra of copper, gold, silver, gallium phosphide, and indium phosphide
[LBL-1125] 24 p2927 N73-33375
ABSORPTIVE INDEX
U ABSORPTIVITY
ABSORPTIVITY
Absorption coefficient and index of refraction data for Pb[1-x]S n[x] Te thin films
[AD-751650] 07 p0832 N73-16747
Two flux radiative transfer model for measuring absorption and scattering coefficients for nonhomogeneous minerals
[RE-451J] 13 p1558 N73-22632
Monochromatic absorption coefficient in narrow regions of oscillatory-rotational spectrum of H2O
[AD-759238] 16 p1946 N73-25743
Measurement of acoustic absorption coefficient of Bidin
[TR-7302.626] 19 p2321 N73-28669

Star cluster data used to obtain absorption values for different galactic longitudes in northern part of Milky Way
20 p2471 N73-29842
Comparison of absorption and scattering coefficients for air
[LA-UR-73-708] 24 p2923 N73-33348

**ABSTRACTS**
Bibliography of abstracts for NASA patents and patent applications
[NASA-SP-7039[01]-SECTION-1]
02 p0244 N73-11982
Annotated bibliography on pulsars taken from Nuclear Science Abstracts for 1971
[TID-3320-SUPPL-2] 03 p0357 N73-12909
Soviet scientific abstracts on physics and mathematics
[JPRS-57242] 03 p0366 N73-12984
Abstracts on physics and mathematics, including aerohydrodynamics, magnetohydrodynamics, thermodynamics, and physics of crystals and semiconductors
[JPRS-57312] 03 p0366 N73-12985
Abstracts on aeronautical, marine, mechanical, automotive, civil, and industrial engineering
[JPRS-57311] 03 p0366 N73-12986
Abstracts and bibliographies on research in laser technology, effects of explosions, geosciences, and particle beams
[AD-749488] 04 p0430 N73-13504
Abstracts from Soviet scientific and technical journals on electronics and electrical engineering
[JPRS-57877] 06 p0647 N73-15256
Abstracts on radiation and health physics
[BNWL-1651-VOL-2-PT-2] 07 p0746 N73-16069
Bibliography and abstracts on upper atmospheric phenomena in inner region of polar caps
[AD-751335] 07 p0796 N73-16473
Abstracts on remote sensing of turbulence and waves in planetary boundary layer
[AD-751110] 07 p0816 N73-16618
Bibliography of Nuclear Science Abstracts from 1964 to 1970
[AED-C-21-10] 08 p0942 N73-17720
Abstracts of experimental studies on superconductivity
[AD-751869] 08 p0952 N73-17794
Abstracts of plasma physics publications
[NASA-CR-130983] 09 p1069 N73-18723
Abstracts on kinetics and thermodynamics of gases interacting with liquid metals
[JPRS-58282] 09 p1098 N73-18964
Abstracts on directionally grown eutectic alloy composites
[AD-754779] 11 p1309 N73-20625
Abstracts of articles on Soviet Bloc research in earth and space sciences
[JPRS-58437] 11 p1338 N73-20860
Tabulation of research reports published in German technical document series during calendar year 1972
[DLR-MITT-73-01] 11 p1352 N73-20971
Cumulative index of abstracts contained in Aeronautical Engineering and Aerodynamics Bibliography for calendar year 1972
[NASA-SP-7037[27]] 15 p1725 N73-23994
Abstracts on properties of semiconductors and semiconductor devices
[AD-758053] 15 p1822 N73-24767
Abstracts of studies in nuclear physics, solid state physics, and plasma physics
[AD-759252] 16 p1947 N73-25756
Literature survey of abstracts on plasma instabilities
[AD-759276] 16 p1951 N73-25787
Abstracts of reports on high temperature research
16 p1974 N73-25960
Abstracts and bibliographic lists of Soviet technical literature on research and development
[AD-758784] 16 p1977 N73-25995
Abstracts and bibliographies of Soviet literature on lasers, explosion effects, particle beams, and geosciences
[AD-762376] 19 p2356 N73-28955
Annotated bibliography on weather modification by precipitation inducement
[PB-220348/7] 21 p2575 N73-30634
Abstracts on research projects inclusive of flight dynamics to heating of swimming pools using solar collector
[ISBN-0-85494-200-9] 21 p2609 N73-30910
Abstracts of research projects on adaptive telemetry systems
[NASA-CR-130228] 22 p2631 N73-31088
ADAM automatic abstracting system for evaluating and improving computer produced abstracts
22 p2636 N73-31126
Abstracts on source encoding for two-dimensional data
[NASA-CR-132796] 22 p2639 N73-31149
Abstracts of NASA-ASRDI publications on aerospace safety research
[NASA-TM-X-71428] 23 p2866 N73-32911

**ABUNDANCE**
Chemical composition and abundance of alpha Centauri visual binary determined from spectral lines
[ROY-OBS-BULL-173] 06 p0719 N73-15870
Rare gas abundances in Apollo 11 rocks 10017 and 10071, and rock age determinations
07 p0842 N73-16818
IMP 6 measurements of light element composition of solar cosmic rays during flares of Apr. and Sept. 1971
[NASA-TM-X-65947] 09 p1080 N73-18814
Consistence of cosmic ray source compulsion with explosive nucleosynthesis
[NASA-TM-X-70448] 21 p2592 N73-30768

**AC [CURRENT]**
U ALTERNATING CURRENT

**AC GENERATORS**
Two dimensional numerical analysis based on nonlinear partial difference equations of cross sections of long alternators
[AD-744985] 01 p0007 N73-10052
Inductive reactances of superconducting synchronous machine
[AD-749526] 05 p0499 N73-14066
Characteristics of conventional alternators and aircraft electrical power systems and comparison with electric systems using superconductors
10 p1109 N73-19036
Characteristics of superconducting electric generators to show effect of electromechanical, electromagnetic, and cryogenic parameters on design
10 p1109 N73-19039
Magnetic field intensity calculations for gap electrical machinery with symmetric and asymmetric windings
[JPRS-58448] 11 p1324 N73-20744
Digital computer program for analyzing electromagnetic design of salient, wound pole alternators
[NASA-TN-D-7258] 12 p1366 N73-21082
Analysis of operation of electric alternator feeding into direct current system through rectifying device
[RAE-LIB-TRANS-1679] 17 p1986 N73-26049

**ACCELERATED LIFE TESTS**
Development of rationale and requirements for conducting accelerated life tests on spacecraft electronic systems
[NASA-CR-129096] 02 p0233 N73-11892
Vacuum life tests on lubricated bearings and slip rings
[ESRO-CR-91] 03 p0307 N73-12504
Comparison of outdoor exposure of elastomers and plastics with exposure in accelerated weathering test chamber using fluorescent source of UV radiation
[ERDE-TR-107] 06 p0688 N73-15600
Development and testing of primary structural elements of windshield system for space shuttle orbiter
[NASA-CR-112234] 06 p0720 N73-15879
Accelerated life tests and reliability predictions for ageing components
[AD-751616] 07 p0805 N73-16529
Fatigue tests to determine service life of catapult structure on C-2 aircraft
[AD-752493] 08 p0868 N73-17028
Formulation of stress strain model for storage batteries
[AD-752257] 08 p0870 N73-17045
Characteristics of carbon, cermet, and wire-wound type potentiometers based on service life and environmental tests
[ECR-30] 08 p0924 N73-17569
Evaluation of polyimide second stage rod seals at high temperatures to determine suitability for application to aircraft systems
[NASA-CR-121124] 08 p0927 N73-17592
Accelerated reliability tests of circuit components by continuous loading method
[AD-752689] 09 p1040 N73-18485
Test plan for extending service life of E-2A arresting gear
[AD-754752] 11 p1267 N73-20284
Development of methods for determining service life of rolling bearings based on fatigue of bearing materials
[NLL-RISLEY-TR-2524-[9091.9F]]
12 p1407 N73-21406
Fatigue life and wear tests of spur gears based on pitting fatigue at pitch circle to compare AISI M-50 and super nitralloy materials
[NASA-TN-D-7261] 12 p1408 N73-21411
Accelerated life test program for space batteries
[NASA-SP-323] 13 p1476 N73-21958
Development of guidelines for spacecraft equipment selection based on quality control and test procedures during manufacturing - Vol. 4
[NASA-CR-128908] 14 p1707 N73-23856
Accelerated life tests of copper/acetone heat pipe for meteorological satellite temperature control, including thermal cycling tests
14 p1719 N73-23948
Cyclic pressure tests of F-4 aircraft forward and aft canopies to determine safe service life after delamination of acrylic sheet
[AD-759349] 16 p1862 N73-25084
Performance tests of nickel cadmium and silver cadmium electric batteries to determine service life and reliability
[NASA-CR-132801] 17 p1985 N73-26046

**ACCELERATION**
Mechanical response of otolith-dependent units of cats to sinusoidal linear rotation
[AMRU-R-69-3] 02 p0132 N73-11068
Static moment and horizontal sinusoidal acceleration effects on stabilization errors in gyrovertical with mixed gyroscope correction characteristics
17 p2060 N73-26661
Single grid accelerator system for electron bombardment type ion thrustor
[NASA-CASE-XLE-10453-2] 18 p2192 N73-27699

**ACCELERATION [PHYSICS]**
NT ANGULAR ACCELERATION
NT DECELERATION
NT HIGH ACCELERATION
NT HIGH GRAVITY ENVIRONMENTS
NT IMPACT ACCELERATION
NT PARTICLE ACCELERATION
NT PLASMA ACCELERATION
NT SPIN REDUCTION
NT TRANSVERSE ACCELERATION
Apparatus for measuring velocity and acceleration of military vehicles
[PHL-1972-5] 01 p0055 N73-10446
Effects of orientation of acceleration vector on burning rate augmentation determined for aluminized composite propellant
[NASA-TN-D-6952] 01 p0116 N73-10962
Effects of propellant composition variables on acceleration-induced burning rate augmentation of solid propellants
[NASA-TN-D-6923] 01 p0117 N73-10966
Theoretical model of utricular otolith and associated neural connections to oculomotor system and their response to angular motion with respect to acceleration in shear
[FPRC-1315] 02 p0132 N73-11070
Cross axis behavior of circular elastic diaphragm accelerometers
[REPT-519] 02 p0177 N73-11438
Testing hydrophone types for acceleration response
[AD-748038] 03 p0338 N73-12758
Electronic transducer for acceleration measurement
[AD-748885] 04 p0423 N73-13451
Control system for rockets during combustion
[REPT-13-PT-2] 04 p0463 N73-13776
Measurements of launch g forces and line tensions in aerial recovery of dummies for long-line loiter personnel retrieval system
[AD-749518] 05 p0497 N73-14045
Lost data channels of acceleration measurements in underground nuclear tests
[UCRL-73665] 05 p0580 N73-14725
Relation between measured C.G. vertical accelerations and loads at T-tail of military aircraft
07 p0851 N73-16904
Nervous system functional changes due to forces of acceleration and weightlessness
[NASA-TT-F-733] 08 p0877 N73-17105
Analysis of motion of gimbal mounted gyroscope during rotor acceleration
08 p0923 N73-17560
Condition of drift invariance of two-stage gyroscope with arbitrary gas-lubricated main bearings in active accelerations
10 p1184 N73-19635
Collection and processing of gust load data obtained from counting accelerometers mounted at center of gravity of various aircraft
[AGARD-R-605] 11 p1235 N73-20023
Quantitative analysis of irreversible portion of radiation damage combined with gamma rays and acceleration
11 p1242 N73-20082
High speed water jets from vertically accelerated cones partially filled with water
[MT-64] 11 p1270 N73-20302
Acquisition of stress data and aerodynamic loads on F-5 aircraft using mechanical strain gages and oscillograph recorders for service life determination
[AD-760567] 20 p2361 N73-28991
Performance of anti-G valve subjected to varying acceleration forces
[AD-760814] 20 p2372 N73-29062
Relative frequency of occurrence of different normal accelerations at the center of gravity of aircraft in turbulence
[ARC-R/M-3714] 24 p2870 N73-32929
Effect of accelerations on active transport of glucose in small intestine of rats
24 p2883 N73-33021

**ACCELERATION STRESSES [PHYSIOLOGY]**
NT CENTRIFUGING STRESS
Analysis of physiological mechanisms contributing to occurrence of motion sickness
01 p0003 N73-10020
Analysis of acceleration forces produced during aerobatic flight and effects of acceleration forces on human body
[FAA-AM-72-28] 02 p0132 N73-11075

Feasibility of multichannel rheography for studying cardiovascular system on centrifuge
03 p0259 N73-12094

Subjective effects of sustained acceleration, including positive, negative, forward, backward, and lateral acceleration effects
06 p0628 N73-15095

Prolonged bed rest and positive radial acceleration effects on human visual response time
[NASA-TN-D-7161] 06 p0630 N73-15117

Human semicircular canal response to rotational stimuli in yaw, pitch, and roll planes of the head
06 p0632 N73-15137

Anti-compensatory oculomotor responses in human visual tracking and vestibulo-ocular mechanism during rotational head movement in flight
06 p0633 N73-15140

Oculogravic illusion factor in theoretical model of pilot control loss in jet aircraft
06 p0633 N73-15142

Vestibular neuron response to rotational stimuli in space flight environment
06 p0634 N73-15150

Effect of accelerations on thiamine S-35 distribution in organs, tissues, and subcellular structures of white mice
07 p0743 N73-16044

Morphological changes in juxtaglomerular apparatus in kidneys of rats during multihour exposure to accelerations in different directions
07 p0743 N73-16045

Effects of hypoxia and acceleration stresses on enzyme activities in erythrocytes and blood plasma
[DLR-FB-72-71] 07 p0746 N73-16070

Transverse acceleration effects on rat hepatocytic structures
10 p1115 N73-19086

Mental and cardiovascular acceleration stress effects on heart rate studied by beta adrenergic blockage
10 p1122 N73-19149

Human pituitary and adrenal hormone reserve in acceleration stress tolerance
10 p1123 N73-19150

Measurements of acceleration stress effects on pilot maneuvering ability and flight control performance
[AMRL-TR-72-3] 10 p1123 N73-19154

Positive pressure breathing for increased human acceleration tolerance
10 p1123 N73-19156

Bradycardia and death in guinea pigs exposed to acceleration overloads after injections of aminothiol group radioprotectors
11 p1239 N73-20057

Transverse acceleration overload effects on mice sensitivity to toxic doses of cysteamine and aminothiol group antiradiation drugs
11 p1239 N73-20061

Functional changes in systemic and cerebral hemodynamics with respect to vestibular stresses accompanying low accelerations
11 p1245 N73-20108

Lower body decompression effects on cardiac cycle and human acceleration tolerance
14 p1608 N73-23037

Acceleration effects on human visual functions under hypoxic conditions
14 p1609 N73-23040

Effects of weightlessness and acceleration on human body during space flight
20 p2365 N73-29022

Morphological changes in rat kidneys exposed to different accelerations
20 p2366 N73-29023

Impact acceleration effects on rabbit central nervous system
20 p2366 N73-29024

Physical/mathematical analyses on human vestibular responses to acceleration stresses
20 p2367 N73-29033

Influence of transverse accelerations on electrolyte composition of plasma and erythrocytes
24 p2884 N73-33030

**ACCELERATION TOLERANCE**

Cellular activation energy effect in rat tolerance to acceleration stress
[AD-749338] 05 p0501 N73-14079

Semicircular canal plugging response in cats to rotary stimulation
06 p0634 N73-15151

Hypodynamia effect on human transverse acceleration tolerance
10 p1114 N73-19083

Sound, light, and proprioceptive stimuli for inhibiting vestibular illusion in man
10 p1115 N73-19087

Composition and effects of radioprotectors on acceleration tolerance, hypoxia toxicity, radiation protection, and dynamic space flight stress in animals
[NASA-TT-F-721] 11 p1239 N73-20054

Effects of antiradiation drug dosage on mice and rat tolerance to transverse acceleration overloads
11 p1239 N73-20055

Resistance of mice to acceleration overloads after injection of aminothiol group radioprotector
11 p1239 N73-20056

Hypoxia and reduced acceleration tolerance of rats after injection of cysteamine radioprotector
11 p1239 N73-20058

Resistance of animals immersed in water to high acceleration
[NASA-TT-F-14828] 11 p1246 N73-20119

High altitude acclimatization effects on mice and rabbit tolerances to hypoxia, acceleration, and high temperature
[NASA-TT-F-14861] 11 p1247 N73-20123

Conditioned reflex motion sickness test of statokinetic fitness for flying personnel
13 p1480 N73-21994

Barany chair rotation for acceleration tolerance testing on flying personnel
13 p1480 N73-21995

Development of aircraft seat for high acceleration tolerance of flight crew personnel by elevating pelvis and legs forward
[AD-756630] 14 p1605 N73-23009

Computation of Coriolis forces in selecting flying personnel for vestibular tolerance
14 p1609 N73-23042

Distribution parameter model for acceleration forces acting on arterial system
[AD-756530] 15 p1743 N73-24128

Aerial combat acceleration environment testing of human performance capability using human centrifuges
[AD-759174] 16 p1869 N73-25134

Acceleration effects on mechanical impedance of human body in supine position
19 p2227 N73-27963

Mathematical simulation study of neuron response to vestibular analyzer exposed to periodically varying acceleration
[NASA-TT-F-15130] 22 p2623 N73-31015

**ACCELEROMETERS**

Uncorrected accelerometer data resulting from San Fernando, California earthquake of Feb. 1971
[PB-208529] 01 p0054 N73-10439

Cross axis behavior of circular elastic diaphragm accelerometers
[REPT-519] 02 p0177 N73-11438

Scripps Institute research on oceanographic instruments, stabilized floating platforms, ocean bottom accelerometers, and surface waves
[AD-748024] 04 p0417 N73-13407

Temperature corrected circuit for gyroscope or accelerometer of digital rebalance type
[NASA-CASE-NPO-13044-1] 04 p0421 N73-13436

Threshold of accelerometer and drag free probe detector
[ONERA-NT-199] 04 p0423 N73-13448

Triaxial accelerometer for determining upper air density, temperature, and pressure
[AD-749881] 05 p0543 N73-14422

Accelerometers, electromyogram sensors, and telemetry system for measuring human body segment motions
[AD-751134] 07 p0751 N73-16104

Adaptive filter for estimating atmospheric density profile during Atmospheric Explorer missions from accelerometer data
[NASA-TM-X-66202] 10 p1154 N73-19388

Collection and processing of gust load data obtained from counting accelerometers mounted at center of gravity of various aircraft
[AGARD-R-605] 11 p1235 N73-20023

Electron and proton radiation effects on Cactus accelerometer electric charge
[ONERA-NT-200] 11 p1294 N73-20503

Determination of ships orientation from accelerometer signals
11 p1319 N73-20703

Laboratory tests of accelerometers used in inertial guidance systems in French military programs
11 p1320 N73-20714

Differential method for evaluating performance of nonlinear accelerometers
11 p1320 N73-20715

Effect of spurious forces on electrostatic suspension of ultrasensitive accelerometers
[ONERA-NT-197] 13 p1530 N73-22397

Repackaging of broadband quartz torsional accelerometers for borehole use
[AD-755852] 13 p1531 N73-22410

Development of guidelines for selection of hardware items for use in manned spacecraft design to obtain five year maintenance-free service life - Vol. 3
[NASA-CR-128907] 14 p1707 N73-23855

NASA space vehicle design criteria on accelerometer applications
[NASA-SP-8102] 17 p2088 N73-26891

Theoretical model of Sparton Model 601 M horizontal velocity gage
[AD-762268] 19 p2302 N73-28508

Procedures for predicting fatigue life of aircraft flying under various load conditions using data obtained by counting accelerometer
20 p2481 N73-29927

Elastic deformation of gimbal suspension on gyroscope nutation, moments acting on spherical rotor in magnetic suspension, and differentiating linear accelerometer
[JPRS-59740] 21 p2547 N73-30420

Differential equations of motion and transfer functions of linear accelerometer for use in selection of instrument parameters
21 p2547 N73-30423

**ACCEPTABILITY**

Verification program for Inflight Blood Collection system
[NASA-CR-128645] 03 p0261 N73-12112

Functional relationship between food preference and frequency of repetitious eating
[AD-749079] 05 p0503 N73-14100

Test programs for TIROS M
[NASA-CR-130165] 07 p0849 N73-16882

Acceptance tests of C 90 MB vibration simulator
[LRBA-PV-15/72/SEV] 09 p1039 N73-18477

Performance verification test plan for Apollo ultraviolet spectrometer experiment
[NASA-CR-128573] 16 p1915 N73-25500

**ACCEPTANCE**

U ACCEPTABILITY

**ACCEPTOR MATERIALS**

Simultaneous donor and acceptor concentration determination, using Hall effect measurements
[ONERA-DERTS-NT-02-31] 05 p0587 N73-14776

Lithium-multivalent acceptor impurity interaction in germanium
12 p1437 N73-21645

Low temperature measurement of heat pulse and ultrasonic wave interaction with stress-split acceptor states in semiconductors
18 p2186 N73-27647

Transport coefficients of donor and acceptor mixtures for epitaxial growth of silicon by sandwich method
18 p2187 N73-27659

**ACCESS TIME**

Airport access and ground travel modes
[PB-212814] 11 p1353 N73-20990

**ACCIDENT INVESTIGATION**

NT AIRCRAFT ACCIDENT INVESTIGATION

Compilation of mishaps in manned space flight program for 1970 to 1971
[NASA-CR-120999] 09 p1090 N73-18897

Application of aircraft crash investigation procedures to railroad passenger train derailment
[FAA-AM-73-1] 19 p2218 N73-27896

**ACCIDENT PREVENTION**

System safety program plan for aviation accident prevention
[AD-746995] 03 p0253 N73-12048

Aircraft accident prevention analysis of air taxi/commuter operations to identify safety factors and enhance safety of operations
[NTSB-AAS-72-9] 05 p0493 N73-14016

Maintenance programs for oxygen systems to prevent accidents
[NASA-CR-120922-VOL-3] 05 p0580 N73-14718

Compilation of mishaps in manned space flight activity
[NASA-CR-120998] 09 p1090 N73-18896

Role of NASA in accident prevention
[NASA-CR-133051] 16 p1977 N73-25989

Objectives, scope of work, and funding requirements of research project for improvement of aircraft safety
[FAA-ED-18-1] 21 p2493 N73-30008

**ACCIDENTS**

NT AIRCRAFT ACCIDENTS
NT AUTOMOBILE ACCIDENTS

Evacuation areas for transportation accidents involving propellant tank pressure bursts
[NASA-TM-X-68277] 20 p2488 N73-29987

**ACCLIMATIZATION**

NT ALTITUDE ACCLIMATIZATION

Human factors investigations and acclimatization research conducted during Tenth Soviet Antarctic Expedition
20 p2407 N73-29348

**ACCOMMODATION**

NT VISUAL ACCOMMODATION

**ACCRETION**

U DEPOSITION

**ACCUMULATORS**

NT SOLAR COLLECTORS

Electrostatic charged particle collector containing stacked electrodes for microwave tube
[NASA-CASE-LEW-11192-1] 04 p0395 N73-13208

Discharge circuit of inductive accumulator for generating short front current pulse
[JPRS-58892] 13 p1504 N73-22190

Design and development of volume accumulator units for thermoelectric reactor coolant loops
[NASA-CR-121245] 18 p2177 N73-27582

**ACCURACY**

Evaluation of ice-water mixture thermocouple reference chamber discussing best operating parameter combination for high accuracy
[RAE-TR-72035] 01 p0058 N73-10475

Digital simulation and angle tracking accuracy of tactical radar with multipath propagation
[AD-748384] 03 p0268 N73-12172

Astrometry for determination of absolute positions of stars and their relative motions from Schmidt plates noting accuracy
07 p0845 N73-16843

Numerical calculation of quantitative characteristics of observation systems
[NAL-TR-301] 09 p1057 N73-18616
Accuracy estimates for syntheses of filters by optimizing mutual uncertainty function in minimax criterion
17 p1997 N73-26151
Spectrophotometry accuracy with Kodak IN, $IIaO_3$ and II aD photographic emulsions
[RR-3] 19 p2301 N73-28502
ACETATES
Engineer design tests of two dust control materials, polyvinyl acetate water emulsion and cationic asphalt-neoprene emulsion
[AD-745086] 01 p0038 N73-10297
ACETONE
Molecular orbital energies in spectra of tervalent titanium chlorocomplexes
13 p1542 N73-22493
Accelerated life tests of copper/acetone heat pipe for meteorological satellite temperature control, including thermal cycling tests
14 p1719 N73-23948
Acetone decomposition by stainless steel and other metal compounds
[AERE-R-7407] 24 p2892 N73-33088
Acetone decomposition by austenitic stainless steel, iron oxide, and chromium oxide
[AERE-R-7408] 24 p2892 N73-33089
ACETYLENE
Molecular beam sampling system for measuring size, size distribution, and particle concentration of carbon particles in acetylene-oxygen flame
[AD-744920] 01 p0118 N73-10971
Vibrationally excited carbon monoxide from reaction of oxygen with acetylene, methylacetylene, and methane
[DREV-TN-2051/72] 11 p1252 N73-20160
Atomic oxygen hydrogen reaction with acetylene, and gas discharge shock tube design
13 p1488 N73-22060
Photographic recording of dynamic behavior of flames in explosive gases caused by ignition of equimolar acetylene-oxygen mixture
[NASA-CR-135672] 23 p2856 N73-32825
ACIDITY
Electrochemical methods for determining acidity standard, atomic weight, stoichiometric composition, and trace contaminants
[NBS-TN-583] 09 p0999 N73-18153
ACIDS
NT AMINO ACIDS
NT ASCORBIC ACID
NT CARBONIC ACID
NT CARBOXYLIC ACIDS
NT DEOXYRIBONUCLEIC ACID
NT FATTY ACIDS
NT GLUTAMIC ACID
NT GLYCINE
NT HEXOGENES [TRADEMARK]
NT HYDRAZOIC ACID
NT HYDROCHLORIC ACID
NT HYDROCYANIC ACID
NT HYDROFLUORIC ACID
NT NICOTINIC ACID
NT NITRIC ACID
NT NUCLEIC ACIDS
NT PEPTIDES
NT PHOSPHORIC ACID
NT RIBONUCLEIC ACIDS
NT SULFURIC ACID
Corrosion tests of candidate rocket engine materials exposed to standard high density acids for liquid propellant compatibility determination
[AD-749965] 06 p0712 N73-15807
Stabilization of aqueous prussic acid during synthesis from ammonia by carbon dioxide
[NASA-TT-F-14691] 07 p0752 N73-16110
Humic soil acid effects in silicate mineral weathering with aluminum migration
[NASA-TT-F-15134] 23 p2754 N73-32034
Usefulness of ERTS-1 MSS data for monitoring coal strip mining, detection of acid mine drainage, and determination of effectiveness of reclamation and abatement procedures in Pennsylvania
[E73-11112] 24 p2915 N73-33269
ACLINAL VALLEYS
U VALLEYS
ACOUSTIC ATTENUATION
NT SHOCK WAVE ATTENUATION
Noise attenuation characteristics of cylindrical suppressors with duct lining composed of honeycomb cells covered with perforated plate
[NASA-TM-X-2652] 01 p0005 N73-10032
Dimpled array liners used as augmentor acoustic devices for controlling low frequency combustion instabilities
[AD-750902] 06 p0731 N73-15963
Interferometric measurement of hypersonic sound wave attenuation in liquid helium transition region
13 p1558 N73-22629
Development of annular acoustically porous elements for installation in exhaust and inlet ducts of turbofan engine to reduce aircraft engine noise intensity
[NASA-CASE-LAR-11141-1] 14 p1600 N73-22975
Attenuation of ultrasonic waves and methods for measuring attenuation
[NLL-RISLEY-TR-2571-[9091.9F]]
15 p1812 N73-24683
Ultrasonic absorption and dielectric loss as function of temperature in heterophase block copolymers
[AD-762452] 20 p2435 N73-29559
Hypersound attenuation in superconducting aluminum and cadmium
23 p2825 N73-32580
Thermodynamic state of thin helium films for precise measurements of third sound velocity and attenuation
24 p2968 N73-33720
ACOUSTIC COMBUSTION
U COMBUSTION STABILITY
ACOUSTIC DELAY LINES
Atmospheric and man made disturbances, resulting in noise pulses of random amplitude affecting delay lines in HF communication
[AD-745184] 01 p0029 N73-10223
Operational principles of ultrasonic devices in radio circuits
[AD-754616] 11 p1263 N73-20248
Design and fabrication of microwave acoustic surface wave delay lines
[AD-754896] 11 p1263 N73-20252
Surface acoustic waves used with devices for parametric signal processing and long delay lines
[AD-755943] 12 p1385 N73-21235
Doppler resolution filter configured as tapped delay line with simple input and output transducers
[AD-755194] 13 p1504 N73-22193
Prototypes of two acoustic delay lines with delays of 0.5 and 7.5 microsec, noting passband enlargement and echo suppression
15 p1757 N73-24239
Bulk elastic wave signals and design of acoustic filter
[AD-760020] 17 p2006 N73-26223
Acousto-optical delay line for UHF pulses with continuously variable delay, based on photon-phonon interaction
18 p2179 N73-27597
Electron beam imaging for manufacturing high rfequency surface acoustic wave transducers
[AD-761625] 19 p2245 N73-28101
Temperature stability of ceramic surface acoustic wave delay devices
[AD-761884] 19 p2327 N73-28723
Structural parameters of magnetoacoustic converters and its position
[AD-764935] 23 p2767 N73-32134
ACOUSTIC DUCTS
Noise attenuation characteristics of cylindrical suppressors with duct lining composed of honeycomb cells covered with perforated plate
[NASA-TM-X-2652] 01 p0005 N73-10032
Performance prediction for acoustically lined engine nacelle design
03 p0250 N73-12019
Noise output of turbofan engine with acoustically treated nacelle
03 p0250 N73-12020
Noise output from quiet engine during simulated takeoff and approach tests
03 p0250 N73-12021
Estimates of reduced noise levels for turbofan engines with sound suppressors
03 p0250 N73-12022
Bessel function analysis on acoustic wave propagation in curved ducts
[NASA-TM-X-2698] 06 p0700 N73-15705
Design of noise source for simulating supersonic spinning modes in duct acoustics
[NASA-CR-2260] 12 p1364 N73-21067
Development of annular acoustically porous elements for installation in exhaust and inlet ducts of turbofan engine to reduce aircraft engine noise intensity
[NASA-CASE-LAR-11141-1] 14 p1600 N73-22975
Annular duct liner curvature for aircraft noise reduction
[NASA-TN-D-7277] 17 p2063 N73-26688
Automatic control system for in-duct cancellation of spinning modes of sound
[NASA-CR-132317] 23 p2819 N73-32540
ACOUSTIC EXCITATION
Application of acoustic emission analysis to nondestructive testing on crack formation
[RFP-TRANS-101] 07 p0821 N73-16656
Analysis of response of structure to acoustic excitation to include vibration of structure, natural frequencies and damping, and noise field characteristics
[ESDU-72001-AMEND-A] 07 p0850 N73-16895
Strains affecting growth rate of edge cracks in acoustically excited panels
[ISVR-TR-59] 13 p1586 N73-22860
Design and performance of acoustic exciter for gas volume modulation in absorption cell
[NASA-CR-124269] 16 p1913 N73-25482
Statistical energy and deterministic analyses on dynamic response of coupled rods to longitudinal acoustic excitation
[AD-760276] 17 p2095 N73-26951
Acoustic pressure radiation from infinite elastic plate excited by point source
19 p2320 N73-28666
Random vibrations of infinite-span plate on rigid supports during cylindrical bending
[AD-761454] 19 p2321 N73-28677
Parametric ion acoustic wave excitation in ionized plasma
23 p2822 N73-32559
ACOUSTIC FATIGUE
Development of aerodynamic structural design data to reduce effects of acoustic fatigue on flat and singly-curved sandwich panels - Part 2
[AGARD-AG-162-PT-2] 05 p0602 N73-14898
Fatigue tests of aluminum alloy specimens used for aircraft structures under simulated acoustic loading conditions
[ESDU-72015] 06 p0723 N73-15899
Numerical analysis of stress in face plates of sandwich panel structures subjected to random acoustic loading
[ESDU-72017] 06 p0723 N73-15900
Noise effects on hearing conservation in aircrew and ground support personnel of aerospace operations
08 p0876 N73-17101
Acoustic fatigue characteristics of flat multi-layered structural panel
[NASA-CR-124079] 13 p1546 N73-22529
Proceedings of conference on acoustic fatigue to show effects of aerodynamic loads, response of structures, structural design, and fatigue test methods
[AGARD-CP-113] 20 p2478 N73-29905
Address on problems of acoustic fatigue
20 p2478 N73-29906
Analysis of response and fatigue characteristics of light alloy integrally machined planks with emphasis on acoustic fatigue properties
20 p2479 N73-29912
Methods for determining aircraft structural response to acoustic fatigue
20 p2479 N73-29913
Analysis of structural response to acoustic loading and preparation of data sheets for various conditions of acoustic loads
20 p2479 N73-29914
Development of method for determining response of box type structures subjected to high intensity acoustic loading
20 p2479 N73-29915
Analysis of intake duct noise of turbofan engine and effect on duct structure due to acoustic fatigue
20 p2479 N73-29916
Analysis of effect of damping on response of structure to acoustic excitation and experimental method for determining damping coefficients
20 p2479 N73-29917
Analysis of programs for acoustic testing of composite material components and development of theory for predicting natual frequencies, mode shapes, and stresses in composite panels
20 p2480 N73-29918
Sonic fatigue characteristics of titanium sandwich structures and numerical analysis of natural frequencies and static stress values
20 p2480 N73-29919
Structural response and endurance tests of aircraft structural components to determine effect of critical environment on acoustic fatigue
20 p2480 N73-29920
Acoustic fatigue tests of aluminum alloy structural elements under narrow-band, random loading with zero mean stress in skin
20 p2480 N73-29921
Application of siren as test technique for determining response and life of aircraft structures subject to engine noise field excitation
20 p2480 N73-29922
Development of experimental program for determining response and sonic fatigue resistance of lightweight aircraft structures
20 p2480 N73-29923
ACOUSTIC GENERATORS
U SOUND GENERATORS
ACOUSTIC IMPEDANCE
Microwave acoustic signal processing with time-variant distributed networks using surface amplifiers
07 p0820 N73-16649
Development of long acoustic damping device for various chamber flow conditions based on nonlinearity of orifice flow upon passage of high intensity wave
15 p1765 N73-24299
Computer program for calculating acoustic impedance of submerged vibrating structure
[AD-762007] 19 p2322 N73-28680
Acoustic pumping used to achieve analogous ac Josephson effect in He2
20 p2385 N73-29164
Development of model for analyzing pressure excitation spectrum and acoustic impedance of sound absorbers in presence of grazing flow
[NASA-TM-X-71418] 21 p2523 N73-30231
ACOUSTIC INSTABILITY
Ion acoustic instability in helium positive column
[AD-745399] 01 p0086 N73-10709

Solid propellant flame as source of amplification for acoustic pressure waves
[AD-746616] 03 p0365 N73-12971
Acoustic combustion instability of solid propellants in radial burner
[AD-755826] 13 p1592 N73-22904
Nonsteady combustion and extinguishment tests to determine acoustic instabilities of solid rocket propellants during combustion
[AD-760788] 18 p2207 N73-27813

ACOUSTIC MEASUREMENTS
Jet aircraft noise of XV-5B V/STOL aircraft as determined by full scale flight test and wind tunnel model tests
[NASA-TM-X-62182] 01 p0004 N73-10029
Noise abatement and measurement, and human response to noise
[PB-210591] 01 p0081 N73-10671
Procedures for determining present and predicted noise exposure at residential construction sites
[PB-210590] 01 p0081 N73-10672
Facility monitoring of stress wave emission as nondestructive testing method
[AD-745729] 01 p0114 N73-10945
Acoustic noise, transmission loss, and reverberation measurements in West Greenland Sea
[AD-746839] 02 p0169 N73-11373
Measurement of axial velocity profiles and resulting acoustical fields of rod under continuous-wave excitation
[AD-747209] 02 p0239 N73-11945
Calculation of acoustic field generated by circular jet in presence of low speed crossflow
[NASA-CR-2169] 03 p0252 N73-12036
Far field noise measurements to determine effects of flow distortion for three different installations on noise from fan designed for turbofan engines
[NASA-TN-D-7076] 03 p0280 N73-12269
Acoustic measurements of aerodynamic noise generated by air jet impinging on large flat board for variable impingement angles, jet velocities, and distances from board
[NASA-TN-D-7075] 04 p0372 N73-13026
Measurement of sound generated by impingement of turbulent jet on elastic plates
[DGLR-PAPER-72-85] 04 p0373 N73-13032
Instrumentation and methods used with acoustic studio scale model
[BBC-1972/34] 04 p0419 N73-13413
Development of remote sensing devices to measure jet exhaust fluctuating density gradients, mean and turbulent velocity, and mean temperature Vol. 6
[AD-749143] 05 p0496 N73-14041
Data analysis on reflected oblique soundings of ionosphere using short pulses
[AD-749766] 05 p0543 N73-14417
Test results of acoustic ranging and bearing measuring system
[AD-749041] 05 p0578 N73-14703
Acoustic signal recorders and electroacoustic measurements in liquids
[JPRS-57778] 05 p0580 N73-14720
Analysis of jet noise produced by supersonic transport aircraft with augmentor wing and four duct burning turbofan engines
[NASA-TM-X-68177] 06 p0619 N73-15028
Screening tests of upper surface blowing on externally blown flaps configurations to obtain noise and turning effectiveness data
[NASA-TM-X-68167] 06 p0620 N73-15030
Analysis of jet aircraft noise propagation near airports and methods for reducing noise intensity
[NASA-TT-F-14655] 06 p0700 N73-15707
Effect of sound absorbing exhaust duct on rear quadrant noise of J-65 engine and contributions of internal and jet components
[NASA-TM-X-2718] 07 p0739 N73-16011
Measurement of noise levels produced by Boeing 737 aircraft and correlation with local meteorological parameters including wind force and direction, temperature, and atmospheric pressure
[FAA-RD-72-145] 07 p0821 N73-16651
Development of theory of aerodynamic noise to analyze jet noise directivity and shear-noise contribution to overall jet noise
[NASA-TN-D-7158] 07 p0821 N73-16654
Performance characteristics of solid state converter system for measuring aircraft noise and sonic boom
[NASA-CR-112260] 09 p0982 N73-18019
Measurement of noise levels produced by F-105 aircraft and analysis of effects on environment and land use
[AD-753113] 09 p0987 N73-18056
Application of sound suppression techniques to OH-6 helicopter and measurement of resultant noise reduction
[AD-753646] 09 p0989 N73-18077
Measurement of indoor and outdoor sound pressure levels at airport control towers during aircraft takeoff and landing
[AD-752535] 09 p1012 N73-18262
Evaluation of aircraft noise pollution level as a predictor of annoyance
[NASA-CR-130920] 09 p1100 N73-18978
Analysis of aircraft noise environment for land areas in vicinity of military air bases
[AD-754111] 10 p1107 N73-19028
Analysis of hydrodynamics of helium isotopes to determine entrainment of sound in moving fluid
10 p1139 N73-19278
Noise measurements and frequency analysis for noise pollution control
[TR-7209.602] 10 p1164 N73-19473
Flow and acoustic characteristics determined for subsonic and supersonic jets and supersonic suppressors
[NASA-CR-131297] 11 p1233 N73-20006
Analysis of noise sources in jet aircraft based on measurement of infrared emission
[NASA-TT-F-14851] 11 p1234 N73-20020
Evaluation of acoustic properties of conventional wind tunnels for analyzing aerodynamically generated noise
[NASA-CR-114575] 11 p1266 N73-20277
Acoustic emission correlation with slow crack growth in polycrystalline ceramics
[AD-754839] 11 p1310 N73-20626
Acoustic measurement methods for evaluating aircraft noise pollution in urban areas
[PB-212875] 11 p1326 N73-20757
Analysis of acoustic properties of jet engine malfunction as means for detecting jet engine burnthrough - Vol. I
[FAA-RD-72-149-VOL-1] 11 p1334 N73-20825
Noise spectrum characteristics and directivity patterns for rotary wings as function of blade tip speed, total rotor thrust, and angle of rotor disc plane
12 p1362 N73-21056
Acoustic measurements of aerodynamic noise generated by externally blown flap lift augmentation system for various aerodynamic configurations
[NASA-TM-X-2776] 12 p1363 N73-21059
Development of system for analyzing aircraft sound levels for areas in vicinity of airports
[FAA-EQ-73-3] 12 p1364 N73-21064
Analysis of common aircraft noise measures in terms of selected human response for jet transport aircraft
[FAA-RD-71-112] 12 p1365 N73-21074
Measurement and analysis of aircraft noise generated by general aviation aircraft during level flyovers
[TR-S-212] 12 p1366 N73-21081
Analysis of transition region of subsonic turbulent jets to determine noise producing potential based on far field acoustic density
[NASA-TN-D-7242] 12 p1428 N73-21573
Calculation of polymer elastic constants using sound speed measurements
[AD-755695] 12 p1429 N73-21586
Analysis of underwater sound signals to show coherence, noise level, and reverberation between vertically separated hydrophones
[AD-755696] 12 p1430 N73-21591
Acoustic measurements of sound pressure levels due to cross flow over face of lift fans on fan-in-wing and V/STOL model transport aircraft
[NASA-CR-114566] 13 p1473 N73-21928
Wind tunnel tests to determine effect of cross flow velocity on jet noise power level using V/STOL model transport
[NASA-CR-114571] 13 p1473 N73-21929
Development of jet noise test facility for flow and acoustic measurements of mean and turbulent velocities in jet flow
[RE-450] 13 p1505 N73-22196
Analysis of effects of aircraft noise in residential communities near London, England airport
[TT-7302] 14 p1599 N73-22966
Analysis of aerodynamic noise produced by rotor operating at supersonic speed
[TT-7213] 14 p1599 N73-22967
Acoustic and physiological investigation of speaker variabilities relative to speech wave parameters
14 p1623 N73-23150
Fundamental acoustic models for synthesis of speech operating on articulatory parameters
14 p1623 N73-23151
Acoustic theory of speech production for definition of terminal analog speech synthesizer configuration using digital signal processing techniques
14 p1623 N73-23152
Model of speech production mechanism based on anatomical structures and physiological natures of articulatory organs
14 p1624 N73-23153
Measurement of monosyllabic speech communication using adaptive methodology
14 p1625 N73-23165
Role of distinctive features in speech production, acoustics, and phonetics
14 p1625 N73-23167
Relation of phonemes to acoustic signals from human vocal tracts as represented by ultrahigh frequency patterns
14 p1631 N73-23218
Porous surface microphones for acoustic measurements in subsonic flow in wind tunnels
[NASA-CR-114593] 14 p1639 N73-23289
Role of microstructure on acoustic emission in deformation of Al-CuAl2 composites
[AD-758378] 14 p1679 N73-23628
Acoustic measurements for large model engine-over-wing configurations with conventional and powered lift, various flap settings, and comparison with engine-under-wing aircraft
[NASA-TM-X-68246] 15 p1735 N73-24070
Analysis of relative intensity profiles of density fluctuations based on acoustic properties of subsonic and supersonic unheated jet flow
[NASA-CR-124563] 16 p1861 N73-25073
Time domain acoustic signal processor for automatic pattern recognition and target discrimination
[AD-757538] 16 p1876 N73-25190
Measured noise level data for proposed airport sites in Florida
[PB-214459/0] 16 p1945 N73-25737
Combination of noise from separate time varying sources
[PB-214250/3] 16 p1945 N73-25738
Analysis of reverberant-field noise produced by three lift fan models operating at various rotor tip speeds
[NASA-TM-X-68243] 17 p1981 N73-26014
Analysis of acoustic factors involved in wind tunnel tests to show contributions from various sources
17 p2009 N73-26247
Wind tunnel tests to determine acoustic properties of helicopter rotor and wind tunnel calibration techniques
[RAE-LIB-TRANS-1683] 17 p2009 N73-26249
Measurement of noise and wake structure of ducted fan with subsonic tip speed to show sound pressure levels and blade wake characteristics
[NASA-CR-132259] 18 p2129 N73-27207
Application of cross-spectral analysis to measurement of contribution of noise sources
[ISAS-493] 18 p2179 N73-27591
Analysis of supersonic jet aircraft noise using fluctuating jet pressures to characterize the sources
[AD-762296] 19 p2222 N73-27923
Measurement of acoustic absorption coefficient of Bidin
[TR-7302.626] 19 p2321 N73-28669
Development of noise standard for permissible noise levels in air traffic control and navigational facilities
[FAA-RD-72-47] 20 p2452 N73-29708
Analysis of fan noise levels for fan in proximity of side and ground plane to determine effects on harmonic frequencies
[NASA-CR-132306] 21 p2495 N73-30023
Measurements of aerodynamic noise produced by modified and standard OH-6A helicopter configurations to determine noise reduction effectiveness
[NASA-TN-D-7216] 21 p2496 N73-30031
Noise standards for habitable houses, rest homes, hospitals, camps, public facilities, and streets in residential areas
[NASA-TT-F-15065] 21 p2503 N73-30088
Development of model for analyzing pressure excitation spectrum and acoustic impedance of sound absorbers in presence of grazing flow
[NASA-TM-X-71418] 21 p2523 N73-30231
Analysis of fluctuating density with high temperature subsonic jet and characteristics of noise radiated to surroundings
[NASA-CR-133789] 21 p2524 N73-30241
Procedures for the measurement and evaluation of noise, noise reduction and control, and current data on noise analysis and control
[EA-7301] 21 p2579 N73-30664
Aero and acoustic design features of single stage fans tested in outdoor acoustic facility
[NASA-TM-X-68289] 21 p2579 N73-30668
Analysis of sound propagation in elliptic ducts to determine acoustic effects produced by variations from symmetry in circular ducts
[NASA-CR-132307] 21 p2579 N73-30672
Analysis of aircraft engine noise sources and characteristics of engine noise produced by turbofan engines
21 p2588 N73-30735
Aerodynamic noise and flow field characteristics of internal flow, jet augmented flap configurations
22 p2612 N73-30937
Reduction of aircraft noise by installing acoustically absorbent material
[NASA-CR-2261] 22 p2613 N73-30941
Calculation procedures for predicting noise-time histories and noise contours for various types of aircraft
[NASA-CR-114649] 23 p2741 N73-31945
Computer programs for predicting the noise-time histories and noise contours for five types of aircraft
[NASA-CR-114650] 23 p2741 N73-31946
Onboard frequency analyzer for measurement and analysis of acoustic and vibration data
[NASA-CR-132305] 23 p2793 N73-32343
Acoustic measurements of aerodynamic noise produced by impingement of jet exhaust on wing and flap of externally blown flap system installed on F-111 aircraft
24 p2875 N73-32964

Aerodynamic noise characteristics of short takeoff aircraft with externally blown flaps and engines mounted over and under wing
24 p2876 N73-32966
Forward velocity effects on jet noise with dominant internal noise source
[NASA-TM-X-71438] 24 p2876 N73-32968
Method for predicting noise generated by deflecting engine exhaust for under-the-wing and over-the-wing versions of externally blown flap configuration
[NASA-TM-X-71449] 24 p2876 N73-32969
Subsonic jet noise measurements by means of directional microphone system
24 p2956 N73-33612

**ACOUSTIC PROPAGATION**
Hydrophone measurement of acoustic propagation and CW signals from underwater explosions in shallow Bering Sea
[AD-745735] 01 p0081 N73-10667
Approximate solution to covariance of plane wave direction and propagation velocity of signals in array processing scheme
[AD-747591] 03 p0267 N73-12160
Method for statistical estimation of magnitude of acoustic power radiated from fluid loaded cylindrical shells
[AD-749361] 05 p0603 N73-14906
Acoustic emission and discontinuous yielding of dead weight in Portevin-Le Chatelier effect
[COO-2204-1] 10 p1190 N73-19680
Optimization of microphone propagation in television studio
[BBC-RD-1973/3] 15 p1749 N73-24173
Fabrication and characterization of monolithic acoustic surface wave amplifiers
15 p1755 N73-24229
Computerized acoustic imaging technique with automatic pattern recognition
[AD-761497] 19 p2240 N73-28060
Application of acoustic transducers for suspending object at center of chamber under near weightless conditions
[NASA-CASE-NPO-13263-1] 22 p2677 N73-31443

**ACOUSTIC PROPERTIES**
NT ACOUSTIC IMPEDANCE
NT ACOUSTIC INSTABILITY
NT ACOUSTIC SCATTERING
NT ACOUSTIC VELOCITY
NT REVERBERATION
NT SOUND INTENSITY
Ground based UH-1 helicopter sonic analyzer for evaluation of effectiveness of using sonic data to diagnose mechanical condition of army helicopter power train components
[AD-745089] 01 p0004 N73-10026
Acoustic emission and crack propagation in single crystal MgO and glass as model ceramic materials
[AD-745000] 01 p0070 N73-10575
Sound wave reflection from sea bed, acoustic properties of sedimentary layer, and application to Baltic Sea
[FOA-3-C-3680-E1] 02 p0164 N73-11331
Effect of external air flowing across exhaust nozzles on jet noise produced by supersonic transport aircraft at high takeoff speeds
[NASA-TM-X-68161] 03 p0250 N73-12027
Research project to analyze and evaluate supersonic jet noise generation and radiation - Vol. 1
[AD-749428] 05 p0495 N73-14035
Definition of supersonic aircraft jet noise generation and methods for reducing noise intensity - Vol. 2
[AD-749137] 05 p0495 N73-14036
Development of unified theory of jet engine noise based on fluctuating motions in fluids - Vol. 3
[AD-749138] 05 p0496 N73-14037
Development of theory for jet noise generated by turbulence, noise radiation from upstream sources, and combustion noise - Vol. 4
[AD-749139] 05 p0496 N73-14038
Analysis of noise sources associated with supersonic jet noise and establishment of effects of refraction on radiated field of sources - Vol. 5 App. 1
[AD-749141] 05 p0496 N73-14039
Analysis of acoustic properties of shock associated noise in narrow band spectrum produced by jet flows - Vol. 5 App. 2
[AD-749142] 05 p0496 N73-14040
Acoustic properties of supersonic jet noise and refraction effects on noise field
[AD-749140] 05 p0581 N73-14728
Acoustic properties of air and sound absorption anomalies due to molecular relaxation
[AD-750220] 05 p0581 N73-14732
Acoustic properties of supersonic fan
[NASA-TN-D-7096] 06 p0619 N73-15025
Properties of amorphous semiconductors
[AD-750163] 06 p0710 N73-15797
Effect of sound absorbing exhaust duct on rear quadrant noise of J-65 engine and contributions of internal and jet components
[NASA-TM-X-2718] 07 p0739 N73-16011
Performance of scanning acoustical imaging telescope at microwave frequencies
07 p0820 N73-16648
Acoustic properties of sound emitted from arbitrary point in parallel or nearly parallel turbulent shear flow confined to region near solid boundaries
[NASA-TN-D-7118] 07 p0821 N73-16653
Development of theory of aerodynamic noise to analyze jet noise directivity and shear-noise contribution to overall jet noise
[NASA-TN-D-7158] 07 p0821 N73-16654
Effect of various physical and operating parameters on noise produced by low pressure ratio propulsive fans operating at subsonic speeds
[NASA-CR-2188] 09 p0980 N73-18011
Wind tunnel tests to determine acoustic properties of semispan wing with externally blown jet flap to include effects of flap size, vertical location and forward speed
[NASA-TM-X-2749] 09 p0985 N73-18041
Acoustic properties of ocean bottom and relevance to sonar performance
[AD-753265] 09 p1032 N73-18429
Analysis of hydrodynamics of helium isotopes to determine entrainment of sound in moving fluid
10 p1139 N73-19278
Acoustic properties and sound pressure of jet flow
[AD-754422] 10 p1144 N73-19321
Evaluation of acoustic properties of conventional wind tunnels for analyzing aerodynamically generated noise
[NASA-CR-114575] 11 p1266 N73-20277
Vibration and acoustic tests for spacecraft electronic equipment design
[NASA-TN-D-7159] 11 p1345 N73-20914
Generation of aerodynamic noise by turbulent wake behind rotary wing airfoil and relationship to drag and lift coefficients
12 p1362 N73-21054
Analysis of helicopter internal and external noise levels for various flight conditions and timing of acoustical spectra
12 p1362 N73-21055
Noise spectrum characteristics and directivity patterns for rotary wings as function of blade tip speed, total rotor thrust, and angle of rotor disc plane
12 p1362 N73-21056
Development of system for analyzing aircraft sound levels for areas in vicinity of airports
[FAA-EQ-73-3] 12 p1364 N73-21064
Analysis of common aircraft noise measures in terms of selected human response for jet transport aircraft
[FAA-RD-71-112] 12 p1365 N73-21074
Acoustic emission signals by fcc phase transition to fct in In-Ti alloys
[SC-DC-72-1650] 12 p1414 N73-21462
Analysis of transition region of subsonic turbulent jets to determine noise producing potential based on far field acoustic density
[NASA-TN-D-7242] 12 p1428 N73-21573
Analysis of underwater sound signals to show coherence, noise level, and reverberation between vertically separated hydrophones
[AD-755696] 12 p1430 N73-21591
Fundamentals of helicopter noise generation and propagation to include noise control procedures and cost effectiveness of noise reduction
14 p1598 N73-22953
Analysis of aerodynamic noise produced by rotor operating at supersonic speed
[TT-7213] 14 p1599 N73-22967
Acoustic feedback of subsonic and supersonic jet impinging on obstacle
[DLR-FB-72-72] 14 p1602 N73-22987
Analysis of vortex shedding from airfoils with application to vortex noise generated by helicopter rotary wings
[AD-757167] 14 p1602 N73-22989
Electroacoustic effects of speech communication circuits on speech intelligibility
[AD-757326] 14 p1633 N73-23236
Computer program for analyzing piezoelectric transducer acoustic surface wave device
[AD-757485] 14 p1642 N73-23320
Acoustic surface wave convolution in piezoelectric crystals with determination of magnitudes of nonlinear coupling constants
[AD-757441] 14 p1682 N73-23648
Quantitative data on propagation and directivity of parametric array in air
[AD-757034] 14 p1693 N73-23737
Acoustic measurements for large model engine-over-wing configurations with conventional and powered lift, various flap settings, and comparison with engine-under-wing aircraft
[NASA-TM-X-68246] 15 p1735 N73-24070
Development of long acoustic damping device for various chamber flow conditions based on nonlinearity of orifice flow upon passage of high intensity wave
15 p1765 N73-24299
Analysis of relative intensity profiles of density fluctuations based on acoustic properties of subsonic and supersonic unheated jet flow
[NASA-CR-124563] 16 p1861 N73-25073
Effects of free stream velocity and incidence angle on aerodynamic and acoustic performance of translating centerbody choked flow inlet
[NASA-TM-X-2773] 16 p1957 N73-25829
Analysis of combustion instability in solid propellant rocket engines and characteristics of acoustic waves in T-burner geometry
16 p1973 N73-25958
Wind tunnel tests to determine acoustic properties of jet augmented lifting flap configuration
[NASA-TT-F-14951] 17 p1983 N73-26030
Analysis of acoustic factors involved in wind tunnel tests to show contributions from various sources
17 p2009 N73-26247
Wind tunnel tests to determine acoustic properties of helicopter rotor and wind tunnel calibration techniques
[RAE-LIB-TRANS-1683] 17 p2009 N73-26249
Measurement of noise and wake structure of ducted fan with subsonic tip speed to show sound pressure levels and blade wake characteristics
[NASA-CR-132259] 18 p2129 N73-27207
Acoustical transducer calibrating system including differential pressure activating device
[NASA-CASE-FRC-10060-1] 18 p2150 N73-27379
Acoustic measurement and recording system for noise generated by air bag automobile safety device
[AD-761836] 19 p2229 N73-27977
Program summary of research project for sonic inlet technology involving design concepts for aerodynamic performance and noise suppression - Vol. 1
[NASA-CR-121126] 19 p2328 N73-28731
Spin energy transfer processes at low temperatures
[AD-762618] 20 p2455 N73-29731
Analysis of acoustic and fluctuating pressure environments for complete flight envelope of space shuttle
[NASA-CR-124347] 20 p2475 N73-29885
Development of statistical methods for determining vibration and acoustic radiation of fluid loaded cylindrical shells
20 p2477 N73-29895
Development of method for calculating near field noise level of free jet and influence of ground effect on noise produced by V/STOL aircraft operation
20 p2478 N73-29907
Application of siren as test technique for determining response and life of aircraft structures subject to engine noise field excitation
20 p2480 N73-29922
Analysis of discrete frequency and broad band noise generation by subsonic rotary wings for vertical takeoff aircraft
[NASA-CR-2077] 21 p2494 N73-30014
Analysis of acoustic properties and aerodynamic characteristics of engine over wing configuration with flow attached and unattached on upper surface of flaps
[NASA-TM-X-71419] 21 p2494 N73-30015
Analysis of fan noise levels for fan in proximity of side and ground plane to determine effects on harmonic frequencies
[NASA-CR-132306] 21 p2495 N73-30023
Analysis of noise problems created by supersonic transport aircraft, conventional aircraft, and short takeoff aircraft to show methods for jet exhaust noise reduction
21 p2495 N73-30024
Development of computer programs to analyze sound power and peak noise levels for turbojet exhaust noise at various velocities
21 p2496 N73-30029
Analysis of fluctuating density with high temperature subsonic jet and characteristics of noise radiated to surroundings
[NASA-CR-133789] 21 p2524 N73-30241
Analysis of sound propagation in elliptic ducts to determine acoustic effects produced by variations from symmetry in circular ducts
[NASA-CR-132307] 21 p2579 N73-30672
Analysis of aircraft engine noise sources and characteristics of engine noise produced by turbofan engines
21 p2588 N73-30735
Evaluation of acoustic radiation from various noise sources in axial fan
[NASA-CR-114576] 22 p2614 N73-30952
Capabilities of surface wave devices as signal processors for spread spectrum communications systems
[AD-763881] 22 p2645 N73-31197
Evaluation of aerodynamic calibration and performance characteristics of anechoic flow facility
[AD-763668] 22 p2647 N73-31212
Far field noise reduction of tilting rotor aircraft based on performance and weight tradeoffs to improve acoustic signatures
[NASA-CR-114648] 23 p2740 N73-31937
Theory for predicting sonic boom intensity and techniques for sonic boom suppression
[FAA-RD-73-4] 23 p2741 N73-31944
Calculation procedures for predicting noise-time histories and noise contours for various types of aircraft
[NASA-CR-114649] 23 p2741 N73-31945

Computer programs for predicting the noise-time histories and noise contours for five types of aircraft
[NASA-CR-114650] 23 p2741 N73-31946
Analysis of jet engine noise to show sources of noise, noise spectra, and use of laminates and composite materials for noise reduction
24 p2875 N73-32962
Characteristics of aerodynamic noise generated by interaction of airstream with flap surface to show location and control of noise sources
24 p2875 N73-32963
Wind tunnel tests to determine acoustic properties of externally blown flap and augmentor wing for short takeoff aircraft configurations
24 p2875 N73-32965
Method for predicting noise generated by deflecting engine exhaust for under-the-wing and over-the-wing versions of externally blown flap configuration
[NASA-TM-X-71449] 24 p2876 N73-32969
Wind tunnel tests to determine acoustic properties of large scale lift fan transport aircraft model
[NASA-TM-X-62284] 24 p2877 N73-32975
Relationship between distribution of outflow of acoustic energy over jet boundary and far-field intensity
[NASA-TN-D-7269] 24 p2905 N73-33181
Theory of electroacoustical images and relationship between geometric form of horn and sound antennas based on acoustic properties
24 p2956 N73-33617

**ACOUSTIC RADIATION**
U SOUND WAVES
**ACOUSTIC SCATTERING**
NT REVERBERATION
Algorithm for underwater echo signals from elastic spherical shell subjected to incident pulse
[AD-746229] 01 p0082 N73-10676
Survey of methods to obtain electromagnetic and acoustic high frequency scattering
[AD-747044] 02 p0143 N73-11158
Acoustic radar scattering in lower atmosphere for measuring wind velocity and direction
02 p0197 N73-11592
Partial wave analysis solutions for acoustic scattering patterns and target recognition in antisubmarine warfare
[AD-750754] 06 p0700 N73-15710
Low frequency underwater sound surface-scattering experiments in Pacific
[AD-752065] 08 p0945 N73-17739
Mathematical model to predict scattering of plane acoustic wave from elastic spherical shell with different fluid media inside and out
[AD-752760] 09 p1067 N73-18708
Stimulated and spontaneous scattering of electromagnetic radiation
[AD-757082] 13 p1559 N73-22639
Analysis of acoustic volume scattering in Bermuda Ocean to show daily variability and diurnal variations
[AD-761976] 19 p2296 N73-28465
Solution of acoustic and electromagnetic scattering problems in exterior domains using integral equations
[NPL-NAC-30] 19 p2314 N73-28608
Underwater scattering of sound waves by submerged viscoelastic cylindrical shell
[AD-761618] 19 p2321 N73-28674
Stimulated Brillouin scattering in shock-compressed fluids
20 p2386 N73-29166
Application of mathematical techniques to problems of interaction of acoustic or electromagnetic waves with complex bodies
[AD-762802] 21 p2581 N73-30685

**ACOUSTIC STABILITY**
U FREQUENCY STABILITY
**ACOUSTIC STREAMING**
Theoretical analysis of ballistic H powder erosion combustion in acoustic stream
14 p1700 N73-23796
Sound beams for position control during manufacturing in space
[NASA-CR-124300] 19 p2321 N73-28671
**ACOUSTIC VELOCITY**
Sound speed and other thermodynamic quantities of dilute aqueous electrolyte solutions by ultrasonic velocimeter comparison technique
[AD-745843] 01 p0081 N73-10669
Elastic properties determination of crystals by sound velocity measurements
[AD-745859] 01 p0089 N73-10733
Acoustic measurements and sound velocity calculations for molten rubidium at high pressures
[AD-746838] 02 p0138 N73-11120
Frequency and line width of Brillouin scattering in aqueous electrolyte solutions
[AD-749354] 04 p0387 N73-13148
Interaction between acoustic velocities and solid propellant combustion with variations in frequency of oscillation, mean pressure, and propellant formulation
[AD-750142] 06 p0712 N73-15809
Prevention of spurious caustics in ray tracing scheme for sound propagation mapping in sea water
[AD-752080] 08 p0944 N73-17735
Sound speed modulation by bubbles in upper ocean
[AD-754372] 11 p1325 N73-20754
High resolution Brillouin spectroscopic study of hypersonic sound velocity and attenuation as function of temperature in acrylic monomers
16 p1944 N73-25731
Calculating acoustic source distributions in turbulent flows when average velocity distribution is known
[NASA-TT-F-14946] 17 p2063 N73-26689
Thermodynamic state of thin helium films for precise measurements of third sound velocity and attenuation
24 p2968 N73-33720

**ACOUSTIC VIBRATIONS**
U SOUND WAVES
**ACOUSTICS**
NT BIOACOUSTICS
NT MICROSONICS
NT PSYCHOACOUSTICS
NT UNDERWATER ACOUSTICS
Dependence of timbre on location in diffuse sound fields
[IZF-1972-15] 02 p0211 N73-11711
Techniques for generation and processing microwave signals using elastic, electromagnetic and carrier space charge waves in solid media
[AD-747047] 02 p0220 N73-11782
Conference proceedings of British Acoustical Society, 1972
[AD-747615] 03 p0338 N73-12756
International conference on acoustical holography
[AD-749337] 04 p0430 N73-13505
Microwave acoustic signal processing with time-variant distributed networks using surface amplifiers
07 p0820 N73-16649
Acoustic combustion instability in solid propellant rockets
[AD-752205] 08 p0970 N73-17926
Hydrodynamic equations of motion for studying sound interaction in transient chemical reactions
[AD-753798] 10 p1191 N73-19628
Acoustic surface wave matched filters
[AD-754283] 11 p1262 N73-20245
Multidimensional representation of personal quality of vowels and their acoustical correlates
14 p1631 N73-23217
Adaptation of Acoustic Research Tank Facility for parametric sonar experiments
[AD-756176] 14 p1634 N73-23249
Measurements and techniques of low temperature acoustic thermometry
[NBS-TN-765] 14 p1666 N73-23518
N wave focusing on principal axis of spherical mirror
[AD-757035] 14 p1692 N73-23736
Acoustic emission from ferrous martensites as function of thermomechanical history
[AD-761220] 18 p2163 N73-27472
Equations for determining pressure profile, forces, and torques on disk pendulum by point source wave theory from acoustics
[NASA-TM-X-69569] 20 p2454 N73-29725

**ACOUSTO-OPTICS**
Acoustic-optical imaging techniques for detecting bubble formation in circulatory system during decompression
[AD-749087] 04 p0424 N73-13457
Electronically tunable acousto-optical filter for laser applications
[AD-752052] 08 p0944 N73-17733
Holographic memory system using argon ion lasers and acoustooptic beam deflectors
[NASA-CR-124084] 09 p1064 N73-18680
Acousto-optic interactions in guided wave structure for optical modulation, deflection and signal processing
[AD-758719] 15 p1752 N73-24198
Acousto-optical isolator for suppressing optical feedback generated laser instabilities
[AD-757914] 15 p1796 N73-24556
Nondestructive test equipment using acousto-optical imaging techniques
[AD-760554] 18 p2152 N73-27397
Acousto-optical delay line for UHF pulses with continuously variable delay, based on photon-phonon interaction
18 p2179 N73-27597

**ACQUISITION**
NT DATA ACQUISITION
NT TARGET ACQUISITION
Design and operation of Aeros satellite attitude control system during acquisition phase
[DGLR-PAPER-72-62] 06 p0721 N73-15885
**ACRYLIC RESINS**
Effect of temperature and flange configurations on critical pressure of 90-degree conical acrylic windows for hydrostatic pressure vessels when subjected to short term loading
[AD-748583] 04 p0440 N73-13583
Free-formed, flanged, acrylic shells for service as external pressure hulls with nominal 36-ft depth
[AD-749029] 05 p0603 N73-14908
Application of correlation equations to evaluate structural strength and reliability of various materials
[AD-753497] 09 p1097 N73-18956
Cyclic pressure tests of F-4 aircraft forward and aft canopies to determine safe service life after delamination of acrylic sheet
[AD-759349] 16 p1862 N73-25084
High resolution Brillouin spectroscopic study of hypersonic sound velocity and attenuation as function of temperature in acrylic monomers
16 p1944 N73-25731
Development of organic glass and plastic materials with improved mechanical and physical properties for use with aircraft canopies and protective coatings
[AD-763263] 21 p2497 N73-30039
**ACRYLONITRILES**
Production of carbon fibers from polyacrylonitrile
[AD-750362] 06 p0688 N73-15604
Evaluation of stabilized precursors for high strength carbon fibers
[AD-755427] 13 p1547 N73-22540
Mass thermal analysis of chemical reactions in conversion of polyacrylonitrile fibers to high modulus, high strength carbon fibers - Vol. 2
[AD-755350] 13 p1549 N73-22549
Polyacrylonitrile precurser fibers for conversion to high modulus, high strength fibers using X ray diffraction analysis
[AD-755351] 13 p1549 N73-22550
**ACTH**
U ADRENOCORTICOTROPIN [ACTH]
**ACTINIDE SERIES**
NT CALIFORNIUM ISOTOPES
NT CURIUM 244
NT NEPTUNIUM
NT PLUTONIUM
NT PLUTONIUM 238
NT RADIUM 226
NT TRANSURANIUM ELEMENTS
NT URANIUM
NT URANIUM 233
**ACTINIDE SERIES COMPOUNDS**
NT PLUTONIUM OXIDES
NT THORIUM COMPOUNDS
NT THORIUM OXIDES
NT URANIUM CARBIDES
NT URANIUM COMPOUNDS
NT URANIUM FLUORIDES
NT URANIUM OXIDES
Optical and magnetic properties of actinide and rare earth ions in insulators and semiconductors
[RLO-2221-T-6-14] 03 p0345 N73-12815
Optimal molecular composition of zirconium phosphate ion exchanger for separation of radioactive actinide series elements
08 p0883 N73-17151
Space disposal of actinide radioactive wastes
[NASA-TM-X-68216] 12 p1426 N73-21562
**ACTINOGRAPHS**
U ACTINOMETERS
**ACTINOMETERS**
NT INFRARED DETECTORS
NT INFRARED SCANNERS
NT INFRARED SPECTROMETERS
NT INFRARED SPECTROPHOTOMETERS
NT MICROWAVE RADIOMETERS
NT PYRANOMETERS
NT RADIOMETERS
NT SOLAR SPECTROMETERS
NT SPECTROHELIOGRAPHS
NT SPECTROPHOTOMETERS
NT SPECTRORADIOMETERS
NT ULTRAVIOLET SPECTROMETERS
NT ULTRAVIOLET SPECTROPHOTOMETERS
Application of polyethylene materials as screens for actinometric instruments to include analysis of physical, mechanical, and optical properties
[NLL-M-22675-(5828.4F)] 01 p0069 N73-10566
Actinometric equipment on Soviet meteorological satellites for thermal radiation measurements of earth atmosphere
[AD-749622] 04 p0479 N73-13920
High resolution film actinometric measurements of ultraviolet irradiation levels during space flight
15 p1741 N73-24112
Potassium ferrioxalate actinometric measurements of solar ultraviolet photobiological energy
15 p1741 N73-24113
Application of airborne actinometric measurements to determine transmission, absorption, and reflection of solar radiation by clouds
20 p2401 N73-29292
Development of actinometric instruments and surface coatings to show performance parameters and construction details
20 p2403 N73-29307
Meteorological, actinometric, and aerological investigations conducted aboard ships of Tenth Soviet Antarctic Expedition
20 p2406 N73-29341
**ACTIVATION [BIOLOGY]**
Factors influencing reactivation of phosphorylated acetylcholine esterase by oximes
[BMVG-FBWT-72-32] 10 p1121 N73-19137
**ACTIVATION ANALYSIS**
NT NEUTRON ACTIVATION ANALYSIS

Application of nuclear and X ray techniques for analysis of environmental pollution samples
[CONF-721002-1] 10 p1161 N73-19443
Annual report 1971-1972 of Interuniversitair Reactor Institute in Netherlands
10 p1195 N73-19721
Radioactive isotope measurements and neutron activation analyses for identifying contaminants in space environment simulator
[NASA-CR-128931] 15 p1815 N73-24709
Application of inorganic exchangers to radiochemical separations on neutron activated high purity materials
[CONF-721069-42] 17 p2050 N73-26584
Separation of short half life O-15 and N-13 isotopes from alkali metals, steels, copper, and indium by gamma activation analysis
[CONF-721069-24] 18 p2160 N73-27453
Photonuclear activation with Ge Li detectors
[AD-761992] 19 p2231 N73-27990

ACTIVATION ENERGY
Determination of activation parameters and microcreep in niobium single crystals at low temperature
[COO-1198-909] 04 p0458 N73-13742
Cellular activation energy effect in rat tolerance to acceleration stress
[AD-749338] 05 p0501 N73-14079

ACTIVE GLACIERS
U GLACIERS

ACTIVE VOLCANOES
U VOLCANOES

ACTIVITY [BIOLOGY]
Research in aerospace and biological sciences
[AD-740761] 01 p0121 N73-11000

ACTIVITY CYCLES [BIOLOGY]
Diurnal changes in human histamine and serotonin metabolism and effects of work-sleep cycle
03 p0258 N73-12089
Activity cycle data for spacecrews of Soyuz 3 to 9 spacecrafts before, during and after space flights
[JPRS-58173] 07 p0746 N73-16068

ACTUATOR DISKS
Evaluation of active and passive rupture disk designs for performance at cryogenic temperatures
[NASA-CR-121118] 14 p1670 N73-23554

ACTUATORS
Redundant hydraulic control system for actuators with three main valve combination
[NASA-CASE-MFS-20944] 04 p0425 N73-13466
Actuator operated by electrolytic drive gas generator and evacuator
[NASA-CASE-NPO-11369] 04 p0425 N73-13467
Manual actuator for exercise machine onboard spacecraft
[NASA-CASE-MFS-21481-1] 06 p0676 N73-15503
Design and performance tests of prototype self-locking actuator
[NASA-CR-124135] 10 p1163 N73-19459
Actuator shaft sealing techniques for long term interplanetary spacecraft missions
[NASA-CR-130927] 10 p1165 N73-19479
Design, development, and evaluation of servoactuator device to include application to optimized system configuration
[NASA-CR-124025] 11 p1297 N73-20524
Effects of sensor deadband and actuator breakout torque control system nonlinearities on performance of Apollo telescope mount pointing capability
[NASA-TN-D-7247] 15 p1834 N73-24868
Optical laser triggering of high voltage spark gap
[IPP-4/102] 17 p2040 N73-26504
Research and development of high performance satellite thermal control louver array actuator including single blade and multiple blade actuation system
[ESRO-CR[P]-247] 18 p2201 N73-27766
Optically actuated two position mechanical mover
[NASA-CASE-NPO-13105-1] 20 p2422 N73-29458
Single channel wheel system with electrohydraulic servoactuators for flight control feel system
22 p2731 N73-31855

ACUITY
NT VISUAL ACUITY

AD/I B
U EXPLORER 24 SATELLITE

AD/I SATELLITE
U EXPLORER 24 SATELLITE

ADAPTATION
NT ACCLIMATIZATION
NT ALTITUDE ACCLIMATIZATION
NT DARK ADAPTATION
NT LIGHT ADAPTATION
NT RETINAL ADAPTATION
Direction-specific adaptation effects acquired by humans in slowly rotating room
[NASA-CR-129063] 01 p0008 N73-10062
Mathematical models for studying vestibuli adaptation to stimuli in humans
[AMRU-R-70-1] 02 p0131 N73-11062
Physiological factors of human vestibular adaptation to flight and space environments
06 p0633 N73-15146
Hypoxia adaptation of rats for increased resistance to toxic atmospheric gases
10 p1116 N73-19100
Survival and reproduction of protozoa in simulated Mars environment
10 p1118 N73-19115
Adaptability and receptivity factors affecting motion sickness susceptibility in pilots
12 p1367 N73-21095
Physiological adjustments to environmental factors
[AD-753913] 13 p1487 N73-22059
Low temperature tolerance and adaptation of biological systems to space environment
[JPRS-59129] 14 p1610 N73-23055
Physiological and hemodynamic adaptations to CO levels and exercise in nonsmoking normal men
[PB-213834/1] 14 p1612 N73-23073
Handedness and adaptation to distortions of size and distance underwater
[AD-759722] 17 p1991 N73-26098
Role of respiratory enzymes on human adaptation to hypoxia
[NASA-TT-F-15058] 21 p2500 N73-30060
Psychoneurological problems in adaptation by man to modified diurnal regimes
24 p2884 N73-33031

ADAPTERS
Fabrication and testing of 22 sounding rockets using solid propellants
[AD-753089] 09 p1092 N73-18911

ADAPTIVE CONTROL
NT LEARNING MACHINES
NT SELF ADAPTIVE CONTROL SYSTEMS
Development of adaptive controller for multivariable systems and application to helicopter system with time varying parameters
[AD-746492] 01 p0002 N73-10007
Hybrid computer identification program for visual display of adaptive control state to human operator
01 p0014 N73-10109
Random Gaussian distribution for input noise approximation in human response tracker modeling
01 p0014 N73-10110
Synthesis of adaptive control tracking systems using Liapunov second method
[NASA-CR-129175] 02 p0150 N73-11220
Adaptive control of linear, noisy systems using two controllers
[AD-746679] 02 p0151 N73-11227
Adaptive Kalman filter approach for identifying submarine trajectory from hydrodynamic parameters
[AD-747515] 02 p0159 N73-11288
Full order adaptive observer for single-input single-output continuous differential system with unknown parameters
[NASA-CR-129172] 02 p0195 N73-11574
Full order adaptive observer for single input, single output, stable, linear differential systems
[NASA-CR-129193] 02 p0195 N73-11575
Bang-bang controller operating in chatter mode for disturbance regulation in linear system
[AD-745896] 02 p0203 N73-11643
Optimal adaptive control of aircraft lateral dynamics in gust presence using Pontryagin principle and cost function
[AASU-314] 03 p0253 N73-12046
Adaptive control systems for phased antenna arrays
[AD-748220] 04 p0390 N73-13174
Automatic monitor for classifying high usage data transmission system circuits
[AD-749268] 04 p0392 N73-13183
Operational control of ramjet engine with fixed nozzle diffuser geometry
[AD-748708] 04 p0465 N73-13787
Adaptive pulse code modulator for speech signals noting coder and decoder
[SRDE-72001] 05 p0514 N73-14174
Research reports on control theory in flight systems
[AD-746296] 05 p0523 N73-14251
Characteristics of nonlinear self adjusting and variable structure automatic flight control system for piloted and pilotless aircraft
[AD-750502] 06 p0624 N73-15062
Development of aircraft control systems based on operator performance, adaptive displays, and coupling of manual with automatic control
[AD-751306] 07 p0741 N73-16026
Algorithm for choosing adaptive loop parameters and adjustment intervals of adaptive control systems
07 p0764 N73-16207
Development of adaptive control system for atmospheric reentry vehicle to meet flying quality requirements
07 p0848 N73-16871
Scientific reports on adaptive control system theory for aerospace engineering
[AD-751941] 08 p0887 N73-17187
Optimization and estimation theory applied to design of automatic navigation system
[AD-751942] 08 p0942 N73-17716
Mathematical and numerical methods for solving spacecraft control problems and mapping of celestial bodies
[NASA-TT-F-731] 10 p1177 N73-19572
Parametric design of aerodynamic control system for compensating artificial satellite orbit perturbations
10 p1178 N73-19580
Numerical method for determining optimal satellite control system with discontinuous links
10 p1178 N73-19581
Numerical solutions for variational control functions of flight dynamics in circular orbits
10 p1178 N73-19582
Maximum principle for determining necessary conditions for optimality when delay depends on state, control, and time
[AD-753675] 10 p1179 N73-19592
Adaptive controllability of dynamical systems in Banach space with bounded operators
[AD-753716] 10 p1179 N73-19593
Human factors criteria for adaptive computer aiding in man-machine control system
[AD-754835] 11 p1250 N73-20147
Application of optimal control theory to design of constant gain filters to minimize weighted average of filtered variances
[AD-755798] 12 p1380 N73-21190
Development and use of synthetic flight trainers based on degree and fidelity of simulation as key design considerations
[AD-754957] 12 p1388 N73-21260
Optimal control and measurement techniques of decentralization for stochastic linear dynamic systems
[AD-754984] 12 p1419 N73-21501
Application of adaptive control algorithms to self adjusting control systems for aeroelastic aircraft, flight vehicle roll, and control during reentry
[AD-756598] 13 p1474 N73-21941
Conferences on optimizing adaptive automatic systems
[JPRS-58809] 14 p1644 N73-23330
Search and optimization capabilities of collective of independent automatic devices
14 p1644 N73-23331
Random search in problems of optimization, identification, and teaching of automatic systems
14 p1644 N73-23333
Synthesis and analysis of systems combining extreme principle of control with correlation processing of signals entering from object being controlled
14 p1644 N73-23334
Development of algorithms for calculating modal trajectory estimate, conditional mean state estimate, and weighted least squares trajectory estimate
[AD-757240] 14 p1684 N73-23665
Adaptive processing filtering and design of digital signals for real time analysis with algorithm derivation
[AD-757229] 14 p1684 N73-23667
Stationary point processes and applications to communications and logistic systems
[AD-758281] 15 p1804 N73-24621
Mathematical models for stochastic feedback processes in optimal adaptive control systems
[AD-757900] 16 p1935 N73-25653
Quantitative evaluations of adaptive physical operator/manipulator control systems
17 p1990 N73-26090
Measurement subsystem parameter optimization to enhance estimates
[AD-759175] 17 p2055 N73-26625
Automative adaptive flight training, using instrument flight maneuvers
[AD-759366] 18 p2112 N73-27080
Constant gain optimal tracking control laws for finite final time
[AD-761091] 18 p2214 N73-27882
Development of analog hardware for flight control system design to control aircraft with uncertain parameters
[NASA-CR-133416] 19 p2220 N73-27909
Versatile ergometer with work load control
[NASA-CASE-MFS-21109-1] 19 p2224 N73-27941
Adaptive control for multivariable systems using reduced dynamic ordering
[NASA-CR-133429] 19 p2314 N73-28607
Parameter plane methods for linear systems with time delay
[AD-761761] 19 p2314 N73-28611
Examples for sequential gradient-restoration algorithm for minimizing functions subject to constraints
[AD-761789] 19 p2315 N73-28618
Design of automatic throttle control for Navy carrier based A-7 E aircraft
[AD-761764] 19 p2329 N73-28740
Development of automatic flight control systems based on adaptive control techniques and variable structure control systems
[AD-763415] 21 p2498 N73-30047
Development of theory for adaptive control of aircraft in atmospheric turbulence using stochastic identification method
[AD-763739] 21 p2498 N73-30051
Stability of multiple loop nonlinear time varying systems
[AD-764631] 23 p2813 N73-32492

ADAPTIVE CONTROL SYSTEMS
U ADAPTIVE CONTROL

ADAPTIVE FILTERS
Matrix method for calculating adaptive pre-whitening filter for radar echo signal processing
01 p0025 N73-10197

Fast Fourier transform digital processor as spectrum analyzer and adaptive filter
01 p0025 N73-10198
Automatic equalizers of telephone channels for fast transmission of digital data
01 p0025 N73-10199
Algorithm for adaptive digital filters of data communication channels
01 p0026 N73-10200
Adaptive filter using minimum variance criteria to estimate state noise covariance
[NASA-TM-X-66080] 01 p0032 N73-10252
Development of adaptive filter technique to minimize effect of noise produced errors in gyrocompasses and production of true azimuth data
[AD-747478] 03 p0329 N73-12685
Algorithms for variable order filters from extensions of spline function concepts
[AD-751124] 07 p0813 N73-16595
Adaptive filter for estimating atmospheric density profile during Atmospheric Explorer missions from accelerometer data
[NASA-TM-X-66202] 10 p1154 N73-19388
Techniques and circuitry for designing adaptive high Q notch filter
[AD-759031] 17 p2004 N73-26210

**ADDERS [CIRCUITS]**
U ADDING CIRCUITS

**ADDING CIRCUITS**
Synthesis of combination adder with group carry circuits
[AD-752816] 09 p1007 N73-18216

**ADDITION RESINS**
NT ACRYLIC RESINS
NT VINYL COPOLYMERS
Viscoelastic properties of styrene butadiene plastic homopolymers and styrene-butadiene-styrene block copolymers
[AD-752622] 08 p0936 N73-17660

**ADDITIVES**
NT ADMIXTURES
NT ANTIICING ADDITIVES
NT ANTIOXIDANTS
NT OIL ADDITIVES
NT PLASTICIZERS
NT PROPELLANT ADDITIVES
NT PROPELLANT BINDERS
NT SOLID ROCKET BINDERS
Substitutional element diffusion coefficients in silicon
[AD-745945] 01 p0089 N73-10735
Performance characteristics of gallium arsenide solar cells with zinc or beryllium ion implantations
[NASA-CR-129199] 02 p0128 N73-11042
Radiation damage recovery characteristics of lithium doped solar silicon cells
[NASA-CR-129183] 02 p0128 N73-11044
Microwave probe studies on chemical additives behavior in nitrogen oxygen plasma
[AD-748469] 04 p0456 N73-13724
Electrical properties of insulating and semiconducting CdF2 with trivalent Ce and Gd codopants
[AD-750937] 06 p0711 N73-15799
Effects of various oxide additives on volume change on melting, surface tension, and viscosity of liquid aluminum oxide
[NASA-CR-120910] 07 p0811 N73-16580
Passivating effects of additives on zinc corrosion in potassium hydroxide solutions
[NASA-TT-F-14693] 08 p0884 N73-17155
Recovery of barium oxide reagent from residue from preparing lubricant additives in centrifuge
[AD-751945] 09 p1042 N73-18500
Elucidation of satellite lines of manganese-doped zinc selenide single crystals in electron paramagnetic resonance spectrum
[AD-753507] 09 p1077 N73-18788
Emulsifying capacity of oils and wearability of additives during contact with water
[AD-754622] 11 p1302 N73-20561
Synthesis of stoichiometric crystals of InP doped with impurities for obtaining semiconductor with desired resistance
[NLL-RRE-TRANS-381-[8036.625]] 11 p1329 N73-20790
Performance characteristics of erbium doped laser glass material
[AD-755683] 12 p1411 N73-21435
Electrical and ionic conductivity of calcium oxide-doped nonstoichiometric cerium dioxide at various temperature ranges
[COO-1441-16] 12 p1416 N73-21473
Vibronic interaction in electron paramagnetic resonance spectra of yttrium and scandium doped single strontium chloride crystals
[NASA-CR-131295] 13 p1561 N73-22653
Industrial application of ion implantation for doped semiconducting structures
[NLL-TRANS-861-[9022.64]] 15 p1759 N73-24257
Surface potential and wear measurements on carbamate, amine, and phosphorothioate lubricant additives
[AD-759126] 17 p2051 N73-26595
Chromium concentration effect on duration and width of luminescent lines in ruby spectrum
[AD-761374] 18 p2191 N73-27692
Drag reduction in fluids by addition of polymer additives
[AD-763824] 22 p2654 N73-31263
Intensity of EPR line spectra as affected by indium doped zinc oxide
[AD-764490] 22 p2708 N73-31684
Effect of FeF2 addition on Hastelloy N compatibility with LiF-BeF2-UF in low temperature convection loop system
[ORNL-TM-4188] 24 p2936 N73-33444
Influence of alloy additives on strength of nickel base alloys at temperatures from 25 to 650 C
[ORNL-TM-4173] 24 p2936 N73-33446

**ADDRESSING**
Effect of multiword addressing with laminated ferrite arrays
[NASA-CR-124372] 21 p2512 N73-30149

**ADENINES**
NT RIBONUCLEIC ACIDS
Adenin-nucleotides NAD[plus] and NADN in skeletal muscles during intensive work and at rest
[NASA-TT-F-14856] 11 p1246 N73-20118

**ADENOSINE TRIPHOSPHATE [ATP]**
Luciferase ATP assay procedure for determining bacterial infections in urinary tract
[NASA-CR-130797] 09 p0992 N73-18096
Automatic device for assaying urine on bacterial adenosine triphosphate content
[NASA-CASE-GSC-11169-2] 23 p2750 N73-32011

**ADENOSINES**
NT ADENOSINE TRIPHOSPHATE [ATP]

**ADHEROMETERS**
U ADHESION TESTS

**ADHESION**
Microstructural studies of adhesion, wear, friction, and lubrication using LEED, Auger emission spectroscopy analysis, and field ion microscopy
[NASA-TM-X-68152] 01 p0058 N73-10471
Statistical analysis of adhesive bond strength as function of plasma treatment of polymer films
[AD-749253] 04 p0440 N73-13587
Research on physics of adhesive joint
[AD-751301] 07 p0805 N73-16530
Analysis of adhesion forces in cutting metals to determine effects of formatting and destruction of adhesive connections on wear of cutting tools
[AD-754041] 11 p1301 N73-20555
Adhesion, friction, and wear behavior of glasses and ionic solids
[NASA-TM-X-68255] 16 p1932 N73-25632
Adhesion criterion in gas solid interface
[NASA-CR-133618] 20 p2374 N73-29075

**ADHESION TESTS**
Technique and instrument for measuring adhesive force
[NLL-TRANS-2863-[9022.81]] 02 p0171 N73-11384
Predictive model for failure times of adhesive bonded aluminum under constant stress
[AD-758845] 16 p1919 N73-25528
Elastomeric silicone adhesive systems for surface insulation attachment to space shuttle 24 p2942 N73-33491

**ADHESIVE BONDING**
Formation mechanism and strength of adhesive bond between polyvinyl acetate and steel
[NLL-RTS-7520] 02 p0190 N73-11543
Low temperature bonding of solar panel materials
[AD-746684] 05 p0553 N73-14493
Structural analysis of laminated aluminum alloy sheets to determine flaw growth behavior in roll diffusion bonded and adhesive bonded structures
[NASA-CR-128844] 10 p1220 N73-19921
Interpretation of ERTS-1 geologic data for Nevada and evaluation of materials used in compiling photomaps
[E73-10398] 11 p1277 N73-20360
Reliability and failure time prediction for titanium adhesive bonds using multiple regression analysis
[AD-754526] 11 p1301 N73-20560
Stress distribution in lap joints under cleavage and tension-shear loading conditions 13 p1584 N73-22843
Joint strength, adhesive ductility of adhesively bonded joints of epoxy resins bonded to aluminum and titanium alloys
[DLR-FB-73-22] 14 p1680 N73-23636
Cyclic debonding of adhesive joints
[NASA-CR-2207] 16 p1932 N73-25631
Aging tests of light alloys bonded with various adhesives and development of new aging test criteria
[RAE-LIB-TRANS-1662] 17 p2043 N73-26528
Adhesive shear stress distribution in elastic plates reinforced by orthotropic elastic layer
[NASA-CR-132273] 17 p2093 N73-26933
Location of adhesive bond failure on Al surface during coupon surface treatment by radioactive tracing
[AD-761073] 18 p2168 N73-27509
Fokker F-28 fellowship structure adhesive bonding processes and quality control methods
[FOK-K-67] 21 p2497 N73-30037
Bibliography of reports dealing with adhesion bonding
[AD-763200] 21 p2553 N73-30471
Reliability analysis and characterization model of adhesive bonds
[AD-763707] 21 p2563 N73-30549
Adhesive bonding of structures and composite materials on advanced turbofan engines 23 p2810 N73-32470
Chemical bonding of solid polymers to metal surfaces and formation of organometallics
[NASA-TM-X-71452] 24 p2929 N73-33390
Stress analysis of adhesive lap joint subjected to tension, shear force, and bending moments for various material properties and thickness of adherents 24 p2988 N73-33877

**ADHESIVES**
NT GLUES
NT PASTES
Technique and instrument for measuring adhesive force
[NLL-TRANS-2863-[9022.81]] 02 p0171 N73-11384
Electrical, mechanical, and thermal properties of transparent optical adhesives
[AD-750571] 06 p0688 N73-15602
Optimization of transparent ethylene terpolymer and compilation of engineering data for use as adhesive in polycarbonate composite aircraft transparencies
[AD-750814] 06 p0689 N73-15611
Design allowables for room temperature vulcanizing silicone rubber based adhesives for attaching reusable surface insulation to space shuttle structures
[NASA-CR-128887] 11 p1308 N73-20615
Development of design data for adhesives for attaching reusable surface insulation on space shuttle
[NASA-CR-128888] 11 p1308 N73-20616
Evaluation of Puller tapes applied to military use
[AD-754925] 11 p1353 N73-20987
Development of low density foamed epoxy adhesives
[Y-1833] 13 p1547 N73-22538
Technical compilation on adhesives and polymeric plastics
[NASA-SP-5961[01]] 14 p1680 N73-23630
Strength, creep, and transmission coefficient of adhesives for attaching strain gages
[AD-761470] 19 p2302 N73-28506
Thermal and ultraviolet vacuum tests on adhesives, thermoplastic, and thermosetting resins for space environment simulation
[RV-106] 19 p2312 N73-28596
Fracture characteristics of adhesive joints
[AD-762457] 19 p2351 N73-28910
High temperature silicone adhesive formulations for thermal protection systems used with space shuttle mission
[NASA-CR-124389] 22 p2688 N73-31533

**ADIABATIC CONDITIONS**
Influence of adiabatic oil compression on power of hydraulic motors and pumps 10 p1111 N73-19055
Adiabatic processes in spiral magnetic field
[UCRL-TRANS-1487] 10 p1189 N73-19679
RF stacking in ISABELLE
[BNL-17274] 10 p1193 N73-19709
Temperatures of various adiabatic and isobaric mixtures of humid atmospheric air with water or ice
[PUBL-SER-B-68] 12 p1465 N73-21866
Development of method for calculating characteristics of laminar boundary layer on nonadiabatic wall of constant temperature in presence of pressure gradients
[ARC-R/M-3233] 15 p1728 N73-24013
Nonadiabatic atmospheric model for short term weather forecasts
[AD-759631] 16 p1939 N73-25690
Explosive fragmentation of heat treated martensitic microstructure steel
[DSL-REPT-532] 17 p2091 N73-26915
Influence of nonadiabatic processes particularly radiative heat influx on numerical weather forecasting 20 p2443 N73-29624
Variational principles for examining adiabatic motions in gaseous sphere and waves in stratified horizontal fluids 21 p2523 N73-30237
Uses of cluster materials and related types in antiferromagnetic cooling by adiabatic magnetization and demagnetization of antiferromagnets
[AD-764620] 23 p2826 N73-32592

**ADIABATIC EQUATIONS**
Analysis of post-Newtonian effects on instability of white dwarf stars, neutron stars, and supermassive stars
[NASA-CR-129241] 03 p0355 N73-12893

**ADJOINTS**
Variational principle of self and non self adjoint linear differential equations
[PB-210374] 02 p0203 N73-11642
Computer code for generating spatial-angular moments of adjoint gamma-ray flux in infinite mediums
[NBS-TN-748] 10 p1193 N73-19702

**ADJUSTING**
Human operator adaptive behavior in slowly changing dynamic system
[AD-748243] 05 p0503 N73-14097

ADJUSTMENT
U ADJUSTING
ADMINISTRATION
U MANAGEMENT
ADMITTANCE
U ELECTRICAL IMPEDANCE
ADMIXTURES
Distribution profiles of admixtures in epitaxial silicon layers prepared with hydrogen of high purity
18 p2187 N73-27661
ADRENAL GLAND
Dystrophic degeneration of suprarenal rat cortex during hypokinesia
13 p1481 N73-22003
ADRENAL METABOLISM
Radioimmunoassays of plasma aldosterone and catecholamine concentrations as human vasomotor regulators
09 p0994 N73-18111
Temperature and noise irradiation effects on human energetic metabolism during vigilance task
10 p1123 N73-19155
Effects of physical training on human enzyme activity, carbohydrate metabolism, cholesterol level, and adrenal function
[NASA-TT-F-14826] 11 p1243 N73-20093
Human hydroxycorticosteroid and aldosterone excretions during hypodynamic space flight conditions
20 p2367 N73-29031
Effect of physical and psychological stress on urinary excretions of adrenal harmones in normal man
[NASA-TT-F-15046] 20 p2368 N73-29043
Water load tests for determining hydration status and adrenal and kidney functions during post flight period
[NASA-TT-F-15091] 22 p2620 N73-30998
ADRENALINE
U EPINEPHRINE
ADRENERGICS
Mental and cardiovascular acceleration stress effects on heart rate studied by beta adrenergic blockage
10 p1122 N73-19149
Increased toxicity of sympathomimetic amine stimulants on spinal reflexes in irradiated frogs
11 p1240 N73-20063
Epinephrine oxidation and indole production during high pressure oxygen poisoning
[AD-759405] 18 p2110 N73-27061
ADRENOCORTICOTROPIN [ACTH]
Human adrenocorticotropin level measurements as indication of adaptation to space flight stress
09 p0993 N73-18109
ADSORPTION
NT CHEMISORPTION
Effect of heat treatment on adsorption properties of titano-silica gel and interactions of adsorbed molecules with silanol groups
[NLL-RTS-7360] 01 p0069 N73-10564
Surface properties study of thermionic electrodes, using quasi-equilibrium model for oxygen reactions with refractory metals
[NASA-CR-129598] 03 p0254 N73-12057
Reaction kinetics when liquid hydrazines adsorbed on supported ruthenium catalyst
[RPE-TR-72/1-PT-5] 05 p0506 N73-14122
Dissociative character of carbon dioxide adsorption on nickel film surfaces
[NLL-TRANS-746-1341-[9022.401]]
06 p0682 N73-15549
Low energy electron diffraction and Auger electron spectroscopy used for determination of structure of adsorbed gases on solid surfaces
[LBL-878] 10 p1193 N73-19708
Adsorption properties of synthetic zeolites
[AD-754324] 11 p1253 N73-20170
Kinetics of decomposition of adsorbed sarin determined microcalorimetrically
[REPT-1972-18] 14 p1616 N73-23091
Photoelectric emission of gallium arsenide from adsorbed layers of cesium and barium oxide
[NLL-DRIC-TRANS-2293-[3623.66]]
15 p1819 N73-24746
Adsorption properties of natural zeolites
[BM-RI-7744] 15 p1820 N73-24753
Computerized prediction and actual carbon dioxide adsorption performance of solid amine resin
[NASA-CR-112324] 16 p1870 N73-25140
Heat capacity of submonolayer helium films adsorbed on exfoliated graphite in very low temperatures
16 p1973 N73-25953
Crystal phonon contribution to free energy of identical atom pairs adsorbed on cubic lattice surface
[AD-759035] 17 p1992 N73-26109
Phase characteristics of submonolayer isotopic mixtures of helium adsorbed on Grafoil
18 p2113 N73-27084
Quantitative deposition by standard techniques of adsorbates containing C and Si
[NASA-CR-124309] 19 p2343 N73-28850
Absorptive equipment for control of air polluting industrial wastes
[PB-221138/1] 21 p2575 N73-30637
Adsorption kinetics of CO on {100} face of molybdenum single crystal
[CEA-CONF-2194] 22 p2684 N73-31499
Reflection intensities of thermal molecular beam on metals and aluminum oxide, to determine gas-solid interaction
[DLR-FB-73-14] 23 p2805 N73-32432
ADVANCED SODIUM COOLED REACTOR
Design and development of volume accumulator units for thermoelectric reactor coolant loops
[NASA-CR-121245] 18 p2177 N73-27582
ADVANCING GLACIERS
U GLACIERS
ADVANCING SHORELINES
U BEACHES
ADVECTION
Conservative finite difference method applied to meteorological advection problems
[NASA-CR-129090] 02 p0204 N73-11653
Meridional wind effects on advection heating in thermosphere during geomagnetic storms
[AD-751921] 08 p0919 N73-17528
Two-dimensional numerical model for simulating formation and dissipation of advection fogs
[NASA-CR-2201] 09 p1060 N73-18648
Numerical advection model for simulating maritime fog
[AD-757328] 14 p1685 N73-23676
AE-B SATELLITE
U EXPLORER 32 SATELLITE
AERATION
Test equipment and procedures for determining foaming and aeration characteristics of aircraft engine lubricants
[AD-747804] 03 p0321 N73-12618
AERIAL EXPLOSIONS
Analysis of shock wave propagation in direction of decreasing air density following aerial explosion
[AD-755173] 12 p1465 N73-21873
Diffuse shock wave reflection from ridged plates, simulating aerial explosion effects on earth surface
[REPT-7/72] 15 p1766 N73-24305
Fluid dynamics of meteor disintegration due to aerodynamic forces in heterogeneous atmosphere
16 p1960 N73-25855
Characteristics of vegetation from existing data for predicting munition height of burst in inaccessible areas
[AD-763179] 21 p2607 N73-30891
AERIAL IMAGERY
U AERIAL PHOTOGRAPHY
AERIAL PHOTOGRAPHY
Noise and error effects on differential pulse code modulation transmission of sampled aerial imagery
01 p0024 N73-10190
On-line computer technique for evaluating reconnaissance image compression algorithms
01 p0024 N73-10191
Determination of boundaries of aircraft and spacecraft data within which water quality can be obtained
[E72-10168] 01 p0044 N73-10349
Evaluation of three types of aerial photographs used in coastal studies of Baja California
[AD-744310] 01 p0052 N73-10421
Aerial photography used to delineate areas of ocean ground water discharge and detect submarine springs along northwest coast of Puerto Rico
[PB-210754] 01 p0052 N73-10426
Evaluation of simultaneous ERTS-1 and aerial photography of Arizona
[E72-10213] 02 p0162 N73-11308
Remote sensing in forestry using aerial and satellite-borne photography and imaging techniques
[E72-10221] 02 p0162 N73-11315
Computerized aerotriangulation with independent models and planimetric point adjustments
02 p0164 N73-11332
Application of aerial photography and photointerpretation to analyzing groundwater conditions under various types of landscape and morphological elements
[NASA-TT-F-681] 02 p0174 N73-11409
Photographic recording of aircraft strike, emphasizing air-to-air encounter
[AD-746837] 02 p0176 N73-11423
Comparison of mapping accuracies obtained by analytic system of aerotriangulation with accuracies obtained using conventional first-order plotting instruments
03 p0294 N73-12391
Photographic aerial survey over underground nuclear test at Amchitka to record changes in bioenvironment
[BMI-171-146] 03 p0296 N73-12411
Automatic plotting of aerial reconnaissance imagery and evaluation of image quality using coherent optical processing techniques
[AD-747803] 03 p0303 N73-12478
Analysis of image coordinate refinement parameters applied to aerial photography of ground areas for improved aero-triangulation
[AD-747799] 03 p0304 N73-12479
Tests and evaluations of methods for recovering ground colors in aerial photographs
[AD-747340] 03 p0304 N73-12481
Comparison of methods for determining transfer functions of black and white aerial photographic films
[AD-747594] 03 p0304 N73-12483
Theory and practice of aerial photography to include aerial triangulation, stereometric methods of photointerpretation, and production of maps
[AD-748871] 04 p0423 N73-13449
Metric calibration of aerial photographic system by method of mixed ranges
[AD-748812] 04 p0423 N73-13452
Application of remotely sensed data to determination of resources and conditions in Susquehanna River Basin
04 p0471 N73-13844
Geology photography infrared imagery, and remote sensing evaluation of Klondike Mining District, Nevada
[NASA-CR-129934] 05 p0537 N73-14371
Delineation of flood plain hazard zones by means of detailed soil surveys and by means of aerial photointerpretation
[PB-211325] 05 p0541 N73-14398
Evaluation of utility of available remote sensor returns in analysis of slope failure phenomena
[AD-750735] 06 p0671 N73-15462
Mapping of distribution of slope failure forms as depicted by remote sensor returns
[AD-750733] 06 p0672 N73-15463
Camera installation for multispectral aerial photography using four electrically driven cameras for synchronous photography
[FOA-2-C-2469-S2] 06 p0672 N73-15469
Application of aerial and spaceborne photography to urban, regional, and management planning
[NASA-CR-130290] 06 p0673 N73-15473
Employment of Earth Resources Technology Satellite capabilities for determining distribution of earth resources
07 p0782 N73-16353
Application of remote sensing from aircraft and spacecraft to geology, hydrology, and geographical data acquisition
07 p0782 N73-16354
Application of airborne and spaceborne photography to determine agricultural and forestry resources
07 p0782 N73-16355
Characteristics and capabilities of remote sensor systems to collect and analyze earth resource data
07 p0783 N73-16361
Application of color photography and infrared photography for determining effects of weather on coffee crop production
07 p0783 N73-16365
Detection of disease in coffee crops using color photography and infrared photography techniques
07 p0783 N73-16366
Comparison of imagery obtained with several types of remote sensors over Test Site 701, Mexico
07 p0783 N73-16367
Analysis of imagery obtained from infrared color and color photography used for highway and railroad engineering applications
07 p0783 N73-16368
Identification of organizations and activities concerning French programs in aerial photography and earth resources technology
07 p0784 N73-16372
Application of aerial photography for remote sensing to include characteristics of cameras, films, and photographic processing
07 p0784 N73-16375
Characteristics of multispectral sensors and methods for interpreting multispectral data obtained during earth resources surveys
07 p0784 N73-16378
Organization and functions of interdisciplinary teams for analyzing and interpreting remotely sensed data on earth resources
07 p0784 N73-16381
Proceedings of conference on earth resources survey systems - Vol. 2
[NASA-TM-X-68912] 07 p0785 N73-16382
Regional agricultural survey using small scale aerial and space photography
07 p0785 N73-16383
Detection of citrus tree anomalies by remote sensing with infrared color aerial photography
07 p0785 N73-16384
Application of color infrared film to measure spatial and temporal changes in vegetation
07 p0788 N73-16406
Analysis of oceanography remote sensing using black and white, color, and color infrared photographic recording
07 p0788 N73-16407
Airborne multispectral scanning of maize canopy to determine temporal characteristics, and relation of leaf area index to spectral response curves
[NASA-CR-130369] 07 p0789 N73-16421
Airborne multispectral scanning of maize canopy to determine density, and comparision to leaf area index
[NASA-CR-130363] 07 p0790 N73-16425
Anomalous scattering effects of haze layer in remote sensing data on corn blight distribution
[NASA-CR-130028] 07 p0790 N73-16428

Comparison of monochrome and color film for air to ground target acquisition
[RAE-TR-72064] 07 p0801 N73-16504
Earth resources surveys and management in California using ERTS-1 and supporting aircraft data
[E73-10027] 08 p0900 N73-17287
Utilization of ERTS-1 and aircraft remotely sensed data for land use inventory and planning in Maryland
[E73-10081] 08 p0901 N73-17293
Application of remote sensors carried in aircraft and satellites to survey extent of usage of recreational facilities
[NASA-CR-130752] 08 p0917 N73-17517
Classification of landforms for land use and regional planning using aerial photographic interpretation
[PB-212774] 08 p0918 N73-17525
Comparison of day and night infrared thermal imagery with results obtained using color photography and multispectral band sensor imagery
[AD-752217] 08 p0919 N73-17535
Photographic and infrared scanning surveys over Harper Lake, California
[AD-752226] 08 p0920 N73-17536
Digital data processing system for infrared video scan
[AD-752069] 08 p0944 N73-17731
Operational system for employment of remote sensing and automated information in urban land management
[NASA-CR-130969] 09 p1030 N73-18410
Multiband airborne remote sensor devices for collecting data on reflective and emissive terrain properties
[AD-752420] 09 p1033 N73-18430
Reference key for error avoidance in aerial photointerpretation
[AD-752437] 09 p1037 N73-18463
Identification and classification of Iowa crop lands using ERTS-1 imagery and aerial photography
[E73-10343] 10 p1148 N73-19342
Relationship between wave parameters and spatial spectrum of aerial photographs of sea surface and electromagnetic method for measuring conductivity of sea surface
[JPRS-58370] 10 p1153 N73-19381
Derivation of algorithms correlating spectra of ocean wave conditions with two dimensional spectra of aerial photographs and radar imagery
10 p1153 N73-19383
Application of remote sensing techniques and laboratory analyses for determining water pollution caused by carbonaceous materials
[NASA-CR-128824] 10 p1154 N73-19387
Correlation and regression analysis of aerial photography and soil samples to determine principal soil limitations
[NASA-CR-131110] 10 p1154 N73-19392
Application of remote sensing and aerial photography to Houston metropolitan area
[NASA-CR-128746] 10 p1159 N73-19431
Strip photography used in simulation study of very low altitude detection of small stationary targets at very slow speeds
[AD-754928] 11 p1250 N73-20146
Development of procedure and system for uniform mapping and monitoring of earth resources and environmental complexes using ERTS-1 imagery
[E73-10350] 11 p1275 N73-20344
Analysis of ERTS-1 data to detect and map areas of tree mortality due to insect outbreaks using color infrared positive transparencies
[E73-10351] 11 p1275 N73-20345
Interpretation of ERTS-1 geologic data for Nevada and evaluation of materials used in compiling photomaps
[E73-10398] 11 p1277 N73-20360
Analysis of ERTS-1 photographic imagery for identification, definition, and mapping, of terrestrial ecosystems in interior Alaska
[E73-10399] 11 p1277 N73-20361
Analysis of ERTS-1 imagery for land use and lake turbidity mapping of Lake Champlain Basin and Vermont
[E73-10432] 11 p1281 N73-20393
Identification of geologic and hydrologic features of Republic of Mali, West Africa using ERTS-1 imagery
[E73-10435] 11 p1281 N73-20395
Soviet method of illumination calculation for aerial survey on color film
[AD-754627] 11 p1295 N73-20508
Effects of atmospheric aerosols on image transfer in aerial photography using polarized light
12 p1400 N73-21356
Space and supporting aircraft photography for interpretation and analysis of non-forest vegetation
[NASA-CR-131585] 13 p1522 N73-22338
Classification of forest land use and detection of forest disturbances using space and high altitude aerial photography
[NASA-CR-131584] 13 p1523 N73-22339
Application of spaceborne photography and aerial photography to ecological resource inventory and analysis of naturally vegetated areas in Arizona
[NASA-CR-131581] 13 p1523 N73-22342
Terrain factor analysis and automatic color coded mapping using image processing methods in estimation of construction time relative to prospective military airfields
[AD-755531] 13 p1526 N73-22367
Compilation of aerial photographs of coastal areas of United States
[AD-755508] 13 p1526 N73-22368
Investigation of optical properties of natural objects and their aerial photographic imaging characteristics
[AD-756603] 13 p1532 N73-22413
Color photographic techniques to study vegetation and terrain, improve mapping methods, and to provide photoelectronic color separation using aerial cameras
[AD-756700] 14 p1668 N73-23536
Color and color infrared aerial photographic detection of Dutch elm disease
16 p1866 N73-25110
Application of sea photo analysis techniques to obtain surface truth descriptors of open ocean from aerial photography
[FAA-RD-72-110] 16 p1905 N73-25412
Urban mapping activities assisted by aerial photography and ground surveying in connection with urban planning and community development
[PB-214305/5] 16 p1915 N73-25494
Classification of aerial photographic image data sets on basis of computable textural features
[AD-759505] 16 p1915 N73-25498
Evaluation of utility of ERTS-1 satellite and aircraft remotely sensed data to integrated processes of state planning and land use in Maryland
[E73-10716] 17 p2019 N73-26323
Analysis of ERTS-1 data for interdisciplinary study of estuarine and coastal oceanography of Block Island Sound and adjacent New York coastal waters
[E73-10736] 17 p2020 N73-26342
Remote sensing techniques for earth resources, water pollution, and vegetation growth
[PUBL-21] 18 p2143 N73-27321
Remote color aerial photography for soil mapping and highway engineering applications
[PB-22037/6] 18 p2148 N73-27363
Algorithm for detecting man-made objects from aerial reconnaissance photographs
[AD-760755] 18 p2153 N73-27402
Application of ERTS-1 and U-2 photography to study of urban land use in Pennsylvania
[PAPER-L17] 19 p2275 N73-28312
Land use mapping and inventory of Houston, Texas using ERTS-1 and high altitude photography
[PAPER-L20] 19 p2276 N73-28315
Aerial and space photographic methods for geographic research
[NASA-TT-F-14966] 19 p2293 N73-28440
Image acquisition and enhancement techniques for oceanographic photography using photo-optical and electronic methods
[AD-761663] 19 p2296 N73-28463
Using infrared aerial photography for detection of forest fires
[AD-762259] 19 p2302 N73-28509
Forest fire detection by airbonre infrared photography
[AD-762265] 19 p2353 N73-28931
Analysis of ERTS data on ice formation in Bering Sea and correlation with ice observations by aerial reconnaissance
[E73-10865] 20 p2392 N73-29216
Application of ERTS data for mapping snow cover in Arizona and California and correlation with aerial photography
[E73-10866] 20 p2392 N73-29217
Sequential photography for coastal oceanography
[AD-760713] 20 p2413 N73-29399
Aerochrome infrared aerial photography over Barro Colorado Island, using multispectral, line scan data for tropical forests
[AD-762583] 20 p2415 N73-29410
Physiographic terrain analysis in Colorado using principles of aerial photointerpretation
20 p2416 N73-29413
Aerial photointerpretation of impact of highway construction on rural area in Thailand
20 p2417 N73-29414
General principles of geological interpretation of remote images of earth surface
21 p2534 N73-30319
Radar aerial survey and significance in combination with high altitude and space geological research techniques
21 p2535 N73-30325
Interpreting and compiling soil maps from aerial and space survey data
21 p2535 N73-30328
Glossary of aerial photography and remote sensing in geology and earth science
[PB-220154/9] 21 p2541 N73-30373
Bibliography of abstracts on remote sensing of water resources
[PB-220163/0] 21 p2542 N73-30383
Application of aerial photography and ERTS imagery to agricultural, forest, and water resources management in Minnesota
[NASA-CR-135483] 22 p2665 N73-31357
Compensation formulas for panoramic aerial photography cameras
[AD-764168] 22 p2676 N73-31431
Scale, haze, and image motion effects on human performance in photointerpretation of aerial photography
[AD-763908] 23 p2752 N73-32024
Aerial photography for detecting cereal crop insect infestation
[PAPER-8076] 23 p2783 N73-32268
Remote sensor data, particularly photography, applied to geological mapping of Rio Grande rift zone
[NASA-CR-135636] 23 p2785 N73-32279
Storage and retrieval of ERTS-1 and underflight imagery of Pennsylvania
[E73-11116] 24 p2916 N73-33273
Sea photo analysis for ocean surface truth descriptors from aircraft
[AD-764858] 24 p2924 N73-33360
Pan-frame system model for panoramic camera in aerial triangulation
24 p2925 N73-33363
Interpretation of aerial photographs to generate category maps and textures
[AD-765526] 24 p2928 N73-33382

**AERIAL RECONNAISSANCE**

Gray scale reproduction capability for characterizing aerial television reconnaissance system
[AD-747632] 03 p0267 N73-12165
Automatic plotting of aerial reconnaissance imagery and evaluation of image quality using coherent optical processing techniques
[AD-747803] 03 p0303 N73-12478
Role of remote sensing in geologic reconnaissance for tunnel-site selection
[AD-748663] 04 p0416 N73-13399
Avionics requirements for multimission, fixed wing, twin engine aircraft designed for search and rescue operations
[AD-750463] 06 p0624 N73-15064
Evaluation of device to train forward air controllers to communicate target locations
[AD-751292] 07 p0751 N73-16103
Statistical three-stage sampling model for estimating resources from remote sensor applications
[NASA-CR-130026] 07 p0800 N73-16494
Methods for lowering cost of environmental aerial surveys
[NASA-CR-124107] 09 p1025 N73-18369
Photointerpretation techniques based on holographic stereogram three dimensional presentations
[AD-753167] 09 p1044 N73-18518
Strip photography used in simulation study of very low altitude detection of small stationary targets at very slow speeds
[AD-754928] 11 p1250 N73-20146
Design and performance of C band airborne data transmission system for aerial reconnaissance
[AD-759184] 16 p1877 N73-25194
C-130 aircraft flights to obtain simulated operation of Skylab multispectral scanner, thermal scanner, and cameras
[E73-10761] 17 p2023 N73-26361
Side-looking radar for aerial imagery of earth surface
[JPRS-59391] 18 p2116 N73-27108
Dynamics and morphology of Beaufort Sea ice determined from satellites, aircraft, and drifting stations
[NASA-TM-X-66291] 18 p2144 N73-27333
Bibliography on geothermal prospecting in arid and semiarid lands
[PB-218830/8] 18 p2148 N73-27359
Thermal surveillance of Cascade range volcanoes using ERTS-1 MSS data, aircraft imaging systems, and ground based DCP
19 p2284 N73-28369
Techniques for creating moving image reconnaissance display
[AD-763789] 21 p2551 N73-30452
Aerial surveillance system for remote detection of real and potential oil spills threatening inland waterways
[PB-221484/9] 22 p2669 N73-31385

**AEROBEE ROCKET VEHICLE**

X ray sources in galactic center and comparison of Aerobee data with Uhuru data
[NASA-TM-X-66114] 03 p0353 N73-12873
Electron beam-induced luminescence studies of thermospheric temperatures and particle densities, using two Aerobee 150 rockets
[AD-749877] 05 p0541 N73-14406
Aerobee-borne spectrometer/monochromator for advanced studies of solar X-ray line emissions and preliminary results
[NASA-CR-130359] 07 p0838 N73-16793
Aerobee rocket observation of ultraviolet line spectra of Delta Scorpii and Zeta Ophiuchi
08 p0958 N73-17838
Design and fabrication of payloads for sounding rockets for use in X ray astronomy
[NASA-CR-130749] 08 p0959 N73-17845
Preflight tests and performance of electronic instrumentation in measuring solar radiation during Aerobee 170 and Black Brant V rockets
[AD-756909] 13 p1532 N73-22412

Sounding rocket injection of controlled beam of energetic electrons into trapping region of magnetosphere
16 p1895 N73-25329
High resolution solar X ray astronomy from Aerobee rockets
[NASA-CR-132984] 16 p1959 N73-25849
X ray astronomy from sounding rockets
[NASA-CR-133211] 16 p1963 N73-25880
Bubble formation analysis in plain and fiber reinforced metals melted and solidified under weightless conditions, using Aerobee and Black Brant rocket vehicles
[NASA-TM-X-64665] 16 p1964 N73-25886
Surface brightness and X ray measurements of Cygnus Loop from Aerobee rocket
[NASA-CR-133098] 17 p2080 N73-26822

**AEROBES**
Ultraviolet space irradiation effects on Aeromonas proteolytica extracellular enzyme production
15 p1741 N73-24111

**AERODYNAMIC AXIS**
U AERODYNAMIC BALANCE

**AERODYNAMIC BALANCE**
Planform shape effects on aerodynamic center location and aeroelasticity of fighter aircraft
[NASA-CR-2117] 13 p1469 N73-21896

**AERODYNAMIC BRAKES**
NT DRAG CHUTES
NT LEADING EDGE SLATS
NT TRAILING-EDGE FLAPS
NT WING FLAPS
Performance prediction for deployable aerodynamic decelerators operating in supersonic wakes using gas dynamics analogy
[AD-751982] 08 p0897 N73-17266
Aerobraking trajectory for return of reusable space tugs
[NASA-CR-124057] 09 p1082 N73-18827

**AERODYNAMIC BUZZ**
U FLUTTER

**AERODYNAMIC CENTER**
U AERODYNAMIC BALANCE

**AERODYNAMIC CHARACTERISTICS**
NT AERODYNAMIC BALANCE
NT AERODYNAMIC DRAG
NT AERODYNAMIC STABILITY
NT INTERFERENCE DRAG
NT INTERFERENCE LIFT
NT JET LIFT
NT LIFT
NT STATIC AERODYNAMIC CHARACTERISTICS
NT ZERO LIFT
Longitudinal and lateral aerodynamic characteristics of cruise missile with swept wing and conventional aft tails at various Mach numbers
[NASA-TN-D-7069] 01 p0001 N73-10002
Force measuremeats on caret and delta wings at high incidence in hypersonic reentry conditions noting comparison with theoretical predictions
[IC-AERO-72-16] 01 p0001 N73-10004
Modeling data developed during manned simulation of large transport aircraft and comparison with training simulator results - Vol. 2
[NASA-CR-114494] 01 p0004 N73-10027
Numerical analysis of aircraft equilibrium spin characteristics based on nonlinear equations of motion and constrained minimization techniques
[NASA-TN-D-6926] 01 p0004 N73-10028
Longitudinal aerodynamic characteristics of large scale model with swept wing and augmented jet flap in ground effect, using 40 x 80 ft wind tunnel
[NASA-TM-X-62174] 01 p0004 N73-10030
Development and characteristics of civilian V/STOL aircraft with application to short haul commercial air traffic
[NASA-TT-F-14629] 01 p0005 N73-10034
Development of computer program for analyzing mono-element and multi-element airfoils at subsonic speed with attached air flow - Vol. 2
[AD-740124] 01 p0031 N73-10242
Computer programs for analysis of axial compressor aerodynamic test data
[AD-744502] 01 p0092 N73-10756
Aerodynamic characteristics of Scout vehicle during launch through high velocity horizontal winds
[NASA-CR-112175] 01 p0108 N73-10888
Wind tunnel analysis of asymmetric yawing moments produced by long pointed fuselage nose shapes at high angles of attack
[NASA-TN-D-7095] 02 p0123 N73-11003
Wind tunnel tests of twin jet afterbody models to determine thrust minus total drag and afterbody drag at Mach numbers to 2.2 and zero degree angle of attack
[NASA-TM-X-2601] 02 p0123 N73-11004
Wind tunnel tests to determine aerodynamic characteristics of two different size blunt 120 degree included angle cones behind 20 degree included angle cone
[NASA-TM-X-2603] 02 p0123 N73-11005
Computer program listings for analysis of main rotor free wake geometry effects on blade air loads and response for helicopters in steady maneuvers - Vol. 2
[NASA-CR-2111] 02 p0124 N73-11006
Flight and wind tunnel tests to determine effects of Reynolds number of installed boattail drag of underwing nacelle
[NASA-TM-X-68162] 02 p0124 N73-11007
Wind tunnel tests and firing tests to determine aerodynamic characteristics and subsonic flight performance of spin stabilized mortar projectile
[AD-746977] 02 p0124 N73-11009
Aerodynamic characteristics of four configurations of rounded shoulder boattail nozzles mounted on F-106B aircraft at subsonic speeds
[NASA-TM-X-2626] 02 p0124 N73-11013
Prediction of lateral directional aerodynamic characteristics for twin engine propeller driven airplane
[NASA-TN-D-6946] 02 p0125 N73-11016
Evaluation of Rayleigh-Ritz anisotropic plate analysis procedure for determining performance of composite wing for aircraft operating in transonic environment
[AD-745129] 02 p0126 N73-11023
Wind tunnel tests to determine drag and performance of disk-gap-band parachutes in wake of Viking reentry vehicle scale model from subsonic to supersonic speeds
[AD-746291] 02 p0126 N73-11026
Influence of split ground belt on aerodynamic characteristics of high lift STOL aircraft with blown flap
[UTIAS-TN-173] 02 p0152 N73-11230
Design, construction, and calibration of closed circuit wind tunnel for study of aerodynamic behavior of precipitation
[UTIAS-TN-181] 02 p0152 N73-11232
Wind tunnel tests to determine stability and control effectiveness of basic configuration of pressure-fed ballistic recoverable booster for space shuttle
[NASA-CR-120073] 02 p0233 N73-11896
Wind tunnel tests to determine aerodynamic characteristics of space shuttle ascent configurations with parallel burn pressure-fed and SRM boosters and tank T3 installation - Vol. 2
[NASA-CR-120084] 02 p0234 N73-11902
Wind tunnel tests to determine aerodynamic characteristics of space shuttle ascent configurations with parallel burn pressure-fed and SRM boosters and tank T4 installation - Vol. 3
[NASA-CR-120085] 02 p0234 N73-11903
Wind tunnel tests to determine aerodynamic characteristics of space shuttle ascent configurations with orbiter, tanks, and booster alone installations - Vol. 5
[NASA-CR-120087] 02 p0234 N73-11905
Effects of location of wing pivot and geometry of wing on static longitudinal aerodynamic characteristics of variable-sweep supersonic fighter aircraft model
[NASA-TM-X-2674] 03 p0247 N73-12000
Analysis of forced-oscillation pitch-damping over small angular amplitude range about nominal angle of attack
[NASA-CR-129522] 03 p0247 N73-12001
Turbofan design parameters for optimal acoustic and aerodynamic performance
03 p0249 N73-12014
Analysis of weight and inertia, aerodynamic derivatives, control characteristics, and stability augmentation systems for various military and civilian aircraft
[NASA-CR-2144] 03 p0252 N73-12039
Development of equations for large amplitude coupled flap-lag motion of hingeless elastic helicopter blades
[NASA-CR-114485] 03 p0252 N73-12043
Wind tunnel tests to determine aerodynamic characteristics of V/STOL aircraft configurations using blowing flapped wing and direct jet lift systems
[NASA-CR-114496] 03 p0282 N73-12284
Calculation of drag of porous lattice plates in turbulent flow
[IC-AERO-72-20] 03 p0284 N73-12300
Analysis of flow distribution around axisymmetric bodies at extreme angles of attack and calculation of pressure distribution for asymmetric steady vortex wake
[AD-747986] 03 p0286 N73-12315
Calculation of coefficient of resistance of sphere at supersonic velocities and measurement of critical point on free flying bodies
[AD-747513] 03 p0287 N73-12324
Characteristics of flow around bluff body at supersonic speed with emphasis on leading shock wave formation and changes in withdrawal value for argon and nitrogen
[AD-747407] 03 p0287 N73-12325
Wind tunnel tests to determine effect of nozzle lateral spacing on afterbody drag and performance of twin-jet afterbody models with cone plug nozzles at supersonic speeds
[NASA-TM-X-2632] 04 p0369 N73-12999
Analysis of aerodynamic interference effects between aircraft and external store carried under wing based on inviscid flow characteristics
[AD-748348] 04 p0370 N73-13005
Development of numerical analysis techniques for determining lifting surface characteristics of circular wings and parabolic wing tips
[AD-748433] 04 p0370 N73-13006
Numerical analysis of pressure distribution at parabolic wing tips on circular wing model based on occurrence of logarithmic sets
[AD-748432] 04 p0370 N73-13007
Application of parameter estimation algorithm to obtain longitudinal aerodynamic derivatives from flight data for XC-142A aircraft in cruise conditions
[NASA-TN-D-7114] 04 p0372 N73-13025
Analysis of minimum time maneuvers by high thrust-to-weight aircraft using optimal control theory to determine open-loop control laws
[AD-748354] 04 p0374 N73-13039
Analysis of model helicopter rotor blade response to random excitation during simulated forward flight using electromechanical apparatus
[AD-748457] 04 p0374 N73-13040
Flight tests to determine lateral-directional handling qualities and roll-sideslip coupling of jet aircraft at high speeds
[AD-748435] 04 p0374 N73-13042
Wind tunnel tests to determine effects of aerodynamic configuration, dimensions, and materials on spinning characteristics of cross parachute
[AD-749010] 04 p0374 N73-13045
Wind tunnel tests of longitudinal aerodynamic characteristics of aspect ratio airfoil with 0.098 chord blowing flap
[NASA-TM-X-2675] 04 p0421 N73-13431
Application of model helicopter rotor experiments to determining dynamic stall of rotary wings and predicting aerodynamic loads developed
05 p0491 N73-14002
Numerical analysis of unsteady aerodynamic forces on helicopter rotor blades to determine lift distribution as function of velocity component normal to blades
05 p0491 N73-14003
Wind tunnel tests to determine aerodynamic and propulsion characteristics of propulsive wing V/STOL configuration at high subsonic speed
[NASA-TM-X-2693] 05 p0493 N73-14020
Longitudinal and lateral data, lateral oscillatory derivatives, and aileron and rudder powers for BAC 221 aircraft
[ARC-CP-1230] 05 p0494 N73-14027
Analysis of compatibility between maneuver load control, relaxed static stability, and flying qualities requirements for various aircraft configurations
[AD-749479] 05 p0495 N73-14032
Numerical analysis of induced velocities of wing with curved axis not perpendicular to velocity of incoming flow
[AD-749843] 05 p0497 N73-14048
Design and fabrication of balloon to carry 3500 pound payload at 60,000 feet altitude for feasibility test of powering free balloon near minimum wind field
[AD-750542] 05 p0498 N73-14052
Calculation method for effect of compressible three dimensional relief on torque required for helicopter rotor
[AD-750179] 05 p0498 N73-14053
Analysis of flow properties in wake of 120 and 140 degree included angle conical bodies and flow characteristics of Viking 75 entry vehicle configuration
[NASA-TN-D-7089] 05 p0527 N73-14285
Performance tests of single stage fan-compressor to evaluate shock-in-rotor blading for jet engine applications requiring high aerodynamic performance and stability
[NASA-CR-120991] 05 p0590 N73-14795
Spacecraft configurations and aerodynamic characteristics of space shuttle systems with two reusable stages
[NASA-CASE-MSC-12433] 05 p0597 N73-14854
Wind tunnel tests to determine aerodynamic characteristics of expendable second stage and payload configurations for reusable space shuttle booster - Vol. 3
[NASA-CR-128674] 05 p0599 N73-14869
Development of procedure for computing normal force, axial force, and pitching moment coefficients with application to space shuttle booster characteristics
[NASA-TN-D-6996] 06 p0614 N73-14988
Aerodynamic characteristics and trajectory analysis of ballistic-type, self-dispersing bomblet based on wind tunnel tests and numerical probability application
[AD-749956] 06 p0615 N73-14993
Aerodynamic characteristics of wing moving close to interface with annular jet flowing from wing surface and impinging on screen
[AD-750933] 06 p0615 N73-14995
Proceedings of conference on fluid dynamics of aircraft stalling to include stall and post-stall aerodynamic characteristics of various military aircraft
[AGARD-CP-102] 06 p0616 N73-14998
Design characteristics and performance of airfoils with high lift at low and medium subsonic speeds and various angles of attack
06 p0616 N73-15004
Analysis of aerodynamic processes occurring in flow past unpowered multi-element airfoils in high lift attitude
06 p0617 N73-15007

Analysis of aerodynamic stall characteristics of wing sections with high lift devices in two dimensional flow
06 p0617 N73-15008
Development of procedure for determining characteristics of high lift systems where viscous effects dominate
06 p0617 N73-15009
Analysis of stall and post-stall characteristics of F-111 aircraft and development of regression techniques to obtain aerodynamic derivatives
06 p0617 N73-15013
Post-stall aerodynamic characteristics of Harrier GR-1 aircraft and development of lift augmenting devices
06 p0618 N73-15014
Development of F-28 transport aircraft wing and analysis characteristics to show effects of boundary layer fences
06 p0618 N73-15015
Wind tunnel tests to obtain pre-flight estimates of stall speed and low air speed performance of Boeing 747 aircraft
06 p0618 N73-15016
Aerodynamic design, engineering development, and flight testing of naval aircraft for operation at high angles of attack
06 p0618 N73-15020
Wind tunnel tests of VTOL lift fan stages to determine changes in thrust characteristics with varations in back pressure imposed on stages by cross flow
[NASA-TM-X-68169] 06 p0620 N73-15031
Mission performance analysis of three supersonic transport configurations and effects of limitations on allowable engine noise
[NASA-TM-X-68178] 06 p0620 N73-15032
Design, stress analysis, and high altitude performance of recovery parachute system
[NASA-CR-130304] 06 p0621 N73-15037
Wind tunnel tests to determine effects of ground proximity on lift, drag, and pitching moment of rectangular wing equipped with jet flaps
[NAL-TR-294] 06 p0621 N73-15038
Theoretical and experimental analyses of aircraft propeller operating under turbulent ambient conditions
[UTIAS-183] 06 p0621 N73-15039
Prediction analysis method to determine influence of geometry parameters on aerodynamic characteristics of body-wing configuration
[DLR-FB-72-63] 06 p0622 N73-15050
Flight tests to determine lateral-directional performance and roll-sideslip coupling of T-33 aircraft at subsonic speed - Vol. 2
[AD-748436] 06 p0622 N73-15051
Analysis of stability characteristics of hingeless rotary wing on flap and lead-lag degrees of freedom of single blade
[AD-750359] 06 p0623 N73-15053
Development and operation of facility for investigating effect of spin on aerodynamic characteristics of shaped charges
[DREV-TN-2037/72] 06 p0649 N73-15271
Research projects to determine aerodynamic characteristics of rotary wings and propellers
[AD-750175] 06 p0656 N73-15326
Hypersonic air flow effects on aerodynamic characteristics of elliptical cones at large angles of attack
[AD-749738] 06 p0657 N73-15335
Cold air experiment in two-dimensional cascade to determine aerodynamic performance of turbine stator blade with suction-surface cooling
[NASA-TM-X-2685] 06 p0713 N73-15818
Method for estimating aerodynamic characteristics of airfoils in compressible inviscid flow based on thickness and camber line parameters
[ESDU-72024] 07 p0735 N73-15981
Wind tunnel determination of supersonic aerodynamic characteristics of variable geometry spacecraft designed for high hypersonic performance
[NASA-TM-X-2703] 07 p0735 N73-15985
Development of nonlinearized solution for aerodynamic characteristics of jet flap lifting surface with span-wise slot near trailing edge
[NASA-CR-2190] 07 p0736 N73-15986
Aerodynamic configurations and characteristics of airfoils designed to reduce formation of shock waves during supersonic flight
[NASA-TT-F-749] 07 p0736 N73-15987
Effects of various leading edge slat devices on static aerodynamic characteristics of twin-jet, swept wing fighter model
[NASA-TN-D-6921] 07 p0736 N73-15988
Method for estimating changes in lift curve, drag, tail lift, and downwash from wing of aircraft due to ground effect in incompressible flow
[ESDU-72023] 07 p0736 N73-15993
Numerical analysis of characteristics of rotary wing aircraft when considered as two coupled rigid bodies representing rotor and fuselage
07 p0737 N73-15994
Development and application of computer programs for evaluating performance of powered-lift STOL aircraft to include static, takeoff, and landing performance
[NASA-TM-X-62217] 07 p0738 N73-16007
Technique for defining aircraft performance model from limited flight test data and predicted aerodynamic and propulsion system characteristics
[NASA-TN-D-7137] 07 p0738 N73-16008
Wind tunnel tests of full scale model of light aircraft to determine effects of configuration changes on aerodynamic characteristics
[NASA-TN-D-6896] 07 p0739 N73-16012
Development of dynamic helicopter performance and control model based on force and rotor aerodynamic equations
[AD-751460] 07 p0740 N73-16022
Physical principles of experimental aeromechanics using wind tunnel tests
[AD-751464] 07 p0773 N73-16280
Aerodynamic characteristics of two-stage, flexible, variable-mass missile with internal flow, discrete masses, and aerodynamic forces in powered flight
07 p0848 N73-16870
System for eliminating roll rate anomalies occurring during flights of slender ballistic reentry vehicles
[SC-DC-72-2244-A] 07 p0849 N73-16883
Effects of nozzle orientation and configuration on roll control and base pressure of hypersonic reentry vehicle
[SC-DC-72-1187-A] 07 p0849 N73-16884
Analysis of aerodynamic characteristics of free, semibounded slipstream of straight-jet laminar gas flames
[NASA-TT-F-14688] 07 p0855 N73-16934
Development of analytical technique for computing performance of arbitrary jet-flapped wing with compensations for variations in wing geometry
[NASA-CR-2179] 08 p0863 N73-16982
Wind tunnel tests of two dimensional wing model with leading edge slat and trailing edge flap
[FAA-AU-862] 08 p0863 N73-16984
Computer program and users manual for calculating aerodynamic characteristics of wing-body combinations at subsonic and supersonic speeds
[FFA-AU-635-PT-2] 08 p0863 N73-16985
Aerodynamic characteristics of biplane wing systems with emphasis on stall matching and induced camber effects which differ from monoplane wing
08 p0864 N73-16987
Conference on flight handling qualities and requirements
08 p0864 N73-16993
Revisions to V/STOL handling qualities based on criteria
08 p0864 N73-16994
Role of theory and calculations in refinement of flying qualities
08 p0865 N73-16999
Predicting flying qualities by wind tunnel tests
08 p0865 N73-17000
Effect of engine failure on aerodynamic characteristics of supersonic aircraft
08 p0865 N73-17003
Analysis of performance potential of buoyant systems and flexible structures for use with short haul passenger transport aircraft
[NASA-TM-X-62168] 08 p0866 N73-17014
Development of methods for predicting performance characteristics of V/STOL aircraft - Vol. 1
[AD-752557] 08 p0869 N73-17033
Analytical techniques for predicting static and dynamic stability, control derivatives, and force and moment coefficients for V/STOL aircraft - Vol. 2
[AD-752558] 08 p0869 N73-17034
Computer program manual for analytical techniques to predict performance of V/STOL aircraft - Vol. 3
[AD-752559] 08 p0869 N73-17035
Literature survey of techniques for predicting performance of V/STOL aircraft- Vol. 4
[AD-752563] 08 p0869 N73-17036
Experimental determination of aerodynamic performance of cooled turbine vanes at gas to coolant temperature ratios up to 2.75
[NASA-TM-X-2733] 08 p0954 N73-17815
Technique for predicting shock envelopes and pressure distributions for two dimensional airfoil at angles of attack producing shock detachment and subsonic flow
[NASA-TN-D-7197] 09 p0979 N73-18001
Effect of ablation on aerodynamic characteristics of blunted slender cone during free flight ablating conditions
[NASA-TN-D-7196] 09 p0979 N73-18002
Evaluation of fluid dynamics of aircraft stalling to determine effects of three dimensional flow, wing sweep back, and high lift devices
[AGARD-AR-49] 09 p0982 N73-18023
Aeroelastic divergence of transport aircraft flying at supersonic speeds and design techniques to eliminate adverse effects
[NASA-CR-112262] 09 p0984 N73-18036
Numerical analysis of aerodynamic characteristics of unsteady, two-dimensional, jet-flapped wing
[AD-752928] 09 p0986 N73-18051
Aerodynamic characteristics of flow around wing profiles
[AD-752686] 09 p0987 N73-18054
Hypersonic and hyperthermic test apparatus for hypersonic vehicle aerodynamic investigations
[VTH-170] 09 p1011 N73-18255
Calculation of outer inviscid flow about rectangular wing moving at supersonic speeds
[NASA-CR-130985] 09 p1013 N73-18269
Effects of chemical nonequilibrium of inviscid flow in windward plane of symmetry for space shuttle orbiter configurations
[NASA-TN-D-7189] 09 p1015 N73-18287
Numerical analysis of inviscid, fully developed structure of lift-generated vortices behind aircraft wings and extension to arbitrary span-loaded distributions
[NASA-TM-X-62224] 09 p1016 N73-18289
Comparison of validity of results obtained by flight simulation with results obtained from actual flight test of short takeoff aircraft
10 p1105 N73-19007
Determination of aircraft aerodynamic characteristics under captive flight conditions and description of test equipment
10 p1105 N73-19010
Wind tunnel tests to determine effects of blade twist and aeroelasticity of rotary wings on tilt rotor performance from hover to Mach 0.7 speed
[NASA-TM-X-68948] 10 p1105 N73-19012
Computerized simulation of aerodynamic characteristics for trailing wire system towed by orbiting aircraft
[AD-753909] 10 p1136 N73-19255
Computerized simulation of spiral curve of wire being towed behind orbiting aircraft
[AD-753908] 10 p1136 N73-19256
Wind tunnel tests to determine effects of nozzle geometry and upper surface blowing on aerodynamic characteristics of 14 percent thick airfoil
[NASA-CR-114560] 11 p1231 N73-19998
Method for computing lifting pressure distribution on wing with partial span, swept control surfaces
[NASA-TN-D-7251] 11 p1232 N73-19999
Wind tunnel tests of scale model of space shuttle orbiter to determine low subsonic aerodynamic characteristics
[NASA-TM-X-2712] 11 p1232 N73-20000
Characteristics of system for providing yaw control of vehicles at high supersonic and hypersonic speeds by deflecting flaps mounted on upper wing surface
[NASA-CASE-LAR-11140-1] 11 p1233 N73-20008
Wind tunnel tests to determine low speed aerodynamic characteristics of large scale V/STOL transport models with lift fan lift-cruise fan propulsion system
[NASA-TM-X-62231] 11 p1233 N73-20014
Flight test of X-22 aircraft to determine longitudinal stability requirements of short takeoff aircraft during terminal area operations
[AD-754840] 11 p1235 N73-20029
Application of parafoil equations of motion to predict flight performance of powered parafoil flight vehicle
[AD-754907] 11 p1236 N73-20034
Annotated bibliography of aerodynamic configurations and characteristics of short takeoff aircraft
[AD-754500] 11 p1236 N73-20037
Tables and graphs on static stability and axial force characteristics of flat faced right circular cylinders at subsonic and supersonic speed
[AD-754920] 11 p1273 N73-20330
Aerodynamic performance of core-engine turbine stator vane tested in two-dimensional cascade of 10 vanes and in single-vane tunnel
[NASA-TM-X-2766] 11 p1333 N73-20823
Static-aerodynamic forces and moments of 162-inch diameter solid rocket booster with and without strakes
[NASA-CR-120090] 11 p1342 N73-20888
Analysis of optimum pressure distribution on multi-element airfoils to obtain conditions for maximum lift coefficient
12 p1355 N73-20996
Development of method for estimating normal force, axial force, and pitching moment coefficients for slender bodies of varying cross section equipped with lifting surfaces
[NASA-TN-D-7228] 12 p1355 N73-20998
Minimum weight design of supersonic aircraft wing with finite element modeling to meet strength, stability, frequency, and flutter requirements
12 p1356 N73-21003
Comparisons between analog and numerical methods for studying response of an aircraft
[PUBL-97] 12 p1357 N73-21007
Presentation of helicopter level flight performance as power coefficient compared with tip speed or advance ratio for range of thrust coefficients
12 p1358 N73-21014
Flight tests of XH-51 helicopter to determine effects of gyroscope and control spring modifications on stability and control
12 p1358 N73-21015

Discussion of speed record establishment by SA-341 helicopter to include aircraft preparation procedures and requirements for successful completion
12 p1358 N73-21018
Review of tilting rotor technology and comparison of tilting rotor performance with standard rotary wings
12 p1359 N73-21027
Proceedings of conference on fluid dynamics of rotary wings and aerodynamic characteristics of rotary wing systems
[AGARD-CP-111] 12 p1359 N73-21031
Analytical and experimental techniques to define geometry of vortex field of hovering rotary wing and effect on rotor performance
12 p1359 N73-21032
Wind tunnel tests of rotary wing to determine retreating blade stall at several preset parameters and effect of reverse flow area
12 p1360 N73-21037
Improvements in basic rotary wing design and tests to determine effects on helicopter performance
12 p1360 N73-21038
Aerodynamic characteristics of rotary wings under axial flow conditions and development of numerical analysis techniques
12 p1360 N73-21039
Development of method for predictiong performance of heavily loaded propellers and rotors in steady hovering flight
12 p1360 N73-21040
Analysis of unsteady aerodynamic environment of rotary wings and research projects to improve understanding of rotor unsteady airfoils
12 p1361 N73-21041
Analysis of unsteady aerodynamic loading on reference section of helicopter rotor blade in axial or hovering flight under compressible flow conditions
12 p1361 N73-21044
Developments in techniques for analyzing boundary layer characteristics of rotary wings based on unsteady viscous-inviscid interaction
12 p1361 N73-21046
Development of concept of circulation control applied to rotary wings to show effects on hover, transition, and high speed cruise performance
12 p1362 N73-21050
Wind tunnel tests to determine effects of nonrotating components on helicopter performance and application for helicopter design optimization
12 p1362 N73-21052
Low speed wind tunnel tests of scale model of space shuttle orbiter to determine longitudinal and lateral-directional aerodynamic characteristics
[NASA-CR-123851] 12 p1460 N73-21829
Trisonic wind tunnel tests to determine force and moment characteristics of space shuttle orbiter and modified external tank and solid rocket booster
[NASA-CR-120089] 12 p1460 N73-21831
Wind tunnel tests to determine viscous normal force, pitching moment, side force and yawing moment on bodies of revolution at incidences up to 90 degrees
[WRE-782[WR/D]] 13 p1470 N73-21902
Numerical analysis of unsteady supersonic characteristics of space shuttle type vehicles using arbitrary finite element technique
[NASA-CR-112296] 13 p1470 N73-21904
Development of coruputer program to predict lift, drag, and center of pressure on bodies of revolution at subsonic, transonic, and supersonic speeds
[AD-754098] 13 p1471 N73-21913
Development of method for calculating potential flow about arbitrary lifting three dimensional bodies with emphasis on bound vorticity and application of Kutta condition
[AD-755480] 13 p1471 N73-21914
Wind tuanel tests of swept augmentor wing aerodynamic characteristics
[NASA-TM-X-62252] 13 p1472 N73-21923
Proceedings of conference on rotary wings to investigate rotor wakes, aerodynamic characteristics at hover and high advance ratio, and aerodynamic noise properties
13 p1473 N73-21931
Gas dynamic simulation of plumes from orbiter propulsion system for determining power-on aerodynamic flight characteristics of orbiter
[NASA-CR-124217] 13 p1581 N73-22814
Analysis of aerodynamic and dynamic properties of rotary wing aircraft for application to design, development, and evaluation of helicopters
[AGARD-LS-63] 14 p1597 N73-22948
Basic dynamics of rotary wings, mechanics of helicopter flight, and aerodynamic characteristics of advanced rotary wing concepts and configurations
14 p1598 N73-22951
Analysis of effects of aerodynamic and dynamic parameters on design synthesis of rotary wings and application of optimization techniques
14 p1598 N73-22958
Flight test procedures for rotary wing aircraft with emphasis on performance and flying qualities
14 p1598 N73-22959
Analysis of aircraft rolling moment derivatives caused by rolling, yawing, and sideslip
[ESDU-66.01.00-AMEND-A-C]
14 p1599 N73-22963
Development of lifting surface theory for statically operating propellers based on vortex-lattice representation
[AD-757264] 14 p1603 N73-22998
Development of theory for wind tunnel boundary upwash interference on symmetrical finite wing with arbitrary lift distribution
[AD-757196] 14 p1652 N73-23397
Wind tunnel tests to determine pressure distribution of space shuttle launch configuration for various combinations of geometric components and Mach number
[NASA-CR-120058] 14 p1709 N73-23872
Analysis of flow pattern on tapered, sweptback wing at Mach numbers between 0.6 and 1.6 and 12 degree angle of incidence
[ARC-R/M-3271] 15 p1726 N73-24004
Numerical analysis of aircraft rolling performance and effect of cross-coupling of lateral and longitudinal motions
[ARC-R/M-3349] 15 p1727 N73-24010
Development of method for calculating downwash interference and longitudinal stability of tandem rotor helicopter
[ARC-R/M-3223] 15 p1729 N73-24022
Flight tests of 45 degree delta cropped wing to determine dynamic lateral stability characteristics
[ARC-R/M-3243] 15 p1729 N73-24027
Performance tests of negative hub reaction turbine with jet flap stator and jet flap rotor
[NASA-CR-2244] 15 p1731 N73-24036
Numerical analysis of aircraft takeoff performance based on phases of takeoff and forces exerted on aircraft as basis for aircraft design
15 p1733 N73-24051
Numerical analysis of minimum time climbing procedure and minimum fuel climbing procedure for typical subsonic aircraft
15 p1733 N73-24052
Wind tunnel tests to determine aerodynamic characteristics of delta wing space shuttle orbiter model at various angles of attack and sideslip
[NASA-TM-X-2748] 15 p1733 N73-24058
Analysis of factors affecting flight of multi-engine aircraft with one engine inoperative
[NASA-TT-F-734] 15 p1734 N73-24060
Two dimensional unsteady separation and stall phenomena over airfoils oscillating in pitch with application to short takeoff aircraft
[AD-758899] 15 p1736 N73-24080
Numerical analysis of steady transonic flows over lifting configurations to show reduced lift in thickness-dominated regime
15 p1765 N73-24302
Application of Kelvin impulse theory for computing lift on airfoils and analysis of circulation around airfoil to produce lift
16 p1851 N73-24997
Wind tunnel tests at Mach 2.0 to determine aerodyaamic characteristics of cambered and uncambered gothic wings
[ARC-R/M-3211] 16 p1852 N73-25003
Wind tunnel tests to determine effect of interference on performance of full span jet flap mounted on trailing edge of high aspect ratio unswept wing
[ARC-R/M-3219] 16 p1852 N73-25005
Analysis of effects of shock induced boundary layer separation in transonic flight and methods for eliminating or reducing effects
[ARC-R/M-3510] 16 p1854 N73-25019
Wind tunnel tests to determine subsonic derivatives for oscillating M-wing planform
[ARC-R/M-3214] 16 p1854 N73-25022
Method for conducting aerodynamic analysis of wing-body-tail configurations in subsonic and supersonic flow - Vol. 1
[NASA-CR-2228-PT-1] 16 p1857 N73-25045
Computer program for conducting aerodynamic analysis of wing-body-tail configurations in subsonic and supersonic flow - Vol. 2
[NASA-CR-2228-PT-2] 16 p1858 N73-25046
Characteristics of Yak 40 aircraft and application for short haul service to isolated areas of USSR
[NASA-TT-F-14943] 16 p1859 N73-25057
Analysis of quiet turbofan short takeoff aircraft for short haul air transportation to show research and development requirements and advanced technology benefits - Vol. 2
[NASA-CR-114613] 16 p1860 N73-25066
Computer programs for design of aircraft control systems based on FORTRAN subroutines for generating aircraft transfer functions in six degrees of freedom
[AD-758781] 16 p1861 N73-25075
Design and development of STOL and V/STOL aircraft to show design requirements, performance characteristics, and air traffic control problems
[PB-217102] 16 p1862 N73-25085
Design studies and model test results of folding-proprotor aircraft concept
[AD-759534] 16 p1862 N73-25086
Wind tunnel tests to determine inflation characteristics of solid, flat, circular model parachutes at subsonic speed and various geometric configurations
[AD-759209] 16 p1863 N73-25087
Aerodynamic characteristics and noise attenuation effects of leading edge serrations on rotary wings
[AD-759028] 16 p1863 N73-25088
Development of flow visualization techniques for determining aerodynamic characteristics of bluff bodies under unsteady flow conditions
[AD-759266] 16 p1892 N73-25311
Aerodynamic design parameters and test performance of two-stage high pressure ratio centrifugal compressor
[AD-759499] 16 p1919 N73-25533
Dynamics of sounding rockets at burnout
[SC-DC-72-1613] 16 p1967 N73-25911
Analysis of nonhomogeneous flow associated with two dimensional propulsive lifting system based on flow with energy addition
[NASA-CR-2250] 17 p1979 N73-25997
Aerodynamic characteristics of space shuttle orbiter model in wind tunnel test
[NASA-TM-X-2786] 17 p1979 N73-25998
Comparison of linearized theories to determine aerodyaamic characteristics of slender wings in supersonic flow
[RAE-LIB-TRANS-1677] 17 p1981 N73-26010
Wind tunnel tests to determine effect on cruise performance of installing long duct refan-engine nacelle on DC 8 aircraft
[NASA-CR-121218] 17 p1982 N73-26023
Aerodynamic characteristics of slender delta wings to show performance under various conditions of airspeed, angle of attack, and ground effect
[NASA-TT-F-14949] 17 p1983 N73-26031
Development of engineering analysis and computer code for predicting space shuttle orbiter longitudinal aerodynamic characteristics during abort separation
[NASA-CR-128974] 17 p2086 N73-26877
Low subsonic aerodynamic characteristics of 60 deg swept delta wing space shuttle orbiter
[NASA-TM-X-2762] 17 p2087 N73-26880
Wind tunnel determination of effect of fin planform on aerodynamic characteristics of wingless missile with aft cruciform controls at Mach 1.60, 2.36, and 2.86
[NASA-TM-X-2774] 18 p2101 N73-26995
Wind tunnel tests to determine effect of asymmetric nose bluntness on aerodynamic characteristics of slender cone at Mach 14
[AD-760807] 18 p2102 N73-26998
Analysis of descent trajectories to determine static and dynamic stability of free-fall stores with freely spinning stabilizer devices
[AD-760677] 18 p2102 N73-26999
Analysis of aerodynamic characteristics affecting selection of short takeoff transport aircraft
18 p2103 N73-27012
Numerical analysis of lift and roll stability of ram air cushion vehicle to determine equations for rolling moment coefficient
[PB-219820/8] 18 p2106 N73-27032
Development of simulation program for determining characteristics of tracked air cushion research vehicle
[PB-218368/9] 18 p2106 N73-27033
Analysis of flow field around 18 inch diameter flat circular parachute model using helium bubble technique
[AD-761098] 18 p2106 N73-27034
Wind tunnel tests to determine aerodynamic characteristics of two missile configurations with common body at transonic and supersonic speeds
[NASA-TM-X-2780] 19 p2218 N73-27891
Evaluation of air cushion vehicle operations over railroad beds and secondary roads and analysis of dynamic response to geometric obstacles
[AD-762169] 19 p2221 N73-27920
Analysis of performance benefits for fighter aircraft by application of maneuver load control and relaxed static stability parameters
[AD-762299] 19 p2222 N73-27922
Analysis of transonic scaling effect on quasi, two-dimensional airfoil model of C-141 aircraft
[AD-762285] 19 p2222 N73-27924
Wind tunnel tests to determine effects of control surface modifications on stability and control of space shuttle orbiter
[NASA-CR-133979] 19 p2346 N73-28870
Aeroelastic and dynamic studies of technology applicable to tilting rotor vertical takeoff aircraft with emphasis on propeller whirl instability - Vol. 1
[NASA-TM-X-69497] 20 p2359 N73-28976
Numerical methods for determining unsteady aerodynamic forces on helicopter rotor blades to show lift distribution as function of velocity component normal to blades
[NASA-TT-F-15039] 20 p2360 N73-28981
Development of equations of motion for longitudinal suspension line wave motion during parachute deployment process
[NASA-TM-X-69498] 20 p2361 N73-28988

Aerodynamic characteristics of high lift wing concepts for application to commercial short takeoff transport aircraft
20 p2479 N73-29908
Design, development, and flight test of stowed folding tilt rotor aircraft and comparison with nonfolding tilt rotor aircraft - Vol. 5
[NASA-CR-114598] 21 p2493 N73-30009
Development of procedures for determining stability parameters of balloons tethered under steady wind conditions
[NASA-TN-D-7222] 21 p2493 N73-30013
Analysis of acoustic properties and aerodynamic characteristics of engine over wing configuration with flow attached and unattached on upper surface of flaps
[NASA-TM-X-71419] 21 p2494 N73-30015
Development of automatic flight control systems based on adaptive control techniques and variable structure control systems
[AD-763415] 21 p2498 N73-30047
Development of data for numerical analysis of aerodynamic performance of jet, blown, and ejector flaps
[AD-763793] 21 p2498 N73-30049
Aero and acoustic design features of single stage fans tested in outdoor acoustic facility
[NASA-TM-X-68289] 21 p2579 N73-30668
Simulation calculations of parachute deployment dynamics process for Viking 75 entry vehicle
[NASA-TN-D-7415] 21 p2600 N73-30841
Wind tunnel tests to determine flow characteristics around sharp-edged slender delta wing at large angles of attack
[NASA-TT-F-15107] 22 p2611 N73-30928
Aerodynamic characteristics of round jet located on center line of bottom of aircraft fuselage and elongated slots for lift augmentation
[NASA-TN-D-7299] 22 p2613 N73-30939
Mathematical model for real-time flight simulation of tilt rotor research aircraft for application to aircraft design, pilot training and proof-of-concept-Vol. 5
[NASA-CR-114614] 22 p2614 N73-30949
Wind tunnel tests to determine static longitudinal, lateral, and directional characteristics of twin-engine light aircraft scale model
[NASA-TN-D-7109] 22 p2614 N73-30951
Aerodynamic characteristics and aircraft performance of jet aircraft during takeoff run
[AD-764314] 22 p2615 N73-30959
Wind tunnel tests to determine drag and stability characteristics of solid flat circular and ringslot parachute models
[AD-764364] 22 p2616 N73-30963
Numerical analysis of laminar unsteady flow around airfoil in viscous, incompressible fluid
22 p2649 N73-31226
Prediction of aerodynamic characteristics of airfoils at transonic speeds including effects of fluid viscosity
[AD-763295] 22 p2654 N73-31260
Flight tests of hydrazine control system performance and its effects on flight behavior of reentry vehicle
[SLA-73-154] 22 p2722 N73-31785
Aerodynamic wind tunnel performance of high bypass pressure ratio fan engine for STOL aircraft
[NASA-TM-X-71445] 23 p2740 N73-31931
Wind tunnel tests to determine static and dynamic stability coefficients for circular cone with various nose bluntness configurations
[AD-765164] 23 p2740 N73-31934
Computer program for analyzing characteristics of parachute-payload system during deployment and trajectory
23 p2740 N73-31936
Stability derivative analysis of tethered balloon in steady wind conditions to determine balloon aerodynamics buoyancy, mass, and static forces resulting from tether cable
[NASA-TN-D-7272] 23 p2743 N73-31955
Wind tunnel tests of high harmonic circulation control rotary wing model to show instruments required and data acquisition procedures
[AD-765320] 23 p2747 N73-31984
Thrust augmentation, lift forces, and mixing properties of two-phase flow propulsion and lift system for ground effect machines
[AD-765332] 23 p2777 N73-32208
Aerodynamic characteristics of flow around elliptic cones at large angles of attack
[AD-764945] 23 p2777 N73-32209
Wind tunnel test program to investigate subsonic through high supersonic aerodynamic characteristics of Lockheed delta lifting orbiter and stage-and-one-half launch vehicle
[NASA-CR-124419] 23 p2849 N73-32770
Aerodynamic characteristics of alternate space shuttle configurations and trajectory analysis with external drop tanks installed
[NASA-CR-124418] 23 p2850 N73-32775
Wind tunnel tests to determine aerodynamic characteristics of three oblique, high aspect ratio wing and body combinations at Mach numbers between 0.60 and 1.40
[NASA-TM-X-62256] 24 p2869 N73-32926
Wind tunnel tests to determine aerodynamic characteristics of oblique wing and body combination at Mach numbers between 0.60 and 1.40
[NASA-TM-X-62207] 24 p2870 N73-32927
Objectives and findings of study to determine applicability of short takeoff aircraft for short-haul air transportation systems
24 p2872 N73-32936
Wind tunnel tests to determine aerodynamic characteristics of upper surface blown jet-flap concept incorporating high-bypass-ratio turbofan engines
24 p2872 N73-32943
Development and evaluation of active control system to provide ride smoothing on short takeoff aircraft
24 p2873 N73-32951
Transonic wind tunnel tests to determine lift, drag, and stability characteristics of F-8 aircraft model with oblique wing
[NASA-TM-X-62273] 24 p2877 N73-32974
Transonic wind tunnel tests to determine effects on flutter of aerodynamic interference between pairs of closely spaced delta wings
[NASA-CR-2331] 24 p2989 N73-33887

**AERODYNAMIC CHORDS**
U AIRFOIL PROFILES

**AERODYNAMIC COEFFICIENTS**

Wind tunnel tests to determine effect of simulated hoar frost on lift coefficient of three aircraft wing configurations
[FFA-AU-902] 01 p0001 N73-10001
Linear and nonlinear parts of slender body of revolution aerodynamic coefficients in supersonic flow, noting influence of incidence on pressure distribution
[DLR-FB-72-42] 01 p0001 N73-10006
Procedure for calculating sectional lift coefficient as function of angle of attack and free stream Reynolds number at angles of attack beyond maximum coefficient of lift
[AD-746505] 01 p0002 N73-10008
Development of computer program for analyzing mono-element and multi-element airfoils at subsonic speed with attached air flow - Vol. 2
[AD-740124] 01 p0031 N73-10242
Influence of drag, pressure, and turbulent distribution on flow of dilute Polyox WSR-301 solutions in circular cylinders
[AD-745763] 01 p0042 N73-10334
Digital visual displays for checking pressure points from wind tunnel models
[ARA-28] 02 p0172 N73-11388
FORTRAN program for calculating aerodynamic coefficients of subsonic aircraft at high speeds
04 p0370 N73-13010
Computer program for determining aerodynamic influence coefficients on interferring wings in unsteady supersonic conditions - programmers manual
[NASA-CR-112185] 04 p0404 N73-13291
Improving method of numerical calculation of aerodynamic coefficients for subsonic lifting surface
[REPT-32] 05 p0491 N73-14004
Computer program for calculating aerodynamic coefficients from trajectory angles of projectiles passing through paper screens
[FOA-2-C-2478-44] 06 p0613 N73-14980
Aerodynamic drag coefficients for conical body in near free molecule and transitional flow regimes
[AD-750042] 06 p0615 N73-14994
Application of blockage correction factors to wind tunnel test measurements on aircraft models
06 p0617 N73-15006
Analysis of aerodynamic processes occurring in flow past unpowered multi-element airfoils in high lift attitude
06 p0617 N73-15007
Design aspects of stall of powered-lift aircraft with externally blown flaps and methods for predicting increment in maximum lift coefficient due to power
06 p0617 N73-15011
Flutter characteristics of thin cantilever wings at transonic and supersonic speeds
[NAL-TR-288] 06 p0618 N73-15022
Procedure for determining rolling moment derivatives of aircraft due to rolling, yawing, and sideslip
[ESDU-AIRCRAFT-06.01.00] 07 p0735 N73-15978
Contribution of straight-tapered swept wing to rolling moment derivative due to yawing under conditions where flow remains fully attached to surface
[ESDU-72021] 07 p0735 N73-15980
Method for estimating aerodynamic characteristics of airfoils in compressible inviscid flow based on thickness and camber line parameters
[ESDU-72024] 07 p0735 N73-15981
Effects of thickness and viscosity considerations on accuracy of aerodynamic coefficients determined for thin wings in inviscid flow conditions
[ESDU-70011-AMEND-A] 07 p0735 N73-15982
Computerized aircraft simulation using aerodynamic coefficient table storage, checkout, and interpolation routines
[NASA-TM-X-62229] 08 p0863 N73-16983
Mathematical models for gas surface interactions and calculating aerodynamic coefficients for simple geometric shapes and high Mach number flow past thin airfoils
[AD-752245] 08 p0899 N73-17278
Supersonic aerodynamic influence coefficients for isolated and parallel interfering coplanar and noncoplanar wings
[NASA-CR-2168] 09 p0979 N73-18003
Transonic wind tunnel tests of two dimensional airfoil fitted with square and convex semicircular blunt bases to determine aerodynamic drag coefficients
[ARL/A-NOTE-336] 10 p1103 N73-18994
Mathematical model of force coefficient and pitching moment by wing-body configuration
[BMVG-FBWT-72-28] 10 p1103 N73-18997
Procedure for developing aerodynamic parameters for use in flight simulator research projects with emphasis on wind tunnel measurements
10 p1105 N73-19008
Drag coefficients for Echo 1 and Explorer 24 spherical surfaces in atomic oxygen over energy range from 4 to 200 eV
[NASA-CR-2233] 10 p1192 N73-19697
Influence of degree of turbulence on aerodynamic coefficients of cascades
10 p1204 N73-19798
Effect of axial velocity ratio on aerodynamic coefficients of compressor cascade in viscous flow
10 p1205 N73-19804
Analysis of optimum pressure distribution on multielement airfoils to obtain conditions for maximum lift coefficient
12 p1355 N73-20996
Presentation of helicopter level flight performance as power coefficient compared with tip speed or advance ratio for range of thrust coefficients
12 p1358 N73-21014
Analysis of effects of Reynolds number on aerodynamic stalling of rotary wings and relationship of Reynolds number to aerodynamic coefficients of blade elements
14 p1598 N73-22957
Wind tunnel tests to determine aerodynamic characteristics of model of sweptback wing with warp distribution to produce constant spanwise coefficient of lift
[ARC-R/M-3385] 15 p1727 N73-24007
Aerodynamic coefficients for calculating transport aircraft performance using wind tunnel and scale models
15 p1732 N73-24046
Evaluation of double integral equation for calculation of wave drag due to volume and aerodynamic lift of slender wings
[ARC-R/M-3221] 16 p1852 N73-25006
Design criteria for slender warped wings with unswept trailing edge with zero load along leading edge and near planar vortex sheet at trailing edge for design lift coefficient
[ARC-R/M-3406] 16 p1852 N73-25008
Survey of aerodynamic derivative measurements for unswept rectangular wings and delta wings with emphasis on main surface pitching moment derivatives
[ARC-R/M-3232] 16 p1855 N73-25024
Measurement of pitching moment derivatives using free oscillation technique on two dimensional airfoils of double wedge section and single wedge section
[ARC-R/M-3234] 16 p1855 N73-25025
Development and characteristics of test equipment for measurement of direct pitching moment derivatives for two dimensional flow at subsonic and supersonic speeds
[ARC-R/M-3257] 16 p1855 N73-25027
Design and characteristics of test equipment for measuring longitudinal oscillatory aerodynamic derivatives in high speed wind tunnel
[ARC-R/M-3260] 16 p1855 N73-25029
Flight tests of XB-70 aircraft to determine skin friction coefficients and boundary layer profiles at Mach numbers up to 2.5
[NASA-TN-D-7220] 16 p1887 N73-25276
Objectives of dynamic tests in low speed wind tunnels and techniques for measuring oscillatory derivatives and transient motion effects
17 p2009 N73-26244
Effect of interference of engine jet on aerodynamic characteristics of lifting surface induced by horizontal or vertical jet
[NASA-TT-F-14956] 17 p2015 N73-26292
Determination of aerodynamic parameters for use in flight simulator research
[NASA-TT-F-14994] 18 p2126 N73-27178
Development of data for numerical analysis of aerodynamic performance of jet, blown, and ejector flaps
[AD-763793] 21 p2498 N73-30049
Wind tunnel tests to determine two dimensional characteristics of airfoil optimized for maximum lift coefficient at various angles of attack
[NASA-TN-D-7071] 22 p2611 N73-30929
Aerodynamic configurations of series of airfoils used in parametric studies of drag-rise Mach number
[ESDU-71020] 22 p2650 N73-31228

Derivation of charts for predicting drag-rise Mach number for airfoils with specified upper surface pressure distribution
[ESDU-71019] 22 p2650 N73-31229

Aerodynamic characteristics of augmentor wings and analysis of augmentation and entrainment in defining a net thrust coefficient
24 p2872 N73-32942

Wind tunnel tests to determine magnitude of adverse ground effects on longitudinal aerodynamic coefficients of powered-lift short takeoff aircraft
24 p2873 N73-32950

AERODYNAMIC CONFIGURATIONS

Longitudinal and lateral aerodynamic characteristics of cruise missile with swept wing and conventional aft tails at various Mach numbers
[NASA-TN-D-7069] 01 p0001 N73-10002

High angle of attack characteristics of high performance aircraft and correlation with dynamic directional-stability parameter
[NASA-TN-D-6993] 01 p0005 N73-10033

Test results of booster and orbiter configurations
[NASA-CR-119994-VOL-4] 01 p0108 N73-10887

Wind tunnel analysis of asymmetric yawing moments produced by long pointed fuselage nose shapes at high angles of attack
[NASA-TN-D-7095] 02 p0123 N73-11003

Flight and wind tunnel tests to determine effects of Reynolds number of installed boattail drag of underwing nacelle
[NASA-TM-X-68162] 02 p0124 N73-11007

Evaluation of Rayleigh-Ritz anisotropic plate analysis procedure for determining performance of composite wing for aircraft operating in transonic environment
[AD-745129] 02 p0126 N73-11023

Basic flight characteristics and specifications of An-2 aircraft and equipment
[AD-746791] 02 p0127 N73-11032

Wind tunnel tests to determine lee surface flow characteristics and aerodynamic heating of space shuttle orbiters at supersonic speed with large angles of attack
[NASA-TN-D-7088] 02 p0233 N73-11890

Wind tunnel tests to determine stability and control effectiveness of basic configuration of pressure-fed ballistic recoverable booster for space shuttle
[NASA-CR-120073] 02 p0233 N73-11896

Wind tunnel tests to determine aerodynamic characteristics of space shuttle ascent configurations with parallel burn pressure-fed and SRM boosters and tank T3 installation - Vol. 2
[NASA-CR-120084] 02 p0234 N73-11902

Development of computer programs for analyzing and predicting properties of transonic flows around certain types of wing-body combinations
[NASA-CR-2157] 03 p0247 N73-11999

Evaluation of helicopter rotary wing configuration consisting of conventional pitch horn linkages inboard and aerodynamic control flap outboard for controllable twist
[AD-747808] 03 p0254 N73-12054

Design, development, and evaluation of helicopter control system using fan in fin configuration for antitorque and directional control
[AD-747806] 03 p0254 N73-12055

Aerodynamic design of Mach 8 contoured nozzle for hypervelocity wind tunnel
[AD-747477] 03 p0281 N73-12278

Wind tunnel simulation of ground effect conditions to determine effect of three dimensional turbulent boundary layer on V/STOL aircraft configurations - Pt. 1
[NASA-CR-114495] 03 p0282 N73-12283

Wind tunnel tests to determine aerodynamic characteristics of V/STOL aircraft configurations using blowing flapped wing and direct jet lift systems
[NASA-CR-114496] 03 p0282 N73-12284

Internal drag lift and pitching moment of ducted body, neglecting post exit flow
[ARC-CP-1211] 03 p0285 N73-12305

Operational test and evaluation of angle of attack system for displaying percentage of lift produced by wing for all flap configurations
[AD-748844] 03 p0304 N73-12485

Analysis of interference heating on surfaces of reentry vehicle configurations and effects of wing sweep, angle of attack, and Reynolds number
[NASA-TM-D-7060] 03 p0364 N73-12964

Wind tunnel tests to determine effect of nozzle lateral spacing on afterbody drag and performance of twin-jet afterbody models with cone plug nozzles at supersonic speeds
[NASA-TM-X-2632] 04 p0369 N73-12999

Development of numerical method for designing minimum drag supersonic wing camber surfaces of arbitrary planform for given lift characteristics
[NASA-TN-D-7097] 04 p0369 N73-13001

Effects of wing camber and twist on longitudinal aerodynamic characteristics of wing-body configuration
[NASA-TN-D-7099] 04 p0369 N73-13002

Analysis of aerodynamic interference effects between aircraft and external store carried under wing based on inviscid flow characteristics
[AD-748348] 04 p0370 N73-13005

Flight tests of rotating cylinder flap on YOV-10 aircraft modified to STOL configuration
[NASA-CR-2135] 04 p0371 N73-13020

Helicopter design data to include kinematic and power diagrams of basic components of helicopter structures
[AD-748751] 04 p0373 N73-13035

Development of auxiliary lifting system to provide ferry capability for entry vehicles
[NASA-CASE-LAR-10574-1] 04 p0400 N73-13257

Proceedings of conference to analyze static and dynamic loads exerted on helicopter rotary wings and application to improved helicopter design
[AGARD-R-595] 05 p0491 N73-14000

Analysis of compatibility between maneuver load control, relaxed static stability, and flying qualities requirements for various aircraft configurations
[AD-749479] 05 p0495 N73-14032

Computer program for designing leading edge slats for producing specified pressure distribution on main airfoil
[AD-749485] 05 p0496 N73-14043

Numerical analysis of two dimensional shock wave resulting from mobile wedge moving with supersonic velocity and specific angle of attack into detonation wave
[AD-749650] 05 p0528 N73-14299

Wind tunnel tests to determine pressure distribution on wing and lower body surface for space shuttle orbiter in launch configuration
[NASA-CR-120075] 05 p0600 N73-14879

IBM 360 and 365 computer program for calculating heat and internal conduction of aerodynamic configurations
[AD-749482] 05 p0606 N73-14931

Aerodynamic characteristics of wing moving close to interface with annular jet flowing from wing surface and impinging on screen
[AD-750933] 06 p0615 N73-14995

Design characteristics and performance of airfoils with high lift at low and medium subsonic speeds and various angles of attack
06 p0616 N73-15004

Aerodynamic configurations of swept wings to improve lift performance at stall in higher range of subsonic speeds
06 p0617 N73-15010

Modifications of Jet Provost and Strikemaster trainer aircraft to provide adequate stall warning without excessive penalty on maximum lift at low speed
06 p0617 N73-15012

Analysis of high subsonic and transonic characteristics of fighter aircraft and factors affecting aerodynamic boundaries for various wing design parameters
06 p0618 N73-15019

Reduction of noise generated by externally blown flaps using slot near trailing edge of flap with low velocity secondary air blown through slot
[NASA-TM-X-68172] 06 p0619 N73-15027

Screening tests of upper surface blowing on externally blown flaps configurations to obtain noise and turning effectiveness data
[NASA-TM-X-68167] 06 p0620 N73-15030

Mission performance analysis of three supersonic transport configurations and effects of limitations on allowable engine noise
[NASA-TM-X-68178] 06 p0620 N73-15032

Analysis and application of load alleviation and mode suppression system for YF-12A aircraft to determine extent of design risks
[NASA-CR-2158] 06 p0620 N73-15033

Performance tests of cargo parachutes with pulled down vents for airdrop of supplies from 500 feet altitude
[AD-750585] 06 p0624 N73-15068

Modification of UH-1 helicopter rotor to determine effects of injecting tip vortex of rotor blade with mass of linearly directed air
[AD-750634] 06 p0625 N73-15074

Design and development of sectionalized main rotor blade for UH-1 helicopter
[AD-750633] 06 p0625 N73-15075

Wind tunnel tests to determine effect of wing planform on generation of sonic boom at various Mach numbers
[NASA-TN-D-7160] 06 p0700 N73-15709

Procedure for designing axisymmetric, transiating, cesterbody inlet bleed system for operation at Mach 3.5
[NASA-CR-2187] 06 p0713 N73-15821

Contribution of straight-tapered swept wing to rolling moment derivative due to yawing under conditions where flow remains fully attached to surface
[ESDU-72021] 07 p0735 N73-15980

Design modifications to improve static performance and lateral-directional dynamic stability of light aircraft
07 p0737 N73-15996

Optimized design of supersonic aircraft wing based on linear combination of weight of wing and aerodynamic drag minimization
07 p0737 N73-15997

Wind tunnel tests of full scale model of light aircraft to determine effects of configuration changes on aerodynamic characteristics
[NASA-TN-D-6896] 07 p0739 N73-16012

Computer program and users manual for calculating aerodynamic characteristics of wing-body combinations at subsonic and supersonic speeds
[FFA-AU-635-PT-2] 08 p0863 N73-16985

Aerodynamic characteristics of biplane wing systems with emphasis on stall matching and induced camber effects which differ from monoplane wing
08 p0864 N73-16987

Aerodynamic configuration and predicted performance of short takeoff aircraft for short haul passenger transportation
[CRANFIELD-AERO-12-PT-1] 08 p0867 N73-17019

Analytical techniques for predicting static and dynamic stability, control derivatives, and force and moment coefficients for V/STOL aircraft - Vol. 2
[AD-752558] 08 p0869 N73-17834

Computer program manual for analytical techniques to predict performance of V/STOL aircraft - Vol. 3
[AD-752559] 08 p0869 N73-17835

Literature survey of techniques for predicting performance of V/STOL aircraft- Vol. 4
[AD-752563] 08 p0869 N73-17836

Concept of nuclear powered ground effect machine for commercial operations in Arctic regions
[NASA-TM-X-2684] 08 p0977 N73-17991

Development of takeoff airworthiness standards for new aircraft designs using motion simulators to compare performance and handling characteristics
[NASA-TN-D-7106] 09 p0983 N73-18031

Detail design features of short takeoff and landing commercial aircraft and impact on design caused by STOL requirement - Part 2
[AERO-13-PT-2] 09 p0984 N73-18033

Design, development, and manufacture of natural shape free flight balloon to include requirements, documentation, testing, and inspection
[AD-753086] 09 p0987 N73-18055

Analysis of effects of rotary wing configuration on aerodynamic noise generation during hovering flight
[AD-753397] 09 p0989 N73-18070

Effects of chemical nonequilibrium of inviscid flow in windward plane of symmetry for space shuttle orbiter configurations
[NASA-TN-D-7189] 09 p1015 N73-18287

Numerical analysis of inviscid, fully developed structure of lift-generated vortices behind aircraft wings and extension to arbitrary span-loaded distributions
[NASA-TM-X-62224] 09 p1016 N73-18289

Wind tunnel tests to determine effects of blade twist and aeroelasticity of rotary wings on tilt rotor performance from hover to Mach 0.7 speed
[NASA-TM-X-68948] 10 p1105 N73-19012

Analysis of requirements for turbofan engines for high speed commercial transport aircraft - Vol. 1
[NASA-CR-121132] 10 p1207 N73-19820

Mission analysis of VTOL passenger transport aircraft to determine optimum engine cycle for minimum direct operating cost
[NASA-TM-X-68186] 10 p1208 N73-19826

Performance tests of axial flow transonic compressor stage with multiple circular arc blades to determine effects of blade shape on efficiency and stall margin
[NASA-TM-X-2731] 11 p1231 N73-19995

Method for computing lifting pressure distribution on wing with partial span, swept control surfaces
[NASA-TN-D-7251] 11 p1232 N73-19999

Annotated bibliography of aerodynamic configurations and characteristics of short takeoff aircraft
[AD-754500] 11 p1236 N73-20037

Wind tunnel tests of space shuttle orbiter in various configurations to determine aerodynamic loads and pressure distributions at range of Mach numbers
[NASA-CR-120066] 11 p1342 N73-20890

Design of airfoil sections for low Reynolds numbers based on requirement to achieve transition upstream of major adverse pressure gradient
12 p1355 N73-20995

Wind tunnel tests to determine aerodynamic characteristics of full scale H-126 aircraft using jet flap principle
[NASA-TN-D-7252] 12 p1355 N73-20997

Development of method for estimating normal force, axial force, and pitching moment coefficients for slender bodies of varying cross section equipped with lifting surfaces
[NASA-TN-D-7228] 12 p1355 N73-20998

Minimum weight design of supersonic aircraft wing with finite element modeling to meet strength, stability, frequency, and flutter requirements
12 p1356 N73-21003

Flight tests of Westland Scout helicopter fitted with reduced scale version of rigid rotor to determine airworthiness and handling characteristics
12 p1358 N73-21017

Survey of problems encountered in prediction of structural design loads and aeroelastic stability margins during development of rotary wing aircraft
12 p1358 N73-21020
Aerodynamic characteristics of circulation controlled rotor and fundamental problems of stopped rotor aircraft
12 p1359 N73-21024
Development of jet-flap rotor and application to heavy helicopter and stoppable rotor designs
12 p1359 N73-21025
Review of tilting rotor technology and comparison of tilting rotor performance with standard rotary wings
12 p1359 N73-21027
Development of advancing blade concept rotary wing and wind tunnel tests of full scale model
12 p1359 N73-21029
Proceedings of conference on fluid dynamics of rotary wings and aerodynamic characteristics of rotary wing systems
[AGARD-CP-111] 12 p1359 N73-21031
Aerodynamic characteristics of rotary wings under axial flow conditions and development of numerical analysis techniques
12 p1360 N73-21039
Analysis of unsteady aerodynamic environment of rotary wings and research projects to improve understanding of rotor unsteady airfoils
12 p1361 N73-21041
Effect of rotary wing airfoil modifications on performance, stability, and control of helicopters
12 p1361 N73-21045
Development of technique for rotor blade design and measurement of pressure distributions along the blade chord and across blade wake near rotor tip in flight
12 p1361 N73-21047
Development of algorithm for calculating inviscid flow about arbitrary planform rotors and application to analyzing various rotary wing configurations
12 p1362 N73-21048
Wind tunnel tests to determine effects of blade twist and aeroelasticity on tilt rotor performance from hover to mach number 0.7
12 p1362 N73-21049
Development of concept of circulation control applied to rotary wings to show effects on hover, transition, and high speed cruise performance
12 p1362 N73-21050
Aerodynamic, dynamic, and aeroelastic problems in rotary wing design for helicopters and V/STOL aircraft with application to hingeless rotor systems
12 p1362 N73-21051
Wind tunnel tests to determine effects of nonrotating components on helicopter performance and application for helicopter design optimization
12 p1362 N73-21052
Acoustic measurements of aerodynamic noise generated by externally blown flap lift augmentation system for various aerodynamic configurations
[NASA-TM-X-2776] 12 p1363 N73-21059
Design, development, and production of low cost remotely piloted vehicles based on innovative approach for aircraft engineering procedures
[P-4902] 12 p1363 N73-21060
Application of maximum likelihood criterion and optimal input design for analyzing flight test data to obtain aircraft stability and control derivatives
[NASA-CR-2200] 12 p1364 N73-21071
Bibliography of supersonic transport aircraft data to include program management, systems engineering, aircraft structures, and operational considerations
[AD-755600] 12 p1365 N73-21076
Development of computer program and algorithm for determining interference between lifting surface elements at various Mach numbers
[NASA-CR-112264] 12 p1390 N73-21272
Wind tunnel tests to determine heat transfer properties of space shuttle orbiter, booster, and launch configurations for various angles of attack and yaw
[NASA-CR-128891] 12 p1460 N73-21830
Numerical analysis of unsteady supersonic characteristics of space shuttle type vehicles using arbitrary finite element technique
[NASA-CR-112296] 13 p1470 N73-21904
Design and aerodynamic characteristics of tilt propeller aircraft for short takeoff and landing operations - Vol. 1
[NASA-CR-114441] 13 p1473 N73-21926
Design and aerodynamic characteristics of tilt propellor aircraft for conducting flight research on V/STOL aircraft - Vol. 2
[NASA-CR-114442] 13 p1473 N73-21927
Fundamentals of rotary wing aerodynamics and application to performance considerations of helicopters
14 p1598 N73-22950
Effects of aeroelasticity on performance of rotary wings and procedures for predicting aerodynamic forces on rotary wing blades
14 p1598 N73-22952
Effects of aerodynamic drag on rotary wing performance and methods for reducing influence of stall and compressibility parameters
14 p1598 N73-22954
Windward surface flow distribution on lifting reentry vehicle configurations at high angles of incidence under hypersonic perfect gas conditions
[AD-756499] 14 p1599 N73-22961
Conceptual designs and aerodynamic configurations of tilting rotor V/STOL aircraft for 1975 to 1980 time period - Vol. 1
[NASA-CR-114437] 14 p1599 N73-22964
Preliminary design of V/STOL tilting rotor aircraft for performance of research flights - Vol. 2
[NASA-CR-114438] 14 p1599 N73-22965
Design and evaluation of two airfoils for helicopter rotors for reduction of rotor power requirements
[NASA-CR-112297] 14 p1601 N73-22977
Development of lifting surface theory for statically operating propellers based on vortex-lattice representation
[AD-757264] 14 p1603 N73-22998
Wind tunnel tests to determine aerodynamic interference between space shuttle orbiter, external tank, and solid rocket booster in ascent configuration
[NASA-CR-120060] 14 p1709 N73-23871
Wind tunnel tests to determine pressure distribution of space shuttle launch configuration for various combinations of geometric components and Mach number
[NASA-CR-120058] 14 p1709 N73-23872
Development of slender body theory for analyzing flow past thin, conically cambered, delta wing with exact boundary conditions
[ARC-R/M-3249] 15 p1726 N73-24002
Wind tunnel tests to determine effects of leading edge modifications on flow and forces on untapered wing with 50 degree leading edge sweep and Mach numbers from 0.60 to 1.20
[ARC-R/M-3270] 15 p1726 N73-24003
Measurements of roll damping derivative of three wing planforms using free light roll balance technique for Mach numbers from 0.7 to 1.4
[ARC-R/M-3274] 15 p1726 N73-24005
Wind tunnel tests to determine aerodynamic characteristics of model of sweptback wing with warp distribution to produce constant spanwise coefficient of lift
[ARC-R/M-3385] 15 p1727 N73-24007
Analysis of flow development over plane, half-wing with cropped-delta planform using surface pressure distributions and oil flow patterns with variations in incidence and Mach number
[ARC-R/M-3286] 15 p1727 N73-24008
Theoretical investigation of longitudinal stability, control, and response characteristics of jet flap aircraft
[ARC-R/M-3272] 15 p1730 N73-24028
Application of conformal mapping procedures for designing airfoil shapes with high design lift coefficients
[AD-757813] 15 p1731 N73-24040
Development and application of aircraft performance prediction methods for subsonic and supersonic transport and fighter aircraft
[AGARD-LS-56] 15 p1732 N73-24042
Parametric and optimization techniques for aircraft design synthesis to show principal lines of data flow for component development
15 p1732 N73-24049
Acoustic measurements for large model engine-over-wing configurations with conventional and powered lift, various flap settings, and comparison with engine-under-wing aircraft
[NASA-TM-X-68246] 15 p1735 N73-24070
Wind tunnel tests to determine time-averaged aerodynamic forces on model of helicopter landing pad to be installed on top of lighthouse
[MAR-SCI-R-106] 15 p1761 N73-24269
Numerical analysis of steady transonic flows over lifting configurations to show reduced lift in thickness-dominated regime
15 p1765 N73-24302
Wind tunnel tests to determine pressure distributions for four percent thick, circular arc, biconvex airfoil at transonic speeds
[ARC-R/M-3180] 16 p1852 N73-25002
Application of slender body theory for calculating minimum values of zero lift wave drag of slender wings with unswept trailing edge
[ARC-R/M-3222] 16 p1852 N73-25007
Supersonic wind tunnel tests to measure overall normal and side forces, rolling, pitching, and yawing moments on canard aircraft
[ARC-R/M-3226] 16 p1853 N73-25011
Research projects in theoretical and practical aerodynamics - Vol. 2
16 p1854 N73-25020
Analysis of effect of localized mass on flutter characteristics of delta wing for various spanwise and chordwise positions for the mass center of gravity
[ARC-R/M-3264] 16 p1855 N73-25030
Nonlinear unsteady small-disturbance theory of inviscid transonic flows for oscillating aerodynamic configurations
[NASA-CR-2258] 16 p1858 N73-25048
Wind tunnel tests to determine inflation characteristics of solid, flat, circular model parachutes at subsonic speed and various geometric configurations
[AD-759209] 16 p1863 N73-25087
Numerical analysis of lift and lift distribution on aircraft wing and trailing vortex flow behind wing
[AD-759262] 16 p1863 N73-25089
Analysis of phenomenon generated by passage of projectile into water to determine effects of accelerations, aerodynamic configurations, and surface motions
16 p1886 N73-25264
Designs of high temperature seals for gaps between structure and aerodynamic control surfaces of space shuttle orbiter
[NASA-CR-128951] 16 p1965 N73-25891
Analysis of effect of turbulence intensity on aerodynamic characteristics of bodies of various shapes to develop method for measuring initial turbulence
[AD-760264] 17 p2015 N73-26297
Effects of addition and position of outboard stabilizers and tail configurations on aerodynamic characteristics of low-wave-drag elliptical body at hypersonic speed
[NASA-TM-X-2747] 18 p2101 N73-26993
Aerodynamic characteristics of two space shuttle concepts with delta wing configurations at hypersonic speed using helium flow visualization technique
[NASA-TN-D-7282] 18 p2102 N73-26997
Review of V/STOL development programs to compare basic characteristics of XC-142A, X-19 and X-22A aircraft under various flight conditions
18 p2103 N73-27003
Design, development, and flight characteristics of VAK 191 B V/STOL strike/reconnaissance aircraft
18 p2103 N73-27006
Propulsive-lift technology program for development of short takeoff aircraft propulsion systems and lift augmentation devices
18 p2103 N73-27009
Design, development, and evaluation of Buffalo/Spey Augmentor-Wing research aircraft using internally blown flap for lift augmentation
18 p2103 N73-27010
Design, fabrication, and flight test of Boeing 727 aircraft nacelle modification to reduce aerodynamic noise levels
[AD-756040] 18 p2108 N73-27048
Integral equations for calculating incompressible potential flows around profiles with suction and blowing
[NASA-TT-F-14962] 18 p2130 N73-27209
Wind tunnel tests to determine control of magnus instabilities with aerodynamic configurations using symmetrical fin and non-finned bodies
19 p2217 N73-27885
Effect of nose shape and tail length on static stability of fin-stabilized projectile at supersonic speeds and various angles of attack
[NASA-TM-X-2831] 19 p2217 N73-27888
Design, development, and characteristics of quiet turbofan short takeoff aircraft for short haul air transportation - Vol. 2
[NASA-CR-114607] 19 p2219 N73-27899
Design and characteristics of augmentor wing cruise blowing valveless system for STOL passenger aircraft to define requirements for test facilities - Vol. 2
[NASA-CR-114570] 19 p2220 N73-27907
Design, reliability analysis, maintainability, and cost effectiveness of expendable rotor blades for UH-1 helicopter rotary wing
[AD-762198] 19 p2222 N73-27926
Development and characteristics of pitch/yaw dynamic stability, forced-oscillation test mechanism for measuring stability derivatives of lifting reentry vehicles
[AD-762286] 19 p2250 N73-28143
Program summary of research project for sonic inlet technology involving design concepts for aerodynamic performance and noise suppression - Vol. 1
[NASA-CR-121126] 19 p2328 N73-28731
Research project for noise suppression of sonic inlets used with turbofan engines and improvement in engine inlet flow characteristics - Vol. 2
[NASA-CR-121127] 19 p2328 N73-28732
Numerical analysis of response of aircraft in three dimensional gust field to obtain aerodynamic load data on fuselage and tail structures
[AD-762511] 20 p2359 N73-28978
Performance tests of twin jet afterbody configurations to determine effect of nozzle spacing, fairing shapes, and angle of attack
[NASA-TM-X-2724] 21 p2491 N73-29994
Polar coordinate method applied to program for calculating aerodynamic loads on oscillating wing configurations in subsonic flow
[SAAB-L-0-R64] 21 p2493 N73-30006
Analysis of acoustic properties and aerodynamic characteristics of engine over wing configuration with flow attached and unattached on upper surface of flaps
[NASA-TM-X-71419] 21 p2494 N73-30015
Development and characteristics of experimental aircraft for demonstrating augmentor wing jet short takeoff concept using modified C-8A aircraft - Vol. 1
[NASA-CR-114503] 21 p2494 N73-30016
Flight tests of modified C-8A aircraft to demonstrate augmentor wing, short takeoff concept - Vol. 2
[NASA-CR-114504] 21 p2494 N73-30017

Design of aircraft with rotatable wing for producing high speed aerodynamic configuration
[NASA-CASE-ARC-10470-2] 21 p2494 N73-30018
Effect of wing aspect ratio and flap span on aerodynamic characteristics of short takeoff model with externally blown jet flap
[NASA-TN-D-7205] 21 p2494 N73-30020
Wind tunnel tests to determine effects of variations in Reynolds number and leading edge configurations on aerodynamic characteristics of STOL transport with externally blown flaps
[NASA-TN-D-7194] 21 p2494 N73-30021
Aerodynamic fuselage rear part configurations for aircraft stability optimization noting pressure distribution and aerodynamic forces
[DLR-FB-72-25] 22 p2612 N73-30931
Aerodynamic noise and flow field characteristics of internal flow, jet augmented flap configurations
22 p2612 N73-30937
Criteria for acceptance of early design information with application to design studies and cost estimates for liquid hydrogen fueled aircraft and remotely piloted vehicles
[NASA-TM-X-62303] 22 p2613 N73-30943
Mathematical model for real-time flight simulation of tilt rotor research aircraft for application to aircraft design, pilot training and proof-of-concept-Vol. 5
[NASA-CR-114614] 22 p2614 N73-30949
Wind tunnel and rotor whirl cage tests to determine stability and control parameters of scale model of tilting rotor aircraft model - Vol. 6
[NASA-CR-114615] 22 p2614 N73-30950
Occurrence and magnitude of surface effect takeoff and landing aircraft skirt flutter
[AD-764137] 22 p2616 N73-30966
Aerodynamic configurations of series of airfoils used in parametric studies of drag-rise Mach number
[ESDU-71020] 22 p2650 N73-31228
Wind tunnel tests to determine flow distribution at inlet locations on aircraft model for various aerodynamic configurations and airspeeds
[NASA-TN-D-7364] 23 p2739 N73-31929
Procedure for evaluating relative economic value of technology factors affecting design, configuration, and operation of hypersonic cruise transport
[NASA-CR-2286] 23 p2743 N73-31953
Flight tests of modified F-106 aircraft to determine installation effects of two aft underwing nacelles housing afterburning J-85 engines
[NASA-TM-X-71439] 23 p2743 N73-31959
Aerodynamic design of inlet stage for two-stage compressor and performance comparison for axial, mixed flow, and centrifugal stage configurations
[NASA-CR-120943] 23 p2829 N73-32610
Aerodynamic characteristics of alternate space shuttle configurations and trajectory analysis with external drop tanks installed
[NASA-CR-124418] 23 p2850 N73-32775
Trisonic wind tunnel tests of baseline launch configuration space shuttle model to determine effects of model parametric variations on static stability characteristics
[NASA-CR-128778] 23 p2851 N73-32783
Wind tunnel tests to determine aerodynamic characteristics of oblique wing and body combination at Mach numbers between 0.60 and 1.40
[NASA-TM-X-62207] 24 p2870 N73-32927
Aerodynamic and performance characteristics of short takeoff aircraft equipped with externally blown flaps
24 p2872 N73-32939
Wind tunnel tests to determine stability and control characteristics of externally blown jet-flap configurations
24 p2872 N73-32940
Aerodynamic characteristics of augmentor wings and analysis of augmentation and entrainment in defining a net thrust coefficient
24 p2872 N73-32942
Wind tunnel tests to determine aerodynamic characteristics of five configurations of short takeoff aircraft wind tunnel models
24 p2872 N73-32944
Flight tests of augmentor-wing jet STOL research aircraft to compare wind tunnel data with flight data for dynamic characteristics and limitations
24 p2874 N73-32954
Wind tunnel tests to determine acoustic properties of externally blown flap and augmentor wing for short takeoff aircraft configurations
24 p2875 N73-32965
Aerodynamic noise characteristics of short takeoff aircraft with externally blown flaps and engines mounted over and under wing
24 p2876 N73-32966
Flight tests of Boeing 727 aircraft to determine effects of modifications on reduction of aerodynamic noise
[FAA-RD-72-40-VOL-3] 24 p2876 N73-32971
Effect of inlet conditions on optimal shape of diffuser based on theory of potential flow of fluid in channels
[AD-765577] 24 p2911 N73-33230

**AERODYNAMIC DRAG**

Wind tunnel tests to determine effect of nozzle lateral spacing on afterbody drag and performance of twin-jet afterbody models with cone plug nozzles at supersonic speeds
[NASA-TM-X-2632] 04 p0369 N73-12999
Application of point position radar data to determine aerodynamic drag of projectile
[AD-750564] 05 p0492 N73-14013
Use of aerodynamic drag for transfer from hyperbolic trajectories to satellite orbits noting spacecraft guidance
[D-149] 05 p0596 N73-14849
Aerodynamic drag of series of spherically-blunted conical bodies with three classes of half-vertex angles under hypersonic flow conditions
[NAL-TR-280] 06 p0613 N73-14978
Computation of drag coefficients for ballistic range models
[DREV-TN-2027/72] 06 p0614 N73-14987
Influence of trailing edge thickness on aerodynamic drag of rectangular wings in transonic and supersonic flow
[DLR-FB-71-85] 06 p0615 N73-14991
Aerodynamic drag coefficients for conical body in near free molecule and transitional flow regimes
[AD-750042] 06 p0615 N73-14994
Application of power method for reducing base drag of long range supersonic aircraft at supersonic speeds
[AD-750950] 06 p0623 N73-15056
Methods for determining air resistance to fragmented shrapnel of different shapes
[FOA-2-A-2539-44] 06 p0653 N73-15304
Aerodynamic drag for streamline bodies at small angles of incidence
[ESDU-BODIES-02.04.00] 07 p0735 N73-15979
Reduction of transonic drag for high performance aircraft by injecting air in rear of aircraft to alter transonic flow distribution on aft section
[AD-751269] 07 p0736 N73-15991
Inverse method for exact analytical solutions for particle motion under central Newtonian gravitational force and atmospheric drag force
[AD-751491] 07 p0847 N73-16865
Analysis of aerodynamic drag on general convex bodies at zero angle of attack during high speed flow in rarefied air
08 p0895 N73-17242
Heat transfer and aerodynamic resistance of in-line smooth walled tube arrays in transverse air flow at high Reynolds number
[NLL-RTS-7689] 09 p1098 N73-18959
Transonic wind tunnel tests of two dimensional airfoil fitted with square and convex semicircular blunt bases to determine aerodynamic drag coefficients
[ARL/A-NOTE-336] 10 p1103 N73-18994
Flow instabilities of supersonic variable ramp inlets at Mach 2 discussing Concorde aircraft intake
[ARC-R/M-3711] 10 p1104 N73-18999
Development of base bleed techniques to reduce Magnus moment on long spinning bodies and improved drag characteristics
[AD-754753] 11 p1232 N73-20002
Computer program for calculating aerodynamic stability and drag of slender aircraft at subsonic and supersonic speeds
[NASA-CR-112229] 13 p1469 N73-21897
Effects of aerodynamic drag on rotary wing performance and methods for reducing influence of stall and compressibility parameters
14 p1598 N73-22954
Drag and stability characteristics of hypersonic blunt nosed conical bodies in gas mixtures
[NASA-CR-131986] 14 p1599 N73-22962
Numerical analysis of drag of streamlined bodies of revolution for various length to diameter ratios
[ESDU-BODIES-02.04.02] 14 p1647 N73-23362
Development and characteristics of analog wake drag evaluation system for use in test section of low speed wind tunnel
[FFA-AU-860] 14 p1648 N73-23368
Equation of motion of sand particle under influence of aerodynamic drag developed in inertial coordinate system
[AD-757724] 14 p1653 N73-23405
Many body theory of aerodynamic forces
16 p1851 N73-24995
Evaluation of double integral equation for calculation of wave drag due to volume and aerodynamic lift of slender wings
[ARC-R/M-3221] 16 p1852 N73-25006
Optimum design of wing-body combinations for zero-lift drag rise at transonic speeds
[ARC-R/M-3279] 16 p1857 N73-25043
Application of laminar flow solutions for heat transfer and flow friction to design of heat exchangers
16 p1886 N73-25266
Effects of variations in fineness ratio and closure ratio on boattail drag of circular arc afterbody models at static conditions and at Mach number of 1.30
[NASA-TN-D-7163] 16 p1957 N73-25830
DC 9 refanned engine nacelle effects on cruise drag considering lateral spacing
[NASA-CR-121219] 17 p1982 N73-26024
Effects of addition and position of outboard stabilizers and tail configurations on aerodynamic characteristics of low-wave-drag elliptical body at hypersonic speed
[NASA-TM-X-2747] 18 p2101 N73-26993
Design and development of two dimensional airfoil with optimum drag divergence characteristics at transonic speeds
[NAL-TR-299] 18 p2101 N73-26994
Effect of air resistance on vibration damping in metal plates
[AD-761591] 19 p2350 N73-28906
Aerodynamic drag on slender bodies in transonic flow
[AD-763437] 21 p2527 N73-30264
Derivation of charts for predicting drag-rise Mach number for airfoils with specified upper surface pressure distribution
[ESDU-71019] 22 p2650 N73-31229
Method for estimating drag-rise mach number of smooth, nonducted, axisymmetric bodies at zero incidence without discontinuities in surface slope
[ESDU-71008] 22 p2650 N73-31230
Aerodynamic drag and lift of airships, noting boundary layer control by suction
24 p2879 N73-32994
Technical conditions for airship development, noting weight reduction, propulsion system performance, and maneuverability improvement
24 p2879 N73-32995
Falling sphere measurement data on atmospheric parameters
[WRE-TN-799[WR/D]] 24 p2958 N73-33639

**AERODYNAMIC FORCES**

NT AERODYNAMIC DRAG
NT AERODYNAMIC LOADS
NT BLAST LOADS
NT GUST LOADS
NT INTERFERENCE LIFT
NT JET LIFT
NT LIFT
NT WING LOADING
NT ZERO LIFT
Digital analysis of dynamic response data, aerodynamic forces and stability derivatives, of free flight models
[ARC-R/M-3699] 03 p0248 N73-12006
Design and development of instrument for measuring aerodynamic loads and fatique characteristics of aircraft structures
[AGARD-R-597] 04 p0371 N73-13019
Development of computer program for generating aerodynamic forces for plane and interfering wings at supersonic speeds
[NASA-CR-112184] 04 p0404 N73-13290
Perturbation approximation method for determining velocity potential and aerodynamic forces of slender body of elliptical cross section in airstream
[AD-748353] 04 p0407 N73-13317
Integration of unsteady aerodynamic forces and pressure distributions in aeroelastic analysis
[NLR-MP-71013-U] 05 p0492 N73-14011
Analysis of velocity profiles in boundary layer produced by incompressible flow during takeoff
06 p0616 N73-15001
Analysis of shock forces generated by opening 35 foot diameter extended-skirt parachute for retardation at 100,000 feet altitude
[AD-749690] 06 p0623 N73-15060
Modifications to helicopter active transmission isolation system to provide method for measuring forces on rotary wing of CH-53 helicopter
[NASA-CR-112245] 09 p0982 N73-18024
Dynamic and aeroelastic problems of stop-rotors of V/STOL aircraft occurring during retracting and stowing of rotary wings
[DLR-FB-72-65-PT-1] 09 p0983 N73-18027
Collection and processing of gust load data obtained from counting accelerometers mounted at center of gravity of various aircraft
[AGARD-R-605] 11 p1235 N73-20023
Numerical analysis of ideal and real gas equations for application to lift generated by helicopter rotors
[AD-754420] 11 p1235 N73-20026
Development of method for estimating normal force, axial force, and pitching moment coefficients for slender bodies of varying cross section equipped with lifting surfaces
[NASA-TN-D-7228] 12 p1355 N73-20998
Calculation and measurement of aerodynamic forces on oscillating airfoil with and without aerodynamic stalling
12 p1361 N73-21042
Influence of various aerodynamic forces on rectangular wing performance with harmonic movement parallel to sieve flow movement
12 p1361 N73-21043
Research projects involving aerodynamics, aerodynamic heating, aerodynamic forces, airframes, structural analysis, and fluid mechanics - Vol. 1
15 p1725 N73-23995
Calculation of aerodynamic forces of bending and torsional vibration on installed vibrating cascade blades
[ARC-R/M-3254] 15 p1728 N73-24015

Aerodynamic forces and trajectories of external stores separated from F-4 aircraft
[AD-757932] 15 p1850 N73-24993
Many body theory of aerodynamic forces
16 p1851 N73-24995
Supersonic wind tunnel tests to measure overall normal and side forces, rolling, pitching, and yawing moments on canard aircraft
[ARC-R/M-3226] 16 p1853 N73-25011
Analysis of effect of localized mass on flutter characteristics of delta wing for various spanwise and chordwise positions for the mass center of gravity
[ARC-R/M-3264] 16 p1855 N73-25030
Development of method for calculating spanwise loading on helicopter rotor blades in forward flight at various azimuth angles
[ARC-R/M-3318] 16 p1856 N73-25032
Method for conducting aerodynamic analysis of wing-body-tail configurations in subsonic and supersonic flow - Vol. 1
[NASA-CR-2228-PT-1] 16 p1857 N73-25045
Computer program for conducting aerodynamic analysis of wing-body-tail configurations in subsonic and supersonic flow - Vol. 2
[NASA-CR-2228-PT-2] 16 p1858 N73-25046
Flight test measurements of control surface hinge moments on X-24 lifting body correlation with wind tunnel data
[NASA-TM-X-2816] 16 p1858 N73-25049
Analysis of aerodynamically induced oscillations of bundled power conductors resulting from effect of wind on transmission power lines
17 p2098 N73-26971
Development of equations of motion for longitudinal suspension line wave motion during parachute depioyment process
[NASA-TM-X-69498] 20 p2361 N73-28988
Analysis of aerodynamic drag on object moving in rarefied gas under nearly free molecular flow conditions
24 p2869 N73-32923
On the effects of viscous interaction for a flat delta wing at incidence
[ARC-CP-1237] 24 p2870 N73-32931
Development of instrument to measure steady and oscillatory aerodynamic forces on sting-mounted model using forced oscillation technique
[ATN-7101] 24 p2926 N73-33366

**AERODYNAMIC HEAT TRANSFER**
NT HYPERSONIC HEAT TRANSFER
Effect of heat transfer level on mechanical properties of elastomeric ablative material used on spherically blunted cones
[NASA-TM-X-2612] 02 p0191 N73-11548
Ablation of graphite surfaces heated in turbulent flow of air or carbon dioxide and development of method for calculating ablation rate
[AD-747727] 03 p0365 N73-12973
Aerothermodynamic wind tunnel tests of space shuttle configurations performed at Mach number 8 for flow distribution and heat transfer under reentry conditions
[NASA-CR-131486] 13 p1583 N73-22834
Heat transfer tests for simple delta wings at Mach numbers 8 and 10.5
[NASA-CR-131485] 13 p1591 N73-22900
Effects of heat transfer on laminar boundary layer development under pressure gradients in compressible flow
[ARC-R/M-3218] 15 p1727 N73-24012
Reduction of photographic heat transfer rate data at wind tunnel test facility
[AD-762928] 20 p2420 N73-29447

**AERODYNAMIC HEATING**
NT SHOCK HEATING
Newton-Raphson techniques for analyzing reentry trajectories for heat minimization and terminal range maximization
[AD-745998] 01 p0106 N73-10882
Development of computer program for simulating performance of space radiator to account for transient and steady state performance
[NASA-CR-128594] 01 p0108 N73-10891
Fortran program for axisymmetric, transient heating and material ablation
[AD-745441] 01 p0118 N73-10975
Wind tunnel tests to determine lee surface flow characteristics and aerodynamic heating of space shuttle orbiters at supersonic speed with large angles of attack
[NASA-TN-D-7088] 02 p0233 N73-11890
Analysis of shock interaction and interference heating on military aerospace vehicles at hypersonic speeds
[AD-747765] 03 p0286 N73-12319
Analysis of interference heating on surfaces of reentry vehicle configurations and effects of wing sweep, angle of attack, and Reynolds number
[NASA-TN-D-7060] 03 p0364 N73-12964
Wind tunnel tests to determine effects of hypersonic flow interaction on thrustor nozzle configurations and procedures to prevent excess heating
[NASA-CR-129914] 05 p0597 N73-14857
IBM 360 and 365 computer program for calculating heat and internal conduction of aerodynamic configurations
[AD-749482] 05 p0606 N73-14931
Aerodynamic heating of supersonic models due to shock wave impingement
[AD-749946] 06 p0655 N73-15324
Numerical analysis of characteristic processes of hyperbolic shock layers generated during atmospheric entry
07 p0768 N73-16242
FORTRAN program for predicting temperature-time histories of hemispherical shells subject to aerodynamic heating
[WRE-TN-783[WR/D]] 09 p1098 N73-18961
Computation of aerodynamic heating for Europa 3 launch vehicle
[TN-ER/02-22/001] 10 p1224 N73-19952
Development of methods for protecting aircraft compartments from aerodynamic heating effects
[AD-754606] 11 p1236 N73-20036
Research projects involving aerodynamics, aerodynamic heating, aerodynamic forces, airframes, structural analysis, and fluid mechanics - Vol. 1
15 p1725 N73-23995
Measurement of aerodynamic heating on nose of Fairey Delta aircraft at 40,000 feet and Mach numbers to 1.65 during climb and level flight
[ARC-R/M-3280] 15 p1725 N73-23996
Research projects involving boundary layer flow, heat transfer during aerodynamic heating, atmospheric turbulence effects, and airframe structural analysis - Vol. 2
15 p1727 N73-24011
Effects of heat transfer on laminar boundary layer development under pressure gradients in compressible flow
[ARC-R/M-3218] 15 p1727 N73-24012
Analysis of wing leading edge buckling due to aerodynamic heating to show effect of shear modulus of material and geometry of leading edge on buckling onset
[ARC-R/M-3197] 16 p1851 N73-25000
Development of equations of motion for energy dissipation phase of shuttle reentry and landing approach - Document 23
[NASA-CR-128960] 16 p1941 N73-25709
Aerodynamic heating analysis on sounding rocket tangent ogive nose wall
[NASA-TM-X-69896] 17 p1979 N73-26001
Strain gage bridge calibrations on wing structure at elevated temperatures to establish thermal and mechanical loads due to aerodynamic heating
[NASA-TN-D-7390] 19 p2348 N73-28883
Development of computer program for solving one dimensional heat flow problem using aerodynamic heating examples
[WRE-TN-884[WR/D]] 19 p2351 N73-28914
Radiant array with as many as 144, 13 inches wide, modular radiant heating units mounted in sets of 3 to comprise each adjustable row
[NASA-CR-124435] 24 p2901 N73-33153
Plasma-sprayed metal-glass and metal-glass fluoride coatings for lubrication
[NASA-TM-X-71432] 24 p2929 N73-33392
Space environment aerodynamic heating tests on mullite and silica fiber surface insulation panels
24 p2940 N73-33476

**AERODYNAMIC INTERFERENCE**
Wind tunnel tests to determine aerodynamic interference between space shuttle orbiter, external tank, and solid rocket booster in ascent configuration
[NASA-CR-120060] 14 p1709 N73-23871
Wind tunnel interference factors for high lift wings in closed wind tunnels
16 p1851 N73-24996
Wind tunnel tests to determine effect of interference on performance of full span jet flap mounted on trailing edge of high aspect ratio unswept wing
[ARC-R/M-3219] 16 p1852 N73-25005
Numerical analysis of wing bending, wing torsion, and aileron rotation at transonic speeds to determine effects on wing-aileron flutter
[ARC-R/M-3258] 16 p1855 N73-25028
Aerodynamic interference between aircraft and external store mounted on elliptical wing under inviscid flow conditions
[AD-759170] 16 p1864 N73-25094
Aerodynamic effects of blade tip clearance in axial flow turbine lifting line for nonuniform flow, calculating lift and induced drag
[REPT-4/1973] 19 p2329 N73-28738
Slotted transonic wind tunnel tests on pitching delta wing enable selection of porpous walls for interference free damping derivatives
[ARC-R/M-3715] 24 p2870 N73-32930

**AERODYNAMIC LIFT**
U LIFT

**AERODYNAMIC LOADS**
NT BLAST LOADS
NT GUST LOADS
Engineering data for aeronautical structures under loads
[ESDU-SS2] 01 p0111 N73-10918
Survey of aerospace industry to determine various techniques used in considering interactions of handling qualities, stability, control, and load alleviation devices on structural loads
[AGARD-R-593] 02 p0125 N73-11020
Analysis of fatigue crack propagation characteristics of steel structures in F-111 aircraft under specific flight loading spectra
[AD-746343] 02 p0127 N73-11033
Statistical analysis of normal acceleration, airspeed, altitude, and flight loads on military aircraft
[AD-747285] 02 p0127 N73-11035
Development of equations for large amplitude coupled flap-lag motion of hingeless elastic helicopter blades
[NASA-CR-114485] 03 p0252 N73-12040
Flight loads data recording system for F-102 aircraft maneuver load analysis for data acquisition and application to development of structural design criteria
[AD-747016] 03 p0253 N73-12047
Development of method for estimating length of atmospheric turbulence patch as function of different turbulence intensities for two or more regions
[NRC-12793] 04 p0370 N73-13009
Design and development of instrument for measuring aerodynamic loads and fatique characteristics of aircraft structures
[AGARD-R-597] 04 p0371 N73-13019
Effects of aerodynamic stall on helicopter rotor blade element in three dimensional rotating environment
[NASA-CR-114489] 04 p0372 N73-13028
Analysis of response of flexible helicopter rotor blade to random loads with vertical velocity component
[AD-746627] 04 p0374 N73-13038
Fatigue crack propagation of aluminum metal sheets under flight simulation loads corresponding to gust spectrum
[NLR-MP-72010-U] 04 p0480 N73-13926
Proceedings of conference to analyze static and dynamic loads exerted on helicopter rotary wings and application to improved helicopter design
[AGARD-R-595] 05 p0491 N73-14000
Application of model helicopter rotor experiments to determining dynamic stall of rotary wings and predicting aerodynamic loads developed
05 p0491 N73-14002
Numerical analysis of unsteady aerodynamic forces on helicopter rotor blades to determine lift distribution as function of velocity component normal to blades
05 p0491 N73-14005
Analysis and application of load alleviation and mode suppression system for YF-12A aircraft to determine extent of design risks
[NASA-CR-2158] 06 p0620 N73-15033
Relation between measured C.G. vertical accelerations and loads at T-tail of military aircraft
07 p0851 N73-16004
Calculation of induced load effects on controllability of rigid and flexible aircraft
08 p0865 N73-17004
Development of computer programs to calculate helicopter rotor tip vortex geometry in hover and forward flight to include calculation of rotor harmonic air loads
[AD-752628] 08 p0869 N73-17032
Measurement of surface pressure fluctuations at two locations on XB-70 aircraft at local Mach number range from 0.35 to 2.45
[NASA-TN-D-7226] 09 p0981 N73-18013
Analysis of airload and blade response of rotary wings to determine sources of rotor vibratory loads in level and maneuvering flight of NH-3A and CH-53A helicopters
[NASA-CR-2225] 10 p1103 N73-18996
Analysis of point vortex approximation of vortex sheet in two space dimensions and application to vortex sheet induced by ellipitcally loaded wing
[AD-755007] 11 p1273 N73-20335
Wind tunnel tests of space shuttle orbiter in various configurations to determine aerodynamic loads and pressure distributions at range of Mach numbers
[NASA-CR-120066] 11 p1342 N73-20890
Tables of reports giving comparative theoretical and experimental aerodynamic loading data relevant to zero- and low-frequency aeroelastic problems
[ARC-R/M-3708] 12 p1356 N73-21000
Survey of problems encountered in prediction of structural design loads and aeroelastic stability margins during development of rotary wing aircraft
12 p1358 N73-21020
Analysis of unsteady aerodynamic loading on reference section of helicopter rotor blade in axial or hovering flight under compressible flow conditions
12 p1361 N73-21044
Structural load reduction of space shuttle booster/orbiter configuration using load relief guidance technique
[NASA-TM-X-64738] 12 p1457 N73-21812
Results of wind tunnel measurements of normal force, pitching moment, and Magnus force and moment on M823 research store with fixed and freely spinning stabilizers
[AD-757658] 13 p1471 N73-21912

Computer graphics for solving three dimensional lifting body potential flow nonlinear equations to determine aerodynamic loads
[DGT-7510] 13 p1474 N73-21939
Numerical analysis of aerodynamic load distribution on swept back wing mounted on infinite circular cylinder fuselage at zero angle of attack
[AD-756075] 13 p1475 N73-21952
Aerodynamic characteristics of helicopters with emphasis on airloads, aeroelasticity, and mechanical instabilities
14 p1597 N73-22949
Effects of aeroelasticity on performance of rotary wings and procedures for predicting aerodynamic forces on rotary wing blades
14 p1598 N73-22952
Analysis of effects of aerodynamic and dynamic parameters on design synthesis of rotary wings and application of optimization techniques
14 p1598 N73-22958
Development of reliability analysis procedure for determining effects of cumulative and maximum operational loads on airplane structures
[AD-757529] 14 p1603 N73-22999
Application of modified slender wing theory to analyze aerodynamic characteristics of slender, lifting, wings with curved leading edges at supersonic speeds
[ARC-R/M-3278] 15 p1727 N73-24006
Wind tunnel tests to determine time-averaged aerodynamic forces on model of helicopter landing pad to be installed on top of lighthouse
[MAR-SCI-R-106] 15 p1761 N73-24269
Calculation of spanwise loading on sweptback wings with trailing edge flaps using data obtained from electric tank tests
[ARC-R/M-3487] 16 p1853 N73-25010
Research projects in theoretical and practical aerodynamics - Vol. 2
16 p1854 N73-25020
Development of numerical procedures for determining velocity potential on triangular wing oscillating harmonically in supersonic flow
[ARC-R/M-3229] 16 p1854 N73-25023
Wind tunnel tests to determine pressure distribution on two dimensional airfoil with pylon mounted stores at subsonic speeds using F-4 aircraft model
[AD-759582] 16 p1859 N73-25053
Optimization of mass distribution of solid beams and panels for structural design of airframes and panels
[AD-759169] 16 p1859 N73-25054
Development of procedures for determining service life of helicopter airframes and rotor blades
[RAE-LIB-TRANS-1520] 17 p1981 N73-26013
Statistical analysis of counting accelerometer data obtained on Navy and Marine fleet aircraft from 1 Jan. 1962 to 1 Jan. 1972
[AD-760321] 17 p1985 N73-26041
Elastic vibrations of aircraft wing caused by distributed load, center of gravity displacement, and rotation using electromodeling techniques
[AD-760965] 18 p2108 N73-27043
Analysis of aircraft structural loads in operational flight to determine effects of pilot performance and aircraft characteristics
[AGARD-R-608] 19 p2218 N73-27895
Application of oscillation theory and mathematical statistics to problems of aircraft structures and aerodynamic loads on aircraft and missiles
[NASA-TT-F-753] 19 p2220 N73-27908
Development of rolling maneuver fatigue load data for F-5 and F-105 aircraft based on statistical flight loads data
[AD-761491] 19 p2221 N73-27915
Strain gage bridge calibrations on wing structure at elevated temperatures to establish thermal and mechanical loads due to aerodynamic heating
[NASA-TN-D-7390] 19 p2348 N73-28883
Acquisition of stress data and aerodynamic loads on F-5 aircraft using mechanical strain gages and oscillograph recorders for service life determination
[AD-760567] 20 p2361 N73-28991
Proceedings of conference on acoustic fatigue to show effects of aerodynamic loads, response of structures, structural design, and fatigue test methods
[AGARD-CP-113] 20 p2478 N73-29905
Development of digital computer program for generating individual component or entire aircraft mass and aerodynamic models for vehicle inelastic bending response analysis
[AD-763701] 21 p2498 N73-30045
Development of damping system to compensate for wind loads on space shuttle vehicle during launch operations
[NASA-CR-124367] 21 p2601 N73-30845
Effects of wind loads on structures and structural design criteria based on wind speed, structural shape, and aerodynamic coefficients
[NLL-LIB-TRANS-1705-[5205.9]]
21 p2602 N73-30857
Computer programs for computing stability characteristics of tethered balloon under steady wind conditions
[NASA-TM-X-2740] 23 p2742 N73-31952

AERODYNAMIC MOMENTS
U STABILITY DERIVATIVES
AERODYNAMIC NOISE
Application of ride-quality criteria to design of commercial helicopters with emphasis on noise and vibration considerations
01 p0003 N73-10015
Jet aircraft noise of XV-5B V/STOL aircraft as determined by full scale flight test and wind tunnel model tests
[NASA-TM-X-62182] 01 p0004 N73-10029
Aircraft maneuvers for reducing sonic boom intensity during horizontal turns
[AD-744859] 02 p0126 N73-11022
Development of procedures for quieting externally-blown-flap noise sources produced by interaction of jet exhaust flow with deployed flaps
[NASA-CR-112166] 04 p0372 N73-13022
Acoustic measurements of aerodynamic noise generated by air jet impinging on large flat board for variable impingement angles, jet velocities, and distances from board
[NASA-TN-D-7075] 04 p0372 N73-13026
Proceedings of symposium on helicopter noise held at Durham, North Carolina Sept. 1971
[AD-748876] 04 p0373 N73-13036
Analysis of acoustic properties of shock associated noise in narrow band spectrum produced by jet flows - Vol. 5 App. 2
[AD-749142] 05 p0496 N73-14040
Acoustic properties of supersonic jet noise and refraction effects on noise field
[AD-749140] 05 p0581 N73-14728
Reduction of noise generated by externally blown flaps using slot near trailing edge of flap with low velocity secondary air blown through slot
[NASA-TM-X-68172] 06 p0619 N73-15027
Screening tests of upper surface blowing on externally blown flaps configurations to obtain noise and turning effectiveness data
[NASA-TM-X-68167] 06 p0620 N73-15030
Wind tunnel tests to determine effect of wing planform on generation of sonic boom at various Mach numbers
[NASA-TN-D-7160] 06 p0700 N73-15709
Acoustic properties of sound emitted from arbitrary point in parallel or nearly parallel turbulent shear flow confined to region near solid boundaries
[NASA-TN-D-7118] 07 p0821 N73-16653
Development of theory of aerodynamic noise to analyze jet noise directivity and shear-noise contribution to overall jet noise
[NASA-TN-D-7158] 07 p0821 N73-16654
Structural vibration and noise effects on man in aerospace operations
[AGARDOGRAPH-151] 08 p0876 N73-17098
Airborne noise in aerospace operations and bioacoustics effects on man
08 p0876 N73-17100
Effect of various physical and operating parameters on noise produced by low pressure ratio propulsive fans operating at subsonic speeds
[NASA-CR-2188] 09 p0980 N73-18011
Flight test measurements and analysis of sonic booms to determine caustics produced by variations in flight speed and to develop method for predicting shock wave-ground intersections
[NASA-CR-2167] 09 p0982 N73-18022
Wind tunnel tests to determine acoustic properties of semispan wing with externally blown jet flap to include effects of flap size, vertical location and forward speed
[NASA-TM-X-2749] 09 p0985 N73-18041
Measurement of noise levels produced by F-105 aircraft and analysis of effects on environment and land use
[AD-753113] 09 p0987 N73-18056
Analysis of effects of rotary wing configuration on aerodynamic noise generation during hovering flight
[AD-753397] 09 p0989 N73-18070
Analysis of aerodynamic noise generated by tips of helicopter rotary wings during acceleration to near sonic speed
[AD-752301] 09 p0989 N73-18072
Application of sound suppression techniques to OH-6 helicopter and measurement of resultant noise reduction
[AD-753646] 09 p0989 N73-18077
Effects of flow turbulence and noise on transition and boundary layer development in aerodynamic wind tunnel tests
[NASA-TT-F-14833] 09 p1066 N73-18702
Application of gas dynamics equations to determine magnitude of pressure rise due to sonic boom in stratified atmosphere
[NASA-TN-D-7105] 11 p1233 N73-20010
Analysis of basic acoustic characteristics and noise reduction potential of upper surface of blown flap
[NASA-CR-112246] 11 p1234 N73-20017
Evaluation of acoustic properties of conventional wind tunnels for analyzing aerodynamically generated noise
[NASA-CR-114575] 11 p1266 N73-20277

Analysis of aerodynamic noise produced by rotary wings and methods for noise reduction based on shed vortex wakes and blade tip modification
12 p1362 N73-21053
Generation of aerodynamic noise by turbulent wake behind rotary wing airfoil and relationship to drag and lift coefficients
12 p1362 N73-21054
Analysis of helicopter internal and external noise levels for various flight conditions and timing of acoustical spectra
12 p1362 N73-21055
Noise spectrum characteristics and directivity patterns for rotary wings as function of blade tip speed, total rotor thrust, and angle of rotor disc plane
12 p1362 N73-21056
Acoustic measurements of aerodynamic noise generated by externally blown flap lift augmentation system for various aerodynamic configurations
[NASA-TM-X-2776] 12 p1363 N73-21059
Design of V/STOL research transport aircraft to achieve low fan noise with high thrust/weight capability of high pressure ratio lift fan system
[NASA-CR-121146] 12 p1364 N73-21065
Analysis of transition region of subsonic turbulent jets to determine noise producing potential based on far field acoustic density
[NASA-TN-D-7242] 12 p1428 N73-21573
Flight tests to determine magnitude of groundtrack overpressure generated by oblique wing transport aircraft at Mach 1.4 and 45,000 feet
[NASA-TM-X-62247] 13 p1472 N73-21922
Wind tunnel tests to determine acoustic properties of externally blown jet flap and augmentor wing short takeoff aircraft concepts
[NASA-TM-X-62251] 13 p1472 N73-21924
Acoustic measurements of sound pressure levels due to cross flow over face of lift fans on fan-in-wing and V/STOL model transport aircraft
[NASA-CR-114566] 13 p1473 N73-21928
Wind tunnel tests to determine effect of cross flow velocity on jet noise power level using V/STOL model transport
[NASA-CR-114571] 13 p1473 N73-21929
Proceedings of conference on rotary wings to investigate rotor wakes, aerodynamic characteristics at hover and high advance ratio, and aerodynamic noise properties
13 p1473 N73-21931
Fundamentals of helicopter noise generation and propagation to include noise control procedures and cost effectiveness of noise reduction
14 p1598 N73-22953
Analysis of aerodynamic noise produced by rotor operating at supersonic speed
[TT-7213] 14 p1599 N73-22967
Analysis of vortex shedding from airfoils with application to vortex noise generated by helicopter rotary wings
[AD-757167] 14 p1602 N73-22989
Noise tests on large scale model of externally blown flap lift augmentation system using mixer nozzle
[NASA-TN-D-7236] 15 p1733 N73-24059
Aerodynamic characteristics and noise attenuation effects of leading edge serrations on rotary wings
[AD-759028] 16 p1863 N73-25088
Analysis of reverberant-field noise produced by three lift fan models operating at various rotor tip speeds
[NASA-TM-X-68243] 17 p1981 N73-26014
Wind tunnel tests to determine acoustic properties of jet augmented lifting flap configuration
[NASA-TT-F-14951] 17 p1983 N73-26030
Effects of turbulence and noise on wind tunnel measurements at transonic speeds
17 p2014 N73-26284
Design, development, and evaluation of Boeing 727 aircraft nacelle to conform to upper noise reduction goals
[FAA-RD-72-40-VOL-2] 18 p2104 N73-27017
Characteristics of long range transport aircraft to include reduction of aircraft engine noise and improved engine response during go-around maneuver
[NASA-CR-121243] 18 p2104 N73-27020
Design, fabrication, and flight test of Boeing 727 aircraft nacelle modification to reduce aerodynamic noise levels
[AD-756040] 18 p2108 N73-27048
Measurement of noise and wake structure of ducted fan with subsonic tip speed to show sound pressure levels and blade wake characteristics
[NASA-CR-132259] 18 p2129 N73-27207
Characteristics of propulsion system for subsonic, long-range transport aircraft designed to meet aerodynamic noise level requirements
[NASA-CR-121242] 18 p2193 N73-27704
Aerodynamic noise of STOL engine-over-wing configuration using nozzle deflector
[NASA-TM-X-2871] 19 p2219 N73-27897
Velocity decay and acoustic characteristics of various nozzle geometries with forward velocity
[NASA-TM-X-68259] 20 p2388 N73-29183

Analysis of discrete frequency and broad band noise generation by subsonic rotary wings for vertical takeoff aircraft
[NASA-CR-2077] 21 p2494 N73-30014
Analysis of fan noise levels for fan in proximity of side and ground plane to determine effects on harmonic frequencies
[NASA-CR-132306] 21 p2495 N73-30023
Measurements of aerodynamic noise produced by modified and standard OH-6A helicopter configurations to determine noise reduction effectiveness
[NASA-TN-D-7216] 21 p2496 N73-30031
Diagnostic techniques for measurement of aerodynamic noise in free field and reverberant environment of wind tunnels
[NASA-CR-114636] 21 p2579 N73-30669
System for reducing noise generated by jet impinging on external flap using injection of secondary air from slot near trailing edge of flap
[NASA-CR-132270] 22 p2611 N73-30930
Aerodynamic noise and flow field characteristics of internal flow, jet augmented flap configurations
22 p2612 N73-30937
Evaluation of acoustic radiation from various noise sources in axial fan
[NASA-CR-114576] 22 p2614 N73-30952
Evaluation of aerodynamic calibration and performance characteristics of anechoic flow facility
[AD-763668] 22 p2647 N73-31212
Local pressure field in turbulent shear flow and its relation to aerodynamic noise generation
[NASA-CR-134493] 22 p2653 N73-31253
Far field noise reduction of tilting rotor aircraft based on performance and weight tradeoffs to improve acoustic signatures
[NASA-CR-114648] 23 p2740 N73-31937
Analysis of human reactions to short takeoff aircraft aerodynamic noise for predicting community acceptance of short haul air service operations
24 p2875 N73-32960
Characteristics of aerodynamic noise generated by interaction of airstream with flap surface to show location and control of noise sources
24 p2875 N73-32963
Acoustic measurements of aerodynamic noise produced by impingement of jet exhaust on wing and flap of externally blown flap system installed on F-111 aircraft
24 p2875 N73-32964
Wind tunnel tests to determine acoustic properties of externally blown flap and augmentor wing for short takeoff aircraft configurations
24 p2875 N73-32965
Method for predicting noise generated by deflecting engine exhaust for under-the-wing and over-the-wing versions of externally blown flap configuration
[NASA-TM-X-71449] 24 p2876 N73-32969
Flight tests of Boeing 727 aircraft to determine effects of modifications on reduction of aerodynamic noise
[FAA-RD-72-40-VOL-3] 24 p2876 N73-32971
Wind tunnel tests to determine acoustic properties of large scale lift fan transport aircraft model
[NASA-TM-X-62284] 24 p2877 N73-32975
Fluid mechanics of hole tone whistle designed as efficient producer of discrete frequency sound
24 p2903 N73-33170

**AERODYNAMIC STABILITY**

Cross flexure sting designed for measuring dynamic stability of slender bodies of revolution with delta wings in supersonic wind tunnel tests
[FFA-AU-637] 01 p0035 N73-10278
Aircraft glide path stability under speed constraint
[ARC-R/M-3705] 03 p0248 N73-12008
Atmospheric turbulence response of reusable space shuttle configuration during ascent flight
[NASA-CR-123952] 03 p0357 N73-12913
Flight tests to determine buffet characteristics of four high performance aircraft during transonic maneuvers
06 p0618 N73-15017
Analysis of stability characteristics of hingeless rotary wing on flap and lead-lag degrees of freedom of single blade
[AD-750359] 06 p0623 N73-15053
Nonlinear instability in flap-lag of rotor blades in forward flight
[NASA-CR-114524] 08 p0867 N73-17017
Analysis of whirl stability boundaries and aerodynamic characteristics of tilting rotors
12 p1356 N73-21004
Analytical and experimental techniques to define geometry of vortex field of hovering rotary wing and effect on rotor performance
12 p1359 N73-21032
Mass distribution analyses for design of low aspect ratio aerodynamic stable fighter wings
[NASA-CR-112232] 13 p1469 N73-21900
Drag and stability characteristics of hypersonic blunt nosed conical bodies in gas mixtures
[NASA-CR-131986] 14 p1599 N73-22962
Aerodynamic stability and control characteristics of X-20 aircraft
[AD-756854] 14 p1710 N73-23877
Structural stability testing of aerospace components under pyrotechnic loading conditions using subscale plastic models
[NASA-CR-128911] 14 p1715 N73-23914
Analytical solution of nonlinear aeroelastic galloping instability, with reference to space shuttle ground wind response, and application to U beams
[DLR-FB-73-18] 21 p2601 N73-30848

**AERODYNAMIC STALLING**

Effects of aerodynamic stall on helicopter rotor blade element in three dimensional rotating environment
[NASA-CR-114489] 04 p0372 N73-13028
Developments in unsteady aerodynamics of helicopter rotary wings to analyze stall flutter, transient effects of interactions, and wake induced instabilities
05 p0491 N73-14001
Analysis of US general aviation accidents caused by stalls and spins for period 1967 to 1969
[NTSB-AAS-72-8] 05 p0493 N73-14018
Proceedings of conference on fluid dynamics of aircraft stalling to include stall and post-stall aerodynamic characteristics of various military aircraft
[AGARD-CP-102] 06 p0616 N73-14998
Analysis of parameters affecting aircraft stall and post stall gyrations to include aerodynamic configurations and pilot performance
06 p0616 N73-14999
Analysis of laminar part of separation bubbles in two dimensional incompressible flow for various shaped objects
06 p0616 N73-15000
Development of method for calculating small separation zones near leading edge of airfoil at incidence
06 p0616 N73-15002
Analysis of aerodynamic stall characteristics of wing sections with high lift devices in two dimensional flow
06 p0617 N73-15008
Aerodynamic configurations of swept wings to improve lift performance at stall in higher range of subsonic speeds
06 p0617 N73-15010
Design aspects of stall of powered-lift aircraft with externally blown flaps and methods for predicting increment in maximum lift coefficient due to power
06 p0617 N73-15011
Modifications of Jet Provost and Strikemaster trainer aircraft to provide adequate stall warning without excessive penalty on maximum lift at low speed
06 p0617 N73-15012
Analysis of stall and post-stall characteristics of F-111 aircraft and development of regression techniques to obtain aerodynamic derivatives
06 p0617 N73-15013
Post-stall aerodynamic characteristics of Harrier GR-1 aircraft and development of lift augmenting devices
06 p0618 N73-15014
Development of F-28 transport aircraft wing and analysis characteristics to show effects of boundary layer fences
06 p0618 N73-15015
Wind tunnel tests to obtain pre-flight estimates of stall speed and low air speed performance of Boeing 747 aircraft
06 p0618 N73-15016
Analysis of aerodynamic buffeting and related phenomena to include development of models for oscillatory rigid-body motion
06 p0618 N73-15018
Wind tunnel tests to determine aircraft post-stall characteristics and to define boundaries for maintaining controlled aircraft flight
[AD-751461] 07 p0740 N73-16023
Evaluation of fluid dynamics of aircraft stalling to determine effects of three dimensional flow, wing sweep back, and high lift devices
[AGARD-AR-49] 09 p0982 N73-18023
Analysis of aerodynamic stall characteristics of airfoils at various angles of attack with application to control forces of H-53 helicopter
[AD-752917] 09 p0986 N73-18053
Calculation and measurement of aerodynamic forces on oscillating airfoil with and without aerodynamic stalling
12 p1361 N73-21042
Aircraft accident involving crash of Turbo Commander aircraft following takeoff and climbout from Greater Pittsburgh Airport, Pennsylvania on 14 Aug. 1972
[NTSB-AAR-73-5] 13 p1474 N73-21936
Analysis of effects of Reynolds number on aerodynamic stalling of rotary wings and relationship of Reynolds number to aerodynamic coefficients of blade elements
14 p1598 N73-22957
Aircraft accident involving attempted takeoff of Sabre Mark 5 aircraft at Sacramento, California airport on 24 Sept. 1972
[NTSB-AAR-73-6] 14 p1602 N73-22985
Wind tunnel tests to determine transient wake velocities behind three stalled wing configurations at Reynolds numbers up to 4.8 million
[AD-763468] 21 p2498 N73-30050
The lift and stalling characteristics of a 35 deg sweptback wing designed to have identical chordwise pressure distributions at all spanwise stations when near maximum lift
[ARC-R/M-3721] 22 p2612 N73-30935
Aircraft accident involving crash of Boeing 737 aircraft during instrument approach to Chicago-Midway Airport, Illinois on 8 December 1972
[NTSB-AAR-73-16] 22 p2614 N73-30947
Helicopter gust response to include unsteady aerodynamic stall effects under short-term, control-fixed conditions
[AD-763957] 22 p2615 N73-30958
Rotating stall in axial flow compressor stages with different types of profiling along blade height and different flow regimes past profile in cascade
[NASA-TT-F-15115] 22 p2709 N73-31698
Characteristics of axial flow compressors to show compressor parameters during pre-stall conditions and techniques for predicting compressor stall conditons
[AD-763816] 22 p2710 N73-31704
Design, development, and evaluation of automatic departure prevention system and stall inhibitor for A-7 aircraft
[AD-764767] 23 p2745 N73-31972

**AERODYNAMIC VEHICLES**

U AIRCRAFT

**AERODYNAMICS**

NT AERODYNAMIC INTERFERENCE
NT AEROTHERMODYNAMICS
NT ROTOR AERODYNAMICS
Annotated bibliography and indexes on aeronautical engineering and aerodynamics - July 1972
[NASA-SP-7037[21]] 02 p0123 N73-11001
Basic flight characteristics and specifications of An-2 aircraft and equipment
[AD-746791] 02 p0127 N73-11032
Aerodynamics structure of swirling flow in short cylindrical combustion chamber
[AD-747455] 03 p0365 N73-12975
Aerospace sciences and flight mechanics research projects
04 p0487 N73-13975
Annotated bibliography and indexes on aeronautical engineering and aerodynamics, September 1972
[NASA-SP-7037[22]] 05 p0491 N73-13999
Wind tunnel tests to determine subsonic aerodynamic characteristics of model of space shuttle orbiter configuration with swept trapezoidal wing and swept fixed glove
[NASA-TM-X-2701] 05 p0491 N73-14005
Research projects in flow mechanics and gas dynamics
05 p0526 N73-14278
Satellite aerodynamics and upper atmospheric density determination from satellite dynamic response
05 p0609 N73-14950
Annotated bibliography and indexes on aeronautical engineering and aerodynamics-October 1972
[NASA-SP-7037[23]] 07 p0735 N73-15984
Role of theoretical studies of flight dynamics in relation to flight testing
08 p0866 N73-17011
Wind tunnel study of turbulent wake flow dynamics
[AD-751970] 08 p0897 N73-17267
Annotated bibliography and indexes on aeronautical engineering and aerodynamics - Nov. 72
[NASA-SP-7037[24]] 09 p0979 N73-17999
Apollo Command Module Aerodynamic Simulation tests in hypersonic flow
[DLR-FB-71-83] 09 p1089 N73-18892
Annotated bibliography and indexes on aeronautical engineering and aerodynamics - Dec. 1972
[NASA-SP-7037[25]] 11 p1231 N73-19992
Annotated bibliography and indexes on aeronautical engineering and aerodynamics - Jan. 1973
[NASA-SP-7037[26]] 11 p1231 N73-19993
Effect of wing span loading on wing trailing vortices
[AD-754055] 11 p1232 N73-20003
Naval research in aerodynamics, ballistics, mathematics, and physics
[AD-754397] 11 p1268 N73-20292
Annotated bibliography and indexes on aeronautical engineering and aerodynamics - February 1973
[NASA-SP-7037[28]] 13 p1469 N73-21895
Fluid mechanics facility in aerodynamics laboratory
[AD-756512] 14 p1646 N73-23350
Cumulative index of abstracts contained in Aeronautical Engineering and Aerodynamics Bibliography for calendar year 1972
[NASA-SP-7037[27]] 15 p1725 N73-23994
Annotated bibliography and indexes on aeronautical engineering and aerodynamics - March, 1973
[NASA-SP-7037[29]] 16 p1851 N73-24998
Annotated bibliography and indexes of aeronautical engineering and aerodynamics - April 1973
[NASA-SP-7037[30]] 18 p2101 N73-26990
Annotated bibliography and indexes on aeronautical engineering and aerodynamics - May 1973
[NASA-SP-7037[31]] 18 p2101 N73-26991

Possibility of similarity solution to describe flow field at juncture of sonic line and shock in flows with high subsonic Mach numbers
[AD-760801] 18 p2132 N73-27224
Analysis of transonic aerodynamics developments to include methods for computing steady and unsteady transonic flows
[AD-761551] 19 p2218 N73-27892
Bibliography of research in radiation physics and aerodynamics
[AD-761633] 19 p2356 N73-28952
Transonic wind tunnel tests of thrust effects on missile aerodynamics
[AD-762576] 20 p2476 N73-29889
Annotated bibliography and indexes on aeronautical engineering and aerodynamics - June 1973
[NASA-SP-7037[32]] 21 p2491 N73-29993
Hydrogen bubble flow visualization technique for study of aerodynamic problems in water flow facilities
[ARL/A-NOTE-338] 21 p2523 N73-30229
Research progress in aerodynamics, propulsion, electronics, instrumentation, and mathematical sciences
21 p2609 N73-30917
Annotated bibliography and indexes on aeronautical engineering and aerodynamics - July 1973
[NASA-SP-7037[33]] 23 p2739 N73-31925
Analysis of unsteady aerodynamics of space shuttle vehicles
[NASA-CR-124424] 23 p2848 N73-32763

**AEROELASTICITY**
Computer program for subsonic lifting surface analysis with static aeroelastic effects
[AD-745894] 02 p0157 N73-11273
Integration of unsteady aerodynamic forces and pressure distributions in aeroelastic analysis
[NLR-MP-71013-U] 05 p0492 N73-14011
Development and characteristics of automatic control system for aeroelastic aircraft using optimal gain in stabilization loops
[AD-750501] 06 p0624 N73-15061
Procedure for predicting aeroelastic behavior of Huber suspension bridge
[NPL-R102] 06 p0726 N73-15926
Influence of aeroelasticity on flight mechanics of flexible aircraft
08 p0864 N73-16991
Prediction of aeroelastic hinge moment effects on stability and control
08 p0866 N73-17006
Development of two dimensional theory for unsteady flow disturbances caused by aeroelastic deformation of thick wing at high subsonic speeds
[NASA-CR-112114] 08 p0896 N73-17258
Dynamic and aeroelastic problems of stop-rotors of V/STOL aircraft occurring during retracting and stowing of rotary wings
[DLR-FB-72-65-PT-1] 09 p0983 N73-18027
Application of computer techniques for determination of flutter characteristics of aircraft and comparison with model matching data analysis
[AGARD-R-596] 09 p0983 N73-18030
Aeroelastic divergence of transport aircraft flying at supersonic speeds and design techniques to eliminate adverse effects
[NASA-CR-112262] 09 p0984 N73-18036
Analysis of effects on in-plane boundary conditions and panel geometry on natural vibration and flutter characteristics of panels exposed to supersonic flow parallel to generators
09 p1094 N73-18933
Dynamic structural design of aeroelastic wind tunnel models using combinatorial flutter analyses
10 p1140 N73-19291
Tables of reports giving comparative theoretical and experimental aerodynamic loading data relevant to zero- and low-frequency aeroelastic problems
[ARC-R/M-3708] 12 p1356 N73-21000
Effect of elastic flapping of rotor blades on stability and control of helicopter equipped with hingeless rotor system
12 p1358 N73-21016
Wind tunnel tests to determine effects of blade twist and aeroelasticity on tilt rotor performance from hover to mach number 0.7
12 p1362 N73-21049
Application of adaptive control algorithms to self adjusting control systems for aeroelastic aircraft, flight vehicle roll, and control during reentry
[AD-756598] 13 p1474 N73-21941
Numerical analysis of panel flutter based on isoperimetric inequality and effect of viscous damping forces
[NASA-CR-131828] 13 p1475 N73-21950
Aerodynamic characteristics of helicopters with emphasis on airloads, aeroelasticity, and mechanical instabilities
14 p1597 N73-22949
Effects of aeroelasticity on performance of rotary wings and procedures for predicting aerodynamic forces on rotary wing blades
14 p1598 N73-22952
Numerical methods for determining effect of aerodynamic lag on bending response of aircraft wings at supersonic speeds
[NAL-TN-36] 15 p1733 N73-24056
Analysis of supersonic, unstalled torsional flutter in cascades of compressor blades to determine position of flutter boundary and aeroelastic instability
[AD-758721] 15 p1827 N73-24809
Wind tunnel tests to determine aeroelastic stability of thin isotropic circular cylindrical shells at subsonic and supersonic air speeds
20 p2359 N73-28975
Aeroelastic and dynamic studies of technology applicable to tilting rotor vertical takeoff aircraft with emphasis on propeller whirl instability - Vol. 1
[NASA-TM-X-69497] 20 p2359 N73-28976
Natural mode vibration analysis of aircraft structural systems by direct and component mode synthesis techniques applied to tilt rotor VTOL aircraft aeroelasticity - Vol. 2
[NASA-TM-X-69496] 20 p2359 N73-28977
Research projects involving aeroelastic stability and response, stability of thin shell structures, and suspension system concept for control of vehicle responses
[AD-762568] 20 p2359 N73-28979
Dynamic and aeroelastic problems of V/STOL aircraft stop-rotors occurring during retracting and stowing of rotor blades
[DLR-FB-73-19] 21 p2496 N73-30035
Analytical solution of nonlinear aeroelastic galloping instability, with reference to space shuttle ground wind response, and application to U beams
[DLR-FB-73-18] 21 p2601 N73-30848
Simplified analysis procedure for determining static and dynamic aeroelastic loads for space shuttle dynamics
[NASA-CR-124370] 22 p2722 N73-31781

**AEROEMBOLISM**
Oxygen breathing in decompression sickness and remedial recompression of human beings
[DRIC-TRANS-3095] 17 p1988 N73-26069
Extreme aeroembolism case and successful therapy in hyperbaric chamber
19 p2227 N73-27959

**AEROGYRO HELICOPTERS**
U XH-51 HELICOPTER

**AEROLOGY**
Aerological data from balloon and rocket flights for Japan and its vicinity - tables for Oct. 1971
01 p0073 N73-10601
Aerological data from balloon and rocket flights for Japan and its vicinity, tables for Dec. 1971, and ozone data, tables for Jan. - Dec. 1971
01 p0073 N73-10603
Aerological data from balloon and rocket flights for Japan and its vicinity-tables for Nov. 1971
01 p0073 N73-10604
Aerological data from balloon and rocket flights for Japan and its vicinity for period from 1966 to 1970
01 p0074 N73-10605
Aerological data from balloon and rocket flights for Japan and vicinity - Jan. 72
06 p0693 N73-15647
Upper atmospheric data of Japan and vicinity Feb. 1972
06 p0693 N73-15648
Aerological climatology based on IRMB weather station data recorded between 1951 and 1965
[PUBL-SER-A-77] 07 p0815 N73-16609
Aerological data from balloon and rocket flights for Japan and vicinity - May 1972
10 p1182 N73-19612
Aerological data from radiosonde observations for Japan and vicinity during 1969 and 1970
10 p1182 N73-19613
Aerological data from flights for Japan - June 1972
10 p1182 N73-19614
Aerological data from balloon and rocket flights for Japan and vicinity - Apr. 1972
10 p1182 N73-19615
Aerological data from balloon and rocket flights for Japan and vicinity
15 p1777 N73-24407
Aerological data from balloon and rocket flights for Japan and vicinity - September 1972
18 p2172 N73-27539
Aerological data from balloon and rocket flights for Japan and vicinity - Aug. 1972
18 p2172 N73-27540
Aerological data from balloon and rocket flights for Japan and vicinity - Oct. 1972
18 p2172 N73-27541
Aerological data from balloon and rocket flights for Japan and vicinity - December 1972
24 p2921 N73-33325
Aerological data from balloon and rocket flights for Japan and vicinity - Nov. 1972
24 p2947 N73-33540
Aerological data from balloon and rocket flights for Japan and vicinity - Jan. 1973
24 p2947 N73-33541

**AEROMAGNETISM**
U GEOMAGNETISM

**AEROMAGNETO FLUTTER**
U FLUTTER

**AERONAUTICAL ENGINEERING**
Titles of all Data Items issued by ESDU to end of 1971
01 p0002 N73-10009
Engineering data for aeronautical structures under loads
[ESDU-SS2] 01 p0111 N73-10918
Annotated bibliography and indexes on aeronautical engineering and aerodynamics - July 1972
[NASA-SP-7037[21]] 02 p0123 N73-11001
Annotated bibliography and indexes on aeronautical engineering and aerodynamics, September 1972
[NASA-SP-7037[22]] 05 p0491 N73-13999
English, French, and Spanish vocabulary of aircraft aeronautical terminology
[DOC-8800-VOL-1] 06 p0616 N73-14996
English, Spanish, and French definitions for international civil aviation terminology
[DOC-8800-VOL-2] 06 p0616 N73-14997
Annotated bibliography and indexes on aeronautical engineering and aerodynamics-October 1972
[NASA-SP-7037[23]] 07 p0735 N73-15984
Aeronautical research for 1971-1972
07 p0856 N73-16943
Annotated bibliography and indexes on aeronautical engineering and aerodynamics - Nov. 72
[NASA-SP-7037[24]] 09 p0979 N73-17999
Annotated bibliography and indexes on aeronautical engineering and aerodynamics - Dec. 1972
[NASA-SP-7037[25]] 11 p1231 N73-19992
Annotated bibliography and indexes on aeronautical engineering and aerodynamics - Jan. 1973
[NASA-SP-7037[26]] 11 p1231 N73-19993
Existing position and future prospects of wind tunnels in European research
[AGARD-AR-60] 11 p1266 N73-20269
Congressional assessment of governmental role in industrial and social aspects of aerospace and related technology
11 p1292 N73-20482
History of German aeronautical development during the first half of the century
11 p1350 N73-20956
Annotated bibliography and indexes on aeronautical engineering and aerodynamics - February 1973
[NASA-SP-7037[28]] 13 p1469 N73-21895
Cumulative index of abstracts contained in Aeronautical Engineering and Aerodynamics Bibliography for calendar year 1972
[NASA-SP-7037[27]] 15 p1725 N73-23994
Annotated bibliography and indexes on aeronautical engineering and aerodynamics - March, 1973
[NASA-SP-7037[29]] 16 p1851 N73-24998
Annotated bibliography and indexes of aeronautical engineering and aerodynamics -April 1973
[NASA-SP-7037[30]] 18 p2101 N73-26990
Annotated bibliography and indexes on aeronautical engineering and aerodynamics - May 1973
[NASA-SP-7037[31]] 18 p2101 N73-26991
Annotated bibliography and indexes on aeronautical engineering and aerodynamics - June 1973
[NASA-SP-7037[32]] 21 p2491 N73-29993
Annotated bibliography and indexes on aeronautical engineering and aerodynamics - July 1973
[NASA-SP-7037[33]] 23 p2739 N73-31925

**AERONAUTICS**
Military technology, research, and development contributions to US aviation advances since 1925 - Exec. Summary
[NASA-CR-129574] 04 p0487 N73-13984
Aeronautically oriented numerical weather prediction activities in Finland during 1970
[TR-2] 08 p0937 N73-17677
Management and organization in aerospace science and technology research
11 p1350 N73-20955
Technical and scientific contributions of German aeronautical societies to aerospace sciences
11 p1350 N73-20957
Economic evaluation of aircraft and spacecraft
[JPRS-60104] 23 p2865 N73-32907

**AERONOMY**
Abstracts of DNA-sponsored reaction rate research programs for FY 72
[AD-747660] 03 p0299 N73-12441
Neutral and ion chemistry of D and E regions symposium papers
[AD-749780] 06 p0668 N73-15430
Atomic and molecular processes in atmospheric environments
[AD-751766] 07 p0795 N73-16468
Association, switching, and rearrangement for positively charged cluster ions at 80 km in upper atmosphere
[AD-751140] 07 p0797 N73-16478
Climatic changes resulting from upper atmosphere perturbation by supersonic aircraft exhausts
[PB-212427] 07 p0816 N73-16612
Atomic and molecular reaction kinetics in upper atmosphere
[AD-753246] 09 p1000 N73-18158
Stratospheric chemical reactions and perturbations caused by supersonic aircraft exhaust
[PB-213111] 11 p1290 N73-20464

Survey on aeronomic dynamics of photochemical reactions caused by supersonic aircraft exhaust
[PB-213126] 11 p1290 N73-20466
Research on aeronomy and upper atmospheric composition and environments
[AD-760576] 18 p2149 N73-27367
Nitric oxide spectral line width for stratospheric aeronomical analysis
[A-114-1973] 23 p2819 N73-32536
Payload and scientific mission of German aeronomy satellite AEROS
[NASA-TT-F-15104] 23 p2850 N73-32779

AEROPHYSICS
U ATMOSPHERIC PHYSICS

AEROS SATELLITE
Design and qualification of hydrazine attitude control engines for Aeros satellite
[DGLR-PAPER-72-79] 06 p0714 N73-15824
Design and operation of Aeros satellite attitude control system during acquisition phase
[DGLR-PAPER-72-62] 06 p0721 N73-15885
Standardization of satellite control systems by using onboard computers, exemplified by proposal for Aeros satellite
[DGLR-PAPER-72-064] 06 p0721 N73-15886
Impedance probe and counter-voltage analyzer used on Aeros satellite for plasma diagnostics experiment
[DGLR-PAPER-72-070] 09 p1036 N73-18455
Layout of scientific experiments in Aeros satellite, including description and function of satellite-borne instruments
[DGLR-PAPER-72-069] 09 p1091 N73-18906
Payload and scientific mission of German aeronomy satellite AEROS
[NASA-TT-F-15104] 23 p2850 N73-32779

AEROSOLS
Determination of optical thickness of aerosols in atmosphere around Salton Sea desert area using ERTS-1 imagery
[E72-10200] 02 p0160 N73-11298
Balloon measurements of aerosol and ozone in Arctic stratosphere
[AD-747256] 02 p0169 N73-11374
True absorption of light by aerosols in atmosphere
[AD-748111] 03 p0299 N73-12437
Nonflammable antifogging agent with low level, nonobjectionable odor and capable of being dispensed from aerosol container for in-flight visibility
[AD-746844] 03 p0321 N73-12617
Cascade impactor network for determining gravimetrically particle size distribution of suspended aerosols in urban areas
[AP-108] 03 p0326 N73-12656
Measurement of spatial distribution of aerosols and water vapor in earth mixing layer using optical radar, particle counters, and rawinsonde
[NASA-TN-D-7103] 04 p0444 N73-13621
Determination of aerosol optical thickness in atmosphere at Salton Sea and San Diego based on ERTS-1 data
[E72-10359] 05 p0534 N73-14347
Light scattering technique for studying Brownian particles
[AD-750110] 06 p0701 N73-15716
Cardiac toxicity of fluoroalkane gases for propelling aerosols in industry and household applications
[AD-751425] 07 p0749 N73-16090
Concentrated aerosol layer at intermediate levels of pure Rayleigh atmosphere
07 p0775 N73-16295
Jet impactor for size separation of aerosol particles
[BMVG-FBWT-72-11] 07 p0805 N73-16526
Operating principles and flight test performance of aerosol counter onboard tethered balloon
[AD-751315] 07 p0816 N73-16619
Nephelometer design and data on total light scatter and backscatter component of extinction of light due to aerosols
08 p0899 N73-17281
ERTS-1 measurement of aerosol content in atmosphere over Salton Sea and desert test sites
[E73-10295] 09 p1020 N73-18328
Models of aerosol dynamics in upper atmosphere
[BNL-17174] 10 p1126 N73-19176
Atmospheric aerosol particles in infrared radiation transfer process
10 p1146 N73-19325
Determination of boundaries confining constant of turbulent coagulation of aerosols
[NLL-RTS-7293] 11 p1269 N73-20297
Detection of smoke pollution in Virginia by photogrammetric and densitometric analysis of ERTS-1 imagery
[E73-10419] 11 p1279 N73-20381
Effects of atmospheric aerosols on image transfer in aerial photography using polarized light
12 p1400 N73-21356
Analysis of global effects created by increase in carbon dioxide and aerosol content in atmosphere
12 p1420 N73-21511
Measurement of distribution of radioactivity in troposphere and stratosphere to determine aerosol dimensions and variation with time
12 p1421 N73-21513
Airborne heated glycerine droplets for fog dispersal
[TOPR-178-3-133-PT-1] 12 p1421 N73-21521
Remote detection and measurement of clear air turbulence using pulsed laser radar
[NASA-CASE-MFS-21244-1] 12 p1422 N73-21523
Determination of aerosol content in atmosphere at Salton Sea test site using ERTS-1 data
[E73-10524] 13 p1517 N73-22291
Size distribution of natural aerosol particles, using terrestrial measurements
[AD-756051] 13 p1528 N73-22381
Radiative light transfer model for aerosol radiance loss in atmospheric photometry
13 p1558 N73-22628
Evaporation of droplets in aerosol jets, by simulation with latex spheres
[BMVG-FBWT-73-5] 14 p1616 N73-23096
Aerosol particle size determination and distribution with aerodynamically focused impactor, applied to coal mine dust
[BMVG-FBWT-73-1] 14 p1667 N73-23533
Dosage device for diluting concentrated aerosols at ratios between 1/60 and 1/800
[BMVG-FBWT-73-2] 14 p1668 N73-23534
Aerodynamic size and mass distribution of aerosol particles determined with spiral centrifuge compared to other precipitators
[BMVG-FBWT-73-3] 14 p1668 N73-23535
Analysis of laser outputs required to initiate gas breakdown when gas contains suspended particles
[AD-757517] 14 p1674 N73-23585
Polycyclic aromatic hydrocarbon aerosol collection using fiber glass and silica gel filters
[NLL-TRANS-1191-[9022.9]-PT-1]
15 p1746 N73-24152
Mesospheric diffuse skylight measurement onboard Centaure sounding rockets launched from Kiruna during August 1969
[ISL-16/72-PT-1] 15 p1781 N73-24439
Working principles of two aerosol particle size spectrometers, based on lateral air jet or asymmetric expansion of aerosol
[BMVG-FBWT-73-6] 15 p1788 N73-24496
Chemical changes during transformation of aerosols to cloud droplets and rain in orographic clouds
15 p1805 N73-24630
HCl acid aerosol production by space shuttle exhaust products and atmosphere
[NASA-CR-132993] 16 p1870 N73-25142
Solid aerosol particle capture by water drops at low Reynolds numbers
[AD-759667] 16 p1872 N73-25157
Analysis of ERTS-1 data to determine aerosol content in atmosphere and comparison with data obtained by sun photometer at Salton Sea, California
[E73-10702] 16 p1903 N73-25394
Survey of atmospheric aerosol concentrations over seas
[PB-214170/3] 16 p1909 N73-25442
Diffuse reflectance theory for estimating optical absorption coefficients of aerosol particles collected on filter surface
[AD-759490] 16 p1946 N73-25744
Aerosol model of atmosphere based on experimental data regarding aerosol attenuation and particle number concentration and size distribution at various heights
[AD-760393] 17 p2030 N73-26429
Electrostatic entrained material measurement system
[NASA-CASE-MFS-22128-1] 17 p2032 N73-26442
Characteristics of zero aerosol sampling tube for aspiration of samples from gas flow with minimum changes in isokinetic coefficient
[AD-759868] 17 p2035 N73-26470
Effect of atmospheric contaminants on laser induced air breakdown
[AD-760175] 17 p2070 N73-26750
Effect of atmospheric stability on vertical spread of airborne pollutants from steady and instantaneous sources in constant stress region
17 p2098 N73-26974
Observability of high altitude aerosol and atmospheric scattering layers by satellite-borne optical detector
[NASA-CR-112309] 18 p2144 N73-27329
Aerosol physical properties from horizon inversion by satellite
[NASA-CR-112311] 18 p2144 N73-27330
Weight measurement of impurities during aspiration of aerosol samples from flow, using zero intake tubes
[AD-762329] 19 p2232 N73-27998
Photogrammetric and densitometric examination of ERTS-1 MSS imagery of Eastern Virginia to determine sources of aerosol pollution
[PAPER-E5] 19 p2269 N73-28269
Measurement of atmospheric aerosol content in Southern California desert areas from ERTS-1 contrast and radiance measurements
[PAPER-I2] 19 p2277 N73-28324
Computed atmospheric effects on ERTS-1 MSS observations
19 p2284 N73-28371
Effects of aerological fine-strength characteristics of vertical distribution of aerosols
[AD-762335] 19 p2299 N73-28485
Propane aerosol dispenser for cold fog dissipation at airfields
[AD-762292] 19 p2317 N73-28635
Numerical analysis of aerosol concentration and deposition flux for several flow configurations with and without electrical force deposition
20 p2386 N73-29172
Mathematical model for shaping aerosol spectrum in troposphere
20 p2389 N73-29194
Determination of earth aerosol albedo using Skylab EREP data
[E73-10871] 20 p2393 N73-29222
Measurement of aerosol content in atmosphere over Salton Sea and desert areas of California
[E73-10947] 21 p2530 N73-30289
Large scale weather modification through spread of carbon black particles in aerosol form in upper atmosphere
[PB-220642/3] 21 p2541 N73-30374
Quantitative analysis of stratospehric aerosol characteristics from Skylab data
[E73-11009] 22 p2660 N73-31314
Measurements of Fe, Mn, Fn, Cu, Ni, and Pb in aerosols and precipitation in clean tropospheric air
[NOAA-TR-ERL-248-APCL-24]
22 p2664 N73-31349
Particle size distribution of coagulated aerosols using computer program
[NPL-NAC-35] 22 p2668 N73-31373
Optical properties of atmospheric aerosols in near infrared region of spectrum
[AD-764135] 22 p2668 N73-31374
Determination of earth aerosol albedo using Skylab data from White Sands, New Mexico
[E73-11080] 23 p2782 N73-32255
Photoelectric sensor for measurement of spectra and concentration of liquid particles in aerosol
[AD-764927] 23 p2794 N73-32353
Aerosol growth kinetics in flow reactor
24 p2901 N73-33159
Quantitative determination of Statospheric aerosol composition over western United States
[E73-11138] 24 p2918 N73-33293

AEROSPACE ENGINEERING
NT AERONAUTICAL ENGINEERING
Aerospace engineering including materials, orbits and trajectories, power sources, satellite geodesy, and structural engineering
[NASA-CR-128329] 01 p0119 N73-10981
Engineering data on new aerospace structural materials with potential use in weapon system
[AD-746761] 02 p0189 N73-11534
Use of space technology to solve medical problems and improve medical equipment
04 p0472 N73-13848
Aerospace technology for solving domestic solid waste disposal, water purification, and water recovery problems
04 p0472 N73-13849
Space technology for developing ground based integrated medical laboratory
04 p0472 N73-13851
Influence of space technology on X ray astronomy
04 p0473 N73-13856
Space technology for ground based economic support and investigating solar system origins
04 p0473 N73-13857
Preparation of solid homogeneous materials in space
04 p0473 N73-13861
Aerospace MHD large scale power generation
04 p0473 N73-13865
Workshop for educating public to space benefits in education
04 p0474 N73-13867
Space technology for solving materials and design problems of earthbased housing
04 p0474 N73-13868
Technical engineering services in support of Nike-Tomahawk sounding rocket vehicles
[NASA-CR-130123] 04 p0478 N73-13906
Chemical processing industries and utilization of NASA technology - conference
[NASA-CR-129827] 05 p0607 N73-14937
Failure analysis of aluminum alloy components with history of failures in aerospace applications
[NASA-CR-2166] 06 p0684 N73-15568
Advanced technology, experimental and instrument design, and mission planning for space shuttle sortie workshop - conference working group reports
[NASA-TM-X-68842] 06 p0719 N73-15867
Report to House Committee on Science and Astronautics on aerospace museum in Western United States
07 p0857 N73-16949
Utilization of scientific and technical personnel by urban governments
[PB-212762] 07 p0860 N73-16979
Facilities engineering for NASA space program
08 p0873 N73-17070

Structural vibrations in aerospace operations and effects on man
08 p0876 N73-17099
Scientific reports on adaptive control system theory for aerospace engineering
[AD-751941] 08 p0887 N73-17187
Cost effectiveness of water reclamation subsystem in advanced aerospace life support systems
[NASA-CR-124098] 09 p0997 N73-18134
Errors in design of mechanisms which result in problems during later development stages
09 p1087 N73-18867
Conference on Air Force science and engineering research
[AD-753072] 09 p1101 N73-18991
Water reclamation and waste disposal technology applied to land use and aerospace engineering
[NASA-CR-128857] 10 p1124 N73-19158
Waste disposal and water reclamation technology for land use and aerospace engineering application
[NASA-CR-128858] 10 p1124 N73-19159
Engineering data on aerospace structural materials - Vol. 1
[AD-755407] 13 p1544 N73-22517
Engineering data on aerospace structural materials - Vol. 2
[AD-755408] 13 p1545 N73-22518
Congressional hearings on NASA technology applications program budget
14 p1721 N73-23966
List of NASA inventions available for licensing in foreign countries
[NASA-SP-7038[01]] 15 p1845 N73-24947
Use of aerospace technology to solve earth based problems
[NASA-CR-132148] 15 p1846 N73-24961
Application of holographic nondestructive testing to experimental production hardware components and structural problems in aerospace engineering
16 p1921 N73-25546
Synopsis of past, present, and future progress in aerospace engineering and manned space exploration
[UTIAS-REV-37] 16 p1976 N73-25979
Zvenigorod Experimental Station optical observations of artificial satellites
[JPRS-59567] 18 p2126 N73-27181
ONERA activities for 1972
19 p2354 N73-28933
Orbital docking technology for spacecraft
[NASA-TT-F-15105] 22 p2716 N73-31741
Capabilities of space processes in ground based experiments at low-g periods
[NASA-CR-124385] 22 p2717 N73-31752
Aerospace distillation water recovery system for reclamation of potable water from domestic wash water
[NASA-TM-X-2896] 22 p2737 N73-31913
Application of aerospace engineering to planetary exploration and spacecraft shielding problems
[NASA-CR-135529] 23 p2858 N73-32836
Research activities for technology transfer and impact studies
[NASA-CR-135720] 23 p2859 N73-32847
Economic evaluation of aircraft and spacecraft
[JPRS-60104] 23 p2865 N73-32907
Description and capabilities of ground Operations Aerospace Language [GOAL]
[NASA-TM-X-69541] 24 p2897 N73-33128
Textbook of Ground Operations Aerospace Language [GOAL]
[NASA-TM-X-69542] 24 p2897 N73-33129

**AEROSPACE ENVIRONMENTS**
NT INTERPLANETARY SPACE
NT INTERSTELLAR SPACE
Development of procedures for determining contamination characteristics of materials which become volatile in space environment
[NASA-CR-130132] 05 p0600 N73-14878
Analysis of natural environment design requirements for space tug to show orbital environmental impacts and short-period atmospheric density variation effects
[NASA-TM-X-64713] 05 p0600 N73-14881
Ice particle formation and lifetime in space environment, affecting Skylab program
05 p0609 N73-14949
Physiological factors of human vestibular adaptation to flight and space environments
06 p0633 N73-15146
Application of remote sensors for determining meteorological and environmental parameters with emphasis on data obtained by satellite infrared sensors
07 p0782 N73-16357
Aerospace medicine for treating abnormal conditions caused by space flight
[NASA-TT-F-735] 09 p0994 N73-18116
Materials for ball bearings for space applications using chromium steel and silver-indium alloy
[REPT-781-4.4] 10 p1166 N73-19490
Research in space biology and medicine
[JPRS-58620] 11 p1243 N73-20094
Human performance and life support engineering for space environment conditions
[AD-754216] 11 p1252 N73-20157
Developing facility on Skylab mission for electromagnetic suspension of small molten spheres in space
[NASA-CR-124134] 11 p1297 N73-20522
Analysis of materials, processing criteria, processing techniques, and apparatus for preparation of composite materials in space
[NASA-CR-124172] 11 p1307 N73-20609
Recalibration of magnetic spectrometer designed to measure 0.1 to 1.0 MeV electron flux in space environment
[AD-755790] 12 p1406 N73-21404
Apollo 16 microbiological experiment on microbial response to aerospace environments - Part B
12 p1452 N73-21762
Device for extravehicular microbe exposures to space environment during Apollo 16 flight
15 p1740 N73-24104
Development, manufacture, and testing of optical beam steerer for use in spaceborne optical radar systems
[NASA-CR-124283] 16 p1884 N73-25246
Utilization of thiophenyl ether disiloxane and trisiloxane as lubricant fluids in severe environment including space
[NASA-CASE-MFS-22411-1] 19 p2304 N73-28532
Glacio-climatic and geophysical rhythms of earth and space
[NASA-TT-F-14985] 19 p2342 N73-28843
Method for predicting degradation of solar array in space radiation environment
[NASA-CR-133738] 21 p2499 N73-30055
Research in physical phenomena of space and planetary environments, and applications of radio technology
[NASA-CR-133856] 21 p2596 N73-30809
External heat transfer problems under space conditions
[NASA-TT-F-783] 21 p2605 N73-30879
Lubricants for use in space environment at high and low temperature and zero gravity - bibliographies
[AD-765300] 23 p2799 N73-32385
Growth of electronic ceramic single crystals from solution as feasibility study for future crystal growth in space environment
[NASA-CR-124443] 23 p2826 N73-32587
Pulling single crystal silicon in space environment
[NASA-CR-124439] 23 p2826 N73-32588
High temperature general purpose furnace for use in space
[NASA-CR-124458] 24 p2991 N73-33905

**AEROSPACE INDUSTRY**
NT AIRCRAFT INDUSTRY
Results from employment workshop program for unemployed aerospace engineers and scientists
[PB-209366] 01 p0022 N73-10168
Research in aerospace and biological sciences
[AD-740761] 01 p0121 N73-11000
Survey of aerospace industry to determine various techniques used in considering interactions of handling qualities, stability, control, and load alleviation devices on structural loads
[AGARD-R-593] 02 p0125 N73-11020
Transfer of unemployed aerospace professionals to small businesses
[NASA-CR-129504] 03 p0366 N73-12979
Major problems associated with use and usefulness of aeronautical test facilities
04 p0400 N73-13258
Research projects conducted by French research facility during 1971 with application to aerospace industry
05 p0611 N73-14966
Congressional hearings on aeronautics and space technology
14 p1721 N73-23967
Pilot program for transfer of aerospace technology to city management
[NASA-CR-131918] 14 p1724 N73-23992
Model for updating aerospace research and development as function of perturbations in program time
[NASA-TM-X-64748] 15 p1845 N73-24948
Project management in aerospace industry
15 p1847 N73-24967
Industrial policy of ESRO noting distribution of contracts, relations with industry, multinational consortiums, and technological research
15 p1848 N73-24975
Air Force objectives for maintaining aerospace superiority
[AD-759566] 17 p2099 N73-26982
Effects of NASA expenditures to aerospace industry as factor of industrial location
18 p2207 N73-27814
Inventory of European aerospace industries on satellite systems
[ESRO-SP-91] 21 p2602 N73-30852
United States cooperation with the USSR and Japan in science and technology
22 p2737 N73-31917
Economic analysis of US aerospace/defense industry
[AD-763242] 22 p2738 N73-31921
Handbook for liquid and solid lubricants in aerospace industry
[NASA-CR-130490] 23 p2796 N73-32365
Abstracts of NASA-ASRDI publications on aerospace safety research
[NASA-TM-X-71428] 23 p2866 N73-32911
Industrial utilization of NASA generated aerospace technology
[NASA-TM-X-71435] 24 p2994 N73-33923

**AEROSPACE MEDICINE**
Aerospace biology research, including physical principles of gravitational biology, such as forces, weight and mass, weightlessness, and size and scale effects
[NASA-CR-128471] 01 p0009 N73-10075
Interactive information system with application in medical area
[NASA-TM-X-66076] 01 p0020 N73-10156
Annotated bibliography and indexes on aerospace medicine and biology - Aug. 1972
[NASA-SP-7011[106]] 02 p0130 N73-11054
Annotated bibliography and indexes on aerospace medicine and biology - July 1972
[NASA-SP-7011[105]] 03 p0256 N73-12073
Prolonged weightlessness for 300 plus days and cardiac performance in primates
[NASA-CR-129512] 03 p0256 N73-12075
Spacecraft environment, radiation, and weightlessness effects on human biological processes in manned space flight
[JPRS-57517] 03 p0256 N73-12076
Supplement to bibliography on Aerospace Medicine and Biology, October 1972
[NASA-SP-7011[107]] 04 p0377 N73-13069
Research and development in Army aviation medical science and problems
[AD-749456] 06 p0631 N73-15129
Physiological stresses and medical criteria for aircrew fatigue
06 p0634 N73-15152
Bibliography of aerospace medicine and biology
[NASA-SP-7011[108]] 07 p0742 N73-16037
Research and development related to space biology and medicine
[JPRS-58010] 07 p0743 N73-16041
Fiftieth anniversary of formation of USSR with synopsis of accomplishments including rocket flights with animals for space medicine research
07 p0743 N73-16042
Applications of aerospace technology in biology and medicine
[NASA-CR-130544] 08 p0871 N73-17047
Conference on occupational medicine support in NASA programs to prevent health and emotional problems in personnel
[NASA-TM-X-69072] 08 p0871 N73-17048
Occupational medicine procedures for personnel in lunar receiving laboratory for Apollo 11 crew members
08 p0871 N73-17049
Medical examinations and protection procedures for NASA employees working in radiologically controlled areas
08 p0871 N73-17050
Medical concepts and functional management in NASA Environmental Health Program
08 p0872 N73-17056
Environmental health measures to prevent cabin atmosphere toxicity and provide drinking water standards in manned space flight applications
08 p0872 N73-17058
Conference on preventive medical and environmental control measures for NASA and aviation industry personnel management
[NASA-TM-X-69073] 08 p0873 N73-17064
Chorioretinal burn hazards of high intensity radiation sources in industry
08 p0873 N73-17071
Structural vibration and noise effects on man in aerospace operations
[AGARDOGRAPH-151] 08 p0876 N73-17098
Prolonged weightlessness effects on physiological functions of dogs
[NASA-TT-F-14672] 08 p0878 N73-17110
Annotated bibliography and indexes on Aerospace Medicine and Biology - December 1972
[NASA-SP-7011[109]] 09 p0992 N73-18094
Conference on human endocrine secretions and hormone metabolisms during space flight stress
[NASA-TM-X-58093] 09 p0993 N73-18104
Aerospace medicine for treating abnormal conditions caused by space flight
[NASA-TT-F-735] 09 p0994 N73-18116
Review of papers presented at Conference on Space Biology and Aerospace Medicine
[JPRS-58345] 09 p0995 N73-18125
Medical and biological problems of manned space flight
[NASA-TT-F-719] 10 p1114 N73-19077
Effects of space flight noise intensities on human physiological functions
10 p1114 N73-19080
Annotated bibliography and indexes on aerospace medicine and biology - January 1973
[NASA-SP-7011[110]] 11 p1238 N73-20052

Feasibility determination for polyethylene packaging of drugs stocked in spacecraft pharmacies
11 p1246 N73-20114
Review of published bibliographical index of Soviet and foreign literature on biomedical problems in space
11 p1246 N73-20115
Annotated bibliography and indexes on aerospace medicine and biology
[NASA-SP-7011[112]] 12 p1367 N73-21087
Medical biological and other problems of space flight
[JPRS-58678] 12 p1367 N73-21089
Review of bibliography on medical and biological research during space flights
12 p1367 N73-21091
NASA contributions to patient monitoring
[NASA-CR-131538] 12 p1373 N73-21138
Diagnostic physiological tests for selection and training of flying personnel
[NASA-TT-F-687] 13 p1479 N73-21981
Physiological stress effects of space flight on human body
[JPRS-57139] 13 p1481 N73-22002
Pathophysiological justifications for using drugs in aerospace medicine
[NASA-TT-F-736] 13 p1484 N73-22033
Analysis of aeromedical factors leading to midair collisions and recommended actions to avoid collisions
[AD-758189] 14 p1604 N73-23005
Research activities in exobiology and aerospace medicine
[JPRS-59015] 14 p1607 N73-23024
USSR conference on exobiology and aerospace medicine
14 p1609 N73-23045
Annotated bibliography and indexes on aerospace medicine and biology for 1961 to 1965
[NASA-TT-F-14662] 14 p1610 N73-23053
Aerospace medicine research, including human tolerance to various stress factors - conferences
[AGARD-CP-110] 14 p1610 N73-23057
NASA programs on life science research in aerospace environments, emphasizing cardiovascular system
14 p1611 N73-23058
Annotated bibliography and indexes on Aerospace Medicine and Biology - February 1973
[NASA-SP-7011[113]] 15 p1739 N73-24099
Annotated bibliography and indexes on aerospace medicine and biology - January 1973
[NASA-SP-7011[111]] 15 p1739 N73-24100
Space biology, space medicine, and human physiology
[NASA-TT-F-14964] 16 p1867 N73-25116
Aerospace biotechnology research projects
[AD-759277] 16 p1869 N73-25135
Annotated bibliography and indexes on Aerospace Medicine and Biology - April 1973
[NASA-SP-7011[114]] 17 p1986 N73-26055
Bibliography of aerospace medicine and biology
[NASA-SP-7011[115]] 18 p2109 N73-27051
Telemetry and investigative methods in space biology
[NASA-TT-F-14996] 18 p2109 N73-27057
Aerospace medicine and exobiology research in support of long term manned space flight
[JPRS-59702] 20 p2365 N73-29021
Application of aerospace medicine research in science and technology
[JPRS-59803] 20 p2368 N73-29040
Bibliography of Russian literature on aviation and space medicine
[JPRS-53329] 20 p2369 N73-29047
Aerospace Medical Research Laboratory handbook to medical monitoring and treatment of environmental stresses
[AD-760813] 20 p2372 N73-29061
Bibliography of aerospace medicine and biology
[NASA-SP-7011[116]] 21 p2500 N73-30059
Soviet research on space biology, aerospace medicine, and human factors engineering
[JPRS-59952] 22 p2618 N73-30983
Studies in hypoxia and phylogenetics by USSR aerospace medical scientist
[NASA-TT-F-15101] 22 p2619 N73-30991
Medically related NASA technology applications and transfer activities
[NASA-CR-135527] 22 p2621 N73-31001
Physiological stress effects of aerospace environment on human body and animals
[NASA-TT-F-15081] 23 p2749 N73-32001
Annotated bibliography and indexes on aerospace medicine and biology - September 1973
[NASA-SP-7011[119]] 24 p2882 N73-33012
Aerospace psychology and physiology
[JPRS-60248] 24 p2882 N73-33014
Aerospace medicine session concerning aviation and space physiology and psychology
24 p2885 N73-33037

**AEROSPACE SCIENCES**
USSR space program accomplishments in fields of geophysics, astronomy, meteorology, oceanography, upper atmosphere, and space sciences
[JPRS-57229] 01 p0104 N73-10864
Scientific research projects in Europe relative to aerospace technology, biology, computer development, physical sciences, and microwaves
[AD-746879] 02 p0246 N73-11996
Congressional hearing to establish national science policy and priorities act of 1972
03 p0367 N73-12991
Proceedings of conference on benefits of space exploration conducted at Huntsville, Alabama Nov. 1971
[NASA-SP-313] 04 p0470 N73-13829
Contributions of science and technology to success of US as world leader
04 p0470 N73-13835
Application of remote sensing techniques for solution of ecological management problems
04 p0471 N73-13838
Aerospace sciences and flight mechanics research projects
04 p0487 N73-13975
Proceedings of conference on automation of scientific research through use of computers
[JPRS-57826] 05 p0516 N73-14199
Research in space physics at University of Iowa
[NASA-CR-129878] 05 p0594 N73-14825
USSR research projects involving meteorology, oceanography, upper atmosphere, space research, and terrestrial geophysics
[JPRS-57777] 05 p0596 N73-14844
Research projects conducted by French research facility during 1971 with application to aerospace industry
05 p0611 N73-14966
International research on aerospace instrumentation systems
[AD-750653] 06 p0675 N73-15493
Soviet Bloc research in astronomy, meteorology, oceanography, geology, and space science
[JPRS-58333] 09 p1085 N73-18852
Organization and research projects for 1971
10 p1229 N73-19988
USSR research projects in meteorology, oceanography, upper atmosphere and space astronomy, and terrestrial geophysics
[JPRS-58609] 11 p1339 N73-20867
Management and organization in aerospace science and technology research
11 p1350 N73-20955
Technical and scientific contributions of German aeronautical societies to aerospace sciences
11 p1350 N73-20957
German cooperation with AGARD research in aerospace sciences
11 p1350 N73-20958
German cooperation in international aeronautical research
11 p1351 N73-20959
Organization, management, and research activities at National Institute for Aerospace Research of the Netherlands
11 p1351 N73-20960
History and organization of German Society for Aerospace Research
11 p1351 N73-20961
Management models for large research institute considering aerospace sciences
11 p1351 N73-20968
USSR research projects in subjects of microclimate, agricultural meteorology, weather forecasting, climate control, and hydrological forecasting
[JPRS-58483] 12 p1420 N73-21510
USSR research projects in meteorology, oceanography, geophysics, upper atmosphere, and extraterrestrial radiation - No. 298
[JPRS-58734] 12 p1458 N73-21817
Proceedings of conference on research and development projects conducted by US Air Force Research and Development Command
[AD-753071] 12 p1467 N73-21890
Research projects in theoretical and practical aerodynamics - Vol. 1
16 p1851 N73-24999
Aerospace research projects
16 p1976 N73-25980
French-Soviet cooperation in space research
[AD-759106] 16 p1978 N73-25996
USSR research projects in geophysics, astronomy, and aerospace subjects - May 1973
[JPRS-59136] 17 p2024 N73-26379
Technology planning objectives and supporting technical goals for Air Force Flight Dynamics Laboratory during Fiscal Year 1974
[AD-762300] 19 p2356 N73-28950
Strategy of space research
[NASA-TT-F-15120] 22 p2716 N73-31745

**AEROSPACE SYSTEMS**
HAL programming language for aerospace computer applications
[NASA-CR-129506] 03 p0270 N73-12191
Papers presented at 7th Aerospace Mechanisms Symposium
[NASA-TM-X-58106] 09 p1087 N73-18866
Management of development and research costs for advancement of technology in aerospace systems
11 p1351 N73-20964
Onboard computers for automatic control of manned aerospace systems considering human factors integration
[AGARD-CP-114] 14 p1710 N73-23881
Exponential probability distribution analysis for extrapolating aerospace system performance statistics from test results
14 p1713 N73-23903
Computerized teleoperator applications in manned aerospace systems
14 p1713 N73-23904
Research projects in theoretical and practical aerodynamics - Vol. 1
16 p1851 N73-24999
Aerospace application of holography through nondestructive testing and flow visualization
16 p1922 N73-25550
Inventory of European aerospace industries on satellite systems
[ESRO-SP-91] 21 p2602 N73-30852
Syntax diagrams handbook for Ground Operations Aerospace Language [GOAL]
[NASA-TM-X-69505] 22 p2639 N73-31148

**AEROSPACE VEHICLES**
Analysis of vibration environment in aerospace and surface vehicles with definitions of effect on human comfort and performance
01 p0003 N73-10021
Development of computer code for determining survivability of aircraft following exposure to radiation from aerial nuclear explosion
[AD-746015] 02 p0215 N73-11738
Analysis of shock interaction and interference heating on military aerospace vehicles at hypersonic speeds
[AD-747765] 03 p0286 N73-12319
Chemical spot tests for identification of titanium and titanium alloys used in aerospace vehicles
[NASA-CASE-LAR-10539-1] 03 p0312 N73-12547
Analysis of factors involved in specification, design, and evaluation of gyroscopes for spaceborne sensor applications
[NASA-SP-8096] 03 p0328 N73-12680
Development of design data for metallic materials, fasteners, joints, and structural elements used in aerospace vehicle design
[AD-748268] 04 p0479 N73-13917
Capabilities and limitations for quantitative nondestructive testing of aerospace structures
[NASA-TM-X-64706] 05 p0552 N73-14483
Thermally stable phosphonitrile elastomers for advanced aerospace structures
[NASA-CR-124008] 06 p0687 N73-15593
Application of control theory to determine time history of thrust profile to achieve optimal maneuvers of aerospace lifting vehicles
[AD-751281] 07 p0850 N73-16891
Buckling modes of four optimized Mars entry aeroshell configurations at angle of attack loadings based on experimental pressure distributions
[NASA-CR-2087] 07 p0852 N73-16907
Frangible glass canister capable of deploying payload in space without dynamically disturbing its contents
09 p1088 N73-18875
Design and characteristics of auxiliary power source to operate electric, hydraulic, and pneumatic subsystems in ramjet powered aerospace vehicles
10 p1110 N73-19048
Fabrication and evaluation of wire harnesses from small gage wire round conductor cables - Vol. 2
[NASA-CR-128846] 11 p1262 N73-20242
Development of structural optimization algorithm used with large finite element program based on displacement method of structural analysis
12 p1356 N73-21005
Conference on high temperature corrosion of alloys for aerospace applications
[AGARD-CP-120] 14 p1675 N73-23597
NATO national reports on high temperature corrosion of aerospace alloys
14 p1678 N73-23618
Development of digital computing system for synthesis and optimization of military flight vehicle preliminary designs
[AD-760568] 18 p2108 N73-27045
Characteristics of carbon fiber composite materials and application for structures with reduced weight, fatigue reduction, and corrosion resistance
18 p2164 N73-27477
Production of fibrous metal composites by rolling of powder with strong reinforcing wires and application to aerospace vehicle structures
18 p2164 N73-27478
Design and manufacturing of composite materials with organic matrices for use in aerospace vehicle structures subjected to high temperatures
18 p2165 N73-27489
Application of high strength structural materials for aerospace vehicles and use of fracture control procedures for improved damage tolerance
20 p2481 N73-29928
Model for energetic solar proton fluxes with applications to earth spacecraft
[NASA-TM-X-70433] 21 p2592 N73-30769

AEROSPACEPLANES
Fundemental aspects of regenerative cooled, upper stage rocket plane with external-burning thrust augmentation
[AD-756498] 13 p1583 N73-22832
Collection generation, and analysis of MIL-HDBK-5 allowable design data for aerospacecraft
[AD-761817] 19 p2347 N73-28877
AEROSTATS
U AIRSHIPS
AEROTHERMODYNAMICS
Wind tunnel tests to determine convective heat distribution for space shuttle configurations based on viscous/inviscid interactions of three dimensional flow fields
[NASA-CR-128586] 01 p0040 N73-10318
Hypervelocity wind tunnel tests of aerothermal characteristics of winged space shuttle booster model
[NASA-TM-X-2642] 01 p0109 N73-10895
Analysis of surface flow, pressures, and heat transfer on two conical delta wings at hypersonic speed and various angles of attack
[NASA-TM-X-2668] 02 p0156 N73-11268
Wind tunnel tests to determine heat transfer and pressure distributions of hemisphere cylinders in hypersonic flow environment
[NASA-TN-D-7104] 05 p0605 N73-14925
Numerical analysis of characteristic processes of hyperbolic shock layers generated during atmospheric entry
07 p0768 N73-16242
Apollo experience report on techniques to define aerothermodynamic environment of Apollo spacecraft during post boost phase and to predict structural temperatures
[NASA-TN-D-7085] 09 p1091 N73-18903
Development of methods for protecting aircraft compartments from aerodynamic heating effects
[AD-754606] 11 p1236 N73-20036
Analysis of requirements, instruments, and procedures for measurement of aircraft temperatures up to Mach 2.3 and altitudes up to 80,000 feet
[AGARD-AG-160-VOL-2] 11 p1294 N73-20499
Effect of nose geometry on aerothermodynamic environment of shuttle entry configurations
[NASA-CR-128873] 11 p1348 N73-20937
Boundary layer transition and heat transfer in aerodynamic and thermic wall deformation
14 p1601 N73-22982
Effects of heating within oblique shock wave on its aerothermodynamic and geometric properties
[DLR-FB-73-21] 16 p1858 N73-25050
Hydrogen/oxygen combustion for simulating reentry aerothermodynamic characteristics
16 p1974 N73-25964
Wind tunnel tests to determine heat transfer and flow distribution of space shuttle configuration at hypersonic speeds simulating atmospheric entry
[NASA-CR-133405] 18 p2201 N73-27772
Wind tunnel tests to analyze aerothermodynamic control problems of space shuttle attitude control system at hypersonic speed
[NASA-CR-133407] 18 p2201 N73-27773
Analysis of surface pressure and cold wall heating rate distributions for large, flat panel at Mach 7 in high temperature wind tunnel
[NASA-TN-D-7275] 21 p2524 N73-30243
Regional extreme atmospheric model for aerothermodynamic calculation of probable vertical temperature profile
[AD-763671] 21 p2540 N73-30369
AEROZINE
Buffered gelled water to control nitrogen tetroxide-aerozine 50-hypergolic fuel fires
[NASA-CR-2198] 10 p1203 N73-19789
AFC [CONTROL]
U AUTOMATIC FREQUENCY CONTROL
AFCS [CONTROL SYSTEM]
U AUTOMATIC FLIGHT CONTROL
AFRICA
Morphology, provenance, and movement of desert sand seas in Africa, Asia, and Australia
[E72-10249] 03 p0289 N73-12349
Chlorophyll and plankton population distribution in upwelling waters off northwest coast of Africa and effects of eolian dust particles on surface water chemistry
[E72-10331] 05 p0531 N73-14319
Eastern Atlantic continental margin study of area between Port Elizabeth and Congo River
[PB-211392] 05 p0541 N73-14399
Geophysical survey of continental shelves off African coast and mapping for oil potential
[PB-211393] 05 p0541 N73-14400
Geological structure of selected areas of East Africa based on ERTS-1 imagery
[E73-10005] 06 p0638 N73-15341
Morphology, provenance, and movement of desert sand seas in Africa, Asia, and Australia
[E73-10058] 07 p0778 N73-16320
Morphology, provenance, and desert sand sea movements in Asia, Australia, and Africa
[E73-10060] 07 p0778 N73-16322
Dynamics of plankton populations in upwelling waters along Arabian Coast, Somali Coast, and Northwest Coast of Africa
[E73-10325] 09 p1024 N73-18357
ERTS-1 imagery of morphology, provenance, and movement of desert sand seas in Africa, Asia, and Australia
[E73-10409] 11 p1278 N73-20371
Morphology, provenance, and movement of desert sand seas in Africa, Asia, and Australia
[E73-10542] 13 p1518 N73-22305
ERTS-1 imagery of plankton populations in upwelling waters off Africa
[E73-10603] 15 p1773 N73-24364
Cosmic ray neutron monitor data for Potchefstroom
[P-2] 15 p1828 N73-24812
Cosmic ray neutron monitor data at Pochefstroom during period from May 1971 to December 1971
[P-1] 15 p1828 N73-24813
ERTS-1 imagery of morphology, provenance, and movement of desert sand areas in Africa, Asia, and Australia
[E73-10710] 17 p2018 N73-26317
ERTS-1 imagery of morphology, provenance, and movement of desert sand seas in Africa, Asia, and Australia
[E73-10786] 18 p2136 N73-27262
Investigation of plankton populations in upwelling waters along NW coast of Africa using ERTS-1 imagery
[E73-10795] 18 p2137 N73-27271
Construction of mosaic map of Morocco, North Africa using ERTS-1 data and comparison with data obtained from Gemini 5 flight
[PAPER-G5] 19 p2263 N73-28236
Morphology, provenance, and movement of desert sand seas in Africa, Asia, and Australia using ERTS-1 data
[PAPER-G8] 19 p2264 N73-28239
ERTS-1 imagery of biomass in upwelling waters along northwest coast of Africa
[PAPER-M15] 19 p2281 N73-28354
Classification of coastal environments along Americas and Africa
[AD-761193] 20 p2415 N73-29412
Mapping lineaments, structures, and lithological formations of African Rift System in Africa and Yemen from ERTS-1 imagery
[E73-11126] 24 p2916 N73-33281
AFRICAN RIFT SYSTEM
Lithological and structural surveys of African rift system using ERTS-1 imagery
[E72-10194] 01 p0046 N73-10373
Mapping of major geological structures of African Rift System using ERTS-1 imagery
[E73-10026] 06 p0660 N73-15360
Mapping of major structural lineaments of Ethiopian rift using ERTS-1 imagery
[E73-10431] 11 p1281 N73-20392
Mapping of major geological structures of African rift system from ERTS-1 imagery
[E73-10622] 15 p1775 N73-24383
Mapping lineaments, structures, and lithological formations of African Rift System in Africa and Yemen from ERTS-1 imagery
[E73-11126] 24 p2916 N73-33281
AFTERBODIES
Wind tunnel tests of twin jet afterbody models to determine thrust minus total drag and afterbody drag at Mach numbers to 2.2 and zero degree angle of attack
[NASA-TM-X-2601] 02 p0123 N73-11004
Wind tunnel tests to determine effect of nozzle lateral spacing on afterbody drag and performance of twin-jet afterbody models with cone plug nozzles at supersonic speeds
[NASA-TM-X-2632] 04 p0369 N73-12999
Effect of plume-induced boundary layer separation on afterbody during powered supersonic flight
[AD-754640] 11 p1272 N73-20326
Separation of incompressible boundary layer from axisymmetric curved afterbody
13 p1509 N73-22226
Performance of Mirage 3 sigma 4 after body
14 p1597 N73-22946
Effect of fineness ratio on boattail drag of circular arc afterbodies having closure ratios of 0.50 with jet exhaust at Mach numbers up to 1.30
[NASA-TN-D-7192] 14 p1701 N73-23802
Factors affecting base flow and jet structure behind cylindrical afterbody with central nozzle at mach 2.0 and turbulent boundary layer conditions
[ARC-R/M-3224] 16 p1851 N73-25001
Effects of variations in fineness ratio and closure ratio on boattail drag of circular arc afterbody models at static conditions and at Mach number of 1.30
[NASA-TN-D-7163] 16 p1957 N73-25830
Performance tests of twin jet afterbody configurations to determine effect of nozzle spacing, fairing shapes, and angle of attack
[NASA-TM-X-2724] 21 p2491 N73-29994
AFTERBURNERS
U AFTERBURNING
AFTERBURNING
Portable sampling and measurement system for determining gaseous emission species in afterburn of turbojet engine at ground level
[AD-747773] 03 p0351 N73-12866
Relation between invariance conditions and characteristics of turbojet engine with afterburner multidimensional control system under variable flight conditions
[AD-749656] 06 p0714 N73-15828
Combustion tests of afterburner performance of circular and parallel V-gutters for range of inlet temperatures to 1800 F
[NASA-TN-D-7212] 09 p1099 N73-18966
Kinetics of afterburning process following injection of oxidizer into high temperature gas flow
[AD-756098] 14 p1719 N73-23951
Experimental cold flow evaluation of ram air cooled plug nozzle concept for afterburning turbojet engines in static altitude facility
[NASA-TM-X-2811] 16 p1956 N73-25823
Combustion tests of various integral, spray-bar and flameholder configurations to determine configuration with maximum combustion efficiency
[NASA-TM-X-2855] 19 p2352 N73-28919
Flight tests of modified F-106 aircraft to determine installation effects of two aft underwing nacelles housing afterburning J-85 engines
[NASA-TM-X-71439] 23 p2743 N73-31959
Influence of combustion chamber, compressor, and afterburner configuration on static performance of two-cycle turbojet engines with high bypass ratio
24 p2973 N73-33756
AFTERGLOWS
NT HELIUM AFTERGLOW
Chemiluminescence of O plus NO2 in afterglow
[NASA-CR-130263] 05 p0539 N73-14383
Microwave excitation of electroacoustic resonances in afterglow plasmas
[AD-759789] 17 p2070 N73-26746
AGC [CONTROL]
U AUTOMATIC GAIN CONTROL
AGE DETERMINATION
U CHRONOLOGY
AGE FACTOR
Changes in electrocardiographs of Rhesus monkeys as function of age
[NASA-TT-F-14675] 07 p0745 N73-16062
Bioelectric activity changes in brains of sleeping children caused by aging factor
13 p1484 N73-22032
AGE HARDENING
U PRECIPITATION HARDENING
AGING [BIOLOGY]
Mathematical model for photosynthetic gas exchanges in growing wheat and radish biopaks of life support systems
03 p0257 N73-12081
Age limits and flight fitness of civil aviation pilots
13 p1481 N73-21999
Influence of personal characteristics on likelihood of decompression sickness
[NASA-CR-135495] 22 p2621 N73-31002
Effects of fatigue, age, and degree of difficulty on eye-hand coordination performance
24 p2887 N73-33051
AGING [MATERIALS]
NT AGING [METALLURGY]
Effect of titanium additions on aging characteristics of Al-Zn-Mg alloy
[AD-746195] 01 p0068 N73-10561
Aging of polyurethane elastomers based on hydroxyl terminated polybutadienes
[ERDE-TR-77] 02 p0192 N73-11554
Sulfur and MOCA cured polyurethane elastomer resistance to water, STF, and STF/water mixture
[ERDE-TR-83-PT-2] 02 p0192 N73-11555
Statistical analysis of thermal stability and service life of electrical insulation
[AD-749925] 05 p0521 N73-14239
Accelerated life tests and reliability predictions for ageing components
[AD-751616] 07 p0805 N73-16529
Correlation of mechanical properties for stored and carton sampled solid rocket propellants
[AD-752612] 08 p0953 N73-17804
Heat treatment and aging behavior of rubbers
[AD-755827] 13 p1548 N73-22548
Aging effects on chemical structure of solid rocket propellant
[AD-759564] 16 p1955 N73-25815
Aging tests of light alloys bonded with various adhesives and development of new aging test criteria
[RAE-LIB-TRANS-1662] 17 p2043 N73-26528
Analysis of loss of high temperature strength in composite materials following aging in room temperature environments
[NASA-CR-124290] 17 p2050 N73-26583
Strain history effects in solid rocket propellant deformation
[AD-764666] 23 p2832 N73-32635
Application of tension stress relaxation measurements to determine physical and mechanical properties of rubber networks during chemical reactions
[RR-204] 24 p2987 N73-33868

AGING [METALLURGY]
Effect of aging time on spallation of 2024-T6 aluminum subjected to impulsive loading
[AD-746955] 05 p0564 N73-14579
Solutioning and aging reactions and effects on microstructure and hardness of niobium-based alloys
[AD-752930] 09 p1049 N73-18558
Aging stability of samarium cobalt magnets
[AD-758806] 16 p1881 N73-25222
Effect of aging heat treatments on mechanical properties of Ti-8Al-1Mo-1V alloy
[AD-760461] 17 p2048 N73-26567
Deformation and aging characteristics of titanium alloys
[AD-763429] 21 p2561 N73-30526
Recrystallization and aging studies of steels
[PB-221302/3] 22 p2687 N73-31526
Effect of aging temperature and time on impact and tensile properties of L-605 cobalt alloy
[ORNL-TM-3734] 24 p2934 N73-33435

AGITATION
NT ULTRASONIC AGITATION

AGRICULTURE
Inventory and management of geological, botanical, and agricultural resources in Wyoming using satellite and airborne imagery and ground control data
[E72-10229] 02 p0163 N73-11322
Analysis and interpretation of ERTS-1 ecologic, geographic, and agricultural data for Tennessee Valley
[E72-10231] 02 p0163 N73-11324
Application of ERTS-1 imagery to agriculture resource and land use evaluation in Mariposa County, Arizona and San Joaquin County, California
[E72-10264] 03 p0291 N73-12363
Side-looking radar for agricultural applications, noting crop identification and growth
03 p0295 N73-12403
Application of ERTS-1 imagery to agricultural practices in Mississippi Delta Region
[E72-10312] 04 p0412 N73-13361
Experimental control of hydrometeorological factors for solution of agrometeorological problems
[JPRS-57637] 04 p0444 N73-13619
Identification of agricultural crops and soil moisture stress in Iowa using ERTS-1 imagery
[E72-10335] 05 p0531 N73-14323
Summary of side-looking radar applications in earth resources noting basic principles of side-looking radar, radar scattering, data handling, and research and development
[ESRO-CR[P]-141] 06 p0641 N73-15200
Automated thematic mapping and interpretation of hydrologic and agricultural resources using ERTS-1 imagery
[E73-10023] 06 p0660 N73-15357
Microanalytic analysis of satellite meteorology on resource utilization, commerce, and agriculture
06 p0692 N73-15637
Comprehension and use of weather forecasts by Wisconsin agricultural groups
06 p0692 N73-15639
ERTS-1 imagery of geology, agriculture, hydrology, and ecology of Niger River Delta, Republic of Mali
[E73-10047] 07 p0777 N73-16309
Applicated of ERTS-1 imagery to agriculture practices in Mississippi Delta region
[E73-10075] 07 p0780 N73-16337
Application of airborne and spaceborne photography to determine agricultural and forestry resources
07 p0782 N73-16355
Regional agricultural survey using small scale aerial and space photography
07 p0785 N73-16383
Application of thermal infrared scanner data to agriculture
07 p0785 N73-16387
Automatic processing of remote sensed data to aid in land use mapping and agricultural conservation
[NASA-CR-130372] 07 p0790 N73-16423
Multidisciplinary analysis of forestry, agriculture, soils, and landforms in Michigan using ERTS-1 imagery
[E73-10310] 09 p1022 N73-18342
Application of ERTS-1 imagery for locating coal refuse deposits, analysis of geologic formations and mapping of agricultural areas in Pennsylvania
[E73-10327] 09 p1024 N73-18358
Application of ERTS-1 imagery to Bureau of Reclamation studies of geology, agriculture, and urban development
[E73-10336] 10 p1147 N73-19337
Agricultural and urban land use mapping of Phoenix Quadrangle based on ERTS-1 imagery
[E73-10340] 10 p1147 N73-19339
Application of ERTS-1 data for identifying ethnic groups, limits of occupancy, and use of physiographic features in Republic of Mali, West Africa
[E73-10434] 11 p1281 N73-20394
Application of ERTS-1 imagery to analysis of agricultural crops and forests in Michigan
[E73-10470] 12 p1395 N73-21307
Mapping of land use in agriculture area of Finney County, Kansas based on ERTS-1 imagery
[E73-10474] 12 p1395 N73-21311
Application of ERTS-1 imagery to identification of agricultural crops, grasslands and forestry in Mississippi Delta Region
[E73-10476] 12 p1395 N73-21313
Application of ERTS-1 data to analysis of agricultural crops, forests, soils, landforms, and acreage estimates in Michigan
[E73-10483] 12 p1396 N73-21320
Development of agrometeorological forecasts with emphasis on optimal decisions on taking preventive measures for frost control
12 p1421 N73-21517
ERTS-1 imagery of Iceland geology, geophysics, hydrology, oceanography, and agriculture
[E73-10535] 13 p1518 N73-22299
Projected data systems requirements for agriculturally oriented earth resources technology satellites in 1980s
[NASA-TM-X-62240] 14 p1660 N73-23472
Application of ERTS-1 data to agricultural practices in Mississippi Delta Region
[E73-10597] 16 p1896 N73-25335
Automated thematic mapping and change detection of hydrological and agricultural resources from ERTS-1 imagery
[E73-10644] 16 p1897 N73-25341
ERTS-1 imagery of strip mining activity in Cumberland Plateau, Tennessee Test Site and agricultural areas in Alabama, Georgia, and Tennessee
[E73-10694] 16 p1902 N73-25386
Analysis of ERTS-1 imagery for crop identification and area estimates in Iowa
[E73-10699] 16 p1903 N73-25391
Agricultural study using microwave radiation from Cosmos 243 satellite over European USSR
[NASA-TT-F-14952] 16 p1944 N73-25732
Application of ERTS-1 data for multidisciplinary analysis of Michigan resources and development of computerized procedure for map coordinates correlation
[E73-10703] 17 p2018 N73-26316
Bibliography on remote sensing for agriculture and geological surveys
[PB-219103/9] 18 p2147 N73-27357
Agricultural analysis of ERTS-1 multispectral band scanner data for Monterey Bay, California
[PAPER-A23] 19 p2262 N73-28230
Analysis of ERTS-1 MSS imagery to determine geologic, hydrologic, oceanographic, and agricultural phenomena in Iceland
[PAPER-G10] 19 p2264 N73-28241
ERTS-1 imagery of land use, agriculture, vegetation, geology, landforms, and hydrology in Central Coastal Zone of California
[PAPER-L4] 19 p2273 N73-28300
Mapping of agricultural land use in Lancaster and Lebandon Counties, Pennsylvania from ERTS-1 digital data
[PAPER-L22] 19 p2276 N73-28317
ERTS-1 detection and monitoring of tectonic and vegetational patterns, urban development, and agricultural processes in Southern California
[PAPER-R4] 19 p2283 N73-28362
ERTS-1 imagery of geology, agriculture, forestry, and hydrology in Iran
19 p2287 N73-28387
Inventories of agriculture, forestry, and rangeland resources based on ERTS-1 imagery
19 p2288 N73-28396
Results of ERTS-1 investigations of agriculture, forestry, and range resources
19 p2289 N73-28406
ERTS-1 imagery of landscape changes, strip mines, timber, agriculture, and water resources in eastern Tennessee
[E73-10843] 19 p2291 N73-28421
Application of ERTS-1 imagery to geologic, hydrologic, agricultural, botanical, and land use studies in Wyoming
[E73-10844] 19 p2291 N73-28422
Application of multispectral scanning to agriculture, oceanography, hydrology, and geology
[ERL/R-246] 19 p2294 N73-28450
Multispectral scanning systems applied to agriculture and forestry
19 p2295 N73-28452
Agricultural and crop identification decisions in Mississippi Delta region of Mississippi using Skylab EREP data
[E73-10870] 20 p2393 N73-29221
Investigation of agricultural practices in Mississippi Delta region of Mississippi using ERTS-1 imagery
[E73-10881] 20 p2394 N73-29232
Monitoring vegetation conditions of direct concern to rangeland and agriculture management in Great Plains Corridor
[E73-10891] 20 p2394 N73-29240
ERTS-1 imagery of villages and cultivation sites in Niger and Upper Volta
[E73-10893] 20 p2395 N73-29242
Geological, hydrological, ecological, and agricultural mapping of Botswana from ERTS-1 photography
[E73-10928] 20 p2399 N73-29277
Articles concerning development and progress in theoretical and applied sciences of leading East European scientific organizations
[JPRS-59756] 20 p2488 N73-29982
Water, agriculture, and soil resources management and planning in California using ERTS-1 imagery
[E73-10935] 21 p2529 N73-30277
In situ spectroradiometric quantification of ERTS-1 imagery of Arizona agriculture
[E73-10967] 21 p2533 N73-30309
Utilization of ERTS-1 imagery for studies of agriculture, forestry, cartography, geography, hydrology, meteorology, geology, and oceanography in Thailand
[E73-10996] 22 p2659 N73-31302
ERTS-1 imagery of geology, botany, agriculture, hydrology, and cultural features of Wyoming
[E73-11022] 22 p2661 N73-31326
Application of aerial photography and ERTS imagery to agricultural, forest, and wate resources management in Minnesota
[NASA-CR-135483] 22 p2665 N73-31357
Identification of agricultural crops in Mississippi Delta from ERTS-1 imagery
[E73-11094] 23 p2783 N73-32261
Agroclimatology study of highlands of eastern Africa
[WMO-339] 24 p2886 N73-33045
Utilization of Skylab EREP data in making agriculturally oriented decisions in Mississippi Delta alluvial plain region
[E73-11125] 24 p2916 N73-33280
Application of ERTS-1 imagery to agriculture, forestry, meteorology, and hydrology in Thailand
[E73-11145] 24 p2918 N73-33299
Agricultural crop identification and land use patterns from Skylab data of California
[E73-11163] 24 p2920 N73-33316

AILERONS
Numerical analysis of wing bending, wing torsion, and aileron rotation at transonic speeds to determine effects on wing-aileron flutter
[ARC-R/M-3258] 16 p1855 N73-25028

AIMP-D
U EXPLORER 33 SATELLITE

AIMP-E
U EXPLORER 35 SATELLITE

AIMP-1
U EXPLORER 33 SATELLITE

AIMP-2
U EXPLORER 35 SATELLITE

AIR
NT COMPRESSED AIR
NT EXPIRED AIR
NT HIGH TEMPERATURE AIR
NT LIQUID AIR
Development of low cost cathode catalysts for air breathing fuel cells containing phosphoric acid electrolyte
[AD-748447] 04 p0376 N73-13059
Chemical evolution of air and hydrogen in turbulent mixing layer
[NASA-TT-F-14633] 04 p0386 N73-13141
Environmental indices covering land, water, and air quality compatible with ERTS-1 imagery
[E72-10330] 05 p0531 N73-14318
Acoustic properties of air and sound absorption anomalies due to molecular relaxation
[AD-750220] 05 p0581 N73-14732
Thermal conductivity of air and nitrogen at high temperatures
[AD-749842] 05 p0607 N73-14934
Optical and energy measurements of strong current discharges in air
[AD-751414] 07 p0830 N73-16729
Land use, water quality, and air quality indices useful to environmental resources managers and data processing equipment and techniques for production of indices
[E73-10376] 10 p1151 N73-19371
Development of environmental indices covering land, water, and air quality in Pennsylvania compatible with ERTS-1 imagery
[E73-10505] 13 p1516 N73-22280
Quantitative data on propagation and directivity of parametric array in air
[AD-757034] 14 p1693 N73-23737
Burning rate of JP-4 and air propellant in closed combustion chamber
[AD-757634] 14 p1720 N73-23954
Hydrocarbon oxidation by metal catalysts and adsorption layer formation on electrode in propane air fuel cell
[AD-758172] 15 p1748 N73-24168
Measurement of heat transfer coefficients of air-glass, argon-glass, and argon-aluminum suspensions
[NASA-CR-2266] 15 p1843 N73-24932
Air breakdown and plasma generation by carbon dioxide laser
[AD-759567] 16 p1951 N73-25785
Effect of atmospheric contaminants on laser induced air breakdown
[AD-760175] 17 p2070 N73-26750

Acoustic measurement and recording system for noise generated by air bag automobile safety device
[AD-761836] 19 p2229 N73-27977

Fourier analysis on ergodic calculations of reaction kinetic rate coefficients in air dissociation and hydrogen oxygen combustion
[AD-762421] 19 p2232 N73-27996

Superconducting magnetic field trapping device for producing magnetic field in air
[NASA-CASE-XNP-01185] 19 p2326 N73-28710

Environmental factors in production and use of energy and effects on air, water, and land
[R-992-RF] 21 p2537 N73-30340

Effect of O2-H2 atmosphere, H2, Ar, and room air on fatigue crack propagation in 4340 steel
[COO-3166-4] 21 p2559 N73-30513

Exact equations for five-component gas mixture transport coefficients as dissociated air model gas
[DLR-FB-72-34] 21 p2580 N73-30678

Atmospheric attenuation of sound transmissions in air
[AD-764286] 22 p2675 N73-31428

Development of land use, water quality, and air quality indices from ERTS-1 imagery for environmental resources management in Susquehanna River Basin and Quantico, Virginia test areas
[E73-11143] 24 p2918 N73-33298

Comparison of absorption and scattering coefficients for air
[LA-UR-73-708] 24 p2923 N73-33348

**AIR BEARINGS**
U GAS BEARINGS

**AIR BLASTS**
U AERIAL EXPLOSIONS

**AIR BREATHING ENGINES**
NT CF-700 ENGINE
NT DUCTED FAN ENGINES
NT GAS TURBINE ENGINES
NT J-57 ENGINE
NT J-65 ENGINE
NT J-75 ENGINE
NT J-85 ENGINE
NT JET ENGINES
NT PULSEJET ENGINES
NT RAMJET ENGINES
NT SUPERSONIC COMBUSTION RAMJET ENGINES
NT TURBOFAN ENGINES
NT TURBOJET ENGINES
NT TURBOPROP ENGINES

Turbulent, transitional, and laminar film cooling of air breathing engine inlet at hypersonic speed noting heat transfer rate measurement
[IC-AERO-72-15] 01 p0041 N73-10323

Development of hydrocarbon fuels and fuel systems for advanced air breathing engines
[AD-746334] 01 p0090 N73-10741

Development and characteristics of hydrogen-based mobile fuel systems and analysis of technical and economic problems in large scale application
[UCRL-51228] 07 p0834 N73-16766

Description of research and air breathing engine test facility at University of Stuttgart
[AD-758150] 15 p1827 N73-24806

Internal performance of mixed compression axisymmetric inlet model at Mach 0.8 to 2.65
[NASA-TN-D-7320] 16 p1955 N73-25817

Development of fiber reinforced composite materials for application to air breathing engines, aeronautical vehicles, and spacecraft components
18 p2166 N73-27491

Analysis of various mixed cycle engines and impact of component choices on application of propulsion system
21 p2590 N73-30747

Monitoring of air breathing engine exhaust gas emissions, pollutants, and atmospheric air pollution propagation
[DLR-MITT-72-14-PT-1] 22 p2694 N73-31584

Hypersonic wind tunnel tests of air breathing engines
23 p2770 N73-32158

Combustion process for airbreathing propulsion using fixed geometry ramjets
23 p2831 N73-32626

**AIR CARGO**

Findings and recommendations of Aviation Advisory Commission on long range needs of Aviation-- Vol. I Vol. 2
[PB-215803] 09 p1101 N73-18983

Analysis of special problems and issues involved in the long range of aviation with emphasis on I aa Vol. 2
[PB-215804] 09 p1101 N73-18984

Stochastic network to model materials handling operations at air cargo terminals
[AD-757629] 14 p1647 N73-23356

Activity network to model cargo flow through air cargo terminal
[AD-757628] 14 p1647 N73-23357

Performance tests of commercial nylon double braided rope for extraction lines
[AD-757209] 14 p1681 N73-23643

GERTS 3Q simulation model and data base for air cargo terminal
[AD-753925] 16 p1885 N73-25257

Proceedings of conference on air transport industry with emphasis on economics, market demand, airlines regulation, and international transportation policy - Vol. 2
[NASA-CR-135635] 23 p2862 N73-32875

Analysis of economic factors involved in air cargo operations and air cargo market development
23 p2863 N73-32881

Analysis of factors involved in developing market for air cargo services
23 p2863 N73-32882

Analysis of air freight rate problems to define roles of Civil Aviation Board and domestic air carriers
23 p2863 N73-32883

Research project to determine factors involved in expansion of air freight traffic and prospects for future expansion
23 p2863 N73-32884

Application of airships to air transportation, noting cost effectiveness
24 p2879 N73-32991

**AIR CONDITIONING**

Solar heating and air conditioning as energy conservation alternatives to nuclear power
[NASA-TM-X-70468] 23 p2748 N73-31990

**AIR CONDITIONING EQUIPMENT**

Technical and economic feasibility of solar powered space heating, air conditioning, and hot water heating systems for residential applications
[NASA-CR-124063] 08 p0968 N73-17911

Applications of heat pumps for recovery of unused heat in factories, air conditioned buildings, and refrigeration plants
[NLL-OA-TRANS-1264-[6196.3]] 15 p1842 N73-24921

Design and development of electric batteries for use with thermoelectric air conditioning systems
[AD-759239] 17 p1986 N73-26051

Analysis of energy separator for application to air conditioning system of E-8 aircraft
[AD-762590] 20 p2364 N73-29014

Design and development of cryptosteady energy separator for application to F-8 aircraft air conditioning system
[AD-762579] 20 p2364 N73-29015

**AIR COOLING**

Influence of various types of air exhaust on cooling effectiveness of trailing edges of gas turbine blades
[AD-745834] 01 p0092 N73-10754

Effusion cooled turbine blade boundary layer velocity and temperature profiles as function of hole distribution
[DGLR-PAPER-72-59] 04 p0427 N73-13479

Cooling efficiency of air discharge on nozzle blades with deflectors
[AD-749654] 05 p0591 N73-14803

Analysis of effect of chord size and cooling methods on cooling requirements for air cooled turbine blades - Vol. I
[NASA-CR-120882-BK-1] 08 p0954 N73-17809

Analysis of effect of chord size and cooling methods on cooling requirements for air cooled turbine blades - Vol. 2
[NASA-CR-120882] 08 p0954 N73-17810

**AIR CURRENTS**
NT JET STREAMS [METEOROLOGY]
NT MERIDIONAL FLOW
NT VERTICAL AIR CURRENTS

Small perturbation theory applied to effects of irregular topography on deflection of wind blowing over industrial area and then residential area and effects on air pollution
[NASA-TM-X-2653] 01 p0074 N73-10610

Trivane measured fluctuations of wind and temperature over an inland lake
22 p2694 N73-31578

Air circulation patterns induced by wind and atmospheric pressure over Lake Superior
[PB-220244/8] 22 p2695 N73-31590

**AIR CUSHION VEHICLES**
U GROUND EFFECT MACHINES

**AIR DEFENSE**
NT ANTIMISSILE DEFENSE

Information theory criteria for electronic jaming and countermeasures for air defense
[FOA-3-C-3644-66] 02 p0140 N73-11133

Detailed digital simulation of Army Missile Command experimental array radar system for air defense against low altitude threats
[AD-749501] 05 p0514 N73-14177

Miss distance radar for air defense weapons testing
[AD-750323] 06 p0642 N73-15210

Radar arrays with no phase shifters for air defense systems
[AD-750328] 06 p0642 N73-15211

Combat use and combat effectiveness of fighter-interceptors
[AD-751512] 12 p1468 N73-21894

Air defense articles written by Soviet military personnel
[AD-755679] 13 p1596 N73-22942

Electronics of antiaircraft defense systems
[AD-761540] 19 p2248 N73-28125

**AIR DENSITY/INJUN EXPLORER B**
U EXPLORER 24 SATELLITE

**AIR DUCTS**

Simulation of interaction between wind-driven rain and annular air curtain dome and analysis of resulting flow distribution
[UTIAS-TN-182] 20 p2388 N73-29187

**AIR FILTERS**

Use of ultrafine fiber filter cloth for removing bacterial contaminants from air
[NASA-TT-F-14940] 15 p1742 N73-24123

Polycyclic aromatic hydrocarbon aerosol collection using fiber glass and silica gel filters
[NLL-TRANS-1191-[9022.9]-PT-1] 15 p1746 N73-24152

Solid amine filter material for humidity control and carbon dioxide removal in space shuttle
[NASA-CR-133963] 18 p2113 N73-27087

One- and two-dimensional analysis of particle deposition in turbulent slot flow with application to self cleaning air filter design
22 p2649 N73-31225

**AIR FLOW**
NT AIR CURRENTS
NT JET STREAMS [METEOROLOGY]
NT MERIDIONAL FLOW
NT VERTICAL AIR CURRENTS

Transverse injection of water and isopropyl alcohol from flat plate into air streams
[AD-741887] 01 p0043 N73-10339

Interference of wing and propeller streams
[AD-745916] 02 p0124 N73-11008

Recirculation flow velocities and temperatures of VTOL lift engines
[DLR-FB-72-50] 02 p0223 N73-11806

Numerical analysis of induced velocities of wing with curved axis not perpendicular to velocity of incoming flow
[AD-749843] 05 p0497 N73-14048

Numerical analysis of thermal resistance of air layers in air permeable clothing
[NLL-DRIC-TRANS-2717-[3623.66]] 05 p0502 N73-14089

Analysis of heat transfer characteristics of hot wire normal to incompressible air flow and influence of frequency on sensitivity and temperature distribution along wire
[WTHD-33] 05 p0605 N73-14922

Flow characteristics around semi-infinite plate with sharp leading edge inserted in hypersonic uniform air stream
[NAL-TR-289T] 06 p0613 N73-14979

Numerical analysis of development of incompressible, symmetrical turbulent wake flows downstream of airfoils using integral method of momentum and energy
[NAL-TR-292] 06 p0614 N73-14986

Hypersonic air flow effects on aerodynamic characteristics of elliptical cones at large angles of attack
[AD-749738] 06 p0657 N73-15335

Numerical simulation of air flow in atmospheric layer over inhomogeneous surface considering wind, temperature, shear stress, and turbulent energy
[AD-751589] 07 p0795 N73-16462

Mass spectrometer for investigating hypersonic air flows in shock tube for application to reentry body problems
[BMVG-FBWT-72-20] 07 p0801 N73-16505

Performance tests to determine effects of increased rotor blade loading on gas turbine operation by reduction of rotor blade inlet diameter
[NASA-TM-X-2730] 08 p0870 N73-17039

Performance test of internal combustion engine to determine effects of pulsed injection of secondary air on exhaust emission levels
[NASA-TM-X-2737] 08 p0969 N73-17920

Calculation of interaction of penetratable shelter belts and ground air flow, including mean horizontal wind profiles and eddy viscosity coefficient
09 p1059 N73-18640

Application of optimal control theory to design of control system for supersonic inlet of turbojet engine
[NASA-TN-D-7188] 09 p1079 N73-18803

Heat transfer and aerodynamic resistance of in-line smooth walled tube arrays in transverse air flow at high Reynolds number
[NLL-RTS-7689] 09 p1098 N73-18959

Performance tests of experimental short length annular combustor using one-side-entry dilution airflow technique
[NASA-TN-D-7225] 09 p1099 N73-18967

Analysis of design flow in open jet wind tunnel and examination of processes for starting supersonic wind tunnels
[ARL/ME-138] 10 p1137 N73-19264

Wind tunnel measurements of nearly homogeneous grid turbulence field with large amplitude temperature fluctuations
10 p1139 N73-19280

Effect of cooling air discharged into air-gas flow of turbine engine to improve effeciency of gas turbine engine operation
[AD-753969] 10 p1210 N73-19840

Numerical analysis of low Reynolds number flow perpendicular to circular cylinder with constant radial suction mass flux at surface
12 p1389 N73-21264

Effect of inlet-air humidity on formation of oxides of nitrogen from a gas turbine combustor under various air inlet temperature conditions
[NASA-TM-X-68209] 12 p1443 N73-21691

Development of mathematical matrix technique for calculating inviscid, rotational, compressible axisymmetric flow field through axial flow compressor
[ME/A-73-1] 13 p1570 N73-22723

Development and evaluation of throat bypass bleed system to increase stable airflow range of sonic mixed-compression inlet
[NASA-TM-X-2779] 14 p1597 N73-22947

Analysis of supersaturation conditions in Mach 7.5 wind tunnel in expansion region of nozzle and technique for visualization of shock waves and shear layers
[ARL/A-139] 14 p1648 N73-23367

Numerical analysis of nonequilibrium nozzle expansions from reservoir at high specific enthalpy
[LOG-J7197] 14 p1649 N73-23375

Analysis of turbulent boundary layer on porous plate and fluid mechanics of adverse free stream pressure gradients
15 p1765 N73-24303

Wind tunnel tests to determine effect of approaching boundary layer on separated flow behind downstream facing step
[NLR-TR-70033-U] 15 p1768 N73-24322

Analysis of relationship between losses in rotating turbine blade and pitch irregularity after nozzle blade
[NLL-CE-TRANS-6113-[9022.09]] 15 p1824 N73-24782

Application of finite element method for analyzing stability of rectangular plates in supersonic air stream
15 p1838 N73-24899

Application of Kelvin impulse theory for computing lift on airfoils and analysis of circulation around airfoil to produce lift
16 p1851 N73-24997

Effect of humidity on laminar recovery temperature measurements during supersonic air flow in wind tunnels
[ARC-R/M-3215] 16 p1857 N73-25042

Analysis of motion of laminar and turbulent viscous vortex rings produced in air by pneumatic actuated piston vortex generator
16 p1886 N73-25265

Characteristics of water waves generated by steady two-dimensional wind at three different speeds over water depth of 19 centimeters
16 p1887 N73-25272

Effect of adjacent jets on turbulent mixing rate of coaxial helium jet in Mach 4 air stream
[NASA-CR-112292] 16 p1888 N73-25281

Airflow distribution control in gas turbine engines
[NASA-CASE-LEW-11593-1] 16 p1955 N73-25816

Analysis of nonhomogeneous flow associated with two dimensional propulsive lifting system based on flow with energy addition
[NASA-CR-2250] 17 p1979 N73-25997

Analysis of minimum run times required for instationary measurements at transonic speeds during wind tunnel tests
17 p2009 N73-26243

Development of alternating direction relaxation method for computing inviscid two dimensional transonic flows through cascades
17 p2012 N73-26268

Analysis of jet penetration and mixing of multiple cold air jets into ducted subsonic heated mainstream flow
[NASA-CR-121217] 17 p2014 N73-26286

Design and operation of sonic velometer using transit times of ultrasonic pulses in air to measure air velocity
17 p2031 N73-26434

Design, development, and evaluation of centrifugal compressor with six to one pressure ratio and two pounds per second air flow
[NASA-CR-120941] 17 p2037 N73-26483

Analysis of flow field around 18 inch diameter flat circular parachute model using helium bubble technique
[AD-761098] 18 p2106 N73-27034

Analysis of local and average heat transfer characteristics of single turbulent air jet impinging on concave surface of hemisphere
[NASA-TM-X-2859] 18 p2206 N73-27806

Apparatus and method for generating large mass flow of high temperature air at hypersonic speeds
[NASA-CASE-LAR-10612-1] 19 p2250 N73-28144

Analysis of flow distribution over three axisymmetric bodies at various angles of attack to determine boundary layer transition point characteristics
19 p2250 N73-28145

Development of improved cooling system for low-flow gas turbine rotor
[AD-761452] 19 p2330 N73-28743

Analysis of rotating stall conditions in axial flow compressors and development of control system to improve flow stability
[AD-762297] 19 p2330 N73-28748

Stability characteristics of stratified and unstratified air flow between two horizontal, infinite disks rotating at slightly different rotation rates
20 p2384 N73-29154

Numerical analysis of steady, two-dimensional, laminar, incompressible, high Reynolds number separated flow past thin airfoils
[NASA-CR-114656] 20 p2388 N73-29185

Simulation of interaction between wind-driven rain and annular air curtain dome and analysis of resulting flow distribution
[UTIAS-TN-182] 20 p2388 N73-29187

Analysis of steady-state and dynamic pressure conditions in F-111 aircraft engine to determine causes of engine compressor stalls
[NASA-TN-D-7328] 20 p2465 N73-29806

Development of computer program for determining airfoil pressure distribution for subcritical attached viscous flow
[NAL-TR-248] 21 p2523 N73-30236

Analysis of surface pressure and cold wall heating rate distributions for large, flat panel at Mach 7 in high temperature wind tunnel
[NASA-TN-D-7275] 21 p2524 N73-30243

Oxidation resistance of selected mechanical carbons at 650 C in dry flowing air
[NASA-TN-D-7381] 21 p2562 N73-30539

Finite element analysis and computer graphics visualization of unsteady flow around pitching and plunging airfoils
[NASA-CR-2249] 22 p2611 N73-30926

Evaluation of acoustic radiation from various noise sources in axial fan
[NASA-CR-114576] 22 p2614 N73-30952

Device for welding hot-wire anemometer components following breakage due to dust particles in air stream
[AERE-R-7304] 22 p2678 N73-31451

Measurement of flow parameters in midspan double-circular-arc section of stator in subsonic flow and comparison with computed performance
[NASA-TN-D-7425] 23 p2740 N73-31932

Shock wave pattern and stability in axial flow supersonic compressor using simulated rotating cascade test facility
23 p2775 N73-32196

Aerodynamic design of inlet stage for two-stage compressor and performance comparison for axial, mixed flow, and centrifugal stage configurations
[NASA-CR-120943] 23 p2829 N73-32610

Flow characteristics of multiple dilution jets mixing with primary airstream for gas turbine combustors
[NASA-TM-X-71426] 23 p2829 N73-32612

Characteristics of low speed air flow over slender, sharp edged delta wing at various angles of attack and effects on longitudinal and lateral stability
24 p2869 N73-32922

Characteristics of aerodynamic noise generated by interaction of airstream with flap surface to show location and control of noise sources
24 p2875 N73-32963

Time resolved measurements of droplet growth in Wilson expansion cloud chamber
24 p2901 N73-33158

Influence of periodic oscillations of mean flow on mean and turbulent structure of fully developed air flow in smooth circular pipe
24 p2902 N73-33161

Relationship between distribution of outflow of acoustic energy over jet boundary and far-field intensity
[NASA-TN-D-7269] 24 p2905 N73-33181

Supersonic stationary flow around atmosphere retained by gravitational force of spherical body
24 p2905 N73-33183

Subsonic air flow pressure drop at interface between two rectilinear ducts noting pressure pulses
[PUBL-133] 24 p2910 N73-33222

Pressure drop in air flow isothermally across bank of helically wound, L-type fin tubes
[PB-220315/6] 24 p2911 N73-33229

**AIR FREIGHT**
U AIR CARGO

**AIR INLETS**
U AIR INTAKES

**AIR INTAKES**
NT ENGINE INLETS
NT HYPERSONIC INLETS
NT SUPERSONIC INLETS

Free molecular flow analysis for hypersonic air inlet configurations of ion engine
[AD-756680] 13 p1571 N73-22732

Experimental investigation of large scale, two dimensional, mixed compression inlet system
[NASA-TN-D-7445] 23 p2739 N73-31928

Adjustable airfoil for reversable cowl flap inlet thrust augmentation
[NASA-CASE-ARC-10754-1] 23 p2831 N73-32624

Characteristics of variable geometry high Mach inlet concepts to reduce jet engine noise on subsonic, long range commercial aircraft
[NASA-CR-134495] 24 p2972 N73-33748

**AIR JETS**

Effect of Reynolds number and frequency on control-surface buzz at high subsonic speeds noting control of flap oscillation by air jets
[ARC-R/M-3702] 03 p0248 N73-12007

Irregularities in flow behavior of parallel air jets behind smoothing grids
[NASA-TT-F-14653] 06 p0654 N73-15311

Experimental investigation of mean flow characteristics of air jets issuing from rectangular orifices
[AD-754225] 10 p1143 N73-19314

Control technology for air cushion passenger vehicle
11 p1352 N73-20969

Literature survey of heat transfer characteristics of single and multiple turbulent air jets impinging on flat plates
[NASA-TM-X-2778] 15 p1842 N73-24927

Effect of adjacent jets on turbulent mixing rate of coaxial helium jet in Mach 4 air stream
[NASA-CR-112292] 16 p1888 N73-25281

Simulation of interaction between wind-driven rain and annular air curtain dome and analysis of resulting flow distribution
[UTIAS-TN-182] 20 p2388 N73-29187

**AIR LAND INTERACTIONS**

Parameterization of atmospheric boundary layer
05 p0574 N73-14664

**AIR LAUNCHING**

Flight tests of disk-gap band parachute behind full-scale simulator of Viking reentry vehicle over maximum range of entry conditions for landing on planet Mars-Vehicle AV-1
[NASA-CR-112176] 04 p0372 N73-13021

Flight tests of disk-gap band parachute behind full-scale simulator of Viking reentry vehicle over maximum range of entry conditions for landing on planet Mars-Vehicle AV-4
[NASA-CR-112179] 04 p0372 N73-13024

**AIR LOCKS**

Air lock mechanism for inserting and removing specimens from vacuum furnace
[NASA-CASE-LAR-10841-1] 03 p0305 N73-12494

Human factors characteristics and geometry of expandable structures for use as airlocks, escape capsules, and crew transfer tunnels on Skylab program
[AD-749131] 06 p0722 N73-15896

Design and development of gas-film seal using shrouded Rayleigh step lift pads at primary sealing face of gas turbine engine
[NASA-CR-121177] 18 p2155 N73-27415

**AIR MASSES**

Mathematical model for acoustic gravity wave excitations moving air masses
05 p0508 N73-14135

Various Belgian climates associated to different air mass origins
[MISC-SER-A-2] 05 p0574 N73-14667

Numerical analysis of gravity wave generation in atmospheric frontal zone
[AD-751638] 07 p0796 N73-16469

Dynamics of horizontal movement of air masses
[NLL-M-22820-[5828.4F]] 16 p1936 N73-25667

Radar observation of air mass circulation in upper atmosphere during IQSY
17 p2023 N73-26364

**AIR NAVIGATION**
NT ALL-WEATHER AIR NAVIGATION
NT AREA NAVIGATION

Numerical control of delta modulated vocal signals in air navigation telecommunication system
01 p0025 N73-10194

Development of air navigation system using moving map display based on holographic storage and display techniques
[AD-745025] 01 p0065 N73-10533

Development and application of correction information to improve accuracy of differential Omega navigation system
[AD-745878] 02 p0208 N73-11691

Compilation of Instrument Flight Rules Off-Airway Non-95 Routes for US and Alaska, November 1972
05 p0577 N73-14696

Analysis of methods for obtaining improved accuracy of aircraft position determination in Discrete Address Beacon system of air navigation
[TN-1972-38] 05 p0577 N73-14697

Characteristics of air traffic control system to include components of system and application of automation to obtain system safety
[MTR-6152-REV-1] 05 p0577 N73-14698

Development and characteristics of terminal area simulation for analysis of air traffic control requirements and improvement in flight safety conditions
[NASA-CR-112195] 05 p0577 N73-14699

Development, characteristics, and applications of Loran C navigation system for air navigation and microsecond clock synchronization
[NBS-MONO-129] 05 p0577 N73-14700

Analysis of Canadian air traffic control system to include human factors aspects, automation, and environmental engineering
[DCIEM-825] 06 p0696 N73-15670

Analysis of Air Traffic Control Radar Beacon System performance and effects on several Air Route Traffic Control Centers
[ECAC-PR-72-023] 06 p0696 N73-15675

Application of propagation theory to analyze development and effectiveness of loran navigation system in Germany
[AD-750006] 06 p0697 N73-15682

Handbook of operating instructions for air navigation systems to include international air routes. Doppler radar, and great circle navigation
[AD-750493] 06 p0697 N73-15684
Demand and trade study related to development of air traffic control system based on geographical regions - Vol. 3
[PB-212180] 06 p0698 N73-15690
Analysis of military helicopter formation flight techniques with emphasis on station keeping based on nominal point coordinate system
[AD-751459] 07 p0740 N73-16021
Survey of Air Traffic Control Beacon System to determine occurrence of excessive interrogation signals within New York air control sector - Final Report
[ECAC-PR-72-031] 07 p0818 N73-16630
Description of Geographical Position Locator system with emphasis on means for automatically reducing position errors
[UCRL-74039] 07 p0818 N73-16631
Kalman filtering applied to surface and air navigation using celestial body coordinates
07 p0860 N73-16973
Evaluation of loran antenna modification to determine effect of increased height on radiated power and system performance
[AD-751978] 08 p0942 N73-17714
Performance tests of various Tacan ground station modifications designed to minimize false distance measuring equipment indications
[FAA-NA-72-63] 09 p1062 N73-18664
Technical evaluation of cartography for use in civil air navigation map displays to determine information elements required to operate in 1975 to 1980 airspace - Vol. 1
[FAA-RD-72-129-VOL-1] 10 p1155 N73-19393
Evaluation of cartographic information for use in civil air navigation map displays to determine information elements required to operate in 1975 to 1980 airspace - Vol. 2
[FAA-RD-72-129-VOL-2] 10 p1155 N73-19394
Proceedings of symposium on flight operations and air traffic control to show problems affecting airports, general aviation, air traffic controllers, and governmental agencies
[DLR-MITT-72-24] 10 p1183 N73-19623
Development of systematic methodology and computer programs for optimal design of national grid of high altitude VHF omnirange navigation systems - Part 2
[FAA-RD-72-118-2-PT-2] 10 p1185 N73-19644
Pilot error analysis for airborne navigation procedures
[AD-754214] 11 p1251 N73-20150
Development and evaluation of discrete address beacon system for air traffic control applications
[FAA-RD-73-12] 11 p1255 N73-20184
Analysis of synchronized discrete address beacon system for improved air traffic control capability
[SD-FR-01] 11 p1256 N73-20189
Proceedings of conference on inertial navigation components and systems with emphasis on concepts and techniques involving cost and performance tradeoffs
[AGARD-CP-116] 11 p1316 N73-20684
Application of loran/inertial hybrid system and Kalman filter algorithm to fixed feedback gain
11 p1318 N73-20701
Fault detection possibilities in integrated navigation system employing Kalman filtering
11 p1320 N73-20712
Life cycle cost analysis of inertial navigation systems for aircraft and air to surface missiles
11 p1320 N73-20717
Analysis of interaction of major elements of Oceanic Air Traffic Control System to determine minimum longitudinal and lateral separation distances
[FAA-RD-73-8] 11 p1321 N73-20719
Analysis of improved signal processing techniques for low frequency, one-way ranging for aircraft radio navigation
[AD-754031] 11 p1322 N73-20727
Functional error analysis and simulation of air traffic control system to support concepts evaluation program
[PB-213148] 11 p1322 N73-20730
Development of navigation system design factors through computerized simulation for application to loran/inertial hybrid system
[AD-754548] 11 p1322 N73-20731
Interrupt handling facilities in AADC system and associated control
[AD-756665] 13 p1498 N73-22142
Development of integrated system for air navigation using radio range measurements and data from onboard inertial sensors for aircraft approach and landing
[NASA-TM-X-62199] 13 p1556 N73-22614
Development of on-board navigation system based on Applications Technology Satellites, Omega navigation systems, and aircraft terminal facilities
[NASA-CR-130213] 13 p1556 N73-22615
Evaluation of VORTAC navigation system accuracies required to support present and anticipated operational uses of system
13 p1557 N73-22616
Statistical analysis of phase data on three Omega navigation stations to determine positioning accuracies - Vol. I
[AD-756024] 13 p1557 N73-22617
Program listings and output data summaries for differential Omega navigation system monitoring and analysis - Vol. 2
[AD-756025] 13 p1557 N73-22618
Analog charts developed during monitoring and analysis of differential Omega navigation system - Vol. 3
[AD-756026] 13 p1557 N73-22619
Development of air navigation system to provide four dimensional guidance for short takeoff aircraft operating in terminal area
[NASA-TM-X-62234] 14 p1687 N73-23686
Analysis of air navigation systems for continental US and overseas flights based on projected traffic loads of 1980 time period
[FAA-ED-04-1] 14 p1687 N73-23688
Proceedings of conference on air traffic control developments and procedures
[AGARD-CP-105] 14 p1687 N73-23689
Air traffic control facilities operated by U.S. military forces and developments in improved air traffic control systems
14 p1687 N73-23690
Comparison of cost, complexity, and cockpit workload for seven area navigation system configurations
14 p1688 N73-23697
Characteristics of airborne area navigation equipment and application to air traffic control functions
14 p1688 N73-23698
Analysis of North Atlantic air route structure to determine impact of inertial navigation and satellite surveillance on separation reduction
14 p1688 N73-23699
Development and characteristics of forward area homing and landing guidance for military aircraft operations
14 p1689 N73-23708
Development of high bandwidth time division communications system to provide ground based, wide area, position location system
14 p1689 N73-23711
Analysis of communications, navigation, and identification equipment for aircraft and proposed system for improvement in capability
14 p1690 N73-23720
Analysis of integrated communications, navigation, and identification system for aircraft operation and proposal for improved capability
14 p1691 N73-23721
Analysis of Loran C signal processing techniques using hybrid simulation procedure
[AD-757586] 14 p1691 N73-23725
Computation of geodetic coordinates of aircraft from two measured distances and height above earth surface
[AD-757541] 15 p1808 N73-24658
Computer program for selection of radio frequencies used in VOR, ILS, and Tacan/DME air navigation systems
[FAA-NA-73-4] 16 p1940 N73-25700
Analysis and digital computer simulation of operational and performance aspects of vertical area navigation system
[FAA-RD-72-125] 16 p1941 N73-25705
Proceedings of conference on precise time and time interval planning for application to hypersonic navigation systems
[AD-758739] 16 p1942 N73-25717
Effects of polar cap absorption events on performance of Omega navigation system operating in high latitudes
[AD-759009] 16 p1942 N73-25718
Equipment route winds and great circle distances for helicopter air routes at 5,000, 10,000, and 18,000 feet - Vol. 1
[AD-760252] 17 p1985 N73-26043
Equipment route winds and great circle distances for helicopter air routes at 5,000, 10,000 and 18,000 feet - Vol. 2
[AD-760253] 17 p1985 N73-26044
Characteristics of airborne radio homing and alerting equipment for use with emergency locator transmitters
[RTCA-SC-124] 17 p2060 N73-26663
Proceedings of conference to develop area navigation system design concept for application to national airspace system for improved air traffic control
17 p2060 N73-26664
Very low frequency timing techniques for Omega navigation system to include operational considerations, path selection, and adjustment procedure
[NASA-CR-133185] 17 p2061 N73-26669
Research projects conducted by organizations of National Research Council of Canada on structural analysis, jet fuels, air pollution, and very low frequency navigation
[DME/NAE-1973[1]] 17 p2098 N73-26970
Development of airborne very low frequency navigation system using radio communications stations and comparison with other air navigation systems
17 p2098 N73-26973
Regulations for promoting safety in air navigation for municipal airport of Hartselle, Alabama
[PB-220087/1] 18 p2127 N73-27185
Analysis of very low frequency radio signals for aircraft area navigation to show capability for continental flight redundancy and reliability
[AD-761498] 19 p2318 N73-28651
Flight tests of VHF Omnirange navigation and Tacan systems to determine bearing error curves
[FAA-RD-72-73] 20 p2452 N73-29710

**AIR PIRACY**

Speech on problem of aircraft hijacking and efforts to prevent hijackers from continuing to conduct air piracy
05 p0611 N73-14970

**AIR POLLUTION**

Mass spectrometer system for monitoring atmospheric constituents and pollutants -operation and maintenance manual
[NASA-CR-128603] 01 p0057 N73-10469
Small perturbation theory applied to effects of irregular topography on deflection of wind blowing over industrial area and then residential area and effects on air pollution
[NASA-TM-X-2653] 01 p0074 N73-10610
Sulfur oxides, smoke, and air pollution tables from Belgian weather stations, Oct. 1971
01 p0075 N73-10619
Influence of meteorological conditions on air pollution
[PB-210381] 01 p0077 N73-10634
Regional air pollution study and air quality control
[PB-210017] 01 p0077 N73-10636
Research plan for regional air pollution study
[PB-210018] 01 p0077 N73-10637
Laboratory facility for regional air pollution study at St. Louis, Missouri
[PB-210019] 01 p0077 N73-10638
Scheduling management, and costs of St. Louis air pollution facility
[PB-210020] 01 p0077 N73-10639
USSR air pollution literature survey on biological effects and health aspects
[PB-209478] 01 p0078 N73-10642
PICK method of particle-in-cell techniques for numerical solution of atmospheric diffusion equation applied to air pollution problems
[PB-209290] 01 p0078 N73-10643
Design and characteristics of instrument for monitoring carbon monoxide content of ambient atmosphere to include operations and maintenance instructions
[NASA-CR-128602] 02 p0172 N73-11394
Modification of atmosphere contamination sensor to include carbon monoxide monitoring capability
[NASA-CR-128604] 02 p0172 N73-11395
Optical radar data for probing atmospheric composition and air pollution particulates
02 p0197 N73-11595
Sulfur oxides, smoke, and air pollution tables from Belgian weather stations, Dec. 1971
02 p0205 N73-11659
Three laser methods of remotely mapping gaseous pollutants of atmosphere
[AD-746280] 02 p0205 N73-11664
Proceedings of conference on environmental toxicology held at Fairborn, Ohio, 31 August, and 1-2 September 1971
[AD-746660] 02 p0207 N73-11676
Proceedings of conference on air pollution, turbulence, and diffusion
[SC-M-71-0913] 03 p0327 N73-12662
Sulfur oxides, smoke, and air pollution tables from Belgian weather stations, Nov. 1971
03 p0327 N73-12663
Control system design criteria to prevent air pollution from volatile fuel storage tank emission
[AD-748009] 03 p0350 N73-12854
Portable sampling and measurement system for determining gaseous emission species in afterburn of turbojet engine at ground level
[AD-747773] 03 p0351 N73-12866
Increase of water vapor in stratosphere due to fleet of SSTs
[AD-748797] 04 p0416 N73-13397
Satellite observation for acquisition and monitoring of planetary radiation, clouds, particles, and air pollution
[DGLR-PAPER-72-81] 04 p0444 N73-13626
Feasibility of monitoring global air pollution using optical sensors installed in orbiting satellites
04 p0471 N73-13840
Application of remotely sensed, multispectral observations for assessment of earth resources and environmental quality in Alabama
04 p0471 N73-13841
Conversion and utilization of solar energy to solve energy shortages and pollution problems on earth
04 p0474 N73-13866

Application of remote sensing techniques to public health
[NASA-CR-129822] 05 p0500 N73-14069
Effects of SO2 decay product toxicity on human physiological functions
05 p0500 N73-14071
Utilization of ERTS-1 imagery in air pollution and marine biology studies of lower Chesapeake Bay and continental shelf of Eastern US
[E72-10367] 05 p0535 N73-14355
Model of turbulent structure and diffusion for studying movement of air pollution
[PB-211897] 05 p0540 N73-14397
Particulate and gaseous pollutant data gathered during 1968 by national, state, and local air surveillance networks
[APTD-0978] 05 p0572 N73-14652
Sulfur oxides, smoke, and air pollution tables from Belgian weather stations, Jan. 1972
05 p0574 N73-14668
Laboratory experiments and mathematical models of nitrogen oxide formation in combustion of fossil fuels
[PB-211480] 05 p0606 N73-14932
Research on chemical reactions, remote sensors, pollution, and transportation
[NASA-CR-61396] 05 p0607 N73-14938
Respiratory models for studying hazards of air pollution
[UR-3490-169] 06 p0630 N73-15121
High concentration sulfur dioxide pollution over Osaka, Japan during summer
[NLL-M-20713-[5828.4F]] 06 p0692 N73-15634
Simulation of emission-dispersion of inert pollutant in lower atmosphere in industrial zones by numerical integration of conservation and pollutant flow equations
06 p0693 N73-15649
Analysis of factors affecting environmental chambers used to study photochemical reactions in lower atmosphere
[PB-212715] 06 p0695 N73-15663
Public health exposure limits to nitrogen oxide, hydrogen chloride, and hydrogen fluoride air pollutants
[AD-751438] 07 p0748 N73-16084
Public health exposure limits for air pollutants
[AD-751437] 07 p0749 N73-16088
Measurement of radioisotopes in air and rain water for areas around Helsinki and Ivalo, Finland
[REPT-11] 07 p0815 N73-16604
Weekend effect in CCN spectra and St. Louis urban heat island
[TN-45] 07 p0815 N73-16606
Climatic changes resulting from upper atmosphere perturbation by supersonic aircraft exhausts
[PB-212427] 07 p0816 N73-16612
Analysis of haze aerosols in rural and urban atmospheres
[PB-212609] 07 p0816 N73-16613
Design and performance of exhaust hood with protective air current outside of hood surface
08 p0872 N73-17063
Anhydrous ammonia for removing nitrogen dioxide from stack emission simulating hydrazine nitrogen tetroxide rocket fuel combustion exhaust
08 p0874 N73-17075
Ozone reaction with mercaptane for elimination of exhaust gas pollution in air
08 p0883 N73-17152
Remote gas filter correlation instrument for monitoring air pollution by satellites
[NASA-CR-112137] 08 p0938 N73-17682
Sulfur oxides, smoke, and air pollution tables from Belgian weather stations, Feb. 1972
08 p0939 N73-17686
Bibliography of USAF reports on air, water, noise, and radiation pollution
[AD-751898] 08 p0940 N73-17699
Measurement methods based on gas chemiluminescence, emphasizing air pollution applications
[AD-753222] 09 p1000 N73-18163
Guide to research in air pollution for 1972
[AP-47] 09 p1060 N73-18649
Developments in air pollution research program
09 p1060 N73-18650
Analysis of air pollution caused by exhaust from military aircraft engines and development of technology for pollutant measurement to meet EPA standards
[AD-753095] 09 p1100 N73-18975
Hypoxia adaptation of rats for increased resistance to toxic atmospheric gases
10 p1116 N73-19100
Toxic effect of indole inhalation on man, mouse, rat, and rabbit organisms
10 p1117 N73-19102
Toxic effects of human exhaled air on mice organisms
10 p1117 N73-19103
Oxidation of atmospheric impurities in space cabin and purity of reclamated water
10 p1117 N73-19104
Atmospheric pollution in Belgium from 1 Apr. 1969 to 31 Mar. 1970
[PUBL-SER-A-78] 10 p1182 N73-19618
X ray fluorescence analysis on air pollution particulate sample
[PB-213366] 11 p1254 N73-20173
Method of measuring amount of carbon monoxide by oxidizing agents to yield carbon dioxide for air pollution control
[NLL-RTS-7573] 11 p1274 N73-20340
Detection of smoke pollution in Virginia by photogrammetric and densitometric analysis of ERTS-1 imagery
[E73-10419] 11 p1279 N73-20381
Carbon dioxide lasers, optical measurement instrumentation and imaging techniques for air pollution detection
[AD-754939] 11 p1303 N73-20574
Portable laser velocimeter for stack velocity measurements
[PB-213263] 11 p1304 N73-20579
Air pollution models, and problem areas in air pollution dispersion modeling
[NASA-SP-322] 11 p1313 N73-20658
Control measures for preventing environmental beryllium contamination
[AP-116] 11 p1313 N73-20659
Occupational hazards and control measures to prevent air pollution from asbestos processing
[AP-117] 11 p1314 N73-20660
Mercury emission control systems for primary mercury facility and for chlor-alkali plant
[AP-118] 11 p1314 N73-20661
Averaging time and maxima for dependent observations
[AD-754788] 11 p1315 N73-20674
Alternate fuels to reduce aircraft exhaust pollutants
[AD-755151] 11 p1332 N73-20815
Effects of transportation combustion products in air pollution
[PB-213034] 11 p1354 N73-20991
Survey on computerized modeling of transportation generated air pollution
[PB-213013] 11 p1354 N73-20992
Analysis of global effects created by increase in carbon dioxide and aerosol content in atmosphere
12 p1420 N73-21511
Analysis of atmospheric pollution parameters to show sources, physiological effects, biological effects, and meteorological effects
12 p1421 N73-21519
Comparison of air pollution from aircraft, automobiles, buses, trucks, railroads, and electric trains in US from 1940-1980
[FAA-EQ-73-2] 12 p1421 N73-21522
Stratospheric photochemical reactions of ozone in relation to climatology and supersonic transport pollution
[NOAA-TM-NESS-47] 12 p1422 N73-21526
Analysis of times series processes for correlation of air pollution data measurements
[AD-754433] 12 p1424 N73-21538
Satellite solar occultation absorption measurements of pollutant concentrations and spectral properties of molecules in infrared region
[REPT-011023-1-T] 12 p1444 N73-21700
Isotopic composition of atmospheric carbon monoxide
[PB-213591] 13 p1527 N73-22378
High altitude measurement of atmospheric pollution from aircraft engine exhaust gases
[NASA-TM-X-68221] 13 p1553 N73-22584
Present and predicted nature, entent, and control of air pollution related to aircraft operations in US
[REPT-72-02452] 13 p1553 N73-22586
Sulfur oxides, smoke, and air pollution tables from Belgian weather stations, Mar. 1972
13 p1553 N73-22587
Sulfur oxides, smoke, and air pollution tables from Belgian weather stations, Apr. 1972
13 p1553 N73-22590
Solid state laser multiwavelength identification and display system for detection and spectrum analysis of air pollutants
[AD-755161] 13 p1554 N73-22598
Collection and measurement of atmospheric contaminants during Skylab AM/MDA unmanned altitude chamber test
[NASA-CR-128903] 13 p1582 N73-22823
Man induced changes in earth climate by environment pollution and heat production
[PB-213676/2] 14 p1613 N73-23074
Estimates of cost of air pollution damage
[AP-85] 14 p1685 N73-23669
Effect of primary-zone water injection on pollutants from combustor burning liquid ASTM A-1 and vaporized propane fuels
[NASA-TN-D-7293] 14 p1718 N73-23943
Threat of stratospheric ozone nonequilibrium by SST nitric oxide exhaust gases
[AD-757059] 14 p1719 N73-23949
Solid phase trace element aerosol concentrations in lowest 34 meters of atmosphere
15 p1771 N73-24343
Air pollution modeling and meteorology for California particularly San Francisco Bay Area
[UCRL-74335] 15 p1806 N73-24635
Summaries of research in plasma sources, hydromagnetic shock waves rotating plasmas, ion cyclotrons, air pollution, and laser diagnostics
[NP-19643] 15 p1817 N73-24727
Analysis of air pollution caused by aircraft engine emissions in vicinity of airport and comparison with air pollution in urban areas
15 p1825 N73-24788
Establishment of criteria for oxides of nitrogen emissions to control air pollution contribution from aircraft operating at major air terminals - Vol. 1
[REPT-1162-1-VOL-1] 15 p1825 N73-24789
Numerical analysis of process for nitrogen oxide formation in aircraft engine exhaust products and development of computer program for application of theory - Vol. 2
[REPT-1162-2-VOL-2] 15 p1825 N73-24790
Pollutant level measurement of exhaust gases from annular swirl can combustor
[NASA-TM-X-68247] 15 p1826 N73-24797
Tunable diode laser for air pollution gas analysis
[PB-214240/5] 16 p1871 N73-25149
Survey of atmospheric aerosol concentrations over seas
[PB-214170/3] 16 p1909 N73-25442
Development of breadboard model correlation interferometer for carbon monoxide pollution experiment
[NASA-CR-112212] 16 p1913 N73-25478
Importance of depth of mixing layer in air pollution studies
[NLL-M-22807-[5828.4F]] 16 p1936 N73-25668
Air pollution of biosphere
[NLL-M-22885-[5828.4F]] 16 p1936 N73-25669
Weather forecasting and measurement of air pollution by laser sounding of atmosphere
[NASA-TT-F-14948] 17 p2026 N73-26391
Electrostatic entrained material measurement system
[NASA-CASE-MFS-22128-1] 17 p2032 N73-26442
Method for calculating ground level concentration of pollutants emitted from high stack based on plume aerodynamics and atmospheric mixing
[PUB-73-3] 17 p2057 N73-26636
Combustor research programs to gain advanced technology for reducing aircraft engine pollution
[NASA-TM-X-68256] 17 p2076 N73-26797
Research projects conducted by organizations of National Research Council of Canada on structural analysis, jet fuels, air pollution, and very low frequency navigation
[DME/NAE-1973[1]] 17 p2098 N73-26970
Effect of atmospheric stability on vertical spread of airborne pollutants from steady and instantaneous sources in constant stress region
17 p2098 N73-26974
Correlation of ERTS-1 data with ground data for determining characteristics of air pollution in Norfolk, Virginia area
[E73-10779] 18 p2135 N73-27255
Nationwide air pollutant trends for hydrocarbons, oxides, and particulates from 1940 to 1970
[AP-115] 18 p2171 N73-27537
Testing association of automotive fuel composition with exhaust reactivity using different engines and gasolines of varied composition
[BM-RI-7756] 18 p2172 N73-27542
Validation of calibration procedure used with climatological models of multiple-source urban air pollution
[PB-218716/9] 18 p2173 N73-27553
Testing reactor-equipped vehicle for assessment of emissions control
[PB-218639/3] 18 p2173 N73-27554
Basic fundamentals of meteorology and their effect on pollutant concentration on highway corridor
[PB-219811/7] 18 p2174 N73-27556
Environmental impact of highway projects as determined by vehicle emission factors
[PB-219812/5] 18 p2174 N73-27557
Contribution of automobiles to air pollution levels in Reading, England
[PB-219602/0] 18 p2175 N73-27563
Relationship between highway traffic parameters and air quality analysis - Vol. 3
[PB-219813/3] 18 p2175 N73-27564
Mathematical approach to estimating highway impact on air quality - Vol. 4
[PB-219814/1] 18 p2175 N73-27565
Interaction between air pollution sources and meteorological conditions and impact on air quality along highway corridor - Vol. 6
[PB-219816/6] 18 p2175 N73-27566
Performance of commercial multiple crystal spectrometer instruments in analyzing particulate matter
[AD-762061] 19 p2231 N73-27994
Photogrammetric and densitometric examination of ERTS-1 MSS imagery of Eastern Virginia to determine sources of aerosol pollution
[PAPER-E5] 19 p2269 N73-28269
Analysis of ERTS-1 imagery to determine meteorological content with emphasis on mesoscale effects of Great Lakes and air pollution dispersion
[PAPER-W17] 19 p2272 N73-28294

Analysis of aircraft emissions and recommendations for reducing impact of aircraft emissions on air pollution
[NREC-1168-1] 20 p2360 N73-28986
Determining diffusion of impurities in atmosphere by mixing properties of turbulence
[NLL-M-23009-[5828.4F]] 20 p2390 N73-29198
Assessment of vehicular air pollution for Tulsa, Oklahoma
20 p2441 N73-29606
Atmospheric pollution due to use of lead iodide in weather modification
[NLL-M-23006-[5828.4F]] 20 p2441 N73-29607
Removal of pollutants from atmosphere by precipitation and clouds
[NLL-M-23010-[5828.4F]] 20 p2441 N73-29608
Influence of ground concentration, hilly terrain, and wind velocity on distribution of pollutants considering initial elevation
20 p2446 N73-29648
Appropriate line profiles for radiation modeling in detection of atmospheric pollutants
[NASA-CR-132303] 20 p2448 N73-29672
Sulfur oxides, smoke, and air pollution tables from Belgian weather stations, Jul. 1972
20 p2449 N73-29686
Analysis of jet engine test cell pollution abatement methods
[AD-763119] 20 p2450 N73-29690
Feasibility of using satellite-borne instruments to detect atmospheric pollution
[PB-220394/1] 21 p2541 N73-30372
Increased optical efficiency of flame photometric detector for detection of SO2 in air
[PB-220480/8] 21 p2551 N73-30453
Theory and operating characteristics of equipment in laser exhaust measurement program
[PB-220429/5] 21 p2556 N73-30493
Theoretical study of thermal structure and dispersion in polluted urban atmosphere
21 p2568 N73-30579
National Environmental Research Center research projects for FY 73 on air pollution and control equipment
[PB-220259/6] 21 p2574 N73-30630
Numerical simulation of chemical reactions in air pollution - Vol. 1
[PB-220456] 21 p2574 N73-30631
User guide for computer simulation model air pollution - Vol. 2
[PB-220457/6] 21 p2574 N73-30632
Bibliography on air pollution from both natural and man-made sources
[AD-761950] 21 p2575 N73-30636
Absorptive equipment for control of air polluting industrial wastes
[PB-221138/1] 21 p2575 N73-30637
Measurements of Fe, Mn, Fu, Cu, Ni, and Pb in aerosols and precipitation in clean tropospheric air
[NOAA-TR-ERL-248-APCL-24]
22 p2664 N73-31349
Theory and application of active and passive remote sensors in air pollution engineering
22 p2671 N73-31395
Airborne measurements of photochemical pollution in California and adjacent waters of Pacific Ocean
[NASA-TM-X-69504] 22 p2694 N73-31581
Methodology for controlling air pollution episodes
[ANL/ES-14] 22 p2694 N73-31583
Monitoring of air breathing engine exhaust gas emissions, pollutants, and atmospheric air pollution propagation
[DLR-MITT-72-14-PT-1] 22 p2694 N73-31584
Chemical and physical characterization of automotive exhaust particulate matter in atmosphere
[PB-221603/4] 22 p2695 N73-31589
Measurement of concentration of volatile and particulate lead compounds in atmosphere at selected road sites
[PB-221663/8] 22 p2695 N73-31592
Methodology for integrating air pollution impact of airport and its environs
[PB-220987/2] 22 p2696 N73-31594
User manual for air quality data handling system
[PB-220985/6] 22 p2696 N73-31595
Impact of highway transportation control strategies on Los Angeles air pollution and quality
[PB-221301/5] 22 p2696 N73-31597
Transportation control measures to improve air quality standards in Greater Houston area by 1977
[PB-221611/7] 22 p2696 N73-31598
Design and performance of remote sensing system for optical sensing of emissions
[PB-221073/0] 22 p2696 N73-31599
Formation of nitric oxide in steady laminar diffusion flame
22 p2727 N73-31825
Proceedings of conference on mathematical modeling of photochemical smog
[PB-221177/9] 23 p2754 N73-32038
Utilization of ERTS data to study air pollution, insect infestation, and water transport in Minnesota
[NASA-CR-135565] 23 p2783 N73-32266
ERTS-1 sensor analysis of air pollution and air pollution related injuries to plant vegetation in metropolitan Minnesota
23 p2784 N73-32269
Research projects to determine effects of exhaust products from aircraft operating in stratosphere on global and local climatic conditions
[UCRL-51336] 23 p2787 N73-32296
Air pollution test and evaluation plan for 1972-77
[PB-221011] 23 p2814 N73-32501
Field program design for verifying photochemical diffusion models
[PB-221300/7] 23 p2814 N73-32502
Feasibility of conducting long-range atmospheric tracer experiments to study transport and diffusion of air pollution plumes
[AD-764893] 23 p2815 N73-32504
Attenuation of solar spectral intensity by pollution in boundary layer of New Haven, Connecticut atmosphere
23 p2833 N73-32641
Emission of air pollutants from combustion of wood wastes
[WSCI-72-1] 23 p2856 N73-32821
Effect of inlet air humidity on exhaust gas emissions of nitrogen oxides in gas turbine combustor
[NASA-TN-D-7396] 23 p2856 N73-32822
Inelastic light scattering from molecular gases with applications to remote detection of air pollutants
24 p2891 N73-33077
Photoelectron spectroscopic analysis of excited hydrogen fluoride in contaminated atmospheres
[AD-764813] 24 p2893 N73-33093
Atmospheric modeling and environmental protection needs for air pollution control
[UCRL-74249] 24 p2922 N73-33341
Measurements of atmospheric lead concentrations in European community and United Kingdom
[EUR-4982] 24 p2949 N73-33555
Sulfur oxides, smoke, and air pollution tables from Belgian weather stations, Aug. 1972
24 p2949 N73-33559
Sulfur oxides, smoke, and air pollution tables from Belgian weather stations, Sep. 1972
24 p2949 N73-33560

**AIR PURIFICATION**
Bibliography on carbon dioxide removal from gases by lithium hydroxide
[CL-1971-15] 04 p0386 N73-13136
Hydrogen peroxide aerosols for decontamination of influenza atmosphere
[NASA-TT-F-15127] 23 p2750 N73-32006
Cost data for modified hydrogen depolarized carbon dioxide concentrator in life support system
[NASA-CR-124462] 24 p2887 N73-33052

**AIR SAMPLING**
Development of automatic air sampling system
[RM-559] 04 p0420 N73-13428
Collection and measurement of atmospheric contaminants during Skylab AM/MDA unmanned altitude chamber test
[NASA-CR-128903] 13 p1582 N73-22823
Polycyclic aromatic hydrocarbon aerosol collection using fiber glass and silica gel filters
[NLL-TRANS-1191-[9022.9]-PT-1]
15 p1746 N73-24152
Contribution of automobiles to air pollution levels in Reading, England
[PB-219602/0] 18 p2175 N73-27563
Quantitative neutron activation analysis of stable elements in air pollution particulates
[AD-764715] 23 p2755 N73-32043
Air pollution test and evaluation plan for 1972-77
[PB-221011] 23 p2814 N73-32501

**AIR SEA INTERACTIONS**
U AIR WATER INTERACTIONS

**AIR SICKNESS**
U MOTION SICKNESS

**AIR TO AIR MISSILES**
Analysis of flow distribution around axisymmetric bodies at extreme angles of attack and calculation of pressure distribution for asymmetric steady vortex wake
[AD-747986] 03 p0286 N73-12315
Performance tests of strapdown air to air tracking system for short range weapons control system
[AD-751654] 07 p0818 N73-16633
Infrared signatures of high performance jet aircraft and evaluation of air to air missile effectiveness
[SLA-73-5271] 24 p2994 N73-33929

**AIR TO AIR ROCKETS**
U AIR TO AIR MISSILES

**AIR TO SURFACE MISSILES**
Computerized simulation of longitudinal cable shapes during deployment from missile away from flying aircraft
[AD-753907] 10 p1135 N73-19254
Life cycle cost analysis of inertial navigation systems for aircraft and air to surface missiles
11 p1320 N73-20717

**AIR TRAFFIC**
Forecasts of military air traffic activity and effect on air traffic control facilities for 1972 through 1983
05 p0493 N73-14014
Aircraft accident prevention analysis of air taxi/commuter operations to identify safety factors and enhance safety of operations
[NTSB-AAS-72-9] 05 p0493 N73-14016
Infrastructural role of airports in Germany and planning for future traffic increase
[DGLR-PAPER-72-034] 06 p0650 N73-15281
Experiences of airline operator regarding developments in flight safety, passenger comfort, schedule adherence, and economy
[DGLR-PAPER-72-037] 06 p0650 N73-15282
Findings and recommendations of Aviation Advisory Commission on long range needs of Aviation-- Vol. 1 Vol. 2
[PB-215803] 09 p1101 N73-18983
Development of procedures for accurately estimating annual air traffic levels at airports without tower control
[SCI-2-2040] 11 p1321 N73-20722
Analysis of trans-Atlantic aircraft movements for 1970 - 1971 period to establish base line for passenger forecasts
13 p1474 N73-21935
Analysis of air passenger traffic on North Atlantic air routes to show development of scheduled and chartered operations
13 p1474 N73-21937
Analysis of impact of major airport operations on economy, ecology, and urban development
13 p1505 N73-22199
Profiles of scheduled air carrier airport operations for top 100 airports in U.S.A.
[REPT-73-00328] 13 p1506 N73-22207
Utilizing Out-of-Kilter Algorithm to evaluate efficiency of passenger capacity of selected air carriers between twenty cities in US
13 p1592 N73-22910
Performance of airfield pavement construction joints under heavy aircraft loads
[FAA-RD-72-106] 16 p1969 N73-25926
User manual for Los Angeles Basin Standard Traffic Model
[FAA-RD-73-89] 21 p2576 N73-30647
Statistical analysis of air traffic conditions predicted for Los Angeles, California area in 1982 - Vol. 1
[MTR-6387-VOL-1] 21 p2577 N73-30653
Statistical analysis of air traffic conditions predicted for Los Angeles, California area in 1982 - Vol. 2
[MTR-6387-VOL-2] 21 p2577 N73-30654
Future of short haul air transport in Western Europe - V/STOL Working Group
[SP-73-001] 22 p2737 N73-31915
Effects of transition from conventional to quiet takeoff and landing air traffic, noting introduction of microwave ILS and area navigation
[MBB-UH-05-73-O] 23 p2817 N73-32525
International civil aviation organization for air traffic forecasting and airport development
23 p2861 N73-32865
World air passenger traffic demand
23 p2862 N73-32868
Proceedings of conference on air transport industry with emphasis on economics, market demand, airlines regulation, and international transportation policy - Vol. 2
[NASA-CR-135635] 23 p2862 N73-32875
Organization, responsibilities, and functions of Civil Aeronautics Board in determining award of air routes to air lines
23 p2863 N73-32880

**AIR TRAFFIC CONTROL**
Development of statistical-probabilistic method of collision probability calculation and application to arbitrary flight paths and vehicle shapes
[AD-744722] 01 p0006 N73-10046
Design of computerized airborne traffic display device with alphanumerical control for aircraft pilots
01 p0014 N73-10112
Runway separation standards according to reaction time of pilot manual control response to air traffic controller communication
01 p0015 N73-10113
ATC surveillance/communication analysis and planning activities from 1 June to 31 Aug. 1972
[FAA-RD-72-107] 01 p0078 N73-10645
Performance of air-to-satellite-to-ground systems for air traffic control
[PB-210378] 01 p0078 N73-10646
Proposed control tower and cockpit visibility readouts based on airport-aircraft information flow system
[AD-744718] 01 p0078 N73-10647
Methods for implementation of man machine interface of digital data links for air traffic control
[AD-744721] 01 p0079 N73-10648
Comparison of age, education, pre-FAA experience, aptitudes, training course performance, and post-Academy attrition rates of male and female trainees
[FAA-AM-72-22] 02 p0135 N73-11094
Self-estimates of distractibility as related to performance decrement on task requiring sustained attention
[FAA-AM-72-25] 02 p0135 N73-11096

Design, development, and evaluation of mockup of control tower for airport traffic control functions
[FAA-NA-72-63] 02 p0152 N73-11235
Simulator test to evaluate use of air traffic control radar beacon code assignment plan to provide interim radar data processing capability
[FAA-RD-72-103] 02 p0207 N73-11681
Evaluation of automated air traffic control system and comparison with operator performance using manual system 02 p0207 N73-11683
Functions of automated system for processing flight data and surveillance functions with development plan for improved capability
[FAA-ED-12-2] 02 p0208 N73-11684
Design, development, and evaluation of airport lighting control panel for airport traffic control towers
[FAA-RD-72-93] 03 p0260 N73-12108
Development and evaluation of instrument landing system with VHF and UHF capability for localizer and glide slope
[AD-747656] 03 p0329 N73-12688
Discrete address radar beacon system for aircraft tracking and traffic control
[FAA-RD-72-117] 04 p0447 N73-13649
Carrier based air trafic control system with enroute trajectory optimization capability and computer-aided marshal reassignment procedure
[AD-748302] 04 p0447 N73-13651
Analysis of flight plans submitted at flight service stations for IFR and VFR flight clearances during calendar year 1971
[AD-748901] 04 p0447 N73-13652
Development of flight path optimization procedure to minimize flight time of aircraft returning to aircraft carrier
[AD-749326] 04 p0447 N73-13653
Compilation of Instrument Flight Rules Off-Airway Non-95 Routes for US and Alaska, November 1972 05 p0577 N73-14696
Analysis of methods for obtaining improved accuracy of aircraft position determination in Discrete Address Beacon system of air navigation
[TN-1972-38] 05 p0577 N73-14697
Characteristics of air traffic control system to include components of system and application of automation to obtain system safety
[MTR-6152-REV-1] 05 p0577 N73-14698
Development and characteristics of terminal area simulation for analysis of air traffic control requirements and improvement in flight safety conditions
[NASA-CR-112195] 05 p0577 N73-14699
Design and development of microwave landing system for operation of civil and military aircraft in conventional and V/STOL configurations
[AD-749505] 05 p0578 N73-14702
Planning process, objectives of program areas, and index of plans for air traffic control system improvements
[AD-750224] 05 p0578 N73-14705
Trailing vortex hazard avoidance of Jumbo jets by airport warning system 05 p0610 N73-14958
Optimal moving target indicator for long range air traffic control surveillance radars
[AD-750747] 06 p0642 N73-15209
Analysis of Canadian air traffic control system to include human factors aspects, automation, and environmental engineering
[DCIEM-825] 06 p0696 N73-15670
Analysis of excessive interrogation signals from Air Traffic Control Radar Beacon System and effect on operation of Jacksonville, Florida center
[ECAC-PR-72-014] 06 p0696 N73-15675
Analysis of excessive interrogation signals from Air Traffic Control Radar Beacon System and effect on operation of Washington, D.C. center
[ECAC-PR-72-022] 06 p0696 N73-15676
Analysis of excessive interrogation signals from Air Traffic Control Radar Beacon System and effect on operation of Los Angeles, California center
[ECAC-PR-72-044] 06 p0696 N73-15677
Analysis of Air Traffic Control Radar Beacon System performance and effects on several Air Route Traffic Control Centers
[ECAC-PR-72-023] 06 p0696 N73-15678
Tabulation of minimum enroute instrument flight rules altitudes over particular routes and intersections - November 1972 06 p0697 N73-15679
Development and characteristics of air traffic control system to show system performance tradeoffs and technonogical alternatives - Vol. I
[PB-212178] 06 p0698 N73-15688
Analysis of technological alternatives involved in development of air traffic control systems - Vol. 2
[PB-212179] 06 p0698 N73-15689
Demand and trade study related to development of air traffic control system based on geographical regions - Vol. 3
[PB-212180] 06 p0698 N73-15690
Air traffic control system development to show factors involved in system selection - Vol. 4
[PB-212181] 06 p0698 N73-15691
Research and development involved in design and implementation of air traffic control system - Vol. 5
[PB-212182] 06 p0698 N73-15692
Effectiveness of training device for air traffic communication and carrier landing control
[AD-751556] 07 p0751 N73-16101
Survey of air traffic control system to determine areas within system susceptible to radio frequency interference effects
[ECAC-PR-72-008] 07 p0818 N73-16629
Survey of Air Traffic Control Beacon System to determine occurrence of excessive interrogation signals within New York air control sector - Final Report
[ECAC-PR-72-031] 07 p0818 N73-16630
Problems of flight safety in air traffic control with increased volume of traffic
[DGLR-PAPER-72-038] 07 p0818 N73-16632
Theory of Kalman filtering and applications to real time tracking systems for air traffic control, satellite observation, and aircraft navigation
[AD-751485] 07 p0818 N73-16634
Research and development in advance electronics including applications to digital computers, air traffic control, and solid state physics
[AD-751308] 07 p0834 N73-16758
Operation and characteristics of primary radar system for air traffic control surveillance
[FAA-ED-02-1] 08 p0885 N73-17163
Receiver synthesis for air traffic moving target indicator with digital signal processing
[AD-751923] 08 p0885 N73-17170
Development of digital fast-time air traffic control conflict prediction models and application to specific air route traffic control situations
[UTIAS-TN-183] 08 p0941 N73-17708
Development of algorithm for multiple hypothesis testing with application to amplitude comparison monopulse radar system in air traffic control operations
[TN-1973-7] 09 p1002 N73-18173
Systems planning for improved airport surveillance radar equipment using dual airborne antenna switching for air traffic control
[FAA-RD-72-136] 09 p1002 N73-18176
Analysis of system concepts, design criteria, operating procedures, and terminal facilities for short haul transportation aircraft and supporting systems
[NASA-TM-X-62235] 10 p1105 N73-19013
Proceedings of symposium on flight operations and air traffic control to show problems affecting airports, general aviation, air traffic controllers, and governmental agencies
[DLR-MITT-72-24] 10 p1183 N73-19623
Characteristics and functions of various types of aircraft landing fields in Germany and development of airfields for improved air safety 10 p1183 N73-19624
Requirements for air traffic control in German air operations and recommendations for improved air traffic control procedures 10 p1183 N73-19628
Evaluation of associative processor in performance of tracking and conflict detection function in real time ATC terminal environment
[PX-6406-REV-A] 10 p1185 N73-19642
Development of computer programs for design of air route networks for improved flight safety - Part I
[FAA-RD-72-118-1-PT-1] 10 p1185 N73-19643
Development of systematic methodology and computer programs for optimal design of national grid of high altitude VHF omnirange navigation systems - Part 2
[FAA-RD-72-118-2-PT-2] 10 p1185 N73-19644
Analysis of effects of automation on productivity and efficiency of air traffic control and flight services
[MTR-6110] 10 p1185 N73-19646
Attrition-retention rates of air traffic control trainees recruited during 1960 to 1963 and 1968 to 1970
[FAA-AM-72-33] 11 p1249 N73-20140
Characteristics of operational airport surveillance radars and methods for improving performance to meet air route surveillance requirements
[ATC-14] 11 p1255 N73-20183
Development and evaluation of discrete address beacon system for air traffic control applications
[FAA-RD-73-12] 11 p1255 N73-20184
Analysis of synchronized discrete address beacon system for improved air traffic control capability
[SD-FR-01] 11 p1256 N73-20189
Development of statistical methods for estimating annual operations at non-tower airports and establishment of standardized estimation procedure
[SCI-2040] 11 p1267 N73-20278
Analysis of interaction of major elements of Oceanic Air Traffic Control System to determine minimum longitudinal and lateral separation distances
[FAA-RD-73-8] 11 p1321 N73-20719
Research and development projects conducted by Federal Aviation Administration to improve air traffic control and flight safety
[FAA-EM-73-2] 11 p1321 N73-20720
Functional error analysis and simulation of air traffic control system to support concepts evaluation program
[PB-213148] 11 p1322 N73-20730
Development and evaluation of aircraft tracking techniques based on radar and beacon target reports from common sensor site
[PX-6392] 12 p1378 N73-21177
Development and evaluation of cross-band radar/beacon system for operation with airport surveillance radar/air traffic control beacon interrogator system
[FAA-RD-73-38] 12 p1379 N73-21182
Development of computer program to analyze air traffic in North Atlantic to show zone traffic at specified instants
[AD-755910] 12 p1426 N73-21557
Capabilities, functions, and conceptual methods of operation for satellite-aided communications system in oceanic air traffic control environment
[FAA-RD-73-41] 12 p1460 N73-21833
Dynamic simulation used to analyze various aspects of STOL aircraft operations within air traffic control system
[FAA-NA-72-95] 13 p1472 N73-21919
Design of multiple beam UHF antenna for air traffic control satellite
[ESRO-CR(P)-199] 13 p1500 N73-22159
Comparison of voice coding technique for satellite-based air traffic control system 14 p1630 N73-23209
Grounding, bonding, and shielding practices for operational reliability enhancement in air traffic control electronic facilities
[FAA-RD-73-51] 14 p1645 N73-23341
Development of mathematical and simulation models to calculate capacity of single runway under instrument flight rules conditions
[MTR-4102-REV-2] 14 p1645 N73-23345
Air traffic control procedures for simultaneous instrument flight rules approaches to set of three parallel runways
[FAA-NA-73-23] 14 p1687 N73-23687
Analysis of air navigation systems for continental US and overseas flights based on projected traffic loads of 1980 time period
[FAA-ED-04-1] 14 p1687 N73-23688
Proceedings of conference on air traffic control developments and procedures
[AGARD-CP-105] 14 p1687 N73-23689
Air traffic control facilities operated by U.S. military forces and developments in improved air traffic control systems 14 p1687 N73-23690
Characteristics of air traffic control system to include description of electronic components and projects for developing improved equipment 14 p1687 N73-23692
Development of automated air traffic control system using computer techniques to provide flight safety for increased air traffic 14 p1687 N73-23693
Organization, functions, and capabilities of automated air traffic control system for Rome, Italy 14 p1687 N73-23694
Integrated SAVVAN, VOR, and DME system for locating and controlling high altitude aircraft 14 p1688 N73-23695
Status and trends of civil air traffic control systems and development of automated network for increased flight safety 14 p1688 N73-23696
Comparison of cost, complexity, and cockpit workload for seven area navigation system configurations 14 p1688 N73-23697
Analysis of North Atlantic air route structure to determine impact of inertial navigation and satellite surveillance on separation reduction 14 p1688 N73-23699
Analysis of terminal air traffic control procedures to determine impact of automation on air traffic controller personnel 14 p1688 N73-23700
Numerical anlaysis of optimal control and sequencing of air traffic control operations in near terminal area 14 p1688 N73-23701
Analysis of short takeoff and landing aircraft landing guidance systems and application of air traffic control procedures for improved sequencing 14 p1688 N73-23703
Development and characteristics of air traffic management system for operation of military aircraft under instrument meteorological conditions 14 p1689 N73-23704
Development and characteristics of microwave landing system with emphasis on functional design requirements for airborne equipment 14 p1689 N73-23705
Development of Doppler microwave landing system and techniques for eliminating effects of multipath transmissions 14 p1689 N73-23706

Development and characteristics of forward area homing and landing guidance for military aircraft operations
14 p1689 N73-23708
Application of artificial satellites for data acquisition and communication functions in air traffic control system
14 p1689 N73-23709
Development of high bandwidth time division communications system to provide ground based, wide area, position location system
14 p1689 N73-23711
Development and characteristics of system for separation and control of aircraft to avoid midair collisions
14 p1690 N73-23712
Performance tests of air traffic control system to determine effectiveness in prevention of midair collisions
14 p1690 N73-23713
Analysis of air traffic controller responses under stress conditions to show effects of accuracy, quality, and comprehensiveness of available data
14 p1690 N73-23714
Analysis of man-machine interfaces and system reliability for air traffic control automation systems
14 p1690 N73-23715
Analysis of interface between controller and computer in automated air traffic control system
14 p1690 N73-23716
Analysis of development program for improving US air traffic control procedures for 1980 time period
14 p1690 N73-23718
Conceptual analysis of improved communication, navigation, and indentification system for military applications
14 p1690 N73-23719
Analysis of communications, navigation, and identification equipment for aircraft and proposed system for improvement in capability
14 p1690 N73-23720
Analysis of integrated communications, navigation, and identification system for aircraft operation and proposal for improved capability
14 p1691 N73-23721
Computer program system for automatic operation and safety backup in ground based ATC system
[FAA-EM-73-7] 15 p1808 N73-24654
Systems analysis of civil airport surface traffic control
[FAA-ED-08-1] 15 p1808 N73-24655
Automation of decision making process in air traffic controllers terminal operations
[FAA-RD-72-63-VOL-3] 15 p1808 N73-24657
Definition and evaluation of three basic alternative national aviation systems based on forecasted increases in aviation demands
[PB-215533/1] 16 p1862 N73-25081
Development and characteristics of air traffic control radar and associated signal and display processing equipment
[FAA-RD-73-35] 16 p1875 N73-25178
Discretely addressable radar beacon system with airborne transponders and ground-air-ground data link for air traffic control
[FAA-RD-73-48] 16 p1940 N73-25701
Proceedings of conference on operational problems of air traffic control beacon system
[FAA-NA-72-80] 16 p1940 N73-25702
Objectives, goals, and program structure of project to improve performance of air traffic and control and navigation facilities within National Airspace System
[FAA-ED-21-2] 16 p1940 N73-25703
Development and application of Airborne Traffic and Situation Display for improved air traffic control
[PB-215714/7] 16 p1942 N73-25715
Forecasts of aviation activity at selected airports to meet needs of planning personnel for future air traffic control operations
17 p1982 N73-26019
Planning of short haul air transportation system based on computer simulation of various concepts
[FAA-QS-73-2] 17 p1983 N73-26026
Interface evaluation of digital simulation facility with system support facility for radar beacon target source for air traffic control
[FAA-NA-73-33] 17 p2009 N73-26248
Evaluation of pilot assurance value of airborne display device for monitoring air traffic in high density terminal airspace
[AD-749280] 17 p2011 N73-26267
Proceedings of conference to develop area navigation system design concept for application to national airspace system for improved air traffic control
17 p2060 N73-26664
Control and display testing for air traffic instrument landing system
[AD-759539] 17 p2060 N73-26667
Application of microwave landing system to provide operational flexibility and improved capacity in terminal area
[FAA-RD-73-143] 18 p2104 N73-27019
Job attitudes of air traffic controllers
[FAA-AM-73-2] 18 p2110 N73-27066
Design technology of aeronautical satellite communication system for air traffic control over Atlantic Ocean
[FAA-ED-17-1] 18 p2115 N73-27104
Analysis of radio communication links for air traffic control operations to show effects of adjacent channel interference and modulation limitations
[FAA-RD-70-71] 18 p2117 N73-27114
Analysis of air space control problems associated with military operations and development of doctrine for improved command and control
[AD-761034] 18 p2176 N73-27573
Analysis of candidate data and surveillance modems for avionics system used in air traffic control system
[AD-758407] 18 p2176 N73-27574
Research and development program plan for air traffic control technology involving data display and data entry
[FAA-ED-16-1] 19 p2318 N73-28647
Automatic aircraft altitude reporting using air traffic control radar beacon system
[FAA-RD-73-44] 19 p2318 N73-28648
Technical evaluation of weather clutter feasibility model to provide air traffic controllers with weather display of air traffic and contour depiction of weather detected by radar
[FAA-NA-73-48] 20 p2376 N73-29094
Airport surface traffic control requirements analysis
[AD-762442] 20 p2383 N73-29147
Development and characteristics of radar system for improved air traffic control
[FAA-RD-73-100] 20 p2452 N73-29703
Development of computer model to simulate air traffic conditions in Los Angeles, California area in 1982
[MTR-6386] 20 p2452 N73-29706
Development of noise standard for permissible noise levels in air traffic control and navigational facilities
[FAA-RD-72-47] 20 p2452 N73-29708
FAA engineering and development program for terminal air traffic control
[FAA-ED-14-2] 21 p2521 N73-30215
Flight plan position extrapolation in automated oceanic air traffic control system
[FAA-RD-73-72] 21 p2576 N73-30648
User manual for Los Angeles Standard Traffic Model computer tapes
[FAA-RD-73-88] 21 p2577 N73-30649
Positional accuracy of aircraft radar targets as displayed in air traffic control airport surveillance radar system
[FAA-NA-72-87-PT-2] 21 p2577 N73-30650
Development of discrete address beacon system for application to air traffic control operations
[FAA-RD-73-101] 21 p2577 N73-30651
Feasibility of ATC radar beacon system based on vehicle surveillance on airport surface in relation to vehicle time of arrival
[AD-763328] 21 p2577 N73-30655
Developments in data systems air traffic control, and solid state physics
[AD-763731] 21 p2587 N73-30727
Introductory background to planning process, objectives, and indexing for twenty two engineering and development programs with FAA
[FAA-ED-00-A] 21 p2609 N73-30918
VFR flight operations in 1972 Los Angeles Basin air traffic model
[FAA-NA-73-51] 22 p2697 N73-31605
Algorithms to determine potential conflicts over oceanic airspace based on vertical, lateral, and longitudinal separation criteria
[FAA-RD-73-73] 22 p2697 N73-31606
Numerical analysis of curved approach paths and landing sequence for multiple aircraft using same terminal facilities to provide maximum system performance
23 p2740 N73-31935
Analysis and simulation of intermittent positive control of air traffic by fully automated ground facility
23 p2816 N73-32511
Evaluation of air traffic control beacon alphanumeric system for automatic operation in low density airport towers and terminal facilities
[FAA-NA-73-54] 23 p2816 N73-32516
Air traffic control evaluation to determine feasibility of combining smaller aircraft into gaps on flow of normal traffic to increase effectiveness of terminal facilites
[FAA-AFS-500-1] 23 p2816 N73-32517
Performance and environmental tests of National Air Space Enroute Stage air traffic control system
[FAA-NA-73-55] 23 p2817 N73-32518
Air traffic control problems created by introduction of large numbers of STOL aircraft into high density terminal area
24 p2874 N73-32956
Development and characteristics of 4-D guidance system for traffic control of STOL aircraft operating in congested areas
24 p2874 N73-32957
Systems analysis of problems created in terminal area by application of short takeoff aircraft for providing high speed, short haul air transportation service
24 p2874 N73-32958
Evaluation of large screen display for automated oceanic air traffic control applications
[FAA-ND-73-75] 24 p2950 N73-33568
Operational evaluation of ARTS 2 radar alphanumeric display subsystem
[FAA-NA-73-77] 24 p2951 N73-33569
Restructuring of oceanic air traffic control airspace jurisdictional boundaries in presence of satellite system
[FAA-RD-73-59] 24 p2951 N73-33570
Computer model of Los Angeles, California air traffic control situation to predict conditions expected by 1982
[AD-765153] 24 p2951 N73-33571

**AIR TRANSPORTATION**

Proceedings of conference on ride qualities of air, surface, and water vehicles with emphasis on human factors engineering for comfort in transportation
[NASA-TM-X-2620] 01 p0002 N73-10012
Analysis of current knowledge regarding ride quality factors in passenger transportation and development of criteria based on human factors engineering
01 p0002 N73-10013
Guidelines and criteria for developing ride quality in air transportation based on external and internal environment conditions
01 p0002 N73-10014
Analysis of research activities conducted to determine criteria for passenger comfort in various methods of transportation
01 p0004 N73-10024
Effects of intraurban V/STOL commuter system on economic, social, and physical environment on San Francisco Bay Area
[NASA-CR-114492] 03 p0366 N73-12982
Traffic environment and operational procedures for intercity STOL transportation system
[NASA-CR-114523] 03 p0367 N73-12990
Analysis of criteria for establishing air transportation curricula in community college based on manpower requirements and industrial needs
04 p0486 N73-13969
Research on air transport with VTOL and STOL aircraft
[PUBL-1352] 06 p0613 N73-14977
National transportation statistics summaries for 1960 to 1970
06 p0732 N73-15969
Findings and recommendations of Aviation Advisory Commission on long range needs of Aviation-- Vol. 1 Vol. 2
[PB-215803] 09 p1101 N73-18983
Analysis of special problems and issues involved in the long range of aviation with emphasis on 1 aa Vol. 2
[PB-215804] 09 p1101 N73-18984
Economic analysis of high density short haul air market to show aircraft requirements, engine development, and funding sources
[NASA-CR-2227] 10 p1106 N73-19017
Proceedings of symposium on flight operations and air traffic control to show problems affecting airports, general aviation, air traffic controllers, and governmental agencies
[DLR-MITT-72-24] 10 p1183 N73-19623
Analysis of airport operations to show importance to community, effect on environment, and application of new technologies for airport development
10 p1183 N73-19625
Design and development of vertical takeoff aircraft configuration for use with air transportation services between major population centers
13 p1471 N73-21916
Survey of passengers flying from Dulles Airport, Virginia during one year period to obtain cross section of typical passengers and destinations
13 p1473 N73-21925
Analysis of trans-Atlantic aircraft movements for 1970 - 1971 period to establish base line for passenger forecasts
13 p1474 N73-21935
Operational decision model for making conditional weather forecasts for airlift supply task
[AD-755403] 13 p1555 N73-22601
Forecasting demand potential for STOL transportation
[NASA-CR-114572] 13 p1595 N73-22932
Application of program evaluation and review technique for planning and management of air transport operations
[NASA-TT-F-742] 16 p1860 N73-25067
Problems of air transport economics and efficiency of air transport utilization in USSR
[NASA-TT-F-741] 16 p1860 N73-25069
Definition and evaluation of three basic alternative national aviation systems based on forecasted increases in aviation demands
[PB-215533/1] 16 p1862 N73-25081
Planning of short haul air transportation system based on computer simulation of various concepts
[FAA-QS-73-2] 17 p1983 N73-26026

Tables of data for airline economic impact computer model f Vol. 2
[AD-749491] 17 p2100 N73-26989
Program definition study for improvement of short haul air transportation to show development requirements and operational constraints - Vol. 2
[FAA-QS-73-1-VOL-2] 18 p2213 N73-27869
Role of air transportation in sparsely developed areas including cost estimates
[PB-219293/8] 18 p2214 N73-27880
Design, development, and characteristics of quiet turbofan short takeoff aircraft for short haul air transportation - Vol. 2
[NASA-CR-114607] 19 p2219 N73-27899
Marketing survey to determine acceptance and utilization of STOL aircraft for short-haul air transportation system - Vol. 4
[NASA-CR-114609] 19 p2219 N73-27901
Analysis of economic factors affecting operation of STOL aircraft for short-haul air transportation system - Vol. 5
[NASA-CR-114610] 19 p2219 N73-27902
Systems analysis of quiet turbofan STOL aircraft for short-haul air transportation operations - Vol. 6
[NASA-CR-114611] 19 p2219 N73-27903
Analysis of passenger acceptance of commercial low-density short haul, air transportation
[NASA-CR-132285] 19 p2226 N73-27950
Resynchronization of circadian rhythms following transmeridian flight observed in two group of students 19 p2227 N73-27958
Effects of two sequential transatlantic flights on circadian rhythm of body function and performance 19 p2227 N73-27964
Analysis of regional aviation system for Southern California with extension to system of global airports to cope with future requirements 22 p2697 N73-31607
Economics, traffic demand, and community acceptance of short haul air transportation system in California Corridor - Vol. 1
[NASA-CR-114634] 23 p2859 N73-32842
Economic factors, financial management, production and marketing for air transport industry
[NASA-CR-135634] 23 p2860 N73-32848
Federal Government participation in development of US air transportation system 23 p2860 N73-32850
Marketing and cost effectiveness in air transportation economics 23 p2860 N73-32855
Economic efficiency in pricing of air transport services 23 p2860 N73-32856
Demand factors in air transportation marketing 23 p2861 N73-32863
Analytical forecasting methods for air passenger traffic 23 p2861 N73-32864
Patterns of behavior of airlines and air travellers in air transportation network and effects on use of satellite airports 23 p2862 N73-32876
Airport establishment and operation with emphasis on regional planning, social factors, and economic forces 23 p2863 N73-32877
Procedures for conducting air traffic forecasts with emphasis on socio-economic and demographic characteristics of population 23 p2863 N73-32879
Organization, responsibilities, and functions of Civil Aeronautics Board in determining award of air routes to air lines 23 p2863 N73-32880
Analysis of economic factors involved in air cargo operations and air cargo market development 23 p2863 N73-32881
Analysis of factors involved in developing market for air cargo services 23 p2863 N73-32882
Analysis of air freight rate problems to define roles of Civil Aviation Board and domestic air carriers 23 p2863 N73-32883
Evaluation of new forms of air transport service for improving short haul air travel market 23 p2863 N73-32887
Federal policy establishing guidelines for US participation in international air transportation services 23 p2865 N73-32902
Improving air transportation to low density population regions
[NASA-CR-114484] 23 p2865 N73-32905
Proceedings of conference on short takeoff and landing aircraft to determine aerodynamic characteristics and short haul transportation applications
[NASA-SP-320] 24 p2871 N73-32934
Analysis of short-haul air transportation requirements to include aircraft development programs, economic factors, and environmental considerations 24 p2871 N73-32935
Technical and economic aspects of airship transportation
[DLR-MITT-72-17] 24 p2879 N73-32989
Application of airships to air transportation, noting cost effectiveness 24 p2879 N73-32991
Use of energy in transportation and implications for future
[P-5025] 24 p2993 N73-33921

**AIR WATER INTERACTIONS**

Development of finite difference scheme for numerical analysis of time dependent seiche oscillating across shallow, infinite channel and transients associated with bottom spiral
[AD-745194] 01 p0053 N73-10428
Macroscale fluctuations in atmospheric and oceanic variables
[AD-744976] 01 p0075 N73-10621
Feasibility of infrared laser/sonar beam communication system between submarine and aircraft and effects of air water interaction
[AD-746106] 02 p0143 N73-11156
Influence of wind stress and bottom friction on spectral response of two layer beta plane ocean currents
[AD-746506] 02 p0168 N73-11367
Influence of ocean on atmospheric circulation noting role of heat, momentum, and water vapor transfer 05 p0573 N73-14662
Wind velocity fluctuations over natural ocean waves, and wind-wave coupling
[AD-749073] 05 p0574 N73-14673
Natural convection in liquid layers of differing density
[AD-750762] 06 p0656 N73-15330
Numerical analysis of ocean circulation effects on transients in atmospheric circulation
[AD-751637] 07 p0796 N73-16470
Gain and impedance measurements on ultrahigh frequency antennas near surface of simulated sea water
[AD-751922] 08 p0890 N73-17205
Confidence intervals for ocean wave spectra for ordinary waves and hurricane sized waves
[AD-752135] 08 p0920 N73-17542
Spectral analysis of turbulent fluctuations over ocean waves
[AD-753624] 10 p1156 N73-19406
Spectral development of wind-generated water waves in laboratory facility
[AD-754113] 11 p1287 N73-20445
Near-surface air and sea-surface temperatures for hurricanes in Gulf of Mexico
[AD-754353] 11 p1315 N73-20677
Analysis of interrelation of ocean and atmosphere based on temperature of surface layer of water in Atlantic and Pacific Oceans 12 p1421 N73-21514
Surface wave interaction and thermal microstructure of sea water
[AD-757425] 14 p1664 N73-23502
PAPA Ocean Weather Station measurements of wind and wave condition in north Pacific Ocean
[AD-757982] 15 p1806 N73-24638
Air water interaction in seasonal circulation variations of Red Sea
[PB-214446/7] 16 p1909 N73-25443
Atmospheric wind fields and circulation effects on Pacific Ocean hydrologic regime
[TT-70-50129] 18 p2171 N73-27538
Influence of atmospheric cyclones on circulation and mixing of sea water in motionless uniformly rotating baroclinic ocean 19 p2258 N73-28202
Wave-related velocity fluctuations over ocean waves as measured from floating instrument platform during BOMEX
[AD-761768] 19 p2296 N73-28461
Regional and time variations in heat transfer from oceanic regions to atmosphere 20 p2389 N73-29195
Methods for studying effect of sea on thermal regime of atmosphere 20 p2445 N73-29636
Computational methods for determining eddy momentum, heat, and fluxes in water-adjoining layer of atmosphere 20 p2445 N73-29637
Application of theoretical model to velocity fields observed over water waves
[AD-764196] 22 p2668 N73-31377
Infrared radiometry and air/sea interaction studies
[AD-763788] 22 p2669 N73-31389
Dynamics of wind driven lake currents and application of vertical cross-section models 23 p2777 N73-32211
Influence of wind drift and capillarity on blockage of short surface waves
[AD-764559] 24 p2924 N73-33358
Influence of solar energy absorption and air water interactions on seasonal thermocline of sea 24 p2957 N73-33623
Measurement of air-sea temperature in relation to incident solar energy 24 p2975 N73-33773

**AIRBORNE EQUIPMENT**

NT AIRBORNE/SPACEBORNE COMPUTERS
Power supply for aircraft data acquisition system time display unit using dc to dc converter
[ARL/ME-NOTE-332] 01 p0006 N73-10049
Impact of technological development on airborne data acquisition system and ground data processing station 01 p0036 N73-10457
Design and performance of multiple channel analog multiplexer for airborne data acquisition system
[ARL/F-NOTE-49] 02 p0145 N73-11172
Principles, installation, and operation of side-looking radar in aircraft and satellites for earth resources sensing
[ESRO-CR[P]-136-VOL-1] 03 p0296 N73-12418
Infrared polarimeter for airborne measurement of terrestrial cloud particle sizes and shapes
[NASA-CR-130119] 03 p0301 N73-12458
Development of airborne instrumentation and application of remote earth observations for determining stream discharge prediction for water management program 04 p0471 N73-13839
Calibration and temperature control system for airborne interferometer
[AD-749876] 06 p0667 N73-15427
Safety calculations for compaction and coolant voiding by airborne fast reactor
[LA-4977] 06 p0699 N73-15695
Application of remote sensing techniques for detecting environmental changes at and near earth surface 07 p0784 N73-16379
Forest fire detection using airborne infrared scanners 07 p0785 N73-16390
Evaluation of aerial survey on terrestrial gamma radiation environment
[EGG-1183-1559] 07 p0793 N73-16447
Airborne radiological measuring system for use in nuclear safety programs and routine surveillance of areas around nuclear facilities
[EGG-1183-1558] 07 p0800 N73-16501
Systems planning for improved airport surveillance radar equipment using dual airborne antenna switching for air traffic control
[FAA-RD-72-136] 09 p1002 N73-18176
Design of airborne electronically steerable phased array system
[NASA-CR-124041] 09 p1007 N73-18219
Survey and mapping Colorado geology using airborne remote sensors
[NASA-CR-130822] 09 p1025 N73-18370
Analysis of effect of mass on operation of airborne superconductor magnetic system with aluminum stabilized conductor 10 p1108 N73-19034
Characteristics of large, lightweight, saddle-coil, superconducting dipole magnet for airborne magnetohydrodynamic generators 10 p1109 N73-19038
Performance estimates for airborne magnetic drum memories
[AD-754933] 11 p1260 N73-20226
Airborne C band pulsed transmitter for instrument landing system 13 p1491 N73-22086
Enhancement of multispectral aircraft scanner data using scan overlap redundancy
[NASA-CR-131587] 13 p1530 N73-22395
High altitude measurement of atmospheric pollution from aircraft engine exhaust gases
[NASA-TM-X-68221] 13 p1553 N73-22584
Feasibility analysis and planning for two aircraft television transmission over Federal Republic of Germany
[DLR-MITT-73-09] 14 p1633 N73-23235
Development and characteristics of microwave landing system with emphasis on functional design requirements for airborne equipment 14 p1689 N73-23705
Development and application of Airborne Traffic and Situation Display for improved air traffic control
[PB-215714/7] 16 p1942 N73-25715
Evaluation of pilot assurance value of airborne display device for monitoring air traffic in high density terminal airspace
[AD-749280] 17 p2011 N73-26267
Application of airborne microwave radiometers for remote monitoring of soil moisture in selected areas of Texas and Oklahoma
[NASA-CR-133102] 17 p2031 N73-26438
Application of airborne microwave radiometry for remote sensing of soil moisture in southwest US
[NASA-TM-X-66265] 17 p2032 N73-26444
Error reduction in two-gimbal, airborne search radar system
[AD-760551] 18 p2119 N73-27131
Measurements of upward radiation flux from ground and atmosphere using airborne spectrophotometer 20 p2400 N73-29284
Airborne observations to determine radiation characteristics of underlying surface and clouds over various types of ground conditions 20 p2400 N73-29285

Application of airborne actinometric measurements to determine transmission, absorption, and reflection of solar radiation by clouds
20 p2401 N73-29292
Development and characteristics of radiometer for airborne measurement of outgoing long wave radiation from earth surface between 8 and 12 microns
20 p2402 N73-29302
Digital data generation and processing in airborne ionospheric research
[AD-763088] 20 p2414 N73-29406
Airborne radiometer for continuously measuring sea water temperature
[NASA-TT-F-15070] 20 p2419 N73-29441
Use of differential magnetometers with mobile carriers for earth magnetic field measurements
22 p2671 N73-31398
Compensation of static fields for ferrosonde magnetometer mounted on mobile carrier
22 p2672 N73-31400
Airborne research management and shuttle sortie planning
[NASA-TM-X-62287] 22 p2715 N73-31729
Compilation, reduction, and correlation of spectrophotometric data obtained during NASA airborne auroral expedition
[NASA-CR-135497] 23 p2785 N73-32278
Annual variations of Garda Lake surface temperature using airborne bolometric equipment and earth based infrared video equipment
[IFA-STR-23] 23 p2787 N73-32298
Airborne aluminum oxide hygrometer for water vapor measurements in atmosphere
[NASA-TM-X-70475] 23 p2792 N73-32341
Digital synchronization of airborne collision avoidance systems
[DGLR-PAPER-73-012] 23 p2817 N73-32519

**AIRBORNE TERRAIN ANALYSIS**
U TERRAIN ANALYSIS

**AIRBORNE/SPACEBORNE COMPUTERS**
Digital simulation model for design of optimal spaceborne computer system
[NASA-CR-128997] 02 p0146 N73-11184
Digital simulation model for central processing unit of spaceborne computer with automatically reconfigurable modular multiprocessor system
[NASA-CR-128996] 02 p0146 N73-11185
Optimal emitter location algorithm using Kalman filtering for computerized airborne direction finding
[AD-745888] 02 p0208 N73-11688
Design and operation of computer for installation onboard satellite
[RAE-LIB-TRANS-1647] 04 p0392 N73-13188
Standardization of satellite control systems by using onboard computers, exemplified by proposal for Aeros satellite
[DGLR-PAPER-72-064] 06 p0721 N73-15886
Design of solar ephemeris synthesizer for LES-8/9 stationkeeping system
[AD-752250] 08 p0965 N73-17891
Mathematical and numerical methods for solving spacecraft control problems and mapping of celestial bodies
[NASA-TT-F-731] 10 p1177 N73-19572
Probabilistic model for estimating efficiency of operational servicing system for control digital computer onboard spacecraft
10 p1177 N73-19575
Feasibility study of spaceborne plated wire memory with associated electronic circuits and components
[REPT-26/1422/EC/MB/VOL-1]
13 p1498 N73-22137
Feasibility study of spaceborne plated wire memory with associated electronic circuits and components
[REPT-26/1422/EC/MB/VOL-2]
13 p1498 N73-22138
Feasibility of advanced digital flight control system using digital processor as main computational element
[AD-757271] 14 p1604 N73-23002
Onboard computers for automatic control of manned aerospace systems considering human factors integration
[AGARD-CP-114] 14 p1710 N73-23881
Computerized integrated control and information management system with graphic display for manned space flight
14 p1710 N73-23882
Design of airborne flight data transmission system for automatic acquisition and tracking
14 p1711 N73-23885
Space station information subsystem for automatic support of manned operations
14 p1711 N73-23887
Feasibility of automated spacecraft monitoring using real time computer telemetry
14 p1711 N73-23888
Simulation model for optimum spaceborne computer system design controlling shuttle booster subsystems
14 p1712 N73-23891
Onboard computer system for in-flight monitoring of space shuttle in support of flight crew
14 p1712 N73-23893
Systems design for spaceborne computer engineering module
14 p1712 N73-23894
Computerized inertialess guidance system for aircraft flight control
14 p1712 N73-23895
Computerized automated avionics system with electronic display for Comet 4 aircraft navigation
14 p1712 N73-23896
Serial digital data bus for integrated avionics system interface
14 p1713 N73-23902
Airborne radio frequency measurements using automatic spectrum analyzer
[AD-758772] 16 p1876 N73-25184
Fundamental characteristics of onboard digital computers and converters
16 p1879 N73-25208
Performance of computerized inertial guidance system for Delta launch vehicle
18 p2208 N73-27819
Lightweight reprogrammable data system for small scientific satellite
18 p2208 N73-27823
Onboard OAO 3 computer for commanding and data processing
18 p2208 N73-27824
Design of two dimensional digital computer for optical image processing onboard spacecraft using liquid crystal circuits
18 p2209 N73-27827
Implementation and development of multiple user on amtran on datacraft dc 6024
[NASA-CR-124330] 19 p2239 N73-28052
Multiprocessing operating system and software for space ultrareliable modular computer
[NASA-CR-124371] 21 p2512 N73-30147
Display device for integrated jet engine instrument system program
[AD-763440] 21 p2550 N73-30450
Spaceborne TR 16 digital computer systems analysis
[BMBW-FBW-72-22] 22 p2639 N73-31152
Integrated data acquisition system for airborne computer
[NASA-TM-X-56018] 23 p2760 N73-32087
Onboard control systems for spacecraft
[JPRS-60179] 23 p2847 N73-32755
Automated monitoring of reliability of onboard computers and simulation of malfunction problem using Markov processes nonuniform in time
23 p2848 N73-32757
Airborne computer role in digital flight control systems, noting systems model, man machine interface, and integration
24 p2878 N73-32982
Design of modular spaceborne digital computer system
[NASA-CR-124171] 24 p2898 N73-33130

**AIRCRAFT**
Human operator model performance in tracking high performance aircraft
[AD-746725] 04 p0381 N73-13101
Thunderstorm probability and supersonic transport safety on flight paths over southern United States during July
[AD-748798] 04 p0445 N73-13628
Pilot warning indicator system of intruder aircraft
[NASA-CASE-ERC-10226-1] 07 p0798 N73-16483
Computerized aircraft simulation using aerodynamic coefficient table storage, checkout, and interpolation routines
[NASA-TM-X-62229] 08 p0863 N73-16983
Laser scattering from curved aluminum and titanium aircraft surfaces in clear atmosphere
08 p0884 N73-17159
Development of computer programs for design of air route networks for improved flight safety - Part 1
[FAA-RD-72-118-1-PT-1] 10 p1185 N73-19643
Comparison of air pollution from aircraft, automobiles, buses, trucks, railroads, and electric trains in US from 1940-1980
[FAA-EQ-73-2] 12 p1421 N73-21522
Aerodynamic characteristics and performance of USSR An-12 turboprop aircraft to include handling technique and flight safety
[AD-756948] 13 p1476 N73-21953
Advanced wiring system for aircraft and space vehicle application
14 p1642 N73-23311
Moments and products measurement of inertia of aircraft weighing up to 300,000 lbs
[AD-758398] 14 p1669 N73-23546
Design and performance of aircraft or spacecraft differential maneuvering simulator
[NASA-TN-D-7304] 16 p1885 N73-25259

**AIRCRAFT ACCIDENT INVESTIGATION**
Selected aircraft accident reports for civil aviation in 1971
[NTSB-BA-72-3] 03 p0251 N73-12034
Reliability design of manned supersonic aircraft considering safety hazards
14 p1711 N73-23883

**AIRCRAFT ACCIDENTS**
Compilation of accident reports involving corporate executive aircraft during 1970
[PB-210247] 01 p0005 N73-10040
Development of statistical-probabilistic method of collision probability calculation and application to arbitrary flight paths and vehicle shapes
[AD-744722] 01 p0006 N73-10046
Statistical analysis of impact injuries to seated human responding to square wave energy absorption of vertical deceleration pulse representing helicopter crash
[AD-745919] 02 p0136 N73-11102
Inflight incident involving number two engine failure on DC 10 aircraft near Tucson International Airport, Arizona on 2 May, 1972
[NTSB-AAR-72-29] 03 p0251 N73-12035
Investigation of midair collision between commercial DC 9 aircraft and Marine Corps F-4B aircraft at Duarte, California on 6 June 1971
[NTSB-AAR-72-26] 03 p0252 N73-12037
Investigation of aircraft accident involving Beech aircraft performing air taxi service to Boise, Idaho on 20 Feb. 1972
[NTSB-AAR-72-25] 03 p0253 N73-12050
Aircraft accident and incident reports for general aviation during 1970
[NTSB-BA-72-5] 04 p0371 N73-13015
Compilation and analysis of selected US civil aviation accidents for calendar year 1971
[NTSB-BA-72-4] 04 p0371 N73-13017
Aircraft accident prevention analysis of air taxi/commuter operations to identify safety factors and enhance safety of operations
[NTSB-AAS-72-9] 05 p0493 N73-14016
Aircraft accident investigation of Boeing 727 crash near Juneau, Alaska, 4 Sept. 71
[NTSB-AAR-72-28] 05 p0493 N73-14017
Analysis of US general aviation accidents caused by stalls and spins for period 1967 to 1969
[NTSB-AAS-72-8] 05 p0493 N73-14018
Investigation of aircraft accidents involving US general aviation turbine powered aircraft for 1970
[NTSB-AMM-72-6] 05 p0493 N73-14019
Compilation of selected aircraft accident reports for US Civil Aviation operations during calendar year 1970 - Issue 5
[PB-211158] 05 p0497 N73-14047
Investigation of crash of L-1011 aircraft near Miami, Florida on 29 Dec. 1972
06 p0619 N73-15024
Investigation of US Army UH-1 helicopter accidents where orientation errors were contributing factor during fiscal year 1969
[AD-749695] 06 p0623 N73-15059
Aircraft accident involving Lear jet model 25 at Victoria, Texas on 18 Jan. 1972
[PB-212484] 06 p0625 N73-15076
Crash of DC-8 aircraft during takeoff from Anchorage International Airport, Alaska on 27 Nov. 1970
[NTSB-AAR-72-12] 07 p0737 N73-15999
Incident involving collision of Boeing 727 aircraft with landing light system at Atlanta International Airport, Georgia on 21 Dec. 1971
[NTSB-AAR-72-22] 07 p0737 N73-16000
Bibliography of aircraft accident reports for US civil aviation operations during calendar year 1971
[NTSB-BA-72-6] 07 p0738 N73-16001
Bibliography of aircraft accident reports for US civil aviation operations during calendar year 1971
[NTSB-BA-72-7] 07 p0738 N73-16002
Aircraft accident involving DH-114 aircraft during attempted landing at Mercedita Airport, Puerto Rico on 24 June, 1972
[NTSB-AAR-72-34] 07 p0738 N73-16004
Aircraft accident involving DC-9 aircraft landing at Fort Lauderdale, Florida airport in marginal weather conditions on 18 May, 1972
[NTSB-AAR-72-31] 07 p0738 N73-16005
Aircraft accident involving Beechcraft 18 aircraft on air taxi flight from Cleveland, Ohio airport on 22 June, 1972
[NTSB-AAR-72-33] 07 p0738 N73-16006
Investigation of disappearance of Cessna 310 aircraft on flight between Anchorage and Juneau, Alaska on 16 Oct. 1972
[NTSB-AAR-73-1] 08 p0867 N73-17018
Analysis of factors affecting crashworthiness of light aircraft to show nature of damage to aircraft and hazards to flight crews
[FAA-TR-FS-70-592-120A] 09 p0984 N73-18032
Investigation of correlation between pilot disorientation and UH-1 helicopter accidents
[AD-753208] 09 p0986 N73-18049
Statistical analysis of engine failure/malfunction accidents for US fixedwing aircraft of general aviation category during 1965 to 1969
[NTSB-AAS-72-10] 10 p1106 N73-19015
Statistical anlaysis of aircraft accidents occurring in US civil aviation during calendar year 1971
[NTSB-BA-73-1] 11 p1234 N73-20015

Inflight incident involving separation of cargo compartment door on DC-10 aircraft near Windsor, Ontario, Canada on 12 June, 1972
[NTSB-AAR-73-2] 12 p1363 N73-21061
Aircraft accident involving Boeing 707 aircraft at San Francisco, California airport following rejected takeoff on 13 Sept. 1972
[NTSB-AAR-73-4] 12 p1363 N73-21062
Aircraft accident involving crash of Turbo Commander aircraft following takeoff and climbout from Greater Pittsburgh Airport, Pennsylvania on 14 Aug. 1972
[NTSB-AAR-73-5] 13 p1474 N73-21936
Analysis of aircraft accidents occurring in US Civil Aviation operations during calendar year 1972
[NTSB-APA-73-1] 14 p1601 N73-22980
Aircraft accident involving attempted takeoff of Sabre Mark 5 aircraft at Sacramento, California airport on 24 Sept. 1972
[NTSB-AAR-73-6] 14 p1602 N73-22985
Analysis of aeromedical factors leading to midair collisions and recommended actions to avoid collisions
[AD-758189] 14 p1604 N73-23005
Aircraft accident involving crash of Cessna 182 aircraft near Duluth, Minnesota airport on 8 Nov. 1972
[NTSB-AAR-73-10] 14 p1604 N73-23006
Aircraft accident reports of US civil aviation accidents occurring during calendar year 1972
[NTSB-BA-73-2] 15 p1734 N73-24064
Aircraft accident involving Boeing 707 aircraft during landing at John F. Kennedy Airport, New York, 12 Dec. 1972
[NTSB-AAR-73-11] 15 p1734 N73-24068
Aircraft accidents involving US civil aviation operations during calendar year 1972 - Vol. 2
[NTSB-BA-73-3] 16 p1860 N73-25064
Aircraft accidents involving US civil aviation operations in calendar year 1971
[PB-214412/9] 16 p1862 N73-25078
Aircraft accident involving midair collision of Convair 340 and DHC-6 near Appleton, Wisconsin on 29 June 1972
[NTSB-AAR-73-9] 17 p1981 N73-26016
Aircraft accident involving crash of DC-9 aircraft during landing following go-round at Fort Worth, Texas Airport on 30 May 1972
[NTSB-AAR-73-3] 17 p1982 N73-26017
Aircraft accident involving crash of Fairchild Hiller FH-227b aircraft near Albany County Airport, New York on 3 March 1972
[NTSB-AAR-73-8] 17 p1982 N73-26018
Reports of aircraft accidents occurring in US civil aviation operations during calendar year 1972 - Issue 3
[NTSB-BA-73-4] 17 p1982 N73-26020
Statistical analysis of aircraft accidents and incidents occurring to US civil and commercial aircraft during calender year 1971 - Supplemental Issue
[NTSB-BA-73-5] 17 p1983 N73-26028
Aircraft accident involving Lear jet aircraft following takeoff from Atlanta, Georgia Airport on 26 Feb. 1973
[NTSB-AAR-73-12] 17 p1984 N73-26036
Analysis of self-destructive tendencies created by psychological stress and relationship to aircraft accidents
[FAA-AM-73-5] 18 p2104 N73-27016
Statistical analysis of aircraft accidents occurring in US civil aviation operations during calendar year 1972 - Issue 4
[NTSB-BA-73-6] 18 p2105 N73-27024
Position reporting and communications systems of aviation and marine rescue operations
[AD-761756] 19 p2228 N73-27967
Analysis of factors affecting approach and landing of aircraft under visual conditions to show causes of misjudgement resulting in aircraft landing accidents
[NASA-TT-F-15054] 20 p2360 N73-28980
Aircraft accident involving crash of TU-144 aircraft at Paris Air Show in 1973
[NASA-TT-F-15062] 20 p2360 N73-28982
Aircraft accident involving L-1011 aircraft crash near Miami, Florida on 29 Dec. 1972 during examination of suspected nose gear malfunction
[NTSB-AAR-73-14] 20 p2360 N73-28984
Probability of aircraft crashing into Boardman nuclear power plant
[PB-220715/7] 21 p2578 N73-30662
Aircraft accident involving ground collision of DC-9 and CV-880 aircraft at O Hare International Airport, Chicago, Illinois on 20 December, 1972
[NTSB-AAR-73-15] 22 p2614 N73-30945
Aircraft accident involving crash of Boeing 737 aircraft during instrument approach to Chicago-Midway Airport, Illinois on 8 December 1972
[NTSB-AAR-73-16] 22 p2614 N73-30947
Aircraft mounted crash location transmitter for emergency signal transmission after crashes
[NASA-CASE-MFS-16609-2] 22 p2631 N73-31084
Statistical analysis of aircraft accidents occurring in US Civil Aviation during calenadar year 1972 - Issue 5
[NTSB-BA-73-7] 23 p2741 N73-31942
Aircraft accident involving Boeing 707 aircraft following aborted takeoff at Kennedy International Airport, New York, on 13 August, 1972
[NTSB-AAR-73-7] 23 p2741 N73-31943
Analysis of flight crew errors contributing to aircraft accidents on P-3 and F-4 aircraft for improved air safety
[AD-764868] 23 p2746 N73-31979
Test data and description of unsymmetrical crash analysis computer program for improved helicopter structural crashworthiness analytical and design techniques - Vol. 2
[AD-764986] 23 p2747 N73-31986
Computer program and mathematical model for predicting dynamic response of helicopter in accident involving vertical and lateral impact
[AD-764985] 24 p2879 N73-32996

**AIRCRAFT ANTENNAS**
Controlled magnetic and electric excitation of airframe of LOH-6A helicopter and measurement of impedance, radiation patterns, and bandwidths
[AD-757143] 14 p1602 N73-22992
Improvements in design of HF communication systems for naval aircraft
[AD-759709] 16 p1878 N73-25200
Radiation characteristics of grounded slotted dielectric slab
[AD-760129] 17 p1999 N73-26165
Analysis of antenna radiation patterns of radio antennas installed on aircraft using high frequency solutions
18 p2115 N73-27098
Radiation from apertures in curved panels
[NASA-CR-2263] 18 p2116 N73-27110
Voltage standing wave ratio measurement and evaluation of aircraft antenna systems
[AD-761031] 18 p2123 N73-27161
Measurements on high and low gain L band aircraft aerials using transmissions from high altitude balloon
[RAE-TR-73008] 20 p2377 N73-29102
Communication antenna isolation
[FAA-RD-73-94] 21 p2507 N73-30119
Dielectric lightweight aircraft radar antenna array
[AD-764685] 23 p2766 N73-32131

**AIRCRAFT APPROACH INSTRUMENTS**
U APPROACH INDICATORS

**AIRCRAFT APPROACH SPACING**
Analysis and recommendations concerning relaxation of spacing requirements for independent IFR parallel approaches into closely spaced runways
[MTR-6282] 19 p2249 N73-28129

**AIRCRAFT BASES**
U MILITARY AIR FACILITIES

**AIRCRAFT BRAKES**
NT LEADING EDGE SLATS
NT TRAILING-EDGE FLAPS
NT WING FLAPS
Evaluation of aluminum runway surface concepts as possible aid to aircraft braking
[NASA-TN-D-7186] 09 p0985 N73-18040

**AIRCRAFT BREATHING APPARATUS**
U BREATHING APPARATUS

**AIRCRAFT CABINS**
U AIRCRAFT COMPARTMENTS

**AIRCRAFT CARRIERS**
Carrier based air trafic control system with enroute trajectory optimization capability and computer-aided marshal reassignment procedure
[AD-748302] 04 p0447 N73-13651
Development of flight path optimization procedure to minimize flight time of aircraft returning to aircraft carrier
[AD-749326] 04 p0447 N73-13653
Development and characteristics of six degree of freedom, fast time predictor model for simulation of F-4 aircraft landing on aircraft carrier
[AD-750294] 05 p0504 N73-14102
Analysis of simulated aircraft landing approach to aircraft carrier to determine display system requirements and to evalute dangerous conditions
[AD-751076] 07 p0819 N73-16635
Flight control improvement of F-8 aircraft relative to carrier takeoff and landing
[AD-753010] 09 p0986 N73-18052
Test plan for extending service life of E-2A arresting gear
[AD-754752] 11 p1267 N73-20284
Laboratory hook bounce test for E-2A arresting gear A-frame
[AD-754753] 11 p1267 N73-20285
Hook bounce test of C-2A aircraft arresting gear A-frame
[AD-754077] 11 p1268 N73-20288
Test plan for extending life of C-2A arresting hook A-frame to 3000 arrested landings
[AD-754076] 11 p1268 N73-20289
Simultaneous equation production functions for decisions pertaining to sea-based tactical air resources
17 p2054 N73-26612
Approach abort optimization in control of aircraft carrier landings
[AD-761617] 19 p2221 N73-27914
Redesign concept for A-7E approach power compensator system, including longitudinal feedback
[AD-761458] 19 p2330 N73-28742
Prototype model for aircraft carrier landing officer
[AD-762728] 20 p2372 N73-29064
Turbo-type energy absorber for aircraft carrier arresting gear
[AD-761502] 21 p2522 N73-30226
Statistical analysis of aircraft carrier wave-off situation based on deck motion and aircraft approach geometry
[AD-764516] 22 p2616 N73-30967

**AIRCRAFT COMMUNICATION**
Speech intelligibility in naval aircraft radio communications
[AD-748202] 03 p0268 N73-12173
Discrete address radar beacon system for aircraft tracking and traffic control
[FAA-RD-72-117] 04 p0447 N73-13649
Satellites for mobile aircraft and ship communications
04 p0472 N73-13852
Diversity techniques for airborne communications in presence of ground reflection multipath
[AD-752249] 08 p0887 N73-17178
TAM-TAM system for use during oceanic, continental, and terminal control area flight
14 p1689 N73-23710
Improvements in design of HF communication systems for naval aircraft
[AD-759709] 16 p1878 N73-25200
Design of avionics digital frequency synthesizer with four phase locked loops for aircraft communication and navigational aids
[AD-759699] 16 p1883 N73-25238
ESRO AEROSAT experiment using stratospheric balloon-borne transponder to relay signals from ground station to aircraft flying over sea
18 p2106 N73-27029
System design and test plan for NASA position location and aircraft communications equipment at C band using USNS Vanguard and ATS 3 and ATS 5 satellites
[NASA-TM-X-70447] 21 p2576 N73-30646
Flight test and evaluation of system for providing precise time signals to aircraft in flight using distance measuring [VORTAC] ground station and cesium beam atomic clock
[FAA-NA-73-23] 21 p2577 N73-30652

**AIRCRAFT COMPARTMENTS**
Acute toxicity of brief exposures to HF, HCl, NO2, and HCN singly and in combination with CO in aircraft cabins
[AD-751442] 07 p0748 N73-16085
Application of normal bivariate distributions and anthropometric correlations for design of workspaces in aircraft
[AD-754780] 11 p1290 N73-20468
Inflight incident involving separation of cargo compartment door on DC-10 aircraft near Windsor, Ontario, Canada on 12 June, 1972
[NTSB-AAR-73-2] 12 p1363 N73-21061
Decomposition products of polyurethane foam related to aircraft cabin flash fires
[AD-763327] 22 p2730 N73-31846
Research and development projects concerning fire hazards in aircraft cabins and design of aircraft compartments to provide greater passenger survivability
[FAA-RD-73-146] 24 p2876 N73-32972

**AIRCRAFT CONFIGURATIONS**
Computer model for determining economic impact of aircraft retrofit on airlines
[FAA-EQ-72-4-VOL-1] 02 p0245 N73-11988
Quiet Engine Program technology application to low noise aircraft development
03 p0249 N73-12013
Analysis of weight and inertia, aerodynamic derivatives, control characteristics, and stability augmentation systems for various military and civilian aircraft
[NASA-CR-2144] 03 p0252 N73-12039
Flight tests to determine buffet characteristics of four high performance aircraft during transonic maneuvers
06 p0618 N73-15017
Digital computer program for parametric analysis and optimization performance aircraft configurations and propulsion concepts
06 p0620 N73-15035
Evaluation of fluid dynamics of aircraft stalling to determine effects of three dimensional flow, wing sweep back, and high lift devices
[AGARD-AR-49] 09 p0982 N73-18023
Analysis of integrated airframe and engine configuration for hypersonic transport at 70,000 feet altitude and Mach 6.0
[NASA-CR-112300] 11 p1234 N73-20022
Analysis of requirements, instruments, and procedures for measurement of aircraft temperatures up to Mach 2.3 and altitudes up to 80,000 feet
[AGARD-AG-160-VOL-2] 11 p1294 N73-20499
Optimization of aircraft structures by finite element modeling and automated structural optimization computer program
[AD-754915] 11 p1344 N73-20905
Proceedings of conference on rotary wing aircraft developments to include operational experience, flight tests, and evaluation of structural concepts
[AGARD-CP-121] 12 p1357 N73-21008

Feasibility of using iron magnetic support to extend cold magnetic balance wind tunnel system to subsonic flow regimes and continuous spinning aircraft configurations
15 p1762 N73-24275
Characteristics of quiet turbofan short takeoff aircraft for short haul air transportation and analysis of economic and sociological factors affecting operation Vol. 1
[NASA-CR-114612] 16 p1860 N73-25065
Wind tunnel stability tests to determine static longitudinal and lateral characteristics of full-scale model of light, single engine, high wing aircraft
[NASA-TN-D-7149] 16 p1860 N73-25068
Design and development of STOL and V/STOL aircraft to show design requirements, performance characteristics, and air traffic control problems
[PB-217102] 16 p1862 N73-25085
Design of dual fuselage aircraft with pivoting wing and horizontal stabilizer to permit yawing of wing in flight for high speed operation
[NASA-CASE-ARC-10470-1] 17 p1980 N73-26005
Aircraft configuration for reducing effects of nose-down pitching moments due to high lift forces, loss of trim lift, and engine-out yawing moments
[NASA-CASE-LAR-11252-1] 17 p1980 N73-26007
Development of aircraft configuration for reduction of jet aircraft noise by exhausting engine gases over upper surface of wing
[NASA-CASE-LAR-11087-1] 17 p1980 N73-26008
Analysis of influence of engine response characteristics on approach and landing performance of aircraft equipped with externally blown flap
[NASA-TM-X-62265[2]] 17 p1982 N73-26022
Proceedings of conference on military applications of V/STOL aircraft to include current and proposed research projects to meet military requirements
[AGARD-CP-126-VOL-1] 18 p2102 N73-27000
Review of V/STOL aircraft research and development programs to increase effectiveness of aircraft and develop mission improvements
18 p2102 N73-27001
Flight test and evaluation of CL-84 tilt-wing V/STOL aircraft with application to specific military roles
18 p2103 N73-27007
Design, development, and evaluation of Boeing 727 aircraft nacelle to conform to upper noise reduction goals
[FAA-RD-72-40-VOL-2] 18 p2104 N73-27017
Calculation of three-dimensional boundary layer flows on aircraft and space shuttle configurations
[NASA-CR-2285] 18 p2130 N73-27214
Wind tunnel tests to determine effects of modified engine nacelle on stability and control characteristics of DC-9 aircraft with emphasis on deep stall regime
[NASA-CR-121220] 19 p2219 N73-27904
Wind tunnel tests to determine effects of slot spoilers on longitudinal and lateral aerodynamic characteristics of twin engine light aircraft
[NASA-TN-D-7315] 21 p2496 N73-30033
Theory for predicting sonic boom intensity and techniques for sonic boom suppression
[FAA-RD-73-4] 23 p2741 N73-31944
Nozzle geometry and forward velocity effects on noise for CTOL engine-over-wing concept
[NASA-TM-X-71453] 24 p2971 N73-33742

**AIRCRAFT CONSTRUCTION**
U AIRCRAFT STRUCTURES

**AIRCRAFT CONTROL**
NT HELICOPTER CONTROL
Bibliography of research on aircraft sidearm control
[AD-745863] 01 p0005 N73-10039
Analysis of weight and inertia, aerodynamic derivatives, control characteristics, and stability augmentation systems for various military and civilian aircraft
[NASA-CR-2144] 03 p0252 N73-12039
Design, development, and evaluation of fluidic emergency thrusters for aircraft stabilization
[NASA-CR-114490] 03 p0252 N73-12041
Optimal adaptive control of aircraft lateral dynamics in gust presence using Pontryagin principle and cost function
[AASU-314] 03 p0253 N73-12046
Stability and control systems for advanced aircraft flight mechanics and safety
[AGARD-AR-48] 04 p0371 N73-13018
Improvement in V/STOL aircraft performance with yaw control augmentation to reduce cross coupling effects
[AD-749489] 04 p0375 N73-13046
Development and characteristics of automatic control system for aeroelastic aircraft using optimal gain in stabilization loops
[AD-750501] 06 p0624 N73-15061
Telecommunication jamming of robot aircraft control system by pulse amplitude modulation or pulse time modulation
[FOA-3-C-3649-66] 06 p0639 N73-15188
Analysis of controllability and steady-state response of parallel-redundant flight control systems
[NASA-CR-130354] 07 p0737 N73-15998
Development of aircraft control systems based on operator performance, adaptive displays, and coupling of manual with automatic control
[AD-751306] 07 p0741 N73-16026
Summaries of papers presented to conference concerning aircraft stability and control
[AGARD-CP-119] 08 p0864 N73-16989
Design criteria for satisfactory stability and control of military aircraft
08 p0865 N73-16996
Influence of load and wing load distribution on lateral and longitudinal maneuverability of aircraft
08 p0865 N73-16998
Prediction of aeroelastic hinge moment effects on stability and control
08 p0866 N73-17006
Criteria for designing manual control system for military transport aircraft
08 p0866 N73-17007
Influence of powered controls on stability and maneuverability
08 p0866 N73-17008
Automatic method for determining stability and control derivatives from flight data
08 p0866 N73-17012
Effect of control force gradient on VTOL visual hovering task
[NASA-TM-X-62230] 08 p0866 N73-17015
Application of modern control theory to design of optimum aircraft controllers
[NASA-TM-X-62208] 08 p0867 N73-17016
Analysis of response of constant-attitude aircraft to atmospheric turbulence
[NASA-CR-2204] 09 p0983 N73-18025
Wind tunnel tests of blowing on circular cylinders applied to aircraft control and braking at low speeds
[ARC-CP-1232] 10 p1104 N73-19000
Aircraft control system for rotary wing aircraft
[NASA-CASE-ERC-10439] 10 p1104 N73-19004
Proceedings of conference on flight test technology to analyze results of flight test and comparison with data obtained using flight simulators for short takeoff aircraft
[DLR-MITT-72-18] 10 p1104 N73-19005
Comparison of simulation and flight test results for automatic short takeoff aircraft landing system
10 p1105 N73-19006
Determination of aircraft aerodynamic characteristics under captive flight conditions and description of test equipment
10 p1105 N73-19010
Situational display system of cathode ray tubes to assist pilot in aircraft control
[NASA-CASE-ERC-10350] 11 p1291 N73-20474
Application of maximum likelihood criterion and optimal input design for analyzing flight test data to obtain aircraft stability and control derivatives
[NASA-CR-2200] 12 p1364 N73-21071
Engine and control problems of light aircraft
14 p1600 N73-22972
Aerodynamic stability and control characteristics of X-20 aircraft
[AD-756854] 14 p1710 N73-23877
Analysis of manual control theory of vertical situation displays for short takeoff aircraft
[NASA-CR-114620] 15 p1734 N73-24061
Flight tests to determine longitudinal aerodynamic parameters of P-1127 aircraft with vectored thrust control
[NASA-TN-D-7296] 15 p1734 N73-24066
Wind tunnel tests to determine aerodynamic characteristics of vectored thrust V/STOL fighter aircraft in transition speed range
[NASA-TN-D-7191] 16 p1858 N73-25047
Wind tunnel stability tests to determine static longitudinal and lateral characteristics of full-scale model of light, single engine, high wing aircraft
[NASA-TN-D-7149] 16 p1860 N73-25068
Computer programs for design of aircraft control systems based on FORTRAN subroutines for generating aircraft transfer functions in six degrees of freedom
[AD-758781] 16 p1861 N73-25075
Computerized design of aircraft control optimization stabilization systems
[NASA-CR-133002] 16 p1935 N73-25653
Development of aerodynamic control system to control flutter over large range of oscillatory frequencies using stability augmentation techniques
[NASA-CASE-LAR-10682-1] 17 p1980 N73-26004
Aircraft configuration for reducing effects of nose-down pitching moments due to high lift forces, loss of trim lift, and engine-out yawing moments
[NASA-CASE-LAR-11252-1] 17 p1980 N73-26007
Aircraft accident involving crash of DC-9 aircraft during landing following go-round at Fort Worth, Texas Airport on 30 May 1972
[NTSB-AAR-73-3] 17 p1982 N73-26017
Analysis of influence of engine response characteristics on approach and landing performance of aircraft equipped with externally blown flap
[NASA-TM-X-62265[2]] 17 p1982 N73-26022
Equations of motion and response curve fitting method for determining transfer function coefficients of longitudinal aircraft motion
[DLR-FB-73-39] 17 p1984 N73-26034
Wind tunnel tests to determine effects of modified engine nacelle on stability and control characteristics of DC-9 aircraft with emphasis on deep stall regime
[NASA-CR-121220] 19 p2219 N73-27904
Handling characteristics of V/STOL aircraft based on data obtained from flight tests, simulator operation, and analytical studies
[AGARD-R-577-PT-2] 19 p2220 N73-27906
Development of analog hardware for flight control system design to control aircraft with uncertain parameters
[NASA-CR-133416] 19 p2220 N73-27909
Development of feedback control in tilt rotor aircraft using swashplate cyclic and collective controls in addition to direct lift control - Vol. 7
[NASA-CR-114600] 21 p2493 N73-30011
Development of theory for adaptive control of aircraft in atmospheric turbulence using stochastic identification method
[AD-763739] 21 p2498 N73-30051
Application of active control technology for suppression of flutter with analysis of effect on B-52 aircraft configuration
[NASA-TM-X-2909] 21 p2603 N73-30864
Development and characteristics of system for integrated control of engine power and aerodynamic configuration of aircraft during landing approach
[NASA-CASE-ARC-10456-1] 22 p2613 N73-30938
Longitudinal stability and control derivatives of XB-70 aircraft to compare flight test and theoretical data
[NASA-TM-X-2881] 22 p2613 N73-30940
Wind tunnel and rotor whirl cage tests to determine stability and control parameters of scale model of tilting rotor aircraft model - Vol. 6
[NASA-CR-114615] 22 p2614 N73-30950
Design of aircraft lateral flight director
[DLR-FB-72-44] 22 p2614 N73-30953
Electronic display devices in aircraft control, noting pilot activation and VTOL control
[DLR-MITT-72-04] 24 p2880 N73-32998
Extrapolation predictive displays for manual path and position control of VTOL aircraft
24 p2880 N73-33000

**AIRCRAFT DESIGN**
NT HELICOPTER DESIGN
Analysis of current knowledge regarding ride quality factors in passenger transportation and development of criteria based on human factors engineering
01 p0002 N73-10013
Guidelines and criteria for developing ride quality in air transportation based on external and internal environment conditions
01 p0002 N73-10014
Flight loads data recording system for F-102 aircraft maneuver load analysis for data acquisition and application to development of structural design criteria
[AD-747016] 03 p0253 N73-12047
Development of numerical method for designing minimum drag supersonic wing camber surfaces of arbitrary planform for given lift characteristics
[NASA-TN-D-7097] 04 p0369 N73-13001
Computer program for design optimization of subsonic swept wing jet transport aircraft
[RAE-TM-AERO-1448] 05 p0494 N73-14026
Aerodynamic design, engineering development, and flight testing of naval aircraft for operation at high angles of attack
06 p0618 N73-15020
Digital computer program for parametric analysis and optimization performance aircraft configurations and propulsion concepts
06 p0620 N73-15035
Technical and economic feasibility of V/STOL lift-fan commercial aircraft for short haul transport applications
[NASA-CR-2184] 06 p0621 N73-15041
Aircraft performance optimization by including flight control system in design
[MBB-UFE-895-72-O] 06 p0622 N73-15048
Avionics requirements for multimission, fixed wing, twin engine aircraft designed for search and rescue operations
[AD-750463] 06 p0624 N73-15064
Design modifications to improve static performance and lateral-directional dynamic stability of light aircraft
07 p0737 N73-15996
Optimized design of supersonic aircraft wing based on linear combination of weight of wing and aerodynamic drag minimization
07 p0737 N73-15997
Development of optimized aircraft structures based on vibratory strain energy distribution using damped forced response
[AD-751809] 07 p0741 N73-16027
Aerodynamic characteristics of biplane wing systems with emphasis on stall matching and induced camber effects which differ from monoplane wing
08 p0864 N73-16987

Design criteria for satisfactory stability and control of military aircraft
08 p0865 N73-16996
Role of theory and calculations in refinement of flying qualities
08 p0865 N73-16999
Role of flight simulation in development of S-3 and F-14 aircraft
08 p0865 N73-17001
Criteria for designing manual control system for military transport aircraft
08 p0866 N73-17007
Development of takeoff airworthiness standards for new aircraft designs using motion simulators to compare performance and handling characteristics
[NASA-TN-D-7106] 09 p0983 N73-18031
Analysis of factors affecting crashworthiness of light aircraft to show nature of damage to aircraft and hazards to flight crews
[FAA-TR-FS-70-592-120A] 09 p0984 N73-18032
Detail design features of short takeoff and landing commercial aircraft and impact on design caused by STOL requirement - Part 2
[AERO-13-PT-2] 09 p0984 N73-18033
Design of simple to fly, constant attitude light general purpose aircraft
[NASA-CR-2208] 09 p0984 N73-18037
Conceptual designs of V/STOL lift fan commercial short haul transport aircraft to determine technical and economic feasibility
[NASA-CR-2183] 09 p0984 N73-18038
Analysis of V/STOL aircraft design and operation to determine effects of noise problems and constraints with emphasis on helicopter performance
[AD-752447] 09 p0989 N73-18073
Preliminary aerodynamic and mechanical design of selected gas generators and lift unit for V/STOL aircraft
[NASA-CR-120972] 10 p1106 N73-19020
Development of techniques for reduction of aircraft noise generated by short takeoff aircraft
[NASA-TM-X-68195] 10 p1106 N73-19021
Analysis of interface between aircraft mechanical power requirements and performance requirements of auxiliary power systems
10 p1110 N73-19049
Application of normal bivariate distributions and anthropometric correlations for design of workspaces in aircraft
[AD-754780] 11 p1290 N73-20468
Optimization of aircraft structures by finite element modeling and automated structural optimization computer program
[AD-754915] 11 p1344 N73-20905
Structural concepts of rotary wing system capabilities to show changes in design of specific vertical takeoff aircraft components
12 p1358 N73-21021
Development and application of composite materials for vertical takeoff aircraft airframes and effect on improved aircraft performance
12 p1359 N73-21023
Design, development, and production of low cost remotely piloted vehicles based on innovative approach for aircraft engineering procedures
[P-4902] 12 p1363 N73-21060
Design of V/STOL research transport aircraft to achieve low fan noise with high thrust/weight capability of high pressure ratio lift fan system
[NASA-CR-121146] 12 p1364 N73-21065
Atmospheric density extremes up to 15,000 feet for design of military aircraft
[AD-755791] 12 p1403 N73-21382
Planform shape effects on aerodynamic center location and aeroelasticity of fighter aircraft
[NASA-CR-2117] 13 p1469 N73-21896
Design and development of vertical takeoff aircraft configuration for use with air transportation services between major population centers
13 p1471 N73-21916
Design and aerodynamic characteristics of tilt propeller aircraft for short takeoff and landing operations - Vol. 1
[NASA-CR-114441] 13 p1473 N73-21926
Design and aerodynamic characteristics of tilt propellor aircraft for conducting flight research on V/STOL aircraft - Vol. 2
[NASA-CR-114442] 13 p1473 N73-21927
V/STOL lift fan commercial short haul transport aircraft for 1980 to 1985 period to include aircraft design, hover control, and cruise performance
[NASA-CR-2185] 13 p1473 N73-21930
Computer graphics for solving three dimensional lifting body potential flow nonlinear equations to determine aerodynamic loads
[DGT-7510] 13 p1474 N73-21939
Designing aircraft for combined effects of vertical, lateral, and longitudinal turbulence by power spectral techniques
[AD-756886] 13 p1475 N73-21951
Conceptual designs and aerodynamic configurations of tilting rotor V/STOL aircraft for 1975 to 1980 time period - Vol. 1
[NASA-CR-114437] 14 p1599 N73-22964
Preliminary design of V/STOL tilting rotor aircraft for performance of research flights - Vol. 2
[NASA-CR-114438] 14 p1599 N73-22965
Design concepts, manufacturing process, weight analysis, and cost estimates for long range transport aircraft using composite structures
[NASA-CR-112253] 14 p1600 N73-22976
Development and application of aircraft performance prediction methods for subsonic and supersonic transport and fighter aircraft
[AGARD-LS-56] 15 p1732 N73-24042
Parametric and optimization techniques for aircraft design synthesis to show principal lines of data flow for component development
15 p1732 N73-24049
Numerical analysis of aircraft takeoff performance based on phases of takeoff and forces exerted on aircraft as basis for aircraft design
15 p1733 N73-24051
Development of two methods for optimizing design of subsonic, swept wing jet transport aircraft
15 p1733 N73-24054
Sonic boom minimization design for supersonic transport aircraft
[NASA-TN-D-7218] 15 p1734 N73-24065
Computer program for developing optimal stability augmentation system for high performance aircraft based on pilot parameters for pitch tracking task
[AD-757879] 15 p1736 N73-24076
Analysis of quiet turbofan short takeoff aircraft for short haul air transportation to show research and development requirements and advanced technology benefits - Vol. 2
[NASA-CR-114613] 16 p1860 N73-25066
Computer programs for design of aircraft control systems based on FORTRAN subroutines for generating aircraft transfer functions in six degrees of freedom
[AD-758781] 16 p1861 N73-25075
Design of dual fuselage aircraft with pivoting wing and horizontal stabilizer to permit yawing of wing in flight for high speed operation
[NASA-CASE-ARC-10470-1] 17 p1980 N73-26005
Aircraft configuration for reducing effects of nose-down pitching moments due to high lift forces, loss of trim lift, and engine-out yawing moments
[NASA-CASE-LAR-11252-1] 17 p1980 N73-26007
Development of formula for determining ideal weight of shell-type aircraft fuselages with body of revolution cross section
[RAE-LIB-TRANS-1688] 17 p1981 N73-26009
Design of aircraft for high reliability and low maintenance costs and maintenance procedures for maximum efficiency
17 p1983 N73-26032
Review of V/STOL aircraft research and development programs to increase effectiveness of aircraft and develop mission improvements
18 p2102 N73-27001
Design, development, and characteristics of Do-31 V/STOL aircraft to include solution of operational problems caused by ground effect and transition flight
18 p2103 N73-27004
Design, development, and evaluation of Buffalo/Spey Augmentor-Wing research aircraft using internally blown flap for lift augmentation
18 p2103 N73-27010
Design, development, and requirements for short takeoff transport aircraft for military applications using civil aircraft production procedures
18 p2103 N73-27011
Analysis of aerodynamic characteristics affecting selection of short takeoff transport aircraft
18 p2103 N73-27012
Analysis of research and development programs involving construction of short takeoff transport aircraft in Germany
18 p2103 N73-27013
Numerical analysis of lift and roll stability of ram air cushion vehicle to determine equations for rolling moment coefficient
[PB-219820/8] 18 p2106 N73-27032
Development of digital computing system for synthesis and optimization of military flight vehicle preliminary designs
[AD-760568] 18 p2108 N73-27045
Design, development, and characteristics of quiet turbofan short takeoff aircraft for short haul air transportation - Vol. 2
[NASA-CR-114607] 19 p2219 N73-27899
Application of oscillation theory and mathematical statistics to problems of aircraft structures and aerodynamic loads on aircraft and missiles
[NASA-TT-F-753] 19 p2220 N73-27908
Design of aircraft with rotatable wing for producing high speed aerodynamic configuration
[NASA-CASE-ARC-10470-2] 21 p2494 N73-30018
Aerodynamic fuselage rear part configurations for aircraft stability optimization noting pressure distribution and aerodynamic forces
[DLR-FB-72-25] 22 p2612 N73-30931
Criteria for acceptance of early design information with application to design studies and cost estimates for liquid hydrogen fueled aircraft and remotely piloted vehicles
[NASA-TM-X-62303] 22 p2613 N73-30943
Mathematical model for real-time flight simulation of tilt rotor research aircraft for application to aircraft design, pilot training and proof-of-concept-Vol. 5
[NASA-CR-114614] 22 p2614 N73-30949
Design of aircraft lateral flight director
[DLR-FB-72-44] 22 p2614 N73-30953
Application of short takeoff aircraft for short haul air transportation with identification of critical technology, economics, and social viability
[NASA-CR-135481] 23 p2741 N73-31941
Procedure for evaluating relative economic value of technology factors affecting design, configuration, and operation of hypersonic cruise transport
[NASA-CR-2286] 23 p2743 N73-31953
Design parameters for optimal cost/cruise performance of subsonic jet transport
23 p2860 N73-32853
Analysis of short-haul air transportation requirements to include aircraft development programs, economic factors, and environmental considerations
24 p2871 N73-32935
Objectives and findings of study to determine applicability of short takeoff aircraft for short-haul air transportation systems
24 p2872 N73-32936
Economic and environmental aspects of short takeoff aircraft used for short-haul air transportation systems
24 p2872 N73-32937
Short takeoff aircraft technology development related to requirements for expanded and improved short-haul air transportation system capabilities
24 p2872 N73-32938
Characteristics and performance of piloted simulator for application as research tool in design and development of experimental aircraft
24 p2874 N73-32955
Program plan to develop criteria for airworthiness standards applied to short takeoff aircraft used as transport service
24 p2875 N73-32959

**AIRCRAFT DETECTION**
Surface based altitude measuring system for accurately measuring altitude of airborne vehicle
[NASA-CASE-ERC-10412-1] 03 p0273 N73-12211
Matrix method for computing radar scattering cross sections of airplanes
[AD-750486] 06 p0643 N73-15217
Analysis of aircraft tracking techniques to show sensitivity of tracking performance to data environment
[AD-753114] 09 p1063 N73-18667
Computer programs for aircraft position and stationary satellite orbit determination from radar range and rate measurements
[ESRO-CR-81] 19 p2318 N73-28650
Aural detection model for detecting low flying aircraft
[AD-764226] 22 p2676 N73-31435

**AIRCRAFT ENGINES**
NT HELICOPTER ENGINES
NT J-52 ENGINE
NT J-58 ENGINE
NT TF-34 ENGINE
Effectiveness of DOD guidelines in determining time of aircraft engine replacements
[AD-745396] 01 p0091 N73-10749
Noise caused by jet exhaust and wing for STOL engine-over-wing configuration
[NASA-TM-X-68159] 02 p0125 N73-11018
Recirculation flow velocities and temperatures of VTOL lift engines
[DLR-FB-72-50] 02 p0223 N73-11806
Conference on reduction and suppression of aircraft engine noise
[NASA-SP-311] 03 p0249 N73-12012
Design and performance of suppressors for acoustic noise reduction in turbofan engines
03 p0249 N73-12015
Performance prediction for acoustically lined engine nacelle design
03 p0250 N73-12019
Development of flow visualization and flow measurement techniques and application to flow problems of turbines, aircraft engines, and missile propulsion
[AD-747613] 03 p0287 N73-12328
Test equipment and procedures for determining foaming and aeration characteristics of aircraft engine lubricants
[AD-747804] 03 p0321 N73-12618
Quasi area rule for heat addition in transonic and supersonic flight including determination of optimum shapes with propulsion to minimize wave drag
[AD-747772] 03 p0352 N73-12867
Theory and operation of various jet aircraft engines
[AD-747406] 03 p0352 N73-12868
Evaluation of current US Air Force aircraft engine status reporting system
[AD-750910] 06 p0624 N73-15067

Computer program for analyzing flow field generated near aircraft engine operating in reverse thrust
[NASA-CR-121147] 09 p1012 N73-18264
Analysis of air pollution caused by exhaust from military aircraft engines and development of technology for pollutant measurement to meet EPA standards
[AD-753095] 09 p1100 N73-18975
Analysis of gas turbine engine requirements and performance when main propulsion system furnishes auxiliary power source
10 p1110 N73-19050
Mission analysis of VTOL passenger transport aircraft to determine optimum engine cycle for minimum direct operating cost
[NASA-TM-X-68186] 10 p1208 N73-19826
Analysis of integrated airframe and engine configuration for hypersonic transport at 70,000 feet altitude and Mach 6.0
[NASA-CR-112300] 11 p1234 N73-20022
Analysis formation of carbon deposits on jet engines and effect on reliability, efficiency, and service life
[AD-754607] 11 p1335 N73-20837
Analysis of gas turbine engine rotor failures as basis for conducting program to provide equipment for protection of passengers and aircraft structures from damage
[NASA-CR-131525] 12 p1443 N73-21692
Modifications of fuel control units in aircraft gas turbine engines for reducing production costs
[NASA-TM-X-68229] 13 p1571 N73-22729
Information and guidance for type certification of aircraft engines as required by Federal Aviation Administration
[FAA-AC-33-2A] 13 p1571 N73-22730
Test rig simulation of gas turbine engine to determine means for minimizing incidence of lubricant sump fires in high speed aircraft engines
[NASA-CR-121158] 13 p1590 N73-22891
Engine and control problems of light aircraft
14 p1600 N73-22972
Development of annular acoustically porous elements for installation in exhaust and inlet ducts of turbofan engine to reduce aircraft engine noise intensity
[NASA-CASE-LAR-11141-1] 14 p1600 N73-22975
Performance of aircraft gas turbine components in hot corrosion environments
14 p1676 N73-23599
Chemical and mechanical properties of aircraft gas turbine engine components
14 p1676 N73-23600
Analysis of parameters affecting choice of engines for transport and combat aircraft during design process
15 p1732 N73-24048
Analysis of factors affecting flight of multi-engine aircraft with one engine inoperative
[NASA-TT-F-734] 15 p1734 N73-24060
Analysis of temperature and pressure parameters associated with recirculated engine exhaust from V/STOL aircraft engines exhausting normal to ground
[NASA-TT-F-14912] 15 p1768 N73-24323
Analysis of factors influencing technical feasibility of operating aircraft on liquid hydrogen fuel
[NASA-TM-X-68242] 15 p1823 N73-24777
Analysis of air pollution caused by aircraft engine emissions in vicinity of airport and comparison with air pollution in urban areas
15 p1825 N73-24788
Establishment of criteria for oxides of nitrogen emissions to control air pollution contribution from aircraft operating at major air terminals - Vol. 1
[REPT-1162-1-VOL-1] 15 p1825 N73-24789
Numerical analysis of process for nitrogen oxide formation in aircraft engine exhaust products and development of computer program for application of theory - Vol. 2
[REPT-1162-2-VOL-2] 15 p1825 N73-24790
Development of computer program to analyze flow conditions in gas turbine compressor for application to reduction of nitrogen oxides from aircraft engine exhaust - Vol. 3
[REPT-1162-3-VOL-3] 15 p1825 N73-24791
Mechanical cross coupling of STOL transport aircraft engines
[CRANFIELD-AERO-14] 16 p1955 N73-25819
Manufacturing processes for aircraft engine parts
[AD-759577] 16 p1958 N73-25837
Analysis of coolant flow in transpiration-cooled vanes
[NASA-TN-D-7341] 16 p1974 N73-25966
Simulator analysis of effect of engine response characteristics on approach and landing operations of powered lift aircraft with externally blown flaps
[NASA-TM-X-62265] 17 p1982 N73-26021
Analysis of techniques and equipment required to conduct test of jet aircraft engine models in wind tunnels
17 p2009 N73-26245
Combustor research programs to gain advanced technology for reducing aircraft engine pollution
[NASA-TM-X-68256] 17 p2076 N73-26797
Propulsive-lift technology program for development of short takeoff aircraft propulsion systems and lift augmentation devices
18 p2103 N73-27009
Wind tunnel tests to determine effects of modified engine nacelle on stability and control characteristics of DC-9 aircraft with emphasis on deep stall regime
[NASA-CR-121220] 19 p2219 N73-27904
Development of method for determining cost functions involving aircraft rework and engine repair programs at military installation
[AD-761475] 19 p2249 N73-28135
Development of turbine engine accessory drive techniques to establish potential systems for lightweight low profile package
[AD-761527] 19 p2330 N73-28741
Performance tests of annular combustor designed for use in low cost turbojet engine
[NASA-TM-X-2857] 19 p2352 N73-28918
Logistic performance data book on propulsion system for KC-135 aircraft to show reliability, maintenance, costs, and problems
[AD-762217] 19 p2357 N73-28962
Logistic performance data book for C-130E aircraft propulsion system to show reliability, maintainability, logistic support costs, and operational problems
[AD-762249] 19 p2357 N73-28964
Analysis of aircraft emissions and recommendations for reducing impact of aircraft emissions on air pollution
[NREC-1168-1] 20 p2360 N73-28986
Analysis of steady-state and dynamic pressure conditions in F-111 aircraft engine to determine causes of engine compressor stalls
[NASA-TN-D-7328] 20 p2465 N73-29806
Buried engines in rear fuselage
21 p2590 N73-30750
Sleep deprivation effects, airborne simulator feel system, bed forms, and V/STOL engine model tests
[DME/NAE-1973[2]] 22 p2731 N73-31853
Research projects to determine effects of exhaust products from aircraft operating in stratosphere on global and local climatic conditions
[UCRL-51336] 23 p2787 N73-32296
Wind tunnel tests to determine aerodynamic loads on flap systems behind engines and vibration modes of flap system
24 p2873 N73-32945
Design and development of quiet, clean propulsion systems for short takeoff aircraft with emphasis on engine noise reduction
24 p2875 N73-32961
Analysis of jet engine noise to show sources of noise, noise spectra, and use of laminates and composite materials for noise reduction
24 p2875 N73-32962
Selection criteria and characteristics of quiet, clean propulsion systems for use with short takeoff aircraft
24 p2876 N73-32967
Computer program for evaluating techniques to improve aircraft engine response systems for application to long range commercial aircraft
[NASA-CR-134496] 24 p2877 N73-32977
Investigations of HT-S/PMR-PI composites for applications to advanced aircraft engines
[NASA-TM-X-71459] 24 p2943 N73-33502

**AIRCRAFT EQUIPMENT**
NT AIRCRAFT HYDRAULIC SYSTEMS
NT AIRCRAFT TIRES
NT BOMBING EQUIPMENT
NT EJECTION SEATS

Development of specifications for design of avionics subsystems to improve reliability
[AD-746029] 01 p0006 N73-10043
Procedure for determining noise levels in flight test measuring systems
01 p0056 N73-10456
Development and evaluation of three axis fluidic airspeed sensor system for use with standard aircraft power supplies
[NASA-CR-112167] 01 p0058 N73-10472
Adaptation of lidar to aircraft and missile rangefinding
[NASA-TT-F-14716] 02 p0181 N73-11466
Development and optimization of fire extinguishers for use in passenger and crew compartments of aircraft
[AD-747496] 03 p0253 N73-12051
Operational tests and evaluation of optical infrared pilot warning system to determine probability of detection versus range
[NASA-CR-129525] 03 p0302 N73-12463
Design criteria for load suspension points, slings, and lifting equipment used on military helicopters
[AD-747814] 03 p0307 N73-12508
Development of adaptive filter technique to minimize effect of noise produced errors in gyrocompasses and production of true azimuth data
[AD-747478] 03 p0329 N73-12685
Technology of aircraft construction to include manufacturing of parts from plastics, ceramics, and nonmetallic materials
[AD-749558] 04 p0374 N73-13044
Aircraft clutch assemblies, ramp roller evaluation at engine input conditions of 26,500 rpm and 1500 hp
[AD-747816] 04 p0427 N73-13481
Development of statistical technique for determining injury reduction capability of energy absorber equipment
[AD-749333] 05 p0497 N73-14044
Design development, and evaluation of hoist for H-3 helicopter rescue system
[AD-750289] 06 p0623 N73-15054
Avionics requirements for multimission, fixed wing, twin engine aircraft designed for search and rescue operations
[AD-750463] 06 p0624 N73-15064
Analysis of heat dissipation and frictional properties of materials used in aircraft brakes
[NASA-CR-121116] 06 p0687 N73-15595
Research projects involving all weather landing systems to include electronic and visual guidance, airborne systems, and data collection
[FAA-ED-07-3] 06 p0697 N73-15680
Analysis of aircraft fire warning system performance and procedures for eliminating false fire warning indications
[AD-751346] 07 p0740 N73-16025
Design, development, and evaluation of flywheel powered hoist for personnel rescue missions conducted by helicopters
[AD-751217] 07 p0741 N73-16029
Feasibility determination of using nematic liquid crystals for aircraft displays
[AD-751667] 07 p0832 N73-16748
Simulation of flight in Concorde for improving characteristic of flight control system
08 p0866 N73-17013
Evaluation of head-up display instrument for providing aircraft vertical guidance during landing approach to comply with noise abatement procedures
[NASA-TM-X-62187] 09 p0982 N73-18021
Analysis of factors affecting crashworthiness of light aircraft to show nature of damage to aircraft and hazards to flight crews
[FAA-TR-FS-70-592-120A] 09 p0984 N73-18032
Avionics requirements for HH-53C helicopter engaged in search and rescue operations
[AD-752625] 09 p0986 N73-18047
UH-1 helicopter test bed program for evaluation of automatic inspection, diagnosis, and prognostic maintenance functions on selected subsystems - Vol. 1
[AD-752890] 09 p0987 N73-18058
Evaluation of conference to investigate current and future development in aircraft electrical and auxiliary power systems
[AGARD-AR-50] 09 p0990 N73-18081
Continuous particle replicator for cloud drops and ice crystals onboard pressurized aircraft
[AD-753091] 09 p1061 N73-18655
Proceedings of conference on application of superconductivity techniques to auxiliary power systems for aircraft and missiles
[AGARD-CP-104] 10 p1108 N73-19030
Characteristics of conventional alternators and aircraft electrical power systems and comparison with electric systems using superconductors
10 p1109 N73-19036
Features and characteristics of superconducting electrical machines and design of synchronous electric generator for airborne use
10 p1109 N73-19040
Characteristics of auxiliary power unit combined with accessory drive to form auxiliary power system for aircraft electric power supply
10 p1110 N73-19045
Design principles of auxiliary power units of secondary power system for operation of aircraft equipment
10 p1110 N73-19046
Analysis of interface between aircraft mechanical power requirements and performance requirements of auxiliary power systems
10 p1110 N73-19049
Air Force research and development programs in aircraft electrical power systems to show planning process for developing specific classes of technology
10 p1111 N73-19052
Application of solid state switching, multiplexing, and electrically programmable logic to aircraft electrical systems
10 p1111 N73-19053
Development of electrical generation and distribution systems for supersonic aircraft using solid state switching and remote control of protective devices
10 p1111 N73-19054
Development of integrated control system for supersonic aircraft based on pneumatic power generation
10 p1111 N73-19056
Numerical analysis of aircraft shock absorber operation to show initial charging, motion, and force parameters during static and dynamic compression of landing gear
[AD-754609] 11 p1236 N73-20031
Design and performance of advanced auxiliary power system for fighter aircraft
[AD-754903] 11 p1238 N73-20049

Analysis of synchronized discrete address beacon system for improved air traffic control capability
[SD-FR-01] 11 p1256 N73-20189
Manual on electromagnetic compatibility and interference between aircraft weapon systems
[AD-754411] 11 p1265 N73-20263
Structural concepts of rotary wing system capabilities to show changes in design of specific vertical takeoff aircraft components
12 p1358 N73-21021
Bibliography of supersonic transport aircraft data to include program management, systems engineering, aircraft structures, and operational considerations
[AD-755600] 12 p1365 N73-21076
Development of halogenated hydrocarbon materials for use as fire and ignition suppressants for aircraft fuel tanks subjected to incendiary ammunition
[AD-755362] 12 p1365 N73-21079
Development of collision avoidance warning system criterion for use with aircraft operating in high density areas
13 p1471 N73-21915
Development of equipment for securing external stores SH-3G helicopter and analysis of failure modes
[AD-757001] 13 p1474 N73-21943
Analysis of H-58 helicopter maintenance to determine removal rate of aircraft equipment and develop failure analysis statistics
[AD-756406] 13 p1475 N73-21945
Cross and square command symbol and video inset generator to display flight command data on aircraft television screen
[AD-755160] 13 p1494 N73-22111
Development, characteristics, and advantages of high voltage direct current electrical systems for aircraft power supplies
[AD-757646] 14 p1604 N73-23001
Development of aircraft seat for high acceleration tolerance of flight crew personnel by elevating pelvis and legs forward
[AD-756630] 14 p1605 N73-23009
Development of hermetically sealed nickel cadmium battery and associated control logic and charger circuit for aircraft applications
[AD-757535] 14 p1606 N73-23017
Economic analysis of integrated time-frequency system for aircraft
14 p1690 N73-23717
Analysis of integrated communications, navigation, and identification system for aircraft operation and proposal for improved capability
14 p1691 N73-23721
Analysis of manual control theory of vertical situation displays for short takeoff aircraft
[NASA-CR-114620] 15 p1734 N73-24061
Development and evaluation of display and control equipment for remotely piloted vehicles
[AD-757761] 15 p1736 N73-24077
Design, development, and testing of inflexible blade, hingeless rotor system with hydraulic rotor control system
[AD-758514] 15 p1736 N73-24081
Purpose, operating principles, and technical description of instrument panel equipment installed on An-24 aircraft
[AD-758751] 15 p1789 N73-24504
Development of inertial smoothing system for control and display applications for VTOL aircraft automatic instrument approach and landing operations
[NASA-TN-D-7271] 15 p1808 N73-24653
Installation of electronic warfare training equipment in rear cockpit of CF-100 aircraft with emphasis on human engineering considerations
[DCIEM-904] 16 p1861 N73-25071
High resolution pulse width modulated parallel channel for forward looking infrared display system
[AD-759224] 16 p1882 N73-25231
Design of landing approach automatic flight control system using optimal feedback techniques
[AD-760125] 17 p1984 N73-26040
Human factors in design of avionics subsystems considering training costs and performance of Air Force personnel
[AD-759583] 17 p1990 N73-26096
Performance tests of four flight-director/attitude indicator displays under three conditions of simulator motion and comparison with flight test results
[AD-760049] 17 p2011 N73-26264
Design of extended Kalman filter for detection and ranging of ground radar from aircraft
[AD-760764] 18 p2123 N73-27158
Flight test of multispectral image dissector camera onboard high altitude aircraft
18 p2209 N73-27835
Analysis of various aircraft antiskid braking systems to determine appropriate antiskid braking system for space shuttle vehicle
[NASA-CR-124349] 19 p2294 N73-28449
Logistic performance data book for bomb navigation avionics system of F-111 aircraft to show support cost, reliability, maintenance, and problems
[AD-762214] 19 p2357 N73-28959
Logistic performance data book on propulsion system for KC-135 aircraft to show reliability, maintenance, costs, and problems
[AD-762217] 19 p2357 N73-28962
Logistic performance data book for C-141A aircraft radio navigation system to show reliability, maintainability, logistics support, and operating problems
[AD-762250] 19 p2358 N73-28971
Logistic performance data book for KC-135 aircraft electrical power system to show reliability, maintainability, logistics support, and operating problems
[AD-762225] 19 p2358 N73-28972
Logistic performance data book for RF-4C photographic reconnaissance system to show reliability, maintainability, logistic support, and operating problems
[AD-762232] 19 p2358 N73-28974
Development of digital flight control system for performing pilot assist augmentation and pilot relief automatic pilot functions
[AD-762521] 20 p2361 N73-28992
Design, development, airworthiness test, and flight test of multiplexing components for fly by wire flight control
[AD-763111] 20 p2362 N73-28996
Analysis of voice command systems for application to military aircraft operation to show manufacturers, specifications, and research projects
[AD-762922] 20 p2362 N73-28998
Design and development of integrated fire and overheat detection and warning system for installation in aircraft nacelle
[AD-762919] 20 p2362 N73-28999
Analysis of energy separator for application to air conditioning system of E-8 aircraft
[AD-762590] 20 p2364 N73-29014
Design and development of cryptosteady energy separator for application to F-8 aircraft air conditioning system
[AD-762579] 20 p2364 N73-29015
Analysis of noise problems created by supersonic transport aircraft, conventional aircraft, and short takeoff aircraft to show methods for jet exhaust noise reduction
21 p2495 N73-30024
Design of integrated aircraft instrumention display system utilizing plasma display/memory unit
[AD-763599] 21 p2550 N73-30446
Techniques for creating moving image reconnaissance display
[AD-763789] 21 p2551 N73-30452
Nonlinear vibrations of pipelines containing pressurized fluids with application to aircraft hydraulic systems
[AD-764154] 22 p2616 N73-30968
Aircraft accident involving Boeing 707 aircraft following aborted takeoff at Kennedy International Airport, New York, on 13 August, 1972
[NTSB-AAR-73-7] 23 p2741 N73-31943
Research and development projects concerning fire hazards in aircraft cabins and design of aircraft compartments to provide greater passenger survivability
[FAA-RD-73-146] 24 p2876 N73-32972
Systems analysis of avionics and aircraft equipment for search and rescue helicopters to determine cost effective improvements - Vol. 7
[AD-764914] 24 p2927 N73-33381
Equipment for removing silver crazing on aircraft glass
[AD-764972] 24 p2944 N73-33510

**AIRCRAFT EXHAUST**

U EXHAUST GASES

**AIRCRAFT FUEL SYSTEMS**

Alternate fuels to reduce aircraft exhaust pollutants
[AD-755151] 11 p1332 N73-20815
Development of fibrous flame arrestor materials to provide explosion and fire protection for aircraft fuel tanks
[AD-759193] 16 p1863 N73-25090

**AIRCRAFT FUELS**

Development of method for determining ethylene dibromide depletion in aviation fuels
[AD-746250] 02 p0221 N73-11791
Vaporization rates of liquid injected into high temperature, supersonic gas flow using aviation gasoline injected by Laval nozzle into air stream
[AD-747456] 03 p0286 N73-12317
Automatic controlled pressure system for onshore fueling of navy aircraft
[AD-748211] 04 p0489 N73-13997
Analysis of factors influencing technical feasibility of operating aircraft on liquid hydrogen fuel
[NASA-TM-X-68242] 15 p1823 N73-24777
Effectiveness of crushed and graded stone aggregate in preventing or retarding rate of flame propagation from fixed ignition source for aircraft fuels
[FAA-NA-73-13] 17 p2097 N73-26962
Comparison of military and civil jet engine fuel specifications and test procedures for fuel performance and quality control
17 p2098 N73-26972
Optimization of supersonic aircraft C3/C4 polymer fuel by normal paraffins containing 10 to 16 carbon atoms
[DLR-FB-73-32] 22 p2708 N73-31689

**AIRCRAFT GUIDANCE**

Development of gradient clearance monitor concept to ascertain glide slope clearance signal
[FAA-RD-72-147] 10 p1185 N73-19645
Development of air navigation system to provide four dimensional guidance for short takeoff aircraft operating in terminal area
[NASA-TM-X-62234] 14 p1687 N73-23686
Air traffic control procedures for simultaneous instrument flight rules approaches to set of three parallel runways
[FAA-NA-73-23] 14 p1687 N73-23687
Analysis of air navigation systems for continental US and overseas flights based on projected traffic loads of 1980 time period
[FAA-ED-04-1] 14 p1687 N73-23688
Characteristics of air traffic control system to include description of electronic components and projects for developing improved equipment
14 p1687 N73-23692
Development of automated air traffic control system using computer techniques to provide flight safety for increased air traffic
14 p1687 N73-23693
Organization, functions, and capabilities of automated air traffic control system for Rome, Italy
14 p1687 N73-23694
Status and trends of civil air traffic control systems and development of automated network for increased flight safety
14 p1688 N73-23696
Comparison of cost, complexity, and cockpit workload for seven area navigation system configurations
14 p1688 N73-23697
Numerical anlaysis of optimal control and sequencing of air traffic control operations in near terminal area
14 p1688 N73-23701
Analysis of short takeoff and landing aircraft landing guidance systems and application of air traffic control procedures for improved sequencing
14 p1688 N73-23703
Development and characteristics of instrument landing system using radioactive materials along runways for glide slope and alignment information
14 p1689 N73-23707
Development and characteristics of forward area homing and landing guidance for military aircraft operations
14 p1689 N73-23708
Application of artificial satellites for data acquisition and communication functions in air traffic control system
14 p1689 N73-23709
Development and characteristics of system for separation and control of aircraft to avoid midair collisions
14 p1690 N73-23712
Performance tests of air traffic control system to determine effectiveness in prevention of midair collisions
14 p1690 N73-23713
Analysis of man-machine interfaces and system reliability for air traffic control automation systems
14 p1690 N73-23715
Analysis of interface between controller and computer in automated air traffic control system
14 p1690 N73-23716
Analysis of development program for improving US air traffic control procedures for 1980 time period
14 p1690 N73-23718
Conceptual analysis of improved communication, navigation, and indentification system for military applications
14 p1690 N73-23719
Analysis of communications, navigation, and identification equipment for aircraft and proposed system for improvement in capability
14 p1690 N73-23720
Characteristics of flight control system for approach flight path control of augmentor wing on powered-lift short takeoff aircraft configuration
[NASA-CR-114574] 15 p1734 N73-24062
Development of perturbation guidance system for maintaining tilting rotor vertical takeoff aircraft on predetermined flight path during takeoff and landing
[NASA-CR-132043] 15 p1735 N73-24072
Analysis and digital computer simulation of operational and performance aspects of vertical area navigation system
[FAA-RD-72-125] 16 p1941 N73-25705
Operational procedures and modes of experimental guidance system for short takeoff aircraft to provide arrival time control and automatic tracking
[NASA-TM-X-62233] 16 p1941 N73-25710
Characteristics of airborne radio homing and alerting equipment for use with emergency locator transmitters
[RTCA-SC-124] 17 p2060 N73-26663

Titan 3c guidance with carousel vehicle borne inertial guidance system
[AD-764729] 23 p2852 N73-32788

**AIRCRAFT HAZARDS**
Methodology for determining climatological probability of aircraft icing throughout Northern Hemisphere
[AD-745098] 01 p0075 N73-10623
Investigation of aircraft accident involving Beech aircraft performing air taxi service to Boise, Idaho on 20 Feb. 1972
[NTSB-AAR-72-25] 03 p0253 N73-12050
Migration corridors for ducks and geese and effects on aviation safety
[AD-748114] 04 p0382 N73-13109
Hazards related to use of jet thrust power
[PB-211593] 05 p0497 N73-14046
Compilation of selected aircraft accident reports for US Civil Aviation operations during calendar year 1970 - Issue 5
[PB-211158] 05 p0497 N73-14047
Trailing vortex hazard avoidance of Jumbo jets by airport warning system
05 p0610 N73-14958
Wind tunnel tests to determine structural integrity of birds under conditions simulating ingestion of birds into inlets of high speed aircraft
[NASA-TM-X-68163] 06 p0629 N73-15114
Aviation hazards of turbulence and shear in stable stratified atmosphere
[CONF-720535-2] 06 p0694 N73-15653
Bibliography of aircraft accident reports for US civil aviation operations during calendar year 1971
[NTSB-BA-72-6] 07 p0738 N73-16001
Aircraft accident involving Beechcraft Queen Air aircraft on takeoff from Albuquerque, New Mexico airport on 19 May, 1972
[NTSB-AAR-72-32] 07 p0738 N73-16003
Doppler effect continuous wave radar for bird hazard detection and aircraft collision avoidance near airfields
[AD-751985] 08 p0885 N73-17168
Probability of aircraft being struck by lightning
[NLL-M-22800-[5828.4F]] 11 p1313 N73-20656
Statistical correlation of gulls and USAF aircraft hazards
[AD-759824] 16 p1863 N73-25092
Aircraft accident involving Lear jet aircraft following takeoff from Atlanta, Georgia Airport on 26 Feb. 1973
[NTSB-AAR-73-12] 17 p1984 N73-26036
Probability of aircraft crashing into Boardman nuclear power plant
[PB-220715/7] 21 p2578 N73-30662

**AIRCRAFT HYDRAULIC SYSTEMS**
Variable-orifice hydraulic mechanism for aircraft gas turbine engine fuel control
[NASA-CASE-LEW-11187-1] 10 p1203 N73-19793
Effects of trapped air on operation of aircraft hydraulic systems and methods for removing air contamination
[NLL-NEL-TT-2420-[6075.461]]
11 p1232 N73-20005
Computerized analysis of aircraft hydraulic system dynamic performance
[AD-757537] 16 p1864 N73-25093

**AIRCRAFT INDUSTRY**
Technology of aircraft construction
[AD-748712] 04 p0374 N73-13043
Findings and recommendations of Aviation Advisory Commission on long range needs of Aviation-- Vol. 1 Vol. 2
[PB-215803] 09 p1101 N73-18983
Large subsonic wind tunnel design for German industry
[REPT-EA-317-A] 13 p1507 N73-22213
Production forecasting for aircraft manufacturer
23 p2862 N73-32872

**AIRCRAFT INSTRUMENTS**
NT ALTIMETERS
NT ANEMOMETERS
NT APPROACH INDICATORS
NT ATTITUDE INDICATORS
NT AUTOMATIC PILOTS
NT GYRO HORIZONS
NT GYROCOMPASSES
NT HOT-WIRE ANEMOMETERS
NT PLAN POSITION INDICATORS
NT POSITION INDICATORS
NT RADIO ALTIMETERS
NT RADIO DIRECTION FINDERS
NT SPACECRAFT POSITION INDICATORS
NT SPEED INDICATORS
NT TACHOMETERS
Design of aircraft flight test instrumentation systems
01 p0055 N73-10451
Operational test and evaluation of angle of attack system for displaying percentage of lift produced by wing for all flap configurations
[AD-748844] 03 p0304 N73-12485
Aircraft horizon and vertical indicator
[NASA-CASE-ERC-10392] 05 p0576 N73-14692
Astronomical techniques for spacecraft orientation and aircraft instrument errors
[JPRS-57704] 05 p0577 N73-14693
Integration of STOL aircraft instruments and approach control for new approach profiles
[DGLR-PAPER-72-096] 06 p0622 N73-15047
Design and tests of counting strain gages for high-g naval aircraft
[AD-750692] 06 p0676 N73-15498
Development and characteristics of cathode ray tube vertical display system for use in all-weather air navigation aircraft
[AD-752510] 08 p0868 N73-17026
Flight test of instrument for determining low airspeeds to evaluate suitability for helicopter airspeed indicator
[AD-753343] 09 p0989 N73-18071
Analysis of aircraft instruments and display devices for approach control and landing of V/STOL aircraft
[AGARD-AR-51] 09 p1034 N73-18439
Atmospheric observation techniques using aircraft infrared radiometers as prototypes for spacecraft remote sensing application
[NOAA-TR-NESS-64] 11 p1293 N73-20494
Wind tunnel tests to determine pressure sensing characteristics of trailing cone device for calibrating aircraft static-pressure systems
[NASA-TN-D-7217] 13 p1470 N73-21906
Development of heads-up flight data display for aircraft approach and landing during all conditions of visibility
14 p1688 N73-23702
Economic analysis of integrated time-frequency system for aircraft
14 p1690 N73-23717
Analysis of manual control theory of vertical situation displays for short takeoff aircraft
[NASA-CR-114620] 15 p1734 N73-24061
Purpose, operating principles, and technical description of instrument panel equipment installed on An-24 aircraft
[AD-758751] 15 p1789 N73-24504
Performance tests of four flight-director/attitude indicator displays under three conditions of simulator motion and comparison with flight test results
[AD-760049] 17 p2011 N73-26264
Display device for integrated jet engine instrument system program
[AD-763440] 21 p2550 N73-30450
Performance tests of hemispherical flow-direction sensor mounted on F-104 aircraft to develop Mach number position error calibration curve
[NASA-TN-D-7461] 23 p2743 N73-31956
Logic and design procedures for multifunction mode switching controls in jet aircraft cockpits
[AD-764617] 23 p2767 N73-32141

**AIRCRAFT LANDING**
NT CRASH LANDING
Development of computer program for complete simulation of factors involved in aircraft takeoff and landing
[AD-741942] 01 p0006 N73-10042
Development of statistical-probabilistic method of collision probability calculation and application to arbitrary flight paths and vehicle shapes
[AD-744722] 01 p0006 N73-10046
Improved pilot performance using simulated pictorial landing display with symbols
01 p0016 N73-10122
Fixed base flight simulator evaluation of wing spoilers for longitudinal flight path control of Cessna aircraft during instrument landing system approach
[NASA-CR-2121] 02 p0125 N73-11015
Development of performance criteria to estimate relative proficiency of aircraft pilots during aircraft carrier qualification training with F-4 aircraft
[AD-746095] 02 p0127 N73-11030
Analysis of effective perceived noise level method for determining airport noise and comparison with actual noise measurements taken during aircraft landings
[UCLA-PAPER-ENG-0872] 03 p0249 N73-12010
Analysis of forces imposed on aircraft wing from landing gear impact in relation to weight of wing, damping, and frequency of periodic load
[AD-747381] 03 p0254 N73-12052
Analysis of instrument system for assisting pilots in making decisions during aircraft takeoff and landing rolls
[FAA-RD-72-112] 03 p0301 N73-12460
Analysis of limitations on helicopter approach and landing during conditions of low visibility
[AD-747732] 03 p0329 N73-12686
Analysis of aircraft pilot experiences during landing approaches in minimum visibility situations
[AD-747654] 03 p0329 N73-12687
Development and evaluation of instrument landing system with VHF and UHF capability for localizer and glide slope
[AD-747656] 03 p0329 N73-12688
Analysis of loading conditions imposed on commercial aircraft during turning maneuvers on ground
[NASA-TN-D-7132] 04 p0372 N73-13027
Operational test and evaluation of four configurations of flight director display for instrument landings based on command heading and command flight path angle
[AD-748244] 04 p0374 N73-13041
Evaluation of approach lighting system for visual guidance of helicopters during instrument flight rules approach and landing operations
[FAA-RD-72-133] 04 p0401 N73-13261
Location of soil types with potential for generating atmospheric sand and dust with application to analysis of V/STOL operational environment
[AD-749462] 05 p0495 N73-14033
Development and characteristics of six degree of freedom, fast time predictor model for simulation of F-4 aircraft landing on aircraft carrier
[AD-750294] 05 p0504 N73-14102
Design and development of microwave landing system for operation of civil and military aircraft in conventional and V/STOL configurations
[AD-749505] 05 p0578 N73-14702
Analysis of air cushion vehicle landing system operation and computation of air flow requirements
[AD-750936] 06 p0625 N73-15069
Aircraft accident involving Lear jet model 25 at Victoria, Texas on 18 Jan. 1972
[PB-212484] 06 p0625 N73-15076
Performance tests of aircraft arresting gear to determine allowable operating restraints on angular displacement and off-center engagements
[NATF-R125] 06 p0649 N73-15268
Measurement of critical atmospheric turbulence for aircraft takeoff and landing
[AD-750131] 06 p0694 N73-15660
Research projects involving all weather landing systems to include electronic and visual guidance, airborne systems, and data collection
[FAA-ED-07-3] 06 p0697 N73-15680
Analysis of position determination accuracy obtainable with microwave landing guidance system
[NASA-TN-D-7116] 06 p0697 N73-15681
Incident involving collision of Boeing 727 aircraft with landing light system at Atlanta International Airport, Georgia on 21 Dec. 1971
[NTSB-AAR-72-22] 07 p0737 N73-16000
Aircraft accident involving DH-114 aircraft during attempted landing at Mercedita Airport, Puerto Rico on 24 June, 1972
[NTSB-AAR-72-34] 07 p0738 N73-16004
Aircraft accident involving DC-9 aircraft landing at Fort Lauderdale, Florida airport in marginal weather conditions on 18 May, 1972
[NTSB-AAR-72-31] 07 p0738 N73-16005
Flight simulator evaluations of flight control, flight path, and airspeed for approach and landing of powered lift jet short takeoff aircraft
[NASA-TM-X-62203] 07 p0739 N73-16014
Bibliography of data on aircraft landings, instrument landings, approach control, glide path systems, display devices, and terminal facilities
[AD-751800] 07 p0740 N73-16024
Effectiveness of training device for air traffic communication and carrier landing control
[AD-751556] 07 p0751 N73-16101
Analysis of simulated aircraft landing approach to aircraft carrier to determine display system requirements and to evalute dangerous conditions
[AD-751076] 07 p0819 N73-16635
Measurement of pilot performance during aircraft landing simulation to determine significance of vertical acceleration cues during approach and landing maneuver
[NASA-TM-X-62236] 08 p0867 N73-17020
Design and development of stability augmentation system to eliminate coupling effects during landing of short takeoff aircraft
[NASA-CR-130543] 08 p0867 N73-17021
Approach light properties for visual discrimination in pilot landing environment
[NASA-TT-F-14667] 08 p0941 N73-17710
Analysis of internal flow conditions of inlet with centerbody retracted for short takeoff and landing aircraft takeoff and approach operations
[NASA-TN-D-7185] 09 p0980 N73-18010
Evaluation of head-up display instrument for providing aircraft vertical guidance during landing approach to comply with noise abatement procedures
[NASA-TM-X-62187] 09 p0982 N73-18021
Development of empirical method for determining optimum reversing coefficient of thrust reversal of jet engines on passenger aircraft
[AD-752814] 09 p0986 N73-18048
Development of criteria for predicting landing impact loads for V/STOL aircraft based on data obtained by flight tests of X-22 aircraft
[AD-753852] 09 p0989 N73-18075
Analysis of aircraft instruments and display devices for approach control and landing of V/STOL aircraft
[AGARD-AR-51] 09 p1034 N73-18439
Comparison of simulation and flight test results for automatic short takeoff aircraft landing system
10 p1105 N73-19006
Command and control of stability of Do-31 aircraft by landing and hovering
[BMVG-FBWT-72-25] 10 p1106 N73-19022

Development of gradient clearance monitor concept to ascertain glide slope clearance signal
[FAA-RD-72-147] 10 p1185 N73-19645
Flight test of X-22 aircraft to determine longitudinal stability requirements of short takeoff aircraft during terminal area operations
[AD-754840] 11 p1235 N73-20029
Analysis of procedures and problems involved in operating helicopters from decks of ships
12 p1357 N73-21010
Analysis of effect of grooved runway configurations on aircraft tire braking traction on flooded runway surfaces
[NASA-TN-D-7215] 12 p1363 N73-21057
Analysis of electromagnetic compatibility of microwave landing guidance system and candidate interim systems
[ECAC-PR-72-069] 12 p1425 N73-21554
Analysis of parameters affecting transition from meteorological visibility range to real visibility range during aircraft landing
[NASA-TT-F-14887] 13 p1556 N73-22607
Analysis of minimum longitudinal stability for large delta wing transport aircraft during landing approach and touchdown using inflight simulator
[TR-5084-F-1-VOL-1] 14 p1601 N73-22984
Development of mathematical and simulation models to calculate capacity of single runway under instrument flight rules conditions
[MTR-4102-REV-2] 14 p1645 N73-23345
Air traffic control procedures for simultaneous instrument flight rules approaches to set of three parallel runways
[FAA-NA-73-23] 14 p1687 N73-23687
Development of heads-up flight data display for aircraft approach and landing during all conditions of visibility
14 p1688 N73-23702
Analysis of short takeoff and landing aircraft landing guidance systems and application of air traffic control procedures for improved sequencing
14 p1688 N73-23703
Development of Doppler microwave landing system and techniques for eliminating effects of multipath transmissions
14 p1689 N73-23706
Development and characteristics of instrument landing system using radioactive materials along runways for glide slope and alignment information
14 p1689 N73-23707
Development and characteristics of forward area homing and landing guidance for military aircraft operations
14 p1689 N73-23708
Development of stability augmentation systems for decoupling response of short takeoff and landing aircraft in longitudinal and lateral-directional flight modes
15 p1732 N73-24041
Methods for evaluating and predicting airfield performance of turbojet and turbofan aircraft operating in conventional and short takeoff modes
15 p1732 N73-24044
Aircraft accident involving Boeing 707 aircraft during landing at John F. Kennedy Airport, New York, 12 Dec. 1972
[NTSB-AAR-73-11] 15 p1734 N73-24068
Development of perturbation guidance system for maintaining tilting rotor vertical takeoff aircraft on predetermined flight path during takeoff and landing
[NASA-CR-132043] 15 p1735 N73-24072
Application of ground effect machine landing systems for recovery of remotely piloted vehicles
[AD-758789] 15 p1736 N73-24079
Development of inertial smoothing system for control and display applications for VTOL aircraft automatic instrument approach and landing operations
[NASA-TN-D-7271] 15 p1808 N73-24653
Development of air traffic control procedure to permit short takeoff aircraft landing along curved approach trajectory and analysis of data transmission requirements
16 p1859 N73-25055
Direct side force control for STOL crosswind landings with analysis of manual and automatic control modes
[AD-759555] 16 p1863 N73-25091
Operational procedures and modes of experimental guidance system for short takeoff aircraft to provide arrival time control and automatic tracking
[NASA-TM-X-62233] 16 p1941 N73-25710
Analysis of control and display device testing for microwave landing system - Vol. 1
[AD-758791] 16 p1942 N73-25713
Development of control and display testing requirements for evaluation of microwave landing system - Vol. 2
[AD-758792] 16 p1942 N73-25714
Analysis of data rate requirements for low visibility approach with scanning beam landing guidance system
[AD-758786] 16 p1942 N73-25719
Aircraft accident involving crash of DC-9 aircraft during landing following go-round at Fort Worth, Texas Airport on 30 May 1972
[NTSB-AAR-73-3] 17 p1982 N73-26017
Analysis of influence of engine response characteristics on approach and landing performance of aircraft equipped with externally blown flap
[NASA-TM-X-62265[2]] 17 p1982 N73-26022
Aircraft accident involving Boeing 747 aircraft during landing at Miami, Florida airport on 15 Dec. 1972 following collision with birds
[NTSB-AAR-73-13] 17 p1983 N73-26029
Design of landing approach automatic flight control system using optimal feedback techniques
[AD-760125] 17 p1984 N73-26040
Flight simulation to determine effects of wind shear on aircraft landings for various commercial and military aircraft
[NASA-CR-2287] 18 p2105 N73-27023
Flight evaluation of glide slope determination during landing approach by reference to diamond shaped figure painted on runway
[NASA-TM-X-2849] 18 p2105 N73-27027
Comparison of automatic short takeoff aircraft landings based on simulation and flight test results
[NASA-TT-F-14995] 18 p2105 N73-27028
Analysis of minimum longitudinal stability for large delta wing transport aircraft during landing approach and touchdown using in-flight simulation techniques
[AD-761120] 18 p2106 N73-27036
Performance tests of visual approach slope indicator [VASI] equipment and systems for improved terminal area effectiveness
[FAA-NA-73-64] 18 p2175 N73-27568
Approach abort optimization in control of aircraft carrier landings
[AD-761617] 19 p2221 N73-27914
Analysis of factors affecting approach and landing of aircraft under visual conditions to show causes of misjudgement resulting in aircraft landing accidents
[NASA-TT-F-15054] 20 p2360 N73-28980
Analysis of pilot performance and short takeoff aircraft characteristics during landing approach
[AD-762566] 20 p2362 N73-29000
Prototype model for aircraft carrier landing officer
[AD-762728] 20 p2372 N73-29064
Evaluation of structural layers in flexible pavement during simulated aircraft traffic
[AD-762131] 20 p2383 N73-29149
Status of civil airline implementation of all-weather landings in Europe and United Kingdom
[MTR-6211] 20 p2452 N73-29711
Flight tests of various steep gradient approaches to ground level short takeoff and landing runway to determine aircraft performance and navigation aids required
[FAA-NA-72-77] 21 p2495 N73-30025
Analysis of landing performance of scale model of C-8 aircraft equipped with air cushion landing system on variety of surfaces including calm and rough water
[NASA-TN-D-7295] 21 p2496 N73-30032
Development of procedures for stabilizing snow to permit helicopter landings
[AD-763231] 21 p2497 N73-30040
Effect of inflated air cushion landing gear on subsonic static stability of high performance aircraft operating out of ground effect
[AD-763365] 21 p2498 N73-30048
Ground based visual aid to alleviate spatial disorientation during takeoff and landing
[FAA-RD-73-26] 21 p2521 N73-30216
Determination of variability of oblique and horizontal visibility for aircraft landing by analysis of experimental data
[NLL-M-23046-[5828.4F]] 21 p2567 N73-30576
Analysis of glide path parameters, approach control system precision, and separation standards for extension of runway capacity under instrument flight rule conditions
[AD-763142] 21 p2578 N73-30657
Development and characteristics of system for integrated control of engine power and aerodynamic configuration of aircraft during landing approach
[NASA-CASE-ARC-10456-1] 22 p2613 N73-30938
Statistical analysis of aircraft carrier wave-off situation based on deck motion and aircraft approach geometry
[AD-764516] 22 p2616 N73-30967
Finite element model of jointed concrete pavement on nonlinear viscous subgrade dynamic interaction of aircraft-pavement systems
[AD-764243] 22 p2647 N73-31213
Effects of snow cover and snow surface conditions on image glide path systems for aircraft approach control
[FAA-RD-72-85] 22 p2697 N73-31602
Numerical analysis of curved approach paths and landing sequence for multiple aircraft using same terminal facilities to provide maximum system performance
23 p2740 N73-31935
Flight paths for short takeoff aircraft landing approach consistent with pilot preference passenger comfort, and microwave landing system limitations
[NASA-TN-D-7298] 23 p2742 N73-31949
Display devices for short takeoff aircraft landing
[DGLR-PAPER-73-038] 23 p2744 N73-31961
Flight control for steep approach landing
[DGLR-PAPER-73-027] 23 p2744 N73-31962
Flight control problems of steep approach landing with direct lift control, exemplified by HFB-320 aircraft
[DGLR-PAPER-73-024] 23 p2744 N73-31965
Cockpit layouts in view of new landing approach methods
[MBB-UH-07-73-O] 23 p2744 N73-31966
Automatic flight control system for curved flight path profiles
[DGLR-PAPER-73-030] 23 p2745 N73-31970
Computerized simulation of DC-8 aircraft during landing approach under wind shear conditions
[AD-764697] 23 p2745 N73-31975
Development and characteristics of air cushion landing system for remotely piloted vehicles
[AD-764774] 23 p2747 N73-31985
Digital computer-generated contact analog landing display
[AD-764764] 23 p2771 N73-32162
Evaluation of approach and landing performance of inertial navigation system with Kalman filter installed in CV-340 aircraft
[NASA-TN-D-7302] 23 p2816 N73-32515
Aircraft landing problems under low visibility weather conditions
[DGLR-PAPER-73-015] 23 p2817 N73-32520
Description of sector-Tacan and DME-supported instrument landing systems
[DGLR-73-019] 23 p2817 N73-32523
Compatible ILS, using microwave frequencies, and precision ILS, using antenna arrays, as improved standard instrument landing systems
[DGLR-PAPER-73-018] 23 p2817 N73-32524
Flight simulation to determine manual control of flight path and airspeed for approach and landing of powered lift jet short takeoff aircraft
24 p2873 N73-32949
Pilot activation in automatic landing by display devices
24 p2880 N73-32999
Meteorological and weather effects on aircraft landings and flights along air lanes and stratospheric wind effects on supersonic transports
[JPRS-60114] 24 p2945 N73-33522
Determination of visibility slant range when landing aircraft in radiation fog
24 p2946 N73-33523

**AIRCRAFT LANDING INSTRUMENTS**
U LANDING INSTRUMENTS

**AIRCRAFT LAUNCHING DEVICES**
Flight control improvement of F-8 aircraft relative to carrier takeoff and landing
[AD-753010] 09 p0986 N73-18052

**AIRCRAFT MAINTENANCE**
Performance tests to determine proficiency of maintenance personnel in servicing fuel start solenoid in UH-1 helicopter
[AD-745163] 0! p0021 N73-10166
Development of usage rate system to determine logistics requirements for military aircraft support
[AD-746482] 0% p0127 N73-11034
Development of computer assisted troubleshooting system for maintenance of helicopters and aircraft using Univac 1108 computer
[AD-748665] 04 p0373 N73-13037
Noise reduction and control in FAA air traffic control, navigational, and service facilities
[J-6250] 04 p0401 N73-13264
Space shuttle design recommendations based on aircraft maintenance experience
[NASA-TM-X-68646] 08 p0965 N73-17888
Aircraft corrosion prevention by addition of potassium dichromate to rinse water
[AD-753214] 09 p0986 N73-18050
Optimum service life determination technique for Naval aircraft
[AD-752747] 09 p0987 N73-18057
UH-1 helicopter test bed program for evaluation of automatic inspection, diagnosis, and prognostic maintenance functions on selected subsystems - Vol. I
[AD-752890] 09 p0987 N73-18058
Accomplishments during evaluation of automatic inspection, diagnostic, and prognostic maintenance system using UH-1 helicopter as test bed - Vol. 2
[AD-752891] 09 p0987 N73-18059
Development of automatic inspection diagnostic and prognostic systems for maintenance of military helicopters - Vol. 1
[AD-752893] 09 p0987 N73-18060
Development of automatic inspection diagnostic and prognostic systems for maintenance of military helicopters - Vol. 2
[AD-752894] 09 p0987 N73-18061
Formulation of automatic inspection, diagnostic, and prognostic system for maintenance of army aircraft - Vol. 1
[AD-752882] 09 p0988 N73-18062
Design and tradeoff studies applied to automatic inspection, diagnostic, and prognostic maintenance system for military aircraft - Vol. 2
[AD-752883] 09 p0988 N73-18063
Technical proposal and development plan for automatic inspection, diagnostic, and prognostic maintenance system for military aircraft - Vol. 3
[AD-752884] 09 p0988 N73-18064

General specification for automatic inspection, diagnostic, and prognostic maintenance system for military aircraft - Vol. 4
[AD-752885] 09 p0988 N73-18065
Computer models for application to automatic inspection, diagnostic, and prognostic system for maintenance of military aircraft - Appendix C
[AD-752886] 09 p0988 N73-18066
Computer output data for automatic inspection, diagnostic, and prognostic system for maintenance of military aircraft - Appendix D
[AD-752887] 09 p0988 N73-18067
Maintenance data tabulations for automatic inspection, diagnostic, and prognostic systems for military aircraft maintenance - Appendix E
[AD-752888] 09 p0988 N73-18068
Cost effectiveness of automatic inspection, diagnostic, and prognostic maintenance system for military aircraft - Appendix F
[AD-752889] 09 p0988 N73-18069
Improvements in military helicopter flight test techniques to provide data for safety, maintainability, and reliability
12 p1357 N73-21013
Analysis of H-58 helicopter maintenance to determine removal rate of aircraft equipment and develop failure analysis statistics
[AD-756406] 13 p1475 N73-21945
Design of aircraft for high reliability and low maintenance costs and maintenance procedures for maximum efficiency
17 p1983 N73-26032
Manpower requirements for aircraft maintenance operations of USAF
[AD-760082] 17 p1991 N73-26097
Structural inspection for maintaining airworthiness of older aircraft
[NASA-TM-X-2845] 17 p2092 N73-26925
Heuristic method for scheduling aircraft maintenance
[AD-761494] 19 p2355 N73-28947
Objectives and performance indicators for aircraft maintenance organizations
[AD-762270] 19 p2356 N73-28951
Cost history of F-111 aircraft airframe system to show logistics organization, support costs, reliability and maintainability, and development problems
[AD-762213] 19 p2356 N73-28958
Logistic performance data book for C-5A aircraft landing gear to show system reliability, maintainability, logistic support cost, and performance data
[AD-762248] 19 p2357 N73-28963
Logistic performance data book for C-130E aircraft propulsion system to show reliability, maintainability, logistic support costs, and operational problems
[AD-762249] 19 p2357 N73-28964
Application of radiation technology and equipment for nondestructive analysis of commercial aircraft structures during aircraft maintenance periods
24 p2952 N73-33579

**AIRCRAFT MODELS**
Role of free-flight models in aircraft research and development
08 p0865 N73-17002
Effects of porous wind tunnel wall corrections on transport aircraft models
14 p1648 N73-23366
NRC 10 ft x 20 ft V/STOL propulsion tunnel for V/STOL engine model testing
22 p2731 N73-31857

**AIRCRAFT NOISE**
NT JET AIRCRAFT NOISE
NT SONIC BOOMS
Noise tests on simulated mixer nozzles and scale models of externally blown flap, lift augmentation system
[NASA-TM-X-2638] 02 p0124 N73-11012
Model for generation of blade-passage noise caused by interaction of rotor wakes with downstream stator blades in fan stage
[NASA-TM-X-2669] 02 p0222 N73-11797
Analysis of effective perceived noise level method for determining airport noise and comparison with actual noise measurements taken during aircraft landings
[UCLA-PAPER-ENG-0872] 03 p0249 N73-12010
Method for computing effects of meteorological conditions on sound in vicinity of subsonic aircraft
[SC-DC-72-1007] 03 p0253 N73-12044
Proceedings of symposium on helicopter noise held at Durham, North Carolina Sept. 1971
[AD-748876] 04 p0373 N73-13036
Data concerning airport development including land use, noise level compatibility, and zoning
[FAA-EQ-72-3-VOL-2] 04 p0401 N73-13267
Noise exposure model MOD-5 - Vol 1
[PB-211979] 05 p0497 N73-14049
Noise exposure model MOD-5 - Vol 2
[PB-211976] 05 p0497 N73-14050
Analysis of jet noise produced by supersonic transport aircraft with augmentor wing and four duct burning turbofan engines
[NASA-TM-X-68177] 06 p0619 N73-15028
Evaluation of subjective annoyance caused by noise generated by turbofan short takeoff aircraft and comparison with noise of conventional takeoff aircraft
[NASA-TN-D-7102] 06 p0621 N73-15040
Effect of nozzle inlet shape, lip thickness, and exit shape and size on subsonic jet noise
[NASA-TM-X-68182] 07 p0821 N73-16655
Noise effects on hearing conservation in aircrew and ground support personnel of aerospace operations
08 p0876 N73-17101
Open jet, wind tunnel operating within anechoic chamber for studying V/STOL noise mechanisms
[AD-751857] 08 p0894 N73-17235
Performance characteristics of solid state converter system for measuring aircraft noise and sonic boom
[NASA-CR-112260] 09 p0982 N73-18019
Analysis of V/STOL aircraft design and operation to determine effects of noise problems and constraints with emphasis on helicopter performance
[AD-752447] 09 p0989 N73-18073
Effects of light aircraft noise on hearing
[NASA-CR-130987] 09 p0992 N73-18095
Unique field-laboratory methodology for assessing human response to noise
[NASA-CR-2221] 09 p0995 N73-18124
Measurement of indoor and outdoor sound pressure levels at airport control towers during aircraft takeoff and landing
[AD-752535] 09 p1012 N73-18262
Evaluation of aircraft noise pollution level as a predictor of annoyance
[NASA-CR-130920] 09 p1100 N73-18978
Analysis of special problems and issues involved in the long range of aviation with emphasis on 1 aa Vol. 2
[PB-215804] 09 p1101 N73-18984
Concepts for achieving low noise levels for V/STOL aircraft
[NASA-CR-120970-VOL-1] 10 p1106 N73-19018
Analysis of aircraft noise environment for land areas in vicinity of military air bases
[AD-754111] 10 p1107 N73-19028
Influence of cockpit noise on hearing in flight crew personnel
[FAA-AM-72-32] 10 p1119 N73-19125
Acoustic measurement methods for evaluating aircraft noise pollution in urban areas
[PB-212875] 11 p1326 N73-20757
Guidelines for urban control of aircraft noise pollution
[PB-213020] 11 p1326 N73-20759
Noise level surveys of seventeen general aviation aircraft including jet and propeller driven types
[FAA-EQ-73-1] 12 p1363 N73-21063
Development of system for analyzing aircraft sound levels for areas in vicinity of airports
[FAA-EQ-73-3] 12 p1364 N73-21064
Measurement and analysis of aircraft noise generated by general aviation aircraft during level flyovers
[TR-S-212] 12 p1366 N73-21081
Analysis of effects of aircraft noise in residential communities near London, England airport
[TT-7302] 14 p1599 N73-22966
Analysis of parameters affecting choice of engines for transport and combat aircraft during design process
15 p1732 N73-24048
Acoustic measurements for large model engine-over-wing configurations with conventional and powered lift, various flap settings, and comparison with engine-under-wing aircraft
[NASA-TM-X-68246] 15 p1735 N73-24070
Technique for realistic prediction and electronic synthesis of helicopter rotor noise
[AD-759955] 17 p1984 N73-26037
Annular duct liner curvature for aircraft noise reduction
[NASA-TN-D-7277] 17 p2063 N73-26688
Electroencephalographic and behavioral responses of humans to aircraft noise during sleep
[NASA-CR-2279] 18 p2109 N73-27058
Guide for airport planning and development to identify and resolve environmental problems caused by air pollution, water pollution, and aircraft noise
[PB-219957/8] 18 p2127 N73-27187
Development of noise index based on slow and fast noise level variation perception, and applied to aircraft noise data
[REPT-3/1973] 19 p2220 N73-27911
Measurement of sound power levels, power spectra, and directivity patterns for jet exit velocities of F-111A aircraft
[NASA-TN-D-7376] 20 p2361 N73-28989
Influence of noise requirements on STOL propulsion systems design
[NASA-TM-X-68280] 20 p2465 N73-29807
Design and tests of lift fan exhaust suppression system for future VTOL aircraft noise goals
[NASA-CR-121108] 20 p2466 N73-29812
Development of method for calculating near field noise level of free jet and influence of ground effect on noise produced by V/STOL aircraft operation
20 p2478 N73-29907
Analysis of acoustic properties and aerodynamic characteristics of engine over wing configuration with flow attached and unattached on upper surface of flaps
[NASA-TM-X-71419] 21 p2494 N73-30015
Development of computer program to predict aerodynamic noise levels of V/STOL aircraft at various points in flight trajectory
[PB-221140/7] 21 p2499 N73-30054
Calculation procedures for predicting noise-time histories and noise contours for various types of aircraft
[NASA-CR-114649] 23 p2741 N73-31945
Computer programs for predicting the noise-time histories and noise contours for five types of aircraft
[NASA-CR-114650] 23 p2741 N73-31946
Middle ear muscle reflex thresholds to various aircraft noises
[AD-764739] 24 p2886 N73-33048

**AIRCRAFT PARTS**
Nondestructive inspection techniques for examining catapult and arresting gear structures on E-2 aircraft
[AD-752492] 08 p0868 N73-17027
Reliability and operational safety of mechanical helicopter transmission boxes
12 p1357 N73-21012
Fail-safe and safe-life design of aircraft components made from Ti-alloys
[NLR-TR-72034-U] 22 p2685 N73-31510

**AIRCRAFT PERFORMANCE**
NT HELICOPTER PERFORMANCE
Simulated STOL aircraft flight to determine effects of cruise and terminal area maneuvers on ride quality and passenger comfort
01 p0003 N73-10016
Modeling data developed during manned simulation of large transport aircraft and comparison with training simulator results - Vol. 2
[NASA-CR-114494] 01 p0004 N73-10027
Numerical analysis of aircraft equilibrium spin characteristics based on nonlinear equations of motion and constrained minimization techniques
[NASA-TN-D-6926] 01 p0004 N73-10028
High angle of attack characteristics of high performance aircraft and correlation with dynamic directional-stability parameter
[NASA-TN-D-6993] 01 p0005 N73-10033
Digital computer program for solution of aircraft longitudinal stability characteristics at or near stall point
[AD-745557] 01 p0005 N73-10037
Development of computer program for complete simulation of factors involved in aircraft takeoff and landing
[AD-741942] 01 p0006 N73-10042
Curves for determining climb performance of aircraft
[ESDU-RJ1/2-AMEND-A] 02 p0124 N73-11011
Weapon delivery accuracy of F-4 aircraft with experimental stick to rudder interconnect to minimize lateral tracking error
[AD-746000] 02 p0126 N73-11027
Analysis of weight and inertia, aerodynamic derivatives, control characteristics, and stability augmentation systems for various military and civilian aircraft
[NASA-CR-2144] 03 p0252 N73-12039
Effects of wing camber and twist on longitudinal aerodynamic characteristics of wing-body configuration
[NASA-TN-D-7099] 04 p0369 N73-13002
Application of parameter estimation algorithm to obtain longitudinal aerodynamic derivatives from flight data for XC-142A aircraft in cruise conditions
[NASA-TN-D-7114] 04 p0372 N73-13025
Performance tests of Andover C short takeoff transport aircraft on grass, concrete and soil landing sites
[ARC-CP-1220] 04 p0373 N73-13034
Analysis of minimum time maneuvers by high thrust-to-weight aircraft using optimal control theory to determine open-loop control laws
[AD-748354] 04 p0374 N73-13039
Flight tests to determine lateral-directional handling qualities and roll-sideslip coupling of jet aircraft at high speeds
[AD-748435] 04 p0374 N73-13042
Improvement in V/STOL aircraft performance with yaw control augmentation to reduce cross coupling effects
[AD-749489] 04 p0375 N73-13046
Development of auxiliary lifting system to provide ferry capability for entry vehicles
[NASA-CASE-LAR-10574-1] 04 p0400 N73-13257
Analysis of compatibility between maneuver load control, relaxed static stability, and flying qualities requirements for various aircraft configurations
[AD-749479] 05 p0495 N73-14032
Analysis of parameters affecting aircraft stall and post stall gyrations to include aerodynamic configurations and pilot performance
06 p0616 N73-14999
Modifications of Jet Provost and Strikemaster trainer aircraft to provide adequate stall warning without excessive penalty on maximum lift at low speed
06 p0617 N73-15012
Post-stall aerodynamic characteristics of Harrier GR-1 aircraft and development of lift augmenting devices
06 p0618 N73-15014

Flight tests to determine buffet characteristics of four high performance aircraft during transonic maneuvers
06 p0618 N73-15017
Analysis of aerodynamic buffeting and related phenomena to include development of models for oscillatory rigid-body motion
06 p0618 N73-15018
Analysis of high subsonic and transonic characteristics of fighter aircraft and factors affecting aerodynamic boundaries for various wing design parameters
06 p0618 N73-15019
Aerodynamic design, engineering development, and flight testing of naval aircraft for operation at high angles of attack
06 p0618 N73-15020
Mission performance analysis of three supersonic transport configurations and effects of limitations on allowable engine noise
[NASA-TM-X-68178] 06 p0620 N73-15032
Analysis and application of load alleviation and mode suppression system for YF-12A aircraft to determine extent of design risks
[NASA-CR-2158] 06 p0620 N73-15033
Digital computer program for parametric analysis and optimization performance aircraft configurations and propulsion concepts
06 p0620 N73-15035
Aircraft performance optimization by including flight control system in design
[MBB-UFE-895-72-O] 06 p0622 N73-15048
Flight tests to determine lateral-directional performance and roll-sideslip coupling of T-33 aircraft at subsonic speed - Vol. 2
[AD-748436] 06 p0622 N73-15051
Procedure for determining rolling moment derivatives of aircraft due to rolling, yawing, and sideslip
[ESDU-AIRCRAFT-06.01.00] 07 p0735 N73-15978
Method for estimating changes in lift curve, drag, tail lift, and downwash from wing of aircraft due to ground effect in incompressible flow
[ESDU-72023] 07 p0736 N73-15993
Design modifications to improve static performance and lateral-directional dynamic stability of light aircraft
07 p0737 N73-15996
Analysis of controllability and steady-state response of parallel-redundant flight control systems
[NASA-CR-130354] 07 p0737 N73-15998
Development and application of computer programs for evaluating performance of powered-lift STOL aircraft to include static, takeoff, and landing performance
[NASA-TM-X-62217] 07 p0738 N73-16007
Technique for defining aircraft performance model from limited flight test data and predicted aerodynamic and propulsion system characteristics
[NASA-TN-D-7137] 07 p0738 N73-16008
Time vector technique for determining stability and control derivatives by simultaneous analysis of two maneuvers which differ by dependent control input
[NASA-TM-X-2722] 07 p0739 N73-16010
Wind tunnel tests to determine aircraft post-stall characteristics and to define boundaries for maintaining controlled aircraft flight
[AD-751461] 07 p0740 N73-16023
Analysis of control and power requirements for X-14 aircraft based on equations of motion with respect to set of axes fixed to aircraft
[NASA-CR-130760] 08 p0864 N73-16988
Conference on flight handling qualities and requirements
08 p0864 N73-16993
Performance tests of F-14 aircraft with jet blast deflector to determine effects of backflow of jet exhaust on aircraft launch operation
[AD-752018] 08 p0867 N73-17023
Development of methods for predicting performance characteristics of V/STOL aircraft - Vol. I
[AD-752557] 08 p0869 N73-17033
Development of takeoff airworthiness standards for new aircraft designs using motion simulators to compare performance and handling characteristics
[NASA-TN-D-7106] 09 p0983 N73-18031
Analysis of V/STOL aircraft design and operation to determine effects of noise problems and constraints with emphasis on helicopter performance
[AD-752447] 09 p0989 N73-18073
Development of mathematical models for C-130 aircraft to predict general trends and probable values for stability derivatives and mode parameters over flight envelope
[AD-753388] 09 p0989 N73-18076
Evaluation of energy maneuverability procedures in aircraft flight path optimization and performance estimation
[AD-754909] 11 p1236 N73-20035
Wind tunnel tests to determine aerodynamic characteristics of full scale H-126 aircraft using jet flap principle
[NASA-TN-D-7252] 12 p1355 N73-20997
Bibliography of supersonic transport aircraft data to include program management, systems engineering, aircraft structures, and operational considerations
[AD-755600] 12 p1365 N73-21076
Analysis of equations of aircraft dynamics and development of analog-digital simulation capability
[AD-755868] 12 p1365 N73-21077
Development of pilot model parameters to provide data base for multiloop, single controller, multi-input analysis of aircraft performance
[AD-755367] 12 p1365 N73-21078
Design and aerodynamic characteristics of tilt propellor aircraft for conducting flight research on V/STOL aircraft - Vol. 2
[NASA-CR-114442] 13 p1473 N73-21927
V/STOL lift fan commercial short haul transport aircraft for 1980 to 1985 period to include aircraft design, hover control, and cruise performance
[NASA-CR-2185] 13 p1473 N73-21930
Aerodynamic characteristics and performance of USSR An-12 turboprop aircraft to include handling technique and flight safety
[AD-756948] 13 p1476 N73-21953
Development of procedure for determining characteristics of aircraft roll coupling moment caused by flow induced by deflected wings and cross flow
[ISAS-488-VOL.-37-NO-14] 14 p1597 N73-22945
Analysis of aircraft rolling moment derivatives caused by rolling, yawing, and sideslip
[ESDU-06.01.00-AMEND-A-C]
14 p1599 N73-22963
Development of computer programs for numerical analysis of spinning aircraft based on Euler integration and minimization by gradient search
[AD-757257] 14 p1602 N73-22990
Simulation of wind gust effects on aircraft
14 p1645 N73-23338
Numerical analysis of aircraft rolling performance and effect of cross-coupling of lateral and longitudinal motions
[ARC-R/M-3349] 15 p1727 N73-24010
Theoretical investigation of longitudinal stability, control, and response characteristics of jet flap aircraft
[ARC-R/M-3272] 15 p1730 N73-24028
Development of stability augmentation systems for decoupling response of short takeoff and landing aircraft in longitudinal and lateral-directional flight modes
15 p1732 N73-24041
Development and application of aircraft performance prediction methods for subsonic and supersonic transport and fighter aircraft
[AGARD-LS-56] 15 p1732 N73-24042
Numerical methods for determining range and radius of action performance of transport and combat aircraft and effects of various parameters on performance
15 p1732 N73-24043
Methods for evaluating and predicting airfield performance of turbojet and turbofan aircraft operating in conventional and short takeoff modes
15 p1732 N73-24044
Development of methods for predicting aircraft flight maneuver and climb performance to show effects of excess power and load factor
15 p1732 N73-24045
Aerodynamic coefficients for calculating transport aircraft performance using wind tunnel and scale models
15 p1732 N73-24046
Mathematical models of aircraft mass and performance
15 p1732 N73-24047
Development of methods for presenting aircraft performance data and comparison of specific methods to show sources of discrepancies
15 p1733 N73-24050
Numerical analysis of aircraft takeoff performance based on phases of takeoff and forces exerted on aircraft as basis for aircraft design
15 p1733 N73-24051
Numerical analysis of minimum time climbing procedure and minimum fuel climbing procedure for typical subsonic aircraft
15 p1733 N73-24052
Development of computer program for determining minimum time trajectory and comparison with gradient method of computation
15 p1733 N73-24053
Development of two methods for optimizing design of subsonic, swept wing jet transport aircraft
15 p1733 N73-24054
Numerical analysis of minimum flight time for sail plane performance while performing cross country flight
[ME-68] 15 p1733 N73-24055
Application of cold thrust augmentation techniques for improved performance of short takeoff aircraft performance
[AD-758202] 15 p1735 N73-24073
Computer program for developing optimal stability augmentation system for high performance aircraft based on pilot parameters for pitch tracking task
[AD-757879] 15 p1736 N73-24076
Characteristics of quiet turbofan short takeoff aircraft for short haul air transportation and analysis of economic and sociological factors affecting operation Vol. 1
[NASA-CR-114612] 16 p1860 N73-25065
Performance of aircraft taxiing on dirt surfaces
[AD-756588] 16 p1861 N73-25077
Design and development of STOL and V/STOL aircraft to show design requirements, performance characteristics, and air traffic control problems
[PB-217102] 16 p1862 N73-25085
Research projects for improving maneuverability and buffet characteristics of fighter aircraft in high subsonic and transonic speed ranges
[NASA-TN-D-7131] 17 p1979 N73-25999
Simulator analysis of effect of engine response characteristics on approach and landing operations of powered lift aircraft with externally blown flaps
[NASA-TM-X-62265] 17 p1982 N73-26021
Statistical analysis of counting accelerometer data obtained on Navy and Marine fleet aircraft from 1 Jan. 1962 to 1 Jan. 1972
[AD-760321] 17 p1985 N73-26041
Proceedings of conference on military applications of V/STOL aircraft to include current and proposed research projects to meet military requirements
[AGARD-CP-126-VOL-1] 18 p2102 N73-27000
Review of V/STOL development programs to compare basic characteristics of XC-142A, X-19 and X-22A aircraft under various flight conditions
18 p2103 N73-27003
Design, development, and characteristics of Do-31 V/STOL aircraft to include solution of operational problems caused by ground effect and transition flight
18 p2103 N73-27004
Design concept, operational performance, and military employment of AV-8A Harrier aircraft
18 p2103 N73-27005
Flight test and evaluation of CL-84 tilt-wing V/STOL aircraft with application to specific military roles
18 p2103 N73-27007
Development of techniques for predicting point and path performance of light aircraft
[NASA-CR-2272] 18 p2105 N73-27022
Development and characteristics of control system for short takeoff transport aircraft for ride-smoothing effect
[NASA-CR-2276] 18 p2105 N73-27026
Analysis of minimum longitudinal stability for large delta wing transport aircraft during landing approach and touchdown using in-flight simulation techniques
[AD-761120] 18 p2106 N73-27036
Flight test F-106 aircraft to determine comparative time advantages of energy optimization climb and acceleration methodology
[AD-760571] 18 p2107 N73-27041
Analysis of three dimensional weakly controlled soaring procedures for increased sailplane performance
19 p2218 N73-27894
Analysis of aircraft structural loads in operational flight to determine effects of pilot performance and aircraft characteristics
[AGARD-R-608] 19 p2218 N73-27895
Systems analysis of quiet turbofan STOL aircraft for short-haul air transportation operations - Vol. 6
[NASA-CR-114611] 19 p2219 N73-27903
Flight tests of F-8C aircraft to determine effects of flaps on buffet characteristics and wing-rock onset at subsonic and supersonic speeds
[NASA-TM-X-2873] 19 p2220 N73-27905
Handling characteristics of V/STOL aircraft based on data obtained from flight tests, simulator operation, and analytical studies
[AGARD-R-577-PT-2] 19 p2220 N73-27906
Design and characteristics of augmentor wing cruise blowing valveless system for STOL passenger aircraft to define requirements for test facilities - Vol. 2
[NASA-CR-114570] 19 p2220 N73-27907
Development of rolling maneuver fatigue load data for F-5 and F-105 aircraft based on statistical flight loads data
[AD-761491] 19 p2221 N73-27915
Analysis of performance benefits for fighter aircraft by application of maneuver load control and relaxed static stability parameters
[AD-762299] 19 p2222 N73-27922
Numerical analysis of response of aircraft in three dimensional gust field to obtain aerodynamic load data on fuselage and tail structures
[AD-762511] 20 p2359 N73-28978
Simulator tests to determine short takeoff transport aircraft terminal area characteristics and longitudinal handling qualities
[MDC-J5575L] 20 p2360 N73-28983
Flight tests of modified C-8A aircraft to demonstrate augmentor wing, short takeoff concept - Vol. 2
[NASA-CR-114504] 21 p2494 N73-30017
Larger aircraft landing approach performance and altitude control during atmospheric turbulence and wind shear
[NLR-TR-72023-U] 21 p2497 N73-30036

Analysis of aircraft stability and control derivatives in turbulent conditions subject to random state disturbance
[AD-763741] 21 p2498 N73-30046

Longitudinal stability and control derivatives of XB-70 aircraft to compare flight test and theoretical data
[NASA-TM-X-2881] 22 p2613 N73-30940

Aerodynamic characteristics and aircraft performance of jet aircraft during takeoff run
[AD-764314] 22 p2615 N73-30959

Takeoff and landing performance characteristics and field length requirements for jet short takeoff transport aircraft with full span, externally blown flaps
[NASA-TN-D-7441] 23 p2741 N73-31939

Wind tunnel tests to determine low speed characteristics of large scale model of F-14A aircraft with emphasis on high lift configuration stability
[NASA-TM-X-62244] 23 p2741 N73-31940

Mathematical model for real time simulation of tilt rotor aircraft to evaluate aircraft performance and handling qualities
[NASA-CR-114601] 23 p2742 N73-31947

Flight test of structural mode control system installed in XB-70 aircraft to determine effectiveness of system under turbulent conditions
[NASA-TN-D-7420] 23 p2742 N73-31950

Stability and control characteristics of XB-70 aircraft at airspeeds up to Mach 3.0 and addition of lateral bobweight as auxiliary stabilization device
[NASA-TM-X-2933] 23 p2743 N73-31958

Rotary wing aircraft steep instrument approach limits
[MBB-UD-101-73-O] 23 p2745 N73-31969

Design, development, and evaluation of automatic departure prevention system and stall inhibitor for A-7 aircraft
[AD-764767] 23 p2745 N73-31972

Pilot rating of fighter aircraft in precision heading task using mathematical model for predicting aircraft performance
[AD-764695] 23 p2745 N73-31973

Mathematical model for predicting pilot rating of aircraft in pitch tracking under gust conditions
[AD-764698] 23 p2746 N73-31976

Flight simulation to determine manual control of flight path and airspeed for approach and landing of powered lift jet short takeoff aircraft
24 p2873 N73-32949

Characteristics and performance of piloted simulator for application as research tool in design and development of experimental aircraft
24 p2874 N73-32955

Effect of artificial longitudinal stability on aircraft performance, based on control configured vehicle concept
24 p2878 N73-32986

**AIRCRAFT PILOTS**

Statistical analysis of air combat situation evaluations conducted by US Navy pilots to detect differences caused by experience
[AD-747519] 03 p0261 N73-12119

Changes in circadian rhythm of aircraft pilot oral body temperature as result of transmeridian flights
[DLR-FB-73-01] 09 p0997 N73-18140

Methods for determining blood alcohol levels in pilots
12 p1371 N73-21124

Impact resistance of crash helmets for agricultural aviation pilots
[ARL/SM-NOTE-390] 22 p2623 N73-31014

**AIRCRAFT POWER SOURCES**
U AIRCRAFT ENGINES

**AIRCRAFT PRODUCTION**

Analysis of factors affecting future of commercial aircraft development to show effects on overall airline operations
23 p2865 N73-32900

**AIRCRAFT PROTUBERANCES**
U PROTUBERANCES

**AIRCRAFT RELIABILITY**

Application of reliability theory to determine risk function, probability of failure, under ultimate load, and wear-out process of aircraft structures
[ARL/SM-REPT-337] 04 p0480 N73-13925

Influence of aircraft reliability regulations on STOL takeoff and landing performance
[MBB-UH-13-72-O] 07 p0740 N73-16018

Reliability design of manned supersonic aircraft considering safety hazards
14 p1711 N73-23883

Effect of gust loads on wing and T-tail airworthiness requirements for short haul aircraft
[FOK-K-66] 16 p1859 N73-25058

Structural inspection for maintaining airworthiness of older aircraft
[NASA-TM-X-2845] 17 p2092 N73-26925

Program plan to develop criteria for airworthiness standards applied to short takeoff aircraft used as transport service
24 p2875 N73-32959

**AIRCRAFT SAFETY**

Development of in-flight fire detection and automatic suppression system for use on military helicopters
[AD-746630] 02 p0127 N73-11037

Inflight incident involving Boeing 747 aircraft encounter with unforecast clear air turbulence during flight from Japan to Hawaii on 12 April 1972
[NTSB-AAR-72-27] 03 p0252 N73-12038

In flight incident involving near miss of Boeing 720 aircraft and Convair 240 aircraft near Front Royal, Virginia on 26 Apr. 1972
[NTSB-AAR-72-30] 03 p0252 N73-12040

Development and optimization of fire extinguishers for use in passenger and crew compartments of aircraft
[AD-747496] 03 p0253 N73-12051

Nonflammable antifogging agent with low level, nonobjectionable odor and capable of being dispensed from aerosol container for in-flight visibility
[AD-746844] 03 p0321 N73-12617

Stability and control systems for advanced aircraft flight mechanics and safety
[AGARD-AR-48] 04 p0371 N73-13018

Development and operating principles of collision warning system for aircraft accident prevention
[NASA-CASE-HQN-10703] 04 p0446 N73-13643

Analysis of US general aviation accidents caused by stalls and spins for period 1967 to 1969
[NTSB-AAS-72-8] 05 p0493 N73-14018

Development, design, fabrication, and testing of a self-generating overheat detection system for USAF aircraft
[AD-749474] 05 p0495 N73-14031

Differential game theory for optimal collision avoidance between two aircraft moving in horizontal plane
[NASA-CR-129988] 05 p0577 N73-14701

Flight simulator tests to define minimum acceptable levels of static longitudinal stability for aircraft landing approach following failure of stability augmentation systems
[NASA-TM-X-62200] 06 p0620 N73-15034

Analysis of position determination accuracy obtainable with microwave landing guidance system
[NASA-TN-D-7116] 06 p0697 N73-15681

Development of halogenated hydrocarbon materials for use as fire and ignition suppressants for aircraft fuel tanks subjected to incendiary ammunition
[AD-755362] 12 p1365 N73-21079

Feasibility of liquid nitrogen fuel tank inerting system on commercial aircraft to prevent fuel tank explosions
[FS-140-72-1] 13 p1473 N73-21934

Development and characteristics of air traffic control radar and associated signal and display processing equipment
[FAA-RD-73-35] 16 p1875 N73-25178

Regulations for promoting safety in air navigation for municipal airport of Hartselle, Alabama
[PB-220087/1] 18 p2127 N73-27185

Installation of XM19 airfield landing mat and ancillary items
[AD-762137] 20 p2383 N73-29148

Procedures for evaluating fatigue quality of aircraft structures based on fatigue life, crack propagation, and rehidual strength
20 p2480 N73-29925

Objectives, scope of work, and funding requirements of research project for improvement of aircraft safety
[FAA-ED-18-1] 21 p2493 N73-30008

Analysis of glide path parameters, approach control system precision, and separation standards for extension of runway capacity under instrument flight rule conditions
[AD-763142] 21 p2578 N73-30657

Safety concerns with shuttle payloads, space stations and space shuttle orbiters
[NASA-CR-134022] 22 p2714 N73-31726

Program plan to develop criteria for airworthiness standards applied to short takeoff aircraft used as transport service
24 p2875 N73-32959

Electrified kerosene and gasoline aviation fuel during passage through pipes and filters of fuel tank reservoir
[AD-764941] 24 p2971 N73-33740

Relationships between performance, safety, cost, and schedule parameters to generate program models for total space program
[NASA-CR-135903] 24 p2993 N73-33919

Relationships between performance, safety, cost, and schedule parameters to generate program models for total space program
[NASA-CR-135902] 24 p2993 N73-33920

**AIRCRAFT SPECIFICATIONS**

Design, developmeat, and requirements for short takeoff transport aircraft for military applications using civil aircraft production procedures
18 p2103 N73-27011

Analysis of research and development programs involving construction of short takeoff transport aircraft in Germany
18 p2103 N73-27013

Three-axis, adjustable loading structure for testing soundness of aircraft skin by applying pressure
[NASA-CASE-FRC-10051-1] 21 p2547 N73-30416

**AIRCRAFT STABILITY**

**NT HOVERING STABILITY**

Simulated STOL aircraft flight to determine effects of cruise and terminal area maneuvers on ride quality and passenger comfort
01 p0003 N73-10016

Digital computer program for solution of aircraft longitudinal stability characteristics at or near stall point
[AD-745557] 01 p0005 N73-10037

Definitions of aircraft longitudinal stability to account for effects of aircraft structure distortion and compressibility effects
[ESDU-00.00.03] 02 p0124 N73-11010

Survey of aerospace industry to determine various techniques used in considering interactions of handling qualities, stability, control, and load alleviation devices on structural loads
[AGARD-R-593] 02 p0125 N73-11020

Aircraft glide path stability under speed constraint
[ARC-R/M-3705] 03 p0248 N73-12008

Analysis of weight and inertia, aerodynamic derivatives, control characteristics, and stability augmentation systems for various military and civilian aircraft
[NASA-CR-2144] 03 p0252 N73-12039

Design, development, and evaluation of fluidic emergency thrusters for aircraft stabilization
[NASA-CR-114490] 03 p0252 N73-12041

Linear differential equations describing aircraft lateral motion in presence of atmospheric turbulence
[AASU-311] 03 p0253 N73-12045

Effects of wing camber and twist on longitudinal aerodynamic characteristics of wing-body configuration
[NASA-TN-D-7099] 04 p0369 N73-13002

Stability and control systems for advanced aircraft flight mechanics and safety
[AGARD-AR-48] 04 p0371 N73-13018

Application of parameter estimation algorithm to obtain longitudinal aerodynamic derivatives from flight data for XC-142A aircraft in cruise conditions
[NASA-TN-D-7114] 04 p0372 N73-13025

Flight tests to determine lateral-directional handling qualities and roll-sideslip coupling of jet aircraft at high speeds
[AD-748435] 04 p0374 N73-13042

Real time hybrid simulation of tied down helicopter for optimal stability control
05 p0494 N73-14024

Flight simulator tests to define minimum acceptable levels of static longitudinal stability for aircraft landing approach following failure of stability augmentation systems
[NASA-TM-X-62200] 06 p0620 N73-15034

Flight tests to determine lateral-directional performance and roll-sideslip coupling of T-33 aircraft at subsonic speed - Vol. 2
[AD-748436] 06 p0622 N73-15051

Characteristics of nonlinear self adjusting and variable structure automatic flight control system for piloted and pilotless aircraft
[AD-750502] 06 p0624 N73-15062

Aerodynamic characteristics of helicopters with sling loads in hovering and near-hovering conditions
[AD-750618] 06 p0625 N73-15073

Procedure for determining rolling moment derivatives of aircraft due to rolling, yawing, and sideslip
[ESDU-AIRCRAFT-06.01.00] 07 p0735 N73-15978

Design modifications to improve static performance and lateral-directional dynamic stability of light aircraft
07 p0737 N73-15996

Digital simulation language for flight dynamic tests, exemplified by Fiat G-91 and Dornier Do-31 aircraft
[BMVG-FBWT-72-21] 07 p0740 N73-16019

Wind tunnel tests to determine aircraft post-stall characteristics and to define boundaries for maintaining controlled aircraft flight
[AD-751461] 07 p0740 N73-16023

Development of automatic system for controlling aircraft under turbulent atmospheric conditions to provide pitch stabilization
[AD-751148] 07 p0741 N73-16028

Analysis of control and power requirements for X-14 aircraft based on equations of motion with respect to set of axes fixed to aircraft
[NASA-CR-130760] 08 p0864 N73-16988

Summaries of papers presented to conference concerning aircraft stability and control
[AGARD-CP-119] 08 p0864 N73-16989

Relationship between mission requirements of piloted aircraft stability and maneuverability
08 p0864 N73-16995

Design criteria for satisfactory stability and control of military aircraft
08 p0865 N73-16996

Prediction of aeroelastic hinge moment effects on stability and control
08 p0866 N73-17006

Influence of powered controls on stability and maneuverability
08 p0866 N73-17008

Artificial stabilization to correct control deficiencies for high performance aircraft
08 p0866 N73-17009
Automatic method for determining stability and control derivatives from flight data
08 p0866 N73-17012
Design and development of stability augmentation system to eliminate coupling effects during landing of short takeoff aircraft
[NASA-CR-130543] 08 p0867 N73-17021
Development of mathematical models for C-130 aircraft to predict general trends and probable values for stability derivatives and mode parameters over flight envelope
[AD-753388] 09 p0989 N73-18076
Planform shape effects on aerodynamic center location and aeroelasticity of fighter aircraft
[NASA-CR-2117] 13 p1469 N73-21896
Computer program for calculating aerodynamic stability and drag of slender aircraft at subsonic and supersonic speeds
[NASA-CR-112229] 13 p1469 N73-21897
Structural influence coefficient matrix for computer simulation of aerodynamic aircraft stability
[NASA-CR-112230] 13 p1469 N73-21898
Analysis of minimum longitudinal stability for large delta wing transport aircraft during landing approach and touchdown using inflight simulator
[TR-5084-F-1-VOL-1] 14 p1601 N73-22984
Development of computer programs for numerical analysis of spinning aircraft based on Euler integration and minimization by gradient search
[AD-757257] 14 p1602 N73-22990
Numerical analysis of aircraft rolling performance and effect of cross-coupling of lateral and longitudinal motions
[ARC-R/M-3349] 15 p1727 N73-24010
Development of stability augmentation systems for decoupling response of short takeoff and landing aircraft in longitudinal and lateral-directional flight modes
15 p1732 N73-24041
Computer program for developing optimal stability augmentation system for high performance aircraft based on pilot parameters for pitch tracking task
[AD-757879] 15 p1736 N73-24076
Application of ground effect machine landing systems for recovery of remotely piloted vehicles
[AD-758789] 15 p1736 N73-24079
Wind tunnel stability tests to determine static longitudinal and lateral characteristics of full-scale model of light, single engine, high wing aircraft
[NASA-TN-D-7149] 16 p1860 N73-25068
Research projects for improving maneuverability and buffet characteristics of fighter aircraft in high subsonic and transonic speed ranges
[NASA-TN-D-7131] 17 p1979 N73-25999
Development of aerodynamic control system to control flutter over large range of oscillatory frequencies using stability augmentation techniques
[NASA-CASE-LAR-10682-1] 17 p1980 N73-26004
Longitudinal stability derivatives from flight data by model with automatic parameter adjustment
[DLR-FB-73-13] 17 p1984 N73-26033
Numerical analysis of lift and roll stability of ram air cushion vehicle to determine equations for rolling moment coefficient
[PB-219820/8] 18 p2106 N73-27032
Design and development of fixed gain control system for longitudinal axis of C-141 aircraft fly-by-wire control
[AD-760763] 18 p2107 N73-27038
Wind tunnel tests to determine effects of modified engine nacelle on stability and control characteristics of DC-9 aircraft with emphasis on deep stall regime
[NASA-CR-121220] 19 p2219 N73-27904
Flight tests of F-8C aircraft to determine effects of flaps on buffet characteristics and wing-rock onset at subsonic and supersonic speeds
[NASA-TM-X-2873] 19 p2220 N73-27905
Handling characteristics of V/STOL aircraft based on data obtained from flight tests, simulator operation, and analytical studies
[AGARD-R-577-PT-2] 19 p2220 N73-27906
Aeroelastic and dynamic studies of technology applicable to tilting rotor vertical takeoff aircraft with emphasis on propeller whirl instability - Vol. 1
[NASA-TM-X-69497] 20 p2359 N73-28976
Numerical analysis of response of aircraft in three dimensional gust field to obtain aerodynamic load data on fuselage and tail structures
[AD-762511] 20 p2359 N73-28978
Analysis of aircraft stability and control derivatives in turbulent conditions subject to random state disturbance
[AD-763741] 21 p2498 N73-30046
Development of theory for adaptive control of aircraft in atmospheric turbulence using stochastic identification method
[AD-763739] 21 p2498 N73-30051
Longitudinal stability and control derivatives of XB-70 aircraft to compare flight test and theoretical data
[NASA-TM-X-2881] 22 p2613 N73-30940
Wind tunnel and rotor whirl cage tests to determine stability and control parameters of scale model of tilting rotor aircraft model - Vol. 6
[NASA-CR-114615] 22 p2614 N73-30950
Flight test of structural mode control system installed in XB-70 aircraft to determine effectiveness of system under turbulent conditions
[NASA-TN-D-7420] 23 p2742 N73-31950
Stability and control characteristics of XB-70 aircraft at airspeeds up to Mach 3.0 and addition of lateral bobweight as auxiliary stabilization device
[NASA-TM-X-2933] 23 p2743 N73-31958
Jet aircraft flight tests for stability derivative determination comparing various measuring techniques
[BMVG-FBWT-73-12] 23 p2745 N73-31971
Computer program for predicting pilot rating of pitch stability of T-33 aircraft under vertical turbulence conditions
[AD-764696] 23 p2745 N73-31974
Computerized simulation of DC-8 aircraft during landing approach under wind shear conditions
[AD-764697] 23 p2745 N73-31975
Mathematical model for predicting pilot rating of aircraft in pitch tracking under gust conditions
[AD-764698] 23 p2746 N73-31976
Development and evaluation of active control system to provide ride smoothing on short takeoff aircraft
24 p2873 N73-32951
Requirements of flight control systems with regard to aircraft stability and attitude control
[DLR-MITT-72-05] 24 p2877 N73-32978
Nonlinear feedback control concepts for variable stability aircraft
24 p2877 N73-32979
Effect of artificial longitudinal stability on aircraft performance, based on control configured vehicle concept
24 p2878 N73-32986
Effects of artificial aircraft stability control on damping, and static stability recovery by controllers
24 p2878 N73-32987
Design of pitching axis control system for aircraft with artificial stability
24 p2878 N73-32988

**AIRCRAFT STRUCTURES**
NT AIRFRAMES
NT FUSELAGES
Analysis of dynamic aircraft landing loads, and a proposal for rational design landing load requirements
01 p0002 N73-10010
Engineering data for aeronautical structures under loads
[ESDU-SS2] 01 p0111 N73-10918
Development and fabrication of graphite polyimide wing box beam
[NASA-CR-123959] 04 p0480 N73-13923
Fatigue behavior of hat section stringer stiffened panels compressed in post-buckling range
[AD-748855] 04 p0482 N73-13938
Fatigue tests of aluminum alloy specimens used for aircraft structures under simulated acoustic loading conditions
[ESDU-72015] 06 p0723 N73-15899
Estimates of LC stress response in aircraft skin panels to random acoustic loads
[ESDU-67028-AMEND-A] 06 p0723 N73-15904
Applicability of composite materials in aircraft structure and engine design
[NASA-TT-F-14648] 07 p0811 N73-16576
Random load fatigue of aircraft structures
[AGARD-CP-118] 07 p0851 N73-16896
Fatigue life assessment of aircraft structures based on random or programmed fatigue tests and loadings
07 p0851 N73-16897
Physical aspects of fatigue damage accumulation, including interaction and sequence effects
07 p0851 N73-16899
Analysis of factors affecting crashworthiness of light aircraft to show nature of damage to aircraft and hazards to flight crews
[FAA-TR-FS-70-592-120A] 09 p0984 N73-18032
Research projects in structural reliability engineering for transport vehicles
12 p1466 N73-21878
Parametric and optimization techniques for aircraft design synthesis to show principal lines of data flow for component development
15 p1732 N73-24049
Flight evaluation of composite for use in aircraft structures
[NASA-TM-X-2761] 17 p2049 N73-26579
Use of reinforced boron and carbon fiber composites in aircraft structures
18 p2165 N73-27484
Construction of glider aircraft using glass fiber and carbon fiber reinforced plastic composite materials for weight reduction and increased strength
18 p2165 N73-27486
Application of composite materials and sandwich structures to reduce vulnerability of aircraft structures to projectile impact
18 p2165 N73-27487
Design and manufacturing of composite materials with organic matrices for use in aerospace vehicle structures subjected to high temperatures
18 p2165 N73-27489
Development of fiber reinforced composite materials for application to air breathing engines, aeronautical vehicles, and spacecraft components
18 p2166 N73-27491
Gluing technology for airframe construction
[AD-761496] 19 p2221 N73-27912
Development of mathematical model for determining replacement criteria for aircraft structural components
[AD-762226] 19 p2222 N73-27921
Strain gage bridge calibrations on wing structure at elevated temperatures to establish thermal and mechanical loads due to aerodynamic heating
[NASA-TN-D-7390] 19 p2348 N73-28883
Summaries of papers presented to AGARD conference on random load fatigue
[AGARD-AR-54] 19 p2348 N73-28884
Analysis of response and fatigue characteristics of light alloy integrally machined planks with emphasis on acoustic fatigue properties
20 p2479 N73-29912
Methods for determining aircraft structural response to acoustic fatigue
20 p2479 N73-29913
Structural response and endurance tests of aircraft structural components to determine effect of critical environment on acoustic fatigue
20 p2480 N73-29920
Application of siren as test technique for determining response and life of aircraft structures subject to engine noise field excitation
20 p2480 N73-29922
Development of experimental program for determining response and sonic fatigue resistance of lightweight aircraft structures
20 p2480 N73-29923
Development of procedures for predicting fatigue life of aircraft structures based on fracture mechanics, crack propagation, and residual static strength anlysis
[AGARD-LS-62] 20 p2480 N73-29924
Procedures for evaluating fatigue quality of aircraft structures based on fatigue life, crack propagation, and residual strength
20 p2480 N73-29925
Procedures for predicting fatigue life of aircraft flying under various load conditions using data obtained by counting accelerometer
20 p2481 N73-29927
Decision methodology on static tests of large aircraft vehicles
[NASA-CR-124366] 21 p2604 N73-30866

**AIRCRAFT SURVIVABILITY**
Application of composite materials and sandwich structures to reduce vulnerability of aircraft structures to projectile impact
18 p2165 N73-27487

**AIRCRAFT TIRES**
Braking effects on aircraft tire tread wear and runway surface characteristics
[NASA-TN-D-6963] 02 p0125 N73-11021
Aircraft tire dynamometer tests to determine effects of tire deflection on rolling resistance and tire life
[AD-746304] 02 p0127 N73-11031
Nondestructive ultrasonic testing of aircraft tires
[AD-747633] 03 p0309 N73-12521
Dynamic testing and structural modeling of aircraft tire properties
[NASA-CR-2219] 09 p0985 N73-18042
Technique for determining mechanical properties of full-size aircraft tires from tests conducted with small-scale model tires
[NASA-CR-2220] 12 p1357 N73-21006
Analysis of effect of grooved runway configurations on aircraft tire braking traction on flooded runway surfaces
[NASA-TN-D-7215] 12 p1363 N73-21057
Performance tests to determine cornering characteristics of cantilever aircraft tire on dry, damp, and flooded runway surfaces over range of yaw angles
[NASA-TN-D-7203] 12 p1363 N73-21058
Performance tests to determine fore and aft elastic response characteristics of aircraft tires with bias ply, bias-belted, and radial-belted design
[NASA-TM-X-69570] 20 p2360 N73-28987
Flight tests of folding sidewall, expandable tires on C-131 aircraft to determine operation of inflation and deflation system
[AD-762730] 20 p2361 N73-28993
Performance tests to determine cornering characteristics of aircraft tire under various runway conditions, ground speeds, and yaw angles with and without braking
[NASA-TN-D-7351] 23 p2742 N73-31948
Design requirements and characteristics of toroidal, continuous wound aircraft tire
[AD-764888] 23 p2746 N73-31977

**AIRCRAFT WAKES**
NT HELICOPTER WAKES
NT PROPELLER SLIPSTREAMS
NT SLIPSTREAMS

Development of wake vortex monitoring system using laser Doppler sensors for analyzing vortex flow field
[NASA-CR-123921] 02 p0152 N73-11229
Results of analytical methods for predicting wing vortex strength compared with results of flight investigation of wake characteristics of several large jet transport aircraft
[NASA-TN-D-6904] 03 p0251 N73-12033
Systems simulation for airport trailing vortex warning system
[NASA-TM-X-64704] 03 p0280 N73-12267
Development of system for predicting movement and decay of aircraft-generated vortices in air corridors near air terminals using meteorological information
[LMSC/HREC-D306226] 06 p0620 N73-15036
Analysis of aircraft trailing vortices to show formation and breakdown for various aircraft wing configurations
[ME/A-72-1] 08 p0895 N73-17247
Chemically reacting wave of aircraft flying at subsonic and supersonic velocity in upper troposphere and stratosphere
[AD-754918] 11 p1287 N73-20447
Flight investigation to determine velocity and persistence characteristics of trailing vortices generated by jumbo jet transport
[NASA-TN-D-7172] 12 p1364 N73-21058
Flight tests to determine characteristics of vortex and turbulent wake generated by DC-10 aircraft for development of air traffic control separation criteria
[REPT-73-00470] 13 p1474 N73-21938
Development of wake vortex avoidance system for airports to reduce hazards caused by aircraft wakes and permit increased utilization of terminal facilities
[FAA-ED-21-1] 14 p1645 N73-23342
Ship model basin for simulating aircraft vortex wake
[AD-758893] 16 p1890 N73-25291
Calculation of wake vortices behind wings of transport aircrafts in holding, takeoff, and landing configurations
[FAA-RD-73-42] 17 p1983 N73-26027
Wake model program for computing wake height and width
[PB-218820/9] 18 p2106 N73-27030
Analysis of pressure distribution on plane ground surface under aircraft flying at low altitude with subsonic velocity
[FFA-AU-634-PT-2] 18 p2129 N73-27206
Analysis of random motions of vortex elements behind aircraft wing and design of vortex arrays to reduce wake-vortex to small aircraft
[NASA-TM-X-62304] 24 p2877 N73-32976

**AIRCREWS**
U FLIGHT CREWS

**AIRFIELD SURFACE MOVEMENTS**
Analysis of loading conditions imposed on commercial aircraft during turning maneuvers on ground
[NASA-TN-D-7132] 04 p0372 N73-13027
Hazards related to use of jet thrust power
[PB-211593] 05 p0497 N73-14046
Systems analysis of civil airport surface traffic control
[FAA-ED-08-1] 15 p1808 N73-24655
Airport surface traffic control requirements analysis
[AD-762442] 20 p2383 N73-29147

**AIRFOIL CHARACTERISTICS**
U AIRFOILS

**AIRFOIL PROFILES**
NT WING PROFILES
NT WING SPAN
Numerical analysis of induced velocities of wing with curved axis not perpendicular to velocity of incoming flow
[AD-749843] 05 p0497 N73-14048
Airfoil with cambered trailing edge section for supersonic flight
[NASA-CASE-LAR-10585-1] 06 p0613 N73-14981
Design characteristics and performance of airfoils with high lift at low and medium subsonic speeds and various angles of attack
06 p0616 N73-15004
Aerodynamic configurations and characteristics of airfoils designed to reduce formation of shock waves during supersonic flight
[NASA-TT-F-749] 07 p0736 N73-15987
Technique for predicting shock envelopes and pressure distributions for two dimensional airfoil at angles of attack producing shock detachment and subsonic flow
[NASA-TN-D-7197] 09 p0979 N73-18001
Wind tunnel tests to determine flow characteristics of stalled two dimensional airfoil
[NASA-CR-130919] 09 p0982 N73-18020
Minimum weight design of supersonic aircraft wing with finite element modeling to meet strength, stability, frequency, and flutter requirements
12 p1356 N73-21003
Modane-Avricux transonic blowdown wind tunnel for two dimensional flow airfoil profile study
[ONERA-NT-203] 15 p1762 N73-24281
Analysis of Kutta-Joukowsky condition in three dimensional flow with application to vortex sheet attachment to wing surface
[NASA-TT-F-14918] 15 p1767 N73-24319

**AIRFOIL SECTIONS**
U AIRFOIL PROFILES

**AIRFOIL THICKNESS**
U AIRFOIL PROFILES

**AIRFOILS**
NT AILERONS
NT CAMBERED WINGS
NT CARET WINGS
NT CRUCIFORM WINGS
NT DELTA WINGS
NT FIXED WINGS
NT FLAPS [CONTROL SURFACES]
NT FLEXIBLE WINGS
NT HORIZONTAL TAIL SURFACES
NT INFINITE SPAN WINGS
NT JET FLAPS
NT LEADING EDGE SLATS
NT LIFTING ROTORS
NT LOW ASPECT RATIO WINGS
NT PARAWINGS
NT PROPELLER BLADES
NT RECTANGULAR WINGS
NT RIGID ROTORS
NT RIGID WINGS
NT RING WINGS
NT ROTARY WINGS
NT SLENDER WINGS
NT SPOILERS
NT SUPERSONIC AIRFOILS
NT SWEPT WINGS
NT SWEPTBACK WINGS
NT THIN AIRFOILS
NT THIN WINGS
NT TILTING ROTORS
NT TIP DRIVEN ROTORS
NT TRAILING-EDGE FLAPS
NT UNCAMBERED WINGS
NT UNSWEPT WINGS
NT VARIABLE SWEEP WINGS
NT WING FLAPS
NT WINGS
Development of computer program for analyzing mono-element and multi-element airfoils at subsonic speed with attached air flow - Vol. 2
[AD-740124] 01 p0031 N73-10242
FORTRAN computer program for annular airfoil pressure distribution at subsonic speeds
[ARC-CP-1217] 03 p0248 N73-12004
Wind tunnel tests of longitudinal aerodynamic characteristics of aspect ratio airfoil with 0.098 chord blowing flap
[NASA-TM-X-2675] 04 p0421 N73-13431
Single stage experimental evaluation of D and E stage design of tandem airfoil rotor and stator blading for compressors
[NASA-CR-121008] 04 p0463 N73-13779
Development of iterative procedure for analysis of arbitrary multi-element airfoils in viscous flow
[AD-749484] 05 p0496 N73-14042
Computer program for designing leading edge slats for producing specified pressure distribution on main airfoil
[AD-749485] 05 p0496 N73-14043
Wing impulse theory applied to determination of propeller slipstream influence on wing aerodynamic characteristics, using airfoil of finite span
[AD-749726] 05 p0498 N73-14051
Numerical analysis of development of incompressible, symmetrical turbulent wake flows downstream of airfoils using integral method of momentum and energy
[NAL-TR-292] 06 p0614 N73-14986
Development of finite difference procedure to calculate steady flows over several classes of airfoils under inviscid transonic flow conditions
[NASA-CR-2186] 06 p0614 N73-14989
Development of two experimental approaches for analyzing two dimensional flow on high lift devices
06 p0617 N73-15005
Analysis of aerodynamic processes occurring in flow past unpowered multi-element airfoils in high lift attitude
06 p0617 N73-15007
Analysis of aerodynamic stall characteristics of wing sections with high lift devices in two dimensional flow
06 p0617 N73-15008
Development of procedure for determining characteristics of high lift systems where viscous effects dominate
06 p0617 N73-15009
Aerodynamic configurations of swept wings to improve lift performance at stall in higher range of subsonic speeds
06 p0617 N73-15010
Coanda effect on plane jet flowing over curved surface considering two dimensional flow over airfoil
[DLR-FB-71-46] 06 p0621 N73-15043
Method for estimating aerodynamic characteristics of airfoils in compressible inviscid flow based on thickness and camber line parameters
[ESDU-72024] 07 p0735 N73-15981
Short takeoff aircraft lift augmentation and prevention of airflow separation on cambered elliptical airfoil section using circulation control
[AD-751045] 07 p0736 N73-15992
Air foils based on utilization of jet flap principle
[AD-751075] 07 p0774 N73-16283
Analysis of uniform jet flow around airfoil with separated shock wave at low supersonic velocities of incident flow
[NASA-TT-F-14813] 08 p0896 N73-17259
Two dimensional cascade test of highly loaded, low solidity, tandem airfoil turbine rotor blade
[NASA-TM-X-2729] 08 p0954 N73-17814
Measurement of unsteady pressures developed on harmonically oscillating wing planform in three dimensional compressible flow
[DLR-FB-72-55] 09 p0980 N73-18007
Analysis of aerodynamic stall characteristics of airfoils at various angles of attack with application to control forces of H-53 helicopter
[AD-752917] 09 p0986 N73-18053
Jet deflection characteristics of jet-flapped airfoil with Coanda deflection surfaces based on velocity distribution and flow angle measurements for static operation
[AD-753618] 09 p0989 N73-18074
Calculation of flow through airfoils in cascade to show pressure distribution under conditions of two dimensional incompressible flow with boundary layer separation at trailing edge
[DLR-FB-72-62] 09 p1014 N73-18276
Numerical solution to transonic airfoil problems
[AD-753390] 09 p1018 N73-18304
Analysis of flow field around two dimensional airfoil of arbitrary shape
[AD-753387] 09 p1019 N73-18320
Transonic wind tunnel tests of two dimensional airfoil fitted with square and convex semicircular blunt bases to determine aerodynamic drag coefficients
[ARL/A-NOTE-336] 10 p1103 N73-18994
Effect of two dimensional suction flows into double intakes on upper surface of Joukowski airfoil for application to vertical takeoff and landing aircraft
[AD-754208] 10 p1104 N73-19003
Wind tunnel tests to determine effects of nozzle geometry and upper surface blowing on aerodynamic characteristics of 14 percent thick airfoil
[NASA-CR-114560] 11 p1231 N73-19998
Design of airfoil sections for low Reynolds numbers based on requirement to achieve transition upstream of major adverse pressure gradient
12 p1355 N73-20995
Analysis of optimum pressure distribution on multi-element airfoils to obtain conditions for maximum lift coefficient
12 p1355 N73-20996
Calculation and measurement of aerodynamic forces on oscillating airfoil with and without aerodynamic stalling
12 p1361 N73-21042
Effect of rotary wing airfoil modifications on performance, stability, and control of helicopters
12 p1361 N73-21045
Development of algorithm for calculating inviscid flow about arbitrary planform rotors and application to analyzing various rotary wing configurations
12 p1362 N73-21048
Generation of aerodynamic noise by turbulent wake behind rotary wing airfoil and relationship to drag and lift coefficients
12 p1362 N73-21054
Effects of aeroelasticity on performance of rotary wings and procedures for predicting aerodynamic forces on rotary wing blades
14 p1598 N73-22952
Iterative method for analyzing feathering characteristics in airfoil whirlwinds
[DEP/PRA/NT/88/72] 14 p1600 N73-22968
Design and evaluation of two airfoils for helicopter rotors for reduction of rotor power requirements
[NASA-CR-112297] 14 p1601 N73-22977
Wall interference effects at Mach 1 on airfoils in transonic wind tunnels
[AD-757534] 14 p1646 N73-23349
Application of integral relations to analyzing inviscid supercritical flow about lifting airfoils with embedded shock wave
[AD-755762] 14 p1651 N73-23390
Numerical analysis of pressure distribution in incompressible flow on two dimensional airfoils near ground
[ARC-R/M-3238] 15 p1726 N73-24000
Application of conformal mapping procedures for designing airfoil shapes with high design lift coefficients
[AD-757813] 15 p1731 N73-24040
Stalling characteristics of airfoil in laminar viscous incompressible fluid with consideration of starting vortex and separation bubble
[AD-758831] 15 p1769 N73-24334
Application of Kelvin impulse theory for computing lift on airfoils and analysis of circulation around airfoil to produce lift
16 p1851 N73-24997
Wind tunnel tests to determine pressure distributions for four percent thick, circular arc, biconvex airfoil at transonic speeds
[ARC-R/M-3180] 16 p1852 N73-25002

Force measurements and pressure distributions on three Gottinger airfoil profiles during transition from laminar to turbulent boundary layer flow
[NASA-TT-F-14959] 17 p1979 N73-26000
Underwater vortex field generation in wake of rectangular airfoil
[NASA-TM-X-62274] 17 p2014 N73-26288
Effects of mass injection of tip vortex on airfoil performance at transonic speeds
[AD-760363] 17 p2016 N73-26304
Design and development of two dimensional airfoil with optimum drag divergence characteristics at transonic speeds
[NAL-TR-299] 18 p2101 N73-26994
Numerical analysis of two dimensional incompressible potential flow around system of arbitrary airfoils using relaxation method
[NAL-TR-309] 18 p2130 N73-27212
Two dimensional flow, low speed wind tunnel tests of trapped vortex-high lift airfoil to reduce blowing requirements for lift augmentation
[AD-762077] 19 p2218 N73-27893
Analysis of transonic scaling effect on quasi, two-dimensional airfoil model of C-141 aircraft
[AD-762285] 19 p2222 N73-27924
Calculation of incompressible potential flow of airfoils by conformal mapping potential flow of lifting circles onto airfoils by double transformations
[ARC-R/M-3717] 21 p2492 N73-30002
Analysis of drag and pressure measurements made in subsonic wind tunnel tests on two annular airfoils noting relation between pressure distribution in compressible flow and at high speed
[ARC-R/M-2718] 21 p2492 N73-30003
Wind tunnel tests to determine transient wake velocities behind three stalled wing configurations at Reynolds numbers up to 4.8 million
[AD-763468] 21 p2498 N73-30050
Development of computer program for determining airfoil pressure distribution for subcritical attached viscous flow
[NAL-TR-248] 21 p2523 N73-30236
Three-dimensional compressible turbulent boundary layer for subsonic and transonic flow over yawed airfoil
[AD-763730] 21 p2526 N73-30258
Measurement of temperatures of airfoil immersed in stream of combustion gases to determine effectiveness of two phase cooling system
[ARL/ME-338] 21 p2605 N73-30876
Finite element analysis and computer graphics visualization of unsteady flow around pitching and plunging airfoils
[NASA-CR-2249] 22 p2611 N73-30926
Wind tunnel tests to determine two dimensional characteristics of airfoil optimized for maximum lift coefficient at various angles of attack
[NASA-TN-D-7071] 22 p2611 N73-30929
Correlation between wind tunnel data and finite difference solutions for viscous and wind tunnel effects in transonic flows over airfoils
[AD-764133] 22 p2612 N73-30936
Numerical analysis of laminar unsteady flow around airfoil in viscous, incompressible fluid
22 p2649 N73-31226
Aerodynamic configurations of series of airfoils used in parametric studies of drag-rise Mach number
[ESDU-71020] 22 p2650 N73-31228
Derivation of charts for predicting drag-rise Mach number for airfoils with specified upper surface pressure distribution
[ESDU-71019] 22 p2650 N73-31229
Prediction of aerodynamic characteristics of airfoils at transonic speeds including effects of fluid viscosity
[AD-763295] 22 p2654 N73-31260
Designing axial compressor airfoils with camber lines of arbitrary shape
[AD-765165] 23 p2832 N73-32636

**AIRFRAME MATERIALS**

Development of procedures for determining contamination characteristics of materials which become volatile in space environment
[NASA-CR-130132] 05 p0600 N73-14878
Crack growth characteristics of steel and structural failure of F-111 aircraft frame
[AD-752223] 08 p0868 N73-17024
Analysis of physiological and toxicological aspects of smoke produced by combustion of aircraft interior materials - Part 1
[FAA-RD-73-50-PT-1] 18 p2104 N73-27014
Physio-chemical analysis of flammability characteristics and thermal degradation of rigid and flexible urethane foams used in aircraft structures - Part 2
[FAA-RD-73-50-PT-2] 18 p2105 N73-27025
Gluing technology for airframe construction
[AD-761496] 19 p2221 N73-27912

**AIRFRAMES**

Application of integral nonlinear programming and random search techniques for determining minimum weight of reinforcing structures commensurate with strength requirements
01 p0112 N73-10929
Application of scatter factors for various Weibull-shaped parameters, fleet sizes, and level of reliability for aircraft structures
[NASA-CR-2100] 01 p0113 N73-10934
Four-phase airframe fatigue program for bending tests of aluminum alloy box beams
[AD-744673] 01 p0114 N73-10943
Application of reliability based static strength criteria system to analysis of C-141 aircraft - Vol. 1
[AD-742260] 02 p0126 N73-11024
Implementation of reliability based strength criteria system for determining service life of C-141 aircraft structures - Vol. 2
[AD-742261] 02 p0126 N73-11025
Analysis of fatigue crack propagation characteristics of steel structures in F-111 aircraft under specific flight loading spectra
[AD-746343] 02 p0127 N73-11033
Development of airframe integrity investigation procedures to determine structural deficiencies and modifications required to airframes for increased service life
[AD-746881] 03 p0253 N73-12049
References on fatigue and fracture of aircraft structures and materials to include instruments, sonic fatigue, and mechanical fasteners
[AD-748100] 03 p0254 N73-12053
Procedures for using liquid crystal tape for thermographic testing of bonded structures for aircraft
[NASA-CR-123932] 03 p0300 N73-12451
Quasi area rule for heat addition in transonic and supersonic flight including determination of optimum shapes with propulsion to minimize wave drag
[AD-747772] 03 p0352 N73-12867
Design and development of instrument for measuring aerodynamic loads and fatique characteristics of aircraft structures
[AGARD-R-597] 04 p0371 N73-13019
Helicopter design data to include kinematic and power diagrams of basic components of helicopter structures
[AD-748751] 04 p0373 N73-13035
Technology of aircraft construction to include manufacturing of parts from plastics, ceramics, and nonmetallic materials
[AD-749558] 04 p0374 N73-13044
Application of reliability theory to determine risk function, probability of failure, under ultimate load, and wear-out process of aircraft structures
[ARL/SM-REPT-337] 04 p0480 N73-13925
Development of aerodynamic structural design data to reduce effects of acoustic fatigue on flat and singly-curved sandwich panels - Part 2
[AGARD-AG-162-PT-2] 05 p0602 N73-14898
Analysis of natural vibration characteristics of plate-beam combination structures during supersonic flight
[NAL-TR-291] 06 p0725 N73-15917
Development of optimized aircraft structures based on vibratory strain energy distribution using damped forced response
[AD-751809] 07 p0741 N73-16027
Nondestructive inspection techniques for examining catapult and arresting gear structures on E-2 aircraft
[AD-752492] 08 p0868 N73-17027
Fatigue tests to determine service life of catapult structure on C-2 aircraft
[AD-752493] 08 p0868 N73-17028
Design parameters for torsion of airframe sandwich strips having trapezoidal, rectangular, and triangular cross sections
[AD-752619] 08 p0868 N73-17029
Procedures for reducing residual stresses in aircraft metal structures reinforced by filamentary composites
[NASA-CR-112207] 08 p0966 N73-17900
Aerodynamic characteristics of flow around wing profiles
[AD-752686] 09 p0987 N73-18054
Experimental determination of high velocity liquid impact damage for application to rain erosion protection of supersonic aircraft
[AD-753381] 09 p1018 N73-18305
Evaluation of airframe fatigue life gage under constant and variable amplitude loading
[AD-753800] 09 p1037 N73-18464
Methods for designing and developing aircraft structural components by riveting, welding, and gluing aluminum alloys parts
[AD-753513] 09 p1041 N73-18491
Fabrication of L-1011 aircraft panels to compare costs and service performance characteristics of PRD-49 and fiberglass
[NASA-CR-112250] 11 p1234 N73-20018
Fatigue damage of helicopter rotary wing structures - bibliographies
[AD-754062] 11 p1235 N73-20027
Development of methods for protecting aircraft compartments from aerodynamic heating effects
[AD-754606] 11 p1236 N73-20036
Development of beryllium-copper bearings for use with stainless steel shafts under high bearing stress levels imposed by airframes
[AD-754759] 11 p1299 N73-20540
Optimization of aircraft structures by finite element modeling and automated structural optimization computer program
[AD-754915] 11 p1344 N73-20905
Theories, numerical methods, and computer programs for determining inviscid three dimensional flow around spherically-capped smooth bodies and wings at supersonic speeds
[AD-753696] 12 p1356 N73-21002
Development of structural optimization algorithm used with large finite element program based on displacement method of structural analysis
12 p1356 N73-21005
Development and application of composite materials for vertical takeoff aircraft airframes and effect on improved aircraft performance
12 p1359 N73-21023
Analysis of aircraft construction methods to compare riveting, welded joints, and bonded joints for structural stability
[AD-755754] 13 p1475 N73-21948
Numerical analysis of panel flutter based on isoperimetric inequality and effect of viscous damping forces
[NASA-CR-131828] 13 p1475 N73-21950
Design, fabrication, and evaluation of boron-epoxy reinforced C-130 center wing boxes
[NASA-CR-112272] 14 p1601 N73-22979
Application of power spectral density method to analyze vibrations induced in aircraft during taxiing
[AD-757283] 14 p1602 N73-22991
Controlled magnetic and electric excitation of airframe of LOH-6A helicopter and measurement of impedance, radiation patterns, and bandwidths
[AD-757143] 14 p1602 N73-22992
Development of reliability analysis procedure for determining effects of cumulative and maximum operational loads on airplane structures
[AD-757529] 14 p1603 N73-22999
Application of holographic interferometry for inspection of large aircraft structures during manufacturing and maintenance
[AD-757510] 14 p1604 N73-23000
Analysis of fatigue performance of titanium alloys and steels to identify variations based on shape parameter for reliability engineering of airframes
[AD-758219] 14 p1605 N73-23008
Application of multipoint excitation for helicopter structural dynamic testing using impedance techniques - Vol. 1
[AD-756389] 14 p1716 N73-23921
Design criteria and analysis procedures to minimize occurrence of major structural failures in airframes due to undetected damage
[AD-757870] 15 p1735 N73-24074
Resonance tests of delta wing aircraft model to determine effect of stiffness changes of wing spars on frequencies and modes of vibration
[ARC-R/M-3268] 16 p1856 N73-25031
Optimization of mass distribution of solid beams and panels for structural design of airframes and panels
[AD-759169] 16 p1859 N73-25054
Design of dual fuselage aircraft with pivoting wing and horizontal stabilizer to permit yawing of wing in flight for high speed operation
[NASA-CASE-ARC-10470-1] 17 p1980 N73-26005
Aircraft configuration for reducing effects of nose-down pitching moments due to high lift forces, loss of trim lift, and engine-out yawing moments
[NASA-CASE-LAR-11252-1] 17 p1980 N73-26007
Development of formula for determining ideal weight of shell-type aircraft fuselages with body of revolution cross section
[RAE-LIB-TRANS-1688] 17 p1981 N73-26009
Analysis of fatigue behavior of airframe components and development of methods for predicting service life of aircraft structures
[RAE-LIB-TRANS-1678] 17 p1981 N73-26012
Development of procedures for determining service life of helicopter airframes and rotor blades
[RAE-LIB-TRANS-1520] 17 p1981 N73-26013
Thesaurus of terms for information on mechanics of structural failure modes and mechanisms for aerospace structures
[NASA-CR-121199] 17 p2091 N73-26917
Identification of sources for specialized information on failure modes and mechanisms of aerospace structures
[NASA-CR-121201] 17 p2091 N73-26919
Bibliography of citations related to problem areas in mechanics of failure in aerospace structures
[NASA-CR-121202] 17 p2091 N73-26920
Analysis of physiological and toxicological aspects of smoke produced by combustion of aircraft interior materials - Part 1
[FAA-RD-73-50-PT-1] 18 p2104 N73-27014
Physio-chemical analysis of flammability characteristics and thermal degradation of rigid and flexible urethane foams used in aircraft structures - Part 2
[FAA-RD-73-50-PT-2] 18 p2105 N73-27025
Evaluation of nondestructive testing techniques for diffusion-bonded titanium alloy aircraft structures using ultrasonic radiation
[AD-760673] 18 p2106 N73-27035

Proceedings of conference on application of composite materials in construction of aerospace vehicles and propulsion systems
[AGARD-CP-112] 18 p2163 N73-27474
Application of boron/epoxy composite materials for airframe construction with specific development of F-111 stabilizer
18 p2164 N73-27480
Application of glass reinforced and carbon reinforced composite materials for helicopter structures and rotary wings
18 p2165 N73-27483
Application of composite materials to reinforce metallic structures for low cost improvement in structural stability of airframes
18 p2165 N73-27485
Analysis of aircraft structural loads in operational flight to determine effects of pilot performance and aircraft characteristics
[AGARD-R-608] 19 p2218 N73-27895
Analysis of effects of flying time on service life of wing fastening knee plates on transport aircraft
[AD-761468] 19 p2221 N73-27919
Effect of friction forces on fatigue breakdown of bolted and riveted joints in airframes
[AD-761446] 19 p2305 N73-28539
Physical properties of aluminum alloys, titanium alloys, and stainless steels for aerospace airframes
[AD-762305] 19 p2311 N73-28587
Cost history of F-111 aircraft airframe system to show logistics organization, support costs, reliability and maintainability, and development problems
[AD-762213] 19 p2356 N73-28958
Logistic performance data book for UH-1F helicopter airframe to show reliability, maintainability, logistic costs, and operational problems
[AD-762251] 19 p2357 N73-28965
Logistic performance data book for C-5A airframe to show reliability, maintainability, logistics support, and operating problems
[AD-762233] 19 p2358 N73-28968
Research projects involving aeroelastic stability and response, stability of thin shell structures, and suspension system concept for control of vehicle responses
[AD-762568] 20 p2359 N73-28979
Procedures for ultrasonic inspection of wing attachment fittings on Viscount aircraft
[TR-7211.621] 20 p2422 N73-29455
Proceedings of conference on acoustic fatigue to show effects of aerodynamic loads, response of structures, structural design, and fatigue test methods
[AGARD-CP-113] 20 p2478 N73-29905
Development of method for determining response of box type structures subjected to high intensity acoustic loading
20 p2479 N73-29915
Effect of environment and stress-cycling on in-service structural failure of airframes and procedures for predicting safe operational conditions
20 p2481 N73-29929
Development of rational analytic theory for analyzing fatigue of airframes based on maximum stress-field parameter and maximum load excursion ratio
20 p2481 N73-29931
Development of procedure for estimating fatigue life of airframes to eliminate errors caused by neglecting effect of stress redistribution after localized yielding
20 p2481 N73-29933
Ground vibration tests of YF-12 aircraft to determine frequency response data, measured node lines, and elastic mode shapes for aircraft components
[NASA-TM-X-2880] 20 p2483 N73-29944
Analysis of flight test procedures for evaluating strength of airframes for aircraft and helicopters
[NASA-TT-F-769] 21 p2494 N73-30019
Application of reinforced fiberglass thermoplastic materials for construction of military aircraft structures
[AD-763470] 21 p2498 N73-30044
Development of digital computer program for generating individual component or entire aircraft mass and aerodynamic models for vehicle inelastic bending response analysis
[AD-763701] 21 p2498 N73-30045
Analysis of equipment and procedures for conducting sonic fatigue tests of airframes at elevated temperatures
[AD-763798] 21 p2498 N73-30052
Pressure fields over hypersonic wing-body configuration at moderate incidence
[AD-763762] 21 p2526 N73-30256
Application of composite materials to construction of helicopter airframes and landing gear
[NASA-CR-112333] 22 p2614 N73-30948
Finite element method to determine post-buckling strength of B-1 aircraft aft intermediate fuselage following combined torque and axial loading
[AD-763813] 22 p2615 N73-30956
Application of fracture prevention principles to airframes to reduce catastrophic failure and increase service life
[AD-764513] 22 p2617 N73-30969
FORTRAN matrix abstraction program for structural analysis of aerospace structures, Vol. 2 - Digital computer program description
[AD-764360] 22 p2640 N73-31158
FORTRAN matrix abstraction program for structural analysis of aerospace structures, Vol. 5 - Engineering user and technical report
[AD-763812] 22 p2640 N73-31159
FORTRAN matrix abstraction program for structural analysis of aerospace structures, Vol. 6 - Digital computer program Phase I description
[AD-764366] 22 p2640 N73-31160
Construction of helicopter airframes and landing gear to show advantages of composite material prototype over metal prototype
[NASA-CR-112333] 23 p2743 N73-31957
Application of reliability analysis to aircraft structures subject to fatigue crack growth and periodic structural inspection
[AD-764775] 23 p2798 N73-32383
Application of radiation technology and equipment for nondestructive analysis of commercial aircraft structures during aircraft maintenance periods
24 p2952 N73-33579

**AIRGLOW**
NT GEOCORONAL EMISSIONS
NT NIGHTGLOW
NT TWILIGHT GLOW
Airborne auroral expedition of November and December 1969
[NASA-CR-128392] 01 p0047 N73-10379
Instrumentation, calibration, and observational data obtained in airglow and auroral expedition aboard CV 990 aircraft
[NASA-CR-129511] 03 p0293 N73-12384
Detection of large cosmic ray showers by atmospheric fluorescence
[NYO-3038-13] 05 p0593 N73-14822
Analysis of dayside auroral characteristics and hydroxyl airglow variations from 1969 airborne auroral expedition
[NASA-CR-130916] 09 p1025 N73-18367
Comparison between measured transmission and emission spectra and calculated spectra in upper atmosphere ozone region
[BMFT-FBW-73-01] 11 p1285 N73-20429
Characteristics of narrow field of view, sensitive photometers and application to measuring air glow, aurora, sun corona, and barium releases
[LA-DC-72-1422] 12 p1406 N73-21399
Research projects conducted by Australian atmospheric physics laboratory to analyze atmospheric radiation, micrometeorology, ozone, airglow, and cloud physics
14 p1659 N73-23465
Photometric measurements of airglow and auroral intensity and ionspheric disturbances by Goose Ionospheric Observatory
[AD-762081] 19 p2297 N73-28471
Atomic oxygen emission line in high resolution spectra of zenith day airglow
23 p2778 N73-32214
Aurora data from Michigan airglow payload and stellar occultation data
[NASA-CR-135718] 23 p2785 N73-32281

**AIRLINE OPERATIONS**
Development of mathematical model to analyze traveler acceptance factors in short haul air carrier operations
01 p0004 N73-10023
Computer model for determining economic impact of aircraft retrofit on airlines
[FAA-EQ-72-4-VOL-1] 02 p0245 N73-11988
Traffic environment and operational procedures for intercity STOL transportation system
[NASA-CR-114523] 03 p0367 N73-12990
Speech on problem of aircraft hijacking and efforts to prevent hijackers from continuing to conduct air piracy
05 p0611 N73-14970
Cost effectiveness analysis of propane operated fog dispersal system and evaluation of runway visual range improvement
[FAA-RD-72-123] 06 p0649 N73-15267
Experiences of airline operator regarding developments in flight safety, passenger comfort, schedule adherence, and economy
[DGLR-PAPER-72-037] 06 p0650 N73-15282
Analysis of excessive interrogation signals from Air Traffic Control Radar Beacon System and effect on operation of Jacksonville, Florida center
[ECAC-PR-72-014] 06 p0696 N73-15675
Analysis of excessive interrogation signals from Air Traffic Control Radar Beacon System and effect on operation of Washington, D.C. center
[ECAC-PR-72-022] 06 p0696 N73-15676
Analysis of excessive interrogation signals from Air Traffic Control Radar Beacon System and effect on operation of Los Angeles, California center
[ECAC-PR-72-044] 06 p0696 N73-15677
Technical documentation to support V/STOL aircraft implementation and utilization based on short haul air transportation requirements - Vol. 2
[NASA-CR-114518] 07 p0739 N73-16009
Analysis of factors affecting development and operation of satellite airport system as method for relieving congestion at metropolitan airports
07 p0765 N73-16216
Findings and recommendations of Aviation Advisory Commission on long range needs of Aviation-- Vol. 1 Vol. 2
[PB-215803] 09 p1101 N73-18983
Analysis of special problems and issues involved in the long range of aviation with emphasis on 1 aa Vol. 2
[PB-215804] 09 p1101 N73-18984
Analysis of system concepts, design criteria, operating procedures, and terminal facilities for short haul transportation aircraft and supporting systems
[NASA-TM-X-62235] 10 p1105 N73-19013
Economic analysis of high density short haul air market to show aircraft requirements, engine development, and funding sources
[NASA-CR-2227] 10 p1106 N73-19017
Analysis of problems in air traffic control caused by expansion of commercial and civil aviation in Germany and proposed actions for improved safety and efficiency
10 p1133 N73-19627
Requirements for air traffic control in German air operations and recommendations for improved air traffic control procedures
10 p1183 N73-19628
Analysis of factors involving commercial application of short takeoff aircraft for short haul airline operations
[NASA-TM-X-62239] 11 p1234 N73-20016
House hearings on air passenger fees, related taxation, and government regulation of commercial airline operations
11 p1352 N73-20970
Development of computer program to analyze air traffic in North Atlantic to show zone traffic at specified instants
[AD-755910] 12 p1426 N73-21557
Long range operational factors affecting commercial aviation industry
13 p1472 N73-21917
Survey of passengers flying from Dulles Airport, Virginia during one year period to obtain cross section of typical passengers and destinations
13 p1473 N73-21925
Analysis of trans-Atlantic aircraft movements for 1970 - 1971 period to establish base line for passenger forecasts
13 p1474 N73-21935
Analysis of air passenger traffic on North Atlantic air routes to show development of scheduled and chartered operations
13 p1474 N73-21937
Analysis of impact of major airport operations on economy, ecology, and urban development
13 p1505 N73-22199
Profiles of scheduled air carrier airport operations for top 100 airports in U.S.A.
[REPT-73-00328] 13 p1506 N73-22207
Present and predicted nature, entent, and control of air pollution related to aircraft operations in US
[REPT-72-02452] 13 p1553 N73-22586
Utilizing Out-of-Kilter Algorithm to evaluate efficiency of passenger capacity of selected air carriers between twenty cities in US
13 p1592 N73-22910
Survey of US tourism potential
13 p1595 N73-22933
Proceedings of conference on short haul air transportation to show development requirements, economic aspects, and urban and environmental impacts
[M73-54] 14 p1600 N73-22974
Analysis of nonfatal injuries to passengers and flight attendants in airline operations during period 1968 through 1971
[NTSB-AAS-73-1] 14 p1601 N73-22983
Analysis of air navigation systems for continental US and overseas flights based on projected traffic loads of 1980 time period
[FAA-ED-04-1] 14 p1687 N73-23688
Development of simulation model and computer code for evaluation of operation of short takeoff aircraft for commercial airline operations
[NASA-CR-114631] 16 p1860 N73-25062
Problems of air transport economics and efficiency of air transport utilization in USSR
[NASA-TT-F-741] 16 p1860 N73-25069
Airport planning studies, and procedures for determining airfield capacity, operations, and delays
[FAA-RD-73-11-VOL-2] 17 p2010 N73-26255
Tables of data for airline economic impact computer model - Vol. 2
[AD-749491] 17 p2100 N73-26989
Development of procedures for determining capacity of airports and causes of airport delays - Vol. 1
[FAA-RD-73-11-VOL-1] 18 p2126 N73-27180
Systems analysis of quiet turbofan STOL aircraft for short-haul air transportation operations - Vol. 6
[NASA-CR-114611] 19 p2219 N73-27903

Analysis of factors affecting feasibility of minimizing runway spacings for increased air terminal operational capacity - Vol. 2
[FAA-RD-72-58-VOL-2] 20 p2452 N73-29709
Statistical analysis of air traffic conditions predicted for Los Angeles, California area in 1982 - Vol. 1
[MTR-6387-VOL-1] 21 p2577 N73-30653
Statistical analysis of air traffic conditions predicted for Los Angeles, California area in 1982 - Vol. 2
[MTR-6387-VOL-2] 21 p2577 N73-30654
Algorithms to determine potential conflicts over oceanic airspace based on vertical, lateral, and longitudinal separation criteria
[FAA-RD-73-73] 22 p2697 N73-31606
Analysis of regional aviation system for Southern California with extension to system of global airports to cope with future requirements
22 p2697 N73-31607
Application of short takeoff aircraft for short haul air transportation with identification of critical technology, economics, and social viability
[NASA-CR-135481] 23 p2741 N73-31941
Aircraft landing problems under low visibility weather conditions
[DGLR-PAPER-73-015] 23 p2817 N73-32520
New type of instrument landing systems, according to ICAO requirements
[DGLR-PAPER-73-011] 23 p2817 N73-32522
Economics, traffic demand, and community acceptance of short haul air transportation system in California Corridor - Vol. 1
[NASA-CR-114634] 23 p2859 N73-32842
Forecast model for predicting economic factors involved in short haul air transportation in California Corridor - Vol. 2
[NASA-CR-114634[1]] 23 p2859 N73-32843
Method for estimating airline operating costs
23 p2860 N73-32851
Formula for computing operating cost of turbine powered transport aircraft
23 p2860 N73-32852
Differential pricing policy in airline operations
23 p2861 N73-32857
Competition effects on air transportation industry economics
23 p2861 N73-32858
Financial sources and airline operations
23 p2861 N73-32859
Estimated costs for additional aircraft in air transport industry
23 p2861 N73-32860
Financial requirements of air transportation industry
23 p2861 N73-32861
Analytic methods for evaluating transportation systems with interacting elements
23 p2861 N73-32867
Economic market structure of airline industry
23 p2862 N73-32869
Functional models for airline operations
23 p2862 N73-32870
Excess capacity in airline industry and operational and financial problems
23 p2862 N73-32871
Production forecasting for aircraft manufacturer
23 p2862 N73-32872
Consumer marketing for airline industry
23 p2862 N73-32873
Concepts of expanding airline marketing strategies
23 p2862 N73-32874
Proceedings of conference on air transport industry with emphasis on economics, market demand, airlines regulation, and international transportation policy - Vol. 2
[NASA-CR-135635] 23 p2862 N73-32875
Patterns of behavior of airlines and air travellers in air transportation network and effects on use of satellite airports
23 p2862 N73-32876
Development and operation of cost accounting system for airport functions to show application of data processing equipment
23 p2863 N73-32878
Procedures for conducting air traffic forecasts with emphasis on socio-economic and demographic characteristics of population
23 p2863 N73-32879
Organization, responsibilities, and functions of Civil Aeronautics Board in determining award of air routes to air lines
23 p2863 N73-32880
Analysis of economic factors involved in air cargo operations and air cargo market development
23 p2863 N73-32881
Analysis of factors involved in developing market for air cargo services
23 p2863 N73-32882
Analysis of air freight rate problems to define roles of Civil Aviation Board and domestic air carriers
23 p2863 N73-32883
Research project to determine factors involved in expansion of air freight traffic and prospects for future expansion
23 p2863 N73-32884
Analysis of commuter air transportation services to define problems and identify methods for improvements in cost effective operations
23 p2863 N73-32885
Operation of low cost local air service carriers to show methods for improving transportation services
23 p2863 N73-32886
Evaluation of new forms of air transport service for improving short haul air travel market
23 p2863 N73-32887
Actions by Civil Aviation Board to regulate and improve commuter air transportation services
23 p2864 N73-32888
Historical and constitutional framework of industry regulation with application to airline operations
23 p2864 N73-32889
Procedures for determining rates charged by airlines to show factors involved in making determinations
23 p2864 N73-32890
Regulatory policies of Civil Aviation Board for controlling operations of commercial airlines
23 p2864 N73-32891
Economic analysis of airline operating without Civil Aviation Board control and comparison with economic status of controlled airlines
23 p2864 N73-32892
Economic aspects of Federal regulation of airline operations to show agencies involved and functions of government organizations
23 p2864 N73-32893
Characteristics of Federal regulation of airline operations and predictions for type and extent of future regulation
23 p2864 N73-32894
Actions of Civil Aviation Board with respect to monopolies and mergers of domestic airline operations
23 p2864 N73-32895
Policy of Department of Transportation with respect to evaluating proposals for airline mergers
23 p2864 N73-32896
Policy of Justice Department with respect to airline merger within context of Federal Aviation Act
23 p2864 N73-32897
Analysis of airline mergers to show effects on management, personnel, and overall airline operations
23 p2865 N73-32898
Advice and assistance provided by Civil Aviation Board to State Department on matters of international air transportation policy
23 p2865 N73-32899
Analysis of factors affecting future of commercial aircraft development to show effects on overall airline operations
23 p2865 N73-32900
Analysis of factors affecting operation of domestic airline to overseas areas
23 p2865 N73-32901
Federal policy establishing guidelines for US participation in international air transportation services
23 p2865 N73-32902
International air transportation policy and application of policy to scheduled and chartered airline services
23 p2865 N73-32903
Economic and environmental aspects of short takeoff aircraft used for short-haul air transportation systems
24 p2872 N73-32937
Short takeoff aircraft technology development related to requirements for expanded and improved short-haul air transportation system capabilities
24 p2872 N73-32938
Short haul aircraft operations in terminal area with concurrent conventional aircraft operations to show methods for improved utilization of facilities
24 p2874 N73-32953
Systems analysis of problems created in terminal area by application of short takeoff aircraft for providing high speed, short haul air transportation service
24 p2874 N73-32958
Restructuring of oceanic air traffic control airspace jurisdictional boundaries in presence of satellite system
[FAA-RD-73-59] 24 p2951 N73-33570

**AIRLINERS**
U COMMERCIAL AIRCRAFT
U PASSENGER AIRCRAFT

**AIRPORT BEACONS**
Comparison tests of strobe and incandescent beacons to determine suitability as replacement for standard rotating airport beacon
[FAA-NA-73-1] 11 p1255 N73-20182
Portable beacon test site for enroute radar coverage in airport vicinity
[FAA-RD-73-49] 15 p1760 N73-24266
Feasibility of ATC radar beacon system based on vehicle surveillance on airport surface in relation to vehicle time of arrival
[AD-763328] 21 p2577 N73-30655

**AIRPORT LIGHTS**
NT RUNWAY LIGHTS
Evaluation of approach lighting system for visual guidance of helicopters during instrument flight rules approach and landing operations
[FAA-RD-72-133] 04 p0401 N73-13261
Incident involving collision of Boeing 727 aircraft with landing light system at Atlanta International Airport, Georgia on 21 Dec. 1971
[NTSB-AAR-72-22] 07 p0737 N73-16000
Comparison tests of strobe and incandescent beacons to determine suitability as replacement for standard rotating airport beacon
[FAA-NA-73-1] 11 p1255 N73-20182

**AIRPORT PLANNING**
Airport planning, economics, computer program, and arena characteristics for short haul, high density transportation systems in 1980 time period
[NASA-CR-114467] 01 p0120 N73-10991
Community/airport economic development model for assisting land use planning near metropolitan airports
[FAA-EQ-72-3-VOL-1] 04 p0400 N73-13259
Sample output for community/aircraft economic development model - programmers manual
[FAA-EQ-72-3-VOL-4] 04 p0401 N73-13260
Data concerning airport development including land use, noise level compatibility, and zoning
[FAA-EC-72-3-VOL-2] 04 p0401 N73-13267
Infrastructural role of airports in Germany and planning for future traffic increase
[DGLR-PAPER-72-034] 06 p0650 N73-15281
Analysis of factors affecting development and operation of satellite airport system as method for relieving congestion at metropolitan airports
07 p0765 N73-16216
Economic feasibility analysis on San Francisco rapid transit system extension to serve airport
[PB-212456] 07 p0860 N73-16978
Characteristics and functions of various types of aircraft landing fields in Germany and development of airfields for improved air safety
10 p1183 N73-19624
Analysis of airport operations to show importance to community, effect on environment, and application of new technologies for airport development
10 p1183 N73-19625
Analysis of technical and economic feasibility of constructing offshore airport in New York Metropolitan area
[FAA-RD-73-45] 11 p1267 N73-20280
Synopsis of factors contributing to airport congestion and flight delays
[REPT-73-00315] 13 p1505 N73-22200
Airport planning recommendations and procedures for San Francisco Bay Area
[REPT-73-00316] 13 p1506 N73-22208
Effective land use of airport-incompatible areas through conversion planning from residential to compatible zones
[FAA-EQ-72-1] 13 p1594 N73-22926
Feasibility analysis for computer-based data communications and/or processing facilities at civil airport
[RAE-TR-72133] 16 p1941 N73-25711
Measured noise level data for proposed airport sites in Florida
[PB-214459/0] 16 p1945 N73-25737
Airport planning studies, and procedures for determining airfield capacity, operations, and delays
[FAA-RD-73-11-VOL-2] 17 p2010 N73-26255
Conceptual development and cost analysis of elevated short takeoff and landing facility for test purposes
[FAA-RD-73-15] 18 p2126 N73-27179
Development of procedures for determining capacity of airports and causes of airport delays - Vol. 1
[FAA-RD-73-11-VOL-1] 18 p2126 N73-27180
Regulations for promoting safety in air navigation for municipal airport of Hartselle, Alabama
[PB-220087/1] 18 p2127 N73-27185
Guide for airport planning and development to identify and resolve environmental problems caused by air pollution, water pollution, and aircraft noise
[PB-219957/8] 18 p2127 N73-27187
Airport construction procedures to include general requirements, construction materials, and operational maintenance
[AD-759243] 18 p2127 N73-27191
Airport siting, design, cost, operation, and implementation for STOL aircraft short-haul air transportation system - Vol. 3
[NASA-CR-114608] 19 p2219 N73-27900
Future of short haul air transport in Western Europe - V/STOL Working Group
[SP-73-001] 22 p2737 N73-31915
Regional airport planning in Germany
[DGLR-PAPER-73-035] 23 p2770 N73-32159
Patterns of behavior of airlines and air travellers in air transportation network and effects on use of satellite airports
23 p2862 N73-32876
Airport establishment and operation with emphasis on regional planning, social factors, and economic forces
23 p2863 N73-32877

**AIRPORT TOWERS**
Design, development, and evaluation of mockup of control tower for airport traffic control functions
[FAA-NA-72-63] 02 p0152 N73-11235
Design, development, and evaluation of airport lighting control panel for airport traffic control towers
[FAA-RD-72-93] 03 p0260 N73-12108

Noise reduction and control in FAA air traffic control, navigational, and service facilities
[J-6250] 04 p0401 N73-13264
Measurement of indoor and outdoor sound pressure levels at airport control towers during aircraft takeoff and landing
[AD-752535] 09 p1012 N73-18262
Development of wake vortex avoidance system for airports to reduce hazards caused by aircraft wakes and permit increased utilization of terminal facilities
[FAA-ED-21-1] 14 p1645 N73-23342
Evaluation of air traffic control beacon alphanumeric system for automatic operation in low-density airport towers and terminal facilities
[FAA-NA-73-54] 23 p2816 N73-32516

**AIRPORTS**
NT HELIPORTS
Soil stabilization during road and airport construction
[AD-748153] 03 p0299 N73-12442
Effectiveness of airborne chemical seeding techniques for airport fog dispersal
[NETL-72-005-1] 04 p0444 N73-13622
Noise exposure model MOD-5 - Vol 2
[PB-211976] 05 p0497 N73-14050
Cost effectiveness analysis of propane operated fog dispersal system and evaluation of runway visual range improvement
[FAA-RD-72-123] 06 p0649 N73-15267
Regional airport planning in Germany, noting infrastructural, economic, safety, and noise problems
[DGLR-PAPER-72-033] 06 p0650 N73-15280
Analysis of jet aircraft noise propagation near airports and methods for reducing noise intensity
[NASA-TT-F-14655] 06 p0700 N73-15707
User manual for computer programs applied to community/airport economic development model - Vol. 3
[FAA-EQ-72-3-VOL-3] 06 p0732 N73-15971
Requirements, basic principles of operation, design, construction, and maintenance of thermal fog dispersal system for airport applications
[FAA-RD-72-138] 07 p0766 N73-16222
Reduction in auxiliary extinguishing agents and systems for aircraft ground fire suppression at military airports
[AD-753069] 09 p1011 N73-18256
Structural design guidance and construction standards for upgrading and extending service life of airport pavements
[FAA-ED-08-2] 10 p1137 N73-19266
Characteristics and functions of various types of aircraft landing fields in Germany and development of airfields for improved air safety
10 p1183 N73-19624
Analysis of airport operations to show importance to community, effect on environment, and application of new technologies for airport development
10 p1183 N73-19625
Criteria on jet blast velocities and effects during operation of commercial aircraft and recommended procedures to reduce adverse impact
[AC-150/5325-6A] 11 p1266 N73-20271
Development of statistical methods for estimating annual operations at non-tower airports and establishment of standardized estimation procedure
[SCI-2040] 11 p1267 N73-20278
Development of procedures for accurately estimating annual air traffic levels at airports without tower control
[SCI-2-2040] 11 p1321 N73-20722
Airport access and ground travel modes
[PB-212814] 11 p1353 N73-20990
Development of system for analyzing aircraft sound levels for areas in vicinity of airports
[FAA-EQ-73-3] 12 p1364 N73-21064
Detection and indentification of major airports in northeastern Kansas and northwestern Missouri
[E73-10471] 12 p1395 N73-21308
Analysis of impact of major airport operations on economy, ecology, and urban development
13 p1505 N73-22199
FAA research and development in airport paving criteria
13 p1506 N73-22205
Profiles of scheduled air carrier airport operations for top 100 airports in U.S.A.
[REPT-73-00328] 13 p1506 N73-22207
Analysis of effects of aircraft noise in residential communities near London, England airport
[TT-7302] 14 p1599 N73-22966
Inspection of Hunter Army Airfield, Savannah, Georgia to determine condition of runways
[AD-757387] 15 p1763 N73-24285
Fog clearing at airports by ground based heating
[AD-757897] 15 p1806 N73-24639
Evaluation of courses of action and costs to reduce aircraft noise levels in vicinity of airports
[PB-215611/5] 16 p1862 N73-25080
Analysis of economics and finances of airport operations to determine procedures for improved management and operation
[REPT-73-01210] 16 p1884 N73-25253
Computer programs for ceiling and visibility forecasting using air terminal weather data
[FAA-RD-73-13] 16 p1937 N73-25677
Optical radar evaluation of techniques for fog dissipation at airports
[AD-758767] 16 p1938 N73-25682
Forecasts of aviation activity at selected airports to meet needs of planning personnel for future air traffic control operations
17 p1982 N73-26019
Review and analysis of air carrier/reliever airport grant allocations and technological forecast of airport demands
[FAA-AV-72-4] 17 p2010 N73-26253
Worldwide airfield climatic data for Eastern Europe and USSR - Part 1
[AD-759794] 17 p2057 N73-26640
Worldwide airfield climatic data for Eastern Europe, and USSR - Part 2
[AD-759795] 17 p2057 N73-26641
Analysis of generated solid wastes and collection systems for San Francisco International Airport
[PB-219372/0] 18 p2127 N73-27189
State airport system plan for Iowa - Volume 1
[PB-217531/3] 18 p2127 N73-27192
State airport system plan for Iowa - Volume 2
[PB-217532/1] 18 p2128 N73-27193
Feasibility of rapid transit service between downtown Washington, D.C. and Dulles Airport in Virginia
[PB-220074/9] 18 p2214 N73-27879
Propane aerosol dispenser for cold fog dissipation at airfields
[AD-762292] 19 p2317 N73-28635
Statistical analysis of meteorological parameters during fog at US airports
[FAA-RD-72-39] 20 p2448 N73-29673
Statistical analysis of air traffic conditions predicted for Los Angeles, California area in 1982 - Vol. 1
[MTR-6387-VOL-1] 21 p2577 N73-30653
Statistical analysis of air traffic conditions predicted for Los Angeles, California area in 1982 - Vol. 2
[MTR-6387-VOL-2] 21 p2577 N73-30654
Aircraft accident involving ground collision of DC-9 and CV-880 aircraft at O Hare International Airport, Chicago, Illinois on 20 December, 1972
[NTSB-AAR-73-15] 22 p2614 N73-30945
Airport environment compatibility plan for Jackson, Tennessee
[PB-221129] 22 p2648 N73-31217
Methodology for integrating air pollution impact of airport and its environs
[PB-220987/2] 22 p2696 N73-31594
Analysis of regional aviation system for Southern California with extension to system of global airports to cope with future requirements
22 p2697 N73-31607
Airport establishment and operation with emphasis on regional planning, social factors, and economic forces
23 p2863 N73-32877
Development and operation of cost accounting system for airport functions to show application of data processing equipment
23 p2863 N73-32878
Procedures for conducting air traffic forecasts with emphasis on socio-economic and demographic characteristics of population
23 p2863 N73-32879

**AIRSHIPS**
Analysis of rigid airship operations for commercial cargo handling in United Kingdom
[CRANFIELD-CTS-3] 20 p2360 N73-28985
Technical and economic aspects of airship transportation
[DLR-MITT-72-17] 24 p2879 N73-32989
History of Zeppelin airships to show uses for civil and military purposes
24 p2879 N73-32990
Application of airships to air transportation, noting cost effectiveness
24 p2879 N73-32991
Flexible airship manufacturing
24 p2879 N73-32992
Technical aspects of airship manufacture and ground and loading operations
24 p2879 N73-32993
Aerodynamic drag and lift of airships, noting boundary layer control by suction
24 p2879 N73-32994
Technical conditions for airship development, noting weight reduction, propulsion system performance, and maneuverability improvement
24 p2879 N73-32995

**AIRSPACE**
Simulation tests of short takeoff transport aircraft to determine airport and air space requirements under normal operating conditions
[NASA-TN-D-7300] 21 p2495 N73-30026
Technology for evaluating ground station sites based on effectiveness in disseminating time synchronization
[FAA-RD-73-102] 23 p2770 N73-32155

**AIRSPEED**
Pilot visual threshold and perception for aircraft movement estimation during unaided visual approach control
01 p0016 N73-10125
Flight test of instrument for determining low airspeeds to evaluate suitability for helicopter airspeed indicator
[AD-753343] 09 p0989 N73-18071
Measurement of low airspeeds with ion beam produced in positive corona discharge based on beam deflection properties
10 p1158 N73-19423
True airspeed sensor for V/STOL aircraft with increased accuracy below 40 knots
[AD-755374] 12 p1406 N73-21403
Position errors in airspeed calibration methods
[NAL-TR-298] 15 p1786 N73-24477
Air or inertial data addition to onboard navigation system for improved air traffic control
16 p1940 N73-25699
Equipment route winds and great circle distances for helicopter air routes at 5,000, 10,000, and 18,000 feet - Vol. 1
[AD-760252] 17 p1985 N73-26043
Design and flight tests of helicopter airspeed indicator
[AD-764240] 22 p2675 N73-31430

**AIRWORTHINESS**
U AIRCRAFT RELIABILITY

**AIRWORTHINESS REQUIREMENTS**
U AIRCRAFT RELIABILITY

**AIRY FUNCTION**
Generalized Airy functions, using one dimensional, time independent, Schroedinger equation
[NASA-CR-129604] 03 p0324 N73-12638

**AJ-10 ENGINE**
Altitude test and performance of Aerojet AJ10-179 liquid rocket engine under vacuum conditions
[AD-763727] 21 p2591 N73-30758

**ALABAMA**
NT TENNESSEE VALLEY [AL-KY-TN]
Visual inspection of runway conditions at Redstone Army Airfield, Huntsville, Ala.
[AD-743857] 01 p0037 N73-10295
Application of remotely sensed, multispectral observations for assessment of earth resources and environmental quality in Alabama
04 p0471 N73-13841
Utilization of ERTS-1 imagery of Alabama to study environmental factors, land use, and geology
[E72-10319] 05 p0530 N73-14310
Application of ERTS-1 MSS imagery to multidisciplinary investigations in Alabama
[E73-10509] 13 p1516 N73-22284
Environmental impact of noise produced by transonic wind tunnel at Arnold Engineering Development Center
[AD-757552] 14 p1646 N73-23351
ERTS-1 imagery of strip mining activity in Cumberland Plateau, Tennessee Test Site and agricultural areas in Alabama, Georgia, and Tennessee
[E73-10694] 16 p1902 N73-25386
Mapping land use and detecting land use change in Montgomery County, Alabama using ERTS-1 data
19 p2285 N73-28378
Multidisciplinary investigations using ERTS-1 data for Alabama
[E73-11137] 24 p2917 N73-33292

**ALARMS**
U WARNING SYSTEMS

**ALASKA**
NT CHENA RIVER BASIN [AK]
NT COOK INLET [AK]
NT PRINCE WILLIAM SOUND [AK]
NT WRANGELL MOUNTAINS [AK]
Data processing of hydrologic conditions using ERTS-1 time lapse imagery of Wrangell Mountains
[E72-10187] 01 p0046 N73-10366
Environmental studies of sedimentation and nearshore marine processes in Cook Inlet, Alaska, and regional study of permafrost regimes in Alaska using ERTS-1 imagery
[E72-10209] 02 p0161 N73-11304
Mapping and detection of snow cover changes on land and on glaciers in Alaska, British Columbia, and Washington using ERTS-1 imagery
[E72-10237] 03 p0288 N73-12337
Prototype volcano surveillance network in Alaska and Cascade Mountains
[E72-10242] 03 p0289 N73-12342
ERTS-1 imagery of permafrost and geologic hazards in Alaska
[E72-10247] 03 p0289 N73-12347
Photographic aerial survey over underground nuclear test at Amchitka to record changes in bioenvironment
[BMI-171-146] 03 p0296 N73-12411
Management of wildlife habitat in Alaska using ERTS-1 imagery
[E72-10293] 04 p0410 N73-13343
Identification of continental crust geostructures and their relation to mineral resources based on ERTS-1 imagery
[E72-10296] 04 p0410 N73-13346
Aircraft accident investigation of Boeing 727 crash near Juneau, Alaska, 4 Sept. 71
[NTSB-AAR-72-28] 05 p0493 N73-14017
Location of archaeological village sites in Alaska by ERTS-1 imagery
[E72-10338] 05 p0532 N73-14326

University of Alaska survey of environment using ERTS-1 imagery
[E72-10341] 05 p0532 N73-14329
Identification, definition, and mapping of terrestrial ecosystems in interior Alaska
[E72-10343] 05 p0532 N73-14331
Survey of seasonal snow cover of Alaska from ERTS-1 imagery
[E72-10344] 05 p0532 N73-14332
ERTS-1 sensing of fall snow melting in Chena River Basin, Alaska
[E72-10345] 05 p0533 N73-14333
Application of ERTS-1 imagery to study of caribou movements and winter dispersal in relation to prevailing snow cover
[E72-10346] 05 p0533 N73-14334
Sea, ice, and surface water circulation in Alaskan Continental Shelf
[E72-10347] 05 p0533 N73-14335
ERTS-1 imagery of surface water circulation in Prince William Sound
[E72-10348] 05 p0533 N73-14336
Mapping of seismically active faults in Alaska using ERTS-1 imagery
[E72-10352] 05 p0533 N73-14340
ERTS-1 data as teaching and research tool in Department of Geology at University of Alaska
[E72-10353] 05 p0534 N73-14341
Environmental analyses of Alaskan arctic and subarctic geology and geomorphology using ERTS-1 imagery
[E72-10370] 05 p0536 N73-14358
Fluvial environment of Arctic coastal plain in Northern Alaska
[AD-749150] 05 p0542 N73-14412
Fluvial environmental charts for Arctic coastal plain in Northern Alaska
[AD-749151] 05 p0542 N73-14413
Crustal deformation propagation in Alaska
[AD-750468] 06 p0671 N73-15461
Investigation of disappearance of Cessna 310 aircraft on flight between Anchorage and Juneau, Alaska on 16 Oct. 1972
[NTSB-AAR-73-1] 08 p0867 N73-17018
ERTS-1 identification of phenological stages and vegetation types in Alaska for land use classification
[E73-10276] 08 p0914 N73-17484
Alaskan arctic and subarctic sediment deposition, permafrost, snow cover, and ice mapping from ERTS-1 imagery
[E73-10279] 08 p0914 N73-17487
Survey and mapping of freeze-up and break-up patterns of seasonal snow and ice covers in Alaska
[E73-10282] 08 p0914 N73-17489
Preparation of mosaic of Alaska using ERTS-1 imagery
[E73-10284] 08 p0914 N73-17490
Application of ERTS-1 imagery to study of caribou movements and winter dispersal in relation to snow cover
[E73-10285] 08 p0914 N73-17491
Fog drop measurement at Barrow, Alaska on chloride sensitive, gelatin-coated glass
[AD-752129] 08 p0940 N73-17705
Mapping seismically active faults in Alaska from ERTS-1 imagery
[E73-10283] 09 p1020 N73-18326
Vegetation map of western Seward Peninsula, Alaska, based on ERTS-1 imagery
[E73-10305] 09 p1022 N73-18337
Identification, analysis, and mapping of terrestrial ecosystems and vegetation types in Alaska based on ERTS-1 imagery
[E73-10306] 09 p1022 N73-18338
Land use management and planning in Alaska using ERTS-1 imagery
[E73-10307] 09 p1022 N73-18339
ERTS-1 imagery of permafrost and geologic hazards in Alaska
[E73-10320] 09 p1023 N73-18352
ERTS-1 imagery of geostructures of Alaskan continental crust and relation to mineral resources
[E73-10321] 09 p1024 N73-18353
Volcano and earthquake surveillance network in Alaska, California, Washington, Hawaii, El Salvador, Nicaragua, Iceland, and Guatemala
[E73-10337] 09 p1025 N73-18365
Air-cushion tankers for transporting Alaskan North Slope oil
[NASA-TM-X-2683] 09 p1100 N73-18981
Management of wildlife habitats in Alaska using ERTS-1 imagery
[E73-10335] 10 p1147 N73-19336
Analysis of ERTS-1 photographic imagery for identification, definition, and mapping, of terrestrial ecosystems in interior Alaska
[E73-10399] 11 p1277 N73-20361
Utilization of ERTS-1 imagery for study of caribou movements and winter dispersal in relation to prevailing Alaskan snow cover
[E73-10401] 11 p1277 N73-20363
Utilization of ERTS-1 imagery as teaching and research tool in Department of Geology at University of Alaska
[E73-10403] 11 p1277 N73-20365
Mapping of seismically active faults in Alaska using ERTS-1 imagery to determine areas of earthquake occurrence
[E73-10405] 11 p1277 N73-20367
Locating archaeological village sites in Alaska from remotely sensed imagery
[E73-10406] 11 p1277 N73-20368
Utilization of ERTS-1 imagery in structural reconnaissance for minerals and oil in Alaska, Canada, Montana, Colorado, New Mexico, and Texas
[E73-10414] 11 p1279 N73-20376
ERTS-1 imagery of sea ice and surface water circulation along Alaskan contiental shelf
[E73-10416] 11 p1279 N73-20378
Survey of seasonal snow and ice covers in Alaska using ERTS-1 imagery
[E73-10438] 11 p1281 N73-20398
Identification of phenological stages and vegetative types from ERTS-1 imagery for land use classification in Alaska
[E73-10439] 11 p1281 N73-20399
Coordination and establishment of centralized facilities and services for University of Alaska ERTS-1 survey of Alaskan environment
[E73-10459] 11 p1284 N73-20417
ERTS-1 imagery of permafrost and geologic hazards in Alaska
[E73-10495] 12 p1397 N73-21331
Mapping permafrost areas of Alaska, correlating snowpack cover of Caribou-Poker Creek with stream runoff, and mapping and inventorying icing on Chena River
[E73-10511] 13 p1516 N73-22286
Aeromagnetic survey of Amchitka Island, Alaska and adjacent insular shelf for studying tertiary volcanic rocks
[USGS-PP-707] 14 p1661 N73-23481
Seismic reflection, refraction, and near bottom observations in Aleutian trench near 173 deg W
[AD-755455] 14 p1664 N73-23508
ERTS-1 imagery of permafrost and geologic hazards in Alaska
[E73-10601] 15 p1772 N73-24362
Application of ERTS-1 imagery to study of caribou movements and winter dispersal in relation to prevailing snow cover in Alaska
[E73-10615] 15 p1774 N73-24376
Mapping of seismically active faults in Alaska from ERTS-1 imagery
[E73-10616] 15 p1774 N73-24377
Identification of phenological stages and vegetative types in Alaska for land use classification
[E73-10618] 15 p1774 N73-24379
ERTS-1 imagery of sea ice and surface water circulation along Alaskan Continental Shelf
[E73-10620] 15 p1775 N73-24381
Identification, definition, and mapping of terrestrial ecosystems in interior Alaska from ERTS-1 imagery
[E73-10634] 15 p1776 N73-24393
Utilization of ERTS-1 data as teaching and research tool in Department of Geology at University of Alaska
[E73-10635] 15 p1776 N73-24394
University of Alaska program for processing ERTS-1 environmental data
[E73-10636] 15 p1776 N73-24395
Survey of seasonal snow cover in Alaska using ERTS-1 imagery
[E73-10637] 15 p1776 N73-24396
Location of archeological village sites in Alaska from ERTS-1 imagery
[E73-10638] 15 p1776 N73-24397
Observation of earthquake associated tilt steps in Central Alaska
[RLO-2229-T-4-2] 15 p1781 N73-24436
Tectonic and structural mapping in Alaska using ERTS-1 imagery
[E73-10685] 16 p1901 N73-25379
Application of ERTS-1 data for development and operation of volcano surveillance network
[E73-10711] 17 p2018 N73-26318
Identification of copper/molybdenum porphyry mineral deposits in characteristic geologic setting in Nevada, Arizona, Colorado, Australia, Alaska, and New Guinea
[E73-10762] 17 p2023 N73-26362
Identification of geostructures of continental crust and relation to mineral resources
[E73-10787] 18 p2136 N73-27263
Wildlife management in Alaska using ERTS-1 data
[E73-10791] 18 p2137 N73-27267
Application of ERTS-1 imagery for vegetative and geologic mapping of western Seward Peninsula, Alaska
[PAPER-A8] 19 p2260 N73-28216
Development of volcano surveillance and early warning system using ERTS-1 data collection system
[PAPER-G9] 19 p2264 N73-28240
Application of ERTS-1 imagery for delineating structural features in Alaska and discovery of active strand in Denali fault
[PAPER-G23] 19 p2266 N73-28254
Application of ERTS-1 imagery to determine geological evidence of mineral and hydrocarbon accumulations in Alaska, Canada, Montana, Colorado, New Mexico, and Texas
[PAPER-G30] 19 p2267 N73-28261
Evaluation of ERTS-1 imagery as tool for management of wildlife habitat in Alaska
[PAPER-W11] 19 p2271 N73-28288
Influence of sea ice on coastal marine environment of Beaufort Sea, Alaska
[PAPER-M7] 19 p2280 N73-28346
ERTS-1 imagery of snow cover on northern foothills of Brooks Range and Wrangell Mountains, Alaska
19 p2285 N73-28374
Application of ERTS-1 imagery for geologic development of natural resources in Alaska
19 p2287 N73-28393
Application of ERTS-1 imagery for multidisciplinary survey to aid in management of Alaskan resources
19 p2288 N73-28394
ERTS-1 imagery of caribou movements and winter habitats in Alaska in relation to prevailing snow cover
[E73-10840] 19 p2290 N73-28418
Utilization of ERTS-1 imagery as teaching and research tool in Department of Geology at University of Alaska
[E73-10841] 19 p2290 N73-28419
Mapping seismically active faults in Alaska using ERTS-1 imagery
[E73-10842] 19 p2291 N73-28420
Sea ice and surface water circulation along Alaskan continental shelf
[E73-10901] 20 p2396 N73-29250
Coordination and establishment of centralized facilities and services for University of Alaska ERTS-1 survey of Alaskan environment
[E73-10904] 20 p2396 N73-29253
ERTS-1 identification of phenological stages and vegetatine types for land use classification in Alaska
[E73-10905] 20 p2396 N73-29254
Survey of freeze-up and breakup patterns of seasonal snow and ice covers in Alaska
[E73-10920] 20 p2398 N73-29269
Identification, definition, and mapping vegetation and terrestrial ecosystems in interior Alaska using ERTS-1 imagery
[E73-10921] 20 p2398 N73-29270
Fabry-Perot interferometer measurements at Ester Dome, Alaska during 1971-73
[NASA-CR-124348] 21 p2538 N73-30351
Identification of geostructures of continental crust from ERTS-1 imagery and relationship to mineral resources in Alaska
[E73-11023] 22 p2662 N73-31327
Prototype DCP volcano surveillance network in Washington, Nicaragua, California, Guatemala, Hawaii, El Salvador, Iceland, and Alaska
[E73-11024] 22 p2662 N73-31328
Management of wildlife habitats in Alaska using ERTS-1 MSS data
[E73-11030] 22 p2662 N73-31334
Identification of geostructures of continental crust in Alaska and relation to mineral resources and exploration
[E73-11035] 22 p2663 N73-31339
ERTS-1 imagery of sea, ice, and surface water circulation along Alaskan continental shelf
[E73-11050] 23 p2779 N73-32226
Identification, definition, and mapping of terrestrial ecosystems in interior Alaska
[E73-11065] 23 p2781 N73-32241
Identification of phenological stages and vegetative types for land use classification in Alaska
[E73-11066] 23 p2781 N73-32242
Analysis and mapping sediment deposition, permafrost areas, snow cover, and icing in Arctic regions of Alaska from ERTS-1 data
[E73-11067] 23 p2781 N73-32243
Tsunami propagation into Fisher-Fitz Hugh complex, Alaska, and Juan de Fuca Strait
23 p2784 N73-32273
Survey of seasonal snow cover of North Slope and Alaska Range from ERTS-1 data
[E73-11086] 24 p2913 N73-33249
Utilization of ERTS-1 data and imagery as teaching and research tool in Department of Geology, University of Alaska
[E73-11128] 24 p2917 N73-33283

ALBEDO
NT EARTH ALBEDO
Mathematical model for calculating scanning angle distribution of planetary albedo gamma rays above 100 MeV
[NASA-TM-X-66117] 03 p0353 N73-12874
Light and ultraviolet albedo of grass and snow including effect of sun altitude, cloud cover, and state of underlying surface on magnitude of albedo
04 p0442 N73-13609
Solar cosmic ray, solar wind, solar flare, and neutron albedo measurements, using mineral detectors onboard Apollo 16
12 p1450 N73-21749
Zonal, hemispherical, and global averages for satellite measurements of albedo and outgoing long wave radiation
[NOAA-TM-NESS-48] 19 p2340 N73-28823

Analysis of albedo of reservoirs from observations of total and reflected radiation measured near floating island stations
20 p2402 N73-29301
Spectral albedos of Galilean satellites from broadband photometry
[LPL-COMMUN-168] 21 p2591 N73-30764
Determination of earth aerosol albedo using Skylab data from White Sands, New Mexico
[E73-11080] 23 p2782 N73-32255
OSO-6 measurements on albedo neutron flux distribution and density
23 p2834 N73-32644
Mariner 9 mapping of Mars surface albedo variations
23 p2840 N73-32693
Stereographic albedo map of Mars south polar region using Mariner 9 video data
23 p2844 N73-32724

**ALCOHOLS**
NT BISPHENOLS
NT ETHYL ALCOHOL
NT GLYCOLS
NT ISOPROPYL ALCOHOL
NT METHYL ALCOHOLS
NT PHENOLS
Thermal conductivities of liquid alcohols at their saturation pressures
[ESDU-67030] 01 p0115 N73-10953
Conference on detection, evaluation, and identification of drugs and alcohol in flying personnel and effects on flight fitness
[AGARD-CP-108] 12 p1368 N73-21102
Pilot performance and sleep patterns in long duration flights and control of hypnotic drug and alcohol use
12 p1369 N73-21107
Alcohol reference method for predicting drug modifications of central nervous system activity and pilot performance decrease
12 p1369 N73-21112
Alcohol induced performance degradation in pilot instrument approach landings
12 p1370 N73-21113
Methods for determining blood alcohol levels in pilots
12 p1371 N73-21124
Comparison of alcohol and diazepam effects on human mental and psychomotor functions
12 p1371 N73-21126

**ALDEHYDES**
NT FORMALDEHYDE

**ALDOSTERONE**
Radioimmunoassays of plasma aldosterone and catecholamine concentrations as human vasomotor regulators
09 p0994 N73-18111
Chromatographic determination of aldosterone level in urine
[RAE-LIB-TRANS-1682] 17 p1987 N73-26061

**ALERTNESS**
Reinforcement effects on human attention and performance in continuous response to visual stimuli
[AD-747798] 04 p0381 N73-13103
Effects of human alertness on vestibular nystagmus habituation
[AD-749352] 05 p0505 N73-14108
Temperature and noise irradiation effects on human energetic metabolism during vigilance task
10 p1123 N73-19155
Stimulating and tranquilizing drug effects on human performance indices
13 p1483 N73-22021

**ALFALFA**
Phenological observations of lilac, honeysuckle, alfalfa, and winter wheat in Rocky Mountain and Columbia Valley Corridors
[E73-10925] 20 p2398 N73-29274

**ALFVEN WAVES**
U MAGNETOHYDRODYNAMIC WAVES

**ALGAE**
NT BLUE GREEN ALGAE
NT CHLORELLA
Absorption and fluorescence spectra of marine and fresh water algae using pulsed N2/Ne dye laser as excitation source
[NASA-CR-62090] 03 p0310 N73-12527
ERTS-1 imagery of algal streaks and flooding in Lake Erie and Michigan and Ohio areas
[E73-10793] 18 p2137 N73-27269
ERTS-1 imagery of algal blooms in Lake Erie and Utah Lake, Ohio
19 p2285 N73-28376
Light beam attenuation in suspensions of algae
20 p2405 N73-29325
ERTS-1 imagery of algal bloom in Lake Erie and upwelling in Lake Michigan
[E73-10932] 21 p2529 N73-30274
Light and carbon dioxide effects on algal life support systems in space flight
[NASA-CR-135796] 24 p2885 N73-33039

**ALGAL BLOOM**
U ALGAE

**ALGEBRA**
NT ADJOINTS
NT BANACH SPACE
NT BINOMIALS
NT CANONICAL FORMS
NT CURRENT ALGEBRA
NT DETERMINANTS
NT EIGENVALUES
NT EIGENVECTORS
NT GROUP THEORY
NT HILBERT SPACE
NT HOMOMORPHISMS
NT JORDAN FORM
NT LIE GROUPS
NT LINEAR EQUATIONS
NT LINEAR TRANSFORMATIONS
NT MATRICES [MATHEMATICS]
NT NONLINEAR EQUATIONS
NT POLYNOMIALS
NT QUADRATIC EQUATIONS
NT STOKES THEOREM [VECTOR CALCULUS]
NT VECTOR SPACES
NT VECTORS [MATHEMATICS]
NT VORTICITY
Library of numerical linear algebra programs
[AD-745430] 01 p0072 N73-10588
Chain geometry theorem for Minkowski space
02 p0203 N73-11641
Abstract algebraic techniques to determine synchronization properties of binary, linear, and maximal length sequences
[AD-744101] 13 p1550 N73-22560
Prosodic signals for parenthesis in algebraic expressions
14 p1629 N73-23207
Presentation of algebra of projections on convex cones in Hilbert space
[AD-761867] 19 p2315 N73-28619

**ALGOL**
Checkout of computer programs for errors, using ALGOL compilers
[NPL-NAC-21] 02 p0147 N73-11189
ALGOL computer program for combined photogrammetric-terrestrial cadastral surveying
02 p0165 N73-11338
TRANSLANG, ALGOL-like language and Burroughs D machine for microprogramming
[NASA-CR-129805] 04 p0393 N73-13196
ALGOL procedures for calculating velocity and pressure distribution on rectangular and triangular planforms oscillating harmonically in supersonic flow - Part 1
[FOK-X-449-PT-1] 13 p1471 N73-21909
ALGOL procedures for calculating velocity and pressure distribution on rectangular and triangular planforms oscillating harmonically in supersonic flow - Part 2
[FOK-X-449-PT-2] 13 p1471 N73-21910
Validation tests for ALGOL 60 compiler
[NPL-NAC-33] 22 p2639 N73-31153
Revised algorithm for constrained optimization using quasi Newton-Raphson method based on recurring factorization of approximation to Hessian matrices
[NPL-NAC-32] 22 p2692 N73-31560

**ALGORITHMS**
Algorithm for reducing redundancy during image transmission
01 p0024 N73-10189
Algorithm for adaptive digital filters of data communication channels
01 p0026 N73-10200
Signal processing algorithms for estimating from radar data characteristics and trajectory parameters of bodies moving in air
[AD-745421] 01 p0029 N73-10227
Reliability analysis of Abel transformation algorithm applied to mass measurement in hypersonic wakes
[ISL-21/70] 01 p0041 N73-10324
Algorithm for determining optimal partition of points into mutually exclusive and exhaustive subsets or clusters according to objective function defined on set of all partitions
[F-4878] 01 p0072 N73-10586
Algorithm for synthesizing mass and stiffness matrices from experimental vibration modes
01 p0119 N73-10983
Hardware design and algorithm for image processing on IDECS/PDP system
[AD-743526] 02 p0174 N73-11414
Survey of field of fault diagnosis and key algorithms and heuristics currently in use
[NASA-CR-129095] 02 p0178 N73-11440
Development of least squares curve-fitting algorithm for simultaneous estimation of small signal gain and saturation intensity in carbon dioxide laser waveguide
[NASA-TM-X-66097] 02 p0181 N73-11468
Algorithm for computing Luenberger canonical form directly for multivariable systems
[NASA-CR-129174] 02 p0195 N73-11576
Heuristic algorithm for mixed integer linear programming problems
[NPL-NAC-18] 02 p0202 N73-11637
Algorithms and FORTRAN 4 data analysis programs for reflectometer diagnosis of thin boundary layer plasma sheaths - users manual
[AD-747041] 02 p0217 N73-11758
Comparison of open and closed loop applications of second order guidance algorithm using minimum distance strategy for Earth-Mars transfer
[NASA-CR-129170] 02 p0227 N73-11830
Walsh transformation for two dimensional correlation and convolution in pattern recognition
[AD-746701] 03 p0272 N73-12207
Algorithms for computerized design of printed circuits with fixed component positions
03 p0278 N73-12255
Construction of extremal controller for high current betatron using stochastic algorithms
[AD-747370] 03 p0281 N73-12279
Algorithm for calculating distribution functions of meteorological parameters by computer technique
[AD-749588] 04 p0446 N73-13642
Algorithms for construction of minimum cost communication networks
[PB-211233] 05 p0514 N73-14178
Automata theory of cubical complexes applied to diagnosis and algorithmic description, noting logic design of ultra LSI
[NASA-CR-130388] 05 p0517 N73-14201
Recognition and parsing algorithms for phrase structure languages
[NLL-SMRE-TRANS-5884-[8313.4]]
06 p0643 N73-15219
Evaluation of ERTS-1 imagery data compression algorithm technique
[E73-10012] 06 p0659 N73-15348
Algorithm for choosing adaptive loop parameters and adjustment intervals of adaptive control systems
07 p0764 N73-16207
Theoretical derivation of finite element solution algorithm for transient energy conservation equation
[NASA-CR-130149] 07 p0813 N73-16593
Algorithms for variable order fiiters from extensions of spline function concepts
[AD-751124] 07 p0813 N73-16595
Application of pattern recognition oriented algorithms for multispectral data analysis software system
[NASA-CR-130757] 08 p0887 N73-17184
Development of digital fast-time air traffic control conflict prediction models and application to specific air route traffic control situations
[UTIAS-TN-183] 08 p0941 N73-17708
Algorithm for targeting finite burn maneuvers
[NASA-TM-X-66180] 08 p0961 N73-17859
Development of algorithm for multiple hypothesis testing with application to amplitude comparison monopulse radar system in air traffic control operations
[TN-1973-7] 09 p1002 N73-18173
Implementation of FORTRAN extended graph algorithmic language for univac 1108 computer
[NASA-CR-130966] 09 p1006 N73-18212
Algorithm for solving pure integer linear programming problem
[NPL-NAC-20-PT-1] 09 p1057 N73-18621
ALGOL 60 subroutine for implementation of modified Newton algorithms for problem solving
[NPL-NAC-24] 09 p1057 N73-18622
Algorithm for adjusting linear and nonlinear classifiers
[BMVG-FBWT-72-5] 09 p1057 N73-18623
Algorithms for iterative solution of unconstrained optimization problems
[NPL-NAC-25] 09 p1058 N73-18625
Algorithms for numerical solution of problems in calculus of variations
[NPL-NAC-28] 09 p1058 N73-18626
Parallel image logical operations using cross correlation
09 p1066 N73-18695
Representations of language recognition problem for theorem prover in first order logic
[NASA-CR-131402] 11 p1310 N73-20632
Gradient-secant algorithm for unconstrained optimization
[NASA-CR-131396] 11 p1310 N73-20633
Simple algorithm for optimal control of systems governed by delayed differential equations
[AD-754379] 11 p1312 N73-20650
Application of loran/inertial hybrid system and Kalman filter algorithm to fixed feedback gain
11 p1318 N73-20701
Development of structural optimization algorithm used with large finite element program based on displacement method of structural analysis
12 p1356 N73-21005
Design of FGRAAL type compiler language for solving graph structure algorithm problems
[NASA-CR-131474] 12 p1382 N73-21204
Algorithm for determining location of moving object by inertial navigation
12 p1419 N73-21500
Algorithm for space vehicle re-orientation through angular velocity control by jet momentum
12 p1425 N73-21555

Maximum likelihood testing algorithm for estimating monopulse radar signal amplitude in air traffic control
[AD-756844] 13 p1493 N73-22105
Three day advance warning system of heating plant failure using algorithmic detection methods
[NASA-CR-131571] 13 p1505 N73-22197
Algorithm for adaptive convergence rate on weak noise components in seismic signal processing
[AD-756904] 13 p1525 N73-22361
Algorithm for calculating Jordan canonical form of matrix
[NASA-CR-131654] 13 p1550 N73-22557
Analysis of algorithms for failure detection, isolation, and correction of redundant inertial instruments in strapdown dodecahedron configuration
[NASA-CR-124234] 13 p1556 N73-22608
Algorithm for determining position of moving object by inertial navigation methods
13 p1556 N73-22613
Discrimination of liquids and glides in automatic speech recognition system using syntactic recognition algorithms in analysis of digital spectrograms
14 p1623 N73-23149
Three stage algorithm for representing human speech by time ordered sets of Hanning cosine modulated wavefunctions
14 p1630 N73-23214
Search and optimization capabilities of collective of independent automatic devices
14 p1644 N73-23331
Algorithms for developing equations yielding root locus diagram
[TT-7303] 14 p1683 N73-23653
Algorithm for determining frequency response of linear control system
[TT-7304] 14 p1683 N73-23654
Search algorithm for component placement problem in computerized design of circuits
[AD-756502] 14 p1684 N73-23663
Development of algorithms for calculating modal trajectory estimate, conditional mean state estimate, and weighted least squares trajectory estimate
[AD-757240] 14 p1684 N73-23665
Computer graphic display system for generating optimal electric propulsion space trajectory
[NASA-CR-130241] 15 p1754 N73-24217
Algorithm for computer processing of Fourier transformations
[AD-758451] 15 p1755 N73-24222
Algorithm for automatic photointerpretation of plant species and stresses in Minnesota imagery
[E73-10639] 15 p1776 N73-24398
Algorithm for computer simulation of Eulerian angles for spacecraft attitude
[NAL-TR-305] 15 p1803 N73-24612
Performance of algorithms for calculating shortest path trees in networks
[NBS-TN-772] 15 p1803 N73-24615
Algorithm for modifying collocation method of solving differential equations
[NASA-TT-F-14800] 15 p1803 N73-24616
Algorithm for computing satellite orientation and tables of gravitational constants used for computations
[NASA-TT-F-14699] 15 p1831 N73-24840
Algorithm and computer program for generating all distinct 2[p-q] fractional factorial designs and applications to design of experiments
[NASA-TN-D-7327] 16 p1934 N73-25650
Algorithm for correcting errors in linear transmission codes
[AD-760154] 17 p2000 N73-26169
Optimal algorithms for processing radar data for trajectory estimation
[AD-759947] 17 p2000 N73-26171
Discrete unitary transforms with fast algorithm for encoding images for transmission
[NASA-CR-132771] 17 p2055 N73-26622
Algorithm for computing unrelieved electromagnetic forces of attraction of rotors in EDG electric motors
17 p2059 N73-26657
Algorithm for computerized spectral analysis on linearly swept signals
[AD-760775] 18 p2120 N73-27138
Algorithm for automatic classification and mapping of earth resources satellite data
[NASA-TM-X-64762] 18 p2144 N73-27332
Extension of combination shift QZ algorithm for solving generalized matrix eigenvalue problem
[NASA-TN-D-7305] 18 p2169 N73-27519
One-level polynomial objective analysis of meteorological fields
[NLL-M-22903-[5828.4F]] 18 p2170 N73-27524
Computer algorithm for calculating orbital trajectories by optimization of equation of motion parameters
18 p2211 N73-27846
Automatic recognition algorithm for liquids and glides
[AD-762377] 19 p2237 N73-28032
Algorithm for discrete transforms for implementing computer programs in radar signal processing
[AD-762437] 19 p2237 N73-28039
Forward algorithm for scheduling process monitor in time sharing computer sample data control
[AD-761668] 19 p2240 N73-28058
Analysis of algorithms for construction of system of diagnostic programs for digital computer complexes
[AD-762310] 19 p2242 N73-28074
Error detecting algorithm for digital control computer
[AD-762241] 19 p2242 N73-28075
Computer programming algorithm for surface line drawing graphics
[AD-762023] 19 p2242 N73-28077
Algorithm for classifying land use categories of ERTS-1 data by textural features
[PAPER-I16] 19 p2279 N73-28337
Application of classification algorithms to ERTS-1 MSS imagery of Texas land and water coastal features
19 p2286 N73-28383
Processes, algorithms, and procedures for extraction and interpretation ERTS-1 data
19 p2290 N73-28412
Algorithm for optimal control problems with bounded state
[AD-761790] 19 p2314 N73-28610
Theory of modified quasilinearization algorithm for optimal control problems with bounded state variables - Part 1
[AD-761786] 19 p2315 N73-28614
Modified quasilinearization algorithm for optimal control problems with bounded state variables - Part 2
[AD-761791] 19 p2315 N73-28615
Examples for sequential gradient-restoration algorithm for minimizing functions subject to constraints
[AD-761789] 19 p2315 N73-28618
Automation of computer controlled robot manipulators
[JPRS-59717] 20 p2371 N73-29051
Evaluation of algorithm for linear inequalities and its applications
[REPT-11] 20 p2437 N73-29576
Nearest neighbor algorithms for pattern classification
[REPT-18] 20 p2438 N73-29582
Algorithms for solving differential-range bearing in rectangular geocentric system of coordinates
20 p2439 N73-29595
Algorithm for solving approximate problem of nonlinear function
[NASA-CR-133728] 20 p2440 N73-29599
Collection of Soviet articles on computer elements and systems
[TT-72-50009] 21 p2512 N73-30150
Algorithm for location of electronic modules on printed circuit board
21 p2513 N73-30156
Functional algorithms for homogeneous general-purpose computer systems
21 p2513 N73-30159
Functional algorithms for homogeneous general-purpose computers in simple situations
21 p2513 N73-30160
Data compression algorithm and techniques for ERTS-1 imagery
[E73-10959] 21 p2532 N73-30301
Algorithms employed in current ERIM data processing scheme
[NASA-CR-134007] 21 p2538 N73-30347
Algorithm for optimization of reliability characteristics of redundant digital computer
[AD-763261] 22 p2640 N73-31156
Branch and search algorithms for knapsack and other computationally related problems
[PB-221436/9] 22 p2641 N73-31165
Algorithm for assembling continuous boundaries and contours from black and white picture for computer processing and photointerpretation
[NPL-COM-66] 22 p2675 N73-31426
Use of Cholesky decomposition technique in feature selection and classification algorithms
[NASA-CR-133990] 22 p2690 N73-31550
Revised algorithm for constrained optimization using quasi Newton-Raphson method based on recurring factorization of approximation to Hessian matrices
[NPL-NAC-32] 22 p2692 N73-31560
Contour plotting algorithm for aerial radiation patterns
[BBC-RD-1973/18] 23 p2755 N73-32045
Recognition algorithm for object localization in pictures
[BMVG-FBWT-73-14] 23 p2760 N73-32091
Algorithms involved in visual shape perception
24 p2886 N73-33050
Algorithm of simple inductive interaction between man and surrounding objects and events
24 p2888 N73-33058
Description of software modules of Image Data Processing System
[NASA-CR-124447] 24 p2897 N73-33123
Wave digital filter design using ladder networks
24 p2899 N73-33145
Application of second-order accurate fluid algorithm for variable spatial grid
[AD-765316] 24 p2910 N73-33225
Application of random walks for search optimization and function space
24 p2944 N73-33514

**ALIGNMENT**
NT SELF ALIGNMENT
Determining optimal runway orientation for minimizing frequency of crosswinds and headwind reversals at Cape Kennedy
[NASA-CR-128995] 01 p0075 N73-10617
Ferromagnetic materials sensor for detecting time varying magnetic field disturbances and positional changes in ferromagnetic objects
[AD-748117] 03 p0338 N73-12757
EPR study of molecular ordering in smectic-A liquid crystals without nematic phases
[NASA-TN-D-7124] 04 p0437 N73-13563
Real time program for alignment of components and subassemblies prior to installation in chamber
[NASA-CR-128712] 07 p0800 N73-16493
Alignment control of high energy laser system and importance of external sources of alignment error
[UCRL-74050] 08 p0929 N73-17609
Methods for determining plane of meridian during initial alignment of inertial systems
10 p1184 N73-19636
Prelaunch alignment of stable platform to desired orientation
[NASA-CR-128802] 10 p1184 N73-19638
Angular alignment of inertial reference by non-directional data from radio aids
[NASA-CR-128806] 10 p1185 N73-19639
Alignment and field distribution of coil currents in storage accelerators using superconducting magnets
[BNL-17272] 10 p1194 N73-19712
Plastic compensating coatings for alignment and assembly of bearing unit
[AD-754591] 11 p1300 N73-20550
Parameters of single-axis floated gyroscopes when used in inertial systems requiring rapid gyrocompassing for alignment
11 p1319 N73-20709
A-7 aircraft airborne, ground, and shipboard inertial navigator alignment methodology
11 p1319 N73-20710
Guide accessories for correctly aligning paper in typewriter to correct typographical errors
[NASA-CASE-MFS-15218-1] 22 p2676 N73-31438
Method of alignment and technology of fabricating RTI-7.5/250 MVTU radio telescope antennas
23 p2838 N73-32675
Design of precision vertical alignment system using laser with gravitationally sensitive cavity
[NASA-CASE-ARC-10444-1] 24 p2930 N73-33397

**ALIPHATIC COMPOUNDS**
NT ACETONE
NT ACETYLENE
NT ACRYLONITRILES
NT ADENINES
NT ADENOSINE TRIPHOSPHATE [ATP]
NT ALKENES
NT ALKYL COMPOUNDS
NT ALLYL COMPOUNDS
NT BUTADIENE
NT BUTENES
NT CARBAMIDES
NT CARBON TETRACHLORIDE
NT CELLULOSE
NT CYCLIC HYDROCARBONS
NT CYCLOBUTANE
NT DEXTRANS
NT DIBUTYL COMPOUNDS
NT DIISOCYANATES
NT ETHANE
NT ETHYL ALCOHOL
NT ETHYLENE
NT ETHYLENEDIAMINE
NT GLUCOSE
NT GLUCOSIDES
NT GLUTAMIC ACID
NT GLYCEROLS
NT GLYCOLS
NT HEXENES
NT HEXOGENES [TRADEMARK]
NT HYDRAZIDES
NT HYDRAZINE NITROFORM
NT HYDRAZINES
NT ISOPROPYL ALCOHOL
NT KETONES
NT LACTATES
NT METHANE
NT METHYL ALCOHOLS
NT METHYL COMPOUNDS
NT METHYL NITRATE
NT METHYLHYDRAZINE
NT MONOSACCHARIDES
NT NUCLEASE
NT PARAFFINS
NT PENTANES
NT PENTANONE
NT PROPANE
NT PROPYL COMPOUNDS
NT PROPYLENE
NT RIBOSE
NT THIOLS
NT URETHANES

Analysis of thermal conductivity of liquid aliphatic hydrocarbons with saturated and unsaturated straight or branch chain carbons
[ESDU-67018] 01 p0116 N73-10955
Analysis of thermal conductivity of liquid halogenated aliphatic hydrocarbons and commercial refrigerants
[ESDU-68024-AMEND-A] 01 p0116 N73-10956

ALKALI HALIDES
NT CESIUM IODIDES
NT POTASSIUM IODIDES
NT SODIUM CHLORIDES
NT SODIUM FLUORIDES
Application of alkali halides for holographic recording and recovery at room temperatures for high density data storage systems
[AD-748027] 03 p0311 N73-12537
Analysis of laser bulk damage in alkali-halides with no self-focusing and measurement of damaging fields considering effects of inclusions on bulk optical strength
05 p0554 N73-14502
Hardening characteristics of alkali halides selected as laser window materials
[AD-749867] 05 p0559 N73-14545
Mechanical properties of polycrystalline alkali halides determined for application to high power infrared laser windows
[AD-752193] 08 p0930 N73-17617
Correlation of materials properties with atomic density concept for alkali halides
[NASA-CR-124095] 09 p0999 N73-18156

ALKALI METALS
NT CESIUM
NT LIQUID SODIUM
NT LITHIUM
NT LITHIUM ISOTOPES
NT POTASSIUM
NT RUBIDIUM
NT RUBIDIUM ISOTOPES
NT SODIUM
NT SODIUM VAPOR
General, nonstationary electron gas equation for noble gas-alkali plasma
[JUL-802-TP] 01 p0085 N73-10704
Charge exchange cross sections for protons and alkali atoms using classical approximation of Gryzinski
[NASA-CR-129262] 03 p0339 N73-12763
Resistance leval indicator used in high temperature alkali tanks
[SFB-MHD-2] 04 p0422 N73-13444
Charge transfer cross sections of alkali metals
[AD-752909] 09 p1000 N73-18161
High field superconductivity in alkali metal [Na, K, Rb, and Cs] intercalates of MoS2
[NASA-TM-X-68206] 11 p1330 N73-20794
Development of high power alkali vapor lamp for laser applications
[AD-755213] 13 p1560 N73-22646
Separation of short half life O-15 and N-13 isotopes from alkali metals, steels, copper, and indium by gamma activation analysis
[CONF-721069-24] 18 p2160 N73-27453
Method for producing alkali metal dispersions of high purity
[NASA-CASE-XNP-08876] 19 p2309 N73-28573
Thermotransport in liquid alkali metal alloys as function of composition
[COO-841-29] 24 p2992 N73-33915

ALKALIES
NT LITHIUM HYDROXIDES
NT POTASSIUM HYDROXIDES
NT SODIUM HYDROXIDES
Homogeneous cyanoethylation of hydrogen cyanide in presence of alkaline catalysts
[NASA-TT-F-14690] 08 p0884 N73-17154
Speed of alkaline polymerization of hydrocyanic acid - Part 1
[NASA-TT-F-14651] 09 p0998 N73-18145
Chemical composition of polymers formed by alkaline polymerization of hydrocyanic acid - Part 2
[NASA-TT-F-14645] 09 p0998 N73-18146
Intensity relations and spectral satellite studies of alkali/foreign gas interactions
13 p1528 N73-22385

ALKALINE BATTERIES
Development of nickel hydroxide electrode for use in rechargeable alkaline batteries
[AD-746335] 01 p0007 N73-10058
Comparison of alkaline manganese-zinc cells with salt-electrolyte cells
[AD-746558] 02 p0129 N73-11051
Sintered Cd-Ni electrodes for alkaline batteries
[AD-754237] 10 p1112 N73-19063
Design of prototype thermal battery incorporating pelletized alkaline heat source
[SC-RR-69-497-A] 12 p1366 N73-21084
Activation and cycling of silver zinc batteries
[AD-761186] 20 p2364 N73-29013

ALKALINE EARTH OXIDES
NT BARIUM OXIDES
NT BERYLLIUM OXIDES
NT CALCIUM OXIDES
NT MAGNESIUM OXIDES

ALKALOIDS
NT ATROPINE

ALKANES
NT ETHANE
NT HEXENES
NT METHANE
NT PARAFFINS
NT PENTANES
NT PROPANE

ALKENES
NT BUTADIENE
NT BUTENES
NT ETHYLENE
NT HEXENES
NT PROPYLENE
Carbonyl formation data at elevated temperatures for estimating storage life of unstabilized polyolefins
[AD-748827] 04 p0438 N73-13572
Thermomechanical analysis of physical transitions and stability of poly[norbornadiene] in nitrogen
[AD-749374] 05 p0566 N73-14396
Mechanisms of oxidation of polyolefins below 150 C
08 p0882 N73-17139
Spectrophotometric analysis of terminal epoxy and olefinic compounds
[TN-287] 15 p1746 N73-24155
Effects of ionizing radiation and high pressure on polymerization processes of fluoroolefins and fluorocarbon compounds
[AD-750151] 16 p1870 N73-25143
Thin layer chromatographic identification and infrared spectrophotometric quantification of antitoxiants used in manufacturing polyolefinic polymers
[REPT-6726] 22 p2625 N73-31029
Optimization of supersonic aircraft C3/C4 polymer fuel by normal paraffins containing 10 to 16 carbon atoms
[DLR-FB-73-32] 22 p2708 N73-31689

ALKYL COMPOUNDS
NT DIBUTYL COMPOUNDS
NT METHYL NITRATE
Protective effects of pyridinium salts against alkyl phosphate poisoning including influence of chemical and aging
[BMVG-FBWT-72-8] 07 p0746 N73-16072
Pharmacological data for aminothiol and indolylalkylamine radioprotectors
11 p1240 N73-20066
Preparation of fluorohydroxy ethers by reacting fluoroalkylene oxides with alkali salt of polyfluoroalkylene diol
[NASA-CASE-MFS-10507] 21 p2505 N73-30101

ALKYNES
NT ACETYLENE

ALL SKY PHOTOGRAPHY
Direct comparison between electric field measurements by Injun 5 satellite and visual aurora data
[NASA-CR-132958] 16 p1906 N73-25416

ALL-WEATHER AIR NAVIGATION
Display systems for all-weather terminal operational capability of V/STOL aircraft
[AGARD-R-594] 02 p0174 N73-11407
Research projects involving all weather landing systems to include electronic and visual guidance, airborne systems, and data collection
[FAA-ED-07-3] 06 p0697 N73-15680
Development and characteristics of cathode ray tube vertical display system for use in all-weather air navigation aircraft
[AD-752510] 08 p0868 N73-17026
Radio navigation system for providing all-weather short baseline navigation capability for Army aeronautical missions
[AD-752466] 08 p0942 N73-17715
Research projects to develop all-weather, low level navigation systems based on one way ranging, range-range navigation techniques
[AD-755205] 12 p1426 N73-21556
Purpose, operating principles, and technical description of instrument panel equipment installed on An-24 aircraft
[AD-758751] 15 p1789 N73-24504
Status of civil airline implementation of all-weather landings in Europe and United Kingdom
[MTR-6211] 20 p2452 N73-29711

ALLOCATIONS
NT RESOURCE ALLOCATION
Optimum allocation of redundancy in system of serially connected subsystems
[NASA-TN-D-7164] 09 p1056 N73-18614
Scope of Federal funding for scientific research and development
[NSF-72-317] 15 p1846 N73-24958
Summary of national patterns of R and D funding and manpower allocations
[NSF-73-303] 15 p1846 N73-24960
Congressional committe report to identify and resolve disagreements in NASA appropriations for Fiscal Year 1974
[H-REPT-93-353] 21 p2607 N73-30892
Congressional hearings concerning appropriations for NASA operations during Fiscal Year 1974 - Part 1
21 p2608 N73-30906
Congressional hearings concerning appropriations for NASA operations during Fiscal Year 1974 - Part 3
21 p2608 N73-30907
Differential pricing policy in airline operations
23 p2861 N73-32857

ALLOYS
NT ALUMINUM ALLOYS
NT ANTIMONY ALLOYS
NT AUSTENITIC STAINLESS STEELS
NT BEARING ALLOYS
NT BERYLLIUM ALLOYS
NT BINARY ALLOYS
NT BISMUTH ALLOYS
NT BORON ALLOYS
NT BRASSES
NT BRONZES
NT CADMIUM ALLOYS
NT CARBON STEELS
NT CHROMIUM ALLOYS
NT CHROMIUM STEELS
NT COBALT ALLOYS
NT COPPER ALLOYS
NT EUTECTIC ALLOYS
NT FERRITIC STAINLESS STEELS
NT GALLIUM ALLOYS
NT GERMANIUM ALLOYS
NT GOLD ALLOYS
NT HASTELLOY [TRADEMARK]
NT HEAT RESISTANT ALLOYS
NT HIGH STRENGTH ALLOYS
NT HIGH STRENGTH STEELS
NT INCONEL [TRADEMARK]
NT INDIUM ALLOYS
NT IRON ALLOYS
NT KAMACITE
NT LEAD ALLOYS
NT LIGHT ALLOYS
NT LIQUID ALLOYS
NT LITHIUM ALLOYS
NT MAGNESIUM ALLOYS
NT MANGANESE ALLOYS
NT MANGANIN [TRADEMARK]
NT MARAGING STEELS
NT MARTENSITIC STAINLESS STEELS
NT MOLYBDENUM ALLOYS
NT NEODYMIUM ALLOYS
NT NICHROME [TRADEMARK]
NT NICKEL ALLOYS
NT NICKEL STEELS
NT NIMONIC ALLOYS
NT NIOBIUM ALLOYS
NT NITINOL ALLOYS
NT OSMIUM ALLOYS
NT PALLADIUM ALLOYS
NT PERMALLOYS [TRADEMARK]
NT PLATINUM ALLOYS
NT RARE EARTH ALLOYS
NT REFRACTORY METAL ALLOYS
NT RHENIUM ALLOYS
NT RHODIUM ALLOYS
NT RUTHENIUM ALLOYS
NT SELENIUM ALLOYS
NT SILICON ALLOYS
NT SILVER ALLOYS
NT STAINLESS STEELS
NT STEELS
NT TANTALUM ALLOYS
NT TERNARY ALLOYS
NT THALLIUM ALLOYS
NT TIN ALLOYS
NT TITANIUM ALLOYS
NT TUNGSTEN ALLOYS
NT UDIMET ALLOYS
NT URANIUM ALLOYS
NT VANADIUM ALLOYS
NT WROUGHT ALLOYS
NT YTTRIUM ALLOYS
NT ZINC ALLOYS
NT ZIRCALOY 2 [TRADEMARK]
NT ZIRCALOYS [TRADEMARK]
NT ZIRCONIUM ALLOYS
Single-step diffusion welding process
[NASA-CASE-LEW-11388-2] 01 p0061 N73-10500
Metallic alloy and aluminide coating for metallic base system
[NASA-CASE-LEW-11696-1] 01 p0061 N73-10502
Crystalline structures, physical properties, chemical properties, and phase characteristics of various metal systems and alloys
[AD-746792] 02 p0189 N73-11532
Directional martensite transformations in steel and alloy development
[AD-748408] 04 p0436 N73-13553
Weldability and properties of materials undergoing electron beam welding
[CRANFIELD-MAT-7] 05 p0551 N73-14474
High temperature ceramic to metal seal capable of operation at 1200 C for 3 to 5 years
[NASA-CR-120831] 05 p0552 N73-14484
Electron-impurity spin interchange model for analyzing magnetic properties of diluted magnetic alloys at low temperatures
08 p0931 N73-17626

Effects of preliminary deformation on superplasticity and other properties of metals and alloys
[JPRS-58097] 09 p1046 N73-18529
Influence of heat treatment on strength properties of EI893L alloy
[JPRS-58137] 09 p1048 N73-18543
Fracture mechanics and structural fatigue of nickel alloys, aluminum alloys, and molybdenum alloys at elevated temperatures
[AD-753687] 09 p1097 N73-18958
Anneal hardening of irradiated molybdenum metals and alloys
[ORO-3612-9] 10 p1173 N73-19545
Microstructure and mechanical properties of precipitation hardened-dispersion strengthened aluminum and titanium alloys and refractory materials
[AD-753910] 10 p1174 N73-19550
Compilation of metallurgical processes for variety of metals and alloys
[NASA-SP-5953(01)] 11 p1306 N73-20593
Volumetric factor of precipitation phase causing X ray diffraction fading in alloys
[JPRS-58761] 12 p1414 N73-21455
Infiltrating porous and particulate materials with metallic alloys
[Y-1846] 12 p1414 N73-21458
Optical properties and electronic structure of metal alloys
[AD-755847] 12 p1441 N73-21675
Analysis of metals and alloys to include superelasticity properties, plastic growth in cracks, strain aging, and strengthening by nuclear gamma resonance
[JPRS-58611] 13 p1540 N73-22477
Development of model for conditions of superplasticity related to maximum interphase surface of fluctuation nuclei of phase transformation
13 p1540 N73-22478
Exoelectronic emission and relationship with various surface properties of metals and alloys
[AD-756943] 13 p1543 N73-22509
Superplastic flow as common phenomenon during plastic deformation of metals and alloys
[AD-756601] 13 p1544 N73-22512
Vacuum brazing-gas quenching process for joining chemical and ordnance munitions materials
[AD-759117] 16 p1919 N73-25531
Potential of hot-isostatic pressing, hydrostatic extrusion and deformable die tube tapering processes to production of titanium tubes
[AD-759504] 16 p1919 N73-25532
Standards for metallic specimens to include methods of mechanical and technological testing
[JPRS-59280] 17 p2044 N73-26538
Mechanical properties and crystal structures of polymorphous metals and alloys
[AD-759753] 17 p2074 N73-26779
Structure and segragation in cast alloys
[AD-761202] 18 p2163 N73-27470
Pressure shaping of steels and alloys
[AD-762308] 19 p2306 N73-28549
Effect of high speed volumetric deformation on ductility of metals and alloys
[AD-762246] 19 p2310 N73-28582
Effect of applied electric field on oxidation/hot corrosion of metals and alloys in molten salt
[AD-762074] 19 p2311 N73-28584
Experimental methods for determining internal damping in metal alloys and identification of factors causing internal damping
[NLL-CE-TRANS-6132-[9022.09]]
20 p2429 N73-29508
Analysis of variations in hardness and microstructure of metals subjected to shock wave pressures
[NLL-NEL-TT-2489-[6075.461]]
20 p2429 N73-29514
Development of procedures for determining molybdenum in iron and steel with emphasis on factors affecting stability and temperature dependence
[TN-303] 20 p2431 N73-29529
Yielding, work hardening, and fracture behavior of ordered and disorded alloys as function of dislocation
[ORO-3935-25] 21 p2559 N73-30514
Formation of solid solutions and fluidity of alloys based on aluminum and titanium
[AD-763491] 21 p2560 N73-30522
Effect of aluminum on fundamental mechanical properties of titanium
[AD-763785] 21 p2560 N73-30524
Theoretical and experimental approach to stress corrosion cracking in metal alloys
21 p2603 N73-30859
Electrical, magnetic, and thermal properties of dilute and concentrated magnetic alloys
[AD-763820] 22 p2707 N73-31682
Properties of materials in high pressure hydrogen at cryogenic, room, and elevated temperatures
[NASA-CR-124394] 22 p2725 N73-31804
Two-step diffusion welding process of unrecrystallized alloys
[NASA-CASE-LEW-11388-1] 23 p2795 N73-32358
Elastic constants for calculating parallel Shockley partial dislocations in ordered alloys and intermetallic compounds
23 p2803 N73-32420
Composition and structural modification of glassy carbon alloys
[AD-764918] 24 p2944 N73-33511

**ALLUVIAL CONES**
U ALLUVIUM

**ALLUVIAL PLAINS**
U FLOOD PLAINS

**ALLUVIUM**
Utilization of ERTS-1 MSS imagery for study of faulting in alluvium of California, Nevada, and Arizona
[E73-10070] 07 p0779 N73-16332
Utilization of Skylab EREP data in making agriculturally oriented decisions in Mississippi Delta alluvial plain region
[E73-11125] 24 p2916 N73-33280

**ALLYL COMPOUNDS**
Monomer polymerization by plasma discharge as thin film for water purification membrane
[NASA-CASE-ARC-10643-1] 20 p2374 N73-29074

**ALMUCANTAR**
U ELEVATION ANGLE

**ALOUETTE SATELLITES**
NT ALOUETTE 1 SATELLITE
NT ALOUETTE 2 SATELLITE
Low energy particle measurements by soft particle spectrometer on ISIS-1 orbiting satellite and relation to production of auroral particles
10 p1146 N73-19329

**ALOUETTE 1 SATELLITE**
Structure and variation of topside ionosphere at mid-latitudes during sunrise period based on Alouette 1 electron density measurements
[AD-748430] 03 p0299 N73-12443

**ALOUETTE 2 SATELLITE**
Comparison of electron temperature from Alouette diffuse resonance observations with those from Alouette 2 electrostatic probe
[NASA-TM-X-66205] 12 p1433 N73-21611

**ALPHA DECAY**
Energy tables for alpha emitting nuclides
[AAEC/TM-631] 17 p2065 N73-26703

**ALPHA PARTICLES**
Analysis of alpha particle observations performed by HEOS 1 satellite and comparison with observations made by Vela 3 and Explorer 34 satellites
01 p0098 N73-10809
Four particle correlations in nuclear alpha structure
[HMI-B-125] 02 p0213 N73-11727
Development of alpha and X ray spectrometers for use on Apollo 15 and 16 flights
[NASA-CR-128649] 03 p0301 N73-12461
Lunar radon emanation measurements, using alpha particle spectrometers on Apollo 16
12 p1451 N73-21754
Alpha particle beam spalling production of aluminum, oxygen, carbon, and beryllium isotopes, and cosmic ray transport theory
13 p1561 N73-22651
Black Brant rocket measurements of proton and alpha particle fluxes
[AD-760138] 17 p2028 N73-26417
Absorbed dose rate and equivalent dose rate investigation for galactic cosmic ray protons and alpha particles in manned spacecraft shields
[ORNL-TM-4029] 17 p2089 N73-26901
Angular distributions of elastically and inelastically scattered 42 MeV alpha particles from Cu-65
[NASA-TN-D-7354] 18 p2181 N73-27611
Performance of OV-5 and OV-6 alpha and proton particle detector
[AD-760147] 19 p2302 N73-28505
Low energy solar flare alpha to proton flux ratios
19 p2337 N73-28804

**ALPHA RADIATION**
U ALPHA PARTICLES

**ALPHANUMERIC CHARACTERS**
NT BINARY DIGITS
Alphanumeric character display device for oscilloscopes
[NASA-CASE-GSC-11582-1] 23 p2765 N73-32120

**ALPS MOUNTAINS [EUROPE]**
Geomorphology, tectonics, and structural relations between Alps and Pyrenees based on ERTS-1 imagery
[E72-10286] 04 p0410 N73-13336
ERTS-1 imagery of geography, geology, and glaciology of Germany and part of Alps Mountains
[E73-10099] 09 p1020 N73-18322
Snow cover survey and vegetation growth in Swiss Alps using ERTS-1 imagery
[E73-10586] 14 p1657 N73-23446
Survey of snow cover and vegetation growth in high mountains of Swiss Alps based on ERTS-1 imagery
[E73-10733] 17 p2020 N73-26339
Analysis of tectonic situation in Alps and Apennine mountains using ERTS-1 imagery of previously inaccessible areas
[PAPER-G27] 19 p2267 N73-28258
ERTS-1 imagery of water pollution, sedimentation, and geology of southeastern France and western Alps
[PAPER-R6] 19 p2283 N73-28364

**ALSEP**
U APOLLO LUNAR SURFACE EXPERIMENTS PACKAGE

**ALTERNATING CURRENT**
Electrical and dimensional characteristics of ac superconducting power transmission circuits
[AD-745846] 01 p0088 N73-10727
Ac measurements of cold worked superconducting niobium-titanium alloy
[CONF-720513-4] 03 p0346 N73-12819
Analysis of alternating current loss mechanisms in superconductors with comparison of performance in coil and cable configurations
10 p1108 N73-19032
Effect of active, inductive and capacitive resistance of elements of asymmetric alternating current battery charger on discharged characteristics of silver zinc batteries
[AD-756955] 13 p1478 N73-21970
Voltage fluctuation of batteries during charging with asymmetrical alternating current
[AD-756557] 13 p1478 N73-21974
Analysis of effects of alternating current on corrosion of iron in aqueous solutions of acidic and neutral salts
[REPT-733] 14 p1675 N73-23590
AC conductivity and dielectric dispersion in amorphous semiconductors
[AD-757097] 14 p1698 N73-23780
Ac susceptibility of powdered samples of SmCo5, YCo5, and NdCo5
[AD-758218] 14 p1700 N73-23794
Magnetic coil design and physical phenomena responsible for ac losses in superconductivity
15 p1761 N73-24273
Superconducting materials for high field ac magnets with one second field risetime
[BMFT-FBT-73-03] 22 p2685 N73-31509

**ALTERNATING CURRENT GENERATORS**
U AC GENERATORS

**ALTERNATORS [GENERATORS]**
U AC GENERATORS

**ALTIMETERS**
NT LASER ALTIMETERS
NT RADIO ALTIMETERS
Effects of tracking system errors of satellite orbit when single station provides satellite tracking in immediate area of altimeter evaluations
[NASA-TM-X-69352] 03 p0301 N73-12457
Analysis of pilot performance in evaluating three types of aircraft altimeters during C-135B simulator flight
[ASD-TR-72-63] 04 p0383 N73-13117
Aircraft instrument errors
05 p0577 N73-14695
Conference on laser and radar altimeter measurement of sea surface topography from space
[NASA-CR-130293] 06 p0661 N73-15369
Design criteria for highly accurate and reliable GEOS-C satellite altimetry system
06 p0661 N73-15370
Effect of sea state and atmospheric parameters on satellite altimeter performance
06 p0662 N73-15372
Sampling function representation for applying satellite-to-ocean altitude altimeter data to geoid
06 p0662 N73-15373
Combined marine astrogravimetry and marine geodetic acoustic techniques for accurate determination of global marine geoid
06 p0662 N73-15374
Sea state effects on altimeter signal scattering and radar wave form estimates
06 p0663 N73-15381
Influence of sea state on short pulse radar satellite altimeter determination of mean surface position
06 p0663 N73-15385
Electrical and performance characteristics of Skylab radar altimeter
06 p0663 N73-15386
Operating characteristics of GEOS-C K band radar altimeter
06 p0663 N73-15387
Service life and reliability of single transmitter and array modular type satellite altimeter systems
06 p0663 N73-15388
Compression of satellite altimeter radar pulses and high resolution sea reflectivity
06 p0663 N73-15389
Numerical analysis on hypothetical satellite altimeter detection of tides and tsunamis
06 p0664 N73-15396
Design and performance of optical altimeter with shaft angle recording
[AD-749964] 06 p0675 N73-15488
Precision yawsonde calibration technique within 0.1 deg accuracy
[AD-758158] 14 p1710 N73-23880
Frequency modulated radar systems for range finding, velocity measurement, and altimeters
16 p1873 N73-25162
Calibration and evaluation of Skylab altimetry for geodetic determination of geoid
[E73-10671] 16 p1900 N73-25366
Development of method for predicting performance of barometric sensing systems used in determining sounding rocket altitude
[NASA-TM-X-65991] 17 p2087 N73-26881

Development of mathematical models for processing Skylab EREP altimeter data
[E73-10801] 18 p2138 N73-27276
Coordination of ground truth and basic altimeter data processing requirements for North Atlantic test area
[E73-10811] 18 p2139 N73-27286
Gravimetry and satellite altimetry for determining earth gravity field
[AD-759536] 18 p2148 N73-27365
Calibration and evaluation of Skylab altimetry for geodetic determination of geoid
[E73-10872] 20 p2393 N73-29223
Development of computer program required in reduction and analysis for calibration of Skylab S-193 altimeter data
[E73-10876] 20 p2393 N73-29227
Acquisition of quick look data from SL-2, SL-3 planning, and development of mathematical models to process S-193 radar altimeter data
[E73-10917] 20 p2398 N73-29266
Bendix AAU 19A/A AIMS altimeters - Standard three inch, counter-drum-point altimeter
[AD-762523] 20 p2420 N73-29446
Calibration and evaluation of Skylab altimetry for geodetic determination of geoid
[E73-11013] 22 p2660 N73-31318
Analysis of terrain properties and topography from Skylab altimetry
[E73-11081] 23 p2782 N73-32256
Calibration and evaluation of Skylab altimetry for geodetic determination of geoid
[E73-11120] 24 p2916 N73-33275

**ALTITUDE**
NT FLIGHT ALTITUDE
NT HIGH ALTITUDE
NT LOW ALTITUDE
Extremes of precipitation aloft mandatory for design of military equipment capable of operating at altitude anywhere in world
[AD-747482] 04 p0445 N73-13629
Sampling function representation for applying satellite-to-ocean altitude altimeter data to geoid
06 p0662 N73-15373
Source and form of altitude errors obtained from antenna/satellite attitude errors
06 p0664 N73-15390
Reference atmosphere mean temperature and altimetric corrections
07 p0859 N73-16963
Influence of altitude and drugs on cerebral circulation in smokers and non-smokers
12 p1371 N73-21125
Venus wind/altitude Doppler radar probe
[NASA-CR-114556] 16 p1962 N73-25871

**ALTITUDE ACCLIMATIZATION**
Physiological effects of high mountain alpinism exercises on human body
07 p0745 N73-16058
High altitude acclimatization effects on mice and rabbit tolerances to hypoxia, acceleration, and high temperature
[NASA-TT-F-14861] 11 p1247 N73-20123
Hemoglobin and erythrocyte increase in rat adaptation to hypoxic hypoxia
13 p1481 N73-22005
Altitude acclimatization period effects on rat resistance to hypoxia
13 p1481 N73-22006
Cardiopulmonary adaptations of man to moderately high altitude
[AD-755192] 14 p1613 N73-23075

**ALTITUDE CONTROL**
Development and characteristics of laser altimeter for use with Apollo Lunar Orbital Experiments Mission
[NASA-CR-128738] 08 p0924 N73-17567
Investigation of fibers and composites applicable to design of high pressure gas storage vessels for satellite altitude control
[RRCM/ED/R/10] 13 p1586 N73-22856
Spacelab configurations noting thermal control, life support, electrical power, communication, and altitude control subsystems
[ESS/SS-399-VOL-2] 17 p2089 N73-26903
Automatic aircraft altitude reporting using air traffic control radar beacon system
[FAA-RD-73-44] 19 p2318 N73-28648
Larger aircraft landing approach performance and altitude control during atmospheric turbulence and wind shear
[NLR-TR-72023-U] 21 p2497 N73-30036

**ALTITUDE SICKNESS**
Review of decompression and altitude sickness noting effects at safe depths/altitudes
[DRIC-TRANS-3035] 13 p1485 N73-22041

**ALTITUDE SIMULATION**
Gastrointestinal proprioceptor effects on high altitude rabbit ocular reflexes
13 p1479 N73-21984
Simulated altitude firing test on solid propellant rocket motor
[NASA-CR-135485] 22 p2710 N73-31705

**ALTITUDE TESTS**
NT HIGH ALTITUDE TESTS
Altitude test and performance of Aerojet AJ10-179 liquid rocket engine under vacuum conditions
[AD-763727] 21 p2591 N73-30758
Altitude test of rocket-borne mass spectrometer cooled by liquid helium in arc heated plasma jet wind tunnel
[DLR-MITT-72-23] 22 p2675 N73-31424

**ALTITUDE TOLERANCE**
Nutrient protein intake of rats and tolerance to acute hypoxia
14 p1608 N73-23035

**ALTOCUMULUS CLOUDS**
U CUMULUS CLOUDS

**ALU [COMPUTER COMPONENTS]**
U ARITHMETIC AND LOGIC UNITS

**ALUMINA**
U ALUMINUM OXIDES

**ALUMINATES**
Visible fluorescence and thermoluminescence of YAlO3 crystals containing Er, Eu, Nd, Tb or Yb and other optically active centers
[AD-759161] 17 p1992 N73-26112
Optical spectra and crystal field parameters of neodymium in lanthanum aluminate
17 p2071 N73-26757

**ALUMINIZING**
U ALUMINUM COATINGS

**ALUMINUM**
Influence of shock compression pressure on critical shear in aluminum, copper, and lead
[AD-745365] 01 p0068 N73-10555
Effects of aluminum addition on explosive behavior of ammonium perchlorate
[AD-745344] 01 p0090 N73-10739
Application of strain compatibility equations to evaluate thermal stresses in unidirectional graphite composites bonded to aluminum structures
[NASA-CR-112162] 02 p0125 N73-11014
Aluminum metallographic method to obtain dislocation etchings and microstructural details
[AD-747086] 02 p0189 N73-11537
Design, development, and evaluation of aluminum-chlorine battery
[AD-747775] 03 p0255 N73-12065
Analysis of crack tip deformation in boron-aluminum sheet and laminar steel sheet resulting from crack propagation
[AD-747760] 03 p0322 N73-12623
Spectral absorption coefficients of argon and silicon and spectral reflectivity of aluminum as function of pressure, temperature, and wave number
[NASA-CR-129300] 03 p0335 N73-12727
Fabrication and properties of structural materials based on ceramic titanium powders alloyed with molybdenum and aluminum
04 p0432 N73-13520
Technology assessment of silicon carbide reinforced composites with aluminum or nickel matrix discussing mechanical resistance at high temperatures
04 p0434 N73-13543
Fatigue crack propagation of aluminum metal sheets under flight simulation loads corresponding to gust spectrum
[NLR-MP-72010-U] 04 p0480 N73-13926
Kinetics of Fe and Al atom oxidation reactions at high temperatures
[AD-749380] 05 p0507 N73-14125
Ultrasonic inspection of aluminum keys used in electric generators
[TR-7206.590] 05 p0551 N73-14473
Hot pressing and hot rolling procedures for producing aluminum reinforced with high strength steel strips
[NLL-TRANS-746-1355-[9022.401]]
05 p0561 N73-14554
Corrosion tests of inhibitors for protection of aluminum
[AD-749705] 06 p0689 N73-15606
Coincidence rate measurements for inelastically scattered electrons and associated bremsstrahlung at intermediate bombarding energies
[NASA-CR-124007] 06 p0702 N73-15723
Fluctuation-induced diamagnetism in bulk Al and Al alloys above superconducting transition temperature
[AD-750275] 06 p0710 N73-15794
Crystallographic fatigue crack growth in aluminum single crystals
[AD-751603] 07 p0810 N73-16567
Spall calculations in one-dimensional hydrodynamics codes using aluminum and high explosives
[LA-5001] 07 p0855 N73-16935
Characteristics of molybdenum disulfide films radio frequency sputtered on aluminum and nickel surfaces at elevated, ambient, and liquid nitrogen temperatures
[NASA-TN-D-7170] 08 p0927 N73-17593
Impact damage caused by polystyrene, aluminum, or iron hypervelocity particles on glass
08 p0934 N73-17651
Reliability of semiconductor devices as influenced by quality of aluminum wire bonds used in assembly
[NASA-CR-124037] 09 p1038 N73-18469
Biological and toxicity effects of aluminum and other chemicals in animals
[ORNL-TIP/TIRC-72-76] 10 p1121 N73-19136
Boron-aluminum radiators for space shuttle orbiters
[NASA-CR-128805] 10 p1164 N73-19468
Low energy fracture process in high strength aluminum alloy 2014T6
[NASA-CR-131099] 10 p1170 N73-19520
Effect of fabrication conditions on mechanical properties of Be-Al monolayer tape and composite specimens
[SC-DR-72-0731] 10 p1175 N73-19559
Dimensions and mechanical properties of elastic spherical shells measured by sound echo signals
10 p1188 N73-19667
Gas chromatographic separation of beryllium [II], copper [II], aluminum [III], and chromium [III] chelates
[NLL-M-22879-[5828.4F]] 11 p1252 N73-20158
Liquid-vapor state of aluminum during electron bombardment
[AD-754449] 11 p1253 N73-20171
X ray detection of incomplete weldment and surface oxidation in welded aluminum spacecraft structures
[NASA-CR-124167] 11 p1298 N73-20536
Theoretical and experimental determination of nonlinear behavior of angleplied boron/aluminum composites
[NASA-TM-X-68205] 11 p1309 N73-20617
Design of despin mechanism noting thermal and stress analysis of beryllium and aluminum as structural materials
[ESRO-CR[P]-226] 13 p1534 N73-22432
Mechanical properties of aluminum stainless steel composites and associated interface microstructures
[AD-756673] 13 p1548 N73-22542
Visual and microscopic studies on corrosion resistance of anodized aluminum sheets
[M72-09-96-REI/BLA/PUT] 14 p1675 N73-23592
Aluminum-gold interaction in thin layers
[NASA-TT-F-14919] 14 p1675 N73-23595
Addition of chromium or aluminum to improve oxidation resistance of nickel and cobalt alloys
14 p1677 N73-23611
Feasibility and cost effectiveness of expendable main rotor blades on UH-1 helicopter
[AD-758464] 15 p1736 N73-24078
Utilization of semiconductor in systematic analysis of Al after subjected to neutron irradiation
[FRNC-CONF-75] 15 p1788 N73-24495
Copper coating of welded aluminum spacecraft structures to resist oxidation and aid detection of incomplete penetration
[NASA-CR-124251] 15 p1791 N73-24515
Scanning electron microscope used in friction tests of polytetrafluoroethylene sliding on aluminum single crystals
[NASA-TN-D-7321] 15 p1791 N73-24520
Nondestructive tests for predicting effect of copper and aluminum microstructure on acoustic emission
[AD-758216] 15 p1800 N73-24587
Feasibility of using RF generated argon plasma for sputter etching Al and SiO2 windows and photoresist
[AD-757878] 15 p1800 N73-24588
Electric field and current in thin aluminum film superconductor near critical temperature
[LNF-72/77] 15 p1821 N73-24759
Measurement of heat transfer coefficients of air-glass, argon-glass, and argon-aluminum suspensions
[NASA-CR-2266] 15 p1843 N73-24932
Aluminum ribbon wire for ultrasonic bonding of semiconductor microelectronic interconnections
[AD-758981] 16 p1881 N73-25223
Evaluation of low cost techniques for forming boron-reinforced aluminum structural shapes from diffusion-bonded flat sheet and plate
[NASA-CR-124279] 16 p1918 N73-25523
Predictive model for failure times of adhesive bonded aluminum under constant stress
[AD-758845] 16 p1919 N73-25528
Helium migration in aluminum matrices under temperature gradients
16 p1926 N73-25586
Production of monolayer boron-aluminum composite materials
[NASA-CR-124278] 16 p1928 N73-25601
Harper-Dorn creep and microstructure of pure aluminum and other metals at high temperature
[LBL-1158] 16 p1928 N73-25604
Ziman theory for calculating electrical conductivity of liquid aluminum
[UCRL-51322] 16 p1929 N73-25605
Evaluation of sandwich structures of titanium and aluminum honeycomb in edgewise compression under static and fatigue loading
[FPL-196] 16 p1969 N73-25927
Graded band gap p-n junction gallium arsenide/gallium aluminum arsenide solar cell
[NASA-CASE-LAR-11174-1] 17 p1985 N73-26047
Design of upper atmosphere chemical release package
[AD-760141] 17 p2028 N73-26416
Plastic properties of alpha-phase Cu-Al single crystals at low and room temperature
17 p2042 N73-26524
Swelling study of metals irradiated by small angle scattering of X rays applied to Al irradiated by fast neutrons
[CEA-CONF-2115] 17 p2045 N73-26543

Stability of refractory compounds in liquid aluminum at high temperatures
[NLL-RTS-7975] 18 p2113 N73-27083
Development of nondestructive inspection procedures for determining quality of welded joints in aluminum spacecraft structures
[NASA-CR-124332] 18 p2156 N73-27420
Development of modeling schemes to predict effect of coalescence on observed growth characteristics during dynamic fracture
[AD-761082] 18 p2204 N73-27790
Design of torque motor with armature windings cast in epoxy cylinder and conductors cast integrally with aluminum mounting ring
18 p2209 N73-27830
High bias tunneling of silicon and aluminum semiconductor junctions
19 p2326 N73-28712
Burning rate, heat transfer, and combustion physics of aluminum in composition of heterogeneous condensed systems
[AD-761609] 19 p2354 N73-28932
Variable measurements in electrolytic production of aluminum
[NLL-TRANS-1059-[9022.04]]
20 p2422 N73-29454
Diffision in niobium of beryllium and aluminum from solid phase at 900 to 1300 deg
[NLL-CE-TRANS-5121-[9022.09]]
20 p2429 N73-29513
Ellipsometric measurements on passive film prior to initiation of breakdown in aluminum
[NASA-CR-132301] 20 p2432 N73-29533
Mechanical properties and crack growth in thick welded plates of aluminum at room and cryogenic temperature
[NASA-TN-D-7377] 20 p2483 N73-29946
Formation of solid solutions and fluidity of alloys based on aluminum and titanium
[AD-763491] 21 p2560 N73-30522
Effect of aluminum on fundamental mechanical properties of titanium
[AD-763785] 21 p2560 N73-30524
Controlling constituent properties for strengthening graphite fiber reinforced aluminum and magnesium composites
[AD-763211] 21 p2563 N73-30548
JERK Monte Carlo program for studying crystal defects in irridiated metals
[CEA-N-1567] 21 p2585 N73-30718
Analysis of threshold penetration of spherical projectiles impacting aluminum single wall targets at hypervelocity speeds
[NASA-TN-D-7308] 21 p2603 N73-30865
Fusion welding of aluminum to steels
[AD-764322] 22 p2678 N73-31454
Reactivity of tungsten in mixture of Hexogen and aluminum in bomb calorimeter
[ICT-12/72] 22 p2730 N73-31845
Chemiluminescence of Al atoms
[AD-765347] 23 p2755 N73-32044
Bonding methods of aluminum beam leaded devices on microcircuit ceramic substrates
[NASA-CR-124434] 23 p2797 N73-32369
Hypersound attenuation in superconducting aluminum and cadmium
23 p2825 N73-32580

## ALUMINUM ALLOYS

Effect of chemical composition, method of heat treatment, and production methods, on corrosion resistance of metal sheets
[AD-742106] 01 p0067 N73-10550
Effect of charge materials, melting condition, and type of melting equipment on hydrogen gas contained in copper alloys
[AD-745845] 01 p0068 N73-10558
Effect of titanium additions on aging characteristics of Al-Zn-Mg alloy
[AD-746195] 01 p0068 N73-10561
Four-phase airframe fatigue program for bending tests of aluminum alloy box beams
[AD-744673] 01 p0114 N73-10943
Electric arc welding of tin and aluminum bronzes and silicon brass
[DRIC-TRANS-2843] 02 p0179 N73-11448
Optical measurements of thin slots milled in edges of aluminum alloy test blocks to determine accuracy of measurement and detectability by operators using high frequency probes
[ARL/MET-NOTE-82-PT-1] 02 p0186 N73-11506
Analysis of fatigue crack growth data obtained in high strength aluminum alloys to separate metallurgical effects from other factors
[AD-745989] 02 p0187 N73-11518
Effects of growth speed and heat treatment on deformation of aligned Ag3 Mg-AgMg and Al-Ag2 Al eutectics at minus 196 to 300 C
[AD-747310] 02 p0190 N73-11541
Effects of molybdenum and tungsten fiber reinforcements on nickel chromium aluminum matrix alloys
[NLL-TRANS-746-1193-[9022.401]]
02 p0191 N73-11546
Neutron irradiation damage in precipitation hardened aluminum alloy component from High Flux Isotope Reactor
[CONF-720604-1] 03 p0313 N73-12555
Bibliographic survey on stress corrosion cracking of high strength aluminum alloys, including oxide effects
[DLR-FB-71-105] 03 p0316 N73-12572
Short time annealing effect under load on aluminum alloy precipitation hardening process
[DLR-FB-71-111] 03 p0316 N73-12573
Wedge procedure for determining stress corrosion cracking susceptibility of 5000 series aluminum alloy sheets
[AD-747944] 03 p0316 N73-12577
Method for evaluating antiseizure properties of aluminum and zinc alloys
[AD-747411] 03 p0317 N73-12587
Ductility theory used as basis for experimental determination of relation between stress and deformation during loading of thin tubular specimens of aluminum alloy AK 6
[AD-747437] 03 p0318 N73-12592
Mechanisms of corrosion fatigue crack propagation in Al-Zn-Mg including effect of cyclic stress waveform
[AD-747709] 03 p0319 N73-12597
Fatigue and crack propagation characteristics of aluminum alloy sheet under controlled cycle stress conditions to simulate fuel tank structural failure
[NASA-CR-128600] 03 p0360 N73-12935
Effects of thermomechanical treatment on mechanical, microstructural, and stress corrosion resistance properties of Al alloys
[AD-748361] 04 p0427 N73-13483
Regular forging and explosive forming effects on mechanical properties of aluminum alloy
[AD-748710] 04 p0427 N73-13484
Fatigue crack propagation in aluminum alloy sheets in environments of dry argon, normal air, distilled water, and aqueous sodium chloride solutions
[NLR-TR-72005-U] 04 p0431 N73-13513
Effects of one dimensional yield strength gradients on plastic zones in notched aluminum specimens
[AD-747783] 04 p0435 N73-13546
Temperature effects on tensile-, fracture toughness-, and crack growth-properties of aluminum alloy forgings
[AD-748257] 04 p0436 N73-13554
Tensile creep tests to determine properties of 7075-T6 aluminum alloy reinforced with unidirectional boron/epoxy
[NBS-TN-722] 04 p0437 N73-13565
Elastic buckling strength of thin walled aluminum alloy tubes fabricated with and without boron/epoxy glass/epoxy composite materials for reinforcement
[NBS-TN-728] 04 p0437 N73-13566
Brittle fracture of polycrystalline disks of alloyed alumina
[AD-748110] 04 p0439 N73-13577
Process for spraying metal coatings on aluminum alloys and resulting antifriction properties
[NLL-TRANS-746-1290-[9022.401]]
05 p0550 N73-14465
High temperature dispersion strengthening of Fe-Al alloys by internal oxidation
[BM-RI-7686] 05 p0562 N73-14564
Effect of heat treatment on fatigue life under gust loads of notched Al-Cu alloy
[ARC-CP-1221] 05 p0563 N73-14571
Experimental determination of fracture strength and critical crack length of 7075-T7351 aluminum alloy plates
[AD-748254] 05 p0563 N73-14575
Improved mechanical properties of aluminum alloys cast at ambient temperature
[AD-750532] 05 p0563 N73-14577
Effect of aging time on spallation of 2024-T6 aluminum subjected to impulsive loading
[AD-746955] 05 p0564 N73-14579
Boron filament splitting in boron aluminum composites caused by water vapor effects
[AD-749971] 05 p0566 N73-14602
Titanium chlorides and alloys and binary Al-Zn alloys
[JPRS-57787] 06 p0683 N73-15559
Composition and structural effects on mechanical properties of superplastic zinc and aluminum binary alloys
06 p0683 N73-15562
Effect of residual compressive stresses on fatigue strength and service life of aluminum alloy 7079 specimens
[NLR-TR-71105-U] 06 p0684 N73-15567
Failure analysis of aluminum alloy components with history of failures in aerospace applications
[NASA-CR-2166] 06 p0684 N73-15568
Fatigue tests of notched and unnotched Ti6Al4V bars compared to other Ti-alloys
[LBF-TM-62/71] 06 p0685 N73-15574
Fatigue strength of notched titanium aluminum vanadium alloy between 1 million and 10 million stress cycles
[LBF-TM-63/71] 06 p0685 N73-15575
Fracture strength of aluminum alloys 7075-T6 and 2024-T3 with surface flaws and corner cracks at holes
[NLR-TR-71033-U] 06 p0685 N73-15576
Effect of sodium chloride solution and distilled water on stress corrosion crack propagation in aluminum alloy 7075
[NLR-TR-71090-U-PT-1] 06 p0685 N73-15577
High strength aluminum alloys by optimizing precipitate microstructure
[AD-750140] 06 p0686 N73-15586
Influence of ingot thermal-mechanical processing on grain size and mechanical properties of 7075 wrought aluminum alloy
[AD-750390] 06 p0686 N73-15588
High temperature oxidation behavior of NiBAl with and without yttrium additions and reaction kinetics of Al2O3 layer growth
[AD-750410] 06 p0686 N73-15589
Fermi surface changes in dilute alloys of aluminum, cadmium, and zinc
[AD-750726] 06 p0709 N73-15786
Fatigue tests of aluminum alloy specimens used for aircraft structures under simulated acoustic loading conditions
[ESDU-72015] 06 p0723 N73-15899
Fatigue tests to determine service life of aluminum alloy lugs with push-fit pins under tensile stress conditions
[ESDU-72020] 06 p0723 N73-15901
Analysis of metallurgical factors and mechanical effects during and subsequent to cold hydrostatic extrusion of magnesium and aluminum alloys
[AD-751739] 07 p0805 N73-16527
Development of differential equation for normal evaporation of nickel-aluminum alloy relating evaporating time to final solute concentration
[NASA-CR-124040] 07 p0808 N73-16558
Evaluation of aluminum 1 by 12 ft extruded light-duty landing mat with symmetrical butt-type end connectors
[AD-752079] 08 p0893 N73-17233
Significance of grain boundary microstructure and pH in chloride ion solution as stress corrosives in 7075 aluminum alloys
[RM-564J] 08 p0931 N73-17624
Evaluation of aluminum strain hardenable alloys for suitability as materials for cartridge cases
[AD-749508] 08 p0933 N73-17640
Liquid hot pressing of silicon carbide whiskers for reinforcing aluminum alloy composites
[AD-752589] 08 p0936 N73-17666
Methods for designing and developing aircraft structural components by riveting, welding, and gluing aluminum alloys parts
[AD-753513] 09 p1041 N73-18491
Seven year tropical exposure test to evaluate corrosion resistance effectiveness of finishing systems for aluminum and magnesium
[AD-752907] 09 p1042 N73-18498
Effect of constant applied stress in crack initiation of aluminum and titanium alloys exposed to salt solution and organic fluids
[NASA-CR-124110] 09 p1045 N73-18525
Aluminum-copper eutectic solidification experiment to be run in M518 multipurpose electric furnace during Skylab mission
[NASA-CR-124103] 09 p1045 N73-18526
Influence of preliminary hot rolling on superplasticity of zinc aluminum eutectoid
09 p1046 N73-18530
Change in flow curves of superplastic aluminum-zinc alloy in different states as function of temperature
09 p1046 N73-18531
Influence of small magnesium additives on effect of superplasticity in aluminum-zinc eutectoid as function of temperature and velocity of deformation
09 p1046 N73-18532
Effect of biaxial strain deformation on dynamic fracture of aluminum alloy
[AD-752832] 09 p1048 N73-18549
Compilation of fracture mechanics data on high strength aluminum alloys, alloy steels, stainless steels, and titanium alloys
[AD-753774] 09 p1049 N73-18554
Corrosion behavior of grain boundary constituents in Al-Zn-Mg alloys
[AD-753273] 09 p1049 N73-18556
Tensile, exfoliation, fatigue, and crack growth properties of heat treated aluminum sheet alloy 7475
[AD-753709] 09 p1050 N73-18560
Interaction between creep and fatigue processes during crack growth in sheet specimens of aluminum alloy at 400 F
[AD-753688] 09 p1050 N73-18562
Time dependent mechanical behavior of boron filament reinforced aluminum composites based on static and dynamic properties
[AD-753706] 09 p1054 N73-18590
Fatigue behavior of directionally-solidified aluminum-nickel eutectic alloy under cyclic torsional loading
[AD-753689] 09 p1055 N73-18600

Strain fields around tapered interference fit steel pins in aluminum and steel alloy plates
[ARL/SM-NOTE-377] 09 p1093 N73-18919
Cavitation-corrosion resistance tests of tin and aluminum bronzes used for marine pumps in synthetic sea water and distilled water
[DRIC-TRANS-3016] 10 p1167 N73-19492
Mechanical and microstructural behavior of Al-Zn alloy in superplastic region at high temperature
10 p1170 N73-19518
Impurities and plastic fracture in aluminum alloys
[NASA-CR-131100] 10 p1171 N73-19521
Fatigue tests of 7075-T6 aluminum alloy under synchronous pulsating triaxial stresses
[AD-754414] 10 p1174 N73-19552
Development of thick-walled, Borsic aluminum alloy ring for use as stiffener in 155 millimeter atomic artillery projectile
[SC-DR-72-0706] 10 p1176 N73-19562
Structural analysis of laminated aluminum alloy sheets to determine flaw growth behavior in roll diffusion bonded and adhesive bonded structures
[NASA-CR-128844] 10 p1220 N73-19921
Carbon dioxide shielded-arc welding with electrodes containing aluminum
[NLL-CE-TRANS-6011-[9022.09]]
11 p1296 N73-20515
Processing techniques for high strength aluminum alloys including ingot processing, solidification and homogenization, and thermal mechanical treatments
[AD-754571] 11 p1307 N73-20606
Analysis of microplasticity of materials used in inertial navigation systems to show friction stress, yield stress, and rate of strain hardening in microstrain region
11 p1317 N73-20692
Effects of hydrogen environment embrittlement of steels and alloys
[NASA-CR-2163] 12 p1412 N73-21444
X ray and electron microscopic analysis of vacuum environment effects on 7075-T6 Al alloy fatigue life, fatigue-crack-growth behavior, and fracture toughness
[NASA-TM-X-69223] 12 p1413 N73-21450
Effects of specimen thickness on fatigue-crack growth and fracture toughness of 7075-T6 and 7178-T6 aluminum alloy plates and sheets
[NASA-TN-D-7173] 12 p1413 N73-21453
Dynamic tear tests for determining fracture resistance properties of aluminum alloys
[AD-755436] 12 p1415 N73-21465
Current-voltage characteristics measured in Al/AlO lead tunneling junctions
[COO-1569-91] 12 p1439 N73-21656
Strength mechanism of stress wave emission in steel and aluminum alloys during tensile testing
[RFP-TRANS-104] 12 p1463 N73-21854
Preliminary evaluation of lithium aluminum electrode for thermal batteries
[AD-757007] 13 p1477 N73-21964
Stress corrosion cracking tests of aluminum alloys in synthetic sea water
[NASA-TM-X-64733] 13 p1488 N73-22062
Determination of corrosion resistance of coatings on low alloy steel and susceptibility to exfoliation of 7178 aluminum alloy using Lawrence corrosion detection gauge
[AD-755163] 13 p1531 N73-22405
Aluminum alloy sheet bonding with steel sheets to form high strength composites
[TN-279] 13 p1533 N73-22421
Stress corrosion cracking in high strength aluminum alloys due to hydrogen embrittlement
13 p1539 N73-22472
Analysis of high temperature stability of reinforcing phase in eutectic composition of aluminum-nickel alloys for various rates of growth
13 p1541 N73-22487
Analysis of electrical conductivity of eutectic solutions of aluminum-nickel alloy using directional crystallization method
13 p1541 N73-22489
Fatigue mechanics studies of fatigue crack propagation in 2024 aluminum alloy panels containing transverse slits
[ARL/SM-379] 13 p1542 N73-22491
Fatigue damage accumulation and incompatible crack front orientation analyzed from aluminum alloys crack propagation test
[NLR-TR-72061-U] 13 p1543 N73-22504
Mechanical strength of multilayer thin metal films
[AD-756582] 13 p1543 N73-22508
Influence of surface conditions on Ti-6Al-4V alloy fatigue life
[AD-755385] 13 p1544 N73-22516
Secondary bending effect on aluminum alloy riveted joint fatigue strength determined by comparetive program fatigue tests
[NLR-TR-72007-U] 13 p1586 N73-22862
Development of galvanic forming techniques and application to production of complex structures requiring accurate dimensions
13 p1593 N73-22918
Development of electron beam welding techniques and application to welding various metal structures
13 p1593 N73-22919
Effects of oxide dispersions and rare earth elements on oxidation of Cr and Al containing alloys
14 p1677 N73-23608
X ray diffraction analysis of Al based rare earth alloys with potential permanent properties
[AD-756245] 14 p1698 N73-23776
Design, development, and manufacture of boron-aluminum alloy for use as space shuttle structural components
[NASA-CR-124242] 14 p1709 N73-23873
Influence of active and passive electrolyte solutions on corrosion of aluminum alloys
15 p1746 N73-24154
Statistical test of difference in fatigue life results in conventional and shot peening in aluminum-titanium alloy
[AD-758624] 15 p1794 N73-24542
Homogenization processing of aluminum alloy ingots during extrusion for changing structure and properties of product
[AD-759245] 16 p1919 N73-25527
Analysis of unidirectionally solidified aluminum alloys to determine properties of random polycrystals, columnar crystals, and growth twin crystals
16 p1927 N73-25594
Evaluation of high strength aluminum alloy plates and forgings
[AD-759557] 16 p1930 N73-25613
Influence of phase composition on mechanical properties of heat resistant vacuum tight cast aluminum alloys
[AD-759645] 16 p1930 N73-25619
Dynamic tear tests for determining fracture mechanics of high strength structural steels and aluminum and titanium alloys
[AD-759351] 16 p1930 N73-25620
Elastic and mechanical properties of Al-Li alloy
[AD-759423] 16 p1931 N73-25625
Fatigue mechanics of boron-aluminum composites under oscillating tensile loads
[AD-757213] 16 p1932 N73-25635
Square sectioned single crystals of Cu-Al alloys at low temperature
17 p2043 N73-26525
Aging tests of light alloys bonded with various adhesives and development of new aging test criteria
[RAE-LIB-TRANS-1662] 17 p2043 N73-26528
Cumulative damage of high strength aluminum alloy under operational loading
[ISD-133] 17 p2046 N73-26553
Laws governing crystallization of ingots with continuous casting in electromagnetic crystallizer
[AD-759230] 17 p2046 N73-26554
Electroslag melting method in casting of aluminum alloy ingot
[AD-759758] 17 p2047 N73-26558
Fast freezing for producing aluminum alloys from consolidated powder
[AD-759828] 17 p2048 N73-26569
Internal friction measurements on brass and aluminum alloys during plastic deformation loading
[AD-760145] 17 p2048 N73-26570
Mechanical properties of alloys on aluminum beryllium base with magnesium
[AD-759876] 17 p2048 N73-26571
Fatigue damage due to seismic loads of materials with different yield strength and various ductility
[NASA-CR-133099] 17 p2091 N73-26916
Evaluation of aluminum honeycomb core landing mat with modified hinges
[AD-758840] 18 p2127 N73-27186
Development of ultrasonic techniques for continuous monitoring of fatigue damage during cyclic testing of metal specimens
[AD-760787] 18 p2156 N73-27422
Low energy electron diffraction and auger spectroscopy of [100] surfaces of aluminum and aluminum-copper alloys
18 p2159 N73-27445
Effect of stress intensity on fatigue crack growth in 5456-H117 aluminum alloys
[AD-760668] 18 p2162 N73-27465
Influence of heat treatment on stress corrosion susceptibility of ternary Al-Zn-Mg alloy
[AD-761207] 18 p2162 N73-27467
Stress corrosion behavior of titanium and aluminum alloys with and without surface layer
[AD-760529] 18 p2163 N73-27469
Analysis of dynamic fracture in aluminum alloys using radial cylindrical wave propagation technique
18 p2202 N73-27778
Analysis of threshold of alternating range of stress intensity factor for producing extremely slow fatigue crack growth in aluminum alloys
18 p2202 N73-27779
Axial load fatigue tests on unnotched specimens of aluminum alloy extrusions following aging specimens
[ARL/SM-NOTE-386] 18 p2203 N73-27780
Physical properties of aluminum alloys, titanium alloys, and stainless steels for aerospace airframes
[AD-762305] 19 p2311 N73-28587
Effect of filament-matrix interfaces on fatigue resistance of boron-aluminum composites
[AD-761658] 19 p2312 N73-28597
Evaluation and characterization of superplastic properties of aluminum, zinc, and titanium alloys in various microstructural conditions
20 p2429 N73-29509
Stress corrosion cracking in aluminum and titanium alloys
[NASA-CR-124352] 20 p2431 N73-29831
Effects of diffusion on aluminum depletion and degradation of NiAl coatings on superalloys
[NASA-TM-X-68274] 20 p2435 N73-29555
Acoustic fatigue tests of aluminum alloy structural elements under narrow-band, random loading with zero mean stress in skin
20 p2480 N73-29921
Development of experimental program for determining response and sonic fatigue resistance of lightweight aircraft structures
20 p2480 N73-29923
High temperature creep of Al alloys tin, and lead at intermediate and low stresses
[LBL-1183] 21 p2559 N73-30512
SQUID magnetometer measurement of fluctuation diamagnetism of Al and Al alloys above superconducting transition temperature
[COO-3156-56] 21 p2559 N73-30515
Stress and corrosion effects on fatigue behavior 7075-T6 aluminum alloy
[AD-763455] 21 p2560 N73-30525
Effects of high temperature cycling on structural properties of boron reinforced aluminum alloys used in spacecraft structures
[NASA-CR-124369] 21 p2562 N73-30541
Thermotransport of copper in liquid Al-Cu alloys
[NASA-TR-R-415] 22 p2625 N73-31030
Argon-arc welding of aluminum and aluminum alloys to steels
[AD-763948] 22 p2679 N73-31458
Tensile and fatigue data for irradiated and unirradiated AISI 310 stainless steel and titanium-5 percent aluminum-2.5 percent tin applied to universal slopes
[NASA-TM-X-2883] 22 p2683 N73-31494
Effect of temperature and extension rate on tensile properties of SAP
[AREAEE-159] 22 p2685 N73-31507
Particle erosion of 2024 aluminum alloys
[AD-764267] 22 p2686 N73-31517
Hot forging of aluminum alloy structural parts
[AD-764618] 23 p2798 N73-32384
Fluctuation diamagnetism of aluminum and aluminum alloys above superconducting transition temperature
23 p2804 N73-32422
Yield and fracture model for Ti-6Al-4V titanium and 7075-T6 aluminum alloys
23 p2804 N73-32423
Crack propagation of 2219-T87 aluminum alloy from 20 K to 422 K
[NASA-CR-134047] 23 p2805 N73-32430
Fatigue life and fracture toughness of 7075-T6 Al alloy in vacuum and air environments
[NASA-TN-D-7262] 23 p2805 N73-32431
Impurity resonances in dilute copper cobalt alloy, aluminum manganese alloy, and copper vanadium alloy at low temperatures
24 p2960 N73-33655

**ALUMINUM CARBIDES**

Fabrication of aluminum-carbon composites
[NASA-CR-121266] 20 p2435 N73-29557

**ALUMINUM COATINGS**

Metallic alloy and aluminide coating for metallic base system
[NASA-CASE-LEW-11696-1] 01 p0061 N73-10502
Evaluation of magnesium-aluminum eutectic to improve combustion efficiency in low burning rate propellants
[NASA-TN-D-7133] 07 p0836 N73-16775
Evaluation of aluminum runway surface concepts as possible aid to aircraft braking
[NASA-TN-D-7186] 09 p0985 N73-18040
Kinetics of phase layer growth during diffusion coating of nickel with aluminum
[AD-760365] 17 p2054 N73-26611
Effects of diffusion on aluminum depletion and degradation of NiAl coatings on superalloys
[NASA-TM-X-68274] 20 p2435 N73-29555
Intermetallic chromium containing nickel aluminide for high temperature corrosion protection of stainless steels
[NASA-CASE-LEW-11267-1] 23 p2803 N73-32414

**ALUMINUM COMPOUNDS**

NT ALUMINATES
NT ALUMINUM CARBIDES
NT ALUMINUM OXIDES
NT ALUMINUM PERCHLORATES
NT ALUMINUM SILICATES
NT CRYOLITE
NT FELDSPARS
NT NEPHELITE
NT SAPPHIRE
Development of gallium aluminum phosphide alloys for electroluminescent diodes
[NASA-CR-112182] 03 p0273 N73-12213

Mass spectra and dissociation energies of high temperature gaseous molecules containing aluminum
[NASA-TN-D-7123] 04 p0386 N73-13138
Crack blunting through fiber matrix debonding in Borsic-aluminum composites
[SC-DC-71-4467] 04 p0438 N73-13568
Laser-induced fluorescence for gas phase oxidation of aluminum atoms
[AD-753839] 10 p1127 N73-19182
Application of boron/aluminum composite material for construction of turbine blades with low notch sensitivity in high cycle fatigue
18 p2166 N73-27497
Enriched aluminide coatings for dispersion strengthened nickel compounds
[NASA-CR-121250] 21 p2558 N73-30506
Mechanical processes for developing metal matrix composite Al/B tubes
[NASA-CR-124407] 23 p2797 N73-32370

ALUMINUM OXIDES
NT SAPPHIRE
Use of quartz and corundum monocrystals to verify dilatometric measurements in USSR
[AD-745840] 01 p0059 N73-10480
Feasibility of hot pressing alumina composites with potassium and barium fluorine micas
[AD-742207] 01 p0071 N73-10584
Hydrolytically grown aluminum oxide films on silicon
[AD-747019] 02 p0193 N73-11564
Thin walled and solid cylinders of alumina and yttria after fast neutron irradiation
[LA-DC-72-535] 03 p0314 N73-12564
Flexural strength of aluminum oxide substrates separated by lasers and diamond sawing
[SC-DC-71-4496] 03 p0321 N73-12613
Growth of hollandite crystal membranes under inert gas pressures
[NASA-CR-121033] 03 p0345 N73-12810
Electrolytic procedure for manufacturing aluminum whisker and pure nickel matrix composites with reinforced fibers
04 p0435 N73-13544
Pressure sintering of beryllium oxide powder blended with aluminum oxide powder
[AD-748389] 04 p0439 N73-13576
X ray analysis of B2O3 effects on composition, porosity, and sorption properties of Al2O3
[NLL-M-22796-[5828.4F]] 06 p0682 N73-15553
Charge trap structure of pyrolytic alumina layer in metal oxide semiconductor capacitor
[AD-751629] 07 p0762 N73-16195
Effects of various oxide additives on volume change on melting, surface tension, and viscosity of liquid aluminum oxide
[NASA-CR-120910] 07 p0811 N73-16580
Analysis of crosslinked epoxy-urethane polymer filled with aluminum oxide particles to determine mechanical and thermodynamic properties
[SC-DR-70-617] 07 p0812 N73-16584
Aluminum rods for gas cooling requirements of satellite attitude and orbit control using hydrazine as low thrust propellant
[RAE-TR-72161] 09 p0991 N73-18086
Environment-sensitive hardness effects on drilling and machining aluminum oxides
[AD-753276] 09 p1053 N73-18586
Deformation processes in forging refractory ceramic oxides
[NASA-CR-131109] 10 p1175 N73-19558
Nickel ion absorption on alumina and titania electrolyte interfaces
[AD-754540] 11 p1253 N73-20167
Kinetics of decomposition of adsorbed sarin determined microcalorimetrically
[REPT-1972-18] 14 p1616 N73-23091
Vaporization thermodynamics of Cr2O3 protective scales under transonic flow conditions
14 p1677 N73-23607
Open circuit voltage measurements on solid beta alumina electrolytic cells
[NASA-TN-D-7322] 15 p1738 N73-24089
Desilification in alumina and cement production by sintering disintegration method
[NLL-LIB-TRANS-1725-[5205.9]]
15 p1746 N73-24150
Effects of aluminum oxide on Raman scattering from nitrogen and oxygen
[AD-758913] 15 p1824 N73-24781
Effects of electron and hole trapping on radiation hardness of aluminum oxide MIS devices
[AD-758696] 16 p1882 N73-25229
Characteristics and production of silicon nitride-alumina sintered materials
[NLL-RTS-7988] 16 p1931 N73-25627
Analysis of aluminum oxide to determine material characterization, particle size distribution, and specific surface area
17 p2050 N73-26582
Microstructure of hot pressed and press forged polycrystalline refractory oxides
[AD-760353] 17 p2053 N73-26606
Determining the effects of ion implantation in aluminum oxide including implanted impurities and crystal damage by electrical resistivity and photoluminescence
17 p2071 N73-26755
Force and wear analysis in ceramic processing for alumina and silicon nitride
[AD-762522] 20 p2436 N73-29561
Creep behavior of polycrystalline aluminum oxide cermets with varying chromium concentrations
[KFK-1753] 21 p2563 N73-30545
Airborne aluminum oxide hygrometer for water vapor measurements in atmosphere
[NASA-TM-X-70475] 23 p2792 N73-32341
Hot pressing behavior of SiC with Al2O3
[AD-764639] 23 p2811 N73-32475

ALUMINUM PERCHLORATES
Combustion process and burning rate of aluminum perchlorate composite propellant
22 p2732 N73-31865

ALUMINUM SILICATES
Splitting aluminosilicates with silicate bacteria for liberation of potassium in soils
[NASA-TT-F-14870] 11 p1286 N73-20437
X ray fluorescence analysis of aluminosilicate refractories
[PB-214233/9] 16 p1932 N73-25636
Humic soil acid effects in silicate mineral weathering with aluminum migration
[NASA-TT-F-15134] 23 p2754 N73-32034
Production of silica, mullite, and alumino silicate reusable surface insulation materials for space shuttle orbiters
[NASA-TM-X-2719] 24 p2938 N73-33461
Alumina silicate based composite materials for space shuttle heat shielding system
24 p2939 N73-33466
Thermal cycling effects on properties of silica, mullite, and alumino-silicate insulation coatings
24 p2941 N73-33487

AMBIENT TEMPERATURE
Design of miniature tactical crystal oscillator for operation at ambient temperature
[AD-749271] 04 p0397 N73-13232
Durability investigation of strain gage pressure transducers subjected to long term pressure cycling at ambient and elevated temperatures
[NASA-CR-120953] 07 p0800 N73-16497
Circadian rhythms of sleep and cerebral temperature in rats chronically exposed to hot environments
[NASA-TT-F-15082] 22 p2620 N73-30994

AMBIT
U FIELD THEORY [PHYSICS]

AMIDES
NT CARBAMIDES
NT POLYIMIDES
NT UREAS

AMINES
NT CATECHOLAMINE
NT CYSTEAMINE
NT DIAMINES
NT ETHYLENEDIAMINE
NT SEROTONIN
Effectiveness of pharmacochemical protective substances on irradiated mice as neutron component increases
[DRIC-TRANS-2961] 06 p0631 N73-15124
Pharmacological data for aminothiol and indolylalkylamine radioprotectors
11 p1240 N73-20066
Aminothiol radioprotector, finam, effect on irradiated animal tissues under various conditions
11 p1242 N73-20085
Computerized prediction and actual carbon dioxide adsorption performance of solid amine resin
[NASA-CR-112324] 16 p1870 N73-25140
Refractory chamber meterials for N2O4/amine propellants
[AD-762531] 20 p2467 N73-29818
Development of chemical process for determining quantity of contamination buried in potting compounds and removable of spores with amine dissolution and plating techniques
[NASA-CR-133645] 21 p2562 N73-30535
Systems design for amine carbon dioxide sorber bed to be used in manned spacecraft
[NASA-CR-111849] 22 p2623 N73-31018

AMINO ACIDS
NT GLUTAMIC ACID
NT GLYCINE
NT PEPTIDES
Extraction and analysis by gas-liquid chromatography of catecholamine metabolites from biological tissue
[AD-745944] 03 p0260 N73-12105
Abiogenic syntheses of aliphatic and aromatic amino acids by ultraviolet radiation
10 p1119 N73-19119
Resistance of mice to acceleration overloads after injection of aminothiol group radioprotector
11 p1239 N73-20056
GAST and GALT aminotransferases activity of dog blood serum following total exposure to gamma rays with stomach or head shielded
11 p1241 N73-20075
Free amino acid excretion in urine as test for early diagnosis of radiation damage in humans
11 p1243 N73-20092
Validity of rapid delta-aminolevulinic acid determination in urine for lead intoxication tests on industrial workers
[NASA-TT-F-14864] 12 p1371 N73-21128
Mass fragmentography-computer for identification and quantitation of amino acids in soil
[NASA-CR-131507] 12 p1376 N73-21159
Nuclear magnetic resonance method for chemical shifts of amino acids and hybrid state of nitrogen atom
[NASA-TT-F-14893] 14 p1694 N73-23750
Concentration, composition, and properties of amino acids found in Cenozoic formations of Japan
[NASA-TT-F-15002] 19 p2293 N73-28439
Development of fluorescent reagent and application to automated assay of amino acids and peptides
[PAPER-76A6-747] 21 p2546 N73-30413
Kinetic deuterium isotope effect in aqueous reaction of methyl radicals with deuterated alpha-alanine and glycine
[NASA-TT-F-15123] 23 p2753 N73-32033
Organic geochemistry of amino acids in sedimentary rocks
[NASA-TT-F-14986] 23 p2787 N73-32295

AMMETERS
Design and performance of ammeter with reversible temperature indicator for recording peak currents
[UCRL-73587] 05 p0547 N73-14446

AMMONIA
NT LIQUID AMMONIA
Stabilization of aqueous prussic acid during synthesis from ammonia by carbon dioxide
[NASA-TT-F-14691] 07 p0752 N73-16110
Anhydrous ammonia for removing nitrogen dioxide from stack emission simulating hydrazine nitrogen tetroxide rocket fuel combustion exhaust
08 p0874 N73-17075
Influence of 100 percent anhydrous ammonia environment on body functions
08 p0875 N73-17088
Nitrogen oxide and ammonia removal from spacecabin atmosphere by catalytic oxidation with ruthenium and adsorption on silica gel
[NASA-CR-2132] 09 p0999 N73-18151
Electrons in metal ammonia solutions - abstracts of conference papers
[AD-752915] 10 p1127 N73-19179
Formation of hydrocyanic acid from mixtures of ammonia, metane and noble gas or hydrogen subjected to UHF waves
[NASA-TT-F-14678] 12 p1376 N73-21162
Hyperoxic atmosphere effect on rat metabolism and elimination of gaseous wastes
13 p1481 N73-22004
Ammonifying ability of denitrifying bacteria of species pseudomonas fluorescens
[NASA-TT-F-15086] 21 p2501 N73-30068
Preflight tests on fluorine/ammonia propellants to be used in Europa 2 transfer stage
[BMFT-FBW-73-07] 21 p2587 N73-30731
Self-induced transparency with CO2 laser pulses in two nondegenerating, vibration-rotation transitions in ammonia gas absorber
[AD-765550] 24 p2932 N73-33417

AMMONIUM COMPOUNDS
NT AMMONIUM NITRATES
NT AMMONIUM PERCHLORATES
Hyperammonemia development in metabolic toxicity of hydrazine
[AD-749519] 05 p0501 N73-14077
Low frequency Raman spectra of ammonium halides measured by double monochromator at high temperature
[NASA-CR-132049] 15 p1747 N73-24160
Conductance of quaternary ammonium salt dispersions in polymeric films
[AD-759073] 17 p2052 N73-26597

AMMONIUM NITRATES
Differential thermal analysis and dilatometry of 4 to 5 years stored ammonium nitrates with amine copper complex additives
[ICT-4/72] 16 p1954 N73-25812
Ion mobility, electrical conductance, and decomposition reactions of ammonium nitrate and ammonium perchlorate oxidizers
[AD-762744] 22 p2626 N73-31041

AMMONIUM PERCHLORATES
Effects of aluminum addition on explosive behavior of ammonium perchlorate
[AD-745344] 01 p0090 N73-10739
Catalyst effects on decomposition kinetics of rocket oxidizer ammonium perchlorate
[AD-746728] 02 p0221 N73-11792
Theoretical study of time-independent and oscillatory combustion of nonmetallized AP/composite propellants
[NASA-CR-129198] 02 p0243 N73-11973
Theory for combustion of ammonium perchlorate propellant
[NASA-TT-F-14720] 04 p0484 N73-13955
Time of flight measurements of vacuum sublimation of ammonium perchlorate
[AD-753219] 09 p1000 N73-18162

Motion picture study to provide combustion mechanism observations of ammonium perchlorate composite propellants
12 p1463 N73-21857
Combustion tests of ammonium perchlorate-binder sandwich structures
[AD-757347] 14 p1719 N73-23952
Analysis of steady state burning of ammonium perchlorate composite solid propellants
[AD-762600] 20 p2465 N73-29803
Ion mobility, electrical conductance, and decomposition reactions of ammonium nitrate and ammonium perchlorate oxidizers
[AD-762744] 22 p2626 N73-31041
Combustion characteristics of polystyrene and oxygen-styrene copolymer with ammonium perchlorate composites
22 p2708 N73-31687
Color schlieren photography of ammonium perchlorate binder sandwich combustion
[AD-764489] 23 p2857 N73-32829
Decomposition of ammonium perchlorate condensate, from electron emission, infrared absorption, and surface structure
[DLR-FB-73-59] 24 p2971 N73-33739

**AMMONOLYSIS**
Growth of bulk gallium nitride crystals by ammonolysis of gallium monochloride
[NASA-CR-112211] 03 p0344 N73-12807

**AMMUNITION**
Wind tunnel tests and firing tests to determine aerodynamic characteristics and subsonic flight performance of spin stabilized mortar projectile
[AD-746977] 02 p0124 N73-11009
Application of point position radar data to determine aerodynamic drag of projectile
[AD-750564] 05 p0492 N73-14013
Evaluation of aluminum strain hardenable alloys for suitability as materials for cartridge cases
[AD-749508] 08 p0933 N73-17640
Bibliography on pyrotechnics
[AD-752700] 09 p1100 N73-18976
Tests of ammunition without cases and with combustible cases to evaluate mechanical and environmental stress effects
[ICT-6/72] 12 p1465 N73-21869

**AMORPHOUS MATERIALS**
Yield strength of rigid polymers, discussing tensile and compression stresses
[D-MAT-180] 05 p0565 N73-14591
Temperature and intensity dependences of photoconductivity and annealing effects in electro-optical properties of amorphous Ge[.5]Te[.5] films
[AD-752024] 08 p0951 N73-17787
Electronic density of state in Weaire model of amorphous solid
[JINR-E4-6589] 12 p1440 N73-21668
Research reports on amorphous, laser window, composite, and gradient materials
[AD-755585] 13 p1545 N73-22521
Influence of plastic deformation on structure and mechanical behavior of glassy amorphous polymers
15 p1801 N73-24595
Vapor quenching in ultra-high vacuum of amorphous silicon films
[AD-758267] 15 p1821 N73-24765
Annealing properties and electron emission of amorphous and crystalline silicon
17 p2072 N73-26760
Amorphous silica material characterizations for thermal reusable insulation of space shuttle orbiter
24 p2939 N73-33470
Nonlinear optical susceptibilities of atoms, molecules, and condensed matter
[AD-764889] 24 p2959 N73-33643

**AMORPHOUS SEMICONDUCTORS**
Crystal structure of tetrahedrally coordinated amorphous semiconductors
[AD-746638] 03 p0346 N73-12821
Superconductor interactions and properties, and amorphous semiconducting and magnetic materials
[NASA-CR-129524] 04 p0457 N73-13731
Effect of structural changes on electrical and magnetic properties of amorphous semiconducting material
[AD-748661] 04 p0460 N73-13751
Electrical conductivity of thin films during nucleation and film growth
[AD-748269] 04 p0460 N73-13756
Band structure and electrical properties of amphorous semiconductors
[AD-749379] 04 p0461 N73-13761
Calorimetric, diffraction, and microscopic examination of evaporated amorphous germanium
[AD-749363] 04 p0461 N73-13762
System characteristics of amorphous semiconductor thin film and electron beam storage devices
[AD-749282] 05 p0587 N73-14778
Analog simulation of electrical conductivity in disordered amorphous semiconductor systems
[AD-749300] 05 p0588 N73-14779
Isothermal compressibility of amorphous semiconductors
[AD-750397] 06 p0709 N73-15785
Properties of amorphous semiconductors
[AD-750163] 06 p0710 N73-15797
Threshold commutation in amorphous semiconductors
[CEA-CONF-1972] 07 p0832 N73-16741
Structural, optical, and electrical properties of amorphous semiconductors
[AD-751084] 07 p0834 N73-16760
Research on amorphous semiconductor materials
[AD-752798] 09 p1074 N73-18761
Photodielectric and conduction properties of amorphous semiconductors
[AD-753053] 09 p1074 N73-18762
Electrical conductivity of amorphous germanium semiconductor with pseudogap structure
[AD-753824] 09 p1076 N73-18784
Spectroscopic studies of electrical and optical properties of amorphous semiconductors
[AD-753903] 10 p1202 N73-19779
Theory of amorphous semiconductors with electronic states in undulatory-graded band-gap model
12 p1438 N73-21650
Electronic structure in disordered amorphous materials and dense helium
[AD-755260] 13 p1567 N73-22701
AC conductivity and dielectric dispersion in amorphous semiconductors
[AD-757097] 14 p1698 N73-23780
Direct current conductivity in amorphous semiconductors
[AD-756783] 14 p1699 N73-23785
Switching processes in selected amorphous compounds
[AD-758133] 14 p1699 N73-23791
Multiple scattering theory and pseudogaps in amorphous covalent semiconductors
[JINR-E4-6747] 15 p1820 N73-24755
Alternating current Hall mobility and electrical conductivity in amorphous threshold switching semiconductors
[AD-759004] 16 p1954 N73-25809
Theoretical and experimental investigations of superconductivity, and amorphous semiconductors, superconductivity and magnetism
[NASA-CR-133234] 17 p2072 N73-26767
Mechanical properties of amorphous semiconductors at high pressures
[AD-759849] 17 p2075 N73-26784
Short-range ordering in amorphous Ge thin films studied by photoemission spectrum analysis as function of film preparation at different substrate temperatures
18 p2190 N73-27680
Electrical and optical properties of amorphous silicon and germanium semiconductors
[AD-760595] 18 p2191 N73-27690
X ray and electron diffraction spectra of amorphous arsenic sellenide semiconductors
[AD-762367] 20 p2463 N73-29792
Electron recording and readout sensitivity characteristics of amorphous semiconductor thin films
[AD-763253] 21 p2585 N73-30719
Observation of amorphous to crystalline transition in vacuum deposited tellurium films using Mossbauer spectroscopy
[AD-763408] 21 p2586 N73-30724
Calculation of density of states in amorphous covalently bonded semiconductors
[AD-763496] 21 p2587 N73-30728
Electrical conductivity measurements in controlled occupancy energy band tails of disordered semiconductors
[AD-763426] 21 p2587 N73-30729
Research in solid state semiconductor physics
[PB-220703/3] 22 p2738 N73-31923
Optical, photoelectric, and structural properties of amorphous B1-Ge thin films
23 p2824 N73-32572
Analysis of electrical switching phenomena in amorphous arsenic telluride-arsenic selenide system
24 p2966 N73-33707
Electrical properties and switching behavior of amorphous semiconductor films
[AD-765346] 24 p2970 N73-33732

**AMORPHOUSNESS**
U CRYSTALLINITY

**AMPERAGE**
U ELECTRIC CURRENT

**AMPHIBIA**
NT FROGS

**AMPHIBOLES**
Constant strain rate deformation of amphibole minerals
[AD-760105] 18 p2149 N73-27372

**AMPLIFICATION**
NT POWER GAIN
NT WAVE AMPLIFICATION
Pulsed gain measurements on CO2 lasers
[AD-751620] 07 p0807 N73-16545
Gain and performance measurement of expanding CO2 laser mixtures at high pressures
[AD-751694] 07 p0807 N73-16547
Influence of flare shapes on element factors and gain as function of scan angle of 40 element linear array at superhigh frequencies
[PHL-1973-10] 14 p1639 N73-23288
Radiation patterns for cavity backed dipole antenna with almost constant gain
[AD-760126] 17 p2005 N73-26216
Optical gain of combustion driven gas dynamic lasers
[AD-760390] 17 p2042 N73-26523
Approximative gain calculations for linear and rectangular arrays using vertically directed noise model
[AD-760690] 18 p2119 N73-27133
Transmitter and receiver antenna gain analysis for optical radar and communication systems
[NASA-TM-X-70423] 19 p2235 N73-28023
Maser amplification of incoherent radiation
[RR-113-PT-1] 24 p2930 N73-33401

**AMPLIFICATION FACTOR**
U AMPLIFICATION

**AMPLIFIER DESIGN**
Instrumentation for photometry, and amplifier and circuit design
[NBS-TN-594-2] 01 p0056 N73-10459
Modification principle for synchronous amplifier to improve sensitivity
[NASA-TT-F-14719] 04 p0395 N73-13213
Technique for selective amplifiers using transistor phase to eliminate induction
[PUBL-1369] 06 p0645 N73-15236
Optimization of fluid amplifier cascades by means of electric equivalent circuit
[CRIF-EL-6] 10 p1142 N73-19304
Design and performance of transistorized broadband logarithmic amplifier using hybrid thick film technology
[ECR-32] 12 p1382 N73-21210
Amplifier design for multiwire proportional chamber signals
[LA-5085] 12 p1383 N73-21215
Doping profile effect on stabilization mechanisms in microwave GaAs reflection amplifiers around X band
19 p2244 N73-28089
Comparative study of TWT and klystron amplifiers for use as power amplifiers in television broadcast satellites
[ESRO-CR[P]-268] 21 p2508 N73-30123
Comparative study of TWT and klystron for use as power amplifier in TV broadcast satellites
[ESRO-CR[P]-271] 22 p2634 N73-31109
Comparative study of TWT and klystron for use as power amplifier in TV broadcast satellites
[ESRO-CR[P]-272] 22 p2634 N73-31110

**AMPLIFIERS**
NT BEAM PLASMA AMPLIFIERS
NT BROADBAND AMPLIFIERS
NT CURRENT AMPLIFIERS
NT DIFFERENTIAL AMPLIFIERS
NT FEEDBACK AMPLIFIERS
NT FLUID AMPLIFIERS
NT INTERMEDIATE FREQUENCY AMPLIFIERS
NT LIGHT AMPLIFIERS
NT LIMITER AMPLIFIERS
NT LINEAR AMPLIFIERS
NT MICROWAVE AMPLIFIERS
NT PARAMETRIC AMPLIFIERS
NT PHOTOMULTIPLIER TUBES
NT POWER AMPLIFIERS
NT PREAMPLIFIERS
NT TRANSISTOR AMPLIFIERS
NT TRAVELING WAVE AMPLIFIERS
Design and performance of C band traveling wave tube amplifier for space communication application
[NASA-CR-112125] 01 p0032 N73-10250
Large aperture seismic array, seismometer and amplifier performance, and seismograph calibration
[AD-745753] 01 p0053 N73-10433
Parametric analysis for estimating spectral spreading of radio frequency amplifier output due to nonlinearities
[SC-DR-72-0330] 03 p0274 N73-12222
Stabilization of base line at output of amplifiers for gamma spectrometry chain
[CEA-N-1514] 03 p0277 N73-12248
Generator of extended duration high voltage pulses for controlling high-gain light amplifier
[CEA-N-1516] 03 p0280 N73-12272
Design, development, and fabrication of L band RF electron beam semiconductor amplifier
[AD-748898] 04 p0396 N73-13224
Integrated circuit operational amplifiers
[AD-749013] 04 p0397 N73-13229
Performance of temperature compensated rocket-borne MOSFET electrometer amplifier for measurement of electron and ion densities in lower ionosphere
[FOA-3-C-3640-E1] 04 p0420 N73-13424
Circuit configuration for high Q factor selective amplifier
[REPT-1370] 05 p0522 N73-14245
Measurement of magnetic field emission of spacecraft power system units at low frequencies
[ESRO-CR-57] 05 p0548 N73-14452
Application of absorber laser amplifier and detector to wide angle low noise optical radar and communication systems
[AD-749543] 05 p0558 N73-14533

Solid state amplifier for bridge circuit of atomic absorption mercury detector
[PB-212658] 07 p0801 N73-16506
Performance of sensing system having inverse function amplifier
[RD/B/M-2306] 08 p0889 N73-17196
Sense amplifier of ferrite coincident core memory
[AD-752817] 09 p1009 N73-18235
Very low noise amplifiers for semiconductor X ray detectors
[CONF-720559-2] 10 p1200 N73-19769
Construction of liquid laser designed for operation as oscillator-amplifier in high brightness mode
[AD-757072] 13 p1538 N73-22457
Feasibility analysis and design of bleachable absorber laser amplifier and detector
[AD-757361] 14 p1672 N73-23571
Research and development progress on solid state microwave oscillator and amplifier
[AD-758244] 15 p1757 N73-24241
Digital reproducing amplifiers for magnetically recording data from airborne processor
[ARL/ME-337] 20 p2376 N73-29090
Considerations for precise measurement of amplifier noise with hot and cold noise standards and mismatch problems
[NBS-TN-640] 24 p2898 N73-33136

**AMPLITUDE DISTRIBUTION ANALYSIS**
Amplitude analysis of mechanical fatigue of structures acted upon by cyclic stresses
[AD-750908] 06 p0729 N73-15947
Analog to digital converter circuit for pulse height analysis
[NASA-CASE-XNP-00477] 19 p2238 N73-28045
Optical modeling of radiation pattern of variable profile antenna operating in Hartman diaphragm mode
23 p2837 N73-32674

**AMPLITUDE MODULATION**
Methods for predicting parametric amplifier input noise temperature degradation for pump AM noise levels undergoing signal interference
[AD-751652] 07 p0763 N73-16197
Detection scheme with threshold learning for amplitude shift keyed signals
[AD-752009] 08 p0886 N73-17171
Detection of time varying signals in amplitude shift keyed signals with additive disturbance
[AD-752008] 08 p0890 N73-17208
Optimization of noise immunity of analog signal transmission channels by preemphasis, exemplified for AM or FM channel
[DLR-FB-73-09] 12 p1379 N73-21188
Modulation transfer functions for linear image formation with partially coherent light
15 p1812 N73-24689
Analysis of major sources of distortion in AM baseband telemetry systems and techniques for optimum baseband design
16 p1874 N73-25169
Analysis of amplitude modulation of ultrasonic sound beam impinging at right angles to turbulent water jet
[RAE-LIB-TRANS-1671] 17 p2063 N73-26686
Amplitude control method for equalizing low level phonemes in satellite voice communication system
18 p2212 N73-27862
Experimental television transmission system with vestigeal sideband amplitude/frequency modulation
[FTZ-44-TBR-33] 22 p2633 N73-31102
Amplitude steered antenna array approximating performance of electronically steered phased array
[NASA-CASE-GSC-11446-1] 23 p2764 N73-32117

**AMPLITUDE PROBABILITY ANALYSIS**
U AMPLITUDE DISTRIBUTION ANALYSIS

**AMPLITUDES**
NT PULSE AMPLITUDE
NT SCATTERING AMPLITUDE
Amplitude analog signals for use with CAMAC coline operation
[EUR-5100-E] 01 p0055 N73-10447
Large amplitude wave study
[COO-3004-3] 04 p0454 N73-13711

**AN-3 AIRCRAFT**
Basic flight characteristics and specifications of An-2 aircraft and equipment
[AD-746791] 02 p0127 N73-11032

**AN-24 AIRCRAFT**
Purpose, operating principles, and technical description of instrument panel equipment installed on An-24 aircraft
[AD-758751] 15 p1789 N73-24504

**ANACLINAL STREAMS**
U STREAMS

**ANACLINAL VALLEYS**
U VALLEYS

**ANALOG CIRCUITS**
Analog signal to discrete time interval converter for control of dc to dc power supplies
[NASA-TM-X-68153] 02 p0128 N73-11043

**ANALOG COMPUTERS**
Transfer function of linearizer for anemometer data
[AD-744975] 01 p0075 N73-10622
Solution of partial differential equations by analog networks
[AD-746929] 03 p0272 N73-12206
Design features and capabilities of quasi analog and hybrid computers
[AD-747579] 03 p0273 N73-12210
Abstracts on theory, design, and applications of analog and digital computers and digital control systems
[JPRS-57529] 04 p0392 N73-13189
Quasi-analog computer proposed for Soviet hydrometeorological service for calculating nonsteady state motion of water in river channels
04 p0443 N73-13618
Obtaining rocket trajectories by anological-hybrid computation
04 p0470 N73-13828
Application of equations of motion to develop analog computer simulation of helicopter rotor system
[AD-754547] 11 p1235 N73-20024
Analog computer models of tracking system errors
14 p1683 N73-23658
Transformation of guided missile computer input/output routine for general purpose applications
[AD-760761] 18 p2121 N73-27147
Control models for diagnosing malfunctions in analog computers
[AD-762220] 20 p2379 N73-29115
Pneumatic analogue decompression computer for real time prediction of safe ascent depth following depth excursion
[DCIEM-884] 22 p2638 N73-31144
Hybrid programmable attitude control electronic analog digital system for preflight and in-flight changes in planetary missions
22 p2731 N73-31859

**ANALOG DATA**
Amplitude analog signals for use with CAMAC online operation
[EUR-5100-E] 01 p0055 N73-10447
Design and performance of multiple channel analog multiplexer for airborne data acquisition system
[ARL/F-NOTE-49] 02 p0145 N73-11172
Analog charts developed during monitoring and analysis of differential Omega navigation system - Vol. 3
[AD-756026] 13 p1557 N73-22619
Thermomagnetic recording of analog signals on CrO2 magnetic tape
[NHK-LABS-NOTE-157] 18 p2116 N73-27112
Technique for hybrid addition of both digital and analog data in troposcatter communication system
[AD-761523] 19 p2236 N73-28030

**ANALOG SIMULATION**
Analog simulation of electrical conductivity in disordered amorphous semiconductor systems
[AD-749300] 05 p0588 N73-14779
Experimental study and analog simulation of steady state and dynamic response of jet interaction proportional fluid amplifier
[AD-751458] 07 p0805 N73-16532
Analog simulation of free piston gasifier tests relative to combustion and friction
[ME-240] 14 p1719 N73-23947
Analog and digital computer simulation study of pulse width modulation in feedback control systems
16 p1883 N73-25242
Analog models of errors in processing navigational information
17 p2059 N73-26660
Aircraft flutter analog simulation noting structural nonlinearity effects
[DLR-FB-73-30] 22 p2615 N73-30954
Mathematical simulation study of neuron response to vestibular analyzer exposed to periodically varying acceleration
[NASA-TT-F-15130] 22 p2623 N73-31015

**ANALOG TO DIGITAL CONVERTERS**
Analog to digital converter with teleprinter for multiple printout of projectile ballistic measurements
[PHL-1972-4] 01 p0032 N73-10245
Automatic analog to digital assembly for measuring electronic equipment characteristics
[CEA-CONF-1966] 03 p0302 N73-12468
Computerized on-line measurement processor for quality control of electronic materials
[CEA-CONF-1967] 03 p0302 N73-12469
Reference manual for SAID (speech analog input to digitizer) hardware system which performs preliminary preprocessing of speech signal before entering into computer
[AD-753012] 09 p1006 N73-18215
Analog digitizer for recording non-recurrent signals
[LRP-57/72] 10 p1132 N73-19226
Slow speed, multiple channel, analog to digital, logging system
[NASA-CR-132954] 15 p1754 N73-24219
Nonrecursive counting digital filter containing shift register
[NASA-CASE-NPO-11821-1] 17 p2000 N73-26175
Feasibility of limb controlled astronaut maneuvering scheme
18 p2110 N73-27063
Analog to digital converter circuit for pulse height analysis
[NASA-CASE-XNP-00477] 19 p2238 N73-28045
Device for semi-automatic digital encoding of graphic data
21 p2513 N73-30157
Performance of acoustic signal data processing and conversion system
[AD-763326] 22 p2700 N73-31628
Radio frequency interference measurements with common digitizer door opened and closed, and influence of various equipments inside room on interference magnitude and intensity
[FAA-NA-73-41] 23 p2757 N73-32061

**ANALOGIES**
NT HYDRAULIC ANALOGIES

**ANALOGS**
Analog reinforcement for reducing stress concentration around hole in plate
[AD-745116] 01 p0071 N73-10578
Determining open-loop response of Reynolds number dependent process as analog of drop-vaporization burning-rate process
[NASA-CR-121167] 11 p1269 N73-20301
Forecasting monthly mean air temperature anomalies by analogs
[NLL-M-22859-[5828.4F]] 11 p1313 N73-20655
Continuous Fourier transform method and apparatus
[NASA-CASE-ARC-10466-1] 12 p1381 N73-21199
Possible analogs around Orientale Basin provide reasonable alternatives to geomorphologic interpretation of volcanism in Descartes highlands - Part D
12 p1453 N73-21768
Sorting analogs to composite-kinematic maps of natural synoptic periods
21 p2573 N73-30618
Analog measurement of useful energy stored in thermocollector several years
24 p2974 N73-33766

**ANALYSIS [MATHEMATICS]**
NT ABEL FUNCTION
NT AIRY FUNCTION
NT ANALYTIC FUNCTIONS
NT ASYMPTOTES
NT BANACH SPACE
NT BINARY INTEGRATION
NT BURGER EQUATION
NT CALCULUS
NT CALCULUS OF VARIATIONS
NT CAUCHY INTEGRAL FORMULA
NT COMBINATORIAL ANALYSIS
NT CONFORMAL MAPPING
NT CONTINUITY [MATHEMATICS]
NT CONVOLUTION INTEGRALS
NT COSINE SERIES
NT DEPENDENT VARIABLES
NT DIFFERENTIAL CALCULUS
NT DIFFERENTIAL EQUATIONS
NT EINSTEIN EQUATIONS
NT ELLIPTIC DIFFERENTIAL EQUATIONS
NT ELLIPTIC FUNCTIONS
NT EXPONENTIAL FUNCTIONS
NT EXTREMUM VALUES
NT FOKKER-PLANCK EQUATION
NT FOURIER ANALYSIS
NT FOURIER SERIES
NT FOURIER TRANSFORMATION
NT FREDHOLM EQUATIONS
NT FUNCTION SPACE
NT FUNCTIONAL ANALYSIS
NT FUNCTIONAL INTEGRATION
NT GAUSS EQUATION
NT GREEN FUNCTION
NT HALF PLANES
NT HALF SPACES
NT HANKEL FUNCTIONS
NT HARMONIC ANALYSIS
NT HARMONIC FUNCTIONS
NT HELMHOLTZ VORTICITY EQUATION
NT HILBERT SPACE
NT HYPERBOLIC FUNCTIONS
NT INTEGRAL CALCULUS
NT INTEGRAL EQUATIONS
NT INTEGRAL TRANSFORMATIONS
NT LAPLACE TRANSFORMATION
NT LEBESGUE THEOREM
NT LEGENDRE FUNCTIONS
NT LIAPUNOV FUNCTIONS
NT LINEAR EQUATIONS
NT MATHIEU FUNCTION
NT MAXIMA
NT MEASURE AND INTEGRATION
NT NEUMANN PROBLEM
NT NONLINEAR EQUATIONS
NT NUMERICAL ANALYSIS
NT NUMERICAL INTEGRATION
NT ORTHOGONAL FUNCTIONS
NT PARABOLIC DIFFERENTIAL EQUATIONS
NT PARTIAL DIFFERENTIAL EQUATIONS
NT PERIODIC FUNCTIONS
NT PHASE-SPACE INTEGRAL
NT POISSON EQUATION
NT POWER SERIES
NT QUADRATIC EQUATIONS
NT RUNGE-KUTTA METHOD
NT SERIES [MATHEMATICS]
NT SINE SERIES
NT SINGULARITY [MATHEMATICS]
NT SPHERICAL HARMONICS
NT STURM-LIOUVILLE THEORY
NT TANGENTS

NT TAYLOR SERIES
NT TESSERAL HARMONICS
NT TRIGONOMETRIC FUNCTIONS
NT VECTOR ANALYSIS
NT VLASOV EQUATIONS
NT VOLTERRA EQUATIONS
NT VORTICITY
NT WEIGHTING FUNCTIONS
NT WIENER HOPF EQUATIONS
NT ZONAL HARMONICS
Analysis methods for studying fatigue in bonded joints of composite materials
[AD-750132] 06 p0728 N73-15939
Numerical integration subroutines built into NASA-JSC computer
[NASA-CR-134021] 22 p2714 N73-31725
ANALYSIS OF VARIANCE
Satellite derived potential coefficients and terrestrial gravity information for estimating geopotential anomaly degree variance
[AD-754236] 11 p1290 N73-20471
Estimation of random error variance from simultaneous radar measurements
[AD-755402] 13 p1494 N73-22114
ANALYTIC FUNCTIONS
Analytic model for teletype communication networks, using queueing theory
[AD-744467] 01 p0028 N73-10222
Analytic model for behavior of neutral and ion chemistry in D region following nuclear burst
[AD-750395] 05 p0543 N73-14416
Global investigation of Einstein space of maximal mobility and Petrov Type 2
[ITF-72-140-P] 15 p1804 N73-24618
Global structure of highly mobile Einstein space of Petrov Type T3
[ITF-72-117-P] 15 p1832 N73-24849
Analytic function of electron temperature measurements in ionosphere by high frequency probe method
20 p2410 N73-29372
Analytic procedure for nonequilibrium boundary layer integral matrix code
[NASA-CR-134039] 22 p2729 N73-31835
ANALYTIC GEOMETRY
NT CYCLOIDS
NT ELLIPSES
NT LOCI
NT OBLATE SPHEROIDS
NT TANGENTS
NT TORUSES
Orthogonal coordinate systems for three dimensional boundary layer calculations on ship hull geometry
[AD-749774] 05 p0529 N73-14301
ANALYTICAL CHEMISTRY
Documentation and examples of radionuclide X ray fluorescence analysis as instrumental analytic method - Part 3
[NASA-TT-F-14635] 05 p0582 N73-14736
Radionuclide X ray fluorescence radiation excitation and applications in analytical chemistry - Part 2
[NASA-TT-F-14634] 05 p0582 N73-14737
Rare earth electronic configurations, physiochemical properties, and implications of analytical chemistry
[IS-2966] 10 p1126 N73-19170
Research and development in analytical chemistry
[AD-758805] 16 p1871 N73-25150
ANALYZERS
NT SIGNAL ANALYZERS
Description, performance specifications, and results of performance tests for Hydrolab 2A portable water quality analyzer
[NOOH-IFS-73006] 01 p0057 N73-10468
Use of cross ratio invariance for analysis and error evaluation in automatic microwave network analyzers
[NBS-TN-623] 03 p0277 N73-12246
Effect of grid transparency and finite collector size on RPA ion temperature and density observations
[NASA-TM-X-66153] 07 p0799 N73-16487
Micrometeoroid analyzer using arrays of interconnected capacitors and ion detector
[NASA-CASE-ARC-10443-1] 11 p1291 N73-20477
ANATOMY
NT ADRENAL GLAND
NT ARTERIES
NT BARORECEPTORS
NT BONES
NT BRAIN
NT CARDIAC VENTRICLES
NT CARDIOVASCULAR SYSTEM
NT CEREBRAL CORTEX
NT CEREBRUM
NT CIRCULATORY SYSTEM
NT COCHLEA
NT COLLAGENS
NT CRANIUM
NT EAR
NT ERYTHROCYTES
NT EYE [ANATOMY]
NT FOVEA
NT GENITOURINARY SYSTEM
NT GLOMERULUS
NT GRAVIRECEPTORS
NT HAND [ANATOMY]
NT HEAD [ANATOMY]
NT HEART
NT HEMATOPOIETIC SYSTEM
NT HUMAN BODY
NT JOINTS [ANATOMY]
NT KIDNEYS
NT LABYRINTH
NT LIMBS [ANATOMY]
NT LIVER
NT LUNGS
NT LYMPHOCYTES
NT MARROW
NT MIDDLE EAR
NT MUSCULOSKELETAL SYSTEM
NT MYOCARDIUM
NT NECK [ANATOMY]
NT OCULOMOTOR NERVES
NT ORGANS
NT OTOLITH ORGANS
NT PHOTORECEPTORS
NT PITUITARY GLAND
NT RESPIRATORY SYSTEM
NT RETINA
NT SEMICIRCULAR CANALS
NT SPLEEN
NT STOMACH
NT TESTES
NT THYROID GLAND
NT VASCULAR SYSTEM
NT VERTEBRAL COLUMN
NT VESTIBULES
Handbook on structural evolution of vestibular apparatus
14 p1609 N73-23044
Computerized simulation of anatomically correct geometrical model of human body
[NASA-CR-134043] 23 p2752 N73-32022
ANDROMEDA GALAXIES
Mathematical model for Andromeda galaxy
[NASA-TT-F-14839] 14 p1704 N73-23830
ANECHOIC CHAMBERS
Instrumentation and methods used with acoustic studio scale model
[BBC-1972/34] 04 p0419 N73-13413
Microwave frequency reflection characteristics of quasi-tapered anechoic chamber for radar echo tests
[AD-754203] 10 p1138 N73-19275
Electromagnetic absorber reflectance and anechoic chamber design for microwave antenna measurements
[FTZ-A-454-TBR-13] 22 p2642 N73-31176
Evaluation of aerodynamic calibration and performance characteristics of anechoic flow facility
[AD-763668] 22 p2647 N73-31212
ANELASTICITY
Experimental methods for determining internal damping in metal alloys and identification of factors causing internal damping
[NLL-CE-TRANS-6132-[9022.09]]
20 p2429 N73-29508
Cyclic mechanical and fatigue properties of ferroanelastic beta prime gold-cadmium
24 p2933 N73-33421
ANEMIAS
Industrial health hazard in chronic exposure to monomethylhydrazine and dose related hemolytic anemia in humans
[AD-751440] 07 p0749 N73-16087
ANEMOMETERS
NT HOT-FILM ANEMOMETERS
NT HOT-WIRE ANEMOMETERS
Transfer function of linearizer for anemometer data
[AD-744975] 01 p0075 N73-10622
Remote recording of speed with laser Doppler anemometry
[RISO-M-1489] 04 p0422 N73-13442
Wind tunnel and atmospheric tests of dynamic performance of anemometers
[AD-747341] 04 p0445 N73-13630
Local quantities in two phase flow measured with anemometer, electrical probe, microthermocouple, and optical sensor techniques
[CEA-CONF-2033] 08 p0897 N73-17263
Lidar anemometry for quick determination of aerological data above launching site prior to rocket firing
[ONERA-TP-1151] 09 p1027 N73-18385
Two-axis fluidic wind measuring devices
[AD-755740] 12 p1425 N73-21550
Cooled film anemometry applied to determination of temperature and velocity distributions in wake of projectiles travelling at hypersonic speeds in free flight range
[DREV-R-648/72] 14 p1648 N73-23365
Laser-Doppler anemometer measurements of turbulence in drag reducing flows
[AD-757075] 14 p1669 N73-23545
Maxometers for measuring peak wind speeds during severe environmental conditions
[NASA-CASE-MFS-20916] 16 p1911 N73-25460
Heating device to prevent icing for windmill type anemometers
[NLL-M-29974-[5828.4F]] 16 p1936 N73-25665
Experimental determination of laminar boundary layer and oscillatory suspension flows by laser anemometry
17 p2012 N73-26271
Multichannel pulse sampling system with pulse anemometers and current meters on oceanographic buoy
[AD-760336] 17 p2030 N73-26426
Wind tunnel tests to determine boundary layer characteristics of air flows using laser light source and thermoanemometer
[NASA-TT-F-14945] 20 p2387 N73-29180
Comparison of laser Doppler measurements of wind velocities and turbulence with measurements by anemometers
[NASA-CR-124355] 21 p2574 N73-30627
Sign determination of laser Doppler anemometer velocity components of two Doppler difference signal components
[REPT-1/1972] 22 p2674 N73-31422
Laser anemometer self aligning reference beam method for measurement of three flow velocity components, with reference beam produced by scattering
[REPT-3/1972] 22 p2674 N73-31423
Trivane measured fluctuations of wind and temperature over an inland lake
22 p2694 N73-31578
ANEMOMETRY
U VELOCITY MEASUREMENT
ANESTHESIA
Respiratory impedance effects on electrical activities of bulbar respiratory neurons, respiratory muscles, and pulmonary ventilation in anesthesized cats
03 p0257 N73-12084
ANGLE OF ATTACK
Procedure for calculating sectional lift coefficient as function of angle of attack and free stream Reynolds number at angles of attack beyond maximum coefficient of lift
[AD-746505] 01 p0002 N73-10008
High angle of attack characteristics of high performance aircraft and correlation with dynamic directional-stability parameter
[NASA-TN-D-6993] 01 p0005 N73-10033
Wind tunnel analysis of asymmetric yawing moments produced by long pointed fuselage nose shapes at high angles of attack
[NASA-TN-D-7095] 02 p0123 N73-11003
Analysis of surface flow, pressures, and heat transfer on two conical delta wings at hypersonic speed and various angles of attack
[NASA-TM-X-2668] 02 p0156 N73-11268
Analysis of forced-oscillation pitch-damping over small angular amplitude range about nominal angle of attack
[NASA-CR-129522] 03 p0247 N73-12001
Analysis of flow around conical body at small angles of attack in uniform supersonic flow of ideal gas
[AD-747408] 03 p0287 N73-12326
Operational test and evaluation of angle of attack system for displaying percentage of lift produced by wing for all flap configurations
[AD-748844] 03 p0304 N73-12485
Computer program for calculating aerodynamic coefficients from trajectory angles of projectiles passing through paper screens
[FOA-2-C-2478-44] 06 p0613 N73-14980
Feasibility of porous jet stretcher nozzle for angle of attack testing of missiles in supersonic wind tunnel
[AD-750867] 06 p0651 N73-15288
Aerodynamic drag for streamline bodies at small angles of incidence
[ESDU-BODIES-02.04.00] 07 p0735 N73-15979
Buckling modes of four optimized Mars entry aeroshell configurations at angle of attack loadings based on experimental pressure distributions
[NASA-CR-2087] 07 p0852 N73-16907
Wind tunnel calibration and requirements for in-flight use of fixed hemispherical head of angle of attack and angle of sideslip sensors
[NASA-TN-D-6986] 09 p0981 N73-18014
Measurement of aerodynamic drag of conical bodies at zero angle of attack in free molecular and near free molecular flow regime
[DLR-FB-72-64] 09 p1014 N73-18278
Evaluation of standardized angle of attack flight training system
[AD-757243] 14 p1615 N73-23090
Analysis of effects of shock induced boundary layer separation in transonic flight and methods for eliminating or reducing effects
[ARC-R/M-3510] 16 p1854 N73-25019
Analysis of Magnus forces on high fineness ratio body of revolution with ogive forebody at varying angles of attack
[AD-759987] 17 p1980 N73-26003
Aerodynamic characteristics of flow around elliptic cones at large angles of attack
[AD-764945] 23 p2777 N73-32209
ANGLES [GEOMETRY]
NT ANGLE OF ATTACK
NT BRAGG ANGLE
NT BREWSTER ANGLE
NT ELEVATION ANGLE
NT SWEEP ANGLE
Rotating generator for angular display of television raster in horizontal and visual simulation systems
[NASA-CASE-FRC-10071-1] 05 p0513 N73-14171

Laser range finding for satellite angular coordinate determination using echo recorded by Schmidt telescope
05 p0557 N73-14523
Multiple element antenna array for receiving Doppler arrival angle spectral measurements in radio astronomy
[AD-751873] 08 p0889 N73-17202
Orifice inclination effect in pressure measurements on hypersonic rarefied flow field of flat plate
10 p1140 N73-19290
Device for measuring angle of arrival of laser beams and predictions of expected results for input apertures and turbulence
[AD-755404] 13 p1538 N73-22464
Determination of Hamaker complex constants in hydrocarbon emulsion films by measurement of contact angles and interfacial tension
[NLL-M-23001-[5828.4F]] 21 p2504 N73-30095

**ANGULAR ACCELERATION**
Neurophysiology and dynamic response of vestibular system to angular and linear acceleration
[DR-215] 02 p0130 N73-11057
Physiological response of cat semicircular canal dependent units to linear acceleration without angular acceleration
[AMRU-R-70-4] 02 p0131 N73-11061
Human performance, physiological effects, and pathological effects of rotary acceleration
06 p0628 N73-15096
Determination of angular acceleration equivalent to effect of coriolis acceleration on receptors of semicircular canals
11 p1246 N73-20112
Effects of alcohol on eye movements and tracking performance during laboratory angular accelerations about yaw and pitch axes
[FAA-AM-72-34] 22 p2619 N73-30989

**ANGULAR CORRELATION**
Device for determining relative angular position of spacecraft and radiating celestial body
[NASA-CASE-GSC-11444-1] 19 p2300 N73-28490

**ANGULAR DISTRIBUTION**
Anisotropy and angular distribution of bremsstrahlung radiation emitted by electrons confined in magnetic mirrors
[ORNL-TM-3821] 04 p0453 N73-13698
Aircraft measurement of long wave radiation brightness and angular distribution
[AD-750945] 05 p0544 N73-14424
Solar wind angular measurements and correlation with solar activity, magnetic storms, plasma flow, in magnetosheath
05 p0593 N73-14821
Angular distributions of elastically and inelastically scattered 42 MeV alpha particles from Cu-65
[NASA-TN-D-7354] 18 p2181 N73-27611
Computer program which uses Monte Carlo technique to compute geometrical factor, and spatial and angular distributions of simulated particles
[NASA-TM-X-70428] 19 p2301 N73-28498
Detection effeciencies of cylindrical detectors for gamma ray photon angular distributions
[NASA-TM-X-70445] 21 p2548 N73-30424

**ANGULAR MOMENTUM**
Problems of solar and stellar spindown and theory, emphasizing angular momentum flux of solar wind
01 p0095 N73-10784
Flow visualization and analytical analysis of momentum roll up of turbulent circular jet
04 p0403 N73-13286
Comsic ray air shower muon momentum spectra, noting dependence on shower primary energy, zenith angle, and arrival directions
13 p1574 N73-22755
Determining important processes for cyclogenesis in extratropical cyclone
17 p2056 N73-26632
Accuracy improvement of angular momentum projection
[NASA-TM-X-2875] 20 p2440 N73-29600
Semiclassical approximation to atom symmetric top rotational excitation
[NASA-CR-133849] 21 p2582 N73-30690

**ANGULAR MOTION**
U ANGULAR VELOCITY

**ANGULAR RESOLUTION**
High angular resolution imaging system for outer planet Grand Tour Mission
[NASA-CR-132013] 14 p1704 N73-23823
Various imaging systems and techniques for possible use aboard Grand Tour Spacecraft
[NASA-CR-132014] 14 p1704 N73-23824
Angular resolution and target discrimination in pulsed search radar
[AD-759350] 17 p1999 N73-26162
Equations for determining ground resolution on surface of earth observed by satellite-borne sensor
[AD-764246] 22 p2668 N73-31375

**ANGULAR VELOCITY**
Problems of solar and stellar spindown and theory, emphasizing changes in angular velocity of surface regions of sun and stars
01 p0095 N73-10785
Problems of solar and stellar spindown and theory, emphasizing angular velocity inside sun and stars
01 p0095 N73-10786
Semicircular canal model with flow visualization chamber for dynamic recording of canal fluid response to angular velocity effects
06 p0634 N73-15153
Development of device for measuring angular rate based on fluidic components for inertial angular rate sensors using vortex principle
[FOA-2-C-2466-54] 06 p0696 N73-15672
Algorithm for space vehicle re-orientation through angular velocity control by jet momentum
12 p1425 N73-21555
Performance of seismic angular vibration transducer using gas rotor
[RAE-TM-IR-128] 13 p1530 N73-22400

**ANHYDRIDES**
NT PEROXIDES
Crystal chemistry of anhydrous and hydrous layer silicates
[NRC-TT-1479] 04 p0458 N73-13734

**ANIMALS**
NT ARTEMIA
NT BATS
NT BIRDS
NT CALVES
NT CARIBOUS
NT CATS
NT CHIMPANZEES
NT DOGS
NT DOLPHINS
NT FISHES
NT FROGS
NT GUINEA PIGS
NT HAMSTERS
NT HUMAN BEINGS
NT INSECTS
NT LARVAE
NT MAMMALS
NT MICE
NT MONKEYS
NT PRIMATES
NT PROTOZOA
NT RABBITS
NT RATS
NT SEALS [ANIMALS]
NT SPORES
NT SWINE
NT TRIBOLIA
NT WHALES
NT WILDLIFE
NT WORMS
Abstracts on microwave radiation effects on human and animal physiological functions and life expectancy
[MBL-1972-6] 01 p0008 N73-10061
Toxic effects of continuous exposure to dichloromethane vapor on dogs, monkeys, rats, and mice
[AD-746295] 02 p0134 N73-11088
Bibliography of wildlife movements and tracking systems
[NASA-CR-130380] 07 p0742 N73-16040
Animal species susceptibility to toxic effects of long term exposure to environmental monomethylhydrazine
[AD-751441] 07 p0748 N73-16086
Toxicity of long term methyl isobutyl ketone exposure in dogs, monkeys, mice, and rats
[NASA-TM-X-69100] 09 p0996 N73-18130
Hyperoxic damage in animal cells, tissues, and organs
10 p1115 N73-19091
Composition and effects of radioprotectors on acceleration tolerance, hypoxia toxicity, radiation protection, and dynamic space flight stress in animals
[NASA-TT-F-721] 11 p1239 N73-20054
Pharmacological measures for prophylactic and restorative treatment of men and animals during space flight
11 p1239 N73-20060
Resistance of animals immersed in water to high acceleration
[NASA-TT-F-14828] 11 p1246 N73-20119
Barotrauma mechanoreceptor reflex effects on animal respiratory and circulatory system
13 p1479 N73-21982
Neurophysiology of sleep and wakefulness in fish, amphibians, birds, and reptiles
13 p1483 N73-22025
Interdependence of slow and rapid brain waves during sleep
13 p1483 N73-22027
Thermal effects of microwave and radio frequency radiation on biological systems
[MBL-1971-7-PT-1] 14 p1609 N73-23048
Voice communication and hearing in acoustic orientation systems of animals at various evolution levels
[DRIC-TRANS-3056] 16 p1867 N73-25121
Evaluation of ERTS-1 imagery as tool for management of wildlife habitat in Alaska
[PAPER-W11] 19 p2271 N73-28288
Influence of solar activity on biological indices and disease of living organisms in biosphere
[NRC-TT-1679] 21 p2592 N73-30771
Physiological stress effects of aerospace environment on human body and animals
[NASA-TT-F-15081] 23 p2749 N73-32001
Analysis of grizzly bear habitats from ERTS-1 photography
[NASA-CR-135776] 24 p2920 N73-33319

**ANIMATION**
U MOTION

**ANISOTROPIC MEDIA**
Water impingement model for raindrop erosion of homogeneous materials
[AD-748790] 04 p0406 N73-13310
Radiation and propagation of electromagnetic waves in anisotropic medium
[NASA-TT-F-743] 08 p0943 N73-17726
Model medium concept in geometric optics for electromagnetic wave propagation in absorbing media
[MPI-PAE/EXTRATERR-60] 08 p0943 N73-17727
Kinetic theory for input impedance of cylindrical dipole antenna in anisotropic plasma
17 p2067 N73-26720
Computer solutions of cylindrical antennas in anisotropic media
22 p2627 N73-31045
Linear and nonlinear wave particle cyclotron interaction for whistler mode waves in anisotropic plasma
[AD-763744] 22 p2705 N73-31668

**ANISOTROPIC PLATES**
Equations of motion for high frequency vibrations of thin crystal plates
[AD-760323] 17 p2095 N73-26948
Structural analysis of unsymmetrically laminated anisotropic plates using linear plate theory and strain-displacement relations
24 p2987 N73-33875

**ANISOTROPIC SHELLS**
Refined theory on deformation effects in anisotropic shells
[AD-747609] 03 p0362 N73-12949
Derivation of equations for multilayer anisotropic shells with lateral shift considered
[AD-762224] 19 p2351 N73-28908

**ANISOTROPY**
NT ELASTIC ANISOTROPY
Anisotropic instability of plasma without permanent magnetic field
02 p0166 N73-11350
Anisotropic nature of toughness due to texture in titanium and titanium alloy plate
[AD-748390] 04 p0435 N73-13549
Directional measurements of solar protons during low solar activity from HEOS A satellite
05 p0593 N73-14818
Interferometric investigation of anisotropy in light speed
10 p1187 N73-19661
Macroscopic interaction between electromagnetic fields and lossy, anisotropic, compressible plasma
10 p1195 N73-19724
Graphical amplitude characteristics of electromagnetic radiation reflected from anisotropic plasma boundary
[AEC-TR-7368] 10 p1196 N73-19734
Colloid thruster producing beams with anisotropic current, specific charge, and mass flow distributions
[AD-754902] 11 p1335 N73-20836
Solar proton anisotropies in interplanetary space as measured by Explorer 35 solid state detectors
13 p1573 N73-22744
Arrival directions and anisotropies of large cosmic ray air showers of primary energy larger than 100,000 TeV
13 p1573 N73-22751
Failure modes for isotropic and anisotropic composite materials
[AD-756889] 14 p1681 N73-23639
Analysis of relationship between texture development and normal anisotropy in cold-rolled, low carbon steel
[NLL-M-21627-[5828.4F]] 15 p1797 N73-24567
Linear anisotropic elastic field equations for interrelations and bounds on moduli in composite materials
[AD-758438] 15 p1801 N73-24601
Interchange stability of anisotropic guiding-center plasma in axisymmetric magnetic trap
[ORNL-TM-4077] 15 p1817 N73-24728
Vlasov equation for studying anisotropy produced instabilities in confined hot electron plasma
[EUR-CEA-FC-664] 15 p1818 N73-24736
Raman scattering by polaritons in anisotropic crystals, including noncollinearity of propagation
[AD-757810] 15 p1822 N73-24769

**ANNEALING**
NT PULSE HEATING
Annealing effect on amorphous silicon nitride protective film defects
[DRIC-TRANS-2902] 02 p0192 N73-11557
Effects of annealing on microstructure and room temperature mechanical properties of 0.100 inch thick ingot-source beryllium sheet
[RFP-1831] 03 p0314 N73-12562
Short time annealing effect under load on aluminum alloy precipitation hardening process
[DLR-FB-71-111] 03 p0316 N73-12573

Effects of polishing on magnetic properties of nickel-zinc ferrite toroids during annealing and procedures to restore original magnetic properties
[AD-747251] 03 p0346 N73-12822
Annealing phase and space charge decay following pulsed irradiation of MOS structures
[AD-748007] 03 p0347 N73-12833
Mechanical properties of types 304 and 304 plus 0.15 percent Ti stainless steel after irradiation at temperatures in range of 400 to 820 C
[ORNL-TM-3733] 05 p0562 N73-14569
Crack formation during stress-relief annealing in heat-affected zones of weld seams in low-alloy steels
[NLL-RISLEY-TR-2507-[9091.9F]] 06 p0676 N73-15499
Temperature and intensity dependences of photoconductivity and annealing effects in electro-optical properties of amorphous Ge[.5]Te[.5] films
[AD-752024] 08 p0951 N73-17787
Development of processing techniques for fabrication of lithium doped solar cells noting behavior during electron irradiation and annealing
[ESRO-CR-94] 09 p0991 N73-18088
Variations of electrical resistance of hydroextruded polycrystalline beryllium in annealing process 10 p1171 N73-19525
Effect of annealing on substructure of cold worked FCC copper alloys and metals
[COO-1431-14] 10 p1173 N73-19540
Influence of annealing on thin films of beta SiC
[AD-755792] 12 p1442 N73-21683
Analysis of high temperature stability of reinforcing phase in eutectic composition of aluminum-nickel alloys for various rates of growth 13 p1541 N73-22487
Analysis of effects of homogenizing annealing on ductility of high strength steel
[NLL-M-21616-[5828.4F]] 15 p1796 N73-24562
Finite deformation of annealed metals including loading and unloading constitutive and second order transitions
[AD-758261] 15 p1799 N73-24586
Annealing properties and electron emission of amorphous and crystalline silicon 17 p2072 N73-26760
Kinetics of change in electrical resistance of thin films annealed in magnetic field at high temperature
[JPRS-59625] 19 p2309 N73-28575
Process for manufacturing synthetic iron and comparison of annealing rate of synthetic iron with conventional iron
[NLL-M-21640-[5828.4F]] 20 p2429 N73-29507
Interstitial and vacancy motion in defect annealing of alpha brass and copper gold alloy by electron irradiation 22 p2683 N73-31489
Annealing effects on room temperature ductility of molybdenum
[CEA-CONF-2236] 24 p2935 N73-33443

**ANNIHILATION REACTIONS**
NT POSITRON ANNIHILATION
Inelastic lepton-nucleon process in Bjorken limit for neutral gluon model
[ILL-[TH]-72-10] 01 p0083 N73-10684
Impulsive plasma accelerator study of plasma acceleration by magnetic field annihilation
[AD-758880] 16 p1950 N73-25780
Uncorrelated jet model in proton-proton and proton-antiproton annihilation integral 18 p2182 N73-27615
Conference on annihilation reactions and gamma ray and universal evolution
[NASA-TM-X-66279] 19 p2331 N73-28753
Annihilation processes as origin of matter-antimatter in universe 19 p2332 N73-28767
Annihilation reactions and gamma ray spectra for studying large scale cosmologic antimatter 19 p2332 N73-28769
Detecting antimatter in universe 19 p2333 N73-28771

**ANNUAL VARIATIONS**
Model of semiannual thermospheric density variations based on latitude-dependent temperature and composition variations
[NASA-TM-X-65835] 01 p0047 N73-10380
Seasonal, altitude, and universal time differences in field-aligned electrons
[NASA-TM-X-66099] 02 p0166 N73-11345
Semi-annual variations in thermospheric density
[NASA-TM-X-66100] 02 p0166 N73-11346
Statistical analysis of geography and seasonal variation effects on intensification of tropical cyclones over western North Pacific Ocean
[AD-746130] 02 p0206 N73-11669
Correlation between solar radiation and monthly and seasonal variations for calculating atmospheric turbidity in Belgium
[PUBL-SER-A-75] 03 p0354 N73-12882
Analysis of natural synoptic seasons prior to winter to determine forecasting indications of extremely warm periods 04 p0442 N73-13605
Monthly and annual percentage levels of wind speed differences computed by using FPS-16 radar/Jimsphere wind profiles for Cape Kennedy
[NASA-TM-X-64712] 05 p0572 N73-14650
Computations of seasonal variations in internal waves and tidal phenomena in northern Atlantic Ocean
[AD-750842] 06 p0670 N73-15452
Annual variations of carbon dioxide concentration in Italian and Scandinavian cities 07 p0859 N73-16966
Diurnal and annual variations in intensity of urban heat island in Austin, Texas
[REPT-34] 08 p0938 N73-17679
Rocket measurements of ozone distribution under varying latitudes and seasonal conditions in stratosphere
[NASA-TM-X-66192] 09 p1028 N73-18391
Relationship between surface temperature anomalies in European USSR and seasonal variations of stratospheric circulation
[NLL-M-22851-[5828.4F]] 11 p1274 N73-20336
Synoptic climatological studies of precipitation in Plateau states from 850, 700, and 500 mb lows during spring
[NOAA-TM-NWS-TDL-48] 13 p1553 N73-22585
Forty year statistical study of geomagnetic data
[AD-756828] 14 p1663 N73-23497
Seasonal transitions in spring and autumn in mesopause region for Northern Hemisphere
[NASA-TT-F-14924] 14 p1685 N73-23672
Survey of seasonal snow cover in Alaska using ERTS-1 imagery
[E73-10637] 15 p1776 N73-24396
Air water interaction in seasonal circulation variations of Red Sea
[PB-214446/7] 16 p1909 N73-25443
Sea surface temperature anomalies and model generated meteorological histories
[NASA-CR-132756] 16 p1938 N73-25679
Analysis of ERTS-1 data for predicting ephemeral and perennial range quantity and quality during normal grazing season in Arizona and California
[E73-10712] 17 p2018 N73-26319
Seasonal variations in tropospheric and stratospheric carbon dioxide concentration determined from commercial aircraft sampling within Northern Hemisphere
[AC-24-PT-3] 17 p2028 N73-26409
Atmospheric wind fields and circulation effects on Pacific Ocean hydrologic regime
[TT-70-50129] 18 p2171 N73-27538
Seasonal changes of littoral transport and beach width of Maryland portion of Chesapeake Bay and resultant effect on protective structures
[PAPER-M1] 19 p2280 N73-28341
Analysis of long term weather variations, climate changes, and atmospheric circulation 20 p2444 N73-29634
Analysis of epochal variations in atmospheric circulation of Northern Hemisphere, atmosphere, and hydrosphere for making long and extra long range hydrometeorological forecasts 20 p2444 N73-29635
Atmospheric circulation for long range weather forecasts 20 p2445 N73-29641
Determination of seasonal, meteorological, and statistical variations in spectral signatures for geological target types from ERTS-1 data
[E73-10933] 21 p2529 N73-30275
Interpretation of seasonal changes in vegetation and soils in Idaho from ERTS-1 imagery
[E73-10936] 21 p2529 N73-30278
ERTS-1 measurements of seasonal changes in reflectance of soils, vegetation, and water in Hidalgo County, Texas
[E73-10946] 21 p2530 N73-30288
Annual variations of Garda Lake surface temperature using airborne bolometric equipment and earth based infrared video equipment
[IFA-STR-23] 23 p2787 N73-32298
Mariner 9 television observations of Mars atmosphere variations 23 p2840 N73-32699
Seasonal ozone variations in ultraviolet spectra of Mars atmosphere 23 p2841 N73-32704
Sources and dispersal patterns of suspended particles in nearshore surface waters of northeast Pacific Ocean and seasonal variation in snow cover in Sierra Nevada Mountains
[E73-11099] 24 p2914 N73-33256
Influence of solar energy absorption and air water interactions on seasonal thermocline of sea 24 p2957 N73-33623

**ANNULAR DRAINAGE PATTERNS**
U DRAINAGE PATTERNS

**ANNULAR FLOW**
Analysis of critical density heat flows during internal heating of annular channels
[AD-743681] 01 p0118 N73-10972
Comparison of turbine annulus mass flow calculations when computed by one- and two-dimensional analysis
[NASA-TM-X-2661] 02 p0156 N73-11264
Development of equations and computer program for determining temperature distribution in walls of three eccentric annuli
[AD-747697] 03 p0287 N73-12322
Low pressure air-water annular flow in horizontal tube
[AERE-R-6687] 06 p0655 N73-15320
Analysis of eddy diffusivity of momentum for heating air in turbulent annular flow and effect of various flow parameters on eddy diffusivities ratio 10 p1139 N73-19279
Prediction of annulus wall boundary layers in axial flow turbomachines 10 p1206 N73-19813
Annulus wall boundary layers in axial flow turbomachine 10 p1206 N73-19814
Laplace transformation and Volterra integral equation for studying heat transfer in laminar flow through pipe with annular space
[NLL-RTS-7525] 11 p1347 N73-20928
Influence of high level of inlet turbulence on performance of annular diffusers having center bodies of uniform diameter and conically diverging walls
[TT-7101] 22 p2652 N73-31243
Jet noise emission and reduction by secondary cold annular flow for SST and military aircraft 23 p2820 N73-32543
Swirling, annular, gas liquid flow down vertical tube 24 p2902 N73-33160

**ANNULAR JETS**
U ANNULAR FLOW
U JET FLOW

**ANNULI**
Development of equations and computer program for determining temperature distribution in walls of three eccentric annuli
[AD-747697] 03 p0287 N73-12322
Solar probe orbit perturbation calculation assuming circular gravitating asteroid ring with center at sun
[ESRO-SR-19] 19 p2344 N73-28856
Steady, supersonic, three dimensional flow in rotating and stationary annular cascades treated by method of characteristics in three independent variables
[DLR-FB-73-12] 21 p2525 N73-30247

**ANODES**
Anodic efficiency of lithium in electrolytic cells
[AD-749009] 04 p0387 N73-13147
Time development of anode surface temperatures for vacuum arc discharges of microsecond duration
[SC-DC-72-2267] 05 p0580 N73-14723
Coaxial anode for gas radiation counter for suppressing background ionization interference
[NASA-CASE-GSC-11492-1] 19 p2301 N73-28497
Position resistive anode wire radiation counters noting counter acting as voltage and current source
[IRI-132-73-02] 19 p2302 N73-28504

**ANODIC COATINGS**
Prototype multi-wafer plasma anodization process
[AD-746003] 01 p0064 N73-10521
Transport properties of anodic oxides in metals 09 p1063 N73-18674
Visual and microscopic studies on corrosion resistance of anodized aluminum sheets
[M72-09-96-REI/BLA/PUT] 14 p1675 N73-23592
Plasma anodization and oxidation of thin metal film semiconductors
[AD-760171] 17 p2052 N73-26600
Structure and composition of anodic coatings formed on magnesium dry cell
[AD-764253] 22 p2618 N73-30980
Anodic oxidation of titanium and its alloys
[LS-254] 22 p2685 N73-31505

**ANODIZING**
Prototype multi-wafer plasma anodization process
[AD-746003] 01 p0064 N73-10521

**ANOMALIES**
U ABNORMALITIES

**ANORTHOSITE**
Natural exoelectron emission of anorthosite rocks from Luna-20
[NASA-TT-F-15116] 24 p2980 N73-33817

**ANS**
U ASTRONOMICAL NETHERLANDS SATELLITE

**ANTARCTIC REGIONS**
Canadian research on atmospheric precipation in antarctic regions and meteorological radar systems
[AD-746604] 04 p0444 N73-13627
Trigonometric leveling and gravimetric survey in Antarctic
[AD-752232] 08 p0920 N73-17540
ERTS-1 imagery of geology in ice free valleys of Antarctica
[E73-10309] 09 p1022 N73-18341
Monitoring Northern Hemisphere transmissions in Antarctica and some oblique sounding systems
[JPRS-58205] 10 p1128 N73-19186
Peculiarities of short wave propagation over long distance radio links connecting Antarctia with Northern Hemisphere 10 p1128 N73-19187
Simulation of monthly variation of local surface energy budget and sub-surface temperature regime in Antarctica 10 p1146 N73-19326

Geological survey and mapping of ice-free valleys of Antarctica from interpretation of ERTS-1 imagery
[E73-10564] 14 p1656 N73-23436
Cosmic ray neutron monitor data for Sanae Antarctica
[S-6] 15 p1827 N73-24811
Cartographic applications of ERTS-1 RBV imagery of Arctic and Antarctic regions
[E73-10651] 16 p1898 N73-25347
ERTS-1 imagery of icebergs and sea ice in Antarctic region
[E73-10686] 16 p1902 N73-25380
Survey of Antarctic icebergs using ERTS-1 imagery
[E73-10692] 16 p1902 N73-25385
Design of reserve master clock for controlling meteorological recording instruments in Antarctic weather stations
[NLL-M-22972-[5828.4F]] 16 p1911 N73-25459
Tables on Antarctic cosmic ray measurements obtained during 1969
[NP-19680] 17 p2080 N73-26824
Ionic migration and weathering in frozen Antarctic soils
[NASA-CR-2283] 18 p2143 N73-27326
General description and scientific results of Tenth Soviet Antarctic Expedition for period 1965 to 1966
[TT70-50072] 20 p2406 N73-29339
Analysis of Tenth Soviet Antarctic Expedition to show preparations, logistic support, and operational accomplishments
20 p2406 N73-29340
Meteorological, actinometric, and aerological investigations conducted aboard ships of Tenth Soviet Antarctic Expedition
20 p2406 N73-29341
Analysis of ice conditions existing in Antarctic waters during Tenth Soviet Antarctic Expedition
20 p2407 N73-29342
Hydrological investigations conducted during Tenth Soviet Antarctic Expedition to determine temperature and salinity of ocean
20 p2407 N73-29343
Hydrographic investigations conducted aboard ships of the Tenth Soviet Antarctic Expedition
20 p2407 N73-29344
Marine geological research of submarine relief and ocean bottom sediments conducted during Tenth Soviet Antarctic Expedition
20 p2407 N73-29345
Radar analysis of ice sheets in Antarctic regions conducted during Tenth Soviet Antarctic Expedition
20 p2407 N73-29346
Clinical medicine and human factors engineering functions conducted during Tenth Soviet Antarctic Expedition
20 p2407 N73-29347
Human factors investigations and acclimatization research conducted during Tenth Soviet Antarctic Expedition
20 p2407 N73-29348
Investigation of oribatid mites found in Antarctic regions during Tenth Soviet Antarctic Expedition
20 p2407 N73-29349
Activities of meteorological section during Tenth Soviet Antarctic Expedition
20 p2408 N73-29350
Marine ice observations during Tenth Soviet Antarctic Expedition to measure formation, growth, disintegration, and physicomechanical properties
20 p2408 N73-29351
Analysis of physicomechanical properties of ice conducted during Tenth Soviet Antarctic Expedition with emphasis on ice cover temperature effects
20 p2408 N73-29352
Hydrological investigations of Davis Sea conducted during Tenth Soviet Antarctic Expedition
20 p2408 N73-29353
Geophysical observations made during Tenth Soviet Antarctic Expedition with emphasis on field strength of long and short wave radio transmission
20 p2408 N73-29354
Technical and support services performed during Tenth Soviet Antarctic Expedition
20 p2408 N73-29355
Analysis of operations at ground station during Tenth Soviet Antarctic Expedition to show equipment requirements and mission accomplishments
20 p2408 N73-29356
Medical analysis of vitamin balance among personnel of Tenth Soviet Antarctic Expedition to show effects on health and acclimatization ability
20 p2408 N73-29357
Analysis of physiological effects of diet on personnel of Tenth Soviet Antarctic Expedition
20 p2409 N73-29358
Analysis of microclimate of living and service quarters during Tenth Soviet Antarctic Expedition
20 p2409 N73-29359
Operations and functions of ground station during Tenth Soviet Antarctic Expedition to obtain meteorological and geophysical data
20 p2409 N73-29360
Functions and operations of ground station during Tenth Soviet Antarctic Expedition including construction procedures and equipment installation
20 p2409 N73-29361
Analysis of ice conditions existing in Alasheyev Bight during Tenth Soviet Antarctic Expedition
20 p2409 N73-29362
Seasonal plankton collections conducted during Tenth Antarctic Expedition
20 p2409 N73-29363
Geologic structure and geomorphology of Antarctic
[TT-67-59071] 21 p2541 N73-30375
Reconnaissance geologic mapping in Dry Valleys of Antarctica using ERTS-1 imagery
[E73-11127] 24 p2916 N73-33282
Automation of processes of gathering and primary processing of scientific information on expeditions of Arctic and Antarctic Scientific Research Institute
24 p2947 N73-33537

**ANTARCTICA**
U ANTARCTIC REGIONS
**ANTENNA ARRAYS**
NT LINEAR ARRAYS
NT STEERABLE ANTENNAS
NT TURNSTILE ANTENNAS

Characteristics of directional dipole antenna array for very high frequency radio interferometer
01 p0027 N73-10213
Computerized simulation of planar phased array of circular waveguide elements
[NASA-CR-123820] 02 p0140 N73-11139
Papers presented at antenna array conference concerning phased arrays and array techniques
[AD-744629] 02 p0149 N73-11209
Papers presented at antenna array conference concerning adaptive arrays, conformal arrays, and component techniques for array antennas
[AD-744630] 02 p0149 N73-11210
Reduction of angle frequency deviation in antenna array by waveguide parameters
[AD-748742] 04 p0389 N73-13164
Radiation parameters of VLF transmitting station NPM, Lualualei, Hawaii with antenna operating in dual or parallel east and west array configuration
[AD-748177] 04 p0390 N73-13172
Adaptive control systems for phased antenna arrays
[AD-748220] 04 p0390 N73-13174
Design and performance of digital ferrite phase shifter for phased array antenna systems
[AD-748431] 04 p0396 N73-13225
Computerized model of arbitrarily orientable Yagi - Uda array for obtaining impedance gain pattern and front-to-back ratios
[AD-751658] 07 p0763 N73-16199
Development of phase control coupling for use with phased array antenna
[NASA-CASE-ERC-10285] 07 p0764 N73-16206
Nonlinear interaction and modulation in parametric acoustic array for spherical wave field
07 p0821 N73-16650
Parametric design optimization for multiple element short backfire antenna array
[AD-751918] 08 p0889 N73-17199
Multiple element antenna array for receiving Doppler arrival angle spectral measurements in radio astronomy
[AD-751873] 08 p0889 N73-17202
Research activities in solid state physics
[AD-753255] 09 p1075 N73-18770
Plural beam antenna with parabolic reflectors
[NASA-CASE-GSC-11013-1] 10 p1133 N73-19234
Method of moments for approximating current distribution in antenna array with arbitrarily located parallel center fed dipoles with terminals in common plane
10 p1133 N73-19236
Interference rejection by adaptive antenna array in spread spectrum communication system
[AD-754444] 11 p1258 N73-20211
Analysis and design by matrix methods of circular antenna arrays consisting of identical parallel dipoles
12 p1382 N73-21205
Optimization and constrained optimization of parallel wire antenna arrays based on directivity, maximum power gain, quality factor, and efficiency index
[AD-755915] 12 p1385 N73-21233
Phase optimization and synthesis of antenna arrays, using variable phase and constrained amplitude excitation
13 p1499 N73-22149
Design of multiple beam UHF antenna for air traffic control satellite
[ESRO-CR[P]-199] 13 p1500 N73-22159
Analytical and computer design of array antennas, and analysis and synthesis of electromagnetic scattering systems
[AD-758768] 15 p1758 N73-24249
Antenna capable of receiving weak communication signal in presence of strong interference
[AD-758690] 15 p1758 N73-24250
Characteristics of antenna arrays of superconducting point contact Josephson junctions
17 p1994 N73-26120
Adaptive beamforming techniques for HF antenna array systems
[AD-760137] 17 p1999 N73-26166
Matrix equation for finite planar antenna arrays
[AD-759008] 17 p2004 N73-26209
Research and development in solid state physics, antenna arrays, and control theory
[AD-760008] 17 p2074 N73-26783
Experimental in-orbit verification of mathematical model for RAE spacecraft gravity gradient dynamics
18 p2208 N73-27825
Adaptive phased antenna array simulation for optimal design of tracking data relay satellite very high frequency beam
18 p2210 N73-27841
Development of low volume, high power radiating transmitter and antenna array to show radiation pattern, antenna gain, and efficiency
[AD-761793] 19 p2245 N73-28098
Computer solution to Hallens equation on half wavelength elements of planar symmetrical antenna arrays
[AD-761471] 19 p2245 N73-28103
Correlation receivers for detecting binary array signals with directional interference
22 p2627 N73-31047
Evaluation of phased array antennas
[AD-764367] 22 p2634 N73-31113
Design considerations and calculations for highly directional medium frequency aerial array
22 p2641 N73-31170
Amplitude steered antenna array approximating performance of electronically steered phased array
[NASA-CASE-GSC-11446-1] 23 p2764 N73-32117
Dielectric lightweight aircraft radar antenna array
[AD-764685] 23 p2766 N73-32131
Theory of electroacoustical images and relationship between geometric form of horn and sound antennas based on acoustic properties
24 p2956 N73-33617

**ANTENNA COMPONENTS**
NT ANTENNA COUPLERS
NT ANTENNA FEEDS

Evaluation of HF/VHF breadboard modeled manpack radio sets
[AD-745918] 02 p0142 N73-11152
Application of digital techniques for control of large antennas used for satellite tracking
[NASA-TM-X-66154] 07 p0754 N73-16127
Numerical analysis of parameters affecting design and characteristics of spiral top loaded antennas
10 p1134 N73-19238
Extension of electromagnetic antenna wave diffraction principle
[AD-759690] 17 p1999 N73-26163
Digital servocontroller for rotating antenna shaft
[NASA-CASE-KSC-10769-1] 18 p2122 N73-27153

**ANTENNA COUPLERS**
NT COUPLING CIRCUITS

Analysis of mutual coupling compensation using microstrip techniques with application to behind-the-array coupling of phased antenna array
[NASA-CR-123819] 02 p0151 N73-11222
Development of electronically tuned automatic antenna matching coupler for radio equipment
[AD-746996] 03 p0274 N73-12227
Optimization and constrained optimization of parallel wire antenna arrays based on directivity, maximum power gain, quality factor, and efficiency index
[AD-755915] 12 p1385 N73-21233
Developmental model of VHF transceiver multicoupler
[AD-755548] 13 p1502 N73-22177

**ANTENNA DESIGN**

Optimized antenna design for medium artillery delivered seismic detection system sensor
[AD-748825] 04 p0396 N73-13219
Lubricant supply for mechanical antenna bearings
[NLL-RISLEY-TR-2308-[9091.9F]]
05 p0550 N73-14463
Antenna systems for Ku band synchronous orbit communication satellite
05 p0608 N73-14941
Optimal design of coherent radar system
06 p0640 N73-15193
Analysis of parameters affecting design of synthetic aperture radar antennas for satellites
[NASA-TM-X-66162] 07 p0755 N73-16130
Characteristics of four types of horn antennas for application as S-band radiometers and modifications to improve beam efficiency
[NASA-CR-2133] 07 p0755 N73-16135
Evaluation of loran antenna modification to determine effect of increased height on radiated power and system performance
[AD-751978] 08 p0942 N73-17714
Design, fabrication, and testing of lightweight, foldable 4.27 meter spacecraft antenna
09 p1087 N73-18870
Numerical analysis of parameters affecting design and characteristics of spiral top loaded antennas
10 p1134 N73-19238
Computer simulation of space station computer-steered high gain antenna
[NASA-CR-128749] 10 p1134 N73-19239
Antenna design and transionospheric propagation relative to space communication - conference
[AD-754061] 11 p1256 N73-20193

Design of low gain L-band orthogonal-mode crossed slot antenna and VHF crossed loop antenna for airborne applications
[NASA-CR-130795] 11 p1261 N73-20237
Optimization and constrained optimization of parallel wire antenna arrays based on directivity, maximum power gain, quality factor, and efficiency index
[AD-755915] 12 p1385 N73-21233
Design of multiple beam UHF antenna for air traffic control satellite
[ESRO-CR[P]-199] 13 p1500 N73-22159
Computer analysis and design of special antenna configurations and characteristics
[AD-756470] 13 p1501 N73-22169
Electrodynamic fundamentals of antenna theory and design
[AD-755689] 13 p1502 N73-22176
Design and performance of low frequency/very low frequency omnidirectional antenna model
[AD-757556] 14 p1643 N73-23324
Evolution of conceptual design of flight hardware for surface electrical Properties experiment - Vol. 1
[NASA-CR-128918] 14 p1705 N73-23835
Collapsible high gain antenna which can be automatically expanded to operating state
[NASA-CASE-KSC-10392] 17 p1993 N73-26117
Design of omnidirectional ultrahigh frequency communication antenna fitted around pole
[AD-760201] 17 p2005 N73-26217
Design and tests of hybrid-mode tracking feed horn
[AD-759834] 18 p2123 N73-27159
Transmitter and receiver antenna gain analysis for optical radar and communication systems
[NASA-TM-X-70423] 19 p2235 N73-28023
Design and performance characteristics of trap loaded cylindrical antennas
21 p2516 N73-30183
Design of high frequency radar antenna equipment for radar stations
[AD-764333] 22 p2632 N73-31093
Design considerations and calculations for highly directional medium frequency aerial array
22 p2641 N73-31170
Omnidirectional polygon reflector antenna with cosecant radiation pattern for TV transmission in SHF range
[FTZ-A-454-TBR-16] 22 p2643 N73-31179
Design and performance of DSS 14 64 m antenna feed system
22 p2732 N73-31861
Dish antenna having switching beamwidth with truncated concave ellipsoid subreflector
[NASA-CASE-GSC-11760-1] 23 p2764 N73-32116
Problems in designing large mirror radio telescopes
[JPRS-60153] 23 p2793 N73-32345

ANTENNA FEEDS
Antenna feed networks for broadbanding very low frequency and low frequency antennas to wide frequency shift keying modulation
[AD-746119] 02 p0151 N73-11226
Reduction of angle frequency deviation in antenna array by waveguide parameters
[AD-748742] 04 p0389 N73-13164
Method of moments for approximating current distribution in antenna array with arbitrarily located parallel center fed dipoles with terminals in common plane
10 p1133 N73-19236
Computerized design of dielectric lenses for phase corrected horn antennas
[AD-753914] 10 p1136 N73-19258
Design and tests of hybrid-mode tracking feed horn
[AD-759834] 18 p2123 N73-27159
Multimode antenna feed system for microwave and broadband communication
[NASA-CASE-GSC-11046-1] 19 p2234 N73-28013
Broadband space feed system for phased array
[AD-763767] 21 p2518 N73-30195
Multimode coaxial feeds for parabolic antennas with large aperture reflectors
[FTZ-A-454-TBR-14] 22 p2642 N73-31177
Design and performance of DSS 14 64 m antenna feed system
22 p2732 N73-31861
Feed displacement effect on double-spherical Cassegrain antenna patterns
[AD-764778] 23 p2767 N73-32139

ANTENNA FIELDS
U ANTENNA RADIATION PATTERNS

ANTENNA RADIATION PATTERNS
NT SIDELOBES
Characteristics of directional dipole antenna array for very high frequency radio interferometer
01 p0027 N73-10213
Antenna pattern calibration for Havana radar systems
01 p0101 N73-10834
Computer program for mapping satellite-borne narrow beam antenna footprints on earth
[NASA-CR-129283] 03 p0265 N73-12149
Dielectric loaded aperture antenna with directive radiation pattern from waveguide
[NASA-CASE-LAR-11084-1] 03 p0273 N73-12216
Radiation patterns of linear phased array focused in near field
[AD-746997] 03 p0274 N73-12226
Frequency characteristics optimization in two dimensional antenna pattern synthesis
[AD-747492] 03 p0276 N73-12242
Radiation pattern characteristics of traveling wave coaxial cable antenna
[AD-749051] 04 p0397 N73-13233
Microwave breakdown at waveguide antenna discharge into ionized gas media
[AD-748830] 04 p0455 N73-13717
RF electric field reflected by finite conducting plane target illuminated by small antenna
[AD-750088] 05 p0514 N73-14183
Synthesis of source distribution on antenna for producing desired radiation patterns
[PB-211348] 05 p0520 N73-14232
Characteristics of shipboard radar antennas, antenna radiation patterns, and automatic target tracking systems
[AD-750871] 06 p0642 N73-15216
Characteristics of four types of horn antennas for application as S-band radiometers and modifications to improve beam efficiency
[NASA-CR-2133] 07 p0755 N73-16135
Effect of electromagnetic scattering from ocean surface on spherical waves of dipole antenna
07 p0761 N73-16184
Waveguide polarizer for horizontal control of antenna radiation patterns
[AD-751449] 07 p0763 N73-16198
Mathematical models for predicting microwave breakdown in fringing field of rectangular slot antenna
[AD-751320] 07 p0763 N73-16202
Parametric design optimization for multiple element short backfire antenna array
[AD-751918] 08 p0889 N73-17199
Evaluation of loran antenna modification to determine effect of increased height on radiated power and system performance
[AD-751978] 08 p0942 N73-17714
Computer program for shape of microwave reflector antenna
[REPT-53199] 10 p1135 N73-19247
Wooded terrain effects on radiation patterns of circular and directional antennas
[FOA-3-A-3747-60] 11 p1255 N73-20179
Numerical analysis of low frequency radiation and scattering from noncircular cylinders with transverse electric polarization
[NASA-CR-2245] 11 p1255 N73-20187
Stereo three dimensional gain pattern formation from plane rectangular antenna characteristics
[AD-754782] 11 p1257 N73-20199
Three dimensional response of directional antenna in elliptically polarized field
[AD-754906] 11 p1257 N73-20202
Lossy earth effects on very high frequency antenna patterns near ground level
[AD-754637] 11 p1257 N73-20204
Computerized simulation of roll and pitch effects on shipboard antenna radiation patterns
[AD-754348] 11 p1258 N73-20212
First order expressions for low angle radiation fields of monopole antenna over irregular ground surface
[AD-756911] 13 p1503 N73-22185
Gain pattern measurements for delta antenna and log periodic antenna configurations
[AD-757619] 14 p1633 N73-23239
VHF broadband directional log periodic antenna study, including pattern and impedance data
[AD-755199] 14 p1643 N73-23323
Evolution of conceptual design of flight hardware for surface electrical Properties experiment - Vol. 1
[NASA-CR-128918] 14 p1705 N73-23835
Characteristics of Hertzian dipole antenna radiation patterns and application to lunar surface and subsurface electrical properties investigation - Vol. 2
[NASA-CR-128919] 14 p1705 N73-23836
Antenna pattern and steering measurements of Wisconsin Test Facility transmissions
[AD-758648] 15 p1752 N73-24200
Analysis of some slow-wave conical log-spiral and helical antennas
[AD-757913] 15 p1757 N73-24242
Transient electromagnetic fields of pulse-excited wire and aperture antennas
16 p1874 N73-25167
Characteristics of antenna arrays of superconducting point contact Josephson junctions
17 p1994 N73-26120
Error analysis for measurements of Mariner Venus Mercury 1973 gain, antenna patterns, and insertion loss of cables
[NASA-CR-133230] 17 p1997 N73-26148
Properties and applications of radar antennas
[AD-759693] 17 p1998 N73-26159
Radiation characteristics of grounded slotted dielectric slab
[AD-760129] 17 p1999 N73-26165
Holographic matched filters for correcting phase heterogeneities in aperture antennas
[JPRS-59253] 17 p2003 N73-26201
Radiation patterns for cavity backed dipole antenna with almost constant gain
[AD-760126] 17 p2005 N73-26216
Analysis of antenna radiation patterns of radio antennas installed on aircraft using high frequency solutions
18 p2115 N73-27098
Radiation patterns of electron plasma waves and reception patterns of monopole antennas
[ISAS-491] 18 p2115 N73-27103
Characteristics of low cost mass producible earth terminal antenna system for broadcast satellite
18 p2122 N73-27152
Design and tests of hybrid-mode tracking feed horn
[AD-759834] 18 p2123 N73-27159
Slot antenna mounted symmetrically on square plate with symmetrical antenna pattern
[AD-762056] 19 p2237 N73-28038
Development of low volume, high power radiating transmitter and antenna array to show radiation pattern, antenna gain, and efficiency
[AD-761793] 19 p2245 N73-28098
Fourier solution for determining radiation patterns of dielectric coated loop antenna
[AD-762041] 19 p2245 N73-28100
Far-field pattern of antenna determined from probe compensated near-field measurements over surface of right circular cylinder enclosing antenna
20 p2375 N73-29084
Hertz vector analysis of spatial structure of cross polarization radiation in axisymmetric parabolic antennas
20 p2377 N73-29096
Computerized simulation of monopulse radar antenna pointing errors due to ground reflection multipath propagation
21 p2507 N73-30114
Efficient technique for determining apparent temperature distributions from antenna temperature measurements
[NASA-CR-2310] 21 p2538 N73-30350
Radar microwave link antenna pattern measurements
[FAA-RD-73-118] 22 p2631 N73-31087
Electromagnetic absorber reflectance and anechoic chamber design for microwave antenna measurements
[FTZ-A-454-TBR-13] 22 p2642 N73-31176
Conception and application of phased arrays
[FTZ-A-454-TBR-15] 22 p2642 N73-31178
Omnidirectional polygon reflector antenna with cosecant radiation pattern for TV transmission in SHF range
[FTZ-A-454-TBR-16] 22 p2643 N73-31179
Contour plotting algorithm for aerial radiation patterns
[BBC-RD-1973/18] 23 p2755 N73-32045
Electromagnetic field problems in inhomogeneous media, radiation patterns, and Eaton lenses for antenna arrays
[NASA-CR-132336] 23 p2757 N73-32060
System for locating lightning strokes by coordination of directional antenna signals
[NASA-CASE-KSC-10729-1] 23 p2763 N73-32110
Design and operational technology associated with radio telescope antennas
[JPRS-59985] 23 p2837 N73-32671
Synchronous-Tracking drive system for automating observations on RTI-7.50/250 MVTU radio telescope
23 p2837 N73-32672
Optical modeling of radiation pattern of variable profile antenna operating in Hartman diaphragm mode
23 p2837 N73-32674

ANTENNAS
NT AIRCRAFT ANTENNAS
NT CASSEGRAIN ANTENNAS
NT CYLINDRICAL ANTENNAS
NT DELTA ANTENNAS
NT DIPOLE ANTENNAS
NT DIRECTIONAL ANTENNAS
NT FURLABLE ANTENNAS
NT HELICAL ANTENNAS
NT HORN ANTENNAS
NT LENS ANTENNAS
NT LOG PERIODIC ANTENNAS
NT LOOP ANTENNAS
NT MICROWAVE ANTENNAS
NT MISSILE ANTENNAS
NT MONOPOLE ANTENNAS
NT MULTIPLE BEAM INTERVAL SCANNERS
NT OMNIDIRECTIONAL ANTENNAS
NT PARABOLIC ANTENNAS
NT RADAR ANTENNAS
NT RADIO ANTENNAS
NT SATELLITE ANTENNAS
NT SLOT ANTENNAS
NT SPACECRAFT ANTENNAS
NT SPHERICAL ANTENNAS
NT SPIRAL ANTENNAS
NT STEERABLE ANTENNAS
NT TURNSTILE ANTENNAS
NT TWO REFLECTOR ANTENNAS
NT WAVEGUIDE ANTENNAS
NT WHIP ANTENNAS

Radiation diagram measurements on antenna model surface for UHF communication to FPL 35F
[FOA-3-C-3678-61] 02 p0139 N73-11130
Boundary value problem of finite tubular antenna in free space and hot isotropic plasma
[AD-746171] 02 p0141 N73-11145
Shipboard antenna height effect on ultrahigh frequency surface of air communication
[AD-748203] 04 p0390 N73-13171
Mathematical model of atmospheric drag distortion of long spinning, flexible antennas
[CRC-1232] 04 p0395 N73-13210
Synthesis of source distribution on antenna for producing desired radiation patterns
[PB-211348] 05 p0520 N73-14232
Computerized simulation of aerodynamic characteristics for trailing wire system towed by orbiting aircraft
[AD-753909] 10 p1136 N73-19255
Energy transfer and behavior of field along biconical antenna
[AD-754386] 11 p1263 N73-20246
Noise sources in towed ELF H-field antenna
[AD-754949] 11 p1263 N73-20250
Analysis of dual reflector antenna system using physical optics and digital computers
[NASA-TM-X-66223] 12 p1379 N73-21183
Investigation of antenna cable responses to pulsed electromagnetic field
[AD-755514] 12 p1385 N73-21234
Research on electromagnetic wave transmission and antennas
[AD-756915] 13 p1496 N73-22126
Calculation and computer program of impedance and far field of short helix antenna above infinite groundplane
[PHL-1972-27] 14 p1619 N73-23110
Antenna measurement of millimeter radio signal propagation through rain
[NASA-CR-132074] 15 p1751 N73-24188
Characteristics of edge mounted coaxial TEM line antenna
[AD-758518] 15 p1758 N73-24252
Multi-impedance loading of linear antennas to improve transmitting and receiving characteristics
21 p2516 N73-30184
Modes of cable vibration compared with pure flexing mode in production of motion induced noise from towed ELF H field antenna
[AD-762936] 22 p2645 N73-31199
Summary of attitude dynamic analysis for IMP-J S/C wire antenna spacecraft
[NASA-TM-X-70465] 22 p2720 N73-31764
Performance data and characteristics of magnetic antennas
[AD-765364] 24 p2899 N73-33141

**ANTHROPOMETRY**
Armed forces anthropometric survey of 6682 Army men
[AD-743465] 01 p0021 N73-10160
Anthropometric survey of US army aviators conducted in 1970
[AD-743528] 01 p0021 N73-10162
Anthropometric data of Japanese Air Self-Defense Force personnel
05 p0502 N73-14091
Anthropometric measurements of military personnel engaged in underwater diving to development standards for design of equipment
[AD-748627] 06 p0637 N73-15175
Color photographic system using grid projector and telecentric lenses for recording contours of human face for aircrew oxygen mask fitting
[RAE-TR-71184] 07 p0750 N73-16099
Multivariate limits for describing cockpit related anthropometric features of aviation personnel
[AD-752032] 08 p0880 N73-17124
Quantitative description of mobility for human torso
[AD-754924] 11 p1251 N73-20151
Anthropometry of Air Force women
[AD-743113] 13 p1484 N73-22034
Anthropometry for protective equipment evaluation and human impact acceleration experiments
14 p1612 N73-23066
Bibliography of anthropometric information for Air Force human factors engineering
[AD-762287] 19 p2229 N73-27978
Mass, volume, center of mass, and mass moment of inertia determined for head and head and neck of human body
[AD-762581] 20 p2372 N73-29065

**ANTIAIRCRAFT MISSILES**
NT NIKE-AJAX MISSILE
NT NIKE-HERCULES MISSILE
NT TERRIER MISSILE
Military training, combat readiness, and antiaircraft defense
[AD-754834] 11 p1352 N73-20980
Electronics of antiaircraft defense systems
[AD-761540] 19 p2248 N73-28125

**ANTIBIOTICS**
Chemical synthesis inhibitor of oceanic species having antibiotic properties
07 p0858 N73-16962

**ANTIBODIES**
Localized shielding effects on antitissue antibody mobilization in irradiated rats
03 p0258 N73-12086

**ANTICHOLINERGICS**
Effects of phosdrin on electrical brain potentials in squirrel monkeys
[FAA-AM-73-3] 18 p2109 N73-27056

**ANTICLINAL MOUNTAINS**
U MOUNTAINS

**ANTICLINAL VALLEYS**
U VALLEYS

**ANTICYCLONES**
Middle latitude anticyclone vertical atmospheric circulation heat sources and sinks, and torques
[REPT-7/1972] 04 p0444 N73-13625
Feasibility determination of Sutcliffe-Petersen development theory to predict development of cyclones and anticyclones at sea level
[NASA-CR-2192] 07 p0815 N73-16605
Blocking anticyclones over Siberia during winter, and meteorological conditions for forecasting their occurrence
13 p1552 N73-22577
Influence of circulation poles and anticyclones on synopticoclimatology
20 p2445 N73-29643

**ANTIDIURETICS**
Radioimmunoassay of urinary antidiuretic hormone excretion in man considering water loading and dehydration effects
09 p0993 N73-18107
Measurement of antidiuretic hormone excretions in human urine as indication of neurosecretory stress response during space flight
09 p0993 N73-18108

**ANTIDOTES**
Protective effects of pyridinium salts against alkyl phosphate poisoning including influence of chemical and aging
[BMVG-FBWT-72-8] 07 p0746 N73-16072

**ANTIFERROMAGNETISM**
Analysis of magnon contribution to total heat current and magneto-elastic coupling in antiferromagnetic materials
16 p1932 N73-25630
Uses of cluster materials and related types in antiferromagnetic cooling by adiabatic magnetization and demagnetization of antiferromagnets
[AD-764620] 23 p2826 N73-32592
Transport coefficient anomalies in antiferromagnetic metals in vicinity of Neel temperature
24 p2933 N73-33424
Affect of antiferromagnetic ordering onset at Neel temperature on transport properties of CeAl, AuHo, and ErCu systems
24 p2933 N73-33425

**ANTIFRICTION BEARINGS**
NT BALL BEARINGS
NT ROLLER BEARINGS
Characteristics of dry rubbing bearings with guide to design and material selection based on specific applications
[ESDU-68018] 01 p0060 N73-10491
Numerical analysis of friction forces developed in ball bearing of pendulum support to show dynamic friction torque and arm of rolling friction
[JPRS-57257] 01 p0062 N73-10507
Performance tests of ball bearings to determine service life during operation without lubrication under various conditions of atmospheres, loads, and speeds
[AD-746034] 01 p0063 N73-10520
Application of metal-polyfluoroethylene bearings in helicopter rotor hinges for operation with and without lubrication
[AD-747428] 03 p0308 N73-12512
Development of method for estimating power required to drive ball bearings in turbine engine based on performance of high speed antifriction bearings
[AD-747600] 03 p0308 N73-12514
Performance of powder metallurgy bronze graphite bearings operating under hydrodynamic conditions at high slipping rates
[AD-747432] 03 p0309 N73-12523
Elastomer inertia effects in compliant surface bearings
[AD-747666] 03 p0309 N73-12524
Elastomer viscoelasticity effects in compliant surface bearings
[AD-747667] 03 p0309 N73-12525
Formula for evaluating durability of plastic bearings based on fatigue wear theory and including friction, elasticity, strength, and pressure factors
[AD-752820] 09 p1040 N73-18480
Numerical analysis of oil film bearing with respect to bushing based in inertial force, viscous force of liquid, and load lifting force exerted by bearing
[AD-752688] 09 p1040 N73-18483
Development of beryllium-copper bearings for use with stainless steel shafts under high bearing stress levels imposed by airframes
[AD-754759] 11 p1299 N73-20540
Defect effect in geometric shape of antifriction bearings on balancing precision of rigid rotors
[AD-754610] 11 p1300 N73-20551
Development of spherical, hydrostatic, compliant bearing for directional gyroscope
11 p1318 N73-20695
Design, development, and evaluation of spherical hydrostatic gas bearing gyroscope for operation in random vibration environment
[AD-755124] 11 p1322 N73-20725
Development of methods for determining service life of rolling bearings based on fatigue of bearing materials
[NLL-RISLEY-TR-2524-[9091.9F]]
12 p1407 N73-21406
Development of virtually zero magnetic bearing for application to electric motor construction
[NASA-CR-130225] 13 p1499 N73-22152
Equations of motion for gyroscopic devices and analysis of effects on accuracy produced by loads and vibrations in supports of gyroscopic instruments
[AD-756337] 13 p1557 N73-22622
Analysis of lubricating oil losses under vacuum conditions and application to antifriction bearings in antenna despin system of Helios solar probe
[NLL-RISLEY-TR-2567-[9091.9F]]
15 p1790 N73-24509
Design, development, and reliability analysis of bearings for turbine pump on nuclear engine for rocket vehicles
[NASA-CR-132227] 15 p1792 N73-24525
Operating characteristics and service life tests of bypass control valve seal and bearing for nuclear engine for rocket vehicles
[NASA-CR-132226] 15 p1792 N73-24526
Increased service life of rolling element radial bearings in nuclear engine for rocket vehicles by liquid hydrogen cooling and bearing modifications
[NASA-CR-132229] 15 p1792 N73-24531
Low temperature tests of elastomeric bearing rotors on OH-58 helicopter
[AD-759957] 17 p2038 N73-26490
Development of optical system for detecting defective components in rotating machinery with emphasis on bearing assemblies
[NASA-CASE-KSC-10752-1] 18 p2154 N73-27407
Effect of lubricant active additives on rolling-element fatigue life using five-ball fatigue tester
[NASA-TN-D-7383] 18 p2156 N73-27417
Numerical analysis of effects on bearing load carrying capacity of opposing surfaces with striated roughness on both surfaces
[AD-761169] 18 p2156 N73-27423
Wear tests of ceramic materials for rolling contact bearings
[AD-761200] 18 p2168 N73-27506
Fatigue life of hybrid antifriction bearings at ultrahigh speeds
[NASA-CASE-LEW-11152-1] 23 p2795 N73-32359
Hollow high strength rolling elements for antifriction bearings fabricated from preformed components
[NASA-CASE-LEW-11026-1] 24 p2928 N73-33383

**ANTIICING ADDITIVES**
Effect of antiicing additives on flammability properties of hydrocarbon fuels used in jet aircraft
[AD-747945] 03 p0349 N73-12852

**ANTIMATTER**
NT ANTINUCLEONS
NT ANTIPROTONS
NT POSITRONS
High energy particle kinetics along boundary of matter-antimatter of universe
[LPTHE-73/5] 14 p1703 N73-23818
Existence of antimatter in Universe
[LPTHE-73/4] 14 p1703 N73-23819
Annihilation processes as origin of matter-antimatter in universe
19 p2332 N73-28767
Annihilation reactions and gamma ray spectra for studying large scale cosmologic antimatter
19 p2332 N73-28769
Detecting antimatter in universe
19 p2333 N73-28771

**ANTIMISSILE DEFENSE**
Computer program for optimum mixed offense weapons system
[AD-746263] 02 p0245 N73-11995
Systems analysis and evaluation of perimeter acquisition radar equipment for use with Safeguard Antiballistic Missile System - Vol. 1B
[AD-748060] 03 p0267 N73-12161
System definition and methodology for selecting perimeter acquisition radar system used with Safeguard Antiballistic Missile System - Vol. 2
[AD-748061] 03 p0267 N73-12162
System definition and criticality analysis of perimeter acquisition radar system used with Safeguard Antiballistic Missile System - Vol. 3 Pt. 1
[AD-748062] 03 p0267 N73-12163
Quality control data and monitoring equipment specifications for hardness testing of antimissile radar defense system
[AD-748063] 03 p0268 N73-12169
Real time software for ballistic missile defense data processing system
[AD-750389] 06 p0644 N73-15234
Control concept utilizing interaction of injected fluid with airstream surrounding missile
[AD-750306] 06 p0722 N73-15894

Constant gain optimal tracking control laws for finite final time
[AD-761091] 18 p2214 N73-27882
Proposed transfer of mission responsibility Army Nike-Hercules Air Defense sites to Army National Guard
[AD-760483] 18 p2214 N73-27883
Development plan for experimental array radar for antimissile defense
[AD-763171] 21 p2509 N73-30132
Statistical decision approach to missile payload discrimination
[AD-764723] 23 p2852 N73-32790

**ANTIMISSILE MISSILES**
Differential game theory applied to military operations, such as antimissile missile problem and air warfare
[BMVG-FBWT-73-9] 19 p2314 N73-28609

**ANTIMONIDES**
NT INDIUM ANTIMONIDES
Pulsed magnetic field apparatus, and microstructure influence on critical current density of superconducting Nb3Sn strips in pulsed fields
[LBL-448] 06 p0708 N73-15778

**ANTIMONY**
Iodoantimonous acid for quantitative yield estimation of antimony trace concentrations by spectrophotometric method
[AREAEE-126] 04 p0433 N73-13531

**ANTIMONY ALLOYS**
Galvanomagnetic and thermoelectric properties of monocrystalline alloys of bismuth and antimony at liquid nitrogen temperature
[AD-745865] 01 p0089 N73-10734
Metal-dielectric phase transitions in Bi-Sb alloys and V2O3
[JPRS-57631] 04 p0433 N73-13525

**ANTIMONY COMPOUNDS**
NT ANTIMONIDES
NT INDIUM ANTIMONIDES

**ANTINUCLEONS**
Antiproton and antinucleon energy spectrum analysis
[LPTHE-73/1] 10 p1191 N73-19691

**ANTIOXIDANTS**
Compatibility with explosives and propellants of natural, butyl and chloroprene rubbers containing Octamine or Flectol H as antioxidants
[ERDE-TN-55] 05 p0565 N73-14592
Stabilization of polyethylene plastics by antioxidants
[AD-753479] 10 p1176 N73-19564
Effect of hypoxia and hyperoxia on rate of blood deoxygenation, and influence of antioxidants in mice
11 p1244 N73-20096

**ANTIPARTICLES**
NT ANTINUCLEONS
NT ANTIPROTONS
NT POSITRONS

**ANTIPROTONS**
Antiproton and antinucleon energy spectrum analysis
[LPTHE-73/1] 10 p1191 N73-19691
Uncorrelated jet model in proton-proton and proton-antiproton annihilation integral
18 p2182 N73-27615

**ANTIRADIATION DRUGS**
Protection of humans from radiation injuries by chemical means
[NRC-TT-1609] 06 p0629 N73-15112
Effectiveness of pharmacochemical protective substances on irradiated mice as neutron component increases
[DRIC-TRANS-2961] 06 p0631 N73-15124
Effectiveness of polymer complex of cysteamine and sulfopropyl ester of dextran as an antiradiation drug on irradiated mice
[DRIC-TRANS-2963] 06 p0631 N73-15125
Composition and effects of radioprotectors on acceleration tolerance, hypoxia toxicity, radiation protection, and dynamic space flight stress in animals
[NASA-TT-F-721] 11 p1239 N73-20054
Effects of antiradiation drug dosage on mice and rat tolerance to transverse acceleration overloads
11 p1239 N73-20055
Resistance of mice to acceleration overloads after injection of aminothiol group radioprotector
11 p1239 N73-20056
Bradycardia and death in guinea pigs exposed to acceleration overloads after injections of aminothiol group radioprotectors
11 p1239 N73-20057
Hypoxia and reduced acceleration tolerance of rats after injection of cysteamine radioprotector
11 p1239 N73-20058
Pathophysiological response reactions of rats to acute hypoxia after injection of cysteamine and aminothiol group radioprotector
11 p1239 N73-20059
Transverse acceleration overload effects on mice sensitivity to toxic doses of cysteamine and aminothiol group antiradiation drugs
11 p1239 N73-20061
Effects of radioprotective drugs on motor evacuatory functions in gastrointestinal tracts of healthy and irradiated rats
11 p1239 N73-20062
Classification of radioprotectors for radiation sickness prevention effects
11 p1240 N73-20065
Pharmacological data for aminothiol and indolylalkylamine radioprotectors
11 p1240 N73-20066
Antiradiation effectiveness of cysteamine in mice under various conditions of gamma radiation
11 p1240 N73-20067
Effectiveness of combined chemical protectors against mixed gamma-neutron radiation with neutron contributions to absorbed dose
11 p1240 N73-20068
Reactivity changes of rats to antiradiation drugs with head and stomach shielded during total irradiation
11 p1241 N73-20072
Mortality rate in antiradiation drug protected mice subjected to gamma radiation overloads
11 p1242 N73-20079
Effect of some radioprotective preparations on motor and evacuator function of gastrointestinal tract of healthy and irradiated rats
[DRIC-TRANS-2962] 12 p1372 N73-21130
Antiradiation drug effects on vestibular analyzer functions
14 p1608 N73-23033

**ANTISEPTICS**
Daylight and disinfectant effects on bacteria survival times on plastic surfaces
[NASA-TT-F-13923] 01 p0009 N73-10069
Chemical synthesis of formaldehyde based disinfectants without penetrating odor and eye and ear irritation properties
[NASA-CASE-NPO-12115-1] 08 p0884 N73-17153

**ANTISKID DEVICES**
Analysis of various aircraft antiskid braking systems to determine appropriate antiskid braking system for space shuttle vehicle
[NASA-CR-124349] 19 p2294 N73-28449

**ANTISUBMARINE WARFARE**
Partial wave analysis solutions for acoustic scattering patterns and target recognition in antisubmarine warfare
[AD-750754] 06 p0700 N73-15710
Kalman filter theory for estimating sonobuoy reference system in antisubmarine warfare
[AD-753608] 10 p1129 N73-19201

**ANTISUBMARINE WARFARE AIRCRAFT**
NT BREGUET 1150 AIRCRAFT
NT CL-84 AIRCRAFT
NT P-3 AIRCRAFT
NT S-3 AIRCRAFT
NT SH-3 HELICOPTER

**ANTITANK MISSILES**
Design, fabrication, manufacture, and verification of composite material rocket engine cases for antitank missiles - Vol. 1
[AD-760566] 18 p2202 N73-27774
Design calculations, tooling sketches, manufacturing and inspection records of composite material rocket engine cases for antitank missiles - Vol. 2
[AD-760569] 18 p2202 N73-27775
Subsonic wind tunnel tests of ring-wing canard configurations for air to surface antitank missiles
[AD-763899] 22 p2723 N73-31788

**ANTONOV AIRCRAFT**
NT AN-2 AIRCRAFT
NT AN-24 AIRCRAFT
Aerodynamic characteristics and performance of USSR An-12 turboprop aircraft to include handling technique and flight safety
[AD-756948] 13 p1476 N73-21953

**ANTONOV AN-24 AIRCRAFT**
U AN-24 AIRCRAFT

**ANXIETY**
Relating test anxiety and trait-state anxiety
[AD-746453] 03 p0260 N73-12104

**APATITES**
U MINERALS

**APERTURES**
Scattering of electromagnetic pulse by rectangular apertures in metal structures
[AD-750381] 06 p0701 N73-15714
Maps of line profile at each position of aperture of neutral hydrogen in NGC 2403 and NGC 4236
[AD-748983] 06 p0719 N73-15872
Analysis of parameters affecting design of synthetic aperture radar antennas for satellites
[NASA-TM-X-66162] 07 p0755 N73-16130
Theory of finite aperture waveguide gas laser resonators representing external reflectors by matrices
[NASA-TM-X-66186] 08 p0929 N73-17608
Optical absorption properties of polycrystalline zinc selenide and cadmium telluride materials for infrared laser windows
[AD-753068] 09 p1044 N73-18512
Procedure for fabricating element with cavity closed by thin wall with precisely shaped slit
[NASA-CASE-LAR-10409-1] 11 p1297 N73-20526
Five possible supernova remnants mapped by aperture synthesis interferometry
12 p1447 N73-21721
Device for measuring angle of arrival of laser beams and predictions of expected results for input apertures and turbulence
[AD-755404] 13 p1538 N73-22464
Real image of aperture-limited, in-line Fraunhofer hologram
16 p1923 N73-25560
Extension of electromagnetic antenna wave diffraction principle
[AD-759690] 17 p1999 N73-26163
Holographic matched filters for correcting phase heterogeneities in aperture antennas
[JPRS-59253] 17 p2003 N73-26201
Apparatus for on-film optical recording of camera lens aperture and focus setting
[NASA-CASE-MSC-12363-1] 17 p2030 N73-26431
Effect of connecting aperture in resonator mirror on radiation power of CO2 laser
[AD-763254] 21 p2555 N73-30484

**APEXES**
Load near apex of lifting swept wing in linearized subsonic flow
[ARC-R/M-3716] 21 p2492 N73-30001

**APNEA**
U RESPIRATION

**APOGEES**
Apogee stage for Europa 3 launch vehicle
15 p1835 N73-24879

**APOLLO FLIGHTS**
NT APOLLO 9 FLIGHT
NT APOLLO 11 FLIGHT
NT APOLLO 12 FLIGHT
NT APOLLO 13 FLIGHT
NT APOLLO 14 FLIGHT
NT APOLLO 15 FLIGHT
NT APOLLO 16 FLIGHT
NT APOLLO 17 FLIGHT
Effect of residual motion smear or image reproduction processes on detail of lunar surface imagery from orbiting command module
[NASA-CR-130378] 07 p0798 N73-16485
Dynamic mass modeling and geophysical analysis of lunar maria based on Apollo tracking data
[NASA-TM-X-65940] 11 p1338 N73-20854

**APOLLO LUNAR SURFACE EXPERIMENTS PACKAGE**
Progress in ALSEP program
[NASA-CR-128597] 01 p0057 N73-10464
ALSEP developments, and environmental and quality control tests
[NASA-CR-128580] 01 p0103 N73-10847
Familiarization course for Apollo 17 flight Lunar Surface Experiments package
[NASA-CR-128636] 03 p0301 N73-12459
Time and motion study of astronaut lunar surface activity on Apollo 16
[NASA-CR-128696] 07 p0842 N73-16825
Lunar cart for carrying experimental payloads between Apollo 11 and lunar roving vehicle
09 p1088 N73-18882
Passive seismic experiment at Descartes landing site of Apollo 16 mission
12 p1449 N73-21741
Active seismic experiment deployed to provide data concerning near-surface structure at Apollo 16 landing site
12 p1450 N73-21742
Apollo 16 lunar surface magnetometer providing measurements of global response of moon to large-scale solar and terrestrial magnetic fields
12 p1450 N73-21743
Permanent magnetic field on lunar surface measured by Apollo 16 lunar portable magnetometer experiment
12 p1450 N73-21744
Far UV camera/spectrograph deployed on lunar surface in Apollo 16 mission
12 p1450 N73-21745
Flat conductors for ALSEP
14 p1642 N73-23315
Evolution of conceptual design of flight hardware for surface electrical Properties experiment - Vol. 1
[NASA-CR-128918] 14 p1705 N73-23835
Characteristics of Hertzian dipole antenna radiation patterns and application to lunar surface and subsurface electrical properties investigation - Vol. 2
[NASA-CR-128919] 14 p1705 N73-23836
Reliability and quality control procedures for development of test equipment used on lunar experiment projects - Vol. 3
[NASA-CR-128920] 14 p1705 N73-23837
Internal lunar properties calculated from surface magnetometer experiments data
[NASA-TM-X-62278] 17 p2082 N73-26842

**APOLLO PROJECT**
Development of alpha and X ray spectrometers for use on Apollo 15 and 16 flights
[NASA-CR-128649] 03 p0301 N73-12461
Application of Apollo Project managerial practices to solution of problems encountered in modern civilization
04 p0470 N73-13834

Effect of Apollo project accomplishments on earth resources surveys and conduct of earth resources investigations in future space missions
07 p0781 N73-16349
Development and characteristics of laser altimeter for use with Apollo Lunar Orbital Experiments Mission
[NASA-CR-128738] 08 p0924 N73-17567
Philosophical and social psychological study of Apollo moon scientist
[NASA-CR-130832] 09 p0995 N73-18122
Papers presented at 7th Aerospace Mechanisms Symposium
[NASA-TM-X-58106] 09 p1087 N73-18866
Apollo experience report to analyze radiation protection problems on earth and in space
[NASA-TN-D-7080] 09 p1090 N73-18899
Apollo experience report on lunar module ascent propulsion subsystem to identify significant technical problems encountered during all phases of program
[NASA-TN-D-7082] 09 p1090 N73-18900
Apollo experience report of structural subsystem, structural configuration, and design verification of lunar module spacecraft
[NASA-TN-D-7084] 09 p1091 N73-18901
Investigation of light flash phenomenon observed by Apollo crews
[NASA-CR-128866] 10 p1213 N73-19867
Apollo experience report on evolution of attitude time line
[NASA-TN-D-7086] 10 p1214 N73-19872
Apollo experience report on causes of stress-corrosion cracking of structural materials and corrective actions
[NASA-TN-D-7111] 10 p1214 N73-19875
Apollo experience report on development of flight simulators for spacecrew training to show functional uses, characteristics, and problems
[NASA-TN-D-7112] 10 p1214 N73-19876
Apollo experience report on propulsion system for descent stage of lunar module with emphasis on throttling capability and cryogenic helium pressurization system
[NASA-TN-D-7143] 10 p1215 N73-19877
Apollo experience report on instrument calibration data to provide correct engineering data for tests and mission support
[NASA-TN-D-7144] 11 p1341 N73-20881
Presidential report on progress and activities of various aerospace programs in 1972 and comments on future mission planning
11 p1352 N73-20975
Accomplishments of Apollo project and objectives of post-Apollo lunar scientific investigations
[LC-72-93379] 12 p1446 N73-21714
Analysis of major problems in early stages of manned spaceflight, Vostok and Mercury flights, and Mars exploration
[NASA-TT-F-14916] 14 p1709 N73-23867
Apollo experience report on engineering simulation in support of Apollo guidance and control system
[NASA-TN-D-7287] 15 p1835 N73-24873
Spares and repair parts support plan for ultraviolet spectrometer Apollo experiment
[NASA-CR-128571] 16 p1885 N73-25260
Performance verification test plan for Apollo ultraviolet spectrometer experiment
[NASA-CR-128573] 16 p1915 N73-25500
Stress analysis verification of structural integrity of Apollo ultraviolet spectrometer experiment
[NASA-CR-128551] 16 p1916 N73-25501
Final nonmetallic materials list for Apollo ultraviolet spectrometer experiment
[NASA-CR-128583] 16 p1916 N73-25502
Qualification plan for the Apollo ultraviolet spectrometer experiment, revision
[NASA-CR-128572] 16 p1916 N73-25503
Exit slit mirrors for Ebert ultraviolet spectrometer Apollo experiment
[NASA-CR-128549] 16 p1916 N73-25504
System safety plan for Apollo ultraviolet spectrometer experiment
[NASA-CR-128576] 16 p1916 N73-25505
Contamination control program plan for Apollo ultraviolet spectrometer experiment
[NASA-CR-128575] 16 p1916 N73-25506
Apollo experience report on development of Apollo digital autopilots for primary attitude control during all phases of lunar landing mission
[NASA-TN-D-7289] 16 p1964 N73-25888
Apollo experience report on design and development of cryogenic storage system and related components
[NASA-TN-D-7288] 16 p1964 N73-25889
Erratic operation of mapping camera extension mechanism on Apollo spacecraft
[NASA-TM-X-69269] 16 p1967 N73-25909
Research in intepretation of lunar data developed during Apollo Program
[NASA-CR-133302] 18 p2190 N73-27679
Apollo experience report on development of design loads criteria, methods, and operational procedures for prelaunch, lift-off, and midboost conditions
[NASA-TN-D-7373] 20 p2474 N73-29875
Apollo experience report on evolution of rendezvous maneuver plan for lunar landing missions
[NASA-TN-D-7388] 20 p2475 N73-29882
Apollo lunar sample return containers for storing and protecting lunar samples
[Y-1867] 21 p2553 N73-30465
Apollo experience report on process of crew procedures development for systems procedures and flight procedures
[NASA-TN-D-7436] 22 p2721 N73-31772
Intra- and extravehicular life support space suite for Apollo astronauts
[NASA-CASE-MSC-12609-1] 23 p2751 N73-32012
Users manual for Apollo cryogenic storage system computer program
[NASA-CR-134054] 23 p2760 N73-32088

**APOLLO SOYUZ TEST PROJECT**

Computer program used for dynamic analysis of Apollo-Salyut/Soyuz docking
09 p1087 N73-18871
Mathematical model of VHF ranging system to analyze performance of Apollo Soyuz test project
[NASA-CR-134063] 23 p2846 N73-32741
Spacecraft mass properties data for use in mission planning for Apollo/Soyuz Test Project
[NASA-TM-X-69502] 24 p2980 N73-33813

**APOLLO SPACECRAFT**

Wind tunnel tests to determine pressure distribution on Apollo command module and Saturn launch vehicle at supersonic and hypersonic speeds
[NASA-TM-X-62117] 04 p0477 N73-13904
Wind tunnel pressure signatures for scale model of Apollo command module
[NASA-TM-X-62047] 04 p0478 N73-13905
Transient thermodynamic simulation of Apollo fuel cell/radiator system for proposed Skylab mission
[NASA-CR-129824] 05 p0598 N73-14860
Use of cyclic struts as energy absorbers for Apollo couch
09 p1088 N73-18881
Dynamic testing for determining flight readiness of Apollo docking system hardware
09 p1089 N73-18885
Apollo Command Module Aerodynamic Simulation tests in hypersonic flow
[DLR-FB-71-83] 09 p1089 N73-18892
Apollo experience report on water landing requirement and two stable flotation attitudes for upright flotation of command module
[NASA-TN-D-7081] 09 p1090 N73-18898
Apollo experience report concerning general design, development, and qualification of launch escape propulsion subsystem
[NASA-TN-D-7083] 09 p1091 N73-18902
Apollo experience report on techniques to define aerothermodynamic environment of Apollo spacecraft during post boost phase and to predict structural temperatures
[NASA-TN-D-7085] 09 p1091 N73-18903
Apollo experience report on design philosophy and experience of Apollo spacecraft electrical power generation system
[NASA-TN-D-7142] 10 p1214 N73-19873
Apollo experience report on procedures and techniques for predicting consumables usage for Apollo missions
[NASA-TN-D-7140] 10 p1214 N73-19874
Apollo experience report on use of pyrotechnic devices in systems of Apollo spacecraft
[NASA-TN-D-7141] 10 p1215 N73-19878
Failure analysis and design criteria for transducers in Apollo environmental control systems
[NASA-CR-128921] 15 p1756 N73-24231
Apollo experience report on design and function of Apollo potable water system supplied as byproduct of fuel cells
[NASA-TN-D-7291] 15 p1835 N73-24874
Apollo experience report on lighting requirements for Apollo command and lunar modules for internal and external lighting
[NASA-TN-D-7290] 16 p1964 N73-25887
Apollo experience report on command and service module reaction control systems
[NASA-TN-D-7151] 16 p1966 N73-25901
Apollo experience report on development of design loads criteria, methods, and operational procedures for prelaunch, lift-off, and midboost conditions
[NASA-TN-D-7373] 20 p2474 N73-29875
Three axis inertial system in Apollo gimbal for fine grain evaluation of strapdown system performance in dynamic environments
[NASA-CR-135484] 22 p2698 N73-31609
Apollo experience report on command and service module instrumentation subsystem to show requirements determination and conceptual design
[NASA-TN-D-7374] 22 p2719 N73-31761
Apollo experience report on service propulsion subsystem development, qualification, and flight performance
[NASA-TN-D-7375] 22 p2719 N73-31763
Development of crew-couch/restraint system and crew load attenuation system for Apollo command module
[NASA-TN-D-7440] 22 p2720 N73-31768
Apollo experience report on reliability of Apollo spacecraft based on application of proven reliability and quality control techniques
[NASA-TN-D-7438] 22 p2720 N73-31769
Apollo experience report on window structural design and verification for command and lunar modules
[NASA-TN-D-7439] 22 p2720 N73-31770
Apollo experience report on equipment storage and stowage arrangement in spacecraft for maximum operational performance
[NASA-TN-D-7434] 22 p2720 N73-31771
Apollo experience report on various phases of post-flight testing of command modules to resolve or minimize anomalies discovered during flight
[NASA-TN-D-7435] 22 p2721 N73-31773
Details and problems of docking technology, mutual aid and rescue for disasters, search and rendezvous means, and cabin atmospheric parameters for Soviet-American flight
[NASA-TT-F-15096] 23 p2844 N73-32726

**APOLLO TELESCOPE MOUNT**

Data processing needs of Apollo Telescope Mount experiment
[NASA-CR-123911] 01 p0030 N73-10232
Effects of sensor deadband and actuator breakout torque control system nonlinearities on performance of Apollo telescope mount pointing capability
[NASA-TN-D-7247] 15 p1834 N73-24868
Thermionic cathode development for Apollo telescope mount camera tube Spares Program
[NASA-CR-124342] 19 p2243 N73-28087
Operation of switching electronic power regulator for Skylab/Apollo telescope mount
[NASA-CR-124445] 23 p2748 N73-31989
Skylab, solar studies, and usefulness of Apollo telescope mount
[NASA-EP-119] 23 p2834 N73-32645

**APOLLO 9 FLIGHT**

Analysis of photography from Apollo 9 flight to determine origin, movement, and dissipation of masses of discolored water near shores of North and South Carolina
07 p0788 N73-16408

**APOLLO 11 FLIGHT**

Lunar cart for carrying experimental payloads between Apollo 11 and lunar roving vehicle
09 p1088 N73-18882
Measurement of line spectra produced by high resolution mass spectrometer and application to identifying organic compounds in samples from Apollo 11 and 12 flights
[NASA-CR-128840] 10 p1160 N73-19436
Pre- and post-Apollo 11 studies on lunar geologic evolution
[NASA-TM-X-65939] 13 p1577 N73-22777
Effect of neutron irradiation on remanent magnetization in Apollo 11 and 12 lunar samples of iron and kamacite
15 p1813 N73-24692
Postflight analysis of Apollo 11 glycol temperature control valve failure
[NASA-TM-X-69200] 17 p2088 N73-26896

**APOLLO 12 FLIGHT**

Effects of Apollo 12 lunar materials on lipid levels, including fatty acids and sterols, of tobacco tissue and slash pine cultures
[NASA-CR-128606] 01 p0008 N73-10063
Evaluation of descent propulsion system for Apollo 12
[NASA-TM-X-68933] 06 p0712 N73-15812
Mineral analysis of lunar samples of crystalline rocks from Apollo 12 flight
[NASA-SP-306] 07 p0844 N73-16837
Measurement of line spectra produced by high resolution mass spectrometer and application to identifying organic compounds in samples from Apollo 11 and 12 flights
[NASA-CR-128840] 10 p1160 N73-19436
Cytological changes in pine tissues treated with lunar materials collected on Apollo 12 quarantine mission
[NASA-CR-128914] 14 p1610 N73-23054
Effect of neutron irradiation on remanent magnetization in Apollo 11 and 12 lunar samples of iron and kamacite
15 p1813 N73-24692
Results of postflight analysis of APS performance during Apollo 12 Mission
[NASA-TM-X-69529] 17 p2083 N73-26850

**APOLLO 13 FLIGHT**

Analysis of inflight performance of Apollo 13 spacecraft guidance, navigation, and control equipment
[NASA-TM-X-69528] 17 p2060 N73-26666

**APOLLO 14 FLIGHT**

Microbial analysis of Apollo 14 astronauts
[NASA-TM-X-58094] 05 p0500 N73-14073
Systems analysis for determining cause of steerable antenna oscillations during Apollo 14 and 15 missions
[NASA-TM-X-68901] 05 p0519 N73-14218
Postflight analysis of Apollo 14 translunar docking anomaly
09 p1089 N73-18884

Analysis of melting, mixing, and solidification of metal matrix composite materials in weightless environment
13 p1594 N73-22921
Neutron activation analysis of cosmic radiation doses in Apollo 14, 15, and 16 astronauts
[NASA-CR-131984] 14 p1612 N73-23070
Temporary loss of Apollo 14 command module color television picture by ground station converter
[NASA-TM-X-69296] 15 p1751 N73-24189
Performance of Apollo 14 lunar module descent propulsion system
[NASA-TM-X-69491] 20 p2466 N73-29813
Bistatic radar experiments during lunar orbit phases of Apollo 14, 15, and 16
[NASA-CR-134003] 21 p2507 N73-30116
Postflight analysis of Apollo 14 flight to show spacecraft performance, launch vehicle performance, and malfunctions occurring during flight
[NASA-TM-X-69536] 24 p2981 N73-33824

APOLLO 15 FLIGHT

Performance tests of scale model of lunar roving vehicle used on Apollo 15 mission to determine vehicle mobility
[NASA-CR-129176] 02 p0152 N73-11234
Analysis of sonic boom pressure signatures recorded during reentry of Apollo 15 command module and correlation with wind tunnel signatures
[NASA-TM-X-62111] 04 p0371 N73-13016
Development and performance of color television equipment developed for use on Apollo 15 mission
04 p0473 N73-13855
Systems analysis for determining cause of steerable antenna oscillations during Apollo 14 and 15 missions
[NASA-TM-X-68901] 05 p0519 N73-14218
Apoll 15 photography of lunar surface
[NASA-TM-X-68910] 05 p0595 N73-14834
Stratigraphy of Apollo 15 drill core
[NASA-TM-X-58101] 05 p0595 N73-14839
Guidance, navigation and control system analysis report for Apollo 15
[NASA-TM-X-68934] 06 p0696 N73-15673
Postflight analysis of Apollo 15 LM APS
[NASA-TM-X-68932] 06 p0712 N73-15813
Time and motion study of lunar surface activity on Apollo 15
[NASA-CR-128695] 07 p0842 N73-16823
Apollo 15 X ray fluorescence experiment
08 p0975 N73-17978
Apollo 15 deployable boom anomaly and subsequent design changes
09 p1087 N73-18868
Analysis of design features and photographic data to determine cause of Apollo 15 main parachute failure
09 p1088 N73-18879
Specifications and characteristics of ground-commanded color television assembly used on Apollo 15 flight
[NASA-CR-128829] 10 p1128 N73-19192
Improving selenodetic control on lunar limb using Apollo 15 transearth photography
[NASA-CR-131264] 11 p1336 N73-20846
Photogrammetric techniques from Apollo 15 and 16 flights to provide accurate measurement of lunar topography
12 p1456 N73-21791
Neutron activation analysis of cosmic radiation doses in Apollo 14, 15, and 16 astronauts
[NASA-CR-131984] 14 p1612 N73-23070
Results of postflight analysis of APS performance during Apollo 15 mission
[NASA-TM-X-69204] 17 p2077 N73-26801
Apollo 15 measurement of cosmic gamma ray spectrum between 0.3 and 27 MeV
19 p2331 N73-28756
Measurement of ionic conductivity and temperature in Apollo 15 plume
[AD-761484] 19 p2353 N73-28924
Bistatic radar experiments during lunar orbit phases of Apollo 14, 15, and 16
[NASA-CR-134003] 21 p2507 N73-30116
Steady state performance of LM-10 Descent Propulsion System during descent phase of Apollo 15 Mission
[NASA-TM-X-69506] 22 p2717 N73-31750
Estimates of moon geometry using lunar orbiter imagery and Apollo laser altimeter data
[NASA-TR-R-407] 23 p2846 N73-32743
Postflight analysis of Apollo 15 flight to determine performance of launch vehicle, spacecraft, and lunar roving vehicle and to analyze malfunctions
[NASA-TM-X-69539] 24 p2981 N73-33819

APOLLO 16 FLIGHT

Free electrophoresis in zero gravity on Apollo 16 flight
[NASA-CR-123920] 02 p0130 N73-11055
Analysis of nutrient intake and absorption during Apollo 16 flight
[NASA-TM-X-58096] 03 p0260 N73-12110
Analysis of radioactivity in lunar samples returned by Apollo 16 flight and relationship to occurrence of solar flares
[NASA-CR-129291] 03 p0354 N73-12886
Postflight trajectory for Apollo/Saturn V AS-511 spent S-4B/IU stage from CSM separation to lunar impact
[NASA-CR-123975] 05 p0594 N73-14826
Failure analysis of malfunction of Apollo 16 television camera monitor on command module
[NASA-TM-X-68930] 06 p0639 N73-15190
Guidance, navigation, and control system performance analysis report for Apollo 16 mission
[NASA-TM-X-68931] 06 p0696 N73-15674
Time and motion study of astronaut lunar surface activity on Apollo 16
[NASA-CR-128696] 07 p0842 N73-16825
Free fluid electrophoresis experiment onboard Apollo 16 flight
[NASA-TM-X-64724] 09 p1000 N73-18157
Performance of LM-11 Descent propulsion System during Apollo 16 Mission
[NASA-CR-128826] 10 p1213 N73-19865
Analysis of off-scale low indications of voltmeters for batteries at initial powerup for Apollo 16 lunar roving vehicle
[NASA-TM-X-69123] 11 p1266 N73-20272
Apollo 16 flight anomaly report to determine cause of burn holes in main parachute canopy
[NASA-TM-X-69127] 11 p1338 N73-20863
Report by Apollo 16 crew that lunar roving vehicle rear steering was inoperative
[NASA-TM-X-69124] 11 p1339 N73-20864
Correlation of sonic boom pressure signatures recorded during reentry of Apollo 16 command module with wind tunnel signatures
[NASA-TM-X-62073] 12 p1365 N73-21073
Preliminary results of Apollo 16 investigations
[NASA-SP-315] 12 p1448 N73-21729
Selection of lunar landing site for Apollo 16
12 p1448 N73-21730
Description of Apollo 16 flight
12 p1448 N73-21731
Topographic mapping of Apollo 16 landing from high resolution photographs by lunar orbiter
12 p1448 N73-21732
Preliminary results of Apollo 16 lunar experiments
12 p1449 N73-21733
Photographic summary for Apollo 16 flight
12 p1449 N73-21734
Observations by astronauts on Apollo 16 flight
12 p1449 N73-21735
Preliminary results of examining lunar rock samples from Apollo 16 flight
12 p1449 N73-21736
Chemical, petrographic, and textural characteristics of Apollo 16 rock and soil samples
12 p1449 N73-21737
Special samples which were collected on Apollo 16 for specific investigations
12 p1449 N73-21738
Unstable component of magnetization found in lunar samples
12 p1449 N73-21739
Soil mechanics for lunar soils near landing site for Apollo 16 mission
12 p1449 N73-21740
Passive seismic experiment at Descartes landing site of Apollo 16 mission
12 p1449 N73-21741
Active seismic experiment deployed to provide data concerning near-surface structure at Apollo 16 landing site
12 p1450 N73-21742
Apollo 16 lunar surface magnetometer providing measurements of global response of moon to large-scale solar and terrestrial magnetic fields
12 p1450 N73-21743
Permanent magnetic field on lunar surface measured by Apollo 16 lunar portable magnetometer experiment
12 p1450 N73-21744
Far UV camera/spectrograph deployed on lunar surface in Apollo 16 mission
12 p1450 N73-21745
Solar wind composition experiment onboard Apollo 16
12 p1450 N73-21746
Plastic and glass detectors for measuring composition and energy spectra of solar cosmic ray nuclei
12 p1450 N73-21747
Solar flare producing large amounts of low energy nuclei measured by Apollo 16
12 p1450 N73-21748
Solar cosmic ray, solar wind, solar flare, and neutron albedo measurements, using mineral detectors onboard Apollo 16
12 p1450 N73-21749
Apollo 16 photography of Gegenschein-Moulton region for libration point determination of Sun-Earth system
12 p1451 N73-21750
UV imagery of earth and moon at varied wavelengths
12 p1451 N73-21751
Gamma ray spectrometer experiment during transearth coast period of Apollo 16 flight
12 p1451 N73-21752
X ray fluorescence spectrometer for orbital mapping of lunar composition and X ray galactic observations
12 p1451 N73-21753
Lunar radon emanation measurements, using alpha particle spectrometers on Apollo 16
12 p1451 N73-21754
Lunar orbital mass spectrometer for lunar atmosphere detection and lunar volcanism search
12 p1451 N73-21755
Apollo 16 particles and fields subsatellite for measuring vector magnetic fields and plasma and energetic particle fluxes
12 p1451 N73-21756
Particles and fields subsatellite magnetometer experiment to calculate lunar interior electrical conductivity
12 p1451 N73-21757
Use of superhigh frequency transponder on Apollo 16 subsatellite to measure lunar gravitational field as preliminary investigation of lunar mass
12 p1451 N73-21758
Bistatic radar investigation of lunar electromagnetic and surface properties from Apollo 16 command and service module
12 p1451 N73-21759
Use of Apollo heat shield window to study dynamic and physical properties of meteoroids
12 p1452 N73-21760
Apollo 16 experiment using biostack to determine effects of heavy nuclei on biological organisms
12 p1452 N73-21761
Apollo 16 microbiological experiment on microbial response to aerospace environments - Part B
12 p1452 N73-21762
Light flash observation experiments conducted by Apollo 16 astronauts - Part C
12 p1452 N73-21763
Apollo 16 visual observations of surface geology from lunar orbit
12 p1452 N73-21764
Relative ages of near side and far side terra plains based on interpretation of Apollo 16 photogeology - Part A
12 p1452 N73-21765
Cayley Formation interpreted as deposited fluidized debris that traveled beyond extent of Imbrium Basin ejecta - Part B
12 p1453 N73-21766
Small scale analogs of Cayley Formation and Descartes Mountains in impact crater-associated deposits - Part C
12 p1453 N73-21767
Possible analogs around Orientale Basin provide reasonable alternatives to geomorphologic interpretation of volcanism in Descartes highlands - Part D
12 p1453 N73-21768
Interpretation of Apollo 16 photography of Orientale Basin deposits under earthshine illumination conditions - Part E
12 p1453 N73-21769
Photogeologic analysis of Apollo 16 metric photography of northern Nectaris Basin - Part F
12 p1453 N73-21770
Structural aspects of distinctive landforms collectively referred to as Imbrium sculpture - Part G
12 p1453 N73-21771
Discovery of previously unknown structural basin and crater on Apollo 16 photography of far side highlands near eastern limb of moon - Part H
12 p1453 N73-21772
Identification of artificial lunar impact craters produced by Ranger 7 and 9 spacecraft and S-4B stage of Apollo 13 and 14 - Part I
12 p1453 N73-21773
Identification of Ranger 7 and 9 impact craters from Apollo 16 photography - Part J
12 p1454 N73-21774
Apollo 16 photography of V-shaped ridges associated with secondary craters - Part K
12 p1454 N73-21775
Morphometric analysis of Apollo 16 photography of lunar craters - Part L
12 p1454 N73-21776
Apollo 16 orbital photography of King Crater and surrounding environment - Part M
12 p1454 N73-21777
Interpretation of ejecta blanket deposition from King Crater photographs
12 p1454 N73-21778
Examination of lunar surface patterns created by volcanic lava flows and impact debris
12 p1454 N73-21779
Volcanic origin of mare ridges and sinuous rilles on lunar surface
12 p1454 N73-21780
Fourier technique for quantitatively classifying lunar rilles by planimetric shape
12 p1455 N73-21781
Origins of fracture patterns in Type 3 marginal premare craters
12 p1455 N73-21782
Stereoscopic photographs for studying low relief mare features of lunar surface
12 p1455 N73-21783

Exogenetic and endogenetic origin of sinuous markings on lunar mare
12 p1455 N73-21784
Near terminator photography of low relief features and mare units of Descartes Region
12 p1455 N73-21785
Distribution of color variations in Mare Nubium and Southern Oceanus Procellarum lunar regions
12 p1455 N73-21786
Analysis of earth based remote sensing data and infrared observations to determine nature of Apollo 16 landing site
12 p1455 N73-21787
Apollo 16 radar echo data for predicting blockiness of lunar surface
12 p1455 N73-21788
Physical and geological aspects of heiligenschein measurements made from Apollo 16 Flight
12 p1455 N73-21789
Use of laser altimetry in Apollo 16 flight to aid in spacecraft position determination and lunar geological investigation
12 p1455 N73-21790
Photogrammetric techniques from Apollo 15 and 16 flights to provide accurate measurement of lunar topography
12 p1456 N73-21791
Use of Apollo 16 photogrammetry to determine frequency distributions of lunar slopes
12 p1456 N73-21792
Astronomical photography of Gum Nebula, galactic clusters, and zodiacal light from Apollo 16 flight
12 p1456 N73-21793
Photographic observations of solar corona by Apollo 16 command module from lunar orbit
12 p1456 N73-21794
BIOSTACK experiment on Apollo 16 for studying combined action of heavy high energy loss nuclei and space flight factors on resting biological systems
14 p1611 N73-23062
Neutron activation analysis of cosmic radiation doses in Apollo 14, 15, and 16 astronauts
[NASA-CR-131984] 14 p1612 N73-23070
Conference on Apollo 16 experiment for measuring microbial response to space environment
[NASA-TM-X-58103] 15 p1740 N73-24102
Design of microbial test system for Apollo 16 mission
15 p1740 N73-24103
Device for extravehicular microbe exposures to space environment during Apollo 16 flight
15 p1740 N73-24104
Operational handling of test equipment for microorganism exposure to space environment
15 p1740 N73-24105
Physiological responses of parasitic worms and their larvae to solar ultraviolet irradiation and space flight stress
15 p1740 N73-24106
Ultraviolet extraterrestrial radiation tolerances of Bacillus subtilis spores and Escherichia coli bacteriophages
15 p1740 N73-24107
Space vacuum and solar ultraviolet irradiation effects on survival of Bacillus subtilis spores
15 p1740 N73-24108
Space flight ultraviolet irradiation effects on Bacillus thuringiensis toxin production capability
15 p1740 N73-24109
Phenotype numbers and survival rates of fungi exposed to space environment during Apollo 16 flight
15 p1740 N73-24110
Ultraviolet space irradiation effects on Aeromonas proteolytica extracellular enzyme production
15 p1741 N73-24111
High resolution film actinometric measurements of ultraviolet irradiation levels during space flight
15 p1741 N73-24112
Potassium ferrioxalate actinometric measurements of solar ultraviolet photobiological energy
15 p1741 N73-24113
Nuclear track dosimetry for monitoring cosmic ray exposure of Apollo 16 astronauts
15 p1741 N73-24114
Lithium fluoride thermoluminescent dosimeter for measuring ionizing radiation exposure during Apollo 16 flight
15 p1741 N73-24115
Data users note for dissemination of Apollo 16 lunar photographs
[NSSDC-73-01] 15 p1785 N73-24468
Apollo 16 lunar maps
[NASA-CR-132066] 15 p1785 N73-24469
Inoperative conditions of rear steering system of lunar roving vehicle on Apollo 16 flight
[NASA-TM-X-69198] 17 p2010 N73-26256
Anomaly report of explosive failure of ground support equipment decontamination unit tank during postflight deactivation of Apollo 16 command module
[NASA-TM-X-69323] 17 p2088 N73-26897
Inertial subsystem warning and coupling data unit failure indications on Apollo 16 mission
[NASA-TM-X-69199] 17 p2089 N73-26898
Postflight analysis of Apollo 16 scanning telescope system to determine cause of uneven drive rates
[NASA-TM-X-69233] 17 p2089 N73-26899
Apollo 16 flight anomaly report on malfunction of water/glycol temperature control circuit
[NASA-TM-X-69234] 17 p2089 N73-26900
Bistatic radar experiments during lunar orbit phases of Apollo 14, 15, and 16
[NASA-CR-134003] 21 p2507 N73-30116
Apollo 16 lunar surface cosmic ray experiment S-152
[NASA-CR-134019] 21 p2592 N73-30770
Postflight analysis of Apollo 16 flight to show spacecraft performance, launch vehicle performance, and malfunctions occuring during flight
[NASA-TM-X-69535] 24 p2981 N73-33823
**APOLLO 17 FLIGHT**
Familiarization course for Apollo 17 flight Lunar Surface Experiments package
[NASA-CR-128636] 03 p0301 N73-12459
Apollo 17 vacuum ultraviolet spectrometer calibration plan
[NASA-CR-128831] 10 p1160 N73-19439
Apollo 17 far ultraviolet scanning spectrometer experiment for lunar atmosphere measurements
[NASA-CR-128835] 10 p1160 N73-19440
Postflight analysis of abnormalities in Apollo 17 flight
[NASA-TM-X-69122] 10 p1211 N73-19850
Evaluation of ultraviolet flux from stars used as inertial-hold pointing directions during Apollo 17 flight
[NASA-CR-128834] 10 p1213 N73-19866
Apollo 17 Calibration Facility safety plan covering ultraviolet spectrometer components
[NASA-CR-128833] 10 p1229 N73-19990
Construction of far ultraviolet Ebert spectrometer for use on Apollo 17 flight to observe lunar atmosphere
[NASA-CR-128889] 11 p1293 N73-20491
Analysis of test films to assess readiness of Apollo 17 radar equipment with emphasis on lunar sounder equipment
[NASA-CR-128883] 11 p1338 N73-20858
Microbiological studies of Apollo 17 command module preflight and postflight samples
[NASA-CR-132022] 14 p1610 N73-23056
Operational and engineering aspects of Apollo 17 lunar landing mission
[NASA-TM-X-69292] 14 p1706 N73-23844
Semiautomatic self-leveling lunar gravimeter for Apollo 17 mission
[NASA-CR-128948] 15 p1787 N73-24490
Historical account of data and theories pertaining to lunar atmosphere prior to Apollo
[NASA-CR-128548] 15 p1833 N73-24863
Supporting research plan for Apollo 17 ultraviolet spectrometer experiment
[NASA-CR-128547] 16 p1916 N73-25507
Lunar roving vehicle/traverse gravimeter experiment motion sensitivity test showing gravity measurements in normal and bypass modes
[NASA-TM-X-69268] 16 p1963 N73-25882
Analysis of Apollo 17 flight to show extravehicular activities, lunar surface experiments, orbital science projects, and spacecraft reentry and recovery
[NASA-TM-X-69527] 17 p2083 N73-26851
Apollo 17 flight plan for prelaunch checkout support and continuous support to be provided during mission - Revision A
[NASA-TM-X-69530] 17 p2083 N73-26853
Failure analysis of telemetry anomalies during Apollo 17 flight
[NASA-TM-X-69367] 18 p2117 N73-27118
Physical and detonation properties of dry blended hexanitrostilbene/Teflon explosive charges used on Apollo 17 seismic experiment
[NASA-CR-133838] 21 p2606 N73-30886
Apollo 17 heat flow and convection experiments
[NASA-TM-X-64772] 22 p2729 N73-31840
Apollo 17 mission at Taurus Littrow with color illustration and summaries
[NASA-EP-102] 24 p2979 N73-33804
Evaluation of launch vehicle, spacecraft, and lunar rover performance during Apollo 17 flight to determine malfunctions and recommend corrective actions
[NASA-TM-X-69534] 24 p2981 N73-33822
**APPARATUS**
U EQUIPMENT
**APPENDAGES**
NT HAND [ANATOMY]
**APPLICATIONS OF MATHEMATICS**
One-dimensional and multi-dimensional inversion techniques for processing remote atmospheric and ionospheric sounding data
[NASA-TM-X-62150] 02 p0196 N73-11585
Mathematical analysis and curve plotting for microwave physics
[AD-747035] 03 p0337 N73-12746
Modification of Ber and Friedman mathematical theory of elasticity
10 p1172 N73-19536
Minimization technique for determining structural parameters of IR and vibrational rotational spectra of H2O
[AD-754612] 11 p1253 N73-20166
Statistical tests for determining Colorado River Basin response to natural or induced changes
[PB-214114/1] 14 p1665 N73-23513
Development of equations of condition necessary for determining coefficients for Runge-Kutta methods used to solve ordinary differential equations
[NASA-CR-130902] 15 p1803 N73-24613
**APPLICATIONS TECHNOLOGY SATELLITES**
NT ATS 1
NT ATS 3
NT ATS 5
NT ATS 6
Definition of experiments for collection of RFI and multipath data for application to synchronous relay satellite
[NASA-CR-128717] 07 p0754 N73-16128
Development of on-board navigation system based on Applications Technology Satellites, Omega navigation systems, and aircraft terminal facilities
[NASA-CR-130213] 13 p1556 N73-22615
Spaceborne prototype model of millimeter wave experiment radiating transmitter for ATS-F spacecraft
[NASA-CR-132760] 16 p1965 N73-25895
ATS ranging and position fixing experiments
[NASA-CR-132755] 16 p1965 N73-25896
Tests of potential thermal degradation of ATS-F radiant cooler form contaminants generated by hydrazine thruster in simulated space
[NASA-CR-132988] 16 p1974 N73-25965
Satellite activities of NOAA
19 p2346 N73-28871
Analysis and Mechanical design of solar array stowage and deployment arrangements for use in Small Applications Technology Satellite spacecraft
[NASA-CR-132800] 22 p2720 N73-31767
Space applications research in astronomy and earth physics
[NASA-SP-331] 22 p2732 N73-31867
Features and planned experiments of Communications Technology Satellite
[CRC-SER-DOC-06-RI/PS-3/1/72]
23 p2847 N73-32754
Observations of amplitude scintillations produced in F region in equatorial areas based on Applications Technology Satellite transmissions
[NASA-TM-X-70478] 24 p2921 N73-33326
**APPROACH**
NT INSTRUMENT APPROACH
Longitudinal stability of Boeing 707 aircraft during steep approach, for noise reduction
[DGLR-PAPER-73-023] 23 p2744 N73-31963
Noise reducing approach and takeoff profiles for short takeoff aircraft
[MBB-UH-06-73-O] 23 p2744 N73-31968
Automatic flight control system for curved flight path profiles
[DGLR-PAPER-73-030] 23 p2745 N73-31970
Flight control display device for producing curved approach profiles in microwave instrument landing systems
[DGLR-PAPER-73-016] 23 p2818 N73-32526
**APPROACH CONTROL**
Pilot visual threshold and perception for aircraft movement estimation during unaided visual approach control
01 p0016 N73-10125
Analysis of limitations on helicopter approach and landing during conditions of low visibility
[AD-747732] 03 p0329 N73-12686
Analysis of aircraft pilot experiences during landing approaches in minimum visibility situations
[AD-747654] 03 p0329 N73-12687
Development and evaluation of instrument landing system with VHF and UHF capability for localizer and glide slope
[AD-747656] 03 p0329 N73-12688
Operational test and evaluation of four configurations of flight director display for instrument landings based on command heading and command flight path angle
[AD-748244] 04 p0374 N73-13041
Evaluation of approach lighting system for visual guidance of helicopters during instrument flight rules approach and landing operations
[FAA-RD-72-133] 04 p0401 N73-13261
Design and development of microwave landing system for operation of civil and military aircraft in conventional and V/STOL configurations
[AD-749505] 05 p0578 N73-14702
Integration of STOL aircraft instruments and approach control for new approach profiles
[DGLR-PAPER-72-096] 06 p0622 N73-15047
Incident involving collision of Boeing 727 aircraft with landing light system at Atlanta International Airport, Georgia on 21 Dec. 1971
[NTSB-AAR-72-22] 07 p0737 N73-16000
Flight simulator evaluations of flight control, flight path, and airspeed for approach and landing of powered lift jet short takeoff aircraft
[NASA-TM-X-62203] 07 p0739 N73-16014
Bibliography of data on aircraft landings, instrument landings, approach control, glide path systems, display devices, and terminal facilities
[AD-751800] 07 p0740 N73-16024
Analysis of simulated aircraft landing approach to aircraft carrier to determine display system requirements and to evalute dangerous conditions
[AD-751076] 07 p0819 N73-16635

Measurement of pilot performance during aircraft landing simulation to determine significance of vertical acceleration cues during approach and landing maneuver
[NASA-TM-X-62236] 08 p0867 N73-17020
Analysis of aircraft instruments and display devices for approach control and landing of V/STOL aircraft
[AGARD-AR-51] 09 p1034 N73-18439
Development of gradient clearance monitor concept to ascertain glide slope clearance signal
[FAA-RD-72-147] 10 p1185 N73-19645
Visual cue reinforcement for skill retention in pilot simulated space vehicle approach and landing performance
[NASA-CR-128912] 14 p1614 N73-23086
Development of mathematical and simulation models to calculate capacity of single runway under instrument flight rules conditions
[MTR-4102-REV-2] 14 p1645 N73-23345
Air traffic control procedures for simultaneous instrument flight rules approaches to set of three parallel runways
[FAA-NA-73-23] 14 p1687 N73-23687
Development of inertial smoothing system for control and display applications for VTOL aircraft automatic instrument approach and landing operations
[NASA-TN-D-7271] 15 p1808 N73-24653
Development of air traffic control procedure to permit short takeoff aircraft landing along curved approach trajectory and analysis of data transmission requirements
16 p1859 N73-25055
Development of equations of motion for energy dissipation phase of shuttle reentry and landing approach - Document 23
[NASA-CR-128960] 16 p1941 N73-25709
Operational procedures and modes of experimental guidance system for short takeoff aircraft to provide arrival time control and automatic tracking
[NASA-TM-X-62233] 16 p1941 N73-25710
Analysis of control and display device testing for microwave landing system - Vol. 1
[AD-758791] 16 p1942 N73-25713
Development of control and display testing requirements for evaluation of microwave landing system - Vol. 2
[AD-758792] 16 p1942 N73-25714
Analysis of data rate requirements for low visibility approach with scanning beam landing guidance system
[AD-758786] 16 p1942 N73-25719
Design of landing approach automatic flight control system using optimal feedback techniques
[AD-760125] 17 p1984 N73-26040
Application of microwave landing system to provide operational flexibility and improved capacity in terminal area
[FAA-RD-73-143] 18 p2104 N73-27019
Flight evaluation of glide slope determination during landing approach by reference to diamond shaped figure painted on runway
[NASA-TM-X-2849] 18 p2105 N73-27027
Comparison of automatic short takeoff aircraft landings based on simulation and flight test results
[NASA-TT-F-14995] 18 p2105 N73-27028
Performance tests of visual approach slope indicator [VASI] equipment and systems for improved terminal area effectiveness
[FAA-NA-73-64] 18 p2175 N73-27568
Status of civil airline implementation of all-weather landings in Europe and United Kingdom
[MTR-6211] 20 p2452 N73-29711
Flight tests of various steep gradient approaches to ground level short takeoff and landing runway to determine aircraft performance and navigation aids required
[FAA-NA-72-77] 21 p2495 N73-30025
Aircraft accident involving crash of Boeing 737 aircraft during instrument approach to Chicago-Midway Airport, Illinois on 8 December 1972
[NTSB-AAR-73-16] 22 p2614 N73-30947
Statistical analysis of aircraft carrier wave-off situation based on deck motion and aircraft approach geometry
[AD-764516] 22 p2616 N73-30967
Flight paths for short takeoff aircraft landing approach consistent with pilot preference passenger comfort, and microwave landing system limitations
[NASA-TN-D-7298] 23 p2742 N73-31949
Flight control for steep approach landing
[DGLR-PAPER-73-027] 23 p2744 N73-31962
Pilot display for monitoring of automatic steep approach
[DGLR-PAPER-73-031] 23 p2744 N73-31964
Cockpit layouts in view of new landing approach methods
[MBB-UH-07-73-O] 23 p2744 N73-31966
Aircraft landing problems under low visibility weather conditions
[DGLR-PAPER-73-015] 23 p2817 N73-32520
New type of instrument landing systems, according to ICAO requirements
[DGLR-PAPER-73-011] 23 p2817 N73-32522
Compatible ILS, using microwave frequencies, and precision ILS, using antenna arrays, as improved standard instrument landing systems
[DGLR-PAPER-73-018] 23 p2817 N73-32524
Flight simulation to determine manual control of flight path and airspeed for approach and landing of powered lift jet short takeoff aircraft
24 p2873 N73-32949
Flight simulation to determine effectiveness of head-up display for improving glide-slope tracking performance during steep visual approach of short takeoff aircraft
24 p2874 N73-32952

**APPROACH INDICATORS**
Approach light properties for visual discrimination in pilot landing environment
[NASA-TT-F-14667] 08 p0941 N73-17710
Development of gradient clearance monitor concept to ascertain glide slope clearance signal
[FAA-RD-72-147] 10 p1185 N73-19645
Analysis of electromagnetic compatibility of microwave landing guidance system and candidate interim systems
[ECAC-PR-72-069] 12 p1425 N73-21554

**APPROPRIATIONS**
Distribution of federal funds for research and development
[NSF-72-317-VOL-21] 09 p1100 N73-18980
NASA appropriations for FY 1974
[H-REPT-93-171] 13 p1595 N73-22929
Hearings concerning NASA appropriations for FY 1974
14 p1721 N73-23960
NASA authorization for fiscal year 1974
[S-REPT-93-179] 15 p1845 N73-24950
Congressional hearings on appropriations for Housing and Urban Development, National Science Foundation, and Veterans organizations for 1974
16 p1976 N73-25978
Hearings concerning fiscal year 1974 appropriations for space shuttle, earth resources program, and SST - Part 2
17 p2099 N73-26977
Hearings concerning appropriations for housing urban development, space, science and VA - Part 1
17 p2099 N73-26978
Congressional appropriations to National Aeronautics and Space Adminstration
[PUB-LAW-91-556] 18 p2213 N73-27872
Recommendations of conference committee concerning Senate admendments to H.R. 8825
[H-REPT-91-316] 19 p2354 N73-28935

**APPROXIMATION**
NT CHEBYSHEV APPROXIMATION
NT FINITE DIFFERENCE THEORY
NT FINITE ELEMENT METHOD
NT HARTREE APPROXIMATION
NT LEAST SQUARES METHOD
NT NEWTON-RAPHSON METHOD
NT RAYLEIGH-RITZ METHOD
NT RELAXATION METHOD [MATHEMATICS]
NT RITZ AVERAGING METHOD
NT SOMMERFELD APPROXIMATION
Least squares polynomial approximation for computer generation of differentiable functions
[USC-113P19-27] 02 p0146 N73-11180
Approximation techniques for descrete dynamic programming problems
[USC-113P19-26] 02 p0146 N73-11181
Eigenfunctionals of linear Boltzmann transport operator in modal approximations
[APS-PH-87] 02 p0195 N73-11580
Successive approximations for solving discrete Bolza problem by dynamic programming
[TR-72-43] 02 p0202 N73-11632
Analysis of approximation methods for solving discrete Bolza problem by dynamic programming, and stability and error properties
[USC-113P19-28] 02 p0202 N73-11633
Bicubic spline approximations over two dimensional region derived with dynamic programming
[USC-113P19-33] 02 p0202 N73-11635
Criteria for optimal approximating functions for experimental test design
[NASA-TM-X-2663] 02 p0202 N73-11636
Spectral line profiles of helium triplet diffuse series and quasi-static approximation for ions and electrons
[NASA-TN-D-6954] 02 p0214 N73-11731
Approximation of diffusion coefficients for charged particles in random magnetic field
[NASA-CR-129523] 03 p0339 N73-12767
Perturbation approximation method for determining velocity potential and aerodynamic forces of slender body of elliptical cross section in airstream
[AD-748353] 04 p0407 N73-13317
Applicability of various laws of statistics of extremal values for approximating empirical distributions of maximum wind velocities
04 p0442 N73-13608
Approximative parameters and probabilistic sequential subsets for modeling linear and renewal sources in communication theory
06 p0639 N73-15186
Approximate dispersion relationship of hydrodynamic waves in thin rotating spherical shells of incompressible fluid pervaded by uniform magnetic field
[MET-O-857] 06 p0699 N73-15702
Low level tuning of approximations, with response variant emerging from standardized high level commands
[NASA-CR-130699] 08 p0891 N73-17210
Approximative solution for photon emission amplitude in soft photon irradiation by electromagnetic wave field
[NASA-TT-F-14686] 09 p1066 N73-18697
Approximative model for diurnal effect on atmospheric density distribution and artificial earth satellite deceleration
10 p1177 N73-19578
Approximative ephemeris calculations for moving celestial objects using coordinates from different points on earth surface
10 p1178 N73-19587
Approximative solution for first boundary value problem of thermal conductivity
[AD-754255] 11 p1349 N73-20947
Approximation method for kinetic Boltzmann equation
12 p1418 N73-21490
Approximation methods for solving hyperbolic partial differential equations of meteorology and oceanography
[GARP-PUBL-10] 16 p1938 N73-25680
Maxwell equation and approximation theory for examining attenuation behavior of coaxial cables with woven outer conductors
[RAE-LIB-TRANS-1642] 17 p1997 N73-26147
Dynamic and adiabatic approximation applied to polarons in uniform magnetic field
17 p2071 N73-26753
Survey of articles dealing with stochastic approximation
[AD-761766] 19 p2314 N73-28613
Approximation of curves and surfaces in three-dimensional space by smooth circular interpolation
21 p2512 N73-30154
Approximation of functions of terminal state of dynamic system and determination of error bounds
21 p2515 N73-30175
Revised algorithm for constrained optimization using quasi Newton-Raphson method based on recurring factorization of approximation to Hessian matrices
[NPL-NAC-32] 22 p2692 N73-31560
Closed form approximation in dissipation integral for incompressible turbulent boundary layers
24 p2908 N73-33204
Integral relations of velocity and thermal boundary layer for approximation purposes
24 p2909 N73-33213

**APPROXIMATION METHODS**
U APPROXIMATION

**APSIDAL ANGLES**
U ANGLES [GEOMETRY]

**APSIDES**
NT APOGEES
NT PERIGEES
NT PERIHELIONS

**APT [PICTURE TRANSMISSION]**
U AUTOMATIC PICTURE TRANSMISSION

**APTITUDE**
Comparison of age, education, pre-FAA experience, aptitudes, training course performance, and post-Academy attrition rates of male and female trainees
[FAA-AM-72-22] 02 p0135 N73-11094
Color aptitude of dyschromatopsia French navigators and pilots
10 p1113 N73-19068

**AQUEOUS SOLUTIONS**
Spectrophotometric determination of aqueous iodine complexed with potassium iodide showing free iodine optimally determined at isosbestic point for solutions
[NASA-CR-128585] 01 p0022 N73-10172
Sound speed and other thermodynamic quantities of dilute aqueous electrolyte solutions by ultrasonic velocimeter comparison technique
[AD-745843] 01 p0081 N73-10669
Frequency and line width of Brillouin scattering in aqueous electrolyte solutions
[AD-749354] 04 p0387 N73-13148
Optical properties and constants of water and aqueous solutions
[NASA-CR-130136] 06 p0699 N73-15700
Effectiveness of sodium hydrocarbonate as means for treating and preventing motion sickness
07 p0745 N73-16057
Technique for predicting corrosion behavior of engineering alloys in aqueous electrolytes with and without chlorides present
[AD-752487] 08 p0933 N73-17638
Gas chromatographic analysis of beryllium in aqueous solutions and biological tissues
[AD-753112] 09 p0996 N73-18131
Rayleigh-Brillouin intensity ratios measured for aqueous electrolytic solutions as function of concentration
[AD-753017] 09 p1001 N73-18166
Corrosion behavior of titanium alloys in chloride solutions
[AD-753573] 09 p1050 N73-18561

Composition effects on stress corrosion cracking of titanium alloys in aqueous environments
[NASA-CR-131872] 13 p1540 N73-22475
Fuel system for thermal nuclear reactor which uses inorganic ion exchanger
[NASA-CASE-LEW-11645-2] 19 p2319 N73-28660
PH influence on hexachloroiridite and hexachloroiridate ions in aqueous solutions
[IRI-133-73-02-PT-2] 21 p2506 N73-30111
Application of phosphorimetry procedures to quantitative chemical analysis of several aqueous solutions
[PAPER-76A6-743] 21 p2546 N73-30409
Growth of electronic ceramic single crystals from solution as feasibility study for future crystal growth in space environment
[NASA-CR-124443] 23 p2826 N73-32587
Stress corrosion cracking in gaseous and aqueous environments
24 p2933 N73-33426
Oxidative stress cracking in nylon fibers immersed in alkaline aqueous medium saturated with molecular oxygen at elevated temperature
24 p2937 N73-33455

**ARC DISCHARGES**
Bibliography of arc discharges in vacuum and gaseous atmospheres
[SC-B-72-3233] 03 p0278 N73-12251
Time development of anode surface temperatures for vacuum arc discharges of microsecond duration
[SC-DC-72-2267] 05 p0580 N73-14723
Design and performance of flash lamps with nanosecond light pulses
[AD-750788] 06 p0701 N73-15720
Properties of plasma stream flowing from pulsed magnetoplasmadynamic arc jet
[ISAS-490] 14 p1695 N73-23756
Technique for measuring hypersonic flow velocity profiles
[NASA-TN-D-7270] 17 p2032 N73-26443
Double discharge high power TEA CO2 laser, noting application of xylene to avoid electric arcs
[LRP-60/73] 18 p2158 N73-27434
Thomson scattering diagnosis on pulsed xenon arc plasma flow
[NASA-TM-X-71443] 24 p2962 N73-33669

**ARC GENERATORS**
Analysis of electronic circuit and performance of spark gap assembly
[CERN-72-6] 04 p0399 N73-13244

**ARC HEATING**
Numerical technique for obtaining solutions to governing equations for gas flowing in axially symmetric constricted-arc heaters
[NASA-TM-X-2700] 07 p0769 N73-16246
High enthalpy arc-heated helium shock tunnel for gas dynamic research
[NASA-TM-X-2814] 16 p1885 N73-25258
Laser Raman spectroscopy for calibrating arc heated wind tunnel flow
[AD-761500] 19 p2231 N73-27989
Measurements of pressure, voltage, and wall heat flux in wall-stabilized arc heater
[NASA-TM-X-69571] 20 p2420 N73-29443

**ARC JET ENGINES**
Numerical technique for obtaining solutions to governing equations for gas flowing in axially symmetric constricted-arc heaters
[NASA-TM-X-2700] 07 p0769 N73-16246
Improving preformance of magnetoplasmadynamic arc rocket engine
[NASA-CASE-LEW-11180-1] 16 p1948 N73-25760

**ARC LAMPS**
Uses of high power arc light sources
[AD-745565] 01 p0033 N73-10259
Design of prototype infrared countermeasure arc lamp
[AD-759752] 17 p2063 N73-26692
Production of high power arc lamp cathodes by casting copper body on thoriated tungsten insert
[NASA-TM-X-2865] 18 p2160 N73-27451
Life tests of niobium coatings used on alkali metal arc lamps
[AD-761204] 18 p2168 N73-27508

**ARC MELTING**
Magnetic field effects in cathode mechanism of electric arc initiation and travel between copper electrodes
[NLL-CE-TRANS-6108-[9022.09]]
15 p1755 N73-24226
Metal refining during vacuum arc melting for lowering nonmetallic inclusions and gases in ingot
21 p2557 N73-30502

**ARC SPRAYING**
Microstructure and mechanical properties of thermal barrier materials produced by arc plasma spraying
[AD-762045] 19 p2312 N73-28598

**ARC WELDING**
NT GAS TUNGSTEN ARC WELDING
NT PLASMA ARC WELDING
Electric arc welding of tin and aluminum bronzes and silicon brass
[DRIC-TRANS-2843] 02 p0179 N73-11448
Effect of heat input and post-weld heat treatment on mild and low alloy steel submerged arc weld deposits
[CRANFIELD-MAT-8] 05 p0551 N73-14475
Low cost arc welding technique for thick sections of HY-150 steels
[NASA-CR-120994] 09 p1039 N73-18472
Effect of angle of inclination on formation of gas cavities in weld root during argon-arc welding
10 p1172 N73-19532
Formation of flaws in seam metal during argon-arc pulse welding
10 p1172 N73-19533
Carbon dioxide shielded-arc welding with electrodes containing aluminum
[NLL-CE-TRANS-6011-[9022.09]]
11 p1296 N73-20515
Electrode metal volatilization and oxidation in gas-shielded arc welding
[DRIC-TRANS-3005] 12 p1408 N73-21415
Low alloy copper welding rods used as welding materials for argon arc welding of copper
[DRIC-TRANS-3008] 12 p1409 N73-21416
Arc welding of joints and hard surfaces using longitudinally notched ceramic rods
[AD-756944] 13 p1535 N73-22435
Electrode metal loss by volatilization in gas-shielded arc welding
[NLL-DRIC-TRANS-3005-[3623.66]]
15 p1790 N73-24511
Irradiation strengthening and fracture embrittlement of A533-B steel and arc weldment metal
[HEDL-SA-323] 16 p1969 N73-25931
Development of procedure for argon arc welding of copper using complex alloy wire and comparison with other welding techniques
[NLL-DRIC-TRANS-3008-[3623.66]]
18 p2154 N73-27404
Arc welding and industrial processing - bibliographies
[AD-760970] 18 p2156 N73-27421
Modified filler metal composite for reducing or eliminating underbread cracking in multipass gas tungsten arc plate welds of T-111
[NASA-CR-121198] 19 p2304 N73-28530
Argon-arc welding of aluminum and aluminum alloys to steels
[AD-763948] 22 p2679 N73-31458
Electrode burn off characteristics of manual metal arc electrodes using continuous and modulated welding current
[CRANFIELD-MAT-9] 24 p2928 N73-33386

**ARCAS ROCKET VEHICLES**
Development and use of three payloads for studying mesospheric parameters, using Arcas rockets
[AD-752241] 08 p0921 N73-17545

**ARCHAEOLOGY**
Location of archaeological village sites in Alaska by ERTS-1 imagery
[E72-10338] 05 p0532 N73-14326
Locating archaeological village sites in Alaska from remotely sensed imagery
[E73-10406] 11 p1277 N73-20368
Location of archeological village sites in Alaska from ERTS-1 imagery
[E73-10638] 15 p1776 N73-24397
Hydrology of prehistoric farming systems in central Arizona ecotone from Skylab EREP data
[E73-11044] 23 p2779 N73-32220

**ARCHES**
Analysis of Michell framework for uniform load between fixed supports
[REPT-1054/73] 13 p1586 N73-22861

**ARCHITECTURE**
Development of construction block in form of container folded from flat sheet and filled with solid material for architectural purposes
[NASA-CASE-MSC-12233-2] 04 p0480 N73-13921
Wind effects on tall building design
[NPL-TECH-MEMO-MAR-SCI-TM-100]
11 p1344 N73-20909
Lumiduc architecture for urban housing
[NASA-TT-F-14963] 17 p2098 N73-26976
Utilization of solar rays as internal light sources in architectural designs
24 p2975 N73-33771

**ARCS**
Reflecting solutions of high order elliptic differential equations in two independent variables across analytic arcs
[NASA-CR-135667] 23 p2812 N73-32483

**ARCTIC OCEAN**
Numerical analysis of stability and convergence conditions based on mathematical model of Arctic Ocean
[AD-745182] 01 p0053 N73-10429
Prediction of long-term temperature fluctuations, July temperature, and annual average temperature of Barents Sea in surface to 200 m layer
[NLL-M-20600-[5828.4F]] 05 p0529 N73-14304
Ray tracing of underwater sound in Arctic Ocean
[AD-752056] 08 p0944 N73-17734
Acoustic transmission loss measurements in Arctic Ocean ice zone by aircraft
[AD-754394] 11 p1325 N73-20755
Prevaling monthly and seasonal surface wind directions for coastal areas around Arctic Ocean
[AD-761074] 18 p2174 N73-27560

**ARCTIC REGIONS**
Remote automatic multipurpose station for collecting oceanographic and meteorological data in Arctic regions
[AD-746496] 01 p0038 N73-10300
Surveillance and mapping of sea ice in Arctic regions based on ERTS-1 imagery
[E72-10199] 02 p0160 N73-11297
Detection and mapping snow cover from ERTS-1 remotely sensed imagery of western US and Arctic
[E72-10202] 02 p0160 N73-11299
Environmental studies of sedimentation and nearshore marine processes in Cook Inlet, Alaska, and regional study of permafrost regimes in Alaska using ERTS-1 imagery
[E72-10209] 02 p0161 N73-11304
Balloon measurements of aerosol and ozone in Arctic stratosphere
[AD-747256] 02 p0169 N73-11374
Arctic technology development program including design and operation of under-ice research submersible
[AD-748228] 04 p0416 N73-13395
Papers on Arctic ionospheric modeling
[AD-748796] 04 p0416 N73-13398
Lake, river, and land-fast sea ice thickness in North American Arctic and subarctic regions during 1968-1969 and 1969-1970
[AD-746256] 04 p0416 N73-13400
Solar and terrestrial radiation regimes over arctic ice packs
[AD-748214] 04 p0467 N73-13808
Environmental analyses of Alaskan arctic and subarctic geology and geomorphology using ERTS-1 imagery
[E72-10370] 05 p0536 N73-14358
Arctic glacier mapping, research, and effects on surroundings
[AD-747001] 06 p0667 N73-15425
Statistical determination of atmospheric temperatures at mandatory pressure levels in North American Arctic for regional extreme model atmosphere
[AD-750170] 06 p0669 N73-15445
Remote automatic multipurpose station for collecting oceanographic and meteorological data in Arctic regions
[AD-751039] 07 p0758 N73-16159
Latitude-time variations of ionospheric electron densities at high latitudes during periods of solar activity
07 p0791 N73-16431
Airborne measurement of ionization cross sections suitable for assessing HF propagation conditions in Arctic ionosphere
[AD-751235] 07 p0797 N73-16480
Nature of weak high latitude X ray sources
[NASA-TM-X-66168] 07 p0839 N73-16796
Aerobee mass spectrometer data on neutral gas composition of Arctic thermosphere
08 p0899 N73-17282
Mapping Arctic sea ice from ERTS-1 MSS imagery
[E73-10278] 08 p0914 N73-17486
Alaskan arctic and subarctic sediment deposition, permafrost, snow cover, and ice mapping from ERTS-1 imagery
[E73-10279] 08 p0914 N73-17487
Arctic ice measurements from airborne microwave radiometers and ground based equipment in Mar. 1971
08 p0971 N73-17937
Civil engineering in Arctic regions using dual channel infrared scanner and infrared photography
[AD-753048] 09 p1037 N73-18461
Effects of ground effect vehicle tests on ecology of arctic tundra in northern Alaska
[AD-751741] 10 p1107 N73-19026
Cold weather tests to determine application of ground effect machines for military logistic purposes in Arctic regions
[AD-753527] 10 p1107 N73-19027
Data from simultaneous satellite measurement of electron and proton precipitation at high latitudes
[NP-19465] 10 p1210 N73-19845
Technology assessment for long range year-round transportation in Arctic
[AD-754381] 11 p1269 N73-20296
Mapping Arctic sea ice from ERTS-1 imagery of Hudson Bay, M'Clure Strait, Beaufort Sea, and Greenland Sea
[E73-10447] 11 p1282 N73-20407
Sea ice dynamics, heat and mass budget of Arctic sea ice, desalinization, thermal and mechanical stresses, bearing capacity of floating ice, and interaction of oil and ice
[AD-754118] 11 p1290 N73-20463
Thematic and photomapping of Arizona CARETS, and polar regions from ERTS-1 imagery
[E73-10463] 12 p1394 N73-21302
Mapping of polar regions using ERTS-1 multispectral photography
[E73-10501] 12 p1398 N73-21337
Development of collision protection equipment for ground effect machines operating in arctic regions
[AD-758359] 14 p1604 N73-23004

Detection and mapping of sea ice in Arctic regions using ERTS-1 RBV and MSS data
[E73-10595] 14 p1658 N73-23452
Integrated analysis of past and present climates of Northern Cumberland and Peninsula
[AD-757270] 15 p1783 N73-24457
Problems associated with instrumentation for Arctic tests
[AD-758170] 15 p1789 N73-24502
Solar and terrestrial radiation fluxes over Arctic pack ice
[AD-758060] 15 p1828 N73-24820
Cartographic applications of ERTS-1 RBV imagery of Arctic and Antarctic regions
[E73-10651] 16 p1898 N73-25347
Effects of polar cap absorption events on performance of Omega navigation system operating in high latitudes
[AD-759009] 16 p1942 N73-25718
Assessment of geological applications of ERTS-1 imagery from selected areas of Canadian Arctic
[PAPER-G11] 19 p2264 N73-28242
Detection and mapping Arctic sea ice from ERTS-1 imagery
[PAPER-M14] 19 p2281 N73-28353
Analog model for arctic ionosphere
[AD-762280] 19 p2299 N73-28484
Statistical determination of temperature at mandatory pressure levels in Arctic region
[AD-761474] 19 p2316 N73-28627
Spectral analysis of wind-wave spectrum at ice edge in Arctic Basin
21 p2573 N73-30621
Application of ERTS-1 data to detection and mapping of sea ice in Beaufort Sea and Bering Sea areas
[E73-11037] 22 p2663 N73-31341
Thermal infrared imagery of North American Arctic for different seasons
[AD-764239] 22 p2668 N73-31376
Analysis and mapping sediment deposition, permafrost areas, snow cover, and icing in Arctic regions of Alaska from ERTS-1 data
[E73-11067] 23 p2781 N73-32243
Automation of processes of gathering and primary processing of scientific information on expeditions of Arctic and Antarctic Scientific Research Institute
24 p2947 N73-33537

**AREA**
Planimetric, topographic, and thematic mapping using remotely sensed imagery
07 p0786 N73-16391

**AREA NAVIGATION**
Comparison of cost, complexity, and cockpit workload for seven area navigation system configurations
14 p1688 N73-23697
Characteristics of airborne area navigation equipment and application to air traffic control functions
14 p1688 N73-23698
Development of high bandwidth time division communications system to provide ground based, wide area, position location system
14 p1689 N73-23711
Feasibility of modifying Tacan/DME system to broadcast digital data for area navigation
[FAA-RD-73-2] 15 p1808 N73-24656
Analysis and digital computer simulation of operational and performance aspects of vertical area navigation system
[FAA-RD-72-125] 16 p1941 N73-25705
Proceedings of conference to develop area navigation system design concept for application to national airspace system for improved air traffic control
17 p2060 N73-26664
Analysis of very low frequency radio signals for aircraft area navigation to show capability for continental flight redundancy and reliability
[AD-761498] 19 p2318 N73-28651
Effects of transition from conventional to quiet takeoff and landing air traffic, noting introduction of microwave ILS and area navigation
[MBB-UH-05-73-O] 23 p2817 N73-32525

**AREND-ROLAND COMET**
Bessel theory for analyzing head and tail regions of dust comets
02 p0228 N73-11846

**ARGENTINA**
Solar eclipse of 4 January 1973, visible in Argentina
06 p0717 N73-15853
Analysis of ERTS-1 data for studies of hydrogeology, geomorphology, and paleoclimatology in Bolivia, Argentina, Chile, and Peru
[PAPER-W1] 19 p2270 N73-28281
Partial annular eclipse of 4 January 1973 in Argentina
[NP-19597] 21 p2597 N73-30811

**ARGON**
NT ARGON ISOTOPES
Rate coefficient data for recombination reaction hydrogen plus oxygen plus argon yields water and argon in mixtures behind incident shock waves
[NASA-TN-D-6990] 01 p0117 N73-10965
Development of steel smelting process using inert argon atmosphere for gas saturation and removal of impurities
[JPRS-57542] 03 p0313 N73-12553
Spectral absorption coefficients of argon and silicon and spectral reflectivity of aluminum as function of pressure, temperature, and wave number
[NASA-CR-129300] 03 p0335 N73-12727
Plastic detectors used to confirm acceleration of argon nuclei to relativistic velocities at Princeton Particle Accelerator
[AD-749863] 05 p0549 N73-14458
Dissociation rate of bromine diatomics in argon heat bath
[NASA-TN-D-7077] 07 p0824 N73-16676
Shock structure characterization of normal ionizing shock waves in argon
[AD-751594] 07 p0829 N73-16719
Physiological effects of argon/oxygen breathing on rats noting carbon dioxide level
10 p1116 N73-19094
Transition moments and associated probabilities, line strengths, and absorption oscillator strengths
[AD-754025] 11 p1252 N73-20163
Free bound, relative continuum-absorption cross sections for first 90 excited S, P, and D states of neutral argon
[AD-754007] 11 p1253 N73-20164
Reaction of nickel oxide with steel in argon and vacuum atmospheres
[AD-754776] 11 p1306 N73-20600
Bronze coating of alloys in argon atmosphere
[AD-753985] 11 p1309 N73-20623
Low alloy copper welding rods used as welding materials for argon arc welding of copper
[DRIC-TRANS-3008] 12 p1409 N73-21416
Bearings for control system of high temperature lithium or argon cooled fast nuclear reactors
[NASA-TM-X-68218] 13 p1534 N73-22429
Raman spectra of Van der Waals complexes in argon, helium, and xenon
[AD-758241] 15 p1748 N73-24171
Measurement of heat transfer coefficients of air-glass, argon-glass, and argon-aluminum suspensions
[NASA-CR-2266] 15 p1843 N73-24932
Analysis of electron number density and collision frequency levels behind reflected shock waves and shock wave interactions in argon
16 p1887 N73-25275
Development of procedure for argon arc welding of copper using complex alloy wire and comparison with other welding techniques
[NLL-DRIC-TRANS-3008-[3623.66]]
18 p2154 N73-27404
One dimensional flow of partially ionized argon in hypersonic nozzle
[AD-760967] 18 p2184 N73-27632
Radical species concentration profiles for methane-oxygen-argon flame
[BM-RI-7766] 18 p2206 N73-27803
Transition model for computing population density profiles of partially ionized argon in source flow expansion
[C-37] 22 p2652 N73-31242
Argon-arc welding of aluminum and aluminum alloys to steels
[AD-763948] 22 p2679 N73-31458
Time resolved measurements of droplet growth in Wilson expansion cloud chamber
24 p2901 N73-33158

**ARGON ISOTOPES**
Increase in laser damage threshold of sapphire surfaces by polishing with energetic argon ion beams
05 p0555 N73-14505
Experiment observing solar neutrinos by neutrino capture reaction, using Ar-37
[BNL-16937] 12 p1445 N73-21707

**ARGON LASERS**
Development of fluid mechanical helium argon ion laser and analysis of improvements in efficiency and power output
[NASA-CR-128397] 01 p0064 N73-10526
Argon laser radiation damage to retina of diabetic and nondiabetic patients
[AD-747058] 04 p0381 N73-13099
Holographic memory system using argon ion lasers and acoustooptic beam deflectors
[NASA-CR-124084] 09 p1064 N73-18680
Design and performance of two color laser Doppler velocimeter for wind tunnels
[NASA-TM-X-62254] 12 p1405 N73-21393
High efficiency ion lasers and high power carbon dioxide lasers through study of improved electrode structures
[AD-757099] 14 p1673 N73-23575
Use of argon-ion laser transverse mode locking to produce high resolution scanning beam
15 p1794 N73-24546
Digital data transmission with argon laser beam through atmosphere to determine error frequency
[FTZ-44-TBR-34] 22 p2681 N73-31478
Electron collision excitation of population inversion in ionic argon lasers
23 p2800 N73-32393

**ARGON PLASMA**
Vibration-translation and vibration-vibration relaxation rates in rapid expansions of N2 and CO2 in argon
[AD-746068] 02 p0216 N73-11751
Techaique for determining influence of axial magnetic field on holdup of argon in coaxially fed argon-helium plasma generated by radio frequency induction
[ORNL-TM-3700] 03 p0341 N73-12779
Low frequency instabilities in hollow cathode magnetoplasma discharge
[AD-750477] 06 p0707 N73-15765
Impulse response of low pressure argon magnetoplasma to excitation by electric field
[NASA-TR-R-400] 07 p0826 N73-16693
Wave transformation region in superhigh frequency argon discharge plasma
[AEC-TR-7339] 07 p0827 N73-16706
Theta pinch generation of ionizing shock waves in argon plasma
[AD-751659] 07 p0829 N73-16721
Laboratory double inverse plasma pinch experiments with argon, hydrogen, and deuterium and relevance to solar flare
07 p0838 N73-16791
Nitrogen exchange between furnace atmosphere and argon plasma arc when melting pure iron
12 p1413 N73-21447
Properties of dense helical microwave plasma source in intense magnetic field
[CEA-EUR-FC-652] 12 p1435 N73-21626
Feasibility of using RF generated argon plasma for sputter etching Al and SiO2 windows and photoresist
[AD-757878] 15 p1800 N73-24588
Equilibrium compositions and thermodynamic properties of mixed plasmas, including argon-hydrogen plasmas at .01 to 100 atmospheres between 2,000 K and 35,000 K
16 p1948 N73-25764
Numerical prediction of turbulent flow in argon cascade arc
[AD-759183] 16 p1950 N73-25783
Argon plasma temperature profile measurement by differential interferometry, based on temperature dependent refractivity
[IPF-71-4] 17 p2069 N73-26737
Spectral absorption and emission coefficient calculations for argon plasmas
[AD-759571] 17 p2070 N73-26748
Microwave probe for observing parametrically excited ion acoustic wave oscillations in argon plasma
[AD-762380] 19 p2325 N73-28705
Collisionless shock waves in argon plasma pinch discharge
[AD-762426] 19 p2325 N73-28707

**ARGON 36**
U ARGON ISOTOPES

**ARGON 40**
U ARGON ISOTOPES

**ARGUMENTS [MATHEMATICS]**
U INDEPENDENT VARIABLES

**ARID LANDS**
Inventory and monitoring of natural vegetation-landform relationships in arid regions of southern Arizona using ERTS-1 imagery
[E72-10184] 01 p0045 N73-10363
Preparation of hydrologic atlases of arid land watersheds using ERTS-1 imagery of Wyoming, Utah, Montana, and New Mexico
[E72-10240] 03 p0288 N73-12340
Distribution and density of phreatophytes and other arid and desert plants
[E72-10243] 03 p0289 N73-12343
Remote sensing of native arid plant distribution using ERTS-1
[E72-10314] 04 p0412 N73-13363
Inventory and monitoring of natural vegetation and related resources in arid environment of Arizona using ERTS-1 imagery
[E72-10360] 05 p0534 N73-14348
Distribution and density of phreatophytes and other arid land plants measured from ERTS-1 imagery
[E73-10094] 08 p0902 N73-17306
Preparation of hydrologic atlases of arid land watersheds using ERTS-1 imagery
[E73-10318] 09 p1023 N73-18350
Identification of native arid plant distribution in Avra Valley, Arizona using ERTS-1 imagery
[E73-10369] 10 p1151 N73-19365
Comparative evaluation of ERTS-1 imagery for inventorying and monitoring vegetation-terrain relationships in arid environments of Arizona
[E73-10413] 11 p1279 N73-20375
Mapping distribution and density of phreatophytes and other arid land plant communities in Arizona using ERTS-1 imagery
[E73-10543] 13 p1518 N73-22306
Determination of arid plant distribution in Arizona from ERTS-1 imagery
[E73-10520] 14 p1654 N73-23413
Inventory and monitoring natural vegetation and related resources in arid environments using ERTS-1 imagery
[E73-10519] 15 p1771 N73-24344

Determination of native desert plant distributions in Avra Valley, Arizona from ERTS-1 MSS imagery
[E73-10659] 16 p1899 N73-25355
Bibliography on geothermal prospecting in arid and semiarid lands
[PB-218830/8] 18 p2148 N73-27359
Inventory and monitoring natural vegetation and plants in arid land of Arizona from satellite-borne photography
[E73-11021] 22 p2661 N73-31325

ARIEL SATELLITES
NT ARIEL 3 SATELLITE

ARIEL 3 SATELLITE
Temporal variations in dawn and dusk 600 km midlatitude trough position measured by RF capacitive probes on Ariel 3
[NASA-TM-X-66253] 15 p1806 N73-24634

ARIP [IMPACT PREDICTION]
U COMPUTERIZED SIMULATION
U IMPACT PREDICTION

ARITHMETIC
NT FLOATING POINT ARITHMETIC

ARITHMETIC AND LOGIC UNITS
Arithmetic and logic units in digital computer for processing of radar, sonar, and communication systems signals
[AD-750665] 06 p0646 N73-15248
Hybrid computer multiplication-division modular unit for ASMODEE minicomputer noting three state gate circuits, integrated circuits, and algorithms
[LAAS-TNPE-73-1-07] 23 p2761 N73-32094

ARIZONA
NT COLORADO PLATEAU [US]
NT PHOENIX QUADRANGLE [AZ]
Geologic mapping of Basin and Range - Colorado Plateau boundary in Arizona using ERTS-1 imagery
[E72-10157] 01 p0044 N73-10347
Landform-vegetation relationships in southern Arizona based on interpretation of ERTS-1 imagery
[E72-10176] 01 p0044 N73-10355
Inventory and monitoring of natural vegetation-landform relationships in arid regions of southern Arizona using ERTS-1 imagery
[E72-10184] 01 p0045 N73-10363
Mineral exploration in Arizona using ERTS-1 imagery
[E72-10197] 01 p0047 N73-10376
In situ spectroradiometric quantification of ERTS-1 imagery of Arizona and Texas
[E72-10173] 01 p0055 N73-10444
Evaluation of simultaneous ERTS-1 and aerial photography of Arizona
[E72-10213] 02 p0162 N73-11308
Detection of regional tectonic structures and mineral exploration in Arizona using ERTS-1 imagery
[E72-10218] 02 p0162 N73-11312
Relationships of vegetation distribution to geomorphic characteristics of landscape and of plant phenological patterns to vegetation identification of satellite imagery of Arizona
[E72-10228] 02 p0163 N73-11321
Land use mapping of Phoenix quadrangle using ERTS-1 imagery
[E72-10236] 03 p0288 N73-12336
Application of ERTS-1 imagery to agriculture resource and land use evaluation in Mariposa County, Arizona and San Joaquin County, California
[E72-10264] 03 p0291 N73-12363
Natural resource inventory in Arizona using ERTS-1 imagery
[E72-10287] 04 p0410 N73-13337
Spectral signatures for dominant desert scrub plant species of Arizona and soil surface backgrounds
[E72-10318] 04 p0413 N73-13367
Inventory and monitoring of natural vegetation and related resources in arid environment of Arizona using ERTS-1 imagery
[E72-10360] 05 p0534 N73-14348
Photointerpretation of ERTS-1 imagery of Arizona with emphasis on porphyry copper deposits occurring at intersection of major faults and igneous intrusions
[E73-10018] 06 p0659 N73-15354
Prediction of range quantity and quality in desert areas of California and Arizona during growing and grazing seasons
[E73-10068] 07 p0779 N73-16330
Utilization of ERTS-1 MSS imagery for study of faulting in alluvium of California, Nevada, and Arizona
[E73-10070] 07 p0779 N73-16332
Geologic investigation of Basin and Range-Colorado Plateau boundary in northwestern and north central Arizona using ERTS-1 and EREP imagery
[E73-10074] 07 p0780 N73-16336
Mapping of soil-vegetation groupings in Arizona using ERTS-1 imagery
[E73-10290] 09 p1020 N73-18327
Application of ERTS-1 data collection platform system in Arizona ecological test site
[E73-10332] 09 p1024 N73-18362
Application of ERTS-1 data collection system platforms in Arizona ecological test site
[E73-10333] 09 p1025 N73-18363
Spectroradiometric quantification of soil moisture in Willcox Playa, Arizona based on ERTS-1 imagery
[E73-10354] 10 p1149 N73-19350
Detection and mapping snow cover in Salt-Verde Watershed of Arizona using ERTS-1 imagery
[E73-10361] 10 p1149 N73-19357
Identification of native arid plant distribution in Avra Valley, Arizona using ERTS-1 imagery
[E73-10369] 10 p1151 N73-19365
Prediction of ephemeral and perennial range quantity and quality during normal grazing season in Arizona based on ERTS-1 imagery
[E73-10377] 10 p1152 N73-19372
Utilization of ERTS-1 imagery to detect and map erosion features and changes in southern Arizona
[E73-10382] 10 p1152 N73-19377
Automated thematic mapping and analysis of terrain in Arizona, Texas, Washington, Utah, Louisiana, and California using ERTS-1 imagery
[E73-10386] 10 p1153 N73-19379
Comparative evaluation of ERTS-1 imagery for inventorying and monitoring vegetation-terrain relationships in arid environments of Arizona
[E73-10413] 11 p1279 N73-20375
ERTS-1 imagery applied to geological and water resources investigations of Basin and Range - Colorado Plateau boundary in northwestern and north central Arizona
[E73-10441] 11 p1282 N73-20401
Natural resources management and inventory of Arizona using ERTS-1 imagery
[E73-10442] 11 p1282 N73-20402
Determination of specific spectral signatures for dominant Arizona desert scrub plant species and soil surface backgrounds
[E73-10466] 11 p1284 N73-20421
Airborne electrical scanning microwave radiometric measurements of soil moisture in Texas, California, and Arizona
[NASA-CR-130204] 11 p1284 N73-20423
Thematic and photomapping of Arizona CARETS, and polar regions from ERTS-1 imagery
[E73-10463] 12 p1394 N73-21302
Photomapping of Phoenix area from ERTS-1 RBV imagery
[E73-10502] 12 p1398 N73-21338
Arizona aeromagnetic map from data of digitally recording proton precession magnetometer
13 p1514 N73-22265
Mapping distribution and density of phreatophytes and other arid land plant communities in Arizona using ERTS-1 imagery
[E73-10543] 13 p1518 N73-22306
ERTS-1 imagery of structural features in Colorado Plateau margin near Flagstaff, Arizona
[E73-10517] 14 p1654 N73-23411
Determination of arid plant distribution in Arizona from ERTS-1 imagery
[E73-10520] 14 p1654 N73-23413
Utilization of ERTS-1 imagery to predict ephemeral and perennial range quality and quantity during normal grazing season in Arizona and California
[E73-10541] 14 p1654 N73-23418
Detection of regional tectonic structures related to mineralization in Arizona
[E73-10591] 14 p1657 N73-23450
Determination of native desert plant distributions in Avra Valley, Arizona from ERTS-1 MSS imagery
[E73-10659] 16 p1899 N73-25355
Application of ERTS-1 imagery to geologic investigations of Basin and Range Colorado Plateau boundary in northwestern and north-central Arizona
[E73-10645] 17 p2017 N73-26312
Analysis of ERTS-1 data for predicting ephemeral and perennial range quantity and quality during normal grazing season in Arizona and California
[E73-10712] 17 p2018 N73-26319
Application of ERTS-1 imagery for inventory and monitoring of natural vegetation and related resources in arid environment
[E73-10728] 17 p2020 N73-26334
In situ spectroradiometric quantification of ERTS-1 data based on Arizona test site and Willcox Playa
[E73-10738] 17 p2021 N73-26344
Identification of copper/molybdenum porphyry mineral deposits in characteristic geologic setting in Nevada, Arizona, Colorado, Australia, Alaska, and New Guinea
[E73-10762] 17 p2023 N73-26362
Application of ERTS-1 and EREP imagery to geologically investigations of Basin and Range-Colorado Plateau boundary in Arizona
[E73-10799] 18 p2138 N73-27275
Mapping snow cover in central Arizona mountains and southern Sierra Nevada of California from ERTS-1 imagery
[E73-10833] 18 p2141 N73-27303
Application of ERTS-1 imagery for vegetation identification in southern Arizona
[PAPER-A7] 19 p2260 N73-28215
Application of ERTS-1 imagery for monitoring accelerated soil erosion in southern Arizona
[PAPER-G7] 19 p2264 N73-28238
Analysis of regional structures in Verde Valley region of central Arizona based on ERTS-1 data
[PAPER-G19] 19 p2265 N73-28250
Application of ERTS-1 imagery and ground mapping in southern basin-range province of California, Nevada, and Arizona to show tectonic control of tertiary minerlization
[PAPER-G21] 19 p2266 N73-28252
Assessment of flood damage in Arizona using ERTS-1 MSS imagery to show extent of inundation and sediment deposition
[PAPER-W6] 19 p2271 N73-28284
Analysis of ERTS-1 imagery of southern Arizona plant communities using electronic satellite image analysis console
[PAPER-W7] 19 p2271 N73-28285
Evaluation of stream flow data for Verde River watershed in central Arizona provided by ERTS-1 imagery
[PAPER-W8] 19 p2271 N73-28286
VICAR image processing system used for enhancement of ERTS-1 images for Arizona geological experiment
[PAPER-I9] 19 p2278 N73-28330
Relationship between in situ spectral reflectance measurements and photometric characteristics of ERTS-1 MSS imagery of Willcox Playa, Arizona
[PAPER-I19] 19 p2279 N73-28340
Application of ERTS data for mapping snow cover in Arizona and California and correlation with aerial photography
[E73-10866] 20 p2392 N73-29217
Field sampling taxonomic units within geomorphic-soil-vegetation mapping units in Arizona
[E73-10889] 20 p2394 N73-29238
Spectral signatures for dominant desert scrub plant species and soil surface backgrounds in Arizona
[E73-10890] 20 p2394 N73-29239
Detection and mapping of soil erosion and flooding in southern Arizona
[E73-10950] 21 p2531 N73-30292
Recognition of geologic framework for ERTS-1 identification of mineral deposits of copper/molybdenum prophyry type in Colorado, Nevada, Arizona, and Australia
[E73-10960] 21 p2532 N73-30302
In situ spectroradiometric quantification of ERTS-1 imagery of Arizona agriculture
[E73-10967] 21 p2533 N73-30309
Application of Skylab multispectral photography and scanner images to geological survey of Basin-and Range-Colorado Plateau boundary in north central and central Arizona
[E73-11000] 22 p2659 N73-31305
Inventory and monitoring natural vegetation and plants in arid land of Arizona from satellite-borne photography
[E73-11021] 22 p2661 N73-31325
Application of Skylab MSS imagery to geological survey of Basin-and-Range-Colorado Plateau boundary in Arizona
[E73-11042] 22 p2664 N73-31343
Detection and mapping snow cover in Arizona and California from ERTS-1 imagery
[E73-11038] 23 p2778 N73-32217
Hydrology of prehistoric farming systems in central Arizona ecotone from Skylab EREP data
[E73-11044] 23 p2779 N73-32220
Application of ERTS-1 and EREP imagery to geological surveys and mapping of Basin and Range - Colorado Plateau boundary in Arizona
[E73-11131] 24 p2917 N73-33286
Utilization of ERTS-1 imagery of topography and drainage patterns for resources inventory and management in Arizona
[E73-11159] 24 p2919 N73-33312
Daytime noise environment in Tucson, Arizona
[EE-SER-40] 24 p2921 N73-33332

ARMATURES
Methods of reducing damping in pneumatic piston drivers used in cryogenic armatures
22 p2678 N73-31449

ARMED FORCES
NT ARMED FORCES [FOREIGN]
NT ARMED FORCES [UNITED STATES]
NT NAVY
Anthropometry of Air Force women
[AD-743113] 13 p1484 N73-22034
On-going research relevant to continuous operations
14 p1723 N73-23983
Hazards of exposure to noise, fumes and vapors in military environment
14 p1723 N73-23985
Work-rest schedules for military tracking crews under prolonged vibration
14 p1723 N73-23986
Air Force objectives for maintaining aerospace superiority
[AD-759566] 17 p2099 N73-26982
Army materiel susceptability to high intensity electromagnetic radiation in radio frequency spectrum
[AD-763141] 21 p2508 N73-30125
Economic analysis of US aerospace/defense industry
[AD-763242] 22 p2738 N73-31921

Data base management information systems and selected Air Force applications
[AD-765203] 23 p2762 N73-32103
**ARMED FORCES (FOREIGN)**
Color vision requirements for German Air Force personnel
10 p1112 N73-19067
Color vision requirements of Canadian Armed Forces, including their standard tests
10 p1113 N73-19070
Color vision requirements of Great Britain's Armed Forces
10 p1113 N73-19072
Training of scientists and engineers for German Department of the Defense
11 p1351 N73-20965
Operational performance of helicopters in French Army
12 p1357 N73-21011
Physiological method for selecting and observing student pilots in Belgian Air Force for motion sickness
12 p1368 N73-21099
Canadian Armed Forces education impact on national development
[DRAE-37] 23 p2859 N73-32845
**ARMED FORCES (UNITED STATES)**
Armed forces anthropometric survey of 6682 Army men
[AD-743465] 01 p0021 N73-10160
Anthropometric survey of US army aviators conducted in 1970
[AD-743528] 01 p0021 N73-10162
Evaluation of current US Air Force aircraft engine status reporting system
[AD-750910] 06 p0624 N73-15067
Survey of industrial hygiene and safety in Air Forces operations
[AD-751897] 08 p0880 N73-17126
Armed Forces science conference report with list of principle authors
[AD-750326] 08 p0977 N73-17992
Armed Forces science conference report with list of principle authors
[AD-750360] 08 p0977 N73-17993
Comparison of accident rates among color defective and normal personnel
10 p1113 N73-19073
Air force radio communication and navigation system development planning
[AD-754930] 11 p1258 N73-20207
Effectiveness and cost of high performance watercraft for selected missions of US Coast Guard
[AD-754917] 11 p1268 N73-20295
Review of Naval research activities
[PB-212475] 11 p1354 N73-20993
Vacuum tube and solid state circuitry in electronic communications equipment for army training school
[AD-759129] 17 p2073 N73-26775
**ARMOR**
Stress corrosion cracking test for armor alloys with self-loading
[AD-746251] 01 p0068 N73-10560
Structural properties of dual hardness steel armor with high hardness and high carbon frontal plates
[AD-759506] 17 p2047 N73-26561
**AROMATIC COMPOUNDS**
Wide Temperature range, nonpolymeric, large molecular weight lubricants based on combination of siloxane and aromatic groups, for equipment near spacecraft nuclear reactors
[NASA-CR-123966] 04 p0447 N73-13654
Tricyclic nitropropene nitronate intermediates in condensation reactions of symmetric trinitrobenzene with cycloalkanones, and with phloroglucinol
[NASA-CR-131288] 11 p1252 N73-20159
Polycondensation syntheses of heat resistant siloxane polymers with fluoro aromatic groups at silicon atoms
[RAE-LIB-TRANS-1669] 17 p1991 N73-26104
High temperature and ultraviolet stability properties of poly[diarylsiloxy]arylazine
[NASA-CASE-ARC-10592-1] 20 p2435 N73-29554
**AROUSAL**
Electroencephalographic and behavioral responses of humans to aircraft noise during sleep
[NASA-CR-2279] 18 p2109 N73-27058
**ARRAYS**
NT ANTENNA ARRAYS
NT LARGE APERTURE SEISMIC ARRAY
NT LINEAR ARRAYS
NT PHASED ARRAYS
NT SOLAR ARRAYS
NT STEERABLE ANTENNAS
NT SYNTHETIC ARRAYS
NT TURNSTILE ANTENNAS
Computer aided analysis on radiative characteristics of sonar transducer with spaced sensor element array
[AD-747281] 03 p0266 N73-12156
Fabrication of monolithic ferrite memory arrays
[NASA-CR-2152] 04 p0398 N73-13238
Digital filter theory for broadband beamforming and hydrophone array steering
[AD-746206] 06 p0641 N73-15201
Heat transfer and aerodynamic resistance of in-line smooth walled tube arrays in transverse air flow at high Reynolds number
[NLL-RTS-7689] 09 p1098 N73-18959
Design of infrared detector array using multielement heterodyne technology
[AD-754443] 11 p1325 N73-20751
Passive electrical dummy load for simulating transducers in large sonar arrays
[AD-755174] 13 p1495 N73-22123
Cosmic ray air shower investigations with Haverah Park array
[HPNL-8] 13 p1573 N73-22749
Design of sonar array using standard amplitude shading technique
[AD-755481] 14 p1633 N73-23241
Quantitative data on propagation and directivity of parametric array in air
[AD-757034] 14 p1693 N73-23737
Fully steerable, decametric array for radio astronomy near Borrego Springs, California
16 p1960 N73-25853
**ARRESTERS**
Performance of lightning and surge suppressors for digital transmission equipment
[AD-752448] 09 p1004 N73-18195
**ARRESTING GEAR**
Design study of arresting gear system for recovery of space shuttle orbiters
[NASA-TM-X-68881] 04 p0401 N73-13265
Performance tests of aircraft arresting gear to determine allowable operating restraints on angular displacement and off-center engagements
[NATF-R125] 06 p0649 N73-15268
Test plan for extending service life of E-2A arresting gear
[AD-754752] 11 p1267 N73-20284
Laboratory hook bounce test for E-2A arresting gear A-frame
[AD-754753] 11 p1267 N73-20285
Hook bounce test of C-2A aircraft arresting gear A-frame
[AD-754077] 11 p1268 N73-20288
Test plan for extending life of C-2A arresting hook A-frame to 3000 arrested landings
[AD-754076] 11 p1268 N73-20289
Turbo-type energy absorber for aircraft carrier arresting gear
[AD-761502] 21 p2522 N73-30226
**ARRHYTHMIA**
Hyperbaric chamber used to determine influence of increased ambient pressure and gas density on cardiac rate in man
[AD-755129] 13 p1487 N73-22058
**ARSENIC**
Ion concentration profiles of injected boron and phosphorus including substitution of arsenic for phosphorus
05 p0522 N73-14249
**ARSENIC COMPOUNDS**
NT ARSENIDES
NT GALLIUM ARSENIDES
NT INDIUM ARSENIDES
NT PROUSTITE
Salvarsan therapy of luetic patients and behavior of Wassermann reaction
[NASA-TT-F-14618] 02 p0133 N73-11076
Thermal stability of amorphous arsenic compound glasses and electron diffraction analyses on semiconducting arsenic selenide films
[AD-752993] 09 p1076 N73-18778
X ray and electron diffraction spectra of amorphous arsenic sellenide semiconductors
[AD-762367] 20 p2463 N73-29792
Analysis of electrical switching phenomena in amorphous arsenic telluride-arsenic selenide system
24 p2966 N73-33707
**ARSENIDES**
NT GALLIUM ARSENIDES
NT INDIUM ARSENIDES
NT PROUSTITE
Crystal growth and magnetic properties of transition metal chalcogenides
[AD-748864] 04 p0459 N73-13748
Isothermal compressibility of amorphous semiconductors
[AD-750397] 06 p0709 N73-15785
**ARTEMIA**
Dosimetric analyses for Biosatellite 2 yeast and artemia radiation exposure experiment
[NASA-CR-127142] 04 p0379 N73-13082
**ARTERIES**
Transducer for converting arterial pulse wave into electric signals
[NASA-CASE-GSC-11531-1] 02 p0135 N73-11097
Analysis of arterial hypoxemia caused by pulmonary malfunctions and regulation of oxygen during exercise and rest
[AD-746979] 04 p0380 N73-13092
Influence of elastic properties of human body on arterial blood pressure measurement
05 p0500 N73-14072
Human arterial elasticity during breathing of reduced partial oxygen atmosphere
13 p1480 N73-21987
Arterial hypertension symptoms in flying personnel
13 p1480 N73-21991
Measurement of arterial pressure under influence of ODNT
[NASA-TT-F-15087] 23 p2749 N73-31998
**ARTERIOSCLEROSIS**
Flight stress effects on cardiovascular reactions of pilots with a theroscleresis
03 p0258 N73-12090
Atherosclerosis and hypertonia under high mountain conditions and seasonal effects
[NASA-TT-F-745] 09 p0995 N73-18121
Changes in vectorcardiograms of atherosclerotic flying personnel after glucose testing
13 p1480 N73-21989
**ARTHROPODS**
NT ARTEMIA
NT INSECTS
NT LARVAE
NT TRIBOLIA
**ARTICULATION**
Fundamental acoustic models for synthesis of speech operating on articulatory parameters
14 p1623 N73-23151
Model of speech production mechanism based on anatomical structures and physiological natures of articulatory organs
14 p1624 N73-23153
Role of distinctive features in speech production, acoustics, and phonetics
14 p1625 N73-23167
**ARTIFACTS**
Upper eye lid position effects in electro-oculograhic vertical eye movement recordings
06 p0633 N73-15143
**ARTIFICIAL CLOUDS**
Release technique for creating large dense vapor clouds in upper atmosphere using thermite formulation of barium metal and barium nitrate
[AD-745980] 01 p0054 N73-10438
Photogrammetric interpetation of barium cloud developments parallel to geomagnetic field
[EGG-1183-5006] 06 p0666 N73-15418
Radar sounding of magnetospheric instability and atmospheric density using barium release clouds
[AD-751567] 07 p0795 N73-16461
High altitude plasma physics and experiments simulating release of artificial plasma clouds in ionosphere
[AD-756684] 13 p1525 N73-22364
Large aperture Fabry-Perot interferometer used to scan barium ion clouds
[AD-757563] 14 p1663 N73-23495
Artificial plasma injection of lithium cloud in program to stimulate electromagnetic cyclotron instabilities in magnetosphere
[AD-760032] 17 p2029 N73-26424
Chemical system for releasing barium to create ion clouds in upper atmosphere and interplanetary space
[NASA-CASE-LAR-10670-1] 21 p2504 N73-30097
**ARTIFICIAL EARS**
Design and performance of wideband artificial ear for calibrating audiometric earphones
[AD-746691] 04 p0382 N73-13112
**ARTIFICIAL GRAVITY**
Effects of simulated artificial gravity on human performance
[NASA-CR-2129] 03 p0260 N73-12111
Results of OFO-A vestibular experiment and requirements of artificial gravity onboard manned spacecraft
[NASA-TT-F-14836] 08 p0961 N73-17861
Spacecraft with artificial gravity and earthlike atmosphere
[NASA-CASE-LEW-11101-1] 23 p2847 N73-32750
**ARTIFICIAL HEART VALVES**
Pu-238 grade fuels for supplying power to artificial heart and circulatory assist devices
[LA-DC-72-473] 03 p0261 N73-12115
**ARTIFICIAL INTELLIGENCE**
Internal structure of SQAP natural language parser for question-answer system
[FOA-P-C-8286-11[64]] 02 p0145 N73-11174
Statistical analysis of air combat situation evaluations conducted by US Navy pilots to detect differences caused by experience
[AD-747519] 03 p0261 N73-12119
Computerized simulation of three dimensional robots using generalized cylinder descriptions
[AD-755139] 11 p1251 N73-20152
Artificial intelligence in integrated circuit control of bionic manipulators
[NASA-CR-131403] 11 p1251 N73-20156
Design and implementation of language for expressing problem solving procedures in artificial intelligence
[NASA-CR-131591] 13 p1497 N73-22130
Radio controlled robots with computer induced artificial intelligence to act as human substitutes under adverse conditions
[NASA-CR-131593] 13 p1550 N73-22558
Papers presented at conference on speech communication and processing
[AD-742236] 14 p1620 N73-23119
Need and feasibility of automatic speech reading machines for blind people
14 p1620 N73-23121

Technical problems of automatic speech reading machines and methods adopted for their solution
14 p1620 N73-23122

Field evaluation of automated reading system for blind that produces synthetic speech from written text by use of computer and special-purpose devices
14 p1620 N73-23123

Word and phrase stress by rule for reading machine that produces synthetic English speech
14 p1620 N73-23124

System for automated speech synthesis from ordinary English text
14 p1620 N73-23125

System for generating speech from English text punched on paper tape using small digital computer and parametric speech synthesizer
14 p1620 N73-23126

Synthesis of letter sounds of alphabet by concatenation of phonemes for digital spelled speech reading machine for blind
14 p1620 N73-23127

Time induced orthogonality for simplified voice control of speech recognition machines
14 p1621 N73-23130

Computer program for machine recognition of distinctive features in words and sentences
14 p1623 N73-23147

Artificial intelligence research projects with emphasis on design, implementation, and integration of system for control of robot
[NASA-CR-131991] 14 p1638 N73-23279

Power of programming features in computer languages
[NASA-CR-131895] 14 p1638 N73-23280

Application of artificial intelligence to control of mobile automatons
[NASA-CR-132996] 16 p1874 N73-25173

Artificial intelligence for identifying practical applications to unmanned spacecraft to explore solar system in 1980 time period - Vol. 1
[NASA-CR-132256] 16 p1962 N73-25873

Development of artificial intelligence for onboard decision making capability of unmanned spacecraft during solar system exploration - Vol. 2
[NASA-CR-132257] 16 p1962 N73-25874

Machine perception of speech and vision
[AD-760153] 17 p2002 N73-26187

Computer interpretation of textured visual outdoor scenes
[AD-759712] 17 p2034 N73-26463

Computer programming for hierarchial robot intelligence system
[AD-761641] 19 p2240 N73-28061

**ARTIFICIAL SATELLITES**
NT AEROS SATELLITE
NT ALOUETTE SATELLITES
NT ALOUETTE 1 SATELLITE
NT ALOUETTE 2 SATELLITE
NT APPLICATIONS TECHNOLOGY SATELLITES
NT ARIEL 3 SATELLITE
NT ASTRONOMICAL NETHERLANDS SATELLITE
NT ATS 1
NT ATS 3
NT ATS 5
NT ATS 6
NT BIOSATELLITE 2
NT COMMUNICATION SATELLITES
NT COSMOS SATELLITES
NT COSMOS 213 SATELLITE
NT COSMOS 224 SATELLITE
NT COSMOS 381 SATELLITE
NT DIADEME SATELLITES
NT EARTH RESOURCES TECHNOLOGY SATELLITE 1
NT EARTH RESOURCES TECHNOLOGY SATELLITES
NT ECHO 1 SATELLITE
NT ENVIRONMENTAL RESEARCH SATELLITES
NT EOLE SATELLITES
NT EROS [SATELLITES]
NT ESRO SATELLITES
NT ESRO 1 SATELLITE
NT ESRO 2 SATELLITE
NT ESSA 8 SATELLITE
NT EXPLORER SATELLITES
NT EXPLORER 12 SATELLITE
NT EXPLORER 18 SATELLITE
NT EXPLORER 21 SATELLITE
NT EXPLORER 24 SATELLITE
NT EXPLORER 27 SATELLITE
NT EXPLORER 31 SATELLITE
NT EXPLORER 32 SATELLITE
NT EXPLORER 33 SATELLITE
NT EXPLORER 34 SATELLITE
NT EXPLORER 35 SATELLITE
NT EXPLORER 38 SATELLITE
NT EXPLORER 40 SATELLITE
NT EXPLORER 41 SATELLITE
NT EXPLORER 49 SATELLITE
NT FRENCH SATELLITES
NT GEODETIC SATELLITES
NT GEOS SATELLITES [ESRO]
NT GEOS 1 SATELLITE
NT GEOS 2 SATELLITE
NT GEOS-C SATELLITE
NT GOE SATELLITES
NT GRAVITY GRADIENT SATELLITES
NT HELIOS SATELLITES
NT HEOS A SATELLITE
NT HEOS B SATELLITE
NT HEOS SATELLITES
NT IMP
NT IMPROVED TIROS OPERATIONAL SATELLITES
NT INJUN 3 SATELLITE
NT INTELSAT SATELLITES
NT INTERCOSMOS SATELLITES
NT ISIS SATELLITES
NT ISIS-A
NT ITOS 1
NT ITOS 2
NT ITOS 3
NT ITOS 4
NT LINCOLN EXPERIMENTAL SATELLITES
NT LUNAR ORBITER
NT LUNAR SATELLITES
NT METEOROLOGICAL SATELLITES
NT METEOSAT SATELLITE
NT MOLNIYA SATELLITES
NT NAVIGATION SATELLITES
NT NIMBUS SATELLITES
NT NIMBUS 2 SATELLITE
NT NIMBUS 3 SATELLITE
NT NIMBUS 4 SATELLITE
NT NIMBUS 5 SATELLITE
NT OAO
NT OGO
NT OGO-A
NT ORBITAL SPACE STATIONS
NT ORBITAL WORKSHOPS
NT OSO
NT OSO-J
NT OSO-1
NT OSO-5
NT OSO-6
NT OSO-7
NT PROTON 1 SATELLITE
NT RADIO ASTRONOMY EXPLORER SATELLITE
NT RELAY SATELLITES
NT SAN MARCO 3 SATELLITE
NT SAS-B
NT SAS-C
NT SPUTNIK SATELLITES
NT SYMPHONIE SATELLITES
NT SYNCHRONOUS METEOROLOGICAL SATELLITE
NT SYNCHRONOUS SATELLITES
NT TIROS M
NT TIROS SATELLITES
NT TRANSIT SATELLITES
NT UHURU SATELLITE
NT UK SATELLITES
NT VANGUARD 3 SATELLITE
NT VELA SATELLITES
NT VENERA SATELLITES
NT VENERA 8 SATELLITE

Numerical integration of artificial satellite orbit perturbation due to planetary gravitational effects, including long period and secular terms
[GRGS-BULL-5] 01 p0105 N73-10868

Secular and long period terms of artificial satellite perturbed equation of motion noting planetary gravitational effects
01 p0105 N73-10870

Tables of data on artificial satellites launched during period 1957 to 1971 to include chronology of manned space flight and emission frequencies of various satellites
[F-22] 01 p0107 N73-10885

Development of occultation satellite system for determining atmospheric pressure at various millibar levels
02 p0198 N73-11601

Position of satellite with respect to earth magnetosphere
[AD-746469] 02 p0232 N73-11883

Development of spacecraft control system using two speed-baised and speed-modulated reaction wheels with resultant momentum nominally oriented along orbit normal
[AD-745961] 02 p0235 N73-11911

Modification to Dynamic Operational Requirements and Cost Analysis Program to perform traffic analyses of automated satellite program - Vol. 5
[NASA-CR-129267] 03 p0270 N73-12187

Analysis of computer programs for plotting geographical and political features of world based on observations from artificial satellites
[NASA-CR-129282] 03 p0356 N73-12903

List of artificial satellites launched between 1 Jan. 1969 and 31 Dec. 1971 giving details of lifetime, orbit, mass, and size
[RAE-TR-72127] 03 p0359 N73-12929

Feasibility of monitoring global air pollution using optical sensors installed in orbiting satellites
04 p0471 N73-13840

Analysis of photographic data obtained during manned and unmanned space flight and application to oceanography, hydrology, geography, and geology
04 p0471 N73-13843

Application of radiophysical methods to study of earth atmosphere and earth resources with satellites
[NASA-TT-F-14642] 05 p0538 N73-14381

Tables of data on artificial satellites launched during period 1957 to 1971 to include chronology of manned space flight and emission frequencies of various satellites
[F-23] 05 p0598 N73-14861

Variational equations for studying rotational motion of orbiting rigid body about its center of mass under conservative and nonconservative torques
07 p0817 N73-16624

Analysis of motion of compound pendulum and two-gimbal gyroscope mounted in artificial satellite with prescribed orbit and constant rate of rotation
07 p0817 N73-16625

Analysis of parametric resonance in rotating crossed-dipole satellites and method for determining regions of instability
07 p0847 N73-16868

Analysis of satellite stability of motion using Liapunov system as applied to flexible bodies
07 p0848 N73-16869

Mathematical and numerical methods for solving spacecraft control problems and mapping of celestial bodies
[NASA-TT-F-731] 10 p1177 N73-19572

Approximative model for diurnal effect on atmospheric density distribution and artificial earth satellite deceleration
10 p1177 N73-19578

Effects of solar pressure and gravity gradient on attitude motions of artificial satellite near far moon side libration point
12 p1447 N73-21722

Capabilities, functions, and conceptual methods of operation for satellite-aided communications system in oceanic air traffic control environment
[FAA-RD-73-41] 12 p1460 N73-21833

Feasibility and costs of orbiting satellite data collection systems
[NASA-CR-130232] 13 p1581 N73-22812

Manufacture of quartz gyroscopes for application to General Relativity Satellite
13 p1593 N73-22920

Development of system for collection and processing of telemetered magnetometer data received from artificial satellite
[GAMMA-17-167S] 14 p1658 N73-23457

Application of artificial satellites for data acquisition and communication functions in air traffic control system
14 p1689 N73-23709

Asymptotic methods for deriving transient backscattered signatures from artificial satellites
[AD-758245] 15 p1751 N73-24192

Artificial satellite motion and tracking
[GRGS-BULL-6] 15 p1832 N73-24846

Artificial satellite equations of motion approximations for photographic and laser tracking optimization
15 p1832 N73-24848

Computerized data processing and graphic display system for artificial satellite
[AD-760304] 17 p2002 N73-26190

Application of pulsed radars for side scanning from artificial earth satellites and numerical analysis of radar operating parameters
18 p2117 N73-27117

Zvenigorod Experimental Station optical observations of artificial satellites
[JPRS-59567] 18 p2126 N73-27181

Application of infrared reconnaissance satellites for detecting missiles and military satellites
[AD-760951] 18 p2152 N73-27395

Soundings and imagings from geostationary satellites and numerical analysis of satellite stability parameters
[NASA-CR-132799] 18 p2200 N73-27761

Semi-analytical solution of oceanic tidal perturbations in motion of artificial satellites
[NASA-TM-X-66298] 18 p2200 N73-27763

Congressional hearings to review NASA program accomplishments and to predict advantages to accrue from space programs
21 p2609 N73-30916

Forces and torques on satellites moving through rarefied plasmas
23 p2847 N73-32752

Application of Runge-Kutta, multi-step, and extrapolation methods for numerical integration of equations of motion on controlled satellite
[NASA-CR-124416] 23 p2848 N73-32762

Determination of perturbing moments due to solar radiation pressure forces acting on body of revolution
[NASA-TT-F-15072] 24 p2976 N73-33780

Satellite motion in gravitational field of nonspherical rotating planet
[NASA-TT-F-15073] 24 p2981 N73-33825

ARTILLERY
Optimized antenna design for medium artillery delivered seismic detection system sensor
[AD-748825] 04 p0396 N73-13219
Development of thick-walled, Borsic aluminum alloy ring for use as stiffener in 155 millimeter atomic artillery projectile
[SC-DR-72-0706] 10 p1176 N73-19562
ARTILLERY FIRE
Artillery sound ranging computer simulations
[AD-745887] 02 p0212 N73-11719
Analysis of standard radiosonde system for accurate measurement of meteorological parameters which affect artillery fire
[AD-747759] 03 p0327 N73-12671
ARTS
NT ABILITIES
ARYL COMPOUNDS
U AROMATIC COMPOUNDS
ASBESTOS
Method for producing asbestos matrix suitable for use in fuel cell or electrolysis cell
[NASA-CASE-MSC-12568-1] 07 p0811 N73-16577
Determination of aerodynamic diameter of latex spheres and asbestos fibers using aerosol spiral centrifuge
[BMVG-FBWT-72-10] 07 p0812 N73-16585
Properties of thermal resistant electrical insulating papers based on inorganic fibers
[NLL-RTS-7740] 10 p1175 N73-19554
Occupational hazards and control measures to prevent air pollution from asbestos processing
[AP-117] 11 p1314 N73-20660
Improving resistance of chrysotile asbestos to potassium hydroxide at temperatures above 100 C
[AD-761512] 19 p2223 N73-27931
ASCENT
NT CLIMBING FLIGHT
ASCENT PROPULSION SYSTEMS
Apollo experience report on lunar module ascent propulsion subsystem to identify significant technical problems encountered during all phases of program
[NASA-TN-D-7082] 09 p1090 N73-18900
Results of postflight analysis of APS performance during Apollo 15 mission
[NASA-TM-X-69204] 17 p2077 N73-26801
Results of postflight analysis of APS performance during Apollo 12 Mission
[NASA-TM-X-69529] 17 p2083 N73-26850
Centaur D-1T improved propulsion and propellant systems
[NASA-TM-X-71436] 23 p2830 N73-32619
ASCENT TRAJECTORIES
Criteria and guidelines for combining loads during ascent phase of space flight
[NASA-SP-8099] 02 p0234 N73-11897
Wind tunnel tests to determine aerodynamic characteristics and aerodynamic interference of various configurations of space shuttle ascent vehicle-Vol. I
[NASA-CR-120083] 02 p0234 N73-11901
Atmospheric turbulence response of reusable space shuttle configuration during ascent flight
[NASA-CR-123952] 03 p0357 N73-12913
Ascent control studies of 049 and ATP parallel burn solid rocket motor shuttle
[NASA-TM-X-64720] 08 p0960 N73-17854
Structural load reduction of space shuttle booster/orbiter configuration using load relief guidance technique
[NASA-TM-X-64738] 12 p1457 N73-21812
Development of computer program for parametric ascent trajectory optimization for application to space shuttle vehicle operation
[NASA-CR-129000] 12 p1458 N73-21815
Effects of ascent trajectory mode and tank disposal method on shuttle payload accommodation
[NASA-TM-X-64773] 21 p2599 N73-30831
Technique for determining fuel optimal, impulsive, fixed time trajectories based on comparison of two neighboring trajectories with application to ascent rendezvous
24 p2978 N73-33799
ASCORBIC ACID
Influence of cysteamine hydrochlorine and vitamin B and C prophylaxis on radiation sickness in humans
11 p1242 N73-20078
ASCR REACTOR
U ADVANCED SODIUM COOLED REACTOR
ASHES
Development of model to describe characteristics of one dimensional lunar ash flow with and without heat transfer effects
[NASA-CR-130697] 08 p0895 N73-17245
ASIA
Morphology, provenance, and movement of desert sand seas in Africa, Asia, and Australia
[E72-10249] 03 p0289 N73-12349
Specific humidity distributions over Northern Hemisphere during monsoon season in Asia at 1000, 850, and 700 mb levels for June and July 1970
[NOTE-9] 05 p0572 N73-14647
Tables of synoptic meteorological observations for Southeast Asian coastal marine areas
[AD-750159] 06 p0694 N73-15658
Morphology, provenance, and movement of desert sand seas in Africa, Asia, and Australia
[E73-10058] 07 p0778 N73-16320
Morphology, provenance, and desert sand sea movements in Asia, Australia, and Africa
[E73-10060] 07 p0778 N73-16322
ERTS-1 imagery of morphology, provenance, and movement of desert sand seas in Africa, Asia, and Australia
[E73-10409] 11 p1278 N73-20371
Morphology, provenance, and movement of desert sand seas in Africa, Asia, and Australia
[E73-10542] 13 p1518 N73-22305
Surface gravity and satellite derived gravimetric geoid of North America, North Atlantic, Eurasia, and Australia
[NASA-TM-X-66238] 15 p1778 N73-24413
ERTS-1 imagery of morphology, provenance, and movement of desert sand areas in Africa, Asia, and Australia
[E73-10710] 17 p2018 N73-26317
ERTS-1 imagery of morphology, provenance, and movement of desert sand seas in Africa, Asia, and Australia
[E73-10786] 18 p2136 N73-27262
Bibliography of articles concerning water balance of monsoon Asia
[CLIMATOL-NOTES-11] 18 p2171 N73-27531
Morphology, provenance, and movement of desert sand seas in Africa, Asia, and Australia using ERTS-1 data
[PAPER-G8] 19 p2264 N73-28239
ASPECT RATIO
NT HIGH ASPECT RATIO
NT LOW ASPECT RATIO
Velocity irregularities in near field of high aspect ratio turbulent jets
[AD-754224] 10 p1143 N73-19315
ASPHERICITY
Electrostatic gyroscope deviations from rotor asphericity with axisymmetric surface
20 p2418 N73-29433
ASPIRATION
U VACUUM
ASSEMBLIES
NT SUBASSEMBLIES
Elastic interface pressure and stress calculations on assemblies of shafts with interference-fit collars
[ESDU-68004-PT-3] 02 p0177 N73-11433
ASSEMBLING
Computer based automation for performing material handling, assembly, and quality control tasks
[AD-752464] 08 p0928 N73-17601
Plastic compensating coatings for alignment and assembly of bearing unit
[AD-754591] 11 p1300 N73-20550
ASSEMBLY
Text, syntax, and description of PL 516 assembler noting ALGOL, one track, one pass syntax, and design philosophy
[NPL-COM-SCI-65] 23 p2761 N73-32093
ASSEMBLY LANGUAGE
Comparing complexity classes of formal languages
[NASA-CR-129294] 03 p0269 N73-12181
Assembly language programs required to interface ALQHA system to IBM telecommunication time sharing operation
[NASA-CR-133853] 22 p2639 N73-31155
Text, syntax, and description of PL 516 assembler noting ALGOL, one track, one pass syntax, and design philosophy
[NPL-COM-SCI-65] 23 p2761 N73-32093
ASSESSMENTS
NT TECHNOLOGY ASSESSMENT
ASSIGNMENT
U ALLOCATIONS
ASSOCIATIONS
U ORGANIZATIONS
ASSURANCE
Management concept for reliability assurance from aerospace industry experience applied to shipbuilding
[MBB-UA-60-72-O] 17 p2099 N73-26980
ASTEROIDS
NT CERES ASTEROID
NT ICARUS ASTEROID
NT VESTA ASTEROID
Results of Meteor Research Program
01 p0101 N73-10831
Dynamics of meteor streams and new asteroid-meteor and comet-meteor associations
01 p0102 N73-10843
Shape and rotation rate of asteroid bodies
02 p0228 N73-11850
Assessment of present state of knowledge of asteroids for identifying mission and target priorities
[NASA-CR-129247] 03 p0354 N73-12889
Resonance capture of Toro asteroid perturbed orbit by earth
[TRITA-EPP-72-19] 07 p0846 N73-16863
Application of infrared detectors for location and identification of asteroids during sky survey activities
[AD-760107] 18 p2198 N73-27745
Solar probe orbit perturbation calculation assuming circular gravitating asteroid ring with center at sun
[ESRO-SR-19] 19 p2344 N73-28856
Theories and definitions of comets and asteroids for proposed recommendations
[NASA-TM-X-71917] 22 p2717 N73-31747
ASTIGMATISM
Weightlessness effects on development of vestibular apparatus and ocular nystagmus in rat, using chronic 2g centrifuge
[NASA-CR-114569] 08 p0878 N73-17112
ASTP
U APOLLO SOYUZ TEST PROJECT
ASTRIONICS
Integrated electronics for European space tug
[HSD-TP-7227-APP-5] 10 p1217 N73-19897
European space tug guidance control rendezvous and integrated electronics
[HSD-TP-7264-VOL-4] 10 p1218 N73-19904
ASTROBEE ROCKET VEHICLES
Astrobee rocket instrumentation for infrared radiation measurements on auroral display
[AD-755823] 12 p1402 N73-21373
ASTROBIOLOGY
U EXOBIOLOGY
ASTROMETRY
Astrometry for determination of absolute positions of stars and their relative motions from Schmidt plates noting accuracy
07 p0845 N73-16843
Astrometric performance of Schmidt plates for stellar positions noting reduction of coordinates
07 p0845 N73-16844
Schmidt telescopes for astrometry discussing correspondence between flat and curved plates
07 p0845 N73-16845
Spatial distribution of stars in area surrounding cluster NGC 6913
20 p2471 N73-29843
ASTRONAUT LOCOMOTION
Dynamic changes in psychophysiological motor efficiency of cosmonauts in flight
[JPRS-57417] 01 p0019 N73-10144
ASTRONAUT MANEUVERING EQUIPMENT
Extravehicular activity support systems and equipment with emphasis on physical operational and performance characteristics of major systems
[NASA-CR-2160] 06 p0718 N73-15858
Feasibility of limb controlled astronaut maneuvering scheme
18 p2110 N73-27063
ASTRONAUT PERFORMANCE
NT BLACKOUT PREVENTION
Astronaut manual performance limits in intravehicular Skylab environment
[NASA-CR-128590] 01 p0019 N73-10150
Time and motion study of lunar surface activity on Apollo 15
[NASA-CR-128695] 07 p0842 N73-16823
Time and motion study of astronaut lunar surface activity on Apollo 16
[NASA-CR-128696] 07 p0842 N73-16825
Psychological assessment techniques for determining astronaut attentional flexibility and associate performance
[NASA-CR-128945] 15 p1744 N73-24136
Human factors analysis of astronaut working conditions in space vehicles
[NASA-TT-F-750] 19 p2225 N73-27946
Contrasting opinions concerning space activity concerning untested physiological effects
[NASA-TT-F-15019] 19 p2342 N73-28842
Apollo experience report on process of crew procedures development for systems procedures and flight procedures
[NASA-TN-D-7436] 22 p2721 N73-31772
Development of flight experiment work performance and workstation interface requirements for Sortie Lab
[NASA-CR-124409] 23 p2845 N73-32733
ASTRONAUT TRAINING
Bioelectric monitoring and motion picture surveying for improved physical training of astronauts
14 p1608 N73-23039
ASTRONAUTICS
Soviet research in meteorology, geophysics, space, and astronomy
[JPRS-57989] 07 p0843 N73-16829
ASTRONAUTS
Cosmic radiation dosage measurements on Apollo astronauts by Lexan dosimetry
[AD-745188] 01 p0013 N73-10101
Microbial analysis of Apollo 14 astronauts
[NASA-TM-X-58094] 05 p0500 N73-14073
Measurement of radiation exposure of astronauts by radiochemical techniques
[NASA-CR-130538] 08 p0878 N73-17114
Light flash observation experiments conducted by Apollo 16 astronauts - Part C
12 p1452 N73-21763
Nuclear track dosimetry for monitoring cosmic ray exposure of Apollo 16 astronauts
15 p1741 N73-24114
Data analysis for predicting human personal hygienic needs during long term space flight
[NASA-CR-128929] 15 p1743 N73-24132
Analytical gas chromatography and mass spectrography for physiological monitoring of astronauts
[NASA-CR-133272] 18 p2110 N73-27059

Radioactivity urinalysis for calculating postflight astronaut cosmic radiation exposure
[NASA-CR-133378] 19 p2224 N73-27939
Laboratory investigation of Coriolis acceleration effects on vestibular apparatus of cosmonauts
[NASA-TT-F-15129] 22 p2620 N73-30993

**ASTRONAVIGATION**
Most probable position in astronomical navigation using celestial body coordinates
07 p0859 N73-16972

**ASTRONOMICAL CATALOGS**
Northern PZT stars observation and astronomical catalogs
01 p0101 N73-10827
Calculation of all occultations by planet Jupiter of stars brighter than magnitude 6.55 for period 1951 to 2000
[NASA-TT-F-14626] 01 p0104 N73-10862
Objective prism survey of entire southern sky within 10th to 13th photographic magnitude range by Schmidt telescope equipped with ultraviolet prism
06 p0717 N73-15851
Annual of National Astronomical Observatory of Columbia for 1972
06 p0717 N73-15852
Aeronautical almanac for period from January to April, 1973
08 p0916 N73-17509
Magnitude and UBV colors for 900 stars brighter than magnitude 5.0 and south of plus 10 deg declination
[ANNALS-7] 08 p0960 N73-17849
Astronomical ephemerides for 1973
08 p0960 N73-17855
Method for determining relative orientation of coordinate axes of stellar catalogs
[AD-751077] 09 p1085 N73-18855
Catalog of proper motion for 691 stars of Southern Hemisphere
11 p1338 N73-20861
Astronomical catalog for 1973
13 p1576 N73-22774
Classification of southern carbon stars using objective prism spectra
16 p1960 N73-25857
Catalog of ultraviolet stellar observations obtained from celescope experiment on OAO 2
[NASA-CR-132196] 16 p1962 N73-25869
Use of Sydney photographic plates to compile astronomical catalog
18 p2196 N73-27725
Tables listing 1970.0 ecliptic coordinates of hot stars
[COMMUN-27] 19 p2344 N73-28857
Hot star catalog listed in constellation alphabetical order
[COMMUN-31] 19 p2344 N73-28858
Astronomical ephemerides for 1974
23 p2838 N73-32679

**ASTRONOMICAL COORDINATES**
Astrometric performance of Schmidt plates for stellar positions noting reduction of coordinates
07 p0845 N73-16844
Astronomical mapping of rotating spiral Maffei galaxy
[AD-752042] 08 p0962 N73-17873
Method for determining relative orientation of coordinate axes of stellar catalogs
[AD-751077] 09 p1085 N73-18855
Development of automated astronomic positioning system using vertically oriented telescope to produce accurate astronomic latitude and longitude
[AD-760108] 17 p2060 N73-26668

**ASTRONOMICAL MAPS**
Schmidt telescopes for compilation of stellar spectra and novae maps, galactic structure, and radial velocities
07 p0846 N73-16856
X ray astronomy and its impact on galactic and extragalactic radio source mapping
17 p2084 N73-26856

**ASTRONOMICAL MODELS**
Model of Crab nebula derived from dual-frequency radio measurements
[AD-744678] 01 p0106 N73-10879
Short-period comets and meteor stream genetic origin discussing formation processes
[TRITA-EPP-72-18] 02 p0231 N73-11880
Conference on stellar chromospheres and their compositions
[NASA-SP-317] 04 p0465 N73-13792
Radiative equilibrium and empirical models for stellar chromospheres
04 p0466 N73-13794
Stellar evolution and atmospheric turbulence dynamics for chromospheric activity model
04 p0466 N73-13799
Summary of physical and theoretical work on stellar chromospheres
04 p0466 N73-13800
Extragalactic radio sources
04 p0468 N73-13815
Model for pulsar radiation mechanism and relativistic plasma
[NP-19402] 07 p0826 N73-16692
Computerized analysis of binary star systems with eclipsing light curves
[NASA-TM-X-66155] 07 p0842 N73-16821
Virial theorem for analyzing structure of clusters in galaxies
08 p0959 N73-17840
Existing stochastic models of galactic magnetic field
[NASA-CR-130158] 08 p0959 N73-17847
Model for ionized part of interstellar medium based on low frequency observations by RAE satellite
08 p0975 N73-17970
Asymptotic behavior of kinetic solar wind model
[AERONOMICA-ACTA-A-108] 09 p1080 N73-18812
Two fluid cosmological model including interaction between matter and radiation
13 p1561 N73-22652
Tensor viral method for modeling and studying pulsars in rapidly rotating magnetosphere
16 p1960 N73-25858
Rotating atmospheric model for Altair
17 p2081 N73-26833
Equations used in analysis of photometric observations of zodiacal light, and zodiacal light models
[NASA-TN-D-7263] 17 p2082 N73-26843
Dynamic particle mass flow model for solar flares
19 p2333 N73-28773
Magnetic field rearrangement model for solar infall-impact flares
19 p2333 N73-28775
Computational method for obtaining models for fast and differentially rotating upper main sequence stars in radiative equilibrium
20 p2470 N73-29838
Theoretical evolution of extremely metal poor stars
20 p2470 N73-29839
High energy astrophysics and solar astronomy
22 p2732 N73-31868
Positron annihilation radiation model for neutron star density in galactic disk
22 p2733 N73-31869
X ray emission in pulsar model for supernovae remnants
22 p2733 N73-31870
Hydrodynamic model for stellar mass ejection and planetary nebula formation
22 p2734 N73-31885
Light curve computations from astrophysical models of W Ursae Majoris systems
23 p2836 N73-32664
Structural, compositional, and photometric model of comet Encke
[NASA-CR-135707] 23 p2845 N73-32737

**ASTRONOMICAL NETHERLANDS SATELLITE**
X ray Astronomical Netherlands Satellite experimental design for soft and hard source identification and spectral analysis
17 p2084 N73-26860

**ASTRONOMICAL OBSERVATORIES**
NT HEAO
NT OAO
NT OSO
NT OSO-J
NT OSO-1
NT OSO-7
Contributions of Smithsonian Astrophysical Observatory to International Satellite Geodesy program
[NASA-CR-128396] 01 p0100 N73-10825
History of Radcliffe Observatory and its scientific research activities and personnel
02 p0152 N73-11231
Influence of space technology on X ray astronomy
04 p0473 N73-13856
Design and operation of Orion orbital astrophysical observatory
[NASA-TT-F-14581] 07 p0766 N73-16221
Control system for automatic orientation and tracking operation of Orien orbital observatory
[NASA-TT-F-14583] 07 p0799 N73-16490
Operating principles of high precision orbiting astronomical observatory manned by nonprofessional cosmonaut astronomer
[NASA-TT-F-14580] 07 p0843 N73-16830
Schmidt telescopes in Southern Hemisphere survey noting possible sites and study of Magellanic clouds
07 p0846 N73-16853
Stellar, planetary, and comet observations at astronomical observatory during 1973
08 p0960 N73-17850
Scientific space mission of small spin stabilized astronomical satellite with X ray and IR experiments
09 p1081 N73-18817
Incorporation of high resolution Fourier transform spectrometer with astronomical telescope at Mauna Kea Observatory, Hawaii
[NASA-CR-131893] 14 p1667 N73-23530
Astronomical studies at Hale Observatories
14 p1704 N73-23828
European Southern Observatory in Chile including research projects, equipment, and management for 1971
15 p1763 N73-24282
Experimental design, research programs, and equipment design activities of Astronomical Space Laboratory for 1971 to 1972
[RAP-01-72] 17 p2011 N73-26261
Observations of lunar behavior in stellar occulation
[PUBL-25] 17 p2081 N73-26836
Astronomical research and instrument development by Professor M. G. Pereira de Barros
17 p2081 N73-26837
Conference on X ray experiments onboard different astronomical observatories for galactic and extragalactic X ray source position and size determination
[ESRO-SP-87] 17 p2084 N73-26855
Comparison of HELOS mission with other X ray astronomy missions
17 p2085 N73-26874
Zvenigorod Experimental Station optical observations of artificial satellites
[JPRS-59567] 18 p2126 N73-27181
Galilean satellites, Venus clouds, and astronomical observatories
[NASA-CR-133826] 21 p2591 N73-30761
Optical seeing tests on Mt. Lemmon, using Polaris telescope from Lick Observatory
[LPL-COMMUN-170] 21 p2592 N73-30766
Solar data on daily total areas of sunspot groups, for Oct. 1972 by Rome, Italy Astronomical Observatory
[BULL-174] 21 p2597 N73-30817
Solar data on daily total areas of sunspot groups, for Nov. 1972 by Rome, Italy Astronomical Observatory
[BULL-175] 21 p2598 N73-30818
History, organization, and functions of Vatican astronomical observatory
22 p2714 N73-31724
Symposium on Gum Nebula and related topics
[NASA-SP-332] 22 p2715 N73-31731
Listing of double star observations for 1900 and 1960
22 p2717 N73-31748
Report of the Astronomer Royal for Scotland for the year ending 31 March 1973
22 p2718 N73-31760
Using UBUH gamma photometry and spectral classifications for 48 stars in monoceros region to study dispersed part of 1 Mon association
23 p2836 N73-32658
Study of known RR Lyrae type variable stars in Messier 3
[REPT-63] 23 p2846 N73-32746
Mission objectives of German astronomical satellite, noting X ray astronomy, IR and UV experiments
[BMBW-FB-W-72-25] 23 p2851 N73-32786
German astronomical satellite configuration and subsystems for launching Scout D vehicle
[BMBW-FB-W-72-26] 23 p2852 N73-32787
Activities of Haystack Observatory, and radio astronomy
[NASA-CR-135773] 24 p2900 N73-33152
Solar data on daily total areas of sunspot groups for Apr. 1973 by Rome Astronomical Observatory
[PUBL-180] 24 p2977 N73-33788
Survey of properties of supernova remnants
24 p2978 N73-33793

**ASTRONOMICAL PHOTOGRAPHY**
Inference of coronal and interplanetary magnetic fields and H-alpha patterns from high resolution photography
01 p0094 N73-10771
Spectroscopy and photography of novae and supernovae
[AD-743955] 01 p0106 N73-10875
Development of photoelectric and photographic standards for Magellanic clouds and analysis of differences in stellar population of regions
02 p0227 N73-11832
Spectroscopic observation of Comets Tago-Sato-Kosaka and Bennett
02 p0228 N73-11848
Photographic observation of Type 1 and Type 2 tail motion in Comet Bennett
02 p0229 N73-11854
Soviet camera for tracking satellites and solving geodetic and geophysical problems
[AD-747135] 03 p0303 N73-12476
Chilean astronomical observations of early star spectra, southern star radial velocities, and minor planet positions
05 p0594 N73-14828
Applications of Schmidt telescopes to study astrometry, photometry, galactic structure, quasars, and stellar spectra
07 p0844 N73-16840
Applications of Tautenburg 134-cm Schmidt telescope noting instrument efficiency and astrophysical statistics
07 p0846 N73-16860
Cameras for photographing meteors in selected sky area
[NASA-CASE-LAR-10226-1] 10 p1158 N73-19419
Astronomical photography of Gum Nebula, galactic clusters, and zodiacal light from Apollo 16 flight
12 p1456 N73-21793
Apollo 16 lunar maps
[NASA-CR-132066] 15 p1785 N73-24469
Use of Sydney photographic plates to compile astronomical catalog
18 p2196 N73-27725

Brightness changes in WZ Cas in photographic and visible light
20 p2471 N73-29844
Construction of rotating photoshutter for use with various astronomical instruments
20 p2471 N73-29850
Electrophotometry, photoelectronic images, converters, and television equipment for studying variable stars
[NASA-TT-F-797] 21 p2594 N73-30783

**ASTRONOMICAL PHOTOMETRY**
NT STELLAR SPECTROPHOTOMETRY
Development of photoelectric and photographic standards for Magellanic clouds and analysis of differences in stellar population of regions
02 p0227 N73-11832
Extended two color photometry of faint stars by telescope with objective grating
[BULL-172] 07 p0842 N73-16819
Applications of Schmidt telescopes to study astrometry, photometry, galactic structure, quasars, and stellar spectra
07 p0844 N73-16840
Application of Schmidt telescopes and three color photometry to galactic clusters, star distribution in galactic disk and halo and galactic white stars.
07 p0845 N73-16842
Galactic brightness distribution obtained by imaging galaxies on Schmidt plates, selecting one as photometric standard and applying microdensitometric scans
07 p0845 N73-16852
Identification of infrared stars using Schmidt telescopes, infrared photometry, and slit spectra
07 p0846 N73-16855
Photometric analysis of violet clouds on planet Mars and determination of monochromatic albedo
09 p1083 N73-18834
Spectrophotometric observations of planet Jupiter to determine ultraviolet absorption for different regions of disk
09 p1083 N73-18835
Photometric and polarimetric measurements of Bruderheim meteorite particles and comparison with astronomical data to determine composition of asteroids
[NASA-CR-131418] 11 p1339 N73-20865
UBV observations of RR Lyrae variable HD 176387
[ROY-OBS-BULL-174] 13 p1578 N73-22787
Brightness changes of MZ Cas and TZ Cas in B- and V-light
20 p2471 N73-29845
Detection of new variable [BD plus 60 deg 2633] from photometric plates
20 p2471 N73-29846
Determination of magnitude and brightness of variable stars by photographic photometry
21 p2594 N73-30786
Multicolor photometric systems for studying physical properties and spectra of variable stars
21 p2594 N73-30790
Optical and ultraviolet methods in astronomy
22 p2734 N73-31882

**ASTRONOMICAL SPECTROSCOPY**
Spectroscopy and photography of novae and supernovae
[AD-743955] 01 p0106 N73-10875
High dispersion Coude spectrograms of zeta Oph and Per, and molecular absorption in interstellar medium
[NASA-TM-X-66073] 02 p0224 N73-11812
Gamma, X ray, ultraviolet, and infrared astronomy noting instrumentation and radiative transfer
[ESRO-SP-75] 04 p0476 N73-13889
Objective prism survey of entire southern sky within 10th to 13th photographic magnitude range by Schmidt telescope equipped with ultraviolet prism
06 p0717 N73-15851
Pros and cons of objective prisms in astronomical spectroscopy noting work in conjunction with Schmidt telescopes and novel techniques
07 p0845 N73-16846
Low intensity H-beta emission from interstellar medium
08 p0975 N73-17973
Spectrometry investigations of planets by USSR astronomical observatories with emphasis on ultraviolet absorption by planetary atmospheres
[NASA-TT-F-747] 09 p1083 N73-18833
High resolution spectral and polarization behavior of solar Type 3 bursts at 34 MHz
13 p1489 N73-22073
Incorporation of high resolution Fourier transform spectrometer with astronomical telescope at Mauna Kea Observatory, Hawaii
[NASA-CR-131893] 14 p1667 N73-23530
Spectroscopic observation of Nova Delphini 1967 in gamma gamma 4,000 to 9,000 region
17 p2080 N73-26825
Spectroscopic observation of metastable helium line in alpha-orionis and interstellar media
17 p2081 N73-26830
HEAO-B cosmic ray experiment for diffuse sky brightness determination
17 p2085 N73-26871
HEAO-C X ray focusing telescopes for spectrometric and polarization studies
17 p2085 N73-26872
Cooled filter wheel spectrometers for short wavelength telescopic observations of faint planetary objects
[NASA-CR-133413] 18 p2197 N73-27739
Design of ultraviolet Explorer satellite for spaceborne astronomy
18 p2210 N73-27838
Development, construction, and operation of polarization fourier spectrometer for conducting astronomical observations
19 p2300 N73-28492
History, organization, and functions of Vatican astronomical observatory
22 p2714 N73-31724

**ASTRONOMICAL TELESCOPES**
NT APOLLO TELESCOPE MOUNT
NT HELIOMETERS
NT PYROHELIOMETERS
NT SPECTROSCOPIC TELESCOPES
NT STRATOSCOPE TELESCOPES
NT X RAY TELESCOPES
Thermal control of scientific instrument package in large scale telescope
05 p0608 N73-14946
Analytical methods for estimating circumferential and longitudinal temperature distributions in large space telescope
[NASA-TN-D-7174] 07 p0855 N73-16931
Development of Large Space Telescope for conducting astronomical observations from unmanned satellites and analysis of constraints and tradeoffs during design phase - Vol. I
[NASA-TM-X-64726-VOL-1] 09 p1035 N73-18449
Mission description and system design for Large Space Telescope used on unmanned satellites - Vol. 2
[NASA-TM-X-64726-VOL-2] 09 p1036 N73-18450
Development and characteristics of optical telescope assembly system for Large Space Telescope based on mission-related and optical parameters - Vol. 3
[NASA-TM-X-64726-VOL-3] 09 p1036 N73-18451
Combination nuclear emulsion/spark chamber gamma ray telescope study of galactic center region
[NASA-CR-130863] 09 p1081 N73-18819
European Southern Observatory in Chile including research projects, equipment, and management for 1971
15 p1763 N73-24282
Design details of photoheliograph thermal concepts
[NASA-CR-124255] 15 p1787 N73-24492
HEAO-C X ray focusing telescopes for spectrometric and polarization studies
17 p2085 N73-26872
HEAO-C soft X ray telescope
17 p2085 N73-26873
Catalog of ultraviolet stellar observations using celescope on OAO 2
[NASA-CR-133259] 17 p2088 N73-26889
Analysis of dynamics of thin primary mirrors for large astronomical telescopes
[NASA-TM-X-2790] 17 p2090 N73-26911
LST phase A design update study
[NASA-TM-X-64763] 19 p2300 N73-28494
Rocket infrared multicolor observations of interplanetary medium H II regions and galactic center region, using Cornell liquid helium cooled rocket telescope
19 p2342 N73-28838
Construction and testing of matched pair solar telescopes
[AD-762274] 20 p2420 N73-29444
Time series on optical pulsar candidates
20 p2469 N73-29831
Analysis of interferometric characteristics of stellar figure sensor for orbiting astronomical telescope
[NASA-CR-132795] 22 p2673 N73-31408
Gamma ray telescope using double Compton process and measuring extraterrestrial gamma ray fluxes in energy range 1-10 MeV
[MPI-PAE/EXTRATERR-74] 22 p2674 N73-31421
History, organization, and functions of Vatican astronomical observatory
22 p2714 N73-31724
Kerber profile Schmidt plates uses in optical combinations with applications to cameras
[OPT-01-72] 23 p2794 N73-32352
Evaluation of control laws and actuator locations for control systems applicable to deformable astronomical telescope mirrors
[NASA-TN-D-7276] 24 p2900 N73-33148
CIT photoheliograph functional verification unit test in Big Bear Solar Observatory vacuum chamber
[NASA-CR-124455] 24 p2925 N73-33364

**ASTRONOMY**
NT INFRARED ASTRONOMY
NT RADAR ASTRONOMY
NT RADIO ASTRONOMY
NT SPACEBORNE ASTRONOMY
NT X RAY ASTRONOMY
Soviet bloc research in astronomy, meteorology, oceanography, geology, and space science - 3 Oct. 1972
[JPRS-57162] 01 p0104 N73-10856
USSR space program accomplishments in fields of geophysics, astronomy, meteorology, oceanography, upper atmosphere, and space sciences
[JPRS-57229] 01 p0104 N73-10864
Activities of Astronomical Council, USSR
[AD-746016] 02 p0232 N73-11884
Soviet Bloc research in astronomy, meteorology, oceanography, geology, and space science - 1 Nov. 1972
[JPRS-57392] 03 p0355 N73-12895
USSR research projects in geosphysics, astronomy, and space - No. 288
[JPRS-57505] 03 p0357 N73-12906
Contributions of astronomy to understanding solar system and initiating manned space flight and exploration
04 p0471 N73-13837
Soviet research on astronomy, meteorology, oceanography, and space science - 27 Dec. 1972
[JPRS-57858] 06 p0717 N73-15856
Soviet research in meteorology, geophysics, space, and astronomy
[JPRS-57989] 07 p0843 N73-16829
Soviet bloc research in astromony, meteorology, oceanography, geology, and space science - 31 Jan. 1973
[JPRS-58112] 08 p0961 N73-17860
Soviet Bloc research in astronomy, meteorology, oceanography, geology, and space science - Feb. 1973
[JPRS-58218] 09 p1085 N73-18851
Soviet Bloc research in astronomy, meteorology, oceanography, geology, and space science
[JPRS-58333] 09 p1085 N73-18852
Particles and fields, upper atmosphere physics, and solar and stellar astronomy
[NASA-CR-130197] 11 p1285 N73-20424
Abstracts of articles on Soviet Bloc research in earth and space sciences
[JPRS-58437] 11 p1338 N73-20860
Research progress in astronomy, space, radio, engineering, and nuclear physics
[NP-19468] 11 p1352 N73-20979
In-depth analysis of UV instruments, nondeployed solar payload, and on-orbit access
[NASA-CR-131892] 13 p1576 N73-22770
Research activities of ESO
13 p1576 N73-22773
Composition and physical characteristics of meteorites and meteoritic craters
[SAO-909-42] 14 p1704 N73-23827
Astronomical studies at Hale Observatories
14 p1704 N73-23828
Research on geodesy, topography, cartography, photography, astronomy, and chemistry
[AD-758290] 15 p1788 N73-24500
Influence of Arabian astronomy on Europe
15 p1829 N73-24828
Holography and optical filtering techniques for structural analysis, material tests, and astronomical observation - conference
[NASA-SP-299] 16 p1920 N73-25540
USSR research projects in geophysics, astronomy, and aerospace subjects - May 1973
[JPRS-59136] 17 p2024 N73-26379
Soviet research in meteorology, oceanography, upper atmosphere, astronomy, and space
[JPRS-59002] 18 p2196 N73-27729
Soviet-bloc research in geophysics, astronomy, and space
[JPRS-59490] 18 p2196 N73-27730
Soviet-bloc research in geophysics, astronomy, and space research
[JPRS-59390] 18 p2196 N73-27733
Astronomical and astrophysical research reports
[PB-219589/9] 18 p2198 N73-27747
Directional low energy gamma ray detector for gamma ray astronomy
[NASA-TM-X-70449] 20 p2419 N73-29442
Soviet bloc research in astronomy, meteorology, oceanography and space science Aug. 1973
[JPRS-59673] 20 p2473 N73-29861
Soviet block research in astronomy meteorology, geology, and space science Aug. 1973
[JPRS-59789] 20 p2473 N73-29863
Soviet bloc research in astronomy, meteorology, oceanography, geology, and space science - September 1973
[JPRS-60035] 22 p2716 N73-31740
Soviet research in meteorology, oceanography, geophysics, astronomy, and space
[JPRS-60165] 23 p2846 N73-32744

**ASTROPHYSICS**
NT SOLAR PHYSICS
Nuclear research, including reaction mechanisms, nuclear astrophysics, isobaric analog, and heavy ions studies
[ANU-P-542] 03 p0339 N73-12769
Conference on stellar chromospheres and their compositions
[NASA-SP-317] 04 p0465 N73-13792

Summary of physical and theoretical work on stellar chromospheres
04 p0466 N73-13800
Astrophysical flow problems, planetary atmospheres, and space radiation
04 p0468 N73-13814
Euler equations of motion of relativistic, perfect-fluid hydrodynamics, and potential application to stellar stability
07 p0840 N73-16806
History of physics with emphasis on nuclear physics and astrophysics
[NASA-TT-F-14670] 07 p0843 N73-16827
Research progress in accelerator and ion source development, detection and computer systems, and various nuclear physics projects
09 p1101 N73-18986
Charged particle transport in turbulent astrophysical plasmas
12 p1432 N73-21606
General conference of European Physical Society on trends in physics
[AD-757261] 14 p1693 N73-23738
Laboratory astrophysics research on defense applications of gas ionization, electron scattering, plasmas, and line broadening
[AD-757721] 14 p1695 N73-23753
Equipment and mission of Astrophysics Institute in Tadzhikistan relative to radar tracking and wind velocity measurement
[AD-756100] 14 p1706 N73-23848
Detailed information of physics subfields and interface areas
[NASA-CR-132050] 15 p1813 N73-24693
Electromagnetic and gravitational wave interaction of black holes
15 p1829 N73-24824
Israel-Carter conjecture of black hole physics and baryon number
15 p1829 N73-24825
Atomic and gas dynamical processes in astrophysical plasmas
17 p2066 N73-26719
Astronomical and astrophysical research reports
[PB-219589/9] 18 p2198 N73-27747
Structure and physics of solar and stellar atmosphere including physical processes in nonstationary stars
[NASA-TT-F-760] 20 p2470 N73-29840
Application of very long-baseline interferometry at Smithsonian Astrophysical Laboratory to geophysical measurements of earth
[NASA-CR-135493] 22 p2666 N73-31365
Space applications research in astronomy and earth physics
[NASA-SP-331] 22 p2732 N73-31867
High energy astrophysics and solar astronomy
22 p2732 N73-31868

**ASYMMETRY**
Calculation of interplanetary magnetic field induced asymmetries in forward stagnation region of solar-wind magnetospheric interaction
07 p0838 N73-16792

**ASYMPTOTES**
Asymptotic behavior of kinetic solar wind model
[AERONOMICA-ACTA-A-108] 09 p1080 N73-18812
Error formulas and asymptotes for vocabulary size determination for one, two, and three parameter rank distribution
[NASA-CR-132023] 14 p1683 N73-23659

**ASYMPTOTIC METHODS**
Asymptotic solution of two-dimensional flow of perfect gas past blunt body at given Mach number
[AD-747545] 03 p0287 N73-12327
Rearrangement collision leading to formation of highly excited hydrogenlike states
[NASA-TM-X-66184] 08 p0945 N73-17743
Solution of temperature distribution in hollow cylinder for asymptotic regime and variable heat conductivity coefficient
[AD-755251] 12 p1465 N73-21872
Asymptotic methods for deriving transient backscattered signatures from artificial satellites
[AD-758245] 15 p1751 N73-24192
Korteweg-deVries equation for studying effect of Landau damping on nonlinear ion acoustic waves
[IPPJ-155] 16 p1949 N73-25775
Solution of laminar natural convection flows of Newtonian fluid in rectangular enclosures by asymptotic expansion
18 p2128 N73-27198
Application of matched asymptotic expansions to lunar and interplanetary trajectories
[NASA-CR-2255] 18 p2197 N73-27738
Derivations of second-order asymptotic boundary value solutions for lunar and interplanetary trajectories
[NASA-CR-2256] 19 p2343 N73-28845
Asymptotic expansion analysis of jet entrainment in incompressible cross flow
24 p2902 N73-33166
Asymptotic expansion analysis of shock supported arrhenius reactions and ignition delay
24 p2903 N73-33172

**ATHENA ROCKET VEHICLE**
Meteorological and ballistics data for launching of Athena rocket flight 134, vehicle H-0043
[AD-749436] 04 p0445 N73-13633
Meteorological data gathered for launching of Athena flight 135
[AD-754557] 11 p1314 N73-20667
Meteorological and ballistics data for launching of Athena rocket vehicle, flight 137, vehicle H-005
[AD-755776] 12 p1424 N73-21542
Meteorological and ballistics data for launching of Athena rocket vehicle, flight 136, vehicle H-009
[AD-755779] 12 p1424 N73-21547
Meteorological and ballistics data for launching of Athena rocket flight 138, vehicle H-008
[AD-758866] 15 p1807 N73-24645
Meteorological and ballistics data for launching Athena rocket flight 139, vehicle H-006
[AD-758867] 15 p1807 N73-24646
Meteorological and ballistic data gathered for launching Athena flight 140
[AD-762160] 19 p2317 N73-28639

**ATHEROSCLEROSIS**
U ARTERIOSCLEROSIS

**ATHLETES**
Influence of time zones on physiological organs and systems and performance of athlete
[NASA-TT-F-14632] 04 p0383 N73-13116

**ATHODYDS**
U RAMJET ENGINES

**ATLANTIC AIRCRAFT**
U BREGUET 1150 AIRCRAFT

**ATLANTIC OCEAN**
Analysis of subbottom acoustic reflection profiles along track line from Monrovia, Liberia to Lesser Antilles
[PB-209872] 01 p0053 N73-10427
Tables on Atlantic tropical cyclone strike probabilities - 24 hour movement
[AD-744916] 01 p0076 N73-10630
Tables on Atlantic tropical cyclone strike probabilities - 48 hour movement
[AD-744917] 01 p0076 N73-10631
Probabilities of forecasting future movement of North Atlantic tropical cyclones
[AD-744918] 01 p0076 N73-10632
ERTS-1 imagery of French shoreline along the Atlantic Ocean and English Channel
[E72-10211] 02 p0161 N73-11306
ERTS-1 imagery of coastal marshland, tidal flats, and littoral transport in French Atlantic waters
[E72-10251] 03 p0289 N73-12351
Descriptions of earthquakes and location of epicenters in US, Alaska, Panama Canal Zone, and Virgin Islands during 1970
03 p0294 N73-12393
Eastern Atlantic continental margin study of area between Port Elizabeth and Congo River
[PB-211392] 05 p0541 N73-14399
Cloud cover maps for North America and western North Atlantic for August, 1972
[AD-749128] 05 p0575 N73-14678
Geothermal data from deep water and bottom sediment measurements in Atlantic and Pacific Oceans
[AD-749983] 06 p0669 N73-15441
Computations of seasonal variations in internal waves and tidal phenomena in northern Atlantic Ocean
[AD-750842] 06 p0670 N73-15452
Mean monthly hurricane heat potential and sea surface temperature changes associated with storm passage for North Atlantic and North Pacific Oceans
[AD-751590] 07 p0790 N73-16429
Small scale interaction between ocean and atmosphere [heat flow, vapor, and momentum]
[AD-751415] 07 p0796 N73-16474
Measurement of diurnal heat budget in tropical Atlantic surface layers
07 p0857 N73-16953
Investigation of phytoplankton populations in waters along eastern coast of US using ERTS-1 imagery and surface measurements
[E73-10097] 08 p0902 N73-17308
ERTS-1 imagery of marshlands and turbid waters of French Atlantic littoral
[E73-10341] 10 p1147 N73-19340
Optical properties of sea water in Atlantic, Pacific, and Caribbean
[AD-753474] 11 p1290 N73-20470
Development of computer program to analyze air traffic in North Atlantic to show zone traffic at specified instants
[AD-755910] 12 p1426 N73-21557
Scenario forecasting of likely air passenger trends to 1976 over North Atlantic routes
[REPT-72-02326] 13 p1472 N73-21918
ERTS-1 imagery of marshes, wetlands, and turbid waters in French Atlantic littoral
[E73-10548] 13 p1518 N73-22307
Total electron content of ionosphere with emphasis on North Atlantic region
[AGARD-AG-166] 13 p1524 N73-22350
Data obtained in Bahama channels and Northwestern Atlantic ocean during Deep Ocean Optical Measurement program
[AD-757332] 14 p1665 N73-23511
Surface gravity and satellite derived gravimetric geoid of North America, North Atlantic, Eurasia, and Australia
[NASA-TM-X-66238] 15 p1778 N73-24413
Physical properties and suspended matter of surface waters in southeastern Atlantic Ocean
[PB-214813/8] 15 p1784 N73-24467
Preparation of equipment and procedures for program to perform broadband noise measurements at sea
[AD-759033] 16 p1877 N73-25195
Large scale interaction of atmospheric circulation with Atlantic Ocean on 30 deg W meridian between April and June 1970
[NLL-M-22854-[5828.4F]] 16 p1894 N73-25321
Temperature anomaly studies along 30 deg W meridian of Atlantic Ocean
[NLL-M-22849-[5828.4F]] 16 p1894 N73-25323
Measurement of chlorophyll and plankton populations of shelf and slope waters off northeastern United States
[E73-10683] 16 p1901 N73-25378
Daily tidal current tables for stations along Atlantic coast of North America - 1973
16 p1904 N73-25403
Effect of general atmospheric circulation of large scale and persistent weather features of Atlantic-Eurasian sector of hemisphere in 1968 to 1970
[NLL-M-22853-[5828.4F]] 16 p1936 N73-25663
Use of ERTS-1 data to apply marine station data to study of productivity along Eastern Self Expanded Waters of US
[E73-10778] 18 p2135 N73-27254
Coordination of ground truth and basic altimeter data processing requirements for North Atlantic test area
[E73-10811] 18 p2139 N73-27286
Parameters affecting design of AEROSAT navigation satellite for aircraft communication and air traffic control
18 p2201 N73-27768
Assessment of ERTS-1 imagery for mapping geologic features of Gaspe Peninsula, Quebec and determination of lithologic lineaments
[PAPER-G28] 19 p2267 N73-28259
Analysis of lineaments and fault traces in Atlantic Coastal Plain of southern Maryland using ERTS-1 imagery
[PAPER-G29] 19 p2267 N73-28260
Analysis of acoustic volume scattering in Bermuda Ocean to show daily variability and diurnal variations
[AD-761976] 19 p2296 N73-28465
Analysis of long term variations in water surface temperature of North Atlantic Ocean
[NLL-M-23016-[5828.4F]] 20 p2390 N73-29200
Random errors of marine meteorological observations by ships in tropical Atlantic Ocean
20 p2447 N73-29659
Analysis of ways and sources for transfer of dust precipitating over Atlantic Ocean
[TT-72-50018] 21 p2541 N73-30376
Statistical analysis of large scale fluctuations in water surface temperature of North Atlantic Ocean
21 p2572 N73-30614

**ATLAS CENTAUR LAUNCH VEHICLE**
Data and design information for Atlas Centaur launched configuration of Tracking and Data Relay Satellite system - Vol. 3
[NASA-CR-130221] 13 p1579 N73-22801
Specifications for Atlas/Centaur 30 Pioneer G Mission
[NASA-TM-X-69267] 16 p1964 N73-25885

**ATLAS LAUNCH VEHICLES**
NT ATLAS CENTAUR LAUNCH VEHICLE
Postflight analysis of Atlas/Centaur - 29 and Intelsat 4 launch and orbit establishment
[NASA-TM-X-68649] 01 p0102 N73-10845

**ATMOSPHERE EXPLORER B**
U EXPLORER 32 SATELLITE

**ATMOSPHERES**
Angular distribution of outgoing shortwave radiation intensity in atmosphere with continuous cloud cover
[AD-753975] 10 p1157 N73-19417

**ATMOSPHERIC ABSORPTION**
U ATMOSPHERIC ATTENUATION

**ATMOSPHERIC ATTENUATION**
NT AURORAL ABSORPTION
Absorption of 4 to 6 mm wavelength band in atmosphere from zenith attenuation measurements
[AD-745951] 02 p0168 N73-11363
Attenuation of carbon dioxide laser beams in atmosphere at various frequencies and method for calculating absorption coefficients from measured data
[FOA-2-A-2542-E3/E4/E6] 02 p0181 N73-11465
Tables for quantitative atmospheric attenuation of 97 HF and DF laser lines and 10 atmospheric models
[AD-747010] 03 p0310 N73-12534
Influence of atmospheric conditions on remote image transfer and interpretation as determined by laboratory measurements
05 p0537 N73-14370

Scattering and absorption effects in atmospheric transmission of infrared radiation
[AD-750084] 05 p0542 N73-14410
Radiation attenuation in atmosphere by water vapor
[NLL-M-20840-[5828.4F]] 05 p0569 N73-14622
Effect of sea state and atmospheric parameters on satellite altimeter performance
06 p0662 N73-15372
Temporal spectra of fluctuations in atmospherically degraded spherical waves
[AD-751304] 07 p0807 N73-16551
Attenuation of nitric oxide dissociation in mesosphere and stratosphere
[PSU-IRL-SCI-407] 08 p0917 N73-17518
Development of model for analyzing propagation of weak normal shock wave through turbulent atmosphere and application to sonic boom characteristics
[NRC-12981] 09 p0983 N73-18028
Dissociation of nitric oxide in mesosphere and stratosphere by attenuation
[AERONOMICA-ACTA-A-112] 09 p1027 N73-18384
Technique for determining atmospheric transmittance of coherent light between two points in terrestrial atmosphere for selected laser frequencies
[AD-753075] 09 p1030 N73-18412
Light and infrared radiation propagation and absorption in atmosphere
[AD-753974] 10 p1158 N73-19418
Analysis of shock wave propagation in direction of decreasing air density following aerial explosion
[AD-755173] 12 p1465 N73-21873
Atmospheric effects on laser propagation and impact on eye safety
[AD-755405] 13 p1485 N73-22044
Dispersion of light intensity logarithm along axis of laser beam propagating in atmosphere
[AD-756094] 13 p1539 N73-22470
Analysis of atmospheric transmission properties of 1.06 microns radiation using neodymium laser
[AD-757249] 14 p1672 N73-23572
Approximate methods for solving spherical transfer equation in spherical case
[AD-759392] 16 p1910 N73-25453
General expression for short term average optical beam spread of initially coherent beam wave propagating in turbulent medium
[AD-759804] 16 p1925 N73-25573
Conference on atmospheric attenuation and rainfall effects on ultrahigh frequency telecommunication systems
[AGARD-CP-107] 17 p1994 N73-26121
Multiple scattering and attenuation of radio signals caused by rainfall
17 p1994 N73-26122
Ultrahigh frequency coherent radio signal transmission for differential phase shift measurements due to vapor and oxygen absorption lines
17 p1995 N73-26131
Restoration of atmospherically degraded laser beam and definition of isoplanatic patch size
[AD-760548] 18 p2158 N73-27437
Obtaining absolute target reflectances by correcting ERTS-1 radiance measurements for variable target irradiance, atmospheric attenuation, and atmospheric backscatter
[PAPER-13] 19 p2277 N73-28325
Analysis of absorption of solar radiation by atmospheric water vapor to determine effects of various atmospheric parameters
20 p2401 N73-29294
Pyranometer measurements of direct and total solar radiation in crops and semiempirical relations
20 p2404 N73-29319
Appropriate line profiles for radiation modeling in detection of atmospheric pollutants
[NASA-CR-132303] 20 p2448 N73-29672
Application of radio astronomical methods for determining attenuation and radio emission of rain from cumulonimbus clouds
21 p2570 N73-30594
Analysis of atmospheric attenuation of circularly polarized electromagnetic radiation from meteorological radar
21 p2570 N73-30595
Characteristics of meteorological radar operating in millimeter wavelength range and methods for improving radar performance
21 p2572 N73-30607
Atmospheric attenuation of sound transmissions in air
[AD-764286] 22 p2675 N73-31428
Water vapor absorption by highly attenuated CO laser lines
[AD-764376] 22 p2682 N73-31485
Atmospheric infrared transmission spectral analysis discussing computed and measured data, and absorption due to atmospheric components
[BMVG-FBWT-73-11] 23 p2787 N73-32297
Atmospheric attenuation of CO2 laser radiation measured by pyroelectric detection noting fog absorption and optical communication application
[LCR-DR-1-72-67/1/R] 23 p2801 N73-32404
Attenuation of solar spectral intensity by pollution in boundary layer of New Haven, Connecticut atmosphere
23 p2833 N73-32641
Solution to equation of radiative transfer for homogeneous atmosphere bounded by perfect specular reflector
[AD-764619] 23 p2857 N73-32830
Thermal blooming of carbon dioxide laser during atmospheric propagation
[AD-765520] 24 p2932 N73-33418

**ATMOSPHERIC BOUNDARY LAYER**

Hydrodynamics of surface layer of atmosphere and micrometeorological processes over flat homogeneous surface
[NLL-M-22574-[5828.4F]] 01 p0072 N73-10593
Simulation of alternate expressions for meteorological phenomena of atmospheric boundary layer - tables
[AD-746247] 02 p0205 N73-11665
Analysis of mean distribution maps for altitude and temperature of tropopause over Northern Hemisphere in Jan. and July between 1957 and 1965
04 p0442 N73-13607
Effects of acoustic gravity wave diffusion on atmospheric boundaries
05 p0508 N73-14136
Ejector-driven multiple jet wind tunnel for simulation of flows in planetary boundary layer
[AD-748903] 05 p0527 N73-14289
Parameterization of atmospheric boundary layer
05 p0574 N73-14664
Abstracts on remote sensing of turbulence and waves in planetary boundary layer
[AD-751110] 07 p0816 N73-16618
Effects of solar activity and geocoronal emissions on atmospheric boundary layer as observed by Prognoz satellite
12 p1461 N73-21840
Structure and dynamics of horizontal roll vortices in planetary boundary layer
15 p1771 N73-24341
Multilevel atmospheric prediction model based on primtiive equations of moiton
[DM-8] 16 p1938 N73-25681
Meteorological processes and FM-CW radar soundings in boundary layer
[AD-759019] 16 p1939 N73-25695
Truncation error dependence on computational diffusion coefficient in atmospheric boundary layer models
[AD-760122] 17 p2029 N73-26420
Two dimensional nonsteady model of nocturnal flow of stable atmosphere over wide, warm, rough city
20 p2441 N73-29604
Theoretical study of thermal structure and dispersion in polluted urban atmosphere
21 p2568 N73-30579
Study of low level boundary layer jet streams for predicting dangerous atmospheric conditions
21 p2573 N73-30622
Dynamic forecast model for studying moisture variation in planetary boundary layer
[PB-220532/6] 21 p2575 N73-30635
Monitoring of air breathing engine exhaust gas emissions, pollutants, and atmospheric air pollution propagation
[DLR-MITT-72-14-PT-1] 22 p2694 N73-31584

**ATMOSPHERIC CHEMISTRY**

Neutral and ion chemistry of D and E regions symposium papers
[AD-749780] 06 p0668 N73-15430
Influence of electron beam irradiation on upper atmospheric chemistry and physics
[AD-753707] 09 p1033 N73-18431
Chemical dynamic model of moist Martian atmosphere
[NASA-CR-130799] 09 p1082 N73-18825
Vapor phase chemistry for producing hydrated ions in upper atmosphere
[AD-753940] 10 p1157 N73-19411
Method of measuring amount of carbon monoxide by oxidizing agents to yield carbon dioxide for air pollution control
[NLL-RTS-7573] 11 p1274 N73-20340
Reaction rate data for atmospheric chemistry, metal atom oxidation, and nuclear fireball
[AD-756674] 13 p1488 N73-22063
Role of biosphere in regulating chemical processes in atmosphere
[AERONOMICA-ACTA-A-116] 13 p1551 N73-22569
Photochemical mechanisms of ozone and energy budget in atmosphere between 10 and 100 km
18 p2133 N73-27233
Development of numerical method for computing transmission functions of atmospheric gases based on exact frequency integration using structure of absorption spectrum
20 p2401 N73-29296
Stratospheric and tropospheric composition and chemical reactions
[AP-12] 21 p2539 N73-30357

**ATMOSPHERIC CIRCULATION**

Atmospheric effects on laser beam propagation
[AD-746053] 01 p0066 N73-10544
Long-term tendencies in atmospheric circulation variations for deveoping long-range hydrometeorological forecasting
[NLL-M-22333-[5828.4F]] 01 p0072 N73-10592
Global distributions of mean January surface wind stress, diabatic heating rate, and rate of moisture addition as simulated in 30-day integration with atmospheric general circulation model
[AD-745752] 01 p0077 N73-10640
Mesospheric circulation and noctilucent clouds
[NASA-TT-F-14712] 01 p0105 N73-10866
Circulation pattern over British Isles and system classification from 1861 to 1971
[MET-O-845B] 02 p0204 N73-11648
Methods for determining atmospheric circulation from satellite pictures
02 p0204 N73-11649
Energy transfers and transformations in atmosphere and chemical tracers of atmospheric circulation
[TID-25731] 03 p0295 N73-12410
Transport of energy over turbulence spectrum of free atmosphere
[AD-747728] 03 p0299 N73-12438
Time series and probability density function analyses of hypothesis that organized motion exists in air flow above naturally occurring water waves
[AD-749045] 04 p0408 N73-13328
Momentum, energy, and mass budgets of stratosphere
[COO-2195-2] 04 p0415 N73-13385
Model for stationary motion of atmosphere in equatorial latitudes based on nonlinear system of equations of hydrothermodynamics
04 p0442 N73-13604
Middle latitude anticyclone vertical atmospheric circulation heat sources and sinks, and torques
[REPT-7/1972] 04 p0444 N73-13625
Mathematical model for acoustic gravity wave excitations moving air masses
05 p0508 N73-14135
Parameterization and its role in atmospheric modeling
[GARP-PUBL-8] 05 p0573 N73-14654
Parameterization in atmospheric circulation models
05 p0573 N73-14655
Parameterization of clouds in numerical circulation model
05 p0573 N73-14657
Two dimensional eddy viscosity coefficients in atmospheric motion noting parameterization of clear air turbulence
05 p0573 N73-14658
Parameterization of gravity waves noting upper boundary conditions
05 p0573 N73-14659
Mesoscale processes in circulation models noting parameterization
05 p0573 N73-14660
Parameterization of turbulent boundary layer in atmospheric circulation model
05 p0573 N73-14661
Influence of ocean on atmospheric circulation noting role of heat, momentum, and water vapor transfer
05 p0573 N73-14662
Energy balance equations for parameterization of hydrological processes effecting atmospheric circulation
05 p0573 N73-14663
Parameterization of near surface mesoscale circulation
05 p0574 N73-14665
Statistical correlations between clear air turbulence and macrosynoptic processes in troposphere and stratosphere
[AD-750514] 06 p0670 N73-15451
Meteorological ground level maps of Northern Hemisphere for fourth quarter in 1971
[QR-4-PT-4] 06 p0691 N73-15628
Model of Venus atmospheric composition, temperature, and circulation based on Mariner 5 and Venera 4, 5, 6, and 7 data
[NASA-TM-X-66140] 06 p0719 N73-15865
Boundary layer approach to analysis of atmospheric motion over surface obstruction
[NASA-CR-2182] 07 p0769 N73-16244
Numerical simulation of air flow in atmospheric layer over inhomogeneous surface considering wind, temperature, shear stress, and turbulent energy
[AD-751589] 07 p0795 N73-16462
Numerical analysis of ocean circulation effects on transients in atmospheric circulation
[AD-751637] 07 p0796 N73-16470
Atmospheric circulation and temperature effects on stratospheric ozone during winter storm period
[AD-751211] 07 p0797 N73-16479
Abstracts on remote sensing of turbulence and waves in planetary boundary layer
[AD-751110] 07 p0816 N73-16618
Effect of solar magnetic sector structure on stratospheric circulation
[NASA-CR-130551] 08 p0916 N73-17505
Divergence at 200 mb level in Southern Hemisphere atmospheric circulation inferred from EOLE data
08 p0918 N73-17523

Atmospheric ozone as circulation tracer in upper troposphere and lower stratosphere
08 p0972 N73-17940
Analysis of energy conservation constraints on circulation of Southern Hemisphere atmosphere and oceans based on radiant, latent, and sensible heat energy transfers
[METEOROL-STUDY-26] 09 p1027 N73-18387
Ellipticity condition of three dimensional partial differential equation as turbulence criterion in atmospheric motion
[AD-746624] 09 p1032 N73-18424
Global response of atmosphere to persistent anomalous pool of warm sea surface temperatures in extratropical Pacific Ocean
[NASA-CR-130179] 10 p1154 N73-19391
Solution for steady state motion of atmosphere about rotating earth
[AD-754248] 10 p1157 N73-19414
Observations of kinematic and thermodynamic fields over Barbados
10 p1180 N73-19596
Relationship between surface temperature anomalies in European USSR and seasonal variations of stratospheric circulation
[NLL-M-22851-[5828.4F]] 11 p1274 N73-20336
Fluctuations of zonal atmospheric circulation in Northern Hemisphere in first half of century
[NLL-M-22855-[5828.4F]] 11 p1274 N73-20337
Mathematical and physical principles for computational schemes atmospheric model
[NASA-CR-131531] 12 p1420 N73-21508
Dynamics of lower thermosphere through comparison of optical observations of motions of vapor trails with radar observations of ionized meteor trails
[NASA-CR-131645] 12 p1420 N73-21509
Computer simulation of global atmospheric circulation in climatological research
[P-4933] 12 p1421 N73-21520
Dynamics of neutral atmosphere in 200 to 500 km height region at low latitudes from incoherent scattering measurements
13 p1513 N73-22263
Research on atmospheric eddy transport
[AD-757692] 14 p1663 N73-23496
Nimbus 3 infrared spectrometric data on global ozone distribution in correlation with atmospheric circulation
[COO-1340-30] 15 p1781 N73-24435
Long fetch technique for simulating neutral atmospheric layers in wind tunnels
[AD-758888] 15 p1784 N73-24462
Automatic methods for measuring cloud motions from digital brightness data from geosynchronous satellites
[AD-757814] 15 p1806 N73-24640
Circulation model for feasibility of modifying earth surface climate at middle and high northern latitudes
[AD-757795] 15 p1807 N73-24641
Large scale interaction of atmospheric circulation with Atlantic Ocean on 30 deg W meridian between April and June 1970
[NLL-M-22854-[5828.4F]] 16 p1894 N73-25321
Temperature anomaly studies along 30 deg W meridian of Atlantic Ocean
[NLL-M-22849-[5828.4F]] 16 p1894 N73-25323
Atmospheric mesostructure model for clear air turbulence
[AD-759787] 16 p1909 N73-25448
Biennial periodicity of blocking systems in atmosphere over Europe-Atlantic region considering cyclonic circulation
[NLL-M-22831-[5828.4F]] 16 p1936 N73-25661
Synoptic meteorology of large dust cloud over west coast of Africa
[NLL-M-22850-[5828.4F]] 16 p1936 N73-25662
Effect of general atmospheric circulation of large scale and persistent weather features of Atlantic-Eurasian sector of hemisphere in 1968 to 1970
[NLL-M-22853-[5828.4F]] 16 p1936 N73-25663
Stability analyses of idealized atmosphere and perfect gas blowing over inviscid liquid
17 p2012 N73-26269
Radar measurement of air mass circulation and meteor trail drift in upper atmosphere during IQSY
[NASA-TT-F-744] 17 p2023 N73-26363
Radar observation of air mass circulation in upper atmosphere during IQSY
17 p2023 N73-26364
Parameterization of meteorological factors for unusual atmospheric circulation in Northern Hemisphere in January 1963
17 p2056 N73-26631
Periodic spectral solutions of combined system of equations of planetary dynamics of atmosphere and hydrosphere
[AD-759857] 17 p2058 N73-26646
Model of atmospheric motion for long-term weather forecasting
[AD-759877] 17 p2058 N73-26651
Nonlinear temperature and vorticity equations for studying convective motions of 4-day zonal circulation of upper Venus atmosphere
17 p2080 N73-26828
Plasma and neutral atmospheric motion in earths polar ionosphere
18 p2132 N73-27229
Atmospheric wind fields and circulation effects on Pacific Ocean hydrologic regime
[TT-70-50129] 18 p2171 N73-27538
Remote determination profiles of atmospheric structure constants and wind velocity along line-of-sight path by statistical inversion procedure
[AD-760805] 18 p2173 N73-27552
Dispersion of tracers in atmosphere from planetary boundary layer to turbopause
[AD-760694] 18 p2174 N73-27559
Abstracts of papers concerning various aspects of meteorology
[AD-760753] 18 p2174 N73-27562
Analysis of ERTS-1 imagery to determine meteorological content with emphasis on mesoscale effects of Great Lakes and air pollution dispersion
[PAPER-W17] 19 p2272 N73-28294
Numerical solution to boundary value problems of hydrodynamic forecasting and atmospheric circulation
[AD-761574] 19 p2317 N73-28640
Winter atmospheric circulation over European sector of Northern Hemisphere in twentieth century
[NLL-M-2337-[5828.4F]] 20 p2391 N73-29205
Exact time-independent solution for rotation of atmosphere about earth
[AD-762486] 20 p2414 N73-29402
Synopticostatistical, numerical, and laboratory procedures for studying dynamics of atmospheric circulation in planetary atmospheres including earth
[TT-70-50052] 20 p2442 N73-29615
Theoretical model for studying circulation and climate of atmosphere
20 p2442 N73-29616
Orthogonal functional analysis of unsteadiness in atmospheric circulation
20 p2442 N73-29617
Solutions to quasisteady problems of dynamic weather forecasting
20 p2442 N73-29618
Statistical properties of atmospheric circulation particularly geopotential fields on global basis
20 p2442 N73-29619
Integral characteristics and models of general atmospheric circulation
20 p2443 N73-29621
Principles of energy transformation in atmospheric circulation
20 p2443 N73-29622
Radiation equilibrium and interaction problems of atmospheric circulation
20 p2443 N73-29623
Nature of zonal and meridional circulation components of troposphere and stratosphere of Northern Hemisphere
20 p2443 N73-29626
Atmospheric ozone transport by atmospheric circulation and vertical air currents
20 p2443 N73-29627
Jet streams for studying kinetics of atmospheric circulation
20 p2444 N73-29628
Circulation structure of stratosphere and troposphere over Southern Hemisphere as determined by rocket soundings
20 p2444 N73-29629
Rocket sounding of two year cyclic variations of zonal wind components in stratosphere and mesosphere up to 100 km
20 p2444 N73-29631
Effect of orography on climatic wind distribution and geopotential fields
20 p2444 N73-29632
Atmospheric circulation effects on precipitation and temperature regimes of USSR and Northern Hemisphere
20 p2444 N73-29633
Analysis of long term weather varjations, climate changes, and atmospheric circulation
20 p2444 N73-29634
Analysis of epochal variations in atmospheric circulation of Northern Hemisphere, atmosphere, and hydrosphere for making long and extra long range hydrometeorological forecasts
20 p2444 N73-29635
Utilization of two rotating vessels to model and analyze certain schemes of atmospheric circulation and heat exchange
20 p2445 N73-29638
Atmospheric circulation of planetary atmospheres
20 p2445 N73-29639
Power spectral analysis of atmospheric circulation types
20 p2445 N73-29640
Atmospheric circulation for long range weather forecasts
20 p2445 N73-29641
Influence of circulation poles and anticyclones on synopticoclimatology
20 p2445 N73-29643
Radioactive tracers for studying atmospheric circulation and synoptic conditions
20 p2446 N73-29644
Atmospheric models for studying typhoon and thundercloud processes
20 p2446 N73-29645
Improved numerical models of mesoscale and small scale effects of atmospheric motion which influence global weather
[AD-762584] 20 p2451 N73-29698
Numerical experiments for solving complete equations of hydrodynamics
[AD-763143] 21 p2539 N73-30339
Three basic forms of cyclonic cloud vortices to trace spirals
[AD-763170] 21 p2540 N73-30363
Analysis of ways and sources for transfer of dust precipitating over Atlantic Ocean
[TT-72-50018] 21 p2541 N73-30376
Predicted weather conditions for USSR during winter of December 1971 through March 1972
[NLL-M-23035-[5828.4F]] 21 p2568 N73-30578
Solar magnetic sector structure related to earth atmospheric circulation during winter
[NASA-CR-133850] 21 p2593 N73-30774
Structure of barotropically unstable disturbances in tropical regions
[AD-764090] 22 p2695 N73-31588
Radiative-conductive heat transfer and circulation of lower Martian atmosphere
[NASA-CR-2318] 23 p2786 N73-32287
Exact solution to nonlinear Euler equations pertaining to problem of thermally stratified compressible fluid motion on rotating sphere with gravitation
[AD-764684] 23 p2788 N73-32308
Feasibility of conducting long-range atmospheric tracer experiments to study transport and diffusion of air pollution plumes
[AD-764893] 23 p2815 N73-32504
Characteristics of constant scaling method for analyzing linear inviscid internal waves in ocean, atmosphere, and experimental tanks
[AD-764579] 24 p2910 N73-33227
Two dimensional time dependent numerical simulation of atmospheric flow over urban area
24 p2911 N73-33235
Mechanism and rates of atmospheric mixing in lower thermosphere including heat input
[NASA-CR-135789] 24 p2920 N73-33321
Sea/land breeze circulation study, using airborne infrared radiation measurements of surface temperature along upper Texas coast
[REPT-36] 24 p2922 N73-33336
Structure of global geopotential fields in connection with quasi-biannual cyclicity in equatorial stratosphere
24 p2947 N73-33533
Balloon sub-system of Eole experiments in Southern Hemisphere lower stratosphere
24 p2948 N73-33547
Numerical weather forecasting noting atmospheric models and circulation
24 p2949 N73-33553
Mathematical model for Northern Hemisphere atmospheric circulation during cold season
[AD-765544] 24 p2950 N73-33562

**ATMOSPHERIC COMPOSITION**
NT ATMOSPHERIC MOISTURE
NT IONOSPHERIC COMPOSITION

Microwave attenuation and neutral gas density profile measurements behind shock waves in air
[AD-745969] 02 p0158 N73-11282
One-dimensional and multi-dimensional inversion techniques for processing remote atmospheric and ionospheric sounding data
[NASA-TM-X-62150] 02 p0196 N73-11585
Mathematical inversion of light scattering data to obtain atmospheric ozone profile
02 p0196 N73-11586
Maximum probability and minimum variance methods for interpreting remote soundings on meteorological structure of atmosphere
02 p0196 N73-11587
Iterative methods and relaxation algorithm for calculating vertical atmospheric structure from noise contaminated infrared spectral measurements
02 p0196 N73-11588
Relaxation method for inverse solution to atmospheric parameters appearing as functions in integrand of radiative transfer equation
02 p0197 N73-11590
Limb radiance inversion using weighting functions and iterative convergence for nonlinear kernel
02 p0197 N73-11591
Optical radar data for probing atmospheric composition and air pollution particulates
02 p0197 N73-11595
Magnetospheric and upper atmospheric physics data obtained during 1971
[AD-746326] 02 p0232 N73-11882
Three-dimensional, two-constituent model for composition characteristics, temperature and mass density of magnetic storm
[NASA-TM-X-66112] 03 p0294 N73-12394
Correlation between solar radiation and monthly and seasonal variations for calculating atmospheric turbidity in Belgium
[PUBL-SER-A-75] 03 p0354 N73-12882

Influence of atmospheric sulfur budget on biosphere
[BNL-16906] 04 p0415 N73-13387
Conference on stellar chromospheres and their compositions
[NASA-SP-317] 04 p0465 N73-13792
Tabulated data on atmospheric ozone density at UCCLE, Belgium, for 1969
[QR-3] 05 p0539 N73-14386
Atmospheric structure of cyclonic and anticyclonic Bora at Split and Zagreb, Yugoslavia
05 p0571 N73-14639
Ozone tables, ozonagrams, and ascent tables for aerological ozone soundings conducted at Hohenpeissenberg, West Germany
[AD-750166] 06 p0670 N73-15446
Daily and monthly meteorological charts for Europe obtained during June, 1972 at Berlin
06 p0691 N73-15629
Daily and monthly meteorological charts for Europe obtained during May, 1972 at Berlin
06 p0692 N73-15631
Development of four-level model of baroclinic atmosphere for predicting geopotential at various isobaric surfaces for Northern Hemisphere
[AD-750496] 06 p0694 N73-15659
Composition, temperature, and optical properties of Jupiter and Saturn atmospheres
[NLL-M-20702-[5828.4F]] 06 p0716 N73-15845
Model of Venus atmospheric composition, temperature, and circulation based on Mariner 5 and Venera 4, 5, 6, and 7 data
[NASA-TM-X-66140] 06 p0719 N73-15865
Diurnal electron content tables obtained at Hawaii during 1971
07 p0789 N73-16419
Radar sounding of magnetospheric instability and atmospheric density using barium release clouds
[AD-751567] 07 p0795 N73-16461
Annual variations of carbon dioxide concentration in Italian and Scandinavian cities
07 p0859 N73-16966
Configuration and requirements for general purpose optical research facility to investigate earth atmosphere from space shuttle orbiter vehicle
[NASA-CR-128732] 08 p0893 N73-17226
Aerobee mass spectrometer data on neutral gas composition of Arctic thermosphere
08 p0899 N73-17282
Derivation of empirical global thermosphere model for magnetically quiet conditions from longitudinally averaged gas densities using expansion in spherical harmonics
[NASA-TM-X-66183] 08 p0917 N73-17512
Tabulated data on atmospheric ozone density at Uccle, Belgium for 1969
08 p0918 N73-17522
Measurement of total oxidants in atmosphere using potassium iodide absorbing solutions
[LR140[AP]] 08 p0937 N73-17674
Ion clusters and atmospheric composition of Venus ultraviolet haze layer
08 p0973 N73-17952
Visual observations of atmospheric structure and land and water surfaces by cosmonauts from manned orbiting space stations
09 p1026 N73-18373
Human ability to note changes in composition of inhaled air
10 p1115 N73-19090
Toxicity of gaseous urine and feces emissions on rat organism
10 p1116 N73-19097
Development of technique for inferring atmospheric ozone information from satellite nadir measurements
[NASA-TR-R-399] 10 p1154 N73-19386
Daily meteorological ground level charts for Northern Hemisphere, January through June, 1971
[SAR-1-PT-1] 10 p1181 N73-19606
Meteorological ground level charts for Northern Hemisphere, April through June, 1971
[QR-2-PT-2] 10 p1181 N73-19607
Atmospheric pollution in Belgium from 1 Apr. 1969 to 31 Mar. 1970
[PUBL-SER-A-78] 10 p1182 N73-19618
Rocket-borne mass spectrometer experiment with cryo-cooled ion source to determine neutral atmosphere composition between 85 and 125 km altitude
[BMFT-FBW-73-03] 11 p1285 N73-20431
Development of numerical model of eddy diffusive transport of emitted gases from space shuttle wake to show chemical reactions between emitted gases and ambient atmosphere
[NASA-TM-X-66215] 11 p1287 N73-20440
Analysis of global effects created by increase in carbon dioxide and aerosol content in atmosphere
12 p1420 N73-21511
Analysis of atmospheric pollution parameters to show sources, physiological effects, biological effects, and meteorological effects
12 p1421 N73-21519
HO radicals produced in reaction of O[3P] with 1-C4H8
[NASA-CR-131590] 13 p1519 N73-22310
Reactions of HO2 with CO and NO, and O[1D] with H2O
[NASA-CR-131603] 13 p1519 N73-22312
Isotopic composition of atmospheric carbon monoxide
[PB-213591] 13 p1527 N73-22378
Role of biosphere in regulating chemical processes in atmosphere
[AERONOMICA-ACTA-A-116] 13 p1551 N73-22569
Properties of lunar atmosphere and ionosphere
13 p1575 N73-22763
Conference on structure and composition of upper atmosphere and planetary atmospheres
[AD-756812] 14 p1662 N73-23489
Cryogenic sampling of atmosphere at 40,000 to 65,000 ft, using modified matrix isolation technique
[AD-757533] 14 p1662 N73-23493
Rocket-borne mass spectrometric measurements of atmospheric ion composition
15 p1779 N73-24421
Nimbus 3 infrared spectrometric data on global ozone distribution in correlation with atmospheric circulation
[COO-1340-30] 15 p1781 N73-24435
HCl acid aerosol production by space shuttle exhaust products and atmosphere
[NASA-CR-132993] 16 p1870 N73-25142
Global distribution of total ozone as determined by Nimbus 3 satellite infrared interferometer spectrometer
16 p1895 N73-25326
Analysis of ERTS-1 data to determine aerosol content in atmosphere and comparison with data obtained by sun photometer at Salton Sea, California
[E73-10702] 16 p1903 N73-25394
Design of chemical pumps for Venus Pioneer mass spectrometer used to determine atmospheric composition of Venus
[NASA-CR-114604] 16 p1918 N73-25519
Instrumentation for determining composition of Venus clouds
[NASA-CR-132766] 16 p1963 N73-25876
Design engineering for radio communication systems considering troposphere transmission characteristics
17 p1995 N73-26128
Instrumentation of San Marco 3 satellite for neutral atmosphere composition experiments
[NASA-TM-X-66269] 17 p2024 N73-26380
Atmospheric sulfur budget for northern Europe with model for deposition variations with distance from source
[AC-17] 17 p2027 N73-26408
Synoptic weathermaps for ground and 500 mb levels obtained in Berlin during January, 1973
17 p2057 N73-26634
Effect of atmospheric stability on vertical spread of airborne pollutants from steady and instantaneous sources in constant stress region
17 p2098 N73-26974
Research on aeronomy and upper atmospheric composition and environments
[AD-760576] 18 p2149 N73-27367
Development and operation of apparatus for sampling particulates in gases in upper atmosphere
[NASA-CASE-HQN-10037-1] 18 p2150 N73-27376
Spectroscopic analysis of atmospheric water vapor at 6943.8 Angstrom line in telluric spectrum
19 p2258 N73-28203
Cost analyses on mass spectrometric and gas chromatographic atmospheric monitoring systems
[NASA-CR-124331] 19 p2315 N73-28622
Analysis of atmospheric temperature inversion conditions and requirements for thermal convection for removal of temperature inversion effects
[NLL-M-23034-[5828.4F]] 20 p2391 N73-29204
Analysis of methods for interpreting satellite radiation measurements to determine physical parameters of atmosphere which affect earth radiation field
20 p2399 N73-29281
Characteristics of vertical structure of temperature and humidity fields in earth atmsophere based on satellite radiation data of earth surface temperature
20 p2399 N73-29282
Measurements of upward radiation flux from ground and atmosphere using airborne spectrophotometer
20 p2400 N73-29284
Airborne observations to determine radiation characteristics of underlying surface and clouds over various types of ground conditions
20 p2400 N73-29285
Analysis of statistical characteristics of ozonosphere to provide additional information in satellite ozonometry and interpretation of satellite results
20 p2400 N73-29287
Development of numerical method for computing transmission functions of atmospheric gases based on exact frequency integration using structure of absorption spectrum
20 p2401 N73-29296
Measurement of aerosol content in atmosphere over Salton Sea and desert areas of California
[E73-10947] 21 p2530 N73-30289
Distribution of odd nitrogen in lower stratosphere and perturbations caused by stratospheric air transport
[NASA-CR-2314] 21 p2536 N73-30336
Stratospheric and tropospheric composition and chemical reactions
[AP-12] 21 p2539 N73-30357
Application of radio astronomy methods for analyzing microwave absorption spectrum and properties of atmospheric cloud formations
21 p2570 N73-30593
Development of system for quantitative evaluation of radio echo intensities received during measurement of atmospheric formations
21 p2572 N73-30609
Mission planning for Pioneer Saturn/Uranus atmospheric probe missions
[NASA-TM-X-2824] 21 p2595 N73-30800
Infrared laboratory studies of synthetic planetary atmospheres
[NASA-CR-133855] 21 p2597 N73-30810
Food heating tests in different atmospheres
[NASA-CR-134040] 22 p2622 N73-31012
Experimental and theoretical IR spectra of atmospheric hydrocarbon gases CO, CO2, and NH4 for occultation sounding
[BMBW-FBW-72-14-PT-2] 22 p2667 N73-31369
Application of spectroscopic methods in remote sensing for determining structure of microwave spectra in earth atmosphere
22 p2692 N73-31563
Rocket-borne mass spectrometer identification of metallic ions during Encke meteor shower
22 p2735 N73-31897
Atmospheric infrared transmission spectral analysis discussing computed and measured data, and absorption due to atmospheric components
[BMVG-FBWT-73-11] 23 p2787 N73-32297
Food consumption and morphollogical indices of blood in white mice with replacement of air nitrogen by inert gases in pressurized chamber
24 p2882 N73-33020
Dynamics of weight change and variations in weight indices of internal organs in white mice as function of atmospheric composition and diet
24 p2883 N73-33022
Biological evaluation of influence of helium-oxygen atmosphere on culture of mammalian cells
24 p2883 N73-33024
Absorbent columns as samplers for organic vapors in atmosphere
24 p2911 N73-33234
Quantitative determination of Statospheric aerosol composition over western United States
[E73-11138] 24 p2918 N73-33293
OGO-6 neutral atmospheric composition experiment
24 p2920 N73-33320
Methods for measuring and elaborating atmospheric phenomena and meteorological yearbook
[EUR-4943] 24 p2949 N73-33554
Falling sphere measurement data on atmospheric parameters
[WRE-TN-799[WR/D]] 24 p2958 N73-33639

**ATMOSPHERIC CONDITIONS**
U METEOROLOGY

**ATMOSPHERIC CONDUCTIVITY**
NT IONOSPHERIC CONDUCTIVITY
Direct measurement of mesosphere and stratosphere electrical conductivity and relaxation time
15 p1779 N73-24419
Auroral bremsstrahlung flux spectra at various atmospheric depths
[NASA-SP-3081] 23 p2786 N73-32293

**ATMOSPHERIC DENSITY**
Model of semiannual thermospheric density variations based on latitude-dependent temperature and composition variations
[NASA-TM-X-65835] 01 p0047 N73-10380
Semi-annual variations in thermospheric density
[NASA-TM-X-66100] 02 p0166 N73-11346
Air density at 200 km heights analyzed from Cosmos 286 rocket orbit decay, emphasizing annual variations and geomagnetic disturbances
[RAE-TR-72071] 03 p0296 N73-12417
Empirical model constructed to account for large atmospheric density variations observed from drag on satellites in upper atmosphere
[AD-748392] 04 p0445 N73-13631
Accuracy of atmospheric density predictions for satellite orbit determination
[D-151] 05 p0596 N73-14850
Accuracy of harmonics of diurnal density variations in thermosphere determined from satellite drag data and Jacchia empirical atmospheric model
[NASA-TM-X-66160] 07 p0790 N73-16427
Rocket and satellite instrument for simulatenous measurements of total mass density and number density of atomic oxygen in lower thermosphere
[AD-751468] 07 p0795 N73-16464
Extreme temperature, pressure, and density of atmosphere between 30 and 80 km
[AD-751874] 08 p0919 N73-17530

Determination of atmospheric density numbers by sounding rocket carrying mass spectrometer with cryo ion source
[BMBW-FBW-72-34] 09 p1027 N73-18381
Adaptive filter for estimating atmospheric density profile during Atmospheric Explorer missions from accelerometer data
[NASA-TM-X-66202] 10 p1154 N73-19388
Approximative model for diurnal effect on atmospheric density distribution and artificial earth satellite deceleration
10 p1177 N73-19578
Numerical analysis of ideal and real gas equations for application to lift generated by helicopter rotors
[AD-754420] 11 p1235 N73-20026
Analysis of semiannual density variation in thermosphere during period of increasing solar activity
[BMFT-FBW-73-02] 11 p1285 N73-20430
Supplemental catalog of atmospheric densities from satellite drag analysis
[NASA-CR-131646] 12 p1398 N73-21341
Extrapolation technique to obtain estimates of mesospheric density, pressure, and temperature
[NASA-CR-2223] 12 p1401 N73-21364
Atmospheric density extremes up to 15,000 feet for design of military aircraft
[AD-755791] 12 p1403 N73-21382
Atmospheric density data derived from SPADES satellite ultrasensitive triaxial accelerometer system
[AD-756831] 13 p1525 N73-22363
Profiles of neutral atmospheric density at high and middle latitudes in Southern Hemisphere from OV1-15
[AD-755396] 13 p1526 N73-22370
Approximation of atmospheric density and winds from radar track of passive inflatable sphere
17 p2057 N73-26633
Model for predicting atmospheric parameters at altitudes between 90 and 2500 km
[NASA-SP-8021] 18 p2143 N73-27325
Reaction time of 27-day density variation in upper atmosphere noting satellite recorded data on drag using regression analysis, cross correlation, and solar spectrum analysis
[BMFT-FBW-73-10] 21 p2538 N73-30352

**ATMOSPHERIC DIFFUSION**
Deviations from diffusive equilibrium and response of atmosphere above 120 km
[NASA-TM-X-66057] 01 p0049 N73-10394
Influence of meteorological conditions on air pollution
[PB-210381] 01 p0077 N73-10634
PICK method of particle-in-cell techniques for numerical solution of atmospheric diffusion equation applied to air pollution problems
[PB-209290] 01 p0078 N73-10643
Effects of acoustic gravity wave diffusion on atmospheric boundaries
05 p0508 N73-14136
Model of turbulent structure and diffusion for studying movement of air pollution
[PB-211897] 05 p0540 N73-14397
Large scale turbulence and diffusion of pollutants in atmosphere
[COO-1585-22] 07 p0793 N73-16449
Temperature influence on atmospheric diffusion and turbulence near ground level
[AD-753350] 09 p1033 N73-18434
Mesospheric diffuse skylight measurement onboard Centaure sounding rockets launched from Kiruna during August 1969
[ISL-16/72-PT-1] 15 p1781 N73-24439
Influence of wind speed and direction, and temperature on radon gas concentration in atmosphere
17 p2017 N73-26309
Numerical solution and internal gravity wave approximation of solar semidiurnal tidal mode behavior in dissipative atmospheres
[NASA-CR-132779] 17 p2025 N73-26383
Method for calculating ground level concentration of pollutants emitted from high stack based on plume aerodynamics and atmospheric mixing
[PUB-73-3] 17 p2057 N73-26636
Atmospheric diffusion of carbon monoxide and lead from expressways
18 p2170 N73-27527
Abstracts of papers concerning various aspects of meteorology
[AD-760753] 18 p2174 N73-27562
NASA/MSFC multilayer diffusion models and computer program for operational prediction of toxic fuel hazards
[NASA-CR-129006] 19 p2239 N73-28050
Model for estimation of turbojet engine exhaust dispersion into atmosphere
[NASA-TN-D-7382] 19 p2254 N73-28174
Determining diffusion of impurities in atmosphere by mixing properties of turbulence
[NLL-M-23009-[5828.4F]] 20 p2390 N73-29198
Distribution of odd nitrogen in lower stratosphere and perturbations caused by stratospheric air transport
[NASA-CR-2314] 21 p2536 N73-30336
Theoretical study of thermal structure and dispersion in polluted urban atmosphere
21 p2568 N73-30579
Field program design for verifying photochemical diffusion models
[PB-221300/7] 23 p2814 N73-32502
Feasibility of conducting long-range atmospheric tracer experiments to study transport and diffusion of air pollution plumes
[AD-764893] 23 p2815 N73-32504

**ATMOSPHERIC ELECTRICITY**
NT AURORAL ELECTROJETS
NT ELECTROJETS
NT EQUATORIAL ELECTROJET
NT IONOSPHERIC CURRENTS
Dourbes [Belgium] Geophysical Observatory data on geomagnetism, ionospheric propagation, seismology, cosmic rays, and atmospheric electricity, Nov. 1971
01 p0050 N73-10401
Dourbes [Belgium] Geophysical Observatory data on geomagnetism, ionospheric propagation, seismology, cosmic rays, and atmospheric electricity, Dec. 1971
01 p0050 N73-10405
Measuring electric field intensities of lightning strokes for determining lightning channel currents
[NASA-CR-2161] 02 p0205 N73-11658
Dourbes [Belgium] Geophysical Observatory data on geomagnetism, ionospheric propagation, seismology, cosmic rays, and atmospheric electricity, Jan. 1972

**SEISMOLOGY IONOSPHERIC PROPAGATION**
03 p0296 N73-12416
Differential magnetometer method for measuring thunderstorm charging currents near cumulus clouds
[AD-750087] 05 p0542 N73-14411
Ground-based measurements of electrical length of vehicle and plume and of atmospheric electricity during Apollo 13 and 14 launches
[NASA-CR-130535] 08 p0916 N73-17503
Dourbes, Belgium, geophysical observatory data on geomagnetism, ionospheric propagation, seismology, cosmic rays, and atmospheric electricity, Feb. 1972
09 p1030 N73-18403
Dourbes, Belgium, geophysical observatory data on geomagnetism, ionospheric propagation, seismology, cosmic rays, and atmospheric electricity, Mar. 1972
09 p1030 N73-18404
Dourbes, Belgium, geophysical observatory data on geomagnetism, ionospheric propagation, seismology, cosmic rays, and atmospheric electricity, Apr. 1972
09 p1030 N73-18405
Dourbes, Belgium, geophysical observatory data on geomagnetism, ionospheric propagation, seismology, cosmic rays, and atmospheric electricity, May 1972
09 p1030 N73-18406
Dourbes, Belgium, geophysical observatory data on geomagnetism, ionospheric propagation, seismology, cosmic rays, and atmospheric electricity, Jun. 1972
09 p1030 N73-18407
Dourbes, Belgium, geophysical observatory data on geomagnetism, ionospheric propagation, seismology, cosmic rays, and atmospheric electricity, Jul. 1972
09 p1030 N73-18408
Geoelectric observations made from three locations in Japan
[REPT-89] 12 p1399 N73-21344
Meteorological instruments to measure atmospheric electricity aboard modified B-57 aircraft
[AD-755400] 13 p1526 N73-22372
Dourbes [Belgium] geophysical observatory data on geomagnetism, ionospheric propagation, seismology, cosmic rays, and atmospheric electricity, Aug. 1972
17 p2028 N73-26411
Dourbes [Belgium] geophysical observatory data on geomagnetism, ionospheric propagation, seismology, cosmic rays, and atmospheric electricity, Sep. 1972
17 p2028 N73-26412
Characteristics of three station network for sensing magnetic and electric fields associated with lightning discharges
[NASA-CR-133400] 18 p2151 N73-27382
Stratospheric electricity due to operating supersonic transport fleets
[AD-763471] 21 p2540 N73-30365
Systems for protection of low altitude tethered balloons from effects of atmospheric electricity
[AD-764651] 23 p2746 N73-31978
Dourbes [Belgium] geophysical observatory data on geomagnetism, ionospheric propagation, seismology, cosmic rays, and atmospheric electricity, Nov. 1972
24 p2924 N73-33353
Geophysical observatory data obtained at Dourbes, Belgium in Dec. 1972 on geomagnetism, ionospheric propagation, seismology, cosmic rays, and atmospheric electricity
24 p2924 N73-33354

**ATMOSPHERIC EMISSION**
U AIRGLOW

**ATMOSPHERIC ENTRY**
NT HYPERBOLIC REENTRY
NT HYPERSONIC REENTRY
NT REENTRY
NT SPACECRAFT REENTRY
Finite difference solution of film cooling as alternate thermal protection system for spacecraft during reentry
[NASA-CR-112192] 01 p0116 N73-10958
Thermal expansion, specific heat, and thermal conductivity of carbon reentry materials to 3000 C
[SC-CR-72-3139] 03 p0320 N73-12610
Guidance method for transition of space shuttle from hypersonic entry to subsonic cruise flight
[NASA-CR-128648] 03 p0357 N73-12905
Calculation of optimal gliding flight paths associated with space shuttle orbiter transition from entry to cruising flight
[NASA-CR-128647] 03 p0359 N73-12922
Destructive and nondestructive tests of carbon-carbon reentry heat shields
[SC-R-71-3354] 03 p0364 N73-12966
Analysis of sonic boom pressure signatures recorded during reentry of Apollo 15 command module and correlation with wind tunnel signatures
[NASA-TM-X-62111] 04 p0371 N73-13016
Microstrip plasma probe as diagnostic tool in atmospheric entry
[AD-749860] 05 p0585 N73-14757
Multicomponent electron collision frequency model for predicting signal attenuation in plasma sheath surrounding reentry vehicle
[AD-750553] 05 p0585 N73-14758
Fused slurry silicide protective coatings for tantalum heat shielding
[NASA-CR-121022] 06 p0688 N73-15599
Solution of viscous shock-layer equations using implicit finite difference scheme for hyperboloid body under conditions simulating atmospheric entry
07 p0768 N73-16238
Numerical analysis of characteristic processes of hyperbolic shock layers generated during atmospheric entry
07 p0768 N73-16242
Radio blackout prevention in atmospheric reentry by chemical injection into vehicle plasma sheath
[AD-753077] 09 p1003 N73-18187
Problem formulation and numerical procedures for solving flow equations for flow distribution of viscous shock layer on nose of shuttle orbiter during reentry - Vol. I
[NASA-CR-128871] 11 p1271 N73-20309
Research projects on wake turbulence and atmospheric boundary layers, turbulent mixing and shear flows, and high temperature gas dynamics
[AD-755273] 13 p1512 N73-22251
Analysis of aerodynamic characteristics of Gemini spacecraft during reentry and comparison with wind tunnel data
[NASA-TM-X-58100] 13 p1577 N73-22786
Spacecraft microbial burden reduction for Jupiter due to atmospheric entry heating
[NASA-CR-132072] 15 p1741 N73-24117
Analysis of atmospheric entry trajectories for manned and unmanned missions to planet Venus
[NASA-TN-D-7316] 16 p1966 N73-25900
Optimal three dimensional trajectories to maximize landing footprint of lifting reentry vehicle using energy approximations based on flight path
[AD-764132] 22 p2615 N73-30960
Application of perturbation method for computing optimal three dimensional reentry trajectories for shuttle-type spacecraft
24 p2978 N73-33798
Entry and impact behavior of isotope heat source for space nuclear power following flight abort to provide safe dispersion
[LA-UR-73-741] 24 p2986 N73-33861

**ATMOSPHERIC ENTRY SIMULATION**
Simulation of rocket plumes and reentry aerothermodynamics using oxygen/hydrogen combustion products
[NASA-CR-128955] 16 p1974 N73-25962
Hydrogen/oxygen combustion for simulating reentry aerothermodynamic characteristics
16 p1974 N73-25964
Experimental determination of electron attachment in high temperature plasma
[AD-763090] 20 p2459 N73-29765
Thermal response of glassy fibrous mullite insulation to entry environment simulation
24 p2940 N73-33478
Simulated reentry heating tests on silica surface insulation material for space shuttle
24 p2940 N73-33482

**ATMOSPHERIC HEAT BUDGET**
Past, present, and projected climate, and heat budget of atmosphere and hydrosphere
[NLL-M-20071-[5828.4F]] 01 p0073 N73-10597
Transport processes governing structure, energy, mass, and momentum of upper atmosphere
[COO-2195-6] 04 p0415 N73-13388
Annual global average earth-atmospheric system radiation balance determined from Nimbus 3 radiation measurements
[NASA-TN-D-7249] 12 p1445 N73-21702
Budget relations of thermal variance and kinetic energy in transition zone from forced to free convection
15 p1771 N73-24342
Regional and time variations in heat transfer from oceanic regions to atmosphere
20 p2389 N73-29195

Computational methods for determining eddy momentum, heat, and fluxes in water-adjoining layer of atmosphere
20 p2445 N73-29637
Influence of solar radiation on thermodynamic balance and biological processes of earth
24 p2975 N73-33770

ATMOSPHERIC HEATING
Rate of solar extreme ultraviolet radiation heating in upper atmosphere
[AD-745305] 01 p0051 N73-10410
Far ultraviolet heating in upper atmosphere variations
[AD-745309] 01 p0051 N73-10411
Global response of atmosphere to persistent anomalous pool of warm sea surface temperatures in extratropical Pacific Ocean
[NASA-CR-130179] 10 p1154 N73-19391
Thermospheric heating due to EUV absorption and Joule dissipation
[AD-758758] 15 p1784 N73-24464
Three dimensional steady state model of thermospheric dynamics with auroral heating
[AD-758733] 15 p1784 N73-24466
Mathematical models for studying atmospheric heating by ozone absorption of sunlight
[NASA-CR-132778] 17 p2024 N73-26382
Mechanism and rates of atmospheric mixing in lower thermosphere including heat input
[NASA-CR-135789] 24 p2920 N73-33321

ATMOSPHERIC IMPURITIES
U AIR POLLUTION

ATMOSPHERIC IONIZATION
NT AURORAL IONIZATION
Various opinions on physical and mental exhaustion caused by atmospheric ion shortage
[NASA-TT-F-14646] 04 p0380 N73-13088
High resolution study of ion mobility spectra and effect on atmospheric ionization
[AD-747687] 04 p0416 N73-13396
Estimating quantity of helium in Venus atmosphere from measured ionization profile
[NASA-TM-X-66128] 04 p0475 N73-13883
Neutral and ion chemistry of D and E regions symposium papers
[AD-749780] 06 p0668 N73-15430
D region ionization during polar cap absorption determined from parachutebornе blunt probe measurements of charged particle conductivity
[AD-750570] 06 p0670 N73-15448
Anomalous F region ionization patterns during winter in dark ionosphere in polar regions
13 p1520 N73-22318
Predicting regular variations in geometric parameters of N[h] profiles and h prime f characteristics of quiet and disturbed ionosphere
13 p1520 N73-22321
Predicting daily variations in geometric parameters of N[h] profiles and h prime f characteristics of quiet and disturbed ionosphere
13 p1520 N73-22322
Predicting geometric parameters of N[h] profiles and h prime f characteristics of F region during disturbances
13 p1520 N73-22323
Predicting arrival angle and skip distance variations of quiet and disturbed ionosphere on basis of N[h] profiles and h prime f characteristics
13 p1520 N73-22324
Long-term prognosis of midday N[h] profiles of F region
13 p1521 N73-22325
Rocket produced infrared emissions for analyzing auroral atmospheric mechanisms
[AD-762206] 19 p2298 N73-28478
Theoretical calculation of heavy particle induced ionization rates during PCA events
[AD-763089] 20 p2415 N73-29407

ATMOSPHERIC MODELS
NT BREADBOARD MODELS
NT DYNAMIC MODELS
NT REFERENCE ATMOSPHERES
Model of semiannual thermospheric density variations based on latitude-dependent temperature and composition variations
[NASA-TM-X-65835] 01 p0047 N73-10380
Physical model of excitation processes and infrared radiation
[AD-745319] 01 p0051 N73-10409
Atmospheric transmittance calculations of laser beams for atmospheric models with water vapor as molecular absorber
[AD-745585] 01 p0065 N73-10532
Numerical weather forecasting methods - atmospheric and weather forcasting models
[NLL-M-20352-[5828.4F]-VOL-2]
01 p0073 N73-10596
Effects of surface anomalies on certain model generated meteorological histories
[NASA-CR-130070] 01 p0074 N73-10612
Barotropic primitive equation model for numerical weather forecasting for tropics
[AD-743729] 01 p0076 N73-10626
Global distributions of mean January surface wind stress, diabatic heating rate, and rate of moisture addition as simulated in 30-day integration with atmospheric general circulation model
[AD-745752] 01 p0077 N73-10640
Combined influence of finite Larmor radius corrections and inertia on stability of infinite slab model
[AD-746060] 02 p0168 N73-11365
Derivation of doubling equations for scattering and transmission functions for a homogeneous isotropically scattering atmosphere using scattering matrix
[USC-113P19-32] 02 p0202 N73-11631
Conservative finite difference method applied to meteorological advection problems
[NASA-CR-129090] 02 p0204 N73-11653
Phase variation and hydrostatic atmospheric models for eta Aquilae
[NASA-TT-F-14717] 02 p0229 N73-11857
Development of mathematical models to analyze stability characteristics of thermally stratified shear flow in atmosphere
[ORO-4199-1] 03 p0296 N73-12414
Tables for quantitative atmospheric attenuation of 97 HF and DF laser lines and 10 atmospheric models
[AD-747010] 03 p0310 N73-12534
Papers on Arctic ionospheric modeling
[AD-748796] 04 p0416 N73-13398
Empirical model constructed to account for large atmospheric density variations observed from drag on satellites in upper atmosphere
[AD-748392] 04 p0445 N73-13631
Inhomogeneous models of Jovian atmosphere with two cloud layers
04 p0468 N73-13817
Luminosity, mass, and elemental abundances of line-blanketed model stellar atmospheres
[NASA-CR-129670] 04 p0469 N73-13825
Model of turbulent structure and diffusion for studying movement of air pollution
[PB-211897] 05 p0540 N73-14397
Auroral substorm model for predicting high frequency radio absorption
[AD-749859] 05 p0542 N73-14408
Parameterization and its role in atmospheric modeling
[GARP-PUBL-8] 05 p0573 N73-14654
Parameterization in atmospheric circulation models
05 p0573 N73-14655
Role of radiation in atmospheric models noting equation of transfer for thermal and solar radiation
05 p0573 N73-14656
Two dimensional eddy viscosity coefficients in atmospheric motion noting parameterization of clear air turbulence
05 p0573 N73-14658
Parameterization of gravity waves noting upper boundary conditions
05 p0573 N73-14659
Mesoscale processes in circulation models noting parameterization
05 p0573 N73-14660
Parameterization of turbulent boundary layer in atmospheric circulation model
05 p0573 N73-14661
Influence of ocean on atmospheric circulation noting role of heat, momentum, and water vapor transfer
05 p0573 N73-14662
Energy balance equations for parameterization of hydrological processes effecting atmospheric circulation
05 p0573 N73-14663
Parameterization of atmospheric boundary layer
05 p0574 N73-14664
Parameterization of near surface mesoscale circulation
05 p0574 N73-14665
Two dimensional dynamical model for fog forecasting for periods up to eight hours on local scale
[AD-750082] 05 p0575 N73-14682
Accuracy of atmospheric density predictions for satellite orbit determination
[D-151] 05 p0596 N73-14850
Computer program for tracing paths of high frequency electromagnetic rays through two-dimensional models of ionosphere
[AWRE-O-34/72] 06 p0644 N73-15228
Statistical determination of atmospheric temperatures at mandatory pressure levels in North American Arctic for regional extreme model atmosphere
[AD-750170] 06 p0669 N73-15445
Mesoscale interaction models for effects of orography on momentum and energy transfer in atmosphere and interaction of solar radiation with earth atmosphere
[AD-750727] 06 p0694 N73-15657
Model of Venus atmospheric composition, temperature, and circulation based on Mariner 5 and Venera 4, 5, 6, and 7 data
[NASA-TM-X-66140] 06 p0719 N73-15865
Possibility of developing theoretical models of disturbed F region, using ground based and spaceborne experiments
[RSD-77] 07 p0789 N73-16417
Accuracy of harmonics of diurnal density variations in thermosphere determined from satellite drag data and Jacchia empirical atmospheric model
[NASA-TM-X-66160] 07 p0790 N73-16427
Extension of US standard atmosphere to region from 80 to 200 km
[NASA-TM-X-66171] 07 p0792 N73-16441
Numerical analysis of gravity wave generation in atmospheric frontal zone
[AD-751638] 07 p0796 N73-16469
Numerical analysis of ocean circulation effects on transients in atmospheric circulation
[AD-751637] 07 p0796 N73-16470
Relationship between vertical velocity in baroclinic model and occurrence of rain and clouds in Finland
[TR-4] 07 p0814 N73-16603
Atmospheric energetics as related to cyclogenesis over eastern United States
[NASA-CR-2189] 07 p0815 N73-16607
Engineering models of Venus atmosphere, based on theory and measured data
[NASA-SP-8011-REV] 07 p0842 N73-16824
Tables on airborne and ground based measurements of optical atmospheric properties in central New Mexico
[AD-751936] 08 p0919 N73-17534
Method for integrating pressure-scaled water-vapor and CO2 absorber masses from surface to sigma levels in Naval primite equation model
[AD-752475] 08 p0921 N73-17544
Probability models of wet and dry days for several stations in Thailand
[THESIS-392] 08 p0938 N73-17684
Model for solution of equations of motion for thermospheric wind - Part 1
[NASA-TM-X-66189] 09 p1028 N73-18393
Eighty atmospheric models for measuring total outgoing radiance of earth-atmosphere system
[NASA-TM-X-66195] 09 p1029 N73-18400
Simultaneous investigations of three-dimensional structure of atmospheric radiation fields using equipment installed on airplanes, balloons, satellites, and ground
[AD-750962] 09 p1030 N73-18411
Evaluation of worldwide empirical ionospheric model to assist in design of satellite navigational system - Vol. 1
[AD-753081] 09 p1031 N73-18419
Evaluation of worldwide empirical ionospheric model to assist in design of satellite navigational system - Vol. 2
[AD-753082] 09 p1031 N73-18420
Evaluation of worldwide empirical ionospheric model to assist in design of satellite navigational system - Vol. 3
[AD-753083] 09 p1032 N73-18421
Atmospheric data from OV1-15 satellite
[AD-753680] 09 p1033 N73-18432
Models for warm and cold conditions of winter stratosphere of polar latitudes
09 p1059 N73-18636
GARP standard data sets for studying behavior of numerical global models noting data acquisition, analysis, and storage
[GARP-PUBL-9] 09 p1061 N73-18652
Multilayer numerical weather prediction model for studying tropical weather systems, including winds, vorticity, and divergence
[AD-752929] 09 p1061 N73-18653
Chemical dynamic model of moist Martian atmosphere
[NASA-CR-130799] 09 p1082 N73-18825
Models of aerosol dynamics in upper atmosphere
[BNL-17174] 10 p1126 N73-19176
Three dimensional density model of thermosphere dynamics
[NASA-TM-X-66206] 10 p1154 N73-19389
Numerical and photochemical models for analyzing transport and trace constituents in stratosphere
[COO-2249-1] 10 p1155 N73-19399
Neutral atmospheric models compatible with satellite orbital decay and incoherent scatter measurements
[NASA-CR-131294] 11 p1285 N73-20427
Atmospheric models for fluid dynamic and chemical impacts of supersonic aircraft on climatology
[PB-212819] 11 p1291 N73-20473
Atmospheric model for acoustic pressure produced in shadow zone by wind and temperature gradients
[AD-754634] 11 p1324 N73-20747
Mid-latitude ionospheric and neutral atmospheric models
[NASA-CR-131547] 12 p1399 N73-21342
Atmospheric model for predicting seasonal and diurnal behavior of D region electron density
[AD-755447] 12 p1403 N73-21383
Mathematical and physical principles for computational schemes atmospheric model
[NASA-CR-131531] 12 p1420 N73-21508
Computer simulation of global atmospheric circulation in climatological research
[P-4933] 12 p1421 N73-21520
Static planar model for explaining structure and thermal conduction heating of chromosphere-corona transition region
12 p1444 N73-21699

Atmospheric noise model with application to low frequency radio navigation receivers
[AD-757275] 13 p1493 N73-22101
Model of equatorial F 2 region ionosphere based on known physical and chemical processes
13 p1514 N73-22268
Long-term prognosis of midday N[h] profiles of F region
13 p1521 N73-22325
Photoelectron transport energy for calculating electron and ion temperatures of ionospheric models
[AD-756241] 13 p1525 N73-22362
Proposed 50 to 100 km revision to US Standard Atmosphere, 1962
[AD-755394] 13 p1526 N73-22371
Numerical forecasts of barometric fields in stratosphere using quasi-geopotential model
13 p1552 N73-22574
Composite maps from 950 mb to 150 mb of relative wind field, mixing ratio R
[AD-755485] 13 p1555 N73-22600
Parametric model of cumulus convection to simulate entire life cycle of different types of cumuli under various environmental conditions
[PB-213623-2] 13 p1555 N73-22602
Numerical model of individual convective clouds used for analysis of cumulus and mesoscale interactions
[PB-213624-0] 13 p1555 N73-22603
Utilization of ERTS-1 data for crop identification and acreage estimation, soil mapping, urban land use, water resources, atmospheric modeling, and earth surface feature identification in Wabash River Basin
[E73-10549] 14 p1655 N73-23422
Analysis and modeling of ionospheric data collected worldwide
[AD-757480] 14 p1662 N73-23491
Phenomenological model of global ionospheric electron density in E, F 1, and F 2 region
[AD-757507] 14 p1663 N73-23498
BOMEX array for longwave radiative transfer model of tropical atmosphere
15 p1770 N73-24339
Representation of Jacchia thermospheric models in spherical harmonics
[NASA-TM-X-66247] 15 p1778 N73-24416
Simulation of asymmetric hurricane with fine mesh multiple grid primitive equation model
15 p1805 N73-24631
Air pollution modeling and meteorology for California particularly San Francisco Bay Area
[UCRL-74335] 15 p1806 N73-24635
Brightness temperature of Venus and absolute flux scale at 608 MHz
[AD-756084] 15 p1832 N73-24853
Polarization of infrared waves due to propagation through atmosphere
16 p1895 N73-25327
Chemical kinetics and atmospheric dynamics data base for digital modeling of climatological aircraft exhaust effects
[PB-214100/0] 16 p1908 N73-25441
Atmospheric mesostructure model for clear air turbulence
[AD-759787] 16 p1909 N73-25448
Development of methods for improving forecasting of precipitation, surface pressure, temperature, and dew point
[NLL-M-22980-[5828.4F]] 16 p1935 N73-25658
Estimation techniques in modified binomial distribution that describes thunderstorms over Cape Kennedy, Florida
[NASA-CR-2280] 16 p1937 N73-25678
Sea surface temperature anomalies and model generated meteorological histories
[NASA-CR-132756] 16 p1938 N73-25679
Multilevel atmospheric prediction model based on primitive equations of moiton
[DM-8] 16 p1938 N73-25681
Nonadiabatic atmospheric model for short term weather forecasts
[AD-759631] 16 p1939 N73-25690
Jovian magnetosphere model with thermal plasma and superimposed radiation belts
[NASA-CR-132960] 16 p1963 N73-25878
Temporal variations in atmospheric electric fields noting propagation and disturbances
[TRITA-EPP-73-02] 17 p2027 N73-26405
Atmospheric sulfur budget for northern Europe with model for deposition variations with distance from source
[AC-17] 17 p2027 N73-26408
Truncation error dependence on computational diffusion coefficient in atmospheric boundary layer models
[AD-760122] 17 p2029 N73-26420
Aerosol model of atmosphere based on experimental data regarding aerosol attenuation and particle number concentration and size distribution at various heights
[AD-760393] 17 p2030 N73-26429
Periodic spectral solutions of combined system of equations of planetary dynamics of atmosphere and hydrosphere
[AD-759857] 17 p2058 N73-26646
Model of atmospheric motion for long-term weather forecasting
[AD-759877] 17 p2058 N73-26651
Hot and cold atmospheres for Vanderberg AFB, California
[NASA-TM-X-64756] 18 p2141 N73-27306
Model for predicting atmospheric parameters at altitudes between 90 and 2500 km
[NASA-SP-8021] 18 p2143 N73-27325
Woomera atmospheric parameters measured during falling sphere ejection from rocket soundings between Feb. and Jun. 1972 noting comparison with atmospheric models
[WRE-TN-787] 18 p2146 N73-27341
Semi-implicit version of numerical weather prediction model developed by Shuman and Hovermale
[NOAA-TM-NWS-NMC-53] 18 p2172 N73-27545
Effect of eddy turbulence in development of models of lower and upper thermosphere
[NASA-TM-X-70431] 19 p2293 N73-28443
Analog model for arctic ionosphere
[AD-762280] 19 p2299 N73-28484
Application of model output statistics to predict ceiling and visibility
[FAA-RD-73-14] 19 p2315 N73-28621
Numerical experiments with five-level global atmospheric prediction model using staggered, spherical, Sigma coordinate system
[AD-761386] 19 p2316 N73-28626
Operational equations model forecasting extratropical cyclogenesis in evaluating the fleet numerical weather center
[AD-761727] 19 p2316 N73-28629
Application of line-blanketed model stellar atmospheres to Sirius
19 p2342 N73-28837
Numerical model to simulate vertical mass transfer and stratification in layer of buoyant convection
20 p2391 N73-29208
Spherically symmetric models for radiance and color of twilight sky calculated for single scatter radiation
[NASA-CR-133739] 20 p2413 N73-29393
Two dimensional nonsteady model of nocturnal flow of stable atmosphere over wide, warm, rough city
20 p2441 N73-29604
Numerical simulation of thunderstorm cell in two and three dimensions
20 p2441 N73-29605
Synopticostatistical, numerical, and laboratory procedures for studying dynamics of atmospheric circulation in planetary atmospheres including earth
[TT-70-50052] 20 p2442 N73-29615
Integral characteristics and models of general atmospheric circulation
20 p2443 N73-29621
Utilization of two rotating vessels to model and analyze certain schemes of atmospheric circulation and heat exchange
20 p2445 N73-29638
Atmospheric models for studying typhoon and thundercloud processes
20 p2446 N73-29645
Model for calulating coherence function for atmospheric turbulence
[NPL-MAR-SCI-R-108] 20 p2449 N73-29675
Upper air numerical forecast model designed to predict tropical macro-scale features
[AD-763102] 20 p2451 N73-29697
Model of wind shear in lower 50 meter section of glide path from low inertia measured data
[NLL-M-23036-[5828.4F]] 21 p2528 N73-30271
Distribution of odd nitrogen in lower stratosphere and perturbations caused by stratospheric air transport
[NASA-CR-2314] 21 p2536 N73-30336
Stochastic model of atmosphere between 30 and 90 km was developed for use in Monte Carlo space shuttle entry studies
[NASA-TM-X-69567] 21 p2536 N73-30337
Atmospheric model of artificial night sky illumination in Italy
21 p2538 N73-30348
Regional extreme atmospheric model for aerothermodynamic calculation of probable vertical temperature profile
[AD-763671] 21 p2540 N73-30369
FORTRAN computer program for computing transmittance of atmosphere in ultraviolet to infrared spectral region
[AD-763721] 21 p2541 N73-30378
Dynamic forecast model for studying moisture variation in planetary boundary layer
[PB-220532/6] 21 p2575 N73-30635
Tilted image dipole model of magnetosphere replacing earth dipole by full internal field expansion
22 p2657 N73-31281
Numerical modeling of upper atmosphere
[ISAS-496-VOL-38-NO-7] 22 p2664 N73-31347
Atmospheric model developed for altitude range of 24 to 500 km
[AD-764303] 22 p2668 N73-31379
Air stress predictions for synoptic scale ice dynamics model
[PB-222057/2] 22 p2669 N73-31388
Atmospheric model for secondary gamma ray production
22 p2733 N73-31871
Atmospheric models for computing radiation effects in ERTS observations
22 p2736 N73-31905
Crop identification, soil mapping, and atmospheric modeling in Wabash River Basin using ERTS-1 data
[E73-11082] 23 p2782 N73-32257
Computer program for modeling E and F region of ionosphere
[AD-764662] 23 p2789 N73-32312
Analytical and numerical model of sea breeze
23 p2814 N73-32496
Numerical weather prediction activities of National Meteorological Center for first half of 1973
23 p2814 N73-32497
Atmospheric models for evaluating nuclear facility sites
[BNWL-1651-VOL-2-PT-1] 24 p2885 N73-33044
Atmospheric modeling and environmental protection needs for air pollution control
[UCRL-74249] 24 p2922 N73-33341
Exact solution to system of forecasting equations of barotropic divergent model of atmosphere
24 p2946 N73-33531
Numerical weather forecasting noting atmospheric models and circulation
24 p2949 N73-33553
Models for predicting wind fields over mountains, and potential radiological fields over Nevada test site
[NOAA-ARLV-351-28] 24 p2949 N73-33556

**ATMOSPHERIC MOISTURE**
Monthly statistics of precipitable water over Australia in atmosphere from 400 mb to surface, determined from daily radiosonde ascents, 1958 through 1969
01 p0074 N73-10609
Correlation of total precipitable water in atmosphere with surface absolute humidity for California and Pacific Ocean islands
[AD-745954] 02 p0206 N73-11666
Meteorological causes and characteristics of dry spells
[NLL-M-20052-[5828.4F]] 05 p0569 N73-14623
Tabulation of relative humidity data obtained from network of weather stations in Switzerland
05 p0572 N73-14645
Measurement of vertical distribution of atmospheric water vapor by ruby laser rod
[PB-211891] 05 p0575 N73-14680
Optical radar system for determining tropospheric water vapor content, based on absorption line shift
[DLR-MITT-72-26] 07 p0815 N73-16608
Measurement of water content of Martian atmosphere by Mars 3 spacecraft
[NASA-TT-F-14815] 08 p0961 N73-17864
Graphical method for determining soil temperature from air temperature and humidity measurements
[NLL-M-22802-[5828.4F]] 11 p1274 N73-20339
Temperatures of various adiabatic and isobaric mixtures of humid atmospheric air with water or ice
[PUBL-SER-B-68] 12 p1465 N73-21866
Analysis of convective cumulus cloud development and numerical relationships of hydrodynamic and thermodynamic concepts of cloud formation
[NLL-M-22840-[5828.4F]] 16 p1936 N73-25666
Ruby laser radar system for measuring spatial density distribution of atmospheric water vapor
17 p2039 N73-26499
Spectroscopic analysis of atmospheric water vapor at 6943.8 Angstrom line in telluric spectrum
19 p2258 N73-28203
Development of numerical methods for computation of vertical divergence of thermal radiation
20 p2400 N73-29290
Analysis of absorption of solar radiation by atmospheric water vapor to determine effects of various atmospheric parameters
20 p2401 N73-29294
Characteristics of vertical distribution of atmospheric moisture using satellite measurements
[AD-763286] 21 p2540 N73-30364
Mean monthly values of turbulent heat and moisture fluxes over oceans
21 p2572 N73-30613
Dynamic forecast model for studying moisture variation in planetary boundary layer
[PB-220532/6] 21 p2575 N73-30635

**ATMOSPHERIC NEUTRON FLUX DENSITY**
U ATMOSPHERIC RADIATION
U NEUTRON FLUX DENSITY

**ATMOSPHERIC NOISE**
U ATMOSPHERICS

**ATMOSPHERIC OPTICS**
Modulation transfer function of atmospheric medium as function of light wavelength
[AD-751641] 07 p0796 N73-16471
Optical apparatus to determine effect of turbulence on modulation transfer function of atmosphere
[AD-757256] 14 p1661 N73-23485
Analysis of ERTS-1 imagery of Los Angeles, California area to determine effects of haze on accuracy of ground truth data
[E73-10691] 16 p1902 N73-25384

Proceedings of conference on actinometry and atmospheric optics to include effects of solar radiation and atmospheric light on photosynthesis
[TT-70-50159] 20 p2399 N73-29280
Introduction to optical communication with lasers
[FTZ-A-465-TBR-8] 22 p2681 N73-31477
Utilization of inverse scattering method to measure transparency of atmosphere in slant direction
22 p2693 N73-31571
Proceedings of conference on electromagnetic and optical properties of sea water for application to surveillance, mapping, communications, and visibility
[AGARD-LS-61] 24 p2956 N73-33619
Radiance distribution as function of depth in upper layers of ocean and numerical analysis of inherent and apparent optical properties
24 p2957 N73-33621

**ATMOSPHERIC PHYSICS**
NT CLOUD PHYSICS
Translation of titles, subtitles, and table of contents for Soviet publication on Problems of Physics of Atmosphere
[NASA-TT-F-14424] 01 p0049 N73-10396
Utilization of ERTS-1 imagery for water depth measurement, mapping of Yellowstone Park, atmospheric effects in Colorado, lake ice surveillance, recreational land use, IFYGL Lake Ontario, image enhancement, water quality monitoring, and oil pollution detection
[E72-10201] 02 p0144 N73-11167
Utilization of ERTS-1 imagery for water depth measurement, mapping of Yellowstone Park, atmospheric effects in Colorado, lake ice surveillance, recreational land use, IFYGL Lake Ontario, image enhancement, water quality monitoring, oil pollution detection, and mapping iron compounds
[E72-10198] 02 p0160 N73-11296
Development of mathematical models to analyze stability characteristics of thermally stratified shear flow in atmosphere
[ORO-4199-1] 03 p0296 N73-12414
Analysis of atmospheric optical properties with application to night vision, infrared radiation, astrogeophysics, and electro-optical physics
[AD-750610] 06 p0669 N73-15443
Analysis of ion current density at central point of charged mass spectrometer during atmospheric and ionospheric sounding
[AD-750483] 06 p0671 N73-15456
Cosmos 121 measurements of total ozone content of earth atmosphere
[JPRS-57976] 07 p0791 N73-16430
Influence of electron beam irradiation on upper atmospheric chemistry and physics
[AD-753707] 09 p1033 N73-18431
Using lasers to study properties of atmosphere
[JPRS-58346] 09 p1060 N73-18647
History and future of scientific attempts to control meteorological processes and climatology
[NLL-M-22821-[5828.4F]] 12 p1420 N73-21506
Effects of solar activity and geocoronal emissions on atmospheric boundary layer as observed by Proguoz satellite
12 p1461 N73-21840
Atmospheric physics and gas dynamics research in Soviet Union
[JPRS-58988] 14 p1649 N73-23377
Research projects conducted by Australian atmospheric physics laboratory to analyze atmospheric radiation, micrometeorology, ozone, airglow, and cloud physics
14 p1659 N73-23465
Two rocket measurements of atmospheric oxygen concentration during twilight
16 p1895 N73-25331
Development of method for remotely determining average transverse wind velocity and atmospheric structure constant along line of sight path
16 p1937 N73-25670
Atmospheric physics of condensation nuclei
[NLL-M-22806-[5828.4F]] 16 p1947 N73-25749
SOM-3 radar design for measuring meteor trail physics and upper atmosphere physical properties
17 p2023 N73-26368
ESRO sounding rocket experiment R-175 in presence of noctilucent clouds on polar summer upper atmosphere structure, composition, and ionization
[AP-7] 17 p2027 N73-26406
Analysis of methods for interpreting satellite radiation measurements to determine physical parameters of atmosphere which affect earth radiation field
20 p2399 N73-29281
Numerical analysis of dependence of transmission function of atmosphere on temperature of radiation source
20 p2402 N73-29299
Meteorological, actinometric, and aerological investigations conducted aboard ships of Tenth Soviet Antarctic Expedition
20 p2406 N73-29341
Development of system for quantitative evaluation of radio echo intensities received during measurement of atmospheric formations
21 p2572 N73-30609
Falling sphere experiment for profiles of basic atmospheric parameters in Woomera, Australia
[WRE-TN-786[WR/D]] 22 p2694 N73-31579
Atmospheric effects in Skylab EREP MSS data
[E73-11118] 23 p2783 N73-32263
Research projects to determine effects of exhaust products from aircraft operating in stratosphere on global and local climatic conditions
[UCRL-51336] 23 p2787 N73-32296
Development and characteristics of apparatus for measuring intensity of electric field in atmosphere
[NASA-CASE-KSC-10730-1] 23 p2790 N73-32318
Analysis of nonlinear atmospheric waves
24 p2912 N73-33236

**ATMOSPHERIC PRESSURE**
Development of occultation satellite system for determining atmospheric pressure at various millibar levels
02 p0198 N73-11601
Effects of atmospheric pressure on thermoluminescence of crystalline powder
[AD-746442] 02 p0219 N73-11770
Development of method for determining response of fluids under high pressure when released to atmosphere using closed form solution and numerical analysis
03 p0282 N73-12289
Temperature, pressure, and related climatological data for Australia - tables for [May, 1972]
04 p0441 N73-13598
Temperature, pressure, and related climatological data for Australia - tables for [April 1972]
04 p0442 N73-13599
Record high air pressure of 1083.8 mb at Lake Agatha, Siberia, on 31 Dec. 1968, and weather phenomena in Northern Hemisphere at end of 1968
[NLL-M-22700-[5828.4F]] 05 p0570 N73-14629
Effects of alterations in barometric pressure on humans
06 p0628 N73-15092
Ozone tables, ozonagrams, and ascent tables for aerological ozone soundings conducted at Hohenpeissenberg, West Germany
[AD-750166] 06 p0670 N73-15446
Two satellite microwave occultation system for determining pressure levels in atmosphere using infrared sensors
07 p0775 N73-16294
Extreme temperature, pressure, and density of atmosphere between 30 and 80 km
[AD-751874] 08 p0919 N73-17530
Characteristics of global atmospheric field at sea level
08 p0938 N73-17683
Computer procedure for analysis of maritime sea-level pressure and wind fields
[NASA-TM-X-69135] 09 p1058 N73-18630
Relationship between solar activity and atmospheric pressure of Northern Hemisphere
[NLL-M-22858-[5828.4F]] 11 p1313 N73-20651
Extrapolation technique to obtain estimates of mesospheric density, pressure, and temperature
[NASA-CR-2223] 12 p1401 N73-21364
Effects of reduced atmospheric pressure, elimination of nitrogen, hypoxia, and exposure to restricted visual environment on range of accommodation and color vision
[NASA-CR-128896] 13 p1484 N73-22037
General expressions for transfer function and coherence relating earth motion and atmospheric pressure variations generated by slowly propagating, partially organized pressure fields
[AD-755527] 13 p1526 N73-22365
Characteristics of carbon dioxide laser operating at atmospheric pressure
[TM-50] 13 p1536 N73-22446
Atmospheric pressure gas lasers
[AD-755477] 13 p1538 N73-22462
Northern Hemisphere ground weather maps for July through December, 1972
[QR-2-PT-2] 15 p1804 N73-24624
Remote barometric altimetry and estimation of meteorological field variables
[AD-759910] 17 p2058 N73-26650
Indirect atmospheric pressure estimation from measurements of height and temperature
[AD-759920] 17 p2059 N73-26653
Relation of local pressure fluctuations to large-scale meteorology, and simulation of acoustic-gravity waves in inhomogeneous media
18 p2170 N73-27528
Influence of atmospheric pressure and temperature on viscosity and density of mineral oil and siloxane liquids
[AD-761590] 19 p2232 N73-27999
Exact time-independent solution for rotation of atmosphere about earth
[AD-762486] 20 p2414 N73-29402
Air circulation patterns induced by wind and atmospheric pressure over Lake Superior
[PB-220244/8] 22 p2695 N73-31590
Detection of low pressure center by viewing cloud pattern and wind direction in ERTS-1 photography
[E73-10978] 24 p2913 N73-33243
Exact solution to system of forecasting equations of barotropic divergent model of atmosphere
24 p2946 N73-33531

**ATMOSPHERIC RADIATION**
NT AIRGLOW
NT AURORAL ARCS
NT AURORAS
NT DAWN CHORUS
NT DAYGLOW
NT GEOCORONAL EMISSIONS
NT NIGHTGLOW
NT RADIO AURORAS
NT RED ARCS
NT SKY RADIATION
NT STRATOSPHERE RADIATION
NT TROPOSPHERIC RADIATION
NT TWILIGHT GLOW
NT WHISTLERS
Computer program for calculating constant dose range in air transport of neutron and photon radiation from point source in atmosphere
[LA-DC-13293] 04 p0453 N73-13700
Role of radiation in atmospheric models noting equation of transfer for thermal and solar radiation
05 p0573 N73-14656
Analysis of atmospheric optical properties with application to night vision, infrared radiation, astrogeophysics, and electro-optical physics
[AD-750610] 06 p0669 N73-15443
Mesoscale variation of outgoing spectral radiation near 15 microns
[AD-757622] 14 p1663 N73-23500
Upper atmospheric neutral hydrogen distribution
15 p1779 N73-24423
Atmospheric radiation transmission research, including aerosol, sky radiance, and electromagnetic field studies
[AD-758771] 15 p1784 N73-24460
Radiometric measuring system for solar activity and atmospheric attenuation and emission
[NASA-CASE-ERC-10276] 17 p2031 N73-26432
Comparison of Nimbus interferometer spectrometer observations and theoretical radiances between 425 to 1450/cm
[NASA-TM-X-66275] 18 p2142 N73-27314
Balloon measurements on atmospheric secondary gamma rays using digitized spark chamber
[NASA-TM-X-66278] 18 p2195 N73-27718
Cerenkov light technique for measuring high energy gamma rays in air showers
19 p2332 N73-28760
Analysis of methods for interpreting satellite radiation measurements to determine physical parameters of atmosphere which affect earth radiation field
20 p2399 N73-29281
Characteristics of vertical structure of temperature and humidity fields in earth atmosphere based on satellite radiation data of earth surface temperature
20 p2399 N73-29282
Development of numerical methods for computation of vertical divergence of thermal radiation
20 p2400 N73-29290
Development of mathematical relationships to determine short-wave thermal radiation under cloudy and cloudless conditions
20 p2401 N73-29291
Application of airborne actinometric measurements to determine transmission, absorption, and reflection of solar radiation by clouds
20 p2401 N73-29292
Balloon sounding program to measure all components of atmospheric radiation balance and analysis of atmospheric stratification
20 p2401 N73-29293
Development of numerical method for determining long wave radiation balance of atmosphere based on effective surface radiation
20 p2401 N73-29295
Development of numerical methods for improving accurracy of calculations of thermal radiation in earth atmosphere
20 p2401 N73-29297
Development of method for determining atmospheric transmission function with allowance for divergence of thermal radiation
20 p2401 N73-29298
Development of empirical relationship between effective terrestrial radiation, ground temperature, and water vapor pressure in the ground air layer for cloudless skies
20 p2402 N73-29300
Performance tests of radiation thermoelements for radiation flux measurements of atmospheric radiation
20 p2403 N73-29308
Short wave radiation regime compared to atmospheric radiation regime for vegetation
20 p2404 N73-29318
Effects of radiation and heat balance of active surface on life processes of plants with emphasis on productivity of cotton
20 p2404 N73-29323
Analysis of temperature and radiation regime above paddie surfaces as obtained by helicopter-borne radiation thermometer
20 p2405 N73-29324

Comparison between measured transmission and emission spectra and calculated spectra in 9.6 micron region of ozone
[NASA-TT-F-15110] 22 p2665 N73-31356
Atmospheric radioactivity measurements for 1972 obtained at Vienna, Austria
[NP-19753] 24 p2922 N73-33339
Measurement of atmospheric radiation levels at low altitude in vincinity of Vienna, Austria during 1972
[NP-19751] 24 p2922 N73-33340
Measurement of neutron energy spectrum at 9 g/sq cm residual atmospheric
[ORNL-TM-3877] 24 p2976 N73-33783

ATMOSPHERIC REFRACTION
NT RADIO WAVE REFRACTION
Mach-Zehnder interferometric determination of nitrogen and oxygen atom specific refractivities during atmospheric entry
[AD-745132] 02 p0138 N73-11114
Ionospheric refractivity influence on electromagnetic wave propagation errors discussing electron density profiles
[DLR-MITT-71-31] 03 p0266 N73-12154
Airborne measurements of optical atmospheric properties and southern Germany during spring 1970
[AD-747490] 03 p0298 N73-12429
Wave propagation and refraction of Type-1 irregularities in equatorial electrojet
[NASA-CR-130382] 07 p0780 N73-16340
Atmospheric refraction effects on geodetic measuAtmospheric rements to celestial bodies
[NASA-CR-131534] 12 p1398 N73-21339
Diurnal cycles of atmospheric refractive index structure function coefficient used to describe scintillation and phase fluctuations of electromagnetic radiation propagated in atmosphere
[AD-755808] 12 p1402 N73-21374
Analysis of ERTS-1 imagery of Los Angeles, California area to determine effects of haze on accuracy of ground truth data
[E73-10691] 16 p1902 N73-25384
Curve fitting method for comparing refractive adjustments in laser satellite ranging
[PB-214447/5] 16 p1909 N73-25445
Comparisons of radar refraction correction computer programs at selected test ranges
[AD-762383] 19 p2297 N73-28470
Using upper air soundings to compute refractive-indcx gradients in lower atmosphere
[AD-762501] 20 p2414 N73-29404
Profiles of atmospheric temperature and optical refractive index structure measured over land and ocean to 3 km above surface
[AD-762460] 20 p2450 N73-29687
Photogrammetric refraction angles through total refraction A
[NASA-TT-F-15074] 24 p2922 N73-33335

ATMOSPHERIC SCATTERING
NT TROPOSPHERIC SCATTERING
Derivation of doubling equations for scattering and transmission functions for a homogeneous isotropically scattering atmosphere using scattering matrix
[USC-113P19-32] 02 p0202 N73-11631
Scintillation reductions in multiwavelength laser propagation by near field transmitter apertures
[AD-747640] 03 p0337 N73-12751
Disposition of scattering layers over polar-regions as observed by OGO-6 airglow photometer
[NASA-CR-130271] 07 p0791 N73-16436
Nephelometer design and data on total light scatter and backscatter component of extinction of light due to aerosols
08 p0899 N73-17281
Observability of high altitude aerosol and atmospheric scattering layers by satellite-borne optical detector
[NASA-CR-112309] 18 p2144 N73-27329
Restorstion of atmospherically degraded laser beam and definition of isoplanatic patch size
[AD-760548] 18 p2158 N73-27437
Development of backscattering diagrams for sources of reflections from clear sky based on signatures from meteorological radar
21 p2571 N73-30600

ATMOSPHERIC SHELLS
U ATMOSPHERIC STRATIFICATION

ATMOSPHERIC STRATIFICATION
Radar techniques for measuring turbulent layers in lower stratosphere and rain in troposphere
02 p0197 N73-11593
High resolution radar scattering data for determining refractive structure in troposphere
02 p0197 N73-11594
Development of occultation satellite system for determining atmospheric pressure at various millibar levels
02 p0198 N73-11601
Numerical analysis and diagnostics of nonradially stratified media applied to distributions lacking spherical symmetry
02 p0200 N73-11614
Development of mathematical models to analyze stability characteristics of thermally stratified shear flow in atmosphere
[ORO-4199-1] 03 p0296 N73-12414
Aircraft measurements of microscale motions and atmospheric structure associated with thin echo layers in stable stratified zones
[AD-749512] 05 p0540 N73-14393
Multipath propagation and phase delay of ultrahigh frequency radio wave caused by atmospheric discontinuity
17 p1994 N73-26124
Aerological ozone sounding
[AD-762291] 19 p2297 N73-28469
Characteristics of vertical structure of temperature and humidity fields in earth atmsophere based on satellite radiation data of earth surface temperature
20 p2399 N73-29282
Application of satellite observation data for determining statistical relationship between cloud field and outgoing short wave radiation in earth atmosphere
20 p2399 N73-29283
Balloon sounding program to measure all components of atmospheric radiation balance and analysis of atmospheric stratification
20 p2401 N73-29293
Ultraviolet evening terminator observations in Martian atmosphere by Mariner 9 space probe
23 p2841 N73-32702

ATMOSPHERIC TEMPERATURE
Aperiodic processes and formation of seasonal temperature and wind fields in stratosphere in Northern Hemisphere, and tropospheric influences
[NLL-M-20086-[5828.4F]] 01 p0043 N73-10342
Variational extrapolation method for wind and atmospheric temperature analysis
[AD-745354] 01 p0051 N73-10413
Comparison of statistical and iteration methods for obtaining vertical temperature profiles from multispectral radiation measurements
02 p0196 N73-11589
High altitude wind and temperature measurement data from meteorological sounding rockets, and radiosondes for May 1971
02 p0204 N73-11651
Infrasonic resonance tube determination of wind and temperature variabilities in lower troposphere
[AD-745912] 02 p0206 N73-11667
Synoptic weather charts of daily and monthly heights and temperature for Northern Hemisphere from Jan. to Dec. 1968
[AD-746659] 02 p0206 N73-11673
Three-dimensional, two-constituent model for composition characteristics, temperature and mass density of magnetic storm
[NASA-TM-X-66112] 03 p0294 N73-12394
Development of system to correct upper atmosphere temperature readings to ambient air temperature
[AD-747973] 03 p0298 N73-12433
Temperature, pressure, and related climatological data for Australia - tables for [May, 1972]
04 p0441 N73-13598
Temperature, pressure, and related climatological data for Australia - tables for [April 1972]
04 p0442 N73-13599
Survey of methods for sounding atmospheric temperature profile by remote measurement
[NASA-CR-130110] 04 p0442 N73-13601
Variability of temperature field of troposphere, stratosphere, and mesosphere in winter
04 p0442 N73-13606
Analysis of mean distribution maps for altitude and temperature of tropopause over Northern Hemisphere in Jan. and July between 1957 and 1965
04 p0442 N73-13607
Errors in air temperature measurement resulting from instrument inertia
04 p0443 N73-13615
Temperature measurement of air layer directly over ocean surface
[NLL-M-20745-[5828.4F]] 05 p0529 N73-14308
Correlation coefficient between D region HF radio wave absorption and 10mb level winds and temperature in Northern Hemisphere
[COO-2195-5] 05 p0539 N73-14384
Relation of solar activity to air temperature and precipitation
[NLL-M-20651-[5828.4F]] 05 p0570 N73-14626
Statistical determination of atmospheric temperatures at mandatory pressure levels in North American Arctic for regional extreme model atmosphere
[AD-750170] 06 p0669 N73-15445
Composition, temperature, and optical properties of Jupiter and Saturn atmospheres
[NLL-M-20702-[5828.4F]] 06 p0716 N73-15845
Model of Venus atmospheric composition, temperature, and circulation based on Mariner 5 and Venera 4, 5, 6, and 7 data
[NASA-TM-X-66140] 06 p0719 N73-15865
Electrical and meteorological experimentation in upper atmosphere of polar regions - bibliography
[AD-751336] 07 p0796 N73-16472
Reference atmosphere mean temperature and altimetric corrections
07 p0859 N73-16963
Analysis of heat supply requirements and heating availability in geographical areas of USSR
[JPRS-58114] 08 p0917 N73-17513
Extreme temperature, pressure, and density of atmosphere between 30 and 80 km
[AD-751874] 08 p0919 N73-17530
Thermal parameters as predictors of precipitation at Ellsworth, S.D.
[AD-753418] 09 p1061 N73-18657
Graphical method for determining soil temperature from air temperature and humidity measurements
[NLL-M-22802-[5828.4F]] 11 p1274 N73-20339
Forecasting monthly mean air temperature anomalies by analogs
[NLL-M-22859-[5828.4F]] 11 p1313 N73-20655
Extrapolation technique to obtain estimates of mesospheric density, pressure, and temperature
[NASA-CR-2223] 12 p1401 N73-21364
Mean temperature lapse rates within lower 300 meters
[NLL-M-22838-[5828.4F]] 12 p1419 N73-21503
Tabular listing of minimum and maximum temperatures for use in specifying fuel and lubricant properties needed in different geographical areas
[AD-756420] 14 p1685 N73-23675
Determining past global climate by determining past trends in surface temperature of earth
[AD-757225] 14 p1686 N73-23683
Operational exploitation of satellite infrared channel radiances in resolution of atmospheric thermal-structure variabilities
[AD-757773] 15 p1782 N73-24443
Northern Hemisphere ground weather maps for July through December, 1972
[QR-2-PT-2] 15 p1804 N73-24624
Satellite infrared channel radiances for resolution of atmospheric thermal structure and developing weather analysis and forecasting system
[AD-758734] 15 p1807 N73-24644
Raman scattering techniques in atmospheric temperature measurements
[NASA-TM-X-68250] 16 p1906 N73-25422
Ice crystal multiplication in convective precipitation considering cloud top temperature
[PB-215626/3] 16 p1908 N73-25439
Data processing techniques for radiometry
[PB-214184/4] 16 p1939 N73-25689
Feasibility of using adaptive estimation for atmospheric temperature forecasting
[AD-759546] 16 p1940 N73-25698
Model for predicting atmospheric parameters at altitudes between 90 and 2500 km
[NASA-SP-8021] 18 p2143 N73-27325
Statistical determination of temperature at mandatory pressure levels in Arctic region
[AD-761474] 19 p2316 N73-28627
Thermal parameters as predictors of precipitation at Carswell AFB, Texas
[AD-762289] 19 p2318 N73-28644
Analysis of atmospheric temperature inversion conditions and requirements for thermal convection for removal of temperature inversion effects
[NLL-M-23034-[5828.4F]] 20 p2391 N73-29204
Characteristics of vertical structure of temperature and humidity fields in earth atmsophere based on satellite radiation data of earth surface temperature
20 p2399 N73-29282
Numerical analysis of dependence of transmission function of atmosphere on temperature of radiation source
20 p2402 N73-29299
Development of empirical relationship between effective terrestrial radiation, ground temperature, and water vapor pressure in the ground air layer for cloudless skies
20 p2402 N73-29300
Methods for studying effect of sea on thermal regime of atmosphere
20 p2445 N73-29636
Numerical forecasting of geopotential, temperature, dew point fields at 850 millibar level
20 p2446 N73-29650
Profiles of atmospheric temperature and optical refractive index structure measured over land and ocean to 3 km above surface
[AD-762460] 20 p2450 N73-29687
Exploitation of satellite observed radiances for increased resolution of atmospheric thermal structure
[AD-762752] 20 p2450 N73-29692
Calculation of temperature fields of solids under conditions of natural heat exchange with atmosphere
[AD-762494] 20 p2486 N73-29968
Regional extreme atmospheric model for aerothermodynamic calculation of probable vertical temperature profile
[AD-763671] 21 p2540 N73-30369
Multiparameter method for forecasting monthly mean air temperature anomalies in U.S.S.R.
[NLL-M-23038-[5828.4F]] 21 p2567 N73-30577
Theoretical study of thermal structure and dispersion in polluted urban atmosphere
21 p2568 N73-30579
Influence of C02 concentration on thermal regime of clear sky
21 p2573 N73-30615
Forecasting mean monthly air temperature anomalies for Oct. in northern part of European territory of USSR
22 p2693 N73-31575

Statistical weather forecasting using Gumbel theory noting application to atmospheric temperature long term effects
[MONO-89] 23 p2814 N73-32500
Radiosonde sounding data for determining vertical atmospheric temperature and humidity profiles
[AD-764949] 23 p2815 N73-32508
Methods for measuring and elaborating atmospheric phenomena and meteorological yearbook
[EUR-4943] 24 p2949 N73-33554
Measurement of air-sea temperature in relation to incident solar energy
24 p2975 N73-33773

**ATMOSPHERIC TIDES**
Derivation of temperature fields from Mariner 9 infrared spectroscopy and calculation of Martian atmospheric tidal pressure and wind fields
[NASA-TM-X-66230] 12 p1458 N73-21818
Phenomenological concepts of earth electrical structure controlled by neutral atmosphere dynamics of stratospheric tides
16 p1895 N73-25330
Formation theory of sporadic E by tidal wind systems
17 p2017 N73-26306
Numerical solution and internal gravity wave approximation of solar semidiurnal tidal mode behavior in dissipative atmospheres
[NASA-CR-132779] 17 p2025 N73-26383
Diurnal temperature variations and upper atmospheric tides
22 p2736 N73-31908
Classical tide calculations for atmospheric response to lunar diurnal component
24 p2979 N73-33810

**ATMOSPHERIC TURBULENCE**
NT CLEAR AIR TURBULENCE
NT GUSTS
NT LOW LEVEL TURBULENCE
Newton-Raphson least squares percentage error method for determining atmospheric turbulence field parameters
[AD-745946] 01 p0078 N73-10641
Variations of microturbulent velocity with atmospheric phase and height in classical Cepheids
[NASA-TM-X-66081] 01 p0105 N73-10867
Turbulence, billows, and gravity waves in high shear region of upper atmosphere during morning twilight, determined by rocket-released lithium cloud
[WRE-TN-670[WR/D]] 02 p0164 N73-11327
Radar techniques for measuring turbulent layers in lower stratosphere and rain in troposphere
02 p0197 N73-11593
Linear differential equations describing aircraft lateral motion in presence of atmospheric turbulence
[AASU-311] 03 p0253 N73-12045
Proceedings of conference on air pollution, turbulence, and diffusion
[SC-M-71-0913] 03 p0327 N73-12662
Development of method for estimating length of atmospheric turbulence patch as function of different turbulence intensities for two or more regions
[NRC-12793] 04 p0370 N73-13009
Effects of turbulence instabilities on laser propagation
[AD-748809] 04 p0450 N73-13677
Stellar evolution and atmospheric turbulence dynamics for chromospheric activity model
04 p0466 N73-13799
Method for predicting flight characteristics of F-5 and A-7 aircraft during atmospheric turbulence using large amplitude flight simulator
[AD-749480] 05 p0495 N73-14030
Acoustic gravity wave generation by transient sources in isothermal atmosphere
05 p0508 N73-14139
Acoustic gravity wave propagation modes in ionosphere and neutral atmosphere following nuclear explosion
[CONTRIB-1799] 05 p0509 N73-14140
Infrasonic wave generation and atmospheric propagation of gravity acoustic waves
05 p0509 N73-14142
Excitation of Lamb atmospheric edge mode by tail of large atmospheric explosion
05 p0509 N73-14143
Detection of tropospheric turbulence and gravitational waves by radar sounding
05 p0510 N73-14151
Model of turbulent structure and diffusion for studying movement of air pollution
[PB-211897] 05 p0540 N73-14397
Aviation hazards of turbulence and shear in stable stratified atmosphere
[CONF-720535-2] 06 p0694 N73-15653
Measurement of critical atmospheric turbulence for aircraft takeoff and landing
[AD-750131] 06 p0694 N73-15660
Development of automatic system for controlling aircraft under turbulent atmospheric conditions to provide pitch stabilization
[AD-751148] 07 p0741 N73-16028
Determination of turbulent structure of atmosphere through analysis of perturbations induced upon radio wave propagation
07 p0775 N73-16292
Large scale turbulence and diffusion of pollutants in atmosphere
[COO-1585-22] 07 p0793 N73-16449
Small scale interaction between ocean and atmosphere [heat flow, vapor, and momentum]
[AD-751415] 07 p0796 N73-16474
Analysis of laser beam scintillation due to atmospheric turbulence
[AD-752565] 08 p0930 N73-17620
Development of model for analyzing propagation of weak normal shock wave through turbulent atmosphere and application to sonic boom characteristics
[NRC-12981] 09 p0983 N73-18028
Interaction between radiative transfer and turbulent exchange in lower layers of atmosphere
[NASA-TT-F-14518] 09 p1026 N73-18378
Effects of earth surface characteristics on cumulus scale convection for stable and unstable boundary layers above relatively dry ground
[AD-752914] 09 p1031 N73-18416
Ellipticity condition of three dimensional partial differential equation as turbulence criterion in atmospheric motion
[AD-746624] 09 p1032 N73-18424
Behavior comparison of certain properties generated by different forms of eddy diffusion term in two dimensional turbulent flow
[AD-753619] 09 p1032 N73-18425
Temperature influence on atmospheric diffusion and turbulence near ground level
[AD-753350] 09 p1033 N73-18434
Effects of turbulence instabilities on laser propagation
[AD-753401] 09 p1044 N73-18515
Analysis of gust alleviation system for short takeoff aircraft for improved performance under random turbulence conditions
[NASA-TN-D-7201] 11 p1233 N73-20013
Stratospheric turbulence as an effect of jet streams, vorticity, temperature gradients, and temperature distribution
[NLL-M-22823-[5828.4F]] 11 p1274 N73-20338
Aerosynoptic wind and temperature conditions contributing to atmospheric turbulence at altitude of 18 km over European USSR
[NLL-M-22822-[5828.4F]] 11 p1274 N73-20342
Statistical properties measurements of atmospheric turbulence at altitudes below 1000 ft over hilly and flat terrain
[LR-567] 11 p1285 N73-20428
Meteorological investigation of stratospheric turbulence using radiosonde data
[NLL-M-22819-[5828.4F]] 12 p1419 N73-21502
Effect of Doppler radar pulse volume on atmospheric turbulence measurements
[AD-755440] 12 p1423 N73-21534
Doppler radar measurement of turbulent air associated with stalactite cloud base zone
[AD-755441] 12 p1423 N73-21535
Doppler radar measurement of atmospheric turbulence structure function
[AD-755439] 12 p1423 N73-21536
Instrumentation and data handling process of NAE T-33 turbulence research aircraft, stationary gas turbine icing problems, and role of plastic deformation in metal powder compaction
[DME/NAE-1972[4]] 12 p1466 N73-21882
Designing aircraft for combined effects of vertical, lateral, and longitudinal turbulence by power spectral techniques
[AD-756886] 13 p1475 N73-21951
Various atmospheric disturbances including turbulence, sonic boom, and shock wave propagation
13 p1514 N73-22271
Method for calculating turbulent fluxes by measuring meteorological parameters at two meter height
13 p1552 N73-22576
Model of symmetric large scale whirl using equations of motion as applied to satellite data
[AD-756096] 13 p1554 N73-22596
Weather forecasting and atmospheric activity detection using meteorological radar and remote sensing equipment
[AD-755438] 13 p1554 N73-22597
Oscillation and supergranulation motions in solar atmosphere
[NASA-CR-131606] 13 p1579 N73-22797
Wind gust effects on STOL type aircraft
14 p1600 N73-22971
Simulation of wind gust effects on aircraft
14 p1645 N73-23338
Optical apparatus to determine effect of turbulence on modulation transfer function of atmosphere
[AD-757256] 14 p1661 N73-23485
Laser beam propagation in turbulent air
[AD-757221] 14 p1673 N73-23574
Laser beam scintillation caused by atmospheric turbulence
[AD-757562] 14 p1674 N73-23580
Research projects involving boundary layer flow, heat transfer during aerodynamic heating, atmospheric turbulence effects, and airframe structural analysis - Vol. 2
15 p1727 N73-24011
Analysis of atmospheric turbulence characteristics to show discrete gust and spectral presentations and to determine limitations of discrete gust approach
[ARC-R/M-3216] 15 p1729 N73-24026
Split-film atmospheric turbulence anemometer evaluation
[NASA-CR-62093] 16 p1914 N73-25485
Development of method for remotely determining average transverse wind velocity and atmospheric structure constant along line of sight path
16 p1937 N73-25670
Effects of rain and atmospheric turbulence on ultrahigh frequency space communication radio line
17 p1996 N73-26143
Development of wind and turbulence model for surface boundary layer based on surface parameters of stability and height
[NASA-CR-2288] 18 p2104 N73-27021
Radar measurement of atmospheric turbulence structure function
18 p2170 N73-27526
Balloon measurements of stellar scintillation for predicting fading on space to ground laser propagation path
18 p2212 N73-27858
Polarization fluctuation of beam wave propagating in random atmosphere
19 p2234 N73-28014
Comparison between ground based atmospheric turbidity network measurements and ERTS-1 MSS channel 4 scene grayness measurements
19 p2284 N73-28373
Effect of eddy turbulence in development of models of lower and upper thermosphere
[NASA-TM-X-70431] 19 p2293 N73-28443
Determining diffusion of impurities in atmosphere by mixing properties of turbulence
[NLL-M-23009-[5828.4F]] 20 p2390 N73-29198
Propagation of multiwavelength laser radiation through atmospheric turbulance
[AD-762516] 20 p2426 N73-29491
Effect of atmospheric turbulence on stability of laser radiation propagation
[AD-763109] 20 p2427 N73-29494
Model for calulating coherence function for atmospheric turbulence
[NPL-MAR-SCI-R-108] 20 p2449 N73-29675
Determination of turbulent velocities in solar photosphere with allowance for influence of instrumental contour
20 p2472 N73-29855
Effects of turbulence in Venus atmosphere on Pioneer Venus radio
[JPL-TM-33-644] 20 p2473 N73-29866
Space vehicle design criteria based on interplanetary charged particle environments
[NASA-CR-124341] 20 p2474 N73-29876
Larger aircraft landing approach performance and altitude control during atmospheric turbulence and wind shear
[NLR-TR-72023-U] 21 p2497 N73-30036
Development of theory for adaptive control of aircraft in atmospheric turbulence using stochastic identification method
[AD-763739] 21 p2498 N73-30051
Application of meteorological radar measurements of atmospheric turbulence using velocities of reflectors located in scattering volume of radar set
21 p2570 N73-30596
Application of radar signatures for analyzing the turbulent flow structure of earth adjacent layers of subfrontal clouds and precipitation
21 p2570 N73-30597
Development of methods for conducting radar measurements of parameters of atmospheric turbulence
21 p2570 N73-30598
Comparison of laser Doppler measurements of wind velocities and turbulence with measurements by anemometers
[NASA-CR-124355] 21 p2574 N73-30627
Methods for obtaining vertical motion signs at various atmospheric levels to explain areas of rain and no rain
[NASA-CR-2304] 22 p2694 N73-31577
Atmospheric circulation and turbulence forecasting
[AD-764919] 23 p2815 N73-32507
Turbulence effects on fireball dynamics
[LA-UR-73-713] 24 p2923 N73-33347
Atmospheric turbulence near tropopause over mountainous terrain
24 p2946 N73-33525
Zones of severe turbulence in troposphere
24 p2946 N73-33527

**ATMOSPHERIC WINDOWS**
Nimbus 4 IRIS spectra in 750-1250/cm atmospheric window region
[NASA-TM-X-66281] 18 p2142 N73-27315

**ATMOSPHERICS**
NT DAWN CHORUS
NT HISS
NT IONOSPHERICS
NT WHISTLERS

Atmospheric observation techniques using aircraft infrared radiometers as prototypes for spacecraft remote sensing application
[NOAA-TR-NESS-64] 11 p1293 N73-20494
Computer control of Atmosphere Explorer spacecraft
[NASA-TM-X-66209] 11 p1341 N73-20884
Atmospheric noise model with application to low frequency radio navigation receivers
[AD-757275] 13 p1493 N73-22101
Radar clutter and false alarm probability by high frequency atmospheric noise
[AD-756842] 13 p1493 N73-22104
High speed digital recording system for VLF and ELF sferic waveforms
[AD-757427] 14 p1669 N73-23544
Computer analysis of digitized sferic data from atmospheric analyzers
[AD-758102] 15 p1783 N73-24453
Digitally recorded sferics waveforms providing ELF attenuation rates for day and night propagation
[AD-760686] 18 p2119 N73-27132
Atmospheric noise measurements from Cosmos 149, 243, 320, and 394 satellites
[NASA-TT-F-14977] 18 p2143 N73-27319
Application of radio wave propagation and radar signatures for analyzing structure of clouds
21 p2569 N73-30589
Application of pulsed Doppler radar for analyzing motion of sources of reflection from clear skies to show effect of wind
21 p2571 N73-30601
USSR research in solid state physics, plasma physics, atmospheric physics, and seismology
[AD-763743] 23 p2866 N73-32918

**ATOM CONCENTRATION**
Organic dye pulsed laser for detecting individual atomic species concentration in upper atmosphere
[AD-747335] 02 p0169 N73-11377

**ATOMIC BATTERIES**
U RADIOISOTOPE BATTERIES

**ATOMIC BEAMS**
Reaction kinetics in pulsed atomic beam generation by laser vaporization of metallic atoms
[AD-748278] 04 p0387 N73-13145
Crossed beam method for measuring photoionization cross section on atomic barium beam
06 p0707 N73-15770

**ATOMIC BOMBS**
U FISSION WEAPONS

**ATOMIC CLOCKS**
Progress report from Bureau International de l Heure for period 1967 to 1971, including earth rotation, atomic time scale, and coordination of time signals
05 p0596 N73-14848
Concepts, physical principles, and design features of frequency standards and clocks
[NBS-TN-616] 10 p1160 N73-19435
Modeling atomic clock performance and detection of abnormal clock behavior
[NBS-TN-636] 12 p1427 N73-21565
Proceedings of conference on precise time and time interval planning for application to hypersonic navigation systems
[AD-758739] 16 p1942 N73-25717
Flight test and evaluation of system for providing precise time signals to aircraft in flight using distance measuring [VORTAC] ground station and cesium beam atomic clock
[FAA-NA-73-23] 21 p2577 N73-30652

**ATOMIC COLLISIONS**
Fabry-Perot laser interferometer for studying atomic collisional rate and ionization relaxation time in helium shock wave
[AD-749553] 04 p0408 N73-13326
Monte Carlo calculations of reaction rates for collisions of H atoms with vibrationally excited HF
[AD-751910] 08 p0884 N73-17157
Research reports on SQUID programs related to fluid mechanics, and atomic and molecular collisions
[AD-752037] 08 p0955 N73-17820
Phase-space theory for electron excitation in slow atomic collisions
[PUBL-73-4] 17 p2064 N73-26699
Inelastic atom-atom scattering within intense laser beam
[AD-761180] 18 p2159 N73-27442
Cross section for collision processes between molecular oxygen and electron with collision energy below 100 eV
[NASA-TT-F-15048] 23 p2821 N73-32550

**ATOMIC ENERGY**
U NUCLEAR ENERGY

**ATOMIC ENERGY LEVELS**
Data tables of atomic spectra derived from optical analyses
[NSRDS-NBS-3-SECT-6] 01 p0082 N73-10677
Ionization and excitation cross section measurements on degenerate helium levels
[NASA-TM-X-66137] 05 p0582 N73-14738
Quantum electrodynamic view of superradiance as competition between stimulated and spontaneous atomic decay
[AD-750005] 05 p0582 N73-14741
Photoionization cross section measurements on excited cesium maser by light beams
[AD-756217] 13 p1564 N73-22677
Spectroscopic analysis of energy transfer in rare earth compounds to determine effect of transfer phenomena on lasing efficiency
[AD-757520] 14 p1673 N73-23579
Design, development, and operation of carbon dioxide-nitrogen-helium laser to show beam characteristics and power output as function of gas mixture
[AD-757263] 14 p1674 N73-23582
Collision cross section of D line radiated into sodium atoms for one 3 P2 state
[NASA-TT-F-14853] 14 p1695 N73-23752
Absolute polarization and microwave optical photoselection spectroscopy of zerofield transitions of triplet state
[AD-759996] 17 p1993 N73-26115
Properties of nuclear gamma ray line emissions during solar flares
19 p2336 N73-28796
Development of method for calculating molar volume and density of molten binary alloys with strongly interacting dissimilar atoms
[NLL-M-21695-[5828.4F]] 20 p2429 N73-29512
Density matrix methods developed and applied in investigation of electronic structure of atoms
[AD-763815] 22 p2709 N73-31692
Atomic structure of stripped heavy ions and their formation and destruction by collisions
[NASA-CR-135704] 23 p2821 N73-32553
Xenon laser terminating on dissociating level
[SLA-73-5285] 24 p2931 N73-33412

**ATOMIC EXCITATIONS**
Excitation of N 1 ultraviolet multiplets by electron impact on atomic nitrogen
[NASA-CR-129087] 02 p0214 N73-11730
Ionization and excitation cross section measurements on degenerate helium levels
[NASA-TM-X-66137] 05 p0582 N73-14738
Electron impact excitation and ionization cross sections of nitrogen atoms
[AD-749807] 05 p0582 N73-14742
Field evaporation model for predicting tungsten surface potential in electric field
[AD-750205] 05 p0588 N73-14786
Reaction kinetics in vibrationally excited nitrogen quenching by atomic oxygen
[AD-752542] 08 p0946 N73-17751
Optical excitation of atomic levels for orientation of nuclei, polarized electron production, and magnetic resonance experiments
[NASA-TT-F-14862] 11 p1326 N73-20765
Spin-orbit interactions with singlet-triplet mixing in excited states of helium
16 p1947 N73-25751
Optical potential approach to electron-atom impact ionization threshold problem
[NASA-TM-X-66282] 18 p2181 N73-27609
Helium excitation and structure of quiescent solar prominences
20 p2472 N73-29859

**ATOMIC EXPLOSIONS**
U NUCLEAR EXPLOSIONS

**ATOMIC GASES**
U MONATOMIC GASES

**ATOMIC MASS**
U ATOMIC WEIGHTS

**ATOMIC PHYSICS**
Long-range forces between atoms at large distances, and weak forces arising from neutrino-antineutrino exchange
[TR-73-049] 03 p0339 N73-12764
Research in physics
[LUNP-7201] 04 p0452 N73-13690
General conference of European Physical Society on trends in physics
[AD-757261] 14 p1693 N73-23738
International conference on fundamental atomic and molecular physics
[AD-757890] 15 p1816 N73-24717

**ATOMIC RECOMBINATION**
NT OXYGEN RECOMBINATION
Searches for interstellar OH and other molecular emission and recombination lines in radio frequency range
[RR-108] 09 p1084 N73-18845

**ATOMIC SPECTRA**
Data tables of atomic spectra derived from optical analyses
[NSRDS-NBS-3-SECT-6] 01 p0082 N73-10677
Atomic line shapes, shifts, and broadening - bibliography for 1889 through Mar. 1972
[NBS-SP-366] 02 p0214 N73-11732
Atomic and molecular spectra of SC stars
04 p0469 N73-13821
Research projects in atomic and molecular spectroscopy
[NASA-CR-131829] 13 p1495 N73-22119
Chemical analysis of iron, steel, and nonmetallic materials
[PB-214230/5] 16 p1929 N73-25609

**ATOMIC STRUCTURE**
Physics research on solid state materials - radiation damage, electronic structure, and magnetic, electrical, surface, low temperature, and lattice properties
[ORNL-4779] 06 p0706 N73-15776
Electron structure of transition metals and alloys
[ONERA-P-144] 09 p1048 N73-18548
Rare earth electronic configurations, physiochemical properties, and implications of analytical chemistry
[IS-2966] 10 p1126 N73-19170
Electronic structure in disordered amorphous materials and dense helium
[AD-755260] 13 p1567 N73-22701
Electronic structure and properties of covalent and polar solids
14 p1697 N73-23773
Statistical mechanics for relating material properties to their atomic and molecular structures
[AD-758257] 15 p1814 N73-24708
Analysis of dynamic Stark effect in laser-atom interactions to show distortion of atomic structure in high intensity laser fields
[CEA-CONF-2135] 20 p2425 N73-29481
Production and characteristics of refractory materials for high temperature applications
[NLL-RTS-7942] 20 p2433 N73-29543

**ATOMIC THEORY**
NT HEISENBERG THEORY

**ATOMIC WEIGHTS**
Correlation of materials properties with atomic density concept for alkali halides
[NASA-CR-124095] 09 p0999 N73-18156

**ATOMIZATION**
U ATOMIZING

**ATOMIZING**
Heat and mass transfer analysis of liquids and air flowing in opposite directions under various atmospheric pressures
[AD-751503] 07 p0856 N73-16938
Model for liquid fuel sprayed into supersonic gaseous stream and two phase flow of dispersed liquid
[AD-753515] 09 p1019 N73-18316
Energy addition from propellant spray combustion to liquid fuel efficiency
[AD-755879] 12 p1443 N73-21687
Atomized particle dispersion in dryer space
[AD-762221] 19 p2233 N73-28005
Effects of accelerating gas flow on atomization characteristics of liquid sprays produced by impinging two liquid jets - Part 1
[NASA-CR-134478] 22 p2652 N73-31247
Secondary atomization produced by accelerating gas flow to show effects on liquid sprays produced by impinging two liquid jets - Part 2
[NASA-CR-134479] 22 p2652 N73-31248

**ATOMS**
NT HELIUM ATOMS
NT HYDROGEN ATOMS
NT METASTABLE ATOMS
NT NITROGEN ATOMS
NT OXYGEN ATOMS
Chemiluminescence of Al atoms
[AD-765347] 23 p2755 N73-32044

**ATP**
U ADENOSINE TRIPHOSPHATE [ATP]

**ATROPHY**
Dystrophic degeneration of suprarenal rat cortex during hypokinesia
13 p1481 N73-22003
Atrophy and metabolic changes in internal organs and skeletal muscles of rats exposed to hypokinesia
14 p1607 N73-23029

**ATROPINE**
Temporary blindness of monkeys caused by combined effects of phosdrin and atropine exposure
[FAA-AM-73-4] 18 p2109 N73-27035

**ATS [SATELLITES]**
U APPLICATIONS TECHNOLOGY SATELLITES

**ATS 1**
Correlation between frequency of magnetic oscillations and geomagnetic disturbances, and low frequency oscillation of earth magnetic field
[NASA-CR-127801] 05 p0537 N73-14372
Correlation between frequency of magnetic oscillations observed by ATS 1 and two indices of geomagnetic disturbance
05 p0537 N73-14373
Low frequency oscillations of earth magnetic field observed by ATS 1
05 p0537 N73-14374
Diurnal electron content tables obtained at Hawaii during 1971
07 p0789 N73-16419
Geomagnetic micropulsations during magnetic storms as observed by ATS 1
12 p1447 N73-21716
Scintillation and polarimeter measurements of ionospheric column using ATS 1
[AD-759533] 16 p1910 N73-25451
Experimental system for conducting ionospheric scintillation measurements using ATS geostationary satellites at 136 and 1550 MHz
[PB-220564/9] 21 p2509 N73-30133

Cataloging of Pc4 and Pc5 micropulsations at ATS-1
[NASA-CR-133847] 21 p2583 N73-30698
ATS 3
Faraday rotation angle phi of radio signal from ATS-C
[AD-753088] 09 p1031 N73-18414
Tornado occurrences related to overshooting cloud-top heights as determined from ATS 3 photographs
[NASA-CR-131875] 13 p1551 N73-22567
VHF/UHF technique for determination of columnar electron contents of plasmasphere and of protonosphere using geostationary satellite transmissions of magnetic storm observations
15 p1770 N73-24338
ATS-3 satellite measurement of ionospheric effects during partial solar eclipses of July 10, 1972
[AD-758855] 15 p1784 N73-24461
Experimental system for conducting ionospheric scintillation measurements using ATS geostationary satellites at 136 and 1550 MHz
[PB-220564/9] 21 p2509 N73-30133
System design and test plan for NASA position location and aircraft communications equipment at C band using USNS Vanguard and ATS 3 and ATS 5 satellites
[NASA-TM-X-70447] 21 p2576 N73-30646
ATS 5
Characteristics of diversity satellite-to-ground communication link measured using ATS 5 15.3 GHz downlink
[NASA-CR-130118] 03 p0265 N73-12144
Design of experiment to measure communication characteristics of wideband satellite to ground communication links
[NASA-CR-130196] 11 p1294 N73-20497
Spin reorientation of nonsymmetric body with energy dissipation, using ATS5
[NASA-CR-131320] 11 p1316 N73-20683
Simultaneous ultrahigh and very high frequency ionospheric effects from ATS 5 at the magnetic equator
[NASA-TM-X-65948] 12 p1378 N73-21173
Thunderstorm cloud height and fading statistics for ATS 5 ultrahigh frequency signal transmission to earth
17 p1996 N73-26141
Ultrahigh frequency precipitation attenuation measurements by ATS 5 weather radar and radiometer
17 p1996 N73-26142
Design, development, and test of NASA-GFSC Position Location and Aircraft Communications Equipment [PLACE]
[NASA-TM-X-66287] 18 p2117 N73-27115
System design and test plan for NASA position location and aircraft communications equipment at C band using USNS Vanguard and ATS 3 and ATS 5 satellites
[NASA-TM-X-70447] 21 p2576 N73-30646
ATS 6
Satellite telecommunication link in health/education experiment using tuned radio frequency receiver
18 p2213 N73-27864
Design, fabrication, and tests of ground station hardware for ATS-F millimeter wave experiment
[NASA-CR-132802] 22 p2673 N73-31409
Application of laser systems to space communication using carbon dioxide laser for two way communication with ATS-F satellite - Vol. 1 Pt. 1
[NASA-CR-132803] 22 p2680 N73-31469
Application of carbon dioxide laser for space communication to include ground equipment, data acquisition, and data processing - Vol. 1 Pt. 2
[NASA-CR-132804] 22 p2681 N73-31470
Requirements for design, fabrication, performance, and testing of optical heterodyne receiver subsystem for use in laser communication system - Vol. 1 Pt. 3
[NASA-CR-132805] 22 p2681 N73-31471
ATTACHMENT
Silicon carbide backward diode with coated lead attachment
[NASA-CASE-ERC-10224-2] 18 p2122 N73-27150
Mechanical attachment of surface insulation tiles to space shuttle structure
24 p2942 N73-33494
ATTACK AIRCRAFT
NT A-4 AIRCRAFT
NT A-6 AIRCRAFT
NT A-7 AIRCRAFT
NT A-37 AIRCRAFT
NT B-1 AIRCRAFT
NT B-52 AIRCRAFT
NT B-57 AIRCRAFT
NT B-70 AIRCRAFT
NT BOMBER AIRCRAFT
NT BREGUET 1150 AIRCRAFT
NT F-14 AIRCRAFT
NT F-15 AIRCRAFT
NT F-100 AIRCRAFT
NT F-102 AIRCRAFT
NT F-104 AIRCRAFT
NT F-105 AIRCRAFT
NT F-106 AIRCRAFT
NT F-111 AIRCRAFT
NT FIGHTER AIRCRAFT
NT GA-5 AIRCRAFT
NT JET PROVOST AIRCRAFT
NT MIRAGE 3 AIRCRAFT
NT OV-10 AIRCRAFT
NT P-1127 AIRCRAFT
NT VULCAN AIRCRAFT
Application of cluster rotation to improvement of existing platforms in strike aircraft
11 p1319 N73-20704
Vertical display techniques for naval all-weather day/night attack aircraft
[AD-755739] 13 p1557 N73-22620
ATTENTION
Self-estimates of distractibility as related to performance decrement on task requiring sustained attention
[FAA-AM-72-25] 02 p0135 N73-11096
Human attention and reaction performance as function of type and latency in response to signal stimulus
[AD-747801] 04 p0382 N73-13110
Cyclically changing temperature effects on monitoring behavior and physiological responses of man
[AD-748451] 05 p0505 N73-14110
ATTENUATION
NT ACOUSTIC ATTENUATION
NT ATMOSPHERIC ATTENUATION
NT AURORAL ABSORPTION
NT MICROWAVE ATTENUATION
NT RADAR ATTENUATION
NT RADIO ATTENUATION
NT SHOCK WAVE ATTENUATION
NT WAVE ATTENUATION
Measurement of sound transmission and attenuation in Tyrrhenian Sea discussing experimental design and results
07 p0858 N73-16959
Attenuation of surface elastic waves as related to mass defects and applied to lunar geology
08 p0958 N73-17837
Maxwell equation and approximation theory for examining attenuation behavior of coaxial cables with woven outer conductors
[RAE-LIB-TRANS-1642] 17 p1997 N73-26147
Diversity and selection effects for improving microwave relay link performance
[AD-756605] 18 p2120 N73-27141
Light beam attenuation in suspensions of algae
20 p2405 N73-29325
Standard coupler effects on EHF attenuation in waveguides with bending moments
[FTZ-A-333-TBR-18] 22 p2632 N73-31096
Nitrogen gas supply system for EHF waveguides to improve attenuation by control of water vapor and oxygen content
[FTZ-A-333-TBR-10] 22 p2642 N73-31175
ATTENUATION COEFFICIENTS
Vertical and horizontal turbulent mixing coefficients of sea water determined from attenuation coefficient
[NLL-RTS-7536] 02 p0160 N73-11294
Characteristics of millimeter attenuation and reflection coefficient measurement system and specifications for waveguide standards fabrication
[NBS-TN-619] 03 p0302 N73-12462
ATTENUATORS
NT POTENTIOMETERS [RESISTORS]
NT RESISTORS
NT THERMISTORS
Rotary vane attenuator with two stators and intermediary rotor, using resistive and orthogonally disposed cards
[NASA-CASE-NPO-11418-1] 04 p0420 N73-13420
Tunable filter system for reducing intermodulation noise in radio transmitter
[AD-754938] 11 p1257 N73-20197
Basic-mode wave attenuator in multimode waveguide
[AD-754516] 11 p1257 N73-20203
Computer-controlled fine attenuators for fine gain adjustments of linear amplifiers
[KFK-1707] 20 p2381 N73-29130
ATTITUDE [INCLINATION]
NT PITCH [INCLINATION]
NT ROLL
NT SATELLITE ORIENTATION
NT YAW
Diurnal variations in ionospheric F region tilts near magnetic equator
[WRE-TN-A-199[AP]] 04 p0414 N73-13384
Diurnal variations in ionospheric tilt near magnetic dip equator due to gravity waves
05 p0512 N73-14160
Design and tests of liquid metal slip ring/solar orientation mechanism
[NASA-CR-120885] 14 p1640 N73-23292
Cartographic evaluation of ERTS-1 orbit and attitude data
[E73-10544] 14 p1654 N73-23419
Spacecraft attitude sensing system design with narrow field of view sensor rotating about spacecraft x-y axis
[NASA-CASE-GSC-10890-1] 21 p2575 N73-30640
ATTITUDE CONTROL
NT DIRECTIONAL CONTROL
NT LATERAL CONTROL
NT LONGITUDINAL CONTROL
NT SATELLITE ATTITUDE CONTROL
NT THRUST VECTOR CONTROL
Simulation control of European SOREL space probe attitude and position
[S-3-1949-VOL-3] 02 p0235 N73-11907
Application of secondary injection to obtain controllable roll moment solid rocket propelled launch vehicles
03 p0350 N73-12856
Analysis of pointing and stability problems of space shuttle sortie mission and application to earth observation and astronomy experiments
[NASA-TM-X-64692] 03 p0355 N73-12892
Characteristics of star field attitude sensor for installation in Pioneer Venus spacecraft
[NASA-CR-114516] 03 p0359 N73-12924
Performance of attitude sensors determined from Skylark 586 payload flight test
[RAE-TR-72066] 03 p0359 N73-12927
Characteristics of thermoelectric outer planet spacecraft attitude propulsion subsystem
[NASA-CR-129795] 04 p0464 N73-13781
Hydrogen oxygen engine for space shuttle attitude control and stationary or pulsed operation
[MBB-UR-158-72-O] 06 p0714 N73-15823
Tests of seat and poppet materials for use in chlorine pentafluoride attitude control system valves
[AD-750873] 06 p0715 N73-15831
Development of computer model to simulate pulse mode performance operation of liquid bipropellant attitude control engines
[AD-752610] 08 p0955 N73-17819
Techniques for determining attitude of rocket axis for vehicle AH 7.886
[AD-751937] 08 p0965 N73-17890
Application of multivariate control theory to design of hierarchial attitude control system for CARD space vehicle
[NASA-CR-124087] 09 p1086 N73-18859
Design criteria for SOREL drag-free space probe discussing attitude control and orbital position estimation
[S-3-1949-VOL-1/2] 09 p1091 N73-18904
Computation of optical sensor output relative to known star magnitudes for attitude control of spacecraft
[NASA-CR-130926] 10 p1212 N73-19859
Apollo experience report on evolution of attitude time line
[NASA-TN-D-7086] 10 p1214 N73-19872
Analysis of Mariner 71 attitude control subsystem flight performance and effects of performance anomalies on subsystem operation
[NASA-CR-131522] 12 p1461 N73-21835
Design of despin mechanism noting angular stiffness, stress analysis, signal transmission, power transmission, instrumentation and ground support equipment
[ESRO-CR[P]-228] 13 p1535 N73-22434
Improved ITOS attitude control system with Hall generator brushless motor and earth-splitting technique
[NASA-TM-X-66232] 14 p1708 N73-23858
Development of electrostatically focused image dissector tube for use in spacecraft attitude control star trackers
[NASA-CR-132153] 15 p1787 N73-24487
Attitude control and auxiliary propulsion for nuclear upper stage of Europa 3 launch vehicle
[TR-TT-4-17/72] 15 p1811 N73-24678
Direct side force control for STOL crosswind landings with analysis of manual and automatic control modes
[AD-759555] 16 p1863 N73-25091
Method for calculating transient thrust and flowrate levels for Mariner type attitude control nitrogen gas jets
[NASA-CR-132987] 16 p1888 N73-25279
Steady-state attitude control propulsion system simulation program
[NASA-CR-128916] 16 p1955 N73-25820
Computer programmers manual for parametric analysis of attitude control propulsion system using converted liquid cryogenics reaction system - Vol. 5 B-3 Part 2
[NASA-CR-133958] 17 p2087 N73-26886
Instrument system to acquire attitude determination data for RAE-B spacecraft
[NASA-CR-132782] 18 p2175 N73-27569
Instrument system to acquire attitude determination data for RAE-B spacecraft
[NASA-CR-132783] 18 p2176 N73-27570
Skylark star-pointing attitude control system using strapdown inertial system
[RAE-TR-71241] 18 p2176 N73-27571
Feasibility demonstration of biowaste propellant resistojet engines for space station attitude control system
[NASA-CR-132269] 18 p2193 N73-27706
Computerized design of variable feedback system for attitude control of hypersonic vehicle
[AD-761493] 19 p2221 N73-27916
Nitrogen and hydrazine leakage of monopropellant ACS valves
[AD-762943] 20 p2423 N73-29465

Test stand for precise measurement of impulse bit and thrust vector of reaction jet thrusters in attitude control system
[NASA-TN-D-7402] 22 p2719 N73-31762
Requirements of flight control systems with regard to aircraft stability and attitude control
[DLR-MITT-72-05] 24 p2877 N73-32978
Digital attitude control system for Explorer 50 satellite
[NASA-TM-X-70488] 24 p2950 N73-33567

ATTITUDE GYROS
NT GYRO HORIZONS
Design and performance of vibratory output gyro using asymmetrical rotor for rocket inertial attitude control
[NAL-TR-290] 04 p0447 N73-13645
Inertial grade instrumentation for precision strapdown reference system
11 p1318 N73-20699
Double-gimbaled control moment gyro system for maintaining Skylab attitude control without excessive fuel consumption after failure of main gyro system
[NASA-TM-X-64746] 14 p1707 N73-23851
Procedures for calculating attitude of rocket from gyroscopic roll, pitch and yaw
[AD-758764] 15 p1809 N73-24659
Rate integrated gyro attitude control system for sounding rockets
18 p2208 N73-27820
Inertial gyro attitude reference system for pitch and yaw control of OAO spacecraft
18 p2208 N73-27821
Gimballed attitude gyros for Symphonie satellite stabilization
[DGLR-PAPER-73-058] 24 p2927 N73-33377

ATTITUDE INDICATORS
NT GYRO HORIZONS
High resolution attitude sensor for sensing spacecraft attitude relative to light source
[NASA-CASE-LAR-10586-1] 02 p0174 N73-11406
Design and fabrication of radar attitude sensing system
[NASA-CR-128684] 04 p0388 N73-13157
Aircraft horizon and vertical indicator
[NASA-CASE-ERC-10392] 05 p0576 N73-14692
Design of attitude line generator for use with aircraft-type television displays
[AD-757620] 14 p1634 N73-23247
Test performance of computerized strapdown inertial attitude reference system
[NASA-TM-X-2848] 20 p2453 N73-29713

ATTITUDE STABILITY
NT DIRECTIONAL STABILITY
NT GYROSCOPIC STABILITY
NT LATERAL STABILITY
NT LONGITUDINAL STABILITY
Attitude stability of dual spin spacecraft with mathematical model covering fuel sloshing, nutation dampers, and flexible bearings
[ESRO-CR-56] 02 p0235 N73-11908
Bearing flexibility effect on triple-spin satellite attitude stability
[ESRO-SN-121] 03 p0359 N73-12926
Stability of dual-spin satellite system during momentum wheel spin-up maneuver
[NASA-CR-130130] 05 p0597 N73-14858
Flight simulator tests to define minimum acceptable levels of static longitudinal stability for aircraft landing approach following failure of stability augmentation systems
[NASA-TM-X-62200] 06 p0620 N73-15034
Mathematical model and analysis of attitude stability and control of spinning flexible satellite in force-free environment
08 p0964 N73-17876
Attitude control of space vehicles using single movable mass to generate control torques with application to cable-connected, artificial gravity configuration
[NASA-CR-124081] 08 p0964 N73-17880
Attitude stability and alignment of magnetically oriented ESRO I satellite
[ESRO-SN-120-ESTEC] 09 p1085 N73-18854
Application of multivariate control theory to design of hierarchial attitude control system for CARD space vehicle
[NASA-CR-124087] 09 p1086 N73-18859
Derivation of equations of motion for small angular displacements from equilibrium position of earth pointing satellite with reaction wheel damping
[ARC-R/M-3276] 16 p1857 N73-25039
Characteristics of spacecraft control systems to provide examples of attitude control and stabilization for manual and automatic operation
[NASA-TT-F-774] 16 p1966 N73-25903
Pointing error sensor in star tracker system for OAO 3 attitude control
18 p2208 N73-27822
Strapped down gyroscope aligned with sun and star tracker optical axis calibrating roll, yaw and pitch values
[NASA-CASE-ARC-10716-1] 23 p2851 N73-32784
Attitude stability of spinning elastic bodies based on modal analysis and criteria for idealized spinning flexible spacecraft
24 p2950 N73-33564
Stellar-inertial measurement system trade study on spacecraft orbital ephemeris and attitude errors for landmark location
[NASA-CR-134042] 24 p2984 N73-33845

ATTRITION [MATERIALS]
U COMMINUTION

AUDIO EQUIPMENT
NT EARPHONES
NT MICROPHONES
Audio equipment for removing impulse noise from audio signals
[NASA-CASE-NPO-11631] 03 p0277 N73-12244
Instrumentation and methods used with acoustic studio scale model
[BBC-1972/34] 04 p0419 N73-13413
Electronic time compressor/expander for audio using digital technology
14 p1621 N73-23129

AUDIO FREQUENCIES
Effect of reverberation and interfering noise on speech intelligibility as determined from physical description of running speech
14 p1631 N73-23219
Analysis and perception of nonspeech marine sounds
[OES-6/72] 22 p2624 N73-31023

AUDIO VISUAL EQUIPMENT
U TRAINING DEVICES
U VISUAL AIDS

AUDIOMETRY
Speech and tone audiometry for testing auditory acuity of flying personnel
13 p1480 N73-21990
Audiometric thresholds for bare headed subjects, or wearing M1 helmet, and experimental helmet
[AD-745121] 13 p1486 N73-22053
Improvements in intelligibility testing reliability using experienced listeners
14 p1625 N73-23166
Effect of reverberation and interfering noise on speech intelligibility as determined from physical description of running speech
14 p1631 N73-23219
Segmentation and classification of speech using low Q single-tuned filters
14 p1631 N73-23220

AUDITORY DEFECTS
Influence of cockpit noise on hearing in flight crew personnel
[FAA-AM-72-32] 10 p1119 N73-19125
Experimental computer-based system of speech training aids for deaf
14 p1626 N73-23178
Visual vocoder for aiding in speech teaching to deaf
14 p1627 N73-23184
Transient responses of hearing aids with compression
14 p1627 N73-23186
Effects of frequency bandwidth and harmonic distortion of speech intelligibility for normal and hearing impaired subjects
14 p1627 N73-23187
Electrotactile sound detector for deaf to detect and localize sounds
14 p1627 N73-23188
Speech discrimination by personnel with hearing loss at 3 kHz in noise
[AD-752974] 16 p1867 N73-25118
Evaluation of hearing protectors for general aviation aircraft
[NASA-CR-133303] 18 p2112 N73-27078

AUDITORY PERCEPTION
Binaural improvement in normal and defective ears in background of other voices
[AD-746101] 01 p0013 N73-10103
Effect of concurrent audio tasks on human operator compensatory tracking performance using manual control system
01 p0018 N73-10139
Dynamic model for pilot manual control ability using aural compensatory tracking
01 p0018 N73-10142
Pure tone thresholds of 24 normal hearing listeners at 11 audiometric frequencies on two [TDH-49 and TDH-39] earphones
[AD-744823] 01 p0080 N73-10663
Development of auditory display of two-dimensional patterns to assist blind persons in pattern identification
[NASA-CASE-HQN-10832-1] 03 p0301 N73-12456
Psychophysical analysis of RF sound perception in human subjects
[AD-747684] 05 p0501 N73-14076
Physical correlations of hearing, auditory system, and hearing loss
06 p0629 N73-15105
Blockage effect in external ear canal on diver auditory perception threshold
[AD-751664] 09 p0996 N73-18132
Speech and tone audiometry for testing auditory acuity of flying personnel
13 p1480 N73-21990
Human perception of musical intervals between simultaneous tones
[IZF-1972-20] 14 p1613 N73-23078
Linguistic and perceptual role of syntactic hypotheses in speech recognition systems
14 p1625 N73-23168
Perceptive evaluation of acoustic signal parts displaying rapid changes and short durations
14 p1625 N73-23170
Psychophysical and statistical experiments on auditory speech perception
14 p1626 N73-23175
Aids for speech perception and speech training
14 p1626 N73-23176
Multidimensional representation of personal quality of vowels and their acoustical correlates
14 p1631 N73-23217
Loudness level perception of human ear and reference level for telephone engineering
[NLL-PO-2831-[9022.81]] 15 p1812 N73-24684
Real time hybrid computer audio synthesis system
[AD-761730] 19 p2228 N73-27968
Analysis and perception of nonspeech marine sounds
[OES-6/72] 22 p2624 N73-31023
Aural detection model for detecting low flying aircraft
[AD-764226] 22 p2676 N73-31435

AUDITORY SENSATION AREAS
Frequency selectivity and two tone inhibition in neural coding of acoustic stimuli
[IZF-1972-25] 14 p1610 N73-23050
Behavioral learning response of cat to electric stimulation of auditory nervous system
[NASA-CR-132047] 15 p1742 N73-24124

AUDITORY SIGNALS
Audio equipment for removing impulse noise from audio signals
[NASA-CASE-NPO-11631] 03 p0277 N73-12244
Test and evaluation of aural signal device to prompt students to scan for aircraft during flight simulator training
[FAA-RD-72-95] 04 p0373 N73-13030
Application of acoustic emission analysis to non-destructive testing on crack formation
[RFP-TRANS-101] 07 p0821 N73-16656
Extraction of formant information from discrete spectrograms in speech recognition processes
14 p1630 N73-23216
Performance of acoustic signal data processing and conversion system
[AD-763326] 22 p2700 N73-31628

AUDITORY STIMULI
Effects of direct auditory feedback of electromyogram on learning to control single unit
[AD-745107] 01 p0021 N73-10165
Development of auditory display of two-dimensional patterns to assist blind persons in pattern identification
[NASA-CASE-HQN-10832-1] 03 p0301 N73-12456
Frequency selectivity and two tone inhibition in neural coding of acoustic stimuli
[IZF-1972-25] 14 p1610 N73-23050
Pilot performance in dual time-sharing tracking task
[AD-755363] 14 p1615 N73-23088
Mathematical models for deriving loudness function from physical evidence without human judgment
[NASA-TN-D-7297] 15 p1742 N73-24121
Cross correlation analysis of stress rhythm during stimuli of varying biological significance
24 p2890 N73-33071

AUDITORY TASKS
Binaural processing of speech intelligibility in light aircraft
[FAA-AM-72-31] 05 p0503 N73-14094
Effect of sleep deprivation and heat stress on human performance in visual and auditory tasks
[OES-8/72] 22 p2624 N73-31024

AUGER EFFECT
Auger electron spectroscopy of surface segregation in binary alloys
[NASA-TN-D-6982] 06 p0683 N73-15564
Technique for obtaining Auger spectra of electron desorbable surface species on time independent basis
[NASA-TN-D-7257] 11 p1252 N73-20161
Auger analysis of chemisorption of various gases to metal surfaces and sliding friction effects on interaction
[NASA-TN-D-7340] 16 p1918 N73-25520
Scanning auger spectroscopy for surface analysis of solid state devices
[AD-760550] 18 p2153 N73-27399
Heat treatment effects on metal black surfaces, and Auger spectra during magnesium and iron oxidation
[RU-20-6] 23 p2769 N73-32146

AUGMENTATION
NT THRUST AUGMENTATION
Augmentation of signal transmission using microwave radio relay systems
[JPRS-58044] 08 p0885 N73-17162

Wind tunnel tests of swept augmentor wing aerodynamic characteristics
[NASA-TM-X-62252] 13 p1472 N73-21923

**AURORAL ABSORPTION**
Auroral substorm model for predicting high frequency radio absorption
[AD-749859] 05 p0542 N73-14408

**AURORAL ACTIVITY**
U AURORAS

**AURORAL ARCS**
NT RED ARCS
Auroral infrasonic sound wave generation and downward propagation into lower atmosphere
05 p0508 N73-14134
Auroral infrasonic shock wave generation by supersonic electrojet arcs
05 p0508 N73-14137
Mass plots of quiet auroral arc positions and precipitation pattern of auroral particles
[R-33] 18 p2141 N73-27310
Distribution of vibrationally excited molecular nitrogen in auroral red arc and effect on ionospheric electron densities
24 p2912 N73-33241

**AURORAL ELECTROJETS**
Auroral infrasonic shock wave generation by supersonic electrojet arcs
05 p0508 N73-14137
Observations of weak infrasound emission during magnetic storms caused by ionospheric auroral electrojets
05 p0508 N73-14138
Measurement of auroral electrojet magnetic activity indices for calendar year 1970
[UAG-22] 18 p2133 N73-27231
Sounding rocket instrument for measuring polar electrojet position and current parameters
[AD-760767] 18 p2152 N73-27396

**AURORAL EMISSION**
U AURORAS
U LIGHT EMISSION

**AURORAL IONIZATION**
Numerical analysis of ionospheric and plasma sheet particle densities, fluxes, and bulk velocities along auroral magnetic field for ion-exosphere model
[A-N-109-1972] 06 p0664 N73-15400

**AURORAL SPECTROSCOPY**
Airborne auroral expedition of November and December 1969
[NASA-CR-128392] 01 p0047 N73-10379
Instrumentation, calibration, and observational data obtained in airglow and auroral expedition aboard CV 990 aircraft
[NASA-CR-129511] 03 p0293 N73-12384
Characteristics of narrow field of view, sensitive photometers and application to measuring air glow, aurora, sun corona, and barium releases
[LA-DC-72-1422] 12 p1406 N73-21399
High time resolution measurements of energetic electrons in auroral breakup using sounding rockets
16 p1895 N73-25324
Electrostatic analyzer and energy spectrum determination methodology used with primary electron spectrometer on Nike-Tomahawk sounding rocket
[NASA-CR-133409] 18 p2151 N73-27389

**AURORAL ZONES**
Relation of Hall current electrojet instability to VLF hiss in auroral zone of magnetic storms
[NASA-CR-130078] 01 p0047 N73-10378
Observations and analysis of VLF radio emissions in auroral zone
[AD-748880] 04 p0416 N73-13393
Low energy particle measurements by soft particle spectrometer on ISIS-1 orbiting satellite and relation to production of auroral particles
10 p1146 N73-19329
Evaluation of field aligned ionospheric currents produced by azimuthal and radial magnetospheric disturbances
[PR-122] 10 p1156 N73-19402
Plasma convection patterns in polar upper ionosphere obtained from Cosmos 184 satellite measurements during magnetic disturbance of 4 Nov. 1967
[PR-130] 10 p1156 N73-19403
Direct comparison between electric field measurements by Injun 5 satellite and visual aurora data
[NASA-CR-132958] 16 p1906 N73-25416
Simultaneous observations of low energy electrons in plasma sheet and in auroral zone
[LMSC-D350709] 22 p2702 N73-31638

**AURORAS**
NT AURORAL ARCS
NT RADIO AURORAS
NT RED ARCS
Synoptic study of field-aligned electron precipitation in auroral regions
[NASA-TM-X-66065] 01 p0049 N73-10392
Analysis of instabilities resulting from interaction of electromagnetic waves with active medium or system
[AD-746893] 02 p0143 N73-11159
Distribution of auroral frequencies in polar regions
[DMI-GEOPHYS-PAPERS-R-28]
02 p0167 N73-11354
Analysis of all-sky photographs and ionograms taken during flights and ground magnetic records from auroral zone stations
[AD-746283] 02 p0205 N73-11663
Time of flight measurement of N2 plus meinel lifetimes
[AD-746157] 02 p0214 N73-11735
Auroral effects on HF radiowave propagation traversing polar regions
[AD-749515] 05 p0540 N73-14392
Numerical analysis of ionospheric and plasma sheet particle densities, fluxes, and bulk velocities along auroral magnetic field for ion-exosphere model
[A-N-109-1972] 06 p0664 N73-15400
Rocket-borne auroral optical measurement of proton and electron precipitation
[SC-RR-72-0543] 07 p0793 N73-16448
Analysis of dayside auroral characteristics and hydroxyl airglow variations from 1969 airborne auroral expedition
[NASA-CR-130916] 09 p1025 N73-18367
Vertical distribution of vibrationally excited molecular nitrogen in thermosphere corresponding to stable auroral red arc
[NASA-TM-X-66194] 09 p1028 N73-18390
Astrobee rocket instrumentation for infrared radiation measurements on auroral display
[AD-755823] 12 p1402 N73-21373
Injun 5 observations of charged particle precipitation over auroral zone during magnetic substorm
13 p1515 N73-22272
Two substorm studies of relations between westward electric fields in outer plasmasphere, auroral activity, and geomagnetic perturbations
[NASA-CR-131497] 13 p1518 N73-22309
Ionospheric investigation of auroral activity using rocket-borne spectrophotometric techniques
[NASA-CR-131484] 13 p1519 N73-22311
Auroral ionospheric measurements from incoherent scatter radar facility
[AD-757358] 14 p1664 N73-23504
Analysis of ground and airborne hydroxyl emission observations in northern polar regions
[NASA-CR-130237] 15 p1777 N73-24408
Analysis of data taken by CV-990 aircraft during 1968 and 1960 auroral expedition
[NASA-CR-114616] 15 p1777 N73-24409
Three dimensional steady state model of thermospheric dynamics with auroral heating
[AD-758733] 15 p1784 N73-24466
Photometric and image intensified TV measurements of auroral precipitation patterns and energy input during rocket experiments at Poker Flats, Alaska in Operation Ice Cap
[AD-760042] 17 p2029 N73-26419
Feasibility of generating artificial auroras by injecting electrons into upper atmosphere
[NASA-CR-133298] 18 p2151 N73-27388
Photometric measurements of airglow and auroral intensity and ionospheric disturbances by Goose Ionospheric Observatory
[AD-762081] 19 p2297 N73-28471
Auroral clutter mapping with Homer backscattering radar to study reaction of upper atmosphere to nuclear explosions
[AD-762012] 19 p2297 N73-28474
High resolution interferometer spectrometer measurements of auroral infrared emissions to simulate high altitude nuclear explosions
[AD-762013] 19 p2297 N73-28475
Rocket produced infrared emissions for analyzing auroral atmospheric mechanisms
[AD-762206] 19 p2298 N73-28478
Infrared emission from chemical and radiative processes to study auroral altitudes
[AD-762318] 19 p2298 N73-28479
Pyrheliometers errors with various aperture angles associated with solar aurora effects
20 p2403 N73-29311
Electron and proton precipitation in different auroral forms from data obtained by TWINS 1 and 2
[NASA-CR-133889] 22 p2667 N73-31367
Compilation, reduction, and correlation of spectrophotometric data obtained during NASA airborne auroral expedition
[NASA-CR-135497] 23 p2785 N73-32278
Aurora data from Michigan airglow payload and stellar occultation data
[NASA-CR-135718] 23 p2785 N73-32281
Analysis of ionograms to determine HF auroral backscatter over bistatic path
24 p2911 N73-33231
Balloon and GEOS satellite observations of auroral X rays from Scandinavia to Greenland
[NP-19738] 24 p2923 N73-33343

**AUSTENITE**
Preparation and homogeneity characteristics of austenitic iron-chromium-nickel alloy at micrometer level of spatial resolution to establish standard reference material
[NBS-SP-260-43] 02 p0186 N73-11511
Reports on electrical and mechanical properties of beryllium, chromium-manganese austenitic steels, and martensitic conversion during deformation
[JPRS-58357] 10 p1171 N73-19524
Effect of warm rolling on mechanical properties of unstable chromium-manganese austenitic steels
10 p1171 N73-19526
Cyclic deformation diagrams of heat resistant and austenitic steels
10 p1219 N73-19914
Structural recrystallization of steels during fast and slow heating to show structural succession caused by different mechanisms of formation of austenite
13 p1541 N73-22481
Cyclic transformation treatments on structural and mechanical properties of austenitic steels
[AD-756240] 13 p1543 N73-22506
Effect of phase instability during low cycle fatigue on plastic deformation in steels
[AD-763235] 22 p2686 N73-31512

**AUSTENITIC STAINLESS STEELS**
Vulnerability mechanism of pearlitic and austenitic steel alloys during plastic deformation
[NLL-RTS-7426] 02 p0184 N73-11493
Influence of high temperature thermomechanical treatment on mechanical properties of austenitic steel
[NLL-M-21480-[5828.4F]] 02 p0186 N73-11504
Correlation of substructure with mechanical properties of 304 and 316 stainless steel plastically deformed at elevated temperatures
03 p0313 N73-12554
Correlation of substructure with mechanical properties of 304 and 316 stainless steel plastically deformed at elevate temperatures
[COO-2107-5] 03 p0315 N73-12568
Creep and stress relaxation tests on Cr-Ni austenitic steel at 700 C
[STU-70-419/U-350-B] 04 p0481 N73-13932
Intergranular corrosion resistance of matching and dissimilar welds in nitrogen-bearing and nitrogen-free austenitic steels
[NLL-TRANS-746-1313-[9022.401]]
05 p0560 N73-14546
Stress corrosion cracking of sensitized austenitic stainless steels in oxygenated high temperature water
[BMI-1927] 05 p0562 N73-14565
Role of cesium in fuel-cladding interaction of austenitic stainless steels mixed with oxide fuels
[EUR-4893] 10 p1187 N73-19657
Effect of passivation and dissolution phenomena on structural corrosion of Cr-Ni stainless steels
[NLL-RISLEY-TR-2500-[9091.9F]]
11 p1305 N73-20586
Effects of heat on embrittlement of austenitic welded joints and welded claddings
[NLL-RISLEY-TR-2508-[9091.9F]]
12 p1407 N73-21405
X ray Mossbauer study of strengthening properties of laves phases in austenitic steels
[JPRS-58852] 13 p1543 N73-22503
Helium embrittlement of austenitic stainless steels
[AI-AEC-13047] 15 p1799 N73-24580
Deformation properties of hot worked Type 304 austenitic stainless steel, Mangalloy, and other steel alloys
[AD-758912] 15 p1800 N73-24592
Various applications of explosive welding
[AD-758844] 16 p1919 N73-25530
High temperature heating effects on structure and ductile properties of austenitic steels
[NLL-M-21563-[5828.4F]] 16 p1926 N73-25584
Formation of cavities in nickel and some austenitic steels irradiated by medium energy heavy ions
[CEA-CONF-2113] 17 p2045 N73-26542
Relationship between microstructure and properties of austenitic stainless steels
[ORO-4044-3] 17 p2045 N73-26545
Fatigue and creep-fatigue behavior of irradiated austenitic stainless steel used in LMFBR design
[ANCR-1096] 19 p2349 N73-28891
Electron microscopic study of stress corrosion cracking behavior of austenitic stainless steel having increased nitrogen content in boiling MgC42
20 p2427 N73-29495
Fatigue and martensitic transformations of austenitic stainless steels
20 p2427 N73-29498
Influence of carbon stabilizing elements and temperature on cold worked austenitic stainless steel corrosion
[CEA-CONF-2119] 21 p2560 N73-30518
Intermetallic chromium containing nickel aluminide for high temperature corrosion protection of stainless steels
[NASA-CASE-LEW-11267-1] 23 p2803 N73-32414
Acetone decomposition by austenitic stainless steel, iron oxide, and chromium oxide
[AERE-R-7408] 24 p2892 N73-33089
Evaluation of welding techniques for austenitic stainless steels for use in liquid metal fast breeder reactors
[ORNL-TM-4055] 24 p2954 N73-33601

**AUSTRALIA**
Monthly mean climatological statistics for surface to 5 mb pressure level over Australia - Dec. 1971
01 p0074 N73-10606
Monthly mean climatological statistics for surface to 5 mb pressure level over Australia - Aug. 1971
01 p0074 N73-10607

Statistical data of tropical cyclones in Australian Region east of 135E from November 1909 to June 1969
01 p0074 N73-10608
Monthly statistics of precipitable water over Australia in atmosphere from 400 mb to surface, determined from daily radiosonde ascents, 1958 through 1969
01 p0074 N73-10609
Geological and geophysical mapping of mineral resources in Australia and New Guinea
02 p0164 N73-11328
Monthly mean climatological statistics from surface to 5 mb level over Australia - January 1972
02 p0204 N73-11654
Meteorological upper air statistics in Australian region
02 p0204 N73-11655
Morphology, provenance, and movement of desert sand seas in Africa, Asia, and Australia
[E72-10249] 03 p0289 N73-12349
Gravimetric map of Australia
[AD-747873] 04 p0417 N73-13405
Temperature, pressure, and related climatological data for Australia - tables for [May, 1972]
04 p0441 N73-13598
Temperature, pressure, and related climatological data for Australia - tables for [April 1972]
04 p0442 N73-13599
Research and development projects conducted to improve weapon systems and to conduct ionospheric and upper atmosphere experiments in Australia
05 p0611 N73-14965
Research and development related to maintaining national standards of measurement of physical quantities in Australia
[NP-19392] 06 p0650 N73-15276
Morphology, provenance, and movement of desert sand seas in Africa, Asia, and Australia
[E73-10058] 07 p0778 N73-16320
Morphology, provenance, and desert sand sea movements in Asia, Australia, and Africa
[E73-10060] 07 p0778 N73-16322
Research projects in plasma physics
[NP-19414] 07 p0828 N73-16710
ERTS-1 imagery of morphology, provenance, and movement of desert sand seas in Africa, Asia, and Australia
[E73-10409] 11 p1278 N73-20371
Morphology, provenance, and movement of desert sand seas in Africa, Asia, and Australia
[E73-10542] 13 p1518 N73-22305
Geomorphic coastal variability for Northwestern Australia
[AD-755154] 13 p1527 N73-22377
Measurements of meteorological parameters at Woomera using falling spheres from February to June 1972
[WRE-TN-787[WR/D]] 14 p1685 N73-23670
Surface gravity and satellite derived gravimetric geoid of North America, North Atlantic, Eurasia, and Australia
[NASA-TM-X-66238] 15 p1778 N73-24413
ERTS-1 imagery of morphology, provenance, and movement of desert sand areas in Africa, Asia, and Australia
[E73-10710] 17 p2018 N73-26317
Identification of copper/molybdenum porphyry mineral deposits in characteristic geologic setting in Nevada, Arizona, Colorado, Australia, Alaska, and New Guinea
[E73-10762] 17 p2023 N73-26362
ERTS-1 imagery of morphology, provenance, and movement of desert sand seas in Africa, Asia, and Australia
[E73-10786] 18 p2136 N73-27262
Geopotential topographies and currents for sea surface off west Australia
[CSIRO-DFO-TP-32] 18 p2143 N73-27323
Woomera atmospheric parameters measured during falling sphere ejection from rocket soundings between Feb. and Jun. 1972 noting comparison with atmospheric models
[WRE-TN-787] 18 p2146 N73-27341
Use of Sydney photographic plates to compile astronomical catalog
18 p2196 N73-27725
Morphology, provenance, and movement of desert sand seas in Africa, Asia, and Australia using ERTS-1 data
[PAPER-G8] 19 p2264 N73-28239
Surface climatological data for Australia - October 1972
20 p2449 N73-29676
Surface climatological data for Australia - September 1972
20 p2449 N73-29677
Monthly mean climatological statistics for surface to 5 mb pressure level over Australia - October 1972
20 p2449 N73-29678
Monthly mean climatological statistics for surface to 5 mb pressure level over Australia - Dec. 1972
20 p2449 N73-29679
Monthly mean climatological statistics for surface to 5 mb pressure level over Australia - September 1972
20 p2449 N73-29680
Monthly mean climatological statistics for surface to 5 mb pressure level over Australia - November 1972
20 p2449 N73-29681
Surface climatological data for Australia - November 1972
20 p2449 N73-29682
Surface climatological data for Australia Dec. 1972
20 p2449 N73-29684
Surface climatological data for Australia - Jan. 1973
20 p2449 N73-29685
Administration, development, and maintenance of NASA tracking network with emphasis on Australia
[NASA-CR-133828] 21 p2521 N73-30214
Recognition of geologic framework for ERTS-1 identification of mineral deposits of copper/molybdenum prophyry type in Colorado, Nevada, Arizona, and Australia
[E73-10960] 21 p2532 N73-30302
Surface climatological data for Australia - August 1972
21 p2574 N73-30626
Sampling strategies for automatic thematic land use mapping of Washington D.C., Maryland counties, and Alice Springs, Australia using Skylab multispectral photography
[E73-11018] 22 p2661 N73-31322
Activities of Australian Bureau of Mineral Resources
24 p2921 N73-33324

AUSTRIA
NT ALPS MOUNTAINS [EUROPE]
Atmospheric radioactivity measurements for 1972 obtained at Vienna, Austria
[NP-19753] 24 p2922 N73-33339
Measurement of atmospheric radiation levels at low altitude in vincinity of Vienna, Austria during 1972
[NP-19751] 24 p2922 N73-33340

AUTOCLAVING
High temperature tests to determine effect of autoclave heat treatment of mechanical properties of cobalt-base alloy HS-31 in prealloyed powder form
[NASA-TN-D-7117] 07 p0809 N73-16559

AUTOCOLLIMATORS
U COLLIMATORS

AUTOCORRELATION
Autocorrelation analysis of velocity structure temporal evolution in solar wind
01 p0094 N73-10775
Autocorrelation evaluation for texture indicator for lunar ground photos
05 p0609 N73-14955
Application of scale autocorrelation coefficients to atmospheric and geophysical measurements
[AD-750476] 06 p0695 N73-15661
Autocorrelation, Chree, and power spectrum analyses of cosmic ray 27-day recurrences
[NP-19466] 08 p0957 N73-17833
Influence of autocorrelation and its parameters on phase manipulated signal passed through n stage resonance filter
09 p1002 N73-18180
Theoretical approach to autodocumentation
10 p1131 N73-19217
Analysis of times series processes for correlation of air pollution data measurements
[AD-754433] 12 p1424 N73-21538
Polarization measurement of whistler-type radio frequency signals by using auto- and cross-correlation functions of horizontal signal components
[CEPHAG-24/72] 13 p1491 N73-22088
Electric field autocorrelations in guiding center plasma
[NASA-CR-133410] 18 p2183 N73-27624
Variability of eigenvectors and eigenvalues using autocorrelation matrices of vertical temperature profiles on regional latitudes
[AD-763145] 21 p2539 N73-30360

AUTOIONIZATION
Calculation of photoionization cross sections near autoionizing lines and theoretical cross sections for beryllium and magnesium
[NASA-CR-130884] 09 p1068 N73-18716

AUTOMATA THEORY
Automata theory for realizing reliable computer logic with fault detection
[AD-745720] 01 p0031 N73-10241
Markov chain model for classifying stochastic automation
02 p0195 N73-11579
Seven families of linear codes for automata
03 p0271 N73-12201
Injections of neighborhood size three and four on set of configurations from infinite one-dimensional tessellation automata of two state cells
[AD-748072] 03 p0272 N73-12209
Abstracts on theory, design, and applications of analog and digital computers and digital control systems
[JPRS-57529] 04 p0392 N73-13189
Soviet abstracts on analog and digital systems, control systems, information theory, and automata theory
[JPRS-57520] 04 p0393 N73-13190
Total machine language conception for sequential automaton from modular evolution
04 p0394 N73-13201
Redundant cells to improve reliability of asynchronous automata
04 p0399 N73-13250
Automata theory of cubical complexes applied to diagnosis and algorithmic description, noting logic design of ultra LSI
[NASA-CR-130388] 05 p0517 N73-14201
Method to automate and represent relief drawings
[AD-750750] 06 p0670 N73-15453
Control theory in game problems, optimization, feedback, and probabilistic automata - conference
[JPRS-58030] 08 p0891 N73-17214
Conference papers on automated methods of computer program documentation
[NASA-TM-X-66196] 10 p1130 N73-19204
Project maintenance and comparison of documentation and automation
10 p1131 N73-19214
Preliminary identification of tools for automatic program annotation [AUTONOTE]
10 p1131 N73-19219
Automated engineering design for development of problem and user-oriented languages
10 p1131 N73-19221
Speaker adaptation to automatic speech recognition system, extracting acoustic and phonetic features from continuous speech
14 p1628 N73-23192
Artificial intelligence research projects with emphasis on design, implementation, and integration of system for control of robot
[NASA-CR-131991] 14 p1638 N73-23279
Computation of optimal parameters of automaton implemented in cryotron medium
21 p2515 N73-30173
Method for iterative reanalysis in automated structural designs using direct stiffness approach
[NASA-TN-D-7357] 23 p2853 N73-32797

AUTOMATIC CONTROL
NT ADAPTIVE CONTROL
NT AUTOMATIC FLIGHT CONTROL
NT AUTOMATIC FREQUENCY CONTROL
NT AUTOMATIC GAIN CONTROL
NT AUTOMATIC LANDING CONTROL
NT CASCADE CONTROL
NT DYNAMIC CONTROL
NT FEEDBACK CONTROL
NT FEEDFORWARD CONTROL
NT LEARNING MACHINES
NT NUMERICAL CONTROL
NT OFF-ON CONTROL
NT OPTIMAL CONTROL
NT PROPORTIONAL CONTROL
NT SELF ADAPTIVE CONTROL SYSTEMS
NT SELF ALIGNMENT
NT SEQUENTIAL CONTROL
NT TIME OPTIMAL CONTROL
Suboptimal sampling and control behavior of human operator in output prediction task for automatic process
01 p0015 N73-10114
Automated technical control system for military communications facility
01 p0027 N73-10207
Design, development, and characteristics of industrial robot machinery to show load capacity, positioning accuracy, power actuators, and method of controls
01 p0060 N73-10486
Capability of training human to control and/or interact with complex electronic or mechanical systems
[AD-746179] 02 p0136 N73-11101
Discrete control of linear distributed systems with specific application to primary mirror for orbiting astronomical observatory
[NASA-TM-X-68855] 02 p0173 N73-11400
Automated planning systems for cold forging production processes
[NLL-NEL-TT-2393-[6075.461]]
02 p0177 N73-11436
Evaluation of automated air traffic control system and comparison with operator performance using manual system
02 p0207 N73-11683
Functions of automated system for processing flight data and surveillance functions with development plan for improved capability
[FAA-ED-12-2] 02 p0208 N73-11684
Specifications for automatic command and control of real time plasma simulation chamber
[GRI/NTP/102] 02 p0216 N73-11747
Atmosphere Explorer Control System for automatic control of AE spacecraft and experiments
[NASA-TM-X-66086] 02 p0232 N73-11888
Catalog of automatic control computer programs including description and use of programs
[LAAS-NT-SIS-72-T-15] 05 p0517 N73-14202
Automatic longitudinal control of closely packed personnel rapid transit vehicles
05 p0610 N73-14962
Development and characteristics of automatic control system for aeroelastic aircraft using optimal gain in stabilization loops
[AD-750501] 06 p0624 N73-15061

Spacecraft control over segment of atmospheric reentry trajectory using on-board computers to preclude deflection beyond atmosphere
[AD-750520] 06 p0719 N73-15871
Automatic systems for analyzing fatigue crack propagation and for conducting constant stress intensity factor fatigue tests with servo-hydraulic machine
[RD/B/N-2013] 06 p0726 N73-15928
Remote automatic multipurpose station for collecting oceanographic and meteorological data in Arctic regions
[AD-751039] 07 p0758 N73-16159
Automatic calculation of runway visual range on airdromes
07 p0814 N73-16599
Periodic health examinations and automatic processing of medical histories for detection and prevention of human diseases
08 p0874 N73-17074
Automated procedures for Passive Immune Agglutination system
[NASA-CR-128731] 08 p0877 N73-17107
Computer based automation for performing material handling, assembly, and quality control tasks
[AD-752464] 08 p0928 N73-17601
Feasibility of solid state electric switch gear for aircraft and spacecraft
[NASA-CR-121140] 09 p1007 N73-18223
Stabilization of nonlinear systems with dither control
[TAE-150] 09 p1009 N73-18239
Design of automated production facility capable of manufacturing beam-lead CMOS integrated circuits
[NASA-CR-124116] 09 p1038 N73-18465
Simulation of logical functions for construction of computerized control system for onboard spacecraft instrumentation
10 p1177 N73-19573
Simulation of program sequencing functions in design of computerized digital control system for onboard spacecraft instrumentation
10 p1177 N73-19574
Computerized control and recording system for magnetic spectrometer
[FRNC-TH-268] 11 p1294 N73-20502
Automatic connection of aerogenerator to electrical network
[NASA-TT-F-14873] 12 p1386 N73-21238
Computerized control of synchrotron beam lines and power supply system
[DNPL/R-22] 12 p1388 N73-21254
Economic effectiveness of production planning and automatic control methods in industry
[JPRS-58680] 12 p1467 N73-21884
Design of automatic system for computer program documentation
[NASA-CR-130231] 13 p1496 N73-22129
Feasibility of automated spacecraft monitoring using real time computer telemetry
14 p1711 N73-23888
Tactical integrated electronic systems for Swedish military aircraft
14 p1711 N73-23889
Computerized simulation of multiloop attitude control system for satellite with flexible booms
14 p1712 N73-23890
Exponential probability distribution analysis for extrapolating aerospace system performance statistics from test results
14 p1713 N73-23903
Modular inverter/converter automatic paralleling and protection system
[NASA-TN-D-7279] 15 p1737 N73-24084
Digital command and simulation of automatic tracking device carrying pulsed laser and receiving telescope
[ONERA-NT-198] 15 p1751 N73-24190
Automatic temperature control for liquid cooled space suit
[NASA-CASE-ARC-10599-1] 17 p1988 N73-26071
Design analysis for reversible, self adaptive manipulator control system
17 p1989 N73-26083
Error analysis on manipulator activation system using reversible self adaptive control mechanism
17 p1989 N73-26084
Digital system for programmed control of maching process for turbine blade foil
[AD-759682] 17 p2077 N73-26804
Comparison of automatic short takeoff aircraft landings based on simulation and flight test results
[NASA-TT-F-14995] 18 p2105 N73-27028
Application of Minuteman guidance computer for numerical processing control
[AD-760757] 18 p2121 N73-27145
Computerized management tools for use in analysis of automatic switching centers and associated tributaries of Autodin communications network
[AD-761479] 19 p2236 N73-28028
Determination of diagnostic nucleus of digital computer
[AD-762264] 19 p2242 N73-28080
Comparison of nondestructive evaluation methods
19 p2303 N73-28518
Automatic aircraft altitude reporting using air traffic control radar beacon system
[FAA-RD-73-44] 19 p2318 N73-28648
Development of method for determining optimum setting of regulators on metal working machinery involved in sintering process
[NLL-M-21642-[5828.4F]] 20 p2428 N73-29505
Ergonomic research and design principles for automatic control and man machine systems
[NASA-TT-F-716] 21 p2502 N73-30079
Automatically operable self-leveling load table with plurality of solenoid valves
[NASA-CASE-MFS-22039-1] 21 p2548 N73-30428
Methods for approximating probability of tracking disruptions in automatic control systems
21 p2565 N73-30564
Equipment for program control of satellite ground station
[DLR-MITT-72-16] 22 p2647 N73-31211
Pilot display for monitoring of automatic steep approach
[DGLR-PAPER-73-031] 23 p2744 N73-31964
Speed control system for dc motor equipped with brushless Hall effect device
[NASA-CASE-MFS-20207-1] 23 p2763 N73-32107
Textbook for engineers for planning control systems for industrial automation
[JPRS-60162] 23 p2797 N73-32373
Similitude theory for design optimization of automatic control systems for aircraft gas turbine engines
[AD-764683] 23 p2832 N73-32631
Automatic control for absorption columns, fluidized bed processors, and continuous fermentation noting enzymatic protein production
[LAAS-PUBL-975] 24 p2892 N73-33090
Automatic control systems with variable coupling between functional elements
24 p2900 N73-33149
Automatic experimenter concept based on evolution strategy
24 p2908 N73-33210
Temperature, shock, vibration, humidity, salt-fog, and electromagnetic tests on automotive disk recorder
24 p2926 N73-33368

**AUTOMATIC CONTROL VALVES**
NT PRESSURE REGULATORS
NT RELIEF VALVES
Operating force of optimal pulsed electrically controlled pneumatic valve
[FOA-2-C-2481-H5] 02 p0148 N73-11203
Design of IDPF servovalve applicable for controlling hydraulic systems
[NAL-TR-303] 15 p1824 N73-24787
Postflight analysis of Apollo 11 glycol temperature control valve failure
[NASA-TM-X-69200] 17 p2088 N73-26896

**AUTOMATIC DATA PROCESSING**
U DATA PROCESSING

**AUTOMATIC FLIGHT CONTROL**
NT AUTOMATIC LANDING CONTROL
Integrated information presentation and control system analysis to determine control and display requirements for contingency operation of jet aircraft - Vol. 3
[AD-740435] 01 p0006 N73-10041
Characteristics of nonlinear self adjusting and variable structure automatic flight control system for piloted and pilotless aircraft
[AD-750502] 06 p0624 N73-15062
Onboard computers for automatic control of manned aerospace systems considering human factors integration
[AGARD-CP-114] 14 p1710 N73-23881
Computerized inertialess guidance system for aircraft flight control
14 p1712 N73-23895
Design of aircraft digital system for automatic flight control
14 p1713 N73-23900
Automatic flight control system AOOSY for satellite control, tested with Azur satellite
[MBB-UA-56-72-O] 18 p2126 N73-27183
Development of automatic flight control systems based on adaptive control techniques and variable structure control systems
[AD-763415] 21 p2498 N73-30047
Automatic flight control system for curved flight path profiles
[DGLR-PAPER-73-030] 23 p2745 N73-31970

**AUTOMATIC FREQUENCY CONTROL**
Construction and testing of dual 10.6 micron CO2 laser AFC heterodyne system
[AD-747947] 03 p0312 N73-12544
Self-tuning electronic filter for maintaining constant bandwidth and center frequency gain
[NASA-CASE-ARC-10264-1] 11 p1261 N73-20231
Speech modulated, single sideband, suppressed carrier systems for speech reception
14 p1630 N73-23215
Automatic frequency control circuit for radiotelegtype receiver-converter
[AD-758686] 16 p1877 N73-25193

**AUTOMATIC GAIN CONTROL**
Self-tuning electronic filter for maintaining constant bandwidth and center frequency gain
[NASA-CASE-ARC-10264-1] 11 p1261 N73-20231

**AUTOMATIC LANDING CONTROL**
Electronic display devices in aircraft control, noting pilot activation and VTOL control
[DLR-MITT-72-04] 24 p2880 N73-32998
Pilot activation in automatic landing by display devices
24 p2880 N73-32999

**AUTOMATIC PATTERN RECOGNITION**
U PATTERN RECOGNITION

**AUTOMATIC PICTURE TRANSMISSION**
Influence of atmospheric conditions on remote image transfer and interpretation as determined by laboratory measurements
05 p0537 N73-14370

**AUTOMATIC PILOTS**
Characteristics of nonlinear self adjusting and variable structure automatic flight control system for piloted and pilotless aircraft
[AD-750502] 06 p0624 N73-15062
Application of autopilot techniques to control and stabilize vibration modes of two space shuttle configurations at liftoff flight condition
[NASA-CR-112202] 06 p0721 N73-15884
Development of automatic system for controlling aircraft under turbulent atmospheric conditions to provide pitch stabilization
[AD-751148] 07 p0741 N73-16028
Linear programming for design of large flexible launch vehicle autopilots
[NASA-CR-124124] 10 p1183 N73-19621
Users manual for COEBRA program for design of launch vehicle autopilots
[NASA-CR-124125] 10 p1183 N73-19622
Synthesis of hover autopilots for rotary wing VTOL aircraft
[NASA-CR-132053] 15 p1735 N73-24071
Apollo experience report on development of Apollo digital autopilots for primary attitude control during all phases of lunar landing mission
[NASA-TN-D-7289] 16 p1964 N73-25888
Development of analog hardware for flight control system design to control aircraft with uncertain parameters
[NASA-CR-133416] 19 p2220 N73-27909
Development of digital flight control system for performing pilot assist augmentation and pilot relief automatic pilot functions
[AD-762521] 20 p2361 N73-28992
Specification of thrust control system for Airbus A 300 B, tested in Boeing 707
24 p2877 N73-32981

**AUTOMATIC ROCKET IMPACT PREDICTORS**
U COMPUTERIZED SIMULATION
U IMPACT PREDICTION

**AUTOMATIC TEST EQUIPMENT**
Assessment of cartographers role in automatic cartography system
[AD-746019] 02 p0169 N73-11376
Automatic test generator for failure detection and localization in logic systems, LADISLAS
03 p0272 N73-12204
Reliability tests of computer elements used in automatic airport weather stations
[AD-747558] 03 p0328 N73-12673
Development of automatic air sampling system
[RM-559] 04 p0420 N73-13428
Trace element detection by automated distillation and ion exchange in neutron activation analysis for As, Cd, Cu, Hg, Se, and Zn
[IRI-133-72-10] 07 p0753 N73-16114
Management of NASA employee health problems by automated medical system
08 p0874 N73-17079
System designs for automating GC/MS analyzing system
[NLL-RTS-7572] 11 p1259 N73-20218
Problems of designing and developing automatic equipment and control systems
[JPRS-58746] 12 p1405 N73-21391
Automatic temperature controller for liquid cooled garment based on total evaporative water loss during exercise
[NASA-TN-D-7311] 16 p1868 N73-25126
Automated visual sensitivity tester for determining visual field sensitivity and blind spot size
[NASA-CASE-ARC-10329-1] 17 p1988 N73-26072
Stability of two coordinate angle tracking optical automatic tracking systems
[AD-762106] 19 p2250 N73-28138
Automatic shot change detector for pre-programmed corrections of film reproduced by telecine
[BBC-RD-1973/10] 22 p2671 N73-31392
Technical equipment for large scale automation of USSR hydrometeorological service
[AD-763956] 22 p2696 N73-31593

**AUTOMATION**
Design, development, and characteristics of industrial robot machinery to show load capacity, positioning accuracy, power actuators, and method of controls
01 p0060 N73-10486

Automated nondestructive testing - bibliography with abstracts
[CE-BIB-227] 01 p0061 N73-10498
Application of optimality criteria to automation of structural design with emphasis on aerospace applications
[NASA-TN-D-7115] 05 p0603 N73-14901
Automated computer index and retrieval system on machining of materials
[AD-752000] 09 p1053 N73-18582
Analysis of effects of automation on productivity and efficiency of air traffic control and flight services
[MTR-6110] 10 p1185 N73-19646
Development of automated air traffic control system using computer techniques to provide flight safety for increased air traffic
14 p1687 N73-23693
Organization, functions, and capabilities of automated air traffic control system for Rome, Italy
14 p1687 N73-23694
Analysis of terminal air traffic control procedures to determine impact of automation on air traffic controller personnel
14 p1688 N73-23700
Automation of decision making process in air traffic controllers terminal operations
[FAA-RD-72-63-VOL-3] 15 p1808 N73-24657

**AUTOMOBILE ACCIDENTS**
Decelerator sled simulation for testing air bag restraint system effects in passenger motor vehicle crash
[PB-212706] 11 p1251 N73-20155

**AUTOMOBILE ENGINES**
Design and evaluation of automobile thermal reactors with ceramic material construction
[NASA-TM-X-68148] 01 p0069 N73-10567
Performance capabilities and cycle life of high specific energy batteries for pollution free electric vehicles
[ANL-7953] 10 p1112 N73-19061
Performance and exhaust emission analysis of Williams research Gas Turbine Hornet automobile engine
[PB-218687/2] 18 p2173 N73-27551
Testing reactor-equipped vehicle for assessment of emissions control
[PB-218639/3] 18 p2173 N73-27554
Modified 1964 Dodge Dart induction system
[PB-218730/0] 18 p2194 N73-27710
Performance of 1972 ford galaxie equipt with rankine cycle power system composed of organic based working fluid and reciprocating expander
[PB-210836] 19 p2329 N73-28739

**AUTOMOBILES**
Driving speed in relation to interactions among automobile driver, roadway variables, and vehicle control
01 p0017 N73-10131
Double steering wheel forcing functions for estimating automobile driver manual control response
01 p0017 N73-10132
Analysis of noise pollution by military vehicles, public transportation, farm equipment, private automobiles, and construction equipment
[AD-747685] 03 p0338 N73-12754
Effect of fuel front-end olefin and midrange volatility on automobile emissions
[BM-RI-7707] 05 p0506 N73-14119
Application of ultrasonic nondestructive tests to vehicle tire compliance measurements
[PB-211892] 05 p0553 N73-14491
High charge and discharge rate lead/acid battery for hybrid heat-engine/electric vehicle
[PB-213257] 13 p1477 N73-21969
Feasibility of emission control devices for motor vehicles
[PB-218942/1] 18 p2174 N73-27555
Environmental impact of highway projects as determined by vehicle emission factors
[PB-219812/5] 18 p2174 N73-27557
Contribution of automobiles to air pollution levels in Reading, England
[PB-219602/0] 18 p2175 N73-27563
Acoustic measurement and recording system for noise generated by air bag automobile safety device
[AD-761836] 19 p2229 N73-27977
Numerical analysis of ice fog produced by automobiles during arctic conditions
20 p2441 N73-29603
Assessment of vehicular air pollution for Tulsa, Oklahoma
20 p2441 N73-29606
Stress-time relations of automobile rear wheel suspension systems, over various road surface conditions, based on power spectral density
[LBF-TB-102] 21 p2553 N73-30468
Automobile exhaust emission surveillance of light-duty vehicles
[PB-220755/3] 21 p2575 N73-30638

**AUTORADIOGRAPHY**
Autoradiograms of deformed silicon and germanium single crystal surfaces
[AD-753039] 09 p1074 N73-18765
Electrochemical and mechanical parameters of localization hydrogen in iron and maraging steel using high resolving power autoradiography
[RAE-LIB-TRANS-1665] 17 p2044 N73-26533

**AUTOROTATION**
Helicopter autorotation capability, noting BO-105 helicopter behavior
05 p0494 N73-14023
Coning motion, autorotation and vortex system of slender missiles
[BMVO-FBWT-72-31] 10 p1103 N73-18998
Analysis of helicopter performance with functioning engines, disengaged transmission, and steady autorotation of coaxial rotary wings
[AD-756592] 13 p1474 N73-21942

**AUTOTROPHS**
Biological mineralization products of human waste for autotroph cultivation
10 p1117 N73-19109

**AUXILIARY ELECTRIC POWER UNITS**
U AUXILIARY POWER SOURCES

**AUXILIARY EQUIPMENT [COMPUTERS]**
NT PLOTTERS
Reference manual for SAID (speech analog input to digitizer) hardware system which performs preliminary preprocessing of speech signal before entering into computer
[AD-753012] 09 p1006 N73-18215
Functional organization of homogeneous computer systems
21 p2514 N73-30165

**AUXILIARY POWER SOURCES**
NT CHEMICAL AUXILIARY POWER UNITS
NT NUCLEAR AUXILIARY POWER UNITS
NT SNAP
NT SNAP 8
NT SNAP 10A
NT SNAP 19
NT SNAP 23
NT SPACE POWER REACTORS
NT SPACE POWER UNIT REACTORS
Developing isotopic thermoelectric generators in USSR
[AD-749528] 05 p0499 N73-14065
Performance of auxiliary power systems for advanced Army rotary wing aircraft
[AD-751854] 08 p0870 N73-17046
Evaluation of conference to investigate current and future development in aircraft electrical and auxiliary power systems
[AGARD-AR-50] 09 p0990 N73-18081
Proceedings of conference on application of superconductivity techniques to auxiliary power systems for aircraft and missiles
[AGARD-CP-104] 10 p1108 N73-19030
Characteristics of auxiliary power unit combined with accessory drive to form auxiliary power system for aircraft electric power supply
10 p1110 N73-19045
Design principles of auxiliary power units of secondary power system for operation of aircraft equipment
10 p1110 N73-19046
Design parameters and characteristics of intermittent pulse jet engine for use as auxiliary power source
10 p1110 N73-19047
Design and characteristics of auxiliary power source to operate electric, hydraulic, and pneumatic subsystems in ramjet powered aerospace vehicles
10 p1110 N73-19048
Analysis of interface between aircraft mechanical power requirements and performance requirements of auxiliary power systems
10 p1110 N73-19049
Analysis of gas turbine engine requirements and performance when main propulsion system furnishes auxiliary power source
10 p1110 N73-19050
Development of integrated control system for supersonic aircraft based on pneumatic power generation
10 p1111 N73-19056
Design and performance of advanced auxiliary power system for fighter aircraft
[AD-754903] 11 p1238 N73-20049
Failure analysis of components of CH-47A auxiliary power plants
[AD-756407] 13 p1478 N73-21975
Development and characteristics of hydrogen-oxygen power unit for application to onboard systems of space shuttle orbiter vehicle
[NASA-TM-X-68262] 20 p2363 N73-29005
Effects of partly filled small gas turbine hydrodynamic converter during starting process of main engines
24 p2973 N73-33759

**AUXILIARY PROPULSION**
Chemical and electric auxiliary propulsion technology of United Kingdom, France, and West Germany
[NASA-CR-128328] 01 p0090 N73-10742
Analytical assessment of potential methods for replenishing auxiliary propulsion onboard orbiting space stations
[NASA-CR-123947] 04 p0461 N73-13764
Evaluation of concept of reverse flow engine for APS engine
[NASA-CR-120881] 04 p0464 N73-13783
Postflight analysis of Apollo 15 LM APS
[NASA-TM-X-68932] 06 p0712 N73-15813
Fuel expulsion efficiency and service life of Arde metallic diaphragm used in Atmospheric Explorer propulsion subsystem
[NASA-TM-X-66191] 09 p1078 N73-18794
Design and development of low pressure auxiliary propulsion system for space shuttle orbiter and booster
[NASA-CR-130796] 09 p1078 N73-18796
Analytical and experimental evaluation of high pressure thrust chamber concepts for hydrogen oxygen auxiliary propulsion for space shuttle vehicle
[NASA-CR-120895] 09 p1079 N73-18800
Design and tests of low pressure thrust chamber concepts for hydrogen oxygen auxiliary propulsion for space shuttle vehicle
[NASA-CR-120896] 09 p1079 N73-18801
Development and characteristics of auxiliary propulsion system for space shuttle applications - Summary
[NASA-CR-128818] 10 p1208 N73-19827
Analysis of requirements for oxygen-hydrogen auxiliary propulsion system for use with space shuttle vehicle concept - Phase A
[NASA-CR-128820] 10 p1208 N73-19828
Comparison and evaluation of competing concepts of auxiliary propulsion concepts for space shuttle applications - Phase B
[NASA-CR-128823] 10 p1208 N73-19829
Evaluation of concepts for integrating reaction control system and orbit maneuvering system of space shuttle vehicle - Phase C
[NASA-CR-128821] 10 p1209 N73-19830
Evaluation of two alternate oxygen-hydrogen auxiliary propulsion system concepts for space shuttle vehicle - Phase D
[NASA-CR-128822] 10 p1209 N73-19831
Evaluation of monopropellant and bipropellant earth storable reaction control systems for application to space shuttle vehicle - Phase C & E
[NASA-CR-128819] 10 p1209 N73-19832
Auxiliary propulsion for space shuttle orbiters
[SEF-NT-3054/71-M] 10 p1209 N73-19835
Combined orbital maneuvering and attitude control propulsion system for space shuttles
[MBB-UR-82-71] 10 p1209 N73-19836
Auxiliary propulsion system for space shuttle orbiter
[REPT-D-9/71-MK/DH] 10 p1209 N73-19837
European space tug auxiliary and main propulsion
[HSD-TP-7264-VOL-3] 10 p1217 N73-19903
Reliability model and associated computer code developed to compute reliability of monopropellant hydrazine spacecraft auxiliary propulsion system as function of time
[NASA-CR-131400] 11 p1333 N73-20821
Specific impulse of auxiliary rocket thrusters using liquefied gases
[NASA-TT-F-14878] 12 p1444 N73-21694
Potential valve closures for space shuttle auxiliary propulsion system
[NASA-CR-120976] 15 p1791 N73-24516
Attitude control and auxiliary propulsion for nuclear upper stage of Europa 3 launch vehicle
[TR-TT-4-17/72] 15 p1811 N73-24678
Eight cm electron bombardment thruster for auxiliary propulsion
[NASA-TM-X-68296] 22 p2709 N73-31694

**AVALANCHE DIODES**
Design and development of wideband TRAPATT amplifier in microstrip configuration for use in phased-array radar modules in S-band
[AD-747050] 02 p0150 N73-11215
Experimental characterization of abrupt junctions in avalanche mode
[LAAS-PUBL-939] 04 p0399 N73-13246
Transferred electron and avalanche diodes and solid state materials, for solid state microwave oscillators and amplifiers
[AD-748241] 04 p0460 N73-13755
Noise measurements on n-junction gold silicon and aluminum silicon diodes at avalanche potential considering leakage current
[FRNC-CONF-29] 05 p0519 N73-14221
GaAs Schottky barrier IMPATT diodes in 20 to 30 GHz frequency range
[NHK-LABS-NOTE-156] 07 p0761 N73-16183
Mathematical model for nonlinear characteristics of avalanche diode
[AD-751974] 08 p0890 N73-17207
Electro-optical control for volt-ampere characteristics of avalanche phototransistors
[JPRS-58321] 09 p1008 N73-18226
Analysis of subharmonically injection locked microwave IMPATT diode oscillators to improve frequency stability and noise characteristics
10 p1133 N73-19237
Operating characteristics of avalanche diode oscillator circuit high efficiency TRAPATT modes
[NASA-CR-131399] 11 p1264 N73-20258

Microwave amplifier circuit for testing avalanche diode
[AD-756520] 13 p1503 N73-22180
Analysis of electromagnetic noise in photodetection system consisting of germanium avalanche photodiode with application to laser range finders
[PHL-1972-24] 14 p1672 N73-23568
Research and development on microwave oscillators, diode structures, and ion implantation and diffusion
[AD-759542] 17 p1998 N73-26161
Characteristics of subharmonically injection locked microwave diode oscillators
[AD-759540] 17 p2004 N73-26208
Design of broadband continuous wave amplifier for phased array
[AD-760545] 18 p2124 N73-27167
S-band power amplifier using high efficiency silicon avalanche diode
[AD-763104] 20 p2381 N73-29135
Theoretical and developmental work on high efficiency avalanche diode sources and amplifiers
[FAA-RD-73-93] 21 p2517 N73-30186
Frequency domain analysis on noise in avalanche diode microwave oscillator
22 p2641 N73-31166
Solid state avalanche diodes for use as microwave amplifiers and oscillators
[NASA-CR-132300] 22 p2642 N73-31172
Noise in microwave semiconductor oscillators and amplifiers
[AD-764259] 22 p2644 N73-31188
Reliability and failure modes of GaAs Gunn and impatt diodes and Si impatt diodes
[AD-763929] 22 p2644 N73-31193
Design and performance of silicon Schottky barrier avalanche diodes
23 p2764 N73-32113

**AVALANCHES**
NT ELECTRON AVALANCHE
Performance of mathematical snowmelt models and statistical analysis of avalanche forecasts
06 p0665 N73-15402
Prediction of sonic boom effect on avalanches to prepare mirage 3 flight over Lavey Valley
[ISL-13/72] 13 p1474 N73-21940
Laser induced damage and avalanche breakdown in transparent insulators
[AD-761168] 18 p2158 N73-27439

**AVERAGE**
NT MEAN
Averaging process for continuum mechanics in two phase flow analysis
[AD-752159] 08 p0898 N73-17273

**AVIATION**
U AERONAUTICS

**AVIATORS**
U AIRCRAFT PILOTS

**AVIONICS**
Integrated information presentation and control system analysis to determine control and display requirements for contingency operation of jet aircraft - Vol. 3
[AD-740435] 01 p0006 N73-10041
Development of specifications for design of avionics subsystems to improve reliability
[AD-746029] 01 p0006 N73-10043
Page replacement algorithm simulations for advanced avionic digital computer programming
[AD-746110] 02 p0147 N73-11196
Space shuttle avionics design and cost analysis
[NASA-CR-123962] 03 p0300 N73-12449
Avionics requirements for multimission, fixed wing, twin engine aircraft designed for search and rescue operations
[AD-750463] 06 p0624 N73-15064
Avionics requirements for HH-53C helicopter engaged in search and rescue operations
[AD-752625] 09 p0986 N73-18047
Analysis of aircraft instruments and display devices for approach control and landing of V/STOL aircraft
[AGARD-AR-51] 09 p1034 N73-18439
Design, construction, and demonstration of airborne, low frequency, phase stable receiver for aircraft navigation
[AD-754027] 10 p1186 N73-19651
Analysis of synchronized discrete address beacon system for improved air traffic control capability
[SD-FR-01] 11 p1256 N73-20189
Reliable functioning of avionic power supply equipment through employment of redundant components
[AD-757152] 14 p1602 N73-22988
Onboard computers for automatic control of manned aerospace systems considering human factors integration
[AGARD-CP-114] 14 p1710 N73-23881
Operational cost and technological development aspects in design of space shuttle avionic systems
14 p1711 N73-23884
Extended computer language for real time simulation of process control in large systems
14 p1712 N73-23892
Serial digital data bus for integrated avionics system interface
14 p1713 N73-23902
Installation of electronic warfare training equipment in rear cockpit of CF-100 aircraft with emphasis on human engineering considerations
[DCIEM-904] 16 p1861 N73-25071
Human factors in design of avionics subsystems considering training costs and performance of Air Force personnel
[AD-759583] 17 p1990 N73-26096
Logistic performance data book for bomb navigation avionics system of F-111 aircraft to show support cost, reliability, maintenance, and problems
[AD-762214] 19 p2357 N73-28959
Analysis of voice command systems for application to military aircraft operation to show manufacturers, specifications, and research projects
[AD-762922] 20 p2362 N73-28998
Development of alternate space shuttle concepts to show modified avionics, vehicle subsystems, and thermal protection system
[NASA-CR-124345] 21 p2601 N73-30844
Extended automatic avionics interference prediction model
[ECAC-PR-73-002] 22 p2631 N73-31086
Space shuttle avionics and GOAL language including impact of error detection and redundancy management
[NASA-CR-134034] 22 p2638 N73-31142
Applications of spread spectrum communications techniques to avionics systems
23 p2756 N73-32058
Systems analysis of avionics and aircraft equipment for search and rescue helicopters to determine cost effective improvements - Vol. 7
[AD-764914] 24 p2927 N73-33381
Alternate concepts study on two and one half stage, stage and one half, and SRM interim booster systems for establishing performance, costs, and schedules
[NASA-CR-124344] 24 p2982 N73-33829

**AVOIDANCE**
NT COLLISION AVOIDANCE

**AVRO 698 AIRCRAFT**
U VULCAN AIRCRAFT

**AXES [COORDINATES]**
U COORDINATES

**AXES [REFERENCE LINES]**
NT AXES OF ROTATION
NT EARTH AXIS

**AXES OF ROTATION**
NT EARTH AXIS
Determination of parameters related to interior of Mercury
[NASA-CR-130981] 09 p1082 N73-18823
Three axes motion simulator for satellite attitude control systems
[ESRO-CR-61] 19 p2249 N73-28132
Quasistationary mode of rotation of spherical rotor of free gyroscope
20 p2418 N73-29427

**AXIAL COMPRESSION LOADS**
Creep buckling of flat plates and cylindrical shells subjected to edge wise and uniform axial compression respectively
[AD-746475] 02 p0240 N73-11952
Nondestructive evaluation of stability of shells and development of mechanical device for crash simulator
04 p0480 N73-13922
Buckling and intial postbuckling of oval cylindrical shells under pure bending and under combined uniform axial compression and bending
[AD-747493] 04 p0482 N73-13939
Analysis of stability of cylindrical shells with filler under axial compression and development of linearized equations of stability
[AD-750953] 05 p0605 N73-14919
Distribution losses in axial compressor over blade cross sections and effects of blade heights
[AD-750931] 06 p0657 N73-15334
Calculation of bifurcation stress in elastic/plastic plate under uniaxial compression
[AD-753136] 09 p1096 N73-18949
Sensitivity of thin-walled compression members to column axis imperfection
[VTH-172] 13 p1587 N73-22863
Experimental analysis of buckling of integrally ring stiffened cylindrical shells under axial compression to determine influence of shell and ring geometry on applicability of linear theory
[AD-755392] 13 p1588 N73-22872
Holographic interferometric measurement of prebuckling deformation in cylindrical shell structures under axial compression
16 p1921 N73-25545
Buckling of cylindrical panels under non-uniform axial compression
[AD-758833] 16 p1971 N73-25946
Computation of buckling of thin walled circular cylinders under axial compression loads
[DLR-FB-73-36] 21 p2604 N73-30868

**AXIAL COMPRESSORS**
U TURBOCOMPRESSORS

**AXIAL FLOW**
Design and experimental performance of axial flow, transonic compressor
[NASA-TM-X-2645] 02 p0123 N73-11002
Development of supersonic cascade and wheel structure for axial flow compressor
[AD-752583] 09 p1079 N73-18804
Development of algorithm for testing gas dynamic design of axial flow compressors with multiple stages
[AD-753519] 09 p1080 N73-18809
Iterative method for calculating axial flow resistance in annular slots of impeller pumps
[NLL-NEL-TT-2422-(6075.461)] 11 p1269 N73-20299
Aerodynamic characteristics of rotary wings under axial flow conditions and development of numerical analysis techniques
12 p1360 N73-21039
Measurement of power spectra of waveforms derived from vibrating blades in axial compressor and application to determine damping factor of blades
[ARC-R/M-3253] 15 p1728 N73-24014
Design and evaluation of multiple circular arc bladed, axial flow transonic compressor rotor
[NASA-TM-X-2697] 15 p1730 N73-24033
Nonuniform flow in front of axial flow compressor stage
[AD-759247] 16 p1891 N73-25303
Wind tunnel tests of short takeoff and landing fan stage model to determine airflow conditions around rotor and stator and stage pressure ratio
[NASA-TM-X-2837] 18 p2192 N73-27701
Comparison of thrust and torque forces on ship propeller blades in oblique and axial flow
[DRIC-TRANS-3205] 21 p2525 N73-30249
Evaluation of acoustic radiation from various noise sources in axial fan
[NASA-CR-114576] 22 p2614 N73-30952
Rotating stall in axial flow compressor stages with different types of profiling along blade height and different flow regimes past profile in cascade
[NASA-TT-F-15115] 22 p2709 N73-31698
Shock wave pattern and stability in axial flow supersonic compressor using simulated rotating cascade test facility
23 p2775 N73-32196
Coefficient of thermal conductivity for composite materials by using axial thermal flow method
23 p2807 N73-32447
Designing axial compressor airfoils with camber lines of arbitrary shape
[AD-765165] 23 p2832 N73-32636

**AXIAL FLOW COMPRESSORS**
U TURBOCOMPRESSORS

**AXIAL FLOW PUMPS**
NT TURBINE PUMPS
Mechanical, friction, and gap-effects on semiaxial turbine pump having different blade arrangements
02 p0178 N73-11439
Rotor design, test apparatus and procedure, and data reduction and evaluation for axial flow pump rotor configurations
[NASA-TN-D-7074] 06 p0613 N73-14982
Prediction of overall and blade-element performance for axial flow pumps
[NASA-CR-2301] 23 p2775 N73-32189

**AXIAL FLOW TURBINES**
Performance tests of single stage, axial flow, transonic compressor over stable operating range at rotative speeds from fifty to one hundred percent of design speed
[NASA-TM-X-2658] 06 p0614 N73-14983
Role of boundary layers in axial flow turbomachines and prediction of their effects
10 p1205 N73-19806
Application of boundary layer fences in turbomachinery
10 p1206 N73-19810
Prediction of annulus wall boundary layers in axial flow turbomachines
10 p1206 N73-19813
Annulus wall boundary layers in axial flow turbomachine
10 p1206 N73-19814
Performance tests of axial flow transonic compressor stage with multiple circular arc blades to determine effects of blade shape on efficiency and stall margin
[NASA-TM-X-2731] 11 p1231 N73-19995
Application of momentum theory to determine performance limits of propellers, and lifting rotors with axes parallel to undisturbed flow
[AD-754072] 11 p1235 N73-20025
Development of mathematical matrix technique for calculating inviscid, rotational, compressible axisymmetric flow field through axial flow compressor
[ME/A-73-1] 13 p1570 N73-22723
Application of three dimensional analysis techniques for determining operating characteristics of axial turbines
15 p1824 N73-24785
Axial flow turbomachine response to upstream disturbances
[AD-759029] 16 p1866 N73-25107
Analytical method for predicting stall flutter of axial-turbomachine blading
[AD-760354] 17 p2078 N73-26813

Aerodynamic effects of blade tip clearance in axial flow turbine lifting line for nonuniform flow, calculating lift and induced drag
[REPT-4/1973] 19 p2329 N73-28738
Numerical analysis of variable pitch compressor rotor blades for reduction of rotor vibrations
[AD-762228] 19 p2330 N73-28746
Analysis of rotating stall conditions in axial flow compressors and development of control system to improve flow stability
[AD-762297] 19 p2330 N73-28748

**AXIAL LOADS**
NT AXIAL COMPRESSION LOADS
Fatigue strength curves for large steel screw threads under axial loading
[ESDU-68045] 01 p0110 N73-10905
Approximation of beam buckling mechanics using axial and transverse loads
[AD-745881] 02 p0219 N73-11775
Fatigue tests on unnotched steel specimens during bending and axial loading
[ESDU-FAT-E.07.04] 02 p0236 N73-11924
One-component strain gage for measuring axial forces on low density wind tunnel models
[DLR-MITT-71-30] 04 p0423 N73-13447
Fatigue properties of sintered test bars for bending and axial loads
[LBF-TM-58/71] 05 p0563 N73-14570
Buckling of flat isotropic plates under uniaxial and biaxial loading
[ESDU-72019] 06 p0724 N73-15908
Shell theory and three dimensional analysis of cylindrical shells subjected to axisymmetric tangential surface loads
13 p1584 N73-22838
Higher-order shell theory for thick circular cylinders under arbitrary load and boundary conditions
[AD-756648] 13 p1589 N73-22885
Computer program for linear instability analyses of biaxially loaded composite structures
[NASA-CR-112226] 15 p1838 N73-24893
Elastic stresses due to axial loads on nozzle intersecting cylindrical shell
[AD-758075] 15 p1841 N73-24916
Analysis of general buckling of pressurized stiffened cylinder under axial load
[ARC-R/M-3198] 16 p1857 N73-25040
Statistical method used to examine stability of cylindrical shell under influence of axial forces
[AD-759394] 16 p1970 N73-25938
Axial load fatigue tests on unnotched specimens of aluminum alloy extrusions following aging specimens
[ARL/SM-NOTE-386] 18 p2203 N73-27780
Numerical analysis of stability of axially compressed cylindrical shells from composite materials under nonstationary heating
18 p2203 N73-27785
Selected articles on gyroscopes and gyromotors
[JPRS-59053] 20 p2417 N73-29420
Equations for determining action and deformation of bearings when force applied to center of gravity of gyromotor rotor
20 p2417 N73-29422
Equations for determining change of axial rigidity as function of component rotor weight
20 p2417 N73-29423

**AXIAL STRAIN**
Measurement of axial velocity profiles and resulting acoustical fields of rod under continuous-wave excitation
[AD-747209] 02 p0239 N73-11945
Self-consistent Pauli corrections in Brueckner-Hartree-Fock calculations
[NASA-TM-X-68197] 10 p1193 N73-19704
Cartesian and curvilinear coordinates for studying axial symmetrical deformation of rotatory bodies
[NLL-M-22827-[5828.4F]] 11 p1344 N73-20907
Higher order theories and solution techniques for moderately thick shells of revolution using Reissner Theory and Legendre functions
13 p1584 N73-22842
Numerical analysis of fatigue strength of steel specimens under symmetric loading cycles
[AD-761469] 19 p2310 N73-28581
Stress and strain relations for elastic and plastic deformation in uniaxial strain
[AD-762536] 20 p2464 N73-29797
Dynamic compressive stress-strain data of polymer foams obtained from uniaxial compressive tests
[AD-762490] 21 p2565 N73-30559

**AXIAL STRESS**
Subsequent yield curves for axial stressed-shear stressed surfaces of annealed SAE 1017 steel
[AD-746474] 02 p0188 N73-11523
Relationships between continuum metal plastic deformation under multiaxial stress and phenomenological dislocation theory
[AD-746187] 02 p0219 N73-11769
Application of least square point matching for stress analysis of shallow, perforated, cylindrical shell subjected to tension, edge moment, or transverse shear
[AD-750942] 06 p0728 N73-15942
Hydraulic biaxial medium-rate tension-torsion testing machine
[REPT-1047/72] 10 p1161 N73-19449
Graphite and epoxy plastic material strength under biaxial stress
[AD-758448] 15 p1801 N73-24600
Statistical theory for fracture of brittle structures subjected to nonuniform polyaxial stresses
[AD-759805] 16 p1970 N73-25936
Optimum edge reinforcement around a circular hole in a flat elastic sheet subjected to axial tensile stress
[ARC-R/M-3723] 21 p2604 N73-30869

**AXISYMMETRIC BODIES**
Calculation of Magnus forces on axisymmetric bodies at small angles of attack with incompressible turbulent boundary layers
[AD-746449] 02 p0157 N73-11270
Analysis of flow distribution around axisymmetric bodies at extreme angles of attack and calculation of pressure distribution for asymmetric steady vortex wake
[AD-747986] 03 p0286 N73-12315
Computer program for calcuating transonic flow about axisymmetric bodies
[AD-752898] 09 p1018 N73-18309
Magnetohydrodynamic equilibrium in axisymmetric torus
[IPPJ-141] 09 p1070 N73-18727
Finite difference method applied to axisymmetric random shells of revolution for unsymmetrical loading
[DRIC-TRANS-2996] 12 p1463 N73-21855
Analysis of flow distribution over three axisymmetric bodies at various angles of attack to determine boundary layer transition point characteristics
19 p2250 N73-28145
Method for estimating drag-rise mach number of smooth, nonducted, axisymmetric bodies at zero incidence without discontinuities in surface slope
[ESDU-71008] 22 p2650 N73-31230
Cavitation inception and separation on axisymmetric bodies in water tunnel
23 p2771 N73-32164

**AXISYMMETRIC DEFORMATION**
U AXIAL STRAIN

**AXISYMMETRIC FLOW**
NT ANNULAR FLOW
Numerical analysis of change in component energies due to three dimensional distortion in homogeneous and initially axisymmetric turbulence
[REPT-72-FM-7] 06 p0652 N73-15298
Solving singular axisymmetric field problem noting applications to electromagnetism and fluid mechanics
[ONERA-NT-207] 10 p1190 N73-19685
Simulation of atmospheric vortex based on boundary conditions and parameter values of strong atmospheric tornadoes and waterspouts
12 p1390 N73-21269
Mass transfer rates of swirling and pulsating flow through axisymmetric duct
[AD-756546] 14 p1652 N73-23396
Numerical analysis of Navier-Stokes equations for steady, viscous, axisymmetric flow with application to flow past pitot tube at low Reynolds numbers
[ARC-R/M-3240] 15 p1725 N73-23998
Flow characteristics of axially symmetrical, supersonic, fully-expanded jet to determine relation between static pressure distributions and jet turbulence
[ARC-R/M-3292] 16 p1857 N73-25038
Numerical analysis of axisymmetrical, viscous, compressible flow around blunt bodies for ideal gases with laminar unseparated boundary layers
17 p2012 N73-26273
Structure of axisymmetric jet in near field for jet noise and impingement schemes
[NASA-CR-121257] 19 p2255 N73-28177
Analysis of viscous effects in low-density nozzle flows using internal laminar layer equations for two dimensional or axisymmetric flow
[AD-761489] 19 p2257 N73-28191
Development of theoretical model for supersonic turbulent near wakes of planar and axisymmetric configuration in supersonic flow
20 p2384 N73-29151
Hydrodynamic stability of axisymmetric free shear layers
24 p2902 N73-33165

**AXISYMMETRY**
U SYMMETRY

**AXLES**
U SHAFTS [MACHINE ELEMENTS]

**AZIDES [INORGANIC]**
Electrical strength of pressed lead azide
10 p1199 N73-19753

**AZIMUTH**
Longitude, latitude, and azimuth determinations using transit instrument
[MITT-99] 01 p0101 N73-10826
Constant azimuth cycloids discussing rotating earth trajectory
07 p0859 N73-16970
Cinetheodolite observations of satellites between 3 and 26 Nov. 1965
[ROE-STS-134] 09 p1091 N73-18907
Computer program to compute geodetic distance and azimuth between two geodetic positions
[P-4950] 14 p1659 N73-23462
Relation between azimuth component of interplanetary magnetic field and geomagnetic field in polar caps
[NASA-CR-133273] 18 p2145 N73-27338

**AZINES**
Nuclear magnetic resonance spectrum analysis for rings inversion rate in benzodiazepine derivatives
[RAE-LIB-TRANS-1628] 17 p1991 N73-26103
High temperature and ultraviolet stability properties of poly[diarylsiloxy]arylazine
[NASA-CASE-ARC-10592-1] 20 p2435 N73-29554

**AZO COMPOUNDS**
NT RDX
Reaction of azotetrazole anion and nitric, sulfuric and hydrochloric acid noting giving of 5-hydrazinotetrazole and 5-azidotetrazole
[ERDE-TN-44] 05 p0507 N73-14123

**AZOLES**
NT INDOLES
NT OXAZOLE
NT PYRROLES

**AZULENE**
Amino acids, urea, guanidine, glycocyamine, and 5-amino 4-imidazole carboxamidine from hydrolysis of azulmic acids
[NASA-TT-F-14640] 04 p0380 N73-13089

**AZUR SATELLITE**
Azur satellite proton and electron telescope measurements in radiation belt, and conclusions regarding magnetospheric processes
[MPI-PAE/EXTRATERR-66] 02 p0226 N73-11821
Raw data processing from proton, alpha particle, and electron flux experiments of Azur satellite
[MPI-PAE/EXTRATERR-76] 09 p1081 N73-18818
Automatic flight control system AOOSY for satellite control, tested with Azur satellite
[MBB-UA-56-72-O] 18 p2126 N73-27183
Azur satellite orbit perturbation recorded from Weilheim-Lichtenau ground station
[BMBW-FBW-72-18] 21 p2597 N73-30816
Azur satellite telemetry data processing - conferences
[BMFT-FB-W-73-04] 24 p2985 N73-33852
Azur satellite telemetry, noting real time and tape telemetry systems
24 p2985 N73-33853
Preprocessing of Azur satellite telemetry data to provide several output tape formats
24 p2985 N73-33854
Time allocation in Azur satellite telemetry data, noting onboard clock and world time deviations on tapes
24 p2985 N73-33855
Selection of Azur satellite additional information for telemetry data processing
24 p2985 N73-33856
Redundancy elimination in Azur satellite telemetry data
24 p2985 N73-33857
Azur satellite attitude determination, based on coordinate transformation matrix and angle measurement
24 p2985 N73-33858
Planning of satellite data computer processing
24 p2986 N73-33860

**A2F AIRCRAFT**
U A-6 AIRCRAFT

**A4D AIRCRAFT**
U A-4 AIRCRAFT


## B


**B STARS**
Balmer and H gamma line profiles for determining electron density in model B stars
[NASA-TM-X-66266] 17 p2082 N73-26840
Far ultraviolet photometry of peculiar B and A stars by OAO 2
22 p2734 N73-31883

**B-1 AIRCRAFT**
Finite element method to determine post-buckling strength of B-1 aircraft aft intermediate fuselage following combined torque and axial loading
[AD-763813] 22 p2615 N73-30956

**B-52 AIRCRAFT**
Logistic performance data book for electronic countermeasures system of B-52G aircraft to show reliability, maintenance, costs, and problems
[AD-762216] 19 p2357 N73-28961
Application of active control technology for suppression of flutter with analysis of effect on B-52 aircraft configuration
[NASA-TM-X-2909] 21 p2603 N73-30864

**B-57 AIRCRAFT**
Meteorological instruments to measure atmospheric electricity aboard modified B-57 aircraft
[AD-755400] 13 p1526 N73-22372

**B-70 AIRCRAFT**
Measurement of surface pressure fluctuations at two locations on XB-70 aircraft at local Mach number range from 0.35 to 2.45
[NASA-TN-D-7226] 09 p0981 N73-18013
Flight-measured base pressure coefficients for thick boundary layer flow over aft-facing step for Mach numbers from 0.4 to 2.5 using XB-70 aircraft
[NASA-TN-D-7202] 15 p1767 N73-24317

Low frequency structural response and damping characteristics of XB-70 aircraft during subsonic and supersonic flight
[NASA-TN-D-7227] 15 p1837 N73-24892
Flight tests of XB-70 aircraft to determine skin friction coefficients and boundary layer profiles at Mach numbers up to 2.5
[NASA-TN-D-7220] 16 p1887 N73-25276
Longitudinal stability and control derivatives of XB-70 aircraft to compare flight test and theoretical data
[NASA-TM-X-2881] 22 p2613 N73-30940
Flight test of structural mode control system installed in XB-70 aircraft to determine effectiveness of system under turbulent conditions
[NASA-TN-D-7420] 23 p2742 N73-31950
Stability and control characteristics of XB-70 aircraft at airspeeds up to Mach 3.0 and addition of lateral bobweight as auxiliary stabilization device
[NASA-TM-X-2933] 23 p2743 N73-31958

**BABBITT METAL**
U BEARING ALLOYS

**BAC AIRCRAFT**
NT CANBERRA AIRCRAFT
NT H-126 AIRCRAFT
NT JET PROVOST AIRCRAFT
NT VISCOUNT AIRCRAFT
Longitudinal and lateral data, lateral oscillatory derivatives, and aileron and rudder powers for BAC 221 aircraft
[ARC-CP-1230] 05 p0494 N73-14027

**BACILLUS**
Ultraviolet extraterrestrial radiation tolerances of Bacillus subtilis spores and Escherichia coli bacteriophages
15 p1740 N73-24107
Space vacuum and solar ultraviolet irradiation effects on survival of Bacillus subtilis spores
15 p1740 N73-24108
Space flight ultraviolet irradiation effects on Bacillus thuringiensis toxin production capability
15 p1740 N73-24109
Thermal inactivation of Bacillus subtilis var. niger spores on Viking lander
[NASA-CR-133223] 17 p1987 N73-26058
Dry heat inactivation of atypical Bacillus subtilis var. niger spores in and on interplanetary space vehicle components
[NASA-CR-133224] 17 p1987 N73-26059
Composition of human gastrointestinal microflora during prolonged isolation
20 p2367 N73-29037

**BACK BAYS**
U BAYS [TOPOGRAPHIC FEATURES]

**BACK INJURIES**
Statistical analysis of occurrence of backache among Royal Air Force flight crews and ground crews to show effects of crew seats on physical comfort
[AD-745177] 01 p0013 N73-10102

**BACKFIRE**
Investigation of backfires and explosions occuring in vacuum pumps of oxygen test stands
[AD-763370] 21 p2554 N73-30474

**BACKGROUND NOISE**
Binaural improvement in normal and defective ears in background of other voices
[AD-746101] 01 p0013 N73-10103
Noise and response complexity effects on human attention and performance in visual perception task
[AD-747797] 04 p0381 N73-13105
Flicker noise and related bulk effects in silicon junction field effect transistors
20 p2461 N73-29774

**BACKGROUND RADIATION**
Solar wind/interstellar gas interactions and Lyman alpha background radiation
[TRITA-EPP-72-03] 01 p0105 N73-10871
Background Lyman alpha radiation and interstellar hydrogen gas taking into account radiative heat transfer
01 p0105 N73-10872
Coaxial anode scheme for reducing background of X ray astronomy proportional counter
[NASA-CR-130127] 04 p0421 N73-13432
Measurements of isotropy of cosmic background radiation at 6 cm determined from apparent sky brightness temperature differences
07 p0838 N73-16789
Galactic and background radiation measurements by rocket-borne submillimeter detectors
07 p0840 N73-16808
OSO-1 experimental design for cosmic X ray sources identification and diffusion background radiation spectroscopy
17 p2084 N73-26861
Red shift energy distribution and black body background distortion theories of universal formation
19 p2333 N73-28770
Far infrared and submillimeter background
[AD-763139] 21 p2598 N73-30823

**BACKSCATTERING**
Radar backscatter produced by chaff cloud as function of position of radar relative to chaff cloud
[AD-744776] 01 p0029 N73-10226
Direct scatter effects from field aligned E and F layer irregularities and scatter from subauroral ionospheric clouds at 19.4 MHz
[AD-746311] 01 p0054 N73-10436
Phase difference between temperature and density in thermosphere
[NASA-TM-X-66119] 03 p0294 N73-12395
Analysis of backscatter from radar transmission and effect of field aligned laminae in both E and F layers of ionosphere
[AD-747027] 03 p0297 N73-12426
Mossbauer spectrometer with high efficiencies in both transmission and backscattering techniques
[NASA-CASE-LAR-11155-1] 04 p0421 N73-13433
Doppler study of microwave backscattering from ocean waves in wind wave tank
[AD-753199] 09 p1032 N73-18422
Correlation of ocean surface parameters with radar backscatter data
[E73-10530] 13 p1517 N73-22295
Optimum techniques for detecting and discriminating backscattered electromagnetic radiation associated with impulse radar concept
[AD-757220] 14 p1636 N73-23267
Asymptotic methods for deriving transient backscattered signatures from artificial satellites
[AD-758245] 15 p1751 N73-24192
Laser observations of dense natural fog to determine backscatter and slant range visibility for aircraft landing operations
[AD-760128] 17 p2041 N73-26511
Development and characteristics of instrument to measure back reflection of laser radiation
17 p2041 N73-26515
Stratospheric backscattering measurements using airborne lidar system onboard Convair 990 aircraft
18 p2132 N73-27227
HF and VHF oblique backscatter and scintillation study at Plum Island
[AD-760783] 18 p2146 N73-27349
Obtaining absolute target reflectances by correcting ERTS-1 radiance measurements for variable target irradiance, atmospheric attenuation, and atmospheric backscatter
[PAPER-I3] 19 p2277 N73-28325
Development of catalogs for backscatter and brightness temperature measurements and atmospheric effects on Skylab S-193 data
[E73-10896] 20 p2395 N73-29245
Preparation of backscatter and brightness temperature measurement catalogs and atmospheric effects on Skylab S-193 data
[E73-10897] 20 p2395 N73-29246
Backscatter spectrum comparisons, including ionospheric inhomogeneity effects
[NASA-CR-133809] 21 p2538 N73-30349
Application of polarized electromagnetic radiation for analyzing parameters of atmospheric formations
21 p2569 N73-30592
Application of radio astronomical methods for determining attenuation and radio emission of rain from cumulonimbus clouds
21 p2570 N73-30594
Development of backscattering diagrams for sources of reflections from clear sky based on signatures from meteorological radar
21 p2571 N73-30600
Doppler and surface effects in backscattered signal fading
22 p2627 N73-31052
Utilization of inverse scattering method to measure transparency of atmosphere in slant direction
22 p2693 N73-31571
Experimental determination of coupling between normal F region ionosphere and protonosphere using radar backscatter techniques at Arecibo, Puerto Rico
23 p2778 N73-32213
Analysis of ionograms to determine HF auroral backscatter over bistatic path
24 p2911 N73-33231
Laser fusion and parameteric instabilities
[COO-3227-18] 24 p2932 N73-33413

**BACKSHORES**
U BEACHES

**BACKWARD WAVE TUBES**
EHF attenuation measurements of helical waveguides, using FSK shuttle pulse method and backward wave oscillator
[FTZ-333-TBR-17] 22 p2643 N73-31182

**BACTERIA**
NT BACILLUS
NT ESCHERICHIA
NT PSEUDOMONAS
NT STAPHYLOCOCCUS
NT STREPTOCOCCUS
Daylight and disinfectant effects on bacteria survival times on plastic surfaces
[NASA-TT-F-13923] 01 p0009 N73-10069
Growth response of bacteria and yeast in high pressure helium-oxygen environment
[AD-745334] 01 p0012 N73-10096
Characteristics of photogenic bacteria - Micrococcus pierantonii
[NASA-TT-F-14439] 02 p0132 N73-11072
Bacterial reduction of organically bound phosphoric acid in blood
[NASA-TT-F-14723] 04 p0379 N73-13080
Planetary quarantine procedures for reduction of microbial burden on spacecraft
[NASA-CR-129793] 04 p0379 N73-13086
Photosynthetic energy conversion in membranes, tissues, and reaction centers of bacteria and viruses
[COO-3162-9] 04 p0380 N73-13091
Differential light scattering patterns for identifying different species of bacteria
08 p0875 N73-17090
Splitting aluminosilicates with silicate bacteria for liberation of potassium in soils
[NASA-TT-F-14870] 11 p1286 N73-20437
Conference on Apollo 16 experiment for measuring microbial response to space environment
[NASA-TM-X-58103] 15 p1740 N73-24102
Enzymatic luminescent bioassay method for determining bacterial levels in urine
[NASA-CASE-GSC-11092-2] 18 p2109 N73-27052
Susceptibility of synthetic engine and transmission lubricants of OH-58 A helicopter to microbal attack
[AD-762176] 19 p2313 N73-28604
Tape cassette bacteria detection system for automatic continuous bacterial detection for monitoring sterility of regenerated water in spacecraft
[NASA-CR-134035] 22 p2620 N73-30996

**BACTERICIDES**
Antimicrobial water reclamation methods for processing human urine
10 p1117 N73-19105
Antimicrobial phenyl preparations for human urine conservation during space flight
10 p1118 N73-19112
Bactericidal activity of human skin at different times of day
11 p1245 N73-20110
Silver-ion bactericidal monitor for Space Shuttle potable water system
[NASA-CR-128884] 11 p1293 N73-20492
Bactericidal properties of sorbents in spacecraft water regeneration system
20 p2367 N73-29038

**BACTERIOLOGY**
Detection of bacteria in biological fluids and foods
[NASA-CASE-GSC-11533-1] 04 p0421 N73-13435
Development of procedures of identification of microorganisms on orbiting spacecraft
[NASA-CR-128747] 10 p1120 N73-19132
Methods for improving bacterial transport media
[NASA-CR-128958] 16 p1866 N73-25113

**BAFFLES**
Pressure loads and damping associated with rigid ring baffles in large cylindrical tanks
[NASA-TN-D-6870] 03 p0282 N73-12285
Simple baffle combustor for heating test facilities
[ARL/ME-334] 10 p1137 N73-19265
Damping of liquid oscillations using flexible ring baffles
[NASA-TM-X-64730] 12 p1390 N73-21273
Performance of baffles as energy dissipation suppressors in liquid filled precessing cavities
16 p1888 N73-25280
Acoustic shielding baffle for determining jet noise source location
[NASA-TN-D-7229] 16 p1944 N73-25734
Floating baffle for tank drain
[NASA-CASE-KSC-10639] 17 p2036 N73-26472

**BAGS**
NT GAS BAGS

**BAILOUT**
Proceedings of symposium to determine requirements and configurations of emergency ejection systems for helicopter crews
[AGARD-AR-62] 23 p2743 N73-31954

**BAKEOUT**
U DEGASSING

**BALANCE**
Evaluation of stability derivatives obtained from dynamic tests of model in cold magnetic balance wind tunnel facility
[NASA-CR-112305] 11 p1267 N73-20279
Radial flow balance in turbomachines
[ONERA-NT-209] 15 p1768 N73-24326
Influence of man on biospheric balance
[JPRS-59366] 18 p2110 N73-27065

**BALANCE EQUATIONS**
U EQUATIONS

**BALANCING**
Data transmission and processing system for balanced air bearing stabilized platform for satellite motion simulator
[ESRO-CR-54] 01 p0037 N73-10287
Static force balancing system attached to lifting body
[NASA-CASE-LAR-10348-1] 03 p0279 N73-12264

**BALL BEARINGS**
Numerical analysis of friction forces developed in ball bearing of pendulum support to show dynamic friction torque and arm of rolling friction
[JPRS-57257] 01 p0062 N73-10507
Ball bearing performance in liquid hydrogen at 30,000 rpm under thrust load of 1780 N
[NASA-TN-D-6981] 02 p0178 N73-11441

Surface active substance effect on contact fatigue life of hardened ball bearing steel
[AD-746040] 03 p0307 N73-12506
Development of method for estimating power required to drive ball bearings in turbine engine based on performance of high speed antifriction bearings
[AD-747600] 03 p0308 N73-12514
Performance tests of ball bearings operating at high dn values
[NAL-TR-284] 04 p0426 N73-13469
Fatigue tests of hot pressed silicon nitride ball bearings
[NASA-TM-X-68174] 06 p0725 N73-15922
Production of ball bearing steel ingots with emphasis on effects of temperature, surface defects, and casting methods
[AD-751252] 07 p0805 N73-16533
Materials for ball bearings for space applications using chromium steel and silver-indium alloy
[REPT-781-4.4] 10 p1166 N73-19490
Effect of ovality of radial thrust bearing balls on axial vibration of rapidly rotating rotor of engine
[AD-754615] 11 p1300 N73-20546
Development of self-contained, solid lubricated ball bearings for operation at high speed - Part 2
[AD-756487] 14 p1671 N73-23557
Oscillographic measurements of friction moments in gas ball bearings
[NLL-RISLEY-TR-2565-[9091.9F]] 15 p1790 N73-24507
Performance tests to determine stress-life exponent for vacuum-processed steel ball bearing operating at 500 F
[NASA-TM-X-68240] 15 p1791 N73-24521
Evaluation of materials for ball bearings intended for use in liquid fluorine and/or FLOX
[NASA-CR-120820] 16 p1917 N73-25516
Endurance and performance tests of bore ball bearings lubrication thrust loaded 120-mm to 3 million DN
[NASA-TM-X-68264] 17 p2037 N73-26479
Experimental evaluation of 150-mm bore ball bearings to 3-million DN using solid and drilled balls
[NASA-TM-X-68265] 17 p2037 N73-26480
Modification of spinning torque apparatus to measure spinning torque on cageless ball thrust bearing using oil jet lubrication or thin surface film only
[NASA-TN-D-7356] 17 p2038 N73-26484
Application of magnetic perturbation technique to nondestructively detect subsurface nonmetallic inclusions in inner races of deep groove ball bearings
[NASA-TM-X-68260] 18 p2155 N73-27410
Performance tests of high speed ball bearings with lead and lead alloy plated retainers operating in liquid hydrogen at 30,000 rpm and 400 pound thrust load
[NASA-TM-X-68268] 18 p2155 N73-27412
Measurement of spinning and rolling torques in angular-contact ball bearing with and without cages under several lubrication regimes
[NASA-TM-X-68271] 18 p2155 N73-27414
Equations for determining action and deformation of bearings when force applied to center of gravity of gyromotor rotor
20 p2417 N73-29422
Equations for determining change of axial rigidity as function of component rotor weight
20 p2417 N73-29423
Low mass rolling element bearing assembly
[NASA-CASE-LEW-11087-1] 21 p2552 N73-30458
Limiting speed and bearing performance of grooved and angular contact ball bearings
[NASA-TT-F-15017] 23 p2796 N73-32364
Fatigue life tests of ball motion and sliding friction in arched outer race ball bearing under thrust load
[NASA-TM-X-71442] 23 p2797 N73-32375

**BALL LIGHTNING**
Oxidation of nitrogen and ball lightning
[AD-763146] 21 p2539 N73-30358

**BALLAST [MASS]**
Inflatable stabilizing system for use on life raft to reduce rocking and preclude capsizing
[NASA-CASE-MSC-12393-1] 17 p1980 N73-26006

**BALLISTIC MISSILES**
NT MINUTEMAN ICBM
NT PERSHING MISSILE
NT POSEIDON MISSILES
NT SHORT RANGE BALLISTIC MISSILES
Solving problems of long-range ballistic missiles - launching, trajectory and flight characteristics, and firing data
[AD-743687] 01 p0109 N73-10898
Use of solid rocket engine as power plant for ballistic missiles
15 p1825 N73-24795
Ballistic design of solid propellant missiles to include analysis of physical properties and determination of reliability
[JPRS-59060] 18 p2200 N73-27759
Development of principles for design, development, and evaluation of ballistic missiles and support systems
[JPRS-51810] 20 p2475 N73-29881

**BALLISTIC RANGES**
Scale model evaluation of fiber glass wedge and parabolic deflector efficiencies in cylindrical ballistic ranges using pressure transducer measurements
[DREV-TN-2031/72] 06 p0649 N73-15270
Optical measuring instruments used at hypervelocity ballistic range facility
[AD-750866] 06 p0651 N73-15284

**BALLISTIC TRAJECTORIES**
Graphs for ballistic transfers to Jupiter, Saturn, and Uranus
[NASA-CR-129162] 02 p0226 N73-11826
Computer program for calculating aerodynamic coefficients from trajectory angles of projectiles passing through paper screens
[FOA-2-C-2478-44] 06 p0613 N73-14980
Computation of drag coefficients for ballistic range models
[DREV-TN-2027/72] 06 p0614 N73-14987
Analysis of development of rocket dynamics
[AD-756962] 13 p1583 N73-22835
Payloads of ballistic trajectories in Mercury orbit, and interplanetary trajectory characteristics for Venus swingbys to Mercury
[NASA-CR-2298] 23 p2846 N73-32745

**BALLISTICS**
NT INTERIOR BALLISTICS
NT TERMINAL BALLISTICS
Analog to digital converter with teleprinter for multiple printout of projectile ballistic measurements
[PHL-1972-4] 01 p0032 N73-10245
Monopulse laser emission study of moving objects during shadow photography
[AD-747607] 03 p0311 N73-12539
Meteorological and ballistics data for launching of Athena rocket flight 134, vehicle H-004J
[AD-749436] 04 p0445 N73-13633
Meteorological and ballistics data for launching 13901 Little John, missile number 2172, round number 684 AM
[AD-749435] 04 p0445 N73-13634
Meteorological and ballistics data for launching 13401 Honest John, missile number 2632, round number 626 ROL
[AD-749434] 04 p0445 N73-13635
Meteorological and ballistics data for launching of Lance Missile 2143, vehicle 159
[AD-749429] 04 p0445 N73-13636
Meteorological and ballistics data for launching of Honest John Laser, missile flight 205, vehicle 624
[AD-749430] 04 p0446 N73-13637
Meteorological and ballistics data for launching of Honest John Missile flight 1755, vehicle 625
[AD-749431] 04 p0446 N73-13638
Meteorological and ballistics data for launching of Lance Missile 2168, vehicle 160
[AD-749432] 04 p0446 N73-13639
Meteorological and ballistics data for launching of Lance Missile 2159, vehicle 161
[AD-749433] 04 p0446 N73-13640
Meteorological and ballistics data for launching of Little John, missile number 3175, round 687 RO
[AD-749439] 05 p0574 N73-14669
Meteorological and ballistics data for launching of Little John, missile number 2253, round 683 RO
[AD-749437] 05 p0574 N73-14670
Meteorological and ballistics data for launching of Honest John, missile number 3116, round 686
[AD-749438] 05 p0574 N73-14671
Meteorological and ballistics data for launching of 11601 Lance Missile number 2154, round number 163 RBL
[AD-752088] 08 p0939 N73-17690
Meteorological and ballistics data for launching of 11602 Lance Missile number 5175, round number 164 ESL
[AD-752090] 08 p0940 N73-17695
Meteorological and ballistics data for launching of 13901 Little John Missile number 1463, round number 692 RG
[AD-752091] 08 p0940 N73-17696
Meteorological and ballistics data for launching of 14101 Little John RIP missile number 12751
[AD-752092] 08 p0940 N73-17697
Meteorological and ballistics data for launching of 13801 Little John ARM-P Ripple, missile numbers 3102, 3142 and 3257, round numbers 693, 694 and 695 RO
[AD-752095] 08 p0940 N73-17698
Meteorological and ballistics data for launching of Lance missile, number 2183, round no. 167 APT
[AD-752098] 08 p0940 N73-17700
Naval research in aerodynamics, ballistics, mathematics, and physics
[AD-754397] 11 p1268 N73-20292
Meteorological and ballistics data for launching of 15001 Little John missile no. 1508, round no. 697 RG
[AD-754558] 11 p1314 N73-20665
Meteorological and ballistics data for launching of 14801 Lance missile no. 2184, round no. 168 APT 9
[AD-754556] 11 p1315 N73-20669
Meteorological and ballistics data for launching of 12802 Lance missile no. 2150, round no. 174 ESL
[AD-754563] 11 p1316 N73-20678
Meteorological and ballistics data for launching of 11602 Lance missile, number 2174, round 181
[AD-755773] 12 p1424 N73-21539
Meteorological and ballistics data for launching of 12893 Lance missile, number 2354, round 182
[AD-755774] 12 p1424 N73-21540
Meteorological and ballistics data for launching of 14101 RIP missile, numbers 12723/12720, rounds 3/4
[AD-755775] 12 p1424 N73-21541
Meteorological and ballistics data for launching of Athena rocket vehicle, flight 137, vehicle H-005
[AD-755776] 12 p1424 N73-21542
Meteorological and ballistics data for launching of Athena rocket vehicle, flight 136, vehicle H-009
[AD-755779] 12 p1424 N73-21547
Meteorological and ballistics data for launching of Lance missile, number 2149, round 180
[AD-755772] 13 p1555 N73-22599
Theoretical analysis of ballistic H powder erosion combustion in acoustic stream
14 p1700 N73-23796
Meteorological and ballistics data for launching of 14101 RIP missile nos. 9623/9034, round nos. 5/6
[AD-758861] 15 p1807 N73-24647
Meteorological and ballistics data for launching of 03702 Honest John missile number 1003, round number 631 AML
[AD-758869] 15 p1807 N73-24650
Meteorological and ballistics data for launching of Honest John missile number 359, round 629,
[AD-758862] 16 p1938 N73-25684
Meteorological and ballistics data for launching of Honest John missile number 627, round 632
[AD-758868] 16 p1938 N73-25685
Meteorological and ballistics data for launching of Honest John, missile number 1002, round 630
[AD-758865] 16 p1938 N73-25686
Meteorological and ballistics data for launching of Lance missile, number 2237, round 185
[AD-758864] 16 p1939 N73-25687
Meteorological and ballistics data for launching of 13401 Honest John missile no. 2542, round no. 634 RMI
[AD-762157] 19 p2317 N73-28633
Meteorological and ballistic data gathered for launching Athena flight 140
[AD-762160] 19 p2317 N73-28639
Score, approach, and major results of study of ballistic mode Mercury orbit missions
[NASA-CR-114617] 22 p2715 N73-31733
Scope, approach, and major results of study of ballistic mode of Mercury orbit missions
[NASA-CR-114618] 22 p2715 N73-31734

**BALLOON FLIGHT**
Iterative method for localizing position of balloon on earth, using interrogating satellite and correcting for errors due to terrestrial rotation
[NASA-TT-F-14702] 03 p0328 N73-12677
Method for localizing position of balloon on earth, using interrogating satellite and correcting for electronic errors in distance measurement
[NASA-TT-F-14707] 03 p0328 N73-12678
High altitude balloon flights for solar cell calibration
[NASA-CR-129794] 04 p0375 N73-13050
Cosmic ray charge and energy spectra above 10 GeV from balloon flight data
08 p0974 N73-17963
Survival of heavy nuclei in cosmic ray source environments from Goddard balloon spectrometer experiment
08 p0974 N73-17964
Detection of high energy gamma rays from Crab nebula pulsar by balloon flight with gas Cerenkov telescope
20 p2467 N73-29822
Identifying heavy primary cosmic ray particles at energies higher than 1 GeV/nucleon by nuclear emulsion balloonborne photometry
[LUIP-CR-73-02] 21 p2593 N73-30778

**BALLOON SOUNDING**
Methane mixing ratios in stratosphere deduced from balloon-observed solar infrared spectra
[AERONOMICA-ACTA-A-105] 01 p0092 N73-10757
Balloon measurements of aerosol and ozone in Arctic stratosphere
[AD-747256] 02 p0169 N73-11374
Systematic error in locating sounding balloon caused by influence of wind
[NASA-TT-F-14704] 03 p0326 N73-12654
Method of arithmetic data processing for restituting geographic components of wind
[NASA-TT-F-14705] 03 p0326 N73-12655
Evidence for one source mechanism for primary cosmic rays and another mechanism for iron nuclei, based on balloon-borne ionization spectrometer
[NASA-TM-X-66149] 06 p0716 N73-15841
Balloon observation of pulsed gamma rays above 250 keV from Crab Nebula pulsar NP 0532
12 p1444 N73-21698

Balloon measurement of gamma ray emission from region of galactic center
16 p1959 N73-25844
Daily summaries for vertical echo sounding of upper atmosphere over Freiburg, Germany during March, 1973
[REPT-321F] 18 p2141 N73-27308
Balloon measurements on atmospheric secondary gamma rays using digitized spark chamber
[NASA-TM-X-66278] 18 p2195 N73-27718
Skyhook balloon flight operations
[AD-761657] 19 p2221 N73-27913
Measurement of mean isotopic composition of even-charge cosmic ray elements using balloon-borne ionization chamber
[NASA-CR-135516] 22 p2711 N73-31711
Balloon observations of solar neutrons by scintillation counter
[NASA-CR-135496] 22 p2712 N73-31714
Balloon flown hodoscopic observations of rapid variations in solar proton flux in 1972
[TR-73-134] 23 p2834 N73-32650
Balloon and GEOS satellite observations of auroral X rays from Scandinavia to Greenland
[NP-19738] 24 p2923 N73-33343
Pilot balloon observations of lower tropospheric winds along upper Texas coast
[REPT-35] 24 p2948 N73-33544

**BALLOONS**
NT HIGH ALTITUDE BALLOONS
NT JIMSPHERE BALLOONS
NT METEOROLOGICAL BALLOONS
NT SKYHOOK BALLOONS
NT TETHERED BALLOONS
Strength, mechanical properties, and deformation analysis of flexible polyethylene balloons
[AD-746308] 02 p0127 N73-11029
Low temperature investigation of polyethylene balloon film mechanical properties and structural factors affecting such properties
[AD-746678] 02 p0194 N73-11572
Iterative method for localizing position of balloon on earth, using interrogating satellite and correcting for errors due to terrestrial rotation and Doppler effect
[NASA-TT-F-14703] 03 p0328 N73-12679
System for controlling torque buildup in suspension of gondola connected to balloon by parachute shroud lines
[NASA-CASE-GSC-11077-1] 04 p0370 N73-13008
Flight tests of disk-gap band parachute behind full-scale simulator of Viking reentry vehicle over maximum range of entry conditions for landing on planet Mars-Vehicle AV-1
[NASA-CR-112176] 04 p0372 N73-13021
Flight tests of disk-gap band parachute behind full-scale simulator of Viking reentry vehicle over maximum range of entry conditions for landing on planet Mars-Vehicle AV-4
[NASA-CR-112179] 04 p0372 N73-13024
Design and fabrication of balloon to carry 3500 pound payload at 60,000 feet altitude for feasibility test of powering free balloon near minimum wind field
[AD-750542] 05 p0498 N73-14052
Design, development, and manufacture of natural shape free flight balloon to include requirements, documentation, testing, and inspection
[AD-753086] 09 p0987 N73-18055
Brittleness determination of low density blown polyethylene film balloons to account for high altitude failure
[AD-757885] 15 p1802 N73-24603
Mixing processes occurring in in-flight balloons with initially separate gases
[AD-760600] 18 p2207 N73-27812
Development of procedures for determining stability parameters of balloons tethered under steady wind conditions
[NASA-TN-D-7222] 21 p2493 N73-30013
Systems for protection of low altitude tethered balloons from effects of atmospheric electricity
[AD-764651] 23 p2746 N73-31978

**BALMER SERIES**
OAO-A2 observations of Be stars, continuous Balmer emission, and interstellar polarization
[NASA-CR-129166] 02 p0226 N73-11828
Balmer and H gamma line profiles for determining electron density in model B stars
[NASA-TM-X-66266] 17 p2082 N73-26840

**BALTIC SEA**
Sound wave reflection from sea bed, acoustic properties of sedimentary layer, and application to Baltic Sea
[FOA-3-C-3680-E1] 02 p0164 N73-11331
Interpretation of meteorological satellite TV pictures of ice in Baltic Sea
[NLL-M-20841-[5828.4F]] 05 p0529 N73-14306
Two-reservoir exchange model for Baltic Sea material balance
[GH-4] 17 p2027 N73-26407

**BALTIC SHIELD [EUROPE]**
Major fracture and fault zones of Baltic Shield and their relationships to mineral deposits
[E72-10297] 04 p0411 N73-13347
Major fracture and fault zones of Baltic Shield in Finland and relationships to mineral deposits
[E73-10682] 16 p1901 N73-25377

**BANACH SPACE**
Adaptive controllability of dynamical systems in Banach space with bounded operators
[AD-753716] 10 p1179 N73-19593
Fixed point theorems and dissipative processes in differential systems of Euclidian space
[NASA-CR-131267] 11 p1310 N73-20631

**BAND STRUCTURE OF SOLIDS**
Optical properties and band structure of solids studied with electroreflectance and other optical modulation
[AD-746271] 01 p0089 N73-10736
Absorption spectra analyses on germanium films for determining band structure transformations
02 p0218 N73-11765
Perturbation approach to strains confined to elastic region with small electronic energy changes
[AD-748085] 03 p0347 N73-12829
Band structure and electrical properties of amphorous semiconductors
[AD-749379] 04 p0461 N73-13761
Influence of band structure on photofield emission from metals
[AD-749828] 05 p0589 N73-14788
X ray and electron energy spectroscopy for analysis on band structure of materials
[NAL-SR-1] 06 p0699 N73-15703
Fermi surface changes in dilute alloys of aluminum, cadmium, and zinc
[AD-750726] 06 p0709 N73-15786
Electronic transport properties in band properties
[AD-752100] 08 p0951 N73-17790
Electron structure of transition metals and alloys
[ONERA-P-144] 09 p1048 N73-18548
Theory of amorphous semiconductors with electronic states in undulatory-graded band-gap model
12 p1438 N73-21650
Optical properties and electronic structure of metal alloys
[AD-755847] 12 p1441 N73-21675
Temperature dependence of mercury telluride band gap
15 p1820 N73-24749
Electronic state density of semiconductor compounds A[3] B[5], using law of dispersion
[AD-758168] 15 p1822 N73-24766
Proceedings of conference on nondestructive testing and materials characterization with emphasis on development of new techniques for materials testing
[AD-760174] 18 p2157 N73-27427
Electron spin resonance measurements on Fermi levels in molybdenum doped rutile during hydrogen treatment
[AD-760735] 18 p2192 N73-27694
Infrared optical reflectivity analysis for determining free carrier parameters of irradiated gallium arsenide
[AD-762273] 20 p2463 N73-29791
Variation of crystal Fermi energy to obtain different charge states in paramagnetic impurity ions for ESP study
[AD-760736] 20 p2464 N73-29798
Optical determination of electronic structure of Au-Cu alloys in disordered and ordered phases
[AD-763239] 21 p2586 N73-30720
Calculation of density of states in amorphous covalently bonded semiconductors
[AD-763496] 21 p2587 N73-30728
Electrical conductivity measurements in controlled occupancy energy band tails of disordered semiconductors
[AD-763426] 21 p2587 N73-30729
Absence of S band energy gap in single crystal niobium
[AD-764906] 23 p2827 N73-32594
Photodielectric techniques for analyzing low temperature band structure of gallium arsenide
24 p2891 N73-33080

**BANDPASS FILTERS**
NT CRYSTAL FILTERS
NT TRACKING FILTERS
High power electronically tunable VHF/UHF bandpass filter for radio frequency interference reduction
[AD-748810] 04 p0390 N73-13168
Development of allpass, highpass, bandpass, and stopband electric filter circuits using only resistors as passive components
[REPT-1404] 05 p0522 N73-14244
Configuration of all pass network with negative real poles and Q factor
[PUBL-1367] 05 p0522 N73-14246
Extreme values of irregularity factor of bandpass filters for realizing steady Gauss processes with one-peak power density spectrum
[LBF-TM-64/72] 05 p0523 N73-14250
X ray bandpass filters for hot transient plasma diagnostics
[AD-752544] 08 p0950 N73-17775
Influence of autocorrelation and its parameters on phase manipulated signal passed through n stage resonance filter
09 p1002 N73-18180
Analysis of effects of nonlinear electronic devices on bandpass signals consisting of modulated sine waves
[CRC-1234] 10 p1128 N73-19189
Design of digital filters for bandpass and low pass applications
[AD-754032] 11 p1265 N73-20266
Analysis of quartz and piezoelectric ceramic components for application in high frequency bandpass filters
[REPT-4.387] 12 p1383 N73-21219
Dispersive delay lines, bandpass filters, and lines with delay above 30 microseconds utilizing Rayleigh surface waves at VHF/UHF frequencies
[REPT-4.427] 12 p1384 N73-21223
Digital quadrature methods for processing bandpass signals
[AD-755473] 13 p1494 N73-22110
Characteristics of tunable bandpass filter with large range of resonant frequency
[AD-756662] 13 p1501 N73-22165
Tapered interdigital transducers as flat bandpass devices
[AD-756935] 13 p1503 N73-22182
Physical and spectral characteristics of infrared solid state dispersion filters
[NASA-TT-F-14838] 13 p1558 N73-22631
Signal to noise ratio determination circuit using bandpass limiter
[NASA-CASE-GSC-11239-1] 16 p1883 N73-25241
Selective bandpass resonators using bandstop resonator pairs for microwave frequency operation
[NASA-CASE-GSC-10990-1] 17 p2003 N73-26195
Techniques and circuitry for designing adaptive high Q notch filter
[AD-759031] 17 p2004 N73-26210
UHF linear phase bandpass filter for communication satellite
[ESRO-CR[P]-253] 19 p2235 N73-28024
Resonator design for low cost microwave bandpass filter
[NHK-LABS-NOTE-162] 20 p2381 N73-29128
Methods of circuit optimization and analysis of advantages and disadvantages of circuit optimization by computer
[AD-763766] 21 p2520 N73-30211
Signal to noise ratios in coherent bandpass limiters
[NASA-CR-135781] 23 p2765 N73-32122
Using optical interference coatings to produce bandpass filters for spectral region
[NASA-CR-135671] 23 p2819 N73-32537

**BANDWIDTH**
NT BROADBAND
NT SPECTRAL LINE WIDTH
Error probability and bandwidth efficiency in digital transmission channel
01 p0025 N73-10193
Bandwidth reduction technique for loran retransmission system
[AD-746055] 02 p0208 N73-11687
Equatorial resonance between electrons and VLF signals, characterized by intrinsic bandwidth
[AD-750865] 06 p0667 N73-15428
Very low frequency propagation effect on minimum shift keying communication system signal transmission
[AD-755122] 11 p1258 N73-20213
Self-tuning electronic filter for maintaining constant bandwidth and center frequency gain
[NASA-CASE-ARC-10264-1] 11 p1261 N73-20231
Accuracy of formant parameter estimation based on method of Prony
14 p1622 N73-23140
Measurement of bandwidth for binary FM and bitternary FM signals
[AD-757139] 14 p1633 N73-23240
Radio frequency bandwidth for satellite frequency modulated television broadcasting
[BBC-RD-1973/19] 24 p2893 N73-33097

**BANG-BANG CONTROL**
U OFF-ON CONTROL

**BANKING FLIGHT**
U TURNING FLIGHT

**BARANY CHAIR**
Barany chair rotation for acceleration tolerance testing on flying personnel
13 p1480 N73-21995

**BARBADOS**
Observations of kinematic and thermodynamic fields over Barbados
10 p1180 N73-19596
Study of tropical oceanic subcloud layer using data from Barbados experiment
10 p1180 N73-19598
Wave-related velocity fluctuations over ocean waves as measured from floating instrument platform during BOMEX
[AD-761768] 19 p2296 N73-28461

**BARBED TRIBUTARIES**
U DRAINAGE PATTERNS

**BARDEEN APPROXIMATION**
U BARRIER LAYERS
U ELECTRICAL PROPERTIES
U SURFACE PROPERTIES

**BARENTS SEA**
Prediction of long-term temperature fluctuations, July temperature, and annual average temperature of Barents Sea in surface to 200 m layer
[NLL-M-20600-[5828.4F]] 05 p0529 N73-14304

**BARIUM**
Release technique for creating large dense vapor clouds in upper atmosphere using thermite formulation of barium metal and barium nitrate
[AD-745980] 01 p0054 N73-10438
Barium release measurements in support of OOSIK experiment
[AD-749016] 04 p0417 N73-13409
Photogrammetric interpetation of barium cloud developments parallel to geomagnetic field
[EGG-1183-5006] 06 p0666 N73-15418
Crossed beam method for measuring photoionization cross section on atomic barium beam
06 p0707 N73-15770
Survey of results from barium cloud releases using shaped charge technique in ionosphere and magnetosphere
[MPI-PAE/EXTRATERR-67] 07 p0794 N73-16454
Radar sounding of magnetospheric instability and atmospheric density using barium release clouds
[AD-751567] 07 p0795 N73-16461
Effect of ionospheric conductivity on barium ion cloud dynamics
[NASA-CR-131533] 12 p1433 N73-21610
High resolution optical measurements of high altitude barium releases at Elgin AFB during January 1971
[AD-756938] 13 p1528 N73-22382
Photoionization cross section of barium and strontium, determined with atomic beam crossed with ultraviolet radiation
[MPI-PAE/EXTRATERR-75] 15 p1781 N73-24440
Striations in large barium ion clouds in two stage process
[AD-757916] 15 p1807 N73-24643
Numerical analysis of barium cloud growth and striation in conducting background
[AD-761828] 19 p2317 N73-28637
Chemical system for releasing barium to create ion clouds in upper atmosphere and interplanetary space
[NASA-CASE-LAR-10670-1] 21 p2504 N73-30097
Striation of ion cloud in Oosik barium release experiment
[LA-UR-73-677] 24 p2923 N73-33349

**BARIUM COMPOUNDS**
NT BARIUM FERRATES
NT BARIUM OXIDES
NT BARIUM TITANATES
Inorganic binders for utilizing high reflectance of BaSO4 in paints
[NASA-TM-X-66082] 02 p0191 N73-11549
Half wave voltage for optimum orientation for barium sodium niobate transverse light modulator
[CRC-1229] 04 p0457 N73-13733
Barium sodium niobate as nonlinear optical material
[AD-758221] 14 p1682 N73-23650
Absorption spectra of laser excited Ba2NaNb5O15 crystal
21 p2585 N73-30714
Potential use of strontium barium metaniobate crystals for electro-optics
[AD-762740] 22 p2687 N73-31520

**BARIUM FERRATES**
Ferroelectric crystal growth in electric, magnetic and vibrational fields
[AD-751204] 07 p0834 N73-16763
Growth of single barium ferrite crystals for magnetic optical devices
[AD-758926] 16 p1953 N73-25807

**BARIUM OXIDES**
Recovery of barium oxide reagent from residue from preparing lubricant additives in centrifuge
[AD-751945] 09 p1042 N73-18500
Photoelectric emission of gallium arsenide from adsorbed layers of cesium and barium oxide
[NLL-DRIC-TRANS-2293-(3623.66)]
15 p1819 N73-24746
Hollow cathode with BaO impregnated, porous tungsten inserts and tips
[NASA-TM-X-71417] 21 p2517 N73-30189

**BARIUM TITANATES**
Fabrication and evaluation of RF sputtered barium titanate thin films for integrated circuit application
[AD-749236] 04 p0397 N73-13227
Convolution of surface acoustic waves on barium titanate crystal
[AD-761880] 19 p2327 N73-28724
Dielectric, ferroelectric barium strontium titanate for electronic tuning
[AD-765417] 23 p2769 N73-32150

**BAROCLINIC WAVES**
Influence of atmospheric cyclones on circulation and mixing of sea water in motionless uniformly rotating baroclinic ocean
19 p2258 N73-28202

**BAROCLINITY**
Long range forecast by means of spectral nonlinear baroclinic model of atmosphere
[AD-754682] 11 p1315 N73-20670
Numerical boundary conditions in baroclinic and barotropic models for forecasting
[DM-9] 19 p2316 N73-28623

**BAROMETERS**
Uncorrected and barometer-corrected, cosmic ray, NM-64 neutron monitor data from Kula, Hawaii, Jan.-Dec. 1971
[AECL-4161] 04 p0467 N73-13804
Highly accurate digital barometer
[NLL-M-22973-[5828.4F]] 16 p1910 N73-25458

**BAROMETRIC PRESSURE**
U ATMOSPHERIC PRESSURE

**BARORECEPTORS**
Barotrauma mechanoreceptor reflex effects on animal respiratory and circulatory system
13 p1479 N73-21982
Evoked compensatory reflex reactions of rabbit ocular and eyelid muscles during hypoxia
13 p1480 N73-21992

**BAROTRAUMA**
Effects of gastrointestinal pressure on rabbit eye nystagmus during barotrauma
13 p1479 N73-21983
Middle ear barotrauma effect on work capacity and flight fitness of flying personnel
13 p1481 N73-22000

**BAROTROPIC FLOW**
Short range forecasting of geopotential and wind for large territory by barotropic divergent
[AD-751422] 07 p0796 N73-16475

**BAROTROPISM**
Numerical boundary conditions in baroclinic and barotropic models for forecasting
[DM-9] 19 p2316 N73-28623
Structure of barotropically unstable disturbances in tropical regions
[AD-764090] 22 p2695 N73-31588

**BARRIER BEACHES**
U BEACHES

**BARRIER FLATS**
U BARRIERS [LANDFORMS]

**BARRIER ISLANDS**
U ISLANDS

**BARRIER LAGOONS**
U LAGOONS

**BARRIER LAKES**
U LAKES

**BARRIER LAYERS**
Potential barrier for neutral excitation at helium liquid-vapor interfaces
[NOTA-INTERNA-375] 01 p0083 N73-10690
Semiconductor theory of barrier layer and point-contact rectifiers
[NASA-TT-F-14708] 02 p0218 N73-11766
Microstructure and mechanical properties of thermal barrier materials produced by arc plasma spraying
[AD-762045] 19 p2312 N73-28598
Polymeric monolayer barrier for thin film Josephson junctions
[NASA-CR-121270] 19 p2326 N73-28715
Application of surface barrier detectors for time measurement of nuclear energy events and comparison of two methods used for timing procedures
22 p2671 N73-31393

**BARRIERS [LANDFORMS]**
Estuary and barrier island studies using ERTS-1 imagery
[E72-10266] 03 p0291 N73-12365
Estuary and barrier island investigations utilizing ERTS-1 imagery
[E73-11041] 22 p2664 N73-31342

**BARS**
NT ELASTIC BARS
NT PRISMATIC BARS
Determining maximum shear stress at hole boundary in axially loaded bar
[ESDU-66011-AMEND-A] 01 p0111 N73-10913
Computerized simulation of heat transfer and elasticity in bars
[PB-213060] 11 p1347 N73-20927
Torsion of an orthotropic, inhomogeneous bar with cylindrical anisotropy including solution by Saint Venant principle
[DRIC-TRANS-2995] 12 p1463 N73-21856

**BARYCENTER**
U CENTER OF GRAVITY

**BARYON RESONANCES**
Mass formula calculations on baryonic resonances using radial excited symmetric quark model
[TR-74-018] 22 p2701 N73-31636

**BARYONS**
NT OMEGA-MESONS
Israel-Carter conjecture of black hole physics and baryon number
15 p1829 N73-24825
Naive quark pair creation model and centrifugal barrier effect in baryon decays
[LPTHE-73/11] 20 p2456 N73-29736
Baryon spectroscopy and regularities between SU[6] and SU[3] mass breaking parameters
[LPTHE-73/21] 21 p2581 N73-30687

**BASALT**
Results of examining 40 maar volcanic cones in western North America
[NASA-CR-129290] 03 p0292 N73-12382
Plagioclase mineralogy of olivine alkaline basalt in Potrillo volcanic field
[NASA-CR-130918] 09 p1025 N73-18368
Thermal conductivity measurements of particulate materials in vacuum using basalt and soda lime glass beads of various size ranges as samples
[NASA-TM-X-64759] 18 p2205 N73-27801
Mass spectrometric determination of rare earth concentration in basaltic rocks and luna sample 14305
[FRNC-TH-335] 21 p2597 N73-30813

**BASE FLOW**
Factors affecting base flow and jet structure behind cylindrical afterbody with central nozzle at mach 2.0 and turbulent boundary layer conditions
[ARC-R/M-3224] 16 p1851 N73-25001

**BASE HEATING**
Test data tabulation, statistical analysis, and heating rate contours for base region thermal environment of Saturn S-2 stage scale model - Vol. 2
[NASA-CR-129010] 20 p2382 N73-29144
Base region thermal environment test of scale model of Saturn S-2 stage - Vol. I
[NASA-CR-129009] 20 p2475 N73-29883

**BASE PRESSURE**
Reduction of transonic drag for high performance aircraft by injecting air in rear of aircraft to alter transonic flow distribution on aft section
[AD-751269] 07 p0736 N73-15991
Predicting base pressure in subsonic two dimensional steady base flow
[DLR-FB-72-57] 09 p1014 N73-18274
Flight-measured base pressure coefficients for thick boundary layer flow over aft-facing step for Mach numbers from 0.4 to 2.5 using XB-70 aircraft
[NASA-TN-D-7202] 15 p1767 N73-24317
Base pressure of bodies of revolution in supersonic gas flow
[AD-762243] 19 p2258 N73-28198

**BASES [FOUNDATIONS]**
U FOUNDATIONS

**BASINS**
U STRUCTURAL BASINS

**BASINS [CONTAINERS]**
Self wave oscillations in variable depth rotating basins discussing second class modes for three cases
07 p0857 N73-16952

**BATHING**
Design, fabrication and acceptance testing of zero gravity whole body shower
[NASA-CR-134066] 22 p2623 N73-31019

**BATHS**
NT SALT BATHS
Influence of immersion in temperature controlled bath on circulation and water balance in human body
[NASA-TT-F-14834] 10 p1119 N73-19124
Measurement of vapor pressure of cryolitic baths
[NLL-TRANS-1034-(9022.04)]
20 p2374 N73-29073

**BATHYMETERS**
Geological charts of Ontong Java Plateau including bathymetric, sedimentary isochron, and structural contour
[AD-743900] 01 p0052 N73-10423
Bathymetry, magnetic, and gravity data for North Pacific Ocean areas collected between 1961 and 1970 - Technical Report 50
[NOAA-TR-NOS-50] 07 p0792 N73-16444
Bathymetry, magnetic, and gravity data for North Pacific Ocean areas collected between 1961 and 1970 - Technical Report 49
[NOAA-TR-NOS-49] 07 p0793 N73-16445
Bathymetry, free air gravity anomaly, and magnetic field intensity data on Strait of Sicily, gathered from 1965 to 1971
[SACLANTCEN-CONF-PROC-7@8 p0915 N73-17501
Deploying airborne laser transmitter/receiver to measure water depth in turbid water
[AD-752486] 08 p0921 N73-17551
Bathymetry, magnetic, and gravity data collected between 1961 and 1969 in North Central Pacific
[NOAA-TR-NOS-51] 09 p1029 N73-18401
Bathymetric survey of Pacific Ocean area for oceanographic data to support underwater acoustic experiment
[AD-752840] 09 p1032 N73-18428
Acoustic transmission loss measurements in Arctic Ocean ice zone by aircraft
[AD-754394] 11 p1325 N73-20755
Mediterranean Sea geophysical survey
[AD-757455] 16 p1910 N73-25452
Development of semi-automatic system for digitizing bathymetry charts for showing ocean bottom contour information
[AD-761647] 19 p2296 N73-28464
Computer program for generation of random bathymetric profiles from oceanographic data
[AD-762070] 19 p2298 N73-28476

**BATHYMETRY**
U BATHYMETERS

**BATS**
Reduction of midair collision hazard with bats through tracking by radar and use of high intensity lights
[AD-764828] 23 p2746 N73-31982

**BATTERIES**
U ELECTRIC BATTERIES

**BATTERY CHARGERS**
Development of nickel hydroxide electrode for use in rechargeable alkaline batteries
[AD-746335] 01 p0007 N73-10058
Effect of active, inductive and capacitive resistance of elements of asymmetric alternating current battery charger on discharged characteristics of silver zinc batteries
[AD-756955] 13 p1478 N73-21970
Voltage fluctuation of batteries during charging with asymmetrical alternating current
[AD-756557] 13 p1478 N73-21974

**BATTERY SEPARATORS**
U SEPARATORS

**BAYES THEOREM**
Bayesian model for stimuli processing in visual space perception
01 p0016 N73-10127
Contradictions and inconsistencies in use of Bayesian approach for production of sampling theory point estimators
[AD-747325] 03 p0325 N73-12650
Bayes theorem for optimal decision and stop models of production processes
13 p1497 N73-22132
Comparisons of maximum likelihood estimator, Bayesian estimator, and known failure rate
[NASA-CR-133227] 17 p2004 N73-26203
Statistical classification of earth resources in remote sensing data
[NASA-CR-128988] 17 p2054 N73-26615
Bayesian reliability demonstration for statistical test development
[AD-765172] 24 p2945 N73-33520

**BAYESIAN STATISTICS**
U BAYES THEOREM

**BAYHEAD BEACHES**
U BEACHES

**BAYS (TOPOGRAPHIC FEATURES)**
NT CHESAPEAKE BAY (US)
NT MONTEREY BAY (CA)
NT SAN FRANCISCO BAY (CA)
Lagrangian computer program for predicting movement and dispersion of pollutant in tidal embayment, and application to Bolinas Lagoon, California
[USGS-582-B] 01 p0048 N73-10389
Pollution hazards from petroleum industries and shipping in Delaware Bay
07 p0857 N73-16948
Study of suspended sediment and aquatic fronts in Delaware Bay using ERTS-1 imagery
[E73-10368] 10 p1150 N73-19364
ERTS-1 imagery of suspended matter and hydrologic interfaces in Delaware Bay
[E73-10515] 14 p1653 N73-23409
Application of ERTS-1 imagery to analysis of suspended sediments and aquatic fronts in Delaware Bay
[PAPER-M3] 19 p2280 N73-28343
Detection of turbidity plumes in Tampa Bay, Florida from ERTS-1 MSS imagery
19 p2287 N73-28388
Identification of suspended sediment, current circulation, water mass boundaries, and waste disposal plumes in Delaware Bay using ERTS-1 imagery
[E73-11164] 24 p2920 N73-33317

**BCC LATTICES**
U BODY CENTERED CUBIC LATTICES

**BE C**
U EXPLORER 27 SATELLITE

**BEACHES**
Variability of coastal processes and resulting shoreline morphology along peninsula of Baja California
[AD-756676] 16 p1907 N73-25432
Influence of ocean waves and meteorological variables on beach erosion at Plum Island, Massachusetts
[AD-759513] 18 p2148 N73-27364
Seasonal changes of littoral transport and beach width of Maryland portion of Chesapeake Bay and resultant effect on protective structures
[PAPER-M1] 19 p2280 N73-28341
ERTS-1 imagery of littoral drift and sedimentation patterns of beach and nearshore areas of Maryland section of Chesapeake Bay
[PAPER-M2] 19 p2280 N73-28342

**BEACON EXPLORER C**
U EXPLORER 27 SATELLITE

**BEACONS**
NT AIRPORT BEACONS
NT RADAR BEACONS
NT RADIO BEACONS
NT RADIO DIRECTION FINDERS
One watt pulsed solid state source for X-band navigational beacons
[TR-70-3] 05 p0518 N73-14213

**BEAM COLUMNS**
U BEAMS [SUPPORTS]
U COLUMNS [SUPPORTS]

**BEAM CURRENTS**
Beam current monitoring system and performance for linear accelerator
[AD-745841] 01 p0038 N73-10299
Pulse modulation characteristics of vidicon beam currents
[DRIC-TRANS-2875] 02 p0174 N73-11413
Production and current measurement of hydrogen ion beam and plasma in duoplasmatron with cusped magnetic field
[NP-19364] 05 p0583 N73-14747
Measurement of signal strength variations in beam currents of vidicon targets
[DRIC-TRANS-2965] 06 p0645 N73-15238
Influence of photoconducting layer thickness on sensitivity of vidicons
[NLL-DRIC-TRANS-2965-[3623.66]] 11 p1261 N73-20233
Measurement of performance of ion exhaust beam current flow for multiply charged ion species using time of flight techniques
[NASA-CR-131841] 17 p2076 N73-26795
Power supply electronic tests on single jet disk type cesium thrustor with beam current feedback control
[LAAS-TNPE-73-T-17] 23 p2831 N73-32629
Supercritical helium cooling of superconducting magnet for use in dc beam line elements
[RHEL/R-258] 24 p2969 N73-33725

**BEAM LEADS**
Development and application of polyimide films for hybrid and beam lead substrates
[AD-745731] 01 p0033 N73-10260
Thermocompression wobble tool bonding of beam lead devices
[SC-DC-72-1197-A] 03 p0306 N73-12501
Ultrasonic torsional welding system for simultaneously bonding beam leads of hybrid integrated circuit device to suitable substrate
[AD-757561] 14 p1671 N73-23559

**BEAM PLASMA AMPLIFIERS**
Design and performance of liquid nitrogen cooled nozzle for producing pulsed cylindrical hydrogen cluster beams
[KFK-1610] 12 p1436 N73-21632

**BEAM SPLITTERS**
Pockels cell for splitting light pulses from NdYAG mode locked pulsed laser
[AD-751532] 07 p0807 N73-16550
Birefringence properties of total reflection of light beam at separation plane
[LPTHE-72/39] 10 p1188 N73-19668
Direct current superconducting beam splitting magnet system
[BNL-17221] 10 p1200 N73-19765

**BEAM SWITCHING**
Systems planning for improved airport surveillance radar equipment using dual airborne antenna switching for air traffic control
[FAA-RD-72-136] 09 p1002 N73-18176
Physical properties of electro-optical switching devices for telecommunication
[REPT-61] 16 p1875 N73-25177
Dish antenna having switching beamwidth with truncated concave ellipsoid subreflector
[NASA-CASE-GSC-11760-1] 23 p2764 N73-32116

**BEAM WAVEGUIDES**
Digital filter theory for broadband beamforming and hydrophone array steering
[AD-746206] 06 p0641 N73-15201
Standard coupler effects on EHF attenuation in waveguides with bending moments
[FTZ-A-333-TBR-18] 22 p2632 N73-31096
Pseudorandom 160 Mbits/s pulse generation, and digital word synchronization, for 640 Mbit/s PCM waveguide error rate measurements
[FTZ-A-442-TBR-38] 22 p2633 N73-31098
Nitrogen gas supply system for EHF waveguides to improve attenuation by control of water vapor and oxygen content
[FTZ-A-333-TBR-10] 22 p2642 N73-31175
Attenuation of circularly bent waveguides with dielectric coatings, noting role of mode filters
[FTZ-A-333-TBR-16] 22 p2643 N73-31181
EHF attenuation measurements of helical waveguides, using FSK shuttle pulse method and backward wave oscillator
[FTZ-333-TBR-17] 22 p2643 N73-31182
Theoretical analysis of grating coupler for application in thin film integrated optical waveguides
22 p2699 N73-31621

**BEAMS**
Propagation of multiwavelength laser radiation through atmospheric turbulance
[AD-762516] 20 p2426 N73-29491
Performance tests of geometrically different sets of dished accelerator grids on ion thruster engines
[NASA-TM-X-71420] 23 p2830 N73-32615

**BEAMS (RADIATION)**
NT ATOMIC BEAMS
NT ELECTRON BEAMS
NT GAMMA RAY BEAMS
NT ION BEAMS
NT LIGHT BEAMS
NT MOLECULAR BEAMS
NT NEUTRON BEAMS
NT PARTICLE BEAMS
NT PHOTON BEAMS
NT PROTON BEAMS
Requirements for heating large Tokamak device with energetic neutral beams
[CONF-720804-2] 06 p0704 N73-15743
Dependence of magnetic effective length and fringe field correction constant on central field flux density for beam transport systems
[LA-DC-72-1121] 10 p1190 N73-19682
Beam focusing optical system consisting of elliptical and parabolic mirrors
[AD-757008] 13 p1560 N73-22643
Use of argon-ion laser transverse mode locking to produce high resolution scanning beam
15 p1794 N73-24546
Beam position monitor which operates by detection of temperature differences
[AERE-M-2372] 17 p2033 N73-26452
Polarization fluctuation of beam wave propagating in random atmosphere
19 p2234 N73-28014
Development of laser amplifier using disks of neodymium glass and measurement of beam amplification for laser beams
[EP-RR-35] 20 p2425 N73-29478
Stability theory of laser beam self focusing
[LA-UR-73-671] 24 p2932 N73-33414

**BEAMS (SUPPORTS)**
NT BOX BEAMS
NT CANTILEVER BEAMS
NT I BEAMS
NT RECTANGULAR BEAMS
Guide for using data on effects of buckling and deflections in beams, struts, and shafts
[ESDU-SS3] 01 p0112 N73-10922
Approximation of beam buckling mechanics using axial and transverse loads
[AD-745881] 02 p0219 N73-11775
Digital computer procedure for analyzing initially bent two span columns
[AD-747075] 02 p0238 N73-11933
Torsion, bending, and shear in concrete beams reinforced with stirrups
[D-10-72] 02 p0238 N73-11938
Procedures for computing upper and lower bounds to bending frequencies and estimates of mode shapes of beams with constant stiffness and mass - Part 1
[AD-747241] 02 p0239 N73-11946
Computer program user guide for determining limits to bending frequencies and mode shape estimates for free nonuniform beams with attached masses - Part 2
[AD-747242] 02 p0239 N73-11947
Evaluation of edge and membrane effects in moderately thick beams by singular perturbation technique
[AD-746985] 02 p0240 N73-11955
Finite element displacement method for studying transient response and dispersive behavior of elastic structures
[AD-747283] 02 p0241 N73-11956
Buckling tests on double T shaped Protenax steel beams
[CRIF-MT-78] 04 p0481 N73-13935
Flexural deformation of laminated beams subjected to initial stresses
[AD-750574] 05 p0604 N73-14912
Elastic properties of thin walled U beam lateral stiffness under flexing torsional stresses
[ISD-130] 09 p1095 N73-18939
Nondestructive methods determining composite beam and plate critical loading
[ENSMP-010] 17 p2094 N73-26940
Application of constrained optimal design approaches for minimum mass designs of damped, linear, continuous sandwich beam
[AD-761881] 19 p2349 N73-28896
Stability of deep beam subjected to concentrated, transverse follower force applied at center of beam
[AD-762124] 19 p2350 N73-28900
Exact solution for free transverse vibrations of annular plate with supported inner and free outer edge-beams
20 p2482 N73-29938
Analytical solution of nonlinear aeroelastic galloping instability, with reference to space shuttle ground wind response, and application to U beams
[DLR-FB-73-18] 21 p2601 N73-30848
Semidirect boundary integral method to obtain numerical solution for elastic stress and strain fields in V-notched beams in pure bending
[NASA-TN-D-7424] 22 p2725 N73-31803
Bonding methods of aluminum beam leaded devices on microcircuit ceramic substrates
[NASA-CR-124434] 23 p2797 N73-32369
Post yield behavior of beam with partial end fixity
[AD-764576] 23 p2855 N73-32813
Dynamic buckling of thin, elastic beam subjected to constant, compressive axial displacement
24 p2987 N73-33871
Development of finite element relations for dynamic structural analysis of linearly elastic beam and plate flexure problems
24 p2987 N73-33873

**BEAMSHAPING**
U COLLIMATION

**BEARING**
LOX-cooled bearing and seal start cycling performance
[MBB-UR-84-71] 10 p1167 N73-19493
Bibliography on various types of bearings
[AD-761960] 19 p2306 N73-28547
**BEARING [DIRECTION]**
Ionospheric disturbance effects on sky wave bearing measurement
05 p0511 N73-14159
**BEARING ALLOYS**
Hot hardness characteristics of ausformed AISI M-50, Matrix 2, WD-65, modified AISI 440-C, and Super Nitralloy
[NASA-TN-D-7244] 15 p1791 N73-24517
Roller bearings technology - material, design, and lubricants
[NASA-TM-X-71441] 24 p2929 N73-33389
**BEARINGS**
NT ANTIFRICTION BEARINGS
NT BALL BEARINGS
NT FOIL BEARINGS
NT GAS BEARINGS
NT JOURNAL BEARINGS
NT LIQUID BEARINGS
NT ROLLER BEARINGS
NT THRUST BEARINGS
Influence of transverse force on impeller bearing rupture of centrifugal pumps
02 p0179 N73-11446
Magnetic bearings for spacecraft applications
[NASA-TM-X-66111] 03 p0306 N73-12499
Vacuum life tests on lubricated bearings and slip rings
[ESRO-CR-91] 03 p0307 N73-12504
Bearing flexibility effect on triple-spin satellite attitude stability
[ESRO-SN-121] 03 p0359 N73-12926
Lubricant supply for mechanical antenna bearings
[NLL-RISLEY-TR-2308-[9091.9F]] 05 p0550 N73-14463
Elastohydrodynamic analysis using power law pressure-viscosity relation
[NASA-TN-D-7121] 06 p0677 N73-15507
Plastic coatings for lining hydrostatic bearings
[AD-750525] 06 p0690 N73-15614
Design of combined hydrostatic and dynamic bearings
[AD-752821] 09 p1040 N73-18479
Bearing design refinement and fluid film bearing studies of solar 10 kW turbo-alternator bearing with 6000 hr test program
[AD-752895] 09 p1042 N73-18496
Nomograph for calculating optimal working characteristics of hydrostatic sliding bearings
[AD-753553] 09 p1042 N73-18501
Design of hydrostatic shaft guide bearings for sodium pumps
[CEA-CONF-2045] 10 p1166 N73-19486
Tests on bearings and seals undergoing repeated starts of turbine pumps
[SEP-NT-3058/71-M] 10 p1167 N73-19494
Laser forming of sliding friction bearings for instrument construction
[AD-753490] 10 p1169 N73-19511
Low mass rolling element bearing with lightweight core and hollow center
[NASA-CASE-LEW-11087-3] 11 p1298 N73-20534
Plastic compensating coatings for alignment and assembly of bearing unit
[AD-754591] 11 p1300 N73-20550
Bearings for control system of high temperature lithium or argon cooled fast nuclear reactors
[NASA-TM-X-68218] 13 p1534 N73-22429
Test rig simulation of gas turbine engine to determine means for minimizing incidence of lubricant sump fires in high speed aircraft engines
[NASA-CR-121158] 13 p1590 N73-22891
Environmental endurance testing of elastomeric pitch change bearing for use on H-1 Aircraft
[AD-758463] 14 p1671 N73-23561
Polybenzimidazole, polyimide, and polyquinoxaline for low wear, lightweight, high strength bearing retainer
[NASA-CR-132217] 15 p1792 N73-24528
Vibration tests of flight control moment gyros and bearing life test fixtures
[NASA-CR-124449] 24 p2926 N73-33365
Fabrication of cermet bearings for control system of high temperature lithium cooled nuclear reactors
[NASA-TM-X-2892] 24 p2953 N73-33595
**BEAT**
U SYNCHRONISM
**BEAT FREQUENCIES**
Beat frequency detector algorithm for multichannel signal analysis
[AD-746682] 03 p0266 N73-12157
Moire patterns in circular carrier frequency photography for observing phase objects
[NASA-CR-130198] 11 p1292 N73-20481
**BEAUFORT SEA [NORTH AMERICA]**
ERTS-1 imagery of inner shelf and coastal sedimentation environment of Beaufort Sea
[E72-10248] 03 p0289 N73-12348
ERTS-1 imagery of inner shelf and coastal sedimentation environment of Beaufort Sea, Alaska
[E73-10412] 11 p1278 N73-20374
Mapping Arctic sea ice from ERTS-1 imagery of Hudson Bay, M'Clure Strait, Beaufort Sea, and Greenland Sea
[E73-10447] 11 p1282 N73-20407
ERTS-1 imagery of inner shelf and coastal sedimentation environment of Beaufort Sea
[E73-10492] 12 p1397 N73-21328
ERTS-1 imagery of inner shelf and coastal sediment transport in Beaufort Sea
[E73-10649] 16 p1897 N73-25345
Dynamics and morphology of Beaufort Sea ice determined from satellites, aircraft, and drifting stations
[NASA-TM-X-66291] 18 p2144 N73-27333
Influence of sea ice on coastal marine environment of Beaufort Sea, Alaska
[PAPER-M7] 19 p2280 N73-28346
Application of ERTS-1 data to detection and mapping of sea ice in Beaufort Sea and Bering Sea areas
[E73-11037] 22 p2663 N73-31341
Mesoscale movement and deformation of sea ice in Beaufort Sea
[E73-11153] 24 p2919 N73-33307
**BED REST**
Prolonged bed rest and positive radial acceleration effects on human visual response time
[NASA-TN-D-7161] 06 p0630 N73-15117
Regulation of vertical posture after Soyuz 6, 7, and 8 flights and after 120-day bed rest experiment
07 p0744 N73-16052
Effect of atmosphere with increased oxygen and carbon dioxide content on human orthostatic tolerance following 10 days of bedrest
07 p0744 N73-16055
Effects of prolonged bed rest on body temperature and heart rate periodicity in man
09 p0994 N73-18113
Prolonged bed rest effects on human blood hormone level periodicities
09 p0994 N73-18114
Physiological stress effects of space flight on human body
[JPRS-57139] 13 p1481 N73-22002
Physiological effects of long term hypodynamic weightlessness simulation on humans
13 p1482 N73-22010
Human horizontal or antiorthostatic position effect in hypodynamic weightlessness test
13 p1482 N73-22011
Human regional blood circulation changes during bed rest experiment
13 p1482 N73-22012
Metabolic changes and cardiac output of humans in hypokinetic bed rest study
13 p1482 N73-22013
Visual acuity changes in humans during hypokinetic bed rest test
13 p1482 N73-22014
Functional reactions of human otorhinolaryngolic organs during hypokinesia
13 p1482 N73-22015
Human pulmonary volume decrease during long term bed rest
13 p1482 N73-22016
Weightlessness simulator for evaluating exercise effects in hypokinetic bed rest test
13 p1482 N73-22018
Exercise and muscle stimulation for preventing metabolism changes during bed rest
13 p1483 N73-22019
Changes in human cerebral circulation during prolonged bed rest test
13 p1483 N73-22020
Long term bed rest effects on human retinal blood circulation and intraocular pressure
14 p1608 N73-23038
Alterations in myocardial contractility induced by bed rest
[NASA-CR-128968] 17 p1986 N73-26056
Physiological motor function measurements for determining optimal bed rest periods
[NASA-TT-F-15144] 23 p2749 N73-32004
Physiological effects on highly trained subjects when confined to bed, deprived of sleep, or allowed to discontinue training
[NASA-CR-134044] 23 p2750 N73-32008
Fluid-electrolyte balance during 120-day bed rest
24 p2883 N73-33028
**BEDROCK**
NT BALTIC SHIELD [EUROPE]
**BEDS [GEOLOGY]**
Sleep deprivation effects, airborne simulator feel system, bed forms, and V/STOL engine model tests
[DME/NAE-1973[2]] 22 p2731 N73-31853
**BEECH AIRCRAFT**
U BEECHCRAFT AIRCRAFT
**BEECHCRAFT AIRCRAFT**
NT BEECHCRAFT 18 AIRCRAFT
Investigation of aircraft accident involving Beech aircraft performing air taxi service to Boise, Idaho on 20 Feb. 1972
[NTSB-AAR-72-25] 03 p0253 N73-12050
Aircraft accident involving Beechcraft Queen Air aircraft on takeoff from Albuquerque, New Mexico airport on 19 May, 1972
[NTSB-AAR-72-32] 07 p0738 N73-16003
Aerial natural radiation survey, using Twin Bonanza Beechcraft
[HASL-269] 17 p2027 N73-26403
**BEECHCRAFT 18 AIRCRAFT**
Aircraft accident involving Beechcraft 18 aircraft on air taxi flight from Cleveland, Ohio airport on 22 June, 1972
[NTSB-AAR-72-33] 07 p0738 N73-16006
**BEETLES**
NT TRIBOLIA
**BEHAVIOR**
NT HUMAN BEHAVIOR
Behavioral and social science advancement in USSR after 50 years
[JPRS-58686] 12 p1467 N73-21883
Mathematical models and physiological mechanisms of goal-directed behavior
[JPRS-60091] 24 p2887 N73-33053
Theory of systems for effective behavior predictions
24 p2887 N73-33054
Approach to construction of formal model of behavior
24 p2887 N73-33055
One class of adaptive systems and results of computer modeling of their self instruction
24 p2887 N73-33056
Expedient functioning of automata with normal and disturbed behavior in experiments on reinforcement selection
24 p2887 N73-33057
Structural, behavioral, and EEG correlates of alimentary motivation
24 p2888 N73-33063
Behavior of dogs when given choice of various reinforcements
24 p2889 N73-33066
Structure and functions of central mechanisms of reinforcement
24 p2889 N73-33067
**BELGIAN CONGO**
U ZAIRE
**BELGIUM**
Hydrometeorologic study of precipitation in Viroin basin, Belgium
[IRMB-PUBL-A-70-2] 01 p0047 N73-10381
Dourbes [Belgium] Geophysical Observatory data on geomagnetism, ionospheric propagation, seismology, cosmic rays, and atmospheric electricity, Nov. 1971
01 p0050 N73-10401
Ionospheric sounding and cosmic ray neutron flux density tables, Dourbes, Belgium, Feb. 1972
01 p0050 N73-10402
Dourbes [Belgium] Geophysical Observatory data on geomagnetism, ionospheric propagation, seismology, cosmic rays, and atmospheric electricity, Dec. 1971
01 p0050 N73-10405
Meteorological parameter table for Belgian weather stations, June 1972
01 p0075 N73-10618
Sulfur oxides, smoke, and air pollution tables from Belgian weather stations, Oct. 1971
01 p0075 N73-10619
Ionospheric sounding and cosmic ray neutron flux density tables, Dourbes, Belgium, Mar. 1972
02 p0166 N73-11352
Sulfur oxides, smoke, and air pollution tables from Belgian weather stations, Dec. 1971
02 p0205 N73-11659
Dourbes [Belgium] Geophysical Observatory data on geomagnetism, ionospheric propagation, seismology, cosmic rays, and atmospheric electricity, Jan. 1972
**SEISMOLOGY IONOSPHERIC PROPAGATION**
03 p0296 N73-12416
Ionospheric sounding and cosmic ray neutron flux density tables, Dourbes, Belgium, Apr. 1972
03 p0297 N73-12420
Sulfur oxides, smoke, and air pollution tables from Belgian weather stations, Nov. 1971
03 p0327 N73-12663
Meteorological parameter tables for Belgian weather stations, Aug. 1972
03 p0327 N73-12664
Synoptic meteorological data for weather stations, Belgium, Oct. 1971
03 p0327 N73-12665
Synoptic meteorological data for weather stations, Belgium, Nov. 1971
03 p0327 N73-12666
Meteorological parameter tables for Belgian weather stations, Sep. 1972
03 p0327 N73-12668

Correlation between solar radiation and monthly and seasonal variations for calculating atmospheric turbidity in Belgium
[PUBL-SER-A-75] 03 p0354 N73-12882
Tabulated data on atmospheric ozone density at UCCLE, Belgium, for 1969
[QR-3] 05 p0539 N73-14386
Ionospheric sounding and cosmic ray neutron flux density tables, Dourbes, Belgium, May 1972
05 p0539 N73-14387
Various Belgian climates associated to different air mass origins
[MISC-SER-A-2] 05 p0574 N73-14667
Sulfur oxides, smoke, and air pollution tables from Belgian weather stations, Jan. 1972
05 p0574 N73-14668
Meteorological parameter tables for Belgian weather stations, Oct. 1972
06 p0694 N73-15654
Aerological climatology based on IRMB weather station data recorded between 1951 and 1965
[PUBL-SER-A-77] 07 p0815 N73-16609
Bibliography of Belgian research reports in fluid mechanics and plasma physics from 1957 to 1972
[NT-32-1972] 07 p0860 N73-16975
Tabulated data on atmospheric ozone density at Uccle, Belgium for 1969
08 p0918 N73-17522
Ionospheric sounding and cosmic ray neutron flux density tables, Dourbes, Belgium, Jun. 1972
08 p0918 N73-17524
Sulfur oxides, smoke, and air pollution tables from Belgian weather stations, Feb. 1972
08 p0939 N73-17686
Meteorological parameter tables for Belgian weather stations, Nov. 1972
08 p0939 N73-17687
Dourbes, Belgium, geophysical observatory data on geomagnetism, ionospheric propagation, seismology, cosmic rays, and atmospheric electricity, Feb. 1972
09 p1030 N73-18403
Dourbes, Belgium, geophysical observatory data on geomagnetism, ionospheric propagation, seismology, cosmic rays, and atmospheric electricity, Mar. 1972
09 p1030 N73-18404
Dourbes, Belgium, geophysical observatory data on geomagnetism, ionospheric propagation, seismology, cosmic rays, and atmospheric electricity, Apr. 1972
09 p1030 N73-18405
Dourbes, Belgium, geophysical observatory data on geomagnetism, ionospheric propagation, seismology, cosmic rays, and atmospheric electricity, May 1972
09 p1030 N73-18406
Dourbes, Belgium, geophysical observatory data on geomagnetism, ionospheric propagation, seismology, cosmic rays, and atmospheric electricity, Jun. 1972
09 p1030 N73-18407
Dourbes, Belgium, geophysical observatory data on geomagnetism, ionospheric propagation, seismology, cosmic rays, and atmospheric electricity, Jul. 1972
09 p1030 N73-18408
Ionospheric sounding and cosmic ray neutron flux density tables, Dourbes, Belgium, Jul. 1972
09 p1030 N73-18409
Meteorological parameter tables for Belgian weather stations, Dec. 1972
09 p1061 N73-18651
Atmospheric pollution in Belgium from 1 Apr. 1969 to 31 Mar. 1970
[PUBL-SER-A-78] 10 p1182 N73-19618
Hydrometeorological study of periodic precipitation variations over Lesse Basin, Belgium
[PUBL-SER-A-76] 12 p1423 N73-21530
Ionospheric sounding and cosmic ray neutron flux density tables, Dourbes, Belgium, Aug. 1972
13 p1524 N73-22354
Sulfur oxides, smoke, and air pollution tables from Belgian weather stations, Mar. 1972
13 p1553 N73-22587
Synoptic meteorological data for weather stations, Belgium, Jan. 1972
13 p1553 N73-22588
Synoptic meteorological data for weather stations, Belgium, Feb. 1972
13 p1553 N73-22589
Sulfur oxides, smoke, and air pollution tables from Belgian weather stations, Apr. 1972
13 p1553 N73-22590
Meteorological parameter tables for Belgian weather stations, Jan. 1973
13 p1553 N73-22591
Ionospheric sounding and cosmic ray neutron flux density tables from Dourbes, Belgium for Oct. 1972
15 p1781 N73-24438
Meteorological parameter tables for Belgian weather stations, Feb. 1973
15 p1806 N73-24636
Ionospheric sounding and cosmic ray neutron flux density tables, Dourbes, Belgium, Sep. 1972
16 p1907 N73-25428
Dourbes [Belgium] geophysical observatory data on geomagnetism, ionospheric propagation, seismology, cosmic rays, and atmospheric electricity, Aug. 1972
17 p2028 N73-26411
Dourbes [Belgium] geophysical observatory data on geomagnetism, ionospheric propagation, seismology, cosmic rays, and atmospheric electricity, Sep. 1972
17 p2028 N73-26412
Meteorological parameter tables for Belgian weather stations, Mar. 1973
17 p2057 N73-26638
Ionospheric sounding and cosmic ray neutron flux density tables, Dourbes, Belgium, Dec. 1972
18 p2146 N73-27342
Ionospheric sounding and cosmic ray neutron flux density tables, Dourbes, Belgium, Nov. 1972
18 p2146 N73-27343
Sulfur oxides, smoke, and air pollution tables from Belgian weather stations, Jul. 1972
20 p2449 N73-29686
Ionospheric sounding and cosmic ray neutron flux density tables, Dourbes, Belgium, Mar. 1973
21 p2539 N73-30354
Ionospheric sounding and cosmic ray neutron flux density tables, Dourbes, Belgium, Apr. 1973
21 p2539 N73-30355
Meteorological parameter tables for Belgian weather stations, May 1973
21 p2574 N73-30628
Ionospheric sounding and cosmic ray neutron flux density tables, Dourbes, Belgium Jun. 1973
24 p2923 N73-33350
Ionospheric sounding and cosmic ray neutron flux density tables, Dourbes, Belgium, Feb. 1973
24 p2923 N73-33351
Geophysical data tables and graphs for Dourbes, Belgium
24 p2924 N73-33352
Dourbes [Belgium] geophysical observatory data on geomagnetism, ionospheric propagation, seismology, cosmic rays, and atmospheric electricity, Nov. 1972
24 p2924 N73-33353
Geophysical observatory data obtained at Dourbes, Belgium in Dec. 1972 on geomagnetism, ionospheric propagation, seismology, cosmic rays, and atmospheric electricity
24 p2924 N73-33354
Sulfur oxides, smoke, and air pollution tables from Belgian weather stations, Aug. 1972
24 p2949 N73-33559
Sulfur oxides, smoke, and air pollution tables from Belgian weather stations, Sep. 1972
24 p2949 N73-33560
Meteorological parameter tables for Belgian weather stations, Apr. 1973
24 p2950 N73-33561

**BELL AIRCRAFT**
NT OH-13 HELICOPTER
NT UH-1 HELICOPTER
NT X-14 AIRCRAFT
NT X-22 AIRCRAFT

**BELL MILITARY AIRCRAFT**
U MILITARY AIRCRAFT

**BELLOWS**
High speed bellows shaft seals for rocket engine turbopumps
03 p0348 N73-12842
LOX-cooled bearing and seal start cycling performance
[MBB-UR-84-71] 10 p1167 N73-19493
Design of welded bellows for cryogenic turbomachinery face seal applications
[NASA-CR-121117] 13 p1533 N73-22423

**BELTED PLAINS**
U PLAINS

**BELTS**
Apparatus for manufacturing polyester drive belts
[NASA-CASE-NPO-13205-1] 22 p2677 N73-31442

**BENCHES**
U SEATS

**BENDING**
NT ELASTIC BENDING
Bending moment at center of strut due to initial curvature under combined action of end loads and equal restraining moments
[ESDU-01.01.12] 01 p0110 N73-10904
Inversion of radio occultation data for planetary atmospheres by bent ray path technique
02 p0198 N73-11598
Fatigue tests on unnotched steel specimens during bending and axial loading
[ESDU-FAT-E.07.04] 02 p0236 N73-11924
Buckling and intial postbuckling of oval cylindrical shells under pure bending and under combined uniform axial compression and bending
[AD-747493] 04 p0482 N73-13939
Effects of various forming factors and process variables on forming of sheet metal products
05 p0551 N73-14476
Endurance of high strength steels subjected to bending
[ESDU-71027] 05 p0561 N73-14561
Axisymmetric bending of round sandwich plate with rigid isotropic layers
[AD-749767] 05 p0604 N73-14915
Secondary bending effect on aluminum alloy riveted joint fatigue strength determined by comparetive program fatigue tests
[NLR-TR-72007-U] 13 p1586 N73-22862
Construction and operation of bend tester at temperature ranges from minus 192 to 650 C
[NASA-TM-X-2853] 18 p2160 N73-27452
Response of general laminated plates to applied loads with coupling between bending and extensional modes of deformation
18 p2165 N73-27488
Distribution of stress across thickness near crack tip in epoxy resin plate subjected to approximate cylindrical bending
20 p2476 N73-29893

**BENDING FATIGUE**
Fatigue tests on solid shafts with interference-fit collars
[ESDU-68005-PT-4] 02 p0177 N73-11434
Calibration of combined bending-torsion fatigue reliability research machines and reliability data reduction
[NASA-CR-72837] 03 p0306 N73-12497
Fatigue properties of sintered test bars for bending and axial loads
[LBF-TM-58/71] 05 p0563 N73-14570
Detection of acoustic emission signals from fatigue cracks during cyclic bend tests
[NASA-TM-X-68228] 12 p1462 N73-21848
Boundary integral equation method for determining plane elasto-plastic analysis of V-notched plate under bending stress
24 p2987 N73-33869

**BENDING MOMENTS**
Graphical solution to bending moment of curved strut subjected to end loads
[ESDU-01.01.14] 02 p0236 N73-11919
Influence of end loads and moments on bending moment of straight strut
[ESDU-01.01.15] 02 p0236 N73-11920
Bending moments at ends of strut due to end load and triangularly distributed side load
[ESDU-01.01.25] 02 p0236 N73-11923
Procedures for computing upper and lower bounds to bending frequencies and estimates of mode shapes of beams with constant stiffness and mass - Part 1
[AD-747241] 02 p0239 N73-11946
Computer program user guide for determining limits to bending frequencies and mode shape estimates for free nonuniform beams with attached masses - Part 2
[AD-747242] 02 p0239 N73-11947
Stress freezing and slicing techniques of photoelasticity to analyze local stresses near deep surface flaws under cylindrical bending fields
[AD-746976] 02 p0240 N73-11950
Analysis of forces imposed on aircraft wing from landing gear impact in relation to weight of wing, damping, and frequency of periodic load
[AD-747381] 03 p0254 N73-12052
Torsional bending and longitudinal vibrations of rotating shafts and application to free vibrations of individual rotor blades, blade cascades, and shrouded blades
[NASA-TT-F-14627] 04 p0372 N73-13029
Mathematical model for bending of hybrid and composite hybrid beams
[CRIF-MT-79] 05 p0603 N73-14902
Numerical methods for determining effect of aerodynamic lag on bending response of aircraft wings at supersonic speeds
[NAL-TN-36] 15 p1733 N73-24056
Numerical analysis of bending of rotating beams with application to linear flap-lag stability of hingeless rotary wings using nonlinear equations
[NASA-TM-X-2770] 15 p1838 N73-24897
Numerical analysis of elasto-plastic bending of plates with V-notch on one edge and subjected to pure bending
[NASA-CR-132225] 15 p1839 N73-24900
Numerical analysis of wing bending, wing torsion, and aileron rotation at transonic speeds to determine effects on wing-aileron flutter
[ARC-R/M-3258] 16 p1855 N73-25028
Derivation of finite element properties in terms of stress functions for structural and nonstructural applications
[AD-762947] 20 p2484 N73-29953
Standard coupler effects on EHF attenuation in waveguides with bending moments
[FTZ-A-333-TBR-18] 22 p2632 N73-31096
Variational method for numerical analysis of bending and supercritical behavior of heterogeneous slightly curved plates
[AD-765543] 24 p2990 N73-33891

**BENDING THEORY**
Stiffness of flat strips in compression under sinusiodally distributed bending couples at their edges
[ESDU-05.01.30-AMEND-A] 14 p1714 N73-23906
Semidirect boundary integral method to obtain numerical solution for elastic stress and strain fields in V-notched beams in pure bending
[NASA-TN-D-7424] 22 p2725 N73-31803

**BENDING VIBRATION**
Analysis of helicopter blade flutter for both hinged and hingeless rotor blades
[AGARD-R-607] 13 p1472 N73-21920
Numerical analysis of panel flutter based on isoperimetric inequality and effect of viscous damping forces
[NASA-CR-131828] 13 p1475 N73-21950

Detailed calculations of natural vibrations of single cylindrically curved open shells
[NASA-TT-F-14979] 19 p2347 N73-28880
Asymmetrical bending and vibration of conical shell finite element
[TR-73-5-2] 24 p2989 N73-33884
BENDS [PHYSIOLOGY]
U DECOMPRESSION SICKNESS
BENZENE
Potassium exchange on sulfocation resins containing divinylbenzene for drinking water regeneration
03 p0257 N73-12078
Nuclear magnetic resonance spectrum analysis for rings inversion rate in benzodiazepine derivatives
[RAE-LIB-TRANS-1628] 17 p1991 N73-26103
Para-benzoquinone dioxime and concentrated mineral acid processed to yield intumescent or fire resistant, heat insulating materials
[NASA-CASE-ARC-10304-1] 17 p2048 N73-26572
BERING SEA
Analysis of ERTS data on ice formation in Bering Sea and correlation with ice observations by aerial reconnaissance
[E73-10865] 20 p2392 N73-29216
Application of ERTS-1 data to detection and mapping of sea ice in Beaufort Sea and Bering Sea areas
[E73-11037] 22 p2663 N73-31341
BERMUDA
Analysis of acoustic volume scattering in Bermuda Ocean to show daily variability and diurnal variations
[AD-761976] 19 p2296 N73-28465
BERNSTEIN ENERGY PRINCIPLE
Theoretical model for electromagnetic coupling of Bernstein modes in vacuum boundary of dense plasma
[COO-2181-10] 06 p0704 N73-15742
BERYLLIUM
Development of proton-activated recession sensor based on migration of beryllium isotope in graphite at high temperature and application to nose cone conditions during reentry
[AD-745454] 01 p0109 N73-10899
Performance characteristics of gallium arsenide solar cells with zinc or beryllium ion implantations
[NASA-CR-129199] 02 p0128 N73-11042
Effects of annealing on microstructure and room temperature mechanical properties of 0.100 inch thick ingot-source beryllium sheet
[RFP-1831] 03 p0314 N73-12562
Kinetics of purification of beryllium through evaporation data acquired during vacuum induction melting
[NASA-CR-123946] 04 p0431 N73-13512
Beryllium and beryllium-lithium complexes in single crystal silicon with acceptor levels 191 and 145 MeV
[NASA-TR-R-395] 04 p0458 N73-13736
Process for making high strength beryllium by hot-pressing extrusion and forging
[RFP-1816] 06 p0684 N73-15570
Fabrication and nondestructive tests of beryllium reinforced metal matrix composites
[AD-750764] 06 p0686 N73-15583
Gas chromatographic analysis of beryllium in aqueous solutions and biological tissues
[AD-753112] 09 p0996 N73-18131
Development of technique for production of beryllium foil with high surface finish
[RFP-1842] 10 p1166 N73-19483
Reports on electrical and mechanical properties of beryllium, chromium-manganese austenitic steels, and martensitic conversion during deformation
[JPRS-58357] 10 p1171 N73-19524
Variations of electrical resistance of hydroextruded polycrystalline beryllium in annealing process
10 p1171 N73-19525
Effect of fabrication conditions on mechanical properties of Be-Al monolayer tape and composite specimens
[SC-DR-72-0731] 10 p1175 N73-19559
Gas chromatographic separation of beryllium [II], copper [II], aluminum [III], and chromium [III] chelates
[NLL-M-22879-[5828.4F]] 11 p1252 N73-20158
Control measures for preventing environmental beryllium contamination
[AF-116] 11 p1313 N73-20659
Fabrication of beryllium compression tubes and structural panels for space shuttle application
[NASA-CR-124245] 13 p1533 N73-22420
Design of despin mechanism noting thermal and stress analysis of beryllium and aluminum as structural materials
[ESRO-CR[P]-226] 13 p1534 N73-22432
Development and testing of beryllium honeycomb sandwich composite panels
[NASA-CR-130648] 15 p1838 N73-24896
Extraction-Photometric methods for determining impurities in beryllium
[JAERI-1222] 17 p2044 N73-26537
Electronic properties of beryllium single crystals with emphasis on microwave surface impedance
18 p2185 N73-27646
Diffision in niobium of beryllium and aluminum from solid phase at 900 to 1300 deg
[NLL-CE-TRANS-5121-[9022.09]]
20 p2429 N73-29513
Control of material or process variables to optimize short time creep behavior of hot pressed beryllium
[AD-763121] 20 p2432 N73-29537
Effect of surface properties on tensile properties of beryllium under hydrostatic pressure
[NEL-537] 22 p2684 N73-31502
Analytical investigation of hexagonal metal deformation with particular application to Ti and Be
[AD-763835] 22 p2686 N73-31518
Ignition properties and combustion physics of beryllium to show effects of various physical parameters and composition of combustion products
24 p2992 N73-33908
BERYLLIUM ALLOYS
Toxicity and safety hazard of dry beryllium copper alloy machining for human operator
08 p0872 N73-17059
Health hazards in using electron beams for welding beryllium alloys
10 p1172 N73-19531
Development of beryllium-copper bearings for use with stainless steel shafts under high bearing stress levels imposed by airframes
[AD-754759] 11 p1299 N73-20540
Analysis of microplasticity of materials used in inertial navigation systems to show friction stress, yield stress, and rate of strain hardening in microstrain region
11 p1317 N73-20692
Effects of heat treatment on Brinell hardness of Co-Be alloy system
[RFP-TRANS-122] 17 p2044 N73-26541
Mechanical properties of alloys on aluminum beryllium base with magnesium
[AD-759876] 17 p2048 N73-26571
Determining mechanical properties of high conductivity metals and alloys
[NASA-CR-133890] 22 p2684 N73-31498
BERYLLIUM COMPOUNDS
NT BERYLLIUM OXIDES
BERYLLIUM OXIDES
Pressure sintering of beryllium oxide powder blended with aluminum oxide powder
[AD-748389] 04 p0439 N73-13576
Performance of translucent beryllium oxide as envelope material for high intensity flash and continuous wave lamps
[AD-751661] 07 p0813 N73-16589
Toxicological properties of rocket exhaust products and blood analysis for beryllium oxide content
[AD-754936] 11 p1248 N73-20131
Physical and chemical characteristics, and biological activity of exhaust from beryllium-fueled motor
[AD-756531] 13 p1485 N73-22042
Calculated power distribution of thermionic, beryllium oxide reflected, fast spectrum reactor
[NASA-TM-X-2838] 19 p2320 N73-28663
BESSEL FUNCTIONS
NT HANKEL FUNCTIONS
BESSEL-BREDICHIN THEORY
Bessel theory for analyzing head and tail regions of dust comets
02 p0228 N73-11846
BETA PARTICLES
Experiments on rotating plasmas for determining magnetohydrodynamic stability at high beta values
[TRITA-EPP-72-33] 09 p1071 N73-18741
Effects of beta radiation on electrical resistivity of mica
[NLL-RTS-7926] 18 p2184 N73-27635
Drift waves in finite beta plasmas
19 p2323 N73-28690
BETATRONS
Construction of extremal controller for high current betatron using stochastic algorithms
[AD-747370] 03 p0281 N73-12279
Computerized design of betatron electromagnet having optimal parameters
[AD-750523] 06 p0651 N73-15289
Digital computer simulation of one-dimensional plasma behavior in plasma betatron
10 p1195 N73-19726
BEVATRON
Bevatron for astrophysical and superheavy element studies with nuclear tracks in solids
[UCB-34-P-189-X-3] 12 p1445 N73-21708
BIAS
NT RESPONSE BIAS
Optimal estimation of measurement biases in Kalman-Schmidt filtering
[AD-753961] 11 p1311 N73-20641
BIBLIOGRAPHIES
Bibliography of research on aircraft sidearm control
[AD-745863] 01 p0005 N73-10039
Annotated bibliography on reaction times in selected human information processing tasks
[AD-745416] 01 p0012 N73-10095
Bibliography on digital image processing information
[AD-745790] 01 p0029 N73-10231
Bibliography of on-line computers in nuclear and thermal power stations from 1960 to June 1972
[CE-BIB-226] 01 p0030 N73-10233
Coastal geology bibliography of New England with punch card reference system
[AD-744001] 01 p0052 N73-10424
Automated nondestructive testing - bibliography with abstracts
[CE-BIB-227] 01 p0061 N73-10498
Bibliography on fiber reinforced plastic composites
[PB-210305] 01 p0071 N73-10585
Annotated bibliography and indexes on aeronautical engineering and aerodynamics - July 1972
[NASA-SP-7037[21]] 02 p0123 N73-11001
Annotated bibliography and indexes on aerospace medicine and biology - Aug. 1972
[NASA-SP-7011[106]] 02 p0130 N73-11054
Bibliography on laser Doppler velocimeter theory and usage
[AD-746634] 02 p0176 N73-11427
Bibliography of Soviet laser research and development
[AD-746339] 02 p0183 N73-11480
Bibliographic survey on yield behavior of metal surfaces
[AD-746473] 02 p0188 N73-11524
Atomic line shapes, shifts, and broadening - bibliography for 1889 through Mar. 1972
[NBS-SP-366] 02 p0214 N73-11732
Bibliography of articles on cosmic X ray astronomy from Astrophysical Journal
[NASA-TM-X-64705] 02 p0230 N73-11869
Bibliography of abstracts for NASA patents and patent applications
[NASA-SP-7039(01)-SECTION-1]
02 p0244 N73-11982
List of scientific and technical reports published by ESRO up to Jul. 1972
[ESRO-SP-88] 02 p0245 N73-11992
Annotated bibliography and indexes on aerospace medicine and biology - July 1972
[NASA-SP-7011[105]] 03 p0256 N73-12073
Bibliography of arc discharges in vacuum and gaseous atmospheres
[SC-B-72-3233] 03 p0278 N73-12251
Bibliography of solid state electronics
[AD-748739] 03 p0279 N73-12262
Bibliographic survey on stress corrosion cracking of high strength aluminum alloys, including oxide effects
[DLR-FB-71-105] 03 p0316 N73-12572
Annotated bibliography of research and development of high temperature stable polymeric systems
[NASA-TM-X-2641] 03 p0320 N73-12608
Annotated bibliography of sintered and hot pressed silicon nitride
[AD-747785] 03 p0322 N73-12624
Bibliography on environmental monitoring for radioactivity
[ORNL-NSIC-101] 03 p0334 N73-12720
Bibliography on controlled fusion and plasma physics
[TID-3557-1971-SUPPL] 03 p0341 N73-12785
Annotated bibliography on pulsars taken from Nuclear Science Abstracts for 1971
[TID-3320-SUPPL-2] 03 p0357 N73-12909
Bibliography on theory, calibration, pyrometric devices, and temperature measurements
[NBS-SP-373] 03 p0364 N73-12962
Bibliography of economic impact of stimulated aerospace technology activity
[NASA-CR-129515] 03 p0366 N73-12981
Supplement to bibliography on Aerospace Medicine and Biology, October 1972
[NASA-SP-7011[107]] 04 p0377 N73-13069
Annotated bibliography with preliminary analysis on dysbaric osteonecrosis
[AD-747258] 04 p0381 N73-13100
Bibliography on effects of underwater environment on tools, equipment, and human performance
[AD-748000] 04 p0384 N73-13122
Bibliography on carbon dioxide removal from gases by lithium hydroxide
[CL-1971-15] 04 p0386 N73-13136
Bibliography on laser development in Soviet Union
[AD-748258] 04 p0430 N73-13499
Literature survey on wave scattering from rough surfaces
[FOA-2-C-2486-E1] 04 p0449 N73-13668
Annotated bibliography and indexes on aeronautical engineering and aerodynamics, September 1972
[NASA-SP-7037[22]] 05 p0491 N73-13999
Human performance measurement - bibliographies
[AD-749100] 05 p0501 N73-14080
Bibliography of research reports and publications issued by Human Engineering Division for April 1946 to December 1970
[AD-749933] 05 p0504 N73-14103
Upper atmospheric disturbance near polar cap - bibliographies
[AD-746298] 05 p0539 N73-14390
Bibliography of literature on radiographic techniques for nondestructive tests
[AD-749258] 05 p0553 N73-14488
Bibliography on fibers and composite materials
[AD-746214] 05 p0566 N73-14595
Bibliography on meteorological phenomena in Switzerland
[REFT-71-II] 05 p0571 N73-14643
Bibliography on meteorological phenomena in Switzerland
[REFT-72-I] 05 p0571 N73-14644

Thrust reversal and thrust vectoring technology review to identify test data and prediction methods
[AD-749476] 05 p0591 N73-14800

Bibliography on radio frequency and microwave radiation effects in biological systems
[AD-750271] 06 p0632 N73-15131

Bibliography on role of vestibular apparatus in compressed air work underwater
[AD-750686] 06 p0632 N73-15133

Soviet bibliography on biocybernetics material received from Jan. to May 1972
[AD-750129] 06 p0636 N73-15167

Bibliography on side-looking radar for remote sensing of earth resources, agriculture, oceanography, geology, hydrology, geography - noting data processing and photointerpretation
[ESRO-CR[P]-142-VOL-7] 06 p0640 N73-15198

Bibliography of publications from OGO E plasma wave investigation
[NASA-CR-130140] 06 p0644 N73-15227

Bibliography on chemical contaminants released in upper atmosphere
[WRE-TM-498[WR/D]-PT-2] 06 p0667 N73-15422

Annotated bibliography of technical characteristics of remote sensors and technological experiments developed under NASA programs for earth observation
[NASA-TM-X-66144] 06 p0674 N73-15482

Annotated bibliography on nuclear energy research in Philippines
[PAEC[A]-7116-SUPPL-4] 06 p0699 N73-15698

Bibliography of heat pipe applications
[BIB-2-72] 06 p0729 N73-15951

Annotated bibliography and indexes on aeronautical engineering and aerodynamics-October 1972
[NASA-SP-7037[23]] 07 p0735 N73-15984

Bibliography of aircraft accident reports for US civil aviation operations during calendar year 1971
[NTSB-BA-72-7] 07 p0738 N73-16002

Bibliography of aerospace medicine and biology
[NASA-SP-7011[108]] 07 p0742 N73-16037

Bibliography of wildlife movements and tracking systems
[NASA-CR-130380] 07 p0742 N73-16040

Electrical and meteorological experimentation in upper atmosphere of polar regions - bibliography
[AD-751336] 07 p0796 N73-16472

Bibliography and abstracts on upper atmospheric phenomena in inner region of polar cape
[AD-751335] 07 p0796 N73-16473

Abstracts of selected reports on heat transfer and fluid dynamics with applicability to oxygen systems
[NASA-SP-3076-VOL-3] 07 p0855 N73-16932

Bibliography of Belgian research reports in fluid mechanics and plasma physics from 1957 to 1972
[NT-32-1972] 07 p0860 N73-16975

Bibliography on capabilities and limitations of chemical milling techniques
[AD-752050] 08 p0928 N73-17597

Bibliography of laser communication systems
[AD-751900] 08 p0929 N73-17612

Bibliography of USAF reports on air, water, noise, and radiation pollution
[AD-751898] 08 p0940 N73-17699

Bibliography of weather predictions and verifications
[AD-751950] 08 p0940 N73-17701

Bibliography on applications of nuclear explosions in mines, chemistry, and gas and oil extraction
[CEA-BIB-129-ADD-1] 08 p0942 N73-17719

Bibliography of Nuclear Science Abstracts from 1964 to 1970
[AED-C-21-10] 08 p0942 N73-17720

Bibliography of nuclear explosion effects on explosives
[ICT-11/71] 08 p0946 N73-17749

Index of bibliographies for patents and patent applications May 1969 through June 1972
[NASA-SP-7039[01]-SECTION-2] 08 p0971 N73-17932

Abstracts and bibliographic lists on major research projects completed in September, 1972
[AD-751956] 08 p0977 N73-17996

Bibliography of armed forces research and development bibliographies - Vol. 1
[AD-752150] 08 p0978 N73-17997

Annotated bibliography of military research and development bibliographies - Vol. 2
[AD-752160] 08 p0978 N73-17998

Annotated bibliography and indexes on aeronautical engineering and aerodynamics - Nov. 72
[NASA-SP-7037[24]] 09 p0979 N73-17999

Annotated bibliography and indexes on Aerospace Medicine and Biology - December 1972
[NASA-SP-7011[109]] 09 p0992 N73-18094

Bibliography on human factors in man machine interactions and systems design
[AD-752800] 09 p0997 N73-18141

Bibliography on techniques for integrating and packaging printed circuits
[AD-752400] 09 p1010 N73-18241

Design, construction, and maintenance of landing fields and runways
[AD-751400] 09 p1012 N73-18263

Research and development of lasers and laser-related equipment in the Soviet Union - bibliography
[AD-753098] 09 p1043 N73-18510

Bibliography on pyrotechnics
[AD-752700] 09 p1100 N73-18976

Bibliography on titanium toxicity in human and animal organisms
[ORNL-TIP/TIRC-72-65] 10 p1120 N73-19135

Annotated bibliography and indexes on aeronautical engineering and aerodynamics - Dec. 1972
[NASA-SP-7037[25]] 11 p1231 N73-19992

Annotated bibliography and indexes on aeronautical engineering and aerodynamics - Jan. 1973
[NASA-SP-7037[26]] 11 p1231 N73-19993

Annotated bibliography of aerodynamic configurations and characteristics of short takeoff aircraft
[AD-754500] 11 p1236 N73-20037

Annotated bibliography and indexes on aerospace medicine and biology - January 1973
[NASA-SP-7011[110]] 11 p1238 N73-20052

Review of published bibliographical index of Soviet and foreign literature on biomedical problems in space
11 p1246 N73-20115

Magnetic tape version of substance-property index and bibliographies
[NBS-TN-760] 11 p1260 N73-20223

Bibliography on infrared photography and infrared films
[AD-754600] 11 p1295 N73-20509

Compilation of metallurgical processes for variety of metals and alloys
[NASA-SP-5953[01]] 11 p1306 N73-20593

Bibliography of AGARD publications
[AGARD-INDEX-52/70-PT-1] 11 p1352 N73-20973

Subject index for AGARD publications bibliography - Part 2
[AGARD-INDEX-52/70-PT-2] 11 p1352 N73-20974

Laser technology, strong explosion effects, geosciences, and particle beams bibliographies
[AD-754946] 11 p1353 N73-20982

Laser technology, strong explosion effects, geosciences, and particle beams - bibliographies
[AD-754962] 11 p1353 N73-20988

Guide to literature of engineering, mathematics and physical science
[AD-754382] 11 p1353 N73-20989

Tables of reports giving comparative theoretical and experimental aerodynamic loading data relevant to zero- and low-frequency aeroelastic problems
[ARC-R/M-3708] 12 p1356 N73-21000

Annotated bibliography and indexes on aerospace medicine and biology
[NASA-SP-7011[112]] 12 p1367 N73-21087

Bibliography on ceramic materials
[AD-755650] 12 p1417 N73-21478

Bibliography on shock waves in solids
[AD-755429] 12 p1441 N73-21679

Annotated bibliography and indexes on aeronautical engineering and aerodynamics - February 1973
[NASA-SP-7037[28]] 13 p1469 N73-21895

Bibliography of citations relating to planetary quarantine from 1966 to 1971
[NASA-CR-131889] 13 p1485 N73-22038

Bibliography of developments in field of picture processing by computers during 1972
[AD-755702] 13 p1499 N73-22146

Government contracts and grants relative to documents on environmental satellites
[NOAA-TM-NESS-46] 13 p1524 N73-22349

Bibliography on use of neutron activation analysis of geochemical samples
[NASA-CR-131831] 13 p1524 N73-22352

Annotated bibliography on holography
[AD-756600] 13 p1531 N73-22408

Marine biology literature compilation for Caribbean Sea and adjacent regions
14 p1607 N73-23022

Literature compilation on marine geology and geophysics for Caribbean Sea and adjacent regions
14 p1607 N73-23023

Annotated bibliography and indexes on aerospace medicine and biology for 1961 to 1965
[NASA-TT-F-14662] 14 p1610 N73-23053

Bibliography of kinetic data in gas phase reactions of nitrogen, oxygen, and nitrogen oxides
[NBS-SP-371] 14 p1616 N73-23094

Literature survey of articles dealing with all aspects of predicting, measuring, and controlling unwanted scattered light in large space telescopes
[NASA-CR-124240] 14 p1667 N73-23531

Bibliography of documents on noise pollution
[NASA-CR-131968] 14 p1692 N73-23734

Cumulative index of abstracts contained in Aeronautical Engineering and Aerodynamics Bibliography for calendar year 1972
[NASA-SP-7037[27]] 15 p1725 N73-23994

Annotated bibliography and indexes on Aerospace Medicine and Biology - February 1973
[NASA-SP-7011[113]] 15 p1739 N73-24099

Annotated bibliography and indexes on aerospace medicine and biology - January 1973
[NASA-SP-7011[111]] 15 p1739 N73-24100

Bibliography of Soviet research and development of lasers
[AD-758259] 15 p1795 N73-24552

Literature survey of heat transfer characteristics of single and multiple turbulent air jets impinging on flat plates
[NASA-TM-X-2778] 15 p1842 N73-24927

Annotated bibliography of reports, articles, and documents introduced into NASA scientific and technical information system in 1972
[NASA-SP-7500[07]] 15 p1845 N73-24946

Annotated bibliography and indexes on aeronautical engineering and aerodynamics - March, 1973
[NASA-SP-7037[29]] 16 p1851 N73-24998

Sixth supplement to bibliography on planetary quarantine with indexes
[NASA-CR-131817] 16 p1866 N73-25112

Marine science newsletters - 1973 annotated bibliography
[NOAA-TM-EDS-NODC-3] 16 p1906 N73-25417

NASA patent abstracts bibliography
[NASA-SP-7039[2]-SECTION-1] 16 p1976 N73-25976

Indexes to patent abstracts bibliography
[NASA-SP-7039[2]-SECTION-2] 16 p1976 N73-25977

Bibliography of JPL reports for 1972
[NASA-CR-132994] 16 p1976 N73-25983

Abstracts and bibliographic lists of Soviet technical literature on research and development
[AD-758784] 16 p1977 N73-25995

Annotated bibliography and indexes on Aerospace Medicine and Biology - April 1973
[NASA-SP-7011[114]] 17 p1986 N73-26055

Bibliography of literature on phase locked loops
[NASA-CR-133225] 17 p2004 N73-26202

Bibliography on welding by electron beam, ultrasonic radiation, laser beam, and friction
[ORNL-TM-4133] 17 p2038 N73-26486

Bibliography on metallic fuels for pyrotechnic compositions
[AD-759761] 17 p2097 N73-26963

Bibliography of management planning and information systems
[AD-758900] 17 p2099 N73-26986

Bibliography of urban area problems
[AD-756500] 17 p2099 N73-26987

Annotated bibliography and indexes of aeronautical engineering and aerodynamics - April 1973
[NASA-SP-7037[30]] 18 p2101 N73-26990

Annotated bibliography and indexes on aeronautical engineering and aerodynamics - May 1973
[NASA-SP-7037[31]] 18 p2101 N73-26991

Bibliography of aerospace medicine and biology
[NASA-SP-7011[115]] 18 p2109 N73-27051

Bibliography of literature concerning electromagnetic and seismic noise and propagation
[PB-217500/8] 18 p2118 N73-27125

Composite materials, ceramics, textiles, and plastics for radomes - bibliographies
[AD-760960] 18 p2118 N73-27126

Bibliography of references on urban hydrology
[PB-219105/4] 18 p2146 N73-27348

Bibliography of remote sensing applications to agriculture, civil engineering, and geology
[PB-219104/7] 18 p2147 N73-27356

Bibliography on geothermal prospecting in arid and semiarid lands
[PB-218830/8] 18 p2148 N73-27359

Arc welding and industrial processing - bibliographies
[AD-760970] 18 p2156 N73-27421

Bibliography of test equipment and procedures for determining physical and mechanical properties of iron and steel products
[PB-219047] 18 p2161 N73-27439

Bibliography of articles concerning water balance of monsoon Asia
[CLIMATOL-NOTES-11] 18 p2171 N73-27531

Mars bibliography, including topography and atmosphere
[AD-759291] 18 p2198 N73-27743

Bibliography on lasers, strong explosions, geosciences, particle beams, and material sciences
[AD-759275] 18 p2215 N73-27884

Bibliography of anthropometric information for Air Force human factors engineering
[AD-762287] 19 p2229 N73-27978

Bibliography on various types of bearings
[AD-761960] 19 p2306 N73-28547

Dye laser bibliography from 1966 to 1972
19 p2307 N73-28559

Literature abstracts for plasma instability research
[UNICP-SR95-PT-2] 19 p2324 N73-28696

Bibliography of research in radiation physics and aerodynamics
[AD-761633] 19 p2356 N73-28952

Abstracts and bibliographies of Soviet literature on lasers, explosion effects, particle beams, and geosciences
[AD-762376] 19 p2356 N73-28955

Bibliography of Russian literature on aviation and space medicine
[JPRS-53329] 20 p2369 N73-29047

Bibliography of Soviet laser developments. Jan. - Mar. 1973
[AD-762569] 20 p2427 N73-29492

Selected bibliography of articles on product liability
[NASA-TM-X-69493] 20 p2488 N73-29985

Bibliography of publications by Cryogenics Division of NBS
[NBS-TN-639] 20 p2488 N73-29988
Annotated bibliography and indexes on aeronautical engineering and aerodynamics - June 1973
[NASA-SP-7037[32]] 21 p2491 N73-29993
Bibliography of aerospace medicine and biology
[NASA-SP-7011[116]] 21 p2500 N73-30059
Microcircuit reliability bibliography
[AD-763764] 21 p2518 N73-30194
Bibliography of lighting theory, instrumentation, and protection
[AD-763667] 21 p2540 N73-30366
Bibliography of water pollution from natural and man-made sources
[AD-761980] 21 p2541 N73-30371
Bibliography of abstracts on remote sensing of water resources
[PB-220163/0] 21 p2542 N73-30383
Bibliography of reports dealing with adhesion bonding
[AD-763200] 21 p2553 N73-30471
Bibliography on etching and chemical machining techniques
[AD-763100] 21 p2554 N73-30472
Bibliography on stress wave emission, 1950-1972
[ARL/MET-BIBL-1] 21 p2557 N73-30500
Bibliography on refractory coatings in industrial processes
[AD-763150] 21 p2563 N73-30547
Annotated bibliography on weather modification by precipitation inducement
[PB-220348/7] 21 p2575 N73-30634
Bibliography on air pollution from both natural and man-made sources
[AD-761950] 21 p2575 N73-30636
Review of resources of fossil and nuclear fuels, solar energy and hydroelectric power
[LRP-63/73] 22 p2617 N73-30975
Annotated bibliography of literature on resource sharing computer networks
[NBS-SP-384] 22 p2638 N73-31140
Uranium-titanium alloys - annotated bibliography
[RFP-2005] 22 p2684 N73-31500
Annotated bibliography and indexes on aeronautical engineering and aerodynamics - July 1973
[NASA-SP-7037[33]] 23 p2739 N73-31925
Bibliography of technical reports of helicopter engines and rotary wings
[AD-764900] 23 p2746 N73-31981
Compilation of operational and mathematical computer programs from NASA programs
[NASA-SP-5962[01]] 23 p2760 N73-32089
Bibliography on computer-aided logical processes
[AD-764400] 23 p2762 N73-32099
Annotated bibliography on microminiaturization electronics
[AD-764800] 23 p2767 N73-32136
Bibliography on capacitor technology
[AD-764825] 23 p2767 N73-32137
Multispectral scanning systems and potential application to earth resources surveys - bibliography
[ERL/R-249-U] 23 p2787 N73-32299
Bibliography of reports on sputtering in industrial processes for applying coatings
[AD-763600] 23 p2798 N73-32379
Bibliography of techniques, procedures, manufacturing methods, time studies, and shop layout in machine shop practice
[AD-765400] 23 p2799 N73-32388
Bibliography of chemical laser publications with tables showing chemical systems exhibiting laser action
[DREV-TN-2080/73] 23 p2801 N73-32403
Bibliography of Italian climatology
[IFA-STR-22] 23 p2814 N73-32499
Annotated bibliography and indexes on aerospace medicine and biology - September 1973
[NASA-SP-7011[119]] 24 p2882 N73-33012
Development of report search code for computer generated bibliographic data in machine readable form
[DSIR-TN-11] 24 p2897 N73-33125
Weibull distribution bibliography, 1957 - 1972
[CE-BIB-235] 24 p2928 N73-33387
Bibliography of manufacturing methods of composite materials
[AD-764600] 24 p2944 N73-33512
Abstracts of reports concerning noise pollution
[NASA-CR-135954] 24 p2956 N73-33618
Light coupling, light modulation, and integrated optics - bibliography
[NASA-TM-X-64787] 24 p2959 N73-33641
Bibliography on plasma generation by lasers
[LS-255] 24 p2964 N73-33688
Cumulative bibliography of research and development projects conducted on heat pipe technology and applications
[NASA-CR-135953] 24 p2991 N73-33900
Bibliography of research projects on heat pipe, development, performance, and application - January through March, 1972
[NASA-CR-135956] 24 p2991 N73-33901
Bibliography of heat pipe research and development projects conducted during April through June 1972
[NASA-CR-135955] 24 p2991 N73-33902
Bibliography of heat pipe research and development projects conducted during July through September, 1972
[NASA-CR-135952] 24 p2991 N73-33903
Supplemental report and bibliographies of heat pipe research projects conducted during calendar year 1971
[NASA-CR-135951] 24 p2991 N73-33904

**BICARBONATES**
U CARBONATES

**BICRYSTALS**
Creep tests and transmission electron microscopic observation of grain boundary structure in stainless steel bicrystals
[CEA-R-4317] 10 p1200 N73-19768

**BICYCLE**

Performance evaluation of training devices for developing human physical fitness
[NASA-CR-134046] 23 p2752 N73-32023

**BIGHORN MOUNTAINS [MT-WY]**

Tectonic analysis of Bighorn Mountains using ERTS-1 imagery
[E72-10310] 04 p0412 N73-13359
Tectonic analysis of Bighorn Mountains using ERTS-1 imagery
[E73-10036] 08 p0900 N73-17288
Vegetation analysis and preparation of tectonic map overlay of Bighorn Mountains region based on ERTS-1 data
[E73-10420] 11 p1279 N73-20382
Utilization of ERTS-1 imagery for tectonic analysis and geological mapping of Bighorn Mountains
[E73-10583] 14 p1657 N73-23443
ERTS-1 imagery of Bighorn-Pryor mountains of Wyoming and Montana applied to analysis of regional tectonic relationships
[E73-10704] 16 p1903 N73-25395
Application of ERTS-1 imagery for tectonic analysis of Bighorn Mountains region and effect of snow cover and low sun angle on identifying topographical features
[E73-10722] 17 p2019 N73-26329
Skylab and EREP remote sensing data for tectonic analysis of Bighorn Mountains of Wyoming and Montana
[E73-10784] 18 p2136 N73-27260
Analysis of geological structure in Bighorn Mountains region of Wyoming and Montana based on multispectral band imagery from ERTS-1 satellite
[PAPER-G31] 19 p2267 N73-28262
Tectonic analysis and mapping of Bighorn Mountains from ERTS-1 imagery
[E73-11049] 23 p2779 N73-32225
Tectonic analysis of Bighorn Mountains of Montana and Wyoming and Black Hills of South Dakota and Wyoming from Skylab imagery
[E73-11131] 24 p2919 N73-33305

**BILLOW CLOUDS**
U CLOUDS [METEOROLOGY]

**BIMETALS**

Effect of high pressure shock waves on mechanical properties of bimetals produced by different cladding techniques
[AD-750958] 06 p0677 N73-15513
Copper brass bimetal cladding layers on steel strips for manufacturing elastic current conducting springs
[NLL-M-21498-[5828.4F]] 06 p0682 N73-15554
Electrical resistance measurement for determining electron state densities in molten germanium-silver and germanium-copper systems
[NLL-M-21613-[5828.4F]] 15 p1746 N73-24153
Microstructural determination of bonding strength of steel bimetal produced by pressure working
[NLL-M-21699-[5828.4F]] 21 p2557 N73-30499

**BINARY ALLOYS**

Thermodynamic properties of transition metal/silicon binary alloys
[NPL-CHEM-18] 03 p0365 N73-12970
Evaporative segregation in binary alloys of Ni-Cr and Ni-Fe systems
[NASA-CR-123993] 05 p0561 N73-14562
Microstructural features of deformation analyzed in two-phase titanium alloys to determine beta phase effect on ductility
06 p0683 N73-15557
Composition and structural effects on mechanical properties of superplastic zinc and aluminum binary alloys
06 p0683 N73-15562
Auger electron spectroscopy of surface segregation in binary alloys
[NASA-TN-D-6982] 06 p0683 N73-15564
Electron structure of transition metals and alloys
[ONERA-P-144] 09 p1048 N73-18548
Steady state creep rate of nickel as effected by binary alloys at increased temperatures
12 p1413 N73-21448
Pseudo-binary crystal model for electron mobility variation with composition of gallium indium arsenide semiconducting alloys
18 p2181 N73-27607
Development of method for calculating molar volume and density of molten binary alloys with strongly interacting dissimilar atoms
[NLL-M-21695-[5828.4F]] 20 p2429 N73-29512
Epitaxic sublimation methods for studying pseudo-binary semiconductor alloys
[AD-763488] 21 p2586 N73-30723

**BINARY CODES**

PCM coding and decoding noting truncated hamming codes and analysis of error rates
[ESRO-TN-112-ESTEC] 05 p0513 N73-14173
Binary code signals produced by electron beam deflection in magnetic fields
12 p1378 N73-21176
Procedure for connected and orthogonal binary random processes with continuous time
22 p2628 N73-31059
Spectral correlation characteristics of pair of orthogonal binary random signals
22 p2628 N73-31060
Data error protection in disturbed binary channels by linear systematic codes, applied to 50 Kbaud telephone channel transmission
[FTZ-A-441-TBR-1] 22 p2632 N73-31097

**BINARY DATA**

Parallel image logical operations using cross correlation
09 p1066 N73-18695
Abstract algebraic techniques to determine synchronization properties of binary, linear, and maximal length sequences
[AD-744101] 13 p1550 N73-22560
Phase modulation of tone and binary signals on carrier waves in communication systems
[NASA-CASE-GSC-11743-1] 18 p2116 N73-27107
Weakly homogeneous binary systems of order two for random search theory
18 p2169 N73-27515
On-line binary scan converter for converting pictorial from computer output to raster form suitable for TV display
19 p2238 N73-28046
Coded transmission of binary data over coherent white Gaussian channels
[AD-761465] 19 p2245 N73-28102
Digital input/output modules for binary signals
[KFK-1688] 20 p2379 N73-29114
Procedure for connected and orthogonal binary random processes with continuous time
22 p2628 N73-31059
Spectral correlation characteristics of pair of orthogonal binary random signals
22 p2628 N73-31060
Monte Carlo simulation of self bit synchronizer for binary overlapping signals
23 p2755 N73-32046

**BINARY DIGITS**

Digital converter for scaling binary number to binary coded decimal number of higher multiple
[NASA-CASE-KSC-10595] 03 p0269 N73-12176
Binary concatenated coding system to measure, count, and record numerical information using minimized number of digits
[NASA-CASE-MSC-14082-1] 07 p0759 N73-16163
Family of m-ary linear feedback shift register with binary logic
[NASA-CASE-NPO-11868] 11 p1264 N73-20254

**BINARY FLUIDS**

Numerical analysis of fluid containment near stagnation point and within self-confined stagnation region for bi-component mixture
[NASA-CR-2172] 03 p0283 N73-12292
Solution of boundary layer equations of chemically reacting flat plate flow of binary gas mixture with Hermitian finite difference method
[DLR-FB-72-58] 07 p0772 N73-16272
Numerical analysis of steady state laminar motion of viscous, incompressible, and binary fluids for rotating flow in cylindrical geometry
18 p2129 N73-27204
Ultrasound and light scattering in diffusing and chemical reacting binary mixture of fluids
23 p2774 N73-32185

**BINARY INTEGRATION**

Shift register with feedback for generating pseudorandom binary sequences
[REPT-6707] 08 p0887 N73-17183

**BINARY MIXTURES**
NT BINARY FLUIDS
NT EUTECTIC ALLOYS
NT EUTECTICS

Equilibrium distribution of helium-4 and helium-3 between the liquid and vapor phases of deuterium 2 and hydrogen 2
[NBS-TN-621] 02 p0137 N73-11109
Analysis of mass transfer through binary, monatomic gas mixture of arbitrary composition contained between two plane parallel surfaces
[COO-2032-10] 03 p0284 N73-12304
Transfer of mass and heat through single component diatomic gas and binary monatomic gas mixture of arbitrary composition
[COO-2032-12] 03 p0364 N73-12968
Tabular data on transport and thermophysical properties of selected binary mixtures in gaseous state
[AD-757528] 14 p1617 N73-23101
Concentration fluctuations in critical region of binary liquid mixture 3-methylpentane-nitroethane
[AD-759740] 16 p1872 N73-25158

Ultrasonic wave propagation in He-Ar and He-Xe mixtures
24 p2956 N73-33614
BINARY STARS
NT ECLIPSING BINARY STARS
Chemical composition and abundance of alpha Centauri visual binary determined from spectral lines
[ROY-OBS-BULL-173] 06 p0719 N73-15870
Chemical composition of line spectra for binary alpha Centauri and determination of abundances
[BULL-173] 07 p0842 N73-16820
Mass-luminosity relationship of binary stars in Hyades cluster
[ROY-OBS-BULL-175] 13 p1578 N73-22788
Analysis of rotational velocities in close visual binary stars
19 p2341 N73-28833
Primordial helium abundance and population II binary stars, measurement technique
20 p2469 N73-29832
Line strengths in spectra of seven double-lined Am binary stars
[BULL-177] 21 p2596 N73-30803
Line strengths in spectra of seven double-lined Am binary stars
[ROY-OBS-BULL-177] 21 p2598 N73-30819
Fundamental data for contact binaries RZ Comae, RZ Tauri and AW UMa
[NASA-TM-X-69614] 22 p2718 N73-31755
BINARY SUMMATORS
U ADDING CIRCUITS
BINARY SYSTEMS [DIGITAL]
U DIGITAL SYSTEMS
BINARY SYSTEMS [MATERIALS]
NT BINARY ALLOYS
NT BINARY FLUIDS
NT BINARY MIXTURES
NT EUTECTIC ALLOYS
NT EUTECTICS
Equations based on theory of elastic moduli of composite materials used to calculate electrical and thermal conductivities of two phase systems
[AD-748304] 04 p0439 N73-13580
Review and compilation of technical data on Lorenz ratio of metals and alloys to include electrical resistivity and thermal conductivity
[NBS-TN-634] 12 p1413 N73-21451
Combustion rates for binary pyrotechnic compositions in rarefied air
[AD-756043] 13 p1591 N73-22898
Thermodynamic properties of solid and molten silicate systems
[NPL-CHEM-21] 15 p1844 N73-24938
Binary boron/lithium system as propellant additive of hybrid rocket engines, noting enthalpy and reaction product density
[DLR-MITT-73-08] 17 p2075 N73-26791
Handbook of phase diagrams of silicate and similar systems comprising oxides and fluorides - Vol. 1
[TT-71-50040] 21 p2564 N73-30556
BINAURAL HEARING
Voice communication and hearing in acoustic orientation systems of animals at various evolution levels
[DRIC-TRANS-3056] 16 p1867 N73-25121
BINDERS [ADHESIVES]
U ADHESIVES
BINDERS [MATERIALS]
NT PROPELLANT BINDERS
NT SOLID ROCKET BINDERS
Inorganic binders for utilizing high reflectance of BaSO4 in paints
[NASA-TM-X-66082] 02 p0191 N73-11549
Effects of rebinders on strength of polyethylene and polymethyl methacrylate
[AD-751615] 07 p0812 N73-16587
Quality control and composition of grinding wheels discussing microstructure and chemistry
[CRIF-MC-45] 13 p1530 N73-22399
Coated reinforced materials, glass antidiffusion films, and metal binders
[AD-758167] 14 p1682 N73-23649
BINOCULAR VISION
Psycho-visual problems associated with monocular, bi-ocular, and binocular visual systems
[AD-749450] 05 p0502 N73-14085
Binocular vision models for designing image distortion compensation system
16 p1920 N73-25534
BINOMIALS
Estimation techniques in modified binomial distribution that describes thunderstorms over Cape Kennedy, Florida
[NASA-CR-2280] 16 p1937 N73-25678
BIOACOUSTICS
Voice and hearing in system of acoustic orientation of animals
[NLL-DRIC-TRANS-3056-[3623.66]]
15 p1739 N73-24101
BIOASSAY
Procedure for assaying enzyme activity in soils and application to presumptive life tests in Martian soil
[NASA-CR-128399] 01 p0008 N73-10059
Soil sampling and microorganism analysis in planetary spacecraft assembly area for prevention of Mars contamination
[NASA-CR-130009] 07 p0745 N73-16059
Animal species susceptibility to toxic effects of long term exposure to environmental monomethylhydrazine
[AD-751441] 07 p0748 N73-16086
Risk scoring system for identifying subjects with high risk to coronary heart disease
08 p0874 N73-17080
Microbiological assay procedures for spacecraft cabling, antennas, solar panels, and thermal blankets
[NASA-CR-130383] 08 p0877 N73-17109
Luciferase ATP assay procedure for determining bacterial infections in urinary tract
[NASA-CR-130797] 09 p0992 N73-18096
Radioimmunoassays of plasma aldosterone and catecholamine concentrations as human vasomotor regulators
09 p0994 N73-18111
Multiple immunoassay system for determining parathyroid hormone, calcitonin, and vitamin D in human blood
09 p0994 N73-18112
Detection of evolutionary organic compounds in extraterrestrial matter
10 p1118 N73-19114
Potassium ferrioxalate actinometric measurements of solar ultraviolet photobiological energy
15 p1741 N73-24113
Enzymatic luminescent bioassay method for determining bacterial levels in urine
[NASA-CASE-GSC-11092-2] 18 p2109 N73-27052
Analytical gas chromatography and mass spectrography for physiological monitoring of astronauts
[NASA-CR-133272] 18 p2110 N73-27059
Procedures and instrumentation for life detection on Mars
[NASA-CR-133186] 19 p2344 N73-28854
Biodetection grinder for sampling aerospace materials for microorganisms
[NASA-TM-X-64765] 20 p2372 N73-29059
Fluorometric 11-hydroxycorticosteroid determination in human blood plasma
[NASA-TT-F-15092] 22 p2619 N73-30990
BIOASTRONAUTICS
Aerospace medicine session concerning aviation and space physiology and psychology
24 p2885 N73-33037
BIOCHEMISTRY
NT BACTERIOLOGY
NT ENZYMOLOGY
NT PHYSIOCHEMISTRY
Procedure for assaying enzyme activity in soils and application to presumptive life tests in Martian soil
[NASA-CR-128399] 01 p0008 N73-10059
Oxygen redox processes in blood coagulation mechanism
03 p0257 N73-12079
Absorption and emission spectra for trace element analyses on biological sample solutions
03 p0258 N73-12093
Spectrometric determination of copper, iron, cobalt, nickel, and manganese complexes in biological samples
13 p1483 N73-22022
Summary of biochemistry and biology research projects
[NASA-CR-135650] 22 p2667 N73-31366
BIODYNAMICS
Conference on operational flight stress effects on human biodynamics and performance
[AGARD-CP-101] 10 p1122 N73-19143
Combined stress effects in human communication and motion sickness biodynamics
10 p1122 N73-19144
Quarterly report of JPL research and development
[NASA-CR-131152] 10 p1227 N73-19975
Construction of remote controlled mechanical manipulators using biodynamic principles
[NASA-TT-F-14889] 12 p1374 N73-21152
BIOELECTRIC POTENTIAL
Electrophysiological sleep patterns of human and animal brains
[NASA-TT-F-740] 13 p1483 N73-22023
Bioelectrical activity differentiations in cat cortex during sleep inhibition
13 p1483 N73-22026
Interdependence of slow and rapid brain waves during sleep
13 p1483 N73-22027
Neuronal changes in cortical motor region cells during pharmacological induced sleep
13 p1483 N73-22028
Somnofunctional mapping of deep brain waves in neurological patients
13 p1484 N73-22029
Thalamic cat cell activities during sleep and wakefulness phases
13 p1484 N73-22030
Bioelectric activity and excitability of cat brain structures during sleep phases
13 p1484 N73-22031
Bioelectric activity changes in brains of sleeping children caused by aging factor
13 p1484 N73-22032
Centripetal acceleration for inhibiting cerebellar rat cortex activity
14 p1608 N73-23030
Comparison of electroencephalographic response patterns in man and monkeys to visually evoked cortical stimuli
[IZF-1972-24] 14 p1609 N73-23049
Effects of phosdrin on electrical brain potentials in squirrel monkeys
[FAA-AM-73-3] 18 p2109 N73-27056
Influence of N-type sound wave pressure rise time on guinea pig cochlear and acoustically evoked potentials
[ISL-31/72] 19 p2224 N73-27940
BIOELECTRICITY
Mechanical response of otolith-dependent units of cats to sinusoidal linear rotation
[AMRU-R-69-3] 02 p0132 N73-11068
Elastomeric extensometer for measuring surface area changes of human body caused by body expansion and contraction
[NASA-CASE-MFS-21049-1] 02 p0173 N73-11405
Neuroelectric oscillation in two parallel, single-unit pathways feeding back on single primary cell
[R-984-RC] 04 p0379 N73-13083
Change in impulse activity of neurons in respiratory center during electric stimulation of vestibular nerve and dorsal roots in spinal cord
24 p2882 N73-33017
State of blood filling and bioelectric activity of grain in circulatory hypoxia in healthy persons and individuals with early forms of autonomic vascular dysfunction
24 p2883 N73-33027
BIOENGINEERING
NT ANTHROPOMETRY
NT BIOINSTRUMENTATION
NT BIOMETRICS
NT BIOTELEMETRY
NT BODY MEASUREMENT [BIOLOGY]
NT ELECTROCARDIOGRAPHY
NT ELECTROENCEPHALOGRAPHY
NT ELECTROMYOGRAPHY
Biomedical electronics and solid state and quantum electronics research
[AD-745968] 02 p0151 N73-11225
Solid state electronics, information systems, plasma and quantum electronics, biomedical electronics, acoustics, and radio sciences
[AD-748281] 04 p0400 N73-13256
Power sources and requirements for human artificial hearts
[COO-2155-4] 05 p0503 N73-14095
Design and development of biomedical prosthetic and electronic devices
[NASA-CR-130022] 07 p0750 N73-16093
Electrocutaneous parameters for designing dynamic tactual communication system
12 p1373 N73-21135
Design of hemoglobin tester, flow ventilation systems, blood viscometer, isotope handling equipment, and blood pressure measuring device
[NASA-TM-X-66214] 12 p1373 N73-21139
Safe handling system for iridium isotopes used in radiation therapy
12 p1374 N73-21143
Bioelectric monitoring and motion picture surveying for improved physical training of astronauts
14 p1608 N73-23039
Biological development of human living environment
[NASA-TT-F-15005] 18 p2111 N73-27067
Interaction concept for improving efficiency of man machine systems
[JPRS-59149] 18 p2111 N73-27070
BIOGENESIS
U BIOLOGICAL EVOLUTION
BIOINSTRUMENTATION
NT BIOTELEMETRY
Design and attachment of skin electrodes in human cardiac monitoring during space flight
03 p0259 N73-12095
Applications of aerospace technology to biomedical research
[NASA-CR-129588] 04 p0378 N73-13071
Obtaining stable oxygen electrodes by coating with plasma catalyzed polymer film
[AD-748422] 04 p0383 N73-13120
Procedures and instrumentation for life detection on Mars
[NASA-CR-133186] 19 p2344 N73-28854
Biodetection grinder for sampling aerospace materials for microorganisms
[NASA-TM-X-64765] 20 p2372 N73-29059
Instrument for measurement of postural equilibrium in human beings
[AD-763096] 20 p2373 N73-29067
NASA bioinstrumentation list for public utilization
[NASA-SP-5958[01]] 23 p2750 N73-32007
BIOLOGICAL ACTIVITY
U ACTIVITY [BIOLOGY]
BIOLOGICAL ANALYSIS
U BIOASSAY
BIOLOGICAL CELLS
U CELLS [BIOLOGY]
BIOLOGICAL CLOCKS
U RHYTHM [BIOLOGY]

**BIOLOGICAL EFFECTS**
NT RELATIVE BIOLOGICAL EFFECTIVENESS [RBE]
Research on biological effects of microwave radiation
[MBL-1972-5] 01 p0008 N73-10060
Biological effectiveness of microwave field and human tolerance
[JPRS-57209] 01 p0009 N73-10073
Exposure distributions for air travelers and radiation workers at 0.54 millirem/year
[AD-743482] 01 p0011 N73-10083
Theoretical study of biological hazards from exposure to ELF electrical fields and potentials
[AD-743480] 01 p0012 N73-10093
Human and animal studies on both ionizing and nonionizing radiations
[PB-210613] 01 p0013 N73-10099
Research in aerospace and biological sciences
[AD-740761] 01 p0121 N73-11000
Annotated bibliography and indexes on aerospace medicine and biology - Aug. 1972
[NASA-SP-7011[106]] 02 p0130 N73-11054
Annotated bibliography and indexes on aerospace medicine and biology - July 1972
[NASA-SP-7011[105]] 03 p0256 N73-12073
Effects of whole body exposure to external radiations, using animal studies applied to man
[CONF-720108-2] 03 p0259 N73-12102
Estimation of censoring, truncation, transformation, and partial data vectors for predicting and measuring assembly performance in biological and physical situations
[NASA-CR-129503] 03 p0323 N73-12632
Conference on biological effects of magnetic fields
[NRC-TT-1545] 05 p0500 N73-14070
Effects of alterations in barometric pressure on humans
06 p0628 N73-15092
Biological effects of Viking Lander spacecraft engine fuel on extraterrestrial life during landing on planet Mars
[NASA-TM-X-2714] 06 p0630 N73-15118
Biosatellite 2 experiments for determining effects of prolonged weightlessness on biological processes
[CONF-720441-1] 06 p0630 N73-15119
Biological effects of microwave irradiation on humans - literature review
[UR-3490-29] 06 p0630 N73-15120
Bibliography on radio frequency and microwave radiation effects in biological systems
[AD-750271] 06 p0632 N73-15131
Bibliography of aerospace medicine and biology
[NASA-SP-7011[108]] 07 p0742 N73-16037
Physiology of depressed metabolic states and gastrointestinal responses to ionizing radiation
[NASA-CR-130381] 07 p0742 N73-16038
Effect of prolonged hypodynamia on rat biology
07 p0744 N73-16050
Abstracts on radiation and health physics
[BNWL-1651-VOL-2-PT-2] 07 p0746 N73-16069
Mortality and blood cell count variation in mice after irradiation with fast neutrons and X rays
[BMVG-FBWT-72-16] 07 p0747 N73-16077
Influence of 100 percent anhydrous ammonia environment on body functions
08 p0875 N73-17088
Occupational hazards and adverse biological effects of ultraviolet radiation
08 p0876 N73-17094
Annotated bibliography and indexes on Aerospace Medicine and Biology - December 1972
[NASA-SP-7011[109]] 09 p0992 N73-18094
Aerospace medicine for treating abnormal conditions caused by space flight
[NASA-TT-F-735] 09 p0994 N73-18116
Monte Carlo radiation transport computer codes for calculating dose distributions and cell survival probabilities
[NASA-CR-130965] 09 p0996 N73-18127
Influence of light flashes from heavy ionizing particles on astronaut nervous system
[LBL-1011] 10 p1120 N73-19134
Biological and toxicity effects of aluminum and other chemicals in animals
[ORNL-TIP/TIRC-72-76] 10 p1121 N73-19136
Annotated bibliography and indexes on aerospace medicine and biology - January 1973
[NASA-SP-7011[110]] 11 p1238 N73-20052
Research in space biology and medicine
[JPRS-58620] 11 p1243 N73-20094
Effect of chronic irradiation of dogs by Co60 gamma rays on level of autoantibodies
11 p1244 N73-20100
Effect of sonic boom on fish and fish eggs during developmental stage
[FAA-RD-73-29] 11 p1247 N73-20121
Annotated bibliography and indexes on aerospace medicine and biology
[NASA-SP-7011[112]] 12 p1367 N73-21087
Review of bibliography on medical and biological research during space flights
12 p1367 N73-21091
Drug effects on vision of flying personnel
12 p1371 N73-21121
Comparison of alcohol and dizepam effects on human mental and psychomotor functions
12 p1371 N73-21126
Apollo 16 experiment using biostack to determine effects of heavy nuclei on biological organisms
12 p1452 N73-21761
Physical and chemical characteristics, and biological activity of exhaust from beryllium-fueled motor
[AD-756531] 13 p1485 N73-22042
Annotated bibliography and indexes on aerospace medicine and biology for 1961 to 1965
[NASA-TT-F-14662] 14 p1610 N73-23053
Biological effects of sleep deprivation, and effects of prolonged work on performance under combat conditions
14 p1723 N73-23989
Annotated bibliography and indexes on Aerospace Medicine and Biology - February 1973
[NASA-SP-7011[113]] 15 p1739 N73-24099
Annotated bibliography and indexes on aerospace medicine and biology - January 1973
[NASA-SP-7011[111]] 15 p1739 N73-24100
Procedures for simulating and studying effects of subgravity on subjects during laboratory experiments and space flight
[NASA-TT-F-14934] 15 p1761 N73-24267
Environmental impact of increased intensities of solar ultraviolet radiation resulting from operation of supersonic transport aircraft
[PB-215524/0] 16 p1862 N73-25079
Modified high pressure system with small sample vessels for conducting biological reactions
[AD-752978] 16 p1885 N73-25256
Annotated bibliography and indexes on Aerospace Medicine and Biology - April 1973
[NASA-SP-7011[114]] 17 p1986 N73-26055
Proving solar activity effect on biosphere by correlation between activity indices with biological indices
[NASA-TT-F-14984] 17 p2079 N73-26821
Significance of biological factors in weathering of rocks and minerals
[NASA-TT-F-14892] 18 p2142 N73-27316
Wing anomalies as result of weightlessness simulation for flour beetle Tribolium confusum
19 p2226 N73-27952
Environmental and medical problems caused by nonionizing radiation
[PB-220851/0] 21 p2509 N73-30134
Influence of solar activity on biological indices and disease of living organisms in biosphere
[NRC-TT-1679] 21 p2592 N73-30771
Annotated bibliography and indexes on aerospace medicine and biology - September 1973
[NASA-SP-7011[119]] 24 p2882 N73-33012
Influence of continuous and discontinuous exposure to carbon monoxide on animals
24 p2882 N73-33019
Biological evaluation of influence of helium-oxygen atmosphere on culture of mammalian cells
24 p2883 N73-33024

**BIOLOGICAL EVOLUTION**
NT ABIOGENESIS
Isotopic composition of carbon in Precambrian graphitoids from various parts of the USSR
[NASA-TT-F-14682] 08 p0918 N73-17520
Biostatistics of genetical processes in human populations
[NASA-CR-131508] 12 p1372 N73-21131
Handbook on structural evolution of vestibular apparatus
14 p1609 N73-23044
State and prospects of biogeocenological research
[JPRS-59395] 18 p2109 N73-27053
Search for biological life forms on Mars and other planets
22 p2619 N73-30985

**BIOLOGICAL MODELS**
U BIONICS

**BIOLOGICAL RHYTHM**
U RHYTHM [BIOLOGY]

**BIOLOGY**
Summaries of research in mathematics, physics, chemistry, biophysics-biochemistry, and biology, and related reports - Weizmann Institute of Science
01 p0119 N73-10977
Research in aerospace, biological, and solar sciences
[AD-746143] 02 p0133 N73-11080
Bibliography of wildlife movements and tracking systems
[NASA-CR-130380] 07 p0742 N73-16040
Applications of aerospace technology in biology and medicine
[NASA-CR-130544] 08 p0871 N73-17047
Bibliography of aerospace medicine and biology
[NASA-SP-7011[116]] 21 p2500 N73-30059
Summary of biochemistry and biology research projects
[NASA-CR-135650] 22 p2667 N73-31366

**BIOLUMINESCENCE**
Characteristics of photogenic bacteria - Micrococcus pierantonii
[NASA-TT-F-14439] 02 p0132 N73-11072
Photometric observations of in situ fluorescence and bioluminescence with Biota in New York Bight
[RM-568J] 13 p1479 N73-21978
NASA supported research in photobiology and photochemistry from 1966 to 1973
[NASA-CR-133459] 19 p2224 N73-27937

**BIOMECHANICS**
U BIODYNAMICS

**BIOMEDICAL DATA**
Neurophysiology and dynamic response of vestibular system to angular and linear acceleration
[DR-215] 02 p0130 N73-11057
Influence of 45 to 60 day space flight on physiological functions of human body
[NASA-CR-129131] 02 p0132 N73-11074
Biomedical electronics and solid state and quantum electronics research
[AD-745968] 02 p0151 N73-11225
Technology utilization in biomedical areas for November 1972
[NASA-CR-129998] 06 p0632 N73-15135
Utilization of aerospace technology in biomedical field - Southwest Research Institute report for Jan. 1973
[NASA-CR-130984] 09 p0992 N73-18097
Technology transfer of biomedical data for use in research of cardiovascular diseases
[NASA-CR-131246] 11 p1238 N73-20053
Review of published bibliographical index of Soviet and foreign literature on biomedical problems in space
11 p1246 N73-20115
Application of systems analysis techniques to improve management controls within biomedical research programs
[NBS-TN-761] 13 p1478 N73-21977
Physical and biomedical research by earth orbiting space stations
[AD-756771] 15 p1743 N73-24126
Space biology, space medicine, and human physiology
[NASA-TT-F-14964] 16 p1867 N73-25116

**BIOMETRICS**
NT ANTHROPOMETRY
NT BODY MEASUREMENT [BIOLOGY]
NT ELECTROCARDIOGRAPHY
NT ELECTROENCEPHALOGRAPHY
NT ELECTROMYOGRAPHY
Transducer for converting arterial pulse wave into electric signals
[NASA-CASE-GSC-11531-1] 02 p0135 N73-11097
Accelerometers, electromyogram sensors, and telemetry system for measuring human body segment motions
[AD-751134] 07 p0751 N73-16104
Computer program for evaluating biological parameters
[ISS-72/4] 10 p1120 N73-19128
Biometric and radiant transfer characteristics of forest vegetation
20 p2405 N73-29328

**BIONICS**
Pattern recognition by devices consisting of arrays of cooperating elements
[PB-211238] 05 p0503 N73-14096
Soviet bibliography on biocybernetics material received from Jan. to May 1972
[AD-750129] 06 p0636 N73-15167
Artificial intelligence in integrated circuit control of bionic manipulators
[NASA-CR-131403] 11 p1251 N73-20156
Binocular vision models for designing image distortion compensation system
16 p1920 N73-25534

**BIOPAKS**
Mathematical model for photosynthetic gas exchanges in growing wheat and radish biopaks of life support systems
03 p0257 N73-12081

**BIOPHYSICS**
NT HEALTH PHYSICS
Biophysics topics involving radiation data inversion problems
02 p0201 N73-11624
Biophysical mechanisms of noninvasive measurement of CVP in man
[NASA-CR-130348] 07 p0742 N73-16039
Detailed information of physics subfields and interface areas
[NASA-CR-132050] 15 p1813 N73-24693
Research on plasma physics, information theory, biophysics, and data processing systems
[AD-765002] 23 p2867 N73-32919

**BIOREGENERATION**
U REGENERATION [PHYSIOLOGY]

**BIOREGENERATIVE LIFE SUPPORT SYSTEMS**
U CLOSED ECOLOGICAL SYSTEMS

**BIOSATELLITE 2**
Dosimetric analyses for Biosatellite 2 yeast and artemia radiation exposure experiment
[NASA-CR-127142] 04 p0379 N73-13082
Biosatellite 2 experiments for determining effects of prolonged weightlessness on biological processes
[CONF-720441-1] 06 p0630 N73-15119

**BIOSATELLITES**
NT BIOSATELLITE 2

**BIOSENSORS**
U BIOINSTRUMENTATION
**BIOSIMULATION**
U BIONICS
**BIOSPHERE**
U EARTH HYDROSPHERE
U LOWER ATMOSPHERE
**BIOSYNTHESIS**
Biosynthesis of unsaturated fatty acids in yeast
[NASA-TT-F-13918] 01 p0009 N73-10068
Effects of hyperoxia on heme biosynthesis
[AD-756836] 15 p1742 N73-24125
**BIOTECHNOLOGY**
Proceedings of conference on manual control to show interplay between man and machine and application of control theory in medicine and psychology
[NASA-CR-131244] 11 p1235 N73-20028
Aerospace biotechnology research projects
[AD-759277] 16 p1869 N73-25135
Interaction concept for improving efficiency of man machine systems
[JPRS-59149] 18 p2111 N73-27070
**BIOTELEMETRY**
Ultrasonic marine biotelemetry transmitter utilizing metal oxide semiconductor integrated circuits
[AD-748605] 04 p0383 N73-13119
Satellite system for tracking of wildlife and birds in natural environment
[NASA-CR-130301] 06 p0627 N73-15090
Accelerometers, electromyogram sensors, and telemetry system for measuring human body segment motions
[AD-751134] 07 p0751 N73-16104
Multichannel medical monitoring system to measure physiological parameters from display device at remote control station
[NASA-CASE-MSC-14180-1] 13 p1486 N73-22045
Telemetry experiments with hibernating bear
[NASA-CR-133926] 22 p2620 N73-31000
**BIOTITE**
Temperature effects on quantitative biotite and nepheline decomposition by weather
[NASA-TT-F-15135] 23 p2754 N73-32035
**BIPLANES**
Aerodynamic characteristics of biplane wing systems with emphasis on stall matching and induced camber effects which differ from monoplane wing
08 p0864 N73-16987
**BIPOLAR TRANSISTORS**
Sensitivity of microwave transistor amplifiers to neutron damage in low noise and high power applications
[SC-R-72-2845] 07 p0762 N73-16190
LINVILL and IBIS programs for calculating gamma radiation damage to biopolar transistors
[CEA-R-4337] 10 p1194 N73-19718
**BIPROPELLANTS**
U LIQUID ROCKET PROPELLANTS
**BIRDFOOT DELTAS**
U DELTAS
**BIRDS**
Feasibility of obtaining estimate of waterfowl production using remote sensing technology
[USGS-IR-215] 02 p0165 N73-11343
Changes in continental migratory bird and wildlife habitats
[E72-10235] 03 p0288 N73-12335
Migration corridors for ducks and geese and effects on aviation safety
[AD-748114] 04 p0382 N73-13109
Satellite system for tracking of wildlife and birds in natural environment
[NASA-CR-130301] 06 p0627 N73-15090
Wind tunnel tests to determine structural integrity of birds under conditions simulating ingestion of birds into inlets of high speed aircraft
[NASA-TM-X-68163] 06 p0629 N73-15114
Monitoring continental migratory bird habitats
[E73-10065] 07 p0779 N73-16327
Doppler effect continuous wave radar for bird hazard detection and aircraft collision avoidance near airfields
[AD-751985] 08 p0885 N73-17168
Study of continental migratory bird habitat changes using ERTS-1 imagery
[E73-10334] 09 p1025 N73-18364
Effect of high intensity laser outputs on behavior and physiology of birds to determine application for reduction of flight hazards
[AD-754269] 11 p1236 N73-20038
Avian hazards to Air Force rocket sled test tract at Holloman AFB, New Mexico
[AD-755833] 12 p1389 N73-21261
Appraisal of changes in migratory bird habitats based on ERTS-1 imagery of North Dakota
[E73-10534] 13 p1518 N73-22298
Statistical correlation of gulls and USAF aircraft hazards
[AD-759824] 16 p1863 N73-25092
Aircraft accident involving Lear jet aircraft following takeoff from Atlanta, Georgia Airport on 26 Feb. 1973
[NTSB-AAR-73-12] 17 p1984 N73-26036
ERTS-1 and aircraft multispectral scanner data for mapping ponds and lakes near Woodworth, North Dakota to determine changes in continental migratory bird habitat
[E73-10714] 17 p2018 N73-26321
Analysis of flight hazards caused by bird strikes on aircraft flying in Panama Canal Zone
[AD-763112] 20 p2362 N73-28997
Appraising changes in continental migratory bird habitats in North Dakota using Skylab EREP system
[E73-10972] 22 p2657 N73-31284
Bird migration patterns using radio transmitters with application to reduction of aircraft hazards during migration in congested air routes
[AD-764830] 23 p2746 N73-31983
Utilization of Skylab EREP system for appraising changes in continental migratory bird habitats
[E73-11079] 23 p2782 N73-32254
**BIREFRINGENCE**
Rotating analyzer method for rapid measurement of polarized light produced by birefringent materials
[AD-750545] 06 p0701 N73-15713
Pockels cell for splitting light pulses from NdYAG mode locked pulsed laser
[AD-751532] 07 p0807 N73-16550
Birefringence properties of total reflection of light beam at separation plane
[LPTHE-72/39] 10 p1188 N73-19668
**BIREFRINGENT COATINGS**
Strain measurement of viscoelastic solid propellant materials with birefringent coating
[NAL-TR-261] 04 p0461 N73-13765
**BISMUTH**
Neutron activation analysis applied to determine bismuth content of meteorites and standard rocks
07 p0840 N73-16809
Quantitative bismuth determination in stainless steels
[PB-214234/7] 16 p1929 N73-25612
Influence of hydrostatic pressure on ductility and fracture mechanics of bismuth and tin-bismuth alloys
[AD-764241] 22 p2686 N73-31514
**BISMUTH ALLOYS**
Galvanomagnetic and thermoelectric properties of monocrystalline alloys of bismuth and antimony at liquid nitrogen temperature
[AD-745865] 01 p0089 N73-10734
Metal-dielectric phase transitions in Bi-Sb alloys and V2O3
[JPRS-57631] 04 p0433 N73-13525
Influence of hydrostatic pressure on ductility and fracture mechanics of bismuth and tin-bismuth alloys
[AD-764241] 22 p2686 N73-31514
**BISMUTH COMPOUNDS**
NT BISMUTH OXIDES
Hall resistivity and electromagnetic properties of bismuth selenide crystals for cryogenic magnetometers
[NASA-TN-D-7057] 03 p0344 N73-12809
Computer processing for calculating optical constants from reflectance data of InBi
05 p0609 N73-14952
Waveguiding in thin silver strip vacuum deposited on bismuth germanium oxide
[AD-750612] 06 p0648 N73-15262
Production of ferromagnetic MnBi thin films by optical control of vacuum deposition and annealing
[KFKI-72-70] 10 p1199 N73-19757
Piezo- and thermo-optical properties of bismuth germanium oxide single crystals
17 p2071 N73-26754
**BISMUTH OXIDES**
Pulse-echo technique for measuring ultrasonic attenuation in Bi12GeO20 single crystals at low temperature
16 p1952 N73-25798
**BISPHENOLS**
Dynamic mechanical analysis of reactions of aromatic diamines with diglycidyl ether of bisphenol A for application to epoxy thermosetting systems
[AD-759995] 17 p2052 N73-26602
**BISTABLE AMPLIFIERS**
U FLIP-FLOPS
**BISTATIC REFLECTIVITY**
Bistatic target areas of three simple targets for seven bistatic angles
[FOA-3-C-3676-E1] 02 p0172 N73-11393
Design, development, and evaluation of bistatic radar processor for synchronizing rotation rate of plan position indicator display
[AD-756515] 13 p1495 N73-22121
**BIT SYNCHRONIZATION**
Optimum design of format synchronizer for ESRO control center
[ESRO-CR[P]-127] 02 p0141 N73-11143
Bit synchronization of PCM communications signal, without separate synchronization channel by digital correlation
[NASA-CASE-NPO-11302-1] 04 p0388 N73-13149
Analysis and simulation of telemetry receivers and bit synchronizers
[NASA-CR-132809] 21 p2507 N73-30120
Synchronization method for pseudorandom binary data sequences in blockwise transmission of nonoverlapping subsequences, based on digital correlation
[FTZ-A-157-TBR-7] 22 p2632 N73-31095
Asynchronous and synchronous time division multiplex systems of 8.448 and 8.192 Mbit/s
[FTZ-442-TBR-40] 22 p2634 N73-31106
Digital synchronization of airborne collision avoidance systems
[DGLR-PAPER-73-012] 23 p2817 N73-32519
**BITERNARY CODE**
Three level transmission code for digital broadcast signal network
[BBC-RD-1973/21] 24 p2894 N73-33101
**BLACK AND WHITE PHOTOGRAPHY**
Analysis of characteristic curves of various black and white photographic films and processing methods for typical conditions
[NASA-TT-F-13920] 01 p0058 N73-10473
Comparison of methods for determining transfer functions of black and white aerial photographic films
[AD-747594] 03 p0304 N73-12483
Feasibility of multispectral signal encoding on black and white film
[AD-749495] 05 p0548 N73-14455
Linear estimation technique for enhancement of black and white images
[AD-760779] 18 p2180 N73-27601
Algorithm for assembling continuous boundaries and contours from black and white picture for computer processing and photointerpretation
[NPL-COM-66] 22 p2675 N73-31426
**BLACK BODY RADIATION**
Physical-statistical inference model using satellite infrared data for estimating cloud distribution from empirical histographs of equivalent black body temperatures
04 p0441 N73-13597
Microwave radiometer technique for detecting and identifying man-made objects and discriminating them from natural objects
[DREO-R-661] 04 p0449 N73-13669
Application of infrared technology for measuring infrared radiation emitted by military aircraft
[AD-749798] 06 p0623 N73-15058
Black body heat capacity and action at distance electrodynamics
[ORO-3992-97] 12 p1429 N73-21578
Black body brightness in horizontal visual range theory
[NASA-TT-F-14930] 15 p1814 N73-24700
Black body temperature of double pyrgeometer with two net radiometers
20 p2403 N73-29313
Numerical analysis of one form of distribution of spectral energy density of thermal radiation
[JPRS-59660] 20 p2485 N73-29958
Satellite infrared radiometer observation of hurricane intensification
22 p2736 N73-31906
**BLACK BRANT SOUNDING ROCKETS**
Preflight tests and performance of electronic instrumentation in measuring solar radiation during Aerobee 170 and Black Brant V rockets
[AD-756909] 13 p1532 N73-22412
Bubble formation analysis in plain and fiber reinforced metals melted and solidified under weightless conditions, using Aerobee and Black Brant rocket vehicles
[NASA-TM-X-64665] 16 p1964 N73-25886
Black Brant rocket measurements of proton and alpha particle fluxes
[AD-760138] 17 p2028 N73-26417
**BLACK HILLS [SD-WY]**
Investigation of forest stress in Black Hills, forest inventory at Atlanta test site, and rangeland inventory at Manitou test site using ERTS-1 imagery
[E72-10219] 02 p0162 N73-11313
Remote detection of insect damage and stress symptoms in forests of Black Hills
07 p0785 N73-16389
Forest and rangeland inventory and forest infestation of Atlanta, Manitou, and Black Hills test sites based on ERTS-1 imagery
[E73-10084] 08 p0901 N73-17296
Inventory of forest and rangeland and detection of insect infestation from ERTS-1 imagery of Black Hills, Atlanta, and Manitou test sites
[E73-10407] 11 p1278 N73-20369
Inventory of forest and rangeland and detection of forest stress at Black Hills, South Dakota, Atlanta, Georgia, and Manitou Forest test sites using ERTS-1 data
[E73-10546] 14 p1655 N73-23421
Inventory of forests and rangelands, including forest stress, at Black Hills, Atlanta, Georgia, and Manitou, Colorado test sites using Skylab EREP
[E73-10587] 14 p1657 N73-23447
Application of ERTS-1 imagery for tectonic analysis of Bighorn Mountains region and effect of snow cover and low sun angle on identifying topographical features
[E73-10722] 17 p2019 N73-26329
Inventroy of forest and rangeland resources at Atlanta, Georgia, Black Hills, South Dakota, and Manitou, Colorado test sites using Skylab EREP imagery
[E73-10749] 18 p2133 N73-27237

Detection and inventory of timber and rangelands and forest stresses in Georgia, Colorado, and Black Hills from ERTS-1 imagery
[E73-10805] 18 p2138 N73-27280
DCP-collected absolute target reflectance measurements to assist interpretation of ERTS-1 imagery of forest stresses in Black Hills, South Dakota
19 p2283 N73-28365
Skylab inventory of forest and rangeland resources and forest stresses at Atlanta Georgia, Manitou, Colorado, and Black Hills test sites
[E73-10895] 20 p2395 N73-29244
Inventory of forest and rangeland resources and stresses at Atlanta, Georgia, Black Hills, South Dakota, and Manitou, Colorado from Skylab EREP
[E73-11040] 23 p2778 N73-32219
Timber identification and inventory and forest management in Colorado, Georgia, Black Hills, California, and Hawaii from ERTS-1 imagery
[E73-11051] 23 p2779 N73-32227
Forest and rangeland inventory and detection of forest stress at Black Hills, South Dakota, Manitou, Colorado, and Atlanta, Georgia test sites
[E73-11052] 23 p2779 N73-32228
Tectonic analysis of Bighorn Mountains of Montana and Wyoming and Black Hills of South Dakota and Wyoming from Skylab imagery
[E73-11151] 24 p2919 N73-33305

**BLACK HOLES [ASTRONOMY]**
Spherical and nonspherical gravitational collapse and Schwarzschild black holes
15 p1829 N73-24822
Global properties of collapsing matter [black holes]
[JINR-E2-6831] 15 p1832 N73-24850
Development of symmetric stress-energy-momentum pseudo-tensor for gravitational fields of Brans-Dicke theory and application to formation of black holes
24 p2978 N73-33800

**BLACK SEA**
Bora on Adriatic and Black Sea coasts - bibliographies
05 p0571 N73-14637

**BLACKOUT [PHYSIOLOGY]**
NT BLACKOUT PREVENTION

**BLACKOUT [PROPAGATION]**
NT ATMOSPHERICS
NT DAWN CHORUS
NT ELECTROMAGNETIC NOISE
NT HISS
NT IONOSPHERICS
NT SHOT NOISE
NT WHISTLERS
Near field characteristics of radio antenna when covered by plasma sheath to determine current distribution, input admittance, and radiation pattern
[NASA-CR-130076] 01 p0024 N73-10184
Multicomponent electron collision frequency model for predicting signal attenuation in plasma sheath surrounding reentry vehicle
[AD-750553] 05 p0585 N73-14758
Development of viscous shock layer analysis to determine nonequilibrium flow distributions of plasma layer during reentry conditions
[NASA-CR-2232] 13 p1491 N73-22085
Calculation of lower bounds of blackout of plasma-covered antennas
[AD-759790] 16 p1881 N73-25227

**BLACKOUT PREVENTION**
Reducing rainfall-induced blackouts by space diversity for millimeter wave, earth satellite communications systems
[AD-747022] 02 p0143 N73-11162

**BLADDERS [MECHANICS]**
U DIAPHRAGMS [MECHANICS]

**BLADE TIPS**
Development of rotary wings with cold, hot, and mixed cycle tip jet propulsion systems and application for torque-free rotor drive system
12 p1359 N73-21026
Procedures for measuring velocity distribution through helicopter rotor blade tip vortex using single full scale rotor blade
12 p1360 N73-21034
Aerodynamic effects of blade tip clearance in axial flow turbine lifting line for nonuniform flow, calculating lift and induced drag
[REPT-4/1973] 19 p2329 N73-28738
Capacitive method for measuring blade tip clearance in running turbocompressors
[DLR-FB-72-40] 23 p2831 N73-32628

**BLASIUS FLOW**
Numerical analysis of effect of boundary layer profile on dynamic response and acoustic radiation of thin, elastic, flat plates
[NASA-TM-X-69568] 21 p2523 N73-30232

**BLAST DEFLECTORS**
Performance tests of F-14 aircraft with jet blast deflector to determine effects of backflow of jet exhaust on aircraft launch operation
[AD-752018] 08 p0867 N73-17023
Criteria on jet blast velocities and effects during operation of commercial aircraft and recommended procedures to reduce adverse impact
[AC-150/5325-6A] 11 p1266 N73-20271

**BLAST LOADS**
Shock tube generated blast loads on panels in steel structures
[REPT-1/72] 02 p0237 N73-11926
Shock wave propagation and attenuation in tunnels noting computer programming based on method of characteristics
[ISL-11/72] 04 p0406 N73-13307
Response of cylindrical shells to traveling load simulation of x ray blow-off impulse
[AD-750536] 06 p0727 N73-15933
Dynamic and static response to blast loads of thin circular plates free or embedded using Timoshenko model and finite difference theory
[ISL-4/72] 09 p1094 N73-18934
Proposed computer program for dynamic analysis of elasto-plastic, thin, isotropic plates of rectangular planform subjected to blast loads
[AD-752449] 09 p1096 N73-18947
Dynamic functions of air blast parameters in detonation of spherical trinitrotoluene charge
[AD-753805] 10 p1187 N73-19659
Containment design calculations for cylindrical vessel wall response to explosion
[SLA-73-508] 24 p2992 N73-33916

**BLASTOFF**
U ROCKET LAUNCHING

**BLEED-OFF**
U PRESSURE REDUCTION

**BLIGHT**
Management and use meteorological satellite data to detect severe storms and crop disease
[NASA-CR-130000] 06 p0693 N73-15642
Meteorological satellites for detecting and aiding southern corn leaf blight disease
06 p0693 N73-15645
Multispectral remote sensing techniques for identification of corn blight disease
[NASA-TM-X-69055] 07 p0745 N73-16064
Handling and analysis of remote sensing data on 1971 corn blight
[NASA-CR-130368] 07 p0759 N73-16164
Anomalous scattering effects of haze layer in remote sensing data on corn blight distribution
[NASA-CR-130028] 07 p0790 N73-16428
Photometric observations of in situ fluorescence and bioluminescence with Biota in New York Bight
[RM-568J] 13 p1479 N73-21978

**BLINDNESS**
NT FLASH BLINDNESS
Design and performance of metal oxide semiconductor analog shift register as image sensor and reading aid for blind persons
[AD-753259] 09 p1075 N73-18776
Blind fish responses to gravitational changes as in parabolic flight
12 p1368 N73-21101
Need and feasibility of automatic speech reading machines for blind people
14 p1620 N73-23121
System of morphemic decomposition for improvement in Braille transcription
14 p1621 N73-23128
Temporary blindness of monkeys caused by combined effects of phosdrin and atropine exposure
[FAA-AM-73-4] 18 p2109 N73-27055

**BLISTERS [PROTUBERANCES]**
U PROTUBERANCES

**BLOCK ISLAND SOUND [RI]**
Analysis of ERTS-1 data for interdisciplinary study of estuarine and coastal oceanography of Block Island Sound and adjacent New York coastal waters
[E73-10735] 17 p2020 N73-26341
Analysis of ERTS-1 data for interdisciplinary study of estuarine and coastal oceanography of Block Island Sound and adjacent New York coastal waters
[E73-10736] 17 p2020 N73-26342
Color enhancement of ERTS-1 imagery of estuarine and coastal oceanography of Block Island Sound and adjacent New York coastal waters
[E73-10819] 18 p2140 N73-27294
Estuarine and coastal oceanography of Block Island Sound and adjacent New York coastal waters
[E73-10968] 21 p2533 N73-30310
Spectroradiometric calibration of EREP imagery and oceanography of Block Island Sound
[E73-11015] 22 p2660 N73-31319

**BLOCKING**
Semicircular canal plugging response in cats to rotary stimulation
06 p0634 N73-15151
Transonic wind tunnel wall effects on boundary layer blocking phenomena
15 p1766 N73-24306
Biennial periodicity of blocking systems in atmosphere over Europe-Atlantic region considering cyclonic circulation
[NLL-M-22831-[5828.4F]] 16 p1936 N73-25661

**BLOCKS**
Capacity of geometric codes and increased effectiveness of semiconductor storage units using number block structures
[JPRS-57251] 02 p0145 N73-11177
Computer program for block analytical aerotriangulation adjustment with independent models
02 p0164 N73-11335
Horizontal accuracy of computerized planimetric block triangulation with independent models
02 p0164 N73-11336
Computerized horizontal block adjustment for aerial mapping using large numbers of points
02 p0165 N73-11337

**BLOOD**
NT ERYTHROCYTES
NT LYMPHOCYTES
Verification program for Inflight Blood Collection system
[NASA-CR-128645] 03 p0261 N73-12112
Bacterial reduction of organically bound phosphoric acid in blood
[NASA-TT-F-14723] 04 p0379 N73-13080
Research on laser irradiation effects, sensory psychophysiology, and human blood processing for military medicine
[AD-749440] 06 p0631 N73-15130
Oxygen content and hydrogen ion concentration in monkey blood after incapacitating ionizing radiation dosage
[AD-750681] 06 p0632 N73-15134
Mortality and blood cell count variation in mice after irradiation with fast neutrons and X rays
[BMVG-FBWT-72-16] 07 p0747 N73-16077
Stabilization methods in collecting and shipping of human sera for chemical analyses
08 p0871 N73-17053
Multiple immunoassay system for determining parathyroid hormone, calcitonin, and vitamin D in human blood
09 p0994 N73-18112
Prolonged bed rest effects on human blood hormone level periodicities
09 p0994 N73-18114
Guide to units and interpretation of blood alcohol measurements
[DCIEM-TM-848] 09 p0995 N73-18120
Effect of hypoxia and hyperoxia on rate of blood deoxygenation, and influence of antioxidants in mice
11 p1244 N73-20096
Effect of hypokinesis of varying duration on fluid-electrolyte metabolism and composition in blood and tissues of animals
11 p1244 N73-20098
Morphological composition of peripheral blood of crew members of Soyuz-9 and Salyut-1
11 p1245 N73-20104
Toxicological properties of rocket exhaust products and blood analysis for beryllium oxide content
[AD-754936] 11 p1248 N73-20131
Methods for determining blood alcohol levels in pilots
12 p1371 N73-21124
Lower body negative pressure for preventing body fluid shifts during weightlessness
13 p1482 N73-22017
Respiratory function and blood acid base equilibrium in human adaptation to high altitude environment
20 p2366 N73-29030
Development and progress in theoretical and scientific disciplines
[JPRS-59769] 20 p2487 N73-29981
Food consumption and morphollogical indices of blood in white mice with replacement of air nitrogen by inert gases in pressurized chamber
24 p2882 N73-33020
Effect of fibrinogen concentration on viscosity of human blood
[DLR-FB-73-54] 24 p2886 N73-33046

**BLOOD CIRCULATION**
NT BRAIN CIRCULATION
NT CARBOXYHEMOGLOBIN
NT ISCHEMIA
NT PULMONARY CIRCULATION
Simulated high altitude determination of interrelation of systematic and cellular responses to acute and chronic hypoxia
[AD-743536] 01 p0010 N73-10081
Circadian rhythm change study of transmeridian flight and medication effects on mildly hypertensive subject
[AD-743300] 01 p0011 N73-10090
Influence of Pervitin in decreasing gas bubbles in blood during decompression
[DLR-FB-72-66] 09 p0994 N73-18117
Influence of immersion in temperature controlled bath on circulation and water balance in human body
[NASA-TT-F-14834] 10 p1119 N73-19124
Effect of transverse overloads and gamma rays at 100 to 200 r on peripheral blood in dogs
11 p1242 N73-20083
Comparison of peripheral blood of acclimatized and nonacclimatized irradiated rats under prolonged conditions of reduced barometric pressure
11 p1243 N73-20088
Change in content of gases in blood when man is exposed to high ambient temperatures
11 p1245 N73-20105
Human regional blood circulation changes during bed rest experiment
13 p1482 N73-22012
Changes in human cerebral circulation during prolonged bed rest test
13 p1483 N73-22020

Lower body decompression effects on cardiac cycle and human acceleration tolerance
14 p1608 N73-23037
Long term bed rest effects on human retinal blood circulation and intraocular pressure
14 p1608 N73-23038
Distribution parameter model for acceleration forces acting on arterial system
[AD-756530] 15 p1743 N73-24128
Numerical solution of viscous fluid flow in finite tube with deformable walls in presence of valves for application to blood circulation process
16 p1867 N73-25117
Temperature interrelationships between rat brain tissues and cerebral blood supply
20 p2366 N73-29026
Human circadian rhythms of blood circulation, respiration and catabolism under flight simulation stress
[DLR-FB-72-49] 21 p2501 N73-30073

BLOOD COAGULATION
Oxygen redox processes in blood coagulation mechanism
03 p0257 N73-12079

BLOOD FLOW
Design of relative velocity blood viscometer
12 p1373 N73-21142
Blood supply to skeletal muscles of rats during hypokinesia
24 p2882 N73-33018

BLOOD PLASMA
Complete activity of lactate dehydrogenase and isoenzymes in plasma and myeloid cells
[NASA-TT-F-14586] 01 p0009 N73-10070
Blood plasma hyperosmolality and antidiuretic hormone inhibition in alcoholic intoxication
[NASA-TT-F-13910] 02 p0133 N73-11079
Behavior of enzyme activities in blood plasma after breathing hyperbaric oxygen
[DLR-FB-71-96] 06 p0635 N73-15163
GAST and GALT aminotransferases activity of dog blood serum following total exposure to gamma rays with stomach or head shielded
11 p1241 N73-20075
Effect of acute and chronic hypercapnia on Ca and inorganic P levels in guinea pig blood plasma and erythrocytes
[AD-749323] 13 p1484 N73-22035
Renin-angiotension system in simulated hypervolemia induced by immersion
[NASA-TT-F-14885] 13 p1484 N73-22036
Influence of transverse accelerations on electrolyte composition of plasma and erythrocytes
24 p2884 N73-33030
Using lower body negative pressure to prevent decrease in volume of circulating plasma during hypokinesia
24 p2885 N73-33036

BLOOD PRESSURE
NT HYPERTENSION
Weight, blood pressure, and intraocular pressure in young healthy males prior to and after 50-km walk
[NASA-TT-F-14557] 02 p0132 N73-11071
Influence of elastic properties of human body on arterial blood pressure measurement
05 p0500 N73-14072
Biophysical mechanisms of noninvasive measurement of CVP in man
[NASA-CR-130348] 07 p0742 N73-16039
Blood pressure and cholesterol level screening for preventing heart diseases in flight crews of commercial airline
08 p0874 N73-17076
Initial systole and dicrotic notch detecting circuitry for monitoring arterial pressure pulse
[NASA-CASE-LEW-11581-1] 09 p0997 N73-18139
Design and performance of strain gage transducer as blood pressure recording device
12 p1374 N73-21144
Effects of hydrostatic water bath pressure on capillary blood pressure and connective tissue dehydration
[NASA-TT-F-14894] 14 p1610 N73-23052
Measurement of arterial pressure under influence of ODNT
[NASA-TT-F-15087] 23 p2749 N73-31998
Measurement of arterial pressure by tachooscilloscope method
[NASA-TT-F-15088] 23 p2751 N73-32016
Functional disturbances during hypokinesia in man
[NASA-TT-F-15148] 24 p2890 N73-33073

BLOOD VESSELS
NT ARTERIES
NT GLOMERULUS

BLOOD VOLUME
Radionuclide measurements on plasma and red cell mass volume losses in Apollo spacecrews
09 p0993 N73-18106
Biophysical properties of human red blood cells exposed to hypobaric hyperoxia
[AD-755783] 14 p1612 N73-23072

BLOWDOWN WIND TUNNELS
Modane-Avrieux transonic blowdown wind tunnel for two dimensional flow airfoil profile study
[ONERA-NT-203] 15 p1762 N73-24281

BLOWING
Vortex sheet and increased lift caused by blowing from leading edges of slender delta wing
[ARC-R/M-3692] 09 p0981 N73-18016
Wind tunnel tests of blowing on circular cylinders applied to aircraft control and braking at low speeds
[ARC-CP-1232] 10 p1104 N73-19000
Integral equations for calculating incompressible potential flows around profiles with suction and blowing
[NASA-TT-F-14962] 18 p2130 N73-27209
Vectored injection into non-adiabatic boundary layer flows including incipient separation
[VPI-AERO-003] 19 p2255 N73-28176

BLUE GREEN ALGAE
Effect of toxic substances on algae by observing photosynthesis determined by oxygen production of algae
[DRIC-TRANS-2991] 10 p1121 N73-19139
Simazine influence on green algae photosynthetic pigments noting chlorophyll luminescence spectra
[DRIC-TRANS-2992] 13 p1485 N73-22040
Influence of blue green algae on crystalline calcium carbonate formation on river rocks
[NASA-TT-F-15028] 20 p2368 N73-29046

BLUFF BODIES
Methods used with fluid mechanics reference data on external flow to predict forces exerted on bodies of non-streamline shape
[ESDU-FME-1] 01 p0039 N73-10304
Characteristics of flow around bluff body at supersonic speed with emphasis on leading shock wave formation and changes in withdrawal value for argon and nitrogen
[AD-747407] 03 p0287 N73-12325
Research facility for studying noise generated by bluff body flow interaction inside ducted fuel combustion system
[AD-754094] 11 p1268 N73-20286
Development of flow visualization techniques for determining aerodynamic characteristics of bluff bodies under unsteady flow conditions
[AD-759266] 16 p1892 N73-25311

BLUNT BODIES
Inverse method for calculating hypersonic flow shock layer around axisymmetrical two-dimensional blunt bodies
[ISL-42/71] 01 p0041 N73-10325
Analysis of diffusive separation in front of blunt body in low density binary mixture of supersonic flows using electron beam densitometer
[AD-745960] 02 p0157 N73-11274
Numerical analysis of viscous-inviscid interaction in supersonic flow around blunt body
[AD-746891] 02 p0160 N73-11293
Effect of heat transfer level on mechanical properties of elastomeric ablative material used on spherically blunted cones
[NASA-TM-X-2612] 02 p0191 N73-11548
Asymptotic solution of two-dimensional flow of perfect gas past blunt body at given Mach number
[AD-747545] 03 p0287 N73-12327
Wake transition of blunt cones in hypersonic flight using schlieren photography and opto-electronic laser system
[ISL-12/72] 03 p0310 N73-12531
Base pressure effect of external shocks or expansions intersecting wake of two dimensional blunt body in supersonic flow
04 p0403 N73-13285
Development of mathematical model for viscous inviscid interaction analysis and solution of boundary layer equations by finite difference scheme
[AD-748342] 04 p0408 N73-13322
Aerodynamic drag of series of spherically-blunted conical bodies with three classes of half-vertex angles under hypersonic flow conditions
[NAL-TR-280] 06 p0613 N73-14978
Aerodynamic drag coefficients for conical body in near free molecule and transitional flow regimes
[AD-750042] 06 p0615 N73-14994
Numerical solution of shock wave interaction with supersonic blunt body flow exemplified by circular cylinder and parabolic body
[DLR-FB-72-68] 07 p0736 N73-15990
Analysis of fin bow shock wave during high speed air flow on blunt fin to determine interaction of vortices and shock waves
[AD-752210] 08 p0898 N73-17274
Finite difference method for calculating three dimensional, unsteady and steady, inviscid gas flows around blunt bodies
[NASA-TT-F-714] 09 p0980 N73-18009
Effects of density measurement electron beam impinging on blunt body in transition flow, noting influence of secondary electrons
[DLR-FB-73-08] 09 p0981 N73-18017
Postflight analysis of AV-2 balloon launched decelerator flight test to determine parachute system operation in wake of blunt body simulating Viking 75 entry vehicle
[NASA-CR-112177] 11 p1233 N73-20011
Postflight analysis of AV-3 balloon launched decelerator flight test to determine parachute system operation in wake of blunt body simulating Viking 75 entry vehicle
[NASA-CR-112178] 11 p1233 N73-20012
User manual for computer program to solve equations of fully coupled viscous, radiating flow at stagnation point of blunt body which may be ablating or non-ablating
[NASA-CR-2237] 11 p1347 N73-20933
Radiative coupled viscous flow past ablating blunt body at hyperbolic entry conditions
[NASA-CR-2236] 11 p1347 N73-20934
Computer automated scheme for solving equations of radiating flow over blunt body with or without ablation
[NASA-CR-2235] 11 p1348 N73-20936
Effects of nose bluntness on natural and induced boundary layer transition on axisymmetric bodies in supersonic flow
[AD-755843] 12 p1393 N73-21295
Theoretical and experimental studies on microwave transmission through hypersonic air plasma generated about blunt wedge
[SC-CR-72-3164] 12 p1434 N73-21621
Finite difference method for blunt body supersonic flow computation
[DLR-FB-73-10] 14 p1650 N73-23381
Viscous shock layer in hypersonic flow of perfect gas past axisymmetric blunt nosed body
15 p1764 N73-24297
Finite difference calculations of laminar flow past blunt-nosed cone with spherical after body injecting mass into air
[AD-758009] 15 p1844 N73-24943
Numerical analysis of real gas effects in supersonic flows over sharp and spherically blunted cones
16 p1887 N73-25274
Numerical analysis of axisymmetrical, viscous, compressible flow around blunt bodies for ideal gases with laminar unseparated boundary layers
17 p2012 N73-26273
Wind tunnel tests to determine effect of asymmetric nose bluntness on aerodynamic characteristics of slender cone at Mach 14
[AD-760807] 18 p2102 N73-26998
Boundary layer electron concentration profiles for entry of blunt nosed slender body into earth atmosphere
[NASA-TN-D-7332] 18 p2182 N73-27620
Analysis of stagnation point on blunt body in massive ablation condition to show effects of absorption coefficient enhancement on mass loss rate
19 p2351 N73-28912
General methods for calculating three dimensional laminar boundary layers over inclined blunt bodies
[AD-763831] 22 p2656 N73-31274
Finite difference solutions for flow equations of three dimensional boundary layer on blunt body
[SLA-73-366-PT-1] 24 p2909 N73-33217

BLUNTNESS
U ELLIPTICITY

BO-105 HELICOPTER
Helicopter autorotation capability, noting BO-105 helicopter behavior
05 p0494 N73-14023
Design optimization and testing of flight control systems for light helicopters, applied to BO-105 helicopter
24 p2878 N73-32985

BOATTAILS
Flight and wind tunnel tests to determine effects of Reynolds number of installed boattail drag of underwing nacelle
[NASA-TM-X-68162] 02 p0124 N73-11007
Aerodynamic characteristics of four configurations of rounded shoulder boattail nozzles mounted on F-106B aircraft at subsonic speeds
[NASA-TM-X-2626] 02 p0124 N73-11013
Effects of variations in fineness ratio and closure ratio on boattail drag of circular arc afterbody models at static conditions and at Mach number of 1.30
[NASA-TN-D-7163] 16 p1957 N73-25830

BODIES OF REVOLUTION
NT CONICAL BODIES
NT CYLINDRICAL BODIES
NT PARABOLIC BODIES
NT ROTATING CYLINDERS
NT ROTATING SPHERES
NT SLENDER CONES
NT SPHERES
NT TORUSES
Linear and nonlinear parts of slender body of revolution aerodynamic coefficients in supersonic flow, noting influence of incidence on pressure distribution
[DLR-FB-72-42] 01 p0001 N73-10006
Linear and nonlinear analysis of static equilibrium stability, and vibrations of shell of revolution subjected to unsymmetric loadings
[AD-745967] 02 p0238 N73-11939
Contour of wave drag optimized bodies of revolution as function of Mach number in hypersonic flow
[DGLR-PAPER-72-108] 04 p0369 N73-13003
Three dimensional laminar boundary layer flow over bodies of revolution
[AD-748282] 04 p0408 N73-13323

Wind tunnel measurement of surface pressure distributions on three bodies of revolution at Mach numbers from 0.7 to 2.02
[AD-749934] 05 p0492 N73-14012
Analysis of aerodynamic drag on general convex bodies at zero angle of attack during high speed flow in rarefied air
08 p0895 N73-17242
User manual and related documentation for six compatible computer programs for structural analysis of ring-stiffened shells of revolution
[NASA-CR-2086] 09 p1094 N73-18930
Development of base bleed techniques to reduce Magnus moment on long spinning bodies and improved drag characteristics
[AD-754755] 11 p1232 N73-20002
Finite difference method applied to axisymmetric random shells of revolution for unsymmetrical loading
[DRIC-TRANS-2996] 12 p1463 N73-21855
Wind tunnel tests to determine viscous normal force, pitching moment, side force and yawing moment on bodies of revolution at incidences up to 90 degrees
[WRE-782[WR/D]] 13 p1470 N73-21902
Development of computer program to predict lift, drag, and center of pressure on bodies of revolution at subsonic, transonic, and supersonic speeds
[AD-754098] 13 p1471 N73-21913
Steady oscillatory irrotational motion of inviscid incompressible fluid described by boundary value problem of elliptic type
[AD-755465] 13 p1512 N73-22252
Numerical analysis of drag of streamlined bodies of revolution for various length to diameter ratios
[ESDU-BODIES-02.04.02] 14 p1647 N73-23362
Prediction of Magnus force and moment coefficients for bodies of revolution
[SC-RR-72-0537] 15 p1731 N73-24039
Numerical solutions for laminar, compressible, three dimensional boundary layer on sharp bodies of revolution at angle of attack with moderate axial spin
[SC-CR-72-3182] 15 p1768 N73-24325
Development of finite difference method for calculating boundary value problem for nonsymmetrical deformation of random shells of revolution
[NLL-DRIC-TRANS-2996-[3623.66]]
15 p1836 N73-24884
Analysis of static, buckling, and vibration characteristics of orthotropic, inhomogeneous shells of revolution
15 p1837 N73-24889
Wind tunnel studies to determine static stability of two bodies of revolution with noses of varying spherical bluntness at Mach 0.6 to 1.5
[AD-758817] 16 p1858 N73-25052
Measurements of pressure distributions, mean velocity profiles, and Reynolds stresses in thick incompressible turbulent boundary layer near tail of body of revolution
[AD-759014] 16 p1892 N73-25310
Analysis of Magnus forces on high fineness ratio body of revolution with ogive forebody at varying angles of attack
[AD-759987] 17 p1980 N73-26003
Vibrational characteristics, mechanical properties, and stress analysis of thin shell structures of various cross sections
[NASA-SP-288] 17 p2092 N73-26924
Wind tunnel tests to determine control of magnus instabilities with aerodynamic configurations using symmetrical fin and non-finned bodies
19 p2217 N73-27885
Base pressure of bodies of revolution in supersonic gas flow
[AD-762243] 19 p2258 N73-28198
Effects of rocket plume simulators on pressure distribution of body of revolution at transonic speeds
[NASA-CR-133916] 22 p2651 N73-31238
Computer program for elastic-plastic dynamic analysis of shells of revolution by finite element method
[AD-764244] 22 p2726 N73-31812

**BODY CENTERED CUBIC LATTICES**
Proceedings of conference on microstructure of titanium, uranium, and zirconium body centered cubic lattices
[AD-748035] 03 p0319 N73-12598
Short range structure of Ti and Zr body centered cubic lattice solid solutions containing omega phase
[AD-755454] 13 p1567 N73-22698
Short range structure of Ti and Zr body centered cubic lattice solid solutions containing omega phase
[AD-755463] 13 p1567 N73-22699
Attenuation and thermal release dislocations by interstitial impurities in bcc lattice metals
[NASA-TT-F-14920] 14 p1675 N73-23596
Constitutive equations for determining elastic deformation twinning in body centered cubic lattice metals at low temperatures
[AD-757042] 14 p1679 N73-23624

**BODY FLUIDS**
NT BLOOD
NT CEREBROSPINAL FLUID
NT ERYTHROCYTES
NT LYMPHOCYTES
NT SALIVA
NT SWEAT
NT URINE
Liquid retention in chlorpropamide therapy and water intoxication of patients
[NASA-TT-F-14597] 02 p0133 N73-11077
Absorption and emission spectra for trace element analyses on biological sample solutions
03 p0258 N73-12093
Computer controlled infusion pump for time varying input of calcium into physiological systems
[NASA-CASE-ARC-10447-1] 05 p0503 N73-14092
Effect of hypokinesis of varying duration on fluid-electrolyte metabolism and composition in blood and tissues of animals
11 p1244 N73-20098
Accuracy of various tracer methods for measuring body water compartments during bed rest
[NASA-TR-R-406] 15 p1744 N73-24133
Fluid-electrolyte balance during 120-day bed rest
24 p2883 N73-33028

**BODY KINEMATICS**
Lower body decompression effects on cardiac cycle and human acceleration tolerance
14 p1608 N73-23037

**BODY MEASUREMENT [BIOLOGY]**
NT ANTHROPOMETRY
Ingestible miniaturized telemetry device for deep body temperature measurements on humans and animals
[NASA-CASE-ARC-10583-1] 05 p0503 N73-14093

**BODY SWAY TEST**
Physical/mathematical analyses on human vestibular responses to acceleration stresses
20 p2367 N73-29033
Human hemodynamic responses and vestibular tolerances to body sway tests
20 p2367 N73-29034

**BODY TEMPERATURE**
Tests to evaluate heat loss from Navy diver suits in water of 55, 45, and 35 F
[AD-747276] 02 p0136 N73-11103
Thermal resistance of clothing noting radiative body heat transfer, air layers, and clothing thickness
[DRIC-TRANS-2920] 03 p0261 N73-12117
Effects of prolonged bed rest on body temperature and heart rate periodicity in man
09 p0994 N73-18113
Changes in circadian rhythm of aircraft pilot oral body temperature as result of transmeridian flights
[DLR-FB-73-01] 09 p0997 N73-18140
Low barometric pressure effects on human thermoregulation function
13 p1480 N73-21996
Influence of He, N2, and N2O environments on physiological parameters of rats
20 p2365 N73-29019
Human body temperature dynamics in adaptation to changed work-sleep cycles
20 p2367 N73-29036
Heat exchange of hand as function of local thermal conditions
[NASA-TT-F-15143] 24 p2885 N73-33043

**BODY TEMPERATURE [NON-BIOLOGICAL]**
U TEMPERATURE

**BODY TEMPERATURE REGULATION**
U THERMOREGULATION

**BODY WEIGHT**
Weight, blood pressure, and intraocular pressure in young healthy males prior to and after 50-km walk
[NASA-TT-F-14557] 02 p0132 N73-11071
Radionuclide measurements on plasma and red cell mass volume losses in Apollo spacecrews
09 p0993 N73-18106
Influence of personal characteristics on likelihood of decompression sickness
[NASA-CR-135495] 22 p2621 N73-31002
Dynamics of weight change and variations in weight indices of internal organs in white mice as function of atmospheric composition and diet
24 p2883 N73-33022

**BODY-WING AND TAIL CONFIGURATIONS**
Pressure measurements on harmonically oscillating wing-tailplane configurations in incompressible speed range noting wind tunnel tests on aircraft models
[DLR-FB-71-52] 04 p0373 N73-13033
Aerodynamic influence coefficient matrix for non-planar wing-body-tail configurations
[NASA-CR-112231] 13 p1469 N73-21899
Method for conducting aerodynamic analysis of wing-body-tail configurations in subsonic and supersonic flow - Vol. 1
[NASA-CR-2228-PT-1] 16 p1857 N73-25045
Computer program for conducting aerodynamic analysis of wing-body-tail configurations in subsonic and supersonic flow - Vol. 2
[NASA-CR-2228-PT-2] 16 p1858 N73-25046

**BODY-WING CONFIGURATIONS**
Mathematical model of unsteady pressure distribution on harmonically oscillating slender cruciform wing and cylindrical body configurations
[DLR-FB-71-87] 06 p0615 N73-14990
Prediction analysis method to determine influence of geometry parameters on aerodynamic characteristics of body-wing configuration
[DLR-FB-72-63] 06 p0622 N73-15050
Computer program and users manual for calculating aerodynamic characteristics of wing-body combinations at subsonic and supersonic speeds
[FFA-AU-635-PT-2] 08 p0863 N73-16985
Technique for predicting shock envelopes and pressure distributions for two dimensional airfoil at angles of attack producing shock detachment and subsonic flow
[NASA-TN-D-7197] 09 p0979 N73-18001
Mathematical model of force coefficient and pitching moment by wing-body configuration
[BMVG-FBWT-72-28] 10 p1103 N73-18997
Numerical analysis of unsteady supersonic characteristics of space shuttle type vehicles using arbitrary finite element technique
[NASA-CR-112296] 13 p1470 N73-21904
Wind tunnel tests to determine static longitudinal aerodynamic characteristics of jet transport wing-body with upper surface blown jet flap for lift augmentation
[NASA-TN-D-7183] 13 p1470 N73-21907
Development of method for calculating potential flow about arbitrary lifting three dimensional bodies with emphasis on bound vorticity and application of Kutta condition
[AD-755480] 13 p1471 N73-21914
Numerical analysis of aerodynamic load distribution on swept back wing mounted on infinite circular cylinder fuselage at zero angle of attack
[AD-756075] 13 p1475 N73-21952
Development of procedure for determining characteristics of aircraft roll coupling moment caused by flow induced by deflected wings and cross flow
[ISAS-488-VOL-37-NO-14] 14 p1597 N73-22945
Optimum design of wing-body combinations for zero-lift drag rise at transonic speeds
[ARC-R/M-3279] 16 p1857 N73-25043
Application of holographic interferometry techniques for determining asymmetric flow distribution encountered near wing-fuselage junction at transonic speed
[AD-759967] 17 p2015 N73-26296
Wind tunnel tests to determine aerodynamic characteristics of three oblique, high aspect ratio wing and body combinations at Mach numbers between 0.60 and 1.40
[NASA-TM-X-62256] 24 p2869 N73-32926

**BOEING AIRCRAFT**
NT B-52 AIRCRAFT
NT BOEING 707 AIRCRAFT
NT BOEING 720 AIRCRAFT
NT BOEING 727 AIRCRAFT
NT BOEING 737 AIRCRAFT
NT BOEING 747 AIRCRAFT
NT C-135 AIRCRAFT
NT CH-47 HELICOPTER
NT X-20 AIRCRAFT

**BOEING MILITARY AIRCRAFT**
U MILITARY AIRCRAFT

**BOEING 707 AIRCRAFT**
Aircraft accident involving Boeing 707 aircraft at San Francisco, California airport following rejected takeoff on 13 Sept. 1972
[NTSB-AAR-73-4] 12 p1363 N73-21062
Aircraft accident involving Boeing 707 aircraft during landing at John F. Kennedy Airport, New York, 12 Dec. 1972
[NTSB-AAR-73-11] 15 p1734 N73-24068
Aircraft accident involving Boeing 707 aircraft following aborted takeoff at Kennedy International Airport, New York, on 13 August, 1972
[NTSB-AAR-73-7] 23 p2741 N73-31943
Longitudinal stability of Boeing 707 aircraft during steep approach, for noise reduction
[DGLR-PAPER-73-023] 23 p2744 N73-31963
Specification of thrust control system for Airbus A 300 B, tested in Boeing 707
24 p2877 N73-32981

**BOEING 720 AIRCRAFT**
Computerized simulation of passenger emergency evacuation efficiency using Boeing 720 aircraft models
[FAA-AM-72-30] 08 p0879 N73-17119

**BOEING 727 AIRCRAFT**
Aircraft accident investigation of Boeing 727 crash near Juneau, Alaska, 4 Sept. 71
[NTSB-AAR-72-28] 05 p0493 N73-14017
Incident involving collision of Boeing 727 aircraft with landing light system at Atlanta International Airport, Georgia on 21 Dec. 1971
[NTSB-AAR-72-22] 07 p0737 N73-16000
Design, development, and evaluation of Boeing 727 aircraft nacelle to conform to upper noise reduction goals
[FAA-RD-72-40-VOL-2] 18 p2104 N73-27017
Design, fabrication, and flight test of Boeing 727 aircraft nacelle modification to reduce aerodynamic noise levels
[AD-756040] 18 p2108 N73-27048
Flight tests of Boeing 727 aircraft to determine effects of modifications on reduction of aerodynamic noise
[FAA-RD-72-40-VOL-3] 24 p2876 N73-32971

**BOEING 737 AIRCRAFT**
Measurement of noise levels produced by Boeing 737 aircraft and correlation with local meteorological parameters including wind force and direction, temperature, and atmospheric pressure
[FAA-RD-72-145] 07 p0821 N73-16651
Aircraft accident involving crash of Boeing 737 aircraft during instrument approach to Chicago-Midway Airport, Illinois on 8 December 1972
[NTSB-AAR-73-16] 22 p2614 N73-30947
**BOEING 747 AIRCRAFT**
Inflight incident involving Boeing 747 aircraft encounter with unforecast clear air turbulence during flight from Japan to Hawaii on 12 April 1972
[NTSB-AAR-72-27] 03 p0252 N73-12038
Wind tunnel tests to obtain pre-flight estimates of stall speed and low air speed performance of Boeing 747 aircraft
06 p0618 N73-15016
Aircraft accident involving Boeing 747 aircraft during landing at Miami, Florida airport on 15 Dec. 1972 following collision with birds
[NTSB-AAR-73-13] 17 p1983 N73-26029
**BOGS**
U MARSHLANDS
**BOILERS**
Computer calculations of two-phase flow transients in once-through steam generators
[CEA-CONF-2009] 06 p0655 N73-15318
Theoretical investigation of rocket steam generator with emphasis on trajectories and spectrum of injected drops and their vaporization for Europa 1 launch vehicle
[DLR-FB-71-36] 09 p1011 N73-18253
Boiler surface coating effects on water heated by solar energy
[NASA-TT-F-14850] 11 p1237 N73-20043
**BOILING**
NT FILM BOILING
NT NUCLEATE BOILING
Boiling inception in trichlorotrifluoroethane during forced convection at high pressures
[NASA-CR-2170] 04 p0485 N73-13960
Effect of crud deposits on frictional pressure drop in boiling channel
[AEEW-R-767] 07 p0820 N73-16645
Void fraction in subcooled trichlorotrifluoroethane boiling at high pressures
[NASA-CR-2241] 14 p1718 N73-23938
Steady state heat and mass transfer in suction boiling
15 p1842 N73-24923
Development of method for calculating bubble conditions in flow of boiling liquid in vertical tubes
[NLL-WH-335-[9091.9F]] 21 p2605 N73-30875
**BOILING WATER REACTORS**
Analysis of forced convection film, transition, and nucleate boiling regions for water with application to boiling water reactor cooling systems
[DSR-73645-80] 13 p1590 N73-22892
Prototype mechanical drive for boiling water reactor in-core out-core neutron flux detectors
[BMBW-FBK-72-25] 22 p2699 N73-31617
**BOLIVIA**
Acquisition of earth resources data for Bolivia using ERTS-1 imagery
[E72-10191] 01 p0046 N73-10370
Regional geologic, tectonic, and volcanic surveys of Bolivia using ERTS-1 imagery
[E73-10286] 08 p0914 N73-17492
ERTS-1 imagery of structural geology and volcanology in Central High Plateau of Bolivian Andes
[E73-10296] 10 p1146 N73-19333
Geological mapping in Bolivia using ERTS-1 imagery
[E73-10614] 15 p1774 N73-24375
Application of ERTS-1 imagery to cartography, geomorphology, agronomy, and hydrology of Bolivia
[E73-10695] 16 p1902 N73-25387
Analysis of ERTS-1 data for studies of hydrogeology, geomorphology, and paleoclimatology in Bolivia, Argentina, Chile, and Peru
[PAPER-W1] 19 p2270 N73-28281
**BOLKOW AIRCRAFT**
NT BO-105 HELICOPTER
**BOLKOW BO-105 HELICOPTER**
U BO-105 HELICOPTER
**BOLLWORMS**
Control of pink bollworm infestation in southern California cotton fields using ERTS-1 remotely sensed imagery
[E72-10285] 04 p0409 N73-13335
Mapping and control of pink cotton bollworm in California
[E73-10073] 07 p0780 N73-16335
Control and mapping of pink bollworm infestations in cotton fields of California desert areas
[E73-10452] 11 p1283 N73-20411
Mapping of cotton fields in Southern California using ERTS-1 data for control of pink bollworm growth
[PAPER-A15] 19 p2261 N73-28223
Utilization of ERTS-1 imagery for mapping and control of pink bollworm in Imperial, Coachella, and Palo Verde Valleys of California
[E73-10858] 19 p2292 N73-28435
**BOLOGRAMS**
U BOLOMETERS
**BOLOMETERS**
Transient and steady state response characteristics of sandwich-type wavelength selective bolometer
[AD-750264] 06 p0675 N73-15496
Calibration of liquid helium-cooled germanium bolometers to determine responsitivity at different chopper frequencies and cryostat temperatures
[BMFT-FBW-73-05] 14 p1666 N73-23524
Bolometric pyrheliometer with balanced resistance bridge and radiation detector having copper wire spiral
20 p2403 N73-29315
**BOLTS**
Tensile and stripping strength data in terms of failure probability for bolts, nuts, screws, and threaded rods
[ESDU-67019] 01 p0110 N73-10908
Numerical analysis of stresses produced in bolt or similar threaded object from application of known tightening torque to bolt head or engaged nut
[ESDU-72022] 05 p0601 N73-14888
Relaxation tests on high temperature bolted metal joints
[NLL-ESB-TRANS-303-[3810.97]]
06 p0683 N73-15555
Twelve simulated bolted flanges during stress relaxation
[NASA-CR-132218] 15 p1792 N73-24527
Improving screwability of titanium bolts with nuts of various materials
[AD-758037] 15 p1794 N73-24541
Device for securing together structural members with axially stretched bolt and nut
[NASA-CASE-GSC-11149-1] 21 p2552 N73-30457
**BOLTZMANN TRANSPORT EQUATION**
Eigenfunctionals of linear Boltzmann transport operator in modal approximations
[APS-PH-87] 02 p0195 N73-11580
Steady-state solutions for discrete-velocity Boltzmann systems in restricted flow region
[AD-748182] 04 p0406 N73-13311
Application of turbulence transport equations to problems in which buoyancy is driving force
[LA-DC-72-705] 06 p0654 N73-15314
Differential energy spectra of cosmic ray protons and helium nuclei dominated by solar modulation of local interstellar spectra, and numerical solutions to transport equation
[NASA-CR-130298] 06 p0715 N73-15837
Proofs for binary collision term in Boltzmann transport equations in kinetic theory of gas and plasma dynamics
[TRITA-EPP-72-25] 07 p0772 N73-16273
Boltzmann equations for kinetic modeling of supersonically flowing electrically excited laser system
[NASA-TM-X-62196] 07 p0806 N73-16538
Transport equations for studying radiative transport through dense plasma
[AD-753245] 09 p1072 N73-18753
Singular limits of Boltzmann equation solutions for describing qualitative and quantitative properties of rarefied gas
[AD-753691] 10 p1143 N73-19312
Numerical methods in theory of rarefied gases with application of Boltzmann equation
[NASA-TT-F-638] 12 p1417 N73-21483
Review of numerical methods used in solving Boltzmann equation
12 p1417 N73-21484
Solution of Boltzmann kinetic equation for relaxation of gas mixture
12 p1418 N73-21486
Method for direct numerical integration of Boltzmann equation
12 p1418 N73-21487
Shock wave structure in gas consisting of ideally elastic, rigid spherical molecules
12 p1418 N73-21488
Solution of relaxation problem for Boltzmann equation by integral iteration method
12 p1418 N73-21489
Approximation method for kinetic Boltzmann equation
12 p1418 N73-21490
Derivation of directional plasma transport equations from Boltzmann equation
[AD-758275] 14 p1697 N73-23768
N-particle kinetic equation for classical gas with central force interactions
20 p2456 N73-29735
Kinetic molecular flow distribution at porous wall using one dimensional steady state Boltzmann equation
[VKI-TN-79] 22 p2654 N73-31259
Application of Boltzmann transport theory for determining penetration of matter by heavy-ion beam
[AD-765315] 23 p2822 N73-32556
Boltzmann transport equation for electron bombardment effects in solids
[AD-764637] 23 p2827 N73-32599
Dynamics of axisymmetric stellar systems applied to collapse and violent relaxation of rotating stellar systems
24 p2977 N73-33792
**BOMB CALORIMETERS**
Reactivity of tungsten in mixture of Hexogen and aluminum in bomb calorimeter
[ICT-12/72] 22 p2730 N73-31845
**BOMBER AIRCRAFT**
NT A-4 AIRCRAFT
NT A-6 AIRCRAFT
NT B-1 AIRCRAFT
NT B-52 AIRCRAFT
NT B-57 AIRCRAFT
NT B-70 AIRCRAFT
NT F-100 AIRCRAFT
NT VULCAN AIRCRAFT
Aerodynamic interference between aircraft and external store mounted on elliptical wing under inviscid flow conditions
[AD-759170] 16 p1864 N73-25094
**BOMBING EQUIPMENT**
Model of pilot-aircraft system for relating pilot tracking performance to overall weapon delivery
[AD-745999] 01 p0006 N73-10045
Logistic performance data book for bomb navigation avionics system of F-111 aircraft to show support cost, reliability, maintenance, and problems
[AD-762214] 19 p2357 N73-28959
Logistics performance data book on bombing and navigation system for A-7D aircraft to show reliability, maintainability, cost, and problems
[AD-762215] 19 p2357 N73-28960
**BOMBS (ORDNANCE)**
Aerodynamic characteristics and trajectory analysis of ballistic-type, self-dispersing bomblet based on wind tunnel tests and numerical probability application
[AD-749956] 06 p0615 N73-14993
Effects of various external stores characteristics, spanwise positions, and Mach number on static longitudinal stability of several military aircraft
[AD-750120] 06 p0624 N73-15063
IBM 7090 computer program for determining values of error sensitivity for dive and glide bombing with free fall weapons
[AD-758420] 15 p1850 N73-24994
System modeling and performance optimization for analyzing parameters and disturbances for dynamic precision weapon delivery - Vol. I
[AD-751505] 16 p1976 N73-25985
Computer programs for conducting mathematical analysis of weapon delivery techniques and performance optimization of aerial delivery weapons - Vol. 2
[AD-751506] 16 p1977 N73-25986
Testing and demonstration of weapon delivery analysis program to determine major contributors to probable error - Vol. 3
[AD-751527] 16 p1977 N73-25987
Determination of bomb range of low drag bombs delivered by fighter aircraft
[AD-762500] 20 p2488 N73-29992
Application of X ray fluoroscopy and radiography for determining presence of bombs in suspicious packages and protection measures for personnel
24 p2952 N73-33586
**BOMBS [PRESSURE GAGES]**
U PRESSURE GAGES
**BOMBS (SAMPLERS)**
U SAMPLERS
**BONDING**
NT ADHESIVE BONDING
NT CERAMIC BONDING
NT EXPLOSIVE WELDING
NT METAL BONDING
NT METAL-METAL BONDING
NT RESIN BONDING
Reduction of peak shear stress in bonded joint
[NASA-CASE-LAR-10900-1] 01 p0061 N73-10499
Application of strain compatibility equations to evaluate thermal stresses in unidirectional graphite composites bonded to aluminum structures
[NASA-CR-112162] 02 p0125 N73-11014
Thermocompression wobble tool bonding of beam lead devices
[SC-DC-72-1197-A] 03 p0306 N73-12501
Analysis methods for studying fatigue in bonded joints of composite materials
[AD-750132] 06 p0728 N73-15939
Fabrication, inspection and tests of fatigue in bonded joints of composite materials
[AD-750133] 06 p0728 N73-15940
Fatigue analysis and fatigue mode studies in bonded joints of composite materials
[AD-750134] 06 p0728 N73-15941
Research on physics of adhesive joint
[AD-751301] 07 p0805 N73-16530
Application of gas-pressure bonding to joining components for convectively cooled turbine blades and vanes
[NASA-CR-121090] 08 p0954 N73-17808
Procedures for reducing residual stresses in aircraft metal structures reinforced by filamentary composites
[NASA-CR-112207] 08 p0966 N73-17900

Methods for designing and developing aircraft structural components by riveting, welding, and gluing aluminum alloys parts
[AD-753513] 09 p1041 N73-18491
Improvement in interlaminar shear strength of organic matrix composites using plasma deposited coupling agents
[AD-753857] 09 p1055 N73-18599
High temperature bonding of sapphire to sapphire by eutectic Al2O3 and ZrO2 mixture to form sapphire rubidium maser cell
[NASA-CASE-GSC-11577-1] 10 p1164 N73-19467
Significant advances in welding, bonding, and joining techniques since 1960
[AD-754262] 10 p1168 N73-19502
Quality control of welded, brazed, and bonded electrical terminations
[BDX-613-613-REV] 12 p1383 N73-21214
Analysis of aircraft construction methods to compare riveting, welded joints, and bonded joints for structural stability
[AD-755754] 13 p1475 N73-21948
Analysis of structural reliability of large scale bonded joints for advanced composite wing to determine service life of boron epoxy to titanium scarf joint
[AD-756893] 14 p1603 N73-22995
Grounding, bonding, and shielding practices for operational reliability enhancement in air traffic control electronic facilities
[FAA-RD-73-51] 14 p1645 N73-23341
Aluminum ribbon wire for ultrasonic bonding of semiconductor microelectronic interconnections
[AD-758981] 16 p1881 N73-25223
Vacuum brazing-gas quenching process for joining chemical and ordnance munitions materials
[AD-759117] 16 p1919 N73-25531
Process of density change in epoxy bonding agents throughout curing process
[RAE-LIB-TRANS-1686] 17 p2049 N73-26576
Strength, creep, and transmission coefficient of adhesives for attaching strain gages
[AD-761470] 19 p2302 N73-28506
Scanning electron microscope examination of wire bonds from high reliability microelectronic devices
[NBS-TN-785] 21 p2549 N73-30432

**BONE MARROW**
Proliferative activity of bone marrow in dogs exposed to three-year chronic gamma irradiation
11 p1244 N73-20102
Leukopenic response of dog bone marrow for evaluating hematopoietic tissue function
13 p1481 N73-22009

**BONES**
NT CEREBRUM
NT CRANIUM
NT MARROW
Effect of calcium-deficient diet on bone structure of pigs and dogs
[NASA-TT-F-13917] 01 p0008 N73-10067
Annotated bibliography with preliminary analysis on dysbaric osteonecrosis
[AD-747258] 04 p0381 N73-13100
Chemical and orthopedic properties of ceramic bone implants in monkeys
[AD-754982] 11 p1248 N73-20134
Ultrasonic bone densitometer for measuring calcium content of bone structures
[NASA-CASE-MFS-20994-1] 21 p2504 N73-30090
Effect of high ambient temperature on calcium content of human bone tissue
24 p2884 N73-33033

**BOOLEAN ALGEBRA**
NT BOOLEAN FUNCTIONS
Algorithm for determining optimal partition of points into mutually exclusive and exhaustive subsets or clusters according to objective function defined on set of all partitions
[P-4878] 01 p0072 N73-10586
Proceedings of conference on multiple-valued logic
[AD-762123] 19 p2240 N73-28063
Boolean functions for logic and mathematic operations in magnetic domain devices
20 p2461 N73-29780

**BOOLEAN FUNCTIONS**
Simplification of Boolean functions adapted to incompletely specified functions
03 p0325 N73-12649

**BOOMS [EQUIPMENT]**
Prototype elbow joint for remote control of heavy duty cargo boom
[AD-749520] 05 p0553 N73-14487
Design development, and evaluation of hoist for H-3 helicopter rescue system
[AD-750289] 06 p0623 N73-15054
Apollo 15 deployable boom anomaly and subsequent design changes
09 p1087 N73-18868
Analysis of thermal static bending forces on deployable interlocked booms and comparison with thermal bending of seamless tubes
[NASA-TN-D-7243] 11 p1345 N73-20915
Development and design of satellite cable boom
[HSD-TP-7356] 12 p1366 N73-21086
Design, development, and testing of foldable beryllium copper alloy elastic tubes for hinges on satellite booms
[ESRO-CR-65] 19 p2346 N73-28874
Extended torsional tests of interlocked bi-stem satellite boom
[NASA-TN-D-7365] 22 p2724 N73-31798

**BOOST**
U ACCELERATION [PHYSICS]

**BOOSTER RECOVERY**
Empirical data on probable sea state conditions to be encountered by space shuttle booster recovery forces
[NASA-TM-X-68631] 07 p0792 N73-16440
Design criteria and aerodynamic characteristics of decelerator parachutes used for recovery of solid rocket boosters used in space shuttle launching
[NASA-CR-124266] 16 p1861 N73-25072
Quantitative tests of space shuttle booster recovery in open seas
[NASA-TM-X-69273] 16 p1965 N73-25892
Bibliography of technical documents pertinent to development of system for recovering space shuttle solid rocket booster motors from ocean
[LPC-DOC-SRM-143] 16 p1965 N73-25899

**BOOSTER ROCKET ENGINES**
NT AJ-10 ENGINE
Simulation for use in dynamics and control analysis during boost from liftoff to orbit insertion
[NASA-CR-128592] 01 p0108 N73-10890
Wind tunnel tests to determine stability and control effectiveness of basic configuration of pressure-fed ballistic recoverable booster for space shuttle
[NASA-CR-120073] 02 p0233 N73-11896
Development and application of systematic procedures for estimating life cycle costs of solid rocket motor booster configurations
[NASA-CR-129255] 03 p0350 N73-12857
Definition of system for expendable second stage and reusable space shuttle booster system - Vol. 2 - Bk. 1
[NASA-CR-128670] 05 p0598 N73-14866
Design criteria and aerodynamic characteristics of decelerator parachutes used for recovery of solid rocket boosters used in space shuttle launching
[NASA-CR-124266] 16 p1861 N73-25072
Bibliography of technical documents pertinent to development of system for recovering space shuttle solid rocket booster motors from ocean
[LPC-DOC-SRM-143] 16 p1965 N73-25899
High energy rocket engines - propellant physical chemistry, propulsion system performance, hydrogen oxygen engines, boosters, nozzles - conferences
[DLR-MITT-72-09] 24 p2972 N73-33749
Booster rocket engines, mentioning 20T-LOX/LH2, 5T-LOX/kerosene, 13T-LOX/LH2, and 1T-N2O4/UDMH engines
24 p2973 N73-33753
Alternate concepts study on two and one half stage, stage and one half, and SRM interim booster systems for establishing performance, costs, and schedules
[NASA-CR-124344] 24 p2982 N73-33829

**BOOSTERS**
Hypervelocity wind tunnel tests of aerothermal characteristics of winged space shuttle booster model
[NASA-TM-X-2642] 01 p0109 N73-10895
Program planning, contract administration, manufacturing, and testing of solid propellant rocket engine for space shuttle booster - Vol. 3
[NASA-CR-124238] 20 p2467 N73-29821

**BOOSTGLIDE VEHICLES**
NT X-20 AIRCRAFT

**BORANES**
NT CARBORANE

**BORES**
U CAVITIES

**BORIDES**
Borides, carbides, and nitrides of silicon oxidation resistant refractory compounds for use in gas turbines and reentry vehicles
14 p1678 N73-23616

**BOROHYDRIDES**
Synthesis and characterization of tetrahydroborates of lanthanum, neodymium, and erbium
[AD-759372] 17 p1992 N73-26110

**BORON**
Analysis of crack tip deformation in boron-aluminum sheet and laminar steel sheet resulting from crack propagation
[AD-747760] 03 p0322 N73-12623
Ion concentration profiles of injected boron and phosphorus including substitution of arsenic for phosphorus
05 p0522 N73-14249
Boron filament splitting in boron aluminum composites caused by water vapor effects
[AD-749971] 05 p0566 N73-14602
Selected abstracts on boron from internaticonference held at Tbilisi
[JPRS-57879] 06 p0687 N73-15596
Tensile strength determined for two commercial boron filaments
[AD-752505] 08 p0936 N73-17663
Time dependent mechanical behavior of boron filament reinforced aluminum composites based on static and dynamic properties
[AD-753706] 09 p1054 N73-18590
Boron-aluminum radiators for space shuttle orbiters
[NASA-CR-128805] 10 p1164 N73-19468
Direct mixing and combustion measurements in ducted, particle-laden jets using boron loaded propellant
[AD-754434] 10 p1224 N73-19956
Theoretical and experimental determination of nonlinear behavior of angleplied boron/aluminum composites
[NASA-TM-X-68205] 11 p1309 N73-20617
Evaluation of upgraded boron fibers in epoxy-matrix composites
[NASA-CR-112266] 12 p1416 N73-21472
Development of compatible titanium alloy for boron reinforced composites
[AD-758294] 14 p1682 N73-23652
Evaluation of low cost techniques for forming boron-reinforced aluminum structural shapes from diffusion-bonded flat sheet and plate
[NASA-CR-124279] 16 p1918 N73-25523
Production of monolayer boron-aluminum composite materials
[NASA-CR-124278] 16 p1928 N73-25601
Neutronic feasibility of fast spectrum space power reactor design concepts using boron control devices
[NASA-TM-X-2821] 16 p1943 N73-25720
Use of reinforced boron and carbon fiber composites in aircraft structures
18 p2165 N73-27484
Performance and fatigue strength of compressor blades fabricated from carbon fiber composites and boron composite wires
18 p2166 N73-27496
Performance and endurance of compressor disks bound with boron composite wires
18 p2167 N73-27499
Chemical vapor deposition process for preparing large diameter carbon-boron monofilaments
[NASA-CR-121229] 18 p2167 N73-27502
Ignition model for predicting ignition delay times of boron particle clouds in oxidizing atmosphere
20 p2484 N73-29955
Effects of high temperature cycling on structural properties of boron reinforced aluminum alloys used in spacecraft structures
[NASA-CR-124369] 21 p2562 N73-30541

**BORON ALLOYS**
Design, development, and manufacture of boron-aluminum alloy for use as space shuttle structural components
[NASA-CR-124242] 14 p1709 N73-23873
Fatigue mechanics of boron-aluminum composites under oscillating tensile loads
[AD-757213] 16 p1932 N73-25635
Cause and prevention of smoky spots occurring on surface of silicon alloyed with boron after chemical polishing
18 p2188 N73-27663
Effect of filament-matrix interfaces on fatigue resistance of boron-aluminum composites
[AD-761658] 19 p2312 N73-28597

**BORON CARBIDES**
B4C-alkali metal carbonates for boronizing steel surfaces
[NLL-RTS-7197] 01 p0069 N73-10562
Mechanical properties of boron carbide reinforced titanium laminates
[AD-745002] 01 p0070 N73-10570
Analysis of boron carbide drum-controlled critical reactor experiment
[NASA-TM-X-2680] 03 p0331 N73-12701
Modified lamination process for developing boron carbide ribbon reinforced titanium matrix composites
[AD-754478] 11 p1309 N73-20618

**BORON CHLORIDES**
Pressure dependent absorption of CO2 laser in BCl3 at 10.6 micron
[DREV-TN-2086/73] 24 p2930 N73-33403

**BORON COMPOUNDS**
NT BORIDES
NT BOROHYDRIDES
NT BORON CARBIDES
NT BORON CHLORIDES
NT BORON OXIDES
NT BORON PHOSPHIDES
NT CARBORANE
NT DIBORANE
Tensile creep tests to determine properties of 7075-T6 aluminum alloy reinforced with unidirectional boron/epoxy
[NBS-TN-722] 04 p0437 N73-13565
Development of process for fabricating dense boron suboxide billets by hot pressing to eliminate decomposition and cracking
[AD-751980] 08 p0936 N73-17662
Thermochemical combustion effects of fuel-rich boron compound as solid rocket propellant
[AD-753105] 09 p1099 N73-18971

Analysis of loss of high temperature strength in composite materials following aging in room temperature environments
[NASA-CR-124290] 17 p2050 N73-26583
Optical and magnetic resonance spectra of uranium borohydride in hafnium borohydride
[AD-759371] 17 p2074 N73-26777
Binary boron/lithium system as propellant additive of hybrid rocket engines, noting enthalpy and reaction product density
[DLR-MITT-73-08] 17 p2075 N73-26791
Application of boron/epoxy composite materials for airframe construction with specific development of F-111 stabilizer
18 p2164 N73-27480
Application of boron/aluminum composite material for construction of turbine blades with low notch sensitivity in high cycle fatigue
18 p2166 N73-27497
Design, fabrication, and test of boron-polyimide reinforced titanium fan disks to operate at high temperatures
18 p2167 N73-27498
Flight tests of CH-47 helicopter to determine structural performance of boron-reinforced epoxy aft rotor blades
[AD-762199] 19 p2222 N73-27927

BORON HYDRIDES
NT CARBORANE

BORON OXIDES
X ray analysis of B2O3 effects on composition, porosity, and sorption properties of Al2O3
[NLL-M-22796-[5828.4F]] 06 p0682 N73-15553
Infrared spectra of aluminum, gallium, and indium suboxide vapors considering frequency oscillations in group 3 suboxides and molecular constants of boron oxide
[AD-752861] 09 p1000 N73-18164
Magnetic properties of iron oxides in boron oxides
[AD-754104] 10 p1202 N73-19780
Silicon additions and borax-glass coatings used to reduce surface hot shortness of copper-bearing steels
[PB-212660] 11 p1307 N73-20607

BORON PHOSPHIDES
Synthesis and characterization of semiconducting diamond and boron phosphide crystals
18 p2186 N73-27648

BOROSILICATE GLASS
Coatings of borosilicate glasses deposited on silicon solar cells by radio frequency sputtering for enhanced protection
[ESRO-CR-68] 09 p0991 N73-18087

BOSE GEOMETRY
Bose model for foreign particle interaction with superfluid helium
20 p2455 N73-29732

BOSE-EINSTEIN STATISTICS
U QUANTUM STATISTICS

BOSONS
NT ALPHA PARTICLES
NT LIGHT BEAMS
NT MESON RESONANCES
NT MESONS
NT PHOTONS
NT PIONS
One boson exchange nucleon-nucleon potential in two nucleon and many nucleon problems
[NOTA-INTERNA-380] 01 p0084 N73-10694
Critical exponents for charged and neutral Bose gases above Lambda points
[AD-756022] 12 p1430 N73-21587
Application of Boson method to quantum field theory computations and mixed state of type 2 superconductors
23 p2825 N73-32582

BOTANY
NT GEOBOTANY
Inventory and management of geological, botanical, and agricultural resources in Wyoming using satellite and airborne imagery and ground control data
[E72-10229] 02 p0163 N73-11322
Application of ERTS-1 imagery to geologic, hydrologic, agricultural, botanical, and land use studies in Wyoming
[E73-10844] 19 p2291 N73-28422
ERTS-1 imagery of geology, botany, agriculture, hydrology, and cultural features of Wyoming
[E73-11022] 22 p2661 N73-31326

BOTSWANA
Geological survey of Botswana using ERTS-1 imagery
[E73-10753] 17 p2022 N73-26356
Geological, hydrological, ecological, and agricultural mapping of Botswana from ERTS-1 photography
[E73-10928] 20 p2399 N73-29277
Geology, hydrology, and ecology of Botswana from ERTS-1 MSS imagery
[E73-10929] 20 p2399 N73-29278

BOUNDARIES
NT FLUID BOUNDARIES
NT FREE BOUNDARIES
NT GAS-SOLID INTERFACES
NT GRAIN BOUNDARIES
NT LIQUID-LIQUID INTERFACES
NT LIQUID-SOLID INTERFACES
NT LIQUID-VAPOR INTERFACES
Meaning coefficients for heat flows and temperature fields of simple shaped bodies with III order boundary conditions
[NLL-M-21522-[5828.4F]] 11 p1347 N73-20929
Multiperipherism and hydrodynamics of multiple processes
[NASA-TT-F-14896] 13 p1561 N73-22656
Boundary conditions and singularities in gravitational collapse and gravitational radiation
[MATSCIENCE-72] 15 p1781 N73-24437

BOUNDARY LAYER COMBUSTION
Laminar chemically reacting boundary layer at solid fuel/gas interface over vaporizing surface
19 p2230 N73-27981

BOUNDARY LAYER CONTROL
NT POROUS BOUNDARY LAYER CONTROL
Boundary layer control under hypersonic flow conditions using tangential injection of gas
[NASA-TT-F-13927] 01 p0041 N73-10320
Computerized design and tests of two-dimensional subsonic short diffusers employing boundary layer control
[NASA-CR-121024] 03 p0283 N73-12294
Development of two experimental approaches for analyzing two dimensional flow on high lift devices
Development of F-28 transport aircraft wing and analysis characteristics to show effects of boundary layer fences
06 p0618 N73-15015
Procedure for designing axisymmetric, translating, centerbody inlet bleed system for operation at Mach 3.5
[NASA-CR-2187] 06 p0713 N73-15821
Systems for controlling boundary layer in hypersonic air intakes
[AD-750513] 06 p0715 N73-15834
Analysis of fin bow shock wave during high speed air flow on blunt fin to determine interaction of vortices and shock waves
[AD-752210] 08 p0898 N73-17274
Numerical analysis of aerodynamic characteristics of unsteady, two-dimensional, jet-flapped wing
[AD-752928] 09 p0986 N73-18051
Boundary layer control for mixing region in three dimensional laminar elliptical jet for thrust augmentation
[AD-754227] 10 p1143 N73-19313
Investigation of low density hypersonic flow by controlled boundary layer removal from nozzle wall
[AD-754276] 11 p1271 N73-20316
Development of high performance, low volume thrust augmentation using combined Coanda inlet and jet flap diffusion techniques
[AD-756895] 13 p1476 N73-21954
Mixing characteristics of steady and intermittent blowing applied to boundary layer control
[AD-758390] 14 p1652 N73-23403
Two dimensional flow, low speed wind tunnel tests of trapped vortex-high lift airfoil to reduce blowing requirements for lift augmentation
[AD-762077] 19 p2218 N73-27893
Numerical analysis of three dimensional boundary layer for various distribution laws of suction intensity on leading edge of wing
[AD-763280] 21 p2497 N73-30038
Aerodynamic drag and lift of airships, noting boundary layer control by suction
24 p2879 N73-32994

BOUNDARY LAYER FLOW
NT BOUNDARY LAYER SEPARATION
NT REATTACHED FLOW
NT SECONDARY FLOW
NT SEPARATED FLOW
Procedure for calculating sectional lift coefficient as function of angle of attack and free stream Reynolds number at angles of attack beyond maximum coefficient of lift
[AD-746505] 01 p0002 N73-10008
Boundary layer control under hypersonic flow conditions using tangential injection of gas
[NASA-TT-F-13927] 01 p0041 N73-10320
Analysis of velocity and temperature distribution in unsteady thermal boundary layer by approximate integral method
[NASA-TN-D-7054] 01 p0117 N73-10967
Analysis of laminar fluid flow between two rotating coaxial disks
[ISAS-485-VOL-37-11] 02 p0155 N73-11257
Analysis of mean velocity, turbulence intensity, and wall heat transfer for conical diffuser coupled to constant diameter recovery section
[NASA-TM-X-2677] 02 p0156 N73-11267
Development of theories for calculating pressure on perturbed plane wall in presence of viscous boundary layer
[AD-746332] 02 p0158 N73-11278
Calculation of Magnus sideforce developed by spinning cylinder at angle of attack considering effects of boundary layer and shed vorticity in crossflow
03 p0247 N73-11998
Development and characteristics of test facility for measuring three dimensional boundary layers on helicopter rotor blade under various conditions
[NASA-CR-112194] 03 p0252 N73-12042
Application of modified compressibility transformation for analyzing variable property turbulent boundary layers and predicting flow properties
[NASA-CR-2147] 03 p0282 N73-12286
Analysis of relaxation of laminar boundary layer to test gas boundary layer over flat plate in expansion tube
[NASA-TR-R-397] 03 p0283 N73-12296
Calculation of heat transfer on turbine blade profiles to determine transition region coordinates in boundary layer flow through gas turbine engine
[AD-747602] 03 p0352 N73-12870
Parametric relations for ordinary and confluent turbulent wall jet flows with external stream velocity and arbitrary pressure distribution
04 p0405 N73-13297
Uniqueness theorem for two-dimensional nonstationary wall boundary layer in incompressible fluid
[AD-748743] 04 p0407 N73-13314
Development of mathematical model for viscous inviscid interaction analysis and solution of boundary layer equations by finite difference scheme
[AD-748342] 04 p0408 N73-13322
Three dimensional laminar boundary layer flow over bodies of revolution
[AD-748282] 04 p0408 N73-13323
Numerical analysis of development of incompressible, symmetrical turbulent wake flows downstream of airfoils using integral method of momentum and energy
[NAL-TR-292] 06 p0614 N73-14986
Analysis of velocity profiles in boundary layer produced by incompressible flow during takeoff
06 p0616 N73-15001
Development of two experimental approaches for analyzing two dimensional flow on high lift devices
06 p0617 N73-15005
Application of power method for reducing base drag of long range supersonic aircraft at supersonic speeds
[AD-750950] 06 p0623 N73-15056
Analysis of unsteady flow over moving boundaries to determine characteristics of boundary layer separation
[AD-750398] 06 p0655 N73-15322
Numerical analysis of three dimensional compressible laminar boundary layer flow characteristics of right circular cone in supersonic and hypersonic flow
[AD-750130] 06 p0656 N73-15331
Short takeoff aircraft lift augmentation and prevention of airflow separation on cambered elliptical airfoil section using circulation control
[AD-751045] 07 p0736 N73-15992
Finite difference solutions for laminar and turbulent boundary layer equations of perfect gases and gas mixtures in chemical equilibrium
07 p0767 N73-16236
Solution of boundary layer equations of chemically reacting flat plate flow of binary gas mixture with Hermitian finite difference method
[DLR-FB-72-58] 07 p0772 N73-16272
High frequency pressure effect on wave propagation along layer of magnetoactive plasma
[AEC-TR-7336] 07 p0826 N73-16698
Computerized prediction of two dimensional wall boundary layer flow from laminar through transition to turbulent regimes
08 p0894 N73-17239
Analysis of downstream mixing of transverse hydrogen injection from single and multiple orifices in Mach 4 boundary layer over flat plate
[NASA-CR-112254] 09 p1015 N73-18285
Effects of earth surface characteristics on cumulus scale convection for stable and unstable boundary layers above relatively dry ground
[AD-752914] 09 p1031 N73-18416
Application of implicit finite-difference method for solution of compressible boundary layer equations
10 p1139 N73-19277
Flow equations for unsteady turbulent boundary layer flow on swept infinite cylinder to show effects of variations in frequency of oscillations
[NASA-TM-X-62242] 10 p1141 N73-19297
Effects of boundary layer flow patterns on upright cascade blade performance
10 p1205 N73-19803
Application of boundary layer fences in turbomachinery
10 p1206 N73-19810
Wind tunnel tests to determine effects of nozzle geometry and upper surface blowing on aerodynamic characteristics of 14 percent thick airfoil
[NASA-CR-114560] 11 p1231 N73-19998
Heat transfer solutions for solids with moving boundaries and for viscous liquid flow
[AD-754639] 11 p1349 N73-20950
Developments in techniques for analyzing boundary layer characteristics of rotary wings based on unsteady viscous-inviscid interaction
12 p1361 N73-21046
Finite difference solution of general class of three-dimensional boundary layer flows
[NASA-CR-112315] 12 p1391 N73-21277
Development of statistical equations for turbulent compressible gas with emphasis on space-time correlations in boundary layer
[AD-755889] 12 p1393 N73-21291

Gas injection of turbulent boundary layer through porous wall
[ONERA-NT-201] 13 p1510 N73-22237
Research projects on hypersonic and rarefied gas flows, separated and reattached wakes, viscous flow, and laminar and turbulent boundary layers with strong blowing
[AD-755276] 13 p1512 N73-22249
Analysis of internal waves generated by passage of body through density stratified medium and effects on mean flow
[AD-755714] 13 p1512 N73-22254
Numerical analysis of drag of streamlined bodies of revolution for various length to diameter ratios
[ESDU-BODIES-02.04.02] 14 p1647 N73-23362
Research projects involving aerodynamics, aerodynamic heating, aerodynamic forces, airframes, structural analysis, and fluid mechanics - Vol. 1
15 p1725 N73-23995
Numerical analysis of pressure distribution in incompressible flow on two dimensional airfoils near ground
[ARC-R/M-3238] 15 p1726 N73-24000
Analysis of flow pattern on tapered, sweptback wing at Mach numbers between 0.6 and 1.6 and 12 degree angle of incidence
[ARC-R/M-3271] 15 p1726 N73-24004
Research projects involving boundary layer flow, heat transfer during aerodynamic heating, atmospheric turbulence effects, and airframe structural analysis - Vol. 2
15 p1727 N73-24011
Effects of heat transfer on laminar boundary layer development under pressure gradients in compressible flow
[ARC-R/M-3218] 15 p1727 N73-24012
Effects of wall jets in still air on flat and curved surfaces under external stream in presence and absence of pressure gradient and initial boundary layer
[ARC-R/M-3252] 15 p1729 N73-24025
Two dimensional unsteady separation and stall phenomena over airfoils oscillating in pitch with application to short takeoff aircraft
[AD-758899] 15 p1736 N73-24080
Analysis of turbulent boundary layer on porous plate and fluid mechanics of adverse free stream pressure gradients
15 p1765 N73-24303
Flight-measured base pressure coefficients for thick boundary layer flow over aft-facing step for Mach numbers from 0.4 to 2.5 using XB-70 aircraft
[NASA-TN-D-7202] 15 p1767 N73-24317
Wind tunnel tests to determine effect of approaching boundary layer on separated flow behind downstream facing step
[NLR-TR-70033-U] 15 p1768 N73-24322
Numerical solutions for laminar, compressible, three dimensional boundary layer on sharp bodies of revolution at angle of attack with moderate axial spin
[SC-CR-72-3182] 15 p1768 N73-24325
Research projects in theoretical and practical aerodynamics - Vol. 1
16 p1851 N73-24999
Measurement of pitching moment derivatives using free oscillation technique on two dimensional airfoils of double wedge section and single wedge section
[ARC-R/M-3234] 16 p1855 N73-25025
Flight tests of XB-70 aircraft to determine skin friction coefficients and boundary layer profiles at Mach numbers up to 2.5
[NASA-TN-D-7220] 16 p1887 N73-25276
Force measurements and pressure distributions on three Gottinger airfoil profiles during transition from laminar to turbulent boundary layer flow
[NASA-TT-F-14959] 17 p1979 N73-26000
Numerical analysis of effect of streamwise coordinate of basic flow on stability characteristics of boundary layer flow
17 p2012 N73-26270
Nonstationary heat and mass transfer developed by transverse flow around cylindrical body to determine conditions at stagnation point
[AD-760396] 17 p2016 N73-26299
Development of wind and turbulence model for surface boundary layer based on surface parameters of stability and height
[NASA-CR-2288] 18 p2104 N73-27021
Interactions of radiation with conductive and convective heat transfer in ablation and boundary layer flow determined by normal mode expansion technique
18 p2128 N73-27200
Wind tunnel investigation of turbulent boundary layer response to lateral surface roughness discontinuities
18 p2129 N73-27202
Influence of CISK process on mass convergence in tropical planetary boundary layer
18 p2171 N73-27529
Vectored injection into non-adiabatic boundary layer flows including incipient separation
[VPI-AERO-003] 19 p2255 N73-28176
Numerical analysis of compressible turbulent boundary layer velocity and temperature profiles with zero pressure gradient
[AD-762152] 19 p2258 N73-28200
Numerical calculation of three dimensional boundary layers by finite difference methods
20 p2384 N73-29156
Analysis of drop trajectories transition of boundary layer structure and flow regime for binary spray flow over upstream surface of isothermal cylinder
20 p2386 N73-29171
Application of finite-difference machine code for analyzing wake-vortex problem in quasi-cylindrical boundary layer approximation
[NASA-TM-X-69495] 20 p2387 N73-29179
Wind tunnel tests to determine boundary layer characteristics of air flows using laser light source and thermoanemometer
[NASA-TT-F-14945] 20 p2387 N73-29180
Effect of surface pressure fluctuations on response of panels underlying attached and separated turbulent boundary layers and shock waves
20 p2479 N73-29910
Effect of ablation modes and flow field distribution on cross hatching phenomenon at supersonic speeds
[TN-85] 20 p2485 N73-29963
Numerical analysis of three dimensional boundary layer for various distribution laws of suction intensity on leading edge of wing
[AD-763280] 21 p2497 N73-30038
Numerical analysis of effect of boundary layer profile on dynamic response and acoustic radiation of thin, elastic, flat plates
[NASA-TM-X-69568] 21 p2523 N73-30232
Analysis of boundary layer and turbulence characteristics inside passages of axial flow inducer and technique for predicting properties of boundary layer
[NASA-CR-121248] 21 p2524 N73-30240
Changes in planetary boundary layer wind profiles
[PB-221752/9] 22 p2697 N73-31601
Analysis of water table simulation of transpirationally cooled nozzle, and formulation of two flow models of water table boundary layer
[NASA-TM-X-2884] 22 p2710 N73-31702
Wind tunnel tests to determine boundary layer flow characteristics in supersonic axisymmetric inlet
[NASA-TM-X-2902] 23 p2739 N73-31926
Flow field solution for boundary layer interaction in confined viscous vortex
23 p2772 N73-32170
High enthalpy hypersonic bounary layer flow
[NASA-CR-135479] 23 p2774 N73-32187
Flow interference between supersonic intake and airframe to show three dimensional separation of boundary layer
23 p2775 N73-32194
Free jet boundary and distribution of flow within planar jet and pressure distribution at flat panel
[NASA-TT-F-15151] 24 p2905 N73-33180
Turbulent shear stress profiles in boundary layer flow at sine wave pressure perturbations
24 p2906 N73-33194
Stability of heterogeneous chemical recombination reactions of free radicals in boundary layer flow past heat conducting wall
24 p2908 N73-33209
Integral relations of velocity and thermal boundary layer for approximation purposes
24 p2909 N73-33213
Boundary layer calculation and wind tunnel model test of ships
24 p2909 N73-33214
Three dimensional incompressible laminar flow in centrifugal toroidal shell
24 p2909 N73-33215

**BOUNDARY LAYER NOISE**

U AERODYNAMIC NOISE
U BOUNDARY LAYERS

**BOUNDARY LAYER SEPARATION**

Incompressible boundary layer flow separation over moving boundaries
[AD-746869] 02 p0159 N73-11292
Three-dimensional flow arising in two dimensional separation bubbles noting flow characteristics in turbulent and laminar layer and in suction or blowing conditions
[IC-AERO-72-19] 05 p0525 N73-14275
Analysis of parameters affecting aircraft stall and post stall gyrations to include aerodynamic configurations and pilot performance
06 p0616 N73-14999
Analysis of laminar part of separation bubbles in two dimensional incompressible flow for various shaped objects
06 p0616 N73-15000
Development of method for calculating small separation zones near leading edge of airfoil at incidence
06 p0616 N73-15002
Analysis of unsteady flow over moving boundaries to determine characteristics of boundary layer separation
[AD-750398] 06 p0655 N73-15322
Three dimensional boundary layer separation and shock wave generation in flow field of supersonic conical intake mounted on fuselage side
[ARL/ME-137] 08 p0863 N73-16981
Couette flows used to determine effect of injection and curvature of walls on flow separation
[AD-753501] 09 p1019 N73-18317
Flow instabilities of supersonic variable ramp inlets at Mach 2 discussing Concorde aircraft intake
[ARC-R/M-3711] 10 p1104 N73-18999
Method for calculating three dimensional turbulent boundary layer separation applied to simple turbomachine case
10 p1205 N73-19808
Effect of plume-induced boundary layer separation on afterbody during powered supersonic flight
[AD-754640] 11 p1272 N73-20326
Partial differential equations for studying laminar boundary layer separations
13 p1508 N73-22221
Analysis of fluid flow over two dimensional flat plate wedge configuration for application to deep submersible vehicles
[NASA-CR-131888] 13 p1510 N73-22233
Calculation of supersonic boundary layer flow separation and reattachment along plane wall with sinusoidal hollow
[REPT-72-4] 14 p1650 N73-23382
Supersonic boundary layer separation and reattachment - finite difference theory solutions
[AD-757062] 14 p1651 N73-23388
Boundary layer separation on flat plate in high supersonic free stream as caused by normal injection of two dimensional sonic or supersonic jet
[AD-757635] 14 p1652 N73-23398
Turbulent boundary layer separation criteria for subsonic and transonic flows
[AD-757531] 14 p1652 N73-23401
Analysis of Kutta-Joukowsky condition in three dimensional flow with application to vortex sheet attachment to wing surface
[NASA-TT-F-14918] 15 p1767 N73-24319
Wind tunnel tests to determine effect of approaching boundary layer on separated flow behind downstream facing step
[NLR-TR-70033-U] 15 p1768 N73-24322
Stalling characteristics of airfoil in laminar viscous incompressible fluid with consideration of starting vortex and separation bubble
[AD-758831] 15 p1769 N73-24334
Analysis of effects of shock induced boundary layer separation in transonic flight and methods for eliminating or reducing effects
[ARC-R/M-3510] 16 p1854 N73-25019
Analytical method for predicting stall flutter of axial-turbomachine blading
[AD-760354] 17 p2078 N73-26813
Structural and gas dynamic parameters at flow separation boundary in compressor cascades
[AD-762238] 19 p2257 N73-28197
Influence of high level of inlet turbulence on performance of annular diffusers having center bodies of uniform diameter and conically diverging walls
[TT-7101] 22 p2652 N73-31243
Investigation of naturally turbulent two dimensional boundary layer undergoing separation
[AD-764512] 22 p2655 N73-31272
Flow interference between supersonic intake and airframe to show three dimensional separation of boundary layer
23 p2775 N73-32194
Incipient boundary layer separation on axiaymmetric compression surfaces of conical body at hypersonic speeds
23 p2775 N73-32195

**BOUNDARY LAYER STABILITY**

Stability of laminar boundary layers
[NASA-CR-128532] 01 p0039 N73-10311
Boundary layer stability on two-layer flat plates using viscous liquid currents
[AD-752696] 09 p1016 N73-18294
Orr-Sommerfeld equation for studying laminar boundary layer stability on elastic surface
[NASA-TT-F-14855] 11 p1270 N73-20307
Analysis of mean and fluctuating flow properties of compressible turbulent boundary layer in shock wave-induced adverse pressure gradient
[NASA-TN-D-7092] 12 p1391 N73-21280
Linear stability analysis on liquid film adjacent to compressible viscous gas stream
[AD-758982] 16 p1889 N73-25290
Numerical analysis of effect of streamwise coordinate of basic flow on stability characteristics of boundary layer flow
17 p2012 N73-26270
Theory for small perturbation laminar boundary layer stability at longitudinally curved walls
24 p2909 N73-33212

**BOUNDARY LAYER TRANSITION**

Accuracy of transitional boundary layer theory in low hypersonic Mach number range
[NASA-CR-2131] 01 p0041 N73-10322
Postflight evaluation of ballistic vehicle flight test boundary layer transition data
[NASA-CR-129045] 03 p0282 N73-12287
Assessing laminar flow on conical vehicles during hyperbolic entry by studying boundary layer transition on ablating cones
[NASA-TM-X-68867] 03 p0283 N73-12293

Analysis of flow distribution around axisymmetric bodies at extreme angles of attack and calculation of pressure distribution for asymmetric steady vortex wake
[AD-747986] 03 p0286 N73-12315
Calculation of heat transfer on turbine blade profiles to determine transition region coordinates in boundary layer flow through gas turbine engine
[AD-747602] 03 p0352 N73-12870
Transonic flow around slender bodies noting wave drag deceleration and boundary layer transition
[ISL-33/71] 04 p0406 N73-13304
Development of iterative procedure for analysis of arbitrary multi-element airfoils in viscous flow
[AD-749484] 05 p0496 N73-14042
Effects of flow turbulence and noise on transition and boundary layer development in aerodynamic wind tunnel tests
[NASA-TT-F-14833] 09 p1066 N73-18702
Finite difference procedure for computing behavior of two-dimensional boundary layers and turbulence model to predict location and extent of transition region
10 p1204 N73-19796
Predictions of boundary layer transition on turbomachine blades
10 p1204 N73-19797
Effects of nose bluntness on natural and induced boundary layer transition on axisymmetric bodies in supersonic flow
[AD-755843] 12 p1393 N73-21295
Analytic model to make comprehensive transition run-out calculations for compressible boundary layer with wall cooling
[AD-756890] 13 p1513 N73-22258
Boundary layer transition and heat transfer in aerodynamic and thermic wall deformation
14 p1601 N73-22982
Force measurements and pressure distributions on three Gottinger airfoil profiles during transition from laminar to turbulent boundary layer flow
[NASA-TT-F-14959] 17 p1979 N73-26000
Influence of free stream Reynolds number on transition in boundary layer on infinite swept wing
17 p2013 N73-26280
Application of methods for prediction of boundary layer transition on sheared wings
17 p2013 N73-26281
Analysis of flow distribution over three axisymmetric bodies at various angles of attack to determine boundary layer transition point characteristics
19 p2250 N73-28145
Analysis of surface pressure and cold wall heating rate distributions for large, flat panel at Mach 7 in high temperature wind tunnel
[NASA-TN-D-7275] 21 p2524 N73-30243
Shadowgraph photography of boundary layer transition of spinning cones
[AD-762564] 22 p2656 N73-31276

**BOUNDARY LAYERS**
NT ATMOSPHERIC BOUNDARY LAYER
NT COMPRESSIBLE BOUNDARY LAYER
NT HYPERSONIC BOUNDARY LAYER
NT INCOMPRESSIBLE BOUNDARY LAYER
NT LAMINAR BOUNDARY LAYER
NT SUPERSONIC BOUNDARY LAYERS
NT THERMAL BOUNDARY LAYER
NT THREE DIMENSIONAL BOUNDARY LAYER
NT TURBULENT BOUNDARY LAYER
NT TWO DIMENSIONAL BOUNDARY LAYER
Remotely operated boundary layer probe for use in three dimensional measurements
[AD-745215] 01 p0059 N73-10481
Nozzle wall boundary layer of helium tunnel
[NASA-TN-D-6965] 02 p0156 N73-11261
Procedure for solving nonconservative projectile penetration problems
[AD-746140] 02 p0219 N73-11774
Calculation of heat transfer on shuttle type configurations including effects of variable entropy at boundary layer edge
[NASA-CR-112180] 04 p0484 N73-13958
Surface pressure distribution on hydrofoil profiles in accelerated cascades, using boundary layer calculations
[REPT-251] 06 p0724 N73-15914
Optimal coordinates and boundary layer theory
07 p0767 N73-16234
Analysis of Magnus sideforce developed by spinning cylinder at angle of attack based on boundary layer and shed vorticity in cross flow
07 p0768 N73-16239
Boundary layer approach to analysis of atmospheric motion over surface obstruction
[NASA-CR-2182] 07 p0769 N73-16244
Simplified steady boundary layer flows at low altitudes, with small Coriolis parameter
07 p0776 N73-16297
Characterization of halo in pinch plasma by image converters and streak camera
[IPP-1/125] 07 p0828 N73-16709
Integration of Galerkin method for solving boundary layer equation with steady incompressible flow
[AD-752203] 08 p0898 N73-17275
Affect of sound and vibration on convective heat transfer and flow distribution on boundary layers of cylindrical bodies
[AD-754006] 10 p1143 N73-19316
Boundary layer effects in turbomachines
[AGARD-AG-164] 10 p1204 N73-19794
Role of boundary layers in axial flow turbomachines and prediction of their effects
10 p1205 N73-19806
Mathematical model for prediction of axial compressor performance including effect of annulus wall boundary layers
10 p1206 N73-19812
Prediction of annulus wall boundary layers in axial flow turbomachines
10 p1206 N73-19813
Annulus wall boundary layers in axial flow turbomachine
10 p1206 N73-19814
Shock wave boundary layer interaction in compressor cascades
10 p1207 N73-19816
Boundary layer behavior in supersonic straight and annular blade cascades of fixed and mobile types
10 p1207 N73-19817
Heat and mass transfer with phase and chemical transformations in reacting boundary layer
[AD-758210] 15 p1748 N73-24165
Transonic wind tunnel wall effects on boundary layer blocking phenomena
15 p1766 N73-24306
Approximate calculation of heat transfer in transpired boundary layers
[AD-759353] 16 p1891 N73-25301
Boundary layer electron concentration profiles for entry of blunt nosed slender body into earth atmosphere
[NASA-TN-D-7332] 18 p2182 N73-27620
Boundary between open and closed magnetospheres of pulsar atmosphere
[AD-761883] 21 p2598 N73-30822
Boundary and shear layers in rotating and stratified fluids
22 p2651 N73-31235
Equilibrium structure of boundary layer between plane magnetic piston and low density plasma
[JUL-890-PP] 22 p2704 N73-31655
Analytic procedure for nonequilibrium boundary layer integral matrix code
[NASA-CR-134039] 22 p2729 N73-31835
Formation of vortices in free boundary layer
[NASA-TT-F-15133] 23 p2774 N73-32188
Remote sensing of ocean current boundary layer in Caribbean Sea from Skylab EREP
[E73-11095] 23 p2783 N73-32262
Fluid dynamics, noting boundary layer theory
[DLR-FB-72-26] 24 p2905 N73-33186
Fluid dynamics, noting boundary layer theory
[DLR-FB-72-27-PT-2] 24 p2907 N73-33202
Magnetospheric plasma flow and magnetospheric boundary layer observations by Vela satellite
[LA-UR-73-732] 24 p2964 N73-33686

**BOUNDARY LUBRICATION**
Oxygen concentration on boundary lubricating characteristics of unformulated C-ether using ball-on-disk sliding friction apparatus
[NASA-TN-D-7155] 07 p0811 N73-16578
Chemistry and physics of thin liquid films in contact with solid substrates and application to boundary lubrication of propulsion systems
[AD-757061] 14 p1670 N73-23556
Investigation of wear behavior and load capacity of journal bearings in transition range from full to boundary lubrication using radioisotopes
[KFK-1569] 15 p1793 N73-24533

**BOUNDARY VALUE PROBLEMS**
NT NEUMANN PROBLEM
Effect of longitudinal slot in circular waveguide
[PB-208160] 01 p0034 N73-10267
Application of periodic Dirichlet problems to analysis of planar theory of elasticity
[AD-741924] 01 p0115 N73-10948
Boundary value problem of finite tubular antenna in free space and hot isotropic plasma
[AD-746171] 02 p0141 N73-11145
Location of poles of scattering matrix
02 p0201 N73-11628
Volterra factorization of Green matrix and imbedding of general linear boundary value problems
[TR-72-48] 02 p0202 N73-11634
Applications of orbital mechanics to aerospace systems and ballistic trajectories
[AD-746706] 02 p0232 N73-11885
Analysis of refraction of gravity water waves based on group velocity and phase velocity relationships
[AD-747982] 03 p0286 N73-12316
Solution of boundary value problems by characteristics equations
[NASA-CR-129256] 03 p0324 N73-12637
Computer methods for solving some boundary value problems dealing with transport phenomena
[AD-747962] 03 p0325 N73-12651
Spline approximation of initial value problem and successive application of finite difference and spline interpolation operators for heat equation
[AD-748774] 04 p0441 N73-13594
Boundary value equations for numerically forecasting weather in area defined by artificial boundaries
[AD-749748] 05 p0576 N73-14689
Series expansion of functions using eigenfunctions and applications to initial and boundary value problems of orbital mechanics
[BMBW-FBW-72-33] 09 p1084 N73-18844
Thermal stress vibrations in prebuckled region of orthotropic trapezoidal plates with two parallel opposite sides and various boundary conditions
[NASA-CR-2174] 09 p1094 N73-18928
Application of theoretical framework of governing equations and extremum principles to classical elasticity and plasticity yield-point problems
[AD-753137] 09 p1096 N73-18948
Calculation of bifurcation stress in elastic/plastic plate under uniaxial compression
[AD-753136] 09 p1096 N73-18949
Geodetic boundary value solution with height anomalies to plus or minus 5 cm and to order e cubed
[NASA-TM-X-66199] 10 p1153 N73-19384
Mologenskys solution of geodetic boundary value problems
[AD-754251] 11 p1287 N73-20444
Solution of Hertz contact problem for case involving indentation of elastic half space by rigid axisymmetric punch under monotonically applied normal force with assumed Coulomb friction
[AD-755071] 11 p1299 N73-20544
Field method for linear static analysis on open branch shells of revolution under asymmetric loads
[NASA-CR-112270] 11 p1311 N73-20638
Application of vibrational methods for solving problems on theory of elasticity
[AD-754668] 11 p1346 N73-20922
Approximative solution for first boundary value problem of thermal conductivity
[AD-754255] 11 p1349 N73-20947
Effect of homogeneous dielectric sphere on electromagnetic radiation from simple sources treated as boundary value problem and solution obtained by technique of dyadic Green functions
[NASA-CR-2211] 12 p1378 N73-21178
Vibratory stability of plate over viscous heat conducting gas layer
[AD-755288] 12 p1393 N73-21293
Steady oscillatory irrotational motion of inviscid incompressible fluid described by boundary value problem of elliptic type
[AD-755465] 13 p1512 N73-22252
Entropy rate admissibility criterion for solutions of hyperbolic conservation laws
[NASA-CR-131812] 13 p1513 N73-22261
Intermediate problem technique used to generate difficult eigenvector and boundary value problem solutions
[AD-756672] 13 p1550 N73-22561
Uniqueness of solution for plane crack problems in linear elastostatics
[AD-756653] 13 p1587 N73-22865
Application of trilinear coordinates to boundary value problems in plane elasticity
[AD-755181] 13 p1588 N73-22876
Numerical solution of one hydrodynamics equation
[AD-756099] 14 p1651 N73-23394
Velocity potential solution of heavy incompressible liquid wave motion
[AD-758251] 15 p1769 N73-24331
Steady state solution of hydromagnetic mode of initial value problem of micropulsations
[AD-757866] 15 p1783 N73-24451
Development of finite difference method for calculating boundary value problem for nonsymmetrical deformation of random shells of revolution
[NLL-DRIC-TRANS-2996-[3623.66]]
15 p1836 N73-24884
Circular geometry and mixed boundary value problems in three dimensional elasticity
[NASA-TN-D-7266] 15 p1837 N73-24891
Optimization of mass distribution of solid beams and panels for structural design of airframes and panels
[AD-759169] 16 p1859 N73-25054
Nonlinear, two point, boundary value problems using Chebyshev polynomial series
17 p2054 N73-26613
Elastic vibrations of aircraft wing caused by distributed load, center of gravity displacement, and rotation using electromodeling techniques
[AD-760965] 18 p2108 N73-27043
Analysis of wake collapse in sea water and stratified fluids with emphasis on final stages of decay
[AD-761622] 19 p2257 N73-28189
Numerical boundary conditions in baroclinic and barotropic models for forecasting
[DM-9] 19 p2316 N73-28623
Numerical solution to boundary value problems of hydrodynamic forecasting and atmospheric circulation
[AD-761574] 19 p2317 N73-28640

Derivations of second-order asymptotic boundary value solutions for lunar and interplanetary trajectories
[NASA-CR-2256] 19 p2343 N73-28845
Analysis of boundary value problem associated with laminar fluid flow
20 p2385 N73-29158
Technique for dealing with problem of elastic domain containing arbitrarily oriented internal crack
[NASA-CR-132289] 20 p2482 N73-29937
Approximation of functions of terminal state of dynamic system and determination of error bounds
21 p2515 N73-30175
Numerical solution of multidimensional linear thermal conductivity problems with complex boundary conditions which occur with heating of metals
[NLL-M-21666-[5828.4F]] 21 p2557 N73-30495
Boundary layer theory for flow and heat transfer problems in turbomachine blades
21 p2590 N73-30751
Boundary value problems involving T-T operators
[AD-763837] 22 p2692 N73-31562
Applications of eigenfunctions for solution of boundary value problems in orbital mechanics
[BMBW-FBW-72-17] 22 p2718 N73-31758
Initial value problems solution on satellite geodesy and orbital mechanics using Hammerstein method for boundary value problem
[BMBW-FBW-72-23] 22 p2718 N73-31759
Boundary conditions and uniqueness in internal gas dynamic flows
23 p2775 N73-32192

**BOW SHOCK WAVES**
U BOW WAVES
U SHOCK WAVES

**BOW WAVES**
Greenstadt binary index criterion for distinguishing between laminar and pulsating bow shock crossings expressed as critical angle between shock normal and magnetic field
[NASA-TM-X-66105] 02 p0225 N73-11817
Numerical analysis of ion dissipation in high Mach number bow shocks
[IPP-6/102] 04 p0405 N73-13300
Correlative studies of effects of solar wind and interplanetary magnetic field on bow shock and geomagnetic cavity
[NASA-CR-129924] 05 p0592 N73-14808
Whistler wave propagation in relation to interplanetary shocks
[NASA-TM-X-66245] 15 p1778 N73-24414

**BOX BEAMS**
Four-phase airframe fatigue program for bending tests of aluminum alloy box beams
[AD-744673] 01 p0114 N73-10943
Mathematical model for bending of hybrid and composite hybrid beams
[CRIF-MT-79] 05 p0603 N73-14902

**BOXES [CONTAINERS]**
Apollo lunar sample return containers for storing and protecting lunar samples
[Y-1867] 21 p2553 N73-30465

**BRADYCARDIA**
Bradycardia and death in guinea pigs exposed to acceleration overloads after injections of aminothiol group radioprotectors
11 p1239 N73-20057
Role of water temperature in bradycardia during facial immersion
[NASA-TT-F-15025] 24 p2890 N73-33072

**BRAGG ANGLE**
Principles and techniques of Bragg diffraction laser beam probing of ultrasonic field
[AD-756521] 13 p1537 N73-22454

**BRAIDED STREAMS**
U STREAMS

**BRAIN**
NT CEREBRAL CORTEX
NT CEREBRUM
Toxic effects of Freon decomposition products on activity of isoenzymes of lactate dehydrogenase in rat brains
03 p0259 N73-12097
Electrophysiological sleep patterns of human and animal brains
[NASA-TT-F-740] 13 p1483 N73-22023
Interdependence of slow and rapid brain waves during sleep
13 p1483 N73-22027
Somnofunctional mapping of deep brain waves in neurological patients
13 p1484 N73-22029
Bioelectric activity and excitability of cat brain structures during sleep phases
13 p1484 N73-22031
Bioelectric activity changes in brains of sleeping children caused by aging factor
13 p1484 N73-22032
Cone model for oxygen diffusion in brain considering spatial tissue/capillary permeability
[RAE-LIB-TRANS-1663] 17 p1987 N73-26060
Effects of phosadrin on electrical brain potentials in squirrel monkeys
[FAA-AM-73-3] 18 p2109 N73-27056
Equipment for implanting electrodes in subcortical structures of cat brain
[NASA-TT-F-15001] 19 p2225 N73-27947
Relation between hyperbaric oxygenation and functional activity of differentiated brain with respect ot glutamic acid metabolism
19 p2227 N73-27960
Temperature interrelationships between rat brain tissues and cerebral blood supply
20 p2366 N73-29026
State of blood filling and bioelectric activity of grain in circulatory hypoxia in healthy persons and individuals with early forms of autonomic vascular dysfunction
24 p2883 N73-33027
Various types of corticopetal influences from deep-seated emotiogenic formations of brain
24 p2889 N73-33068

**BRAIN CIRCULATION**
Influence of altitude and drugs on cerebral circulation in smokers and non-smokers
12 p1371 N73-21125

**BRAKES [FOR ARRESTING MOTION]**
NT AERODYNAMIC BRAKES
NT AIRCRAFT BRAKES
NT DRAG CHUTES
NT LEADING EDGE SLATS
NT TRAILING-EDGE FLAPS
NT WING FLAPS
Analysis of heat dissipation and frictional properties of materials used in aircraft brakes
[NASA-CR-121116] 06 p0687 N73-15595
Brake clearance controlling mechanism with split bush screwed into body and with components as springing elements
[AD-742704] 13 p1533 N73-22424
Chloride and water permeability parameters for hydraulic brake hose testing
[AD-748083] 13 p1546 N73-22530
Sprag solenoid brake with cylindrical chamber
[NASA-CASE-MFS-21846-1] 14 p1670 N73-23552
Aircraft accident involving Boeing 747 aircraft during landing at Miami, Florida airport on 15 Dec. 1972 following collision with birds
[NTSB-AAR-73-13] 17 p1983 N73-26029
Analysis of various aircraft antiskid braking systems to determine appropriate antiskid braking system for space shuttle vehicle
[NASA-CR-124349] 19 p2294 N73-28449

**BRAKING**
Wind tunnel tests of blowing on circular cylinders applied to aircraft control and braking at low speeds
[ARC-CP-1232] 10 p1104 N73-19000
Analysis of effect of grooved runway configurations on aircraft tire braking traction on flooded runway surfaces
[NASA-TN-D-7215] 12 p1363 N73-21057
Dependences between braking and precession moments acting on spherical rotor in magnetic suspension
21 p2547 N73-30422

**BRANCHING [PHYSICS]**
Molecular branching ratio method for intensity calibration of optical systems in far ultraviolet
[NASA-TM-X-66070] 01 p0103 N73-10853
Mathematical model for energy distribution in waveguide bifurcations
[DLR-FB-71-17] 05 p0520 N73-14224

**BRASSES**
Electric arc welding of tin and aluminum bronzes and silicon brass
[DRIC-TRANS-2843] 02 p0179 N73-11448
Effect of hydrostatic pressure on plasticity of L-62 copper-zinc brass and LS-59-1 brass
[NLL-NEL-TT-2398-[6075.461]] 02 p0185 N73-11497
Influence of preliminary deformation on superplasticity of alpha brasses and pure copper
09 p1047 N73-18534
Internal friction measurements on brass and aluminum alloys during plastic deformation loading
[AD-760145] 17 p2048 N73-26570
Plastic deformation in alpha-brasses
20 p2427 N73-29497
Interstitial and vacancy motion in defect annealing of alpha brass and copper gold alloy by electron irradiation
22 p2683 N73-31489
Elastic and shape memory properties of beta-brass alloys at various temperatures
[AD-764472] 22 p2686 N73-31515

**BRAYTON CYCLE**
Analysis of terrestrial nuclear hazards involving zirconium hydride reactor-Brayton power module for all phases of space base program - Vol. 3 Pt. 2
[NASA-CR-123839] 02 p0209 N73-11697
Preliminary design of heat exchanger and duct assembly for Brayton cycle space power system
[NASA-CR-121011] 05 p0605 N73-14923
Performance and cost effectiveness of isotope Brayton space power system
[NASA-TM-X-68145] 06 p0626 N73-15081
Motor starting characteristics of Brayton electric engine using static inverter
[NASA-TM-X-2738] 09 p0990 N73-18080
Modifications and test performance of 2 to 15 kilowatt Brayton cycle electrical subsystem
[NASA-TM-X-2757] 09 p0990 N73-18083
Effects of backlash and dead band on temperature control of primary loop of conceptual nuclear Brayton space powerplant
[NASA-TM-X-2754] 09 p1064 N73-18679
Design, development, fabrication, and test of coolant circulating pump assemblies for use in Brayton cycle space power system
[NASA-CR-2176] 11 p1297 N73-20529
Design, development, and test of two types of pivoted pad journal bearings and spiral groove thrust bearing for use with Brayton cycle power unit
[NASA-CR-121098] 12 p1408 N73-21410
Vibration response of gas bearing rotor-supports to sinusoidal and random vibrations in Brayton rotating unit turbogenerator
[NASA-CR-2177] 13 p1534 N73-22427
Reduction of random vibration response data for NASA Brayton rotating unit turbogenerator
[NASA-CR-121178] 13 p1534 N73-22428
Performance of gas lubricated nonconforming pivoted-pad journal bearings and flexibly mounted spiral groove thrust bearing designed for Brayton cycle rotating unit
[NASA-TM-X-2765] 15 p1738 N73-24086
Operational performance of electrical subsystem for Brayton power conversion system
[NASA-TM-X-2810] 15 p1738 N73-24088
Design, fabrication, and performance tests of foil journal bearings for application to Brayton cycle turbo-alternator-compressor
[NASA-CR-2243] 19 p2304 N73-28529
Design and evaluation of mini-Brayton compressor-alternator-turbine system for spacecraft power supplies
[NASA-CR-133810] 21 p2553 N73-30463

**BRAZIL**
Tables of earth magnetic field intensity measurements at Sao Jose dos Campos, Brazil
[AD-747060] 04 p0415 N73-13389
Analysis of remote sensing of earth resources program conducted by Brazil
07 p0783 N73-16364

**BRAZING**
Ultrasonic scanner for inspection and evaluation of in-place brazed tube joints
[NASA-TM-X-64702] 02 p0178 N73-11445
Effects of high temperature brazing and thermal cycling on mechanical properties of Hastelloy X
[NASA-TM-X-2704] 04 p0433 N73-13529
Production of ceramic-metal compounds by contact-reactive brazing for increasing mechanical strength
10 p1163 N73-19462
Compilation of eutectics and melting point minima for binary combinations of metals for refractory metal brazing
[NASA-TM-X-68190] 10 p1172 N73-19537
Test equipment and methods for nondestructive inspection of welded, brazed, and composite structures
[NASA-SP-5952[02]] 11 p1297 N73-20528
Electric resistance spot welding and brazing for producing metal bonds with superior mechanical and structural characteristics
[NASA-CASE-LAR-11072-1] 11 p1298 N73-20535
Quality control of welded, brazed, and bonded electrical terminations
[BDX-613-613-REV] 12 p1383 N73-21214
Preflight, inflight, and post flight operations evaluation analyses for Skylab exothermic brazing experiment facility - Appendix G
[NASA-CR-61386-APP-G] 14 p1708 N73-23861
Metallurgical and mechanical properties of joints treated by weld-braze joining process
[NASA-TN-D-7281] 15 p1798 N73-24573
Vacuum brazing-gas quenching process for joining chemical and ordnance munitions materials
[AD-759117] 16 p1919 N73-25531
Causes of defects in silver-brazed steel joints
[AD-762120] 19 p2305 N73-28541

**BREADBOARD MODELS**
Evaluation of HF/VHF breadboard modeled manpack radio sets
[AD-745918] 02 p0142 N73-11152
Spacecraft communications terminal breadboard components
[NASA-CR-128859] 11 p1255 N73-20181
Prototypes of two acoustic delay lines with delays of 0.5 and 7.5 microsec, noting passband enlargement and echo suppression
15 p1757 N73-24239
Development of breadboard model correlation interferometer for carbon monoxide pollution experiment
[NASA-CR-112212] 16 p1913 N73-25478
Design, fabrication, and tests of breadboard model of earth orbital, rotating gradiometer
[NASA-CR-112215] 23 p2792 N73-32340

**BREAKAWAY**
U BOUNDARY LAYER SEPARATION

**BREAKDOWN**
High vacuum breakdown initiated field emission between technically pure electrodes
[AD-747586] 03 p0338 N73-12753

Thermal instability and secondary breakdown prediction for low frequency power transistor
[AD-751852] 08 p0890 N73-17203
Test data on liquid dielectric breakdown mechanisms
[AD-752819] 09 p1053 N73-18585
Characteristics of second breakdown in germanium gold diodes
[AD-755425] 12 p1385 N73-21230
Effects of acceleration or retardation on electric strength of gas
[AD-755848] 12 p1429 N73-21584
Effect of atmospheric contaminants on laser induced air breakdown
[AD-760175] 17 p2070 N73-26750
Ionizing wave transport in streamer breakdown of gas
[JPRS-59474] 18 p2183 N73-27622

**BREAKERS [ELECTRIC]**
U CIRCUIT BREAKERS

**BREAKWATERS**
Effects of vertical jet breakwaters on wind generated deep water waves
[AD-748190] 05 p0528 N73-14293

**BREATHING**
NT HIGH ALTITUDE BREATHING
NT OXYGEN BREATHING
Design and performance of breathing metabolic simulator
04 p0472 N73-13850
Helium/oxygen breathing effects on rat gas exchange and musculoskeletal heat control
10 p1115 N73-19093
Physiological effects of argon/oxygen breathing on rats noting carbon dioxide level
10 p1116 N73-19094

**BREATHING APPARATUS**
NT OXYGEN MASKS
NT UNDERWATER BREATHING APPARATUS
Influence of liquid oxygen on chromate coated aluminum tubing of breathing apparatus
[AD-752030] 08 p0936 N73-17661
NO2 and UDMH absorbing properties of rocket propellant gas mask canisters
[AD-752538] 10 p1203 N73-19791
Design and performance of demand regulated liquid breathing systems for mammalian respiration
13 p1478 N73-21976
Breathing apparatus for parachutists
[AD-756554] 15 p1745 N73-24141
Decomposition of compounds adsorbed in charcoal of manned spacecraft breathing system
[NASA-CR-134013] 21 p2504 N73-30092

**BREECHES**
U CLOSURES

**BREEDER REACTORS**
Carbon dioxide gas turbine cycles for sodium cooled fast breeder reactor
[BMBW-FBK-72-17] 03 p0334 N73-12722
Fabrication and characteristics of ceramic-metal multilayers for inclusion in experimental breeder reactor
[LA-5021-PR] 07 p0820 N73-16646
Nuclear calculations for gas core breeder reactor configurations
19 p2319 N73-28656
Triple wall tube exchanger/steam generator for sodium cooled fast breeder reactor
[BMBW-FBK-72-28] 22 p2699 N73-31619

**BREGUET AIRCRAFT**
NT BREGUET 941 AIRCRAFT
NT BREGUET 1150 AIRCRAFT

**BREGUET 941 AIRCRAFT**
Flight tests for determining handling qualities and operational characteristics of Breguet 941 STOL aircraft
18 p2103 N73-27008

**BREGUET 1150 AIRCRAFT**
Description of Breguet 1150 to be used as European earth resources survey aircraft noting sensor payload
21 p2538 N73-30353

**BREMSSTRAHLUNG**
Production and research applications of magnetic bremsstrahlung
[BNL-TR-480] 04 p0452 N73-13689
Anisotropy and angular distribution of bremsstrahlung radiation emitted by electrons confined in magnetic mirrors
[ORNL-TM-3821] 04 p0453 N73-13698
Coincidence rate measurements for inelastically scattered electrons and associated bremsstrahlung at intermediate bombarding energies
[NASA-CR-124007] 06 p0702 N73-15723
Differential cross section of emitted photon in suprathermal proton bremsstrahlung
08 p0974 N73-17966
Bremsstrahlung for enhancing far infrared laser scattering from theta pinch plasma
[AD-753404] 09 p1073 N73-18755
Bremsstrahlung theory for relativistic plasma properties
[AEC-TR-7348] 12 p1434 N73-21618
Polarization of bremsstrahlung from electron-ion collisions by magnetically confined electrons
[ORNL-TM-4103] 17 p2067 N73-26726
Photonuclear activation with Ge L1 detectors
[AD-761992] 19 p2231 N73-27990
Hard X radiation from solar flares caused by bremsstrahlung of nonthermal electron streams
19 p2335 N73-28789
Dense plasma focus using CO2 laser scattering and infrared bremsstrahlung emission
[COO-2233-2] 22 p2703 N73-31652
Bremsstrahlung radiation from beam of electrons in solar chromosphere, and total energy of solar flares
[NASA-CR-133943] 22 p2711 N73-31710
Auroral bremsstrahlung flux spectra at various atmospheric depths
[NASA-SP-3081] 23 p2786 N73-32293

**BREWSTER ANGLE**
Design of Brewster angle acousto-optic modulator for high power mode locked C02 laser
[AD-751680] 07 p0807 N73-16544

**BRICKS**
Development of construction block in form of container folded from flat sheet and filled with solid material for architectural purposes
[NASA-CASE-MSC-12233-2] 04 p0480 N73-13921

**BRIDGES**
Comparison of extreme floods statistically predicted for highway bridge design in Pennsylvania to actual floods caused by hurricane Agnes
[PB-220888/2] 21 p2575 N73-30639

**BRIDGES [STRUCTURES]**
Procedure for predicting aeroelastic behavior of Huber suspension bridge
[NPL-R102] 06 p0726 N73-15926

**BRIGHTNESS**
Legibility and recognition by test groups of displayed signals differing by brightness or color
[DLR-FB-71-57] 06 p0674 N73-15484
Black body brightness in horizontal visual range theory
[NASA-TT-F-14930] 15 p1814 N73-24700
Surface brightness and X ray measurements of Cygnus Loop from Aerobee rocket
[NASA-CR-133098] 17 p2080 N73-26822
Neon line strength measurements using coherent laser spectroscopy
[NASA-CR-133406] 18 p2114 N73-27096

**BRIGHTNESS DISCRIMINATION**
Bloch law error in visual perception of capacitor discharge brightness
[AD-749452] 05 p0505 N73-14109
Galactic brightness distribution obtained by imaging galaxies on Schmidt plates, selecting one as photometric standard and applying microdensitometric scans
07 p0845 N73-16852
Photometric measurements on human sensitivity to optical luminosity considering seasonal and monthly fluctuations
14 p1692 N73-23732
Automated visual sensitivity tester for determining visual field sensitivity and blind spot size
[NASA-CASE-ARC-10329-1] 17 p1988 N73-26072
Visibility and optimum light characteristics of marks for sighting devices
20 p2368 N73-29039

**BRIGHTNESS TEMPERATURE**
Radio observations of distribution of chromospheric brightness temperature
[AD-747021] 04 p0467 N73-13809
Measurements of isotropy of cosmic background radiation at 6 cm determined from apparent sky brightness temperature differences
07 p0838 N73-16789
Radio frequency measurement of brightness temperature and radar cross sections for explaining subsurface and atmospheric properties of Venus
07 p0840 N73-16803
Infrared measurement of brightness temperature of Martian surface by Mars-3 automatic interplanetary station
[NASA-TT-F-14837] 10 p1211 N73-19852
Microwave emissivity and sea brightness temperatures of surface waves
[AD-753533] 11 p1287 N73-20443
Characteristics of thermal radiation of Greenland ice measurements by Cosmos-243
[NASA-TT-F-14953] 15 p1780 N73-24427
Development of catalogs for backscatter and brightness temperature measurements and atmospheric effects on Skylab S-193 data
[E73-10896] 20 p2395 N73-29245
Preparation of backscatter and brightness temperature measurement catalogs and atmospheric effects on Skylab S-193 data
[E73-10897] 20 p2395 N73-29246
Microwave imagery of Great Lake ice formations
22 p2736 N73-31903

**BRILLOUIN EFFECT**
Frequency and line width of Brillouin scattering in aqueous electrolyte solutions
[AD-749354] 04 p0387 N73-13148
Rayleigh-Brillouin intensity ratios measured for aqueous electrolytic solutions as function of concentration
[AD-753017] 09 p1001 N73-18166
High resolution Brillouin spectroscopic study of hypersonic sound velocity and attenuation as function of temperature in acrylic monomers
16 p1944 N73-25731
Stimulated Brillouin scattering in shock-compressed fluids
20 p2386 N73-29166
Manufacturing of high efficiency ultrasonic wave transducer for light modulation using Brillouin effect
[REPT-4.473] 23 p2820 N73-32544

**BRITISH AIRCRAFT CORP AIRCRAFT**
U BAC AIRCRAFT

**BRITTLE MATERIALS**
Strength of brittle matrix materials reinforced with steel fibers or whiskers
[NLL-CE-TRANS-6145-[9022.09]]
20 p2434 N73-29545
Nondestructive tests of brittle ceramic materials
[AD-764795] 23 p2811 N73-32477
Plastic flow and fracture mechanics of brittle cuperious oxide and gamma 2Cu-Al compounds under high pressure
24 p2967 N73-33709

**BRITTLENESS**
Fracture measurement in high strength brittle ceramic materials
[AECL-3677] 03 p0361 N73-12944
Brittle fracture of polycrystalline disks of alloyed alumina
[AD-748110] 04 p0439 N73-13577
Plastic deformation of brittle materials by machining
[AD-753027] 09 p1041 N73-18494
Relationship between brittle and plastic fracture of high strength steels owing to void dynamics
[NASA-CR-131101] 10 p1171 N73-19522
Silicon additions and borax-glass coatings used to reduce surface hot shortness of copper-bearing steels
[PB-212660] 11 p1307 N73-20607
Analysis of metal transition into brittle state with determination of impact strength
[AD-758252] 14 p1679 N73-23627
Brittleness determination of low density blown polyethylene film balloons to account for high altitude failure
[AD-757885] 15 p1802 N73-24603
Statistical theory for fracture of brittle structures subjected to nonuniform polyaxial stresses
[AD-759805] 16 p1970 N73-25936
Fracture mechanics applied to analysis of brittle fracture of unidirectional and angle-ply composites
[AD-760361] 17 p2053 N73-26610

**BROADBAND**
Comparison of European and United States of America reproduced broadband microwave components
[FOA-3-A-3750-E6] 02 p0148 N73-11204
Antenna feed networks for broadbanding very low frequency and low frequency antennas to wide frequency shift keying modulation
[AD-746119] 02 p0151 N73-11226
Computer aided broadband impedance matching technique using comparison reflectometer
[NASA-CR-129567] 04 p0398 N73-13237
Long life broadband transistor amplifier chain for very high frequency range
[AD-752444] 09 p1004 N73-18194
Radio frequency interference rejection of broadband communication system receiver
[AD-756590] 13 p1492 N73-22096
Channel measurement techniques, modeling multipath structure of line-of-sight tropospheric paths, and prediction of spread spectrum modem performance as function of multipath conditions
[AD-755922] 13 p1494 N73-22115
Theory for third harmonic generation due to broad band optical pulses in picosecond time region
[AD-757211] 14 p1693 N73-23742
Broadband characteristics of open sleeve dipole antenna mounted in front of metallic reflector
[AD-758755] 15 p1758 N73-24251
Hardware design, implementation, and test results of two wideband channel accommodation
[NASA-CR-124267] 16 p1875 N73-25182
Development of linear power transistors and design of broadband UHF amplifiers from these transistors
[AD-757558] 17 p2006 N73-26227
Multimode antenna feed system for microwave and broadband communication
[NASA-CASE-GSC-11046-1] 19 p2234 N73-28013
Broadband space feed system for phased array
[AD-763767] 21 p2518 N73-30195

**BROADBAND AMPLIFIERS**
Design and construction of broadband combinable amplifier using stripline techniques for UHF amplification
[AD-747404] 04 p0396 N73-13218
Design and performance of transistorized broadband logarithmic amplifier using hybrid thick film technology
[ECR-32] 12 p1382 N73-21210
Electronic digital data synchronizing and instrumentation amplification techniques
[AD-763797] 21 p2509 N73-30131

**BROADCASTING**
Systems analysis of radio-TV satellite for coverage of West Germany and west European areas with German language
14 p1710 N73-23876
Multiplexing still picture broadcasting by cable system
[NHK-LABS-NOTE-158] 18 p2115 N73-27099
Statistical weather analysis for optimum picture quality design of satellite television broadcasting system
18 p2115 N73-27101
Direct satellite FM-TV broadcasting experiment, with receiver operating near threshold and with 24 and 32 MHz IF band widths
[ESRO-CR[P]-251] 18 p2117 N73-27119
Direct satellite FM-TV broadcasting experiment, with receiver operating near threshold and with 20 MHz IF bandwidth
[ESRO-CR[P]-252] 18 p2117 N73-27120
Packet switching, bilateral broadcasting, and burst random access capabilities
[AD-761544] 19 p2237 N73-28035
Transmitter network synthesis by calculating coverage parameters of broadcast
[BBC-RD-1973/11] 22 p2626 N73-31044
Television broadcasting wave depolarization measurement for multiple utilization of assigned frequencies
[FTZ-A-455-TBR-36] 22 p2633 N73-31101
Experimental television transmission system with vestigeal sideband amplitude/frequency modulation
[FTZ-44-TBR-33] 22 p2633 N73-31102
Usability of 42 and 85 GHz mm waves for terrestrial television broadcasting
[FTZ-455-TBR-37] 22 p2634 N73-31107
Television broadcasting and communication systems using communication satellites, noting space law and regional coverage
23 p2757 N73-32068
Three level transmission code for digital broadcast signal network
[BBC-RD-1973/21] 24 p2894 N73-33101
Direct TV broadcasting communication satellites
[DGLR-PAPER-73-040] 24 p2895 N73-33112
Direct broadcasting TV satellite solar arrays, and heat budget subsystems
[DGLR-PAPER-73-051] 24 p2986 N73-33865
Direct broadcasting TV communication satellite temperature control by louvers, heat pipes, radiators, heat storage, and coatings
[DGLR-PAPER-73-052] 24 p2986 N73-33866
**BROKEN CLOUDS**
U CLOUDS [METEOROLOGY]
**BROMIDES**
NT DIBROMIDES
NT HYDROBROMIDES
NT POTASSIUM BROMIDES
**BROMINE**
Dissociation rate of bromine diatomics in argon heat bath
[NASA-TN-D-7077] 07 p0824 N73-16676
**BROMINE COMPOUNDS**
NT DIBROMIDES
NT HYDROBROMIDES
NT POTASSIUM BROMIDES
Effects of chemical fire extinguishing agents containing bromotrifluoromethane on cardiovascular and nervous systems of dogs, monkeys, and baboons
[AGARD-R-599] 08 p0877 N73-17106
**BRONZES**
Electric arc welding of tin and aluminum bronzes and silicon brass
[DRIC-TRANS-2843] 02 p0179 N73-11448
Electrolytic preparation and evaluation of mixed sodium-iron tungsten bronzes
[AD-746248] 02 p0188 N73-11522
Electric arc bonding of aluminum bronze onto clean steel surface
[AD-747768] 03 p0307 N73-12510
Performance of powder metallurgy bronze graphite bearings operating under hydrodynamic conditions at high slipping rates
[AD-747432] 03 p0309 N73-12523
Mechanical properties, machinability, and corrosion characteristics of 80-10-10 high leaded tin bronze alloy
[PB-211945] 05 p0563 N73-14576
Influence of surface finishing on adherence of radio frequency sputtered molybdenum disulfide on silver, gold, copper, and bronze
[NASA-TN-D-7169] 07 p0804 N73-16523
Cavitation-corrosion resistance tests of tin and aluminum bronzes used for marine pumps in synthetic sea water and distilled water
[DRIC-TRANS-3016] 10 p1167 N73-19492
Bronze coating of alloys in argon atmosphere
[AD-753985] 11 p1309 N73-20623
**BROWNIAN MOVEMENTS**
Light scattering technique for studying Brownian particles
[AD-750110] 06 p0701 N73-15716
**BRUDERHEIM METEORITE**
Photometric and polarimetric measurements of Bruderheim meteorite particles and comparison with astronomical data to determine composition of asteroids
[NASA-CR-131418] 11 p1339 N73-20865
**BRUSH [BOTANY]**
Remote sensing of native arid plant distribution using ERTS-1
[E72-10314] 04 p0412 N73-13363
Spectral signatures for dominant desert scrub plant species of Arizona and soil surface backgrounds
[E72-10318] 04 p0413 N73-13367
**BRUSHES**
Very bright field ionization and evaporation ion sources for use in ion probes of scanning instruments
[IPP-9/6] 10 p1194 N73-19717
**BUBBLE CHAMBERS**
Development of method for automatically scanning bubble chamber films based on optical system for detecting information points as vertices
[CEA-R-4329] 03 p0302 N73-12465
Maximum likelihood determination of electron tracks in propane, propane-Freon, and hydrogen-neon bubble chambers
[JINR-P10-6868] 17 p2066 N73-26712
Determination of electron track parameters in propane bubble chamber based on least-squares method
[JINR-P10-6869] 17 p2066 N73-26713
**BUBBLES**
Effect of bubble inclusions on mechanical properties of cast polymethyl methacrylate
[AD-746862] 03 p0321 N73-12616
Test equipment and procedures for determining foaming and aeration characteristics of aircraft engine lubricants
[AD-747804] 03 p0321 N73-12618
Reaction engines with shrouded nozzles, reaction engines for boats, and thermodynamics of hot air bubble cooling in liquid
[JPRS-57308] 04 p0404 N73-13292
Differential-difference equation describing thermodynamic interactions of hot air bubbling cooling in surrounding liquid
04 p0404 N73-13294
Bubble distributions in quiescent ocean calculated from bubble transport equation
[AD-749046] 04 p0408 N73-13329
Acoustic-optical imaging techniques for detecting bubble formation in circulatory system during decompression
[AD-749087] 04 p0424 N73-13457
Bubble frequencies of air gun sources for at-sea experiments
[AD-748586] 04 p0451 N73-13680
Three-dimensional flow arising in two dimensional separation bubbles noting flow characteristics in turbulent and laminar layer and in suction or blowing conditions
[IC-AERO-72-19] 05 p0525 N73-14275
Effects of gas bubbles in decompression pathology of humans
[AD-748229] 06 p0631 N73-15126
Inherent statistical properties of bubble field in two phase flow determined by correlation functions
[EUR-4840] 06 p0655 N73-15319
Behavior of gas occlusions in arterial heat pipes
[NASA-CR-114531] 06 p0730 N73-15958
Laser Doppler velocity measurement of turbid and bubbly flow media
[UTIAS-TN-185-PT-2] 09 p1043 N73-18506
Sound speed modulation by bubbles in upper ocean
[AD-754372] 11 p1325 N73-20754
Vapor deposition for epitaxial film growth of bubble domain materials
[AD-754958] 11 p1332 N73-20813
Model for prediction of pressure within recirculation bubble of attached jet
13 p1507 N73-22216
Growth of cavitation bubbles and boiling bubbles
[AD-760719] 18 p2132 N73-27225
Bubble transport theory applied to upper ocean
[AD-761999] 19 p2257 N73-28194
Development of method for calculating bubble conditions in flow of boiling liquid in vertical tubes
[NLL-WH-335-[9091.9F]] 21 p2605 N73-30875
Equations describing dynamical motions of small cavitation bubbles in liquids
[AD-764075] 22 p2656 N73-31277
**BUCKLING**
NT CREEP BUCKLING
NT ELASTIC BUCKLING
NT EULER BUCKLING
NT THERMAL BUCKLING
Guide for using data on effects of buckling and deflections in beams, struts, and shafts
[ESDU-SS3] 01 p0112 N73-10922
Buckled states of thin, flat, rectanguar elastic plate subjected to constant compressive thrust
[AD-744993] 01 p0113 N73-10938
Buckling of constant flexural rigid composite struts
[ESDU-01.01.23] 02 p0236 N73-11921
Buckling characteristics of perfect and imperfect circular cylindrical shells subjected to dynamic axial loading
[NASA-CR-129086] 02 p0237 N73-11927
Digital computer procedure for analyzing initially bent two span columns
[AD-747075] 02 p0238 N73-11933
Creep buckling of flat plates and cylindrical shells subjected to edge wise and uniform axial compression respectively
[AD-746475] 02 p0240 N73-11952
Elastic buckling strength of thin walled aluminum alloy tubes fabricated with and without boron/epoxy glass/epoxy composite materials for reinforcement
[NBS-TN-728] 04 p0437 N73-13566
Buckling tests on double T shaped Protenax steel beams
[CRIF-MT-78] 04 p0481 N73-13935
Buckling and intial postbuckling of oval cylindrical shells under pure bending and under combined uniform axial compression and bending
[AD-747493] 04 p0482 N73-13939
Analysis of volume changes in composite wrought iron associated with fiber buckling
[AD-749711] 05 p0567 N73-14606
Use of data items on buckling of plates and compression panels manufactured from isotropic materials
[ESDU-72012] 06 p0723 N73-15906
Modified Flugge equations for buckling of circular cylindrical shells, using membrane theory of shells
[REPT-248] 06 p0724 N73-15911
Variational principle for calculating buckling of thin clamped free circular cylindrical shells subjected to wind load
[TT-7113] 06 p0725 N73-15916
Buckling analysis of elastic plate floating on water and stressed uniformly along periphery of internal hole
[AD-750594] 06 p0728 N73-15943
Theory for nonlinear collapse analysis of shells with general shape
[AD-751702] 07 p0853 N73-16916
Static perturbation method of studying nonlinear equilibrium and stability problems of structural systems and elements
09 p1093 N73-18921
Calculation of bifurcation stress in elastic/plastic plate under uniaxial compression
[AD-753136] 09 p1096 N73-18949
Analysis of structural response of light aircraft to crash loadings based on dynamic buckling of discretely stiffened shells
10 p1219 N73-19910
Movement of trench boundary relative to colliding plates in conjunction with down-buckling of descending plate corner
[NASA-TM-X-66212] 11 p1286 N73-20439
Addition of three-dimensional isoparametric elements to NASTRAN structural analysis program
[NASA-CR-112269] 11 p1345 N73-20916
Buckling and vibration behavior of tensioned sheets with elliptical openings
13 p1584 N73-22840
Buckling of stiffened cylindrical shells subjected to combined axial compression, normal pressure, bending, and shear loads
13 p1585 N73-22847
Theory and user manual for computer program to determine buckling behavior of arbitrarily loaded shells of revolution with actual initial imperfections
[AD-756545] 13 p1587 N73-22866
Buckling of shells under combined loading and thermal stresses
[AD-756494] 13 p1589 N73-22883
Inelastic buckling of eccentrically loaded simply supported columns of rectangular and circular cross sections
[AD-756186] 13 p1589 N73-22887
Analysis for stresses and buckling of heated composite stiffened structures
[NASA-CR-112227] 15 p1838 N73-24894
Analysis of wing leading edge buckling due to aerodynamic heating to show effect of shear modulus of material and geometry of leading edge on buckling onset
[ARC-R/M-3197] 16 p1851 N73-25000
Analysis of general buckling of pressurized stiffened cylinder under axial load
[ARC-R/M-3198] 16 p1857 N73-25040
Holographic interferometric measurement of prebuckling deformation in cylindrical shell structures under axial compression
16 p1921 N73-25545
Buckling of cylindrical panels under non-uniform axial compression
[AD-758833] 16 p1971 N73-25946
Collocation method for numerical solution of buckling of conical shells under hydrostatic pressure
[AD-758834] 16 p1971 N73-25947
Static and dynamic buckling of nonhomogeneous cylindrical shells
17 p2090 N73-26912

Buckling and structural response of two magnesium ring stiffened conical shells subjected to uniform external pressure
[NASA-TN-D-7303] 17 p2092 N73-26926
Laminated composite cylindrical shell buckling strength criteria
[AD-759537] 17 p2095 N73-26944
Energy criteria for predicting dynamic buckling of structures
[AD-760158] 17 p2096 N73-26954
Numerical analysis of stability of axially compressed cylindrical shells from composite materials under nonstationary heating
18 p2203 N73-27785
Effects of shear, rotatory inertia and inplane forces on transverse vibration of thin plates, and effect of shear on buckling
19 p2347 N73-28879
Development of numerical procedures for buckling analysis of truncated conical shells with rigid edge constraint using load displacement criterion
20 p2477 N73-29894
Buckling behavior of composite cylinders to compressive loads
[NASA-CR-132264] 20 p2483 N73-29945
Development of linear analysis method for predicting buckling of composite structures with arbitrary uniform cross section
[NASA-CR-2216] 21 p2603 N73-30863
Computation of buckling of thin walled circular cylinders under axial compression loads
[DLR-FB-73-36] 21 p2604 N73-30868
Numerical analysis of buckling characteristics of ring-stiffened, oval, orthotropic, cylindrical shells
[AD-763369] 21 p2604 N73-30872
Finite element method to determine post-buckling strength of B-1 aircraft aft intermediate fuselage following combined torque and axial loading
[AD-763813] 22 p2615 N73-30956
Creep induced buckling of infinitely long sandwich panel under uniform pressure and uniform temperature
[AD-764311] 22 p2725 N73-31810
Inelastic buckling of deep spherical shell subject to uniformly distributed external pressure
[AD-764085] 22 p2726 N73-31815
Test equipment to prevent buckling of small diameter specimens during compression tests
[NASA-CASE-LAR-10440-1] 23 p2790 N73-32323
Engineering programming information for digital computer program developed to analyze buckling characteristics of shell structures - Vol. 5
[NASA-CR-2273-VOL-5] 23 p2854 N73-32805
Dynamic buckling of thin, elastic beam subjected to constant, compressive axial displacement
24 p2987 N73-33871
Analysis of internal buckling of fibers in viscoelastic composite plate based on linear material responses and small deflection theory
24 p2987 N73-33874

**BUDGETING**
NT FEDERAL BUDGETS
Production of software in NASA within predictable schedule and budget constraints and reasonable tolerances - App. C
[NASA-CR-129818] 05 p0516 N73-14191
Congressional hearings on NASA technology applications program budget
14 p1721 N73-23966

**BUDGETS**
Research project requirements and 1973 budget forecast for French Space Laboratory
[AD-03-72] 23 p2866 N73-32915

**BUFFER STORAGE**
Microprogrammed control, buffer store, and storage control units for all applications digital computer for signal processing in radar, sonar, and communication systems
[AD-748996] 05 p0520 N73-14227
On-line programming to measure correlations in plasma using fast buffer memory and digital analysis
[IPPJ-T-12] 09 p1070 N73-18729

**BUFFETING**
Flight tests to determine buffet characteristics of four high performance aircraft during transonic maneuvers
06 p0618 N73-15017
Analysis of aerodynamic buffeting and related phenomena to include development of models for oscillatory rigid-body motion
06 p0618 N73-15018
Wind tunnel tests to predict full scale aircraft buffet loads during buffet boundary penetration using scale flutter model of fighter aircraft with variable sweep wings
[NASA-TN-D-7066] 07 p0851 N73-16905
Research projects for improving maneuverability and buffet characteristics of fighter aircraft in high subsonic and transonic speed ranges
[NASA-TN-D-7131] 17 p1979 N73-25999
Flight tests of F-8C aircraft to determine effects of flaps on buffet characteristics and wing-rock onset at subsonic and supersonic speeds
[NASA-TM-X-2873] 19 p2220 N73-27905
Aerothermodynamic study of air cushion vehicles buffeting noting dynamical stability, nonlinear behavior, and similitude law
[NT-33-1973] 24 p2870 N73-32933

**BUILDING MATERIALS**
U CONSTRUCTION MATERIALS

**BUILDING STRUCTURES**
U BUILDINGS

**BUILDINGS**
Acquisition of data concerning urban housing quality using remotely sensed imagery
07 p0786 N73-16393
Analysis of temperature conditions in hermetically sealed room to determine human tolerances under various climatic conditions
[FOA-1-A-1527-76] 07 p0854 N73-16924
Summer room heating in buildings with large window glass surfaces
[NASA-TT-F-14849] 11 p1349 N73-20944
Measurement of effects of sonic booms on light building structures for various building configurations
[RAE-LIB-TRANS-1633] 17 p1981 N73-26011
Lumiduc architecture for urban housing
[NASA-TT-F-14963] 17 p2098 N73-26976
Radio frequency shadow calculation for airspace obstruction of radar reception considering Fresnel diffraction
[AG-5082-E-1] 20 p2377 N73-29097

**BULK MODULUS**
Technique for determining bulk modulus and associated loss factor of elastomeric and plastic materials
[AD-752483] 08 p0935 N73-17659
Microwave Doppler shift technique for measuring dynamic bulk modulus of dielectric materials including solid propellants
[NASA-CR-131743] 13 p1546 N73-22532
Computation of bulk moduli of synthetic hydrocarbon hydraulic fluid
[AD-760776] 18 p2163 N73-27471

**BULKHEADS**
Axisymmetric oscillation of partially liquid-filled cylindrical shell container having hemispherical bulkheads
[NASA-TN-D-7318] 16 p1969 N73-25925

**BUMPERS**
Analysis of bumper plate penetration by meteoroid and subsequent phenomena
[NASA-CR-124061] 08 p0966 N73-17894
Meteoroid impact resistance of bumper protected laminated spacecraft mainwalls
[NASA-CR-2262] 14 p1714 N73-23909

**BUNCHING**
NT ELECTRON BUNCHING
Bunch lengthening and power losses due to vacuum chamber walls
[DESY-72/72] 17 p2010 N73-26258

**BUOYANCY**
Application of turbulence transport equations to problems in which buoyancy is driving force
[LA-DC-72-705] 06 p0654 N73-15314
Microbiological investigation of neutral buoyancy simulator for weightless space environment testing
[NASA-TM-X-64736] 12 p1371 N73-21127

**BUOYS**
Requirements for remote buoys, transmitting to ERTS-A
05 p0608 N73-14943
Hydrodynamic and weight loads of self-contained buoy stations for oceanographic research in strong current areas
09 p1059 N73-18638
R/V Knorr cruise in Oct. 1970 to deploy and recover instrumented deep sea moorings
[AD-754796] 11 p1288 N73-20455
Analysis of errors in wind measurements from ocean data buoys
[AD-757981] 14 p1686 N73-23685
Multichannel pulse sampling system with pulse anemometers and current meters on oceanographic buoy
[AD-760336] 17 p2030 N73-26426
Robot buoy for study of relation between marine environment and weather in Sea of Japan
[NLL-M-23049-[5828.4F]] 21 p2567 N73-30573

**BURGER EQUATION**
Numerical method of characteristics for unsteady propagation processes considering dissipative terms in equations for supersonic mixing processes
[NASA-TT-F-14825] 15 p1767 N73-24320
Saddle point method for exact wave plane solution of Burger equation in shock zone
[AD-758409] 15 p1814 N73-24706
Applications of Wiener-Hermite expansion to theories of hydrodynamical turbulence
23 p2771 N73-32167

**BURNERS**
Acoustic combustion instability of solid propellants in radial burner
[AD-755826] 13 p1592 N73-22904

**BURNING**
U COMBUSTION

**BURNING PROCESS**
U COMBUSTION

**BURNING RATE**
Effects of orientation of acceleration vector on burning rate augmentation determined for aluminized composite propellant
[NASA-TN-D-6952] 01 p0116 N73-10962
Effects of propellant composition variables on acceleration-induced burning rate augmentation of solid propellants
[NASA-TN-D-6923] 01 p0117 N73-10966
Analysis of transient and steady-state combustion processes in hybrid rocket system based on gaseous oxidizer flowing within tube of solid fuel
[NASA-CR-112201] 02 p0242 N73-11968
Numerical analysis of nonlinear longitudinal combustion instability in metallized solid propellant rocket engines - Vol. 1
[AD-748415] 04 p0462 N73-13767
Numerical analysis of nonlinear longitudinal combustion instability in metallized solid propellant rocket engines - Vol. 2
[AD-748417] 04 p0462 N73-13768
Microwave continuous measuring technique for solid propellant burning rates rapid depressurization, emphasizing carboxyl terminated polybutadiene and ammonium perchlorate composite
[AD-748256] 04 p0462 N73-13769
Interaction between acoustic velocities and solid propellant combustion with variations in frequency of oscillation, mean pressure, and propellant formulation
[AD-750142] 06 p0712 N73-15809
Development of physical model to determine mechanism of condensed phase reaction in combustion of double base rocket propellants
07 p0853 N73-16921
Influence of ammonia perchlorate binder and surface microstructure on combustion velocity development in solid composite propellants
[ONERA-TP-1167] 10 p1222 N73-19941
Determining open-loop response of Reynolds number dependent process as analog of drop-vaporization burning-rate process
[NASA-CR-121167] 11 p1269 N73-20301
Combustion rates for binary pyrotechnic compositions in rarefied air
[AD-756043] 13 p1591 N73-22898
Burning rate of JP-4 and air propellant in closed combustion chamber
[AD-757634] 14 p1720 N73-23954
Analysis of flame front propagation in porous propellant charges to show wave propagation speed and mass fraction of propellant burned during flame propagation
[AD-762063] 19 p2353 N73-28928
Burning rate, heat transfer, and combustion physics of aluminum in composition of heterogeneous condensed systems
[AD-761609] 19 p2354 N73-28932
Effects of additives on high speed ignition and combustion characteristics of slurry fuels using magnesium and lithium fluoride
[AD-762615] 20 p2465 N73-29802
Analysis of steady state burning of ammonium perchlorate composite solid propellants
[AD-762600] 20 p2465 N73-29803
Mechanism of super burning of catalyzed double based propellants
[AD-763786] 21 p2606 N73-30887
Combustion characteristics of polystyrene and oxygen-styrene copolymer with ammonium perchlorate composites
22 p2708 N73-31687
Magnetic field effects on burning rate of solid rocket propellants
[AD-763894] 22 p2730 N73-31847
Combustion process and burning rate of aluminum perchlorate composite propellant
22 p2732 N73-31865

**BURNOUT**
Initial temperature effects on diffusion burning of hydrogen flame in closed channel with supersonic flow
[NASA-TT-F-14844] 10 p1141 N73-19295
Dynamics of sounding rockets at burnout
[SC-DC-72-1613] 16 p1967 N73-25911

**BURNS [INJURIES]**
Chorioretinal burn hazards of high intensity radiation sources in industry
08 p0873 N73-17071

**BURNTHROUGH [FAILURE]**
Analysis of acoustic properties of jet engine malfunction as means for detecting jet engine burnthrough - Vol. 1
[FAA-RD-72-149-VOL-1] 11 p1334 N73-20825

**BURSTS**
NT RADIO BURSTS
NT SOLAR RADIO BURSTS
NT TYPE 2 BURSTS
NT TYPE 3 BURSTS
NT TYPE 4 BURSTS
NT TYPE 5 BURSTS

**BUSHINGS**
Elastic stresses in flat plates, strips, and lugs due to interference-fit pins or bushes
[ESDU-71011] 01 p0111 N73-10916

Performance characteristics of self lubricating sintered sulfureiron material used for bushings in naval aircraft
[AD-748175] 03 p0319 N73-12603

**BUTADIENE**
Viscoelastic properties of styrene butadiene plastic homopolymers and styrene-butadiene-styrene block copolymers
[AD-752622] 08 p0936 N73-17660

**BUTENES**
Comparison of rheological equations of state and constrained shear recovery results for two polyisobutylene melts
[RR-203] 24 p2891 N73-33078

**BUTT JOINTS**
Improvements in welding techniques to increase productivity and quality of performance of bonded joints
[JPRS-58291] 10 p1163 N73-19460
Butt welding of titanium alloy rings and flanges to improve mechanical properties
10 p1163 N73-19463
Effect of internal weld defects on fatigue behavior in mild structural steel butt welded connections
[PB-220896/5] 21 p2554 N73-30475

**BUTYLENE**
U BUTENES

**BY-PRODUCTS**
Quantum yields of O[D-1] in ozone photolysis near 310 nm
[NASA-CR-122206] 18 p2142 N73-27311

**BYPASSES**
Narrow band equivalent circuit for two-port network using cascaded, lossless transmission lines and lossless shunt elements
[APS-EL-30] 02 p0150 N73-11221
Structural changes in high bypass ratio engines for fan noise reduction to jet noise level
03 p0249 N73-12017
Shunted junction model applied to point contact Josephson junctions, using dc characteristics as function of temperature, contact pressure, and RF power
[AD-754082] 11 p1331 N73-20801
Development and evaluation of throat bypass bleed system to increase stable airflow range of sonic mixed-compression inlet
[NASA-TM-X-2779] 14 p1597 N73-22947
Characterization of electromagnetic pulse shunt protective devices
[AD-763886] 22 p2644 N73-31191


## C


**C BAND**
Design and performance of C band traveling wave tube amplifier for space communication application
[NASA-CR-112125] 01 p0032 N73-10250
Spectral analysis of data from C band radar tracking GEOS 2 satellite and development of data compaction method
[NASA-CR-62085] 13 p1490 N73-22082
Determination of ship positions in broad ocean areas using C band radar tracking data
[NASA-CR-62086] 13 p1491 N73-22083
Utilization of C band instrumentation radars during GEOS 2 program
[NASA-CR-62087] 13 p1491 N73-22084
C band waveguide phased array
[AD-763214] 21 p2517 N73-30193
System design and test plan for NASA position location and aircraft communications equipment at C band using USNS Vanguard and ATS 3 and ATS 5 satellites
[NASA-TM-X-70447] 21 p2576 N73-30646

**C-2 AIRCRAFT**
Fatigue tests to determine service life of catapult structure on C-2 aircraft
[AD-752493] 08 p0868 N73-17028
Hook bounce test of C-2A aircraft arresting gear A-frame
[AD-754077] 11 p1268 N73-20288

**C-5 AIRCRAFT**
Logistic performance data book for C-5A aircraft landing gear to show system reliability, maintainability, logistic support cost, and performance data
[AD-762248] 19 p2357 N73-28963
Logistic performance data book for C-5A airframe to show reliability, maintainability, logistics support, and operating problems
[AD-762233] 19 p2358 N73-28968
Exhaust blast velocities and temperatures at ground level for various aircraft and wing tip vortex velocity for C-5 aircraft
[AD-764228] 22 p2616 N73-30961

**C-142 AIRCRAFT**
U XC-142 AIRCRAFT

**C-130 AIRCRAFT**
Design, fabrication, and flight tests of boron-epoxy reinforced C-130E center wing boxes
[NASA-CR-112126] 04 p0370 N73-13011
Development of mathematical models for C-130 aircraft to predict general trends and probable values for stability derivatives and mode parameters over flight envelope
[AD-753388] 09 p0989 N73-18076
Design, fabrication, and evaluation of boron-epoxy reinforced C-130 center wing boxes
[NASA-CR-112272] 14 p1601 N73-22979
Suitability determination of redesigned XW18 membrane as expedient surfacing for waterproofing and dustproofing hastily prepared airfields for operations of C-130 aircraft
[AD-761089] 18 p2127 N73-27190
Logistic performance data book for C-130E aircraft propulsion system to show reliability, maintainability, logistic support costs, and operational problems
[AD-762249] 19 p2357 N73-28964

**C-131 AIRCRAFT**
In-flight simulator [TIFS] of C-131 aircraft with capability of varying six degrees of freedom
[AD-750745] 06 p0651 N73-15286
Flight tests of folding sidewall, expandable tires on C-131 aircraft to determine operation of inflation and deflation system
[AD-762730] 20 p2361 N73-28993

**C-135 AIRCRAFT**
Analysis of pilot performance in evaluating three types of aircraft altimeters during C-135B simulator flight
[ASD-TR-72-63] 04 p0383 N73-13117
Application of power spectral density method to analyze vibrations induced in aircraft during taxiing
[AD-757283] 14 p1602 N73-22991
Root mean square center of gravity accelerations and undercarriage forces for taxiing KC-135 tanker aircraft
[CRANFIELD-AERO-15] 16 p1859 N73-25060
Logistic performance data book on propulsion system for KC-135 aircraft to show reliability, maintenance, costs, and problems
[AD-762217] 19 p2357 N73-28962
Logistic performance data book for KC-135 aircraft electrical power system to show reliability, maintainability, logistics support, and operating problems
[AD-762225] 19 p2358 N73-28972

**C-141 AIRCRAFT**
Application of reliability based static strength criteria system to analysis of C-141 aircraft - Vol. 1
[AD-742260] 02 p0126 N73-11024
Implementation of reliability based strength criteria system for determining service life of C-141 aircraft structures - Vol. 2
[AD-742261] 02 p0126 N73-11025
Design and development of fixed gain control system for longitudinal axis of C-141 aircraft fly-by-wire control
[AD-760763] 18 p2107 N73-27038
Numerical analysis of supercritical flow about C-141 aircraft wing using finite difference, relaxation algorithm
[NASA-TN-D-6933] 19 p2217 N73-27889
Analysis of transonic scaling effect on quasi, two-dimensional airfoil model of C-141 aircraft
[AD-762285] 19 p2222 N73-27924
Logistic performance data book for C-141A aircraft radio navigation system to show reliability, maintainability, logistics support, and operating problems
[AD-762250] 19 p2358 N73-28971

**C-160 AIRCRAFT**
Statistical evaluation of meteorological ice formation parameters: free moisture content, drop diameters, and temperature, obtained from Transall C-160 flights
[MBB-UH-11-72-O] 07 p0739 N73-16016

**CABIN ATMOSPHERES**
NT SPACECRAFT CABIN ATMOSPHERES

**CABLES**
Development and design of satellite cable boom
[HSD-TP-7356] 12 p1366 N73-21086
Cable guide and restraint device for reefing tubes in uniform manner
[NASA-CASE-LAR-10129-1] 16 p1917 N73-25512
Cable fabrication and encapsulation inclusive of, string-pulling machine and solder sleeve processing
[BDX-613-775] 21 p2553 N73-30467

**CABLES [ROPES]**
Experimental and analytical studies of highway cable barrier and digital simulation of vehicle redirection
[NRC-12694] 01 p0119 N73-10978
Analysis of wind induced vibration in vertical cantilever beam and square sagging suspended cable
[AD-750550] 05 p0604 N73-14913
Cable connected spinning spacecraft, canonical and Lagrange equations, and urban mass transportation
05 p0610 N73-14961
Variable principle for analyzing torsion of fluted bar with rope like cross section
[AD-752059] 08 p0928 N73-17598
Computerized simulation of spiral curve of wire being towed behind orbiting aircraft
[AD-753908] 10 p1136 N73-19256
Rotational injection moulding for designing polythene sheathed closures on large size cables
[REPT-6713] 10 p1164 N73-19474
Design, fabrication, and evaluation of mechanical devices for supporting external stores on military helicopters
[AD-755532] 13 p1535 N73-22436
Modes of cable vibration compared with pure flexing mode in production of motion induced noise from towed ELF H field antenna
[AD-762936] 22 p2645 N73-31199

**CADASTRAL MAPPING**
ALGOL computer program for combined photogrammetric-terrestrial cadastral surveying
02 p0165 N73-11338

**CADMIUM**
Hydrogen embrittlement of cadmium coated steels due to paint stripping
[AD-747634] 03 p0319 N73-12599
Solid cadmium embrittlement in A-7 aircraft failure of six shaft and one horn fracture surfaces
[AD-756906] 13 p1545 N73-22525
Corrosion prevention mechanism of benzotriazole inhibitors for zinc and cadmium
[DRIC-TRANS-3080] 17 p2046 N73-26552
Hypersound attenuation in superconducting aluminum and cadmium
23 p2825 N73-32580
Transverse magneto-resistance and Hall resistivity in pure cadmium and in dilute crystal alloys of Cd-Ag and Cd-In
23 p2825 N73-32585

**CADMIUM ALLOYS**
Fermi surface changes in dilute alloys of aluminum, cadmium, and zinc
[AD-750726] 06 p0709 N73-15786
Cyclic mechanical and fatigue properties of ferroanelastic beta prime gold-cadmium alloy
[NASA-CR-131843] 16 p1969 N73-25929
Transverse magneto-resistance and Hall resistivity in pure cadmium and in dilute crystal alloys of Cd-Ag and Cd-In
23 p2825 N73-32585

**CADMIUM COMPOUNDS**
NT CADMIUM FLUORIDES
NT CADMIUM SELENIDES
NT CADMIUM SULFIDES
NT CADMIUM TELLURIDES
Cadmium and germanium compounds chalcopyrite semiconductor materials for infrared optics
[AD-759556] 16 p1945 N73-25742

**CADMIUM FLUORIDES**
Electrical properties of insulating and semiconducting CdF2 with trivalent Ce and Gd codopants
[AD-750937] 06 p0711 N73-15799

**CADMIUM NICKEL BATTERIES**
U NICKEL CADMIUM BATTERIES

**CADMIUM SELENIDES**
Application of gas transport method for analyzing p-n junction in cadmium selenide monocrystal
[AD-750506] 06 p0711 N73-15800
Tunneling characteristics of thin cadmium selenide, zinc selenide, and cadmium telluride evaporated semiconductor films
12 p1438 N73-21652
Photoelectric solar converter using cadmium sulfide and cadmium selenide tablets or thin films
[AD-756594] 13 p1476 N73-21960

**CADMIUM SILVER BATTERIES**
U SILVER CADMIUM BATTERIES

**CADMIUM SULFIDES**
Argon laser for spin-flip Raman scattering study in cadmium sulfide at liquid helium temperature
[AD-746219] 02 p0219 N73-11768
Kapton covered cadmium sulfide solar cell performance tests in aerospace and earth atmosphere environments
[ONERA-DERTS-NT-02-32] 03 p0255 N73-12062
Theoretical and experimental investigations of CdS single crystals photovoltaic cells
[NASA-CR-129675] 04 p0457 N73-13730
Measurement of picosecond laser pulse width using two-photon conductivity in GaAs and three-photon conductivity in CdS
[AD-750414] 06 p0710 N73-15798
Photoconductivity of cadmium sulfide crystals excited by mode-locked neodymium laser pulses
[AD-753677] 09 p1077 N73-18786
Photoelectric solar converter using cadmium sulfide and cadmium selenide tablets or thin films
[AD-756594] 13 p1476 N73-21960
Effectiveness of solar cells based on CdS-Cu-xS heterojunctions
[AD-756602] 13 p1478 N73-21971
Electric, photoelectric, and electroluminescence properties of Cu contacts on CdS surface
[AD-756876] 13 p1504 N73-22187
Optical and electronic properties of single crystal Cu2S-CdS photovoltaic cells
[NASA-CR-121228] 15 p1738 N73-24091
Thermoelectric and photothermoelectric effects in semiconductors
15 p1819 N73-24747
Technique for determination of conductivity profile in diffusion layer of CdS electroacoustic transducers
[AD-758450] 15 p1822 N73-24773
Spin-flip Raman scattering in cadmium sulfide
[AD-764699] 23 p2827 N73-32598

**CADMIUM TELLURIDES**
Growth of single crystal CdTe materials for use in infrared electro-optic devices
[AD-749368] 05 p0588 N73-14783
Optical absorption properties of polycrystalline zinc selenide and cadmium telluride materials for infrared laser windows
[AD-753068] 09 p1044 N73-18512
Tunneling characteristics of thin cadmium selenide, zinc selenide, and cadmium telluride evaporated semiconductor films
12 p1438 N73-21652
Development of cadmium telluride modulator for infrared laser communication system
[NASA-CR-112321] 15 p1795 N73-24549
Mercury cadmium telluride 10.6-micron photodiode
[AD-762167] 19 p2248 N73-28122

**CALCIUM**
NT CALCIUM ISOTOPES
Effect of calcium-deficient diet on bone structure of pigs and dogs
[NASA-TT-F-13917] 01 p0008 N73-10067
Computer controlled infusion pump for time varying input of calcium into physiological systems
[NASA-CASE-ARC-10447-1] 05 p0503 N73-14092
Effect of acute and chronic hypercapnia on Ca and inorganic P levels in guinea pig blood plasma and erythrocytes
[AD-749323] 13 p1484 N73-22035
Ultrasonic bone densitometer for measuring calcium content of bone structures
[NASA-CASE-MFS-20994-1] 21 p2504 N73-30090
Effect of high ambient temperature on calcium content of human bone tissue
24 p2884 N73-33033

**CALCIUM CARBONATES**
Influence of blue green algae on crystalline calcium carbonate formation on river rocks
[NASA-TT-F-15028] 20 p2368 N73-29046

**CALCIUM COMPOUNDS**
NT CALCIUM CARBONATES
NT CALCIUM OXIDES
NT CALCIUM TUNGSTATES
NT PEROVSKITES
NT SCHEELITE

**CALCIUM ISOTOPES**
Calcium metabolism determination in rats by measuring argon isotope in exhaled air after neutron irradiation
[NASA-CR-128816] 10 p1120 N73-19130

**CALCIUM METABOLISM**
Calcium metabolism determination in rats by measuring argon isotope in exhaled air after neutron irradiation
[NASA-CR-128816] 10 p1120 N73-19130

**CALCIUM OXIDES**
Electrical and ionic conductivity of calcium oxide-doped nonstoichiometric cerium dioxide at various temperature ranges
[COO-1441-16] 12 p1416 N73-21473

**CALCIUM TUNGSTATES**
Effects of high energy radiations in laser materials of calcium tungstates
[AD-753534] 09 p1044 N73-18519

**CALCIUM 45**
U CALCIUM ISOTOPES

**CALCULATION**
U COMPUTATION

**CALCULATORS**
Electronic desk calculator for automatic X ray spectrometry data processing
[Y-1854] 10 p1132 N73-19231
Special purpose slide rule to compute free space propagation delay between synchronous satellite and points on earth surface
[NBS-TN-638] 22 p2638 N73-31139

**CALCULUS**
NT CONTINUITY [MATHEMATICS]
NT COSINE SERIES
NT DIFFERENTIAL CALCULUS
NT FOURIER SERIES
NT INTEGRAL CALCULUS
NT POWER SERIES
NT SERIES [MATHEMATICS]
NT SINE SERIES
NT TAYLOR SERIES
NT VECTOR ANALYSIS
NT VORTICITY
Elements of numerical calculus
[ISS-72/13-PT-1] 10 p1179 N73-19590

**CALCULUS OF VARIATIONS**
Variational extrapolation method for wind and atmospheric temperature analysis
[AD-745354] 01 p0051 N73-10413
HILTOP - variational calculus program for generating electric propulsion data on rendezvous missions to comet Encke
[NASA-CR-114491] 01 p0104 N73-10857
Variational problem for computation of maximum thrust nozzles
[AD-746618] 03 p0351 N73-12864
Algorithms for numerical solution of problems in calculus of variations
[NPL-NAC-28] 09 p1058 N73-18626
Variational and Schelkunoff methods for analyzing microwave propagation in magnetoplasma filled waveguides
16 p1947 N73-25757

**CALIBRATING**
NT WIND TUNNEL CALIBRATION
Large aperture seismic array, seismometer and amplifier performance, and seismograph calibration
[AD-745753] 01 p0053 N73-10433
Calibration of rotating sand erosion test apparatus simulating turbocompressor wear
[AD-743309] 01 p0059 N73-10483
Molecular branching ratio method for intensity calibration of optical systems in far ultraviolet
[NASA-TM-X-66070] 01 p0103 N73-10853
Piston manometer as absolute standard for vacuum gage calibration in 2 to 300 millitorr range
[NASA-TN-D-7059] 02 p0173 N73-11402
Procedures, techniques, and equipment for calibrating luminous intensity, luminous flux, and color temperature of incandescent lamps
[NBS-TN-594-3] 02 p0174 N73-11408
Establishment of radiometric calibration technique to permit absolute reflectance characteristics of ground targets to be determined from ERTS-1 data
[E72-10255] 03 p0290 N73-12355
High altitude balloon flights for solar cell calibration
[NASA-CR-129794] 04 p0375 N73-13050
Design and performance of wideband artificial ear for calibrating audiometric earphones
[AD-746691] 04 p0382 N73-13112
Signal ratio measurements for determining terminal invariant parameters in microwave system calibration
[SC-DR-72-0315] 04 p0395 N73-13216
Metric calibration of aerial photographic system by method of mixed ranges
[AD-748812] 04 p0423 N73-13452
Swinging ball viscosimeter design and calibration for water viscosity measurements
[AD-745252] 04 p0424 N73-13456
Calibration of aerodynamic wind tunnel with supersonic nozzle flow
[AD-749513] 05 p0524 N73-14264
Radiometric calibration technique to permit absolute reflectance characteristics of ground targets to be determined from ERTS-1 data
[E72-10326] 05 p0530 N73-14314
Method for calibrating visible channel of satellite radiometer from orbit by using sunlit area as calibration target
[NOAA-TR-NESS-62] 05 p0547 N73-14441
Dynamic calibration of gas flowmeters by impedance measurement in oscillating flow
[ARC-CP-1224] 05 p0548 N73-14451
Mathematical solution to compressive bulk formation for calibrating ring test specimens using constant interface friction factor
[AD-750885] 06 p0675 N73-15492
Design and performance of miniaturized electric field meters for wind tunnel measurements
[AD-750148] 06 p0675 N73-15495
Energy calibration of Orion spectrograph for operation in wavelength range from 2000 to 3800
[NASA-TT-F-14584] 07 p0799 N73-16491
Organometallic and physical property standards for diluent oil calibration
[NBS-TN-751] 08 p0883 N73-17150
Calibration of flow in working section of hypersonic blowdown wind tunnel to include test equipment required and techniques used
[ARA-30] 08 p0892 N73-17225
Development of procedure for predicting time interval of single clock and matrix equation for optimum weighting coefficients
[NBS-TN-626] 08 p0923 N73-17565
Ozone and nonreactive gas calibration of mass spectrometer with modified helium-cooled ion sources
[BMBW-FBW-72-32] 09 p1034 N73-18440
Quantitative schlieren photography with semishadow of edge in photograph allowing calibration
[WB-2/72] 09 p1037 N73-18459
Design and calibration of liquid metal calorimeter for high temperature operation
[AD-752443] 09 p1037 N73-18462
Fabrication and calibration of Tomahawk sounding rocket payload for magnetic field measurements in ionosphere
[AD-754246] 10 p1157 N73-19413
Apollo 17 vacuum ultraviolet spectrometer calibration plan
[NASA-CR-128831] 10 p1160 N73-19439
Apollo 17 Calibration Facility safety plan covering ultraviolet spectrometer components
[NASA-CR-128833] 10 p1229 N73-19990
Radiometric calibration technique to permit absolute reflectance characteristics of ground targets to be determined from ERTS-1 imagery
[E73-10349] 11 p1274 N73-20343
Calibration of missile infrared track and acquisition system
[AD-754944] 11 p1295 N73-20507
Advanced procedures for self alignment and calibration of inertial platforms
11 p1319 N73-20706
Establishment of radiometric calibration technique to permit absolute reflectance characteristics of ground targets to be determined from ERTS-1 data
[E73-10458] 12 p1394 N73-21300
Recalibration of magnetic spectrometer designed to measure 0.1 to 1.0 MeV electron flux in space environment
[AD-755790] 12 p1406 N73-21404
Calibration and operational characteristics of highly sensitive microwave radiometers
[AD-756563] 13 p1531 N73-22406
Calibration of target acquisition system using infrared tracking
[AD-756845] 13 p1595 N73-22937
Calorimetric calibration method for commercial power monitor used with high power microwave generators
[PB-213970/7] 14 p1669 N73-23548
Cross calibration tests of ultraviolet spectrometer
[NASA-CR-128628] 15 p1789 N73-24506
Calibration and evaluation of Skylab altimetry for geodetic determination of geoid
[E73-10671] 16 p1900 N73-25366
Multispectral scanner system for Earth Resources Technology Satellites
[NASA-CR-132758] 16 p1912 N73-25474
Validation of calibration procedure used with climatological models of multiple-source urban air pollution
[PB-218716/9] 18 p2173 N73-27553
Calibrator for biaxial electronic platforms designed to measure postural equilibrium
[AD-763093] 20 p2372 N73-29066
Calibration and evaluation of Skylab altimetry for geodetic determination of geoid
[E73-10872] 20 p2393 N73-29223
Development of computer program required in reduction and analysis for calibration of Skylab S-193 altimeter data
[E73-10876] 20 p2393 N73-29227
Calibration of vacuum gauges for measuring total and partial pressures in ultrahigh vacuum region
[NASA-CASE-XGS-07752] 21 p2544 N73-30390
Calibration and evaluation of Skylab altimetry for geodetic determination of geoid
[E73-11013] 22 p2660 N73-31318
Spectroradiometric calibration of EREP imagery and oceanography of Block Island Sound
[E73-11015] 22 p2660 N73-31319
Sample-and-hold circuit for monitoring system calibration
[AD-764242] 22 p2676 N73-31434
Mobile test chamber for calibration of fixed incore radiation detectors
[BMBW-FBK-72-26] 22 p2699 N73-31618
EMR 549-120 image dissector test and calibration noting geometrical and photometric tube properties
[ELEC-010-72] 23 p2766 N73-32127
Optomechanical tests equipment for D2B satellite vacuum chamber calibration
[OPT-005-72] 23 p2770 N73-32160
Hydrazine engine tests and small bipropellant engine calibration in Molsink facility
23 p2858 N73-32837
Dynamic calibration of inertial navigation system using extended Kalman filtering and command torquing of platform gyros
24 p2950 N73-33566

**CALIFORNIA**
NT CASCADE RANGE [CA-OR-WA]
NT COACHELLA VALLEY [CA]
NT GREAT BASIN [US]
NT IMPERIAL VALLEY [CA]
NT MONTEREY BAY [CA]
NT PALO VERDE VALLEY [CA]
NT SACRAMENTO VALLEY [CA]
NT SAN FRANCISCO BAY [CA]
NT SIERRA NEVADA MOUNTAINS [CA]
NT SOUTHERN CALIFORNIA
Ocean water color assessment of Monterey Bay, California, from ERTS-1 RBV and MSS imagery
[E72-10190] 01 p0046 N73-10369
Uncorrected accelerometer data resulting from San Fernando, California earthquake of Feb. 1971
[PB-208529] 01 p0054 N73-10439
Atmospheric measurement of photochemical smog reactions in San Francisco Bay area
[PB-210422] 01 p0077 N73-10635
Determination of optical thickness of aerosols in atmosphere around Salton Sea desert area using ERTS-1 imagery
[E72-10200] 02 p0160 N73-11298
Geological fracture mapping based on enhancement of ERTS-1 snow cover imagery of Massachusetts, Connecticut, and Feather River/Lake Tahoe area
[E72-10205] 02 p0161 N73-11302
Monitoring and surveillance of state of eutrophication of inland lakes in California and Nevada
[E72-10207] 03 p0288 N73-12330
ERTS-1 imagery of structures and lithology of Northern California Coast Ranges and Sacramento Valley, California
[E72-10214] 03 p0288 N73-12332

Monitoring plant development in California rangeland environments using ERTS-1 and supporting aircraft data
[E72-10263] 03 p0290 N73-12362
Application of ERTS-1 imagery to agriculture resource and land use evaluation in Mariposa County, Arizona and San Joaquin County, California
[E72-10264] 03 p0291 N73-12363
Handbook on weather patterns over Point Mugu, California
[AD-747641] 03 p0327 N73-12672
Effects of intraurban V/STOL commuter system on economic, social, and physical environment on San Francisco Bay Area
[NASA-CR-114492] 03 p0366 N73-12982
Control of pink bollworm infestation in southern California cotton fields using ERTS-1 remotely sensed imagery
[E72-10285] 04 p0409 N73-13335
Iron absorption band analysis for discrimination of iron-rich zones in California and Nevada
[E72-10294] 04 p0410 N73-13344
Earthquake epicenters and fault intersections in central and southern California
[E72-10304] 04 p0411 N73-13353
ERTS-1 imagery of California coastal nearshore processes
[E72-10316] 04 p0413 N73-13365
Acquisition and analysis of California coastal ground truth data for correlation with ERTS-1 imagery
[E72-10321] 04 p0413 N73-13369
Determination of aerosol optical thickness in atmosphere at Salton Sea and San Diego based on ERTS-1 data
[E72-10359] 05 p0534 N73-14347
ERTS-1 imagery of California nearshore processes including estuarine flushing, currents, season river discharges, and sediment dispersion
[E72-10363] 05 p0535 N73-14351
Remote sensing techniques for regional planning and managing earth resources, particularly water resources in California
[NASA-CR-129917] 05 p0536 N73-14361
Remote sensing of California water systems
05 p0536 N73-14362
Use of ERTS data to manage and solve social problems associated with earth resources in California
05 p0536 N73-14363
Remote sensing data for determining land use potential of northern California coastal zone
05 p0536 N73-14365
Impact of California Water Project on environmental quality and resources in southern California
05 p0537 N73-14368
Seasonal flow patterns of coastal currents along Oregon-Northern California coast
[AD-749077] 05 p0541 N73-14403
Graphical summary of weather and sea conditions along California coast
[AD-749781] 05 p0576 N73-14690
Acquisition and analysis of coastal ground data for correlation with ERTS-1 imagery of Monterey Bay and Santa Barbara Channel areas of California
[E73-10043] 07 p0776 N73-16306
Prediction of range quantity and quality in desert areas of California and Arizona during growing and grazing seasons
[E73-10068] 07 p0779 N73-16330
Utilization of ERTS-1 MSS imagery for study of faulting in alluvium of California, Nevada, and Arizona
[E73-10070] 07 p0779 N73-16332
Mapping and control of pink cotton bollworm in California
[E73-10073] 07 p0780 N73-16335
Earth resources surveys and management in California using ERTS-1 and supporting aircraft data
[E73-10027] 08 p0900 N73-17287
Repetitive ERTS-1 imagery of surface water variability and flooding along rivers and low-lying areas in Virginia, Iowa, and California
[E73-10046] 08 p0900 N73-17289
Development of system for mapping and monitoring natural ecosystems and environmental complexes from ERTS-1 imagery of California, Nevada, Four Corners Area, Louisiana, and Colorado Plateau
[E73-10289] 08 p0915 N73-17495
Photographic and infrared scanning surveys over Harper Lake, California
[AD-752226] 08 p0920 N73-17536
Identification and interpretation of tectonic features of Colorado, California, and Sonora, Mexico
[E73-10275] 09 p1020 N73-18324
ERTS-1 measurement of aerosol content in atmosphere over Salton Sea and desert test sites
[E73-10295] 09 p1020 N73-18328
Volcano and earthquake surveillance network in Alaska, California, Washington, Hawaii, El Salvador, Nicaragua, Iceland, and Guatemala
[E73-10337] 09 p1025 N73-18365
Operational system for employment of remote sensing and automated information in urban land management
[NASA-CR-130969] 09 p1030 N73-18410
Measurement of coastal currents and processes and seaward extent of suspended sediment transport in waters of California
[E73-10375] 10 p1151 N73-19370
Automated thematic mapping and analysis of terrain in Arizona, Texas, Washington, Utah, Louisiana, and California using ERTS-1 imagery
[E73-10386] 10 p1153 N73-19379
Integrated state-wide information management system for water quality control for California
10 p1228 N73-19982
ERTS-1 detection of oil pollution in Gulf of Mexico and in waters off Salem, Massachusetts and Oakland, California
[E73-10396] 11 p1276 N73-20358
Identification and interpretation of tectonic features and mercury deposited in California coast ranges and western transverse ranges
[E73-10446] 11 p1282 N73-20406
Control and mapping of pink bollworm infestations in cotton fields of California desert areas
[E73-10452] 11 p1283 N73-20411
Classification of land use in California using textural information in ERTS-1 MSS imagery
[E73-10461] 11 p1284 N73-20419
Airborne electrical scanning microwave radiometric measurements of soil moisture in Texas, California, and Arizona
[NASA-CR-130204] 11 p1284 N73-20423
Technique for processing and compressing ERTS-1 imagery of California
[E73-10465] 12 p1394 N73-21303
ERTS-1 imagery of structural and lithological properties of Northern Coast Ranges and Sacramento Valley, california
[E73-10478] 12 p1396 N73-21315
Acquisition and analysis of coastal ground truth data in pacific water off California for correlation with ERTS-1 imagery
[E73-10482] 12 p1396 N73-21319
Remote sensing techniques for managing California earth resources
[NASA-CR-131392] 12 p1399 N73-21347
Land use, urban development, and regional planning for Los Angeles County based on photointerpretation of MSS imagery and multispectral information extraction
[E73-10486] 13 p1515 N73-22277
Analysis of digital microdensitometer data from ERTS-1 imagery of San Francisco, California
[E73-10521] 13 p1517 N73-22289
Determination of aerosol content in atmosphere at Salton Sea test site using ERTS-1 data
[E73-10524] 13 p1517 N73-22291
ERTS-1 imagery of California nearshore sediment transport, coastal processes, and tidal currents
[E73-10525] 13 p1517 N73-22292
Earth resources study for California
[NASA-CR-131579] 13 p1523 N73-22345
Utilization of ERTS-1 imagery to predict ephemeral and perennial range quality and quantity during normal grazing season in Arizona and California
[E73-10541] 14 p1654 N73-23418
Thermal surveillance of active volcanoes in Washington, California, and Iceland
[E73-10556] 14 p1655 N73-23428
Structural and lithological investigation of Northern Coast Ranges and Sacramento Valley, California
[E73-10577] 14 p1656 N73-23438
Acquisition and analysis of coastal ground truth data of Santa Monica Bay, Santa Barbara Channel, and Monterey Bay for correlation with ERTS-1 imagery
[E73-10607] 15 p1773 N73-24368
Data compression technique for ERTS-1 imagery of Montreal and Lake St. John, Canada, Orange County, California, San Pedro/Long Beach, California, and Chesapeake Bay
[E73-10625] 15 p1775 N73-24385
Air pollution modeling and meteorology for California particularly San Francisco Bay Area
[UCRL-74335] 15 p1806 N73-24635
Paleomagnetic study of Mano Lake, California to determine secular variations during past 30,000 years
16 p1895 N73-25325
Mapping and monitoring natural ecosystems and environmental complexes and estimation of rice crop yield in California and Louisiana from ERTS-1 imagery
[E73-10669] 16 p1899 N73-25364
Analysis of ERTS-1 imagery of Los Angeles, California area to determine effects of haze on accuracy of ground truth data
[E73-10691] 16 p1902 N73-25384
Analysis of ERTS-1 imagery to determine structural and lithological characteristics of northern coast ranges and Sacramento Valley, California
[E73-10698] 16 p1903 N73-25390
Analysis of ERTS-1 data to determine aerosol content in atmosphere and comparison with data obtained by sun photometer at Salton Sea, California
[E73-10702] 16 p1903 N73-25394
Analysis of ERTS-1 data for predicting ephemeral and perennial range quantity and quality during normal grazing season in Arizona and California
[E73-10712] 17 p2018 N73-26319
Evaluation of ERTS-1 image data compression technique
[E73-10717] 17 p2019 N73-26324
Analysis of ERTS-1 imagery to interpret three seasonal nearshore processes along California coast
[E73-10727] 17 p2020 N73-26333
Forest sampling and timber inventory in California from ERTS-1 imagery
[E73-10743] 17 p2021 N73-26348
Application of ERTS-1 data for identification of ice formations in Lake Erie and snow mapping in American River basin
[E73-10750] 17 p2022 N73-26353
Analysis of generated solid wastes and collection systems for San Francisco International Airport
[PB-219372/0] 18 p2127 N73-27189
Application of ERTS-1 imagery for seismic conditions and recent fault formations in eastern California and western and central Nevada
[E73-10769] 18 p2134 N73-27245
Identification of major fault zone along California-Nevada state line from ERTS-1 MSS imagery
[E73-10773] 18 p2135 N73-27249
EREP 463 imagery of fault tectonics and earthquake hazards in peninsular ranges of southern California
[E73-10781] 18 p2136 N73-27257
Hot and cold atmospheres for Vanderberg AFB, California
[NASA-TM-X-64756] 18 p2141 N73-27306
Detection and identification of crops in Imperial Valley, California using ERTS-1 sequential imagery and remote sensing techniques
[PAPER-A2] 19 p2259 N73-28210
Application of ERTS-1 imagery for identification of ecological analogs of natural vegetation and food crops in California, Colorado, and Louisiana
[PAPER-A6] 19 p2260 N73-28214
Application of ERTS-1 imagery and aerial photography for monitoring forage crop resources in California
[PAPER-A11] 19 p2260 N73-28219
Application of ERTS-1 imagery for inventory of wildland resources in northern California
[PAPER-A12] 19 p2261 N73-28220
Identification of fire hazards in San Pablo test site area in California using ERTS-1 data and aerial photography
[PAPER-A18] 19 p2261 N73-28225
Evaluation of ERTS-1 data for production of land use stratifications and crop inventory process in San Joaquin County, California
[PAPER-A24] 19 p2262 N73-28231
Analysis of ERTS-1 imagery to determine enhancement of ground fracture detail produced by snow cover
[PAPER-G12] 19 p2264 N73-28243
Application of ERTS-1 imagery and ground mapping in southern basin-range province of California, Nevada, and Arizona to show tectonic control of tertiary minerlization
[PAPER-G21] 19 p2266 N73-28252
Mapping of snow cover in western areas of US based on ERTS-1 data
[PAPER-W18] 19 p2272 N73-28295
ERTS-1 imagery of land use, agriculture, vegetation, geology, landforms, and hydrology in Central Coastal Zone of California
[PAPER-L4] 19 p2273 N73-28300
Urban development and regional planning for Los Angeles County, California using ERTS-1 imagery
[PAPER-L18] 19 p2275 N73-28313
Application of ERTS-1 data to geomorphotectonics, earthquake studies, and mineral exploration at Los Angeles, California, and New Jersey coastal plain
19 p2284 N73-28367
Application of ERTS-1 for mapping California, identifying natural resources, and developing programs for environmental improvement
19 p2287 N73-28390
Application of ERTS-1 data to water resources management in State of California
19 p2289 N73-28403
Uniform mapping and monitoring of natural ecosystems and environments in California, Louisiana, and Colorado from ERTS-? imagery
[E73-10839] 19 p2290 N73-28417
Application of ERTS data for mapping snow cover in Arizona and California and correlation with aerial photography
[E73-10866] 20 p2392 N73-29217
Identification and interpretation of tectonics from ERTS-1 imagery of California, Mexico, and Baja California
[E73-10875] 20 p2393 N73-29226
Mapping rice crops of California and Louisiana and natural vegetation of Colorado Plateau from Skylab photography
[E73-10885] 20 p2394 N73-29236

Photomapping of rice crops and natural vegetation in Louisiana and California from Skylab EREP imagery
[E73-10916] 20 p2397 N73-29265
Water, agriculture, and soil resources management and planning in California using ERTS-1 imagery
[E73-10935] 21 p2529 N73-30277
Measurement of aerosol content in atmosphere over Salton Sea and desert areas of California
[E73-10947] 21 p2530 N73-30289
Simulation of San Andreas fault for determining relative motion of plates
[NASA-TM-X-70439] 21 p2537 N73-30338
Uniform mapping of rice crops in Louisiana and California and desert vegetation in southwestern Colorado from Skylab imagery
[E73-10979] 22 p2657 N73-31286
Prototype DCP volcano surveillance network in Washington, Nicaragua, California, Guatemala, Hawaii, El Salvador, Iceland, and Alaska
[E73-11024] 22 p2662 N73-31328
Airborne measurements of photochemical pollution in California and adjacent waters of Pacific Ocean
[NASA-TM-X-69504] 22 p2694 N73-31581
Detection and mapping snow cover in Arizona and California from ERTS-1 imagery
[E73-11038] 23 p2778 N73-32217
Timber identification and inventory and forest management in Colorado, Georgia, Black Hills, California, and Hawaii from ERTS-1 imagery
[E73-11051] 23 p2779 N73-32227
Uniform mapping and monitoring of natural ecosystems and environmental complexes of Colorado Plateau and Sierra-Lahontan areas and estimation of rice crop yields in California and Louisiana
[E73-11070] 23 p2781 N73-32246
Development of multistage forest sampling inventory system using ERTS-1 data for Trinity Alps in California
[E73-11092] 23 p2782 N73-32259
Multistage survey of forests in Trinity Alps of California from Skylab EREP data
[E73-11093] 23 p2783 N73-32260
Uniform mapping of vegetation and rice in Colorado Plateau, Sierra-Lahontan, California, and Louisiana coastal plain from Skylab multispectral photography
[E73-11149] 24 p2919 N73-33303
Agricultural crop identification and land use patterns from Skylab data of California
[E73-11163] 24 p2920 N73-33316

**CALIFORNIUM**
NT CALIFORNIUM ISOTOPES

**CALIFORNIUM ISOTOPES**
Californium-252 isotope as neutron source for activation analysis
03 p0263 N73-12128
Time of flight spectroscopy for X ray coincidence measurements on californium isotopic fission yield
[AD-753542] 10 p1195 N73-19722

**CALIFORNIUM 252**
U CALIFORNIUM ISOTOPES

**CALORIMETERS**
NT BOMB CALORIMETERS
Differential scanning calorimeter for solid state reaction analysis in pure metals and alloys
[EUR-4802-D] 01 p0055 N73-10449
Design and calibration of liquid metal calorimeter for high temperature operation
[AD-752443] 09 p1037 N73-18462
Precision closed bomb calorimeter for monitoring electrically or mechanically actuated flame and gas producing devices
[NASA-CR-131371] 11 p1295 N73-20510
Calorimeter for measuring high temperature specific heat of Ti and Ti based alloys during intermetallic phase
[AD-754954] 11 p1306 N73-20599
Standards for calorimeter measurement of laser beam absorption by graphite cones
[CEA-CONF-2056] 12 p1411 N73-21432
Hadronic component of cosmic ray shower and relation to shower size, using calorimeter
13 p1574 N73-22757
Kinetics of decomposition of adsorbed sarin determined microcalorimetrically
[REPT-1972-18] 14 p1616 N73-23091
Construction and operation of calorimeters for heat of solution and low temperature heat capacitance measurements
[USGS-PP-755] 16 p1912 N73-25470
Absolute calorimeter for high power TEA-CO2 infrared laser output power measurement, consisting of plastic covered copper plate and thermocouple
[LRP-59/73] 18 p2158 N73-27433
Measurement of quantum yields using chemistry, laser technology, photodetector instrumentation, and calorimetry
[PAPER-76A6-742] 21 p2546 N73-30408

**CALORIMETRY**
U HEAT MEASUREMENT

**CALUTRONS**
U CYCLOTRONS

**CALVES**
Inhibiting and activating effect of mono- and bi-quaternary pyridioxide reactivators on bovine erythrocyte cell membrane
[BMVG-FBWT-72-9] 10 p1121 N73-19138

**CAMBER**
NT CONICAL CAMBER
NT WING CAMBER

**CAMBERED WINGS**
Wind tunnel tests at Mach 2.0 to determine aerodynamic characteristics of cambered and uncambered gothic wings
[ARC-R/M-3211] 16 p1852 N73-25003
Development of formulas for calculating gradients and ordinates of camber surfaces of sweptback wings of arbitrary planform with subsonic leading edges and specified load distribution
[ARC-R/M-3217] 16 p1852 N73-25004

**CAMERA SHUTTERS**
Development and characteristics of cyclically operable, optical shutter for use as focal plane shutter for transmitting single radiation pulses
[NASA-CASE-NPO-10758] 05 p0545 N73-14427
In-flight photography of projectiles using film-image synchronized, rotating-slit shuttered drum field camera
[LA-DC-72-909] 10 p1161 N73-19445
Electromechanical focal plane shutters for spectrographic and color schlieren camera systems
[DREV-TN-1997/72] 15 p1785 N73-24475
Development of rotary solenoid shutter drive assembly and inertia damper for use with cameras mounted in satellites
[NASA-CASE-GSC-11560-1] 17 p2003 N73-26198
Optoelectronic shutters with opening times of 0.05 nsec for image converters
[IPF-72-5] 17 p2033 N73-26456
Construction of rotating photoshutter for use with various astronomical instruments
20 p2471 N73-29850

**CAMERA TUBES**
NT IMAGE DISSECTOR TUBES
NT IMAGE ORTHICONS
NT RETURN BEAM VIDICONS
NT VIDICONS
Effects of camera lense photosensitivity on signal loss in vidicon tubes
[AD-750530] 05 p0549 N73-14459
Design modifications to WX-5419B SEC camera tube
[NASA-CR-130934] 10 p1160 N73-19434
Increase in resolving power of camera tubes by changing form and size of electron gun aperture noting electron beam density distribution
[DRIC-TRANS-3025] 13 p1500 N73-22160
Philips 25 mm electron bombarded silicon tube tests, including photocathode sensitivity, dark current, and square wave response
[AD-758360] 15 p1758 N73-24246
Method and equipment for testing lag response in television camera tubes
[AD-763339] 22 p2644 N73-31186
Photocathode for high resolution streak camera tube
[UCID-16218] 24 p2898 N73-33137

**CAMERAS**
NT FRAMING CAMERAS
NT HIGH SPEED CAMERAS
NT I2S CAMERAS
NT MULTISPECTRAL BAND CAMERAS
NT PANORAMIC CAMERAS
NT SCHMIDT CAMERAS
NT TELEVISION CAMERAS
Spectral resolution and image enhancement by focusing of lense optics
[TPD-1972-0-2] 01 p0079 N73-10655
Functional design of electrostatic camera system for application on outer planets explorers
[NASA-CR-129093] 02 p0173 N73-11399
Photographic recording of aircraft strike, emphasizing air-to-air encounter
[AD-746837] 02 p0176 N73-11423
Camera with laser driven Kerr cell having fast time resolution
[DESY-72/14] 04 p0422 N73-13438
Velocity determination of shell fragments, using FORTRAN routines for evaluating film from drum camera
[FOA-2-C-2475-11[44]] 06 p0643 N73-15222
Design and performance of heat camera using indium antimony and germanium mercury infrared detectors
[FOA-2-A-2540-52] 06 p0700 N73-15704
Development of infrared camera for detecting wilt root disease in coconut trees
07 p0783 N73-16369
Application of aerial photography for remote sensing to include characteristics of cameras, films, and photographic processing
07 p0784 N73-16375
First-order geometrical optics analysis of quasi-microscope planetary landers
[NASA-TN-D-7129] 07 p0800 N73-16498
Fourier theory of using grating to extend dynamic range of laser far field camera
[UCRL-51255] 07 p0806 N73-16542
Tests and equipment for measuring performance characteristics of camera systems for space applications
[NASA-CR-128825] 10 p1160 N73-19438
Geodetic quality determination of Soviet satellite data, using camera sites at Riga, Uzhgorod, and Helsinki
[AD-754070] 11 p1287 N73-20446
Analysis of internal precisions and external accuracies of various stereometric systems consisting of single stereometric camera
12 p1404 N73-21384
Multistage forest surveys from Skylab EREP multispectral band scanner and camera imagery
[E73-10531] 13 p1517 N73-22296
Spin scan camera photography of Jupiter from rotating outer planet orbiters
[NASA-TM-X-62260] 15 p1830 N73-24836
Satellite tracking camera for geometric geodesy
[PUBL-27] 16 p1913 N73-25479
C-130 aircraft flights to obtain simulated operation of Skylab multispectral scanner, thermal scanner, and cameras
[E73-10761] 17 p2023 N73-26361
Apparatus for on-film optical recording of camera lens aperture and focus setting
[NASA-CASE-MSC-12363-1] 17 p2030 N73-26431
Integration of spectrometer capability with imagery function of facsimile cameras for use on planetary landers
[NASA-CASE-LAR-11207-1] 19 p2300 N73-28496
Formulation of image quality prediction criteria for Viking lander camera
[NASA-TM-X-2802] 21 p2548 N73-30425
Hewitt camera satellite tracking at Earlyburn, England, between 1 Jan. and 31 May 1973
[ROE-STS-153] 21 p2602 N73-30850
Real time three dimensional motion picture camera using holography
[NASA-TR-R-409] 22 p2673 N73-31413
Silicon vidicon camera for slow scan operation onboard Mariner spacecraft
22 p2732 N73-31862
Characteristics of direct-coupled photodetector-preamplifier for use in facsimile camera for improved sensitivity and reduced mechanical complexity
[NASA-TN-D-7338] 23 p2769 N73-32148
Mechanical exposure interlock device for preventing film overexposure in oscilloscope camera
[NASA-CASE-LAR-10319-1] 23 p2790 N73-32322
Metric cartographic potential of geostationary/geosynchronous satellite camera
24 p2912 N73-33238
Characteristics of lenses and ports for underwater imaging systems to compare depth of field and relative aperture for several lens port combinations
24 p2958 N73-33635

**CAMOUFLAGE**
Radiation mechanisms of camouflaged body coupled radio transmitters
[AD-759927] 17 p2000 N73-26173

**CAMS**
Numerical procedures for designing cams with radial followers for conditions of straight line travel and flat faced followers with faces normal to direction of motion
[ESDU-66009] 01 p0060 N73-10490
Numerical analysis of contact stresses between cam and follower mechanisms for combinations of materials, surface finish, and lubrication conditions
[ESDU-66002] 01 p0060 N73-10492
Numerical analysis of performance of sinusoidal acceleration cams using radial followers and no opening or closing ramps
[ESDU-66026-AMEND-A] 01 p0060 N73-10494
Development of design criteria for maximum horsepower to be transmitted using cycloidal cam transmission and application to marine gas turbine engines
[AD-754822] 11 p1301 N73-20554

**CANADA**
NT LABRADOR
NT ROCKY MOUNTAINS [NORTH AMERICA]
Description of magnetic and seismic facility at Great Whale River, Canada and analysis of data acquired during calendar year 1969 - Vol. 43, No. 3
[M70-43/3] 01 p0043 N73-10343
Description of equipment installed in magnetic and seismic observatory at Mould Bay, Canada and analysis of data acquired during 1969 - Vol 43. No. 4
[M70-43/4] 01 p0043 N73-10344
Description of magnetic and seismic facility at Baker Lake, Canada and analysis of data acquired during calendar year 1969 - Vol. 43, No. 2
[M70-43/2] 01 p0044 N73-10345
Three component aeromagnetic survey of British Columbia and northeastern Pacific Ocean to determine magnetic anomalies - Vol. 42, No. 7
[M70-42/7] 01 p0044 N73-10346
Water resources survey and river monitoring in Canada using ERTS-1 imagery
[E72-10230] 02 p0163 N73-11323
Mapping and detection of snow cover changes on land and on glaciers in Alaska, British Columbia, and Washington using ERTS-1 imagery
[E72-10237] 03 p0288 N73-12337

Canadian research on atmospheric precipation in antarctic regions and meteorological radar systems
[AD-746604] 04 p0444 N73-13627
Description of Telesat-A including operations and test plans
[NASA-TM-X-68927] 05 p0595 N73-14835
Ice problems in Canada, estimates of economic significance of problems, and order of priorities of research programs and management
[REPT-17] 07 p0788 N73-16412
Color vision requirements of Canadian Armed Forces, including their standard tests
10 p1113 N73-19070
Computer control and data acquisition of tidal model of St. Lawrence River
[MH-110] 11 p1259 N73-20221
Utilization of ERTS-1 imagery in structural reconnaissance for minerals and oil in Alaska, Canada, Montana, Colorado, New Mexico, and Texas
[E73-10414] 11 p1279 N73-20376
Mapping Arctic sea ice from ERTS-1 imagery of Hudson Bay, M'Clure Strait, Beaufort Sea, and Greenland Sea
[E73-10447] 11 p1282 N73-20407
Canadian radio telemetry installation in conjuction with seismic array system
12 p1377 N73-21169
ERTS-1 retransmission of water level data collected at remote locations in Canada
[E73-10469] 12 p1395 N73-21306
Data retransmission from Canadian water gauging stations using ERTS-1
[E73-10479] 12 p1396 N73-21316
ERTS-1 retransmission of water resources data collected from remote regions of Canada
[E73-10504] 13 p1515 N73-22279
Information dissemination services of technical information service of National Research Council of Canada
15 p1753 N73-24211
Data compression technique for ERTS-1 imagery of Montreal and Lake St. John, Canada, Orange County, California, San Pedro/Long Beach, California, and Chesapeake Bay
[E73-10625] 15 p1775 N73-24385
Atomic materials research in Canada
[AECL-4353] 17 p2065 N73-26711
Application of ERTS-1 imagery for hydrometric and hydrographic surveys of Canada
[E73-10777] 18 p2135 N73-27253
Environmental factors influencing Canadian industrial growth
[DRAE-34] 18 p2207 N73-27815
Assessment of geological applications of ERTS-1 imagery from selected areas of Canadian Arctic
[PAPER-G11] 19 p2264 N73-28242
Assessment of ERTS-1 imagery for mapping geologic features of Gaspe Peninsula, Quebec and determination of lithologic lineaments
[PAPER-G28] 19 p2267 N73-28259
Application of ERTS-1 imagery to determine geological evidence of mineral and hydrocarbon accumulations in Alaska, Canada, Montana, Colorado, New Mexico, and Texas
[PAPER-G30] 19 p2267 N73-28261
Utilization of ERTS-1 imagery for coastal oceanography in British Columbia
19 p2286 N73-28384
Research activities for DREV during 1972
[DREV-692/73] 19 p2307 N73-28553
Acquisition of land use, soil moisture, and hydrological data of Ontario, Canada and Syracuse, New York for Skylab-3
[E73-10888] 20 p2394 N73-29237
Pilot knee ejection clearances for Canadian military aircrafts
[DCIEM-936] 23 p2741 N73-31938
Wave propagation and amplification of tsunami in Canada
23 p2784 N73-32272
Tsunami propagation into Fisher-Fitz Hugh complex, Alaska, and Juan de Fuca Strait
23 p2784 N73-32273
Canadian Armed Forces education impact on national development
[DRAE-37] 23 p2859 N73-32845
Role of electrical processes in thunderstorms of Canadian prairies
24 p2912 N73-33242

**CANADAIR AIRCRAFT**
NT CL-84 AIRCRAFT
**CANADAIR CF-104 AIRCRAFT**
U F-104 AIRCRAFT
**CANADAIR CL-84 AIRCRAFT**
U CL-84 AIRCRAFT
**CANARD CONFIGURATIONS**
Supersonic wind tunnel tests to measure overall normal and side forces, rolling, pitching, and yawing moments on canard aircraft
[ARC-R/M-3226] 16 p1853 N73-25011
Analysis of performance benefits for fighter aircraft by application of maneuver load control and relaxed static stability parameters
[AD-762299] 19 p2222 N73-27922
Aircraft accident involving crash of TU-144 aircraft at Paris Air Show in 1973
[NASA-TT-F-15062] 20 p2360 N73-28982
Subsonic wind tunnel tests of ring-wing canard configurations for air to surface antitank missiles
[AD-763899] 22 p2723 N73-31788
**CANBERRA AIRCRAFT**
Comparison of gust velocities derived from accelerations of Canberra and Vulcan aircraft noting acceleration and wing loading power spectra
[ARC-CP-1244] 22 p2615 N73-30955
**CANBERRA BOMBER**
U B-57 AIRCRAFT
**CANCER**
Rotating target providing high yield neutrons by He-4 reaction for cancer therapy
[NASA-TM-X-68179] 07 p0746 N73-16067
Routine proctosigmoidoscopic examinations of asymptotic NASA personnel for cancer prevention
08 p0872 N73-17061
**CANISTERS**
U CANS
**CANNONS**
U GUNS [ORDNANCE]
**CANONICAL FORMS**
Algorithm for computing Luenberger canonical form directly for multivariable systems
[NASA-CR-129174] 02 p0195 N73-11576
Discussion of Sturm-Liouville theory and canonical system of arbitrary number of differential equations
[NASA-TT-F-14696] 08 p0937 N73-17671
Arguments on symplectic matrices group of canonical differential equations
[NASA-TT-F-14806] 11 p1311 N73-20637
Symplectic matrices and structures of sets of unstable canonical systems with periodic coefficients
[NASA-TT-F-14810] 11 p1311 N73-20639
Algorithm for calculating Jordan canonical form of matrix
[NASA-CR-131654] 13 p1550 N73-22557
Classification of ERTS-1 MSS data by canonical analysis
[PAPER-I18] 19 p2279 N73-28339
Application of cononical perturbation theory to nonconservative systems
20 p2470 N73-29835
Canonical analysis applied to processing and interpreting MSS data with digital computers
[E73-11104] 24 p2915 N73-33261
**CANOPIES**
Cyclic pressure tests of F-4 aircraft forward and aft canopies to determine safe service life after delamination of acrylic sheet
[AD-759349] 16 p1862 N73-25084
Development of organic glass and plastic materials with improved mechanical and physical properties for use with aircraft canopies and protective coatings
[AD-763263] 21 p2497 N73-30039
**CANS**
Extrusion can for extruding ceramics under heat and pressure
[NASA-CASE-NPO-10812] 04 p0425 N73-13464
Frangible glass canister capable of deploying payload in space without dynamically disturbing its contents
09 p1088 N73-18875
NO2 and UDMH absorbing properties of rocket propellant gas mask canisters
[AD-752538] 10 p1203 N73-19791
**CANTILEVER BEAMS**
Interrelation of divergence, flutter and autoparametric resonance in cantilever beams
[AD-746695] 03 p0285 N73-12311
Shock tests on rectangular steel beams, relation of tension-compression properties to moment-curvature equation, and viscoelastic cantilever beam response to shock
[AD-748656] 04 p0482 N73-13941
Analysis of wind induced vibration in vertical cantilever beam and square sagging suspended cable
[AD-750550] 05 p0604 N73-14913
Lateral bending torsion vibrations of thin cantilever beam under parametric excitation
[AD-750546] 06 p0727 N73-15934
Application of Ritz-Galerkin method and complementary energy to problems in theory of nonconservative elastic stability
[AD-750575] 06 p0729 N73-15945
Stress corrosion cracking of steel double cantilever beam specimens produced by loading sequence in aqueous environment
[AD-752215] 08 p0933 N73-17637
Behavior of cantilevered beam of elastic foundation subjected to following force
[NASA-CR-131608] 13 p1588 N73-22877
Cantilever beam tests for determining strength of tungsten carbide-cobalt alloys
16 p1927 N73-25591
Application of perturbation theory and Ritz energy method for analyzing nonlinear flexural gyrations of untwisted, rotating cantilevered blade vibrating in plane of rotation
16 p1968 N73-25923
Feasibility of using Galkerin method to control cantilevered beam subjected to nonconservative force
17 p2091 N73-26913
Finite element calculation of tapered double cantilever beam modulus of elasticity for sharp blunted cracks
[NLR-TR-72083-U] 17 p2094 N73-26941
Approximate solution for free vibrations of rotating uniform cantilever beams
[NASA-TM-X-62299] 24 p2989 N73-33885
**CANTILEVER MEMBERS**
NT CANTILEVER BEAMS
Flutter characteristics of thin cantilever wings at transonic and supersonic speeds
[NAL-TR-288] 06 p0618 N73-15022
**CANTILEVER WINGS**
U WINGS
**CAPACITANCE**
Satterthwaite approximation distribution for resistance capacitance integrated Chi-squared noise
[AD-747208] 02 p0150 N73-11217
Capacitance analysis of electromagnetic coupling response in transmission lines and cables
[SC-RR-72-0299] 04 p0458 N73-13741
Circuit with differential amplifier for synthesizing capacitance multiplier with microminiaturized feedback components
[NASA-CASE-NPO-11948-1] 06 p0647 N73-15255
Solution of Laplace equation in space bounded by flat and sinusoidal surface for determination of precision of noncontacting capacitive wave transducers
[AD-752021] 09 p1008 N73-18229
Hardware phase of digital capacitance measuring system
[REPT-2873-2143-116] 15 p1754 N73-24218
Design of second order resistance capacitance filters
24 p2898 N73-33133
**CAPACITANCE SWITCHES**
Volt-ampere characteristics of deformed niobium semiconductor memory switch
[COO-3169-12] 12 p1441 N73-21673
**CAPACITORS**
High energy capacitors of six designs for moderate repetition rate
[AD-746991] 02 p0150 N73-11214
Fabricating Ga-As-phosphide mis capacitors using dielectric-growth processes and radiation studies
[AD-747663] 03 p0275 N73-12232
Fabrication of thin film silicon integrated square wave oscillator circuit capacitors
[AD-749266] 04 p0397 N73-13231
Magnetic probes and instrumentation of capacitive discharges
[AD-748610] 04 p0423 N73-13450
Evaluation of high temperature, space vacuum performance of electrical materials, capacitors, and compression sealed pyrolytic boron nitride slot insulation
[NASA-CR-120785] 05 p0518 N73-14216
Hydrostatic pressure technique for improving dielectric properties of inorganic glasses used as capacitor materials
[AD-750393] 05 p0521 N73-14236
Surface and PCM temperature measurement of capacitors during melting and solidification
05 p0608 N73-14945
Design and safety procedures for operating high voltage capacitor bank
[AD-750535] 09 p1008 N73-18231
Techniques for casting large area polysulfone film capacitors onto thick aluminum substrates for application as meteoroid impact sensors
[NASA-CR-128862] 10 p1160 N73-19441
Micrometeoroid analyzer using arrays of interconnected capacitors and ion detector
[NASA-CASE-ARC-10443-1] 11 p1291 N73-20477
Insulated electrode for electrocardiographic recording without paste electrolyte
[NASA-CASE-MSC-14339-1] 12 p1374 N73-21151
Multilayer and disk type, ceramic chip capacitors for thick and thin film hybrid circuits
[ECR-28] 12 p1383 N73-21211
Integrated microcircuits and complementary four-phase logic system
[NASA-CASE-MSC-14240-1] 12 p1386 N73-21240
Temporal variations in dawn and dusk 600 km midlatitude trough position measured by RF capacitive probes on Ariel 3
[NASA-TM-X-66253] 15 p1806 N73-24634
Fabrication and analysis of metal insulator semiconductor capacitors for radiation vulnerability studies
16 p1880 N73-25217
Electrical properties of thin sputtered aluminum-silica capacitors
[NASA-CR-121165] 16 p1880 N73-25220
Effects of ion implantation displacement damage in silicon diodide insulator of MIS capacitor
[AD-758695] 16 p1881 N73-25228
Electrical response of capacitor triggered by shock wave effect on Fermi energy level
[AD-759059] 16 p1883 N73-25239
Guidelines for selection and application of three types of tantalum electrolytic capacitors for design of circuits in spacecraft components
[NASA-TM-X-64755] 17 p2003 N73-26200

Manufacturing of metal insulator semiconductor capacitors on single crystal silicon substrates
[AD-760009] 17 p2005 N73-26214
Electrical properties and radiation resistance of capacitor insulation
[ORNL-4842] 21 p2563 N73-30544
Bibliography on capacitor technology
[AD-764825] 23 p2767 N73-32137
Dielectric, ferroelectric barium strontium titanate for electronic tuning
[AD-765417] 23 p2769 N73-32150

**CAPACITY**
Excess capacity in airline industry and operational and financial problems
23 p2862 N73-32871

**CAPE KENNEDY LAUNCH COMPLEX**
Determining optimal runway orientation for minimizing frequency of crosswinds and headwind reversals at Cape Kennedy
[NASA-CR-128995] 01 p0075 N73-10617
Monthly and annual percentage levels of wind speed differences computed by using FPS-16 radar/Jimsphere wind profiles for Cape Kennedy
[NASA-TM-X-64712] 05 p0572 N73-14650
List of facilities and environmental measurements to be monitored in support of Skylab 2 at Launch Complex 39
[NASA-TM-X-68916] 07 p0849 N73-16879
Hand book on ionizing radiation protection policies at Kennedy Space Center
[NASA-TM-X-69410] 10 p1120 N73-19133
Reliability aspects of ground support equipment at Kennedy Space Center
[NASA-CR-131362] 11 p1265 N73-20268
Summary of KSC program for investigating reliability of ground support activities
[NASA-CR-131361] 11 p1297 N73-20521
Instructions for implementing safety program for KSC
[NASA-TM-X-69219] 12 p1467 N73-21885
Guide for preparation of contractor safety plans at Cape Kennedy Space Center
[NASA-TM-X-69492] 20 p2488 N73-29986
Normal probabilities for Cape Kennedy wind components - monthly reference periods for all flight azimuths for altitudes from 0 to 70 kilometers
[NASA-TM-X-64771] 21 p2574 N73-30625
Environmental sanitation handbook for occupational medicine and health procedures at Kennedy Space Center
[NASA-TM-X-69522] 23 p2752 N73-32020
Glossary of acronyms, abbreviations, initials, code words and phrases used at John F. Kennedy Space Center
[NASA-TM-X-69523] 23 p2866 N73-32908

**CAPILLARY CIRCULATION**
U CAPILLARY FLOW

**CAPILLARY FLOW**
Analytical and test program for establishing feasibility of multichamber pulsed-capillary viscometer
[NASA-CR-120982] 02 p0173 N73-11401
Capillary flow through partially saturated fibrous wicks in heat pipes
[AD-763427] 21 p2527 N73-30263
Thermally assisted cavitation by localized fluctuations in capillary forces
[NASA-TM-X-70458] 22 p2728 N73-31834
Laminar dispersion for measuring ethane binary diffusion coefficients in methane filled capillaries
24 p2891 N73-33079

**CAPILLARY TUBES**
Transition Poiseuille flow through long cylindrical capillary
13 p1508 N73-22224

**CAPILLARY WAVES**
NT BAROCLINIC WAVES
NT GRAVITY WAVES

**CAPSULES [SPACECRAFT]**
U SPACE CAPSULES

**CAPTIVE TESTS**
NT STATIC TESTS
Determination of aircraft aerodynamic characteristics under captive flight conditions and description of test equipment
10 p1105 N73-19010

**CAPTURE CROSS SECTIONS**
U ABSORPTION CROSS SECTIONS

**CAPTURE EFFECT**
Resonance capture of Toro asteroid perturbed orbit by earth
[TRITA-EPP-72-19] 07 p0846 N73-16863
Solid aerosol particle capture by water drops at low Reynolds numbers
[AD-759667] 16 p1872 N73-25157

**CARBAMATES [TRADENAME]**
NT URETHANES

**CARBAMIDES**
Physicomechanical and antifriction behavior of polycaproamide and Caprolon surfaces
[NLL-RISLEY-TR-2360-[9091.9F]]
05 p0550 N73-14464

**CARBIDES**
NT ALUMINUM CARBIDES
NT BORON CARBIDES
NT CHROMIUM CARBIDES
NT HAFNIUM CARBIDES
NT MOLYBDENUM CARBIDES
NT NIOBIUM CARBIDES
NT SILICON CARBIDES
NT TITANIUM CARBIDES
NT TUNGSTEN CARBIDES
NT URANIUM CARBIDES
NT ZIRCONIUM CARBIDES
Development of chemical model to present properties of carbides for localized and nonlocalized conditions of electrons in crystal structure
[NLL-RTS-7334] 01 p0069 N73-10565
Compilation of reports on transition metal carbides for period 1956 to 1972
[CE-BIB-228] 04 p0437 N73-13560
Synthesis and high rate deposition of ceramics and dispersion stengthened alloys
[AD-750413] 06 p0685 N73-15580
Development of powder metallurgy nickel-base superalloy for application at 1800 to 2000 F
[NASA-CR-121099] 09 p1047 N73-18537
Solid phase interactions in cobalt-carbide systems
[NLL-LTI-746-1338-[9022.401]]
12 p1415 N73-21468
Borides, carbides, and nitrides of silicon oxidation resistant refractory compounds for use in gas turbines and reentry vehicles
14 p1678 N73-23616
Phonon scattering by conduction electrons in transition metal carbides
[COO-1198-937] 16 p1947 N73-25755
Thermal analysis of carbon migration in carbide and oxycarbide systems
[AERE-R-6897] 21 p2606 N73-30885
Specific electrical resistance of metal-carbide two-phase system to show effect of porosity and metal content on electrical properties
23 p2807 N73-32444
Application of protective layers of refractory oxides and carbide onto high strength fiber substrates
[NASA-CR-134466] 23 p2810 N73-32467
Chemical and physical properties of graphite and carbide-graphite composites developed by powder metallurgy
[LA-5147] 24 p2936 N73-33448
Refractory metal carbide/metal oxide composites for thermal insulation
[LA-5136] 24 p2943 N73-33504
Magnetic and specific heat measurements of carbides, nitrides, and uranium and thorium sulfides
[CEA-R-4453] 24 p2943 N73-33506

**CARBOHYDRATE METABOLISM**
NT HYPOGLYCEMIA
Mathematical model for in vivo study of glucose homeostasis in humans
[NASA-CR-129171] 02 p0130 N73-11056
Toxic effects of Freon decomposition products on activity of isoenzymes of lactate dehydrogenase in rat brains
03 p0259 N73-12097
Effects of physical training on human enzyme activity, carbohydrate metabolism, cholesterol level, and adrenal function
[NASA-TT-F-14826] 11 p1243 N73-20093

**CARBOHYDRATES**
NT ADENINES
NT ADENOSINE TRIPHOSPHATE [ATP]
NT CELLULOSE
NT DEXTRANS
NT GLUCOSE
NT GLUCOSIDES
NT MONOSACCHARIDES
NT RIBOSE

**CARBON**
NT CARBON ISOTOPES
NT CHARCOAL
High temperature reaction of carbon with refractory compounds of groups 4, 5, and 6
[NLL-RTS-7425] 01 p0022 N73-10171
Structural characterizations and key property measurements of glassy carbons
[AD-745347] 01 p0070 N73-10574
Measurement of electron density in carbon plasma created by heating solid target with laser radiation
[AD-746221] 01 p0086 N73-10715
Molecular beam sampling system for measuring size, size distribution, and particle concentration of carbon particles in acetylene-oxygen flame
[AD-744920] 01 p0118 N73-10971
Formation of chaoite and other crystal forms of carbon by CO2 laser irradiation of solid carbons
[AD-747020] 02 p0193 N73-11565
Pyrolysis of glassy carbons in inert atmosphere from copolymers of furfuryl alcohol
[AD-746883] 02 p0194 N73-11570
Source of C3 in comets
02 p0228 N73-11842
Formation processes for C3 or C2 in comets
02 p0228 N73-11843
Effect of chemical vapor deposition on properties of carbon-felt carbon-matrix composites at high temperature
[SC-DC-71-4395] 03 p0320 N73-12609
Thermal expansion, specific heat, and thermal conductivity of carbon reentry materials to 3000 C
[SC-CR-72-3139] 03 p0320 N73-12610
Carbon black additives used to improve heat-aging resistance in silicone rubber vulcanizates
[AD-747769] 03 p0321 N73-12619
Pyrolytic carbon deposition in steady state fluidized beds
[AD-748223] 03 p0323 N73-12631
Crystal structure of polymorphic form of carbon similar to chaoite
[AD-747476] 03 p0347 N73-12828
Destructive and nondestructive tests of carbon-carbon reentry heat shields
[SC-R-71-3354] 03 p0364 N73-12966
Permeability of fine-pored carbons as function of mean pressure temperature and gas properties
[AD-749362] 05 p0499 N73-14064
Processes leading to carbon formation in premixed laminar flames of various fuels
08 p0882 N73-17144
Investigation for attenuation and extinction in interaction between laser beams and flowing particulate clouds
[RM-567] 08 p0929 N73-17605
CMB-13 research on carbon and graphite
[NASA-CR-130539] 08 p0935 N73-17652
Synthesis of SiC single crystals free from carbon particle inclusions
[AD-752227] 08 p0952 N73-17792
Friction, wear, and transfer of carbon and graphite to copper, chromium, and aluminum metal surfaces in vacuum
[NASA-TN-D-7206] 09 p1039 N73-18475
Lowering of ionization potentials of hydrogen and carbon atoms immersed in high temperature and high density thermal plasma
[AD-753247] 09 p1072 N73-18752
Removal and separation of particles by crystallization in carbon-naphthalene system
[AD-753056] 09 p1076 N73-18777
Mechanical and thermal properties and oxidation resistance of seal ring carbon graphite materials with resin impregnants
[NASA-CR-120955] 10 p1165 N73-19480
Improved carbon graphite materials for high temperature self-acting seals
[NASA-CR-121092] 10 p1165 N73-19481
Research and development with glassy carbon
[AD-755146] 11 p1310 N73-20629
Analysis formation of carbon deposits on jet engines and effect on reliability, efficiency, and service life
[AD-754607] 11 p1335 N73-20837
Effects of carbon and copper on magnetic properties of iron and iron-silicon alloys
[NASA-TT-F-14857] 12 p1428 N73-21574
Variations of relative abundances of helium, carbon, nitrogen, oxygen, and iron-group nuclei in solar cosmic rays and their relationship to solar particle acceleration
[NASA-TM-X-66228] 12 p1445 N73-21706
Analysis of strain aging process in high carbon quenched steels caused by plastic deformation of martensite and migration of carbon to crystal defects in microstructure
13 p1541 N73-22484
Research on carbon, graphite, and phenolic resin binders
[NASA-CR-131483] 13 p1547 N73-22539
Model testing of gases, powders, and carbon particles in vibration combustion studies
[AD-755712] 13 p1591 N73-22902
Coagulation of carbon particles in premixed flames
[AD-755693] 13 p1592 N73-22907
Corona equilibrium model for ionization state distributions in carbon, aluminum, copper, and tungsten plasmas
[AD-758357] 14 p1696 N73-23767
Physical and mechanical properties of glassy carbons
[AD-757765] 15 p1802 N73-24606
Classification of southern carbon stars using objective prism spectra
16 p1960 N73-25857
Vapor composition and chemical reactions of carbon atoms and molecules from graphite and tantalum carbide heated by laser radiation
[SLA-73-57] 17 p1992 N73-26107
Calorimetric measurements on X ray penetration through thin carbon foils
[AD-761826] 19 p2322 N73-28679
Quantitative deposition by standard techniques of adsorbates containing C and Si
[NASA-CR-124309] 19 p2343 N73-28850
Electromicroscopic analysis of Nb3Sn bands to determine effect of carbon doping on current carrying capacity
[NLL-M-23057-[5828.4F]] 20 p2434 N73-29544
Determination of limiting solubility of carbon in cobalt in solid state
[NLL-M-21664-[5828.4F]] 21 p2504 N73-30096
Large scale weather modification through spread of carbon black particles in aerosol form in upper atmosphere
[PB-220642/3] 21 p2541 N73-30374

Influence of carbon stabilizing elements and temperature on cold worked austenitic stainless steel corrosion
[CEA-CONF-2119] 21 p2560 N73-30918
Oxidation resistance of selected mechanical carbons at 650 C in dry flowing air
[NASA-TN-D-7381] 21 p2562 N73-30539
Thermal analysis of carbon migration in carbide and oxycarbide systems
[AERE-R-6897] 21 p2606 N73-30885
Physical and mechanical properties of carbon produced from furfural alcohol resins
[AD-763499] 23 p2810 N73-32472
Metal-loaded carbon and graphite cloth reinforced composites from polymer blends
[AD-764630] 23 p2811 N73-32474
Direct charge state measurements of low energy solar carbon and oxygen in interplanetary space
[TR-73-132] 23 p2834 N73-32648
Carbon-oxygen fuel cell of solid carbon anode, nickel gauze cathode, and flamed electrolytes
24 p2880 N73-33001
Simultaneous determination of carbon, hydrogen, and nitrogen in organic compounds
[UCID-16198] 24 p2892 N73-33085
Mass loss rate of carbon and graphite at high temperature
[LA-5223-PR] 24 p2943 N73-33503
Composition and structural modification of glassy carbon alloys
[AD-764918] 24 p2944 N73-33511
Kinematic properties of carbon stars
24 p2977 N73-33791
Explosive carbon burning effects of observed nuclei in solar system and constraints on supernova explosions
[LA-UR-73-489] 24 p2992 N73-33911
Screening factor which reduces densities at which carbon ignition can occur in helium, exhausted carbon, and oxygen stellar core models
[UCRL-74669-REV-1] 24 p2992 N73-33913

**CARBON ARCS**
Uses of high power arc light sources
[AD-745565] 01 p0033 N73-10259

**CARBON COMPOUNDS**
NT ALUMINUM CARBIDES
NT BORON CARBIDES
NT CALCIUM CARBONATES
NT CARBIDES
NT CARBONATES
NT CHROMIUM CARBIDES
NT HAFNIUM CARBIDES
NT LEXAN [TRADEMARK]
NT MOLYBDENUM CARBIDES
NT NIOBIUM CARBIDES
NT POLYCARBONATES
NT SILICON CARBIDES
NT SODIUM CARBONATES
NT TITANIUM CARBIDES
NT TUNGSTEN CARBIDES
NT URANIUM CARBIDES
NT ZIRCONIUM CARBIDES
Publications of carbon and graphite research results
[NYO-1710-106] 05 p0565 N73-14590
Photolysis of perfluorodienes and diacyl fluorides to produce high molecular weight perfluorocarbon polyether gums
[NASA-CR-130552] 08 p0883 N73-17149
Carbon refractory composites for application in rocket motor nozzles, propulsion structures, and planetary atmospheric entry shells
[NASA-CR-131745] 13 p1547 N73-22533

**CARBON DIOXIDE**
Vibration-translation and vibration-vibration relaxation rates in rapid expansions of N2 and CO2 in argon
[AD-746068] 02 p0216 N73-11751
Photodissociative excitation of carbon dioxide as source of atomic oxygen in Martian atmosphere
[NASA-TM-X-66088] 02 p0229 N73-11856
Computerized simulation of carbon dioxide partial pressure in spacecraft environment for wide range of operating conditions - Vol. 1
[NASA-CR-128630] 02 p0233 N73-11893
Development of simulation models for computerized simulation of carbon dioxide partial pressure in spacecraft environment - Vol. 2
[NASA-CR-128631] 02 p0233 N73-11894
Analytical analysis of graphite interaction with carbon dioxide at high temperature
[AD-747556] 03 p0264 N73-12141
Carbon dioxide gas turbine cycles for sodium cooled fast breeder reactor
[BMBW-FBK-72-17] 03 p0334 N73-12722
Oxygen, carbon dioxide, nitrogen, and noble gases for environment suitable for humans
06 p0628 N73-15093
Atmospheric control studies, emphasizing carbon dioxide problem
06 p0629 N73-15108
Gas laser measurements of absorptive losses introduced by water vapor and carbon dioxide for laser emission lines in 7-6 to 10-9 vibrational bands
[AD-749823] 06 p0681 N73-15542
Dissociative character of carbon dioxide adsorption on nickel film surfaces
[NLL-TRANS-746-1341-[9022.401]]
06 p0682 N73-15549
Stabilization of aqueous prussic acid during synthesis from ammonia by carbon dioxide
[NASA-TT-F-14691] 07 p0752 N73-16110
He-Xe tunable laser measurement of infrared line shape and CO2 absorption spectra
[AD-751230] 07 p0808 N73-16556
Method for integrating pressure-scaled water-vapor and CO2 absorber masses from surface to sigma levels in Naval primite equation model
[AD-752475] 08 p0921 N73-17544
Absolute intensity, polarization, and relative line intensities of rotational Raman scattering spectra from nitrogen, oxygen, and carbon dioxide
[NASA-CR-121091] 08 p0946 N73-17746
Infrared interferometer spectrophotometer for infrared spectra measurement of CO2 in atmospheres of Earth and Venus
08 p0973 N73-17954
Change in content of gases in blood when man is exposed to high ambient temperatures
11 p1245 N73-20105
Method of measuring amount of carbon monoxide by oxidizing agents to yield carbon dioxide for air pollution control
[NLL-RTS-7573] 11 p1274 N73-20340
Carbon dioxide shielded-arc welding with electrodes containing aluminum
[NLL-CE-TRANS-6011-[9022.09]]
11 p1296 N73-20515
Analysis of global effects created by increase in carbon dioxide and aerosol content in atmosphere
12 p1420 N73-21511
Electron scattering spectra of low state CO2 in energy-loss range 7 to 10 eV
[NASA-CR-132202] 17 p2064 N73-26697
Development of design information for molecular sieve sorbants regenerative CO2-removal systems for manned spacecraft
[NASA-CR-2277] 19 p2225 N73-27948
Oscillation relaxation time of CO2 molecular energy levels in temperature intervals 300 to 600 K.
[AD-762436] 19 p2323 N73-28688
Regenerable CO2 sorbent formulation and fabrication for extravehicular activity
[NASA-CR-114632] 20 p2371 N73-29054
Temperature dependence of several vibrational relaxation processes in DF-CO2 mixtures
[AD-762925] 20 p2374 N73-29078
Interaction of titanium nitrides with oxygen and carbon dioxide
[NASA-TT-F-15108] 22 p2625 N73-31035
CO2 laser and spectrophone for CO2 and water vapor absorption measurements
22 p2679 N73-31462
Physical behavior of water and carbon dioxide on Mars
24 p2984 N73-33843

**CARBON DIOXIDE CONCENTRATION**
Annual variations of carbon dioxide concentration in Italian and Scandinavian cities
07 p0859 N73-16966
Physiological effects of argon/oxygen breathing on rats noting carbon dioxide level
10 p1116 N73-19094
Seasonal variations in tropospheric and stratospheric carbon dioxide concentration determined from commercial aircraft sampling within Northern Hemisphere
[AC-24-PT-3] 17 p2028 N73-26409
Influence of C02 concentration on thermal regime of clear sky
21 p2573 N73-30615
Toxicological aspects of carbon dioxide exposure in chronic hypercapnia
[AD-763394] 22 p2621 N73-31005
Liquid carbon dioxide in Martian polar laminated surface layers
23 p2840 N73-32698

**CARBON DIOXIDE LASERS**
CO2 laser radiation damage to surface of infrared laser optical material
[DREV-TN-2013/72] 01 p0064 N73-10524
Stable mode-locking and pulse coupling of longitudinal discharge carbon dioxide laser with single electro-optical element
[AD-744996] 01 p0064 N73-10528
Construction of carbon dioxide transversely excited atmospheric laser and application to absorption studies of laser induced plasmas
[AD-745842] 01 p0066 N73-10542
Analysis of applications for infrared, carbon dioxide, and chemical laser devices with emphasis on window materials and absorption mechanics
[AD-745927] 01 p0067 N73-10546
Feasibility study for laser transponder onboard SOREL space probe
[ESRO-CR[P]-123] 02 p0149 N73-11207
Analysis of dependence of refractive index of gas discharge medium in carbon dioxide laser on amplitude of discharge current
[NLL-DRIC-TRANS-2815-[3623.66]]
02 p0180 N73-11459
Plasma parameters in carbon dioxide laser discharge
[DREV-TN-2025/72] 02 p0181 N73-11464
Attenuation of carbon dioxide laser beams in atmosphere at various frequencies and method for calculating absorption coefficients from measured data
[FOA-2-A-2542-E3/E4/E6] 02 p0181 N73-11465
Development of least squares curve-fitting algorithm for simultaneous estimation of small signal gain and saturation intensity in carbon dioxide laser waveguide
[NASA-TM-X-66097] 02 p0181 N73-11468
Window material for high power carbon dioxide infrared lasers
[AD-746500] 02 p0182 N73-11473
Direct generation of far infrared power through laser action on rotational transitions in molecular gases
[AD-745984] 02 p0182 N73-11476
Electrically excited, high power, molecular gas lasers
[AD-746148] 02 p0182 N73-11478
Reflectivity measurements with 10.6 micrometer infrared radiation from CO2 laser
[AD-746238] 02 p0183 N73-11482
Formation of chaoite and other crystal forms of carbon by CO2 laser irradiation of solid carbons
[AD-747020] 02 p0193 N73-11565
Extremely short, high power pulses from electron beam controlled CO2 laser amplifier
[LA-DC-72-447] 03 p0310 N73-12528
Construction and testing of dual 10.6 micron CO2 laser AFC heterodyne system
[AD-747947] 03 p0312 N73-12544
Carbon dioxide lasers used for heating of dense arc plasmas to several million degrees
[UCLA-34-P-157-X-3] 03 p0342 N73-12788
Thermal decay of magnetically confined fully ionized arc plasma heated with pulsed CO2 laser energy
[UCLA-34-P-157-X-4] 03 p0342 N73-12789
RESALE-2 and INHALE computer code modifications for detecting radiative power of C02 in detector
[AD-748293] 04 p0430 N73-13500
Analysis of surface damage mechanisms to mirrors and mirror coatings resulting from irradiation by pulsed carbon dioxide lasers
05 p0556 N73-14519
CO2 laser model study of electron beam
[AD-750314] 06 p0680 N73-15532
Measurement of infrared emission spectra of liquid cyclopentane derivatives excited by carbon dioxide laser
[AD-750480] 06 p0681 N73-15544
Absorption of carbon dioxide laser radiation by gaseous sulfur hexafluorine in air boundary layers
[AD-751016] 06 p0681 N73-15546
Design of Brewster angle acousto-optic modulator for high power mode locked C02 laser
[AD-751680] 07 p0807 N73-16544
Pulsed gain measurements on CO2 lasers
[AD-751620] 07 p0807 N73-16545
Gain and performance measurement of expanding CO2 laser mixtures at high pressures
[AD-751694] 07 p0807 N73-16547
Development and characteristics of stable master oscillator carbon dioxide laser system
[AD-752219] 08 p0930 N73-17614
Systems and techniques of experiment to establish air-to-ground CO2 laser heterodyne link
[NASA-TM-X-65946] 09 p1043 N73-18507
High resolution transmittance curves for spectral region 320 to 1400 wavenumbers and attenuation of CO2 laser radiation
[AD-753076] 09 p1043 N73-18511
High power output from carbon dioxide laser and effects of higher order transverse and longitudinal mode excitation
[AD-753402] 09 p1045 N73-18521
Frequency stable Q switched carbon dioxide laser oscillators, free-running and injection locked pulsed lasers, and optical heterodyne measurements of frequency stability
[AD-753605] 09 p1045 N73-18523
High resistivity gallium arsenide window material for high power carbon dioxide lasers emitting at 10.6 micrometers
[AD-752783] 09 p1048 N73-18550
Design and performance of carbon dioxide laser amplifier with double discharge electrode geometry
[DREV-TN-2022/72] 10 p1134 N73-19240
Characteristics of carbon dioxide laser for use as interferometric and light scattering plasma diagnostic radiation source
[LRP-54/72] 10 p1168 N73-19504
Effects of heavy particle external ionization source on carbon dioxide laser efficiency
[COO-2007-24] 10 p1169 N73-19509
CO2/N2 laser applied to CO2 excited state population study during supersonic nozzle expansion
[ONERA-NT-204] 10 p1169 N73-19510
Continuous wave CO2 laser radiation effects on semiconductor materials
[AD-753918] 10 p1202 N73-19785

Evaluation of cold cathode materials for sealed off carbon dioxide lasers to show power output and service life
[NASA-CR-130202] 11 p1302 N73-20564
Review of 10.6 micrometer detection techniques
[DREV-TN-2052/73] 11 p1302 N73-20567
Design and performance of transverse excited atmospheric carbon dioxide lasers
[AD-754544] 11 p1303 N73-20572
Carbon dioxide lasers, optical measurement instrumentation and imaging techniques for air pollution detection
[AD-754939] 11 p1303 N73-20574
Analysis of inversion medium of quasi-stationary carbon dioxide laser to show molecules in vibrational and rotational states
12 p1410 N73-21424
Nonlinear pulse interaction in CO2 lasers
[AD-755919] 12 p1411 N73-21436
CO2 laser communications for army tactical applications
[AD-756866] 13 p1496 N73-22124
Characteristics of carbon dioxide laser operating at atmospheric pressure
[TM-50] 13 p1536 N73-22446
Theoretical model developed for carbon dioxide laser operating in short pumping time, gain switched, mode-locked mode of operation
[AD-756456] 13 p1537 N73-22452
Atmospheric pressure gas lasers
[AD-755477] 13 p1538 N73-22462
Design, development, and characteristics of atmospheric pressure, double discharge carbon dioxide laser
[AD-756517] 13 p1539 N73-22467
Plasma diagnostic visualization with pulsed carbon dioxide TEA laser and liquid crystal infrared detector, noting spark discharges
[ISL-18/72] 13 p1563 N73-22668
Design of tunable carbon dioxide laser using integrated optics technique
[AD-757088] 14 p1672 N73-23569
High efficiency ion lasers and high power carbon dioxide lasers through study of improved electrode structures
[AD-757099] 14 p1673 N73-23575
Optical performance evaluation of infrared transmitting materials
[AD-756825] 14 p1673 N73-23576
Carbon dioxide laser based on Na catalyzed combustion of CO with N2O
[AD-757585] 14 p1674 N73-23584
Significant population inversion in flow structure behind blast wave
[AD-757881] 15 p1795 N73-24555
Gallium arsenide epitaxial thin films as active elements for electrooptic modulation of carbon dioxide laser radiation
[AD-757792] 15 p1796 N73-24559
CO2 waveguide laser as master oscillator for high resolution optical radar application
[AD-758706] 15 p1796 N73-24561
Collisionless plasma with two stream coupling of corona and core in C02 laser-heated pellets
[AD-757790] 15 p1818 N73-24740
Development of 10.6 micrometer range gated upconversion imaging laser radar receiver with 150 by 150 resolution elements
[AD-759077] 16 p1915 N73-25495
Performance of CO2 laser excited by H-3 [neutron, proton] reaction
16 p1920 N73-25536
Reaction rate effect on gain and power of CO2-N2 gasdynamic laser in presence of H2 and H2O
[TAE-176] 16 p1920 N73-25539
Mathematical model for calculating time required for continuous wave CO2 laser to perforate thin metal sheets
[REPT-534] 16 p1923 N73-25562
Influence on output power of coupling orifice of CO2 gas laser cavity operating in mode of excitation by microsecond pulses
16 p1923 N73-25563
Design and performance of stable CO and CO2 lasers
[AD-758774] 16 p1924 N73-25568
Design and performance of carbon dioxide laser communication system
[AD-759483] 16 p1924 N73-25572
CO2 laser study of ZrO-Y2O3 phase diagram
16 p1931 N73-25629
Plasma diagnostics with infrared schlieren and interferometric techniques using TEA-CO2 laser, exemplified by electric spark transient response
[ISL-19/72] 16 p1950 N73-25779
Air breakdown and plasma generation by carbon dioxide laser
[AD-759567] 16 p1951 N73-25785
High power CO2 tea laser for use as plasma diagnostic radiation source
[LRP-54/72] 17 p2040 N73-26505
Computation of laser gain as function of time in CO2 gas lasers
[LA-5151] 17 p2040 N73-26508
CO2 laser-plasma heating and diagnostic scattering experiments
[LA-5167-MS] 17 p2040 N73-26509
Numerical analysis of stationary internal structure of plasma in homogeneous carbon dioxide laser discharge
[DREV-TN-2061/73] 18 p2157 N73-27430
Absolute calorimeter for high power TEA-CO2 infrared laser output power measurement, consisting of plastic covered copper plate and thermocouple
[LRP-59/73] 18 p2158 N73-27433
Double discharge high power TEA CO2 laser, noting application of xylene to avoid electric arcs
[LRP-60/73] 18 p2158 N73-27434
Design of tunable waveguide carbon dioxide laser for optical heterodyne communication system between satellites
18 p2212 N73-27860
Carbon dioxide laser frequency stability data for receiver design optimization
18 p2212 N73-27861
Mercury cadmium telluride 10.6-micron photodiode
[AD-762167] 19 p2248 N73-28122
Carbon dioxide laser for heating hypersonic wind tunnel flow
[AD-761506] 19 p2249 N73-28134
Electric discharges in supersonic high pressure gas flow to improve carbon dioxide laser power
[ISL-20/72] 19 p2307 N73-28560
Kinetic model and computerized simulation of DF-carbon dioxide chemical transfer laser
[AD-762284] 19 p2309 N73-28571
Wavelength profilometer based on phase-ranging with VHF - modulated C02 laser
[AD-762453] 20 p2415 N73-29411
Kinetics of chemically pumped CO2 and CH2N2-CO2 photolysis laser systems
20 p2424 N73-29469
Estimation of electron drift velocity and characteristic energy as function of electric field strength in carbon dioxide laser gas mixtures
[TN-280] 20 p2425 N73-29477
Cold cathode materials for constructing sealed off CO2 lasers
[NASA-TN-D-7307] 20 p2425 N73-29480
Double exposure interferograms of discharge region of transverse electrically-excited atmospheric pressure CO2 lasers
[UCRL-13547] 20 p2425 N73-29483
Characteristics of carbon dioxide lasers and application for transmission of data
21 p2554 N73-30479
Molecular population inversion by Laval nozzle expansion in N2/He/carbon dioxide laser
[DLR-FB-72-21] 21 p2554 N73-30480
Effect of connecting aperture in resonator mirror on radiation power of CO2 laser
[AD-763254] 21 p2555 N73-30484
Development of mirror material for carbon monoxide and carbon dioxide lasers
[AD-763795] 21 p2556 N73-30490
CO2 laser and spectrophone for CO2 and water vapor absorption measurements
22 p2679 N73-31462
Application of laser systems to space communication using carbon dioxide laser for two way communication with ATS-F satellite - Vol. 1 Pt. 1
[NASA-CR-132803] 22 p2680 N73-31469
Application of carbon dioxide laser for space communication to include ground equipment, data acquisition, and data processing - Vol. 1 Pt. 2
[NASA-CR-132804] 22 p2681 N73-31470
Requirements for design, fabrication, performance, and testing of optical heterodyne receiver subsystem for use in laser communication system - Vol. 1 Pt. 3
[NASA-CR-132805] 22 p2681 N73-31471
Dense plasma focus using CO2 laser scattering and infrared bremsstrahlung emission
[COO-2233-2] 22 p2703 N73-31652
Performance of ac power supply developed for CO2 laser system
[NASA-CASE-GSC-11222-1] 23 p2800 N73-32391
Dynamic processes for laser emission in pulsed pumping of transversely excited atmospheric carbon dioxide laser
[DREV-TN-2036/73] 23 p2800 N73-32396
Operation of Laflamme double-discharge laser structure up to pressures of several atmospheres
[DREV-TN-2092/73] 23 p2800 N73-32397
Atmospheric attenuation of CO2 laser radiation measured by pyroelectric detection noting fog absorption and optical communication application
[LCR-DR-1-72-67/1/R] 23 p2801 N73-32404
Infrared detection of zero pi pulses generated by mode locked CO2 lasers
[AD-764692] 23 p2802 N73-32406
Integrated optics design principles of tunable CO2 laser
[AD-764638] 23 p2802 N73-32408
Liquid crystal infrared detectors for plasma diagnostics and flow visualization using CO2 laser impulses
[BMVG-FBWT-73-16] 23 p2823 N73-32564
Laser ignition of pyrotechnic compositions being considered as drag reducing fumers
[AD-765415] 23 p2858 N73-32834
Induced reactions in gas mixtures using carbon dioxide laser pulses and electrical discharges
24 p2930 N73-33400
Pressure dependent absorption of CO2 laser in BCl3 at 10.6 micron
[DREV-TN-2086/73] 24 p2930 N73-33403
Self-induced transparency with CO2 laser pulses in two nondegenerating, vibration-rotation transitions in ammonia gas absorber
[AD-765550] 24 p2932 N73-33417
Thermal blooming of carbon dioxide laser during atmospheric propagation
[AD-765520] 24 p2932 N73-33418

**CARBON DIOXIDE REMOVAL**
Computer prediction of performance of sorbent beds for CO2 or water removal
[NASA-CR-112098] 01 p0022 N73-10173
Bibliography on carbon dioxide removal from gases by lithium hydroxide
[CL-1971-15] 04 p0386 N73-13136
Methodology for estimating costs and estimates for 3 carbon dioxide concentrators
[NASA-CR-123960] 04 p0486 N73-13971
Hydrogen depolarized cell for removing CO2 in spacecraft life support systems
[NASA-CR-131868] 13 p1486 N73-22047
Computerized prediction and actual carbon dioxide adsorption performance of solid amine resin
[NASA-CR-112324] 16 p1870 N73-25140
Cost estimates for carbon dioxide concentrators in spacecraft life support systems
[NASA-CR-124302] 18 p2111 N73-27073
Alkali metal carbonate-bicarbonate solid gas reaction for removing CO2 from atmosphere of EVA life support system
[NASA-CR-114661] 22 p2622 N73-31013
Systems design for amine carbon dioxide sorber bed to be used in manned spacecraft
[NASA-CR-111849] 22 p2623 N73-31018
Cost data for modified hydrogen depolarized carbon dioxide concentrator in life support system
[NASA-CR-124462] 24 p2887 N73-33052

**CARBON DIOXIDE TENSION**
NT HYPERCAPNIA

**CARBON FIBER REINFORCED PLASTICS**
Structural design and load tests on carbon fiber reinforced plastic VC-10 aileron control strut
[ARC-CP-1229] 05 p0603 N73-14903
Properties of graphite fiber/polycarbonate and glass fiber/polycarbonate composites as influenced by heat treatment
[AD-757763] 15 p1802 N73-24605
High temperature carbon polymeric composite materials
[AD-759963] 17 p2052 N73-26598

**CARBON FIBERS**
Evaluation of disubstituted perylene compounds as monomers for high temperature polymers and as possible binders for carbon fibers
[AD-746626] 02 p0139 N73-11122
Unidirectional and bidirectional carbon fiber/epoxy resin composites for cryogenic vessels
[NASA-CR-120899] 02 p0192 N73-11533
Nondestructive measurement of modulus of elasticity of carbon fibers
[AD-749011] 04 p0440 N73-13585
Mechanical properties data and fabrication technology for filament wound graphite/epoxy resin pressure vessels
[NASA-CR-120951] 05 p0602 N73-14897
Structural design and load tests on carbon fiber reinforced plastic VC-10 aileron control strut
[ARC-CP-1229] 05 p0603 N73-14903
Production of carbon fibers and reinforced plastics in British installations
[FOA-2-C-2468-91] 06 p0687 N73-15594
Production of carbon fibers from polyacrylonitrile
[AD-750362] 06 p0688 N73-15604
Production of large carbon fibers by impregnation with phenolic resin and carbonizing composite fiber
[NPL-IMS-18] 09 p1052 N73-18580
Drop impact strength and toughness of glass and carbon fiber composite materials
[AD-753101] 09 p1054 N73-18595
Carbon fiber reinforced metal structures for space shuttles
[SOR-W-13] 10 p1167 N73-19495
Mechanical and physical properties of discontinuous thermoset carbon fiber reinforced plastic composites
[AD-754034] 11 p1309 N73-20622
Role of titanium in fabricating magnesium-graphite fiber composites with improved strength and stiffness
[AD-754570] 11 p1310 N73-20627
Transverse tension strength and stiffness of unidirectional carbon fiber reinforced plastic
[RAE-TR-72129] 12 p1416 N73-21477
Evaluation of stabilized precursors for high strength carbon fibers
[AD-755427] 13 p1547 N73-22540

Mass thermal analysis of chemical reactions in conversion of polyacrylonitrile fibers to high modulus, high strength carbon fibers - Vol. 2
[AD-755350] 13 p1549 N73-22549
Polyacrylonitrile precurser fibers for conversion to high modulus, high strength fibers using X ray diffraction analysis
[AD-755351] 13 p1549 N73-22550
Investigation of fibers and composites applicable to the design of high pressure vessels for satellites
[MAN-NT-10/72] 13 p1586 N73-22859
Improved resin adhesion by depositing silicon carbide whiskers on carbon fibers
[AD-757659] 14 p1681 N73-23642
Compressive strength and modulus of unidirectional carbon fiber reinforced plastic laminates
[RAE-TR-72096] 17 p2050 N73-26587
Characteristics of carbon fiber composite materials and application for structures with reduced weight, fatigue reduction, and corrosion resistance
18 p2164 N73-27477
Application of glass composites, all carbon composites, and PRD-49 organic fiber material for airframe and spacecraft construction
18 p2164 N73-27482
Application of glass reinforced and carbon reinforced composite materials for helicopter structures and rotary wings
18 p2165 N73-27483
Use of reinforced boron and carbon fiber composites in aircraft structures
18 p2165 N73-27484
Construction of glider aircraft using glass fiber and carbon fiber reinforced plastic composite materials for weight reduction and increased strength
18 p2165 N73-27486
Application of glass and carbon fiber reinforced structures for gas turbine engine components to operate in high temperature environments
18 p2166 N73-27495
Performance and fatigue strength of compressor blades fabricated from carbon fiber composites and boron composite wires
18 p2166 N73-27496
Chemical vapor deposition process for preparing large diameter carbon-boron monofilaments
[NASA-CR-121229] 18 p2167 N73-27502
Strength of brittle matrix materials reinforced with steel fibers or whiskers
[NLL-CE-TRANS-6145-[9022.09]]
20 p2434 N73-29545
Compressive strength and deformation properties of unidirectionally carbon fiber reinforced plastic under uniaxial compression
20 p2434 N73-29550
Carbon fiber/cobalt/chromium system tensile and high temperature strength noting different solidification modes
[DLR-FB-73-37] 21 p2560 N73-30519
Fabrication and properties of carbon-fiber glass composites and methods for improving mechanical properties
[ARL/MET-NOTE-85] 21 p2561 N73-30533
Shear, flexural, and tensile strength performance of carbon fiber composites made from epoxy, phenolic, polyester, and polyimide resins
[AQD/NM-000198] 22 p2689 N73-31536
Internal pressure vessels with filament of carbon fibers and epoxy resins
[NASA-CR-121138] 22 p2724 N73-31799

**CARBON ISOTOPES**
Isotopic composition of carbon in Precambrian graphitoids from various parts of the USSR
[NASA-TT-F-14682] 08 p0918 N73-17520
Isotopic composition of carbon in carbonaceous rocks from oil field of Belorussia as indication of their origin
[NASA-TT-F-14938] 15 p1780 N73-24426

**CARBON MONOXIDE**
Analysis of energy transfer processes in molecular lasers
[AD-745368] 01 p0066 N73-10537
High temperature oxidation reactions of carbon monoxide and methane in oxygen-rich atmospheres in turbulent flow reactor
[AD-746284] 02 p0138 N73-11116
Vertical distribution and dissociation of methane in stratosphere and CO production
[A-N-103-1972] 02 p0164 N73-11329
Design and characteristics of instrument for monitoring carbon monoxide content of ambient atmosphere to include operations and maintenance instructions
[NASA-CR-128602] 02 p0172 N73-11394
Modification of atmosphere contamination sensor to include carbon monoxide monitoring capability
[NASA-CR-128604] 02 p0172 N73-11395
Measurement of pollutant levels of nitrogen oxides, unburned hydrocarbons, and carbon monoxide for annular, swirl can combustor
[NASA-TM-X-68160] 02 p0243 N73-11974
Detection and measurement of carbon monoxide in atmosphere
[PB-211265] 05 p0575 N73-14677
Oxygen, carbon monoxide, and fuel toxicity
06 p0628 N73-15101
Acute toxicity of brief exposures to HF, HCl, NO2, and HCN singly and in combination with CO in aircraft cabins
[AD-751442] 07 p0748 N73-16085
Search for interstellar C[14]O
[AD-751912] 08 p0962 N73-17870
Analysis of gaseous emissions from J-85 engine at various fuel-air ratios, engine speeds, and simulated altitude conditions
[NASA-TM-X-2726] 08 p0969 N73-17921
Mariner 6 and 7 flybys measuring hot CO on Mars with ultraviolet scanning spectrometers
08 p0973 N73-17955
Interstellar CO in ultraviolet spectrum of Zeta Ophiuchi
08 p0975 N73-17972
Recombination coefficients of electrons with hydrogen and carbon monoxide ions
[NASA-CR-131107] 10 p1192 N73-19699
Carbon monoxide content in exhaled air and blood carboxyhemoglobin in subjects confined to insulating protective gear
11 p1245 N73-20106
Vibrationally excited carbon monoxide from reaction of oxygen with acetylene, methylacetylene, and methane
[DREV-TN-2051/72] 11 p1252 N73-20160
Method of measuring amount of carbon monoxide by oxidizing agents to yield carbon dioxide for air pollution control
[NLL-RTS-7573] 11 p1274 N73-20340
Hyperoxic atmosphere effect on rat metabolism and elimination of gaseous wastes
13 p1481 N73-22004
Isotopic composition of atmospheric carbon monoxide
[PB-213591] 13 p1527 N73-22378
Physiological and hemodynamic adaptations to CO levels and exercise in nonsmoking normal men
[PB-213834/1] 14 p1612 N73-23073
Data tables on nonmetallic materials for offgassing CO and hydrocarbons in 5 psia O2
[NASA-TM-X-64745] 14 p1680 N73-23631
Mass spectrographic determination of ions and neutral reactions in glow discharge of helium-sulfur dioxide-carbon monoxide
[BM-RI-7747] 15 p1747 N73-24157
Infrared fluorescent low level carbon monoxide analyzer
[PB-213846/7] 15 p1747 N73-24163
Electron collision processes in atmospheric gases of oxygen, carbon monoxide, and nitrogen oxide
[AD-757841] 15 p1748 N73-24170
Effect of carbon monoxide on time perception
[PB-214651/2] 16 p1868 N73-25123
Development of breadboard model correlation interferometer for carbon monoxide pollution experiment
[NASA-CR-112212] 16 p1913 N73-25478
Atmospheric diffusion of carbon monoxide and lead from expressways
18 p2170 N73-27527
CO releases at high altitude to determine atmospheric N2 vibrational temperature
[AD-762316] 19 p2298 N73-28480
Molecular absorption coefficients for H20-N2 mixtures as measured by Co laser
[AD-760140] 19 p2308 N73-28561
Adsorption kinetics of CO on [100] face of molybdenum single crystal
[CEA-CONF-2194] 22 p2684 N73-31499
Vibrational cross section resonances of excited state in nitrogen and carbon monoxide
[AD-764596] 23 p2754 N73-32042
Influence of continuous and discontinuous exposure to carbon monoxide on animals
24 p2882 N73-33019

**CARBON MONOXIDE LASERS**
Absorptive losses in carbon monoxide laser emission lines
[AD-746170] 02 p0182 N73-11479
Dispersion characteristics of plasma instabilities in carbon monoxide plasma
[AD-748470] 04 p0456 N73-13723
Design of electron gun and laser cavity for carbon monoxide lasers
[AD-752818] 08 p0931 N73-17623
Mechanism for formation of inverse population of oscillatory levels in gas discharge carbon monoxide laser
[AD-753559] 09 p1045 N73-18520
Model of pulsed CO/N2 molecular laser system with emphasis on mixture components and temperature variation
[AD-755197] 14 p1673 N73-23573
Design and performance of stable CO and CO2 lasers
[AD-758774] 16 p1924 N73-25568
Cooled carbon monoxide laser for pulsed operation with pressure up to 1 atmosphere using electron beam for gas excitation
[AD-759755] 16 p1924 N73-25570
Molecular laser model for pulsed carbon monoxide/nitrogen system
[AD-759509] 16 p1924 N73-25571
Measurement of vibrational temperatures in carbon monoxide laser
[AD-759237] 16 p1925 N73-25575
Formation mechanism of vibrational level population inversion in gas discharge CO lasers
[AD-759679] 16 p1925 N73-25578
Results of investigations of CO lasers
[AD-759861] 17 p2041 N73-26512
Design, fabrication, and performance evaluation of CO laser
[AD-762334] 19 p2308 N73-28568
Water vapor absorption by highly attenuated CO laser lines
[AD-764376] 22 p2682 N73-31485

**CARBON MONOXIDE POISONING**
Hypokinetic disturbances of rats after exposure to carbon monoxide
13 p1481 N73-22007
Tolerance of hypokinetic rats to carbon monoxide exposure
14 p1609 N73-23043

**CARBON STEELS**
Stress state and deformation characteristics of hardening carbon steel with decreasing temperatures
[AD-746723] 02 p0188 N73-11527
Influence of carbon content and structural state on abrasive wear resistance of iron alloys
[AD-747078] 02 p0190 N73-11539
Buckling tests on double T shaped Protenax steel beams
[CRIF-MT-78] 04 p0481 N73-13935
Producing niobium carbide coatings on carbon steels and hard composite alloys
[NLL-TRANS-746-1314-[9022.401]]
05 p0560 N73-14547
Random fatigue tests on normalized carbon steel with 0.7 percent carbon
07 p0851 N73-16902
Macroscopic and microscopic approach to fracture and hardness of carbon steels
[COO-3084-10] 08 p0932 N73-17630
Analysis of fatigue damage cumulation of low carbon steel specimens with transverse hole using two step rotating bending tests and block loading sequence
[TAE-164] 09 p1093 N73-18922
Hydrocompression treatment to lower residual stresses in weld joints of forge-welded carbon steel vessels
10 p1163 N73-19461
Low carbon steel for studying dissolution behavior of Fe3C particles under rapid heating and short time temperature conditions
[AD-753928] 11 p1307 N73-20602
Effect of molybdenum addition on physicomechanical properties of titanium-carbon-nickel composite alloys
[NLL-LTI-746-1422-[9022.401]]
15 p1797 N73-24565
Analysis of relationship between texture development and normal anisotropy in cold-rolled, low carbon steel
[NLL-M-21627-[5828.4F]] 15 p1797 N73-24567
Influence of variation in cylinder geometry on fragmentation and mode of fracture of internally detonated carbon steel cylinders
[DSL-REPT-533] 16 p1969 N73-25930
Effect of microstructure on elastic limit of low carbon alloy and low carbon steels
[RAE-LIB-TRANS-1700] 17 p2044 N73-26534
Fatigue strength and other mechanical properties of medium carbon steels chromed by gaseous and vapor phase methods
[DRIC-TRANS-2156] 17 p2046 N73-26550
Environmental tests of zinc-rich coatings applied to carbon steels
[NASA-TN-D-7336] 18 p2160 N73-27450
Effect of copper and silicon on selected mechanical properties of hot rolled medium carbon steels
[BM-RI-7777] 21 p2558 N73-30504

**CARBON TETRACHLORIDE**
Preparation of tetraperchlorate of methane by displacement of halogen from carbon tetrahalides using halogen perchlorates
[NASA-CR-129168] 02 p0137 N73-11106

**CARBONACEOUS METEORITES**
Neutron activation analysis applied to determine bismuth content of meteorites and standard rocks
07 p0840 N73-16809
Vapor condensation of Ni-Fe phases and paleomagnetic records in carbonaceous chondrites
17 p2017 N73-26310

**CARBONACEOUS ROCKS**
NT COAL

**CARBONATES**
NT CALCIUM CARBONATES
NT LEXAN [TRADEMARK]
NT POLYCARBONATES
NT SODIUM CARBONATES
Dry sliding friction characteristics of iron ceramic materials using solid lubricants
04 p0432 N73-13517

Application of remote sensing techniques and laboratory analyses for determining water pollution caused by carbonaceous materials
[NASA-CR-128824] 10 p1154 N73-19387
Chemical and physical properties of synthetic polyurethane polymer prepared by reacting hydroxy carbonate with organic diisocyanate
[NASA-CASE-MFS-10512] 21 p2505 N73-30099
Alkali metal carbonate-bicarbonate solid gas reaction for removing CO2 from atmosphere of EVA life support system
[NASA-CR-114661] 22 p2622 N73-31013

CARBONIC ACID
Compatibility of Ti and Ni alloys, stainless steels, Al, tungsten carbide, butyl, and Ep rubbers with hydrazine noting decomposition rates and effects of carbonic acid
[ESRO-CR-85-PT-2] 13 p1569 N73-22712

CARBONIZATION
Production of large carbon fibers by impregnation with phenolic resin and carbonizing composite fiber
[NPL-IMS-18] 09 p1052 N73-18580
Polyacrylonitrile precurser fibers for conversion to high modulus, high strength fibers using X ray diffraction analysis
[AD-755351] 13 p1549 N73-22550
Deposition process investigation of steady-state fluid beds to observe carbonization of pyrolytic materials
[AD-757118] 14 p1682 N73-23647
Precursor carbons and molding of graphites
[Y-1857] 24 p2954 N73-33598

CARBONYL COMPOUNDS
Measurement of carbonyls and noncarbonyl oxygenates in exhaust from gasoline fuels
[BM-RI-7675] 02 p0137 N73-11110
Determination and identification of gases in powdered carbonyl nickel
[NLL-LTI-746-1353-[9022.401]] 12 p1412 N73-21439

CARBORANE
Nine poly carborane-siloxane, high temperature elastomers differing in chemical structure, using torsional braid analysis
[AD-748931] 04 p0440 N73-13586
Glass transistion characteristics and compatibility of linear poly carborane-siloxane series plastics
[AD-749385] 05 p0566 N73-14597
Thermomechanical behavior and structure of poly[carborane-siloxane]s containing icosahedral cages in nitrogen environment
[AD-749364] 05 p0566 N73-14598
Infrared and NMB spectra of poly[carborane-siloxane] s containing icosahedral cages in nitrogen environment
[AD-749386] 05 p0566 N73-14599
Relationship of molecular structure to thermo-oxidative stability of carborane-siloxane polymers with icosohedral CB10H10C cages
[AD-749820] 05 p0567 N73-14610
Carborane burning catalysts for solid propellants
[AD-755379] 13 p1489 N73-22068

CARBOXYHEMOGLOBIN
Carbon monoxide content in exhaled air and blood carboxyhemoglobin in subjects confined to insulating protective gear
11 p1245 N73-20106

CARBOXYL GROUP
Conversion of 2-methyl 5-ethyl pyridine compound into 5-ethyl picoline acid by different methods
[DRIC-TRANS-2951] 06 p0638 N73-15178

CARBOXYLIC ACIDS
NT HEXOGENES [TRADEMARK]
NT NICOTINIC ACID
Stability constants and distribution of tin IV complexes by anion exchange resin with carboxylic acids
[AREAEE-128] 07 p0824 N73-16679
Wear inhibition of carboxylic acids in synthetic lubricating oils on ester basis
[DLR-FB-73-43] 15 p1793 N73-24536
Stable polyimide synthesis from mixtures of monomeric diamines and polycarboxylic acid esters
[NASA-CASE-LEW-11325-1] 19 p2229 N73-27980
Fluorinated esters of polycarboxylic acid and lubricating compositions for use at extreme temperature
[NASA-CASE-MFS-21040-1] 21 p2505 N73-30098
Kinetic deuterium isotope effect in aqueous reaction of methyl radicals with deuterated alpha-alanine and glycine
[NASA-TT-F-15123] 23 p2753 N73-32033

CARCINOMA
U CANCER

CARDIAC VENTRICLES
Gaussian curve simulation of multiple-dipole model of ventricular depolarization
[TH-71-E-25] 03 p0261 N73-12116

CARDIOGRAPHY
NT ELECTROCARDIOGRAPHY

CARDIOLOGY
Dynamic electrocardiographic standardization for detecting cardiac risk factor in personnel
08 p0873 N73-17066
Long term exercise effects on cardiovascular response in NASA personnel with periodic ergometric evaluation
08 p0873 N73-17067
Development of instantaneous reading tachometer for measuring electrocardiogram signal rate
[NASA-CASE-MFS-20418] 15 p1785 N73-24473

CARDIOTACHOMETERS
Development of electrocardiogram protection circuits to prevent accidental electrocution and digital cardiotachometer system to display heart rate
13 p1594 N73-22924
Measurement of arterial pressure by tachooscilloscope method
[NASA-TT-F-15088] 23 p2751 N73-32016

CARDIOVASCULAR SYSTEM
NT ARTERIES
NT CARDIAC VENTRICLES
NT ERYTHROCYTES
NT GLOMERULUS
NT HEART
NT HEMATOPOIETIC SYSTEM
NT LYMPHOCYTES
NT MYOCARDIUM
High altitude effects on cerebral and cardiovascular systems of monkeys
[AD-745891] 02 p0134 N73-11085
Effects of gravitational and inertial forces on cardiovascular and respiratory dynamics
[NASA-CR-129603] 03 p0256 N73-12074
Standard requirements for ultrasonic Doppler probes of cardiovascular systems in medical monitoring functions
03 p0257 N73-12083
Transverse acceleration effects on human cardiovascular system
03 p0258 N73-12088
Flight stress effects on cardiovascular reactions of pilots with a therosclerosis
03 p0258 N73-12090
Feasibility of multichannel rheography for studying cardiovascular system on centrifuge
03 p0259 N73-12094
Cardiac toxicity of fluoroalkane gases for propelling aerosols in industry and household applications
[AD-751425] 07 p0749 N73-16090
Cardiovascular effects of fluorocarbon exposure, emphasizing epinephrine sensitivity
[AD-751427] 07 p0749 N73-16091
Cardiovascular and respiratory systems reactions in cosmonauts during space flight
10 p1114 N73-19079
Technology transfer of biomedical data for use in research of cardiovascular diseases
[NASA-CR-131246] 11 p1238 N73-20053
Techniques for determining effects of prolonged weightlessness on cardiovascular system of subhuman primates
[NASA-CR-131890] 13 p1479 N73-21980
Distribution parameter model for acceleration forces acting on arterial system
[AD-756530] 15 p1743 N73-24128
Instrumentation and techniques for determining effects of gravitational and inertial forces on cardiovascular and respiratory dynamics
[NASA-CR-133212] 16 p1867 N73-25119
Lower body decompression effects on human cardiovascular hemodynamic system
20 p2367 N73-29032
Fluid dynamic aspects of cardiovascular behavior during low frequency whole-body vibration such as encountered by astronauts during launch and reentry
[NASA-CR-133843] 21 p2501 N73-30069
Evaluation of energy expenditures and reactions of cardiovascular and respiratory systems to physical work
[NASA-TT-F-15090] 23 p2749 N73-31997
Measurement of arterial pressure by tachooscilloscope method
[NASA-TT-F-15088] 23 p2751 N73-32016
Role of extracardial innervation in compensation of orthostatic load
24 p2883 N73-33023
Mathematical model and digital computer simulation of cardiovascular control system response to ergometer exercise
24 p2886 N73-33049

CARDS
NT PUNCHED CARDS
Evaluation of magnetic cards with cylindrical domains for application to magnetic circuits, noting domain propagation
[LCR-71-232/1/R] 16 p1945 N73-25736

CARET WINGS
Force measurements on caret and delta wings at high incidence in hypersonic reentry conditions noting comparison with theoretical predictions
[IC-AERO-72-16] 01 p0001 N73-10004
Analysis of optimum nozzle thrust deflection angles in cruising flight
[ARC-CP-1222] 05 p0590 N73-14796
Two and three dimensional flow field characteristics of lower surfaces of caret wings
[AASU-327] 21 p2491 N73-29997

CARGO
NT AIR CARGO
Advanced technology hoist-drive system applicable to helicopter cargo hoists with capacities ranging from 12.5 to 50 tons
[AD-746629] 04 p0377 N73-13067
Cost effectiveness of transporting military cargo by air versus surface modes
[AD-750848] 06 p0732 N73-15974
Fuel consumption profiles of passenger and freight transportation modes
[P-4935] 14 p1721 N73-23962
Attached manipulator system for simulating and demonstrating shuttle manipulator cargo handling operations under weightless conditions
[NASA-CR-133964] 18 p2126 N73-27176
Ship to shore transportation of military cargo using tethered balloons
[AD-765352] 23 p2747 N73-31987

CARGO AIRCRAFT
NT BREGUET 941 AIRCRAFT
NT C-2 AIRCRAFT
NT C-5 AIRCRAFT
NT C-130 AIRCRAFT
NT C-131 AIRCRAFT
NT C-135 AIRCRAFT
NT C-141 AIRCRAFT
NT C-160 AIRCRAFT
NT DC 3 AIRCRAFT
NT F-27 AIRCRAFT
Development and characteristics of dual cargo hook system for use on military transport helicopters
12 p1358 N73-21022
Performance of fibrous concrete pavement materials under cargo aircraft and roadway vehicle loads
[AD-741357] 13 p1547 N73-22537

CARGO SHIPS
NT TANKER SHIPS

CARIBBEAN SEA
ERTS A spectrophotographic measurement of water pollution in Charlotte Amalie harbor, St. Thomas
[NASA-CR-130008] 07 p0792 N73-16437
Oceanographic data collection on Caribbean Sea and Gulf of Mexico environments
[AD-752494] 10 p1156 N73-19404
Water depth measurement and mapping of shallow water features of Little Baham Bank using ERTS-1 imagery
[E73-10388] 11 p1275 N73-20350
Optical properties of sea water in Atlantic, Pacific, and Caribbean
[AD-753474] 11 p1290 N73-20470
Marine biology literature compilation for Caribbean Sea and adjacent regions
14 p1607 N73-23022
Literature compilation on marine geology and geophysics for Caribbean Sea and adjacent regions
14 p1607 N73-23023
Remote detection of oceanic eddies in Lesser Antilles using ERTS-1 imagery
[E73-10592] 14 p1657 N73-23451
Calculation of water depth in Caribbean from ERTS-1 MSS data
[E73-10566] 15 p1771 N73-24346
Application of ERTS-1 return beam vidicon and multispectral scanner imagery for ocean water color assessment in Caribbean Sea
[E73-10726] 17 p2019 N73-26332
ERTS-1 I2S imagery of Virgin Islands
[E73-10767] 18 p2134 N73-27243
Topographic mapping of Caribbean Sea surface by GEOS-C satellite
[AD-759041] 18 p2147 N73-27354
Oceanographic features in the lee of the windward and leeward islands: ERTS and ship data
[PAPER-M12] 19 p2281 N73-28351
Estimation of water depth off Great Bahama Bank using ERTS-1 imagery
[PAPER-M19] 19 p2282 N73-28357
Calculation of water depth off Little Bahama Bank from ERTS-1 data for use in upgrading and mapping world navigation charts of shallow waters
[PAPER-M20] 19 p2282 N73-28358
ERTS-1 detection of oceanic eddies in Lesser Antilles
[E73-10922] 20 p2398 N73-29271
Assessment of water color in Caribbean from ERTS-1 RBV and MSS imagery.
[E73-11006] 22 p2660 N73-31311
Atlas presenting oceanographic data collected during Barbados oceanograpic and meteorological experiment
22 p2666 N73-31362
Remote sensing of ocean current boundary layer in Caribbean Sea from Skylab EREP
[E73-11095] 23 p2783 N73-32262

CARIBOUS
Application of ERTS-1 imagery to study of caribou movements and winter dispersal in relation to prevailing snow cover
[E72-10346] 05 p0533 N73-14334

Application of ERTS-1 imagery to study of caribou movements and winter dispersal in relation to snow cover
[E73-10285] 08 p0914 N73-17491
Utilization of ERTS-1 imagery for study of caribou movements and winter dispersal in relation to prevailing Alaskan snow cover
[E73-10401] 11 p1277 N73-20363
Application of ERTS-1 imagery to study of caribou movements and winter dispersal in relation to prevailing snow cover in Alaska
[E73-10615] 15 p1774 N73-24376
ERTS-1 imagery of caribou movements and winter habitats in Alaska in relation to prevailing snow cover
[E73-10840] 19 p2290 N73-28418

**CAROTENE**
Chemiotaxionomic survey of carotenoid pigments in several species and groups of Basidiomycetes
[NASA-TT-F-14858] 11 p1246 N73-20117

**CARRIER FREQUENCIES**
Noise immunity of optical communication lines with frequency and time multiplexing subcarriers
[JPRS-57178] 02 p0181 N73-11467
Analysis of problems and effects in reducing sampling frequency in 625 line television digital codes to improve transmission
[REPT-1972/36] 05 p0507 N73-14129
Automatic carrier acquisition system for phase locked loop receiver
[NASA-CASE-NPO-11628-1] 21 p2506 N73-30113

**CARRIER INJECTION**
Effects of electron-hole scattering on mobility to carriers in silicon at high injected carrier densities
01 p0087 N73-10718
Millimeter wave image conversion panel using p-i-n diode structures for carrier injection and bulk conductivity modulation
[AD-747409] 03 p0276 N73-12241

**CARRIER MOBILITY**
NT ELECTRON MOBILITY
NT HOLE MOBILITY
Carrier mobility in epitaxial silicon film deposited on spinel crystal surface
[NLL-TRANS-2768-[9022.81]]
05 p0585 N73-14761
Current carrier mobility near charged semiconductor surface
[AD-758973] 16 p1953 N73-25804
Alternating current Hall mobility and electrical conductivity in amorphous threshold switching semiconductors
[AD-759004] 16 p1954 N73-25809

**CARRIER MODULATION**
U MODULATION

**CARRIER ROCKETS**
U LAUNCH VEHICLES

**CARRIER SYSTEMS**
U WIRELESS COMMUNICATIONS

**CARRIER WAVES**
Spectrum analysis program for computing power spectrum of angle modulated high frequency carrier wave
[NASA-CR-128984] 17 p1997 N73-26145
Phase modulation of tone and binary signals on carrier waves in communication systems
[NASA-CASE-GSC-11743-1] 18 p2116 N73-27107
Noise tolerant radio telegraphy, using orthogonal carrier modulation
[FTZ-455-TBR-39] 22 p2634 N73-31108

**CARTESIAN COORDINATES**
Construction of continuous rate field in plane steady state plastic flow in bi-cylindrical system of coordinates
[NLL-M-21519-[5828.4F]] 11 p1310 N73-20630
Cartesian and curvilinear coordinates for studying axial symmetrical deformation of rotatory bodies
[NLL-M-22827-[5828.4F]] 11 p1344 N73-20907
Determining mean and covariance errors in alpha-beta filter operating in Cartesian coordinates
[AD-759011] 16 p1935 N73-25656
Computer solution of transformation parameters between two Cartesian coordinate systems from sets of coordinates given in both systems
[NASA-CR-132210] 17 p2055 N73-26621

**CARTRIDGE ACTUATED DEVICES**
U ACTUATORS
U EXPLOSIVE DEVICES

**CARTRIDGES**
Evaluation of aluminum strain hardenable alloys for suitability as materials for cartridge cases
[AD-749508] 08 p0933 N73-17640

**CARTS**
Lunar cart for carrying experimental payloads between Apollo 11 and lunar roving vehicle
09 p1088 N73-18882

**CASCADE CONTROL**
L2 stability in low and high frequency distributed feedback systems
[NASA-CR-129599] 03 p0277 N73-12245
Numerical analysis of variable pitch compressor rotor blades for reduction of rotor vibrations
[AD-762228] 19 p2330 N73-28746

**CASCADE FLOW**
Influence of coriolis effect on energy transfer in mixed flow rotor cascades
[ARC-R/M-3703] 03 p0285 N73-12306
Development of design data for cascades of flat plate guide vanes suitable for use in ninety degree elbows in ducts of circular cross section
[ESDU-AERO-00.02.09] 04 p0403 N73-13284
Improvement of turbojet engine performance analysis by plotting parameters of two shaft turbojet engine operation
[AD-749058] 04 p0465 N73-13789
Calculation of compressible flow in three dimensional cascade of turbomachine blades using stream line curvature technique
[ARC-R/M-3704] 05 p0527 N73-14287
Secondary flow phenomena and associated losses in high-deflection turbine rotor cascade
[AD-750183] 05 p0528 N73-14300
Calculating trajectories of solid particles entrained by fluid flow in turbine and compressor stators
[AD-749547] 05 p0591 N73-14799
Static and wind tunnel tests to determine performance of four cowl cascade thrust reverser configurations at forward velocity
[NASA-TM-X-2665] 07 p0835 N73-16773
Calculation of flow through airfoils in cascade to show pressure distribution under conditions of two dimensional incompressible flow with boundary layer separation at trailing edge
[DLR-FB-72-62] 09 p1014 N73-18276
Analysis of two dimensional cascade flow of double circular arc blades at transonic speed with various camber angles and pitch-chord ratios
[NAL-TR-300] 09 p1014 N73-18279
Experimental investigation of two dimensional cascade flow tests for three cascade configurations - Vol. 4
[NASA-CR-121101] 09 p1015 N73-18282
Three dimensional solid particle trajectories through stationary and rotating turbine cascades
[AD-753364] 09 p1080 N73-18808
Influence of degree of turbulence on aerodynamic coefficients of cascades
10 p1204 N73-19798
Analytical approach for loss and deflection behavior of cascades in transonic flow including axial mass flow variation
10 p1204 N73-19800
Singularity method for calculating incompressible flow through cascades with separation
10 p1205 N73-19802
Effect of axial velocity ratio on aerodynamic coefficients of compressor cascade in viscous flow
10 p1205 N73-19804
Influence of axial velocity density ratio on compressor cascade performance in compressible flow
10 p1205 N73-19805
Experiments with cascade secondary flows
10 p1206 N73-19811
Shock wave boundary layer interaction in compressor cascades
10 p1207 N73-19816
Boundary layer behavior in supersonic straight and annular blade cascades of fixed and mobile types
10 p1207 N73-19817
High speed schlieren film of pulsating flow in transonic turbine cascade
10 p1207 N73-19818
Flow theory calculation of pogo instability in inducer cascades
[NASA-CR-131415] 11 p1271 N73-20313
Numerical analysis of gas flow ahead of supersonic cascade
[AD-756079] 14 p1650 N73-23385
Analysis of transonic potential flow through oscillating unstaggered thin plate cascade
[AD-757255] 14 p1701 N73-23806
Calculation of aerodynamic forces of bending and torsional vibration on installed vibrating cascade blades
[ARC-R/M-3254] 15 p1728 N73-24015
Analysis of supersonic, unstalled torsional flutter in cascades of compressor blades to determine position of flutter boundary and aeroelastic instability
[AD-758721] 15 p1827 N73-24809
Development of alternating direction relaxation method for computing inviscid two dimensional transonic flows through cascades
17 p2012 N73-26268
Wake effects in transpiration cooling of gas turbine blades
[AD-759191] 17 p2078 N73-26806
Irrotational planar supersonic cascade ideal gas flow computation using method of characteristics
[DLR-FB-73-34] 21 p2491 N73-29998
Heat transfer between gas and turbine casing in intervane channels of stators and guide vanes
[NASA-TT-F-15051] 21 p2588 N73-30737
Stoichiometric gas turbines using hot cascades, aerodynamic cascades, and combustor rigs
[EDR-7460] 21 p2589 N73-30746
Supersonic flow configurations at inlet and exit of infinite two dimensional straight cascade of flat plates
22 p2652 N73-31244
Rotating stall in axial flow compressor stages with different types of profiling along blade height and different flow regimes past profile in cascade
[NASA-TT-F-15115] 22 p2709 N73-31698
Shock wave pattern and stability in axial flow supersonic compressor using simulated rotating cascade test facility
23 p2775 N73-32196
Thermodynamic state in cascade argon arc after initiation of step increase in electrode voltage from initial steady-state D.C. level
24 p2990 N73-33893

**CASCADE RANGE [CA-OR-WA]**
Prototype volcano surveillance network in Alaska and Cascade Mountains
[E72-10242] 03 p0289 N73-12342
Thermal surveillance of volcanoes of Cascade Range and Iceland using ERTS-1 imagery and data collection platforms
[E72-10246] 03 p0289 N73-12346
Thermal surveillance of volcanoes of Cascade Range and Iceland using ERTS-1 DCP systems and imagery
[E73-10317] 09 p1023 N73-18349
Mapping and detection of snow cover on land and glaciers in Cascade Range using ERTS-1 imagery
[E73-10379] 10 p1152 N73-19374
Thermal surveillance of Cascade range volcanoes using ERTS-1 MSS data, aircraft imaging systems, and ground based DCP
19 p2284 N73-28369
Snow cover surveys of Sierra Nevada, Cascades, and Wasatch mountains using Skylab EREP data
[E73-11036] 22 p2663 N73-31340
Aerial thermal infrared surveillance of active volcanoes in northern Cascade Range
[E73-11100] 24 p2914 N73-33257

**CASCADE WIND TUNNELS**
Cascade tests of highly loaded multistage fan drive turbine configurations
[NASA-CR-2171] 07 p0836 N73-16778
Two dimensional cascade test of highly loaded, low solidity, tandem airfoil turbine rotor blade
[NASA-TM-X-2729] 08 p0954 N73-17814
Aerodynamic performance of core-engine turbine stator vane tested in two-dimensional cascade of 10 vanes and in single-vane tunnel
[NASA-TM-X-2766] 11 p1333 N73-20823
Methods of testing rotating components of turbomachines compared with tests on complete turbomachines
[AGARD-AG-167] 17 p2077 N73-26800

**CASCADES**
Method of characteristics for analyzing supersonic flow past oscillating flat plate cascades with leading edge locus
[AD-745838] 01 p0042 N73-10332
Development of supersonic cascade and wheel structure for axial flow compressor
[AD-752583] 09 p1079 N73-18804
Effects of boundary layer flow patterns on upright cascade blade performance
10 p1205 N73-19803
Mathematical models for calculating subcritical and supercritical compressible flow about blade cascades
14 p1649 N73-23378

**CASCADES [FLUID DYNAMICS]**
U FLUID DYNAMICS

**CASCODE MOSFET**
U FIELD EFFECT TRANSISTORS

**CASE HISTORIES**
Conference on occupational medicine support in NASA programs to prevent health and emotional problems in personnel
[NASA-TM-X-69072] 08 p0871 N73-17048
Multiphase health screening and medical history questionnaire for preventive/occupational physical examinations
08 p0871 N73-17052
Automated medical history questionnaire for screening industrial personnel and scheduling physical examinations
08 p0872 N73-17060
Periodic health examinations and automatic processing of medical histories for detection and prevention of human diseases
08 p0874 N73-17074
Automated medical record system for identifying and managing medical problems for Navy
08 p0875 N73-17087
Articles on methodology and historical importance of scientific research in creativity
[TT-70-57147-2] 21 p2502 N73-30075

**CASES [CONTAINERS]**
NT ROCKET ENGINE CASES
Tests of ammunition without cases and with combustible cases to evaluate mechanical and environmental stress effects
[ICT-6/72] 12 p1465 N73-21869
Development of analytical and experimental techniques for determining heat transfer characteristics of solid propellant rocket engine storage container system
[AD-758515] 15 p1827 N73-24807

Manipulator kinematics in selecting geometrical shapes of containers and chambers
17 p1990 N73-26087

CASING
Structural stability of gun launched finned projectile motor case
[AD-754378] 11 p1344 N73-20906

CASSEGRAIN ANTENNAS
Dual frequency feed systems for Cassegrainian antennas
[NASA-CASE-NPO-13091-1] 03 p0273 N73-12214
Feed displacement effect on double-spherical Cassegrain antenna patterns
[AD-764778] 23 p2767 N73-32139

CASSEGRAIN OPTICS
Design of Schmidt telescope with possibility of converting to Cassegrain configuration and noting achromatic corrector and angular resolution
07 p0846 N73-16858
Design and construction of 3.5 m telescope in Italy
16 p1911 N73-25466

CASSIOPEIA A
Rocket-borne instrument detection of X ray flux from iron line of Cassiopeia A
[NASA-TM-X-66216] 11 p1336 N73-20843
Mapping of Perseus arm feature in spectrum of Cassiopeia A
[AD-757687] 15 p1832 N73-24854

CASTING
NT SLIP CASTING
Casting techniques for preparation of multiple U-233 metal target disks
[RFP-1848] 03 p0314 N73-12563
Laboratory manual on technology of polycondensation plastics including methods of preparation, analysis, and properties
[AD-747014] 03 p0321 N73-12615
Improved mechanical properties of aluminum alloys cast at ambient temperature
[AD-750532] 05 p0563 N73-14577
Direct casting for producing cast superalloy tungsten or columbium alloy fiber composites with high strength
[NASA-TM-X-2782] 15 p1798 N73-24572
Casting and heat treatments for fabricating ductile superconducting copper base alloys
[CALT-822-51] 22 p2707 N73-31678
Characteristics of silicon carbide samples produced by hot casting under pressure
23 p2808 N73-32450

CASTING SOLVENTS
U PLASTICIZERS

CASTINGS
Characteristics of high performance metal castings and procedures for improving reliability
[AD-748462] 04 p0436 N73-13557
Volumetric analysis and dilatometric study of ferrite magnesium cast iron during heat treatment
[AD-749627] 05 p0563 N73-14572
Ultrasonic inspection and control of cast steel parts for use as machine gears
[TR-7210.617] 10 p1164 N73-19471
Processing techniques for high strength aluminum alloys including ingot processing, solidification and homogenization, and thermal mechanical treatments
[AD-754571] 11 p1307 N73-20606
Directional crystallization in eutectic alloys used on casting turbine blades
[AD-759422] 16 p1931 N73-25624
Laws governing crystallization of ingots with continuous casting in electromagnetic crystallizer
[AD-759230] 17 p2046 N73-26554
Structure and segragation in cast alloys
[AD-761202] 18 p2163 N73-27470
Formation of in situ composites by directional solidification
[AD-765348] 23 p2805 N73-32435

CATABOLISM
Transverse acceleration effects on dioxyribonucleic acid catabolism in rat spleen and liver
03 p0257 N73-12080
Human circadian rhythms of blood circulation, respiration and catabolism under flight simulation stress
[DLR-FB-72-49] 21 p2501 N73-30073

CATALASE
Gas environment effect on catalase cryolysis
10 p1119 N73-19121

CATALOGS (PUBLICATIONS)
NT ASTRONOMICAL CATALOGS
Catalog of automatic control computer programs including description and use of programs
[LAAS-NT-SIS-72-T-15] 05 p0517 N73-14202
Catalog of batteries for Navy weapon systems
[AD-751018] 06 p0627 N73-15087
Preparation of hydrologic atlases of arid land watersheds using ERTS-1 imagery
[E73-10318] 09 p1023 N73-18350
Catalogue of selected remote sensing data for New Jersey environment protection and management
[E73-10383] 11 p1275 N73-20347
Supplemental catalog of atmospheric densities from satellite drag analysis
[NASA-CR-131646] 12 p1398 N73-21341
Data catalog of Nimbus 4 satellite performance capacity, experimentation, and instrumentation - Vol. 2
[NASA-TM-X-69889] 13 p1580 N73-22805
Data catalog of Nimbus 4 satellite performance capacity, experimentation, and instrumentation - Vol. 6
[NASA-TM-X-69893] 13 p1580 N73-22809
Catalog of data in World Data Center C2 for Geomagnetism
14 p1658 N73-23456
Catalog of international rocket and satellite launching data
18 p2199 N73-27750
Development of catalogs for backscatter and brightness temperature measurements and atmospheric effects on Skylab S-193 data
[E73-10896] 20 p2395 N73-29245
Preparation of backscatter and brightness temperature measurement catalogs and atmospheric effects on Skylab S-193 data
[E73-10897] 20 p2395 N73-29246
Pennsylvania State University library catalogue for remotely sensed digital data tapes
[E73-11115] 24 p2916 N73-33272

CATALYSIS
Nitrogen oxide and ammonia removal from spacecabin atmosphere by catalytic oxidation with ruthenium and adsorption on silica gel
[NASA-CR-2132] 09 p0999 N73-18151

CATALYSTS
NT ELECTROCATALYSTS
Performance of hydrocarbon oxidation catalysts as adsorbed layer promoter
[AD-746258] 02 p0138 N73-11117
Catalyst effects on decomposition kinetics of rocket oxidizer ammonium perchlorate
[AD-746728] 02 p0221 N73-11792
Evaluation of cooled, flightweight gaseous hydrogen-oxygen reaction control thrusters to determine catalytic igniter operational limits and performance - Vol. I
[NASA-CR-120869] 03 p0350 N73-12858
Gas chromatographic method for quantitative analysis on hydrazine and its breakdown products at catalytic activity levels
[NASA-TT-F-14722] 04 p0386 N73-13137
Reaction kinetics when liquid hydrazines adsorbed on supported ruthenium catalyst
[RPE-TR-72/1-PT-5] 05 p0506 N73-14122
Plasma sprayed catalyst coatings for low pressure polymerization of ethylene
[AD-750718] 05 p0568 N73-14613
Monolithic catalyst bed for monopropellant hydrazine decomposition
[NASA-CR-132983] 16 p1914 N73-25486
Base metal catalysts as platinum substitutes in petroleum refining and automobile emission devices
[NMAB-297] 18 p2113 N73-27088
Mossbauer spectra of ferrite catalysts used in oxidative dehydrogenation
[NASA-CR-133740] 21 p2506 N73-30108
Mechanism of super burning of catalyzed double based propellants
[AD-763786] 21 p2606 N73-30887

CATALYTIC ACTIVITY
Proton magnetic resonance spectra of ribonuclease A inhibitor complexes, noting effect on catalytic activity
[BMVG-FBWT-72-13] 07 p0747 N73-16074
Carbon dioxide laser based on Na catalyzed combustion of CO with N2O
[AD-757585] 14 p1674 N73-23584

CATARACTS
Literature review of experimental studies to assess relationship of exposure to microwaves and subsequent development of cataracts
[UR-3490-103] 06 p0631 N73-15123

CATCHMENT AREAS
U WATERSHEDS

CATECHOLAMINE
NT EPINEPHRINE
Extraction and analysis by gas-liquid chromatography of catecholamine metabolites from biological tissue
[AD-745944] 03 p0260 N73-12105
Radioimmunoassays of plasma aldosterone and catecholamine concentrations as human vasomotor regulators
09 p0994 N73-18111

CATHODE RAY TUBES
Investigating polymers for suitability of use as light valve display device called deformographic storage display tube
[AD-744689] 01 p0033 N73-10258
Military applications of single gun color cathode ray tubes in display devices
[AD-748385] 04 p0396 N73-13222
Improved multibeam cathode ray tube for real time display of infrared reconnaissance data
[AD-749475] 05 p0520 N73-14228
Design of digital controlled thin cathode tube screen for computer output display
[AD-751745] 07 p0762 N73-16193
Performance of large screen tactical display systems in training devices using cathode ray tubes
[AD-751559] 07 p0767 N73-16228
Development and characteristics of cathode ray tube vertical display system for use in all-weather air navigation aircraft
[AD-752510] 08 p0868 N73-17026
Auxiliary corrective windings for increased resolution and decreased distortions in cathode ray tubes
[AD-751879] 08 p0889 N73-17201
New and revised test methods for cathode ray electron storage tubes
[AD-754139] 11 p1263 N73-20251
Situational display system of cathode ray tubes to assist pilot in aircraft control
[NASA-CASE-ERC-10350] 11 p1291 N73-20474
Development and characteristics of flat, thin, cathode ray tube with digital switching for beam deflection and positioning
[AD-755938] 12 p1384 N73-21227
Data entry and edit monitor using rear ported CRT display device
[AD-756934] 13 p1498 N73-22140
Analysis of ultraviolet emitting fiber optic faceplate cathode ray tubes
[AD-755509] 13 p1503 N73-22181
Cathodochromic storage and display for television systems
[NASA-CR-130236] 15 p1756 N73-24233
Rare earth oxysulfide luminescent films for use in CRT screens
[AD-758760] 16 p1954 N73-25808
Research and development of thin cathode ray display tubes
[AD-762115] 19 p2246 N73-28108
X ray inspection and quality control of AEG cathode life-tests tubes after 44,000/hr life for prediction of communication satellite traveling wave tube durability
[ESRO-TM-148-ESTEC] 19 p2305 N73-28536
Digital address thin display tube to meet Army requirements for computer-output display
[AD-763933] 23 p2762 N73-32100
Design of computer controlled cathode ray tube display screen for flight simulator
[AD-764762] 23 p2767 N73-32140

CATHODES
NT CELL CATHODES
NT COLD CATHODES
NT HOLLOW CATHODES
NT HOT CATHODES
NT PHOTOCATHODES
NT PHOTOMULTIPLIER TUBES
NT THERMIONIC CATHODES
Thermionic emission from oxide-coated cathodes at low temperatures
[AD-747319] 02 p0150 N73-11218
Preparation of thin film metal fluoride electrodes from elemental constituents to obtain high purity and variations in size and shape
[NASA-TM-X-2690] 04 p0386 N73-13140
Energy distribution measurement of experimental thin film emission cathodes to determine acceptability as low energy monoenergetic flood source
[AD-749556] 04 p0397 N73-13228
Dished high perveance grids on throttlable 15 cm hollow cathode ion thruster
[NASA-CR-121038] 04 p0464 N73-13782
Classification and glow discharge with hollow cathodes
[AD-755412] 12 p1385 N73-21231
Performance of rhenium alloy electron tube cathodes
[AD-755828] 12 p1385 N73-21232
Distribution functions of spot diameter for single and multicathode discharges in vacuum
[TH-73-E-32] 14 p1643 N73-23328
Oxygen gas production during stand and discharge in silver zinc batteries
[NASA-CR-128933] 15 p1738 N73-24087
Research in plasma acceleration, hollow cathode physics, and plasma dynamics
[NASA-CR-131270] 15 p1817 N73-24725
Characteristics of ion rocket engine with combination keeper electrode and electron baffle
[NASA-CASE-NPO-11880] 15 p1824 N73-24783
Physical nature of electron emission from tin oxide cathode sources
16 p1947 N73-25750
Production of high power arc lamp cathodes by casting copper body on thoriated tungsten insert
[NASA-TM-X-2865] 18 p2160 N73-27451
Development of field emitter cathodes for electron beam devices
[AD-762322] 20 p2381 N73-29134
Spectrochemical analysis of nonconducting materials using cathodes from sample in Grim glow discharge tube
[NASA-TT-F-15031] 20 p2454 N73-29723

CATIONS
NT METAL IONS

CATS
Dynamic response of vestibular nuclei neurons of decerebrated cats subjected to sinusoidal rotation
[AMRU-R-70-2] 02 p0130 N73-11059

Asymmetric response of cat semicircular canal neurons to symmetric sinusoidal rotation
[AMRU-R-69-2] 02 p0130 N73-11060
Physiological response of cat semicircular canal dependent units to linear acceleration without angular acceleration
[AMRU-R-70-4] 02 p0131 N73-11061
Mechanical response of otolith-dependent units of cats to sinusoidal linear rotation
[AMRU-R-69-3] 02 p0132 N73-11068
Effects of intraperitoneally administered hydrazine on electrophysiology, general behavior, and performance of cats
[AD-746014] 02 p0133 N73-11081
Monomethylhydrazine effects on evoked cerebral neuroelectric responses in unanesthetized cat
[AD-746302] 02 p0133 N73-11082
Respiratory impedance effects on electrical activities of bulbar respiratory neurons, respiratory muscles, and pulmonary ventilation in anesthesized cats
03 p0257 N73-12084
Semicircular canal plugging response in cats to rotary stimulation
06 p0634 N73-15151
Bioelectric activity and excitability of cat brain structures during sleep phases
13 p1484 N73-22031
Behavioral learning response of cat to electric stimulation of auditory nervous system
[NASA-CR-132047] 15 p1742 N73-24124
Equipment for implanting electrodes in subcortical structures of cat brain
[NASA-TT-F-15001] 19 p2225 N73-27947

**CATTLE**
NT CALVES

**CAUCHY INTEGRAL FORMULA**
Structural analysis of two bonded half planes with finite crack perpendicular to and passing through interface
[NASA-CR-2181] 07 p0852 N73-16910

**CAUCHY PROBLEM**
Riemann-Hilbert solution to steady state crack propagation in orthotropic solid
[AD-754529] 11 p1332 N73-20810
Analysis of equations of finite elasticity to show nonapplicability of rest state constraint associated with strain energy function
[AD-764667] 23 p2855 N73-32817

**CAUSTICS**
U ALKALIES

**CAVITATION**
U CAVITATION FLOW

**CAVITATION CORROSION**
Apparatus for low temperature cavitation testing of materials at increased static pressure
[AD-748108] 03 p0304 N73-12482
Experimental data on baffled and unbaffled vibratory cavitation damage tests
[PB-211899] 05 p0525 N73-14270
Cavitation-corrosion resistance tests of tin and aluminum bronzes used for marine pumps in synthetic sea water and distilled water
[DRIC-TRANS-3016] 10 p1167 N73-19492
Analysis of physical properties of liquids on cavitation erosion to provide basis for developing modeling laws to reduce cavitation damage
24 p2904 N73-33175

**CAVITATION FLOW**
Numerical solution of steady state cavitation flows
[AD-745346] 01 p0042 N73-10331
Equations for fully cavitating flow of fluid past flat plate hydrofoil running below free surface with consideration of transverse gravity effects
[AD-746484] 02 p0157 N73-11272
Causes and mechanisms of cavitating inducer instabilities
[NASA-CR-123939] 04 p0405 N73-13299
Cavitation compliance from pulsing tests on rocket turbopumps
[NASA-CR-123963] 04 p0426 N73-13468
Similarity law analysis on flow noise due to cavity resonator
[AD-749673] 05 p0581 N73-14731
Kinetic energy of abrasive particles knocked from metal surface during impact
[AD-750500] 06 p0655 N73-15321
Supercavitating jet flapped hydrofoil with drag reduction due to combined effects of foil camber jet flap
[REPT-249] 06 p0724 N73-15912
Cavitation in liquid cryogens with determination of flow and thermodynamic conditions of cavitating hydrofoil
[NASA-CR-2156] 07 p0770 N73-16255
Computer program to evaluate effect of closed-jet tunnel test on force coefficents of cambered, sharp-nosed, fully cavitating, two dimensional hydrofoil section
[AD-755423] 13 p1512 N73-22250
Schlieren method adapted as flow visualization technique to study cavitation development on axisymmetric bodies in water tunnel
[AD-757078] 14 p1652 N73-23402
Cavitation data on surface irregularities applied to design problems
[AD-759030] 17 p2015 N73-26295
Growth of cavitation bubbles and boiling bubbles
[AD-760719] 18 p2132 N73-27225
Restoration of obliterated stamped serial numbers by ultrasonically induced cavitation in water
[NASA-TM-X-68257] 18 p2213 N73-27866
Thermodynamic behavior of liquid hydrogen and nitrogen cavitation in ogives
[NASA-CR-2242] 19 p2251 N73-28153
Fluid mass flow rate measurements using cavitating Venturi tubes noting application to liquid rocket propellant
[DLR-FB-72-33] 21 p2525 N73-30245
Environmental effects on headform cavitation inception
[AD-763367] 21 p2527 N73-30261
Modeling flow cavitation in water
[PB-220531/8] 21 p2528 N73-30268
Development of method for calculating bubble conditions in flow of boiling liquid in vertical tubes
[NLL-WH-335-[9091.9F]] 21 p2605 N73-30875
Differential solution to problem of nonlinear cavitational flow around channel plates by gravity fluid
22 p2651 N73-31239
Equations describing dynamical motions of small cavitation bubbles in liquids
[AD-764075] 22 p2656 N73-31277
Cavitation inception and separation on axisymmetric bodies in water tunnel
23 p2771 N73-32164
Analysis of physical properties of liquids on cavitation erosion to provide basis for developing modeling laws to reduce cavitation damage
24 p2904 N73-33175

**CAVITIES**
Swirling cavity flow breakdown along axis of swirling water flow in circular pipe
[REPT-250] 06 p0724 N73-15913
Electron bunching in drift area of two cavity klystrons via one dimensional approximation, using electron beam disk model
[AD-751073] 07 p0763 N73-16204
Field emission, high intensity electron gun, single RF cavity, and compression system
[IPPJ-T-11] 09 p1011 N73-18249
Low mass rolling element bearing with lightweight core and hollow center
[NASA-CASE-LEW-11087-3] 11 p1298 N73-20534
Nature of power losses in RF superconducting cavities at low and high temperatures
[SLAC-PUB-963] 12 p1383 N73-21213
Transonic wind tunnel corrections for slotted or perforated walls
14 p1649 N73-23373
Visualization of flow deviation by cylindrical wall cavities
14 p1649 N73-23374
Calculation of supersonic boundary layer flow separation and reattachment along plane wall with sinusoidal hollow
[REPT-72-4] 14 p1650 N73-23382
Cavity temperature and flow characteristics in gas-core reactor for testing fissioning uranium plasmas
[NASA-TM-X-2797] 15 p1809 N73-24662
Polarization effects in photon echoes and in anisotropic mirror laser cavities
18 p2157 N73-27429
Soil burrowing mole apparatus
[NASA-CASE-XNP-07169] 23 p2796 N73-32362

**CAVITY RESONATORS**
Helmholtz resonator damping device for suppressing rocket combustion instability
03 p0349 N73-12845
Similarity law analysis on flow noise due to cavity resonator
[AD-749673] 05 p0581 N73-14731
Suitibility of Nb surfaces in superconducting RF cavities
[KFK-EXT-3/72-3] 06 p0709 N73-15781
Feasibility of developing stirred chemical reactor laser cavity based on perfectly stirred reactor concept
[AD-751299] 07 p0807 N73-16549
Cavity resonators for measuring cryogenic propellant content in space shuttle orbiter tanks under weightlessness
10 p1162 N73-19452
Ultrashort pulse generation from mode locked carbon dioxide laser by resonant acoustic loss modulator
[DREV-TN-2024/72] 11 p1302 N73-20566
Calculating resonance frequency of cylindrical cavity frequency meter
[REPT-6659] 14 p1666 N73-23522
Design and performance of acoustic exciter for gas volume modulation in absorption cell
[NASA-CR-124269] 16 p1913 N73-25482
Electromagnetic wave propagation in inhomogeneous plasmas exemplified by cavity resonators and positive column in magnetic field
[IPF-72-8] 17 p2069 N73-26742
Radio frequency resonant cavity mode analysis technique for fluid mass quantity gauging of space shuttle orbiter tankage
[NASA-CR-133393] 18 p2151 N73-27390
Infrared tunable dye laser with nonlinear wavelength mixing crystal in optical cavity
[NASA-CASE-ARC-10463-1] 23 p2763 N73-32111
PDP 8/I data acquisition and averaging program for synchronous hot-wire measurements in mouth of flow excited cavity resonator
[AD-764851] 23 p2795 N73-32357
Enhanced electron field emission in resonant niobium superconducting cavity
[AD-765336] 24 p2970 N73-33733

**CDC COMPUTERS**
NT CDC 1604 COMPUTER
NT CDC 6000 SERIES COMPUTERS
NT CDC 6600 COMPUTER

**CDC 6000 SERIES COMPUTERS**
NT CDC 6600 COMPUTER

**CDC 1604 COMPUTER**
Speech display simulation system, using CDC 1604 computer
14 p1627 N73-23183

**CDC 6000 SERIES COMPUTERS**
General purpose linkage editor for CDC 6000 series computers
[AD-764044] 22 p2725 N73-31809
Computer programming procedure for linking independent CDC 6000 series computers
[NASA-CR-2296] 23 p2760 N73-32090

**CDC 6600 COMPUTER**
Users manual for network analysis program
[AD-752600] 08 p0892 N73-17218
CDC 6600 computer analysis of numerical stabilizer effects on computing time for second order accurate schemes
[AD-753165] 09 p1018 N73-18308

**CEILINGS [METEOROLOGY]**
Application of model output statistics to predict ceiling and visibility
[FAA-RD-73-14] 19 p2315 N73-28621
Utilization of inverse scattering method to measure transparency of atmosphere in slant direction
22 p2693 N73-31571

**CEILOMETERS**
U CLOUD HEIGHT INDICATORS

**CELESCOPES**
Catalog of ultraviolet stellar observations obtained from celescope experiment on OAO 2
[NASA-CR-132196] 16 p1962 N73-25869
Catalog of ultraviolet stellar observations using celescope on OAO 2
[NASA-CR-133259] 17 p2088 N73-26889

**CELESTIAL BODIES**
NT A STARS
NT ANDROMEDA GALAXIES
NT AREND-ROLAND COMET
NT ASTEROIDS
NT B STARS
NT BINARY STARS
NT BRUDERHEIM METEORITE
NT CARBONACEOUS METEORITES
NT CASSIOPEIA A
NT CEPHEID VARIABLES
NT CERES ASTEROID
NT CHONDRITES
NT COMET TAILS
NT COMETS
NT CRAB NEBULA
NT EARLY STARS
NT EARTH [PLANET]
NT ECLIPSING BINARY STARS
NT EXTRASOLAR PLANETS
NT GALAXIES
NT GIANT STARS
NT HOT STARS
NT ICARUS ASTEROID
NT INFRARED STARS
NT IRON METEORITES
NT JUPITER [PLANET]
NT LATE STARS
NT MAIN SEQUENCE STARS
NT MARS [PLANET]
NT MERCURY [PLANET]
NT METEORITES
NT METEOROID SHOWERS
NT METEOROIDS
NT MICROMETEOROIDS
NT MILKY WAY GALAXY
NT MOON
NT NATURAL SATELLITES
NT NEBULAE
NT NEPTUNE [PLANET]
NT NEUTRON STARS
NT NOVAE
NT O STARS
NT PLANETARY NEBULAE
NT PLANETS
NT PULSARS
NT QUASARS
NT RADIO GALAXIES
NT RADIO METEORS
NT RADIO SOURCES [ASTRONOMY]
NT RADIO STARS
NT REFERENCE STARS
NT SATURN [PLANET]
NT SOLAR SYSTEM
NT SPIRAL GALAXIES
NT STAR CLUSTERS

NT STARS
NT SUN
NT SUPERGIANT STARS
NT SUPERNOVAE
NT T TAURI STARS
NT TAURID METEOROIDS
NT TEKTITES
NT TUNGUSK METEORITE
NT URANUS [PLANET]
NT VARIABLE STARS
NT VENUS [PLANET]
NT VESTA ASTEROID
NT VIRGO STAR CLUSTER
NT WHITE DWARF STARS
NT ZODIACAL DUST
Catalog of 383 celestial objects emitting infrared radiation near 10 microns
[AD-743891] 01 p0106 N73-10878
Space electronics, data transmission, orientation of celestial objects, and research instruments
01 p0119 N73-10979
Catalog of micron celestial objects
[AD-747776] 04 p0476 N73-13894
Stellar, planetary, and comet observations at astronomical observatory during 1973
08 p0960 N73-17850
Approximative ephemeris calculations for moving celestial objects using coordinates from different points on earth surface
10 p1178 N73-19587
Tables on structure of interstellar masers and quasars
14 p1704 N73-23826
Device for determining relative angular position of spacecraft and radiating celestial body
[NASA-CASE-GSC-11444-1] 19 p2300 N73-28490
Symposium on Gum Nebula and related topics
[NASA-SP-332] 22 p2715 N73-31731
Optical and ultraviolet methods in astronomy
22 p2734 N73-31882

CELESTIAL GEODESY
Atmospheric refraction effects on geodetic measuAtmospheric rements to celestial bodies
[NASA-CR-131534] 12 p1398 N73-21339
Some results of astro-gravimetric leveling in USSR
[AD-755881] 14 p1664 N73-23503
Development of satellite geodesy technique for accurate determination of three dimensional coordinates of ground stations
[NASA-CR-132251] 15 p1778 N73-24412
Development of automated astronomic positioning system using vertically oriented telescope to produce accurate astronomic latitude and longitude
[AD-760108] 17 p2060 N73-26668

CELESTIAL MECHANICS
Calculation of all occultations by planet Jupiter of stars brighter than magnitude 6.55 for period 1951 to 2000
[NASA-TT-F-14626] 01 p0104 N73-10862
Finite series expansion study on motion of Mercury perihelion
[PB-213059] 11 p1339 N73-20870
Numerical integration techniques for solution of orbital elements of moon and planets
[AD-755164] 14 p1707 N73-23850
Influence of Arabian astronomy on Europe
15 p1829 N73-24828
Galactic nucleus map at ten microns with few arc second resolutions
[LPL-COMMUN-169] 21 p2592 N73-30765
Quasirelativistic theory of two-body motion in Euclidean space and Newtonian time
[AD-763431] 21 p2598 N73-30827
Range points in relativistic test of celestial mechanics in Mariner 9 Doppler tracking data analysis for Mars gravity
23 p2842 N73-32710
Celestial mechanics for Mariner 9 space probe
24 p2983 N73-33836

CELESTIAL NAVIGATION
NT ASTRONAVIGATION
Astronomical techniques for spacecraft orientation
05 p0577 N73-14694
Handbook of operating instructions for air navigation systems to include international air routes, Doppler radar, and great circle navigation
[AD-750493] 06 p0697 N73-15684
Celestial navigation method using astronomical refraction effects
07 p0859 N73-16971
Most probable position in astronomical navigation using celestial body coordinates
07 p0859 N73-16972
Development of automated astronomic positioning system using vertically oriented telescope to produce accurate astronomic latitude and longitude
[AD-760108] 17 p2060 N73-26668

CELESTIAL OBSERVATION
U ASTRONOMY

CELL CATHODES
Electrolytic preparation and evaluation of mixed sodium-iron tungsten bronzes
[AD-746248] 02 p0188 N73-11522

CELLS [BIOLOGY]
NT CARBOXYHEMOGLOBIN
NT CHROMOSOMES
NT COLLAGENS
NT ERYTHROCYTES
NT HEMOGLOBIN
NT LYMPHOCYTES
NT MACROPHAGES
NT NEURONS
Complete activity of lactate dehydrogenase and isoenzymes in plasma and myeloid cells
[NASA-TT-F-14586] 01 p0009 N73-10070
Simulated high altitude determination of interrelation of systematic and cellular responses to acute and chronic hypoxia
[AD-743536] 01 p0010 N73-10081
Energy comparisons for lethal doses of gamma radiation and visible light with energy of basal cell metabolism
[AD-746750] 04 p0381 N73-13102
Internally deposited radioisotope effects on cell populations in mammals
[NYO-3970-29] 05 p0500 N73-14074
Cellular activation energy effect in rat tolerance to acceleration stress
[AD-749338] 05 p0501 N73-14079
Transverse acceleration effects on rat hepatocytic structures
10 p1115 N73-19086
Thalamic cat cell activities during sleep and wakefulness phases
13 p1484 N73-22030
Physiological regeneration of corneal epithelial mice cells exposed to strong magnetic fields
14 p1608 N73-23034
Mechanisms of oxygen toxicity at cellular level
[AD-758725] 16 p1868 N73-25124
Single body theory for weightlessness simulation, applied to simple cell model
19 p2227 N73-27961
Microscopic morphological changes in dog cardiac muscle after chronic gamma irradiation
20 p2366 N73-29027
Biological evaluation of influence of helium-oxygen atmosphere on culture of mammalian cells
24 p2883 N73-33024

CELLULOSE
Biodegradation of cellulose fibers and reclamation of single cell protein from refuse through fermentation process
[NASA-CR-130300] 06 p0630 N73-15115
Pyrolysis and combustion of cellulosic materials
08 p0883 N73-17147
Pyrolysis products of flame retardant treated cellulose
19 p2351 N73-28913

CELLULOSE NITRATE
Ignition and deflagration of in nitrocellulose based solid propellants
[AD-756880] 13 p1570 N73-22720

CEMENTATION
Kinetic study of copper cementation on iron
[BM-RI-7761] 15 p1791 N73-24519

CEMENTS
Desilification in alumina and cement production by sintering disintegration method
[NLL-LIB-TRANS-1725-[5205.9]]
15 p1746 N73-24150
Lime-cement combination for soil stabilization in road and airfield construction
[AD-762552] 22 p2690 N73-31545

CEMS SYSTEM
U CENTRAL ELECTRONIC MANAGEMENT SYSTEM

CENSUS
Census cities experiment in detection of urban change and land use
[E73-10490] 12 p1397 N73-21326
Census cities experiment in detection of urban development and land use from ERTS-1 imagery
[E73-10538] 13 p1518 N73-22302

CENTAUR LAUNCH VEHICLE
NT ATLAS CENTAUR LAUNCH VEHICLE
Postflight analysis of Atlas/Centaur - 29 and Intelsat 4 launch and orbit establishment
[NASA-TM-X-68649] 01 p0102 N73-10845
Liquid hydrogen reorientation in fuel tanks of Centaur launch vehicle using low level accelerations with and without internal baffles
[NASA-TN-D-7168] 07 p0770 N73-16252
History and future of Titan/Centaur launch vehicle
[NASA-TM-X-68249] 15 p1835 N73-24877
Centaur D-1T improved propulsion and propellant systems
[NASA-TM-X-71436] 23 p2830 N73-32619
Cryogenic tanking and partial jettison tests of Centaur launch vehicle and Centaur standard shroud to develop insulation, purge, and vent systems
[NASA-TM-X-71455] 24 p2984 N73-33850

CENTAUR VEHICLE
U CENTAUR LAUNCH VEHICLE

CENTAURUS CONSTELLATION
Use of objective grating for extension of magnitudes and colors beyond those available photoelectrically
[ROY-OBS-BULL-172] 06 p0674 N73-15486
Chemical composition and abundance of alpha Centauri visual binary determined from spectral lines
[ROY-OBS-BULL-173] 06 p0719 N73-15870
Chemical composition of line spectra for binary alpha Centauri and determination of abundances
[BULL-173] 07 p0842 N73-16820

CENTER OF GRAVITY
SOS - computer program for calculating weight, center of gavity, and inertias of asymmetrical missiles
[AD-749251] 05 p0601 N73-14885
Variational equations for studying rotational motion of orbiting rigid body about its center of mass under conservative and nonconservative torques
07 p0817 N73-16624
Magnus forces on center of gravity and rotational startup response of self-spinning rotor in subsonic air stream
[AD-755108] 11 p1232 N73-20001
Equations for determining action and deformation of bearings when force applied to center of gravity of gyromotor rotor
20 p2417 N73-29422

CENTRAL AMERICA
Application of ERTS-1 data for development and operation of volcano surveillance network
[E73-10711] 17 p2018 N73-26318
Development of volcano surveillance and early warning system using ERTS-1 data collection system
[PAPER-G9] 19 p2264 N73-28240
Ground-based radiation thermometry mapping of volcanology in Central America
[E73-10937] 21 p2529 N73-30279

CENTRAL ATLANTIC REGION [US]
Mapping land use and land use change in Central Atlantic Region using ERTS-1 imagery
[E72-10241] 03 p0288 N73-12341
Land use mapping and change detection in Central Atlantic Regional Ecological Test Site based on ERTS-1 MSS imagery
[E73-10034] 06 p0661 N73-15367
Development of standards for classification, mapping and scientific analysis of land use and land use change in Central Atlantic Region Ecological Test Site using ERTS-1 imagery
[E73-10347] 10 p1148 N73-19346
Thematic and photomapping of Arizona CARETS, and polar regions from ERTS-1 imagery
[E73-10463] 12 p1394 N73-21302
Prototype regional environmental information system based on ERTS-1 imagery of Central Atlantic Regional Ecological Test Site
[E73-10497] 12 p1397 N73-21333
Land use mapping of Central Atlantic Region using ERTS-1 imagery
[E73-10557] 14 p1655 N73-23429
Land use change and classification using ERTS-1 imagery of Central Atlantic Regional Ecological Test Site
[PAPER-L6] 19 p2274 N73-28302
Linking land use and environmental processes in Central Atlantic Region using ERTS-1 data
[PAPER-L7] 19 p2274 N73-28303
Land cover and land use mapping of Central Atlantic Region shoreline zone using ERTS-1 imagery
[PAPER-L8] 19 p2274 N73-28304

CENTRAL ELECTRONIC MANAGEMENT SYSTEM
Design of aircraft digital system for automatic flight control
14 p1713 N73-23900
Human factors in design of aircraft in-flight monitoring and automatic landing system for low weather operation
14 p1713 N73-23901

CENTRAL NERVOUS SYSTEM
NT BRAIN
NT CEREBRAL CORTEX
NT CEREBRUM
NT SPINAL CORD
NT THALAMUS
Lesions of nervous system and vascular embolisms in decompression sickness
[AD-743330] 01 p0010 N73-10076
Clinical study of 56 cases with neurological symptoms in decompression sickness
[AD-744298] 01 p0011 N73-10086
Monomethylhydrazine effects on evoked cerebral neuroelectric responses in unanesthetized cat
[AD-746302] 02 p0133 N73-11082
High altitude effects on cerebral and cardiovascular systems of monkeys
[AD-745891] 02 p0134 N73-11085
End organs, central nervous system connections, and static and dynamic characteristics of vestibular system
06 p0629 N73-15103
Syringomyelia in central nervous system affecting flying fitness
14 p1611 N73-23061
Impact acceleration effects on rabbit central nervous system
20 p2366 N73-29024

CENTRAL NERVOUS SYSTEM DEPRESSANTS
Effects of antimotion sickness drugs, placebos, and secobarbital on postural equilibrium functions at sea level and at simulated altitudes of 12,000 feet
[AD-748192] 05 p0504 N73-14105

Alcohol reference method for predicting drug modifications of central nervous system activity and pilot performance decrease
12 p1369 N73-21112

CENTRAL NERVOUS SYSTEM STIMULANTS
Hashish smoking effects on human oxygen consumption during physical stress and safe driving ability
12 p1370 N73-21115

CENTRAL PROCESSING UNITS
NT ARITHMETIC AND LOGIC UNITS
Large scale integration techniques for computer multiprocessing system
[NASA-CR-128395] 01 p0030 N73-10234
Digital simulation model for central processing unit of spaceborne computer with automatically reconfigurable modular multiprocessor system
[NASA-CR-128996] 02 p0146 N73-11185
Baseline design of central multiprocessor for manned space station application
[NASA-CR-124151] 11 p1259 N73-20219

CENTRIFUGAL COMPRESSORS
Performance tests of low-pressure-ratio centrifugal compressor with four different diffuser configurations
[NASA-TN-D-7237] 11 p1231 N73-19997
Design and fabrication of backswept impeller vane island diffuser, and advanced-concepts compressor rig
[NASA-CR-120942] 11 p1298 N73-20531
Aerodynamic design parameters and test performance of two-stage high pressure ratio centrifugal compressor
[AD-759499] 16 p1919 N73-25533
Design, development, and evaluation of centrifugal compressor with six to one pressure ratio and two pounds per second air flow
[NASA-CR-120941] 17 p2037 N73-26483
Analysis of operation of single stage, high pressure centrifugal compressor during closed loop flow of various gases
[AD-761608] 19 p2331 N73-28750
Design and operating principles of base plate for regulating performance of radial centrifugal machines
[NLL-NEL-TT-2476-[6075.461]] 20 p2382 N73-29137
Isothermal forging of titanium centrifugal compressor impeller
[AD-764266] 22 p2678 N73-31455

CENTRIFUGAL FORCE
Analysis of swirling jet of gas injected into vacuum and effect of centrifugal force on separation of constituents
[ISAS-487-VOL-37-NO-13] 05 p0526 N73-14283
Human performance, physiological effects, and pathological effects of rotary acceleration
06 p0628 N73-15096
Mathematical model for dense rotating plasma with centrifugal expansion instability at high beta values
[TRITA-EPP-72-28] 09 p1071 N73-18740

CENTRIFUGAL PUMPS
Influence of transverse force on impeller bearing rupture of centrifugal pumps
02 p0179 N73-11446
Analysis, design, fabrication, and performance tests to determine effects of impeller blade clearance on efficiency of centrifugal pumps
[NASA-CR-120815] 03 p0305 N73-12493

CENTRIFUGES
NT HUMAN CENTRIFUGES
Determination of aerodynamic diameter of latex spheres and asbestos fibers using aerosol spiral centrifuge
[BMVG-FBWT-72-10] 07 p0812 N73-16585
Method for calculating magnetic field map of magnetic suspension in ultracentrifuge
[LNF-72/49] 10 p1138 N73-19272
Aerodynamic size and mass distribution of aerosol particles determined with spiral centrifuge compared to other precipitators
[BMVG-FBWT-73-3] 14 p1668 N73-23535
Theory and applications of centrifugal extraction process based on numerical analysis of flow characteristics of liquid residue
[NLL-RTS-7990] 15 p1790 N73-24512
Three dimensional incompressible laminar flow in centrifugal toroidal shell
24 p2909 N73-33215

CENTRIFUGING
Molecular diffusion in mixing binary flow and separation of uranium isotopes by fixed wall centrifugation
06 p0653 N73-15302
General equations for describing molecular diffusion in vortex flow and possible application to isotopic separation by fixed wall centrifugation
[FRNC-TH-213] 08 p0897 N73-17262
Recovery of barium oxide reagent from residue from preparing lubricant additives in centrifuge
[AD-751945] 09 p1042 N73-18500
Theory and applications of centrifugal extraction process based on numerical analysis of flow characteristics of liquid residue
[NLL-RTS-7990] 15 p1790 N73-24512
Ultracentrifugation of biological materials
[NASA-CR-114673] 23 p2750 N73-32009

CENTRIFUGING STRESS
Centripetal acceleration for inhibiting cerebellar rat cortex activity
14 p1608 N73-23030

CEPHEID VARIABLES
Transformations for converting b-y color excesses for Cepheids into B-V excesses
[NASA-TM-X-66061] 01 p0103 N73-10854
Variations of microturbulent velocity with atmospheric phase and height in classical Cepheids
[NASA-TM-X-66081] 01 p0105 N73-10867
OAO 2 observations used to determine relationship between visual and ultraviolet variations in C-4 155-nm line in Beta Cephei
08 p0975 N73-17974
Ultraviolet photometry of eclipsing Cephei variable star by OAO 2
22 p2734 N73-31884

CERAMAL PROTECTIVE COATINGS
U CERMETS
U PROTECTIVE COATINGS

CERAMALS
U CERMETS

CERAMIC BONDING
Improvements in welding techniques to increase productivity and quality of performance of bonded joints
[JPRS-58291] 10 p1163 N73-19460
Production of ceramic-metal compounds by contact-reactive brazing for increasing mechanical strength
10 p1163 N73-19462
Metal-ceramic bonding detailing dry soldering method
[FTZ-A-97-TBR-2] 22 p2678 N73-31453
Bonding methods of aluminum beam leaded devices on microcircuit ceramic substrates
[NASA-CR-124434] 23 p2797 N73-32369
Ceramic to metal bonding, noting improvement of Mo-Mn silicate method, and use of interfacially active metals
[BMFT-FB-T-73/07] 23 p2798 N73-32377
Ceramic reinforced mullite thermal protection system design for space shuttle surface
24 p2942 N73-33495

CERAMIC COATINGS
Effective thermal conductivities of four metal-ceramic composite coatings in hydrogen-oxygen rocket firings
[NASA-TN-D-7055] 01 p0116 N73-10961
Plasma sprayed catalyst coatings for low pressure polymerization of ethylene
[AD-750718] 05 p0568 N73-14613
Using Plamya-62 acetylene cutting torch for spraying ceramics
10 p1172 N73-19530
Bibliography on ceramic materials
[AD-755650] 12 p1417 N73-21478
Optimization of basic ceramic insulation for space shuttle orbiters - Part 2
[NASA-CR-112257] 13 p1546 N73-22531
Microstructure and mechanical properties of thermal barrier materials produced by arc plasma spraying
[AD-762045] 19 p2312 N73-28598
Radiometric emittance measurements on reusable external insulation materials
24 p2939 N73-33473
Design of rigid ceramic foam insulation for space shuttle surface thermal protection
24 p2942 N73-33493
Flexible ceramic mat surface insulation for space shuttle thermal protection system design
24 p2942 N73-33497

CERAMIC NUCLEAR FUELS
Characteristic property data for plutonia molybdenum radioisotopic cermet fuel
[LA-4976] 06 p0698 N73-15694
Computerized simulation of stainless steel clad uranium oxide plutonium oxide fuel pin behavior in reactor core
[ORNL-4825] 07 p0819 N73-16640
Development of plutonium dioxide molybdenum cermet nuclear fuels
[MLM-1905] 07 p0820 N73-16643
Fabrication and performance of uranium carbide and uranium dioxide thermionic reactor fuels
[GULF-GA-A-12251] 24 p2954 N73-33599

CERAMICS
NT CERAMIC NUCLEAR FUELS
NT PORCELAIN
Design and evaluation of automobile thermal reactors with ceramic material construction
[NASA-TM-X-68148] 01 p0069 N73-10567
Research and development of ceramic systems for use as structural components in hypersonic missile applications
[AD-745744] 01 p0071 N73-10580
Electrostriction in ferroelectric ceramics
[AD-745821] 01 p0089 N73-10731
Development of efficient high power NDY ceramic laser material
[AD-746521] 02 p0184 N73-11491
Refractory glass ceramics for gas turbines
[NPL-IMS-17] 02 p0192 N73-11556
Densification of ceramic materials and mechanical behavior of ceramic materials with emphasis on fracture energies
[AD-745909] 02 p0193 N73-11561
Influence of fast neutron damage to ceramic insulators on thermionic reactor design
[LA-DC-72-523] 03 p0333 N73-12716
Single crystal growth of ceramic oxides and compound semiconductors in space
[NASA-CR-123951] 03 p0344 N73-12806
Research data on dielectrics, refractory materials, plastics, ceramics, and glasses
[AD-746686] 03 p0347 N73-12827
Determining elastic compliance, piezoelectric constant, and dielectric constant by mechanically driving polarized ceramic bar
[AD-748357] 03 p0348 N73-12839
Fracture measurement in high strength brittle ceramic materials
[AECL-3677] 03 p0361 N73-12944
Technology of aircraft construction to include manufacturing of parts from plastics, ceramics, and nonmetallic materials
[AD-749558] 04 p0374 N73-13044
Extrusion can for extruding ceramics under heat and pressure
[NASA-CASE-NPO-10812] 04 p0425 N73-13464
Lead lanthanum zirconate titanate ceramics as intracavity tuning elements in rhodamine 6G dye laser
[SC-RR-72-0273] 04 p0429 N73-13493
Nonlinear characteristics of polarized ferroelectric ceramics in operational environment
[AD-748198] 04 p0438 N73-13571
Electrical resistivity of space electric power insulating materials
[LA-4978] 05 p0498 N73-14058
Sonar equipment research project to include determination of temperature and heat dissipation characteristics of ceramics used in high frequency projectors
[AD-749960] 05 p0515 N73-14187
High temperature ceramic to metal seal capable of operation at 1200 C for 3 to 5 years
[NASA-CR-120831] 05 p0552 N73-14484
Thermal shock resistant hafnia ceramic materials
[NASA-CASE-LAR-10894-1] 05 p0564 N73-14584
Fracture behavior of silicon nitride and silicon carbide ceramics
[NASA-CR-129671] 05 p0564 N73-14585
Increased heat and impact resistance of ceramics made of zirconium dioxide reinforced with mullite whiskers
[JPRS-57770] 05 p0565 N73-14588
Electrically conducting ceramics to heat biowaste propellants to 2000 K in resistojet thrustors for space station application
[NASA-CR-112159] 06 p0635 N73-15161
Determination of optical/mechanical properties of low expansion glass ceramic material for use as lightweight substrate for primary mirror on large spaceborne telescope
[NASA-CR-130141] 06 p0674 N73-15481
Fabricating lamellar ceramic-based composites with synthetic fluorine mica
[AD-750353] 06 p0688 N73-15601
Application of powder metallurgical techniques to fabrication of reaction-bonded Si3N4 for use as high temperature engineering ceramic
[AD-750096] 06 p0688 N73-15603
Development of ceramic materials for construction of full scale, high pressure, hypersonic facility for testing aircraft and missile models
[AD-751298] 07 p0812 N73-16588
Fabrication and characteristics of ceramic-metal multilayers for inclusion in experimental breeder reactor
[LA-5021-PR] 07 p0820 N73-16646
Chemical process for producing continuous fine superconducting filaments
[AD-751545] 07 p0832 N73-16746
Solid ceramic electrolyte system for measuring redox conditions in high temperature gas mixing
[NASA-TM-X-58105] 08 p0892 N73-17224
Development of process for fabricating dense boron suboxide billets by hot pressing to eliminate decomposition and cracking
[AD-751980] 08 p0936 N73-17662
Evaluation of ceramic materials for application as high temperature gas bearing material
[AD-753858] 09 p1042 N73-18499
Alloying and thermal treatment for improving mechanical properties of ceramics
[AD-753124] 09 p1055 N73-18597
Deformation processes in forging refractory ceramic oxides
[NASA-CR-131109] 10 p1175 N73-19558
Commercial applications of rare earth elements in ceramics, glasses, and nuclear technology
[IS-2967] 10 p1175 N73-19561
Chemical and orthopedic properties of ceramic bone implants in monkeys
[AD-754982] 11 p1248 N73-20134
Reduction of orange peel and extended defect formation in ceramics
[AD-754837] 11 p1303 N73-20576

Failure mechanics and compressive biaxial strength of ceramics
[AD-754826] 11 p1309 N73-20621
Acoustic emission correlation with slow crack growth in polycrystalline ceramics
[AD-754839] 11 p1310 N73-20626
Research projects in metals and ceramics
[ORNL-4820] 11 p1330 N73-20796
Polarization and thermionic emission effects on resistivity measurements for metal oxide electrical insulators at high temperatures
[HEDL-TME-72-73] 12 p1386 N73-21243
Bibliography on ceramic materials
[AD-755650] 12 p1417 N73-21478
Arc welding of joints and hard surfaces using longitudinally notched ceramic rods
[AD-756944] 13 p1535 N73-22435
Material tests to determine characteristics of fiber reinforced ceramic matrix composites
[AD-757063] 13 p1544 N73-22513
Status of research on gas discharge, liquid crystal display systems, and ferroelectric ceramics in Europe
[AD-757649] 14 p1668 N73-23538
Vapor deposition techniques for preparation of nickel foil and various ceramic materials
[AD-758389] 14 p1679 N73-23625
Properties of piezoelectric lead zirconate titanate ceramic resonator material produced by adding lead niobates to material
[AD-757617] 14 p1681 N73-23644
High temperature testing of silicon carbide ceramics for use in gas turbine vanes
[AD-757796] 15 p1802 N73-24602
Monolithic light emitting diode display devices
[AD-758853] 16 p1882 N73-25232
Adhesion, friction, and wear behavior of glasses and ionic solids
[NASA-TM-X-68255] 16 p1932 N73-25632
Proof testing of ceramic materials for component lifetimes
[AD-759373] 17 p2051 N73-26590
Wear tests of ceramic materials for rolling contact bearings
[AD-761200] 18 p2168 N73-27506
Temperature stability of ceramic surface acoustic wave delay devices
[AD-761884] 19 p2327 N73-28723
Force and wear analysis in ceramic processing for alumina and silicon nitride
[AD-762522] 20 p2436 N73-29561
Theoretical treatment of neutron irradiation caused crystal lattice defects in ceramic materials
[AECL-4375] 20 p2462 N73-29788
Research projects to develop and evaluate ceramic materials in areas of refactory structural ceramics and solid electrolyte ceramics
[NASA-CR-133741] 21 p2562 N73-30540
Crack propagation in glass and ceramic materials
[AD-764045] 22 p2690 N73-31543
Thermal properties of ceramics for design of sonar arrays
[AD-764572] 23 p2758 N73-32071
Synthesis of polycrystalline oxide ceramic laser rods
[AD-765345] 23 p2802 N73-32413
Mechanism of grain growth in ceramics
[NASA-CR-135673] 23 p2804 N73-32425
Method for determining heat capacity of ceramic materials by measuring heat transfer during condensation process
23 p2807 N73-32445
Nondestructive tests of brittle ceramic materials
[AD-764795] 23 p2811 N73-32477
Glass ceramic foam materials for space shuttle heat shielding system
24 p2938 N73-33464

**CEREBRAL CORTEX**
Dynamics of some characteristics of induced potential of optical region in cerebral cortex in rabbits with increasing hypoxia
11 p1244 N73-20103
Bioelectrical activity differentiations in cat cortex during sleep inhibition
13 p1483 N73-22026
Centripetal acceleration for inhibiting cerebellar rat cortex activity
14 p1608 N73-23030
Comparison of electroencephalographic response patterns in man and monkeys to visually evoked cortical stimuli
[IZF-1972-24] 14 p1609 N73-23049

**CEREBROSPINAL FLUID**
Effects of monomethylhydrazine on blood and cerebrospinal fluid glucose in anesthetized monkeys
[AD-751232] 07 p0749 N73-16092

**CEREBRUM**
Monomethylhydrazine effects on evoked cerebral neuroelectric responses in unanesthetized cat
[AD-746302] 02 p0133 N73-11082
Dynamics of nitrogenous cerebral metabolites accompanying repeated hypothermia and subsequent self-heating
11 p1244 N73-20097
Influence of altitude and drugs on cerebral circulation in smokers and non-smokers
12 p1371 N73-21125
Changes in human cerebral circulation during prolonged bed rest test
13 p1483 N73-22020
Circadian rhythms of sleep and cerebral temperature in rats chronically exposed to hot environments
[NASA-TT-F-15082] 22 p2620 N73-30994

**CERENKOV COUNTERS**
Night sky Cerenkov detector for measuring electromagnetic radiation produced by high energy cosmic rays
[AD-746734] 03 p0354 N73-12883
Ionization chamber/Cerenkov counter measurements of heavy cosmic ray flux and composition
[NASA-CR-130921] 09 p1080 N73-18811
Results from Nottingham cosmic ray air shower muon detector
13 p1574 N73-22756
Detection of high energy gamma rays from Crab nebula pulsar by balloon flight with gas Cerenkov telescope
20 p2467 N73-29822

**CERENKOV EFFECT**
U CERENKOV RADIATION

**CERENKOV RADIATION**
Method for obtaining ultraviolet source using Cerenkov radiation
[AD-746174] 02 p0182 N73-11477
Experiment, theory, and simulation of Cerenkov ion acoustic radiation generated by pseudowaves
[ORO-4211-2] 03 p0342 N73-12791
Energy loss method for calculating synchrotron-Cerenkov radiation of relativistic electrons in cold magnetoplasma
[AD-755387] 13 p1564 N73-22675
Cerenkov light technique for measuring high energy gamma rays in air showers
19 p2332 N73-28760

**CERES ASTEROID**
Analysis of asteroids selected for space mission objectives to show significant parameters
[NASA-CR-129248] 03 p0355 N73-12890

**CERIUM**
Influence of microdoping with cerium on quality of fractures in structural steels
09 p1047 N73-18535

**CERIUM COMPOUNDS**
NT CERIUM OXIDES

**CERIUM OXIDES**
ESR spectra of paramagnetic hole centers in CeO2 after ultraviolet irradiation
[AD-746036] 02 p0220 N73-11778
Thermodynamic analysis of nonstoichiometric cerium dioxide in temperature range from 700 to 1500 C and reduced atmospheric pressure conditions
[COO-1441-18] 10 p1175 N73-19560
Oxygen vacancy model for transport properties of defective cerium oxides structure
[COO-1441-9] 10 p1199 N73-19759
Electrical and ionic conductivity of calcium oxide-doped nonstoichiometric cerium dioxide at various temperature ranges
[COO-1441-16] 12 p1416 N73-21473
Electrical conductivity of sintered nonstoichiometric CeO(2-x) as function of temperature
[COO-1441-17] 12 p1416 N73-21474
Electron irradiation effect on transmission properties of ceria doped solar cell cover glass
[NASA-TN-D-7245] 15 p1737 N73-24082

**CERMETS**
Performance of powder metallurgy bronze graphite bearings operating under hydrodynamic conditions at high slipping rates
[AD-747432] 03 p0309 N73-12523
Physical, technological, and wear resistant properties of naturally alloyed metal ceramic material developed from iron powder
[AD-747626] 03 p0322 N73-12626
Development, production, and application of friction cermet and metal plastics materials
[AD-747575] 03 p0323 N73-12630
PUO2-Mo cermet spheres for use as isotopic power fuels
[MCM-1887] 03 p0333 N73-12715
Analysis of microstructure of radio frequency-sputtered, thin lead-dielectric cermet films using transmission electron microscopy
[NASA-TR-R-393] 03 p0345 N73-12811
Production engineering methods for metal ceramic structural materials and parts
[JPRS-57487] 04 p0431 N73-13515
Orthorhombic chromium carbide for increased strength of sintered iron ceramic structural material
04 p0432 N73-13516
Dry sliding friction characteristics of iron ceramic materials using solid lubricants
04 p0432 N73-13517
Sintering temperature and tungsten content effects on volumetric shrinkage of ferrotungsten alloy briquets
04 p0432 N73-13518
Cold plastic deformation process for manufacturing molds and stamps from sintered metal powder ceramic blanks
04 p0432 N73-13519
Fabrication and properties of structural materials based on ceramic titanium powders alloyed with molybdenum and aluminum
04 p0432 N73-13520
Design and technical characteristics of rotary automatic devices for pressing and gauging of metal ceramic structural parts
04 p0432 N73-13524
Analysis of microstructure and optical properties of thin lead dielectric cermet films
10 p1175 N73-19555
Development of method for fabricating cermets and analysis of various compositions to show electrical and physical properties
[NASA-CASE-NPO-13120-1] 14 p1679 N73-23629
Creep behavior of polycrystalline aluminum oxide cermets with varying chromium concentrations
[KFK-1753] 21 p2563 N73-30545
Physical and mechanical properties of cermets to include methods for altering characteristics for specific industrial applications
23 p2809 N73-32459
Fabrication of cermet bearings for control system of high temperature lithium cooled nuclear reactors
[NASA-TM-X-2892] 24 p2953 N73-33595

**CERTIFICATION**
Information and guidance for type certification of aircraft engines as required by Federal Aviation Administration
[FAA-AC-33-2A] 13 p1571 N73-22730

**CESIUM**
Geomagnetic measurement using cesium Z-magnetometer aboard nonmagnetic schooner Zarya
[JPRS-58040] 08 p0925 N73-17579
Cesium oxide/cesium solutions as sources of oxygen and cesium for improved thermionic converter performance
[NASA-CR-121119] 08 p0942 N73-17717
Operational frequency stability of rubidium and cesium frequency standards
[NASA-TN-D-7063] 08 p0943 N73-17724
Development of two cell cesium optically pumped gradient magnetometer
[AD-753060] 09 p1037 N73-18460
Role of cesium in fuel-cladding interaction of austenitic stainless steels mixed with oxide fuels
[EUR-4893] 10 p1187 N73-19657
Production of iodine isotope by high energy bombardment of cesium heat pipe causing spallation reaction
[NASA-CASE-LEW-11390-2] 11 p1326 N73-20763
Photoionization cross section measurements on excited cesium maser by light beams
[AD-756217] 13 p1564 N73-22677
Spherical harmonic analysis of Cosmos-321 geomagnetic survey
14 p1659 N73-23463
Photoelectric emission of gallium arsenide from adsorbed layers of cesium and barium oxide
[NLL-DRIC-TRANS-2293-[3623.66]]
15 p1819 N73-24746
Feasibility of potassium-cesium mixture for seeding magnetohydrodynamic combustion plasma
[PB-214314/7] 16 p1865 N73-25102
Ionization mechanisms in cesium
24 p2932 N73-33419

**CESIUM COMPOUNDS**
NT CESIUM IODIDES

**CESIUM ENGINES**
Cesium engine testing laboratories at ONERA, France
[ONERA-NT-21/6046-SNE] 05 p0524 N73-14263
Power supply electronic tests on single jet disk type cesium thrustor with beam current feedback control
[LAAS-TNPE-73-T-17] 23 p2831 N73-32629

**CESIUM HALIDES**
NT CESIUM IODIDES

**CESIUM IODIDES**
Optical transmission measurements of single crystal and polycrystal CsI
[NASA-TM-X-66178] 08 p0951 N73-17784
Handbook on scintillation counters with emphasis on cesium iodide scintillators for HEAO experiments
[NASA-TM-X-64741] 13 p1530 N73-22398
Discrimination between high energy cosmic ray electrons and interacting protons using cesium iodide
[NASA-TM-X-70446] 20 p2435 N73-29556

**CESIUM ION**
Vibrational energy distribution of positive Cs ions in output from Cs2O2 chemical laser
[DREV-TN-2019/72] 06 p0679 N73-15522

**CESIUM PLASMA**
Debye parameters of nonideal cesium plasma reached in shock tube
[AD-754015] 10 p1198 N73-19749
Direct current conductivity of cesium plasma in magnetic field
22 p2702 N73-31645

**CESSNA AIRCRAFT**
NT A-37 AIRCRAFT

Fixed base flight simulator evaluation of wing spoilers for longitudinal flight path control of Cessna aircraft during instrument landing system approach
[NASA-CR-2121] 02 p0125 N73-11015
Investigation of disappearance of Cessna 310 aircraft on flight between Anchorage and Juneau, Alaska on 16 Oct. 1972
[NTSB-AAR-73-1] 08 p0867 N73-17018
Aircraft accident involving crash of Cessna 182 aircraft near Duluth, Minnesota airport on 8 Nov. 1972
[NTSB-AAR-73-10] 14 p1604 N73-23006

**CESSNA MILITARY AIRCRAFT**
U MILITARY AIRCRAFT

**CF-104 AIRCRAFT**
U F-104 AIRCRAFT

**CF-700 ENGINE**
Pressures and temperatures on the lower surfaces of an externally blown flap system during full-scale ground tests
[NASA-TN-D-7138] 06 p0614 N73-14984

**CFRP**
U CARBON FIBER REINFORCED PLASTICS

**CH-53 HELICOPTER**
U H-53 HELICOPTER

**CH-3 HELICOPTER**
Design development, and evaluation of hoist for H-3 helicopter rescue system
[AD-750289] 06 p0623 N73-15054

**CH-47 HELICOPTER**
Construction of pitch link in CH-47 helicopter control system using composite materials of graphite, glass, and carbon-steel
[AD-747337] 02 p0127 N73-11036
Foreign process for developing spiral bevel gear for CH-47 helicopter
[AD-747857] 03 p0309 N73-12522
Effect of dynamic absorbers and damping on noise generated by CH-47 helicopter rotor transmission
[AD-752579] 08 p0868 N73-17031
Measurement of vibration levels in CH-47 helicopter at pilot seat, control stick, rudder pedals, instrument panel, and human interface points
[AD-761199] 18 p2107 N73-27040
Flight tests of CH-47 helicopter to determine structural performance of boron-reinforced epoxy aft rotor blades
[AD-762199] 19 p2222 N73-27927
Failure analysis of synchronizing drive shaft adapter on CH-47A helicopter for improved reliability and cost reduction
[AD-763186] 21 p2497 N73-30041
Analysis of failure modes of blades on CH-47 helicopter rotary wings for improved helicopter reliability and cost reduction
[AD-763187] 21 p2497 N73-30042

**CHAFF**
Radar backscatter produced by chaff cloud as function of position of radar relative to chaff cloud
[AD-744776] 01 p0029 N73-10226

**CHAIRS**
U SEATS

**CHALCOGENIDES**
NT ALUMINUM OXIDES
NT BARIUM OXIDES
NT BERYLLIUM OXIDES
NT BISMUTH OXIDES
NT BORON OXIDES
NT CADMIUM SELENIDES
NT CADMIUM SULFIDES
NT CADMIUM TELLURIDES
NT CALCIUM OXIDES
NT CARBON DIOXIDE
NT CARBON MONOXIDE
NT CHROMIUM OXIDES
NT COBALT OXIDES
NT COPPER SULFIDES
NT DIOXIDES
NT FLINT
NT GALLIUM SELENIDES
NT GERMANIUM OXIDES
NT HAFNIUM OXIDES
NT HEAVY WATER
NT HEMATITE
NT HYDROGEN PEROXIDE
NT HYDROGEN SULFIDE
NT IRON OXIDES
NT LEAD OXIDES
NT LEAD SELENIDES
NT LEAD SULFIDES
NT LEAD TELLURIDES
NT LITHIUM OXIDES
NT MAGNESIUM OXIDES
NT MANGANESE OXIDES
NT MERCURY TELLURIDES
NT METAL OXIDES
NT MOLYBDENUM DISULFIDES
NT MOLYBDENUM SULFIDES
NT NEPHELITE
NT NICKEL OXIDES
NT NIOBIUM OXIDES
NT NITRIC OXIDE
NT NITROGEN DIOXIDE
NT NITROGEN OXIDES
NT NITROGEN TETROXIDE
NT NITROUS OXIDES
NT OXIDES
NT PEROXIDES
NT PLUTONIUM OXIDES
NT PYROXENES
NT QUARTZ
NT RUTILE
NT SAPPHIRE
NT SCHEELITE
NT SELENIDES
NT SILICON DIOXIDE
NT SILICON OXIDES
NT SULFIDES
NT SULFUR OXIDES
NT TANTALUM OXIDES
NT TELLURIDES
NT THORIUM OXIDES
NT TIN OXIDES
NT TIN TELLURIDES
NT TITANIUM OXIDES
NT URANIUM OXIDES
NT VANADIUM OXIDES
NT YTTRIUM OXIDES
NT ZINC OXIDES
NT ZINC SELENIDES
NT ZINC SULFIDES
NT ZIRCONIUM OXIDES
Development and characteristics of Si-As-Te glasses containing Ag and Se as constituent of chalcogenic glasses
[AD-749958] 05 p0567 N73-14603
Analysis of on-state in chalcogenide threshold switches
[AD-756273] 15 p1821 N73-24763

**CHAMBERS**
Nondestructive tests of welds in regenerative chambers
[NASA-CR-120980-APP] 06 p0677 N73-15509

**CHANCE-VOUGHT MILITARY AIRCRAFT**
U MILITARY AIRCRAFT

**CHANNEL FLOW**
NT OPEN CHANNEL FLOW
Limit process expansion techniques used to analyze fully developed turbulent incompressible flow in infinitely long channel with plane parallel walls
[AD-746112] 02 p0158 N73-11283
Optimal inlet parameters for magnetohydrodynamic channel using combustion products of kerosene and gaseous oxygen
[AD-748750] 04 p0376 N73-13057
Mixed convection in reactor channel utilizing sodium as working fluid
[CEA-CONF-2001] 06 p0654 N73-15317
Stabilizing and destabilizing effects of Coriolis body force on turbulent wall layers in two dimensional channel flow
07 p0768 N73-16243
Perturbation method for separated laminar incompressible flows in divergent channels
16 p1886 N73-25268
Thermohydrodynamic stability in channel flow heat and mass transfer considering variable cross section area
[AD-758748] 16 p1889 N73-25289
Analysis of characteristics of initially plane, strong shock wave propagating into conical convergence using multi-crystal piezoelectric probe
21 p2522 N73-30228
Experimental observations of upstream disturbances in flow of two fluids over obstacle in channel
[AD-763759] 21 p2526 N73-30259
Differential solution to problem of nonlinear cavitational flow around channel plates by gravity fluid
22 p2651 N73-31239
Numerical integration techniques for shock discontinuity in one dimensional unsteady channel flow
[PUBL-138] 22 p2654 N73-31258
Laminar secondary Taylor-Goertler vortex flow in rectangular cross section channel
[AD-764503] 22 p2655 N73-31268
Heat transfer in slit-like channels
[AD-762793] 22 p2730 N73-31851
Turbulent gas-solid electrohydrodynamic flow into channel
23 p2772 N73-32172
Effect of high polymer drag reducing additives on longitudinal turbulent dispersion coefficient for two dimensional open channel flow
24 p2902 N73-33164
Parallel heat conducting viscous gas flow in flat channel with sine wave wall perturbation
24 p2906 N73-33189

**CHANNEL MULTIPLIERS**
Low energy electron detection by channel multiplier
[CONF-720404-VOL-1] 19 p2322 N73-28682
Titanium dioxide doped, silicon rubber, potting compound for satellite-borne channel multipliers noting doping effects, performance tests, and space applications
24 p2927 N73-33378
Titanium dioxide doped silicone rubber potting compound for satellite-borne channel multipliers
24 p2927 N73-33379

**CHANNELS**
Propagation path simulator for channel between Tracking and Data Relay Satellite and user spacecraft
[NASA-CR-130173] 11 p1255 N73-20185

**CHANNELS [DATA TRANSMISSION]**
Digital computer techniques for filtering and transmission of telecommunication data
01 p0025 N73-10192
Error probability and bandwidth efficiency in digital transmission channel
01 p0025 N73-10193
Operational performance and transmission measurements on worldwide Defense Communications System network
01 p0027 N73-10208
Integral equation for calculating influence of linear channels on correlation processing of noise signals
12 p1378 N73-21180
Adaptive maximum likelihood receiver for digital communication channels
16 p1873 N73-25163
High resolution pulse width modulated parallel channel for forward looking infrared display system
[AD-759224] 16 p1882 N73-25231
Precision and reliability characteristics of combined gyroscopic and correction channel
17 p2059 N73-26659
Assessment of communication channels for maritime satellite systems using broad beam and multiple beam antennas for satellite-ship links
18 p2117 N73-27121
Coded transmission of binary data over coherent white Gaussian channels
[AD-761465] 19 p2245 N73-28102
Determining necessary number of channels in maritime communications satellite network
20 p2440 N73-29597
Some design features of distributed general-purpose computer systems
21 p2514 N73-30170
Data error protection in disturbed binary channels by linear systematic codes, applied to 50 Kbaud telephone channel transmission
[FTZ-A-441-TBR-1] 22 p2632 N73-31097
High density bipolar encoder and decoder for code transparent digital channels
[FTZ-44-TBR-35] 22 p2633 N73-31103

**CHANNELTRONS**
U CHANNEL MULTIPLIERS

**CHAOTIC CLOUD PATTERNS**
U CLOUDS [METEOROLOGY]

**CHAPLYGIN EQUATION**
Solution of Chaplygin equation by straight line method to describe gas flow around profile at high subsonic speed with local supersonic curved shock wave
[AD-753557] 09 p1019 N73-18318

**CHAPMAN SHEAR LAYER**
U SHEAR LAYERS

**CHAPMAN-JOUGET FLAME**
U CHEMICAL EQUILIBRIUM
U DETONATION
U FLAME PROPAGATION

**CHARACTER RECOGNITION**
Analysis of sampling mechanism and operation of automatic normalization of character patterns
[REPT-726] 05 p0516 N73-14195
Method for quantitative print quality evaluation of large amount of data with determination based on requirements of optical character readers
[REPT-731] 14 p1637 N73-23276
Algorithm for assembling continuous boundaries and contours from black and white picture for computer processing and photointerpretation
[NPL-COM-66] 22 p2675 N73-31426

**CHARACTERISTIC EQUATIONS**
U EIGENVALUES
U EIGENVECTORS

**CHARACTERISTIC FUNCTIONS**
U EIGENVALUES
U EIGENVECTORS

**CHARACTERISTIC METHOD**
U METHOD OF CHARACTERISTICS

**CHARACTERISTICS**
Apollo Command Module Aerodynamic Simulation tests in hypersonic flow
[DLR-FB-71-83] 09 p1089 N73-18892

**CHARACTERIZATION**
Statistical mechanics for relating material properties to their atomic and molecular structures
[AD-758257] 15 p1814 N73-24708

**CHARACTERS**
U SYMBOLS

**CHARCOAL**
Decomposition of compounds adsorbed in charcoal of manned spacecraft breathing system
[NASA-CR-134013] 21 p2504 N73-30092

**CHARGE CARRIERS**
NT FREE ELECTRONS
NT HOLES [ELECTRON DEFICIENCIES]
NT MAJORITY CARRIERS
NT MINORITY CARRIERS

Numerical analysis of signal trapping effects in neutron irradiated p-n junctions as function of frequency
[SC-DC-72-1237] 05 p0587 N73-14772
Hydro and aerodynamic phenomena in liquid dielectric conduction through charge carrier injection
[NLL-PO-2890-[9022.81]] 11 p1269 N73-20298
Effect of charge carrier heating on volt-ampere characteristics of thermoelectric indicators of microwave emissions
[AD-756561] 13 p1531 N73-22407
Carrier lifetime measurement by photoconductive decay method
[NBS-TN-736] 13 p1563 N73-22685
Influence of carrier lifetime in semiconductor material on its performance as radiation detector
[NASA-CR-121187] 14 p1697 N73-23775
Charge carrier transport properties in p-type germanium semiconductors
[AD-757232] 14 p1698 N73-23783
Nonlinear dynamic resistance and light emission associated with carrier generation by impact ionization in Gunn domains
15 p1794 N73-24543
Measurements of excess carriers in intrinsic germanium
[AD-758211] 15 p1822 N73-24772
Variation of crystal Fermi energy to obtain different charge states in paramagnetic impurity ions for ESP study
[AD-760736] 20 p2464 N73-29798

**CHARGE DISTRIBUTION**
Theoretical studies of solid surfaces, electron diffraction experiments, and electronic charge distribution
[AD-750481] 06 p0711 N73-15802
Least squares representation for charge distribution on monopole antenna immersed in dissipative medium
[AD-753092] 09 p1008 N73-18230
Critical exponents for charged and neutral Bose gases above Lambda points
[AD-756022] 12 p1430 N73-21587
Charge neutralization and echo analysis using electron gun in magnetosphere onboard sounding rocket during Electron Echo 1 experiment
19 p2258 N73-28204

**CHARGE EXCHANGE**
Charge exchange cross sections for protons and alkali atoms using classical approximation of Gryzinski
[NASA-CR-129262] 03 p0339 N73-12763
Regge pole model for charge exchange processes using isospin amplitudes and daughter trajectories
[TUETP-73-4] 14 p1694 N73-23747
Direct charge state measurements of low energy solar carbon and oxygen in interplanetary space
[TR-73-132] 23 p2834 N73-32648

**CHARGE SEPARATION**
U POLARIZATION [CHARGE SEPARATION]

**CHARGE TRANSFER**
Electrical and transport properties in polycyclic semiconductor compounds
[AD-745988] 02 p0219 N73-11771
Noise measurements on n-junction gold silicon and aluminum silicon diodes at avalanche potential considering leakage current
[FRNC-CONF-29] 05 p0519 N73-14221
Two-phase charge-coupled shift registers
[NASA-CR-2148] 07 p0761 N73-16187
Factors affecting design of charge-coupled image sensors
[AD-758741] 16 p1882 N73-25234
Electrical properties of solid-solid interfaces for charge transfer phenomena used in image transducer and metal-semiconductor devices
18 p2123 N73-27156

**CHARGED PARTICLES**
NT ALPHA PARTICLES
NT ANTIPROTONS
NT ARGON PLASMA
NT BETA PARTICLES
NT CESIUM PLASMA
NT COLD PLASMAS
NT COLLISIONLESS PLASMAS
NT CONDUCTION ELECTRONS
NT COSMIC PLASMA
NT DEUTERIUM PLASMA
NT DEUTERONS
NT ELECTRON PLASMA
NT ELECTRONS
NT FREE ELECTRONS
NT HELIUM PLASMA
NT HIGH ENERGY ELECTRONS
NT HIGH TEMPERATURE PLASMAS
NT HOT ELECTRONS
NT HYDROGEN PLASMA
NT MAGNETICALLY TRAPPED PARTICLES
NT METAL IONS
NT METALLIC PLASMAS
NT NONEQUILIBRIUM PLASMAS
NT NONUNIFORM PLASMAS
NT NUCLEI [NUCLEAR PHYSICS]
NT OUTER RADIATION BELT
NT PARTONS
NT PHOTOELECTRONS
NT PLASMA CLOUDS
NT PLASMA LAYERS
NT PLASMA SHEATHS
NT PLASMA SLABS
NT PLASMAS [PHYSICS]
NT POLARONS
NT POSITRONS
NT PROTON BELTS
NT PROTONS
NT RADIATION BELTS
NT RAREFIED PLASMAS
NT RECOIL PROTONS
NT RELATIVISTIC PLASMAS
NT ROTATING PLASMAS
NT SOLAR ELECTRONS
NT SOLAR PROTONS
NT SOLAR WIND
NT THERMAL PLASMAS
NT TOROIDAL PLASMAS
NT TRITONS
Theoretical and experimental analysis of charged metal particle detection in jet engine exhaust by cylindrical electrostatic probe
[AD-745540] 01 p0091 N73-10753
Approximation of diffusion coefficients for charged particles in random magnetic field
[NASA-CR-129523] 03 p0339 N73-12767
Charged particle energy deposition calculations for radiobiological system
[ORO-3798-52] 04 p0380 N73-13090
Electrostatic charged particle collector containing stacked electrodes for microwave tube
[NASA-CASE-LEW-11192-1] 04 p0395 N73-13208
Paramagnetic resonance energy for accelerating charged particles
[NLL-RTS-7598] 05 p0579 N73-14715
Large silver halide single crystals as charged particle track detectors in regions of damaged lattice
05 p0609 N73-14951
Radial diffusion of charged particles and splitting of drift shells surrounding earth
[AD-750741] 06 p0668 N73-15437
Approximate second invariant for charged particle trapped in field of magnetic dipole
[AD-750860] 06 p0701 N73-15715
Spreading of charged particles from point source in magnetic dipole field
[AD-750703] 06 p0703 N73-15732
Distribution of charged particles in magnetic field for determining superhigh frequency wave absorption by palsma
[AEC-TR-7321] 08 p0949 N73-17768
Ultraviolet and charged particle irradiation of solar cell coverslide materials and conductive coatings for Helios satellites
[NASA-TM-X-65945] 09 p1051 N73-18571
Low energy particle measurements by soft particle spectrometer on ISIS-1 orbiting satellite and relation to production of auroral particles
10 p1146 N73-19329
Solution to Klein-Gordon and Dirac equations for charged particles in two noncollinear electromagnetic waves
[AD-754307] 11 p1327 N73-20769
Charged particle and magnetic field research using ATS 1 and Mariner measurements
[NASA-CR-131269] 11 p1338 N73-20857
Precipitation of auroral and ring current particles in magnetosphere by artificial plasma injection
[AD-755352] 12 p1403 N73-21381
Analysis of conditions leading to generation of cosmic rays by acceleration of charged particles caused by electromagnetic field of pulsars
[PPG-144] 12 p1445 N73-21703
Injun 5 observations of charged particle precipitation over auroral zone during magnetic substorm
13 p1515 N73-22272
Comparison of charged particle conductivities measured in very low ionosphere with atmospheric parameters and high frequency radio wave absorption measurements
[NASA-CR-131604] 13 p1519 N73-22313
Effects of energetic charged particle irradiation of solar system material
[NASA-CR-132045] 15 p1831 N73-24845
Conference on wave-particle interactions in magnetosphere and wave amplification for communications
[AD-759071] 16 p1909 N73-25450
Unique approach for deriving cosmic ray diffusion equation for charged particles in static, random magnetic field
[NASA-TM-X-66263] 16 p1959 N73-25848
Data processing and analysis of charged particle experiment on OGO-5 spacecraft
[NASA-CR-132761] 16 p1962 N73-25870
Dating of ocean floor rocks and investigation of kinetic processes in lunar regolith
17 p2017 N73-26307
High energy particles in cosmic radiation sources
[CONF-710974-6] 17 p2080 N73-26823
Computer program for calculating characteristics of charged particles beam transported through focusing and bending magnets
[NASA-TN-D-7352] 18 p2121 N73-27143
Pulse radiolysis of biphenyl solutions in cyclohexane noting life distribution of biphenyl ions
[IRI-133-72-07] 19 p2323 N73-28686
Composition and energy spectra of energetic particles emitted during solar flares
19 p2337 N73-28800
Magnetic field structure effects on coronal propagation of solar charged particle event
19 p2338 N73-28808
Energetic particle storage in solar corona
19 p2338 N73-28809
Vacuum/tissue interface effect on biological energy absorption from charged particle track
20 p2366 N73-29028
Photometric determination of charge spectrum of low energy primary cosmic rays in stack of nuclear photographic emulsions
20 p2468 N73-29823
Solid state dectors for indicating energy and point of impact of charged particles
[ISS-72/7] 21 p2548 N73-30431
Scattering by charged particle density fluctuations of plasma for zero magnetic field
[NASA-CR-133808] 21 p2582 N73-30694
Coherent charged particle propagation in magnetic fields
[NASA-CR-135492] 22 p2702 N73-31639
Cosmic ray charged particle interactions with matter
[AD-764833] 23 p2821 N73-32555
Development of fixed pole solution for pion-pion scattering amplitude and comparison with high energy data
[ILL-[TH]-73-15] 24 p2960 N73-33657

**CHARGING**
Charge characteristics of sealed nickel cadmium and lead acid batteries
[PB-221475/7] 22 p2618 N73-30981

**CHARPY IMPACT TEST**
Charpy toughness of discontinuous fiber reinforced plastics under nonuniform interfacial shear stress
[SC-DR-72-0260] 03 p0320 N73-12611
Ductility as criterion of performance of quenched and tempered steel
[AD-751534] 07 p0810 N73-16568
Instruments for recording force deflection from Charpy impact tests on metals
[REPT-527] 13 p1585 N73-22852
Low energy blow technique to determine dimensional changes and development of cracking in Charpy V-notch impact test
[CRANFIELD-MAT-10] 24 p2988 N73-33880

**CHARRING**
Differential equations for charring ablator with thermal nonequilibrium, chemical kinetics, and mass transfer
[NASA-TN-D-7180] 16 p1974 N73-25961

**CHARTS**
NT FLOW CHARTS
NT GRAPHS [CHARTS]
NT METEOROLOGICAL CHARTS

**CHEBYSHEV APPROXIMATION**
Equations showing relationship between temperature and vapor pressure of liquids emphasizing vapor pressure measurement and Chebyshev polynomials
[NPL-CHEM-19] 06 p0638 N73-15179
Nonlinear, two point, boundary value problems using Chebyshev polynomial series
17 p2054 N73-26613

**CHECKOUT**
Checkout of computer programs for errors, using ALGOL compilers
[NPL-NAC-21] 02 p0147 N73-11189
Fine pitched, rolling gear checking systems
[BDX-613-563-REV] 03 p0306 N73-12500
TD-1A satellite ground checkout stations noting spacecraft communication and data transmission
[ESRO-TM-140-ESTEC] 04 p0402 N73-13277
Europa 3 launch vehicle checkout system
10 p1138 N73-19274
Program debugging and monitoring facilities for improving diagnostic capability of compiler
[NBS-TN-763] 12 p1381 N73-21197
Skylab rescue space vehicle flight readiness test
[NASA-TM-X-69519] 23 p2850 N73-32777

**CHECKOUT EQUIPMENT**
U TEST EQUIPMENT

**CHELATE COMPOUNDS**
U CHELATES

**CHELATES**
Gas chromatographic separation of beryllium [II], copper [II], aluminum [III], and chromium [III] chelates
[NLL-M-22879-[5828.4F]] 11 p1252 N73-20158
Chemical composition and structure of metal surface corrosion protective chelate coatings
[DRIC-TRANS-3020] 14 p1616 N73-23095
Chemical equilibrium constants for n-ethylethylenediamine and 2-(ethylthio)-ethylamine complex reactions
[PB-213951/8] 14 p1618 N73-23104
Corrosion and protective properties of organic complex-forming agents which produce insoluble chelate compounds with various metal surfaces
[DRIC-TRANS-3079] 17 p2046 N73-26551

CHEMICAL ANALYSIS
NT ELECTROPHOTOMETRY
NT GAS ANALYSIS
NT GAS SPECTROSCOPY
NT MICROANALYSIS
NT NEUTRON ACTIVATION ANALYSIS
NT OZONOMETRY
NT QUALITATIVE ANALYSIS
NT QUANTITATIVE ANALYSIS
NT SPECTROSCOPIC ANALYSIS
NT URINALYSIS
NT VOLUMETRIC ANALYSIS
Description, performance specifications, and results of performance tests for Hydrolab 2A portable water quality analyzer
[NOOH-IFS-73006] 01 p0057 N73-10468
Application of ultraviolet absorption, gas-liquid chromatography, and gravimetric analysis to determine diphenylamine and ethyl centralite in solid rocket propellant
[TN-267] 02 p0221 N73-11786
Development of method for determining ethylene dibromide depletion in aviation fuels
[AD-746250] 02 p0221 N73-11791
Development and characteristics of coulometric detector for conducting chromatographic analyses
[NLL-TRANS-857-[9022.64]] 05 p0545 N73-14425
Analysis of crosslinked epoxy-urethane polymer filled with aluminum oxide particles to determine mechanical and thermodynamic properties
[SC-DR-70-617] 07 p0812 N73-16584
Stabilization methods in collecting and shipping of human sera for chemical analyses 08 p0871 N73-17053
Water sample analysis for identifying sources of mercury pollution of Great Lakes 08 p0876 N73-17096
Chemical analysis of krypton and xenon isotopes in three meteorites and for melt extractions on samples of five terrestrial sedimentary rocks 08 p0958 N73-17836
Determination of impurities in titanium tetrachloride by infrared spectroscopy, emission spectra, and chemical analysis
[NLL-RTS-7725] 09 p1045 N73-18524
Proficiency of X ray fluorescence spectrospectory and wet chemical techniques in measuring trace copper impurities in beryllium foils
[SC-RR-72-0722] 10 p1126 N73-19175
Chemiotaxionomic survey of carotenoid pigments in several species and groups of Basidiomycetes
[NASA-TT-F-14858] 11 p1246 N73-20117
Micrometeoroid analyzer using arrays of interconnected capacitors and ion detector
[NASA-CASE-ARC-10443-1] 11 p1291 N73-20477
Urinalysis methodology for detection of abusive and therapeutic drugs in man 12 p1370 N73-21117
Chromatographic and polarographic methods for determining metabolic levels of hypnotic drugs in blood plasma and urine of man 12 p1370 N73-21118
Mass fragmentography-computer for identification and quantitation of amino acids in soil
[NASA-CR-131507] 12 p1376 N73-21159
Saturation of zirconium iodide with nitrogen and oxygen and analysis of effects on mechanical properties, deformation, and microstructure 13 p1541 N73-22488
Analysis of metallic compounds produced by reduction of material of simulated lunar composition as basis for origin of metallic mounds on lunar glasses
[NASA-CR-131870] 13 p1576 N73-22769
Chemical composition and structure of metal surface corrosion protective chelate coatings
[DRIC-TRANS-3020] 14 p1616 N73-23095
Development of method for determining zinc dialkyl diaryl dithiophosphate in lubricating oils
[AD-757605] 14 p1671 N73-23563
Data tables on nonmetallic materials for offgassing CO and hydrocarbons in 5 psia O2
[NASA-TM-X-64745] 14 p1680 N73-23631
Chemical analyses of orthopyroxene and clinopyroxene composition of chondrites
[NASA-TM-X-62259] 15 p1830 N73-24835
Preventive maintenance of internal combustion engines and transmissions using spectrochemical oil analysis techniques
[PB-216168/5] 16 p1919 N73-25525
Chemical analysis of iron, steel, and nonmetallic materials
[PB-214230/5] 16 p1929 N73-25609
Correction factor technique for X ray fluorescent analysis on stainless steel
[PB-214231/3] 16 p1929 N73-25611
Comparison of military and civil jet engine fuel specifications and test procedures for fuel performance and quality control 17 p2098 N73-26972
Analysis of tungsten in tungsten steel by precipitation with cinchonine and spectrophotometric measurement of hydroquinone color
[AD-762122] 19 p2310 N73-28579
Synthesis and properties of perchloroaromatic compounds
[AD-763125] 20 p2375 N73-29081
Development and characteristics of device for head space analysis used with dual column gas chromatographs
[NLL-M-23025-[5828.4F]] 20 p2417 N73-29415
Analysis of chemical and electrochemical processes occurring on titanium sheet metal surfaces during oxidation at room temperature by electron-diffraction method
[NLL-RTS-7888] 20 p2428 N73-29503
Development of procedures for determining molybdenum in iron and steel with emphasis on factors affecting stablity and temperature dependence
[TN-303] 20 p2431 N73-29529
Proceedings of conference on accuracy in spectrophotometry and luminescence measurements
[NBS-SP-378] 21 p2544 N73-30396
Procedures for accurate measurement of molar absorptivities to show sources of determinant error and methods for elimination of errors
[PAPER-76A5-734] 21 p2545 N73-30403
Procedures for standardization in clinical spectrophotometric and fluorometric measurements
[PAPER-76A5-735] 21 p2545 N73-30404
Measurement of quantum yields using chemistry, laser technology, photodetector instrumentation, and calorimetry
[PAPER-76A6-742] 21 p2546 N73-30408
Application of fluorescence spectroscopy for analyzing macromolecules of proteins and nucleic acids
[PAPER-76A6-744] 21 p2546 N73-30410
Development of fluorometric methods for analysis of biological compounds based on production of fluorescence by enzymic reaction
[PAPER-76A6-745] 21 p2546 N73-30411
Absorption and fluorescence of inorganic glasses and polycrystalline discs doped by heavy metal ions
[PAPER-76A6-746] 21 p2546 N73-30412
Development of fluorescent reagent and application to automated assay of amino acids and peptides
[PAPER-76A6-747] 21 p2546 N73-30413
Analysis of various organic compounds in solution and inorganic ions in glasses as possible fluorescence standard reference materials
[PAPER-76A6-748] 21 p2547 N73-30414
Chemical analysis of structure and strength of polymeric glasses, elastomers, fibers, and solid polymeric systems with high degree of crosslinking
[AD-763398] 21 p2564 N73-30555
Rapid determination of diphenylamine and dinitrotoluene in single base propellants by ultraviolet spectrophotometry analysis
[TM-51] 21 p2587 N73-30730
Hydrographic, chemical, and optical observations from Legs 4 and 5, YALOC-71 in vicinity of Panama Basin
[AD-763591] 22 p2669 N73-31386
High temperature decomposition of propylene in single pulse shock tube to determine products of decomposition and rate of decomposition
[TAE-172] 23 p2754 N73-32036
Post mission data analysis of Surveyor 5, 6, and 7 chemical data
[NASA-CR-135900] 24 p2979 N73-33802
Analysis of isotopic composition of chemical elements in solar structure using photospheric and sunspot spectra
[NP-19727] 24 p2981 N73-33826
CHEMICAL ATTACK
NT INTERGRANULAR CORROSION
Corrosion behavior of interstitial alloying elements in canning steels for sodium cooled fast breeder reactor
[NLL-RISLEY-TR-2444-[9091.9F]] 02 p0209 N73-11693
Passivating effects of additives on zinc corrosion in potassium hydroxide solutions
[NASA-TT-F-14693] 08 p0884 N73-17155
Compatibility of Ti and Ni alloys, stainless steels, Al, tungsten carbide, butyl, and Ep rubbers with hydrazine noting decomposition rates and effects of carbonic acid
[ESRO-CR-85-PT-2] 13 p1569 N73-22712
Physical and chemical properties of nickel alloys following cyclic and isothermal oxidation
[NASA-TN-D-7267] 14 p1675 N73-23594
Stainless steel and Hastelloy corrosion by boron trifluoride, air, and argon mixtures
[ORNL-TM-4172] 24 p2892 N73-33087
CHEMICAL AUXILIARY POWER UNITS
Construction, operation, and applications of fuel cells to show advantages and limitations
[NASA-SP-5115] 17 p1985 N73-26045
CHEMICAL BONDS
NT COVALENT BONDS
Far infrared laser spectroscopy of spin clusters in linear magnetic system of cobalt chloride compound
[AD-756264] 13 p1566 N73-22691
CHEMICAL CLEANING
Cause and prevention of smoky spots occurring on surface of silicon alloyed with boron after chemical polishing 18 p2188 N73-27663
Kinetics of gas pickling and epitaxial growth of semiconductor materials 18 p2188 N73-27664
Active cleaning technique for removing contaminants from optical surfaces in space
[NASA-CR-124374] 21 p2583 N73-30697
CHEMICAL COMPOSITION
NT CARBON DIOXIDE CONCENTRATION
Potassium argon age, and chemical composition of glasses from Bosumtwi crater in Ghana
[NASA-TT-F-14496] 01 p0049 N73-10398
Determination of comet chemical nature from comet spectral energy 02 p0228 N73-11847
Statistical analysis of stream meteor composition 02 p0229 N73-11851
Research data on cometary structure and characteristics particularly Lyman alpha emission 02 p0229 N73-11853
Influence of chemical composition, non-metallic impurities, and production methods on physical properties of molten high alloy steels and special alloys
[AD-747394] 03 p0316 N73-12579
Gas chromatographic method for quantitative analysis on hydrazine and its breakdown products at catalytic activity levels
[NASA-TT-F-14722] 04 p0386 N73-13137
Nine poly carborane-siloxane, high temperature elastomers differing in chemical structure, using torsional braid analysis
[AD-748931] 04 p0440 N73-13586
Procedure for estimating changes in composition resulting from evaporation during storage of liquid oxygen
[NASA-TM-X-2686] 05 p0498 N73-14056
Development and characteristics of Si-As-Te glasses containing Ag and Se as constituent of chalcogenic glasses
[AD-749958] 05 p0567 N73-14603
X ray analysis of B2O3 effects on composition, porosity, and sorption properties of Al2O3
[NLL-M-22796-[5828.4F]] 06 p0682 N73-15553
Chemical composition and abundance of alpha Centauri visual binary determined from spectral lines
[ROY-OBS-BULL-173] 06 p0719 N73-15870
Influence of chemical composition and molecular structure of liquid lubricant on its performance
[NASA-TM-X-68183] 07 p0804 N73-16521
Chemical composition of line spectra for binary alpha Centauri and determination of abundances
[BULL-173] 07 p0842 N73-16820
Chemical synthesis inhibitor of oceanic species having antibiotic properties 07 p0858 N73-16962
Chemical composition of polymers formed by alkaline polymerization of hydrocyanic acid - Part 2
[NASA-TT-F-14645] 09 p0998 N73-18146
Quantitative analysis and identification of chemical properties of minerals in Japanese placer platinoids
[NASA-TT-F-14625] 09 p1048 N73-18547
Charge composition of cosmic rays for elements silicon to nickel
[LUIP-CR-72-16] 09 p1069 N73-18721
Ionization chamber/Cerenkov counter measurements of heavy cosmic ray flux and composition
[NASA-CR-130921] 09 p1080 N73-18811
Stress effects on element balance in human waste for life support recycling system 10 p1117 N73-19107
Chemical composition stability of Chlorella biomass during prolonged cultivation 10 p1117 N73-19108
Low energy fracture process in high strength aluminum alloy 2014T6
[NASA-CR-131099] 10 p1170 N73-19520
Effects of excessive HfC on mechanical properties of W-Re-Hf-C alloys
[NASA-TN-D-7210] 11 p1305 N73-20588
High temperature research on effects of chemical variation and processing variables on properties of wrought cobalt-base-NASA alloy
[NASA-CR-121189] 12 p1414 N73-21457
Chemical, petrographic, and textural characteristics of Apollo 16 rock and soil samples 12 p1449 N73-21737
Composition effects on stress corrosion cracking of titanium alloys in aqueous environments
[NASA-CR-131872] 13 p1540 N73-22475
Aging effects on chemical structure of solid rocket propellant
[AD-759564] 16 p1955 N73-25815
Computer program and numerical technique for calculating chemical composition of stirred reactor
[AD-751462] 16 p1974 N73-25967
Effect of Al-Zn-Mg-Cu alloy composition variations on fracture strength and tensile properties
[RAE-TR-72173] 17 p2046 N73-26549
Data processing system for elastomer development
[AD-759902] 17 p2052 N73-26603

Structure, composition, and electrophysical properties of autoepitaxial silicon layers from vapor-gas tetrachloride mixture
18 p2186 N73-27653
Theoretical evolution of extremely metal poor stars
20 p2470 N73-29839
Effects of solvent composition in quenching fluorescence of Pr[3 plus] ions in aprotic solvents
[CRC-TN-657] 21 p2505 N73-30104
Expected gamma ray emission spectra from lunar surface for range of chemical compositions
[NASA-TM-X-70453] 21 p2595 N73-30796
Chemical composition of lunar soil samples obtained by Lunik 20 lunar probe
[NASA-TT-F-15100] 22 p2716 N73-31744
Composition and structural modification of glassy carbon alloys
[AD-764918] 24 p2944 N73-33511

CHEMICAL COMPOUNDS
Low temperature addition reactions of hydrogen and oxygen atoms with chemical compounds through creation of secondary valence
[NASA-TT-F-14643] 06 p0703 N73-15729
Gas chromatographic and mass spectrometric determinations of trace elements in human breath samples
[AD-750141] 09 p1000 N73-18159
Radio blackout prevention in atmospheric reentry by chemical injection into vehicle plasma sheath
[AD-753077] 09 p1003 N73-18187

CHEMICAL EFFECTS
Detection of vegetation damage associated with highways and highway facilities with reference to stress caused by chemicals and alteration to ground water table
[E72-10288] 04 p0410 N73-13338
Effect of atmospheric stability on vertical spread of airborne pollutants from steady and instantaneous sources in constant stress region
17 p2098 N73-26974

CHEMICAL ELEMENTS
NT ALKALI METALS
NT ALUMINUM
NT ANTIMONY
NT ARGON
NT ARGON ISOTOPES
NT ARSENIC
NT BARIUM
NT BERYLLIUM
NT BISMUTH
NT BORON
NT BROMINE
NT CADMIUM
NT CALCIUM
NT CALCIUM ISOTOPES
NT CALIFORNIUM ISOTOPES
NT CARBON
NT CARBON ISOTOPES
NT CERIUM
NT CESIUM
NT CHARCOAL
NT CHLORINE
NT CHROMIUM
NT COBALT
NT COBALT 60
NT COPPER
NT COPPER ISOTOPES
NT CURIUM 244
NT DEUTERIUM
NT DEUTERIUM PLASMA
NT DYSPROSIUM
NT ERBIUM
NT FLUORINE
NT GADOLINIUM
NT GALLIUM
NT GERMANIUM
NT GOLD
NT HAFNIUM
NT HALOGENS
NT HELIUM
NT HELIUM ATOMS
NT HELIUM FILM
NT HELIUM ISOTOPES
NT HOLMIUM
NT HYDROGEN
NT HYDROGEN ATOMS
NT HYDROGEN IONS
NT HYDROGEN ISOTOPES
NT HYDROGEN PLASMA
NT INDIUM
NT IODINE
NT IODINE ISOTOPES
NT IRIDIUM
NT IRON
NT IRON 57
NT ISOTOPES
NT LANTHANUM
NT LEAD [METAL]
NT LIGHT ELEMENTS
NT LIQUID HELIUM
NT LIQUID HYDROGEN
NT LIQUID NITROGEN
NT LIQUID SODIUM
NT LITHIUM
NT LITHIUM ISOTOPES
NT MAGNESIUM
NT MANGANESE
NT MERCURY [METAL]
NT MERCURY VAPOR
NT METALLOIDS
NT MOLYBDENUM
NT NEODYMIUM
NT NEON
NT NEPTUNIUM
NT NICKEL
NT NICKEL ISOTOPES
NT NIOBIUM
NT NITROGEN
NT NITROGEN ATOMS
NT NITROGEN IONS
NT NITROGEN ISOTOPES
NT NUCLIDES
NT OSMIUM
NT OXYGEN ISOTOPES
NT PALLADIUM
NT PLATINUM
NT PLATINUM BLACK
NT PLUTONIUM
NT PLUTONIUM 238
NT POTASSIUM
NT PRASEODYMIUM
NT RADIOACTIVE ISOTOPES
NT RADIUM 226
NT RADON
NT RARE EARTH ELEMENTS
NT RARE GASES
NT REFRACTORY METALS
NT RHODIUM
NT RUBIDIUM
NT RUBIDIUM ISOTOPES
NT RUTHENIUM
NT SAMARIUM
NT SELENIUM
NT SILICON
NT SILVER
NT SODIUM
NT SODIUM VAPOR
NT STRONTIUM
NT SULFUR
NT TANTALUM
NT TELLURIUM
NT THALLIUM
NT THULIUM
NT TIN
NT TITANIUM
NT TRACE ELEMENTS
NT TRANSURANIUM ELEMENTS
NT TRITIUM
NT TUNGSTEN
NT URANIUM
NT URANIUM 233
NT VANADIUM
NT XENON
NT YTTERBIUM
NT ZINC
NT ZIRCONIUM
Design of radiometric emittance measurement system for use at high temperatures
[NASA-CR-123968] 04 p0420 N73-13421
Isotopic composition of chemical elements in solar atmosphere
[AD-758769] 18 p2198 N73-27748
Decomposition of compounds adsorbed in charcoal of manned spacecraft breathing system
[NASA-CR-134013] 21 p2504 N73-30092

CHEMICAL ENGINEERING
Chemical processing industries and utilization of NASA technology - conference
[NASA-CR-129827] 05 p0607 N73-14937
Research reports for various engineering sciences and materials and metallurgy
14 p1721 N73-23961

CHEMICAL EQUILIBRIUM
Nonequilibrium combustion products for calculating rocket engine performance and chemical kinetics of combustion processes
[AD-750169] 06 p0715 N73-15835
Computer program for determining thermodynamic and transport properties of complex mixtures to include rocket performance, shock properties, and detonation properties
[NASA-TN-D-7056] 06 p0730 N73-15954
Chemical composition stability of Chlorella biomass during prolonged cultivation
10 p1117 N73-19108
Role of biosphere in regulating chemical processes in atmosphere
[AERONOMICA-ACTA-A-116] 13 p1551 N73-22569
Chemical equilibrium constants for n-ethylethylenediamine and 2-[ethylthio]-ethylamine complex reactions
[PB-213951/8] 14 p1618 N73-23104
Corona equilibrium model for ionization state distributions in carbon, aluminum, copper, and tungsten plasmas
[AD-758357] 14 p1696 N73-23767
Convergence improvement in equilibrium calculation using Newton-Raphson method for C, H, N, F system, noting monomethylhydrazine/Fe mixture
[ICT-3/72] 18 p2192 N73-27696
Tables and graphs of thermodynamic and transport properties of gaseous CF4 in chemical equilibrium
[NASA-TN-D-7181] 18 p2206 N73-27805
Rate-controlled method of constrained equilibrium applied to chemically reactive open systems
[FML-PUBL-73-6] 22 p2625 N73-31031
Equilibrium concentration and catalytic decomposition products of hydrazine at elevated temperatures and pressures
[NASA-CR-135478] 23 p2753 N73-32031

CHEMICAL EXPLOSIONS
NT GAS EXPLOSIONS
Evacuation areas for transportation accidents involving propellant tank pressure bursts
[NASA-TM-X-68277] 20 p2488 N73-29987

CHEMICAL EXTINGUISHERS
U FIRE EXTINGUISHERS

CHEMICAL FUELS
NT AEROZINE
NT AIRCRAFT FUELS
NT GASOLINE
NT HIGH ENERGY FUELS
NT HYDROCARBON FUELS
NT HYDROGEN FUELS
NT JET ENGINE FUELS
NT JP-4 JET FUEL
NT JP-5 JET FUEL
NT METAL FUELS
NT SLURRY PROPELLANTS
Problems of using metallurgical and chemical materials in direct conversion systems
[UCRL-73560] 03 p0333 N73-12718
Biological effects of Viking Lander spacecraft engine fuel on extraterrestrial life during landing on planet Mars
[NASA-TM-X-2714] 06 p0630 N73-15118

CHEMICAL INDICATORS
Evaluation of methods for detection of fluorine-containing missile oxidizers
[AD-756525] 13 p1569 N73-22713

CHEMICAL KINETICS
U REACTION KINETICS

CHEMICAL LASERS
Application of flow field models, combustion, mixing, and nonequilibrium chemistry data to development of chemical lasers
[AD-745419] 01 p0066 N73-10536
Analysis of applications for infrared, carbon dioxide, and chemical laser devices with emphasis on window materials and absorption mechanics
[AD-745927] 01 p0067 N73-10546
Generation spectrum of excited DF molecules obtained during chemical reactions in D2/F2/N2/O2 laser system
[NLL-DRIC-TRANS-2816-[3623.66]]
02 p0180 N73-11458
Model of diffusion-type, HF chemical laser
[AD-745952] 02 p0183 N73-11484
Operating characteristics of small pulsed HF chemical lasers
[AD-747210] 03 p0310 N73-12533
Tables for quantitative atmospheric attenuation of 97 HF and DF laser lines and 10 atmospheric models
[AD-747010] 03 p0310 N73-12534
Quantitative analysis of HF chemical CW laser including influence of stimulated emission on reacting medium
[AD-746685] 03 p0311 N73-12535
Developments in laser technology to include chemical lasers, electric discharge lasers, high power glass lasers, and laser techniques
[AD-748178] 04 p0429 N73-13498
RESALE-2 and INHALE computer code modifications for detecting radiative power of C02 in detector
[AD-748293] 04 p0430 N73-13500
Analysis of conditions required to obtain laser action based on chemical reactions
[DREV-TN-2004/72] 05 p0557 N73-14520
Vibrational energy distribution of positive Cs ions in output from Cs2O2 chemical laser
[DREV-TN-2019/72] 06 p0679 N73-15522
Output and power characteristics of CS2/O2 chemical laser with flow transverse to optical axis
[DREV-R-684/72] 06 p0679 N73-15527
LLL studies of various lasers and analysis of laser produced plasmas
[UCRL-50022-1] 07 p0806 N73-16541
Analytical and experimental determination of reaction mechanisms involved in HN3 plus CO2 laser
[AD-751634] 07 p0807 N73-16546
Feasibility of developing stirred chemical reactor laser cavity based on perfectly stirred reactor concept
[AD-751299] 07 p0807 N73-16549
Development of infrared chemiluminescence technique to measure rates of energy transfer reactions and application to chemical lasers
[AD-751930] 08 p0929 N73-17611
Chemical and molecular laser research
[AD-754792] 11 p1303 N73-20575
Predicted multiline continuous wave power output from perfectly stirred reactor chemical laser
[AD-755904] 12 p1411 N73-21433

Analysis of elementary, exothermic, atom-molecule reactions for application as laser materials for chemical lasers
[AD-756686] 14 p1673 N73-23578
Reaction kinetics of CF3 I flash photolysis iodine laser
[AD-760806] 18 p2158 N73-27436
Research and development on chemical and molecular lasers
[AD-760701] 18 p2158 N73-27438
Kinetics of chemically pumped CO2 and CH2N2-CO2 photolysis laser systems
20 p2424 N73-29469
Design of high power continuous wave HF chemical laser
[DREV-TN-2060/73] 20 p2425 N73-29475
Theoretical performance of HCl continuous wave chemical laser
[AD-762924] 20 p2427 N73-29493
Using simple numerical model of CW chemical laser to study output power
[AD-763169] 21 p2555 N73-30485
Chemical and energy transfer reactions in hydrogen fluoride chemical laser system
[AD-763715] 21 p2556 N73-30491
Simulated emission predictions and measurement of H2 pressure effects on pulsed H2-F2 laser outputs
[AD-763716] 21 p2556 N73-30492
Method of characteristics laser and mixing program for examining chemical laser flows and reactants in axial and lateral pressure gradients
[AD-763906] 22 p2682 N73-31482
Arc-driven N2CS2 mixing gas-dynamic laser
[AD-763898] 22 p2682 N73-31483
Development and application of mathematical models for chemical and gas lasers - Part I
[AD-763905] 22 p2682 N73-31484
Bibliography of chemical laser publications with tables showing chemical systems exhibiting laser action
[DREV-TN-2080/73] 23 p2801 N73-32403
Chemical transfer laser development
[AD-764814] 23 p2802 N73-32409
Gain measurements of excited iodine atom decay rates in photochemical iodine laser
[UCRL-TRANS-10692] 24 p2931 N73-33409

**CHEMICAL MACHINING**
NT ELECTROCHEMICAL MACHINING
Manual of chemical processes related to spacecraft development technology
[NASA-TM-X-2635] 05 p0506 N73-14117
Bibliography on capabilities and limitations of chemical milling techniques
[AD-752050] 08 p0928 N73-17597
Chemical machining of steels, iron, nickel, cobalt, copper, and light alloys
18 p2161 N73-27454
Bibliography on etching and chemical machining techniques
[AD-763100] 21 p2554 N73-30472

**CHEMICAL MILLING**
U CHEMICAL MACHINING

**CHEMICAL PROPERTIES**
NT ACIDITY
NT HEAT OF COMBUSTION
NT HEAT OF VAPORIZATION
NT SALINITY
NT THERMOCHEMICAL PROPERTIES
Effect of heat treatment on adsorption properties of titano-silica gel and interactions of adsorbed molecules with silanol groups
[NLL-RTS-7360] 01 p0069 N73-10564
Chemical and physical properties of three petroleum resistant elastomers suitable for use under low temperature conditions
[AD-745900] 02 p0194 N73-11569
Influence of neutron irradiation on physical and chemical properties of vanadium
[IS-2833] 03 p0314 N73-12558
Chemical and physiochemical properties of wear resistant steels
[AD-749601] 05 p0563 N73-14573
Chemical stability, electrochemical properties and wetting characteristics of polyvinyl and polyethylene membrane separators for alkaline silver zinc batteries
[NASA-CR-130154] 07 p0741 N73-16030
Microphotometer analysis of absorption spectra, physical and chemical properties of NO2 system in Martian atmosphere
07 p0752 N73-16107
Chemical flame inhibitors for examining chemical microstructure of normal CH4, O2, Ar, and Halon inhibited flames
[BM-RI-7723] 09 p1034 N73-18438
Limiting stabilities and thickening properties of phthalocyanine lubricants in different dispersion media
[AD-752827] 09 p1040 N73-18484
Thermodynamic analysis of nonstoichiometric cerium dioxide in temperature range from 700 to 1500 C and reduced atmospheric pressure conditions
[COO-1441-18] 10 p1175 N73-19560
Chemical characteristics of mushroom pigments and mycological classifications
[NASA-TT-F-14865] 11 p1247 N73-20124
Hydrodynamic and chemical properties of stratospheric aircraft wake
[PB-213114] 11 p1290 N73-20465
Effect of flaws on chemical, electrical, mechanical, and masking properties of Si3N4 films
[NLL-DRIC-TRANS-2902-[3623.66]]
11 p1329 N73-20789
Physical and chemical characteristics, and biological activity of exhaust from beryllium-fueled motor
[AD-756531] 13 p1485 N73-22042
Physical and chemical nature of N2O flow decay in liquid propellants
[AD-755378] 13 p1489 N73-22070
Chemical and mechanical properties of aircraft gas turbine engine components
14 p1676 N73-23600
Effect of crystallization kinetics on physical and chemical properties of polymers particularly polyethylene
[AD-750157] 16 p1953 N73-25802
Synthesis and properties of perchloroaromatic compounds
[AD-763125] 20 p2375 N73-29081
Chemical and physical properties of synthetic polyurethane polymer prepared by reacting hydroxy carbonate with organic diisocyanate
[NASA-CASE-MFS-10512] 21 p2505 N73-30099
Chemical and physical characterization of automotive exhaust particulate matter in atmosphere
[PB-221603/4] 22 p2695 N73-31589
Properties and structure of polymers crystallized from stirred dilute solutions and sheared polymer melts
22 p2706 N73-31673
Physical and chemical properties of JP-4 jet fuel for 1972
[AD-764690] 23 p2828 N73-32605
Research in dynamics of thin films polymer chemistry mechanical and chemical properties of materials
[NASA-CR-135697] 23 p2865 N73-32906
Chemical and elastic properties of fluorinated polyurethanes
[NASA-CASE-NPO-10767-1] 24 p2891 N73-33076
Chemical and physical properties of graphite and carbide-graphite composites developed by powder metallurgy
[LA-5147] 24 p2936 N73-33448
Convective heating effects on properties of glassy surface insulation coatings
24 p2941 N73-33488

**CHEMICAL PROPULSION**
NT HYBRID PROPULSION
Chemical and electric auxiliary propulsion technology of United Kingdom, France, and West Germany
[NASA-CR-128328] 01 p0090 N73-10742
Performance, stability, and design of aerospike engines and engine system components
[NASA-TM-X-64690] 03 p0348 N73-12840
Research reports on chemical propulsion systems and performance engineering
03 p0348 N73-12841
Advanced concepts in conventional chemical rocketry
[AD-750554] 06 p0714 N73-15827
Advanced measurement techniques for determining compatibility of materials with propellants
[NASA-CR-130546] 08 p0953 N73-17800
Comparison of chemical [hydrazine and aerozine], electrothermal, electrostatic, and radioisotopic propulsion systems, emphasizing performance and configurations
[ESRO-CR-25-PT-A] 08 p0955 N73-17818
Cost effectiveness and mission value comparisons of three propulsion systems for delivery of advanced probe spacecraft
[NASA-TM-X-2751] 09 p1079 N73-18802
Onboard spacecraft thermoelectric and chemical propulsion systems - Pt. 2
[JPRS-58612-2-PT-2] 10 p1209 N73-19834
Combined chemical solar electric transfer stage for inserting Europa 3 satellites into twenty-four hour orbits
[MBB-UR-V-49-71] 15 p1832 N73-24851

**CHEMICAL REACTION CONTROL**
Controlled gaseous oxidations of organic compounds
08 p0882 N73-17141

**CHEMICAL REACTIONS**
NT AMMONOLYSIS
NT ATOMIC RECOMBINATION
NT CARBONIZATION
NT DECARBONATION
NT DEHYDROGENATION
NT DEIONIZATION
NT DENITROGENATION
NT DEOXIDIZING
NT ELECTROCHEMICAL OXIDATION
NT ENDOTHERMIC REACTIONS
NT FERMENTATION
NT FLUORINATION
NT HALOGENATION
NT HYDROGENATION
NT HYDROLYSIS
NT ION RECOMBINATION
NT NITRIDING
NT OXIDATION
NT OXYGEN RECOMBINATION
NT OXYGENATION
NT PHOSPHORYLATION
NT PHOTOCHEMICAL REACTIONS
NT PHOTODECOMPOSITION
NT PHOTOLYSIS
NT PHOTOSYNTHESIS
NT PYROLYSIS
NT RADIOLYSIS
NT REDUCTION [CHEMISTRY]
NT SULFATION
NT THERMAL DISSOCIATION
NT TITRATION
High temperature reaction of carbon with refractory compounds of groups 4, 5, and 6
[NLL-RTS-7425] 01 p0022 N73-10171
Modification of uncoupled radiation analysis of diffusion-type chemical laser to determine lasing diatomics of radiatively saturated medium
[AD-745311] 01 p0065 N73-10534
Application of flow field models, combustion, mixing, and nonequilibrium chemistry data to development of chemical lasers
[AD-745419] 01 p0066 N73-10536
Macroscopic models of quasi-chemical reactions, dielectric relaxation, and deformation energy
01 p0087 N73-10719
Rate coefficient data for recombination reaction hydrogen plus oxygen plus argon yields water and argon in mixtures behind incident shock waves
[NASA-TN-D-6990] 01 p0117 N73-10965
Chemorheology of Viton B fluorocarbon elastomer by kinetic analysis of chemical stress relaxation, and infrared and gel permeation chromatography analysis
01 p0119 N73-10985
Chemical and physical properties of three petroleum resistant elastomers suitable for use under low temperature conditions
[AD-745900] 02 p0194 N73-11569
Determination of functionality distribution of prepolymers used for rocket binders
[NASA-CR-129505] 03 p0262 N73-12121
Multistep chemical processes for water decomposition, using nuclear heat for producing hydrogen
[EUR-4776-E] 03 p0263 N73-12132
Analytical analysis of graphite interaction with carbon dioxide at high temperature
[AD-747556] 03 p0264 N73-12141
Formation of nitrous oxide molecules from ion-molecule reactions following sea level nuclear burst
[AD-746958] 03 p0298 N73-12428
Chemical spot tests for identification of titanium and titanium alloys used in aerospace vehicles
[NASA-CASE-LAR-10539-1] 03 p0312 N73-12547
Chemical evolution of air and hydrogen in turbulent mixing layer
[NASA-TT-F-14633] 04 p0386 N73-13141
Susceptibility of model polymer with diagonal viscosity and weak interaction
[COO-3161-2] 04 p0387 N73-13142
Calculation of vibrational energy level distributions of hydrogen fluoride formed during atomic fluoride reaction with molecular hydrogen
[AD-748291] 04 p0387 N73-13146
Reaction of Fe-Ni-Cr alloys with oxygen-containing sodium
[IS-T-508] 04 p0433 N73-13534
Chemical reaction of Si, SiC, and Si-SiC mixtures in CO and N at high temperature
[AD-747718] 04 p0438 N73-13569
Isotope chemistry studies, including bulk density and vapor pressure measurements
[COO-3498-2] 05 p0506 N73-14121
Reaction of azotetrazole anion and nitric, sulfuric and hydrochloric acid noting giving of 5-hydrazinotetrazole and 5-azidotetrazole
[ERDE-TN-44] 05 p0507 N73-14123
Analysis of conditions required to obtain laser action based on chemical reactions
[DREV-TN-2004/72] 05 p0557 N73-14520
Development of process for obtaining iron whiskers and description of mechanical and physical properties
[IIS-142-VOL-22-4] 05 p0586 N73-14766
Fluid dynamic and chemical processes occurring in solid propellant gas generator
[AD-749144] 05 p0589 N73-14790
Research on chemical reactions, remote sensors, pollution, and transportation
[NASA-CR-61396] 05 p0607 N73-14938
Synthesis and high rate deposition of ceramics and dispersion stengthened alloys
[AD-750413] 06 p0685 N73-15580
Chemical surface reactions, phase transformations, and reaction kinetics in flow systems
[AD-750172] 06 p0712 N73-15808
Chemical reactions from combustion of unmixed gases
[NASA-TT-F-14360] 06 p0730 N73-15956
Design and operation of galvanic cells involving solid electrolytes to determine accuracy in thermochemical measurements
[LBL-839] 07 p0742 N73-16034
Method of characteristics for analyzing three dimensional, steady supersonic, nonequilibrium,

chemically reacting flow of thermally perfect gases in exhaust nozzle
07 p0768 N73-16240
Chemical analysis, production, and physical properties of polyimide syntactic foam
[SC-DC-72-2297] 07 p0812 N73-16583
Chemical process for producing continuous fine superconducting filaments
[AD-751545] 07 p0832 N73-16746
Synthesis of superconducting intercalated and intermetallic compounds
[AD-751497] 07 p0833 N73-16751
Self-cycling fluid heater for heating continuous fluid stream to ultrahigh temperatures to facilitate chemical reactions
[NASA-CASE-MSC-15567-1] 07 p0853 N73-16918
Polymer gas reactions in air pollutants such as NO2 and SO2 as function of pressure, UV light, temperature, and morphology
08 p0882 N73-17140
One- and two-D core theories for analyzing ducted mixing and burning of coaxial streams
08 p0896 N73-17253
Development of infrared chemiluminescence technique to measure rates of energy transfer reactions and application to chemical lasers
[AD-751930] 08 p0929 N73-17611
Laser frequency modulation, molecular lasers, superconducting lasers, and laser induced instabilities in fluids
[AD-752633] 08 p0931 N73-17621
Plasticization of polyvinyl chloride with various reagents and effect on physicomechanical properties of systems
[AD-751875] 08 p0935 N73-17656
Kinetics and rate constant of reaction OH[v equals 0] plus O3 yields HO2 plus O2
[NASA-CR-130858] 09 p0999 N73-18152
Mass spectrometric analysis of reactions of nitrogen oxide and nitrogen dioxide with hydrogen peroxide at 25 C
[NASA-CR-130831] 09 p0999 N73-18155
N2O photolyzed at 2139 A producing O[1 D] atoms in H2O and CO
[NASA-CR-130976] 09 p1029 N73-18398
Hydrodynamic equations of motion for studying sound interaction in transient chemical reactions
[AD-753798] 10 p1191 N73-19688
Development of method for extending low temperature strain limit of rubber-based solid propellants by induced plasticization
10 p1203 N73-19788
Development of semi-empirical expression for specific surface oxidation rate of soot for application to design of combustion chambers
10 p1223 N73-19943
Computer program for calculating structure and supersonic combustion flow with chemical reactions and shock waves
[NASA-CR-112303] 11 p1271 N73-20311
Development of numerical model of eddy diffusive transport of emitted gases from space shuttle wake to show chemical reactions between emitted gases and ambient atmosphere
[NASA-TM-X-66215] 11 p1287 N73-20440
Atmospheric models for fluid dynamic and chemical impacts of supersonic aircraft on climatology
[PB-212819] 11 p1291 N73-20473
Solid phase interactions in cobalt-carbide systems
[NLL-LTI-746-1338-[9022.401]]
12 p1415 N73-21468
Transfer phenomena in reacting gas mixtures
12 p1418 N73-21492
Perturbation of Maxwellian distribution in chemically reacting gas mixtures
12 p1418 N73-21493
Calculation of thermodynamic and transport properties for chemically reacting gases
[AD-756597] 13 p1488 N73-22064
CSTR system for measuring ozone reactions in lower atmosphere
13 p1514 N73-22269
HO radicals produced in reaction of O[3P] with 1-C4H8
[NASA-CR-131590] 13 p1519 N73-22310
Reactions of HO2 with CO and NO, and O[1D] with H2O
[NASA-CR-131603] 13 p1519 N73-22312
Mass thermal analysis of chemical reactions in conversion of polyacrylonitrile fibers to high modulus, high strength carbon fibers - Vol. 2
[AD-755350] 13 p1549 N73-22549
Chemical process for production of polyisobutylene compounds and application as solid rocket propellant binder
[NASA-CASE-NPO-10893] 13 p1568 N73-22710
Analysis of metallic compounds produced by reduction of material of simulated lunar composition as basis for origin of metallic mounds on lunar glasses
[NASA-CR-131870] 13 p1576 N73-22769
Chemical equilibrium constants for n-ethylethylenediamine and 2-[ethylthio]-ethylamine complex reactions
[PB-213951/8] 14 p1618 N73-23104
Analysis of effects of alternating current on corrosion of iron in aqueous solutions of acidic and neutral salts
[REPT-733] 14 p1675 N73-23590
Aluminum-gold interaction in thin layers
[NASA-TT-F-14919] 14 p1675 N73-23595
Thermodynamic stability diagrams of high temperature O2 corrosion reactions
14 p1676 N73-23602
Analysis of kinetic and transport factors governing interfacial mass transfer rates in high temperature systems
[AD-758256] 14 p1720 N73-23959
Heat and mass transfer with phase and chemical transformations in reacting boundary layer
[AD-758210] 15 p1748 N73-24165
Physical and chemical processes of solidification of fusion welds and its effects on weldability
[NLL-T1780/GC/72-[9022.305]]
15 p1790 N73-24508
Microhardness and corrosion resistance of Zr-Nb alloy prepared by reaction of ZrC with Nb2O5
[BARC-612] 15 p1799 N73-24583
Analysis of polymerization mechanism and fabrication of polyimide/graphite fiber composites using A-type polyimide prepolymers as matrix
[NASA-TM-X-2798] 15 p1801 N73-24597
Chemical changes during transformation of aerosols to cloud droplets and rain in orographic clouds
15 p1805 N73-24630
Stability constants for chloride complexes of palladium [II]
[AD-758684] 16 p1871 N73-25151
Development of procedure for estimating solid phase occurrence during oxidation of heavy metal sulfides
[NLL-M-22913-[5828.4F]] 16 p1926 N73-25581
Influence of titanium ions on magnetic properties of manganese-zinc ferrites
[NLL-TRANS-862-[9022.64]]
16 p1931 N73-25626
Vapor composition and chemical reactions of carbon atoms and molecules from graphite and tantalum carbide heated by laser radiation
[SLA-73-57] 17 p1992 N73-26107
Materials research covering properties, structure, and synthesis
[AD-760021] 17 p2100 N73-26988
Chemical reactions of urea with carbohydrazide in smelts and aqueous solutions
[ICT-5/72] 18 p2114 N73-27090
Inorganic halogen oxidizer chemistry
[AD-760696] 18 p2114 N73-27092
Selective growth of epitaxial silicon layers in chloride process
18 p2188 N73-27668
Characteristics of crystal growth on embossed substrates to show chemical reactions for reducing number of lattice defects
18 p2189 N73-27671
Analysis of heat exchange between liquid and bodies on which liquid flows during catalytic chemical reactions on surface of bodies
[AD-761607] 19 p2353 N73-28927
Preparation of stable polyurethane polymer by reacting polymer with diisocyanate
[NASA-CASE-MFS-10506] 21 p2505 N73-30100
Preparation of polyurethane polymer by reacting hydroxy polyformal with organic diisocyanate
[NASA-CASE-MFS-10509] 21 p2505 N73-30103
Development of fluorescent reagent and application to automated assay of amino acids and peptides
[PAPER-76A6-747] 21 p2546 N73-30413
Chemical and energy transfer reactions in hydrogen fluoride chemical laser system
[AD-763715] 21 p2556 N73-30491
Numerical simulation of chemical reactions in air pollution - Vol. 1
[PB-220456] 21 p2574 N73-30631
Rate-controlled method of constrained equilibrium applied to chemically reactive open systems
[FML-PUBL-73-6] 22 p2625 N73-31031
Interaction of titanium nitrides with oxygen and carbon dioxide
[NASA-TT-F-15108] 22 p2625 N73-31035
Method of characteristics laser and mixing program for examining chemical laser flows and reactants in axial and lateral pressure gradients
[AD-763906] 22 p2682 N73-31482
Utilization of lithium p-lithiphenoxide to prepare star polymers
[NASA-CASE-NPO-10998-1] 23 p2753 N73-32029
Cross sections for reactions of atmospheric ions with atomic oxygen
[AD-765333] 23 p2789 N73-32316
Solid-phase interaction of refractory metals and refractory compounds at high temperature using electron beam heater
23 p2808 N73-32455
Interaction of powders of carbides of zirconium, niobium, and molybdenum with silicon using X ray and chemical analysis to determine reaction products
23 p2809 N73-32461
Radiolytic preparation of anhydrous tin [2] chloride
[NASA-TM-X-2927] 24 p2891 N73-33082
Asymptotic expansion analysis of shock supported arrhenius reactions and ignition delay
24 p2903 N73-33172
Stability of heterogeneous chemical recombination reactions of free radicals in boundary layer flow past heat conducting wall
24 p2908 N73-33209
Induced reactions in gas mixtures using carbon dioxide laser pulses and electrical discharges
24 p2930 N73-33400
Application of tension stress relaxation measurements to determine physical and mechanical properties of rubber networks during chemical reactions
[RR-204] 24 p2987 N73-33868

**CHEMICAL REACTORS**
Development of hydrocarbon fuels and fuel systems for advanced air breathing engines
[AD-746334] 01 p0090 N73-10741
Computerized simulation models for thermal exhaust reactors
22 p2727 N73-31824
Aerosol growth kinetics in flow reactor
24 p2901 N73-33159

**CHEMICAL RELAXATION**
U MOLECULAR RELAXATION

**CHEMICAL SHIFT**
U CHEMICAL EQUILIBRIUM

**CHEMICAL TESTS**
NT CHEMICAL ANALYSIS
NT ELECTROPHOTOMETRY
NT GAS ANALYSIS
NT GAS SPECTROSCOPY
NT MICROANALYSIS
NT NEUTRON ACTIVATION ANALYSIS
NT OZONOMETRY
NT QUALITATIVE ANALYSIS
NT QUANTITATIVE ANALYSIS
NT SALT SPRAY TESTS
NT SPECTROSCOPIC ANALYSIS
NT URINALYSIS
NT VOLUMETRIC ANALYSIS
Chemical spot tests for identification of titanium and titanium alloys used in aerospace vehicles
[NASA-CASE-LAR-10539-1] 03 p0312 N73-12547
Methods for determining blood alcohol levels in pilots
12 p1371 N73-21124
Validity of rapid delta-aminolevulinic acid determination in urine for lead intoxication tests on industrial workers
[NASA-TT-F-14864] 12 p1371 N73-21128
Chemical spot test for identifying magnesium or magnesium alloys used in aerospace applications
[NASA-CASE-LAR-10953-1] 18 p2160 N73-27446
Chemical determination of organic nitrate additive in diesel engine fuel
[AD-762177] 19 p2328 N73-28730

**CHEMILUMINESCENCE**
Method for producing chemiluminescent materials using rhodamine C and material properties
[NASA-TT-F-14423] 01 p0023 N73-10175
Chemiluminescence of O plus NO2 in afterglow
[NASA-CR-130263] 05 p0539 N73-14383
Development of infrared chemiluminescence technique to measure rates of energy transfer reactions and application to chemical lasers
[AD-751930] 08 p0929 N73-17611
Measurement methods based on gas chemiluminescence, emphasizing air pollution applications
[AD-753222] 09 p1000 N73-18163
Emission rate constant for infrared chemiluminescent reaction of oxygen with nitric oxide
[NASA-CR-132157] 15 p1747 N73-24158
Kinetics of far ultraviolet chemiluminescence of exhaust plumes
[AD-760584] 18 p2114 N73-27093
Hydrocarbon chemistry and chemiluminescence in high altitude plumes
[AD-760793] 18 p2114 N73-27094
Chemiluminescent emissions from trimethylaluminium, iron pentacarbonyl, and lead tetraethyl upon reaction with oxygen
[AD-762317] 19 p2233 N73-28087
Laser motivated studies of chemiluminescence in metal oxides and nitrides
21 p2554 N73-30477
Chemiluminescence of Al atoms
[AD-765347] 23 p2755 N73-32044
Lectures presented at International Conference on Chemiluminescence
[AD-765525] 24 p2893 N73-33094

**CHEMISORPTION**
Determination of surface structure of metal crystals by chemisorption method
[NLL-TRANS-746-1340-[9022.401]]
06 p0682 N73-15548
Saturation of zirconium iodide with nitrogen and oxygen and analysis of effects on mechanical properties, deformation, and microstructure
13 p1541 N73-22488
Auger analysis of chemisorption of various gases to metal surfaces and sliding friction effects on interaction
[NASA-TN-D-7340] 16 p1918 N73-25520
Electronic structure of solid surfaces
[AD-762372] 19 p2328 N73-28727

**CHEMISTRY**
Summaries of research in mathematics, physics, chemistry, biophysics-biochemistry, and biology, and related reports - Weizmann Institute of Science
01 p0119 N73-10977
Chemistry research program for Air Force
[AD-749544] 05 p0507 N73-14124
High, medium, and low energy physics, mathematics and computers, chemistry, and metallurgy and materials research
[IS-2800] 10 p1189 N73-19678
Research projects in solid state chemistry and materials science
[AECL-4351] 16 p1871 N73-25145
Systems theory in analysis and system of analytical quantity ranges
[NASA-TT-F-15029] 20 p2423 N73-29460
Research and development progress in solid state physics, chemistry, electronics, and materials science
[AD-763501] 21 p2610 N73-30924
Scientific research projects in engineering, chemistry, and social sciences
23 p2859 N73-32844
Fort Lauderdale Workshop on chemistry and meteorology
[WASH-1217] 24 p2923 N73-33342
**CHEMONUCLEAR PROPULSION**
U CHEMICAL PROPULSION
U NUCLEAR PROPULSION
**CHEMOTHERAPY**
Salvarsan therapy of luetic patients and behavior of Wassermann reaction
[NASA-TT-F-14618] 02 p0133 N73-11076
Pharmacological measures for prophylactic and restorative treatment of men and animals during space flight
11 p1239 N73-20060
Hypothermy effects on drug actions in physiological rabbit functions
11 p1240 N73-20064
Drug therapy effects on flying effectiveness and psychosomatic fitness of flying personnel
12 p1369 N73-21103
Chemotherapy for air crews in Great Britain
12 p1369 N73-21105
Effects of human biorhythms on chemotherapy and drug evaluation
12 p1370 N73-21119
Suitability of insulin dependent and oral drug dependent diabetics as navigation personnel
12 p1371 N73-21120
Drug effects on vision of flying personnel
12 p1371 N73-21121
Flight safety factors in prescribing tranquilizing drugs for flying personnel
12 p1371 N73-21123
**CHENA RIVER BASIN [AK]**
ERTS-1 imagery of snow cover and break-up characteristics in Chena River Basin, Alaska
[E73-10292] 08 p0915 N73-17497
ERTS-1 imagery of ice break-up characteristics of Chena River Basin
[E73-10400] 11 p1277 N73-20362
Mapping permafrost areas of Alaska, correlating snowpack cover of Caribou-Poker Creek with stream runoff, and mapping and inventorying icing on Chena River
[E73-10511] 13 p1516 N73-22286
ERTS-1 imagery of snow cover break-up in Chena River Basin, Alaska
[E73-10619] 15 p1774 N73-24380
ERTS-1 imagery of snow melt in Chena River Basin of Alaska
[E73-10903] 20 p2396 N73-29252
Snowmelt model for Chena River Basin
[E73-11085] 24 p2913 N73-33248
**CHESAPEAKE BAY [US]**
Sediment pattern correlations with inflow and tidal action in Chesapeake Bay based on ERTS-1 imagery
[E72-10169] 01 p0044 N73-10350
Analysis of ERTS-1 MSS data for color variations in Great Lakes and Chesapeake Bay to determine if multispectral imagery usable for locating and mapping extent of distinct water masses
[E72-10224] 02 p0163 N73-11318
Digital precision processing of ERTS-1 imagery of Chesapeake Bay
[E72-10292] 04 p0410 N73-13342
Sediment pattern correlation with tidal and inflow action in Chesapeake Bay using ERTS-1 data
[E72-10334] 05 p0531 N73-14322
Utilization of ERTS-1 imagery in air pollution and marine biology studies of lower Chesapeake Bay and continental shelf of Eastern US
[E72-10367] 05 p0535 N73-14355
ERTS-1 imagery of wetlands ecology in Maryland, Georgia, and Chesepeake Bay test sites
[E73-10288] 08 p0915 N73-17494
Correlation of chlorophyll and suspended sediments in Chesapeake Bay to ERTS-1 imagery
[E73-10424] 11 p1280 N73-20385
Mapping wetlands ecology of Chesapeake Bay, South Carolina, and Georgia from ERTS-1 imagery
[E73-10507] 13 p1516 N73-22282
Relation of chlorophyll and suspended sediment content in lower Chesapeake Bay to ERTS-1 imagery and application of marine station data to study of productivity along eastern shelf waters of US
[E73-10593] 15 p1772 N73-24358
Data compression technique for ERTS-1 imagery of Montreal and Lake St. John, Canada, Orange County, California, San Pedro/Long Beach, California, and Chesapeake Bay
[E73-10625] 15 p1775 N73-24385
Sediment pattern correlation with inflow and tidal action in Chesapeake Bay
[E73-10623] 16 p1896 N73-25336
Movement of suspended particle and solute concentrations with inflow and tidal action in Chesapeake Bay
[E73-10662] 16 p1899 N73-25358
Use of ERTS-1 data to apply marine station data to study of productivity along Eastern Self Expanded Waters of US
[E73-10778] 18 p2135 N73-27254
Seasonal changes of littoral transport and beach width of Maryland portion of Chesapeake Bay and resultant effect on protective structures
[PAPER-M1] 19 p2280 N73-28341
ERTS-1 imagery of littoral drift and sedimentation patterns of beach and nearshore areas of Maryland section of Chesapeake Bay
[PAPER-M2] 19 p2280 N73-28342
Correlation of ERTS-1 multispectral imagery with suspended matter and chlorophyll in lower Chesapeake Bay
[PAPER-M4] 19 p2280 N73-28344
Relation of chlorophyll and suspended sediments in waters of lower Chesapeake Bay to ERTS-1 imagery
[E73-10851] 19 p2292 N73-28429
Computer interpretation of multispectral data of Chesapeake Bay, Lake Pontchartrain, Louisiana, and lower Mississippi Valley
[E73-11007] 22 p2660 N73-31312
Collection of phytoplankton and chlorophyll samples from waters of Chesapeake Bay
[E73-11154] 24 p2919 N73-33308
**CHILDREN**
Absorption of fructose in saline mixture used for enteritis therapy of children
[NASA-TT-F-14596] 02 p0133 N73-11078
Bioelectric activity changes in brains of sleeping children caused by aging factor
13 p1484 N73-22032
Meteorological conditions and infection of upper respiratory tract in children
[NLL-M-22866-[5828.4F]] 16 p1866 N73-25109
Satellite telecommunications systems for childhood education
[NASA-CR-133028] 16 p1869 N73-25131
**CHILE**
Night cloud cover and meteorological parameter variations determined at La Silla, Chile, in 1970
[ESO-BULL-9] 01 p0075 N73-10620
European Southern Observatory in Chile including research projects, equipment, and management for 1971
15 p1763 N73-24282
Analysis of ERTS-1 data for studies of hydrogeology, geomorphology, and paleoclimatology in Bolivia, Argentina, Chile, and Peru
[PAPER-W1] 19 p2270 N73-28281
Seasonal climatology of Chilean sea coast
[AD-765355] 23 p2815 N73-32506
**CHILLING**
U COOLING
**CHIMES**
U AUDITORY SIGNALS
**CHIMNEYS**
Method for calculating ground level concentration of pollutants emitted from high stack based on plume aerodynamics and atmospheric mixing
[PUB-73-3] 17 p2057 N73-26636
**CHIMPANZEES**
NT MONKEYS
Scientific and engineering studies for Physiology of Chimpanzees in Orbit Program
[NASA-CR-131374] 11 p1248 N73-20129
Interface requirements for design and development of Physiology of Chimpanzees in Orbit experiment
[NASA-CR-131397] 11 p1248 N73-20130
**CHINA**
NT CHINESE PEOPLES REPUBLIC
Tables of synoptic meteorological observations for Okinawa, Sakishima Islands, and southern East China Sea
[AD-753216] 09 p1061 N73-18656
Synoptic marine meteorological observations of Chinese and Taiwan coastal areas - Vol. 2
[AD-760333] 17 p2058 N73-26647
Summaries of synoptic meteorological observations for Chinese - Philippine coastal marine areas
[AD-762423] 19 p2318 N73-28645
**CHINA [COMMUNIST] MAINLAND**
U CHINESE PEOPLES REPUBLIC
**CHINESE PEOPLES REPUBLIC**
Synoptic marine meteorological observations of Chinese and Taiwan coastal areas - Vol. 2
[AD-760333] 17 p2058 N73-26647
**CHINOOK HELICOPTER**
U CH-47 HELICOPTER
**CHIPS**
Methods for chip mounting and establishing electrical connections in miniaturized printed circuits and thick and thin film hybrid circuits
[ECR-27] 08 p0891 N73-17212
**CHIRAL DYNAMICS**
Field theory model for unified strong and electromagnetic interactions
09 p1066 N73-18701
**CHIRP**
NT CHIRP SIGNALS
**CHIRP SIGNALS**
Frequency modulated [chirped] optical pulses in subpicosecond to microsecond pulse length range
15 p1812 N73-24686
**CHLORATES**
Analysis of chlorate candle generated oxygen
[AD-762276] 19 p2231 N73-27992
**CHLORELLA**
Chemical composition stability of Chlorella biomass during prolonged cultivation
10 p1117 N73-19108
Effects of atmospheric oxygen concentration on Chlorella photosynthesis
14 p1608 N73-23032
Photosynthesis of chlorella
20 p2405 N73-29326
**CHLORIDES**
NT BORON CHLORIDES
NT CARBON TETRACHLORIDE
NT COPPER CHLORIDES
NT DICHLORIDES
NT HYDROCHLORIC ACID
NT HYDROGEN CHLORIDES
NT IRON CHLORIDES
NT LITHIUM CHLORIDES
NT POTASSIUM CHLORIDES
NT SILVER CHLORIDES
NT SODIUM CHLORIDES
NT TETRACHLORIDES
NT TITANIUM CHLORIDES
Dry sliding friction characteristics of iron ceramic materials using solid lubricants
04 p0432 N73-13517
Effect of chloride ion additions on dissolution behavior of Fe-Ni alloys in sulfuric acid
[AD-751258] 07 p0811 N73-16574
Thermodynamics of molten mixtures of lithium chloride-potassium chloride at 640 C
[AD-752087] 08 p0970 N73-17925
Corrosion behavior of titanium alloys in chloride solutions
[AD-753573] 09 p1050 N73-18561
Chloride and water permeability parameters for hydraulic brake hose testing
[AD-748083] 13 p1546 N73-22530
Vibronic interaction in electron paramagnetic resonance spectra of yttrium and scandium doped single strontium chloride crystals
[NASA-CR-131295] 13 p1561 N73-22653
Far infrared laser spectroscopy of spin clusters in linear magnetic system of cobalt chloride compound
[AD-756264] 13 p1566 N73-22691
Sulfur, sodium, and chloride contaminants in gas turbines
14 p1677 N73-23610
Stability constants for chloride complexes of palladium [II]
[AD-758684] 16 p1871 N73-25151
Magnetic susceptibilities of NiCl2.6H2O
[AD-759417] 17 p2046 N73-26555
Selective growth of epitaxial silicon layers in chloride process
18 p2188 N73-27668
Ellipsometric measurements on passive film prior to initiation of breakdown in aluminum
[NASA-CR-132301] 20 p2432 N73-29533
Radiolytic preparation of anhydrous tin [2] chloride
[NASA-TM-X-2927] 24 p2891 N73-33082
Mass spectra of doublets in samarium and gadolinium chlorides
24 p2959 N73-33648
**CHLORINE**
Design, development, and evaluation of aluminum-chlorine battery
[AD-747775] 03 p0255 N73-12065
Calculation of heat of evaporation of liquid chlorine into calorimeter for rocket propulsion
[AD-755894] 12 p1466 N73-21874
Gas proportional counting of chlorine-36 in iron and iron meteorites
23 p2835 N73-32656
**CHLORINE COMPOUNDS**
NT ALUMINUM PERCHLORATES
NT AMMONIUM PERCHLORATES
NT BORON CHLORIDES
NT CARBON TETRACHLORIDE
NT CHLORATES
NT CHLORIDES
NT CHLORINE FLUORIDES
NT COPPER CHLORIDES
NT DICHLORIDES
NT HYDROCHLORIC ACID
NT IRON CHLORIDES

NT LITHIUM CHLORIDES
NT PERCHLORATES
NT POTASSIUM CHLORIDES
NT SILVER CHLORIDES
NT SODIUM CHLORIDES
NT TETRACHLORIDES
NT TITANIUM CHLORIDES
Toxicity of atmospheric dichloromethane levels in simulated space cabin atmosphere on dogs, rats, mice, and monkeys
[NASA-TM-X-69099] 09 p0996 N73-18129
Effect of toxic substances on algae by observing photosynthesis determined by oxygen production of algae
[DRIC-TRANS-2991] 10 p1121 N73-19139
PH influence on hexachloroiridite and hexachloroiridate ions in aqueous solutions
[IRI-133-73-02-PT-2] 21 p2506 N73-30111
CHLORINE FLUORIDES
Tests of seat and poppet materials for use in chlorine pentafluoride attitude control system valves
[AD-750873] 06 p0715 N73-15831
Symptomatic and pathological information from acute toxicity exposure of chlorine pentafluoride
[AD-751452] 07 p0747 N73-16078
CHLOROAROMATICS
Synthesis and properties of perchloroaromatic compounds
[AD-763125] 20 p2375 N73-29081
CHLOROPHYLLS
ERTS-1 remote sensing of chlorophyll measurements in upwelling areas of oceans
[E72-10196] 01 p0047 N73-10375
Chlorophyll and plankton population distribution in upwelling waters off northwest coast of Africa and effects of eolian dust particles on surface water chemistry
[E72-10331] 05 p0531 N73-14319
Correlation of chlorophyll and suspended sediments in Chesapeake Bay to ERTS-1 imagery
[E73-10424] 11 p1280 N73-20385
Hydrophobic iminoxyl radicals as uncouplers of photophosphorylation in choloroplasts
[NASA-TT-F-14819] 12 p1376 N73-21160
Relation of chlorophyll and suspended sediment content in lower Chesapeake Bay to ERTS-1 imagery and application of marine station data to study of productivity along eastern shelf waters of US
[E73-10593] 15 p1772 N73-24358
Measurement of chlorophyll and plankton populations of shelf and slope waters off northeastern United States
[E73-10683] 16 p1901 N73-25378
Correlation of ERTS-1 multispectral imagery with suspended matter and chlorophyll in lower Chesapeake Bay
[PAPER-M4] 19 p2280 N73-28344
Relation of chlorophyll and suspended sediments in waters of lower Chesapeake Bay to ERTS-1 imagery
[E73-10851] 19 p2292 N73-28429
Relation of sea truth data from Cape Cod, Massachusetts, and Charleston, South Carolina on plankton composition and chlorophyll values with ERTS-1 data
[E73-10907] 20 p2397 N73-29256
Differentiation of ocean multispectral data obtained by satellite for chlorophyll content
22 p2736 N73-31904
Collection of phytoplankton and chlorophyll samples from waters of Chesapeake Bay
[E73-11154] 24 p2919 N73-33308
CHLOROPRENE RESINS
Engineer design tests of two dust control materials, polyvinyl acetate water emulsion and cationic asphalt-neoprene emulsion
[AD-745086] 01 p0038 N73-10297
CHOKES [RESTRICTIONS]
Feasibility determination for application of principle of corresponding states to two phase choked flow
[NASA-TM-X-68193] 10 p1141 N73-19299
Flow characteristics of radial inward choked flow of liquid nitrogen stream
[NASA-TM-X-68283] 20 p2387 N73-29181
CHOLESTEROL
Blood pressure and cholesterol level screening for preventing heart diseases in flight crews of commercial airline
08 p0874 N73-17076
Influence of repeated test and dietary counseling on hypercholesterolemia control in NASA employees
08 p0875 N73-17081
Iridescence and selective reflection of cholesteric liquid crystals according to various models
[BMVG-FBWT-72-27] 10 p1190 N73-19684
Absorption of bile acids and cholesterol by polymers
10 p1227 N73-19976
Effects of physical training on human enzyme activity, carbohydrate metabolism, cholesterol level, and adrenal function
[NASA-TT-F-14826] 11 p1243 N73-20093
CHOLINERGIC BLOCKING AGENTS
U ANTICHOLINERGICS
CHOLINERGICS
NT ANTICHOLINERGICS
Transverse acceleration effects on rat gastrointestinal response to drugs
10 p1114 N73-19085
CHOLINESTERASE
Factors influencing reactivation of phosphorylated acetylcholine esterase by oximes
[BMVG-FBWT-72-32] 10 p1121 N73-19137
Inhibiting and activating effect of mono- and bi-quaternary pyridioxide reactivators on bovine erythrocyte cell membrane
[BMVG-FBWT-72-9] 10 p1121 N73-19138
Cholinesterase reactivator as antidote in human organophosphate poisoning
13 p1480 N73-21998
CHONDRITES
NT BRUDERHEIM METEORITE
NT CARBONACEOUS METEORITES
Analysis of carbonaceous Migei chondrite for content of polynucleotide
[NASA-TT-F-14683] 08 p0962 N73-17868
Particle shape and magnetism of chondrite meteorites
[NASA-TM-X-63942] 10 p1212 N73-19862
Chemical analyses of orthopyroxene and clinopyroxene composition of chondrites
[NASA-TM-X-62259] 15 p1830 N73-24835
CHONDRULE
Element abundances in meteoritic chondrules by neutron activation analysis
12 p1446 N73-21713
CHORUS [DAWN PHENOMENON]
U DAWN CHORUS
CHORUS PHENOMENON
U DAWN CHORUS
CHROMATES
NT POTASSIUM CHROMATES
Chemical reactions involved with molybdenum, tungsten, vanadium, and chromium additives in hydrogen-oxygen flames seeded with potassium
[AD-743514] 01 p0023 N73-10179
CHROMATOGRAPHY
Chromatographic determination of gaseous metabolites released by man during reduced food intake
03 p0258 N73-12091
Gas chromatographic separation of beryllium [II], copper [II], aluminum [III], and chromium [III] chelates
[NLL-M-22879-[5828.4F]] 11 p1252 N73-20158
Self-scanning chromatographic-fluorographic drug detector with optical readout system
[NASA-CASE-ARC-10633-1] 13 p1486 N73-22048
Chromatographic determination of aldosterone level in urine
[RAE-LIB-TRANS-1682] 17 p1987 N73-26061
Chromatographic determination of urine corticosteroids
[RAE-LIB-TRANS-1694] 17 p1987 N73-26062
CHROME
U CHROMIUM
CHROMIUM
Roentgenographic measurement of coefficient of thermal expansion for chromium and solid chromium based solutions
[AD-747399] 03 p0317 N73-12580
Abrasive wear resistance of vapor plated chrome coatings
[AD-749769] 05 p0567 N73-14605
Influence of volatile compounds on high temperature oxidation of Cr and Cr alloys
[TM-49] 06 p0684 N73-15566
Influence of heat treatment on physical properties of iron- and chromium-doped rutile
[RR-107] 09 p1073 N73-18760
Effect of warm rolling on mechanical properties of unstable chromium-manganese austenitic steels
10 p1171 N73-19326
Gas chromatographic separation of beryllium [II], copper [II], aluminum [III], and chromium [III] chelates
[NLL-M-22879-[5828.4F]] 11 p1252 N73-20158
Atomic absorption spectrophotometric analysis of chromium in stainless steels
[AD-755809] 13 p1545 N73-22522
Addition of chromium or aluminum to improve oxidation resistance of nickel and cobalt alloys
14 p1677 N73-23611
EPR in Cr[3 plus] in Li2Ge7O15
[AD-757884] 15 p1822 N73-24768
Fatigue strength and other mechanical properties of medium carbon steels chromed by gaseous and vapor phase methods
[DRIC-TRANS-2156] 17 p2046 N73-26550
Analysis of structural-eutectic transformations in liquid phase of metal-metal and metal-semiconductor systems
[NLL-M-21665-[5828.4F]] 21 p2557 N73-30496
Creep behavior of polycrystalline aluminum oxide cermets with varying chromium concentrations
[KFK-1753] 21 p2563 N73-30545
Thermodynamic stability diagrams for iron, nickel, and chromium in fused sodium hydroxide
22 p2625 N73-31028
Heat treated chromium doped rutile for L-band traveling wave masers
[RR-111] 24 p2930 N73-33402
Temperature dependence of spin-Hamiltonian parameters for chromium doped rutile
[RR-110] 24 p2968 N73-33721
CHROMIUM ALLOYS
NT CHROMIUM STEELS
High temperature and fatigue tests to determine effects of heat resistant coatings on mechanical and physical properties of nickel-chromium-iron alloys
[NLL-TRANS-746-1236-[9022.401]]
02 p0185 N73-11500
Analysis of structural changes during heating and elongation of two-phase, high chromium content Cr-Ni-Fe alloys over ranges of temperature and concentration
[NLL-TRANS-746-1153-[9022.401]]
02 p0185 N73-11501
Preparation and homogeneity characteristics of austenitic iron-chromium-nickel alloy at micrometer level of spatial resolution to establish standard reference material
[NBS-SP-260-43] 02 p0186 N73-11511
TD nickel chromium, dispersion-strengthened alloy for thermal protection system of space shuttle
[NASA-CR-120796] 02 p0187 N73-11512
Effects of molybdenum and tungsten fiber reinforcements on nickel chromium aluminum matrix alloys
[NLL-TRANS-746-1193-[9022.401]]
02 p0191 N73-11546
Chromium superalloy damage and temperature effects
[NASA-TN-D-7073] 03 p0312 N73-12549
Effect of mechanical-thermal pretreatments on time-to-rupture and creep strength of nickel-chromium steels
[KFK-1535] 03 p0313 N73-12557
Roentgenographic measurement of coefficient of thermal expansion for chromium and solid chromium based solutions
[AD-747399] 03 p0317 N73-12580
Recrystallization processes of sheet nichrome containing zirconium dioxide inclusions
[AD-747603] 03 p0318 N73-12589
Dispersion hardening of complex chromium nickel alloy by zirconium dioxide
04 p0432 N73-13523
Diffusion creep and creep degradation in precipitation hardened TD-NiCr alloy
[NASA-TN-D-7079] 04 p0433 N73-13530
Electric field effects on oxidation mechanisms of metals and alloys
[AD-748297] 04 p0436 N73-13558
Creep and stress relaxation tests on Cr-Ni austenitic steel at 700 C
[STU-70-419/U-350-B] 04 p0481 N73-13932
Structure and phase composition of electrodeposited iron-nickel-chromium alloys analyzed by X ray spectroscopy and electron microscopy
[NLL-TRANS-746-1327-[9022.401]]
05 p0560 N73-14551
Evaporative segregation in binary alloys of Ni-Cr and Ni-Fe systems
[NASA-CR-123993] 05 p0561 N73-14562
Beta-phase effect on ductility of two-phase titanium alloys and calorimetric determination of atomic ordering effects in Ni2Cr alloy
[JPRS-57578] 06 p0683 N73-15556
Calorimetric determination of atomic ordering effects in alloy Ni2Cr
06 p0683 N73-15558
Influence of volatile compounds on high temperature oxidation of Cr and Cr alloys
[TM-49] 06 p0684 N73-15566
Dispersion effects of heat resistant metal oxides
[AD-754760] 11 p1306 N73-20595
Solid state and fusion resistance spot welding of TD-NiCr sheet
[NASA-TN-D-7256] 12 p1412 N73-21443
Effect of yttrium, lanthanum, and cerium additives on oxidation kinetics of nickel-chromium based alloys
[JPRS-58777] 13 p1542 N73-22497
Effects of oxide dispersions and rare earth elements on oxidation of Cr and Al containing alloys
14 p1677 N73-23608
Change in fine structure of nickel-chromium heat resistant alloys during creep
[AD-759233] 16 p1971 N73-25939
Thermodynamic properties of solid alloys of chromium with nickel and iron
[COO-1791-4] 21 p2559 N73-30516
Carbon fiber/cobalt/chromium system tensile and high temperature strength noting different solidification modes
[DLR-FB-73-37] 21 p2560 N73-30519
Mechanical and physical property tests of TD-NiCr [Ni-20Cr-2ThO2] alloy sheet
[NASA-CR-121221] 22 p2683 N73-31493
Potentiostatic tests for determining range of crevice corrosion susceptibility in chromium modified cupronickel alloys
[AD-762596] 22 p2687 N73-31524

Thermodynamic property measurements of solid chromium sesquioxide and chromium in solid alloys with iron and nickel
[TID-26322] 24 p2934 N73-33433
**CHROMIUM CARBIDES**
Orthorhombic chromium carbide for increased strength of sintered iron ceramic structural material
04 p0432 N73-13516
Hot pressing of chromium carbide alloy matrice tools for cold drawing of pipes
04 p0432 N73-13522
**CHROMIUM COMPOUNDS**
NT CHROMATES
NT CHROMIUM CARBIDES
NT CHROMIUM OXIDES
NT POTASSIUM CHROMATES
**CHROMIUM OXIDES**
Thermogravimetric analysis of reduction of oxides of nickel and chromium
[NASA-TM-X-2688] 06 p0684 N73-15565
Formation and failure of chromium sesquioxide on cobalt-base alloy L-605 during oxidation at high temperatures
[NASA-TN-D-7255] 12 p1414 N73-21454
Vaporization thermodynamics of Cr2O3 protective scales under transonic flow conditions
14 p1677 N73-23607
Acetone decomposition by austenitic stainless steel, iron oxide, and chromium oxide
[AERE-R-7408] 24 p2892 N73-33089
**CHROMIUM STEELS**
Microstructural analysis of high-chromium martensitic semiferritic and ferritic steel phase transformations and thermal expansion coefficient determination
[AD-749522] 04 p0436 N73-13559
**CHROMOSOMES**
Computer technique for automatic analysis of planar characteristics of chromosome patterns in microscopic observations
[JPRS-57118] 04 p0379 N73-13085
Radiation effects on human chromosomal aberrations in peripheral blood lymphocytes
14 p1609 N73-23041
Machine assisted human chromosome karyotyping and aberration for radiation damage
[ANL-7960-PT-2] 17 p1988 N73-26068
**CHROMOSPHERE**
Synoptic charts and catalogs of solar activity centers and chromospheric filaments
01 p0099 N73-10817
Analysis of chromospheric patterns produced by changes in interplanetary and geomagnetic fields
[AD-745100] 01 p0106 N73-10877
Radiative equilibrium and empirical models for stellar chromospheres
04 p0466 N73-13794
Ground based line spectra analyses for determining stellar chromospheres
04 p0466 N73-13795
Spaceborne ultraviolet emission lines in stellar sources as chromospheric indicators
04 p0466 N73-13796
Solar atmospheric heating model for mechanical heating in stellar chromospheres
04 p0466 N73-13797
Radiative mass flow transfer model for inhomogeneous structure of chromosphere
04 p0466 N73-13798
Stellar evolution and atmospheric turbulence dynamics for chromospheric activity model
04 p0466 N73-13799
Summary of physical and theoretical work on stellar chromospheres
04 p0466 N73-13800
Radio observations of distribution of chromospheric brightness temperature
[AD-747021] 04 p0467 N73-13809
Static planar model for explaining structure and thermal conduction heating of chromosphere-corona transition region
12 p1444 N73-21699
Computer program to analyze solar observational data
[AD-755921] 14 p1703 N73-23815
Observation analysis of August 1972 solar flares using spectrophotographic techniques
[NASA-CR-132195] 16 p1963 N73-25881
Bremsstrahlung radiation from beam of electrons in solar chromosphere, and total energy of solar flares
[NASA-CR-133943] 22 p2711 N73-31710
**CHRONIC CONDITIONS**
Chronic disease health trends and mortality rates in employee population of NASA Goddard Space Flight Center
08 p0875 N73-17086
**CHRONOGRAPHS**
U CHRONOMETERS
**CHRONOLOGY**
NT GEOCHRONOLOGY
Reference to aerospace-related events for 1970
[NASA-SP-4015] 14 p1705 N73-23833
Dating of ocean floor rocks and investigation of kinetic processes in lunar regolith
17 p2017 N73-26307
**CHRONOMETERS**
Design of reserve master clock for controlling meteorological recording instruments in Antarctic weather stations
[NLL-M-22972-[5828.4F]] 16 p1911 N73-25459
Nucleocosmochrometers for short lived Pb-205 s-process nucleosynthesis study
[AD-760535] 18 p2182 N73-27618
**CHRONOPHOTOGRAPHY**
Data processing of hydrologic conditions using ERTS-1 time lapse imagery of Wrangell Mountains
[E72-10187] 01 p0046 N73-10366
Time-lapse data processing for dynamic hydrologic conditions at Mt. Rainier, Washington
[E73-10582] 15 p1772 N73-24356
Analysis of time-lapse data processing for dynamic hydrologic conditions based on ERTS-1 imagery and aerial photography
[E73-10729] 17 p2020 N73-26335
Time lapse processing of dynamic hydrologic conditions
[E73-11054] 23 p2780 N73-32230
**CHRONOTRONS**
U PULSE RATE
U TIME LAG
**CHUGGING**
U COMBUSTION STABILITY
**CINEFLUOROGRAPHY**
U MOTION PICTURES
U RADIOGRAPHY
**CINEMATOGRAPHY**
Reception of positive color television images using negative color motion picture film
[NLL-DRIC-TRANS-2835-[3623.66]]
11 p1291 N73-20480
Bioelectric monitoring and motion picture surveying for improved physical training of astronauts
14 p1608 N73-23039
Investigation of vocal cord regulatory mechanism of register, pitch, and intensity of voice during singing
14 p1632 N73-23225
K. E. Tsiolkovskiy as film consultant
[NASA-TT-F-14890] 14 p1708 N73-23865
**CINERADIOGRAPHY**
U MOTION PICTURES
U RADIOGRAPHY
**CINETHEODOLITES**
Cinetheodolite observations of satellites between 30 Nov. 1965 and 17 Jan. 1966
[ROE-STS-136] 09 p1091 N73-18909
Cinetheodolite observations of satellites between 18 and 31 Jan. 1966
[ROE-STS-137] 09 p1091 N73-18910
Cinetheodolite satellite tracking at Earlyburn between 15 and 18 Feb. 1966
[ROE-STS-142] 13 p1582 N73-22829
Cinetheodolite satellite tracking at Earlyburn between 19 Feb. and 1 Mar. 1966
[ROE-STS-143] 13 p1583 N73-22830
Cinetheodolite satellite tracking at Earlyburn between 2 and 10 Mar. 1966
[ROE-STS-148] 15 p1836 N73-24882
Contraves cinetheodolite optical system modification
[SC-DR-72-0754] 16 p1914 N73-25487
Cinetheodolite satellite tracking at Earlyburn between 11 and 29 Mar. 1966
[ROE-STS-149] 17 p2089 N73-26905
**CIRCADIAN RHYTHMS**
Circadian rhythm change study of transmeridian flight and medication effects on mildly hypertensive subject
[AD-743300] 01 p0011 N73-10090
Influence of time zones on physiological organs and systems and performance of athlete
[NASA-TT-F-14632] 04 p0383 N73-13116
Changes in circadian rhythm of aircraft pilot oral body temperature as result of transmeridian flights
[DLR-FB-73-01] 09 p0997 N73-18140
Circadian phase relationships of physiological functions of isolated monkeys subjected to varying photoperiod phases
12 p1367 N73-21088
Effects of work-rest schedules, circadian rhythms, continuous work, and sleep loss on sustained performance
14 p1723 N73-23988
Experimental research in underwater medicine, flight stress, and pilot selection
[DLR-FB-73-15] 19 p2226 N73-27951
Resynchronization of circadian rhythms following transmeridian flight observed in two group of students
19 p2227 N73-27958
Effects of two sequential transatlantic flights on circadian rhythm of body function and performance
19 p2227 N73-27964
Rhythm disturbances in sleep and wakefulness cycles of Soyuz 3 and 9 crews before, during, and after space flight
[NASA-TT-F-15103] 20 p2369 N73-29048
Time shift effects on human 17-hydroxy corticosteroid diurnal excretion noting transmeridian flights
[DLR-FB-73-58] 21 p2501 N73-30070
Preflight and flight stress analysis, its relation to circadian rhythms measured in pilot physiological parameters
[DLR-FB-72-39] 21 p2501 N73-30071
Human circadian rhythms of blood circulation, respiration and catabolism under flight simulation stress
[DLR-FB-72-49] 21 p2501 N73-30073
Circadian rhythms of sleep and cerebral temperature in rats chronically exposed to hot environments
[NASA-TT-F-15082] 22 p2620 N73-30994
Human psychomotor performance circadian rhythm variations after transmeridian flight noting time shift effect
[DLR-FB-73-52] 22 p2624 N73-31022
Psychoneurological problems in adaptation by man to modified diurnal regimes
24 p2884 N73-33031
**CIRCLES (GEOMETRY)**
Flanged and circular data sheet-sections, beyond limit of proportionality
[ESDU-01.06.00] 01 p0110 N73-10903
Calculation of incompressible potential flow of airfoils by conformal mapping potential flow of lifting circles onto airfoils by double transformations
[ARC-R/M-3717] 21 p2492 N73-30002
**CIRCUIT BOARDS**
Infrared nondestructive testing techniques used to detect unbonded areas in laminated structures and incipient failures in electrical circuit boards
[AD-746233] 02 p0175 N73-11419
Development and characteristics of polyimide impregnated laminates with fiberglass cloth backing for application as printed circuit broads
[NASA-CASE-MFS-20408] 03 p0320 N73-12604
Design and operation of programmable logic tester for high speed static testing of circuit boards
[REPT-6570] 04 p0420 N73-13422
Welding leads of integrated circuits to printed circuit boards
[AD-749838] 05 p0523 N73-14254
Printed circuit boards for microminiaturized electronic manufacturing
[AD-750918] 06 p0648 N73-15265
Processes for developing high quality multilayer printed wiring boards
[BDX-613-382-REV] 07 p0762 N73-16189
Device for bending leads projecting from printed circuit boards
[NASA-CASE-MFS-22133-1] 09 p1039 N73-18473
Photoresist fabrication of printed circuit boards
[BDX-613-496] 12 p1387 N73-21245
Techniques for packaging and mounting printed circuit boards
[NASA-CASE-MFS-21919-1] 16 p1883 N73-25243
Computerized design of printed circuit boards
[AD-762021] 19 p2247 N73-28114
Printed wire routing on multilayer circuit boards
20 p2380 N73-29122
Algorithm for location of electronic modules on printed circuit board
21 p2513 N73-30156
Viscoelastic shock absorbing mount for electrical circuit board
[NASA-CASE-NPO-13253-1] 22 p2677 N73-31445
Fast heuristic techniques for placing and wiring printed circuit boards
24 p2898 N73-33134
**CIRCUIT BREAKERS**
Feasibility of solid state electric switch gear for aircraft and spacecraft
[NASA-CR-121140] 09 p1007 N73-18223
Self-healing fuse development
[NASA-CR-121244] 21 p2517 N73-30191
**CIRCUIT DIAGRAMS**
Circuit and plug register diagrams for printout converter
[PHL-1972-4] 02 p0144 N73-11168
Control circuit for nuclear thermionic converter power source for spacecraft
[NASA-CASE-NPO-13114-1] 04 p0448 N73-13656
Circuit configuration for high Q factor selective amplifier
[REPT-1370] 05 p0522 N73-14245
Configuration of all pass network with negative real poles and Q factor
[PUBL-1367] 05 p0522 N73-14246
Boundary test procedure for determining characteristics and design of integrated transistor-transistor logic circuits
[AD-749604] 05 p0523 N73-14253
Diagram solutions of circuits forming high frequency electromagnetic fields in plasma devices
[AEC-TR-7326] 07 p0826 N73-16696
Design and development of universal voice processor system
[NASA-CR-128739] 08 p0885 N73-17161
Integrated circuit designs for self controlling electrical heater
[NASA-TN-D-7248] 15 p1786 N73-24479
Elements of block diagrams for automatic radio tracking systems
16 p1875 N73-25179

Techniques and circuitry for designing adaptive high Q notch filter
[AD-759031] 17 p2004 N73-26210
Design of tubular thermoelectric module for astronuclear power conversion system
[NASA-CR-121210] 19 p2319 N73-28659
CIRCUIT PROTECTION
Performance of lightning and surge suppressors for digital transmission equipment
[AD-752448] 09 p1004 N73-18195
Overvoltage protection network for electrical equipment
[NASA-CASE-ARC-10197-1] 20 p2380 N73-29124
Characterization of electromagnetic pulse shunt protective devices
[AD-763886] 22 p2644 N73-31191
Application of diffusion bonding to electronic interconnection of flatpack leads
[NASA-CR-124460] 24 p2934 N73-33429
CIRCUIT RELIABILITY
Redundancy reduction for logic circuits by error correcting codes to improve method of increasing circuit reliability
04 p0399 N73-13249
Redundant cells to improve reliability of asynchronous automata
04 p0399 N73-13250
Performance and reliability of large scale integrated circuits
[AD-750577] 06 p0646 N73-15250
Accelerated reliability tests of circuit components by continuous loading method
[AD-752689] 09 p1040 N73-18485
Analysis of methods of fault diagnosis used with logic circuits and effect of procedures on structure of circuit assemblies
[NLL-PO-2913-[9022.81]] 15 p1759 N73-24255
Microcircuit reliability bibliography
[AD-763764] 21 p2518 N73-30194
Strength of printed circuit joints for reliability, based on electrical resistivity
[DLR-FB-73-33] 24 p2899 N73-33140
CIRCUITS
NT ADDING CIRCUITS
NT ANALOG CIRCUITS
NT CIRCULATORS [PHASE SHIFT CIRCUITS]
NT COINCIDENCE CIRCUITS
NT COUPLING CIRCUITS
NT DELAY CIRCUITS
NT DIGITAL INTEGRATORS
NT ELECTRIC BRIDGES
NT EQUIVALENT CIRCUITS
NT FEEDBACK CIRCUITS
NT FLIP-FLOPS
NT FLUID SWITCHING ELEMENTS
NT FLUIDIC CIRCUITS
NT GATES [CIRCUITS]
NT INTEGRATED CIRCUITS
NT ITERATIVE NETWORKS
NT LC CIRCUITS
NT LIMITER CIRCUITS
NT LOGIC CIRCUITS
NT MAGNETIC CIRCUITS
NT MATRICES [CIRCUITS]
NT MICROWAVE CIRCUITS
NT MIXING CIRCUITS
NT NEGATIVE RESISTANCE CIRCUITS
NT PHASE DETECTORS
NT PHASE SHIFT CIRCUITS
NT POWER SUPPLY CIRCUITS
NT PRINTED CIRCUITS
NT RC CIRCUITS
NT SCALERS
NT SWITCHING CIRCUITS
NT THRESHOLD GATES
NT TRANSISTOR CIRCUITS
NT TRANSMISSION CIRCUITS
NT TRIGGER CIRCUITS
NT WHEATSTONE BRIDGES
Fast periodic steady state analysis of nonlinear large signal electronic circuits
[AD-745639] 01 p0034 N73-10271
Comparison of quasi-Newton methods for dc analysis of electronic circuits
[AD-746391] 01 p0035 N73-10274
Instrumentation for photometry, and amplifier and circuit design
[NBS-TN-594-2] 01 p0056 N73-10459
Narrow band equivalent circuit for two-port network using cascaded, lossless transmission lines and lossless shunt elements
[APS-EL-30] 02 p0150 N73-11221
Harmonic functions for determining currents and voltages in nonlinear electrical circuit
[AD-748231] 03 p0276 N73-12243
Stabilization of base line at output of amplifiers for gamma spectrometry chain
[CEA-N-1514] 03 p0277 N73-12248
Graphical method for solving interference problem in asynchronous circuit
[CEA-CONF-1961] 03 p0277 N73-12249
Temperature corrected circuit for gyroscope or accelerometer of digital rebalance type
[NASA-CASE-NPO-13044-1] 04 p0421 N73-13436
Circuit theory research in Europe
[AD-749346] 05 p0523 N73-14252
Thermochromic compositions for detecting heat levels in electronic circuits and devices
[NASA-CASE-NPO-10764-1] 05 p0545 N73-14428
Reliability data for hybrid microcircuit discrete components
[NASA-TM-X-64686] 07 p0764 N73-16208
FORTRAN program for handling radiation effects circuit analysis problems
[AD-751519] 07 p0765 N73-16213
Utilization of oil dischargers in high voltage pulse circuits
[AD-751170] 07 p0765 N73-16214
Irradiation of three low power microcircuits by Co-60 gamma radiation, low and high energy electrons, and neutrons
[NASA-CR-130750] 08 p0891 N73-17215
Automatic through-insulation welding of small-diameter solid conductor wires to facilitate production of miniature electronic assemblies
[NASA-CR-130751] 08 p0927 N73-17591
Initial systole and dicrotic notch detecting circuitry for monitoring arterial pressure pulse
[NASA-CASE-LEW-11581-1] 09 p0997 N73-18139
Discharge circuit of inductive accumulator for generating short front current pulse
[JPRS-58892] 13 p1504 N73-22190
Electroacoustic effects of speech communication circuits on speech intelligibility
[AD-757326] 14 p1633 N73-23236
Design and analysis of Type 2 correlation-extreme systems composed of control circuits and gages for measuring random functions
14 p1644 N73-23335
Design, construction, and electrical circuits for radiosondes to study warm cloud development
[AD-758073] 14 p1686 N73-23684
Noise properties and circuits to cancel noise in gas parametric amplifiers
15 p1756 N73-24230
Electric modulator circuit for controlling output power of commercial laser
[LA-5166-MS] 17 p2040 N73-26507
Development of electrical circuitry for analysis of stress deformation state of delta wing model based on discrete design diagram
[AD-760948] 18 p2108 N73-27044
Universal program for optimizing parameters of electrical circuits
21 p2515 N73-30174
Electrodeless lamp circuit driven by induction
[NASA-CASE-MFS-21214-1] 21 p2516 N73-30181
Automatic speech level meter on voice frequency telephone circuit
[REPT-6648] 22 p2672 N73-31402
Sample-and-hold circuit for monitoring system calibration
[AD-764242] 22 p2676 N73-31434
Program for generating transfer functions of electrical network circuits
[AD-764809] 23 p2762 N73-32102
CIRCULAR CONES
Computerized stability derivative calculations for oscillating parabolic ogives and circular cones in transonic flow field using iterative procedure
[NASA-CR-124033] 07 p0769 N73-16249
Finite difference solution of three-dimensional compressible boundary layer equations for circular cones at angle of attack
[NASA-CR-112316] 12 p1391 N73-21276
Finite difference solution to right angle circular cone streamline swallowing phenomenon during supersonic and hypersonic flow
13 p1508 N73-22218
CIRCULAR CYLINDERS
Numerical analysis of finite-strength, isentropic pressure waves transverse to axis of circular cylinder
[NASA-CR-2138] 01 p0041 N73-10321
Fatigue strength data for thick steel and aluminum alloy cylinders under internal pressure
[ESDU-67014] 01 p0110 N73-10910
Curves for determining maximum combined stresses in long circular cylindrical shells with flat head closure under uniform pressure only
[ESDU-66010] 01 p0111 N73-10912
Convective heat transfer for Newtonian fluid cross flow over circular cylinder
[ESDU-69004-AMEND-A] 02 p0241 N73-11962
Analysis of eddies and lift forces created on vertical circular cylinder by oscillatory flow conditions
[AD-748078] 03 p0287 N73-12329
Wave forces on horizontal circular cylinder subjected to train of gravity waves
[AD-747332] 03 p0362 N73-12951
Literature survey for action of applied magnetic field on conducting liquid in circular cylindrical container
[AE-447] 04 p0450 N73-13674
High speed mechanics research, including circular cylindrical shell buckling and hydrofoil profiles
06 p0724 N73-15910
Modified Flugge equations for buckling of circular cylindrical shells, using membrane theory of shells
[REPT-248] 06 p0724 N73-15911
Visualization of longitudinal vortices in stagnation area of circular cylinder in turbulent flow with splitting plate
07 p0771 N73-16264
Measurement of microscale turbulence and turbulent flow intensity of dilute polymer solutions about circular cylinders
[AD-751640] 07 p0774 N73-16284
Circular cylindrical shell pressure limits
[PB-212638] 07 p0852 N73-16912
Analysis of flow distribution around harmonically oscillating circular cylinder under two dimensional flow conditions
[DLR-FB-72-56] 09 p1014 N73-18277
Elastic-plastic behavior of thick-walled circular cylinders under internal pressure
[AD-753121] 09 p1097 N73-18952
Wind tunnel tests of blowing on circular cylinders applied to aircraft control and braking at low speeds
[ARC-CP-1232] 10 p1104 N73-19000
Numerical analysis of low Reynolds number flow perpendicular to circular cylinder with constant radial suction mass flux at surface
12 p1389 N73-21264
Investigation of cracks in radial plane of solid right circular cylinder
13 p1584 N73-22841
Higher-order shell theory for thick circular cylinders under arbitrary load and boundary conditions
[AD-756648] 13 p1589 N73-22885
Construction of transfer functions in problems of weak shock interactions with cylindrical and spherical surfaces
14 p1715 N73-23913
Wind tunnel tests to determine aeroelastic stability of thin isotropic circular cylindrical shells at subsonic and supersonic air speeds
20 p2359 N73-28975
Far-field pattern of antenna determined from probe compensated near-field measurements over surface of right circular cylinder enclosing antenna
20 p2375 N73-29084
Computation of buckling of thin walled circular cylinders under axial compression loads
[DLR-FB-73-36] 21 p2604 N73-30868
Unidirectional periodic flow about circular cylinders
[AD-764487] 22 p2656 N73-31273
Analysis of transient wave motion in liquid filled cylinders
23 p2773 N73-32179
CIRCULAR ORBITS
NT STATIONARY ORBITS
Numerical solutions for variational control functions of flight dynamics in circular orbits
10 p1178 N73-19582
CIRCULAR PLATES
Curves for determining maximum elastic stresses and deflections for initially flat circular plates of uniform thickness under uniform pressure with various edge conditions
[ESDU-65002] 01 p0112 N73-10923
Axisymmetric bending of round sandwich plate with rigid isotropic layers
[AD-749767] 05 p0604 N73-14915
Dynamic and static response to blast loads of thin circular plates free or embedded using Timoshenko model and finite difference theory
[ISL-4/72] 09 p1094 N73-18934
Post buckling behavior of circular plate following heating at center and heating at edge and effects of restraints on final configuration
[ARC-R/M-3245] 15 p1730 N73-24031
Nonlinear deflections of circular plate with varying thickness
22 p2723 N73-31794
CIRCULAR POLARIZATION
Investigation of emissivity and circular polarization of synchrotron radiation
[NASA-CR-131526] 12 p1457 N73-21811
Development of exact circular polarization in short helical antennas by conducting disk at helix end
[DLR-FB-73-46] 17 p1998 N73-26156
Analysis of atmospheric attenuation of circularly polarized electromagnetic radiation from meteorological radar
21 p2570 N73-30595
Improvement of instrument landing systems with respect to multipath propagation effects and surface reflections
[DGLR-PAPER-73-017] 23 p2817 N73-32321
CIRCULAR SHELLS
Buckling characteristics of perfect and imperfect circular cylindrical shells subjected to dynamic axial loading
[NASA-CR-129086] 02 p0237 N73-11927
Variational principle for calculating buckling of thin clamped free circular cylindrical shells subjected to wind load
[TT-7113] 06 p0725 N73-15916
Application of three dimensional theory of elasticity to dynamic response of freely supported circular cylindrical shell
06 p0725 N73-15921

Noise intensities of rectangular and circular supersonic nozzle geometries
[NASA-CR-130964] 09 p1067 N73-18704
Shell equations for orthotropic, circular cylinders during axially symmetric, harmonic motion
16 p1968 N73-25918
Stability of freely supported circular cylindrical shell subjected to random stresses
[AD-761541] 19 p2350 N73-28901
Vibration stability contact and interfacial crack propagation for partially delaminated layered circular cylindrical shells
20 p2476 N73-29891
Impact of thin elastic circular shell on surface of compressible fluid
[AD-763259] 21 p2526 N73-30252

CIRCULAR TUBES
Parameters and secondary factors governing forced convective heat transfer and turbulent flow in circular tubes
[ESDU-67016] 02 p0242 N73-11964
Darcy-Weisback equation for investigating solid-liquid flow in noncircular pipes
[BM-RI-7725] 09 p1013 N73-18271
Calculation of flows in subsonic and transonic portions of circular nozzles
[NASA-TT-F-14847] 11 p1270 N73-20308
Hot-wire anemometer measurements of turbulence and shear stress in circular tube flow
[KFK-1642] 12 p1392 N73-21286
Equations of motion for studying convection transport processes in strongly curved tubes
13 p1509 N73-22227
Steady laminar flow of viscous fluid in circular tube entrance
22 p2650 N73-31232
Influence of periodic oscillations of mean flow on mean and turbulent structure of fully developed air flow in smooth circular pipe
24 p2902 N73-33161
Continuity and Navier-Stokes equations for analyzing viscous flow heat transfer in curved tubes
24 p2902 N73-33162
Cooling of 60 to 400 cm length circular tubes with superfluid helium
[KFK-1786] 24 p2992 N73-33910

CIRCULATION
NT ATMOSPHERIC CIRCULATION
NT BLOOD CIRCULATION
NT BRAIN CIRCULATION
NT CARBOXYHEMOGLOBIN
NT ISCHEMIA
NT PERIPHERAL CIRCULATION
NT PULMONARY CIRCULATION
NT WATER CIRCULATION
Recirculation flow velocities and temperatures of VTOL lift engines
[DLR-FB-72-50] 02 p0223 N73-11806
Model for prediction of pressure within recirculation bubble of attached jet
13 p1507 N73-22216

CIRCULATORS [PHASE SHIFT CIRCUITS]
Design of high power air cooled microwave S band junction circulator using YIG rod and boron nitride transformers
[AD-751743] 07 p0762 N73-16194
Strip transmission line circulators using ferrites, noting new densification method for polycrystalline ferrimagnetic materials
[REPT-8.422] 12 p1384 N73-21222
Wideband SHF ferrite microelectronics
19 p2236 N73-28025

CIRCULATORY SYSTEM
NT ARTERIES
NT GLOMERULUS
NT VASCULAR SYSTEM
Acoustic-optical imaging techniques for detecting bubble formation in circulatory system during decompression
[AD-749087] 04 p0424 N73-13457
Pathogenesis of some respiratory and circulatory reactions accompanying drop in barometric pressure
07 p0743 N73-16047

CIRRUS CLOUDS
Application of ERTS-1 multispectral scanner data for detecting thin cirrus and clear air turbulence
[PAPER-E14B] 19 p2270 N73-28279

CITIES
Evaporation and vertical transfer of water vapor in urban areas
[NLL-M-20842-[5828.4F]] 05 p0570 N73-14625
Propagation model for V/STOL aircraft noise in urban area
[PB-211953] 05 p0581 N73-14729
Diurnal and annual variations in intensity of urban heat island in Austin, Texas
[REPT-34] 08 p0938 N73-17679
Influence of urban and suburban area on wind and temperature profiles at Austin, Texas
[REPT-33] 08 p0938 N73-17680
Investigation of urban heat island phenomena in Austin, Texas, using two-dimensional, time-dependent, earth atmosphere mathematical model
[REPT-32] 08 p0938 N73-17681
Utilization of ERTS-1 imagery for mapping extent of Pleistocene glaciation and delineation of small urban areas in Wyoming
[E73-10425] 11 p1280 N73-20386
Census cities experiment in detection of urban change and land use
[E73-10490] 12 p1397 N73-21326
Census cities experiment in detection of urban development and land use from ERTS-1 imagery
[E73-10538] 13 p1518 N73-22302
Pilot program for transfer of aerospace technology to city management
[NASA-CR-131918] 14 p1724 N73-23992
Location of archeological village sites in Alaska from ERTS-1 imagery
[E73-10638] 15 p1776 N73-24397
Cartographic evaluation of ERTS-1 imagery for area of Bristol, England to show natural and man-made features
[E73-10739] 17 p2021 N73-26345
Inadvertent modification of cloud formation and weather by St. Louis area - Project Metromex 1
[PB-218678/1] 18 p2173 N73-27549
Validation of calibration procedure used with climatological models of multiple-source urban air pollution
[PB-218716/9] 18 p2173 N73-27553
Application of ERTS-1 and U-2 photography to study of urban land use in Pennsylvania
[PAPER-L17] 19 p2275 N73-28312
Seasonal variations of vegetation, circulation patterns in Lake Pontchartrain, and urban neighborhood quality in Louisiana from ERTS-1 imagery
[E73-10838] 19 p2290 N73-28416
Influence of image position on urban place detection in ERTS-1 imagery of Kansas and Missouri
[E73-10971] 21 p2533 N73-30312
Detection of urban street patterns in ERTS-1 imagery of Lincoln, Nebraska
[E73-10976] 21 p2534 N73-30315
Two dimensional time dependent numerical simulation of atmospheric flow over urban area
24 p2911 N73-33235
Skylab photography of recreational land and urban resources in Oakland County, Michigan
[E73-11150] 24 p2919 N73-33304

CITRUS TREES
Detection of citrus tree anomalies by remote sensing with infrared color aerial photography
07 p0785 N73-16384
Early detection of insect infestations and density/distribution of host citrus trees along Rio Grande River in Texas
[E73-11073] 23 p2782 N73-32248
Early detection of insect infestations and density/distribution of host citrus trees in Texas
[E73-11074] 23 p2782 N73-32249
Detection of insect infestations and density/distribution of host citrus trees in Texas
[E73-11075] 23 p2782 N73-32250
Detection of insect infestations and density/distribution of host citrus trees in Texas
[E73-11077] 23 p2782 N73-32252

CIVIL AVIATION
NT YAK 40 AIRCRAFT
Selected aircraft accident reports for civil aviation in 1971
[NTSB-BA-72-3] 03 p0251 N73-12034
Compilation and analysis of selected US civil aviation accidents for calendar year 1971
[NTSB-BA-72-4] 04 p0371 N73-13017
Analysis of flight plans submitted at flight service stations for IFR and VFR flight clearances during calendar year 1971
[AD-748901] 04 p0447 N73-13652
Contributions of military technology, research, and development to civil aviation programs - Vol. 1
[NASA-CR-129572] 04 p0487 N73-13982
Military technology, research, and development contributions to civil aviation programs - Vol. 2
[NASA-CR-129573] 04 p0487 N73-13983
Identification of human factors research projects in support of civil aviation for accomplishment by NASA research centers
05 p0493 N73-14015
Compilation of selected aircraft accident reports for US Civil Aviation operations during calendar year 1970 - Issue 5
[PB-211158] 05 p0497 N73-14047
English, Spanish, and French definitions for international civil aviation terminology
[DOC-8800-VOL-2] 06 p0616 N73-14997
Bibliography of aircraft accident reports for US civil aviation operations during calendar year 1971
[NTSB-BA-72-6] 07 p0738 N73-16001
Bibliography of aircraft accident reports for US civil aviation operations during calendar year 1971
[NTSB-BA-72-7] 07 p0738 N73-16002
Conference on preventive medical and environmental control measures for NASA and aviation industry personnel management
[NASA-TM-X-69073] 08 p0873 N73-17064
Technical evaluation of cartography for use in civil air navigation map displays to determine information elements required to operate in 1975 to 1980 airspace - Vol. 1
[FAA-RD-72-129-VOL-1] 10 p1155 N73-19393
Evaluation of cartographic information for use in civil air navigation map displays to determine information elements required to operate in 1975 to 1980 airspace - Vol. 2
[FAA-RD-72-129-VOL-2] 10 p1155 N73-19394
Analysis of general aviation activities in Germany and recommendations for flight control procedures to reduce aircraft accident hazards
10 p1183 N73-19626
Analysis of problems in air traffic control caused by expansion of commercial and civil aviation in Germany and proposed actions for improved safety and efficiency
10 p1183 N73-19627
Requirements for air traffic control in German air operations and recommendations for improved air traffic control procedures
10 p1183 N73-19628
Statistical anlaysis of aircraft accidents occurring in US civil aviation during calendar year 1971
[NTSB-BA-73-1] 11 p1234 N73-20015
US civil airmen statistics
[AD-754271] 11 p1251 N73-20153
Drug screening data for civil aviation personnel obtained by urinalyses
12 p1369 N73-21104
Long range operational factors affecting commercial aviation industry
13 p1472 N73-21917
Scenario forecasting of likely air passenger trends to 1976 over North Atlantic routes
[REPT-72-02326] 13 p1472 N73-21918
Survey of passengers flying from Dulles Airport, Virginia during one year period to obtain cross section of typical passengers and destinations
13 p1473 N73-21925
Synopsis of factors contributing to airport congestion and flight delays
[REPT-73-00315] 13 p1505 N73-22200
Profiles of scheduled air carrier airport operations for top 100 airports in U.S.A.
[REPT-73-00328] 13 p1506 N73-22207
Airport planning recommendations and procedures for San Francisco Bay Area
[REPT-73-00316] 13 p1506 N73-22208
Effective land use of airport-incompatible areas through conversion planning from residential to compatible zones
[FAA-EQ-72-1] 13 p1594 N73-22926
Analysis of aircraft accidents occurring in US Civil Aviation operations during calendar year 1972
[NTSB-APA-73-1] 14 p1601 N73-22980
Aircraft accident reports of US civil aviation accidents occurring during calendar year 1972
[NTSB-BA-73-2] 15 p1734 N73-24064
FAA communications system description for 1973
[FAA-RD-73-36] 15 p1750 N73-24186
Systems analysis of civil airport surface traffic control
[FAA-ED-08-1] 15 p1808 N73-24655
Aircraft accidents involving US civil aviation operations during calendar year 1972 - Vol. 2
[NTSB-BA-73-3] 16 p1860 N73-25064
Aircraft accidents involving US civil aviation operations in calendar year 1971
[PB-214412/9] 16 p1862 N73-25078
Definition and evaluation of three basic alternative national aviation systems based on forecasted increases in aviation demands
[PB-215533/1] 16 p1862 N73-25081
Air or inertial data addition to onboard navigation system for improved air traffic control
16 p1940 N73-25699
Feasibility analysis for computer-based data communications and/or processing facilities at civil airport
[RAE-TR-72133] 16 p1941 N73-25711
Shortcomings in Government organization for civil aviation
[PB-215426/8] 16 p1977 N73-25994
Reports of aircraft accidents occurring in US civil aviation operations during calendar year 1972 - Issue 3
[NTSB-BA-73-4] 17 p1982 N73-26020
Program definition study for improvement of short haul air transportation facilities - Vol. 1
[FAA-QS-73-1-VOL-1] 17 p1983 N73-26025
Statistical analysis of aircraft accidents and incidents occurring to US civil and commercial aircraft during calender year 1971 - Supplemental Issue
[NTSB-BA-73-5] 17 p1983 N73-26028
Design of aircraft for high reliability and low maintenance costs and maintenance procedures for maximum efficiency
17 p1983 N73-26032
Statistical analysis of aircraft accidents occurring in US civil aviation operations during calendar year 1972 - Issue 4
[NTSB-BA-73-6] 18 p2105 N73-27024
Marketing survey to determine acceptance and utilization of STOL aircraft for short-haul air transportation system - Vol. 4
[NASA-CR-114609] 19 p2219 N73-27901

Statistical analysis of Civil Aviation midair collisions occurring during period January 1964 to December 1971
[MTR-6334] 22 p2614 N73-30946
Statistical analysis of aircraft accidents occurring in US Civil Aviation during calenadar year 1972 - Issue 5
[NTSB-BA-73-7] 23 p2741 N73-31942
International civil aviation organization for air traffic forecasting and airport development
23 p2861 N73-32865
Application of airships to air transportation, noting cost effectiveness
24 p2879 N73-32991
Acquisition of conditions of icing on modern civil transport aircraft from flight data
24 p2946 N73-33528

CL-595 HELICOPTER
U XH-51 HELICOPTER

CL-84 AIRCRAFT
Flight test and evaluation of CL-84 tilt-wing V/STOL aircraft with application to specific military roles
18 p2103 N73-27007

CLADDING
Influence of neutron irradiation on damage to fuel cladding and reactor structural materials
[HEDL-SA-317] 03 p0332 N73-12709
Cladding materials research, including Pt-Rh-W alloy and Ir properties and Ir purification
[ORNL-TM-3865] 04 p0453 N73-13696
Heat transfer coefficient between fuel and cladding as parameter for calculating fuel rod temperature
[NLL-WINDSCALE-497-[9091.9F]]
05 p0578 N73-14706
Effect of high pressure shock waves on mechanical properties of bimetals produced by different cladding techniques
[AD-750958] 06 p0677 N73-15513
Copper brass bimetal cladding layers on steel strips for manufacturing elastic current conducting springs
[NLL-M-21498-[5828.4F]] 06 p0682 N73-15554
Relations between fuel swelling and clad strain for cylindrical uranium dioxide pins with niobium zirconium cladding
[NASA-TM-X-2717] 07 p0819 N73-16638
Hydrogen embrittlement of tantalum alloy cladding for uranium mononitride nuclear fuel pins at high temperatures
[NASA-TM-X-2732] 09 p1063 N73-18675
Results of uranium dioxide-tungsten irradiation test and post-test examination
[NASA-TM-X-2709] 09 p1063 N73-18677
Irradiation damage to tungsten rhenium and tungsten rhenium hafnium claddings of uranium nitride fuel pins
[ORNL-TM-3895] 10 p1186 N73-19653
Role of cesium in fuel-cladding interaction of austenitic stainless steels mixed with oxide fuels
[EUR-4893] 10 p1187 N73-19657
Computer program for modeling UO2 cladding strain resulting from irradiation
[NASA-TM-X-68281] 20 p2453 N73-29715

CLARK Y AIRFOIL
U AIRFOIL PROFILES

CLASSICAL MECHANICS
NT CELESTIAL MECHANICS
NT MINIMUM VARIANCE ORBIT DETERMINATION
NT ORBITAL MECHANICS
Phase-space theory for electron excitation in slow atomic collisions
[PUBL-73-4] 17 p2064 N73-26699

CLASSIFICATIONS
NT INDEXES [DOCUMENTATION]
Classification and pattern recognition of short lived events using ERTS-1 imagery
[E72-10183] 01 p0045 N73-10362
Circulation pattern over British Isles and system classification from 1861 to 1971
[MET-O-845B] 02 p0204 N73-11648
Procedure for defining spectrally separable classes for soil survey research
[NASA-CR-130031] 07 p0791 N73-16434
Classification of landforms for land use and regional planning using aerial photographic interpretation
[PB-212774] 08 p0918 N73-17525
Classification of plasma instability including stable and unstable disturbances
[TRITA-EPP-72-23] 09 p1070 N73-18734
Identification and classification of Iowa crop lands using ERTS-1 imagery and aerial photography
[E73-10343] 10 p1148 N73-19342
Classification of radioprotectors for radiation sickness prevention effects
11 p1240 N73-20065
Classification of meteoroids according to density and beginning height, and meteor stream search
[NASA-CR-131177] 11 p1337 N73-20851
Classification of meteoroids according to density and beginning height
[CONTRIB-14] 11 p1337 N73-20852
Meteoroid stream search among photographic meteors
[CONTRIB-15] 11 p1337 N73-20853
Automatic land use classification based on optical density and shapes from ERTS-1 imagery
[E73-10816] 18 p2140 N73-27291
Algorithm for classifying land use categories of ERTS-1 data by textural features
[PAPER-I16] 19 p2279 N73-28337
Identification and classification of clouds from ERTS-1 photography
[E73-10977] 21 p2534 N73-30316
Minimum distance classification based on multispectral scanner data using density estimators and Kullback-Leibler numbers as distance measures
[NASA-CR-133796] 21 p2566 N73-30569
Use of spatial information for improving classification accuracy of remotely sensed data
[NASA-CR-133988] 22 p2637 N73-31130
Radar detection of underground objects using polarization for target classification
[AD-763155] 23 p2758 N73-32069
Minimizing probability of incorrectory classifying spectral observations from multispectral band scanners
[NASA-CR-134058] 23 p2812 N73-32486
Infrared quantitative spectral star classification system
23 p2836 N73-32665

CLASSIFIERS
Sample classification accuracy of minimum distance and maximum likelihood classifiers and parametric and nonparametric classifiers in remote sensing
[NASA-CR-130030] 07 p0799 N73-16489
Algorithm for adjusting linear and nonlinear classifiers
[BMVG-FBWT-72-5] 09 p1057 N73-18623

CLASSIFYING
Depths of reflection zone characteristics for classifying ultrasonic echoes in weld testing
[NLL-CE-TRANS-5993-[9022.09]]
11 p1324 N73-20742

CLAYS
Measurements of thermal conductivity in boulder clay and effects of soil moisture conductivity
[NASA-TT-F-14664] 07 p0793 N73-16446
Hydroponic cultivation of plants on clay filters from human mineralized feces
10 p1117 N73-19110

CLEAN ROOMS
Environmentally controlled suit for working in sterile chamber
[NASA-CASE-LAR-10076-1] 11 p1249 N73-20137
Design of anesthetic flow valve canister system for exhaust gas absorption and laminar ventilation system for operating rooms
12 p1373 N73-21141

CLEANERS
NT AIR FILTERS
Sanitizing agents for cleansing and decontaminating spacecraft environment
[NASA-CR-128591] 01 p0019 N73-10149

CLEANING
Cleaning processes and postcleaning inspection procedures for meeting oxygen system cleaning requirements
[NASA-SP-3072] 06 p0634 N73-15155
Procedures for cleaning materials and producing corrosion resistant epoxy plastics
[AD-752039] 08 p0936 N73-17664
Dermatological testing of personal hygiene cleansing agents and laundry detergents for possible use in Skylab Program
[NASA-CR-128880] 11 p1250 N73-20143
Laboratory demonstration model of active cleaning technique device
[NASA-CR-124335] 21 p2582 N73-30696

CLEAR AIR TURBULENCE
Inflight incident involving Boeing 747 aircraft encounter with unforecast clear air turbulence during flight from Japan to Hawaii on 12 April 1972
[NTSB-AAR-72-27] 03 p0252 N73-12038
Aircraft measurements of microscale motions and atmospheric structure associated with thin echo layers in stable stratified zones
[AD-749512] 05 p0540 N73-14393
Two dimensional eddy viscosity coefficients in atmospheric motion noting parameterization of clear air turbulence
05 p0573 N73-14658
Statistical correlations between clear air turbulence and macrosynoptic processes in troposphere and stratosphere
[AD-750514] 06 p0670 N73-15451
Abstracts on remote sensing of turbulence and waves in planetary boundary layer
[AD-751110] 07 p0816 N73-16618
Modulator/demodulator for probing and analyzing forward scatter path at 15 GHz to clear air turbulence
[AD-753090] 09 p1030 N73-18413
Remote detection and measurement of clear air turbulence using pulsed laser radar
[NASA-CASE-MFS-21244-1] 12 p1422 N73-21523
Occurrence of violent clear air turbulence near Kustanay on 27 July, 1971
13 p1552 N73-22579
Effectiveness of infrared radiometer and digital recording equipment as clear air turbulence warning system
[AD-757501] 14 p1685 N73-23677
Atmospheric mesostructure model for clear air turbulence
[AD-759787] 16 p1909 N73-25448
Instability of internal waves in stratified nonviscous jet stream
[AD-761373] 18 p2149 N73-27368
Application of ERTS-1 multispectral scanner data for detecting thin cirrus and clear air turbulence
[PAPER-E14B] 19 p2270 N73-28279
Kelvin-Helmholtz instabilities in mesoscale wind and temperature structure during clear air turbulence
[AD-763084] 20 p2413 N73-29397
Application of microwave radar for monitoring tropopause level to determine dynamic instability and turbulence generation in clear atmosphere
[NOAA-TR-ERL-243-WPL-21] 22 p2665 N73-31353
Dependence of clear air turbulence on evolution of baric field and effect on synoptic forecasting
24 p2946 N73-33526

CLEARANCES
Pilot knee ejection clearances for Canadian military aircrafts
[DCIEM-936] 23 p2741 N73-31938
Capacitive method for measuring blade tip clearance in running turbocompressors
[DLR-FB-72-40] 23 p2831 N73-32628

CLEAVAGE
Electron fractography of cleavage in metal crystals discussing crack propagation
[NLR-TR-71047-U] 02 p0187 N73-11513

CLIMATE
Interdependence of lake ice and climate in central North America
[E72-10362] 05 p0535 N73-14350
Martinique climate variations noting wind circulation, cyclones and tropical storms recorded from various weather stations and meteorological satellites
[MONO-86] 07 p0815 N73-16610
Atmospheric models for fluid dynamic and chemical impacts of supersonic aircraft on climatology
[PB-212819] 11 p1291 N73-20473
Theoretical model for studying circulation and climate of atmosphere
20 p2442 N73-29616
GARP subprograms including numerical experimentation, GATE climate, and oceanography
24 p2949 N73-33557

CLIMATOLOGY
NT MICROCLIMATOLOGY
Past, present, and projected climate, and heat budget of atmosphere and hydrosphere
[NLL-M-20071-[5828.4F]] 01 p0073 N73-10597
Monthly mean climatological statistics for surface to 5 mb pressure level over Australia - Dec. 1971
01 p0074 N73-10606
Monthly mean climatological statistics for surface to 5 mb pressure level over Australia - Aug. 1971
01 p0074 N73-10607
Statistical data of tropical cyclones in Australian Region east of 135E from November 1909 to June 1969
01 p0074 N73-10608
Monthly statistics of precipitable water over Australia in atmosphere from 400 mb to surface, determined from daily radiosonde ascents, 1958 through 1969
01 p0074 N73-10609
Macroscale fluctuations in atmospheric and oceanic variables
[AD-744976] 01 p0075 N73-10621
Methodology for determining climatological probability of aircraft icing throughout Northern Hemisphere
[AD-745098] 01 p0075 N73-10623
Global distributions of surface albedo, planetary albedo, and total precipitation - supplementary data for Dec., Jan., and Feb.
[AD-744633] 01 p0076 N73-10628
Meteorological data from radiosondes at Berlin
02 p0204 N73-11650
Monthly mean climatological statistics from surface to 5 mb level over Australia - January 1972
02 p0204 N73-11654
Reference file of local factors affecting weather at Ramey AFB, Puerto Rico
[AD-746026] 02 p0205 N73-11661
Reference file of factors affecting weather at Kelly AFB, Texas
[AD-746028] 02 p0205 N73-11662
Handbook on weather patterns over Point Mugu, California
[AD-747641] 03 p0327 N73-12672
Temperature, pressure, and related climatological data for Australia - tables for [May, 1972]
04 p0441 N73-13598
Temperature, pressure, and related climatological data for Australia - tables for [April 1972]
04 p0442 N73-13599
Experiment in climatic zoning of coast of Gulf of Riga
04 p0443 N73-13610

Satellite observation for acquisition and monitoring of planetary radiation, clouds, particles, and air pollution
[DGLR-PAPER-72-81] 04 p0444 N73-13626
Solar and terrestrial radiation regimes over arctic ice packs
[AD-748214] 04 p0467 N73-13808
Potential of data on radioisotopes in atmosphere for determining climatological parameters
[NLL-M-9221-[5828.4F]] 05 p0529 N73-14305
Effects of changes in ocean currents and motion on climatology
[NLL-M-22797-[5828.4F]] 05 p0529 N73-14307
Climate changes caused by human activities and need for international studies
[NLL-M-22770-[5828.4F]] 05 p0570 N73-14628
Meteorology and climatology of Northern Hemisphere during calendar year 1972 - Vol. 128 No. 4
05 p0570 N73-14631
Stratospheric weather maps for Northern Hemisphere based on rawinsonde and rocketsonde observations - Vol. 124, No. 3
05 p0570 N73-14632
Annual report of meteorological observations conducted by weather stations in Switzerland during calendar year 1970
05 p0572 N73-14646
Nearly instantaneous precipitation rates measured in several locations of world to determine point frequencies of occurrence
[AD-749878] 05 p0575 N73-14681
Graphical summary of weather and sea conditions along California coast
[AD-749781] 05 p0576 N73-14690
European climatological maps constructed from ESSA 8 satellite photographic observations during first quarter of 1972
06 p0691 N73-15630
Synoptic meteorological weather charts for Northern Hemisphere obtained at ground level, 500 mb, and 850 mb during July, 1972, at Berlin
06 p0692 N73-15635
Mesoscale interaction models for effects of orography on momentum and energy transfer in atmosphere and interaction of solar radiation with earth atmosphere
[AD-750727] 06 p0694 N73-15657
Application of remote sensing techniques to study of climatology of urban-regional systems
07 p0786 N73-16394
Classification, description, and statistical treatment of European large-scale weather patterns
[NLL-M-9145-[5828.4F]] 07 p0814 N73-16600
Aerological climatology based on IRMB weather station data recorded between 1951 and 1965
[PUBL-SER-A-77] 07 p0815 N73-16609
Climatic changes resulting from upper atmosphere perturbation by supersonic aircraft exhausts
[PB-212427] 07 p0816 N73-16612
Annual climatological measurements of evaporation in Panama Canal Zone
[AD-751782] 07 p0817 N73-16621
Analysis of heat supply requirements and heating availability in geographical areas of USSR
[JPRS-58114] 08 p0917 N73-17513
Climatological summaries for Denmark and Faroe Islands for 1967
[ISBN-87-7478-060-3] 08 p0937 N73-17675
Characteristics of global atmospheric field at sea level
08 p0938 N73-17683
Survey of climatological conditions in Martinique
[MN-MONO-86] 09 p1060 N73-18644
Articles on meteorology and hydrology
[JPRS-58133] 09 p1060 N73-18646
Revision of tropical cyclone climatology by satellite data for northern Pacific Ocean
[AD-753584] 09 p1061 N73-18658
Meteorological and climatological radiosonde observations
10 p1180 N73-19601
Statistical analysis of rainfall frequency in central Valais
[REPT-28] 10 p1181 N73-19609
Engineering analysis of tornado structures and occurrence climatology
[SC-M-72-0688] 10 p1182 N73-19617
Fluctuations of zonal atmospheric circulation in Northern Hemisphere in first half of century
[NLL-M-22855-[5828.4F]] 11 p1274 N73-20337
Influence on volcanic eruption exerted by particular weather and climatic situations
[NLL-M-22864-[5828.4F]] 11 p1313 N73-20652
Synoptic-climatological method for long range forecast of heavy rain for European USSR
[NLL-M-22865-[5828.4F]] 11 p1313 N73-20653
History and future of scientific attempts to control meteorological processes and climatology
[NLL-M-22821-[5828.4F]] 12 p1420 N73-21506
USSR research projects in subjects of microclimate, agricultural meteorology, weather forecasting, climate control, and hydrological forecasting
[JPRS-58483] 12 p1420 N73-21510
Computer simulation of global atmospheric circulation in climatological research
[P-4933] 12 p1421 N73-21520
Stratospheric photochemical reactions of ozone in relation to climatology and supersonic transport pollution
[NOAA-TM-NESS-47] 12 p1422 N73-21526
Annual, monthly, and hourly rainfall for Hilo, Hawaii
[UHMET-72-03] 12 p1422 N73-21527
Long term climatological study of meteorological parameters for Northern Hemisphere
13 p1551 N73-22565
Optimum utilization of long range forecasts and climatology in making economic decisions
13 p1552 N73-22573
Time-space analysis of asynchronous meteorological data
13 p1552 N73-22575
Synoptic climatological studies of precipitation in Plateau states from 850, 700, and 500 mb lows during spring
[NOAA-TM-NWS-TDL-48] 13 p1553 N73-22585
Italian thermal conditions affecting acceleration tolerance and psychomotor performance of flying personnel
14 p1612 N73-23068
Man induced changes in earth climate by environment pollution and heat production
[PB-213676/2] 14 p1613 N73-23074
Modification of Japan climate by environmental pollution
[AD-757487] 14 p1686 N73-23678
Tables of climatological conditions for selected areas of Virginia
[PB-213881/3] 14 p1686 N73-23681
Tree ring chronology for constructing paleoclimatology of North America and Europe
[AD-757486] 14 p1686 N73-23682
Determining past global climate by determining past trends in surface temperature of earth
[AD-757225] 14 p1686 N73-23683
Integrated analysis of past and present climates of Northern Cumberland and Peninsula
[AD-757270] 15 p1783 N73-24457
Circulation model for feasibility of modifying earth surface climate at middle and high northern latitudes
[AD-757795] 15 p1807 N73-24641
Chemical kinetics and atmospheric dynamics data base for digital modeling of climatological aircraft exhaust effects
[PB-214100/0] 16 p1908 N73-25441
Analysis of meteorological parameters and climatological effects leading to heavy icing of ships
[NLL-M-22981-[5828.4F]] 16 p1935 N73-25657
Effect of general atmospheric circulation of large scale and persistent weather features of Atlantic-Eurasian sector of hemisphere in 1968 to 1970
[NLL-M-22853-[5828.4F]] 16 p1936 N73-25663
TAXIR information retrieval system for analyzing climatic conditions on east slope of Colorado front range
[PB-214341/0] 16 p1939 N73-25688
Handbook on climatology of USSR
[AD-759244] 16 p1939 N73-25694
ERTS-1 imagery of geological, climatological, and volcanic activities in Iceland
[E73-10713] 17 p2018 N73-26320
Meteorological tables and charts on Berlin temperature
17 p2057 N73-26635
Worldwide airfield climatic data for Eastern Europe and USSR - Part I
[AD-759794] 17 p2057 N73-26640
Worldwide airfield climatic data for Eastern Europe, and USSR - Part 2
[AD-759795] 17 p2057 N73-26641
Catalogue indexes to local weather forecasts
[AD-760091] 17 p2058 N73-26648
Frequency and duration of extreme surface temperatures and effects on missile systems development in hot-dry climates
[AD-759899] 17 p2059 N73-26652
Bibliography of articles concerning water balance of monsoon Asia
[CLIMATOL-NOTES-11] 18 p2171 N73-27531
Evaluation of radiometric computations in infrared window and water vapor absorption band regions based on 4-D atmospheric models
[NASA-CR-129007] 18 p2172 N73-27546
Analysis of ERTS-1 data for studies of hydrogeology, geomorphology, and paleoclimatology in Bolivia, Argentina, Chile, and Peru
[PAPER-W1] 19 p2270 N73-28281
Analysis of cause of nonlinear relationship between solar constant and solar activity to show possible climatic consequences
[NLL-M-23053-[5828.4F]] 20 p2390 N73-29201
Effects of solar activity on present day changes of climate
[NLL-M-23005-[5828.4F]]. 20 p2442 N73-29612
Daily and monthly weather charts for Northern Hemisphere and Berlin, Germany for February, 1973
20 p2442 N73-29614
Analysis of long term weather variations, climate changes, and atmospheric circulation
20 p2444 N73-29634
Hydrological and meteorological forecasting and climate control
[JPRS-59052] 20 p2446 N73-29647
Surface climatological data for Australia - October 1972
20 p2449 N73-29676
Surface climatological data for Australia - September 1972
20 p2449 N73-29677
Monthly mean climatological statistics for surface to 5 mb pressure level over Australia - October 1972
20 p2449 N73-29678
Monthly mean climatological statistics for surface to 5 mb pressure level over Australia - Dec. 1972
20 p2449 N73-29679
Monthly mean climatological statistics for surface to 5 mb pressure level over Australia - September 1972
20 p2449 N73-29680
Monthly mean climatological statistics for surface to 5 mb pressure level over Australia - November 1972
20 p2449 N73-29681
Surface climatological data for Australia - November 1972
20 p2449 N73-29682
Surface climatological data for Australia Dec. 1972
20 p2449 N73-29684
Surface climatological data for Australia - Jan. 1973
20 p2449 N73-29685
Improved numerical models of mesoscale and small scale effects of atmospheric motion which influence global weather
[AD-762584] 20 p2451 N73-29698
Solar activity effects on terrestrial climate
[AD-762227] 20 p2468 N73-29827
Photographic recordings and meteorological data obtained by Environmental Research Satellite during January 1973
20 p2475 N73-29879
Photographic recordings and meteorological data obtained by Environmental Research Satellite During June 1973
20 p2475 N73-29880
Statistical procedures for hydrometeorological and weather forecasting and climate control
[JPRS-59580] 21 p2572 N73-30612
Surface climatological data for Australia - August 1972
21 p2574 N73-30626
Daily hemispheric mosaics by satellite for use in selection of climatological data
22 p2693 N73-31576
Guide to worldwide standard weather and climatological summaries
[PB-221354/4] 22 p2696 N73-31596
Bibliography of Italian climatology
[IFA-STR-22] 23 p2814 N73-32499
Seasonal climatology of Chilean sea coast
[AD-765355] 23 p2815 N73-32506
Agroclimatology study of highlands of eastern Africa
[WMO-339] 24 p2886 N73-33045
Deficiencies in development of hydrometeorological science
24 p2947 N73-33536
Methods for measuring and elaborating atmospheric phenomena and meteorological yearbook
[EUR-4943] 24 p2949 N73-33554
Meteorological parameter tables for Belgian weather stations, Apr. 1973
24 p2950 N73-33561

**CLIMBING FLIGHT**

Curves for determining climb performance of aircraft
[ESDU-RJ1/2-AMEND-A] 02 p0124 N73-11011
Low speed pull-up maneuvers for slender wing transport aircraft with stability and control augmentation
[ARC-CP-1231] 04 p0369 N73-13004
Development of methods for predicting aircraft flight maneuver and climb performance to show effects of excess power and load factor
15 p1732 N73-24045
Numerical analysis of minimum time climbing procedure and minimum fuel climbing procedure for typical subsonic aircraft
15 p1733 N73-24052

**CLINICAL MEDICINE**

Use of Ringers lactate solution in pre- and postoperative fluid therapy
[NASA-TT-F-14600] 01 p0009 N73-10071
Tracking tests as quantitative measurements of neuromuscular functions in clinical applications
01 p0015 N73-10118
Microelectrophoresis of human erthyrocytes as diagnostic tool in gynecology and obstetrics
[NASA-TT-F-14587] 04 p0378 N73-13077
Argon laser radiation damage to retina of diabetic and nondiabetic patients
[AD-747058] 04 p0381 N73-13099
Use of space technology to solve medical problems and improve medical equipment
04 p0472 N73-13848

Blood lipid diagnostic and therapeutic measures to prevent heart disease in humans
08 p0874 N73-17073
Risk scoring system for identifying subjects with high risk to coronary heart disease
08 p0874 N73-17080
Clinical analysis of relationship between VPB and mortality rate in patient with acute myocardial infractions
08 p0875 N73-17083
Automated medical record system for identifying and managing medical problems for Navy
08 p0875 N73-17087
Clinical practice and problems associated with urine analysis
08 p0875 N73-17089
Survey of industrial hygiene and safety in Air Forces operations
[AD-751897] 08 p0880 N73-17126
Luciferase ATP assay procedure for determining bacterial infections in urinary tract
[NASA-CR-130797] 09 p0992 N73-18096
Influence of Pervitin in decreasing gas bubbles in blood during decompression
[DLR-FB-72-66] 09 p0994 N73-18117
Studies of biomedical applications of NASA technology
[NASA-CR-130809] 09 p0997 N73-18135
Clinical procedures for selecting pilot personnel based on predisposition to motion sickness
12 p1367 N73-21094
Tracking tasks for clinical evaluation of human movement disorders
[NASA-CR-132275] 18 p2111 N73-27069
Heat pipe production of high purity radioiodine for thyroid measurements
[NASA-CASE-LEW-11390-3] 19 p2248 N73-28128
Use of therapeutic exercise for treatment of functional vascular disorders and occlusive lesions of arteries and veins
[NASA-TT-F-15043] 20 p2368 N73-29045
Hygienic importance and toxicity of manganese oxides, and clinical medicine of chronic manganese exposure
[NASA-TT-F-15000] 21 p2501 N73-30067
Spectrophotometric procedures applied to medical services in clinical chemistry laboratories and analysis of sources of error in diagnoses
[PAPER-76A5-736] 21 p2545 N73-30405
Water load tests for determining hydration status and adrenal and kidney functions during post flight period
[NASA-TT-F-15091] 22 p2620 N73-30998
Surgical liquification pump for removing macerated tissue from eye
[NASA-CASE-LEW-12051-1] 23 p2749 N73-32000
Prototype automatic sleep analyzer for clinical applications
[NASA-CR-134049] 23 p2793 N73-32346

**CLOCKS**
NT ATOMIC CLOCKS
NT CHRONOMETERS
Development of procedure for predicting time interval of single clock and matrix equation for optimum weighting coefficients
[NBS-TN-626] 08 p0923 N73-17565
Fault-tolerant clock apparatus for use in digital logic systems which maintains output pulses during component failure
[NASA-CASE-MSC-12531-1] 13 p1528 N73-22386
Standard digital data clock-rate generator with programmable digital phase shift for data transmission from communication satellites
[AD-764049] 22 p2635 N73-31117

**CLOSE PACKED LATTICES**
Coincidence structural unit models for grain boundaries in HCP metals
[AD-756884] 13 p1545 N73-22520

**CLOSED BASINS**
U STRUCTURAL BASINS

**CLOSED CIRCUIT TELEVISION**
Development of spacecraft docking system for optical alignment of spacecraft using television camera system
[NASA-CASE-MSC-12559-1] 17 p2086 N73-26879

**CLOSED CYCLES**
Performance of closed cycle MHD generators
[AD-747661] 03 p0255 N73-12068
Closed cycle magnetohydrodynamics - conference paper abstracts
[TH-72-E-29] 04 p0453 N73-13703
Bibliography of literature on phase locked loops
[NASA-CR-133225] 17 p2004 N73-26202
Analysis of operation of single stage, high pressure centrifugal compressor during closed loop flow of various gases
[AD-761608] 19 p2331 N73-28750
Digital phase-locked loop for accumulator output signal phase-locked to input signal
[NASA-CASE-GSC-11623-1] 22 p2646 N73-31202
Effect of FeF2 addition on Hastelloy N compatibility with LiF-BeF2-UF in low temperature convection loop system
[ORNL-TM-4188] 24 p2936 N73-33444

**CLOSED ECOLOGICAL SYSTEMS**
Recorded observations of crew member activities during Tektite 2 underwater habitability study
[NASA-CR-130034] 07 p0750 N73-16094
Habitability factors during long-term space and undersea missions in confined habitats
[NASA-CR-130537] 08 p0879 N73-17123
Stress effects on element balance in human waste for life support recycling system
10 p1117 N73-19107
Cosmonaut adaptation to dehydrated food products and effects on human waste cycle
10 p1118 N73-19113
Spacecraft with artificial gravity and earthlike atmosphere
[NASA-CASE-LEW-11101-1] 23 p2847 N73-32750

**CLOSED FAULTS**
U GEOLOGICAL FAULTS

**CLOSED FOLDS**
U FOLDS [GEOLOGY]

**CLOSED LOOP SYSTEMS**
U FEEDBACK CONTROL

**CLOSURES**
Ultrasonic testing of closures for rocket HEAT 66 mm L1A2
[TM-52] 20 p2423 N73-29462

**CLOTH**
U FABRICS

**CLOTHING**
NT COTTON FIBERS
NT GLOVES
NT GOGGLES
NT HELMETS
NT PRESSURE SUITS
NT PROTECTIVE CLOTHING
NT SPACE SUITS
Thermal resistance of clothing noting radiative body heat transfer, air layers, and clothing thickness
[DRIC-TRANS-2920] 03 p0261 N73-12117
Numerical analysis of thermal resistance of air layers in air permeable clothing
[NLL-DRIC-TRANS-2717-[3623.66]]
05 p0502 N73-14089
Examination of physical processes governing heat transfer through air-penetrable clothing in wind
[DRIC-TRANS-2921] 06 p0636 N73-15166
Spectroscopic studies of luminescence emitted by dyes irradiated by lasers
[AD-750377] 06 p0680 N73-15535

**CLOUD CHAMBERS**
Supersaturation and condensation in cloud chamber expansion
[AD-745348] 01 p0058 N73-10478
Streamer chamber for visual observation of proton-proton interactions in accelerator
[BNL-17273] 10 p1138 N73-19271
Cloud chamber study of cosmic ray air shower multicore structure
15 p1827 N73-24810
Time resolved measurements of droplet growth in Wilson expansion cloud chamber
24 p2901 N73-33158

**CLOUD COVER**
Night cloud cover and meteorological parameter variations determined at La Silla, Chile, in 1970
[ESO-BULL-9] 01 p0075 N73-10620
Physical-statistical inference model using satellite infrared data for estimating cloud distribution from empirical histographs of equivalent black body temperatures
04 p0441 N73-13597
Synoptic cloud cover observations for computing probability of clear lines of sight through atmosphere to ground
[P-4883] 04 p0444 N73-13620
Theoretical statistical distribution model representing worldwide cloud cover
[NASA-TM-X-64714] 05 p0573 N73-14653
Cloud cover maps for North America and western North Atlantic for August, 1972
[AD-749128] 05 p0575 N73-14678
Using photos exposed through two spherical mirrors to obtain cloud base heights
[NASA-TT-F-14668] 09 p1060 N73-18643
Continuous particle replicator for cloud drops and ice crystals onboard pressurized aircraft
[AD-753091] 09 p1061 N73-18655
Angular distribution of outgoing shortwave radiation intensity in atmosphere with continuous cloud cover
[AD-753975] 10 p1157 N73-19417
Application of photointerpretation and photogrammetry to analysis of cloud cover type and motion
[NASA-TM-X-64710] 12 p1404 N73-21385
Model of symmetric large scale whirl using equations of motion as applied to satellite data
[AD-756096] 13 p1554 N73-22596
ESSA 8 photographic observations of European cloud cover for third quarter of 1972
[QR-3-PT-3] 15 p1804 N73-24623
Automatic methods for measuring cloud motions from digital brightness data from geosynchronous satellites
[AD-757814] 15 p1806 N73-24640
Development of methods for improving forecasting of precipitation, surface pressure, temperature, and dew point
[NLL-M-22980-[5828.4F]] 16 p1935 N73-25658
Techniques for improving accuracy of numerical 24-hour cloud cover forecasts in sparse data areas using satellite data
[AD-759986] 17 p2058 N73-26644
Scanning radiometer imagery of Northern Hemisphere cloud cover obtained during May, 1973 by enivornmental satellite
18 p2171 N73-27535
Calculation of cloud cover from vertical velocity data supplied by meteorological satellites
[AD-761545] 19 p2317 N73-28634
Radiation regime of forest vegetation under plant cover and open areas under various weather conditions
20 p2405 N73-29329
Radiation equilibrium and interaction problems of atmospheric circulation
20 p2443 N73-29623
Radiation equilibrium and grayness of clouds
20 p2448 N73-29665
Comparison of surface cloud cover observations and cloud cover estimates determined by satellite measurements for Southeast Asia
[AD-763098] 20 p2451 N73-29695
Effect of vertical structure of flows on cloudiness of intertropical convergence zone
[NLL-M-23045-[5828.4F]] 21 p2567 N73-30575
Sulfuric acid in Venus clouds by photolytic decomposition of hydrogen bromide
[LPL-COMMUN-171] 21 p2592 N73-30767
Specifications of infrared detector for cloud cover determination
[BMVG-FBWT-73-13] 23 p2793 N73-32349
Present status in meteorological satellites, wind observation, cloud cover, and the imagery compared with predictions made in 1962
24 p2949 N73-33552

**CLOUD GLACIATION**
Ice crystal multiplication in convective precipitation considering cloud top temperature
[PB-215626/3] 16 p1908 N73-25439
Silver iodide particle size effect on water condensation for artificial precipitation
[AD-758857] 17 p1993 N73-26114
Mariner 9 spectroscopic evidence for H2O ice clouds in Martian atmosphere
[NASA-TM-X-66289] 18 p2142 N73-27312

**CLOUD HEIGHT INDICATORS**
Comparison of rawinsonde data with baroclinic cloud motion pictures
[NOAA-TM-NESS-43] 01 p0074 N73-10611
Forecasting altitude of lower cloud boundary after time intervals of 6, 9, and 12 hours
24 p2946 N73-33524

**CLOUD PHOTOGRAPHS**
Seeding experiment effects on hurricane Ginger, Sep. 1971, analyzed from ATS 3 photographs
[SMRP-RP-106] 03 p0326 N73-12657
Processing techniques for deducing cloud motion vectors from overlapped portions of pairs of satellite
[NASA-CR-130115] 03 p0326 N73-12660
Satellite cloud photographs of BOMEX area
04 p0442 N73-13600
Estimation of average daily rainfall from satellite photographs
[NOAA-TM-NESS-44] 09 p1060 N73-18645
Tornado occurrences related to overshooting cloud-top heights as determined from ATS 3 photographs
[NASA-CR-131875] 13 p1551 N73-22567
Satellite cloud photography for predicting rainfall in Sudan
[AD-757733] 15 p1783 N73-24452
Exploration of natural landscape using TV pictures from meteorological satellites
[NASA-TT-F-14965] 17 p2025 N73-26389
Cloud cover mosaics developed from environmental satellite imagery for April, 1973
18 p2171 N73-27534

**CLOUD PHOTOGRAPHY**
Comparison of rawinsonde data with baroclinic cloud motion pictures
[NOAA-TM-NESS-43] 01 p0074 N73-10611
Data catalog for Nimbus 4 from 1 March to 30 April 1971
[NASA-TM-X-68840] 03 p0326 N73-12658
Using photos exposed through two spherical mirrors to obtain cloud base heights
[NASA-TT-F-14668] 09 p1060 N73-18643
Application of photointerpretation and photogrammetry to analysis of cloud cover type and motion
[NASA-TM-X-64710] 12 p1404 N73-21385
Stereophotography of rain clouds using panoramic rotating-lens cameras
[AD-757882] 15 p1807 N73-24642
Cloud data for November and December 1972, obtained by environmental satellite imagery
18 p2171 N73-27536
Visible infrared spin-scan radiometer system for earth and cloud cover photography by synchronous meteorological satellite
18 p2209 N73-27834

Identification and classification of clouds from ERTS-1 photography
[E73-10977] 21 p2534 N73-30316
Detection of low pressure center by viewing cloud pattern and wind direction in ERTS-1 photography
[E73-10978] 24 p2913 N73-33243
Wind estimation by photographic tracking of clouds on images from synchronous meteorological satellites
24 p2948 N73-33546

CLOUD PHYSICS
Design and development of zero-gravity atmospheric cloud physics experiment laboratory for installation in orbiting spacecraft
[NASA-CR-128998] 03 p0280 N73-12270
Vertical air gust velocities and turbulence spectral structure around and within cumulonimbus clouds
[AD-748518] 04 p0445 N73-13632
Microphysical and meteorological data on fog cycle in California valley
[AD-750086] 05 p0576 N73-14685
Condensation nuclei measurements noting counters and importance to cloud physics
07 p0859 N73-16964
Moment equations for describing evolution of droplet populations in convection clouds
10 p1180 N73-19595
Effect of ionospheric conductivity on barium ion cloud dynamics
[NASA-CR-131533] 12 p1433 N73-21610
Instrumentation to aid radar investigations of cloud and precipitation physics
[AD-755401] 13 p1555 N73-22606
Research projects conducted by Australian atmospheric physics laboratory to analyze atmospheric radiation, micrometeorology, ozone, airglow, and cloud physics
14 p1659 N73-23465
Computer programs for numerical approximation of selected meteorological parameters related to cloud physics
[AD-757623] 14 p1686 N73-23680
Analysis of improved numerical solutions to stochastic collection equation for cloud droplets
15 p1805 N73-24629
Atmospheric physics of condensation nuclei
[NLL-M-22806-[5828.4F]] 16 p1947 N73-25749
Inadvertent modification of cloud formation and weather by St. Louis area - Project Metromex I
[PB-218678/1] 18 p2173 N73-27549
Numerical analysis of barium cloud growth and striation in conducting background
[AD-761828] 19 p2317 N73-28637
Cloud physics studies using Skylab S-191 filter wheel infrared spectrometer data
[E73-10880] 20 p2394 N73-29231
Zero-gravity cloud physics laboratory for space shuttle payload planning
[NASA-CR-129002] 20 p2449 N73-29674
Meteorological radar analysis of convective cloud evolution
22 p2693 N73-31570
Analysis of aircraft measurements of long-wave radiation fluxes, water content, and temperature in presence of stratified and stratocumulus clouds
22 p2693 N73-31574
Theory of drop growth by condensation for cloud physics application
[AD-764258] 22 p2695 N73-31586
One dimensional elastic collision problem in which two approaching masses are separated by elastic particle
[AD-764514] 22 p2726 N73-31814
Application of Skylab EREP data to cloud physics investigations
[E73-11057] 23 p2780 N73-32233
Simultaneous satellite observations of infrared and reflected energy measured to infer convective activity of tropical cloud clusters
[NOAA-TM-NESS-50] 23 p2814 N73-32498

CLOUD SEEDING
Seeding experiment effects on hurricane Ginger, Sep. 1971, analyzed from ATS 3 photographs
[SMRP-RP-106] 03 p0326 N73-12657
Effectiveness of airborne chemical seeding techniques for airport fog dispersal
[NETL-72-005-1] 04 p0444 N73-13622
Bibliography on chemical contaminants released in upper atmosphere
[WRE-TM-498[WR/D]-PT-2] 06 p0667 N73-15422
Life cycles of natural and hygroscopically seeded warm tropical cumuli
[AD-750889] 06 p0695 N73-15662
Monitoring weather conditions for cloud seeding control
[E73-10059] 07 p0778 N73-16321
Use of hygroscopic materials and ionic surfactants as warm fog for dispersants
[AD-753635] 07 p0817 N73-16622
DCS platform monitoring of weather conditions for cloud seeding control
[E73-10095] 08 p0902 N73-17307
Utilization of ERTS-1 imagery for monitoring weather conditions for cloud seeding control
[E73-10489] 12 p1397 N73-21325
Time dependent two-dimensional atmospheric model used to test hypothesis of increased precipitation downwind from cloud seeding area
[AD-755724] 12 p1425 N73-21551
Three dimensional growth rates of seeded Florida cumulus
[UM-RSMAS-73029] 14 p1661 N73-23480
Organic compounds for nucleating supercooled water
[AD-758002] 15 p1748 N73-24169
Development of facilities and processing for determining increase in mean seasonal runoff due to cloud seeding in San Juan Mountains, Colorado
16 p1859 N73-25056
Computerized simulation of maritime cumulus clouds considering meteorological parameters and cloud seeding
[AD-759368] 16 p1939 N73-25693
Ground based silver iodide cloud seeding for modifying snowfall in northern Rockies near Montana
[PB-2180512] 18 p2173 N73-27548
Numerical analysis of barium cloud growth and striation in conducting background
[AD-761828] 19 p2317 N73-28637
Analysis of radar data to determine characteristics of precipitation belts resulting from weather modification practices
21 p2571 N73-30603
Annotated bibliography on weather modification by precipitation inducement
[PB-220348/7] 21 p2575 N73-30634
Monitoring weather conditions in Colorado for cloud seeding control
[E73-11071] 24 p2913 N73-33245

CLOUD STREETS
U CLOUDS [METEOROLOGY]

CLOUDS
NT ARTIFICIAL CLOUDS
NT CIRRUS CLOUDS
NT CLOUDS [METEOROLOGY]
NT CONVECTION CLOUDS
NT CUMULONIMBUS CLOUDS
NT CUMULUS CLOUDS
NT MAGELLANIC CLOUDS
NT NOCTILUCENT CLOUDS
NT PLASMA CLOUDS
NT STRATOCUMULUS CLOUDS
NT STRATUS CLOUDS
NT VENUS CLOUDS
Investigation for attenuation and extinction in interaction between laser beams and flowing particulate clouds
[RM-567] 08 p0929 N73-17605
Photometric profiles of dust particle size and dust cloud origins during dust storms on Mars as reported by Mars 3 Automatic Interplanetary Station
[NASA-TT-F-14818] 08 p0962 N73-17866
Ignition model for predicting ignition delay times of boron particle clouds in oxidizing atmosphere
20 p2484 N73-29955

CLOUDS [METEOROLOGY]
NT ARTIFICIAL CLOUDS
NT CIRRUS CLOUDS
NT CONVECTION CLOUDS
NT CUMULONIMBUS CLOUDS
NT CUMULUS CLOUDS
NT NOCTILUCENT CLOUDS
NT STRATOCUMULUS CLOUDS
NT STRATUS CLOUDS
Monitor for electric fields of cloud formations in particular area
[NASA-CASE-KSC-10731-1] 01 p0056 N73-10461
Study of 4-day retrograde rotation of external cloud layer of Venus
[NASA-TT-F-14710] 02 p0230 N73-11864
Infrared polarimeter for airborne measurement of terrestrial cloud particle sizes and shapes
[NASA-CR-130119] 03 p0301 N73-12458
Cost effectiveness analysis of propane operated fog dispersal system and evaluation of runway visual range improvement
[FAA-RD-72-123] 06 p0649 N73-15267
Airborne spectrometer measurements of cloud droplet size
[NASA-CR-130138] 06 p0693 N73-15650
Requirements, basic principles of operation, design, construction, and maintenance of thermal fog dispersal system for airport applications
[FAA-RD-72-138] 07 p0766 N73-16222
Measurement of cloud base temperature with infrared detector and comparison with lidar and radiosonde results
[BMVG-FBWT-72-17] 07 p0815 N73-16611
Analysis of cloud formations, ozone distribution, and meteorological data from Nimbus 4 satellite observations
[NASA-TM-X-66190] 09 p1028 N73-18392
Effect of cloud conditions on satellite infrared spectrometer temperature retrievals
[NOAA-TR-NESS-63] 09 p1034 N73-18435
Photometric analysis of violet clouds on planet Mars and determination of monochromatic albedo
09 p1083 N73-18834
Study of tropical oceanic subcloud layer using data from Barbados experiment
10 p1180 N73-19598
Doppler radar measurement of turbulent air associated with stalactite cloud base zone
[AD-755441] 12 p1423 N73-21535
Design, construction, and electrical circuits for radiosondes to study warm cloud development
[AD-758073] 14 p1686 N73-23684
Mathematical models and computer simulation for predicting spectral parameters of radar echoes from rain clouds
[STC-TM-308] 15 p1750 N73-24180
Analysis of improved numerical solutions to stochastic collection equation for cloud droplets
15 p1805 N73-24629
Chemical changes during transformation of aerosols to cloud droplets and rain in orographic clouds
15 p1805 N73-24630
Synoptic meteorology of large dust cloud over west coast of Africa
[NLL-M-22850-[5828.4F]] 16 p1936 N73-25662
Influence of electric forces in development and dissipation of clouds and fog
[AD-758925] 16 p1938 N73-25683
Laser observations of dense natural fog to determine backscatter and slant range visibility for aircraft landing operations
[AD-760128] 17 p2041 N73-26511
Evaluation of electrogasdynamic concept for dispersal of warm fog based on injection of charged water droplets into fog
[ASRC-PUBL-207] 20 p2382 N73-29140
Application of satellite observation data for determining statistical relationship between cloud field and outgoing short wave radiation in earth atmosphere
20 p2399 N73-29283
Analysis of sky back radiation intensity measurements for clear and overcast skies conducted at different angles of elevation above the horizon by day and night
20 p2400 N73-29286
Development of mathematical relationships to determine short-wave thermal radiation under cloudy and cloudless conditions
20 p2401 N73-29291
Application of airborne actinometric measurements to determine transmission, absorption, and reflection of solar radiation by clouds
20 p2401 N73-29292
Removal of pollutants from atmosphere by precipitation and clouds
[NLL-M-23010-[5828.4F]] 20 p2441 N73-29608
Identification and classification of clouds from ERTS-1 photography
[E73-10977] 21 p2534 N73-30316
Three basic forms of cyclonic cloud vortices to trace spirals
[AD-763170] 21 p2540 N73-30363
Application of radio wave propagation and radar signatures for analyzing structure of clouds
21 p2569 N73-30589
Application of polarized electromagnetic radiation for analyzing parameters of atmospheric formations
21 p2569 N73-30592
Application of radio astronomy methods for analyzing microwave absorption spectrum and properties of atmospheric cloud formations
21 p2570 N73-30593
Procedure for determining lower cloud boundaries using dual range meteorological radar operating in vertical sounding mode
21 p2572 N73-30610
Design and development of meteorological radar for detecting hail-bearing clouds
21 p2572 N73-30611
Effect of television camera and radiometer resolution on accuracy of cloud quantity determinations from satellites
22 p2693 N73-31569
Daily hemispheric mosaics by satellite for use in selection of climatological data
22 p2693 N73-31576
Nimbus 4 satellite infrared spectra for analyzing cloud spectral effects
22 p2736 N73-31907
Application of Skylab EREP data to cloud physics investigations
[E73-11057] 23 p2780 N73-32233
Development and characteristics of apparatus for measuring intensity of electric field in atmosphere
[NASA-CASE-KSC-10730-1] 23 p2790 N73-32318
Meteorological radar observations of clouds and precipitation
[AD-764934] 23 p2815 N73-32510

CLUMPS
Delineation of clustered points in two dimensions by measuring perimeters of convex hulls and applicability in fields of geology and geochemistry
[BM-RI-7565] 05 p0568 N73-14616
Cluster seeking techniques in pattern recognition
[REPT-10] 20 p2437 N73-29575

CLUSTERS
U CLUMPS

CLUTCHES
Performance of high speed overriding clutch assemblies for helicopters
[AD-747807] 03 p0308 N73-12518
Aircraft clutch assemblies, ramp roller evaluation at engine input conditions of 26,500 rpm and 1500 hp
[AD-747816] 04 p0427 N73-13481
CLUTTER
First-order statistics of terrain clutter
[AD-750668] 06 p0641 N73-15205
Evaluation of improved quantizer detector modification to production common digitizer
[FAA-RD-73-54] 15 p1750 N73-24181
COACHELLA VALLEY (CA)
Utilization of ERTS-1 imagery for monitoring land use change and regional planning in Coachella Valley, California
[PAPER-L5] 19 p2273 N73-28301
Utilization of ERTS-1 imagery for mapping and control of pink bollworm in Imperial, Coachella, and Palo Verde Valleys of California
[E73-10858] 19 p2292 N73-28435
COAGULATION
NT BLOOD COAGULATION
Determination of boundaries confining constant of turbulent coagulation of aerosols
[NLL-RTS-7293] 11 p1269 N73-20297
Coagulation of carbon particles in premixed flames
[AD-755693] 13 p1592 N73-22907
Particle size distribution of coagulated aerosols using computer program
[NPL-NAC-35] 22 p2668 N73-31373
COAL
Application of ERTS-1 imagery to fracture related mine safety hazards in coal mining industry in Indiana
[E72-10193] 01 p0046 N73-10372
Mapping ecological effects of coal strip mining in Ohio
[E72-10256] 03 p0290 N73-12356
Environmental and ecological effects of coal strip mining in Ohio
[E73-10003] 06 p0658 N73-15339
Application of ERTS-1 imagery to fracture related mine safety hazards in coal mining industry in Indiana and Illinois
[E73-10096] 09 p1020 N73-18321
Application of ERTS-1 imagery for locating coal refuse deposits, analysis of geologic formations and mapping of agricultural areas in Pennsylvania
[E73-10327] 09 p1024 N73-18358
Application of ERTS-1 imagery to fracture related mine safety hazards in coal mining industry in Indiana and Illinois
[E73-10371] 10 p1151 N73-19366
Ecological effects of coal strip mining in Ohio
[E73-10430] 11 p1281 N73-20391
Trace element analysis of coal by neutron activation
[NASA-TM-X-68208] 12 p1431 N73-21596
Feasibility of detecting subsurface coal fires in Wyoming and Montana from ground observation, aerial photography, and satellite imagery
13 p1528 N73-22384
Detection, monitoring, and mapping coal strip mining and reclamation in Ohio from ERTS-1 imagery
[E73-10641] 16 p1896 N73-25338
Application of ERTS-1 imagery to fracture related mine safety hazards in coal mining industry in Indiana
[E73-10776] 18 p2135 N73-27252
Identification and mapping of coal refuse banks in Pennsylvania anthracite coal fields from ERTS-1 data
[PAPER-L24] 19 p2276 N73-28319
Test equipment and procedure for determining electrical conductivity of stream of hot powdered fuel during combustion process
[JPRS-59752] 20 p2485 N73-29960
Application of ERTS-1 imagery to study of fracture-related safety hazards in Indiana coal mining industry
[E73-10970] 21 p2533 N73-30311
Technologies for production and utilization of petroleum, natural gas, oil shale and coal
[BM-IC-8612] 21 p2536 N73-30335
Application of ERTS-1 imagery to fracture-related mine safety hazards in Ohio coal mining industry
[E73-11034] 22 p2663 N73-31338
Mapping of anthracite wastes from mining in Pennsylvania
[E73-11107] 24 p2915 N73-33264
Usefulness of ERTS-1 MSS data for monitoring coal strip mining, detection of acid mine drainage, and determination of effectiveness of reclamation and abatement procedures in Pennsylvania
[E73-11112] 24 p2915 N73-33269
Application of ERTS-1 imagery to fracture related coal mine safety hazards and environmental problems in mining in Indiana
[E73-11148] 24 p2918 N73-33302
COALESCENCE
U COALESCING
COALESCING
Cumulus cloud modification with coalescence attempts
[NOAA-TM-ERL-OD-14] 24 p2947 N73-33539
COANDA EFFECT
Mathematical models for developing Coanda eductors for pneumatic conveying systems used in underground excavation
[AD-749088] 05 p0552 N73-14485
Coanda effect on plane jet flowing over curved surface considering two dimensional flow over airfoil
[DLR-FB-71-46] 06 p0621 N73-15043
Jet deflection characteristics of jet-flapped airfoil with Coanda deflection surfaces based on velocity distribution and flow angle measurements for static operation
[AD-753618] 09 p0989 N73-18074
Development of high performance, low volume thrust augmentation using combined Coanda inlet and jet flap diffusion techniques
[AD-756895] 13 p1476 N73-21954
Coanda effect with jet displacement over planar, concave, and convex walls
[AD-764506] 22 p2655 N73-31270
Wind tunnel tests of high harmonic circulation control rotary wing model to show instruments required and data acquisition procedures
[AD-765320] 23 p2747 N73-31984
Wind tunnel tests of large scale subsonic jet transport with upper surface blowing flap system for lift augmentation
[NASA-TM-X-62296] 24 p2876 N73-32973
COASTAL CURRENTS
ERTS-1 imagery of California nearshore processes including estuarine flushing, currents, season river discharges, and sediment dispersion
[E72-10363] 05 p0535 N73-14351
Generation and stabilization of coastal wave induced circulation and longshore current patterns
[AD-750291] 06 p0671 N73-15458
Applications of multicolor dye tracers and multispectral photography to coastal water mapping
[AD-754437] 12 p1403 N73-21378
Dynamics of wind driven lake currents and application of vertical cross-section models
23 p2777 N73-32211
COASTAL DUNES
U DUNES
COASTAL ECOLOGY
Application of ERTS-1 imagery data to protection and management of New Jersey coastal environment
[E72-10178] 01 p0045 N73-10357
Mapping, evaluation, and monitoring of coastal and saline wetlands ecology and shallow water environments using ERTS-1 imagery
[E72-10290] 04 p0410 N73-13340
Fluvial environment of Arctic coastal plain in Northern Alaska
[AD-749150] 05 p0542 N73-14412
Identification and mapping of coastal vegetation species in ERTS-1 imagery of Delaware
[E73-10007] 06 p0658 N73-15343
Application of multispectral data processing to Delaware coastal wetlands vegetation mapping
[E73-10069] 07 p0779 N73-16331
Application of ERTS-1 imagery to protection and management of New Jersey coastal environment
[E73-10330] 10 p1147 N73-19335
Mapping northern Atlantic coastal marshlands of Maryland, Delaware, and Virginia using ERTS-1 imagery
[E73-10363] 10 p1150 N73-19359
Application of ecological, geological, and oceanographic ERTS-1 imagery to coastal resources management and planning in Delaware
[E73-10426] 11 p1280 N73-20387
Remote sensing techniques for water management and land use classification in California coastal zone considering river deltas
12 p1400 N73-21357
Application of ecological, geological, and oceanographic ERTS-1 imagery to Delaware coastal resources management and planning
[E73-10631] 15 p1776 N73-24391
Application of ERTS-1 data to develop and implement utilization of living marine resources in Mississippi Sound
[E73-10707] 16 p1904 N73-25398
Analysis of ERTS-1 imagery to interpret three seasonal nearshore processes along California coast
[E73-10727] 17 p2020 N73-26333
Analysis of ERTS-1 data for interdisciplinary study of estuarine and coastal oceanography of Block Island Sound and adjacent New York coastal waters
[E73-10735] 17 p2020 N73-26341
Analysis of ERTS-1 data for interdisciplinary study of estuarine and coastal oceanography of Block Island Sound and adjacent New York coastal waters
[E73-10736] 17 p2020 N73-26342
Application of ERTS-1 imagery for identifying and mapping rivers, agricultural areas, forest, mineral resources, and water conditions in Thailand
[E73-10746] 17 p2021 N73-26350
Application of ERTS-1 imagery for determining availability and distribution of menhaden within Mississippi Sound adjacent waters
[E73-10751] 17 p2022 N73-26354
Use of ERTS-1 data to apply marine station data to study of productivity along Eastern Self Expanded Waters of US
[E73-10778] 18 p2135 N73-27254
Application of ERTS-1 imagery for defining ice formations, ocean currents, beach erosion, and estuarine circulation
[E73-10780] 18 p2136 N73-27256
Mapping of Atlantic coastal marshlands of Maryland and Georgia using ERTS-1 imagery
[PAPER-E7] 19 p2269 N73-28271
Analysis of coastal vegetation species in Delaware Bay, Delaware based on ERTS-1 imagery and high altitude photography
[PAPER-E8] 19 p2269 N73-28272
Analysis of ERTS-1 imagery of New Jersey coastal resources to assist in resource management and allocation of funds for environmental control
[PAPER-E9] 19 p2269 N73-28273
ERTS-1 imagery for monitoring dumping of municipal and industrial wastes in New York Bight
[PAPER-E10] 19 p2269 N73-28274
Analysis of erosion along Niigata Beach, and development of improved methods of erosion control based on ERTS-1 imagery
[PAPER-E14A] 19 p2270 N73-28278
Analysis of ERTS-1 multispectral scanner imagery to determine polluted and turbid water masses in Osaka Bay, Japan
[PAPER-E14C] 19 p2270 N73-28280
COASTAL MARSHES
U MARSHLANDS
COASTAL PLAINS
Remote sensing data for determining land use potential of northern California coastal zone
05 p0536 N73-14365
Fluvial environment of Arctic coastal plain in Northern Alaska
[AD-749150] 05 p0542 N73-14412
Fluvial environmental charts for Arctic coastal plain in Northern Alaska
[AD-749151] 05 p0542 N73-14413
Seismic reflection and refraction surveys of thickness of coastal plain sediments in Virginia
[PB-212604] 07 p0794 N73-16455
ERTS-1 imagery of marshlands and turbid waters of French Atlantic littoral
[E73-10341] 10 p1147 N73-19340
Mapping southeastern coastal marshlands and wetlands of South Carolina and Georgia using ERTS-1 imagery
[E73-10362] 10 p1150 N73-19358
Location of wet areas and detection of potential locust breeding sites using ERTS-1 imagery of Red Sea coastal plain of Saudi Arabia
[E73-10462] 12 p1394 N73-21301
Application of ERTS-1 data to management and protection of New Jersey coastal environment
[E73-10527] 14 p1654 N73-23415
Analysis of lineaments and fault traces in Atlantic Coastal Plain of southern Maryland using ERTS-1 imagery
[PAPER-G29] 19 p2267 N73-28260
Application of ERTS-1 data to protection and management of New Jersey coastal environment
[E73-11031] 22 p2662 N73-31335
COASTAL WATER
Estuarine and coastal oceanography of Block Island Sound and adjacent New York coastal waters based on ERTS-1 multispectral band scanner imagery
[E72-10171] 01 p0044 N73-10352
Interdisciplinary study of estuarine and coastal oceanography of Block Island Sound and New York Bight area using ERTS-1 imagery
[E72-10172] 01 p0044 N73-10353
Coastal geology bibliography of New England with punch card reference system
[AD-744001] 01 p0052 N73-10424
Aerial photography used to delineate areas of ocean ground water discharge and detect submarine springs along northwest coast of Puerto Rico
[PB-210754] 01 p0052 N73-10426
ERTS-1 imagery of French shoreline along the Atlantic Ocean and English Channel
[E72-10211] 02 p0161 N73-11306
ERTS-1 imagery of inner shelf and coastal sedimentation environment of Beaufort Sea
[E72-10248] 03 p0289 N73-12348
Estuarine coastal water dynamics controlling sediment transport and plume development in Long Island Sound
[E72-10250] 03 p0289 N73-12350
ERTS-1 imagery of coastal marshland, tidal flats, and littoral transport in French Atlantic waters
[E72-10251] 03 p0289 N73-12351
Dynamic behavior of coastal sedimentation in Lions Gulf
[E72-10289] 04 p0410 N73-13339
ERTS-1 imagery of California coastal nearshore processes
[E72-10316] 04 p0413 N73-13365
Acquisition and analysis of California coastal ground truth data for correlation with ERTS-1 imagery
[E72-10321] 04 p0413 N73-13369

Multispectral imagery of estuarine and coastal oceanography of Block Island Sound and adjacent New York coastal waters using ERTS-1 imagery
[E73-10010] 06 p0659 N73-15346
Application of ERTS-1 MSS imagery to coastal engineering planning and construction
[E73-10050] 07 p0777 N73-16312
ERTS-1 imagery of estuarine and coastal water dynamics controlling sediment transport and plume development in Long Island Sound
[E73-10093] 08 p0902 N73-17305
Surface water circulation in Prince William Sound using ERTS-1 imagery
[E73-10291] 08 p0915 N73-17496
ERTS-1 imagery of marshlands and turbid waters of French Atlantic littoral
[E73-10341] 10 p1147 N73-19340
Identification of marsh vegetation and coastal land use in Delaware from ERTS-1 imagery
[E73-10367] 10 p1150 N73-19363
Measurement of coastal currents and processes and seaward extent of suspended sediment transport in waters of California
[E73-10375] 10 p1151 N73-19370
Estuarine and coastal water dynamics controlling sediment transport and plume development in Long Island Sound
[E73-10378] 10 p1152 N73-19373
ERTS-1 imagery of inner shelf and coastal sedimentation environment of Beaufort Sea, Alaska
[E73-10412] 11 p1278 N73-20374
ERTS-1 imagery of sea ice and surface water circulation along Alaskan contiental shelf
[E73-10416] 11 p1279 N73-20378
Acquisition and analysis of coastal ground truth data in pacific water off California for correlation with ERTS-1 imagery
[E73-10482] 12 p1396 N73-21319
ERTS-1 imagery of inner shelf and coastal sedimentation environment of Beaufort Sea
[E73-10492] 12 p1397 N73-21328
Mapping of coastal sedimentation and related processes in Cook Inlet, Alaska and distribution and environmental interrelationships of permafrost terrain
[E73-10421] 13 p1515 N73-22275
ERTS-1 imagery of California nearshore sediment transport, coastal processes, and tidal currents
[E73-10525] 13 p1517 N73-22292
ERTS-1 imagery of marshes, wetlands, and turbid waters in French Atlantic littoral
[E73-10548] 13 p1518 N73-22307
Application of ERTS-1 data to management and protection of New Jersey coastal environment
[E73-10527] 14 p1654 N73-23415
Geophysical survey off Surinam coast including seismics, magnetics, and gravity
[SP-6] 14 p1660 N73-23476
Numerical simulation of free-boundary shoreline under hurrican action
15 p1770 N73-24337
Acquisition and analysis of coastal ground truth data of Santa Monica Bay, Santa Barbara Channel, and Monterey Bay for correlation with ERTS-1 imagery
[E73-10607] 15 p1773 N73-24368
Estuarine and coastal water dynamics controlling sediment transport and plume development in Long Island Sound
[E73-10627] 15 p1775 N73-24387
ERTS-1 imagery of inner shelf and coastal sediment transport in Beaufort Sea
[E73-10649] 16 p1897 N73-25345
ERTS-1 detection and measurement of coastal marshes in Houston area test site
[E73-10676] 16 p1900 N73-25371
Determination of coastal water types around Monterey Bay, California by analysis of ERTS-1 MSS data
[E73-10677] 16 p1901 N73-25372
Measurement of chlorophyll and plankton populations of shelf and slope waters off northeastern United States
[E73-10683] 16 p1901 N73-25378
Variability of coastal processes and resulting shoreline morphology along peninsula of Baja California
[AD-756676] 16 p1907 N73-25432
Research and development in coastal engineering
[AD-759283] 17 p2028 N73-26413
Color enhancement of ERTS-1 imagery of estuarine and coastal oceanography of Block Island Sound and adjacent New York coastal waters
[E73-10819] 18 p2140 N73-27294
Littoral transport of sedimention coastal region of France
[E73-10822] 18 p2140 N73-27297
Land cover and land use mapping of Central Atlantic Region shoreline zone using ERTS-1 imagery
[PAPER-L8] 19 p2274 N73-28304
Comparison of conventional maps of southeastern Massachusetts to ERTS-1 imagery of coastal and submarine geology and hydrology
[PAPER-M18] 19 p2282 N73-28356
Application of classification algorithms to ERTS-1 MSS imagery of Texas land and water coastal features
19 p2286 N73-28383
Utilization of ERTS-1 imagery for coastal oceanography in British Columbia
19 p2286 N73-28384
Application of ERTS-1 imagery to study of coastal areas and processes
19 p2286 N73-28386
Utilization of ERTS-1 data for regulation, protection, and management of New Jersey coastal environment
[E73-10845] 19 p2291 N73-28423
Correlation of coastal ground truth data from Southern California waters with ERTS imagery
[E73-10864] 20 p2392 N73-29215
Surface circulation of coastal waters of Prince William Sound Alaska
[E73-10902] 20 p2396 N73-29251
Relation of sea truth data from Cape Cod, Massachusetts, and Charleston, South Carolina on plankton composition and chlorophyll values with ERTS-1 data
[E73-10907] 20 p2397 N73-29256
Classification of coastal environments along Americas and Africa
[AD-761193] 20 p2415 N73-29412
Synoptic meteorological data for Philippine coastal marine surfaces
[AD-762424] 20 p2450 N73-29688
Synoptic meteorological data for Philippine and Vietnam coastal marine surfaces
[AD-762425] 20 p2450 N73-29689
Estuarine and coastal oceanography of Block Island Sound and adjacent New York coastal waters
[E73-10968] 21 p2533 N73-30310
Skylab monitoring of gamefish in coastal waters off of Florida
[E73-10997] 22 p2659 N73-31303
Application of ERTS-1 data to protection and management of New Jersey coastal environment
[E73-11031] 22 p2662 N73-31335
Multispectral band scanner reconnaissance of Pacific Ocean off Oregon coast
[AD-763428] 23 p2789 N73-32311
Sources and dispersal patterns of suspended particles in nearshore surface waters of northeast Pacific Ocean and seasonal variation in snow cover in Sierra Nevada Mountains
[E73-11099] 24 p2914 N73-33256
ERTS-1 monitoring of turbidity, color, boundaries, circulation, and pollution dispersion in Delaware coastal waters
[E73-11147] 24 p2918 N73-33301

**COASTS**
Evaluation of three types of aerial photographs used in coastal studies of Baja California
[AD-744310] 01 p0052 N73-10421
Experiment in climatic zoning of coast of Gulf of Riga
04 p0443 N73-13610
Seasonal flow patterns of coastal currents along Oregon-Northern California coast
[AD-749077] 05 p0541 N73-14403
Pressure patterns chronology with Bora on Adriatic coast from 1 Jan. 1956 to 31 Dec. 1965
05 p0571 N73-14640
Graphical summary of weather and sea conditions along California coast
[AD-749781] 05 p0576 N73-14690
Tables of synoptic meteorological observations of Japan coastal marine areas
[AD-754773] 11 p1314 N73-20668
Compilation of aerial photographs of coastal areas of United States
[AD-755508] 13 p1526 N73-22368
Geomorphic coastal variability for Northwestern Australia
[AD-755154] 13 p1527 N73-22377
Identification of marshland vegetation and coastal land use in Delaware from ERTS-1 imagery
[E73-10516] 14 p1653 N73-23410
Coastline induced Loran C anomalies
[AD-757142] 14 p1691 N73-23724
Prevaling monthly and seasonal surface wind directions for coastal areas around Arctic Ocean
[AD-761074] 18 p2174 N73-27560
Seasonal climatology of Chilean sea coast
[AD-765355] 23 p2815 N73-32506
ERTS-1 observation of marshy ocean coast areas and sedimentary material
[NASA-TT-F-13063] 24 p2922 N73-33333

**COATING**
NT ANODIZING
NT ELECTROPLATING
NT ENCAPSULATING
NT METALLIZING
Determination of corrosion resistance of coatings on low alloy steel and susceptibility to exfoliation of 7178 aluminum alloy using Lawrence corrosion detection gauge
[AD-755163] 13 p1531 N73-22405

**COATINGS**
NT ALUMINUM COATINGS
NT ANODIC COATINGS
NT BIREFRINGENT COATINGS
NT CERAMIC COATINGS
NT ELECTROPLATING
NT ENAMELS
NT ENCAPSULATING
NT GLASS COATINGS
NT GOLD COATINGS
NT INORGANIC COATINGS
NT MAGNETIC FILMS
NT METAL COATINGS
NT METALLIZING
NT NICKEL COATINGS
NT PAINTS
NT PLASTIC COATINGS
NT PROTECTIVE COATINGS
NT RUBBER COATINGS
NT SPRAYED COATINGS
NT THERMAL CONTROL COATINGS
Determination of quality of zinc phosphate coatings by measurement of electrode potential
[AD-745094] 01 p0070 N73-10571
Development of surfaces and coatings for solar energy conversion systems
[NASA-TT-F-14650] 06 p0688 N73-15598
Ultraviolet and charged particle irradiation of solar cell coverslide materials and conductive coatings for Helios satellites
[NASA-TM-X-65945] 09 p1051 N73-18571
Development of graphite-matrix fuels for booster assemblies in reactor cores
09 p1063 N73-18669
Improved silicide coatings for refractory metals employed in space shuttles and gas turbine engine components
[NASA-CASE-LEW-11179-1] 13 p1540 N73-22474
Specific heat measurements of He-4 monolayers on sintered and gas monolayer coated copper
16 p1973 N73-25957
Solar absorber coatings for use with spaceborne Vuilleumier cycle cryogenic refrigerators
[AD-760577] 18 p2167 N73-27505
Attenuation of circularly bent waveguides with dielectric coatings, noting role of mode filters
[FTZ-A-333-TBR-16] 22 p2643 N73-31181
Contrast color coating for meteoroid impact position locator for space vehicles
[NASA-CASE-LAR-10629-1] 23 p2793 N73-32348

**COAXIAL CABLES**
Analysis of coupling characteristics and crosswalk between electric cables used in naval environments
[AD-742971] 01 p0032 N73-10253
Radiation pattern characteristics of traveling wave coaxial cable antenna
[AD-749051] 04 p0397 N73-13233
Loading effect of probes used in coaxial waveguide experimental coupler
[AD-749060] 05 p0521 N73-14233
Development and characteristics of hermetically sealed coaxial package for containing microwave semiconductor components
[NASA-CASE-GSC-10791-1] 05 p0550 N73-14469
Baseband equalization system for correcting response characteristics of high quality coaxial transmission lines
[UCRL-73943] 07 p0756 N73-16141
Surface transfer impedance measurements for determining shielding characteristics of coaxial cables
[AD-753678] 09 p1009 N73-18237
Phase delay control system for stabilizing signals passing through coaxial cables
[NASA-CASE-NPO-13138-1] 11 p1262 N73-20238
Characteristics of edge mounted coaxial TEM line antenna
[AD-758518] 15 p1758 N73-24252
Coaxial connector for standard hardware program
[AD-758649] 16 p1882 N73-25233
Improving optical compatibility of lidar transmitter-receiver
[NASA-TM-X-64753] 16 p1923 N73-25561
Maxwell equation and approximation theory for examining attenuation behavior of coaxial cables with woven outer conductors
[RAE-LIB-TRANS-1642] 17 p1997 N73-26147
Optimum design of insulating intersheaths between radio frequency cable braids
[RAE-TR-72151] 17 p1998 N73-26154
Differential geometry scaling method for determining electromagnetic field of coaxial waveguide coupler
[AD-760157] 17 p2006 N73-26222
Coaxial anode for gas radiation counter for suppressing background ionization interference
[NASA-CASE-GSC-11492-1] 19 p2301 N73-28497
Shielding analysis of joints and connectors in coaxial cables
[AD-761825] 21 p2518 N73-30201

**COAXIAL FLOW**
One- and two-D core theories for analyzing ducted mixing and burning of coaxial streams
08 p0896 N73-17253
Model scale air jets for sound study of coaxial circular jets
[FAA-RD-71-101-VOL-1] 20 p2454 N73-29721
Correlation parameters for velocity, temperature and concentration of coaxial, heterogeneous, compressible free jet cores
24 p2907 N73-33201

**COAXIAL PLASMA ACCELERATORS**
Computer analysis of tapered coaxial plasma gun electrodes
[AD-747057] 03 p0343 N73-12797

Analysis of performance of pulsed coaxial guns based on snowplow model allowing for variable initial mass-loading distribution
10 p1111 N73-19057
Study of ionizing wave in coaxial plasma guns to explain plasma-neutral gas interaction
[TRITA-EPP-72-31] 16 p1950 N73-25778
Snowplow calculations of acceleration and compression in coaxial plasma accelerator with focusing equipment
[IFP-72-4] 17 p2069 N73-26740
Current density, flow velocity, and mass density in coaxial annular plasma Hall accelerator
[DLR-FB-73-45] 22 p2705 N73-31663
Scattering of ruby laser beam by plasma focus of coaxial gun
[CEA-R-4430] 24 p2931 N73-33411

**COAXIAL TRANSMISSION**
U COAXIAL CABLES
U TRANSMISSION

**COBALT**
NT COBALT 60
Ferromagnetic resonance in iron and hexagonal close packed cobalt lattices
[AD-753841] 09 p1076 N73-18783
X ray attenuation coefficients in absorption spectra of titanium, iron, cobalt, nickel, copper, and zinc
[UCRL-73923] 10 p1189 N73-19675
Solid phase interactions in cobalt-carbide systems
[NLL-LTI-746-1338-[9022.401]] 12 p1415 N73-21468
Electromechanical energy conversion devices using both conventional and rare-earth cobalt permanent magnet materials
[AD-756433] 13 p1501 N73-22168
Design of ironless armature torque motor using samarium cobalt permanent magnets
[NASA-CR-130224] 13 p1532 N73-22416
Cantilever beam tests for determining strength of tungsten carbide-cobalt alloys
16 p1927 N73-25591
Magnetic properties of cobalt rare earth thin films
16 p1951 N73-25790
Determination of limiting solubility of carbon in cobalt in solid state
[NLL-M-21664-[5828.4F]] 21 p2504 N73-30096

**COBALT ALLOYS**
Analysis of cobalt alloys containing samarium additives to determine effects on saturation magnetization, residual magnetization, and coercive forces
[NLL-M-21478-[5828.4F]] 02 p0185 N73-11499
Magnetic properties and crystalline structures of rare earth-cobalt alloys
[AD-748270] 04 p0436 N73-13555
Magnetic intermetallic cobalt-rare earth compounds for electromechanical energy converters
[AD-750338] 06 p0645 N73-15242
High temperature tests to determine effect of autoclave heat treatment of mechanical properties of cobalt-base alloy HS-31 in prealloyed powder form
[NASA-TN-D-7117] 07 p0809 N73-16559
Physical property changes of rare earth cobalt magnet materials in temperature range up to 1000 C
[AD-753572] 10 p1201 N73-19778
Dispersion effects of heat resistant metal oxides
[AD-754760] 11 p1306 N73-20595
Analysis of KC-135 flight samples of Star-J Satellite solidified in near-zero gravity
[NASA-CR-124179] 11 p1308 N73-20610
Formation and failure of chromium sesquioxide on cobalt-base alloy L-605 during oxidation at high temperatures
[NASA-TN-D-7255] 12 p1414 N73-21454
High temperature research on effects of chemical variation and processing variables on properties of wrought cobalt-base-NASA alloy
[NASA-CR-121189] 12 p1414 N73-21457
Analysis of precipitation process in cobalt-tungsten-titanium alloys using electron microscope and X ray imaging techniques
13 p1541 N73-22483
Addition of chromium or aluminum to improve oxidation resistance of nickel and cobalt alloys
14 p1677 N73-23611
Comparison of cobalt alloys and nickel alloys relative to hot corrosion resistance
14 p1677 N73-23612
Ac susceptibility of powdered samples of SmCo5, YCo5, and NdCo5
[AD-758218] 14 p1700 N73-23794
Degradation and reuse of radiative-thermal protection materials for space shuttle
[NASA-CR-123587] 14 p1709 N73-23866
Magnetic properties of highly dispersed iron-cobalt-nickel alloy powders
[NLL-LTI-746-1419-[9022.401]] 15 p1797 N73-24566
Cyclic furnace tests of nickel-, cobalt-, and iron-base alloys oxidation resistance considering scale spalling
[NASA-TM-X-68252] 16 p1870 N73-25144
Effects of heat treatment on Brinell hardness of Co-Be alloy system
[RFP-TRANS-122] 17 p2044 N73-26541
Carbon fiber/cobalt/chromium system tensile and high temperature strength noting different solidification modes
[DLR-FB-73-37] 21 p2560 N73-30519
Thermal cycling effects on structure of cobalt-niobium eutectic alloys
[AD-763706] 21 p2560 N73-30521
Method for fabricating samarium cobalt permanent magnets
[BM-RI-7784] 21 p2580 N73-30679
Correlation of X ray and electron microscope data for fatigue in nickel and cobalt alloys
[AD-764282] 22 p2686 N73-31513
Cobalt-tungsten alloys with superior strength at elevated temperatures
[NASA-CASE-LEW-10436-1] 23 p2803 N73-32415
Effect of aging temperature and time on impact and tensile properties of L-605 cobalt alloy
[ORNL-TM-3734] 24 p2934 N73-33435

**COBALT COMPOUNDS**
NT COBALT OXIDES
Rare earth-cobalt permanent magnet materials processing
[AD-748264] 04 p0451 N73-13679
Crystal growth and magnetic properties of transition metal chalcogenides
[AD-748864] 04 p0459 N73-13748
Processing methods for rare earth cobalt compounds as permanent magnets
[AD-754951] 11 p1325 N73-20749
Far infrared laser spectroscopy of spin clusters in linear magnetic system of cobalt chloride compound
[AD-756264] 13 p1566 N73-22691
Materials processing method for optimization of rare earth cobalt compounds as permanent magnets
[AD-760777] 18 p2180 N73-27599

**COBALT ISOTOPES**
NT COBALT 60

**COBALT OXIDES**
Optical properties of films based on tin dioxide and cobalt oxides
[AD-755250] 12 p1417 N73-21479

**COBALT 60**
Oxidation resistance of capsule materials for cobalt 60 power and heat source
[DP-1300] 05 p0498 N73-14057
Effect of chronic irradiation of dogs by Co60 gamma rays on level of autoantibodies
11 p1244 N73-20100
Development and characteristics of instrument landing system using radioactive materials along runways for glide slope and alignment information
14 p1689 N73-23707

**COCHLEA**
Influence of N-type sound wave pressure rise time on guinea pig cochlear and acoustically evoked potentials
[ISL-31/72] 19 p2224 N73-27940

**COCKPIT SIMULATORS**
Comparison of contact analog channel display with conventional indicators in cockpit simulator
[DGLR-PAPER-72-100] 04 p0422 N73-13445
Summary of conference on flight simulation
08 p0864 N73-16992
Comparative evaluation of cockpit displays considering human factors and aircraft control data
[NASA-TT-F-14846] 11 p1234 N73-20019
Guidelines for assessing acceptability of pilot ground trainer devices based on simulated aircraft maneuvers
[FAA-NA-73-15] 20 p2382 N73-29139

**COCKPITS**
Survey of electronic cockpit displays, noting human factors, head-up, head-down and eyeglass display, and related technology
[DLR-FB-72-43] 01 p0058 N73-10474
Methods of evaluating electronic cockpit display devices, emphasizing control, psychology, physiology, and subjective rating
[DGLR-PAPER-72-97] 04 p0383 N73-13118
Problems of cockpit environment
08 p0864 N73-16990
Multivariate limits for describing cockpit related anthropometric features of aviation personnel
[AD-752032] 08 p0880 N73-17124
Influence of cockpit noise on hearing in flight crew personnel
[FAA-AM-72-32] 10 p1119 N73-19125
Application of normal bivariate distributions and anthropometric correlations for design of workspaces in aircraft
[AD-754780] 11 p1290 N73-20468
Cockpit display evaluation methods
[DLR-FB-73-03] 12 p1406 N73-21400
Computerized design of fighter aircraft cockpit electronic control system considering man machine interaction
14 p1714 N73-23905
High g Approach for cockpit design
[AD-757216] 15 p1744 N73-24138
Tachistoscopic investigation on electronic and electromechanical cockpit display for performance comparison
[DLR-FB-73-27] 21 p2496 N73-30034
Development of organic glass and plastic materials with improved mechanical and physical properties for use with aircraft canopies and protective coatings
[AD-763263] 21 p2497 N73-30039
Cockpit layouts in view of new landing approach methods
[MBB-UH-07-73-O] 23 p2744 N73-31966
Logic and design procedures for multifunction mode switching controls in jet aircraft cockpits
[AD-764617] 23 p2767 N73-32141

**COD AIRCRAFT**
U C-2 AIRCRAFT

**CODERS**
Design and performance of optical altimeter with shaft angle recording
[AD-749964] 06 p0675 N73-15488
Binary code signals produced by electron beam deflection in magnetic fields
12 p1378 N73-21176
Design and implementation of adaptive delta modulator with integrated circuit hardware for encoding of speech signals
14 p1621 N73-23132
Device for semi-automatic digital encoding of graphic data
21 p2513 N73-30157
Convolutional encoder and decoder for PCM telemetry
[ESRO-CR-165] 22 p2634 N73-31111

**CODES**
Capacity of geometric codes and increased effectiveness of semiconductor storage units using number block structures
[JPRS-57251] 02 p0145 N73-11177
Operational principles and applications of address code communication systems
14 p1619 N73-23114

**CODING**
NT DECODING
NT REDUNDANCY ENCODING
NT SIGNAL ENCODING
Space shuttle orbiter subsystems, formats and format trees, and coding of sample format - Vol. 3
[NASA-CR-128578] 01 p0019 N73-10147
Seven families of linear codes for autoinata
03 p0271 N73-12201
Application of graph theory to network analysis and coding problems in communication systems
[AD-748290] 04 p0391 N73-13178
Analysis of digital information coding procedures with application to control of synchronization errors in data transmission on pulse code modulation systems
[NLL-TRANS-2825-[9022.81]] 05 p0507 N73-14127
Binary concatenated coding system to measure, count, and record numerical information using minimized number of digits
[NASA-CASE-MSC-14082-1] 07 p0759 N73-16163
Color vision requirements for air crew personnel of future, including coding evaluation
[AMRL-TR-71-116] 10 p1113 N73-19076
Source encoding using delta modulation
[NASA-CR-131228] 10 p1127 N73-19185
Computer code for generating spatial-angular moments of adjoint gamma-ray flux in infinite mediums
[NBS-TN-748] 10 p1193 N73-19702
Apparatus and digital technique for coding rate data
[NASA-CASE-LAR-10128-1] 11 p1259 N73-20217
Source coding, modulation/channel coding, and systems techniques for application to teleconferencing over high data rate digital communication satellite links
[NASA-CR-114561] 11 p1342 N73-20889
Color coding scheme for hierarchically representing cartographic symbology
[AD-740606] 13 p1497 N73-22134
Coding systems in geographic data maps
13 p1523 N73-22343
FORTRAN-4 computer program for compiling irradiation data on UN and UC fuel pins
[NASA-TM-X-68226] 13 p1558 N73-22625
Feasibility of hybrid voice coding system for speech transmission
[AD-756519] 14 p1637 N73-23272
Algorithm for correcting errors in linear transmission codes
[AD-760154] 17 p2000 N73-26169
Coded transmission of binary data over coherent white Gaussian channels
[AD-761465] 19 p2245 N73-28102
Research progress in coding, synchronization, data processing, and communication systems
[AD-762542] 20 p2379 N73-29117
Multifold Euclidean geometry codes
[NASA-CR-133529] 20 p2439 N73-29590
Comprehensive computer code for collapse of general shape shells
[AD-762543] 20 p2484 N73-29951
Semi-automatic device for encoding three dimensional models
21 p2513 N73-30158
Abstracts on source encoding for two-dimensional data
[NASA-CR-132796] 22 p2639 N73-31149

**COEFFICIENT OF FRICTION**
Performance of gas lubricated thrust bearing based on minimum surface damage and low value of friction coefficient
[AD-753018] 09 p1041 N73-18493
Effect of wall suction on turbulent pipe flow friction coefficient
[AD-757584] 14 p1653 N73-23406
Performance tests to determine cornering characteristics of aircraft tire under various runway conditions, ground speeds, and yaw angles with and without braking
[NASA-TN-D-7351] 23 p2742 N73-31948
Boundary layer friction data under ion pumped vacuum
[NASA-CR-135480] 23 p2796 N73-32366
Comparison of theories for skin friction coefficient in turbulent compressible boundary layers
24 p2907 N73-33203
Frictional processes, electric contact resistance, and wear of pin on disk friction pair
[NASA-TT-F-15049] 24 p2929 N73-33391

**COEFFICIENTS**
NT AERODYNAMIC COEFFICIENTS
NT ATTENUATION COEFFICIENTS
NT COEFFICIENT OF FRICTION
NT COHERENCE COEFFICIENT
NT CORRELATION COEFFICIENTS
NT COUPLING COEFFICIENTS
NT DIFFUSION COEFFICIENT
NT DISCHARGE COEFFICIENT
NT FLOW COEFFICIENTS
NT HEAT TRANSFER COEFFICIENTS
NT NOZZLE THRUST COEFFICIENTS
NT RECOMBINATION COEFFICIENT
NT SCATTERING COEFFICIENTS
Fourier coefficients of Eisenstein series of the second degree
[NASA-TT-F-14937] 16 p1934 N73-25648
Analysis on Fourier coefficients of second degree Eisenstein series
[NASA-TT-F-14936] 16 p1934 N73-25649
Transport coefficient anomalies in antiferromagnetic metals in vicinity of Neel temperature
24 p2933 N73-33424

**COERCIVITY**
Analysis of cobalt alloys containing samarium additives to determine effects on saturation magnetization, residual magnetization, and coercive forces
[NLL-M-21478-[5828.4F]] 02 p0185 N73-11499

**COGNITION**
Cognitive functioning test to measure human performance in underwater diving stress
[AD-748036] 04 p0382 N73-13108
Combined noise and vibration effects on human mental and psychomotor performance
[AMRL-TR-71-115] 10 p1122 N73-19147
Human psychomotor and cognitive performance in humid environment
[AD-756835] 15 p1745 N73-24142

**COHERENCE**
Coherence statistics of horizontal wind speed as measured by micrometeorological mast array
16 p1937 N73-25675
Model for calulating coherence function for atmospheric turbulence
[NPL-MAR-SCI-R-108] 20 p2449 N73-29675

**COHERENCE COEFFICIENT**
Estimation of magnitude-squared coherence function spectrum
[AD-743945] 01 p0029 N73-10225

**COHERENT ELECTROMAGNETIC RADIATION**
NT COHERENT LIGHT
Research on electron beam devices, quantum electronic devices, plasmas, and solid state microwave devices
[AD-760033] 17 p2041 N73-26517

**COHERENT LIGHT**
Analysis of laser beam scintillation due to atmospheric turbulence
[AD-752565] 08 p0930 N73-17620
Technique for determining atmospheric transmittance of coherent light between two points in terrestrial atmosphere for selected laser frequencies
[AD-753075] 09 p1030 N73-18412
Review of coherent optical data processing
09 p1065 N73-18685
Parallel image processing including electronic, noncoherent, and coherent methods
09 p1065 N73-18691
Design concepts for on-board coherent optical image processor
09 p1066 N73-18694
Measurement of stimulated emission cross section of neodymium laser based on laser threshold gain and inverted population
[AD-753901] 10 p1170 N73-19514
Dispersion of light intensity logarithm along axis of laser beam propagating in atmosphere
[AD-756094] 13 p1539 N73-22470
Development of optical and digital techniques for application to synthetic holograms recorded with suboptical sources
[AD-756506] 14 p1674 N73-23583
Spatial filtering techniques in connection with coherent light optical data processing
[LCR-DR-1-71-253/1/R] 15 p1754 N73-24220
Holographic investigations using pulsed lasers
[AD-761977] 19 p2308 N73-28565

**COHERENT RADAR**
Optimal design of coherent radar system
06 p0640 N73-15193
Optimization of radar acquisition of moving targets by blind speed zone eliminations
[AD-753963] 11 p1256 N73-20195
Ultrahigh frequency coherent radar as moving target indicator
[AD-757565] 16 p1877 N73-25191

**COHERENT RADIATION**
NT COHERENT ELECTROMAGNETIC RADIATION
NT COHERENT LIGHT
Construction of carbon dioxide transversely excited atmospheric laser and application to absorption studies of laser induced plasmas
[AD-745842] 01 p0066 N73-10542
Analysis of dependence of refractive index of gas discharge medium in carbon dioxide laser on amplitude of discharge current
[NLL-DRIC-TRANS-2815-[3623.66]]
02 p0180 N73-11459
Analysis of conditions created by intense laser beam focused on plasma with application as plasma diagnostic technique
[DREV-R-676/72] 02 p0181 N73-11463
Analysis of dispersion, correlation and structural functions in amplitude and phase of laser being propagated into turbulent atmosphere
02 p0181 N73-11470
Improving divergence in ruby laser radiation by holographic transformation of light field coherence
[AD-746646] 02 p0183 N73-11486
Abstracts of papers presented at conference on coherence and quantum optics
[AD-746712] 02 p0183 N73-11487
Conditions of coherence in diffraction spectra produced in liquids on ultrasonic standing waves
[NASA-TT-F-13925] 02 p0211 N73-11713
Frequency stability characteristics of single frequency neodymium YAG laser system with coherent ultrashort pulses for high resolution imaging
[AD-747967] 03 p0312 N73-12543
Analysis of laser light scattered from marginally stable hydrogen plasma
[INR-P-1377] 04 p0429 N73-13491
Tunable radiation obtained across wide region of electromagnetic spectrum using parametric amplifier
[AD-748849] 04 p0429 N73-13497
Second order coherence function discriminating between thermal and laser radiation
[ONERA-NT-196] 04 p0450 N73-13675
Effects of turbulence instabilities on laser propagation
[AD-748809] 04 p0450 N73-13677
Procedures and equipment for measuring angular distribution of laser beam scattering by evolving water vapor
[NLL-M-22457-[5828.4F]] 05 p0554 N73-14497
Proceedings of symposium on laser radiation damage to transparent dielectrics, plasma formation at dielectric surfaces, and damage morphology of thin film coatings
[NBS-SP-372] 05 p0554 N73-14498
Characteristics of optical glass materials with specific resistance to effects of laser radiation
05 p0554 N73-14499
Development of interaction gradient concept and application to laser radiation damage to quartz crystals, fused quartz, and laser glass samples
05 p0554 N73-14500
Effects of stoichiometry variation, heat treatment, impurity, and color center content of electrooptic crystals and kinetics of index damage process
05 p0554 N73-14501
Analysis of laser induced surface damage to glass materials at Brewster angle and near normal incidence
05 p0554 N73-14503
Analysis of entrance and exit surface laser induced radiation damage on sapphire crystal samples as function of beam size and divergence at surfaces
05 p0555 N73-14504
Surface damage to gallium arsenide surfaces from radiation by ruby and neodymium-glass lasers
05 p0555 N73-14507
Analysis of time dependent, self focusing optical beams with elliptical constant intensity contours
05 p0555 N73-14509
Effect of glass laser radiation on borosilicate crown glass, fused silica, and flint glass with estimates of Kerr effect and electrostriction processes
05 p0555 N73-14510
Analysis of self focusing damage in laser rods with subnanosecond pulse
05 p0555 N73-14511
Analysis of damage to thin films and substrate surfaces during irradiation by Q switched ruby laser
05 p0556 N73-14512
Measurement of damage thresholds for multiple layer dielectric mirrors for laser pulses of twenty nanoseconds and twenty picoseconds duration
05 p0556 N73-14513
Analysis of laser damage to thin film coatings caused by radiation from Q switched ruby laser
05 p0556 N73-14514
Analysis of damage threshold and damage mode from laser radiation for multilayer and periodic inhomogeneous film systems
05 p0556 N73-14515
Analysis of fundamental absorption properties of laser window materials and limitations imposed by uncontrolled impurities
05 p0556 N73-14516
Pressure induced optical distortion in high power, infrared laser system windows and determination of figures of merit based on minimum thickness
05 p0556 N73-14517
Analysis of surface damage mechanisms to mirrors and mirror coatings resulting from irradiation by pulsed carbon dioxide lasers
05 p0556 N73-14519
Investigation of 106 micron propagation phenomena
[AD-749504] 05 p0581 N73-14727
Quantum electrodynamic view of superradiance as competition between stimulated and spontaneous atomic decay
[AD-750005] 05 p0582 N73-14741
Coherent optical processing of phased array radar data, using electron beam addressed, potassium dideuterium phosphate modulator
05 p0610 N73-14957
Structural effects of various optical coatings on single shot laser induced damage threshold using pulsed neodymium glass laser
[AD-749852] 06 p0680 N73-15531
Application of quasistatic theory of spectral line broadening to predict values for laser radiation
[AD-750156] 06 p0681 N73-15541
Absorption of carbon dioxide laser radiation by gaseous sulfur hexafluorine in air boundary layers
[AD-751016] 06 p0681 N73-15546
Characteristics and operation of videocoherent system for improved target acquisition and measurement of target velocity
07 p0755 N73-16133
Design and development of multichannel laser remote control system using modulated helium-neon laser as transmitter and light collector as receiving antenna
[NASA-CASE-LAR-10311-1] 07 p0806 N73-16536
Proceedings of conference to determine research projects for development of lasers for optical communications applications
[PB-212692] 07 p0807 N73-16543
Pockels cell for splitting light pulses from NdYAG mode locked pulsed laser
[AD-751532] 07 p0807 N73-16550
Temporal spectra of fluctuations in atmospherically degraded spherical waves
[AD-751304] 07 p0807 N73-16551
Evaluation of infrared laser beams using thin membrane type displays of cholestric liquid crystals
[AD-752201] 08 p0930 N73-17616
Development of electronically tunable dye laser with capability for producing two randomly accessible and simultaneous frequencies
[AD-752053] 08 p0933 N73-17641
Analysis of plasmas produced by high power laser beam irradiation of beryllium, carbon, and polyethylene targets
[IPPJ-142] 08 p0947 N73-17754
Development of optical equipment including image converters and infrared detectors employing coherent radiation
[AD-753275] 09 p1067 N73-18711
Pair of coherent frequency-hopped/pseudo noise frequency synthesizers
[AD-753399] 10 p1135 N73-19252
Variation of laser radiation intensity along axis of unstable optical cavity with partially transmitting mirrors or gratings
[AD-753902] 10 p1170 N73-19515
Intensity stabilization and development of tunable ultranarrowband dye laser
[AD-754112] 10 p1170 N73-19517
Development of techniques for frequency tripling laser radiation based on mixtures of metal vapors and inert gases
[AD-754096] 11 p1304 N73-20581
Coherent behavior of Josephson junction arrays
[BNL-17232] 12 p1441 N73-21671
Experimental facility for measuring rotational Raman scattering cross sections of nitrogen and oxygen at 10.6 microns
[AD-757111] 14 p1617 N73-23098
Homodyne interferometer for measuring phase variations of laser beam wave front
[AD-756885] 14 p1668 N73-23539
Performance capabilities of erbium lasers and tabulation of laser materials to show chemical composition, mode of operation, frequency and output characteristics
[PHL-1973-12] 14 p1672 N73-23565

Analysis of atmospheric transmission properties of 1.06 microns radiation using neodymium laser
[AD-757249] 14 p1672 N73-23572
Laser beam scintillation caused by atmospheric turbulence
[AD-757562] 14 p1674 N73-23580
Analysis of acoustical amplitude and frequency modulation techniques of continuous wave helium-neon laser for optical communication applications
[AD-757672] 14 p1674 N73-23581
Analysis of laser outputs required to initiate gas breakdown when gas contains suspended particles
[AD-757517] 14 p1674 N73-23585
Analysis of effects of high power lasers to include interactions with plasma, metals, dielectrics, semiconductors, and gases
[AD-755820] 14 p1674 N73-23586
Theory for third harmonic generation due to broad band optical pulses in picosecond time region
[AD-757211] 14 p1693 N73-23742
Performance tests of copper vapor laser and analysis of relaxation of metastable lower levels
15 p1794 N73-24544
General expression for short term average optical beam spread of initially coherent beam wave propagating in turbulent medium
[AD-759804] 16 p1925 N73-25573
Tunable infrared parametric oscillators and coherent spectroscopy
[AD-759408] 16 p1945 N73-25741
Application of matched filtering techniques for detection of mode locked laser signals
17 p2039 N73-26496
Electron beam, quantum electronics, and solid state devices for useful frequency extension into microwave and optical frequencies
[AD-759066] 17 p2041 N73-26510
Development and characteristics of instrument to measure back reflection of laser radiation
17 p2041 N73-26515
Analysis of changes in amplitudes and frequencies of laser oscillations due to effect of weak reflected signal
17 p2041 N73-26516
Numerical analysis of stationary internal structure of plasma in homogeneous carbon dioxide laser discharge
[DREV-TN-2061/73] 18 p2157 N73-27430
Development of laser model for analyzing pulsed excitation of molecules in discharge and nonequilibrium discharge of supersonic flow in vacuum
[JPRS-59040] 18 p2158 N73-27432
Restoration of atmospherically degraded laser beam and definition of isoplanatic patch size
[AD-760548] 18 p2158 N73-27437
Coherent laser light measurement of ceramic material surface roughness
[AD-761198] 18 p2168 N73-27512
Effect of transverse pumping distribution on energetics and profiles of thermo-optical distortions of laser in solution of rhodamine dye
[NLL-M-23052-[5828.4F]] 20 p2424 N73-29472
Development of nitrogen-laser-pumped tunable-dye laser for application as spectroscopic light source
20 p2424 N73-29473
Development of laser amplifier using disks of neodymium glass and measurement of beam amplification for laser beams
[EP-RR-35] 20 p2425 N73-29478
Effect of atmospheric turbulence on stability of laser radiation propagation
[AD-763109] 20 p2427 N73-29494
Development and characteristics of radar receiver for detecting coherent and incoherent optical signals against background of noise
22 p2630 N73-31075
Coherent charged particle propagation in magnetic fields
[NASA-CR-135492] 22 p2702 N73-31639
Operation of Laflamme double-discharge laser structure up to pressures of several atmospheres
[DREV-TN-2092/73] 23 p2800 N73-32397
Application of laser energy to induce homogeneous exchange reaction of hydrogen and deuterium
24 p2930 N73-33399
Induced reactions in gas mixtures using carbon dioxide laser pulses and electrical discharges
24 p2930 N73-33400
Application of incoherent and coherent light sources for underwater illumination and comparison of efficiency for various conditions
24 p2958 N73-33633

**COHERENT SCATTERING**
HCN laser study of coherent scattering from waves in plasma confinement and heating experiments
[IPP-4/39] 12 p1435 N73-21631
Approximative model for coherent electromagnetic wave scattering from bounded plasma waves
[IPP-4/48] 17 p2067 N73-26728

**COHERENT SOUND**
U SOUND WAVES

**COHERENT SOURCES**
U COHERENT RADIATION
U RADIATION SOURCES

**COHERENT TRANSMISSION**
U COHERENT RADIATION

**COHESION**
Thin film physics, cohesive and dielectric properties, and solid state theory
[COO-623-190] 12 p1439 N73-21658

**COILS**
Numerical analysis of elastic stresses and deflections of helical compression springs made of round wire
[ESDU-65005] 01 p0112 N73-10926
Analysis of factors affecting choice of material and manufacturing methods for production of helical compression springs
[ESDU-65006] 01 p0112 N73-10927
Bumpy torus magnet facility with 12 superconducting coils, each 19 cm and capable of 3.0 tesla on their axes
[NASA-TM-X-68165] 06 p0648 N73-15266
Superconductors in marine technology, including coils, solenoids, and magnetic systems
[AD-755711] 13 p1567 N73-22702

**COIN AIRCRAFT**
NT F-5 AIRCRAFT
NT OV-10 AIRCRAFT

**COINCIDENCE CIRCUITS**
Pion electroproduction cross section measured near threshold by coincidence experiments
[NOTA-INTERNA-383-A] 01 p0084 N73-10696
Extended applications and improvement of 4 pi beta-gamma coincidence method in standardization of radionuclides
[RR-730] 06 p0702 N73-15724

**COKE AIRCRAFT**
U AN-24 AIRCRAFT

**COLD CATHODE TUBES**
NT PHOTOMULTIPLIER TUBES

**COLD CATHODES**
Evaluation of cold cathode materials for sealed off carbon dioxide lasers to show power output and service life
[NASA-CR-130202] 11 p1302 N73-20564
Fabrication of cold cathode optoelectronic electron emitter with emission properties suitable for practical applications
[AD-760601] 18 p2123 N73-27162
Cold cathode materials for constructing sealed off CO2 lasers
[NASA-TN-D-7307] 20 p2425 N73-29480
Cold cathode discharge tube with pressurized gas cell for meteoroid detection in space
[NASA-CASE-LAR-10483-1] 23 p2791 N73-32327

**COLD FLOW TESTS**
Cold flow tests of factors affecting noise suppression and thrust loss of divergent lobe supersonic jet noise suppressor
[NASA-TM-X-2820] 18 p2101 N73-26992

**COLD FORMING**
U COLD WORKING

**COLD HARDENING**
Stress state and deformation characteristics of hardening carbon steel with decreasing temperatures
[AD-746723] 02 p0188 N73-11527
Phase structure of crystallizing nickel tin alloy melt during cooling
[JPRS-58681] 12 p1414 N73-21456

**COLD PLASMAS**
Application of reductive perturbation method to electromagnetic waves propagating in cold electron plasma
[IPPJ-136] 02 p0216 N73-11745
Boundary value solution for current distribution on infinite tubular antenna in cold collisionless plasma
[NASA-CR-130297] 06 p0640 N73-15194
Analysis of sinusoidally varying point induced charge potential in cold, homogeneous, and boundless magnetoplasma
[GRI/TP/109] 06 p0703 N73-15733
Excitation of electromagnetic waves in cold plasma contained in metal waveguide by electron beam
[AEC-TR-7333] 07 p0827 N73-16704
Propagation of magnetohydrodynamic waves in cold plasma inclined to ionosphere and applied to geomagnetic pulsation study
[PR-119] 10 p1156 N73-19401
Wave-wave coupling in cold beam/cold plasma system
12 p1433 N73-21608
Energy loss method for calculating synchrotron-Cerenkov radiation of relativistic electrons in cold magnetoplasma
[AD-755387] 13 p1564 N73-22675
Excitation of longitudinal waves in collisionless and cold plasma in presence of uniform magnetic field
[AD-756477] 14 p1696 N73-23764
Theoretical analysis of ion cyclotron wave dynamics in cold plasma
[IPPJ-150] 15 p1816 N73-24722
Artificial plasma injection of lithium cloud in program to stimulate electromagnetic cyclotron instabilities in magnetosphere
[AD-760032] 17 p2029 N73-26424
Transient response of stratified cold plasma to infinite plane impulsive electromagnetic wave incident vertically on ionization
21 p2582 N73-30693
Millimeter wave polarimeters and Cotton-Mouton effect in plasmas
[EUR-CEA-FC-675] 24 p2965 N73-33694

**COLD TOLERANCE**
Low temperature tolerance and adaptation of biological systems to space environment
[JPRS-59129] 14 p1610 N73-23055

**COLD WALLS**
U WALLS

**COLD WEATHER**
Simulation of monthly variation of local surface energy budget and sub-surface temperature regime in Antarctica
10 p1146 N73-19326

**COLD WEATHER TESTS**
Cold weather tests to determine application of ground effect machines for military logistic purposes in Arctic regions
[AD-753527] 10 p1107 N73-19027
Cold weather construction practices relative to men, materials, and equipment
[AD-745395] 13 p1506 N73-22206
Problems associated with instrumentation for Arctic tests
[AD-758170] 15 p1789 N73-24502
Cold weather tests on military equipment
[AD-761105] 18 p2214 N73-27881
Analysis of Tenth Soviet Antarctic Expedition to show preparations, logistic support, and operational accomplishments
20 p2406 N73-29340

**COLD WORKING**
NT EXPLOSIVE FORMING
Effects of axially symmetric deformation of metal on mechanical and physical properties of samples
[AD-745551] 01 p0063 N73-10513
Automated planning systems for cold forging production processes
[NLL-NEL-TT-2393-[6075.461]]
02 p0177 N73-11436
Metal temperature effect on friction factor in cold rolling within 20 to 250 C
[AD-746935] 02 p0180 N73-11455
Analysis of hydrogen diffusion in alpha-iron in six degree to seventy seven degrees Kelvin using magnetic after-effect technique
[COO-1198-903] 03 p0314 N73-12561
Influence of grain size and cold working on static corrosion of Incoloy 800 alloy in superheated steam
[EURFNR-965] 03 p0315 N73-12570
Cold plastic deformation process for manufacturing molds and stamps from sintered metal powder ceramic blanks
04 p0432 N73-13519
Critical cold work for grain coarsening of equiaxed alpha Ti-5Al-2.5Sn alloy heated at 1144 K for one hr after plastic tensile deformation
[AD-748352] 04 p0435 N73-13550
Effects of various forming factors and process variables on forming of sheet metal products
05 p0551 N73-14476
Analysis of metallurgical factors and mechanical effects during and subsequent to cold hydrostatic extrusion of magnesium and aluminum alloys
[AD-751739] 07 p0805 N73-16527
Effect of annealing on substructure of cold worked FCC copper alloys and metals
[COO-1431-14] 10 p1173 N73-19540
Shear instabilities and tensile fracture characteristics of cold worked 1080 pearlitic steel
[AD-755102] 11 p1307 N73-20604
Effect of viscous lubricants on metal flow during cold reverse extrusion
[AD-743242] 13 p1533 N73-22425
Plastic deformation of cold worked metals
[AD-762468] 19 p2310 N73-28583

**COLLAGENS**
Hydroxyproline determination in collagen-like plasma and urine
[NASA-TT-F-15093] 22 p2620 N73-30997

**COLLAPSE**
Approximative prediction for elastic collapse of spherical shell with flat spot region under external pressure
[NASA-CR-130961] 09 p1096 N73-18946
Collapse of homogeneous fluid mass immersed in vertically stratified fluid
[AD-757995] 15 p1769 N73-24330
Numerical analysis of collapse of homogeneous fluid mass in stratified fluid
[AD-763657] 21 p2526 N73-30257
Collapsible piston for hypervelocity gun
[NASA-CASE-MSC-13789-1] 23 p2769 N73-32152

**COLLECTION**
Automatic liquid collection and disposal system
[NASA-CASE-LAR-11071-1] 09 p1039 N73-18474

**COLLECTORS**
U ACCUMULATORS

**COLLEGES**
U UNIVERSITIES

**COLLIMATION**
Refocusing of spent axisymmetric beam in klystron tubes for optimal entry into multistage depressed potential collector
[NASA-CR-121114] 05 p0519 N73-14217

**COLLIMATORS**
Design and performance of optical altimeter with shaft angle recording
[AD-749964] 06 p0675 N73-15488
Beam position monitor which operates by detection of temperature differences
[AERE-M-2372] 17 p2033 N73-26452
HEAO-A integrated modulation collimator experiment for determining angular sizes and celestial position of X ray sources
17 p2085 N73-26867
Focusing optical collimator for high resolution scanning of electromagnetic radiations, neutrons, and other particles
[NASA-CASE-MFS-20932-1] 18 p2150 N73-27380
Collimator for analyzing spatial location of near and distant sources of radiation
[NASA-CASE-MFS-20546-2] 21 p2543 N73-30389

**COLLISION AVOIDANCE**
Flight tests of transponder correlation ranging equipment for use in airborne collision avoidance system
[AD-746448] 02 p0175 N73-11416
Application of time frequency techniques to improve navigation of ships and reduce risk of collision
[NASA-TT-F-14718] 02 p0207 N73-11679
In flight incident involving near miss of Boeing 720 aircraft and Convair 240 aircraft near Front Royal, Virginia on 26 Apr. 1972
[NTSB-AAR-72-30] 03 p0252 N73-12040
Development and operating principles of collision warning system for aircraft accident prevention
[NASA-CASE-HQN-10703] 04 p0446 N73-13643
Differential game theory for optimal collision avoidance between two aircraft moving in horizontal plane
[NASA-CR-129988] 05 p0577 N73-14701
Doppler effect continuous wave radar for bird hazard detection and aircraft collision avoidance near airfields
[AD-751985] 08 p0885 N73-17168
Development of computer programs for design of air route networks for improved flight safety - Part 1
[FAA-RD-72-118-1-PT-1] 10 p1185 N73-19643
Analysis of interaction of major elements of Oceanic Air Traffic Control System to determine minimum longitudinal and lateral separation distances
[FAA-RD-73-8] 11 p1321 N73-20719
Analysis of aircraft pilot capability to visually detect other aircraft in air to air situation as collision avoidance feasibility
[FAA-RD-73-40] 12 p1374 N73-21145
Performance tests to determine capability of aircraft pilots to avoid midair collisions based on visual perception of target and information from pilot warning indicator
12 p1374 N73-21146
Photographic recording of aircraft in near midair collision conditions to determine feasibility of collision avoidance based on visual perception of pilot
[CDC-JL-5] 12 p1374 N73-21147
Analysis of flight tests to determine range of visual detection of aircraft as basis for visual perception to avoid midair collisions
12 p1374 N73-21148
Development of collision avoidance warning system criterion for use with aircraft operating in high density areas
13 p1471 N73-21915
Proceedings of conference on air traffic control developments and procedures
[AGARD-CP-105] 14 p1687 N73-23689
Air traffic control facilities operated by U.S. military forces and developments in improved air traffic control systems
14 p1687 N73-23690
Status and trends of civil air traffic control systems and development of automated network for increased flight safety
14 p1688 N73-23696
Numerical anlaysis of optimal control and sequencing of air traffic control operations in near terminal area
14 p1688 N73-23701
Development and characteristics of air traffic management system for operation of military aircraft under instrument meteorological conditions
14 p1689 N73-23704
Development and characteristics of system for separation and control of aircraft to avoid midair collisions
14 p1690 N73-23712
Performance tests of air traffic control system to determine effectiveness in prevention of midair collisions
14 p1690 N73-23713
Analysis of development program for improving US air traffic control procedures for 1980 time period
14 p1690 N73-23718
Computerized multistage decision process for radar operator aid in collision avoidance trajectory control
14 p1711 N73-23886
Development and characteristics of electronic signalling system and data processing equipment for warning systems to avoid midair collisions between aircraft
[NASA-CASE-LAR-10717-1] 21 p2576 N73-30641
Reduction of midair collision hazard with bats through tracking by radar and use of high intensity lights
[AD-764828] 23 p2746 N73-31982
Bird migration patterns using radio transmitters with application to reduction of aircraft hazards during migration in congested air routes
[AD-764830] 23 p2746 N73-31983
Digital synchronization of airborne collision avoidance systems
[DGLR-PAPER-73-012] 23 p2817 N73-32519
Evaluation of large screen display for automated oceanic air traffic control applications
[FAA-ND-73-75] 24 p2950 N73-33568

**COLLISION PARAMETERS**
NT COLLISION RATES
Differential scattering from collision of metastable atoms of He[2 3S] with molecules of N2 and O2
[NASA-TT-F-14801] 15 p1815 N73-24712
Collisional effects on ion distribution function and potential in Tonks-Langmuir plasma sheath problem
20 p2457 N73-29745
Cross section for collision processes between molecular oxygen and electron with collision energy below 100 eV
[NASA-TT-F-15048] 23 p2821 N73-32550
Application of laser energy to induce homogeneous exchange reaction of hydrogen and deuterium
24 p2930 N73-33399

**COLLISION RATES**
Measurement of effective collision frequency in RF heating through decay instability in Q device plasma
[CONF-720705-2] 07 p0755 N73-16136

**COLLISION WARNING DEVICES**
U COLLISION AVOIDANCE
U WARNING SYSTEMS

**COLLISIONAL PLASMAS**
Computerized simulation of wave field distributions in collisional plasma
22 p2703 N73-31646

**COLLISIONLESS PLASMAS**
Numerical simulation of one-dimensional collisionless plasma phenomena - users manual
[AD-745423] 01 p0085 N73-10706
Influence of inhomogeneity on structure of collisionless turbulent shock wave in high beta infinite plasma
[AD-746467] 02 p0217 N73-11756
Computerized simulation of nonlinear evolution of high frequency, flute-like plasma microinstabilities
[ORNL-TM-3812] 03 p0341 N73-12781
Computerized simulation of whistler instabilities in anisotropic collisionless plasmas
[AD-748176] 03 p0344 N73-12805
Lagrangian method used for describing small signal wave propagation and nonlinear wave interaction in warm collisionless plasmas
[NASA-CR-129922] 05 p0583 N73-14744
Numerical simulation and study of collisional plasmas and shock tube phenomena
[COO-3086-15] 05 p0583 N73-14748
Particle loss rate from mirror machines, and radiation coupling in dense plasmas
[COO-2181-9] 06 p0704 N73-15744
Fast electron production by absorption of shf wave in collisionless plasma
[AEC-TR-7331] 07 p0827 N73-16700
Collisionless ion acoustic shocks with high Mach number in plasma
[IPPJ-119] 08 p0948 N73-17765
Model of shock wave propagation parallel to external magnetic field in hot collisionless plasma with turbulent dissipation based on garden hose instability
[MPI-PAE/EXTRATERR-69] 09 p1071 N73-18736
Penning discharge along magnetic field in collision-free plasma to simulate geomagnetic flux tube conditions
[TRITA-EPP-72-13] 10 p1189 N73-19676
Striction and thermal mechanisms of superhigh frequency, self stress in collisionless plasma
[AEC-TR-7374] 10 p1196 N73-19733
Superhigh frequency emission of collisionless magnetized plasma on its interaction with pumping wave in microwave range
[AEC-TR-7373] 10 p1197 N73-19736
Structure of large amplitude stationary hydromagnetic disturbance in collisionless plasma
12 p1432 N73-21604
Computer simulation of collisionless plasma with self-electric and magnetic interactions
[COO-2200-1] 12 p1434 N73-21619
Description of linear wave propagation in hot collisionless plasmas using Vlasov and Maxwell equations
[NASA-CR-131496] 13 p1562 N73-22663
Excitation of longitudinal waves in collisionless and cold plasma in presence of uniform magnetic field
[AD-756477] 14 p1696 N73-23764
Collisionless plasma with two stream coupling of corona and core in C02 laser-heated pellets
[AD-757790] 15 p1818 N73-24740
Coupling of magnetic pulse to initially magnetized collisionless plasma
16 p1948 N73-25759
Observation of laminar electrostatic shock waves in collisionless plasma generated by ion beam
[IPPJ-156] 16 p1949 N73-25771
Reverse deflection and contraction of plasma beam entering a curved magnetic field
[TRITA-EPP-72-32] 17 p2068 N73-26735
Drift waves in finite beta plasmas
19 p2323 N73-28690
Collisionless shock waves in argon plasma pinch discharge
[AD-762426] 19 p2325 N73-28707
Laboratory analysis of high Beta collision-free plasma shock waves
20 p2457 N73-29749
Nonlinear Schrodinger equation for studying nonlinear wave modulation in magnetized collisionless plasma
[IPPJ-162] 20 p2458 N73-29755
Large amplitude electron plasma wave with trailing wave train in collisionless plasma
[IPPJ-163] 20 p2458 N73-29756
Shear stabilization of collisionless drift wave instability
[IPPJ-166] 20 p2459 N73-29759
Linear ion acoustic waves in density gradient in collisionless discharge plasma
[ORO-4338-2] 22 p2702 N73-31640
Nonlinear small-amplitude behavior of collisionless plasma
23 p2822 N73-32561
Measurement of turbulence in collisionless oblique plasma shock by scattered ruby laser light
24 p2961 N73-33665
Mathematical model for noncollisional plasma
[FRNC-TH-329] 24 p2963 N73-33679
Plasma transport properties and confinement
[COO-2168-5] 24 p2965 N73-33696

**COLLISIONS**
NT ATOMIC COLLISIONS
NT COULOMB COLLISIONS
NT INELASTIC COLLISIONS
NT IONIC COLLISIONS
NT METEORITE COLLISIONS
NT MIDAIR COLLISIONS
NT MOLECULAR COLLISIONS
NT PARTICLE COLLISIONS
Penetration and wake formation in interstellar cloud collision
16 p1961 N73-25862
Aircraft accident involving ground collision of DC-9 and CV-880 aircraft at O Hare International Airport, Chicago, Illinois on 20 December, 1972
[NTSB-AAR-73-15] 22 p2614 N73-30945

**COLLOCATION**
Algorithm for modifying collocation method of solving differential equations
[NASA-TT-F-14800] 15 p1803 N73-24616
Collocation method for numerical solution of buckling of conical shells under hydrostatic pressure
[AD-758834] 16 p1971 N73-25947

**COLLOIDAL PROPELLANTS**
Colloidal thrustor propellant performance discussing thrustor design and propellant choice
[ESRO-CR-53] 03 p0349 N73-12851
Anomalous rheological characteristics of high-internal-phase-ratio emulsions containing 97 to 98 percent liquid fuel as dispersed phase
[AD-758908] 15 p1823 N73-24779

**COLLOIDS**
NT AEROSOLS
NT COLLOIDAL PROPELLANTS
NT FOG
Method for studying absorption spectra of colloidal solutions
[NASA-TT-F-14497] 01 p0023 N73-10177
Magnetic fluid preparation by grinding and concentrating pyrophoric antiferromagnetic iron oxide colloidals
[BM-RI-7702] 05 p0580 N73-14721
Design and tests of advanced colloid thruster system components
[AD-749961] 05 p0591 N73-14801
Colloid thruster producing beams with anisotropic current, specific charge, and mass flow distributions
[AD-754902] 11 p1335 N73-20836

**COLONIES**
Systems engineering study for proposed lunar colony
[NASA-CR-129164] 02 p0152 N73-11236

**COLOR**
NT IRIDESCENCE
NT WATER COLOR
Color naming latencies with brief exposures of individual Stroop and control stimuli
[AD-745106] 01 p0012 N73-10094
Acyclic color rings of planar graphs
[AD-747662] 03 p0325 N73-12652
Television reviewing conditions, including contrast handling requirements of color TV display
[BBC-1972/37] 06 p0638 N73-15182

Legibility and recognition by test groups of displayed signals differing by brightness or color
[DLR-FB-71-57] 06 p0674 N73-15484
Phytoplankton density determination from ocean color measurements
08 p0972 N73-17939
Distribution of color variations in Mare Nubium and Southern Oceanus Procellarum lunar regions
12 p1455 N73-21786
Terrain factor analysis and automatic color coded mapping using image processing methods in estimation of construction time relative to prospective military airfields
[AD-755531] 13 p1526 N73-22367
Multichannel ocean color data analysis to produce color maps
[TRW-21123-6001-RU-00] 18 p2144 N73-27328
Chemical spot test for identifying magnesium or magnesium alloys used in aerospace applications
[NASA-CASE-LAR-10953-1] 18 p2160 N73-27446
Comparison of color index and formation conditions of cluster and field galaxies
[NLL-RTS-8000] 21 p2593 N73-30780
Contrast color coating for meteoroid impact position locator for space vehicles
[NASA-CASE-LAR-10629-1] 23 p2793 N73-32348

**COLOR BLINDNESS**
U COLOR VISION

**COLOR CENTERS**
Coloring memory crystals by electron bombardment and KCl, Na, Cl for thermoelectric cooling for high density optical memory
[AD-765391] 23 p2762 N73-32105

**COLOR PERCEPTION**
U COLOR VISION

**COLOR PHOTOGRAPHY**
Use of TV equipment for converting color negative cinefilm into color positive image
[DRIC-TRANS-2835] 02 p0174 N73-11412
Tests and evaluations of methods for recovering ground colors in aerial photographs
[AD-747340] 03 p0304 N73-12481
Color film spectroscopy for quantitative optical radiation detection
[EGG-1183-5015] 06 p0674 N73-15483
Application of color photography and infrared photography for determining effects of weather on coffee crop production
07 p0783 N73-16365
Detection of disease in coffee crops using color photography and infrared photography techniques
07 p0783 N73-16366
Comparison of imagery obtained with several types of remote sensors over Test Site 701, Mexico
07 p0783 N73-16367
Analysis of imagery obtained from infrared color and color photography used for highway and railroad engineering applications
07 p0783 N73-16368
Detection of citrus tree anomalies by remote sensing with infrared color aerial photography
07 p0785 N73-16384
Analysis of oceanography remote sensing using black and white, color, and color infrared photographic recording
07 p0788 N73-16407
Relationship between maize canopy density and reflected energy determined from color and color infrared photographs
[NASA-CR-130370] 07 p0790 N73-16422
Comparison of monochrome and color film for air to ground target acquisition
[RAE-TR-72064] 07 p0801 N73-16504
Spurious image and color rendition problems in producing multicolor holograms
[AD-751560] 07 p0801 N73-16508
Soviet method of illumination calculation for aerial survey on color film
[AD-754627] 11 p1295 N73-20508
Technique for reproducing negative color film in telecine
[BBC-RD-1973/2] 14 p1666 N73-23517
Color photographic techniques to study vegetation and terrain, improve mapping methods, and to provide photoelectronic color separation using aerial cameras
[AD-756700] 14 p1668 N73-23536
Color and color infrared aerial photographic detection of Dutch elm disease
16 p1866 N73-25110
Application of ERTS-1 RBV and multispectral scanner imagery for assessment of ocean water color
[E73-10718] 17 p2019 N73-26325
Pseudocolor transformation of ERTS-1 imagery of Monterey Bay-San Francisco, California area
[PAPER-112] 19 p2278 N73-28333
Image acquisition and enhancement techniques for oceanographic photography using photo-optical and electronic methods
[AD-761663] 19 p2296 N73-28463
Research needs in ocean color data analysis
[NASA-TM-X-70466] 22 p2665 N73-31355
Apollo 17 mission at Taurus Littrow with color illustration and summaries
[NASA-EP-102] 24 p2979 N73-33804

**COLOR TELEVISION**
Development of system for eliminating constant luminance failure in color television systems by modifying coding process
[BBC-1972/29] 01 p0023 N73-10180
Development of graphical method for determining chromaticity and relative luminance of test color reproduced by color television display
[BBC-1972/30] 01 p0023 N73-10182
Television picture quality dependence on color tone change from phase shift of color carrier
[NLL-TRANS-2870-[9022.81]] 02 p0139 N73-11125
Military applications of single gun color cathode ray tubes in display devices
[AD-748385] 04 p0396 N73-13222
Encoding action of pair of dichroic gratings suitable for single tube color television camera
[BBC-1972/32] 04 p0419 N73-13414
Development and performance of color television equipment developed for use on Apollo 15 mission
04 p0473 N73-13855
Specification for group delay variation in upper video band of television transmission system based on chrominance pulse tests
[BBC-1972/39] 06 p0638 N73-15181
Specifications and characteristics of ground-commanded color television assembly used on Apollo 15 flight
[NASA-CR-128829] 10 p1128 N73-19192
Reception of positive color television images using negative color motion picture film
[NLL-DRIC-TRANS-2835-[3623.66]] 11 p1291 N73-20480
Video tape recorder with scan conversion playback for color television signals
[NASA-CASE-NPO-10166-1] 13 p1490 N73-22076
Television readout devices for color display of data and picture blending
[NLL-PO-2958-[9022.81]] 15 p1755 N73-24225
Cathodochromic storage and display for television systems
[NASA-CR-130236] 15 p1756 N73-24233
Space shuttle visual simulation system design study
[NASA-CR-128940] 15 p1760 N73-24265

**COLOR VISION**
Influence of illumination color, viewing distance, and turbidity on underwater vision
[AD-743756] 01 p0012 N73-10092
Literature review on psychophysiological factors affecting visual perception of colored signal light
[AD-746297] 02 p0133 N73-11083
Color vision requirements for flying personnel of various armed forces - conferences
[AGARD-CP-99] 10 p1112 N73-19065
Three color receptors of Young-Helmholtz and opponent color types of information processing
10 p1112 N73-19066
Color vision requirements for German Air Force personnel
10 p1112 N73-19067
Color aptitude of dyschromatopsia French navigators and pilots
10 p1113 N73-19068
Color vision testing and selection procedures for flying personnel since World War I
10 p1113 N73-19069
Color vision requirements of Canadian Armed Forces, including their standard tests
10 p1113 N73-19070
Standardization of tests and classification of color perception abnormalities in military personnel
10 p1113 N73-19071
Color vision requirements of Great Britain's Armed Forces
10 p1113 N73-19072
Comparison of accident rates among color defective and normal personnel
10 p1113 N73-19073
Color vision tests as predictive indicators of flying task performance
10 p1113 N73-19074
Helicopter flying in poor light and featureless terrain and color vision abnormality
10 p1113 N73-19075
Color vision requirements for air crew personnel of future, including coding evaluation
[AMRL-TR-71-116] 10 p1113 N73-19076
Proceedings of symposium on color vision, color perception, visual acuity, and psychophysiology
[AD-754328] 11 p1249 N73-20136
Effects of reduced atmospheric pressure, elimination of nitrogen, hypoxia, and exposure to restricted visual environment on range of accommodation and color vision
[NASA-CR-128896] 13 p1484 N73-22037
Literature review on human macular pigment absorption and density spectrum of cone receptor
[IZF-1972-17] 14 p1609 N73-23046
Chromatic induction and spatial intraocular straylight effects in human perception of contrast colors
[IZF-1972-19] 14 p1692 N73-23730
Color vision standards for flying military aircrews
[FPRC/1319] 19 p2225 N73-27942
Relationship between intermediate medium, and transformation and contrast phenomena
[NASA-TT-F-15035] 20 p2371 N73-29055

**COLORADO**
NT COLORADO PLATEAU [US]
Visual inspection of runway conditions at Butts Army Airfield, Fort Carson, Colorado
[AD-743859] 01 p0037 N73-10293
Utilization of ERTS-1 imagery for water depth measurement, mapping of Yellowstone Park, atmospheric effects in Colorado, lake ice surveillance, recreational land use, IFYGL Lake Ontario, image enhancement, water quality monitoring, and oil pollution detection
[E72-10201] 02 p0144 N73-11167
Utilization of ERTS-1 imagery for water depth measurement, mapping of Yellowstone Park, atmospheric effects in Colorado, lake ice surveillance, recreational land use, IFYGL Lake Ontario, image enhancement, water quality monitoring, oil pollution detection, and mapping iron compounds
[E72-10198] 02 p0160 N73-11296
Analysis of ERTS-1 imagery for Colorado environments using automatic data processing techniques
[E72-10204] 02 p0161 N73-11301
Gravity observations near San Juan Moutains in Colorado
[PB-211430] 05 p0340 N73-14395
Interdisciplinary analysis of ERTS-1 multispectral data of Colorado mountain areas using automatic data processing techniques
[E73-10033] 06 p0661 N73-15366
Analysis of ERTS-1 imagery for identification and discrimination of geological, hydrological, and mineral phenomena in western and central Colorado
[E73-10041] 07 p0776 N73-16304
Forest and rangeland inventory and forest infestation of Atlanta, Manitou, and Black Hills test sites based on ERTS-1 imagery
[E73-10084] 08 p0901 N73-17296
Identification and interpretation of tectonic features of Colorado, California, and Sonora, Mexico
[E73-10275] 09 p1020 N73-18324
Survey and mapping Colorado geology using airborne remote sensors
[NASA-CR-130822] 09 p1025 N73-18370
Interdisciplinary analysis of ERTS-1 imagery for Colorado mountain areas using ADP techniques
[E73-10348] 10 p1148 N73-19347
Utilization of ERTS-1 imagery in structural reconnaissance for minerals and oil in Alaska, Canada, Montana, Colorado, New Mexico, and Texas
[E73-10414] 11 p1279 N73-20376
Analysis of ERTS-1 imagery for identification and discrimination of geological and hydrological phenomena in central and western Colorado
[E73-10422] 11 p1280 N73-20383
Interdisciplinary analysis of Skylab EREP MSS photography of vegetative and geomorphological cover types in Colorado Mountains
[E73-10533] 13 p1517 N73-22297
Ecology, hydrology, geomorphology, and terrain modeling of Colorado mountain environments from ERTS-2 data
[E73-10551] 14 p1655 N73-23424
Inventory of forests and rangelands, including forest stress, at Black Hills, Atlanta, Georgia, and Manitou, Colorado test sites using Skylab EREP
[E73-10587] 14 p1657 N73-23447
Use of remotely sensed data to solve water resource problems of Wolf Creek Watershed, Colorado
[NASA-CR-129001] 14 p1660 N73-23479
Statistical tests for determining Colorado River Basin response to natural or induced changes
[PB-214114/1] 14 p1665 N73-23513
Geologic, mineral, and water resources investigations in western Colorado using ERTS-1 imagery
[E73-10608] 15 p1773 N73-24369
Geologic mapping of Bonanza Test Site Colorado using remotely sensed data
[NASA-CR-132231] 15 p1780 N73-24433
Development of facilities and processing for determining increase in mean seasonal runoff due to cloud seeding in San Juan Mountains, Colorado
16 p1859 N73-25056
Commercial application of ERTS-1 imagery in structural reconnaissance for minerals and petroleum
[E73-10700] 16 p1903 N73-25392
TAXIR information retrieval system for analyzing climatic conditions on east slope of Colorado front range
[PB-214341/0] 16 p1939 N73-25688
Identification of copper/molybdenum porphyry mineral deposits in characteristic geologic setting in Nevada, Arizona, Colorado, Australia, Alaska, and New Guinea
[E73-10762] 17 p2023 N73-26362
Inventroy of forest and rangeland resources at Atlanta, Georgia, Black Hills, South Dakota, and Manitou, Colorado test sites using Skylab EREP imagery
[E73-10749] 18 p2133 N73-27237
Detection and inventory of timber and rangelands and forest stresses in Georgia, Colorado, and Black Hills from ERTS-1 imagery
[E73-10805] 18 p2138 N73-27280

Interpretation of geologic, mineral, and water resources in western Colorado from ERTS-1 imagery
[E73-10814] 18 p2139 N73-27289
Application of ERTS-1 imagery for identification of ecological analogs of natural vegetation and food crops in California, Colorado, and Louisiana
[PAPER-A6] 19 p2260 N73-28214
Analysis of ERTS-1 multispectral data by automatic pattern recognition procedures for geological mapping of San Juan Basin, Colorado
[PAPER-G25] 19 p2267 N73-28256
Application of ERTS-1 imagery to determine geological evidence of mineral and hydrocarbon accumulations in Alaska, Canada, Montana, Colorado, New Mexico, and Texas
[PAPER-G30] 19 p2267 N73-28261
Identification and discrimination of geological and hydrological phenomena in central and western Colorado using ERTS-1 imagery
[E73-10837] 19 p2290 N73-28415
Uniform mapping and monitoring of natural ecosystems and environments in California, Louisiana, and Colorado from ERTS-2 imagery
[E73-10839] 19 p2290 N73-28417
Skylab multispectral data for selected cover types in Colorado Mountains
[E73-10878] 20 p2393 N73-29229
Skylab inventory of forest and rangeland resources and forest stresses at Atlanta Georgia, Manitou, Colorado, and Black Hills test sites
[E73-10895] 20 p2395 N73-29244
Skylab MSS imagery of selected cover types in Colorado Mountains
[E73-10914] 20 p2397 N73-29263
Geologic, mineral, and water resources of western Colorado from Skylab EREP data
[E73-10918] 20 p2398 N73-29267
Geological surveys of Colorado from Skylab EREP photography
[E73-10919] 20 p2398 N73-29268
Regional environmental impact from oil shale development on private and public lands in Wyoming, Colorado, and Utah - Vol. 1
[EIS-AA-72-5242-D-1-VOL-1] 20 p2410 N73-29367
Energy alternatives to prototype oil shale leasing program for Wyoming, Colorado, and Utah - Vol. 2
[EIS-AA-72-5242-D-2-VOL-2] 20 p2410 N73-29368
Description of proposed leases for oil-shale program in Wyoming, Utah, and Colorado, and potential environmental impacts - Vol. 3
[EIS-AA-72-5242-D-3-VOL-3] 20 p2410 N73-29369
Physiographic terrain analysis in Colorado using principles of aerial photointerpretation 20 p2416 N73-29413
Recognition of geologic framework for ERTS-1 identification of mineral deposits of copper/molybdenum prophyry type in Colorado, Nevada, Arizona, and Australia
[E73-10960] 21 p2532 N73-30302
Gravity station data for upper part of Arkansas Valley area in Colorado
[PB-220865/0] 21 p2542 N73-30385
Uniform mapping of rice crops in Louisiana and California and desert vegetation in southwestern Colorado from Skylab imagery
[E73-10979] 22 p2657 N73-31286
Skylab imagery of terrain surface moisture, vegetation, and forestation in Colorado and Oregon
[E73-11001] 22 p2659 N73-31306
Analysis of geology, ecology, and hydrology of Colorado mountains from Skylab multispectral photography and data
[E73-11002] 22 p2659 N73-31307
Geologic and mineral and water resources of western Colorado from Skylab multispectral photography
[E73-11010] 22 p2660 N73-31315
Interdisciplinary analysis of Colorado Rocky Mountain environments using ADP techniques
[E73-11039] 23 p2778 N73-32218
Inventory of forest and rangeland resources and stresses at Atlanta, Georgia, Black Hills, South Dakota, and Manitou, Colorado from Skylab EREP
[E73-11040] 23 p2778 N73-32219
Identification and discrimination of geological, hydrological, and mineralogical phenomena in central and western Colorado from ERTS-1 data
[E73-11047] 23 p2779 N73-32223
Timber identification and inventory and forest management in Colorado, Georgia, Black Hills, California, and Hawaii from ERTS-1 imagery
[E73-11051] 23 p2779 N73-32227
Forest and rangeland inventory and detection of forest stress at Black Hills, South Dakota, Manitou, Colorado, and Atlanta, Georgia test sites
[E73-11052] 23 p2779 N73-32228
Multidisciplinary research on water depth measurement, Yellowstone Park, atmospheric effects, lake ice surveillance, recreational land use, IFYGL, image enhancement, water quality, oil pollution detection, and mapping iron compounds from ERTS-1 data
[E73-11119] 23 p2783 N73-32264
Monitoring weather conditions in Colorado for cloud seeding control
[E73-11071] 24 p2913 N73-33245
Geology, mineral deposits, and water resources of western Colorado from Skylab EREP data
[E73-11130] 24 p2917 N73-33285
Identification of selected forest and vegetation cover in Colorado Mountains from Skylab EREP data
[E73-11132] 24 p2917 N73-33287

**COLORADO PLATEAU [US]**

Geologic mapping of Basin and Range - Colorado Plateau boundary in Arizona using ERTS-1 imagery
[E72-10157] 01 p0044 N73-10347
Study of crustal structure from eastern Sierra Nevada to Colorado Plateau using ERTS-1 imagery
[E72-10192] 01 p0046 N73-10371
ERTS-1 imagery of crustal structure of area from eastern Sierra Nevada to Colorado Plateau
[E73-10028] 06 p0660 N73-15361
Geologic investigation of Basin and Range-Colorado Plateau boundary in northwestern and north central Arizona using ERTS-1 and EREP imagery
[E73-10074] 07 p0780 N73-16336
Development of system for mapping and monitoring natural ecosystems and environmental complexes from ERTS-1 imagery of California, Nevada, Four Corners Area, Louisiana, and Colorado Plateau
[E73-10289] 08 p0915 N73-17495
ERTS-1 imagery of crustal structure of strip from eastern Sierra Nevada to Colorado Plateau
[E73-10355] 10 p1149 N73-19351
ERTS-1 imagery applied to geological and water resources investigations of Basin and Range - Colorado Plateau boundary in northwestern and north central Arizona
[E73-10441] 11 p1282 N73-20401
ERTS-1 imagery of structural features in Colorado Plateau margin near Flagstaff, Arizona
[E73-10517] 14 p1654 N73-23411
ERTS-1 imagery of crustal structure of strip from eastern Sierra Nevada to Colorado Plateau
[E73-10529] 14 p1654 N73-23416
Application of ERTS-1 imagery to geologic investigations of Basin and Range Colorado Plateau boundary in northwestern and north-central Arizona
[E73-10645] 17 p2017 N73-26312
Application of ERTS-1 MSS imagery to study of tectonics and crustal structure of area from eastern Sierra Nevada to Colorado Plateau
[E73-10774] 18 p2135 N73-27250
Application of ERTS-1 and EREP imagery to geologically investigations of Basin and Range-Colorado Plateau boundary in Arizona
[E73-10799] 18 p2138 N73-27275
Mapping rice crops of California and Louisiana and natural vegetation of Colorado Plateau from Skylab photography
[E73-10885] 20 p2394 N73-29236
ERTS-1 reconnaissance of crustal structure of strip from eastern Sierra Nevada to Colorado Plateau
[E73-10985] 22 p2658 N73-31292
Application of Skylab multispectral photography and scanner images to geological survey of Basin-and Range-Colorado Plateau boundary in north central and central Arizona
[E73-11000] 22 p2659 N73-31305
Application of Skylab MSS imagery to geological survey of Basin-and-Range-Colorado Plateau boundary in Arizona
[E73-11042] 22 p2664 N73-31343
Uniform mapping and monitoring of natural ecosystems and environmental complexes of Colorado Plateau and Sierra-Lahontan areas and estimation of rice crop yields in California and Louisiana
[E73-11070] 23 p2781 N73-32246
Application of ERTS-1 and EREP imagery to geological surveys and mapping of Basin and Range - Colorado Plateau boundary in Arizona
[E73-11131] 24 p2917 N73-33286
Uniform mapping of vegetation and rice in Colorado Plateau, Sierra-Lahontan, California, and Louisiana coastal plain from Skylab multispectral photography
[E73-11149] 24 p2919 N73-33303

**COLORATION**
U COLOR

**COLORIMETRY**

Specific wavelength colorimeter for measuring given solute concentration in test sample
[NASA-CASE-MSC-14081-1] 09 p1035 N73-18443
Analysis of tungsten in tungsten steel by precipitation with cinchonine and spectrophotometric measurement of hydroquinone color
[AD-762122] 19 p2310 N73-28579

**COLUMNS [PROCESS ENGINEERING]**

Automatic control for absorption columns, fluidized bed processors, and continuous fermentation noting enzymatic protein production
[LAAS-PUBL-975] 24 p2892 N73-33090

**COLUMNS [SUPPORTS]**

Sensitivity of thin-walled compression members to column axis imperfection
[VTH-172] 13 p1587 N73-22863
Inelastic buckling of eccentrically loaded simply supported columns of rectangular and circular cross sections
[AD-756186] 13 p1589 N73-22887

**COMBAT**

Application of night vision technology helicopter night scouts 10 p1226 N73-19970
Combat use and combat effectiveness of fighter-interceptors
[AD-751512] 12 p1468 N73-21894
Biological effects of sleep deprivation, and effects of prolonged work on performance under combat conditions 14 p1723 N73-23989
Computerized simulation of tactical ground surveillance system
[AD-761805] 19 p2240 N73-28059
Combat job performance and training for air cavalry aeroscout pilot and aeroscout observer
[AD-755505] 23 p2753 N73-32027

**COMBINATIONS [MATHEMATICS]**

Universal cellular network for combinational switching functions with simple failure testing 03 p0278 N73-12252

**COMBINATORIAL ANALYSIS**
NT COMBINATIONS [MATHEMATICS]
NT FACTORIALS
NT PARTITIONS [MATHEMATICS]
NT PERMUTATIONS

Criteria for selected response surface methodology design variants in human performance research
[AD-748236] 05 p0503 N73-14099

**COMBINED STRESS**

Curves for determining maximum combined stresses in long circular cylindrical shells with flat head closure under uniform pressure only
[ESDU-66010] 01 p0111 N73-10912
Buckling and intial postbuckling of oval cylindrical shells under pure bending and under combined uniform axial compression and bending
[AD-747493] 04 p0482 N73-13939
Circular cylindrical shell pressure limits
[PB-212638] 07 p0852 N73-16912
Combined stress effects in human communication and motion sickness biodynamics 10 p1122 N73-19144
Combined heat, noise, and vibration effects on aircrew performance
[AMRL-TR-71-113] 10 p1122 N73-19146
Combined noise and vibration effects on human mental and psychomotor performance
[AMRL-TR-71-115] 10 p1122 N73-19147
Measures to determine psychophysiological reactions of military flight crews to flying stress 10 p1122 N73-19148
Temperature and noise irradiation effects on human energetic metabolism during vigilance task 10 p1123 N73-19155

**COMBUSTIBILITY**
U FLAMMABILITY

**COMBUSTIBLE FLOW**

Analysis of parameters involved in flow of combustion to produce stable propagation and efficient fuel consumption
[NLL-T1873/BGC/73-[9022.305]] 21 p2605 N73-30874
Characteristics of weakly turbulent flame with high activation energy and comparison with laminar flame spread
[AD-763340] 21 p2606 N73-30889

**COMBUSTION**
NT AFTERBURNING
NT BOUNDARY LAYER COMBUSTION
NT DEFLAGRATION
NT FUEL COMBUSTION
NT HYDROCARBON COMBUSTION
NT PROPELLANT COMBUSTION
NT SOLID PROPELLANT IGNITION
NT SUPERSONIC COMBUSTION

Theoretical study of time-independent and oscillatory combustion of nonmetallized AP/composite propellants
[NASA-CR-129198] 02 p0243 N73-11973
Solid propellant flame as source of amplification for acoustic pressure waves
[AD-746616] 03 p0365 N73-12971
Chemical reactions from combustion of unmixed gases
[NASA-TT-F-14360] 06 p0730 N73-15956
Device for detection of combustion light preceding gaseous explosions
[NASA-CASE-LAR-10739-1] 07 p0798 N73-16484
Chemical and physical properties and thermal decomposition products of certain natural fibers and synthetic materials
[AD-751899] 08 p0935 N73-17658
Combustion tests of afterburner performance of circular and parallel V-gutters for range of inlet temperatures to 1800 F
[NASA-TN-D-7212] 09 p1099 N73-18966
Thermochemical combustion effects of fuel-rich boron compound as solid rocket propellant
[AD-753105] 09 p1099 N73-18971
Analysis of stage-by-stage combustion process of methane in air
[AD-752862] 09 p1100 N73-18974
Interdependence of combustion processes and physico-mechanical behavior of solid fuels
[AD-754827] 11 p1333 N73-20817

Apollo 16 flight anomaly report to determine cause of burn holes in main parachute canopy
[NASA-TM-X-69127] 11 p1338 N73-20863
Computations of turbulent mixing and combustion of swirling jets in coaxial stream
[NASA-CR-2231] 11 p1348 N73-20935
Nonsteady combustion and extinguishment effects, including external thermal radiation effects, steady flame temperature, and L-stability limit
[AD-755860] 12 p1442 N73-21686
Safety hazards related to ignition and combustion in oxygen systems
[NASA-TM-X-68223] 12 p1464 N73-21861
Perturbation analysis of combustion and burning of initially unmixed reactants
[AD-755214] 13 p1592 N73-22906
Combustion tests of ammonium perchlorate-binder sandwich structures
[AD-757347] 14 p1719 N73-23952
Burning rate of JP-4 and air propellant in closed combustion chamber
[AD-757634] 14 p1720 N73-23954
Fourier analysis on ergodic calculations of reaction kinetic rate coefficients in air dissociation and hydrogen oxygen combustion
[AD-762421] 19 p2232 N73-27996
Numerical analysis and computerized simulation of open combustion processes and flame stability
[AD-762360] 19 p2353 N73-28925
Combustibility and toxicity of metals and alloys
[AD-764287] 22 p2621 N73-31003
Oxygen index method for evaluating flammability of organic polymeric materials
[DSL-REPT-561] 22 p2729 N73-31836
Smoke generation data on organic polymeric materials
[DSL-REPT-560] 22 p2729 N73-31837
Emission of air pollutants from combustion of wood wastes
[WSCI-72-1] 23 p2856 N73-32821
Color schlieren photography of ammonium perchlorate binder sandwich combustion
[AD-764489] 23 p2857 N73-32829
Explosive carbon burning effects of observed nuclei in solar system and constraints on supernova explosions
[LA-UR-73-489] 24 p2992 N73-33911

**COMBUSTION CHAMBERS**

Effects of fuel nozzle design on performance of annular combustor using natural gas fuel
[NASA-TN-D-7072] 02 p0223 N73-11805
Stability of small amplitude oscillations in combustion chambers for one and three dimensional problems
[AD-746132] 02 p0224 N73-11807
Measurement of pollutant levels of nitrogen oxides, unburned hydrocarbons, and carbon monoxide for annular, swirl can combustor
[NASA-TM-X-68160] 02 p0243 N73-11974
Aerodynamics structure of swirling flow in short cylindrical combustion chamber
[AD-747455] 03 p0365 N73-12975
Measuring flame temperature in exhaust nozzle and combustion chamber by pyrometer
04 p0420 N73-13425
Data dump of space shuttle orbiter maneuvering engine performance, weight, envelope, and interface pressure requirements for propellant combinations
[NASA-CR-128675] 04 p0464 N73-13784
Fabrication and acceptance tests of FLOX/MMH engine assemblies
[NASA-CR-130288] 06 p0712 N73-15814
Analysis of factors affecting cooling of liners in gas turbine combustion chambers
[NAL-TR-196] 06 p0713 N73-15819
Analysis of combustion liner wall temperatures under steady-state and convective heat balance conditions and comparison with experimental values
[NASA-TM-X-2711] 06 p0730 N73-15959
Test facility for combustion flow in open cycle magnetohydrodynamic generator
[AD-751251] 07 p0742 N73-16036
Analysis of flow characteristics of asymmetric annular diffuser with wall bleed capability and application to gas turbine combustors
[NASA-TM-X-2710] 07 p0770 N73-16251
Analysis of thermal failures in combustion chambers of J-57 jet engine and system for detecting burnthrough prior to engine case rupture
[FAA-NA-72-92] 07 p0835 N73-16772
Tests of high pressure combustor exhaust emissions with improved air-atomizing and conventional pressure-atomizing fuel nozzle
[NASA-TN-D-7154] 07 p0855 N73-16929
Simultaneous film and convection cooling of plate inserted in exhaust stream of gas turbine combustor
[NASA-TN-D-7156] 07 p0855 N73-16930
Analysis of turbulent diffusion in rocket combustion chamber to determine Lagrangian correlation coefficient and intensity of turbulence in chamber
08 p0967 N73-17908
Effect of fuel zoning and fuel nozzle design on exhaust pollution emissions at ground idle conditions for double-annular ram-induction combustor for turbofan engines
[NASA-CR-121094] 08 p0968 N73-17916
Combustion efficiency of annular turbojet combustor using heated natural gas as fuel
[NASA-TM-X-2742] 09 p1098 N73-18960
Performance tests of experimental short length annular combustor using one-side-entry dilution airflow technique
[NASA-TN-D-7225] 09 p1099 N73-18967
Tests of combustion chamber with burner device using system of transverse air streams for flame stabilization
[AD-753518] 09 p1100 N73-18977
Simple baffle combustor for heating test facilities
[ARL/ME-334] 10 p1137 N73-19265
Development and characteristics of molecular beam mass spectrometer system for sampling rocket engine combustion chambers
[NASA-CR-130933] 10 p1137 N73-19267
Research facility for studying noise generated by bluff body flow interaction inside ducted fuel combustion system
[AD-754094] 11 p1268 N73-20286
Development and mixing of coaxial fluid jet with axisymmetric swirling vortex flow in cylindrical chamber
[AD-754613] 11 p1272 N73-20324
Structural design criteria for ramjet combustion chamber
[PB-212691] 11 p1335 N73-20838
Calculation of heat transfer coefficients of laminar incompressible boundary layer to corrugated wall, with application to combustion chamber liquid film cooling
[DLR-FB-73-07] 12 p1465 N73-21868
Chemical analysis of products in combustion chamber of nitrogen tetroxide/aerozine rocket engine during preignition, ignition, and postignition conditions
[NASA-CR-128898] 13 p1590 N73-22890
Problems associated with advanced, small, high temperature rise combustors
[AD-757173] 14 p1702 N73-23808
Excitation of low frequency instability during powder combustion of rocket engine
14 p1718 N73-23942
Pollutant level measurement of exhaust gases from annular swirl can combustor
[NASA-TM-X-68247] 15 p1826 N73-24797
Pressure effects on tangential-injection film cooling in combustor exhaust stream
[NASA-TM-X-2809] 15 p1843 N73-24931
Linear stability analysis on liquid film adjacent to compressible viscous gas stream
[AD-758982] 16 p1889 N73-25290
Airflow distribution control in gas turbine engines
[NASA-CASE-LEW-11593-1] 16 p1955 N73-25816
Analysis of factors causing nitrogen oxides in exhaust gases of gas turbine engines and development of models of flow in gas turbine combustor
[NASA-CR-132959] 16 p1955 N73-25821
Combustor research programs to gain advanced technology for reducing aircraft engine pollution
[NASA-TM-X-68256] 17 p2076 N73-26797
Analysis of thermal fatigue in nontubular regeneratively cooled combustion chambers and prediction of thermal cycle life capability - Vol. 1
[AD-760582] 18 p2194 N73-27715
Analysis of thermal fatigue in nontubular regeneratively cooled combustion chambers and development of life prediction techniques - Vol. 2
[AD-760583] 18 p2194 N73-27716
Mixing and ignition of enclosed supersonic diffusion flames
[AD-760804] 18 p2207 N73-27811
Prediction of acoustic pressure wave oscillations in T burner combustors
[AD-762153] 19 p2328 N73-28728
Performance tests of annular combustor designed for use in low cost turbojet engine
[NASA-TM-X-2857] 19 p2352 N73-28918
Gaseous propellant combustion and injector/chamber design guidelines
[NASA-CR-121234] 20 p2464 N73-29799
Refractory chamber meterials for N2O4/amine propellants
[AD-762531] 20 p2467 N73-29818
Swirl can, full-annulus combustion chambers for high performance gas turbine engines
[NASA-CASE-LEW-11326-1] 21 p2579 N73-30665
Analysis of parameters involved in flow of combustion to produce stable propagation and efficient fuel consumption
[NLL-T1873/BGC/73-[9022.305]] 21 p2605 N73-30874
High performance annular combustion chambers for use in turboreactors
22 p2709 N73-31696
Monograph for design and development of combustion chambers for liquid propellant rocket engines
[NASA-SP-8087] 22 p2709 N73-31697
Design of high temperature combustor for use as solid fuel MHD generator and thermodynamic analysis of combustion conditions
[AD-764153] 22 p2730 N73-31848
Hydrodynamic simulation using flow field visualization for combustor study
23 p2831 N73-32625
Combustion process for airbreathing propulsion using fixed geometry ramjets
23 p2831 N73-32626
Technique for predicting high frequency stability characteristics of gaseous-propellant rocket combustion system
[NASA-TN-D-7406] 23 p2831 N73-32627
Emission abatement in aircraft gas turbine combustor with low mass emissions
[AD-764987] 23 p2833 N73-32638
Forward velocity effects on jet noise with dominant internal noise source
[NASA-TM-X-71438] 24 p2876 N73-32968
Influence of combustion chamber, compressor, and afterburner configuration on static performance of two-cycle turbojet engines with high bypass ratio
24 p2973 N73-33756

**COMBUSTION CONTROL**

Analysis of factors affecting combustion performance requirements of gas turbine engines and methods for improving gas turbine operation
21 p2606 N73-30882

**COMBUSTION EFFICIENCY**

Effects of fuel nozzle design on performance of annular combustor using natural gas fuel
[NASA-TN-D-7072] 02 p0223 N73-11805
Performance, combustion stability, and combustion efficiency of aerospike rocket engines
03 p0349 N73-12847
Combustion efficiency of FLOX/polyethylene hybrid propellants
[DGLR-PAPER-72-86] 04 p0462 N73-13766
Comparison of combustion characteristics of ASTM A-1, propane, and natural gas fuels in annular turbojet combustor
[NASA-TN-D-7135] 07 p0835 N73-16771
Evaluation of magnesium-aluminum eutectic to improve combustion efficiency in low burning rate propellants
[NASA-TN-D-7133] 07 p0836 N73-16775
Utilization of inorganic metal-oxidizer materials in solid rocket propellants resulting in increased combustion efficiency
[NASA-CASE-NPO-11975-1] 08 p0953 N73-17802
Combustion efficiency of annular turbojet combustor using heated natural gas as fuel
[NASA-TM-X-2742] 09 p1098 N73-18960
Thermal combustion requirements for burner devices of human vegetative waste products
10 p1118 N73-19111
Analytical models for ignition and complete combustion of aluminized slurry fuels in ramjet engines
[AD-754117] 10 p1203 N73-19792
Factors affecting tangential fuel injector design and their effect on efficiency of supersonic combustion processes
[NASA-CR-112302] 11 p1334 N73-20829
Analysis formation of carbon deposits on jet engines and effect on reliability, efficiency, and service life
[AD-754607] 11 p1335 N73-20837
Energy addition from propellant spray combustion to liquid fuel efficiency
[AD-755879] 12 p1443 N73-21687
Analog simulation of free piston gasifier tests relative to combustion and friction
[ME-240] 14 p1719 N73-23947
Effect of fuel vapor concentrations on combustion emissions and performance using experimental turbojet combustor segment
[NASA-TM-X-2800] 15 p1843 N73-24933
Combustion tests of various integral, spray-bar and flameholder configurations to determine configuration with maximum combustion efficiency
[NASA-TM-X-2855] 19 p2352 N73-28919
Analysis of factors affecting combustion performance requirements of gas turbine engines and methods for improving gas turbine operation
21 p2606 N73-30882
Application of gas analysis techniques to determine combustion efficiency in turbine engines and rocket engine combustion chambers
[AGARD-AG-168] 22 p2728 N73-31830

**COMBUSTION HEAT**

U HEAT OF COMBUSTION

**COMBUSTION INSTABILITY**

U COMBUSTION STABILITY

**COMBUSTION PHYSICS**

Modification of uncoupled radiation analysis of diffusion-type chemical laser to determine lasing diatomics of radiatively saturated medium
[AD-745311] 01 p0065 N73-10534
Analysis of transient and steady-state combustion processes in hybrid rocket system based on gaseous oxidizer flowing within tube of solid fuel
[NASA-CR-112201] 02 p0242 N73-11968
Determination of point of ignition and ignition delay period for single drop of fuel under specified conditions of temperature and vapor
[AD-745868] 02 p0244 N73-11979
Effect of antiicing additives on flammability properties of hydrocarbon fuels used in jet aircraft
[AD-747945] 03 p0349 N73-12852

Analysis of subsonic and supersonic burning in ramjet combustors to determine effects of nozzle configurations
[AD-747030] 03 p0351 N73-12862
Analysis of motion of chemically active gases to determine heat and mass transfer in turbulent jet system during diffusion combustion
[AD-747571] 03 p0365 N73-12976
Development of description for phenomenon of intrinsic unstable combustion in gas rocket
04 p0483 N73-13948
Analysis of reaction kinetics, combustion physics, and propellant properties of fuel elements used with rocket and ramjet engines
05 p0590 N73-14793
Development and characteristics of hydrogen-based mobile fuel systems and analysis of technical and economic problems in large scale application
[UCRL-51228] 07 p0834 N73-16766
Development of physical model to determine mechanism of condensed phase reaction in combustion of double base rocket propellants
07 p0853 N73-16921
Analysis of laminar hydrogen, ethylene, and propylene air diffusion flames burning in weightless environment
[NASA-TN-D-7165] 07 p0855 N73-16933
Theoretical analysis of reaction kinetics limitations leading to extinction of counterflow diffusion flame
[AD-751053] 07 p0856 N73-16940
Papers presented at conference on mechanisms of pyrolysis, oxidation, and burning of organic materials
[NBS-SP-357] 08 p0880 N73-17129
Kinetics and mechanisms of gas phase combustion, flames, and flame suppression
08 p0882 N73-17143
Fluorocarbon combustion and theories on fluorine supported combustion kinetics
08 p0883 N73-17145
Models for candle-like flames produced by burning of polymers
08 p0883 N73-17146
Pyrolysis and combustion of cellulosic materials
08 p0883 N73-17147
Surface pyrolysis boundary condition for combustion of polymers
08 p0883 N73-17148
Development of model to describe flow process, energy transfer, and flame front propagation during combustion of porous propellant charges
08 p0968 N73-17910
Combustion instability of solid rocket propellants
[AD-753835] 09 p1078 N73-18795
Mixing and ignition of hydrogen jets injected normally into supersonic two dimensional flow and effect on combustion performance of hyersonic ramjet engine
[ONERA-TP-973] 09 p1098 N73-18962
Dynamic behavior of flames in explosive acetylene oxygen mixture
[NASA-CR-130963] 09 p1099 N73-18973
Development and characteristics of molecular beam mass spectrometer system for sampling rocket engine combustion chambers
[NASA-CR-130933] 10 p1137 N73-19267
Spectroscopic measurements of flame composition an temperature of composite solid propellants during unstable combustion
10 p1222 N73-19939
Topler method for studying structure of turbulent diffusion flames
[NASA-TT-F-14842] 10 p1223 N73-19945
Topler schlieren photographic study of diffusion flame structure
[NASA-TT-F-14843] 10 p1223 N73-19946
Effect of prevaporization of jet fuels on exhaust emission levels produced in turbojet combustor segment
[NASA-TM-X-68194] 10 p1224 N73-19949
Motion picture study to provide combustion mechanism observations of ammonium perchlorate composite propellants
12 p1463 N73-21857
Chemical analysis of products in combustion chamber of nitrogen tetroxide/aerozine rocket engine during preignition, ignition, and postignition conditions
[NASA-CR-128898] 13 p1590 N73-22890
Formation of large polymers in vacuum plumes of large rocket engines following combustion of hydrogen and oxygen under adiabatic conditions
[RM-571] 13 p1590 N73-22893
Analysis of tangential mode, nonlinear wave motion in liquid propellant rocket engine using two phase detonation wave as reaction model
[NASA-CR-121194] 14 p1718 N73-23944
Analysis of kinetic and transport factors governing interfacial mass transfer rates in high temperature systems
[AD-758256] 14 p1720 N73-23959
Characteristics of solid propellant rocket engine with controlled rate of thrust buildup operating in vacuum environment
[NASA-CASE-NPO-11559] 15 p1824 N73-24784
Analysis of conditions under which coupling occurs between structure of combustion front and periodic oscillations
[NLL-M-22985-[5828.4F]] 15 p1842 N73-24922
Combustion phenomena in reinforced plastics ablation under simulated atmospheric reentry using plasma arc jets
[ONERA-NT-195] 15 p1844 N73-24939
Analysis of combustion instability in solid propellant rocket engines and characteristics of acoustic waves in T-burner geometry
16 p1973 N73-25958
Test equipment and experimental procedures for determining effects of turbulent flow on ignition properties of gasoline and air mixture
[NLL-RTS-7883] 18 p2128 N73-27194
Nonsteady combustion and extinguishment tests to determine acoustic instabilities of solid rocket propellants during combustion
[AD-760788] 18 p2207 N73-27813
Combustion tests of various integral, spray-bar and flameholder configurations to determine configuration with maximum combustion efficiency
[NASA-TM-X-2855] 19 p2352 N73-28919
Burning rate, heat transfer, and combustion physics of aluminum in composition of heterogeneous condensed systems
[AD-761609] 19 p2354 N73-28932
Effects of additives on high speed ignition and combustion characteristics of slurry fuels using magnesium and lithium fluoride
[AD-762615] 20 p2465 N73-29802
Ignition model for predicting ignition delay times of boron particle clouds in oxidizing atmosphere
20 p2484 N73-29955
Test equipment and procedure for determining electrical conductivity of stream of hot powdered fuel during combustion process
[JPRS-59752] 20 p2485 N73-29960
Analysis of parameters involved in flow of combustion to produce stable propagation and efficient fuel consumption
[NLL-T1873/BGC/73-[9022.305]]
21 p2605 N73-30874
Analysis of ignition properties of hypergolic fluids under low pressure conditions to determine relations of time, temperature, and thermodynamic properties
21 p2605 N73-30878
Analysis of ignition characteristics of high velocity hydrocarbon diffusion flames and comparison with ignition properties of hydrogen
21 p2605 N73-30881
Characteristics of weakly turbulent flame with high activation energy and comparison with laminar flame spread
[AD-763340] 21 p2606 N73-30889
Combustion characteristics of polystyrene and oxygen-styrene copolymer with ammonium perchlorate composites
22 p2708 N73-31687
Application of gas analysis techniques to determine combustion efficiency in turbine engines and rocket engine combustion chambers
[AGARD-AG-168] 22 p2728 N73-31830
Combustion process and burning rate of aluminum perchlorate composite propellant
22 p2732 N73-31865
Combustion and expansion of propane-air mixtures near bottom of short cylinder to generate air vortex rings for removing air from cylinder
[AD-764613] 23 p2777 N73-32207
Ignition properties and combustion physics of beryllium to show effects of various physical parameters and composition of combustion products
24 p2992 N73-33908

**COMBUSTION PRODUCTS**
Design and evaluation of automobile thermal reactors with ceramic material construction
[NASA-TM-X-68148] 01 p0069 N73-10567
Molecular beam sampling system for measuring size, size distribution, and particle concentration of carbon particles in acetylene-oxygen flame
[AD-744920] 01 p0118 N73-10971
Chemical spray scrubber for cleaning toxic products from rocket exhaust gases
[AD-747023] 02 p0224 N73-11810
Numerical prediction of exhaust products released to stratosphere during supersonic flight along definite air routes
[NASA-TT-F-14622] 04 p0371 N73-13013
Detection of C, H, and Ni in Pu metal by hot extrusion-combustion method
[FOA-VOL-6-NO-10] 05 p0506 N73-14115
Nonequilibrium combustion products for calculating rocket engine performance and chemical kinetics of combustion processes
[AD-750169] 06 p0715 N73-15835
Anhydrous ammonia for removing nitrogen dioxide from stack emission simulating hydrazine nitrogen tetroxide rocket fuel combustion exhaust
08 p0874 N73-17075
Modification of jet engine fuels to reduce emissions of nitrogen oxides from jet aircraft turbine engines
[AD-752581] 08 p0953 N73-17803
Analysis of gaseous emissions from J-85 engine at various fuel-air ratios, engine speeds, and simulated altitude conditions
[NASA-TM-X-2726] 08 p0969 N73-17921
Analysis of air pollution caused by exhaust from military aircraft engines and development of technology for pollutant measurement to meet EPA standards
[AD-753095] 09 p1100 N73-18975
Changes in oxygen consumption in rats after inoculation with polymer combustion products
10 p1116 N73-19096
Development of techniques for reducing exhaust emissions from turbine engines
[NASA-TM-X-68192] 10 p1208 N73-19824
Handbook on thermodynamic and thermophysical properties of high propellant combustion products
[AD-754329] 11 p1253 N73-20165
Analysis formation of carbon deposits on jet engines and effect on reliability, efficiency, and service life
[AD-754607] 11 p1335 N73-20837
Effects of transportation combustion products in air pollution
[PB-213034] 11 p1354 N73-20991
Survey on computerized modeling of transportation generated air pollution
[PB-213013] 11 p1354 N73-20992
Effect of inlet-air humidity on formation of oxides of nitrogen from a gas turbine combustor under various air inlet temperature conditions
[NASA-TM-X-68209] 12 p1443 N73-21691
Chemical analysis of products in combustion chamber of nitrogen tetroxide/aerozine rocket engine during preignition, ignition, and postignition conditions
[NASA-CR-128898] 13 p1590 N73-22890
Formation of large polymers in vacuum plumes of large rocket engines following combustion of hydrogen and oxygen under adiabatic conditions
[RM-571] 13 p1590 N73-22893
J-57 combustor exhaust odor intensity and chemical composition considering inlet parameters, fuel types, and nozzle shapes
[NASA-CR-121159] 14 p1616 N73-23093
Effect of primary-zone water injection on pollutants from combustor burning liquid ASTM A-1 and vaporized propane fuels
[NASA-TN-D-7293] 14 p1718 N73-23943
Polycyclic aromatic hydrocarbon aerosol collection using fiber glass and silica gel filters
[NLL-TRANS-1191-[9022.9]-PT-1]
15 p1746 N73-24152
Analysis of air pollution caused by aircraft engine emissions in vicinity of airport and comparison with air pollution in urban areas
15 p1825 N73-24788
Establishment of criteria for oxides of nitrogen emissions to control air pollution contribution from aircraft operating at major air terminals - Vol. 1
[REPT-1162-1-VOL-1] 15 p1825 N73-24789
Numerical analysis of process for nitrogen oxide formation in aircraft engine exhaust products and development of computer program for application of theory - Vol. 2
[REPT-1162-2-VOL-2] 15 p1825 N73-24790
Development of computer program to analyze flow conditions in gas turbine compressor for application to reduction of nitrogen oxides from aircraft engine exhaust - Vol. 3
[REPT-1162-3-VOL-3] 15 p1825 N73-24791
Comparison of nitrogen oxide emissions produced by hydrogen combustion with emissions produced by jet engine fuels at simulated cruise conditions
[NASA-TM-X-68258] 18 p2206 N73-27804
Analysis of aircraft emissions and recommendations for reducing impact of aircraft emissions on air pollution
[NREC-1168-1] 20 p2360 N73-28986
Development of computerized, theoretical model to predict characteristics of emissions from gas turbine engine combustors
[AD-762935] 20 p2467 N73-29819
Mathematical models for analyzing origin and distribution of combustion generated pollutants in gas turbines
[NASA-CR-121208] 21 p2590 N73-30754
Research projects to determine effects of exhaust products from aircraft operating in stratosphere on global and local climatic conditions
[UCRL-51336] 23 p2787 N73-32296
Sensory odor tests of exhaust from turbojet engine combustor operating at simulated idle conditions
[NASA-TM-X-71429] 23 p2829 N73-32613

**COMBUSTION STABILITY**
NT FLAME STABILITY
Suppression devices for controlling acoustic combustion instability in solid propellant engines
[AD-743701] 01 p0090 N73-10740
Performance, stability, and design of aerospike engines and engine system components
[NASA-TM-X-64690] 03 p0348 N73-12840
Combustion stability with hydrogen-oxygen liquid rocket propellants
03 p0349 N73-12844

Helmholtz resonator damping device for suppressing rocket combustion instability
03 p0349 N73-12845
Performance, combustion stability, and combustion efficiency of aerospike rocket engines
03 p0349 N73-12847
Theoretical analysis of rotating two phase detonation in liquid propellant rocket engine
04 p0461 N73-13763
Numerical analysis of nonlinear longitudinal combustion instability in metallized solid propellant rocket engines - Vol. 1
[AD-748415] 04 p0462 N73-13767
Numerical analysis of nonlinear longitudinal combustion instability in metallized solid propellant rocket engines - Vol. 2
[AD-748417] 04 p0462 N73-13768
Development of description for phenomenon of intrinsic unstable combustion in gas rocket
04 p0483 N73-13948
Instabilities in gaseous hydrogen-liquid oxygen rocket engine noting influence of pressure and concentration
[DLR-FB-71-47] 06 p0711 N73-15805
Interaction between acoustic velocities and solid propellant combustion with variations in frequency of oscillation, mean pressure, and propellant formulation
[AD-750142] 06 p0712 N73-15809
Mathematical model for unsteady one dimensional reaction waves during combustion of gas mixtures including application to air-propane mixture
[DLR-FB-71-66] 06 p0731 N73-15962
Dimpled array liners used as augmentor acoustic devices for controlling low frequency combustion instabilities
[AD-750902] 06 p0731 N73-15963
Combustion stability and gas dynamic research
[AD-750466] 06 p0731 N73-15964
Prediction of three-dimensional liquid-propellant rocket nozzle admittances
[NASA-CR-121129] 08 p0954 N73-17807
Acoustic combustion instability in solid propellant rockets
[AD-752205] 08 p0970 N73-17926
Combustion instability of solid rocket propellants
[AD-753835] 09 p1078 N73-18795
Electrothermal acoustics model for predicting and suppressing combustion instability in rocket motors
[AD-753111] 09 p1079 N73-18807
ONERA results of work to determine response of solid propellant to pressure and velocity fluctuations
[ONERA-TP-1165] 09 p1098 N73-18963
Turbulence and combustion stability in gas turbines
[AD-753062] 09 p1099 N73-18972
Hybrid rocket interior ballistics and heat transfer limited model
[AD-754769] 11 p1335 N73-20833
Mathematical techniques for studying high frequency nonlinear longitudinal combustion instability in liquid propellant rocket engines
12 p1443 N73-21689
Nonacoustic combustion instability of composite solid propellants
[AD-755825] 13 p1569 N73-22715
Combustion transients of solid rocket propellants
[AD-757234] 13 p1591 N73-22899
Model testing of gases, powders, and carbon particles in vibration combustion studies
[AD-755712] 13 p1591 N73-22902
Combustion instability in gas-fired T-burner
[AD-755824] 13 p1591 N73-22903
Acoustic combustion instability of solid propellants in radial burner
[AD-755826] 13 p1592 N73-22904
Droplet combustion at high pressures with unsteady effects
[AD-757227] 14 p1720 N73-23957
Improved version of modified machine gun for use as combustion stability rating device with various rocket combustors
[NASA-TM-X-2792] 15 p1842 N73-24928
Afterburner instability vortex shedding model for air breathing turbojet combustion
[AD-758890] 16 p1957 N73-25834
Combustion stability theory for solid propellant treated as elastic body
[AD-759819] 16 p1975 N73-25973
Prediction of acoustic pressure wave oscillations in T burner combustors
[AD-762153] 19 p2328 N73-28728
Combustion instability analysis of solid propellants
[AD-762841] 20 p2464 N73-29801
Performance analysis and high frequency combustion stability of high pressure rocket motor
20 p2484 N73-29956
Technique for predicting high frequency stability characteristics of gaseous-propellant rocket combustion system
[NASA-TN-D-7406] 23 p2831 N73-32627
Role of solid phase heterogeneity on low pressure L-star instability of nonmetallized rocket propellants
[NASA-CR-135766] 24 p2970 N73-33735

**COMBUSTION TEMPERATURE**
Calculating flame temperatures at constant pressure and volume
[ARL/ME-NOTE-341] 22 p2729 N73-31838
Ignition properties and combustion physics of beryllium to show effects of various physical parameters and composition of combustion products
24 p2992 N73-33908

**COMBUSTION WAVES**
U FLAME PROPAGATION

**COMBUSTORS**
U COMBUSTION CHAMBERS

**COMET NUCLEI**
Monochromatic isophote determination of particle distribution in bright comet
22 p2735 N73-31898

**COMET TAILS**
Solar wind interaction with Comet Bennett during period 23 March to 5 April 1970
[NASA-TM-X-66087] 02 p0224 N73-11813
Comet probe for analyzing properties of solar wind and direction of type 1 comet tails
02 p0228 N73-11845
Bessel theory for analyzing head and tail regions of dust comets
02 p0228 N73-11846
Photographic observation of Type 1 and Type 2 tail motion in Comet Bennett
02 p0229 N73-11854
Dust tail of comet Seki-Lines mapped isophotometrically for relative intensities
23 p2836 N73-32662

**COMET 4 AIRCRAFT**
Computerized automated avionics system with electronic display for Comet 4 aircraft navigation
14 p1712 N73-23896

**COMETS**
NT AREND-ROLAND COMET
NT COMET NUCLEI
NT COMET TAILS
Results of Meteor Research Program
01 p0101 N73-10831
Dynamics of meteor streams and new asteroid-meteor and comet-meteor associations
01 p0102 N73-10843
HILTOP - variational calculus program for generating electric propulsion data on rendezvous missions to comet Encke
[NASA-CR-114491] 01 p0104 N73-10857
Proceedings of conference on comets, University of Arizona - Apr. 1970
[NASA-CR-129110] 02 p0227 N73-11833
Existence of icy-conglomerate cometary nucleus
02 p0227 N73-11835
Structure of cometary nucleus
02 p0227 N73-11836
Infrared observations of comets, 1969g and 1969i
02 p0227 N73-11837
Infrared observations of comets Ikeya-Seki [1965f] and Bennett [1969i]
02 p0227 N73-11838
Nature and origin of cometary heads
02 p0228 N73-11839
Photometric observations of comets
02 p0228 N73-11840
L alpha photometry of Comet Bennett
02 p0228 N73-11841
Source of C3 in comets
02 p0228 N73-11842
Formation processes for C3 or C2 in comets
02 p0228 N73-11843
Ionization of gas emitted by comets
02 p0228 N73-11844
Determination of comet chemical nature from comet spectral energy
02 p0228 N73-11847
Spectroscopic observation of Comets Tago-Sato-Kosaka and Bennett
02 p0228 N73-11848
Influence of nongravitational effects on accurate prediction of comet orbits
02 p0228 N73-11849
Feasibility of flyby or rendezvous cometary mission
02 p0229 N73-11852
Research data on cometary structure and characteristics particularly Lyman alpha emission
02 p0229 N73-11853
Mass spectrometer identification of positive metal ions in Comet Encke beta Taurids meteor shower
[NASA-TM-X-66084] 02 p0229 N73-11855
Short-period comets and meteor stream genetic origin discussing formation processes
[TRITA-EPP-72-18] 02 p0231 N73-11880
Four periodic comets (Encke, dArrest, Kopff, and Halley) for comet rendezvous mission study
[NASA-CR-129820] 04 p0469 N73-13823
Ionizing flow in solar wind passage through cometary coma
[TRITA-EPP-71-33] 06 p0716 N73-15842
Approximate analytic and numerical methods for describing encounter of star with sun-comet system and resulting gravitational perturbations of cometary orbits
07 p0840 N73-16805

Development of computerized multistage failure process simulation to evaluate risk in solar electric space mission
[NASA-CR-131518] 12 p1457 N73-21813
Theories and definitions of comets and asteroids for proposed recommendations
[NASA-TM-X-71917] 22 p2717 N73-31747
Projected space missions to comets and scientific goals
22 p2735 N73-31899
Structural, compositional, and photometric model of comet Encke
[NASA-CR-135707] 23 p2845 N73-32737

**COMMAND AND CONTROL**
Specifications for automatic command and control of real time plasma simulation chamber
[GRI/NTP/102] 02 p0216 N73-11747
Design and development of electronic equipment for antiaircraft defense to include radio equipment, command and control, and electronic countermeasures
[AD-748709] 04 p0400 N73-13254
Digitized grammar for signal analysis and speech recognition accuracy in command and control system
[AD-746333] 06 p0643 N73-15218
Analysis of excessive interrogation signals from Air Traffic Control Radar Beacon System and effect on operation of Jacksonville, Florida center
[ECAC-PR-72-014] 06 p0696 N73-15675
Analysis of excessive interrogation signals from Air Traffic Control Radar Beacon System and effect on operation of Washington, D.C. center
[ECAC-PR-72-022] 06 p0696 N73-15676
Analysis of excessive interrogation signals from Air Traffic Control Radar Beacon System and effect on operation of Los Angeles, California center
[ECAC-PR-72-044] 06 p0696 N73-15677
Command and control of stability of Do-31 aircraft by landing and hovering
[BMVG-FBWT-72-25] 10 p1106 N73-19022
Survivability analysis of command and control communication systems
[AD-755846] 13 p1495 N73-22116
Performance analysis and conceptual design of waveform and modem to provide jamming-resistant command and control data link for ground station control of drone aircraft
[AD-756933] 13 p1496 N73-22125
Medium speed mass random access memory module to operate in airborne or tactical field environment with command and control system computer
[AD-755937] 13 p1498 N73-22144
Automation of technical control centers for operation and maintenance of Armed Forces defense communication system
[AD-757551] 14 p1635 N73-23255
Conceptual analysis of improved communication, navigation, and indentification system for military applications
14 p1690 N73-23719
Computerized integrated control and information management system with graphic display for manned space flight
14 p1710 N73-23882
Goals, objectives, tasks, and reporting channels of project management organization
15 p1846 N73-24963
Project management in aerospace industry
15 p1847 N73-24967
Project management system and application of management method
15 p1847 N73-24968
Project control at ESTEC, noting network analysis, phased project planning, cost control, and contract management
15 p1848 N73-24981
Requirements, functions, and tasks of project control teams within European space program
15 p1848 N73-24982
Integrated project control for ESRO satellite management
15 p1849 N73-24985
Analysis of air space control problems associated with military operations and development of doctrine for improved command and control
[AD-761034] 18 p2176 N73-27573
Onboard OAO 3 computer for commanding and data processing
18 p2208 N73-27824
Wideband communication command and control modem
[AD-762281] 19 p2238 N73-28042
Analysis of voice command systems for application to military aircraft operation to show manufacturers, specifications, and research projects
[AD-762922] 20 p2362 N73-28998

**COMMAND GUIDANCE**
Relocatable assembler and loader systems for Minuteman guidance computer
[AD-760758] 18 p2121 N73-27148

**COMMAND MODULES**
Wind tunnel tests to determine pressure distribution on Apollo command module and Saturn launch vehicle at supersonic and hypersonic speeds
[NASA-TM-X-62117] 04 p0477 N73-13904

Wind tunnel pressure signatures for scale model of Apollo command module
[NASA-TM-X-62047] 04 p0478 N73-13905
Failure analysis of malfunction of Apollo 16 television camera monitor on command module
[NASA-TM-X-68930] 06 p0639 N73-15190
Effect of residual motion smear or image reproduction processes on detail of lunar surface imagery from orbiting command module
[NASA-CR-130378] 07 p0798 N73-16485
Apollo Command Module Aerodynamic Simulation tests in hypersonic flow
[DLR-FB-71-83] 09 p1089 N73-18892
Apollo experience report on water landing requirement and two stable flotation attitudes for upright flotation of command module
[NASA-TN-D-7081] 09 p1090 N73-18898
Correlation of sonic boom pressure signatures recorded during reentry of Apollo 16 command module with wind tunnel signatures
[NASA-TM-X-62073] 12 p1365 N73-21073
Microbiological studies of Apollo 17 command module preflight and postflight samples
[NASA-CR-132022] 14 p1610 N73-23056
Apollo experience report on lighting requirements for Apollo command and lunar modules for internal and external lighting
[NASA-TN-D-7290] 16 p1964 N73-25887
Apollo experience report on command and service module reaction control systems
[NASA-TN-D-7151] 16 p1966 N73-25901
Anomaly report of explosive failure of ground support equipment decontamination unit tank during postflight deactivation of Apollo 16 command module
[NASA-TM-X-69323] 17 p2088 N73-26897
Apollo experience report on command and service module instrumentation subsystem to show requirements determination and conceptual design
[NASA-TN-D-7374] 22 p2719 N73-31761
Development of crew-couch/restraint system and crew load attenuation system for Apollo command module
[NASA-TN-D-7440] 22 p2720 N73-31768
Apollo experience report on window structural design and verification for command and lunar modules
[NASA-TN-D-7439] 22 p2720 N73-31770

**COMMAND SERVICE MODULES**
Postflight trajectory for Apollo/Saturn V AS-511 spent S-4B/IU stage from CSM separation to lunar impact
[NASA-CR-123975] 05 p0594 N73-14826
Erasable-memory programs for guidance computers in command and lunar modules
[NASA-CR-128689] 07 p0817 N73-16626

**COMMAND SYSTEMS**
U COMMAND GUIDANCE

**COMMAND-CONTROL**
U COMMAND AND CONTROL

**COMMERCE**
Microanalytic analysis of satellite meteorology on resource utilization, commerce, and agriculture
06 p0692 N73-15637
Commercial application of ERTS-1 imagery in structural reconnaissance for minerals and petroleum
[E73-10700] 16 p1903 N73-25392
Analysis of rigid airship operations for commercial cargo handling in United Kingdom
[CRANFIELD-CTS-3] 20 p2360 N73-28985

**COMMERCIAL AIRCRAFT**
NT BOEING 707 AIRCRAFT
NT BOEING 720 AIRCRAFT
NT BOEING 727 AIRCRAFT
NT BOEING 737 AIRCRAFT
NT BOEING 747 AIRCRAFT
NT COMET 4 AIRCRAFT
NT CV-340 AIRCRAFT
NT CV-990 AIRCRAFT
NT DC 3 AIRCRAFT
NT DC 8 AIRCRAFT
NT DC 9 AIRCRAFT
NT DC 10 AIRCRAFT
NT EUROPEAN AIRBUS
NT F-28 TRANSPORT AIRCRAFT
NT L-1011 AIRCRAFT
NT LEAR JET AIRCRAFT
NT SUPERSONIC COMMERCIAL AIR TRANSPORT
NT TU-144 AIRCRAFT
Development and characteristics of civilian V/STOL aircraft with application to short haul commercial air traffic
[NASA-TT-F-14629] 01 p0005 N73-10034
Conservation of fossil fuels in commercial aviation by using hydrogen
[NASA-CR-112204] 02 p0125 N73-11019
Effect on pilot performance and comfort of active vibration isolation system for commercial transport pilot seat
[NASA-CR-2146] 03 p0260 N73-12109
Analysis of loading conditions imposed on commercial aircraft during turning maneuvers on ground
[NASA-TN-D-7132] 04 p0372 N73-13027
Aircraft accident prevention analysis of air taxi/commuter operations to identify safety factors and enhance safety of operations
[NTSB-AAS-72-9] 05 p0493 N73-14016
Technical documentation to support V/STOL aircraft implementation and utilization based on short haul air transportation requirements - Vol. 2
[NASA-CR-114518] 07 p0739 N73-16009
Design principles of gas turbine and piston engines for commercial aircraft
[AD-751510] 07 p0837 N73-16783
Detail design features of short takeoff and landing commercial aircraft and impact on design caused by STOL requirement - Part 2
[AERO-13-PT-2] 09 p0984 N73-18033
Development of empirical method for determining optimum reversing coefficient of thrust reversal of jet engines on passenger aircraft
[AD-752814] 09 p0986 N73-18048
Proceedings of symposium on flight operations and air traffic control to show problems affecting airports, general aviation, air traffic controllers, and governmental agencies
[DLR-MITT-72-24] 10 p1183 N73-19623
Analysis of problems in air traffic control caused by expansion of commercial and civil aviation in Germany and proposed actions for improved safety and efficiency
10 p1183 N73-19627
Analysis of requirements for turbofan engines for high speed commercial transport aircraft - Vol. 1
[NASA-CR-121132] 10 p1207 N73-19820
Preliminary design assessment of turbofan engines for installation on high speed commercial transport aircraft - Vol. 2
[NASA-CR-121133] 10 p1207 N73-19821
Propulsion system requirements for aircraft engines installed in high speed commercial transport aircraft - Vol. 3
[NASA-CR-121134] 10 p1207 N73-19822
Design of perforated tube uniform distribution of fire extinguishing agent into commercial air transport compartments
[FAA-NA-73-3] 11 p1233 N73-20009
Analysis of factors involving commercial application of short takeoff aircraft for short haul airline operations
[NASA-TM-X-62239] 11 p1234 N73-20016
House hearings on air passenger fees, related taxation, and government regulation of commercial airline operations
11 p1352 N73-20970
Long range operational factors affecting commercial aviation industry
13 p1472 N73-21917
Survey of passengers flying from Dulles Airport, Virginia during one year period to obtain cross section of typical passengers and destinations
13 p1473 N73-21925
Performance tests on commercial transport aircraft engines to determine factors contributions to engine malfunctions
[FS-140-72-2] 13 p1473 N73-21933
Characteristics of single linear inertia exciter and multichannel recording equipment for flight flutter tests on Meteor aircraft
[ARC-R/M-3247] 16 p1855 N73-25026
Definition and evaluation of three basic alternative national aviation systems based on forecasted increases in aviation demands
[PB-215533/1] 16 p1862 N73-25081
Program definition study for improvement of short haul air transportation facilities - Vol. 1
[FAA-QS-73-1-VOL-1] 17 p1983 N73-26025
Statistical analysis of aircraft accidents and incidents occurring to US civil and commercial aircraft during calender year 1971 - Supplemental Issue
[NTSB-BA-73-5] 17 p1983 N73-26028
Design of aircraft for high reliability and low maintenance costs and maintenance procedures for maximum efficiency
17 p1983 N73-26032
Program definition study for improvement of short haul air transportation to show development requirements and operational constraints - Vol. 2
[FAA-QS-73-1-VOL-2] 18 p2213 N73-27869
Marketing survey to determine acceptance and utilization of STOL aircraft for short-haul air transportation system - Vol. 4
[NASA-CR-114609] 19 p2219 N73-27901
Fail-safe and safe-life design of aircraft components made from Ti-alloys
[NLR-TR-72034-U] 22 p2685 N73-31510
Development of US commercial air transport industry
23 p2860 N73-32849
Federal Government participation in development of US air transportation system
23 p2860 N73-32850
Proceedings of conference on air transport industry with emphasis on economics, market demand, airlines regulation, and international transportation policy - Vol. 2
[NASA-CR-135635] 23 p2862 N73-32875
Analysis of factors affecting future of commercial aircraft development to show effects on overall airline operations
23 p2865 N73-32900
Application of radiation technology and equipment for nondestructive analysis of commercial aircraft structures during aircraft maintenance periods
24 p2952 N73-33579

**COMMERCIAL AVIATION**
U CIVIL AVIATION
U COMMERCIAL AIRCRAFT

**COMMINUTION**
NT GRINDING (COMMINUTION)
Dispersion strengthened nickel-yttria sheet alloy produced from comminuted powders
[NASA-TM-X-68245] 15 p1798 N73-24576

**COMMITTEE ON SPACE RESEARCH**
Summary of COSPAR meetings and reports on news from national and international organizations about rockets and propelled vehicles
24 p2994 N73-33922

**COMMUNICATING**
NT AIRCRAFT COMMUNICATION
NT ELECTROCUTANEOUS COMMUNICATION
NT GROUND-AIR-GROUND COMMUNICATIONS
NT INFORMATION DISSEMINATION
NT LIP READING
NT UNDERGROUND COMMUNICATION
NT VERBAL COMMUNICATION
Experimental design formulated for alternative modes of man-computer dialogue
[AD-760010] 18 p2118 N73-27129

**COMMUNICATION**
NT INFORMATION DISSEMINATION
NT UNDERWATER COMMUNICATION
NT VERBAL COMMUNICATION
Use of skin analyzer as communication channel in controlling activity
04 p0378 N73-13074
Systems and studies for direct TV reception from satellite in Germany
[DGLR-PAPER-72-50] 04 p0389 N73-13160
Electromagnetic technology for radar, air traffic control, and communication systems
[AD-756482] 13 p1493 N73-22107
Measurements and predictions of loss and multipath variations for microwave troposcatter communication link
[AD-757553] 14 p1635 N73-23256
Development technology for communication systems
[JPRS-59221] 15 p1750 N73-24184
Computation oriented communications network using computer resources
[AD-758098] 15 p1752 N73-24197
Stationary point processes and applications to communications and logistic systems
[AD-758281] 15 p1804 N73-24621
Research progress in general physics, plasma dynamics, and communication sciences and engineering
[AD-759747] 17 p2099 N73-26983

**COMMUNICATION CABLES**
NT BEAM WAVEGUIDES
NT COAXIAL CABLES
NT WAVEGUIDES
Influence of temperature on cable parameter variations in wideband transmission system
[REPT-6670] 01 p0034 N73-10268
Combination satellite television system with local cable system for Federal Post Office
[NASA-TT-F-14660] 06 p0640 N73-15195
Fabrication and encapsulation processes for multiconductor cables
[BDX-613-740] 10 p1134 N73-19245
Improved fabrication and encapsulation techniques for multiconductor cables
[BDX-613-687] 10 p1134 N73-19246
Analysis of aerodynamically induced oscillations of bundled power conductors resulting from effect of wind on transmission power lines
17 p2098 N73-26971
Multiplexing still picture broadcasting by cable system
[NHK-LABS-NOTE-158] 18 p2115 N73-27099
Process for making RF shielded cable connector assemblies and resulting structures
[NASA-CASE-GSC-11215-1] 19 p2243 N73-28083
Cable television, emphasizing juridical and economical aspects in various nations
23 p2757 N73-32067

**COMMUNICATION EQUIPMENT**
NT CLOSED CIRCUIT TELEVISION
NT RADIO RECEIVERS
NT SATELLITE TELEVISION
NT SPACECRAFT TELEVISION
NT SUPERHETERODYNE RECEIVERS
NT TRANSMITTER RECEIVERS
Development of communication system for transmitting differential phase shift keyed signals from input data bits without timing or phase reference signals
[NASA-CASE-MSC-14065-1] 01 p0028 N73-10215

ATC surveillance/communication analysis and planning activities from 1 June to 31 Aug. 1972
[FAA-RD-72-107] 01 p0078 N73-10645
Characteristics and operation of educational satellite networks
[NASA-CR-129257] 03 p0265 N73-12148
Design and development of closed-loop, digital data communication system using optimum number of interconnecting wires
[NASA-CASE-MSC-13912-1] 03 p0266 N73-12151
Design, development, and evaluation of three channel interference cancellation system for use with ultrahigh frequency communication systems
[AD-747802] 03 p0267 N73-12158
Satellites for mobile aircraft and ship communications
04 p0472 N73-13852
Establishment of radar information transmission network for dissemination of meteorological data
[NLL-M-22692-[5828.4F]] 05 p0307 N73-14128
Test range for Symphonie satellite antennas and onboard communication equipment
[DGLR-PAPER-72-89] 06 p0640 N73-15199
Effectiveness of training device for air traffic communication and carrier landing control
[AD-751536] 07 p0751 N73-16101
Characteristics of data-aided carrier tracking loop used for tracking carrier in angle modulated communications system
[NASA-CASE-NPO-11282] 07 p0764 N73-16205
Mariner Mars 1971 radio frequency subsystem to provide communication link between spacecraft and Deep Space Instrumentation Facility
[NASA-CR-130866] 08 p0885 N73-17164
Performance of piezoelectric transducer for seismic communication in mine environment
[AD-752218] 08 p0885 N73-17169
Design of klystron microwave amplifier tube for troposcatter communication system
[AD-752075] 08 p0890 N73-17204
Speech tests and typical naval noise spectra for use in evaluating voice communication equipment
[AD-753207] 09 p1003 N73-18185
Performance of lightning and surge suppressors for digital transmission equipment
[AD-752448] 09 p1004 N73-18195
Analysis of effects of nonlinear electronic devices on bandpass signals consisting of modulated sine waves
[CRC-1234] 10 p1128 N73-19189
Doppler compensated communication system for locating supersonic transport position
[NASA-CASE-GSC-10087-4] 11 p1254 N73-20174
Handbook on defense and commercial communication systems
[AD-755917] 12 p1380 N73-21191
Capabilities, functions, and conceptual methods of operation for satellite-aided communications system in oceanic air traffic control environment
[FAA-RD-73-41] 12 p1460 N73-21833
Design of communication repeater subsystems for advanced multifunctional communications satellites
[NASA-CR-132296] 13 p1581 N73-22819
Design and development of telecommunications equipment for use with Tracking and Data Relay Satellite System - Vol. 2
[NASA-CR-130217] 13 p1582 N73-22821
Reliable functioning of avionic power supply equipment through employment of redundant components
[AD-757152] 14 p1602 N73-22988
Development and characteristics of audio response unit for use with telephone exchange to answer tax inquiries from subscribers
14 p1632 N73-23229
Frequency division multiplexer for operation in double or single sideband channel
[NASA-CR-124250] 14 p1640 N73-23293
Application of artificial satellites for data acquisition and communication functions in air traffic control system
14 p1689 N73-23709
Development of high bandwidth time division communications system to provide ground based, wide area, position location system
14 p1689 N73-23711
Analysis of communications, navigation, and identification equipment for aircraft and proposed system for improvement in capability
14 p1690 N73-23720
Analysis of integrated communications, navigation, and identification system for aircraft operation and proposal for improved capability
14 p1691 N73-23721
Feasibility analysis for computer-based data communications and/or processing facilities at civil airport
[RAE-TR-72133] 16 p1941 N73-25711
Design, development, and evaluation of optical detectors used in high speed digital laser communication links
[NASA-CR-132772] 17 p2032 N73-26446
Vacuum tube and solid state circuitry in electronic communications equipment for army training school
[AD-759129] 17 p2073 N73-26775
Position reporting and cmmunications systems of aviation and marine rescue operations
[AD-761756] 19 p2228 N73-27967
Radio transmitter and receiver design procedures for elimination of mutual radio frequency interference as function of total link selectivity
[SRDE-72023] 19 p2235 N73-28018
Communication antenna isolation
[FAA-RD-73-94] 21 p2507 N73-30119
Identification of Polish institutes involved in electron tube development and recommendations for changes in research projects
21 p2608 N73-30899
Polish research projects on piezoelectronic and acoustoelectronic equipment with specific application to computers and communication systems
21 p2608 N73-30901
Performance tests for Naval global communications system equipment
[AD-764485] 22 p2635 N73-31116
Capabilities of surface wave devices as signal processors for spread spectrum communications systems
[AD-763881] 22 p2645 N73-31197
Proceedings of conference on spread spectrum techniques and application to digital communications systems
[AGARD-LS-58] 23 p2756 N73-32053
Principles and operation of spread spectrum communication system with application to satellite communication systems
23 p2756 N73-32056
Applications of spread spectrum communications techniques to avionics systems
23 p2756 N73-32058

COMMUNICATION SATELLITES
NT INTELSAT SATELLITES
NT MOLNIYA SATELLITES
NT RELAY SATELLITES
NT SYMPHONIE SATELLITES
Propagation characteristics of satellite-borne television transmitter and ground receiver for communication satellite system
[NASA-CR-123909] 01 p0028 N73-10214
Telecommunications by satellite, and operation of Intelsat network
[NLL-TRANS-2860-[9022.81]]
02 p0139 N73-11126
Multipath propagation between aeronautical relay satellite in synchronous earth orbit and aircraft flying over ocean
[NASA-TM-X-66094] 02 p0141 N73-11140
Satellite communications and defense
[AD-746165] 02 p0142 N73-11147
Development and characteristics of four spacecraft configurations for communications satellite applications - Vol. 1
[NASA-CR-120873-VOL-1] 02 p0234 N73-11899
Development and characteristics of four spacecraft configurations for communications satellite applications - Vol. 2
[NASA-CR-120873-VOL-2] 02 p0236 N73-11915
Coherent multiplexing and radio relay array systems for satellite communication with small terminals
[AD-747488] 03 p0268 N73-12171
Design of high frequency mercury ion engine for application to communication satellite stationkeeping
[DGLR-PAPER-72-88] 03 p0351 N73-12861
Application of unmanned spacecraft for research purposes to show benefits from Communication and Navigation satellites and Earth Observation satellites
04 p0470 N73-13830
Satellites for mobile aircraft and ship communications
04 p0472 N73-13852
Revolutionization of communications by satellite systems
04 p0472 N73-13854
Advances in educational communication and meteorology as derived from satellite technology
04 p0474 N73-13869
Design of systems for utilizing communication satellite data in education
04 p0474 N73-13873
Computer program for geostationary orbit avoidance by radio relay transmitting antennas
[PB-211500] 05 p0514 N73-14179
Description of Telesat-A including operations and test plans
[NASA-TM-X-68927] 05 p0595 N73-14835
Methods for predicting parametric amplifier input noise temperature degradation for pump AM noise levels undergoing signal interference
[AD-751652] 07 p0763 N73-16197
Evaluation of Halo and Hummingbird satellites for lunar libration point satellite to provide tracking and communications link with far side of moon
[NASA-CR-130135] 07 p0844 N73-16836
German needs for television transmission via satellite
[DGLR-PAPER-72-051] 09 p1003 N73-18183
Source coding, modulation/channel coding, and systems techniques for application to teleconferencing over high data rate digital communication satellite links
[NASA-CR-114561] 11 p1342 N73-20889
Design of communication repeater subsystems for advanced multifunctional communications satellites
[NASA-CR-132296] 13 p1581 N73-22819
System parameters for satellite communications system to provide remote area telephone and television service
[REPT-6741] 14 p1619 N73-23109
Systems analysis of radio-TV satellite for coverage of West Germany and west European areas with German language
14 p1710 N73-23876
Electrical properties and performance of satellite group terminal system
[STC-TM-332] 15 p1749 N73-24178
Communication satellite systems for educational television vision
[NASA-TT-F-775] 15 p1845 N73-24953
Phased project planning and development for operational space missions referring to NASA meteorological and communication satellite programs
15 p1848 N73-24978
Satellite telecommunications systems for childhood education
[NASA-CR-133028] 16 p1869 N73-25131
Geostationary satellite trajectory optimization by low thrust resistojet propulsion
[AASU-323] 16 p1967 N73-25913
Design and testing of high power microwave components for communications satellites
[NASA-CR-120927] 17 p1998 N73-26152
Direct satellite FM-TV broadcasting experiment, with receiver operating near threshold and with 24 and 32 MHz IF band widths
[ESRO-CR[P]-251] 18 p2117 N73-27119
Direct satellite FM-TV broadcasting experiment, with receiver operating near threshold and with 20 MHz IF bandwidth
[ESRO-CR[P]-252] 18 p2117 N73-27120
Assessment of communication channels for maritime satellite systems using broad beam and multiple beam antennas for satellite-ship links
18 p2117 N73-27121
Analysis of candidate data and surveillance modems for avionics system used in air traffic control system
[AD-758407] 18 p2176 N73-27574
UHF linear phase bandpass filter for communication satellite
[ESRO-CR[P]-253] 19 p2235 N73-28024
Solid polymer electrolyte regenerative fuel cells for communication satellites
[AD-762923] 20 p2365 N73-29016
Stability of multistation satellite communications system
[JPRS-59753] 20 p2376 N73-29092
Characteristics of Orbita-2 satellite communications system
[JPRS-59751] 20 p2376 N73-29093
Capabilities and limitations of communication satellite data transmission for conducting conferences
[NASA-CR-133591] 20 p2377 N73-29098
Legal considerations of satellite communications system for teleconferencing applications
[NASA-CR-133592] 20 p2377 N73-29099
Development of analytical capabilities for determining use of satellite communications technology for professional education and medical services
[NASA-CR-133359] 20 p2377 N73-29100
Design, development, and control of large scale educational telecommunication system using satellites
[NASA-CR-133646] 20 p2377 N73-29104
Errors in determining ionosphere parameters and characteristics of ionospheric inhomogeities by signals from satellite mounted radio station, Maiak
20 p2410 N73-29373
Determining necessary number of channels in maritime communications satellite network
20 p2440 N73-29597
Orbit calculations for communication satellite using communications ground terminal minicomputer
[AD-762510] 20 p2474 N73-29874
Performance and growth capability of orbital test satellite for European communication satellite program
[DGLR-PAPER-73-044] 21 p2602 N73-30849
Satellite based system for L band precision positioning
[NASA-CR-62095] 22 p2697 N73-31604
Priority basis for satellite applications to communications, navigation, and surveillance for aircraft over contiguous US
[NASA-CR-132794] 22 p2722 N73-31784
Television broadcasting and communication systems using communication satellites, noting space law and regional coverage
23 p2757 N73-32068
Features and planned experiments of Communications Technology Satellite
[CRC-SER-DOC-06-RI/PS-3/1/72]
23 p2847 N73-32754
Direct TV broadcasting communication satellites
[DGLR-PAPER-73-040] 24 p2895 N73-33112
Central ground station and local receivers for direct TV broadcasting satellite system
[DGLR-PAPER-73-055] 24 p2895 N73-33114
European communication satellite and orbital test satellite transponders
[DGLR-PAPER-73-057] 24 p2896 N73-33116

Use of mercury ion engines for attitude control of communication satellites
[DGLR-PAPER-73-048] 24 p2986 N73-33863
Mechanical drives for communication satellite antennas and solar arrays
[DGLR-PAPER-73-050] 24 p2986 N73-33864
Direct broadcasting TV satellite solar arrays, and heat budget subsystems
[DGLR-PAPER-73-051] 24 p2986 N73-33865
Direct broadcasting TV communication satellite temperature control by louvers, heat pipes, radiators, heat storage, and coatings
[DGLR-PAPER-73-052] 24 p2986 N73-33866
Aims, prospects, organization, and financing of EUROSAT S.A.
24 p2994 N73-33930

**COMMUNICATION SYSTEMS**
U TELECOMMUNICATION
**COMMUNICATION THEORY**
NT SYLLABLES
NT WORDS [LANGUAGE]
Analysis of single channel phase communication system based on statistical communication theory with application to direction finding
12 p1425 N73-21553
Statistical models for smoothing environmental economics and communications data
13 p1549 N73-22554
Papers presented at conference on speech communication and processing
[AD-742236] 14 p1620 N73-23119
System for automated speech synthesis from ordinary English text
14 p1620 N73-23125
System for generating speech from English text punched on paper tape using small digital computer and parametric speech synthesizer
14 p1620 N73-23126
System of morphemic decomposition for improvement in Braille transcription
14 p1621 N73-23128
Electronic time compressor/expander for audio using digital technology
14 p1621 N73-23129
Evaluation of various parameters in spoken digits recognition
14 p1622 N73-23144
Use of orthogonal Walsh and Hadamard transforms to reduce bit rate for speech communication
14 p1624 N73-23159
Measurement of monosyllabic speech communication using adaptive methodology
14 p1625 N73-23165
Prosodic signals for parenthesis in algebraic expressions
14 p1629 N73-23207
Review of geomagnetic micropulsation modes for possible communications application
[AD-759380] 16 p1878 N73-25203
Proceedings of conference on spread spectrum techniques and application to digital communications systems
[AGARD-LS-58] 23 p2756 N73-32053
Fundamental concepts of communication theory to include transmission of continuous signals and use of discrete time signals
23 p2756 N73-32054
Characteristics of digital communication systems and processing of bandpass digital signals using spread spectrum techniques for data transmission
23 p2756 N73-32055
Principles and operation of spread spectrum communication system with application to satellite communication systems
23 p2756 N73-32056
Performance of spread spectrum communication systems to include effects of various forms of channel noise and synchronization aspects of system
23 p2756 N73-32057
Applications of spread spectrum communications techniques to avionics systems
23 p2756 N73-32058
Interference control in radio link operation
24 p2895 N73-33110
**COMMUNITIES**
Location of archaeological village sites in Alaska by ERTS-1 imagery
[E72-10338] 05 p0532 N73-14326
User manual for computer programs applied to community/airport economic development model - Vol. 3
[FAA-EQ-72-3-VOL-3] 06 p0732 N73-15971
Locating archaeological village sites in Alaska from remotely sensed imagery
[E73-10406] 11 p1277 N73-20368
Noise pollution effects on human communities
[PB-213021] 11 p1325 N73-20756
ERTS-1 imagery of villages and cultivation sites in Niger and Upper Volta
[E73-10893] 20 p2395 N73-29242
**COMMUTATION**
Threshold commutation in amorphous semiconductors
[CEA-CONF-1972] 07 p0832 N73-16741
Determination of dynamic zone sparkless commutation for linear and sinusoidal load current changes in dc machines
[NLL-RTS-7771] 18 p2122 N73-27149
**COMMUTATORS**
Solid state commutator design for radiosonde set AN/AMQ-9
[AD-763085] 20 p2381 N73-29132
**COMPACTNESS**
U VOID RATIO
**COMPARATORS**
Numerical comparator for indicating error in measurement transformations
[PUBL-1361] 06 p0690 N73-15615
Extraction of beginning and ending of pulse trains
16 p1883 N73-25244
Instrumented methods for finding variable stars on sky photographs
21 p2594 N73-30784
**COMPARISON**
Comparison of alkaline manganese-zinc cells with salt-electrolyte cells
[AD-746558] 02 p0129 N73-11051
**COMPARTMENTS**
NT AIR LOCKS
NT AIRCRAFT COMPARTMENTS
NT ANECHOIC CHAMBERS
NT COMMAND MODULES
NT PRESSURE CHAMBERS
NT PRESSURIZED CABINS
NT SPACECRAFT CABINS
NT TEST CHAMBERS
NT VACUUM CHAMBERS
**COMPASSES**
NT GYROCOMPASSES
**COMPATIBILITY**
Psychological stresses and crew compatibility during interplanetary spacecraft flight
[JPRS-57878] 06 p0629 N73-15113
Advanced measurement techniques for determining compatibility of materials with propellants
[NASA-CR-130546] 08 p0953 N73-17800
Data and design criteria on dynamic compatibility of fluorine with metals
[AD-756908] 13 p1489 N73-22071
Chemical compatibility of materials used for lithium cooled space power reactor concept at high temperature
[NASA-TN-D-7259] 15 p1809 N73-24660
Effect of FeF2 addition on Hastelloy N compatibility with LiF-BeF2-UF in low temperature convection loop system
[ORNL-TM-4188] 24 p2936 N73-33444
Compatability of tantalum alloys fuel capsules and [Pu-238]O2 fuels in radioisotopic thermoelectric generators
[LA-UR-73-764] 24 p2955 N73-33610
**COMPENSATION**
Model for awarding hazardous pay to employees
08 p0876 N73-17095
**COMPENSATORS**
Computation of optimal output-feedback compensators for linear time-invariant systems
[NASA-CR-130988] 09 p1056 N73-18607
Mathematical programming used in computer-aided-compensator design for control system
[NASA-CR-2248] 16 p1934 N73-25651
Optimal compensation of linear multivariable systems with structurally constrained dynamic compensators
22 p2690 N73-31548
**COMPENSATORY TRACKING**
Random Gaussian distribution for input noise approximation in human response tracker modeling
01 p0014 N73-10110
Tracking tests as quantitative measurements of neuromuscular functions in clinical applications
01 p0015 N73-10118
Visual display format effects on pilot describing functions in manual tracking performance
01 p0016 N73-10123
Magnetic data tapes containing measurements of pilot scanning behavior, control response and vehicle response during simulated instrument landing approaches
01 p0016 N73-10124
Human physiological and psychological responses in long time exposure to simulated space station atmosphere as observed by critical tracking task
01 p0017 N73-10133
Hypoxia stress effects on human operator performance in unstable tracking task using manual control
01 p0018 N73-10138
Effect of concurrent audio tasks on human operator compensatory tracking performance using manual control system
01 p0018 N73-10139
Attention sharing effects on human operator performing simultaneously dynamic compensatory tracking control tasks
01 p0018 N73-10140
Motion cue effects on pilot manual control tracking task
01 p0018 N73-10141
Dynamic model for pilot manual control ability using aural compensatory tracking
01 p0018 N73-10142
Computerized fast Fourier transform technique for measuring human performance in compensatory tracking task
[AD-748659] 05 p0501 N73-14078
Pupil enlargement in relation to operator stress during adaptive critical tracking task
[AD-749075] 05 p0501 N73-14081
Compensatory oculogravic response of eye movement direction during slow head rotation
06 p0634 N73-15148
Study of differences between left and right hand performance in compensatory tracking task
[RAE-TR-72117] 07 p0750 N73-16098
Linear rating scale for selecting tracking task parameters by subjective operator
[AD-752036] 08 p0880 N73-17125
Adaptive tracking task for evaluating drug after-effects on human flight performance
12 p1369 N73-21109
Pilot performance in dual time-sharing tracking task
[AD-755363] 14 p1615 N73-23088
Human visual/motor response to tracking task during long term confinement in simulated space station
[NASA-CR-2240] 15 p1744 N73-24134
Tracking tasks for clinical evaluation of human movement disorders
[NASA-CR-132275] 18 p2111 N73-27069
Design and performance of optically stabilized telescope pointing system using digital star tracker
[NASA-TN-D-7204] 18 p2125 N73-27173
Adaptive control system for compensatory positioning of optical tracking telescope
18 p2210 N73-27842
Constant gain optimal tracking control laws for finite final time
[AD-761091] 18 p2214 N73-27882
**COMPETITION**
Sports medicine - parameters necessary for maintaining competitive form
12 p1370 N73-21114
Competition effects on air transportation industry economics
23 p2861 N73-32858
**COMPILATION [COMPUTERS]**
U COMPILERS
**COMPILER PROGRAMS**
U COMPILERS
**COMPILERS**
Use, implementation, and maintenance procedures for data reconfiguration service compiler coded in PL/1
[AD-745751] 01 p0031 N73-10243
Checkout of computer programs for errors, using ALGOL compilers
[NPL-NAC-21] 02 p0147 N73-11189
Program debugging and monitoring facilities for improving diagnostic capability of compiler
[NBS-TN-763] 12 p1381 N73-21197
Design of FGRAAL type compiler language for solving graph structure algorithm problems
[NASA-CR-131474] 12 p1382 N73-21204
SCEPTRE translator providing point-to-point input of one dimensional mechanical systems
[AD-755166] 13 p1498 N73-22141
ILLIAC 4 and parallel assembler, Pandora
[AD-757779] 14 p1639 N73-23286
Manual for TMGL self-describing metalanguage with bootstrapping feature
[ESRO-SP-86] 19 p2239 N73-28054
Compiler optimization techniques
[NASA-TM-X-69499] 21 p2512 N73-30148
Validation tests for ALGOL 60 compiler
[NPL-NAC-33] 22 p2639 N73-31153
Text, syntax, and description of PL 516 assembler noting ALGOL, one track, one pass syntax, and design philosophy
[NPL-COM-SCI-65] 23 p2761 N73-32093
FORTRAN-WATFIV compiler noting differences with FORTRAN G and H extended and usefulness in program debugging
[LAAS-NT-SIS-73-T-04] 23 p2761 N73-32095
**COMPLEX SYSTEMS**
Limiting performance of large systems subject to steady state and transient inputs
[NASA-CR-112293] 11 p1265 N73-20261
Application of Liapunov function for analysis of finite stability of complex system in limited range of parameters
[NASA-TT-F-14869] 11 p1311 N73-20640
General Monte Carlo simulation model for estimating large scale system reliability and availability
24 p2928 N73-33385
**COMPLEX VARIABLES**
NT AIRY FUNCTION
NT ANALYTIC FUNCTIONS
NT CAUCHY INTEGRAL FORMULA
NT CONFORMAL MAPPING
NT ELLIPTIC FUNCTIONS
NT EXPONENTIAL FUNCTIONS
NT HANKEL FUNCTIONS
NT HARMONIC FUNCTIONS
NT HYPERBOLIC FUNCTIONS
NT LEGENDRE FUNCTIONS

NT MATHIEU FUNCTION
NT ORTHOGONAL FUNCTIONS
NT SINGULARITY [MATHEMATICS]
NT SPHERICAL HARMONICS
COMPLEXITY
NT TASK COMPLEXITY
COMPLIANCE [ELASTICITY]
U MODULUS OF ELASTICITY
COMPONENT RELIABILITY
Failure tolerant computer design noting component reliability
05 p0517 N73-14206
Computer program models for reliability prediction of electronic and electromechanical components
[NLL-RISLEY-TR-2329-[9091.9F]]
06 p0676 N73-15501
Reliability data for hybrid microcircuit discrete components
[NASA-TM-X-64686] 07 p0764 N73-16208
Rocket engines and components
[AD-754320] 10 p1210 N73-19839
Failure analysis of components of CH-47A auxiliary power plants
[AD-756407] 13 p1478 N73-21975
Structural and failure rate models for reliability analysis of electrical systems
[AD-758396] 14 p1671 N73-23560
Electron-proton spectrometer component derating
[NASA-CR-128706] 17 p2033 N73-26450
Methods of testing rotating components of turbomachines compared with tests on complete turbomachines
[AGARD-AG-167] 17 p2077 N73-26800
Behavior of hazard rate function of two component parallel systems
19 p2305 N73-28537
Reliability improvement by redundancy in electronic systems
[RAE-TR-72200] 21 p2520 N73-30208
Vibration design loads for component dynamic magnification factors of space shuttle
[NASA-CR-124337] 21 p2601 N73-30842
Component testing and analysis in program to evaluate metal shear web selectively reinforced with filamentary composites for space shuttle application
[NASA-CR-132322] 22 p2721 N73-31776
Onboard control systems for spacecraft
[JPRS-60179] 23 p2847 N73-32755
Automated monitoring of reliability of onboard computers and simulation of malfunction problem using Markov processes nonuniform in time
23 p2848 N73-32757
Reliability evaluation of radiation hardened dual nand gates
[AD-765173] 24 p2900 N73-33151
General Monte Carlo simulation model for estimating large scale system reliability and availability
24 p2928 N73-33385
COMPONENTS
Search algorithm for component placement problem in computerized design of circuits
[AD-756502] 14 p1684 N73-23663
Thermal stabilization of component dimensions for gyro devices
[AD-763148] 21 p2549 N73-30441
Component design and draw tooling of Pt heat source liner bodies
[MLM-1972] 24 p2955 N73-33608
COMPOSITE MATERIALS
NT CARBON FIBER REINFORCED PLASTICS
NT CERMETS
NT COMPOSITE PROPELLANTS
NT LAMINATES
NT METAL MATRIX COMPOSITES
NT REINFORCED PLASTICS
NT WHISKER COMPOSITES
Initial yield surfaces of unidirectional fiber-reinforced composites
[AD-745176] 01 p0070 N73-10572
Reflection and propagation of plane waves in fiber reinforced materials
[AD-745358] 01 p0070 N73-10576
Analog reinforcement for reducing stress concentration around hole in plate
[AD-745116] 01 p0071 N73-10578
Stress field intensity in opening interface crack in composite materials
[AD-746033] 01 p0071 N73-10583
Feasibility of hot pressing alumina composites with potassium and barium fluorine micas
[AD-742207] 01 p0071 N73-10584
Bibliography on fiber reinforced plastic composites
[PB-210305] 01 p0071 N73-10585
Static, ballistic, and impact behavior of glass/graphite drive shaft sections to determine suitability for heavy lift helicopters
[AD-743938] 01 p0091 N73-10752
Application of strain compatibility equations to evaluate thermal stresses in unidirectional graphite composites bonded to aluminum structures
[NASA-CR-112162] 02 p0125 N73-11014
Construction of pitch link in CH-47 helicopter control system using composite materials of graphite, glass, and carbon-steel
[AD-747337] 02 p0127 N73-11036
Development of hard TiC-Ni alloys for use as cutting tools
[NLL-TRANS-746-1226-[9022.401]]
02 p0185 N73-11496
Failure analysis and fracture modes of carbon epoxy composites
[NASA-CR-121000] 02 p0191 N73-11550
Unidirectional and bidirectional carbon fiber/epoxy resin composites for cryogenic vessels
[NASA-CR-120899] 02 p0192 N73-11553
Glass fiber reinforced composite materials for developing prototype missile fuselages
[AD-746288] 02 p0193 N73-11560
Development of nondestructive test procedures for determining properties of multidirectional fiber reinforced resin matrix composites
[AD-746592] 02 p0193 N73-11562
Development and evaluation of space shuttle main landing gear door constructed of boron/epoxy composite material ribs on titanium panel
[NASA-CR-112172] 02 p0233 N73-11889
Buckling of constant flexural rigid composite struts
[ESDU-01.01.23] 02 p0236 N73-11921
Analysis of short time response of cylindrical, elastic segment to shock wave engulfment based on focusing effects due to curved geometry
[AD-745962] 02 p0238 N73-11940
Fabrication of helicopter rotary wings from composite materials of stainless steel liner overwrapped with fiberglass
[NASA-CR-112191] 03 p0251 N73-12031
Explosive welding process for producing molybdenum wire reinforced columbium alloy composites
[NASA-CR-123937] 03 p0305 N73-12490
Application of metal-polyfluoroethylene bearings in helicopter rotor hinges for operation with and without lubrication
[AD-747428] 03 p0308 N73-12512
Development and characteristics of multilayer insulations for long term cryogenic storage
[NASA-CR-123938] 03 p0320 N73-12606
Influence of temperature on creep and strength characteristics of organic PRD49 fiber/epoxy composites
[NASA-TN-D-7120] 03 p0320 N73-12607
Effect of chemical vapor deposition on properties of carbon-felt carbon-matrix composites at high temperature
[SC-DC-71-4395] 03 p0320 N73-12609
Analysis of crack tip deformation in boron-aluminum sheet and laminar steel sheet resulting from crack propagation
[AD-747760] 03 p0322 N73-12623
Design, development, and evaluation of pressurized purge system for reusable space shuttles and fabrication of multilayer insulation systems
[NASA-CR-123942] 03 p0358 N73-12914
Technology of aircraft construction to include manufacturing of parts from plastics, ceramics, and nonmetallic materials
[AD-749558] 04 p0374 N73-13044
Compilation of reports on transition metal carbides for period 1956 to 1972
[CE-BIB-228] 04 p0437 N73-13560
Development, characteristics, and applications of composite materials containing inorganic fiber or metal fiber reinforcement
[NLL-RTS-7657] 04 p0437 N73-13561
Tensile creep tests to determine properties of 7075-T6 aluminum alloy reinforced with unidirectional boron/epoxy
[NBS-TN-722] 04 p0437 N73-13565
Development and fabrication of graphite polyimide wing box beam
[NASA-CR-123959] 04 p0480 N73-13923
Electrical resistivity of space electric power insulating materials
[LA-4978] 05 p0498 N73-14058
Analysis of damage threshold and damage mode from laser radiation for multilayer and periodic inhomogeneous film systems
05 p0556 N73-14515
Hot pressing and hot rolling procedures for producing aluminum reinforced with high strength steel strips
[NLL-TRANS-746-1355-[9022.401]]
05 p0561 N73-14554
Mechanical properties of thin films of Ni-SiO
[NLL-TRANS-746-1329-[9022.401]]
05 p0564 N73-14582
Development and characteristics of composite materials with emphasis on non-aerospace applications
[NASA-CR-129989] 05 p0565 N73-14587
Bibliography on fibers and composite materials
[AD-746214] 05 p0566 N73-14595
Elastic modulus of composite polyblends and polymers having phase inversion
[AD-749973] 05 p0566 N73-14601
Boron filament splitting in boron aluminum composites caused by water vapor effects
[AD-749971] 05 p0566 N73-14602
Fabrication of Nb-Ti and Al composite for use in superconducting rod
[COO-3311-1] 05 p0587 N73-14775
Photoelastic methods of stress analysis applied to fiber reinforced composites
05 p0602 N73-14892
Analysis of fatigue behavior of composite-reinforced, integrally stiffened metal panels and effects of temperature on adhesive substances
[NASA-CR-112148] 05 p0602 N73-14899
Limit equilibrium of axially symmetrical shells made from multilayered structurally-orthotropic and uniform material
[AD-747715] 05 p0603 N73-14905
Stability of three-layer plates with elastoviscous core subject to time-dependent loads
[AD-749746] 05 p0605 N73-14918
Approximate method to analyze plane stress, orthotropic, linear viscoelastic problems under isothermal conditions for metal-epoxy composites
05 p0607 N73-14939
Optimal design of baseline configuration for solar array panel with deployable beam
[NASA-CR-130287] 06 p0626 N73-15079
Analysis of heat dissipation and frictional properties of materials used in aircraft brakes
[NASA-CR-121116] 06 p0687 N73-15595
Selection of resin matrices for composites with improved unidirectional strength
[NASA-TM-X-68166] 06 p0687 N73-15597
Fabricating lamellar ceramic-based composites with synthetic fluorine mica
[AD-750353] 06 p0688 N73-15601
Stress singularities associated with crack inclined to bimaterial interface
[AD-750367] 06 p0689 N73-15607
Continuum theory for wave propagation in laminated composites applied to propagation parallel to laminates
[AD-750504] 06 p0689 N73-15608
Thermal degradation process and char forming characteristics of polymers and composites
[AD-750396] 06 p0689 N73-15612
Elastic waves in reinforced composite materials
[AD-750983] 06 p0689 N73-15613
Shearing mode stress intensity for finite length crack in bimaterial composite
[AD-750498] 06 p0727 N73-15937
Analysis methods for studying fatigue in bonded joints of composite materials
[AD-750132] 06 p0728 N73-15939
Fabrication, inspection and tests of fatigue in bonded joints of composite materials
[AD-750133] 06 p0728 N73-15940
Fatigue analysis and fatigue mode studies in bonded joints of composite materials
[AD-750134] 06 p0728 N73-15941
Fiber properties of simple and complex S-glass/epoxy composites under biaxial loading
[UCRL-73772] 07 p0812 N73-16582
Theory of plates and shields to include response of structurally loaded shells of cylindrical and spherical configurations
[AD-751502] 07 p0852 N73-16913
Analysis of environmental effects on physical, mechanical, and thermodynamic properties of various multilayer insulation materials - Vol. I
[NASA-CR-120978] 08 p0934 N73-17648
Analysis of environmental effects on physical, mechanical, and thermodynamic properties of various multilayer insulation materials - Vol. 2
[NASA-CR-120979] 08 p0934 N73-17649
Statistical analysis of strength and fracture characteristics of materials with application to fiber composites using Weibull density functions
[JPL-TM-33-580] 08 p0934 N73-17650
Application of neutron radiography for inspection of fiber glass composite structures
[AD-752457] 08 p0936 N73-17665
Mechanical properties of unidirectionally solidified, in-situ grown composites
[ONERA-TP-1147] 09 p1051 N73-18570
Numerical solution for stress concentration factors in isotropic and layered composites with parallel and collinear cracks
[WB-5/72] 09 p1052 N73-18576
Survey of heavy duty composite materials, development, manufacturing, costs, and applications
09 p1052 N73-18577
Electrical properties of reinforced dielectrics, magnetic permeabilities of multicomponent materials, and electromagnetic waves in fibrous dielectrics
[AD-752693] 09 p1053 N73-18583
Terminal ballistic performance of fiber glass epoxy composite material for aerodynamic control surfaces
[AD-752918] 09 p1053 N73-18584
Internal stress field and elastic moduli of fibrous compositions
[AD-752866] 09 p1053 N73-18587
Bench tests of wear resistance and antifriction properties of epoxy compounds
[AD-752868] 09 p1054 N73-18588
Optimal design of elastic bodies using fiberglass reinforced plastics or fibers with high modulus of elasticity
[AD-753040] 09 p1054 N73-18589

Analysis of complex moduli of uniaxially fiber reinforced materials containing viscoelastic matrix and elastic fibers
[AD-753699] 09 p1054 N73-18591
Experimental and analytical determination of elastic constants for some fiber reinforced composite materials
[AD-753575] 09 p1055 N73-18602
Notch stress finite element method for loaded elastic cores, applicable to compositesor welded joints
[ISD-129] 09 p1095 N73-18938
Stress analysis of uniaxial steel wire-plastic composite material, using finite element method
[ISD-131] 09 p1095 N73-18940
Effects of substrates on stability of superconductor and electrical properties of superconductors for various conditions
10 p1108 N73-19031
Carbon fiber reinforced metal structures for space shuttles
[SOR-W-13] 10 p1167 N73-19495
Thermal vacuum environment tests of materials used in space technology to determine effect of ultraviolet radiation on contaminative properties
[NASA-CR-122374] 10 p1175 N73-19556
Effect of fabrication conditions on mechanical properties of Be-Al monolayer tape and composite specimens
[SC-DR-72-0731] 10 p1175 N73-19559
Design and fabrication of fiberglass, graphite, and maraging steel composite motor cases
[AD-753959] 10 p1176 N73-19569
Fatigue tests to determine plastic deformations in composite materials
10 p1219 N73-19913
Technology for applying advanced fibers or resins to high performance high pressure filament-wound pressure vessels
[NASA-TM-X-68196] 10 p1220 N73-19923
Composite material for cargo door of space shuttle
[R-1525] 10 p1221 N73-19928
Creep properties of composite, plastic reinforced polyester concretes
[AD-752454] 10 p1221 N73-19930
Test equipment and methods for nondestructive inspection of welded, brazed, and composite structures
[NASA-SP-5952[02]] 11 p1297 N73-20528
High-speed oscillating and thermal resistance tests of 25 self-lubricating composites
[AD-755112] 11 p1299 N73-20539
Analysis of materials, processing criteria, processing techniques, and apparatus for preparation of composite materials in space
[NASA-CR-124172] 11 p1307 N73-20609
Development of polyphenylquinoxaline graphite fiber reinforced composites for structural materials
[NASA-CR-121109] 11 p1308 N73-20611
Optimal tensile strength composition for molding compounds of epoxy resin reinforced with glass fibers
[AD-754763] 11 p1309 N73-20620
Mechanical and physical properties of discontinuous thermoset carbon fiber reinforced plastic composites
[AD-754034] 11 p1309 N73-20622
Abstracts on directionally grown eutectic alloy composites
[AD-754779] 11 p1309 N73-20625
Development and application of composite materials for vertical takeoff aircraft airframes and effect on improved aircraft performance
12 p1359 N73-21023
Ni/ZrO2 composite material for designing high strength thermal switches
[HIT-527] 12 p1383 N73-21212
Thermal design of filamentary composite materials for primary structures on space shuttles
[NASA-CR-124206] 12 p1415 N73-21469
Evaluation of upgraded boron fibers in epoxy-matrix composites
[NASA-CR-112266] 12 p1416 N73-21472
Superconducting properties and damage susceptibility of composite wire conductors
[BNL-17222] 12 p1439 N73-21660
Limit equilibrium of axially symmetrical shells made from multilayered structurally-orthotropic and uniform materials
[NI.I.-DRIC-TRANS-2854-[3623.66]] 12 p1462 N73-21844
Material tests to determine characteristics of fiber reinforced ceramic matrix composites
[AD-757063] 13 p1544 N73-22513
Research reports on amorphous, laser window, composite, and gradient materials
[AD-755585] 13 p1545 N73-22521
Composite materials for use as internal LH2 tank insulation for reusable boosters
[NASA-CR-124222] 13 p1546 N73-22528
Acoustic fatigue characteristics of flat multi-layered structural panel
[NASA-CR-124079] 13 p1546 N73-22529
Fracture toughness and strength of diboride composites treated with metallic additives
[NASA-CR-131877] 13 p1547 N73-22535
Photon mean free path control of radiative heat transfer in composite materials
[AD-757140] 13 p1548 N73-22544
Three-dimensional finite element analysis of stress concentration near holes in laminated composites
[AD-756454] 13 p1548 N73-22545
Development of high strength composite tungsten alloy and silicon carbide filaments for high temperature applications
[AD-756867] 13 p1549 N73-22551
Mechanical properties and behavior of heat resistant alloys semiconductors, polymers and composite materials
[AD-755660] 13 p1549 N73-22552
Ultrasonic testing of Teflon and composite materials considering phase velocity
[AD-756385] 13 p1560 N73-22642
Fatigue behavior of composite-reinforced, integrally stiffened metal panels
[NASA-CR-112148] 13 p1585 N73-22853
Investigation of fibers and composites applicable to design of high pressure gas storage vessels for satellite altitude control
[RRCM/ED/R/10] 13 p1586 N73-22856
Investigation of fibers and composites applicable to the design of high pressure vessels for satellites
[MAN-NT-10/72] 13 p1586 N73-22859
Development and application of composite materials for weight reduction of space shuttle structural hardware
13 p1593 N73-22917
Design concepts, manufacturing process, weight analysis, and cost estimates for long range transport aircraft using composite structures
[NASA-CR-112255] 14 p1600 N73-22976
Design, fabrication, and evaluation of boron-epoxy reinforced C-130 center wing boxes
[NASA-CR-112272] 14 p1601 N73-22979
Development of boron composite materials for construction of aircraft landing gear for A-37 aircraft - Vol. 1
[AD-756922] 14 p1603 N73-22996
Design, fabrication, and test of boron composite material landing gear for use as main landing gear on A-37 aircraft - Vol. 2
[AD-756923] 14 p1603 N73-22997
Development of self-contained, solid lubricated ball bearings for operation at high speed - Part 2
[AD-756487] 14 p1671 N73-23557
High strength tungsten fiber reinforced oxidation resistant niobium alloy composites for use in gas turbine engines at 2000 F
[AD-757380] 14 p1678 N73-23620
Failure modes for isotropic and anisotropic composite materials
[AD-756889] 14 p1681 N73-23639
Development of compatible titanium alloy for boron reinforced composites
[AD-758294] 14 p1682 N73-23652
Fabrication of full-size structural rings from composite materials
[NASA-CR-124253] 15 p1793 N73-24532
Direct casting for producing cast superalloy tungsten or columbium alloy fiber composites with high strength
[NASA-TM-X-2782] 15 p1798 N73-24572
Vacuum effects on mechanical properties of composite heat ablator and solid problem material
15 p1801 N73-24594
Mathematical models for surface ablation of silica-reinforced composites
15 p1801 N73-24596
Linear anisotropic elastic field equations for interrelations and bounds on moduli in composite materials
[AD-758438] 15 p1801 N73-24601
Properties of graphite fiber/polycarbonate and glass fiber/polycarbonate composites as influenced by heat treatment
[AD-757763] 15 p1802 N73-24605
Composite constructions of reinforced plastics with improved rain erosion resistance
[AD-758650] 15 p1803 N73-24610
Composite conductors of 19-Nb3Sn filaments in normal metal matrix, using heat treatment
[BNL-17425] 15 p1821 N73-24756
Propagation of shear waves in layered composites
[SCL-RR-72-0351] 15 p1839 N73-24905
Development of fibrous flame arrestor materials to provide explosion and fire protection for aircraft fuel tanks
[AD-759193] 16 p1863 N73-25090
Production of monolayer boron-aluminum composite materials
[NASA-CR-124278] 16 p1928 N73-25601
Fatigue mechanics of boron-aluminum composites under oscillating tensile loads
[AD-757213] 16 p1932 N73-25635
Numerical analysis of load absorption of two adjacent filaments in fiber-reinforced material
[AD-759729] 16 p1933 N73-25639
Effect of interface in aluminum, boron, and silicon carbide coated boron on mechanical properties
[AD-759204] 16 p1933 N73-25641
Dynamic compression and release of simple homogeneous mechanical mixtures of solids in phase change
[AD759150] 16 p1933 N73-25644
Correspondence principle for vibration analyses on viscoelastic bodies with loss tangents
[AD-759260] 16 p1971 N73-25943
Flight evaluation of composite for use in aircraft structures
[NASA-TM-X-2761] 17 p2049 N73-26579
Analysis of loss of high temperature strength in composite materials following aging in room temperature environments
[NASA-CR-124290] 17 p2050 N73-26583
High performance vulcanized elastomers produced by nitrile and silicone rubber covulcanization
[RAE-TR-72184] 17 p2050 N73-26588
Mechanical property determination and fracture mechanics of fiber reinforced composite materials
[D-MAT-178] 17 p2051 N73-26589
Melt-grown, oxide-metal composites for high field electron emission testing
[AD-759507] 17 p2051 N73-26592
Strength of randomly oriented short fiber composite laminates
[AD-759827] 17 p2051 N73-26594
High temperature carbon polymeric composite materials
[AD-759963] 17 p2052 N73-26598
Scattered light photoelastic method for predicting stress distribution in composite epoxy glass structures
[AD-759900] 17 p2052 N73-26601
Effects of high intensity electrical currents on advanced composites
[AD-760352] 17 p2053 N73-26605
Evaluation of GRP rod and rope materials and associated end fittings
[AD-759931] 17 p2053 N73-26607
Fracture mechanics applied to analysis of brittle fracture of unidirectional and angle-ply composites
[AD-760361] 17 p2053 N73-26610
Stress analysis of elastic plane containing elastic inclusion using singular integral equations
[NASA-CR-132272] 17 p2093 N73-26934
Vibrations of stiffened composite shells
[AD-759375] 17 p2095 N73-26946
Proceedings of conference on nondestructive testing and materials characterization with emphasis on development of new techniques for materials testing
[AD-760174] 18 p2157 N73-27427
Proceedings of conference on application of composite materials in construction of aerospace vehicles and propulsion systems
[AGARD-CP-112] 18 p2163 N73-27474
Physical and mechanical properties of high-strength, high-modulus reinforcing fibers and organic resin composite materials
18 p2164 N73-27475
Analysis of properties of fiber reinforced materials with plastic and metallic matrix composition and application to gas turbine engines
18 p2164 N73-27476
Characteristics of carbon fiber composite materials and application for structures with reduced weight, fatigue reduction, and corrosion resistance
18 p2164 N73-27477
Production of fibrous metal composites by rolling of powder with strong reinforcing wires and application to aerospace vehicle structures
18 p2164 N73-27478
Design of filamentary composite materials for application to construction of airframes and spacecraft structures
18 p2164 N73-27479
Application of boron/epoxy composite materials for airframe construction with specific development of F-111 stabilizer
18 p2164 N73-27480
Application of composite materials for structural purposes to show limitations and failure characteristics
18 p2164 N73-27481
Application of glass composites, all carbon composites, and PRD-49 organic fiber material for airframe and spacecraft construction
18 p2164 N73-27482
Application of glass reinforced and carbon reinforced composite materials for helicopter structures and rotary wings
18 p2165 N73-27483
Use of reinforced boron and carbon fiber composites in aircraft structures
18 p2165 N73-27484
Application of composite materials to reinforce metallic structures for low cost improvement in structural stability of airframes
18 p2165 N73-27485
Application of composite materials and sandwich structures to reduce vulnerability of aircraft structures to projectile impact
18 p2165 N73-27487
Response of general laminated plates to applied loads with coupling between bending and extensional modes of deformation
18 p2165 N73-27488

Design and manufacturing of composite materials with organic matrices for use in aerospace vehicle structures subjected to high temperatures
18 p2165 N73-27489
Application of reinforced composite materials for construction of aeronautical gas turbine engines
18 p2165 N73-27490
Development of fiber reinforced composite materials for application to air breathing engines, aeronautical vehicles, and spacecraft components
18 p2166 N73-27491
Production of lamellar and fibrous composite materials from directional solidification of eutectic alloys and application to gas turbine blades and vanes
18 p2166 N73-27492
Application of directionally solidified eutectics for design and construction of gas turbine engines
18 p2166 N73-27493
Application of glass and carbon fiber reinforced structures for gas turbine engine components to operate in high temperature environments
18 p2166 N73-27495
Performance and fatigue strength of compressor blades fabricated from carbon fiber composites and boron composite wires
18 p2166 N73-27496
Application of boron/aluminum composite material for construction of turbine blades with low notch sensitivity in high cycle fatigue
18 p2166 N73-27497
Design, fabrication, and test of boron-polyimide reinforced titanium fan disks to operate at high temperatures
18 p2167 N73-27498
Performance and endurance of compressor disks bound with boron composite wires
18 p2167 N73-27499
Failure analysis of fiber reinforced composite rocket engine case using distortional energy and maximum strain theories of failure
18 p2167 N73-27500
Process for developing flame retardant elastomeric composition textiles for use in space suits
[NASA-CASE-MSC-14331-1] 18 p2167 N73-27501
Micromechanical failure criteria for tensile and shear strengths of composites
[AD-761221] 18 p2167 N73-27504
Coherent laser light measurement of ceramic material surface roughness
[AD-761198] 18 p2168 N73-27512
Design, fabrication, manufacture, and verification of composite material rocket engine cases for antitank missiles - Vol. 1
[AD-760566] 18 p2202 N73-27774
Design calculations, tooling sketches, manufacturing and inspection records of composite material rocket engine cases for antitank missiles - Vol. 2
[AD-760569] 18 p2202 N73-27775
Development of unidirectional fiber composite materials with emphasis on improving compressive strength
[NASA-CR-112334] 18 p2203 N73-27784
Numerical analysis of stability of axially compressed cylindrical shells from composite materials under nonstationary heating
18 p2203 N73-27785
Stress analysis of impact in composite plates
[NASA-CR-121110] 18 p2203 N73-27786
Flight tests of CH-47 helicopter to determine structural performance of boron-reinforced epoxy aft rotor blades
[AD-762199] 19 p2222 N73-27927
Analysis of thermophysical properties of plasma sprayed materials for use as thermal insulation coating on rocket nozzles
[NASA-CR-121144] 19 p2311 N73-28590
Tensor analysis of strength and failure of composite materials
[AD-761994] 19 p2313 N73-28600
Design and tests of composite propulsion feedlines for cryogenic space vehicles - Vol. 1
[NASA-CR-121137-VOL-1] 19 p2346 N73-28868
Design and tests of composite propulsion feedlines for cryogenic space vehicles - Vol. 2
[NASA-CR-121137-VOL-2] 19 p2346 N73-28869
Bonded half planes containing an arbitrarily oriented crack
[NASA-CR-132290] 19 p2348 N73-28888
Load absorption and interaction of two elastic filaments in fiber reinforced composite material
20 p2433 N73-29542
Composite materials studies, including compressive strength and reinforced plastics
[JPRS-59610] 20 p2434 N73-29549
Microtribometric study of self-lubricating composite materials on polymers
20 p2435 N73-29553
Fabrication of aluminum-carbon composites
[NASA-CR-121266] 20 p2435 N73-29557
General continuum theory with microstructure for wave propagation in elastic laminated composites in two dimensional case
[AD-762609] 20 p2436 N73-29562
Fabricating lamellar ceramic-based composites with controllable properties by hot pressing of gamma AL2O3/Ba-mica
[AD-762839] 20 p2436 N73-29563
Analysis of programs for acoustic testing of composite material components and development of theory for predicting natual frequencies, mode shapes, and stresses in composite panels
20 p2480 N73-29918
Wave propagation and impact in composite materials
[NASA-CR-121226] 20 p2482 N73-29935
Interaction between parallel cracks in layered composites
[NASA-CR-132287] 20 p2482 N73-29936
Buckling behavior of composite cylinders to compressive loads
[NASA-CR-132264] 20 p2483 N73-29945
Application of composite materials in development of tilting rotor for vertical takeoff aircraft - Vol. 6
[NASA-CR-114599] 21 p2493 N73-30010
Fabrication and properties of carbon-fiber glass composites and methods for improving mechanical properties
[ARL/MET-NOTE-85] 21 p2561 N73-30533
Effects of high temperature cycling on structural properties of boron reinforced aluminum alloys used in spacecraft structures
[NASA-CR-124369] 21 p2562 N73-30541
Performed investigations and results on composite materials in space
[NASA-CR-124365] 21 p2562 N73-30542
Controlling constituent properties for strengthening graphite fiber reinforced aluminum and magnesium composites
[AD-763211] 21 p2563 N73-30548
Determining mechanical properties of composite materials using computers
[AD-763708] 21 p2563 N73-30550
Effect of temperature and strain rate on tensile properties of aluminum-boron, epoxy-boron, and epoxy-graphite composites
[AD-763656] 21 p2564 N73-30551
Fatigue properties of high strength high modulus graphite /glass/epoxy matrix composites
[AD-763760] 21 p2564 N73-30552
Maximizing impact strength of advanced graphite composites without affecting other directional strength properties
[AD-763376] 21 p2564 N73-30553
Optimization method for minimum weight design of structures made from fiber reinforced composites
[AD-763732] 21 p2565 N73-30558
Application of composite materials to construction of helicopter airframes and landing gear
[NASA-CR-112333] 22 p2614 N73-30948
Application of divergent beam X ray microdiffraction technique for measuring residual and impressed stresses and strains in iron-silicon alloy transformer sheet
[NBS-MONOGRAPH-130] 22 p2672 N73-31407
Superconducting materials for high field ac magnets with one second field risetime
[BMFT-FBT-73-03] 22 p2685 N73-31509
Advanced material composites for use as insulations for space shuttle LH2 tanks
[NASA-CR-124388] 22 p2688 N73-31532
Shear, flexural, and tensile strength performance of carbon fiber composites made from epoxy, phenolic, polyester, and polyimide resins
[AQD/NM-000198] 22 p2689 N73-31536
Finite element analysis of behavior of filamentary composite plates with cutouts
[AD-764362] 22 p2689 N73-31538
Fracture and fatigue properties of composite materials
[AD-764356] 22 p2689 N73-31540
Fracture toughness of homogeneous isotropic composites
[AD-764070] 22 p2689 N73-31541
Application of fiber glass reinforced plastic materials for ground handling of aviation fuels and hazards of static electricity caused by plastic materials
[AD-764358] 22 p2709 N73-31693
Design of metal shear web selectively reinforced with filamentary composites for space shuttle application
[NASA-CR-132320] 22 p2721 N73-31774
Component fabrication of metal shear web selectively reinforced with filamentary composites for space shuttle application
[NASA-CR-132321] 22 p2721 N73-31775
Component testing and analysis in program to evaluate metal shear web selectively reinforced with filamentary composites for space shuttle application
[NASA-CR-132322] 22 p2721 N73-31776
Construction of helicopter airframes and landing gear to show advantages of composite material prototype over metal prototype
[NASA-CR-112333] 23 p2743 N73-31957
Factors affecting miniature izod impact strength of tungsten-fiber-metal-matrix composites
[NASA-TN-D-7393] 23 p2804 N73-32427
Formation of in situ composites by directional solidification
[AD-765348] 23 p2805 N73-32435
Development of continuum theory with microstructure for wave propagation in composite materials
23 p2806 N73-32438
Propagation of waves in layered composites
23 p2806 N73-32439
Application of hot pressing, hot extruding, and sintering processes for production of composite materials
[JPRS-59873] 23 p2807 N73-32441
Specific electrical resistance of metal-carbide two-phase system to show effect of porosity and metal content on electrical properties
23 p2807 N73-32444
Thermophysical properties of synthetic resin-base materials with fillers to show errors in development of mathematical relationships
23 p2807 N73-32446
Coefficient of thermal conductivity for composite materials by using axial thermal flow method
23 p2807 N73-32447
Production and characteristics of highly dispersed composite powders on copper base containing metal carbides by reducing copper carbonate with hydrogen
23 p2808 N73-32451
Adhesive bonding of structures and composite materials on advanced turbofan engines
23 p2810 N73-32470
Metal-loaded carbon and graphite cloth reinforced composites from polymer blends
[AD-764630] 23 p2811 N73-32474
Behavior of impact-generated elastic stress waves propagating in rods of unidirectional composite material
23 p2852 N73-32792
Plasma-sprayed metal-glass and metal-glass fluoride coatings for lubrication
[NASA-TM-X-71432] 24 p2929 N73-33392
Extension of linear elastic fracture mechanics from homogeneous isotropic metallic alloys to heterogeneous anisotropic advanced fiber composites
[NASA-CR-132337] 24 p2937 N73-33456
Fabrication and evaluation of composite thermal engine insulation
[NASA-CR-124457] 24 p2938 N73-33458
Production of silica, mullite, and alumino silicate reusable surface insulation materials for space shuttle orbiters
[NASA-TM-X-2719] 24 p2938 N73-33461
Glass ceramic foam materials for space shuttle heat shielding system
24 p2938 N73-33464
Alumina silicate based composite materials for space shuttle heat shielding system
24 p2939 N73-33466
Silica fiber materials for surface insulation of space shuttle orbiters
24 p2939 N73-33467
Radiant heat transfer in surface insulation materials for space shuttle orbiter
24 p2939 N73-33468
Hafnium pigmentation for mullite composite thermophysical optimization
24 p2939 N73-33469
Mechanical and thermophysical characteristics of nonmetallic insulation materials for space shuttle orbiter surface
24 p2939 N73-33471
Porosity analysis on silica and mullite composite surface insulation tiles
24 p2939 N73-33472
Radiometric emittance measurements on reusable external insulation materials
24 p2939 N73-33473
Microstructure of mullite composite fibers
24 p2940 N73-33474
Space environment simulation tests on space shuttle reusable surface insulation materials
[NASA-TM-X-2720] 24 p2940 N73-33475
Space environment aerodynamic heating tests on mullite and silica fiber surface insulation panels
24 p2940 N73-33476
Plasma jet wind tunnel tests on space shuttle surface insulation materials
24 p2940 N73-33479
Plasma arc thermal cycling tests on surface insulation materials for space shuttle
24 p2940 N73-33480
Cyclic convective heating evaluation of surface insulation materials for space shuttles
24 p2940 N73-33481
Acoustic, reentry, and structural load environment tests on mullite insulation for space shuttle
24 p2941 N73-33483
Meteoroid impact simulation tests on bonded fiber/aluminum skin panels for space shuttle insulation
24 p2941 N73-33485
Sea salt and radiant heat effects on crystalline properties of mullite/silica composite thermal insulation for space shuttle
24 p2941 N73-33486
Thermal and structural performance tests on space shuttle orbiter surface insulation materials
24 p2941 N73-33489

Ceramic reinforced mullite thermal protection system design for space shuttle surface
24 p2942 N73-33495
Thermostructural evaluation of mullite and silica composite materials for space shuttle surface insulation system design
24 p2942 N73-33498
Radiative emittance measurements on surface insulation coatings in plasma jet wind tunnel
24 p2943 N73-33501
Investigations of HT-S/PMR-PI composites for applications to advanced aircraft engines
[NASA-TM-X-71459] 24 p2943 N73-33502
Mechanical and thermophysical properties of composite materials
[LA-5173] 24 p2943 N73-33505
Bibliography of manufacturing methods of composite materials
[AD-764600] 24 p2944 N73-33512

**COMPOSITE PROPELLANTS**
Solid phase reaction and fuel component effects on composite propellant combustion
[NASA-CR-112083] 01 p0089 N73-10738
Effects of orientation of acceleration vector on burning rate augmentation determined for aluminized composite propellant
[NASA-TN-D-6952] 01 p0116 N73-10962
Theoretical study of time-independent and oscillatory combustion of nonmetallized AP/composite propellants
[NASA-CR-129198] 02 p0243 N73-11973
Influence of ammonia perchlorate binder and surface microstructure on combustion velocity development in solid composite propellants
[ONERA-TP-1167] 10 p1222 N73-19941
Analysis of steady state burning of ammonium perchlorate composite solid propellants
[AD-762600] 20 p2465 N73-29803
Rate theory for determining failure accumulation in composite propellants
[AD-763806] 21 p2588 N73-30733
Combustion process and burning rate of aluminum perchlorate composite propellant
22 p2732 N73-31865

**COMPOSITE STRUCTURES**
NT LAMINATES
Development and characteristics of composite materials with emphasis on non-aerospace applications
[NASA-CR-129989] 05 p0565 N73-14587
Analysis of fatigue behavior of composite-reinforced, integrally stiffened metal panels and effects of temperature on adhesive substances
[NASA-CR-112148] 05 p0602 N73-14899
Analysis of natural vibration characteristics of plate-beam combination structures during supersonic flight
[NAL-TR-291] 06 p0725 N73-15917
Analysis of fatigue and fail-safe characteristics of composite-reinforced, stiffened metal panels to determine residual strength
[NASA-CR-2136] 07 p0852 N73-16909
Application of neutron radiography for inspection of fiber glass composite structures
[AD-752457] 08 p0936 N73-17665
Development and application of design synthesis methodology for composite structures
[AD-752158] 08 p0936 N73-17667
Analysis of structural properties produced by selective reinforcement of aluminum compression panels with unidirectional boron epoxy composite materials
[NASA-CR-2145] 08 p0966 N73-17895
Procedures for reducing residual stresses in aircraft metal structures reinforced by filamentary composites
[NASA-CR-112207] 08 p0966 N73-17900
Methods for designing and developing aircraft structural components by riveting, welding, and gluing aluminum alloys parts
[AD-753513] 09 p1041 N73-18491
Time dependent mechanical behavior of boron filament reinforced aluminum composites based on static and dynamic properties
[AD-753706] 09 p1054 N73-18590
Improvement in interlaminar shear strength of organic matrix composites using plasma deposited coupling agents
[AD-753857] 09 p1055 N73-18599
Development of thick-walled, Borsic aluminum alloy ring for use as stiffener in 155 millimeter atomic artillery projectile
[SC-DR-72-0706] 10 p1176 N73-19562
Analysis of fundamental behavior of fiber reinforced plastic composite structures to determine
[AD-754249] 10 p1177 N73-19570
Development of design concepts for metal-lines, glass-fiber composite pressure vessels and comparison with homogeneous metal pressure vessels
[NASA-TM-X-68198] 10 p1220 N73-19922
Fabrication of L-1011 aircraft panels to compare costs and service performance characteristics of PRD-49 and fiberglass
[NASA-CR-112250] 11 p1234 N73-20018
Development of composite structures for spacecraft to serve as anti-meteoroid device
[NASA-CASE-LAR-10788-1] 11 p1341 N73-20880
Extensional vibrations of simply supported composite plate strips
[AD-756868] 13 p1587 N73-22867
Research projects conducted as part of NASA programs during period May 1970 through May 1972
[NASA-TM-X-64723] 13 p1593 N73-22915
Development and application of composite materials for weight reduction of space shuttle structural hardware
13 p1593 N73-22917
Design concepts, manufacturing process, weight analysis, and cost estimates for long range transport aircraft using composite structures
[NASA-CR-112255] 14 p1600 N73-22976
Analysis of structural reliability of large scale bonded joints for advanced composite wing to determine service life of boron epoxy to titanium scarf joint
[AD-756893] 14 p1603 N73-22995
Development of stability matrices of displacement type for multilayer sandwich beam, rectangular, and triangular plate elements
14 p1714 N73-23908
Computer program for linear instability analyses of biaxially loaded composite structures
[NASA-CR-112226] 15 p1838 N73-24893
Analysis for stresses and buckling of heated composite stiffened structures
[NASA-CR-112227] 15 p1838 N73-24894
Evaluation of low cost techniques for forming boron-reinforced aluminum structural shapes from diffusion-bonded flat sheet and plate
[NASA-CR-124279] 16 p1918 N73-25523
Analysis of optimal configurations for thin walled, axisymmetric, laminated shells based on shell configuration, loading, fiber alignment, and material properties of composite structure
16 p1969 N73-25924
Evaluation of sandwich structures of titanium and aluminum honeycomb in edgewise compression under static and fatigue loading
[FPL-196] 16 p1969 N73-25927
Nondestructive methods determining composite beam and plate critical loading
[ENSMP-010] 17 p2094 N73-26940
Response of general laminated plates to applied loads with coupling between bending and extensional modes of deformation
18 p2165 N73-27488
Fracture control method for composite tanks with load sharing liners
[NASA-CR-120918] 19 p2348 N73-28889
Fracture mechanics for Interfacial crack between adhesively bonded dissimiliar materials
20 p2477 N73-29898
Fokker F-28 fellowship structure adhesive bonding processes and quality control methods
[FOK-K-67] 21 p2497 N73-30037
Development of linear analysis method for predicting buckling of composite structures with arbitrary uniform cross section
[NASA-CR-2216] 21 p2603 N73-30863
Application of composite materials to construction of helicopter airframes and landing gear
[NASA-CR-112333] 22 p2614 N73-30948
Construction of helicopter airframes and landing gear to show advantages of composite material prototype over metal prototype
[NASA-CR-112333] 23 p2743 N73-31957
Response of laminated elastic plate to planar impact loads using vibratory modes to develop transient response solution
23 p2853 N73-32795
Structural optimization procedures applied to design of simply supported, corrugated hat stiffened composite panel under uniaxial compression
[NASA-CR-132314] 23 p2853 N73-32798
Procedure for structural analysis of stiffened shells of revolution to describe computer program and types of shapes and cross sections of specimens - Vol. 2
[NASA-CR-2273-VOL-2] 23 p2854 N73-32802
Analysis of internal buckling of fibers in viscoelastic composite plate based on linear material responses and small deflection theory
24 p2987 N73-33874

**COMPOSITES**
U COMPOSITE MATERIALS

**COMPOSITION (PROPERTY)**
NT ATMOSPHERIC COMPOSITION
NT ATMOSPHERIC MOISTURE
NT ATOM CONCENTRATION
NT CARBON DIOXIDE CONCENTRATION
NT CHEMICAL COMPOSITION
NT CONCENTRATION (COMPOSITION)
NT GAS COMPOSITION
NT IONOSPHERIC COMPOSITION
NT LUNAR COMPOSITION
NT METEORITIC COMPOSITION
NT METEOROID CONCENTRATION
NT MOISTURE CONTENT
NT PLANETARY COMPOSITION
NT PLASMA COMPOSITION
Rings of Saturn, their composition, and their thickness
[NASA-TT-F-14617] 02 p0230 N73-11867
Dielectric properties of pure and doped insulating materials
[COO-623-182] 12 p1439 N73-21662

**COMPOUND HELICOPTERS**
NT S-67 HELICOPTER

**COMPRESSED AIR**
Shock wave generation with rechargeable compressed air bottles for large diameter shock tunnel
[REPT-2/72] 02 p0151 N73-11228
Bibliography on role of vestibular apparatus in compressed air work underwater
[AD-750686] 06 p0632 N73-15133

**COMPRESSED GAS**
NT HIGH PRESSURE OXYGEN
Simulation of flow of compressible gas through water channel of varying cross section
[AD-749134] 04 p0408 N73-13327
Analysis of compressibility of polytetrafluoroethylene when subjected to single stage and two stage shock loading
[NLL-NEL-TT-2491-(6075.461)] 20 p2386 N73-29170

**COMPRESSIBILITY**
External friction effects on compressibility of metal powders
[AD-747722] 03 p0317 N73-12583
Compactibility, shrinkage, and microhardness of electrolytic titanium powders obtained at low temperatures from melts
04 p0432 N73-13521
Isothermal compressibility of amorphous semiconductors
[AD-750397] 06 p0709 N73-15785
Equation of state for compressibility of helium, nitrogen, and their mixtures
[JPRS-57923] 07 p0752 N73-16111
Field emission, high intensity electron gun, single RF cavity, and compression system
[IPPJ-T-11] 09 p1011 N73-18249
Effect of undissolved air on compressibility of transmitting medium in hydraulic circuits
[NLL-NEL-TT-2426-(6075.461)] 15 p1763 N73-24289

**COMPRESSIBILITY EFFECTS**
Development of techniques for measuring oscillatory derivatives in wind tunnels and analysis of wind tunnel effects on results
[ARC-R/M-3319] 15 p1729 N73-24020
Characteristics of secondary flows around and downstream of protuberances in laminar boundary layers and conditions for development of turbulence
22 p2649 N73-31222

**COMPRESSIBLE BOUNDARY LAYER**
Hypersonic axisymmetric turbulent boundary layer compression in adverse pressure gradient along cylindrical axisymmetric body
[NASA-CR-112247] 07 p0770 N73-16253
Application of implicit finite-difference method for solution of compressible boundary layer equations
10 p1139 N73-19277
Analytic model to make comprehensive transition run-out calculations for compressible boundary layer with wall cooling
[AD-756890] 13 p1513 N73-22258
Compressible turbulent boundary layer in zero-pressure gradient nozzle flow for zero, moderate, and severe heat transfer conditions
[AD-757330] 14 p1651 N73-23391
Three-dimensional compressible turbulent boundary layer for subsonic and transonic flow over yawed airfoil
[AD-763730] 21 p2526 N73-30258
Integral method for analyzing two-dimensional and axisymmetric compressible and three-dimensional incompressible turbulent boundary layer
23 p2772 N73-32169
Comparison of theories for skin friction coefficient in turbulent compressible boundary layers
24 p2907 N73-33203

**COMPRESSIBLE FLOW**
NT TRANSONIC FLOW
Calculating laminar viscous, compressible flows
[NASA-TN-D-6998] 01 p0040 N73-10313
Finite element procedure for predicting unsteady compressible gas flow in one spatial dimension
[AD-746234] 02 p0157 N73-11276
Development of formula for calculating natural frequencies of cantilever plate in fluid medium
[AD-747206] 02 p0241 N73-11958
Modification of Navier-Stokes equation for hypersonic compressible flow to eliminate need for specifying far field and/or boundary condition parameters
[AD-747644] 03 p0287 N73-12321
Interference theory in slotted wind tunnels extended to subsonic rectangular wind tunnels with ventilated tool, longitudinal slots and perforated screens of arbitrary porosity
[ARC-R/M-3706] 05 p0492 N73-14007
Calculation of compressible flow in three dimensional cascade of turbomachine blades using stream line curvature technique
[ARC-R/M-3704] 05 p0527 N73-14287

Effect of space-time integral of thermodynamic pressure on thermodynamic potential for compressible, adiabatic flow
[NASA-TM-X-66139] 05 p0606 N73-14926
Method for estimating aerodynamic characteristics of airfoils in compressible inviscid flow based on thickness and camber line parameters
[ESDU-72024] 07 p0735 N73-15981
Finite difference solution for supersonic laminar flow over two dimensional compression corner
08 p0894 N73-17241
Force and pressure distribution measurements on wing-body combination with wing of low aspect ratio in compressible flow
[DLR-FB-72-08] 09 p0980 N73-18008
Stability of steady state of compressible viscous fluid
[AD-752692] 09 p1016 N73-18295
Heat exchange and drag during turbulent flow of compressible gas
[AD-753046] 09 p1017 N73-18300
Influence of axial velocity density ratio on compressor cascade performance in compressible flow
10 p1205 N73-19805
Development of computer program for solving fully compressible, two-dimensional hydrodynamics problems using flux-corrected transport algorithms
[AD-754736] 11 p1271 N73-20315
Development of statistical equations for turbulent compressible gas with emphasis on space-time correlations in boundary layer
[AD-755889] 12 p1393 N73-21291
Effects of aerodynamic drag on rotary wing performance and methods for reducing influence of stall and compressibility parameters
14 p1598 N73-22954
Mathematical models for calculating subcritical and supercritical compressible flow about blade cascades
14 p1649 N73-23378
Increased propulsive efficiency through improved secondary flow capacity in double flow turbojets
[NASA-TT-F-14904] 14 p1701 N73-23803
Effects of heat transfer on laminar boundary layer development under pressure gradients in compressible flow
[ARC-R/M-3218] 15 p1727 N73-24012
Nonlinear partial differential equations for studying viscous compressible corner flow at subsonic and supersonic Mach numbers
15 p1764 N73-24294
Mach number effect on motion of sphere in compressible low Reynolds number flow
15 p1765 N73-24298
Transonic perturbation equation for studying steady compressible flow past lifting and nonlifting wings at high subsonic Mach numbers
[NASA-CR-2246] 15 p1766 N73-24312
Numerical solutions for laminar, compressible, three dimensional boundary layer on sharp bodies of revolution at angle of attack with moderate axial spin
[SC-CR-72-3182] 15 p1768 N73-24325
Calculation of two-dimensional turbulent skin friction under arbitrary compressible flow conditions
[AD-757872] 15 p1769 N73-24329
Development of mathematical formula for growth of compressible, turbulent boundary layers on isothermal and adiabatic walls
[ARC-R/M-3191] 16 p1853 N73-25013
Development of mathematical procedures for determining turbulent boundary layer in arbitrary pressure gradient
[ARC-R/M-3207] 16 p1854 N73-25017
Numerical analysis of axisymmetrical, viscous, compressible flow around blunt bodies for ideal gases with laminar unseparated boundary layers
17 p2012 N73-26273
Numerical analysis of compressible turbulent boundary layer velocity and temperature profiles with zero pressure gradient
[AD-762152] 19 p2258 N73-28200
Analysis of compressibility of polytetrafluoroethylene when subjected to single stage and two stage shock loading
[NLL-NEL-TT-2491-[6075.461]]
20 p2386 N73-29170
Analysis of compressible three-dimensional turbulent flow over yawed cone
22 p2649 N73-31227
Second order thermal boundary layer theory for steady, laminar, compressible flow over cambered two dimensional or rotational bodies
[DLR-FB-73-31] 22 p2653 N73-31256
Numerical analysis of boundary conditions of time dependent viscous compressible flow based on small perturbation of Navier-Stokes equation
23 p2773 N73-32176
Analysis of transient wave motion in liquid filled cylinders
23 p2773 N73-32179
Exact solution to nonlinear Euler equations pertaining to problem of thermally stratified compressible fluid motion on rotating sphere with gravitation
[AD-764684] 23 p2788 N73-32308

**COMPRESSIBLE FLUIDS**
Analysis of free transverse oscillations of closed prismatic shell of flexible rectangular panels and filled with compressible inviscid liquid
[AD-755416] 14 p1716 N73-23927
Analysis of convective cumulus cloud development and numerical relationships of hydrodynamic and thermodynamic concepts of cloud formation
[NLL-M-22840-[5828.4F]] 16 p1936 N73-25666
Approximate method for calculating echo signal of finite spherical pulse from elastic cylindrical shell in compressible fluid
16 p1969 N73-25928
Finite difference solution to thermoacoustic convection of fluids in low gravity environment
[NASA-CR-2269] 17 p2014 N73-26289
Mathematical model for calculating transient flow of compressible condensable fluid mixtures in open channels
[UCID-16170] 19 p2255 N73-28181
Stimulated Brillouin scattering in shock-compressed fluids
20 p2386 N73-29166
Impact of thin elastic circular shell on surface of compressible fluid
[AD-763259] 21 p2526 N73-30252

**COMPRESSING**
Thermocompression wobble tool bonding of beam lead devices
[SC-DC-72-1197-A] 03 p0306 N73-12501
Feasibility of gun launched projectile to produce magnetic flux compression
[AD-755103] 11 p1325 N73-20750
Free piston shock tube driver using two stage compression techinque with intermediate diaphragm
[FFA-AU-765] 12 p1376 N73-21161
Theoretical analysis of flow recompression, reattachment, and redevelopment associated with supersonic laminar flow past rearward facing step
20 p2385 N73-29162

**COMPRESSION BUCKLING**
U BUCKLING

**COMPRESSION LOADS**
NT AXIAL COMPRESSION LOADS
NT IMPACT LOADS
Buckled states of thin, flat, rectanguar elastic plate subjected to constant compressive thrust
[AD-744993] 01 p0113 N73-10938
Buckling characteristics of perfect and imperfect circular cylindrical shells subjected to dynamic axial loading
[NASA-CR-129086] 02 p0237 N73-11927
Weakening and fracture of glass reinforced plastics during compression under conditions of one-sided heating
[AD-748526] 04 p0439 N73-13581
Fatigue behavior of hat section stringer stiffened panels compressed in post-buckling range
[AD-748855] 04 p0482 N73-13938
Stability of three-layer plates with elastoviscous core subject to time-dependent loads
[AD-749746] 05 p0605 N73-14918
Semi-infinite homogeneous response to shear and compressional line sources
[UCRL-51233] 06 p0667 N73-15420
Effect of residual compressive stresses on fatigue strength and service life of aluminum alloy 7079 specimens
[NLR-TR-71105-U] 06 p0684 N73-15567
Stiffness of flat strips in compression under sinusoidally distributed bending couples at their edges
[ESDU-02.01.30-AMEND-A] 06 p0723 N73-15905
Hysteresis behavior of glass fiber reinforced plastic specimens under compressive cyclic loading
[AD-753823] 10 p1176 N73-19566
Comprehensive and tensile load tests on three-inch cubes of concrete
[AD-756926] 14 p1715 N73-23919
Analysis of general buckling of pressurized stiffened cylinder under axial load
[ARC-R/M-3198] 16 p1857 N73-25040
Carrying capacity of cylindrical shells under dynamic loads
[AD-759103] 16 p1971 N73-25944
Numerical analysis of stability of axially compressed cylindrical shells from composite materials under nonstationary heating
18 p2203 N73-27785
Analysis of properties of powder materials subjected to compressive forces and development of equations of state for determining mechanical properties
[NLL-NEL-RR-2474-[6075.461]]
21 p2603 N73-30858
Numerical analysis of buckling characteristics of ring-stiffened, oval, orthotropic, cylindrical shells
[AD-763369] 21 p2604 N73-30872
Dynamic buckling of thin, elastic beam subjected to constant, compressive axial displacement
24 p2987 N73-33871

**COMPRESSION TESTERS**
U COMPRESSION TESTS

**COMPRESSION TESTS**
Analysis of stability of cylindrical shells with filler under axial compression and development of linearized equations of stability
[AD-750953] 05 p0605 N73-14919
Mathematical solution to compressive bulk formation for calibrating ring test specimens using constant interface friction factor
[AD-750885] 06 p0675 N73-15492
Hydrocompression treatment to lower residual stresses in weld joints of forge-welded carbon steel vessels
10 p1163 N73-19461
Compressive tests on cubical test specimens of cast concrete
[AD-756927] 14 p1715 N73-23920
Evaluation of sandwich structures of titanium and aluminum honeycomb in edgewise compression under static and fatigue loading
[FPL-196] 16 p1969 N73-25927
Compression tests of pure Ti and Ti alloy deformation properties
[RAE-LIB-TRANS-1657] 17 p2043 N73-26529
Dynamic compressive stress-strain data of polymer foams obtained from uniaxial compressive tests
[AD-762490] 21 p2565 N73-30559
Test equipment to prevent buckling of small diameter specimens during compression tests
[NASA-CASE-LAR-10440-1] 23 p2790 N73-32323
Test fixture design for boron-aluminum and beryllium test panels
[NASA-CR-124401] 23 p2792 N73-32337
Method for determining stress and displacements infinite plate with hole of various shapes under uniform tension of compression
24 p2988 N73-33882

**COMPRESSION WAVES**
Plane compression wave in pressure field of electrical discharge into water
[AD-754614] 11 p1324 N73-20746

**COMPRESSIVE STRENGTH**
Elastic stresses in single lap joints under compression or tension
[ESDU-67008] 01 p0111 N73-10920
Compressive stress-strain properties of aircraft materials
[ESDU-00.01.01-AMEND-A] 06 p0723 N73-15902
Numerical analysis of incompressible linearly compressible viscoelastic creep and relaxation for plastic materials
[AD-752067] 08 p0967 N73-17903
Failure mechanics and compressive biaxial strength of ceramics
[AD-754826] 11 p1309 N73-20621
Stability of cylindrical shells with consideration of initial imperfections
[AD-757728] 15 p1840 N73-24909
Measurement of elastic moduli and compressive yield strength for Ni3[Al,X] alloy single crystals
16 p1927 N73-25589
Experimental determination of compressive behavior of linear induction motor reaction rail
[NASA-TM-X-69276] 17 p2011 N73-26263
Compressive strength and modulus of unidirectional carbon fiber reinforced plastic laminates
[RAE-TR-72096] 17 p2050 N73-26587
Development of unidirectional fiber composite materials with emphasis on improving compressive strength
[NASA-CR-112334] 18 p2203 N73-27784
Composite materials studies, including compressive strength and reinforced plastics
[JPRS-59610] 20 p2434 N73-29549
Buckling behavior of composite cylinders to compressive loads
[NASA-CR-132264] 20 p2483 N73-29945

**COMPRESSOR BLADES**
Analysis, design, fabrication, and performance tests to determine effects of impeller blade clearance on efficiency of centrifugal pumps
[NASA-CR-120815] 03 p0305 N73-12493
Multiple tone acoustic radiations phenomenon in transonic fans
[ARC-CP-1226] 05 p0580 N73-14726
Distribution losses in axial compressor over blade cross sections and effects of blade heights
[AD-750931] 06 p0657 N73-15334
Oscillographic pressure measuring system for flow structure in compressor impeller bladings
[NASA-TT-F-14647] 06 p0673 N73-15480
Analysis of stresses in compressor blades with emphasis on conditions in dove tail joints at base of blades
[AD-750497] 06 p0727 N73-15936
Development of supersonic cascade and wheel structure for axial flow compressor
[AD-752583] 09 p1079 N73-18804
Development of algorithm for testing gas dynamic design of axial flow compressors with multiple stages
[AD-753519] 09 p1080 N73-18809
Effects of boundary layer flow patterns on upright cascade blade performance
10 p1205 N73-19803

Effect of axial velocity ratio on aerodynamic coefficients of compressor cascade in viscous flow
10 p1205 N73-19804
Performance tests of axial flow transonic compressor stage with multiple circular arc blades to determine effects of blade shape on efficiency and stall margin
[NASA-TM-X-2731] 11 p1231 N73-19995
Computer program for use in design of axial compressor airfoils suitable for operation at high subsonic and supersonic Mach numbers
[AD-756879] 13 p1536 N73-22442
Vibration damping ability of steel compressor blades subjected to different heat treatments
[AD-743119] 13 p1543 N73-22502
Protection of titanium microstructure with intermediate nickel barrier to prevent abrasion and crack propagation on turbine compressor blades
[AD-758276] 14 p1682 N73-23651
Design and evaluation of multiple circular arc bladed, axial flow transonic compressor rotor
[NASA-TM-X-2697] 15 p1730 N73-24033
Performance test of compressor stage with cantilevered stator and rotating inner shroud under stator at rotor tip speed of 1600 feet per second
[NASA-CR-121141] 15 p1825 N73-24794
Analysis of supersonic, unstalled torsional flutter in cascades of compressor blades to determine position of flutter boundary and aeroelastic instability
[AD-758721] 15 p1827 N73-24809
Performance data for single stage axial flow compressor with tandem airfoil blading
[NASA-CR-121145] 16 p1955 N73-25818
Dynamic characteristics of solid particles in particulate flow through turbine and compressor cascades
17 p2013 N73-26278
Performance and fatigue strength of compressor blades fabricated from carbon fiber composites and boron composite wires
18 p2166 N73-27496
Process for welding compressor and turbine blades to rotors and discs of jet engines
[NASA-CASE-LEW-10533-1] 19 p2303 N73-28515
Design and operating principles of base plate for regulating performance of radial centrifugal machines
[NLL-NEL-TT-2476-[6075.461]]
20 p2382 N73-29137
Investigations of HT-S/PMR-PI composites for applications to advanced aircraft engines
[NASA-TM-X-71459] 24 p2943 N73-33502

**COMPRESSOR EFFICIENCY**
Analysis of data obtained in evaluation tests of circumferential airflow uniformity entering combustors from two advanced engine compressors
[NASA-CR-121009] 05 p0526 N73-14276
Data tables and computer generated profile plots obtained in evaluation tests of circumferential airflow uniformity entering combustors from two advanced engine compressors
[NASA-CR-121010] 05 p0526 N73-14277
Flow characteristics of tandem bladed compressor stators at various inlet incidence angles
[NASA-TM-X-2734] 08 p0863 N73-16986

**COMPRESSOR ROTORS**
Development of supersonic cascade and wheel structure for axial flow compressor
[AD-752583] 09 p1079 N73-18804
Design and aerodynamic performance of low speed fan stage for low noise turboengine
[NASA-CR-121148] 12 p1364 N73-21070
Three dimensional particle trajectories in compressible gas flow in rotating cascade
[AD-757162] 14 p1701 N73-23807
Performance test of compressor stage with cantilevered stator and rotating inner shroud under stator at rotor tip speed of 1600 feet per second
[NASA-CR-121141] 15 p1825 N73-24794
Design, development, and evaluation of centrifugal compressor with six to one pressure ratio and two pounds per second air flow
[NASA-CR-120941] 17 p2037 N73-26483
Holographic visualization of flow field within transonic compressor rotor
[NASA-CR-121112] 18 p2130 N73-27215
Energy transfer control and compressor bleed concepts of remote lift fan control
[NASA-TM-X-2863] 21 p2590 N73-30749
Numerical analysis of dynamics of constant speed rotor with three dimensional rotary inertia using eight degree of freedom model with coupled linear and angular motion
22 p2676 N73-31437
Effects of blade tip clearance and leading edge sweepback of compressor rotor blades on inducer performance and blade pressure loading
[NASA-CR-72712] 23 p2739 N73-31930

**COMPRESSORS**
NT CENTRIFUGAL COMPRESSORS
NT SUPERSONIC COMPRESSORS
NT TRANSONIC COMPRESSORS
NT TURBOCOMPRESSORS
Computation principles and methods of free-piston expander-compressors
05 p0552 N73-14481
Analysis of thermomechanical compressor to include principles of operation and specific applications
05 p0552 N73-14482
Turbulent transport models for designing compressors and gas turbines
[AD-751757] 07 p0837 N73-16786
Analysis of dynamics of free-piston expander-compressor machinery
18 p2156 N73-27416
Performance and endurance of compressor disks bound with boron composite wires
18 p2167 N73-27499
Design of standard, special purpose air, and refrigeration screw compressors
[NLL-NEL-TT-2460-[6075.461]]
20 p2422 N73-29452
Steady state analysis of energy transfer control and compressor concepts of remote lift fan control
[NASA-TM-X-2876] 21 p2590 N73-30753

**COMPTON EFFECT**
Sum rule for photoproduction amplitudes in isovector Compton scattering and inconsistency of free fermion parton model in deep inelastic limit
[NUB-2169] 07 p0823 N73-16673
Design and performance of Compton diode radiation detector
[SC-DR-72-0118] 10 p1134 N73-19242
Electron correlation and band structure in solids using X ray Compton effect
15 p1820 N73-24751
Gamma ray telescope using double Compton process and measuring extraterrestrial gamma ray fluxes in energy range 1-10 MeV
[MPI-PAE/EXTRATERR-74] 22 p2674 N73-31421
K shell Compton scattering on tin and gold at 145 keV and gold at 320 keV
24 p2960 N73-33654

**COMPUTATION**
NT MINIMUM VARIANCE ORBIT DETERMINATION
NT ORBIT CALCULATION
Computation of optical sensor output relative to known star magnitudes for attitude control of spacecraft
[NASA-CR-130926] 10 p1212 N73-19859
Free stream pressure gradient effects on accuracy of turbulent boundary layer calculations
22 p2648 N73-31219
Computation of characteristics of tracking disruption
22 p2691 N73-31558
Formula for computing operating cost of turbine powered transport aircraft
23 p2860 N73-32852

**COMPUTER COMPONENTS**
Large scale integration techniques for computer multiprocessing system
[NASA-CR-128395] 01 p0030 N73-10234
Method of determining reliability of computer components and subsystems
[AD-747080] 02 p0148 N73-11198
Design and fabrication of magnetic logic circuits using ferrite delay elements
[NASA-CR-112198] 03 p0277 N73-12247
Reliability tests of computer elements used in automatic airport weather stations
[AD-747558] 03 p0328 N73-12673
Design and functional description of digital computer system
[FOA-3-C-3657-63] 06 p0643 N73-15220
Operational models for analyzing digital control system between computer and information sources
10 p1177 N73-19576
Hardware manual for Space Ultrareliable Modular Computer-Demonstration Vehicle including assembly, physical and basic electrical tests
[NASA-CR-124205] 12 p1380 N73-21195
Feasibility study of spaceborne plated wire memory with associated electronic circuits and components
[REPT-26/1422/EC/MB/VOL-2]
13 p1498 N73-22138
Collection of Soviet articles on computer elements and systems
[TT-72-50009] 21 p2512 N73-30150
Transient response of devices operating in cryotron computing medium and determination of their speed
21 p2515 N73-30176
Formal method for converting logical descriptions of cryotron circuits of asynchronous automata into differential equations
21 p2515 N73-30177
FORTRAN-WATFIV compiler noting differences with FORTRAN G and H extended and usefulness in program debugging
[LAAS-NT-SIS-73-T-04] 23 p2761 N73-32095

**COMPUTER DESIGN**
Functional design criteria for multiprocessor computer system to provide computational capability for space station
[NASA-CR-128601] 01 p0030 N73-10235
Development and design of small real time computers for information systems
[FOA-2-C-2484-E5] 02 p0145 N73-11175
Technology of small computer systems for industrial automation and control
[FOA-2-C-2485-E5] 02 p0145 N73-11176
Digital simulation model for design of optimal spaceborne computer system
[NASA-CR-128997] 02 p0146 N73-11184
Large scale integrated circuits used for designing 128 words x 72 bits/word memory
[REPT-1404] 03 p0272 N73-12205
Design and operation of computer for installation onboard satellite
[RAE-LIB-TRANS-1647] 04 p0392 N73-13188
Design and development of integrated magnetic memories
04 p0394 N73-13203
Computation, design, and manufacture of integrated circuits for application to computer construction and operation
[JPRS-57333] 04 p0398 N73-13239
Development of specifications for minicomputer hardware and software for NASA applications - App. A
[NASA-CR-129816] 05 p0515 N73-14189
Multiprogram structure of HRS-101 digital computer
05 p0516 N73-14194
Failure tolerant computer design noting component reliability
05 p0517 N73-14206
Simulation of logical functions for construction of computerized control system for onboard spacecraft instrumentation
10 p1177 N73-19573
Simulation of program sequencing functions in design of computerized digital control system for onboard spacecraft instrumentation
10 p1177 N73-19574
Baseline design of central multiprocessor for manned space station application
[NASA-CR-124151] 11 p1259 N73-20219
Research activities of electronic laboratory in development of inertial navigation systems to include applications for space missions and commercial aviation
11 p1316 N73-20686
Design, functional operation, and recommended expansion and enhancements for Space Ultrareliable Modular Computer interpretive simulator
[NASA-CR-124202] 12 p1380 N73-21194
Computer design of sequential synchronous circuits and multiple output logical networks
[CEA-R-4294] 12 p1387 N73-21246
Feasibility study of spaceborne plated wire memory with associated electronic circuits and components
[REPT-26/1422/EC/MB/VOL-2]
13 p1498 N73-22138
Design of multiple output analog computer for hot-wire anemometer signal processing
[AD-756532] 13 p1498 N73-22143
Systems design for spaceborne computer engineering module
14 p1712 N73-23894
Specifications for design of P-channel MOS computers
[AD-759189] 16 p1884 N73-25249
Design of two dimensional digital computer for optical image processing onboard spacecraft using liquid crystal circuits
18 p2209 N73-27827
Asynchronous control modules for digital computer design
[AD-762345] 19 p2241 N73-28067
Analysis of languages for design of digital computers
[AD-762381] 19 p2241 N73-28071
Algorithm for optimization of reliability characteristics of redundant digital computer
[AD-763261] 22 p2640 N73-31156
Angle tracking computer for experimental array radar system
[AD-764224] 23 p2758 N73-32070
Hybrid computer multiplication-division modular unit for ASMODEE minicomputer noting three state gate circuits, integrated circuits, and algorithms
[LAAS-TNPE-73-I-07] 23 p2761 N73-32094
Design of modular spaceborne digital computer system
[NASA-CR-124171] 24 p2898 N73-33130

**COMPUTER GRAPHICS**
Nomographic procedure to calculate gas flow parameters at subsonic, sonic, and supersonic velocities
[AD-745898] 02 p0157 N73-11275
Screen touching device for computer graphic display operation
[RHEL/R-248] 03 p0271 N73-12194
Implementation of FORTRAN-extended graph algorithmic language for Univac 1108
[NASA-CR-129907] 04 p0393 N73-13198
Man machine communication techniques for improving problem solving capability
[AD-748240] 04 p0394 N73-13207
Computer graphics for theoretical geography with spatial analysis of surface topology
[AD-749377] 05 p0543 N73-14418

Interactive graphics solution, PDQ 3, to Laplace and Poisson equations
[AD-749252] 05 p0569 N73-14621
Computer generation of patterns for analysis of human visual perception of form
[FOA-2-C-2473-52] 06 p0643 N73-15224
Computer subroutine for drawing networks of latitude and longitude lines by plotter
[EDFB-IBP-72-7-PT-2] 06 p0667 N73-15421
Design of digital controlled thin cathode tube screen for computer output display
[AD-751745] 07 p0762 N73-16193
Automatic computer mapping of infrared scanner data of terrain classes in Yellowstone National Park
07 p0787 N73-16400
Multispectral data and computer processing technique for mapping soil patterns and multispectral radiation changes from corn crop canopy
[NASA-CR-130035] 07 p0789 N73-16420
On-line computer graphics for display of magnetic tape data from digital computer
[IPPJ-T-10] 08 p0887 N73-17179
Computer network modeling system for planning data management in voice communication
[AD-752797] 09 p1006 N73-18210
Implementation of FORTRAN extended graph algorithmic language for univac 1108 computer
[NASA-CR-130966] 09 p1006 N73-18212
Graphical techniques for developing photoplastic record card system
[AD-753602] 10 p1162 N73-19453
Display device for real time display of computer generated half tone pictures
[AD-753672] 11 p1260 N73-20224
Graphical computers and computing techniques for real time aid in human problem solving tests
[AD-754282] 11 p1260 N73-20227
Computerized video display for processing spark and bubble chamber photographs
[JPRS-58713] 12 p1381 N73-21202
Computer-derived synoptic weather forecast maps
[AD-755898] 12 p1423 N73-21532
Computer graphics for solving three dimensional lifting body potential flow nonlinear equations to determine aerodynamic loads
[DGT-7510] 13 p1474 N73-21939
Data entry and edit monitor using rear ported CRT display device
[AD-756934] 13 p1498 N73-22140
Subroutine package for FORTRAN communication with graphic video system
[R-1015-NIH] 14 p1637 N73-23274
Survey of easy methods of developing easy computer systems useable by everyman
[P-4962] 14 p1638 N73-23278
Automatic data processing techniques for computer graphics and image processing
[AD-757530] 14 p1638 N73-23284
Development of automated drafting and digitizing system for preparing concept, experimental, prototype, and production mechanical drawings
[AD-755502] 14 p1671 N73-23558
Manual for FORTRAN program designed to plot output graphs using IBM 1130 computer
[NASA-TM-X-64744] 15 p1753 N73-24213
Computer graphic display system for generating optimal electric propulsion space trajectory
[NASA-CR-130241] 15 p1754 N73-24217
Modular graphic programs for computerized design
[MBB-UA-79-72-O] 17 p2001 N73-26181
Computerized data processing and graphic display system for artificial satellite
[AD-760304] 17 p2002 N73-26190
Symbol designs for graphic symbol subset of ASCII in warning and control systems
[AD-759807] 17 p2004 N73-26206
Real time computer technique for mission control and schedule planning
18 p2211 N73-27852
Real time hybrid computer audio synthesis system
[AD-761730] 19 p2228 N73-27968
Computer programming algorithm for surface line drawing graphics
[AD-762023] 19 p2242 N73-28077
Computer maps of land use in Titusville, Florida
[E73-10852] 20 p2391 N73-29209
Collection of Soviet articles on computer elements and systems
[TT-72-50009] 21 p2512 N73-30150
Users manual for interactive digital image processing and graphic display system
[NASA-TM-X-70472] 23 p2760 N73-32084
Computerized image processing and graphic display system
[NASA-TM-X-70473] 23 p2760 N73-32085
Generation of line-containing picture samples from gray level pictures using contrast gradient
[BMVG-FBWT-73-10] 23 p2761 N73-32092
Computerized graphics testbed for photointerpretation
[AD-764353] 23 p2761 N73-32096
Computerized laser position detector and optical stereo display system
24 p2897 N73-33121

**COMPUTER METHODS**
U COMPUTER PROGRAMS

**COMPUTER PROGRAMMING**
NT MICROPROGRAMMING
NT MULTIPROGRAMMING
NT ON-LINE PROGRAMMING
Review of commonly used programming languages and their ranges of applicability
[NASA-TT-F-14610] 01 p0030 N73-10237
Corrector module and spacecraft dynamics program
[NASA-CR-130108] 01 p0031 N73-10238
CDC computer program for solving two-dimensional, two-fluid magnetohydrodynamic equations
[AD-745854] 01 p0086 N73-10713
Calculation of direction of magnetic moments of two permanent magnets in ESRO 1 satellite
[NASA-TT-F-14499] 01 p0109 N73-10896
FORTRAN program for plotting attenuation of air-filled rectangular waveguide
[AD-746108] 02 p0142 N73-11153
Development and application of computer program for simulation of continuous systems expressed as ordinary differential and logical equations
[EUR-4836-E] 02 p0144 N73-11169
Page replacement algorithm simulations for advanced avionic digital computer programming
[AD-746110] 02 p0147 N73-11196
Data sheet for prediction of loaded hydrodynamic journal bearing performance
[ESDU-69002-AMEND-A] 02 p0177 N73-11432
Sampled data frequency response method for analyzing control system performance, and compensator improvement program for designing Saturn 5/S1-C compensators
[NASA-CR-123917] 02 p0195 N73-11573
Automated thematic mapping using multispectral and spatial pattern recognition techniques on ERTS-1 imagery
[E72-10281] 03 p0292 N73-12379
Users manual for interpretive computer program implementation on large computer
[NBS-TN-552] 04 p0393 N73-13193
TRANSLANG, ALGOL-like language and Burroughs D machine for microprogramming
[NASA-CR-129805] 04 p0393 N73-13196
Modified programming language for X ray diffraction analysis by special purpose computer using internal counting
[AD-748828] 04 p0459 N73-13747
Computer controlled infusion pump for time varying input of calcium into physiological systems
[NASA-CASE-ARC-10447-1] 05 p0503 N73-14092
Proceedings of conference on automation of scientific research through use of computers
[JPRS-57826] 05 p0516 N73-14199
Digital correction techniques for ERTS-1 imagery
[E72-10365] 05 p0535 N73-14353
Approximative parameters and probabilistic sequential subsets for modeling linear and renewal sources in communication theory
06 p0639 N73-15186
SCEPTRE support program - revised users manual using FORTRAN
[AD-751518] 07 p0764 N73-16211
Theoretical derivation of finite element solution algorithm for transient energy conservation equation
[NASA-CR-130149] 07 p0813 N73-16593
Computerized simulation of stainless steel clad uranium oxide plutonium oxide fuel pin behavior in reactor core
[ORNL-4825] 07 p0819 N73-16640
Computer program for calculating equations of state, thermodynamic functions, and opacities of plasmas
[AD-751607] 07 p0829 N73-16723
Computer program for calculating equations of state, thermodynamic functions, and opacities of plasmas
[AD-751608] 07 p0829 N73-16724
Computerized aircraft simulation using aerodynamic coefficient table storage, checkout, and interpolation routines
[NASA-TM-X-62229] 08 p0863 N73-16983
Computerized multivariate scheduling of physical examinations for NASA personnel in clinical intervention program
08 p0873 N73-17068
On-line dialog and testing program for control of real time FORTRAN program
08 p0887 N73-17182
Frequency multiplier based on snapoff diode and computer program for evaluating performance
08 p0888 N73-17189
Users manual for network analysis program
[AD-752600] 08 p0892 N73-17218
Computer program for solving radiation-hydrodynamic problems in complex geometries
[AD-752066] 08 p0970 N73-17929
Programmable computer interface for computer aided measurement and control instrumentation systems
[NASA-TN-D-7148] 09 p1005 N73-18205
Software module for teletypes connected to HP ALOHA SYSTEM multiplexer
[NASA-CR-130492] 09 p1006 N73-18213
ILLIAC 4 systems characteristics and programming manual
[NASA-CR-2159] 10 p1132 N73-19225
FORTRAN program for computing XYZ potential flow about three-dimensional bodies of arbitrary shape
[AD-754429] 10 p1143 N73-19317
Simulation of program sequencing functions in design of computerized digital control system for on-board spacecraft instrumentation
10 p1177 N73-19574
Computer code for generating spatial-angular moments of adjoint gamma-ray flux in infinite mediums
[NBS-TN-748] 10 p1193 N73-19702
Computation of optical sensor output relative to known star magnitudes for attitude control of spacecraft
[NASA-CR-130926] 10 p1212 N73-19859
Computer control and data acquisition of tidal model of St. Lawrence River
[MH-110] 11 p1259 N73-20221
Fire control computer program for Poseidon missile failure data processing
[AD-754426] 11 p1260 N73-20230
Inclusion problem for monadic recursion schemes
[NASA-CR-131292] 11 p1311 N73-20634
Statistical analysis and computer techniques
[NBS-TN-756] 11 p1311 N73-20635
Problems of multiprogramming for special purpose computers
[JPRS-58571] 12 p1381 N73-21201
Programming language for writing programs conforming to standards of structured programming and modular design
[NASA-CR-131473] 12 p1381 N73-21203
Processing digital radar data base to create simulated mapping-radar scope images
[AD-755722] 13 p1495 N73-22118
Diagnostic computer system for fault diagnosis of digital circuits
13 p1496 N73-22128
SCEPTRE translator providing point-to-point input of one dimensional mechanical systems
[AD-755166] 13 p1498 N73-22141
Computer technique for obtaining near field cross section views of ultrasonic field
[AD-756537] 13 p1502 N73-22170
Radio controlled robots with computer induced artificial intelligence to act as human substitutes under adverse conditions
[NASA-CR-131593] 13 p1550 N73-22558
Software requirements and testing for Minuteman 3 missile system
[AD-757212] 13 p1583 N73-22833
Development of PDP 8 computer programs for medical biological laboratory in Netherlands
[MBL-1972-4] 14 p1637 N73-23275
Computer program for analyzing piezoelectric transducer acoustic surface wave device
[AD-757485] 14 p1642 N73-23320
FORTRAN code for solving time dependent neutron transport equation in three-dimensional geometry by Monte Carlo method
[AD-756290] 14 p1691 N73-23728
Interfacing and programming of minicomputer for Doppler spectrum analysis
[NOAA-TR-ERL-241-AL-7] 14 p1692 N73-23733
Computation oriented communications network using computer resources
[AD-758098] 15 p1752 N73-24197
Manual for FORTRAN program designed to plot output graphs using IBM 1130 computer
[NASA-TM-X-64744] 15 p1753 N73-24213
Computer programs for design of aircraft control systems based on FORTRAN subroutines for generating aircraft transfer functions in six degrees of freedom
[AD-758781] 16 p1861 N73-25075
Software validation for guided missile computer
[AD-759263] 16 p1879 N73-25213
Alternating direction implicit magnetohydrodynamic code for simulating laser plasmas
[SC-DR-72-0733] 16 p1949 N73-25776
Manual of CDC 6400 computer program for predicting nozzleless rocket motor internal ballistics
[AD-759559] 16 p1958 N73-25838
Rendezvous targeting program for space shuttle missions
[NASA-CR-128963] 16 p1965 N73-25898
Techniques used for software reliability determination and evaluation
[AD-760144] 17 p2002 N73-26185
Relationship between page size, program behavior, and page fetch frequency in storage hierarchy systems
[AD-760001] 17 p2002 N73-26186
Broad based computer science research and development, including speech understanding systems and techniques for I/O capability extension
[AD-760024] 17 p2002 N73-26189
Marshall system for aerospace system simulation
[NASA-CR-124288] 17 p2010 N73-26252
Computer code to calculate ionization distribution for polar ionosphere
[AD-760044] 17 p2029 N73-26423
FORTRAN program for solution of linear or non-linear constrained optimization problems
[NASA-TM-X-62282] 17 p2055 N73-26619

Computer solution of transformation parameters between two Cartesian coordinate systems from sets of coordinates given in both systems
[NASA-CR-132210] 17 p2055 N73-26621
Computer manual for transpiration cooling analysis on gas turbine blades
[AD-759192] 17 p2078 N73-26807
Development of programming technique for processing Skylab MSS data
[E73-10765] 18 p2134 N73-27242
Analytical technique and computer program for evaluation of airbreathing propulsion exhaust nozzle performance
[AD-760541] 18 p2194 N73-27712
Advantages and disadvantages of using computers in engineering linguistics
[JPRS-59397] 18 p2213 N73-27870
Quadratic programming with regularization for analyzing polymer molecular weight distribution
[AD-761818] 19 p2234 N73-28009
Interface microprogramming for radar array signal processing computer
[AD-762439] 19 p2238 N73-28041
Processing quantities of multispectra data gathered by scanner systems using hybrid computers
[NASA-CR-133976] 19 p2239 N73-28048
Computer programming for hierarchial robot intelligence system
[AD-761641] 19 p2240 N73-28061
Computer programming for sequential machine design
[AD-762163] 19 p2241 N73-28069
Procedures for checking storage and transmission of instrumental, numerical, and address information in digital computer
[AD-762245] 19 p2242 N73-28073
Compilation of diagnostic programs developed for digital computer malfunctions analysis
[AD-762237] 19 p2242 N73-28076
Computer programming algorithm for surface line drawing graphics
[AD-762023] 19 p2242 N73-28077
Modification of input/output procedures to computer code for structural analysis of general shells
[AD-761806] 19 p2350 N73-28905
Computer analysis to three structural shell problems, including linear stress, free vibration, bifurcation buckling, elastic and inelastic collapse, and transient response
[AD-762946] 20 p2483 N73-29949
Polar coordinate method applied to program for calculating aerodynamic loads on oscillating wing configurations in subsonic flow
[SAAB-L-0-R64] 21 p2493 N73-30006
Installation standards for NASA Aerospace Safety Information System [NASIS] data base management system - Vol. 1
[NASA-CR-134455] 21 p2511 N73-30139
Overviews of NASA Aerospace Safety Information [NASIS] to introduce system features and component capabilities - Vol. 2
[NASA-CR-134456] 21 p2511 N73-30140
Data set specifications for NASA Aerospace Safety Information System [NASIS] to show standard format for every data set required by system - Vol. 3
[NASA-CR-134457] 21 p2511 N73-30141
Design specifications for programs and modules within NASA Aerospace Safety Information System [NASIS] - Vol. 4
[NASA-CR-134458] 21 p2511 N73-30142
Characteristics and operation of retrieval command subsystem for NASA Aerospace Safety Information System [NASIS] - Vol. 5
[NASA-CR-134459] 21 p2511 N73-30143
Definition and functions of message terms used in NASA Aerospace Safety Information System [NASIS] - Vol. 6
[NASA-CR-134460] 21 p2511 N73-30144
Operation specifications, Installation, and Modifications of NASA Aerospace Safety Information System [NASIS] - Vol. 7
[NASA-CR-134461] 21 p2511 N73-30145
Development of data base administrator user guide for use with NASA Aerospace Safety Information System [NASIS] - Vol. 8
[NASA-CR-134462] 21 p2512 N73-30146
Collection of Soviet articles on computer elements and systems
[TT-72-50009] 21 p2512 N73-30150
FAA engineering and development program for terminal air traffic control
[FAA-ED-14-2] 21 p2521 N73-30215
Programming implementation of Taylor series method for numerical solution of ordinary differential equations
[NASA-TM-X-70438] 21 p2566 N73-30567
Programs for control of SEL 86 radar operating system
[AD-763940] 22 p2635 N73-31119
Installation standards for NASA Aerospace Safety Information System [NASIS] data base management system using IBM 360-1370 OS MVT computer - Vol. 1
[NASA-CR-134470] 22 p2637 N73-31132
Overviews of NASA Aerospace Safety Information System [NASIS] to introduce system features and capability of IBM 360/370 OS MVT computer - Vol. 2
[NASA-CR-134471] 22 p2637 N73-31133
Data set specifications for NASA Aerospace Safety Information System [NASIS] to show formats used with IBM 360/370 OS MVT computer - Vol. 3
[NASA-CR-134472] 22 p2637 N73-31134
Design specifications for programs and modules within NASA Aerospace Safety Information System [NASIS] using IBM 360/370 OS MV computer - Vol. 4
[NASA-CR-134473] 22 p2637 N73-31135
Characteristics and operation of retrieval command subsystem for NASA Aerospace Safety Information System [NASIS] using IBM 360/370 OS MVT computer - Vol. 5
[NASA-CR-134474] 22 p2637 N73-31136
Definition and functions of message terms used in NASA Aerospace Safety Information System [NASIS] using IBM 360/370 OS MVT computer - Vol. 6
[NASA-CR-134475] 22 p2637 N73-31137
Development of data base administrator user guide for use with NASA Aerospace Safety Information System [NASIS] using IBM 360/370 OS MVT computer - Vol. 7
[NASA-CR-134476] 22 p2637 N73-31138
Large scale computer programming procedure called DIALOG for Univac 1100
[NASA-CR-134032] 22 p2638 N73-31143
Pneumatic analogue decompression computer for real time prediction of safe ascent depth following depth excursion
[DCIEM-884] 22 p2638 N73-31144
Validation tests for ALGOL 60 compiler
[NPL-NAC-33] 22 p2639 N73-31153
Assembly language programs required to interface ALOHA system to IBM telecommunication time sharing operation
[NASA-CR-133853] 22 p2639 N73-31155
Branch and search algorithms for knapsack and other computationally related problems
[PB-221436/9] 22 p2641 N73-31165
Computer interpretation of multispectral data of Chesapeake Bay, Lake Pontchartrain, Louisiana, and lower Mississippi Valley
[E73-11007] 22 p2660 N73-31312
Users manual for interactive digital image processing and graphic display system
[NASA-TM-X-70472] 23 p2760 N73-32084
Execution time optimization for IBM 360 FORTRAN production programs
[NASA-TM-X-70477] 23 p2760 N73-32086
Compilation of operational and mathematical computer programs from NASA programs
[NASA-SP-5962[01]] 23 p2760 N73-32089
Recognition algorithm for object localization in pictures
[BMVG-FBWT-73-14] 23 p2760 N73-32091
Computer science and technology research programs
[AD-764659] 23 p2762 N73-32101
Program for generating transfer functions of electrical network circuits
[AD-764809] 23 p2762 N73-32102
Computer science and data processing in Japan
[AD-764853] 23 p2763 N73-32106
Three level Boolean digital simulation program for logic circuits noting topological matrix circuit representation and simplified temporal simulation
[LAAS-SL-73-I-08] 23 p2769 N73-32149
User manual for shell theory automated for rotational structures [STAR 2B, 2V] - Vol. 3
[NASA-CR-2273-VOL-3] 23 p2854 N73-32803
Computer programs for analyzing satellite communication links
[REPT-6806] 24 p2895 N73-33108
Urban planning and development in east central Florida from ERTS-1 processed data
[E73-11083] 24 p2913 N73-33246
Coordination and establishment of centralized facilities and services for University of Alaska ERTS survey of Alaskan environment
[E73-11088] 24 p2913 N73-33250
Computer codes for calculating trace contaminant effects on stratospheric transport processes
[COO-2249-2] 24 p2923 N73-33345
Computer code for thermal/hydraulic stress analysis on liquid metal zirconium hydride reactor core
[AI-AEC-13065] 24 p2954 N73-33596

**COMPUTER PROGRAMS**
- NT COMPILERS
- NT COMPUTER SYSTEMS PROGRAMS
- NT EDITING ROUTINES [COMPUTERS]
- NT INPUT/OUTPUT ROUTINES
- NT MULTIPLE OUTPUT PROGRAMS
- NT OPERATING SYSTEMS [COMPUTERS]
- NT SUBROUTINE LIBRARIES [COMPUTERS]
- NT SUBROUTINES

Computer program for measuring specific radioisotopes contained in human body
[AD-745578] 01 p0010 N73-10078
Hybrid computer identification program for visual display of adaptive control state to human operator 01 p0014 N73-10109
Interactive information system with application in medical area
[NASA-TM-X-66076] 01 p0020 N73-10156
Hydraulic transients in cooling water system of thermal power plants, figures and computer programs
[PUBL-101-PT-2] 01 p0041 N73-10327
Lagrangian computer program for predicting movement and dispersion of pollutant in tidal embayment, and application to Bolinas Lagoon, California
[USGS-582-B] 01 p0048 N73-10389
Computation of thermochemical ablation rates of pyrolytic graphite surfaces using FORTRAN 4 computer code - Vol. 1
[AD-745440] 01 p0071 N73-10579
Algorithm for determining optimal partition of points into mutually exclusive and exhaustive subsets or clusters according to objective function defined on set of all partitions
[P-4878] 01 p0072 N73-10586
FORTRAN program for numerical solution of steady state matrix Riccati equation of quadratic cost optimal control problem
[AD-745862] 01 p0072 N73-10589
PICK method of particle-in-cell techniques for numerical solution of atmospheric diffusion equation applied to air pollution problems
[PB-209290] 01 p0078 N73-10643
Flow behavior of integrated circuits in bipolar transistors
[CEA-CONF-1971] 01 p0087 N73-10722
Computer programs for analysis of axial compressor aerodynamic test data
[AD-744502] 01 p0092 N73-10756
Computer program for rapid reduction of Vela satellite data on solar X rays
[AD-743921] 01 p0100 N73-10822
HILTOP - variational calculus program for generating electric propulsion data on rendezvous missions to comet Encke
[NASA-CR-114491] 01 p0104 N73-10857
Development of computer program for simulating performance of space radiator to account for transient and steady state performance
[NASA-CR-128594] 01 p0108 N73-10891
Application of integral nonlinear programming and random search techniques for determining minimum weight of reinforcing structures commensurate with strength requirements
01 p0112 N73-10929
Thermal analysis routine with capability for performing thermal analysis of systems containing flowing fluids
[NASA-CR-128593] 01 p0117 N73-10963
FORTRAN 4 program to compute thermochemical ablation rates of pyrolytic graphite surfaces as function of surface temperature and pressure including flow charts and program listings
[AD-744854] 01 p0117 N73-10969
Airport planning, economics, computer program, and arena characteristics for short haul, high density transportation systems in 1980 time period
[NASA-CR-114467] 01 p0120 N73-10991
Computer program listings for analysis of main rotor free wake geometry effects on blade air loads and response for helicopters in steady maneuvers - Vol. 2
[NASA-CR-2111] 02 p0124 N73-11006
Computer program for determining solar array output characteristics while accounting for effects of temperature,incidence angle on solar arrays
[NASA-CR-130109] 02 p0129 N73-11045
Development and application of computer program for simulation of continuous systems expressed as ordinary differential and logical equations
[EUR-4836-E] 02 p0144 N73-11169
Checkout of computer programs for errors, using ALGOL compilers
[NPL-NAC-21] 02 p0147 N73-11189
Computer program for subsonic lifting surface analysis with static aeroelastic effects
[AD-745894] 02 p0157 N73-11273
Computerized aerotriangulation with independent models and planimetric point adjustments
02 p0164 N73-11332
Development of computer programs for aerotriangulation with independent models
02 p0164 N73-11333
Computer program for strip tripangulation by independent models in aerial photogrammetry
02 p0164 N73-11334
Computer program for block analytical aerotriangulation adjustment with independent models
02 p0164 N73-11335
Horizontal accuracy of computerized planimetric block triangulation with independent models
02 p0164 N73-11336
Computerized horizontal block adjustment for aerial mapping using large numbers of points
02 p0165 N73-11337
ALGOL computer program for combined photogrammetric-terrestrial cadastral surveying
02 p0165 N73-11338

Users information and computer program for hydrodynamic-numerical model for oceanographic analyses
[AD-745760] 02 p0167 N73-11358
Programs and techniques for statistical analysis and reduction of ionospheric physics data
[AD-745966] 02 p0167 N73-11360
Two FORTRAN 4 computer programs for general combination of satellite and gravity data for position and gravity field determinations
[AD-746305] 02 p0168 N73-11364
Computer program for calculating gravimetric deflections of the vertical in central zone
[AD-747136] 02 p0170 N73-11380
FORTRAN program for calculating geostrophic trajectories
[FOA-4-C-4469-A1] 02 p0204 N73-11656
Computer program for analyzing dynamics of propellant feedlines
[NASA-CR-123913] 02 p0220 N73-11785
Operational procedure for computer program to calculate design point characteristics of gas generator or turbojet lift engine for V/STOL applications
[NASA-TM-X-2656] 02 p0222 N73-11794
Computer aided photogrammetric analysis of lunar topography
[AD-744867] 02 p0232 N73-11881
Aerospace Vehicle Synthesis Program for simulating space shuttles
[NASA-CR-129135] 02 p0232 N73-11886
Atmosphere Explorer Control System for automatic control of AE spacecraft and experiments
[NASA-TM-X-66086] 02 p0232 N73-11888
Digital computer procedure for analyzing initially bent two span columns
[AD-747075] 02 p0238 N73-11933
Development of computer programs to provide finite element method solutions to problems involving elastic and inelastic structures
[AD-746175] 02 p0239 N73-11942
Computer program user guide for determining limits to bending frequencies and mode shape estimates for free nonuniform beams with attached masses - Part 2
[AD-747242] 02 p0239 N73-11947
Computer program for optimum mixed offense weapons system
[AD-746263] 02 p0245 N73-11995
FORTRAN computer program for annular airfoil pressure distribution at subsonic speeds
[ARC-CP-1217] 03 p0248 N73-12004
Statistical analysis of air combat situation evaluations conducted by US Navy pilots to detect differences caused by experience
[AD-747519] 03 p0261 N73-12119
Computer program for mapping satellite-borne narrow beam antenna footprints on earth
[NASA-CR-129283] 03 p0265 N73-12149
REPRI program using Monte Carlo techniques for support compatibility studies for space station
[NASA-CR-123948] 03 p0268 N73-12174
FORTRAN 4 programs and subroutines for generating potential parameters from energy dependence of elastic scattering cross sections
[NASA-CR-129179] 03 p0269 N73-12180
Capabilities of Dynamic Operational Requirements and Cost Analysis Program for space mission planning - Vol. 1
[NASA-CR-129263] 03 p0269 N73-12183
Guide for coding Dynamic Operational Requirements and Cost Analysis Program to show subroutines and flow charts - Vol. 2
[NASA-CR-129264] 03 p0270 N73-12184
Program listing for Dynamic Operational Requirements and Cost Analysis Program to provide space mission planning and project management capability - Vol. 3
[NASA-CR-129265] 03 p0270 N73-12185
Description of functions and capabilities of Dynamic Operational Requirements and Cost Analysis Program - Vol. 4
[NASA-CR-129266] 03 p0270 N73-12186
Modification to Dynamic Operational Requirements and Cost Analysis Program to perform traffic analyses of automated satellite program - Vol. 5
[NASA-CR-129267] 03 p0270 N73-12187
User guide for Dynamic Operational Requirements and Cost Analysis Program for space mission planning and project management - Vol. 1
[NASA-CR-123378] 03 p0270 N73-12188
Programmer manual for Dynamic Operational Requirements and Cost Analysis Program for space mission planning and project management - Vol. 2
[NASA-CR-123379] 03 p0270 N73-12189
Program listing for Dynamic Operational Requirements and Cost Analysis Program to provide space mission planning and project management capability - Vol. 3
[NASA-CR-123380] 03 p0270 N73-12190
ALGOL program for lift distribution determination on thin wing in subsonic flow
[NLR-TR-70088-U] 03 p0274 N73-12224
FORTRAN computer program for solar simulator optimization
[DLR-FB-71-34] 03 p0281 N73-12277
Development of computer program for estimating reliability of self-repair and fault-tolerant systems with respect to selected system and mission parameters
[NASA-CASE-NPO-13086-1] 03 p0305 N73-12495
Automatic sequential processing, technique for unsupervised classification, or clustering, of multispectral remote sensing data, using digital computer program
[NASA-CR-128999] 03 p0323 N73-12633
Development of system for encoding outputs from several omnidirectional antennas and processing into modified signal to provide angle of arrival data for direction finding
[AD-747501] 03 p0329 N73-12684
Computer program for high temperature structural design methods for LMFBR components
[ORNL-TM-3845] 03 p0333 N73-12712
Computer analysis of tapered coaxial plasma gun electrodes
[AD-747057] 03 p0343 N73-12797
Computer codes for determining X ray filter/sound state detector response curves
[AD-748465] 03 p0344 N73-12804
Development of equations and mathematical models for decision making concerning military logistics, aircraft, space parts, and support equipment
[AD-747972] 03 p0368 N73-12997
FORTRAN program for calculating aerodynamic coefficients of subsonic aircraft at high speeds
04 p0370 N73-13010
Implementation of FORTRAN-extended graph algorithmic language for Univac 1108
[NASA-CR-129907] 04 p0393 N73-13198
Formulation for Performance Analysis and Design Synthesis [PADS] computer program
[NASA-CR-128677] 04 p0394 N73-13199
Assembler language program for Fourier transform spectroscopy with PDP 11 computer
[MSC-1743] 04 p0394 N73-13200
Development of computer program for generating aerodynamic forces for plane and interfering wings at supersonic speeds
[NASA-CR-112184] 04 p0404 N73-13290
Computer program for determining aerodynamic influence coefficients on interferring wings in unsteady supersonic conditions - programmers manual
[NASA-CR-112185] 04 p0404 N73-13291
CCAMIN, computer program for fitting time of arrival and shock peak overpressure versus slant range in gas
[AD-749332] 04 p0409 N73-13330
Analysis of temperature sensitive paints to determine validity of coating technique and development of methods for predicting areas of high thermal gradients
[AD-749582] 04 p0409 N73-13331
F-02 experiment onboard OGO-6, and computer program for analysis of raw data
[NASA-CR-130128] 04 p0414 N73-13376
Design and operation of programmable logic tester for high speed static testing of circuit boards
[REPT-6570] 04 p0420 N73-13422
RESALE-2 and INHALE computer code modifications for detecting radiative power of C02 in detector
[AD-748293] 04 p0430 N73-13500
Computer program for propagation and thermal blooming of pulsed, focused laser beams
[AD-748991] 04 p0430 N73-13503
Computer program for evaluating effects of conical light beams through interference filters, tilting filter, and energy distribution variations across beam
[WRE-TN-710[AP]] 04 p0449 N73-13665
X ray system for solving structure of crystals by diffraction techniques
[NASA-CR-129908] 04 p0458 N73-13737
Computer program for determining precision interplanetary trajectories
[NASA-CR-128655] 04 p0475 N73-13884
Numerical integration computer program based on integrating only perturbations in cartesian coordinates
[AD-747588] 04 p0476 N73-13890
Development of FORTRAN computer program for solving free axisymmetric vibration of cylindrical shells of arbitrary shape
[AD-748655] 04 p0482 N73-13942
Development of computational techniques for design optimization of thermal protection systems for space shuttle vehicle
[NASA-CR-128618] 04 p0484 N73-13951
Computer program for design optimization of subsonic swept wing jet transport aircraft
[RAE-TM-AERO-1448] 05 p0494 N73-14026
Computer program for geostationary orbit avoidance by radio relay transmitting antennas
[PB-211500] 05 p0514 N73-14179
Development of economical ways of integrating and interfacing new storage devices and data processing programs into computer systems - App. B
[NASA-CR-129817] 05 p0515 N73-14190
Production of software in NASA within predictable schedule and budget constraints and reasonable tolerances - App. C
[NASA-CR-129818] 05 p0516 N73-14191
FORTRAN 4 computer program for one-dimensional stress wave analysis of linear viscoelastic rock
[BM-IC-8563] 05 p0516 N73-14197
Development and application of computer programs as instructional methods for physics laboratory experiments
05 p0516 N73-14198
Catalog of automatic control computer programs including description and use of programs
[LAAS-NT-SIS-72-T-15] 05 p0517 N73-14202
Hardware and software requirements, and program operations and descriptions for cartographic data base program - manual
[AD-749498] 05 p0540 N73-14394
Computer program for calculating forces and energy in magnet systems
[ANL-TKK/RJL-2] 05 p0580 N73-14722
Computer program manual for optimal design of advanced thrust vector control for missile trajectory
[AD-749127] 05 p0590 N73-14798
SOS - computer program for calculating weight, center of gavity, and inertias of asymmetrical missiles
[AD-749251] 05 p0601 N73-14885
IBM 360 and 365 computer program for calculating heat and internal conduction of aerodynamic configurations
[AD-749482] 05 p0606 N73-14931
Computer program for solution of transient thermal problems in electrical power systems using concept of temperature calculations by analogy
[PB-211904] 05 p0607 N73-14933
Limited survey of general purpose finite element computer programs, including structural analysis
05 p0608 N73-14944
SMAC with two manual methods and one computer program with queueing simulation up to five parallel servers or up to three series servers
05 p0610 N73-14956
Digital computer program for parametric analysis and optimization performance aircraft configurations and propulsion concepts
06 p0620 N73-15035
FORTRAN computer program for calculating radar maximum range
[AD-749686] 06 p0642 N73-15208
Recognition and parsing algorithms for phrase structure languages
[NLL-SMRE-TRANS-5884-[8313.4]]
06 p0643 N73-15219
Computer program for tracing paths of high frequency electromagnetic rays through two-dimensional models of ionosphere
[AWRE-O-34/72] 06 p0644 N73-15228
Computer programs for curve-of-growth analysis using dimensions of stellar lines as input
[ROY-OBS-BULL-171] 06 p0644 N73-15230
Real time software for ballistic missile defense data processing system
[AD-750389] 06 p0644 N73-15234
Computer program models for reliability prediction of electronic and electromechanical components
[NLL-RISLEY-TR-2329-[9091.9F]]
06 p0676 N73-15501
Digital computer program for determining mean rainfall over areas by use of Thiessen method
[PB-211232] 06 p0694 N73-15655
Development of method for analysis and assessment of turbofan engine performance
[CRANFIELD-SME-2] 06 p0712 N73-15811
Description of computer program, main subroutines, input, output, and program requirements of Goddard Brouwer Orbit Bulletin
[NASA-TM-X-66141] 06 p0719 N73-15869
Environmental factors affecting OAO and related computer programs for data processing and scheduling observations
[NASA-TM-X-66145] 06 p0721 N73-15882
Computer program for dynamic structural analyses on three dimensional framework and pipework systems
[TRG-1409-REV-1] 06 p0726 N73-15929
Computer program for determining thermodynamic and transport properties of complex mixtures to include rocket performance, shock properties, and detonation properties
[NASA-TN-D-7056] 06 p0730 N73-15954
User manual for computer programs applied to community/airport economic development model - Vol. 3
[FAA-EQ-72-3-VOL-3] 06 p0732 N73-15971
Development and application of computer programs for evaluating performance of powered-lift STOL aircraft to include static, takeoff, and landing performance
[NASA-TM-X-62217] 07 p0738 N73-16007
Development of computer program for calculating flow field resulting from sonic boom focusing
[NASA-CR-2127] 07 p0739 N73-16013
FM distortion and FASP computer program for design and analysis of linear dynamic systems
[NASA-CR-130272] 07 p0754 N73-16125
Computer program for orbit comparison plots - users manual
[NASA-TM-X-66164] 07 p0759 N73-16165
Computer program to simulate FET transistor logic circuit performances and properties
07 p0762 N73-16191
Real time program for alignment of components and subassemblies prior to installation in chamber
[NASA-CR-128712] 07 p0800 N73-16493

Computer program to determine compressible fluid flow with friction across face seals and through narrow solts
[NASA-TN-D-6787] 07 p0803 N73-16518
METROC computer program for producing wind and thermodynamic data from raw upper atmospheric data
[AD-751780] 07 p0816 N73-16616
Erasable-memory programs for guidance computers in command and lunar modules
[NASA-CR-128689] 07 p0817 N73-16626
Computer program ELECTRA used to compute paraxial particle trajectories in axially symmetric electrostatic fields
[SGAE-2007] 07 p0824 N73-16678
Computer computation of spectral data for Josephson junction circuit
[NBS-TN-627] 07 p0832 N73-16740
User manual and source listings for computer programs to solve problems in analysis of in-flight thrust reversers
[AD-751526] 07 p0837 N73-16785
Computerized analysis of binary star systems with eclipsing light curves
[NASA-TM-X-66155] 07 p0842 N73-16821
Computer program for solving problems involving transient heat conduction and convection in continua
[NASA-CR-130148] 07 p0854 N73-16927
Fourier series and fourier integral formulations for improving spectrum analysis and display computer program
[AD-752113] 08 p0886 N73-17177
Mathematical programs for direct problem solving
[NASA-SP-5913[02]] 08 p0887 N73-17180
Computer programs for solution of systems of linear algebraic equations
[NASA-CR-2173] 08 p0887 N73-17181
Computer software to enable any general purpose computer with A/D conversion capability to be used as PSK receiver for low-data rate telemetry processing
[NASA-CR-130174] 08 p0887 N73-17185
Computer program for p-n junction diode simulation
08 p0887 N73-17186
Computer based automation for performing material handling, assembly, and quality control tasks
[AD-752464] 08 p0928 N73-17601
Computer programs for differential curve of growth analysis of solar type stars
[BULL-171] 08 p0960 N73-17848
Logical flow and guidelines for constructing low thrust orbit determination computer program
[NASA-CR-112256] 08 p0961 N73-17862
Computer programmer manual for NASA structural analysis program
[NASA-SP-223[01]] 08 p0966 N73-17892
Fast computer program for prediction of nonequilibrium rocket plume properties
[AD-751984] 08 p0970 N73-17927
Application of computer techniques for determination of flutter characteristics of aircraft and comparison with model matching data analysis
[AGARD-R-596] 09 p0983 N73-18030
Computer models for application to automatic inspection, diagnostic, and prognostic system for maintenance of military aircraft - Appendix C
[AD-752886] 09 p0988 N73-18066
Computer output data for automatic inspection, diagnostic, and prognostic system for maintenance of military aircraft - Appendix D
[AD-752887] 09 p0988 N73-18067
Digital computer routines for calculation of radar/radio tropospheric absorption and noise temperature
[AD-753197] 09 p1004 N73-18193
Computer program for fitting and model selection of two-level factorial replication-free experiments
[NASA-TM-X-2706] 09 p1005 N73-18201
Computer programs for information retrieval and data analysis
[NASA-SP-5955[01]] 09 p1005 N73-18204
Management, processing, and handling of French FR-1 satellite very low frequency data
[GRI/NTP/100] 09 p1005 N73-18207
FORTRAN programs for statistical analysis of signal and linear and nonlinear systems
[ANTHRO-MITT-3/72] 09 p1006 N73-18208
Computer program for analyzing flow field generated near aircraft engine operating in reverse thrust
[NASA-CR-121147] 09 p1012 N73-18264
Computer program for compact transpiration cooling with free jet tests and theory comparison
[AD-753109] 09 p1017 N73-18299
Computer program for calculating dynamic FORTRAN response of piping network to sinusoidal excitation
[AD-752743] 09 p1017 N73-18302
Computer program for calcuating transonic flow about axisymmetric bodies
[AD-752898] 09 p1018 N73-18309
User manual and related documentation for six compatible computer programs for structural analysis of ring-stiffened shells of revolution
[NASA-CR-2086] 09 p1094 N73-18930
Proposed computer program for dynamic analysis of elasto-plastic, thin, isotropic plates of rectangular planform subjected to blast loads
[AD-752449] 09 p1096 N73-18947
Finite element method of continuum and structural analysis using computer programs - users manual
[AD-753120] 09 p1097 N73-18951
FORTRAN program for predicting temperature-time histories of hemispherical shells subject to aerodynamic heating
[WRE-TN-783[WR/D]] 09 p1098 N73-18961
Computer program for evaluating biological parameters
[ISS-72/4] 10 p1120 N73-19128
Computer program for estimating position and shape of surface shadow zone in sonar operations
[AD-753443] 10 p1129 N73-19200
Conference papers on automated methods of computer program documentation
[NASA-TM-X-66196] 10 p1130 N73-19204
Program documentation with advanced data management systems
10 p1130 N73-19205
AUTOFLOW flow chart system for improved documentation and maintenance of scientific applications
10 p1130 N73-19206
BELLFLOW flow chart system for accurate automatic program documentation
10 p1130 N73-19207
Automated system for generating program documentation
10 p1130 N73-19208
Integration of system specifications and program coding as basis for final system documentation
10 p1130 N73-19209
Problems involved in computer program documentation and automation
10 p1130 N73-19210
Automatic editing of manuals for computer program documentation
10 p1130 N73-19211
Automated computer program documentation as feature of total system design
10 p1131 N73-19212
COSMIC history and essentials for computer program documentation
10 p1131 N73-19215
DOCMNT, documentation program, using META-SYMBOL assembly language on XDS 930 computer
10 p1131 N73-19216
Tree-structured information file and its subprogram subtree
10 p1132 N73-19223
Program for logic design of digital counters or sequential circuits
[NASA-CR-2212] 10 p1132 N73-19230
Computer program for shape of microwave reflector antenna
[REPT-53199] 10 p1135 N73-19247
Computer program for analysis of ERTS-1 MSS imagery of haze in Southern California test area
[E73-10346] 10 p1148 N73-19345
Characteristics and applications of computer codes for determining weight, center of gravity, and inertia of nuclear engine for rocket vehicles
[TID-26022] 10 p1186 N73-19652
Computer program to reduce X ray scattering data from cubic alloys by regression analysis
[ORNL-4828] 10 p1194 N73-19716
Computer program for analysis of mass spectra of GaTe and GaSe
[ISS-72/11] 10 p1199 N73-19754
Modified GRACY magnet program for computing magnetization effects in superconducting magnets
[BNL-17219] 10 p1201 N73-19772
Description and operation guide for DSAS illumination and moon conflict programs
[NASA-TM-X-66200] 10 p1213 N73-19863
Development of computer program to size launch vehicles for optimal trajectories and application for general purpose branched trajectory optimization
[NASA-CR-128725] 10 p1214 N73-19869
Development of computer program to predict transient and steady state performance and heat transfer characteristics of pulsing gaseous propellant rocket engine
[NASA-CR-128748] 10 p1214 N73-19871
IBM 360 FORTRAN computer program for three dimensional stress analysis of structural parts
[AD-753617] 10 p1221 N73-19932
NASTRAN computer program for determining stress cencentration at holes in isotropic finite strips
[AD-753574] 10 p1221 N73-19933
Model of n-conductor transmission lines for SCEPTRE computer program
[AD-754964] 11 p1265 N73-20265
Computer program for calculating structure and supersonic combustion flow with chemical reactions and shock waves
[NASA-CR-112303] 11 p1271 N73-20311
Computer program for three dimensional inlet and analysis of capture area, ram force, spillage force, and surface pressure force
[NASA-CR-112304] 11 p1271 N73-20312
Computer radiation interaction program for calculating material response to X ray and electron beam impact
[AD-755147] 11 p1327 N73-20767
Development of dynamic losds computation capability for application to unified flexible spacecraft simulation program
[NASA-CR-124168] 11 p1340 N73-20878
Program formulation for weight/sizing design synthesis computer program for application to space shuttle development - Vol. 1
[NASA-CR-128867] 11 p1343 N73-20894
Program description of computerized analysis for space shuttle weight analysis to include flow chart and subroutine linkages - Vol. 2
[NASA-CR-128868] 11 p1343 N73-20895
User manual for weight/sizing design synthesis computer program for application to space shuttle payloads - Vol. 3
[NASA-CR-128869] 11 p1343 N73-20896
MASS computer models for analyzing space shuttles and space shuttle payload operations
[NASA-CR-112286] 11 p1343 N73-20897
Addition of three-dimensional isoparametric elements to NASTRAN structural analysis program
[NASA-CR-112269] 11 p1345 N73-20916
User manual for computer program to solve equations of fully coupled viscous, radiating flow at stagnation point of blunt body which may be ablating or non-ablating
[NASA-CR-2237] 11 p1347 N73-20933
Computer automated scheme for solving equations of radiating flow over blunt body with or without ablation
[NASA-CR-2235] 11 p1348 N73-20936
Theories, numerical methods, and computer programs for determining inviscid three dimensional flow around spherically-capped smooth bodies and wings at supersonic speeds
[AD-753696] 12 p1356 N73-21002
Digital computer program for analyzing electromagnetic design of salient, wound pole alternators
[NASA-TN-D-7258] 12 p1366 N73-21082
Programming language for writing programs conforming to standards of structured programming and modular design
[NASA-CR-131473] 12 p1381 N73-21203
Computer modification of MOS transistor mathematical models
[CEA-R-4332] 12 p1383 N73-21218
Computer program for producing and updating wiring lists for use in development and production of electronic equipment
[ECR-31] 12 p1386 N73-21239
Three dimensional supersonic flow program for calculating flow field about cone at zero angle of attack
[NASA-CR-112301] 12 p1391 N73-21282
User manual for computer program of potential flow calculation about three-dimensional lifting bodies
[AD-755933] 12 p1393 N73-21292
Development of computer program to analyze air traffic in North Atlantic to show zone traffic at specified instants
[AD-755910] 12 p1426 N73-21557
OSUGOP computer program for adjusting geometrical or optical satellite observations
[NASA-CR-131532] 12 p1448 N73-21728
Development of computer program for parametric ascent trajectory optimization for application to space shuttle vehicle operation
[NASA-CR-129000] 12 p1458 N73-21815
TACOS finite computer program for analyzing dynamic transient response of cylindrical obese shells
[SC-RR-72-0454] 12 p1463 N73-21852
ALGOL procedures for calculating velocity and pressure distribution on rectangular and triangular planforms oscillating harmonically in supersonic flow - Part 1
[FOK-X-449-PT-1] 13 p1471 N73-21909
ALGOL procedures for calculating velocity and pressure distribution on rectangular and triangular planforms oscillating harmonically in supersonic flow - Part 2
[FOK-X-449-PT-2] 13 p1471 N73-21910
Design of automatic system for computer program documentation
[NASA-CR-130231] 13 p1496 N73-22129
Color coding scheme for hierarchically representing cartographic symbology
[AD-740606] 13 p1497 N73-22134
Computer analysis and design of special antenna configurations and characteristics
[AD-756470] 13 p1501 N73-22169
Computerized analysis of noise quality on microwave equipment
[AD-756862] 13 p1504 N73-22192
FORTRAN program for solution of large, sparse unsymmetric systems of linear equations
[AD-755878] 13 p1550 N73-22563
FORTRAN-4 computer program for compiling irradiation data on UN and UC fuel pins
[NASA-TM-X-68226] 13 p1558 N73-22625

GUERAP computer code for accurately measuring off axis rejection characteristics of optical system - users manual
[AD-755353] 13 p1560 N73-22645
Theory and user manual for computer program to determine buckling behavior of arbitrarily loaded shells of revolution with actual initial imperfections
[AD-756545] 13 p1587 N73-22866
Computer program for finite element stress wave analysis
[AD-755393] 13 p1587 N73-22871
User manual for finite element program for analysis of deformations of thin elastic membranes
[AD-755953] 13 p1588 N73-22874
Engineer manual for use of MAGIC 3 automated general purpose program for structural analysis
[AD-755368] 13 p1588 N73-22879
User manual for MAGIC 3 automated general purpose program for structural analysis
[AD-755369] 13 p1589 N73-22880
Programmer manual for use with MAGIC 3 automated general purpose program for structural analysis
[AD-755370] 13 p1589 N73-22881
HEPROP - a computer program for thermophysical properties of helium
[REPT-1046/72] 13 p1591 N73-22896
Calculation and computer program of impedance and far field of short helix antenna above infinite groundplane
[PHL-1972-27] 14 p1619 N73-23110
Word recognition by Walsh transform computer program
14 p1622 N73-23143
Computer program for machine recognition of distinctive features in words and sentences
14 p1623 N73-23147
Real time software speech synthesis
14 p1624 N73-23160
Three stage algorithm for representing human speech by time ordered sets of Hanning cosine modulated wavefunctions
14 p1630 N73-23214
Speech modulated, single sideband, suppressed carrier systems for speech reception
14 p1630 N73-23215
Artificial intelligence research projects with emphasis on design, implementation, and integration of system for control of robot
[NASA-CR-131991] 14 p1638 N73-23279
Computer program for spectral unfolding, using optimization function
[AD-755190] 14 p1638 N73-23281
User manual for turbulent boundary layer and turbulent separation prediction methods used in streamtube curvature computer program
[NASA-CR-112240] 14 p1649 N73-23376
Computer program to compute geodetic distance and azimuth between two geodetic positions
[P-4950] 14 p1659 N73-23462
Computer program for calculating individual characteristic values and associated solutions of Mathieu equation
[VUB-STR-1] 14 p1683 N73-23655
Computer programs for numerical approximation of selected meteorological parameters related to cloud physics
[AD-757623] 14 p1686 N73-23680
Computer program to analyze solar observational data
[AD-755921] 14 p1703 N73-23815
Systems design for spaceborne computer engineering module
14 p1712 N73-23894
Computer programs for analysis of shell structures in general and fiber reinforced rocket engine cases
[AD-756465] 14 p1716 N73-23926
Spacecraft advanced radiator design system program for environmental control in long duration space flights
[NASA-CR-128913] 14 p1719 N73-23946
Computer program for developing optimal stability augmentation system for high performance aircraft based on pilot parameters for pitch tracking task
[AD-757879] 15 p1736 N73-24076
ADMAP computer manipulation program for processing electric propulsion trajectory data generated by low thrust optimization program, HILTOP
[NASA-CR-130242] 15 p1754 N73-24216
Computer program for determining radiative flux and flux divergence through nonisothermal gas
[NASA-CR-112307] 15 p1766 N73-24310
User manual for Streamtube Curvature Analysis program to predict pressure distribution about nacelle at transonic speeds - Vol. 1
[NASA-CR-112239-1] 15 p1767 N73-24313
User manual for Streamtube Curvature Analysis program to predict pressure distribution about nacelle at transonic speeds - Vol. 2
[NASA-CR-112239-2] 15 p1767 N73-24314
User manual for Streamtube Curvature Analysis program to predict pressure distribution about nacelle at transonic speeds - appendix
[NASA-CR-112239-3] 15 p1767 N73-24315
Computer program for extracting features from remotely sensed data presented in digital image form
[NASA-TN-D-7312] 15 p1778 N73-24410
Computer program for dual throat, electromagnetic dc conduction pumps
[NASA-CR-121204] 15 p1791 N73-24518
Computer program system for automatic operation and safety backup in ground based ATC system
[FAA-EM-73-7] 15 p1808 N73-24654
Computer programs for weight, center of gravity, and mass moment of inertia calculations and documentation for NERVA
[NASA-CR-132221] 15 p1810 N73-24666
Fluid dynamic computer programs for NERVA turbopump
[NASA-CR-132222] 15 p1810 N73-24670
Computer program for analyzing kinematical responses of structures caused by excitations for use in NERVA program
[NASA-CR-132214] 15 p1810 N73-24671
Computer programs for analyses of free or forced undamped vibrations of rolling contact supported rotors
[NASA-CR-132220] 15 p1810 N73-24672
Error analysis of computer calculation of magnetic field intensity and magnetic parameter
15 p1813 N73-24696
Numerical analysis of process for nitrogen oxide formation in aircraft engine exhaust products and development of computer program for application of theory - Vol. 2
[REPT-1162-2-VOL-2] 15 p1825 N73-24790
Development of computer program to analyze flow conditions in gas turbine compressor for application to reduction of nitrogen oxides from aircraft engine exhaust - Vol. 3
[REPT-1162-3-VOL-3] 15 p1825 N73-24791
Computer program for linear instability analyses of biaxially loaded composite structures
[NASA-CR-112226] 15 p1838 N73-24893
Computer program for thermal stress and instability analyses of structures
[NASA-CR-112228] 15 p1838 N73-24895
Formulation and checkout problems for computer code for analyzing large deflection elastic-plastic dynamic response of stiffened shells of revolution
[NASA-CR-132044] 15 p1839 N73-24902
IBM 7090 computer program for determining values of error sensitivity for dive and glide bombing with free fall weapons
[AD-758420] 15 p1850 N73-24994
Development of simulation model and computer code for evaluation of operation of short takeoff aircraft for commercial airline operations
[NASA-CR-114631] 16 p1860 N73-25062
Computer program for calculating Concorde aircraft flight profiles for various flight procedures and atmospheric conditions
[RAE-TR-72102] 16 p1861 N73-25074
Development of flight simulator system to show position of joystick displacement
[NASA-CASE-NPO-11497] 16 p1878 N73-25206
Evaluation of computer program for analyzing radiation effects on complex semiconductor devices and microcircuits
[AD-758883] 16 p1882 N73-25237
Computer programs for predicting supersonic and hypersonic interference flow fields and heating
[NASA-TM-X-2725] 16 p1889 N73-25285
Algorithm and computer program for generating all distinct 2[p-q] fractional factorial designs and applications to design of experiments
[NASA-TN-D-7327] 16 p1934 N73-25650
Program for one level objective analysis of meteorological fields by optimal interpolation
[NLL-M-22883-[5828.4F]] 16 p1936 N73-25664
Computer programs for ceiling and visibility forecasting using air terminal weather data
[FAA-RD-73-13] 16 p1937 N73-25677
Feasibility analysis for computer-based data communications and/or processing facilities at civil airport
[RAE-TR-72133] 16 p1941 N73-25711
User manual for one-dimensional plasma diagnostics computer program
[AD-758809] 16 p1950 N73-25784
Steady-state attitude control propulsion system simulation program
[NASA-CR-128916] 16 p1955 N73-25820
Rocket nozzle coolant channel thermal analysis program
[NASA-CR-132185] 16 p1957 N73-25832
Computer program and numerical technique for calculating chemical composition of stirred reactor
[AD-751462] 16 p1974 N73-25967
Computer program for thermodynamic equilibrium calculations
[PB-214372/5] 16 p1975 N73-25971
Computer program for shock and blast loading characteristics high explosive projectile detonation in aircraft
[AD-759002] 16 p1975 N73-25972
User guide for computer program to analyze compact transpiration cooling system proposed for hypersonic reentry vehicles
[AD-759698] 16 p1975 N73-25974
Computer programs for conducting mathematical analysis of weapon delivery techniques and performance optimization of aerial delivery weapons - Vol. 2
[AD-751506] 16 p1977 N73-25986
Testing and demonstration of weapon delivery analysis program to determine major contributors to probable error - Vol. 3
[AD-751527] 16 p1977 N73-25987
Spectrum analysis program for computing power spectrum of angle modulated high frequency carrier wave
[NASA-CR-128984] 17 p1997 N73-26145
Flow diagrams and listings for SAP and PLTGEN programs
[NASA-CR-128985] 17 p1997 N73-26146
Computer program for dynamic analysis of shells of revolution
[NASA-CR-132752] 17 p2001 N73-26177
Development of multielement data reduction analysis software package for use with differential maneuvering simulator
[NASA-TM-X-2705] 17 p2001 N73-26178
Progress report, abstracts, and principle results of research project to develop computer software
[NASA-CR-130209] 17 p2001 N73-26180
Computer programs, documentation, procedures, and design criteria for small to medium data base packages
[AD-760103] 17 p2003 N73-26194
CONSHOC computer program for locating shock waves and contours of flow variables in finite difference flow fields
[AD-759898] 17 p2016 N73-26301
Programs for comparing experimental data with mathematical models with respect to magnetic activity
[AD-760117] 17 p2029 N73-26422
Computer programs for solving metal working equations by considering mechanical properties
[AD-759830] 17 p2038 N73-26491
Computer programmers manual for mathematical model used in design of cryogenic supply systems for space shuttles and spacecraft - Vol. 5 B-2 Part 1
[NASA-CR-133956] 17 p2087 N73-26884
Development of computer program for space shuttle orbit injection propulsion system to generate parametric feed system pressure histories - Vol. 5 B-4
[NASA-CR-133957] 17 p2087 N73-26885
Computer programmers manual for parametric analysis of attitude control propulsion system using converted liquid cryogenics reaction system - Vol. 5 B-3 Part 2
[NASA-CR-133958] 17 p2087 N73-26886
Computer program for designing minimum mass wings under flutter, strength and minimum gage constraints
[NASA-TN-D-7264] 17 p2092 N73-26927
Laminated composite cylindrical shell buckling strength criteria
[AD-759537] 17 p2095 N73-26944
Development of computer program for subsonic and shock-free transonic flow solution on hub-shroud midchannel flow surface of turbomachine - Vol. 1
[NASA-TN-D-7343] 18 p2102 N73-26996
Wake model program for computing wake height and width
[PB-218820/9] 18 p2106 N73-27030
Program for reducing data from high resolution mass spectrometer
[NASA-TM-X-2847] 18 p2113 N73-27089
Computer program for calculating characteristics of charged particles beam transported through focusing and bending magnets
[NASA-TN-D-7352] 18 p2121 N73-27143
TOPAL computer program for investigating metal-liquid thermal interactions under shock tube conditions
[GRO/44/91/26-PT-1] 18 p2125 N73-27174
Computer program for predicting invisicd, transonic flow field about isolated nacelles
[NASA-CR-112271] 18 p2130 N73-27211
One-level polynomial objective analysis of meteorological fields
[NLL-M-22903-[5828.4F]] 18 p2170 N73-27524
Software description and program documentation for strapdown inertial reference unit system
[NASA-CR-128965] 18 p2175 N73-27567
DOPEX-1D2C steepest descent and one-dimensional two constraint radiation shield optimization code
[NASA-TM-X-2836] 18 p2177 N73-27579
Computer codes for designing volume accumulator units
[NASA-CR-121246] 18 p2178 N73-27583
Computer program incorporating capability to perform free vibration analysis for natural frequencies
[AD-761370] 18 p2204 N73-27792
Formulation and development of computer analysis for calculating streamlines and pressure distributions around two-dimensional isolated nacelles at transonic speeds
[NASA-CR-2217] 19 p2217 N73-27890
Update of input instructions for operation of FORTRAN computer code TEMOD
[NASA-CR-121225] 19 p2239 N73-28047

NASA/MSFC multilayer diffusion models and computer program for operational prediction of toxic fuel hazards
[NASA-CR-129006] 19 p2239 N73-28050
Computer program problems and possible solutions
[AD-762141] 19 p2242 N73-28072
Computer solution to Hallens equation on half wavelength elements of planar symmetrical antenna arrays
[AD-761471] 19 p2245 N73-28103
Computer analysis of ERTS-1 MSS data for identification and mapping of soils, vegetation, and water resources in Lynn County, Texas
19 p2287 N73-28392
Computer code for calculating time series of earth tidal gravity and tilt
[AD-762275] 19 p2297 N73-28468
Comparisons of radar refraction correction computer programs at selected test ranges
[AD-762383] 19 p2297 N73-28470
Computer program for generation of random bathymetric profiles from oceanographic data
[AD-762070] 19 p2298 N73-28476
Computer program which uses Monte Carlo technique to compute geometrical factor, and spatial and angular distributions of simulated particles
[NASA-TM-X-70428] 19 p2301 N73-28498
Computer analysis of binary and ternary titanium and niobium alloys
[AD-761814] 19 p2311 N73-28585
Computer programs for aircraft position and stationary satellite orbit determination from radar range and rate measurements
[ESRO-CR-81] 19 p2318 N73-28650
FORTRAN 4 computer program for calculating critical speeds of rotating shafts
[NASA-TN-D-7385] 19 p2347 N73-28881
Computer program for estimating peak static pressure from internal explosions in closed vessels
[AD-762402] 19 p2350 N73-28907
Development of computer program for solving one dimensional heat flow problem using aerodynamic heating examples
[WRE-TN-884(WR/D)] 19 p2351 N73-28914
Computation of skin friction and heat transfer on sharp cone in axisymmetric turbulent hypersonic flow
[AD-761602] 19 p2353 N73-28929
Development of analytic models for describing differential models of attack helicopters supporting a battalion task force - Vol. 1
[AD-762432] 19 p2356 N73-28956
Computer program for identifying and classifying sensor signals
[AD-762567] 20 p2379 N73-29118
Development of computer programs for designing engine inlets for VTOL and STOL aircraft based on axisymmetric potential flow parameter
[NASA-TM-X-68278] 20 p2388 N73-29182
Analytical model and computer program for studying disturbances of liquid propellants in feedline systems
[NASA-CR-124308] 20 p2388 N73-29188
Computer program to compute MF sky-wave interference
[BBC-RD-1973/8] 20 p2391 N73-29206
Development of computer program required in reduction and analysis for calibration of Skylab S-193 altimeter data
[E73-10876] 20 p2393 N73-29227
Development of computer method for solving axisymmetric variational problems of theory of treatment of metals by pressure
[NLL-M-21659-[5828.4F]] 20 p2430 N73-29517
Digital calculations in classification portion of Hybrid Pattern Recognition System [HYMPS] program
[REPT-2] 20 p2437 N73-29567
Computer program for modeling UO2 cladding strain resulting from irradiation
[NASA-TM-X-68281] 20 p2453 N73-29715
Air Force Rocket Propulsion Laboratory computer programs
[AD-763094] 20 p2467 N73-29817
Computer program for application of phase change technique to thin sections with heating on both sides
[NASA-TN-D-7193] 20 p2485 N73-29965
Development of digital computer program for generating individual component or entire aircraft mass and aerodynamic models for vehicle inelastic bending response analysis
[AD-763701] 21 p2498 N73-30045
Development of computer program to predict aerodynamic noise levels of V/STOL aircraft at various points in flight trajectory
[PB-221140/7] 21 p2499 N73-30054
Development of electronic computer process for analyzing contact stress oscillograms
[NLL-M-21662-[5828.4F]] 21 p2511 N73-30136
Multiprocessing operating system and software for space ultrareliable modular computer
[NASA-CR-124371] 21 p2512 N73-30147
Universal program for optimizing parameters of electrical circuits
21 p2515 N73-30174
Algorithms employed in current ERIM data processing scheme
[NASA-CR-134007] 21 p2538 N73-30347
FORTRAN computer program for computing transmittance of atmosphere in ultraviolet to infrared spectral region
[AD-763721] 21 p2541 N73-30378
Analysis of ductile flow of metal during extrusion process with application to manufacture of cable sheathing
[NLL-M-21661-[5828.4F]] 21 p2557 N73-30498
JERK Monte Carlo program for studying crystal defects in irridiated metals
[CEA-N-1567] 21 p2585 N73-30718
Integrated digital flight control system for rotational and translational control of space shuttle orbiters
[NASA-CR-134001] 21 p2600 N73-30835
Improvements to operational capabilities of NASTRAN
[NASA-CR-132283] 21 p2603 N73-30861
Statistical analysis of NASA multivariate spectrum analysis program performance after modifications
[NASA-CR-134011] 22 p2620 N73-30995
FORTRAN program for calculating thermodynamic properties of complex gas molecules
[AD-762614] 22 p2626 N73-31042
FORTRAN program for prediction of tropospheric radio transmission loss over irregular terrain
[AD-764476] 22 p2635 N73-31115
Headlamp research program for extrapolation/interpolation of surface values from predefined grid
[LTR-ST-602] 22 p2637 N73-31129
Feasibility analysis of GOAL to HAL language translator for use with space shuttle
[NASA-CR-134033] 22 p2638 N73-31141
FORTRAN matrix abstraction program for structural analysis of aerospace structures, Vol. 2 - Digital computer program description
[AD-764360] 22 p2640 N73-31158
FORTRAN matrix abstraction program for structural analysis of aerospace structures, Vol. 5 - Engineering user and technical report
[AD-763812] 22 p2640 N73-31159
FORTRAN matrix abstraction program for structural analysis of aerospace structures, Vol. 6 - Digital computer program Phase 1 description
[AD-764366] 22 p2640 N73-31160
Manipulation of digital computer source program for terminal ballistics of gun launched guided projectiles
[AD-764225] 22 p2640 N73-31161
Numerical studies of unsteady two dimensional subsonic flows using ICE method
[NASA-TM-X-68288] 22 p2651 N73-31240
Particle size distribution of coagulated aerosols using computer program
[NPL-NAC-35] 22 p2668 N73-31373
Computer program for analyzing general nonaxisymmetric and nonsynchronous transient and steady-state performance of flexible rotor bearing system
[NASA-CR-121276] 22 p2677 N73-31440
Electron transport in gas discharge lasers
[LA-5134-MS] 22 p2681 N73-31474
Use of Cholesky decomposition technique in feature selection and classification algorithms
[NASA-CR-133990] 22 p2690 N73-31550
Modular program RSYST for simplifying handling of reactor and shielding problems
[CONF-721018-22] 22 p2699 N73-31615
Earth satellite orbit calculation with integration program
[BMBW-FBW-72-16] 22 p2718 N73-31757
BOPACE program for advanced thermal-elastic-plastic-creep structural analysis
[NASA-CR-124390] 22 p2725 N73-31805
Computer program for use with thermal-elastic-plastic-creep structural analyzer for structural analysis of spacecraft and propulsion systems - Vol. 2
[NASA-CR-124391] 22 p2725 N73-31806
Application of structural computer program for analysis of creep stress in thrust chamber liner - Vol.3
[D5-17266-3-VOL-3] 22 p2725 N73-31807
General purpose linkage editor for CDC 6000 series computers
[AD-764044] 22 p2725 N73-31809
Computer program for elastic-plastic dynamic analysis of shells of revolution by finite element method
[AD-764244] 22 p2726 N73-31812
Proceedings of conference on structural analysis with application to ships, guns, hydrofoils, marine propellers, and radar antennas
[AD-764508] 22 p2726 N73-31818
General purpose computer program for inelastic dynamic response of plane structure
[PB-221260/3] 22 p2727 N73-31823
Computer program for calculation of steady, state and/or transient thermal environments for space system during lunar surface, deep space, or thermal vacuum
[NASA-CR-134031] 22 p2729 N73-31842
Digital computer program for nonlinear steady state of transient analysis of heat conduction in three dimensional solids
[WAPD-TM-1080] 22 p2729 N73-31843
Computer program for analyzing characteristics of parachute-payload system during deployment and trajectory
23 p2740 N73-31936
Computer programs for predicting the noise-time histories and noise contours for five types of aircraft
[NASA-CR-114650] 23 p2741 N73-31946
Computer programs for computing stability characteristics of tethered balloon under steady wind conditions
[NASA-TM-X-2740] 23 p2742 N73-31952
Test data and description of unsymmetrical crash analysis computer program for improved helicopter structural crashworthiness analytical and design techniques - Vol. 2
[AD-764986] 23 p2747 N73-31986
Compilation of operational and mathematical computer programs from NASA programs
[NASA-SP-5962[01]] 23 p2760 N73-32089
Simulation of process of dropwise condensation using digital computer
23 p2774 N73-32186
PDP 8/I data acquisition and averaging program for synchronous hot-wire measurements in mouth of flow excited cavity resonator
[AD-764851] 23 p2795 N73-32357
Condensation method and computer program for reducing truncation errors for vibration analysis of complex structures
[NASA-CR-124446] 23 p2812 N73-32484
Comparison of digital computer programs for numerical solution of ordinary differential equations
[NASA-TM-X-64781] 23 p2813 N73-32487
Multidimensional linear system parameter estimation computer program using least squares method evaluating mathematical model stability, observability and real time operation
[LAAS-AS-73-1-06] 23 p2813 N73-32491
Computerized design of axial compressor
[AD-764733] 23 p2832 N73-32633
Computer program for design of axial compressor
[AD-764734] 23 p2832 N73-32634
IBM 1130 computer programs for astrophysics optical data processing noting optical systems simulation and stellar density theoretical estimates
[CALC-01-72] 23 p2846 N73-32747
Theoretical analysis background for shell theory automated for rotational structures [STARS-2] program - Vol. 1
[NASA-CR-2273-VOL-1] 23 p2854 N73-32801
Procedure for structural analysis of stiffened shells of revolution to describe computer program and types of shapes and cross sections of specimens - Vol. 2
[NASA-CR-2273-VOL-2] 23 p2854 N73-32802
Engineering programming information for digital computer program developed for structural analysis of shells - Vol. 4
[NASA-CR-2273-VOL-4] 23 p2854 N73-32804
Engineering programming information for digital computer program developed to analyze buckling characteristics of shell structures - Vol. 5
[NASA-CR-2273-VOL-5] 23 p2854 N73-32805
Engineering programming information for digital computer program developed to analyze vibration effects on shell structures - Vol. 6
[NASA-CR-2273-VOL-6] 23 p2854 N73-32806
Satellite programs for computer program applied to structural analysis of shells to include user and programming information - Vol. 7
[NASA-CR-2273-VOL-7] 23 p2854 N73-32807
Computer program for evaluating techniques to improve aircraft engine response systems for application to long range commercial aircraft
[NASA-CR-134496] 24 p2877 N73-32977
Computer program and mathematical model for predicting dynamic response of helicopter in accident involving vertical and lateral impact
[AD-764985] 24 p2879 N73-32996
Computer program for calculating roll-up solar array performance characteristics
[NASA-CR-135898] 24 p2880 N73-33003
TENEX computer system, ARPA network, and computer language design for robot development
[NASA-CR-135899] 24 p2897 N73-33124
Computer solutions for potential and viscous flow calculations for engine inlets
[NASA-TM-X-71457] 24 p2905 N73-33184
Computer programs for processing multispectral scanner data of Susquehanna River Basin
[E73-11114] 24 p2915 N73-33271
Heat transfer-lifetime code for SNAP reactor analysis
[AI-AEC-13076-VOL-5] 24 p2955 N73-33604
Library of 28-group neutron cross sections designed for SNAP reactor analysis
[AI-AEC-13076-VOL-4] 24 p2955 N73-33605
COLFTAR real time electro-optical system for generating optical Fourier transforms of two-dimensional video signals
24 p2956 N73-33613
Computer programs for analyzing optical properties of sea water
24 p2958 N73-33638

Computer program for correcting solar intensity measurements in elliptical sunspots for stray light
[NP-19735] 24 p2977 N73-33785
COMPUTER SIMULATION
U COMPUTERIZED SIMULATION
COMPUTER STORAGE DEVICES
NT BUFFER STORAGE
NT CORE STORAGE
NT FLIP-FLOPS
NT MAGNETIC CORES
NT MAGNETIC DISKS
NT MAGNETIC DRUMS
NT MAGNETIC TAPES
NT RANDOM ACCESS MEMORY
NT REGISTERS [COMPUTERS]
Fabrication of integrated magnetic storage devices by vapor deposition of gold on copper substrate
01 p0031 N73-10239
Capacity of geometric codes and increased effectiveness of semiconductor storage units using number block structures
[JPRS-57251] 02 p0145 N73-11177
Survey and analysis of high density mass storage devices and systems for Navy fleet material
[AD-747134] 02 p0146 N73-11179
Large scale integrated circuits used for designing 128 words x 72 bits/word memory
[REPT-1404] 03 p0272 N73-12205
Technology assessment for thin film development of magneto-optical manganese bismuth memory
04 p0394 N73-13202
Design and development of integrated magnetic memories
04 p0394 N73-13203
Design of low power high performance MOS random access memory unit
[NASA-CR-123943] 04 p0457 N73-13732
Development of economical ways of integrating and interfacing new storage devices and data processing programs into computer systems - App. B
[NASA-CR-129817] 05 p0515 N73-14190
Statistical and deterministic tests for failure analysis of sequential computer storage devices
05 p0517 N73-14203
System characteristics of amorphous semiconductor thin film and electron beam storage devices
[AD-749282] 05 p0587 N73-14778
Review of high density computer storage devices for recorded data
[AD-753626] 09 p1007 N73-18217
Production of integrated toroidal magnetic memories of 500 bits/sq cm, including electric and magnetic testing
[REPT-1541] 10 p1133 N73-19232
Design and performance of electron beam storage tube for computer random access memory
[AD-753929] 10 p1136 N73-19257
Feasibility study of spaceborne plated wire memory with associated electronic circuits and components
[REPT-26/1422/EC/MB/VOL-1]
13 p1498 N73-22137
Feasibility study of spaceborne plated wire memory with associated electronic circuits and components
[REPT-26/1422/EC/MB/VOL-2]
13 p1498 N73-22138
Design, fabrication, and evaluation of electron beam addressable, high information density memory tube
[AD-756936] 13 p1500 N73-22161
Magnetic bubble garnet materials for thin film storage devices
[AD-755546] 13 p1568 N73-22705
Plated thin magnetic film wire element for high speed main memories
[REPT-732] 14 p1619 N73-23112
High density optical memory
[AD-759032] 17 p2002 N73-26184
Iron-doped lithium niobate as holographic storage medium
[AD-760343] 17 p2042 N73-26518
Fabrication of binary-addressable scan conversion storage tube
[AD-761099] 18 p2124 N73-27168
High density optical memory and electron spin dependent trapping and tunneling processes in KCl and KCl-NaCl
20 p2460 N73-29768
Large scale integration for users and suppliers within circuit technology, manufacturing techniques for bipolar devices and semiconductors memory arrays
[PB-221013/6] 21 p2520 N73-30212
Design of integrated aircraft instrumention display system utilizing plasma display/memory unit
[AD-763599] 21 p2550 N73-30446
Electron recording and readout sensitivity characteristics of amorphous semiconductor thin films
[AD-763253] 21 p2585 N73-30719
Combined micrographic and computerized data storage and search system for information processing
[DSIS-TN-13] 23 p2760 N73-32083
Coloring memory crystals by electron bombardment and KCl, Na, Cl for thermoelectric cooling for high density optical memory
[AD-765391] 23 p2762 N73-32105
Evaluation of computer storage requirements for TV camera tubes with signal encoding test program
[ELEC-011-72] 23 p2794 N73-32350
Fabrication of updated block data composer and holographic storage array for breadboard holographic read/write memory system
[NASA-CR-124442] 23 p2801 N73-32399
COMPUTER SYSTEMS DESIGN
Functional design criteria for multiprocessor computer system to provide computational capability for space station
[NASA-CR-128601] 01 p0030 N73-10235
Serial digital data bus for integrated avionics system interface
14 p1713 N73-23902
Techniques for designing balanced, extensible computer systems
[AD-763117] 20 p2380 N73-29120
Modular interactive data acquisition system for nonexperts
[NBS-TN-790] 21 p2511 N73-30138
Collection of Soviet articles on computer elements and systems
[TT-72-50009] 21 p2512 N73-30150
Application of computer systems for effective investigation of mathematical models in mechanical engineering
21 p2513 N73-30155
Functional algorithms for homogeneous general-purpose computer systems
21 p2513 N73-30159
Functional algorithms for homogeneous general-purpose computers in simple situations
21 p2513 N73-30160
Effect of basic indices of computer system on expected cost savings
21 p2513 N73-30161
Calculation of technical and economic indices of high-power homogeneous general-purpose computer systems
21 p2513 N73-30162
Comparative performance of homogeneous computer systems and computers
21 p2514 N73-30163
Functional organization of homogeneous computer systems
21 p2514 N73-30165
Control-oriented linear homogeneous computer system
21 p2514 N73-30166
Commutator and interaction unit of elementary machines in control-oriented homogeneous computer system
21 p2514 N73-30167
Interrupt system of control-oriented homogeneous computer system
21 p2514 N73-30168
Complex of elements of control-oriented homogeneous computer system
21 p2514 N73-30169
Some design features of distributed general-purpose computer systems
21 p2514 N73-30170
Methods for manufacturing computer systems elements and programming methods
[TT-71-50054/1] 21 p2516 N73-30180
Design techniques for data base oriented computer networks for information flow
[AD-763791] 22 p2640 N73-31163
COMPUTER SYSTEMS PROGRAMS
NT INPUT/OUTPUT ROUTINES
NT OPERATING SYSTEMS [COMPUTERS]
NT SUBROUTINE LIBRARIES [COMPUTERS]
Data processing systems and computer networks
[AD-746509] 01 p0031 N73-10244
Physiological data acquisition system software
[AD-746874] 02 p0148 N73-11200
Computer method for largest number of ground station communication functions
[AD-748881] 04 p0390 N73-13166
Multiprogram structure of HRS 101 digital computer and program package for statistical measured data selection and real time presentation
[JPRS-57696] 05 p0516 N73-14192
Program package for statistical measured data selection and visual presentation in real time
05 p0516 N73-14193
Methodology for computer software documentation
[NASA-TM-X-66161] 07 p0759 N73-16162
Research progress in accelerator and ion source development, detection and computer systems, and various nuclear physics projects
09 p1101 N73-18986
Syntax-directed documentation for PL360
10 p1131 N73-19213
Software conceptual designs for space shuttle simulator requirements
[NASA-CR-128882] 11 p1266 N73-20270
Proposal for hierarchical description of software systems
[NASA-TN-D-7200] 12 p1381 N73-21200
Functional characteristics and test methodology for DMS
[AD-748811] 13 p1497 N73-22136
Survey of easy methods of developing easy computer systems useable by everyman
[P-4962] 14 p1638 N73-23278
Extended computer language for real time simulation of process control in large systems
14 p1712 N73-23892
Development of multielement data reduction analysis software package for use with differential maneuvering simulator
[NASA-TM-X-2705] 17 p2001 N73-26178
Progress report, abstracts, and principle results of research project to develop computer software
[NASA-CR-130209] 17 p2001 N73-26180
Methods for manufacturing computer systems elements and programming methods
[TT-71-50054/1] 21 p2516 N73-30180
ADAM automatic abstracting system for evaluating and improving computer produced abstracts
22 p2636 N73-31126
Robot computer problem solving system which represents robot exploration vehicle in simulated Mars environment
[NASA-CR-133942] 22 p2638 N73-31146
Adaptive speech synthesizer operation and associated software
24 p2894 N73-33106
System software for fault-tolerant digital computer
24 p2896 N73-33120
User manual for Image Data Processing System, language and control system for processing image data
[NASA-CR-124438] 24 p2897 N73-33122
Description of software modules of Image Data Processing System
[NASA-CR-124447] 24 p2897 N73-33123
Design of modular spaceborne digital computer system
[NASA-CR-124171] 24 p2898 N73-33130
COMPUTER TECHNIQUES
On-line computer technique for evaluating reconnaissance image compression algorithms
01 p0024 N73-10191
Real time computerized message switching and data transmission systems for military communications network
01 p0026 N73-10206
Automated technical control system for military communications facility
01 p0027 N73-10207
Automatic data processing in meteorological services
[NLL-M-20789-[5828.4F]] 01 p0072 N73-10591
Computer techniques for pseudocolor image enhancement
[P-4870] 01 p0080 N73-10657
Empirical corrections for quantitative multi-element analyses using combined wavelenth- and energy-dispersive systems
[NASA-TM-X-66103] 02 p0137 N73-11113
Technology of small computer systems for industrial automation and control
[FOA-2-C-2485-E5] 02 p0145 N73-11176
Least squares polynomial approximation for computer generation of differentiable functions
[USC-113P19-27] 02 p0146 N73-11180
Computer subroutines for propagating experimental numerical errors, rounding off numbers, checking validity of assumptions, and finding weak links in experiments
03 p0323 N73-12636
Computer system for control of electronics measuring devices and numerical information processing of measurements
[CEA-CONF-1968] 03 p0333 N73-12713
Development of computer assisted troubleshooting system for maintenance of helicopters and aircraft using Univac 1108 computer
[AD-748665] 04 p0373 N73-13037
Computer technique for automatic analysis of planar characteristics of chromosome patterns in microscopic observations
[JPRS-57418] 04 p0379 N73-13085
Computer techniques for prediction and analysis of OTH radar operation
[AD-748588] 04 p0390 N73-13170
Design of interactive program to teach accounting techniques
[NASA-CR-129674] 04 p0393 N73-13192
Man machine communication techniques for improving problem solving capability
[AD-748240] 04 p0394 N73-13207
Computer aided broadband impedance matching technique using comparison reflectometer
[NASA-CR-129567] 04 p0398 N73-13237
Minicomputer application in processing underwater sound signals
[AD-749095] 05 p0514 N73-14176
ELDO computing facilities noting data links and operating procedures
[ELDO-TN-25] 05 p0518 N73-14209
Computational techniques for design optimization of thermal protection for space shuttle
[NASA-CR-128658] 05 p0598 N73-14863
Computer technique for stereo image processing of Mariner 9 spacecraft color photographs
[NASA-CR-130305] 06 p0644 N73-15226

Mathematical and computer methods of cartography
[BULL-56] 06 p0666 N73-15415
Research on gas chromatography with computer techniques and mass spectrometer methods
[FOA-1-C-1412-34] 06 p0672 N73-15471
Test of computerized analysis method for interpreting ERTS 1 photographs of soils and vegetation
[NASA-CR-130021] 07 p0791 N73-16435
Development of computerized speech recognition and voice communication system
[AD-752244] 08 p0886 N73-17172
Land use classification, utilizing remote multispectral scanner data and computer analysis techniques over Lafayette, Indiana
[NASA-CR-130759] 08 p0917 N73-17516
Computer network with random access storage for teletype data transmission system
[NASA-CR-130500] 09 p1006 N73-18214
Computer procedure for analysis of maritime sea-level pressure and wind fields
[NASA-TM-X-69135] 09 p1058 N73-18630
Application of integrated circuit technology and digital computer techniques to electric control of jet engines
[NAL-TR-281] 09 p1078 N73-18799
Computer techniques and test facilities for structural engineering at German university institute
[ISD-119] 09 p1095 N73-18935
Computer-based pupil/tracking monitoring system for Mesa Public Schools, Mesa Arizona
10 p1228 N73-19985
Computer communications systems
[AD-754461] 11 p1260 N73-20225
Graphical computers and computing techniques for real time aid in human problem solving tests
[AD-754282] 11 p1260 N73-20227
Computer mapping of Michigan recreational land use using ERTS-1 data
[E73-10392] 11 p1276 N73-20354
Construction of cartographic scanner/plotter for computer aided mapping
[AD-754648] 11 p1288 N73-20452
Computer control of Atmosphere Explorer spacecraft
[NASA-TM-X-66209] 11 p1341 N73-20884
Computerized control of synchrotron beam lines and power supply system
[DNPL/R-22] 12 p1388 N73-21254
Application of computerized series manipulation system to planetary theory using recursive linearization
12 p1447 N73-21715
Computer techniques for fitting electron density profiles to oblique path VLF propagation data
[AD-757341] 13 p1492 N73-22098
Three-dimensional finite element studies
[AD-755539] 13 p1571 N73-22734
Real time, adaptive isolated-word speech recognition system using minicomputer to time normalize word duration
14 p1622 N73-23141
Decoding of information in acoustic waveform of human speech using signal processing techniques
14 p1623 N73-23148
Phoneme recognition of continuants in connected English speech by computer
14 p1630 N73-23208
Development and characteristics of computer controlled voice response system
14 p1632 N73-23227
Computer simulation to demonstrate feasibility of delta modulation as method for encoding control signals of voiced speech synthesizer
14 p1632 N73-23231
Design of speech-understanding computer system
[AD-757049] 14 p1637 N73-23270
Design specifications for shipborne real time environmental data processing system
[AD-757458] 14 p1638 N73-23283
Development of automated drafting and digitizing system for preparing concept, experimental, prototype, and production mechanical drawings
[AD-755502] 14 p1671 N73-23558
Development of automated air traffic control system using computer techniques to provide flight safety for increased air traffic
14 p1687 N73-23693
Analysis of interface between controller and computer in automated air traffic control system
14 p1690 N73-23716
Performance evaluation of two-dimensional slot nozzle ejector with variable area mixing sections
[NASA-CR-2251] 15 p1730 N73-24034
Electronic computer processing of data stored in data banks
15 p1753 N73-24212
Design and programming techniques for space shuttle software
[NASA-CR-128971] 16 p1879 N73-25211
Mathematical programming used in computer-aided-compensator design for control system
[NASA-CR-2248] 16 p1934 N73-25651
Structural design of computer controlled manipulator for remote handling
17 p1989 N73-26079
Multichannel ocean color data analysis to produce color maps
[TRW-21123-6001-RU-00] 18 p2144 N73-27328
Attitude computer facility for unmanned satellite control from ground base
18 p2211 N73-27848
Computerized ground-air-ground information system for error estimation and alignment of spacecraft attitude sensors
18 p2211 N73-27849
Computerized support system for complex spacecraft mission scheduling
18 p2211 N73-27851
Control computer for correcting ERTS video data electron beam recorder errors at ground base
18 p2211 N73-27853
Organizational subsystems of information computer center for automatic systems control
[AD-761480] 19 p2240 N73-28057
Research and development program plan for air traffic control technology involving data display and data entry
[FAA-ED-16-1] 19 p2318 N73-28647
Computerized data processing system for sampling, labeling, and digital recording of optical measurements
[AD-762332] 19 p2322 N73-28678
Generation and physical characteristics of ERTS MSS system corrected computer compatible tapes
[NASA-TM-X-70426] 20 p2410 N73-29366
Test performance of computerized strapdown inertial attitude reference system
[NASA-TM-X-2848] 20 p2453 N73-29713
Compiler optimization techniques
[NASA-TM-X-69499] 21 p2512 N73-30148
Application of computer systems in solution of complex problems of planning in mechanical engineering
21 p2512 N73-30151
Digital computer techniques for determining changes in brightness periods of variable stars
21 p2595 N73-30792
Computer courses for professional training of programmers and operators
21 p2609 N73-30914
D region blunt probe data analysis using hybrid computer techniques
[NASA-CR-135646] 22 p2639 N73-31147
Computerized photon counting technique for recording optical images
22 p2700 N73-31622
Scene analysis and computer perception with breadboard Mars robot operating in laboratory environment containing rocks of various sizes
[NASA-CR-135711] 23 p2770 N73-32156
Experimental radio and radar studies on lunar and planetary atmospheres and surfaces, interplanetary medium, and software and hardware conceptions
[NASA-CR-135670] 23 p2845 N73-32734
Development of report search code for computer generated bibliographic data in machine readable form
[DSIS-TN-11] 24 p2897 N73-33125
Automatic hybrid interactive information storage and search system
[DSIS-TN-13] 24 p2897 N73-33126

**COMPUTERIZED CONTROL**
U NUMERICAL CONTROL

**COMPUTERIZED DESIGN**
Numerical optimization techniques for computer-aided design of distributed, lumped, active networks
[AD-745640] 01 p0035 N73-10272
Computerized design of support structure for missile fuse using finite element structural analysis program - Part I
[AD-743879] 01 p0115 N73-10947
Algorithms for computerized design of printed circuits with fixed component positions
03 p0278 N73-12255
Computerized design and tests of two-dimensional subsonic short diffusers employing boundary layer control
[NASA-CR-121024] 03 p0283 N73-12294
Performance of high speed overriding clutch assemblies for helicopters
[AD-747807] 03 p0308 N73-12518
Computer program for design optimization of subsonic swept wing jet transport aircraft
[RAE-TM-AERO-1448] 05 p0494 N73-14026
Design of microwave power transistor for providing power amplification in 1350 to 1850 MHz
[AD-749789] 05 p0521 N73-14237
Computer program for optimal design of advanced thrust vector control of missile trajectory
[AD-749126] 05 p0590 N73-14797
Computer program manual for optimal design of advanced thrust vector control for missile trajectory
[AD-749127] 05 p0590 N73-14798
Computerized design of betatron electromagnet having optimal parameters
[AD-750523] 06 p0651 N73-15289
Scattering characterization inputs in computerized design of wideband linear amplifiers for pulse operation
[LBL-772] 07 p0762 N73-16188
Turbulent transport models for designing compressors and gas turbines
[AD-751757] 07 p0837 N73-16786
Characteristics of Performance Analysis and Design Synthesis computer program for determining size of launch vehicles for optimal trajectories - Vol. 2, Pt. 1
[NASA-CR-128678] 09 p1083 N73-18831
Description of QL module Performance Analysis and Design Synthesis computer program for determining optimal trajectory of launch vehicles - Vol. 2, Pt. 2
[NASA-CR-128657] 09 p1083 N73-18832
Production of integrated toroidal magnetic memories of 500 bits/sq cm, including electric and magnetic testing
[REPT-1541] 10 p1133 N73-19232
Computerized design of dielectric lenses for phase corrected horn antennas
[AD-753914] 10 p1136 N73-19258
Computer analysis and design of special antenna configurations and characteristics
[AD-756470] 13 p1501 N73-22169
Computerized design optimization program for microwave circuits
[AD-756875] 13 p1504 N73-22191
Computer program for use in design of axial compressor airfoils suitable for operation at high subsonic and supersonic Mach numbers
[AD-756879] 13 p1536 N73-22442
Search algorithm for component placement problem in computerized design of circuits
[AD-756502] 14 p1684 N73-23663
Computerized design of fighter aircraft cockpit electronic control system considering man machine interaction
14 p1714 N73-23905
Parametric and optimization techniques for aircraft design synthesis to show principal lines of data flow for component development
15 p1732 N73-24049
Analytical and computer design of array antennas, and analysis and synthesis of electromagnetic scattering systems
[AD-758768] 15 p1758 N73-24249
Application of digital computer for aerodynamic design and automatic control of wind tunnel with flexible walls
[ARC-R/M-3187] 16 p1857 N73-25041
Automated design optimization of supersonic airplane wing structures under dynamic constraints
[NASA-CR-112319] 16 p1860 N73-25063
Modular graphic programs for computerized design
[MBB-UA-79-72-O] 17 p2001 N73-26181
Computerized design of power amplifier
[SLA-73-153] 17 p2004 N73-26204
Computerized design of Smith chart and power amplifier
[AD-759701] 17 p2004 N73-26205
Computerized design of polarization interferometer
[AD-760564] 18 p2180 N73-27602
Computerized design of electron beam semiconductor short pulse generator
[AD-761111] 18 p2191 N73-27693
Computer programming for sequential machine design
[AD-762163] 19 p2241 N73-28069
Computerized design of hollow dipole antennas for measuring nuclear electromagnetic pulse
[AD-761801] 19 p2244 N73-28096
Computerized design of printed circuit boards
[AD-762021] 19 p2247 N73-28114
Design of dynamic and rotary machines - Vol. 2
[AD-762441] 19 p2306 N73-28543
Development of computer program for optimum design of submarine hulls with frame stiffened cylindrical structures
[AD-761643] 19 p2349 N73-28893
Improvements to operational capabilities of NASTRAN
[NASA-CR-132283] 21 p2603 N73-30861
Criteria for acceptance of early design information with application to design studies and cost estimates for liquid hydrogen fueled aircraft and remotely piloted vehicles
[NASA-TM-X-62303] 22 p2613 N73-30943
Performance of computer generated binary and kinoform holograms
22 p2680 N73-31464
Computerized design of multilayer thin film filters
[WRE-TN-903[AP]] 23 p2759 N73-32082
Bibliography on computer-aided logical processes
[AD-764400] 23 p2762 N73-32099
Space shuttle guidance, navigation, and control design equations
[NASA-TM-X-69524] 23 p2816 N73-32514
Computerized design of axial compressor
[AD-764733] 23 p2832 N73-32633
Computer program for design of axial compressor
[AD-764734] 23 p2832 N73-32634
Computer aided design of optimal control systems
24 p2896 N73-33119
Computer programs for three dimensional civil engineering lattice structures noting matrix methods, computerized design, and repetitive lattices
[CRIF-MT-82] 24 p2989 N73-33889

**COMPUTERIZED SIMULATION**
NT ANALOG SIMULATION
NT DIGITAL SIMULATION

Evaluation of minimum aircraft flying speed by digital simulation
[AD-745861] 01 p0005 N73-10038
Visual image generation as textured flight information resembling retinal images for airborne flight simulation
01 p0017 N73-10128
Conference on development of multiple computer system for data processing and simulation
[AD-743937] 01 p0031 N73-10240
Computerized simulation of pulsed HF laser pumped by H2 and F2 chain reaction
[AD-745425] 01 p0065 N73-10531
Numerical simulation of one-dimensional collisionless plasma phenomena - users manual
[AD-745423] 01 p0085 N73-10706
Computer simulations of split interstitial equilibrium positions and binding energies in tungsten crystals
[AD-745839] 01 p0088 N73-10728
Computerized simulation of planar phased array of circular waveguide elements
[NASA-CR-123820] 02 p0140 N73-11139
Computerized simulation of maximum likelihood decoding algorithm
[NASA-TR-R-396] 02 p0141 N73-11141
Computerized radar target return data processing and identification system
[AD-746323] 02 p0142 N73-11148
Multidimensional Fourier transformation model for human visual pattern recognition in computerized simulation
[AD-745995] 02 p0147 N73-11195
Data sheet for prediction of loaded hydrodynamic journal bearing performance
[ESDU-69002-AMEND-A] 02 p0177 N73-11432
Artillery sound ranging computer simulations
[AD-745887] 02 p0212 N73-11719
Computerized simulation of instability response of magnetized two ion species plasma to low frequency electric field oscillations
[AD-746109] 02 p0217 N73-11757
Monte Carlo method for computer simulation of copper crystal surface dynamics
[AD-745872] 02 p0220 N73-11780
Aerospace Vehicle Synthesis Program for simulating space shuttles
[NASA-CR-129135] 02 p0232 N73-11886
Computerized simulation of carbon dioxide partial pressure in spacecraft environment for wide range of operating conditions - Vol. 1
[NASA-CR-128630] 02 p0233 N73-11893
Development of simulation models for computerized simulation of carbon dioxide partial pressure in spacecraft environment - Vol. 2
[NASA-CR-128631] 02 p0233 N73-11894
Whole body counter efficiency calculations using NaI[Tl] detector for measuring point sources
[KFKI-72-30] 03 p0261 N73-12114
Computerized simulation of artificial robot interaction behavior with complex environment
[NASA-CR-129526] 03 p0269 N73-12179
Computerized simulation of faulty logic circuits
03 p0271 N73-12198
Computerized simulation for failure analysis of logic circuits
03 p0271 N73-12199
Variance of Monte Carlo estimates reduced by correlated and antithetic sampling and illustrated by queueing simulation
[NA-70-21] 03 p0324 N73-12643
Antithetic and control variate sampling methods for probability estimation in simulation, with telephony traffic example
[NA-71-41] 03 p0324 N73-12645
Combinations of antithetic sampling methods to determine minimum variance linear combination, with queueing simulation example
[NA-72-49] 03 p0325 N73-12646
Antithetic sampling for variance reduction in stochastic system simulation
[NA-72-57] 03 p0325 N73-12647
Combination of several sampling methods to simulate queueing systems
[NA-72-58] 03 p0325 N73-12648
Computer methods for solving some boundary value problems dealing with transport phenomena
[AD-747962] 03 p0325 N73-12651
Computer simulation of ion heating by pulsed microwaves
[CONF-720705-1] 03 p0336 N73-12739
Computerized simulation of nonlinear evolution of high frequency, flute-like plasma microinstabilities
[ORNL-TM-3812] 03 p0341 N73-12781
Computerized simulation of ion acoustic wave and pseudowave generation in plasma including grid effects
[ORO-4211-1] 03 p0342 N73-12792
Computerized simulation of whistler instabilities in anisotropic collisionless plasmas
[AD-748176] 03 p0344 N73-12805
Sample output for community/aircraft economic development model - programmers manual
[FAA-EQ-72-3-VOL-4] 04 p0401 N73-13260
Computerized simulation of electron-electron collisional effects in plasma
[COO-3086-14] 04 p0454 N73-13709
Real time hybrid simulation of tied down helicopter for optimal stability control
05 p0494 N73-14024
Computerized simulation of gravity wave perturbed traveling ionospheric disturbances using radio ray paths
05 p0512 N73-14163
Computerized simulation of optical stellar observations and data reduction to determine diurnal polar motion
[AD-748460] 05 p0541 N73-14401
Computerized simulation of squall line structure and maintenance, based on convectively unstable air mass, vertical shear of horizontal wind, and lifting mechanism
[REPT-72-5] 05 p0572 N73-14651
Computerized simulation of thunderstorm rainfall characteristics
[PB-211806] 05 p0575 N73-14679
Computer program for optimal design of advanced thrust vector control of missile trajectory
[AD-749126] 05 p0590 N73-14797
Transient thermodynamic simulation of Apollo fuel cell/radiator system for proposed Skylab mission
[NASA-CR-129824] 05 p0598 N73-14860
Computer program for calculating aerodynamic coefficients from trajectory angles of projectiles passing through paper screens
[FOA-2-C-2478-44] 06 p0613 N73-14980
Computation of drag coefficients for ballistic range models
[DREV-TN-2027/72] 06 p0614 N73-14987
Computerized simulation of inductor performance constraints
[AD-749685] 06 p0646 N73-15249
Computerized simulation of data compression using ERTS-1 MSS digital tapes
[E73-10011] 06 p0659 N73-15347
Computerized simulation of electromagnetic wave coupling modes in plasma diagnostics
[AD-750138] 06 p0706 N73-15763
Computerized simulation of nonlinear and turbulent plasma behavior
[AD-750715] 06 p0707 N73-15766
Hybrid computer simulation used for analysis of integral lift-fan engine being considered for VTOL applications
[NASA-TM-X-2691] 06 p0713 N73-15817
Computer program to simulate FET transistor logic circuit performances and properties
07 p0762 N73-16191
Computerized model of arbitrarily orientable Yagi - Uda array for obtaining impedance gain pattern and front-to-back ratios
[AD-751658] 07 p0763 N73-16199
Augmentation and improvement of information management system simulation model
[NASA-CR-128718] 07 p0765 N73-16218
Computerized simulation of shrouded propeller low field in cross flow using vortex lattice models
[AD-751463] 07 p0773 N73-16274
Computerized simulation of stainless steel clad uranium oxide plutonium oxide fuel pin behavior in reactor core
[ORNL-4825] 07 p0819 N73-16640
Computer modeling of space charge flow in electrogasdynamic generator
[AD-751632] 07 p0829 N73-16720
Computerized aircraft simulation using aerodynamic coefficient table storage, checkout, and interpolation routines
[NASA-TM-X-62229] 08 p0863 N73-16983
Pilot performance during simulated standard instrument procedure turn with and without predictor display
[NASA-TM-X-62201] 08 p0879 N73-17118
Computerized simulation of passenger emergency evacuation efficiency using Boeing 720 aircraft models
[FAA-AM-72-30] 08 p0879 N73-17119
Computer program for p-n junction diode simulation
08 p0887 N73-17186
Computerized prediction of two dimensional wall boundary layer flow from laminar through transition to turbulent regimes
08 p0894 N73-17239
Computerized simulation of global communication system
[AD-753115] 09 p1003 N73-18186
Nonparametric method of pattern recognition using computer simulation
[NASA-CR-130824] 09 p1005 N73-18203
Simple method for developing computer models for digital and analog integrated circuits
[AD-753413] 09 p1008 N73-18232
Simulation and evaluation of proposed path selection systems for autonomous Martian Roving vehicle
[NASA-CR-130978] 09 p1010 N73-18242
Computerized simulation of inhomogeneous plasma response to impulse electric field excitation
[AD-753104] 09 p1072 N73-18746
Computer program used for dynamic analysis of Apollo-Salyut/Soyuz docking
09 p1087 N73-18871
Analysis of control and simulation methods for space shuttle manipulator
09 p1089 N73-18889
Computer simulation of space station computer-steered high gain antenna
[NASA-CR-128749] 10 p1134 N73-19239
Computerized simulation of longitudinal cable shapes during deployment from missile away from flying aircraft
[AD-753907] 10 p1135 N73-19254
Computerized simulation of aerodynamic characteristics for trailing wire system towed by orbiting aircraft
[AD-753909] 10 p1136 N73-19255
Computerized simulation of spiral curve of wire being towed behind orbiting aircraft
[AD-753908] 10 p1136 N73-19256
Active optics simulation system for designing mirror control system for large space telescope
[NASA-CR-112259] 10 p1159 N73-19433
Time integration of transient equations in shaft dynamics analysis
[AD-754341] 10 p1168 N73-19500
Computerized simulation of parallel plate pulsed transversely excited atmospheric pressure laser
[DREV-TN-2054/72] 10 p1168 N73-19503
LINVILL and IBIS programs for calculating gamma radiation damage to biopolar transistors
[CEA-R-4337] 10 p1194 N73-19718
Computerized simulation of solution to maintenance and logistics problems of gas turbine engines
[AD-753622] 10 p1210 N73-19838
Application of equations of motion to develop analog computer simulation of helicopter rotor system
[AD-754547] 11 p1235 N73-20024
Computerized simulation of three dimensional robots using generalized cylinder descriptions
[AD-755139] 11 p1251 N73-20152
Computerized simulation of instrument limited angular measurement errors in phased array radar
[AD-754922] 11 p1257 N73-20201
Computerized simulation of roll and pitch effects on shipboard antenna radiation patterns
[AD-754348] 11 p1258 N73-20212
Computerized simulation of orbital assembly dynamics and interactions with geometrical appendages
[NASA-CR-124169] 11 p1259 N73-20220
Development of simulator for training personnel in underwater terrain navigation and reconnaissance
[AD-754091] 11 p1322 N73-20729
Functional error analysis and simulation of air traffic control system to support concepts evaluation program
[PB-213148] 11 p1322 N73-20730
Kinematic equations for unified flexible spacecraft simulation program
[NASA-CR-124170] 11 p1340 N73-20877
Development of dynamic loads computation capability for application to unified flexible spacecraft simulation program
[NASA-CR-124168] 11 p1340 N73-20878
Computerized simulation of terminal homing missile trajectory
[AD-754543] 11 p1344 N73-20904
Computerized simulation of heat transfer and elasticity in bars
[PB-213060] 11 p1347 N73-20927
Survey on computerized modeling of transportation generated air pollution
[PB-213013] 11 p1354 N73-20992
Computerized simulation of aircraft as radar target
[AD-755854] 12 p1380 N73-21189
Validation and verification of computer simulation models
[P-4891] 12 p1381 N73-21196
Computer simulation of global atmospheric circulation in climatological research
[P-4933] 12 p1421 N73-21520
Computer simulation of collisionless plasma with self-electric and magnetic interactions
[COO-2200-1] 12 p1434 N73-21619
Development of computerized training aid for research and development managers based on spacecraft design operations
[NASA-TN-D-7238] 12 p1466 N73-21880
Computer program for calculating aerodynamic stability and drag of slender aircraft at subsonic and supersonic speeds
[NASA-CR-112229] 13 p1469 N73-21897
Structural influence coefficient matrix for computer simulation of aerodynamic aircraft stability
[NASA-CR-112230] 13 p1469 N73-21898
Computerized simulation of plume shapes produced by axially symmetric nozzle geometry
[AD-756380] 13 p1511 N73-22241
Estimating distance to thunderstorms using computerized simulation of ground wave atmospherics
13 p1551 N73-22566

Development of computer programs for numerical analysis of spinning aircraft based on Euler integration and minimization by gradient search
[AD-757257] 14 p1602 N73-22990
Computerized simulation of ion collection by ionospheric probe
[AD-757481] 14 p1662 N73-23492
Computer simulation of nonlinear saturation of parametric decay instability in weak turbulence limit
[AD-757265] 14 p1696 N73-23766
Neutron scattering, computerized simulation, and magnetic resonance techniques for studying phase transitions in magnetic materials
[AD-757223] 14 p1698 N73-23782
Computerized simulation of multiloop attitude control system for satellite with flexible booms
14 p1712 N73-23890
Simulation model for optimum spaceborne computer system design controlling shuttle booster subsystems
14 p1712 N73-23891
Dynamic structural analysis of helicopter structures using single point excitation techniques - Vol. 2
[AD-756390] 14 p1716 N73-23922
Dynamic structural analysis of helicopter structures using free-body response techniques - Vol. 3
[AD-756391] 14 p1716 N73-23923
Mathematical models and computer simulation for predicting spectral parameters of radar echoes from rain clouds
[STC-TM-308] 15 p1750 N73-24180
Digital command and simulation of automatic tracking device carrying pulsed laser and receiving telescope
[ONERA-NT-198] 15 p1751 N73-24190
Computer simulation techniques to determine equilibrium positions and binding energies of inert gas atoms implanted in tungsten crystal
[AD-758501] 15 p1799 N73-24585
Computer simulation to evaluate methods for determining threshold stimulus levels for impact sensitivity tests
[NASA-TM-X-64087] 15 p1801 N73-24598
Algorithm for computer simulation of Eulerian angles for spacecraft attitude
[NAL-TR-305] 15 p1803 N73-24612
Computerized simulation of plasmas in controlled thermonuclear fusion devices
[SU-799-X-1] 15 p1817 N73-24730
Computer manual for experimental array radar ear system simulation program
[AD-758922] 16 p1877 N73-25197
Analysis of dual lane runway operations at high density airport terminals using computerized simulation techniques
[ATC-17] 16 p1885 N73-25254
GERTS 3Q simulation model and data base for air cargo terminal
[AD-753925] 16 p1885 N73-25257
Analysis and digital computer simulation of operational and performance aspects of vertical area navigation system
[FAA-RD-72-125] 16 p1941 N73-25705
Alternating direction implicit magnetohydrodynamic code for simulating laser plasmas
[SC-DR-72-0733] 16 p1949 N73-25776
Steady-state attitude control propulsion system simulation program
[NASA-CR-128916] 16 p1955 N73-25820
Simulation studies of missile and rocket systems using digital, analog, and hybrid computers
[AD-759226] 16 p1967 N73-25914
Marshall system for aerospace system simulation
[NASA-CR-124288] 17 p2010 N73-26252
Point defense missile simulation program
[AD-759969] 17 p2099 N73-26985
Analysis of descent trajectories to determine static and dynamic stability of free-fall stores with freely spinning stabilizer devices
[AD-760677] 18 p2102 N73-26999
Elastic vibrations of aircraft wing caused by distributed load, center of gravity displacement, and rotation using electromodeling techniques
[AD-760965] 18 p2108 N73-27043
Development of electrical circuitry for analysis of stress deformation state of delta wing model based on discrete design diagram
[AD-760948] 18 p2108 N73-27044
Development and characteristics of hybrid loran and inertial navigation system as alternative to high precision navigation sensors
[AD-761027] 18 p2176 N73-27572
Computer simulation and optimization code for nuclear space power systems for thermoelectric power generation
[NASA-TM-X-2860] 18 p2178 N73-27586
Computerized simulation of belt pinch experiments including plasma external circuit interactions
[LRP-61/73] 18 p2183 N73-27626
Computerized management tools for use in analysis of automatic switching centers and associated tributaries of Autodin communications network
[AD-761479] 19 p2236 N73-28028
Computerized simulation of mobile tracking radar performance
[AD-762338] 19 p2238 N73-28043
Analysis of packet switching network by computerized simulation
[NPL-COM-SCI-64] 19 p2239 N73-28053
Computerized simulation of tactical ground surveillance system
[AD-761805] 19 p2240 N73-28059
Computerized simulation of optical pattern recognition and image processing system
[AD-761882] 19 p2241 N73-28065
Kinetic model and computerized simulation of DF-carbon dioxide chemical transfer laser
[AD-762284] 19 p2309 N73-28571
Computerized simulation of cyclotron resonant electrons interaction with narrow band whistler wave along magnetospheric duct for VLF emission triggering
19 p2340 N73-28827
Numerical analysis and computerized simulation of open combustion processes and flame stability
[AD-762360] 19 p2353 N73-28925
Numerical analysis of military helicopters and air defense weapons to define operations in support of battalion task force combat - Vol. 2
[AD-762433] 19 p2356 N73-28957
Computer simulation of aircraft motions and propulsion system dynamics for YF-12 aircraft under supersonic conditions
[NASA-TM-X-62245] 20 p2361 N73-28990
Computer simulated loading of Army Brigade and equipment into several medium short takeoff transport aircraft configurations
[AD-762916] 20 p2362 N73-29002
Analysis of quantized signal dependent control of continuous process by computerized simulation
20 p2378 N73-29110
Numerical simulation of thunderstorm cell in two and three dimensions
20 p2441 N73-29605
Development of computer model to simulate air traffic conditions in Los Angeles, California area in 1982
[MTR-6386] 20 p2452 N73-29706
Computerized simulation of temperatures on Centaur standard shroud during heated jettison tests
[NASA-TM-X-68273] 20 p2485 N73-29962
Computerized simulation of monopulse radar antenna pointing errors due to ground reflection multipath propagation
21 p2507 N73-30114
Basic programming language for simulation of digital devices
21 p2514 N73-30164
Analytical methods, thermal model, and user manual for extravehicular mobility unit routines
[NASA-CR-134005] 21 p2521 N73-30218
Analytical methods, thermal model, and user manual for extravehicular mobility unit routines
[NASA-CR-134006] 21 p2521 N73-30219
Simulated emission predictions and measurement of H2 pressure effects on pulsed H2-F2 laser outputs
[AD-763716] 21 p2556 N73-30492
Numerical simulation of chemical reactions in air pollution - Vol. 1
[PB-220456] 21 p2574 N73-30631
User guide for computer simulation model air pollution - Vol. 2
[PB-220457/6] 21 p2574 N73-30632
Two dimensional analysis of electron-ion streaming instabilities using computerized simulation
[AD-763336] 21 p2583 N73-30703
Analysis and simulation of Mariner Mars 1971 scan platform, and spacecraft dynamic interaction
[NASA-CR-133793] 21 p2600 N73-30837
Computer simulation of multipacket-switched data communication network operating with revised link and node protocol
[NPL-COM-68] 22 p2634 N73-31112
Experimental observations and numerical simulation of Weissenberg climbing effect
22 p2649 N73-31220
Computerized simulation of wave field distributions in collisional plasma
22 p2703 N73-31646
Computerized simulation models for thermal exhaust reactors
22 p2727 N73-31824
Computerized simulation of DC-8 aircraft during landing approach under wind shear conditions
[AD-764697] 23 p2745 N73-31975
Computerized simulation of interactions of VTOL aircraft taking off from or landing on deck of ship moving in irregular or random seaway
[AD-764865] 23 p2746 N73-31980
Computerized simulation of anatomically correct geometrical model of human body
[NASA-CR-134043] 23 p2752 N73-32022
High precision external spur gear inspection and computerized simulation of manufacturing-inspection process
[AD-764588] 23 p2799 N73-32389
Logistics of orbital vehicle servicing computer specification to improve utilization of space shuttle and tug
[NASA-CR-135709] 23 p2845 N73-32736
IBM 1130 computer programs for astrophysics optical data processing noting optical systems simulation and stellar density theoretical estimates
[CALC-01-72] 23 p2846 N73-32747
Computerized simulation of weapon system terminal ballistics and impact effectiveness
[AD-764884] 23 p2867 N73-32921
Simulation of System 10 computer operation for performance evaluation
[ARL/SM-392] 24 p2897 N73-33127
Computer model of Los Angeles, California air traffic control situation to predict conditions expected by 1982
[AD-765153] 24 p2951 N73-33571
Computerized simulation of inhomogeneous plasma excitation by electric field impulse
24 p2961 N73-33660
Digital simulation of plasma generation in Tokamak device
[EUR-CEA-FC-683] 24 p2963 N73-33677
Computerized simulation of electrostatic inertial plasma confinement device
[AD-763826] 24 p2966 N73-33703
Performance calculation of arbitrarily switched gas turbines by simulation with building block system on digital computer
24 p2973 N73-33758

COMPUTERS
NT AIRBORNE/SPACEBORNE COMPUTERS
NT ANALOG COMPUTERS
NT CDC 1604 COMPUTER
NT CDC 6000 SERIES COMPUTERS
NT CDC 6600 COMPUTER
NT DIGITAL COMPUTERS
NT HONEYWELL COMPUTERS
NT HYBRID COMPUTERS
NT IBM COMPUTERS
NT IBM 360 COMPUTER
NT IBM 1130 COMPUTER
NT ILLIAC 4 COMPUTER
NT MINICOMPUTERS
NT PARALLEL COMPUTERS
NT PDP COMPUTERS
NT PDP 8 COMPUTER
NT PDP 10 COMPUTER
NT SEL COMPUTERS
NT SEQUENTIAL COMPUTERS
NT UNIVAC COMPUTERS
NT UNIVAC 1108 COMPUTER
Fluidic elements and hydraulic impulse techniques for information processing equipment
02 p0140 N73-11135
Resource sharing computer communication networks and some aspects of distributed computation
[AD-749378] 05 p0518 N73-14210
Cooperation of Eastern European countries in computer and medical research
[JPRS-58063] 08 p0976 N73-17987
Baseline design of central multiprocessor for manned space station application
[NASA-CR-124151] 11 p1259 N73-20219
Mass fragmentography-computer for identification and quantitation of amino acids in soil
[NASA-CR-131507] 12 p1376 N73-21159
Experimental design formulated for alternative modes of man-computer dialogue
[AD-760010] 18 p2118 N73-27129
Technical facilities for data links in teleautomatic queueing system
[JPRS-59662] 19 p2235 N73-28022
Interface organization of local data control systems with M-6000 ASVT-M computer hardware complex
[JPRS-59612] 19 p2239 N73-28051
Principles of construction, technical characteristics, and functions of several checking general-purpose computers
[AD-762212] 19 p2243 N73-28082
Articles concerning development and progress in theoretical and applied sciences of leading East European scientific organizations
[JPRS-59756] 20 p2488 N73-29982
Geophysical meeting, third generation computers, and computer courses
[JPRS-59825] 21 p2609 N73-30911
Characteristics and equipment for third generation computers
21 p2609 N73-30913
Computer code which reorganizes old FORTRAN programs so that statement numbers are added sequentially and extraneous statements are deleted
[NASA-TM-X-62286] 22 p2636 N73-31128
Computer science and data processing in Japan
[AD-764853] 23 p2763 N73-32106

CONCAVITY
Effects of successive concave optical gratings in spectrograph on X ray diffraction patterns
[AD-757014] 13 p1580 N73-22640

CONCENTRATING
Pilot selection by means of concentration stress test
19 p2226 N73-27957

**CONCENTRATION [COMPOSITION]**
NT ATMOSPHERIC MOISTURE
NT ATOM CONCENTRATION
NT CARBON DIOXIDE CONCENTRATION
NT METEOROID CONCENTRATION
NT MOISTURE CONTENT
Model 735 dissolved oxygen analyzer for continuous measurement of dissolved oxygen concentration in shallow fresh water
[NOAA-IFS-73003] 01 p0057 N73-10465
MINOS DOM oxygen monitor for measuring dissolved oxygen in sea water to depths of 3000 meters
[NOAA-IFS-73004] 01 p0057 N73-10466
Dissolved oxygen analyzer for measuring dissolved oxygen concentration in industrial water systems
[NOAA-IFS-73005] 01 p0057 N73-10467
Temperature and concentration dependence of Debye-Waller factor for superconducting Nb-Zr alloy system
[BNL-TR-483] 03 p0315 N73-12569
Simultaneous donor and acceptor concentration determination, using Hall effect measurements
[ONERA-DERTS-NT-02-31] 05 p0587 N73-14776
X ray fluorescence analysis for determining lead content of paint on pencils in Goddard supply system
08 p0876 N73-17097
Specific wavelength colorimeter for measuring given solute concentration in test sample
[NASA-CASE-MSC-14081-1] 09 p1035 N73-18443
Satellite solar occultation absorption measurements of pollutant concentrations and spectral properties of molecules in infrared region
[REPT-011023-1-T] 12 p1444 N73-21700
Radical species concentration profiles for methane-oxygen-argon flame
[BM-RI-7766] 18 p2206 N73-27803
Concentration, composition, and properties of amino acids found in Cenozoic formations of Japan
[NASA-TT-F-15002] 19 p2293 N73-28439
Influence of ground concentration, hilly terrain, and wind velocity on distribution of pollutants considering initial elevation
20 p2446 N73-29648
Neutron activation analysis of Ga concentration in Ga-Se
[CONF-721069-41] 21 p2506 N73-30110

**CONCENTRATORS**
Cost estimates for carbon dioxide concentrators in spacecraft life support systems
[NASA-CR-124302] 18 p2111 N73-27073

**CONCENTRIC CYLINDERS**
Application of variational principle to laminar flow and heat transfer between concentric cylinders
[REPT-5/1972] 03 p0285 N73-12307
Four moment method for studying thermal conductivity in rarefied gas confined in concentric cylinders
16 p1973 N73-25955
Free surface secondary flow of Newtonian liquid between rotating concentric cylinders
24 p2906 N73-33188

**CONCORDE AIRCRAFT**
Processing of Concorde digitally recorded data
01 p0056 N73-10453
Measurement of ray paths and ground overpressures produced by Concorde aircraft during supersonic flight
[R/D-896] 06 p0618 N73-15021
French aircraft development program including Concorde, Airbus, and Corvette, as well as economic study
06 p0622 N73-15045
Simulation of flight in Concorde for improving characteristic of flight control system
08 p0866 N73-17013
Reliability design of manned supersonic aircraft considering safety hazards
14 p1711 N73-23883
Computer program for calculating Concorde aircraft flight profiles for various flight procedures and atmospheric conditions
[RAE-TR-72102] 16 p1861 N73-25074
Directional equipment for suppressing noise of Concorde propellers during high speed flight
22 p2613 N73-30942

**CONCRETES**
Torsion, bending, and shear in concrete beams reinforced with stirrups
[D-10-72] 02 p0238 N73-11938
Ground erosion on grassland and concrete by vertical takeoff of Do-31 aircraft
[BMVG-FBWT-72-26] 10 p1107 N73-19023
Finite element method computation of 1:5 scale model prestressed concrete high temperature nuclear reactor pressure vessel
[ISD-120] 10 p1221 N73-19927
Creep properties of composite, plastic reinforced polyester concretes
[AD-752454] 10 p1221 N73-19930
Cold weather construction practices relative to men, materials, and equipment
[AD-745395] 13 p1506 N73-22206
Field problems of concrete containing randomly oriented, uniformly distributed, short fibers
[AD-741358] 13 p1547 N73-22536
Performance of fibrous concrete pavement materials under cargo aircraft and roadway vehicle loads
[AD-741357] 13 p1547 N73-22537
Performance of fibrous reinforced concrete overlay test slabs as runways at Tampa International Airport, Florida
[FAA-RD-72-119] 14 p1680 N73-23634
Comprehensive and tensile load tests on three-inch cubes of concrete
[AD-756926] 14 p1715 N73-23919
Compressive tests on cubical test specimens of cast concrete
[AD-756927] 14 p1715 N73-23920
Strengthening of keyed longitudinal construction joints in rigid pavements
[AD-759570] 18 p2204 N73-27789

**CONDENSATES**
Vapor condensation by homogeneous nucleation in supersonic nozzle flows
17 p1991 N73-26101
Explaining differences in composition of terrestrial planets and moon by accretion during condensation
[NASA-CR-132209] 17 p2083 N73-26854
Quadrupole mass spectrometer for direct sampling of atmospheric gases and condensation products
[AD-764238] 22 p2676 N73-31433
Development and characteristics of device for removing condensate from heat exchangers with straight through gas flow
[NASA-CASE-MSC-14143-1] 23 p2856 N73-32823
Decomposition of ammonium perchlorate condensate, from electron emission, infrared absorption, and surface structure
[DLR-FB-73-59] 24 p2971 N73-33739

**CONDENSATION**
Supersaturation and condensation in cloud chamber expansion
[AD-745348] 01 p0058 N73-10478
Tricyclic nitropropene nitronate intermediates in condensation reactions of symmetric trinitrobenzene with cycloalkanones, and with phloroglucinol
[NASA-CR-131288] 11 p1252 N73-20159
Analysis of condensation effects in supersonic nozzle flows for homogeneous and heterogeneous nucleation conditions
18 p2128 N73-27195

**CONDENSATION PUMPS**
Simultaneous determination of carbon, hydrogen, and nitrogen in organic compounds
[UCID-16198] 24 p2892 N73-33085

**CONDENSATION TRAILS**
U CONTRAILS

**CONDENSER RADIATORS**
U CONDENSERS [LIQUIFIERS]
U HEAT RADIATORS

**CONDENSERS [LIQUIFIERS]**
NT JET CONDENSERS
Condensation of gas phase of fast flowing droplet gas mixture of potassium and application to operating magnetohydrodynamic generators
[NASA-TT-F-14609] 07 p0770 N73-16254
Development and characteristics of device for removing condensate from heat exchangers with straight through gas flow
[NASA-CASE-MSC-14143-1] 23 p2856 N73-32823

**CONDENSING**
NT FILM CONDENSATION
Mass transfer rates at flat water surface measured during evaporation and condensation
[COO-2032-11] 03 p0263 N73-12135
Derivation of formulas for calculating interfacial thermal resistance and condensation coefficient during condensation of metal vapors
[AD-748048] 03 p0365 N73-12972
Numerical computations for quiescent solar prominence formation by condensation from solar corona
04 p0465 N73-13790
Partial condensation and fractionation for analysis on mixture of hydrogen, methane, and ethane
[NASA-TT-F-14681] 07 p0752 N73-16109
Corrosion behavior of structural materials during condensation of alkylphenol with formalin and ammonia
[AD-751249] 07 p0753 N73-16119
Elementary processes of precipitation particle formation
[AD-751501] 07 p0816 N73-16615
Condensation nuclei measurements noting counters and importance to cloud physics
07 p0859 N73-16964
Atmospheric physics of condensation nuclei
[NLL-M-22806-[5828.4F]] 16 p1947 N73-25749
Silver iodide particle size effect on water condensation for artificial precipitation
[AD-758857] 17 p1993 N73-26114
Effects of condensation on gas velocity in free jet expansion
[AD-762503] 21 p2527 N73-30266
Theory of drop growth by condensation for cloud physics application
[AD-764258] 22 p2695 N73-31586
Simulation of process of dropwise condensation using digital computer
23 p2774 N73-32186

**CONDITIONED RESPONSES**
U CONDITIONING [LEARNING]

**CONDITIONING**
High temperature tolerance of rats under normal conditions, after thermal conditioning and combined with drugs
11 p1244 N73-20099

**CONDITIONING [LEARNING]**
Overview of literature concerning retention of learned skills with emphasis on space flight skill retention
[NASA-CR-128611] 01 p0020 N73-10152
Behavioral learning response of cat to electric stimulation of auditory nervous system
[NASA-CR-132047] 15 p1742 N73-24124
Use of motivational relations to find acceptor of action with conditioned stimuli
24 p2888 N73-33064
Relation of conditioned reactions to evaluation of results of forthcoming reinforcement
24 p2889 N73-33065
Orientative-investigative reaction as factor changing configuration of evoked potentials during repeated light flashes
24 p2889 N73-33070

**CONDITIONS**
NT ADIABATIC CONDITIONS
NT CHRONIC CONDITIONS
NT FLIGHT CONDITIONS
NT KUTTA-JOUKOWSKI CONDITION
NT NONEQUILIBRIUM CONDITIONS
NT RUNWAY CONDITIONS

**CONDUCTANCE**
U RESISTANCE

**CONDUCTING FLUIDS**
Literature survey for action of applied magnetic field on conducting liquid in circular cylindrical container
[AE-447] 04 p0450 N73-13674
Magnetohydrodynamic analysis of instability due to discontinuity in conductivity and solitary waves of finite amplitude in conducting fluid
15 p1816 N73-24721

**CONDUCTING MEDIA**
U CONDUCTORS

**CONDUCTION BANDS**
Electrical and transport properties in polycyclic semiconductor compounds
[AD-745988] 02 p0219 N73-11771
Photodielectric recombination and trapping model for low temperature n-type epitaxial gallium arsenide
[NASA-CR-130764] 08 p0950 N73-17779
Diagnostic technique for determining excess free carrier lifetime and ambipolar diffusion coefficient in localized regions within semiconductors
24 p2966 N73-33706

**CONDUCTION ELECTRONS**
Effect of magnetic rupture on low frequency electroconductivity and weakly damped electromagnetic waves in metals with closed Fermi surfaces
[KHFTI-71-1] 06 p0684 N73-15569

**CONDUCTIVE HEAT TRANSFER**
Sweat rate and heat conductance in thermoregulatory system during rest and exercise
[NASA-TT-F-14562] 01 p0009 N73-10074
Numerical solution of parabolic partial differential equations with reference to eddy heat conduction in ocean
[AD-746205] 02 p0167 N73-11362
Finite element solution for axisymmetric transient heat conduction and thermal stress problems
[AD-747523] 03 p0362 N73-12950
Finite difference theory and Monte Carlo method for heat conduction and convection problems
[KFK-1554] 03 p0364 N73-12965
Thermal blooming of laser beams in viscous and thermally conductive fluids
[AD-748994] 04 p0431 N73-13508
IBM 360 and 365 computer program for calculating heat and internal conduction of aerodynamic configurations
[AD-749482] 05 p0606 N73-14931
Application of splitting method for numerical analysis of heat conducting gas flows in curvilinear coordinates
[NASA-TT-F-14658] 09 p1015 N73-18288
Computerized simulation of heat transfer and elasticity in bars
[PB-213060] 11 p1347 N73-20927
Heat transfer solutions for solids with moving boundaries and for viscous liquid flow
[AD-754639] 11 p1349 N73-20950
Static planar model for explaining structure and thermal conduction heating of chromosphere-corona transition region
12 p1444 N73-21699
Increase in heat exchange rate between thermometric sensing element and cryogenic fluid
[NASA-TM-X-68251] 16 p1913 N73-25477
Solution of inverse problem of transient heat conduction using Laplace transformation
16 p1973 N73-25954
Analysis of uniform heat energy generation and conduction heat transfer for semi-infinite thin plate with air blowing over one surface and insulated on other
16 p1973 N73-25959

Interactions of radiation with conductive and convective heat transfer in ablation and boundary layer flow determined by normal mode expansion technique
18 p2128 N73-27200
Conductive heat pipes from laboratory to space
[NASA-TM-X-62290] 19 p2352 N73-28917
Measurement of heat conductivity of He 3 and He 4 at superflow temperature
[JINR-P8-7008] 24 p2992 N73-33912
CONDUCTIVITY METERS
NT ELECTRICAL CONDUCTIVITY METERS
CONDUCTORS
NT AIRCRAFT ANTENNAS
NT CASSEGRAIN ANTENNAS
NT DELTA ANTENNAS
NT DIPOLE ANTENNAS
NT DIRECTIONAL ANTENNAS
NT ELECTRIC CONDUCTORS
NT ELECTRIC WIRE
NT ELECTROLYTES
NT EXPLODING WIRES
NT FLAT CONDUCTORS
NT HELICAL ANTENNAS
NT HORN ANTENNAS
NT ION EXCHANGE MEMBRANE ELECTROLYTES
NT LENS ANTENNAS
NT LOG PERIODIC ANTENNAS
NT LOOP ANTENNAS
NT MICROWAVE ANTENNAS
NT MISSILE ANTENNAS
NT MOLTEN SALT ELECTROLYTES
NT MONOPOLE ANTENNAS
NT MULTIPLE BEAM INTERVAL SCANNERS
NT OMNIDIRECTIONAL ANTENNAS
NT PARABOLIC ANTENNAS
NT PHOTOCONDUCTORS
NT RADAR ANTENNAS
NT RADIO ANTENNAS
NT SLOT ANTENNAS
NT SPIRAL ANTENNAS
NT STEERABLE ANTENNAS
NT SUPERCONDUCTORS
NT THERMAL CONDUCTORS
NT TURNSTILE ANTENNAS
NT TWO REFLECTOR ANTENNAS
NT WAVEGUIDE ANTENNAS
Exact solutions for electromagnetic inverse problem for perfectly conducting body with consideration of uniqueness problem and case of spherically symmetric dielectric body
02 p0200 N73-11616
Potential theory for determining electromagnetic field caused by radial electron emission near conducting sphere
[AD-753664] 09 p1068 N73-18714
Mineral insulated conductors for inorganic magnet coils for withstanding high radiation dosage
[LA-DC-72-1106] 10 p1189 N73-19677
Maxwell equation and approximation theory for examining attenuation behavior of coaxial cables with woven outer conductors
[RAE-LIB-TRANS-1642] 17 p1997 N73-26147
Matrix methods for determining nature of eigencurrents and eigenfields in conducting bodies
[AD-761456] 19 p2321 N73-28675
Ferrite memory arrays from pre-formed metal conductors
[NASA-CASE-LAR-10994-1] 21 p2562 N73-30536
CONES
NT CIRCULAR CONES
NT CONICAL BODIES
NT NOSE CONES
NT ROCKET NOSE CONES
NT SLENDER CONES
Generalized method of contraction cone design and low speed velocity distribution
[NASA-TN-D-6962] 01 p0036 N73-10283
Coning motion, autorotation and vortex system of slender missiles
[BMVG-FBWT-72-31] 10 p1103 N73-18998
Numerical calculation of flow fields produced by lifting elliptic cone, lifting three dimensional wing, and lifting delta wings
[NASA-CR-131089] 10 p1139 N73-19282
Nusselt-type analysis of laminar film condensation inside truncated rotating cone, emphasizing heat transfer performance
[AD-758513] 15 p1845 N73-24945
Presentation of algebra of projections on convex cones in Hilbert space
[AD-761867] 19 p2315 N73-28619
CONFERENCES
Proceedings of conference on ride qualities of air, surface, and water vehicles with emphasis on human factors engineering for comfort in transportation
[NASA-TM-X-2620] 01 p0002 N73-10012
Conference on manual control systems for human operator modeling and display systems in man machine environments
[NASA-SP-281] 01 p0013 N73-10104
Conference on expanded aerospace telecommunication system requirements and digital data transmission methods
[AGARD-CP-103] 01 p0024 N73-10187
Conference on development of multiple computer system for data processing and simulation
[AD-743937] 01 p0031 N73-10240
Conference on magnetic structure of interplanetary and solar magnetic fields and solar wind
[NASA-SP-308] 01 p0092 N73-10760
Papers presented at antenna array conference concerning phased arrays and array techniques
[AD-744629] 02 p0149 N73-11209
Papers presented at antenna array conference concerning adaptive arrays, conformal arrays, and component techniques for array antennas
[AD-744630] 02 p0149 N73-11210
One-dimensional and multi-dimensional inversion techniques for processing remote atmospheric and ionospheric sounding data
[NASA-TM-X-62150] 02 p0196 N73-11585
Proceedings of conference on environmental toxicology held at Fairborn, Ohio, 31 August, and 1-2 September 1971
[AD-746660] 02 p0207 N73-11676
Proceedings of conference on comets, University of Arizona - Apr. 1970
[NASA-CR-129110] 02 p0227 N73-11833
Conference on reduction and suppression of aircraft engine noise
[NASA-SP-311] 03 p0249 N73-12012
Neutron activation analysis using gamma ray spectroscopy for determination of trace elements and short-lived nuclides
[BMBW-FBK-72-13] 03 p0262 N73-12122
Proceedings of Zero Gradient Synchrotron Workshops
[ANL/HEP-7208-VOL-1] 03 p0281 N73-12276
Proceedings of conference on air pollution, turbulence, and diffusion
[SC-M-71-0913] 03 p0327 N73-12662
Conference proceedings of British Acoustical Society, 1972
[AD-747615] 03 p0338 N73-12756
Conference on mechanics of deformed solids
[AD-748046] 03 p0362 N73-12954
Proceedings of symposium on helicopter noise held at Durham, North Carolina Sept. 1971
[AD-748876] 04 p0373 N73-13036
Distance measurement using electromagnetic radiation, range finders, and relaied geodetic research - conference summary
[AD-748067] 04 p0418 N73-13411
International conference on acoustical holography
[AD-749337] 04 p0430 N73-13505
Papers presented at conference on processing of superalloys
[AD-748159] 04 p0436 N73-13552
Closed cycle magnetohydrodynamics - conference paper abstracts
[TH-72-E-29] 04 p0453 N73-13703
Conference on research in nonchemical energy sources in nuclear fusion and plasma physics
[AD-748265] 04 p0456 N73-13725
Conference on stellar chromospheres and their compositions
[NASA-SP-317] 04 p0465 N73-13792
Proceedings of conference on benefits of space exploration conducted at Huntsville, Alabama Nov. 1971
[NASA-SP-313] 04 p0470 N73-13829
Proceedings of conference to analyze static and dynamic loads exerted on helicopter rotary wings and application to improved helicopter design
[AGARD-R-595] 05 p0491 N73-14000
Flight mechanics of rotary wing aircraft
[DLR-MITT-71-15] 05 p0493 N73-14021
Conference on biological effects of magnetic fields
[NRC-TT-1545] 05 p0500 N73-14070
Conference on acoustic gravity wave effects in atmospheric transmission of radio communication signals
[AGARD-CP-115] 05 p0508 N73-14131
Proceedings of symposium on laser radiation damage to transparent dielectrics, plasma formation at dielectric surfaces, and damage morphology of thin film coatings
[NBS-SP-372] 05 p0554 N73-14498
Parameterization and its role in atmospheric modeling
[GARP-PUBL-8] 05 p0573 N73-14654
Preliminary results from HEOS A satellite in electron and proton events, solar wind and interplanetary magnetic field measurement, and propagation of charged particles
[ESRO-SP-74] 05 p0592 N73-14813
Chemical processing industries and utilization of NASA technology - conference
[NASA-CR-129827] 05 p0607 N73-14937
Proceedings of conference on fluid dynamics of aircraft stalling to include stall and post-stall aerodynamic characteristics of various military aircraft
[AGARD-CP-102] 06 p0616 N73-14998
Conference on laser and radar altimeter measurement of sea surface topography from space
[NASA-CR-130293] 06 p0661 N73-15369
Conference on dynamic wave effects on satellite-borne sea surface measurements
[NASA-CR-129993] 06 p0664 N73-15392
Neutral and ion chemistry of D and E regions symposium papers
[AD-749780] 06 p0668 N73-15430
International research on aerospace instrumentation systems
[AD-750653] 06 p0675 N73-15493
Conference on environmental effects on mechanical failures
[AD-750411] 06 p0677 N73-15512
Selected abstracts on boron from internatioconference held at Tbilisi
[JPRS-57879] 06 p0687 N73-15596
Lectures on partial differential equations and numerical analysis presented at International Congress on Mathematics
[FOA-2-C-2470-11] 06 p0690 N73-15618
Crystal growth from vapor phases and epitaxy, and applications to semiconductors and microelectronics - conference review
[AD-750654] 06 p0710 N73-15793
Proceedings of Space Shuttle Sortie Workshop
[NASA-TM-X-68841] 06 p0719 N73-15866
Advanced technology, experimental and instrument design, and mission planning for space shuttle sortie workshop - conference working group reports
[NASA-TM-X-68842] 06 p0719 N73-15867
Research and development projects compiled at Army science conference
[AD-750300] 06 p0732 N73-15973
Liapunov functions for analyzing stability properties of various large scale electrical power systems - conferences
07 p0760 N73-16169
Proceedings of 1972 GOMAC conference on microcircuit applications
[AD-751316] 07 p0765 N73-16212
Proceedings of conference on management of information analysis centers
[COSATI-72-1] 07 p0766 N73-16224
Laminar and turbulent boundary layers, including hypersonic flow, wall flow and stagnation area
[DLR-MITT-71-13] 07 p0770 N73-16256
Cranfield fluidics conference of Uppsala, Sweden
[AD-751186] 07 p0774 N73-16287
Proceedings of conference on earth resources survey systems to show applications of remote sensing to agriculture, forestry, oceanography, and urban development - Vol. 1
[NASA-SP-283-VOL-1] 07 p0781 N73-16348
Proceedings of conference on earth resources survey systems - Vol. 2
[NASA-TM-X-68912] 07 p0785 N73-16382
Proceedings of conference to determine research projects for development of lasers for optical communications applications
[PB-212692] 07 p0807 N73-16543
Applications of Schmidt telescopes to study astrometry, photometry, galactic structure, quasars, and stellar spectra
07 p0844 N73-16840
Random load fatigue of aircraft structures
[AGARD-CP-118] 07 p0851 N73-16896
Summaries of papers presented to conference concerning aircraft stability and control
[AGARD-CP-119] 08 p0864 N73-16989
Conference on occupational medicine support in NASA programs to prevent health and emotional problems in personnel
[NASA-TM-X-69072] 08 p0871 N73-17048
Conference on preventive medical and environmental control measures for NASA and aviation industry personnel management
[NASA-TM-X-69073] 08 p0873 N73-17064
Conference on occupational and environmental medical services provided to NASA employees
[NASA-TM-X-69074] 08 p0874 N73-17078
Papers presented at conference on mechanisms of pyrolysis, oxidation, and burning of organic materials
[NBS-SP-357] 08 p0880 N73-17129
Control theory in game problems, optimization, feedback, and probabilistic automata - conference
[JPRS-58030] 08 p0891 N73-17214
Papers presented at conference on lightning and static electricity
[AD-752551] 08 p0922 N73-17552
Research on remote sensing applications and satellite observation data - conferences
[NASA-SP-312] 08 p0971 N73-17934
Armed Forces science conference report with list of principle authors
[AD-750326] 08 p0977 N73-17992
Armed Forces science conference report with list of principle authors
[AD-750360] 08 p0977 N73-17993
Conference on human endocrine secretions and hormone metabolisms during space flight stress
[NASA-TM-X-58093] 09 p0993 N73-18104
Review of papers presented at Conference on Space Biology and Aerospace Medicine
[JPRS-58345] 09 p0995 N73-18125
Papers presented at conference on halogenated fire extinguishing agents
[AD-753218] 09 p1001 N73-18168

Conference on parallel image processing for earth observation systems
[NASA-TM-X-66175] 09 p1065 N73-18684
Cryogenics, superconductors, and electromagnets - conference
[AD-753456] 09 p1067 N73-18705
Papers presented at conference on physics of low temperature plasma
[AD-753061] 09 p1072 N73-18745
Papers presented at 7th Aerospace Mechanisms Symposium
[NASA-TM-X-58106] 09 p1087 N73-18866
Summary of conference on stress corrosion testing methods
[AGARD-AR-52] 09 p1094 N73-18931
Conference on Air Force science and engineering research
[AD-753072] 09 p1101 N73-18991
Proceedings of conference on flight test technology to analyze results of flight test and comparison with data obtained using flight simulators for short takeoff aircraft
[DLR-MITT-72-18] 10 p1104 N73-19005
Proceedings of conference on application of superconductivity techniques to auxiliary power systems for aircraft and missiles
[AGARD-CP-104] 10 p1108 N73-19030
Color vision requirements for flying personnel of various armed forces - conferences
[AGARD-CP-99] 10 p1112 N73-19065
Conference on operational flight stress effects on human biodynamics and performance
[AGARD-CP-101] 10 p1122 N73-19143
Electrons in metal ammonia solutions - abstracts of conference papers
[AD-752915] 10 p1127 N73-19179
Conference papers on automated methods of computer program documentation
[NASA-TM-X-66196] 10 p1130 N73-19204
Conference of ERTS-1 performance, and application
[NASA-TM-X-66193] 10 p1155 N73-19396
Proceedings of symposium on flight operations and air traffic control to show problems affecting airports, general aviation, air traffic controllers, and governmental agencies
[DLR-MITT-72-24] 10 p1183 N73-19623
Heat transfer from radioisotope generator, using organic fluids
[CEA-CONF-2042] 10 p1224 N73-19950
Proceedings of conference on manual control to show interplay between man and machine and application of control theory in medicine and psychology
[NASA-CR-131244] 11 p1235 N73-20028
Conference on human visual search and perception
[AD-754327] 11 p1248 N73-20133
Antenna design and transionospheric propagation relative to space communication - conference
[AD-754061] 11 p1256 N73-20193
Proceedings of conference on inertial navigation components and systems with emphasis on concepts and techniques involving cost and performance tradeoffs
[AGARD-CP-116] 11 p1316 N73-20684
Interrelationships between energy, resources, and environment, conference summary
[PB-213031] 11 p1333 N73-20820
Proceedings of conference on rotary wing aircraft developments to include operational experience, flight tests, and evaluation of structural concepts
[AGARD-CP-121] 12 p1357 N73-21008
Proceedings of conference on fluid dynamics of rotary wings and aerodynamic characteristics of rotary wing systems
[AGARD-CP-111] 12 p1359 N73-21031
Predictability of motion sickness in pilot selection - conferences
[AGARD-CP-109] 12 p1367 N73-21092
Conference on detection, evaluation, and identification of drugs and alcohol in flying personnel and effects on flight fitness
[AGARD-CP-108] 12 p1368 N73-21102
Conference on pulsed high-beta plasmas
[IPP-1/127] 12 p1435 N73-21627
Annual AGARD meeting in Brussels, Belgium
12 p1466 N73-21881
Scientific conferences held in east Europe
[JPRS-58769] 12 p1467 N73-21886
Proceedings of conference on rotary wings to investigate rotor wakes, aerodynamic characteristics at hover and high advance ratio, and aerodynamic noise properties
13 p1473 N73-21931
Proceedings of NASA/Goddard Battery Workshop, first day
[NASA-TM-X-69240] 13 p1476 N73-21956
Proceedings of NASA/Goddard Battery Work Shop, second day
[NASA-TM-X-69239] 13 p1476 N73-21957
Proceedings of conference on short haul air transportation to show development requirements, economic aspects, and urban and environmental impacts
[M73-54] 14 p1600 N73-22974
USSR conference on exobiology and aerospace medicine
14 p1609 N73-23045
Aerospace medicine research, including human tolerance to various stress factors - conferences
[AGARD-CP-110] 14 p1610 N73-23057
Papers presented at conference on speech communication and processing
[AD-742236] 14 p1620 N73-23119
Conference papers on flat conductor cable technology and applications
[NASA-TM-X-64716] 14 p1640 N73-23294
Conferences on optimizing adaptive automatic systems
[JPRS-58809] 14 p1644 N73-23330
Conference on heat transfer and fluid mechanics
[AD-758404] 14 p1653 N73-23404
Conference on structure and composition of upper atmosphere and planetary atmospheres
[AD-756812] 14 p1662 N73-23489
Conference on high temperature corrosion of alloys for aerospace applications
[AGARD-CP-120] 14 p1675 N73-23597
Conference on liquid crystals
[AD-757224] 14 p1699 N73-23789
Conference on human performance under sustained work, and interdisciplinary research
[AD-744782] 14 p1723 N73-23981
Conference papers on thermionic power generation
[AD-758620] 15 p1739 N73-24098
Conference on Apollo 16 experiment for measuring microbial response to space environment
[NASA-TM-X-58103] 15 p1740 N73-24102
Proceedings of conference on pattern information processing
[PB-214617/3] 15 p1743 N73-24129
Summaries of papers presented at conference on optical communication systems
[PB-214778/3] 15 p1752 N73-24199
Conference on military research and numerical analysis
[AD-758145] 15 p1804 N73-24620
International conference on fundamental atomic and molecular physics
[AD-757890] 15 p1816 N73-24717
Brief summaries of 13th International Congress of Theoretical and Applied Mechanics
[NASA-CR-132236] 15 p1846 N73-24955
Conference on project management and project control
[ESRO-SP-90] 15 p1846 N73-24962
Conference on wave-particle interactions in magnetosphere and wave amplification for communications
[AD-759071] 16 p1909 N73-25450
Holography and optical filtering techniques for structural analysis, material tests, and astronomical observation - conference
[NASA-SP-299] 16 p1920 N73-25540
Proceedings of conference on operational problems of air traffic control beacon system
[FAA-NA-72-80] 16 p1940 N73-25702
Conference on atmospheric attenuation and rainfall effects on ultrahigh frequency telecommunication systems
[AGARD-CP-107] 17 p1994 N73-26121
Papers presented at conference on microwave transistors
[AD-760315] 17 p2005 N73-26213
Meissner effects and magnetization curves for superconductors - conference
[LA-5115] 17 p2010 N73-26257
Franco-Soviet conference on conjugate points, noting analyses of Pc 1 geomagnetic micropulsations
[CEP-AG-10/73] 17 p2026 N73-26395
Proceedings of conference to develop area navigation system design concept for application to national airspace system for improved air traffic control
17 p2060 N73-26664
Conference on growth and synthesis of semiconductor crystals and films
[JPRS-59208] 17 p2072 N73-26762
Conference on X ray experiments onboard different astronomical observatories for galactic and extragalactic X ray source position and size determination
[ESRO-SP-87] 17 p2084 N73-26855
Proceedings of conference on military applications of V/STOL aircraft to include current and proposed research projects to meet military requirements
[AGARD-CP-126-VOL-1] 18 p2102 N73-27000
Conference on communications policy research from 17 to 18 November 1972, Washington, D.C.
[PB-218981/9] 18 p2118 N73-27124
Proceedings of conference on application of composite materials in construction of aerospace vehicles and propulsion systems
[AGARD-CP-112] 18 p2163 N73-27474
Conference on technology utilization in spacecraft guidance, ground operations, communications and navigation systems, and sensor development
[NASA-SP-326] 18 p2207 N73-27816
Conference on uses and toxicity of halogenated fire extinguishing agents
[PB-218448/9] 18 p2214 N73-27875
Proceedings of conference on multiple-valued logic
[AD-762123] 19 p2240 N73-28063
Proceedings of conference on free turbulent shear flows - Vol. 1
[NASA-SP-321-VOL-1] 19 p2252 N73-28154
Proceedings of conference on significant results obtained from ERTS-1 - Vol. 1, Parts A and B
[E73-10824] 19 p2259 N73-28207
Proceedings of conference on significant results obtained by ERTS-1 - Vol. 2
[E73-10825] 19 p2287 N73-28389
Conference on significant results obtained from ERTS-1 MSS and RBV data - Vol. 3
[E73-10826] 19 p2289 N73-28405
Conference on annihilation reactions and gamma ray and universal evolution
[NASA-TM-X-66279] 19 p2331 N73-28753
Conference on solar high energy interactions
[NASA-TM-X-66290] 19 p2333 N73-28772
Summaries of papers presented to AGARD conference on random load fatigue
[AGARD-AR-54] 19 p2348 N73-28884
Capabilities and limitations of communication satellite data transmission for conducting conferences
[NASA-CR-133591] 20 p2377 N73-29098
Legal considerations of satellite communications system for teleconferencing applications
[NASA-CR-133592] 20 p2377 N73-29099
Proceedings of conference on solar proton event of Nov. 1969
[AD-763081] 20 p2468 N73-29830
Proceedings of conference on acoustic fatigue to show effects of aerodynamic loads, response of structures, structural design, and fatigue test methods
[AGARD-CP-113] 20 p2478 N73-29905
General problems with psychology in scientific and technical creativity
[TT-70-57147-1] 21 p2502 N73-30074
Articles on methodology and historical importance of scientific research in creativity
[TT-70-57147-2] 21 p2502 N73-30075
Presentations on psychological models, cybernetics, methodology, and applications to teaching
[TT-70-57147-3] 21 p2502 N73-30076
Conference on contact surface requirements for electric contacts and connectors
[AD-763213] 21 p2519 N73-30203
Papers presented at meeting of Soviet-American working group on remote sensing of natural environment from space
[JPRS-59739] 21 p2534 N73-30317
Proceedings of international conference on remote sensing of environment
[NASA-CR-133784] 21 p2540 N73-30370
Proceedings of conference on accuracy in spectrophotometry and luminescence measurements
[NBS-SP-378] 21 p2544 N73-30396
Conference on flux pumps and ac superconducting components
[CONF-720908] 21 p2580 N73-30674
Social, philosophical, and humanistic impacts of possible existence of extraterrestrial life
[NASA-SP-328] 21 p2596 N73-30807
Symposium on Gum Nebula and related topics
[NASA-SP-332] 22 p2715 N73-31731
Proceedings of symposium to determine requirements and configurations of emergency ejection systems for helicopter crews
[AGARD-AR-62] 23 p2743 N73-31954
Proceedings of conference on spread spectrum techniques and application to digital communications systems
[AGARD-LS-58] 23 p2756 N73-32053
Worldwide conference on data base management systems
[AD-765204] 23 p2762 N73-32104
Conference on cosmic ray and solar particle diffusion and concentration in interstellar space
[NASA-CR-135528] 23 p2834 N73-32646
Proceedings of conference on air transport industry with emphasis on economics, market demand, airlines regulation, and international transportation policy - Vol. 2
[NASA-CR-135635] 23 p2862 N73-32875
Proceedings of conference on short takeoff and landing aircraft to determine aerodynamic characteristics and short haul transportation applications
[NASA-SP-320] 24 p2871 N73-32934
Requirements of flight control systems with regard to aircraft stability and attitude control
[DLR-MITT-72-05] 24 p2877 N73-32978
Technical and economic aspects of airship transportation
[DLR-MITT-72-17] 24 p2879 N73-32989
Electronic display devices in aircraft control, noting pilot activation and VTOL control
[DLR-MITT-72-04] 24 p2880 N73-32998
Lectures presented at International Conference on Chemiluminescence
[AD-765525] 24 p2893 N73-33094
Fort Lauderdale Workshop on chemistry and meteorology
[WASH-1217] 24 p2923 N73-33342
Proceedings of Second Conference on Climatic Impact Assessment Program, November 14-17, 1972
[PB-221166/2] 24 p2924 N73-33357

Conference on waste glass recovery and re-use in secondary products
[NASA-CR-135792] 24 p2938 N73-33460
Conference on hydrologic research in representative and experimental basins
24 p2947 N73-33538
Meteorological services, satellites, and numerical weather forecasting
[WMO-342] 24 p2948 N73-33550
Proceedings of conference on radiation safety and protection in industrial applications
[DHEW-PUBL-[FDA]73-8012] 24 p2951 N73-33574
Proceedings of conference on electromagnetic and optical properties of sea water for application to surveillance, mapping, communications, and visibility
[AGARD-LS-61] 24 p2956 N73-33619
High energy rocket engines - propellant physical chemistry, propulsion system performance, hydrogen oxygen engines, boosters, nozzles - conferences
[DLR-MITT-72-09] 24 p2972 N73-33749
Turbojet and turbine engine performance optimalization by configuration variations, and auxiliary turbine engine converter problem
[DLR-MITT-73-05] 24 p2973 N73-33755
Conference on use of solar energy in Mediterranean
[BULL-22] 24 p2974 N73-33762
Azur satellite telemetry data processing - conferences
[BMFT-FB-W-73-04] 24 p2985 N73-33852

**CONFIDENCE LIMITS**
Survivability and confidence assessment of military weapon systems with reference to tactics, threat, and environment
[AD-746061] 02 p0235 N73-11913
Computerized information processing for radar system by subdivisions and multiple decision making processes
04 p0389 N73-13158
Applications of least squares method to analysis of parameters and confidence region determination
[LAAS-NT-SIS-72-T-08] 04 p0441 N73-13593
Accelerated life tests and reliability predictions for ageing components
[AD-751616] 07 p0805 N73-16529
Confidence intervals for ocean wave spectra for ordinary waves and hurricane sized waves
[AD-752135] 08 p0920 N73-17542
Estimating confidence intervals of probability of rare events as function of scale of sample
[AD-751953] 08 p0939 N73-17693
Validation and verification of computer simulation models
[P-4891] 12 p1381 N73-21196
Pattern recognition as statistical analysis of confidence level in forensic trace element identification
[IRI-133-72-11] 19 p2240 N73-28056
Statistical analysis of upper confidence levels for system failure rates
[AD-761758] 19 p2314 N73-28612

**CONFIGURATION MANAGEMENT**
Control of modifications in projects noting contractors and customers viewpoints
15 p1849 N73-24986

**CONFINEMENT**
Observation window for internal gas confining chamber
[NASA-CASE-NPO-10890] 03 p0279 N73-12265
Electronic detectors and computer software for analyzing human electroencephalographs in isolated environment
[AD-751272] 07 p0751 N73-16105

**CONFIRMATION**
U PROVING

**CONFORMAL MAPPING**
Application of conformal mapping procedures for designing airfoil shapes with high design lift coefficients
[AD-757813] 15 p1731 N73-24040
Conformal mapping technique for two-dimensional porous media and jet impingement heat transfer
[NASA-TM-X-68276] 20 p2485 N73-29961
Calculation of incompressible potential flow of airfoils by conformal mapping potential flow of lifting circles onto airfoils by double transformations
[ARC-R/M-3717] 21 p2492 N73-30002

**CONFORMAL TRANSFORMATIONS**
U CONFORMAL MAPPING

**CONGO (KINSHASA)**
U ZAIRE

**CONGRESS**
Hearings concerning research and development requirements for future energy needs
01 p0119 N73-10980
Research and development of advanced energy sources for United States of America
01 p0120 N73-10988
Congressional hearing on 1973 fiscal budget for Department of Transportation
01 p0120 N73-10989
Congressional hearing to establish national science policy and priorities act of 1972
03 p0367 N73-12991
Congressional hearings to establish government supported projects for fire research and safety
04 p0487 N73-13981
Congressional hearings on earthbound potential utilization of solar energy
05 p0592 N73-14812
Report to House Committee on Science and Astronautics on aerospace museum in Western United States
07 p0857 N73-16949
Proceedings of Congressional committee on use of recycled materials in NASA programs and requirement for recycling legislation for environmental and economy improvement
11 p1308 N73-20614
House hearings on air passenger fees, related taxation, and government regulation of commercial airline operations
11 p1352 N73-20970
Congressional hearings on research and development of environmentally safe electric power production
11 p1352 N73-20976
Congressional study on historical background of energy research and development
13 p1594 N73-22928
NASA appropriations for FY 1974
[H-REPT-93-171] 13 p1595 N73-22929
Congressional hearings on NASA budgetary authorizations for 1974
13 p1595 N73-22930
Planning and budgeting in lightweight fighter prototype development for military aviation
13 p1595 N73-22934
Hearings concerning NASA appropriations for FY 1974
14 p1721 N73-23960
Observations of various organizations and individuals on certain aspects of federal support of problem oriented research
[B-133183] 14 p1721 N73-23964
Congressional hearings on Skylab program, Apollo/Soyuz test project; and other planned space missions
14 p1721 N73-23965
Congressional hearings on NASA technology applications program budget
14 p1721 N73-23966
Congressional hearings on aeronautics and space technology
14 p1721 N73-23967
Hearings concerning energy problems of US
14 p1721 N73-23969
NASA authorization for fiscal year 1974
[S-REPT-93-179] 15 p1845 N73-24950
Congressional hearings on appropriations for Housing and Urban Development, National Science Foundation, and Veterans organizations for 1974
16 p1976 N73-25978
Hearings concerning fiscal year 1974 appropriations for space shuttle, earth resources program, and SST - Part 2
17 p2099 N73-26977
Hearings concerning appropriations for housing urban development, space, science and VA - Part 1
17 p2099 N73-26978
Congressional appropriations to National Aeronautics and Space Administration
[PUB-LAW-91-556] 18 p2213 N73-27872
Recommendations of conference committee concerning Senate admendments to H.R. 8825
[H-REPT-91-316] 19 p2354 N73-28935
Congressional hearing concerning GAO cost analysis of NASA estimates for space shuttle
19 p2354 N73-28936
Congressional committe report to identify and resolve disagreements in NASA appropriations for Fiscal Year 1974
[H-REPT-93-353] 21 p2607 N73-30892
Congressional hearings concerning appropriations for NASA operations during Fiscal Year 1974 - Part 1
21 p2608 N73-30906
Congressional hearings concerning appropriations for NASA operations during Fiscal Year 1974 - Part 3
21 p2608 N73-30907
Congressional hearings to review NASA program accomplishments and to predict advantages to accrue from space programs
21 p2609 N73-30916
Congressional hearing on national program to establish international metric system as official and standard system for United States commerce and industry
21 p2610 N73-30920
Index of subjects presented during Congressional hearings involving NASA appropriations for Fiscal Year 1974
21 p2610 N73-30921
Congressional hearings on legislation for conversion to metric system of weights and meaures in United States
21 p2610 N73-30922
Congressional hearing to determine causes of malfunctions of Skylab space vehicle
22 p2737 N73-31914
Congressional hearings on cost of space shuttle program to show differences between Government Accounting Office and NASA projections
22 p2737 N73-31916
Senate hearings concerning GAO analysis of space shuttle cost estimates
22 p2738 N73-31919
Congressional hearings on Federal policy, plans, and organization for support and utilization of science and technology
24 p2994 N73-33924
Congressional hearings on causes and implications of impending shortages of gasoline, heating oil, diesel fuel, jet fuel, and electricity
24 p2994 N73-33928

**CONGRUENCES**
Right congruences and semisimplicity for Rees matrix semigroups
[AD-754816] 11 p1312 N73-20645

**CONICAL BODIES**
NT SLENDER CONES
Wind tunnel tests to determine aerodynamic characteristics of two different size blunt 120 degree included angle cones behind 20 degree included angle cone
[NASA-TM-X-2603] 02 p0123 N73-11005
Numerical analysis of motion of inviscid fluid flow around pointed elliptic cone at incidence using fluid flow equations in conservation law form
[NASA-CR-129178] 02 p0154 N73-11251
Analysis of flow around conical body at small angles of attack in uniform supersonic flow of ideal gas
[AD-747408] 03 p0287 N73-12326
Optimum configuration of supersonic propelling nozzle for air driven two stage ejector stage with conical mixing chamber
[AD-747584] 03 p0352 N73-12869
Heat transfer and surface pressure measurements at supersonic speeds on conical delta wings with sharp leading edges
[ARC-CP-1212] 05 p0492 N73-14008
Characteristics of microwave antenna with conical reflectors to generate plane wave front
[NASA-CASE-NPO-11661] 05 p0507 N73-14130
Analysis of flow properties in wake of 120 and 140 degree included angle conical bodies and flow characteristics of Viking 75 entry vehicle configuration
[NASA-TN-D-7089] 05 p0527 N73-14285
Aerodynamic drag of series of spherically-blunted conical bodies with three classes of half-vertex angles under hypersonic flow conditions
[NAL-TR-280] 06 p0613 N73-14978
Aerodynamic drag coefficients for conical body in near free molecule and transitional flow regimes
[AD-750042] 06 p0615 N73-14994
Numerical analysis of three dimensional compressible laminar boundary layer flow characteristics of right circular cone in supersonic and hypersonic flow
[AD-750130] 06 p0656 N73-15331
Hypersonic air flow effects on aerodynamic characteristics of elliptical cones at large angles of attack
[AD-749738] 06 p0657 N73-15335
Effect of nonuniform upstream flow conditions on shock shape and surface pressure distribution on two dimensional pointed bodies
08 p0895 N73-17244
Measurement of aerodynamic drag of conical bodies at zero angle of attack in free molecular and near free molecular flow regime
[DLR-FB-72-64] 09 p1014 N73-18278
Penetration of truncated cones into ductile targets
[DREV-R-655/72] 09 p1093 N73-18926
High speed water jets from vertically accelerated cones partially filled with water
[MT-64] 11 p1270 N73-20302
Three dimensional supersonic flow program for calculating flow field about cone at zero angle of attack
[NASA-CR-112301] 12 p1391 N73-21282
Finite difference method for evaluating supersonic flow over sharp cone
[AD-755862] 12 p1392 N73-21290
Wind tunnel tests to determine pressure sensing characteristics of trailing cone device for calibrating aircraft static-pressure systems
[NASA-TN-D-7217] 13 p1470 N73-21906
Drag and stability characteristics of hypersonic blunt nosed conical bodies in gas mixtures
[NASA-CR-131986] 14 p1599 N73-22962
Analysis of viscous hypersonic flow around slender sharp wedges and unyawed cones
[AD-757037] 14 p1650 N73-23386
Numerical analysis of real gas effects in supersonic flows over sharp and spherically blunted cones
16 p1887 N73-25274
Sequential spark method for measuring cone wake velocity profiles
[AD-759159] 16 p1893 N73-25317
Analysis of characteristics of supersonic flow of helium around right circular cones at zero angle of attack and Mach numbers from 1.5 to 30.0
[NASA-SP-3078] 18 p2130 N73-27208
Development of numerical procedures for buckling analysis of truncated conical shells with rigid edge constraint using load displacement criterion
20 p2477 N73-29894

Wind tunnel tests to determine static and dynamic stability coefficients for circular cone with various nose bluntness configurations
[AD-765164] 23 p2740 N73-31934
Incipient boundary layer separation on axisymmetric compression surfaces of conical body at hypersonic speeds
23 p2775 N73-32195
Static pressure and heat transfer rate distributions on conical bodies at hypersonic speeds laminar and turbulent flow conditions
[AD-764983] 23 p2777 N73-32204
Aerodynamic characteristics of flow around elliptic cones at large angles of attack
[AD-764945] 23 p2777 N73-32209
Flow characteristics of merged layer regime in hypersonic, low density flow past semi-infinite sharp cone
24 p2903 N73-33168
CONICAL CAMBER
Development of slender body theory for analyzing flow past thin, conically cambered, delta wing with exact boundary conditions
[ARC-R/M-3249] 15 p1726 N73-24002
CONICAL FLARE
U CONES
CONICAL FLOW
Subsonic diffusers having ribs aligned transverse to flow direction for separation control
13 p1508 N73-22225
Pressure recovery performance of conical diffusers at high subsonic speeds and range of geometries
[NASA-CR-2299] 22 p2611 N73-30927
Study of supersonic conical flow by solving exact conical flow equations
[ISAD-4980-VOL-38-NO-9] 22 p2651 N73-31236
CONICAL NOZZLES
Performance tests of twin jet afterbody configurations to determine effect of nozzle spacing, fairing shapes, and angle of attack
[NASA-TM-X-2724] 21 p2491 N73-29994
Method of characteristics for studying flow field produced by underexpanded jet exhausted from conical nozzle into cylindrical tube
24 p2904 N73-33173
CONICAL SHELLS
Collocation method for numerical solution of buckling of conical shells under hydrostatic pressure
[AD-758834] 16 p1971 N73-25947
Buckling and structural response of two magnesium ring stiffened conical shells subjected to uniform external pressure
[NASA-TN-D-7303] 17 p2092 N73-26926
Asymmetrical bending and vibration of conical shell finite element
[TR-73-5-2] 24 p2989 N73-33884
CONICS
NT ELLIPSES
CONIFERS
Remote sensing techniques for evaluating vigor loss in black spruce due to eastern dwarf mistletoe
[NASA-CR-131582] 13 p1523 N73-22341
CONJUGATE POINTS
Franco-Soviet conference on conjugate points, noting analyses of Pc 1 geomagnetic micropulsations
[CEP-AG-10/73] 17 p2026 N73-26395
Polarization of Pc1 micropulsations observed in the same hemisphere, and in conjugate points
17 p2026 N73-26398
CONJUGATES
NT CONJUGATE POINTS
CONJUGATION
High percentage of zero elements of sparse matrix methods based on orthogonality and conjugacy
[NASA-CR-133231] 17 p2054 N73-26617
CONNECTICUT
Geological fracture mapping based on enhancement of ERTS-1 snow cover imagery of Massachusetts, Connecticut, and Feather River/Lake Tahoe area
[E72-10205] 02 p0161 N73-11302
Analysis of ERTS-1 imagery using electronic satellite image analysis console to display and measure snowfield extent, glacier development, and hydrologic features
[E73-10415] 11 p1279 N73-20377
Land use in northern megalopolis of Massachusetts, Connecticut, and Rhode Island
[E73-10506] 13 p1516 N73-22281
Land use of northern megalopolis of Massachusetts, Connecticut, and Rhode Island from ERTS-1 imagery
[E73-10630] 15 p1776 N73-24390
Application of ERTS-1 imagery to determine land use in Massachusetts, Connecticut, and Rhode Island
[E73-10723] 17 p2019 N73-26330
Mapping and digitization of land use in northern megalopolis of Masssachusetts, Connecticut, and Rhode Island using ERTS-1 data
[PAPER-L12] 19 p2274 N73-28308
ERTS-1 imagery of plume development where Connecticut River flows into Long Island Sound
[PAPER-M5] 19 p2280 N73-28345
Regional land use planning and management in Tri-State area from ERTS-1 MSS photography
[E73-10986] 22 p2658 N73-31293
Attenuation of solar spectral intensity by pollution in boundary layer of New Haven, Connecticut atmosphere
23 p2833 N73-32641
CONNECTIONS
U JOINTS [JUNCTIONS]
CONNECTIVE TISSUE
NT COLLAGENS
NT MARROW
CONNECTORS
NT ELECTRIC CONNECTORS
NT UMBILICAL CONNECTORS
Squib actuated disconnect for spacecraft coupling to launch vehicle
[NASA-CASE-NPO-13172-1] 08 p0969 N73-17917
Process for making RF shielded cable connector assemblies and resulting structures
[NASA-CASE-GSC-11215-1] 19 p2243 N73-28083
Shielding analysis of joints and connectors in coaxial cables
[AD-761825] 21 p2518 N73-30201
CONNECTORS [ELECTRIC]
U ELECTRIC CONNECTORS
CONOIDS
U CONICAL BODIES
CONSEQUENT LAKES
U LAKES
CONSEQUENT STREAMS
U STREAMS
CONSEQUENT VALLEYS
U VALLEYS
CONSERVATION
Conservation of fossil fuels in commercial aviation by using hydrogen
[NASA-CR-112204] 02 p0125 N73-11019
Proceedings of Congressional committee on use of recycled materials in NASA programs and requirement for recycling legislation for environmental and economy improvement
11 p1308 N73-20614
CONSERVATION EQUATIONS
Stochastic solutions of conservative dynamic systems such as particle accelerators and storage rings
[LAAS-PUBL-935] 02 p0203 N73-11640
Conservative finite difference method applied to meteorological advection problems
[NASA-CR-129090] 02 p0204 N73-11653
Simulation of emission-dispersion of inert pollutant in lower atmosphere in industrial zones by numerical integration of conservation and pollutant flow equations
06 p0693 N73-15649
Theoretical derivation of finite element solution algorithm for transient energy conservation equation
[NASA-CR-130149] 07 p0813 N73-16593
Conservation equations for analyzing supersonic and mixing flow regimes of supersonic ejectors
08 p0895 N73-17249
Total energy equation for coherent response of the plasma to linear wave fields
[JUL-895-TP] 20 p2459 N73-29760
CONSERVATION LAWS
Gauge invariance, conservation laws, and Korteweg-deVries equation for class of nonlinear partial differential equations
[IPPJ-138] 04 p0440 N73-13589
Entropy rate admissibility criterion for solutions of hyperbolic conservation laws
[NASA-CR-131812] 13 p1513 N73-22261
CONSOLES
NT REMOTE CONSOLES
CONSTANT SPEED PROPELLERS
U VARIABLE PITCH PROPELLERS
CONSTANTS
NT GRAVITATIONAL CONSTANT
NT GRUNEISEN CONSTANT
NT SOLAR CONSTANT
NT TIME CONSTANT
Tables of conversion factors and physical constants in International System of Units
[NASA-SP-7012] 17 p2098 N73-26969
CONSTELLATIONS
NT CENTAURUS CONSTELLATION
NT CYGNUS CONSTELLATION
NT LYRAE CONSTELLATION
NT ORION CONSTELLATION
NT SCORPIUS CONSTELLATION
Interstellar CO in ultraviolet spectrum of Zeta Ophiuchi
08 p0975 N73-17972
CONSTITUTIONAL DIAGRAMS
U PHASE DIAGRAMS
CONSTITUTIVE EQUATIONS
Constitutive equations for materials with memory
[AD-753460] 10 p1201 N73-19774
Constitutive equations for determining elastic deformation twinning in body centered cubic lattice metals at low temperatures
[AD-757042] 14 p1679 N73-23624
Constitutive equations for studying finite elastic-plastic deformation of ductile metals
[AD-761635] 19 p2310 N73-28578
Inequalities satisfied by strain energy functions for isotopic elastic material
[AD-761624] 19 p2315 N73-28616
CONSTRAINTS
NT METEOROLOGICAL PARAMETERS
Design, development, and evaluation of aircrew restraint system for forward-facing, nonejection seat for military aircraft
[AD-746631] 02 p0128 N73-11038
Subroutines for optimization of criteria under constraints using gradient projection method and HEATHER computer program
[LAAS-NI-CH-72-03] 02 p0147 N73-11191
Target maneuvers and sensor noise effects on proportional navigation systems noting Kalman filtering
[AASU-316] 03 p0329 N73-12681
Computerized simulation of inductor performance constraints
[AD-749685] 06 p0646 N73-15249
Minimax approximation to frequency responsive nonrecursive digital filter
[AD-750767] 06 p0648 N73-15263
Algorithms for iterative solution of unconstrained optimization problems
[NPL-NAC-25] 09 p1058 N73-18625
Comparison of effectiveness of yielding and elastic restraint systems for crash protection to show effects of slack and yield at constant load
[ARL/SM-382] 15 p1837 N73-24890
Development and characteristics of inflatable airbag restraint system for use in general aviation aircraft
[FAA-RD-73-3] 16 p1868 N73-25127
Cable guide and restraint device for reefing tubes in uniform manner
[NASA-CASE-LAR-10129-1] 16 p1917 N73-25512
Development of restraint system for securing personnel to ergometer while exercising under weightless conditions
[NASA-CASE-MFS-21046-1] 18 p2150 N73-27377
Requirements for mobility aids and restraint devices for use by personnel of space shuttle - Vol. 4
[NASA-CR-133994] 22 p2622 N73-31009
CONSTRICTIONS
Flow characteristics associated with laminar oscillating flow in horizontal tube containing mild axisymmetric constriction
23 p2772 N73-32175
CONSTRUCTION
Cold weather construction practices relative to men, materials, and equipment
[AD-745395] 13 p1506 N73-22206
Performance of airfield pavement construction joints under heavy aircraft loads
[FAA-RD-72-106] 16 p1969 N73-25926
CONSTRUCTION MATERIALS
Polymer optimization with molecular relaxation processes for preparing vibration damping plastic materials
[RAE-LIB-TRANS-1646] 04 p0386 N73-13135
Production engineering methods for metal ceramic structural materials and parts
[JPRS-57487] 04 p0431 N73-13515
Space technology for solving materials and design problems of earthbased housing
04 p0474 N73-13868
Development of construction block in form of container folded from flat sheet and filled with solid material for architectural purposes
[NASA-CASE-MSC-12233-2] 04 p0480 N73-13921
Oxidation resistance of capsule materials for cobalt 60 power and heat source
[DP-1300] 05 p0498 N73-14057
Development and characteristics of composite materials with emphasis on non-aerospace applications
[NASA-CR-129989] 05 p0565 N73-14587
Compatibility and safety of materials for liquid and gaseous oxygen systems
[NASA-CR-120922-VOL-1] 05 p0579 N73-14716
Construction materials and electrolytes for electrochemical fuel cells
[AD-750152] 06 p0627 N73-15089
Development of ceramic materials for construction of full scale, high pressure, hypersonic facility for testing aircraft and missile models
[AD-751298] 07 p0812 N73-16588
Structural design guidance and construction standards for upgrading and extending service life of airport pavements
[FAA-ED-08-2] 10 p1137 N73-19266
Mechanical and thermal properties and oxidation resistance of seal ring carbon graphite materials with resin impregnants
[NASA-CR-120955] 10 p1165 N73-19480
Improved carbon graphite materials for high temperature self-acting seals
[NASA-CR-121092] 10 p1165 N73-19481
Thermal vacuum environment tests of materials used in space technology to determine effect of ultraviolet radiation on contaminative properties
[NASA-CR-122374] 10 p1175 N73-19556
Apollo experience report on causes of stress-corrosion cracking of structural materials and corrective actions
[NASA-TN-D-7111] 10 p1214 N73-19875
Handbook for design of isogrid, triangular integrated stiffened structures for spacecraft structures and components
[NASA-CR-124075] 10 p1219 N73-19911

Application of vibrational methods for solving problems on theory of elasticity
[AD-754668] 11 p1346 N73-20922
Engineering data on aerospace structural materials - Vol. 1
[AD-755407] 13 p1544 N73-22517
Engineering data on aerospace structural materials - Vol. 2
[AD-755408] 13 p1545 N73-22518
Emplacement and maintenance of dust control materials for military aircraft and helicopter landing facilities
[AD-756179] 14 p1647 N73-23359
Effects of environmental stresses on materials used in constructing glide reentry vehicles
14 p1676 N73-23601
Refractory metal alloys with protective coatings for use in structural components of turbine engines
14 p1678 N73-23614
Final nonmetallic materials list for Apollo ultraviolet spectrometer experiment
[NASA-CR-128583] 16 p1916 N73-25502
Analysis of heat transfer properties and thermophysical properties of materials used for aircraft and spacecraft construction
[AGARD-R-606] 16 p1975 N73-25965
Airport construction procedures to include general requirements, construction materials, and operational maintenance
[AD-759243] 18 p2127 N73-27191
Application of composite materials for structural purposes to show limitations and failure characteristics
18 p2164 N73-27481
Neutron emission spectra from protons impinging on spacecraft structural materials
[NASA-TN-D-7386] 20 p2468 N73-29825
Hydrogen diffusion and hydrogen induced cracking of structural materials
[COO-3166-5] 21 p2604 N73-30867
Research and development projects concerning fire hazards in aircraft cabins and design of aircraft compartments to provide greater passenger survivability
[FAA-RD-73-146] 24 p2876 N73-32972

**CONSUMERS**
Consumer marketing for airline industry
23 p2862 N73-32873
Concepts of expanding airline marketing strategies
23 p2862 N73-32874

**CONSUMPTION**
NT FUEL CONSUMPTION
NT OXYGEN CONSUMPTION
NT WATER CONSUMPTION

**CONTACT RESISTANCE**
Frictional processes, electric contact resistance, and wear of pin on disk friction pair
[NASA-TT-F-15049] 24 p2929 N73-33391
Contact resistance of thermoelectric semiconductors by increasing switching layers
[AD-765769] 24 p2959 N73-33646

**CONTACTORS**
Tray hydraulic research, using cyclic operation of plate columns for gas-liquid contact
[PB-211853] 05 p0507 N73-14126

**CONTACTS (ELECTRIC)**
U ELECTRIC CONTACTS

**CONTAINERS**
Soil impact test with spherical nuclear reactor containment model for fracture strength observations
[NASA-TM-X-68180] 07 p0819 N73-16641
Design and development of diborane shipping container
[NASA-CR-130808] 09 p1038 N73-18466
Fabrication of plastic encapsulated metal containers by rotational molding process
[AD-753344] 10 p1168 N73-19499
Temperature and internal pressure response of nuclear waste disposal container following impact on earth
[NASA-CR-121186] 16 p1943 N73-25721
Heat transfer characteristics of container stored rocket motor
[AD-764536] 24 p2974 N73-33760

**CONTAMINANTS**
NT RADIOACTIVE CONTAMINANTS
NT TRACE CONTAMINANTS
Mass spectrometer system for monitoring atmospheric constituents and pollutants -operation and maintenance manual
[NASA-CR-128603] 01 p0057 N73-10469
Measurement of pollutant levels of nitrogen oxides, unburned hydrocarbons, and carbon monoxide for annular, swirl can combustor
[NASA-TM-X-68160] 02 p0243 N73-11974
Particulate and gaseous pollutant data gathered during 1968 by national, state, and local air surveillance networks
[APTD-0978] 05 p0572 N73-14652
Bibliography on chemical contaminants released in upper atmosphere
[WRE-TM-498(WR/D)-PT-2] 06 p0667 N73-15422
Effects and prevention of possible mercury pollution from failure of solar electric propulsion spacecraft using mercury propellant
[NASA-CR-130286] 06 p0717 N73-15855
Large scale turbulence and diffusion of pollutants in atmosphere
[COO-1585-22] 07 p0793 N73-16449
Reflectance spectra of contaminants in space simulation chamber
[NASA-CR-128716] 07 p0799 N73-16486
Spectroscopic and chromatographic analysis of outgassing contaminants in potting compound and paint
[NASA-CR-124227] 13 p1488 N73-22061
Prevention of N2O4 flow decay by means of contaminant removal through distillation and filtration
[AD-755380] 13 p1569 N73-22717
Collection and measurement of atmospheric contaminants during Skylab AM/MDA unmanned altitude chamber test
[NASA-CR-128903] 13 p1582 N73-22823
Sulfur, sodium, and chloride contaminants in gas turbines
14 p1677 N73-23610
Radioactive isotope measurements and neutron activation analyses for identifying contaminants in space environment simulator
[NASA-CR-128931] 15 p1815 N73-24709
Analysis of air pollution caused by aircraft engine emissions in vicinity of airport and comparison with air pollution in urban areas
15 p1825 N73-24788
Development of chemical process for determining quantity of contamination buried in potting compounds and removable of spores with amine dissolution and plating techniques
[NASA-CR-133645] 21 p2562 N73-30535
Active cleaning technique for removing contaminants from optical surfaces in space
[NASA-CR-124374] 21 p2583 N73-30697
Survey of contaminants and impurities in propellant grade hydrazine
[AD-764365] 22 p2626 N73-31040

**CONTAMINATION**
NT FUEL CONTAMINATION
NT SPACECRAFT CONTAMINATION
Space simulation study of plume contamination in reaction control thruster
[NASA-TM-X-68149] 01 p0090 N73-10743
Contamination avoidance devices for poppet-type shutoff valves
[NASA-CR-121125] 09 p1039 N73-18471
Microbial contamination studies for spacecraft assemblies
[NASA-CR-131086] 10 p1119 N73-19123
Terrestrial quarantine considerations for unmanned sample return missions
[NASA-CR-132071] 15 p1742 N73-24118
Kinetic of interstital contamination and defect growth in fused slurry silicide coated columbium alloys
[NASA-TN-D-7324] 18 p2160 N73-27448
Metabolism and propagation of microbial contamination in planetary atmospheres
[NASA-CR-133638] 20 p2369 N73-29049
Contamination tests of Vacuum Chamber A and cryogenic/vacuum study of quartz crystal microbalance
[NASA-TM-X-64776] 21 p2521 N73-30220
Analysis of data from quartz crystal microbalance contamination monitors on Skylab
[NASA-TM-X-64778] 22 p2673 N73-31412
Contamination of sensors installed in spacecraft and recommendations for eliminating or correcting
[NASA-TM-X-70487] 24 p2926 N73-33367

**CONTINENTAL SHELVES**
ERTS-1 imagery of inner shelf and coastal sedimentation environment of Beaufort Sea
[E72-10248] 03 p0289 N73-12348
Sea, ice, and surface water circulation in Alaskan Continental Shelf
[E72-10347] 05 p0533 N73-14335
Utilization of ERTS-1 imagery in air pollution and marine biology studies of lower Chesapeake Bay and continental shelf of Eastern US
[E72-10367] 05 p0535 N73-14355
Eastern Atlantic continental margin study of area between Port Elizabeth and Congo River
[PB-211392] 05 p0541 N73-14399
Geophysical survey of continental shelves off African coast and mapping for oil potential
[PB-211393] 05 p0541 N73-14400
Sea ice and surface water circulation in Cook Inlet, Alaska, and along continental shelves
[E73-10370] 11 p1275 N73-20346
ERTS-1 imagery of inner shelf and coastal sedimentation environment of Beaufort Sea, Alaska
[E73-10412] 11 p1278 N73-20374
ERTS-1 imagery of sea ice and surface water circulation along Alaskan contiental shelf
[E73-10416] 11 p1279 N73-20378
Relation of chlorophyll and suspended sediment content in lower Chesapeake Bay to ERTS-1 imagery and application of marine station data to study of productivity along eastern shelf waters of US
[E73-10593] 15 p1772 N73-24358
ERTS-1 imagery of sea ice and surface water circulation along Alaskan Continental Shelf
[E73-10620] 15 p1775 N73-24381
ERTS-1 imagery of inner shelf and coastal sediment transport in Beaufort Sea
[E73-10649] 16 p1897 N73-25345
Measurement of chlorophyll and plankton populations of shelf and slope waters off northeastern United States
[E73-10683] 16 p1901 N73-25378
Structural framework of Sunda Shelf and vicinity
[PB-218671/6] 18 p2146 N73-27346
Sea ice and surface water circulation along Alaskan continental shelf
[E73-10901] 20 p2396 N73-29250
ERTS-1 imagery of sea, ice, and surface water circulation along Alaskan continental shelf
[E73-11050] 23 p2779 N73-32226

**CONTINENTS**
NT AFRICA
NT ASIA
NT AUSTRALIA
NT EUROPE
NT NORTH AMERICA
NT SOUTH AMERICA
Identification of geostructures of continental crust and relation to mineral resources
[E73-10496] 12 p1397 N73-21332

**CONTINUITY [MATHEMATICS]**
Continuation from deep inelastic electron scattering to deep electron-positron annihilation
[NOTA-INTERNA-378] 01 p0084 N73-10692
Continuation method for solving eigenvalue problems and finding roots of polynomials
[TAE-152] 09 p1057 N73-18617
Continuity and Navier-Stokes equations for analyzing viscous flow heat transfer in curved tubes
24 p2902 N73-33162

**CONTINUOUS NOISE**
Detectors for signals in non-Guassian additive noise
19 p2235 N73-28016

**CONTINUOUS RADIATION**
Analysis of reaction mechanisms involved in chemical and continuous wave lasers based on carbon disulfide/oxygen system
[DREV-R-656/72] 01 p0064 N73-10525
Hydrophone measurement of acoustic propagation and CW signals from underwater explosions in shallow Bering Sea
[AD-745735] 01 p0081 N73-10667
Derivation of equations governing modulation of continuous wave whistler-mode transition by resonant particles
[AD-751043] 07 p0797 N73-16482
Performance of translucent beryllium oxide as envelope material for high intensity flash and continuous wave lamps
[AD-751661] 07 p0813 N73-16589
Continuous wave CO2 laser radiation effects on semiconductor materials
[AD-753918] 10 p1202 N73-19785
Design, construction, and evaluation of 12.2 GHz, 4.0 kW-CW coupled-cavity traveling wave tube for satellite-borne television broadcast transmitters
[NASA-CR-120920] 12 p1382 N73-21209
Multiple line output from tunable CW dye lasers
[AD-757772] 15 p1796 N73-24557
Spaceborne prototype model of millimeter wave experiment radiating transmitter for ATS-F spacecraft
[NASA-CR-132760] 16 p1965 N73-25895
Electromagnetic and strong interactions processes for producing diffuse cosmic gamma continuum radiation
19 p2332 N73-28763
Using simple numerical model of CW chemical laser to study output power
[AD-763169] 21 p2555 N73-30485
Continuous low dose gamma irradiation effects on cell population kinetics of mice lymphoid tissue
[NASA-CR-135723] 23 p2749 N73-31999
Industrial applications of radiation technology for conducting nondestructive tests
24 p2952 N73-33578

**CONTINUOUS WAVE LASERS**
Continuous wave dye laser for studying interaction of electromagnetic radiation with matter
[AD-762370] 19 p2309 N73-28572
Design of high power continuous wave HF chemical laser
[DREV-TN-2060/73] 20 p2425 N73-29475
Theoretical performance of HCl continuous wave chemical laser
[AD-762924] 20 p2427 N73-29493

**CONTINUOUS WAVE RADAR**
Doppler effect continuous wave radar for bird hazard detection and aircraft collision avoidance near airfields
[AD-751985] 08 p0885 N73-17168
Remote sensing with meteorological radar equipment
[AD-753813] 09 p1004 N73-18197
Calibration and electromagnetic field mapping for continuous wave test facility
[AD-757638] 14 p1647 N73-23358

**CONTINUOUS WAVES**
U CONTINUOUS RADIATION

**CONTINUUM FLOW**
Data acquisition system for S-1 wind tunnel with continuous subsonic/supersonic flow
[WRE-TN-784(WR/D)] 09 p1010 N73-18248
**CONTINUUM MECHANICS**
Development of general mixed finite element models of nonlinear thermomechanical response of dissipative media
[AD-745994] 02 p0239 N73-11944
Analysis of vibration characteristics of laminated plates and modifications of plate theory to produce results consistent with continuum theory
[AD-746951] 02 p0240 N73-11949
Conservation laws and entropy production inequality applied to continuum thermodynamics
[AD-748654] 04 p0485 N73-13965
Continuum theory for wave propagation in laminated composites applied to propagation parallel to laminates
[AD-750504] 06 p0689 N73-15608
Unified theory of thermoviscoplasticity of crystalline solids
[AD-751293] 07 p0833 N73-16756
Averaging process for continuum mechanics in two phase flow analysis
[AD-752159] 08 p0898 N73-17273
Lectures on properties and characteristics of rotating and stratified fluids
[AD-754066] 11 p1272 N73-20320
Finite element formulation and thermoelastoviscoplasticity theory for solving problems in nonlinear continuum mechanics
[AD-754952] 11 p1331 N73-20805
Derivation of perturbed equations of motion and heat conduction for thermoelastic solid using finite element method
[AD-754542] 11 p1346 N73-20919
Principle of virtual work applied to continuum mechanics
[AD-758727] 15 p1841 N73-24919
Continuum methods for studying solar wind interaction with interstellar neutral particles
18 p2194 N73-27717
Decimetric radio continuum maps of three extended galactic supernova remnants and Cygnus Loop
19 p2342 N73-28839
Continuum electrostatic probe theory for collision-dominated plasma
[PB-222088/7] 22 p2706 N73-31669
Fundamental concepts and statistical foundation of mechanics of continuous medium
[AD-764370] 22 p2727 N73-31820
Potential representation theorem for diatomic elastic dielectric displacement and polarization fields
24 p2959 N73-33649
**CONTINUUMS**
Low frequency radio continuum arising in inner magnetosphere from trapped and untrapped electrons
07 p0775 N73-16291
Finite element method of continuum and structural analysis using computer programs - users manual
[AD-753120] 09 p1097 N73-18951
Development of continuum theory with microstructure for wave propagation in composite materials
23 p2806 N73-32438
**CONTOURS**
Numerical solutions for jets impinging on curved surfaces
[NASA-CR-129136] 02 p0154 N73-11252
Contour of wave drag optimized bodies of revolution as function of Mach number in hypersonic flow
[DGLR-PAPER-72-108] 04 p0369 N73-13003
Color photographic system using grid projector and telecentric lenses for recording contours of human face for aircrew oxygen mask fitting
[RAE-TR-71184] 07 p0750 N73-16099
Contour plotting algorithm for aerial radiation patterns
[BBC-RD-1973/18] 23 p2755 N73-32045
**CONTRACT MANAGEMENT**
Conference on project management and project control
[ESRO-SP-90] 15 p1846 N73-24962
Integration of projects and contracts into program of research and development center
15 p1847 N73-24965
Organization and management of ESRO 4 satellite project noting planning and contractor relations
15 p1847 N73-24970
Comparison of management, planning and control for Nimrod avionics system and hospital projects
15 p1847 N73-24971
Control of modifications in projects noting contractors and customers viewpoints
15 p1849 N73-24986
Contract requirements, negotiation, and management within European space program
15 p1849 N73-24987
Incentive schemes as contract management tool noting use in ESRO 4 satellite project
15 p1849 N73-24989
**CONTRACT NEGOTIATION**
Contract requirements, negotiation, and management within European space program
15 p1849 N73-24987
Policy of Department of Transportation with respect to evaluating proposals for airline mergers
23 p2864 N73-32896
**CONTRACTION**
Generalized method of contraction cone design and low speed velocity distribution
[NASA-TN-D-6962] 01 p0036 N73-10283
Elastomeric extensometer for measuring surface area changes of human body caused by body expansion and contraction
[NASA-CASE-MFS-21049-1] 02 p0173 N73-11405
Flow through supersonic Laval nozzle with several contractions
24 p2909 N73-33216
**CONTRACTORS**
Guide for preparation of contractor safety plans at Cape Kennedy Space Center
[NASA-TM-X-69492] 20 p2488 N73-29986
**CONTRACTS**
Analysis of F-15 contract structure and contribution to effective program management
[AD-750849] 06 p0732 N73-15975
Government contracts and grants relative to documents on environmental satellites
[NOAA-TM-NESS-46] 13 p1524 N73-22349
Managing contract specification system for satellite projects
15 p1847 N73-24974
Degree of innovation and risk in product development contracts
15 p1849 N73-24988
Policies and guidelines for awarding weapons systems acquisition contracts
[AD-761443] 19 p2356 N73-28949
**CONTRAILS**
Dynamics of lower thermosphere through comparison of optical observations of motions of vapor trails with radar observations of ionized meteor trails
[NASA-CR-131645] 12 p1420 N73-21509
Design of upper atmosphere chemical release package
[AD-760141] 17 p2028 N73-26416
**CONTRAST**
NT IMAGE CONTRAST
NT PHASE CONTRAST
Model for inherent contrast conditions in full-form objects
10 p1226 N73-19966
Measurement of atmospheric aerosol content in Southern California desert areas from ERTS-1 contrast and radiance measurements
[PAPER-I2] 19 p2277 N73-28324
**CONTROL**
Sampled data frequency response method for analyzing control system performance, and compensator improvement program for designing Saturn 5/S1-C compensators
[NASA-CR-123917] 02 p0195 N73-11573
Compensating and matching short period seismometers for laboratory inertial guidance and control
[AD-748245] 04 p0424 N73-13455
Error analysis of lunar control by orbital triangulation
04 p0468 N73-13813
Fume component tests to determine welders safe breathing level through ventilation
[ITR-1] 09 p1038 N73-18467
Application of statistical analysis techniques in telecommunication, tracking, and control
[AD-758260] 15 p1751 N73-24193
Extraction of beginning and ending of pulse trains
16 p1883 N73-25244
**CONTROL DATA [COMPUTERS]**
Minicomputer for controlling data transfer between process instrumentation and on-line computer
[HMI-B-123] 02 p0145 N73-11171
**CONTROL DEVICES**
U CONTROL EQUIPMENT
**CONTROL EQUIPMENT**
NT CONTROL STICKS
NT CRYOSTATS
NT PRESSURE REGULATORS
NT SPEED REGULATORS
NT TELEOPERATORS
NT THERMOSTATS
Flow control valve for high temperature fluids
[NASA-CASE-NPO-11951-1] 01 p0061 N73-10501
Digital control system for Baum folding machine providing automatic counting and machine shutoff
[NASA-CASE-LAR-10688-1] 02 p0178 N73-11442
Construction of extremal controller for high current betatron using stochastic algorithms
[AD-747370] 03 p0281 N73-12279
Design of cryogenic flow control components for Saturn 5 S-1C launch vehicle
03 p0349 N73-12850
Design and operation of programmable logic tester for high speed static testing of circuit boards
[REPT-6570] 04 p0420 N73-13422
Installation, operation, and maintenance procedures for optical figure sensor and associated electronic controls
[NASA-CR-130125] 04 p0421 N73-13429
Control circuit for nuclear thermionic converter power source for spacecraft
[NASA-CASE-NPO-13114-1] 04 p0448 N73-13656





Design technique for control systems of large space telescope mirrors
[NASA-TN-D-7090] 05 p0522 N73-14247
Transistorized control unit for neutron spectrometers or diffractometers
[BARC-591] 05 p0547 N73-14447
Performance tests of hydromechanical fuel control system for J-85 engine
[NASA-TN-D-7198] 09 p0990 N73-18082
Control equipment for sterilization facility used to thermally inactivate microbes on interplanetary space vehicle components
[NASA-CR-131103] 10 p1119 N73-19122
Design and development of brushless, direct drive solar array reorientation control system for satellites
[NASA-CR-130153] 11 p1261 N73-20236
Phase delay control system for stabilizing signals passing through coaxial cables
[NASA-CASE-NPO-13138-1] 11 p1262 N73-20238
Comparison of computed torque method and conventional position servo computer controlled manipulator
[NASA-CR-131521] 12 p1381 N73-21198
Problems of designing and developing automatic equipment and control systems
[JPRS-58746] 12 p1405 N73-21391
Design, development, and operation of remote control system for Large Space Telescope
[NASA-TM-X-64740] 12 p1405 N73-21394
Analysis and design of capsule landing system and surface vehicle control system for Mars exploration
[NASA-CR-131515] 12 p1459 N73-21825
Design and performance of demand regulated liquid breathing systems for mammalian respiration
13 p1478 N73-21976
Mass and momentum of control signals in switching mechanism of fluid bistable amplifiers
[AD-756583] 13 p1511 N73-22243
Bearings for control system of high temperature lithium or argon cooled fast nuclear reactors
[NASA-TM-X-68218] 13 p1534 N73-22429
Time base stability and intermachine compatibility in wideband laser recording systems
13 p1536 N73-22444
Algorithm for determining frequency response of linear control system
[TT-7304] 14 p1683 N73-23654
Feasibility of using computer system for echo detection and identification of moving targets
[AD-758266] 15 p1751 N73-24191
Integrated circuit designs for self controlling electrical heater
[NASA-TN-D-7248] 15 p1786 N73-24479
Design, fabrication, and test of electronic engine control system for small turboshaft engines
[AD-758173] 15 p1827 N73-24805
Interferometer prism and control system for precisely determining direction to remote light source
[NASA-CASE-ARC-10278-1] 16 p1911 N73-25463
Neutronic feasibility of fast spectrum space power reactor design concepts using boron control devices
[NASA-TM-X-2821] 16 p1943 N73-25720
Feasibility of emission control devices for motor vehicles
[PB-218942/1] 18 p2174 N73-27555
Asynchronous control modules for digital computer design
[AD-762345] 19 p2241 N73-28067
National Environmental Research Center research projects for FY 73 on air pollution and control equipment
[PB-220259/6] 21 p2574 N73-30630
Absorptive equipment for control of air polluting industrial wastes
[PB-221138/1] 21 p2575 N73-30637
Development and characteristics of variable ratio, mixed-mode, bilateral master-slave control system for space shuttle remote manipulator system
[NASA-CASE-MSC-14245-1] 21 p2599 N73-30832
Design and analysis of Viking Orbiter 1975 guidance and control system
[NASA-CR-135649] 21 p2600 N73-30836
Directional equipment for suppressing noise of Concorde propellers during high speed flight
22 p2613 N73-30942
Fluidic to hydromechanical interface for application to gas turbine engine control system
[AD-764368] 22 p2675 N73-31429
Monitoring and control of fuel cell system by digital computer
[NASA-TM-X-2923] 23 p2748 N73-31994
Reference material for thermal simulation system for programmers, temperature controls, power regulator, peripheral equipment, and radiant array purchased parts
[NASA-CR-124437] 24 p2901 N73-33155
Fabrication of cermet bearings for control system of high temperature lithium cooled nuclear reactors
[NASA-TM-X-2892] 24 p2953 N73-33595
**CONTROL MOMENT GYROSCOPES**
Evaluation of control moment gyro steering laws for use on HEAO spacecraft
[NASA-TM-X-64727] 11 p1321 N73-20718

Double-gimbaled control moment gyro system for maintaining Skylab attitude control without excessive fuel consumption after failure of main gyro system
[NASA-TM-X-64746] 14 p1707 N73-23851
Vibration tests of flight control moment gyros and bearing life test fixtures
[NASA-CR-124449] 24 p2926 N73-33365
CONTROL RODS
Molybdenum reflector reactivity and space power reactor control
[NASA-TM-X-2922] 23 p2819 N73-32533
CONTROL SIMULATION
Simulation control of European SOREL space probe attitude and position
[S-3-1949-VOL-3] 02 p0235 N73-11907
Payload deployment aspects of control system optimization of spacecraft maneuvers involved in stationkeeping and docking - Vol. 1
[NASA-CR-124050] 09 p1086 N73-18860
Mathematical and numerical methods for solving spacecraft control problems and mapping of celestial bodies
[NASA-TT-F-731] 10 p1177 N73-19572
Probabilistic model for estimating efficiency of operational servicing system for control digital computer onboard spacecraft
10 p1177 N73-19575
Apollo experience report on engineering simulation in support of Apollo guidance and control system
[NASA-TN-D-7287] 15 p1835 N73-24873
CONTROL STABILITY
Design and development of active control system for air cushion vehicle to reduce or eliminate effects of excessive vertical vibratory acceleration
[NASA-CASE-LAR-10531-1] 04 p0372 N73-13023
Computerized design of aircraft control optimization stabilization systems
[NASA-CR-133002] 16 p1935 N73-25653
Characteristics of spacecraft control systems to provide examples of attitude control and stabilization for manual and automatic operation
[NASA-TT-F-774] 16 p1966 N73-25903
Stability of two-loop dead-time feedback control systems
[DLR-FB-72-45] 22 p2646 N73-31204
CONTROL STICKS
Bibliography of research on aircraft sidearm control
[AD-745863] 01 p0005 N73-10039
Tracking performance during whole-body vibration with side-mounted and center mounted control sticks
[AD-761798] 19 p2228 N73-27971
CONTROL SURFACES
NT AILERONS
NT FLAPS [CONTROL SURFACES]
NT GUIDE VANES
NT HORIZONTAL TAIL SURFACES
NT JET FLAPS
NT LEADING EDGE SLATS
NT SPOILERS
NT TRAILING-EDGE FLAPS
NT WING FLAPS
Computer program for subsonic lifting surface analysis with static aeroelastic effects
[AD-745894] 02 p0157 N73-11273
Incompressible boundary layer flow separation over moving boundaries
[AD-746869] 02 p0159 N73-11292
Method for computing lifting pressure distribution on wing with partial span, swept control surfaces
[NASA-TN-D-7251] 11 p1232 N73-19999
Characteristics of system for providing yaw control of vehicles at high supersonic and hypersonic speeds by deflecting flaps mounted on upper wing surface
[NASA-CASE-LAR-11140-1] 11 p1233 N73-20008
Flight test measurements of control surface hinge moments on X-24 lifting body correlation with wind tunnel data
[NASA-TM-X-2816] 16 p1858 N73-25049
Numerical analysis of lift and lift distribution on aircraft wing and trailing vortex flow behind wing
[AD-759262] 16 p1863 N73-25089
Designs of high temperature seals for gaps between structure and aerodynamic control surfaces of space shuttle orbiter
[NASA-CR-128951] 16 p1965 N73-25891
Wind tunnel tests to determine effects of control surface modifications on stability and control of space shuttle orbiter
[NASA-CR-133979] 19 p2346 N73-28870
CONTROL SYSTEMS
U CONTROL
CONTROL THEORY
Development of adaptive controller for multivariable systems and application to helicopter system with time varying parameters
[AD-746492] 01 p0002 N73-10007
Control theory model for pilot decision making based on estimated state of linear plant
01 p0014 N73-10107
Bang-bang controller operating in chatter mode for disturbance regulation in linear system
[AD-745896] 02 p0203 N73-11643
Reliability probability analysis on ergatic process in spacecraft control during approach and docking with orbital station
03 p0258 N73-12087
Identification of unknown parameters of multiple input/output, linear, constant, discrete time system from measurements made on inputs and outputs
[AD-747693] 03 p0325 N73-12653
Optical control theory and energy-state approximation to determine parameters for minimum time flight path of supersonic aircraft
[AD-748219] 03 p0329 N73-12689
Analysis of minimum time maneuvers by high thrust-to-weight aircraft using optimal control theory to determine open-loop control laws
[AD-748354] 04 p0374 N73-13039
Research reports on control theory in flight systems
[AD-746296] 05 p0523 N73-14251
Application of control theory to design of actual systems
[AD-750490] 06 p0691 N73-15626
Development of aircraft control systems based on operator performance, adaptive displays, and coupling of manual with automatic control
[AD-751306] 07 p0741 N73-16026
Application of singular perturbation of ordinary differential equations to control system design
07 p0761 N73-16181
Application of modern control theory to design of optimum aircraft controllers
[NASA-TM-X-62208] 08 p0867 N73-17016
Scientific reports on adaptive control system theory for aerospace engineering
[AD-751941] 08 p0887 N73-17187
Control theory in game problems, optimization, feedback, and probabilistic automata - conference
[JPRS-58030] 08 p0891 N73-17214
Computation of optimal output-feedback compensators for linear time-invariant systems
[NASA-CR-130988] 09 p1056 N73-18607
Application of optimal control theory to design of control system for supersonic inlet of turbojet engine
[NASA-TN-D-7188] 09 p1079 N73-18803
Man machine systems, control theory, nuclear geophysics, and research instrumentation
[RISO-M-1509] 10 p1137 N73-19263
Maximum principle for determining necessary conditions for optimality when delay depends on state, control, and time
[AD-753675] 10 p1179 N73-19592
Limiting performance of large systems subject to steady state and transient inputs
[NASA-CR-112293] 11 p1265 N73-20261
Evaluation of control moment gyro steering laws for use on HEAO spacecraft
[NASA-TM-X-64727] 11 p1321 N73-20718
Optimal control and measurement techniques of decentralization for stochastic linear dynamic systems
[AD-754984] 12 p1419 N73-21501
Feedback control techniques for proportional target interception and acceleration
[AD-755795] 13 p1578 N73-22794
Synchronizing control of drag-cup gyro motor using dynamic gas bearing
[NAL-TR-304] 15 p1756 N73-24232
Effectiveness of controllers for dynamic systems modeled by ordinary differential equations
[NASA-CR-132054] 15 p1759 N73-24259
Mathematical programming used in computer-aided-compensator design for control system
[NASA-CR-2248] 16 p1934 N73-25651
Design of manipulator mechanisms with manual, bioelectric, and automatic control systems
[NASA-TT-F-14336] 17 p1989 N73-26073
Research and development in solid state physics, antenna arrays, and control theory
[AD-760008] 17 p2074 N73-26783
Proceedings of conference on multiple-valued logic
[AD-762123] 19 p2240 N73-28063
Theory of modified quasilinearization algorithm for optimal control problems with bounded state variables - Part I
[AD-761786] 19 p2315 N73-28614
Mathematical technique for optimal control problems with initial conditions
[AD-762253] 19 p2315 N73-28620
Control models for diagnosing malfunctions in analog computers
[AD-762220] 20 p2379 N73-29115
Analysis of aircraft stability and control derivatives in turbulent conditions subject to random state disturbance
[AD-763741] 21 p2498 N73-30046
Decentralized control of stochastic large scale systems
[NASA-CR-133857] 21 p2519 N73-30207
Psychological concept for developing cybernetic control devices
[JPRS-60103] 23 p2752 N73-32019
Stability of multiple loop nonlinear time varying systems
[AD-764631] 23 p2813 N73-32492
Evaluation of control laws and actuator locations for control systems applicable to deformable astronomical telescope mirrors
[NASA-TN-D-7276] 24 p2900 N73-33148
CONTROL UNITS [COMPUTERS]
Asynchronous control circuits for digital systems representation and modular design
03 p0272 N73-12202
Probabilistic model for estimating efficiency of operational servicing system for control digital computer onboard spacecraft
10 p1177 N73-19575
Operational models for analyzing digital control system between computer and information sources
10 p1177 N73-19576
Control-oriented linear homogeneous computer system
21 p2514 N73-30166
Commutator and interaction unit of elementary machines in control-oriented homogeneous computer system
21 p2514 N73-30167
Interrupt system of control-oriented homogeneous computer system
21 p2514 N73-30168
Complex of elements of control-oriented homogeneous computer system
21 p2514 N73-30169
CONTROL VALVES
Evaluation of high response electrohydraulic digital control valve for application to flight control systems
[NASA-CR-124178] 11 p1297 N73-20523
Design of pyrotechnical gas generator for gate valve control
[AD-754963] 11 p1301 N73-20556
Performance of anti-G valve subjected to varying acceleration forces
[AD-760814] 20 p2372 N73-29062
Dual stage check valve for cryogenic supply systems used in space flight environmental control system
[NASA-CASE-MSC-13587-1] 21 p2552 N73-30459
Design of valves for reactor coolant system of nuclear powered aircraft
[SLA-73-221] 24 p2929 N73-33393
CONTROLLABILITY
Survey of aerospace industry to determine various techniques used in considering interactions of handling qualities, stability, control, and load alleviation devices on structural loads
[AGARD-R-593] 02 p0125 N73-11020
Calculation of induced load effects on controllability of rigid and flexible aircraft
08 p0865 N73-17004
Control technology for air cushion passenger vehicle
11 p1352 N73-20969
Development, manufacture, and testing of optical beam steerer for use in spaceborne optical radar systems
[NASA-CR-124283] 16 p1884 N73-25246
Flight tests for determining handling qualities and operational characteristics of Breguet 941 STOL aircraft
18 p2103 N73-27008
CONTROLLED ATMOSPHERES
NT INERT ATMOSPHERE
NT SPACECRAFT CABIN ATMOSPHERES
Universal humidity chart allowing humidity and energy calculations for any mixture of monatomic and diatomic gases at pressures encountered in saturation diving
[AD-746162] 02 p0207 N73-11675
Cyclically changing temperature effects on monitoring behavior and physiological responses of man
[AD-748451] 05 p0505 N73-14110
Thermoregulation reactions of rats in hypoxic atmosphere with nitrogen and helium dilution
07 p0743 N73-16046
Effect of atmosphere with increased oxygen and carbon dioxide content on human orthostatic tolerance following 10 days of bedrest
07 p0744 N73-16055
Nitrogen oxide and ammonia removal from spacecabin atmosphere by catalytic oxidation with ruthenium and adsorption on silica gel
[NASA-CR-2132] 09 p0999 N73-18151
Human nitrogen and water/salt metabolisms in controlled regenerative atmosphere
10 p1115 N73-19089
Hyperbaric chamber used to determine influence of increased ambient pressure and gas density on cardiac rate in man
[AD-755129] 13 p1487 N73-22058
Temperature and humidity control in air quality modeling for optimal life support system of spacecraft cabin
15 p1743 N73-24131
Fire suppression and extinguishment techniques in oxygen enriched atmospheres
[NASA-CR-121150] 15 p1842 N73-24926
CONTROLLED FUSION
Bibliography on controlled fusion and plasma physics
[TID-3557-1971-SUPPL] 03 p0341 N73-12785

Possible uses of pulsed lasers for controlled fusion, plasma heating, and creation of controlled nuclear microexplosions
[UCRL-73931] 10 p1186 N73-19654
Neodymium-glass laser system production of plasmas for research on controlled thermonuclear fusion
15 p1794 N73-24545
Motivation, planning, and management of research and development programs using controlled thermonuclear fusion as examples
15 p1846 N73-24964
Magnetic mirrors for controlled nuclear fusion
[IAEA/SM-170/49] 19 p2320 N73-28665

**CONTROLLED STABILITY**
U CONTROL
U STABILITY

**CONTROLLERS**
NT SERVOMECHANISMS
NT SERVOMOTORS
Optimal adaptive control of aircraft lateral dynamics in gust presence using Pontryagin principle and cost function
[AASU-314] 03 p0253 N73-12046

**CONVAIR MILITARY AIRCRAFT**
U MILITARY AIRCRAFT

**CONVAIR 340 AIRCRAFT**
U CV-340 AIRCRAFT

**CONVAIR 990 AIRCRAFT**
U CV-990 AIRCRAFT

**CONVAIR 880 AIRCRAFT**
Aircraft accident involving ground collision of DC-9 and CV-880 aircraft at O Hare International Airport, Chicago, Illinois on 20 December, 1972
[NTSB-AAR-73-15] 22 p2614 N73-30945

**CONVECTION**
NT FORCED CONVECTION
NT FREE CONVECTION
Convection and mixing of stratified fluids in rotating tank
[NASA-TR-R-392] 01 p0039 N73-10312
Mixed convection in reactor channel utilizing sodium as working fluid
[CEA-CONF-2001] 06 p0654 N73-15317
Evolution of stars with suppressed core convection
[NASA-TM-X-68944] 08 p0959 N73-17846
Plasma convection patterns in polar upper ionosphere obtained from Cosmos 184 satellite measurements during magnetic disturbance of 4 Nov. 1967
[PR-130] 10 p1156 N73-19403
Two-dimensional curve fitting technique for analyzing data acquired by Doppler radar and application to study of convective storms
[AD-755946] 12 p1424 N73-21537
Equations of motion for studying convection transport processes in strongly curved tubes
13 p1509 N73-22227
Parametric model of cumulus convection to simulate entire life cycle of different types of cumuli under various environmental conditions
[PB-213623-2] 13 p1555 N73-22602
Numerical model of individual convective clouds used for analysis of cumulus and mesoscale interactions
[PB-213624-0] 13 p1555 N73-22603
Convection velocity measurements in polar upper ionsphere made by Cosmos 184 Satellite during moderate magnetic disturbance
15 p1780 N73-24430
Numerical model of dry and wet cumulus convection
17 p2056 N73-26630
Skylab experiments on convection and molten metal flow and solidification under reduced gravity
[NASA-CR-124329] 19 p2343 N73-28852

**CONVECTION CLOUDS**
NT CIRRUS CLOUDS
NT CUMULONIMBUS CLOUDS
NT STRATOCUMULUS CLOUDS
NT STRATUS CLOUDS
Geostationary satellite observation of convective tropical cloud trajectories and velocity
07 p0814 N73-16602
Moment equations for describing evolution of droplet populations in convection clouds
10 p1180 N73-19595
Precipitation of rain drops from convective clouds over tropical Atlantic Ocean
[NLL-M-22848-[5828.4F]] 16 p1935 N73-25660
Effect of vertical structure of flows on cloudiness of intertropical convergence zone
[NLL-M-23045-[5828.4F]] 21 p2567 N73-30575

**CONVECTION CURRENTS**
Magnetospheric convection, currents feeding polar cap ionosphere, and interplanetary magnetic fields
[NASA-CR-130124] 04 p0413 N73-13375
Nonlinear temperature and vorticity equations for studying convective motions of 4-day zonal circulation of upper Venus atmosphere
17 p2080 N73-26828
Effect of vertical structure of flows on cloudiness of intertropical convergence zone
[NLL-M-23045-[5828.4F]] 21 p2567 N73-30575

**CONVECTIVE FLOW**
Design and development of device to prevent geysering during convective circulation of cryogenic fluids
[NASA-CASE-KSC-10615] 03 p0304 N73-12486
Evolutionary sequences for high-mass stars from zero-age main sequence to end of core helium burning, computed with Ledoux criterion for convective instability
[NASA-TM-X-68914] 07 p0841 N73-16814
Numerical analysis of time dependent natural convection flow within horizontal cylinder based on quasi-compressible Navier-Stokes equations
[NASA-TM-X-69220] 12 p1391 N73-21278
Stability of horizontal layer of binary gas mixture in porous medium with different upper and lower boundary temperatures
16 p1886 N73-25263
Finite difference solution to thermoacoustic convection of fluids in low gravity environment
[NASA-CR-2269] 17 p2014 N73-26289
Solution of laminar natural convection flows of Newtonian fluid in rectangular enclosures by asymptotic expansion
18 p2128 N73-27198
Convection and dispersion patterns associated with stationary and nonstationary fluid transport
18 p2129 N73-27205
Retrevial of dispersive and convective transport phenomena in fluids using time domain analysis
[NASA-TN-D-7240] 19 p2255 N73-28178
Numerical approach to study of convective and semi-convective stability
20 p2470 N73-29836
Characteristics of natural convection induced in cylindrical layer of fluid by uniform heating from below
24 p2902 N73-33163
Heat transfer and wavelength measurement for axisyanmetric flow of fluid layer heated from below
24 p2903 N73-33167

**CONVECTIVE HEAT TRANSFER**
Convective heat transfer for Newtonian fluid cross flow over circular cylinder
[ESDU-69004-AMEND-A] 02 p0241 N73-11962
Parameters and secondary factors governing forced convective heat transfer and turbulent flow in circular tubes
[ESDU-67016] 02 p0242 N73-11964
Forced convective heat transfer for single phase, Newtonian fluid flow in smooth, straight, constant area circular tube
[ESDU-68007-PT-3] 02 p0242 N73-11965
Forced convection heat transfer and burnout measurements with twisted tapes in tubular heat exchangers
[RT/ING-[71]9] 03 p0364 N73-12969
Turbulent convective heat transfer in horizontal liquid layers with volume heating - pt. 1
[DLR-FB-71-39-PT-1] 05 p0606 N73-14927
Turbulent convective heat transfer in horizontal liquid layers with volume heating noting turbulent convection mechanism - Pt. 2
[DLR-FB-71-40-PT-2] 05 p0606 N73-14928
Natural convection in liquid layers of differing density
[AD-750762] 06 p0656 N73-15330
Simultaneous film and convection cooling of plate inserted in exhaust stream of gas turbine combustor
[NASA-TN-D-7156] 07 p0855 N73-16930
Free convection effects in laminar two dimensional wake above isothermal vertical plate cooled by natural convection
08 p0894 N73-17240
Application of gas-pressure bonding to joining components for convectively cooled turbine blades and vanes
[NASA-CR-121090] 08 p0954 N73-17808
Affect of sound and vibration on convective heat transfer and flow distribution on boundary layers of cylindrical bodies
[AD-754006] 10 p1143 N73-19316
Oscillatory and nonoscillatory solutions to equations on nonlinear saturation of convective heat transfer
[AD-754228] 10 p1179 N73-19594
Numerical analysis of time dependent natural convection flow within horizontal cylinder based on quasi-compressible Navier-Stokes equations
[NASA-TM-X-69220] 12 p1391 N73-21278
Convective heat transfer and heat exchange during phase transformation in chemically reacting systems
[AD-756095] 13 p1488 N73-22066
Model developed for opposed free and forced convection flow around heated cylinder
[AD-757993] 15 p1844 N73-24942
Upper bound on heat transfer across porous fluid layer heated from below
16 p1973 N73-25956
Analysis of uniform heat energy generation and conduction heat transfer for semi-infinite thin plate with air blowing over one surface and insulated on other
16 p1973 N73-25959
Interactions of radiation with conductive and convective heat transfer in ablation and boundary layer flow determined by normal mode expansion technique
18 p2128 N73-27200
Analysis of heat exchange between liquid and bodies on which liquid flows during catalytic chemical reactions on surface of bodies
[AD-761607] 19 p2353 N73-28927
Numerical model to simulate vertical mass transfer and stratification in layer of buoyant convection
20 p2391 N73-29208
Convective heat transfer determination for nose region of space shuttle entry configurations, using three dimensional flow field study
[NASA-CR-134057] 23 p2851 N73-32782
Characteristics of natural convection induced in cylindrical layer of fluid by uniform heating from below
24 p2902 N73-33163
Convective heating tests on joints and gaps between surface insulation tiles
24 p2940 N73-33477
Cyclic convective heating evaluation of surface insulation materials for space shuttles
24 p2940 N73-33481
Convective heating effects on properties of glassy surface insulation coatings
24 p2941 N73-33488

**CONVERGENCE**
Influence of CISK process on mass convergence in tropical planetary boundary layer
18 p2171 N73-27529
Convergence improvement in equilibrium calculation using Newton-Raphson method for C, H, N, F system, noting monomethylhydrazine/Fe mixture
[ICT-3/72] 18 p2192 N73-27696

**CONVERGENT-DIVERGENT NOZZLES**
Performance comparison of double cornered plug nozzle with conventional convergent-divergent rocket nozzle
[AD-750591] 06 p0714 N73-15830
Numerical analysis of viscous, compressible, and heat conducting fluid flow patterns in rotating nozzles
07 p0768 N73-16241
Temperature and electrical conductivity of nonequilibrium ionizing gas-particle flow through convergent-divergent nozzle geometry
08 p0947 N73-17752
Effects of nozzle geometry and diaphragm location on starting process in Ludwieg tubes
[AD-755357] 13 p1511 N73-22248
Isentropic frictionless equilibrium flow of evaporating two phase mixtures with low vapor content in convergent-divergent nozzles
[SFB-MHD-5] 22 p2653 N73-31254

**CONVERSION**
Interrelation of martensitic conversion during deformation and structural properties of trip steel
10 p1171 N73-19527

**CONVERSION TABLES**
Tables of conversion factors and physical constants in International System of Units
[NASA-SP-7012] 17 p2098 N73-26969

**CONVERTAPLANES**
U V/STOL AIRCRAFT

**CONVERTERS**
Performance characteristics of solid state converter system for measuring aircraft noise and sonic boom
[NASA-CR-112260] 09 p0982 N73-18019
Automatic frequency control circuit for radiotelemetype receiver-converter
[AD-758686] 16 p1877 N73-25193
Low cost highly sensitive 12 GHz low noise converter for communication between broadcast satellites and ground stations
[NHK-LABS-NOTE-161] 20 p2380 N73-29127

**CONVEXITY**
Delineation of clustered points in two dimensions by measuring perimeters of convex hulls and applicability in fields of geology and geochemistry
[BM-RI-7565] 05 p0568 N73-14616
Presentation of algebra of projections on convex cones in Hilbert space
[AD-761867] 19 p2315 N73-28619

**CONVEYORS**
Mathematical models for developing Coanda eductors for pneumatic conveying systems used in underground excavation
[AD-749088] 05 p0552 N73-14485

**CONVOLUTION INTEGRALS**
Systematic convolutional codes for PCM telemetry
[NASA-TM-X-66085] 02 p0140 N73-11138

**CONVOLUTIONS [MATHEMATICS]**
U CONVOLUTION INTEGRALS

**COOK INLET [AK]**
Sea ice and surface water circulation in Cook Inlet, Alaska, and along continental shelves
[E73-10370] 11 p1275 N73-20346
Mapping of coastal sedimentation and related processes in Cook Inlet, Alaska and distribution and environmental interrelationships of permafrost terrain
[E73-10421] 13 p1515 N73-22275
Mapping permafrost areas of Alaska, correlating snowpack cover of Caribou-Poker Creek with stream

runoff, and mapping and inventorying icing on Chena River
[E73-10511] 13 p1516 N73-22286
ERTS-1 imagery of sea surface circulation and sediment transport in Cook Inlet, Alaska
[PAPER-M8] 19 p2280 N73-28347
Sediment distribution, water currents, and water circulation in Cook Inlet, Alaska
[PAPER-M9] 19 p2281 N73-28348

COOLANTS
NT ENGINE COOLANTS
Cold air experiment in two-dimensional cascade to determine aerodynamic performance of turbine stator blade with suction-surface cooling
[NASA-TM-X-2685] 06 p0713 N73-15818

COOLING
NT AIR COOLING
NT FILM COOLING
NT GAS COOLING
NT LIQUID COOLING
NT QUENCHING [COOLING]
NT REGENERATIVE COOLING
NT SODIUM COOLING
NT SUPERCOOLING
NT SURFACE COOLING
NT SWEAT COOLING
NT THERMOELECTRIC COOLING
Cooling rates of neutron stars with maximum and zero superfluidity
[NASA-TM-X-66101] 02 p0230 N73-11866
Heat transfer and cooling of electronic components and equipment
[AD-746431] 03 p0279 N73-12259
Mathematical model for wall cooling in laminar hypersonic boundary layer
07 p0770 N73-16258
Electron cooling in F2 region at low and midlatitudes, caused by electron-ion collisions and electron impact induced transitions
[RSD-74] 07 p0789 N73-16413
Articles on experimental and theoretical studies of heat transfer and cooling problems of gas turbines
[AD-751513] 07 p0837 N73-16782
Evaluation of sex difference in thermal sensitivity in men and women
[NASA-CR-114564] 08 p0878 N73-17113
Design of katathermometer for measuring environmental cooling effects in simulated space flight
14 p1608 N73-23036
Chilldown tests on single stage inducer test rig
[NASA-CR-132212] 15 p1762 N73-24278
Heat transfer characteristics of impingement-cooled turbine rotor blade
[NASA-TM-X-2791] 15 p1843 N73-24929
Velocity and heat transfer analysis in channels with porous wall for cooling turbine blades
[AD-758782] 16 p1957 N73-25833
Volumetric temperature fields of internally cooled rotating blade
[AD-759246] 16 p1958 N73-25841
Models for radiative heating and cooling and ozone photochemistry in stratosphere
[NASA-CR-132777] 17 p2025 N73-26385
Performance evaluation of model energy separators
[AD-764585] 23 p2798 N73-32381

COOLING FINS
Free convection effects in laminar two dimensional wake above isothermal vertical plate cooled by natural convection
08 p0894 N73-17240

COOLING SYSTEMS
Transients in cooling water systems of thermal power plant discussing mathematical models, computer programs and experiments
[PUBL-101-PT-1] 01 p0041 N73-10326
Hydraulic transients in cooling water system of thermal power plants, figures and computer programs
[PUBL-101-PT-2] 01 p0041 N73-10327
Heat sink and cooling system concepts for space shuttle baseline thermal protection systems
[NASA-CR-123912] 01 p0107 N73-10884
Proceedings of conference to define research requirements for problems involving waste heat transfer from large thermal sources into the environment
02 p0166 N73-11348
Design, development, and performance tests of long pulse liquid laser oscillator and circulatory subsystem
[AD-747964] 03 p0311 N73-12536
Demonstration of duct cooling concept with gaseous hydrogen/oxygen propellant in high pressure thruster - Vol. 2
[NASA-CR-120870] 03 p0350 N73-12859
Light shield and cooling apparatus for high intensity ultraviolet lamps
[NASA-CASE-LAR-10089-1] 04 p0426 N73-13474
Cooling systems using cold gas transfer closed loops in 15 to 80 K temperature range
[DLR-MITT-71-09] 04 p0485 N73-13964
Experimental determination of aerodynamic performance of cooled turbine vanes at gas to coolant temperature ratios up to 2.75
[NASA-TM-X-2733] 08 p0954 N73-17815
Design of porous cooled medium surface to maintain specified design temperature while subjected to uniform heating from external source
[NASA-TN-D-7176] 08 p0969 N73-17919
Aluminum rods for gas cooling requirements of satellite attitude and orbit control using hydrazine as low thrust propellant
[RAE-TR-72161] 09 p0991 N73-18086
Design and tests of passive radiative cooler for spacecraft
09 p1088 N73-18873
Flight tests of portable diaphragm liquid pump for astronaut cooling
09 p1089 N73-18883
Fluid flow analysis in mold heating and cooling control loop
[BDX-613-742] 10 p1142 N73-19303
Development of methods for protecting aircraft compartments from aerodynamic heating effects
[AD-754606] 11 p1236 N73-20036
Design, development, fabrication, and test of coolant circulating pump assemblies for use in Brayton cycle space power system
[NASA-CR-2176] 11 p1297 N73-20529
Increased service life of rolling element radial bearings in nuclear engine for rocket vehicles by liquid hydrogen cooling and bearing modifications
[NASA-CR-132229] 15 p1792 N73-24531
Design of expansion joint unit for coolant piping loop of reactor thermoelectric system - SNAP program
[NASA-CR-121209] 15 p1809 N73-24663
Analysis of coolant flow in transpiration-cooled vanes
[NASA-TN-D-7341] 16 p1974 N73-25966
User guide for computer program to analyze compact transpiration cooling system proposed for hypersonic reentry vehicles
[AD-759698] 16 p1975 N73-25974
Barometric gravity tube discharger for liquid cooling of rocket exhaust gas and analysis of improvement with air vent
[DLR-MITT-73-10] 17 p2011 N73-26262
Helium cooled current leads in refrigerated superconductive magnet system
[DESY-72/65] 17 p2073 N73-26769
Design, development, and fabrication of radiator structure for use with thermoelectric space power systems
[NASA-CR-121222] 17 p2088 N73-26892
Apollo 16 flight anomaly report on malfunction of water/glycol temperature control circuit
[NASA-TM-X-69234] 17 p2089 N73-26900
Development of methods for calculating cooling requirements for gas turbine engines with initial gas temperatures of 750 to 800 C
[AD-760964] 18 p2194 N73-27713
Analysis of thermal fatigue in nontubular regeneratively cooled combustion chambers and prediction of thermal cycle life capability - Vol. 1
[AD-760582] 18 p2194 N73-27715
Temperature characteristics of film cooled and nonfilm cooled vanes incorporating impingement cooling
[NASA-TM-X-2819] 18 p2205 N73-27798
Development of improved cooling system for low-flow gas turbine rotor
[AD-761452] 19 p2330 N73-28743
One dimensional stationary analysis of air cooled, ducted gas turbines nozzle vanes
[AD-761451] 19 p2330 N73-28744
Analysis of earth storable bimodal engine using earth storable propellants and operating in either monopropellant or bipropellant mode
[BELL-8706-933005] 20 p2466 N73-29811
Measurement of temperatures of airfoil immersed in stream of combustion gases to determine effectiveness of two phase cooling system
[ARL/ME-338] 21 p2605 N73-30876
External heat transfer problems under space conditions
[NASA-TT-F-783] 21 p2605 N73-30879
Design, development, and fabrication of liquid cooled space suit using ice pack heat sink - Vol. 1
[NASA-CR-114624-VOL-1] 22 p2622 N73-31006
Operating instructions for functional model icepack heat sink subsystem for cooling system of space suit - Vol. 2
[NASA-CR-114624-VOL-2] 22 p2728 N73-31829
Design of valves for reactor coolant system of nuclear powered aircraft
[SLA-73-221] 24 p2929 N73-33393
Supercritical helium cooling of superconducting magnet for use in dc beam line elements
[RHEL/R-258] 24 p2969 N73-33725

COORDINATE SYSTEMS
U COORDINATES

COORDINATE TRANSFORMATIONS
Nonlinear transformation relating rectangular coordinates to range instrumentation coordinates in guided missile tracking system
[AD-746637] 02 p0144 N73-11163
Navigation with hyperbolic coordinates, and coordinate transformation to geographic and grid coordinates
[SER-C/DISS-176] 10 p1185 N73-19647
Computer solution of transformation parameters between two Cartesian coordinate systems from sets of coordinates given in both systems
[NASA-CR-132210] 17 p2055 N73-26621
Time coordinate transformation for processing asynoptic meteorological data
24 p2945 N73-33521
Azur satellite attitude determination, based on coordinate transformation matrix and angle measurement
24 p2985 N73-33838

COORDINATES
NT ASTRONOMICAL COORDINATES
NT CARTESIAN COORDINATES
NT GEODETIC COORDINATES
NT HYPERBOLIC COORDINATES
NT INERTIAL COORDINATES
NT LAGRANGE COORDINATES
NT PLANETOCENTRIC COORDINATES
NT POLAR COORDINATES
Orthogonal coordinate systems for three dimensional boundary layer calculations on ship hull geometry
[AD-749774] 05 p0529 N73-14301
Finite difference solution to diffusion equation in spherical coordinates
[SCL-DR-72-0017] 06 p0691 N73-15623
Optimal coordinates and boundary layer theory
07 p0767 N73-16234
Most probable position in astronomical navigation using celestial body coordinates
07 p0859 N73-16972
Kalman filtering applied to surface and air navigation using celestial body coordinates
07 p0860 N73-16973
Approximative ephemeris calculations for moving celestial objects using coordinates from different points on earth surface
10 p1178 N73-19587
OSUGOP computer program for adjusting geometrical or optical satellite observations
[NASA-CR-131532] 12 p1448 N73-21728
Application of trilinear coordinates to boundary value problems in plane elasticity
[AD-755181] 13 p1588 N73-22876
Equations of motion for shell developed in general orthogonal coordinates using Hamilton principle
[AD-755239] 13 p1588 N73-22878
Determining accuracy of three dimensional geodetic nets compiled from satellite observations
[NASA-TT-F-776] 16 p1906 N73-25418
Algorithms for solving differential-range bearing in rectangular geocentric system of coordinates
20 p2439 N73-29595
Kinematics of orientation in rotating coordinate system and determination of orientation of instrument trihedrons
[JPRS-59162] 20 p2451 N73-29700
Kinematics of stability of orientation in rotating coordinate system signal processing
20 p2451 N73-29702
Smithsonian astrophysical observatory reference system
[NASA-CR-133829] 21 p2522 N73-30222
System for locating lightning strokes by coordination of directional antenna signals
[NASA-CASE-KSC-10729-1] 23 p2763 N73-32110
Mars surface mapping with Mariner 9 aerographic coordinate system
23 p2843 N73-32720

COORDINATION POLYMERS
Glass transition characteristics and compatibility of linear poly carborane-siloxane series plastics
[AD-749385] 05 p0566 N73-14597

COPERNICUS SPACECRAFT
U OAO 3

COPILOTS
U AIRCRAFT PILOTS

COPOLYMERS
Viscoelastic properties of styrene butadiene plastic homopolymers and styrene-butadiene-styrene block copolymers
[AD-752622] 08 p0936 N73-17660
Characteristics of HALAR fluoropolymer as versatile insulation material
14 p1640 N73-23298
Ultrasonic absorption and dielectric loss as function of temperature in heterophase block copolymers
[AD-762452] 20 p2425 N73-29559

COPPER
NT COPPER ISOTOPES
Influence of shock compression pressure on critical shear in aluminum, copper, and lead
[AD-745365] 01 p0068 N73-10555
High temperature strength and stability of tungsten reinforced copper
[AD-745700] 01 p0071 N73-10581
Recognition of geologic framework for copper porphyry-type deposits on ERTS-1 imagery
[E72-10210] 02 p0161 N73-11305
Monte Carlo method for computer simulation of copper crystal surface dynamics
[AD-745872] 02 p0220 N73-11780
Tight binding interpolation representing transition and noble metal s, p, and d bands applied to Mo and Cu
[IS-T-515] 04 p0434 N73-13535

Photointerpretation of ERTS-1 imagery of Arizona with emphasis on porphyry copper deposits occurring at intersection of major faults and igneous intrusions
[E73-10018] 06 p0659 N73-15354
Recognition of geologic framework of copper and molybdenum porphyry deposits on ERTS-1 imagery of Navada and Utah
[E73-10020] 06 p0659 N73-15356
Pack rolling effects on bond strength between Nb and Cu
[AD-750511] 06 p0678 N73-15517
Influence of surface finishing on adherence of radio frequency sputtered molybdenum disulfide on silver, gold, copper, and bronze
[NASA-TN-D-7169] 07 p0804 N73-16523
Low temperature resistivity of high purity copper wire in high magnetic fields
[U-235] 08 p0943 N73-17725
Influence of preliminary deformation on superplasticity of alpha brasses and pure copper
09 p1047 N73-18534
X ray attenuation coefficients in absorption spectra of titanium, iron, cobalt, nickel, copper, and zinc
[UCRL-73923] 10 p1189 N73-19675
Deformation and different orientation effects on lattice defect energies in copper crystals
[JUL-855-FF] 10 p1194 N73-19713
Interactions of copper lattice atoms with holes, dislocations, and interstitial atoms
[JUL-857-FF] 10 p1194 N73-19714
Gas chromatographic separation of beryllium [II], copper [II], aluminum [III], and chromium [III] chelates
[NLL-M-22879-[5828.4F]] 11 p1252 N73-20158
Search for porphyry copper deposits in Pakistani Baluchistan using ERTS-1 imagery
[E73-10410] 11 p1278 N73-20372
Sliding friction experiments in air with polycrystalline copper and ruby riders
[NASA-TN-D-7232] 11 p1298 N73-20530
Role of plastic deformation process in sliding wear of pure Cu and Cu-Al alloy against Type 440 C in cryogenic fuels
[NASA-TN-D-7253] 11 p1305 N73-20591
Creep processes in vacuum sintered copper and silver
12 p1407 N73-21407
Effects of carbon and copper on magnetic properties of iron and iron-silicon alloys
[NASA-TT-F-14857] 12 p1428 N73-21574
Recognition of characteristic geological structures associated with mineral deposits of copper molybdenum porphyry type
[E73-10526] 13 p1517 N73-22293
Measurement of thermal changes encountered during plastic deformation of copper using photon detection system
[AD-756416] 13 p1543 N73-22510
Accelerated life tests of copper/acetone heat pipe for meteorological satellite temperature control, including thermal cycling tests
14 p1719 N73-23948
Magnetic field effects in cathode mechanism of electric arc initiation and travel between copper electrodes
[NLL-CE-TRANS-6108-[9022.09]]
15 p1755 N73-24226
Copper coating of welded aluminum spacecraft structures to resist oxidation and aid detection of incomplete penetration
[NASA-CR-124251] 15 p1791 N73-24515
Kinetic study of copper cementation on iron
[BM-RI-7761] 15 p1791 N73-24519
Nondestructive tests for predicting effect of copper and aluminum microstructure on acoustic emission
[AD-758216] 15 p1800 N73-24587
Creep test measurement of stresses generated during high temperature oxidation of copper and nickel
16 p1926 N73-25588
Measurement of work functions of copper and copper-nickel single crystals at low pressures and determination of thermionic emission constant
16 p1927 N73-25593
Service life extension of cyclically loaded copper specimens by application of electroplated layers of nickel
16 p1927 N73-25595
Specific heat measurements of He-4 monolayers on sintered and gas monolayer coated copper
16 p1973 N73-25957
Identification of copper/molybdenum porphyry mineral deposits in characteristic geologic setting in Nevada, Arizona, Colorado, Australia, Alaska, and New Guinea
[E73-10762] 17 p2023 N73-26362
Plastic properties of alpha-phase Cu-Al single crystals at low and room temperature
17 p2042 N73-26524
Identification of geomorphic features related to known porphyry copper deposit in Pakistan using ERTS-1 imagery
[PAPER-G17] 19 p2265 N73-28248
Development of techniques for welding copper and copper-base alloys with application to waveguides in electron accelerator facility
[SLAC-PUB-1095] 19 p2305 N73-28533
X ray diffraction analysis of single crystals of high purity copper subjected to shock loading
[AD-762146] 19 p2311 N73-28586
Exploration for copper porphyry deposits in West Pakistan using ERTS-1 imagery
[E73-10954] 21 p2531 N73-30296
Recognition of geologic framework for ERTS-1 identification of mineral deposits of copper/molybdenum prophyry type in Colorado, Nevada, Arizona, and Australia
[E73-10960] 21 p2532 N73-30302
Effect of copper and silicon on selected mechanical properties of hot rolled medium carbon steels
[BM-RI-7777] 21 p2558 N73-30504
Temperature effects on copper plasticity failure, noting hydrogen role
[DRIC-TRANS-3009] 22 p2685 N73-31508
Superconductivity of copper containing small amounts of niobium
[CALT-822-50] 22 p2707 N73-31679
X ray and electron microscopic studies on fatigue life of copper and copper zinc polycrystals
23 p2803 N73-32416
Fatigue behavior of annealed high-conductivity copper and effects of single and periodic intermediate surface layer removal
23 p2803 N73-32419
Wavelength modulation spectra of copper, gold, silver, gallium phosphide, and indium phosphide
[LBL-1125] 24 p2927 N73-33375

**COPPER ALLOYS**
NT BRASSES
NT BRONZES
NT MANGANIN [TRADEMARK]
Effect of charge materials, melting condition, and type of melting equipment on hydrogen gas contained in copper alloys
[AD-745845] 01 p0068 N73-10558
Oxidation rate and compatibility of tungsten filament copper matrix composites
[AD-745324] 01 p0069 N73-10569
Effect of heat treatment on fatigue life under gust loads of notched Al-Cu alloy
[ARC-CP-1221] 05 p0563 N73-14571
Analysis of wear resistance of copper alloyed, magnesium cast iron by reciprocating motion of different friction pairs
[AD-750519] 06 p0687 N73-15590
Effect of degree of saturation on susceptibility to onset of plastic instability in pure shear for solid solution of copper-zinc system
[COO-2048-6-PT-2] 08 p0967 N73-17901
Aluminum-copper eutectic solidification experiment to be run in M518 multipurpose electric furnace during Skylab mission
[NASA-CR-124103] 09 p1045 N73-18526
Effect of annealing on substructure of cold worked FCC copper alloys and metals
[COO-1431-14] 10 p1173 N73-19540
X ray diffraction analysis on microstructure defects in explosively loaded copper germanium alloy
[COO-1431-15] 10 p1173 N73-19541
Mossbauer analysis of spin arrangements in gold iron and copper iron alloys at low temperature
[AD-754140] 10 p1202 N73-19787
Properties of zinc-copper-titanium alloys to include microstructure composition, mechanical properties, and effects of hot and cold deformation
[NLL-M-22842-[5828.4F]] 11 p1304 N73-20583
Role of plastic deformation process in sliding wear of pure Cu and Cu-Al alloy against Type 440 C in cryogenic fuels
[NASA-TN-D-7253] 11 p1305 N73-20591
Silicon additions and borax-glass coatings used to reduce surface hot shortness of copper-bearing steels
[PB-212660] 11 p1307 N73-20607
Low alloy copper welding rods used as welding materials for argon arc welding of copper
[DRIC-TRANS-3008] 12 p1409 N73-21416
Copper alloys with necessary heat resistance and electrical conductance for use as welding electrodes
[AD-758618] 15 p1800 N73-24590
Measurement of work functions of copper and copper-nickel single crystals at low pressures and determination of thermionic emission constant
16 p1927 N73-25593
Corrosion resistant copper zinc alloys for desalinization systems
[PB-215265/0] 16 p1929 N73-25610
X ray analyses of atomic structures in diffusion zones of copper nickel alloys and copper silver alloys
[AD-759195] 16 p1930 N73-25616
Square sectioned single crystals of Cu-Al alloys at low temperature
17 p2043 N73-26525
Internal oxidation of dilute Cu-Ti alloys at 700 to 900 C
[AD-759382] 17 p2047 N73-26557
Development of procedure for argon arc welding of copper using complex alloy wire and comparison with other welding techniques
[NLL-DRIC-TRANS-3008-[3623.66]]
18 p2154 N73-27404
Low energy electron diffraction and auger spectroscopy of [100] surfaces of aluminum and aluminum-copper alloys
18 p2159 N73-27445
Production of high power arc lamp cathodes by casting copper body on thoriated tungsten insert
[NASA-TM-X-2865] 18 p2160 N73-27451
Development of techniques for welding copper and copper-base alloys with application to waveguides in electron accelerator facility
[SLAC-PUB-1095] 19 p2305 N73-28533
Optical determination of electronic structure of Au-Cu alloys in disordered and ordered phases
[AD-763239] 21 p2586 N73-30720
Thermotransport of copper in liquid Al-Cu alloys
[NASA-TR-R-415] 22 p2625 N73-31030
Interstitial and vacancy motion in defect annealing of alpha brass and copper gold alloy by electron irradiation
22 p2683 N73-31489
Determining mechanical properties of high conductivity metals and alloys
[NASA-CR-133890] 22 p2684 N73-31498
Determining thermodynamic properties of liquid copper-magnesium alloys by magnesium vapor pressure
[BARC-613] 22 p2685 N73-31504
Precipitation hardening of copper alloys and iron
[AD-764150] 22 p2686 N73-31516
Potentiostatic tests for determining range of crevice corrosion susceptibility in chromium modified cupronickel alloys
[AD-762596] 22 p2687 N73-31524
Casting and heat treatments for fabricating ductile superconducting copper base alloys
[CALT-822-51] 22 p2707 N73-31678
Isothermal and athermal martensitic transformation in beta copper zinc alloys
23 p2803 N73-32417
Reflectometer for measuring compositional modulation of copper based alloys at room temperature
23 p2803 N73-32418
Short-term tensile and low-cycle fatigue behavior of zirconium-copper at 482C to 593C
[NASA-CR-121260] 24 p2934 N73-33430
Impurity resonances in dilute copper cobalt alloy, aluminum manganese alloy, and copper vanadium alloy at low temperatures
24 p2960 N73-33655

**COPPER CHLORIDES**
Measurement of resonant second harmonic generation in exciton of copper chloride and zinc oxide using Q-switched ruby laser
20 p2424 N73-29474

**COPPER COMPOUNDS**
NT COPPER CHLORIDES
NT COPPER SULFIDES
Crystal growth and magnetic properties of transition metal chalcogenides
[AD-748864] 04 p0459 N73-13748
Discharge compositions of gas laser emissions from mercury and copper halides
[AD-749938] 05 p0559 N73-14541
Variation of electric conductivity and thermal emf at fusion of copper chalcogenides
[AD-756088] 13 p1566 N73-22694
Plastic flow and fracture mechanics of brittle cuperious oxide and gamma 2Cu-Al compounds under high pressure
24 p2967 N73-33709

**COPPER ISOTOPES**
Angular distributions of elastically and inelastically scattered 42 MeV alpha particles from Cu-65
[NASA-TN-D-7354] 18 p2181 N73-27611

**COPPER SULFIDES**
Optical and electronic properties of single crystal Cu2S-CdS photovoltaic cells
[NASA-CR-121228] 15 p1738 N73-24091

**CORDAGE**
Variable principle for analyzing torsion of fluted bar with rope like cross section
[AD-752059] 08 p0928 N73-17598
Performance tests of commercial nylon double braided rope for extraction lines
[AD-757209] 14 p1681 N73-23643

**CORDITE**
U COLLOIDAL PROPELLANTS
U DOUBLE BASE PROPELLANTS

**CORE FLOW**
Wake development on models of elliptic, rectangular, swept and delta planforms when plunged in water
[ARC-CP-1238] 24 p2870 N73-32932

**CORE SAMPLING**
Stratigraphy of Apollo 15 drill core
[NASA-TM-X-58101] 05 p0595 N73-14839

**CORE STORAGE**
Sense amplifier of ferrite coincident core memory
[AD-752817] 09 p1009 N73-18235
Hypermatrix core storage problem solved by triangularization method
[ISD-112] 09 p1058 N73-18624
Development of nickel-iron plated wires for computer memories
[ME-72-6] 13 p1498 N73-22139

Effects of chemical etching on magnetic and storage properties of Permalloy memory films
18 p2178 N73-27589
CORES
NT EARTH CORE
NT HONEYCOMB CORES
NT LUNAR CORE
NT MAGNETIC CORES
NT REACTOR CORES
CORIOLIS EFFECT
Dynamic model of rotating spacecraft force effects on human vestibular system
01 p0015 N73-10119
Effect of space flight on origin, physiological function, and amelioration of coriolis illusion in semicircular canal
[AMRU-R-70-6] 02 p0131 N73-11063
Hypoxia effects on human vestibular tolerance during exposure to coriolis accelerations
03 p0258 N73-12092
Influence of coriolis effect on energy transfer in mixed flow rotor cascades
[ARC-R/M-3703] 03 p0285 N73-12306
Approximate dispersion relationship of hydrodynamic waves in thin rotating spherical shells of incompressible fluid pervaded by uniform magnetic field
[MET-O-857] 06 p0699 N73-15702
Simplified steady boundary layer flows at low altitudes, with small Coriolis parameter
07 p0776 N73-16297
Determination of angular acceleration equivalent to effect of coriolis acceleration on receptors of semicircular canals
11 p1246 N73-20112
Biaxial simulator imposing standardized coriolis stimuli for selection, test, and rehabilitation of motion sick pilots
12 p1368 N73-21098
Application of perturbation theory and Ritz energy method for analyzing nonlinear flexural gyrations of untwisted, rotating cantilevered blade vibrating in plane of rotation
16 p1968 N73-25923
Laboratory investigation of Coriolis acceleration effects on vestibular apparatus of cosmonauts
[NASA-TT-F-15129] 22 p2620 N73-30993
CORN
Meteorological satellites for detecting and aiding southern corn leaf blight disease
06 p0693 N73-15645
Multispectral remote sensing techniques for identification of corn blight disease
[NASA-TM-X-69055] 07 p0745 N73-16064
Handling and analysis of remote sensing data on 1971 corn blight
[NASA-CR-130368] 07 p0759 N73-16164
Multispectral data and computer processing technique for mapping soil patterns and multispectral radiation changes from corn crop canopy
[NASA-CR-130035] 07 p0789 N73-16420
Anomalous scattering effects of haze layer in remote sensing data on corn blight distribution
[NASA-CR-130028] 07 p0790 N73-16428
Atmospheric effects on recognition of rice and corn in ERTS-1 imagery of Sacramento Valley
[E73-10390] 11 p1276 N73-20352
Identification of corn harvesting in Finney County, Kansas from ERTS-1 imagery
[E73-10472] 12 p1395 N73-21309
Spectral characteristics of normal and nutrient-deficient maize leaves
[NASA-CR-132145] 15 p1742 N73-24119
Absorption of direct solar radiation in maize as function of leaf area index and sums altitude
20 p2404 N73-29320
CORNERS
Finite difference solution for supersonic laminar flow over two dimensional compression corner
08 p0894 N73-17241
Nonlinear partial differential equations for studying viscous compressible corner flow at subsonic and supersonic Mach numbers
15 p1764 N73-24294
CORONA DISCHARGES
U ELECTRIC CORONA
CORONAS
NT ELECTRIC CORONA
NT SOLAR CORONA
Static planar model for explaining structure and thermal conduction heating of chromosphere-corona transition region
12 p1444 N73-21699
Variations in solar wind He-4 ion abundance occurring primarily in lower corona
23 p2834 N73-32643
CORPUSCULAR RADIATION
NT BETA PARTICLES
NT CYCLOTRON RADIATION
NT ELECTRON BEAMS
NT ELECTRON PRECIPITATION
NT ELECTRON RADIATION
NT ION CYCLOTRON RADIATION
NT PRIMARY COSMIC RAYS
NT RADIATION BELTS
NT SOLAR CORPUSCULAR RADIATION
NT SOLAR COSMIC RAYS
NT SOLAR ELECTRONS
NT SOLAR PROTONS
Cosmos-378 data on solar cosmic ray penetration into earth polar caps
24 p2976 N73-33782
CORRECTION
NT OPTICAL CORRECTION PROCEDURE
Digital correction techniques for ERTS-1 imagery
[E72-10206] 02 p0161 N73-11303
Reference atmosphere mean temperature and altimetric corrections
07 p0859 N73-16963
Diffraction correction calculations for rectangular ultrasonic transducer
[AD-754677] 11 p1263 N73-20247
Effects of porous wind tunnel wall corrections on transport aircraft models
14 p1648 N73-23366
Transonic wind tunnel corrections for slotted or perforated walls
14 p1649 N73-23373
Kirchhoff approximation correction for application to electromagnetic wave scattering by rough surfaces
[NASA-CR-112263] 16 p1875 N73-25180
CORRELATION
NT ANGULAR CORRELATION
NT AUTOCORRELATION
NT CORRELATION COEFFICIENTS
NT CORRELATION DETECTION
NT CROSS CORRELATION
NT DATA CORRELATION
NT SIGNAL ANALYSIS
NT STATISTICAL CORRELATION
Correlation of total precipitable water in atmosphere with surface absolute humidity for California and Pacific Ocean islands
[AD-745954] 02 p0206 N73-11666
Correlation of assessed maximum oxygen intake with predicted performance in running events
[AD-746867] 04 p0380 N73-13093
Correlation properties of Gaussian random processes under nonlinear transformations
09 p1057 N73-18619
On-line programming to measure correlations in plasma using fast buffer memory and digital analysis
[IPPJ-T-12] 09 p1070 N73-18729
Correlation of sonic boom pressure signatures recorded during reentry of Apollo 16 command module with wind tunnel signatures
[NASA-TM-X-62073] 12 p1365 N73-21073
Correlation functions for displacements in semiboundless isotropic elastic media
[ITF-72-78-P] 12 p1429 N73-21579
Critical exponents for charged and neutral Bose gases above Lambda points
[AD-756022] 12 p1430 N73-21587
Simplified procedures for correlation of experimentally measured and predicted thrust chamber performance
[NASA-CR-131519] 12 p1442 N73-21685
Method for determining correlation function of normalized random processes
13 p1504 N73-22189
Correlation of solar magnetograms with interplanetary magnetic field
[NASA-CR-131607] 13 p1577 N73-22775
Correlation processing of phase modulated signals
14 p1619 N73-23115
Synthesis and analysis of systems combining extreme principle of control with correlation processing of signals entering from object being controlled
14 p1644 N73-23334
Design and analysis of Type 2 correlation-extreme systems composed of control circuits and gages for measuring random functions
14 p1644 N73-23335
Method for calculating correlation functions of diurnal precipitation totals and their space time variability over uniform relief
21 p2573 N73-30619
Correlation parameters for velocity, temperature and concentration of coaxial, heterogeneous, compressible free jet cores
24 p2907 N73-33201
CORRELATION COEFFICIENTS
Correlation techniques and measurements of surface wave height statistics
[NASA-CR-2153] 04 p0405 N73-13298
Correlation coefficient between D region HF radio wave absorption and 10mb level winds and temperature in Northern Hemisphere
[COO-2195-5] 05 p0539 N73-14384
Application of scale autocorrelation coefficients to atmospheric and geophysical measurements
[AD-750476] 06 p0695 N73-15661
Six-day variation in cosmic ray intensity recorded at different astronomical observatories
07 p0859 N73-16967
Prediction of F 2 region critical frequencies from spatial and temporal correlation data
13 p1520 N73-22320
Time dependent correlation functions between magnetohydrodyuamics and space transport coefficients
13 p1562 N73-22660
Estimates of meteorological autocorrelation and cross-correlation functions
[NLL-M-22887-[5828.4F]] 16 p1934 N73-25646
Specialized digital computer for correlation analysis
[AD-761586] 19 p2241 N73-28066
CORRELATION DETECTION
Correlation methods for radio signal processing in presence of interference noise
09 p1002 N73-18181
Linear filtration effect on correlation properties of phase manipulated signals
12 p1378 N73-21175
Phase detector with time correlation integrator for frequency multiplexed signals
[NASA-CASE-GSC-11744-1] 14 p1640 N73-23291
Digital filter with dither for correlation detection of weak signal in jamming environment
[AD-757013] 14 p1643 N73-23325
Correlation receivers for detecting binary array signals with directional interference
22 p2627 N73-31047
CORRELATION FUNCTIONS
U CORRELATION
CORRELATORS
NT IMAGE CORRELATORS
Onboard digital correlator for spacecraft VLF radio wave studies
04 p0423 N73-13446
Design and operation of coherent analyzer
[NASA-TT-F-14595] 06 p0673 N73-15476
Digital optical hybrid correlator for processing pulse Doppler and wideband radar signals
[AD-751695] 07 p0756 N73-16143
Noise characteristics of functional correlators using nonlinear elements with exponential characteristics
12 p1386 N73-21241
Construction method for radio signal correlators using Fourier transformation
13 p1497 N73-22131
Hybrid autocorrelator for high altitude incoherent scatter observations
20 p2417 N73-29417
CORRIDORS
NT GREAT PLAINS CORRIDOR [NORTH AMERICA]
CORROSION
NT CAVITATION CORROSION
NT ELECTROCHEMICAL CORROSION
NT INTERGRANULAR CORROSION
NT SCALE [CORROSION]
NT STRESS CORROSION
Oxidation rate and compatibility of tungsten filament copper matrix composites
[AD-745324] 01 p0069 N73-10569
Deterioration in sea water of materials and underwater system components
[AD-747245] 02 p0194 N73-11567
Chemical diffusion coefficient of oxygen in mixed niobates to determine feasibility of modifying oxide defect structures to enhance oxidation protection of elevated temperature materials
[AD-746834] 03 p0316 N73-12574
Effects of sodium salts on hot corrosion mechanism in Ni-8Cr-6Al
[AD-748349] 04 p0435 N73-13551
Corrosion kinetics of Ti-Pd alloy in HCl at room temperature determined by radioactive tracer method
[NLL-TRANS-746-1328-[9022.401]] 05 p0505 N73-14112
Corrosion behavior of structural materials during condensation of alkylphenol with formalin and ammonia
[AD-751249] 07 p0753 N73-16119
Influence of Na2SO4 oxidation of Ni-20Cr-2ThO2 gas turbine corrosion
[AD-751259] 07 p0810 N73-16573
Dispersion effects of heat resistant metal oxides
[AD-754760] 11 p1306 N73-20595
Effect of reverse abrasive friction exoelectron emission and steel corrosion
[AD-754666] 11 p1307 N73-20603
Preparation of metal-oxide-hydroxide protective layers under controlled pO2-pH2O-T conditions
[AD-755729] 13 p1544 N73-22514
Analysis of effects of alternating current on corrosion of iron in aqueous solutions of acidic and neutral salts
[REPT-733] 14 p1675 N73-23590
Physical and chemical properties of nickel alloys following cyclic and isothermal oxidation
[NASA-TN-D-7267] 14 p1675 N73-23594
Conference on high temperature corrosion of alloys for aerospace applications
[AGARD-CP-120] 14 p1675 N73-23597
High temperature corrosion scale for heat resistant alloys
14 p1676 N73-23598
Performance of aircraft gas turbine components in hot corrosion environments
14 p1676 N73-23599
Thermodynamic stability diagrams of high temperature O2 corrosion reactions
14 p1676 N73-23602
Comparison of cobalt alloys and nickel alloys relative to hot corrosion resistance
14 p1677 N73-23612

Influence of active and passive electrolyte solutions on corrosion of aluminum alloys
15 p1746 N73-24154
Microhardness and corrosion resistance of Zr-Nb alloy prepared by reaction of ZrC with Nb2O5
[BARC-612] 15 p1799 N73-24583
Corrosion fatigue crack growth of high strength steels in hydrogen and water/water vapor environments
[AD-759088] 16 p1930 N73-25615
Effect of heat treatment on corrosion of titanium alloy
[AD-759626] 16 p1931 N73-25621
Effect of applied electric field on oxidation/hot corrosion of metals and alloys in molten salt
[AD-762074] 19 p2311 N73-28584
Wedging corrosion and mass transport in sodium/zirconium/stainless steel system at high temperature - Part 1
[RD/B/N-2521-PT-1] 21 p2559 N73-30517
Influence of carbon stabilizing elements and temperature on cold worked austenitic stainless steel corrosion
[CEA-CONF-2119] 21 p2560 N73-30518
Stress and corrosion effects on fatigue behavior 7075-T6 aluminum alloy
[AD-763455] 21 p2560 N73-30525
Stainless steel and Hastelloy corrosion by boron trifluoride, air, and argon mixtures
[ORNL-TM-4172] 24 p2892 N73-33087
Electrochemical study of corrosion of high strength alloys in contact with Zircaloy-4
[BMI-X-10260] 24 p2936 N73-33449

**CORROSION PREVENTION**
Calculated relationships of potential distribution over ship hulls for electrochemical protection from seawater corrosion
[DRIC-TRANS-2877] 02 p0149 N73-11208
Corrosion control design optimizing layouts, orientation, location, and configuration
[BNWL-SA-3817-REV-1] 04 p0434 N73-13539
Effect of transition zone on mechanical properties of high strength steel after cladding with thin layer of highly ductile material
[NLL-TRANS-746-1323-[9022.401]] 05 p0560 N73-14552
Passivating effects of additives on zinc corrosion in potassium hydroxide solutions
[NASA-TT-F-14693] 08 p0884 N73-17155
Aircraft corrosion prevention by addition of potassium dichromate to rinse water
[AD-753214] 09 p0986 N73-18050
Conductive, lusterless coatings for light metals with improved corrosion durability
[AD-753360] 09 p1054 N73-18594
Chemical composition and structure of metal surface corrosion protective chelate coatings
[DRIC-TRANS-3020] 14 p1616 N73-23095
Mossbauer spectroscopy studies of passivation and corrosion inhibition of metals
[AD-757705] 14 p1679 N73-23626
Corrosion and protective properties of organic complex-forming agents which produce insoluble chelate compounds with various metal surfaces
[DRIC-TRANS-3079] 17 p2046 N73-26551
Corrosion prevention mechanism of benzotriazole inhibitors for zinc and cadmium
[DRIC-TRANS-3080] 17 p2046 N73-26552
Dry inert gas glove box for handling of hygroscopic and corrosive materials in spectroscopic and lasers experiments
[CRC-1244] 21 p2548 N73-30430

**CORROSION RESISTANCE**
NT OXIDATION RESISTANCE
Effect of chemical composition, method of heat treatment, and production methods, on corrosion resistance of metal sheets
[AD-742106] 01 p0067 N73-10550
Laboratory tests to determine corrosion failure mechanisms in electronic equipment exposed to humid tropical environments
[AD-747757] 03 p0279 N73-12261
Influence of grain size and cold working on static corrosion of Incoloy 800 alloy in superheated steam
[EURFNR-965] 03 p0315 N73-12570
Improved oxidation resistance of dispersion strengthened nickel-chromium alloys and thermomechanical procedure to produce course grain microstructure
[AD-748266] 04 p0436 N73-13556
Intergranular corrosion resistance of matching and dissimilar welds in nitrogen-bearing and nitrogen-free austenitic steels
[NLL-TRANS-746-1313-[9022.401]] 05 p0560 N73-14546
Effect of ruthenium on passivating capacity and corrosion resistance of titanium
[NLL-TRANS-746-1375-[9022.401]] 05 p0560 N73-14550
Procedures for cleaning materials and producing corrosion resistant epoxy plastics
[AD-752039] 08 p0936 N73-17664
Seven year tropical exposure test to evaluate corrosion resistance effectiveness of finishing systems for aluminum and magnesium
[AD-752907] 09 p1042 N73-18498
Cavitation-corrosion resistance tests of tin and aluminum bronzes used for marine pumps in synthetic sea water and distilled water
[DRIC-TRANS-3016] 10 p1167 N73-19492
Determination of corrosion resistance of coatings on low alloy steel and susceptibility to exfoliation of 7178 aluminum alloy using Lawrence corrosion detection gauge
[AD-755163] 13 p1531 N73-22405
Fracture toughness and aqueous stress corrosion resistance of high strength commercial Ti alloy
[NLR-TR-72107-U] 13 p1542 N73-22492
Visual and microscopic studies on corrosion resistance of anodized aluminum sheets
[M72-09-96-REI/BLA/PUT] 14 p1675 N73-23592
Corrosion resistant materials for nozzle guide vanes and turbine blades subject to vanadium containing fuel combustion
14 p1678 N73-23613
Methods of oxidation and corrosion resistance in refractory metal alloys used in gas turbine engines
14 p1678 N73-23617
NATO national reports on high temperature corrosion of aerospace alloys
14 p1678 N73-23618
Corrosion resistant copper zinc alloys for desalinization systems
[PB-215265/0] 16 p1929 N73-25610
Corrosion resistant properties of titanium alloys
[AD-759621] 16 p1931 N73-25622
Corrosion resistance of gas turbine components of power plant fueled with shredded refuse
[PB-221095/3] 21 p2591 N73-30759
Potentiostatic tests for determining range of crevice corrosion susceptibility in chromium modified cupronickel alloys
[AD-762596] 22 p2687 N73-31524

**CORROSION TESTS**
NT SALT SPRAY TESTS
Corrosion behavior of interstitial alloying elements in canning steels for sodium cooled fast breeder reactor
[NLL-RISLEY-TR-2444-[9091.9F]] 02 p0209 N73-11693
Corrosion tests of inhibitors for protection of aluminum
[AD-749705] 06 p0689 N73-15606
Corrosion tests of candidate rocket engine materials exposed to standard high density acids for liquid propellant compatibility determination
[AD-749965] 06 p0712 N73-15807
Corrosion of heat pipes
[NASA-TT-F-14689] 08 p0969 N73-17918
Corrosion behavior of titanium alloys in chloride solutions
[AD-753573] 09 p1050 N73-18561
Summary of conference on stress corrosion testing methods
[AGARD-AR-52] 09 p1094 N73-18931
Effect of oxygen on corrosion of niobium and tantalum by liquid lithium at 600 C
[ORNL-TM-4069] 17 p2045 N73-26547

**CORRUGATED PLATES**
Pressure drop in plate heat exchangers with corrugations
[NLL-RTS-7505] 02 p0241 N73-11960
Fatigue behavior of corrugated panels, riveted along corrugations, subjected to cyclic compressive critical loads
[PUBL-1351] 06 p0724 N73-15915
Calculation of heat transfer coefficients of laminar incompressible boundary layer to corrugated wall, with application to combustion chamber liquid film cooling
[DLR-FB-73-07] 12 p1465 N73-21868
Determination of flutter characteristics for arbitrary yaw angles with two types of corrugation-stiffened panels
[NASA-CR-2265] 14 p1714 N73-23910

**CORRUGATING**
Effects of surface corrugation in horn antenna power loss
[NASA-CR-2317] 23 p2756 N73-32059

**CORSAIR AIRCRAFT**
U A-7 AIRCRAFT

**CORTEXES**
Neuronal changes in cortical motor region cells during pharmacological induced sleep
13 p1483 N73-22028

**CORTICOSTEROIDS**
NT ALDOSTERONE
NT HYDROXYCORTICOSTEROID
Chromatographic determination of urine corticosteroids
[RAE-LIB-TRANS-1694] 17 p1987 N73-26062

**CORUNDUM**
U ALUMINUM OXIDES

**COSINE**
U TRIGONOMETRIC FUNCTIONS

**COSINE SERIES**
Function generators for producing complex vibration mode patterns used to identify vibration mode data
[NASA-CASE-LAR-10310-1] 11 p1263 N73-20253

**COSMIC DUST**
NT INTERPLANETARY DUST
NT ZODIACAL DUST
Monochromatic isophote determination of particle distribution in bright comet
22 p2735 N73-31898

**COSMIC GASES**
NT INTERSTELLAR GAS
Characteristics of solar wind and interaction with interstellar plasma and magnetic field
01 p0099 N73-10811

**COSMIC PLASMA**
Observations of solar plasma using interplanetary scintillation techniques and radio scattering methods
01 p0097 N73-10801
Variations of interplanetary scintillation index with wavelength in accordance with smooth, power law spectrum of plasma fluctuations
01 p0097 N73-10802
Effect of sputtering corotating source of thin solar plasma streams on electron content of solar wind
01 p0098 N73-10805
Analysis of solar wind composition obtained by plasma analyzers mounted on various spacecraft
01 p0098 N73-10806
Analysis of isotopic composition of solar wind based on collecting foils and lunar material
01 p0098 N73-10807
Characteristics of solar wind and interaction with interstellar plasma and magnetic field
01 p0099 N73-10811
Ionization of gas emitted by comets
02 p0228 N73-11844
Analyses of solar wind plasma data obtained by Explorer 33 and Explorer 35
[NASA-CR-129923] 05 p0592 N73-14807
Hydromagnetic waves and trapped particle discontinuities in magnetopause
[NASA-TM-X-66146] 06 p0665 N73-15405
Perpendicular fast reverse shock wave found in interplanetary plasma and magnetic field data from Explorers 33 and 35
[NASA-TM-X-70451] 21 p2523 N73-30235
Self-contamination of manned orbiting spacecraft from plasma gas or particulate matter
[NASA-CR-133836] 21 p2601 N73-30843
Forces and torques on satellites moving through rarefied plasmas
23 p2847 N73-32752

**COSMIC RADIATION**
U COSMIC RAYS

**COSMIC RADIO WAVES**
U EXTRATERRESTRIAL RADIO WAVES

**COSMIC RAY SHOWERS**
Detection of large cosmic ray showers by atmospheric fluorescence
[NYO-3038-13] 05 p0593 N73-14822
Physics of high energy particles, cosmic showers, modulation of cosmic rays, high atmospheric meteorology, and application of solar radiation to other areas
[NP-19366] 10 p1211 N73-19847
Results of multijoule air shower fluorescence experiment
13 p1573 N73-22743
Cosmic ray air shower investigations with Haverah Park array
[HPNL-8] 13 p1573 N73-22749
Large cosmic ray air shower, primary energy spectrum, obtained from structure, size, and flux measurements
13 p1573 N73-22750
Arrival directions and anisotropies of large cosmic ray air showers of primary energy larger than 100,000 TeV
13 p1573 N73-22751
Nuclear interaction models for cosmic ray air showers to determine lateral distribution of particles and fluctuations in particle densities
13 p1574 N73-22752
Ground antenna total electric field strength of RF emission from cosmic ray air showers at three VHF frequencies
13 p1574 N73-22753
Muon production altitude in cosmic ray air showers from lateral and angular muon separation from shower core, and geomagnetic effects on muon charge ratio
13 p1574 N73-22754
Comsic ray air shower muon momentum spectra, noting dependence on shower primary energy, zenith angle, and arrival directions
13 p1574 N73-22755
Results from Nottingham cosmic ray air shower muon detector
13 p1574 N73-22756
Hadronic component of cosmic ray shower and relation to shower size, using calorimeter
13 p1574 N73-22757
Cloud chamber study of cosmic ray air shower multicore structure
15 p1827 N73-24810

**COSMIC RAYS**
NT COSMIC RAY SHOWERS
NT PRIMARY COSMIC RAYS
NT SECONDARY COSMIC RAYS
NT SOLAR COSMIC RAYS

Dourbes [Belgium] Geophysical Observatory data on geomagnetism, ionospheric propagation, seismology, cosmic rays, and atmospheric electricity, Nov. 1971
01 p0050 N73-10401
Ionospheric sounding and cosmic ray neutron flux density tables, Dourbes, Belgium, Feb. 1972
01 p0050 N73-10402
Dourbes [Belgium] Geophysical Observatory data on geomagnetism, ionospheric propagation, seismology, cosmic rays, and atmospheric electricity, Dec. 1971
01 p0050 N73-10405
Uncorrected and barometer-corrected hourly rate data on cosmic ray neutrons at Deep River, Ontario - 1960
[AECL-4209] 01 p0092 N73-10758
Development of method for distinguishing between phenomena related to solar wind and those related to solar extreme ultraviolet emission
01 p0099 N73-10816
References to measurements of cosmic ray intensity in and above atmosphere during solar cycles and high energy cosmic ray interactions at sea level
[AD-745331] 01 p0100 N73-10821
Ionospheric sounding and cosmic ray neutron flux density tables, Dourbes, Belgium, Mar. 1972
02 p0166 N73-11352
Spectrum of total diffuse and discrete cosmic gamma ray background over 0.3 to 27 MeV range
[NASA-TM-X-66104] 02 p0225 N73-11818
Geophysical and space data reported from sites throughout the world
[AD-746290] 02 p0226 N73-11822
Bibliography of articles on cosmic X ray astronomy from Astrophysical Journal
[NASA-TM-X-64705] 02 p0230 N73-11869
Dourbes [Belgium] Geophysical Observatory data on geomagnetism, ionospheric propagation, seismology cosmic rays, and atmospheric electricity, Jan. 1972
SEISMOLOGY IONOSPHERIC PROPAGATION
03 p0296 N73-12416
Ionospheric sounding and cosmic ray neutron flux density tables, Dourbes, Belgium, Apr. 1972
03 p0297 N73-12420
Positive diffuse cosmic gamma ray flux measurements for energies to 100 MeV range
[NASA-TM-X-66109] 03 p0353 N73-12877
Uncorrected and barometer-corrected cosmic neutron data for Deep River, Canada - Jan. to Dec. 1959
[AECL-4149] 03 p0353 N73-12878
Uncorrected and barometer-corrected cosmic neutron data taken at Canadian stations - Sept. to Dec. 1971
[AECL-4148] 03 p0353 N73-12879
Total air ionization and tissue dose rate in atmosphere
[HASL-254] 03 p0353 N73-12881
Night sky Cerenkov detector for measuring electromagnetic radiation produced by high energy cosmic rays
[AD-746734] 03 p0354 N73-12883
Production of gamma rays from decay of neutral pions produced by interstellar cosmic ray interactions
[NASA-TM-X-66120] 04 p0467 N73-13803
Uncorrected and barometer-corrected, cosmic ray, NM-64 neutron monitor data from Kula, Hawaii, Jan.-Dec. 1971
[AECL-4161] 04 p0467 N73-13804
Hourly rates corrected for atmospheric temperature and pressure from four cosmic ray stations in Canada
[AECL-4077] 04 p0467 N73-13805
Ionospheric sounding and cosmic ray neutron flux density tables, Dourbes, Belgium, May 1972
05 p0539 N73-14387
Pioneer 10 observations of galactic cosmic ray intensity from 1.0 to 2.0 AU heliocentric radial range
[AD-748614] 05 p0593 N73-14823
Comprehensive listing of ground-based cosmic ray detectors
[AD-749865] 05 p0594 N73-14824
Geophysics and space data bulletin
[AD-749815] 05 p0597 N73-14852
Differential energy spectra of cosmic ray protons and helium nuclei dominated by solar modulation of local interstellar spectra, and numerical solutions to transport equation
[NASA-CR-130298] 06 p0715 N73-15837
Equipment, data processing, and results of Intercosmos observations of cosmic rays
[JPRS-57913] 06 p0716 N73-15839
Diurnal variation amplitude and phase data of cosmic rays in 1962 and 1964-65
[AD-750870] 06 p0716 N73-15844
Nature of weak high latitude X ray sources
[NASA-TM-X-66168] 07 p0839 N73-16796
Total gamma ray production rate per hydrogen atom from neutral pion decay in interstellar cosmic ray interactions, and calculation of molecular hydrogen amount
[NASA-TM-X-66167] 07 p0839 N73-16798
Laser-probe mass spectrometric analysis of solar wind, cosmogenic, and radiogenic gases in Apollo 12, 14, and 15 samples
[NASA-CR-130029] 07 p0841 N73-16811
Six-day variation in cosmic ray intensity recorded at different astronomical observatories
07 p0859 N73-16967
Ionospheric sounding and cosmic ray neutron flux density tables, Dourbes, Belgium, Jun. 1972
08 p0918 N73-17524
Low energy cosmic ray protons from nuclear interactions of cosmic rays with interstellar medium
[NASA-TM-X-66181] 08 p0956 N73-17829
Autocorrelation, Chree, and power spectrum analyses of cosmic ray 27-day recurrences
[NP-19466] 08 p0957 N73-17833
Tables of cosmic ray MT-64 muon monitor measurements from solar rotation 1867 to solar rotation 1879
[AECL-4207] 08 p0957 N73-17834
Possibility of current sheets serving as pathways for transport of cosmic rays in solar corona
08 p0973 N73-17958
Cosmic ray phenomenon of quiettime electron increases
08 p0974 N73-17962
Cosmic ray charge and energy spectra above 10 GeV from balloon flight data
08 p0974 N73-17963
Survival of heavy nuclei in cosmic ray source environments from Goddard balloon spectrometer experiment
08 p0974 N73-17964
Cosmic radiation dosage for estimating manned spacecraft shielding requirements
09 p0992 N73-18101
Design of multiwire proportional chamber systems using electromagnetic delay lines for cosmic ray experiments
[RM-569] 09 p1011 N73-18251
Dourbes, Belgium, geophysical observatory data on geomagnetism, ionospheric propagation, seismology, cosmic rays, and atmospheric electricity, Feb. 1972
09 p1030 N73-18403
Dourbes, Belgium, geophysical observatory data on geomagnetism, ionospheric propagation, seismology, cosmic rays, and atmospheric electricity, Mar. 1972
09 p1030 N73-18404
Dourbes, Belgium, geophysical observatory data on geomagnetism, ionospheric propagation, seismology, cosmic rays, and atmospheric electricity, Apr. 1972
09 p1030 N73-18405
Dourbes, Belgium, geophysical observatory data on geomagnetism, ionospheric propagation, seismology, cosmic rays, and atmospheric electricity, May 1972
09 p1030 N73-18406
Dourbes, Belgium, geophysical observatory data on geomagnetism, ionospheric propagation, seismology, cosmic rays, and atmospheric electricity, Jun. 1972
09 p1030 N73-18407
Dourbes, Belgium, geophysical observatory data on geomagnetism, ionospheric propagation, seismology, cosmic rays, and atmospheric electricity, Jul. 1972
09 p1030 N73-18408
Ionospheric sounding and cosmic ray neutron flux density tables, Dourbes, Belgium, Jul. 1972
09 p1030 N73-18409
Charge composition of cosmic rays for elements silicon to nickel
[LUIP-CR-72-16] 09 p1069 N73-18721
Ionization chamber/Cerenkov counter measurements of heavy cosmic ray flux and composition
[NASA-CR-130921] 09 p1080 N73-18811
Breakdown of quasi-linear derivation of kinetic equation describing cosmic ray distribution function in random magnetic field
[NASA-TM-X-65949] 09 p1081 N73-18815
Neutron flux spectra induced in the earth atmosphere by galactic cosmic rays
[NASA-CR-131158] 10 p1210 N73-19844
Investigation of light flash phenomenon observed by Apollo crews
[NASA-CR-128866] 10 p1213 N73-19867
Impact calculation of heavy nuclei of cosmic rays
11 p1243 N73-20089
Microdosimetric pattern of galactic heavy primaries dissipation in tissues during space flight
[NASA-CR-131467] 12 p1372 N73-21132
Characteristics of photomultiplier tubes and application to optics, biophysics, radiometry, and astronomy for detecting weak light flows
[AD-755874] 12 p1384 N73-21226
Analysis of conditions leading to generation of cosmic rays by acceleration of charged particles caused by electromagnetic field of pulsars
[PPG-144] 12 p1445 N73-21703
Cosmic ray disturbances following solar flare occurrences in August 1972 recorded by neutron monitoring
12 p1446 N73-21709
Influence of cosmic rays on temperature and ionization rate of interstellar gas
[MPI-PAE/EXTRATERR-72] 12 p1446 N73-21710
Apollo 16 experiment using biostack to determine effects of heavy nuclei on biological organisms
12 p1452 N73-21761
Analysis of techniques for shielding manned space vehicles against protons and alpha particles from Van Allen belt, solar flares, and cosmic rays
[NASA-CR-131517] 12 p1461 N73-21841
Development of multiwire proportional chamber for high resolution spatial detector in cosmic ray investigations and analysis of operating parameters
[NASA-CR-128899] 13 p1506 N73-22210
Ionospheric sounding and cosmic ray neutron flux density tables, Dourbes, Belgium, Aug. 1972
13 p1524 N73-22354
Alpha particle beam spalling production of aluminum, oxygen, carbon, and beryllium isotopes, and cosmic ray transport theory
13 p1561 N73-22651
Solar-geophysical activity associated with major ground level cosmic ray event of 24 January 1971
[UAG-24-PT-1] 13 p1572 N73-22737
Solar-geophysical activity associated with major ground level solar cosmic ray event of 1 September 1971
[UAG-24-PT-2] 13 p1572 N73-22738
Confinement of ultrarelativistic cosmic rays to galactic disk as result of interactions with hydromagnetic waves
13 p1572 N73-22739
Radiation monitor for cosmic X ray experiment on OSO-1
[NASA-CR-130206] 13 p1573 N73-22747
Measurements of galactic cosmic ray dose and geomagnetically trapped radiation from OV 1-4 satellite
[AD-756924] 13 p1575 N73-22761
Electron flux measurements from Cosmos 490 satellite
14 p1660 N73-23477
Geophysical and space data bulletin
[AD-755839] 14 p1706 N73-23849
Nuclear track dosimetry for monitoring cosmic ray exposure of Apollo 16 astronauts
15 p1741 N73-24114
Ionospheric sounding and cosmic ray neutron flux density tables from Dourbes, Belgium for Oct. 1972
15 p1781 N73-24438
Cosmic ray neutron monitor data for Sanae Antarctica
[S-6] 15 p1827 N73-24811
Cosmic ray neutron monitor data for Potchefstroom
[P-2] 15 p1828 N73-24812
Cosmic ray neutron monitor data at Pochefstroom during period from May 1971 to December 1971
[P-1] 15 p1828 N73-24813
OSO-5 X ray detector measurement of diffuse cosmic ray energy spectrum from 14 to 200 keV
[NASA-TM-X-66252] 15 p1828 N73-24815
Intercosmos satellite observation of cosmic rays
15 p1828 N73-24817
Measurements of differential energy spectra in cosmic ray protons and solar cycle variations of atmospheric secondary protons
[NASA-CR-132056] 15 p1828 N73-24818
Ionospheric sounding and cosmic ray neutron flux density tables, Dourbes, Belgium, Sep. 1972
16 p1907 N73-25428
Development and characteristics of solid state cosmic ray telescope for use on IMP F and G missions
[NASA-CR-132767] 16 p1912 N73-25473
Unique approach for deriving cosmic ray diffusion equation for charged particles in static, random magnetic field
[NASA-TM-X-66263] 16 p1959 N73-25848
Relationship between peaks of cosmic radiation and ischemic heart disease
[NASA-TT-F-14992] 17 p1987 N73-26065
Dourbes [Belgium] geophysical observatory data on geomagnetism, ionospheric propagation, seismology, cosmic rays, and atmospheric electricity, Aug. 1972
17 p2028 N73-26411
Dourbes [Belgium] geophysical observatory data on geomagnetism, ionospheric propagation, seismology, cosmic rays, and atmospheric electricity, Sep. 1972
17 p2028 N73-26412
Depth profiles of galactic cosmic ray produced radionuclides in lunar samples
17 p2079 N73-26814
Polarization measurements of cosmic ray muons arriving at sea level with different energies and from different zenith angles
17 p2079 N73-26815
Cosmic rays in earth magnetic field
[NASA-TT-F-756] 17 p2079 N73-26819
High energy particles in cosmic radiation sources
[CONF-710974-6] 17 p2080 N73-26823
Tables on Antarctic cosmic ray measurements obtained during 1969
[NP-19680] 17 p2080 N73-26824
OSO-1 experimental design for cosmic X ray sources identification and diffusion background radiation spectroscopy
17 p2084 N73-26861
HEAO-B cosmic ray experiment for diffuse sky brightness determination
17 p2085 N73-26871

Ionospheric sounding and cosmic ray neutron flux density tables, Dourbes, Belgium, Dec. 1972
18 p2146 N73-27342
Ionospheric sounding and cosmic ray neutron flux density tables, Dourbes, Belgium, Nov. 1972
18 p2146 N73-27343
Spatial distribution of soft X ray and EUV emission associated with chromospheric flare of importance 1B August 2, 1972
[NASA-TM-X-66299] 18 p2195 N73-27720
Pioneer-10 measurements of differential and integral cosmic ray gradients between 1 and 3 AU
[NASA-TM-X-66293] 18 p2197 N73-27736
Definition study of X ray background experiment on HEAO A
[AD-759738] 18 p2198 N73-27742
Design and performance of lightweight cosmic radiation experiment for Pioneer Jupiter mission
18 p2210 N73-27837
Apollo 15 measurement of cosmic gamma ray spectrum between 0.3 and 27 MeV
19 p2331 N73-28756
Electromagnetic and strong interactions processes for producing diffuse cosmic gamma continuum radiation
19 p2332 N73-28763
Metagalactic orgin of cosmic rays and gamma ray astronomy
19 p2332 N73-28764
Production of gamma rays from explosive nucleosynthesis and low energy cosmic ray scattering
19 p2332 N73-28765
Interaction of ultrahigh energy cosmic rays protons with relicit radiation in extragalactic space
19 p2332 N73-28766
Measuring ionizing radiation in near-earth space
[NASA-TT-F-754] 19 p2340 N73-28825
Discrimination between high energy cosmic ray electrons and interacting protons using cesium iodide
[NASA-TM-X-70446] 20 p2435 N73-29556
Energy spectra of six cosmic gamma-ray bursts in regions of 0.1 to 1.2 MeV
[NASA-TM-X-70427] 20 p2468 N73-29824
Magnetic storm effects on cosmic ray intensity
[AD-762223] 20 p2468 N73-29826
Changes in cosmic ray intensity over last solar modulation cycle
[AD-760789] 20 p2468 N73-29828
Calculations of cosmic ray effective cut-off rigidities in real magnetic field
[AD-763124] 20 p2468 N73-29829
Space vehicle design criteria based on interplanetary charged particle environments
[NASA-CR-133600] 20 p2473 N73-29865
Ionospheric sounding and cosmic ray neutron flux density tables, Dourbes, Belgium, Mar. 1973
21 p2539 N73-30354
Ionospheric sounding and cosmic ray neutron flux density tables, Dourbes, Belgium, Apr. 1973
21 p2539 N73-30355
Stratospheric electricity due to operating supersonic transport fleets
[AD-763471] 21 p2540 N73-30365
Consistence of cosmic ray source compulsion with explosive nucleosynthesis
[NASA-TM-X-70448] 21 p2592 N73-30768
Apollo 16 lunar surface cosmic ray experiment S-152
[NASA-CR-134019] 21 p2592 N73-30770
Spallation reactions of light nuclei during galactic cosmic radiation interaction with interstellar gas
[FRNC-TH-333] 21 p2597 N73-30812
Monte Carlo simulation of nuclear-electromagnetic cascade development and energy response of ionization of spectrometers
[NASA-CR-133999] 22 p2672 N73-31406
Testing of power spectrum-diffusion coefficient relations of cosmic rays at low energies
22 p2711 N73-31706
Measurement of mean isotopic composition of even-charge cosmic ray elements using balloon-borne ionization chamber
[NASA-CR-135516] 22 p2711 N73-31711
Primary and secondary nuclei production in cosmic rays
22 p2733 N73-31872
Ionization loss in galactic cosmic ray electron spectrum caused by proton interactions
22 p2733 N73-31873
Solar energy effect in galactic cosmic ray modulation
22 p2733 N73-31875
Solar magnetic field effects on galactic cosmic ray spectrum
22 p2733 N73-31877
Earth albedo neutrons and cosmic ray neutron decay from 10 to 100 MeV
[NASA-CR-135645] 23 p2789 N73-32315
Cosmic ray charged particle interactions with matter
[AD-764833] 23 p2821 N73-32555
Differential energy spectra of cosmic ray protons and helium nuclei
23 p2833 N73-32640
Conference on cosmic ray and solar particle diffusion and concentration in interstellar space
[NASA-CR-135528] 23 p2834 N73-32646
One-dimensional time dependent diffusion convection model analysis of cosmic ray modulation during solar maximum
[TR-73-131] 23 p2834 N73-32647
Physical theory of coherent cosmic ray propagation in random magnetic fields
[TR-73-133] 23 p2834 N73-32649
Hodoscope measurements of cosmic ray electron spectra
[TR-73-135] 23 p2834 N73-32651
Source and diffusion of cosmic rays greater than 4.5 GV in interstellar medium measured by proportional counter-scintillation counter stack
[TR-73-136] 23 p2835 N73-32652
IMP-7 measurement of very low energy cosmic ray energy spectra and concentration during solar flares
[TR-73-138] 23 p2835 N73-32654
Ionospheric soundiag and cosmic ray neutron flux density tables, Dourbes, Belgium Jan. 1973
24 p2923 N73-33350
Ionospheric sounding and cosmic ray neutron flux density tables, Dourbes, Belgium, Feb. 1973
24 p2923 N73-33351
Dourbes [Belgium] geophysical observatory data on geomagnetism, ionospheric propagation, seismology, cosmic rays, and atmospheric electricity. Nov. 1972
24 p2924 N73-33353
Geophysical observatory data obtained at Dourbes, Belgium in Dec. 1972 on geomagnetism, ionospheric propagation, seismology, cosmic rays, and atmospheric electricity
24 p2924 N73-33354
Characteristics of steady galactic winds created by escape of cosmic rays from galaxy
24 p2975 N73-33775
Satellite measurement of cosmic ray abundances and spectra in charge range 2 equal to or less than 7 equal to or less than 10
[NASA-CR-135786] 24 p2976 N73-33777
LUIN, code for calculation of cosmic ray propagation in atmosphere
[HASL-275] 24 p2977 N73-33784
Sources, absorption, and detection of cosmic gamma rays
[MPI-PAE/EXTRATERR-83] 24 p2977 N73-33789

COSMOGONY
U COSMOLOGY

COSMOLOGY
Development of cosmological models based on Einstein field equations with random perturbations of long wave lengths superimposed on unperturbed models
[AD-747505] 03 p0357 N73-12911
Derivation of closed formula for relation between luminosity and red shift in expanding Friedman universe
07 p0840 N73-16802
Research projects for ground-based and space-based astronomy to show present capabilities and future potential
[PB-212965] 12 p1458 N73-21819
Two fluid cosmological model including interaction between matter and radiation
13 p1561 N73-22652
Relating glaciation cycles to cosmic rhythms
[NASA-TT-F-14827] 14 p1659 N73-23469
High energy particle kinetics along boundary of matter-antimatter of universe
[LPTHE-73/5] 14 p1703 N73-23818
Bulk viscosity in relativistic homogeneous isotropic cosmologies
17 p2081 N73-26829
Annihilation reactions and gamma ray spectra for studying large scale cosmologic antimatter
19 p2332 N73-28769

COSMONAUTS
Analysis of cosmonaut emotional stress as determined by physiological and behavioral responses
[NASA-TT-F-14654] 03 p0261 N73-12113
Operating principles of high precision orbiting astronomical observatory manned by nonprofessional cosmonaut astronomer
[NASA-TT-F-14580] 07 p0843 N73-16830
Indices of emotional stress in cosmonauts during Voskhod 2 and Soyuz flights
[JPRS-58039] 08 p0877 N73-17104
Role of cosmonaut in spacecraft control
09 p0997 N73-18137
Morphological composition of peripheral blood of crew members of Soyuz-9 and Salyut-1
11 p1245 N73-20104
Role of cosmonaut in man-spacecraft system, and psychological aspects in training cosmonauts as operators
[NASA-TT-F-727] 12 p1372 N73-21129
Phytological and physiological problems caused by rest-work cycles of cosmonauts during space flight
[NASA-TT-F-14990] 17 p1990 N73-26093
Cosmonaut earth observations from space
[JPRS-59831] 21 p2595 N73-30793
Scheduling of work-rest cycle for cosmonauts during space flights
22 p2618 N73-30984
Cosmonaut activities onboard orbiting space stations
[NASA-TT-F-15152] 23 p2850 N73-32778

COSMOS
Analysis of development of cosmos, universe, mankind, and space exploration
04 p0470 N73-13833

COSMOS SATELLITES
NT COSMOS 213 SATELLITE
NT COSMOS 224 SATELLITE
NT COSMOS 381 SATELLITE
NT INTERCOSMOS SATELLITES
Tracking and orbit calculation of Cosmos 316 to determine upper atmospheric wind
[RAE-TR-72062] 02 p0235 N73-11910
Air density at 200 km heights analyzed from Cosmos 286 rocket orbit decay, emphasizing annual variations and geomagnetic disturbances
[RAE-TR-72071] 03 p0296 N73-12417
Soviet Cosmos satellite and rocket programs
[NASA-TT-F-14641] 04 p0478 N73-13913
Photoelectron effect on second positive system of nitrogen bands in daytime glow of atmosphere from Cosmos 224 data
05 p0536 N73-14360
Optical satellite tracking of Cosmos and other artificial satellites, Edinburgh, Aug. 1972
[ROE-STS-129] 05 p0601 N73-14883
Optical satellite tracking of Cosmos and other artificial satellites, Edinburgh, Sep. 1972
[ROE-STS-130] 05 p0601 N73-14884
Design and employment of Soviet satellite of Cosmos series
[AD-749725] 05 p0601 N73-14886
Optical satellite tracking of Cosmos and other artificial satellites, Edinburgh, Oct. 1972
[ROE-STS-133] 06 p0722 N73-15891
Cosmos 121 measurements of total ozone content of earth atmosphere
[JPRS-57976] 07 p0791 N73-16430
Cosmos measurements of ion concentration in earth atmosphere
07 p0792 N73-16439
Cosmos 434 measurement of oscillations in ion concentration levels in earth ionosphere at 200 to 1300 km altitudes
09 p1028 N73-18394
Optical satellite tracking of Cosmos and other artificial satellites, Edinburgh, Nov. 1972
[ROE-STS-135] 09 p1091 N73-18908
Energy spectra of ionospheric photoelectrons measured in 30 to 150 eV range from Cosmos 348 satellite in summer 1970
[PR-107] 10 p1155 N73-19400
Plasma convection patterns in polar upper ionosphere obtained from Cosmos 184 satellite measurements during magnetic disturbance of 4 Nov. 1967
[PR-130] 10 p1156 N73-19403
Detection of intermediate size magnetic anomalies in Cosmos-49 and OGO-2, 4, and 6 data
[NASA-TM-X-66225] 12 p1401 N73-21368
Optical satellite tracking of Cosmos and other artificial satellites, Edinburgh, Dec. 1972
[ROE-STS-138] 13 p1582 N73-22824
Spherical harmonic analysis of Cosmos-321 geomagnetic survey
14 p1659 N73-23463
Electron flux measurements from Cosmos 490 satellite
14 p1660 N73-23477
Upper atmospheric neutral hydrogen distribution
15 p1779 N73-24423
Convection velocity measurements in polar upper ionsphere made by Cosmos 184 Satellite during moderate magnetic disturbance
15 p1780 N73-24430
Optical satellite tracking of Cosmos aad other artificial satellites, Edinburgh, Feb. 1973
[ROE-STS-147] 15 p1836 N73-24881
Interactions between radio brightness and surface conditions of oceans based on Cosmos 243 data
[NASA-TT-F-14954] 16 p1904 N73-25401
Agricultural study using microwave radiation from Cosmos 243 satellite over European USSR
[NASA-TT-F-14952] 16 p1944 N73-25732
Optical satellite tracking of Cosmos and other artificial satellites, Edinburgh, Jan. 1973
[ROE-STS-141] 16 p1967 N73-25912
Cosmos-187 measurement of ion drift velocity in upper ionosphere during magnetic storms
17 p2024 N73-26381
Atmospheric noise measurements from Cosmos 149, 243, 320, and 394 satellites
[NASA-TT-F-14977] 18 p2143 N73-27319
Cosmos 243 measurements of radioemission properties of land surfaces
[NASA-TT-F-14978] 18 p2143 N73-27320
Optical satellite tracking of Cosmos and other artificial satellites, Edinburgh, Jan. 1973
[ROE-STS-151] 19 p2346 N73-28872

Optical satellite tracking of Cosmos and other artificial satellites, Edinburgh, Apr. 1973
[ROE-STS-152] 19 p2346 N73-28873
Ion drift measurements from Cosmos 184 during 3 Nov. 1967 magnetic storm
20 p2410 N73-29371
Ion analyzer onboard Cosmos 348 for measuring ion temperature and horizontal gradients
20 p2411 N73-29376
Optical satellite tracking of Cosmos and other artificial satellites, Edinburgh, May 1973
[ROE-STS-154] 21 p2602 N73-30851
Cosmos-378 data on solar cosmic ray penetration into earth polar caps
24 p2976 N73-33782
Measurement of night-sky brightness in visible and ultraviolet spectral regions using photometers on Cosmos-51 satellite
[NASA-TT-F-15153] 24 p2980 N73-33815

**COSMOS 213 SATELLITE**
Measurement of night-sky brightness in visible and ultraviolet spectral regions using photometers on Cosmos-51 and Cosmos-213 satellites
[NASA-TT-F-15154] 24 p2980 N73-33814

**COSMOS 224 SATELLITE**
Cosmos 224 observations of N2 ions during medium solar activity
03 p0293 N73-12389

**COSMOS 381 SATELLITE**
Cosmos 381 measurement of ionospheric electron concentration using impedance probe
15 p1779 N73-24422

**COSPAR (COMMITTEE)**
U COMMITTEE ON SPACE RESEARCH

**COSSERAT SURFACES**
Influence of reference geometry on response of elastic shells within scope of nonlinear theory of elastic Cosserat surface
[AD-745291] 01 p0114 N73-10942

**COST ANALYSIS**
Effects of decision models and operational characteristics on economic expenses associated with use of predictive weather information
[NASA-CR-128401] 01 p0073 N73-10600
Space shuttle avionics design and cost analysis
[NASA-CR-123962] 03 p0300 N73-12449
Cost analysis and design of possible fusion reactor coil systems
[UCRL-73187] 03 p0336 N73-12741
Development and application of systematic procedures for estimating life cycle costs of solid rocket motor booster configurations
[NASA-CR-129255] 03 p0350 N73-12857
Analysis of space program costs and launch vehicle traffic based on either expendable, partially reusable, or fully reusable launch vehicle fleet
[NASA-CR-125847] 03 p0355 N73-12896
Payload data bank, space shuttle program risk analysis, reusable launch vehicles, and cost analysis
[NASA-CR-126170] 03 p0355 N73-12897
Projected space missions and space transportation system with payload and cost analysis for space shuttle system - Vol. 2
[NASA-CR-129571] 04 p0487 N73-13978
Analysis of economic merits of three alternative space transportation systems for use during 1980 time period - Vol. 3
[NASA-CR-129569] 04 p0487 N73-13979
Economic analysis of space transportation system for use during 1980 time period based on various configurations of space shuttle and space tug - Executive Summary
[NASA-CR-129570] 04 p0487 N73-13980
Production and costs of producing reliable semiconductor integrated circuits
[AD-749834] 05 p0521 N73-14240
Economic analysis on capital investment for transportation modes
[PB-212307] 07 p0860 N73-16976
Statistical supplement for capital investment in transportation modes
[PB-212308] 07 p0860 N73-16977
Methods for lowering cost of environmental aerial surveys
[NASA-CR-124107] 09 p1025 N73-18369
Quantitative, qualitative, and cost analyses of ERTS-1 imagery
[REPT-11215-1-F] 09 p1025 N73-18371
Environmental factors and cost problems of selecting optimum sanitary landfill site for solid waste disposal
[NASA-CR-128744] 10 p1124 N73-19157
Design and fabrication of wraparound contact silicon solar cells
[NASA-CR-121003] 11 p1237 N73-20044
Life cycle cost analysis of inertial navigation systems for aircraft and air to surface missiles
11 p1320 N73-20717
Proceedings of conference on economic aspects of space shuttle system to show basis for cost effectiveness determinations and system selection
[NASA-CR-131421] 11 p1337 N73-20848
Economic analysis of space tug operations to include tug definition, spacecraft configurations, payload effects, and costing logic - Vol. 1
[NASA-CR-124142] 11 p1343 N73-20899
Comparative analysis of space tug concepts to show overall approach and data generation - Vol. 2, Pt. 1
[NASA-CR-124143] 11 p1343 N73-20900
Economic principles for cost effectiveness and cost benefit analysis of space tug operations - Vol. 2, Pt. 2
[NASA-CR-124144] 11 p1343 N73-20901
Development of data base to show space tug characteristics, costs, and performance for comparison of concepts - Vol. 2 Appendix
[NASA-CR-124146] 11 p1344 N73-20902
Cost analysis of single stage space tug operations with several types of liquid propellant rocket engine propulsion systems - Vol. 3
[NASA-CR-124147] 11 p1344 N73-20903
Cost analysis of oxygen supply equipment and recovery systems for orbital space stations
[NASA-CR-124175] 12 p1373 N73-21137
Feasibility and costs of orbiting satellite data collection systems
[NASA-CR-130232] 13 p1581 N73-22812
FCC transition splices and cost comparison of FCC vs. RCC
14 p1641 N73-23304
Integrated microform-machine processing system and costs of using such systems
15 p1753 N73-24206
Cost analysis of various solid propellant rocket engines for use with space shuttle - Vol. 4
[NASA-CR-124239] 15 p1826 N73-24802
Price trends affecting research and development at academic institutions
[NSF-72-310] 15 p1846 N73-24959
Cost estimating and price analysis in European satellite projects
15 p1849 N73-24984
Design of aircraft for high reliability and low maintenance costs and maintenance procedures for maximum efficiency
17 p1983 N73-26032
Cost analysis of oxygen recovery subsystems for life support systems
[NASA-CR-124304] 18 p2112 N73-27075
Cost analysis of mass spectrometers and gas chromatographs for life support atmosphere monitoring
[NASA-CR-124306] 18 p2112 N73-27076
Characteristics of low cost mass producible earth terminal antenna system for broadcast satellite
18 p2122 N73-27152
Analysis of cost data for fabrication of large solid rocket engine cases based on process complexity factor
[NASA-CR-133412] 18 p2200 N73-27764
Costs, physical characteristics, and performance of urban transportation systems
[PB-219254/0] 18 p2214 N73-27878
Development of method for determining cost functions involving aircraft rework and engine repair programs at military installation
[AD-761475] 19 p2249 N73-28135
Cost analyses on mass spectrometric and gas chromatographic atmospheric monitoring systems
[NASA-CR-124331] 19 p2315 N73-28622
Congressional hearing concerning GAO cost analysis of NASA estimates for space shuttle
19 p2354 N73-28936
Statistical analysis of naval experience in fixed-price incentive contract management for aircraft and missile procurement
[AD-761396] 19 p2355 N73-28946
Cost history of F-111 aircraft airframe system to show logistics organization, support costs, reliability and maintainability, and development problems
[AD-762213] 19 p2356 N73-28958
Analysis of rigid airship operations for commercial cargo handling in United Kingdom
[CRANFIELD-CTS-3] 20 p2360 N73-28985
Congressional hearings on cost of space shuttle program to show differences between Government Accounting Office and NASA projections
22 p2737 N73-31916
Senate hearings concerning GAO analysis of space shuttle cost estimates
22 p2738 N73-31919
Construction of reliability cost-model
[NASA-TM-X-64777] 23 p2797 N73-32372
Design and cost analysis of space shuttle systems - Vol. 2, Part 1
[NASA-CR-124417] 23 p2850 N73-32772
Design and cost analysis of space shuttle systems - Vol. 2, Part 2
[NASA-CR-124422] 23 p2850 N73-32773
Development and operation of cost accounting system for airport functions to show application of data processing equipment
23 p2863 N73-32878
Operation of low cost local air service carriers to show methods for improving transportation services
23 p2863 N73-32886
Procedures for determining rates charged by airlines to show factors involved in making determinations
23 p2864 N73-32890
Regulatory policies of Civil Aviation Board for controlling operations of commercial airlines
23 p2864 N73-32891
Optimization of control and damping system for fighter aircraft with quadratic cost function
24 p2877 N73-32980
Alternate concepts study on two and one half stage, stage and one half, and SRM interim booster systems for establishing performance, costs, and schedules
[NASA-CR-124344] 24 p2982 N73-33829
Results of tug turnaround cost study and space transportation system abort modes and effects study
[NASA-CR-135765] 24 p2983 N73-33833
Relationships between performance, safety, cost, and schedule parameters to generate program models for total space program
[NASA-CR-135903] 24 p2993 N73-33919
Relationships between performance, safety, cost, and schedule parameters to generate program models for total space program
[NASA-CR-135902] 24 p2993 N73-33920
Cost analysis of large research institutes in Germany
[DLR-FB-73-64] 24 p2995 N73-33931

**COST EFFECTIVENESS**
Feasibility of thermal energy storage and solar heating as means of conservation and more efficient utilization of electric power
[PB-210359] 01 p0118 N73-10976
Cost effective data security safeguards in personal information databanks
[P-4871] 02 p0145 N73-11178
Cost effectiveness criteria and parametric data for friction welding of missile systems hardware
[AD-747838] 04 p0427 N73-13482
Cost effectiveness of infrared inspection and maintenance of ARTCC electrical equipment
[C-208] 04 p0447 N73-13648
Optimization and cost factors for cryogenic and superconducting magnets in plasma physics
[IPP-4/96] 04 p0458 N73-13740
Operational effectiveness of jet flight training simulator
[AD-750248] 06 p0636 N73-15170
Technical and economical factors of satellite television reception
[NASA-TT-F-14659] 06 p0640 N73-15196
Cost effectiveness of high speed ground transportation system using tracked air cushion vehicles for access to Los Angeles airport
[PB-212023] 06 p0651 N73-15290
Cost effectiveness of transporting military cargo by air versus surface modes
[AD-750848] 06 p0732 N73-15974
Cost effectiveness of automatic inspection, diagnostic, and prognostic maintenance system for military aircraft - Appendix F
[AD-752889] 09 p0988 N73-18069
Cost effectiveness of water reclamation subsystem in advanced aerospace life support systems
[NASA-CR-124098] 09 p0997 N73-18134
Powder metallurgy methods to increase cost effectiveness of titanium raw materials processing
[JPRS-58217] 09 p1048 N73-18542
Cost effectiveness and mission value comparisons of three propulsion systems for delivery of advanced probe spacecraft
[NASA-TM-X-2751] 09 p1079 N73-18802
Interrelationships between energy, resources, and environment, conference summary
[PB-213031] 11 p1333 N73-20820
Economic analysis of space tug operations to include tug definition, spacecraft configurations, payload effects, and costing logic - Vol. 1
[NASA-CR-124142] 11 p1343 N73-20899
Management of development and research costs for advancement of technology in aerospace systems
11 p1351 N73-20964
Fundamentals of helicopter noise generation and propagation to include noise control procedures and cost effectiveness of noise reduction
14 p1598 N73-22953
Cost effectiveness analysis of helicopter transmission components to determine effect of extended overhaul life up to 6,000 hours
[AD-758465] 14 p1604 N73-23007
Operational cost and technological development aspects in design of space shuttle avionic systems
14 p1711 N73-23884
Development of cost effective program for training naval fixed wing pilots in 1974 to 1986 time period - Vol. 1
[AD-756638] 15 p1745 N73-24143
Development of cost effective program for training naval fixed wing pilots in 1974 to 1986 time period - Vol. 2
[AD-756639] 15 p1745 N73-24144
Development of cost effective program for training naval fixed wing pilots in 1974 to 1986 time period - Vol. 3
[AD-756640] 15 p1745 N73-24145
Human factors in design of avionics subsystems considering training costs and performance of Air Force personnel
[AD-759583] 17 p1990 N73-26096

Ground terminal optimization and cost effectiveness of satellite television broadcasting
18 p2115 N73-27100

Delta vehicle configuration changes and performance increases considering cost effectiveness
18 p2208 N73-27818

Design, reliability analysis, maintainability, and cost effectiveness of expendable rotor blades for UH-1 helicopter rotary wing
[AD-762198] 19 p2222 N73-27926

Technical and economical effiency of thermionic cathode
[AD-761535] 19 p2248 N73-28121

Examination of man machine systems efficiency in relation to cost criteria
21 p2503 N73-30087

Effect of basic indices of computer system on expected cost savings
21 p2513 N73-30161

Calculation of technical and economic indices of high-power homogeneous general-purpose computer systems
21 p2513 N73-30162

Comparative performance of homogeneous computer systems and computers
21 p2514 N73-30163

Cost effective measures for preventing solar proton interference with interplanetary spacecraft operation
22 p2732 N73-31863

Economic benefits of electrochemical fuel cells
[NASA-TT-F-15147] 23 p2748 N73-31991

Design parameters for optimal cost/cruise performance of subsonic jet transport
23 p2860 N73-32853

Principles of functional economic analysis
23 p2860 N73-32854

Differential pricing policy in airline operations
23 p2861 N73-32857

Financial sources and airline operations
23 p2861 N73-32859

Application of airships to air transportation, noting cost effectiveness
24 p2879 N73-32991

Cost effectiveness of silica insulation in space shuttle thermal protection system design
24 p2942 N73-33496

**COST ESTIMATES**

Projections for superconductor costs for dc fusion magnets
[BNL-16748] 03 p0335 N73-12735

Cost estimates for base basing, space shuttles, and systems analysis
[NASA-CR-125985] 03 p0359 N73-12921

Design techniques for estimating cost of flight vehicle structures
[AD-747007] 03 p0367 N73-12994

Cost estimates and design of electron synchrotron injector for high energy rings
[DNPL/R-13] 04 p0401 N73-13268

Methodology for estimating costs and estimates for 3 carbon dioxide concentrators
[NASA-CR-123960] 04 p0486 N73-13971

Project planning and cost estimates for Europa 3 launch vehicle
07 p0850 N73-16889

Statistical analysis on expense increase funding for technological systems
11 p1351 N73-20963

Methods of improving cost estimating techniques in NASA and DOD
12 p1466 N73-21877

Design concepts, manufacturing process, weight analysis, and cost estimates for long range transport aircraft using composite structures
[NASA-CR-112255] 14 p1600 N73-22976

Design and cost estimate of high altitude wind power plant
[NASA-TT-F-14903] 14 p1605 N73-23011

Model for estimating impact of manned EVA costs on future payloads - Vol. 3
[NASA-CR-128928] 14 p1614 N73-23083

Estimates of cost of air pollution damage
[AP-85] 14 p1685 N73-23669

Model for estimating cost of unmanned lunar and planetary exploration programs
[NASA-CR-131897] 14 p1705 N73-23840

Model for updating aerospace research and development as function of perturbations in program time
[NASA-TM-X-64748] 15 p1845 N73-24948

Cost estimating and price analysis in European satellite projects
15 p1849 N73-24984

Production cost optimization for thermoelectric solar cell
[AD-759812] 16 p1865 N73-25104

Cost estimating method for life support systems of manned earth orbital programs
[NASA-CR-124305] 18 p2111 N73-27072

Cost estimates for carbon dioxide concentrators in spacecraft life support systems
[NASA-CR-124302] 18 p2111 N73-27073

Methodology for predicting relevant contributions of cost elements in development of water recovery systems
[NASA-CR-124303] 18 p2111 N73-27074

Models of air, river and highway transportation for developing areas
[PB-219292/0] 18 p2214 N73-27877

Role of air transportation in sparsely developed areas including cost estimates
[PB-219293/8] 18 p2214 N73-27880

Program development requirements for selected Astronomy Sortie Missions concept to show rationale and explanations of guidelines and assumptions - Vol. 4
[NASA-CR-124046] 20 p2474 N73-29872

Method for estimating airline operating costs
23 p2860 N73-32851

Formula for computing operating cost of turbine powered transport aircraft
23 p2860 N73-32852

Estimated costs for additional aircraft in air transport industry
23 p2861 N73-32860

Procedures for determining rates charged by airlines to show factors involved in making determinations
23 p2864 N73-32890

Cost data for modified hydrogen depolarized carbon dioxide concentrator in life support system
[NASA-CR-124462] 24 p2887 N73-33052

**COST REDUCTION**

Algorithms for construction of minimum cost communication networks
[PB-211233] 05 p0514 N73-14178

Possible reduction of NASA payload costs
[NASA-TM-X-62223] 07 p0844 N73-16835

Design, development, and production of low cost remotely piloted vehicles based on innovative approach for aircraft engineering procedures
[P-4902] 12 p1363 N73-21060

Design of all digital low data rate communication system with potential cost reduction
[NASA-CR-130234] 13 p1490 N73-22077

Data recording and data interchange for reducing data processing costs
15 p1753 N73-24207

Feasibility and cost benefits of nuclear-powered standardized spacecraft
[NASA-CR-133743] 21 p2601 N73-30846

**COSTS**

NT FREIGHT COSTS
NT LOW COST

Scheduling management, and costs of St. Louis air pollution facility
[PB-210020] 01 p0077 N73-10639

Interrelation of logistics cost in managing nickel cadmium batteries
[AD-750907] 06 p0733 N73-15977

Launch program cost comparisons of restartable high energy upper stage rocket engine
[NASA-CR-130275] 07 p0835 N73-16768

Costs of space tug refurbishment
[NASA-CR-130366] 07 p0841 N73-16815

Survey of heavy duty composite materials, development, manufacturing, costs, and applications
09 p1052 N73-18577

Resource requirements for single-stage earth-orbital vehicle
[NASA-CR-124091] 09 p1086 N73-18858

**COTTON**

NT COTTON FIBERS

Control of pink bollworm infestation in southern California cotton fields using ERTS-1 remotely sensed imagery
[E72-10285] 04 p0409 N73-13335

Mapping and control of pink cotton bollworm in California
[E73-10073] 07 p0780 N73-16335

Control and mapping of pink bollworm infestations in cotton fields of California desert areas
[E73-10452] 11 p1283 N73-20411

Mapping of cotton fields in Southern California using ERTS-1 data for control of pink bollworm growth
[PAPER-A15] 19 p2261 N73-28223

Utilization of ERTS-1 imagery for mapping and control of pink bollworm in Imperial, Coachella, and Palo Verde Valleys of California
[E73-10858] 19 p2292 N73-28435

**COTTON FIBERS**

Flame retardant treatments for cotton fabrics and polypropylene fibers
19 p2230 N73-27982

**COUCHES**

Use of cyclic struts as energy absorbers for Apollo couch
09 p1088 N73-18881

Development of crew-couch/restraint system and crew load attenuation system for Apollo command module
[NASA-TN-D-7440] 22 p2720 N73-31768

**COUETTE FLOW**

Couette flows used to determine effect of injection and curvature of walls on flow separation
[AD-753501] 09 p1019 N73-18317

Nonoscillatory characteristics of Taylor vortices occurring in Couette flows based on evolution of eigenvalues and analytic continuation - Part 3
[AD-754480] 12 p1392 N73-21289

Numerical analysis of stability of flows of viscoelastic fluids for three conditions
19 p2251 N73-28146

**COULOMB COLLISIONS**

Influence of Coulomb collisions on plasma ion relaxation in confined circular stabilized magnetic mirror
[EUR-CEA-FC-640] 03 p0341 N73-12783

Rearrangement collision leading to formation of highly excited hydrogenlike states
[NASA-TM-X-66184] 08 p0945 N73-17743

Physical properties of Coulomb collisions
[IPPJ-151] 16 p1949 N73-25773

Fokker-Planck study of Coulomb collisions in plasma confined by mirror magnetic configurations
[EUR-CEA-FC-687] 24 p2964 N73-33691

**COULOMB POTENTIAL**

Charged particle motion in nonhomogeneous field with Coulomb potential
[NOTA-INTERNA-383-B] 01 p0084 N73-10697

Perturbed angular correlation measurements on attenuations caused by rare earth nuclei implantation into metals
18 p2184 N73-27638

**COULOMETERS**

Development and characteristics of coulometric detector for conducting chromatographic analyses
[NLL-TRANS-857-[9022.64]] 05 p0545 N73-14425

**COUNTERMEASURES**

NT CHAFF
NT ELECTRONIC COUNTERMEASURES
NT JAMMING

Design of prototype infrared countermeasure arc lamp
[AD-759752] 17 p2063 N73-26692

Degradation, dispersion and movement of oil slicks by wind and ocean as factors influencing applicability of countermeasures
[WMO-359] 23 p2787 N73-32300

**COUNTERS**

NT CERENKOV COUNTERS
NT ELECTRON COUNTERS
NT GEIGER COUNTERS
NT NEUTRON COUNTERS
NT NEUTRON SPECTROMETERS
NT PARTICLE TELESCOPES
NT PROPORTIONAL COUNTERS
NT QUANTUM COUNTERS
NT RADIATION COUNTERS
NT SCINTILLATION COUNTERS
NT SPARK CHAMBERS

Design of logic counters and scalers based on continued quotients for digital function generators
03 p0278 N73-12253

Application of continued fractions to rational scale counter design
05 p0517 N73-14208

Operating principles and flight test performance of aerosol counter onboard tethered balloon
[AD-751315] 07 p0816 N73-16619

Frequency division with binary ripple counters to provide any integral division ratio
[AD-754030] 11 p1260 N73-20229

Electronic strain level counter on in-flight aircraft
[NASA-CASE-LAR-10756-1] 17 p2090 N73-26910

Lightning flash counter measurements in Finland during 1972
[REPT-43] 20 p2412 N73-29390

**COUNTING CIRCUITS**

NT SCALERS

**COUPLED MODES**

Theoretical model for electromagnetic coupling of Bernstein modes in vacuum boundary of dense plasma
[COO-2181-10] 06 p0704 N73-15742

Computerized simulation of electromagnetic wave coupling modes in plasma diagnostics
[AD-750138] 06 p0706 N73-15763

Plasma instability saturation by resonant mode coupling of shock waves
[AD-751538] 07 p0829 N73-16722

Formulation, evaluation, and demonstration of various procedures for analytically coupling two or more substructures to obtain modal data for assembly
[NASA-CR-112252] 10 p1215 N73-19881

Coupled modes on dielectric image waveguide
12 p1382 N73-21206

**COUPLERS**

NT ANTENNA COUPLERS
NT COUPLING CIRCUITS

Loading effect of probes used in coaxial waveguide experimental coupler
[AD-749060] 05 p0521 N73-14233

Slot line transitions to coaxial line and to microstrip
[AD-761765] 19 p2244 N73-28095

**COUPLES**

Simple thickness modes for couple stress theory for laminated media
[AD-759133] 16 p1933 N73-25642

**COUPLING**

NT COUPLES
NT CROSS COUPLING
NT MICROWAVE COUPLING
NT OPTICAL COUPLING

Capacitance analysis of electromagnetic coupling response in transmission lines and cables
[SC-RR-72-0299] 04 p0458 N73-13741
Fourier and Galerkin techniques for analyzing discontinuities and coupling phenomena in microstrip lines
[AD-750737] 06 p0648 N73-15264
Magnetic couplings and magnetomechanical transmissions for airtight manipulator design
17 p1989 N73-26086
Automatic control systems with variable coupling between functional elements
24 p2900 N73-33149

COUPLING CIRCUITS
Development of electronically tuned automatic antenna matching coupler for radio equipment
[AD-746996] 03 p0274 N73-12227
Radiometer quadrature control and measuring system using optical coupling circuitry
[NASA-CASE-MFS-21660-1] 04 p0421 N73-13434
Equivalent circuit network synthesis for branch guide directional couplers
[PB-212651] 08 p0889 N73-17198
Relationship between power distribution and tolerance sensitivity in linear, two-terminal electric network
[NLL-PO-2895-[9022.81]] 15 p1759 N73-24253
Analysis of power loss for coupled transmission and reaction resonator circuits
[AD-762252] 19 p2248 N73-28126
Design and performance of series power combiner for microwave solid state amplifiers
[AD-764728] 23 p2766 N73-32130

COUPLING COEFFICIENTS
Electromechanical coupling coefficient of interdigital surface wave transducer on piezoelectric ceramic
[AD-761879] 19 p2246 N73-28105

COUPLINGS
Design, development, and evaluation of flexible drive shaft coupling used for propulsion of HH-2D helicopter
[AD-746502] 01 p0063 N73-10519
Computation of tensile stress in shackles assuming elastic deformation
[NPL-NAC-17] 02 p0179 N73-11447
Development of epoxy resin lubricant sealant for hermetic sealing of threaded joints on pipes
[AD-752825] 09 p1040 N73-18486
Evaluation of structural capabilities of Marman V-band coupling and flange with Conoseal gasket for use with 75K NERVA propellant lines
[NASA-CR-132219] 15 p1792 N73-24529

COVALENT BONDS
Electronic structure and properties of covalent and polar solids
14 p1697 N73-23773
Multiple scattering theory and pseudogaps in amorphous covalent semiconductors
[JINR-E4-6747] 15 p1820 N73-24755

COVARIANCE
Approximate solution to covariance of plane wave direction and propagation velocity of signals in array processing scheme
[AD-747591] 03 p0267 N73-12160
Necessity of probability conservation law in quantum theories of gravitation
12 p1393 N73-21296
Estimates of meteorological autocorrelation and cross-correlation functions
[NLL-M-22887-[5828.4F]] 16 p1934 N73-25646
Determining mean and covariance errors in alpha-beta filter operating in Cartesian coordinates
[AD-759011] 16 p1935 N73-25656

COVES
U BAYS [TOPOGRAPHIC FEATURES]

COWELL METHOD
U NUMERICAL INTEGRATION

CRAB NEBULA
Meter wavelength observations of Crab nebula pulsar using very long base-line interferometry techniques
[NASA-TM-X-66071] 01 p0103 N73-10852
Model of Crab nebula derived from dual-frequency radio measurements
[AD-744678] 01 p0106 N73-10879
Balloon observation of pulsed gamma rays above 250 keV from Crab Nebula pulsar NP 0532
12 p1444 N73-21698
Attenuation of X rays emitted by supernovae remnants and Crab Nebula
[NASA-TM-X-64722] 12 p1445 N73-21701
Measurement of cosmic gamma ray emission from galactic center, Crab nebula, and diffuse radiation
19 p2331 N73-28757
European measurements of diffuse flux and Crab pulsar NP 0532
19 p2331 N73-28758
Detection of high energy gamma rays from Crab nebula pulsar by balloon flight with gas Cerenkov telescope
20 p2467 N73-29822

CRACK FORMATION
U CRACK INITIATION

CRACK INITIATION
Ultrasonic method for detecting onset of fatigue damage in metal specimens
[AD-745978] 02 p0175 N73-11418
Four basic types of metal fatigue with distinctive modes of crack initiation and growth
[AD-746121] 02 p0187 N73-11519
Correspondance between energy criterion for fracture and mathematical modeling of strain effects at tip of cracks
[AD-746010] 02 p0239 N73-11943
Lowered ductility and crack initiation in neutron irradiated steels after tensile testing
[STU-70-419/U-350-A] 04 p0433 N73-13533
Crack formation during stress-relief annealing in heat-affected zones of weld seams in low-alloy steels
[NLL-RISLEY-TR-2507-[9091.9F]] 06 p0676 N73-15499
Effect of constant applied stress in crack initiation of aluminum and titanium alloys exposed to salt solution and organic fluids
[NASA-CR-124110] 09 p1045 N73-18525
Crack tip plasticity and fracture initiation criteria
[COO-3084-16] 10 p1221 N73-19926
Precipitate size and distribution effects on fatigue crack initiation and propagation in high strength steel
[AD-759048] 16 p1971 N73-25940
Crack initiation and fatigue fracture in overload mechanism of solid structures
[AD-760007] 17 p2048 N73-26568
Statistical analysis of crack growth in various materials resulting from variable loads
[AD-761445] 19 p2349 N73-28895
Techniques for controlling time to fatigue crack initiation in design of aircraft structures and application of residual stress analyses
20 p2481 N73-29930
Application of growth rate data and analytical retardation models for predicting crack growth under variable amplitude loading
20 p2481 N73-29932
Fatigue crack tip deformation and fatigue crack propagation
21 p2602 N73-30854
Hydrogen diffusion and hydrogen induced cracking of structural materials
[COO-3166-5] 21 p2604 N73-30867
Strain energy density and surface layer energy for crack-like ellipse
[NASA-CR-132338] 24 p2988 N73-33879

CRACK PROPAGATION
Stress history effect on incubation time for stress corrosion crack growth in E-4340 HR steel
[AD-745308] 01 p0068 N73-10553
Stress corrosion cracking test for armor alloys with self-loading
[AD-746251] 01 p0068 N73-10560
Acoustic emission and crack propagation in single crystal MgO and glass as model ceramic materials
[AD-745000] 01 p0070 N73-10575
Stress field intensity in opening interface crack in composite materials
[AD-746033] 01 p0071 N73-10583
Application of dynamic photoelasticity to analyze crack branching in homalite sheets
[AD-744661] 01 p0114 N73-10940
Crack propagation and arrest in impacted, edge cracked, tension plates analyzed by dynamic photoelasticity
[AD-745792] 01 p0114 N73-10946
Analysis of fatigue crack propagation characteristics of steel structures in F-111 aircraft under specific flight loading spectra
[AD-746343] 02 p0127 N73-11033
Electron fractography of cleavage in metal crystals discussing crack propagation
[NLR-TR-71047-U] 02 p0187 N73-11513
Fatigue crack propagation in 2024-T3 aluminum alloy sheet in vacuum and air
[NLR-TR-71032-U] 02 p0187 N73-11514
Analysis of fatigue crack growth data obtained in high strength aluminum alloys to separate metallurgical effects from other factors
[AD-745989] 02 p0187 N73-11518
Scanning electron microscope study of fracture and crack propagation in metals
[AD-746125] 02 p0187 N73-11520
Nonmetallic inclusion effects on crack growth rate in two alloy steels
[AD-746950] 02 p0189 N73-11530
Low cycle fatigue crack propagation characteristics of high strength alloys with high levels of fracture toughness
[AD-747243] 02 p0190 N73-11538
Computer program to determine crack propagation characteristics of ultra high strength steel under various load cycles
[ARL/SM-NOTE-376] 02 p0237 N73-11930
Application of acoustic emission testing to yielding, fracture, slow and fast crack growth
[AD-746261] 02 p0239 N73-11941
References on fatigue and fracture of aircraft structures and materials to include instruments, sonic fatigue, and mechanical fasteners
[AD-748100] 03 p0254 N73-12053
Bibliographic survey on stress corrosion cracking of high strength aluminum alloys, including oxide effects
[DLR-FB-71-105] 03 p0316 N73-12572
Effect of neutron irradiation on fatigue crack propagation in stainless steel samples at high temperatures using fracture mechanics approach
[AD-747950] 03 p0316 N73-12578
Effects of surface layer on plastic deformation and crack propagation, using Fe-Si alloys
[AD-748098] 03 p0318 N73-12594
Mechanisms of corrosion fatigue crack propagation in Al-Zn-Mg including effect of cyclic stress waveform
[AD-747709] 03 p0319 N73-12597
Fracture and fatigue crack propagation characteristics of annealed titanium alloy plate
[AD-748644] 03 p0319 N73-12600
Analysis of crack tip deformation in boron-aluminum sheet and laminar steel sheet resulting from crack propagation
[AD-747760] 03 p0322 N73-12623
X ray diffraction analysis of crack propagation in deformed, notched, wedge shaped silicon crystal
[AD-746275] 03 p0346 N73-12820
Analysis of crack propagation properties of solid rocket propellants based on relation between crack tip stress intensity factor and crack velocity
[AD-747531] 03 p0350 N73-12853
Fatigue and crack propagation characteristics of aluminum alloy sheet under controlled cycle stress conditions to simulate fuel tank structural failure
[NASA-CR-128600] 03 p0360 N73-12935
Fatigue crack propagation in aluminum alloy sheets in environments of dry argon, normal air, distilled water, and aqueous sodium chloride solutions
[NLR-TR-72005-U] 04 p0431 N73-13513
Stress corrosion cracking in saline water of TA6V and TU2 titanium alloys
[ONERA-P-145] 04 p0435 N73-13545
Effect of thickness on sustained load crack propagation in Ti-6Al-4V alloy tested in 3-1/2 percent NaCl solution
[AD-748591] 04 p0435 N73-13548
Fatigue crack propagation of aluminum metal sheets under flight simulation loads corresponding to gust spectrum
[NLR-MP-72010-U] 04 p0480 N73-13926
Development of method for determining critical stress intensity for crack propagation and application to reactor components
[RD/B/N-2143] 04 p0481 N73-13934
Microwave coupled stripline, surface crack detector, using pair of conductors over ground to support propagation in two orthogonal TEM modes
[AD-749799] 05 p0549 N73-14462
Experimental determination of fracture strength and critical crack length of 7075-T7351 aluminum alloy plates
[AD-748254] 05 p0563 N73-14575
Environmental fatigue crack propagation in titanium sheet alloys in atmospheres of argon, normal air, distilled water, and salt solution
[NLR-TR-72019-U] 05 p0602 N73-14894
Propagation of fatigue cracks in gas-tungsten-arc welded 304 stainless steels
[HEDL-SA-329] 06 p0677 N73-15510
Fracture strength of aluminum alloys 7075-T6 and 2024-T3 with surface flaws and corner cracks at holes
[NLR-TR-71033-U] 06 p0685 N73-15576
Subcritical crack propagation in pressure vessel plates due to cyclic loads and stresses
[NASA-CR-120834] 06 p0725 N73-15920
Automatic systems for analyzing fatigue crack propagation and for conducting constant stress intensity factor fatigue tests with servo-hydraulic machine
[RD/B/N-2013] 06 p0726 N73-15928
Crystallographic fatigue crack growth in aluminum single crystals
[AD-751603] 07 p0810 N73-16567
Crack growth study and effects of change in spectrum severity and shape on fatigue behavior under random loading
07 p0851 N73-16898
Fatigue crack propagation under flight simulation loading at 10, 1, and 0.1 cycles per second
07 p0851 N73-16900
Structural analysis of two bonded half planes with finite crack perpendicular to and passing through interface
[NASA-CR-2181] 07 p0852 N73-16910
Crack growth characteristics of steel and structural failure of F-111 aircraft frame
[AD-752223] 08 p0868 N73-17024
Measurement of fatigue crack propagation rates in heat treated steels
[PB-212208] 08 p0932 N73-17635
Direct current electrical resistance crack monitoring technique for detection of crack propagation in steels
[PB-212206] 08 p0933 N73-17636
Electrical resistance measurements on crack propagation in fracture toughness specimens under variety of environmental and loading conditions
[MG/54/71] 08 p0966 N73-17899
Hydrogen adsorption and diffusion, and subcritical crack growth in high strength steels and nickel alloys
[NASA-CR-130979] 09 p1046 N73-18528

Interaction between creep and fatigue processes during crack growth in sheet specimens of aluminum alloy at 400 F
[AD-753688] 09 p1050 N73-18562
Numerical analysis of stress and deformation at crack tip for case where finite plastic zone exists along crack line
[NAL-TR-293] 09 p1092 N73-18918
Development of three stage model for fatigue failure of structure with several critical regions for initial failure
[ARL/SM-NOTE-338] 09 p1093 N73-18924
Effect of strain hardening on fatigue crack resistance after single cycle peak overload in Ti-6Al-4V Ti alloy
[AD-753899] 10 p1174 N73-19553
Apollo experience report on causes of stress-corrosion cracking of structural materials and corrective actions
[NASA-TN-D-7111] 10 p1214 N73-19875
Development of crack propagation gases based on plating and etching processes and application to center notch, edge notch, and cleavage type specimens
[AD-754762] 11 p1295 N73-20511
Quantitative analysis of hydrogen-induced slow crack growth in low alloy steel in gaseous hydrogen and distilled water environments
[NASA-TM-X-62253] 11 p1305 N73-20589
Acoustic emission correlation with slow crack growth in polycrystalline ceramics
[AD-754839] 11 p1310 N73-20626
Riemann-Hilbert solution to steady state crack propagation in orthotropic solid
[AD-754529] 11 p1332 N73-20810
Effect of load variables on fatigue crack growth at room temperture in Ti-6Al-4V alloy
[NASA-CR-2239] 11 p1345 N73-20913
Seminumerical analysis of three dimensional elastic properties of finite geometry solids with traction-free cracks
[NASA-TN-D-7213] 11 p1345 N73-20917
Analysis of crack nucleation and crack propagation caused by formal separation of impact ductility into components
[AD-754620] 11 p1346 N73-20926
Large diameter, carbon-carbon composite, monofilaments from pyrolysis of organic precursor resins
[NASA-CR-120973] 12 p1408 N73-21414
X ray and electron microscopic analysis of vacuum environment effects on 7075-T6 Al alloy fatigue life, fatigue-crack-growth behavior, and fracture toughness
[NASA-TM-X-69223] 12 p1413 N73-21450
Material selection determined from mathematical model of crack growth and failure
[NASA-TN-D-7221] 12 p1413 N73-21452
Effects of specimen thickness on fatigue-crack growth and fracture toughness of 7075-T6 and 7178-T6 aluminum alloy plates and sheets
[NASA-TN-D-7173] 12 p1413 N73-21453
Effect of surface layer stress on plastic deformation and crack propagation of steel
[AD-755844] 12 p1415 N73-21467
Aluminum and tin alloys for stress corrosion cracking and fatigue crack growth studies pertinent to spacecraft and booster pressure vessels
[NASA-CR-120823] 12 p1462 N73-21846
Analysis of fracture and crack growth properties of 304 stainless steel to determine suitability as material for cryogenic fluid storage pressure vessels
[NASA-CR-121025] 12 p1462 N73-21847
Analysis of metals and alloys to include superelasticity properties, plastic growth in cracks, strain aging, and strengthening by nuclear gamma resonance
[JPRS-58611] 13 p1540 N73-22477
Fatigue mechanics studies of fatigue crack propagation in 2024 aluminum alloy panels containing transverse slits
[ARL/SM-379] 13 p1542 N73-22491
Fatigue damage accumulation and incompatible crack front orientation analyzed from aluminum alloys crack propagation test
[NLR-TR-72061-U] 13 p1543 N73-22504
Fracture mechanics evaluation of effect of explosive bonding on fatigue crack growth in aluminum plates
[AD-756423] 13 p1544 N73-22511
Stress wave diffraction models for crack propagation induced by dynamic loads
13 p1584 N73-22839
Closed form solution using four harmonic functions for elastic solid with plane crack subjected to concentrated shears parallel to edge of crack
[NASA-CR-112317] 13 p1585 N73-22848
Effect of biaxial loading on flaw growth rate of aluminum alloys used in space shuttle cryogenic tankage
[NASA-CR-128904] 13 p1586 N73-22855
Strains affecting growth rate of edge cracks in acoustically excited panels
[ISVR-TR-59] 13 p1586 N73-22860
Fatigue crack propagation and retardation experiments using polymethyl methacrylate
[AD-756490] 14 p1681 N73-23641
Protection of titanium microstructure with intermediate nickel barrier to prevent abrasion and crack propagation on turbine compressor blades
[AD-758276] 14 p1682 N73-23651
Stress analysis of plates with part circular and flat bottomed cracks and various flaw depths using stress intensity factors from photoelastic data
[NASA-CR-132015] 14 p1715 N73-23915
Survey of electron fractography in field of fatigue cracking, ductile fracture, cleavage, and stress corrosion
[NLR-TR-72029-U] 14 p1715 N73-23916
Assumed stress hybrid finite element method for fracture mechanics and elastic-plastic analysis
[AD-757523] 14 p1717 N73-23931
Center cracked tension specimen for determining plane stress fracture mechanics in metal plates
[AD-757654] 14 p1717 N73-23933
Fatigue tests on Comet aircraft pressure cabin to determine effects of pressure cycles on structural stability of cabin windows
[ARC-R/M-3248] 15 p1728 N73-24017
Design criteria and analysis procedures to minimize occurrence of major structural failures in airframes due to undetected damage
[AD-757870] 15 p1735 N73-24074
Asymptotic finite-deformation analysis of elastostatic field near tip of crack
[AD-757777] 15 p1840 N73-24908
Corrosion fatigue crack growth of high strength steels in hydrogen and water/water vapor environments
[AD-759088] 16 p1930 N73-25615
Phenomenological analysis of interaction of creep and fatigue
16 p1968 N73-25922
Modified boundary collocation method for crack fracture mechanics analysis on cylindrical section
[AD-758849] 16 p1970 N73-25932
Effects of stress concentration ahead of running crack in sheets with centrally located hole
[AD-759734] 16 p1972 N73-25950
Effect of martensitic microstructure on fatigue life and crack propagation characteristics of high strength steels
[S-253] 17 p2044 N73-26536
Application of principles of fracture mechanics to problem of preventing brittle fracture in sheet structures
[RAE-LIB-TRANS-1648] 17 p2092 N73-26921
Stress analysis of pressurized shallow cylindrical shell containing two collinear axial cracks of equal length
[NASA-CR-132271] 17 p2093 N73-26932
Stress analysis of elastic plane containing elastic inclusion using singular integral equations
[NASA-CR-132272] 17 p2093 N73-26934
Finite element calculation of tapered double cantilever beam modulus of elasticity for sharp blunted cracks
[NLR-TR-72083-U] 17 p2094 N73-26941
Effects of mechanical and metallurgical factors on crack propagation and ductile fracturing resistance of steels
[PB-218919] 18 p2161 N73-27458
Accelerated test technique for determination of K ISCC in steels
[PB-217215/3] 18 p2161 N73-27460
Instability model for stress corrosion and fatigue crack propagation in 4340 steel
[AD-761148] 18 p2162 N73-27461
Effect of stress intensity on fatigue crack growth in 5456-H117 aluminum alloys
[AD-760668] 18 p2162 N73-27465
Crack growth in viscoelastic polymers
[AD-759379] 18 p2168 N73-27513
Analysis of threshold of alternating range of stress intensity factor for producing extremely slow fatigue crack growth in aluminum alloys
18 p2202 N73-27779
Development of modeling schemes to predict effect of coalescence on observed growth characteristics during dynamic fracture
[AD-761082] 18 p2204 N73-27790
Analysis of collocation data using approximation method and fracture mechanics
[AD-761102] 18 p2204 N73-27791
Bonded half planes containing an arbitrarily oriented crack
[NASA-CR-132290] 19 p2348 N73-28888
Crack arresting in single edge notch A533 B steel at room temperature
[HSSTP-TR-27] 19 p2349 N73-28892
Metallurgical and environmental factors influencing stress corrosion cracking
[AD-762541] 20 p2431 N73-29528
Compact, portable nondestructive test instrument for susceptability determination to stress corrosion cracking
[AD-762777] 20 p2433 N73-29538
Vibration stability contact and interfacial crack propagation for partially delaminated layered circular cylindrical shells
20 p2476 N73-29891
Fracture mechanics for Interfacial crack between adhesively bonded dissimiliar materials
20 p2477 N73-29898
Mechanical properties and crack growth in thick welded plates of aluminum at room and cryogenic temperature
[NASA-TN-D-7377] 20 p2483 N73-29946
Effect of O2-H2 atmosphere, H2, Ar, and room air on fatigue crack propagation in 4340 steel
[COO-3166-4] 21 p2559 N73-30513
Effect of stress on fatigue crack propagation in metals
[AD-763776] 21 p2560 N73-30523
Rate theory for determining failure accumulation in composite propellants
[AD-763806] 21 p2588 N73-30733
Fatigue crack tip deformation and fatigue crack propagation
21 p2602 N73-30854
Application of fracture prevention principles to airframes to reduce catastrophic failure and increase service life
[AD-764513] 22 p2617 N73-30969
Environmental fatigue crack propagation in Ti-Al-Sn
[NLR-TR-72093-U] 22 p2686 N73-31511
Crack propagation in glass and ceramic materials
[AD-764045] 22 p2690 N73-31543
Application of reliability analysis to aircraft structures subject to fatigue crack growth and periodic structural inspection
[AD-764775] 23 p2798 N73-32383
Crack propagation of 2219-T87 aluminum alloy from 20 K to 422 K
[NASA-CR-134047] 23 p2805 N73-32430
Fatigue - crack growth of Ti-6 Al-2 Cb-1 Ta-0.8 Mo alloy in air and sea water environment
[AD-765318] 23 p2805 N73-32433
Interaction of advancing crack with pre-existing diffusion bonded microcracks in Ti-AlV alloy composites
[AD-765166] 23 p2811 N73-32476
Crack propagation velocities in NaCl crystals
23 p2826 N73-32586
Crack closure phenomenon in fatigue using Ti-6Al-4V titanium alloy
[NASA-CR-2319] 23 p2853 N73-32800
Effects of surface layer on plastic deformation and crack propagation
[AD-765519] 24 p2937 N73-33453

**CRACKING [FRACTURING]**

NT STRESS CORROSION CRACKING

Atomistic approach to modeling crack tips
[AD-746711] 02 p0220 N73-11784
Stress corrosion cracking of sensitized austenitic stainless steels in oxygenated high temperature water
[BMI-1927] 05 p0562 N73-14565
Effect of sodium chloride solution and distilled water on stress corrosion crack propagation in aluminum alloy 7075
[NLR-TR-71090-U-PT-1] 06 p0685 N73-15577
Aircraft accident involving Beechcraft 18 aircraft on air taxi flight from Cleveland, Ohio airport on 22 June, 1972
[NTSB-AAR-72-33] 07 p0738 N73-16006
Structural analysis of two bonded half planes with finite crack perpendicular to and passing through interface
[NASA-CR-2181] 07 p0852 N73-16910
Development of method and equipment for detecting cracks in materials with porous subsurface matrix covered by impervious coating
[NASA-CASE-MSC-14187-1] 08 p0923 N73-17564
Stress corrosion cracking of steel double cantilever beam specimens produced by loading sequence in aqueous environment
[AD-752215] 08 p0933 N73-17637
Static and fatigue loading tests of bonded lap joints to determine crack length leading to failure of joint
[NASA-CR-112219] 08 p0966 N73-17896
Stress-corrosion cracking of zirconium alloys in nuclear reactor environment
09 p1063 N73-18670
Stress-corrosion cracking of zirconium alloy fuel element sheaths subjected to tension stress in iodine vapor environment
09 p1063 N73-18671
Photoelastic analysis of plane polyester specimens containing fatigue crack to determine effect of plastic yielding on stress distribution near crack
[TAE-155] 09 p1093 N73-18923
Application of Schwarz-Neumann alternating method to stress intensity solutions of edge and surface crack problems
[NASA-CR-112299] 11 p1345 N73-20912
Mechanical properties and stress corrosion cracking of 431 stainless steel alloy at low temperatures
[NASA-TM-X-64729] 12 p1412 N73-21441
Improved silicide coatings for refractory metals employed in space shuttles and gas turbine engine components
[NASA-CASE-LEW-11179-1] 13 p1540 N73-22474
Application of crack opening stretch concept to fracture problems
13 p1585 N73-22846

Seam weld cracking in lithium hydride shielding of SNAP 8 reactor after irradiation
[NASA-CR-121157] 14 p1691 N73-23726
Development of photoelastic stress freezing and slicing method to determine stress intensity around surface flaws
[AD-758140] 14 p1717 N73-23934
Modified filler metal composite for reducing or eliminating underbread cracking in multipass gas tungsten arc plate welds of T-111
[NASA-CR-121198] 19 p2304 N73-28530
Statistical analysis of crack growth in various materials resulting from variable loads
[AD-761445] 19 p2349 N73-28895
Theoretical and experimental approach to stress corrosion cracking in metal alloys
21 p2603 N73-30859
Embrittlement and cracking of steels
[CEA-BIB-204] 22 p2685 N73-31506
Stress corrosion cracking of steels in liquid ammonia environments
24 p2932 N73-33420
Stress corrosion cracking in gaseous and aqueous environments
24 p2933 N73-33426

**CRACKS**
NT MICROCRACKS
NT SURFACE CRACKS
Stress singularities associated with crack inclined to bimaterial interface
[AD-750367] 06 p0689 N73-15607
Shearing mode stress intensity for finite length crack in bimaterial composite
[AD-750498] 06 p0727 N73-15937
Numerical solution for stress concentration factors in isotropic and layered composites with parallel and collinear cracks
[WB-5/72] 09 p1052 N73-18576
Crack size and grain size dependence of brittle fracture stress
[AD-753525] 09 p1076 N73-18781
Effects of circular inclusion of different elastic material on stress stage of cracked flat plates
[AD-754211] 10 p1222 N73-19936
Fracture toughness of flat elastic cracked plate with elastic circular inclusion
[AD-754210] 10 p1222 N73-19937
Detection of acoustic emission signals from fatigue cracks during cyclic bend tests
[NASA-TM-X-68228] 12 p1462 N73-21848
Development of approximate equation for determining stress intensities for quarter circular cracks emanating from circular hole in sheet material
[AD-757550] 14 p1716 N73-23928
Fracture mechanics of elastic interactions between cracks and inclusions in composite materials
[NASA-CR-132292] 19 p2312 N73-28593
Edge cracks in infinite strip
[NASA-CR-132288] 19 p2348 N73-28885
Interaction between circular inclusion and arbitrarily oriented crack
[NASA-CR-132291] 19 p2348 N73-28886
Orthotropic effects in cracked cylindrical shell
[NASA-CR-132295] 19 p2348 N73-28887
Development of fatigue cracks in flat plates under action of cyclic loads
[AD-761584] 19 p2351 N73-28911
Distribution of stress across thickness near crack tip in epoxy resin plate subjected to approximate cylindrical bending
20 p2476 N73-29893
Elastic stress analysis of aluminum-epoxy plate with crack normal to interfaces
20 p2478 N73-29901
Interaction between parallel cracks in layered composites
[NASA-CR-132287] 20 p2482 N73-29936
Technique for dealing with problem of elastic domain containing arbitrarily oriented internal crack
[NASA-CR-132289] 20 p2482 N73-29937

**CRAFT**
U VEHICLES

**CRANES**
Design development, and evaluation of hoist for H-3 helicopter rescue system
[AD-750289] 06 p0623 N73-15054

**CRANIUM**
Vestibular function loss in man after unilateral section of eighth cranial nerve
[NASA-CR-129672] 04 p0379 N73-13084

**CRASH INJURIES**
Statistical analysis of impact injuries to seated human responding to square wave energy absorption of vertical deceleration pulse representing helicopter crash
[AD-745919] 02 p0136 N73-11102
Application of aircraft crash investigation procedures to railroad passenger train derailment
[FAA-AM-73-1] 19 p2218 N73-27896

**CRASH LANDING**
Aircraft accident involving attempted takeoff of Sabre Mark 5 aircraft at Sacramento, California airport on 24 Sept. 1972
[NTSB-AAR-73-6] 14 p1602 N73-22985
Analysis of high velocity spacecraft crash landing on planetary surfaces for possible encapsulated microorganism release
[NASA-CR-131835] 16 p1966 N73-25904
Crew survival after emergency landing or ditching in unpopulated areas
[NASA-TT-F-15047] 20 p2371 N73-29053

**CRASHES**
NT CRASH LANDING
Investigation of crash of L-1011 aircraft near Miami, Florida on 29 Dec. 1972
06 p0619 N73-15024
Aircraft accident involving crash of Turbo Commander aircraft following takeoff and climbout from Greater Pittsburgh Airport, Pennsylvania on 14 Aug. 1972
[NTSB-AAR-73-5] 13 p1474 N73-21936
Aircraft accident involving crash of TU-144 aircraft at Paris Air Show in 1973
[NASA-TT-F-15062] 20 p2360 N73-28982
Aircraft accident involving L-1011 aircraft crash near Miami, Florida on 29 Dec. 1972 during examination of suspected nose gear malfunction
[NTSB-AAR-73-14] 20 p2360 N73-28984

**CRATERING**
NT PROJECTILE CRATERING

**CRATERS**
NT LUNAR CRATERS
NT METEORITE CRATERS
Discovery of previously unknown structural basin and crater on Apollo 16 photography of far side highlands near eastern limb of moon - Part H
12 p1453 N73-21772
Martian surface cratering analysis using Mariner 9 observations
23 p2839 N73-32688

**CRAZING**
U SURFACE CRACKS

**CREATININE**
Elimination of creatinine in urine during prolonged hypokinesia
24 p2884 N73-33029

**CREATION**
U CREATIVITY

**CREATIVITY**
General problems with psychology in scientific and technical creativity
[TT-70-57147-1] 21 p2502 N73-30074

**CREEP ANALYSIS**
Effects of diffusional creep on particle morphology of polycrystalline alloys strengthened by second-phase particles
[NASA-TN-D-7177] 09 p1047 N73-18536
Constant-stress irradiation creep capsules for application of load to several graphite samples by single pneumatic bellows
[BNWL-SA-4199] 17 p2050 N73-26586
Fatigue design, below and within creep range
[AD-762619] 20 p2432 N73-29536
Thermal and electrical properties of titanium alloyed with vanadium and high temperature creep of metal with fcc lattice
[JPRS-59623] 22 p2683 N73-31490
High temperature creep of metals with face centered cubic lattice
22 p2683 N73-31492
Steady state creep in orthotropic materials
22 p2724 N73-31795

**CREEP BUCKLING**
Theoretical analysis of snap-through buckling of nonshallow toggle truss structure in creep
[AD-756188] 13 p1589 N73-22888

**CREEP DIAGRAMS**
Creep measurements on metals for calculating stress-strain-time relaxation curves
02 p0186 N73-11507
Deformation mechanism diagrams and creep of tungsten lamp filaments
[AD-755230] 12 p1441 N73-21680
Phenomenological analysis of interaction of creep and fatigue
16 p1968 N73-25922

**CREEP PROPERTIES**
NT TENSILE CREEP
Fast reactor irradiation effects on creep behavior of annealed type 316 stainless steels
[HEDL-SA-300] 03 p0314 N73-12559
Time controlled creep-fatigue interaction for type 403 stainless steels at high temperature
[ORNL-4757] 03 p0315 N73-12565
Relationship between structure and high temperature creep and creep rupture of metals
[SU-326-P-17-X-3] 03 p0315 N73-12566
Influence of temperature on creep and strength characteristics of organic PRD49 fiber/epoxy composites
[NASA-TN-D-7120] 03 p0320 N73-12607
Influence of creep damage on low cycle thermal-mechanical fatigue behavior of two tantalum base alloys
[NASA-CR-121001] 04 p0431 N73-13514
Diffusion creep and creep degradation in precipitation hardened TD-NiCr alloy
[NASA-TN-D-7079] 04 p0433 N73-13530
Determination of activation parameters and microcreep in niobium single crystals at low temperature
[COO-1198-909] 04 p0458 N73-13742
Numerical analysis of incompressible linearly compressible viscoelastic creep and relaxation for plastic materials
[AD-752067] 08 p0967 N73-17903
Interaction between creep and fatigue processes during crack growth in sheet specimens of aluminum alloy at 400 F
[AD-753688] 09 p1050 N73-18562
Methods for bounding life of structures subjected to constant loads and temperature within creep range
[RD/B/N-2257] 10 p1220 N73-19925
Creep properties of composite, plastic reinforced polyester concretes
[AD-752454] 10 p1221 N73-19930
Creep processes in vacuum sintered copper and silver
12 p1407 N73-21407
Steady state creep rate of nickel as effected by binary alloys at increased temperatures
12 p1413 N73-21448
Strengthening of zirconium alloys in creep through interaction of mobile dislocations and gas bubbles
[AECL-4252] 12 p1415 N73-21464
Tensile properties and creep behavior of tungsten alloys dispersion strengthened by ZrO2
16 p1927 N73-25590
Harper-Dorn creep and microstructure of pure aluminum and other metals at high temperature
[LBL-1158] 16 p1928 N73-25604
Change in fine structure of nickel-chromium heat resistant alloys during creep
[AD-759233] 16 p1971 N73-25939
Thermal expansion instability and effect on creep properties of polyurethane
[AD-762458] 19 p2313 N73-28602
Fatigue and creep-fatigue behavior of irradiated austenitic stainless steel used in LMFBR design
[ANCR-1096] 19 p2349 N73-28891
Equations for creep and stress relaxation in nickel-based alloy bolted joints subjected to vibration
[AD-761455] 19 p2349 N73-28897
Control of material or process variables to optimize short time creep behavior of hot pressed beryllium
[AD-763121] 20 p2432 N73-29537
High temperature creep of Al alloys tin, and lead at intermediate and low stresses
[LBL-1183] 21 p2559 N73-30512
Creep properties of aligned silver-magnesium eutectic alloy
[AD-763375] 21 p2561 N73-30531
Creep behavior of polycrystalline aluminum oxide cermets with varying chromium concentrations
[KFK-1753] 21 p2563 N73-30545
Vacuum creep behavior of tantalum alloys and tungsten
[NASA-CR-134481] 22 p2684 N73-31496
Creep tests of fine-grained polycrystalline ice under uniaxial and multiaxial stress conditions to predict time-dependent deformational behavior
22 p2723 N73-31791
Computer program for use with thermal-elastic-plastic-creep structural analyzer for structural analysis of spacecraft and propulsion systems - Vol. 2
[NASA-CR-124391] 22 p2725 N73-31806
Application of structural computer program for analysis of creep stress in thrust chamber liner - Vol.3
[D5-17266-3-VOL-3] 22 p2725 N73-31807
Creep induced buckling of infinitely long sandwich panel under uniform pressure and uniform temperature
[AD-764311] 22 p2725 N73-31810
High temperature creep resistance of Ti alloys
[AD-765784] 24 p2937 N73-33454
Creep characterization tests on stainless steels
[ORNL-TM-4105] 24 p2954 N73-33597

**CREEP RESISTANCE**
U CREEP STRENGTH

**CREEP RUPTURE STRENGTH**
Effects of irradiation microstructure and creep rupture properties of annealed and cold worked type 316 stainless steel
[CONF-720604-4] 03 p0314 N73-12560
Stress-rupture strength of turbine blade root joints at elevated temperature and prolonged stress loads
[AD-749589] 04 p0465 N73-13788
Comparative inter-laboratory creep rupture tests on temperature measurement and control
[PB-211172] 06 p0674 N73-15487
Data compiled in international comparative creep rupture program using two types of steel as test materials
[PB-211174] 06 p0685 N73-15578
Creep rupture tests of Inconel 702 tubes at high temperatures and internal helium pressures to determine service life
[NASA-TM-X-2728] 08 p0932 N73-17628
Creep rupture tests of Hastelloy-X tubes at high temperatures and internal helium pressures to determine service life
[NASA-TM-X-2727] 08 p0932 N73-17629

Tin alloying effects on plastic deformation, mechanical, and stress-rupture properties of Ni-Cr alloys
[JPRS-58159] 09 p1048 N73-18546
Stress-rupture strength testing and principles of creep-rupture in heat resistant alloys
[JPRS-58760] 13 p1542 N73-22494
Investigation of creep rupture strength and plastic properties of heat resistant alloys
13 p1542 N73-22496
Effect of thermal cycling of structure and properties of directionally solidified eutectic composite
[NASA-CR-121249] 21 p2562 N73-30537
Laws governing stress-rupture strength for structural materials under conditions of cyclic loading
[AD-764665] 23 p2854 N73-32810

**CREEP STRENGTH**
Development of methods for determining relationships between shapes of creep curves and changes in structure of metal specimens by exponential function of real order
[NLL-NEL-TT-2404-[6075.461]]
02 p0185 N73-11498
Effect of mechanical-thermal pretreatments on time-to-rupture and creep strength of nickel-chromium steels
[KFK-1535] 03 p0313 N73-12557
Influence of creep strain on elastic modulus, crystallographic orientation, and density of POCO graphite
[LA-DC-13292] 03 p0321 N73-12614
Fabrication and creep strength of precipitation hardened heat resistant alloys
[ITE-MITT-7/1972] 06 p0684 N73-15572
Analysis of short time elevated temperature properties of platinum, rhodium, and palladium alloys
[NLL-M-22799-[5828.4F]] 11 p1304 N73-20582
Strengthening of zirconium alloys in creep through interaction of mobile dislocations and gas bubbles
[AECL-4252] 12 p1415 N73-21464
Development of procedure for designing elevated temperature structures to achieve safety factors and structural integrity of room temperature conditions
[NASA-CR-124232] 13 p1585 N73-22851

**CREEP TESTS**
Development of methods for determining relationships between shapes of creep curves and changes in structure of metal specimens by exponential function of real order
[NLL-NEL-TT-2404-[6075.461]]
02 p0185 N73-11498
Creep tests of beta titanium alloy IVT-1 over range of temperatures and stresses
[AD-747090] 02 p0189 N73-11536
Tensile creep tests to determine properties of 7075-T6 aluminum alloy reinforced with unidirectional boron/epoxy
[NBS-TN-722] 04 p0437 N73-13565
Creep and stress relaxation tests on Cr-Ni austenitic steel at 700 C
[STU-70-419/U-350-B] 04 p0481 N73-13932
Intergranular deformation in creep elongation of platium rhodium alloys
[AD-753508] 10 p1173 N73-19546
Creep tests and transmission electron microscopic observation of grain boundary structure in stainless steel bicrystals
[CEA-R-4317] 10 p1200 N73-19768
Analysis of short time elevated temperature properties of platinum, rhodium, and palladium alloys
[NLL-M-22799-[5828.4F]] 11 p1304 N73-20582
Method of life prediction for nickel-based Udimet alloy by high temperature creep/fatigue testing
[NASA-CR-120958] 12 p1462 N73-21845
Creep test measurement of stresses generated during high temperature oxidation of copper and nickel
16 p1926 N73-25588
Creep tests of fine-grained polycrystalline ice under uniaxial and multiaxial stress conditions to predict time-dependent deformational behavior
22 p2723 N73-31791
Correlation of creep rate with microstructural changes during high temperature creep
[NASA-CR-135698] 23 p2804 N73-32426
Heat to heat variation in fatigue and creep-fatigue behavior of AISI Type 304 stainless steel, and fatigue behavior of type 308 stainless steel weld material
[ANCR-1097] 24 p2936 N73-33450
Creep fracture properties of weld repaired cast titanium alloy
[AD-765185] 24 p2937 N73-33451

**CRESTATRONS**
U TRAVELING WAVE TUBES

**CRESTS**
U WAVES

**CREVASSES**
NT GLACIERS

**CREVICES**
U CRACKS

**CREWS**
NT FLIGHT CREWS
NT SPACECREWS
Problems involved in achieving harmony in life and work of small groups applied to prolonged space flights
24 p2884 N73-33032

**CRICKETS**
NT TRIBOLIA

**CRITERIA**
NT STRUCTURAL DESIGN CRITERIA
Criteria for selected response surface methodology design variants in human performance research
[AD-748236] 05 p0503 N73-14099
Psychometric criteria for pilot performance in F-4 aircraft fleet
[AD-755184] 14 p1614 N73-23087

**CRITICAL EXPERIMENTS**
Analysis of boron carbide drum-controlled critical reactor experiment
[NASA-TM-X-2680] 03 p0331 N73-12701
Flow configurations for maximum nuclear criticality eigenvalue in gas core reactor
[NASA-CR-121191] 18 p2177 N73-27578

**CRITICAL FLOW**
Critical flow study in gas-liquid flow, using numerical models for predicting critical flow rate
[AEC-TR-7309] 03 p0284 N73-12303
Survey of data involving design of equipment for two phase flow of cryogenic fluids based on critical flow rate
[NASA-CR-130793] 09 p1013 N73-18270

**CRITICAL FREQUENCIES**
Prediction of F 2 region critical frequencies*from spatial and temporal correlation data
13 p1520 N73-22320

**CRITICAL LOADING**
Experimental determination of fracture strength and critical crack length of 7075-T7351 aluminum alloy plates
[AD-748254] 05 p0563 N73-14575
Fatigue behavior of corrugated panels, riveted along corrugations, subjected to cyclic compressive critical loads
[PUBL-1351] 06 p0724 N73-15915
Nondestructive methods determining composite beam and plate critical loading
[ENSMP-010] 17 p2094 N73-26940

**CRITICAL MACH NUMBER**
U CRITICAL VELOCITY
U MACH NUMBER

**CRITICAL PATH METHOD**
Project control in ESRO program
05 p0611 N73-14973

**CRITICAL POINT**
Multiplicative renormalization group used to compute critical indices in d equals 4 minus sigma dimensions
[NOTA-INTERNA-384] 01 p0080 N73-10661
Field theoretical model for critical behavor of helium 4 above critical point
[NOTA-INTERNA-374] 01 p0083 N73-10689
Bifurcations, for second order recurrence, related to passing through critical case such as real multiplier having modulus equal to one
[LAAS-PUBL-934] 02 p0203 N73-11639
Heat transfer at critical point, jet turbulence, and vortex systems
[AD-747294] 02 p0244 N73-11981
Regularity in phase transitions of magnetic and liquid-gas systems
[COO-1112-63] 03 p0364 N73-12967

**CRITICAL PRESSURE**
Circular cylindrical shell pressure limits
[PB-212638] 07 p0852 N73-16912
Freezing points of crystalline polymers determined as functions of pressure and temperature
[AD-759007] 17 p2051 N73-26591

**CRITICAL REYNOLDS NUMBER**
U CRITICAL VELOCITY
U REYNOLDS NUMBER

**CRITICAL SPEED**
U CRITICAL VELOCITY

**CRITICAL STRESS**
U CRITICAL LOADING

**CRITICAL TEMPERATURE**
Thermophysical properties of helium-4 under various conditions of temperature and pressure
[NASA-CR-128445] 02 p0242 N73-11966
Superconducting properties of crystalline films of aluminum on silicon, considering fluctuating critical temperatures
[BNL-17240] 12 p1441 N73-21672
Electric field and current in thin aluminum film superconductor near critical temperature
[LNF-72/77] 15 p1821 N73-24759
Freezing points of crystalline polymers determined as functions of pressure and temperature
[AD-759007] 17 p2051 N73-26591

**CRITICAL VELOCITY**
Critical velocity and patterns of stationary motion of filament
[JPRS-57813] 06 p0652 N73-15293
Critical velocity study of stationary motion, using loop filament in viscous medium
06 p0652 N73-15295
Liquid helium experiments on ac Josephson effect in superfluid helium and superfluid critical velocities
16 p1944 N73-25728
Experiments on velocity distribution and critical velocity of rotating hydrogen plasma
[TRITA-EPP-73-06] 17 p2068 N73-26736
FORTRAN 4 computer program for calculating critical speeds of rotating shafts
[NASA-TN-D-7385] 19 p2347 N73-28881

**CROP GROWTH**
Mathematical model for photosynthetic gas exchanges in growing wheat and radish biopaks of life support systems
03 p0257 N73-12081
Impact of accurate long range weather forecasts on Wisconsin pea production
06 p0693 N73-15640
Application of color photography and infrared photography for determining effects of weather on coffee crop production
07 p0783 N73-16365
Mapping of cotton fields in Southern California using ERTS-1 data for control of pink bollworm growth
[PAPER-A15] 19 p2261 N73-28223
Application of ERTS-1 data for analysis of agricultural crops and forests in Michigan
19 p2262 N73-28228
Preparation of recognition map to determine crop species and mensuration accuracy in Sacramento Valley, California
[PAPER-A22] 19 p2262 N73-28229
Agricultural analysis of ERTS-1 multispectral band scanner data for Monterey Bay, California
[PAPER-A23] 19 p2262 N73-28230
Quantitative evaluation of computer processed ERTS-1 MSS data classifications to identify major agricultural crops in Illinois
[PAPER-A25] 19 p2262 N73-28232
Environmental study of Lake Champlain and Vermont land use based on ERTS-1 imagery
[PAPER-E11] 19 p2270 N73-28275
Multispectral scanning systems applied to agriculture and forestry
19 p2295 N73-28452
Xenon lamp light sources for plant growth research
20 p2403 N73-29314
Optimal use of solar energy for high capacity crop growth
20 p2404 N73-29317
Comparative studies of photosynthetic activity of pure and mixed crops during vegetative period
20 p2404 N73-29321
Influence of solar radiation in mountainous areas on crop capacity and grain yield of spring wheat
20 p2406 N73-29335
Uniform mapping and monitoring of natural ecosystems and environmental complexes of Colorado Plateau and Sierra-Lahontan areas and estimation of rice crop yields in California and Louisiana
[E73-11070] 23 p2781 N73-32246
Light and carbon dioxide effects on algal life support systems in space flight
[NASA-CR-135796] 24 p2885 N73-33039
Production of vegetables in arid zones using controlled solar greenhouses
24 p2975 N73-33768

**CROP IDENTIFICATION**
Crop identification and acreage measurement in Idaho, Missouri, Kansas, and South Dakota using ERTS-1 imagery
[E72-10179] 01 p0045 N73-10358
Identification and mapping geologic, soil, agriculture, geographic, and land use features using ERTS-1 imagery of Central US
[E72-10232] 02 p0163 N73-11325
Crop identification, acreage estimation, urban land use, soil mapping, and earth resources identification in Wabash River Basin using ERTS-1 imagery
[E72-10208] 03 p0288 N73-12331
Identification of agricultural crops and soil moisture stress in Iowa using ERTS-1 imagery
[E72-10335] 05 p0531 N73-14323
Crop identification and acreage measurement in Missouri, Kansas, South Dakota, and Idaho using ERTS-1 imagery
[E72-10336] 05 p0531 N73-14324
Soil mapping, crop identification, and rangeland assessment in Great Plains using ERTS-1 multisensor imagery
[E72-10369] 05 p0536 N73-14357
Crop identification and acreage estimation using ERTS-1 MSS imagery of northern Illinois
[E73-10039] 07 p0776 N73-16302
Crop identification through interpretation of multiband and multidate photography
07 p0785 N73-16385
Sample classification accuracy of minimum distance and maximum likelihood classifiers and parametric and nonparametric classifiers in remote sensing
[NASA-CR-130030] 07 p0799 N73-16489
Evaluation of ERTS-1 imagery of major crops and soil associations for selected sites in central United States
[E73-10323] 09 p1024 N73-18355

Crop identification and acreage measurement in Missouri, Kansas, South Dakota, and Idaho based on ERTS-1 imagery and aerial photography
[E73-10328] 09 p1024 N73-18359
Identification and classification of Iowa crop lands using ERTS-1 imagery and aerial photography
[E73-10343] 10 p1148 N73-19342
Crop identification, soil mapping, water resources, and urban land use analysis in Wabash River Basin based on ERTS-1 imagery
[E73-10364] 10 p1150 N73-19360
Atmospheric effects on recognition of rice and corn in ERTS-1 imagery of Sacramento Valley
[E73-10390] 11 p1276 N73-20352
Application of ERTS-1 imagery to analysis of agricultural crops and forests in Michigan
[E73-10470] 12 p1395 N73-21307
Identification of corn harvesting in Finney County, Kansas from ERTS-1 imagery
[E73-10472] 12 p1395 N73-21309
Application of ERTS-1 imagery to identification of agricultural crops, grasslands and forestry in Mississippi Delta Region
[E73-10476] 12 p1395 N73-21313
Crop identification and land acreage measurement in Kansas using ERTS-1 imagery
[E73-10514] 13 p1517 N73-22288
Utilization of ERTS-1 data for crop identification and acreage estimation, soil mapping, urban land use, water resources, atmospheric modeling, and earth surface feature identification in Wabash River Basin
[E73-10549] 14 p1655 N73-23422
Analysis of ERTS-1 imagery for crop identification and area estimates in Iowa
[E73-10699] 16 p1903 N73-25391
Utilization of ERTS-1 imagery for crop identification and acreage measurement in South Dakota, Kansas, Missouri, and Idaho
[E73-10734] 17 p2020 N73-26340
Application of ERTS-1 imagery for identifying and mapping rivers, agricultural areas, forest, mineral resources, and water conditions in Thailand
[E73-10746] 17 p2021 N73-26350
Application of ERTS-1 data to crop identification, land use, and engineering geology
[E73-10792] 18 p2137 N73-27268
Interpretation of ERTS-1 data to determine acreage of winter wheat in Kansas based on multispectral band scanner data
[PAPER-A1] 19 p2259 N73-28209
Detection and identification of crops in Imperial Valley, California using ERTS-1 sequential imagery and remote sensing techniques
[PAPER-A2] 19 p2259 N73-28210
Digital analysis of ERTS-1 imagery for southeastern South Dakota to determine cultivated areas and to identify crops
[PAPER-A3] 19 p2259 N73-28211
Application of ERTS-1 imagery for identifying citrus groves and rice fields in Valencia region of Eastern Spain
[PAPER-A4] 19 p2260 N73-28212
Application of ERTS-1 imagery for determining rice growing areas in Philippines and assessment of crop condition
[PAPER-A5] 19 p2260 N73-28213
Application of ERTS-1 imagery for identification of ecological analogs of natural vegetation and food crops in California, Colorado, and Louisiana
[PAPER-A6] 19 p2260 N73-28214
Application of ERTS-1 imagery and aerial photography for monitoring forage crop resources in California
[PAPER-A11] 19 p2260 N73-28219
Detection of phenological event for specific forest and crop types using ERTS-1 imagery
[PAPER-A19] 19 p2261 N73-28226
Application of ERTS-1 data for analysis of agricultural crops and forests in Michigan
19 p2262 N73-28228
Preparation of recognition map to determine crop species and mensuration accuracy in Sacramento Valley, California
[PAPER-A22] 19 p2262 N73-28229
Agricultural analysis of ERTS-1 multispectral band scanner data for Monterey Bay, California
[PAPER-A23] 19 p2262 N73-28230
Evaluation of ERTS-1 data for production of land use stratifications and crop inventory process in San Joaquin County, California
[PAPER-A24] 19 p2262 N73-28231
Quantitative evaluation of computer processed ERTS-1 MSS data classifications to identify major agricultural crops in Illinois
[PAPER-A25] 19 p2262 N73-28232
ERTS-1 detection of plant diseases and nutrient deficiencies, soil types and moisture levels, forests, and crop identification in Mississippi Delta
[E73-10849] 19 p2292 N73-28427
Agricultural and crop identification decisions in Mississippi Delta region of Mississippi using Skylab EREP data
[E73-10870] 20 p2393 N73-29221
Identification of rice fields in Philippes from ERTS-1 imagery
[E73-10908] 20 p2397 N73-29257
Identification and classification of agricultural crops and forest inventory in Iowa from ERTS-1 imagery
[E73-10927] 20 p2398 N73-29276
Comparison of ERTS-1 spectral reflectance measurements of major crops and soil associations for selected sites in Iowa, Kansas, North Dakota, and Texas
[E73-10981] 22 p2657 N73-31288
Crop identification and acreage measurement in Missouri and Idaho from ERTS-1 imagery
[E73-10982] 22 p2658 N73-31289
Selected reclamation studies on geology and crop inventory using ERTS-1 imagery of lower Missouri region
[E73-11027] 22 p2662 N73-31331
Mathematical model for identification of crops from directional reflectance
[NASA-CR-133989] 22 p2691 N73-31555
Crop identification, soil mapping, and atmospheric modeling in Wabash River Basin using ERTS-1 data
[E73-11082] 23 p2782 N73-32257
Identification of agricultural crops in Mississippi Delta from ERTS-1 imagery
[E73-11094] 23 p2783 N73-32261
Delineation of major terrain features, land uses, and crop species in Tennessee Valley through computerized analysis
[E73-11089] 24 p2913 N73-33251
Agricultural crop identification and land use patterns from Skylab data of California
[E73-11163] 24 p2920 N73-33316

**CROP VIGOR**
Multispectral remote sensing techniques for identification of corn blight disease
[NASA-TM-X-69055] 07 p0745 N73-16064
Application of color photography and infrared photography for determining effects of weather on coffee crop production
07 p0783 N73-16365
Application of ERTS-1 imagery for determining rice growing areas in Philippines and assessment of crop condition
[PAPER-A5] 19 p2260 N73-28213

**CROPLANDS**
U FARMLANDS

**CROPS**
NT WHEAT
identification of phenological events, rangelands, and crops using ERTS-1 imagery
[E72-10351] 05 p0533 N73-14339
ERTS-1 MSS imagery of Great Plains rangeland, croplands, and land systems
[E73-10076] 07 p0780 N73-16338
Detection of disease in coffee crops using color photography and infrared photography techniques
07 p0783 N73-16366
Application of ERTS-1 data to analysis of agricultural crops, forests, soils, landforms, and acreage estimates in Michigan
[E73-10483] 12 p1396 N73-21320
Collection and processing of ground truth crop and field data for Skylab-3
[E73-10879] 20 p2394 N73-29230
ERTS-1 measurements of major crops and soil associations in Indiana, North Dakota, Iowa, Nebraska, Kansas, and Texas
[E73-11155] 24 p2919 N73-33309

**CROSS CORRELATION**
Digital on-line spectrum analysis using cross correlation and fast Fourier transformation techniques
[ARC-CP-1225] 09 p1006 N73-18209
Parallel image logical operations using cross correlation
09 p1066 N73-18695
Polarization measurement of whistler-type radio frequency signals by using auto- and cross-correlation functions of horizontal signal components
[CEPHAG-24/72] 13 p1491 N73-22088
Least squares and cross correlation procedure for determining absolute timing of pulsars
13 p1575 N73-22765
Geomagnetic latitude distribution of stationary Pc3 micropulsation statistical properties from power spectra cross correlations
17 p2026 N73-26397
Frequency response of structural systems excited by transient and random loads using cross correlation and spectral analysis techniques
[ISVR-TR-57] 18 p2180 N73-27598
Magnitude, spectra, and cross correlations for plasma fluctuations in Kaufman thruster
[NASA-TM-X-71421] 23 p2830 N73-32616

**CROSS COUPLING**
Theoretical analysis of linear semi-infinite array of uniformly spaced elements to determine mutual coupling effects
[AD-745799] 01 p0034 N73-10263
Mechanical cross coupling of STOL transport aircraft engines
[CRANFIELD-AERO-14] 16 p1955 N73-25819

**CROSS FAULTS**
U GEOLOGICAL FAULTS

**CROSS FLOW**
Convective heat transfer for Newtonian fluid cross flow over circular cylinder
[ESDU-69004-AMEND-A] 02 p0241 N73-11962
Calculation of acoustic field generated by circular jet in presence of low speed crossflow
[NASA-CR-2169] 03 p0252 N73-12036
Flow visualization and analytical analysis of momentum roll up of turbulent circular jet
04 p0403 N73-13286
Wind tunnel tests of VTOL lift fan stages to determine changes in thrust characteristics with varations in back pressure imposed on stages by cross flow
[NASA-TM-X-68169] 06 p0620 N73-15031
Analysis of Magnus sideforce developed by spinning cylinder at angle of attack based on boundary layer and shed vorticity in cross flow
07 p0768 N73-16239
Analysis of downstream mixing of transverse hydrogen injection from single and multiple orifices in Mach 4 boundary layer over flat plate
[NASA-CR-112254] 09 p1015 N73-18285
Semiempirical model for development of round turbulent jet in cross flow using asymptotic solution for jet excess velocity
[NLR-TR-71107-U] 10 p1142 N73-19307
Wind tunnel tests to determine effect of cross flow velocity on jet noise power level using V/STOL model transport
[NASA-CR-114571] 13 p1473 N73-21929
Analysis of aerodynamic interference resulting from jet issuing normal to chordal plane of two dimensional wing in crossflow conditions
13 p1508 N73-22223
Development of procedure for determining characteristics of aircraft roll coupling moment caused by flow induced by deflected wings and cross flow
[ISAS-488-VOL-37-NO-14] 14 p1597 N73-22945
Numerical analysis of incompressible laminar boundary layer on infinite swept wing with arbitrary velocity and suction distribution
[ARC-R/M-3241] 16 p1854 N73-25018
Nonstationary heat and mass transfer developed by transverse flow around cylindrical body to determine conditions at stagnation point
[AD-760396] 17 p2016 N73-26299
Ionic diffusion in electron boundary layer of spotless discharge crossing nitrogen magnetohydrodynamic flow
[IPF-72-3] 17 p2069 N73-26739
Development of theoretical model for determining flow characteristics of round jet in incompressible cross-flow based on matched asymptotic expansion
[NASA-CR-132324] 23 p2775 N73-32191
Asymptotic expansion analysis of jet entrainment in incompressible cross flow
24 p2902 N73-33166

**CROSS SECTIONS**
Computer technique for obtaining near field cross section views of ultrasonic field
[AD-756537] 13 p1502 N73-22170
Differential cross sections in photodisintegration of helium-3
16 p1947 N73-25753
Application of laser energy to induce homogeneous exchange reaction of hydrogen and deuterium
24 p2930 N73-33399

**CROSSED FIELDS**
Higher-temperature limit for turbulent heating of plasma by cross-field current
[ORO-4211-4] 03 p0342 N73-12787
Fast radial motion of toroidal plasma column in transverse magnetic field resulting in controlled displacement of plasma column
[NP-19401] 06 p0705 N73-15754
Nonlinear time dependent phenomena in JxB devices applicable to MHD power generators and electric propulsion engines
[AD-751943] 08 p0956 N73-17826
Steady state hot-ion plasma produced by crossed electric and magnetic fields
[NASA-TM-X-2783] 12 p1433 N73-21613

**CROSSLINKING**
Analysis of crosslinked epoxy-urethane polymer filled with aluminum oxide particles to determine mechanical and thermodynamic properties
[SC-DR-70-617] 07 p0812 N73-16584
Chemical analysis of structure and strength of polymeric glasses, elastomers, fibers, and solid polymeric systems with high degree of crosslinking
[AD-763398] 21 p2564 N73-30555

**CROSSTALK**
Analysis of coupling characteristics and crosswalk between electric cables used in naval environments
[AD-742971] 01 p0032 N73-10253
Analytical prediction of crosstalk in multi-wire digital data transmission
14 p1641 N73-23301

**CRUCIBLES**
Feasibility of using yttrium oxide crucible to induction melt titanium
[AD-754092] 11 p1306 N73-20597

**CRUCIFORM WINGS**
Mathematical model of unsteady pressure distribution on harmonically oscillating slender cruciform wing and cylindrical body configurations
[DLR-FB-71-87] 06 p0615 N73-14990

**CRUDE OIL**
Set of variables crucial to economic outcome of petroleum exploration
[NASA-CR-129595] 04 p0488 N73-13991
Two stochastic models for petroleum exploration
[NASA-CR-129611] 04 p0488 N73-13992
Air-cushion tankers for transporting Alaskan North Slope oil
[NASA-TM-X-2683] 09 p1100 N73-18981
Commercial utility of ERTS-1 imagery in structural reconnaissance of Precambrian Shield for minerals and petroleum
[E73-10523] 14 p1654 N73-23414
Isotopic composition of carbon in carbonaceous rocks from oil field of Belorussia as indication of their origin
[NASA-TT-F-14938] 15 p1780 N73-24426
Commercial application of ERTS-1 imagery in structural reconnaissance for minerals and petroleum
[E73-10700] 16 p1903 N73-25392
Analysis of ERTS-1 imagery of Northern Coast Ranges and Sacramento Valley, California for locating mercury deposits and oil and gas fields
[PAPER-G18] 19 p2265 N73-28249
Application of ERTS-1 imagery to determine geological evidence of mineral and hydrocarbon accumulations in Alaska, Canada, Montana, Colorado, New Mexico, and Texas
[PAPER-G30] 19 p2267 N73-28261
Earthquakes and volcanoes caused by subterranean explosions provoked by petroleum or natural gas
[NASA-TT-F-15095] 21 p2536 N73-30334
Technologies for production and utilization of petroleum, natural gas, oil shale and coal
[BM-IC-8612] 21 p2536 N73-30335
Problems and prospects for marine transportation of oil
[NASA-CR-133854] 21 p2553 N73-30464

**CRUISE MISSILES**
Longitudinal and lateral aerodynamic characteristics of cruise missile with swept wing and conventional aft tails at various Mach numbers
[NASA-TN-D-7069] 01 p0001 N73-10002

**CRUISING FLIGHT**
Calculation of optimal gliding flight paths associated with space shuttle orbiter transition from entry to cruising flight
[NASA-CR-128647] 03 p0359 N73-12922
Analysis of optimum nozzle thrust deflection angles in cruising flight
[ARC-CP-1222] 05 p0590 N73-14796

**CRUSADER AIRCRAFT**
U F-8 AIRCRAFT

**CRUSTS**
NT EARTH CRUST
NT LUNAR CRUST

**CRYODEPOSITS**
Degradation of cold optical systems on orbiting spacecraft by cryodeposition
[AD-756772] 13 p1560 N73-22644

**CRYOGENIC EQUIPMENT**
Unidirectional and bidirectional carbon fiber/epoxy resin composites for cryogenic vessels
[NASA-CR-120899] 02 p0192 N73-11553
Rocket-borne mass spectrometer experiment with cryo-cooled ion source to determine neutral atmosphere composition between 85 and 125 km altitude
[BMFT-FBW-73-03] 11 p1285 N73-20431
Design of welded bellows for cryogenic turbomachinery face seal applications
[NASA-CR-121117] 13 p1533 N73-22423
Inductive reactances of direct sequence of synchronous machine with ferromagnetic screen
[AD-759879] 17 p2039 N73-26494
Cryogenic stability and reliability of operating Nb3Sn coils in helium gas environment
[IPP-4/100] 17 p2063 N73-26690
Industrial applications of cryogenic technology
[AD-762315] 20 p2455 N73-29728
Dual stage check valve for cryogenic supply systems used in space flight environmental control system
[NASA-CASE-MSC-13587-1] 21 p2552 N73-30459
Design of dc brushless motor driven mixer unit for use in cryogenic fluids
[NASA-CR-120963] 22 p2647 N73-31209
Methods of reducing damping in pneumatic piston drivers used in cryogenic armatures
22 p2678 N73-31449

**CRYOGENIC FLUID STORAGE**
Development and characteristics of multilayer insulations for long term cryogenic storage
[NASA-CR-123938] 03 p0320 N73-12606
Design, development, and evaluation of pressurized purge system for reusable space shuttles and fabrication of multilayer insulation systems
[NASA-CR-123942] 03 p0358 N73-12914
Procedure for estimating changes in composition resulting from evaporation during storage of liquid oxygen
[NASA-TM-X-2686] 05 p0498 N73-14056
Liquid hydrogen reorientation in fuel tanks of Centaur launch vehicle using low level accelerations with and without internal baffles
[NASA-TN-D-7168] 07 p0770 N73-16252
Effect of biaxial loading on flaw growth rate of aluminum alloys used in space shuttle cryogenic tankage
[NASA-CR-128904] 13 p1586 N73-22855
Liquid hydrogen booster propellant tank internal insulation system for use in reusable spacecraft
[NASA-CR-121102] 15 p1842 N73-24925
Apollo experience report on design and development of cryogenic storage system and related components
[NASA-TN-D-7288] 16 p1964 N73-25889
Development of computer program and data base for design of cryogenic systems used in space shuttles and spacecraft - Vol. 5 B-1
[NASA-CR-133955] 17 p2087 N73-26883
Computer programmers manual for mathematical model used in design of cryogenic supply systems for space shuttles and spacecraft - Vol. 5 B-2 Part 1
[NASA-CR-133956] 17 p2087 N73-26884
Computer programmers manual for parametric analysis of attitude control propulsion system using converted liquid cryogenics reaction system - Vol. 5 B-3 Part 2
[NASA-CR-133958] 17 p2087 N73-26886
Analysis of parameters for optimization of cryogenic supply system for space shuttles - Vol. 6
[NASA-CR-133959] 17 p2087 N73-26887
Analysis of space shuttle cryogenic fluid storage system to determine heat absorption capability and design of radiators for additional cooling capability - Vol. 4
[NASA-CR-133952] 17 p2088 N73-26895
Evaluation of candidate systems for cryogenic fuel supply system used on space shuttle vehicle - Vol. 3
[NASA-CR-128994] 18 p2199 N73-27752
Analysis of transient pressures in externally pressurized cryogenic hydrogen and oxygen tanks to determine effects of design variables on pressure response
[NASA-CR-133962] 18 p2199 N73-27755
Development of integrated mathematical model for optimization of cryogenic fluid storage and supply systems for spacecraft - Vol. 5A-1
[NASA-CR-133953] 18 p2199 N73-27757
Cyclically heated auxiliary chamber for heating and mixing stored fluids
[NASA-CASE-ARC-10442-1] 21 p2547 N73-30415
Development and application of self evacuating multilayer insulation system for application to space shuttle orbiter liquid hydrogen tanks
[NASA-CR-121166] 21 p2606 N73-30883
Use of nickel steels for cryogenic tanks
[AD-763947] 22 p2679 N73-31457
Cryogenic tanking and partial jettison tests of Centaur launch vehicle and Centaur standard shroud to develop insulation, purge, and vent systems
[NASA-TM-X-71455] 24 p2984 N73-33850

**CRYOGENIC FLUIDS**
NT FLOX
NT LIQUID HELIUM
NT LIQUID HYDROGEN
NT LIQUID NITROGEN
NT LIQUID OXYGEN
NT SOLIDIFIED GASES
Fluid mechanics and dynamic energy separation in steady flow, nonsteady flow, and cryptosteady flow
[AD-747316] 03 p0286 N73-12314
Design and development of device to prevent geysering during convective circulation of cryogenic fluids
[NASA-CASE-KSC-10615] 03 p0304 N73-12486
Performance evaluation of volumetric and mass cryogenic turbine flowmeters
[NBS-TN-624] 04 p0420 N73-13426
Pump for cryogenic liquids using magnetocaloric material
[NASA-CASE-LEW-11672-1] 05 p0551 N73-14479
Theoretical and parametric study of inductive magnetohydrodynamic converters including design of cryogenic experimental 4 kW converter
[DLR-FB-71-74] 06 p0706 N73-15757
Cavitation in liquid cryogens with determination of flow and thermodynamic conditions of cavitating hydrofoil
[NASA-CR-2156] 07 p0770 N73-16255
Survey of data involving design of equipment for two phase flow of cryogenic fluids based on critical flow rate
[NASA-CR-130793] 09 p1013 N73-18270
Role of plastic deformation process in sliding wear of pure Cu and Cu-Al alloy against Type 440 C in cryogenic fuels
[NASA-TN-D-7253] 11 p1305 N73-20591
Effects of low Bond number sloshing on thermal stratification of cryogenic liquids
12 p1391 N73-21283
Calibration of liquid helium-cooled germanium bolometers to determine responsitivity at different chopper frequencies and cryostat temperatures
[BMFT-FBW-73-05] 14 p1666 N73-23524
Application of cryogenic and superconductive systems for propulsion of ships
[AD-758431] 14 p1694 N73-23746
Cryogenic cooling methods for spaceborne systems
[AD-755780] 14 p1720 N73-23958
Analysis of cryogenic supply system for space shuttle vehicles and evaluation of candidate systems - Vol. 1
[NASA-CR-128992] 18 p2199 N73-27756
Design of dc brushless motor driven mixer unit for use in cryogenic fluids
[NASA-CR-120963] 22 p2647 N73-31209

**CRYOGENIC MAGNETS**
Optimization and cost factors for cryogenic and superconducting magnets in plasma physics
[IPP-4/96] 04 p0458 N73-13740

**CRYOGENIC ROCKET PROPELLANTS**
NPSH technique for two phase pumping of cryogenic propellants in turbopumps and rocket engines
03 p0348 N73-12843
Shuttle reaction control system cryogenic liquid distribution system
[NASA-TM-X-68913] 07 p0834 N73-16765
Development and characteristics of auxiliary propulsion system for space shuttle applications - Summary
[NASA-CR-128818] 10 p1208 N73-19827
Analysis of parameters for optimization of cryogenic supply system for space shuttles - Vol. 6
[NASA-CR-133959] 17 p2087 N73-26887
Design and development of optimized cryogenic fuel supply systems for space shuttle vehicles - Vol. 2
[NASA-CR-128993] 18 p2199 N73-27751
Evaluation of candidate systems for cryogenic fuel supply system used on space shuttle vehicle - Vol. 3
[NASA-CR-128994] 18 p2199 N73-27752
Design and tests of composite propulsion feedlines for cryogenic space vehicles - Vol. 1
[NASA-CR-121137-VOL-1] 19 p2346 N73-28868
Design and tests of composite propulsion feedlines for cryogenic space vehicles - Vol. 2
[NASA-CR-121137-VOL-2] 19 p2346 N73-28869

**CRYOGENIC STORAGE**
Development and evaluation of internal insulation materials for use with liquid hydrogen tanks on space shuttle
[NASA-CR-123928] 02 p0191 N73-11547
Erythrocyte preservation in blood transfusion practice by cryogenic freezing with polyvinylpyrrolidone
[NASA-TT-F-14590] 04 p0378 N73-13076
Production methods for preventing deterioration of freeze-dried foods
[NASA-CR-128915] 14 p1614 N73-23085
Analysis of cryogenic supply system for space shuttle vehicles and evaluation of candidate systems - Vol. 1
[NASA-CR-128992] 18 p2199 N73-27756
Users manual for Apollo cryogenic storage system computer program
[NASA-CR-134054] 23 p2760 N73-32088

**CRYOGENICS**
Galvanomagnetic and thermoelectric properties of monocrystalline alloys of bismuth and antimony at liquid nitrogen temperature
[AD-745865] 01 p0089 N73-10734
Mechanical property and stress corrosion evaluation of Custom 455 stainless steel alloy at cryogenic temperatures
[NASA-TM-X-64682] 02 p0186 N73-11509
Hall resistivity and electromagnetic properties of bismuth selenide crystals for cryogenic magnetometers
[NASA-TN-D-7057] 03 p0344 N73-12809
Technology for determining mechanical properties of single crystal and polycrystals at low temperature
[AD-748744] 03 p0348 N73-12838
Design of cryogenic flow control components for Saturn 5 S-1C launch vehicle
03 p0349 N73-12850
Research trends in steels with reduced nickel content for cryogenic applications
[NLL-TRANS-746-1266-[9022.401]]
05 p0561 N73-14556
Performance tests on cryogenic insulation materials for nuclear radiation shielding
[NASA-CR-2162] 05 p0578 N73-14707
Preparation, testing, and use of superconductive fixed point devices incorporating lead, indium, aluminum, zinc, or cadmium as standard reference materials
[NBS-SP-260-44] 06 p0707 N73-15768
Cryogenic research and development on slush hydrogen heat transfer and hydrocarbon suspension
[NASA-CR-130362] 06 p0729 N73-15950
Cryogenic instrumentation for present and possible future large scale systems operating at liquid hydrogen temperatures
[LA-DC-72-855] 07 p0832 N73-16743
Cryogenic shock tubes for studying shock wave interactions and generating large Mach number flows
[AD-753134] 09 p1012 N73-18261
Cryogenics, superconductors, and electromagnets - conference
[AD-753456] 09 p1067 N73-18705
Application of superconducting coils for energy storage and determination of optimizing parameters for inductive energy storage
10 p1109 N73-19042

Gas environment effect on catalase cryolysis
10 p1119 N73-19121
Design and fabrication of cryogenic gravity meter
[AD-754242] 10 p1162 N73-19455
Thermoelectricity and refrigeration at low temperature
[AD-753405] 10 p1190 N73-19687
State of superconducting science in Switzerland
[AD-754235] 10 p1202 N73-19781
Spectrometric measurements of cryogenic helium 4 scattering angle and momentum transfer
[CONF-720833-10] 12 p1440 N73-21669
Cryogenics applications for development of superconducting levitated system of high speed ground transportation
[NBS-TN-635] 14 p1645 N73-23344
Cryogenic sampling of atmosphere at 40,000 to 65,000 ft, using modified matrix isolation technique
[AD-757533] 14 p1662 N73-23493
Evaluation of cryogenic devices for application in surveillance, radiation detection, and communications
[AD-756175] 14 p1668 N73-23537
Evaluation of active and passive rupture disk designs for performance at cryogenic temperatures
[NASA-CR-121118] 14 p1670 N73-23554
General conference of European Physical Society on trends in physics
[AD-757261] 14 p1693 N73-23738
Cryobiological and space biological studies
[JPRS-59129] 15 p1742 N73-24120
Cryogenic superconducting magnetic suspension and balance facility designs
15 p1761 N73-24272
Increase in heat exchange rate between thermometric sensing element and cryogenic fluid
[NASA-TM-X-68251] 16 p1913 N73-25477
Personnel and laboratory listing in low temperature research
[AD-757651] 16 p1953 N73-25805
Apparatus for measuring thermal conductivities to 2 degrees K used for measurements in single crystal halides as function of dislocation density
[AD-759552] 17 p2034 N73-26462
Cryogenic heat exchanger for removal of waste heat from spacecraft environmental control life support system
[NASA-CR-124301] 18 p2111 N73-27071
Spin energy transfer processes at low temperatures
[AD-762618] 20 p2455 N73-29731
Bibliography of publications by Cryogenics Division of NBS
[NBS-TN-639] 20 p2488 N73-29988
Loss reduction in high voltage LC oscillator circuits by applying cryogenic temperatures
[BMBW-FBK-72-31] 22 p2704 N73-31659
Flight tests of cryogenically cooled hygrometer
[AD-764718] 23 p2794 N73-32354

**CRYOLITE**
Measurement of vapor pressure of cryolitic baths
[NLL-TRANS-1034-[9022.04]]
20 p2374 N73-29073

**CRYOPUMPING**
Experimental analysis of two phase liquid oxygen pumping
[NASA-TN-D-7451] 24 p2972 N73-33747

**CRYOSORPTION**
U SORPTION

**CRYOSTATS**
Improved dilatometer with helium cryostat for low temperature measurements
[AD-747555] 03 p0304 N73-12484
Metal cryostat for studying superconductors in liquid helium
[IPP-4/95] 17 p2072 N73-26766

**CRYOTRONS**
Computation of optimal parameters of automaton implemented in cryotron medium
21 p2515 N73-30173
Transient response of devices operating in cryotron computing medium and determination of their speed
21 p2515 N73-30176
Formal method for converting logical descriptions of cryotron circuits of asynchronous automata into differential equations
21 p2515 N73-30177

**CRYSTAL DEFECTS**
NT CRYSTAL DISLOCATIONS
NT EDGE DISLOCATIONS
NT POINT DEFECTS
NT VACANCIES [CRYSTAL DEFECTS]
Using specific heat method to study vacancies
[AD-743695] 01 p0088 N73-10725
Error analysis on residual stress location for X ray diffraction analyses on crystal lattices
[AD-746488] 01 p0089 N73-10732
Annealing effect on amorphous silicon nitride protective film defects
[DRIC-TRANS-2902] 02 p0192 N73-11557
Using Lang X ray scanning technique for studying crystallographic defect generation in commutation transistors during fabrication
[CEA-CONF-1981] 03 p0274 N73-12220
Defect structures of GaAs by transmission and black reflection X ray topographic analysis
[AD-746895] 03 p0337 N73-12747
X ray diffraction analysis of crack propagation in deformed, notched, wedge shaped silicon crystal
[AD-746275] 03 p0346 N73-12820
Spatial distribution of radiation defects in silicon irradiated by protons, deuterons, and alpha particles
[AD-748734] 04 p0459 N73-13749
Stress behavior of lithium fluoride crystals exposed to shock wave impact
[AD-748267] 04 p0460 N73-13757
In pile neutron irradiation damage in graphite at high temperature
[CEA-CONF-1894] 07 p0820 N73-16644
Measurement of volume relaxation and crystal defects associated with interstitial ion in X irradiated KBr during isothermal annealing
07 p0831 N73-16735
Defect structure of semiconducting III-V compounds and determination of vibrational properties of imperfect systems
[AD-751052] 07 p0834 N73-16762
Photodielectric recombination and trapping model for low temperature n-type epitaxial gallium arsenide
[NASA-CR-130764] 08 p0950 N73-17779
Nuclear magnetic resonance technique to obtain calibrations of charged defects in semiconducting compounds
[NASA-CR-112224] 08 p0950 N73-17781
Synthesis of SiC single crystals free from carbon particle inclusions
[AD-752227] 08 p0952 N73-17792
Internal friction and crystal defects of magnesium oxide crystals
09 p1063 N73-18673
Magnetic impurities and boundary effects in metals and superfluids
[AD-753100] 09 p1074 N73-18763
Electrical resistivity measurements on defect concentrations in zinc selenide single crystals
[AD-753043] 09 p1074 N73-18764
Autoradiograms of deformed silicon and germanium single crystal surfaces
[AD-753039] 09 p1074 N73-18765
X ray diffraction analysis on microstructure defects in explosively loaded copper germanium alloy
[COO-1431-15] 10 p1173 N73-19541
Structural models for grain boundary dislocations and ledges in crystal defects
[COO-3158-12] 10 p1173 N73-19544
Deformation and different orientation effects on lattice defect energies in copper crystals
[JUL-855-FF] 10 p1194 N73-19713
Interactions of copper lattice atoms with holes, dislocations, and interstitial atoms
[JUL-857-FF] 10 p1194 N73-19714
Positron annihilation center decrease through migrating anion vacancies in thermal annealing of radiation damaged sodium chloride crystals
[CONF-720530-6] 10 p1194 N73-19715
Oxygen vacancy model for transport properties of defective cerium oxides structure
[COO-1441-9] 10 p1199 N73-19759
Numerical analyses on elastic displacement field and point defect interactions in anisotropic cubic crystals
[JUL-836-FF] 10 p1200 N73-19767
Reduction of orange peel and extended defect formation in ceramics
[AD-754837] 11 p1303 N73-20576
Effect of flaws on chemical, electrical, mechanical, and masking properties of Si3N4 films
[NLL-DRIC-TRANS-2902-[3623.66]]
11 p1329 N73-20789
Theoretical model for current flux motion and pinning in superconducting niobium crystal lattice
[COO-3169-11] 12 p1440 N73-21663
Performance prediction model and scaling laws for flux pinning in superconducting niobium zirconium and niobium titanium alloys
[COO-3169-13] 12 p1440 N73-21664
Flux line lattice effect on critical current in plastically deformed single niobium crystal
[COO-3169-14] 12 p1440 N73-21665
Analysis of strain aging process in high carbon quenched steels caused by plastic deformation of martensite and migration of carbon to crystal defects in microstructure
13 p1541 N73-22484
Influence of defects and impurities on nucleation and growth of oriented films by evaporation
[NASA-CR-2234] 13 p1559 N73-22636
Storage time loss in metal oxide capacitors caused by surface damage in silicon wafer
[AD-756250] 13 p1566 N73-22690
Attenuation and thermal release dislocations by interstitial impurities in bcc lattice metals
[NASA-TT-F-14920] 14 p1675 N73-23596
Neutron irradiation damage in indium arsenide semiconductors and effect on electrical crystal properties
[AD-757468] 14 p1699 N73-23792
Thermally activated deformation of crystalline solids
[PB-214537/3] 15 p1823 N73-24774
Determining the effects of ion implantation in aluminum oxide including implanted impurities and crystal damage by electrical resistivity and photoluminescence
17 p2071 N73-26755
Kinetic of interstital contamination and defect growth in fused slurry silicide coated columbium alloys
[NASA-TN-D-7324] 18 p2160 N73-27448
Experimental analysis of disappearance phenomena of packing defects in silicon epitaxial films during thermal oxidation in wet oxygen
18 p2187 N73-27662
Electromicroscopic analysis of Nb3Sn bands to determine effect of carbon doping on current carrying capacity
[NLL-M-23057-[5828.4F]] 20 p2434 N73-29544
Relation of electrical properties of thin films of TiO to defect structure
20 p2460 N73-29766
JERK Monte Carlo program for studying crystal defects in irridiated metals
[CEA-N-1567] 21 p2585 N73-30718
Interstitial and vacancy motion in defect annealing of alpha brass and copper gold alloy by electron irradiation
22 p2683 N73-31489
High temperature deformation and fracture behavior of T-111 and ASTAR-811C over temperature range of 982 to 2205 C
[NASA-CR-72859] 22 p2688 N73-31530
Temperature dependence and measurement of crystalline electric fields at ytterbium impurities in thulium metal
[AD-764633] 23 p2827 N73-32596

**CRYSTAL DISLOCATIONS**
NT EDGE DISLOCATIONS
Small etching pits in epitaxial layer of gallium arsenide caused by accumulation of impurities
[DRIC-TRANS-2928] 06 p0709 N73-15782
Dislocation damping in cu single crystals of controlled substructure, and ultrasonic attenuation data
[AD-750712] 06 p0711 N73-15801
Structural models for grain boundary dislocations and ledges in crystal defects
[COO-3158-12] 10 p1173 N73-19544
Kinetic theory of stress-strain relations and temperature induced dislocation in crystal lattices
[AD-753576] 10 p1201 N73-19777
Solutions to diffusion along grain boundaries and dislocations for finite source
[NLL-CE-TRANS-6043-[9022.09]]
11 p1329 N73-20785
Dislocation mobilities and densities in copper, lead, and zinc crystals
[CALT-767-P-3-27] 12 p1440 N73-21666
Attenuation and thermal release dislocations by interstitial impurities in bcc lattice metals
[NASA-TT-F-14920] 14 p1675 N73-23596
High temperature effects on dislocation mobility of LiF single crystals
18 p2185 N73-27642
Elastic constants for calculating parallel Shockley partial dislocations in ordered alloys and intermetallic compounds
23 p2803 N73-32420
Point, line, and planar defects in metal crystals
[COO-3158-17] 24 p2968 N73-33723

**CRYSTAL FILTERS**
Design and performance of stacked crystal filters for frequency control and signal processing
[AD-765416] 23 p2758 N73-32074
Infrared tunable dye laser with nonlinear wavelength mixing crystal in optical cavity
[NASA-CASE-ARC-10463-1] 23 p2763 N73-32111

**CRYSTAL GROWTH**
NT CZOCHRALSKI METHOD
NT EPITAXY
NT HYDROTHERMAL CRYSTAL GROWTH
Development and characteristics of alkali halide window for application to infrared laser systems
[AD-744998] 01 p0065 N73-10530
Molten single crystal silver compounds for studying photographic sensitivity
[AD-746294] 02 p0175 N73-11421
Empirical procedure for predicting growth of ice crystals, grauple, and hail by diffusion
[AD-746451] 02 p0205 N73-11660
Growths and applications of compound semiconductor materials and devices
[AD-746882] 02 p0220 N73-11783
Laser induced infrared quantum counter upconversion experiments utilizing rare earth ions in single crystals
[AD-747415] 03 p0312 N73-12546
Growth of bulk gallium nitride crystals by ammonolysis of gallium monochloride
[NASA-CR-112211] 03 p0344 N73-12807
Growth of hollandite crystal membranes under inert gas pressures
[NASA-CR-121033] 03 p0345 N73-12810
Crystal growth and magnetic properties of transition metal chalcogenides
[AD-748864] 04 p0459 N73-13748
Crystal growing of iron monosulfide, crystallographic studies on titanium oxide semiconductor,

emission of zinc selenide diode, and electroreflectance of gallium arsenide
[AD-748336] 04 p0459 N73-13750
Czochralski technique for growing GaAs and III and V semiconductor crystals
[AD-748344] 04 p0461 N73-13759
Validity determination for cold tip theory of whisker growth
[AD-749038] 04 p0461 N73-13760
Growth of single crystal CdTe materials for use in infrared electro-optic devices
[AD-749368] 05 p0588 N73-14783
Luminescence of ZnSe and ZnS crystals compared to electroluminescence of MS and MIS structures, preparation of heterojunction structures, and solution growth of wafers
[AD-749135] 05 p0588 N73-14784
Single crystal growth of indium antimonide
05 p0608 N73-14940
Rutile crystal growth, and hydrogen kinetics, electronic, and optical properties
[AD-748298] 06 p0709 N73-15789
Crystal growth from vapor phases and epitaxy, and applications to semiconductors and microelectronics - conference review
[AD-750654] 06 p0710 N73-15793
Kinetics of quartz crystal growth and radiation effects on quartz resonators
[AD-750467] 06 p0711 N73-15803
Reaction diffusion method used for growing semiconductive two-layer structures of zinc telluride on zinc selenide
[AD-751476] 07 p0833 N73-16752
Ferroelectric crystal growth in electric, magnetic and vibrational fields
[AD-751204] 07 p0834 N73-16763
Growth and characterization of crystals and metallic whiskers in zero gravity environment during Skylab and Apollo flights
[NASA-CR-124065] 08 p0950 N73-17778
Synthesis of SiC single crystals free from carbon particle inclusions
[AD-752227] 08 p0952 N73-17792
Growth of FeS[x] and NbO2 single crystals
[AD-753270] 09 p1074 N73-18768
Growths of barium and strontium niobate laser materials for electro-optical Q-switching of visible and near infrared radiation
[AD-752445] 09 p1076 N73-18779
Electron microscopic analysis of epitaxial growth and nucleation in condensed gas crystals
[AD-753108] 10 p1201 N73-19773
HCL processing effects on electrical stability and quality of thermally grown SiO2
[AD-754110] 10 p1202 N73-19786
Growth of large-area silicon ribbons for application to large area solar cells and arrays
10 p1228 N73-19981
Magnetic field effect on hydrated glucose crystal growth
[AD-754618] 11 p1254 N73-20172
Applications of holographic system with interferometric capabilities for crystal growth analysis
[AD-754737] 11 p1294 N73-20504
Helium crystal growth in preferred orientations
[AD-754442] 11 p1330 N73-20797
Melt stoichiometry and growth of yttrium vanadate polarizer material
[AD-754650] 11 p1332 N73-20809
Synthesis of compound semiconducting materials and application to planar microwave acoustic equipment using gallium arsenide thin films as active layer
[AD-755947] 12 p1442 N73-21684
Growth of multiply sensitized Ho YLF crystals as laser materials
[AD-755530] 13 p1538 N73-22461
Single crystals of hematitic Fe2O3 grown from Na2B4O7 and occuring as plates, rods, hoppers, and equidimensional solid crystals
[AD-755349] 13 p1567 N73-22697
Electrical and physical properties of low temperature grown cubic gallium nitride films
[AD-755237] 13 p1567 N73-22704
Magnetic bubble garnet materials for thin film storage devices
[AD-755546] 13 p1568 N73-22705
New methods for growth and characterization of GaAs and mixed semiconductor crystals
[AD-756259] 14 p1698 N73-23777
Growth of iron whiskers by hydrogen reduction of iron halide salts
[AD-757588] 14 p1699 N73-23788
Preflight, inflight, and post flight operations evaluation analyses for Skylab gallium arsenide single crystal growth facility - Appendix J
[NASA-CR-61386-APP-J] 14 p1708 N73-23863
Development and characteristics of nonmetallic electro-optic materials for electronic applications
[AD-758528] 15 p1760 N73-24261
Growth and hardening of potassium chloride single crystals for infrared laser windows
[AD-757893] 15 p1795 N73-24550
Effect of helium gas bubbles on grain boundary motion in vapor deposited gold foil samples
[RD/B/N-2430] 15 p1798 N73-24578
Analysis of unidirectionally solidified aluminum alloys to determine properties of random polycrystals, columnar crystals, and growth twin crystals
16 p1927 N73-25594
Growth of single barium ferrite crystals for magnetic optical devices
[AD-758926] 16 p1953 N73-25807
Design of high temperature and high pressure furnace for crystal growth
[AD-759786] 16 p1954 N73-25811
Photoluminescence, thermoluminescence, photoconductivity, and electrical conductivity measurements in heavily doped ZnS-Cu, In phosphors
17 p2071 N73-26759
Conference on growth and synthesis of semiconductor crystals and films
[JPRS-59208] 17 p2072 N73-26762
Growth of single crystals of rhenium and iridium dioxides
[NASA-CR-133213] 17 p2072 N73-26768
Topology and kinetics of grain growth
[AD-760580] 18 p2162 N73-27468
Synthesis and characterization of semiconducting diamond and boron phosphide crystals
18 p2186 N73-27648
Effect of growth conditions and properties of silicon films deposited by chloride method
18 p2187 N73-27658
Production of silicon nitride layers on silicon by growth from gas phase and properties of resulting layers
18 p2189 N73-27670
Characteristics of crystal growth on embossed substrates to show chemical reactions for reducing number of lattice defects
18 p2189 N73-27671
Growth of monocrystalline films of silicon base
18 p2189 N73-27672
Effect of various growth and doping parameters on GaN for LED applications
[NASA-CR-132263] 18 p2189 N73-27676
Physical phenomena related to crystal growth in space environment
[NASA-CR-2281] 18 p2189 N73-27677
Experimental analysis of rutile properties including crystal growth, hydrogen diffusion, and magnetic resonance determination of defects
[AD-760667] 18 p2190 N73-27684
Growth of rutile single crystals by chemical vapor transport
[AD-760733] 18 p2191 N73-27687
Heat transfer and temperature oscillations in chemical vapor transport crystal growth
[AD-760732] 18 p2191 N73-27688
Growth of yttrium orthovanadate large single crystals
[AD-761094] 18 p2191 N73-27689
Characteristics of single crystals of metals with melting points and effects of crystal growth under zero-gravity conditions
[NASA-CR-124354] 20 p2432 N73-29532
Shape of crystal interface and impurity striations in single crystals of silicon grown by Czochralski method
[NLL-RRE-TRANS-387-[8036.625]]
20 p2460 N73-29771
Radiative heat transfer of single crystal surface at phase transition boundary during Czochralski crystal growth
[NLL-RRE-TRANS-386-[8036.625]]
20 p2460 N73-29772
Single orthoferrite crystal growth by crucibleless zone melting, including optical absorption spectra
20 p2461 N73-29777
Characterization and growth of GaAs crystals by gradient freeze and traveling heater methods
[AD-763761] 21 p2586 N73-30722
Research projects involving development and application of semiconductor materials and process for measuring properties of semiconductors at high pressures
21 p2607 N73-30894
Polycrystals and monocrystals of ice grown from KCl solution
[CONTRIB-1247] 22 p2646 N73-31203
Mechanism of grain growth in ceramics
[NASA-CR-135673] 23 p2804 N73-32425
Oxygen grain boundary diffusion and grain growth in pure dense MgO
[NASA-CR-135719] 23 p2810 N73-32466
Growth of electronic ceramic single crystals from solution as feasibility study for future crystal growth in space environment
[NASA-CR-124443] 23 p2826 N73-32587
Pulling single crystal silicon in space environment
[NASA-CR-124439] 23 p2826 N73-32588
Growth of potassium tantalate single crystals
[AD-764902] 23 p2828 N73-32603
Chemical vapor deposition of reproducible device quality ferrimagnetic films
[NASA-CR-132325] 24 p2891 N73-33083

**CRYSTAL LATTICES**
NT BODY CENTERED CUBIC LATTICES
NT CLOSE PACKED LATTICES
NT CUBIC LATTICES
NT FACE CENTERED CUBIC LATTICES
Development of chemical model to present properties of carbides for localized and nonlocalized conditions of electrons in crystal structure
[NLL-RTS-7334] 01 p0069 N73-10565
Lattice potential topography for 180 degree boundary in Perovskite ferroelectrics
[AD-742109] 01 p0088 N73-10724
Error analysis on residual stress location for X ray diffraction analyses on crystal lattices
[AD-746488] 01 p0089 N73-10732
Interstitial impurity diffusion coefficients and crystal lattice defects in cubic alloys
[AD-746949] 02 p0188 N73-11529
Annealing effect on amorphous silicon nitride protective film defects
[DRIC-TRANS-2902] 02 p0192 N73-11557
Pseudopotential analysis of interaction between conduction electrons and metal lattice fi-ld
[ITJ-16] 04 p0433 N73-13532
Dynamic theory of crystal lattices and linear theory of elasticity and piezoelectricity
[AD-749111] 05 p0588 N73-14780
X ray analysis to determine occurrence of metal surface texturing as result of sliding friction
[NASA-TN-D-7136] 06 p0677 N73-15508
Formula for calculating intensity of elastic and inelastic X ray scattering in crystal lattice of vanadium
[NASA-TT-F-13913] 06 p0708 N73-15775
Computation of neutron star mass based on crystal arrangement of particles
08 p0974 N73-17965
Ferromagnetic resonance in iron and hexagonal close packed cobalt lattices
[AD-753841] 09 p1076 N73-18783
Deformation and different orientation effects on lattice defect energies in copper crystals
[JUL-855-FF] 10 p1194 N73-19713
Interactions of copper lattice atoms with holes, dislocations, and interstitial atoms
[JUL-857-FF] 10 p1194 N73-19714
Electronic spectra of benzophenone crystals and low temperature spectra of ketones
[AD-753380] 10 p1201 N73-19775
Spectroscopic analyses of molecular energy levels in crystals
[AD-753382] 10 p1201 N73-19776
Kinetic theory of stress-strain relations and temperature induced dislocation in crystal lattices
[AD-753576] 10 p1201 N73-19777
Theoretical model for current flux motion and pinning in superconducting niobium crystal lattice
[COO-3169-11] 12 p1440 N73-21663
Multiphonon infrared absorption by crystal inclusions of optical window materials
[AD-756080] 13 p1537 N73-22453
Characteristics of crystal growth on embossed substrates to show chemical reactions for reducing number of lattice defects
18 p2189 N73-27671
Site sets in point groups applicable to lattice complex classification
[NBS-MONOGRAPH-134] 18 p2190 N73-27678
Shape of crystal interface and impurity striations in single crystals of silicon grown by Czochralski method
[NLL-RRE-TRANS-387-[8036.625]]
20 p2460 N73-29771
Theoretical treatment of neutron irradiation caused crystal lattice defects in ceramic materials
[AECL-4375] 20 p2462 N73-29788
Analysis of nuclear matter under assumption that nucleons are arranged in lattice
24 p2960 N73-33656

**CRYSTAL OPTICS**
Optical activity and Raman scattering in sodium nitrite crystals
16 p1952 N73-25792
OSO-1 Bragg crystal spectrometer for solar and stellar X ray source analysis
17 p2084 N73-26863
Holographic interferometric analysis of thermal response in ferroelectric crystal to laser radiation
[AD-764703] 23 p2820 N73-32547

**CRYSTAL OSCILLATORS**
NT PIEZOELECTRIC CRYSTALS
Design and fabrication of high stability, temperature compensated, crystal oscillator for advanced SSB communication equipment
[AD-745914] 02 p0149 N73-11212
Temperature controlled piezoelectric crystal oscillator with digital integrated circuitry for timing of pulses
[AECL-4160] 04 p0396 N73-13217
Design of miniature tactical crystal oscillator for operation at ambient temperature
[AD-749271] 04 p0397 N73-13232
Development of single sideband quartz crystals for use in temperature compensated crystal oscillators
[AD-749642] 06 p0646 N73-15244
Use of torsional pendulum as high pressure gage and determination of viscosity of helium gas at high pressures
[NASA-TN-D-7241] 14 p1667 N73-23528
Tactical miniature crystal oscillators
[AD-759484] 17 p2004 N73-26207

Design of stable temperature compensated crystal oscillator for voice communication system
[AD-759938] 17 p2006 N73-26220
CRYSTAL RECTIFIERS
Operational performance of breadboarded silicon controlled rectifier series inverter circuitry for ion thruster power supply
[NASA-TM-X-2699] 06 p0626 N73-15082
Pulse voltage distribution over series connected silicon rectifiers
[AD-750969] 06 p0648 N73-15260
CRYSTAL STRUCTURE
Development of chemical model to present properties of carbides for localized and nonlocalized conditions of electrons in crystal structure
[NLL-RTS-7334] 01 p0069 N73-10565
Multiple ion interaction energy and metal structure distribution
01 p0087 N73-10721
Computer simulations of split interstitial equilibrium positions and binding energies in tungsten crystals
[AD-745839] 01 p0088 N73-10728
Crystalline structures, physical properties, chemical properties, and phase characteristics of various metal systems and alloys
[AD-746792] 02 p0189 N73-11532
Formation of chaoite and other crystal forms of carbon by CO2 laser irradiation of solid carbons
[AD-747020] 02 p0193 N73-11565
Structural properties of glass, using X ray and neutron diffraction methods
[AD-747311] 02 p0194 N73-11568
Crystal structure of tetrahedrally coordinated amorphous semiconductors
[AD-746638] 03 p0346 N73-12821
Crystal structure of polymorphic form of carbon similar to chaoite
[AD-747476] 03 p0347 N73-12828
Pseudopotential analysis of interaction between conduction electrons and metal lattice field
[ITJ-16] 04 p0433 N73-13532
Crystal chemistry of anhydrous and hydrous layer silicates
[NRC-TT-1479] 04 p0458 N73-13734
X ray system for solving structure of crystals by diffraction techniques
[NASA-CR-129908] 04 p0458 N73-13737
Neutron diffraction and single crystal X ray determination of rare earth-cobalt-iron intermetallic magnetic structure
[AD-748429] 04 p0460 N73-13754
Calorimetric, diffraction, and microscopic examination of evaporated amorphous germanium
[AD-749363] 04 p0461 N73-13762
X ray apparatus for investigating hydrogen induced changes in fine crystalline structure of Ni powders and electrolytic films
[NLL-TRANS-746-1294-[9022.401]]
05 p0505 N73-14113
Analysis of lattice spacings and changes in platinum metals as function of temperature and applied pressure
[NLL-TRANS-746-1316-[9022.401]]
05 p0561 N73-14558
Measurements of work function of [110] and [111] faces of crystal from solid solution of osmium in tungsten
[NLL-TRANS-746-1315-[9022.401]]
05 p0585 N73-14760
Standard X ray powder diffraction patterns
[NBS-MONO-25-SECT-10] 05 p0586 N73-14767
High resolution spectral reflectance of potassium chlorides and bromides at room temperature in far ultraviolet yields new structures
[NOTA-INTERNA-402] 05 p0587 N73-14777
Design and fabrication of X ray diffractometer and application to determination of residual stresses in polycrystalline samples
[NAL-TN-34] 06 p0672 N73-15467
Determination of surface structure of metal crystals by chemisorption method
[NLL-TRANS-746-1340-[9022.401]]
06 p0682 N73-15548
X ray and electron diffraction analysis of A[3]B[5] semiconductor crystal structure
[AD-750966] 06 p0709 N73-15787
Structural, optical, and electrical properties of amorphous semiconductors
[AD-751084] 07 p0834 N73-16760
Thermal stability of amorphous arsenic compound glasses and electron diffraction analyses on semiconducting arsenic selenide films
[AD-752993] 09 p1076 N73-18778
Effect of annealing on substructure of cold worked FCC copper alloys and metals
[COO-1431-14] 10 p1173 N73-19540
Structural models for grain boundary dislocations and ledges in crystal defects
[COO-3158-12] 10 p1173 N73-19544
Crystal structures, electrical properties, and electronic applications of metal selenides
[JPRS-58293] 10 p1198 N73-19752
Temperature-modulated reflectivity in fundamental edge region of GaTe
[ISS-72/2] 10 p1199 N73-19755
Crystal structure and mechanical and physical properties of polymide S-6 - Nylon
[AD-753967] 11 p1309 N73-20624
Chemical, petrographic, and textural characteristics of Apollo 16 rock and soil samples
12 p1449 N73-21737
Analysis of fracture of mixed viscous-brittle breakage of polycrystal using raster electron microscope
13 p1540 N73-22479
Coincidence structural unit models for grain boundaries in HCP metals
[AD-756884] 13 p1545 N73-22520
Short range structure of Ti and Zr body centered cubic lattice solid solutions containing omega phase
[AD-755454] 13 p1567 N73-22698
Short range structure of Ti and Zr body centered cubic lattice solid solutions containing omega phase
[AD-755463] 13 p1567 N73-22699
Structures and optical absorption spectra of mercury telluride/cadmium telluride thin films
[AD-756093] 13 p1568 N73-22709
Analysis of relationship between texture development and normal anisotropy in cold-rolled, low carbon steel
[NLL-M-21627-[5828.4F]] 15 p1797 N73-24567
Computer simulation techniques to determine equilibrium positions and binding energies of inert gas atoms implanted in tungsten crystal
[AD-758501] 15 p1799 N73-24585
Influence of plastic deformation on structure and mechanical behavior of glassy amorphous polymers
15 p1801 N73-24595
Crystal structure and electroluminescence of ZnSe films
[NLL-PO-2921-[9022.81]] 15 p1819 N73-24745
Papers on crystallography and liquid and solid structures
[NASA-CR-132048] 15 p1820 N73-24752
Adsorption properties of natural zeolites
[BM-RI-7744] 15 p1820 N73-24753
Effect of heat treatment on structure and properties of stainless steels
[NLL-M-21566-[5828.4F]] 16 p1926 N73-25585
Analysis of unidirectionally solidified aluminum alloys to determine properties of random polycrystals, columnar crystals, and growth twin crystals
16 p1927 N73-25594
Thermal conductivity of complex dielectric crystals at high temperature
16 p1952 N73-25796
High density optical memory
[AD-759032] 17 p2002 N73-26184
Mechanical properties and crystal structures of polymorphous metals and alloys
[AD-759753] 17 p2074 N73-26779
Analysis of wave propagation in double-layered piezoelectric system using two cadmium selenide and cadmium sulfide crystals
18 p2115 N73-27102
Frequency effect of magnetocrystalline anisotropy in nickel ferrous ferrites determined by torque measurements
18 p2159 N73-27443
Piezobirefringence measurements on amorphous and crystalline semiconductors with zincblende, wurtzite, and rocksalt structures
18 p2184 N73-27637
Growth and crystal structure of Si, Ge, and GaAs thin films
[JPRS-59279-PT-2] 18 p2186 N73-27650
Structure, composition, and electrophysical properties of autoepitaxial silicon layers from vapor-gas tetrachloride mixture
18 p2186 N73-27653
Analysis of optimal conditions of selective growth of epitaxial layers of germanium and silicon
18 p2188 N73-27669
Production of silicon nitride layers on silicon by growth from gas phase and properties of resulting layers
18 p2189 N73-27670
Characteristics of crystal growth on embossed substrates to show chemical reactions for reducing number of lattice defects
18 p2189 N73-27671
Growth of monocrystalline films of silicon base
18 p2189 N73-27672
Procedure for obtaining monocrystalline layers of silicon by rheotaxial methods
18 p2189 N73-27673
Site sets in point groups applicable to lattice complex classification
[NBS-MONOGRAPH-134] 18 p2190 N73-27678
Structural and superconducting transition temperature of evaporated aluminum films as function of grain size
[NASA-CR-133450] 19 p2326 N73-28716
Development of low energy diffraction system for observing surface structure of low-index single crystal metal surfaces with and without absorbates
20 p2429 N73-29510
Characteristics of single crystals of metals with melting points and effects of crystal growth under zero-gravity conditions
[NASA-CR-124354] 20 p2432 N73-29532
X ray and electron diffraction spectra of amorphous arsenic selleride semiconductors
[AD-762367] 20 p2463 N73-29792
Diopside submicroscopical twinning in lunar and experimentally deformed pyroxenes
[NASA-CR-133271] 20 p2486 N73-29970
Thermodynamic, structural, and magnetization phenomena during hydrogen reaction with RCo5 type systems
22 p2625 N73-31033
Temperature effects on structures and mechanical properties of polysulfone and poly[216-dimethyl] phenylene oxide
22 p2688 N73-31528
Research on preparation, structure, and optical properties of glass
[AD-763338] 22 p2689 N73-31537
Properties and structure of polymers crystallized from stirred dilute solutions and sheared polymer melts
22 p2706 N73-31673
Effect of scandium, yttrium, and lantham oxides on properties of nickel ferrite
23 p2809 N73-32460
Optical, photoelectric, and structural properties of amorphous B1-Ge thin films
23 p2824 N73-32572
Off-diagonal long range crystalline order and vortex lattices in Bose system
24 p2967 N73-33708
CRYSTAL SURFACES
Crystal phonon contribution to free energy of identical atom pairs adsorbed on cubic lattice surface
[AD-759035] 17 p1992 N73-26109
Annealing properties and electron emission of amorphous and crystalline silicon
17 p2072 N73-26760
Low energy electron diffraction and auger spectroscopy of [100] surfaces of aluminum and aluminum-copper alloys
18 p2159 N73-27445
Analysis of optimal conditions of selective growth of epitaxial layers of germanium and silicon
18 p2188 N73-27669
Electron scattering and secondary emission from tungsten crystal surface
[AD-761876] 19 p2328 N73-28726
Lattice dynamics of crystals surfaces
[AD-764644] 23 p2827 N73-32600
CRYSTALLINITY
Mineral analysis of lunar samples of crystalline rocks from Apollo 12 flight
[NASA-SP-306] 07 p0844 N73-16837
CRYSTALLITES
Effects of atmospheric pressure on thermoluminescence of crystalline powder
[AD-746442] 02 p0219 N73-11770
CRYSTALLIZATION
NT RECRYSTALLIZATION
Removal and separation of particles by crystallization in carbon-naphthalene system
[AD-753056] 09 p1076 N73-18777
Temperature field calculations on cylinder solidification in axial and radial axial heat transfer
[AD-755871] 13 p1591 N73-22901
Influence of surface preparation, surface texture, and initial oxidation on metal surface crystallization
14 p1676 N73-23603
Directional crystallization in eutectic alloys used on casting turbine blades
[AD-759422] 16 p1931 N73-25624
Effect of crystallization kinetics on physical and chemical properties of polymers particularly polyethylene
[AD-750157] 16 p1953 N73-25802
Laws governing crystallization of ingots with continuous casting in electromagnetic crystallizer
[AD-759230] 17 p2046 N73-26554
Cristobalite transformation effects on tensile strength of silica surface insulation materials
24 p2943 N73-33500
CRYSTALLOGRAPHY
Influence of creep strain on elastic modulus, crystallographic orientation, and density of POCO graphite
[LA-DC-13292] 03 p0321 N73-12614
Environmental tests of crystallographic and stress corrosive properties of reactor related metal alloys
[AECL-4353] 09 p1063 N73-18668
Papers on crystallography and liquid and solid structures
[NASA-CR-132048] 15 p1820 N73-24752
Influence of supersaturation on nucleation behavior in continuous agitated cooling crystallizers
[WTHD-44] 16 p1953 N73-25799
Data tables and photographs of gaas epitaxial layer perfections as influenced by substrate disorientation
18 p2189 N73-27675
Site sets in point groups applicable to lattice complex classification
[NBS-MONOGRAPH-134] 18 p2190 N73-27678
CRYSTALS
NT BICRYSTALS
NT CRYSTAL OSCILLATORS
NT CRYSTALLITES
NT IONIC CRYSTALS

NT LIQUID CRYSTALS
NT METAL CRYSTALS
NT PIEZOELECTRIC CRYSTALS
NT POLYCRYSTALS
NT QUARTZ CRYSTALS
NT SINGLE CRYSTALS
NT WHISKERS [SINGLE CRYSTALS]
Elastic properties determination of crystals by sound velocity measurements
[AD-745859] 01 p0089 N73-10733
Failure analysis of crystals exposed to laser emissions
[AD-747730] 03 p0347 N73-12830
Modulation of infrared laser emission using gallium arsenide crystal
[AD-749631] 04 p0430 N73-13507
Measurements of positron lifetime distributions used to characterize plastic deformation in crystals
[COO-2128-2] 06 p0708 N73-15779
Laser induced damage in ruby and sapphire crystals at 6943 A
[AD-751928] 08 p0930 N73-17613
Green function for analyzing light scattering in crystals
[AD-757070] 14 p1693 N73-23741
Physical properties of electronic materials, devices, and thin films
[AD-758197] 14 p1700 N73-23793
Correlation between Ge crystal and spectrometer properties of Ge[L1] detector made from Ge crystal
[AECL-4369] 19 p2327 N73-28718
Absorption spectra of laser excited Ba2NaNb5O15 crystal
21 p2585 N73-30714
Potential use of strontium barium metaniobate crystals for electro-optics
[AD-762740] 22 p2687 N73-31520
Improved high frequency performance of mixer diodes by use of Mott barrier
[AD-765182] 24 p2899 N73-33143

CSM
U COMMAND SERVICE MODULES

CUBES [MATHEMATICS]
Stability of various equilibrium states in cubed incompressible neo-Hookean material subjected to pure homogeneous deformation
[AD-758700] 16 p1970 N73-25937

CUBIC LATTICES
NT BODY CENTERED CUBIC LATTICES
NT FACE CENTERED CUBIC LATTICES
Nonlinear theory using fourth order Hugoniot curves for compression shocks in cubic crystals
01 p0087 N73-10720
Interstitial impurity diffusion coefficients and crystal lattice defects in cubic alloys
[AD-746949] 02 p0188 N73-11529
Time evolution of quantum lattice system Hamiltonian discussing automorphism of suitable algebra
[NOTA-INTERNA-393] 03 p0340 N73-12774
Numerical analyses on elastic displacement field and point defect interactions in anisotropic cubic crystals
[JUL-836-FF] 10 p1200 N73-19767
Temperature dependence of second-order elastic constants of cubic crystalline materials derived on basis of quasiharmonic anisotropic continuum model
24 p2968 N73-33717

CUES
Analysis of reaction time to different visual cuing methods in large displays during secondary task performance
[AD-747688] 03 p0262 N73-12120
Visual cue reinforcement for skill retention in pilot simulated space vehicle approach and landing performance
[NASA-CR-128912] 14 p1614 N73-23086

CUESTAS
U RIDGES

CULTURAL RESOURCES
Cultural resources interpretation and map revision from ERTS-1 RBV and MSS imagery of Washington state
[E72-10276] 03 p0291 N73-12374
Cultural interpretation and map revisions from ERTS-1 imagery
[E73-10052] 07 p0777 N73-16314
ERTS-1 imagery of geology, botany, agriculture, hydrology, and cultural features of Wyoming
[E73-11022] 22 p2661 N73-31326

CULTURE [SOCIAL SCIENCES]
Contributions of science and technology to success of US as world leader
04 p0470 N73-13835
Analysis of Marxist-Leninist theory based on data in cybernetics, information theory, systems analysis, and semiotics
24 p2993 N73-33918

CULTURE TECHNIQUES
Automatic inoculating device for agar trays using cotton swab or loop
[NASA-CASE-LAR-11074-1] 07 p0750 N73-16096
Time periods for nutrient solution exchange in optimal biomass yield on porous aggregate
10 p1117 N73-19106
Chemical composition stability of Chlorella biomass during prolonged cultivation
10 p1117 N73-19108
Biological mineralization products of human waste for autotroph cultivation
10 p1117 N73-19109
Hydroponic cultivation of plants on clay filters from human mineralized feces
10 p1117 N73-19110
Development of procedures of identification of microorganisms on orbiting spacecraft
[NASA-CR-128747] 10 p1120 N73-19132

CUMULATIVE DAMAGE
Application of cumulative damage theory to internal stress caused by cyclic loading in notched bars
[LBF-FB-100/72] 06 p0726 N73-15930
Cumulative damage of high strength aluminum alloy under operational loading
[ISD-133] 17 p2046 N73-26553

CUMULONIMBUS CLOUDS
Vertical air gust velocities and turbulence spectral structure around and within cumulonimbus clouds
[AD-748518] 04 p0445 N73-13632
Investigation of thunderstorm potential in cold air cumulonimbi over northwestern Europe during winter
[AD-749493] 05 p0574 N73-14674
Analysis of radar data for time variability of cumulonimbus clouds in shower and thunderstorm stages
21 p2569 N73-30587
Application of polarized radar signals for analyzing structure of cumulonimbus clouds
21 p2569 N73-30588
Application of radar techniques for determining microstructure parameters of cumulonimbus clouds
21 p2569 N73-30591
Application of radio astronomical methods for determining attenuation and radio emission of rain from cumulonimbus clouds
21 p2570 N73-30594

CUMULUS CLOUDS
Artificial radioactivity of cumulus clouds moving horizontally and touching peaks of Mt. Olympus
[AEC-TR-7308] 03 p0296 N73-12413
Differential magnetometer method for measuring thunderstorm charging currents near cumulus clouds
[AD-750087] 05 p0542 N73-14411
Parameterization of clouds in numerical circulation model
05 p0573 N73-14657
Life cycles of natural and hygroscopically seeded warm tropical cumuli
[AD-750889] 06 p0695 N73-15662
Variation in maximum intensity of precipitation falling from stratiform and cumulus clouds
13 p1552 N73-22581
Parametric model of cumulus convection to simulate entire life cycle of different types of cumuli under various environmental conditions
[PB-213623-2] 13 p1555 N73-22602
Numerical model of individual convective clouds used for analysis of cumulus and mesoscale interactions
[PB-213624-0] 13 p1555 N73-22603
Analysis of convective cumulus cloud development and numerical relationships of hydrodynamic and thermodynamic concepts of cloud formation
[NLL-M-22840-[5828.4F]] 16 p1936 N73-25666
Comparison of cumulus parameterization techniques in numerical integration of easterly wave
16 p1937 N73-25674
Computerized simulation of maritime cumulus clouds considering meteorological parameters and cloud seeding
[AD-759368] 16 p1939 N73-25693
Numerical model of dry and wet cumulus convection
17 p2056 N73-26630
Numerical time dependent model for simulating lifecycle of cumuli under different environmental conditions
18 p2170 N73-27525
Cumulus cloud modification with coalescence attempts
[NOAA-TM-ERL-OD-14] 24 p2947 N73-33539

CURING
Sulfur and MOCA cured polyurethane elastomer resistance to water, STF, and STF/water mixture
[ERDE-TR-83-PT-2] 02 p0192 N73-11555
Nonsporicidal methods for solvent degradation of cured RTV 41 silicon potting compound and chemical curing effects on decontamination properties
[NASA-CR-130720] 08 p0878 N73-17111
Diisocyanate cure rate stabilization with hydroxy-terminated polybutadiene binders
[AD-759960] 17 p2052 N73-26599
Dynamic mechanical analysis of reactions of aromatic diamines with diglycidyl ether of bisphenol A for application to epoxy thermosetting systems
[AD-759995] 17 p2052 N73-26602

CURIUM
NT CURIUM 244

CURIUM ISOTOPES
NT CURIUM 244

CURIUM 244
Use of Cm-244 as radioisotope power fuel in electric power conversion systems
[CONF-720519-1] 03 p0333 N73-12717
Cm-244 development as isotopic power fuels
[ORNL-TM-4035] 10 p1187 N73-19658

CURL [VECTORS]
NT VORTICITY

CURRENT ALGEBRA
Finiteness of radiative corrections to semileptonic decays in unified gauge theories
[TR-74-021] 22 p2701 N73-31637

CURRENT AMPLIFIERS
NT PHOTOMULTIPLIER TUBES
Analog model for minority charge carrier diffusion to base contact of bipolar transistor with current amplification
[NLL-TRANS-2861-[9022.81]]
02 p0148 N73-11201
Evaluation of direct current amplifiers for radiation measurements
[CEA-N-1580] 15 p1757 N73-24237

CURRENT CONVERTERS [AC TO DC]
Development of serial to parallel digital to analogue converter to obtain stable d.c. voltage from three digits of computing counter twelve digit display
[REPT-6702] 05 p0516 N73-14196

CURRENT DENSITY
Pulsed magnetic field apparatus, and microstructure influence on critical current density of superconducting Nb3Sn strips in pulsed fields
[LBL-448] 06 p0708 N73-15778
Radiation effects on current density of superconducting magnets in fusion reactor
[CLM-R-120] 10 p1199 N73-19760
Technique and equipment for sputtering using apertured electrode and pulsed substrate bias
[NASA-CASE-LEW-10920-1] 15 p1797 N73-24569
Current density, flow velocity, and mass density in coaxial annular plasma Hall accelerator
[DLR-FB-73-45] 22 p2705 N73-31663
Fluxon coupling force measurements on superconducting dc transformers noting film thickness and silicon monoxide layer
24 p2898 N73-33135

CURRENT DISTRIBUTION
Current distribution estimates for microwave power tube with depressed multistage collector
[NASA-TM-X-2651] 01 p0032 N73-10251
Flow behavior of integrated circuits in bipolar transistors
[CEA-CONF-1971] 01 p0087 N73-10722
Boundary value solution for current distribution on infinite tubular antenna in cold collisionless plasma
[NASA-CR-130297] 06 p0640 N73-15194
Variation of Rayleigh wave reflection coefficient of different interdigital transducer configurations with electric loads
07 p0831 N73-16737
Method of moments for approximating current distribution in antenna array with arbitrarily located parallel center fed dipoles with terminals in common plane
10 p1133 N73-19236
Alignment and field distribution of coil currents in storage accelerators using superconducting magnets
[BNL-17272] 10 p1194 N73-19712
Coil configuration influence on current distribution of superconducting dipoles and quadrupoles
[BNL-17168] 10 p1201 N73-19771
Theoretical model for current flux motion and pinning in superconducting niobium crystal lattice
[COO-3169-11] 12 p1440 N73-21663
Performance prediction model and scaling laws for flux pinning in superconducting niobium zirconium and niobium titanium alloys
[COO-3169-13] 12 p1440 N73-21664
Current distribution in flooded, porous electrodes
[NASA-CR-131839] 16 p1864 N73-25098
Ionospheric electric field and current distributions, assuming certain time variable convection field profiles at 1250 km
[TRITA-EPP-73-03] 16 p1907 N73-25429
Equilibrium pattern and control of plasma current distribution in diffuse pinch configuration
[IPPJ-158] 16 p1949 N73-25770
Determination of dynamic zone sparkless commutation for linear and sinusoidal load current changes in dc machines
[NLL-RTS-7771] 18 p2122 N73-27149
Computer solution to Hallens equation on half wavelength elements of planar symmetrical antenna arrays
[AD-761471] 19 p2245 N73-28103

CURRENT REGULATORS
Design of integrated circuit with two amplifiers and feedback stabilization for single channel gyrator
[NASA-CASE-MFS-22343-1] 09 p1008 N73-18224
Width modulated pulse rebalance electronics loop for strapdown gyroscope
[NASA-CR-124333] 19 p2318 N73-28649
Control circuit for reducing bias voltage and radiation sensitivity of photomultiplier
[NASA-CASE-ARC-10593-1] 21 p2517 N73-30187

**CURRENT SHEETS**
Current sheet magnetic field model for computing three dimensional currents flowing in solar corona
01 p0093 N73-10764
Physical model for determining structure of neutral sheets in solar corona
01 p0093 N73-10765

**CURRENT STABILIZERS**
U CURRENT REGULATORS

**CURRENTS [OCEANOGRAPHY]**
U WATER CURRENTS

**CURTISS-WRIGHT MILITARY AIRCRAFT**
U MILITARY AIRCRAFT

**CURVATURE**
Two degree inverted flexure from single block of material
[NASA-CASE-ARC-10345-1] 03 p0305 N73-12488
Application of fourier analysis, information theory, or curvature analysis to determine information content of curved line
[MITT-128] 05 p0538 N73-14376
Bessel function analysis on acoustic wave propagation in curved ducts
[NASA-TM-X-2698] 06 p0700 N73-15705
Short curved wall, axisymmetric subsonic diffusers, using slot suction to prevent flow separation
[NASA-CR-2209] 11 p1270 N73-20305
Annular duct liner curvature for aircraft noise reduction
[NASA-TN-D-7277] 17 p2063 N73-26688
Optimization of parallel plate relativistic particle analyzer by reducing z variation of point source image at detector surface
19 p2301 N73-28501

**CURVE FITTING**
Development of least squares curve-fitting algorithm for simultaneous estimation of small signal gain and saturation intensity in carbon dioxide laser waveguide
[NASA-TM-X-66097] 02 p0181 N73-11468
Least squares curve fitting method for smoothing pressure distribution data for various cross sections of circular cylinder
[WRE-TN-688[WR/D]] 02 p0195 N73-11577
Computer programs for curve-of-growth analysis using dimensions of stellar lines as input
[ROY-OBS-BULL-171] 06 p0644 N73-15230
Existence and uniqueness of solutions obtained from streamline curvature method of calculating flow through turbomachines for several operating points of Rolls-Royce compressor
[ARC-CP-1234] 09 p1016 N73-18293
Universal curves which relate general properties of two-dimensional boundary layers on turbomachine blades
10 p1204 N73-19795
Two-dimensional curve fitting technique for analyzing data acquired by Doppler radar and application to study of convective storms
[AD-755946] 12 p1424 N73-21537
Least squares adjustment of geometrical global satellite network data
[NASA-CR-131535] 12 p1459 N73-21823
Standardized stress strain curves
[ESDU-00.01.00] 14 p1675 N73-23588
Smoothing technique for analyzing frequency response of aircraft in flight and on ground
[RAE-LIB-TRANS-1703] 17 p2054 N73-26616
Least squares fitting of bicubic spline surfaces to general data at arbitrary points noting householder orthogonal transformation, solution stability, and ranking
[NPL-NAC-22] 23 p2813 N73-32489

**CURVED PANELS**
Dynamic frequency response of curved or flat honeycomb sandwich panels having cores of negligible flexural stiffness
[ESDU-72016] 06 p0723 N73-15898
Analysis of effects on in-plane boundary conditions and panel geometry on natural vibration and flutter characteristics of panels exposed to supersonic flow parallel to generators
09 p1094 N73-18933
Detailed calculations of natural vibrations of single cylindrically curved open shells
[NASA-TT-F-14979] 19 p2347 N73-28880

**CURVED SURFACES**
U CONTOURS
U SHAPES
U SURFACES

**CURVES [GEOMETRY]**
NT CYCLOIDS
Mathematical analysis and curve plotting for microwave physics
[AD-747035] 03 p0337 N73-12746
Application of fourier analysis, information theory, or curvature analysis to determine information content of curved line
[MITT-128] 05 p0538 N73-14376
Approximation of curves and surfaces in three-dimensional space by smooth circular interpolation
21 p2512 N73-30154

**CUSHIONCRAFT GROUND EFFECT MACHINE**
Cost effectiveness of high speed ground transportation system using tracked air cushion vehicles for access to Los Angeles airport
[PB-212023] 06 p0651 N73-15290

**CUSPS**
NT CUSPS [MATHEMATICS]
Particle entry measurements from IMP 5 of polar or dayside cusp
08 p0972 N73-17949

**CUSPS [MATHEMATICS]**
Characteristic oscillations of plasma in point cusp
[IPPJ-133] 02 p0215 N73-11743

**CUTANEOUS PERCEPTION**
U TOUCH

**CUTTERS**
NT DRILLS
NT SAWS
Tool positioning holder for grinding by ball nose milling cutter
[NASA-CASE-LAR-10450-1] 01 p0061 N73-10504
Development of hard TiC-Ni alloys for use as cutting tools
[NLL-TRANS-746-1226-[9022.401]]
02 p0185 N73-11496
Adjustable hole cutter for forming circular openings
[NASA-CASE-MFS-22649-1] 23 p2797 N73-32376

**CUTTING**
NT METAL CUTTING
NT MILLING [MACHINING]
NT SPARK MACHINING

**CV-340 AIRCRAFT**
Aircraft accident involving midair collision of Convair 340 and DHC-6 near Appleton, Wisconsin on 29 June 1972
[NTSB-AAR-73-9] 17 p1981 N73-26016
Evaluation of approach and landing performance of inertial navigation system with Kalman filter installed in CV-340 aircraft
[NASA-TN-D-7302] 23 p2816 N73-32515

**CV-990 AIRCRAFT**
Instrumentation, calibration, and observational data obtained in airglow and auroral expedition aboard CV 990 aircraft
[NASA-CR-129511] 03 p0293 N73-12384
Soil moisture measurements for microwave radiometers onboard Convair 990 aircraft
08 p0971 N73-17935
Analysis of data taken by CV-990 aircraft during 1968 and 1960 auroral expedition
[NASA-CR-114616] 15 p1777 N73-24409
Wind tunnel tests to measure axial and tangential velocity profiles in near wake vortices of semi-span model of Convair 990 aircraft model using laser Doppler velocimeter
[NASA-TM-X-62294] 21 p2524 N73-30244

**CW RADAR**
U CONTINUOUS WAVE RADAR

**CYANIDES**
Weekend effect in CCN spectra and St. Louis urban heat island
[TN-45] 07 p0815 N73-16606
HCN laser for interferometric measurements in Tokamak machine
[EUR-CEA-FC-670] 22 p2681 N73-31475

**CYANO COMPOUNDS**
NT DIISOCYANATES
NT ISOCYANATES
Synthesis and characterization of 4,5-dicyano oxazole, low hydrogen content fuel for satisfying flame temperature criteria for gas dynamic laser
[AD-746342] 02 p0221 N73-11790

**CYANOPHYTA**
U BLUE GREEN ALGAE

**CYBERNETICS**
Soviet abstracts on analog and digital systems, control systems, information theory, and automata theory
[JPRS-57520] 04 p0393 N73-13190
Impact of cybernetics on management of business organizations
[NASA-CR-129728] 04 p0488 N73-13993
Soviet bibliography on biocybernetics material received from Jan. to May 1972
[AD-750129] 06 p0636 N73-15167
Cybernetic application of computers in personnel training
[AD-751145] 09 p0998 N73-18143
Cybernetic integration of experiments into CVT system
[NASA-CR-124150] 12 p1373 N73-21136
Application of cybernetics and systems analysis techniques to economic problems in USSR
[JPRS-58935] 15 p1845 N73-24951
Presentations on psychological models, cybernetics, methodology, and applications to teaching
[TT-70-57147-3] 21 p2502 N73-30076
Psychological concept for developing cybernetic control devices
[JPRS-60103] 23 p2752 N73-32019
Principles of construction for class of models of intelligent behavior
24 p2888 N73-33059
Experimental evaluation of model of motor behavior
24 p2888 N73-33060
Application of random walks for search optimization and function space
24 p2944 N73-33514

**CYCLES**
NT ACTIVITY CYCLES [BIOLOGY]
NT BRAYTON CYCLE
NT RANKINE CYCLE
NT SOLAR CYCLES
NT STIRLING CYCLE
NT STRESS CYCLES
NT SUNSPOT CYCLE
NT THERMODYNAMIC CYCLES
NT WORK-REST CYCLE
LOX-cooled bearing and seal start cycling performance
[MBB-UR-84-71] 10 p1167 N73-19493

**CYCLIC ACCELERATORS**
NT BETATRONS
NT BEVATRON
NT SYNCHROCYCLOTRONS
NT SYNCHROTRONS

**CYCLIC HYDROCARBONS**
NT CYCLOBUTANE
Thermomechanical analysis of physical transitions and stability of poly[norbornadiene] in nitrogen
[AD-749374] 05 p0566 N73-14596
Thermodynamic properties of cycloalkane and cyclobutane epoxy compounds for synthetic high energy fuels
[AD-760156] 17 p1993 N73-26116
Corrosion prevention mechanism of benzotriazole inhibitors for zinc and cadmium
[DRIC-TRANS-3080] 17 p2046 N73-26552
Para-benzoquinone dioxime and concentrated mineral acid processed to yield intumescent or fire resistant, heat insulating materials
[NASA-CASE-ARC-10304-1] 17 p2048 N73-26572

**CYCLIC LOADS**
Computer program to determine crack propagation characteristics of ultra high strength steel under various load cycles
[ARL/SM-NOTE-376] 02 p0237 N73-11930
Iterative algorithm for determining thermal instabilities in viscoelastic rod under cyclic loads
[AD-746470] 02 p0240 N73-11953
Numerical analysis of dynamic buckling modes of elastic systems under intensive loading in finite time segment
03 p0360 N73-12937
Tray hydraulic research, using cyclic operation of plate columns for gas-liquid contact
[PB-211853] 05 p0507 N73-14126
Elastoplastic deformation of steel samples under cyclic loads during torsion tests
[AD-749768] 05 p0604 N73-14914
Subcritical crack propagation in pressure vessel plates due to cyclic loads and stresses
[NASA-CR-120834] 06 p0725 N73-15920
Application of cumulative damage theory to internal stress caused by cyclic loading in notched bars
[LBF-FB-100/72] 06 p0726 N73-15930
Amplitude analysis of mechanical fatigue of structures acted upon by cyclic stresses
[AD-750908] 06 p0729 N73-15947
Comparison of methods for adapting hydrazine-oxygen fuel cells to cyclic pressure effects of hydrostatic pressure environment
[AD-753802] 10 p1112 N73-19062
Material testing system with load sensor for applying and measuring cyclic tensile and compressive loads to test specimens
[NASA-CASE-MFS-20673] 11 p1291 N73-20476
Axial extension in directionally solidified eutectic of solid cross section during cyclic torsion
[AD-755891] 12 p1417 N73-21481
Detection of acoustic emission signals from fatigue cracks during cyclic bend tests
[NASA-TM-X-68228] 12 p1462 N73-21848
Cyclic pressure tests of F-4 aircraft forward and aft canopies to determine safe service life after delamination of acrylic sheet
[AD-759349] 16 p1862 N73-25084
Coherent optical correlation techniques for detection of microstructural surface alterations during cyclic stressing
16 p1923 N73-25558
Service life extension of cyclically loaded copper specimens by application of electroplated layers of nickel
16 p1927 N73-25595
Cyclic mechanical and fatigue properties of ferroanelastic beta prime gold-cadmium alloy
[NASA-CR-131843] 16 p1969 N73-25929
Development of test equipment for random and constant amplitude loading on resonant and electrohydraulic fatigue machines
[RAE-TR-72226] 17 p2009 N73-26250
Standards for metallic specimens to include methods of mechanical and technological testing
[JPRS-59280] 17 p2044 N73-26538
Development of ultrasonic techniques for continuous monitoring of fatigue damage during cyclic testing of metal specimens
[AD-760787] 18 p2156 N73-27422

Analysis of threshold of alternating range of stress intensity factor for producing extremely slow fatigue crack growth in aluminum alloys
18 p2202 N73-27779
Axial load fatigue tests on unnotched specimens of aluminum alloy extrusions following aging specimens
[ARL/SM-NOTE-386] 18 p2203 N73-27780
Numerical analysis of fatigue strength of steel specimens under symmetric loading cycles
[AD-761469] 19 p2310 N73-28581
Development of fatigue cracks in flat plates under action of cyclic loads
[AD-761584] 19 p2351 N73-28911
Effect of environment and stress-cycling on in-service structural failure of airframes and procedures for predicting safe operational conditions
20 p2481 N73-29929
Thermal stress ratcheting of structures subjected to mechanical and cyclic thermal stresses
22 p2723 N73-31790
Laws governing stress-rupture strength for structural materials under conditions of cyclic loading
[AD-764665] 23 p2854 N73-32810

**CYCLING**
U CYCLES

**CYCLOBUTANE**
Thermodynamic properties of cycloalkane and cyclobutane epoxy compounds for synthetic high energy fuels
[AD-760156] 17 p1993 N73-26116

**CYCLOIDS**
Constant azimuth cycloids discussing rotating earth trajectory
07 p0859 N73-16970

**CYCLONES**
NT HURRICANES
NT TYPHOONS
Tables on Atlantic tropical cyclone strike probabilities - 24 hour movement
[AD-744916] 01 p0076 N73-10630
Tables on Atlantic tropical cyclone strike probabilities - 48 hour movement
[AD-744917] 01 p0076 N73-10631
Probabilities of forecasting future movement of North Atlantic tropical cyclones
[AD-744918] 01 p0076 N73-10632
Statistical analysis of geography and seasonal variation effects on intensification of tropical cyclones over western North Pacific Ocean
[AD-746130] 02 p0206 N73-11669
Feasibility determination of Sutcliffe-Peterssen development theory to predict development of cyclones and anticyclones at sea level
[NASA-CR-2192] 07 p0815 N73-16605
Atmospheric energetics as related to cyclogenesis over eastern United States
[NASA-CR-2189] 07 p0815 N73-16607
Technique for using satellite pictures to analyze and forecast tropical cyclone intensities
[NOAA-TM-NESS-45] 10 p1182 N73-19611
Long term meteorological study of intensity and movement of tropical cyclones and typhoons in western North Pacific
[AD-754349] 11 p1315 N73-20676
Determining important processes for cyclogenesis in extratropical cyclone
17 p2056 N73-26632
Influence of atmospheric cyclones on circulation and mixing of sea water in motionless uniformly rotating baroclinic ocean
19 p2258 N73-28202
Analog scheme for analyzing meteorological parameters to determine their predictive value for forecasting intensity changes in western North Pacific tropical cyclones
[AD-761726] 19 p2316 N73-28625
Circulation and mixing of sea water due to stationary and transitory axisymmetric atmospheric cyclones
[AD-763930] 22 p2669 N73-31383

**CYCLOTRIMETHYLENE TRINITRAMINE**
U RDX

**CYCLOTRON FREQUENCY**
Low frequency oscillations in Penning discharge under conditions of cyclotron ion source
[NASA-TT-F-14649] 06 p0703 N73-15736
Microwave discharge plasma in magnetic fields greater than cyclotron
[AEC-TR-7372] 10 p1196 N73-19735
Stablity of plasma rotating in crossed electrical and magnetic fields
[NASA-TT-F-15021] 20 p2458 N73-29752

**CYCLOTRON RADIATION**
NT ION CYCLOTRON RADIATION
Target design for cyclotron irradiation using iodine nucleus
[NASA-TM-X-68156] 02 p0214 N73-11733
Fast flux neutron source for cyclotron simulation of reactor core
[AERE-R-6626] 04 p0402 N73-13269

**CYCLOTRON RESONANCE**
Cyclotron resonance caused by electromagnetic waves incident on high density gaseous plasma
[IPPJ-134] 02 p0215 N73-11742
Equatorial resonance between electrons and VLF signals, characterized by intrinsic bandwidth
[AD-750865] 06 p0667 N73-15428
High power radio frequency ion heating effects on harmonics of ion cyclotron radiation
[ORO-3871-7] 08 p0889 N73-17197
Dynamic model for calculating radio frequency absorption in perpendicular ion cyclotron resonance heating of hydrogen deuterium plasma
[IPPJ-146] 09 p1070 N73-18730
Artificial plasma injection of lithium cloud in program to stimulate electromagnetic cyclotron instabilities in magnetosphere
[AD-760032] 17 p2029 N73-26424
Computerized simulation of cyclotron resonant electrons interaction with narrow band whistler wave along magnetospheric duct for VLF emission triggering
19 p2340 N73-28827
Linear and nonlinear wave particle cyclotron interaction for whistler mode waves in anisotropic plasma
[AD-763744] 22 p2705 N73-31668
Cyclotron resonance linewidth in semiconductors
24 p2968 N73-33716

**CYCLOTRONS**
NT SYNCHROCYCLOTRONS
Operational problems and scientific research activities at cyclotron
[AD-751539] 07 p0767 N73-16230
Magnetic field measurements of Lewis Research Center cyclotron using Hall effect magnetic field transducer
[NASA-TM-X-2692] 07 p0824 N73-16677
Analysis of electron cyclotron heating characteristics and generation of hot electron plasma in magnetic mirror trap by microwaves
[IPPJ-140] 08 p0947 N73-17755
Axial injection of Grenoble cyclotron for multicharged heavy ion injection
[FRNC-CONF-59] 10 p1138 N73-19270
Interaction between drifting streams of electrons with transverse cyclotron motions and electromagnetic fields
[NASA-CR-130208] 13 p1504 N73-22188
Ordinary wave penetration of infinite magnetoplasma slabs
[IPPJ-154] 16 p1949 N73-25772
Cyclotron damping by suprathermal fluxes of protons and electrons in interplanetary medium
[NASA-TM-X-66254] 16 p1959 N73-25847

**CYGNUS CONSTELLATION**
Balloon-borne X ray telescope survey of Cygnus region on 10 June and 17 July 1969 in 20 to 300 keV energy range
07 p0840 N73-16804
Stellar X ray temporal variations from observations of Sco X-1 and Cyg X-1
08 p0974 N73-17969
Observations of neutral hydrogen absorption spectrum of Cygnus X-3
[AD-752497] 09 p1085 N73-18856
Radio and optical data on outburst in Cygnus constellation
[AD-756464] 15 p1833 N73-24862
Earth rotation aperture synthesis technique and polarized interferometry for determining polarized intensity distributions of Cygnus A at 8300 and 9600 MHz
16 p1961 N73-25865
Surface brightness and X ray measurements of Cygnus Loop from Aerobee rocket
[NASA-CR-133098] 17 p2080 N73-26822
Rocket-borne survey of Cygnus region in energy range from 2 to 20 keV
17 p2081 N73-26831
Decimetric radio continuum maps of three extended galactic supernova remnants and Cygnus Loop
19 p2342 N73-28839

**CYLINDERS**
Numerical solution for cylindrical symmetrical diffusion problem
[FOA-1-C-1409-92] 06 p0653 N73-15306
Magnus effect in supersonic laminar boundary layer on spinning body of revolution
[SC-DC-72-1173] 07 p0772 N73-16269
Sprag solenoid brake with cylindrical chamber
[NASA-CASE-MFS-21846-1] 14 p1670 N73-23552
Theoretical and experimental analysis of flow induced by harmonic oscillation of rods with arbitrary cross sections containing incompressible, viscous, Newtonian fluid
23 p2774 N73-32183

**CYLINDRICAL AFTERBODIES**
U AFTERBODIES
U CYLINDRICAL BODIES

**CYLINDRICAL ANTENNAS**
Least squares representation for charge distribution on monopole antenna immersed in dissipative medium
[AD-753092] 09 p1008 N73-18230
Design and performance characteristics of trap loaded cylindrical antennas
21 p2516 N73-30183
Computer solutions of cylindrical antennas in anisotropic media
22 p2627 N73-31045

**CYLINDRICAL BODIES**
NT ROTATING CYLINDERS
Heat transfer rate measurements on cone cylinder models and in separated regions behind axially symmetric backward facing step
[AD-735744] 01 p0037 N73-10290
Computer analysis of temperature distributions in circular and rectangular bodies exposed to thermal radiation from nuclear weapon explosions
[AD-745727] 01 p0084 N73-10699
Computer program for stress, stability, and vibration analyses of segmented, ring-stiffened, branched shells of rotation
[NASA-CR-2116] 02 p0237 N73-11931
Analysis of short time response of cylindrical, elastic segment to shock wave engulfment based on focusing effects due to curved geometry
[AD-745962] 02 p0238 N73-11940
Calculation of Magnus sideforce developed by spinning cylinder at angle of attack considering effects of boundary layer and shed vorticity in crossflow
03 p0247 N73-11998
Calculation of coefficient of resistance of sphere at supersonic velocities and measurement of critical point on free flying bodies
[AD-747513] 03 p0287 N73-12324
Pressure loss coefficients for fluid flowing through orifice plates, perforated plates, and cylindrical tubes
[ESDU-72010] 04 p0403 N73-13279
Nonisothermal stationary flow of viscoplastic liquid between two concentric cylinders
[AD-748908] 04 p0408 N73-13321
Analytic solution for temperature distribution in thermally insulated cylinder bar to determine time-variable thermal stresses
[DGLR-PAPER-72-112] 04 p0485 N73-13963
Wind tunnel tests to determine heat transfer and pressure distributions of hemisphere cylinders in hypersonic flow environment
[NASA-TN-D-7104] 05 p0605 N73-14925
Analysis of lee side vortex flow distribution about ogive-cylinderfrustum-cylinder at various angles of attack and Mach numbers - Vol. I
[NASA-CR-123997-VOL-1] 06 p0653 N73-15307
Compilation of computed parameters resulting from analysis of lee side vortex flow distribution about ogive-cylinder-frustum-cylinder at various angles of attack and Mach numbers - Vol. 2
[NASA-CR-123997-VOL-2] 06 p0653 N73-15308
Supersonic flow past solid cylindrical and circular jet barriers on flat plates
[AD-750522] 06 p0656 N73-15327
Firing tests to determine cratering produced by impact of flat ended, high density metal cylinders striking mild steel plate targets
[DREV-TN-2034/72] 06 p0726 N73-15927
Analysis of Magnus sideforce developed by spinning cylinder at angle of attack based on boundary layer and shed vorticity in cross flow
07 p0768 N73-16239
Hypersonic axisymmetric turbulent boundary layer compression in adverse pressure gradient along cylindrical axisymmetric body
[NASA-CR-112247] 07 p0770 N73-16253
Flow field measurements around ogive-cylinder at angles of attack to 15 degrees and Mach numbers 3.52 and 4.07
[AD-752025] 08 p0898 N73-17268
Current collection characteristics of moving cylindrical Langmuir probe for range of probe speeds and potentials applicable to earth and planetary measurements
[NASA-TM-X-66177] 08 p0924 N73-17571
Effects of spatially varying curvature on dynamics of cylindrical panels and stiffened cylindrical shell structures
[AD-752590] 08 p0967 N73-17907
Analysis of complex moduli of uniaxially fiber reinforced materials containing viscoelastic matrix and elastic fibers
[AD-753699] 09 p1054 N73-18591
Flow equations for unsteady turbulent boundary layer flow on swept infinite cylinder to show effects of variations in frequency of oscillations
[NASA-TM-X-62242] 10 p1141 N73-19297
Laminar heat transfer problem on spheres and cylinders solved by laminar boundary layer theory
[VKI-TN-84] 10 p1142 N73-19306
Affect of sound and vibration on convective heat transfer and flow distribution on boundary layers of cylindrical bodies
[AD-754006] 10 p1143 N73-19316
Tables and graphs on static stability and axial force characteristics of flat faced right circular cylinders at subsonic and supersonic speed
[AD-754920] 11 p1273 N73-20330
Pitot pressure survey of laminar boundary layer on supersonic spinning ogive cylinder
[AD-755694] 12 p1393 N73-21294
Continuous measurement of residual stress in thin cylindrical pieces using deflection-etching techniques
[CRIF-MC-47] 12 p1409 N73-21418

Solution of temperature distribution in hollow cylinder for asymptotic regime and variable heat conductivity coefficient
[AD-755251] 12 p1465 N73-21872
Perturbation theory for determining potential of point source current in cylindrical cell
[AD-756666] 13 p1501 N73-22166
Temperature field calculations on cylinder solidification in axial and radial axial heat transfer
[AD-755871] 13 p1591 N73-22901
Transfer matrix techniques for vibration analysis of curved skin-stringer structures with tuned elastomeric dampers
[AD-758220] 14 p1605 N73-23010
Development of formulas for elastic behavior of axisymmetrically loaded cylindrical and spherical pressure vessels under various load conditions
[AD-758496] 14 p1717 N73-23936
Discontinuous functions in problems of strength and stability of elongated cylindrical panels with finite deflections
[AD-758621] 15 p1841 N73-24918
Model developed for opposed free and forced convection flow around heated cylinder
[AD-757993] 15 p1844 N73-24942
Factors affecting base flow and jet structure behind cylindrical afterbody with central nozzle at mach 2.0 and turbulent boundary layer conditions
[ARC-R/M-3224] 16 p1851 N73-25001
Admittance of axial slot backed by cylindrical cavity inside infinite cylinder
[AD-759568] 16 p1946 N73-25748
Influence of variation in cylinder geometry on fragmentation and mode of fracture of internally detonated carbon steel cylinders
[DSL-REPT-533] 16 p1969 N73-25930
Modified boundary collocation method for crack fracture mechanics analysis on cylindrical section
[AD-758849] 16 p1970 N73-25932
Buckling of cylindrical panels under non-uniform axial compression
[AD-758833] 16 p1971 N73-25946
Development of formula for determining ideal weight of shell-type aircraft fuselages with body of revolution cross section
[RAE-LIB-TRANS-1688] 17 p1981 N73-26009
Nonstationary heat and mass transfer developed by transverse flow around cylindrical body to determine conditions at stagnation point
[AD-760396] 17 p2016 N73-26299
Numerical analysis of temperature and stresses in cylindrical body heated with constant heat flow
[NLL-M-21601-[5828.4F]] 18 p2205 N73-27794
Analysis of axial conduction current induced in infinitely long cylinder in free space with small resistivity by incident electromagnetic plane wave
[AD-762165] 19 p2246 N73-28106
Velocity and temperature development in entrance region between two rotating concentric cylinders
[AD-762049] 19 p2256 N73-28187
Electrodeposition of cylindrical magnetic films
[JPRS-59626] 19 p2305 N73-28534
Fracture characteristics of small cylindrical bodies partly prefragmented by external notching subject to detonation of high explosive filling
[REPT-545-PT-1] 20 p2483 N73-29943
Development of methods for analyzing thermal stress, heat conduction, structural theory, and thermoelastic wave propagation
[AD-762479] 20 p2484 N73-29952
Linear and nonlinear theory of elasticity used to determine deformation of cylinder and piston of high strength steel under influence of high pressure
[AD-763971] 22 p2687 N73-31519
Creep induced buckling of infinitely long sandwich panel under uniform pressure and uniform temperature
[AD-764311] 22 p2725 N73-31810
Reliability of circular electrical connectors
[AD-765609] 24 p2899 N73-33144
Interactions between fluid flow and mechanical oscillators, using vibrating steel wire and cylindrical body
[DLR-FB-73-42] 24 p2909 N73-33218

**CYLINDRICAL CHAMBERS**

Calculating resonance frequency of cylindrical cavity frequency meter
[REPT-6659] 14 p1666 N73-23522

**CYLINDRICAL SHELLS**

Development of procedure for determining maximum and minimum stresses produced by uniform pressure on unpierced torispherical closure of cylindrical shell
[ESDU-67017] 01 p0110 N73-10911
Curves for determining maximum combined stresses in long circular cylindrical shells with flat head closure under uniform pressure only
[ESDU-66010] 01 p0111 N73-10912
Free vibrations of complex system of ring with added mass, connected to thin spherical or cylindrical shell
01 p0112 N73-10930
Transient response of finite longitudinally-layered cylindrical membrane shell impacted by longitudinal axisymmetric loads
[TAE-154] 02 p0237 N73-11929
Safe carrying loads of external pressure for cylindrical shells
02 p0238 N73-11935
Creep buckling of flat plates and cylindrical shells subjected to edge wise and uniform axial compression respectively
[AD-746475] 02 p0240 N73-11952
Forced steady state response of cylindrical shell immersed in acoustic fluid bounded by elastic half space
[AD-747705] 03 p0337 N73-12750
Residual stresses and mechanical properties in circumferentially wrapped composite cylinders
[SC-DC-72-1291] 03 p0361 N73-12942
Finite analysis of effects of varying radii of circumferential fillets in transition of cylindrical shells
[ORNL-TM-3766] 03 p0361 N73-12943
Equilibrium stability of orthotropic cylindrical shell
[AD-747724] 03 p0362 N73-12948
Procedures for analyzing very thick walled cylindrical shells used in constructing hydrospace simulators
[AD-747963] 03 p0362 N73-12952
Elastic buckling strength of thin walled aluminum alloy tubes fabricated with and without boron/epoxy glass/epoxy composite materials for reinforcement
[NBS-TN-728] 04 p0437 N73-13566
Analysis of ring and stringer stiffness parameters and proportions for axially compressed stiffened isotropic cylinders with and without internal pressure
[NASA-CR-2165] 04 p0481 N73-13930
Buckling and intial postbuckling of oval cylindrical shells under pure bending and under combined uniform axial compression and bending
[AD-747493] 04 p0482 N73-13939
Finite element model for class 4 flextensional underwater transducer shell
[AD-748187] 04 p0482 N73-13940
Development of FORTRAN computer program for solving free axisymmetric vibration of cylindrical shells of arbitrary shape
[AD-748655] 04 p0482 N73-13942
Results of ultrasonic inspection of cast steel cylinders
[TR-7208.594] 05 p0551 N73-14471
Effects of pulse shape on transient response of cylindrical shells and generation of shear waves in cylindrical shells
[NASA-CR-112221] 05 p0602 N73-14891
Method for statistical estimation of magnitude of acoustic power radiated from fluid loaded cylindrical shells
[AD-749361] 05 p0603 N73-14906
Analysis of stability of cylindrical shells with filler under axial compression and development of linearized equations of stability
[AD-750953] 05 p0605 N73-14919
Elastic wave propagation in cylindrical shells
[NASA-CR-112222] 06 p0724 N73-15909
Variational principle for calculating buckling of thin clamped free circular cylindrical shells subjected to wind load
[TT-7113] 06 p0725 N73-15916
Application of three dimensional theory of elasticity to dynamic response of freely supported circular cylindrical shell
06 p0725 N73-15921
Mathematical model for resonant vibration of cylindrical shells using the Rayleigh-Ritz method
[DLR-FB-71-92] 06 p0727 N73-15931
Response of cylindrical shells to traveling load simulation of x ray blow-off impulse
[AD-750336] 06 p0727 N73-15933
Application of least square point matching for stress analysis of shallow, perforated, cylindrical shell subjected to tension, edge moment, or transverse shear
[AD-750942] 06 p0728 N73-15942
Procedures for determining shell stability under various types of dynamic loads
07 p0852 N73-16906
Circular cylindrical shell pressure limits
[PB-212638] 07 p0852 N73-16912
Theory of plates and shields to include response of structurally loaded shells of cylindrical and spherical configurations
[AD-751502] 07 p0852 N73-16913
Analytic models to calculate electrostatic fields produced inside cylinders and spheres by internal electromagnetic pulses
[AD-753014] 09 p1067 N73-18709
Rayleigh-Ritz modal vibration analysis for ring and/or stringer stiffened noncircular cylindrical shells with arbitrary end conditions
[NASA-CR-2151] 09 p1094 N73-18927
Effect of eccentricity of reinforcement upon stability of cylindrical shells
[AD-752691] 09 p1096 N73-18943
Numerical analysis of displacement of cylindrical shell subjected to cylindrical wave in acoustic medium
10 p1219 N73-19918
Brittle fracture and fatigue of cylindrical hollow bodies with offset seams and stiffeners
[NLL-RISLEY-TR-2527-[9001.9F]]
11 p1344 N73-20908
TACOS finite computer program for analyzing dynamic transient response of cylindrical obese shells
[SC-RR-72-0454] 12 p1463 N73-21852
Shell theory and three dimensional analysis of cylindrical shells subjected to axisymmetric tangential surface loads
13 p1584 N73-22838
Buckling of stiffened cylindrical shells subjected to combined axial compression, normal pressure, bending, and shear loads
13 p1585 N73-22847
Theory and user manual for computer program to determine buckling behavior of arbitrarily loaded shells of revolution with actual initial imperfections
[AD-756545] 13 p1587 N73-22866
Experimental analysis of buckling of integrally ring stiffened cylindrical shells under axial compression to determine influence of shell and ring geometry on applicability of linear theory
[AD-755392] 13 p1588 N73-22872
Buckling of shells under combined loading and thermal stresses
[AD-756494] 13 p1589 N73-22883
Higher-order shell equations for vibrations of thick orthotropic circular cylindrical shells
[AD-756649] 13 p1589 N73-22884
Stability of cylindrical shell stiffened by frames and loaded with external pressure
[AD-757726] 14 p1717 N73-23929
Development of equations of motion for vibration frequencies of cantilever and elastically supported-free thin circular cylindrical shell
15 p1837 N73-24887
Stability of cylindrical shells with consideration of initial imperfections
[AD-757728] 15 p1840 N73-24909
Effect of stress state nonhomogeneity and initial imperfections on stability of cylindrical shells
[AD-758027] 15 p1840 N73-24910
Effect of arrangement of stiffening ribs for cylindrical shell on critical load value
[AD-758029] 15 p1840 N73-24912
Structural stability of thin imperfect cylindrical shells as determined by statistical analysis
[AD-758030] 15 p1840 N73-24913
Equations for structural stability of orthotropic plates and cylindrical shells
[AD-758327] 15 p1840 N73-24914
Elastic stresses due to axial loads on nozzle intersecting cylindrical shell
[AD-758075] 15 p1841 N73-24916
Analysis of general buckling of pressurized stiffened cylinder under axial load
[ARC-R/M-3198] 16 p1857 N73-25040
Holographic interferometric measurement of prebuckling deformation in cylindrical shell structures under axial compression
16 p1921 N73-25545
Shell equations for orthotropic, circular cylinders during axially symmetric, harmonic motion
16 p1968 N73-25918
Love- and Donnell-type equations for investigating thermal stresses in ring-reinforced oval cylindrical shells subjected to heat inputs
16 p1968 N73-25920
Axisymmetric oscillation of partially liquid-filled cylindrical shell container having hemispherical bulkheads
[NASA-TN-D-7318] 16 p1969 N73-25925
Approximate method for calculating echo signal of finite spherical pulse from elastic cylindrical shell in compressible fluid
16 p1969 N73-25928
Variational principle for studying elastic-plastic instability of ring stiffened cylindrical shells under external pressure
[AD-757750] 16 p1970 N73-25935
Statistical method used to examine stability of cylindrical shell under influence of axial forces
[AD-759394] 16 p1970 N73-25938
Carrying capacity of cylindrical shells under dynamic loads
[AD-759103] 16 p1971 N73-25944
Fabrication and testing of thin walled cylinders made from tungsten lead composite
[LA-511] 17 p2038 N73-26485
Static and dynamic buckling of nonhomogeneous cylindrical shells
17 p2090 N73-26912
Vibrational characteristics, mechanical properties, and stress analysis of thin shell structures of various cross sections
[NASA-SP-288] 17 p2092 N73-26924
Analysis of dynamic stability of elastic orthotropic cylindrical shell to determine shell parameters, shear moduli, and buckling mode
17 p2093 N73-26930
Stress analysis of pressurized shallow cylindrical shell containing two collinear axial cracks of equal length
[NASA-CR-132271] 17 p2093 N73-26932
Laminated composite cylindrical shell buckling strength criteria
[AD-759537] 17 p2095 N73-26944
Vibrations of stiffened composite shells
[AD-759375] 17 p2095 N73-26946

Numerical analysis of stability of axially compressed cylindrical shells from composite materials under nonstationary heating
18 p2203 N73-27785
Statistical analysis of load-carrying capacity of smooth cylindrical shells
[AD-760946] 18 p2204 N73-27787
Analysis of local and average heat transfer characteristics of single turbulent air jet impinging on concave surface of hemisphere
[NASA-TM-X-2859] 18 p2206 N73-27806
Nonlinear programming algorithms for variable design of structural cylindrical shell
[AD-761645] 19 p2240 N73-28062
Underwater scattering of sound waves by submerged viscoelastic cylindrical shell
[AD-761618] 19 p2321 N73-28674
Detailed calculations of natural vibrations of single cylindrically curved open shells
[NASA-TT-F-14979] 19 p2347 N73-28880
Orthotropic effects in cracked cylindrical shell
[NASA-CR-132295] 19 p2348 N73-28887
Stability of freely supported circular cylindrical shell subjected to random stresses
[AD-761541] 19 p2350 N73-28901
Stability of cylindrical shell under nonuniform radial loads
[AD-762242] 19 p2351 N73-28909
Dynamical response of cylindrical shells due to moving excitations
20 p2476 N73-29892
Nonlinear parametric vibrations of closed cylindrical shells
20 p2482 N73-29939
Numerical analysis of buckling characteristics of ring-stiffened, oval, orthotropic, cylindrical shells
[AD-763369] 21 p2604 N73-30872
Resonant vibration structural analysis of cylindrical sandwich shells
[TUB-IR-1972/2] 22 p2725 N73-31808
Optimum structural design of discretely ring-stiffened cylindrical shell
23 p2853 N73-32794
Fourth order partial differential equations governing deformation of circular cylindrical shells
[AD-764560] 23 p2854 N73-32809
Optimal design of submerged elastic cylindrical shells for maximum pressure
[AD-764578] 23 p2855 N73-32814

**CYLINDRICAL TANKS**
Measurement of fluid velocity and surface deformation during fluid discharge from rotating cylindrical tank
13 p1509 N73-22232
Axisymmetric oscillation of partially liquid-filled cylindrical shell container having hemispherical bulkheads
[NASA-TN-D-7318] 16 p1969 N73-25925

**CYLINDRICAL WAVES**
Numerical analysis of displacement of cylindrical shell subjected to cylindrical wave in acoustic medium
10 p1219 N73-19918
Design and performance of liquid nitrogen cooled nozzle for producing pulsed cylindrical hydrogen cluster beams
[KFK-1610] 12 p1436 N73-21632
Analysis of dynamic fracture in aluminum alloys using radial cylindrical wave propagation technique
18 p2202 N73-27778

**CYLINDROIDS**
U CYLINDRICAL BODIES

**CYSTEAMINE**
Effectiveness of polymer complex of cysteamine and sulfopropyl ester of dextran as an antiradiation drug on irradiated mice
[DRIC-TRANS-2963] 06 p0631 N73-15125
Effects of antiradiation drug dosage on mice and rat tolerance to transverse acceleration overloads
11 p1239 N73-20055
Hypoxia and reduced acceleration tolerance of rats after injection of cysteamine radioprotector
11 p1239 N73-20038
Antiradiation effectiveness of cysteamine in mice under various conditions of gamma radiation
11 p1240 N73-20067
Elimination of toxic cysteamine in organisms and method for prolonging its radioprotective effect
11 p1240 N73-20069
Gamma radiation effects on toxic cysteamine elimination in irradiated and nonirradiated mice
11 p1240 N73-20070
Influence of cysteamine hydrochlorine and vitamin B and C prophylaxis on radiation sickness in humans
11 p1242 N73-20078
Effect of cysteamine combined with adrenalin and phenamine on reparative processes following irradiation and overload
11 p1242 N73-20081
Exposure to gamma rays from Co-60 and transverse loads and effectiveness of cysteamine and AET protection
11 p1242 N73-20086

**CYTOCHROMES**
Isocyanide spin label for studying conformational transitions in cytochrome c, emphasizing heme group
[NASA-TT-F-14623] 03 p0259 N73-12099
Toxic effects of chronic exposure to dichloromethane in liver microsomal cytochromes
[NASA-TM-X-69101] 09 p0996 N73-18128
Molecular organization of active center of microsomal cytochrome P-450
[NASA-TT-F-15042] 20 p2368 N73-29042

**CYTOLOGY**
Energy comparisons for lethal doses of gamma radiation and visible light with energy of basal cell metabolism
[AD-746750] 04 p0381 N73-13102
Cytological changes in pine tissues treated with lunar materials collected on Apollo 12 quarantine mission
[NASA-CR-128914] 14 p1610 N73-23054

**CZECHOSLOVAKIA**
Procedures and facilities in Czechoslovakia for determining pollution of rain water
[NLL-M-22857-[5828.4F]] 15 p1805 N73-24627

**CZOCHRALSKI METHOD**
Czochralski technique for growing GaAs and III and V semiconductor crystals
[AD-748344] 04 p0461 N73-13759

# D

**D LINES**
Collision cross section of D line radiated into sodium atoms for one 3 P2 state
[NASA-TT-F-14853] 14 p1695 N73-23752

**D REGION**
Inversion of VLF-LF sounder data to obtain D region electron density distributions
02 p0201 N73-11626
Electromagnetic cross modulation and very low frequency propagation techniques for measuring acoustic gravity waves in ionospheric D region
05 p0511 N73-14153
Correlation coefficient between D region HF radio wave absorption and 10mb level winds and temperature in Northern Hemisphere
[COO-2195-5] 05 p0539 N73-14384
Analytic model for behavior of neutral and ion chemistry in D region following nuclear burst
[AD-750395] 05 p0543 N73-14416
Neutral and ion chemistry of D and E regions symposium papers
[AD-749780] 06 p0668 N73-15430
D region ionization during polar cap absorption determined from parachuteborne blunt probe measurements of charged particle conductivity
[AD-750570] 06 p0670 N73-15448
Electron density profiles of D region
[RSD-76] 07 p0789 N73-16415
Atmospheric model for predicting seasonal and diurnal behavior of D region electron density
[AD-755447] 12 p1403 N73-21383
Design and implementation of experimental system for receiving and recording partially reflected echoes from D region
[PSU-IRL-SCI-414] 15 p1778 N73-24417
Determination of D region electron density distributions from radio propagation data
[AD-759018] 16 p1909 N73-25449
ESRO sounding rocket experiment R-175 in presence of noctilucent clouds on polar summer upper atmosphere structure, composition, and ionization
[AP-7] 17 p2027 N73-26406
Experimental systems for automatic receiving and recording of echoes from D region
[AD-760362] 17 p2030 N73-26428
Ionosphere D and F region high frequency ray propagation effects and design of high frequency dynamic phase metering instruments
20 p2375 N73-29083
D region blunt probe data analysis using hybrid computer techniques
[NASA-CR-135646] 22 p2639 N73-31147

**DACRON [TRADEMARK]**
Development and characteristics of multilayer insulations for long term cryogenic storage
[NASA-CR-123938] 03 p0320 N73-12606

**DAEMO [DATA ANALYSIS]**
U DATA PROCESSING
U DATA REDUCTION
U DATA TRANSMISSION

**DAMAGE**
NT CUMULATIVE DAMAGE
NT FIRE DAMAGE
NT FLOOD DAMAGE
NT IMPACT DAMAGE
NT METEORITIC DAMAGE
NT RADIATION DAMAGE
NT RAIN IMPACT DAMAGE
Superconducting properties and damage susceptibility of composite wire conductors
[BNL-17222] 12 p1439 N73-21660

**DAMPING**
NT ELASTIC DAMPING
NT LANDAU DAMPING
NT VIBRATION DAMPING
NT VISCOUS DAMPING
Cataloging elastomer stiffness and damping properties in terms of viscoelastic model constants
[NASA-CR-120965] 01 p0113 N73-10931
Analysis of forced-oscillation pitch-damping over small angular amplitude range about nominal angle of attack
[NASA-CR-129522] 03 p0247 N73-12001
Pressure loads and damping associated with rigid ring baffles in large cylindrical tanks
[NASA-TN-D-6870] 03 p0282 N73-12285
Damping of accelerated isothermal superfluid helium flow by roton polarization
[NOTA-INTERNA-395] 03 p0336 N73-12743
Application of finite element method to nonconservative stability problems with damping
[AD-748086] 04 p0483 N73-13945
Dislocation damping in cu single crystals of controlled substructure, and ultrasonic attenuation data
[AD-750712] 06 p0711 N73-15801
Subharmonic angular motion response in asymmetric missile trajectory analysis
[AD-749787] 06 p0722 N73-15893
Damping in porcelain enamel coatings at elevated temperatures
[AD-752317] 09 p1055 N73-18598
Hydraulic damping of sensors of differential manometers of dynamic pressure logs
10 p1184 N73-19637
Finite element technique for elastic stability under nonconservative forces and internal and external damping
[AD-755101] 11 p1346 N73-20925
Lower hybrid frequency damping of longitudinal plasma oscillations and plasma heating
[EUR-CEA-FC-657] 12 p1433 N73-21614
Development of empirical structural damping law for space shuttle by dynamic analysis of vibration test data
[NASA-CR-124203] 12 p1460 N73-21828
Measurements of roll damping derivative of three wing planforms using free light roll balance technique for Mach numbers from 0.7 to 1.4
[ARC-R/M-3274] 15 p1726 N73-24005
Measurement of power spectra of waveforms derived from vibrating blades in axial compressor and application to determine damping factor of blades
[ARC-R/M-3253] 15 p1728 N73-24014
Development of long acoustic damping device for various chamber flow conditions based on nonlinearity of orifice flow upon passage of high intensity wave
15 p1765 N73-24299
Nutation damper for use on spinning body
[NASA-CASE-GSC-11205-1] 16 p1917 N73-25513
Cyclotron damping by suprathermal fluxes of protons and electrons in interplanetary medium
[NASA-TM-X-66254] 16 p1959 N73-25847
Variational principle for studying elastic-plastic instability of ring stiffened cylindrical shells under external pressure
[AD-757750] 16 p1970 N73-25935
Development of electrical circuit for suppressing oscillations across inductor operating in resonant mode
[NASA-CASE-ERC-10403-1] 17 p2007 N73-26228
Spatial growth properties of parametric and backscattering plasma instabilities
[AD-761173] 18 p2184 N73-27631
Experimental methods for determining internal damping in metal alloys and identification of factors causing internal damping
[NLL-CE-TRANS-6132-[9022.09]]
20 p2429 N73-29508
Analysis of pitch damping moment for hovering helicopter rotary wing and development of formula for calculating pitch damping derivative
[NASA-TT-F-15010] 21 p2495 N73-30027
Development of damping system to compensate for wind loads on space shuttle vehicle during launch operations
[NASA-CR-124367] 21 p2601 N73-30845
Methods of reducing damping in pneumatic piston drivers used in cryogenic armatures
22 p2678 N73-31449
Development of program for obtaining resonant frequencies, modal amplitudes, and damping of structure from sinusoidal force-controlled vibration test
[NASA-TM-X-2789] 22 p2724 N73-31802
Damping and saturation of second order electron plasma wave echo
24 p2961 N73-33662

**DAMPING FACTOR**
U DAMPING

**DAMPING IN PITCH**
U DAMPING
U PITCH [INCLINATION]

**DAMPING IN ROLL**
U DAMPING
U ROLL

**DAMPING IN YAW**
U DAMPING
U YAW

DAMPING TESTS
Applicability of composite materials in aircraft structure and engine design
[NASA-TT-F-14648] 07 p0811 N73-16576
Development of dissipative energy approach for predicting damping of four component space shuttle model using modal parameters for individual components
12 p1459 N73-21827

DAMPNESS
U MOISTURE CONTENT

DAMS
Environmental and ecological impact of construction and operation of dam and impoundment on Sangamon River in Illinois
[E72-10216] 02 p0162 N73-11310
Effect of dam construction and staged filling of reservoirs in Illinois on environment and ecology
[E72-10217] 02 p0162 N73-11311
Utilization of ERTS-1 imagery in national program for inspection of dams
[E72-10322] 04 p0413 N73-13370
ERTS-1 imagery in national program for inspection of dams
[AD-754579] 11 p1288 N73-20449
Environmental and ecological impact of construction and operation of Oakley Dam and Friends Creek impoundment located on Sangamon River in East Central Illinois
[E73-10484] 12 p1396 N73-21321
Environmental and ecological impact of construction and operation of Oakley Dam and Friends Creek impoundment located on Sangamon River in East Central Illinois
[E73-10655] 16 p1898 N73-25351
Environmental and ecological impact of construction and operation of Oakley Dam and Friends Creek Impoundment located on Sangamon River in East central Illinois
[E73-10882] 20 p2394 N73-29233
Effect of construction and staged filling of Oakley Dam and Friends Creek impoundment in Illinois on environment and ecology
[E73-11124] 24 p2916 N73-33279

DANGER
U HAZARDS

DARK ADAPTATION
Influence of illumination on electro-oculographic measurements of human eye potential
[AMRU-R-71-1] 02 p0131 N73-11064

DARKENING
NT LIMB DARKENING

DARKNESS
Dark side illumination of Saturns ring by scattering
[REPT-13] 10 p1212 N73-19855

DART TURBOPROP ENGINES
U TURBOPROP ENGINES

DASSAULT AIRCRAFT
NT MIRAGE 3 AIRCRAFT

DASSAULT MIRAGE 3 AIRCRAFT
U MIRAGE 3 AIRCRAFT

DATA ACQUISITION
Acquisition and reduction of data acquired from superconducting magnetic suspension and balance facility
[NASA-CR-112186] 01 p0035 N73-10276
Acquisition of earth resources data for Bolivia using ERTS-1 imagery
[E72-10191] 01 p0046 N73-10370
Development of airborne flight data acquisition and data processing systems
[AGARD-LS-50] 01 p0055 N73-10450
In-flight data acquisition and processing systems
01 p0056 N73-10452
Impact of technological development on airborne data acquisition system and ground data processing station
01 p0056 N73-10457
Head echoes of meteoroids
01 p0102 N73-10840
Data acquisition and storage system for computerized physiological monitoring system
[AD-746872] 02 p0148 N73-11199
Physiological data acquisition system software
[AD-746874] 02 p0148 N73-11200
On-line data acquisition and instrumentation improvements for transonic turbine test rig
[AD-746727] 02 p0175 N73-11422
Digital acquisition of acoustic signals and digital analysis of acoustic and oceanographic data
[AD-746204] 02 p0212 N73-11720
Instrumentation, calibration, and observational data obtained in airglow and auroral expedition aboard CV 990 aircraft
[NASA-CR-129511] 03 p0293 N73-12384
Development of design data for cascades of flat plate guide vanes suitable for use in ninety degree elbows in ducts of circular cross section
[ESDU-AERO-00.02.09] 04 p0403 N73-13284
Development and characteristics of self-contained, portable data acquisition system for conducting marine and ecological research
04 p0471 N73-13842
Analysis of photographic data obtained during manned and unmanned space flight and application to oceanography, hydrology, geography, and geology
04 p0471 N73-13843
Performance of ERTS data collection system in total system context
[E72-10328] 05 p0530 N73-14316
Mission flight performance, and data acquisition of data-90 launch vehicle and InterPlanetary Monitoring Platform-H
[NASA-TM-X-68929] 05 p0595 N73-14836
Remote sensors for data acquisition on soils, water conditions, microclimatic conditions, flora, and land use
05 p0609 N73-14948
Coding data of 2565 individual human altitude chamber tests
[NASA-CR-114550] 07 p0746 N73-16066
Data 620 minicomputer system performance in acquiring and processing data
[AD-751636] 07 p0759 N73-16167
Acquisition and analysis of coastal ground data for correlation with ERTS-1 imagery of Monterey Bay and Santa Barbara Channel areas of California
[E73-10043] 07 p0776 N73-16306
Analysis of effects of various parameters inherent in remote sensors to show distortions and errors produced in remotely sensed data
07 p0784 N73-16380
Organization and functions of interdisciplinary teams for analyzing and interpreting remotely sensed data on earth resources
07 p0784 N73-16381
Development and application of field data collection techniques for remote sensing applications
07 p0785 N73-16386
Acquisition of data concerning urban housing quality using remotely sensed imagery
07 p0786 N73-16393
Performance of ERTS data collection system in total system context
[E73-10091] 08 p0902 N73-17303
Data acquisition system for S-1 wind tunnel with continuous subsonic/supersonic flow
[WRE-TN-784[WR/D]] 09 p1010 N73-18248
Basic mechanism underlying generation of Moire patterns in line scanner data acquisition
[NASA-CR-130829] 09 p1035 N73-18442
GARP standard data sets for studying behavior of numerical global models noting data acquisition, analysis, and storage
[GARP-PUBL-9] 09 p1061 N73-18652
US civil airmen statistics
[AD-754271] 11 p1251 N73-20153
Instrumented dolphins for surveying oceanographic parameters and relaying information to tracking aircraft
[AD-754761] 11 p1256 N73-20191
Computer control and data acquisition of tidal model of St. Lawrence River
[MH-110] 11 p1259 N73-20221
Acquisition and analysis of coastal ground truth data in pacific water off California for correlation with ERTS-1 imagery
[E73-10482] 12 p1396 N73-21319
Performance of ERTS data collection system in total system context
[E73-10494] 12 p1397 N73-21330
Remote sensing techniques for acquiring hydrological resource information to be used in California water management
12 p1399 N73-21350
Feasibility of remote sensing techniques for hydrology and watershed management in California
12 p1399 N73-21351
LORAMS design for remotely collecting weather data
[AD-756682] 13 p1554 N73-22594
On-site digital accumulation and storage of hydrometerological data for use in data acquisition systems
[PB-214185/1] 13 p1555 N73-22604
Data catalog tables and pictorial montages from Nimbus 4 satellite observation
[NASA-TM-X-69891] 13 p1580 N73-22807
Feasibility and costs of orbiting satellite data collection systems
[NASA-CR-130232] 13 p1581 N73-22812
Procedures for testing rotary wing aircraft models in wind tunnels to include design of test facilities, cost of models and facilities, and methods for obtaining data
14 p1598 N73-22955
Acquisition and processing ERTS-1 water resources data for south Florida
[E73-10560] 14 p1656 N73-23432
Development of system for collection and processing of telemetered magnetometer data received from artificial satellite
[GAMMA-17-1675] 14 p1658 N73-23457
Data collection problems for small documentary centers
15 p1753 N73-24208
Tracking and data system report for Mariner Mars 1971 mission
[NASA-CR-132955] 15 p1761 N73-24270
Superconducting magnetic suspension and balance facility data acquisition and data reduction errors
15 p1762 N73-24274
Acquisition and analysis of coastal ground truth data of Santa Monica Bay, Santa Barbara Channel, and Monterey Bay for correlation with ERTS-1 imagery
[E73-10607] 15 p1773 N73-24368
Characteristics of single linear inertia exciter and multichannel recording equipment for flight flutter tests on Meteor aircraft
[ARC-R/M-3247] 16 p1855 N73-25026
Establishment of data management system for ERTS-1 data by National Marine Fisheries Service Engineering Laboratory
[E73-10720] 17 p2019 N73-26327
Acquisition of ground truth and meteorological data in Michigan for Skylab-3 mission
[E73-10748] 17 p2022 N73-26352
Plans for collection of ground truth data for Skylab-2 mission
[E73-10759] 17 p2022 N73-26359
C-130 aircraft flights to obtain simulated operation of Skylab multispectral scanner, thermal scanner, and cameras
[E73-10761] 17 p2023 N73-26361
Acquisition of ground truth data in Ohio for Skylab EREP
[E73-10757] 18 p2133 N73-27239
Acquisition of weather and ground truth data for Skylab EREP experiments
[E73-10797] 18 p2137 N73-27273
Advantages of collecting data in south Florida using ERTS data collection platforms
[E73-10803] 18 p2138 N73-27278
Development and characteristics of electronic data recording equipment for shipboard oceanography data acquisition and processing
[IFS-73010] 18 p2151 N73-27384
Global station coordinate solution based upon camera and laser data
[NASA-TM-X-70422] 19 p2249 N73-28130
Evaluation of quality of ERTS-1 data produced during initial months of operation
19 p2259 N73-28208
Analysis of ERTS-1 data pertaining to Delaware River Basin observations to determine performance of data collection system
[PAPER-W10] 19 p2271 N73-28287
Data acquisition of multispectral scanning noting geology, hydrology, soil sceince, and mapping applications
19 p2295 N73-28451
Acquisition of stress data and aerodynamic loads on F-5 aircraft using mechanical strain gages and oscillograph recorders for service life determination
[AD-760567] 20 p2361 N73-28991
Collection, storage, and retrieval of data by computer at High Field Magnet Laboratory
[EP-RR-28] 20 p2379 N73-29113
Collection and processing of ground truth crop and field data for Skylab-3
[E73-10879] 20 p2394 N73-29230
Acquisition of Skylab data and determination of surface water areas from digital data
[E73-10912] 20 p2397 N73-29261
Acquisition of quick look data from SL-2, SL-3 planning, and development of mathematical models to process S-193 radar altimeter data
[E73-10917] 20 p2398 N73-29266
Procedures for predicting fatigue life of aircraft flying under various load conditions using data obtained by counting accelerometer
20 p2481 N73-29927
Modular interactive data acquisition system for nonexperts
[NBS-TN-790] 21 p2511 N73-30138
Acquisition of ground truth data and site selection for SL-3 EREP experiments in South Dakota
[E73-10945] 21 p2530 N73-30287
Procedures for the measurement and evaluation of noise, noise reduction and control, and current data on noise analysis and control
[EA-7301] 21 p2579 N73-30664
RALPH - on-line data acquisition and analysis system for processing gamma ray and coincidence data
[NASA-TM-X-69507] 22 p2639 N73-31151
Acquisition of ground truth data for Skylab overflights
[E73-11012] 22 p2660 N73-31317
Flight instrumentation for academic acquisition of aircraft flight performance and characteristics
[AD-764479] 22 p2675 N73-31427
First Earth Resources Technology Satellite: system, status, and results
[NASA-TM-X-70462] 22 p2720 N73-31765
Wind tunnel tests of high harmonic circulation control rotary wing model to show instruments required and data acquisition procedures
[AD-765320] 23 p2747 N73-31984
Integrated data acquisition system for airborne computer
[NASA-TM-X-56018] 23 p2760 N73-32087
Acquisition of ground truth data for test site
[E73-11014] 23 p2778 N73-32216

Development of timing device for conserving batteries on remote data collection platform by generating synchronous time windows
[NASA-CASE-GSC-11182-1] 23 p2849 N73-32769
Acquisition of ground truth and processing of Skylab EREP data
[E73-11152] 24 p2919 N73-33306

**DATA ADAPTIVE EVALUATOR/MONITOR**
U DATA PROCESSING
U DATA REDUCTION
U DATA TRANSMISSION

**DATA ANALYSIS**
U DATA PROCESSING
U DATA REDUCTION

**DATA BASES**
Magnetic data tapes containing measurements of pilot scanning behavior, control response and vehicle response during simulated instrument landing approaches
01 p0016 N73-10124
Data base containing objectively-correlated solar measurements used to obtain parameters for flare prediction
[AD-749869] 06 p0716 N73-15843
Automated medical record system for identifying and managing medical problems for Navy
08 p0875 N73-17087
Rate distortion theory for providing privacy transformations in data banks
[P-4952] 14 p1619 N73-23113
GERTS 3Q simulation model and data base for air cargo terminal
[AD-753925] 16 p1885 N73-25257
Design techniques for data base oriented computer networks for information flow
[AD-763791] 22 p2640 N73-31163
Data base management information systems and selected Air Force applications
[AD-765203] 23 p2762 N73-32103
Worldwide conference on data base management systems
[AD-765204] 23 p2762 N73-32104

**DATA COLLECTION PLATFORMS**
Thermal surveillance of volcanoes of Cascade Range and Iceland using ERTS-1 imagery and data collection platforms
[E72-10246] 03 p0289 N73-12346
Performance of ERTS data collection system in total system context
[E72-10328] 05 p0530 N73-14316
Performance of ERTS data collection system in total system context
[E73-10091] 08 p0902 N73-17303
Data collection and relay system for monitoring hydrologic conditions in south and central Florida
[E73-10092] 08 p0902 N73-17304
DCS platform monitoring of weather conditions for cloud seeding control
[E73-10095] 08 p0902 N73-17307
Thermal surveillance of volcanoes of Cascade Range and Iceland using ERTS-1 DCP systems and imagery
[E73-10317] 09 p1023 N73-18349
Application of ERTS-1 data collection platform system in Arizona ecological test site
[E73-10332] 09 p1024 N73-18362
Application of ERTS-1 data collection system platforms in Arizona ecological test site
[E73-10333] 09 p1025 N73-18363
ERTS-1 relayed water resources data collected from Delaware River Basin
[E73-10451] 12 p1394 N73-21299
ERTS-1 retransmission of water level data collected at remote locations in Canada
[E73-10469] 12 p1395 N73-21306
Data retransmission from Canadian water gauging stations using ERTS-1
[E73-10479] 12 p1396 N73-21316
Development of data relay network for monitoring hydrologic conditions collected for south and central Florida
[E73-10491] 12 p1397 N73-21327
Performance of ERTS data collection system in total system context
[E73-10494] 12 p1397 N73-21330
ERTS-1 retransmission of water resources data collected from remote regions of Canada
[E73-10504] 13 p1515 N73-22279
Establishment of prototype volcano surveillance network using ERTS data collection platforms
[E73-10545] 14 p1654 N73-23420
Investigation of marine environment of northern Gulf of California using ERTS data collection platforms
[E73-10550] 14 p1655 N73-23423
Prototype surveillance network of volcanoes in Western Hemisphere using data from ERTS data collection platforms
[E73-10558] 14 p1655 N73-23430
Reservoir and water management in Maine using ERTS-1 data collection platforms and imagery
[E73-10585] 14 p1657 N73-23445
Advantages of collecting data in south Florida using ERTS data collection platforms
[E73-10803] 18 p2138 N73-27278
DCP-collected absolute target reflectance measurements to assist interpretation of ERTS-1 imagery of forest stresses in Black Hills, South Dakota
19 p2283 N73-28365
Thermal surveillance of Cascade range volcanoes using ERTS-1 MSS data, aircraft imaging systems, and ground based DCP
19 p2284 N73-28369
Design, fabrication, production and testing of data collection platforms and platform field test sets for Earth Resources Program
[E73-11008] 22 p2660 N73-31313
Prototype DCP volcano surveillance network in Washington, Nicaragua, California, Guatemala, Hawaii, El Salvador, Iceland, and Alaska
[E73-11024] 22 p2662 N73-31328
Balloon sub-system of Eole experiments in Southern Hemisphere lower stratosphere
24 p2948 N73-33547

**DATA COMPRESSORS**
U DATA REDUCTION
U DATA TRANSMISSION

**DATA CONTROL SYSTEMS**
U DATA SYSTEMS

**DATA CONVERSION ROUTINES**
NT SUBROUTINES

**DATA CONVERTERS**
NT ANALOG TO DIGITAL CONVERTERS
NT DIGITAL TO ANALOG CONVERTERS
Circuit and plug register diagrams for printout converter
[PHL-1972-4] 02 p0144 N73-11168
Digital converter for scaling binary number to binary coded decimal number of higher multiple
[NASA-CASE-KSC-10595] 03 p0269 N73-12176
On-line binary scan converter for comverting pictorial from computer output to raster form suitable for TV display
19 p2238 N73-28046

**DATA CORRELATION**
NT SIGNAL ANALYSIS
Acquisition and analysis of California coastal ground truth data for correlation with ERTS-1 imagery
[E72-10321] 04 p0413 N73-13369
Acquisition and analysis of coastal ground data for correlation with ERTS-1 imagery of Monterey Bay and Santa Barbara Channel areas of California
[E73-10043] 07 p0776 N73-16306
Data correlation for varying times of wind tunnel tests
[AD-751957] 08 p0893 N73-17228
Independent radar systems using information processing, data correlation, and telecommunication
09 p1002 N73-18179
Two dimensional Fourier transform and digital correlation for image processing
[BMVG-FBWT-72-1] 10 p1179 N73-19591
Correlation of ocean surface parameters with radar backscatter data
[E73-10530] 13 p1517 N73-22295
Acquisition and analysis of coastal ground truth data of Santa Monica Bay, Santa Barbara Channel, and Monterey Bay for correlation with ERTS-1 imagery
[E73-10607] 15 p1773 N73-24368
Correlation of ERTS-1 data with in situ water quality measurements around Virgin Islands
[E73-10626] 15 p1775 N73-24386
Evaluation of digital correction techniques for ERTS-1 imagery
[E73-10705] 16 p1903 N73-25396
Correction factor technique for X ray fluorescent analysis on stainless steel
[PB-214231/3] 16 p1929 N73-25611
Estimation of random process correlation functions, and statistical and sampling errors
17 p2026 N73-26399
Correlation of coastal ground truth data from Southern California waters with ERTS imagery
[E73-10864] 20 p2392 N73-29215
Spatial normalized correlation function of total atmospheric ozone content
20 p2448 N73-29669
Development of guidelines for definition of relevant information content in data classes
[NASA-CR-124356] 20 p2488 N73-29990
Synchronization method for pseudorandom binary data sequences in blockwise transmission of nonoverlapping subsequences, based on digital correlation
[FTZ-A-157-TBR-7] 22 p2632 N73-31095

**DATA HANDLING SYSTEMS**
U DATA SYSTEMS

**DATA LINKS**
Automatic monitor for classifying high usage data transmission system circuits
[AD-749268] 04 p0392 N73-13183
Speed independent control structures for digital systems
05 p0517 N73-14207
Analysis of cloud console devices used in displaying meteorological satellite imagery
[AD-750085] 05 p0575 N73-14684
Characteristics of two channel telemetry system with two data rate channels for high and low data rate communication
[NASA-CASE-NPO-11572] 07 p0754 N73-16121
Mariner Mars 1971 radio frequency subsystem to provide communication link between spacecraft and Deep Space Instrumentation Facility
[NASA-CR-130866] 08 p0885 N73-17164
Systems planning for improved airport surveillance radar equipment using dual airborne antenna switching for air traffic control
[FAA-RD-72-136] 09 p1002 N73-18176
Performance and theory of operation of High Speed Sequential Decoder
[NASA-TM-X-62241] 11 p1260 N73-20222
Source coding, modulation/channel coding, and systems techniques for application to teleconferencing over high data rate digital communication satellite links
[NASA-CR-114561] 11 p1342 N73-20889
Performance analysis and conceptual design of waveform and modem to provide jamming-resistant command and control data link for ground station control of drone aircraft
[AD-756933] 13 p1496 N73-22125
TAM-TAM system for use during oceanic, continental, and terminal control area flight
14 p1689 N73-23710
Discretely addressable radar beacon system with airborne transponders and ground-air-ground data link for air traffic control
[FAA-RD-73-48] 16 p1940 N73-25701
Automatic accounting system for transfer of data from terminals to computer
[NASA-CASE-NPO-11456] 17 p2001 N73-26176
Adaptive phased antenna array simulation for optimal design of tracking data relay satellite very high frequency beam
18 p2210 N73-27841
Optimization of global ground data transmission network for spacecraft communications
18 p2210 N73-27843
Satellite telecommunication link in health/education experiment using tuned radio frequency receiver
18 p2213 N73-27864
Technical facilities for data links in teleautomatic queueing system
[JPRS-59662] 19 p2235 N73-28022
Computer simulation of multipacket-switched data communication network operating with revised link and node protocol
[NPL-COM-68] 22 p2634 N73-31112
Computer programs for analyzing satellite communication links
[REPT-6806] 24 p2895 N73-33108

**DATA MANAGEMENT**
Development of Earth Resources Information Storage, Transformation, Analysis, and Retrieval system through NASA research project
[NASA-CR-61392] 01 p0049 N73-10399
Data management system for prediction of Naval student pilot performances
[AD-744984] 02 p0136 N73-11104
Computerized file management system for library reference searches
[UCRL-73355-REV-1] 03 p0271 N73-12193
Use of ERTS data to manage and solve social problems associated with earth resources in California
05 p0536 N73-14363
Legal liability of US Government in handling meteorological data obtained by satellites
06 p0692 N73-15638
Computer network modeling system for planning data management in voice communication
[AD-752797] 09 p1006 N73-18210
Program documentation with advanced data management systems
10 p1130 N73-19205
Data distribution subsystem for space shuttle orbiters
[NT-SES/11/71/030] 10 p1133 N73-19233
Vehicle telemetry measurements for Skylab 2 spacecraft and identification of data sources
[NASA-TM-X-69142] 10 p1216 N73-19887
Integrated electronics for European space tug
[HSD-TP-7227-APP-5] 10 p1217 N73-19897
Processing, analysis, and management of ERTS-1 data for selected disciplines and areas
[E73-10387] 11 p1275 N73-20349
Design of compatible modular data management systems
[AD-749910] 13 p1497 N73-22133
Functional characteristics and test methodology for DMS
[AD-748811] 13 p1497 N73-22136
Coding systems in geographic data maps
13 p1523 N73-22343
Data management systems, instrumentation concepts, and biotechnology laboratory for earth orbital experiment program and requirements study - Vol. 8
[NASA-CR-112332] 13 p1577 N73-22785
Implementation strategy for vocal data management system
14 p1629 N73-23206

Development of methods for presenting aircraft performance data and comparison of specific methods to show sources of discrepancies
15 p1733 N73-24050
Information dissemination services to industry
15 p1753 N73-24210
Associative approach test model data management system
[AD-750147] 16 p1879 N73-25209
Development of guidelines for definition of relevant information content in data classes
[NASA-CR-124356] 20 p2488 N73-29990
Installation standards for NASA Aerospace Safety Information System [NASIS] data base management system - Vol. 1
[NASA-CR-134455] 21 p2511 N73-30139
Overviews of NASA Aerospace Safety Information [NASIS] to introduce system features and component capabilities - Vol. 2
[NASA-CR-134456] 21 p2511 N73-30140
Data set specifications for NASA Aerospace Safety Information System [NASIS] to show standard format for every data set required by system - Vol. 3
[NASA-CR-134457] 21 p2511 N73-30141
Design specifications for programs and modules within NASA Aerospace Safety Information System [NASIS] - Vol. 4
[NASA-CR-134458] 21 p2511 N73-30142
Characteristics and operation of retrieval command subsystem for NASA Aerospace Safety Information System [NASIS] - Vol. 5
[NASA-CR-134459] 21 p2511 N73-30143
Definition and functions of message terms used in NASA Aerospace Safety Information System [NASIS] - Vol. 6
[NASA-CR-134460] 21 p2511 N73-30144
Operation specifications, Installation, and Modifications of NASA Aerospace Safety Information System [NASIS] - Vol. 7
[NASA-CR-134461] 21 p2511 N73-30145
Development of data base administrator user guide for use with NASA Aerospace Safety Information System [NASIS] - Vol. 8
[NASA-CR-134462] 21 p2512 N73-30146
Installation standards for NASA Aerospace Safety Information System [NASIS] data base management system using IBM 360-1370 OS MVT computer - Vol. 1
[NASA-CR-134470] 22 p2637 N73-31132
Overviews of NASA Aerospace Safety Information System [NASIS] to introduce system features and capability of IBM 360/370 OS MVT computer - Vol. 2
[NASA-CR-134471] 22 p2637 N73-31133
Data set specifications for NASA Aerospace Safety Information System [NASIS] to show formats used with IBM 360/370 OS MVT computer - Vol. 3
[NASA-CR-134472] 22 p2637 N73-31134
Design specifications for programs and modules within NASA Aerospace Safety Information System [NASIS] using IBM 360/370 OS MV computer - Vol. 4
[NASA-CR-134473] 22 p2637 N73-31135
Characteristics and operation of retrieval command subsystem for NASA Aerospace Safety Information System [NASIS] using IBM 360/370 OS MVT computer - Vol. 5
[NASA-CR-134474] 22 p2637 N73-31136
Definition and functions of message terms used in NASA Aerospace Safety Information System [NASIS] using IBM 360/370 OS MVT computer - Vol. 6
[NASA-CR-134475] 22 p2637 N73-31137
Development of data base administrator user guide for use with NASA Aerospace Safety Information System [NASIS] using IBM 360/370 OS MVT computer - Vol. 7
[NASA-CR-134476] 22 p2637 N73-31138
Worldwide conference on data base management systems
[AD-765204] 23 p2762 N73-32104

**DATA PROCESSING**

- NT CENTRAL ELECTRONIC MANAGEMENT SYSTEM
- NT DATA CORRELATION
- NT DATA REDUCTION
- NT DATA RETRIEVAL
- NT DATA SMOOTHING
- NT DATA STORAGE
- NT KARHUNEN-LOEVE EXPANSION
- NT MULTIPROCESSING [COMPUTERS]
- NT OPTICAL DATA PROCESSING
- NT PARALLEL PROCESSING [COMPUTERS]
- NT SIGNAL ANALYSIS
- NT SIGNAL PROCESSING
- NT VOICE DATA PROCESSING

Sleep stage classification analysis on heart rate data recordings
[AD-740946] 01 p0021 N73-10167
Bibliography on digital image processing information
[AD-745790] 01 p0029 N73-10231
Data processing needs of Apollo Telescope Mount experiment
[NASA-CR-123911] 01 p0030 N73-10232
Conference on development of multiple computer system for data processing and simulation
[AD-743937] 01 p0031 N73-10240
Use, implementation, and maintenance procedures for data reconfiguration service compiler coded in PL/I
[AD-745751] 01 p0031 N73-10243
Data processing systems and computer networks
[AD-746509] 01 p0031 N73-10244
Data processing of hydrologic conditions using ERTS-1 time lapse imagery of Wrangell Mountains
[E72-10187] 01 p0046 N73-10366
Digital data analysis of traveling ionospheric disturbances
[AD-746314] 01 p0054 N73-10441
Processing of Concorde digitally recorded data
01 p0056 N73-10453
Analysis of deterministic and random flight data
01 p0056 N73-10455
Automatic data processing in meteorological services
[NLL-M-20789-[5828.4F]] 01 p0072 N73-10591
Transfer function of linearizer for anemometer data
[AD-744975] 01 p0075 N73-10622
Digital data coding instructions for underwater acoustics and environmental data bank
[AD-746507] 01 p0082 N73-10675
Data handling theory, telemetry, and signal frequency determination for signal reconnaissance
[FOA-3-C-3653-66] 02 p0140 N73-11134
Fluidic elements and hydraulic impulse techniques for information processing equipment
02 p0140 N73-11135
Computerized radar target return data processing and identification system
[AD-746323] 02 p0142 N73-11148
Design of signal processing computer using arithmetic parallelism
[AD-745950] 02 p0142 N73-11150
Management, storage, and computation of FR-1 satellite very low frequency data
[GRI/NTP/101] 02 p0146 N73-11187
Modification of Minuteman digital computer system to provide for single channel autoanalyzer waveform analysis
[AD-746264] 02 p0147 N73-11197
Analysis of ERTS-1 imagery for Colorado environments using automatic data processing techniques
[E72-10204] 02 p0161 N73-11301
Evaluation of data compression technique for ERTS-1 multispectral imagery
[E72-10226] 02 p0163 N73-11319
Analysis and interpretation of ERTS-1 ecologic, geographic, and agricultural data for Tennessee Valley
[E72-10231] 02 p0163 N73-11324
Two FORTRAN 4 computer programs for general combination of satellite and gravity data for position and gravity field determinations
[AD-746305] 02 p0168 N73-11364
Performance of equipment and software of SAAC [LASA] system
[AD-745874] 02 p0169 N73-11375
One-dimensional and multi-dimensional inversion techniques for processing remote atmospheric and ionospheric sounding data
[NASA-TM-X-62150] 02 p0196 N73-11585
Mathematical inversion of light scattering data to obtain atmospheric ozone profile
02 p0196 N73-11586
Automatic pattern recognition of urban land use and land use change
[E72-10244] 03 p0289 N73-12344
Conceptual design of operational earth resources ground processing systems
[NASA-CR-129605] 03 p0293 N73-12383
Analyzing and processing remotely sensed earth resources data
[NASA-CR-61399] 03 p0293 N73-12390
Analysis of data generated by combined bending-torsion fatigue reliability research machines using probabilistic-graphically and phenomenological techniques
[NASA-CR-72839] 03 p0306 N73-12498
Automatic sequential processing, technique for unsupervised classification, or clustering, of multispectral remote sensing data, using digital computer program
[NASA-CR-128999] 03 p0323 N73-12633
Computer system for control of electronics measuring devices and numerical information processing of measurements
[CEA-CONF-1968] 03 p0333 N73-12713
Payload data bank, space shuttle program risk analysis, reusable launch vehicles, and cost analysis
[NASA-CR-126170] 03 p0355 N73-12897
Computerized information processing for radar system by subdivisions and multiple decision making processes
04 p0389 N73-13158
Computer method for largest number of ground station communication functions
[AD-748881] 04 p0390 N73-13166
Fast acquisition methods for TDMA
[AD-748882] 04 p0390 N73-13167
Digital precision processing of ERTS-1 imagery of Chesapeake Bay
[E72-10292] 04 p0410 N73-13342
Automatic identification of land uses in Milwaukee, Wisconsin using ERTS-1 imagery
[E72-10307] 04 p0412 N73-13356
Digitizing of topographic maps for electronic data processing
[MITT-130] 04 p0414 N73-13379
Proposals for application of data processing to education in Germany
[BMBW-FB-DV-72-05] 04 p0488 N73-13995
Alternatives in complement and structure of NASA teleprocessing resources for years 1975 through 1985 including options of minicomputers, mass storage devices, and software development
[NASA-CR-129825] 05 p0515 N73-14188
ELDO computing facilities noting data links and operating procedures
[ELDO-TN-25] 05 p0518 N73-14209
Digital correction techniques for ERTS-1 imagery
[E72-10365] 05 p0535 N73-14353
Digital facility for handling and processing remotely sensed earth resources data
05 p0537 N73-14369
Operation and data processing system of long period strain seismographs with wave discrimination
[AD-748232] 05 p0549 N73-14460
Data processing and recording applications in tensile testing of thermoplastics
[ERDE-TR-99] 05 p0565 N73-14593
Computer processing for calculating optical constants from reflectance data of InBi
05 p0609 N73-14952
Summary of side-looking radar applications in earth resources noting basic principles of side-looking radar, radar scattering, data handling, and research and development
[ESRO-CR[P]-141] 06 p0641 N73-15200
Digital filter theory for broadband beamforming and hydrophone array steering
[AD-746206] 06 p0641 N73-15201
Development of evaluation method for determining effectiveness of data compression techniques for radar landmass simulation
[AD-750695] 06 p0642 N73-15214
RAF operating procedures for ICL 7020 Remote computer terminal
[RAE-TR-72086] 06 p0644 N73-15231
Arithmetic and logic units in digital computer for processing of radar, sonar, and communication systems signals
[AD-750665] 06 p0646 N73-15248
Computerized simulation of data compression using ERTS-1 MSS digital tapes
[E73-10011] 06 p0659 N73-15347
Evaluation of ERTS-1 imagery data compression algorithm technique
[E73-10012] 06 p0659 N73-15348
Interdisciplinary analysis of ERTS-1 multispectral data of Colorado mountain areas using automatic data processing techniques
[E73-10033] 06 p0661 N73-15366
Mathematical and computer methods of cartography
[BULL-56] 06 p0666 N73-15415
Reduction and analysis of trapped and precipitating electron data from OGO 6 spectrometer experiment F-16
[NASA-CR-130137] 06 p0718 N73-15863
Research progress in electronic equipment, data processing, plasma physics, and information systems
[AD-750669] 06 p0732 N73-15976
Electronic detectors and computer software for analyzing human electroencephalographs in isolated environment
[AD-751272] 07 p0751 N73-16105
Earth resources laboratory data system for analyzing and processing multispectral, radiometric, photographic, and passive microwave imagery data
[NASA-CR-128693] 07 p0758 N73-16160
Handling and analysis of remote sensing data on 1971 corn blight
[NASA-CR-130368] 07 p0759 N73-16164
Telemetry data processing systems for experiments flown on Injun 5 satellite, OV-3 satellite, OV-4 satellite, OV-5 satellite, OV-6 satellite, and OV-15 satellite
[AD-751508] 07 p0759 N73-16166
Data 620 minicomputer system performance in acquiring and processing data
[AD-751636] 07 p0759 N73-16167
Digital data processing portion of Dartmouth ionosonde network used to analyze traveling ionospheric disturbances
07 p0775 N73-16290
Time-lapse data processing of ERTS-1 imagery for dynamic hydrologic conditions
[E73-10035] 07 p0776 N73-16299
Digital processing of ERTS-1 imagery of Tennessee Valley
[E73-10054] 07 p0778 N73-16316
Computer processing, enhancement, and recognition of ERTS imagery of Tennessee Valley
[E73-10056] 07 p0778 N73-16318
Application of multispectral data processing to Delaware coastal wetlands vegetation mapping
[E73-10069] 07 p0779 N73-16331

Analysis of effects of various parameters inherent in remote sensors to show distortions and errors produced in remotely sensed data
07 p0784 N73-16380
Organization and functions of interdisciplinary teams for analyzing and interpreting remotely sensed data on earth resources
07 p0784 N73-16381
Automatic processing of remote sensed data to aid in land use mapping and agricultural conservation
[NASA-CR-130372] 07 p0790 N73-16423
Analysis of light ion mass spectrometer data from OGO-E experiment
[NASA-CR-130156] 07 p0791 N73-16432
Fourier amplitude spectra for earthquake ground motions and structural response accelerations
[PB-212603] 07 p0794 N73-16458
Results of multiprocessor systems design review
[NASA-CR-124026] 07 p0848 N73-16873
Principles of spacecraft telemetry data management
[ESRO-TN-121-ESOC] 08 p0885 N73-17166
On-line computer graphics for display of magnetic tape data from digital computer
[IPPJ-T-10] 08 p0887 N73-17179
Digital processing of ERTS-1 imagery
[E73-10080] 08 p0901 N73-17292
Evaluation of data compression techniques for ERTS-1 MSS imagery
[E73-10287] 08 p0915 N73-17493
Computer analysis of quasi-sinusoidal geomagnetic variations at geomagnetic midlatitude
[AD-752229] 08 p0920 N73-17543
Digital data processing system for infrared video scan
[AD-752069] 08 p0944 N73-17731
Pioneer space probe system design and development, ground support system, tracking and communication, and data processing
[NASA-SP-279-VOL-2] 08 p0964 N73-17882
Analysis of data from charged particle experiment of Explorer 34 satellite and Explorer 35 satellite
[NASA-CR-130171] 08 p0976 N73-17985
Application of computer techniques for determination of flutter characteristics of aircraft and comparison with model matching data analysis
[AGARD-R-596] 09 p0983 N73-18030
Data processing for synthetic aperture radar used as satellite-borne earth resources remote sensor
[NASA-CR-2193] 09 p1005 N73-18202
Computer programs for information retrieval and data analysis
[NASA-SP-5955[01]] 09 p1005 N73-18204
Programmable computer interface for computer aided measurement and control instrumentation systems
[NASA-TN-D-7148] 09 p1005 N73-18205
Hybrid computer program for processing several channels of sweep frequency data simultaneously
[NASA-TM-X-2753] 09 p1005 N73-18206
Management, processing, and handling of French FR-1 satellite very low frequency data
[GRI/NTP/100] 09 p1005 N73-18207
Computer network modeling system for planning data management in voice communication
[AD-752797] 09 p1006 N73-18210
Software module for teletypes connected to HP ALOHA SYSTEM multiplexer
[NASA-CR-130492] 09 p1006 N73-18213
Analysis of dayside auroral characteristics and hydroxyl airglow variations from 1969 airborne auroral expedition
[NASA-CR-130916] 09 p1025 N73-18367
Data processing in reducing effort of mechanical testing polymers for flexural deformation and displacement
[ERDE-TR-111] 09 p1052 N73-18578
Application of data processing to flexural and tensile tests on rubber
[ERDE-TR-114] 09 p1052 N73-18579
Iterative method for refining diagnostic procedures, and applications to geological surveys
09 p1056 N73-18613
Raw data processing from proton, alpha particle, and electron flux experiments of Azur satellite
[MPI-PAE/EXTRATERR-76] 09 p1081 N73-18818
Analysis of design features and photographic data to determine cause of Apollo 15 main parachute failure
09 p1088 N73-18879
Three color receptors of Young-Helmholtz and opponent color types of information processing
10 p1112 N73-19066
Electronic desk calculator for automatic X ray spectrometry data processing
[Y-1854] 10 p1132 N73-19231
Precision geometric and radiometric correction of bulk digital ERTS-1 imagery by digital techniques
[E73-10342] 10 p1148 N73-19341
Interdisciplinary analysis of ERTS-1 imagery for Colorado mountain areas using ADP techniques
[E73-10348] 10 p1148 N73-19347
Computer processing of multispectral imagery of India
[E73-10373] 10 p1151 N73-19368
Land use, water quality, and air quality indices useful to environmental resources managers and data processing equipment and techniques for production of indices
[E73-10376] 10 p1151 N73-19371
Automated thematic mapping and analysis of terrain in Arizona, Texas, Washington, Utah, Louisiana, and California using ERTS-1 imagery
[E73-10386] 10 p1153 N73-19379
Radar arithmetic signal processing element with digital filter and Fourier transformation for moving target indication
[AD-754060] 11 p1258 N73-20206
Processing, analysis, and management of ERTS-1 data for selected disciplines and areas
[E73-10387] 11 p1275 N73-20349
Processing of IFYGL data for Lake Ontario and its drainage basin
[E73-10393] 11 p1276 N73-20355
Coordination and establishment of centralized facilities and services for University of Alaska ERTS-1 survey of Alaskan environment
[E73-10459] 11 p1284 N73-20417
Construction of cartographic scanner/plotter for computer aided mapping
[AD-754648] 11 p1288 N73-20452
Quality control for rawinsonde data dissemination to ships
[NOAA-TM-NWS-NMC-52] 11 p1314 N73-20663
Technique for processing and compressing ERTS-1 imagery of California
[E73-10465] 12 p1394 N73-21303
Characterization of wetlands and marshlands by automatic processing of ERTS-1 data
[E73-10467] 12 p1394 N73-21304
Acquisition and analysis of coastal ground truth data in pacific water off California for correlation with ERTS-1 imagery
[E73-10482] 12 p1396 N73-21319
Application of ERTS-1 data to analysis of agricultural crops, forests, soils, landforms, and acreage estimates in Michigan
[E73-10483] 12 p1396 N73-21320
Remote sensing and automatic data processing techniques for earth resources survey in California
12 p1399 N73-21348
Digital systems for automatic processing of remote earth resources sensing data
12 p1400 N73-21355
Least squares adjustment of geometrical global satellite network data
[NASA-CR-131535] 12 p1459 N73-21823
Design of compatible modular data management systems
[AD-749910] 13 p1497 N73-22133
Techniques and software for digital enhancement of radiographs
[NASA-CR-2213] 13 p1497 N73-22135
Design of multiple output analog computer for hot-wire anemometer signal processing
[AD-756532] 13 p1498 N73-22143
Digital technique for picture processing
[AD-755701] 13 p1499 N73-22145
Bibliography of developments in field of picture processing by computers during 1972
[AD-755702] 13 p1499 N73-22146
Structure analysis of digital picture processing system
[AD-755699] 13 p1499 N73-22147
Three day advance warning system of heating plant failure using algorithmic detection methods
[NASA-CR-131571] 13 p1505 N73-22197
Analysis of digital microdensitometer data from ERTS-1 imagery of San Francisco, California
[E73-10521] 13 p1517 N73-22289
Use of digitized remote sensor data and automatic data processing techniques in preparation of forest cover mapping to aid in forest resources management
[NASA-CR-131578] 13 p1523 N73-22344
Automatic processing of ERTS-1 data for physiography and geologic mapping of San Juan Basin, Colorado
[NASA-CR-131577] 13 p1524 N73-22346
Evaluation of data processing systems for Alaskan and Norwegian seismic arrays
[AD-756905] 13 p1525 N73-22360
Algorithm for adaptive convergence rate on weak noise components in seismic signal processing
[AD-756904] 13 p1525 N73-22361
Time-space analysis of asynchronous meteorological data
13 p1552 N73-22575
Filtered lunar ranging data, and unfiltered photon detections
[NASA-CR-131498] 13 p1576 N73-22771
Low order terms of cepstrum for compact digital form of continuous speech
14 p1628 N73-23195
Development of processing satellite data to show quantity of data and time required for various techniques
[BMFT-FBW-73-04] 14 p1638 N73-23277
Network data handling system, including software release and global weather data base
[AD-757686] 14 p1638 N73-23282
Design specifications for shipborne real time environmental data processing system
[AD-757458] 14 p1638 N73-23283
Automatic data processing techniques for computer graphics and image processing
[AD-757530] 14 p1638 N73-23284
Acquisition and processing ERTS-1 water resources data for south Florida
[E73-10560] 14 p1656 N73-23432
Development of processing and information extraction techniques for Skylab multispectral band scanner data
[E73-10563] 14 p1656 N73-23435
Evaluation of ERTS-1 imagery and automatic data processing techniques for characterization of wetlands and marshlands
[E73-10576] 14 p1656 N73-23437
Identification and mapping of land use classes in Kansas City area by machine processing of ERTS-1 data
[E73-10578] 14 p1656 N73-23439
Evaluation of compression technique for ERTS-1 data tapes
[E73-10589] 14 p1657 N73-23449
Data processing and image enhancement of ERTS-1 MSS data for Kansas
[E73-10596] 14 p1658 N73-23453
Development of system for collection and processing of telemetered magnetometer data received from artificial satellite
[GAMMA-17-167S] 14 p1658 N73-23457
Data analysis from A-37 aircraft flights to evaluate electronic strain-level counter as fatigue damage monitor
[AD-757210] 14 p1668 N73-23540
Design of airborne flight data transmission system for automatic acquisition and tracking
14 p1711 N73-23885
Telemetry preprocessing language for telemetry data processing
[NASA-TM-X-66248] 15 p1750 N73-24183
Data recording and data interchange for reducing data processing costs
15 p1753 N73-24207
Electronic computer processing of data stored in data banks
15 p1753 N73-24212
ADMAP computer manipulation program for processing electric propulsion trajectory data generated by low thrust optimization program, HILTOP
[NASA-CR-130242] 15 p1754 N73-24216
Time-lapse data processing for dynamic hydrologic conditions at Mt. Rainier, Washington
[E73-10582] 15 p1772 N73-24356
Data compression technique for ERTS-1 imagery of Montreal and Lake St. John, Canada, Orange County, California, San Pedro/Long Beach, California, and Chesapeake Bay
[E73-10625] 15 p1775 N73-24385
Processing techniques for ERTS-1 imagery of Tennessee Valley
[E73-10633] 15 p1776 N73-24392
University of Alaska program for processing ERTS-1 environmental data
[E73-10636] 15 p1776 N73-24395
Analysis of data taken by CV-990 aircraft during 1968 and 1960 auroral expedition
[NASA-CR-114616] 15 p1777 N73-24409
Use of ERTS multispectral data to solve development and management problems of agricultural resources in Lynn County, Texas
[NASA-CR-132956] 15 p1778 N73-24411
Computer analysis of digitized sferic data from atmospheric analyzers
[AD-758102] 15 p1783 N73-24453
Data processing in project control illustrated by cost and network analysis and resource allocation modules
15 p1848 N73-24983
Analysis of performance of Honeywell Information System 6000 series computer
[AD-759808] 16 p1879 N73-25212
Automated thematic mapping and change detection of hydrological and agricultural resources from ERTS-1 imagery
[E73-10644] 16 p1897 N73-25341
Computerized interpretation of ERTS-1 data for forest management in Minnesota
[E73-10687] 16 p1902 N73-25381
Evaluation of digital correction techniques for ERTS-1 imagery
[E73-10705] 16 p1903 N73-25396
Classification of aerial photographic image data sets on basis of computable textural features
[AD-759505] 16 p1915 N73-25498
Data processing techniques for radiometry
[PB-214184/4] 16 p1939 N73-25689
Data processing and analysis of charged particle experiment on OGO-5 spacecraft
[NASA-CR-132761] 16 p1962 N73-25870
Image processing techniques and applications to Earth Resources Technology Satellite program
[NASA-CR-124285] 16 p1967 N73-25910

Telemetry data from data processing system for spherical electrostatic analyzer experiment onboard ISIS-A satellite
[AD-760148] 17 p2001 N73-26179
Computerized data processing and graphic display system for artificial satellite
[AD-760304] 17 p2002 N73-26190
Tactical routing indicator look-up and header preparation device
[AD-759944] 17 p2002 N73-26192
Computer programs, documentation, procedures, and design criteria for small to medium data base packages
[AD-760103] 17 p2003 N73-26194
Evaluation of ERTS-1 image data compression technique
[E73-10717] 17 p2019 N73-26324
Establishment of data management system for ERTS-1 data by National Marine Fisheries Service Engineering Laboratory
[E73-10720] 17 p2019 N73-26327
Evaluation of ERTS-1 image sensor spatial resolution in photographic form
[E73-10721] 17 p2019 N73-26328
Evaluation of ERTS-1 image data compression techniques to show four ERTS MSS tapes recorded on single compressed tape
[E73-10730] 17 p2020 N73-26336
Theodolitic errors in processing time dependent geodetic data
[AD-760109] 17 p2029 N73-26421
Analog - digital near real time image processing system
17 p2031 N73-26433
Computer interpretation of textured visual outdoor scenes
[AD-759712] 17 p2034 N73-26463
Development of techniques for processing Skylab multispectral scanner data and comparison with ERTS-1 and aircraft scanner data processed by same technique
[E73-10758] 17 p2036 N73-26473
Data processing system for elastomer development
[AD-759902] 17 p2052 N73-26603
Statistical classification of earth resources in remote sensing data
[NASA-CR-128988] 17 p2054 N73-26615
Analog models of errors in processing navigational information
17 p2059 N73-26660
Development of programming technique for processing Skylab MSS data
[E73-10765] 18 p2134 N73-27242
State of readiness to process and reduce Skylab EREP digital data
[E73-10798] 18 p2138 N73-27274
Development of mathematical models for processing Skylab EREP altimeter data
[E73-10801] 18 p2138 N73-27276
Coordination of ground truth and basic altimeter data processing requirements for North Atlantic test area
[E73-10811] 18 p2139 N73-27286
Mathematical models for processing Skylab S-193 radar altimeter data
[E73-10812] 18 p2139 N73-27287
Statistical processing of Nimbus infrared data for synoptic atmospheric climatology
18 p2170 N73-27523
ESRO 1A [Aurorae] satellite dynamic model derived from attitude sensor data using smoothing factor in spline function subroutine
[RA-SAT-3.4-C-006] 18 p2201 N73-27767
Onboard OAO 3 computer for commanding and data processing
18 p2208 N73-27824
Interface microprogramming for radar array signal processing computer
[AD-762439] 19 p2238 N73-28041
Onboard processing for data collection satellite systems
[NASA-CR-132792] 19 p2239 N73-28049
Forward algorithm for scheduling process monitor in time sharing computer sample data control
[AD-761668] 19 p2240 N73-28058
Design of communications processor for access control to computer system
[AD-761804] 19 p2241 N73-28064
Computerized simulation of optical pattern recognition and image processing system
[AD-761882] 19 p2241 N73-28065
Synchronized digital communication system
[NASA-CASE-XNP-03623] 19 p2243 N73-28084
Design of fast Fourier transform digital processor
[AD-761803] 19 p2245 N73-28097
Evaluation of quality of ERTS-1 data produced during initial months of operation
19 p2259 N73-28208
Application of ERTS-1 imagery for identifying citrus groves and rice fields in Valencia region of Eastern Spain
[PAPER-A4] 19 p2260 N73-28212
Analysis of ERTS-1 multispectral data by automatic pattern recognition procedures for geological mapping of San Juan Basin, Colorado
[PAPER-G25] 19 p2267 N73-28256
Processing and interpretation of ERTS-1 MSS data for Lake Livingston, Texas
[PAPER-I8] 19 p2278 N73-28329
Comparison between geophysical and ERTS data processing techniques
[PAPER-I13] 19 p2278 N73-28334
Analysis of ERTS-1 imagery by combining human and computer interpretation capabilities
[PAPER-I14] 19 p2279 N73-28335
Digital data processing of ERTS-1 MSS imagery of water masses in Delaware Bay
19 p2286 N73-28380
Development of land management programs based on ERTS-1 imagery and computer compatible tapes for machine processing of data
19 p2288 N73-28397
Processes, algorithms, and procedures for extraction and interpretation ERTS-1 data
19 p2290 N73-28412
Machine processing of ERTS-1 radiometric and ground truth data and calibration of radiometers
[E73-10855] 19 p2292 N73-28432
Development of semi-automatic system for digitizing bathymetry charts for showing ocean bottom contour information
[AD-761647] 19 p2296 N73-28464
Integral and spectral flux calculations of long wave radiation in atmosphere, using computers
[AD-761579] 19 p2298 N73-28477
Computerized data processing system for sampling, labeling, and digital recording of optical measurements
[AD-762332] 19 p2322 N73-28678
Test data tabulation, statistical analysis, and heating rate contours for base region thermal environment of Saturn S-2 stage scale model - Vol. 2
[NASA-CR-129010] 20 p2382 N73-29144
Data processing and extraction techniques for Skylab S-192 MSS data
[E73-10859] 20 p2391 N73-29210
Development of extraction and processing techniques for Skylab S-192 MSS data
[E73-10860] 20 p2391 N73-29211
Collection and processing of ground truth crop and field data for Skylab-3
[E73-10879] 20 p2394 N73-29230
Image data compression using digital holography
[AD-762931] 20 p2426 N73-29487
Digital precision processing of ERTS-1 imagery of Monterey Bay, California
[E73-10948] 21 p2530 N73-30290
Data compression algorithm and techniques for ERTS-1 imagery
[E73-10959] 21 p2532 N73-30301
Digital correction techniques for ERTS-1 imagery of Baltimore, Maryland
[E73-10963] 21 p2533 N73-30305
Algorithms employed in current ERIM data processing scheme
[NASA-CR-134007] 21 p2538 N73-30347
Processing of multispectral scanned data noting imaging techniques and user operations
[ERL/R-245] 21 p2539 N73-30356
Data analysis, feature extraction, and pattern recognition for automatic target classification
[AD-763493] 21 p2550 N73-30449
Identification of conjugate, or corresponding points in multitemporal imagery for obtaining coefficients of misregistration
[NASA-CR-133640] 21 p2566 N73-30565
Operational processing of solar proton monitor data from ITOS
[NOAA-TM-NESS-49] 21 p2592 N73-30772
Dispersion of angular coordinate estimate during digital processing of radar data based on application of discrete Markov chains
22 p2628 N73-31058
Procedure for connected and orthogonal binary random processes with continuous time
22 p2628 N73-31059
Spectral correlation characteristics of pair of orthogonal binary random signals
22 p2628 N73-31060
Design of programming language for image processing
22 p2636 N73-31124
D region blunt probe data analysis using hybrid computer techniques
[NASA-CR-135646] 22 p2639 N73-31147
Abstracts on source encoding for two-dimensional data
[NASA-CR-132796] 22 p2639 N73-31149
RALPH - on-line data acquisition and analysis system for processing gamma ray and coincidence data
[NASA-TM-X-69507] 22 p2639 N73-31151
Statistical processing of Pioneer front film data - Part 1
[NASA-CR-132797] 22 p2665 N73-31351
User manual for air quality data handling system
[PB-220985/6] 22 p2696 N73-31595
Performance of acoustic signal data processing and conversion system
[AD-763326] 22 p2700 N73-31628
Injun 5 satellite extended mission analysis discussing experiments, data processing telemetry, and geophysical data
[BMBW-FBW-72-24] 22 p2722 N73-31786
Users manual for digital image processing system
[AD-764280] 23 p2761 N73-32097
Computer science and technology research programs
[AD-764659] 23 p2762 N73-32101
Worldwide conference on data base management systems
[AD-765204] 23 p2762 N73-32104
Computer science and data processing in Japan
[AD-764853] 23 p2763 N73-32106
Time lapse processing of dynamic hydrologic conditions
[E73-11054] 23 p2780 N73-32230
Development of processing and extraction techniques for Skylab EREP MSS data
[E73-11078] 23 p2782 N73-32253
User manual for Image Data Processing System, language and control system for processing image data
[NASA-CR-124438] 24 p2897 N73-33122
Description of software modules of Image Data Processing System
[NASA-CR-124447] 24 p2897 N73-33123
Speech and picture processing
[AD-764968] 24 p2898 N73-33131
Urban planning and development in east central Florida from ERTS-1 processed data
[E73-11083] 24 p2913 N73-33246
Coordination and establishment of centralized facilities and services for University of Alaska ERTS survey of Alaskan environment
[E73-11088] 24 p2913 N73-33250
Delineation of major terrain features, land uses, and crop species in Tennessee Valley through computerized analysis
[E73-11089] 24 p2913 N73-33251
Analysis of ERTS-1 MSS data for West Pakistan
[E73-11097] 24 p2914 N73-33254
Comparison of preprocessing and classification techniques for pattern recognition applications to MSS data
[E73-11103] 24 p2915 N73-33260
Canonical analysis applied to processing and interpreting MSS data with digital computers
[E73-11104] 24 p2915 N73-33261
Operational system for processing both imagery and computer compatible tapes of ERTS-1 and aerial data of Pennsylvania
[E73-11105] 24 p2915 N73-33262
Photointerpretation and digital data mapping of land use in Pennsylvania
[E73-11106] 24 p2915 N73-33263
Correction of banding in ERTS-1 MSS digital data
[E73-11108] 24 p2915 N73-33265
Thematic mapping of land use near Harrisburg, Pennsylvania from ERTS-1 digital data
[E73-11109] 24 p2915 N73-33266
Computer programs for processing multispectral scanner data of Susquehanna River Basin
[E73-11114] 24 p2915 N73-33271
Data processing and information extraction techniques for Skylab S-192 data
[E73-11142] 24 p2918 N73-33297
Acquisition of ground truth and processing of Skylab EREP data
[E73-11152] 24 p2919 N73-33306
Processing ERTS-1 MSS digital data of Susquehanna River Basin
[E73-11165] 24 p2920 N73-33318
Analysis of data on ionospheric parameters gathered by multi-probe rockets
[AD-764781] 24 p2924 N73-33356
Time coordinate transformation for processing asynoptic meteorological data
24 p2945 N73-33521
Data processing role of weather stations, polar and synchronous satellites in global experiments
24 p2948 N73-33549
Post mission data analysis of Surveyor 5, 6, and 7 chemical data
[NASA-CR-135900] 24 p2979 N73-33802
Azur satellite telemetry data processing - conferences
[BMFT-FB-W-73-04] 24 p2985 N73-33852
Preprocessing of Azur satellite telemetry data to provide several output tape formats
24 p2985 N73-33854
Selection of Azur satellite additional information for telemetry data processing
24 p2985 N73-33856
Redundancy elimination in Azur satellite telemetry data
24 p2985 N73-33857
Planning of satellite data computer processing
24 p2986 N73-33860

**DATA PROCESSING EQUIPMENT**
NT AIRBORNE/SPACEBORNE COMPUTERS
NT ANALOG COMPUTERS
NT AUXILIARY EQUIPMENT [COMPUTERS]

NT CDC 1604 COMPUTER
NT CDC 6600 SERIES COMPUTERS
NT COMPUTERS
NT DATA PROCESSING TERMINALS
NT DIGITAL COMPUTERS
NT HONEYWELL COMPUTERS
NT HYBRID COMPUTERS
NT IBM COMPUTERS
NT IBM 360 COMPUTER
NT IBM 1130 COMPUTER
NT ILLIAC 4 COMPUTER
NT MINICOMPUTERS
NT PARALLEL COMPUTERS
NT PDP 8 COMPUTER
NT PDP 10 COMPUTER
NT SEL COMPUTERS
NT SEQUENTIAL COMPUTERS
NT UNIVAC COMPUTERS
NT UNIVAC 1108 COMPUTER

Data transmission and processing system for balanced air bearing stabilized platform for satellite motion simulator
[ESRO-CR-54] 01 p0037 N73-10287

Development of airborne flight data acquisition and data processing systems
[AGARD-LS-50] 01 p0055 N73-10450

In-flight data acquisition and processing systems
01 p0056 N73-10452

Selection of dynamic data processing systems
01 p0056 N73-10454

Impact of technological development on airborne data acquisition system and ground data processing station
01 p0056 N73-10457

Simulator test to evaluate use of air traffic control radar beacon code assignment plan to provide interim radar data processing capability
[FAA-RD-72-103] 02 p0207 N73-11681

Functions of automated system for processing flight data and surveillance functions with development plan for improved capability
[FAA-ED-12-2] 02 p0208 N73-11684

Flight loads data recording system for F-102 aircraft maneuver load analysis for data acquisition and application to development of structural design criteria
[AD-747016] 03 p0253 N73-12047

Development and characteristics of data decoder to process convolution encoded information
[NASA-CASE-NPO-11371] 03 p0269 N73-12177

Development of method for automatically scanning bubble chamber films based on optical system for detecting information points as vertices
[CEA-R-4329] 03 p0302 N73-12465

Automatic plotting of aerial reconnaissance imagery and evaluation of image quality using coherent optical processing techniques
[AD-747803] 03 p0303 N73-12478

Characteristics of digital data processor using pulse from clock source to derive binary singles to show state of various indicators in processor
[NASA-CASE-GSC-10975-1] 04 p0392 N73-13187

Man machine communication techniques for improving problem solving capability
[AD-748240] 04 p0394 N73-13207

Proceedings of conference on automation of scientific research through use of computers
[JPRS-57826] 05 p0516 N73-14199

Onboard data processing system for Helios solar probe
[DGLR-PAPER-72-092] 06 p0644 N73-15229

Development of automatic inspection diagnostic and prognostic systems for maintenance of military helicopters - Vol. 1
[AD-752893] 09 p0987 N73-18060

Development of automatic inspection diagnostic and prognostic systems for maintenance of military helicopters - Vol. 2
[AD-752894] 09 p0987 N73-18061

Formulation of automatic inspection, diagnostic, and prognostic system for maintenance of army aircraft - Vol. 1
[AD-752882] 09 p0988 N73-18062

Design and tradeoff studies applied to automatic inspection, diagnostic, and prognostic maintenance system for military aircraft - Vol. 2
[AD-752883] 09 p0988 N73-18063

Technical proposal and development plan for automatic inspection, diagnostic, and prognostic maintenance system for military aircraft - Vol. 3
[AD-752884] 09 p0988 N73-18064

General specification for automatic inspection, diagnostic, and prognostic maintenance system for military aircraft - Vol. 4
[AD-752885] 09 p0988 N73-18065

Computer models for application to automatic inspection, diagnostic, and prognostic system for maintenance of military aircraft - Appendix C
[AD-752886] 09 p0988 N73-18066

Computer output data for automatic inspection, diagnostic, and prognostic system for maintenance of military aircraft - Appendix D
[AD-752887] 09 p0988 N73-18067

Maintenance data tabulations for automatic inspection, diagnostic, and prognostic systems for military aircraft maintenance - Appendix E
[AD-752888] 09 p0988 N73-18068

Design characteristics of data handling equipment for ITOS D and E meteorological satellites - Vol. 2
[NASA-CR-130161] 09 p1087 N73-18864

Interface data processing system for telecommunication computer network
[AD-754441] 11 p1260 N73-20228

Analysis of ERTS-1 imagery using electronic satellite image analysis console to display and measure snowfield extent, glacier development, and hydrologic features
[E73-10415] 11 p1279 N73-20377

Feasibility and costs of orbiting satellite data collection systems
[NASA-CR-130232] 13 p1581 N73-22812

Development of optical and digital techniques for application to synthetic holograms recorded with suboptical sources
[AD-756506] 14 p1674 N73-23583

Integrated microform-machine processing system and costs of using such systems
15 p1753 N73-24206

Design and construction of multifunction display man/machine interface for use with IBM 360 system - Vol. 1
[NASA-CR-128934] 15 p1754 N73-24214

Design and construction of multifunction display man/machine interface for use with IBM 360 system - Vol. 2
[NASA-CR-128935] 15 p1754 N73-24215

PDP 8 computer interfaces for tropospheric radio propagation measurements
[AD-759700] 16 p1879 N73-25214

Automatic accounting system for transfer of data from terminals to computer
[NASA-CASE-NPO-11456] 17 p2001 N73-26176

Interface message processors for ARPA computer network
[AD-760023] 17 p2003 N73-26193

Development and characteristics of electronic data recording equipment for shipboard oceanography data acquisition and processing
[IFS-73010] 18 p2151 N73-27384

Procedures for checking storage and transmission of instrumental, numerical, and address information in digital computer
[AD-762245] 19 p2242 N73-28073

Principles of construction, technical characteristics, and functions of several checking general-purpose computers
[AD-762212] 19 p2243 N73-28082

Research progress in coding, synchronization, data processing, and communication systems
[AD-762542] 20 p2379 N73-29117

Real time thermoplastic modulator for coherent optical processing
[AD-762920] 20 p2379 N73-29119

Procedures and equipment for automatic reception and processing of meteorological data
[NLL-M-23015-[5828.4F]] 20 p2441 N73-29609

Development and evaluation of on-line spatial light modulator for application as input transducer for real-time optical data processing system
[NASA-CR-124375] 21 p2508 N73-30121

Development of electronic computer process for analyzing contact stress oscillograms
[NLL-M-21662-[5828.4F]] 21 p2511 N73-30136

Installation standards for NASA Aerospace Safety Information System [NASIS] data base management system - Vol. 1
[NASA-CR-134455] 21 p2511 N73-30139

Overviews of NASA Aerospace Safety Information [NASIS] to introduce system features and component capabilities - Vol. 2
[NASA-CR-134456] 21 p2511 N73-30140

Data set specifications for NASA Aerospace Safety Information System [NASIS] to show standard format for every data set required by system - Vol. 3
[NASA-CR-134457] 21 p2511 N73-30141

Design specifications for programs and modules within NASA Aerospace Safety Information System [NASIS] - Vol. 4
[NASA-CR-134458] 21 p2511 N73-30142

Characteristics and operation of retrieval command subsystem for NASA Aerospace Safety Information System [NASIS] - Vol. 5
[NASA-CR-134459] 21 p2511 N73-30143

Definition and functions of message terms used in NASA Aerospace Safety Information System [NASIS] - Vol. 6
[NASA-CR-134460] 21 p2511 N73-30144

Operation specifications, Installation, and Modifications of NASA Aerospace Safety Information System [NASIS] - Vol. 7
[NASA-CR-134461] 21 p2511 N73-30145

Development of data base administrator user guide for use with NASA Aerospace Safety Information System [NASIS] - Vol. 8
[NASA-CR-134462] 21 p2512 N73-30146

Multiprocessing operating system and software for space ultrareliable modular computer
[NASA-CR-124371] 21 p2512 N73-30147

Optical data and image display recorder/processor
[NASA-CASE-GSC-11553-1] 22 p2631 N73-31089

ADAM automatic abstracting system for evaluating and improving computer produced abstracts
22 p2636 N73-31126

Computer code which reorganizes old FORTRAN programs so that statement numbers are added sequentially and extraneous statements are deleted
[NASA-TM-X-62286] 22 p2636 N73-31128

Installation standards for NASA Aerospace Safety Information System [NASIS] data base management system using IBM 360-1370 OS MVT computer - Vol. 1
[NASA-CR-134470] 22 p2637 N73-31132

Overviews of NASA Aerospace Safety Information System [NASIS] to introduce system features and capability of IBM 360/370 OS MVT computer - Vol. 2
[NASA-CR-134471] 22 p2637 N73-31133

Data set specifications for NASA Aerospace Safety Information System [NASIS] to show formats used with IBM 360/370 OS MVT computer - Vol. 3
[NASA-CR-134472] 22 p2637 N73-31134

Design specifications for programs and modules within NASA Aerospace Safety Information System [NASIS] using IBM 360/370 OS MV computer - Vol. 4
[NASA-CR-134473] 22 p2637 N73-31135

Characteristics and operation of retrieval command subsystem for NASA Aerospace Safety Information System [NASIS] using IBM 360/370 OS MVT computer - Vol. 5
[NASA-CR-134474] 22 p2637 N73-31136

Definition and functions of message terms used in NASA Aerospace Safety Information System [NASIS] using IBM 360/370 OS MVT computer - Vol. 6
[NASA-CR-134475] 22 p2637 N73-31137

Development of data base administrator user guide for use with NASA Aerospace Safety Information System [NASIS] using IBM 360/370 OS MVT computer - Vol. 7
[NASA-CR-134476] 22 p2637 N73-31138

Technical equipment for large scale automation of USSR hydrometeorological service
[AD-763956] 22 p2696 N73-31593

Computerized graphics testbed for photointerpretation
[AD-764353] 23 p2761 N73-32096

Interface message processor for digital computer network
[AD-763734] 23 p2761 N73-32098

Development and operation of cost accounting system for airport functions to show application of data processing equipment
23 p2863 N73-32878

Research on plasma physics, information theory, biophysics, and data processing systems
[AD-765002] 23 p2867 N73-32919

DATA PROCESSING TERMINALS
Revised description and specification for CAMAC modular data processing system used with on-line digital computers
[EUR-4100-E-REV-1972] 01 p0032 N73-10246

RAF operating procedures for ICL 7020 Remote computer terminal
[RAE-TR-72086] 06 p0644 N73-15231

Technology base for multiplexed data bus subsystem design for space shuttles
[NASA-CR-124030] 07 p0848 N73-16874

Design of prototype quad redundant data terminal and associated multiplexer/demultiplexer units
[NASA-CR-124127] 10 p1130 N73-19203

TAM-TAM system for use during oceanic, continental, and terminal control area flight
14 p1689 N73-23710

Annotated bibliography of literature on resource sharing computer networks
[NBS-SP-384] 22 p2638 N73-31140

DATA PROCESSORS
U DATA PROCESSING EQUIPMENT

DATA READOUT SYSTEMS
U DATA SYSTEMS
U DISPLAY DEVICES

DATA RECORDING
Processing of Concorde digitally recorded data
01 p0056 N73-10453

Polar ionospheric geophysical data recording at Kiruna, Sweden, during Apr.-Jun. 1972
06 p0667 N73-15424

Hydrology of Sicilian Channel recorded onboard S.S. Dectra in 1969
07 p0858 N73-16958

Low cost magnetic tape recording system for test instrumentation use
[AD-757011] 13 p1493 N73-22102

Catalog of meteorological and geomorphological data acquired from Nimbus 2 satellite
[NASA-TM-X-69886] 14 p1707 N73-23852

Data recording and data interchange for reducing data processing costs
15 p1753 N73-24207

Design and implementation of experimental system for receiving and recording partially reflected echoes from D region
[PSU-IRL-SCI-414] 15 p1778 N73-24417

Characteristics of single linear inertia exciter and multichannel recording equipment for flight flutter tests on Meteor aircraft
[ARC-R/M-3247] 16 p1855 N73-25026

Experimental systems for automatic receiving and recording of echoes from D region
[AD-760362] 17 p2030 N73-26428

Apparatus for on-film optical recording of camera lens aperture and focus setting
[NASA-CASE-MSC-12363-1] 17 p2030 N73-26431
Digital reproducing amplifiers for magnetically recording data from airborne processor
[ARL/ME-337] 20 p2376 N73-29090
Peculiarities of common deep point composite tapes
[JPRS-59754] 20 p2439 N73-29591
Analysis of structural response to acoustic loading and preparation of data sheets for various conditions of acoustic loads
20 p2479 N73-29914

DATA REDUCTION
NT DATA SMOOTHING
Acquisition and reduction of data acquired from superconducting magnetic suspension and balance facility
[NASA-CR-112186] 01 p0035 N73-10276
Analysis of deterministic and random flight data
01 p0056 N73-10455
Computer program for rapid reduction of Vela satellite data on solar X rays
[AD-743921] 01 p0100 N73-10822
Results from synoptic year
01 p0102 N73-10837
Results from simultaneous radar-television observations
01 p0102 N73-10838
Precise reduction of Super-Schmidt meteors
01 p0102 N73-10841
Analysis of range and range rate tracking data from satellite to satellite for geodetic applications
[AD-741683] 01 p0106 N73-10881
Programs and techniques for statistical analysis and reduction of ionospheric physics data
[AD-745966] 02 p0167 N73-11360
Iterative methods and relaxation algorithm for calculating vertical atmospheric structure from noise contaminated infrared spectral measurements
02 p0196 N73-11588
High resolution radar scattering data for determining refractive structure in troposphere
02 p0197 N73-11594
Abel integral transform and ray tracing methods for radio occultation data inversion to obtain refractive index profiles of planetary atmospheres
02 p0197 N73-11596
Inversion of radio occultation data for planetary atmospheres by bent ray path technique
02 p0198 N73-11598
Culling of redundant earth data for geophysical model fitting
02 p0200 N73-11620
Application of stochastic inverse theory for solutions to linear system of integral equations representing reduced gross earth data
02 p0201 N73-11621
Biophysics topics involving radiation data inversion problems
02 p0201 N73-11624
Comparative evolution of inverse problems and various mathematical methods used
02 p0201 N73-11629
Chronological development of multidimensional inversion techniques
02 p0202 N73-11630
Random number generators and use of estimators of probability density functions in data analysis
[NASA-CR-129507] 03 p0269 N73-12178
Fast digital noise filter capable of locating spectral peaks and shoulders by using techniques of convoluting integers
[NASA-TM-X-64707] 03 p0273 N73-12212
Calibration of combined bending-torsion fatigue reliability research machines and reliability data reduction
[NASA-CR-72837] 03 p0306 N73-12497
Graphical and analytical methods for describing earth magnetic field using satellite and ground based observational data
04 p0414 N73-13382
Data analysis on reflected oblique soundings of ionosphere using short pulses
[AD-749766] 05 p0543 N73-14417
Solar eclipse prediction, ionospheric reflection, ionospheric data reduction, and microwave acoustics
[AD-749882] 06 p0668 N73-15432
Reduction and analysis of trapped and precipitating electron data from OGO 6 spectrometer experiment F-16
[NASA-CR-130137] 06 p0718 N73-15863
Transform coding and block quantization for remote aircraft scanner data and digitized satellite imagery compression
[NASA-CR-130365] 07 p0759 N73-16161
Characteristics of multispectral sensors and methods for interpreting multispectral data obtained during earth resources surveys
07 p0784 N73-16378
METROC computer program for producing wind and thermodynamic data from raw upper atmospheric data
[AD-751780] 07 p0816 N73-16616
Mathematical models for reducing force of gravity values from earth relief to external surface
[AD-752235] 08 p0920 N73-17538
OSO 5 spectrophotometer design, solar EUV data acquired, and data reduction
[NASA-CR-130159] 08 p0956 N73-17828
Real time data display and postflight analysis
[NASA-CR-128836] 10 p1132 N73-19229
Technique for processing and compressing ERTS-1 imagery of California
[E73-10465] 12 p1394 N73-21303
Reduction of random vibration response data for NASA Brayton rotating unit turbogenerator
[NASA-CR-121178] 13 p1534 N73-22428
Development of processing satellite data to show quantity of data and time required for various techniques
[BMFT-FBW-73-04] 14 p1638 N73-23277
Analysis of magnetospheric data obtained by satellite sounding
[AD-755390] 14 p1665 N73-23516
Gyroscope noise measurements and data analysis
[AD-756977] 14 p1691 N73-23723
ADMAP computer manipulation program for processing electric propulsion trajectory data generated by low thrust optimization program, HILTOP
[NASA-CR-130242] 15 p1754 N73-24216
Superconducting magnetic suspension and balance facility data acquisition and data reduction errors
15 p1762 N73-24274
Analysis of plasma sheath ion current data measured by electric probes on third flight of Trailblazer 2
[AD-758763] 15 p1836 N73-24883
Evaluation of ERTS-1 image data compression techniques
[E73-10647] 16 p1897 N73-25343
Computerized analysis of electro-optical polymer relaxation data
[AD-759421] 17 p1992 N73-26111
Evaluation of ERTS-1 image data compression techniques to show four ERTS MSS tapes recorded on single compressed tape
[E73-10730] 17 p2020 N73-26336
Program for reducing data from high resolution mass spectrometer
[NASA-TM-X-2847] 18 p2113 N73-27089
State of readiness to process and reduce Skylab EREP digital data
[E73-10798] 18 p2138 N73-27274
Radiometer image data compression system with zero error wideband ground link transmission
18 p2212 N73-27863
Data compression and storage techniques for ERTS-1 image data
[E73-10853] 19 p2292 N73-28430
Data compression preserving statistical independence
[NASA-TM-X-70419] 19 p2313 N73-28606
Development of extraction and processing techniques for Skylab S-192 MSS data
[E73-10860] 20 p2391 N73-29211
Image data compression using digital holography
[AD-762931] 20 p2426 N73-29487
Data reduction procedure for quantitative electron probe microanalysis
[NBS-TN-769] 21 p2549 N73-30433
ADAM automatic abstracting system for evaluating and improving computer produced abstracts
22 p2636 N73-31126
Use of spatial information for improving classification accuracy of remotely sensed data
[NASA-CR-133988] 22 p2637 N73-31130
D region blunt probe data analysis using hybrid computer techniques
[NASA-CR-135646] 22 p2639 N73-31147
Celestial mechanics analysis on Mariner 9 Doppler tracking data for determining Mars gravitational field
23 p2841 N73-32706
Mariner 9 Doppler tracking short data arcs for determining Mars gravitational field
23 p2841 N73-32707
Mariner 9 Doppler tracking data filtering method for determining Mars gravity
23 p2841 N73-32708
Doppler data range change measurements for Mariner 9 celestial mechanics experiment
23 p2842 N73-32709
Post mission data analysis of Surveyor 5, 6, and 7 chemical data
[NASA-CR-135900] 24 p2979 N73-33802

DATA RETRIEVAL
Development of Earth Resources Information Storage, Transformation, Analysis, and Retrieval System based on NASA training program in systems engineering
[NASA-CR-61394] 01 p0050 N73-10400
Procedure for repairing and recovering voice data from heat damaged magnetic tapes
[NASA-CASE-MSC-14219-1] 07 p0755 N73-16132
Development of processing satellite data to show quantity of data and time required for various techniques
[BMFT-FBW-73-04] 14 p1638 N73-23277
Atmospheric effects on ERTS-1 data and advanced data extraction techniques
[PAPER-II] 19 p2277 N73-28323
Collection, storage, and retrieval of data by computer at High Field Magnet Laboratory
[EP-RR-28] 20 p2379 N73-29113
Data processing and extraction techniques for Skylab S-192 MSS data
[E73-10859] 20 p2391 N73-29210
Characteristics and operation of retrieval command subsystem for NASA Aerospace Safety Information System [NASIS] - Vol. 5
[NASA-CR-134459] 21 p2511 N73-30143
Definition and functions of message terms used in NASA Aerospace Safety Information System [NASIS] - Vol. 6
[NASA-CR-134460] 21 p2511 N73-30144
Operation specifications, Installation, and Modifications of NASA Aerospace Safety Information System [NASIS] - Vol. 7
[NASA-CR-134461] 21 p2511 N73-30145
Development of data base administrator user guide for use with NASA Aerospace Safety Information System [NASIS] - Vol. 8
[NASA-CR-134462] 21 p2512 N73-30146
Characteristics and operation of retrieval command subsystem for NASA Aerospace Safety Information System [NASIS] using IBM 360/370 OS MVT computer - Vol. 5
[NASA-CR-134474] 22 p2637 N73-31136
Definition and functions of message terms used in NASA Aerospace Safety Information System [NASIS] using IBM 360/370 OS MVT computer - Vol. 6
[NASA-CR-134475] 22 p2637 N73-31137
Development of data base administrator user guide for use with NASA Aerospace Safety Information System [NASIS] using IBM 360/370 OS MVT computer - Vol. 7
[NASA-CR-134476] 22 p2637 N73-31138
Storage and retrieval of ERTS-1 and underflight imagery of Pennsylvania
[E73-11116] 24 p2916 N73-33273

DATA SAMPLING
Signal to noise ratio performance of optimum digitalized FM demodulator
01 p0025 N73-10195
Sampled data frequency response method for analyzing control system performance, and compensator improvement program for designing Saturn 5/S1-C compensators
[NASA-CR-123917] 02 p0195 N73-11573
Sampling function representation for applying satellite-to-ocean altitude altimeter data to geoid
06 p0662 N73-15373
Sample classification accuracy of minimum distance and maximum likelihood classifiers and parametric and nonparametric classifiers in remote sensing
[NASA-CR-130030] 07 p0799 N73-16489
Survey of easy methods of developing easy computer systems useable by everyman
[P-4962] 14 p1638 N73-23278
Pseudo-Nyquist analysis technique for hybrid sampled-data control systems
[NASA-CR-2345] 24 p2984 N73-33847

DATA SMOOTHING
Least squares curve fitting method for smoothing pressure distribution data for various cross sections of circular cylinder
[WRE-TN-688[WR/D]] 02 p0195 N73-11577
Missile trajectory smoothed by Kalman method using data from several cameras, radars, and Doppler receivers
[WRE-TN-705[T]] 02 p0227 N73-11831
Smoothing functions of range and range rate measurements from earth orbiting satellites
[NASA-TM-X-66126] 04 p0475 N73-13881
Compression of satellite altimeter radar pulses and high resolution sea reflectivity
06 p0663 N73-15389
Smoothing properties of neutral functional differential equations
[NASA-CR-130748] 08 p0936 N73-17668
Statistical models for smoothing environmental economics and communications data
13 p1549 N73-22554
Numerical smoothing and interpolation methods noting spline function method
[ONERA-NT-205] 15 p1804 N73-24619
Smoothing technique for analyzing frequency response of aircraft in flight and on ground
[RAE-LIB-TRANS-1703] 17 p2054 N73-26616
Use of regularization method for interpolation and differentiation of experimental data
[NLL-M-21660-[5828.4F]] 21 p2565 N73-30561
Data smoothing and error detection based on linear interpolation
[NASA-CR-133984] 22 p2637 N73-31131

DATA STORAGE
Development of Earth Resources Information Storage, Transformation, Analysis, and Retrieval system through NASA research project
[NASA-CR-61392] 01 p0049 N73-10399
Development of Earth Resources Information Storage, Transformation, Analysis, and Retrieval

System based on NASA training program in systems engineering
[NASA-CR-61394] 01 p0050 N73-10400
Development of air navigation system using moving map display based on holographic storage and display techniques
[AD-745025] 01 p0065 N73-10533
Survey and analysis of high density mass storage devices and systems for Navy fleet material
[AD-747134] 02 p0146 N73-11179
Data acquisition and storage system for computerized physiological monitoring system
[AD-746872] 02 p0148 N73-11199
Application of alkali halides for holographic recording and recovery at room temperatures for high density data storage systems
[AD-748027] 03 p0311 N73-12537
Development of holographic storage and retrieval system for aerial chart information display in cockpit environment
[AD-748648] 03 p0330 N73-12690
Momentum wheel design for spacecraft attitude control and magnetic drum and head system for data storage
[NASA-CASE-NPO-11481] 04 p0446 N73-13644
Reliable source of high quality magnetic bubble materials
[AD-749806] 05 p0589 N73-14787
Magnetic bubble circuits for satellite data storage
[AD-750660] 06 p0644 N73-15232
Review of high density computer storage devices for recorded data
[AD-753626] 09 p1007 N73-18217
Compensation of vidicon signal dark component
[DRIC-TRANS-2967] 13 p1491 N73-22089
Design, fabrication, and evaluation of electron beam addressable, high information density memory tube
[AD-756936] 13 p1500 N73-22161
Data collection problems for small documentary centers
15 p1753 N73-24208
Electronic computer processing of data stored in data banks
15 p1753 N73-24212
Relationship between page size, program behavior, and page fetch frequency in storage hierarchy systems
[AD-760001] 17 p2002 N73-26186
Data compression and storage techniques for ERTS-1 image data
[E73-10853] 19 p2292 N73-28430
Comparison of photographic digital recording systems using laser technology
[AD-761521] 19 p2308 N73-28563
Collection, storage, and retrieval of data by computer at High Field Magnet Laboratory
[EF-RR-28] 20 p2379 N73-29113
Mariner 9 space probe storage subsystem for flight performance
[NASA-CR-133653] 20 p2475 N73-29884
Data manipulation and sensing in plasma display/storage panel
[AD-763110] 22 p2641 N73-31164
Automatic hybrid interactive information storage and search system
[DSIS-TN-13] 24 p2897 N73-33126
Storage and retrieval of ERTS-1 and underflight imagery of Pennsylvania
[E73-11116] 24 p2916 N73-33273

**DATA SYSTEMS**
Development of Earth Resources Information Storage, Transformation, Analysis, and Retrieval system through NASA research project
[NASA-CR-61392] 01 p0049 N73-10399
Transfer function of linearizer for anemometer data
[AD-744975] 01 p0075 N73-10622
Data management system for prediction of Naval student pilot performances
[AD-744984] 02 p0136 N73-11104
Cost effective data security safeguards in personal information databanks
[P-4871] 02 p0145 N73-11178
Modification of Minuteman digital computer system to provide for single channel autoanalyzer waveform analysis
[AD-746264] 02 p0147 N73-11197
Star sensor/mapper with two data channels with memory for SAS-B
[NASA-CR-129192] 02 p0173 N73-11403
Optical and digital data processing and handling of SLR imagery
[ESRO-CR[P]-139-VOL-4] 03 p0297 N73-12419
Development of map storage and display system using volume holography using iron-doped lithium niobate
[AD-748002] 03 p0311 N73-12541
Program package for statistical measured data selection and visual presentation in real time
05 p0516 N73-14193
Digital facility for handling and processing remotely sensed earth resources data
05 p0537 N73-14369
Handling and analysis of remote sensing data on 1971 corn blight
[NASA-CR-130368] 07 p0759 N73-16164
Telemetry data processing systems for experiments flown on Injun 5 satellite, OV-3 satellite, OV-4 satellite, OV-5 satellite, OV-6 satellite, and OV-15 satellite
[AD-751508] 07 p0759 N73-16166
Principles of spacecraft telemetry data management
[ESRO-TN-121-ESOC] 08 p0885 N73-17166
Development of algorithm for multiple hypothesis testing with application to amplitude comparison monopulse radar system in air traffic control operations
[TN-1973-7] 09 p1002 N73-18173
Computer network modeling system for planning data management in voice communication
[AD-752797] 09 p1006 N73-18210
Computer network with random access storage for teletype data transmission system
[NASA-CR-130500] 09 p1006 N73-18214
Design of prototype quad redundant data terminal and associated multiplexer/demultiplexer units
[NASA-CR-124127] 10 p1130 N73-19203
Standards and procedures for generation of operational display formats for use in Mission Control Center display control system
[NASA-CR-128843] 10 p1132 N73-19228
Computerized positron scintillation camera data acquisition and display system for linear accelerator facility
[UCRL-51288] 10 p1161 N73-19447
Multiple phase shift keying communications for improving carrier tracking efficiency and data detection performance
[NASA-CASE-NPO-13103-1] 11 p1255 N73-20180
Methods employed to obtain datum position and velocity information for evaluation of inertial navigation systems and identification of error sources
11 p1320 N73-20716
Preparation of urban land use inventories by automated processing of ERTS MSS data
[NASA-CR-131576] 13 p1524 N73-22347
Evaluation of data processing systems for Alaskan and Norwegian seismic arrays
[AD-756905] 13 p1525 N73-22360
Automated processing system for mechanical property test data of composite solid propellants and binders
[AD-755515] 13 p1569 N73-22714
Projected data systems requirements for agriculturally oriented earth resources technology satellites in 1980s
[NASA-TM-X-62240] 14 p1660 N73-23472
Microfilm system and update for acquisition, storage, and retrieval of solid propellant mechanical behavior data
[AD-757245] 14 p1700 N73-23799
Design of airborne flight data transmission system for automatic acquisition and tracking
14 p1711 N73-23885
Development of methods for presenting aircraft performance data and comparison of specific methods to show sources of discrepancies
15 p1733 N73-24050
Functions of small industrial information center
15 p1752 N73-24203
Integrated microform-machine processing system and costs of using such systems
15 p1753 N73-24206
Data collection problems for small documentary centers
15 p1753 N73-24208
Evaluation of digital correction techniques for ERTS-1 imagery
[E73-10705] 16 p1903 N73-25396
Establishment of data management system for ERTS-1 data by National Marine Fisheries Service Engineering Laboratory
[E73-10720] 17 p2019 N73-26327
Data base of electron and proton spectrometer, Orbiting Geophysical Observatory, and fluxgate magnetometer experiments
[UCRL-51314] 17 p2033 N73-26453
Corsa 1 and 2 instruments, experimental design, and data systems for X ray astronomy
17 p2084 N73-26864
Lightweight reprogrammable data system for small scientific satellite
18 p2208 N73-27823
Interface organization of local data control systems with M-6000 ASVT-M computer hardware complex
[JPRS-59612] 19 p2239 N73-28051
Organizational subsystems of information computer center for automatic systems control
[AD-761480] 19 p2240 N73-28057
Analysis of algorithms for construction of system of diagnostic programs for digital computer complexes
[AD-762310] 19 p2242 N73-28074
Design of fast Fourier transform digital processor
[AD-761803] 19 p2245 N73-28097
Procedures and equipment for automatic reception and processing of meteorological data
[NLL-M-23015-[5828.4F]] 20 p2441 N73-29609
Mariner 9 space probe storage subsystem for flight performance
[NASA-CR-133653] 20 p2475 N73-29884
Development of guidelines for definition of relevant information content in data classes
[NASA-CR-124356] 20 p2488 N73-29990
Installation standards for NASA Aerospace Safety Information System [NASIS] data base management system - Vol. 1
[NASA-CR-134455] 21 p2511 N73-30139
Overviews of NASA Aerospace Safety Information [NASIS] to introduce system features and component capabilities - Vol. 2
[NASA-CR-134456] 21 p2511 N73-30140
Data set specifications for NASA Aerospace Safety Information System [NASIS] to show standard format for every data set required by system - Vol. 3
[NASA-CR-134457] 21 p2511 N73-30141
Design specifications for programs and modules within NASA Aerospace Safety Information System [NASIS] - Vol. 4
[NASA-CR-134458] 21 p2511 N73-30142
Processing of multispectral scanned data noting imaging techniques and user operations
[ERL/R-245] 21 p2539 N73-30356
Developments in data systems air traffic control, and solid state physics
[AD-763731] 21 p2587 N73-30727
Installation standards for NASA Aerospace Safety Information System [NASIS] data base management system using IBM 360-1370 OS MVT computer - Vol. 1
[NASA-CR-134470] 22 p2637 N73-31132
Overviews of NASA Aerospace Safety Information System [NASIS] to introduce system features and capability of IBM 360/370 OS MVT computer - Vol. 2
[NASA-CR-134471] 22 p2637 N73-31133
Data set specifications for NASA Aerospace Safety Information System [NASIS] to show formats used with IBM 360/370 OS MVT computer - Vol. 3
[NASA-CR-134472] 22 p2637 N73-31134
Design specifications for programs and modules within NASA Aerospace Safety Information System [NASIS] using IBM 360/370 OS MV computer - Vol. 4
[NASA-CR-134473] 22 p2637 N73-31135
Integrated data acquisition system for airborne computer
[NASA-TM-X-56018] 23 p2760 N73-32087
Pseudo-Nyquist analysis technique for hybrid sampled-data control systems
[NASA-CR-2345] 24 p2984 N73-33847

**DATA TRANSMISSION**
NT AUTOMATIC PICTURE TRANSMISSION
Algorithm for reducing redundancy during image transmission
01 p0024 N73-10189
Noise and error effects on differential pulse code modulation transmission of sampled aerial imagery
01 p0024 N73-10190
Automatic equalizers of telephone channels for fast transmission of digital data
01 p0025 N73-10199
Algorithm for adaptive digital filters of data communication channels
01 p0026 N73-10200
Real time computerized message switching and data transmission systems for military communications network
01 p0026 N73-10206
Development of communication system for transmitting differential phase shift keyed signals from input data bits without timing or phase reference signals
[NASA-CASE-MSC-14065-1] 01 p0028 N73-10215
Data transmission and processing system for balanced air bearing stabilized platform for satellite motion simulator
[ESRO-CR-54] 01 p0037 N73-10287
Development of Earth Resources Information Storage, Transformation, Analysis, and Retrieval System based on NASA training program in systems engineering
[NASA-CR-61394] 01 p0050 N73-10400
Space electronics, data transmission, orientation of celestial objects, and research instruments
01 p0119 N73-10979
Figure series for digital data presentation
[IZF-1972-11] 02 p0145 N73-11170
Minicomputer for controlling data transfer between process instrumentation and on-line computer
[HMI-B-123] 02 p0145 N73-11171
Design and development of closed-loop, digital data communication system using optimum number of interconnecting wires
[NASA-CASE-MSC-13912-1] 03 p0266 N73-12151
Instruction manual for Model 600F Data Transmission Test Set
[NASA-TM-X-68833] 03 p0301 N73-12453
Arithmetic codes for error control in digital computation and data transmission
[AD-748201] 04 p0394 N73-13206
TD-1A satellite ground checkout stations noting spacecraft communication and data transmission
[ESRO-TM-140-ESTEC] 04 p0402 N73-13277
Analysis of sampling mechanism and operation of automatic normalization of character patterns
[REPT-726] 05 p0516 N73-14195
Error performances of several digital signaling methods as function of specified signal to noise ratio
05 p0609 N73-14953

Adaptive routing techniques for message switching computer-communication networks
[AD-749678] 06 p0646 N73-15246
Characteristics of two channel telemetry system with two data rate channels for high and low data rate communication
[NASA-CASE-NPO-11572] 07 p0754 N73-16121
Technology base for multiplexed data bus subsystem design for space shuttles
[NASA-CR-124030] 07 p0848 N73-16874
Data collection and relay system for monitoring hydrologic conditions in south and central Florida
[E73-10092] 08 p0902 N73-17304
Analysis of data from charged particle experiment of Explorer 34 satellite and Explorer 35 satellite
[NASA-CR-130171] 08 p0976 N73-17985
Software module for teletypes connected to HP ALOHA SYSTEM multiplexer
[NASA-CR-130492] 09 p1006 N73-18213
Computer network with random access storage for teletype data transmission system
[NASA-CR-130500] 09 p1006 N73-18214
Proceedings of conference on laser beam data transmission and development of laser information systems
[AD-753944] 10 p1169 N73-19513
Analysis of soundings and imaging measurements obtained from geostationary satellites during 1 Nov. 1972 to 31 Jan. 1973
[NASA-CR-130175] 10 p1215 N73-19884
Vehicle telemetry measurements for Skylab 2 spacecraft and identification of data sources
[NASA-TM-X-69142] 10 p1216 N73-19887
Performance of digital voice transmission system with modulator-demodulator network
[AD-754921] 11 p1258 N73-20210
Computer communications systems
[AD-754461] 11 p1260 N73-20225
Handbook on defense and commercial communication systems
[AD-755917] 12 p1380 N73-21191
ERTS-1 retransmission of water level data collected at remote locations in Canada
[E73-10469] 12 p1395 N73-21306
Data retransmission from Canadian water gauging stations using ERTS-1
[E73-10479] 12 p1396 N73-21316
Development of data relay network for monitoring hydrologic conditions collected for south and central Florida
[E73-10491] 12 p1397 N73-21327
Feedback queueing model with interference caused retransmission for space to surface data transmission
[AD-756568] 13 p1492 N73-22093
Fault tolerant data transmission and multiplexing system using digital system
[AD-756485] 13 p1493 N73-22100
Channel measurement techniques, modeling multipath structure of line-of-sight tropospheric paths, and prediction of spread spectrum modem performance as function of multipath conditions
[AD-755922] 13 p1494 N73-22115
ERTS-1 retransmission of water resources data collected from remote regions of Canada
[E73-10504] 13 p1515 N73-22279
Development of Tracking and Data Relay Satellite system concept for service of low, medium, and high data rate user spacecraft - Vol. I
[NASA-CR-130219] 13 p1579 N73-22799
Burst random access channel for satellite computerized data transmission system
[AD-756226] 14 p1635 N73-23252
Analysis of modifications of ALOHA random access channel by considering synchronization among users
[AD-756227] 14 p1637 N73-23271
TAM-TAM system for use during oceanic, continental, and terminal control area flight
14 p1689 N73-23710
Telemetry and transmission system with programmed sampling and multiplexing
[NASA-CASE-GSC-11388-1] 15 p1750 N73-24187
Design and performance of C band airborne data transmission system for aerial reconnaissance
[AD-759184] 16 p1877 N73-25194
Estimation of signal-to-noise ratio in spacecraft data channel
16 p1879 N73-25207
Development and application of Airborne Traffic and Situation Display for improved air traffic control
[PB-215714/7] 16 p1942 N73-25715
Automatic accounting system for transfer of data from terminals to computer
[NASA-CASE-NPO-11456] 17 p2001 N73-26176
Specifications for interconnection of host and interface message processor
[AD-759433] 17 p2001 N73-26182
Multichannel pulse sampling system with pulse anemometers and current meters on oceanographic buoy
[AD-760336] 17 p2030 N73-26426
Recursive scheme for computing system availability from component elements
[AD-759809] 17 p2055 N73-26623
Analysis of candidate data and surveillance modems for avionics system used in air traffic control system
[AD-761522] 18 p2176 N73-27574
Radiometer image data compression system with zero error wideband ground link transmission
18 p2212 N73-27863
Spread spectrum modulation technique for use in airborne relay communication link
[AD-761522] 19 p2236 N73-28027
Packet switching, bilateral broadcasting, and burst random access capabilities
[AD-761564] 19 p2237 N73-28035
Analysis of packet switching network by computerized simulation
[NPL-COM-SCI-64] 19 p2239 N73-28053
Coded transmission of binary data over coherent white Gaussian channels
[AD-761465] 19 p2245 N73-28102
Development of analytical capabilities for determining use of satellite communications technology for professional education and medical services
[NASA-CR-133359] 20 p2377 N73-29100
Facsimile data transmitted simultaneously with television
[NHK-LABS-NOTE-160] 20 p2377 N73-29103
Geoisochronous satellites for obtaining and transmitting meteorological data
20 p2447 N73-29658
Electronic digital data synchronizing and instrumentation amplification techniques
[AD-763797] 21 p2509 N73-30131
Characterictics of carbon dioxide lasers and application for transmission of data
21 p2554 N73-30479
Characteristics and equipment for third generation computers
21 p2609 N73-30913
Data transmission interference after television field synchronizing signal
[BBC-RD-1973/12] 22 p2627 N73-31049
Synchronization method for pseudorandom binary data sequences in blockwise transmission of nonoverlapping subsequences, based on digital correlation
[FTZ-A-157-TBR-7] 22 p2632 N73-31095
Asynchronous and synchronous time division multiplex systems of 8.448 and 8.192 Mbit/s
[FTZ-442-TBR-40] 22 p2634 N73-31106
Computer simulation of multipacket-switched data communication network operating with revised link and node protocol
[NPL-COM-68] 22 p2634 N73-31112
Standard digital data clock-rate generator with programmable digital phase shift for data transmission from communication satellites
[AD-764049] 22 p2635 N73-31117
Assembly language programs required to interface ALOHA system to IBM telecommunication time sharing operation
[NASA-CR-133853] 22 p2639 N73-31155
Digital data transmission with argon laser beam through atmosphere to determine error frequency
[FTZ-44-TBR-34] 22 p2681 N73-31478
Fundamental concepts of communication theory to include transmission of continuous signals and use of discrete time signals
23 p2756 N73-32054
Characteristics of digital communication systems and processing of bandpass digital signals using spread spectrum techniques for data transmission
23 p2756 N73-32055
Principles and operation of spread spectrum communication system with application to satellite communication systems
23 p2756 N73-32056
Performance of spread spectrum communication systems to include effects of various forms of channel noise and synchronization aspects of system
23 p2756 N73-32057

**DATING**
U CHRONOLOGY
U TIME MEASUREMENT

**DAWN CHORUS**
Operational characteristics of sky noise measuring instruments and analysis of discrepancies in data acquired by each instrument
[NASA-CR-133415] 18 p2151 N73-27383

**DAYGLOW**
Cosmos 224 observations of N2 ions during medium solar activity
03 p0293 N73-12389
Photoelectron effect on second positive system of nitrogen bands in daytime glow of atmosphere from Cosmos 224 data
05 p0536 N73-14360
Dayglow measurements of upper atmosphere by Orbiting Astronomical Observatory A-2
[AD-752228] 08 p0920 N73-17539

**DAYTIME**
Daytime ionospheric attenuation of very low frequency signal transmission over Greenland ice
[AD-746636] 04 p0389 N73-13161
Analysis of dayside auroral characteristics and hydroxyl airglow variations from 1969 airborne auroral expedition
[NASA-CR-130916] 09 p1025 N73-18367
Optical atmospheric data in daytime, using airborne instrument measurements
[AD-754898] 11 p1289 N73-20458
Spectral energy distribution of Pamir plants at different altitudes above sea level in relation to mountain plant characteristics
20 p2406 N73-29336

**DC [CURRENT]**
U DIRECT CURRENT

**DC 3 AIRCRAFT**
Camera installation for multispectral aerial photography using four electrically driven cameras for synchronous photography
[FOA-2-C-2469-52] 06 p0672 N73-15469

**DC 8 AIRCRAFT**
Crash of DC-8 aircraft during takeoff from Anchorage International Airport, Alaska on 27 Nov. 1970
[NTSB-AAR-72-12] 07 p0737 N73-15999
Wind tunnel tests to determine effect on cruise performance of installing long duct refan-engine nacelle on DC 8 aircraft
[NASA-CR-121218] 17 p1982 N73-26023
Design of landing approach automatic flight control system using optimal feedback techniques
[AD-760125] 17 p1984 N73-26040
Computerized simulation of DC-8 aircraft during landing approach under wind shear conditions
[AD-764697] 23 p2745 N73-31975

**DC 9 AIRCRAFT**
Investigation of midair collision between commercial DC 9 aircraft and Marine Corps F-4B aircraft at Duarte, California on 6 June 1971
[NTSB-AAR-72-26] 03 p0252 N73-12037
Aircraft accident involving DC-9 aircraft landing at Fort Lauderdale, Florida airport in marginal weather conditions on 18 May, 1972
[NTSB-AAR-72-31] 07 p0738 N73-16005
Feasibility of liquid nitrogen fuel tank inerting system on commercial aircraft to prevent fuel tank explosions
[FS-140-72-1] 13 p1473 N73-21934
Aircraft accident involving crash of DC-9 aircraft during landing following go-round at Fort Worth, Texas Airport on 30 May 1972
[NTSB-AAR-73-3] 17 p1982 N73-26017
DC 9 refanned engine nacelle effects on cruise drag considering lateral spacing
[NASA-CR-121219] 17 p1982 N73-26024
Wind tunnel tests to determine effects of modified engine nacelle on stability and control characteristics of DC-9 aircraft with emphasis on deep stall regime
[NASA-CR-121220] 19 p2219 N73-27904
Aircraft accident involving ground collision of DC-9 and CV-880 aircraft at O Hare International Airport, Chicago, Illinois on 20 December, 1972
[NTSB-AAR-73-15] 22 p2614 N73-30945

**DC 10 AIRCRAFT**
Inflight incident involving number two engine failure on DC 10 aircraft near Tucson International Airport, Arizona on 2 May, 1972
[NTSB-AAR-72-29] 03 p0251 N73-12035
Inflight incident involving separation of cargo compartment door on DC-10 aircraft near Windsor, Ontario, Canada on 12 June, 1972
[NTSB-AAR-73-2] 12 p1363 N73-21061
Flight tests to determine characteristics of vortex and turbulent wake generated by DC-10 aircraft for development of air traffic control separation criteria
[REPT-73-00470] 13 p1474 N73-21938

**DE HAVILLAND AIRCRAFT**
NT COMET 4 AIRCRAFT
Aircraft accident involving DH-114 aircraft during attempted landing at Mercedita Airport, Puerto Rico on 24 June, 1972
[NTSB-AAR-72-34] 07 p0738 N73-16004
Aircraft accident involving midair collision of Convair 340 and DHC-6 near Appleton, Wisconsin on 29 June 1972
[NTSB-AAR-73-9] 17 p1981 N73-26016
Development and characteristics of experimental aircraft for demonstrating augmentor wing jet short takeoff concept using modified C-8A aircraft - Vol. I
[NASA-CR-114503] 21 p2494 N73-30016
Flight tests of modified C-8A aircraft to demonstrate augmentor wing, short takeoff concept - Vol. 2
[NASA-CR-114504] 21 p2494 N73-30017

**DE HAVILLAND DH 106 AIRCRAFT**
U COMET 4 AIRCRAFT

**DE LAVAL NOZZLES**
U CONVERGENT-DIVERGENT NOZZLES

**DEACCLIMATIZATION**
U ACCLIMATIZATION

**DEACTIVATION**
Collisional deactivation rate constants for oxygen by minor atmospheric constituents and other gases
[DREV-TN-2010/72] 01 p0082 N73-10682
Shock deactivation cross sections of metastable barium and thallium atoms in shock tube
[MPI-PAE/EXTRATERR-65] 02 p0214 N73-11734
Theoretical model of optical excitation, emission, and deactivation properties of Meinel band system of nitrogen
[AD-753396] 09 p1069 N73-18722
Gas environment effect on catalase cryolysis
10 p1119 N73-19121

**DEADWEIGHT**
U STATIC LOADS
**DEAFNESS**
U AUDITORY DEFECTS
**DEBRIS**
NT RADIOACTIVE DEBRIS
Erosional latitudinal debris distribution on Mars surface
23 p2839 N73-32689
**DEBUGGING**
U CHECKOUT
**DEBYE LENGTH**
Temperature and concentration dependence of Debye-Waller factor for superconducting Nb-Zr alloy system
[BNL-TR-483] 03 p0315 N73-12569
Debye parameters of nonideal cesium plasma reached in shock tube
[AD-754015] 10 p1198 N73-19749
**DEBYE TEMPERATURE**
U SPECIFIC HEAT
**DEBYE-SCHERER METHOD**
Debye polarization theory for determining electromagnetic wave propagation in sea
24 p2957 N73-33622
**DECARBONATION**
Ferritic steels resistant to high temperature and decarburization by Na
[CEA-CONF-2118] 17 p2044 N73-26539
**DECAY**
NT ALPHA DECAY
NT BIOLUMINESCENCE
NT CHEMILUMINESCENCE
NT ELECTROLUMINESCENCE
NT ELECTRON EMISSION
NT EMISSION
NT FIELD EMISSION
NT FLUORESCENCE
NT INCANDESCENCE
NT ION EMISSION
NT LIGHT EMISSION
NT LUMINESCENCE
NT NEUTRON DECAY
NT NEUTRON EMISSION
NT NUCLEAR FISSION
NT OPTICAL RESONANCE
NT PARTICLE EMISSION
NT PHOSPHORESCENCE
NT PHOTOELECTRIC EFFECT
NT PHOTOELECTRIC EMISSION
NT PHOTOIONIZATION
NT PHOTOLUMINESCENCE
NT PHOTOPRODUCTION
NT PLASMA DECAY
NT RADIO EMISSION
NT RADIOACTIVE DECAY
NT SECONDARY EMISSION
NT SOLAR RADIO BURSTS
NT SOLAR RADIO EMISSION
NT SPECTRAL EMISSION
NT THERMAL EMISSION
NT THERMIONIC EMISSION
NT THERMOLUMINESCENCE
NT TYPE 2 BURSTS
NT TYPE 3 BURSTS
NT TYPE 4 BURSTS
NT TYPE 5 BURSTS
NT X RAY FLUORESCENCE
Inclusive spectra at large transverse momentum for study of massive decay resonances
[TUETP-73-6] 14 p1694 N73-23748
**DECAY RATES**
NT ELECTRON DECAY RATE
Computerized analysis of droplet size effect on erosion rate in wet steam turbine stage
[PB-211901] 05 p0527 N73-14292
Decay times of type 3 solar radio bursts
19 p2338 N73-28811
Gain measurements of excited iodine atom decay rates in photochemical iodine laser
[UCRL-TRANS-10692] 24 p2931 N73-33409
**DECELERATION**
NT SPIN REDUCTION
Transonic flow around slender bodies noting wave drag deceleration and boundary layer transition
[ISL-33/71] 04 p0406 N73-13304
Deceleration method for rapid deceleration of mobile parts in vibration simulators
[LRBA-NT-8/72/SEV] 05 p0548 N73-14449
Approximative model for diurnal effect on atmospheric density distribution and artificial earth satellite deceleration
10 p1177 N73-19578
Decelerator sled simulation for testing air bag restraint system effects in passenger motor vehicle crash
[PB-212706] 11 p1251 N73-20155
Deceleration and vertical motion of gas puff released into upper atmosphere
[AD-757867] 15 p1782 N73-24450
Comparison of effectiveness of yielding and elastic restraint systems for crash protection to show effects of slack and yield at constant load
[ARL/SM-382] 15 p1837 N73-24890
Formation and structure of vortex rings formed by stream deceleration
22 p2653 N73-31251
**DECELERATORS**
U BRAKES [FOR ARRESTING MOTION]
**DECIDUOUS TREES**
Color and color infrared aerial photographic detection of Dutch elm disease
16 p1866 N73-25110
Light effects on organic matter balance of oak underwood growing in forest understorey
20 p2405 N73-29330
Influence of light conditions and understorey tree death on organic matter loss balance in oak underwood
20 p2405 N73-29331
Measurements of radiation characteristics in multistoreyed overmature oak grove
20 p2405 N73-29332
Spectrophotometric measurements of spectral composition of conifer and decidous forests
20 p2406 N73-29337
**DECIMALS**
Digital converter for scaling binary number to binary coded decimal number of higher multiple
[NASA-CASE-KSC-10595] 03 p0269 N73-12176
**DECISION ELEMENTS**
U LOGICAL ELEMENTS
**DECISION MAKING**
Control theory model for pilot decision making based on estimated state of linear plant
01 p0014 N73-10107
Suboptimal sampling and control behavior of human operator in output prediction task for automatic process
01 p0015 N73-10114
Effects of decision models and operational characteristics on economic expenses associated with use of predictive weather information
[NASA-CR-128401] 01 p0073 N73-10600
Statistical analysis of air combat situation evaluations conducted by US Navy pilots to detect differences caused by experience
[AD-747519] 03 p0261 N73-12119
Analysis of instrument system for assisting pilots in making decisions during aircraft takeoff and landing rolls
[FAA-RD-72-112] 03 p0301 N73-12460
Development of equations and mathematical models for decision making concerning military logistics, aircraft, space parts, and support equipment
[AD-747972] 03 p0368 N73-12997
Computerized information processing for radar system by subdivisions and multiple decision making processes
04 p0389 N73-13158
Procedures for constructing and analyzing combat models for planning and executing naval combat operations
[JPRS-57404] 04 p0393 N73-13194
Management planning models for decision making under conditions of uncertainty
[NASA-CR-129592] 04 p0487 N73-13986
Control over social change through anticipatory project assessment
[NASA-CR-129830] 05 p0611 N73-14968
Decision making behavior of sonar operator in target detection and reporting
[AD-750761] 06 p0637 N73-15174
Development of decision models for choosing techniques and procedures to obtain information for investment decisions in natural resources programs
07 p0783 N73-16363
Model for awarding hazardous pay to employees
08 p0876 N73-17095
Choice reaction tasks for discriminating individual skill potentials in information handling situations
[AD-752073] 08 p0878 N73-17115
Linear rating scale for selecting tracking task parameters by subjective operator
[AD-752036] 08 p0880 N73-17125
Relation between top managers in Federal agencies and operations research/management science groups
[NASA-CR-130668] 08 p0976 N73-17980
Impact on political and organizational policy and decision making of operations research/management science
[NASA-CR-130667] 08 p0976 N73-17981
Conceptual framework for analysis for aiding policy analyst and policy researcher in empirical investigations into policy phenomena
[NASA-CR-130669] 08 p0976 N73-17982
Reliability of search strategies for information retrieval by aerospace personnel
[AD-751977] 08 p0977 N73-17995
Development of algorithm for multiple hypothesis testing with application to amplitude comparison monopulse radar system in air traffic control operations
[TN-1973-7] 09 p1002 N73-18173
Proceedings of seminar on organization of NASA to show areas of responsibility, resource allocation, and program management
[NASA-CR-131087] 10 p1225 N73-19958
Analysis of NASA programs during post-Apollo period to show organization of field centers, planning activities, operational activities, and resources utilization
[NASA-CR-131931] 12 p1466 N73-21879
Multicriteria tables and relevance tree techniques in decision making and technological forecasting
12 p1467 N73-21889
Motivational patterns underlying devolunteering by submarine graduate school personnel
[AD-749324] 13 p1487 N73-22054
Bayes theorem for optimal decision and stop models of production processes
13 p1497 N73-22132
Optimum utilization of long range forecasts and climatology in making economic decisions
13 p1552 N73-22573
Probabilities models of organizational behavior and human subjective performance
[IZF-1973-3] 14 p1613 N73-23076
Pilot performance in dual time-sharing tracking task
[AD-755363] 14 p1615 N73-23088
Probabilistic model of planetary contamination for deciding spacecraft quarantine standards and procedures
[NASA-CR-132001] 14 p1704 N73-23829
Space station information subsystem for automatic support of manned operations
14 p1711 N73-23887
Simulation of pilot decision making process in manual landing operation during fog
14 p1713 N73-23898
Monte Carlo simulation for man machine task sequencing considering pilot performance degradation
14 p1713 N73-23899
Automation of decision making process in air traffic controllers terminal operations
[FAA-RD-72-63-VOL-3] 15 p1808 N73-24657
Systems engineering as decision making tool using space system as example
15 p1847 N73-24972
Application of program evaluation and review technique for planning and management of air transport operations
[NASA-TT-F-742] 16 p1860 N73-25067
Development of artificial intelligence for onboard decision making capability of unmanned spacecraft during solar system exploration - Vol. 2
[NASA-CR-132257] 16 p1962 N73-25874
Simultaneous equation production functions for decisions pertaining to sea-based tactical air resources
17 p2054 N73-26612
Judge ranking projects for resource allocations
[AD-761392] 19 p2355 N73-28945
Statistical analysis of naval experience in fixed-price incentive contract management for aircraft and missile procurement
[AD-761396] 19 p2355 N73-28946
Decision methodology on static tests of large aircraft vehicles
[NASA-CR-124366] 21 p2604 N73-30866
Multi-criteria resource allocation decision aid
23 p2812 N73-32480
Implications of technology assessment function for effective public decision making process
[NASA-CR-135782] 23 p2866 N73-32914
Utilization of Skylab EREP data in making agriculturally oriented decisions in Mississippi Delta alluvial plain region
[E73-11125] 24 p2916 N73-33280
Utilization of decision and value theory concepts by helicopter pilots to plan attacks
24 p2950 N73-33565
**DECISION THEORY**
NT STATISTICAL DECISION THEORY
Statistical estimation and decision techniques applied to time series and multivariate analyses for communication, tracking, and physiological monitoring
[AD-749542] 05 p0569 N73-14620
Multiple phase shift keying communications for improving carrier tracking efficiency and data detection performance
[NASA-CASE-NPO-13103-1] 11 p1255 N73-20180
Model for analyzing Markovian decision processes with unobservable states and costs
[P-4917] 12 p1419 N73-21495
Markovian decision processes with limited state observability and unobservable costs
[P-4925] 12 p1419 N73-21496
Operational decision model for making conditional weather forecasts for airlift supply task
[AD-755403] 13 p1555 N73-22601
Pilot level decision analysis of thermionic reactor development strategy for nuclear electric propulsion
[NASA-CR-133035] 16 p1943 N73-25725
Decision graphs for information processing
[AD-761877] 19 p2242 N73-28078
**DECODERS**
Computerized simulation of maximum likelihood decoding algorithm
[NASA-TR-R-396] 02 p0141 N73-11141
SAL storage for AN/UPA-59/60 IFF [identification friend or foe] decoders for displaying aircraft targets
[AD-746445] 02 p0208 N73-11685

Design and construction of decoder for processing signals from multiwire proportional chamber
[LA-5073] 12 p1388 N73-21256
Convolutional encoder and decoder for PCM telemetry
[ESRO-CR-165] 22 p2634 N73-31111
Digital decoder for processing Barker coded pulses in incoherent scatter observations of ionosphere
23 p2778 N73-32212

**DECODING**
Development and characteristics of data decoder to process convolution encoded information
[NASA-CASE-NPO-11371] 03 p0269 N73-12177
PCM coding and decoding noting truncated hamming codes and analysis of error rates
[ESRO-TN-112-ESTEC] 05 p0513 N73-14173
Decoding of information in acoustic waveform of human speech using signal processing techniques
14 p1623 N73-23148
Multifold Euclidean geometry codes
[NASA-CR-133529] 20 p2439 N73-29590
High density bipolar encoder and decoder for code transparent digital channels
[FTZ-44-TBR-35] 22 p2633 N73-31103

**DECOMPOSITION**
NT AMMONOLYSIS
NT PHOTODECOMPOSITION
NT PHOTODISSOCIATION
NT PHOTOLYSIS
NT PROPELLANT DECOMPOSITION
NT RADIOLYSIS
Breakup of liquid jet injected normal to supersonic airstream
[AD-747494] 04 p0406 N73-13309
Reaction kinetics when liquid hydrazines adsorbed on supported ruthenium catalyst
[RPE-TR-72/1-PT-5] 05 p0506 N73-14122
Long-term storability and decomposition kinetics of monopropellant formulations containing hydrazine, hydrazine azide, and ammonia
[AD-750900] 06 p0711 N73-15806
Oxidative degradation of polymers and organic compounds via unimolecular decomposition of peroxy radicals
08 p0882 N73-17138
Temperature effects on hydrogen decomposition of wall surface coatings
[NASA-TM-X-2735] 08 p0946 N73-17748
Thermodynamic equilibrium calculations for uranium hexafluoride decomposition at high temperatures
10 p1126 N73-19168
Susceptibility of synthetic engine and transmission lubricants of OH-58 A helicopter to microbal attack
[AD-762176] 19 p2313 N73-28604
Decomposition of compounds adsorbed in charcoal of manned spacecraft breathing system
[NASA-CR-134013] 21 p2504 N73-30092
Decomposition of hydrogen sulfide, in electrical discharge, to elemental sulfur
[BM-RI-7780] 21 p2505 N73-30105
Preparation of lithium oxide, [Li3O2] by decomposition of anhydrous lithium hydroxide
[NASA-TM-X-2888] 21 p2506 N73-30107
Ion mobility, electrical conductance, and decomposition reactions of ammonium nitrate and ammonium perchlorate oxidizers
[AD-762744] 22 p2626 N73-31041
Temperature effects on quantitative biotite and nepheline decomposition by weather
[NASA-TT-F-15135] 23 p2754 N73-32035
High temperature decomposition of propylene in single pulse shock tube to determine products of decomposition and rate of decomposition
[TAE-172] 23 p2754 N73-32036
Acetone decomposition by stainless steel and other metal compounds
[AERE-R-7407] 24 p2892 N73-33088
Acetone decomposition by austenitic stainless steel, iron oxide, and chromium oxide
[AERE-R-7408] 24 p2892 N73-33089
Decomposition of ammonium perchlorate condensate, from electron emission, infrared absorption, and surface structure
[DLR-FB-73-59] 24 p2971 N73-33739

**DECOMPRESSION**
U PRESSURE REDUCTION

**DECOMPRESSION SICKNESS**
Lesions of nervous system and vascular embolisms in decompression sickness
[AD-743330] 01 p0010 N73-10076
Clinical study of 56 cases with neurological symptoms in decompression sickness
[AD-744298] 01 p0011 N73-10086
Correlation of respiratory distress and ultrasonic transmission with severe decompression sickness in hampsters
[AD-743475] 01 p0012 N73-10091
Annotated bibliography with preliminary analysis on dysbaric osteonecrosis
[AD-747258] 04 p0381 N73-13100
Acoustic-optical imaging techniques for detecting bubble formation in circulatory system during decompression
[AD-749087] 04 p0424 N73-13457
Effects of gas bubbles in decompression pathology of humans
[AD-748229] 06 p0631 N73-15126
Pathogenesis of some respiratory and circulatory reactions accompanying drop in barometric pressure
07 p0743 N73-16047
Analysis of mechanisms of human tolerance to lower body decompression
07 p0744 N73-16054
Influence of Pervitin in decreasing gas bubbles in blood during decompression
[DLR-FB-72-66] 09 p0994 N73-18117
Review of decompression and altitude sickness noting effects at safe depths/altitudes
[DRIC-TRANS-3035] 13 p1485 N73-22041
Oxygen breathing in decompression sickness and remedial recompression of human beings
[DRIC-TRANS-3095] 17 p1988 N73-26069
Pure oxygen and oxygen/nitrogen atmospheres for preventing decompression disease in astronauts
20 p2366 N73-29029
Influence of personal characteristics on likelihood of decompression sickness
[NASA-CR-135495] 22 p2621 N73-31002
Hematology of miniature pigs after rapid decompression
[DLR-FB-73-63] 24 p2886 N73-33047

**DECONTAMINATION**
NT SPACECRAFT STERILIZATION
Chemical spray scrubber for cleaning toxic products from rocket exhaust gases
[AD-747023] 02 p0224 N73-11810
Microbial burden estimation for planning planetary quarantine of advanced spacecraft
[NASA-CR-131845] 13 p1485 N73-22039
Contamination control program plan for Apollo ultraviolet spectrometer experiment
[NASA-CR-128575] 16 p1916 N73-25506
Development of chemical process for determining quantity of contamination buried in potting compounds and removable of spores with amine dissolution and plating techniques
[NASA-CR-133645] 21 p2562 N73-30535

**DEEP SPACE**
NT INTERPLANETARY SPACE
NT INTERSTELLAR SPACE

**DEEP SPACE INSTRUMENTATION FACILITY**
Progress in Deep Space Network for November and December 1972
[NASA-CR-130721] 08 p0884 N73-17160

**DEEP SPACE NETWORK**
Directory of principal tracking facilities used by NASA to include Deep Space Network and several radio telescopes - Vol. 1
[NASA-CR-130071] 01 p0036 N73-10279
Telecommunications systems design techniques for deep space network application
[NASA-CR-129108] 02 p0140 N73-11137
Progress in development of Deep Space Network
[NASA-CR-129831] 05 p0523 N73-14258
Progress in Deep Space Network for November and December 1972
[NASA-CR-130721] 08 p0884 N73-17160
Development and characteristics of traveling wave maser amplifier for use in radio astronomy and deep space communication experiments
[REPT-107] 09 p1043 N73-18504
Progress in deep space network - Jan. and Feb. 1973
[NASA-CR-131493] 13 p1490 N73-22081
Tracking and data system support for Pioneer 6, 7, 8, and 9 missions
[NASA-CR-131818] 15 p1831 N73-24838
Progress in DSN flight project support, research and technology, and network engineering
[NASA-CR-133032] 16 p1874 N73-25172
Low phase noise frequency divider for use with deep space network communication system
[NASA-CASE-NPO-11569] 17 p2007 N73-26229
DSN progress in planetary flight support
[NASA-CR-133651] 20 p2473 N73-29867
Deep Space Network tracking support of planetary and interplanetary flight projects - Vol. 17
[NASA-CR-135708] 23 p2757 N73-32064

**DEER**
NT CARIBOUS

**DEFECTS**
NT AUDITORY DEFECTS
NT CRYSTAL DEFECTS
NT CRYSTAL DISLOCATIONS
NT EDGE DISLOCATIONS
NT INCLUSIONS
NT POINT DEFECTS
NT SURFACE DEFECTS
NT VACANCIES [CRYSTAL DEFECTS]
Interstitial impurity diffusion coefficients and crystal lattice defects in cubic alloys
[AD-746949] 02 p0188 N73-11529
Stereoradiography study of depth and geometrical dimensions of internal flaws in weldments
[AD-749459] 04 p0428 N73-13486
Formation of flaws in seam metal during argon-arc pulse welding
10 p1172 N73-19533
Creation of discontinuities in high strength steels to evaluate effects on mechanical properties of welds
[AD-755524] 13 p1535 N73-22437
Effect of internal weld defects on fatigue behavior in mild structural steel butt welded connections
[PB-220896/5] 21 p2554 N73-30475

**DEFENSE COMMUNICATIONS SATELLITE SYSTEM**
Satellite communications and defense
[AD-746165] 02 p0142 N73-11147

**DEFENSE COMMUNICATIONS SYSTEM [DCS]**
Operational performance and transmission measurements on worldwide Defense Communications System network
01 p0027 N73-10208

**DEFENSE INDUSTRY**
Measure, criteria, and procedure for radar track and search allocation
[AD-757172] 14 p1635 N73-23257

**DEFENSE PROGRAM**
Energy requirements of Department of Defense and identification of research and development activities
[AD-754824] 11 p1333 N73-20819
Critique of methods for allocation of resources for defense projects
[AD-753817] 11 p1354 N73-20994

**DEFLAGRATION**
Ignition and deflagration of in nitrocellulose based solid propellants
[AD-756880] 13 p1570 N73-22720
Experimental determination of composite solid propellant deflagration and component processes
[AD-757066] 14 p1701 N73-23800
Analysis of low speed deflagration of initially unmixed reactants under irreversible, two-step chain reaction
[AD-762459] 19 p2353 N73-28930

**DEFLATING**
U INFLATABLE STRUCTURES
U PRESSURE REDUCTION

**DEFLECTION**
Guide for using data on effects of buckling and deflections in beams, struts, and shafts
[ESDU-SS3] 01 p0112 N73-10922
Curves for determining maximum elastic stresses and deflections for initially flat circular plates of uniform thickness under uniform pressure with various edge conditions
[ESDU-65002] 01 p0112 N73-10923
Maximum deflection and stresses for initially flat circular plates under uniform pressure
[ESDU-65003] 01 p0112 N73-10924
Plumb line deflection calculations for European triangulation network using astronomical observations
[MITT-122] 05 p0538 N73-14377
Instruments for recording force deflection from Charpy impact tests on metals
[REPT-527] 13 p1585 N73-22852
Laser beam divergence and measurement of nanosecond laser pulses
[AD-764702] 23 p2802 N73-32407

**DEFLECTORS**
NT BLAST DEFLECTORS
Cooling efficiency of air discharge on nozzle blades with deflectors
[AD-749654] 05 p0591 N73-14803
Scale model evaluation of fiber glass wedge and parabolic deflector efficiencies in cylindrical ballistic ranges using pressure transducer measurements
[DREV-TN-2031/72] 06 p0649 N73-15270
Holographic memory system using argon ion lasers and acoustooptic beam deflectors
[NASA-CR-124084] 09 p1064 N73-18680
Aerodynamic noise of STOL engine-over-wing configuration using nozzle deflector
[NASA-TM-X-2871] 19 p2219 N73-27897

**DEFOCUSING**
Optical performance evaluation of infrared transmitting materials
[AD-756825] 14 p1673 N73-23576
Radial collapse of dense plasma spindle focus in z-pinch geometry
[LA-5178-MS] 22 p2704 N73-31656

**DEFORMATION**
NT AXIAL STRAIN
NT ELASTIC BENDING
NT ELASTIC BUCKLING
NT ELASTIC DEFORMATION
NT PLASTIC DEFORMATION
NT STATIC DEFORMATION
NT TENSILE DEFORMATION
Effects of axially symmetric deformation of metal on mechanical and physical properties of samples
[AD-745551] 01 p0063 N73-10513
Analysis of sensitivity of elevated temperature deformation of nickel alloy to grain size and shape under tension and creep conditions
[NASA-CR-128403] 01 p0067 N73-10549
Macroscopic models of quasi-chemical reactions, dielectric relaxation, and deformation energy
01 p0087 N73-10719
Numerical analysis of stress field in semi-infinite elastic-plastic medium under generalized plane deformation
[AD-746046] 01 p0115 N73-10951

Influence of inlet deformation on characteristics of ejector jet devices operating on incompressible fluids
[AD-747079] 02 p0179 N73-11454
Stress state and deformation characteristics of hardening carbon steel with decreasing temperatures
[AD-746723] 02 p0188 N73-11527
Analysis of stress formation and changes in physical properties of pipes during rotary swaging using explosion or pulsed magnetic field energy
[AD-747454] 03 p0308 N73-12516
Refined theory on deformation effects in anisotropic shells
[AD-747609] 03 p0362 N73-12949
Determination of temperature and residual stresses and deformations caused by welding process
[AD-749529] 04 p0428 N73-13487
Elastoplastic stress concentration and deformations in perforated plates
[ONERA-NT-193] 04 p0482 N73-13936
Application of finite element method to determine deformation of elastic plates, shells, and membranes
[AD-749565] 04 p0483 N73-13946
Stress deformation in anisotropic elastic thin walled shells
[AD-749955] 05 p0604 N73-14911
Crustal deformation propagation in Alaska
[AD-750468] 06 p0671 N73-15461
Correction of axisymmetric deformations in space telescope mirrors by thermally induced elastic strains
[NASA-TM-X-2673] 06 p0672 N73-15472
Effects of interstitial solute content on deformation kinetics in hot extrusion of titanium aluminum vanadium alloy
[AD-750556] 06 p0677 N73-15511
Procedures for determining shell stability under various types of dynamic loads
07 p0852 N73-16906
Effect of oxygen concentration on deformation of Ti-V alloys and on critical resolved shear stress of Ti-40V
[AD-752082] 08 p0933 N73-17642
High temperature deformation of polycrystalline halide microstructures by infrared lasers
[AD-751655] 08 p0944 N73-17730
Effect of degree of saturation on susceptibility to onset of plastic instability in pure shear for solid solution of copper-zinc system
[COO-2048-6-PT-2] 08 p0967 N73-17901
Effects of preliminary deformation on superplasticity and other properties of metals and alloys
[JPRS-58097] 09 p1046 N73-18529
Influence of preliminary deformation on superplasticity of alpha brasses and pure copper
09 p1047 N73-18534
Elastoplastic bending of cracked plates including effects of crack closure
[NASA-CR-112268] 09 p1092 N73-18915
Sheba triangular thin shell element application to calculation of coding towers, toruses, and roofs
[ISD-127] 09 p1095 N73-18936
Reports on electrical and mechanical properties of beryllium, chromium-manganese austenitic steels, and martensitic conversion during deformation
[JPRS-58357] 10 p1171 N73-19524
Interrelation of martensitic conversion during deformation and structural properties of trip steel
10 p1171 N73-19527
Deformation processes in forging refractory ceramic oxides
[NASA-CR-131109] 10 p1175 N73-19558
Numerical analysis of displacement of cylindrical shell subjected to cylindrical wave in acoustic medium
10 p1219 N73-19918
Numerical analysis of finite deformation of elastoplastic solids
[NASA-CR-2199] 10 p1220 N73-19924
Elastoplastic deformation of slender rod subjected to impact loads
[AD-754241] 10 p1221 N73-19935
Deformation of gamma and epsilon phases in intermetallic compounds by extrusion method
[AD-754523] 11 p1307 N73-20605
Seminumerical analysis of three dimensional elastic properties of finite geometry solids with traction-free cracks
[NASA-TN-D-7213] 11 p1345 N73-20917
Stress analysis of elastoplastic state of thin circular plate subjected to axisymmetric loading
[AD-753983] 11 p1346 N73-20920
Deformation mechanism diagrams and creep of tungsten lamp filaments
[AD-755230] 12 p1441 N73-21680
Vibration analysis of shallow spherical sandwich shells based on effects of thickness-shear deformation and rotary inertia
12 p1462 N73-21843
Effect of deformation performed during heat treatment on structure and mechanical properties of EI437B alloy
13 p1541 N73-22485
Effect of transverse shear deformation on large amplitude free vibrations of plates and cylindrical panels
13 p1584 N73-22845
Analysis of large deflections of rectangular plates with nonlinear elasticity and hollow shells with hinge-supported edges under external normal pressure uniformly distributed over surface
[AD-756103] 13 p1587 N73-22870
User manual for finite element program for analysis of deformations of thin elastic membranes
[AD-755953] 13 p1588 N73-22874
Variational principle for finite deformations of quasi-shallow shells
[AD-756187] 13 p1589 N73-22886
Determination of temperature distributions and deformations of rectangular plates with circular elastic inclusions
[AD-756183] 14 p1717 N73-23930
Numerical analysis of effects of heating unidimensional plate under nonlinear boundary conditions
[NLL-M-21618-[5828.4F]] 15 p1764 N73-24290
Finite deformation of annealed metals including loading and unloading constitutive and second order transitions
[AD-758261] 15 p1799 N73-24586
Deformation properties of hot worked Type 304 austenitic stainless steel, Mangalloy, and other steel alloys
[AD-758912] 15 p1800 N73-24592
Analysis of general buckling of pressurized stiffened cylinder under axial load
[ARC-R/M-3198] 16 p1857 N73-25040
Coherent optical correlation techniques for detection of microstructural surface alterations during cyclic stressing
16 p1923 N73-25558
Compression tests of pure Ti and Ti alloy deformation properties
[RAE-LIB-TRANS-1657] 17 p2043 N73-26529
Development of electrical circuitry for analysis of stress deformation state of delta wing model based on discrete design diagram
[AD-760948] 18 p2108 N73-27044
Effect of high speed volumetric deformation on ductility of metals and alloys
[AD-762246] 19 p2310 N73-28582
Development of doubly curved triangular finite element for use in small deformation analysis of thin shells containing cutouts and irregular boundaries
[RE-453] 19 p2347 N73-28882
Response of thick rectangular plate of incompressible, isotropic elastic material to tensile forces applied to opposite faces
[AD-761941] 19 p2350 N73-28903
Deformation of dry steel surfaces during high velocity sliding contact
20 p2427 N73-29496
Development of method for analyzing stress deformation state of metal during process of lengthwise rolling of tubes
[NLL-M-21655-[5828.4F]] 20 p2428 N73-29501
Analysis of effects of plastic deformation on internal structure of austenitic steels as shown by anomalies in tensile stress-strain curves
[NLL-M-23029-[5828.4F]] 20 p2428 N73-29504
Analysis of fracture and creep properties of metals after extension under conditions of hydrostatic pressure as function of time
[NLL-NEL-TT-2475-[6075.461]]
20 p2429 N73-29515
Effect of high hydrostatic pressure on flow stress of 18-8 stainless steel
[NLL-NEL-TT-2458-[6075.461]]
20 p2430 N73-29516
Development of computer method for solving axisymmetric variational problems of theory of treatment of metals by pressure
[NLL-M-21659-[5828.4F]] 20 p2430 N73-29517
Compressive strength and deformation properties of unidirectionally carbon fiber reinforced plastic under uniaxial compression
20 p2434 N73-29550
Development of numerical procedures for buckling analysis of truncated conical shells with rigid edge constraint using load displacement criterion
20 p2477 N73-29894
Analysis of effects of hydrostatic pressure on yield stress, flow stress, and ductility of metals
[NLL-NEL-TT-2488-[6075.461]]
20 p2478 N73-29904
Derivation of finite element properties in terms of stress functions for structural and nonstructural applications
[AD-762947] 20 p2484 N73-29953
Deformation and aging characteristics of titanium alloys
[AD-763429] 21 p2561 N73-30526
Analysis of state of mechanically heterogeneous material during deformation using optically sensitive coatings
[NLL-M-21653-[5828.4F]] 21 p2602 N73-30856
Computer program for analysis of nonlinear deformation and fatigue response of components subjected to complex load histories
[AD-763780] 21 p2604 N73-30870
Numerical analysis of buckling characteristics of ring-stiffened, oval, orthotropic, cylindrical shells
[AD-763369] 21 p2604 N73-30872
Linear and nonlinear theory of elasticity used to determine deformation of cylinder and piston of high strength steel under influence of high pressure
[AD-763971] 22 p2687 N73-31519
Creep tests of fine-grained polycrystalline ice under uniaxial and multiaxial stress conditions to predict time-dependent deformational behavior
22 p2723 N73-31791
Experimental and theoretical model of deformation and densification of sintered powder metallurgy compacts
24 p2933 N73-33422

**DEFORMETERS**
Development of strain gage mounting assembly for amplifying measurable deformation applied to strain gage
[NASA-CASE-NPO-13170-1] 19 p2300 N73-28495

**DEGASSING**
NT DEOXYGENATION
Effect of charge materials, melting condition, and type of melting equipment on hydrogen gas contained in copper alloys
[AD-745845] 01 p0068 N73-10558
Hole area for evacuating and degassing of far ultraviolet sounding rocket photometer
[MPI-PAE/EXTRATERR-68] 02 p0174 N73-11411

**DEGRADATION**
NT THERMAL DEGRADATION
NT WAVE DEGRADATION
High amplitude gamma current pulse degradation of semiconductor devices
[SC-RR-72-0515] 04 p0399 N73-13245
Degradation of ultraviolet photometry systems on Nimbus 3 and 4 satellites
[NASA-TM-X-66148] 06 p0721 N73-15883
Nonsporicidal methods for solvent degradation of cured RTV 41 silicon potting compound and chemical curing effects on decontamination properties
[NASA-CR-130720] 08 p0878 N73-17111

**DEGREES OF FREEDOM**
Theoretical relationships among displacement, velocity, acceleration, and cue duration for single degree of freedom flight simulator system during sharp onset acceleration profile
[AD-752222] 08 p0893 N73-17230
Calculation of effect of short-term impulse loads on structures with finite and infinite numbers of degrees of freedom
[AD-756959] 13 p1587 N73-22868
Derivation of differential equations of motion to analyze characteristics of three degree of freedom bodies joined by elastic tether
[NASA-CR-124259] 15 p1839 N73-24903
Numerical analysis of dynamics of constant speed rotor with three dimensional rotary inertia using eight degree of freedom model with coupled linear and angular motion
22 p2676 N73-31437

**DEHYDRATED FOOD**
Cosmonaut adaptation to dehydrated food products and effects on human waste cycle
10 p1118 N73-19113

**DEHYDROGENATION**
Vapor phase heteroepitaxial growth of silicon germanium alloys by hydrogen reduction of tetrachlorides
20 p2460 N73-29767
Mossbauer spectra of ferrite catalysts used in oxidative dehydrogenation
[NASA-CR-133740] 21 p2506 N73-30108

**DEICING**
Heating device to prevent icing for windmill type anemometers
[NLL-M-29974-[5828.4F]] 16 p1936 N73-25665

**DEIONIZATION**
Ion recombination loss in high intensity radiation dosimetry
[REPT-736] 17 p2064 N73-26698
Tantalum surface bounding of helium discharge plasma considering resonant ion neutralization
[AD-753520] 22 p2706 N73-31670

**DEKATRONS**
U COUNTERS

**DELAMINATING**
Crack blunting through fiber matrix debonding in Borsic-aluminum composites
[SC-DC-71-4467] 04 p0438 N73-13568

**DELAWARE**
NT DELAWARE RIVER BASIN [US]
Near real time water resources data from Delaware Bay for use in river basin management
[E72-10239] 03 p0288 N73-12339
Identification and mapping of coastal vegetation species in ERTS-1 imagery of Delaware
[E73-10007] 06 p0658 N73-15343
Application of multispectral data processing to Delaware coastal wetlands vegetation mapping
[E73-10069] 07 p0779 N73-16331
Utilization of ERTS-1 imagery for water resources management in Delaware River Basin
07 p0787 N73-16404
Pollution hazards from petroleum industries and shipping in Delaware Bay
07 p0857 N73-16948

Mapping northern Atlantic coastal marshlands of Maryland, Delaware, and Virginia using ERTS-1 imagery
[E73-10363] 10 p1150 N73-19359
Identification of marsh vegetation and coastal land use in Delaware from ERTS-1 imagery
[E73-10367] 10 p1150 N73-19363
Study of suspended sediment and aquatic fronts in Delaware Bay using ERTS-1 imagery
[E73-10368] 10 p1150 N73-19364
Application of ecological, geological, and oceanographic ERTS-1 imagery to coastal resources management and planning in Delaware
[E73-10426] 11 p1280 N73-20387
ERTS-1 relayed water resources data collected from Delaware River Basin
[E73-10451] 12 p1394 N73-21299
ERTS-1 imagery of suspended matter and hydrologic interfaces in Delaware Bay
[E73-10515] 14 p1653 N73-23409
Identification of marshland vegetation and coastal land use in Delaware from ERTS-1 imagery
[E73-10516] 14 p1653 N73-23410
Application of ecological, geological, and oceanographic ERTS-1 imagery to Delaware coastal resources management and planning
[E73-10631] 15 p1776 N73-24391
Aerial photography and multispectral analysis for mapping of Delaware coastal marshes
16 p1905 N73-25414
State of Delaware and New York City using space age management for social problems
[NASA-TM-X-66296] 18 p2213 N73-27873
Analysis of coastal vegetation species in Delaware Bay, Delaware based on ERTS-1 imagery and high altitude photography
[PAPER-E8] 19 p2269 N73-28272
Application of ERTS-1 imagery to analysis of suspended sediments and aquatic fronts in Delaware Bay
[PAPER-M3] 19 p2280 N73-28343
Digital data processing of ERTS-1 MSS imagery of water masses in Delaware Bay
19 p2286 N73-28380
Application of ecological, geological, and oceanographic ERTS-1 imagery to Delaware coastal recources management and planning
[E73-10934] 21 p2529 N73-30276
Mapping coastal vegetation and wetlands use for Delaware from ERTS-1 imagery
[E73-11146] 24 p2918 N73-33300
ERTS-1 monitoring of turbidity, color, boundaries, circulation, and pollution dispersion in Delaware coastal waters
[E73-11147] 24 p2918 N73-33301
Identification of suspended sediment, current circulation, water mass boundaries, and waste disposal plumes in Delaware Bay using ERTS-1 imagery
[E73-11164] 24 p2920 N73-33317

**DELAWARE RIVER BASIN [US]**
Analysis of ERTS-1 data pertaining to Delaware River Basin observations to determine performance of data collection system
[PAPER-W10] 19 p2271 N73-28287

**DELAY**
Synopsis of factors contributing to airport congestion and flight delays
[REPT-73-00315] 13 p1505 N73-22200
High strength steel delayed failure analysis including hydrogen embrittlement
[NLR-TR-72113-U] 14 p1715 N73-23917

**DELAY CIRCUITS**
Development of delay cable to display simultaneous signals in nanosecond region in single trace on oscilloscope
[IPPJ-T-9] 04 p0395 N73-13212
Design of multiwire proportional chamber systems using electromagnetic delay lines for cosmic ray experiments
[RM-569] 09 p1011 N73-18251

**DELAY LINES**
NT ACOUSTIC DELAY LINES
Development of delay cable to display simultaneous signals in nanosecond region in single trace on oscilloscope
[IPPJ-T-9] 04 p0395 N73-13212
Waveguiding in thin silver strip vacuum deposited on bismuth germanium oxide
[AD-750612] 06 p0648 N73-15262
Development of acoustic surface wave, multiple-tap, delay line structure using sputtered zinc oxide piezoelectric films on metal interdigital arrays on silicon surface
[AD-753674] 09 p1009 N73-18238
S band magnetoelastic transmission-type delay line design using YIG birefringent device
[REPT-8.445] 12 p1384 N73-21220
Dispersive delay lines, bandpass filters, and lines with delay above 30 microseconds utilizing Rayleigh surface waves at VHF/UHF frequencies
[REPT-4.427] 12 p1384 N73-21223
Magnetoelastic transmission delay lines for S band noting insertion loss reduction
[REPT-8.425] 13 p1491 N73-22087
Accuracy estimates for syntheses of filters by optimizing mutual uncertainty function in minimax criterion
17 p1997 N73-26151

**DELTA ANTENNAS**
Boundary value solution for current distribution on infinite tubular antenna in cold collisionless plasma
[NASA-CR-130297] 06 p0640 N73-15194
Gain pattern measurements for delta antenna and log periodic antenna configurations
[AD-757619] 14 p1633 N73-23239

**DELTA DAGGER AIRCRAFT**
U F-102 AIRCRAFT

**DELTA DART AIRCRAFT**
U F-106 AIRCRAFT

**DELTA LAUNCH VEHICLE**
Mission flight performance, and data acquisition of data-90 launch vehicle and InterPlanetary Monitoring Platform-H
[NASA-TM-X-68929] 05 p0595 N73-14836
Configuration data and design development for Delta 2914 launched Tracking and Data Relay Satellite system - Vol. 2
[NASA-CR-130220] 13 p1579 N73-22800
Delta vehicle configuration changes and performance increases considering cost effectiveness
18 p2208 N73-27818
Performance of computerized inertial guidance system for Delta launch vehicle
18 p2208 N73-27819
Test objectives and mission planning for extended long tank Delta Launch Vehicle
[NASA-CR-133644] 20 p2475 N73-29886
Model 2914 series Delta launch vehicle configuration
[NASA-TM-X-70455] 21 p2599 N73-30833
Wind tunnel test program to investigate subsonic through high supersonic aerodynamic characteristics of Lockheed delta lifting orbiter and stage-and-one-half launch vehicle
[NASA-CR-124419] 23 p2849 N73-32770

**DELTA MODULATION**
Numerical control of delta modulated vocal signals in air navigation telecommunication system
01 p0025 N73-10194
Source encoding using delta modulation
[NASA-CR-131228] 10 p1127 N73-19185
Design and implementation of adaptive delta modulator with integrated circuit hardware for encoding of speech signals
14 p1621 N73-23132
Voicing adaptive speech digitization technique with delta modulation for effective operation at 9600 bits/second
14 p1621 N73-23133
Computer simulation to demonstrate feasibility of delta modulation as method for encoding control signals of voiced speech synthesizer
14 p1632 N73-23231

**DELTA WINGS**
Force measurements on caret and delta wings at high incidence in hypersonic reentry conditions noting comparison with theoretical predictions
[IC-AERO-72-16] 01 p0001 N73-10004
Computation of steady conical flow past a yawed slender delta wing with leading edge separation using vortex sheet model and Newton-Raphson iteration
[IC-AERO-72-17] 01 p0001 N73-10005
Cross flexure sting designed for measuring dynamic stability of slender bodies of revolution with delta wings in supersonic wind tunnel tests
[FFA-AU-637] 01 p0035 N73-10278
Wind tunnel static stability and control data for delta wing booster of scale model of space shuttle
[NASA-CR-119994-VOL-3] 01 p0107 N73-10886
Analysis of surface flow, pressures, and heat transfer on two conical delta wings at hypersonic speed and various angles of attack
[NASA-TM-X-2668] 02 p0156 N73-11268
Surface pressure measurements over model delta wing undergoing oscillatory deformation in low speed wind tunnel
[ARC-R/M-3693] 03 p0248 N73-12005
Heat transfer and surface pressure measurements at supersonic speeds on conical delta wings with sharp leading edges
[ARC-CP-1212] 05 p0492 N73-14008
Prediction of pressure gradient on delta wing between uniform and nonuniform supersonic inviscid flow
[ARC-CP-1228] 05 p0492 N73-14010
Wave drag reduction on delta wings at zero lift as function of displacement of maximum thickness in spanwise direction
[DLR-FB-71-61] 06 p0621 N73-15044
Analysis of natural vibration characteristics of plate-beam combination structures during supersonic flight
[NAL-TR-291] 06 p0725 N73-15917
Angles of attack for shock wave detachment from sharp leading edge of five delta wing models with flat compression surfaces
[AD-752206] 08 p0898 N73-17271
Vortex sheet and increased lift caused by blowing from leading edges of slender delta wing
[ARC-R/M-3692] 09 p0981 N73-18016
Method of characteristics solution of flow field on lee side of flat plate delta wing with supersonic leading edges
[AD-753389] 09 p1019 N73-18319
Numerical calculation of flow fields produced by lifting elliptic cone, lifting three dimensional wing, and lifting delta wings
[NASA-CR-131089] 10 p1139 N73-19282
Methods for determining inviscid three dimensional flow about smooth shapes at supersonic speeds
[AD-753695] 10 p1143 N73-19311
Wind tunnel tests to determine oscillatory longitudinal derivatives of thin delta wing with 0.8 aspect ratio over range of incidences
[ATN-7105] 13 p1470 N73-21903
ALGOL procedures for calculating velocity and pressure distribution on rectangular and triangular planforms oscillating harmonically in supersonic flow - Part 1
[FOK-X-449-PT-1] 13 p1471 N73-21909
ALGOL procedures for calculating velocity and pressure distribution on rectangular and triangular planforms oscillating harmonically in supersonic flow - Part 2
[FOK-X-449-PT-2] 13 p1471 N73-21910
Heat transfer tests for simple delta wings at Mach numbers 8 and 10.5
[NASA-CR-131485] 13 p1591 N73-22900
Visualization and integral methods for studying three-dimensional supersonic flow separation on delta wing
14 p1600 N73-22970
Analysis of minimum longitudinal stability for large delta wing transport aircraft during landing approach and touchdown using inflight simulator
[TR-5084-F-1-VOL-1] 14 p1601 N73-22984
Development of slender body theory for analyzing flow past thin, conically cambered, delta wing with exact boundary conditions
[ARC-R/M-3249] 15 p1726 N73-24002
Analysis of flow development over plane, half-wing with cropped-delta planform using surface pressure distributions and oil flow patterns with variations in incidence and Mach number
[ARC-R/M-3286] 15 p1727 N73-24008
Effect of jet stream blowing downwards from lower surface of slender delta wing to obtain lift augmentation for takeoff and landing
[ARC-R/M-3288] 15 p1727 N73-24009
Flight tests of 45 degree delta cropped wing to determine dynamic lateral stability characteristics
[ARC-R/M-3243] 15 p1729 N73-24027
Wind tunnel measurements of direct pitching damping and stiffness derivatives for delta wing and swept wing planforms
[ARC-R/M-3419] 16 p1853 N73-25009
Development of numerical procedures for determining velocity potential on triangular wing oscillating harmonically in supersonic flow
[ARC-R/M-3229] 16 p1854 N73-25023
Analysis of effect of localized mass on flutter characteristics of delta wing for various spanwise and chordwise positions for the mass center of gravity
[ARC-R/M-3264] 16 p1855 N73-25030
Resonance tests of delta wing aircraft model to determine effect of stiffness changes of wing spars on frequencies and modes of vibration
[ARC-R/M-3268] 16 p1856 N73-25031
Aerodynamic characteristics of slender delta wings to show performance under various conditions of airspeed, angle of attack, and ground effect
[NASA-TT-F-14949] 17 p1983 N73-26031
Low subsonic aerodynamic characteristics of 60 deg swept delta wing space shuttle orbiter
[NASA-TM-X-2762] 17 p2087 N73-26880
Aerodynamic characteristics of two space shuttle concepts with delta wing configurations at hypersonic speed using helium flow visualization technique
[NASA-TN-D-7282] 18 p2102 N73-26997
Analysis of minimum longitudinal stability for large delta wing transport aircraft during landing approach and touchdown using in-flight simulation techniques
[AD-761120] 18 p2106 N73-27036
Development of electrical circuitry for analysis of stress deformation state of delta wing model based on discrete design diagram
[AD-760948] 18 p2108 N73-27044
Experimental determination of bound vortex lines and flow in vicinity of trailing edge of slender delta wing
[NASA-TT-F-15012] 18 p2131 N73-27217
Pressure fields over hypersonic wing-body configuration at moderate incidence
[AD-763762] 21 p2526 N73-30256
Wind tunnel tests to determine flow characteristics around sharp-edged slender delta wing at large angles of attack
[NASA-TT-F-15107] 22 p2611 N73-30928
Characteristics of low speed air flow over slender, sharp edged delta wing at various angles of attack and effects on longitudinal and lateral stability
24 p2869 N73-32922

On the effects of viscous interaction for a flat delta wing at incidence
[ARC-CP-1237] 24 p2870 N73-32931
Transonic wind tunnel tests to determine effects on flutter of aerodynamic interference between pairs of closely spaced delta wings
[NASA-CR-2331] 24 p2989 N73-33887

**DELTAIC COASTAL PLAINS**
U COASTAL PLAINS

**DELTAS**
NT MISSISSIPPI DELTA [LA]
ERTS-1 observations of plant growth and annual flooding in Inland Delta of Niger River in Mali
[E73-10436] 11 p1281 N73-20396
Numerical model of circulation processes of fjord estuary
[AD-755233] 14 p1664 N73-23506
Analysis of interactions between marine water and freshwater at river mouth for understanding dissemination of sediment
[AD-755158] 14 p1664 N73-23507

**DEMAGNETIZATION**
Magnetooptical measurements of demagnetizing fields in cylindrical magnetic films
[JPRS-59624] 19 p2321 N73-28670
Uses of cluster materials and related types in antiferromagnetic cooling by adiabatic magnetization and demagnetization of antiferromagnets
[AD-764620] 23 p2826 N73-32592

**DEMAND [ECONOMICS]**
Demand factors in air transportation marketing
23 p2861 N73-32863
World air passenger traffic demand
23 p2862 N73-32868

**DEMODULATION**
Acoustic demodulation of predistorted pulsed carriers
[AD-752237] 08 p0945 N73-17738
Interpolative estimation for error reduction during video signal demodulation in noise environment
[NASA-CR-131873] 13 p1490 N73-22080
Robust detection schemes for time varying signals in additive noise
23 p2756 N73-32051

**DEMODULATORS**
NT FREQUENCY COMPRESSION DEMODULATORS
NT MODEMS
NT PHASE DEMODULATORS
NT PHASE LOCK DEMODULATORS
Modulator/demodulator for probing and analyzing forward scatter path at 15 GHz to clear air turbulence
[AD-753090] 09 p1030 N73-18413
Signal to noise ratio of frequency locked loop FM demodulator
16 p1874 N73-25168

**DEMONSTRATION**
U PROVING

**DENDRITIC DRAINAGE**
U DRAINAGE PATTERNS

**DENITROGENATION**
Pure oxygen and oxygen/nitrogen atmospheres for preventing decompression disease in astronauts
20 p2366 N73-29029

**DENMARK**
Papers on research conducted at Riso in nuclear physics
[RISO-256] 03 p0367 N73-12993
Climatological summaries for Denmark and Faroe Islands for 1967
[ISBN-87-7478-060-3] 08 p0937 N73-17675
Oceanographical observations from Danish light vessels and coastal stations - 1972
[ISBN-87-7478-080-6] 20 p2412 N73-29386
Rude Skov Geophysical Observatory magnetic results, 1969
[ISBN-37-7478-065-4] 20 p2412 N73-29388
Yearbook of meteorological parameters measured for Denmark and Faroe Islands - 1968
20 p2449 N73-29683

**DENSE PLASMAS**
Soft X ray level inversions in dense aluminum plasma produced by laser bombardment
[CONF-720404-VOL.4] 19 p2322 N73-28684
X ray emission from dense plasma focus device
[AD-761800] 19 p2325 N73-28703

**DENSIFICATION**
Strip transmission line circulators using ferrites, noting new densification method for polycrystalline ferrimagnetic materials
[REPT-8.422] 12 p1384 N73-21222

**DENSITOMETERS**
NT MICRODENSITOMETERS
Analysis of diffusive separation in front of blunt body in low density binary mixture of supersonic flows using electron beam densitometer
[AD-743960] 02 p0157 N73-11274
Automatic raster scanning microdensitometer measurement of luminosity profiles and density of lenticular galaxies in Virgo Cluster
16 p1961 N73-25859
Photographic equidensitometry of two phase and low density flows
[DLR-MITT-73-02] 17 p2015 N73-26293
Development of transmissometer for measuring optical transmission through aircraft jet engine exhausts
[AD-760050] 17 p2035 N73-26467
Use of computer-controlled two-dimensional film densitometer for analysis of photographs of chemical releases at high altitudes
[AD-763082] 20 p2413 N73-29398
Ultrasonic bone densitometer for measuring calcium content of bone structures
[NASA-CASE-MFS-20994-1] 21 p2504 N73-30090

**DENSITY**
Distribution and density of phreatophytes and other arid land plants measured from ERTS-1 imagery
[E73-10094] 08 p0902 N73-17306

**DENSITY [MASS/VOLUME]**
NT ATMOSPHERIC DENSITY
NT GAS DENSITY
High temperature density determinations of Li, using gamma radiation attenuation technique
[ORO-3604-7] 03 p0263 N73-12134
Three-dimensional, two-constituent model for composition characteristics, temperature and mass density of magnetic storm
[NASA-TM-X-66112] 03 p0294 N73-12394
Lunar surface layer density from radar measurements by satellites and automatic stations
[D-17] 06 p0639 N73-15185
Classification of meteoroids according to density and beginning height, and meteor stream search
[NASA-CR-131177] 11 p1337 N73-20851
Classification of meteoroids according to density and beginning height
[CONTRIB-14] 11 p1337 N73-20852
Density and temperature profiles of HI lines in interstellar dust clouds
12 p1448 N73-21723
Effect of hydraulic fluid density on system performance
[NLL-NEL-TT-2427-[6075.461]]
15 p1763 N73-24287
Density analysis of quartz grains to determine rock damage from small charge blasting in granite
[BM-RI-7751] 18 p2144 N73-27327
Influence of atmospheric pressure and temperature on viscosity and density of mineral oil and siloxane liquids
[AD-761590] 19 p2232 N73-27999
Dielectric constant and loss tangent of Eccofoam PT at various packing densities
[NASA-CR-133550] 19 p2312 N73-28594
Solar type 3 radio burst position measurements for coronal density determination
19 p2338 N73-28812
Bar shaped density wave theory of barred spiral galaxies
19 p2341 N73-28835
Calculation of density of states in amorphous covalently bonded semiconductors
[AD-763496] 21 p2587 N73-30728

**DENSITY [NUMBER/VOLUME]**
NT ELECTRON DENSITY [CONCENTRATION]
NT ELECTRON DENSITY PROFILES
NT ELECTRON DISTRIBUTION
NT ION DENSITY [CONCENTRATION]
NT IONOSPHERIC ELECTRON DENSITY
NT IONOSPHERIC ION DENSITY
NT MAGNETOSPHERIC ELECTRON DENSITY
NT MAGNETOSPHERIC PROTON DENSITY
NT METEOROID CONCENTRATION
NT PACKING DENSITY
NT PARTICLE DENSITY [CONCENTRATION]
NT PLASMA DENSITY
NT PROTON DENSITY [CONCENTRATION]
Mass spectrometer and ion source for flight experiment measurements of thermosphere number density
08 p0899 N73-17283
Density profiles of supersonic jet target of hydrogen-deuterium in vacuum
[LA-UR-73-231] 17 p2010 N73-26260

**DENSITY [RATE/AREA]**
U FLUX DENSITY

**DENSITY DISTRIBUTION**
Computation of lunar gravitational field expansion coefficients utilizing Cassini equator inclination and radial lunar density distribution values
[NASA-TT-F-14605] 01 p0104 N73-10858
Rocket measurements of ozone distribution under varying latitudes and seasonal conditions in stratosphere
[NASA-TM-X-66192] 09 p1028 N73-18391
Critical exponents for charged and neutral Bose gases above Lambda points
[AD-756022] 12 p1430 N73-21587
Cloud chamber study of cosmic ray air shower multicore structure
15 p1827 N73-24810
Measurement of density distribution and patterns of stowing mixture in hydraulic installations by radiometric scanning
[ITJ-35] 21 p2549 N73-30436
Transition model for computing population density profiles of partially ionized argon in source flow expansion
[C-37] 22 p2652 N73-31242

**DENSITY MEASUREMENT**
NT X RAY DENSITY MEASUREMENT
Analysis of density of water in forms of ice, water and steam, liquid and gaseous heavy water, and sea water
[ESDU-68010-AMEND-A] 01 p0038 N73-10302
Phase difference between temperature and density in thermosphere
[NASA-TM-X-66119] 03 p0294 N73-12395
Photographic film density and density distribution measurements, and mean square deviation of density and energy spectrum
[NASA-TT-F-14614] 04 p0420 N73-13427
Effects of density measurement electron beam impinging on blunt body in transition flow, noting influence of secondary electrons
[DLR-FB-73-08] 09 p0981 N73-18017
Automatic raster scanning microdensitometer measurement of luminosity profiles and density of lenticular galaxies in Virgo Cluster
16 p1961 N73-25859
Process of density change in epoxy bonding agents throughout curing process
[RAE-LIB-TRANS-1686] 17 p2049 N73-26576
Method for determining density of impacting particles by using Hugoniot curves
[NASA-CASE-LAR-11059-1] 17 p2082 N73-26838
Measurement of density distribution and patterns of stowing mixture in hydraulic installations by radiometric scanning
[ITJ-35] 21 p2549 N73-30436

**DENTISTRY**
Unified approach to biomechanics of dental implantology
10 p1227 N73-19977

**DEOXIDIZING**
Physical and chemical properties of steel surfaces exposed to deoxidation products
[AD-747828] 04 p0435 N73-13547

**DEOXYGENATION**
Effect of hypoxia and hyperoxia on rate of blood deoxygenation, and influence of antioxidants in mice
11 p1244 N73-20096

**DEOXYRIBONUCLEIC ACID**
Transverse acceleration effects on dioxyribonucleic acid catabolism in rat spleen and liver
03 p0257 N73-12080

**DEPENDENCE**
NT SPATIAL DEPENDENCIES
NT TIME DEPENDENCE

**DEPENDENT VARIABLES**
Input signal dynamics for analyzing gain stability and linearity of electronic circuit working with large signals
[INR-1371] 04 p0398 N73-13240

**DEPLOYMENT**
Computerized simulation of longitudinal cable shapes during deployment from missile away from flying aircraft
[AD-753907] 10 p1135 N73-19254

**DEPOLARIZATION**
Gaussian curve simulation of multiple-dipole model of ventricular depolarization
[TH-71-E-25] 03 p0261 N73-12116
Graphite oxide and fluorides as depolarizers in lithium organic electrolytic cells
[AD-755159] 13 p1477 N73-21968
Hydrogen depolarized cell for removing CO2 in spacecraft life support systems
[NASA-CR-131868] 13 p1486 N73-22047
Nonspherical raindrop depolarization of electromagnetic wave in ultrahigh frequency radio link
17 p1994 N73-26123
Rain depolarization of linearly and circularly polarized microwaves
17 p1995 N73-26127
Television broadcasting wave depolarization measurement for multiple utilization of assigned frequencies
[FTZ-A-455-TBR-36] 22 p2633 N73-31101
Measurements of Rayleigh scattering and depolarization ratio for atoms in gaseous state
[NASA-TN-D-7442] 23 p2819 N73-32539
Propagation path depolarization caused by precipitation
[NASA-CR-132818] 24 p2895 N73-33107

**DEPOLARIZERS**
U DEPOLARIZATION

**DEPOSITION**
NT ANODIZING
NT ELECTRODEPOSITION
NT ELECTROPLATING
NT VACUUM DEPOSITION
NT VAPOR DEPOSITION
Nickel zinc ferrite powders deposited on ceramic substrates by arc plasma spraying
[AD-747771] 03 p0307 N73-12509
Pyrolytic carbon deposition in steady state fluidized beds
[AD-748223] 03 p0323 N73-12631
Optimum conditions for depositing aluminum and silicon hydroxides on titanium dioxide particles
[NLL-RTS-7638] 04 p0425 N73-13460

Dual wavelength system for monitoring film deposition
[NASA-CASE-MFS-20675] 17 p2070 N73-26751
Influence of silicon particle deposition on volt-ampere characteristics of p-n junctions
18 p2186 N73-27652
Quantitative deposition by standard techniques of adsorbates containing C and Si
[NASA-CR-124309] 19 p2343 N73-28850
Numerical analysis of aerosol concentration and deposition flux for several flow configurations with and without electrical force deposition
20 p2386 N73-29172
One- and two-dimensional analysis of particle deposition in turbulent slot flow with application to self cleaning air filter design
22 p2649 N73-31225

**DEPOSITS**
NT CRYODEPOSITS
Effect of crud deposits on frictional pressure drop in boiling channel
[AEEW-R-767] 07 p0820 N73-16645
Chemistry of deposits and their precursors in jet turbine fuel systems
[AD-754459] 11 p1332 N73-20816
Temperature rise at heat transfer surfaces caused by magnetite, humus, calcium, and copper deposits
[AE-459] 15 p1844 N73-24937

**DEPRESSANTS**
NT CENTRAL NERVOUS SYSTEM DEPRESSANTS

**DEPRESSIONS [TOPOGRAPHY]**
U STRUCTURAL BASINS

**DEPRESSURIZATION**
U PRESSURE REDUCTION

**DEPRIVATION**
NT SLEEP DEPRIVATION

**DEPTH**
Stereoradiography study of depth and geometrical dimensions of internal flaws in weldments
[AD-749459] 04 p0428 N73-13486

**DEPTH MEASUREMENT**
MINOS DOM oxygen monitor for measuring dissolved oxygen in sea water to depths of 3000 meters
[NOAA-IFS-73004] 01 p0057 N73-10466
Numerical analysis of Pacific Ocean bottom signal reflection losses using underwater explosive sound sources and multilayered acoustic absorption model
[AD-748199] 04 p0450 N73-13676
Aerial snow gaging, using transmitted terrain gamma radiation
[EGG-1183-1557] 07 p0800 N73-16500
Deploying airborne laser transmitter/receiver to measure water depth in turbid water
[AD-752486] 08 p0921 N73-17551
Water depth measurement and mapping of shallow water features of Little Baham Bank using ERTS-1 imagery
[E73-10388] 11 p1275 N73-20350
Development of semi-automatic system for digitizing bathymetry charts for showing ocean bottom contour information
[AD-761647] 19 p2296 N73-28464
Cup-type snow gage, using kerosene to prevent evaporation
[NLL-M-23051-[5828.4F]] 21 p2567 N73-30572

**DEPTH PERCEPTION**
U SPACE PERCEPTION

**DERIVATION**
Partial derivative analysis using equations of motion for recovering gravity anomalies from satellite observations
[NASA-CR-130240] 14 p1661 N73-23483

**DERIVATION CALCULUS**
U DIFFERENTIAL CALCULUS

**DESALINIZATION**
Sea ice dynamics, heat and mass budget of Arctic sea ice, desalinization, thermal and mechanical stresses, bearing capacity of floating ice, and interaction of oil and ice
[AD-754118] 11 p1290 N73-20463
Corrosion resistant copper zinc alloys for desalinization systems
[PB-215265/0] 16 p1929 N73-25610

**DESCENT**
NT PARACHUTE DESCENT

**DESCENT PROPULSION SYSTEMS**
Biological effects of Viking Lander spacecraft engine fuel on extraterrestrial life during landing on planet Mars
[NASA-TM-X-2714] 06 p0630 N73-15118
Evaluation of descent propulsion system for Apollo 12
[NASA-TM-X-68933] 06 p0712 N73-15812
Performance of LM-11 Descent propulsion System during Apollo 16 Mission
[NASA-CR-128826] 10 p1213 N73-19865
Apollo experience report on propulsion system for descent stage of lunar module with emphasis on throttling capability and cryogenic helium pressurization system
[NASA-TN-D-7143] 10 p1215 N73-19877
Steady state performance of LM-10 Descent Propulsion System during descent phase of Apollo 15 Mission
[NASA-TM-X-69506] 22 p2717 N73-31750

**DESCENT TRAJECTORIES**
NT REENTRY TRAJECTORIES
Aerodynamic characteristics and trajectory analysis of ballistic-type, self-dispersing bomblet based on wind tunnel tests and numerical probability application
[AD-749956] 06 p0615 N73-14993
Performance tests of cargo parachutes with pulled down vents for airdrop of supplies from 500 feet altitude
[AD-750585] 06 p0624 N73-15068
Space vehicle descent into Mars, Jupiter, and Venus atmospheres
[NASA-TT-F-768] 07 p0844 N73-16838
Mesh gradient technique for numerical optimization of descent trajectories
[NASA-TM-X-68181] 08 p0937 N73-17670
Nomographs for predicting aerodynamic performance of air launched stores
[AD-754428] 11 p1353 N73-20981
Application of optimal control technology to design of controller for space shuttle descent
[NASA-CR-124183] 12 p1459 N73-21824
Aerodynamic interference between aircraft and external store mounted on elliptical wing under inviscid flow conditions
[AD-759170] 16 p1864 N73-25094
System modeling and performance optimization for analyzing parameters and disturbances for dynamic precision weapon delivery - Vol. 1
[AD-751505] 16 p1976 N73-25985
Computer programs for conducting mathematical analysis of weapon delivery techniques and performance optimization of aerial delivery weapons - Vol. 2
[AD-751506] 16 p1977 N73-25986
Testing and demonstration of weapon delivery analysis program to determine major contributors to probable error - Vol. 3
[AD-751527] 16 p1977 N73-25987
Analysis of descent trajectories to determine static and dynamic stability of free-fall stores with freely spinning stabilizer devices
[AD-760677] 18 p2102 N73-26999
Optimal three dimensional trajectories to maximize landing footprint of lifting reentry vehicle using energy approximations based on flight path
[AD-764132] 22 p2615 N73-30960

**DESENSITIZING**
Determination of susceptibility limits and desensitization of solid state electronic equipment to power line transients
[AD-762403] 19 p2246 N73-28110

**DESERTS**
Determination of optical thickness of aerosols in atmosphere around Salton Sea desert area using ERTS-1 imagery
[E72-10200] 02 p0160 N73-11298
Distribution and density of phreatophytes and other arid and desert plants
[E72-10243] 03 p0289 N73-12343
Morphology, provenance, and movement of desert sand seas in Africa, Asia, and Australia
[E72-10249] 03 p0289 N73-12349
Spectral signatures for dominant desert scrub plant species of Arizona and soil surface backgrounds
[E72-10318] 04 p0413 N73-13367
Mapping of remote desert dune fields using ERTS-1 imagery
[E73-10009] 06 p0659 N73-15345
Morphology, provenance, and movement of desert sand seas in Africa, Asia, and Australia
[E73-10058] 07 p0778 N73-16320
Morphology, provenance, and desert sand sea movements in Asia, Australia, and Africa
[E73-10060] 07 p0778 N73-16322
Prediction of range quantity and quality in desert areas of California and Arizona during growing and grazing seasons
[E73-10068] 07 p0779 N73-16330
ERTS-1 detection of potential locust breeding sites in Saudi Arabian desert
[E73-10098] 08 p0902 N73-17309
ERTS-1 measurement of aerosol content in atmosphere over Salton Sea and desert test sites
[E73-10295] 09 p1020 N73-18328
ERTS-1 imagery of morphology, provenance, and movement of desert sand seas in Africa, Asia, and Australia
[E73-10409] 11 p1278 N73-20371
Control and mapping of pink bollworm infestations in cotton fields of California desert areas
[E73-10452] 11 p1283 N73-20411
Determination of specific spectral signatures for dominant Arizona desert scrub plant species and soil surface backgrounds
[E73-10466] 11 p1284 N73-20421
Morphology, provenance, and movement of desert sand seas in Africa, Asia, and Australia
[E73-10542] 13 p1518 N73-22305
Determination of native desert plant distributions in Avra Valley, Arizona from ERTS-1 MSS imagery
[E73-10659] 16 p1899 N73-25353
ERTS-1 imagery of morphology, provenance, and movement of desert sand areas in Africa, Asia, and Australia
[E73-10710] 17 p2018 N73-26317
ERTS-1 imagery of morphology, provenance, and movement of desert sand seas in Africa, Asia, and Australia
[E73-10786] 18 p2136 N73-27262
Application of ERTS-1 imagery to determine dynamics of distribution and density of phreatophytes and other arid land plant communities
[E73-10790] 18 p2137 N73-27266
Mapping of wildland vegetation in Great Basin area of Nevada using ERTS-1 imagery
[E73-10813] 18 p2139 N73-27288
Morphology, provenance, and movement of desert sand seas in Africa, Asia, and Australia using ERTS-1 data
[PAPER-G8] 19 p2264 N73-28239
Measurement of atmospheric aerosol content in Southern California desert areas from ERTS-1 contrast and radiance measurements
[PAPER-I2] 19 p2277 N73-28324
ERTS-1 imagery of desertification, hydrology, vegetation, forage, and water resources in Republic of Mali
[PAPER-R5] 19 p2283 N73-28363
Spectral signatures for dominant desert scrub plant species and soil surface backgrounds in Arizona
[E73-10890] 20 p2394 N73-29239
Measurement of aerosol content in atmosphere over Salton Sea and desert areas of California
[E73-10947] 21 p2530 N73-30289
Uniform mapping of rice crops in Louisiana and California and desert vegetation in southwestern Colorado from Skylab imagery
[E73-10979] 22 p2657 N73-31286
Production of vegetables in arid zones using controlled solar greenhouses
24 p2975 N73-33768
Solar still greenhouse for using desalinated water to produce vegetables in arid regions
24 p2975 N73-33769

**DESIGN**
Design and launch support for high altitude sounding rocket payloads
[AD-745977] 02 p0235 N73-11914
Design of sonar array using standard amplitude shading technique
[AD-755481] 14 p1633 N73-23241

**DESIGN OF EXPERIMENTS**
U EXPERIMENTAL DESIGN

**DESORPTION**
Sorption and desorption of ethylene oxide and methyl bromide gases on polymeric materials during sterilization
03 p0257 N73-12082
Method of thermal desorption used to determine specific surfaces in powder metallurgy
[NLL-TRANS-746-1287-[9022.401]]
06 p0682 N73-15547
Technique for obtaining Auger spectra of electron desorbable surface species on time independent basis
[NASA-TN-D-7257] 11 p1252 N73-20161

**DESPINNING**
U SPIN REDUCTION

**DESTRUCTIVE TESTS**
Fatigue tests of steel screw threads with large root radii under axial loading to determine fatigue strength and point of failure
[ESDU-67020-AMEND-A] 01 p0110 N73-10906
Destructive and nondestructive tests of carbon-carbon reentry heat shields
[SC-R-71-3354] 03 p0364 N73-12966

**DETECTION**
NT AIRCRAFT DETECTION
NT CORRELATION DETECTION
NT FOREST FIRE DETECTION
NT HAZE DETECTION
NT MISSILE DETECTION
NT RADAR DETECTION
NT SIGNAL DETECTION
NT TARGET RECOGNITION
Detection of bacteria in biological fluids and foods
[NASA-CASE-GSC-11533-1] 04 p0421 N73-13435

**DETECTORS**
Optimized antenna design for medium artillery delivered seismic detection system sensor
[AD-748825] 04 p0396 N73-13219
Design and fabrication of flight weight ultrasonic contact sensor leak detection system
[NASA-TM-X-68909] 05 p0546 N73-14431
Device for detection of combustion light preceding gaseous explosions
[NASA-CASE-LAR-10739-1] 07 p0798 N73-16484
Optical imaging system for increasing light absorption efficiency of imaging detector
[NASA-CASE-ARC-10194-1] 11 p1324 N73-20741
Simulation testing of detector for digitally encoded multifrequency tones
[REPT-6755] 18 p2116 N73-27113

Automatic shot change detector for pre-programmed corrections of film reproduced by telecine
[BBC-RD-1973/10] 22 p2671 N73-31392
Cold cathode discharge tube with pressurized gas cell for meteoroid detection in space
[NASA-CASE-LAR-10483-1] 23 p2791 N73-32327
Leak detector with high vacuum seals
[NASA-CASE-LAR-11237-1] 23 p2793 N73-32344
Sensitivity of gravitational detector with positive electromechanical transducers
[ITF-72-90-E] 24 p2926 N73-33374

**DETERGENTS**
Dermatological testing of personal hygiene cleansing agents and laundry detergents for possible use in Skylab Program
[NASA-CR-128880] 11 p1250 N73-20143

**DETERMINANTS**
Law of formation of determinants of maximum value
[NRC-TT-1605] 06 p0690 N73-15617

**DETERMINATION**
U MEASUREMENT

**DETONABLE GAS MIXTURES**
Simulation of rocket plumes and reentry aerothermodynamics using oxygen/hydrogen combustion products
[NASA-CR-128955] 16 p1974 N73-25962
Reflected wave detonation of gaseous mixture in shock tube for simulating hydrogen/oxygen rocket plume
16 p1974 N73-25963
Hydrogen/oxygen combustion for simulating reentry aerothermodynamic characteristics
16 p1974 N73-25964

**DETONATION**
Effects of aluminum addition on explosive behavior of ammonium perchlorate
[AD-745344] 01 p0090 N73-10739
Theoretical analysis of rotating two phase detonation in liquid propellant rocket engine
04 p0461 N73-13763
Initiation and propagation of low-velocity detonation in confined energetic liquids
[AD-748438] 04 p0485 N73-13966
Shock initiation of reaction in RDX/TNT, nitromethane explosives, and double base propellants
[ERDE-TR-103] 05 p0606 N73-14930
Sonic boom nitroglycerin resistance noting shock simulation and sonic boom effect on detonation
[ISL-14/72] 07 p0822 N73-16658
Calculation of two dimensional gas dynamic flows with detonation using Lagrange variables
[JPRS-58699] 12 p1391 N73-21281
Creation shape and flow of tridimensional spark by focused radiation
[NASA-CR-2230] 15 p1766 N73-24311
Computer program for shock and blast loading characteristics high explosive projectile detonation in aircraft
[AD-759002] 16 p1975 N73-25972
Fracture characteristics of small cylindrical bodies partly prefragmented by external notching subject to detonation of high explosive filling
[REPT-545-PT-1] 20 p2483 N73-29943
Development of technique and apparatus for optically detonating insensitive high explosives
[NASA-CASE-NPO-11743-1] 20 p2485 N73-29959

**DETONATION WAVES**
Measurement of shock and detonation wave pressures by means of shock-induced polarization of Plexiglas disks
[TL-1972-4] 02 p0155 N73-11254
Numerical analysis of two dimensional shock wave resulting from mobile wedge moving with supersonic velocity and specific angle of attack into detonation wave
[AD-749650] 05 p0528 N73-14299
Lateral gas expansion behind explosive detonating slab
[ISL-19/71] 09 p1016 N73-18291
Analysis of tangential mode, nonlinear wave motion in liquid propellant rocket engine using two phase detonation wave as reaction model
[NASA-CR-121194] 14 p1718 N73-23944
Analysis of interaction of detonation wave with boundary gas based on formation of low velocity detonation wave
20 p2384 N73-29153
Two phase detonation in fuel sprays suspended in gaseous oxidizing atmospheres
20 p2484 N73-29957
Time evolution of finite power density blast waves
[AD-763834] 22 p2656 N73-31278
Nearly spherical constant power detonation waves driven by focused laser beam in gas
23 p2772 N73-32171

**DETONATORS**
Reliability of safety and arming mechanism for NASA/LSPE program
[NASA-CR-131985] 14 p1719 N73-23953

**DEUTERIUM**
Equilibrium distribution of helium-4 and helium-3 between the liquid and vapor phases of deuterium 2 and hydrogen 2
[NBS-TN-621] 02 p0137 N73-11109
Model for behavior of solid deuterium slab under laser irradiation
[LA-DC-72-415] 03 p0310 N73-12530
Laser-plasma coupling and laser absorption by solid deuterium
[UCRL-50022-2] 10 p1169 N73-19506
Nuclear resonance investigation in niobium-hydrogen and niobium-deuterium systems
[JUL-853-FF] 10 p1193 N73-19707
Gas phase recombination of hydrogen and deuterium atoms
[NASA-CR-131417] 11 p1252 N73-20162
Deuterium absorption line in extraterrestrial radiation from galactic center
[AD-754079] 11 p1340 N73-20873
Monte Carlo calculations on reaction kinetics in hydrogen, deuterium, and fluoride interactions
[AD-758759] 16 p1872 N73-25153
Influence of zirconium additions on diffusivity and solubility of hydrogen and deuterium in niobium alloys at high temperature
[BNWL-SA-4473] 17 p2065 N73-26706
Deuterium abundance for proving neutron loss before nucleosynthesis
19 p2332 N73-28768
Design of line-tunable pulsed hydrogen fluoride/deuterium fluoride laser
[AD-764709] 23 p2802 N73-32410
Spectrometric measurement of D/H ratio in Jupiter atmosphere
24 p2978 N73-33797

**DEUTERIUM COMPOUNDS**
NT HEAVY WATER
Generation spectrum of excited DF molecules obtained during chemical reactions in D2/F2/N2/O2 laser system
[NLL-DRIC-TRANS-2816-[3623.66]]
02 p0180 N73-11458
Vibrational relaxation of DF behind incident shock waves
[AD-756462] 13 p1562 N73-22658
Kinetic model and computerized simulation of DF-carbon dioxide chemical transfer laser
[AD-762284] 19 p2309 N73-28571
Temperature dependence of several vibrational relaxation processes in DF-CO2 mixtures
[AD-762925] 20 p2374 N73-29078

**DEUTERIUM OXIDES**
U HEAVY WATER

**DEUTERIUM PLASMA**
High speed ballistic injection of solid spherical pellet of deuterium into thermonuclear reactor plasma to analyze dynamics of pellet evaporation
[AD-751294] 07 p0830 N73-16726
Containment of deuterium plasma in magnetic mirror well
[UCRL-74087] 08 p0949 N73-17769

**DEUTERONS**
Preliminary studies of reaction yielding triton pion from proton deuteron interaction
[NASA-TM-X-68187] 07 p0823 N73-16674
Thermodynamic and kinetic behavior of protons and deuterons in regular and heavy ice
[NASA-TT-F-14692] 08 p0946 N73-17744

**DEVIATION**
Deviation from rotational symmetry of electric arcs in transverse magnetic fields
[AD-754022] 11 p1328 N73-20778

**DEVICES**
Design and development of biomedical prosthetic and electronic devices
[NASA-CR-130022] 07 p0750 N73-16093

**DEVITRIFICATION**
U CRYSTALLIZATION

**DEW**
Development of methods for improving forecasting of precipitation, surface pressure, temperature, and dew point
[NLL-M-22980-[5828.4F]] 16 p1935 N73-25658
Numerical forecasting of geopotential, temperature, dew point fields at 850 millibar level
20 p2446 N73-29650

**DEWAR SYSTEMS**
U CRYOGENIC EQUIPMENT

**DEWETTING**
U DRYING

**DEXTRANS**
Effectiveness of polymer complex of cysteamine and sulfopropyl ester of dextran as an antiradiation drug on irradiated mice
[DRIC-TRANS-2963] 06 p0631 N73-15125

**DH 106 AIRCRAFT**
U COMET 4 AIRCRAFT

**DIABATIC PROCESSES**
U HEAT TRANSFER

**DIABETES MELLITUS**
Argon laser radiation damage to retina of diabetic and nondiabetic patients
[AD-747058] 04 p0381 N73-13099
Suitability of insulin dependent and oral drug dependent diabetics as navigation personnel
12 p1371 N73-21120

**DIADEME SATELLITES**
Optomechanical tests equipment for D2B satellite vacuum chamber calibration
[OPT-005-72] 23 p2770 N73-32160

**DIAGNOSIS**
Logic comparison of failure diagnosis for digital systems
03 p0272 N73-12203
Microelectrophoresis of human erthyrocytes as diagnostic tool in gynecology and obstetrics
[NASA-TT-F-14587] 04 p0378 N73-13077
Dynamic electrocardiographic standardization for detecting cardiac risk factor in personnel
08 p0873 N73-17066
Periodic health examinations and automatic processing of medical histories for detection and prevention of human diseases
08 p0874 N73-17074
Clinical practice and problems associated with urine analysis
08 p0875 N73-17089
Portable telephone system for transmission of electroencephalographical data diagnostic center
[NASA-CR-128877] 11 p1255 N73-20186
Failure and diagnosis of faults in logic and combinational circuits of digital computers
[AD-754029] 11 p1265 N73-20264
Magnetosphere diagnostics using naturally occurring ELF and VLF waves
[R-34] 18 p2141 N73-27309

**DIAGRAMS**
NT CIRCUIT DIAGRAMS
NT CREEP DIAGRAMS
NT FEYNMAN DIAGRAMS
NT NYQUIST DIAGRAM
NT PHASE DIAGRAMS
NT S-N DIAGRAMS
NT STRESS-STRAIN DIAGRAMS
Phototransistor with base collector junction diode for integration into photo sensor arrays
[NASA-CASE-MFS-20407] 10 p1133 N73-19235
Multiperipherism and hydrodynamics of multiple processes
[NASA-TT-F-14896] 13 p1561 N73-22656

**DIAL SATELLITE**
Nutation and damping theory of Dial satellite after last stage separation
[DLR-FB-72-74] 12 p1461 N73-21842

**DIAMAGNETISM**
Magnetism in solids - magnetic moments, propertism of diamagnetism and paramagnetism, and coexistence of superconductivity and ferromagnetism
[ITJ-13] 04 p0449 N73-13670
Fluctuation-induced diamagnetism in bulk Al and Al alloys above superconducting transition temperature
[AD-750275] 06 p0710 N73-15794
Total and induced magnetic fields line structure within Moon and diamagnetic cavity based on asymmetric theory of lunar induction
[NASA-CR-114545] 06 p0718 N73-15860
Meissner effects and magnetization curves for superconductors - conference
[LA-5115] 17 p2010 N73-26257
SQUID magnetometer measurement of fluctuation diamagnetism of Al and Al alloys above superconducting transition temperature
[COO-3156-56] 21 p2559 N73-30515
Fluctuation diamagnetism of aluminum and aluminum alloys above superconducting transition temperature
23 p2804 N73-32422

**DIAMINES**
NT ETHYLENEDIAMINE
Dynamic mechanical analysis of reactions of aromatic diamines with diglycidyl ether of bisphenol A for application to epoxy thermosetting systems
[AD-759995] 17 p2052 N73-26602
Stable polyimide synthesis from mixtures of monomeric diamines and polycarboxylic acid esters
[NASA-CASE-LEW-11325-1] 19 p2229 N73-27980

**DIAMOND WINGS**
U LOW ASPECT RATIO WINGS
U SWEPT WINGS

**DIAMONDS**
Simplified technique and device for producing industrial grade synthetic diamonds
[NASA-CASE-MFS-20698-2] 10 p1163 N73-19457
Synthesis and characterization of semiconducting diamond and boron phosphide crystals
18 p2186 N73-27648
Epitaxial growth of diamond on diamond from vapor at subatmospheric pressures
[AD-761630] 19 p2327 N73-28722

**DIAPHRAGMS**
Diaphragm rupture effects on expanding flow in evacuated tube
[AD-752605] 08 p0899 N73-17277

**DIAPHRAGMS [MECHANICS]**
Cross axis behavior of circular elastic diaphragm accelerometers
[REPT-519] 02 p0177 N73-11438
Development of differential pressure control system using motion of mechanical diaphragms to operate electric switch
[NASA-CASE-MFS-14216] 04 p0419 N73-13418
Fuel expulsion efficiency and service life of Arde metallic diaphragm used in Atmospheric Explorer propulsion subsystem
[NASA-TM-X-66191] 09 p1078 N73-18794

Analysis of residual stresses in pressure displacement converter diaphragm occurring during manufacturing
16 p1968 N73-25921
High pressure compressed gas magnetic diaphragm rupture system for generating megagauss magnetic field
[JPRS-59459] 18 p2179 N73-27593
Device for observing diaphragm surface vibration angular displacement based on two dimensional schlieren techniques
[REPT-10/1972] 22 p2674 N73-31420

**DIATOMIC GASES**
Transfer of mass and heat through single component diatomic gas and binary monatomic gas mixture of arbitrary composition
[COO-2032-12] 03 p0364 N73-12968
Flow distribution of low Reynolds number, high enthalpy viscous flow of diatomic gas through conical nozzles
[DGLR-PAPER-72-110] 04 p0405 N73-13302
Numerical analysis of one-dimensional isentropic flow of thermally perfect, calorically imperfect diatomic gas
[ESDU-S.00.01.10-AMEND-A]
07 p0767 N73-16233
Numerical analysis of one dimensional isentropic flow of thermally perfect, calorically imperfect diatomic gas
[ESDU-S.00.01.10-AMEND-A]
14 p1648 N73-23364
Energy transfer reactions of electronically excited atomic and diatomic specspecies
[AD-762201] 19 p2298 N73-28481

**DIATOMIC MOLECULES**
Nuclear magnetic resonance spectroscopy to measure order parameter in diatomic molecule rotational ordering transitions
[NOTA-INTERNA-376] 01 p0083 N73-10691
Equations of motion for calculating collision dynamics of diatomic molecules
[NASA-CR-131527] 12 p1431 N73-21594
Predissociation by rotation and curve crossing in diatomic molecules
[NASA-CR-131262] 15 p1747 N73-24159
Computer program for determining rotational line intensity of diatomic molecules -users manual
[NASA-TN-D-7268] 21 p2582 N73-30689
Potential representation theorem for diatomic elastic dielectric displacement and polarization fields
24 p2959 N73-33649

**DIBORANE**
Evaluation of boundary cooled rocket engines for development of space storable propellant combination of oxygen difluoride/diborane
[NASA-CR-129260] 03 p0350 N73-12855
Design, development, and tests of liquid diborane
[NASA-CR-130303] 06 p0676 N73-15502
Design and development of diborane shipping container
[NASA-CR-130808] 09 p1038 N73-18466
Instruction manual for safe and efficient use of 200-pound diborane shipping container
[NASA-CR-131290] 11 p1296 N73-20519
Fracture toughness and strength of diboride composites treated with metallic additives
[NASA-CR-131877] 13 p1547 N73-22535

**DIBROMIDES**
Development of method for determining ethylene dibromide depletion in aviation fuels
[AD-746250] 02 p0221 N73-11791

**DIBUTYL COMPOUNDS**
Aerosol growth kinetics in flow reactor
24 p2901 N73-33159

**DICHLORIDES**
Toxic effects of continuous exposure to dichloromethane vapor on dogs, monkeys, rats, and mice
[AD-746295] 02 p0134 N73-11088
Effects of continuous methylene chloride exposure on spontaneous activity of mice for two weeks
[AD-751435] 07 p0748 N73-16082
Toxic effects of chronic exposure to dichloromethane in liver microsomal cytochromes
[NASA-TM-X-69101] 09 p0996 N73-18128

**DICHROISM**
Encoding action of pair of dichroic gratings suitable for single tube color television camera
[BBC-1972/32] 04 p0419 N73-13414

**DICHROMATES**
U CHROMATES

**DICTIONARIES**
English, French, and Spanish vocabulary of aircraft aeronautical terminology
[DOC-8800-VOL-1] 06 p0616 N73-14996
Dictionary-handbook on properties and uses of fuels, lubricating materials, and special liquids
[AD-750484] 06 p0712 N73-15810
Thesaurus of terms for information on mechanics of structural failure modes and mechanisms for aerospace structures
[NASA-CR-121199] 17 p2091 N73-26917
Glossary of aerial photography and remote sensing in geology and earth science
[PB-220154/9] 21 p2541 N73-30373
Glossary of acronyms, abbreviations, initials, code words and phrases used at John F. Kennedy Space Center
[NASA-TM-X-69523] 23 p2866 N73-32908

**DIELECTRIC CONSTANT**
U PERMITTIVITY

**DIELECTRIC MATERIALS**
U DIELECTRICS

**DIELECTRIC PERMEABILITY**
Evolution of conceptual design of flight hardware for surface electrical Properties experiment - Vol. I
[NASA-CR-128918] 14 p1705 N73-23835
Characteristics of Hertzian dipole antenna radiation patterns and application to lunar surface and subsurface electrical properties investigation - Vol. 2
[NASA-CR-128919] 14 p1705 N73-23836

**DIELECTRIC POLARIZATION**
Electrical and luminescence phenomena in pure and dope lithium Floride
[ORNL-4850] 19 p2230 N73-27985
Potential representation theorem for diatomic elastic dielectric displacement and polarization fields
24 p2959 N73-33649

**DIELECTRIC PROPERTIES**
NT PERMITTIVITY
Macroscopic models of quasi-chemical reactions, dielectric relaxation, and deformation energy
01 p0087 N73-10719
Exact solutions for electromagnetic inverse problem for perfectly conducting body with consideration of uniqueness problem and case of spherically symmetric dielectric body
02 p0200 N73-11616
Discharge rate and electrical breakdown in polyethylene, polystyrene, polymethyl methacrylate, and polyvinyl chloride
[SC-T-72-2509] 03 p0273 N73-12217
Determining elastic compliance, piezoelectric constant, and dielectric constant by mechanically driving polarized ceramic bar
[AD-748357] 03 p0348 N73-12839
Metal-dielectric phase transitions in Bi-Sb alloys and V2O3
[JPRS-57631] 04 p0433 N73-13525
Hydrostatic pressure technique for improving dielectric properties of inorganic glasses used as capacitor materials
[AD-750393] 05 p0521 N73-14236
Optical and dielectric properties of liquid glycerol, tetradecane, and heptadecane
[ORO-3861-6] 06 p0647 N73-15259
Behavior of dielectric constant and loss factor of zeolite with various degrees of hydration
[AD-753512] 09 p1055 N73-18603
Photodielectric and conduction properties of amorphous semiconductors
[AD-753053] 09 p1074 N73-18762
Techniques for casting large area polysulfone film capacitors onto thick aluminum substrates for application as meteoroid impact sensors
[NASA-CR-128862] 10 p1160 N73-19441
Application of dielectric constant measurements to interpretation of radar imagery of Michigan ground truth for lake ice
[E73-10391] 11 p1276 N73-20353
Application of dielectric constant measurements to interpretation of radar imagery of ground truth
[E73-10429] 11 p1280 N73-20390
Dielectric properties of pure and doped insulating materials
[COO-623-182] 12 p1439 N73-21662
Electric strength breakdown in insulating dielectric liquids
[AD-755756] 13 p1548 N73-22546
Measured element factor of linear array for various waveguide radiating elements
[PHL-1973-1] 14 p1639 N73-23287
AC conductivity and dielectric dispersion in amorphous semiconductors
[AD-757097] 14 p1698 N73-23780
Piezoelectric and pyroelectric properties of polymer electrets
[AD-758730] 16 p1933 N73-25638
Relation of electrostatic oscillations in lossfree plasma to dispersion and energy equation
[IPPJ-152] 16 p1949 N73-25768
Nondestructive measurement of dielectric properties of slab-type materials
[AD-762359] 19 p2312 N73-28599
Ultrasonic absorption and dielectric loss as function of temperature in heterophase block copolymers
[AD-762452] 20 p2435 N73-29559
Properties of dielectric layers of negative electrosensitive resin noting masking capability and application to MOS circuit manufacturing
[REPT-5.497] 23 p2765 N73-32124

**DIELECTRICS**
NT RADOME MATERIALS
Electromagnetic wave transmission in space-time varying dielectrics and plasmas
[AD-746676] 02 p0144 N73-11165
Effect of purification of transparent dielectrics from dust on breakdown threshold under action of laser irradiation
[AD-748230] 03 p0338 N73-12760
Analysis of microstructure of radio frequency-sputtered, thin lead-dielectric cermet films using transmission electron microscopy
[NASA-TR-R-393] 03 p0345 N73-12811
Research data on dielectrics, refractory materials, plastics, ceramics, and glasses
[AD-746686] 03 p0347 N73-12827
Development and characteristics of electrical insulation material with potential to withstand 80 kilovolts
[BDX-613-502-REV] 04 p0398 N73-13242
Electrical conductivity methods for measuring effects of high energy radiation on dielectric hydrocarbon liquids
[HMI-B-117] 04 p0452 N73-13693
Proceedings of symposium on laser radiation damage to transparent dielectrics, plasma formation at dielectric surfaces, and damage morphology of thin film coatings
[NBS-SP-372] 05 p0554 N73-14498
Measurement of damage thresholds for multiple layer dielectric mirrors for laser pulses of twenty nanoseconds and twenty picoseconds duration
05 p0556 N73-14513
Photoconductivity of thin dielectric films induced by X ray irradiation
[UCRL-73974] 05 p0586 N73-14770
Slot transmission line on dielectric substrate
[AD-751657] 07 p0763 N73-16196
Damage thresholds of multilayered dielectric reflecting mirrors subjected to nanosecond laser pulses
[AD-751265] 07 p0808 N73-16553
Multiple beam interval scanners with dual-antennas and circular artificial dielectric lenses to provide spot beam coverage of contiguous 48 states
[NASA-CR-130168] 08 p0888 N73-17192
High voltage distribution fields of two component dielectrics in rotational series or parallel arrangements
08 p0888 N73-17193
Properties of thin dielectric TiO2 films produced by chemical vapor deposition
[NASA-CR-130763] 08 p0950 N73-17780
Electromagnetic wave interactions in stratified and space-time periodic dielectric or plasma streams
[AD-753690] 09 p1004 N73-18196
Electrical properties of reinforced dielectrics, magnetic permeabilities of multicomponent materials, and electromagnetic waves in fibrous dielectrics
[AD-752693] 09 p1053 N73-18583
Test data on liquid dielectric breakdown mechanisms
[AD-752819] 09 p1053 N73-18585
Computerized design of dielectric lenses for phase corrected horn antennas
[AD-753914] 10 p1136 N73-19258
Methods of charging/discharging in scanning electron microscopy of dielectrics to preserve resolution and contrast
[DRIC-TRANS-2970] 10 p1162 N73-19451
Dielectric susceptibilities of potassium chloride to lithium and hydroxyl, sodium chloride to hydroxyl, and rubidium chloride to cyanides
[COO-3151-14] 10 p1200 N73-19763
Hydro and aerodynamic phenomena in liquid dielectric conduction through charge carrier injection
[NLL-PO-2890-[9022.81]] 11 p1269 N73-20298
Mathematical model for calculating breakdown voltage of solid homogeneous dielectric solid during thermal breakdown
[NLL-CE-TRANS-5560-[9022.09]]
11 p1329 N73-20786
Effect of homogeneous dielectric sphere on electromagnetic radiation from simple sources treated as boundary value problem and solution obtained by technique of dyadic Green functions
[NASA-CR-2211] 12 p1378 N73-21178
Coupled modes on dielectric image waveguide
12 p1382 N73-21206
Microwave Doppler shift technique for measuring dynamic bulk modulus of dielectric materials including solid propellants
[NASA-CR-131743] 13 p1546 N73-22532
Analysis of effects of high power lasers to include interactions with plasma, metals, dielectrics, semiconductors, and gases
[AD-755820] 14 p1674 N73-23586
Scanning electron microscope effects on charging properties of dielectric materials
[NLL-DRIC-TRANS-2970-[3623.66]]
15 p1785 N73-24470
Design technique to reduce absorption in multilayer dielectric mirrors using optical interference coatings
15 p1812 N73-24688
Harmonic generation in electromagnetic wave propagating in isotropic dielectric
[AD-758911] 16 p1877 N73-25198
Analysis of electron number density and collision frequency levels behind reflected shock waves and shock wave interactions in argon
16 p1887 N73-25275
Radiation characteristics of grounded slotted dielectric slab
[AD-760129] 17 p1999 N73-26165
Development of equipment and method for electrifying dielectric to determine electrostatic properties
[NASA-CASE-MFS-22129-1] 17 p2003 N73-26197

Fourier solution for determining radiation patterns of dielectric coated loop antenna
[AD-762041] 19 p2245 N73-28100
Wave amplification in dielectrics
[AD-762283] 19 p2309 N73-28570
Image converter based on multilayer semiconductor dielectric structures
[JPRS-59636] 19 p2326 N73-28714
Theory of dielectric function in magnetized plasma
[AD-762512] 20 p2459 N73-29764
Design and fabrication of two dimensional dielectric lens contained in parallel plate waveguide system in multibeam antenna study
[NASA-CR-132793] 22 p2641 N73-31171
Effect of homogeneous dielectric sphere on electromagnetic radiation from simple source
22 p2646 N73-31201
Bulk semiconductor dielectric waveguide functional circuits
[AD-763888] 22 p2707 N73-31681
Calculation of evanescent-wave gain in TE sub Om and TM Om of optical fibers
[CRC-1247] 23 p2769 N73-32147

**DIES**
Effective tooling designs for producing precision forging using rib and web type configurations
[AD-745991] 02 p0179 N73-11449
Development of extruding machine for producing parts with complicated shapes, high degree of mass, and requiring precision surfaces
[AD-751146] 07 p0805 N73-16534
Procedure for measuring flow stresses of metals during closed die forging
[AD-752588] 08 p0928 N73-17602
Isothermal forging of titanium centrifugal compressor impeller
[AD-764266] 22 p2678 N73-31455

**DIESEL ENGINES**
Chemical determination of organic nitrate additive in diesel engine fuel
[AD-762177] 19 p2328 N73-28730

**DIETS**
Effect of calcium-deficient diet on bone structure of pigs and dogs
[NASA-TT-F-13917] 01 p0008 N73-10067
Therapeutic value of mineral water diets especially Karlsbad Muhlbrunn water
[NASA-TT-F-14620] 04 p0379 N73-13079
Influence of repeated test and dietary counseling on hypercholesterolemia control in NASA employees
08 p0875 N73-17081
Stress effects on element balance in human waste for life support recycling system
10 p1117 N73-19107
Nutrient protein intake of rats and tolerance to acute hypoxia
14 p1608 N73-23035
Analysis of physiological effects of diet on personnel of Tenth Soviet Antarctic Expedition
20 p2409 N73-29358
Dynamics of weight change and variations in weight indices of internal organs in white mice as function of atmospheric composition and diet
24 p2883 N73-33022

**DIFFERENCE EQUATIONS**
Differential-difference equation describing thermodynamic interactions of hot air bubbling cooling in surrounding liquid
04 p0404 N73-13294
Explicit difference method for steady two dimensional or axisymmetric hypersonic flow
[DGLR-PAPER-72-66] 04 p0405 N73-13303
Difference equations for numerical weather forecasting
[AD-759620] 16 p1939 N73-25692

**DIFFERENCES**
Geometrical interpretation of 2n-th central difference using simple recursive functions
[NASA-CR-133965] 22 p2691 N73-31554

**DIFFERENTIAL ALGEBRA**
U DIFFERENTIAL CALCULUS
U MATRICES [MATHEMATICS]

**DIFFERENTIAL AMPLIFIERS**
Integrated circuit differential amplifier for magnetic probe measurements
[LRP-55/72] 10 p1134 N73-19241

**DIFFERENTIAL ANALYZERS**
U ANALOG COMPUTERS

**DIFFERENTIAL CALCULUS**
Use of regularization method for interpolation and differentiation of experimental data
[NLL-M-21660-[5828.4F]] 21 p2565 N73-30561

**DIFFERENTIAL EQUATIONS**
NT BURGER EQUATION
NT COSINE SERIES
NT ELLIPTIC DIFFERENTIAL EQUATIONS
NT FOKKER-PLANCK EQUATION
NT GAUSS EQUATION
NT HELMHOLTZ VORTICITY EQUATION
NT PARABOLIC DIFFERENTIAL EQUATIONS
NT PARTIAL DIFFERENTIAL EQUATIONS
NT POISSON EQUATION
NT VLASOV EQUATIONS
NT VORTICITY EQUATIONS
Differential equations for transient response of one dimensional, ablative thermal protection system, including thermal nonequilibrium, mass transfer, and chemical kinetics
[NASA-TM-X-68853] 02 p0137 N73-11108
Full order adaptive observer for single-input single-output continuous differential system with unknown parameters
[NASA-CR-129172] 02 p0195 N73-11574
Full order adaptive observer for single input, single output, stable, linear differential systems
[NASA-CR-129193] 02 p0195 N73-11575
Perturbation theory for developing eigenvalues and eigenfunctions in power series expansion for Hill differential equation
02 p0195 N73-11581
Variational principle of self and non self adjoint linear differential equations
[PB-210374] 02 p0203 N73-11642
Linear differential equations describing aircraft lateral motion in presence of atmospheric turbulence
[AASU-311] 03 p0253 N73-12045
Iterative solution for characteristic exponents of linear differential equations with periodic coefficients
[ARC-CP-1218] 03 p0324 N73-12642
Differential-difference equation describing thermodynamic interactions of hot air bubbling cooling in surrounding liquid
04 p0404 N73-13294
Differential equation for trajectories in exact form
[LNF-71/81] 04 p0450 N73-13671
Equation for normal freezing for ideal ternary liquid solutions solidified into ideal solid solutions of pseudobinary type
[NASA-CR-129935] 05 p0562 N73-14563
Differential equations for studying dynamic characteristics of motor with separate excitation regulated by negative resistance feed
[PUBL-1368] 06 p0645 N73-15237
Nyquist criterion for control loops, using linear functional differential equations and transfer functions
[NRC-TT-1612] 06 p0690 N73-15622
Estimates of differential functions for proving system stability
07 p0761 N73-16179
Application of singular perturbation of ordinary differential equations to control system design
07 p0761 N73-16181
Theorems for proving consistency of singular perturbations in physical systems with parasitic elements
07 p0761 N73-16182
Perturbed nonlinear differential equations applied to integral manifolds
[NASA-CR-130277] 07 p0813 N73-16592
Smoothing properties of neutral functional differential equations
[NASA-CR-130748] 08 p0936 N73-17668
Numerical solution of linear differential equations describing dynamic response of vehicles
[TT-7212-PT-1] 08 p0937 N73-17669
Discussion of Sturm-Liouville theory and canonical system of arbitrary number of differential equations
[NASA-TT-F-14696] 08 p0937 N73-17671
Oscillation and nonoscillation in solutions of standard linear sets of differential equations
[NASA-TT-F-14809] 08 p0937 N73-17672
Linear differential equations for analyzing viscoelastic properties and mechanical behavior of high polymers
08 p0966 N73-17898
Conditions necessary to insure stationarity in solution process for stochastic differential equations
[NASA-CR-130779] 09 p1056 N73-18606
Differential games, nonlinear sequential machines, hyperbolic partial differential equations, and iterative solutions
[JPRS-58069] 09 p1056 N73-18609
Definitions of linearizable objects and applications in differential games of pursuit
09 p1056 N73-18610
Theorems regarding oscillation and nonoscillation conditions for canonic linear sets of differential equations
[NASA-TT-F-14816] 09 p1057 N73-18615
Application of averaging method to biaxial gyrostabilizer analysis
10 p1159 N73-19429
Efficiency of numerical integration methods for differential equations
10 p1178 N73-19585
Survey on numerical integration methods for differential equations
10 p1178 N73-19586
Liapunov solutions to linear differential equations with periodic coefficients
[NASA-TT-F-14835] 10 p1179 N73-19588
Oscillatory and nonoscillatory solutions to equations on nonlinear saturation of convective heat transfer
[AD-754228] 10 p1179 N73-19594
Node voltage method for analyzing nonlinear electric networks with lumped parameters
[NLL-TRANS-2865-[9022.81]]
11 p1264 N73-20255
Fixed point theorems and dissipative processes in differential systems of Euclidian space
[NASA-CR-131267] 11 p1310 N73-20631
Arguments on symplectic matrices group of canonical differential equations
[NASA-TT-F-14806] 11 p1311 N73-20637
Symplectic matrices and structures of sets of unstable canonical systems with periodic coefficients
[NASA-TT-F-14810] 11 p1311 N73-20639
Simple algorithm for optimal control of systems governed by delayed differential equations
[AD-754379] 11 p1312 N73-20650
Integration of nonlinear differential equations describing one-dimensional steady flow across normal shock wave, considering transport, degree of freedom relaxation, and chemical reactions
[DLR-FB-72-54] 12 p1392 N73-21288
Theorems for oscillatory solutions to differential equations
[NASA-TT-F-14883] 12 p1419 N73-21498
Existence of periodic solutions for nonautonomous neutral functional differential equations
[NASA-CR-131887] 13 p1550 N73-22556
Effectiveness of controllers for dynamic systems modeled by ordinary differential equations
[NASA-CR-132054] 15 p1759 N73-24259
Development of equations of condition necessary for determining coefficients for Runge-Kutta methods used to solve ordinary differential equations
[NASA-CR-130902] 15 p1803 N73-24613
Runge-Kutta-Nystrom formulas of eighth and lower order derived for special second order differential equations
[NASA-TR-R-410] 15 p1803 N73-24614
Algorithm for modifying collocation method of solving differential equations
[NASA-TT-F-14800] 15 p1803 N73-24616
Mathematical design of electric filters using linear differential equations
[AD-757544] 16 p1881 N73-25225
Differential equations for analyzing nonstationary incompressible viscous fluid flow in elastic cylindrical tube
17 p2014 N73-26290
System of differential equations of hydraulics and heat transfer for porous body, reactor core
[JPRS-59775] 20 p2453 N73-29714
Approximation of functions of terminal state of dynamic system and determination of error bounds
21 p2515 N73-30175
Formal method for converting logical descriptions of cryotron circuits of asynchronous automata into differential equations
21 p2515 N73-30177
Programming implementation of Taylor series method for numerical solution of ordinary differential equations
[NASA-TM-X-70438] 21 p2566 N73-30567
Differential solution to problem of nonlinear cavitational flow around channel plates by gravity fluid
22 p2651 N73-31239
Analysis and optimization of cyclic methods in orbit calculation
[NASA-CR-132806] 22 p2691 N73-31559
Comparison of digital computer programs for numerical solution of ordinary differential equations
[NASA-TM-X-64781] 23 p2813 N73-32487
Development of procedures for simultaneous structure and parameter identification of linear dynamical systems
[TAE-173] 23 p2854 N73-32808
Differential approximation and numerical integration methods for analyzing behavior of wall stabilized electric arcs with radiative transport
[AD-765207] 23 p2857 N73-32831
The prediction of instabilities of linear differential equations with periodic coefficients
[ARC-R/M-3713] 24 p2945 N73-33518

**DIFFERENTIAL GEOMETRY**
NT LIE GROUPS
NT TENSOR ANALYSIS

**DIFFERENTIAL INTERFEROMETRY**
Laser interferometric equipment for vibration and distance to surface measurement of mass memory magnetic disk floating heads
[LCR-71-216/1/R] 17 p2034 N73-26461
Argon plasma temperature profile measurement by differential interferometry, based on temperature dependent refractivity
[IPF-71-4] 17 p2069 N73-26737
Sign determination of laser Doppler anemometer velocity components of two Doppler difference signal components
[REPT-1/1972] 22 p2674 N73-31422

**DIFFERENTIAL OPERATORS**
U DIFFERENTIAL EQUATIONS
U OPERATORS [MATHEMATICS]

**DIFFERENTIAL PRESSURE**
Analysis of pressure distribution around hemisphere at supersonic speeds with emphasis on differential pressure measurements
[ARC-R/M-3237] 15 p1729 N73-24023

**DIFFERENTIAL THERMAL ANALYSIS**
Computer programs for differential curve of growth analysis of solar type stars
[BULL-171] 08 p0960 N73-17848

Mass thermal analysis of chemical reactions in conversion of polyacrylonitrile fibers to high modulus, high strength carbon fibers - Vol. 2
[AD-755350] 13 p1549 N73-22549
Differential thermal analysis and dilatometry of 4 to 5 years stored ammonium nitrates with amine copper complex additives
[ICT-4/72] 16 p1954 N73-25812

DIFFRACTION
NT ELECTRON DIFFRACTION
NT FRESNEL DIFFRACTION
NT NEUTRON DIFFRACTION
NT WAVE DIFFRACTION
NT X RAY DIFFRACTION
Conditions of coherence in diffraction spectra produced in liquids on ultrasonic standing waves
[NASA-TT-F-13925] 02 p0211 N73-11713
Diffraction of light by ultrasonic waves and intensity of diffraction spectrum
[NASA-TT-F-13926] 02 p0212 N73-11714
Determination of paleotectonic principal stress orientation and spacings of joints in outcrops, and development of optical diffraction analysis method
[BM-RI-7706] 06 p0665 N73-15409
Diffraction technique for determining three dimensional frequency spectra of photographic images
[AD-751418] 07 p0822 N73-16663
Electromagnetic transients in plasmas and ray techniques for radiation and diffraction of electromagnetic waves
[AD-756484] 13 p1493 N73-22099
Interferometrically controlled ruling machine for manufacturing optical diffraction gratings
[AD-758898] 16 p1946 N73-25745
Diffractive excitation model for evaluation of inelastic part of proton-proton unitarity equation
18 p2182 N73-27614
Nondiffractive models with n squared approximately 1/s
18 p2182 N73-27616

DIFFRACTION GRATINGS
U GRATINGS [SPECTRA]

DIFFRACTION PATTERNS
High speed photography of electro-optical fringe patterns for measuring pulsed electric field between Kerr cell electrodes
[SC-DC-72-1375] 04 p0399 N73-13243
Design and fabrication of X ray diffractometer and application to determination of residual stresses in polycrystalline samples
[NAL-TN-34] 06 p0672 N73-15467
Differential light scattering patterns for identifying different species of bacteria
08 p0875 N73-17090
Thematic mapping and terrain analysis using diffraction patterns of ERTS-1 imagery
[E73-10385] 10 p1153 N73-19378
Topographic interpretation of uranium alloy X ray diffraction patterns
[SC-T-72-2467] 10 p1173 N73-19543
Computerized acoustic imaging technique with automatic pattern recognition
[AD-761497] 19 p2240 N73-28060

DIFFRACTION TELESCOPES
U SPECTROSCOPIC TELESCOPES

DIFFRACTOMETERS
Transistorized control unit for neutron spectrometers or diffractometers
[BARC-591] 05 p0547 N73-14447
Design and fabrication of X ray diffractometer and application to determination of residual stresses in polycrystalline samples
[NAL-TN-34] 06 p0672 N73-15467
Dual purpose optical instrument capable of simultaneously acting as spectrometer and diffractometer
[NASA-CASE-XNP-05231] 19 p2300 N73-28491

DIFFUSE RADIATION
Positive diffuse cosmic gamma ray flux measurements for energies to 100 MeV range
[NASA-TM-X-66109] 03 p0353 N73-12877
OSO-J experimental design, and equipment for soft X ray sources and diffuse components in 0.01 to 2.0 keV range
17 p2085 N73-26865
Structure and origin of soft diffuse X rays below 1 KeV
19 p2331 N73-28754
Measurement of spectral flux density of universal diffuse X ray background between 2 and 200 KeV
19 p2331 N73-28755
Measurement of cosmic gamma ray emission from galactic center, Crab nebula, and diffuse radiation
19 p2331 N73-28757
European measurements of diffuse flux and Crab pulsar NP 0532
19 p2331 N73-28758
Origin of diffuse X ray and gamma ray background
19 p2332 N73-28762
Interaction of ultrahigh energy cosmic rays protons with relicit radiation in extragalactic space
19 p2332 N73-28766
Measurement of light scattering at various angles using point spread function and modulation transformation function techniques
24 p2957 N73-33629
Application of Fourier techniques to calculate spread of scattered light for circular spot, Gaussian profile, and linear stripe cases
24 p2958 N73-33632

DIFFUSERS
Analysis of mean velocity, turbulence intensity, and wall heat transfer for conical diffuser coupled to constant diameter recovery section
[NASA-TM-X-2677] 02 p0156 N73-11267
Computerized design and tests of two-dimensional subsonic short diffusers employing boundary layer control
[NASA-CR-121024] 03 p0283 N73-12294
Procedure for predicting performance characteristics of second throat diffusers in ejector systems
08 p0895 N73-17250
Performance tests of low-pressure-ratio centrifugal compressor with four different diffuser configurations
[NASA-TN-D-7237] 11 p1231 N73-19997
Short curved wall, axisymmetric subsonic diffusers, using slot suction to prevent flow separation
[NASA-CR-2209] 11 p1270 N73-20305
Time dependent flow field model for subsonic diffuser section of supersonic inlet
[AD-758803] 16 p1957 N73-25835
Flow characteristics behind diffusers in wind tunnels
[AD-763257] 21 p2525 N73-30251
Pressure recovery performance of conical diffusers at high subsonic speeds and range of geometries
[NASA-CR-2299] 22 p2611 N73-30927
Transmitting and reflecting diffuser
[NASA-CASE-LAR-10385-3] 23 p2819 N73-32538
Effect of inlet conditions on optimal shape of diffuser based on theory of potential flow of fluid in channels
[AD-765577] 24 p2911 N73-33230

DIFFUSION
NT ATMOSPHERIC DIFFUSION
NT ELECTRON DIFFUSION
NT GASEOUS DIFFUSION
NT IONIC DIFFUSION
NT MAGNETIC DIFFUSION
NT MOLECULAR DIFFUSION
NT PARTICLE DIFFUSION
NT PLASMA DIFFUSION
NT SURFACE DIFFUSION
NT THERMAL DIFFUSION
NT TURBULENT DIFFUSION
Analog model for minority charge carrier diffusion to base contact of bipolar transistor with current amplification
[NLL-TRANS-2861-[9022.81]]
02 p0148 N73-11201
Diffusion metallizing and service life of gas turbine engine blades
[NASA-TT-F-13914] 02 p0223 N73-11801
Effects of interatomic forces on diffusion mechanisms in silver cadmium alloys, silver indium alloys and silver lead alloys
[CEA-R-4292] 03 p0333 N73-12714
Diffusion creep and creep degradation in precipitation hardened TD-NiCr alloy
[NASA-TN-D-7079] 04 p0433 N73-13530
Effects of diffusional creep on particle morphology of polycrystalline alloys strengthened by second-phase particles
[NASA-TN-D-7177] 09 p1047 N73-18536
Dispersion of tracers in atmosphere from planetary boundary layer to turbopause
[AD-760694] 18 p2174 N73-27559
Diffusion across modified polyethylene separator in heat sterilizable silver zinc battery
[NASA-CR-133601] 20 p2363 N73-29007
Theoretical analysis of plastic flow and diffusion during sintering of Life, Ag, and Ni systems
20 p2428 N73-29499
Matrix equations of radiation diffusion
20 p2472 N73-29857
Self diffusion in liquid metals conducted over wide temperature intervals
[COO-841-30] 24 p2934 N73-33434

DIFFUSION BONDING
U DIFFUSION WELDING

DIFFUSION COEFFICIENT
Fricks equation for determining diffusion profiles in two impure semiconductors
[CEA-CONF-1970] 01 p0087 N73-10723
Substitutional element diffusion coefficients in silicon
[AD-745945] 01 p0089 N73-10735
Pitch angle diffusion coefficient for cosmic rays in static random magnetic field
[NASA-TM-X-66077] 01 p0100 N73-10819
Interstitial impurity diffusion coefficients and crystal lattice defects in cubic alloys
[AD-746949] 02 p0188 N73-11529
Chemical diffusion coefficient of oxygen in mixed niobates to determine feasibility of modifying oxide defect structures to enhance oxidation protection of elevated temperature materials
[AD-746834] 03 p0316 N73-12574
Conductivity profiles determined for beryllium diffused silicon for calculating diffusion coefficients
[NASA-CR-129169] 03 p0320 N73-12605
Approximation of diffusion coefficients for charged particles in random magnetic field
[NASA-CR-129523] 03 p0339 N73-12767
Ion mobility expression and diffusion coefficient of plasma in crossed electric and magnetic fields
[NASA-TT-F-14523] 07 p0825 N73-16689
Diffusion coefficients for zinc electrode in potassium hydroxide solutions
[AD-753096] 09 p0991 N73-18092
Calculation of transport and equilibrium properties of simple gases with m-6-8 potential function
[NBS-TN-628] 10 p1125 N73-19167
Determination of diffusion coefficient of hydrogen through nickel and iron-nickel alloys
[UCRL-TRANS-10651] 12 p1415 N73-21463
SOM-1 radar measurement of diffusion in meteor zones
17 p2023 N73-26370
Truncation error dependence on computational diffusion coefficient in atmospheric boundary layer models
[AD-760122] 17 p2029 N73-26420
Experimental analysis of rutile properties including crystal growth, hydrogen diffusion, and magnetic resonance determination of defects
[AD-760667] 18 p2190 N73-27684
Exact equations for five-component gas mixture transport coefficients as dissociated air model gas
[DLR-FB-72-34] 21 p2580 N73-30678
Testing of power spectrum-diffusion coefficient relations of cosmic rays at low energies
22 p2711 N73-31706
Laminar dispersion for measuring ethane binary diffusion coefficients in methane filled capillaries
24 p2891 N73-33079
Diagnostic technique for determining excess free carrier lifetime and ambipolar diffusion coefficient in localized regions within semiconductors
24 p2966 N73-33706

DIFFUSION EFFECT
U DIFFUSION

DIFFUSION FLAMES
Theoretical analysis of reaction kinetics limitations leading to extinction of counterflow diffusion flame
[AD-751053] 07 p0856 N73-16940
Initial temperature effects on diffusion burning of hydrogen flame in closed channel with supersonic flow
[NASA-TT-F-14844] 10 p1141 N73-19295
Topler method for studying structure of turbulent diffusion flames
[NASA-TT-F-14842] 10 p1223 N73-19945
Topler schlieren photographic study of diffusion flame structure
[NASA-TT-F-14843] 10 p1223 N73-19946
Mixing and ignition of enclosed supersonic diffusion flames
[AD-760804] 18 p2207 N73-27811
Formation of nitric oxide in steady laminar diffusion flame
22 p2727 N73-31825

DIFFUSION PUMPS
Computer controlled infusion pump for time varying input of calcium into physiological systems
[NASA-CASE-ARC-10447-1] 05 p0503 N73-14092
Pumping system of space environment simulation vacuum chamber noting vacuum and diffusion pumps, valves, cryogenic section, and automatic control system
[ESDO-TN-113-ESTEC] 05 p0524 N73-14262

DIFFUSION THEORY
Correlation length for interplanetary magnetic field fluctuations
[NASA-TM-X-66138] 05 p0595 N73-14841
Numerical solution for cylindrical symmetrical diffusion problem
[FOA-1-C-1409-92] 06 p0653 N73-15306
Finite difference solution to diffusion equation in spherical coordinates
[SCL-DR-72-0017] 06 p0691 N73-15623
Multicomponent diffusion theory as applied to oxidation, corrosion, and sulfation of complex heat resistant alloys
14 p1677 N73-23609
Unique approach for deriving cosmic ray diffusion equation for charged particles in static, random magnetic field
[NASA-TM-X-66263] 16 p1959 N73-25848

DIFFUSION WELDING
Single-step diffussion welding process
[NASA-CASE-LEW-11388-2] 01 p0061 N73-10500
Development of diffusion welding technique for TD-NiCr metal sheet and effect on creep-rupture shear strength
[NASA-TN-D-7153] 07 p0804 N73-16520
Vacuum-diffusion welding units
10 p1163 N73-19464
Diffusion bonding of plasma sprayed boron reinforced magnesium monolayer tapes by hot pressing
[SC-DR-72-0677] 10 p1166 N73-19488
Developments in vacuum diffusion welding methods and metallurgical applications of solar energy
[NLL-M-22830-[5828.4F]] 11 p1304 N73-20584

Measurements of Mossbauer absorption spectra to investigate diffusion mechanism of iron in beta-titanium
12 p1413 N73-21449
Evaluation of nondestructive testing techniques for diffusion-bonded titanium alloy aircraft structures using ultrasonic radiation
[AD-760673] 18 p2106 N73-27035
Microstructural determination of bonding strength of steel bimetal produced by pressure working
[NLL-M-21699-[5828.4F]] 21 p2557 N73-30499
Two-step diffusion welding process of unrecrystallized alloys
[NASA-CASE-LEW-11388-1] 23 p2795 N73-32358
Interaction of advancing crack with pre-existing diffusion bonded microcracks in Ti-AlV alloy composites
[AD-765166] 23 p2811 N73-32476
Application of diffusion bonding to electronic interconnection of flatpack leads
[NASA-CR-124460] 24 p2934 N73-33429
DIFFUSIVITY
Analysis of eddy diffusivity of momentum for heating air in turbulent annular flow and effect of various flow parameters on eddy diffusivities ratio
10 p1139 N73-19279
Influence of zirconium additions on diffusivity and solubility of hydrogen and deuterium in niobium alloys at high temperature
[BNWL-SA-4473] 17 p2065 N73-26706
DIFLUORO COMPOUNDS
NT POLYTETRAFLUOROETHYLENE
DIGESTIVE SYSTEM
NT GASTROINTESTINAL SYSTEM
NT INTESTINES
NT RECTUM
NT STOMACH
NT TEETH
DIGITAL COMMAND SYSTEMS
Digitized grammar for signal analysis and speech recognition accuracy in command and control system
[AD-746333] 06 p0643 N73-15218
Digital command and simulation of automatic tracking device carrying pulsed laser and receiving telescope
[ONERA-NT-198] 15 p1751 N73-24190
DIGITAL COMMUNICATION
U PULSE COMMUNICATION
DIGITAL COMPUTERS
NT CDC 1604 COMPUTER
NT CDC 6000 SERIES COMPUTERS
NT CDC 6600 COMPUTER
NT HONEYWELL COMPUTERS
NT IBM 360 COMPUTER
NT IBM 1130 COMPUTER
NT ILLIAC 4 COMPUTER
NT MINICOMPUTERS
NT PARALLEL COMPUTERS
NT PDP COMPUTERS
NT PDP 8 COMPUTER
NT PDP 10 COMPUTER
NT SEL COMPUTERS
NT SEQUENTIAL COMPUTERS
NT UNIVAC 1108 COMPUTER
Automata theory for realizing reliable computer logic with fault detection
[AD-745720] 01 p0031 N73-10241
Revised description and specification for CAMAC modular data processing system used with on-line digital computers
[EUR-4100-E-REV-1972] 01 p0032 N73-10246
Digital mimicomputer, D-17B, for NSQ-10 Minuteman I missile guidance system
[AD-746008] 02 p0147 N73-11193
Page replacement algorithm simulations for advanced avionic digital computer programming
[AD-746110] 02 p0147 N73-11196
Modification of Minuteman digital computer system to provide for single channel autoanalyzer waveform analysis
[AD-746264] 02 p0147 N73-11197
Digital converter for scaling binary number to binary coded decimal number of higher multiple
[NASA-CASE-KSC-10595] 03 p0269 N73-12176
PERT planning run time reduction with special purpose cellular logic computer
03 p0271 N73-12195
Synthesis of digital unit of variable structure in all purpose digital selection system
[AD-747726] 03 p0272 N73-12208
Abstracts on theory, design, and applications of analog and digital computers and digital control systems
[JPRS-57529] 04 p0392 N73-13189
Digital computer for variable active attenuation equalizer and associated impedance simulating network for unloaded cables
[REPT-6650] 04 p0398 N73-13236
Multiprogram structure of HRS 101 digital computer and program package for statistical measured data selection and real time presentation
[JPRS-57696] 05 p0516 N73-14192
Multiprogram structure of HRS-101 digital computer
05 p0516 N73-14194
Review of macrocellular research for digital computers, noting parallel computers
05 p0517 N73-14205
Microprogrammed control, buffer store, and storage control units for all applications digital computer for signal processing in radar, sonar, and communication systems
[AD-748996] 05 p0520 N73-14227
Minicomputer for digital measuring system for hydrophone calibration
[AD-749927] 05 p0549 N73-14461
Design and functional description of digital computer system
[FOA-3-C-3657-63] 06 p0643 N73-15220
Characterizing sequences and fault detection in sequential computers
[AD-750266] 06 p0644 N73-15233
Arithmetic and logic units in digital computer for processing of radar, sonar, and communication systems signals
[AD-750665] 06 p0646 N73-15248
Reliability analysis of digital computer used in system for ship navigation
[AD-750990] 06 p0697 N73-15687
Fabrication and performance of real-time jet engine simulator for development of jet engine components and control systems
[NAL-TR-283] 06 p0713 N73-15820
Application of on-board digital computers for stabilization of missile and rocket control systems
[JPRS-57893] 06 p0721 N73-15881
Application of digital techniques for control of large antennas used for satellite tracking
[NASA-TM-X-66154] 07 p0754 N73-16127
Research and development in advance electronics including applications to digital computers, air traffic control, and solid state physics
[AD-751308] 07 p0834 N73-16758
On-line computer graphics for display of magnetic tape data from digital computer
[IPPJ-T-10] 08 p0887 N73-17179
Digital on-line spectrum analysis using cross correlation and fast Fourier transformation techniques
[ARC-CP-1225] 09 p1006 N73-18209
Synthesis of combination adder with group carry circuits
[AD-752816] 09 p1007 N73-18216
Optical data processing of dielectric particle trajectory detector data using flying spot scanner on-line to computer
[BMVG-FBWT-72-34] 09 p1036 N73-18457
Digital image processing for processing pictures from space vehicles
09 p1065 N73-18687
Application of integrated circuit technology and digital computer techniques to electric control of jet engines
[NAL-TR-281] 09 p1078 N73-18799
Probabilistic model for estimating efficiency of operational servicing system for control digital computer onboard spacecraft
10 p1177 N73-19575
Operational models for analyzing digital control system between computer and information sources
10 p1177 N73-19576
Human factors criteria for adaptive computer aiding in man-machine control system
[AD-754835] 11 p1250 N73-20147
Interface data processing system for telecommunication computer network
[AD-754441] 11 p1260 N73-20228
Failure and diagnosis of faults in logic and combinational circuits of digital computers
[AD-754029] 11 p1265 N73-20264
Digital computer program for analyzing electromagnetic design of salient, wound pole alternators
[NASA-TN-D-7258] 12 p1366 N73-21082
Analysis of dual reflector antenna system using physical optics and digital computers
[NASA-TM-X-66223] 12 p1379 N73-21183
On-line digital computer control of NERVA
12 p1426 N73-21558
Interrupt handling facilities in AADC system and associated control
[AD-756665] 13 p1498 N73-22142
Fault-tolerant clock apparatus for use in digital logic systems which maintains output pulses during component failure
[NASA-CASE-MSC-12531-1] 13 p1528 N73-22386
Structure and signal processing capabilities of special speech processor
14 p1631 N73-23222
Tactical integrated electronic systems for Swedish military aircraft
14 p1711 N73-23889
Design of aircraft digital system for automatic flight control
14 p1713 N73-23900
Computerized teleoperator applications in manned aerospace systems
14 p1713 N73-23904
Algorithm for computer processing of Fourier transformations
[AD-758451] 15 p1755 N73-24222
Fundamental characteristics of onboard digital computers and converters
16 p1879 N73-25208
Research and development progress on electronic equipment, integrated circuits, semiconductors, and digital computers
[AD-759180] 16 p1884 N73-25251
Digital computer model to predict spectral irradiance on ground target from sun and sky
[AD-758877] 16 p1945 N73-25739
Specifications for interconnection of host and interface message processor
[AD-759433] 17 p2001 N73-26182
Application of Minuteman guidance computer for numerical processing control
[AD-760757] 18 p2121 N73-27145
Specialized digital computer for correlation analysis
[AD-761586] 19 p2241 N73-28066
Asynchronous control modules for digital computer design
[AD-762345] 19 p2241 N73-28067
Analysis of electronic digital computer inaccuracies
[AD-762235] 19 p2241 N73-28068
Analysis of languages for design of digital computers
[AD-762381] 19 p2241 N73-28071
Procedures for checking storage and transmission of instrumental, numerical, and address information in digital computer
[AD-762245] 19 p2242 N73-28073
Analysis of algorithms for construction of system of diagnostic programs for digital computer complexes
[AD-762310] 19 p2242 N73-28074
Error detecting algorithm for digital control computer
[AD-762241] 19 p2242 N73-28075
Compilation of diagnostic programs developed for digital computer malfunctions analysis
[AD-762237] 19 p2242 N73-28076
Statistical prediction of malfunction in digital computer
[AD-762263] 19 p2242 N73-28079
Determination of diagnostic nucleus of digital computer
[AD-762264] 19 p2242 N73-28080
Signal processing digital computer for microprogramming all applications computer
[AD-761610] 19 p2242 N73-28081
Velocity integration in navigational digital computers
20 p2440 N73-29596
Digital computer calculation of molecular hydrogen-atomic hydrogen interaction energy and electric dipole moment
[NASA-TM-X-2839] 20 p2455 N73-29733
Spaceborne TR 16 digital computer systems analysis
[BMBW-FBW-72-22] 22 p2639 N73-31152
Algorithm for calculating correcting signals in flight control systems with high speed digital computer
[AD-764310] 22 p2640 N73-31157
Manipulation of digital computer source program for terminal ballistics of gun launched guided projectiles
[AD-764225] 22 p2640 N73-31161
Digital computer program for nonlinear steady state of transient analysis of heat conduction in three dimensional solids
[WAPD-TM-1080] 22 p2729 N73-31843
Monitoring and control of fuel cell system by digital computer
[NASA-TM-X-2923] 23 p2748 N73-31994
Interface message processor for digital computer network
[AD-763734] 23 p2761 N73-32098
Design of computer controlled cathode ray tube display screen for flight simulator
[AD-764762] 23 p2767 N73-32140
Comparison of digital computer programs for numerical solution of ordinary differential equations
[NASA-TM-X-64781] 23 p2813 N73-32487
System software for fault-tolerant digital computer
24 p2896 N73-33120
DIGITAL DATA
Kalman filtering algorithm for detecting continuous wave interference signals in digital telecommunications
01 p0027 N73-10210
Digital data analysis of traveling ionospheric disturbances
[AD-746314] 01 p0054 N73-10441
Processing of Concorde digitally recorded data
01 p0056 N73-10453
Methods for implementation of man machine interface of digital data links for air traffic control
[AD-744721] 01 p0079 N73-10648
Figure series for digital data presentation
[IZF-1972-11] 02 p0145 N73-11170
Digital precision processing of ERTS-1 imagery of Chesapeake Bay
[E72-10292] 04 p0410 N73-13342
Digitizing of topographic maps for electronic data processing
[MITT-130] 04 p0414 N73-13379

Phase coherent frequency synthesizer for improving digital voice and data transmission in communication systems
04 p0472 N73-13853
Development and characteristics for automatically displaying digits in any desired order using optical techniques
[NASA-CASE-XKS-00348] 05 p0518 N73-14215
Digital facility for handling and processing remotely sensed earth resources data
05 p0537 N73-14369
Computerized simulation of data compression using ERTS-1 MSS digital tapes
[E73-10011] 06 p0659 N73-15347
Digital data processing portion of Dartmouth ionosonde network used to analyze traveling ionospheric disturbances
07 p0775 N73-16290
Digital signal processing applied to ocean bottom seismic reflection data
[PB-212155] 07 p0794 N73-16456
Digital coding and modulation processes in radio transmission
[NLL-PO-2832-[9022.81]] 11 p1254 N73-20177
Processing digital radar data base to create simulated mapping-radar scope images
[AD-755722] 13 p1495 N73-22118
Analysis of digital microdensitometer data from ERTS-1 imagery of San Francisco, California
[E73-10521] 13 p1517 N73-22289
Analytical prediction of crosstalk in multi-wire digital data transmission
14 p1641 N73-23301
Digital recreational land use mapping in Oakland County, Michigan
[E73-10570] 15 p1772 N73-24350
University of Alaska program for processing ERTS-1 environmental data
[E73-10636] 15 p1776 N73-24395
Computer analysis of digitized sferic data from atmospheric analyzers
[AD-758102] 15 p1783 N73-24453
Feasibility of modifying Tacan/DME system to broadcast digital data for area navigation
[FAA-RD-73-2] 15 p1808 N73-24656
Identification and mapping of soils, vegetation, and water resources in Texas from ERTS-1 MSS digital data
[E73-10670] 16 p1899 N73-25365
State of readiness to process and reduce Skylab EREP digital data
[E73-10798] 18 p2138 N73-27274
Digital system for precision geometric and radiometric correction of ERTS-1 RBV and MSS images
[E73-10827] 18 p2140 N73-27299
Differential pulse code modulation of digital video signals
[BBC-RD-1973/7] 19 p2234 N73-28011
Technique for hybrid addition of both digital and analog data in troposcatter communication system
[AD-761523] 19 p2236 N73-28030
Digital land use mapping in Oakland Country, Michigan using ERTS-1 data
[PAPER-L21] 19 p2276 N73-28316
Digital data processing of ERTS-1 MSS imagery of water masses in Delaware Bay
19 p2286 N73-28380
System for displaying low resolution digital grayscale images of ladar target imaging system
[DREV-TN-2075/73] 19 p2307 N73-28552
Acquisition of Skylab data and determination of surface water areas from digital data
[E73-10912] 20 p2397 N73-29261
Digital data generation and processing in airborne ionospheric research
[AD-763088] 20 p2414 N73-29406
Design, operation, and maintence of digital recording CW system for Minuteman 2 missiles
[AD-763115] 20 p2488 N73-29991
Digital precision processing of ERTS-1 imagery of Monterey Bay, California
[E73-10948] 21 p2530 N73-30290
Standard digital data clock-rate generator with programmable digital phase shift for data transmission from communication satellites
[AD-764049] 22 p2635 N73-31117
Characteristics of digital communication systems and processing of bandpass digital signals using spread spectrum techniques for data transmission
23 p2756 N73-32055
Threshold selection for interpretation of digital pictures
[AD-764736] 24 p2898 N73-33132
Operational system for processing both imagery and computer compatible tapes of ERTS-1 and aerial data of Pennsylvania
[E73-11105] 24 p2915 N73-33262
Correction of banding in ERTS-1 MSS digital data
[E73-11108] 24 p2915 N73-33265
Pennsylvania State University library catalogue for remotely sensed digital data tapes
[E73-11115] 24 p2916 N73-33272
Processing ERTS-1 MSS digital data of Susquehanna River Basin
[E73-11165] 24 p2920 N73-33318

**DIGITAL FILTERS**
Digital computer techniques for filtering and transmission of telecommunication data
01 p0025 N73-10192
Fast Fourier transform digital processor as spectrum analyzer and adaptive filter
01 p0025 N73-10198
Automatic equalizers of telephone channels for fast transmission of digital data
01 p0025 N73-10199
Algorithm for adaptive digital filters of data communication channels
01 p0026 N73-10200
Fast digital noise filter capable of locating spectral peaks and shoulders by using techniques of convoluting integers
[NASA-TM-X-64707] 03 p0273 N73-12212
Research on speech recognition, spectrum analyzers and design of digital filters
[AD-748212] 04 p0396 N73-13223
Digital filter theory for broadband beamforming and hydrophone array steering
[AD-746206] 06 p0641 N73-15201
Minimax approximation to frequency responsive nonrecursive digital filter
[AD-750767] 06 p0648 N73-15263
Digital implementation of high frequency cutoff filter for spacecraft control system optimization based on word length, sampling rate, accuracy, and computing time requirements - Vol. 2
[NASA-CR-124051] 09 p1086 N73-18861
Dither, large suitably fluctuating component, in digital matched filters
[AD-753808] 10 p1135 N73-19249
Digital filtering techniques
[NASA-CR-124166] 11 p1264 N73-20256
Design of digital filters for bandpass and low pass applications
[AD-754032] 11 p1265 N73-20266
Modelling error sensitivity of digital filters for alignment of inertial platforms
11 p1319 N73-20708
Effects of small LSI packages and modularity on development of digital filters
[AD-755657] 12 p1385 N73-21228
Automatic formant and fundamental frequency extraction from digital inverse filter formulation
14 p1622 N73-23139
Digital filter with dither for correlation detection of weak signal in jamming environment
[AD-757013] 14 p1643 N73-23325
Performance of digital matched filter receiver designed to receive biphase modulated signal in presence of interference
[AD-756841] 14 p1643 N73-23326
Design of mathematical filters with finite precision
16 p1934 N73-25647
Nonrecursive counting digital filter containing shift register
[NASA-CASE-NPO-11821-1] 17 p2000 N73-26175
Recursive digital filters in moving target indicator of phased array radars
[AD-759901] 18 p2118 N73-27128
Design of fast Fourier transform digital processor
[AD-761803] 19 p2245 N73-28097
Floating point system quantization errors in digital control systems
[NASA-CR-124382] 22 p2638 N73-31145
Computer enhancement of radiographs using digital filtering techniques
[NASA-CR-124393] 22 p2673 N73-31414
Mathematical voice model for a priori digital speech analysis
24 p2894 N73-33104
Statistical design of nonrecursive digital filters for signal processing
[AD-764595] 24 p2899 N73-33142
Wave digital filter design using ladder networks
24 p2899 N73-33145

**DIGITAL INTEGRATORS**
Digital circuit optimization by time multiplexing component devices
22 p2646 N73-31200
Economics and performance characteristics of high speed digital integrated circuits used in nuclear instrumentation
[LBL-1750] 24 p2900 N73-33150

**DIGITAL RADAR SYSTEMS**
Spatial distribution model of reflectivity in storm cells for digital radar data
[NASA-TM-X-66118] 03 p0327 N73-12661
Receiver synthesis for air traffic moving target indicator with digital signal processing
[AD-751923] 08 p0885 N73-17170
Radar arithmetic signal processing element with digital filter and Fourier transformation for moving target indication
[AD-754060] 11 p1258 N73-20206
Simulation of digital radar landmass simulator
[AD-756219] 14 p1634 N73-23250
Digital radar landmass simulation for determining optimum specification of digital radar training devices
[AD-758363] 15 p1763 N73-24284
Signal modulation and digital processing for real time radar operation
[AD-762438] 19 p2238 N73-28040

**DIGITAL SIMULATION**
Digital simulation model for design of optimal spaceborne computer system
[NASA-CR-128997] 02 p0146 N73-11184
Digital simulation model for central processing unit of spaceborne computer with automatically reconfigurable modular multiprocessor system
[NASA-CR-128996] 02 p0146 N73-11185
Digital simulations of Joule heating and heat transfer processes in amorphous semiconductor switches
[AD-746278] 02 p0219 N73-11776
Digital simulation and angle tracking accuracy of tactical radar with multipath propagation
[AD-748384] 03 p0268 N73-12172
Detailed digital simulation of Army Missile Command experimental array radar system for air defense against low altitude threats
[AD-749501] 05 p0514 N73-14177
Digital simulation language for flight dynamic tests, expemplified by Fiat G-91 and Dornier Do-31 aircraft
[BMVG-FBWT-72-21] 07 p0740 N73-16019
Digital computer simulation of one-dimensional plasma behavior in plasma betatron
10 p1195 N73-19726
Digital simulation method to study wind tunnel model ship configurations
[AD-755005] 11 p1273 N73-20333
Description of maneuvering aircraft trajectory by second-order non-Gaussian process verified by digital simulation
[TAE-167] 14 p1683 N73-23656
Mathematical models for human performance in manned spacecraft control
14 p1712 N73-23897
Serpentine teleoperator device for simulating intravehicular and extravehicular activities in space
[NASA-TR-R-414] 16 p1879 N73-25210
Analog and digital computer simulation study of pulse width modulation in feedback control systems
16 p1883 N73-25242
Simulation testing of detector for digitally encoded multifrequency tones
[REPT-6755] 18 p2116 N73-27113
Vision model for robot object recognition system
[NASA-CR-133458] 19 p2224 N73-27936
Digital simulation of multicorrelated random processes and its applications
[NASA-CR-62092] 21 p2565 N73-30563
Three level Boolean digital simulation program for logic circuits noting topological matrix circuit representation and simplified temporal simulation
[LAAS-SL-73-I-08] 23 p2769 N73-32149
Simulated launch countdown, liftoff, and flight test to demonstrate compatibility of Skylab rescue space vehicle systems, ground support, and off-site support facilities
[NASA-TM-X-69520] 23 p2850 N73-32776
Mathematical model and digital computer simulation of cardiovascular control system response to ergometer exercise
24 p2886 N73-33049

**DIGITAL SYSTEMS**
NT DIGITAL RADAR SYSTEMS
Simulation techniques for determining broadcast quality of digital sound signals produced by pulse code modulation transmission system
[BBC-1972/31] 01 p0024 N73-10183
Digital telecommunication techniques and network planning for aerospace systems
01 p0024 N73-10188
Development and characteristics of digital beamformer for narrowband sonar systems
[AD-745302] 01 p0029 N73-10224
Uncorrected accelerometer data resulting from San Fernando, California earthquake of Feb. 1971
[PB-208529] 01 p0054 N73-10439
Ionosonde using solid state analog components and digital arrays for continuously monitoring ionosphere
[AD-745965] 02 p0167 N73-11359
Digital visual displays for checking pressure points from wind tunnel models
[ARA-28] 02 p0172 N73-11388
Digital control system for Baum folding machine providing automatic counting and machine shutoff
[NASA-CASE-LAR-10688-1] 02 p0178 N73-11442
Digital acquisition of acoustic signals and digital analysis of acoustic and oceanographic data
[AD-746204] 02 p0212 N73-11720
Digital second order, phase locked loop with counter driven by stable clock pulse source
[NASA-CASE-NPO-11905-1] 03 p0270 N73-12192
Asynchronous control circuits for digital systems representation and modular design
03 p0272 N73-12202
Logic comparison of failure diagnosis for digital systems
03 p0272 N73-12203

Characteristics of digital data processor using pulse from clock source to derive binary singles to show state of various indicators in processor
[NASA-CASE-GSC-10975-1] 04 p0392 N73-13187
Arithmetic codes for error control in digital computation and data transmission
[AD-748201] 04 p0394 N73-13206
Temperature corrected circuit for gyroscope or accelerometer of digital rebalance type
[NASA-CASE-NPO-13044-1] 04 p0421 N73-13436
Analysis of digital information coding procedures with application to control of synchronization errors in data transmission on pulse code modulation systems
[NLL-TRANS-2825-[9022.81]] 05 p0507 N73-14127
Development of serial to parallel digital to analogue converter to obtain stable d.c. voltage from three digits of computing counter twelve digit display
[REPT-6702] 05 p0516 N73-14196
Speed independent control structures for digital systems 05 p0517 N73-14207
Simplified model for comparative evaluation of effectiveness of integrated circuits in digital equipment
[AD-749640] 05 p0518 N73-14211
Digital phase measuring device for mutual phase position of two signals, emphasizing LF and VLF waves
[AD-750472] 06 p0675 N73-15497
Digital processing of ERTS-1 imagery of Tennessee Valley
[E73-10054] 07 p0778 N73-16316
Development of highly accurate and reliable telemeter system utilizing integrated circuits
[AD-752481] 08 p0886 N73-17176
Development of solid state magnetic digital temperature transducer - Vol. 1
[NASA-CR-133832] 08 p0923 N73-17556
Multichannel digital spectrometer for measuring ion temperature of Circe 25-kW device
[EUR-CEA-FC-641] 08 p0925 N73-17582
Acceptance tests of direct current high precision digital voltmeter
[LRBA-PV-11/520/SIE] 09 p1008 N73-18227
DONAR system for digitizing ultrashort sonic wave trains from pulse echo systems
[NASA-CR-130883] 09 p1013 N73-18266
Theoretical and experimental analysis of digital processing in various communication systems 10 p1127 N73-19183
Program for logic design of digital counters or sequential circuits
[NASA-CR-2212] 10 p1132 N73-19230
Digital address thin display tube with resolution of 55 holes per inch
[AD-753604] 10 p1135 N73-19250
Digital photometer for recording measurements of ionospheric disturbances
[AD-754436] 10 p1157 N73-19415
Digital flight director for precise aircraft control
[AD-754028] 11 p1322 N73-20726
Piezoelectric quartz crystals used as digital transducers in completely digital detection systems for monitoring gas streams 12 p1382 N73-21208
Development and characteristics of flat, thin, cathode ray tube with digital switching for beam deflection and positioning
[AD-755938] 12 p1384 N73-21227
Digital systems for automatic processing of remote earth resources sensing data 12 p1400 N73-21355
Research projects to develop all-weather, low level navigation systems based on one way ranging, range-range navigation techniques
[AD-755205] 12 p1426 N73-21556
Design of all digital low data rate communication system with potential cost reduction
[NASA-CR-130234] 13 p1490 N73-22077
Digital quadrature methods for processing bandpass signals
[AD-755473] 13 p1494 N73-22110
Diagnostic computer system for fault diagnosis of digital circuits 13 p1496 N73-22128
Structure analysis of digital picture processing system
[AD-755699] 13 p1499 N73-22147
Improved spectral digital frequency synthesizer
[AD-756864] 13 p1501 N73-22164
Characteristics of tunable bandpass filter with large range of resonant frequency
[AD-756662] 13 p1501 N73-22165
Feasibility of advanced digital flight control system using digital processor as main computational element
[AD-757271] 14 p1604 N73-23002
Application of digital signal processing to design of phase vocoder analyzer 14 p1621 N73-23131
Speech synthesis using Hadamard-Walsh transform 14 p1624 N73-23158
Use of orthogonal Walsh and Hadamard transforms to reduce bit rate for speech communication 14 p1624 N73-23159
Diagnostic evaluation of intelligibility in digital vocoders 14 p1624 N73-23161
Subjective evaluation of differential pulse code modulation using speech goodness rating scale 14 p1624 N73-23162
High speed digital recording system for VLF and ELF sferic waveforms
[AD-757427] 14 p1669 N73-23544
Hardware phase of digital capacitance measuring system
[REPT-2873-2143-116] 15 p1754 N73-24218
Interactive digital processing of optical data in investigations of pattern recognition techniques
[AD-758517] 15 p1755 N73-24223
Highly accurate digital barometer
[NLL-M-22973-[5828.4F]] 16 p1910 N73-25458
Low phase noise frequency divider for use with deep space network communication system
[NASA-CASE-NPO-11569] 17 p2007 N73-26229
Digital system for programmed control of maching process for turbine blade foil
[AD-759682] 17 p2077 N73-26804
A priori digital speech analysis
[AD-762029] 19 p2237 N73-28037
Synchronized digital communication system
[NASA-CASE-XNP-03623] 19 p2243 N73-28084
Comparison of photographic digital recording systems using laser technology
[AD-761521] 19 p2308 N73-28563
Development of digital flight control system for performing pilot assist augmentation and pilot relief automatic pilot functions
[AD-762521] 20 p2361 N73-28992
Design, development, airworthiness test, and flight test of multiplexing components for fly by wire flight control
[AD-763111] 20 p2362 N73-28996
Modelling, analysis, and applications of class of all digital phase locked loops 20 p2375 N73-29082
Digital reproducing amplifiers for magnetically recording data from airborne processor
[ARL/ME-337] 20 p2376 N73-29090
Quasi-optimum digital phase locked loops derived by nonlinear estimation theory 20 p2380 N73-29121
Analysis of statistical properties of filtered summed maximum length digital sequences 20 p2436 N73-29564
Digital precision processing of ERTS-1 imagery of Monterey Bay, California
[E73-10948] 21 p2530 N73-30290
Procedure for connected and orthogonal binary random processes with continuous time 22 p2628 N73-31059
Digital signal processor for use with experimental MICOM array radar
[AD-764227] 22 p2635 N73-31121
Digital detector for measuring liquid helium level
[PB-221313] 22 p2676 N73-31436
Hybrid programmable attitude control electronic analog digital system for preflight and in-flight changes in planetary missions 22 p2731 N73-31859
Digital error probalities of binary receivers in presence of intersymbol interference in fading channels 23 p2755 N73-32049

**DIGITAL TECHNIQUES**

Conference on expanded aerospace telecommunication system requirements and digital data transmission methods
[AGARD-CP-103] 01 p0024 N73-10187
Error probability and bandwidth efficiency in digital transmission channel 01 p0025 N73-10193
Digital receiver for detecting moderate data rate phase-shift keyed signals in real time 01 p0025 N73-10196
Feasibility of all-digital implementation of world-wide analog communications systems 01 p0027 N73-10209
Lunar Orbiter photographic and photometric data enhancement - framelet joining, digitization, data improvement, and statistical error analysis
[NASA-CR-128581] 01 p0057 N73-10463
Digital correction techniques for ERTS-1 imagery
[E72-10206] 02 p0161 N73-11303
Design and development of closed-loop, digital data communication system using optimum number of interconnecting wires
[NASA-CASE-MSC-13912-1] 03 p0266 N73-12151
Automatic sequential processing, technique for unsupervised classification, or clustering, of multispectral remote sensing data, using digital computer program
[NASA-CR-128999] 03 p0323 N73-12633
Development and characteristics for automatically displaying digits in any desired order using optical techniques
[NASA-CASE-XKS-00348] 05 p0518 N73-14215
Digital correction techniques for ERTS-1 imagery
[E72-10365] 05 p0535 N73-14353
Application of digital techniques for control of large antennas used for satellite tracking
[NASA-TM-X-66154] 07 p0754 N73-16127
Digital processing of ERTS-1 imagery
[E73-10080] 08 p0901 N73-17292
Theoretical and experimental analysis of digital processing in various communication systems 10 p1127 N73-19183
Precision geometric and radiometric correction of bulk digital ERTS-1 imagery by digital techniques
[E73-10342] 10 p1148 N73-19341
Apparatus and digital technique for coding rate data
[NASA-CASE-LAR-10128-1] 11 p1259 N73-20217
Evaluation of high response electrohydraulic digital control valve for application to flight control systems
[NASA-CR-124178] 11 p1297 N73-20523
Techniques and software for digital enhancement of radiographs
[NASA-CR-2213] 13 p1497 N73-22135
Digital technique for picture processing
[AD-755701] 13 p1499 N73-22145
Digital correction techniques for ERTS-1 MSS imagery
[E73-10503] 13 p1515 N73-22278
Survey of digital speech processing activity in US and abroad 14 p1620 N73-23120
Electronic time compressor/expander for audio using digital technology 14 p1621 N73-23129
Digital pattern classification for automatic recognition of English language speech
[AD-757492] 14 p1636 N73-23262
Digital techniques for reducing variance in reflected rain signals
[METEOROL-STUDY-25] 16 p1875 N73-25181
Analysis of digital communication systems disturbed by non-Gaussian noise 19 p2235 N73-28017
Rectification of ERTS-1 multispectral imagery using digital techniques
[PAPER-16] 19 p2277 N73-28327
Application of digital techniques to processing of ERTS-1 MSS and RBV image data
[PAPER-17] 19 p2278 N73-28328
Digital enhancement of ERTS-1 MSS data for maximum image visibility
[PAPER-110] 19 p2278 N73-28331
Geometric aspects in digital analysis of multispectral scanner data
[NASA-CR-133641] 21 p2511 N73-30137
Digital correction techniques for ERTS-1 imagery of Baltimore, Maryland
[E73-10963] 21 p2533 N73-30305
Digital methods of television signal timing corrections
[BBC-RD-1973/15] 22 p2627 N73-31048
Digital phase-locked loop for accumulator output signal phase-locked to input signal
[NASA-CASE-GSC-11623-1] 22 p2646 N73-31202
Precision geometric and radiometric correction of bulk digital ERTS-1 imagery of Baltimore, Maryland by digital method
[E73-11019] 22 p2661 N73-31323
Digital attitude control system for Explorer 50 satellite
[NASA-TM-X-70488] 24 p2950 N73-33567
Digital spectrum analysis for turbulent plasma diagnostics
[AD-765549] 24 p2966 N73-33704

**DIGITAL TO ANALOG CONVERTERS**

Development of coupled operational amplifier circuits with emphasis on wiring for current signals and influence of errors due to coupling
[AD-743690] 01 p0033 N73-10257
Development of serial to parallel digital to analogue converter to obtain stable d.c. voltage from three digits of computing counter twelve digit display
[REPT-6702] 05 p0516 N73-14196
Digitizer performance under conditions of linear and circular antenna polarization
[FAA-NA-73-49] 20 p2376 N73-29095
Digital to analog converter for sampled signal reconstruction
[NASA-CASE-MSC-12458-1] 23 p2759 N73-32081

**DIGITAL TO VOICE TRANSLATORS**

Voicing adaptive speech digitization technique with delta modulation for effective operation at 9600 bits/second 14 p1621 N73-23133

**DIGITAL TRANSDUCERS**

Elastic surface wave encoders and decoders for use in secure, antijam command, control, and communications systems
[AD-758762] 16 p1919 N73-25529
Computer technique for transferring digital television signal to punched tape
[BBC-RD-1973/6] 19 p2238 N73-28044
Electromechanical coupling coefficient of interdigital surface wave transducer on piezoelectric ceramic
[AD-761879] 19 p2246 N73-28105
Digital to analog converter for sampled signal reconstruction
[NASA-CASE-MSC-12458-1] 23 p2759 N73-32081

DIGITIZERS
U ANALOG TO DIGITAL CONVERTERS
DIGITS
NT BINARY DIGITS
DIHEDRAL EFFECT
U LATERAL STABILITY
DIISOCYANATES
Chemical and physical properties of synthetic polyurethane polymer prepared by reacting hydroxy carbonate with organic diisocyanate
[NASA-CASE-MFS-10512] 21 p2505 N73-30099
Preparation of stable polyurethane polymer by reacting polymer with diisocyanate
[NASA-CASE-MFS-10506] 21 p2505 N73-30100
Preparation of polyurethane polymer by reacting hydroxy polyformal with organic diisocyanate
[NASA-CASE-MFS-10509] 21 p2505 N73-30103
DILATATION
U STRETCHING
DILATATIONAL WAVES
Effect of pressure gradients on supersonic turbulent boundary layers and effect of dilation on Reynolds stresses
[IC-AERO-72-21] 07 p0736 N73-15989
DILATOMETERS
U EXTENSOMETERS
DILATOMETRY
Use of quartz and corundum monocrystals to verify dilatometric measurements in USSR
[AD-745840] 01 p0059 N73-10480
Improved dilatometer with helium cryostat for low temperature measurements
[AD-747555] 03 p0304 N73-12484
Microstructural analysis of high-chromium martensitic semiferritic and ferritic steel phase transformations and thermal expansion coefficient determination
[AD-749522] 04 p0436 N73-13559
Volumetric analysis and dilatometric study of ferrite magnesium cast iron during heat treatment
[AD-749627] 05 p0563 N73-14572
Differential thermal analysis and dilatometry of 4 to 5 years stored ammonium nitrates with amine copper complex additives
[ICT-4/72] 16 p1954 N73-25812
DILUTION
Investigation of He-3 impurities in He-4 for development of microscopic theory of He-3 quasiparticles
12 p1375 N73-21155
Dosage device for diluting concentrated aerosols at ratios between 1/60 and 1/800
[BMVG-FBWT-73-2] 14 p1668 N73-23534
Dispersion and dilution of jet aircraft exhaust at high altitudes
[NASA-TM-X-71451] 24 p2971 N73-33743
DIMENSIONAL ANALYSIS
Physiology and dimensional analysis of semicircular canal
[AMRU-R-69-1] 02 p0130 N73-11058
Comparison of turbine annulus mass flow calculations when computed by one- and two-dimensional analysis
[NASA-TM-X-2661] 02 p0156 N73-11264
Multiperipherism and hydrodynamics of multiple processes
[NASA-TT-F-14896] 13 p1561 N73-22656
DIMENSIONAL MEASUREMENT
Resistance leval indicator used in high temperature alkali tanks
[SFB-MHD-2] 04 p0422 N73-13444
DIMENSIONAL STABILITY
NT SHELL STABILITY
NT STRUCTURAL STABILITY
DIMENSIONLESS NUMBERS
NT FROUDE NUMBER
NT HARTMANN NUMBER
NT MACH NUMBER
NT NUSSELT NUMBER
NT PRANDTL NUMBER
NT REYNOLDS NUMBER
NT SIMILARITY NUMBERS
DIMENSIONS
NT DEPTH
NT FILM THICKNESS
NT HEIGHT
NT RADII
NT THICKNESS
Choice of suitable manufacturing dimensions for parallel axis straight spur and helical gears
[ESDU-66001] 01 p0060 N73-10493
Data for major dimension determination for straight spur and helical gears
[ESDU-68040-AMEND-A] 02 p0176 N73-11428
Functional dependence of semicircular canal on physical size
06 p0633 N73-15139
Dimensions and mechanical properties of elastic spherical shells measured by sound echo signals
10 p1188 N73-19667
Fourier technique for quantitatively classifying lunar rilles by planimetric shape
12 p1455 N73-21781
DIODES
NT AVALANCHE DIODES
NT CRYSTAL RECTIFIERS
NT GERMANIUM DIODES
NT GUNN DIODES
NT JUNCTION DIODES
NT LIGHT EMITTING DIODES
NT PARAMETRIC DIODES
NT PHOTODIODES
NT PLASMA DIODES
NT SCHOTTKY DIODES
NT THERMIONIC DIODES
NT TUNNEL DIODES
NT VARACTOR DIODES
GaAs wafer development, diode construction, and resonator design
[AD-746655] 02 p0150 N73-11213
Development of gallium aluminum phosphide alloys for electroluminescent diodes
[NASA-CR-112182] 03 p0273 N73-12213
Fabrication processes for silicon Schottky barrier diodes
[FRNC-TH-179] 03 p0274 N73-12218
Display system consisting of light emitting diode arrays monolithically fabricated on single wafers of GaP
[AD-746993] 03 p0274 N73-12225
Single crystal alpha SiC for GEISHA device with electron carrier velocity up to 8,200,000 cm/sec on 10 to 17th power/cu cm uncompensated n-type crystals
[AD-747270] 03 p0275 N73-12228
Investigation of nonlinearities in X band IMPATT reflection amplifiers
[AD-747796] 03 p0275 N73-12231
Diode passivation techniques and fabrication of semiconductor targets that are stable under electron beam bombardment for use in L band amplifiers
[AD-747868] 03 p0276 N73-12237
Materials and devices for generation, amplification, and millimeter wave energies
[NASA-CR-130113] 03 p0334 N73-12724
Construction of electron beam semiconductor pulse amplifier and radio frequency amplifier diode
[AD-748892] 04 p0461 N73-13758
Development of temperature compensated light source with components and circuitry for maintaining luminous intensity independent of temperature variations
[NASA-CASE-ARC-10467-1] 05 p0518 N73-14214
Development of high power diode microcircuits
[SC-CR-72-3142] 05 p0519 N73-14219
Automatic measurement of frequency stability of microwave Gunn diode oscillators at low temperatures noting graphs of power and frequency against time
[SRDE-72013] 05 p0520 N73-14226
Feasibility determination for use of p-i-n diodes as switching elements to control impulse signals in strip transmission line
[AD-749125] 05 p0520 N73-14229
Solving problem of noise in single and double injection diodes
[AD-750186] 06 p0645 N73-15240
Application of light emitting diodes to pumping of solid-state laser rods
[AD-750576] 06 p0681 N73-15545
Millimeter wave mixer with small metallic wafer embedded with diodes
[NASA-CR-124060] 08 p0925 N73-17581
Design, fabrication, and test of flight qualified heat pipe diode for Advanced Thermal Control Flight Experiment
[NASA-CR-114526] 08 p0968 N73-17915
Noise characteristics of functional correlators using nonlinear elements with exponential characteristics
12 p1386 N73-21241
Conduction processes in field driven semiconductor p-i-n diodes
12 p1437 N73-21643
Low injection reverse recovery switching phenomena in lithium-drifted silicon PIN diodes
13 p1499 N73-22148
Reliability tests of reverse biased semiconductor diodes under electron beam bombardment conditions
[AD-755449] 13 p1502 N73-22171
Fabrication of monolithic light emitting diode display system on single wafers of gallium phosphide
[AD-755204] 13 p1502 N73-22172
Light emitting diode pumped Nd/YAG lasers
[NASA-CR-124225] 13 p1536 N73-22645
Hot electron effects in SCL diodes and MOSFETS
13 p1565 N73-22680
High isolation RF signal selection switches
[NASA-CASE-NPO-13081-1] 14 p1618 N73-23106
Monolithic light emitting diode display devices
[AD-758853] 16 p1882 N73-25232
Formation of current filaments in thin film silicon-on-sapphire diodes
16 p1952 N73-25795
Silicon carbide backward diode with coated lead attachment
[NASA-CASE-ERC-10224-2] 18 p2122 N73-27150
Fabrication of array of silicon diodes for application in electron beam semiconductor device
[AD-760602] 18 p2124 N73-27164
Effect of various growth and doping parameters on GaN for LED applications
[NASA-CR-132263] 18 p2189 N73-27676
Real time measurement of three-dimensional position of light emitting diodes
[AD-762028] 19 p2241 N73-28070
Research and development of electronic equipment for night combat surveillance
[AD-762351] 19 p2302 N73-28507
Laboratory model of distributed pin diode millimeter wave phase shifter
[AD-762572] 20 p2381 N73-29136
Determination of thermal characteristics of electroluminescent diode
[NASA-TM-X-70440] 21 p2517 N73-30190
Susceptibility of X band point-contact diodes to microwave radiation
[AD-763364] 21 p2518 N73-30197
Luminescent diode and liquid crystal display devices for telephony, using COS/MOS and TTL logic
[FTZ-421-TBR-4] 22 p2633 N73-31105
Minority carrier lifetime and switching time of step recovery diode for pulse generators in microwave equipment
[FTZ-A-651-TBF-3] 22 p2643 N73-31180
Dynamic characteristics of microwave synchronized oscillators
22 p2643 N73-31185
Second breakdown in diodes and transistors from intense ionizing radiation
[AD-763951] 22 p2644 N73-31192
Minority carrier lifetime control in n-type base regions of gallium diffused silicon power thyristors and diodes
[BMFT-FB-T-73-05] 23 p2765 N73-32123
Effects of nuclear radiation on reverse bias electrical characteristics of silicon power diodes
[NASA-TN-D-7423] 23 p2821 N73-32554
Improved high frequency performance of mixer diodes by use of Mott barrier
[AD-765182] 24 p2899 N73-33143
Holographic interferometric measurement of plasma density in electron beam diode
[SLA-73-5483] 24 p2927 N73-33376
Coupling efficiency of GaAlAs diode pumped Nd-YAG laser
24 p2930 N73-33398
DIOXIDES
NT CARBON DIOXIDE
NT FLINT
NT HYDROGEN PEROXIDE
NT QUARTZ
NT SILICON DIOXIDE
Increased heat and impact resistance of ceramics made of zirconium dioxide reinforced with mullite whiskers
[JPRS-57770] 05 p0565 N73-14588
Dual gas correlation spectrometer measurements of sulfur dioxide and nitrogen dioxide in industrial area of southern California
[PB-210717] 05 p0575 N73-14676
High concentration sulfur dioxide pollution over Osaka, Japan during summer
[NLL-M-20713-[5828.4F]] 06 p0692 N73-15634
DIPHENYL COMPOUNDS
Application of ultraviolet absorption, gas-liquid chromatography, and gravimetric analysis to determine diphenylamine and ethyl centralite in solid rocket propellant
[TN-267] 02 p0221 N73-11786
Rapid determination of diphenylamine and dinitrotoluene in single base propellants by ultraviolet spectrophotometry analysis
[TM-51] 21 p2587 N73-30730
DIPOLE ANTENNAS
Mathematical model to simulate sphere-centered thin dipole antenna
[AD-745285] 01 p0034 N73-10264
Numerical solutions for small cone angles of modified dipole antennas
[AD-745979] 02 p0149 N73-11211
Analysis of mutual coupling compensation using microstrip techniques with application to behind-the-array coupling of phased antenna array
[NASA-CR-123819] 02 p0151 N73-11222
Resonance excitation by dipole antenna inside hollow cylindrical, cold, uniform, isotropic plasma
[CRC-1230] 04 p0388 N73-13150
VHF omnidirectional antenna developed as printed current panel from flat plate dipole with low aspect ratio
[TR-72-34] 07 p0756 N73-16142
Effect of electromagnetic scattering from ocean surface on spherical waves of dipole antenna
07 p0761 N73-16184
Gain and impedance measurements on ultrahigh frequency antennas near surface of simulated sea water
[AD-751922] 08 p0890 N73-17205
Hallens integral equation for current on dipole antennas in homogeneous isotropic media
[AD-752474] 08 p0890 N73-17206
Explosive generator source, switching and matching networks, and bent dipole antenna
[AD-751907] 08 p0894 N73-17234
Analysis and design by matrix methods of circular antenna arrays consisting of identical parallel dipoles
12 p1382 N73-21205
Electrodynamic fundamentals of antenna theory and design
[AD-755689] 13 p1502 N73-22176

Three-term solution for integral equation of current along thin cylindrical dipole antenna
[AD-758192] 14 p1643 N73-23327
Characteristics of Hertzian dipole antenna radiation patterns and application to lunar surface and subsurface electrical properties investigation - Vol. 2
[NASA-CR-128919] 14 p1705 N73-23836
Broadband characteristics of open sleeve dipole antenna mounted in front of metallic reflector
[AD-758755] 15 p1758 N73-24251
Radiation patterns for cavity backed dipole antenna with almost constant gain
[AD-760126] 17 p2005 N73-26216
Kinetic theory for input impedance of cylindrical dipole antenna in anisotropic plasma
17 p2067 N73-26720
Radiation patterns of electron plasma waves and reception patterns of monopole antennas
[ISAS-491] 18 p2115 N73-27103
Distribution of current in coupled dipole antennas in homogeneous isotropic media
[AD-761167] 18 p2124 N73-27169
Computerized design of hollow dipole antennas for measuring nuclear electromagnetic pulse
[AD-761801] 19 p2244 N73-28096
Dipole receiver characteristics in presence of sea water
[AD-763722] 22 p2644 N73-31187

**DIPOLE MOMENTS**
NT ELECTRIC MOMENTS
NT MAGNETIC MOMENTS
Dipole configuration of pulsed superconducting synchrotron magnet
[KFK-1354] 04 p0458 N73-13739
Core polarization and mesonic exchange current modifications of nuclear magnetic dipole operator
[COO-3001-32] 17 p2064 N73-26701

**DIPOLES**
Analysis of steady state flow of solar wind and effect on magnetic field of dipole
[NASA-TT-F-15071] 22 p2711 N73-31709

**DIRAC EQUATION**
Simulation of high frequency instabilities, using Dirac delta functions
[ORNL-TM-3447] 03 p0342 N73-12790
Ising model for free spinless particles satisfying one dimensional Dirac equation
[AD-747736] 03 p0347 N73-12834
Solution to Klein-Gordon and Dirac equations for charged particles in two noncollinear electromagnetic waves
[AD-754307] 11 p1327 N73-20769

**DIRECT CURRENT**
Estimation of radio frequency power required to induce direct current in strong magnetic field of thermonuclear fusion device
[IPPJ-135] 02 p0216 N73-11746
C-shaped and symmetric dc and RF, voltage-biased superconducting quantum interference devices
[FOA-2-B-2034-E1] 02 p0218 N73-11763
Electrostatic repulsion criteria for dc high voltage spark breakdown of gas
[ORO-4211-5] 03 p0336 N73-12742
Design of power supply voltage monitor for measuring multiple dc voltages simultaneously
[AD-748829] 04 p0424 N73-13453
Development of serial to parallel digital to analogue converter to obtain stable d.c. voltage from three digits of computing counter twelve digit display
[REPT-6702] 05 p0516 N73-14196
Performance tests of differential dc voltmeter
[LRBA-PV-9/520/SIE] 05 p0548 N73-14450
Direct current electrical resistance crack monitoring technique for detection of crack propagation in steels
[PB-212206] 08 p0933 N73-17636
Microwave surface impedance of thin niobium superconducting films subjected to varying dc magnetic fields
12 p1438 N73-21649
Development, characteristics, and advantages of high voltage direct current electrical systems for aircraft power supplies
[AD-757646] 14 p1604 N73-23001
Direct current conductivity in amorphous semiconductors
[AD-756783] 14 p1699 N73-23785
Evaluation of direct current amplifiers for radiation measurements
[CEA-N-1580] 15 p1757 N73-24237
Determination of dynamic zone sparkless commutation for linear and sinusoidal load current changes in dc machines
[NLL-RTS-7771] 18 p2122 N73-27149
Direct current conductivity of cesium plasma in magnetic field
22 p2702 N73-31645
Powerplexer for distribution of dc power levels to loads which require different voltages
[NASA-CASE-MSC-12396-1] 23 p2747 N73-31988
Supercritical helium cooling of superconducting magnet for use in dc beam line elements
[RHEL/R-258] 24 p2969 N73-33725

**DIRECT LIFT CONTROLS**
Flight control problems of steep approach landing with direct lift control, exemplified by HFB-320 aircraft
[DGLR-PAPER-73-024] 23 p2744 N73-31965

**DIRECT POWER GENERATORS**
NT ALKALINE BATTERIES
NT ELECTROSTATIC GENERATORS
NT FUEL CELLS
NT HYDROGEN OXYGEN FUEL CELLS
NT MAGNESIUM CELLS
NT MAGNETOHYDRODYNAMIC GENERATORS
NT METAL AIR BATTERIES
NT NICKEL ZINC BATTERIES
NT PHOTOELECTRIC GENERATORS
NT PRIMARY BATTERIES
NT RADIOISOTOPE BATTERIES
NT REGENERATIVE FUEL CELLS
NT SNAP 10A
NT SNAP 19
NT SNAP 23
NT SOLAR CELLS
NT THERMAL BATTERIES
NT THERMIONIC CONVERTERS
NT THERMOELECTRIC GENERATORS
NT ZINC-OXYGEN BATTERIES
Development of materials and construction processes for improved efficiency of photoelectric converters
04 p0375 N73-13048
Magnetic intermetallic cobalt-rare earth compounds for electromechanical energy converters
[AD-750338] 06 p0645 N73-15242
Operational characteristics of semiconductor photoconverters as power supply sources for space vehicles
[AD-753063] 09 p1074 N73-18766
Direct thermal energy conversion using thermal absorption principle
[NASA-CASE-ARC-10461-1] 11 p1347 N73-20931
Thermodynamic effects on liquid metal magnetohydrodynamic converter flow
[AD-761548] 20 p2459 N73-29762

**DIRECTION FINDERS [RADIO]**
U RADIO DIRECTION FINDERS

**DIRECTIONAL ANTENNAS**
NT DIPOLE ANTENNAS
NT HELICAL ANTENNAS
NT HORN ANTENNAS
NT LENS ANTENNAS
NT LOG PERIODIC ANTENNAS
NT LOOP ANTENNAS
NT PARABOLIC ANTENNAS
NT RADAR ANTENNAS
NT SLOT ANTENNAS
NT STEERABLE ANTENNAS
NT TWO REFLECTOR ANTENNAS
Design and construction of hydrostatic azimuth thrust bearing for tracking antenna of very large size
[NASA-CR-130930] 10 p1165 N73-19478
Wooded terrain effects on radiation patterns of circular and directional antennas
[FOA-3-A-3747-60] 11 p1255 N73-20179
Three dimensional response of directional antenna in elliptically polarized field
[AD-754906] 11 p1257 N73-20202
Analysis of directional antenna transmission line networks
[AD-756567] 13 p1501 N73-22163
Design considerations and calculations for highly directional medium frequency aerial array
22 p2641 N73-31170

**DIRECTIONAL CONTROL**
NT THRUST VECTOR CONTROL
Equivalent circuit network synthesis for branch guide directional couplers
[PB-212651] 08 p0889 N73-17198

**DIRECTIONAL STABILITY**
NT GYROSCOPIC STABILITY
Methods for determining plane of meridian during initial alignment of inertial systems
10 p1184 N73-19636
Wind tunnel tests to determine directional and longitudinal stability of Javelin aircraft model at transonic speeds
[ARC-R/M-3403] 16 p1853 N73-25012

**DIRECTIVITY**
Digital measurements of underwater sound transducer directivity index using hydrophone array
[AD-758639] 16 p1945 N73-25740

**DIRECTORIES**
U INDEXES [DOCUMENTATION]

**DIRICHLET PROBLEM**
Application of periodic Dirichlet problems to analysis of planar theory of elasticity
[AD-741924] 01 p0115 N73-10948

**DIRIGIBLES**
U AIRSHIPS

**DISCHARGE COEFFICIENT**
Measurement of laminar fluid flow through orifice meters to determine discharge coefficients and head losses
[NLL-NEL-TT-2457-[6075.461]]
20 p2386 N73-29169

**DISCHARGE TUBES**
U GAS DISCHARGE TUBES

**DISCHARGERS**
Utilization of oil dischargers in high voltage pulse circuits
[AD-751170] 07 p0765 N73-16214

**DISCONNECT DEVICES**
Squib actuated disconnect for spacecraft coupling to launch vehicle
[NASA-CASE-NPO-13172-1] 08 p0969 N73-17917
Development of low profile flat conductor cable connecting device and permanent splice methods for use in spacecraft component electrical systems - Vol. 1
[NASA-CR-128845] 11 p1262 N73-20241

**DISCONNECTORS**
U DISCONNECT DEVICES

**DISCONTINUITY**
NT SHOCK DISCONTINUITY
Computation of loading on sweptback wings noting extra collocation points
[ARC-CP-1213] 03 p0247 N73-12002
Fourier and Galerkin techniques for analyzing discontinuities and coupling phenomena in microstrip lines
[AD-750737] 06 p0648 N73-15264
Hydromagnetic waves and trapped particle discontinuities in magnetopause
[NASA-TM-X-66146] 06 p0665 N73-15405

**DISCOVERING**
U EXPLORATION

**DISCRETE FUNCTIONS**
Exponential stability of discrete time composite systems with periodic and non-periodic sampling operation
07 p0761 N73-16178
Design of digital filters for bandpass and low pass applications
[AD-754032] 11 p1265 N73-20266
Discrete method for variational problems in treatment of metals by pressure
[NLL-M-21663-[5828.4F]] 21 p2557 N73-30497

**DISCRIMINATION**
NT BRIGHTNESS DISCRIMINATION
NT SENSORY DISCRIMINATION
NT TACTILE DISCRIMINATION
NT VISUAL DISCRIMINATION

**DISEASED VEGETATION**
U BLIGHT

**DISEASES**
NT ANEMIAS
NT ARTERIOSCLEROSIS
NT CANCER
NT CARBON MONOXIDE POISONING
NT DIABETES MELLITUS
NT EDEMA
NT HEART DISEASES
NT INFECTIOUS DISEASES
NT INFLUENZA
NT KIDNEY DISEASES
NT LEAD POISONING
NT PNEUMONIA
NT RADIATION SICKNESS
NT SYPHILIS
NT TOXIC DISEASES
Absorption of fructose in saline mixture used for enteritis therapy of children
[NASA-TT-F-14596] 02 p0133 N73-11078
Detection of plant diseases and nutrient deficiencies, soil types, and moisture levels in Tennessee using ERTS-1 imagery
[E72-10320] 04 p0413 N73-13368
Remote sensing techniques for detection and prevention of Rocky Mountain spotted fever, Encephalitis, Malaria, and Red Tide environmental health problems
[NASA-CR-128727] 07 p0745 N73-16060
Detection of disease in coffee crops using color photography and infrared photography techniques
07 p0783 N73-16366
Detection of citrus tree anomalies by remote sensing with infrared color aerial photography
07 p0785 N73-16384
Chronic disease health trends and mortality rates in employee population of NASA Goddard Space Flight Center
08 p0875 N73-17086
Detection of plant and forest diseases, nutrient deficiencies, soil types, and soil moisture levels from ERTS-1 imagery of Tennessee
[E73-10311] 09 p1022 N73-18343
Detection of plant diseases and nutrient deficiencies, soil types, and moisture levels from ERTS-1 imagery of Tennessee and Kentucky
[E73-10468] 12 p1395 N73-21305
Detection of ponderosa pine tree stresses from insects or diseases using multispectral photography
[NASA-CR-131586] 13 p1522 N73-22337
Syringomyelia in central nervous system affecting flying fitness
14 p1611 N73-23061
Utilization of ERTS-1 imagery to detect plant diseases, nutrient deficiencies, soil types, and moisture levels in Tennessee
[E73-10640] 15 p1776 N73-24399

Color and color infrared aerial photographic detection of Dutch elm disease
16 p1866 N73-25110
ERTS-1 detection of plant diseases and nutrient deficiencies, soil types and moisture levels, forests, and crop identification in Mississippi Delta
[E73-10849] 19 p2292 N73-28427
Influence of solar activity on biological indices and disease of living organisms in biosphere
[NRC-TT-1679] 21 p2592 N73-30771
Detection of plant diseases, soil moisture, drainage patterns, forestry types, and sedimentation in Tennessee from ERTS-1 imagery
[E73-11091] 23 p2782 N73-32258
DISHES
U PARABOLIC REFLECTORS
DISINFECTANTS
U ANTISEPTICS
DISINTEGRATION
Analysis of gas turbine engine rotor failures as basis for conducting program to provide equipment for protection of passengers and aircraft structures from damage
[NASA-CR-131525] 12 p1443 N73-21692
DISKS [SHAPES]
NT ACTUATOR DISKS
NT ROTATING DISKS
Radar observation of disk-shaped models of proposed nuclear heat source module
[NASA-TM-X-62262] 14 p1601 N73-22978
Finite element calculation of two-dimensional heating and melting of disks and applications to laser effects
[AD-757189] 14 p1719 N73-23950
Bar shaped density wave theory of barred spiral galaxies
19 p2341 N73-28835
Ultrasonic inspection and control for laminated steel disc
[TR-73-2-640] 20 p2423 N73-29461
Temperature, shock, vibration, humidity, salt-fog, and electromagnetic tests on automotive disk recorder
24 p2926 N73-33368
DISLOCATIONS [MATERIALS]
NT CRYSTAL DISLOCATIONS
NT EDGE DISLOCATIONS
Aluminum metallographic method to obtain dislocation etchings and microstructural details
[AD-747086] 02 p0189 N73-11537
Relationships between continuum metal plastic deformation under multiaxial stress and phenomenological dislocation theory
[AD-746187] 02 p0219 N73-11769
Internal friction and crystal defects of magnesium oxide crystals
09 p1063 N73-18673
Dislocation distribution in fatigued metals, including mean stress effects and Cu alloy single crystals
[AD-755227] 13 p1544 N73-22515
Dynamics of dislocation pinning by impurity atoms during dynamic strain aging
[AD-760574] 18 p2162 N73-27466
DISORDERS
Use of therapeutic exercise for treatment of functional vascular disorders and occlusive lesions of arteries and veins
[NASA-TT-F-15043] 20 p2368 N73-29045
DISORIENTATION
NT DISORDERS
Investigation of US Army UH-1 helicopter accidents where orientation errors were contributing factor during fiscal year 1969
[AD-749695] 06 p0623 N73-15059
Investigation of correlation between pilot disorientation and UH-1 helicopter accidents
[AD-753208] 09 p0986 N73-18049
DISPERSING
Sources and dispersal patterns of suspended sediments in nearshore surface waters of Northeast Pacific Ocean and Hawaiian Islands based on ERTS-1 imagery
[E72-10271] 03 p0291 N73-12370
Helicopter downwash for dispersing fogs of 500 to 600 feet in depth
[AD-753357] 09 p1062 N73-18661
Air Force heating system for fog dispersal
[AD-754900] 11 p1315 N73-20675
Field tests of electrogasdynamic fog dispersal concept in Panama Canal Zone
[FAA-RD-73-33-PT-1-PT-2] 17 p2010 N73-26254
Convection and dispersion patterns associated with stationary and nonstationary fluid transport
18 p2129 N73-27205
On-line interactive computer solution of dispersion equations
22 p2636 N73-31123
Dispersion and dilution of jet aircraft exhaust at high altitudes
[NASA-TM-X-71451] 24 p2971 N73-33743
DISPERSION PRECIPITATION HARDENING
U PRECIPITATION HARDENING
DISPERSIONS
NT AEROSOLS
NT COLLOIDAL PROPELLANTS
NT COLLOIDS
NT EMULSIONS
NT FOG
NT LIQUID-GAS MIXTURES
NT NUCLEAR EMULSIONS
NT PHOTOGRAPHIC EMULSIONS
NT SMOKE
Detergent with glyceryl esthers and oil as protective coating to prevent fogging of space suit visor
[NASA-CASE-MSC-13530-2] 02 p0137 N73-11107
Laser method for measuring axial solute dispersion in turbulent pipe flow
[AD-753801] 09 p1019 N73-18314
Tabulation of plasma dispersion function with first derivative using postive imaginary part
[AD-753986] 11 p1328 N73-20780
Tabulation of plasma dispersion function and first derivative using saddle point method
[AD-754002] 11 p1328 N73-20781
Airborne heated glycerine droplets for fog dispersal
[TOPR-178-3-133-PT-1] 12 p1421 N73-21521
Effects of oxide dispersions and rare earth elements on oxidation of Cr and Al containing alloys
14 p1677 N73-23608
Ion-ion hybrid resonance dispersion relation
[IPPJ-157] 16 p1949 N73-25774
Method for producing alkali metal dispersions of high purity
[NASA-CASE-XNP-08876] 19 p2309 N73-28573
DISPLACEMENT
Tsai method for seismic discrimination, using parameterized reduced displacement potential function
[AD-749894] 05 p0542 N73-14407
Displacement damage to infrared detectors from high energy neutrons
[AD-751540] 07 p0802 N73-16510
Holographic interferometry from coherent laser light to detect three dimensional displacements
[UCRL-51241] 07 p0806 N73-16540
Numerical analysis of vertical and lateral motion of road vehicle trains with arbitrary number of components
[TT-7211] 08 p0892 N73-17220
Stress and displacement of structures consisting of alternatingly elastic and hyperbolic paraboloidal shells with rectangular planform
[PB-212649] 08 p0967 N73-17902
Stresses and displacements of elastic-plastic trusses
[AD-758726] 15 p1841 N73-24920
Bimetallic fluid displacement apparatus for stirring and heating stored gases and liquids
[NASA-CASE-ARC-10441-1] 21 p2552 N73-30461
Feed displacement effect on double-spherical Cassegrain antenna patterns
[AD-764778] 23 p2767 N73-32139
DISPLACEMENT MEASUREMENT
Development of procedure for measuring sinusoidal vibration displacement amplitude using laser homodyne system
[RM-5603] 03 p0310 N73-12526
DISPLAY DEVICES
NT ANEMOMETERS
NT APPROACH INDICATORS
NT FLOW DIRECTION INDICATORS
NT GYRO HORIZONS
NT HEAD-UP DISPLAYS
NT HOT-FILM ANEMOMETERS
NT HOT-WIRE ANEMOMETERS
NT KINOFORM
NT PLAN POSITION INDICATORS
NT POSITION INDICATORS
NT RADIO DIRECTION FINDERS
NT SPACECRAFT POSITION INDICATORS
NT SPEED INDICATORS
NT TACHOMETERS
Integrated information presentation and control system analysis to determine control and display requirements for contingency operation of jet aircraft - Vol. 3
[AD-740435] 01 p0006 N73-10041
Power supply for aircraft data acquisition system time display unit using dc to dc converter
[ARL/ME-NOTE-332] 01 p0006 N73-10049
Conference on manual control systems for human operator modeling and display systems in man machine environments
[NASA-SP-281] 01 p0013 N73-10104
Hybrid computer identification program for visual display of adaptive control state to human operator
01 p0014 N73-10109
Design of computerized airborne traffic display device with alphanumerical control for aircraft pilots
01 p0014 N73-10112
Predictive display with continuous parameter tracking for quasi-linear model of human pilot transfer function in closed loop system
01 p0015 N73-10120
Optimal control model for predicting display requirements in pilot landing performance
01 p0016 N73-10121
Improved pilot performance using simulated pictorial landing display with symbols
01 p0016 N73-10122
Visual display format effects on pilot describing functions in manual tracking performance
01 p0016 N73-10123
Utilization of simplified man machine interface concept to manage and control complex space system involving multiple redundant computers that control multiple redundant systems - Vol. I
[NASA-CR-128576] 01 p0019 N73-10145
Space shuttle orbiter subsystems and control and display data required for crew operations - Vol. 2
[NASA-CR-128577] 01 p0019 N73-10146
Control and display sequences for four space shuttle orbiter mission phases - Vol. 4
[NASA-CR-128579] 01 p0019 N73-10148
Investigating polymers for suitability of use as light valve display device called deformographic storage display tube
[AD-744689] 01 p0033 N73-10258
Analysis of gray scale image storage techniques in electroluminescent and photoconductor image conversion panels
[AD-745758] 01 p0033 N73-10261
Development of mosaic image conversion panels sensitive to ultraviolet, X ray, near infrared, and visible light
[AD-745757] 01 p0033 N73-10262
Proposed control tower and cockpit visibility readouts based on airport-aircraft information flow system
[AD-744718] 01 p0078 N73-10647
Digital visual displays for checking pressure points from wind tunnel models
[ARA-28] 02 p0172 N73-11388
Display systems for all-weather terminal operational capability of V/STOL aircraft
[AGARD-R-594] 02 p0174 N73-11407
Acoustic holographic signals for designing underground geological viewing system
[AD-746498] 02 p0184 N73-11490
Perfluorostyrene syntheses, magnetic tapes, titration cell, mill work positioner, superconducting microbridges, position display device, and numbering machine
[NBS-TN-744] 02 p0245 N73-11991
Analysis of reaction time to different visual cuing methods in large displays during secondary task performance
[AD-747688] 03 p0262 N73-12126
Gray scale reproduction capability for characterizing aerial television reconnaissance system
[AD-747632] 03 p0267 N73-12165
Screen touching device for computer graphic display operation
[RHEL/R-248] 03 p0271 N73-12194
Display system consisting of light emitting diode arrays monolithically fabricated on single wafers of GaP
[AD-746993] 03 p0274 N73-12225
Dc electroluminescent flat panel display with Zn, Cu, S, and Mn films
[AD-746632] 03 p0275 N73-12229
Operational test and evaluation of angle of attack system for displaying percentage of lift produced by wing for all flap configurations
[AD-748844] 03 p0304 N73-12485
Recording of holographic visual display elements in dichromated gelation
[AD-746859] 03 p0310 N73-12532
Development of holographic storage and retrieval system for aerial chart information display in cockpit environment
[AD-748648] 03 p0330 N73-12690
Monolithic display using metal oxide semiconducting circuits and liquid crystal layer
[CEA-CONF-1991] 03 p0345 N73-12814
Operational test and evaluation of four configurations of flight director display for instrument landings based on command heading and command flight path angle
[AD-748244] 04 p0374 N73-13041
Methods of evaluating electronic cockpit display devices, emphasizing control, psychology, physiology, and subjective rating
[DGLR-PAPER-72-97] 04 p0383 N73-13118
Military applications of single gun color cathode ray tubes in display devices
[AD-748385] 04 p0396 N73-13222
Comparison of contact analog channel display with conventional indicators in cockpit simulator
[DGLR-PAPER-72-100] 04 p0422 N73-13445
Development of scaling counter for use as laser interferometer readout system to obtain improved length measurement capabilities
[BDX-613-703] 04 p0429 N73-13492
Rotating generator for angular display of television raster in horizontal and visual simulation systems
[NASA-CASE-FRC-10071-1] 05 p0513 N73-14171
Program package for statistical measured data selection and visual presentation in real time
05 p0516 N73-14193
Development and characteristics for automatically displaying digits in any desired order using optical techniques
[NASA-CASE-XKS-00348] 05 p0518 N73-14215
Performance tests and service life of electroluminescent film display device
[AD-749790] 05 p0521 N73-14235
Legibility and recognition by test groups of displayed signals differing by brightness or color
[DLR-FB-71-57] 06 p0674 N73-15484

Development of aircraft control systems based on operator performance, adaptive displays, and coupling of manual with automatic control
[AD-751306] 07 p0741 N73-16026
Design of digital controlled thin cathode tube screen for computer output display
[AD-751745] 07 p0762 N73-16193
Feasibility determination of using nematic liquid crystals for aircraft displays
[AD-751667] 07 p0832 N73-16748
Three axis addressing techniques for matrix display panels
[AD-751666] 07 p0833 N73-16749
Feasibility of developing liquid crystal display system
[AD-751747] 07 p0833 N73-16753
Technology transfer in nondestructive testing and visual displays
[NASA-CR-130302] 07 p0856 N73-16941
Development and characteristics of cathode ray tube vertical display system for use in all-weather air navigation aircraft
[AD-752510] 08 p0868 N73-17026
Analysis of fixed base simulator tests to determine effects of two horizontal display panel locations and three map orientations on manual piloting performance
[NASA-TM-X-62198] 08 p0892 N73-17223
Applications of visual display systems developed by aerospace technology
[NASA-CR-130634] 08 p0924 N73-17566
Motion sickness in fixed-base car simulator with moving visual display
[FPRC-1310] 09 p0995 N73-18119
Design of three color plasma panel display device capable of operating at three intensity levels
[AD-752442] 09 p1009 N73-18236
Design of multiwire proportional chamber systems using electromagnetic delay lines for cosmic ray experiments
[RM-569J] 09 p1011 N73-18251
Analysis of aircraft instruments and display devices for approach control and landing of V/STOL aircraft
[AGARD-AR-51] 09 p1034 N73-18439
Accuracy of method of constant stimuli for studying sensory capabilities of man in relation to display systems
[AD-753009] 10 p1121 N73-19141
Digital address thin display tube with resolution of 55 holes per inch
[AD-753604] 10 p1135 N73-19250
Comparative evaluation of cockpit displays considering human factors and aircraft control data
[NASA-TT-F-14846] 11 p1234 N73-20019
Proceedings of conference on manual control to show interplay between man and machine and application of control theory in medicinc and psychology
[NASA-CR-131244] 11 p1235 N73-20028
Display device for real time display of computer generated half tone pictures
[AD-753672] 11 p1260 N73-20224
Situational display system of cathode ray tubes to assist pilot in aircraft control
[NASA-CASE-ERC-10350] 11 p1291 N73-20474
Electroluminescent characteristics of vacuum deposited zinc sulfide films for airborne electronic displays
[AD-754781] 11 p1332 N73-20811
Influence of displays on image interpreter performance in investigating characteristics of pictorial content of reference material
[AD-754567] 11 p1353 N73-20984
Development and characteristics of flat, thin, cathode ray tube with digital switching for beam deflection and positioning
[AD-755938] 12 p1384 N73-21227
Cockpit display evaluation methods
[DLR-FB-73-03] 12 p1406 N73-21400
Flashlight adaptation of ultraviolet source for illuminating fluorescent map
[AD-755435] 12 p1429 N73-21585
Multichannel medical monitoring system to measure physiological parameters from display device at remote control station
[NASA-CASE-MSC-14180-1] 13 p1486 N73-22045
Millimeter wave image conversion system for optical display of objects obscured by fog or rain
13 p1489 N73-22074
Data entry and edit monitor using rear ported CRT display device
[AD-756934] 13 p1498 N73-22140
Reduction of nonuniformity of electron beam displacement on vidicon screen at raster edges
[DRIC-TRANS-2966] 13 p1500 N73-22156
Time base stability and intermachine compatibility in wideband laser recording systems
13 p1536 N73-22444
Vertical display techniques for naval all-weather day/night attack aircraft
[AD-755739] 13 p1557 N73-22620
Liquid crystal applications as electronic, electro-optic, and diagnostic materials
[AD-755831] 13 p1567 N73-22703
Visible pitch display for extracting frequency by filtering, converting sine waves to pulse train, and showing pulse interval as function of time
14 p1626 N73-23177
Three parameter speech display, including phonemes, pitch, and loudness
14 p1627 N73-23182
Speech display simulation system, using CDC 1604 computer
14 p1627 N73-23183
Design of circular symbol and video inset generator for television display devices
[AD-757621] 14 p1634 N73-23246
Design of attitude line generator for use with aircraft-type television displays
[AD-757620] 14 p1634 N73-23247
Method for quantitative print quality evaluation of large amount of data with determination based on requirements of optical character readers
[REPT-731] 14 p1637 N73-23276
Plasma cell array for capacitor-coupled shift register
[AD-758310] 14 p1639 N73-23285
Status of research on gas discharge, liquid crystal display systems, and ferroelectric ceramics in Europe
[AD-757649] 14 p1668 N73-23538
Flight control system using tactile displays under instrument flying conditions
[AD-757344] 14 p1669 N73-23543
Analysis of manual control theory of vertical situation displays for short takeoff aircraft
[NASA-CR-114620] 15 p1734 N73-24061
Development and evaluation of display and control equipment for remotely piloted vehicles
[AD-757761] 15 p1736 N73-24077
Design and construction of multifunction display man/machine interface for use with IBM 360 system - Vol. 1
[NASA-CR-128934] 15 p1754 N73-24214
Design and construction of multifunction display man/machine interface for use with IBM 360 system - Vol. 2
[NASA-CR-128935] 15 p1754 N73-24215
Television readout devices for color display of data and picture blending
[NLL-PO-2958-[9022.81]] 15 p1755 N73-24225
Cathodochromic storage and display for television systems
[NASA-CR-130236] 15 p1756 N73-24233
Space shuttle visual simulation system design study
[NASA-CR-128940] 15 p1760 N73-24265
Automatic scanning and display eddy current system for nondestructive testing of printed circuit boards
[ARL/MET-NOTE-84] 15 p1786 N73-24478
Development of inertial smoothing system for control and display applications for VTOL aircraft automatic instrument approach and landing operations
[NASA-TN-D-7271] 15 p1808 N73-24653
Conceptual design study for teleoperator visual system
[NASA-CR-124273] 16 p1869 N73-25133
High resolution pulse width modulated parallel channel for forward looking infrared display system
[AD-759224] 16 p1882 N73-25231
Monolithic light emitting diode display devices
[AD-758853] 16 p1882 N73-25232
Cockpit and control display design criteria for tactical STOL and V/STOL aircraft
[AD-758787] 16 p1914 N73-25489
Development of control and display testing requirements for evaluation of microwave landing system - Vol. 2
[AD-758792] 16 p1942 N73-25714
Development and application of Airborne Traffic and Situation Display for improved air traffic control
[PB-215714/7] 16 p1942 N73-25715
Differences in speed of mentally processing displays containing information about right and left
[AD-759723] 17 p1988 N73-26070
Modular graphic programs for computerized design
[MBB-UA-79-72-O] 17 p2001 N73-26181
Processing and displaying techniques for optical images
[AD-759038] 17 p2001 N73-26183
Performance tests of four flight-director/attitude indicator displays under three conditions of simulator motion and comparison with flight test results
[AD-760049] 17 p2011 N73-26264
Evaluation of pilot assurance value of airborne display device for monitoring air traffic in high density terminal airspace
[AD-749280] 17 p2011 N73-26267
Control and display testing for air traffic instrument landing system
[AD-759539] 17 p2060 N73-26667
Radar equipment components for fire control vehicle
[AD-761534] 19 p2237 N73-28031
Research and development of thin cathode ray display tubes
[AD-762115] 19 p2246 N73-28108
Semiconductor image conversion panels using millimeter diodes
[AD-762116] 19 p2246 N73-28109
Analysis and enhancement of ERTS-1 hydrology imagery using electronic satellite image analysis console
[PAPER-115] 19 p2279 N73-28336
Device for displaying and recording angled views of samples to be viewed by microscope
[NASA-CASE-GSC-11690-1] 19 p2301 N73-28499
System for displaying low resolution digital grayscale images of ladar target imaging system
[DREV-TN-2075/73] 19 p2307 N73-28552
Tachistoscopic investigation on electronic and electromechanical cockpit display for performance comparison
[DLR-FB-73-27] 21 p2496 N73-30034
Design of integrated aircraft instrumention display system utilizing plasma display/memory unit
[AD-763599] 21 p2550 N73-30446
Display device for integrated jet engine instrument system program
[AD-763440] 21 p2550 N73-30450
Techniques for creating moving image reconnaissance display
[AD-763789] 21 p2551 N73-30452
Luminescent diode and liquid crystal display devices for telephony, using COS/MOS and TTL logic
[FTZ-421-TBR-4] 22 p2633 N73-31105
Data manipulation and sensing in plasma display/storage panel
[AD-763110] 22 p2641 N73-31164
Effective x-y addressed, liquid crystal display panel
[AD-763927] 22 p2646 N73-31206
Display devices for short takeoff aircraft landing
[DGLR-PAPER-73-038] 23 p2744 N73-31961
Pilot display for monitoring of automatic steep approach
[DGLR-PAPER-73-031] 23 p2744 N73-31964
Cockpit layouts in view of new landing approach methods
[MBB-UH-07-73-O] 23 p2744 N73-31966
Digital address thin display tube to meet Army requirements for computer-output display
[AD-763933] 23 p2762 N73-32100
Alphanumeric character display device for oscilloscopes
[NASA-CASE-GSC-11582-1] 23 p2765 N73-32120
Properties of liquid crystals noting use in display devices, light modulation, image converters, and nondestructive testing
[LCR-DR-1-71-223/1/R] 23 p2765 N73-32125
Design of computer controlled cathode ray tube display screen for flight simulator
[AD-764762] 23 p2767 N73-32140
Transparent switchboard which permits optical display devices to be adapted for use in man machine communications
[NASA-CASE-MSC-13746-1] 23 p2768 N73-32143
Flight control display device for producing curved approach profiles in microwave instrument landing systems
[DGLR-PAPER-73-016] 23 p2818 N73-32526
Production and performance of bleached holographic lenses
[AD-764701] 23 p2821 N73-32548
Electronic display devices in aircraft control, noting pilot activation and VTOL control
[DLR-MITT-72-04] 24 p2880 N73-32998
Pilot activation in automatic landing by display devices
24 p2880 N73-32999
Extrapolation predictive displays for manual path and position control of VTOL aircraft
24 p2880 N73-33000
Computerized laser position detector and optical stereo display system
24 p2897 N73-33121
Coordination and establishment of centralized facilities and services for University of Alaska ERTS survey of Alaskan environment
[E73-11088] 24 p2913 N73-33250
Evaluation of large screen display for automated oceanic air traffic control applications
[FAA-ND-73-75] 24 p2950 N73-33568
Operational evaluation of ARTS 2 radar alphanumeric display subsystem
[FAA-NA-73-77] 24 p2951 N73-33569

**DISPLAY SYSTEMS**
U DISPLAY DEVICES

**DISPOSAL**
NT WASTE DISPOSAL

**DISRUPTING**
Computation of characteristics of tracking disruption
22 p2691 N73-31558

**DISSIPATION**
NT ENERGY DISSIPATION
NT OHMIC DISSIPATION
Least squares representation for charge distribution on monopole antenna immersed in dissipative medium
[AD-753092] 09 p1008 N73-18230

**DISSIPATORS**
U DISSIPATION

**DISSOCIATION**
NT AUTOIONIZATION
NT GAS DISSOCIATION
NT PHOTODISSOCIATION

NT THERMAL DISSOCIATION
Nuclear energy in hydrogen production by water dissociation method
[EUR-4838] 06 p0699 N73-15699
Dissociation rate of bromine diatomics in argon heat bath
[NASA-TN-D-7077] 07 p0824 N73-16676
Dissociation of HBr behind shock waves and at temperatures from 1450 to 2300 K in pure HBr
[AD-753395] 10 p1143 N73-19310
Low carbon steel for studying dissolution behavior of Fe3C particles under rapid heating and short time temperature conditions
[AD-753928] 11 p1307 N73-20602
Predissociation by rotation and curve crossing in diatomic molecules
[NASA-CR-131262] 15 p1747 N73-24159

**DISSOLUTION**
U DISSOLVING

**DISSOLVING**
Effect of chloride ion additions on dissolution behavior of Fe-Ni alloys in sulfuric acid
[AD-751258] 07 p0811 N73-16574
Apparatus for mixing two or more liquids under zero gravity conditions
[NASA-CASE-LAR-10195-1] 10 p1163 N73-19458
Effect of passivation and dissolution phenomena on structural corrosion of Cr-Ni stainless steels
[NLL-RISLEY-TR-2500-(9091.9F)] 11 p1305 N73-20586

**DISSYMMETRY**
U ASYMMETRY

**DISTANCE**
NT DEBYE LENGTH
NT MISS DISTANCE
NT MISSILE RANGES
NT OPTICAL SLANT RANGE
NT RADAR RANGE
NT RANGE AND RANGE RATE TRACKING
Method for localizing position of balloon on earth, using interrogating satellite and correcting for electronic errors in distance measurement
[NASA-TT-F-14707] 03 p0328 N73-12678
Psychophysical functions of range and time estimates by ground and aerial observers
[AD-747271] 04 p0380 N73-13094

**DISTANCE MEASURING EQUIPMENT**
NT ALTIMETERS
NT LASER RANGE FINDERS
NT OPTICAL RANGE FINDERS
NT RADIO ALTIMETERS
NT RANGE FINDERS
Procedures for operating and modulating beam of laser locating devices
[AD-747003] 02 p0184 N73-11492
Development, characteristics, and evaluation of electronic distance measuring instrument
[AD-746017] 02 p0208 N73-11690
Analysis of position determination accuracy obtainable with microwave landing guidance system
[NASA-TN-D-7116] 06 p0697 N73-15681
Performance of radio distance finding net using polygonometric grid
[AD-748866] 06 p0697 N73-15683
Performance tests of various Tacan ground station modifications designed to minimize false distance measuring equipment indications
[FAA-NA-72-65] 09 p1062 N73-18664
Apparatus for determining distance to lighting strokes from single station by magnetic and electric field sensing antennas
[NASA-CASE-KSC-10698] 11 p1254 N73-20175
Atmospheric effects on light distance finder measurements
[AD-763505] 21 p2581 N73-30682
Pilot plant tests of Luch radio distance finder
[AD-763416] 22 p2698 N73-31612
Description of sector-Tacan and DME-supported instrument landing systems
[DGLR-73-019] 23 p2817 N73-32523
Capacitive method for measuring blade tip clearance in running turbocompressors
[DLR-FB-72-40] 23 p2831 N73-32628

**DISTANCE PERCEPTION**
U SPACE PERCEPTION

**DISTILLATION**
Distillation method for quantitative determination of oxygen solubility in sodium
[NLL-RISLEY-TR-2424-(9091.9F)] 02 p0136 N73-11105
Trace element detection by automated distillation and ion exchange in neutron activation analysis for As, Cd, Cu, Hg, Se, and Zn
[IRI-133-72-10] 07 p0753 N73-16114
Removal of lithium from 1040 C aged tantalum alloy by liquid ammonia and vacuum distillation techniques
[NASA-TM-X-2775] 11 p1305 N73-20590
Prevention of N2O4 flow decay by means of contaminant removal through distillation and filtration
[AD-755380] 13 p1569 N73-22717
Evaporator for vacuum distillation/vapor filtration water reclamation on manned space flight
[NASA-CR-124397] 23 p2796 N73-32367

**DISTILLATION EQUIPMENT**
U shaped heated tube for distillation and purification of liquid metals
[NASA-CASE-XNP-08124-2] 04 p0385 N73-13129
Aerospace distillation water recovery system for reclamation of potable water from domestic wash water
[NASA-TM-X-2896] 22 p2737 N73-31913

**DISTORTION**
NT FLOW DISTORTION
NT SIGNAL DISTORTION
NT SURFACE DISTORTION
Divers adjustment to underwater distortion
[AD-744936] 01 p0021 N73-10163
Numerical analysis of thin skew plates using tensor-matrix techniques for elastic isotropic body
[NLL-RTS-7401] 02 p0236 N73-11916
Mathematical model of atmospheric drag distortion of long spinning, flexible antennas
[CRC-1232] 04 p0395 N73-13210
Focusing effects of distortion of near sonic shocks by weakly turbulent layers with random temperature and pressure variations
[AD-752472] 08 p0899 N73-17279
Effects of frequency bandwidth and harmonic distortion of speech intelligibility for normal and hearing impaired subjects
14 p1627 N73-23187
Binocular vision models for designing image distortion compensation system
16 p1920 N73-25534
Geometric distortion characteristics and calibration problems RBV television system onboard Earth Resources Technology Satellites
[PB-218393/7] 18 p2118 N73-27123
Stability effects of steady state circumferential distortions of inlet total temperature and pressure
[NASA-TM-X-71431] 23 p2829 N73-32614

**DISTRIBUTING**
Optimal control of shuttle system consisting of single infinite capacity carrier transporting passengers between two terminals
[P-4979] 19 p2355 N73-28940

**DISTRIBUTION**
Distribution and density of phreatophytes and other arid and desert plants
[E72-10243] 03 p0289 N73-12343
Distribution and density of phreatophytes and other arid land plants measured from ERTS-1 imagery
[E73-10094] 08 p0902 N73-17306
Erosional latitudinal debris distribution on Mars surface
23 p2839 N73-32689

**DISTRIBUTION [PROPERTY]**
NT ANGULAR DISTRIBUTION
NT ANTENNA RADIATION PATTERNS
NT CHARGE DISTRIBUTION
NT CURRENT DISTRIBUTION
NT DIFFRACTION PATTERNS
NT ELECTRON DENSITY PROFILES
NT ELECTRON DISTRIBUTION
NT ENERGY DISTRIBUTION
NT FLOW DISTRIBUTION
NT FORCE DISTRIBUTION
NT FREQUENCY DISTRIBUTION
NT HOLE DISTRIBUTION [MECHANICS]
NT INTERFERENCE LIFT
NT ION DISTRIBUTION
NT LOAD DISTRIBUTION [FORCES]
NT MASS DISTRIBUTION
NT MOMENT DISTRIBUTION
NT NEUTRON DISTRIBUTION
NT PRESSURE DISTRIBUTION
NT RADIAL DISTRIBUTION
NT RADIATION DISTRIBUTION
NT SIDELOBES
NT SPATIAL DISTRIBUTION
NT SPECTRAL ENERGY DISTRIBUTION
NT STAR DISTRIBUTION
NT STRESS CONCENTRATION
NT TEMPERATURE DISTRIBUTION
NT VELOCITY DISTRIBUTION
NT VERTICAL DISTRIBUTION
Nearest neighbor algorithms for pattern classification
[REPT-18] 20 p2438 N73-29582

**DISTRIBUTION FUNCTIONS**
Calculation of neutron energy and flux distributions from D-D reactions in plasma focus and Z pinch discharges
[AD-745955] 02 p0217 N73-11755
Summation method for computing vocabulary size for two parameter rank distribution
[NASA-CR-129806] 04 p0393 N73-13197
Algorithm for calculating distribution functions of meteorological parameters by computer technique
[AD-749588] 04 p0446 N73-13642
Distribution function inequalities in order statistics
[NASA-CR-130962] 09 p1058 N73-18627
Grid excitation and digitized probe measurements for oscilloscopic display of phase space diagram distribution functions of plasma waves
[IPPJ-147] 09 p1070 N73-18732
Breakdown of quasi-linear derivation of kinetic equation describing cosmic ray distribution function in random magnetic field
[NASA-TM-X-65949] 09 p1081 N73-18815
Distribution of lunar craters as a function of their diameter
12 p1457 N73-21806
Definition of equivalent peak level in objective speech level measurement
14 p1625 N73-23163
Distribution functions of spot diameter for single and multicathode discharges in vacuum
[TH-73-E-32] 14 p1643 N73-23328
Weibull distribution bibliography, 1957 - 1972
[CE-BIB-235] 24 p2928 N73-33387

**DISTRIBUTION MOMENTS**
NT MEAN
NT VARIANCE [STATISTICS]
Moment equations for describing evolution of droplet populations in convection clouds
10 p1180 N73-19595
Computer code for generating gamma ray moments
[AD-761839] 19 p2323 N73-28689

**DISTRICT OF COLUMBIA**
Vertical distribution of atmospheric water vapor and ozone over District of Columbia during 1969 and 1970
[AD-751535] 07 p0795 N73-16465
Application of ERTS-1 imagery to thematic mapping of Washington-Baltimore corridors
[E73-10500] 12 p1398 N73-21336
Urban impact on areas of maximum environmental quality in Washington Metropolitan Area, 1971
[PB-214544/9] 16 p1977 N73-25993
Sampling strategies in thematic land use mapping of Maryland, Virginia, and District of Columbia using Skylab EREP data
[E73-10823] 18 p2140 N73-27298
Feasibility of rapid transit service between downtown Washington, D.C. and Dulles Airport in Virginia
[PB-220074/9] 18 p2214 N73-27879
Utilization of ERTS-1 imagery and data for land use, regional planning, and urban development in Metropolitan Washington area
19 p2285 N73-28377
Computer processing of Skylab MSS data for land use mapping of Baltimore, Maryland-Washington, D.C. area
[E73-10913] 20 p2397 N73-29262
Sampling strategies for automatic thematic land use mapping of Washington D.C., Maryland counties, and Alice Springs, Australia using Skylab multispectral photography
[E73-11018] 22 p2661 N73-31322

**DISTURBANCE THEORY**
U PERTURBATION THEORY

**DISTURBING FUNCTIONS**
Disturbing functions of artificial satellite orbit perturbation by solar and lunar gravitational effects
01 p0105 N73-10869
Gyro suspension systems including axis disturbance probability factors, bearing friction, astatic gyro gimbal errors with drift, and horizontal pendulum energy dissipation
[JPRS-57504] 05 p0546 N73-14432
Experimental determination of probability factors of disturbances relative to principal axis of gyroscope
05 p0546 N73-14433
Orbit perturbations due to solar radiation pressure, including disturbing force of satellites with large area to mass ratio
05 p0610 N73-14959
Formulation of disturbing function for computing lunisolar perturbations in satellite motion
[NASA-CR-130743] 08 p0941 N73-17709

**DITCHING [EXCAVATION]**
U EXCAVATION

**DITHERS**
Dither, large suitably fluctuating component, in digital matched filters
[AD-753808] 10 p1135 N73-19249
Digital filter with dither for correlation detection of weak signal in jamming environment
[AD-757013] 14 p1643 N73-23325

**DITHIOLS**
U THIOLS

**DIURNAL RHYTHMS**
U CIRCADIAN RHYTHMS

**DIURNAL VARIATIONS**
Diurnal variations of sunspot classification, areas, and magnetic fields for June and July 1972
[BULL-171] 01 p0092 N73-10759
Diurnal changes in human histamine and serotonin metabolism and effects of work-sleep cycle
Methods for acquiring meteorological parameter data and procedures for analyzing wind data
[AD-747480] 03 p0298 N73-12432
Diurnal variations in ionospheric F region tilts near magnetic equator
[WRE-TN-A-199[AP]] 04 p0414 N73-13384
Diurnal variations in ionospheric tilt near magnetic dip equator due to gravity waves
05 p0512 N73-14160

Computerized simulation of optical stellar observations and data reduction to determine diurnal polar motion
[AD-748460] 05 p0541 N73-14401
Diurnal variations of precipitation and surface wind for North Carolina
[PB-211614] 05 p0576 N73-14688
Diurnal variation amplitude and phase data of cosmic rays in 1962 and 1964-65
[AD-750870] 06 p0716 N73-15844
Accuracy of harmonics of diurnal density variations in thermosphere determined from satellite drag data and Jacchia empirical atmospheric model
[NASA-TM-X-66160] 07 p0790 N73-16427
Equatorial magnetic storm-time variation data from Hermanus, Kakioka, Honolulu, and San Juan
[NASA-TM-X-66174] 08 p0917 N73-17511
Computer analysis of quasi-sinusoidal geomagnetic variations at geomagnetic midlatitude
[AD-752229] 08 p0920 N73-17543
Diurnal and annual variations in intensity of urban heat island in Austin, Texas
[REPT-34] 08 p0938 N73-17679
Diurnal cycles of high absolute humidity at earth surface, using dew point and temperature measurements
[AD-753078] 09 p1061 N73-18654
Magnetic results 1969, Eskdalemuir, Hartland and Lerwick observatories, emphasizing diurnal values
[BULL-3] 10 p1145 N73-19323
Tidal and lunar data for Point Mugu, San Nicholas Island, and Barking Sands areas for 1973
[AD-752892] 10 p1156 N73-19407
Approximative model for diurnal effect on atmospheric density distribution and artificial earth satellite deceleration
10 p1177 N73-19578
Observation of eastward diurnal driving forces in thermospheric superrotation phenomenon
[NASA-TM-X-66222] 11 p1286 N73-20438
Diurnal cycles of atmospheric refractive index structure function coefficient used to describe scintillation and phase fluctuations of electromagnetic radiation propagated in atmosphere
[AD-755808] 12 p1402 N73-21374
Diurnal cardiac rhythm fluctuation for cardiovascular evaluation of flight personnel
13 p1480 N73-21997
Predicting daily variations in geometric parameters of N[h] profiles and h prime f characteristics of quiet and disturbed ionosphere
13 p1520 N73-22322
Table of hourly and daily values of geomagnetic field declination and intensity recorded at Eskdalemuir, Hartland, and Lerwick Observatories, England, in 1969
[GEOMAGNETIC-BULL-3] 13 p1525 N73-22356
Diurnal and hourly geomatnetic variations recorded at Thule Geophysical Observatory, Greenland, in 1947
13 p1525 N73-22357
Dirunal and hourly geomagnetic variations recorded at Thule Geophysical Observatory, Greenland, in 1949
13 p1525 N73-22359
Diurnal geomagnetic variations
[AD-755787] 13 p1526 N73-22369
Inferring polarity of interplanetary magnetic field from observations of diurnal variation of polar geomagnetic fields
[NASA-CR-131609] 13 p1527 N73-22379
Forty year statistical study of geomagnetic data
[AD-756828] 14 p1663 N73-23497
Solid phase trace element aerosol concentrations in lowest 34 meters of atmosphere
15 p1771 N73-24343
Solar diurnal and semidiurnal variations in coamic ray neutron monitor data
[NP-19650] 15 p1828 N73-24819
Changes in diurnal variations of pilot performance in flight simulator compared with performance after transatlantic flights
[DLR-FB-73-25] 16 p1868 N73-25122
Measurement of auroral electrojet magnetic activity indices for calendar year 1970
[UAG-22] 18 p2133 N73-27231
Daily summaries for vertical echo sounding of upper atmosphere over Freiburg, Germany during March, 1973
[REPT-321F] 18 p2141 N73-27308
Global characteristics in diurnal components of OGO-6 neutral mass spectrometer measurements of thermosphere
[NASA-TM-X-66295] 18 p2145 N73-27335
Ionospheric total electron content during magnetic storm, 14-17 Dec. 1971
[KGO-728] 18 p2146 N73-27344
Solar particle contributions to diurnal variations of neutron intensity in upper atmosphere
[AD-760950] 18 p2146 N73-27350
Method for calculating correlation functions of diurnal precipitation totals and their space time variability over uniform relief
21 p2573 N73-30619
Analysis of daily variation of geomagnetic field for eight quiet days of IGY
23 p2777 N73-32210
Analytical theory for diurnal polar motion as forced response to lunisolar torques
[NASA-TM-X-70470] 23 p2785 N73-32284
Diurnal and hourly geomagnetic variations recorded at Godhavn Geophysical Observatory during 1966
[ISBN-87-7478-066-2] 23 p2788 N73-32302
Diurnal and hourly geomagnetic variations recorded at Thule Geophysical Observatory, Greenland, in 1966
[ISBN-87-7478-069-7] 23 p2788 N73-32303
Predicting day-to-day variability of mid-latitude ionosphere for application to HF propagation predictions
[AD-764711] 23 p2789 N73-32310
Classical tide calculations for atmospheric response to lunar diurnal component
24 p2979 N73-33810

**DIVERGENCE**
Divergence at 200 mb level in Southern Hemisphere atmospheric circulation inferred from EOLE data
08 p0918 N73-17523
Best channel selection in terms of divergence and minimizing probability of misclassification
[REPT-5] 20 p2437 N73-29569
Interclass divergence with fixed number of channels and probability of misclassification
[REPT-5] 20 p2437 N73-29570
Divergence and necessary conditions for extremums associated with dimension reducing transformation matrix
20 p2438 N73-29577
Multivariate statistical analysis including divergence, probability of misclassification, information theory, and matrix analysis
[NASA-CR-128990] 20 p2438 N73-29578
Sufficient statistics for divergence and brattacharyya distance
[REPT-13] 20 p2438 N73-29579
Sufficient statistics for divergence and probability of misclassification
[REPT-14] 20 p2438 N73-29580
Perturbation and sensitivity inequalities in divergence calculations
[REPT-20] 20 p2438 N73-29584
Maximum likelihood procedure used for classification problem involving equivalence classes and constant divergence
[REPT-23] 20 p2439 N73-29587
Laser beam divergence and measurement of nanosecond laser pulses
[AD-764702] 23 p2802 N73-32407

**DIVERGENT NOZZLES**
Shrouded divergent body attached to exhaust nozzle for jet noise suppression
[NASA-CASE-LEW-11286-1] 12 p1364 N73-21066
Aerodyanmic tests and noise levels of slot nozzle with V gutter reverser for STOL
[NASA-TM-X-2758] 12 p1365 N73-21072
Cold flow tests of factors affecting noise suppression and thrust loss of divergent lobe supersonic jet noise suppressor
[NASA-TM-X-2820] 18 p2101 N73-26992

**DIVIDERS**
Experimental and analytical studies of highway cable barrier and digital simulation of vehicle redirection
[NRC-12694] 01 p0119 N73-10978

**DIVING [UNDERWATER]**
Underwater submersion and prolonged underwater submersion effects on diver tactile sensitivity
[AD-743709] 01 p0010 N73-10082
Visual evoked cortical response as measure of stress in naval environment, using rapid flash rates
[AD-744934] 01 p0011 N73-10088
Divers adjustment to underwater distortion
[AD-744936] 01 p0021 N73-10163
Mental functions of aquanauts during and after exposure to depths up to 160 m
04 p0378 N73-13073
Cognitive functioning test to measure human performance in underwater diving stress
[AD-748036] 04 p0382 N73-13108
Effect of breathing hydrogen at depths greater than 1000 feet on speech intelligibility
[AD-749320] 04 p0392 N73-13184
Effect of breathing hydrogen at 200 feet below sea level on speech intelligibility
[AD-749322] 04 p0392 N73-13186
Deep diving pulmonary functions of man using different breathing gas densities
[AD-749028] 05 p0501 N73-14082
Apparent object movement due to optical distortion produced by head movement under water
[AD-749319] 05 p0502 N73-14086
Performance of battery powered electrically heated suit for recoanaissance divers
[AD-749847] 05 p0504 N73-14101
Calculation of minimum safe inspired gas temperature limits for deep diving
[AD-748197] 05 p0504 N73-14104
Visual evoked responses from divers subjected to hyperbaric conditions simulating depths to 1200 feet breathing various gas mixtures
[AD-749325] 06 p0631 N73-15127
Bibliography on role of vestibular apparatus in compressed air work underwater
[AD-750686] 06 p0632 N73-15133
Feasibility determination of cutaneous communication system for working divers
[AD-750268] 06 p0636 N73-15169
Anthropometric measurements of military personnel engaged in underwater diving to development standards for design of equipment
[AD-748627] 06 p0637 N73-15175
Underwater divers and speech communication problems
[AD-751665] 07 p0757 N73-16150
Phonetic analysis of underwater diver speech and standardization for intelligibility
[AD-751662] 07 p0757 N73-16153
Blockage effect in external ear canal on diver auditory perception threshold
[AD-751664] 09 p0996 N73-18132
Human factors guide for design of diver-operated hand and power tools
[AD-753262] 09 p1041 N73-18489
Training procedure for improving divers distance estimation ability in clear and turbid water
[AD-752976] 10 p1121 N73-19140
Diver monitoring system for physiologic studies in all hyperbaric environments
[AD-754399] 11 p1251 N73-20154
Ergometer to measure divers physiological hyperbaric stresses at all explorable depths
[AD-754401] 11 p1295 N73-20513
Improving distance under water and long-term effectiveness of training
[AD-752979] 16 p1869 N73-25128
Handedness and adaptation to distortions of size and distance underwater
[AD-759722] 17 p1991 N73-26098

**DIVOT [VOICE TRANSLATORS]**
U DIGITAL TO VOICE TRANSLATORS

**DME-A SATELLITE**
U EXPLORER 31 SATELLITE

**DNA**
U DEOXYRIBONUCLEIC ACID

**DO-31 AIRCRAFT**
Results of aerodynamic jet interference tests for Do-31 aircraft and application to future VSTOL development for lift-loss calculation
[BMVG-FBWT-72-22] 09 p0985 N73-18044
Far and near sound fields of Do-31 aircraft, and noise reduction for future VSTOL aircraft
[BMVG-FBWT-72-23] 09 p0985 N73-18045
Landing loads of Do-31 aircraft in vertical landing, noting undercarriage reactions and sinking speed
[BMVG-FBWT-72-24] 09 p0986 N73-18046
Command and control of stability of Do-31 aircraft by landing and hovering
[BMVG-FBWT-72-25] 10 p1106 N73-19022
Ground erosion on grassland and concrete by vertical takeoff of Do-31 aircraft
[BMVG-FBWT-72-26] 10 p1107 N73-19023
Hot gas recirculation in Do-31 aircraft from scale model to aircraft and trends for future developments of V/STOL aircraft
[BMVG-FBWT-72-29] 10 p1107 N73-19024
Mathematical model of transition flight and application to Do-31 aircraft
[BMVG-FBWT-72-30] 10 p1107 N73-19025
Design, development, and characteristics of Do-31 V/STOL aircraft to include solution of operational problems caused by ground effect and transition flight
18 p2103 N73-27004
DO-31 aircraft integrated flight control system for vertical velocity regulation in gliding, noting signal processing requirements
24 p2878 N73-32983

**DOCKING**
U SPACECRAFT DOCKING

**DOCUMENT STORAGE**
Computerized file management system for library reference searches
[UCRL-73355-REV-1] 03 p0271 N73-12193
Utility of Goddard Trajectory Determination System Solar/Lunar/Planetary ephemeris files
[NASA-TM-X-66185] 08 p0976 N73-17983

**DOCUMENTATION**
Classification system for indexing and retrieving documents on structural analysis
[ESDU-00.00.01] 01 p0112 N73-10928
Publications of carbon and graphite research results
[NYO-1710-106] 05 p0565 N73-14590
Bibliography of publications from OGO E plasma wave investigation
[NASA-CR-130140] 06 p0644 N73-15227
Methodology for computer software documentation
[NASA-TM-X-66161] 07 p0759 N73-16162
Conference papers on automated methods of computer program documentation
[NASA-TM-X-66196] 10 p1130 N73-19204
Program documentation with advanced data management systems
10 p1130 N73-19205
AUTOFLOW flow chart system for improved documentation and maintenance of scientific applications
10 p1130 N73-19206

BELLFLOW flow chart system for accurate automatic program documentation
10 p1130 N73-19207
Automated system for generating program documentation
10 p1130 N73-19208
Integration of system specifications and program coding as basis for final system documentation
10 p1130 N73-19209
Problems involved in computer program documentation and automation
10 p1130 N73-19210
Automatic editing of manuals for computer program documentation
10 p1130 N73-19211
Automated computer program documentation as feature of total system design
10 p1131 N73-19212
Syntax-directed documentation for PL360
10 p1131 N73-19213
Project maintenance and comparison of documentation and automation
10 p1131 N73-19214
COSMIC history and essentials for computer program documentation
10 p1131 N73-19215
DOCMNT, documentation program, using META-SYMBOL assembly language on XDS 930 computer
10 p1131 N73-19216
Theoretical approach to autodocumentation
10 p1131 N73-19217
Integrated documentation approach using on-line programming
10 p1131 N73-19218
Preliminary identification of tools for automatic program annotation [AUTONOTE]
10 p1131 N73-19219
Automated documentation for mission analysis and trajectory simulation program
10 p1131 N73-19220
Automated engineering design for development of problem and user-oriented languages
10 p1131 N73-19221
Program analysis for documentation in FORTRAN
10 p1132 N73-19222
Scan processor and symbol scanner for program documentation
10 p1132 N73-19224
Tabulation of research reports published in German technical document series during calendar year 1972
[DLR-MITT-73-01] 11 p1352 N73-20971
Design of automatic system for computer program documentation
[NASA-CR-130231] 13 p1496 N73-22129
Computer program problems and possible solutions
[AD-762141] 19 p2242 N73-28072
Documentation of electrohydrodynamics research
[NASA-CR-133456] 19 p2255 N73-28180

**DOCUMENTS**
NT ABSTRACTS
NT BIBLIOGRAPHIES
NT CATALOGS [PUBLICATIONS]
NT ENGINEERING DRAWINGS
NT HANDBOOKS
NT MANUALS
NT PERIODICALS
NT PROCEEDINGS
NT RECORDS
NT SUPPLEMENTS
NT TEXTBOOKS
NT TEXTS
Annotated bibliography of reports, articles, and documents introduced into NASA scientific and technical information system in 1972
[NASA-SP-7500(07)] 15 p1845 N73-24946
Foreign reports on environmental pollution
[PB-218839/9] 18 p2148 N73-27360
Foreign reports on environmental pollution legislative, economic, and social aspects
[PB-218858/9] 18 p2148 N73-27361

**DOGHOUSES**
U PROTUBERANCES

**DOGS**
Effect of calcium-deficient diet on bone structure of pigs and dogs
[NASA-TT-F-13917] 01 p0008 N73-10067
Hyperammonemia development in metabolic toxicity of hydrazine
[AD-749519] 05 p0501 N73-14077
Morphological changes in testes and spermatogenesis process of dogs subjected to chronic and combined gamma irradiation
07 p0743 N73-16048
Prolonged weightlessness effects on physiological functions of dogs
[NASA-TT-F-14672] 08 p0878 N73-17110
Vestibular analyzer functions in dogs after prolonged ionizing irradiation
10 p1115 N73-19088
Influence of shielding head and anterior stomach on course of radiation sickness in dogs subjected to total lethal gamma irradiation
11 p1241 N73-20073
GAST and GALT aminotransferases activity of dog blood serum following total exposure to gamma rays with stomach or head shielded
11 p1241 N73-20075
Effect of transverse overloads and gamma rays at 100 to 200 r on peripheral blood in dogs
11 p1242 N73-20083
Clinical hematological indices for evaluating vibration effect [70 Hz, 0.4 cm amplitude] on radiation reaction in dogs
11 p1242 N73-20084
Morphological changes in liver of dogs subjected to chronic gamma radiation
11 p1244 N73-20101
Leukopenic response of dog bone marrow for evaluating hematopoietic tissue function
13 p1481 N73-22009
Influence of isolated heating of spinal column on respiratory rate and panting in dogs
[NASA-TT-F-14998] 18 p2109 N73-27054
Behavior of dogs when given choice of various reinforcements
24 p2889 N73-33066

**DOLPHINS**
Instrumented dolphins for surveying oceanographic parameters and relaying information to tracking aircraft
[AD-754761] 11 p1256 N73-20191

**DOMAINS**
NT MAGNETIC DOMAINS
Solution of acoustic and electromagnetic scattering problems in exterior domains using integral equations
[NPL-NAC-30] 19 p2314 N73-28608

**DOMES [STRUCTURAL FORMS]**
NT RADOMES
Development of formulas for elastic behavior of axisymmetrically loaded cylindrical and spherical pressure vessels under various load conditions
[AD-758496] 14 p1717 N73-23936

**DONNELL EQUATIONS**
Love- and Donnell-type equations for investigating thermal stresses in ring-reinforced oval cylindrical shells subjected to heat inputs
16 p1968 N73-25920

**DONOR MATERIALS**
Simultaneous donor and acceptor concentration determination, using Hall effect measurements
[ONERA-DERTS-NT-02-31] 05 p0587 N73-14776
Transport coefficients of donor and acceptor mixtures for epitaxial growth of silicon by sandwich method
18 p2187 N73-27659

**DOORS**
Development and evaluation of space shuttle main landing gear door constructed of boron/epoxy composite material ribs on titanium panel
[NASA-CR-112172] 02 p0233 N73-11889
Composite material for cargo door of space shuttle
[R-1525] 10 p1221 N73-19928

**DOPING [ADDITIVES]**
U ADDITIVES

**DOPPLER EFFECT**
Application of Doppler-shifted fourth sound techniques for analyzing current states in rotating superfluid helium contained in superleak
[AD-745316] 01 p0118 N73-10974
Iterative method for localizing position of balloon on earth, using interrogating satellite and correcting for errors due to terrestrial rotation and Doppler effect
[NASA-TT-F-14703] 03 p0328 N73-12679
Doppler shift measurement of local velocities in flowing medium
[NRC-TT-1592] 06 p0654 N73-15312
Biophysical mechanisms of noninvasive measurement of CVP in man
[NASA-CR-130348] 07 p0742 N73-16039
Doppler frequency of interplanetary radar signal from earth to another planet or to space probe determined according to general relativity
[NASA-CR-130147] 07 p0755 N73-16131
Power spectrum computation for phototube current of laser Doppler velocimeter
[NASA-TM-X-68184] 07 p0824 N73-16675
Multiple element aatenna array for receiving Doppler arrival angle spectral measurements in radio astronomy
[AD-751873] 08 p0889 N73-17202
Ionospheric electron content measurements by Faraday effect and dispersive Doppler effect
[BMBW-FBW-72-31] 09 p1027 N73-18380
Doppler study of microwave backscattering from ocean waves in wind wave tank
[AD-753199] 09 p1032 N73-18422
Laser Doppler velocity measurement of turbid and bubbly flow media
[UTIAS-TN-185-PT-2] 09 p1043 N73-18506
Application of laser Doppler velocimeter for flow measurements
[AD-753243] 09 p1044 N73-18513
Laser Doppler anemometer for measuring steam and water velocities in two phase flow
[UTIAS-TN-184-PT-1] 10 p1141 N73-19293
Laser-Doppler velocity measurement of large particles in two-phase gas-solid nozzle flow
[VKI-TN-81] 10 p1142 N73-19305
Doppler compensated communication system for locating supersonic transport position
[NASA-CASE-GSC-10087-4] 11 p1254 N73-20174
Method for interpreting Doppler effect measurements and determining their precision
[NASA-TM-X-68199] 11 p1323 N73-20736
Laser Doppler velocimeter for simultaneously measuring orthogonal fluid velocity components without flow field perturbation
[NASA-CASE-ARC-10637-1] 12 p1405 N73-21390
Design and performance of two color laser Doppler velocimeter for wind tunnels
[NASA-TM-X-62254] 12 p1405 N73-21393
Surface wave device to correlate acoustic velocity and to correct signal phases from pulse bursts
[AD-755198] 13 p1502 N73-22175
Doppler resolution filter configured as tapped delay line with simple input and output transducers
[AD-755194] 13 p1504 N73-22193
Application of laser Doppler velocimeter for measurement of central vortex filament in wind tunnel test section
[NASA-TM-X-62243] 13 p1536 N73-22448
Influence of rain on airborne Doppler velocity sensor performance
[AD-757509] 14 p1668 N73-23541
Development of Doppler microwave landing system and techniques for eliminating effects of multipath transmissions
14 p1689 N73-23706
Whistler wave propagation in relation to interplanetary shocks
[NASA-TM-X-66245] 15 p1778 N73-24414
Doppler shift measurements at 16 GHz over transhorizon path to estimate tropospheric wind velocity
[AD-760119] 17 p1999 N73-26164
Generalized radar equations and Doppler shift in Fresnel region
18 p2115 N73-27097
Radar measurement of atmospheric turbulence structure function
18 p2170 N73-27526
Doppler difference monochromatic baseline interferometry for tracking lunar roving vehicle
18 p2210 N73-27844
Ground station S band tracking in Doppler mode for calibrating Mariner 9 in deep space
18 p2210 N73-27845
Doppler return spectra from rough ocean surface
19 p2320 N73-28667
Suppression of Doppler ambiguities in pulsed random signal radar
20 p2375 N73-29086
Extensions to short arc geodetic adjustment for reduction of Doppler operations in satellite geodesy
[AD-760791] 20 p2414 N73-29401
Wind tunnel tests to measure axial and tangential velocity profiles in near wake vortices of semi-span model of Convair 990 aircraft model using laser Doppler velocimeter
[NASA-TM-X-62294] 21 p2524 N73-30244
Position of earth spin axis with respect to crust computed on basis of Doppler satellite observations
[AD-763362] 21 p2542 N73-30381
Measurement capabilities of one dimensional laser Doppler velocimeter system
[NASA-TM-X-64774] 21 p2548 N73-30427
Comparison of laser Doppler measurements of wind velocities and turbulence with measurements by anemometers
[NASA-CR-124355] 21 p2574 N73-30627
Using average transmission and self-indication ratio measurements to investigate temperature dependence of resonance self-shielding effect in depleted uranium and tantalum
[NASA-TM-X-69565] 21 p2585 N73-30715
Doppler and surface effects in backscattered signal fading
22 p2627 N73-31052
Doppler shift arising from radiating body rotation at extreme relativistic speeds
22 p2714 N73-31721
Doppler data range change measurements for Mariner 9 celestial mechanics experiment
23 p2842 N73-32709
Mariner 9 range and Doppler data analyses for relativistic time delay effects
23 p2842 N73-32711
Doppler study of plasma column changes at solar elongation in Mariner 9 tracking path
23 p2842 N73-32715
Wing tip vortex measurements with laser Doppler velocimeter
[NASA-CR-124444] 24 p2869 N73-32924
Feasibility of using Doppler techniques for determining location of ground based emitters causing RFI with low orbiting satellites
[NASA-TM-X-70483] 24 p2895 N73-33109
Frequency modulation method for simultaneous recording of signals reflected from ionosphere
24 p2895 N73-33111

**DOPPLER NAVIGATION**
Characteristics of navigation satellite system and analysis of operation of translocation subsystem
[AD-754173] 10 p1186 N73-19650

Design and development of radio receiver for navigation satellite - Vol. 1
[AD-755149] 11 p1321 N73-20723
Design and development of low cost radio receiver for navigation satellite - Vol. 2
[AD-755150] 11 p1321 N73-20724
Characterization of multipath and Doppler fading in earth scatter communication, navigation, and radar links 24 p2894 N73-33102

DOPPLER RADAR
Development of digital method for smoothing and differentiating output of Doppler radar 01 p0024 N73-10186
Errors in Doppler residuals of Mariner 6 and 7 Martian atmospheric occultation data 02 p0198 N73-11599
Error analysis on Doppler data associated with bent ray path radio occultation of planetary atmospheres 02 p0196 N73-11600
Doppler radar frequency attenuation in horizontally polarized field over forest
[AD-748104] 04 p0389 N73-13163
Procedures for measuring radar cross section areas of extremely small objects in superhigh frequency ranges
[AD-749788] 05 p0515 N73-14186
X-band pulsed-Doppler radar measurement of radial velocity spectra in Arizona light showers
[PB-211388] 05 p0574 N73-14675
Lightweight, low power combat surveillance Doppler radar
[AD-750370] 06 p0642 N73-15212
Capabilities and projected accuracy of various satellite tracking systems 06 p0662 N73-15379
Digital optical hybrid correlator for processing pulse Doppler and wideband radar signals
[AD-751695] 07 p0756 N73-16143
Effect of Doppler radar pulse volume on atmospheric turbulence measurements
[AD-755440] 12 p1423 N73-21534
Doppler radar measurement of turbulent air associated with stalactite cloud base zone
[AD-755441] 12 p1423 N73-21535
Doppler radar measurement of atmospheric turbulence structure function
[AD-755439] 12 p1423 N73-21536
Two-dimensional curve fitting technique for analyzing data acquired by Doppler radar and application to study of convective storms
[AD-755946] 12 p1424 N73-21537
Application of ultrafast laser pulses to high resolution imaging radar systems
[AD-758059] 15 p1795 N73-24551
Venus wind/altitude Doppler radar probe
[NASA-CR-114556] 16 p1962 N73-25871
Relativistic effects in satellite dynamics and Doppler tracking
[AD-762400] 19 p2344 N73-28859
Application of pulsed Doppler radar for analyzing motion of sources of reflection from clear skies to show effect of wind 21 p2571 N73-30601

DORMANT VEGETATION
U VEGETATION
DORNIER AIRCRAFT
NT DO-31 AIRCRAFT
DORNIER DO-31 AIRCRAFT
U DO-31 AIRCRAFT
DOSAGE
NT RADIATION DOSAGE
NT SUBLETHAL DOSAGE
Effects of human biorhythms on chemotherapy and drug evaluation 12 p1370 N73-21119
DOSE
U DOSAGE
DOSIMETERS
NT THRESHOLD DETECTORS [DOSIMETERS]
Dosimetric determination of absorbed gamma and neutron radiation on human phantom
[AD-743005] 01 p0010 N73-10077
Cosmic radiation dosage measurements on Apollo astronauts by Lexan dosimetry
[AD-745188] 01 p0013 N73-10101
Dosimetric analyses for Biosatellite 2 yeast and artemia radiation exposure experiment
[NASA-CR-127142] 04 p0379 N73-13082
Preparation and processing of nuclear emulsions for radiation measurement systems
[AD-756826] 13 p1562 N73-22657
Nuclear track dosimetry for monitoring cosmic ray exposure of Apollo 16 astronauts 15 p1741 N73-24114
Lithium fluoride thermoluminescent dosimeter for measuring ionizing radiation exposure during Apollo 16 flight 15 p1741 N73-24115

DOUBLE BASE PROPELLANTS
NT DOUBLE BASE ROCKET PROPELLANTS
Shock initiation of reaction in RDX/TNT, nitromethane explosives, and double base propellants
[ERDE-TR-103] 05 p0606 N73-14930

DOUBLE BASE ROCKET PROPELLANTS
Development of physical model to determine mechanism of condensed phase reaction in combustion of double base rocket propellants 07 p0853 N73-16921
Mechanism of super burning of catalyzed double based propellants
[AD-763786] 21 p2606 N73-30887
DOUBLE SIDEBAND TRANSMISSION
System performance with single and double sideband doppler low level receiver maintenance simulation
[FAA-RD-72-67] 07 p0818 N73-16627
Frequency division multiplexer for operation in double or single sideband channel
[NASA-CR-124250] 14 p1640 N73-23293
DOUGLAS AIRCRAFT
NT A-4 AIRCRAFT
NT DC 3 AIRCRAFT
NT DC 8 AIRCRAFT
NT DC 9 AIRCRAFT
NT DC 10 AIRCRAFT
DOUGLAS DC-3 AIRCRAFT
U DC 3 AIRCRAFT
DOUGLAS DC-8 AIRCRAFT
U DC 8 AIRCRAFT
DOUGLAS DC-9 AIRCRAFT
U DC 9 AIRCRAFT
DOUGLAS MILITARY AIRCRAFT
U MILITARY AIRCRAFT
DOVAP
U DOPPLER EFFECT
DOWNWASH
Dissipation of fog using helicopter downwash
[AD-744471] 01 p0076 N73-10629
Helicopter downwash for dispersing fogs of 500 to 600 feet in depth
[AD-753357] 09 p1062 N73-18661
Development of actuator disc theory for predicting time-averaged downwash distribution and response characteristics of helicopter rotors in forward flight 12 p1360 N73-21033
Analysis of unsteady aerodynamic loading on reference section of helicopter rotor blade in axial or hovering flight under compressible flow conditions 12 p1361 N73-21044
Development of method for calculating downwash interference and longitudinal stability of tandem rotor helicopter
[ARC-R/M-3223] 15 p1729 N73-24022
Tabular data from helicopter downdraft fog dispersal experiments
[AD-762189] 19 p2318 N73-28643
Exhaust blast velocities and temperatures at ground level for various aircraft and wing tip vortex velocity for C-5 aircraft
[AD-764228] 22 p2616 N73-30961
DRAG
NT AERODYNAMIC DRAG
NT FRICTION DRAG
NT INTERFERENCE DRAG
NT MINIMUM DRAG
NT SATELLITE DRAG
NT WAVE DRAG
Ion drag and winds aloft in high latitudes
[NASA-TM-X-66083] 02 p0165 N73-11340
Calculation of drag of porous lattice plates in turbulent flow
[IC-AERO-72-20] 03 p0284 N73-12300
Viscous drag reduction caused by polymer injection in developing turbulent boundary layer
[AD-747274] 03 p0285 N73-12310
Low speed wind tunnel tests on slender variable sweep wing of lift, drag, and pitching moments
[ARC-CP-1227] 05 p0492 N73-14009
Drag coefficients for Echo 1 and Explorer 24 spherical surfaces in atomic oxygen over energy range from 4 to 200 eV
[NASA-CR-2233] 10 p1192 N73-19697
DRAG BALANCE
U AERODYNAMIC BALANCE
DRAG CHUTES
Flight tests of disk-gap band parachute behind full-scale simulator of Viking reentry vehicle over maximum range of entry conditions for landing on planet Mars-Vehicle AV-1
[NASA-CR-112176] 04 p0372 N73-13021
Flight tests of disk-gap band parachute behind full-scale simulator of Viking reentry vehicle over maximum range of entry conditions for landing on planet Mars-Vehicle AV-4
[NASA-CR-112179] 04 p0372 N73-13024
Flight test of 55 foot diameter disk-gap parachute trailing behind bluff body, planetary aeroshell and attached instrument payload
[NASA-TM-X-2671] 06 p0621 N73-15042
Analysis of shock forces generated by opening 35 foot diameter extended-skirt parachute for retardation at 100,000 feet altitude
[AD-749690] 06 p0623 N73-15060
Postflight analysis of AV-2 balloon launched decelerator flight test to determine parachute system operation in wake of blunt body simulating Viking 75 entry vehicle
[NASA-CR-112177] 11 p1233 N73-20011
Postflight analysis of AV-3 balloon launched decelerator flight test to determine parachute system operation in wake of blunt body simulating Viking 75 entry vehicle
[NASA-CR-112178] 11 p1233 N73-20012
Analysis of size, weight, and packaging requirments for aerodynamic decelerator for recovery of expended solid propellant rocket engines used to launch space shuttle vehicles - Vol. 2, Book 5
[NASA-CR-123730] 15 p1826 N73-24801
DRAG COEFFICIENT
U AERODYNAMIC COEFFICIENTS
U AERODYNAMIC DRAG
DRAG DEVICES
NT AERODYNAMIC BRAKES
NT DRAG CHUTES
NT LEADING EDGE SLATS
NT SPOILERS
NT TRAILING-EDGE FLAPS
NT WING FLAPS
DRAG EFFECT
U DRAG
DRAG MEASUREMENT
Procedure for solving nonconservative projectile penetration problems
[AD-746140] 02 p0219 N73-11774
Measurement of hypersonic free molecular sphere drag at varying wall temperature ratios
[AD-748618] 04 p0407 N73-13320
Drag measurement in wake of oscillating cylinder at low Reynolds number using hot-wire technique
[DLR-FB-71-42] 09 p0981 N73-18015
Measurement of lift, drag, and pitching moments in wing section for range of flap deflections under two-dimensional flow conditions
[ARC-CP-1233] 09 p0981 N73-18018
Development and characteristics of analog wake drag evaluation system for use in test section of low speed wind tunnel
[FFA-AU-860] 14 p1648 N73-23368
Analysis of drag and pressure measurements made in subsonic wind tunnel tests on two annular airfoils noting relation between pressure distribution in compressible flow and at high speed
[ARC-R/M-2718] 21 p2492 N73-30003
Measurement of drag, lift and pitching moments on slender winged low aspect ratio gothic planforms at subsonic speed
[ARC-R/M-3720] 21 p2492 N73-30005
Drag measurement of parallel flat plates and perpendicular disks in supersonic free molecular flow
[DLR-FB-73-17] 21 p2525 N73-30248
Reaction time of 27-day density variation in upper atmosphere noting satellite recorded data on drag using regression analysis, cross correlation, and solar spectrum analysis
[BMFT-FBW-73-10] 21 p2538 N73-30352
Derivation of charts for predicting drag-rise Mach number for airfoils with specified upper surface pressure distribution
[ESDU-71019] 22 p2650 N73-31229
Method for estimating drag-rise mach number of smooth, nonducted, axisymmetric bodies at zero incidence without discontinuities in surface slope
[ESDU-71008] 22 p2650 N73-31230
DRAG REDUCTION
Review and evaluation of theories on turbulent drag reduction by polymeric additives
[AD-746107] 02 p0158 N73-11277
Drag reduction and diffusion accompanying thin slit injections of drag reducing polymer into water turbulent boundary layer of flat plate at high Reynolds number
[AD-747248] 03 p0285 N73-12312
Quasi area rule for heat addition in transonic and supersonic flight including determination of optimum shapes with propulsion to minimize wave drag
[AD-747772] 03 p0352 N73-12867
Application of power method for reducing base drag of long range supersonic aircraft at supersonic speeds
[AD-750950] 06 p0625 N73-15056
Supercavitating jet flapped hydrofoil with drag reduction due to combined effects of foil camber jet flap
[REPT-249] 06 p0724 N73-15912
Reduction of transonic drag for high performance aircraft by injecting air in rear of aircraft to alter transonic flow distribution on aft section
[AD-751269] 07 p0736 N73-15991
Rotating disk measurement of drag reduction and shear properties of various dilute polymers
[AD-751532] 07 p0773 N73-16281
Effects of drag reducing polymer on turbulent boundary layer of submerged flat plates
[AD-753215] 13 p1513 N73-22260
Effect of fineness ratio on boattail drag of circular arc afterbodies having closure ratios of 0.50 with jet exhaust at Mach numbers up to 1.30
[NASA-TN-D-7192] 14 p1701 N73-23802
Characteristics of dilute gas-solids suspensions in drag reducing flow
[NASA-CR-2267] 16 p1888 N73-25277
Syntheses of polystyrene polymers with skin friction reduction in dilute solutions
[AD-761600] 19 p2233 N73-28008

Drag reduction in fluids by addition of polymer additives
[AD-763824] 22 p2654 N73-31263
Reduction of friction drag in polymers
[AD-757012] 23 p2777 N73-32205
Aerodynamic drag and lift of airships, noting boundary layer control by suction
24 p2879 N73-32994
Effect of high polymer drag reducing additives on longitudinal turbulent dispersion coefficient for two dimensional open channel flow
24 p2902 N73-33164

DRAGULATORS
U BRAKES [FOR ARRESTING MOTION]

DRAINAGE
Prediting mean annual runoff from solar activity
[NLL-M-20715-[5828.4F]] 05 p0529 N73-14303
Hydrological information from ERTS-1 imagery for design of highway drainage structure in Maine
[E73-10014] 06 p0659 N73-15350
Geographical, physicomathematical, and hydrological engineering treatment of river runoff in USSR
[TT-70-50058] 07 p0781 N73-16346
Processing of IFYGL data for Lake Ontario and its drainage basin
[E73-10393] 11 p1276 N73-20355
Land use, forest density, soil mapping, erosion, drainage, and salinity limitations in Greece from ERTS-1 data
[E73-10969] 22 p2657 N73-31283
Usefulness of ERTS-1 MSS data for monitoring coal strip mining, detection of acid mine drainage, and determination of effectiveness of reclamation and abatement procedures in Pennsylvania
[E73-11112] 24 p2915 N73-33269

DRAINAGE PATTERNS
Remote sensing of rapid mass wastage, mudflow, and debris slide
[NASA-CR-130379] 07 p0792 N73-16443
Interpretation of ERTS-1 imagery of man made culture and revision of small-scale maps
[E73-10536] 13 p1518 N73-22300
Hydrological investigation of drainage basin characteristics from ERTS-1 imagery for improved regression estimates of water flow
[E73-10652] 16 p1898 N73-25348
Application of ERTS-1 imagery for inventory and monitoring of natural vegetation and related resources in arid environment
[E73-10728] 17 p2020 N73-26334
Stream and river drainage network analysis from Skylab imagery
[E73-10818] 18 p2140 N73-27293
Application of ERTS-1 imagery for analysis of terrestrial water balance of Lake Ontario and drainage basin
[PAPER-W15] 19 p2272 N73-28292
Interpretation of land use and stream drainage in Pawnee River Basin, Kansas
[E73-11005] 22 p2660 N73-31310
Detection of plant diseases, soil moisture, drainage patterns, forestry types, and sedimentation in Tennessee from ERTS-1 imagery
[E73-11091] 23 p2782 N73-32258
Utilization of ERTS-1 imagery of topography and drainage patterns for resources inventory and management in Arizona
[E73-11159] 24 p2919 N73-33312
Conference on hydrologic research in representative and experimental basins
24 p2947 N73-33538

DRAINING
U DRAINAGE

DRAWING
Production of thin walled tubes by drawing and rolling
[NLL-M-21689-[5828.4F]] 20 p2421 N73-29448

DRAWINGS
NT ENGINEERING DRAWINGS

DRIFT [INSTRUMENTATION]
Sources responsible for long term drift of He-Ne lasers
[AD-749055] 05 p0558 N73-14535
Motion of gyroscope in cardan suspension in drift mode during platform oscillations
10 p1184 N73-19634
Condition of drift invariance of two-stage gyroscope with arbitrary gas-lubricated main bearings in active accelerations
10 p1184 N73-19635

DRIFT RATE
Ionospheric soundings in USSR for IQSY
04 p0413 N73-13374
Radio frequency electron drift velocity and parametric instability in plasma heating
[CONF-720705-4] 07 p0756 N73-16138
Parallel wavelength effects on drift waves in collisional potassium Q machine plasmas
12 p1432 N73-21607
Longitudinal source drift measure of PC 1 geomagnetic micropulsation source by signal correlation of spaced receivers
[CEPHAG-22/72] 13 p1524 N73-22353
Extension of drift instability theory to plasmas of arbitrary beta
[NASA-CR-131880] 14 p1695 N73-23758
Sector radio measurements of meteor trail drifts by low frequency radar transmissions
17 p2023 N73-26369
Error drift projection for ERTS orbit maintenance calculation using ground tracking data
18 p2211 N73-27847

DRILLING
Environment-sensitive hardness effects on drilling and machining aluminum oxides
[AD-753276] 09 p1053 N73-18586

DRILLS
Designing laser drill to correct beam wandering during drilling
[AD-759966] 17 p2006 N73-26224
Auger-type soil penetrometer for burrowing into soil formations
[NASA-CASE-XNP-05530] 23 p2790 N73-32321

DROGUE PARACHUTES
U DRAG CHUTES

DROGUES
U TOWED BODIES

DRONE AIRCRAFT
Computerized simulation of aircraft as radar target
[AD-753854] 12 p1380 N73-21189
Performance analysis and conceptual design of waveform and modem to provide jamming-resistant command and control data link for ground station control of drone aircraft
[AD-756933] 13 p1496 N73-22125
Feasibility of modifying supersonic drone configuration into remotely controlled research vehicle
[NASA-CR-112323] 15 p1733 N73-24057

DRONE HELICOPTERS
U DRONE AIRCRAFT
U HELICOPTERS

DRONE VEHICLES
NT DRONE AIRCRAFT

DROP SIZE
Computerized analysis of droplet size effect on erosion rate in wet steam turbine stage
[PB-211901] 05 p0527 N73-14292
Theoretical investigation of rocket steam generator with emphasis on trajectories and spectrum of injected drops and their vaporization for Europa 1 launch vehicle
[DLR-FB-71-36] 09 p1011 N73-18253
Moment equations for describing evolution of droplet populations in convection clouds
10 p1180 N73-19595
Analysis of breakup length and breakup pattern for jets of liquids of different viscosity and surface tension ejected vertically downward into atmosphere
[NLL-RTS-8049] 15 p1764 N73-24291
Theory of drop growth by condensation for cloud physics application
[AD-764258] 22 p2695 N73-31586
Time resolved measurements of droplet growth in Wilson expansion cloud chamber
24 p2901 N73-33158

DROP TESTS
Soil impact test with spherical nuclear reactor containment model for fracture strength observations
[NASA-TM-X-68180] 07 p0819 N73-16641
Drop impact strength and toughness of glass and carbon fiber composite materials
[AD-753101] 09 p1054 N73-18595

DROP WEIGHT TESTS
U DROP TESTS

DROPS [LIQUIDS]
NT RAINDROPS
Ignition site and ignition delay time for spherical fuel droplets
[NLL-RTS-7169] 02 p0241 N73-11959
Oscillatory combustion and fuel vaporization tests to determine thermodynamic properties of droplets under various conditions
[NASA-CR-120974] 02 p0242 N73-11971
Estimation of impact pressures of drops against solid surface
[AD-748731] 03 p0363 N73-12956
Airborne spectrometer measurements of cloud droplet size
[NASA-CR-130138] 06 p0693 N73-15650
Dynamics of water drop evaporated by heating with laser pulse
[AD-752822] 09 p1001 N73-18167
Growth rate of liquid droplets formed in supersaturated vapors
[AD-753074] 09 p1017 N73-18301
Development of droplet monitoring probe for use in analysis of droplet propagation in mixed-phase fluid stream
[NASA-CASE-NPO-10985] 11 p1291 N73-20478
Evaporation of droplets in aerosol jets, by simulation with latex spheres
[BMVG-FBWT-73-5] 14 p1616 N73-23096
Design and construction of waterdrop generator with remote control of drop mass and interval
[NBS-TN-776] 14 p1645 N73-23343
Droplet combustion at high pressures with unsteady effects
[AD-757227] 14 p1720 N73-23957
Analysis of breakup length and breakup pattern for jets of liquids of different viscosity and surface tension ejected vertically downward into atmosphere
[NLL-RTS-8049] 15 p1764 N73-24291
Chemical changes during transformation of aerosols to cloud droplets and rain in orographic clouds
15 p1805 N73-24630
Effects of accelerating gas flow on atomization characteristics of liquid sprays produced by impinging two liquid jets - Part 1
[NASA-CR-134478] 22 p2652 N73-31247
Secondary atomization produced by accelerating gas flow to show effects on liquid sprays produced by impinging two liquid jets - Part 2
[NASA-CR-134479] 22 p2652 N73-31248
Analysis of equal-size droplet injection in fluid flow, noting fuel injection
[DLR-MITT-72-19] 22 p2710 N73-31703
Simulation of process of dropwise condensation using digital computer
23 p2774 N73-32186
Theoretical studies of growth of marine fog droplets
[AD-764597] 23 p2815 N73-32503

DROPSONDES
Wind determination in tropics by balloon carrying dropsondes using Omega navigation system
24 p2948 N73-33548

DROUGHT
Evaluation of hydrology and vegetation in Sahelian zone of Mali, Mauritania, and Senegal during dry season/drought period based on ERTS-1 imagery
[E73-10488] 12 p1396 N73-21324

DROUGHT CONDITIONS
U DROUGHT

DROWSINESS
U SLEEP

DRUG THERAPY
U CHEMOTHERAPY

DRUGS
NT ADRENERGICS
NT ANTIBIOTICS
NT ANTICHOLINERGICS
NT ANTIDIURETICS
NT ANTIDOTES
NT ANTIRADIATION DRUGS
NT ATROPINE
NT CENTRAL NERVOUS SYSTEM DEPRESSANTS
NT CENTRAL NERVOUS SYSTEM STIMULANTS
NT CHOLINERGICS
NT EPINEPHRINE
NT HISTAMINES
NT INSULIN
NT MOTION SICKNESS DRUGS
NT NARCOTICS
NT PENTOBARBITAL SODIUM
NT SEDATIVES
NT STIMULANT
NT TRANQUILIZERS
Guinea pigs used to determine effect of intramuscular injections of drugs on fall-out and Bekhterev nystagmus occurring after unilateral and bilateral labyrinthectomies
07 p0744 N73-16049
High temperature tolerance of rats under normal conditions, after thermal conditioning and combined with drugs
11 p1244 N73-20099
Feasibility determination for polyethylene packaging of drugs stocked in spacecraft pharmacies
11 p1246 N73-20114
In vitro metabolism of antipyrine in rats
[NASA-TT-F-14868] 11 p1246 N73-20116
Metixenum and Meclocin under double blind comparison test conditions against motion sickness
12 p1368 N73-21100
Conference on detection, evaluation, and identification of drugs and alcohol in flying personnel and effects on flight fitness
[AGARD-CP-108] 12 p1368 N73-21102
Drug screening data for civil aviation personnel obtained by urinalyses
12 p1369 N73-21104
Residual effects of hypnotic drugs on human nervous function and performance
12 p1369 N73-21106
Pilot performance and sleep patterns in long duration flights and control of hypnotic drug and alcohol use
12 p1369 N73-21107
Physiological aspects of sleep induction in aircrews after prolonged flight times
12 p1369 N73-21108
Adaptive tracking task for evaluating drug after-effects on human flight performance
12 p1369 N73-21109
Effects of isoniazid treatment on pilot performance
12 p1369 N73-21111
Sports medicine - parameters necessary for maintaining competitive form
12 p1370 N73-21114
Urinalysis methodology for detection of abusive and therapeutic drugs in man
12 p1370 N73-21117

Opthalmological examination of antimalarial drugs effects on performance of navigation personnel
12 p1371 N73-21122

Influence of altitude and drugs on cerebral circulation in smokers and non-smokers
12 p1371 N73-21125

Pathophysiological justifications for using drugs in aerospace medicine
[NASA-TT-F-736] 13 p1484 N73-22033

Self-scanning chromatographic-fluorographic drug detector with optical readout system
[NASA-CASE-ARC-10633-1] 13 p1486 N73-22048

DRUMLINS
U GLACIAL DRIFT

DRUMS [CONTAINERS]
Bending stresses produced by internal pressure in thin walled hollow cylinders with out-of-round cross section
[NLL-CE-TRANS-6040-[9022.09]]
20 p2478 N73-29902

DRY CELLS
NT MAGNESIUM CELLS
NT NICKEL ZINC BATTERIES

DRY FRICTION
Antifriction interaction between metals and steels on polyamide surfaces
[NLL-RTS-7378] 04 p0425 N73-13461

Gyro suspension systems including axis disturbance probability factors, bearing friction, astatic gyro gimbal errors with drift, and horizontal pendulum energy dissipation
[JPRS-57504] 05 p0546 N73-14432

Influence of dry friction in suspension bearings on motion of gyroscope with forced gimbal rotation
05 p0546 N73-14434

DRY HEAT
Thermoradiation sterilization of naturally occurring microorganisms in soil from Kennedy Space Center
[NASA-CR-132197] 16 p1904 N73-25404

Thermal inactivation of Bacillus subtilis var. niger spores on Viking lander
[NASA-CR-133223] 17 p1987 N73-26058

Dry heat inactivation of atypical Bacillus subtilis var. niger spores in and on interplanetary space vehicle components
[NASA-CR-133224] 17 p1987 N73-26059

DRYERS [EQUIPMENT]
U DRYING APPARATUS

DRYING
Drying chamber for photographic sheet material
[NASA-CASE-GSC-11074-1] 19 p2300 N73-28489

Application of holographic interferometry for detecting dewetted zones in solid rocket propellants
[AD-764470] 22 p2708 N73-31690

DRYING APPARATUS
Atomized particle dispersion in dryer space
[AD-762221] 19 p2233 N73-28005

DSIF [INSTRUMENTATION FACILITY]
U DEEP SPACE INSTRUMENTATION FACILITY

DTA [ANALYSIS]
U DIFFERENTIAL THERMAL ANALYSIS

DTMB-111 GROUND EFFECT MACHINE
U GROUND EFFECT MACHINES

DTMB-430 GROUND EFFECT MACHINE
U GROUND EFFECT MACHINES

DUAL SPIN SPACECRAFT
Attitude stability criteria and nutation decay times of dual-spin satellite with large flexible solar array
[AD-743258] 01 p0109 N73-10897

Attitude stability of dual spin spacecraft with mathematical model covering fuel sloshing, nutation dampers, and flexible bearings
[ESRO-CR-56] 02 p0235 N73-11908

Stability of dual-spin satellite system during momentum wheel spin-up maneuver
[NASA-CR-130130] 05 p0597 N73-14858

Attitude dynamics of nearly spherical dual spin satellite with asymmetrical bodies, orbital results for OSO 7, and critical mass properties
07 p0848 N73-16877

Device for automatically balancing spinning spacecraft
17 p2059 N73-26654

DUCTED BODIES
Internal drag lift and pitching moment of ducted body, neglecting post exit flow
[ARC-CP-1211] 03 p0285 N73-12305

DUCTED FAN ENGINES
Bench testing ducted fan engines under conditions close to those of flight
[AD-742376] 13 p1505 N73-22198

DUCTED FANS
DC 9 refanned engine nacelle effects on cruise drag considering lateral spacing
[NASA-CR-121219] 17 p1982 N73-26024

Measurement of noise and wake structure of ducted fan with subsonic tip speed to show sound pressure levels and blade wake characteristics
[NASA-CR-132259] 18 p2129 N73-27207

Far field sound propagation calculation for ducted fan rotor-stator interaction
[NRC-13260] 18 p2179 N73-27592

Aerodynamic characteristics of low speed flight using heavily loaded ducted fans, single bladed hovering rotor, and tensioned sheets with cutouts
[AD-764264] 22 p2616 N73-30964

DUCTED FLOW
Pressure changes in fluid flow along duct with sudden enlargement of area
[ESDU-72011] 04 p0403 N73-13281

Development of design data for cascades of flat plate guide vanes suitable for use in ninety degree elbows in ducts of circular cross section
[ESDU-AERO-00.02.09] 04 p0403 N73-13284

Analysis procedure for three dimensional, subsonic, duct flow
[AD-748649] 04 p0407 N73-13313

Analysis of turbulent fluid flow through rectangular conduit with large aspect ratio and development of mechanical energy-balance equations
[WTHD-27] 05 p0526 N73-14279

One- and two-D core theories for analyzing ducted mixing and burning of coaxial streams
08 p0896 N73-17253

Techniques for determining dynamic characteristics of hydraulic duct for predicting low frequency vibrations of liquid propellant rocket engines
[ONERA-TP-1160] 09 p1015 N73-18281

Linearized theory for MPD duct flows with exterior magnetic fields and Hall effect
[DLR-FB-72-67] 09 p1069 N73-18726

Development of numerical procedure for solving gas dynamics of pulsating, compressible flow in propulsive duct
12 p1389 N73-21266

Finite difference formulation for sound propagation in two-dimensional soft-walled duct with uniform flow
[NASA-TM-X-68295] 20 p2454 N73-29722

Analysis of sound propagation in elliptic ducts to determine acoustic effects produced by variations from symmetry in circular ducts
[NASA-CR-132307] 21 p2579 N73-30672

Finite difference theory of noise propagation in turbofan engine ducts
[NASA-TN-D-7339] 24 p2972 N73-33744

DUCTED PROPELLERS
U SHROUDED PROPELLERS

DUCTILITY
Lowered ductility and crack initiation in neutron irradiated steels after tensile testing
[STU-70-419/U-350-A] 04 p0433 N73-13533

Beta-phase effect on ductility of two-phase titanium alloys and calorimetric determination of atomic ordering effects in Ni2Cr alloy
[JPRS-57578] 06 p0683 N73-15556

Microstructural features of deformation analyzed in two-phase titanium alloys to determine beta phase effect on ductility
06 p0683 N73-15557

Ductility as criterion of performance of quenched and tempered steel
[AD-751534] 07 p0810 N73-16568

Phenomenological criterion for uniaxial yield of ductile materials
[AD-752573] 08 p0952 N73-17795

Metallurgical evaluations of factors influencing ductility of aged T-111
[NASA-CR-120865] 09 p1047 N73-18540

Electron probe microanalysis of ductile metal bond to Ti alloy disc
[AECL-4251] 10 p1172 N73-19535

Rate and time dependent yield behavior of ductile polycarbonates
[AD-753941] 10 p1177 N73-19571

Characteristics of metal drawing processes based on hypotheses of plane cross sections and deformation zone equilibrium conditions
[NLL-M-21553-[5828.4F]] 11 p1296 N73-20518

High temperature heating effects on structure and ductile properties of austenitic steels
[NLL-M-21563-[5828.4F]] 16 p1926 N73-25584

Effect of fast reactor irradiation on ductility of annealed stainless steels
[HEDL-SA-310] 16 p1929 N73-25606

Relationships between fracture strength, flow stress, and material ductility in high strength steels
[AD-761217] 18 p2162 N73-27463

Effect of high speed volumetric deformation on ductility of metals and alloys
[AD-762246] 19 p2310 N73-28582

Analysis of effects of hydrostatic pressure on yield stress, flow stress, and ductility of metals
[NLL-NEL-TT-2488-[6075.461]]
20 p2478 N73-29904

Analytical investigation of hexagonal metal deformation with particular application to Ti and Be
[AD-763835] 22 p2686 N73-31518

Effect of rare earth metals on macrostructure, microstructure, strength, and ductility of cast titanium samples
23 p2809 N73-32458

Annealing effects on room temperature ductility of molybdenum
[CEA-CONF-2236] 24 p2935 N73-33443

DUCTS
NT ACOUSTIC DUCTS
NT AIR DUCTS

Flow coupled diffusion and velocity profiles for steady laminar flow in circular duct
13 p1509 N73-22231

Transmission of wave energy in curved ducts
[NASA-TM-X-68287] 20 p2377 N73-29101

Secondary flow in curved channel of square cross section
[AD-764502] 22 p2655 N73-31267

Zero leakage separable and semipermanent ducting joints for space flight vehicles
[NASA-CR-124386] 22 p2722 N73-31780

DUMMY LOADS
U IMPEDANCE
U OUTPUT

DUMPING
ERTS-1 monitoring of water quality and ocean dumping
[E73-10573] 15 p1772 N73-24353

DUNES
Mapping of remote desert dune fields using ERTS-1 imagery
[E73-10009] 06 p0659 N73-15345

Morphology, provenance, and movement of desert sand seas in Africa, Asia, and Australia
[E73-10542] 13 p1518 N73-22305

ERTS-1 imagery of morphology, provenance, and movement of desert sand areas in Africa, Asia, and Australia
[E73-10710] 17 p2018 N73-26317

Morphology, provenance, and movement of desert sand seas in Africa, Asia, and Australia using ERTS-1 data
[PAPER-G8] 19 p2264 N73-28239

Wind erosion and dune formations in Mars surface topography
[CONTRIB-2353] 23 p2839 N73-32691

Dune barrier erosion due to storms and wave activity near Mosquito Lagoon, Kennedy Space Center
[NASA-CR-135775] 24 p2922 N73-33337

DUNGEYS WIND SHEAR MECHANISM
U WIND SHEAR

DUOPLASMATRONS
Production and current measurement of hydrogen ion beam and plasma in duoplasmatron with cusped magnetic field
[NP-19364] 05 p0583 N73-14747

DUPLICATING
U REPRODUCTION [COPYING]

DURABILITY
Durability test of Hughes SIT-5
[NASA-TM-X-68155] 02 p0223 N73-11802

Performance and endurance testing of 6 kW organic Rankine cycle power conversion system
[SAN-651-130] 08 p0870 N73-17042

DURATION
U TIME

DUST
NT COSMIC DUST
NT INTERPLANETARY DUST
NT LUNAR DUST
NT ZODIACAL DUST

Engineer design tests of two dust control materials, polyvinyl acetate water emulsion and cationic asphalt-neoprene emulsion
[AD-745086] 01 p0038 N73-10297

Spectrophotometric analysis of Orion nebula emission spectra with dust lanes in hydrogen region
[AD-745314] 01 p0104 N73-10863

Establishment of takeoff and landing environment criteria for V/STOL aircraft with emphasis on airborne particle concentration
[AD-749463] 05 p0495 N73-14034

Chlorophyll and plankton population distribution in upwelling waters off northwest coast of Africa and effects of eolian dust particles on surface water chemistry
[E72-10331] 05 p0531 N73-14319

Experimental study of aerodynamic effects on erosion
[AD-749286] 05 p0539 N73-14388

Application of dual-scatter laser velocimeter to measure particle velocity distribution in hypersonic dust erosion facility
[AD-752225] 08 p0930 N73-17618

Photometric profiles of dust particle size and dust cloud origins during dust storms on Mars as reported by Mars 3 Automatic Interplanetary Station
[NASA-TT-F-14815] 08 p0962 N73-17866

Nature of blue clearings on Martian photographs in short wave region
[NASA-TT-F-14820] 11 p1338 N73-20856

Emplacement and maintenance of dust control materials for military aircraft and helicopter landing facilities
[AD-756179] 14 p1647 N73-23359

Synoptic meteorology of large dust cloud over west coast of Africa
[NLL-M-22850-[5828.4F]] 16 p1936 N73-25662

Structure of dust storms determined from ITOS-1 television pictures
[NLL-M-23033-[5828.4F]] 21 p2528 N73-30272

Analysis of ways and sources for transfer of dust precipitating over Atlantic Ocean
[TT-72-50018] 21 p2541 N73-30376

Wind erosion and dune formations in Mars surface topography
[CONTRIB-2353] 23 p2839 N73-32691
DWARF STARS
NT WHITE DWARF STARS
DYE LASERS
Characteristics of dye lasers with emphasis on lasing mechanism of dyes
[PHL-1973-2] 14 p1672 N73-23566
Development of laser head for simultaneous optical pumping of several dye lasers
[NASA-CASE-LAR-11341-1] 16 p1923 N73-25564
Development of nitrogen-laser-pumped tunable-dye laser for application as spectroscopic light source
20 p2424 N73-29473
Infrared tunable dye laser with nonlinear wavelength mixing crystal in optical cavity
[NASA-CASE-ARC-10463-1] 23 p2763 N73-32111
DYES
Frequency shift of flash lamp pumped dye laser with two Fabry-Perot interferometer wavelength selectors
01 p0064 N73-10527
Organic dyes for improving light intensity of Nd YAG laser pump system
[AD-747401] 03 p0312 N73-12545
Lead lanthanum zirconate titanate ceramics as intracavity tuning elements in rhodamine 6G dye laser
[SC-RR-72-0273] 04 p0429 N73-13493
Near infrared laser action for Kodak organic dyes using linear flash lamp for excitation
[AD-748863] 04 p0429 N73-13496
Spectroscopic studies of luminescence emitted by dyes irradiated by lasers
[AD-750377] 06 p0680 N73-15535
Intensity stabilization and development of tunable ultranarrowband dye laser
[AD-754112] 10 p1170 N73-19517
Applications of multicolor dye tracers and multispectral photography to coastal water mapping
[AD-754437] 12 p1403 N73-21378
Development of flow visualization technique using fluorescent dye to simulate smoke lines in water
[AD-761499] 19 p2257 N73-28192
Dye laser bibliography from 1966 to 1972
19 p2307 N73-28559
Research on near-infrared dye lasers
[AD-762354] 20 p2426 N73-29485
Optical transitions between energy states of solute organic dye
[AD-762607] 20 p2426 N73-29489
Use of dye flow visualization techniques in small water tunnel
[ARL/A-NOTE-339] 21 p2523 N73-30230
DYNA-SOAR SPACE GLIDER
U X-20 AIRCRAFT
DYNAMIC CHARACTERISTICS
NT AERODYNAMIC DRAG
NT AERODYNAMIC STABILITY
NT AIRCRAFT STABILITY
NT ATTITUDE STABILITY
NT BOUNDARY LAYER STABILITY
NT COMBUSTION STABILITY
NT CONTROL STABILITY
NT DIRECTIONAL STABILITY
NT DRAG
NT DYNAMIC STABILITY
NT FLAME STABILITY
NT FLOW CHARACTERISTICS
NT FLOW DISTRIBUTION
NT FLOW STABILITY
NT FLOW VELOCITY
NT FREQUENCY STABILITY
NT FRICTION DRAG
NT GYROSCOPIC STABILITY
NT HOVERING STABILITY
NT INTERFERENCE DRAG
NT INTERFERENCE LIFT
NT JET LIFT
NT LATERAL STABILITY
NT LIFT
NT LONGITUDINAL STABILITY
NT LOW SPEED STABILITY
NT MAGNETOHYDRODYNAMIC STABILITY
NT MINIMUM DRAG
NT ROTARY STABILITY
NT SATELLITE DRAG
NT SPACECRAFT STABILITY
NT TRANSIENT RESPONSE
NT WAVE DRAG
NT ZERO LIFT
Solar phenomenon, based on dynamo model
[PUBL-5] 05 p0592 N73-14809
Differential equations for studying dynamic characteristics of motor with separate excitation regulated by negative resistance feed
[PUBL-1368] 06 p0645 N73-15237
Application of three dimensional theory of elasticity to dynamic response of freely supported circular cylindrical shell
06 p0725 N73-15921
General relaxation theory for liquid behavior under dynamic conditions
[NASA-CR-2141] 07 p0769 N73-16245
Technique for determining plasma drifts, applied to dynamic processes in topside F region
07 p0774 N73-16288
Dynamic behavior of externally pressurized foil bearings, including film response to step reduction in tension
[AD-751604] 07 p0805 N73-16531
Fourier theory of using grating to extend dynamic range of laser far field camera
[UCRL-51255] 07 p0806 N73-16542
Analysis of motion of dynamically unbalanced linear acceleration gyrointegrator
08 p0923 N73-17559
Dynamic testing and structural modeling of aircraft tire properties
[NASA-CR-2219] 09 p0985 N73-18042
Design of combined hydrostatic and dynamic bearings
[AD-752821] 09 p1040 N73-18479
Computer program used for dynamic analysis of Apollo-Salyut/Soyuz docking
09 p1087 N73-18871
Radioresistance recovery rate with combined exposure to ionizing radiation and dynamic factors [vibration and acceleration]
11 p1242 N73-20080
Operating characteristics of avalanche diode oscillator circuit high efficiency TRAPATT modes
[NASA-CR-131399] 11 p1264 N73-20258
Mathematical models for measuring operating functions and performance of gyroscope with two degrees of freedom
11 p1318 N73-20696
Influence of axial impact loads on dynamic properties and strain wave speeds in polycarbonate Lexan
[AD-755457] 12 p1417 N73-21482
Computerized analysis of aircraft hydraulic system dynamic performance
[AD-757537] 16 p1864 N73-25093
Flapping- and squeeze-duty design criteria for full journal bearings under dynamic duty
[WTHD-45] 16 p1917 N73-25514
Dynamic characteristics of solid particles in particulate flow through turbine and compressor cascades
17 p2013 N73-26278
Sensitivity of low weight CPNE for planetary composition analysis
[NASA-CR-132208] 17 p2032 N73-26448
Design parameters and dynamic characteristics of navigational instruments
[JPRS-59254] 17 p2059 N73-26656
Precision and reliability characteristics of combined gyroscopic and correction channel
17 p2059 N73-26659
Analytical and experimental dynamic behavior of tethered balloons
[AD-762210] 19 p2222 N73-27925
Performance of commercial multiple crystal spectrometer instruments in analyzing particulate matter
[AD-762061] 19 p2231 N73-27994
Correlation between Ge crystal and spectrometer properties of Ge[L1] detector made from Ge crystal
[AECL-4369] 19 p2327 N73-28718
Dynamic spectra of solar type 3 radio bursts at kilometer wavelengths
19 p2338 N73-28810
Sensitivity and structural peculiarities of underwater pyranometers
20 p2447 N73-29660
Four dimensional processing of a synchronously arriving meteorological data based on dynamic statistical approach
20 p2447 N73-29664
Operating principles of various types of photodetectors
21 p2594 N73-30787
Vibration design loads for component dynamic magnification factors of space shuttle
[NASA-CR-124337] 21 p2601 N73-30842
Computer program for analyzing general nonaxisymmetric and nonsynchronous transient and steady-state performance of flexible rotor bearing system
[NASA-CR-121276] 22 p2677 N73-31440
Dynamic behavior and stability classification of one-dimensional wave propagation systems
24 p2893 N73-33096
Two component force dynamometer and tool control system for dynamic machine tool research
[NASA-TM-X-64786] 24 p2926 N73-33371
Design of precision vertical alignment system using laser with gravitationally sensitive cavity
[NASA-CASE-ARC-10444-1] 24 p2930 N73-33397
Behavior of macroscopic quantum interferometer composed of superconducting tin rings containing two Josephson junctions
24 p2967 N73-33710
DYNAMIC CONTROL
Operator visual perception mapping during parameter adjustment in dynamic control system
01 p0017 N73-10129
Numerical solutions for variational control functions of flight dynamics in circular orbits
10 p1178 N73-19582
Adaptive controllability of dynamical systems in Banach space with bounded operators
[AD-753716] 10 p1179 N73-19593
Extended computer language for real time simulation of process control in large systems
14 p1712 N73-23892
DYNAMIC LOADS
NT AERODYNAMIC LOADS
NT BLAST LOADS
NT CYCLIC LOADS
NT GUST LOADS
NT IMPACT LOADS
NT LANDING LOADS
NT ROLLING CONTACT LOADS
NT SHOCK LOADS
NT THRUST LOADS
NT TRANSIENT LOADS
NT VIBRATORY LOADS
NT WING LOADING
Wave propagation in half space due to interior point load parallel to surface
[AD-747306] 02 p0170 N73-11381
Steady state response of semi-infinite solid with overlying semi-infinite fluid subjected to moving point load at supersonic speed
[AD-747252] 03 p0286 N73-12313
Punch-loading technique effects on mechanical properties of composites reinforced with glass fibers
[REPT-1042/72] 10 p1176 N73-19563
Stress wave diffraction models for crack propagation induced by dynamic loads
13 p1584 N73-22839
Fracture mechanics of polycarbonates and polyimides under dynamic loads
[AD-759917] 17 p2053 N73-26608
Electrical properties of silicon under dynamic loading
18 p2185 N73-27639
Development of computer program for determining ultimate optimum behavior of dynamically loaded structural-mechanical system
[NASA-CR-2268] 18 p2203 N73-27783
Simplified analysis procedure for determining static and dynamic aeroelastic loads for space shuttle dynamics
[NASA-CR-124370] 22 p2722 N73-31781
Mathematical models for determining dynamic response of strain sensitive materials and structure to dynamic loads
22 p2724 N73-31797
Plastic response of metals under dynamic loading
[AD-765522] 24 p2937 N73-33452
DYNAMIC MODELS
Conference on manual control systems for human operator modeling and display systems in man machine environments
[NASA-SP-281] 01 p0013 N73-10104
Human operator model for man machine control behavior in biodynamic flight environment
01 p0014 N73-10105
Nonlinear multiparameter control model for human operator as vehicle controller
01 p0014 N73-10106
Control theory model for pilot decision making based on estimated state of linear plant
01 p0014 N73-10107
Input adaptive behavior model of human operator in pursuit tracking task
01 p0014 N73-10108
Hybrid computer identification program for visual display of adaptive control state to human operator
01 p0014 N73-10109
Matrix methods for dynamic modeling of human operator performance using Liapunov functions
01 p0014 N73-10111
Manual control model structure for industrial management of man machine systems
01 p0015 N73-10115
Dynamic model for nonlinear simulation of human postural control system using sticks
01 p0015 N73-10116
Nonlinear model relating neural input to force and muscle contraction in human ankle joint
01 p0015 N73-10117
Dynamic model of rotating spacecraft force effects on human vestibular system
01 p0015 N73-10119
Predictive display with continuous parameter tracking for quasi-linear model of human pilot transfer function in closed loop system
01 p0015 N73-10120
Optimal control model for predicting display requirements in pilot landing performance
01 p0016 N73-10121
Solar atmospheric heating model for mechanical heating in stellar chromospheres
04 p0466 N73-13797
Semicircular canal model with flow visualization chamber for dynamic recording of canal fluid response to angular velocity effects
06 p0634 N73-15153
Microscopic dipole model for lattice dynamics in transition metals
08 p0950 N73-17782

Dynamic performance criteria for power actuating components of electrohydraulic actuation servosystem
[NASA-TM-X-2736] 09 p0990 N73-18079
Dynamic model of solar flare emission sources
13 p1572 N73-22742
Model testing of gases, powders, and carbon particles in vibration combustion studies
[AD-755712] 13 p1591 N73-22902
Fundamental acoustic models for synthesis of speech operating on articulatory parameters
14 p1623 N73-23151
Generative model for prosody of connected speech in Japanese
14 p1624 N73-23154
Segmentation and classification of speech using low Q single-tuned filters
14 p1631 N73-23220
Application of kinetic theory to collisionless regions of polar and solar winds
[AERONOMICA-ACTA-A-N-115-1973]
14 p1702 N73-23812
Ship model basin for simulating aircraft vortex wake
[AD-758893] 16 p1890 N73-25291
Model for dynamic analysis of gas core reactor system
[NASA-CR-121253] 18 p2177 N73-27581
Pseudo-binary crystal model for electron mobility variation with composition of gallium indium arsenide semiconducting alloys
18 p2181 N73-27607
ESRO 1A [Aurorae] satellite dynamic model derived from attitude sensor data using smoothing factor in spline function subroutine
[RA-SAT-3.4-C-006] 18 p2201 N73-27767
Elastic plate model for earthquakes
22 p2737 N73-31912
Simulation procedures in plasma physics
[JUL-CONF-7] 24 p2963 N73-33680
Dynamic model gravity compensation method for satellite orbit determination
[AD-765551] 24 p2982 N73-33828

**DYNAMIC MODULUS OF ELASTICITY**
Influence of epoxide resin space lattice thickness on dynamic modulus of elasticity
[NASA-TT-F-14913] 14 p1680 N73-23633
Compressive strength and modulus of unidirectional carbon fiber reinforced plastic laminates
[RAE-TR-72096] 17 p2050 N73-26587

**DYNAMIC PROGRAMMING**
Approximation techniques for descrete dynamic programming problems
[USC-113P19-26] 02 p0146 N73-11181
Successive approximations for solving discrete Bolza problem by dynamic programming
[TR-72-43] 02 p0202 N73-11632
Analysis of approximation methods for solving discrete Bolza problem by dynamic programming, and stability and error properties
[USC-113P19-28] 02 p0202 N73-11633
Bicubic spline approximations over two dimensional region derived with dynamic programming
[USC-113P19-33] 02 p0202 N73-11635
Problems of radar network scheduling to track satellites
[AD-751290] 07 p0757 N73-16152
Mathematical programs for direct problem solving
[NASA-SP-5913[02]] 08 p0887 N73-17180
Mathematical models on various modes of functioning in linear dynamic programming
[NASA-TT-F-685] 12 p1419 N73-21499
Time optimal control in stochastic dynamic systems
20 p2436 N73-29565

**DYNAMIC PROPERTIES**
U DYNAMIC CHARACTERISTICS

**DYNAMIC RESPONSE**
NT TRANSIENT RESPONSE
Selection of dynamic data processing systems
01 p0056 N73-10454
Neurophysiology and dynamic response of vestibular system to angular and linear acceleration
[DR-215] 02 p0130 N73-11057
Steady state response of semi-infinite fluid-solid interface subjected to subsonic and intersonic load velocities
[AD-747253] 02 p0159 N73-11287
Dynamic response analysis of analog fluid amplifiers
[AD-746274] 02 p0179 N73-11450
Digital analysis of dynamic response data, aerodynamic forces and stability derivatives, of free flight models
[ARC-R/M-3699] 03 p0248 N73-12006
Measurement technique for determining sensitivity and radiated power of oscillator radio receiver
[AD-748826] 04 p0389 N73-13165
Optical feedback technique to extend frequency response of solid state detector systems
[NASA-TM-X-2676] 04 p0421 N73-13430
Shock tests on rectangular steel beams, relation of tension-compression properties to moment-curvature equation, and viscoelastic cantilever beam response to shock
[AD-748656] 04 p0482 N73-13941
Human operator adaptive behavior in slowly changing dynamic system
[AD-748243] 05 p0503 N73-14097
Dynamic calibration of gas flowmeters by impedance measurement in oscillating flow
[ARC-CP-1224] 05 p0548 N73-14451
Dynamic response of fluid-solid interface to supersonic disturbance
[AD-750253] 05 p0604 N73-14917
Satellite aerodynamics and upper atmospheric density determination from satellite dynamic response
05 p0609 N73-14950
Estimates of LC stress response in aircraft skin panels to random acoustic loads
[ESDU-67028-AMEND-A] 06 p0723 N73-15904
Application of three dimensional theory of elasticity to dynamic response of freely supported circular cylindrical shell
06 p0725 N73-15921
Response of cylindrical shells to traveling load simulation of x ray blow-off impulse
[AD-750336] 06 p0727 N73-15933
Mathematical model for tracked air cushion vehicle and guideway to determine vertical dynamic response of vehicle and guideway system to high speed vehicle passage
07 p0737 N73-15995
Baseband equalization system for correcting response characteristics of high quality coaxial transmission lines
[UCRL-73943] 07 p0756 N73-16141
Experimental study and analog simulation of steady state and dynamic response of jet interaction proportional fluid amplifier
[AD-751458] 07 p0805 N73-16532
Dynamic electrocardiographic standardization for detecting cardiac risk factor in personnel
08 p0873 N73-17066
Assessment of luminous and spectral sensitivity and electro-optical properties of image tubes
[BARC-610] 08 p0888 N73-17194
Low level tuning of approximations, with response variant emerging from standardized high level commands
[NASA-CR-130699] 08 p0891 N73-17210
Numerical solution of linear differential equations describing dynamic response of vehicles
[TT-7212-PT-1] 08 p0937 N73-17669
Computer program for calculating dynamic FORTRAN response of piping network to sinusoidal excitation
[AD-752743] 09 p1017 N73-18302
Dynamic response of fluidic circuits with blocked and orifice terminated lines
[AD-753384] 09 p1018 N73-18307
Application of statistical methods for determination of dynamic system parameters influence on spectrum of natural frequencies
[AD-752695] 09 p1067 N73-18707
Nonlinear dynamic response of thin, clamped hemispherical shell subjected to suddenly applied pressure
[AD-752795] 09 p1096 N73-18950
Time integration of transient equations in shaft dynamics analysis
[AD-754341] 10 p1168 N73-19500
Natural frequencies and dynamic response of NERVA engine thrust train
[NASA-CR-132224] 15 p1809 N73-24664
Low frequency structural response and damping characteristics of XB-70 aircraft during subsonic and supersonic flight
[NASA-TN-D-7227] 15 p1837 N73-24892
Formulation and checkout problems for computer code for analyzing large deflection elastic-plastic dynamic response of stiffened shells of revolution
[NASA-CR-132044] 15 p1839 N73-24902
Derivation of differential equations of motion to analyze characteristics of three degree of freedom bodies joined by elastic tether
[NASA-CR-124259] 15 p1839 N73-24903
Dynamic performance of beam deflection fluid amplifiers
[AD-759211] 16 p1891 N73-25306
Theory of dynamic viscous pressure interaction applied to surface ablation by sublimation
[AD-759186] 16 p1967 N73-25915
Smoothing technique for analyzing frequency response of aircraft in flight and on ground
[RAE-LIB-TRANS-1703] 17 p2054 N73-26616
Dynamic response of Mach 2.5 supersonic mixed compression axisymmetric inlet operating with turbofan engine
[NASA-TM-X-2833] 18 p2193 N73-27709
Dynamic response of light partitions to sonic boom noting theoretical computation and scale model tests
[ISL-23/72] 19 p2220 N73-27910
Calculation of dynamic response of ship structural members consisting of beams and rectangular plates
[AD-762008] 19 p2350 N73-28902
Transient thermal response of globe thermometers in relation to heat transfer parameters
[DCIEM-859] 20 p2418 N73-29431
Dynamical response of cylindrical shells due to moving excitations
20 p2476 N73-29892
Methods for determining aircraft structural response to acoustic fatigue
20 p2479 N73-29913
Dynamic and aeroelastic problems of V/STOL aircraft stop-rotors occurring during retracting and stowing of rotor blades
[DLR-FB-73-19] 21 p2496 N73-30035
Design, dynamic response, and operation of electric pressure difference transducer
[NLL-TRANS-2976-[9022.81]]
21 p2543 N73-30387
Development of damping system to compensate for wind loads on space shuttle vehicle during launch operations
[NASA-CR-124367] 21 p2601 N73-30845
Loading criteria for tracked air cushion vehicle guiderails and methods for calculating dynamic responses of double-span, beam-type guide rails
[PB-221688/5] 22 p2617 N73-30971
Numerical analysis of dynamics of constant speed rotor with three dimensional rotary inertia using eight degree of freedom model with coupled linear and angular motion
22 p2676 N73-31437
Mathematical models for determining dynamic response of strain sensitive materials and structure to dynamic loads
22 p2724 N73-31797
General purpose computer program for inelastic dynamic response of plane structure
[PB-221260/3] 22 p2727 N73-31823
Dynamic response of short haul aircraft to gust loads
[FOK-K66] 23 p2744 N73-31960
Two dimensional elastic-plastic hydrodynamics code for calculating dynamic response of semiconductor configuration to electron loading
[AD-763943] 23 p2826 N73-32590

**DYNAMIC STABILITY**
NT AERODYNAMIC STABILITY
NT AIRCRAFT STABILITY
NT ATTITUDE STABILITY
NT BOUNDARY LAYER STABILITY
NT COMBUSTION STABILITY
NT CONTROL STABILITY
NT DIRECTIONAL STABILITY
NT FLAME STABILITY
NT FLOW STABILITY
NT FREQUENCY STABILITY
NT GYROSCOPIC STABILITY
NT HOVERING STABILITY
NT LATERAL STABILITY
NT LONGITUDINAL STABILITY
NT LOW SPEED STABILITY
NT MAGNETOHYDRODYNAMIC STABILITY
NT ROTARY STABILITY
NT SPACECRAFT STABILITY
Methods for increasing stability of rotors with gas bearings
[AD-745858] 01 p0063 N73-10517
Theoretical analysis of ablation effects on dynamic stability of reentry vehicles
04 p0477 N73-13899
Stability of three-layer plates with elastoviscous core subject to time-dependent loads
[AD-749746] 05 p0605 N73-14918
Dynamics of satellite gravitational stabilization systems with gyrodamping
[AD-750555] 06 p0722 N73-15892
Application of Liapunov function for analysis of finite stability of complex system in limited range of parameters
[NASA-TT-F-14869] 11 p1311 N73-20640
Dynamic stability information for space shuttles, high performance military aircraft, and short takeoff aircraft at high angles of attack
[NASA-CR-114583] 13 p1505 N73-22201
Numerical analysis of resonance interactions in dynamic stability of elastic shells under compression
[AD-756237] 14 p1715 N73-23918
Superconducting electromagnetic suspension and balance and supersonic wind tunnel facility for dynamic stability studies
[NASA-CR-132255] 15 p1761 N73-24271
Experimental in-orbit verification of mathematical model for RAE spacecraft gravity gradient dynamics
18 p2208 N73-27825
Forced oscillation test equipment for measuring dynamic stability of roll velocity on lifting bodies
[AD-762258] 19 p2250 N73-28139
Numerical analysis of dynamics of constant speed rotor with three dimensional rotary inertia using eight degree of freedom model with coupled linear and angular motion
22 p2676 N73-31437
Dynamic stability of harmonically varying forced vibrations of thin spherical shell submerged in acoustic medium medium
22 p2723 N73-31792
Aerothermodynamic study of air cushion vehicles buffeting noting dynamical stability, nonlinear behavior, and similitude law
[NT-33-1973] 24 p2870 N73-32933
Resonance stabilization of air cushion between liquid and oscillation source
[IPP-2/209] 24 p2963 N73-33674

DYNAMIC STRUCTURAL ANALYSIS
Nonalgorithmic methods for determination of strength, oscillations and static and dynamic stability of deformable systems
[AD-745426] 01 p0114 N73-10939
Application of dynamic photoelasticity to analyze crack branching in homalite sheets
[AD-744661] 01 p0114 N73-10940
Structural dynamic behavior of laminated plates and shells composed of bonded elastic orthotropic layers
[AD-745336] 01 p0114 N73-10944
Algorithm for synthesizing mass and stiffness matrices from experimental vibration modes
01 p0119 N73-10983
Procedure for predicting structural and acoustic response of full scale structures to sonic booms using scale models and laboratory techniques
[FAA-RD-72-116] 03 p0251 N73-12029
Design and development of instrument for measuring aerodynamic loads and fatique characteristics of aircraft structures
[AGARD-R-597] 04 p0371 N73-13019
Development of structural dynamics model of space shuttle and evaluation of structural and hydroelastic analysis methods
[NASA-CR-112196] 04 p0478 N73-13911
Application of reliability theory to determine risk function, probability of failure, under ultimate load, and wear-out process of aircraft structures
[ARL/SM-REPT-337] 04 p0480 N73-13925
Development of FORTRAN computer program for solving free axisymmetric vibration of cylindrical shells of arbitrary shape
[AD-748655] 04 p0482 N73-13942
Buckling modes of four optimized Mars entry aeroshell configurations at angle of attack loadings based on experimental pressure distributions
[NASA-CR-2087] 07 p0852 N73-16907
Theory of plates and shields to include response of structurally loaded shells of cylindrical and spherical configurations
[AD-751502] 07 p0852 N73-16913
Crack growth characteristics of steel and structural failure of F-111 aircraft frame
[AD-752223] 08 p0868 N73-17024
Procedure for applying structure-fluid interactions effect to dynamic frequency response calculations for submerged structures
[AD-752484] 08 p0967 N73-17906
Effects of spatially varying curvature on dynamics of cylindrical panels and stiffened cylindrical shell structures
[AD-752590] 08 p0967 N73-17907
Development of three stage model for fatigue failure of structure with several critical regions for initial failure
[ARL/SM-NOTE-338] 09 p1093 N73-18924
Methods for calculation of eigenvalues and eigenvectors of non-Hermitian matrices for dynamic structural analysis
[ISD-128] 09 p1095 N73-18937
Proposed computer program for dynamic analysis of elasto-plastic, thin, isotropic plates of rectangular planform subjected to blast loads
[AD-752449] 09 p1096 N73-18947
Static and dynamic analyses on fracture mechanics of polyester plastic sheet
[AD-749098] 09 p1097 N73-18954
Dynamic structural design of aeroelastic wind tunnel models using combinatorial flutter analyses
10 p1140 N73-19291
Analysis of structural response of light aircraft to crash loadings based on dynamic buckling of discretely stiffened shells
10 p1219 N73-19910
NASTRAN computer program for determining stress concentration at holes in isotropic finite strips
[AD-753574] 10 p1221 N73-19933
Development of dynamic loads computation capability for application to unified flexible spacecraft simulation program
[NASA-CR-124168] 11 p1340 N73-20878
Holographic interferometric testing of laminate and composite structures for internal voids and material defects
[BDX-613-812] 12 p1410 N73-21429
TACOS finite computer program for analyzing dynamic transient response of cylindrical obese shells
[SC-RR-72-0454] 12 p1463 N73-21852
Structural influence coefficient matrix for computer simulation of aerodynamic aircraft stability
[NASA-CR-112230] 13 p1469 N73-21898
Aerodynamic influence coefficient matrix for nonplanar wing-body-tail configurations
[NASA-CR-112231] 13 p1470 N73-21901
Two methods for derivation of structural expansion for ground state energy of simple metal
[NASA-CR-131833] 13 p1565 N73-22687
Application of multipoint excitation for helicopter structural dynamic testing using impedance techniques - Vol. 1
[AD-756389] 14 p1716 N73-23921
Dynamic structural analysis of helicopter structures using single point excitation techniques - Vol. 2
[AD-756390] 14 p1716 N73-23922
Dynamic structural analysis of helicopter structures using free-body response techniques - Vol. 3
[AD-756391] 14 p1716 N73-23923
Dynamic structural analysis of helicopter subsystems based on equations for combination of mobility matrices - Vol. 4
[AD-756392] 14 p1716 N73-23924
Analysis of static, buckling, and vibration characteristics of orthotropic, inhomogeneous shells of revolution
15 p1837 N73-24889
Elastic structural models for dynamics and control of advanced space vehicles
[NASA-CR-124272] 16 p1967 N73-25908
Design of manipulator mechanisms with manual, bioelectric, and automatic control systems
[NASA-TT-F-14336] 17 p1989 N73-26073
Systems engineering for design of two dimensional automatic manipulator control system using reversible follow-up
17 p1989 N73-26081
Dynamic finite element analysis of nonlinear oscillations of multi-degree of freedom structural systems
[ISD-136] 17 p2094 N73-26943
Statistical energy and deterministic analyses on dynamic response of coupled rods to longitudinal acoustic excitation
[AD-760276] 17 p2095 N73-26951
Energy criteria for predicting dynamic buckling of structures
[AD-760158] 17 p2096 N73-26954
Frequency response of structural systems excited by transient and random loads using cross correlation and spectral analysis techniques
[ISVR-TR-57] 18 p2180 N73-27598
Numerical analysis of effect of boundary layer profile on dynamic response and acoustic radiation of thin, elastic, flat plates
[NASA-TM-X-69568] 21 p2523 N73-30232
Dynamic structural analysis of fully articulated rotor blade on helicopter rotary wing for three degrees of freedom
[AD-763934] 22 p2615 N73-30957
Computer program for elastic-plastic dynamic analysis of shells of revolution by finite element method
[AD-764244] 22 p2726 N73-31812
Definition of criteria and techniques of design, analysis, and test for using single major structural test article for performing dynamic, fatigue, and static testing
[NASA-CR-124404] 23 p2853 N73-32799
Development of finite element relations for dynamic structural analysis of linearly elastic beam and plate flexure problems
24 p2987 N73-33873

DYNAMIC TESTS
Dynamic testing for determining flight readiness of Apollo docking system hardware
09 p1089 N73-18885
Dynamic testing procedures for strapdown sensors with motion induced error torques
[NASA-CR-124126] 10 p1185 N73-19641
Dynamic tear tests for determining fracture mechanics of high strength structural steels and aluminum and titanium alloys
[AD-759351] 16 p1930 N73-25620
Dynamic tests of seat belt system, seat belt/shoulder harness system, and seat belt airbag system for aircraft
[FAA-NA-73-30] 20 p2371 N73-29052
Dynamic testing of fabrics and Mylar in shock tubes
[NASA-CR-132284] 23 p2770 N73-32157
Dynamic flight simulation of Symphonie satellite attitude control system
[DGLR-PAPER-73-045] 24 p2986 N73-33862

DYNAMICS
Cardinal equations of dynamics
10 p1188 N73-19665

DYNAMOMETERS
Aircraft tire dynamometer tests to determine effects of tire deflection on rolling resistance and tire life
[AD-746304] 02 p0127 N73-11031
Dynamometer thrust measurements of electrostatic mercury electron bombardment ion engine ESKA 18 P
[DLR-FB-73-48] 17 p2077 N73-26803
Two component force dynamometer and tool control system for dynamic machine tool research
[NASA-TM-X-64786] 24 p2926 N73-33371

DYNAMOS
U ROTATING GENERATORS

DYSPROSIUM
Analysis of effect of dysprosium oxide on the physical properties of nickel-zinc ferrite materials
[NLL-TRANS-746-1284-[9022.401]] 06 p0682 N73-15550
Superconducting energy gap structure and physical properties of dysprosium-dysprosium oxide-lead tunnel junctions
[AD-753847] 09 p1077 N73-18790
Magnetic properties of powdered samples of $Dy_2Ti_2O_7$
[NASA-TM-X-68219] 12 p1428 N73-21575
Kerr magnetooptical effect in nickel, gadolinium, and dysprosium at temperatures between 10 and 300 K in 1 to 5 eV energy range
12 p1437 N73-21644


## E


E LAYERS
U E REGION
E REGION
NT SPORADIC E LAYER
Direct scatter effects from field aligned E and F layer irregularities and scatter from subauroral ionospheric clouds at 19.4 MHz
[AD-746311] 01 p0054 N73-10436
Excitation and deexcitation of vibration in gases by oxygen and nitrogen atoms in E region of earth atmosphere
[AD-745925] 01 p0054 N73-10437
Quasi-equilibrium states of E-layer
[UCRL-51151] 03 p0296 N73-12415
Daily summaries for vertical echo sounding of upper atmosphere over Freiburg, Germany - Aug. 1972
[REPT-314-F] 04 p0414 N73-13380
Daily summaries for vertical echo sounding of upper atmosphere over Freiburg, Germany - Sept. 1972
[REPT-315-F] 04 p0414 N73-13381
Daily summaries for vertical echo sounding of upper atmosphere over Freiburg, Germany - July 1972
[REPT-313-F] 05 p0538 N73-14380
Ionospheric propagation data for E and F regions, India - Jan. 1971
[RTRC-A188] 06 p0664 N73-15397
Ionospheric propagation data for E and F regions, India - Feb. 1971
[RTRC-A189] 06 p0664 N73-15398
Ionospheric propagation data for E and F regions, India - March 1971
[RTRC-A190] 06 p0664 N73-15399
Neutral and ion chemistry of D and E regions symposium papers
[AD-749780] 06 p0668 N73-15430
Cyclic variations in Es layer with 11 year cycle of solar activity
13 p1521 N73-22329
Fading frequency characteristics of Es layer
13 p1521 N73-22330
Daily summaries for vertical echo sounding of upper atmosphere over Freiburg Germany, January 1973
[REPT-319-F] 14 p1659 N73-23460
Daily summaries for vertical echo sounding of upper atmosphere over Freiburg, Germany, December 1972
[REPT-318-F] 14 p1659 N73-23461
Daily summaries for vertical echo sounding of upper atmosphere over Freiburg, Germany - February 1973
[REPT-320-F] 15 p1777 N73-24406
Measurement of positive ion composition in midlatitude sporadic E layer using rocket-borne ion mass spectrometer
[NASA-TM-X-66276] 18 p2142 N73-27313
Ionogram observations supporting chemical release studies in E region
[AD-762927] 20 p2415 N73-29409
Daily summaries for vertical echo sounding of upper atmosphere over Freiburg, Germany - April 1973
[REPT-322-F] 21 p2537 N73-30342
Daily summaries for vertical echo sounding of upper atmosphere over Freiburg, Germany - May 1973
[REPT-323-F] 21 p2537 N73-30343
Daily summaries for vertical echo sounding of upper atmosphere over Freiburg, Germany - June 1973
[REPT-324-F] 21 p2537 N73-30344
Solving equations of motion for behavior of plasma clouds in layered model ionosphere
[MPI-PAE/EXTRATERR-73] 22 p2704 N73-31658
Computer program for modeling E and F region of ionosphere
[AD-764662] 23 p2789 N73-32312
Daily summaries for vertical echo sounding of upper atmosphere over Freiburg, Germany - July 1973
24 p2920 N73-33322

E-2 AIRCRAFT
Nondestructive inspection techniques for examining catapult and arresting gear structures on E-2 aircraft
[AD-752492] 08 p0868 N73-17027
Test plan for extending service life of E-2A arresting gear
[AD-754752] 11 p1267 N73-20284

EAR
NT COCHLEA
NT LABYRINTH
NT MIDDLE EAR
NT SEMICIRCULAR CANALS
NT VESTIBULES
Physical correlations of hearing, auditory system, and hearing loss
06 p0629 N73-15105
Functional reactions of human otorhinolaryngolic organs during hypokinesia
13 p1482 N73-22015

Dichotic signs of recognition of speech elements in normals, temporal lobectomies, and hemispherectomies
14 p1626 N73-23174
Loudness level perception of human ear and reference level for telephone engineering
[NLL-PO-2831-(9022.81)] 15 p1812 N73-24684

EAR PROTECTORS
Interchangeability of earmuff cushions with respect to sound attenuation, including noise-pressure measurements
[IZF-1973-1] 14 p1692 N73-23729
Evaluation of hearing protectors for general aviation aircraft
[NASA-CR-133303] 18 p2117 N73-27078

EARLY STARS
NT T TAURI STARS
Chilean astronomical observations of early star spectra, southern star radial velocities, and minor planet positions
05 p0594 N73-14828
Line spectra and spectral energy distribution of early type stars
05 p0594 N73-14829
Radio telescope observation of low velocity interstellar neutral atomic hydrogen in direction of early type stars
19 p2342 N73-28836

EARLY WARNING SYSTEMS
Development of volcano surveillance and early warning system using ERTS-1 data collection system
[PAPER-G9] 19 p2264 N73-28240

EARPHONES
Pure tone thresholds of 24 normal hearing listeners at 11 audiometric frequencies on two [TDH-49 and TDH-39] earphones
[AD-744823] 01 p0080 N73-10663
Design and performance of wideband artificial ear for calibrating audiometric earphones
[AD-746691] 04 p0382 N73-13112

EARTH [PLANET]
Power spectra of interplanetary magnetic field near earth bow shock
01 p0096 N73-10792
Dynamic determination of equatorial radius of earth
[NASA-TM-X-66151] 06 p0666 N73-15411
Multispectral band survey and mapping of earth in 18 days
[E73-10044] 07 p0777 N73-16307
Secular magnetic variation and inner zone of energetic fields of earth
[AD-751284] 07 p0795 N73-16463
Resonance capture of Toro asteroid perturbed orbit by earth
[TRITA-EPP-72-19] 07 p0846 N73-16863
Combination of satellite and gravimetric data for analysis of terrestrial gravity field blocks
[NASA-CR-130176] 10 p1153 N73-19380
Geodetic boundary value solution with height anomalies to plus or minus 5 cm and to order e cubed
[NASA-TM-X-66199] 10 p1153 N73-19384
Annual global average earth-atmospheric system radiation balance determined from Nimbus 3 radiation measurements
[NASA-TN-D-7249] 12 p1445 N73-21702
UV imagery of earth and moon at varied wavelengths
12 p1451 N73-21751
Survey of earth geomagnetic field
[AD-759837] 17 p2030 N73-26427
Gravimetry and satellite altimetry for determining earth gravity field
[AD-759536] 18 p2148 N73-27365
Glacio-climatic and geophysical rhythms of earth and space
[NASA-TT-F-14985] 19 p2342 N73-28843
Statistical properties of atmospheric circulation particularly geopotential fields on global basis
20 p2442 N73-29619
Solar activity effects on terrestrial climate
[AD-762227] 20 p2468 N73-29827
Inertial navigation methods to determine coordinates of moving object in vicinity of earth
21 p2576 N73-30644
Analysis of steady state flow of solar wind and effect on magnetic field of dipole
[NASA-TT-F-15071] 22 p2711 N73-31709
Modification of world dynamics model to account for pollution abatement
[NASA-TM-X-2832] 23 p2866 N73-32910
Field measurements and earth model of polar motion
[NASA-TT-F-15066] 24 p2922 N73-33334
Heliotechnique for utilizing solar energy on earth
24 p2974 N73-33763

EARTH ALBEDO
Global distributions of surface albedo, planetary albedo, and total precipitation - supplementary data for Dec., Jan., and Feb.
[AD-744633] 01 p0076 N73-10628
Energy exchange between earth and space from meteorological satellite measurements of infrared radiant emittance and reflected and scattered solar radiation
[NASA-CR-130152] 07 p0780 N73-16341
Balloon measurements on neutron energy and angular distributions in earth albedo
[NASA-CR-130019] 07 p0823 N73-16666
Determination of earth aerosol albedo using Skylab EREP data
[E73-10871] 20 p2393 N73-29222
Earth albedo neutrons and cosmic ray neutron decay from 10 to 100 MeV
[NASA-CR-135645] 23 p2789 N73-32315

EARTH ATMOSPHERE
NT D REGION
NT E REGION
NT EXOSPHERE
NT F REGION
NT F 1 REGION
NT F 2 REGION
NT FREE ATMOSPHERE
NT IONOSPHERE
NT LOWER ATMOSPHERE
NT LOWER IONOSPHERE
NT MAGNETOPAUSE
NT MAGNETOSPHERE
NT MESOPAUSE
NT MESOSPHERE
NT MIDLATITUDE ATMOSPHERE
NT OUTER RADIATION BELT
NT OZONOSPHERE
NT PROTON BELTS
NT RADIATION BELTS
NT SPORADIC E LAYER
NT THERMOSPHERE
NT TROPOPAUSE
NT TROPOSPHERE
NT UPPER IONOSPHERE
Atmospheric transmittance from sun and sky radiance measurements with Nimbus E infrared temperature profile radiometer prototype used at Mauna Loa Observatory
[NOAA-TR-NESS-61] 01 p0048 N73-10391
Translation of titles, subtitles, and table of contents for Soviet publication on Problems of Physics of Atmosphere
[NASA-TT-F-14424] 01 p0049 N73-10396
Upward and downward radiance calculations for numerous detector locations in atmosphere and ocean
[AD-745282] 01 p0076 N73-10627
Annotated bibliography of atmospheric sounding, geophysics, and plasma physics
[AD-745168] 01 p0121 N73-10997
Determination of optical thickness of aerosols in atmosphere around Salton Sea desert area using ERTS-1 imagery
[E72-10200] 02 p0160 N73-11298
True absorption of light by aerosols in atmosphere
[AD-748111] 03 p0299 N73-12437
Radiative heating rates measured for global atmosphere
[COO-2195-4] 04 p0415 N73-13386
Measurement of spatial distribution of aerosols and water vapor in earth mixing layer using optical radar, particle counters, and rawinsonde
[NASA-TN-D-7103] 04 p0444 N73-13621
Ray tracing method for calculating paths of acoustic and gravity waves in atmosphere
05 p0508 N73-14133
Determination of aerosol optical thickness in atmosphere at Salton Sea and San Diego based on ERTS-1 data
[E72-10359] 05 p0534 N73-14347
Application of radiophysical methods to study of earth atmosphere and earth resources with satellites
[NASA-TT-F-14642] 05 p0538 N73-14381
Infrared absorption bands of nitrous oxide in earth atmosphere
[AD-749879] 05 p0541 N73-14405
Detection and measurement of carbon monoxide in atmosphere
[PB-211265] 05 p0575 N73-14677
Airborne survey of very high frequency interference levels over residential areas on American west coast
[SD-72-SA-0100-VOL-1] 06 p0640 N73-15197
Analysis of pole tide fluctuations in earth atmosphere and ocean
[NLL-M-20647-[5828.4F]] 06 p0657 N73-15336
Concentrated aerosol layer at intermediate levels of pure Rayleigh atmosphere
07 p0775 N73-16295
Haze-free and cloud-free lines-of-sight through atmosphere
[AD-751264] 07 p0796 N73-16476
Investigation of urban heat island phenomena in Austin, Texas, using two-dimensional, time-dependent, earth atmosphere mathematical model
[REPT-32] 08 p0938 N73-17681
ERTS-1 measurement of aerosol content in atmosphere over Salton Sea and desert test sites
[E73-10295] 09 p1020 N73-18328
Soviet space stations for providing earth space photographs used for earth atmosphere and earth surface analysis
[JPRS-58055-1-PT-1] 09 p1026 N73-18372
Spectrophotometric observation of earth atmosphere and underlying surfaces near twilight horizon from manned spacecraft
09 p1026 N73-18375
Atmospheric effects on remotely sensed radiation measurements
[NASA-CR-130828] 09 p1028 N73-18389
Eighty atmospheric models for measuring total outgoing radiance of earth-atmosphere system
[NASA-TM-X-66195] 09 p1029 N73-18400
Radio telescope and satellite studies of atmosphere, ionosphere, and magnetosphere under disturbed conditions produced by enhanced solar activity
[AD-754252] 10 p1157 N73-19410
Neutron flux spectra induced in the earth atmosphere by galactic cosmic rays
[NASA-CR-131158] 10 p1210 N73-19844
Atmospheric effects on recognition of rice and corn in ERTS-1 imagery of Sacramento Valley
[E73-10390] 11 p1276 N73-20352
Atmospheric effects on ERTS-1 imagery and spatial resolution of MSS data
[E73-10394] 11 p1276 N73-20356
Monte Carlo transport routine for standard atmosphere to altitude of 90 km
[LA-5089] 12 p1422 N73-21529
Determination of aerosol content in atmosphere at Salton Sea test site using ERTS-1 data
[E73-10524] 13 p1517 N73-22291
Proposed 50 to 100 km revision to US Standard Atmosphere, 1962
[AD-755394] 13 p1526 N73-22371
High altitude measurement of atmospheric pollution from aircraft engine exhaust gases
[NASA-TM-X-68221] 13 p1553 N73-22584
Nonlinear acoustic and gravity waves in earth atmosphere
[TR-48] 14 p1659 N73-23466
Atmospheric effects on ERTS-1 imagery for land use mapping
[E73-10568] 15 p1771 N73-24348
Influence of atmosphere pathlengths on ERTS-1 MSS imagery acquired over southwestern Kansas
[E73-10763] 18 p2133 N73-27240
Atmospheric effects on ERTS-1 data and advanced data extraction techniques
[PAPER-I1] 19 p2277 N73-28323
Measurement of atmospheric aerosol content in Southern California desert areas from ERTS-1 contrast and radiance measurements
[PAPER-I2] 19 p2277 N73-28324
Computed atmospheric effects on ERTS-1 MSS observations
19 p2284 N73-28371
Atmospheric effects on radiometric measurements using EREP of Skylab
[E73-10857] 19 p2292 N73-28434
Numerical analysis of dependence of transmission function of atmosphere on temperature of radiation source
20 p2402 N73-29299
Orgin of jet streams in earth atmosphere
20 p2446 N73-29652
Spectral density of infrared radiation reflected by earth atmosphere
21 p2539 N73-30361
Atmospheric absorption line parameters for infrared-active molecules occurring naturally in terrestrial atmosphere
[AD-762904] 21 p2542 N73-30382
Atmospheric effects on Skylab MSS data for Williamston, Michigan
[E73-11043] 22 p2664 N73-31344
Application of spectroscopic methods in remote sensing for determining structure of microwave spectra in earth atmosphere
22 p2692 N73-31563

EARTH AXIS
Computerized simulation of optical stellar observations and data reduction to determine diurnal polar motion
[AD-748460] 05 p0541 N73-14401
Calculation of shape of earth magnetopause for various orientations of solar wind stream with respect to earth dipole axis
16 p1895 N73-25328
Position of earth spin axis with respect to crust computed on basis of Doppler satellite observations
[AD-763362] 21 p2542 N73-30381

EARTH CORE
Flow characteristics in earth liquid core
[NRC-TT-1635] 16 p1904 N73-25402

EARTH CRUST
Study of crustal structure from eastern Sierra Nevada to Colorado Plateau using ERTS-1 imagery
[E72-10192] 01 p0046 N73-10371
Seismological effects of explosions and earthquakes and structural dynamics of earth crust and upper mantle
[AD-746031] 01 p0054 N73-10435
Homogeneous density effects for calculating earth crust structure from gravitational anomalous masses
[AD-746018] 03 p0297 N73-12427
Identification of continental crust geostructures and their relation to mineral resources based on ERTS-1 imagery
[E72-10296] 04 p0410 N73-13346

Attenuation calculations for extremely low frequency and very low frequency electromagnetic wave propagations in earth crust
[AD-748331] 06 p0641 N73-15306
ERTS-1 imagery of crustal structure of area from eastern Sierra Nevada to Colorado Plateau
[E73-10028] 06 p0660 N73-15361
Crustal deformation propagation in Alaska
[AD-750468] 06 p0671 N73-15461
ERTS-1 imagery of geostructures of Alaskan continental crust and relation to mineral resources
[E73-10321] 09 p1024 N73-18353
ERTS-1 imagery of crustal structure of strip from eastern Sierra Nevada to Colorado Plateau
[E73-10355] 10 p1149 N73-19351
Geological structure effect on seismic wave propagation in earth and upper mantle
[AD-753110] 10 p1156 N73-19408
Mapping of seismically active faults in Alaska using ERTS-1 imagery to determine areas of earthquake occurrence
[E73-10405] 11 p1277 N73-20367
Movement of trench boundary relative to colliding plates in conjunction with down-buckling of descending plate corner
[NASA-TM-X-66212] 11 p1286 N73-20439
Crustal structure from high resolution seismic refraction profile across transition zone from Basin and Range provinces into Middle Rocky Mountains
[AD-753850] 11 p1289 N73-20462
Identification of geostructures of continental crust and relation to mineral resources
[E73-10496] 12 p1397 N73-21332
ERTS-1 imagery of crustal structure of strip from eastern Sierra Nevada to Colorado Plateau
[E73-10529] 14 p1654 N73-23416
Observation of earthquake associated tilt steps in Central Alaska
[RLO-2229-T-4-2] 15 p1781 N73-24436
Identification of geostructures of continental crust and relation to mineral resources
[E73-10787] 18 p2136 N73-27263
Effect of microflora on exogenous dynamics of weathering and crust development
[NASA-TT-F-15032] 20 p2411 N73-29383
Position of earth spin axis with respect to crust computed on basis of Doppler satellite observations
[AD-763362] 21 p2542 N73-30381
ERTS-1 reconnaissance of crustal structure of strip from eastern Sierra Nevada to Colorado Plateau
[E73-10985] 22 p2658 N73-31292
Identification of geostructures of continental crust from ERTS-1 imagery and relationship to mineral resources in Alaska
[E73-11023] 22 p2662 N73-31327
Identification of geostructures of continental crust in Alaska and relation to mineral resources and exploration
[E73-11035] 22 p2663 N73-31339

EARTH CURRENTS
U TELLURIC CURRENTS

EARTH ENVIRONMENT
University of Alaska survey of environment using ERTS-1 imagery
[E72-10341] 05 p0532 N73-14329
Isotope effects for environmental monitoring and control
[ORNL-IIC-39] 06 p0703 N73-15730
Phenomenological concepts of earth electrical structure controlled by neutral atmosphere dynamics of stratospheric tides
16 p1895 N73-25330
Application of satellite-borne remote sensors to survey of earth resources and environment
[NASA-TM-X-68266] 20 p2412 N73-29384

EARTH FIGURE
U GEODESY

EARTH HYDROSPHERE
Past, present, and projected climate, and heat budget of atmosphere and hydrosphere
[NLL-M-20071-[5828.4F]] 01 p0073 N73-10597
Influence of atmospheric sulfur budget on biosphere
[BNL-16906] 04 p0415 N73-13387
Role of biosphere in regulating chemical processes in atmosphere
[AERONOMICA-ACTA-A-116] 13 p1551 N73-22569
Proving solar activity effect on biosphere by correlation between activity indices with biological indices
[NASA-TT-F-14984] 17 p2079 N73-26821
Influence of man on biospheric balance
[JPRS-59366] 18 p2110 N73-27065
Ecological forecasting and optimizing biosphere
[JPRS-59729] 20 p2409 N73-29364

EARTH LIMB
Limb radiance inversion using weighting functions and iterative convergence for nonlinear kernel
02 p0197 N73-14591

EARTH MANTLE
Seismological effects of explosions and earthquakes and structural dynamics of earth crust and upper mantle
[AD-746031] 01 p0054 N73-10435
Geological comparison of moon and earth
12 p1457 N73-21810

EARTH MOTION
Response spectra of earthquake motion accelerograms
[PB-212602] 07 p0794 N73-16457
Laser tracking of satellite for measuring polar motion and solid earth tide
22 p2737 N73-31911

EARTH MOVEMENTS
NT EARTHQUAKES
Analysis of propagating and non-propagating motions produced by earth tides and earth rates and effects on inertial instrument performance
[AD-748274] 03 p0330 N73-12691
General expressions for transfer function and coherence relating earth motion and atmospheric pressure variations generated by slowly propagating, partially organized pressure fields
[AD-755527] 13 p1526 N73-22365
Mathematical procedure for calculating tectonic plate movement and the secular shift of the mean pole
[NASA-TM-X-66272] 17 p2024 N73-26376
Polar motion and earth tides applicable to satellite studies of earth elasticity
[NASA-CR-133414] 18 p2145 N73-27339
Efficient separation of two major spectral components in polar motion data for short time windows
18 p2196 N73-27724
Morphology, provenance, and movement of desert sand seas in Africa, Asia, and Australia using ERTS-1 data
[PAPER-G8] 19 p2264 N73-28239
Map of vertical crustal movements of Eastern Europe and ebb and tide studies
21 p2609 N73-30912
Analytical theory for diurnal polar motion as forced response to lunisolar torques
[NASA-TM-X-70470] 23 p2785 N73-32284

EARTH ORBITS
NT APOGEES
NT PERIGEES
Evaluation of five candidate navigation systems for earth orbit missions
[NASA-CR-128582] 01 p0102 N73-10846
Analysis of nuclear safety aspects in transport of nuclear payloads to and from earth orbit by space shuttle - Vol. 4 Pt. 1
[NASA-CR-123847] 02 p0210 N73-11700
Analysis of space rescue mission capability of Earth Orbit Shuttle and concepts for increasing capability- Vol. 2 Pt. 1
[NASA-CR-129104] 02 p0231 N73-11872
Design and development of space shuttle system for delivering payload to earth orbit or celestial orbit
[NASA-CASE-MSC-12391] 03 p0354 N73-12884
Charts for selecting suitable earth orbits for solar observations from space shuttles
[NASA-TM-X-64709] 05 p0595 N73-14840
Accuracy of geopotential solutions from resonant satellites
[NASA-TM-X-66147] 06 p0665 N73-15410
Error analyses of satellite orbital parameters based on simulations of observational variances, observation equations, and normal equations
[NASA-CR-130357] 06 p0720 N73-15878
Development of mathematical model to represent small motions relative to inertial reference coordinate system of spacecraft in low, circular earth orbit
07 p0847 N73-16867
Resource requirements for single-stage earth-orbital vehicle
[NASA-CR-124091] 09 p1086 N73-18858
Orbital evolution and stability analysis for earth and lunar orbiter trajectories
[AD-754738] 11 p1339 N73-20869
Performance characteristics of vehicles traveling in near-earth orbits at super-satellite velocities
[AD-757522] 14 p1710 N73-23878
Earth-based orbit determination for SEP spacecraft in multistation tracking
[NASA-CR-132154] 15 p1830 N73-24832
Habitability study of earth orbital space stations
[NASA-CR-124276] 16 p1869 N73-25132
Cost estimating method for life support systems of manned earth orbital programs
[NASA-CR-124305] 18 p2111 N73-27072
Application of pulsed radars for side scanning from artificial earth satellites and numerical analysis of radar operating parameters
18 p2117 N73-27117
Earth satellite orbit calculation with integration program
[BMBW-FBW-72-16] 22 p2718 N73-31757
Design, fabrication, and tests of breadboard model of earth orbital, rotating gradiometer
[NASA-CR-112215] 23 p2792 N73-32340

EARTH PLANETARY STRUCTURE
Application of stochastic inverse theory for solutions to linear system of integral equations representing reduced gross earth data
02 p0201 N73-11621
Homogeneous density effects for calculating earth crust structure from gravitational anomalous masses
[AD-746018] 03 p0297 N73-12427
Absolute gravity measurements using earth tides for analyzing earth structure
[AD-748529] 05 p0544 N73-14423

Vegetation analysis and preparation of tectonic map overlay of Bighorn Mountains region based on ERTS-1 data
[E73-10420] 11 p1279 N73-20382
Application of ERTS-1 imagery for mapping major geological structural trends and mineralization zones in Utah and Nevada
[E73-10701] 16 p1903 N73-25393
Application of ERTS-1 imagery for tectonic analysis of Bighorn Mountains region and effect of snow cover and low sun angle on identifying topographical features
[E73-10722] 17 p2019 N73-26329
Evolution of earth and moon tectonic elements
[NASA-TT-F-14947] 17 p2083 N73-26848
FORTRAN 4 program for determining transient tangential electric field and vertical magnetic dipole for stratified earth model
[PB-221240/5] 23 p2788 N73-32304

EARTH RADIATION
U TERRESTRIAL RADIATION

EARTH RESOURCES
NT ALFALFA
NT ARID LANDS
NT COAL
NT CORN
NT COTTON
NT CRUDE OIL
NT DESERTS
NT FARM CROPS
NT FORESTS
NT GEOTHERMAL RESOURCES
NT GLACIERS
NT GRAINS (FOOD)
NT ICEBERGS
NT LAKES
NT LAND ICE
NT LAVA
NT RANGE RESOURCES
NT RIVERS
NT ROCKS
NT SANDS
NT SHALES
NT TRIBUTARIES
NT VEGETATION
NT WATER RESOURCES
NT WETLANDS
Soviet Meteor meteorological satellite system and applications in weather forecasting, geological surveys, and exploration of earth resources
[NLL-M-22683-[5828.4F]] 01 p0073 N73-10599
Crop identification, acreage estimation, urban land use, soil mapping, and earth resources identification in Wabash River Basin using ERTS-1 imagery
[E72-10208] 03 p0288 N73-12331
Conceptual design of operational earth resources ground processing systems
[NASA-CR-129605] 03 p0293 N73-12383
Analyzing and processing remotely sensed earth resources data
[NASA-CR-61399] 03 p0293 N73-12390
Potential application of SLR to remote sensing of earth resources
[ESRO-CR[P]-138] 03 p0295 N73-12401
Characteristics and imagery of side-looking radar
03 p0295 N73-12402
Side-looking radar for agricultural applications, noting crop identification and growth
03 p0295 N73-12403
Side-looking radar applications to forestry management, and timber inventory and identification
03 p0295 N73-12404
Principles, installation, and operation of side-looking radar in aircraft and satellites for earth resources sensing
[ESRO-CR[P]-136-VOL-1] 03 p0296 N73-12418
Natural resource inventory in Arizona using ERTS-1 imagery
[E72-10287] 04 p0410 N73-13337
Remote sensing of Thailand earth resources using ERTS-1 imagery
[E72-10298] 04 p0411 N73-13348
Management of earth resources in France and Spain through automatic mapping inventory
[E72-10303] 04 p0411 N73-13352
Environmental and resource study of Kansas using ERTS-1 imagery
[E72-10305] 04 p0412 N73-13354
Investigation of natural resources in remote and unexplored areas of Venezuela using ERTS-1 remotely sensed imagery
[E72-10311] 04 p0412 N73-13360
Multidisciplinary analysis of Michigan resources utilizing ERTS-1 imagery
[E72-10313] 04 p0412 N73-13362
Application of remotely sensed, multispectral observations for assessment of earth resources and environmental quality in Alabama
04 p0471 N73-13841
Application of remotely sensed data to determination of resources and conditions in Susquehanna River Basin
04 p0471 N73-13844
Impact of California Water Project on environmental quality and resources in southern California
05 p0537 N73-14368

Digital facility for handling and processing remotely sensed earth resources data
05 p0537 N73-14369
Possibilities of assessing global environmental quality in relation to future prosperity of man, for Global Environmental Monitoring System
[BULL-10] 05 p0538 N73-14379
Application of radiophysical methods to study of earth atmosphere and earth resources with satellites
[NASA-TT-F-14642] 05 p0538 N73-14381
Bibliography on side-looking radar for remote sensing of earth resources, agriculture, oceanography, geology, hydrology, geography - noting data processing and photointerpretation
[ESRO-CR[P]-142-VOL-7] 06 p0640 N73-15198
Application of ERTS-1 imagery to evaluation and management of Wyoming natural resources
[E73-10037] 07 p0776 N73-16300
Surveying and mapping earth resources over large areas utilizing ERTS-1 imagery
[E73-10049] 07 p0777 N73-16311
Value of ERTS-1 imagery in resource evaluation on national scale in South Africa
[E73-10071] 07 p0779 N73-16333
Proceedings of conference on earth resources survey systems to show applications of remote sensing to agriculture, forestry, oceanography, and urban development - Vol. I
[NASA-SP-283-VOL-1] 07 p0781 N73-16348
Accomplishments of United Nations in providing earth resources data to developing nations
07 p0783 N73-16370
Organization, planning, and development of remote sensor programs for Canada
07 p0784 N73-16371
Identification of organizations and activities concerning French programs in aerial photography and earth resources technology
07 p0784 N73-16372
Analysis of factors affecting design and application of remote sensors for earth observation
07 p0784 N73-16376
Characteristics of radar equipment and microwave radiometers to show application to earth resources surveys
07 p0784 N73-16377
Characteristics of multispectral sensors and methods for interpreting multispectral data obtained during earth resources surveys
07 p0784 N73-16378
Application of remote sensing techniques for detecting environmental changes at and near earth surface
07 p0784 N73-16379
Analysis of effects of various parameters inherent in remote sensors to show distortions and errors produced in remotely sensed data
07 p0784 N73-16380
Organization and functions of interdisciplinary teams for analyzing and interpreting remotely sensed data on earth resources
07 p0784 N73-16381
Remote sensing of areas in Italy using infrared scanners for thermal radiation map
07 p0859 N73-16968
Problems of environmental pollution and natural resource depletion caused by man
[JPRS-58113] 08 p0879 N73-17121
Earth resource survey using remote sensing techniques to improve land use and management in Michigan
[NASA-CR-130758] 08 p0917 N73-17514
Data processing for synthetic aperture radar used as satellite-borne earth resources remote sensor
[NASA-CR-2193] 09 p1005 N73-18202
Spaceborne remote sensing for agricultural and forest resource surveys
[NASA-CR-130798] 09 p1026 N73-18376
Utilization of artificial satellites and spacecraft for surveying and mapping earth resources
[NASA-TT-F-739] 09 p1026 N73-18377
Earth resources requirements for Skylab missions - Appendix B
[NASA-TM-X-69137] 09 p1029 N73-18402
Development of techniques for evaluation of ERTS-1 imagery of natural resources in remote and unexplored areas of Venezuela
[E73-10481] 12 p1396 N73-21318
Remote sensing techniques for managing California earth resources
[NASA-CR-131392] 12 p1399 N73-21347
Remote sensing and automatic data processing techniques for earth resources survey in California
12 p1399 N73-21348
Digital systems for automatic processing of remote earth resources sensing data
12 p1400 N73-21355
Earth resources study for California
[NASA-CR-131579] 13 p1523 N73-22345
Government contracts and grants relative to documents on environmental satellites
[NOAA-TM-NESS-46] 13 p1524 N73-22349
Earth resources remote seasing project using multispectral band scanners to detect and measure thermal radiation from ground vegetation
[NASA-CR-124219] 13 p1529 N73-22393
Passive microwave radiometry and its application to earth resources surveys
[ESRO-CR-116] 13 p1530 N73-22402
Multispectral scanning systems and potential application to earth resources, noting radiation sources, atmospheric effects, and sensor techniques
[ERL/R-243-U] 13 p1531 N73-22403
Multispectral scanning systems and potential application to earth resources noting spectral properties of common earth materials
[ERL/R-244-U] 13 p1531 N73-22404
Investigation of optical properties of natural objects and their aerial photographic imaging characteristics
[AD-756603] 13 p1532 N73-22413
Earth observation experiments identified during earth orbital experiment program and requirements study - Vol. 6
[NASA-CR-112330] 13 p1577 N73-22783
Uniform mapping of earth resources and environmental complexes from Skylab imagery
[E73-10532] 14 p1654 N73-23417
Uniform mapping of earth resources and environmental complexes from Skylab imagery
[E73-10562] 14 p1656 N73-23434
Application of Skylab and EREP imagery for uniform mapping of earth resources and environmental complexes
[E73-10706] 16 p1904 N73-25397
Application of ERTS-1 data for multidisciplinary analysis of Michigan resources and development of computerized procedure for map coordinates correlation
[E73-10703] 17 p2018 N73-26316
Earth resources survey applications of space shuttle sortie mode
[NASA-CR-132207] 17 p2026 N73-26394
Land use models for Houston area
[NASA-CR-128991] 17 p2098 N73-26975
Remote sensing techniques for earth resources, water pollution, and vegetation growth
[PUBL-21] 18 p2143 N73-27321
Bibliography of remote sensing applications to agriculture, civil engineering, and geology
[PB-219104/7] 18 p2147 N73-27356
Development and employment of orbital space stations to conduct earth resources surveys and provide space manufacturing facilities
[JPRS-59650] 18 p2199 N73-27754
Proceedings of conference on significant results obtained from ERTS-1 - Vol. 1, Parts A and B
[E73-10824] 19 p2259 N73-28207
Proceedings of conference on significant results obtained by ERTS-1 - Vol. 2
[E73-10825] 19 p2287 N73-28389
Data acquisition of multispectral scanning noting geology, hydrology, soil sceince, and mapping applications
19 p2295 N73-28451
Solution of earth resources and environmental quality problems using ERT-1 MSS data
[E73-10899] 20 p2395 N73-29248
Investigation of land use and earth resources using Skylab EREP
[E73-10964] 21 p2533 N73-30306
Papers presented at meeting of Soviet-American working group on remote sensing of natural environment from space
[JPRS-59739] 21 p2534 N73-30317
Assessment of US and USSR technology and instrumentation for obtaining, transmitting, and processing earth images from space
21 p2534 N73-30318
General principles of geological interpretation of remote images of earth surface
21 p2534 N73-30319
Solution of certain regional geological problems using space photography
21 p2534 N73-30320
Application of space photography for small-scale mapping and analysis of farm lands
21 p2535 N73-30326
Determination of optimal spectral intervals for remote sensing of earth surface from space
21 p2535 N73-30327
Processing of multispectral scanned data noting imaging techniques and user operations
[ERL/R-245] 21 p2539 N73-30356
Proceedings of international conference on remote sensing of environment
[NASA-CR-133784] 21 p2540 N73-30370
Review of resources of fossil and nuclear fuels, solar energy and hydroelectric power
[LRP-63/73] 22 p2617 N73-30975
Space applications research in astronomy and earth physics
[NASA-SP-331] 22 p2732 N73-31867
Multispectral scanning systems and potential application to earth resources surveys - bibliography
[ERL/R-249-U] 23 p2787 N73-32299
European program in multispectral scanning systems and application to earth resources surveys
[ERL/R-247-U] 23 p2787 N73-32301
Study of terrestrial resources by satellites, and international law
[NASA-TT-F-15094] 23 p2846 N73-32740
Utilization of Skylab imagery as information service for investigating land use and natural resources in New York
[E73-11113] 24 p2915 N73-33270
Activities of Australian Bureau of Mineral Resources
24 p2921 N73-33324

**EARTH RESOURCES EXPERIMENT PACKAGE**
U EREP

**EARTH RESOURCES OBSERVATION SATELLITES**
U EROS [SATELLITES]

**EARTH RESOURCES PROGRAM**

Development of Earth Resources Information Storage, Transformation, Analysis, and Retrieval system through NASA research project
[NASA-CR-61392] 01 p0049 N73-10399
Development of Earth Resources Information Storage, Transformation, Analysis, and Retrieval System based on NASA training program in systems engineering
[NASA-CR-61394] 01 p0050 N73-10400
Evaluation of image dissector sensor for Earth Resources program
[NASA-CR-130131] 05 p0547 N73-14443
Earth resources laboratory data system for analyzing and processing multispectral, radiometric, photographic, and passive microwave imagery data
[NASA-CR-128693] 07 p0758 N73-16160
Global earth resource program for Germany
[DGLR-PAPER-72-072] 09 p1101 N73-18989
ERTS-1 performance during orbits 0 to 1300
[NASA-CR-130178] 11 p1286 N73-20435
Satellite monitoring of open pit mining operations
[BM-IC-8530] 15 p1780 N73-24432
Processing and enhancement of Earth Resources Program photography
[NASA-CR-131819] 15 p1787 N73-24491
Mapping techniques using imagery from ERTS and EROS programs
[PAPER-L2] 19 p2273 N73-28298
Results of ERTS-1 investigations of agriculture, forestry, and range resources
19 p2289 N73-28406
ERTS-1 investigations of environmental quality and pollution
19 p2290 N73-28409
Significant results from marine resources and ocean surveys of discipline overall ERTS program
19 p2290 N73-28411
Aim, methodology, technological requirements, and flexibility of future multispectral scanning programs
19 p2295 N73-28456
Application of satellite-borne remote sensors to survey of earth resources and environment
[NASA-TM-X-68266] 20 p2412 N73-29384
Mapping and mosaic applications of ERTS-1 MSS imagery
[E73-10957] 21 p2532 N73-30299
Summary of research projects in Earth Resources Data Analysis Program
[NASA-CR-133982] 22 p2664 N73-31348
Analysis of grizzly bear habitats from ERTS-1 photography
[NASA-CR-135776] 24 p2920 N73-33319
Technical consulting services for earth resources program
[NASA-CR-135793] 24 p2921 N73-33330

**EARTH RESOURCES SURVEY AIRCRAFT**

Aircraft and spacecraft observation of riverbed formation and flow patterns
04 p0472 N73-13846
Objectives of NASA Earth Resources Survey Program to include types of sensors used and data acquired by aircraft, spacecraft, and ground observations
07 p0782 N73-16351
Analysis of NASA Earth Resources Program to include ERTS satellites, Skylab program, and earth resources survey aircraft
07 p0782 N73-16359
Design and development of two long wavelength, focal plane, and cooler assemblies for use in multispectral scanner installed in earth observations aircraft
[NASA-CR-128743] 10 p1137 N73-19262
Mission planning for European earth resources survey aircraft
[ESRO-CR[P]-117] 14 p1661 N73-23484
Fokker F-27 as European earth resources survey aircraft noting design, remote sensors, and program
[ESRO-CR[P]-128] 17 p1984 N73-26035
Requirements of earth resources aircraft facility for remote sensing of European terrain
[ESRO-CR-97] 20 p2413 N73-29394
Description of Breguet 1150 to be used as European earth resources survey aircraft noting sensor payload
21 p2538 N73-30353
Performances and limitations of geological remote sensing from earth resources survey aircraft and satellites
[BMBW-FBW-72-28] 22 p2667 N73-31370

**EARTH RESOURCES SURVEY PROGRAM**

Passive microwave radiometry for remote sensing of earth resources and environmental monitoring programs
[ESRO-CR-75] 19 p2295 N73-28458

Directory of European activities in remote sensing of earth resources
[ESRO/JPPC-73-20-ADD-1] 22 p2667 N73-31372
EARTH RESOURCES TECHNOLOGY SATELLITE 1
Geologic mapping of Basin and Range - Colorado Plateau boundary in Arizona using ERTS-1 imagery
[E72-10157] 01 p0044 N73-10347
Utilization of ERTS-1 imagery for state and local agency management and planning in North Carolina
[E72-10167] 01 p0044 N73-10348
Determination of boundaries of aircraft and spacecraft data within which water quality can be obtained
[E72-10168] 01 p0044 N73-10349
Sediment pattern correlations with inflow and tidal action in Chesapeake Bay based on ERTS-1 imagery
[E72-10169] 01 p0044 N73-10350
Evaluation of ERTS-1 imagery for hydrologic information in Sierra Nevada Mountains and Lake Ontario
[E72-10170] 01 p0044 N73-10351
Estuarine and coastal oceanography of Block Island Sound and adjacent New York coastal waters based on ERTS-1 multispectral band scanner imagery
[E72-10171] 01 p0044 N73-10352
Interdisciplinary study of estuarine and coastal oceanography of Block Island Sound and New York Bight area using ERTS-1 imagery
[E72-10172] 01 p0044 N73-10353
Mapping and managing soil and range resources in Sand Hills Region of Nebraska using ERTS-1 imagery
[E72-10175] 01 p0044 N73-10354
Landform-vegetation relationships in southern Arizona based on interpretation of ERTS-1 imagery
[E72-10176] 01 p0044 N73-10355
Monitoring rural landscape changes in eastern Tennessee through interpretation of ERTS-1 imagery
[E72-10177] 01 p0045 N73-10356
Application of ERTS-1 imagery data to protection and management of New Jersey coastal environment
[E72-10178] 01 p0045 N73-10357
Crop identification and acreage measurement in Idaho, Missouri, Kansas, and South Dakota using ERTS-1 imagery
[E72-10179] 01 p0045 N73-10358
Interpretation and mapping large scale structural lineaments in Precambrian shield areas and basins containing younger sediments using ERTS-1 imagery
[E72-10180] 01 p0045 N73-10359
Mapping iron compounds in Wind River Range using ERTS-1 multispectral scanner imagery
[E72-10181] 01 p0045 N73-10360
Monitoring by ERTS-1 imagery for resource inventory, planning, land use zoning, and resource development in Oregon
[E72-10182] 01 p0045 N73-10361
Classification and pattern recognition of short lived events using ERTS-1 imagery
[E72-10183] 01 p0045 N73-10362
Inventory and monitoring of natural vegetation-landform relationships in arid regions of southern Arizona using ERTS-1 imagery
[E72-10184] 01 p0045 N73-10363
Uniform mapping and monitoring of natural ecosystems and environmental complexes from ERTS-1 imagery
[E72-10185] 01 p0046 N73-10364
Development of multistage forest sampling inventory system using ERTS-1 imagery
[E72-10186] 01 p0046 N73-10365
Data processing of hydrologic conditions using ERTS-1 time lapse imagery of Wrangell Mountains
[E72-10187] 01 p0046 N73-10366
Land use mapping of northern megalopolis using ERTS-1 imagery
[E72-10188] 01 p0046 N73-10367
Meteorological data from ERTS-1 high resolution multispectral photography
[E72-10189] 01 p0046 N73-10368
Ocean water color assessment of Monterey Bay, California, from ERTS-1 RBV and MSS imagery
[E72-10190] 01 p0046 N73-10369
Acquisition of earth resources data for Bolivia using ERTS-1 imagery
[E72-10191] 01 p0046 N73-10370
Study of crustal structure from eastern Sierra Nevada to Colorado Plateau using ERTS-1 imagery
[E72-10192] 01 p0046 N73-10371
Application of ERTS-1 imagery to fracture related mine safety hazards in coal mining industry in Indiana
[E72-10193] 01 p0046 N73-10372
Lithological and structural surveys of African rift system using ERTS-1 imagery
[E72-10194] 01 p0046 N73-10373
Updating and adding detail to Minnesota Land Management Information Systems utilizing ERTS-1 imagery
[E72-10195] 01 p0047 N73-10374
ERTS-1 remote sensing of chlorophyll measurements in upwelling areas of oceans
[E72-10196] 01 p0047 N73-10375
Mineral exploration in Arizona using ERTS-1 imagery
[E72-10197] 01 p0047 N73-10376
In situ spectroradiometric quantification of ERTS-1 imagery of Arizona and Texas
[E72-10173] 01 p0055 N73-10444
In situ spectroradiometric quantification of ERTS-1 MSS and RBV imagery
[E72-10174] 01 p0055 N73-10445
Requirements for remote buoys, transmitting to ERTS-A
05 p0608 N73-14943
Utilization of ERTS-1 imagery for water resources management in Delaware River Basin
07 p0787 N73-16404
Test of computerized analysis method for interpreting ERTS 1 photographs of soils and vegetation
[NASA-CR-130021] 07 p0791 N73-16435
ERTS A spectrophotographic measurement of water pollution in Charlotte Amalie harbor, St. Thomas
[NASA-CR-130008] 07 p0792 N73-16437
ERTS-1 imagery in national program for inspection of dams
[AD-754579] 11 p1288 N73-20449
Interpretation of geologic map of Fannin County, Texas, prepared by ADP techniques from ERTS MSS data
[NASA-CR-131574] 13 p1522 N73-22333
Urban land use mapping of San Francisco Bay area by machine processing of ERTS-1 multispectral data
[NASA-CR-131589] 13 p1522 N73-22334
Automatic processing of ERTS-1 data for physiography and geologic mapping of San Juan Basin, Colorado
[NASA-CR-131577] 13 p1524 N73-22346
Analysis of telemetry data from prelaunch, launch, and flight activation phases of ERTS-1 spacecraft
[NASA-CR-130150] 13 p1581 N73-22817
Flight performance analysis of ERTS-1 spacecraft components during orbits 1300 to 2600
[NASA-CR-130207] 13 p1581 N73-22818
Utilization of ERTS-1 remotely sensed imagery for land use evaluation and planning in Power River Basin, Wyoming
14 p1653 N73-23407
ERTS-1 data for effective monitoring and management of surface water on earth
[NASA-TM-X-66237] 14 p1659 N73-23468
Multispectral band scanner for Earth Resources Technology Satellite A imagery
18 p2209 N73-27831
Video bandwith tape recorder for ERTS A imagery
18 p2209 N73-27833
Cartographic quality of ERTS-1 RBV and MSS imagery
[PAPER-L1] 19 p2273 N73-28297
Land use mapping of Phoenix Quadrangle, Arizona from ERTS-1 Photography
[PAPER-L3] 19 p2273 N73-28299
Utilization of ERTS-1 imagery for monitoring land use change and regional planning in Coachella Valley, California
[PAPER-L5] 19 p2273 N73-28301
Land use change and classification using ERTS-1 imagery of Central Atlantic Regional Ecological Test Site
[PAPER-L6] 19 p2274 N73-28302
Linking land use and environmental processes in Central Atlantic Region using ERTS-1 data
[PAPER-L7] 19 p2274 N73-28303
Land cover and land use mapping of Central Atlantic Region shoreline zone using ERTS-1 imagery
[PAPER-L8] 19 p2274 N73-28304
Timber inventory and land use in Province of Huelva-Spain based on ERTS-1 imagery
[PAPER-L9] 19 p2274 N73-28305
Geographic applications of ERTS-1 data to landscape changes in eastern Tennessee
[PAPER-L10] 19 p2274 N73-28306
Identification of soil associations in western South Dakota using ERTS-1 imagery
[PAPER-L11] 19 p2274 N73-28307
Mapping and digitization of land use in northern megalopolis of Massachusetts, Connecticut, and Rhode Island using ERTS-1 data
[PAPER-L12] 19 p2274 N73-28308
Land use inventory and mapping in Wyoming from ERTS-1 data
[PAPER-L13] 19 p2274 N73-28309
Utilization of ERTS-1 imagery and data for land use mapping and management in Minnesota
[PAPER-L14] 19 p2275 N73-28310
Utilization of ERTS-1 data for inventory of critical land resources for regional land use planning in Wisconsin
[PAPER-L16] 19 p2275 N73-28311
Application of ERTS-1 and U-2 photography to study of urban land use in Pennsylvania
[PAPER-L17] 19 p2275 N73-28312
Urban development and regional planning for Los Angeles County, California using ERTS-1 imagery
[PAPER-L18] 19 p2275 N73-28313
Preparation of urban land use inventories of Wisconsin and Indiana by machine-processing of ERTS-1 MSS data
[PAPER-L19] 19 p2275 N73-28314
Land use mapping and inventory of Houston, Texas using ERTS-1 and high altitude photography
[PAPER-L20] 19 p2276 N73-28315
Digital land use mapping in Oakland Country, Michigan using ERTS-1 data
[PAPER-L21] 19 p2276 N73-28316
Mapping of agricultural land use in Lancaster and Lebandon Counties, Pennsylvania from ERTS-1 digital data
[PAPER-L22] 19 p2276 N73-28317
Use of temporal dimension in classifying and mapping central Peansylvania area from ERTS-1 MSS data
[PAPER-L23] 19 p2276 N73-28318
Identification and mapping of coal refuse banks in Pennsylvania anthracite coal fields from ERTS-1 data
[PAPER-L24] 19 p2276 N73-28319
Forest management in Minnesota using automatic interpretation of ERTS-1 data
[PAPER-L25] 19 p2276 N73-28320
Utilization of ERTS-1 data for land use and resources survey in Michigan
[PAPER-L26] 19 p2276 N73-28321
Terrain classification maps of Yellowstone Park from ERTS-1 imagery
[PAPER-L27] 19 p2277 N73-28322
Atmospheric effects on ERTS-1 data and advanced data extraction techniques
[PAPER-I1] 19 p2277 N73-28323
Measurement of atmospheric aerosol content in Southern California desert areas from ERTS-1 contrast and radiance measurements
[PAPER-I2] 19 p2277 N73-28324
Obtaining absolute target reflectances by correcting ERTS-1 radiance measurements for variable target irradiance, atmospheric attenuation, and atmospheric backscatter
[PAPER-I3] 19 p2277 N73-28325
Masking of ERTS-1 RBV images to reduce stationary residual inaccuracies in radiometric shading corrections
[PAPER-I4] 19 p2277 N73-28326
Rectification of ERTS-1 multispectral imagery using digital techniques
[PAPER-I6] 19 p2277 N73-28327
Application of digital techniques to processing of ERTS-1 MSS and RBV image data
[PAPER-I7] 19 p2278 N73-28328
Processing and interpretation of ERTS-1 MSS data for Lake Livingston, Texas
[PAPER-I8] 19 p2278 N73-28329
VICAR image processing system used for enhancement of ERTS-1 images for Arizona geological experiment
[PAPER-I9] 19 p2278 N73-28330
Enhancement of ERTS-1 images by density slicing and application to mapping of Yucca trees in Mojave Desert of Southern California and Nevada
[PAPER-I11] 19 p2278 N73-28332
Pseudocolor transformation of ERTS-1 imagery of Monterey Bay-San Francisco, California area
[PAPER-I12] 19 p2278 N73-28333
Comparison between geophysical and ERTS data processing techniques
[PAPER-I13] 19 p2278 N73-28334
Analysis of ERTS-1 imagery by combining human and computer interpretation capabilities
[PAPER-I14] 19 p2279 N73-28335
Analysis and enhancement of ERTS-1 hydrology imagery using electronic satellite image analysis console
[PAPER-I15] 19 p2279 N73-28336
Algorithm for classifying land use categories of ERTS-1 data by textural features
[PAPER-I16] 19 p2279 N73-28337
Automatic recognition of terrain types from ERTS-1 MSS imagery
[PAPER-I17] 19 p2279 N73-28338
Classification of ERTS-1 MSS data by canonical analysis
[PAPER-I18] 19 p2279 N73-28339
Relationship between in situ spectral reflectance measurements and photometric characteristics of ERTS-1 MSS imagery of Wilcox Playa, Arizona
[PAPER-I19] 19 p2279 N73-28340
Seasonal changes of littoral transport and beach width of Maryland portion of Chesapeake Bay and resultant effect on protective structures
[PAPER-M1] 19 p2280 N73-28341
ERTS-1 imagery of littoral drift and sedimentation patterns of beach and nearshore areas of Maryland section of Chesapeake Bay
[PAPER-M2] 19 p2280 N73-28342
Application of ERTS-1 imagery to analysis of suspended sediments and aquatic fronts in Delaware Bay
[PAPER-M3] 19 p2280 N73-28343
Correlation of ERTS-1 multispectral imagery with suspended matter and chlorophyll in lower Chesapeake Bay
[PAPER-M4] 19 p2280 N73-28344
ERTS-1 imagery of plume development where Connecticut River flows into Long Island Sound
[PAPER-M5] 19 p2280 N73-28345
Influence of sea ice on coastal marine environment of Beaufort Sea, Alaska
[PAPER-M7] 19 p2280 N73-28346

ERTS-1 imagery of sea surface circulation and sediment transport in Cook Inlet, Alaska
[PAPER-M8] 19 p2280 N73-28347
Sediment distribution, water currents, and water circulation in Cook Inlet, Alaska
[PAPER-M9] 19 p2281 N73-28348
Distribution and movement of suspended sediment in Gulf of Mexico off Texas coast
[PAPER-M10] 19 p2281 N73-28349
Oceanographic mapping of distribution and flow of water masses in northern Gulf of California by use of ERTS-1 imagery and optical models
[PAPER-M11] 19 p2281 N73-28350
Detection of ocean currents in eastern Gulf of Mexico using ERTS-1 imagery
[PAPER-M13] 19 p2281 N73-28352
Detection and mapping Arctic sea ice from ERTS-1 imagery
[PAPER-M14] 19 p2281 N73-28353
ERTS-1 imagery of biomass in upwelling waters along northwest coast of Africa
[PAPER-M15] 19 p2281 N73-28354
Application of ERTS-1 imagery to harvest model of menhaden fishing industry in Mississippi Sound
[PAPER-M17] 19 p2282 N73-28355
Comparison of conventional maps of southeastern Massachusetts to ERTS-1 imagery of coastal and submarine geology and hydrology
[PAPER-M18] 19 p2282 N73-28356
Estimation of water depth off Great Bahama Bank using ERTS-1 imagery
[PAPER-M19] 19 p2282 N73-28357
Calculation of water depth off Little Bahama Bank from ERTS-1 data for use in upgrading and mapping world navigation charts of shallow waters
[PAPER-M20] 19 p2282 N73-28358
Application of ERTS-1 data to North Carolina forest and water resources management
[PAPER-R1] 19 p2282 N73-28359
Resources and land use management and planning in Oregon using ERTS-1 data
[PAPER-R2] 19 p2282 N73-28360
Application of ERTS-1 imagery to resource management in Ohio
[PAPER-R3] 19 p2283 N73-28361
ERTS-1 detection and monitoring of tectonic and vegetational patterns, urban development, and agricultural processes in Southern California
[PAPER-R4] 19 p2283 N73-28362
ERTS-1 imagery of desertification, hydrology, vegetation, forage, and water resources in Republic of Mali
[PAPER-R5] 19 p2283 N73-28363
ERTS-1 imagery of water pollution, sedimentation, and geology of southeastern France and western Alps
[PAPER-R6] 19 p2283 N73-28364
DCP-collected absolute target reflectance measurements to assist interpretation of ERTS-1 imagery of forest stresses in Black Hills, South Dakota
19 p2283 N73-28365
Application of ERTS-1 TV imagery to map-making
19 p2283 N73-28366
Application of ERTS-1 data to geomorphotectonics, earthquake studies, and mineral exploration at Los Angeles, California, and New Jersey coastal plain
19 p2284 N73-28367
ERTS-1 surveillance of volcanic areas of Southern Italy
19 p2284 N73-28368
Thermal surveillance of Cascade range volcanoes using ERTS-1 MSS data, aircraft imaging systems, and ground based DCP
19 p2284 N73-28369
Geological survey of New Mexico based on ERTS-1 imagery
19 p2284 N73-28370
Computed atmospheric effects on ERTS-1 MSS observations
19 p2284 N73-28371
Comparison between ground based atmospheric turbidity network measurements and ERTS-1 MSS channel 4 scene grayness measurements
19 p2284 N73-28373
ERTS-1 imagery of snow cover on northern foothills of Brooks Range and Wrangell Mountains, Alaska
19 p2285 N73-28374
Monitoring and classifying eutrophication of inland lakes in Michigan using ERTS-1 imagery
19 p2285 N73-28375
ERTS-1 imagery of algal blooms in Lake Erie and Utah Lake, Ohio
19 p2285 N73-28376
Utilization of ERTS-1 imagery and data for land use, regional planning, and urban development in Metropolitan Washington area
19 p2285 N73-28377
Mapping land use and detecting land use change in Montgomery County, Alabama using ERTS-1 data
19 p2285 N73-28378
Land use management in Minnesota by automatic interpretation of ERTS-1 MSS data
19 p2285 N73-28379
Digital data processing of ERTS-1 MSS imagery of water masses in Delaware Bay
19 p2286 N73-28380
Contrast enhancement of ERTS-1 imagery by photographic techniques and methods
19 p2286 N73-28381
Resectioning programs developed to provide precision annotation of predetermined primary land sampling units on ERTS-1 MSS imagery
19 p2286 N73-28382
Application of classification algorithms to ERTS-1 MSS imagery of Texas land and water coastal features
19 p2286 N73-28383
Utilization of ERTS-1 imagery for coastal oceanography in British Columbia
19 p2286 N73-28384
Relationship between ERTS-1 fisheries distribution information and selected oceanographic parameters in Mississippi Sound
19 p2286 N73-28385
Application of ERTS-1 imagery to study of coastal areas and processes
19 p2286 N73-28386
ERTS-1 imagery of geology, agriculture, forestry, and hydrology in Iran
19 p2287 N73-28387
Detection of turbidity plumes in Tampa Bay, Florida from ERTS-1 MSS imagery
19 p2287 N73-28388
Conference on significant results obtained from ERTS-1 MSS and RBV data - Vol. 3
[E73-10826] 19 p2289 N73-28405
Application of ERTS-1 imagery to land use inventory and management and mapping techniques
19 p2289 N73-28407
Mineral resources, geological structures, and landform surveys from ERTS-1 imagery
19 p2289 N73-28408
Utilization of ERTS-1 imagery and data for water resources surveys and management
19 p2290 N73-28410
Processes, algorithms, and procedures for extraction and interpretation ERTS-1 data
19 p2290 N73-28412
ERTS-1 applications in land use, geologic interpretation, resources survey, and pollution monitoring
19 p2290 N73-28413
Analysis of Milwaukee county, Wisconsin land use by machine processing of ERTS-1 remotely sensed data
[NASA-CR-133643] 20 p2412 N73-29385
ERTS-1 sensor analysis of air pollution and air pollution related injuries to plant vegetation in metropolitan Minnesota
23 p2784 N73-32269
ERTS-1 observation of marshy ocean coast areas and sedimentary material
[NASA-TT-F-15063] 24 p2922 N73-33333

**EARTH RESOURCES TECHNOLOGY SATELLITES**
NT EARTH RESOURCES TECHNOLOGY SATELLITE 1
Application of unmanned spacecraft for research purposes to show benefits from Communication and Navigation satellites and Earth Observation satellites
04 p0470 N73-13830
Earth resource surveys for management and development of resources in Ohio
04 p0472 N73-13845
Aircraft and spacecraft observation of riverbed formation and flow patterns
04 p0472 N73-13846
Use of ERTS data to manage and solve social problems associated with earth resources in California
05 p0536 N73-14363
Four band multispectral scanner system for ERTS
[NASA-CR-130111] 05 p0546 N73-14430
Vibration tests of magnetic control assembly for Nimbus and ERTS satellites
[NASA-CR-130143] 06 p0673 N73-15478
Employment of Earth Resources Technology Satellite capabilities for determining distribution of earth resources
07 p0782 N73-16353
Analysis of NASA Earth Resources Program to include ERTS satellites, Skylab program, and earth resources survey aircraft
07 p0782 N73-16359
Analysis of earth resources information systems using satellites as sensor platforms to show type of data obtained and data reduction procedures
07 p0782 N73-16360
Remote sensing of Minnesota lakes and forests using ERTS-1
[NASA-CR-130548] 08 p0916 N73-17502
Quantitative, qualitative, and cost analyses of ERTS-1 imagery
[REPT-11215-1-F] 09 p1025 N73-18371
Data processing requirements for ERTS
09 p1065 N73-18689
Parallel optical data processing for earth resources satellite mission
09 p1065 N73-18690
Mechanical component screening for multispectral scanner mirror mechanism used on Earth Resources Technology Satellite
09 p1087 N73-18872
Magnetic tape transport unit for ERTS recording instruments - Vol. 1
[NASA-CR-130186] 10 p1129 N73-19194
Recording instruments for Earth Resources Technology Satellites - Vol. 2
[NASA-CR-130187] 10 p1129 N73-19195
Conference of ERTS-1 performance, and application
[NASA-TM-X-66193] 10 p1155 N73-19396
ERTS-1 performance during orbits 0 to 1300
[NASA-CR-130178] 11 p1286 N73-20435
ERTS-1 imagery of flood damage to farmlands in South Dakota
[NASA-CR-131641] 12 p1401 N73-21361
Technical utilization of advanced equipment for oceanological exploitation by US
[JPRS-58696] 12 p1401 N73-21363
Preparation of urban land use inventories by automated processing of ERTS MSS data
[NASA-CR-131576] 13 p1524 N73-22347
Projected data systems requirements for agriculturally oriented earth resources technology satellites in 1980s
[NASA-TM-X-62240] 14 p1660 N73-23472
ERTS/Nimbus satellite observations of electron flux levels as function of solar cycle
[NASA-TM-X-66236] 14 p1703 N73-23814
Use of ERTS multispectral data to solve development and management problems of agricultural resources in Lynn County, Texas
[NASA-CR-132956] 15 p1778 N73-24411
Atmospheric effects on remote sensing of nonuniform temperature sources applied to Skylab and ERTS missions
[NASA-CR-129004] 16 p1905 N73-25413
Application of remote sensing techniques of ERTS and other sources for solution of environmental problems in Oregon
[NASA-CR-133034] 16 p1906 N73-25420
Multispectral scanner system for Earth Resources Technology Satellites
[NASA-CR-132758] 16 p1912 N73-25474
Image processing techniques and applications to Earth Resources Technology Satellite program
[NASA-CR-124285] 16 p1967 N73-25910
Geometric distortion characteristics and calibration problems RBV television system onboard Earth Resources Technology Satellites
[PB-218393/7] 18 p2118 N73-27123
Algorithm for automatic classification and mapping of earth resources satellite data
[NASA-TM-X-64762] 18 p2144 N73-27332
Performance of return beam vidicon multispectral camera system for remote ERTS imagery
18 p2209 N73-27832
Proceedings of conference on significant results obtained from ERTS-1 - Vol. 1, Parts A and B
[E73-10824] 19 p2259 N73-28207
Evaluation of quality of ERTS-1 data produced during initial months of operation
19 p2259 N73-28208
Detection and identification of crops in Imperial Valley, California using ERTS-1 sequential imagery and remote sensing techniques
[PAPER-A2] 19 p2259 N73-28210
Digital enhancement of ERTS-1 MSS data for maximum image visibility
[PAPER-I10] 19 p2278 N73-28331
Oceanographic features in the lee of the windward and leeward islands: ERTS and ship data
[PAPER-M12] 19 p2281 N73-28351
Mapping of strip mine areas in southeastern Ohio from ERTS-1 imagery
19 p2284 N73-28372
Proceedings of conference on significant results obtained by ERTS-1 - Vol. 2
[E73-10825] 19 p2287 N73-28389
Analysis of ERTS-1 to include specifications of sensors, data acquisition, orbital mechanics, and data processing
19 p2287 N73-28391
Generation and physical characteristics of ERTS MSS system corrected computer compatible tapes
[NASA-TM-X-70426] 20 p2410 N73-29366
Application of aerial photography and ERTS imagery to agricultural, forest, and water resources management in Minnesota
[NASA-CR-133483] 22 p2665 N73-31357
Performances and limitations of geological remote sensing from earth resources survey aircraft and satellites
[BMBW-FBW-72-28] 22 p2667 N73-31370
First Earth Resources Technology Satellite: system, status, and results
[NASA-TM-X-70462] 22 p2720 N73-31765
Utilization of ERTS data to study air pollution, insect infestation, and water transport in Minnesota
[NASA-CR-135565] 23 p2783 N73-32266

ERTS analysis of geological relationships of Precambrian Greenstone belts and Troctolite series rocks of Minnesota
23 p2784 N73-32271

**EARTH ROTATION**
Iterative method for localizing position of balloon on earth, using interrogating satellite and correcting for errors due to terrestrial rotation
[NASA-TT-F-14702] 03 p0328 N73-12677
Iterative method for localizing position of balloon on earth, using interrogating satellite and correcting for errors due to terrestrial rotation and Doppler effect
[NASA-TT-F-14703] 03 p0328 N73-12679
Progress report from Bureau International de l Heure for period 1967 to 1971, including earth rotation, atomic time scale, and coordination of time signals
05 p0596 N73-14848
Rotational tidal waves due to earth rotation explained by Poincare problem solving
07 p0857 N73-16951
Influence of bottom topography and earth rotation of wind-driven circulation in Mediterranean Sea
07 p0858 N73-16956
Solution for steady state motion of atmosphere about rotating earth
[AD-754248] 10 p1157 N73-19414
Earth rotation aperture synthesis technique and polarized interferometry for determining polarized intensity distributions of Cygnus A at 8300 and 9600 MHz
16 p1961 N73-25865
Smithsonian astrophysical observatory reference system
[NASA-CR-133829] 21 p2522 N73-30222

**EARTH SATELLITES**
NT AEROS SATELLITE
NT ALOUETTE SATELLITES
NT ALOUETTE 1 SATELLITE
NT ALOUETTE 2 SATELLITE
NT APPLICATIONS TECHNOLOGY SATELLITES
NT ARIEL 3 SATELLITE
NT ASTRONOMICAL NETHERLANDS SATELLITE
NT ATS 1
NT ATS 3
NT ATS 5
NT ATS 6
NT BIOSATELLITE 2
NT COMMUNICATION SATELLITES
NT COSMOS SATELLITES
NT COSMOS 213 SATELLITE
NT COSMOS 224 SATELLITE
NT COSMOS 381 SATELLITE
NT DIADEME SATELLITES
NT EARTH RESOURCES TECHNOLOGY SATELLITE 1
NT EARTH RESOURCES TECHNOLOGY SATELLITES
NT ECHO 1 SATELLITE
NT ENVIRONMENTAL RESEARCH SATELLITES
NT EOLE SATELLITES
NT EROS [SATELLITES]
NT ESRO SATELLITES
NT ESRO 1 SATELLITE
NT ESRO 2 SATELLITE
NT ESRO 4 SATELLITE
NT ESSA 8 SATELLITE
NT EXPLORER SATELLITES
NT EXPLORER 12 SATELLITE
NT EXPLORER 18 SATELLITE
NT EXPLORER 21 SATELLITE
NT EXPLORER 24 SATELLITE
NT EXPLORER 27 SATELLITE
NT EXPLORER 31 SATELLITE
NT EXPLORER 32 SATELLITE
NT EXPLORER 33 SATELLITE
NT EXPLORER 34 SATELLITE
NT EXPLORER 35 SATELLITE
NT EXPLORER 38 SATELLITE
NT EXPLORER 40 SATELLITE
NT EXPLORER 41 SATELLITE
NT EXPLORER 49 SATELLITE
NT FRENCH SATELLITES
NT GEODETIC SATELLITES
NT GEOS SATELLITES [ESRO]
NT GEOS 1 SATELLITE
NT GEOS 2 SATELLITE
NT GEOS-C SATELLITE
NT GOE SATELLITES
NT HELIOS SATELLITES
NT HEOS A SATELLITE
NT HEOS B SATELLITE
NT HEOS SATELLITES
NT IMP
NT IMPROVED TIROS OPERATIONAL SATELLITES
NT INJUN 3 SATELLITE
NT INTELSAT SATELLITES
NT INTERCOSMOS SATELLITES
NT ISIS-A
NT ITOS 1
NT ITOS 2
NT ITOS 3
NT ITOS 4
NT LINCOLN EXPERIMENTAL SATELLITES
NT METEOROLOGICAL SATELLITES
NT METEOSAT SATELLITE
NT MOLNIYA SATELLITES
NT MOON
NT NAVIGATION SATELLITES
NT NIMBUS SATELLITES
NT NIMBUS 2 SATELLITE
NT NIMBUS 3 SATELLITE
NT NIMBUS 4 SATELLITE
NT NIMBUS 5 SATELLITE
NT OAO
NT OGO
NT OGO-A
NT OSO
NT OSO-J
NT OSO-1
NT OSO-5
NT OSO-6
NT OSO-7
NT PROTON 1 SATELLITE
NT RADIO ASTRONOMY EXPLORER SATELLITE
NT RELAY SATELLITES
NT SAN MARCO 3 SATELLITE
NT SPUTNIK SATELLITES
NT SYMPHONIE SATELLITES
NT SYNCHRONOUS METEOROLOGICAL SATELLITE
NT TIROS M
NT TIROS SATELLITES
NT TRANSIT SATELLITES
NT UHURU SATELLITE
NT VANGUARD 3 SATELLITE
NT VELA SATELLITES
NT VENERA SATELLITES
NT VENERA 8 SATELLITE
Thermal sounding experiment by Meteor satellite
[NASA-TT-F-14493] 01 p0104 N73-10861
Smoothing functions of range and range rate measurements from earth orbiting satellites
[NASA-TM-X-66126] 04 p0475 N73-13881
Geodetic use of earth satellites
[NASA-TT-F-732] 06 p0665 N73-15408
Definition of experiments for collection of RFI and multipath data for application to synchronous relay satellite
[NASA-CR-128717] 07 p0754 N73-16128
Tidal effects in motion of earth satellites and Love parameters of earth
[NASA-TM-X-66173] 08 p0961 N73-17858
European satellites to be launched between 1980 and 1990
[NASA-TT-F-14695] 08 p0965 N73-17887
Utilization of artificial satellites and spacecraft for surveying and mapping earth resources
[NASA-TT-F-739] 09 p1026 N73-18377
Feasibility of efficient multiamplitude communication in earth satellite systems
10 p1228 N73-19983
Interface requirements for design and development of Physiology of Chimpanzees in Orbit experiment
[NASA-CR-131397] 11 p1248 N73-20130
Computerized simulation of orbital assembly dynamics and interactions with geometrical appendages
[NASA-CR-124169] 11 p1259 N73-20220
Determining preliminary orbital elements of earth satellite from angle-only observations
[AD-755399] 13 p1578 N73-22793
Earth satellite orbit perturbation due to fluid tidal effects and temporal geopotential variations
[GROS-BULL-7] 14 p1706 N73-23847
Determining accuracy of three dimensional geodetic nets compiled from satellite observations
[NASA-TT-F-776] 16 p1906 N73-25418
Early orbit capability of Goddard Trajectory Determination System for earth satellites
[NASA-TM-X-66286] 18 p2197 N73-27734
Estimation of severe attenuation of radio signals due to precipitation at 2 cm on earth satellite paths
20 p2375 N73-29085
Juridical problems in use of stationary orbits for artificial earth satellites
[JPRS-59819] 20 p2473 N73-29862
Feasibility of using Doppler techniques for determining location of ground based emitters causing RFI with low orbiting satellites
[NASA-TM-X-70483] 24 p2895 N73-33109

**EARTH SHAPE**
U GEODESY

**EARTH SURFACE**
Hankel function for calculating radio wave diffraction around earth surface
[AD-742108] 01 p0028 N73-10221
Visible fluorescence of earth surface materials and potential applications in remote sensing
[PB-210621] 01 p0053 N73-10434
Application of Backus-Gilbert method to electrical conductivity problem
02 p0200 N73-11619
Culling of redundant earth data for geophysical model fitting
02 p0200 N73-11620
Correlation of total precipitable water in atmosphere with surface absolute humidity for California and Pacific Ocean islands
[AD-745954] 02 p0206 N73-11666
Atmospheric effects on thermal radiation from tropospheric nuclear explosion to ground target
[AD-745884] 05 p0539 N73-14389
Proceedings of conference on earth resources survey systems to show applications of remote sensing to agriculture, forestry, oceanography, and urban development - Vol. I
[NASA-SP-283-VOL-1] 07 p0781 N73-16348
Formation of seismic waves in surface soils during underground explosions
[AD-751070] 07 p0797 N73-16481
Mathematical models for reducing force of gravity values from earth relief to external surface
[AD-752235] 08 p0920 N73-17538
Soviet space stations for providing earth space photographs used for earth atmosphere and earth surface analysis
[JPRS-58055-1-PT-1] 09 p1026 N73-18372
Visual observations of atmospheric structure and land and water surfaces by cosmonauts from manned orbiting space stations
09 p1026 N73-18373
Analysis of space photographs of earth surface
09 p1026 N73-18374
Spectrophotometric observation of earth atmosphere and underlying surfaces near twilight horizon from manned spacecraft
09 p1026 N73-18375
Diurnal cycles of high absolute humidity at earth surface, using dew point and temperature measurements
[AD-753078] 09 p1061 N73-18654
Propagation of geomagnetic micropulsations into two layer conducting earth
[AD-755428] 12 p1402 N73-21375
Radar system for electromagnetic subsurface profiling
[PB-213892/0] 14 p1665 N73-23514
Diffuse shock wave reflection from ridged plates, simulating aerial explosion effects on earth surface
[REPT-7/72] 15 p1766 N73-24305
Circulation model for feasibility of modifying earth surface climate at middle and high northern latitudes
[AD-757795] 15 p1807 N73-24641
Determining accuracy of three dimensional geodetic nets compiled from satellite observations
[NASA-TT-F-776] 16 p1906 N73-25418
Geomorphological structure of earth surface from spaceborne photography
[NASA-TT-F-14968] 17 p2025 N73-26388
Earth surface scattering model for multiphase prediction of radiowave communication between earth satellites
[NASA-CR-132791] 18 p2116 N73-27109
Visible infrared spin-scan radiometer system for earth and cloud cover photography by synchronous meteorological satellite
18 p2209 N73-27834
Determination of earth aerosol albedo using Skylab EREP data
[E73-10871] 20 p2393 N73-29222
Cosmonaut earth observations from space
[JPRS-59831] 21 p2595 N73-30793

**EARTH TIDES**
Analysis of propagating and non-propagating motions produced by earth tides and earth rates and effects on inertial instrument performance
[AD-748274] 03 p0330 N73-12691
Effects of changes in ocean currents and motion on climatology
[NLL-M-22797-[5828.4F]] 05 p0529 N73-14307
Absolute gravity measurements using earth tides for analyzing earth structure
[AD-748529] 05 p0544 N73-14423
Tidal effects in motion of earth satellites and Love parameters of earth
[NASA-TM-X-66173] 08 p0961 N73-17858
Determination of earth tidal amplitude and phase from orbital perturbations of Beacon Explorer C spacecraft
[NASA-TM-X-70420] 20 p2409 N73-29365
Polar motion and earth tides from Beacon Explorer C
[NASA-TM-X-70460] 22 p2664 N73-31350

**EARTH-MARS TRAJECTORIES**
Comparison of open and closed loop applications of second order guidance algorithm using minimum distance strategy for Earth-Mars transfer
[NASA-CR-129170] 02 p0227 N73-11830

**EARTH-MOON SYSTEM**
Transit time measurements between earth and moon by transportable pulsed laser system
[NASA-CR-130986] 09 p1042 N73-18502

**EARTHQUAKES**
Seismological effects of explosions and earthquakes and structural dynamics of earth crust and upper mantle
[AD-746031] 01 p0054 N73-10435
Uncorrected accelerometer data resulting from San Fernando, California earthquake of Feb. 1971
[PB-208529] 01 p0054 N73-10439

Detection and classification of earthquakes and nuclear explosions by Swedish observatory
[FOA-4-A-4503-T8/S] 01 p0101 N73-10828
Possible shock effect associated with seaquakes
[NASA-TM-X-66096] 02 p0166 N73-11344
Descriptions of earthquakes and location of epicenters in US, Alaska, Panama Canal Zone, and Virgin Islands during 1970
03 p0294 N73-12393
Computing theoretical amplitude ratio of shear waves to compressional waves using double-couple representations of earthquakes
[AD-747763] 03 p0299 N73-12436
Earthquake epicenters and fault intersections in central and southern California
[E72-10304] 04 p0411 N73-13353
Utilization of ERTS-1 imagery to study short-lived events such as fires, volcanism, storms, and earthquakes
[E73-10025] 06 p0660 N73-15359
Method for whitening spectra of teleseismic P waves for determining event depths
[AD-750781] 06 p0671 N73-15455
Seismological wave spectra for differentiating between earthquakes and explosions
[AD-749874] 06 p0671 N73-15457
Earthquake prediction and control through satellite relay telemetry of seismic data
07 p0787 N73-16399
Response spectra of earthquake motion accelerograms
[PB-212602] 07 p0794 N73-16457
Fourier amplitude spectra for earthquake ground motions and structural response accelerations
[PB-212603] 07 p0794 N73-16458
Seismic detection of nuclear explosions and earthquakes
[AD-751243] 08 p0918 N73-17526
Volcano and earthquake surveillance network in Alaska, California, Washington, Hawaii, El Salvador, Nicaragua, Iceland, and Guatemala
[E73-10337] 09 p1025 N73-18365
Location of earthquake epicenters and major fault zones in Nevada using ERTS-1 imagery
[E73-10338] 09 p1025 N73-18366
Mapping of seismically active faults in Alaska using ERTS-1 imagery to determine areas of earthquake occurrence
[E73-10405] 11 p1277 N73-20367
Observation of earthquake associated tilt steps in Central Alaska
[RLO-2229-T-4-2] 15 p1781 N73-24436
Earth dynamic filtering algorithm for earthquake prediction and Love number determination
16 p1896 N73-25333
Pattern recognition and detection of short-lived events such as storms, forest fires, volcanoes, and earthquakes using ERTS-1 data
[E73-10678] 16 p1901 N73-25373
Application of ERTS-1 data for development and operation of volcano surveillance network
[E73-10711] 17 p2018 N73-26318
ERTS-1 imagery of western portion of Nicaragua following December 1972 earthquake to determine lineaments of fault systems related to earthquake
[PAPER-G24] 19 p2266 N73-28255
Application of ERTS-1 data to geomorphotectonics, earthquake studies, and mineral exploration at Los Angeles, California, and New Jersey coastal plain
19 p2284 N73-28367
Analysis of Rayleigh wave dispersion in continental path and development of filters for vertical high gain seismometer
[AD-761795] 19 p2296 N73-28462
Application of Skylab imagery to analysis of fault tectonics and earthquake hazards in Peninsular Ranges of Southern California
[E73-10863] 20 p2392 N73-29214
Tsunami of Ust-Kamchatsk after December 15, 1971 earthquate
20 p2447 N73-29656
Earthquakes and volcanoes caused by subterranean explosions provoked by petroleum or natural gas
[NASA-TT-F-15095] 21 p2536 N73-30334
Application of Skylab imagery to analysis of fault tectonics and earthquake hazards in Peninsular Ranges of Southern California
[E73-10999] 22 p2659 N73-31304
Elastic plate model for earthquakes
22 p2737 N73-31912
Identification and interpretation of tectonic features from ERTS-1 imagery of Southern California and Baja California
[E73-11084] 24 p2913 N73-33247
Application of Skylab imagery to analysis of fault tectonics and earthquake hazards in Peninsular Ranges, Southern California
[E73-11134] 24 p2917 N73-33289

**EBERT SPECTROMETERS**
Construction of far ultraviolet Ebert spectrometer for use on Apollo 17 flight to observe lunar atmosphere
[NASA-CR-128889] 11 p1293 N73-20491

**EBF**
U EXTERNALLY BLOWN FLAPS

**EBULLITION**
U BOILING

**ECCENTRICITY**
Dynamic behavior of eccentric rotating shaft subject to linearly varying or constant tension
13 p1532 N73-22414

**ECHELON FAULTS**
U GEOLOGICAL FAULTS

**ECHO PROJECT**
Compendium of worldwide satellite communications programs to Aug. 1971
[NASA-TM-X-70435] 21 p2599 N73-30834

**ECHO SATELLITES**
NT ECHO 1 SATELLITE

**ECHO 1 SATELLITE**
Drag coefficients for Echo 1 and Explorer 24 spherical surfaces in atomic oxygen over energy range from 4 to 200 eV
[NASA-CR-2233] 10 p1192 N73-19697

**ECHOES**
NT CLUTTER
NT LUNAR RADAR ECHOES
NT RADAR ECHOES
NT RADIO ECHOES
NT SIGNAL REFLECTION
NT VENUS RADAR ECHOES
Characterization of electron plasma wave echoes
[EUR-CEA-FC-639] 07 p0828 N73-16711
Dimensions and mechanical properties of elastic spherical shells measured by sound echo signals
10 p1188 N73-19667
Polarization effects in photon echoes and in anisotropic mirror laser cavities
18 p2157 N73-27429
Charge neutralization and echo analysis using electron gun in magnetosphere onboard sounding rocket during Electron Echo 1 experiment
19 p2258 N73-28204
Damping and saturation of second order electron plasma wave echo
24 p2961 N73-33662

**ECLIPSES**
NT SOLAR ECLIPSES
Observations of Jovian satellite eclipse
[NASA-CR-130292] 06 p0717 N73-15849

**ECLIPSING BINARY STARS**
Photoelectric observation of eclipsing variable stars TY Ursae Majoris and AZ Virginis including spectral classification for WY Cancri, AZ Virginis, and TZ Bootis
04 p0468 N73-13818
OAO 2 observations of LY Aur
[NASA-TM-X-66131] 04 p0475 N73-13880
Computerized analysis of binary star systems with eclipsing light curves
[NASA-TM-X-66155] 07 p0842 N73-16821
Optical identification of pulsed X ray source in eclipsing binary system
[NASA-CR-130923] 09 p1082 N73-18824
Ultraviolet photometry of eclipsing Cephei variable star by OAO 2
22 p2734 N73-31884
Light curve computations from astrophysical models of W Ursae Majoris systems
23 p2836 N73-32664
Photoelectric light curves of eclipsing binary star systems EE Aquarii and AE Phoenicis
23 p2837 N73-32667

**ECLIPTIC**
Tables listing 1970.0 ecliptic coordinates of hot stars
[COMMUN-27] 19 p2344 N73-28857

**ECOLOGICAL SYSTEMS**
U ECOLOGY

**ECOLOGY**
NT COASTAL ECOLOGY
Environmental and ecological impact of construction and operation of dam and impoundment on Sangamon River in Illinois
[E72-10216] 02 p0162 N73-11310
Effect of dam construction and staged filling of reservoirs in Illinois on environment and ecology
[E72-10217] 02 p0162 N73-11311
Analysis and interpretation of ERTS-1 ecologic, geographic, and agricultural data for Tennessee Valley
[E72-10231] 02 p0163 N73-11324
Feasibility of obtaining estimate of waterfowl production using remote sensing technology
[USGS-IR-215] 02 p0163 N73-11343
Mapping ecological effects of coal strip mining in Ohio
[E72-10256] 03 p0290 N73-12356
Environmental and ecological impact of construction and staged filling of reservoirs in Illinois
[E72-10309] 04 p0412 N73-13358
Application of remote sensing techniques for solution of ecological management problems
04 p0471 N73-13838
Development and characteristics of self-contained, portable data acquisition system for conducting marine and ecological research
04 p0471 N73-13842
Environmental and ecological effects of coal strip mining in Ohio
[E73-10003] 06 p0658 N73-15339
ERTS-1 imagery of geology, agriculture, hydrology, and ecology of Niger River Delta, Republic of Mali
[E73-10047] 07 p0777 N73-16309
Conference on environmental, social, economic, and ecological effects of nuclear electric power generation
[TID-25857] 07 p0793 N73-16450
Problems of environmental pollution and natural resource depletion caused by man
[JPRS-58113] 08 p0879 N73-17121
Environmental and ecological impact of construction and filling of reservoir on Sangamon River in Illinois
[E73-10082] 08 p0901 N73-17294
ERTS-1 imagery of wetlands ecology in Maryland, Georgia, and Chesepeake Bay test sites
[E73-10288] 08 p0915 N73-17494
Application of ERTS-1 data collection platform system in Arizona ecological test site
[E73-10332] 09 p1024 N73-18362
Application of ERTS-1 data collection system platforms in Arizona ecological test site
[E73-10333] 09 p1025 N73-18363
Application of NASA developed techniques, photographic film, and photographic equipment to ecological problems
[NASA-SP-5099] 09 p1034 N73-18437
Development of standards for classification, mapping and scientific analysis of land use and land use change in Central Atlantic Region Ecological Test Site using ERTS-1 imagery
[E73-10347] 10 p1148 N73-19346
Development of procedure and system for uniform mapping and monitoring of earth resources and environmental complexes using ERTS-1 imagery
[E73-10350] 11 p1275 N73-20344
Analysis of ERTS-1 photographic imagery for identification, definition, and mapping, of terrestrial ecosystems in interior Alaska
[E73-10399] 11 p1277 N73-20361
Ecological effects of coal strip mining in Ohio
[E73-10430] 11 p1281 N73-20391
Application of remote sensing to Pantano Wash for balance between environment and urban growth for Tucson
[NASA-CR-131279] 11 p1286 N73-20436
Environmental and ecological impact of construction and operation of Oakley Dam and Friends Creek impoundment located on Sangamon River in East Central Illinois
[E73-10484] 12 p1396 N73-21321
Prototype regional environmental information system based on ERTS-1 imagery of Central Atlantic Regional Ecological Test Site
[E73-10497] 12 p1397 N73-21333
Mapping wetlands ecology of Chesapeake Bay, South Carolina, and Georgia from ERTS-1 imagery
[E73-10507] 13 p1516 N73-22282
Ecology, hydrology, geomorphology, and terrain modeling of Colorado mountain environments from ERTS-2 data
[E73-10551] 14 p1655 N73-23424
Energetic role of trade wind inversion in tropical subalpine ecosystem
15 p1806 N73-24633
Environmental and ecological impact of construction and operation of Oakley Dam and Friends Creek impoundment located on Sangamon River in East Central Illinois
[E73-10655] 16 p1898 N73-25351
Application of ERTS-1 imagery to determine ecological effects of strip mining in eastern Ohio
[PAPER-E2] 19 p2268 N73-28266
Environmental and ecological impact of construction and operation of Oakley Dam and Friends Creek Impoundment located on Sangamon River in East central Illinois
[E73-10882] 20 p2394 N73-29233
Environmental and ecological impact of major construction of reservoirs in Illinois
[E73-10892] 20 p2395 N73-29241
Geological, hydrological, ecological, and agricultural mapping of Botswana from ERTS-1 photography
[E73-10928] 20 p2399 N73-29277
Geology, hydrology, and ecology of Botswana from ERTS-1 MSS imagery
[E73-10929] 20 p2399 N73-29278
Ecological forecasting and optimizing biosphere
[JPRS-59729] 20 p2409 N73-29364
Application of ecological, geological, and oceanographic ERTS-1 imagery to Delaware coastal resources management and planning
[E73-10934] 21 p2529 N73-30276
Analysis of geology, ecology, and hydrology of Colorado mountains from Skylab multispectral photography and data
[E73-11002] 22 p2659 N73-31307
Interdisciplinary analysis of Colorado Rocky Mountain environments using ADP techniques
[E73-11039] 23 p2778 N73-32218
Effect of construction and staged filling of Oakley Dam and Friends Creek impoundment in Illinois on environment and ecology
[E73-11124] 24 p2916 N73-33279

Influence of solar radiation on thermodynamic balance and biological processes of earth
24 p2975 N73-33770

ECONOMIC ANALYSIS
Economic analysis of reducing and controlling environmental noise
[PB-206726] 01 p0081 N73-10666
Computer model for determining economic impact of aircraft retrofit on airlines
[FAA-EQ-72-4-VOL-1] 02 p0245 N73-11988
Bibliography of economic impact of stimulated aerospace technology activity
[NASA-CR-129515] 03 p0366 N73-12981
Market research, economic analysis, and technology of conventional STOL aircraft in Europe
[DGLR-PAPER-72-54] 06 p0622 N73-15046
Catalog of economic, social, and educational institutions in Houston Area Test Site
[NASA-CR-128719] 07 p0856 N73-16944
Vehicle selection and economic analysis for European space tug
[HSD-TP-7227-APP-2] 10 p1216 N73-19894
European space tug development including analyses of performance, economics, weights, reliability, and costs
[HSD-TP-7264-VOL-6] 10 p1218 N73-19906
Economic analysis of integrated time-frequency system for aircraft
14 p1690 N73-23717
Application of cybernetics and systems analysis techniques to economic problems in USSR
[JPRS-58935] 15 p1845 N73-24951
Effect of scientific and technical progress on economic control parameters in USSR
[JPRS-58976] 15 p1845 N73-24952
Economic analysis of US aerospace/defense industry
[AD-763242] 22 p2738 N73-31921
Forecast model for predicting economic factors involved in short haul air transportation in California Corridor - Vol. 2
[NASA-CR-114634[1]] 23 p2859 N73-32843
Economic factors, financial management, production and marketing for air transport industry
[NASA-CR-135634] 23 p2860 N73-32848
Principles of functional economic analysis
23 p2860 N73-32854
Marketing and cost effectiveness in air transportation economics
23 p2860 N73-32855
Economic efficiency in pricing of air transport services
23 p2860 N73-32856
Competition effects on air transportation industry economics
23 p2861 N73-32858
Economic risk analysis for propeller STOL transport market
23 p2861 N73-32866
Regulatory policies of Civil Aviation Board for controlling operations of commercial airlines
23 p2864 N73-32891
Economic analysis of airline operating without Civil Aviation Board control and comparison with economic status of controlled airlines
23 p2864 N73-32892
Characteristics of Federal regulation of airline operations and predictions for type and extent of future regulation
23 p2864 N73-32894
Analysis of factors affecting future of commercial aircraft development to show effects on overall airline operations
23 p2865 N73-32900
Analysis of factors affecting operation of domestic airline to overseas areas
23 p2865 N73-32901

ECONOMIC DEVELOPMENT
Economic analysis of airline operating without Civil Aviation Board control and comparison with economic status of controlled airlines
23 p2864 N73-32892

ECONOMIC FACTORS
Measurement of research and development and technological progress impact on national economic growth - Part 1
[NASA-CR-129502] 03 p0366 N73-12980
Economic analysis of space shuttle transportation system based on tradeoffs, alternatives, and variations in spacecraft design - Vol. 1
[NASA-CR-129568] 04 p0487 N73-13977
Utilization of ERTS-1 imagery for evaluation of Iranian playas as potential locations for economic and engineering development
[E73-10067] 07 p0779 N73-16329
Ice problems in Canada, estimates of economic significance of problems, and order of priorities of research programs and management
[REPT-17] 07 p0788 N73-16412
Economic analysis on capital investment for transportation modes
[PB-212307] 07 p0860 N73-16976
Statistical supplement for capital investment in transportation modes
[PB-212308] 07 p0860 N73-16977
Economic feasibility analysis on San Francisco rapid transit system extension to serve airport
[PB-212456] 07 p0860 N73-16978
Conceptual framework for analysis for aiding policy analyst and policy researcher in empirical investigations into policy phenomena
[NASA-CR-130669] 08 p0976 N73-17982
Economic factors affecting titanium powder metallurgy research and development
09 p1047 N73-18539
Impact of radiometry and photometry on economic, social and environmental problems
[NBS-TN-594-4] 11 p1292 N73-20488
Technical and economic problems and possibilities of developing titanium powder metallurgy
[NLL-LTI-746-1336-[9022.401]]
12 p1411 N73-21438
Economic effectiveness of production planning and automatic control methods in industry
[JPRS-58680] 12 p1467 N73-21884
Long range operational factors affecting commercial aviation industry
13 p1472 N73-21917
Cold weather construction practices relative to men, materials, and equipment
[AD-745395] 13 p1506 N73-22206
Congressional study of future governmental role in scientific and technological research and development
13 p1594 N73-22927
Procedure for evaluating relative economic value of technology factors affecting design, configuration, and operation of hypersonic cruise transport
[NASA-CR-2286] 23 p2743 N73-31953
Economic market structure of airline industry
23 p2862 N73-32869
Analysis of short-haul air transportation requirements to include aircraft development programs, economic factors, and environmental considerations
24 p2871 N73-32935
Technical and economic aspects of airship transportation
[DLR-MITT-72-17] 24 p2879 N73-32989

ECONOMICS
NT DEMAND [ECONOMICS]
Effects of decision models and operational characteristics on economic expenses associated with use of predictive weather information
[NASA-CR-128401] 01 p0073 N73-10600
Relative economic advantages of 3 STOL aircraft concepts for short haul, high density transportation systems in 1980 time period
[NASA-CR-114466] 01 p0120 N73-10990
Airport planning, economics, computer program, and arena characteristics for short haul, high density transportation systems in 1980 time period
[NASA-CR-114467] 01 p0120 N73-10991
Joint meetings in Sweden on business economics, industrial economics, and scientific theory
[FOA-P-C-8280-10] 02 p0244 N73-11984
Utilization of ERTS-1 multispectral photography in evaluating Iranian playas as potential locations for economic and engineering development
[E72-10270] 03 p0291 N73-12369
Space technology for ground based economic support and investigating solar system origins
04 p0473 N73-13857
Projected space missions and space transportation system with payload and cost analysis for space shuttle system - Vol. 2
[NASA-CR-129571] 04 p0487 N73-13978
Analysis of economic merits of three alternative space transportation systems for use during 1980 time period - Vol. 3
[NASA-CR-129569] 04 p0487 N73-13979
Potential economic benefits of improvements in weather forecasting, using satellites and computers
[NASA-CR-129991] 05 p0571 N73-14635
Congressional hearings on earthbound potential utilization of solar energy
05 p0592 N73-14812
French aircraft development program including Concorde, Airbus, and Corvette, as well as economic study
06 p0622 N73-15045
Legal liabilities and impact of satellite meteorology on agricultural crops and economics
[NASA-CR-129994] 06 p0692 N73-15636
Impact of accurate long range weather forecasts on Wisconsin pea production
06 p0693 N73-15640
User manual for computer programs applied to community/airport economic development model - Vol. 3
[FAA-EQ-72-3-VOL-3] 06 p0732 N73-15971
Development of decision models for choosing techniques and procedures to obtain information for investment decisions in natural resources programs
07 p0783 N73-16363
Economic analysis of high density short haul air market to show aircraft requirements, engine development, and funding sources
[NASA-CR-2227] 10 p1106 N73-19017
Impact of technological progress on economic development
[NASA-CR-131289] 11 p1352 N73-20977
Role of USSR scientific centers in economic development
[JPRS-58683] 12 p1467 N73-21887
Psychological, physiological, and work hygiene problems in ergonomic technology
[JPRS-58792] 13 p1486 N73-22030
Statistical models for smoothing environmental economics and communications data
13 p1549 N73-22554
Optimum utilization of long range forecasts and climatology in making economic decisions
13 p1552 N73-22573
Problems of air transport economics and efficiency of air transport utilization in USSR
[NASA-TT-F-741] 16 p1860 N73-25069
Analysis of economics and finances of airport operations to determine procedures for improved management and operation
[REPT-73-01210] 16 p1884 N73-25253
Analysis of economic factors affecting operation of STOL aircraft for short-haul air transportation system - Vol. 5
[NASA-CR-114610] 19 p2219 N73-27902
Operational reliability and economics for instrumentation particularly electric pumps
[AD-762321] 19 p2306 N73-28545
Evaluation of Iranian playas as potential locations for economic and engineering development
[E73-11026] 22 p2662 N73-31330
Airport establishment and operation with emphasis on regional planning, social factors, and economic forces
23 p2863 N73-32877
Analysis of economic factors involved in air cargo operations and air cargo market development
23 p2863 N73-32881
Analysis of factors involved in developing market for air cargo services
23 p2863 N73-32882
Economic evaluation of aircraft and spacecraft
[JPRS-60104] 23 p2865 N73-32907

ECONOMY
Cosmization of Soviet economy
[NASA-TT-F-13958] 14 p1705 N73-23839
Methodological principles of economy of ocean
[JPRS-59741] 20 p2487 N73-29980

ECOSYSTEMS
Uniform mapping and monitoring of natural ecosystems and environmental complexes from ERTS-1 imagery
[E72-10185] 01 p0046 N73-10364
Identification, definition, and mapping of terrestrial ecosystems in interior Alaska
[E72-10343] 05 p0532 N73-14331
Development of system for mapping and monitoring natural ecosystems and environmental complexes from ERTS-1 imagery of California, Nevada, Four Corners Area, Louisiana, and Colorado Plateau
[E73-10289] 08 p0915 N73-17495
Identification, analysis, and mapping of terrestrial ecosystems and vegetation types in Alaska based on ERTS-1 imagery
[E73-10306] 09 p1022 N73-18338
Determination of ecosystem-vegetation boundaries from ERTS-1 imagery of Tennessee
[E73-10417] 11 p1279 N73-20379
Identification, definition, and mapping of terrestrial ecosystems in interior Alaska from ERTS-1 imagery
[E73-10634] 15 p1776 N73-24393
Mapping and monitoring natural ecosystems and environmental complexes and estimation of rice crop yield in California and Louisiana from ERTS-1 imagery
[E73-10669] 16 p1899 N73-25364
Uniform mapping and monitoring of natural ecosystems and environments in California, Louisiana, and Colorado from ERTS-2 imagery
[E73-10839] 19 p2290 N73-28417
Identification, definition, and mapping vegetation and terrestrial ecosystems in interior Alaska using ERTS-1 imagery
[E73-10921] 20 p2398 N73-29270
Hydrology of prehistoric farming systems in central Arizona ecotone from Skylab EREP data
[E73-11044] 23 p2779 N73-32220
Identification, definition, and mapping of terrestrial ecosystems in interior Alaska
[E73-11065] 23 p2781 N73-32241
Uniform mapping and monitoring of natural ecosystems and environmental complexes of Colorado Plateau and Sierra-Lahontan areas and estimation of rice crop yields in California and Louisiana
[E73-11070] 23 p2781 N73-32246
Correlation of ERTS-1 imagery signatures with water balance ecosystem and geology of select playa lake basins in West Texas
[E73-11102] 24 p2914 N73-33259

EDDIES
U VORTICES

EDDY CURRENTS
Optical measurements of thin slots milled in edges of aluminum alloy test blocks to determine accuracy of measurement and detectability by operators using high frequency probes
[ARL/MET-NOTE-82-PT-1] 02 p0186 N73-11506

Analysis of eddies and lift forces created on vertical circular cylinder by oscillatory flow conditions
[AD-748078] 03 p0287 N73-12329
Numerical and perturbation theory solutions for evaluating performance of eddy current flowmeters
[BNWL-SA-4236] 03 p0302 N73-12470
Analogous specimen-coil-arrangements in eddy current testing
[ARL/MET-REPT-88] 04 p0420 N73-13423
Calculation of interaction of penetratable shelter belts and ground air flow, including mean horizontal wind profiles and eddy viscosity coefficient
09 p1059 N73-18640
Research on atmospheric eddy transport.
[AD-757692] 14 p1663 N73-23496
Automatic scanning and display eddy current system for nondestructive testing of printed circuit boards
[ARL/MET-NOTE-84] 15 p1786 N73-24478
Magnetic particle inspection of large or irregularly shaped parts by assuring optimum magnetic flux densities
[AD-759207] 16 p1882 N73-25236
Eddy-current inspection for locating subsurface flaws in electrical conductors
19 p2303 N73-28522
Computational methods for determining eddy momentum, heat, and fluxes in water-adjoining layer of atmosphere
20 p2445 N73-29637

**EDDY DIFFUSION**
U TURBULENT DIFFUSION

**EDDY VISCOSITY**
Numerical solution of parabolic partial differential equations with reference to eddy heat conduction in ocean
[AD-746205] 02 p0167 N73-11362
Two dimensional eddy viscosity coefficients in atmospheric motion noting parameterization of clear air turbulence
05 p0573 N73-14658
Mathematical model for eddy viscosity in turbulent boundary layer on flat plates
07 p0771 N73-16262
Effectiveness of eddy viscosity models for coaxial and two-dimensional jets with and without coflowing stream
[AD-759576] 16 p1890 N73-25298
Compressible turbulent boundary layer solutions using eddy viscosity models
[AD-759164] 16 p1891 N73-25307
Kinematic eddy viscosity model which accounts for influence of density variations and preturbulence
19 p2252 N73-28159
Relationship between eddy-transport and second-order closure models for stratified media and for vortices
19 p2253 N73-28161
Predictions of axisymmetric free turbulent shear flows using generalized eddy viscosity approach
19 p2253 N73-28163
Local eddy viscosity model for turbulent shear flow
19 p2254 N73-28168

**EDEMA**
Centrineurogenic etiology for pulmonary changes of high altitude pulmonary edema
[AD-756940] 15 p1743 N73-24127
Measurement of pulmonary extravascular water volume during exposure to simulated high altitude
[AD-763355] 22 p2621 N73-31004

**EDGE DISLOCATIONS**
Application of Schwarz-Neumann alternating method to stress intensity solutions of edge and surface crack problems
[NASA-CR-112299] 11 p1345 N73-20912
Nonlinear deflections of circular plate with varying thickness
22 p2723 N73-31794

**EDGE LOADING**
Creep buckling of flat plates and cylindrical shells subjected to edge wise and uniform axial compression respectively
[AD-746475] 02 p0240 N73-11952
Solution of axisymmetric finite deformation equations for arbitrary shallow orthotropic shell of revolution subjected to uniform pressure and edge loading
13 p1584 N73-22844

**EDGES**
NT LEADING EDGES
NT SHARP LEADING EDGES
NT TRAILING EDGES
Effects of free edge shear stresses on failure of fiber-reinforced angle ply laminates
[AD-747343] 03 p0322 N73-12625

**EDITING ROUTINES [COMPUTERS]**
General purpose linkage editor for CDC 6000 series computers
[AD-764044] 22 p2725 N73-31809

**EDUCATION**
NT ASTRONAUT TRAINING
NT FLIGHT TRAINING
NT PILOT TRAINING
Legal restraints on dissemination of instructional materials by educational communications systems
[NASA-CR-129271] 03 p0366 N73-12983
Workshop for educating public to space benefits in education
04 p0474 N73-13867
Advances in educational communication and meteorology as derived from satellite technology
04 p0474 N73-13869
Design of systems for utilizing communication satellite data in education
04 p0474 N73-13873
Analysis of criteria for establishing air transportation curricula in community college based on manpower requirements and industrial needs
04 p0486 N73-13969
Proposals for application of data processing to education in Germany
[BMBW-FB-DV-72-05] 04 p0488 N73-13995
Development and application of computer programs as instructional methods for physics laboratory experiments
05 p0516 N73-14198
Vocational/technical and adult education, emphasizing status, trends, and issues related to electronic delivery
[NASA-CR-130532] 08 p0971 N73-17933
Cybernetic application of computers in personnel training
[AD-751145] 09 p0998 N73-18143
Development of scientific centers in USSR during past 50 years and considerations for future development
[JPRS-58596] 11 p1267 N73-20281
Utilization of ERTS-1 imagery as teaching and research tool in Department of Geology at University of Alaska
[E73-10403] 11 p1277 N73-20365
Training of scientists and engineers for German Department of the Defense
11 p1351 N73-20965
Electronic procedures for selecting and teaching students at Moscow Institute of Electronic Engineering
[JPRS-58550] 12 p1386 N73-21242
Mathematical models for educational planning and personnel selection in Soviet Union
[JPRS-58793] 12 p1419 N73-21497
Development of computerized training aid for research and development managers based on spacecraft design operations
[NASA-TN-D-7238] 12 p1466 N73-21880
Utilization of ERTS-1 data as teaching and research tool in Department of Geology at University of Alaska
[E73-10635] 15 p1776 N73-24394
Communication satellite systems for educational television vision
[NASA-TT-F-775] 15 p1845 N73-24953
Graduate education of administrators for public service
[NASA-CR-133036] 16 p1976 N73-25984
Utilization of ERTS-1 imagery as teaching and research tool in Department of Geology at University of Alaska
[E73-10841] 19 p2290 N73-28419
Design, development, and control of large scale educational telecommunication system using satellites
[NASA-CR-133646] 20 p2377 N73-29104
Geophysical meeting, third generation computers, and computer courses
[JPRS-59825] 21 p2609 N73-30911
Computer courses for professional training of programmers and operators
21 p2609 N73-30914
Flight instrumentation for academic acquisition of aircraft flight performance and characteristics
[AD-764479] 22 p2675 N73-31427
Canadian Armed Forces education impact on national development
[DRAE-37] 23 p2859 N73-32845
Delphi forecasts of utilization and social impacts of large-scale educational telecommunications technology
[NASA-CR-135477] 23 p2866 N73-32909
Skylab education program for high school students - Vol. 1
[NASA-EP-110] 24 p2980 N73-33811
Skylab education program for high school students - Vol. 2
[NASA-EP-111] 24 p2980 N73-33812

**EDUCATIONAL TELEVISION**
Satellite telecommunications systems for childhood education
[NASA-CR-133028] 16 p1869 N73-25131

**EEG [ELECTROENCEPHALOGRAMS]**
U ELECTROENCEPHALOGRAPHY

**EFFECTIVE PERCEIVED NOISE LEVELS**
Analysis of effective perceived noise level method for determining airport noise and comparison with actual noise measurements taken during aircraft landings
[UCLA-PAPER-ENG-0872] 03 p0249 N73-12010
Noise level surveys of seventeen general aviation aircraft including jet and propeller driven types
[FAA-EQ-73-1] 12 p1363 N73-21063
Aerodynamic tests and noise levels of slot nozzle with V gutter reverser for STOL
[NASA-TM-X-2758] 12 p1365 N73-21072
Analysis of common aircraft noise measures in terms of selected human response for jet transport aircraft
[FAA-RD-71-112] 12 p1365 N73-21074
Development of noise index based on slow and fast noise level variation perception, and applied to aircraft noise data
[REPT-3/1973] 19 p2220 N73-27911

**EFFECTIVENESS**
NT COST EFFECTIVENESS
NT SYSTEM EFFECTIVENESS
Pilot ground training proficiency of flight simulators
[AD-755681] 18 p2112 N73-27081
Effectiveness of braided wire electromagnetic shielding against magnetic field penetration
[AD-761823] 19 p2246 N73-28111

**EFFECTORS**
U CONTROL EQUIPMENT

**EFFERENT NERVOUS SYSTEMS**
Effects of radioprotective drugs on motor evacuatory functions in gastrointestinal tracts of healthy and irradiated rats
11 p1239 N73-20062

**EFFICIENCY**
NT COMBUSTION EFFICIENCY
NT COMPRESSOR EFFICIENCY
NT ENERGY CONVERSION EFFICIENCY
NT NOZZLE EFFICIENCY
NT POWER EFFICIENCY
NT PROPELLER EFFICIENCY
NT PROPULSIVE EFFICIENCY
NT THERMODYNAMIC EFFICIENCY
NT TRANSMISSION EFFICIENCY
Examination of man machine systems efficiency in relation to cost criteria
21 p2503 N73-30087
Coupling efficiency of GaAlAs diode pumped Nd-YAG laser
24 p2930 N73-33398

**EFFLUENTS**
Two-dimensional submerged slot jets to diffuse thermally buoyant water jets into moving water stream
[PB-213461/7] 14 p1651 N73-23395
Dispersion predictions for effluents from exhaust gases from Saturn 5 and Scout-Algol 3 launch vehicles
[NASA-TM-X-2935] 24 p2921 N73-33327

**EFFUSIVES**
NT LAVA

**EGGS**
Effect of sonic boom on fish and fish eggs during developmental stage
[FAA-RD-73-29] 11 p1247 N73-20121

**EIGENFUNCTIONS**
U EIGENVECTORS

**EIGENSTATES**
U EIGENVECTORS

**EIGENVALUES**
Perturbation theory for developing eigenvalues and eigenfunctions in power series expansion for Hill differential equation
02 p0195 N73-11581
Solution of boundary value problems by characteristics equations
[NASA-CR-129256] 03 p0324 N73-12637
Continuation method for solving eigenvalue problems and finding roots of polynomials
[TAE-152] 09 p1057 N73-18617
Methods for calculation of eigenvalues and eigenvectors of non-Hermitian matrices for dynamic structural analysis
[ISD-128] 09 p1095 N73-18937
Extension of combination shift QZ algorithm for solving generalized matrix eigenvalue problem
[NASA-TN-D-7305] 18 p2169 N73-27519
Matrix methods for determining nature of eigencurrents and eigenfields in conducting bodies
[AD-761456] 19 p2321 N73-28675
Variability of eigenvectors and eigenvalues using autocorrelation matrices of vertical temperature profiles on regional latitudes
[AD-763145] 21 p2539 N73-30360

**EIGENVECTORS**
Eigenfunctionals of linear Boltzmann transport operator in modal approximations
[APS-PH-87] 02 p0195 N73-11580
Perturbation theory for developing eigenvalues and eigenfunctions in power series expansion for Hill differential equation
02 p0195 N73-11581
Solution of boundary value problems by characteristics equations
[NASA-CR-129256] 03 p0324 N73-12637
Statistical eigenfunctions used for analysis and prediction of sea level surges
04 p0443 N73-13611
Methods for calculation of eigenvalues and eigenvectors of non-Hermitian matrices for dynamic structural analysis
[ISD-128] 09 p1095 N73-18937
Intermediate problem technique used to generate difficult eigenvector and boundary value problem solutions
[AD-756672] 13 p1550 N73-22561

Variability of eigenvectors and eigenvalues using autocorrelation matrices of vertical temperature profiles on regional latitudes
[AD-763145] 21 p2539 N73-30360
Applications of eigenfunctions for solution of boundary value problems in orbital mechanics
[BMBW-FBW-72-17] 22 p2718 N73-31758

**EINSTEIN EQUATIONS**
Development of cosmological models based on Einstein field equations with random perturbations of long wave lengths superimposed on unperturbed models
[AD-747505] 03 p0357 N73-12911
Universal repulsive component in gravity
[ORO-3992-94] 05 p0539 N73-14385
Global investigation of Einstein space of maximal mobility and Petrov Type 2
[ITF-72-140-P] 15 p1804 N73-24618
Spherical and nonspherical gravitational collapse and Schwarzschild black holes
15 p1829 N73-24822
Wave and Einstein equations for studying scaler waves and tensor perturbations in Mixmaster Universe
15 p1829 N73-24823
Global structure of highly mobile Einstein space of Petrov Type T3
[ITF-72-117-P] 15 p1832 N73-24849
Event horizon and T-S solutions to Einstein vacuum field equation
[RIFP-177] 16 p1934 N73-25652

**EJECTION**
NT STELLAR MASS EJECTION

**EJECTION INJURIES**
Nonfatal ejection vertebral fracture comparison between US, British, and Swedish armed services
14 p1611 N73-23059

**EJECTION SEATS**
Development of fluidic control system for stabilizing aircraft ejection seat in pitch plane during rocket motor burn portion of ejection sequence
[AD-747630] 03 p0254 N73-12056
Aircrew escape autogyro ejector seat/flight vehicle
09 p1089 N73-18890
Pilot knee ejection clearances for Canadian military aircrafts
[DCIEM-936] 23 p2741 N73-31938
Proceedings of symposium to determine requirements and configurations of emergency ejection systems for helicopter crews
[AGARD-AR-62] 23 p2743 N73-31954

**EJECTORS**
Analysis of critical conditions of gas ejectors at large pressure drops within framework of ideal-gas dynamics
[AD-750536] 06 p0656 N73-15328
Designs and performance predictions for high performance supersonic ejector systems
[AGARDOGRAPH-163] 08 p0895 N73-17248
Conservation equations for analyzing supersonic and mixing flow regimes of supersonic ejectors
08 p0895 N73-17249
Procedure for predicting performance characteristics of second throat diffusers in ejector systems
08 p0895 N73-17250
Ejector flow model for predicting performance characteristics of supersonic ejector systems
08 p0896 N73-17251
Semiempiricial methods for designing ejectors for various applications
08 p0896 N73-17252
Theory of two phase gas-liquid and liquid-gas flow for bladed machines and ejectors
[AD-755713] 12 p1409 N73-21419
Four VTOL propulsion concepts compared parametrically for subsonic applications with three types of aircrafts
[NASA-TM-X-68279] 20 p2466 N73-29810
Static tests of cylindrical ejectors using afterburning turbojet gas generators
[NASA-TM-X-52565] 23 p2830 N73-32622

**EKMAN LAYER**
U BOUNDARY LAYER TRANSITION

**EL SALVADOR**
Volcano and earthquake surveillance network in Alaska, California, Washington, Hawaii, El Salvador, Nicaragua, Iceland, and Guatemala
[E73-10337] 09 p1025 N73-18365
Prototype DCP volcano surveillance network in Washington, Nicaragua, California, Guatemala, Hawaii, El Salvador, Iceland, and Alaska
[E73-11024] 22 p2662 N73-31328

**ELASTIC ANISOTROPY**
Numerical analyses on elastic displacement field and point defect interactions in anisotropic cubic crystals
[JUL-836-FF] 10 p1200 N73-19767
Finite element methods used for characterizing linear, anisotropic elastic solids
[AD-756513] 13 p1587 N73-22869

**ELASTIC BARS**
Numerical analysis of torsion characteristics of bar with constant section in shape of circular ring or circular sector
[NLL-DRIC-TRANS-2995-[3623.66]]
15 p1837 N73-24885

**ELASTIC BENDING**
Elastoplastic bending of cracked plates including effects of crack closure
[NASA-CR-112268] 09 p1092 N73-18915

**ELASTIC BODIES**
Procedures for calculating sonic fields radiated and diffracted by elastic bodies and passage of sound through elastic plates and shells - Vol. 1
[JPRS-58146-1-PT-1] 09 p1015 N73-18283
Procedures for calculating sonic fields radiated and diffracted by elastic bodies and passage of sound through elastic plates and shells - Vol. 2
[JPRS-58146-2-PT-2] 09 p1015 N73-18284
Stability of thin elastic tube of infinite length containing rotating inviscid, incompressible fluid flow
13 p1508 N73-22222
Behavior of cantilevered beam of elastic foundation subjected to following force
[NASA-CR-131608] 13 p1588 N73-22877
Modal analysis for Liapunov stability of rotating elastic bodies
[NASA-CR-124258] 15 p1839 N73-24904
Device for measuring tensile forces applied to tension members
[NASA-CASE-MFS-21728-1] 16 p1912 N73-25467
Nonlinear forced vibrations of elastic structures excited by disturbing force as harmonic function of time
[AD-758810] 16 p1970 N73-25934
Stress analysis of elastic plane containing elastic inclusion using singular integral equations
[NASA-CR-132272] 17 p2093 N73-26934
Analysis of state of mechanically heterogeneous material during deformation using optically sensitive coatings
[NLL-M-21653-[5828.4F]] 21 p2602 N73-30856
Application of finite element analysis techniques to determine characteristics of curved elements in thin, elastic shells
24 p2987 N73-33872

**ELASTIC BUCKLING**
Approximation of beam buckling mechanics using axial and transverse loads
[AD-745881] 02 p0219 N73-11775
Flexural deformation of laminated beams subjected to initial stresses
[AD-750574] 05 p0604 N73-14912
Buckling of flat isotropic plates under uniaxial and biaxial loading
[ESDU-72019] 06 p0724 N73-15908
Experimental analysis of buckling of integrally ring stiffened cylindrical shells under axial compression to determine influence of shell and ring geometry on applicability of linear theory
[AD-755392] 13 p1588 N73-22872
Structural stability tests studying buckling of rectangular boron reinforced aluminum plates
[ENSMP-007] 15 p1840 N73-24907
Nondestructive methods determining composite beam and plate critical loading
[ENSMP-010] 17 p2094 N73-26940
Analysis of buckling behavior of viscoelastic structural member
[PB-221835/2] 22 p2726 N73-31817

**ELASTIC COLLISIONS**
U ELASTIC SCATTERING

**ELASTIC CONSTANTS**
U ELASTIC PROPERTIES

**ELASTIC CYLINDERS**
Analysis of short time response of cylindrical, elastic segment to shock wave engulfment based on focusing effects due to curved geometry
[AD-745962] 02 p0238 N73-11940
Design, development, and testing of foldable beryllium copper alloy elastic tubes for hinges on satellite booms
[ESRO-CR-65] 19 p2346 N73-28874
Application of Galerkin method in nonconservative stability problems relating to thin elastic plates and slender elastic rods
[NRC-TT-1673] 21 p2603 N73-30860

**ELASTIC DAMPING**
Elastic gyro rotor with stable orientation of readout axis by point mass system
07 p0817 N73-16623
Variational method for approximate solutions to elastic stability problem with dissipative forces
[AD-754532] 11 p1346 N73-20918

**ELASTIC DEFORMATION**
NT ELASTIC BENDING
NT ELASTIC BUCKLING
Strain rate and temperature dependence of glass fiber reinforced and unreinforced epoxy resins and deformation mechanisms
[REPT-1040/72] 01 p0069 N73-10568
Computation of tensile stress in shackles assuming elastic deformation
[NPL-NAC-17] 02 p0179 N73-11447
Validity of generalized theory of small elastico-deformations
[AD-747296] 02 p0241 N73-11957
Analysis of defects in metals produced by high speed extrusion
[AD-752867] 09 p1041 N73-18488
Approximative prediction for elastic collapse of spherical shell with flat spot region under external pressure
[NASA-CR-130961] 09 p1096 N73-18946
Constitutive equations for determining elastic deformation twinning in body centered cubic lattice metals at low temperatures
[AD-757042] 14 p1679 N73-23624
Stability of various equilibrium states in cubed incompressible neo-Hookean material subjected to pure homogeneous deformation
[AD-758700] 16 p1970 N73-25937
Numerical technique for determining thermo-elastic deformations in segment of hollow cylinder subjected to varying forces
[AECL-4308] 17 p2094 N73-26939
Velocities of elastic waves during deformation and failure of rocks under compression
[AD-759393] 18 p2149 N73-27374
Development of method for predicting crater profiles produced in ductile materials by impact of rigid projectiles at ballistic velocities
[DREV-R-686/73] 18 p2203 N73-27782
Constitutive equations for studying finite elastic-plastic deformation of ductile metals
[AD-761635] 19 p2310 N73-28578
Effect of elastic deformation of gimbal suspension on motion of gyroscope
20 p2418 N73-29424
Bending stresses produced by internal pressure in thin walled hollow cylinders with out-of-round cross section
[NLL-CE-TRANS-6040-[9022.09]]
20 p2478 N73-29902
Influence of elastic deformation of gimbal suspension on frequency of nutation of gyroscope
21 p2547 N73-30421
Analysis of ductile flow of metal during extrusion process with application to manufacture of cable sheathing
[NLL-M-21661-[5828.4F]] 21 p2557 N73-30498
Fourth order partial differential equations governing deformation of circular cylindrical shells
[AD-764560] 23 p2854 N73-32809

**ELASTIC MEDIA**
Application of periodic Dirichlet problems to analysis of planar theory of elasticity
[AD-741924] 01 p0115 N73-10948
Development of computer programs to provide finite element method solutions to problems involving elastic and inelastic structures
[AD-746175] 02 p0239 N73-11942
Structural analysis of two bonded half planes with finite crack perpendicular to and passing through interface
[NASA-CR-2181] 07 p0852 N73-16910
Analysis of particle erosion of solid surfaces using model of erosion pit nucleation and growth for solid spherical particles impacting on plane surface of elastic half space
[AD-752221] 08 p0935 N73-17657
Procedures for calculating sonic fields radiated and diffracted by elastic bodies and passage of sound through elastic plates and shells - Vol. 1
[JPRS-58146-1-PT-1] 09 p1015 N73-18283
Procedures for calculating sonic fields radiated and diffracted by elastic bodies and passage of sound through elastic plates and shells - Vol. 2
[JPRS-58146-2-PT-2] 09 p1015 N73-18284
Effects of circular inclusion of different elastic material on stress stage of cracked flat plates
[AD-754211] 10 p1222 N73-19936
Seminumerical analysis of three dimensional elastic properties of finite geometry solids with traction-free cracks
[NASA-TN-D-7213] 11 p1345 N73-20917
Construction of discrete models of nonlinear wave phenomena in elastic rods based on finite element analysis of shock waves in hyperelastic solids
[AD-754953] 11 p1346 N73-20921
Energy release integral equation for finite elastic and viscoelastic materials
[CONF-720930-1] 12 p1463 N73-21851
Ray tracing method for kinematic analysis of mechanical waves in nonlinear elastic materials
[AD-760438] 17 p2096 N73-26955
Development of method for predicting crater profiles produced in ductile materials by impact of rigid projectiles at ballistic velocities
[DREV-R-686/73] 18 p2203 N73-27782
Technique for dealing with problem of elastic domain containing arbitrarily oriented internal crack
[NASA-CR-132289] 20 p2482 N73-29937

**ELASTIC MODULUS**
U MODULUS OF ELASTICITY

**ELASTIC PLATES**
Curves for determining maximum elastic stresses and deflections for initially flat circular plates of uniform thickness under uniform pressure with various edge conditions
[ESDU-65002] 01 p0112 N73-10923
Buckled states of thin, flat, rectangular elastic plate subjected to constant compressive thrust
[AD-744993] 01 p0113 N73-10938

Measurement of sound generated by impingement of turbulent jet on elastic plates
[DGLR-PAPER-72-85] 04 p0373 N73-13032
Calculation of harmonic vibrations of elastic rectangular plates supported at two edges and reinforced vertically with eccentric ribs
[AD-748906] 04 p0483 N73-13944
Buckling analysis of elastic plate floating on water and stressed uniformly along periphery of internal hole
[AD-750594] 06 p0728 N73-15943
Principal relationships of theory of elastic orthotropic plates of variable rigidity with consideration of transverse shear
[AD-752708] 09 p1095 N73-18942
Application of vibrational methods for solving problems on theory of elasticity
[AD-754668] 11 p1346 N73-20922
Adhesive shear stress distribution in elastic plates reinforced by orthotropic elastic layer
[NASA-CR-132273] 17 p2093 N73-26933
Extensional equations of motion of isotropic, elastic plate, using Legendre polynomials
[AD-760325] 17 p2096 N73-26957
Acoustic pressure radiation from infinite elastic plate excited by point source
19 p2320 N73-28666
Application of Galerkin method in nonconservative stability problems relating to thin elastic plates and slender elastic rods
[NRC-TT-1673] 21 p2603 N73-30860
Elastic plate model for earthquakes
22 p2737 N73-31912
Response of laminated elastic plate to planar impact loads using vibratory modes to develop transient response solution
23 p2853 N73-32795
Dynamic analysis of free vibrations of rectangular elastic plate with central circular hole
[AD-765361] 23 p2855 N73-32816

**ELASTIC PROPERTIES**
NT AEROELASTICITY
NT ANELASTICITY
NT DYNAMIC MODULUS OF ELASTICITY
NT ELASTOPLASTICITY
NT HYDROELASTICITY
NT MAGNETOSTRICTION
NT MODULUS OF ELASTICITY
NT PHOTOELASTICITY
NT PROPORTIONAL LIMIT
NT THERMOELASTICITY
NT THERMOVISCOELASTICITY
NT VISCOELASTICITY

Elastic properties determination of crystals by sound velocity measurements
[AD-745859] 01 p0089 N73-10733
Elastic stresses in single lap joints under compression or tension
[ESDU-67008] 01 p0111 N73-10920
Numerical analysis of elastic stresses and deflections of helical compression springs made of round wire
[ESDU-65005] 01 p0112 N73-10926
Analysis of factors affecting choice of material and manufacturing methods for production of helical compression springs
[ESDU-65006] 01 p0112 N73-10927
Structural dynamic behavior of laminated plates and shells composed of bonded elastic orthotropic layers
[AD-745336] 01 p0114 N73-10944
Elastic interface pressure and stress calculations on assemblies of shafts with interference-fit collars
[ESDU-68004-PT-3] 02 p0177 N73-11433
Cross axis behavior of circular elastic diaphragm accelerometers
[REPT-519] 02 p0177 N73-11438
Complex variable method of planar elastic stress for lubricated rectangular seal
02 p0178 N73-11444
Development of methods for determining relationships between shapes of creep curves and changes in structure of metal specimens by exponential function of real order
[NLL-NEL-TT-2404-[6075.461]]
02 p0185 N73-11498
Analysis of vibration characteristics of laminated plates and modifications of plate theory to produce results consistent with continuum theory
[AD-746951] 02 p0240 N73-11949
Time dependent inelastic behavior of metals and metal structures
[AD-746340] 02 p0240 N73-11951
Development of formula for calculating natural frequencies of cantilever plate in fluid medium
[AD-747206] 02 p0241 N73-11958
Recovery of elastic properties and internal friction of hydrostatically extruded molybdenum with 0 to 80 percent deformation
[AD-747515] 03 p0317 N73-12586
Numerical analysis of dynamic buckling modes of elastic systems under intensive loading in finite time segment
03 p0360 N73-12937
Variational principles of elastic theory
03 p0360 N73-12938
Conference on mechanics of deformed solids
[AD-748046] 03 p0362 N73-12954
Influence of elastic properties of human body on arterial blood pressure measurement
05 p0500 N73-14072
Elastic properties and internal friction of hydrostatically extruded molybdenum
[AD-749539] 05 p0563 N73-14574
J integral relationship between elastic stress and concentration factors for inelastic fracture criterion of sharp notch
[CONF-720806-2] 05 p0569 N73-14617
Dynamic theory of crystal lattices and linear theory of elasticity and piezoelectricity
[AD-749111] 05 p0588 N73-14780
Application of three dimensional theory of elasticity to dynamic response of freely supported circular cylindrical shell
06 p0725 N73-15921
Application of Ritz-Galerkin method and complementary energy to problems in theory of nonconservative elastic stability
[AD-750575] 06 p0729 N73-15945
Nonlinear electroelastic equations for small fields superposed on bias
[AD-751624] 07 p0853 N73-16914
Variable principle for analyzing torsion of fluted bar with rope like cross section
[AD-752059] 08 p0928 N73-17598
Effect of degree of saturation on susceptibility to onset of plastic instability in pure shear for solid solution of copper-zinc system
[COO-2048-6-PT-2] 08 p0967 N73-17901
Experimental and analytical determination of elastic constants for some fiber reinforced composite materials
[AD-753575] 09 p1055 N73-18602
Photoelastic analysis of plane polyester specimens containing fatigue crack to determine effect of plastic yielding on stress distribution near crack
[TAE-155] 09 p1093 N73-18923
Application of theoretical framework of governing equations and extremum principles to classical elasticity and plasticity yield-point problems
[AD-753137] 09 p1096 N73-18948
Elastic-plastic behavior of thick-walled circular cylinders under internal pressure
[AD-753121] 09 p1097 N73-18952
Modification of Ber and Friedman mathematical theory of elasticity
10 p1172 N73-19536
Ultrasonic measurements of elastic constants of polycrystalline alloys of iron in vanadium
[AD-753615] 10 p1174 N73-19547
Fatigue tests to determine plastic deformations in composite materials
10 p1219 N73-19913
Stability criteria for incompressible elastic materials
[AD-753459] 10 p1221 N73-19931
Stress analysis of elastoplastic state of thin circular plate subjected to axisymmetric loading
[AD-753983] 11 p1346 N73-20920
Calculation of polymer elastic constants using sound speed measurements
[AD-755695] 12 p1429 N73-21586
Analysis of elastic properties of Invar and Elinvar alloys at various temperatures
13 p1540 N73-22480
Investigation of cracks in radial plane of solid right circular cylinder
13 p1584 N73-22841
Stress distribution in lap joints under cleavage and tension-shear loading conditions
13 p1584 N73-22843
Analysis of large deflections of rectangular plates with nonlinear elasticity and hollow shells with hinge-supported edges under external normal pressure uniformly distributed over surface
[AD-756103] 13 p1587 N73-22870
Application of trilinear coordinates to boundary value problems in plane elasticity
[AD-755181] 13 p1588 N73-22876
Influence of epoxide resin space lattice thickness on dynamic modulus of elasticity
[NASA-TT-F-14913] 14 p1680 N73-23633
Effects of O2 on mechanical properties, elastic limit, and tension resistance of nonferrous metals
[EURISOTOP-59] 15 p1798 N73-24577
Effects of elasticity on lunar rotation
[NASA-CR-132046] 15 p1831 N73-24844
Circular geometry and mixed boundary value problems in three dimensional elasticity
[NASA-TN-D-7266] 15 p1837 N73-24891
Stability of loaded equilibrium configuration of elastic bodies
[AD-757856] 15 p1841 N73-24917
Effects of wing structural elasticity on accumulation of fatigue damage during aircraft flight in turbulence
[AD-759634] 16 p1862 N73-25082
Elastic and mechanical properties of Al-Li alloy
[AD-759423] 16 p1931 N73-25625
Temperature dependence of elastic constants and Debye temperature of NaCl and KCl single crystals
[NASA-TT-F-14932] 16 p1933 N73-25801
Effect of microstructure on elastic limit of low carbon alloy and low carbon steels
[RAE-LIB-TRANS-1700] 17 p2044 N73-26534
Analysis of structural stability of shells weakened by holes to develop numerical analysis of stress concentration
17 p2093 N73-26929
Forced vibrations of disturbed elastic systems during random loading
[AD-759866] 17 p2095 N73-26950
Elastic properties of oxides and application for temperature compensated materials with large piezoelectric moduli
[AD-760766] 18 p2190 N73-27681
Response of thick rectangular plate of incompressible, isotropic elastic material to tensile forces applied to opposite faces
[AD-761941] 19 p2350 N73-28903
Performance tests to determine fore and aft elastic response characteristics of aircraft tires with bias ply, bias-belted, and radial-belted design
[NASA-TM-X-69570] 20 p2360 N73-28987
Analysis of physical and mechanical properties of nonmagnetic steels and suitability for producing tubes and forgings
[NLL-M-21647-[5828.4F]] 20 p2422 N73-29451
Analysis of effects of plastic deformation on internal structure of austenitic steels as shown by anomalies in tensile stress-strain curves
[NLL-M-23029-[5828.4F]] 20 p2428 N73-29504
Analysis of relationships of dissociation elasticity of vanadium mononitride to composition and temperature based on thermodynamic theory of nonstoichiometric compounds
[NLL-M-21638-[5828.4F]] 20 p2428 N73-29506
Elastic stress analysis of aluminum-epoxy plate with crack normal to interfaces
20 p2478 N73-29901
Modified particle in cell method for solving two dimensional nonlinear elasticity problems
[AD-762362] 20 p2483 N73-29948
Elastic and shape memory properties of beta-brass alloys at various temperatures
[AD-764472] 22 p2686 N73-31515
Linear and nonlinear theory of elasticity used to determine deformation of cylinder and piston of high strength steel under influence of high pressure
[AD-763971] 22 p2687 N73-31519
Nonlinear elastic and thermoelastic properties of single crystals of refractory materials
[COO-3418-9] 22 p2689 N73-31535
Effect of oxides on elastic properties of glasses
[AD-764080] 22 p2689 N73-31539
Elastic constants for calculating parallel Shockley partial dislocations in ordered alloys and intermetallic compounds
23 p2803 N73-32420
Elastic constants and electrical transition in Ti2O3 and V doped Ti2O3
23 p2824 N73-32577
Elastic-plastic theory at finite strain
[AD-764557] 23 p2855 N73-32815
Analysis of equations of finite elasticity to show nonapplicability of rest state constraint associated with strain energy function
[AD-764667] 23 p2855 N73-32817
Chemical and elastic properties of fluorinated polyurethanes
[NASA-CASE-NPO-10767-1] 24 p2891 N73-33076
Attitude stability of spinning elastic bodies based on modal analysis and criteria for idealized spinning flexible spacecraft
24 p2950 N73-33564
Temperature dependence of second-order elastic constants of cubic crystalline materials derived on basis of quasiharmonic anisotropic continuum model
24 p2968 N73-33717

**ELASTIC SCATTERING**
Asymptotic behavior of elastic form factors and light cone expansion for matrix elements
[TR-73-039] 01 p0083 N73-10683
Formula for calculating intensity of elastic and inelastic X ray scattering in crystal lattice of vanadium
[NASA-TT-F-13913] 06 p0708 N73-15775
Elastic scattering of He on LiF crystal surfaces
[NRC-TT-1652] 17 p2072 N73-26764
Angular distributions of elastically and inelastically scattered 42 MeV alpha particles from Cu-65
[NASA-TN-D-7354] 18 p2181 N73-27611
I.S.R. elastic proton-proton scattering data and Gribovs Reggeon calculus
[LPTHE-73/13] 20 p2456 N73-29737
Regularity in dip positions of elastic differential cross sections
[LPTPE-73/18] 20 p2456 N73-29741

**ELASTIC SHEETS**
Application of dynamic photoelasticity to analyze crack branching in homalite sheets
[AD-744661] 01 p0114 N73-10940
Frictionless plane contact between elastic layer on elastic half space with compression loads by frictionless rigid stamp
[WB-1/72] 09 p1040 N73-18478

Static and dynamic analyses on fracture mechanics of polyester plastic sheet
[AD-749098] 09 p1097 N73-18954
Optimum edge reinforcement around a circular hole in a flat elastic sheet subjected to axial tensile stress
[ARC-R/M-3723] 21 p2604 N73-30869
ELASTIC SHELLS
Algorithm for underwater echo signals from elastic spherical shell subjected to incident pulse
[AD-746220] 01 p0082 N73-10676
Influence of reference geometry on response of elastic shells within scope of nonlinear theory of elastic Cosserat surface
[AD-745291] 01 p0114 N73-10942
Numerical analysis of natural vibration modes of thin elastic shells to determine orthogonality of reactions
04 p0481 N73-13931
Recent results in general theory of elastic shells
[AD-749091] 05 p0603 N73-14907
Stress deformation in anisotropic elastic thin walled shells
[AD-749955] 05 p0604 N73-14911
Analysis of external loads and states of deformation in light elastic structures
[PB-212011] 07 p0852 N73-16911
Mathematical model to predict scattering of plane acoustic wave from elastic spherical shell with different fluid media inside and out
[AD-752760] 09 p1067 N73-18708
Dimensions and mechanical properties of elastic spherical shells measured by sound echo signals
10 p1188 N73-19667
Shell theories by direct approach based on Cosserat surface theory
[AD-754803] 11 p1346 N73-20924
Higher order theories and solution techniques for moderately thick shells of revolution using Reissner Theory and Legendre functions
13 p1584 N73-22842
Numerical analysis of resonance interactions in dynamic stability of elastic shells under compression
[AD-756237] 14 p1715 N73-23918
Approximate method for calculating echo signal of finite spherical pulse from elastic cylindrical shell in compressible fluid
16 p1969 N73-25928
Effect of imperfections on behavior of thin elastic shells subject to loads
[AD-761448] 19 p2349 N73-28899
Impact of thin elastic circular shell on surface of compressible fluid
[AD-763259] 21 p2526 N73-30252
Wave propagation in thin elastic shells
22 p2723 N73-31793
Nonlinear analysis for thin elastic shells using modal expansion method of linear vibration analysis extended to nonlinear analog
23 p2852 N73-32793
Optimal design of submerged elastic cylindrical shells for maximum pressure
[AD-764578] 23 p2855 N73-32814
ELASTIC STABILITY
U DAMPING
ELASTIC STRENGTH
U PROPORTIONAL LIMIT
ELASTIC SYSTEMS
Application of vibrational methods for solving problems on theory of elasticity
[AD-754668] 11 p1346 N73-20922
Comparison of effectiveness of yielding and elastic restraint systems for crash protection to show effects of slack and yield at constant load
[ARL/SM-382] 15 p1837 N73-24890
Derivation of differential equations of motion to analyze characteristics of three degree of freedom bodies joined by elastic tether
[NASA-CR-124259] 15 p1839 N73-24903
ELASTIC WAVES
NT AERODYNAMIC NOISE
NT AIRCRAFT NOISE
NT BAROCLINIC WAVES
NT COMPRESSION WAVES
NT DETONATION WAVES
NT DILATATIONAL WAVES
NT ELECTROSTATIC WAVES
NT ENGINE NOISE
NT GRAVITY WAVES
NT IONIC WAVES
NT JET AIRCRAFT NOISE
NT LAMB WAVES
NT LOVE WAVES
NT MAGNETOACOUSTIC WAVES
NT MAGNETOELASTIC WAVES
NT MAGNETOHYDRODYNAMIC STABILITY
NT MAGNETOHYDRODYNAMIC WAVES
NT NOISE (SOUND)
NT NORMAL SHOCK WAVES
NT OBLIQUE SHOCK WAVES
NT P WAVES
NT PHONONS
NT PLASMA WAVES
NT RAYLEIGH WAVES
NT S WAVES
NT SEISMIC WAVES
NT SHOCK WAVES
NT SONIC BOOMS
NT SOUND WAVES
NT STRESS WAVES
NT ULTRASONIC RADIATION
Reflection and transmission of large amplitude shockless waves at interface with semi-infinite medium
[AD-746642] 04 p0483 N73-13947
Elastic waves in reinforced composite materials
[AD-750983] 06 p0689 N73-15613
Elastic wave propagation in cylindrical shells
[NASA-CR-112222] 06 p0724 N73-15909
Lateral inertia effects on elastic-plastic wave propagation in slender rods
[AD-750102] 06 p0728 N73-15938
Attenuation of surface elastic waves as related to mass defects and applied to lunar geology
08 p0958 N73-17837
Analysis of linear elastic wave propagation normal to laminations of periodically laminated porous composite
[AD-753900] 10 p1221 N73-19934
Application of finite element method to stress wave in plates
[NASA-CR-112294] 11 p1345 N73-20911
Experimental verification of output signal to noise ratio and time of arrival estimate of tapped delay line matched filter using surface elastic waves
12 p1377 N73-21171
Elastic and piezoelectric surface waves guided by thin films
[AD-758688] 15 p1823 N73-24776
Analysis of large amplitude elastic wave interaction in bounded medium
16 p1968 N73-25919
Bulk elastic wave signals and design of acoustic filter
[AD-760020] 17 p2006 N73-26223
Ray tracing method for kinematic analysis of mechanical waves in nonlinear elastic materials
[AD-760438] 17 p2096 N73-26955
Velocities of elastic waves during deformation and failure of rocks under compression
[AD-759393] 18 p2149 N73-27374
Plane elastic wave propagation through movable wall, calculating flow distribution behind wall
[DLR-FB-72-59] 21 p2525 N73-30246
ELASTICITY
U ELASTIC PROPERTIES
ELASTICIZERS
U PLASTICIZERS
ELASTODYNAMICS
NT ELASTIC DAMPING
NT ELASTOHYDRODYNAMICS
Elastic structural models for dynamics and control of advanced space vehicles
[NASA-CR-124272] 16 p1967 N73-25908
ELASTOHYDRODYNAMICS
Analytical method to compute squeeze film thickness, pressure, and load relations between rigid ball and rigid groove when lubricated by fluid with exponential pressure-viscosity relationship
[NASA-CR-2139] 01 p0062 N73-10506
Elastohydrodynamic analysis using power law pressure-viscosity relation
[NASA-TN-D-7121] 06 p0677 N73-15507
Elastohydrodynamic traction measurements and lubricant film thickness determination for high speed rolling-sliding contacts
[AD-750752] 06 p0678 N73-15520
Analysis of electrical contact occurrences between rolling surfaces with application to elastohydrodynamic lubrication
[NASA-TN-D-7134] 06 p0690 N73-15620
Surface roughness effects on elastohydrodynamic lubrication
[NASA-CR-2195] 07 p0804 N73-16522
Analysis of parameters and elastohydrodynamic principles affecting lubrication of transmission components with application to helicopter mechanical drive systems
[NASA-TM-X-68215] 12 p1364 N73-21069
Rheological behavior of lubricant in rolling and sliding elastohydrodynamic lubricated contact
[NASA-CR-2206] 12 p1408 N73-21413
Elastohydrodynamic theory for predicting spin friction of ball in nonconforming groove, using rheological model
[NASA-TN-D-7280] 15 p1790 N73-24514
Modification of spinning torque apparatus to measure spinning torque on cageless ball thrust bearing using oil jet lubrication or thin surface film only
[NASA-TN-D-7356] 17 p2038 N73-26484
Development of empirical elastohydrodynamic film thickness formula for predicting minimum film thickness occurring in heavily load contacts
[NASA-TM-X-68267] 18 p2155 N73-27411
Measurement of spinning and rolling torques in angular-contact ball bearing with and without cages under several lubrication regimes
[NASA-TM-X-68271] 18 p2155 N73-27414
ELASTOMERS
NT CHLOROPRENE RESINS
NT VITON RUBBER [TRADEMARK]
NT VULCANIZED ELASTOMERS
Cataloging elastomer stiffness and damping properties in terms of viscoelastic model constants
[NASA-CR-120965] 01 p0113 N73-10931
Preparation of thermally and chemically stable fluoropolymers
[AD-747257] 02 p0139 N73-11121
Sulfur and MOCA cured polyurethane elastomer resistance to water, STF, and STF/water mixture
[ERDE-TR-83-PT-2] 02 p0192 N73-11555
Chemical and physical properties of three petroleum resistant elastomers suitable for use under low temperature conditions
[AD-745900] 02 p0194 N73-11569
Assessment of materials compatibility data for hydrazine monopropellant propulsion systems of space shuttle vehicle in multicycle extended life applications
[NASA-CR-128491] 02 p0221 N73-11788
Elastomer inertia effects in compliant surface bearings
[AD-747666] 03 p0309 N73-12524
Elastomer viscoelasticity effects in compliant surface bearings
[AD-747667] 03 p0309 N73-12525
Synthesis of polyfluoroalkoxy phosphazenes
[AD-747344] 04 p0438 N73-13570
Time temperature superposition in heterophase block copolymers, using viscoelastic behavior of styrene-butadiene-styrene block
[AD-748213] 04 p0438 N73-13574
Nine poly carborane-siloxane, high temperature elastomers differing in chemical structure, using torsional braid analysis
[AD-748931] 04 p0440 N73-13586
Thermally stable phosphonitrile elastomers for advanced aerospace structures
[NASA-CR-124008] 06 p0687 N73-15593
Comparison of outdoor exposure of elastomers and plastics with exposure in accelerated weathering test chamber using fluorescent source of UV radiation
[ERDE-TR-107] 06 p0688 N73-15600
Technique for determining bulk modulus and associated loss factor of elastomeric and plastic materials
[AD-752483] 08 p0935 N73-17659
Vacuum effects on mechanical behavior of filled elastomeric spacecraft materials
13 p1546 N73-22527
Synthesis of fire resistant phosphonitrilic plastics and elastomers for marine applications
[AD-755188] 13 p1548 N73-22547
Environmental endurance testing of elastomeric pitch change bearing for use on H-1 Aircraft
[AD-758463] 14 p1671 N73-23561
Material composition effects on ablation performance of low density elastomer ablators, such as nylon and hollow silica and phenolic spheres
[NASA-TN-D-7246] 14 p1719 N73-23945
Low temperature tests of elastomeric bearing rotors on OH-58 helicopter
[AD-759957] 17 p2038 N73-26490
Data processing system for elastomer development
[AD-759902] 17 p2052 N73-26603
Modified particle in cell method for solving two dimensional nonlinear elasticity problems
[AD-762362] 20 p2483 N73-29948
Liquid jet impact against elastomeric materials
[PB-220972/4] 21 p2528 N73-30269
Constant strain rate tensile tests to determine long-time dynamic compatibility of elastomeric materials with hydrazine
[NASA-CR-133794] 21 p2562 N73-30538
Elastomers for service with engine lubricants and hydraulic fluids
[AD-762800] 21 p2564 N73-30554
Thermal and mechanical properties of low density elastomeric ablation material
[NASA-CR-132281] 23 p2809 N73-32463
Improved flame resistance of spandex elastic elastomeric fibers
[NASA-CR-128505] 23 p2809 N73-32464
Development of high temperature resistant elastomeric sealant
[AD-764589] 23 p2811 N73-32473
Elastomeric silicone adhesive systems for surface insulation attachment to space shuttle
24 p2942 N73-33491
ELASTOPLASTICITY
Elastoplastic stress concentration and deformations in perforated plates
[ONERA-NT-193] 04 p0482 N73-13936
Elasto-viscoplastic behavior of structures subjected to complex loads and thermal gradients
[ONERA-NT-194] 04 p0482 N73-13937
Elastoplastic deformation of steel samples under cyclic loads during torsion tests
[AD-749768] 05 p0604 N73-14914
Proposed computer program for dynamic analysis of elasto-plastic, thin, isotropic plates of rectangular planform subjected to blast loads
[AD-752449] 09 p1096 N73-18947
Numerical analysis of finite deformation of elastoplastic solids
[NASA-CR-2199] 10 p1220 N73-19924

Elastoplastic deformation of slender rod subjected to impact loads
[AD-754241] 10 p1221 N73-19935
Numerical analysis of elasto-plastic bending of plates with V-notch on one edge and subjected to pure bending
[NASA-CR-132225] 15 p1839 N73-24900
Formulation and checkout problems for computer code for analyzing large deflection elastic-plastic dynamic response of stiffened shells of revolution
[NASA-CR-132044] 15 p1839 N73-24902
Elastic-plastic analysis of wheel rolling on rigid track
[AD-764575] 23 p2855 N73-32812
Boundary integral equation method for determining plane elasto-plastic analysis of V-notched plate under bending stress
24 p2987 N73-33869
Theory of elasto-plastic flow applied to work hardening, anisotropy, plastic compressibility and noncontinuous loading in Quasi-linear form
[NASA-CR-2321] 24 p2989 N73-33886

**ELASTOSTATICS**
Mapping-collocation method for elastostatic stress analysis of orthotropic rectangular plates with centrally located traction-free cracks
[NASA-TN-D-7119] 03 p0360 N73-12933
Mathematical and mechanical consideration of finite strip compressed between two rough rigid stamps
[NASA-CR-112318] 13 p1585 N73-22849
Uniqueness of solution for plane crack problems in linear elastostatics
[AD-756653] 13 p1587 N73-22865
Edge cracks in infinite strip
[NASA-CR-132288] 19 p2348 N73-28885

**ELECTRETS**
Piezoelectric and pyroelectric properties of polymer electrets
[AD-758730] 16 p1933 N73-25638

**ELECTRIC APPLIANCES**
U ELECTRIC EQUIPMENT

**ELECTRIC ARCS**
NT CARBON ARCS
Electric arc bonding of aluminum bronze onto clean steel surface
[AD-747768] 03 p0307 N73-12510
Theory and applications of induction arc
[AD-750742] 06 p0706 N73-15761
Displacement of electric arc by magnetron-produced pulsed high frequency heating
[BMVG-FBWT-72-19] 08 p0943 N73-17728
Opposed electrode, parallel gap, and percussive arc monitoring systems
[BDX-613-544] 10 p1134 N73-19244
Deviation from rotational symmetry of electric arcs in transverse magnetic fields
[AD-754022] 11 p1328 N73-20778
Effects of acceleration or retardation on electric strength of gas
[AD-755848] 12 p1429 N73-21584
Magnetic field effects in cathode mechanism of electric arc initiation and travel between copper electrodes
[NLL-CE-TRANS-6108-[9022.09]] 15 p1755 N73-24226
Physical processes occurring in vortex stabilized arcs with and without applied axial magnetic fields
[AD-759187] 16 p1892 N73-25313
Mathematical model for turbulent flow in electric arc
[AD-759572] 16 p1950 N73-25781
Properties of arc disharges heated by induction and direct current electromagnetic field
[AD-760808] 18 p2183 N73-27629
Differential approximation and numerical integration methods for analyzing behavior of wall stabilized electric arcs with radiative transport
[AD-765207] 23 p2857 N73-32831

**ELECTRIC BATTERIES**
NT ALKALINE BATTERIES
NT MAGNESIUM CELLS
NT METAL AIR BATTERIES
NT NICKEL CADMIUM BATTERIES
NT NICKEL ZINC BATTERIES
NT PRIMARY BATTERIES
NT SILVER CADMIUM BATTERIES
NT SILVER ZINC BATTERIES
NT STORAGE BATTERIES
NT THERMAL BATTERIES
NT ZINC-OXYGEN BATTERIES
Design, development, and evaluation of aluminum-chlorine battery
[AD-747775] 03 p0255 N73-12065
Development of lithium-nickel sulfide electric storage battery for operation at high discharge rates and low temperatures
[AD-749861] 05 p0500 N73-14067
Performance of battery powered electrically heated suit for reconnaissance divers
[AD-749847] 05 p0504 N73-14101
Internal impedance of lead accumulator starting batteries
[FOA-3-C-3667-94] 06 p0626 N73-15077
Catalog of batteries for Navy weapon systems
[AD-751018] 06 p0627 N73-15087
Development and characteristics of electric storage battery using lithium-silver chloride couple
[SC-DC-72-2298] 07 p0742 N73-16033
Development of test probe device for simultaneous determination of condition of cells in multi-cell storage battery
[NASA-CASE-MFS-20761-1] 08 p0869 N73-17037
Identification and preparation of materials for use as nonporous solid ionic conductors in rechargeable high energy battery at low temperatures
[NASA-CR-120964] 09 p0990 N73-18078
Performance tests of electric batteries to determine effect of negative limited cell on battery service life
[NASA-CR-130932] 10 p1111 N73-19060
Performance capabilities and cycle life of high specific energy batteries for pollution free electric vehicles
[ANL-7953] 10 p1112 N73-19061
Analysis of off-scale low indications of voltmeters for batteries at initial powerup for Apollo 16 lunar roving vehicle
[NASA-TM-X-69123] 11 p1266 N73-20272
Accelerated life test program for space batteries
[NASA-SP-323] 13 p1476 N73-21958
Optimized construction of thermoelectric cooling batteries
[AD-757467] 14 p1606 N73-23016
Performance of prototype lithium-inorganic electrolyte battery
[AD-758856] 16 p1865 N73-25101
Design and development of electric batteries for use with thermoelectric air conditioning systems
[AD-759239] 17 p1986 N73-26051
Use of lithium/sulfur batteries as load-leveling devices in electrical utility networks
[ANL-7958] 21 p2499 N73-30058
High energy batteries based on aprotic organic electrolytes
[AD-763140] 21 p2506 N73-30112
Development of timing device for conserving batteries on remote data collection platform by generating synchronous time windows
[NASA-CASE-GSC-11182-1] 23 p2849 N73-32769

**ELECTRIC BRIDGES**
NT WHEATSTONE BRIDGES
Perfluorostyrene syntheses, magnetic tapes, titration cell, mill work positioner, superconducting microbridges, position display device, and numbering machine
[NBS-TN-744] 02 p0245 N73-11991
Pulsed piezoresistive gage bridge operating in NIM configuration
[LA-4939] 03 p0303 N73-12471
Solid state amplifier for bridge circuit of atomic absorption mercury detector
[PB-212658] 07 p0801 N73-16506

**ELECTRIC CELLS**
Performance tests of electric batteries to determine effect of negative limited cell on battery service life
[NASA-CR-130932] 10 p1111 N73-19060

**ELECTRIC CHARGE**
NT ELECTRIC DIPOLES
NT ELECTROSTATIC CHARGE
NT ION CHARGE
NT SPACE CHARGE
Methods of charging/discharging in scanning electron microscopy of dielectrics to preserve resolution and contrast
[DRIC-TRANS-2970] 10 p1162 N73-19451
Electric charge, momentum, and mass of elliptic universe
[AD-756902] 13 p1561 N73-22649
Scanning electron microscope effects on charging properties of dielectric materials
[NLL-DRIC-TRANS-2970-[3623.66]] 15 p1785 N73-24470

**ELECTRIC CIRCUITS**
U CIRCUITS

**ELECTRIC COILS**
NT MAGNETIC COILS
Analogous specimen-coil-arrangements in eddy current testing
[ARL/MET-REPT-88] 04 p0420 N73-13423
Formulas for measurement of impedance of single-layer induction coils
[IAE-2120] 08 p0889 N73-17195
Performance of ion cyclotron plasma generator using radio frequency coil for plasma control
[NASA-TN-D-7187] 09 p1069 N73-18725
Coversion data for transition from english to metric system for design and fabrication of transformers
[NASA-CR-133932] 22 p2700 N73-31624

**ELECTRIC CONDUCTORS**
Electrical parameters of large rectangular conductor immersed in cavity of electric motor
[REPT-122] 05 p0586 N73-14765
Copper brass bimetal cladding layers on steel strips for manufacturing elastic current conducting springs
[NLL-M-21498-[5828.4F]] 06 p0682 N73-15554
Production and evaluation of magnetic and electrical materials capable of operating in 800 to 1600 F temperature range for advanced space electric power systems
[NASA-CR-2224] 09 p0990 N73-18084
Analysis of alternating current loss mechanisms in superconductors with comparison of performance in coil and cable configurations
10 p1108 N73-19032
Numerical analysis of multiple conductor transmission line with arbitrarily positioned impedances in series with each wire
[SC-R-72-2695] 12 p1386 N73-21244
Direct current conductivity in amorphous semiconductors
[AD-756783] 14 p1699 N73-23785
Theory for electrical resistivity in wire braid coaxial conduction at low and high radio frequencies
[RAE-TR-72153] 17 p1998 N73-26155
Improved injector with porous plug for bubbles of gas into feed lines of electrically conductive liquid
[NASA-CASE-NPO-11377] 18 p2154 N73-27406
Eddy-current inspection for locating subsurface flaws in electrical conductors
19 p2303 N73-28522
Electrical conductivity of materials and determination of resistivity
[NASA-TT-F-15067] 21 p2579 N73-30667

**ELECTRIC CONNECTORS**
Performance of wire bound electrical connectors used in integrated and hybrid circuits and low power semiconductor devices
[AD-748788] 04 p0396 N73-13220
Sum of two scattering matrices connected together by two hybrid circuits
[NLL-M-22701-[5828.4F]] 05 p0568 N73-14614
Development of low profile flat conductor cable connecting device and permanent splice methods for use in spacecraft component electrical systems - Vol. I
[NASA-CR-128845] 11 p1262 N73-20241
Cost comparison of flat versus round conductor cable based on spacecraft electric wiring system specifications - Vol. 3
[NASA-CR-128847] 11 p1262 N73-20243
Microscopic analysis of silver diffusion into gold plate on electrical connector
[AD-755123] 11 p1263 N73-20249
Development, characteristics, and applications of flat conductor cable to include methods and facilities for fabrication
13 p1593 N73-22916
Conference papers on flat conductor cable technology and applications
[NASA-TM-X-64716] 14 p1640 N73-23294
Manufacturing and quality control of FCC harnesses with design and installation requirements
14 p1641 N73-23302
Military specifications for flat connectors and cables
14 p1641 N73-23306
No-strip-crimp connection for flat electrical signal cables
14 p1641 N73-23308
Application of ANSI Y14.5 rules to designing connectors for interchangeability
14 p1641 N73-23309
Techniques and hardware for facilitating use of flexible flat conductor cable in commercial air transports
14 p1641 N73-23310
Survey of source availability for FCC and/or FCC connectors
14 p1642 N73-23312
Aluminum ribbon wire for ultrasonic bonding of semiconductor microelectronic interconnections
[AD-758981] 16 p1881 N73-25223
Coaxial connector for standard hardware program
[AD-758649] 16 p1882 N73-25233
Conference on contact surface requirements for electric contacts and connectors
[AD-763213] 21 p2519 N73-30203
Evaluation of single wire termination system capable of interconnection to various multicontact connectors
[AD-764248] 22 p2644 N73-31190
Cable driver and technique for testing shielding effectiveness of exterior connectors for Pershing missile cable shields
[AD-764236] 22 p2645 N73-31196
Electroforming of aluminum solar cell contacts
[AD-764816] 23 p2748 N73-31995
Reliability of circular electrical connectors
[AD-765609] 24 p2899 N73-33144

**ELECTRIC CONTACTS**
Methods for chip mounting and establishing electrical connections in miniaturized printed circuits and thick and thin film hybrid circuits
[ECR-27] 08 p0891 N73-17212
Design and fabrication of wraparound contact silicon solar cells
[NASA-CR-121003] 11 p1237 N73-20044
Electric, photoelectric, and electroluminescence properties of Cu contacts on CdS surface
[AD-756876] 13 p1504 N73-22187
Development, characteristics, and applications of flat conductor cable to include methods and facilities for fabrication
13 p1593 N73-22916

Flat conductor cable connectors with individually sealed contacts
14 p1641 N73-33307
Conference on contact surface requirements for electric contacts and connectors
[AD-763213] 21 p2519 N73-30203
ELECTRIC CONTROL
Application of integrated circuit technology and digital computer techniques to electric control of jet engines
[NAL-TR-281] 09 p1078 N73-18799
ELECTRIC CORONA
Measurement of low airspeeds with ion beam produced in positive corona discharge based on beam deflection properties
10 p1158 N73-19423
Analysis of factors affecting quality of electrostatic printing processes and procedures to improve product
[AD-755259] 12 p1409 N73-21420
ELECTRIC CURRENT
NT ALTERNATING CURRENT
NT ARC DISCHARGES
NT AURORAL ELECTROJETS
NT BEAM CURRENTS
NT CARBON ARCS
NT DIRECT CURRENT
NT EDDY CURRENTS
NT ELECTRIC ARCS
NT ELECTRIC CORONA
NT ELECTRIC DISCHARGES
NT ELECTRIC SPARKS
NT ELECTRODELESS DISCHARGES
NT ELECTROJETS
NT EQUATORIAL ELECTROJET
NT GAS DISCHARGES
NT GLOW DISCHARGES
NT HIGH CURRENT
NT IONOSPHERIC CURRENTS
NT LIGHTNING
NT MULTIPACTOR DISCHARGES
NT PENNING DISCHARGE
NT RADIO FREQUENCY DISCHARGE
NT RING CURRENTS
NT TELLURIC CURRENTS
NT THRESHOLD CURRENTS
NT TOROIDAL DISCHARGE
Various types of energy transformation into electric energy
[AD-746549] 03 p0255 N73-12063
Harmonic functions for determining currents and voltages in nonlinear electrical circuit
[AD-748231] 03 p0276 N73-12243
Construction of extremal controller for high current betatron using stochastic algorithms
[AD-747370] 03 p0281 N73-12279
Gauge invariant atomic orbitals and current conservatism within quantum mechanical formalism
[NASA-CR-129246] 03 p0339 N73-12762
Design and performance of ammeter with reversible temperature indicator for recording peak currents
[UCRL-73587] 05 p0547 N73-14446
Current collection characteristics of moving cylindrical Langmuir probe for range of probe speeds and potentials applicable to earth and planetary measurements
[NASA-TM-X-66177] 08 p0924 N73-17571
Light generated current output of vertical multijunction solar cell
[AD-754901] 11 p1238 N73-20047
Operating characteristics of avalanche diode oscillator circuit high efficiency TRAPATT modes
[NASA-CR-131399] 11 p1264 N73-20258
Current-voltage, load, and spectral characteristics of p- and n-type GaAs
[NASA-TT-F-14859] 11 p1330 N73-20793
Quasi-particle pair interference current in superconducting weak links of Josephson junctions
[AD-754081] 11 p1331 N73-20803
Flux line lattice effect on critical current in plastically deformed single niobium crystal
[COO-3169-14] 12 p1440 N73-21665
Numerical calculation of current-voltage characteristics for ionized plasma containing negative ions with unequal electron and ion temperatures
[LOG-J7146] 13 p1563 N73-22667
Three-term solution for integral equation of current along thin cylindrical dipole antenna
[AD-758192] 14 p1643 N73-23327
Pulsed electron motion equations for surface current analysis on conducting sphere
[AD-757190] 14 p1694 N73-23745
Phase shift model for induced voltage in current carrying superconducting thin films in superimposed ac and dc magnetic fields including radio and microwave frequency ranges
15 p1820 N73-24748
Current carrier mobility near charged semiconductor surface
[AD-758973] 16 p1953 N75-25604
Distribution of current in coupled dipole antennas in homogeneous isotropic media
[AD-761167] 18 p2124 N73-27169
Analysis of axial conduction current induced in infinitely long cylinder in free space with small resistivity by incident electromagnetic plane wave
[AD-762165] 19 p2246 N73-28106
Matrix methods for determining nature of eigencurrents and eigenfields in conducting bodies
[AD-761456] 19 p2321 N73-28675
Load-carrying and thermal characteristics of flat conductor cable
[NASA-TM-X-64767] 20 p2380 N73-29125
Electrode burn off characteristics of manual metal arc electrodes using continuous and modulated welding current
[CRANFIELD-MAT-9] 24 p2928 N73-33386
Linear and nonlinear theory of Hall current instability
24 p2962 N73-33667
Electromagnetic characteristics of single crystal niobium, niobium alloy, and molybdenum alloy superconductors
[AD-765368] 24 p2970 N73-33731
ELECTRIC DIPOLES
Gaussian curve simulation of multiple-dipole model of ventricular depolarization
[TH-71-E-25] 03 p0261 N73-12116
Two sector, superconducting dipole in direct current
[LNF-72/6] 04 p0458 N73-13738
Microscopic dipole model for lattice dynamics in transition metals
08 p0950 N73-17782
ELECTRIC DISCHARGES
NT ARC DISCHARGES
NT CARBON ARCS
NT ELECTRIC ARCS
NT ELECTRIC CORONA
NT ELECTRIC SPARKS
NT ELECTRODELESS DISCHARGES
NT GAS DISCHARGES
NT GLOW DISCHARGES
NT LIGHTNING
NT MULTIPACTOR DISCHARGES
NT PENNING DISCHARGE
NT RADIO FREQUENCY DISCHARGE
NT TOROIDAL DISCHARGE
Measurement of partial discharges in electrical insulating materials and application to quality control of manufactured electric equipment
[NLL-CE-TRANS-5844-[9022.09]]
02 p0191 N73-11545
Voltage characteristics of electrical discharges over long air gaps
[AD-746853] 02 p0213 N73-11723
Discharge rate and electrical breakdown in polyethylene, polystyrene, polymethyl methacrylate, and polyvinyl chloride
[SC-T-72-2509] 03 p0273 N73-12217
Effect of purification of transparent dielectrics from dust on breakdown threshold under action of laser irradiation
[AD-748230] 03 p0338 N73-12760
Dynamics of laser triggered spark discharge channel with nanosecond pulse formation
[AD-747510] 03 p0343 N73-12799
Magnetic probes and instrumentation of capacitive discharges
[AD-748610] 04 p0423 N73-13450
Analysis of electron beam induced discharge in nitrogen at high pressure
[NLL-DRIC-TRANS-2857-[3623.66]]
05 p0579 N73-14714
Relation of gas kinetic particle pressure and discharge field in plasma heating by pulsed longitudinal current
[AEC-TR-7330] 07 p0826 N73-16697
Optical and energy measurements of strong current discharges in air
[AD-751414] 07 p0830 N73-16729
Utilization of superconductors to store and discharge electric energy
10 p1109 N73-19041
Effects of electromagnetic forces, energy radiation, and discharge losses on design of superconducting coils for energy storage elements
10 p1109 N73-19043
Plane compression wave in pressure field of electrical discharge into water
[AD-754614] 11 p1324 N73-20746
Oxygen gas production during stand and discharge in silver zinc batteries
[NASA-CR-128933] 15 p1738 N73-24087
Volt-ampere characteristics of enclosed keeper hollow cathode discharge
[NASA-TM-X-2799] 15 p1825 N73-24792
Ionic diffusion in electron boundary layer of spotless discharge crossing nitrogen magnetohydrodynamic flow
[IPF-72-3] 17 p2069 N73-26739
Electric discharges in supersonic high pressure gas flow to improve carbon dioxide laser power
[ISL-20/72] 19 p2307 N73-28560
Excitation and relaxation processes in H2O discharges and lasers
20 p2424 N73-29471
Double exposure interferograms of discharge region of transverse electrically-excited atmospheric pressure CO2 lasers
[UCRL-13547] 20 p2425 N73-29483
Decomposition of hydrogen sulfide, in electrical discharge, to elemental sulfur
[BM-RI-7780] 21 p2505 N73-30101
Electron beam stabilized electrical discharge gas lasers
[AD-763409] 21 p2555 N73-30487
Electron beam stabilized electrical discharge HF laser
[AD-763464] 21 p2556 N73-30489
Electric discharge in turbulent flowing gas
[AD-764468] 22 p2655 N73-31265
Guidance of high voltage electrical breakdown streamers by laser induced ionization in air
[AD-763827] 22 p2705 N73-31665
Systems for protection of low altitude tethered balloons from effects of atmospheric electricity
[AD-764651] 23 p2746 N73-31978
Electrical discharge metastable detector for helium afterglows
[AD-765210] 23 p2823 N73-32570
Experimental and theoretical study of electro-erosion of metals
24 p2933 N73-33423
ELECTRIC ENERGY STORAGE
Development of lithium-nickel sulfide electric storage battery for operation at high discharge rates and low temperatures
[AD-749861] 05 p0500 N73-14067
Utilization of superconductors to store and discharge electric energy
10 p1109 N73-19041
ELECTRIC EQUIPMENT
Measurement of partial discharges in electrical insulating materials and application to quality control of manufactured electric equipment
[NLL-CE-TRANS-5844-[9022.09]]
02 p0191 N73-11545
Cost effectiveness of infrared inspection and maintenance of ARTCC electrical equipment
[C-208] 04 p0447 N73-13648
Development of temperature compensated light source with components and circuitry for maintaining luminous intensity independent of temperature variations
[NASA-CASE-ARC-10467-1] 05 p0518 N73-14214
Development of numerical procedures for determining instantaneous values of current and voltage in nonlinear electrical circuits
[NLL-DRIC-TRANS-2145-[3623.66]]
05 p0522 N73-14241
Measurement of sinusoidal waves in flumes with transducers using non-contacting capacitive sensing
[NRC-MI-836] 05 p0522 N73-14243
Development and characteristics of hermetically sealed coaxial package for containing microwave semiconductor components
[NASA-CASE-GSC-10791-1] 05 p0550 N73-14469
Characteristics of carbon, cermet, and wire-wound type potentiometers based on service life and environmental tests
[ECR-30] 08 p0924 N73-17569
Effects of substrates on stability of superconductor and electrical properties of superconductors for various conditions
10 p1108 N73-19031
Characteristics of superconducting electric generators to show effect of electromechanical, electromagnetic, and cryogenic parameters on design
10 p1109 N73-19039
Application of superconducting coils for energy storage and determination of optimizing parameters for inductive energy storage
10 p1109 N73-19042
Development of low profile flat conductor cable connecting device and permanent splice methods for use in spacecraft component electrical systems - Vol. 1
[NASA-CR-128845] 11 p1262 N73-20241
Fabrication and evaluation of wire harnesses from small gage wire round conductor cables - Vol. 2
[NASA-CR-128846] 11 p1262 N73-20242
Cost comparison of flat versus round conductor cable based on spacecraft electric wiring system specifications - Vol. 3
[NASA-CR-128847] 11 p1262 N73-20243
Design, development, fabrication, and test of coolant circulating pump assemblies for use in Brayton cycle space power system
[NASA-CR-2176] 11 p1297 N73-20529
Characteristics of instrument for measuring and recording water flow and modifications for improved operation
12 p1421 N73-21518
Guidelines for design and development of electrical and electronic components and systems used in spacecraft construction to obtain long service life - Vol. 2
[NASA-CR-128906] 14 p1707 N73-23854
Development of guidelines for selection of hardware items for use in manned spacecraft design to obtain five year maintenance-free service life - Vol. 3
[NASA-CR-128907] 14 p1707 N73-23855
Operational performance of electrical subsystem for Brayton power conversion system
[NASA-TM-X-2810] 15 p1738 N73-24088

Electrical equipment of nuclear upper stage for Europa 3 launch vehicle
[TR-TT-4-16/72] 15 p1811 N73-24677
Electrical instrumentation development for spark source mass spectroscopy
[PB-214212] 16 p1871 N73-25147
Inductance of cryogenic synchronous equipment with damping system
[AD-759235] 16 p1884 N73-25250
Guidelines for selection and application of three types of tantalum electrolytic capacitors for design of circuits in spacecraft components
[NASA-TM-X-64755] 17 p2003 N73-26200
Superconductive materials for military rotating electrical machinery
[AD-760330] 17 p2074 N73-26782
Analysis of power consumption and switching times of micropower complementary bipolar transistor inverters
18 p2125 N73-27172
Comparative evaluation of conventional and solid state simulators for A-7 aircraft electrical system
[AD-762295] 19 p2250 N73-28142
Operational reliability and economics for instrumentation particularly electric pumps
[AD-762321] 19 p2306 N73-28545
Analysis of methods for determining thermoelectric cooling and heating devices using pure resistance principle
[AD-762324] 19 p2353 N73-28926
Design, development, and evaluation of zinc-oxygen battery with mechanically rechargeable feature
[AD-762573] 20 p2364 N73-29012
Overvoltage protection network for electrical equipment
[NASA-CASE-ARC-10197-1] 20 p2380 N73-29124
Design, dynamic response, and operation of electric pressure difference transducer
[NLL-TRANS-2976-[9022.81]]
21 p2543 N73-30387
Design and evaluation of mini-Brayton compressor-alternator-turbine system for spacecraft power supplies
[NASA-CR-133810] 21 p2553 N73-30463
Peel, shear, and tensile strength measurements of transistor header lead welds
[BDX-613-871] 22 p2642 N73-31173
Climatized electrical equipment for tropical and cold climates
[AD-764393] 23 p2766 N73-32128

**ELECTRIC FIELD STRENGTH**

Spectroscopic examination of electric field intensity and ion temperature of turbulent plasma
[AEC-TR-7375] 12 p1434 N73-21623
Ground antenna total electric field strength of RF emission from cosmic ray air showers at three VHF frequencies
13 p1574 N73-22753
Direct comparison between electric field measurements by Injun 5 satellite and visual aurora data
[NASA-CR-132958] 16 p1906 N73-25416

**ELECTRIC FIELDS**

Magnetotelluric analysis of geological structure of various locations in Rhine River Valley, Germany
[GAMMA-20] 01 p0048 N73-10388
Monitor for electric fields of cloud formations in particular area
[NASA-CASE-KSC-10731-1] 01 p0056 N73-10461
Formation of electric fields during friction of lubricating oil on metal surface
[AD-745433] 01 p0062 N73-10511
Charged particle motion in nonhomogeneous field with Coulomb potential
[NOTA-INTERNA-383-B] 01 p0084 N73-10697
Confinement of electron-free plasmas in quadrupole RF electric trap
[NASA-TM-X-65719] 01 p0085 N73-10703
Electric field oscillations in upstream solar wind, using OGO-5 observations
01 p0096 N73-10789
Simultaneous observations of plasma waves from electric field instruments on Pioneer 9 and OGO 5 to illustrate difference between near-earth and deep space conditions
01 p0096 N73-10795
Seasonal, altitude, and universal time differences in field-aligned electrons
[NASA-TM-X-66099] 02 p0166 N73-11345
Analysis of exact and approximate methods for solving inverse scattering problem for transmission lines
02 p0199 N73-11612
Computerized simulation of instability response of magnetized two ion species plasma to low frequency electric field oscillations
[AD-746109] 02 p0217 N73-11757
Numerical analysis of electrical field of capacitance generator to determine potential at points in gas gap
[AD-747570] 03 p0256 N73-12069
Calculation of unsteady electric field produced by radio waves in lower half space
[AD-747731] 03 p0267 N73-12164
Electric field noise phenomena observed by S3-A spacecraft near plasmapause during magnetic storm
[NASA-CR-129243] 03 p0293 N73-12388
Role of azimuthal electric fields in toroidal transport
[IPP-6/105] 03 p0336 N73-12737
Procedures for producing electric fields in conductive media at extremely low frequencies
[AD-748303] 04 p0391 N73-13177
High speed photography of electro-optical fringe patterns for measuring pulsed electric field between Kerr cell electrodes
[SC-DC-72-1375] 04 p0399 N73-13243
Electric field effects on oxidation mechanisms of metals and alloys
[AD-748297] 04 p0436 N73-13558
RF electric field in electron ion plasma condenser with and without magnetic field
[EUR-CEA-FC-638] 04 p0454 N73-13707
RF electric field reflected by finite conducting plane target illuminated by small antenna
[AD-750088] 05 p0514 N73-14183
Measurement of sinusoidal waves in flumes with transducers using non-contacting capacitive sensing
[NRC-MI-836] 05 p0522 N73-14243
Field evaporation model for predicting tungsten surface potential in electric field
[AD-750205] 05 p0588 N73-14786
Effect of external electric field on optical absorption of GaSe and GaTe single crystals and solid solutions
[AD-749750] 05 p0589 N73-14789
Comparing properties of open magnetosphere and its electric field to simple model of dipole in constant field
[NASA-TM-X-66132] 05 p0595 N73-14842
Design and performance of miniaturized electric field meters for wind tunnel measurements
[AD-750148] 06 p0675 N73-15495
Analysis of forces in electrostatic gyroscope with spherical rotor and development of equations to calculate electrical forces
06 p0695 N73-15666
Particle motion in magnetic mirror with high frequency electric field
[COO-2181-7] 06 p0703 N73-15731
Electric field amplitude within superhigh frequency wave absorption by plasma using Stark effect analysis
[FTI-413] 06 p0705 N73-15750
Computer program ELECTRA used to compute paraxial particle trajectories in axially symmetric electrostatic fields
[SGAE-2007] 07 p0824 N73-16678
Impulse response of low pressure argon magnetoplasma to excitation by electric field
[NASA-TR-R-400] 07 p0826 N73-16693
Laboratory experiments with high frequency excitation electric fields
[CONF-720705-3] 07 p0827 N73-16701
High voltage distribution fields of two component dielectrics in rotational series or parallel arrangements
08 p0888 N73-17193
Rocket-borne instrument for ionospheric electric field measurements
[AD-751926] 08 p0920 N73-17537
Plasma heating by turbulent pulsation of electric field
[NASA-TT-F-14673] 08 p0947 N73-17758
Probe measurements of dc electric fields from IMP 1
08 p0973 N73-17950
Magnetospheric convection theory for substorm growth and expansion
[NASA-CR-130499] 09 p1032 N73-18423
Analytic models to calculate electrostatic fields produced inside cylinders and spheres by internal electromagnetic pulses
[AD-753014] 09 p1067 N73-18709
Computerized simulation of inhomogeneous plasma response to impulse electric field excitation
[AD-753104] 09 p1072 N73-18746
Analysis of alternating current loss mechanisms in superconductors with comparison of performance in coil and cable configurations
10 p1108 N73-19032
Linear and nonlinear plasma response to impulse electric field
10 p1195 N73-19725
Operating properties of RF resonant plasma with high-intensity electric field
[ITF-72-77-E] 10 p1197 N73-19739
Apparatus for determining distance to lighting strokes from single station by magnetic and electric field sensing antennas
[NASA-CASE-KSC-10698] 11 p1254 N73-20175
Satellite-borne electric field measurement in magnetosphere
[NASA-CR-131419] 11 p1287 N73-20442
Analysis of electrical charge generated by helicopter rotor operating near particulate matter with seeded vortex
[AD-755282] 12 p1366 N73-21080
Electron temperature and density profiles obtained with Skylark rocket-borne double electrostatic probes
[TRITA-EPP-72-14-REV] 12 p1402 N73-21370
Random walk theory for studying electron avalanche formation in helium electric fields
[NASA-TN-D-7224] 12 p1433 N73-21612
Two substorm studies of relations between westward electric fields in outer plasmasphere, auroral activity, and geomagnetic perturbations
[NASA-CR-131497] 13 p1518 N73-22309
Electric strength breakdown in insulating dielectric liquids
[AD-755756] 13 p1548 N73-22546
Controlled magnetic and electric excitation of airframe of LOH-6A helicopter and measurement of impedance, radiation patterns, and bandwidths
[AD-757143] 14 p1602 N73-22992
Two fluid models with neglected mass rotation and overestimated electric field role
[TH-72-E-28] 14 p1695 N73-23755
Fringing field effect minimization in parallel plate electrostatic spectrograph taking into account condenser plate thickness
15 p1788 N73-24499
Hartree approximation of extra conductivity in quasi-superconducting thin films considering nonlinear external field effect
[LNF-72/76] 15 p1821 N73-24758
Electric field induced instability in transition metal compounds
[AD-758270] 15 p1822 N73-24771
Ionospheric electric field and current distributions, assuming certain time variable convection field profiles at 1250 km
[TRITA-EPP-73-03] 16 p1907 N73-25429
Influence of electric forces in development and dissipation of clouds and fog
[AD-758925] 16 p1938 N73-25683
Temporal variations in atmospheric electric fields noting propagation and disturbances
[TRITA-EPP-73-02] 17 p2027 N73-26405
Quantitative modeling of electric fields induced in magetosphere by changes in magnetospheric magnetic field
[AD-760058] 17 p2029 N73-26418
Effects of electric and magnetic fields on nucleation and growth of metallic thin films
[USC-113-P-22-3] 17 p2045 N73-26546
Characteristics of three station network for sensing magnetic and electric fields associated with lightning discharges
[NASA-CR-133400] 18 p2151 N73-27382
Electron gas behavior and density in constant electric and magnetic fields
[AD-760587] 18 p2182 N73-27617
Electric field autocorrelations in guiding center plasma
[NASA-CR-133410] 18 p2183 N73-27624
Computerized simulation of belt pinch experiments including plasma external circuit interactions
[LRP-61/73] 18 p2183 N73-27626
Effect of applied electric field on oxidation/hot corrosion of metals and alloys in molten salt
[AD-762074] 19 p2311 N73-28584
Electrostatic suspension of conducting sphere in electric field between electrodes
[JPRS-59675] 20 p2380 N73-29123
Numerical analysis of aerosol concentration and deposition flux for several flow configurations with and without electrical force deposition
20 p2386 N73-29172
Circulation in high latitude thermosphere due to electric fields and joule heating
20 p2391 N73-29203
Sounding rocket measurements of high latitude dayside electric fields and low energy particles
[NASA-TM-X-70450] 20 p2413 N73-29392
Estimation of electron drift velocity and characteristic energy as function of electric field strength in carbon dioxide laser gas mixtures
[TN-280] 20 p2425 N73-29477
Interaction to second order of electrostatic and electromagnetic fields with semi-infinite plasma
20 p2457 N73-29747
Complex variable theory used in representation of electric field of longitudinal waves in plasma
[AD-762905] 20 p2459 N73-29763
Dynamic electric field profiles in electron beam semiconductor devices
[AD-763296] 21 p2517 N73-30192
High latitude electric fields and modulations related to interplanetary magnetic field parameters
[NASA-TM-X-70444] 21 p2535 N73-30331
Analysis of linear and nonlinear stage of ion-acoustic instability in low pressure discharge in helium
[AD-763590] 21 p2584 N73-30707
Development of nonlinear stochastic equations for turbulent field with application to simple electron plasma
[AD-763438] 21 p2584 N73-30710
Technique for reducing ambient electric field generated by inductive voltages in extreme low frequency magnetic field generators
[AD-764531] 23 p2768 N73-32142
Development and characteristics of apparatus for measuring intensity of electric field in atmosphere
[NASA-CASE-KSC-10730-1] 23 p2790 N73-32318
Temperature dependence and measurement of crystalline electric fields at ytterbium impurties in thulium metal
[AD-764633] 23 p2827 N73-32596

One-dimensional analysis of electric fields and electric potential near photo emitting plate emmersed in solar wind plasma
23 p2858 N73-32839
Role of electrical processes in thunderstorms of Canadian prairies
24 p2912 N73-33242
Neutral injection heating of plasma
[CONF-730705-3] 24 p2965 N73-33700
Computerized simulation of electrostatic inertial plasma confinement device
[AD-763826] 24 p2966 N73-33703
Electrified kerosene and gasoline aviation fuel during passage through pipes and filters of fuel tank reservoir
[AD-764941] 24 p2971 N73-33740

ELECTRIC FILTERS
NT BANDPASS FILTERS
NT CRYSTAL FILTERS
NT DIGITAL FILTERS
NT INFRARED FILTERS
NT LINEAR FILTERS
NT LOW PASS FILTERS
NT MICROWAVE FILTERS
NT OPTICAL FILTERS
NT RADAR FILTERS
NT RADIO FILTERS
NT TRACKING FILTERS
NT WAVEGUIDE FILTERS

Superconductive tunable filter having broad tuning range with inductance and capacitance varied simultaneously
[AD-749237] 04 p0397 N73-13226
Relations between signal shaping noise and timing resolution in nuclear particle detection
[NASA-CR-129613] 04 p0452 N73-13688
Development of allpass, highpass, bandpass, and stopband electric filter circuits using only resistors as passive components
[REPT-1404] 05 p0522 N73-14244
Mathematical design of electric filters using linear differential equations
[AD-757544] 16 p1881 N73-25225
Design of continuous lumped parameter linear filters
[AD-757545] 16 p1881 N73-25226
Filter for third order phase locked loops in signal receivers
[NASA-CASE-NPO-11941-1] 18 p2125 N73-27171
Design of second order resistance capacitance filters
24 p2898 N73-33133

ELECTRIC FUSES
Self-healing fuse development
[NASA-CR-121244] 21 p2517 N73-30191

ELECTRIC GENERATORS
NT AC GENERATORS
NT ALKALINE BATTERIES
NT DIRECT POWER GENERATORS
NT DYNAMOMETERS
NT ELECTROSTATIC GENERATORS
NT FUEL CELLS
NT HYDROGEN OXYGEN FUEL CELLS
NT MAGNESIUM CELLS
NT MAGNETOHYDRODYNAMIC GENERATORS
NT METAL AIR BATTERIES
NT NICKEL ZINC BATTERIES
NT PHOTOELECTRIC GENERATORS
NT PRIMARY BATTERIES
NT RADIOISOTOPE BATTERIES
NT REGENERATIVE FUEL CELLS
NT ROTATING GENERATORS
NT SNAP 10A
NT SNAP 19
NT SNAP 23
NT SOLAR CELLS
NT SOLAR GENERATORS
NT THERMAL BATTERIES
NT THERMIONIC CONVERTERS
NT THERMOELECTRIC GENERATORS
NT TURBOGENERATORS
NT ZINC-OXYGEN BATTERIES

Analog signal to discrete time interval converter for control of dc to dc power supplies
[NASA-TM-X-68153] 02 p0128 N73-11043
Use of Cm-244 as radioisotope power fuel in electric power conversion systems
[CONF-720519-1] 03 p0333 N73-12717
Problems of using metallurgical and chemical materials in direct conversion systems
[UCRL-73560] 03 p0333 N73-12718
Ultrasonic inspection of aluminum keys used in electric generators
[TR-7206.590] 05 p0551 N73-14473
Performance and endurance testing of 6 kW organic Rankine cycle power conversion system
[SAN-651-130] 08 p0870 N73-17042
Modifications and test performance of 2 to 15 kilowatt Brayton cycle electrical subsystem
[NASA-TM-X-2757] 09 p0990 N73-18083
Development of superconducting homopolar machines with multiple discs and superconducting field winding using liquid metals for armature sliding contacts
10 p1109 N73-19037
Features and characteristics of superconducting electrical machines and design of synchronous electric generator for airborne use
10 p1109 N73-19040
Numerical analysis of voltage spectra of electric inverters with pulse width modulation
[NLL-RTS-7639] 11 p1261 N73-20235
Automatic connection of aerogenerator to electrical network
[NASA-TT-F-14873] 12 p1386 N73-21238
Beta-1 and Beta-2 isotopic electrical generators as power sources for weather stations
[AD-755834] 12 p1428 N73-21572
Operational performance of electrical subsystem for Brayton power conversion system
[NASA-TM-X-2810] 15 p1738 N73-24088
Methods of generating supernarrow pulses
[NLL-DRIC-TRANS-2934-[3623.66]]
16 p1910 N73-25455
Slip parameter for unsteady flow in EHD generators
[AD-759971] 17 p2070 N73-26749
Design, development, and fabrication of radiator structure for use with thermoelectric space power systems
[NASA-CR-121222] 17 p2088 N73-26892
Critical characteristics of gas turbine powered generator
[AD-762200] 19 p2223 N73-27933
Design, development, and performance tests of wind driven, propeller operated electric generation station
[NASA-TT-F-15037] 20 p2363 N73-29004
Design, development, and operation of wind-powered electric generators for commercial electric power applications
[NASA-TT-F-15068] 20 p2364 N73-29008
Development and construction of wind driven electric power generators for specific European areas
[NASA-TT-F-15050] 20 p2364 N73-29009
Performance of pure plutonium oxide fuel under operational conditions
[LA-5160-MS] 21 p2578 N73-30660
Development of aerodynamic transmission system for use with wind driven electric generators
[NASA-TT-F-15131] 22 p2618 N73-30976
Cryocooling and electric capacity of refrigerator/electric generator space power unit
[NASA-TM-X-71433] 23 p2748 N73-31992
Device for converting electromagnetic wave energy into electric power
[NASA-CASE-GSC-11394-1] 23 p2763 N73-32109
Brushless electromechanical generator for sine and cosine functions
[NASA-CASE-LAR-11389-1] 23 p2765 N73-32121

ELECTRIC IGNITION
Internal impedance of lead accumulator starting batteries
[FOA-3-C-3667-94] 06 p0626 N73-15077

ELECTRIC IMPULSES
U ELECTRIC PULSES

ELECTRIC LEADS
U ELECTRIC WIRE

ELECTRIC MOMENTS
Digital computer calculation of molecular hydrogen-atomic hydrogen interaction energy and electric dipole moment
[NASA-TM-X-2839] 20 p2455 N73-29733

ELECTRIC MOTORS
NT INDUCTION MOTORS
NT SYNCHRONOUS MOTORS
NT TORQUE MOTORS

Use of unidirectional glass plastics for wound structures of electrical machines and equipment
[AD-748737] 04 p0400 N73-13252
Electric parameter of rectangular superconductors immersed in cavities of electric motors
[REPT-123] 05 p0586 N73-14764
Electrical parameters of large rectangular conductor immersed in cavity of electric motor
[REPT-122] 05 p0586 N73-14765
Electromechanical response of induction triphase motor to voltage perturbation in feeder network
[PUBL-1362] 06 p0647 N73-15254
Response of triphase induction motor to perturbations caused by power interruptions
[PUBL-1360] 06 p0677 N73-15504
High charge and discharge rate lead/acid battery for hybrid heat-engine/electric vehicle
[PB-213257] 13 p1477 N73-21969
Development of virtually zero magnetic bearing for application to electric motor construction
[NASA-CR-130225] 13 p1499 N73-22152
Mechanical drives of electrical motors
[AD-756705] 14 p1642 N73-23319
Algorithm for computing unrelieved electromagnetic forces of attraction of rotors in EDG electric motors
17 p2059 N73-26657
Design, development, fabrication, and test of propulsion system for free balloon using electric motor and 35.4 foot propeller
[AD-760754] 18 p2107 N73-27042
Speed control system for dc motor equipped with brushless Hall effect device
[NASA-CASE-MFS-20207-1] 23 p2763 N73-32107

ELECTRIC NETWORKS
Development of computer model to analyze effects of temperature variations on six basic electronic components
[AD-745189] 01 p0033 N73-10256
Numerical optimization techniques for computer-aided design of distributed, lumped, active networks
[AD-745640] 01 p0035 N73-10272
Comparison of quasi-Newton methods for dc analysis of electronic circuits
[AD-746391] 01 p0035 N73-10274
Node voltage method for analyzing nonlinear electric networks with lumped parameters
[NLL-TRANS-2865-[9022.81]]
11 p1264 N73-20255
Network analysis of transmission line analogs for stacked piezoelectric crystal vibrators
[AD-754545] 11 p1330 N73-20799
Automatic connection of aerogenerator to electrical network
[NASA-TT-F-14873] 12 p1386 N73-21238
Computer design of sequential synchronous circuits and multiple output logical networks
[CEA-R-4294] 12 p1387 N73-21246
Systems of nonlinear equations connecting capacity and potential at node-points of electrical network
[NLL-PO-2922-[9022.81]] 15 p1759 N73-24256
Analysis of packet switching network by computerized simulation
[NPL-COM-SCI-64] 19 p2239 N73-28053
Use of lithium/sulfur batteries as load-leveling devices in electrical utility networks
[ANL-7958] 21 p2499 N73-30058
Entropy problem in passive networks
[AD-763752] 21 p2520 N73-30209
Methods of circuit optimization and analysis of advantages and disadvantages of circuit optimization by computer
[AD-763766] 21 p2520 N73-30211
Program for generating transfer functions of electrical network circuits
[AD-764809] 23 p2762 N73-32102

ELECTRIC POTENTIAL
NT BIOELECTRIC POTENTIAL
NT COULOMB POTENTIAL
NT LOW VOLTAGE
NT SPIKE POTENTIALS

Determination of quality of zinc phosphate coatings by measurement of electrode potential
[AD-745094] 01 p0070 N73-10571
Potential barrier for neutral excitation at helium liquid-vapor interfaces
[NOTA-INTERNA-375] 01 p0083 N73-10690
Calculated relationships of potential distribution over ship hulls for electrochemical protection from seawater corrosion
[DRIC-TRANS-2877] 02 p0149 N73-11208
Harmonic functions for determining currents and voltages in nonlinear electrical circuit
[AD-748231] 03 p0276 N73-12243
Mechanisms for increases in saturation voltage as result of neutron radiation
[SC-DR-72-0418] 04 p0467 N73-13806
Pulse voltage distribution over series connected silicon rectifiers
[AD-750969] 06 p0648 N73-15260
Development of test probe device for simultaneous determination of condition of cells in multi-cell storage battery
[NASA-CASE-MFS-20761-1] 08 p0869 N73-17037
Limitations and applications of electrostatic probes with floating potential for measurements of plasmas with low frequency oscillations
08 p0947 N73-17757
Perturbation method for calculating voltage and impedance response of Josephson point contacts to external HF currents
[AD-751911] 08 p0951 N73-17786
Design and safety procedures for operating high voltage capacitor bank
[AD-750535] 09 p1008 N73-18231
Instability of rotating plasmas at beta value before reaching critical velocity
[TRITA-EPP-73-01] 12 p1436 N73-21636
Voltage fluctuation of batteries during charging with asymmetrical alternating current
[AD-756557] 13 p1478 N73-21974
Compensation of vidicon signal dark component
[DRIC-TRANS-2967] 13 p1491 N73-22089
Perturbation theory for determining potential of point source current in cylindrical cell
[AD-756666] 13 p1501 N73-22166
Computing rotor potential of electrostatic gyroscope
13 p1556 N73-22610
Numerical calculation of current-voltage characteristics for ionized plasma containing negative ions with unequal electron and ion temperatures
[LOG-17146] 13 p1563 N73-22667
Empirical equations for calculating photovoltaic characteristics of solar cell array
[NASA-CR-130248] 15 p1737 N73-24085
Systems of nonlinear equations connecting capacity and potential at node-points of electrical network
[NLL-PO-2922-[9022.81]] 15 p1759 N73-24256

Determination of electric potential field and aerodynamic moments for steady rarefied plasma flow past solid sphere
15 p1816 N73-24720
Electric field and current in thin aluminum film superconductor near critical temperature
[LNF-72/77] 15 p1821 N73-24759
Inversion layer silicon solar cells with induced junctions
[NASA-CR-131840] 16 p1865 N73-25100
Numerical calculation of electric potential resulting from charged parallel plates of equal width - Part I
[AD-761866] 19 p2321 N73-28676
Measurements of pressure, voltage, and wall heat flux in wall-stabilized arc heater
[NASA-TM-X-69571] 20 p2420 N73-29443
Technique for reducing ambient electric field generated by inductive voltages in extreme low frequency magnetic field generators
[AD-764531] 23 p2768 N73-32142
One-dimensional analysis of electric fields and electric potential near photo emitting plate emmersed in solar wind plasma
23 p2858 N73-32839

**ELECTRIC POWER**
Photoelectric, thermoelectric, and thermoemission methods of converting solar to electrical energy
[AD-747293] 02 p0129 N73-11050
Extraterrestrial space for supplying earth with vanishing minerals, materials, and needed electric power
04 p0473 N73-13863
Utilization of space technology to supply earth demands for thermal and electric energy
04 p0473 N73-13864
Experimental investigations of two-dimensional flow problems and electric power generation in open cycle vortex MHD generator
[BM-RI-7699] 05 p0583 N73-14746
Congressional hearings on research and development of environmentally safe electric power production
11 p1352 N73-20976
Characteristics of nickel-zinc electric battery and application to propulsion of hybrid electric surface vehicles
[AD-756431] 13 p1477 N73-21963
Analysis of power consumption and switching times of micropower complementary bipolar transistor inverters
18 p2125 N73-27172
Magnetohydrodynamic generator for combined magnetohydrodynamic electric power plant with first generation open cycle
[AD-764925] 23 p2748 N73-31996

**ELECTRIC POWER CONVERSION**
U ELECTRIC GENERATORS

**ELECTRIC POWER PLANTS**
NT NUCLEAR POWER PLANTS
Aircraft gas turbine engines in electric and transport power plants
[AD-745832] 01 p0007 N73-10055
Bibliography of on-line computers in nuclear and thermal power stations from 1960 to June 1972
[CE-BIB-226] 01 p0030 N73-10233
Liapunov functions for analyzing stability properties of various large scale electrical power systems - conferences
07 p0760 N73-16169
Stability analysis of electric power systems
07 p0760 N73-16170
Liapunov direct method for studying transient stability of multimachine power system
07 p0760 N73-16171
Output stability analysis on nonlinear feedback and transient power systems
07 p0760 N73-16172
Stability margins for electrical power systems with perturbations in its multiareas
07 p0760 N73-16173
Liapunov type methods for checking dynamic security in power system stability theory
07 p0760 N73-16174
Mathematical models for analyzing synchronous functions of multimachine electrical power systems
07 p0760 N73-16175
Principle and vector Liapunov functions for studying stability in large scale dynamic systems
07 p0760 N73-16176
Algebraic criteria for connective stability of large scale dynamic systems subjected to structural perturbations
07 p0760 N73-16177
Exponential stability of discrete time composite systems with periodic and non-periodic sampling operation
07 p0761 N73-16178
Solar electric power plants in unmanned spacecraft
[NASA-CR-131360] 11 p1333 N73-20824
Gas turbine power plants in future urban energy planning
[RE-439J] 13 p1593 N73-22912
Design, development, and evaluation of organic, Rankine cycle power plant
[AD-757632] 14 p1606 N73-23018
Functional characteristics and operating data of experimental, aerodynamic three-phase electric power plant constructed in Crimea
[NASA-TT-F-14933] 15 p1761 N73-24268
Portable open cycle fuel cell power plant capable of operation on military fuels
[AD-764285] 22 p2618 N73-30979

**ELECTRIC POWER SUPPLIES**
NT SPACECRAFT POWER SUPPLIES
Thermodynamic equilibria and carbon deposition in carbon-hydrogen-oxygen system of high temperature fuel cells
[ARL/ME-NOTE-333] 01 p0006 N73-10048
Power supply for aircraft data acquisition system time display unit using dc to dc converter
[ARL/ME-NOTE-332] 01 p0006 N73-10049
Development, characteristics, and application of solar electric power generators used in USSR spacecraft - Part I
[AD-741524] 01 p0007 N73-10056
Voltage sensor counter as three-phase power disturbance monitor
[AD-746169] 02 p0129 N73-11049
Optimum switching of large number of low voltage power generating elements with nonlinear volt-ampere characteristics
[AD-747560] 03 p0275 N73-12233
Aerospace MHD large scale power generation
04 p0473 N73-13865
Development of procedures for regulating voltage in power systems for conditions of remote electric transmissions and operation of electro-receivers
[AD-748233] 05 p0499 N73-14060
Physical properties and performance of radioisotope power generator Tristan
[CONF-710444-11] 06 p0627 N73-15083
Electromechanical response of induction triphase motor to voltage perturbation in feeder network
[PUBL-1362] 06 p0647 N73-15254
Computer modeling of space charge flow in electrogasdynamic generator
[AD-751632] 07 p0829 N73-16720
Design parameters that contribute to cycle life of sealed, heat-sterilized silver oxide-zinc cells
[NASA-CR-130723] 08 p0869 N73-17038
Evaluation of conference to investigate current and future development in aircraft electrical and auxiliary power systems
[AGARD-AR-50] 09 p0990 N73-18081
Proceedings of conference on application of superconductivity techniques to auxiliary power systems for aircraft and missiles
[AGARD-CP-104] 10 p1108 N73-19030
Development of high magnetic fields using superconductors with high current densities and application to power conversion and energy storage
10 p1108 N73-19035
Characteristics of conventional alternators and aircraft electrical power systems and comparison with electric systems using superconductors
10 p1109 N73-19036
Development of superconducting homopolar machines with multiple discs and superconducting field winding using liquid metals for armature sliding contacts
10 p1109 N73-19037
Characteristics of superconducting electric generators to show effect of electromechanical, electromagnetic, and cryogenic parameters on design
10 p1109 N73-19039
Features and characteristics of superconducting electrical machines and design of synchronous electric generator for airborne use
10 p1109 N73-19040
Characteristics of power generating systems and application in missiles for production of hydraulic and electric energy
10 p1110 N73-19044
Characteristics of auxiliary power unit combined with accessory drive to form auxiliary power system for aircraft electric power supply
10 p1110 N73-19045
Design principles of auxiliary power units of secondary power system for operation of aircraft equipment
10 p1110 N73-19046
Analysis of interface between aircraft mechanical power requirements and performance requirements of auxiliary power systems
10 p1110 N73-19049
Analysis of gas turbine engine requirements and performance when main propulsion system furnishes auxiliary power source
10 p1110 N73-19050
Air Force research and development programs in aircraft electrical power systems to show planning process for developing specific classes of technology
10 p1111 N73-19052
Application of solid state switching, multiplexing, and electrically programmable logic to aircraft electrical systems
10 p1111 N73-19053
Development of electrical generation and distribution systems for supersonic aircraft using solid state switching and remote control of protective devices
10 p1111 N73-19054
Apollo experience report on design philosophy and experience of Apollo spacecraft electrical power generation system
[NASA-TN-D-7142] 10 p1214 N73-19873
Research and development program with space electric power systems
[LA-4690] 11 p1238 N73-20046
Development, characteristics, and advantages of high voltage direct current electrical systems for aircraft power supplies
[AD-757646] 14 p1604 N73-23001
Construction, operation, and applications of fuel cells to show advantages and limitations
[NASA-SP-5115] 17 p1985 N73-26045
Test methods for evaluating electrical power supply characteristics
[AD-759926] 17 p2005 N73-26218
Development of electrical circuit for suppressing oscillations across inductor operating in resonant mode
[NASA-CASE-ERC-10403-1] 17 p2007 N73-26228
Thick film microelectronic amplifier module for space instruments
[RAE-LIB-TRANS-1643-PT-1] 17 p2007 N73-26233
Dc to dc converter for electronic equipment power source
[AD-762181] 19 p2223 N73-27934
Logistic performance data book for KC-135 aircraft electrical power system to show reliability, maintainability, logistics support, and operating problems
[AD-762225] 19 p2358 N73-28972
Design, development, and performance tests of wind driven, propeller operated electric generation station
[NASA-TT-F-15037] 20 p2363 N73-29004
Design, development, and application of 10,000 watt solar array panel for application to three possible space missions and review of solar cell technology
[NASA-CR-133616] 20 p2363 N73-29006
Design, development, and operation of wind-powered electric generators for commercial electric power applications
[NASA-TT-F-15068] 20 p2364 N73-29008
Development and construction of wind driven electric power generators for specific European areas
[NASA-TT-F-15050] 20 p2364 N73-29009
Development of aerodynamic transmission system for use with wind driven electric generators
[NASA-TT-F-15131] 22 p2618 N73-30976
Powerplexer for distribution of dc power levels to loads which require different voltages
[NASA-CASE-MSC-12396-1] 23 p2747 N73-31988
Operation of switching electronic power regulator for Skylab/Apollo telescope mount
[NASA-CR-124445] 23 p2748 N73-31989
Low ripple klystron power supply for experimental array radar transmitter
[AD-765515] 24 p2881 N73-33010

**ELECTRIC POWER TRANSMISSION**
Electrical and dimensional characteristics of ac superconducting power transmission circuits
[AD-745846] 01 p0088 N73-10727
Computer program for solution of transient thermal problems in electrical power systems using concept of temperature calculations by analogy
[PB-211904] 05 p0607 N73-14933
Remote sensing equipment to ensure efficiency in microwave electric power transmission to remote receiving stations
[NASA-CASE-MFS-21470-1] 11 p1264 N73-20257
Powerplexer for distribution of dc power levels to loads which require different voltages
[NASA-CASE-MSC-12396-1] 23 p2747 N73-31988

**ELECTRIC PROPULSION**
NT ARC JET ENGINES
NT ELECTROMAGNETIC PROPULSION
NT ELECTROSTATIC PROPULSION
NT ION PROPULSION
NT PLASMA PROPULSION
NT SOLAR ELECTRIC PROPULSION
Chemical and electric auxiliary propulsion technology of United Kingdom, France, and West Germany
[NASA-CR-128328] 01 p0090 N73-10742
Development and characteristics of radioisotope safety devices for use with electric propulsion system - Vol. 1
[NASA-CR-114505] 01 p0090 N73-10745
Design, development, and characteristics of radioisotope shielding systems for use with spacecraft electric propulsion system - Vol. 2
[NASA-CR-114506] 01 p0091 N73-10746
Design and analysis of radioisotope shield for thermionic power supply used in spacecraft electric propulsion systems - Vol. 3
[NASA-CR-114507] 01 p0091 N73-10747
HILTOP - variational calculus program for generating electric propulsion data on rendezvous missions to comet Encke
[NASA-CR-114491] 01 p0104 N73-10857
Analysis of performance capability improvement for Pioneer F and G spacecraft using electric thrust subsystem
[NASA-CR-114514] 02 p0222 N73-11798

Silicon-controlled, rectifier series, resonant inverter, power conditioning for electric propulsion from solar array
[NASA-CR-120928] 02 p0223 N73-11804
Nonlinear time dependent phenomena in JxB devices applicable to MHD power generators and electric propulsion engines
[AD-751943] 08 p0956 N73-17826
Development of computerized multistage failure process simulation to evaluate risk in solar electric space mission
[NASA-CR-131518] 12 p1457 N73-21813
Mission engineering analysis of nuclear-thermionic electric propulsion spacecraft for unmanned interplanetary and geocentric mission
[NASA-CR-131599] 13 p1570 N73-22724
Mission engineering analysis of nuclear-thermionic electric propulsion spacecraft for unmanned interplanetary and geocentric missions
[NASA-CR-131600] 13 p1570 N73-22725
ADMAP computer manipulation program for processing electric propulsion trajectory data generated by low thrust optimization program, HILTOP
[NASA-CR-130242] 15 p1754 N73-24216
Pilot level decision analysis of thermionic reactor development strategy for nuclear electric propulsion
[NASA-CR-133035] 16 p1943 N73-25725
Control of 30 centimeter diameter mercury bombardment thruster
[NASA-TM-X-68297] 21 p2588 N73-30738
Exhaust pressure and density of pulsed thrustor systems
[NASA-TM-X-68299] 21 p2589 N73-30740
Thermodynamic analysis of MHW space electric power generator with plutonium dioxide heat source
[LA-5202-MS] 22 p2699 N73-31616

**ELECTRIC PULSES**
One watt pulsed solid state source for X-band navigational beacons
[TR-70-3] 05 p0518 N73-14213
Discharge circuit of inductive accumulator for generating short front current pulse
[JPRS-58892] 13 p1504 N73-22190
Extraction of beginning and ending of pulse trains
16 p1883 N73-25244

**ELECTRIC RELAYS**
Transformation of relay contact networks in logic gate circuits for failure analysis
05 p0522 N73-14248
Relationship of relay intermodulation products and constriction resistance with relay life
[AD-755923] 12 p1385 N73-21236
Design and tests of hybrid microelectronics solid state relay for 2500 volts isolation and minus 120 C to 80 C thermal cycling range
[NASA-TM-X-68248] 15 p1756 N73-24235
Static parameters of mechanical model of thin film electrostatic relay
21 p2514 N73-30171

**ELECTRIC ROCKET ENGINES**
NT ARC JET ENGINES
NT CESIUM ENGINES
NT ELECTROSTATIC ENGINES
NT ELECTROTHERMAL ENGINES
NT ION ENGINES
NT PLASMA ENGINES
NT RESISTOJET ENGINES
Design, stress analysis, and reliability evaluation of electric rocket engines
[AD-745427] 01 p0091 N73-10751
Design parameters of space propulsion ramjet engine using plasma accelerator
[AD-759290] 16 p1958 N73-25840
High voltage solar array for ion thruster electric propulsion system
[NASA-TM-X-71462] 24 p2880 N73-33002

**ELECTRIC SPARKS**
Dynamics of laser triggered spark discharge channel with nanosecond pulse formation
[AD-747510] 03 p0343 N73-12799
Analysis of electronic circuit and performance of spark gap assembly
[CERN-72-6] 04 p0399 N73-13244
Design and performance of flash lamps with nanosecond light pulses
[AD-750788] 06 p0701 N73-15720
Plasma diagnostics with infrared schlieren and interferometric techniques using TEA-CO2 laser, exemplified by electric spark transient response
[ISL-19/72] 16 p1950 N73-25779

**ELECTRIC STIMULI**
Physiological and pathological responses of humans exposed to electricity
[NASA-CR-128422] 01 p0008 N73-10065
Behavioral learning response of cat to electric stimulation of auditory nervous system
[NASA-CR-132047] 15 p1742 N73-24124
Cross correlation analysis of stress rhythm during stimuli of varying biological significance
24 p2890 N73-33071

**ELECTRIC STRAIN GAGES**
U STRAIN GAGES

**ELECTRIC SWITCHES**
NT CRYOTRONS
NT THERMOSTATS
Digital simulations of Joule heating and heat transfer processes in amorphous semiconductor switches
[AD-746278] 02 p0219 N73-11776
Development of differential pressure control system using motion of mechanical diaphragms to operate electric switch
[NASA-CASE-MFS-14216] 04 p0419 N73-13418
Contacts between chalcogenide glasses, metals and semiconductors
[AD-752560] 08 p0952 N73-17797
Ni/ZrO2 composite material for designing high strength thermal switches
[HIT-527] 12 p1383 N73-21212
Electronic switching phenomena in organic thin films
[AD-755267] 12 p1442 N73-21682
Analysis of on-state in chalcogenide threshold switches
[AD-756273] 15 p1821 N73-24763
Electric switches for closing high voltage, high Q LC circuits, determining breakdown voltage and open and closed contact resistance
[BMBW-FBK-72-32] 22 p2704 N73-31660

**ELECTRIC TERMINALS**
Quality control of welded, brazed, and bonded electrical terminations
[BDX-613-613-REV] 12 p1383 N73-21214
Relationship between power distribution and tolerance sensitivity in linear, two-terminal electric network
[NLL-PO-2895-[9022.81]] 15 p1759 N73-24253
Helium cooled current leads in refrigerated superconductive magnet system
[DESY-72/65] 17 p2073 N73-26769
Evaluation of single wire termination system capable of interconnection to various multicontact connectors
[AD-764248] 22 p2644 N73-31190

**ELECTRIC WELDING**
NT ARC WELDING
NT ELECTRON BEAM WELDING
NT GAS TUNGSTEN ARC WELDING
NT PLASMA ARC WELDING
Electrical resistance butt welder for welding fine gauge tungsten/rhenium thermocouple wire
[NASA-CASE-LAR-10103-1] 05 p0550 N73-14468
Electric resistance spot welding and brazing for producing metal bonds with superior mechanical and structural characteristics
[NASA-CASE-LAR-11072-1] 11 p1298 N73-20535
Process for welding compressor and turbine blades to rotors and discs of jet engines
[NASA-CASE-LEW-10533-1] 19 p2303 N73-28515
Optimized electric welding technique for silicon solar cell arrays
[LCR-DR-1-72-52/1/R] 21 p2553 N73-30470

**ELECTRIC WIRE**
NT BEAM LEADS
NT EXPLODING WIRES
Analysis of coupling characteristics and crosswalk between electric cables used in naval environments
[AD-742971] 01 p0032 N73-10253
Torque measurement of flat polyimide cable crossing hinge or satellite solar array
[ESRO-TN-114-ESTEC] 05 p0603 N73-14904
Hypervelocity impact tests of Skylab electrical cables for simulation of micrometeoroid environment
[NASA-TN-D-7178] 07 p0761 N73-16186
Low temperature resistivity of high purity copper wire in high magnetic fields
[U-235] 08 p0943 N73-17725
Device for bending leads projecting from printed circuit boards
[NASA-CASE-MFS-22133-1] 09 p1039 N73-18473
Development of low profile flat conductor cable connecting device and permanent splice methods for use in spacecraft component electrical systems - Vol. 1
[NASA-CR-128845] 11 p1262 N73-20241
Fabrication and evaluation of wire harnesses from small gage wire round conductor cables - Vol. 2
[NASA-CR-128846] 11 p1262 N73-20242
Cost comparison of flat versus round conductor cable based on spacecraft electric wiring system specifications - Vol. 3
[NASA-CR-128847] 11 p1262 N73-20243
Electrically conductive wire storage in plastic capsule that allows for unfolding
[NASA-CASE-LAR-10168-1] 13 p1499 N73-22151
Development, characteristics, and applications of flat conductor cable to include methods and facilities for fabrication
13 p1593 N73-22916
Theory for electrical resistivity in wire braid coaxial conduction at low and high radio frequencies
[RAE-TR-72153] 17 p1998 N73-26155
Volt-ampere characteristics of heated electric wire during cryogenic cooling in liquid helium
[AD-759958] 17 p2005 N73-26211
Scanning electron microscope examination of wire bonds from high reliability microelectronic devices
[NBS-TN-785] 21 p2549 N73-30432
Thermal aging of plastic insulated silver-plated copper aircraft electrical wire
[AD-764731] 23 p2767 N73-32135

**ELECTRIC WIRING**
U ELECTRIC WIRE
U WIRING

**ELECTRICAL BREAKDOWN**
U ELECTRICAL FAULTS

**ELECTRICAL CONDUCTIVITY**
U ELECTRICAL RESISTIVITY

**ELECTRICAL CONDUCTIVITY METERS**
Particles and fields subsatellite magnetometer experiment to calculate lunar interior electrical conductivity
12 p1451 N73-21757

**ELECTRICAL ENERGY**
U ELECTRIC POWER

**ELECTRICAL ENGINEERING**
Abstracts from Soviet scientific and technical journals on electronics and electrical engineering
[JPRS-57877] 06 p0647 N73-15256
Research projects in radio and electronic engineering
[AD-752845] 09 p1008 N73-18228
Electronic procedures for selecting and teaching students at Moscow Institute of Electronic Engineering
[JPRS-58550] 12 p1386 N73-21242
Economic effectiveness of production planning and automatic control methods in industry
[JPRS-58680] 12 p1467 N73-21884
Research reports for various engineering sciences and materials and metallurgy
14 p1721 N73-23961
Multipath rainfall measurements for planning ultrahigh frequency radio link
17 p1996 N73-26137
Research conducted in School of Electrical Engineering at Purdue University during 1972
18 p2213 N73-27871
Tandem electronic voice switching system
[FAA-RD-73-133] 21 p2519 N73-30206

**ELECTRICAL FAULTS**
NT SHORT CIRCUITS
Electrical overstress failures in silicon semiconductor devices
[AD-747795] 03 p0275 N73-12230
Surge divertor breakdown voltage characteristics
[AD-747622] 03 p0276 N73-12236
Electrostatic repulsion criteria for dc high voltage spark breakdown of gas
[ORO-4211-5] 03 p0336 N73-12742
Effect of purification of transparent dielectrics from dust on breakdown threshold under action of laser irradiation
[AD-748230] 03 p0338 N73-12760
Mathematical models for predicting microwave breakdown in fringing field of rectangular slot antenna
[AD-751320] 07 p0763 N73-16202
Mathematical model for calculating breakdown voltage of solid homogeneous dielectric solid during thermal breakdown
[NLL-CE-TRANS-5560-[9022.09]]
11 p1329 N73-20786
Electric strength breakdown in insulating dielectric liquids
[AD-755756] 13 p1548 N73-22546
Analysis of methods of fault diagnosis used with logic circuits and effect of procedures on structure of circuit assemblies
[NLL-PO-2913-[9022.81]] 15 p1759 N73-24255
Fault detection test methods in combinational digital logic networks
[AD-760543] 18 p2121 N73-27146
Electrical and thermal breakdown properties of tantalum oxide and hafnium oxides capacitors
22 p2641 N73-31168
Time-resolved voltage breakdown in insulators due to 2-MeV electronics
[UCRL-51372] 24 p2898 N73-33138

**ELECTRICAL IMPEDANCE**
NT CONTACT RESISTANCE
NT ELECTRICAL RESISTANCE
Theoretical analysis of linear semi-infinite array of uniformly spaced elements to determine mutual coupling effects
[AD-745799] 01 p0034 N73-10263
Internal impedance of lead accumulator starting batteries
[FOA-3-C-3667-94] 06 p0626 N73-15077
FORTRAN subroutine for plotting computer determined transmission line parameters on Smith chart
[AD-751019] 06 p0645 N73-15243
Ionospheric transfer impedance of rocket-borne quadrupole probe near lower hybrid resonance
[NRC-TT-1614] 06 p0666 N73-15414
Variation of Rayleigh wave reflection coefficient of different interdigital transducer configurations with electric loads
07 p0831 N73-16737
Formulas for measurement of impedance of single-layer induction coils
[IAE-2120] 08 p0889 N73-17195
Perturbation method for calculating voltage and impedance response of Josephson point contacts to external HF currents
[AD-751911] 08 p0951 N73-17786

Surface transfer impedance measurements for determining shielding characteristics of coaxial cables
[AD-753678] 09 p1009 N73-18237
Load impedance and electromagnetic radar echo scattering
[AD-754899] 11 p1258 N73-20209
Passive electrical dummy load for simulating transducers in large sonar arrays
[AD-755174] 13 p1495 N73-22123
Cylindrical chamber for simulating electrical impedance of whip antenna
[AD-757141] 13 p1501 N73-22167
Kinetic theory for input impedance of cylindrical dipole antenna in anisotropic plasma
17 p2067 N73-26720

ELECTRICAL INSULATION
Measurement of partial discharges in electrical insulating materials and application to quality control of manufactured electric equipment
[NLL-CE-TRANS-5844-[9022.09]]
02 p0191 N73-11545
Development and characteristics of electrical insulation material with potential to withstand 80 kilovolts
[BDX-613-502-REV] 04 p0398 N73-13242
Electrical resistivity of space electric power insulating materials
[LA-4978] 05 p0498 N73-14058
Influence of humidity on thermal life determination of electrical insulation
[AD-749926] 05 p0521 N73-14238
Statistical analysis of thermal stability and service life of electrical insulation
[AD-749925] 05 p0521 N73-14239
Plastic sheaths as lightning conductors for insulating communication cables
[AD-750642] 06 p0647 N73-15252
Radiation damage of electrically insulating polymeric materials used in electrotechnology
[AD-753367] 09 p1001 N73-18169
Properties of thermal resistant electrical insulating papers based on inorganic fibers
[NLL-RTS-7740] 10 p1175 N73-19554
Polarization and thermionic emission effects on resistivity measurements for metal oxide electrical insulators at high temperatures
[HEDL-TME-72-73] 12 p1386 N73-21243
Spectral analysis of nonconducting siliceous materials by luminescent discharge
[CEA-CONF-2060] 12 p1405 N73-21397
Procedure for making insulating foil for use in multilayer insulating system
[NASA-CASE-LEW-11484-1] 13 p1532 N73-22415
Characteristics of HALAR fluoropolymer as versatile insulation material
14 p1640 N73-23298
Laser induced damage and avalanche breakdown in transparent insulators
[AD-761168] 18 p2158 N73-27439
Spectrochemical analysis of nonconducting materials using cathodes from sample in Grim glow discharge tube
[NASA-TT-F-15031] 20 p2454 N73-29723
Electrical properties and radiation resistance of capacitor insulation
[ORNL-4842] 21 p2563 N73-30544
Development of stored charge device using field effect transistor technology
[NASA-CASE-NPO-11136-2] 22 p2617 N73-30974
Time-resolved voltage breakdown in insulators due to 2-MeV electronics
[UCRL-51372] 24 p2898 N73-33138

ELECTRICAL LEADS
U ELECTRIC CONDUCTORS

ELECTRICAL MEASUREMENT
NT POLAROGRAPHY
Determination of KOH loss in ESRO 4 nickel cadmium batteries by electrical measurements
[ESRO-CR[P]-132] 04 p0375 N73-13054
Equatorial electrojet measurement made by Cosmos 321 and magnetic observatories
04 p0414 N73-13377
Design of power supply voltage monitor for measuring multiple dc voltages simultaneously
[AD-748829] 04 p0424 N73-13453
Design and performance of ammeter with reversible temperature indicator for recording peak currents
[UCRL-73587] 05 p0547 N73-14446
Operating principles of RF biased SQUID systems
[NBS-TN-629] 06 p0708 N73-15773
Use of Josephson devices to measure low frequency magnetic fields and voltages
[LBL-845] 06 p0708 N73-15777
Ground-based measurements of electrical length of vehicle and plume and of atmospheric electricity during Apollo 13 and 14 launches
[NASA-CR-130535] 08 p0916 N73-17503
Design and performance of voltage transducers for Mariner spacecraft solar cells
[NASA-CR-132250] 15 p1756 N73-24234
Experimental determination of width of near anode region in knudsen mode of thermionic converter having variable interelectrode gap filled by Ba plus Cs mixture
[AD-760394] 17 p2062 N73-26682
Coversion data for transition from english to metric system for design and fabrication of transformers
[NASA-CR-133932] 22 p2700 N73-31624

ELECTRICAL PROPERTIES
NT CAPACITANCE
NT CARRIER MOBILITY
NT CHARGE DISTRIBUTION
NT CONTACT RESISTANCE
NT DIELECTRIC PROPERTIES
NT ELECTRIC MOMENTS
NT ELECTRICAL IMPEDANCE
NT ELECTRICAL RESISTANCE
NT ELECTRICAL RESISTIVITY
NT ELECTRON MOBILITY
NT ELECTROSTRICTION
NT FERROELECTRICITY
NT HOLE MOBILITY
NT INDUCTANCE
NT IONOSPHERIC CONDUCTIVITY
NT MAGNETORESISTIVITY
NT PERMITTIVITY
NT PHOTOCONDUCTIVITY
NT PHOTOVOLTAIC EFFECT
NT PIEZOELECTRICITY
NT PLASMA CONDUCTIVITY
NT POLARIZATION CHARACTERISTICS
NT PYROELECTRICITY
NT SUPERCONDUCTIVITY
Results of testing and characterization of battery plates for nickel cadmium cells
[NASA-CR-130094] 01 p0006 N73-10050
Electrical and mechanical properties of vector magnetometer in HELIOS experiments for interplanetary magnetic field observations
[GAMMA-21] 01 p0048 N73-10384
Small rocket wire deployment for simulating electrical properties of large rocket engine to study lightning triggering or diversion
[AD-746309] 01 p0078 N73-10644
Electronic and thermodynamic properties of dense plasma interacting with metallic and nonmetallic materials
[CEA-R-4268] 01 p0085 N73-10705
Electrical properties of p-n junctions formed by ion implantation into GaAs and [Ga,In]As
[NASA-CR-112200] 01 p0087 N73-10717
Electrical and dimensional characteristics of ac superconducting power transmission circuits
[AD-745846] 01 p0088 N73-10727
Optical measurements of thin slots milled in edges of aluminum alloy test blocks to determine accuracy of measurement and detectability by operators using high frequency probes
[ARL/MET-NOTE-82-PT-1] 02 p0186 N73-11506
Electrical-, thermal-, and magnetic-properties of zirconium and niobium carbide solid solutions
[AD-746217] 02 p0219 N73-11772
Network synthesis and analysis of thermoelectric generators to show relation between physical properties and elements of internal structure
[AD-747617] 03 p0256 N73-12071
Computer aided analysis on radiative characteristics of sonar transducer with spaced sensor element array
[AD-747281] 03 p0266 N73-12156
Development of materials and construction processes for improved efficiency of photoelectric converters
04 p0375 N73-13048
Evaluation of dielectric insulation and etched junction contact techniques for fabrication of wraparound contact silicon solar cells
[NASA-CR-121021] 04 p0375 N73-13051
Design and development of rechargeable zinc/air electric battery
[AD-748434] 04 p0377 N73-13064
Development and characteristics of electrical insulation material with potential to withstand 80 kilovolts
[BDX-613-502-REV] 04 p0398 N73-13242
Electrical characterization of complex microcircuits for amplifiers, comparators, and regulators
[AD-748242] 04 p0400 N73-13255
Superconductor interactions and properties, and amorphous semiconducting and magnetic materials
[NASA-CR-129524] 04 p0457 N73-13731
Secondary ionic emission procedure for studying semiconductor properties
[CEA-CONF-1969] 04 p0459 N73-13745
Electrical properties of MOS field effect transistors and Schottky barrier photodiode
[AD-748862] 04 p0459 N73-13746
Crystal growing of iron monosulfide, crystallographic studies on titanium oxide semiconductor, emission of zinc selenide diode, and electroreflectance of gallium arsenide
[AD-748336] 04 p0459 N73-13750
Effect of structural changes on electrical and magnetic properties of amorphous semiconducting material
[AD-748661] 04 p0460 N73-13751
Band structure and electrical properties of amphorous semiconductors
[AD-749379] 04 p0461 N73-13761
Development of procedures for regulating voltage in power systems for conditions of remote electric transmissions and operation of electro-receivers
[AD-748233] 05 p0499 N73-14060
Evaluation of high temperature, space vacuum performance of electrical materials, capacitors, and compression sealed pyrolytic boron nitride slot insulation
[NASA-CR-120785] 05 p0518 N73-14216
Effects of low frequency background noise on electrical properties of semiconductor materials and components
05 p0519 N73-14222
Electrical characterization of silicon materials by lifetime, ionized impurity concentration, and noise measurement
05 p0519 N73-14223
Configuration of all pass network with negative real poles and Q factor
[PUBL-1367] 05 p0522 N73-14246
Influence of substrate temperature on properties of epitaxial layers of GaAs during growth
[NLL-RRE-TRANS-370-[8036.625]]
05 p0585 N73-14763
Electric parameter of rectangular superconductors immersed in cavities of electric motors
[REPT-123] 05 p0586 N73-14764
Electrical parameters of large rectangular conductor immersed in cavity of electric motor
[REPT-122] 05 p0586 N73-14765
Electrical and structural criteria for design optimization of integrated circuits
[AD-750947] 06 p0648 N73-15261
Electrical and performance characteristics of Skylab radar altimeter
06 p0663 N73-15386
Electrical, mechanical, and thermal properties of transparent optical adhesives
[AD-750571] 06 p0688 N73-15602
Optical and electrical properties of amorphous germanium and silicon semiconductors
[AD-748856] 06 p0709 N73-15788
Properties of amorphous semiconductors
[AD-750163] 06 p0710 N73-15797
Electrical properties of insulating and semiconducting CdF2 with trivalent Ce and Gd codopants
[AD-750937] 06 p0711 N73-15799
Application of gas transport method for analyzing p-n junction in cadmium selenide monocrystal
[AD-750506] 06 p0711 N73-15800
Development and characteristics of electric storage battery using lithium-silver chloride couple
[SC-DC-72-2298] 07 p0742 N73-16033
Design and operation of galvanic cells involving solid electrolytes to determine accuracy in thermochemical measurements
[LBL-839] 07 p0742 N73-16034
Development and characteristics of long life, high energy density, sealed zinc oxygen secondary battery for military communications application
[AD-751751] 07 p0742 N73-16035
Room temperature electrical properties of SiGe thermoelectric alloys
[SC-DC-72-1020] 07 p0812 N73-16581
Physical and electrical transport properties of VO2 near its semiconductor-to-metal transition
[AD-751524] 07 p0834 N73-16759
Structural, optical, and electrical properties of amorphous semiconductors
[AD-751084] 07 p0834 N73-16760
Mathematical model for nonlinear characteristics of avalanche diode
[AD-751974] 08 p0890 N73-17207
Design of three color plasma panel display device capable of operating at three intensity levels
[AD-752442] 09 p1009 N73-18236
Electrical properties of reinforced dielectrics, magnetic permeabilities of multicomponent materials, and electromagnetic waves in fibrous dielectrics
[AD-752693] 09 p1053 N73-18583
Measurement methods for semiconductor materials, process control, and devices
[AD-753642] 09 p1076 N73-18785
Potentiostatic polarization method for stress corrosion tests on cracking susceptibility of materials
[AD-754205] 10 p1174 N73-19549
Crystal structures, electrical properties, and electronic applications of metal selenides
[JPRS-58293] 10 p1198 N73-19752
Electrical strength of pressed lead azide
10 p1199 N73-19753
Spectroscopic studies of electrical and optical properties of amorphous semiconductors
[AD-753903] 10 p1202 N73-19779
HCL processing effects on electrical stability and quality of thermally grown SiO2
[AD-754110] 10 p1202 N73-19786
Analysis of optimum mass and heat transfer in electrochemical fuel cells to show effects on fuel cell output
[AD-754258] 11 p1238 N73-20051
Effect of flaws on chemical, electrical, mechanical, and masking properties of Si3N4 films
[NLL-DRIC-TRANS-2902-[3623.66]]
11 p1329 N73-20789

Conduction processes in field driven semiconductor p-i-n diodes
12 p1437 N73-21643
Material properties of thin single crystal silicon films on insulator/polycrystalline silicon substrates
[AD-756646] 13 p1503 N73-22179
Electric, photoelectric, and electroluminescence properties of Cu contacts on CdS surface
[AD-756876] 13 p1504 N73-22187
Investigation of electrical properties of vanadium nitrides as effected by nitrogen content
13 p1540 N73-22473
Variations in electrical properties of silicon films on sapphire using MOS Hall technique
13 p1564 N73-22679
Electrical and physical properties of low temperature grown cubic gallium nitride films
[AD-755237] 13 p1567 N73-22704
Electrical characteristics of FCC determined in context of multiple transmission lines theory
14 p1640 N73-23300
Radiation damage in semiconductor devices and changes in electrical properties
[AD-755690] 14 p1698 N73-23778
Study of electrical properties of amorphous semiconductors using Green's function
[AD-757432] 14 p1699 N73-23786
Optical and electronic properties of single crystal Cu2S-CdS photovoltaic cells
[NASA-CR-121228] 15 p1738 N73-24091
Electrical properties and performance of satellite group terminal system
[STC-TM-332] 15 p1749 N73-24178
Electrical characteristics of flush-mounted multimode slot antenna with scan capability
[AD-757990] 15 p1757 N73-24244
Relationship between power distribution and tolerance sensitivity in linear, two-terminal electric network
[NLL-PO-2895-[9022.81]] 15 p1759 N73-24253
Scanning electron microscope effects on charging properties of dielectric materials
[NLL-DRIC-TRANS-2970-[3623.66]]
15 p1785 N73-24470
Electrical properties of thin sputtered aluminum-silica capacitors
[NASA-CR-121165] 16 p1880 N73-25220
Development and characteristics of gate-assisted, turn-off thyristor for high voltage and current operation
[NASA-CR-121161] 16 p1880 N73-25221
Electrical response of capacitor triggered by shock wave effect on Fermi energy level
[AD-759059] 16 p1883 N73-25239
Electrical properties of silicon semiconductor under shock loads
[AD-759003] 16 p1971 N73-25945
Properties and applications of radar antennas
[AD-759693] 17 p1998 N73-26159
Comparison of plasma probe and predicted electrical properties of rocket exhaust plume
17 p2031 N73-26436
Effects of high intensity electrical currents on advanced composites
[AD-760352] 17 p2053 N73-26605
Metallurgical and electrical properties of thin film Pb[0.9]Sn[0.1]Se photoconductive infrared detectors
[AD-758519] 17 p2064 N73-26693
Electrical properties of semiconducting film configurations with contacts to chalcogenide glasses
[AD-760335] 17 p2074 N73-26781
Electrical conductivity and carrier lifetimes in gold doped silicon wafer
[AD-760150] 17 p2075 N73-26789
Electrical properties of solid-solid interfaces for charge transfer phenomena used in image transducer and metal-semiconductor devices
18 p2123 N73-27156
Electrical properties of silicon under dynamic loading
18 p2185 N73-27639
Electronic properties of beryllium single crystals with emphasis on microwave surface impedance
18 p2185 N73-27646
Electrical, optical, and structural properties of RF triode-sputtered gold films
18 p2186 N73-27649
Structure, composition, and electrophysical properties of autoepitaxial silicon layers from vapor-gas tetrachloride mixture
18 p2186 N73-27653
Effect of growth conditions and properties of silicon films deposited by chloride method
18 p2187 N73-27658
Electrical and optical properties of amorphous silicon and germanium semiconductors
[AD-760595] 18 p2191 N73-27690
Analysis of electrical properties, structure, values of passive elements, and operating mode of hybrid neuristor lines
[AD-762311] 19 p2247 N73-28120
MHD generator performance limitation from electrical properties, including conductivity and Hall parameter
19 p2319 N73-28655
Electrical properties of MIS semiconductors and application as infrared detectors
[AD-761510] 19 p2327 N73-28719
Electrical and optical properties of irradiated mercury cadmium telluride semiconductors
[AD-761488] 19 p2327 N73-28721
Development of lead/lead oxide solid electrolyte cell and evaluation of electrical properties in terms of equivalent circuit for cell
20 p2363 N73-29003
Electromicroscopic analysis of Nb3Sn bands to determine effect of carbon doping on current carrying capacity
[NLL-M-23057-[5828.4F]] 20 p2434 N73-29544
Relation of electrical properties of thin films of TiO to defect structure
20 p2460 N73-29766
Sensitivity and optoelectronic properties of semiconductor heterojunctions
20 p2460 N73-29770
Electrical properties and radiation resistance of capacitor insulation
[ORNL-4842] 21 p2563 N73-30544
NBS methods for measuring properties of semiconductor materials, process control, and devices
[NBS-TN-788] 21 p2585 N73-30717
Development of stored charge device using field effect transistor technology
[NASA-CASE-NPO-11156-2] 22 p2617 N73-30974
Electrical properties of dry rocks
[NASA-CR-133886] 22 p2666 N73-31364
Thermal and electrical properties of titanium alloyed with vanadium and high temperature creep of metal with fcc lattice
[JPRS-59623] 22 p2683 N73-31490
Thermal conductivity and electrical properties of titanium alloyed with vanadium at 100 to 350 K
22 p2683 N73-31491
Optical and electrical properties of amorphous Si and their dependence on thermal history
23 p2807 N73-32440
Effect of addition of transition metals on cast zirconium to show changes in microstructure, macrostructure, microhardness, and electrical resistance
23 p2809 N73-32457
Characteristics of hydrazine-oxygen fuel cell operating under moderate temperature conditions and various power density concentrations
[AD-764530] 24 p2881 N73-33009
Analysis of electrical switching phenomena in amorphous arsenic telluride-arsenic selenide system
24 p2966 N73-33707
Electrical properties and switching behavior of amorphous semiconductor films
[AD-765346] 24 p2970 N73-33732

**ELECTRICAL RESISTANCE**
NT CONTACT RESISTANCE
Computer program to simulate FET transistor logic circuit performances and properties
07 p0762 N73-16191
Direct current electrical resistance crack monitoring technique for detection of crack propagation in steels
[PB-212206] 08 p0933 N73-17636
Electrical resistance measurements on crack propagation in fracture toughness specimens under variety of environmental and loading conditions
[MG/54/71] 08 p0966 N73-17899
High temperature electric resistance wire strain gages
[NASA-CR-112241] 09 p1035 N73-18446
Development of method for determining conductivity of surface layer of sea by recording field of remote transmitters operating in superlong wavelength range
10 p1153 N73-19382
Variations of electrical resistance of hydroextruded polycrystalline beryllium in annealing process
10 p1171 N73-19525
Synthesis of stoichiometric crystals of InP doped with impurities for obtaining semiconductor with desired resistance
[NLL-RRE-TRANS-381-[8036.625]]
11 p1329 N73-20790
Electrical resistance of thick film ruthenium dioxide resistor circuits
[AD-756254] 14 p1644 N73-23337
Electrical resistance measurement for determining electron state densities in molten germanium-silver and germanium-copper systems
[NLL-M-21613-[5828.4F]] 15 p1746 N73-24153
Nonlinear dynamic resistance and light emission associated with carrier generation by impact ionization in Gunn domains
15 p1794 N73-24543
Microwave surface resistance of niobium tantalum - and lead indium-superconducting alloys considering thermodynamic vortices
[AD-757875] 15 p1822 N73-24770
Termination resistance as standard for calibrating low noise temperature in electronic equipment
[NASA-TT-F-15016] 19 p2243 N73-28086
Radio frequency source resistance measuring instruments of varied design
[NASA-CASE-NPO-11291-1] 21 p2543 N73-30388
Specific electrical resistance of metal-carbide two-phase system to show effect of porosity and metal content on electrical properties
23 p2807 N73-32444

**ELECTRICAL RESISTIVITY**
NT IONOSPHERIC CONDUCTIVITY
NT MAGNETORESISTIVITY
NT PHOTOCONDUCTIVITY
NT PLASMA CONDUCTIVITY
NT SUPERCONDUCTIVITY
Sheet resistivity and Hall effect study of zinc ions implanted in chromium-doped gallium arsenide
[NASA-CR-112199] 01 p0087 N73-10716
Application of Backus-Gilbert method to electrical conductivity problem
02 p0200 N73-11619
Electrical resistance of lubricating film in friction of various metals
[AD-747451] 03 p0308 N73-12515
Conductivity profiles determined for beryllium diffused silicon for calculating diffusion coefficients
[NASA-CR-129169] 03 p0320 N73-12605
Equations based on theory of elastic moduli of composite materials used to calculate electrical and thermal conductivities of two phase systems
[AD-748304] 04 p0439 N73-13580
Electrical conductivity methods for measuring effects of high energy radiation on dielectric hydrocarbon liquids
[HMI-B-117] 04 p0452 N73-13693
Electrical conductivity of thin films during nucleation and film growth
[AD-748269] 04 p0460 N73-13756
Electrical resistivity of space electric power insulating materials
[LA-4978] 05 p0498 N73-14058
Analog simulation of electrical conductivity in disordered amorphous semiconductor systems
[AD-749300] 05 p0588 N73-14779
Electrical conductivity of ocean basement determined from measurements of geomagnetic time variations on sea floor off Southern California
[AD-749931] 06 p0668 N73-15431
Selection and preliminary evaluation of 2 hollandites, 1 titanate, and 1 tungstate as potential solid conductors of alkali ions
[NASA-TN-D-7157] 06 p0708 N73-15774
Development of theory for time dependent magnetic fields inside Moon and diamagnetic cavity caused by interplanetary eletromagnetic field fluctuation
[NASA-CR-114546] 06 p0718 N73-15861
Low temperature resistivity of high purity copper wire in high magnetic fields
[U-235] 08 p0943 N73-17725
Theoretical study of sunspots and electrical and thermal conductivities of solar magnetoplasma
[AD-752230] 08 p0962 N73-17872
Viscosity and electrical resistivity of molten glass over wide temperature range
[AD-753480] 09 p1055 N73-18604
Electric conductivity of high density xenon plasma
[AD-753489] 09 p1073 N73-18756
Photodielectric and conduction properties of amorphous semiconductors
[AD-753053] 09 p1074 N73-18762
Electrical resistivity measurements on defect concentrations in zinc selenide single crystals
[AD-753043] 09 p1074 N73-18764
Temperature and thickness effects on electrical conductivity of amorphous germanium semiconducting films
[AD-753827] 09 p1076 N73-18782
Electrical conductivity of amorphous germanium semiconductor with pseudogap structure
[AD-753824] 09 p1076 N73-18784
Relationship between wave parameters and spatial spectrum of aerial photographs of sea surface and electromagnetic method for measuring conductivity of sea surface
[JPRS-58370] 10 p1153 N73-19381
Computing electrical conductivity of thermal plasma taking nonelastic collisions into account
[AD-753972] 10 p1198 N73-19746
Polarization and thermionic emission effects on resistivity measurements for metal oxide electrical insulators at high temperatures
[HEDL-TME-72-73] 12 p1386 N73-21243
Review and compilation of technical data on Lorenz ratio of metals and alloys to include electrical resistivity and thermal conductivity
[NBS-TN-634] 12 p1413 N73-21451
Electrical and ionic conductivity of calcium oxide-doped nonstoichiometric cerium dioxide at various temperature ranges
[COO-1441-16] 12 p1416 N73-21473
Electrical conductivity of sintered nonstoichiometric CeO[2-x] as function of temperature
[COO-1441-17] 12 p1416 N73-21474
Electrical conductivity of ThO2 at room and high temperatures and in high intensity gamma radiation fields
[BNWL-1671] 12 p1416 N73-21475
Modification of resistive transition in superconductors by thermodynamic fluctuations
12 p1438 N73-21648

Analysis of electrical conductivity of eutectic solutions of aluminum-nickel alloy using directional crystallization method
13 p1541 N73-22489
Thermal and electrical conductivity of Nd-Y alloy system at room temperature
[AD-756595] 13 p1566 N73-22693
Variation of electric conductivity and thermal emf at fusion of copper chalcogenides
[AD-756088] 13 p1566 N73-22694
Effects of various gases on conductivity of four organic semiconductors at very low pressures
[REPT-1972-19] 14 p1697 N73-23772
AC conductivity and dielectric dispersion in amorphous semiconductors
[AD-757097] 14 p1698 N73-23780
Schumann resonance frequencies and electrical conductivity of mesosphere [40 to 100 km] from ELF spectra
[AD-758775] 15 p1784 N73-24463
Electric field induced instability in transition metal compounds
[AD-758270] 15 p1822 N73-24771
Technique for determination of conductivity profile in diffusion layer of CdS electroacoustic transducers
[AD-758450] 15 p1822 N73-24773
Ziman theory for calculating electrical conductivity of liquid aluminum
[UCRL-51322] 16 p1929 N73-25605
Evaluation of potting compounds by electrical resistivity techniques using continuous current monitoring device
[AD-759005] 16 p1933 N73-25643
Alternating current Hall mobility and electrical conductivity in amorphous threshold switching semiconductors
[AD-759004] 16 p1954 N73-25809
Theory for electrical resistivity in wire braid coaxial conduction at low and high radio frequencies
[RAE-TR-72153] 17 p1998 N73-26155
Conductance of quaternary ammonium salt dispersions in polymeric films
[AD-759073] 17 p2052 N73-26597
Resistivity and ion energy distribution in turbulent plasma heating
[COO-3165-3] 17 p2067 N73-26727
Determining the effects of ion implantation in aluminum oxide including implanted impurities and crystal damage by electrical resistivity and photoluminesence
17 p2071 N73-26755
Internal lunar properties calculated from surface magnetometer experiments data
[NASA-TM-X-62278] 17 p2082 N73-26842
Effects of beta radiation on electrical resistivity of mica
[NLL-RTS-7926] 18 p2184 N73-27635
Molecular mechanisms of conduction and polarization in water vapor, liquid water, and ice
[AD-762060] 19 p2231 N73-27993
Thermal conductivity and electrical resistivity ATJS graphite
[AD-762301] 19 p2313 N73-28601
Electric conductivity of water extracts from soil as measure of ionic strength
[NASA-TT-F-15044] 20 p2411 N73-29377
Influence of applied stress, magnetic and electric fields, and impurity concentration on electrical conductance of n-type germanium at very low temperatures
[RR-738] 20 p2462 N73-29783
Test equipment and procedure for determining electrical conductivity of stream of hot powdered fuel during combustion process
[JPRS-59752] 20 p2485 N73-29960
Magnetic variation station for recording geomagnetic variations on ocean bottom
21 p2547 N73-30419
Electrical conductivity of materials and determination of resistivity
[NASA-TT-F-15067] 21 p2579 N73-30667
Temperature effects and effect of addition of lithium fluoride on conductivity of magnesium oxide
[NLL-M-23040-[5828.4F]] 21 p2585 N73-30711
Electrical conduction in nondegenerate, nonsymmetrical, epitaxial semiconducting films
21 p2585 N73-30713
Electrical conductivity measurements in controlled occupancy energy band tails of disordered semiconductors
[AD-763426] 21 p2587 N73-30729
Ion mobility, electrical conductance, and decomposition reactions of ammonium nitrate and ammonium perchlorate oxidizers
[AD-762744] 22 p2626 N73-31041
Performance calculation for Schottky field effect transistor on resistive substrate
22 p2641 N73-31167
Design of second order resistance capacitance filters
24 p2898 N73-33133
Strength of printed circuit joints for reliability, based on electrical resistivity
[DLR-FB-73-33] 24 p2899 N73-33140

**ELECTRICALLY SUSPENDED GYROSCOPES**
U ELECTROSTATIC GYROSCOPES

**ELECTRICITY**
NT ALTERNATING CURRENT
NT ATMOSPHERIC ELECTRICITY
NT AURORAL ELECTROJETS
NT ELECTROJETS
NT EQUATORIAL ELECTROJET
NT GEOELECTRICITY
NT IONOSPHERIC CURRENTS
NT STATIC ELECTRICITY
NT TELLURIC CURRENTS
Congressional hearings on causes and implications of impending shortages of gasoline, heating oil, diesel fuel, jet fuel, and electricity
24 p2994 N73-33928

**ELECTRO-OPTICAL EFFECT**
High speed photography of electro-optical fringe patterns for measuring pulsed electric field between Kerr cell electrodes
[SC-DC-72-1375] 04 p0399 N73-13243

**ELECTRO-OPTICS**
Stable mode-locking and pulse coupling of longitudinal discharge carbon dioxide laser with single electro-optical element
[AD-744996] 01 p0064 N73-10528
Demountable electro-optical system tests for improving pattern threshold recognition device
[AD-745915] 02 p0147 N73-11194
Application of alkali halides for holographic recording and recovery at room temperatures for high density data storage systems
[AD-748027] 03 p0311 N73-12537
Development of map storage and display system using volume holography using iron-doped lithium niobate
[AD-748002] 03 p0311 N73-12541
Effects of stoichiometry variation, heat treatment, impurity, and color center content of electrooptic crystals and kinetics of index damage process
05 p0554 N73-14501
Growth of single crystal CdTe materials for use in infrared electro-optic devices
[AD-749368] 05 p0588 N73-14783
Analysis of atmospheric optical properties with application to night vision, infrared radiation, astrogeophysics, and electro-optical physics
[AD-750610] 06 p0669 N73-15443
Rotating analyzer method for rapid measurement of polarized light produced by birefringent materials
[AD-750545] 06 p0701 N73-15713
Analysis of intensity distribution of radiation focussed by zone plate optics and computation of radiation flux on sensor area centered about optical axis
[AD-751516] 07 p0822 N73-16661
Assessment of luminous and spectral sensitivity and electro-optical properties of image tubes
[BARC-610] 08 p0888 N73-17194
Electro-optical control for volt-ampere characteristics of avalanche phototransistors
[JPRS-58321] 09 p1008 N73-18226
Laser method for measuring axial solute dispersion in turbulent pipe flow
[AD-753801] 09 p1019 N73-18314
Magneto-optical and electro-optical approaches for meeting time memory demands
09 p1065 N73-18688
Testing point dipole electro-optic model by application to lead titanate
[AD-753467] 09 p1075 N73-18773
Growths of barium and strontium niobate laser materials for electro-optical Q-switching of visible and near infrared radiation
[AD-752445] 09 p1076 N73-18779
Research progress in electro-optics, plasma physics, microwaves, wave propagation, telecommunication, data processing
[AD-753710] 09 p1102 N73-18993
Evaluation of electro-optic direction sensor
[NASA-CR-130928] 10 p1160 N73-19437
Response of optico-electronic scanning system with antiphase connection of radiation detector elements
12 p1405 N73-21395
Electronic optical transfer function analyzer using scanning image dissection system to produce representative output signal
[NASA-CASE-MFS-21672-1] 13 p1558 N73-22630
Liquid crystal applications as electronic, electro-optic, and diagnostic materials
[AD-755831] 13 p1567 N73-22703
Feasibility of integrated optics for use in high capacity, multi-GHz telecommunications
[AD-757342] 14 p1635 N73-23254
Development and characteristics of nonmetallic electro-optic materials for electronic applications
[AD-758528] 15 p1760 N73-24261
Physical properties of electro-optical switching devices for telecommunication
[REPT-61] 16 p1875 N73-25177
Hybrid optical processing system
16 p1922 N73-25552
Measurement of control mechanism of accommodation-vergence eye movement system in human eyes using electro-optical measuring instrument
21 p2500 N73-30062
Development and evaluation of on-line spatial light modulator for application as input transducer for real-time optical data processing system
[NASA-CR-124375] 21 p2508 N73-30121
Development of semiconductor electro-optical devices in Poland with emphasis on management planning and research projects to establish capability
21 p2608 N73-30898
Potential use of strontium barium metaniobate crystals for electro-optics
[AD-762740] 22 p2687 N73-31520
Opto-electronic instruments for spacecraft
[JPRS-60199-1-PT-1] 24 p2926 N73-33372
Opto-electronic instruments for spacecraft
[JPRS-60199-2-PT-2] 24 p2926 N73-33373
COLFTAR real time electro-optical system for generating optical Fourier transforms of two-dimensional video signals
24 p2956 N73-33613

**ELECTROACOUSTIC TRANSDUCERS**
NT HYDROPHONES
NT MICROPHONES
Acoustic signal recorders and electroacoustic measurements in liquids
[JPRS-57778] 05 p0580 N73-14720
Evaluation of device for rapid detection and location of shallow subsurface tunnels and excavations
[AD-752086] 08 p0919 N73-17531
Technique for determination of conductivity profile in diffusion layer of CdS electroacoustic transducers
[AD-758450] 15 p1822 N73-24773
Elimination of principal source of energy loss in microwave acoustic transducers
16 p1880 N73-25216
Digital measurements of underwater sound transducer directivity index using hydrophone array
[AD-758639] 16 p1945 N73-25740
Application of acoustic transducers for suspending object at center of chamber under near weightless conditions
[NASA-CASE-NPO-13263-1] 22 p2677 N73-31443
Structural parameters of magnetoacoustic converters and its position
[AD-764935] 23 p2767 N73-32134

**ELECTROACOUSTIC WAVES**
Acoustic signal recorders and electroacoustic measurements in liquids
[JPRS-57778] 05 p0580 N73-14720
Nonlinear interaction and modulation in parametric acoustic array for spherical wave field
07 p0821 N73-16650
Influence of magnetoacoustic oscillations on electromagnetic excitation of shear acoustic waves
[COO-3150-4] 10 p1190 N73-19681
Theory of electroacoustical images and relationship between geometric form of horn and sound antennas based on acoustic properties
24 p2956 N73-33617

**ELECTROCARDIOGRAMS**
U ELECTROCARDIOGRAPHY

**ELECTROCARDIOGRAPHY**
Electronic instruments for continuous cardiovascular systems measurements
[NASA-TT-F-14492] 01 p0020 N73-10154
Design and attachment of skin electrodes in human cardiac monitoring during space flight
03 p0259 N73-12095
Electrocardiogram recordings on magnetic tape for computerized analysis
[AD-748105] 04 p0384 N73-13124
Threshold circuits with feedback channels for cardiac R-wave detection in electrocardiographic heart rate monitoring
[NASA-TN-D-7152] 06 p0635 N73-15158
Changes in electrocardiographs of Rhesus monkeys as function of age
[NASA-TT-F-14675] 07 p0745 N73-16062
Dynamic electrocardiography in periodic health examinations for detection of cardiac abnormalities
08 p0873 N73-17065
Dynamic electrocardiographic standardization for detecting cardiac risk factor in personnel
08 p0873 N73-17066
Electrocardiographic stress testing for determining influence of occupational and other stresses on ischemic heart disease
08 p0875 N73-17082
Insulated electrode for electrocardiographic recording without paste electrolyte
[NASA-CASE-MSC-14339-1] 12 p1374 N73-21151
Development of electrocardiogram protection circuits to prevent accidental electrocution and digital cardiotachometer system to display heart rate
13 p1594 N73-22924
Development of instantaneous reading tachometer for measuring electrocardiogram signal rate
[NASA-CASE-MFS-20418] 15 p1785 N73-24473

**ELECTROCATALYSTS**
Development of low cost cathode catalysts for air breathing fuel cells containing phosphoric acid electrolyte
[AD-748447] 04 p0376 N73-13059

**ELECTROCHEMICAL CELLS**
NT ALKALINE BATTERIES
NT ELECTRIC BATTERIES

NT FUEL CELLS
NT HYDROGEN OXYGEN FUEL CELLS
NT MAGNESIUM CELLS
NT METAL AIR BATTERIES
NT NICKEL CADMIUM BATTERIES
NT NICKEL ZINC BATTERIES
NT PRIMARY BATTERIES
NT REGENERATIVE FUEL CELLS
NT SILVER CADMIUM BATTERIES
NT SILVER ZINC BATTERIES
NT STORAGE BATTERIES
NT THERMAL BATTERIES
NT ZINC-OXYGEN BATTERIES
Gravitational effects on electrochemical batteries
[NASA-CR-129091] 02 p0128 N73-11039
Design, development, and evaluation of aluminum-chlorine battery
[AD-747775] 03 p0255 N73-12065
Improved electrochemical storage batteries for spacecraft
[NASA-TM-X-66129] 04 p0375 N73-13049
Development of test probe device for simultaneous determination of condition of cells in multi-cell storage battery
[NASA-CASE-MFS-20761-1] 08 p0869 N73-17037
HF cell performance over different operating conditions after storage
[SC-CR-72-3156] 12 p1366 N73-21085
Hydrogen depolarized cell for removing CO2 in spacecraft life support systems
[NASA-CR-131868] 13 p1486 N73-22047
Electrochemical process for recovery of oxygen from atmospheres of manned space capsules
[NASA-CR-114573] 16 p1869 N73-25130
Economic benefits of electrochemical fuel cells
[NASA-TT-F-15147] 23 p2748 N73-31991
Porous electrode for use in electrochemical cells
[NASA-CASE-GSC-11368-1] 23 p2763 N73-32108
Feasibility of electrochemical silver/silver iodide/iodine battery
[SC-RR-72-0386] 24 p2881 N73-33006

**ELECTROCHEMICAL CORROSION**
Calculated relationships of potential distribution over ship hulls for electrochemical protection from seawater corrosion
[DRIC-TRANS-2877] 02 p0149 N73-11208
Technique for predicting corrosion behavior of engineering alloys in aqueous electrolytes with and without chlorides present
[AD-752487] 08 p0933 N73-17638

**ELECTROCHEMICAL MACHINING**
Effect of electrochemical machining on mechanical properties of gas turbine engine blades made of MA-2 alloy
[AD-762497] 20 p2483 N73-29950

**ELECTROCHEMICAL OXIDATION**
Performance of hydrocarbon oxidation catalysts as adsorbed layer promoter
[AD-746258] 02 p0138 N73-11117
Periodic passivation of nickel electrode and changes in properties of cathodic deposits during electrodeposition of nickel using reversible current
[NLL-TRANS-746-1317-[9022.401]] 05 p0560 N73-14549
Propane oxidation using electrochemical mass spectrometry
[AD-762356] 20 p2374 N73-29077
Oxidation of nitrogen and ball lightning
[AD-763146] 21 p2539 N73-30358

**ELECTROCHEMISTRY**
NT ELECTROLYSIS
Electrochemical effects of low temperature operation on zinc air battery performance
[AD-749270] 04 p0377 N73-13068
Gas phase chromatographic study of electrosorbed cyclic hydrocarbon intermediates on fuel cell electrode during oxidation
[AD-750391] 05 p0500 N73-14068
Electrochemical analysis of cathodic hydrogen absorption by iron and steel
[BARC-585] 05 p0506 N73-14116
Production and properties of special purpose synthetic fibers
[AD-749059] 05 p0567 N73-14607
High energy density primary batteries using CuF2/LiAsF6-MF/Li electrochemical system
[NASA-CR-120857] 07 p0741 N73-16032
Technique for predicting corrosion behavior of engineering alloys in aqueous electrolytes with and without chlorides present
[AD-752487] 08 p0933 N73-17638
Thermodynamics of molten mixtures of lithium chloride-potassium chloride at 640 C
[AD-752087] 08 p0970 N73-17925
Electrochemical methods for determining acidity standard, atomic weight, stoichiometric composition, and trace contaminants
[NBS-TN-583] 09 p0999 N73-18153
Electrochemical permeation technique and scanning electron microscopy used to determine hydrogen embrittlement in ferrous materials
[AD-752828] 09 p1049 N73-18557
Present international status of research and development of electrochemistry and fuel cells
[AD-755106] 11 p1238 N73-20048
Mass spectra of electrochemical propane oxidation
[AD-755254] 12 p1376 N73-21166
Synthesis, thermodynamics, and electrochemical properties of graphite fluorides
[AD-755934] 12 p1377 N73-21167
Design and evaluation of electrochemical nitrogen-hydrogen separator for use in spacecraft nitrogen generator
[NASA-CR-114580] 13 p1534 N73-22431
Electrochemical and mechanical parameters of localization hydrogen in iron and maraging steel using high resolving power autoradiography
[RAE-LIB-TRANS-1665] 17 p2044 N73-26533
Analysis of chemical and electrochemical processes occurring on titanium sheet metal surfaces during oxidation at room temperature by electron-diffraction method
[NLL-RTS-7888] 20 p2428 N73-29503
Spectrophotometric analysis of electrochemical reactions on transparent mercury/platinum electrode
[AD-763265] 22 p2626 N73-31043
Lithium anode cells operating at room temperature using electrolytic solutions in inorganic solutions
[AD-763478] 23 p2754 N73-32039
High temperature electrochemical devices incorporating solid oxygen electrolytes for metallurgical processing
[AD-764769] 23 p2806 N73-32436
Electrochemical system with solid electrolyte for regenerating oxygen from CO2 and H2O
24 p2882 N73-33015
Electrochemical study of corrosion of high strength alloys in contact with Zircaloy-4
[BMI-X-10260] 24 p2936 N73-33449

**ELECTROCONDUCTIVITY**
Electroconductivity of system I-Me4NI and comparison with conductivity of iodine solutions of KI and RbI
[NASA-TT-F-13911] 01 p0022 N73-10174
Effect of magnetic rupture on low frequency electroconductivity and weakly damped electromagnetic waves in metals with closed Fermi surfaces
[KHFTI-71-1] 06 p0684 N73-15569
Mineral concentration in ground and river waters of Porkhov determined from their specific electroconductivity
[NASA-TT-F-14991] 17 p1992 N73-26105

**ELECTROCUTANEOUS COMMUNICATION**
Electrocutaneous parameters for designing dynamic tactual communication system
12 p1373 N73-21135

**ELECTRODELESS DISCHARGES**
Electrodeless high frequency discharges in xenon at pressures up to 40 atmospheres
[AD-751944] 08 p0949 N73-17774

**ELECTRODEPOSITION**
NT ELECTROPLATING
Periodic passivation of nickel electrode and changes in properties of cathodic deposits during electrodeposition of nickel using reversible current
[NLL-TRANS-746-1317-[9022.401]] 05 p0560 N73-14549
Structure and phase composition of electrodeposited iron-nickel-chromium alloys analyzed by X ray spectroscopy and electron microscopy
[NLL-TRANS-746-1327-[9022.401]] 05 p0560 N73-14551
Nickel ion absorption on alumina and titania electrolyte interfaces
[AD-754540] 11 p1253 N73-20167
Development of galvanic forming techniques and application to production of complex structures requiring accurate dimensions
13 p1593 N73-22918
Electrodeposition of cylindrical magnetic films
[JPRS-59626] 19 p2305 N73-28534

**ELECTRODERMAL RESPONSE**
U GALVANIC SKIN RESPONSE

**ELECTRODES**
NT ANODES
NT CATHODES
NT CELL CATHODES
NT COLD CATHODES
NT HOLLOW CATHODES
NT HOT CATHODES
NT PHOTOCATHODES
NT PHOTOMULTIPLIER TUBES
NT PLASMA ELECTRODES
NT THERMIONIC CATHODES
Development of nickel hydroxide electrode for use in rechargeable alkaline batteries
[AD-746335] 01 p0007 N73-10058
Determination of quality of zinc phosphate coatings by measurement of electrode potential
[AD-745094] 01 p0070 N73-10571
Surface properties study of thermionic electrodes, using quasi-equilibrium model for oxygen reactions with refractory metals
[NASA-CR-129598] 03 p0254 N73-12057
Development of porous electrode materials for plasma generators and effects of blowing protective gases through plasma
[AD-747369] 03 p0255 N73-12066
Changes in porous structure of nickel electrode substrates due to changes in manufacturing processes
[AD-748109] 03 p0255 N73-12067
Design and attachment of skin electrodes in human cardiac monitoring during space flight
03 p0259 N73-12095
Total correction of ohmic drop with transfer function of interphase electrode-solution equalling one
[UCRL-TRANS-10618] 03 p0263 N73-12129
High vacuum breakdown initiated field emission between technically pure electrodes
[AD-747586] 03 p0338 N73-12753
Obtaining stable oxygen electrodes by coating with plasma catalyzed polymer film
[AD-748422] 04 p0383 N73-13120
Preparation of thin film metal fluoride electrodes from elemental constituents to obtain high purity and variations in size and shape
[NASA-TM-X-2690] 04 p0386 N73-13140
Gas phase chromatographic study of electrosorbed cyclic hydrocarbon intermediates on fuel cell electrode during oxidation
[AD-750391] 05 p0500 N73-14068
Periodic passivation of nickel electrode and changes in properties of cathodic deposits during electrodeposition of nickel using reversible current
[NLL-TRANS-746-1317-[9022.401]] 05 p0560 N73-14549
Characterization of non-aqueous electrolytes and solid electrodes
[AD-750079] 06 p0638 N73-15180
Physical properties of porous nickel strips used as electrodes in electro-vacuum equipment and methods for controlling expansion during production
[NLL-TRANS-746-1342-[9022.401]] 06 p0682 N73-15551
Development and characteristics of long life, high energy density, sealed zinc oxygen secondary battery for military communications application
[AD-751751] 07 p0742 N73-16035
Behavior of graphite electrodes in organic electrolytes
[UCRL-TRANS-1476] 08 p0870 N73-17043
Operational characteristics of carbon manganese dioxide electrode for metal air battery
[AD-751693] 09 p0991 N73-18089
Diffusion coefficients for zinc electrode in potassium hydroxide solutions
[AD-753096] 09 p0991 N73-18092
Opposed electrode, parallel gap, and percussive arc monitoring systems
[BDX-613-544] 10 p1134 N73-19244
Carbon dioxide shielded-arc welding with electrodes containing aluminum
[NLL-CE-TRANS-6011-[9022.09]] 11 p1296 N73-20515
Electrode structures for transverse excitation produced HF lasers
[DREV-TN-2047/73] 11 p1302 N73-20565
Insulated electrode for electrocardiographic recording without paste electrolyte
[NASA-CASE-MSC-14339-1] 12 p1374 N73-21151
Preliminary evaluation of lithium aluminum electrode for thermal batteries
[AD-757007] 13 p1477 N73-21964
Effect of zinc on function of acid electrode
[NASA-TT-F-14922] 14 p1605 N73-23012
Cathode degradation in platinum black fuel cell
[AD-757714] 14 p1606 N73-23019
Low temperature performance of air electrodes for use in zinc-air and metal-air battery systems
[AD-758171] 14 p1607 N73-23021
Low cost oxygen electrode for phosphoric acid fuel cell
[AD-758179] 15 p1739 N73-24095
Electrode metal loss by volatilization in gas-shielded arc welding
[NLL-DRIC-TRANS-3005-[3623.66]] 15 p1790 N73-24511
Copper alloys with necessary heat resistance and electrical conductance for use as welding electrodes
[AD-758618] 15 p1800 N73-24590
Characteristics of ion rocket engine with combination keeper electrode and electron baffle
[NASA-CASE-NPO-11880] 15 p1824 N73-24783
Current distribution in flooded, porous electrodes
[NASA-CR-131839] 16 p1864 N73-25098
Characteristics and evaluation of electrodes for use in thermionic converters - Phase 2
[NASA-CR-131838] 16 p1943 N73-25723
Silicon carbide backward diode with coated lead attachment
[NASA-CASE-ERC-10224-2] 18 p2122 N73-27150
Equipment for implanting electrodes in subcortical structures of cat brain
[NASA-TT-F-15001] 19 p2225 N73-27947
Technique and requirements for projection welding using single large electrode
[NLL-M-23048-[5828.4F]] 21 p2552 N73-30456
Oxygen exchange between solid electrolyte and platinum electrode in flowing gas
22 p2617 N73-30972
Spectrophotometric analysis of electrochemical reactions on transparent mercury/platinum electrode
[AD-763265] 22 p2626 N73-31043

Effects of inclusions and voids in welding electrodes and welding materials on quality of welded joints
22 p2678 N73-31447
Porous electrode for use in electrochemical cells
[NASA-CASE-GSC-11368-1] 23 p2763 N73-32108
Electrode burn off characteristics of manual metal arc electrodes using continuous and modulated welding current
[CRANFIELD-MAT-9] 24 p2928 N73-33386

**ELECTRODYNAMICS**
NT ELECTROHYDRODYNAMICS
NT ELECTROMECHANICS
NT QUANTUM ELECTRODYNAMICS
Theoretical analysis for predicting onset of Kelvin-Helmholtz instability
[NASA-CR-114499] 03 p0363 N73-12961
Black body heat capacity and action at distance electrodynamics
[ORO-3992-97] 12 p1429 N73-21578
Field tests of electrogasdynamic fog dispersal concept in Panama Canal Zone
[FAA-RD-73-33-PT-1-PT-2] 17 p2010 N73-26254
Analysis of longitudinal end effects on constant and traveling wave MHD generators by electrodynamics
[SFB-MHD-7] 22 p2705 N73-31662

**ELECTRODYNAMOMETERS**
U DYNAMOMETERS

**ELECTROENCEPHALOGRAM**
U ELECTROENCEPHALOGRAPHY

**ELECTROENCEPHALOGRAPHY**
Frequency discriminator for on-line measurements of entrainment and synchronization in EEG signals as related to human alertness
[NASA-CR-129173] 02 p0135 N73-11091
Electronic detectors and computer software for analyzing human electroencephalographs in isolated environment
[AD-751272] 07 p0751 N73-16105
Use of photostimulation in electroencephalographic tests of flying personnel and candidates at flight schools
11 p1245 N73-20111
Portable telephone system for transmission of electroencephalographical data diagnostic center
[NASA-CR-128877] 11 p1255 N73-20186
Neurophysiology of sleep and wakefulness in fish, amphibians, birds, and reptiles
13 p1483 N73-22025
Electroencephalographic and behavioral responses of humans to aircraft noise during sleep
[NASA-CR-2279] 18 p2109 N73-27058
Effect of simulated sonic booms and overpressure on EEG waveform patterns and disturbance judgments
[FAA-RD-73-115] 21 p2500 N73-30066
Recording human electroencephalogram under influence of muscle noise
24 p2883 N73-33025
Structural, behavioral, and EEG correlates of alimentary motivation
24 p2888 N73-33063
Correlation between primary response and late slow oscillation of evoked potential in response to light in awake and anesthetized rabbits
24 p2889 N73-33069
Orientative-investigative reaction as factor changing configuration of evoked potentials during repeated light flashes
24 p2889 N73-33070
Cross correlation analysis of stress rhythm during stimuli of varying biological significance
24 p2890 N73-33071

**ELECTROEROSION**
U SPARK MACHINING

**ELECTROEXPLOSIVE DEVICES**
U INITIATORS [EXPLOSIVES]

**ELECTROFORMING**
Development of galvanic forming techniques and application to production of complex structures requiring accurate dimensions
13 p1593 N73-22918
Electroforming of aluminum solar cell contacts
[AD-764816] 23 p2748 N73-31995
Electroforming used for manufacture of hollow wind tunnel models and nozzles
[DLR-FB-73-40] 24 p2929 N73-33395

**ELECTROGENERATORS**
U ELECTRIC GENERATORS

**ELECTROHYDRAULIC CONTROL**
U ELECTRIC CONTROL
U HYDRAULIC CONTROL

**ELECTROHYDRODYNAMICS**
Results of experiments with working model of electrodynamic heat pipe
[NASA-CR-114498] 03 p0363 N73-12960
Slip parameter for unsteady flow in EHD generators
[AD-759971] 17 p2070 N73-26749
Static characteristics of electrohydrodynamic inverted converters
[AD-760966] 18 p2183 N73-27630
Documentation of electrohydrodynamics research
[NASA-CR-133456] 19 p2255 N73-28180
Experimental and theoretical applications to electrohydrodynamic heat pipe research
[NASA-CR-114646] 22 p2729 N73-31839
Turbulent gas-solid electrohydrodynamic flow into channel
23 p2772 N73-32172

**ELECTROJETS**
NT AURORAL ELECTROJETS
NT EQUATORIAL ELECTROJET
Afternoon depression of geomagnetic H field on quiet days near magnetic equator in Indian zone
[AER-73-03] 14 p1658 N73-23459

**ELECTROLUMINESCENCE**
Analysis of gray scale image storage techniques in electroluminescent and photoconductor image conversion panels
[AD-745758] 01 p0033 N73-10261
Development of mosaic image conversion panels sensitive to ultraviolet, X ray, near infrared, and visible light
[AD-745757] 01 p0033 N73-10262
Development of gallium aluminum phosphide alloys for electroluminescent diodes
[NASA-CR-112182] 03 p0273 N73-12213
Dc electroluminescent flat panel display with Zn, Cu, S, and Mn films
[AD-746632] 03 p0275 N73-12229
Performance tests and service life of electroluminescent film display device
[AD-749790] 05 p0521 N73-14235
Luminescence of ZnSe and ZnS crystals compared to electroluminescence of MS and MIS structures, preparation of heterojunction structures, and solution growth of wafers
[AD-749135] 05 p0588 N73-14784
Electroluminescent characteristics of vacuum deposited zinc sulfide films for airborne electronic displays
[AD-754781] 11 p1332 N73-20811
Electric, photoelectric, and electroluminescence properties of Cu contacts on CdS surface
[AD-756876] 13 p1504 N73-22187
Crystal structure and electroluminescence of ZnSe films
[NLL-PO-2921-[9022.81]] 15 p1819 N73-24745
Determination of thermal characteristics of electroluminescent diode
[NASA-TM-X-70440] 21 p2517 N73-30190
Photographing method for manufacturing multicolor electroluminescent chips
[AD-764943] 24 p2944 N73-33509
Rare earth doped gallium phosphide preparation with application to electroluminescence noting physical and chemical properties
24 p2969 N73-33729

**ELECTROLUMINESCENT LAMPS**
U ELECTROLUMINESCENCE
U LUMINAIRES

**ELECTROLYSIS**
Performance of prototype monopropellant engines using electrolytic ignition system
[AD-745993] 02 p0224 N73-11808
Solid polymer for water electrolysis system to generate oxygen and hydrogen in manned space station
[NASA-CR-112183] 04 p0375 N73-13052
Electrolytic procedure for manufacturing aluminum whisker and pure nickel matrix composites with reinforced fibers
04 p0435 N73-13544
X ray apparatus for investigating hydrogen induced changes in fine crystalline structure of N1 powders and electrolytic films
[NLL-TRANS-746-1294-[9022.401]]
05 p0505 N73-14113
Design and performance of prototype nitrogen/oxygen supply unit using water/hydrazine electrolysis to provide cabin leakage makeup in manned spacecraft
[NASA-CR-128688] 06 p0635 N73-15159
Long term performance test on electrolytic oxygen generator for manned test chamber
[NASA-CR-128687] 06 p0635 N73-15160
Design, development, and operation of water electrolysis system to provide gaseous hydrogen and oxygen for satellite propulsion system
[AD-755384] 13 p1571 N73-22735
Analysis of effects of alternating current on corrosion of iron in aqueous solutions of acidic and neutral salts
[REPT-733] 14 p1675 N73-23590

**ELECTROLYTE METABOLISM**
Physiological regulatory mechanisms of water and electrolyte levels in human body in high temperature environment
[NASA-TT-F-13915] 01 p0008 N73-10066

**ELECTROLYTES**
NT ION EXCHANGE MEMBRANE ELECTROLYTES
NT MOLTEN SALT ELECTROLYTES
Sound speed and other thermodynamic quantities of dilute aqueous electrolyte solutions by ultrasonic velocimeter comparison technique
[AD-745843] 01 p0081 N73-10669
Performance of lithium battery with inorganic electrolyte
[AD-746633] 02 p0129 N73-11052
Design, development, and evaluation of aluminum-chlorine battery
[AD-747775] 03 p0255 N73-12065
Design and development of rechargeable zinc/air electric battery
[AD-748434] 04 p0377 N73-13064
Frequency and line width of Brillouin scattering in aqueous electrolyte solutions
[AD-749354] 04 p0387 N73-13148
Development of lithium-nickel sulfide electric storage battery for operation at high discharge rates and low temperatures
[AD-749861] 05 p0500 N73-14067
Construction materials and electrolytes for electrochemical fuel cells
[AD-750152] 06 p0627 N73-15089
Characterization of non-aqueous electrolytes and solid electrodes
[AD-750079] 06 p0638 N73-15180
Development and characteristics of electric storage battery using lithium-silver chloride couple
[SC-DC-72-2298] 07 p0742 N73-16033
Design and operation of galvanic cells involving solid electrolytes to determine accuracy in thermochemical measurements
[LBL-839] 07 p0742 N73-16034
Development and characteristics of long life, high energy density, sealed zinc oxygen secondary battery for military communications application
[AD-751751] 07 p0742 N73-16035
Behavior of graphite electrodes in organic electrolytes
[UCRL-TRANS-1476] 08 p0870 N73-17043
Solid ceramic electrolyte system for measuring redox conditions in high temperature gas mixing
[NASA-TM-X-58105] 08 p0892 N73-17224
Technique for predicting corrosion behavior of engineering alloys in aqueous electrolytes with and without chlorides present
[AD-752487] 08 p0933 N73-17638
Rayleigh-Brillouin intensity ratios measured for aqueous electrolytic solutions as function of concentration
[AD-753017] 09 p1001 N73-18166
Electrical screening procedure for solid ionic conductors
[NASA-TN-D-7146] 09 p1073 N73-18758
Performance tests of electric batteries to determine effect of negative limited cell on battery service life
[NASA-CR-130932] 10 p1111 N73-19060
Transient hot-wire measurement of thermal conductivity of electrolytic solutions
[RISO-264] 10 p1126 N73-19173
Development of low melting fused salt electrolytes
[AD-755528] 13 p1477 N73-21965
Temperature dependence of sparingly soluble electrolytes and nonelectrolytes
[AD-757504] 14 p1617 N73-23102
Electrolytes for hydrocarbon air fuel cells
[AD-758180] 15 p1739 N73-24096
Influence of active and passive electrolyte solutions on corrosion of aluminum alloys
15 p1746 N73-24154
Performance of prototype lithium-inorganic electrolyte battery
[AD-758856] 16 p1865 N73-25101
Development of lead/lead oxide solid electrolyte cell and evaluation of electrical properties in terms of equivalent circuit for cell
20 p2363 N73-29003
Solid polymer electrolyte regenerative fuel cells for communication satellites
[AD-762923] 20 p2365 N73-29016
Materials for immobilization of electrolyte in pellet-type thermal batteries
[SC-RR-66-202-A] 22 p2618 N73-30978
High temperature electrochemical devices incorporating solid oxygen electrolytes for metallurgical processing
[AD-764769] 23 p2806 N73-32436
Carbon-oxygen fuel cell of solid carbon anode, nickel gauze cathode, and flamed electrolyte.
24 p2880 N73-33001
Electrochemical system with solid electrolyte for regenerating oxygen from CO2 and H2O
24 p2882 N73-33015

**ELECTROLYTIC CELLS**
Hull cell investigation of throwing powers of various nickel plating baths
[NLL-RTS-7294] 01 p0067 N73-10548
Comparison of alkaline manganese-zinc cells with salt-electrolyte cells
[AD-746558] 02 p0129 N73-11051
Development of low cost cathode catalysts for air breathing fuel cells containing phosphoric acid electrolyte
[AD-748447] 04 p0376 N73-13059
Anodic efficiency of lithium in electrolytic cells
[AD-749009] 04 p0387 N73-13147
Actuator operated by electrolytic drive gas generator and evacuator
[NASA-CASE-NPO-11369] 04 p0425 N73-13467
Construction materials and electrolytes for electrochemical fuel cells
[AD-750152] 06 p0627 N73-15089
Design and operation of galvanic cells involving solid electrolytes to determine accuracy in thermochemical measurements
[LBL-839] 07 p0742 N73-16034

Thermodynamics of oxygen solubility in lanthanum uranium oxide measured on solid state electrolytic cell
[KFK-1649] 12 p1376 N73-21163
Development of phosphoric acid fuel cells operating on hydrogen produced from thermocracking or steam reforming of hydrocarbon
[AD-755206] 13 p1477 N73-21966
Graphite oxide and fluorides as depolarizers in lithium organic electrolytic cells
[AD-755159] 13 p1477 N73-21968
Open circuit voltage measurements on solid beta alumina electrolytic cells
[NASA-TN-D-7322] 15 p1738 N73-24089
Development of lead/lead oxide solid electrolyte cell and evaluation of electrical properties in terms of equivalent circuit for cell
20 p2363 N73-29003

**ELECTROLYTIC GRINDING**
U ELECTROCHEMICAL MACHINING

**ELECTROLYTIC POLISHING**
U ELECTROPOLISHING

**ELECTROMAGNETIC ABSORPTION**
NT AURORAL ABSORPTION
NT PHOTOABSORPTION
NT POLAR CAP ABSORPTION
NT ULTRAVIOLET ABSORPTION
NT X RAY ABSORPTION
Application of high pass broadband filters to absorption spectrophotometry
[IRI-133-72-08] 03 p0274 N73-12223
True absorption of light by aerosols in atmosphere
[AD-748111] 03 p0299 N73-12437
Effect of external electric field on optical absorption of GaSe and GaTe single crystals and solid solutions
[AD-749750] 05 p0589 N73-14789
Laser-plasma coupling and laser absorption by solid deuterium
[UCRL-50022-2] 10 p1169 N73-19506
Optical imaging system for increasing light absorption efficiency of imaging detector
[NASA-CASE-ARC-10194-1] 11 p1324 N73-20741
Quantum mechanics for describing operational properties of gas laser containing saturable absorber in resonator
12 p1409 N73-21421
Low temperature optical absorption of some unusual intermetallic compounds
12 p1438 N73-21646
Laser light absorption characteristics of laser produced hydrogen plasma
[AD-756524] 13 p1538 N73-22458
Parallel layer model for hydromagnetic wave absorption in magnetospheric tail plasma
15 p1779 N73-24420
Multispectral remote sensing techniques for measuring light absorption, scattering, and particle concentrations in water
[AD-759668] 16 p1914 N73-25491
Horizontal radio link system for measuring ultrahigh frequency absorption spectrum due to rain
17 p1995 N73-26130
Gas, chemical, and solid lasers for producing controlled thermonuclear fusion
[LA-UR-73-224] 19 p2307 N73-28558
Winter anomalous radio wave absorption days at 32 N, and prevalent solar radiation
[AD-762191] 20 p2378 N73-29105
Electromagnetic absorber reflectance and anechoic chamber design for microwave antenna measurements
[FTZ-A-454-TBR-13] 22 p2642 N73-31176

**ELECTROMAGNETIC COMPATIBILITY**
Effect of various technical and operational factors on electromagnetic compatibility of radars operating in 2700 to 2900 MHz frequency band
[ECAC-PR-71-033] 04 p0388 N73-13155
Procedures for producing electric fields in conductive media at extremely low frequencies
[AD-748303] 04 p0391 N73-13177
Electromagnetic compatibility of very high frequency/frequency modulated radio equipment in tactical site selection
[AD-749186] 04 p0391 N73-13179
Analysis of electromagnetic interference between satellite frequency modulated television signal and television signal for commercial broadcasting
[NHK-LABS-NOTE-153] 07 p0754 N73-16123
Electromagnetic compatibility of avionic weapon system
[AD-754412] 11 p1265 N73-20262
Manual on electromagnetic compatibility and interference between aircraft weapon systems
[AD-754411] 11 p1265 N73-20263
Analysis of electromagnetic compatibility of microwave landing guidance system and candidate interim systems
[ECAC-PR-72-069] 12 p1425 N73-21554
Contractual requirements for submission of electromagnetic compatibility and interference control plan for government procurement
[AD-761975] 19 p2237 N73-28033
Army materiel susceptability to high intensity electromagnetic radiation in radio frequency spectrum
[AD-763141] 21 p2508 N73-30125

**ELECTROMAGNETIC CONTROL**
U ELECTROMAGNETS
U REMOTE CONTROL

**ELECTROMAGNETIC DEDUCTION**
U MAGNETIC INDUCTION

**ELECTROMAGNETIC FIELDS**
NT FAR FIELDS
Theoretical study of biological hazards from exposure to ELF electrical fields and potentials
[AD-743480] 01 p0012 N73-10093
Spurious signals introduced into system from external cabling in electromagnetic pulse environment
[AWRE-O-47/71] 01 p0034 N73-10270
Operating force of optimal pulsed electrically controlled pneumatic valve
[FOA-2-C-2481-H5] 02 p0148 N73-11203
Numerical analysis of inverse scattering problem applied to far field relations between incident and scattered radiation in presence of scattering object
02 p0200 N73-11613
Cyclotron resonance caused by electromagnetic waves incident on high density gaseous plasma
[IPPJ-134] 02 p0215 N73-11742
Ionized continuum flows and collisionless plasmas in electric boundary layers on flat plates and cylindrical bodies
[AD-746094] 02 p0217 N73-11753
Method of electroprofiling utilizing natural electromagnetic fields in subsonic frequency range
[AD-747557] 03 p0298 N73-12431
Effects of magnetic and electric coupling parameters on terminal response shielding of braided-shield cables exposed to external electromagnetic fields
[AD-748387] 04 p0396 N73-13221
Penetrating ionizing space radiations with diversity in energy range of both particulate and electromagnetic components
06 p0628 N73-15100
Total and induced magnetic fields line structure within Moon and diamagnetic cavity based on asymmetric theory of lunar induction
[NASA-CR-114545] 06 p0718 N73-15860
Equations and graphs on electromagnetic field parameters
[UCRL-51245] 07 p0756 N73-16140
Diagram solutions of circuits forming high frequency electromagnetic fields in plasma devices
[AEC-TR-7326] 07 p0826 N73-16696
Approximative solution for photon emission amplitude in soft photon irradiation by electromagnetic wave field
[NASA-TT-F-14686] 09 p1066 N73-18697
Potential theory for determining electromagnetic field caused by radial electron emission near conducting sphere
[AD-753664] 09 p1068 N73-18714
Solving singular axisymmetric field problem noting applications to electromagnetism and fluid mechanics
[ONERA-NT-207] 10 p1190 N73-19685
Macroscopic interaction between electromagnetic fields and lossy, anisotropic, compressible plasma
10 p1195 N73-19724
Energy transfer and behavior of field along biconical antenna
[AD-754386] 11 p1263 N73-20246
Investigation of antenna cable responses to pulsed electromagnetic field
[AD-755514] 12 p1385 N73-21234
Interaction between drifting streams of electrons with transverse cyclotron motions and electromagnetic fields
[NASA-CR-130208] 13 p1504 N73-22188
Study of effects of solar activity on geophysical phenomena using numerical techniques
13 p1514 N73-22264
Electromagnetic superconducting force producing coil for positioning models in wind tunnel
15 p1762 N73-24276
Transient electromagnetic fields of pulse-excited wire and aperture antennas
16 p1874 N73-25167
Differential geometry scaling method for determining electromagnetic field of coaxial waveguide coupler
[AD-760157] 17 p2006 N73-26222
Algorithm for computing unrelieved electromagnetic forces of attraction of rotors in EDG electric motors
17 p2059 N73-26657
Einstein-Bonner nonsymmetric field theory of gravity and electromagnetic fields
[AD-761482] 19 p2295 N73-28460
Electromagnetic fields in inhomogeneous media for analysis of scattering and propagation problems and for lense studying
[NASA-CR-132286] 19 p2321 N73-28672
Matrix methods for determining nature of eigencurrents and eigenfields in conducting bodies
[AD-761456] 19 p2321 N73-28675
Signal transmission in visible and infrared portions of electromagnetic spectrum of cloud free, lines of sight through atmosphere at Grand Forks, Fargo, and Minot, North Dakota
[AD-763083] 20 p2415 N73-29408
Earthquakes and volcanoes caused by subterranean explosions provoked by petroleum or natural gas
[NASA-TT-F-15095] 21 p2536 N73-30334
Traveling wave of magnetic field having variable phase velocity and amplitude during movement of liquid metal in expanding channel
[AD-763159] 21 p2583 N73-30702
Uncompensated dc MHD generator, with longitudinal end effect
[SFB-MHD-6] 22 p2704 N73-31661
Electromagnetic field problems in inhomogeneous media, radiation patterns, and Eaton lenses for antenna arrays
[NASA-CR-132336] 23 p2757 N73-32060
Low power electromagnetic flowmeter system producing zero output signal for zero flow
[NASA-CASE-ARC-10362-1] 23 p2791 N73-32326

**ELECTROMAGNETIC INTERACTIONS**
NT PLASMA-ELECTROMAGNETIC INTERACTION
Long-range forces between atoms at large distances, and weak forces arising from neutrino-antineutrino exchange
[TR-73-049] 03 p0339 N73-12764
Absorption, reflection, and scattering of electromagnetic waves by plasma media as electronic countermeasures in radar detection
[FOA-3-C-3652-66] 06 p0639 N73-15189
Effect of displacements of suspended mass on accuracy of electromagnetic load cell and selection of parameters for increased accuracy
06 p0696 N73-15668
Interaction of intense relativistic electron beam with axial and convergent magnetic guide fields
07 p0820 N73-16647
Nonlinear interaction and modulation in parametric acoustic array for spherical wave field
07 p0821 N73-16650
Field theory model for unified strong and electromagnetic interactions
09 p1066 N73-18701
Electromagnetic wave interactions in p type ferromagnetic semiconductors
10 p1198 N73-19751
Photonuclear giant resonance data summary
[NBS-SP-380] 12 p1427 N73-21564
Electromagnetic and gravitational wave interaction of black holes
15 p1829 N73-24824
Relativistic particle motion in electromagnetic wave traveling in direction of uniform static magnetic field
[NASA-CR-132781] 18 p2181 N73-27610
Analysis of axial conduction current induced in infinitely long cylinder in free space with small resistivity by incident electromagnetic plane wave
[AD-762165] 19 p2246 N73-28106
Electromagnetic and strong interactions processes for producing diffuse cosmic gamma continuum radiation
19 p2332 N73-28763
Monte Carlo simulation of nuclear-electromagnetic cascade development and energy response of ionization of spectrometers
[NASA-CR-133999] 22 p2672 N73-31406

**ELECTROMAGNETIC INTERFERENCE**
NT ATMOSPHERICS
NT BLACKOUT [PROPAGATION]
NT CROSSTALK
NT DAWN CHORUS
NT ELECTROMAGNETIC NOISE
NT HISS
NT IONOSPHERICS
NT JAMMING
NT RADIO FREQUENCY INTERFERENCE
NT SHOT NOISE
NT WHISTLERS
NT WHITE NOISE
Intermodulation interference effects of metal surface transmitters and receivers in near field locations of transmission system
01 p0027 N73-10212
Computer program for evaluating effects of conical light beams through interference filters, tilting filter, and energy distribution variations across beam
[WRE-TN-710[AP]] 04 p0449 N73-13665
Low frequency magnetic field interference of dc/dc regulators and transformers
[ESRO-CR-58] 05 p0499 N73-14059
Effects of acoustic gravity waves following nuclear explosion on ionospheric electron density and high frequency communications
05 p0513 N73-14170
Measurement of magnetic field emission of spacecraft power system units at low frequencies
[ESRO-CR-57] 05 p0548 N73-14452
Analysis of electromagnetic interference between satellite frequency modulated television signal and television signal for commercial broadcasting
[NHK-LABS-NOTE-153] 07 p0754 N73-16123
Manual on electromagnetic compatibility and interference between aircraft weapon systems
[AD-754411] 11 p1265 N73-20263
Electromagnetic interference of power conditioners for solar electric propulsion
[NASA-CR-133229] 17 p2076 N73-26798
Magnetic field interference of transformers for dc/dc converters for spacecraft power supplies
[ESRO-CR-84] 19 p2223 N73-27930

Compensation of static fields for ferrosonde magnetometer mounted on mobile carrier
22 p2672 N73-31400
**ELECTROMAGNETIC MEASUREMENT**
NT ELECTROMAGNETIC NOISE MEASUREMENT
Electromagnetic cross modulation and very low frequency propagation techniques for measuring acoustic gravity waves in ionospheric D region
05 p0511 N73-14153
**ELECTROMAGNETIC NOISE**
NT ATMOSPHERICS
NT DAWN CHORUS
NT HISS
NT IONOSPHERICS
NT SHOT NOISE
NT WHISTLERS
NT WHITE NOISE
Audio equipment for removing impulse noise from audio signals
[NASA-CASE-NPO-11631] 03 p0277 N73-12244
Radio auroras and nighttime magnetic field disturbances
[AD-750019] 05 p0543 N73-14415
Solving problem of noise in single and double injection diodes
[AD-750186] 06 p0645 N73-15240
Development of pulsed power strain gage system for use in presence of high amplitude electrical noise
[SC-DC-72-1413] 07 p0801 N73-16503
Electromagnetic interference identification in infrared line scan imaging patterns
[DREO-TN-72-25] 07 p0821 N73-16652
Existence of natural radio noise between electron plasma frequency and upper hybrid resonance frequency as detected by long electric antennas of IMP-6 satellite
[NASA-CR-130273] 07 p0843 N73-16832
Analysis of subharmonically injection locked microwave IMPATT diode oscillators to improve frequency stability and noise characteristics
10 p1133 N73-19237
Ionospheric noise created by electromagnetic wave propagation through turbulent plasma sheath
[AD-754904] 11 p1328 N73-20782
Characteristics of photomultiplier tubes and application to optics, biophysics, radiometry, and astronomy for detecting weak light flows
[AD-755874] 12 p1384 N73-21226
Noise scattered into receiving antenna system by turbulent plasma
[AD-756829] 13 p1492 N73-22094
Equipment for continuous recording of natural electromagnetic noise of extremely low frequencies
[AD-757482] 14 p1634 N73-23244
Analysis of electromagnetic noise in photodetection system consisting of germanium avalanche photodiode with application to laser range finders
[PHL-1972-24] 14 p1672 N73-23568
Effects of vehicle ignition noise on VHF/UHF band terminals
[STC-TM-340] 15 p1749 N73-24179
Azimuthal and diurnal high frequency backscatter and terrestrial radio noise
[AD-758776] 16 p1876 N73-25185
Bibliography of literature concerning electromagnetic and seismic noise and propagation
[PB-217500/8] 18 p2118 N73-27125
Operational characteristics of sky noise measuring instruments and analysis of discrepancies in data acquired by each instrument
[NASA-CR-133415] 18 p2151 N73-27383
Low cost highly sensitive 12 GHz low noise converter for communication between broadcast satellites and ground stations
[NHK-LABS-NOTE-161] 20 p2380 N73-29127
Noise in microwave semiconductor oscillators and amplifiers
[AD-764259] 22 p2644 N73-31188
Modes of cable vibration compared with pure flexing mode in production of motion induced noise from towed ELF H field antenna
[AD-762936] 22 p2645 N73-31199
Performance of spread spectrum communication systems to include effects of various forms of channel noise and synchronization aspects of system
23 p2756 N73-32057
RAE-1 measurements of thunderstorms and ground-based radio noise
[NASA-CR-132810] 23 p2757 N73-32062
**ELECTROMAGNETIC NOISE MEASUREMENT**
Double probe measurements of electromagnetic noise spectra due to thermodynamic plasma density fluctuations for plasma diagnostics
06 p0706 N73-15758
Gyroscope noise measurements and data analysis
[AD-756977] 14 p1691 N73-23723
**ELECTROMAGNETIC PROPAGATION**
U ELECTROMAGNETIC WAVE TRANSMISSION
**ELECTROMAGNETIC PROPERTIES**
NT ABSORPTIVITY
NT BIREFRINGENCE
NT BRIGHTNESS
NT COLOR
NT DICHROISM
NT ELECTRICAL PROPERTIES
NT ELECTROMAGNETIC ABSORPTION
NT FARADAY EFFECT
NT IRIDESCENCE
NT KERR MAGNETOOPTICAL EFFECT
NT LUMINOSITY
NT OPACITY
NT OPTICAL PROPERTIES
NT OPTICAL REFLECTION
NT PHOSPHORESCENCE
NT PHOTOCONDUCTIVITY
NT PHOTOELASTICITY
NT PHOTOELECTRIC EFFECT
NT PHOTOELECTRIC EMISSION
NT PHOTOIONIZATION
NT PHOTOVOLTAIC EFFECT
NT RADIANCE
NT REFLECTANCE
NT REFRACTIVITY
NT SKY BRIGHTNESS
NT STELLAR LUMINOSITY
NT TRANSLUCENCE
NT TRANSMISSIVITY
NT TRANSMITTANCE
NT TRANSPARENCE
NT TURBIDITY
Numerical integration procedure for determining electromagnetic structure of interplanetary space
01 p0093 N73-10768
Measuring electromagnetic parameters of soil samples in VHF/UHF range to determine properties that limit target detection
[AD-747346] 03 p0299 N73-12439
Response of triphase induction motor to perturbations caused by power interruptions
[PUBL-1360] 06 p0677 N73-15504
Off-shell asymptotic behavior of electromagnetic form factors of composite particle
[TR-73-070] 06 p0703 N73-15728
Dynamic interface effects on electromagnetic response of magnetic semiconductors
[AD-755861] 12 p1442 N73-21681
Bistatic radar investigation of lunar electromagnetic and surface properties from Apollo 16 command and service module
12 p1451 N73-21759
Electromagnetic properties of plane slab of finite thickness immersed in uniform magnetic field
[VTH-169] 13 p1559 N73-22637
Electromagnetic dispersion relation for two counterstreaming ion beams flowing parallel to direct current magnetic field
[NASA-CR-132953] 15 p1814 N73-24701
Direct determination of electromagnetic reflection properties of smooth brackish water by remote measurement technique
[PB-221372/6TR-48] 22 p2635 N73-31122
FORTRAN 4 program for determining transient tangential electric field and vertical magnetic dipole for stratified earth model
[PB-221240/5] 23 p2788 N73-32304
**ELECTROMAGNETIC PROPULSION**
Integrated magnetic suspension and propulsion system characteristics
[BNL-16909] 04 p0402 N73-13271
**ELECTROMAGNETIC PULSES**
Ionospheric modification of electromagnetic pulse from nuclear explosions
[SC-RR-72-0400] 06 p0699 N73-15697
Scattering of electromagnetic pulse by rectangular apertures in metal structures
[AD-750381] 06 p0701 N73-15714
Circuits for pulse generation in magnetic plasma pinch
[AD-751250] 07 p0830 N73-16732
Pulsed power burnout tests of hand gate circuits
[AD-752540] 08 p0892 N73-17219
Observation of propagation characteristics of electromagnetic pulse-type signals at altitudes between 100 and 280 km - 30 Oct. 1971
[LA-4947] 08 p0918 N73-17521
Analytic models to calculate electrostatic fields produced inside cylinders and spheres by internal electromagnetic pulses
[AD-753014] 09 p1067 N73-18709
Development of electromagnetic pulse sounding probe for detection and delineation of geological anomalies in hard rock medium
[AD-754847] 11 p1288 N73-20454
Electronic pulse generators producing 10 picosec duration pulses with several hundred MHz repetition rates
[DRIC-TRANS-2934] 12 p1379 N73-21185
Investigation of antenna cable responses to pulsed electromagnetic field
[AD-755514] 12 p1385 N73-21234
Turbulence spectra of magnetic pulsating nonisothermal plasma
[AEC-TR-7379] 12 p1434 N73-21622
Calibration and electromagnetic field mapping for continuous wave test facility
[AD-757638] 14 p1647 N73-23358
Radar system for electromagnetic subsurface profiling
[PB-213892/0] 14 p1665 N73-23514
Computerized design of hollow dipole antennas for measuring nuclear electromagnetic pulse
[AD-761801] 19 p2244 N73-28096
Analysis of axial conduction current induced in infinitely long cylinder in free space with small resistivity by incident electromagnetic plane wave
[AD-762165] 19 p2246 N73-28106
Assembly and operation of direct-drive pulser used in minuteman in-place electromagnetic pulse test program
[AD-763114] 20 p2476 N73-29887
Modulation of high frequency oscillation period by symmetric and asymmetric signals
22 p2630 N73-31079
Characterization of electromagnetic pulse shunt protective devices
[AD-763886] 22 p2644 N73-31191
**ELECTROMAGNETIC PUMPS**
Hydrodynamic instability effects on performance of electromagnetic pump under certain operating conditions
[FRNC-CONF-46] 10 p1166 N73-19485
Computer program for dual throat, electromagnetic dc conduction pumps
[NASA-CR-121204] 15 p1791 N73-24518
Parametric instabilities generated by electromagnetic pump in quiescent plasma device
[AD-759543] 16 p1951 N73-25786
Performance characteristics prediction of linearly oscillating electromagnetic pump
24 p2928 N73-33384
**ELECTROMAGNETIC RADIATION**
NT AIRGLOW
NT BLACK BODY RADIATION
NT BREMSSTRAHLUNG
NT CERENKOV RADIATION
NT COHERENT ELECTROMAGNETIC RADIATION
NT COHERENT LIGHT
NT COMET TAILS
NT CYCLOTRON RADIATION
NT DAYGLOW
NT ELECTROMAGNETIC PULSES
NT EXTRATERRESTRIAL RADIO WAVES
NT FAR INFRARED RADIATION
NT FAR ULTRAVIOLET RADIATION
NT GALACTIC RADIO WAVES
NT GAMMA RAY BEAMS
NT GAMMA RAYS
NT GEGENSCHEIN
NT GEOCORONAL EMISSIONS
NT INFRARED RADIATION
NT LIGHT [VISIBLE RADIATION]
NT LIGHT BEAMS
NT LONG WAVE RADIATION
NT LYMAN ALPHA RADIATION
NT LYMAN BETA RADIATION
NT MICROWAVE EMISSION
NT MICROWAVES
NT MILLIMETER WAVES
NT MONOCHROMATIC RADIATION
NT NEAR INFRARED RADIATION
NT NEAR ULTRAVIOLET RADIATION
NT NIGHTGLOW
NT PHOTON BEAMS
NT PLANETARY RADIATION
NT POLARIZED ELECTROMAGNETIC RADIATION
NT POLARIZED LIGHT
NT RADIO BURSTS
NT RADIO EMISSION
NT RADIO WAVES
NT SHORT WAVE RADIATION
NT SKY RADIATION
NT SKY WAVES
NT SOLAR RADIO BURSTS
NT SOLAR RADIO EMISSION
NT SOLAR X-RAYS
NT SUBMILLIMETER WAVES
NT SUNLIGHT
NT SYNCHROTRON RADIATION
NT TERRESTRIAL RADIATION
NT THERMAL RADIATION
NT TROPOSPHERIC RADIATION
NT TWILIGHT GLOW
NT TYPE 2 BURSTS
NT TYPE 3 BURSTS
NT TYPE 4 BURSTS
NT TYPE 5 BURSTS
NT ULTRAVIOLET RADIATION
NT X RAYS
NT ZODIACAL LIGHT
Modified scalar Debye potentials for electromagnetic waves in spherical gravity and spherical media
[AD-746047] 01 p0081 N73-10673
Electromagnetic wave propagation from oscillating source in suddenly created plasma
[AD-746329] 02 p0142 N73-11151
Analysis of instabilities resulting from interaction of electromagnetic waves with active medium or system
[AD-746893] 02 p0143 N73-11159
Application of reductive perturbation method to electromagnetic waves propagating in cold electron plasma
[IPPJ-136] 02 p0216 N73-11745

Diffraction of acoustic and electromagnetic waves on wavy surfaces
[AD-748037] 03 p0268 N73-12168
Numerical analysis on electromagnetic wave scattering from periodic surface with arbitrary profile
[AD-747491] 03 p0268 N73-12170
Night sky Cerenkov detector for measuring electromagnetic radiation produced by high energy cosmic rays
[AD-746734] 03 p0354 N73-12883
Generation and propagation of low frequency electromagnetic waves in cold collisional plasma
[AD-747092] 04 p0389 N73-13162
Resonance effects anomalous electromagnetic wave propagation in plasma
[NASA-CR-129673] 04 p0454 N73-13704
Capacitance analysis of electromagnetic coupling response in transmission lines and cables
[SC-RR-72-0299] 04 p0458 N73-13741
Characteristics of microwave antenna with conical reflectors to generate plane wave front
[NASA-CASE-NPO-11661] 05 p0507 N73-14130
Comparison of ionospheric radio wave propagation and acoustic gravity wave propagation
05 p0508 N73-14132
Analysis of quasi-periodic modulation of L-bursts in decametric radiation from planet Jupiter
05 p0594 N73-14833
Bibliography on radio frequency and microwave radiation effects in biological systems
[AD-750271] 06 p0632 N73-15151
Procedures and equipment for analyzing field strengths transmitted at extremely low frequencies and measurement of radial magnetic component
[REPT-72-4-ADD] 06 p0664 N73-15401
Theoretical model for electromagnetic coupling of Bernstein modes in vacuum boundary of dense plasma
[COO-2181-10] 06 p0704 N73-15742
High energy electrons and surface expansion in plasma targets heated by electromagnetic radiation
[LA-4986] 06 p0704 N73-15745
Computerized simulation of electromagnetic wave coupling modes in plasma diagnostics
[AD-750138] 06 p0706 N73-15763
Development of theory for time dependent magnetic fields inside Moon and diamagnetic cavity caused by interplanetary eletromagnetic field fluctuation
[NASA-CR-114546] 06 p0718 N73-15861
Helmholtz equation for solving electromagnetic wave functions of parabolic plasma density profiles
[AD-751669] 07 p0757 N73-16151
Radiation and propagation of electromagnetic waves in anisotropic medium
[NASA-TT-F-743] 08 p0943 N73-17726
Electromagnetic radiation screening of semiconductor devices for long life applications
[NASA-CR-124119] 09 p1073 N73-18757
Electromagnetic wave penetration into plasma at lower hybrid frequencies
[AEC-TR-7378] 10 p1196 N73-19732
Graphical amplitude characteristics of electromagnetic radiation reflected from anisotropic plasma boundary
[AEC-TR-7368] 10 p1196 N73-19734
Electromagnetic wave interactions in p type ferromagnetic semiconductors
10 p1198 N73-19751
Solution to Klein-Gordon and Dirac equations for charged particles in two noncollinear electromagnetic waves
[AD-754307] 11 p1327 N73-20769
Electromagnetic waves propagation and impedance analysis of double stream interaction in semiconductors
[NASA-CR-131293] 11 p1329 N73-20791
Operant behavior of rhesus monkeys in presence of extremely low frequency, low intensity magnetic and electric fields
[AD-754058] 12 p1372 N73-21134
Effect of homogeneous dielectric sphere on electromagnetic radiation from simple sources treated as boundary value problem and solution obtained by technique of dyadic Green functions
[NASA-CR-2211] 12 p1378 N73-21178
Characteristics of electromagnetic radiation with emphasis on radiobiology and procedures to reduce undesirable physiological and environmental effects
[JPRS-58783] 12 p1379 N73-21184
Diurnal cycles of atmospheric refractive index structure function coefficient used to describe scintillation and phase fluctuations of electromagnetic radiation propagated in atmosphere
[AD-755808] 12 p1402 N73-21374
Correlation functions for displacements in semiboundless isotropic elastic media
[ITF-72-78-P] 12 p1429 N73-21579
Influence of collisions on incoherent scattering spectrum of nonequilibrium inhomogeneous absorbing plasma
[CEA-R-4351] 12 p1436 N73-21633
Electromagnetic transients in plasmas and ray techniques for radiation and diffraction of electromagnetic waves
[AD-756484] 13 p1493 N73-22099
Longitudinal source drift measure of PC 1 geomagnetic micropulsation source by signal correlation of spaced receivers
[CEPHAG-22/72] 13 p1524 N73-22353
Stimulated and spontaneous scattering of electromagnetic radiation
[AD-757082] 13 p1559 N73-22639
Analysis of radome design techniques and development of specifications for radome construction
[AGARD-AR-53] 14 p1618 N73-23108
Propagation of electromagnetic waves through turbulent media using transport theory
[AD-757491] 14 p1634 N73-23245
Generation of electromagnetic waves and interactions with plasma media
[AD-757901] 15 p1781 N73-24441
Electromagnetic wave scattering from snow, ice, and sea ice
[AD-758071] 15 p1783 N73-24454
Dispersion relations for electromagnetic waves propagating in partially ionized gases immersed in dc magnetic field
[AD-757865] 15 p1819 N73-24743
Electromagnetic wave propagation in nonuniform waveguides with perfect conducting walls
16 p1874 N73-25170
Geometrical optical analysis for determining point source location of electromagnetic signal reflected from ionosphere
[AD-759488] 16 p1877 N73-25196
Review of research in electromagnetic radiation
[AD-759990] 17 p2008 N73-26235
Nonlinear optical susceptibilities for electromagnetic wave coupling of semiconductors
17 p2071 N73-26758
Analysis of antenna radiation patterns of radio antennas installed on aircraft using high frequency solutions
18 p2115 N73-27098
Measurement of electromagnetic wave diffraction by finite plane-parallel waveguide system
18 p2117 N73-27116
Plasma modification associated with electromagnetic waves and parametric instabilities within ionosphere - Parts 1 and 2
[AD-760809] 18 p2147 N73-27351
Focusing optical collimator for high resolution scanning of electromagnetic radiations, neutrons, and other particles
[NASA-CASE-MFS-20932-1] 18 p2150 N73-27380
Development of laser model for analyzing pulsed excitation of molecules in discharge and nonequilibrium discharge of supersonic flow in vacuum
[JPRS-59040] 18 p2158 N73-27432
Relativistic particle motion in electromagnetic wave traveling in direction of uniform static magnetic field
[NASA-CR-132781] 18 p2181 N73-27610
Method and apparatus for measuring electromagnetic radiation
[NASA-CASE-LEW-11159-1] 19 p2299 N73-28488
Wave amplification in dielectrics
[AD-762283] 19 p2309 N73-28570
Continuous wave dye laser for studying interaction of electromagnetic radiation with matter
[AD-762370] 19 p2309 N73-28572
Research projects in environmental and electromagnetic technologies
[AD-761483] 19 p2355 N73-28948
Accessibility of plane electromagnetic wave to lower hybrid resonance of inhomogeneous, magnetized plasma column
[IPP-IV-51] 20 p2459 N73-29761
Electromagnetic radiation trapped in magnetosphere above plasma frequency
[NASA-CR-133837] 21 p2540 N73-30367
Application of radio astronomy methods for analyzing microwave absorption spectrum and properties of atmospheric cloud formations
21 p2570 N73-30593
Application of mathematical techniques to problems of interaction of acoustic or electromagnetic waves with complex bodies
[AD-762802] 21 p2581 N73-30685
Transient response of stratified cold plasma to infinite plane electromagnetic wave
21 p2582 N73-30692
Transient response of stratified cold plasma to infinite plane impulsive electromagnetic wave incident vertically on ionization
21 p2582 N73-30693
Use of passive radar to determine range to target emitting radio signal
22 p2630 N73-31077
Energy spectrum and autocorrelation function of random processes at output of key detector
22 p2630 N73-31078
Anomalous nonlinear dissipation of high frequency radio waves in plasma
[JPRS-59883] 22 p2631 N73-31083
Relativistic particle motion in nonuniform electromagnetic waves
[NASA-CR-133888] 22 p2632 N73-31092
Propagation of electromagnetic signals through ionized media
[AD-764281] 22 p2635 N73-31114
Effect of homogeneous dielectric sphere on electromagnetic radiation from simple source
22 p2646 N73-31201
Nonlinear interactions of electromagnetic waves in parametric plasmas
[JPRS-59883] 22 p2703 N73-31647
Observations of decametric radiation of Jupiter with very-long-baseline interferometer
23 p2836 N73-32659
Pulsar magnetospheric model where radiation is produced near surface of neutron star
[NASA-CR-135587] 23 p2844 N73-32731
Propagation of random electromagnetic waves
24 p2894 N73-33103
Function of National Institute for Occupational Safety and Health in industrial radiation safety
24 p2953 N73-33592
Debye polarization theory for determining electromagnetic wave propagation in sea
24 p2957 N73-33622

**ELECTROMAGNETIC SCATTERING**

NT IONOSPHERIC F-SCATTER PROPAGATION
NT LIGHT SCATTERING
NT MICROWAVE SCATTERING
NT MIE SCATTERING
NT RAMAN SPECTRA
NT RAYLEIGH SCATTERING
NT THOMSON SCATTERING
NT X RAY SCATTERING
Fredholm equations for low frequency scattering by imperfectly conducting obstacles
[AD-746048] 01 p0082 N73-10674
Survey of methods to obtain electromagnetic and acoustic high frequency scattering
[AD-747044] 02 p0143 N73-11158
Numerical analysis of inverse scattering problem applied to far field relations between incident and scattered radiation in presence of scattering object
02 p0200 N73-11613
Three-dimensional electromagnetic inverse scattering identity based on physical optics approximation for monostatic scattered far field cross section of perfect conductors
02 p0200 N73-11615
Exact solutions for electromagnetic inverse problem for perfectly conducting body with consideration of uniqueness problem and case of spherically symmetric dielectric body
02 p0200 N73-11616
Solution of n-dimensional scattering problem by means of k-space formulation of field equations
02 p0201 N73-11623
Numerical analysis on electromagnetic wave scattering from periodic surface with arbitrary profile
[AD-747491] 03 p0268 N73-12170
Development of relaxation method and inverse method for solving problems of electromagnetic scattering
[AD-749954] 05 p0515 N73-14184
Scattering of electromagnetic pulse by rectangular apertures in metal structures
[AD-750381] 06 p0701 N73-15714
Effect of electromagnetic scattering from ocean surface on spherical waves of dipole antenna
07 p0761 N73-16184
Matrix solution for one dimensional model of radiation field arising from multiple scattered photons in planetary atmosphere
[NASA-CR-130755] 08 p0943 N73-17722
Statistical models of electromagnetic scattering from radar targets
[AD-753936] 11 p1256 N73-20192
Optical design of radar antenna configurations with desired scattering patterns
[AD-755914] 12 p1380 N73-21193
Analytical and computer design of array antennas, and analysis and synthesis of electromagnetic scattering systems
[AD-758768] 15 p1758 N73-24249
Kirchhoff approximation correction for application to electromagnetic wave scattering by rough surfaces
[NASA-CR-112263] 16 p1873 N73-25180
Extension of electromagnetic antenna wave diffraction principle
[AD-759690] 17 p1999 N73-26163
Earth surface scattering model for multiphase prediction of radiowave communication between earth satellites
[NASA-CR-132791] 18 p2116 N73-27109
Numerical solution for two dimensional electromagnetic scattering
[AD-760773] 18 p2119 N73-27137
Solution of acoustic and electromagnetic scattering problems in exterior domains using integral equations
[NPL-NAC-30] 19 p2314 N73-28608
Scattering of electromagnetic waves from planar and rough oscillating surfaces
22 p2627 N73-31046
Intergral equations for incident electromagnetic wave scattering by slotted spherical antenna
[AD-764880] 23 p2758 N73-32075
Statistical modeling of electromagnetic scattering from radar targets
24 p2893 N73-33099

**ELECTROMAGNETIC SHIELDING**
NT RADIO FREQUENCY SHIELDING
Effects of magnetic and electric coupling parameters on terminal response shielding of braided-shield cables exposed to external electromagnetic fields
[AD-748387] 04 p0396 N73-13221
Surface transfer impedance measurements for determining shielding characteristics of coaxial cables
[AD-753678] 09 p1009 N73-18237
Grounding, bonding, and shielding practices for operational reliability enhancement in air traffic control electronic facilities
[FAA-RD-73-51] 14 p1645 N73-23341
Electromagnetic shielding and hardening of radio communication systems against atmospheric nuclear burst effects
[AD-758403] 15 p1751 N73-24196
Detection and measurement of radio frequency interference and methods of logic circuit protection
[NLL-PO-2928-[9022.81]] 15 p1759 N73-24254
Shielding effectiveness of exterior shield and connector assemblies on Lance umbilical cables
[AD-761078] 18 p2201 N73-27771
Effectiveness of braided wire electromagnetic shielding against magnetic field penetration
[AD-761823] 19 p2246 N73-28111
Shielding analysis of joints and connectors in coaxial cables
[AD-761825] 21 p2518 N73-30201

**ELECTROMAGNETIC SHOCK TUBES**
U SHOCK TUBES

**ELECTROMAGNETIC SPECTRA**
NT BALMER SERIES
NT D LINES
NT ELECTRONIC SPECTRA
NT FRAUNHOFER LINES
NT H ALPHA LINE
NT H BETA LINE
NT H GAMMA LINE
NT H LINES
NT INFRARED SPECTRA
NT K LINES
NT LINE SPECTRA
NT MICROWAVE SPECTRA
NT RAMAN SPECTRA
NT SOLAR SPECTRA
NT STELLAR SPECTRA
NT TELLURIC LINES
NT UBV SPECTRA
NT ULTRAVIOLET SPECTRA
NT VIBRATIONAL SPECTRA
NT X RAY SPECTRA
Application of electromagnetic sensors for remote sensing of oceanographic processes to determine available resources
07 p0782 N73-16356
Analysis of factors affecting design and application of remote sensors for earth observation
07 p0784 N73-16376

**ELECTROMAGNETIC WAVE FILTERS**
NT ELECTRIC FILTERS
NT INFRARED FILTERS
NT MICROWAVE FILTERS
NT OPTICAL FILTERS
NT RADAR FILTERS
NT WAVEGUIDE FILTERS
Computerized design of dielectric lenses for phase corrected horn antennas
[AD-753914] 10 p1136 N73-19258
Application of optimal control theory to design of constant gain filters to minimize weighted average of filtered variances
[AD-755798] 12 p1380 N73-21190

**ELECTROMAGNETIC WAVE TRANSMISSION**
NT DOUBLE SIDEBAND TRANSMISSION
NT IONOSPHERIC F-SCATTER PROPAGATION
NT IONOSPHERIC PROPAGATION
NT LIGHT SCATTERING
NT LIGHT TRANSMISSION
NT MICROWAVE ATTENUATION
NT MICROWAVE TRANSMISSION
NT MULTIPATH TRANSMISSION
NT RADAR TRANSMISSION
NT RADIO ATTENUATION
NT RADIO TRANSMISSION
NT SCATTER PROPAGATION
NT SHORT WAVE RADIO TRANSMISSION
NT SINGLE SIDEBAND TRANSMISSION
NT TELEVISION TRANSMISSION
Measurement and analysis of depolarization and differential attenuation during propagation of millimeter wave signals through rain
[NASA-CR-130107] 01 p0028 N73-10217
Electromagnetic wave transmission in space-time varying dielectrics and plasmas
[AD-746676] 02 p0144 N73-11165
Cyclotron resonance caused by electromagnetic waves incident on high density gaseous plasma
[IPPJ-134] 02 p0215 N73-11742
Conference on acoustic gravity wave effects in atmospheric transmission of radio communication signals
[AGARD-CP-115] 05 p0508 N73-14131
Auroral infrasonic sound wave generation and downward propagation into lower atmosphere
05 p0508 N73-14134
Mathematical model for acoustic gravity wave excitations moving air masses
05 p0508 N73-14135
Theoretical plasma perturbation model for calculating coupling effects between acoustic gravity waves and electromagnetic waves in ionospheric disturbances
05 p0512 N73-14162
Development of relaxation method and inverse method for solving problems of electromagnetic scattering
[AD-749954] 05 p0515 N73-14184
Loading effect of probes used in coaxial waveguide experimental coupler
[AD-749060] 05 p0521 N73-14233
Absorption, reflection, and scattering of electromagnetic waves by plasma media as electronic countermeasures in radar detection
[FOA-3-C-3652-66] 06 p0639 N73-15189
Attenuation calculations for extremely low frequency and very low frequency electromagnetic wave propagations in earth crust
[AD-748331] 06 p0641 N73-15206
OGO-D electromagnetic wave propagation measurements with whistler and hiss formations in plasmasphere
[NASA-CR-130351] 07 p0754 N73-16126
Equations and graphs on electromagnetic field parameters
[UCRL-51245] 07 p0756 N73-16140
High frequency pressure effect on wave propagation along layer of magnetoactive plasma
[AEC-TR-7336] 07 p0826 N73-16698
High frequency wave field pressure effect on Langmuir monochromatic plasma oscillations
[AEC-TR-7337] 07 p0827 N73-16707
Model medium concept in geometric optics for electromagnetic wave propagation in absorbing media
[MPI-PAE/EXTRATERR-60] 08 p0943 N73-17727
Rotational polarization of electromagnetic waves propagating in magnetized plasma
[JAERI-M-4640] 08 p0948 N73-17766
Electromagnetic wave interactions in stratified and space-time periodic dielectric or plasma streams
[AD-753690] 09 p1004 N73-18196
Diffusion random model for statistical analysis of light propagation in turbulent medium
09 p1066 N73-18698
Development of method for determining conductivity of surface layer of sea by recording field of remote transmitters operating in superlong wavelength range
10 p1153 N73-19382
Propagation pattern of shock waves emitted by solar flares occurring in active region of McMath No. 9740 from 23 Oct. - 4 Nov. 1968
[NASA-TM-X-66227] 12 p1445 N73-21705
Research on electromagnetic wave transmission and antennas
[AD-756915] 13 p1496 N73-22126
Harmonic generation in electromagnetic wave propagating in isotropic dielectric
[AD-758911] 16 p1877 N73-25198
Electromagnetic wave propagation in inhomogeneous plasmas exemplified by cavity resonators and positive column in magnetic field
[IPF-72-8] 17 p2069 N73-26742
Calculation of Mie differential scattering cross section of spherical particles with complex refractivity, for mm wave propagation through precipitation
[FTZ-A-455-TBR-35] 22 p2633 N73-31100
Comparison between measured transmission and emission spectra and calculated spectra in 9.6 micron region of ozone
[NASA-TT-F-15110] 22 p2665 N73-31356
Sine wave propagation in lossy plasmas
[AD-764721] 23 p2758 N73-32073

**ELECTROMAGNETIC WAVES**
U ELECTROMAGNETIC RADIATION

**ELECTROMAGNETICS**
U ELECTROMAGNETISM

**ELECTROMAGNETISM**
Electromagnetic technology for radar, air traffic control, and communication systems
[AD-756482] 13 p1493 N73-22107
Itinerant electron magnetism in ZrZn2 phase
[REPT-735] 16 p1944 N73-25733
Admittance of axial slot backed by cylindrical cavity inside infinite cylinder
[AD-759568] 16 p1946 N73-25748
Spin energy transfer processes at low temperatures
[AD-762618] 20 p2455 N73-29731
Debye polarization theory for determining electromagnetism of sea surface
24 p2957 N73-33620

**ELECTROMAGNETS**
NT HIGH FIELD MAGNETS
NT SUPERCONDUCTING MAGNETS
Development of superconducting magnet system for magnetohydrodynamic power generation
[AD-745321] 01 p0032 N73-10247
Ising ferromagnet thermodynamic equilibrium states in low temperature regions
[NOTA-INTERNA-381] 01 p0080 N73-10660
Magnetic bearings for spacecraft applications
[NASA-TM-X-66111] 03 p0306 N73-12499
Asymmetric magnetic yoke for shaping uniform field in electromagnets
[NP-19359] 04 p0450 N73-13673
Computerized design of betatron electromagnet having optimal parameters
[AD-750523] 06 p0651 N73-15289
Effect of displacements of suspended mass on accuracy of electromagnetic load cell and selection of parameters for increased accuracy
06 p0696 N73-15668
Cryogenics, superconductors, and electromagnets - conference
[AD-753456] 09 p1067 N73-18705
Analysis of stresses in magnet windings due to thermal contraction and temperature gradient stresses and impregnation with epoxy resins to reduce effects
[RHEL/R-264-PT-1] 20 p2435 N73-29558

**ELECTROMECHANICAL DEVICES**
Equivalent circuit of electromechanical or magnetohydrodynamic converter with traveling magnetic field
[AD-747611] 03 p0256 N73-12072
Design and performance of segmented magnetic torque converter for mechanical drives
[AD-753541] 10 p1167 N73-19498
Electromechanical energy conversion devices using both conventional and rare-earth cobalt permanent magnet materials
[AD-756433] 13 p1501 N73-22168
Design and construction of waterdrop generator with remote control of drop mass and interval
[NBS-TN-776] 14 p1645 N73-23343
Electromechanical actuator for producing mechanical force and/or motion in response to electrical signals
[NASA-CASE-NPO-11738-1] 21 p2516 N73-30185
Brushless electromechanical generator for sine and cosine functions
[NASA-CASE-LAR-11389-1] 23 p2765 N73-32121

**ELECTROMECHANICS**
Derivation of minimum dimension sets of discrete coordinate and hybrid coordinate equations of motion for hinge connected rigid bodies assembled in tree topology
[NASA-CR-129950] 05 p0602 N73-14900

**ELECTROMETERS**
Performance of temperature compensated rocketborne MOSFET electrometer amplifier for measurement of electron and ion densities in lower ionosphere
[FOA-3-C-3640-E1] 04 p0420 N73-13424
Design and performance of miniaturized electric field meters for wind tunnel measurements
[AD-750148] 06 p0675 N73-15495

**ELECTROMOTIVE FORCES**
Variation of electric conductivity and thermal emf at fusion of copper chalcogenides
[AD-756088] 13 p1566 N73-22694
Open circuit voltage measurements on solid beta alumina electrolytic cells
[NASA-TN-D-7322] 15 p1738 N73-24089
Electromotive force measurements for determining oxygen concentration in liquid sodium
[NLL-CE-TRANS-6073-[9022.09]] 15 p1746 N73-24148
Effect of irradiation on absolute thermal EMF of alloys, metals, and thermocouple materials
[NASA-TT-F-15015] 19 p2309 N73-28574

**ELECTROMYOGRAMS**
U ELECTROMYOGRAPHY

**ELECTROMYOGRAPHS**
U ELECTROMYOGRAPHY

**ELECTROMYOGRAPHY**
Effects of direct auditory feedback of electromyogram on learning to control single unit
[AD-745107] 01 p0021 N73-10165
Accelerometers, electromyogram sensors, and telemetry system for measuring human body segment motions
[AD-751134] 07 p0751 N73-16104
Investigation of vocal cord regulatory mechanism of register, pitch, and intensity of voice during singing
14 p1632 N73-23225

**ELECTRON ACCELERATORS**
NT BETATRONS
Development and characteristics of synchrotrons with steady-state field in energy range of 35 to 300 giga electron volts
[JPRS-57489] 03 p0280 N73-12271
Development of beam bunching method for injection into pulse excited accelerating cavity
[BNL-16945] 04 p0402 N73-13273
Nuclear research projects with fast electron accelerator and theoretical physics of neutron decay reactions
04 p0452 N73-13687
Design of pulsed electron beam accelerator with multiple Mylar stripline modules
[AD-751593] 07 p0766 N73-16227

Pulsed electron accelerators with energies of 20 to 50 MeV
[JPRS-58160] 09 p1011 N73-18252
Propagation and merging of high current relativistic electron beams in particle accelerator facility
[AD-760344] 17 p2011 N73-26266
Problems of electron accelerator scattering experiments
[CONF-710974-7] 17 p2065 N73-26708

**ELECTRON ATTACHMENT**
Perturbation theoretical and graphical representation of vertical ionization energies and electron affinities of free molecules
08 p0916 N73-17506
Experimental determination of electron attachment in high temperature plasma
[AD-763090] 20 p2459 N73-29765

**ELECTRON AVALANCHE**
Experimental characterization of abrupt junctions in avalanche mode
[LAAS-PUBL-939] 04 p0399 N73-13246
Random walk theory for studying electron avalanche formation in helium electric fields
[NASA-TN-D-7224] 12 p1433 N73-21612

**ELECTRON BEAM WELDING**
Power density as control parameter for electron beam welding
[LA-DC-72-581] 03 p0306 N73-12502
Influence of steam on fusion in electron beam welding
[DRIC-TRANS-2927] 03 p0307 N73-12505
Effect of joint orientation relative to gravitational field direction during electron beam welding
[JPRS-57281] 04 p0426 N73-13476
Weldability and properties of materials undergoing electron beam welding
[CRANFIELD-MAT-7] 05 p0551 N73-14474
Health hazards in using electron beams for welding beryllium alloys
10 p1172 N73-19531
Pulsed electron beam heating for optimal penetration and forming of welds
[AD-754684] 11 p1301 N73-20557
Research projects conducted as part of NASA programs during period May 1970 through May 1972
[NASA-TM-X-64723] 13 p1593 N73-22915
Development of electron beam welding techniques and application to welding various metal structures
13 p1593 N73-22919

**ELECTRON BEAMS**
Intense relativistic electron beam physics
[AD-745369] 01 p0086 N73-10710
Analysis of diffusive separation in front of blunt body in low density binary mixture of supersonic flows using electron beam densitometer
[AD-745960] 02 p0157 N73-11274
High pressure nitrogen gas discharge initiated by fast electron beams of 100 to 300 keV energies
[DRIC-TRANS-2857] 02 p0212 N73-11716
Diode passivation techniques and fabrication of semiconductor targets that are stable under electron beam bombardment for use in L band amplifiers
[AD-747868] 03 p0276 N73-12237
Characteristics of infrared photodetectors manufactured from semiconductor material irradiated by electron beam
[NASA-CASE-LAR-10728-1] 03 p0300 N73-12445
Extremely short, high power pulses from electron beam controlled CO2 laser amplifier
[LA-DC-72-447] 03 p0310 N73-12528
Device for converting optical images into electron beams
[NASA-CASE-GSC-11602-1] 04 p0395 N73-13214
Design, development, and fabrication of L band RF electron beam semiconductor amplifier
[AD-748898] 04 p0396 N73-13224
Development of beam bunching method for injection into pulse excited accelerating cavity
[BNL-16945] 04 p0402 N73-13273
Nonhomogeneity effects of magnetic field on plasma heating by electron beam in mirror trap of probkotron type
[SFTI-1] 04 p0454 N73-13710
Refocusing of spent axisymmetric beam in klystron tubes for optimal entry into multistage depressed potential collector
[NASA-CR-121114] 05 p0519 N73-14217
Analysis of swirling jet of gas injected into vacuum and effect of centrifugal force on separation of constituents
[ISAS-487-VOL-37-NO-13] 05 p0526 N73-14283
Electron beam-induced luminescence studies of thermospheric temperatures and particle densities, using two Aerobee 150 rockets
[AD-749877] 05 p0541 N73-14406
Analysis of electron beam induced discharge in nitrogen at high pressure
[NLL-DRIC-TRANS-2857-(3623.66)]
05 p0579 N73-14714
Permanent electron beam radiation effects on thin film single junction quantum interferometer devices
[AD-749065] 05 p0582 N73-14740
System characteristics of amorphous semiconductor thin film and electron beam storage devices
[AD-749282] 05 p0587 N73-14778
Feasibility of electron beam excited, high pressure recombination laser
[AD-750777] 06 p0680 N73-15530
CO2 laser model study of electron beam
[AD-750314] 06 p0680 N73-15532
Design of pulsed electron beam accelerator with multiple Mylar stripline modules
[AD-751593] 07 p0766 N73-16227
Interaction of intense relativistic electron beam with axial and convergent magnetic guide fields
07 p0820 N73-16647
Excitation of electromagnetic waves in cold plasma contained in metal wavequide by electron beam
[AEC-TR-7333] 07 p0827 N73-16704
Auxiliary corrective windings for increased resolution and decreased distortions in cathode ray tubes
[AD-751879] 08 p0889 N73-17201
Development and characteristics of electron beam excited high pressure mercury dissociation laser
[AD-752465] 08 p0930 N73-17619
Plasma wave generation in ionosphere by rocket-borne electron beam accelerator
08 p0947 N73-17753
Effects of density measurement electron beam impinging on blunt body in transition flow, noting influence of secondary electrons
[DLR-FB-73-08] 09 p0981 N73-18017
Electron beam irradiation capabilities of facility for materials and structures testing
[AD-752762] 09 p1012 N73-18260
Design and performance of electron beam storage tube for computer random access memory
[AD-753929] 10 p1136 N73-19257
Return current induced in bounded plasma by electron beam injection
[SC-RR-72-0669] 10 p1196 N73-19729
Relativistic electron beam for thermonuclear heating of plasma media
[AD-754621] 11 p1329 N73-20783
Binary code signals produced by electron beam deflection in magnetic fields
12 p1378 N73-21176
Correction of scanning beam velocity nonuniformity in vidicons by deflection of current pulse
[DRIC-TRANS-2758] 12 p1384 N73-21224
Development and characteristics of flat, thin, cathode ray tube with digital switching for beam deflection and positioning
[AD-755938] 12 p1384 N73-21227
Design equations for electron beam, semiconductor amplifiers with large area diodes to enhance power output
[AD-755806] 12 p1385 N73-21229
Wave interactions between plasma-electron beam system in magnetic fields
[AEC-TR-7355] 12 p1434 N73-21616
Relativistic electron beam equilibria in cylindrical plasma geometry
[IPP-6/111] 12 p1435 N73-21630
Reduction of nonuniformity of electron beam displacement on vidicon screen at raster edges
[DRIC-TRANS-2966] 13 p1500 N73-22156
Design, fabrication, and evaluation of electron beam addressable, high information density memory tube
[AD-756936] 13 p1500 N73-22161
Interaction between drifting streams of electrons with transverse cyclotron motions and electromagnetic fields
[NASA-CR-130208] 13 p1504 N73-22188
Recombination electron beam-excited plasma into pulsed laser of high peak power
[AD-756681] 13 p1537 N73-22455
Electron beam optics for measuring density and temperature of aerodynamic gas flow
[ONERA-PUBL-146] 13 p1559 N73-22635
Delivery of electron beam to X ray target in 50 nanoseconds
[AD-755456] 14 p1646 N73-23347
Design and performance of high intensity pulsed electron beam system
[FOA-2-C2579-E8] 15 p1788 N73-24493
Electron beam probing technique for measuring hypersonic rarefied gas density, vibration, and rotational temperature
[ONERA-P-146] 15 p1788 N73-24497
Modulation of electron beam by laser beam in thin film with production of light
15 p1795 N73-24548
Etch pit study of motion and generation of dislocations in electron irradiated metals and effect of point defects on mechanical properties of metals
[COO-1367-50] 15 p1799 N73-24579
Cooled carbon monoxide laser for pulsed operation with pressure up to 1 atmosphere using electron beam for gas excitation
[AD-759755] 16 p1924 N73-25570
Feasibility study to develop recombining electron beam-excited plasma into pulsed laser of exceptionally high peak power
[AD-759399] 16 p1925 N73-25579
Theoretical prediction of thermal stress waves in metal conductors induced by relativistic electron beam
16 p1926 N73-25587
Electron beam semiconductor S-band amplifier
[AD-759948] 17 p2005 N73-26212
Ion and electron beam techniques for fabricating integrated optics circuits
[AD-760051] 17 p2008 N73-26237
Intense electron beam generation, transport, and diagnosis to acquire technology for construction of advanced X ray source
[AD-760038] 17 p2011 N73-26265
Propagation and merging of high current relativistic electron beams in particle accelerator facility
[AD-760344] 17 p2011 N73-26266
Spectroscopic methods used for analysis of beam-plasma instability
[LBL-1531] 17 p2068 N73-26732
Fabrication of array of silicon diodes for application in electron beam semiconductor device
[AD-760602] 18 p2124 N73-27164
Total cross sections for electron positron annihilation producing hadron pair
[NOTA-INTERNA-420] 18 p2181 N73-27613
Stabilization of ion acoustic waves by electron trapping
[AD-761174] 18 p2183 N73-27628
Theoretical treatment of Schwarz-Hora effect in which electron beam passing through crystal is modulated by laser light and reproduces it on striking nonluminescent target
18 p2185 N73-27643
Computerized design of electron beam semiconductor short pulse generator
[AD-761111] 18 p2191 N73-27693
Electron beam heating of theta pinch plasma
[AD-762418] 19 p2326 N73-28708
Electron beam flouorescence diagnostics of ternary gas mixture of nitrogen, helium, and hydrogen
[AD-762930] 20 p2374 N73-29079
Development of field emitter cathodes for electron beam devices
[AD-762322] 20 p2381 N73-29134
Stability of microwaves generated by intense relativistic electron beam in rippled magnetic field
[AD-763337] 21 p2508 N73-30126
Dynamic electric field profiles in electron beam semiconductor devices
[AD-763296] 21 p2517 N73-30192
Electron beam semiconductor S-band amplifier
[AD-763223] 21 p2518 N73-30200
Electron beam stabilized electrical discharge gas lasers
[AD-763409] 21 p2555 N73-30487
Electron beam stabilized electrical discharge HF laser
[AD-763464] 21 p2556 N73-30489
Stabilization of electron streams in Type 3 solar radio bursts
[NASA-CR-133844] 21 p2593 N73-30776
Bremsstrahlung radiation from beam of electrons in solar chromosphere, and total energy of solar flares
[NASA-CR-133943] 22 p2711 N73-31710
Solid-phase interaction of refractory metals and refractory compounds at high temperature using electron beam heater
23 p2808 N73-32455
Use of electron beam for preionization in Z-pinch experiment
[AD-765313] 23 p2823 N73-32568
Holographic interferometric measurement of plasma density in electron beam diode
[SLA-73-5483] 24 p2927 N73-33376
Electron beam devices, quantum electronic devices, plasmas, and solid state devices
[AD-764808] 24 p2932 N73-33415
Electron beam energy loss in plasma
[LA-5269-MS] 24 p2964 N73-33684
Plasma heating by electron beam
[COO-3165-4] 24 p2965 N73-33699

**ELECTRON BOMBARDMENT**
Electron bombardment and energy losses in beryllium, aluminum, copper, tin, gadolinium, and lead
[AD-747077] 02 p0215 N73-11739
Electron bombarded semiconductor short pulse generator
[AD-748090] 03 p0276 N73-12239
Optical properties of thin film deposited by electron bombardment
[NPL-OP-MET-13] 03 p0340 N73-12775
Electron transport properties in space environment and spacecraft shielding
[NASA-CR-123998] 06 p0702 N73-15722
Fabrication and tests of 2.5-centimeter Kaufman electron bombardment microthruster
[NASA-TM-X-2708] 07 p0836 N73-16774
Influence of electron beam irradiation on upper atmospheric chemistry and physics
[AD-753707] 09 p1033 N73-18431
Production of stimulated emission in vacuum ultraviolet using molecular xenon gas excited by relativistic electron beam
[AD-753483] 09 p1045 N73-18522
Liquid-vapor state of aluminum during electron bombardment
[AD-754449] 11 p1253 N73-20171
Production of iodine isotope by high energy bombardment of cesium heat pipe causing spallation reaction
[NASA-CASE-LEW-11390-2] 11 p1326 N73-20763

Computer radiation interaction program for calculating material response to X ray and electron beam impact
[AD-755147] 11 p1327 N73-20767
Reliability tests of reverse biased semiconductor diodes under electron beam bombardment conditions
[AD-755449] 13 p1502 N73-22171
Philips 25 mm electron bombarded silicon tube tests, including photocathode sensitivity, dark current, and square wave response
[AD-758360] 15 p1758 N73-24246
Design and performance of high intensity pulsed electron beam system
[FOA-2-C2579-E8] 15 p1788 N73-24493
Etch pit study of motion and generation of dislocations in electron irradiated metals and effect of point defects on mechanical properties of metals
[COO-1367-50] 15 p1799 N73-24579
Fluxgate magnetometer for measuring magnetic flux density of several electron-bombardment ion thrusters
[NASA-TM-X-68239] 15 p1826 N73-24796
High density optical memory
[AD-759032] 17 p2002 N73-26184
Dynamic properties of neutral excitations in electron bombarded superfluid helium
18 p2181 N73-27606
Single grid accelerator system for electron bombardment type ion thrustor
[NASA-CASE-XLE-10453-2] 18 p2192 N73-27699
Eight cm electron bombardment thruster for auxiliary propulsion
[NASA-TM-X-68296] 22 p2709 N73-31694
Coloring memory crystals by electron bombardment and KCl, Na, Cl for thermoelectric cooling for high density optical memory
[AD-765391] 23 p2762 N73-32105
High voltage pulse for igniting electron bombardment mercury ion thruster
[NASA-TM-X-71425] 23 p2765 N73-32119
Boltzmann transport equation for electron bombardment effects in solids
[AD-764637] 23 p2827 N73-32599
Ignition of mini-atomic bomb to produce thermonuclear power with capacitor produced electron beams
24 p2907 N73-33199

**ELECTRON BUNCHING**
Development of beam bunching method for injection into pulse excited accelerating cavity
[BNL-16945] 04 p0402 N73-13273
Electron bunching in drift area of two cavity klystrons via one dimensional approximation, using electron beam disk model
[AD-751073] 07 p0763 N73-16204
Analysis of single electron bunch transfer tolerance for intersecting storage accelerators
[BNL-17275] 10 p1194 N73-19711

**ELECTRON CAPTURE**
Charge exchange cross sections for protons and alkali atoms using classical approximation of Gryzinski
[NASA-CR-129262] 03 p0339 N73-12763
Measurement of electron density in cylindrical electrostatic confinement device
24 p2961 N73-33664
High field emission and capture of electrons and holes at zinc centers in N-P and P-N junctions
24 p2966 N73-33705

**ELECTRON COLLISIONS**
U ELECTRON SCATTERING

**ELECTRON COUNTERS**
Low energy electron detection by channel multiplier
[CONF-720404-VOL-1] 19 p2322 N73-28682

**ELECTRON DECAY RATE**
Radio frequency electron drift velocity and parametric instability in plasma heating
[CONF-720705-4] 07 p0756 N73-16138
Model of electrons artificially injected into inner radiation belt by Starfish nuclear explosion
[NASA-TM-X-66211] 11 p1336 N73-20842

**ELECTRON DENSITY [CONCENTRATION]**
NT ELECTRON DENSITY PROFILES
NT IONOSPHERIC ELECTRON DENSITY
NT MAGNETOSPHERIC ELECTRON DENSITY
Measurement of electron density in carbon plasma created by heating solid target with laser radiation
[AD-746221] 01 p0086 N73-10715
Transition from supersonic to subsonic solar wind by increased density at corona base
01 p0095 N73-10779
Spectral form of irregularities in electron density causing interplanetary scintillation of small angular diameter radio sources
01 p0098 N73-10804
Effect of sputtering corotating source of thin solar plasma streams on electron content of solar wind
01 p0098 N73-10805
Correlation between geomagnetic field increases or storm commencements with variations in electron content of solar wind
01 p0098 N73-10810
Microwave signal interaction with plasma medium
[AD-746677] 02 p0144 N73-11164
Mid-latitude depletions in electron and total ion density by direct and indirect techniques
[NASA-TM-X-66089] 02 p0165 N73-11341
Structure and variation of topside ionosphere at mid-latitudes during sunrise period based on Alouette 1 electron density measurements
[AD-748430] 03 p0299 N73-12443
Analysis of linear and nonlinear properties of density gradient driven drift waves instability using single-ended Q-machine
[AD-747852] 03 p0344 N73-12803
Mapping electron number density distribution in nonequilibrium shock layer with kinetic and radiative processes coupled to gas dynamics
[AD-748833] 04 p0407 N73-13312
Experimental determination of electron density in absorbing layer of laser produced plasmas
[JUL-820-PP] 04 p0454 N73-13706
Full wave solution for electron density perturbations caused by gravity waves in F2 region
05 p0509 N73-14145
Interferometric determination for distribution of electron density of two colliding laser plasmas
[AD-749618] 05 p0584 N73-14754
Laser heating of dense plasma through excitation of parametric instabilities
[AD-749970] 05 p0584 N73-14756
Measurement of energy spectra of high energy trapped protons using nuclear emulsions exposed on low altitude polar orbiting satellites
[AD-750474] 06 p0669 N73-15438
CO2 laser model study of electron beam
[AD-750314] 06 p0680 N73-15532
Electron cooling in F2 region at low and midlatitudes, caused by electron-ion collisions and electron impact induced transitions
[RSD-74] 07 p0789 N73-16413
Electron density profiles of D region
[RSD-76] 07 p0789 N73-16415
Diurnal electron content tables obtained at Hawaii during 1971
07 p0789 N73-16419
Hyperfine electron density fluctuation in stabilized hydrogen arc laser
08 p0943 N73-17723
Electron density profiles from Mariner 5 and solar wind maintenance of nighttime Venus ionosphere
08 p0973 N73-17951
Evaluation of type 3 solar radio burst theories using low frequency satellite observations
08 p0974 N73-17961
Cosmic ray phenomenon of quiettime electron increases
08 p0974 N73-17962
Computer simulation of whistler turbulence and velocity space diffusion in magnetospheric type plasma
[AD-753196] 09 p1031 N73-18415
Electron density, electron and ion temperature, and ion composition values obtained during eclipse on 7 Mar. 1970
[UILU-ENG-73-2501] 10 p1154 N73-19390
Analysis of radio phase differences for determining electron concentration in solar corona
10 p1177 N73-19577
Electron density and temperature measurements on negative glow plasma
12 p1433 N73-21609
Quenching of beam plasma instability by mode mixing at density discontinuity
[AD-755658] 12 p1436 N73-21637
Electronic density of state in Weaire model of amorphous solid
[JINR-E4-6589] 12 p1440 N73-21668
Development of viscous shock layer analysis to determine nonequilibrium flow distributions of plasma layer during reentry conditions
[NASA-CR-2232] 13 p1491 N73-22085
Electron density irregularities and evening anomalies in midlatitude nighttime F region
13 p1514 N73-22270
Energy loss method for calculating synchrotron-Cerenkov radiation of relativistic electrons in cold magnetoplasma
[AD-755387] 13 p1564 N73-22675
Ionosonde virtual height observations based on first order, electron density profile from incoherent scatter
[UILU-ENG-73-2503] 14 p1661 N73-23482
Potential and electron density studies in inertial electrostatic plasma confinement devices
[AD-757228] 14 p1696 N73-23763
Electrical resistance measurement for determining electron state densities in molten germanium-silver and germanium-copper systems
[NLL-M-21613-[5828.4F]] 15 p1746 N73-24153
VHF/UHF technique for determination of columnar electron contents of plasmasphere and of protonosphere using geostationary satellite transmissions of magnetic storm observations
15 p1770 N73-24338
Temporal variations in dawn and dusk 600 km midlatitude trough position measured by RF capacitive probes on Ariel 3
[NASA-TM-X-66253] 15 p1806 N73-24634
Electron density determination in thermodynamic equilibrium behind reflected shock wave in air, using microwave reflectometer in shock tube
[ISL-43/71] 16 p1889 N73-25288
Amplitudes and widths of Gaussian distributions of electron density in wakes of hypervelocity projectiles flown in air and nitrogen at various pressures
[AD-759065] 16 p1893 N73-25316
Features deduced from radio propagation measurements of electron content in solar wind storms
16 p1959 N73-25843
Holographic interferometry using pulsed ruby lasers to measure electron density in toroidal plasmas
[REPT-72-70] 17 p2069 N73-26743
Balmer and H gamma line profiles for determining electron density in model B stars
[NASA-TM-X-66266] 17 p2082 N73-26840
Electrostatic analyzer and energy spectrum determination methodology used with primary electron spectrometer on Nike-Tomahawk sounding rocket
[NASA-CR-133409] 18 p2151 N73-27389
Boundary layer electron concentration profiles for entry of blunt nosed slender body into earth atmosphere
[NASA-TN-D-7332] 18 p2182 N73-27620
Secondary electron densities in two-electrode interspace in ac current present during multipactor discharge
[REPT-73-74] 19 p2244 N73-28091
ISIS-A electro static probe measurements of electron concentration and temperature of plasmapause at mid-latitudes
[NASA-TM-X-70429] 19 p2293 N73-28442
Microwave measurements of electron density profiles in mirror contained plasma
[UCRL-51348] 19 p2323 N73-28685
Electron concentration and temperature measurements, using cylindrical Langmuir probes
20 p2410 N73-29374
Total electron content studies of radio waves of ionosphere
[AD-762481] 20 p2414 N73-29403
Exhaust pressure and density of pulsed thrustor systems
[NASA-TM-X-68299] 21 p2589 N73-30740
Indications of dayside midlatitude plasma trough by ISIS-1 electrostatic probe measurements of electron density and temperature in photonosphere
[NASA-TM-X-70436] 21 p2595 N73-30797
Profile inversion technique for determination of electron density from wave interaction data
[AD-764297] 22 p2668 N73-31378
Measurement of electron density in cylindrical electrostatic confinement device
24 p2961 N73-33664

**ELECTRON DENSITY PROFILES**
Ionospheric refractivity influence on electromagnetic wave propagation errors discussing electron density profiles
[DLR-MITT-71-31] 03 p0266 N73-12154
Magnetic storm effects on topside ionospheric electron density profiles in low and equatorial latitudes
[PSU-IRL-SCI-399] 06 p0666 N73-15412
Radio frequency impedance probe measurement of ionspheric electron density profiles using Veronique rocket for sounding
06 p0667 N73-15423
Mathematical models of midlatitude bottomside electron density profiles
[AD-751267] 07 p0796 N73-16477
Photoionization of room temperature gas by radiation from hot plasma in electromagnetic T-Tubes
07 p0825 N73-16684
Electron temperature and density profiles obtained with Skylark rocket-borne double electrostatic probes
[TRITA-EPP-72-14-REV] 12 p1402 N73-21370
Theory of electron density distribution induced at metal surface by small static external charge distribution
[AD-758380] 15 p1814 N73-24707
Determination of D region electron density distributions from radio propagation data
[AD-759018] 16 p1909 N73-25449
Plasma wave decay effects on solar type 3 radio burst profiles at low frequencies
19 p2339 N73-28815
Development and characteristics of test equipment for determining temperature and electron density of plasma based on derivation of absorption coefficients
[NASA-CASE-ARC-10598-1] 20 p2458 N73-29750

**ELECTRON DETECTORS**
U ELECTRON COUNTERS

**ELECTRON DIFFRACTION**
Microstructural studies of adhesion, wear, friction, and lubrication using LEED, Auger emission spectroscopy analysis, and field ion microscopy
[NASA-TM-X-68152] 01 p0058 N73-10471
Pseudopotential analysis of interaction between conduction electrons and metal lattice field
[ITJ-16] 04 p0433 N73-13532
X ray and electron diffraction analysis of A[3]B[5] semiconductor crystal structure
[AD-750966] 06 p0709 N73-15787
Theoretical studies of solid surfaces, electron diffraction experiments, and electronic charge distribution
[AD-750481] 06 p0711 N73-15802

Refracted electron beam temperature as indication of lead sulfide purity
[AD-753556] 09 p1077 N73-18787
Low energy electron diffraction and Auger electron spectroscopy used for determination of structure of adsorbed gases on solid surfaces
[LBL-878] 10 p1193 N73-19708
Lattice dynamical calculation for soft mode semiconductor surface reconstruction
[AD-758723] 16 p1953 N73-25806
Low energy electron diffraction and auger spectroscopy of [100] surfaces of aluminum and aluminum-copper alloys
18 p2159 N73-27445
Development of low energy diffraction system for observing surface structure of low-index single crystal metal surfaces with and without absorbates
20 p2429 N73-29510

**ELECTRON DIFFUSION**
Characterization of electron plasma wave echoes
[EUR-CEA-FC-639] 07 p0828 N73-16711

**ELECTRON DISTRIBUTION**
NT ELECTRON DENSITY PROFILES
Quasi-equilibrium states of E-layer
[UCRL-51151] 03 p0296 N73-12415
Angular distribution of photoemitted electrons from activated p-type gallium arsenide surfaces
[AD-750364] 06 p0645 N73-15239
Effect of distortion of energy distribution function of electrons measured with spherical probe
[AD-750961] 06 p0706 N73-15760
Distribution of charged particles in magnetic field for determining superhigh frequency wave absorption by palsma
[AEC-TR-7321] 08 p0949 N73-17768
Proton 1 rocket charged particle spectrometer for measuring energy spectrum and electron and proton distribution above 20 keV
[NP-19462] 10 p1161 N73-19444
Comparison of hot electron distribution between two magnetically confined plasmas
12 p1431 N73-21599
Increase in resolving power of camera tubes by changing form and size of electron gun aperture noting electron beam density distribution
[DRIC-TRANS-3025] 13 p1500 N73-22160
Electron density distribution in viscous flows as applied to Trailblazer 2 reentry vehicle
[AD-755397] 13 p1564 N73-22674
Development and characteristics of test equipment for determining temperature and electron density of plasma based on derivation of absorption coefficients
[NASA-CASE-ARC-10598-1] 20 p2458 N73-29750

**ELECTRON EMISSION**
NT FIELD EMISSION
NT PHOTOELECTRIC EMISSION
NT SECONDARY EMISSION
Error analysis of line intensity measurements on plasmas with electron temperature fluctuations
[AD-748474] 04 p0456 N73-13722
Crystal growing of iron monosulfide, crystallographic studies on titanium oxide semiconductor, emission of zinc selenide diode, and electroreflectance of gallium arsenide
[AD-748336] 04 p0459 N73-13750
Exo-electron emission testing of material fatigue
[AD-748272] 05 p0549 N73-14457
Potential theory for determining electromagnetic field caused by radial electron emission near conducting sphere
[AD-753664] 09 p1068 N73-18714
Calculation of high energy electron emission from metal target irridiated by gamma flux field
[NASA-TM-X-2756] 10 p1192 N73-19698
Data from simultaneous satellite measurement of electron and proton precipitation at high latitudes
[NP-19465] 10 p1210 N73-19845
Effect of reverse abrasive friction exoelectron emission and steel corrosion
[AD-754666] 11 p1307 N73-20603
Physical nature of electron emission from tin oxide cathode sources
16 p1947 N73-25750
Phase-space theory for electron excitation in slow atomic collisions
[PUBL-73-4] 17 p2064 N73-26699
Annealing properties and electron emission of amorphous and crystalline silicon
17 p2072 N73-26760
Fabrication of cold cathode optoelectronic electron emitter with emission properties suitable for practical applications
[AD-760601] 18 p2123 N73-27162
Fast electron production by protons trapped in sunspot magnetic field as energy source for solar flares
19 p2333 N73-28774
Positions and sizes of solar type 3 radio bursts associated with electron propagation in interplanetary space
19 p2339 N73-28818
Heat treatment effects on metal black surfaces, and Auger spectra during magnesium and iron oxidation
[RU-20-6] 23 p2769 N73-32146
Temperature relationship of work function of silicon carbide for application to direct conversion of thermal energy to electrical energy
23 p2807 N73-32443
Natural exoelectron emission of anorthosite rocks from Luna-20
[NASA-TT-F-15116] 24 p2980 N73-33817

**ELECTRON ENERGY**
NT ELECTRON STATES
Analysis of dependence of refractive index of gas discharge medium in carbon dioxide laser on amplitude of discharge current
[NLL-DRIC-TRANS-2815-[3623.66]]
02 p0180 N73-11459
Development and characteristics of synchrotrons with steady-state field in energy range of 35 to 300 giga electron volts
[JPRS-57489] 03 p0280 N73-12271
Electron temperatures and thermal conduction in high energy theta pinches
[LA-4930] 03 p0341 N73-12780
Measurement of plasma ultraviolet radiation for determining collisional momentum transfer cross sections in accelerator
[AD-747339] 03 p0344 N73-12802
Energy distributions of field-emitted electrons from p-type silicon surfaces
[AD-747067] 03 p0346 N73-12825
F-02 experiment onboard OGO-6, and computer program for analysis of raw data
[NASA-CR-130128] 04 p0414 N73-13376
Analysis of heating of electron component of magnetoplasma due to localized time varying magnetic field perturbations
[AD-747094] 04 p0415 N73-13390
Numerical analysis of transition frequency and phase excess in double-diffused bipolar transistors
[NLL-TRANS-860-[9022.64]]
05 p0518 N73-14212
Electron energy distribution of semiconductor cold-cathode
[AD-750611] 06 p0646 N73-15247
X ray and electron energy spectroscopy for analysis on band structure of materials
[NAL-SR-1] 06 p0699 N73-15703
Electron transport properties in space environment and spacecraft shielding
[NASA-CR-123998] 06 p0702 N73-15722
Effect of distortion of energy distribution function of electrons measured with spherical probe
[AD-750961] 06 p0706 N73-15760
Electron heating in F region by high power radio frequency beam detected by intensity changes in atomic oxygen nightglow
07 p0775 N73-16293
Isotropic models for determining effect of velocity distribution on electron temperature in ionospheric plasma
[NASA-TM-X-66157] 07 p0791 N73-16433
Electron temperature fluctuations of ionized plasma in Q device
[AD-751256] 07 p0830 N73-16731
Electron and excitation temperature measurements in plasma jets stabilized by air and oxygen
[AD-752694] 09 p1071 N73-18743
Probe measurements of electron energy in glow discharge of nitrogen plasma and air
[AD-752871] 09 p1071 N73-18744
Electron temperature and density profiles obtained with Skylark rocket-borne double electrostatic probes
[TRITA-EPP-72-14-REV] 12 p1402 N73-21370
Correlation energy of quantum mechanical electron gas in intense magnetic field
[NUB-2178] 12 p1431 N73-21597
Comparison of electron temperature from Alouette diffuse resonance observations with those from Alouette 2 electrostatic probe
[NASA-TM-X-66205] 12 p1433 N73-21611
Spectrometric analysis of pulsed X ray sources and detectors
[AD-755845] 12 p1436 N73-21639
High efficiency ion lasers and high power carbon dioxide lasers through study of improved electrode structures
[AD-757099] 14 p1673 N73-23575
Electron energy loss spectra and scattering cross sections
[NASA-CR-132174] 15 p1749 N73-24172
Time varying ac arcs or positive columns in discharges in gas mixtures
[AD-758232] 15 p1818 N73-24738
High time resolution measurements of energetic electrons in auroral breakup using sounding rockets
16 p1895 N73-25324
Sounding rocket injection of controlled beam of energetic electrons into trapping region of magnetosphere
16 p1895 N73-25329
Measurement of vibrational temperatures in carbon monoxide laser
[AD-759237] 16 p1925 N73-25575
Energy tables for alpha emitting nuclides
[AAEC/TM-631] 17 p2065 N73-26703
Properties of energetic electrons accelerated during solar flare flashes
19 p2333 N73-28777
Analytic function of electron temperature measurements in ionosphere by high frequency probe method
20 p2410 N73-29372
Indications of dayside midlatitude plasma trough by ISIS-1 electrostatic probe measurements of electron density and temperature in photonosphere
[NASA-TM-X-70436] 21 p2595 N73-30797
Simultaneous observations of low energy electrons in plasma sheet and in auroral zone
[LMSC-D350709] 22 p2702 N73-31638
Tantalum surface bounding of helium discharge plasma considering resonant ion neutralization
[AD-753520] 22 p2706 N73-31670

**ELECTRON FLUX**
U ELECTRONS
U FLUX [RATE]

**ELECTRON FLUX DENSITY**
Numerical analysis of transition frequency and phase excess in double-diffused bipolar transistors
[NLL-TRANS-860-[9022.64]]
05 p0518 N73-14212
Electron flux density recorded onboard HEOS 1 in 1969 and 1970, discussing solar activity effects and comparing proton flux density
05 p0593 N73-14816
Low energy electron measurements by VELA satellite plasma probes and spacecraft potential
[LA-DC-72-1481] 19 p2324 N73-28695
Ionization loss in galactic cosmic ray electron spectrum caused by proton interactions
22 p2733 N73-31873
Integrated solar-quiet interplanetary electron spectrum obtained by Explorer 41 satellite
22 p2733 N73-31874

**ELECTRON GAS**
General, nonstationary electron gas equation for noble gas-alkali plasma
[JUL-802-TP] 01 p0085 N73-10704
Correlation energy of quantum mechanical electron gas in intense magnetic field
[NUB-2178] 12 p1431 N73-21597
Electron gas behavior and density in constant electric and magnetic fields
[AD-760587] 18 p2182 N73-27617
Gas dynamic and Langmuir probe analysis of weakly ionized plasma jet
23 p2822 N73-32557
Characteristics of bulk and surface modes in simple metals using modified self-consistent linear response theory
24 p2933 N73-33427
Thermodynamic properties of electron gas in magnetic fields of varying strengths to include magnetic susceptibility, internal energy, and specific heat
24 p2990 N73-33896

**ELECTRON GUNS**
Design of electron gun and laser cavity for carbon monoxide lasers
[AD-752818] 08 p0931 N73-17623
Field emission, high intensity electron gun, single RF cavity, and compression system
[IPPJ-T-11] 09 p1011 N73-18249
Increase in resolving power of camera tubes by changing form and size of electron gun aperture noting electron beam density distribution
[DRIC-TRANS-3025] 13 p1500 N73-22160
Development of hollow cathode plasma electron gun for gas lasers
[AD-757086] 14 p1672 N73-23570
Cold test data for various dual helix circuit structures for electron guns
[AD-758458] 15 p1758 N73-24245
Application of high power electron tube technology to cylindrical electron gun design
[AD-760047] 17 p2006 N73-26226
Electron gun for pre-ionization of high beta toroidal pinch system
[IPPJ-164] 20 p2458 N73-29757
Dual beam electron gun broad bands transmitter tube
[AD-763226] 21 p2518 N73-30198
Electron beam emitting device using secondary emission from cathode in low pressure gas discharge
[AD-764952] 23 p2767 N73-32138

**ELECTRON IMPACT**
Cross section measurements for electron impact at low energies in molecular gases
[AD-747304] 02 p0139 N73-11123
Low energy electron impact excitation and ionization rate coefficients for atmospheric nitrogen and oxygen
[AD-747244] 02 p0170 N73-11378
Excitation of N I ultraviolet multiplets by electron impact on atomic nitrogen
[NASA-CR-129087] 02 p0214 N73-11730
Feasibility analysis of laboratory experiment on ionic excitation cross section by electron impact on laser produced plasmas
[ESRO-SN-122] 15 p1818 N73-24737
Optical potential approach to electron-atom impact ionization threshold problem
[NASA-TM-X-66282] 18 p2181 N73-27609

**ELECTRON INTENSITY**
U ELECTRON FLUX DENSITY
**ELECTRON INTERACTIONS**
U ELECTRON SCATTERING
**ELECTRON IONIZATION**
U IONIZATION
**ELECTRON IRRADIATION**
Measurement of ultraviolet and far ultraviolet transmission of transparent materials during high energy electron irradiation
[NASA-CR-129297] 03 p0334 N73-12726
Effects of electron irradiation and temperature on 1 ohm-cm and 10 ohm-cm solar cells
[NASA-TM-X-66231] 12 p1366 N73-21083
Experimental techniques for achieving high flux, high energy electron irradiation
[AD-749856] 13 p1561 N73-22654
Empirical equations for calculating photovoltaic characteristics of solar cell array
[NASA-CR-130248] 15 p1737 N73-24085
Electron irradiation damage as function of accelerating voltage, time, and temperature in stainless steel
[COO-2119-3] 15 p1799 N73-24581
**ELECTRON MASS**
Missing mass spectrum structures for meson resonances in S, T, U, region
[NUB-2167] 07 p0823 N73-16671
**ELECTRON MICROSCOPES**
Scanning electron microscopy applied to surface fracture mechanics study, composite materials, and powder metallurgy
[DLR-MITT-71-32] 03 p0315 N73-12571
Electron fractography of stress corrosion fracture surfaces of aircraft materials as high strength steels, Al-Zn-Mg, Al-Cu and Ti alloys
[NLR-TR-71038-U] 03 p0361 N73-12945
X ray diffraction pattern and electron microscopy of polycarbonate filled with MoS2
[AD-749731] 05 p0567 N73-14604
Application of scanning electron microscope to friction and wear studies
[DLR-FB-71-70] 06 p0674 N73-15485
Surveyor 3 lunar probe television mirror pit X ray analysis and scanning electron microscopy for micrometeoroid impact study
[ONERA-NT-01-15] 07 p0847 N73-16864
Argon ion gun for cleaning surfaces and specimens for use in electron spectrometer
[ECRC/N486] 10 p1125 N73-19165
Methods of charging/discharging in scanning electron microscopy of dielectrics to preserve resolution and contrast
[DRIC-TRANS-2970] 10 p1162 N73-19451
Analysis of microstructure and optical properties of thin lead dielectric cermet films
10 p1175 N73-19555
Creep tests and transmission electron microscopic observation of grain boundary structure in stainless steel bicrystals
[CEA-R-4317] 10 p1200 N73-19768
Electron microscopic analysis of epitaxial growth and nucleation in condensed gas crystals
[AD-753108] 10 p1201 N73-19773
Analysis of precipitation process in cobalt-tungsten-titanium alloys using electron microscope and X ray imaging techniques
13 p1541 N73-22483
Scanning electron microscope effects on charging properties of dielectric materials
[NLL-DRIC-TRANS-2970-[3623.66]]
15 p1785 N73-24470
Scanning electron microscope used in friction tests of polytetrafluoroethylene sliding on aluminum single crystals
[NASA-TN-D-7321] 15 p1791 N73-24520
Analysis of fractures in materials using scanning electron microscopes
[AD-759287] 16 p1930 N73-25617
Studies of electron mirror microscopy and its application to superconductivity and magnetism
16 p1952 N73-25797
Near infrared, electron microscopic, ESR, and magnetic susceptibility measurements
[ORO-4049-3] 17 p2065 N73-26705
Development of procedure for aligning pole piece system of magnetic electron microscope
[NLL-M-23011-[5828.4F]] 20 p2417 N73-29416
Scanning electron microscope examination of wire bonds from high reliability microelectronic devices
[NBS-TN-785] 21 p2549 N73-30432
Comparison of film and video as the recording medium in high voltage electron microscopy
[NPL-IMS-20] 21 p2549 N73-30438
Correlation of X ray and electron microscope data for fatigue in nickel and cobalt alloys
[AD-764282] 22 p2686 N73-31513
**ELECTRON MICROSCOPY**
U ELECTRON MICROSCOPES
**ELECTRON MOBILITY**
Analysis of conditions created by intense laser beam focused on plasma with application as plasma diagnostic technique
[DREV-R-676/72] 02 p0181 N73-11463
Numerical analysis of transition frequency and phase excess in double-diffused bipolar transistors
[NLL-TRANS-860-[9022.64]]
05 p0518 N73-14212
Pseudo-binary crystal model for electron mobility variation with composition of gallium indium arsenide semiconducting alloys
18 p2181 N73-27607
Theoretical calculation of surface mobility in MOS surface inversion layers at room temperature
23 p2825 N73-32578
**ELECTRON MULTIPLIERS**
U PHOTOMULTIPLIER TUBES
**ELECTRON OPTICS**
Electron optics and target study for improved pattern threshold recognition device
[AD-746246] 02 p0147 N73-11192
Microstructural analysis of nickel-base alloy WAZ-20 using qualitative and quantitative electron optical techniques
[NASA-TN-D-7209] 09 p1047 N73-18541
Improved electron optics and target for pattern threshold recognition device
[AD-762164] 19 p2247 N73-28117
Development of procedure for aligning pole piece system of magnetic electron microscope
[NLL-M-23011-[5828.4F]] 20 p2417 N73-29416
**ELECTRON ORBITALS**
Gauge invariant atomic orbitals and current conservatism within quantum mechanical formalism
[NASA-CR-129246] 03 p0339 N73-12762
**ELECTRON OSCILLATIONS**
Hyperfine electron density fluctuation in stabilized hydrogen arc laser
08 p0943 N73-17723
Electron wave amplitude oscillation in plasma due to initial spatial disturbance
[IPPJ-143] 09 p1070 N73-18728
**ELECTRON PARAMAGNETIC RESONANCE**
ESR spectra of paramagnetic hole centers in CeO2 after ultraviolet irradiation
[AD-746036] 02 p0220 N73-11778
EPR study of molecular ordering in smectic-A liquid crystals without nematic phases
[NASA-TN-D-7124] 04 p0437 N73-13563
Electron paramagnetic resonance studies of viscous nematic liquid crystal using vanadyl acetyl acetonate and nitroxides as paramagnetic probes
[NASA-TN-D-7122] 04 p0437 N73-13564
Electron paramagnetic resonance spectra of trivalent titanium ions in used silica
[NLL-RTS-7523] 05 p0564 N73-14583
Excited state paramagnetic resonance interpretation of Zeeman effects in optical spectra of neodymium and erbium containing impurity ions
[AD-750343] 06 p0700 N73-15712
Electron paramagnetic resonance and formed free radical investigation of ionizing radiation damage by sulfur-containing aliphatic compounds, pyridoxine, and proteins
[BMVG-FBWT-72-6] 07 p0753 N73-16115
Design of tunable electron paramagnetic resonance spectrometer with quartz stabilization
13 p1565 N73-22684
Microwave preamplifier induction for electron spin resonance spectroscopy
14 p1666 N73-23521
EPR in Cr[3 plus] in Li2Ge7O15
[AD-757884] 15 p1822 N73-24768
Electron paramagnetic resonance of dilute magnetic alloys including Mg-Gd, and noble metal-rare earth
17 p2071 N73-26756
Optical and magnetic resonance spectra of uranium borohydride in hafnium borohydride
[AD-759371] 17 p2074 N73-26777
Electron spin resonance studies in single crystals of CaS and CdS
[AD-760803] 18 p2191 N73-27691
Electron spin resonance measurements on Fermi levels in molybdenum doped rutile during hydrogen treatment
[AD-760735] 18 p2192 N73-27694
Electron spin resonance and synchrotron radiation energy in magnetoactive plasma
[AD-762319] 19 p2326 N73-28709
Variation of crystal Fermi energy to obtain different charge states in paramagnetic impurity ions for ESP study
[AD-760736] 20 p2464 N73-29798
Intensity of EPR line spectra as affected by indium doped zinc oxide
[AD-764490] 22 p2708 N73-31684
**ELECTRON PATHS**
U ELECTRON TRAJECTORIES
**ELECTRON PHONON INTERACTIONS**
Generalized vector meson dominance model derived from extended quark model with electron proton inelastic scattering
[TUEP-72-43] 07 p0823 N73-16669
Pressure effects on phonon spectrum, electron-phonon interaction strength, and electron-phonon coupling function in Pb-In superconductors using electron tunneling
07 p0831 N73-16739
Effect of electron-phonon interaction on temperature dependence of paramagnetic susceptibility in metals
[AD-753984] 11 p1331 N73-20804
**ELECTRON PLASMA**
Derivation of nonlinear Schroedinger equation for electron plasma waves
[IPPJ-137] 04 p0441 N73-13590
RF electric field in electron ion plasma condenser with and without magnetic field
[EUR-CEA-FC-638] 04 p0454 N73-13707
Microwave reflection from electron density ramps produced behind shock waves in nitrogen oxygen mixtures
07 p0824 N73-16682
Existence of natural radio noise between electron plasma frequency and upper hybrid resonance frequency as detected by long electric aniennas of IMP-6 satellite
[NASA-CR-130273] 07 p0843 N73-16832
Comparison of hot electron distribution between two magnetically confined plasmas
12 p1431 N73-21599
Synchrotron radiation from magnetically confined hot electron plasma
12 p1432 N73-21605
Electron density and temperature measurements on negative glow plasma
12 p1433 N73-21609
Relativistic electron beam equilibria in cylindrical plasma geometry
[IPP-6/111] 12 p1435 N73-21630
Vlasov equation for studying anisotropy produced instabilities in confined hot electron plasma
[EUR-CEA-FC-664] 15 p1818 N73-24736
Damping and saturation of second order electron plasma wave echo
24 p2961 N73-33662
**ELECTRON PRECIPITATION**
Synoptic study of field-aligned electron precipitation in auroral regions
[NASA-TM-X-66065] 01 p0049 N73-10392
Low energy electron precipitation observed as function of substorm phase by polar satellites
[NASA-TM-X-66063] 01 p0049 N73-10393
Reduction and analysis of trapped and precipitating electron data from OGO 6 spectrometer experiment F-16
[NASA-CR-130137] 06 p0718 N73-15863
Rocket-borne auroral optical measurement of proton and electron precipitation
[SC-RR-72-0543] 07 p0793 N73-16448
Electron acceleration mechanism during geomagnetic tail collapse associated with substorm activity
[UNH-73-04] 15 p1779 N73-24418
Effects of season altitude and pitch angle on electron precipitation from OGO-D data
[NASA-TM-X-66260] 16 p1962 N73-25868
Mass plots of quiet auroral arc positions and precipitation pattern of auroral particles
[R-33] 18 p2141 N73-27310
Electron and proton precipitation in different auroral forms from data obtained by TWINS 1 and 2
[NASA-CR-133889] 22 p2667 N73-31367
**ELECTRON PROBES**
Characteristics and vibrational test of structural test unit for electron-proton spectrometer under simulated flight conditions
[NASA-CR-128699] 08 p0924 N73-17573
Electron probe microanalysis of ductile metal bond to Ti alloy disc
[AECL-4251] 10 p1172 N73-19535
Electron-proton spectrometer providing signals for determining energy
[NASA-CR-128850] 11 p1293 N73-20493
Low energy particles on front detector in coincidence in electron spectrometer on OV1-13 satellite
[AD-755789] 12 p1406 N73-21401
Characteristics of electron-proton spectrometer to measure geomagnetically trapped radiation in geostationary orbit at 6.6 earth radii in outer radiation belt
[NASA-CR-132786] 18 p2150 N73-27381
Data reduction procedure for quantitative electron probe microanalysis
[NBS-TN-769] 21 p2549 N73-30433
**ELECTRON RADIATION**
NT BETA PARTICLES
NT ELECTRON BEAMS
Anisotropy and angular distribution of bremsstrahlung radiation emitted by electrons confined in magnetic mirrors
[ORNL-TM-3821] 04 p0453 N73-13698
Effects of Jupiter high energy electron environment on gates and MOSFET performance
[AD-756215] 13 p1502 N73-22178
Radiation patterns of electron plasma waves and reception patterns of monopole antennas
[ISAS-491] 18 p2115 N73-27103
Evidence of electron acceleration and type 3 radio bursts during solar flares
19 p2337 N73-28805
Chromospheric type 3 radio burst acceleration of solar electrons and coronal streamer
19 p2340 N73-28821

**ELECTRON RECOMBINATION**
NT RADIATIVE RECOMBINATION
Photodielectric recombination and trapping model for low temperature n-type epitaxial gallium arsenide
[NASA-CR-130764] 08 p0950 N73-17779
Recombination coefficients of electrons with hydrogen and carbon monoxide ions
[NASA-CR-131107] 10 p1192 N73-19699
Electron recombination with hydrogen ions
[NASA-CR-131108] 10 p1192 N73-19700
Photodielectric techniques for analyzing low temperature band structure of gallium arsenide
24 p2891 N73-33080

**ELECTRON RING ACCELERATORS**
U STORAGE RINGS [PARTICLE ACCELERATORS]

**ELECTRON SCATTERING**
Continuation from deep inelastic electron scattering to deep electron-positron annihilation
[NOTA-INTERNA-378] 01 p0084 N73-10692
Pion electroproduction cross section measured near threshold by coincidence experiments
[NOTA-INTERNA-383-A] 01 p0084 N73-10696
Numerical analysis of inverse scattering problem at fixed angular momentum for noniocal separable interactions
02 p0199 N73-11611
Determination of longitudinal cross section in inelastic electron proton scattering in Delta[1236] resonance region
02 p0213 N73-11728
Computerized simulation of electron-electron collisional effects in plasma
[COO-3086-14] 04 p0454 N73-13709
Thermal conductivity measurements of electron and phonon scattering behavior in low temperature solids
[COO-1629-31] 04 p0485 N73-13961
Free electron production by Raman scattering in initial phase of laser produced plasma
[IPP-4/40] 05 p0583 N73-14745
Multicomponent electron collision frequency model for predicting signal attenuation in plasma sheath surrounding reentry vehicle
[AD-750553] 05 p0585 N73-14758
Coincidence rate measurements for inelastically scattered electrons and associated bremsstrahlung at intermediate bombarding energies
[NASA-CR-124007] 06 p0702 N73-15723
Electron positron annihilation structure functions calculated with light cone operator product expansions and Callan-Symanzik equation
[ILL-[TH]-72-12] 07 p0823 N73-16670
Survey of theoretical models used to discuss final hadronic states produced in inelastic electron-hadron scattering
[ILL-[TH]-73-2] 12 p1430 N73-21593
Thermodynamics of light scattering from Eulerian fluid, and electron scattering by atomic hydrogen
13 p1558 N73-22627
Laboratory astrophysics research on defense applications of gas ionization, electron scattering, plasmas, and line broadening
[AD-757721] 14 p1695 N73-23753
Electron collision processes in atmospheric gases of oxygen, carbon monoxide, and nitrogen oxide
[AD-757841] 15 p1748 N73-24170
Electron correlation and band structure in solids using X ray Compton effect
15 p1820 N73-24751
Electron scattering spectra of low state CO2 in energy-loss range 7 to 10 eV
[NASA-CR-132202] 17 p2064 N73-26697
Research in electron and ion collisions and radiation dosimetry
[ORNL-4811] 17 p2064 N73-26700
Problems of electron accelerator scattering experiments
[CONF-710974-7] 17 p2065 N73-26708
Optical models for electron scattering from atoms and molecules
18 p2181 N73-27608
Electron scattering and secondary emission from tungsten crystal surface
[AD-761876] 19 p2328 N73-28726
Cross section data for collision processes between molecular oxygen and electrons
[NASA-TT-F-15011] 19 p2354 N73-28934
Electron collision processes in ionosphere
[UILU-ENG-73-2504] 23 p2784 N73-32276
Electron collision excitation of population inversion in ionic argon lasers
23 p2800 N73-32393

**ELECTRON SPIN**
Electron-impurity spin interchange model for analyzing magnetic properties of diluted magnetic alloys at low temperatures
08 p0931 N73-17626
Electron spin overlap model for quantitative analyses on magnetic spectra of coordination compounds with unpaired electrons
08 p0945 N73-17740
High density optical memory and electron spin dependent trapping and tunneling processes in KCl and KCl-NaCl
20 p2460 N73-29768

**ELECTRON SPIN RESONANCE**
U ELECTRON PARAMAGNETIC RESONANCE

**ELECTRON STATES**
Electronic state density of semiconductor compounds A[3] B[5], using law of dispersion
[AD-758168] 15 p1822 N73-24766
Spin-orbit interactions with singlet-triplet mixing in excited states of helium
16 p1947 N73-25751
Influence of electronic states, electronic transport, and radiative transitions on luminescent defects in pure and doped single crystal compound semiconductors
[AD-764278] 22 p2708 N73-31683
Electron network model of solid interfaces, surface defects, planar defects, and thin films
23 p2825 N73-32584

**ELECTRON SWEEPING**
U SWEEP FREQUENCY

**ELECTRON TELESCOPES**
U PARTICLE TELESCOPES

**ELECTRON TEMPERATURE**
U ELECTRON ENERGY

**ELECTRON TRAJECTORIES**
Quantum corrections to trajectories of radiating fast electrons in magnetic field
[NASA-TT-F-14495] 01 p0083 N73-10688
Maximum likelihood determination of electron tracks in propane, propane-Freon, and hydrogen-neon bubble chambers
[JINR-P10-6868] 17 p2066 N73-26712
Determination of electron track parameters in propane bubble chamber based on least-squares method
[JINR-P10-6869] 17 p2066 N73-26713

**ELECTRON TRANSFER**
Absorption spectra analyses on germanium films for determining band structure transformations
02 p0218 N73-11765
Analysis of single electron bunch transfer tolerance for intersecting storage accelerators
[BNL-17275] 10 p1194 N73-19711
Nonlinear and parametric effects on synchronization and mixing of electron transfer microwave oscillators
18 p2123 N73-27155

**ELECTRON TRANSITIONS**
Quantum corrections to trajectories of radiating fast electrons in magnetic field
[NASA-TT-F-14495] 01 p0083 N73-10688
Laser transitions in pulsed neodymium yttrium-aluminum garnet emission
[AD-746218] 02 p0181 N73-11472
Quantum electrodynamic view of superradiance as competition between stimulated and spontaneous atomic decay
[AD-750005] 05 p0582 N73-14741
Analysis of nonequilibrium in excited levels of electric ARC heated potassium vapor injected into argon/helium gas flow passing through supersonic nozzle
[AD-750943] 05 p0585 N73-14759
Photon-echo generation and behavior
[AD-750155] 06 p0681 N73-15540
Observations and characteristics of 1.35-cm emissions of water vapor in galactic sources
07 p0837 N73-16787
Production of laser output by excitation of hydrogen chloride vibrational levels using electron impact
[AD-752631] 08 p0930 N73-17615
Development and characteristics of electron beam excited high pressure mercury dissociation laser
[AD-752465] 08 p0930 N73-17619
Synthesis of A to X bands of OH and a to X bands of O2 for studying electronic transitions, rational branch structure, and rotational transition probabilities
[DREV-TN-2012/72] 08 p0945 N73-17742
Mechanism for formation of inverse population of oscillatory levels in gas discharge carbon monoxide laser
[AD-753559] 09 p1045 N73-18520
Theoretical model of optical excitation, emission, and deactivation properties of Meinel band system of nitrogen
[AD-753396] 09 p1069 N73-18722
Analyses of vibrational levels by least squares method for determining transition moment probabilities in nitrogen band
[AD-753394] 09 p1075 N73-18774
Time dependent scattering theory for evaluating transition cross sections in atomic helium collision with charged particle
[NASA-CR-131265] 11 p1326 N73-20761
Design, development, and characteristics of continuous wave laser using organic dyes
[AD-756514] 13 p1539 N73-22466
Analysis of elementary, exothermic, atom-molecule reactions for application as laser materials for chemical lasers
[AD-756686] 14 p1673 N73-23578
Spectroscopic analysis of energy transfer in rare earth compounds to determine effect of transfer phenomena on lasing efficiency
[AD-757520] 14 p1673 N73-23579
Neon line strength measurements using coherent laser spectroscopy
[NASA-CR-133406] 18 p2114 N73-27095
Soft X ray level inversions in dense aluminum plasma produced by laser bombardment
[CONF-720404-VOL-4] 19 p2322 N73-28684
High frequency satellite lines in X ray spectra of heavy ions
[CONF-720404-VOL-3] 19 p2323 N73-28687
Spectroscopic determination of induced emission cross section of 3 P 0 yields 3 F 2 and P 0 yields 3 H 6 transitions of Pr[3 plus] ion in SeCl2 and SnCl2
[CRC-1243] 21 p2579 N73-30671
Influence of electronic states, electronic transport, and radiative transitions on luminescent defects in pure and doped single crystal compound semiconductors
[AD-764278] 22 p2708 N73-31683
Elastic constants and electrical transition in Ti2O3 and V doped Ti2O3
23 p2824 N73-32577

**ELECTRON TUBES**
NT CAMERA TUBES
NT CATHODE RAY TUBES
NT CELESCOPES
NT IMAGE DISSECTOR TUBES
NT IMAGE ORTHICONS
NT KLYSTRONS
NT MAGNETRONS
NT MICROWAVE OSCILLATORS
NT MICROWAVE TUBES
NT RETURN BEAM VIDICONS
NT THERMIONIC DIODES
NT THYRATRONS
NT TRAVELING WAVE TUBES
NT VACUUM TUBES
NT VIDICONS
Demountable electro-optical system tests for improving pattern threshold recognition device
[AD-745915] 02 p0147 N73-11194
Design and performance of electron beam storage tube for computer random access memory
[AD-753929] 10 p1136 N73-19257
New and revised test methods for cathode ray electron storage tubes
[AD-754139] 11 p1263 N73-20251
Performance of shipping container for electron tube in shock and vibration tests
[AD-754926] 11 p1301 N73-20558
Performance of rhenium alloy electron tube cathodes
[AD-755828] 12 p1385 N73-21232
Designing laser drill to correct beam wandering during drilling
[AD-759966] 17 p2006 N73-26224
Application of high power electron tube technology to cylindrical electron gun design
[AD-760047] 17 p2006 N73-26226
Fabrication of binary-addressable scan conversion storage tube
[AD-761099] 18 p2124 N73-27168
Development of field emitter cathodes for electron beam devices
[AD-762322] 20 p2381 N73-29134
Identification of Polish institutes involved in electron tube development and recommendations for changes in research projects
21 p2608 N73-30899

**ELECTRON TUNNELING**
Characteristics of ion transport in silicon dioxide, interface phenomena, and photoelectric method of storing charge in floating gate MOS memory
[AD-746999] 03 p0346 N73-12823
Photoelectric tunnel currents in metal-insulator-metal diodes
[AD-751758] 07 p0763 N73-16201
Pressure effects on phonon spectrum, electron-phonon interaction strength, and electron-phonon coupling function in Pb-In superconductors using electron tunneling
07 p0831 N73-16739
Superconducting energy gap structure and physical properties of dysprosium-dysprosium oxide-lead tunnel junctions
[AD-753847] 09 p1077 N73-18790
Tunneling characteristics of thin cadmium selenide, zinc selenide, and cadmium telluride evaporated semiconductor films
12 p1438 N73-21652
Tunneling biases into interfaces of semiconductor junctions
[AD-755656] 12 p1441 N73-21676
Application of electron tunneling process to superconductor technology
[AD-756081] 13 p1566 N73-22692
Analysis of tunneling in metal semiconductor junctions
18 p2185 N73-27640
High bias tunneling of silicon and aluminum semiconductor junctions
19 p2326 N73-28712
High density optical memory and electron spin dependent trapping and tunneling processes in KCl and KCl-NaCl
20 p2460 N73-29768

Quasiparticle tunneling into superconducting transition metals
[AD-764905] 23 p2826 N73-32591
ELECTRON-ION RECOMBINATION
NT RADIATIVE RECOMBINATION
Ionospheric F-region electron recombination, heating, and electron production
17 p2017 N73-26311
ELECTRONIC AMPLIFIERS
U AMPLIFIERS
ELECTRONIC CONTROL
Operation of electronic telephone exchange in France
[NLL-PO-2957-[9022.81]] 15 p1749 N73-24175
Structural design of computer controlled manipulator for remote handling
17 p1989 N73-26079
Design of electrohydraulic control system for underwater manipulator with position feedback
17 p1989 N73-26085
Bioelectric control system design for reversible slave mechanism manipulator using single muscle input
17 p1990 N73-26088
Motor function modeling of human arm by manipulator using myoelectric control pulses
17 p1990 N73-26091
ELECTRONIC COUNTERMEASURES
NT CHAFF
Information theory criteria for electronic jaming and countermeasures for air defense
[FOA-3-C-3644-66] 02 p0140 N73-11133
Reconnaissance and surveillance countermeasures for radio electronic facilities
03 p0266 N73-12152
Jamming of surveillance radar station by airborne electronic countermeasures
[FOA-3-C-3645-66] 06 p0639 N73-15187
Absorption, reflection, and scattering of electromagnetic waves by plasma media as electronic countermeasures in radar detection
[FOA-3-C-3652-66] 06 p0639 N73-15189
Power handling capability and electrical breakdown characteristics of electronic countermeasure antennas
[AD-751309] 07 p0758 N73-16154
Radio blackout prevention in atmospheric reentry by chemical injection into vehicle plasma sheath
[AD-753077] 09 p1003 N73-18187
Installation of electronic warfare training equipment in rear cockpit of CF-100 aircraft with emphasis on human engineering considerations
[DCIEM-904] 16 p1861 N73-25071
Logistic performance data book for electronic countermeasures system of B-52G aircraft to show reliability, maintenance, costs, and problems
[AD-762216] 19 p2357 N73-28961
ELECTRONIC EQUIPMENT
NT AVALANCHE DIODES
NT CRYOTRONS
NT CRYSTAL RECTIFIERS
NT ELECTRONIC FILTERS
NT ELECTRONIC MODULES
NT ELECTRONIC PACKAGING
NT ELECTRONIC RECORDING SYSTEMS
NT ELECTRONIC TRANSDUCERS
NT FIELD EFFECT TRANSISTORS
NT GALLIUM ARSENIDE LASERS
NT GERMANIUM DIODES
NT JUNCTION DIODES
NT JUNCTION TRANSISTORS
NT METAL OXIDE SEMICONDUCTORS
NT MINIATURE ELECTRONIC EQUIPMENT
NT MIS [SEMICONDUCTORS]
NT NEURISTORS
NT PARAMETRIC DIODES
NT PHOTODIODES
NT PHOTOTRANSISTORS
NT PHOTOVOLTAIC CELLS
NT RUBY LASERS
NT SEMICONDUCTOR DEVICES
NT SEMICONDUCTOR LASERS
NT SILICON TRANSISTORS
NT SOLID STATE DEVICES
NT SOLID STATE LASERS
NT SPACECRAFT ELECTRONIC EQUIPMENT
NT THERMISTORS
NT THYRISTORS
NT TRANSISTOR AMPLIFIERS
NT TRANSISTORS
NT VARACTOR DIODES
Development of specifications for design of avionics subsystems to improve reliability
[AD-746029] 01 p0006 N73-10043
Development and characteristics of vehicle detection system with all active elements carried by moving vehicle
[NASA-CASE-NPO-11850-1] 01 p0032 N73-10248
Development of computer model to analyze effects of temperature variations on six basic electronic components
[AD-745189] 01 p0033 N73-10256
Microminiaturization and reliability of electronic radio equipment
[AD-745828] 01 p0034 N73-10265
Survey on materials and manufacturing processes for solid state electronic devices
[AD-745745] 01 p0034 N73-10266
Development of differential phase shift keyed signal receiver to resolve differential phase shift in incoming signal
[NASA-CASE-MSC-14066-1] 01 p0034 N73-10269
Space electronics, data transmission, orientation of celestial objects, and research instruments
01 p0119 N73-10979
Three channel analog electronic warning system for control of nuclear plant
[NLL-WH-334-[9091.9F]] 02 p0144 N73-11166
Analysis of mutual coupling compensation using microstrip techniques with application to behind-the-array coupling of phased antenna array
[NASA-CR-123819] 02 p0151 N73-11222
Deterioration in sea water of materials and underwater system components
[AD-747245] 02 p0194 N73-11567
Development and characteristics of data decoder to process convolution encoded information
[NASA-CASE-NPO-11371] 03 p0269 N73-12177
Heat transfer and cooling of electronic components and equipment
[AD-746431] 03 p0279 N73-12259
Transient radiation effects and damage to semiconductor devices and electronic equipment
[AD-746851] 03 p0279 N73-12260
Laboratory tests to determine corrosion failure mechanisms in electronic equipment exposed to humid tropical environments
[AD-747757] 03 p0279 N73-12261
Bibliography of solid state electronics
[AD-748739] 03 p0279 N73-12262
Automatic analog to digital assembly for measuring electronic equipment characteristics
[CEA-CONF-1966] 03 p0302 N73-12468
Computerized on-line measurement processor for quality control of electronic materials
[CEA-CONF-1967] 03 p0302 N73-12469
Computer system for control of electronics measuring devices and numerical information processing of measurements
[CEA-CONF-1968] 03 p0333 N73-12713
Closed loop fuel control techniques using electronic circuitry to sense pressure relationships at turbine engine compressor discharge
[AD-747805] 03 p0351 N73-12865
Tasks analyses to determine technical personnel requirements for maintenance of Navy microelectronic shipboard equipment
[AD-748040] 04 p0384 N73-13123
Characteristics of digital data processor using pulse from clock source to derive binary singles to show state of various indicators in processor
[NASA-CASE-GSC-10975-1] 04 p0392 N73-13187
Development of delay cable to display simultaneous signals in nanosecond region in single trace on oscilloscope
[IPPJ-T-9] 04 p0395 N73-13212
Computation, design, and manufacture of integrated circuits for application to computer construction and operation
[JPRS-57333] 04 p0398 N73-13239
Development of troubleshooting skills to isolate causes of malfunctions in complex electronic assemblies
[BDX-613-337-REV] 04 p0398 N73-13241
Analysis of electronic circuit and performance of spark gap assembly
[CERN-72-6] 04 p0399 N73-13244
Design of ground electronic equipment shelters in mobile systems for military ground support application
[AD-748808] 04 p0400 N73-13253
Solid state electronics, information systems, plasma and quantum electronics, biomedical electronics, acoustics, and radio sciences
[AD-748281] 04 p0400 N73-13256
German central ground station including layout and equipment
[DLR-MITT-71-05] 04 p0402 N73-13276
Installation, operation, and maintenance procedures for optical figure sensor and associated electronic controls
[NASA-CR-130125] 04 p0421 N73-13429
Electronic transducer for acceleration measurement
[AD-748885] 04 p0423 N73-13451
Construction of electron beam semiconductor pulse amplifier and radio frequency amplifier diode
[AD-748892] 04 p0461 N73-13758
Space manufacturing of biological and electronic materials
04 p0473 N73-13862
Development and characteristics for automatically displaying digits in any desired order using optical techniques
[NASA-CASE-XKS-00348] 05 p0518 N73-14215
Thermoelectric processes in electronic devices and possibilities for use in small-size, very low frequency devices
[AD-749611] 05 p0520 N73-14231
Thermochromic compositions for detecting heat levels in electronic circuits and devices
[NASA-CASE-NPO-10764-1] 05 p0545 N73-14428
Abstracts from Soviet scientific and technical journals on electronics and electrical engineering
[JPRS-57877] 06 p0647 N73-15256
Application of small digital computer to improve operation of electronic maintenance system
[Y-1837] 06 p0647 N73-15258
Operating, principles of RF biased SQUID systems
[NBS-TN-629] 06 p0708 N73-15773
Research progress in electronic equipment, data processing, plasma physics, and information systems
[AD-750669] 06 p0732 N73-15976
Development of phase control coupling for use with phased array antenna
[NASA-CASE-ERC-10285] 07 p0764 N73-16206
Development of compact, ultrafast streaking camera to include power requirements, electronic circuitry, and performance analysis
[UCRL-73734] 07 p0801 N73-16502
Reliability engineering methods for electronic components
[FTL-A-A16-1] 07 p0803 N73-16517
Design and development of universal voice processor system
[NASA-CR-128739] 08 p0885 N73-17161
Quality control tests of small scale integration electronic components to determine diverging quality levels among manufacturers
[ECR-24] 08 p0891 N73-17213
Evaluation of device for rapid detection and location of shallow subsurface tunnels and excavations
[AD-752086] 08 p0919 N73-17531
Vocational/technical and adult education, emphasizing status, trends, and issues related to electronic delivery
[NASA-CR-130532] 08 p0971 N73-17933
Survey of electronic research projects
[AD-753700] 09 p1010 N73-18240
Operational descriptions of some electronics and nuclear laboratories in Poland
[AD-752772] 09 p1011 N73-18257
Development and characteristics of scientific instrument package for use with Large Space Telescope - Vol. 4
[NASA-TM-X-64726-VOL-4] 09 p1036 N73-18452
Fast electronics technology in signal processing
[CEA-CONF-1897] 10 p1129 N73-19196
Crystal structures, electrical properties, and electronic applications of metal selenides
[JPRS-58293] 10 p1198 N73-19752
Research activities of electronic laboratory in development of inertial navigation systems to include applications for space missions and commercial aviation
11 p1316 N73-20686
Relationship of relay intermodulation products and constriction resistance with relay life
[AD-755923] 12 p1385 N73-21236
Computer program for producing and updating wiring lists for use in development and production of electronic equipment
[ECR-31] 12 p1386 N73-21239
Preflight tests and performance of electronic instrumentation in measuring solar radiation during Aerobee 170 and Black Brant V rockets
[AD-756909] 13 p1532 N73-22412
Characteristics of signal conditioning electronics for vector velocity laser velocimeter
[NASA-CR-131475] 13 p1538 N73-22459
Research and development progress in telecommunications and electronics engineering
[REPT-73-00567] 14 p1619 N73-23111
Development and characteristics of voltmeter and electronic suppression circuit for high accuracy readings
[REPT-6734] 14 p1656 N73-23519
Tactical integrated electronic systems for Swedish military aircraft
14 p1711 N73-23889
Computerized design of fighter aircraft cockpit electronic control system considering man machine interaction
14 p1714 N73-23905
Development and characteristics of nonmetallic electro-optic materials for electronic applications
[AD-758528] 15 p1760 N73-24261
Design, fabrication, and test of electronic engine control system for small turboshaft engines
[AD-758173] 15 p1827 N73-24805
Research and development progress on electronic equipment, integrated circuits, semiconductors, and digital computers
[AD-759180] 16 p1884 N73-25251
Device for locating electrically nonlinear objects and determining distance to object by FM signal transmission
[NASA-CASE-KSC-10108] 16 p1911 N73-25461
Development of electronic circuit for measurement transducer power supply to be used for liquid level measurement in liquid propellant rocket engines
[NASA-CASE-MFS-21698-1] 17 p2003 N73-26196

Development of equipment and method for electrifying dielectric to determine electrostatic properties
[NASA-CASE-MFS-22129-1] 17 p2003 N73-26197
Vacuum tube and solid state circuitry in electronic communications equipment for army training school
[AD-759129] 17 p2073 N73-26775
Electronic strain level counter on in-flight aircraft
[NASA-CASE-LAR-10756-1] 17 p2090 N73-26910
Simulation of complex microelectronic module functions in Delta Sigma Speech Coder containing analogue and digital elements
[AD-761206] 18 p2119 N73-27136
Development and characteristics of electronic data recording equipment for shipboard oceanography data acquisition and processing
[IFS-73010] 18 p2151 N73-27384
Dc to dc converter for electronic equipment power source
[AD-762181] 19 p2223 N73-27934
Contractual requirements for submission of electromagnetic compatibility and interference control plan for government procurement
[AD-761975] 19 p2237 N73-28033
Termination resistance as standard for calibrating low noise temperature in electronic equipment
[NASA-TT-F-15016] 19 p2243 N73-28086
Determination of susceptibility limits and desensitization of solid state electronic equipment to power line transients
[AD-762403] 19 p2246 N73-28110
Tabulation of environmental tests on microelectronic devices
[AD-761951] 19 p2247 N73-28113
Electronics of antiaircraft defense systems
[AD-761540] 19 p2248 N73-28125
Analysis and enhancement of ERTS-1 hydrology imagery using electronic satellite image analysis console
[PAPER-I15] 19 p2279 N73-28336
Research and development of electronic equipment for night combat surveillance
[AD-762351] 19 p2302 N73-28507
Calibrator for biaxial electronic platforms designed to measure postural equilibrium
[AD-763093] 20 p2372 N73-29066
Research and development of electronic equipment and techniques
[AD-763729] 21 p2520 N73-30210
Development of discrete address beacon system for application to air traffic control operations
[FAA-RD-73-101] 21 p2577 N73-30651
Inductive plasma pulverization for protecting mechanical and electronic components
[CEA-CONF-2111] 21 p2583 N73-30701
Development of semiconductor electro-optical devices in Poland with emphasis on management planning and research projects to establish capability
21 p2608 N73-30898
Polish institutes involved in research and development of microwave tubes and recommendations for new research projects
21 p2608 N73-30900
Research progress in aerodynamics, propulsion, electronics, instrumentation, and mathematical sciences
21 p2609 N73-30917
Applications of mathematics to design and development of electronic equipment, microelectronic devices, and lasers
24 p2900 N73-33147
Opto-electronic instruments for spacecraft
[JPRS-60199-1-PT-1] 24 p2926 N73-33372
Opto-electronic instruments for spacecraft
[JPRS-60199-2-PT-2] 24 p2926 N73-33373
Analysis of linear systems to show characteristics and to evaluate distortion on basis of quadratic criteria
24 p2944 N73-33515
Bayesian reliability demonstration for statistical test development
[AD-765172] 24 p2945 N73-33520
Development, fabrication, and evaluation of heat pipe thermal conditioning panels for temperature control of spacecraft electronic equipment - Technical Report
[NASA-CR-124451] 24 p2991 N73-33898

**ELECTRONIC EQUIPMENT TESTS**
Vibration, functional, and electronic equipment tests of ESKA 18 electrostatic ion engine prototype
[DGLR-PAPER-72-87] 06 p0714 N73-15826
Development and evaluation of cross-band radar/beacon system for operation with airport surveillance radar/air traffic control beacon interrogator system
[FAA-RD-73-38] 12 p1379 N73-21182
Design of high temperature integrated circuit holders
[BAH/DS/AG/R-412/1] 13 p1500 N73-22158
Test set for signal conditioner modules
[NASA-CASE-KSC-10750-1] 14 p1667 N73-23527
Fault detection test methods in combinational digital logic networks
[AD-760543] 18 p2121 N73-27146
Method and equipment for testing lag response in television camera tubes
[AD-763339] 22 p2644 N73-31186
Power supply electronic tests on single jet disk type cesium thrustor with beam current feedback control
[LAAS-TNPE-73-T-17] 23 p2831 N73-32629

**ELECTRONIC FILTERS**
Loss coefficients and spectral density of random processes in noise filters
09 p1066 N73-18699
Liquid crystal Fourier plane filter for real time optical image processing
[NASA-CR-130185] 10 p1188 N73-19670
Self-tuning electronic filter for maintaining constant bandwidth and center frequency gain
[NASA-CASE-ARC-10264-1] 11 p1261 N73-20231
Accuracy estimates for syntheses of filters by optimizing mutual uncertainty function in minimax criterion
17 p1997 N73-26151
Application of matched filtering techniques for detection of mode locked laser signals
17 p2039 N73-26496

**ELECTRONIC LEVELS**
U ELECTRON ENERGY
U ENERGY LEVELS

**ELECTRONIC MODULES**
Corrector module and spacecraft dynamics program
[NASA-CR-130108] 01 p0031 N73-10238
Asynchronous control circuits for digital systems representation and modular design
03 p0272 N73-12202
Service life and reliability of single transmitter and array modular type satellite altimeter systems
06 p0663 N73-15388
Methods for chip mounting and establishing electrical connections in miniaturized printed circuits and thick and thin film hybrid circuits
[ECR-27] 08 p0891 N73-17212
Quality control tests of small scale integration electronic components to determine diverging quality levels among manufacturers
[ECR-24] 08 p0891 N73-17213
Systems design for spaceborne computer engineering module
14 p1712 N73-23894
Thick film microelectronic amplifier module for space instruments
[RAE-LIB-TRANS-1643-PT-1]
17 p2007 N73-26233
Development of mechanical linkage for lifting pin-supported electronic packages from electronic circuit boards without damage to connector pins
[NASA-CASE-NPO-13157-1] 17 p2036 N73-26475
Simulation of complex microelectronic module functions in Delta Sigma Speech Coder containing analogue and digital elements
[AD-761206] 18 p2119 N73-27136
Design of tubular thermoelectric module for astronuclear power conversion system
[NASA-CR-121210] 19 p2319 N73-28659
Digital input/output modules for binary signals
[KFK-1688] 20 p2379 N73-29114
Algorithm for location of electronic modules on printed circuit board
21 p2513 N73-30156

**ELECTRONIC PACKAGING**
Package enabling simulation of random samples from discrete and continuous distribution
01 p0072 N73-10587
Packaging techniques for miniaturized thick film networks
[BDX-613-363-REV] 03 p0277 N73-12250
Development and characteristics of hermetically sealed coaxial package for containing microwave semiconductor components
[NASA-CASE-GSC-10791-1] 05 p0550 N73-14469
Quality control tests of small scale integration electronic components to determine diverging quality levels among manufacturers
[ECR-24] 08 p0891 N73-17213
Bibliography on techniques for integrating and packaging printed circuits
[AD-752400] 09 p1010 N73-18241
Techniques for packaging and mounting printed circuit boards
[NASA-CASE-MFS-21919-1] 16 p1883 N73-25243
Packaging of precision quartz crystal resonators and effect on aging and thermal hysteresis
[AD-763215] 21 p2519 N73-30202
Application of diffusion bonding to electronic interconnection of flatpack leads
[NASA-CR-124460] 24 p2934 N73-33429

**ELECTRONIC RECORDING SYSTEMS**
Data analysis from A-37 aircraft flights to evaluate electronic strain-level counter as fatigue damage monitor
[AD-757210] 14 p1668 N73-23540
Video cassette recording techniques and commerical aspects
23 p2757 N73-32066

**ELECTRONIC SIGNAL MEASUREMENT**
U SIGNAL MEASUREMENT

**ELECTRONIC SPECTRA**
Electronic spectra of benzophenone crystals and low temperature spectra of ketones
[AD-753380] 10 p1201 N73-19775
Analysis of electron spectroscopy considering line widths, resolution, X ray emission, and quantum mechanics
[UUIP-752] 17 p2034 N73-26460
Molecular structure studied by electron spectroscopy emphasizing X ray induced spectra
[UUIP-754] 17 p2066 N73-26715

**ELECTRONIC STRUCTURE**
U ATOMIC STRUCTURE

**ELECTRONIC SWITCHES**
U SWITCHING CIRCUITS

**ELECTRONIC TRANSDUCERS**
Performance of seismic angular vibration transducer using gas rotor
[RAE-TM-IR-128] 13 p1530 N73-22400
Design and performance of voltage transducers for Mariner spacecraft solar cells
[NASA-CR-132250] 15 p1756 N73-24234

**ELECTRONICS**
Research projects in radio and electronic engineering
[AD-752845] 09 p1008 N73-18228
Survey of electronic research projects
[AD-753700] 09 p1010 N73-18240
Navy research reports on electronics, optical physics, and information systems
[PB-215342/7] 16 p1977 N73-25992
Electronic design of rubidium-87 maser
[NASA-CR-132770] 17 p2040 N73-26502
Optical electron excitation cross section measurements of nitrogen at high temperatures
[AD-762257] 19 p2232 N73-28000
Research and development progress in solid state physics, chemistry, electronics, and materials science
[AD-763501] 21 p2610 N73-30924
Method for comparing photo-electronic and photographic detectors based on product of signal to noise ratio times spatial bandwidth
24 p2958 N73-33634
Techniques for long range vision underwater using range-gating and dual-scan with parallax techniques
24 p2958 N73-33636

**ELECTRONS**
NT CONDUCTION ELECTRONS
NT FREE ELECTRONS
NT HIGH ENERGY ELECTRONS
NT HOT ELECTRONS
NT PHOTOELECTRONS
NT POLARONS
NT SOLAR ELECTRONS
Quantum corrections to trajectories of radiating fast electrons in magnetic field
[NASA-TT-F-14495] 01 p0083 N73-10688
Vela 4 observation of solar wind electron average thermal characteristics
01 p0094 N73-10776
Perigee rotation effects on orbit-integrated proton and electron fluxes for AE-C orbit
[NASA-TM-X-66059] 01 p0103 N73-10855
Spectral line profiles of helium triplet diffuse series and quasi-static approximation for ions and electrons
[NASA-TN-D-6954] 02 p0214 N73-11731
On variational relationships between solar wind parameters, magnetospheric magnetic activity, and magnetospheric storm electrons
02 p0225 N73-11820
Experimental design for X ray and electron pulse production
[ISL-10/72] 03 p0303 N73-12472
Analysis of electron and proton fluxes encountered during nominal Tiros-N trajectories
[NASA-TM-X-66107] 03 p0357 N73-12908
Charged particle concentrations and plasma temperatures of liquid or film electrode discharges in mercury vapor
[AD-750559] 06 p0706 N73-15759
Coupling between ionosphere and protonosphere and effects on long term variations of ionospheric electron content
07 p0775 N73-16296
Determination of path latitude and electron concentration along path of whistlers in magnetosphere
[NASA-CR-130353] 07 p0781 N73-16345
Fast electron production by absorption of shf wave in collisionless plasma
[AEC-TR-7331] 07 p0827 N73-16700
Electron-proton spectrometer for Skylab radiation dose measurements
[NASA-CR-128702] 08 p0925 N73-17575
Excitation and propagation of free flow electron waves in plasma
[IPPJ-145] 09 p1070 N73-18731
Electrons in metal ammonia solutions - abstracts of conference papers
[AD-752915] 10 p1127 N73-19179
Formation of quiet time slot, dividing radiation belt electrons into inner and outer zone
10 p1145 N73-19324
Energy distributions of electrons in radiation-induced helium plasmas
[NASA-CR-130980] 10 p1195 N73-19727
Quality control procedures for Skylab electron-proton spectrometer equipment and parts
[NASA-CR-128853] 11 p1292 N73-20484

Safety analysis of EPS electron-proton spectrometer
[NASA-CR-128851] 11 p1292 N73-20485
Performance tests of electron-proton spectrometer for design verification
[NASA-CR-128852] 11 p1292 N73-20486
Design of electron-proton spectrometer for mounting externally on Skylab CSM
[NASA-CR-128814] 11 p1293 N73-20490
Electron and proton radiation effects on Cactus accelerometer electric charge
[ONERA-NT-200] 11 p1294 N73-20503
Comparison of simultaneous particle detector and search coil magnetometer measurements of precipitating particles and field aligned currents from OGO-D
[NASA-TM-X-66224] 12 p1401 N73-21367
Total electron content of ionosphere with emphasis on North Atlantic region
[AGARD-AG-166] 13 p1524 N73-22350
Electron flux measurements from Cosmos 490 satellite
14 p1660 N73-23477
ERTS/Nimbus satellite observations of electron flux levels as function of solar cycle
[NASA-TM-X-66236] 14 p1703 N73-23814
Calculation of intensities of VLF hiss generated from electrons in lower magnetosphere
[NASA-TM-X-66255] 15 p1780 N73-24428
Development of classical electron theory
15 p1815 N73-24710
Effects of electron and hole trapping on radiation hardness of aluminum oxide MIS devices
[AD-758696] 16 p1882 N73-25229
Absolute electron yields and spectral characteristics of X ray induced photoemission from metals
[AD-750875] 16 p1928 N73-25599
Low energy electron detection by channel multiplier
[CONF-720404-VOL-1] 19 p2322 N73-28682
Discrimination between high energy cosmic ray electrons and interacting protons using cesium iodide
[NASA-TM-X-70446] 20 p2435 N73-29556
Large amplitude electron plasma wave with trailing wave train in collisionless plasma
[IPPJ-163] 20 p2458 N73-29756
Space vehicle design criteria based on interplanetary charged particle environments
[NASA-CR-133600] 20 p2473 N73-29865
User guide to microfilm records of data obtained in energetic particle experiment with OGO-5
[UCRL-51307] 22 p2639 N73-31150
Electron transport in high density fully ionized liquid metals
[NASA-CR-135648] 22 p2684 N73-31497
LASNEX equations for self-generated magnetic fields and nonthermal electrons in laser produced plasmas
[UCRL-74110] 22 p2703 N73-31653
Cross section for collision processes between molecular oxygen and electron with collision energy below 100 eV
[NASA-TT-F-15048] 23 p2821 N73-32550

**ELECTROPHORESIS**
Free electrophoresis in zero gravity on Apollo 16 flight
[NASA-CR-123920] 02 p0130 N73-11055
Microelectrophoresis of human erthyrocytes as diagnostic tool in gynecology and obstetrics
[NASA-TT-F-14587] 04 p0378 N73-13077
Free electrophoresis space experiment design for weightlessness environments
[NASA-CR-123972] 05 p0502 N73-14090
Free fluid electrophoresis experiment onboard Apollo 16 flight
[NASA-TM-X-64724] 09 p1000 N73-18157
Design of electrophoretic mass screening tester for sickle cell anemia
12 p1373 N73-21140
Electrophoresis in plasmas, with dc gas discharges
[AD-757886] 15 p1818 N73-24739
Electrophoretic flow coating technique for heating oil storage tanks
[NLL-OA-TRANS-833-[6196.3]]
16 p1870 N73-25139

**ELECTROPHOTOMETERS**
Model of electrophotometer for recording ratio of two light currents
[AD-750595] 06 p0675 N73-15494
Star electrophotometer for operation in photon-counting regime
20 p2471 N73-29849
Photoelectronic devices for amplifying brightness image of variable stars
21 p2594 N73-30788

**ELECTROPHOTOMETRY**
Fundamental problems of photoelectric photometry
[PUBL-4] 17 p2031 N73-26439
Simultaneous electrophotometric and spectral observations of N De1 in 1967
20 p2471 N73-29848

**ELECTROPHYSICS**
NT ELECTRO-OPTICS
Large helium systems for superconducting power applications and high energy physics
[BNL-17228] 10 p1200 N73-19764
Variation of electrophysical parameters of epitaxial films of germanium as result of gas etching
18 p2188 N73-27665
High temperature research of thermophysical and electrophysical properties of matter and pilot plant with magnetohydrodynamic power generator
[JPRS-59983] 22 p2728 N73-31831
High temperature research of thermophysical and electrophysical properties of matter
22 p2728 N73-31832

**ELECTROPHYSIOLOGY**
Effects of intraperitoneally administered hydrazine on electrophysiology, general behavior, and performance of cats
[AD-746014] 02 p0133 N73-11081
Electrophysiological sleep patterns of human and animal brains
[NASA-TT-F-740] 13 p1483 N73-22023
Analysis of electronystagmograms for healthy persons in labyrinthal calorization tests
24 p2883 N73-33026

**ELECTROPLATING**
Physical properties of porous nickel strips used as electrodes in electro-vacuum equipment and methods for controlling expansion during production
[NLL-TRANS-746-1342-[9022.401]]
06 p0682 N73-15551
Procedure for fabricating element with cavity closed by thin wall with precisely shaped slit
[NASA-CASE-LAR-10409-1] 11 p1297 N73-20526
Analysis of adhesion strength of electroless nickel plating on Type 4340 steel to determine optimum plating conditions and to certify bond strength
[Y-1838] 12 p1414 N73-21459
Development of nickel-iron plated wires for computer memories
[ME-72-6] 13 p1498 N73-22139
Surveys of electroplating methods and techniques generated from NASA programs
[NASA-SP-5114] 13 p1533 N73-22426
Technique and equipment for sputtering using apertured electrode and pulsed substrate bias
[NASA-CASE-LEW-10920-1] 15 p1797 N73-24569
Service life extension of cyclically loaded copper specimens by application of electroplated layers of nickel
16 p1927 N73-25595

**ELECTROPOLISHING**
Fatigue behavior of annealed high-conductivity copper and effects of single and periodic intermediate surface layer removal
23 p2803 N73-32419

**ELECTROREFINING**
Compactibility, shrinkage, and microhardness of electrolytic titanium powders obtained at low temperatures from melts
04 p0432 N73-13521
Preparation of magnesium-yttrium alloys by electroduction of yttrium oxide dissolved in yttrium fluoride-lithium fluoride bath
[BM-RI-7722] 07 p0809 N73-16560
Variable measurements in electrolytic production of aluminum
[NLL-TRANS-1059-[9022.04]]
20 p2422 N73-29454

**ELECTROSEISMIC EFFECT**
U ELECTRIC CURRENT
U SEISMIC WAVES

**ELECTROSLAG PROCESS**
Electroslag melting method in casting of aluminum alloy ingot
[AD-759758] 17 p2047 N73-26558

**ELECTROSTATIC CHARGE**
Effectiveness of relaxation chamber and static charge reducer in dissipating electrostatic charge during JP-5 refueler loading
[AD-748995] 04 p0462 N73-13772
Analysis of electrical charge generated by helicopter rotor operating near particulate matter with seeded vortex
[AD-755282] 12 p1366 N73-21080
Electrostatic discharge effects in JFET performance and reliability in low humidity environment
[BDX-613-815] 12 p1383 N73-21217
Effect of spurious forces on electrostatic suspension of ultrasensitive accelerometers
[ONERA-NT-197] 13 p1530 N73-22397
Development of equipment and method for electrifying dielectric to determine electrostatic properties
[NASA-CASE-MFS-22129-1] 17 p2003 N73-26197
Electrostatic entrained material measurement system
[NASA-CASE-MFS-22128-1] 17 p2032 N73-26442
Electrostatic suspension of conducting sphere in electric field between electrodes
[JPRS-59675] 20 p2380 N73-29123
Characteristics of electrostatic discharges in liquids to show importance of transport and discharge mechanisms for boundary surface phenomena and particle discharge
[NLL-M-23041-[5828.4F]] 21 p2516 N73-30182

**ELECTROSTATIC ENGINES**
Vibration, functional, and electronic equipment tests of ESKA 18 electrostatic ion engine prototype
[DGLR-PAPER-72-87] 06 p0714 N73-15826

**ELECTROSTATIC EROSION**
U SPARK MACHINING

**ELECTROSTATIC FIELDS**
U ELECTRIC FIELDS

**ELECTROSTATIC GENERATORS**
Numerical analysis of electrical field of capacitance generator to determine potential at points in gas gap
[AD-747570] 03 p0256 N73-12069
Procedure for determining temperature distribution along linear dimension of stator of electrostatic generator
[AD-747425] 03 p0256 N73-12070
Improved electrostatic accelerator with increased terminal voltage capacity
[UR-NSRL-71] 16 p1885 N73-25255

**ELECTROSTATIC GYROSCOPES**
Analysis of forces in electrostatic gyroscope with spherical rotor and development of equations to calculate electrical forces
06 p0695 N73-15666
Mathematical models for measuring inertial qualities of spherical gyroscope rotors with electric suspension
11 p1317 N73-20691
Development of electrostatic gyro systems
11 p1318 N73-20698
Development of strapdown electrically suspended gyroscope components for increased readout accuracy
[NASA-CR-112206] 11 p1321 N73-20721
Computing rotor potential of electrostatic gyroscope
13 p1556 N73-22610
Influence of orthogonal gimbal axes of electrostatic gyroscope when rotor potential is zero
20 p2417 N73-29421

**ELECTROSTATIC PLASMA**
U PLASMAS [PHYSICS]

**ELECTROSTATIC PROBES**
Transient current overshoot to electrostatic probe in slightly ionized plasma
[PB-210383] 01 p0086 N73-10714
Theoretical and experimental analysis of charged metal particle detection in jet engine exhaust by cylindrical electrostatic probe
[AD-745540] 01 p0091 N73-10753
Numerical analysis of Langmuir wave spectra development in turbulent plasma
[JINR-P9-6432] 04 p0455 N73-13712
Plasma diagnostics by means of collision dominated spherical electrostatic probes including mathematical model
[DLR-FB-71-41] 06 p0705 N73-15756
Effect of distortion of energy distribution function of electrons measured with spherical probe
[AD-750961] 06 p0706 N73-15760
Electrostatic probes in spacecraft flow field for measuring plasma sheath density during atmospheric reentry
07 p0825 N73-16683
Current collection characteristics of moving cylindrical Langmuir probe for range of probe speeds and potentials applicable to earth and planetary measurements
[NASA-TM-X-66177] 08 p0924 N73-17571
Limitations and applications of electrostatic probes with floating potential for measurements of plasmas with low frequency oscillations
08 p0947 N73-17757
Double electrostatic probe for measuring plasma density, temperature, and velocity
[NASA-TN-D-7223] 09 p1070 N73-18733
Langmuir measurements of thermodynamic lead vapor properties
[IS-2871] 10 p1173 N73-19542
Electron temperature and density profiles obtained with Skylark rocket-borne double electrostatic probes
[TRITA-EPP-72-14-REV] 12 p1402 N73-21370
Interpretation of signals from cylindrical Langmuir probe for diagnosis of properties of streaming laser-produced plasma
12 p1431 N73-21600
Research and development of French programs for FR-1, impedance and electrostatic probes, and very low frequency wave propagation
[GRI/NTP/103] 13 p1595 N73-22936
Electrostatic analyzer and energy spectrum determination methodology used with primary electron spectrometer on Nike-Tomahawk sounding rocket
[NASA-CR-133409] 18 p2151 N73-27389
ISIS-A electro static probe measurements of electron concentration and temperature of plasmapause at mid-latitudes
[NASA-TM-X-70429] 19 p2293 N73-28442
Indications of dayside midlatitude plasma trough by ISIS-1 electrostatic probe measurements of electron density and temperature in photonosphere
[NASA-TM-X-70436] 21 p2595 N73-30797
Continuum electrostatic probe theory for collision-dominated plasma
[PB-222088/7] 22 p2706 N73-31669
Gas dynamic and Langmuir probe analysis of weakly ionized plasma jet
23 p2822 N73-32557

**ELECTROSTATIC PROPULSION**
NT ION PROPULSION

Comparison of chemical [hydrazine and aerozine], electrothermal, electrostatic, and radioisotopic propulsion systems, emphasizing performance and configurations
[ESRO-CR-25-PT-A] 08 p0955 N73-17818
Deleterious effects of electrostatic rocket exhaust [cesium, mercury] and materials of rocket construction on spacecraft surfaces
[NASA-CR-131092] 10 p1208 N73-19823

**ELECTROSTATIC WAVES**
Low loss coupling method for RF heating of plasma ions by electrostatic ion cyclotron waves
[IPP-4/30] 16 p1948 N73-25763
Relation of electrostatic oscillations in lossfree plasma to dispersion and energy equation
[IPPJ-152] 16 p1949 N73-25768
Observation of laminar electrostatic shock waves in collisionless plasma generated by ion beam
[IPPJ-156] 16 p1949 N73-25771
Dispersion of electrostatic ion plasma waves near harmonics of ion cyclotron frequency
17 p2066 N73-26716

**ELECTROSTATICS**
Functional design of electrostatic camera system for application on outer planets explorers
[NASA-CR-129093] 02 p0173 N73-11399
Electrostatic repulsion criteria for dc high voltage spark breakdown of gas
[ORO-4211-5] 03 p0336 N73-12742
Conversion of electrical signals into hydraulic signals using electrostatic hydraulic converter with no moving parts
[AD-751246] 07 p0759 N73-16168
Nonlinear electroelastic equations for small fields superposed on bias
[AD-751624] 07 p0853 N73-16914
Analysis of factors affecting quality of electrostatic printing processes and procedures to improve product
[AD-755259] 12 p1409 N73-21420
Warm fog modification by electrostatically charged particles
[AD-754100] 12 p1423 N73-21531
Hard copy of visible speech in real time using electrostatic matrix recorder
14 p1631 N73-23224
Parallel plate electrostatic spectrograph as relativistic particle analyzer
15 p1788 N73-24498
Fringing field effect minimization in parallel plate electrostatic spectrograph taking into account condenser plate thickness
15 p1788 N73-24499
Theory of electron density distribution induced at metal surface by small static external charge distribution
[AD-758380] 15 p1814 N73-24707
Development of equipment and method for electrifying dielectric to determine electrostatic properties
[NASA-CASE-MFS-22129-1] 17 p2003 N73-26197
Electrostatic gyroscope deviations and imbalance
[JPRS-59651] 20 p2418 N73-29432
Electrostatic gyroscope deviations from rotor asphericity with axisymmetric surface
20 p2418 N73-29433
Rundown time and rotor imbalance of electrostatic gyroscope with spherical rigid rotor
20 p2419 N73-29434
Static parameters of mechanical model of thin film electrostatic relay
21 p2514 N73-30171
Piezoelectric pressure transducers for shock tubes, noting electrostatic calibrator
[ARC-CP-1240] 24 p2910 N73-33221
Measurement of electron density in cylindrical electrostatic confinement device
24 p2961 N73-33664

**ELECTROSTRICTION**
Electrostriction in ferroelectric ceramics
[AD-745821] 01 p0089 N73-10731
Convolution of surface acoustic waves on barium titanate crystal
[AD-761880] 19 p2327 N73-28724

**ELECTROTHERMAL ENGINES**
NT ARC JET ENGINES
NT PLASMA ENGINES
NT RESISTOJET ENGINES
Electrothermal acoustics model for predicting and suppressing combustion instability in rocket motors
[AD-753111] 09 p1079 N73-18807
Current technology in ion and electrothermal propulsion systems and components
[NASA-TM-X-71434] 23 p2830 N73-32618

**ELECTROWINNING**
Preparation of magnesium-yttrium alloys by electroduction of yttrium oxide dissolved in yttrium fluoride-lithium fluoride bath
[BM-RI-7722] 07 p0809 N73-16560

**ELEMENT ABUNDANCE**
U ABUNDANCE

**ELEMENTARY EXCITATIONS**
NT EXCITONS
NT MAGNONS
NT PHONONS
NT PLASMONS
NT POLARONS
Elementary excitation spectrum of superfluid helium
10 p1198 N73-19750
Quasi-particle pair interference current in superconducting weak links of Josephson junctions
[AD-754081] 11 p1331 N73-20803
Investigation of He-3 impurities in He-4 for development of microscopic theory of He-3 quasiparticles
12 p1375 N73-21155
Quasiparticle tunneling into superconducting transition metals
[AD-764905] 23 p2826 N73-32591

**ELEMENTARY PARTICLE INTERACTIONS**
NT ELECTRON CAPTURE
NT MESON-NUCLEON INTERACTIONS
NT NUCLEON-NUCLEON INTERACTIONS
Characteristics of electrostatic discharges in liquids to show importance of transport and discharge mechanisms for boundary surface phenomena and particle discharge
[NLL-M-23041-[5828.4F]] 21 p2516 N73-30182
Finiteness of radiative corrections to semileptonic decays in unified gauge theories
[TR-74-021] 22 p2701 N73-31637

**ELEMENTARY PARTICLES**
NT ALPHA PARTICLES
NT ANTINUCLEONS
NT ANTIPROTONS
NT BARYON RESONANCES
NT BARYONS
NT BETA PARTICLES
NT BOSONS
NT CONDUCTION ELECTRONS
NT DEUTERONS
NT ELECTRONS
NT FAST NEUTRONS
NT FERMIONS
NT FREE ELECTRONS
NT HADRONS
NT HIGH ENERGY ELECTRONS
NT HOT ELECTRONS
NT LEPTONS
NT LIGHT BEAMS
NT MESON RESONANCES
NT MESONS
NT NEUTRINOS
NT NEUTRON BEAMS
NT NEUTRONS
NT NUCLEONS
NT OMEGA-MESONS
NT PARTONS
NT PHOTOELECTRONS
NT PHOTONS
NT PIONS
NT POLARONS
NT POSITRONS
NT PROTONS
NT QUARKS
NT RECOIL PROTONS
NT SOLAR ELECTRONS
NT SOLAR PROTONS
NT THERMAL NEUTRONS
Development of inverse scattering problem and approach to nonrelativistic problem at fixed angular momentum
02 p0199 N73-11608
Detection and measurement of cosmic ray charge spectrum for nuclei heavier than iron with relation to nucleosynthesis and mechanics of supernova
[NASA-TM-X-58102] 03 p0352 N73-12872

**ELEVATION ANGLE**
Ionospheric range error given by expansion expression in terms of elevation angle and moment of refractivity distribution
[NASA-TM-X-66159] 07 p0790 N73-16426
Cinetheodolite observations of satellites between 3 and 26 Nov. 1965
[ROE-STS-134] 09 p1091 N73-18907

**ELIMINATION**
Hyperoxia effects on elimination of carbon monoxide, ammonia, ketones, and aldehydes by rats
03 p0256 N73-12077

**ELLIPSES**
Rotational tidal waves due to earth rotation explained by Poincare problem solving
07 p0857 N73-16951

**ELLIPSOIDS**
Quasigeoid heights and deflections of vertical for reference field of level ellipsoid
[AD-748528] 06 p0668 N73-15434
Electric charge, momentum, and mass of elliptic universe
[AD-756902] 13 p1561 N73-22649
Computer program to compute geodetic distance and azimuth between two geodetic positions
[P-4950] 14 p1659 N73-23462

**ELLIPSOMETERS**
Characteristics of ellipsometer and techniques for measuring thin films including computer program for determination of optical constants and thickness of film
[NASA-TM-X-64742] 12 p1405 N73-21392
Ellipsometric measurements on passive film prior to initiation of breakdown in aluminum
[NASA-CR-132301] 20 p2432 N73-29533

**ELLIPTIC DIFFERENTIAL EQUATIONS**
Variable directions method for solving numerical weather forecasting problems
[AD-752336] 10 p1182 N73-19620
Reflecting solutions of high order elliptic differential equations in two independent variables across analytic arcs
[NASA-CR-135667] 23 p2812 N73-32483

**ELLIPTIC FUNCTIONS**
Elliptical integral expressions for magnetic field due to current loop
[ORNL-TM-4023] 12 p1429 N73-21581

**ELLIPTIC INTEGRALS**
U ELLIPTIC FUNCTIONS

**ELLIPTICAL CYLINDERS**
Vortex generation and propagation under perfect slip flow conditions, for thin elliptical cylinder
24 p2908 N73-33206

**ELLIPTICAL GALAXIES**
Flat circular plates of particular mass density, representing spiral or flat elliptical galaxeis
19 p2341 N73-28830
Random distributions and position angle measurements of elliptical and spiral galaxies
20 p2469 N73-29833
Gas flow and wind velocity in elliptical and cluster galaxies
24 p2978 N73-33795

**ELLIPTICAL ORBITS**
NT APOGEES
NT PERIGEES
NT PERIHELIONS
NT TRANSFER ORBITS

**ELLIPTICAL POLARIZATION**
Polarized ellipticity of VLF signals in radio fields
[AD-753085] 09 p1003 N73-18190
Three dimensional response of directional antenna in elliptically polarized field
[AD-754906] 11 p1257 N73-20202

**ELLIPTICITY**
Aerodynamic characteristics of flow around elliptic cones at large angles of attack
[AD-764945] 23 p2777 N73-32209

**ELONGATION**
Stability analysis for spinning flow of cylindrical liquid polymer filament with memory function
[AD-755065] 11 p1273 N73-20332
Determination of elongation in flanges during H-beam rolling
[NLL-M-21639-[5828.4F]] 21 p2552 N73-30455

**EMANATION**
U EMISSION

**EMBOLISMS**
NT AEROEMBOLISM

**EMBRITTLEMENT**
Procedure for measuring effect of hydrogen content on toughness and sustained load cracking resistance of titanium alloys including results obtained for Ti-6Al-4V
[AD-746443] 02 p0187 N73-11517
Electrochemical permeation technique and scanning electron microscopy used to determine hydrogen embrittlement in ferrous materials
[AD-752828] 09 p1049 N73-18557
Hydrogen embrittlement of tantalum alloy cladding for uranium mononitride nuclear fuel pins at high temperatures
[NASA-TM-X-2732] 09 p1063 N73-18675
Effects of hydrogen environment embrittlement of steels and alloys
[NASA-CR-2163] 12 p1412 N73-21444
Stress corrosion cracking in 410 stainless steel due to hydrogen embrittlement
13 p1539 N73-22471
Stress corrosion cracking in high strength aluminum alloys due to hydrogen embrittlement
13 p1539 N73-22472
Solid cadmium embrittlement in A-7 aircraft failure of six shaft and one horn fracture surfaces
[AD-756906] 13 p1545 N73-22525
Effect of residual impurity element on sensitivity of low alloy steels to radiation induced embrittlement
[AD-756625] 14 p1679 N73-23622
High strength steel delayed failure analysis including hydrogen embrittlement
[NLR-TR-72113-U] 14 p1715 N73-23917
Helium embrittlement of austenitic stainless steels
[AI-AEC-13047] 15 p1799 N73-24580
Effect of stress corrosion cracking and hydrogen embrittlement on failure of high strength spacecraft fasteners
[AD-758754] 15 p1800 N73-24591
Irradiation strengthening and fracture embrittlement of A533-B steel and arc weldment metal
[HEDL-SA-323] 16 p1969 N73-25931
Analysis of embrittlement in zone refined iron and Armco iron after charging with hydrogen to determine cause of reaction
[RAE-LIB-TRANS-1666] 17 p2043 N73-26530
Embrittlement and cracking of steels
[CEA-BIB-204] 22 p2685 N73-31506
Thermal embrittlement of 4340 steels at high temperatures
[AD-763900] 22 p2687 N73-31521

Susceptibility of Zircaloy 4 and niobium base alloy to hydrogen embrittlement at elevated temperature
[LA-5169] 24 p2936 N73-33447
EMBRYOLOGY
Effect of sonic boom on fish and fish eggs during developmental stage
[FAA-RD-73-29] 11 p1247 N73-20121
EMBRYOS
Comparison of development of auditory vesicle in frog embryos under weightless and terrestrial conditions
[NASA-TT-F-14624] 01 p0009 N73-10072
EMERGENCIES
Aircraft accident involving Boeing 707 aircraft at San Francisco, California airport following rejected takeoff on 13 Sept. 1972
[NTSB-AAR-73-4] 12 p1363 N73-21062
Silent alarm system for mutiple room facility or school
[NASA-CASE-NPO-11307-1] 21 p2519 N73-30205
Requirements and equipment for space shuttle emergency intravehicular activity and effectiveness of emergency procedures - Vol. 5
[NASA-CR-133995] 22 p2622 N73-31010
EMERGENCY LIFE SUSTAINING SYSTEMS
Personnel protection and emergencies handling for oxygen systems
[NASA-CR-120922-VOL-4] 05 p0580 N73-14719
Crew safety for in-flight spacecraft emergencies
[NASA-TT-F-14997] 18 p2111 N73-27068
Crew survival after emergency landing or ditching in unpopulated areas
[NASA-TT-F-15047] 20 p2371 N73-29053
EMISSION
NT BIOLUMINESCENCE
NT CHEMILUMINESCENCE
NT ELECTROLUMINESCENCE
NT ELECTRON EMISSION
NT FIELD EMISSION
NT FLUORESCENCE
NT HYDROXYL EMISSION
NT INCANDESCENCE
NT ION EMISSION
NT LIGHT EMISSION
NT LUMINESCENCE
NT MICROWAVE EMISSION
NT NEUTRON EMISSION
NT OPTICAL RESONANCE
NT PARTICLE EMISSION
NT PHOSPHORESCENCE
NT PHOTOELECTRIC EFFECT
NT PHOTOELECTRIC EMISSION
NT PHOTOIONIZATION
NT PHOTOLUMINESCENCE
NT RADIO BURSTS
NT RADIO EMISSION
NT SECONDARY EMISSION
NT SOLAR RADIO BURSTS
NT SOLAR RADIO EMISSION
NT SPECTRAL EMISSION
NT THERMAL EMISSION
NT THERMIONIC EMISSION
NT THERMOLUMINESCENCE
NT TYPE 2 BURSTS
NT TYPE 3 BURSTS
NT TYPE 4 BURSTS
NT TYPE 5 BURSTS
NT X RAY FLUORESCENCE
Theoretical model of optical excitation, emission, and deactivation properties of Meinel band system of nitrogen
[AD-753396] 09 p1069 N73-18722
EMISSION SPECTRA
Temperature measurements on vibrational excited microwave discharged nitrogen
[AD-746327] 02 p0138 N73-11118
Laser luminescence and shock heating for hydrogen fluoride vibrational relaxation measurements in shock tube
[AD-745953] 02 p0138 N73-11119
Fourier spectrometer for measuring absolute spectral intensity of emissions from earth and other planets
[NASA-TT-F-14425] 02 p0172 N73-11397
Stress wave emission nondestructive inspection technique for detecting flaw criticality in structural parts
[AD-747225] 02 p0176 N73-11426
Activation analysis of prompt gamma ray emission spectra for trace element determination
03 p0262 N73-12123
Infrared spectral emittance data, and infrared spectrometry studies
[NASA-CR-128646] 03 p0335 N73-12730
Secondary ionic emission procedure for studying semiconductor properties
[CEA-CONF-1969] 04 p0459 N73-13745
Interferometric observations of neutral hydrogen emission line of compact galaxy 2 Zw 40
[AD-747993] 04 p0477 N73-13896
Measurement of infrared emission spectra of liquid cyclopentane derivatives excited by carbon dioxide laser
[AD-750480] 06 p0681 N73-15544
Solution of ionization and thermal equilibrium equations for gas clouds in quasars and Seyfert galaxies ionized by ultraviolet radiation sources
07 p0839 N73-16801
Valence electron model for calculating ionization energies and excited levels in photoelectron- and absorption-spectra
08 p0945 N73-17741
Determination of impurities in titanium tetrachloride by infrared spectroscopy, emission spectra, and chemical analysis
[NLL-RTS-7725] 09 p1045 N73-18524
Measurements of emission coefficient of uranium plasmas
[NASA-CR-131319] 11 p1327 N73-20772
Jovian emission spectrum analysis for temperature and ammonia profiles, and Martian infrared limb profile analysis for atmospheric temperature and water vapor
[NASA-CR-131266] 11 p1337 N73-20847
Dynamic model of solar flare emission sources
13 p1572 N73-22742
Nondestructive tests for predicting effect of copper and aluminum microstructure on acoustic emission
[AD-758216] 15 p1800 N73-24587
Collection of marine fluorescence data from Atlantic, Gulf, and Pacific sites
[NASA-CR-114579] 16 p1867 N73-25115
Balloon measurement of gamma ray emission from region of galactic center
16 p1959 N73-25844
Generation of laboratory spectra at photon energies from highly ionized atoms
[AD-758606] 16 p1960 N73-25851
Design of high intensity atomic emission line sources in vacuum ultraviolet region for atmospheric gas trace detection
[AP-11] 17 p2034 N73-26459
Millimeter polarization spectra of solar activities for estimating chromospheric magnetic fields
19 p2334 N73-28780
Solar burst observations at millimeter wavelengths
19 p2334 N73-28781
Gamma ray and neutron emissions during solar flares
19 p2336 N73-28795
Composition and energy spectra of energetic particles emitted during solar flares
19 p2337 N73-28800
Expected gamma ray emission spectra from lunar surface for range of chemical compositions
[NASA-TM-X-70453] 21 p2595 N73-30796
Observations of recombination line emission in direction of supernova remnants
[AD-762002] 21 p2598 N73-30825
EMISSIVITY
Investigation of emissivity and circular polarization of synchrotron radiation
[NASA-CR-131526] 12 p1457 N73-21811
Exoelectronic emission and relationship with various surface properties of metals and alloys
[AD-756943] 13 p1543 N73-22509
Emissivities of metals and compounds in liquid state at fusion temperatures
[NASA-CR-133521] 19 p2309 N73-28576
Techniques and associated instrumentation for high temperature emissivity measurements
[NASA-CR-124423] 23 p2792 N73-32339
EMISSOGRAPHS
U ACTINOMETERS
U RECORDING INSTRUMENTS
EMITTANCE
Design of radiometric emittance measurement system for use at high temperatures
[NASA-CR-123968] 04 p0420 N73-13421
Characteristics of cryogenic interferometric spectrometer and application to measuring low level emittance or absorption in optical elements
05 p0556 N73-14518
EMITTERS
NT THERMIONIC CATHODES
NT THERMIONIC EMITTERS
Inverted geometry transistor for use with monolithic integrated circuit
[NASA-CASE-ARC-10330-1] 23 p2763 N73-32112
EMOTIONAL FACTORS
Analysis of cosmonaut emotional stress as determined by physiological and behavioral responses
[NASA-TT-F-14654] 03 p0261 N73-12113
Indices of emotional stress in cosmonauts during Voskhod 2 and Soyuz flights
[JPRS-58039] 08 p0877 N73-17104
EMOTIONS
Influence of emotional states on human operator performance and efficiency
21 p2503 N73-30085
Various types of corticopetal influences from deep-seated emotiogenic formations of brain
24 p2889 N73-33068
EMPLOYMENT
Workshop for teaching professional unemployed personnel competitive job searching techniques
[PB-209367] 01 p0020 N73-10159
Results from employment workshop program for unemployed aerospace engineers and scientists
[PB-209366] 01 p0022 N73-10168
EMULSIONS
NT NUCLEAR EMULSIONS
NT PHOTOGRAPHIC EMULSIONS
Emulsifying capacity of oils and wearability of additives during contact with water
[AD-754622] 11 p1302 N73-20561
Orientation of molecules of soil soluble surfactant in absorption layers on liquid-liquid interface
[NLL-M-22998-[5828.4F]] 20 p2373 N73-29068
Determination of complex Hamaker constants of molecular interactions in black hydrocarbon emulsion films
[NLL-M-2300-[5828.4F]] 20 p2373 N73-29069
Effects of properties of organic phase on thickness and intermolecular interaction of black hydrocarbon films
[NLL-M-22999-[5828.4F]] 20 p2373 N73-29070
Determination of Hamaker complex constants in hydrocarbon emulsion films by measurement of contact angles and interfacial tension
[NLL-M-23001-[5828.4F]] 21 p2504 N73-30095
ENAMELS
White porcelain enamal thermal control coating for spacecraft
[NASA-CR-124459] 24 p2938 N73-33459
ENCAPSULATING
List of metallic melting bodies for temperature determinations from 30 to 1555 degrees Celsius
[JUL-871-RB] 08 p0932 N73-17631
Platinum-rhodium-tungsten alloys for encapsulating space isotopic heat sources
[ORNL-4813] 08 p0932 N73-17632
Fabrication and encapsulation processes for multiconductor cables
[BDX-613-740] 10 p1134 N73-19245
Improved fabrication and encapsulation techniques for multiconductor cables
[BDX-613-687] 10 p1134 N73-19246
Fabrication of plastic encapsulated metal containers by rotational molding process
[AD-753344] 10 p1168 N73-19499
Production and performance of strain gage embedded in boron/epoxy materials
[AD-759548] 16 p1915 N73-25493
Cable fabrication and encapsulation inclusive of, string-pulling machine and solder sleeve processing
[BDX-613-775] 21 p2553 N73-30467
X ray inspection of losses in high voltage transformers encapsulated by epoxy resins noting thermal cycling effects and stresses
24 p2881 N73-33008
ENCLOSURES
Development of procedure for determining maximum and minimum stresses produced by uniform pressure on unpierced torispherical closure of cylindrical shell
[ESDU-67017] 01 p0110 N73-10911
Solution of laminar natural convection flows of Newtonian fluid in rectangular enclosures by asymptotic expansion
18 p2128 N73-27198
ENCODERS
U CODERS
ENCODING
U CODING
END MORAINES
U GLACIAL DRIFT
ENDOCRINE GLANDS
NT ADRENAL GLAND
NT PITUITARY GLAND
NT THYROID GLAND
ENDOCRINE SECRETIONS
NT ALDOSTERONE
NT HORMONES
NT HYDROXYCORTICOSTEROID
NT INSULIN
Conference on human endocrine secretions and hormone metabolisms during space flight stress
[NASA-TM-X-58093] 09 p0993 N73-18104
Measurements of endocrine metabolic responses to space flight stress on Apollo 14 and Apollo 15 crewmen
09 p0993 N73-18105
Radioimmunoassay of urinary antidiuretic hormone excretion in man considering water loading and dehydration effects
09 p0993 N73-18107
Measurement of antidiuretic hormone excretions in human urine as indication of neurosecretory stress response during space flight
09 p0993 N73-18108
Water immersion model for simulating renin, aldosterone, and natriuresis effects of prolonged weightlessness on man
09 p0993 N73-18110
Influence of long duration flight missions on metabolic and endocrine functions of pilots and navigators
10 p1123 N73-19152
ENDOGENOUS CONDITIONS
U PHYSIOLOGY

**ENDOTHERMIC REACTIONS**
Endothermic decomposition in jet engine exhaust reaction
[AD-758200] 14 p1618 N73-23105
**ENEMY PERSONNEL**
Development of electronic detection system for remotely determining number and movement of enemy personnel
[NASA-CASE-ARC-10097-2] 16 p1873 N73-25160
**ENERGETIC PARTICLE EXPLORER A**
U EXPLORER 12 SATELLITE
**ENERGY**
Fluid mechanics and dynamic energy separation in steady flow, nonsteady flow, and cryptosteady flow
[AD-747316] 03 p0286 N73-12314
Transport of energy over turbulence spectrum of free atmosphere
[AD-747728] 03 p0299 N73-12438
Environmental factors in production and use of energy and effects on air, water, and land
[R-992-RF] 21 p2537 N73-30340
Flight tests of cockpit meter instrumentation system displaying aircraft specific energy and energy rate
[AD-763450] 21 p2550 N73-30448
**ENERGY ABSORPTION**
NT AURORAL ABSORPTION
NT ELECTROMAGNETIC ABSORPTION
NT MOLECULAR ABSORPTION
NT PHOTOABSORPTION
NT POLAR CAP ABSORPTION
NT SELF ABSORPTION
NT THERMAL ABSORPTION
NT THERMALIZATION [ENERGY ABSORPTION]
NT ULTRAVIOLET ABSORPTION
NT X RAY ABSORPTION
Energy-absorbing efficiency of ply-tear webbings and discussion of warp and weft count and binder property effects
[RAE-TR-72051] 01 p0113 N73-10936
Performance tests of crash protective seat belts using energy absorbers to allow system to yield at constant force
[ARL/SM-340] 06 p0619 N73-15023
High energy absorption docking system design for docking large spacecraft
[NASA-CASE-MFS-20863] 17 p2086 N73-26876
Metal shearing energy absorber
[NASA-CASE-HQN-10638-1] 21 p2552 N73-30460
Influence of solar energy absorption and air water interactions on seasonal thermocline of sea
24 p2957 N73-33623
**ENERGY BANDS**
NT CONDUCTION BANDS
Energy calibration of Orion spectrograph for operation in wavelength range from 2000 to 3800
[NASA-TT-F-14584] 07 p0799 N73-16491
**ENERGY BUDGETS**
NT ATMOSPHERIC HEAT BUDGET
NT HEAT BUDGET
Momentum, energy, and mass budgets of stratosphere
[COO-2195-2] 04 p0415 N73-13385
Energy exchange between earth and space from meteorological satellite measurements of infrared radiant emittance and reflected and scattered solar radiation
[NASA-CR-130152] 07 p0780 N73-16341
Atmospheric energetics as related to cyclogenesis over eastern United States
[NASA-CR-2189] 07 p0815 N73-16607
Simulation of monthly variation of local surface energy budget and sub-surface temperature regime in Antarctica
10 p1146 N73-19326
Apollo experience report on procedures and techniques for predicting consumables usage for Apollo missions
[NASA-TN-D-7140] 10 p1214 N73-19874
Photochemical mechanisms of ozone and energy budget in atmosphere between 10 and 100 km
18 p2133 N73-27233
Energy budget of pumice desert surface under clear skies during summer
[PB-218791/2] 18 p2146 N73-27347
**ENERGY CONVERSION**
Photoelectric, thermoelectric, and thermoemission methods of converting solar to electrical energy
[AD-747293] 02 p0129 N73-11050
Activities to develop radioisotope energy conversion systems
[ORNL-TM-3687] 03 p0332 N73-12705
Research on closed cycle MHD power generation for converting heat into electricity
[RT/ING-(7) ]20] 03 p0341 N73-12784
Photosynthetic energy conversion in membranes, tissues, and reaction centers of bacteria and viruses
[COO-3162-9] 04 p0380 N73-13091
Conversion and utilization of solar energy to solve energy shortages and pollution problems on earth
04 p0474 N73-13866
Conversion of solar energy to pollution free power
04 p0474 N73-13870
Development of surfaces and coatings for solar energy conversion systems
[NASA-TT-F-14650] 06 p0688 N73-15598
Kinetic energy and X ray conversion in plasma heated by laser
[AD-751048] 07 p0830 N73-16733
Performance and endurance testing of 6 kW organic Rankine cycle power conversion system
[SAN-651-130] 08 p0870 N73-17042
Formulation of stress strain model for storage batteries
[AD-752257] 08 p0870 N73-17045
Analysis of energy conservation constraints on circulation of Southern Hemisphere atmosphere and oceans based on radiant, latent, and sensible heat energy transfers
[METEOROL-STUDY-26] 09 p1027 N73-18387
Electromechanical energy conversion devices using both conventional and rare-earth cobalt permanent magnet materials
[AD-756433] 13 p1501 N73-22168
Analysis of liquid metal magnetohydrodynamic energy conversion systems to determine performance limits and identify system parameters
[AD-757065] 14 p1606 N73-23013
Applications of solar energy to heat and power requirements
[NASA-CR-133101] 17 p2079 N73-26818
Techniques for improving performance of gallium arsenide solar cells by ion implantation
[NASA-CR-135510] 22 p2618 N73-30977
Device for converting electromagnetic wave energy into electric power
[NASA-CASE-GSC-11394-1] 23 p2763 N73-32109
Design of floating platforms to capture and use solar radiation
24 p2974 N73-33764
Heliothermic conversion of solar radiation for industrial use
24 p2975 N73-33767
**ENERGY CONVERSION EFFICIENCY**
Operation of plasma accelerator in quasi-steady mode to determine ratio of energy deposition into kinetic and thermal modes
[NASA-CR-128408] 01 p0035 N73-10275
Feasibility of using photovoltaic cells to convert laser energy into electrical energy
[LA-DC-72-468] 03 p0255 N73-12061
Design and performance of cylindrical silicon germanium thermoelectric generators
06 p0626 N73-15080
Gas turbine power plants in future urban energy planning
[RE-439] 13 p1593 N73-22912
Solar heating and air conditioning as energy conservation alternatives to nuclear power
[NASA-TM-X-70468] 23 p2748 N73-31990
Characteristics of hydrazine-oxygen fuel cell operating under moderate temperature conditions and various power density concentrations
[AD-764530] 24 p2881 N73-33009
**ENERGY CONVERTERS**
U DIRECT POWER GENERATORS
**ENERGY DENSITY**
U FLUX DENSITY
**ENERGY DISSIPATION**
Influence of cavity radius on energy dissipation rate in liquid filled spherical cavities
01 p0040 N73-10319
Electron bombardment and energy losses in beryllium, aluminum, copper, tin, gadolinium, and lead
[AD-747077] 02 p0215 N73-11739
Experimental determination of energy loss rate of fast ions in dense plasma and comparison of results with predictions of Spitzer formula
[UCRL-51175] 03 p0342 N73-12793
Gyro suspension systems including axis disturbance probability factors, bearing friction, astatic gyro gimbal errors with drift, and horizontal pendulum energy dissipation
[JPRS-57504] 05 p0546 N73-14432
Effect of energy dissipation on drift of horizontal pendulum on vibrating base with application to gyroscopic suspension systems
05 p0546 N73-14436
Particle production and energy dissipation in stationary fusion plasma
[FOA-4-C-4465-25] 06 p0703 N73-15734
Mathematical model for energy losses and velocity distribution in laminar boundary layers, using quadrature formulas
07 p0770 N73-16257
Elastic-plastic solution for calculating influence of energy dissipation on drawn wire fatigue
[AD-752017] 08 p0928 N73-17600
Calculation of energy deposition distributions for simple geometries
[NASA-TN-D-7195] 08 p0957 N73-17832
Spin reorientation of nonsymmetric body with energy dissipation, using ATS5
[NASA-CR-131320] 11 p1316 N73-20683
Finite difference solution of flow and energy losses of pure gases in separation nozzle geometry
[KFK-1630] 12 p1392 N73-21285
Energy release integral equation for finite elastic and viscoelastic materials
[CONF-720930-1] 12 p1463 N73-21851
Storage time loss in metal oxide capacitors caused by surface damage in silicon wafer
[AD-756250] 13 p1566 N73-22690
Magnetic coil design and physical phenomena responsible for ac losses in superconductivity
15 p1761 N73-24273
Elimination of principal source of energy loss in microwave acoustic transducers
16 p1880 N73-25216
Performance of baffles as energy dissipation suppressors in liquid filled precessing cavities
16 p1888 N73-25280
Procedures for reducing loss mechanism in plasma jet engine
[AD-759272] 16 p1958 N73-25839
Measurement of beam divergence of 30-cm dished grids
[NASA-TM-X-68286] 20 p2466 N73-29808
Ionization loss in galactic cosmic ray electron spectrum caused by proton interactions
22 p2733 N73-31873
Evaluation of energy expenditures and reactions of cardiovascular and respiratory systems to physical work
[NASA-TT-F-15090] 23 p2749 N73-31997
Effects of surface corrugation in horn antenna power loss
[NASA-CR-2317] 23 p2756 N73-32059
Closed form approximation in dissipation integral for incompressible turbulent boundary layers
24 p2908 N73-33204
Electron beam energy loss in plasma
[LA-5269-MS] 24 p2964 N73-33684
**ENERGY DISTRIBUTION**
NT SPECTRAL ENERGY DISTRIBUTION
Numerical analysis of quantum mechanical theory of scattering of particle by spherically symmetrical potential
02 p0199 N73-11610
FORTRAN 4 programs and subroutines for generating potential parameters from energy dependence of elastic scattering cross sections
[NASA-CR-129179] 03 p0269 N73-12180
Energy distributions of field-emitted electrons from p-type silicon surfaces
[AD-747067] 03 p0346 N73-12825
Mathematical model for energy distribution in waveguide bifurcations
[DLR-FB-71-17] 05 p0520 N73-14224
Vibrational energy distribution of positive Cs ions in output from Cs2O2 chemical laser
[DREV-TN-2019/72] 06 p0679 N73-15522
Energy deposition in parallel plate plasma accelerators operated in quasi-steady mode
10 p1195 N73-19723
Energy distributions of electrons in radiation-induced helium plasmas
[NASA-CR-130980] 10 p1195 N73-19727
Energy requirements of Department of Defense and identification of research and development activities
[AD-754824] 11 p1333 N73-20819
Porous structure and surface energy of evaporated metal thin films
13 p1565 N73-22683
Theoretical study of fluid dynamic energy separation
15 p1764 N73-24292
Red shift energy distribution and black body background distortion theories of universal formation
19 p2333 N73-28770
**ENERGY EXCHANGE**
U ENERGY TRANSFER
**ENERGY LEVELS**
NT ATOMIC ENERGY LEVELS
NT ELECTRON STATES
NT GROUND STATE
NT INTERMOLECULAR FORCES
NT MOLECULAR ENERGY LEVELS
Multiple ion interaction energy and metal structure distribution
01 p0087 N73-10721
Solid state laser induced excitation of HF second vibration rotation energy levels
15 p1794 N73-24547
Optical transitions between energy states of solute organic dye
[AD-762607] 20 p2426 N73-29489
K sheli Compton scattering on tin and gold at 145 keV and gold at 320 keV
24 p2960 N73-33654
**ENERGY LOSSES**
U ENERGY DISSIPATION
**ENERGY METHODS**
NT BERNSTEIN ENERGY PRINCIPLE
NT STRAIN ENERGY METHODS
Application of energy concepts for prediction of pavement system performance
23 p2770 N73-32153
**ENERGY REQUIREMENTS**
Hearings concerning research and development requirements for future energy needs
01 p0119 N73-10980

Energy variation principle for specific inductance geometry in stable toroidal plasma generation
[NYO-1480-182] 06 p0704 N73-15741
Congressional hearings concerning critical energy needs
08 p0977 N73-17989
Congressional study on historical background of energy research and development
13 p1594 N73-22928
Hearings concerning energy problems of US
14 p1721 N73-23969
Review of resources of fossil and nuclear fuels, solar energy and hydroelectric power
[LRP-63/73] 22 p2617 N73-30975
Use of energy in transportation and implications for future
[P-5025] 24 p2993 N73-33921

**ENERGY SOURCES**

Theoretical analysis of energy supply to quiet solar wind
01 p0094 N73-10773
Research and development of advanced energy sources for United States of America
01 p0120 N73-10988
Method for technical evaluation of controlled nuclear fusion for energy production
[NP-19152] 03 p0332 N73-12707
Conference on research in nonchemical energy sources in nuclear fusion and plasma physics
[AD-748265] 04 p0456 N73-13725
Nuclear energy in hydrogen production by water dissociation method
[EUR-4838] 06 p0699 N73-15699
Physical and chemical energy sources for earth, sea, and space
[AD-753828] 09 p0992 N73-18093
Interrelationships between energy, resources, and environment, conference summary
[PB-213031] 11 p1333 N73-20820
Analysis of methods for meeting national energy requirements with emphasis on technology for using solar energy
[NASA-TM-X-68230] 13 p1573 N73-22748
Energy alternatives to prototype oil shale leasing program for Wyoming, Colorado, and Utah - Vol. 2
[EIS-AA-72-5242-D-2-VOL-2]
20 p2410 N73-29368
Sources of energy for ball lightning
[NASA-TT-F-15097] 23 p2786 N73-32289
Solar energy, thermonuclear energy, and fossile fuel energy sources
[UCRL-74697] 24 p2881 N73-33005
Hydrogen and other synthetic fuels
[TID-26136] 24 p2971 N73-33738

**ENERGY SPECTRA**

NT ELECTRONIC SPECTRA
NT NEUTRON SPECTRA
Absorption spectra analyses on germanium films for determining band structure transformations
02 p0218 N73-11765
Energization of electrons in ionosphere and magnetoplasma by wave particle interaction
[AD-747093] 04 p0415 N73-13391
X ray and electron energy spectroscopy for analysis on band structure of materials
[NAL-SR-1] 06 p0699 N73-15703
Differential energy spectra of cosmic ray protons and helium nuclei dominated by solar modulation of local interstellar spectra, and numerical solutions to transport equation
[NASA-CR-130298] 06 p0715 N73-15837
Balloon borne measurement of cosmic ray electron spectrum from 10 to 200 GeV
[NASA-TM-X-66182] 08 p0956 N73-17830
Cosmic ray charge and energy spectra above 10 GeV from balloon flight data
08 p0974 N73-17963
Frequency spectrum of laser scattering from dense plasma focus
[AD-753705] 09 p1073 N73-18754
Energy spectra of ionospheric photoelectrons measured in 30 to 150 eV range from Cosmos 348 satellite in summer 1970
[PR-107] 10 p1155 N73-19400
Proton 1 rocket charged particle spectrometer for measuring energy spectrum and electron and proton distribution above 20 keV
[NP-19462] 10 p1161 N73-19444
Antiproton and antinucleon energy spectrum analysis
[LPTHE-73/1] 10 p1191 N73-19691
Large cosmic ray air shower, primary energy spectrum, obtained from structure, size, and flux measurements
13 p1573 N73-22750
OSO-5 X ray detector measurement of diffuse cosmic ray energy spectrum from 14 to 200 keV
[NASA-TM-X-66252] 15 p1828 N73-24815
Measurements of differential energy spectra in cosmic ray protons and solar cycle variations of atmospheric secondary protons
[NASA-CR-132056] 15 p1828 N73-24818
Low temperature energy spectrum near roton minimum region in superfluid helium
17 p2064 N73-26696
Energy spectra analysis for heavy nuclei charge compositions in galactic cosmic rays
[NASA-TM-X-66136] 17 p2079 N73-26817
Mathematical models for studying energy spectra and nonlinear surface waves of ocean
[AD-759541] 18 p2149 N73-27371
Energy spectra of six cosmic gamma-ray bursts in regions of 0.1 to 1.2 MeV
[NASA-TM-X-70427] 20 p2468 N73-29824
Energy spectra of solar cosmic rays
22 p2733 N73-31876
Structure of isolated solar flare point
22 p2734 N73-31880
Auroral bremsstrahlung flux spectra at various atmospheric depths
[NASA-SP-3081] 23 p2786 N73-32293
Differential energy spectra of cosmic ray protons and helium nuclei
23 p2833 N73-32640
Flux and energy spectrum of fast neutrons and gamma rays at balloon altitudes
23 p2833 N73-32642
IMP-7 measurement of very low energy cosmic ray energy spectra and concentration during solar flares
[TR-73-138] 23 p2835 N73-32654
Satellite measurement of cosmic ray abundances and spectra in charge range 2 equal to or less than 7 equal to or less than 10
[NASA-CR-135786] 24 p2976 N73-33777

**ENERGY STORAGE**

NT ELECTRIC ENERGY STORAGE
NT HEAT STORAGE
Design of coils and switches for superconducting magnetic energy storage and transfer
[LA-DC-72-470] 03 p0345 N73-12816
Shock heating of plasmas based on superposed superconducting circuits and magnetic energy storage
[TRITA-EPP-72-29] 07 p0829 N73-16717
Vibration simulation of space probe model, superconducting energy storage coil
[LA-DC-72-724] 07 p0832 N73-16742
Development of high magnetic fields using superconductors with high current densities and application to power conversion and energy storage
10 p1108 N73-19035
Application of superconducting coils for energy storage and determination of optimizing parameters for inductive energy storage
10 p1109 N73-19042
Effects of electromagnetic forces, energy radiation, and discharge losses on design of superconducting coils for energy storage elements
10 p1109 N73-19043
Performance tests of electric batteries to determine effect of negative limited cell on battery service life
[NASA-CR-130932] 10 p1111 N73-19060
RF stacking in ISABELLE
[BNL-17274] 10 p1193 N73-19709
Design of repetitively pulsed inductive energy storage systems
[AD-755359] 14 p1606 N73-23014
Weight optimization for energy storage, coil, cryogen, and dewar
[AD-755360] 17 p1986 N73-26054
Proton energy spectra analysis of solar flare for determining altitude limitations on coronal particle storage
19 p2338 N73-28807
Energetic particle storage in solar corona
19 p2338 N73-28809
Development of stored charge device using field effect transistor technology
[NASA-CASE-NPO-11156-2] 22 p2617 N73-30974
Problems and applications of superconductive energy storage
[NASA-TT-F-15109] 22 p2707 N73-31676
Energy storage in electronically excited solid helium
[NASA-CR-135716] 23 p2820 N73-32541
Analog measurement of useful energy stored in thermocollector several years
24 p2974 N73-33766

**ENERGY STORAGE DEVICES**

U ENERGY STORAGE

**ENERGY TRANSFER**

Operation of plasma accelerator in quasi-steady mode to determine ratio of energy deposition into kinetic and thermal modes
[NASA-CR-128408] 01 p0035 N73-10275
Calculation of hydromagnetic wave induced energy transfer in solar wind
01 p0094 N73-10777
Two fluid, solar wind model of energy transfer
01 p0095 N73-10782
Low energy electron impact excitation and ionization rate coefficients for atmospheric nitrogen and oxygen
[AD-747244] 02 p0170 N73-11378
Energy transfers and transformations in atmosphere and chemical tracers of atmospheric circulation
[TID-25731] 03 p0295 N73-12410
Design of coils and switches for superconducting magnetic energy storage and transfer
[LA-DC-72-470] 03 p0345 N73-12816
Charged particle energy deposition calculations for radiobiological system
[ORO-3798-52] 04 p0380 N73-13090
Vibrational energy transfer in gas lasers
[AD-748858] 04 p0387 N73-13143
Numerical analysis of Langmuir wave spectra development in turbulent plasma
[JINR-P9-6432] 04 p0455 N73-13712
Energy transfer in laminar hypersonic boundary layers by hydrogen combustion
07 p0771 N73-16260
Energy exchange between earth and space from meteorological satellite measurements of infrared radiant emittance and reflected and scattered solar radiation
[NASA-CR-130152] 07 p0780 N73-16341
Polystyrene energy transfer studies using nitrostyrene compounds
[TN-257] 09 p0999 N73-18149
Charge transfer cross sections of alkali metals
[AD-752909] 09 p1000 N73-18161
Simulation of monthly variation of local surface energy budget and sub-surface temperature regime in Antarctica
10 p1146 N73-19326
RF stacking in ISABELLE
[BNL-17274] 10 p1193 N73-19709
Energy transfer and behavior of field along biconical antenna
[AD-754386] 11 p1263 N73-20246
Kinetic energy transfer in multiple jet mixing flow of duct inlet
[AD-758836] 16 p1891 N73-25305
Energy exchange characteristics of desert, meadow, forest, and marsh sites
[PB-218825/8] 18 p2173 N73-27550
Analysis of thermodynamic conditions for rapid start up of high temperature, gas loaded heat pipe
[NASA-TM-X-2840] 18 p2205 N73-27800
Energy transfer reactions of electronically excited atomic and diatomic specspecies
[AD-762201] 19 p2298 N73-28481
Evaluation of statistical energy analysis methods for vibrating structures
[NASA-CR-124322] 19 p2349 N73-28890
Principles of energy transformation in atmospheric circulation
20 p2443 N73-29622
Spin energy transfer processes at low temperatures
[AD-762618] 20 p2455 N73-29731
Energy transfer by fluctuations in plasma
20 p2457 N73-29743
Interactions between rare earth ions in yttrium compound crystals
[AD-762363] 20 p2463 N73-29793
Chemical and energy transfer reactions in hydrogen fluoride chemical laser system
[AD-763715] 21 p2556 N73-30491
Energy transfer control and compressor bleed concepts of remote lift fan control
[NASA-TM-X-2863] 21 p2590 N73-30749
Steady state analysis of energy transfer control and compressor concepts of remote lift fan control
[NASA-TM-X-2876] 21 p2590 N73-30753
Statistical study of nonlinear energy transfer interactions in turbulence models
22 p2649 N73-31224
Strategy of space research
[NASA-TT-F-15120] 22 p2716 N73-31745
Energy transfer in methyl fluoride
23 p2824 N73-32575
Vibrational energy transfer between connected substructures under random excitation
[NASA-CR-124450] 24 p2988 N73-33878

**ENGINE CONTROL**

NT TURBOJET ENGINE CONTROL
Dynamics and control analysis of turbofan lift engines
[NASA-TM-X-68175] 06 p0713 N73-15815
Relation between invariance conditions and characteristics of turbojet engine with afterburner multidimensional control system under variable flight conditions
[AD-749656] 06 p0714 N73-15828
Application of integrated circuit technology and digital computer techniques to electric control of jet engines
[NAL-TR-281] 09 p1078 N73-18799
Development of electro-hydrofluidic transducer for control of turbine engines
[AD-762298] 19 p2330 N73-28745
Development and characteristics of system for integrated control of engine power and aerodynamic configuration of aircraft during landing approach
[NASA-CASE-ARC-10456-1] 22 p2613 N73-30938

**ENGINE COOLANTS**

Turbulent, transitional, and laminar film cooling of air breathing engine inlet at hypersonic speed noting heat transfer rate measurement
[IC-AERO-72-15] 01 p0041 N73-10323

**ENGINE DESIGN**

NT ROCKET ENGINE DESIGN
Technology for developing hydrogen-oxygen thruster for space shuttle ACPS
[NASA-TM-X-68146] 01 p0090 N73-10744

Operational procedure for computer program to calculate design point characteristics of gas generator or turbojet lift engine for V/STOL applications
[NASA-TM-X-2656] 02 p0222 N73-11794
Design, development, and evaluation of turbine for small, low-cost turbofan engine
[NASA-TM-X-68157] 02 p0223 N73-11803
Development of closed cycle, vortex stabilized nuclear lightbulb engine to show basic design concepts and operating principles
[NASA-CR-129298] 03 p0330 N73-12695
Design and performance characteristics of small scale model of nuclear lightbulb engine for testing in nuclear furnace reactor
[NASA-CR-129296] 03 p0331 N73-12697
Performance, stability, and design of aerospike engines and engine system components
[NASA-TM-X-64690] 03 p0348 N73-12840
Design of high frequency mercury ion engine for application to communication satellite stationkeeping
[DGLR-PAPER-72-88] 03 p0351 N73-12861
Reaction engines with shrouded nozzles, reaction engines for boats, and thermodynamics of hot air bubble cooling in liquid
[JPRS-57308] 04 p0404 N73-13292
Direct reaction engines for water surface vessels, using admixture of air and outboard water
04 p0404 N73-13295
Design studies for integral lift, high bypass ratio fan engine using Lycoming 502 core and MQT power turbine, for advanced commercial V/STOL aircraft
[NASA-CR-120992] 04 p0426 N73-13471
Analysis of factors affecting cooling of liners in gas turbine combustion chambers
[NAL-TR-196] 06 p0713 N73-15819
Fabrication and performance of real-time jet engine simulator for development of jet engine components and control systems
[NAL-TR-283] 06 p0713 N73-15820
Applicability of composite materials in aircraft structure and engine design
[NASA-TT-F-14648] 07 p0811 N73-16576
Performance tests to determine effects of reducing turbine blade thickness on turbine engine performance
[NASA-TN-D-7128] 07 p0836 N73-16776
Design principles of gas turbine and piston engines for commercial aircraft
[AD-751510] 07 p0837 N73-16783
Engine cycle, configuration, and design requirements
[NASA-CR-120970-VOL-2] 10 p1106 N73-19019
Design and fabrication of fiberglass, graphite, and maraging steel composite motor cases
[AD-753959] 10 p1176 N73-19569
Characteristics and applications of computer codes for determining weight, center of gravity, and inertia of nuclear engine for rocket vehicles
[TID-26022] 10 p1186 N73-19652
Analysis of requirements for turbofan engines for high speed commercial transport aircraft - Vol. 1
[NASA-CR-121132] 10 p1207 N73-19820
Preliminary design assessment of turbofan engines for installation on high speed commercial transport aircraft - Vol. 2
[NASA-CR-121133] 10 p1207 N73-19821
Propulsion system requirements for aircraft engines installed in high speed commercial transport aircraft - Vol. 3
[NASA-CR-121134] 10 p1207 N73-19822
Development of techniques for reducing exhaust emissions from turbine engines
[NASA-TM-X-68192] 10 p1208 N73-19824
Design and performance of gas turbines for hydrofoils
[AD-753890] 11 p1334 N73-20830
Design and performance of nuclear rocket engine
[LA-5057] 12 p1428 N73-21570
Elements, units and characteristics of solid rocket engines
[AD-755411] 12 p1444 N73-21697
Modifications of fuel control units in aircraft gas turbine engines for reducing production costs
[NASA-TM-X-68229] 13 p1571 N73-22729
Information and guidance for type certification of aircraft engines as required by Federal Aviation Administration
[FAA-AC-33-2A] 13 p1571 N73-22730
Engine interface control for coordinating engine and component design activities
[NASA-CR-132215] 15 p1809 N73-24665
Summary of engine design and analytical studies to mature 1137400E engine baseline
[NASA-CR-132230] 15 p1810 N73-24667
Mathematical model for radiation analysis and shielding for 1137400E NERVA engine
[NASA-CR-132228] 15 p1810 N73-24668
Simple performance calculation method for LH2/LOX engines with different cycles
[NASA-TM-X-64749] 15 p1824 N73-24786
Design parameters of space propulsion ramjet engine using plasma accelerator
[AD-759290] 16 p1958 N73-25840
Preliminary design analysis of quiet integral fan lift engines for VTOL transport applications in next decade
[NASA-CR-120969] 17 p2076 N73-26796
Design, materials, fabrication, and testing in DART thruster technology development
[LA-5017-MS] 17 p2077 N73-26802
Proceedings of conference on application of composite materials in construction of aerospace vehicles and propulsion systems
[AGARD-CP-112] 18 p2163 N73-27474
Application of reinforced composite materials for construction of aeronautical gas turbine engines
18 p2165 N73-27490
Production of lamellar and fibrous composite materials from directional solidification of eutectic alloys and application to gas turbine blades and vanes
18 p2166 N73-27492
Application of directionally solidified eutectics for design and construction of gas turbine engines
18 p2166 N73-27493
Directional solidification of eutectic alloys and application to turbine blades and gas turbine engine components
18 p2166 N73-27494
Design of gas turbines for furnishing hot gases for turbine drives and analysis of limitations imposed by thermal stresses
[NASA-SP-8081] 18 p2193 N73-27705
Performance data for three turbofan engine configurations with noise reduction features tested over range of flight conditions
[NASA-CR-121258] 18 p2193 N73-27707
Natural environment design requirement for solar electric power stage based on radiation atmospheric conditions at orbital altitudes
[NASA-TM-X-64761] 18 p2193 N73-27708
Development, characteristics, and performance of ion thruster engine for attitude control and stationkeeping of synchronous satellite
[NASA-CR-121183] 19 p2329 N73-28736
Development of turbine engine accessory drive techniques to establish potential systems for lightweight low profile package
[AD-761527] 19 p2330 N73-28741
Structural analysis of mechanical rhombic drives for machines operating on Stirling cycle
[AD-761594] 19 p2330 N73-28749
Performance tests of annular combustor designed for use in low cost turbojet engine
[NASA-TM-X-2857] 19 p2352 N73-28918
Development and characteristics of hydrogen-oxygen power unit for application to onboard systems of space shuttle orbiter vehicle
[NASA-TM-X-68262] 20 p2363 N73-29005
Gaseous propellant combustion and injector/chamber design guidelines
[NASA-CR-121234] 20 p2464 N73-29799
Influence of noise requirements on STOL propulsion systems design
[NASA-TM-X-68280] 20 p2465 N73-29807
Performance of 30 cm ion thrusters with dished accelerator grids
[NASA-TM-X-68294] 21 p2589 N73-30744
Analysis of various mixed cycle engines and impact of component choices on application of propulsion system
21 p2590 N73-30747
Modification of Olympus turbojet engine to meet supersonic civil transport requirements
21 p2590 N73-30752
Transonic jet engine for ingesting air without compressor
[AD-763173] 21 p2591 N73-30756
Analysis of factors affecting combustion performance requirements of gas turbine engines and methods for improving gas turbine operation
21 p2606 N73-30882
Similitude theory for design optimization of automatic control systems for aircraft gas turbine engines
[AD-764683] 23 p2832 N73-32631
Design and development of quiet, clean propulsion systems for short takeoff aircraft with emphasis on engine noise reduction
24 p2875 N73-32961
Fabrication and evaluation of composite thermal engine insulation
[NASA-CR-124457] 24 p2938 N73-33458
Basic problems of liquid fueled rocket engines
[JPRS-60208] 24 p2972 N73-33745
Design characteristics of solid propellant rocket engines
24 p2972 N73-33746
Performance calculation of arbitrarily switched gas turbines by simulation with building block system on digital computer
24 p2973 N73-33758

**ENGINE FAILURE**

Influence of inlet distortions on turbojet and ingestion engine stability
[AD-745852] 01 p0092 N73-10755
Inflight incident involving number two engine failure on DC 10 aircraft near Tucson International Airport, Arizona on 2 May, 1972
[NTSB-AAR-72-29] 03 p0251 N73-12035
Investigation of aircraft accident involving Beech aircraft performing air taxi service to Boise, Idaho on 20 Feb. 1972
[NTSB-AAR-72-25] 03 p0253 N73-12050
Effect of engine failure on aerodynamic characteristics of supersonic aircraft
08 p0865 N73-17003
Statistical analysis of engine failure/malfunction accidents for US fixedwing aircraft of general aviation category during 1965 to 1969
[NTSB-AAS-72-10] 10 p1106 N73-19015
Performance tests on J-52 turbojet engines to determine acceptable compressor stall margin
[AD-755152] 11 p1334 N73-20832
Analysis of steady-state and dynamic pressure conditions in F-111 aircraft engine to determine causes of engine compressor stalls
[NASA-TN-D-7328] 20 p2465 N73-29806

**ENGINE INLETS**

Wind tunnel tests to determine structural integrity of birds under conditions simulating ingestion of birds into inlets of high speed aircraft
[NASA-TM-X-68163] 06 p0629 N73-15114
Analysis of internal flow conditions of inlet with centerbody retracted for short takeoff and landing aircraft takeoff and approach operations
[NASA-TN-D-7185] 09 p0980 N73-18010
Application of optimal control theory to design of control system for supersonic inlet of turbojet engine
[NASA-TN-D-7188] 09 p1079 N73-18803
Suppression of turbine engine inlet noise
[AD-753000] 09 p1079 N73-18806
Effect of inlet-air humidity on formation of oxides of nitrogen from a gas turbine combustor under various air inlet temperature conditions
[NASA-TM-X-68209] 12 p1443 N73-21691
Wind tunnel tests to determine effect of tip vortex of forward mounted wing on engine inlet ingestion
[NASA-TM-X-68225] 13 p1473 N73-21932
Performance tests of terminal shock and restart control system of two dimensional twin-duct compression inlet
[NASA-TM-X-2818] 16 p1956 N73-25824
Program summary of research project for sonic inlet technology involving design concepts for aerodynamic performance and noise suppression - Vol. 1
[NASA-CR-121126] 19 p2328 N73-28731
Research project for noise suppression of sonic inlets used with turbofan engines and improvement in engine inlet flow characteristics - Vol. 2
[NASA-CR-121127] 19 p2328 N73-28732
Analysis of internal noise field of two axisymmetric sonic inlet models for noise suppression of turbofan engine inlets - Vol. 3
[NASA-CR-121128] 19 p2329 N73-28733
Method to increase full-scale inlet/engine system testing capability of AEDC 16-ft transonic wind tunnel
[AD-762912] 20 p2383 N73-29146
Development of computer programs for designing engine inlets for VTOL and STOL aircraft based on axisymmetric potential flow parameter
[NASA-TM-X-68278] 20 p2388 N73-29182
Analysis of intake duct noise of turbofan engine and effect on duct structure due to acoustic fatigue
20 p2479 N73-29916
Computer solutions for potential and viscous flow calculations for engine inlets
[NASA-TM-X-71457] 24 p2905 N73-33184
Characteristics of variable geometry high Mach inlet concepts to reduce jet engine noise on subsonic, long range commercial aircraft
[NASA-CR-134495] 24 p2972 N73-33748

**ENGINE NOISE**

Conference on reduction and suppression of aircraft engine noise
[NASA-SP-311] 03 p0249 N73-12012
Structural changes in high bypass ratio engines for fan noise reduction to jet noise level
03 p0249 N73-12017
Noise output of turbofan engine with acoustically treated nacelle
03 p0250 N73-12020
Noise output from quiet engine during simulated takeoff and approach tests
03 p0250 N73-12021
Research project to analyze and evaluate supersonic jet noise generation and radiation - Vol. 1
[AD-749428] 05 p0495 N73-14035
Definition of supersonic aircraft jet noise generation and methods for reducing noise intensity - Vol. 2
[AD-749137] 05 p0495 N73-14036
Development of unified theory of jet engine noise based on fluctuating motions in fluids - Vol. 3
[AD-749138] 05 p0496 N73-14037
Development of theory for jet noise generated by turbulence, noise radiation from upstream sources, and combustion noise - Vol. 4
[AD-749139] 05 p0496 N73-14038
Analysis of noise sources associated with supersonic jet noise and establishment of effects of refraction on radiated field of sources - Vol. 5 App. 1
[AD-749141] 05 p0496 N73-14039
Development of remote sensing devices to measure jet exhaust fluctuating density gradients, mean and turbulent velocity, and mean temperature Vol. 6
[AD-749143] 05 p0496 N73-14041

Analysis of jet noise produced by supersonic transport aircraft with augmentor wing and four duct burning turbofan engines
[NASA-TM-X-68177] 06 p0619 N73-15028
Effect of sound absorbing exhaust duct on rear quadrant noise of J-65 engine and contributions of internal and jet components
[NASA-TM-X-2718] 07 p0739 N73-16011
Suppression of turbine engine inlet noise
[AD-753000] 09 p1079 N73-18806
Analysis of aircraft noise environment for land areas in vicinity of military air bases
[AD-754111] 10 p1107 N73-19028
Analysis of parameters affecting choice of engines for transport and combat aircraft during design process
15 p1732 N73-24048
Performance data for three turbofan engine configurations with noise reduction features tested over range of flight conditions
[NASA-CR-121258] 18 p2193 N73-27707
Modifications of turbojet engine with ejector to reduce jet engine exhaust noise
[NASA-TM-X-2841] 19 p2217 N73-27887
Analysis of acoustic properties and aerodynamic characteristics of engine over wing configuration with flow attached and unattached on upper surface of flaps
[NASA-TM-X-71419] 21 p2494 N73-30015
Development of computer programs to analyze sound power and peak noise levels for turbojet exhaust noise at various velocities
21 p2496 N73-30029
Diagnostic techniques for measurement of aerodynamic noise in free field and reverberant environment of wind tunnels
[NASA-CR-114636] 21 p2579 N73-30669
Analysis of aircraft engine noise sources and characteristics of engine noise produced by turbofan engines
21 p2588 N73-30735
Design and characteristics of expansion chamber mufflers for reducing exhaust noise generated by helicopters
[NASA-TN-D-7309] 22 p2700 N73-31623
Scaling laws to predict supersonic jet noise generated by rectangular and axisymmetric nozzles
[PB-221855/0] 22 p2700 N73-31629
Acoustic tests of supersonic tip speed fan with acoustic treatment and rotor casing slots and its performance in reducing engine noise
[NASA-CR-134501] 23 p2828 N73-32608
Noise comparison of two STOL pressure ratio fans with 15 and 42 rotor blades
[NASA-TM-X-2891] 23 p2829 N73-32609
Effect of noise constraints on engine cycle optimization for long-haul transports
[NASA-TM-X-71447] 23 p2830 N73-32620
Analysis of jet engine noise to show sources of noise, noise spectra, and use of laminates and composite materials for noise reduction
24 p2875 N73-32962
Characteristics of variable geometry high Mach inlet concepts to reduce jet engine noise on subsonic, long range commercial aircraft
[NASA-CR-134495] 24 p2972 N73-33748

**ENGINE PARTS**

Wide Temperature range, nonpolymeric, large molecular weight lubricants based on combination of siloxane and aromatic groups, for equipment near spacecraft nuclear reactors
[NASA-CR-123966] 04 p0447 N73-13654
Components and performance of solid propellant rocket engines
[AD-752865] 08 p0956 N73-17823
Performance of aircraft gas turbine components in hot corrosion environments
14 p1676 N73-23599
Chemical and mechanical properties of aircraft gas turbine engine components
14 p1676 N73-23600
Photoelastic stress analysis of NERVA structures
[NASA-CR-132213] 15 p1810 N73-24673
Manufacturing processes for aircraft engine parts
[AD-759577] 16 p1958 N73-25837
Adhesive bonding of structures and composite materials on advanced turbofan engines
23 p2810 N73-32470

**ENGINE STARTERS**

Motor starting characteristics of Brayton electric engine using static inverter
[NASA-TM-X-2738] 09 p0990 N73-18080

**ENGINE TESTING LABORATORIES**

Cesium engine testing laboratories at ONERA, France
[ONERA-NT-21/6046-SNE] 05 p0524 N73-14263
Bench testing ducted fan engines under conditions close to those of flight
[AD-742376] 13 p1505 N73-22198
Design of test facility for turbofan engines at subsonic operation
[AD-757197] 14 p1646 N73-23352

**ENGINE TESTS**

NT COLD FLOW TESTS

Aerodynamic component test results of Fan C, high-bypass-ratio, low-aerodynamic loading, single stage fan
[NASA-CR-120981] 02 p0222 N73-11799
Pulse performance data for small monopropellant and hypergolic bipropellant rocket engines
03 p0349 N73-12846
Optimization of engines for commercial Mach 0.85 transport using advanced turbine cooling methods
[NASA-TM-X-68173] 06 p0619 N73-15029
Fabrication and acceptance tests of FLOX/MMH engine assemblies
[NASA-CR-130288] 06 p0712 N73-15814
Fabrication and evaluation of cooled-gas pyrometer for application in hypersonic research engine program
[NASA-TM-X-2715] 07 p0800 N73-16496
Motor starting characteristics of Brayton electric engine using static inverter
[NASA-TM-X-2738] 09 p0990 N73-18080
Development of standard uncertainty methology for analysis of gas turbine engine performance characteristics
[AD-755356] 13 p1571 N73-22733
Application of three dimensional analysis techniques for determining operating characteristics of axial turbines
15 p1824 N73-24785
Test parameters and methods used in Soviet Union for jet engines
[AD-760963] 18 p2194 N73-27714
Durability test of five cm diameter ion thruster for 9700 hours
[NASA-TM-X-68284] 21 p2589 N73-30741
Regeneratively cooled rocket engine tests with space storable propellants
[NASA-CR-133915] 22 p2708 N73-31688

**ENGINEERING**

Research facilities, and educational and research programs of Institute of Industrial Science, University of Tokyo
01 p0035 N73-10277
Utilization of ERTS-1 multispectral photography in evaluating Iranian playas as potential locations for economic and engineering development
[E72-10270] 03 p0291 N73-12369
Application of ERTS-1 MSS imagery to coastal engineering planning and construction
[E73-10050] 07 p0777 N73-16312
Utilization of ERTS-1 imagery for evaluation of Iranian playas as potential locations for economic and engineering development
[E73-10067] 07 p0779 N73-16329
Development of land use-peak runoff classification system for highway engineering in Maryland
[E73-10100] 08 p0902 N73-17310
Surface properties and gas-solid interface phenomena in engineering materials
[AD-753099] 09 p1000 N73-18165
Civil engineering in Arctic regions using dual channel infrared scanner and infrared photography
[AD-753048] 09 p1037 N73-18461
Training of scientists and engineers for German Department of the Defense
11 p1351 N73-20965
Advantages and disadvantages of using computers in engineering linguistics
[JPRS-59397] 18 p2213 N73-27870
Utilization of Skylab EREP data for highway engineering in Maine
[E73-10909] 20 p2397 N73-29258
Evaluation of Iranian playas as potential locations for economic and engineering development
[E73-11026] 22 p2662 N73-31330
Scientific research projects in engineering, chemistry, and social sciences
23 p2859 N73-32844

**ENGINEERING DEVELOPMENT**

U PRODUCT DEVELOPMENT

**ENGINEERING DRAWINGS**

Space technology for solving materials and design problems of earthbased housing
04 p0474 N73-13868
Preliminary design drawings of expendable second stage reusable space shuttle booster to define specific payloads and configurations - Vol. 7
[NASA-CR-128662] 05 p0599 N73-14873
Application of ANSI Y14.5 rules to designing connectors for interchangeability
14 p1641 N73-23309
Development of automated drafting and digitizing system for preparing concept, experimental, prototype, and production mechanical drawings
[AD-755502] 14 p1671 N73-23558

**ENGINEERING MANAGEMENT**

Advanced NASA and DOD technology management techniques, and application to NATO programs for defense and civil needs
06 p0732 N73-15968
Analysis of NASA programs during post-Apollo period to show organization of field centers, planning activities, operational activities, and resources utilization
[NASA-CR-131931] 12 p1466 N73-21879

Application of ERTS-1 imagery and aerial photography to missions of US Corps of Engineers
19 p2289 N73-28400
Engineering procedures, blasting, and water level regulation for flood prevention and ice jam control on Daestr and Dubossary Reservoirs
21 p2573 N73-30620
Analysis of current operations concepts of NASA and DoD to improve utilization of resources
[NASA-CR-135705] 23 p2844 N73-32729

**ENGINES**

NT AIR BREATHING ENGINES
NT AJ-10 ENGINE
NT ARC JET ENGINES
NT BOOSTER ROCKET ENGINES
NT CESIUM ENGINES
NT CF-700 ENGINE
NT DIESEL ENGINES
NT DUCTED FAN ENGINES
NT ELECTRIC ROCKET ENGINES
NT ELECTROSTATIC ENGINES
NT ELECTROTHERMAL ENGINES
NT GAS TURBINE ENGINES
NT HELICOPTER ENGINES
NT HYBRID PROPELLANT ROCKET ENGINES
NT HYDRAZINE ENGINES
NT HYDROGEN OXYGEN ENGINES
NT INTERNAL COMBUSTION ENGINES
NT ION ENGINES
NT J-2 ENGINE
NT J-52 ENGINE
NT J-57 ENGINE
NT J-58 ENGINE
NT J-65 ENGINE
NT J-75 ENGINE
NT J-85 ENGINE
NT JET ENGINES
NT LIQUID PROPELLANT ROCKET ENGINES
NT LITHERGOL ROCKET ENGINES
NT NUCLEAR ENGINE FOR ROCKET VEHICLES
NT NUCLEAR LIGHTBULB ENGINES
NT NUCLEAR ROCKET ENGINES
NT PISTON ENGINES
NT PLASMA ENGINES
NT PULSEJET ENGINES
NT RAMJET ENGINES
NT RESTARTABLE ROCKET ENGINES
NT RETROROCKET ENGINES
NT REUSABLE ROCKET ENGINES
NT ROCKET ENGINES
NT SOLID PROPELLANT ROCKET ENGINES
NT SUPERSONIC COMBUSTION RAMJET ENGINES
NT TF-34 ENGINE
NT TURBINE ENGINES
NT TURBOFAN ENGINES
NT TURBOJET ENGINES
NT TURBOPROP ENGINES
NT UPPER STAGE ROCKET ENGINES

Design, development, and evaluation of solar electric thrust vector control system for ion engine array
[NASA-CR-130622] 08 p0953 N73-17806
Calculation of heat removed by gas refrigerators and heat engines
[AD-762261] 19 p2306 N73-28544
Optimal engine selection for ground support equipment
[AD-763663] 21 p2591 N73-30757

**ENGLAND**

Cartographic evaluation of ERTS-1 imagery for area of Bristol, England to show natural and man-made features
[E73-10739] 17 p2021 N73-26345

**ENGLISH ELECTRIC AIRCRAFT**

NT CANBERRA AIRCRAFT

**ENGLISH ELECTRIC CANBERRA AIRCRAFT**

U CANBERRA AIRCRAFT

**ENGLISH LANGUAGE**

English, French, and Spanish vocabulary of aircraft aeronautical terminology
[DOC-8800-VOL-1] 06 p0616 N73-14996
Elastic matching, automatic error correction in English language words of any length
[NPL-COM-SCI-63-SUPPL.] 18 p2121 N73-27144

**ENGRAVING**

Fabricating miniature fluidic elements using photochemical engraving
04 p0426 N73-13472

**ENHANCEMENT**

U AUGMENTATION

**ENLARGING**

U EXPANSION

**ENTHALPY**

Calorimetric analysis of low temperature heat capacities and high temperature enthalpies for sodium chromate
[BM-RI-7691] 05 p0605 N73-14924
Enthalpy values for reaction of retarding mononucleotides with ribonuclease and thermodynamic parameters for enzyme inhibitor interactions
[FMVG-FBWT-72-12] 07 p0747 N73-16073

Values for standard heats and Gibbs free energies of formation, entropies, and enthalpies for rare earth elements
[NBS-TN-270-7] 14 p1616 N73-23092
Experiments in shock tunnel driven MHD generator designed for high enthalpy extraction
[AD-757771] 15 p1819 N73-24741
Atomic oxygen reaction with nickel at elevated temperatures
[NASA-TM-X-62295] 20 p2431 N73-29524
High enthalpy hypersonic bounary layer flow
[NASA-CR-135479] 23 p2774 N73-32187

ENTOMOLOGY
Investigation of oribatid mites found in Antarctic regions during Tenth Soviet Antarctic Expedition
20 p2407 N73-29349

ENTRAINMENT
Asymptotic expansion analysis of jet entrainment in incompressible cross flow
24 p2902 N73-33166

ENTRENCHED STREAMS
U STREAMS

ENTROPY
Analysis of entropy rate admissibility criterion for solutions of hyperbolic conservation laws
[NASA-CR-129594] 04 p0484 N73-13956
Calculation of heat transfer on shuttle type configurations including effects of variable entropy at boundary layer edge
[NASA-CR-112180] 04 p0484 N73-13958
Phase transition and entropy behavior of solid He-3
[COO-1569-96] 12 p1439 N73-21654
Entropy rate admissibility criterion for solutions of hyperbolic conservation laws
[NASA-CR-131812] 13 p1513 N73-22261
Values for standard heats and Gibbs free energies of formation, entropies, and enthalpies for rare earth elements
[NBS-TN-270-7] 14 p1616 N73-23092
Formulation of second law of thermodynamics for system in thermal nonequilibrium by assumption of relationship between entropy and temperature
[AD-759970] 17 p2097 N73-26964
Development of entropy coded adaptive differential pulse code modulation systems for speech signals
[AD-762606] 20 p2378 N73-29109
Entropy problem in passive networks
[AD-763752] 21 p2520 N73-30209

ENVIRONMENT EFFECTS
Utilization of ERTS-1 imagery of Alabama to study environmental factors, land use, and geology
[E72-10319] 05 p0530 N73-14310
Effect of friction and external environment on fatigue strength of medium C steels
[AD-749749] 05 p0564 N73-14580
Environmental and ecological effects of coal strip mining in Ohio
[E73-10003] 06 p0658 N73-15339
Environmental factors affecting OAO and related computer programs for data processing and scheduling observations
[NASA-TM-X-66145] 06 p0721 N73-15882
Conference on environmental, social, economic, and ecological effects of nuclear electric power generation
[TID-25857] 07 p0793 N73-16450
Environmental and ecological impact of construction and filling of reservoir on Sangamon River in Illinois
[E73-10082] 08 p0901 N73-17294
Development of standards for classification, mapping and scientific analysis of land use and land use change in Central Atlantic Region Ecological Test Site using ERTS-1 imagery
[E73-10347] 10 p1148 N73-19346
Environmental and ecological impact of construction and operation of Oakley Dam and Friends Creek impoundment located on Sangamon River in East Central Illinois
[E73-10484] 12 p1396 N73-21321
Environmental effects and plans for controlling urban TACV noise levels
13 p1506 N73-22209
Mapping of coastal sedimentation and related processes in Cook Inlet, Alaska and distribution and environmental interrelationships of permafrost terrain
[E73-10421] 13 p1515 N73-22275
Effects of environmental stresses on materials used in constructing glide reentry vehicles
14 p1676 N73-23601
Estimates of cost of air pollution damage
[AP-85] 14 p1685 N73-23669
Environmental and ecological impact of construction and operation of Oakley Dam and Friends Creek impoundment located on Sangamon River in East Central Illinois
[E73-10655] 16 p1898 N73-25351
Application of Skylab EREP imagery to fracture-related mine safety hazards and environmental problems in mining
[E73-10802] 18 p2138 N73-27277
Environmental factors influencing Canadian industrial growth
[DRAE-34] 18 p2207 N73-27815
Linking land use and environmental processes in Central Atlantic Region using ERTS-1 data
[PAPER-L7] 19 p2274 N73-28303
Environmental and ecological impact of construction and operation of Oakley Dam and Friends Creek Impoundment located on Sangamon River in East central Illinois
[E73-10882] 20 p2394 N73-29233
Environmental and ecological impact of major construction of reservoirs in Illinois
[E73-10892] 20 p2395 N73-29241
Direct and indirect environmental factors affecting functional state of operators
21 p2503 N73-30084
Environmental and medical problems caused by nonionizing radiation
[PB-220851/0] 21 p2509 N73-30134
Environmental effects on headform cavitation inception
[AD-763367] 21 p2527 N73-30261
Environmental factors in production and use of energy and effects on air, water, and land
[R-992-RF] 21 p2537 N73-30340
Fatigue life and fracture toughness of 7075-T6 Al alloy in vacuum and air environments
[NASA-TN-D-7262] 23 p2805 N73-32431
Effect of construction and staged filling of Oakley Dam and Friends Creek impoundment in Illinois on environment and ecology
[E73-11124] 24 p2916 N73-33279
Proceedings of Second Conference on Climatic Impact Assessment Program, November 14-17, 1972
[PB-221166/2] 24 p2924 N73-33357

ENVIRONMENT MANAGEMENT
Application of ERTS-1 data to management and protection of New Jersey coastal environment
[E73-10527] 14 p1654 N73-23415
Relevance of ERTS-1 imagery to land use, resources, and environment management in Ohio
[E73-10621] 15 p1775 N73-24382
Man and natural environment protection and management
[JPRS-59369] 18 p2110 N73-27064
Coordination and establishment of centralized facilities and services for University of Alaska ERTS-1 survey of Alaskan environment
[E73-10904] 20 p2396 N73-29253
Airport environment compatibility plan for Jackson, Tennessee
[PB-221129] 22 p2648 N73-31217
Coordination and establishment of centralized facilities and services for University of Alaska ERTS survey of Alaskan environment
[E73-11088] 24 p2913 N73-33250

ENVIRONMENT POLLUTION
NT AIR POLLUTION
NT WATER POLLUTION
Descriptions of Federal Government environmental research and development facilities
[PB-209751] 02 p0153 N73-11239
Inventory listing of Federal Government environmental research facilities
[PB-209752] 02 p0153 N73-11240
Aerial surveillance techniques for measuring gaseous environmental pollution from nuclear power plant
[WERLV-1] 03 p0334 N73-12721
Environmental pollution monitoring for radioactive isotope laboratory
[MLM-1922] 03 p0340 N73-12770
Application of remotely sensed, multispectral observations for assessment of earth resources and environmental quality in Alabama
04 p0471 N73-13841
Development of steps and procedures for determining and evaluating environmental quality through use of remote sensors
07 p0782 N73-16358
Detection, identification, measurement, and monitoring environmental pollution by remote sensing devices and techniques
07 p0786 N73-16397
Problems of environmental pollution and natural resource depletion caused by man
[JPRS-58113] 08 p0879 N73-17121
Effects of ground effect vehicle tests on ecology of arctic tundra in northern Alaska
[AD-751741] 10 p1107 N73-19026
Environmental factors and cost problems of selecting optimum sanitary landfill site for solid waste disposal
[NASA-CR-128744] 10 p1124 N73-19157
Application of nuclear and X ray techniques for analysis of environmental pollution samples
[CONF-721002-1] 10 p1161 N73-19443
Impact of radiometry and photometry on economic, social and environmental problems
[NBS-TN-594-4] 11 p1292 N73-20488
Control measures for preventing environmental beryllium contamination
[AP-116] 11 p1313 N73-20659
Environmental quality program, environmental forecasting program, and seabed assessment program for international decade of ocean exploration
12 p1400 N73-21359
Man induced changes in earth climate by environment pollution and heat production
[PB-213676/2] 14 p1613 N73-23074
Modification of Japan climate by environmental pollution
[AD-757487] 14 p1686 N73-23678
Development of environmental indices covering land, water, and air quality compatible with ERTS-1 imagery for two test sites in Pennsylvania
[E73-10709] 16 p1904 N73-25400
Guide for airport planning and development to identify and resolve environmental problems caused by air pollution, water pollution, and aircraft noise
[PB-219957/8] 18 p2127 N73-27187
Foreign reports on environmental pollution
[PB-218839/9] 18 p2148 N73-27360
Foreign reports on environmental pollution legislative, economic, and social aspects
[PB-218858/9] 18 p2148 N73-27361
Application of ERTS-1 imagery to determine ecological effects of strip mining in eastern Ohio
[PAPER-E2] 19 p2268 N73-28266
ERTS-1 investigations of environmental quality and pollution
19 p2290 N73-28409
ERTS-1 applications in land use, geologic interpretation, resources survey, and pollution monitoring
19 p2290 N73-28413

ENVIRONMENT PROTECTION
Application of remote sensing techniques for solution of ecological management problems
04 p0471 N73-13838
Research activities of Battelle Institute
07 p0856 N73-16942
Technology application team program
[NASA-CR-130990] 09 p1100 N73-18979
Application of ERTS-1 imagery to protection and management of New Jersey coastal environment
[E73-10330] 10 p1147 N73-19335
Application of ERTS-1 data to management and protection of New Jersey coastal environment
[E73-10527] 14 p1654 N73-23415
Man and natural environment protection and management
[JPRS-59369] 18 p2110 N73-27064
Analysis of ERTS-1 imagery of New Jersey coastal resources to assist in resource management and allocation of funds for environmental control
[PAPER-E9] 19 p2269 N73-28273
Analysis of erosion along Niigata Beach, and development of improved methods of erosion control based on ERTS-1 imagery
[PAPER-E14A] 19 p2270 N73-28278
Application of ERTS-1 for mapping California, identifying natural resources, and developing programs for environmental improvement
19 p2287 N73-28390
Solution to problem of endangered living space
[NRC-TT-1636] 20 p2371 N73-29057
Legal and administrative measures adopted by U.S.S.R. for protection of environment
[JPRS-59436] 20 p2486 N73-29971
System of legal protection for environment of U.S.S.R.
20 p2486 N73-29972
Normative acts relating to legal protection of natural areas in U.S.S.R.
20 p2487 N73-29973
Planning and supervision of production activities for purpose of protecting environment in U.S.S.R.
20 p2487 N73-29974
Supervision of use and protection of natural resources according to Soviet legislation
20 p2487 N73-29975
Atmospheric modeling and environmental protection needs for air pollution control
[UCRL-74249] 24 p2922 N73-33341

ENVIRONMENT SIMULATION
NT ALTITUDE SIMULATION
NT SPACE ENVIRONMENT SIMULATION
NT THERMAL SIMULATION
NT WEIGHTLESSNESS SIMULATION
Computerized simulation of artificial robot interaction behavior with complex environment
[NASA-CR-129526] 03 p0269 N73-12179
Lunar laser reflector specifications and fabrication, noting test equipment thermal control, and lunar environment simulation
05 p0558 N73-14529
Simulation of emission-dispersion of inert pollutant in lower atmosphere in industrial zones by numerical integration of conservation and pollutant flow equations
06 p0693 N73-15649
Procedures for simulating and studying effects of subgravity on subjects during laboratory experiments and space flight
[NASA-TT-F-14934] 15 p1761 N73-24267
Simulation studies and design of GARP Global Experiment
[NASA-TM-X-69613] 22 p2694 N73-31582
Users manual for photochemical smog simulation diffusion/kinetics code
[PB-220243/0] 22 p2697 N73-31600

ENVIRONMENT SIMULATORS
NT SOLAR SIMULATORS
NT SPACE SIMULATORS
Design and performance of photostat for simulating Mars environment
10 p1118 N73-19117
Human habitability data for zero gravity environmental architecture
[NASA-TM-X-69322] 15 p1744 N73-24135
Performance of neodymium-yag optical data transmission system and development of channel simulator
18 p2212 N73-27859
ENVIRONMENTAL CHAMBERS
U TEST CHAMBERS
ENVIRONMENTAL CONTROL
Economic analysis of reducing and controlling environmental noise
[PB-206726] 01 p0081 N73-10666
Radiation ecological aspects of environmental pollution and control for human safety
[EUR-4800-D-F-I-E-PT-2] 01 p0082 N73-10680
Bibliography on environmental monitoring for radioactivity
[ORNL-NSIC-101] 03 p0334 N73-12720
Control system design criteria to prevent air pollution from volatile fuel storage tank emission
[AD-748009] 03 p0350 N73-12854
Environmental control unit for damage control suit system for use during shipboard operations
[AD-749025] 04 p0384 N73-13125
Absorption cycle refrigeration system for environmental control of space station
[NASA-CR-123970] 05 p0598 N73-14859
Capabilities and limitations of man as element in closed loop control system under normal environmental conditions
06 p0629 N73-15107
Atmospheric control studies, emphasizing carbon dioxide problem
06 p0629 N73-15108
Isotope effects for environmental monitoring and control
[ORNL-IIC-39] 06 p0703 N73-15730
Remote sensing techniques for detection and prevention of Rocky Mountain spotted fever, Encephalitis, Malaria, and Red Tide environmental health problems
[NASA-CR-128727] 07 p0745 N73-16060
Medical concepts and functional management in NASA Environmental Health Program
08 p0872 N73-17056
Industrial hygiene, radiological health, and spacecraft sanitation studies in NASA Environmental Health Program
08 p0872 N73-17057
Conference on preventive medical and environmental control measures for NASA and aviation industry personnel management
[NASA-TM-X-69073] 08 p0873 N73-17064
Anhydrous ammonia for removing nitrogen dioxide from stack emission simulating hydrazine nitrogen tetroxide rocket fuel combustion exhaust
08 p0874 N73-17075
Environmentally controlled suit for working in sterile chamber
[NASA-CASE-LAR-10076-1] 11 p1249 N73-20137
Conservational and rational use of natural resources and wildlife to preserve biosphere environment
[JPRS-58429] 11 p1250 N73-20145
Control measures for preventing environmental beryllium contamination
[AP-116] 11 p1313 N73-20659
Occupational hazards and control measures to prevent air pollution from asbestos processing
[AP-117] 11 p1314 N73-20660
Mercury emission control systems for primary mercury facility and for chlor-alkali plant
[AP-118] 11 p1314 N73-20661
Guidelines for urban control of aircraft noise pollution
[PB-213020] 11 p1326 N73-20759
Interrelationships between energy, resources, and environment, conference summary
[PB-213031] 11 p1333 N73-20820
Congressional hearings on research and development of environmentally safe electric power production
11 p1352 N73-20976
Acute and subacute inhalation toxicity experiments with organic solvents, rocket propellants, and various hydrocarbons in confined environments
[NASA-CR-131675] 13 p1485 N73-22043
Effective land use of airport-incompatible areas through conversion planning from residential to compatible zones
[FAA-EQ-72-1] 13 p1594 N73-22926
Spacecraft advanced radiator design system program for environmental control in long duration space flights
[NASA-CR-128913] 14 p1719 N73-23946
Failure analysis and design criteria for transducers in Apollo environmental control systems
[NASA-CR-128921] 15 p1756 N73-24231
Analysis of energy separator for application to air conditioning system of E-8 aircraft
[AD-762590] 20 p2364 N73-29014
Solution to problem of endangered living space
[NRC-TT-1636] 20 p2371 N73-29057
Improved water and air quality and land use in Poland
20 p2487 N73-29977
Operational principles and functions of mnemonic diagrams in controlled system
21 p2503 N73-30083
Space shuttle environmental and thermal control/life support system
[NASA-CR-134009] 21 p2504 N73-30091
Dual stage check valve for cryogenic supply systems used in space flight environmental control system
[NASA-CASE-MSC-13587-1] 21 p2552 N73-30459
Environmental sanitation handbook for occupational medicine and health procedures at Kennedy Space Center
[NASA-TM-X-69522] 23 p2752 N73-32020
Spacecraft with artificial gravity and earthlike atmosphere
[NASA-CASE-LEW-11101-1] 23 p2847 N73-32750
Production of vegetables in arid zones using controlled solar greenhouses
24 p2975 N73-33768
ENVIRONMENTAL ENGINEERING
Application of remote sensing techniques for detecting environmental changes at and near earth surface
07 p0784 N73-16379
Development of computer program to optimize space shuttle environmental and thermal control life support system
[NASA-CR-128736] 08 p0964 N73-17883
Environmental engineering for conservation of ocean resources
[PB-212634] 11 p1290 N73-20467
Physiological adjustments to environmental factors
[AD-753913] 13 p1487 N73-22059
Application of ERTS-1 imagery and aerial photography to missions of US Corps of Engineers
19 p2289 N73-28400
Ergonomic solution to organizational problems of human living conditions and activities
21 p2502 N73-30080
Remote sensing techniques in Michigan for resource management and environmental protection in both public and private interests
[NASA-CR-135639] 23 p2785 N73-32282
Natural evironment criteria for high energy astronomy observatory
[NASA-TM-X-64784] 24 p2979 N73-33807
ENVIRONMENTAL INDEX
Application of Skylab and EREP imagery for uniform mapping of earth resources and environmental complexes
[E73-10706] 16 p1904 N73-25397
Development of environmental indices covering land, water, and air quality compatible with ERTS-1 imagery for two test sites in Pennsylvania
[E73-10709] 16 p1904 N73-25400
ENVIRONMENTAL LABORATORIES
Self contained automated primate research laboratory to study physiological effects of space environment weightlessness on monkeys
[NASA-CR-131642] 12 p1387 N73-21250
ENVIRONMENTAL QUALITY
NT WATER QUALITY
Development of automatic air sampling system
[RM-559] 04 p0420 N73-13428
Environmental indices covering land, water, and air quality compatible with ERTS-1 imagery
[E72-10330] 05 p0531 N73-14318
Impact of California Water Project on environmental quality and resources in southern California
05 p0537 N73-14368
Possibilities of assessing global environmental quality in relation to future prosperity of man, for Global Environmental Monitoring System
[BULL-10] 05 p0538 N73-14379
Particulate and gaseous pollutant data gathered during 1968 by national, state, and local air surveillance networks
[APTD-0978] 05 p0572 N73-14652
Role of NASA in area of environmental quality
[NASA-CR-133049] 16 p1907 N73-25426
Urban impact on areas of maximum environmental quality in Washington Metropolitan Area, 1971
[PB-214544/9] 16 p1977 N73-25993
Environmental impact of highway projects as determined by vehicle emission factors
[PB-219812/5] 18 p2174 N73-27557
ERTS-1 investigations of environmental quality and pollution
19 p2290 N73-28409
Solution of earth resources and environmental quality problems using ERT-1 MSS data
[E73-10899] 20 p2395 N73-29248
Polish environmental protection policy and materials for semiconductor radiation detectors
[JPRS-59523] 20 p2487 N73-29976
Land use change and environmental quality in urban areas, emphasizing flood plains and wetlands
[PB-220742/1] 22 p2669 N73-31382
ENVIRONMENTAL RESEARCH SATELLITES
Cloud data for November and December 1972, obtained by environmental satellite imagery
18 p2171 N73-27536
Photographic recordings and meteorological data obtained by Environmental Research Satellite during January 1973
20 p2475 N73-29879
Photographic recordings and meteorological data obtained by Environmental Research Satellite During June 1973
20 p2475 N73-29880
ENVIRONMENTAL SURVEYS
Assessment of technology for environmental impact studies
[AD-754458] 13 p1527 N73-22376
Environmental impact of noise produced by transonic wind tunnel at Arnold Engineering Development Center
[AD-757552] 14 p1646 N73-23351
Regional environmental impact from oil shale development on private and public lands in Wyoming, Colorado, and Utah - Vol. 1
[EIS-AA-72-5242-D-1-VOL-1]
20 p2410 N73-29367
Energy alternatives to prototype oil shale leasing program for Wyoming, Colorado, and Utah - Vol. 2
[EIS-AA-72-5242-D-2-VOL-2]
20 p2410 N73-29368
Description of proposed leases for oil-shale program in Wyoming, Utah, and Colorado, and potential environmental impacts - Vol. 3
[EIS-AA-72-5242-D-3-VOL-3]
20 p2410 N73-29369
Remote sensing methods for earth observation missions by aircraft and satellites
22 p2736 N73-31900
ENVIRONMENTAL TEMPERATURE
U AMBIENT TEMPERATURE
ENVIRONMENTAL TESTS
NT COLD WEATHER TESTS
NT CORROSION TESTS
NT HIGH TEMPERATURE TESTS
NT LOW TEMPERATURE TESTS
NT SALT SPRAY TESTS
NT UNDERWATER TESTS
Analysis of research activities conducted to determine criteria for passenger comfort in various methods of transportation
01 p0004 N73-10024
ALSEP developments, and environmental and quality control tests
[NASA-CR-128580] 01 p0103 N73-10847
Heat test program for general protuberance shapes on flat plate
[NASA-CR-128400] 01 p0116 N73-10959
Development and characteristics of test facility for measuring three dimensional boundary layers on helicopter rotor blade under various conditions
[NASA-CR-112194] 03 p0252 N73-12042
Bibliography on environmental monitoring for radioactivity
[ORNL-NSIC-101] 03 p0334 N73-12720
Wind tunnel and atmospheric tests of dynamic performance of anemometers
[AD-747341] 04 p0445 N73-13630
Environmental fatigue crack propagation in titanium sheet alloys in atmospheres of argon, normal air, distilled water, and salt solution
[NLR-TR-72019-U] 05 p0602 N73-14894
Evaluation of polyimide second stage rod seals at high temperatures to determine suitability for application to aircraft systems
[NASA-CR-121124] 08 p0927 N73-17592
Significance of grain boundary microstructure and pH in chloride ion solution as stress corrosives in 7075 aluminum alloys
[RM-564J] 08 p0931 N73-17624
Analysis of environmental effects on physical, mechanical, and thermodynamic properties of various multilayer insulation materials - Vol. 1
[NASA-CR-120978] 08 p0934 N73-17648
Analysis of environmental effects on physical, mechanical, and thermodynamic properties of various multilayer insulation materials - Vol. 2
[NASA-CR-120979] 08 p0934 N73-17649
Environmental salt spray tests of closed pore insulation for space shuttle orbiter thermal protection system
[RM-570] 09 p1051 N73-18572
Environmental tests of crystallographic and stress corrosive properties of reactor related metal alloys
[AECL-4353] 09 p1063 N73-18668
Environmental and flight readiness tests of scanning mirror for infrared sensors
09 p1089 N73-18888
Nonlinear programming of multifilter phase-lock loops at low signal-to-noise environments
[NASA-CR-131237] 10 p1127 N73-19184
Environmental tests and failure modes for microelectric devices
[AD-753256] 10 p1135 N73-19253
Multiaxes vibration device for making vibration tests along orthogonal axes of test specimen
[NASA-CASE-MFS-20242] 10 p1158 N73-19421

Thermal vacuum environment tests of materials used in space technology to determine effect of ultraviolet radiation on contaminative properties
[NASA-CR-122374] 10 p1175 N73-19556
Tests of ammunition without cases and with combustible cases to evaluate mechanical and environmental stress effects
[ICT-6/72] 12 p1465 N73-21869
Evaluation of ground effect machines under various environmental conditions to determine feasibility as rescue vehicles by Coast Guard
[AD-755409] 13 p1475 N73-21947
Solar array development discussing manufacturing, design qualification tests in aerospace environments, and comparison between fold-up and roll-up types
[RAE-TR-72109] 13 p1476 N73-21959
Stress corrosion cracking tests of aluminum alloys in synthetic sea water
[NASA-TM-X-64733] 13 p1488 N73-22062
High temperature environmental testing of gas-metal interactions to simulate severe operating conditions
14 p1677 N73-23606
Design of microbial test system for Apollo 16 mission
15 p1740 N73-24103
Device for extravehicular microbe exposures to space environment during Apollo 16 flight
15 p1740 N73-24104
Corrosion fatigue crack growth of high strength steels in hydrogen and water/water vapor environments
[AD-759088] 16 p1930 N73-25615
Influence of gaseous atmospheres on aluminum alloy, titanium, and refractory alloy fatigue striations
[ONERA-NT-192] 17 p2045 N73-26548
Environmental and performance tests of thermoelectric materials
[MMM-2473-342] 17 p2050 N73-26585
Environmental tests of interocean acoustic release devices and performance of correlation echo sounder processor
[RN-1008] 18 p2151 N73-27385
Environmental tests of zinc-rich coatings applied to carbon steels
[NASA-TN-D-7336] 18 p2160 N73-27450
Tabulation of environmental tests on microelectronic devices
[AD-761951] 19 p2247 N73-28113
Research projects in environmental and electromagnetic technologies
[AD-761483] 19 p2355 N73-28948
Environmental effects on headform cavitation inception
[AD-763367] 21 p2527 N73-30261
Environmental tests on Symphonie model momentum flywheel
[ESRO-CR-96] 21 p2553 N73-30469
Environmental fatigue crack propagation in Ti-Al-Sn
[NLR-TR-72093-U] 22 p2686 N73-31511
Properties of materials in high pressure hydrogen at cryogenic, room, and elevated temperatures
[NASA-CR-124394] 22 p2725 N73-31804
Performance and environmental tests of National Air Space Enroute Stage air traffic control system
[FAA-NA-73-55] 23 p2817 N73-32518
Space environment simulation tests on space shuttle reusable surface insulation materials
[NASA-TM-X-2720] 24 p2940 N73-33475
Plasma jet wind tunnel tests on space shuttle surface insulation materials
24 p2940 N73-33479
Thermal-vacuum tests of flight model spacecraft to determine performance and reliability based on malfunction analysis
[NASA-TN-D-7408] 24 p2984 N73-33851
Bench and thermal-vacuum testing of superconductors and heat pipe systems to determine failure characteristics
[NASA-TN-D-7395] 24 p2992 N73-33909

**ENVIRONMENTS**
NT AEROSPACE ENVIRONMENTS
NT CHROMOSPHERE
NT EARTH ENVIRONMENT
NT EXTRATERRESTRIAL ENVIRONMENTS
NT HIGH ALTITUDE ENVIRONMENTS
NT HIGH GRAVITY ENVIRONMENTS
NT HIGH TEMPERATURE ENVIRONMENTS
NT INTERPLANETARY SPACE
NT INTERSTELLAR SPACE
NT IONOSPHERE
NT JUPITER ATMOSPHERE
NT LOW TEMPERATURE ENVIRONMENTS
NT LOWER IONOSPHERE
NT LUNAR ATMOSPHERES
NT LUNAR ENVIRONMENT
NT MAGNETOPAUSE
NT MAGNETOSPHERE
NT MARINE ENVIRONMENTS
NT MARS ATMOSPHERE
NT MARS ENVIRONMENT
NT MESOPAUSE
NT MESOSPHERE
NT MIDLATITUDE ATMOSPHERE
NT PLANETARY ATMOSPHERES
NT PLANETARY ENVIRONMENTS
NT ROTATING ENVIRONMENTS
NT SOLAR ATMOSPHERE
NT SPACECRAFT ENVIRONMENTS
NT STELLAR ATMOSPHERES
NT THERMAL ENVIRONMENTS
Uniform mapping and monitoring of natural ecosystems and environmental complexes from ERTS-1 imagery
[E72-10185] 01 p0046 N73-10364
Environmental and ecological impact of construction and operation of dam and impoundment on Sangamon River in Illinois
[E72-10216] 02 p0162 N73-11310
Effect of dam construction and staged filling of reservoirs in Illinois on environment and ecology
[E72-10217] 02 p0162 N73-11311
ERTS-1 imagery of Lake Champlain and Vermont environments
[E72-10225] 03 p0288 N73-12333
Environmental and resource study of Kansas using ERTS-1 imagery
[E72-10305] 04 p0412 N73-13354
Environmental and ecological impact of construction and staged filling of reservoirs in Illinois
[E72-10309] 04 p0412 N73-13358
Development of system for mapping and monitoring natural ecosystems and environmental complexes from ERTS-1 imagery of California, Nevada, Four Corners Area, Louisiana, and Colorado Plateau
[E73-10289] 08 p0915 N73-17495
Coordination and establishment of centralized facilities and services for University of Alaska ERTS-1 survey of Alaskan environment
[E73-10459] 11 p1284 N73-20417
Uniform mapping of earth resources and environmental complexes from Skylab imagery
[E73-10532] 14 p1654 N73-23417
Uniform mapping of earth resources and environmental complexes from Skylab imagery
[E73-10562] 14 p1656 N73-23434
Mapping and monitoring natural ecosystems and environmental complexes and estimation of rice crop yield in California and Louisiana from ERTS-1 imagery
[E73-10669] 16 p1899 N73-25364
Uniform mapping and monitoring of natural ecosystems and environments in California, Louisiana, and Colorado from ERTS-2 imagery
[E73-10839] 19 p2290 N73-28417

**ENZYME ACTIVITY**
NT FERMENTATION
Procedure for assaying enzyme activity in soils and application to presumptive life tests in Martian soil
[NASA-CR-128399] 01 p0008 N73-10059
Complete activity of lactate dehydrogenase and isoenzymes in plasma and myeloid cells
[NASA-TT-F-14586] 01 p0009 N73-10070
Effects of hypoxia and acceleration stresses on enzyme activities in erythrocytes and blood plasma
[DLR-FB-72-71] 07 p0746 N73-16070
Gas environment effect on catalase cryolysis
10 p1119 N73-19121
Inhibiting and activating effect of mono- and bi-quaternary pyridioxide reactivators on bovine erythrocyte cell membrane
[BMVG-FBWT-72-9] 10 p1121 N73-19138
Effects of physical training on human enzyme activity, carbohydrate metabolism, cholesterol level, and adrenal function
[NASA-TT-F-14826] 11 p1243 N73-20093
Ultraviolet space irradiation effects on Aeromonas proteolytica extracellular enzyme production
15 p1741 N73-24111
Enzymatic luminescent bioassay method for determining bacterial levels in urine
[NASA-CASE-GSC-11092-2] 18 p2109 N73-27052
Variations of cell enzymes, glucose, cholesterol, and 17-hydroxycorticosteroid in blood during physical work noting physical training dependence
[DLR-FB-72-48] 21 p2501 N73-30072
Automatic control for absorption columns, fluidized bed processors, and continuous fermentation noting enzymatic protein production
[LAAS-PUBL-975] 24 p2892 N73-33090

**ENZYMES**
NT CATALASE
NT CHOLINESTERASE
NT NUCLEASE
Behavior of enzyme activities in blood plasma after breathing hyperbaric oxygen
[DLR-FB-71-96] 06 p0635 N73-15163
Protein sterilization of firefly luciferase without denaturation
[NASA-CASE-GSC-10225-1] 18 p2113 N73-27086
Role of respiratory enzymes on human adaptation to hypoxia
[NASA-TT-F-15058] 21 p2500 N73-30060
Development of fluorometric methods for analysis of biological compounds based on production of fluorescence by enzymic reaction
[PAPER-76A6-745] 21 p2546 N73-30411

**ENZYMOLOGY**
Proton magnetic resonance spectra and calorimetry of interactions between ions, inhibitors, and substrates with two ribonucleases
[BMVG-FBWT-72-7] 07 p0746 N73-16071
Enthalpy values for reaction of retarding mononucleotides with ribonuclease and thermodynamic parameters for enzyme inhibitor interactions
[FMVG-FBWT-72-12] 07 p0747 N73-16073
Proton magnetic resonance spectra of ribonuclease A inhibitor complexes, noting effect on catalytic activity
[BMVG-FBWT-72-13] 07 p0747 N73-16074

**EOLE SATELLITES**
Eole and support operations planning
[NASA-TT-F-14709] 03 p0249 N73-12011
EOLE satellite tracking of meteorological balloons released in Southern Hemisphere to trace horizontal motion of air masses
[NASA-TM-X-66152] 06 p0694 N73-15651
Divergence at 200 mb level in Southern Hemisphere atmospheric circulation inferred from EOLE data
08 p0918 N73-17523
Balloon sub-system of Eole experiments in Southern Hemisphere lower stratosphere
24 p2948 N73-33547

**EPE-A**
U EXPLORER 12 SATELLITE

**EPHEMERIDES**
NT PLANET EPHEMERIDES
Annual of National Astronomical Observatory of Columbia for 1972
06 p0717 N73-15852
Aeronautical almanac for period from January to April, 1973
08 p0916 N73-17509
Astronomical ephemerides for 1973
08 p0960 N73-17855
Proper motions for 3478 faint stars
[NASA-CR-130693] 09 p1085 N73-18850
Calculation of ephemeris for Navy navigation satellites
[AD-753807] 09 p1092 N73-18914
Tidal and lunar data for Point Mugu, San Nicholas Island, and Barking Sands areas for 1973
[AD-752892] 10 p1156 N73-19407
Description and operation guide for DSAS illumination and moon conflict programs
[NASA-TM-X-66200] 10 p1213 N73-19863
Astronomical catalog for 1973
13 p1576 N73-22774
Calculating position of moon as function of time using numerical techniques
[AD-761651] 21 p2598 N73-30821
Astronomical ephemerides for 1974
23 p2838 N73-32679

**EPHEMERIS TIME**
Strict geometric determination of ephemeris time, positions, and apparent directions of moon against stellar background
[AD-750307] 06 p0671 N73-15460
Greenwich time report for the Royal Greenwich Observatory Time and Latitude Service during period of January to March 1972
08 p0960 N73-17856
Approximative ephemeris calculations for moving celestial objects using coordinates from different points on earth surface
10 p1178 N73-19587
Stellar-inertial measurement system trade study on spacecraft orbital ephemeris and attitude errors for landmark location
[NASA-CR-134042] 24 p2984 N73-33845

**EPINEPHRINE**
Cardiovascular effects of fluorocarbon exposure, emphasizing epinephrine sensitivity
[AD-751427] 07 p0749 N73-16091
Effect of cysteamine combined with adrenalin and phenamine on reparative processes following irradiation and overload
11 p1242 N73-20081
Epinephrine oxidation and indole production during high pressure oxygen poisoning
[AD-759405] 18 p2110 N73-27061

**EPITAXY**
Magnetically uniaxial rare earth garnets grown on substrates, using liquid phase epitaxial dipping technique
[AD-745903] 02 p0220 N73-11781
Nucleation and film growth mechanisms in heteroepitaxial semiconductor
[AD-748424] 04 p0460 N73-13753
Influence of substrate temperature on properties of epitaxial layers of GaAs during growth
[NLL-RRE-TRANS-370-(8036.625)] 05 p0585 N73-14763
Small etching pits in epitaxial layer of gallium arsenide caused by accumulation of impurities
[DRIC-TRANS-2928] 06 p0709 N73-15782
Electron microscopic analysis of epitaxial growth and nucleation in condensed gas crystals
[AD-753108] 10 p1201 N73-19773

Homoepitaxial films of GaAs deposited from vapor phase
[AD-754821] 11 p1331 N73-20800
Vapor deposition for epitaxial film growth of bubble domain materials
[AD-754958] 11 p1332 N73-20813
Binary and ternary system epitaxial crystal growth from liquid phase to obtain high purity, electroluminescent, and infrared detector materials
12 p1441 N73-21674
Vapor phase epitaxy of gallium arsenide
[AD-755434] 12 p1441 N73-21678
Preparation techniques and quality control of GaAs substrates for use in epitaxy
13 p1566 N73-22688
Nucleation and film growth mechanisms in heteroepitaxial semiconductor thin films
[AD-755529] 12 p1568 N73-22706
Characterization of thin films produced by epitaxial growth of magnetic rare earth compounds
[AD-755165] 13 p1568 N73-22707
Vapor epitaxial deposition of yttrium-iron garnet thin films on substrates using iron and yttrium chloride separated fluxes
15 p1821 N73-24762
Growth and crystal structure of Si, Ge, and GaAs thin films
[JPRS-59279-PT-2] 18 p2186 N73-27650
Thermodynamic analysis of Si film growth rate in vertical reactor
18 p2186 N73-27651
Structure, composition, and electrophysical properties of autoepitaxial silicon layers from vapor-gas tetrachloride mixture
18 p2186 N73-27653
Utilization of sandwich method to obtain epitaxial layers of Si, GaAs, and heteroepitaxial GaAs-Ge
18 p2186 N73-27654
Mechanism of silicon autoepitaxy during transport in sandwich process
18 p2187 N73-27655
Low temperature epitaxial development of Ge and Si layers by chloride method
18 p2187 N73-27656
Growth and properties of epitaxial silicon films treated with hydrogen of high purity
18 p2187 N73-27657
Transport coefficients of donor and acceptor mixtures for epitaxial growth of silicon by sandwich method
18 p2187 N73-27659
Alloying epitaxial layers of silicon with boron and arsenic using gas discharge
18 p2187 N73-27660
Distribution profiles of admixtures in epitaxial silicon layers prepared with hydrogen of high purity
18 p2187 N73-27661
Kinetics of gas pickling and epitaxial growth of semiconductor materials
18 p2188 N73-27664
Effects of crystallization conditions on properties of autoepitaxial and heteroepitaxial layers of silicon obtained by hydride pyrolysis
18 p2188 N73-27667
Selective growth of epitaxial silicon layers in chloride process
18 p2188 N73-27668
Analysis of optimal conditions of selective growth of epitaxial layers of germanium and silicon
18 p2188 N73-27669
Procedure for obtaining monocrystalline layers of silicon by rheotaxial methods
18 p2189 N73-27673
Flow velocity, GeCl4 concentration, and temperature effects on growth and morphology of autoepitaxial Ge films
18 p2189 N73-27674
Epitaxial growth of diamond on diamond from vapor at subatmospheric pressures
[AD-761630] 19 p2327 N73-28722
Vapor phase heteroepitaxial growth of silicon germanium alloys by hydrogen reduction of tetrachlorides
20 p2460 N73-29767
Growth of high quality, single crystalline, Pb Sn Te by vapor-phase epitaxy for infrared detectors
[AD-762344] 20 p2463 N73-29795
Electrical conduction in nondegenerate, nonsymmetrical, epitaxial semiconducting films
21 p2585 N73-30713
Epitaxic sublimation methods for studying pseudobinary semiconductor alloys
[AD-763488] 21 p2586 N73-30723
Evaluation of Gallium nitride for active microwave devices
[AD-763413] 21 p2586 N73-30726
Thermal effects on planar epitaxial silicon power transistors
[AD-763903] 22 p2645 N73-31194

EPNL
U EFFECTIVE PERCEIVED NOISE LEVELS

EPOCHS
U TIME MEASUREMENT

EPOXIDES
U EPOXY COMPOUNDS

EPOXY COMPOUNDS
NT ETHYLENE OXIDE
Approximate method to analyze plane stress, orthotropic, linear viscoelastic problems under isothermal conditions for metal-epoxy composites
05 p0607 N73-14939
Bench tests of wear resistance and antifriction properties of epoxy compounds
[AD-752868] 09 p1054 N73-18588
Optimal tensile strength composition for molding compounds of epoxy resin reinforced with glass fibers
[AD-754763] 11 p1309 N73-20620
Evaluation of upgraded boron fibers in epoxy-matrix composites
[NASA-CR-112266] 12 p1416 N73-21472
Development of low density foamed epoxy adhesives
[Y-1833] 13 p1547 N73-22538
Influence of epoxide resin space lattice thickness on dynamic modulus of elasticity
[NASA-TT-F-14913] 14 p1680 N73-23633
Spectrophotometric analysis of terminal epoxy and olefinic compounds
[TN-287] 15 p1746 N73-24155
Production and performance of strain gage embedded in boron/epoxy materials
[AD-759548] 16 p1915 N73-25493
Thermodynamic properties of cycloalkane and cyclobutane epoxy compounds for synthetic high energy fuels
[AD-760156] 17 p1993 N73-26116
Process of density change in epoxy bonding agents throughout curing process
[RAE-LIB-TRANS-1686] 17 p2049 N73-26576
Design of torque motor with armature windings cast in epoxy cylinder and conductors cast integrally with aluminum mounting ring
18 p2209 N73-27830
Fracture mechanics for interfacial crack between adhesively bonded dissimiliar materials
20 p2477 N73-29898

EPOXY RESINS
Strain rate and temperature dependence of glass fiber reinforced and unreinforced epoxy resins and deformation mechanisms
[REPT-1040/72] 01 p0069 N73-10568
Unidirectional and bidirectional carbon fiber/epoxy resin composites for cryogenic vessels
[NASA-CR-120899] 02 p0192 N73-11553
Development of direct method for determining complex modulus of linear viscoelastic materials as function of frequency
[UTIAS-159] 02 p0237 N73-11928
Tensile creep tests to determine properties of 7075-T6 aluminum alloy reinforced with unidirectional boron/epoxy
[NBS-TN-722] 04 p0437 N73-13565
Mechanical properties data and fabrication technology for filament wound graphite/epoxy resin pressure vessels
[NASA-CR-120951] 05 p0602 N73-14897
High tensile strength epoxy system for filament winding
[UCRL-73773] 07 p0812 N73-16586
Analysis of structural properties produced by selective reinforcement of aluminum compression panels with unidirectional boron epoxy composite materials
[NASA-CR-2145] 08 p0966 N73-17895
Development of epoxy resin lubricant sealant for hermetic sealing of threaded joints on pipes
[AD-752825] 09 p1040 N73-18486
Improvement in interlaminar shear strength of organic matrix composites using plasma deposited coupling agents
[AD-753857] 09 p1055 N73-18599
Technology for applying advanced fibers or resins to high performance high pressure filament-wound pressure vessels
[NASA-TM-X-68196] 10 p1220 N73-19923
Epoxy resins for use in superconducting magnets at liquid helium temperatures
[RHEL/R-251] 12 p1416 N73-21476
Design, fabrication, and evaluation of boron-epoxy reinforced C-130 center wing boxes
[NASA-CR-112272] 14 p1601 N73-22979
Design, fabrication, and test of boron composite material landing gear for use as main landing gear on A-37 aircraft - Vol. 2
[AD-756923] 14 p1603 N73-22997
Effects of environmental variables on physical, thermal, and mechanical properties of resin matrix and metal matrix composite materials
[AD-757524] 14 p1681 N73-23640
Graphite and epoxy plastic material strength under biaxial stress
[AD-758448] 15 p1801 N73-24600
Radiation damage in epoxy materials of reduced viscosity
[RHEL/R-249] 16 p1932 N73-25634
Analysis of loss of high temperature strength in composite materials following aging in room temperature environments
[NASA-CR-124290] 17 p2050 N73-26583
Dynamic mechanical analysis of reactions of aromatic diamines with diglycidyl ether of bisphenol A for application to epoxy thermosetting systems
[AD-759995] 17 p2052 N73-26602
Application of boron/epoxy composite materials for airframe construction with specific development of F-111 stabilizer
18 p2164 N73-27480
Flight tests of CH-47 helicopter to determine structural performance of boron-reinforced epoxy aft rotor blades
[AD-762199] 19 p2222 N73-27927
Analysis of stresses in magnet windings due to thermal contraction and temperature gradient stresses and impregnation with epoxy resins to reduce effects
[RHEL/R-264-PT-1] 20 p2435 N73-29558
Distribution of stress across thickness near crack tip in epoxy resin plate subjected to approximate cylindrical bending
20 p2476 N73-29893
Fatigue properties of high strength high modulus graphite /glass/epoxy matrix composites
[AD-763760] 21 p2564 N73-30552
Influence of epoxy resins on mechanical properties of superconducting windings
[RHEL/R-265-PT-2] 22 p2689 N73-31534
Internal pressure vessels with filament of carbon fibers and epoxy resins
[NASA-CR-121138] 22 p2724 N73-31799
X ray inspection of losses in high voltage transformers encapsulated by epoxy resins noting thermal cycling effects and stresses
24 p2881 N73-33008

EQUATIONS
Numerical method of characteristics for unsteady propagation processes considering dissipative terms in equations for supersonic mixing processes
[NASA-TT-F-14825] 15 p1767 N73-24320

EQUATIONS OF MOTION
NT EULER EQUATIONS OF MOTION
NT HELMHOLTZ VORTICITY EQUATION
NT HYDRODYNAMIC EQUATIONS
NT KINEMATIC EQUATIONS
NT KINETIC EQUATIONS
NT NAVIER-STOKES EQUATION
NT REYNOLDS EQUATION
Numerical analysis of aircraft equilibrium spin characteristics based on nonlinear equations of motion and constrained minimization techniques
[NASA-TN-D-6926] 01 p0004 N73-10028
Digital computer program for solution of aircraft longitudinal stability characteristics at or near stall point
[AD-745557] 01 p0005 N73-10037
Development of finite difference scheme for numerical analysis of time dependent seiche oscillating across shallow, infinite channel and transients associated with bottom spiral
[AD-745194] 01 p0053 N73-10428
Numerical analysis of stability and convergence conditions based on mathematical model of Arctic Ocean
[AD-745182] 01 p0053 N73-10429
Integral relationships in planar problem of gas lubrication including applications and approximate solutions
[AD-745833] 01 p0063 N73-10515
Lagrangian theory of internal ocean wave interaction
[AD-746149] 02 p0169 N73-11371
Sphere free motion in rotating fluid noting Taylor instability existence
[DLR-FB-71-32] 03 p0285 N73-12309
Analysis of minimum time maneuvers by high thrust-to-weight aircraft using optimal control theory to determine open-loop control laws
[AD-748354] 04 p0374 N73-13039
Effect of internal spinning fly wheel on air launched missile stability and resulting launch disturbance
[AD-749027] 04 p0375 N73-13047
Determining parameters of rocket capable of 8 km/sec using simplified equations of motion
[REPT-13] 04 p0463 N73-13775
Analysis of interaction between fluid and discrete particles in turbulent flow field and development of equations of motion
[WTHD-32] 05 p0526 N73-14280
Derivation of minimum dimension sets of discrete coordinate and hybrid coordinate equations of motion for hinge connected rigid bodies assembled in tree topology
[NASA-CR-129950] 05 p0602 N73-14900
Dynamic response of fluid-solid interface to supersonic disturbance
[AD-750253] 05 p0604 N73-14917
Equations of compass motion of three axis gyrostabilizer in gyrocompass mode based on initial placement error of platform in horizontal plane
06 p0695 N73-15667
Subharmonic angular motion response in asymmetric missile trajectory analysis
[AD-749787] 06 p0722 N73-15893

Application of equations of motion to investigate effects of mode shape and coning angle on stability boundaries of hingeless helicopter rotor blades
[NASA-CR-114525] 07 p0739 N73-16015
Normal pressure gradients in hypersonic boundary layers, including systematic derivation of equations of motion and energy equations
07 p0771 N73-16259
Integration of equations of motion for three dimensional turbulent boundary layer
07 p0771 N73-16261
Analysis of motion of compound pendulum and two-gimbal gyroscope mounted in artificial satellite with prescribed orbit and constant rate of rotation
07 p0817 N73-16625
Analysis of control and power requirements for X-14 aircraft based on equations of motion with respect to set of axes fixed to aircraft
[NASA-CR-130760] 08 p0864 N73-16988
Averaging process for continuum mechanics in two phase flow analysis
[AD-752159] 08 p0898 N73-17273
Construction of main fundamental solution of gravity equation
[AD-752233] 08 p0922 N73-17553
Equations of motion for calculating flexible rotor influence on two gimbaled gyroscope motion
08 p0922 N73-17554
Inertially coupled equations of motion for analyzing pitching and yawing motions of nonrolling wind tunnel model
[AD-752208] 08 p0926 N73-17586
Development of empirical method for determining optimum reversing coefficient of thrust reversal of jet engines on passenger aircraft
[AD-752814] 09 p0986 N73-18048
Application of splitting method for numerical analysis of heat conducting gas flows in curvilinear coordinates
[NASA-TT-F-14658] 09 p1015 N73-18288
Model for solution of equations of motion for thermospheric wind - Part I
[NASA-TM-X-66189] 09 p1028 N73-18393
Effects of earth surface characteristics on cumulus scale convection for stable and unstable boundary layers above relatively dry ground
[AD-752914] 09 p1031 N73-18416
Ellipticity condition of three dimensional partial differential equation as turbulence criterion in atmospheric motion
[AD-746624] 09 p1032 N73-18424
Equations of motion for elastic tire rolling on ground and forces exerted by tire assuming absence of slippage between tire and ground
[AD-752697] 09 p1040 N73-18482
Cardinal equations of dynamics
10 p1188 N73-19665
Hydrodynamic equations of motion for studying sound interaction in transient chemical reactions
[AD-753798] 10 p1191 N73-19688
Application of parafoil equations of motion to predict flight performance of powered parafoil flight vehicle
[AD-754907] 11 p1236 N73-20034
Development of computer program for solving fully compressible, two-dimensional hydrodynamics problems using flux-corrected transport algorithms
[AD-754736] 11 p1271 N73-20315
Guidance equations for present and advanced techniques
[AD-754923] 11 p1322 N73-20728
Analysis of equations of aircraft dynamics and development of analog-digital simulation capability
[AD-755868] 12 p1365 N73-21077
Finite difference solution of three-dimensional compressible boundary layer equations for circular cones at angle of attack
[NASA-CR-112316] 12 p1391 N73-21276
Equations of motion for calculating collision dynamics of diatomic molecules
[NASA-CR-131527] 12 p1431 N73-21594
Stochastic derivation of equations of motion for deformable particles immersed in Newtonian fluids
[WTHD-46] 12 p1431 N73-21595
Equations of motion in wave solutions for cold collisional plasma
[AD-755388] 12 p1437 N73-21640
Motion and orbital direction of particle in Kerr gravitational field
[NASA-TR-R-403] 12 p1458 N73-21816
Equations of motion for studying convection transport processes in strongly curved tubes
13 p1509 N73-22227
Applying sequential estimation technique of system identification to determination of unknown coefficients in vertical plane equation of motion of hydrofoil
[AD-755738] 13 p1512 N73-22253
Derivation of equations governing temporal and spatial variation for amplitudes and phase of capillary and gravity waves in case of second harmonic resonance
[AD-756218] 13 p1513 N73-22262
Study of effects of solar activity on geophysical phenomena using numerical techniques
13 p1514 N73-22264
Model of symmetric large scale whirl using equations of motion as applied to satellite data
[AD-756096] 13 p1554 N73-22596
Equations of motion for gyroscopic devices and analysis of effects on accuracy produced by loads and vibrations in supports of gyroscopic instruments
[AD-756337] 13 p1557 N73-22622
Effects of solar, lunar, and earth gravity perturbations on synchronous satellite
13 p1576 N73-22767
Application of variational equations for analysis of rapidly spinning triaxial body moving in elliptical orbit
[NASA-CR-131871] 13 p1581 N73-22813
Numerical analysis of satellite stability parameters with application to stability of Skylab satellite
[NASA-CR-124223] 13 p1581 N73-22815
Equations of motion for shell developed in general orthogonal coordinates using Hamilton principle
[AD-755239] 13 p1588 N73-22878
Equation of motion of sand particle under influence of aerodynamic drag developed in inertial coordinate system
[AD-757724] 14 p1653 N73-23405
Partial derivative analysis using equations of motion for recovering gravity anomalies from satellite observations
[NASA-CR-130240] 14 p1661 N73-23483
Pulsed electron motion equations for surface current analysis on conducting sphere
[AD-757190] 14 p1694 N73-23745
Numerical analysis of thermoelastic state of shells subjected to thermal impact on the surface of the shell
14 p1715 N73-23912
Dynamic structural analysis of helicopter structures using single point excitation techniques - Vol. 2
[AD-756390] 14 p1716 N73-23922
Dynamic structural analysis of helicopter subsystems based on equations for combination of mobility matrices - Vol. 4
[AD-756392] 14 p1716 N73-23924
Artificial satellite motion and tracking
[GRGS-BULL-6] 15 p1832 N73-24846
Translational-rotational magnetized satellite equations of motion in geomagnetic field
15 p1832 N73-24847
Description of canonical set of equations which governs behavior of n-body spacecraft connected by dissipative elastic joints
[NASA-CR-132155] 15 p1835 N73-24872
Derivation of equations of motion for small angular displacements from equilibrium position of earth pointing satellite with reaction wheel damping
[ARC-R/M-3276] 16 p1857 N73-25039
Solution of thick axisymmetric turbulent boundary layer and turbulent flow equations
[AD-759015] 16 p1892 N73-25309
Multilevel atmospheric prediction model based on primtiive equations of moiton
[DM-8] 16 p1938 N73-25681
Numerical analysis of space navigation parameters for interplanetary Mars spacecraft based on equations of motion of spacecraft
[NASA-TT-F-14897] 16 p1940 N73-25704
Equations of motion for describing physical picture of anomalous ordinary wave propagation in magnetoplasma
[IPPJ-153] 16 p1949 N73-25767
Linear stability analyses for four satellite configurations using passive elements for attitude control
16 p1964 N73-25883
Numerical analysis of nonstationary three dimensional motion of reentry vehicles entering atmosphere at hypersonic speeds
16 p1965 N73-25897
Shell equations for orthotropic, circular cylinders during axially symmetric, harmonic motion
16 p1968 N73-25918
Correspondence principle for vibration analyses on viscoelastic bodies with loss tangents
[AD-759260] 16 p1971 N73-25943
Analysis of projectile aerodynamic coefficients based on yawsonde and radar imagery data obtained during flight tests
[AD-759482] 17 p1980 N73-26002
Static and dynamic buckling of nonhomogeneous cylindrical shells
17 p2090 N73-26912
Extensional equations of motion of isotropic, elastic plate, using Legendre polynomials
[AD-760325] 17 p2096 N73-26957
Interaction of hypersonic source flow and axisymmetric free jet with rarefied background as examined by equations of motion
[AD-761149] 18 p2131 N73-27218
Mathematical models for studying energy spectra and nonlinear surface waves of ocean
[AD-759541] 18 p2149 N73-27371
Computer algorithm for calculating orbital trajectories by optimization of equation of motion parameters
18 p2211 N73-27846
Numerical transformation of basic equation for two parameter flow
[AD-762104] 19 p2257 N73-28195
Vinti equations of motion solved for position and velocity of orbiting satellite
[NASA-TM-X-70418] 19 p2343 N73-28846
Development of equations of motion for longitudinal suspension line wave motion during parachute deployment process
[NASA-TM-X-69498] 20 p2361 N73-28988
Numerically integrated equations of motion of N particles under mutual gravitation attraction
20 p2390 N73-29202
Influence of elastic deformation of gimbal suspension on frequency of nutation of gyroscope
21 p2547 N73-30421
Differential equations of motion and transfer functions of linear accelerometer for use in selection of instrument parameters
21 p2547 N73-30423
Equations describing dynamical motions of small cavitation bubbles in liquids
[AD-764075] 22 p2656 N73-31277
Turbulent, surface, and internal motions of ocean
[AD-763804] 22 p2670 N73-31390
Separation of variables in special Hamilton-Jacobi equation and application to dynamical problem of constrained on moving surface
[NASA-TR-R-405] 22 p2691 N73-31557
Solving equations of motion for behavior of plasma clouds in layered model ionosphere
[MPI-PAE/EXTRATERR-73] 22 p2704 N73-31658
Finite difference method and equations of motion for studying nonlinear vibrations of one and two degree of freedom spring mass systems
22 p2724 N73-31796
Fundamental concepts and statistical foundation of mechanics of continuous medium
[AD-764370] 22 p2727 N73-31820
Mathematical model for predicting pilot rating of aircraft in pitch tracking under gust conditions
[AD-764698] 23 p2746 N73-31976
Equations of motion formulated to compute transient response of multi-mass flexible rotors
[NASA-CR-2300] 23 p2797 N73-32374
Application of Runge-Kutta, multi-step, and extrapolation methods for numerical integration of equations of motion on controlled satellite
[NASA-CR-124416] 23 p2848 N73-32762
Equations of motion for Lincoln Experimental Satellites with gimbaled momentum wheel and gyroscope to analyze attitude control dynamics
[AD-765548] 24 p2986 N73-33867
Effect of friction term on equations of motion of liquid helium and measurement of temperature along axis of channel carrying supercritical heat current
24 p2990 N73-33894

**EQUATIONS OF STATE**
**NT HUGONIOT EQUATION OF STATE**

Three different equations of state used for computing stress-strain curves of rubber in tension
[AD-747664] 03 p0322 N73-12621
Computing equation of state parameters for material which undergoes phase transition
[AD-746611] 03 p0346 N73-12824
Analysis of entropy rate admissibility criterion for solutions of hyperbolic conservation laws
[NASA-CR-129594] 04 p0484 N73-13956
Equation of state for compressibility of helium, nitrogen, and their mixtures
[JPRS-57923] 07 p0752 N73-16111
Computer program for calculating equations of state, thermodynamic functions, and opacities of plasmas
[AD-751607] 07 p0829 N73-16723
Computer program for calculating equations of state, thermodynamic functions, and opacities of plasmas
[AD-751608] 07 p0829 N73-16724
Physics of Gruneisen parameter for solids analyzed from view of conceptual and physical contributions
[AD-751130] 07 p0834 N73-16761
Equation of state for helium and nitrogen mixture
[AD-753964] 11 p1253 N73-20169
Liquid-vapor state of aluminum during electron bombardment
[AD-754449] 11 p1253 N73-20171
Analysis of oscillating gas flow in open-ended pipe caused by piston operating at or near resonant frequency
[AD-754647] 11 p1272 N73-20321
Free piston shock tube driver using two stage compression techinque with intermediate diaphragm
[FFA-AU-765] 12 p1376 N73-21161
Calculations of equations of state for zero-temperature white dwarf and neutron stars
12 p1447 N73-21719
Validity of CGL equations in solar wind problems of exosphere
[AD-756501] 13 p1575 N73-22760
Equations of state for hydrogen including low temperature regions
[UCID-16095] 19 p2230 N73-27986
Analysis of properties of powder materials subjected to compressive forces and development of equations of state for determining mechanical properties
[NLL-NEL-RR-2474-[6075.461]]
21 p2603 N73-30858

Comparison of rheological equations of state and constrained shear recovery results for two polyisobutylene melts
[RR-203] 24 p2891 N73-33078
EQUATORIAL ELECTROJET
Equatorial electrojet measurement made by Cosmos 321 and magnetic observatories
04 p0414 N73-13377
Wave propagation and refraction of Type-1 irregularities in equatorial electrojet
[NASA-CR-130382] 07 p0780 N73-16340
Explorer 31 measurements of photoelectron escape fluxes for equatorial and midlatitude regions
[NASA-TM-X-68921] 07 p0789 N73-16416
Ionospheric irregularities by low-frequency electrostatic gradient-driven instabilities and their nonlinear evolution in equatorial electrojet plasma
08 p0900 N73-17284
EQUATORIAL ORBITS
NT STATIONARY ORBITS
EQUATORS
NT MAGNETIC EQUATOR
Radio wave scintillations at equatorial regions
[NASA-TM-X-66074] 01 p0028 N73-10218
Model for stationary motion of atmosphere in equatorial latitudes based on nonlinear system of equations of hydrothermodynamics
04 p0442 N73-13604
Equatorial magnetic storm-time variation data from Hermanus, Kakioka, Honolulu, and San Juan
[NASA-TM-X-66174] 08 p0917 N73-17511
Ionospheric fading effects on microwave space communication links in equatorial zone
18 p2212 N73-27855
EQUILIBRIUM
Analysis of approximate transport properties of high temperature air in dissociation equilibrium
[ESDU-00.01.07-AMEND-A] 07 p0853 N73-16919
Relativistic electron beam equilibria in cylindrical plasma geometry
[IPP-6/111] 12 p1435 N73-21630
Principle of virtual work applied to continuum mechanics
[AD-758727] 15 p1841 N73-24919
Calibrator for biaxial electronic platforms designed to measure postural equilibrium
[AD-763093] 20 p2372 N73-29066
Instrument for measurement of postural equilibrium in human beings
[AD-763096] 20 p2373 N73-29067
EQUILIBRIUM DIAGRAMS
U PHASE DIAGRAMS
EQUILIBRIUM EQUATIONS
Variational principles of elastic theory
03 p0360 N73-12938
Solution of ionization and thermal equilibrium equations for gas clouds in quasars and Seyfert galaxies ionized by ultraviolet radiation sources
07 p0839 N73-16801
Principle of virtual work and displacement
10 p1188 N73-19664
Development of linear system of equations for computing errors of volume fractions or partial pressures at calculated equilibrium compositions
[NRC-TT-1665] 17 p2096 N73-26960
EQUILIBRIUM FLOW
Numerical solution of steady state cavitation flows
[AD-745346] 01 p0042 N73-10331
Plasma flow effects on axisymmetric equilibria in toroidal geometry
[IPP-6/107] 07 p0828 N73-16708
Analysis of measurable and ideal quantities of nozzle beams skimmed from parallel equilibrium gas flows
[DLR-FB-72-51] 09 p1014 N73-18275
Analysis of conditions for equilibrium of multi-component liquid at surface of solid body with allowance for selective adsorption at interphase boundaries
[NLL-M-21577-[5828.4F]] 16 p1885 N73-25261
Equilibrium limits of molten zirconium nitride flow over nickel-cobalt solid coating
[NLL-M-21572-[5828.4F]] 16 p1926 N73-25583
Analytical and experimental investigation of turbulent mixing flow in pressure gradient to determine existence of equilibrium flows in streams of helium and nitrogen
23 p2774 N73-32184
EQUILIBRIUM METHODS
Static perturbation method of studying nonlinear equilibrium and stability problems of structural systems and elements
09 p1093 N73-18921
EQUINOXES
Rocket sounding of zonal wind field structure in stratosphere and lower mesosphere of tropical zone during equinoxes
21 p2573 N73-30617
EQUIPMENT
Bibliography on effects of underwater environment on tools, equipment, and human performance
[AD-748000] 04 p0384 N73-13122
Service life and operation of military equipment in subzero Siberian environments
[AD-756478] 13 p1554 N73-22595
Coordination and establishment of centralized facilities and services for University of Alaska ERTS survey of Alaskan environment
[E73-11088] 24 p2913 N73-33250
EQUIPMENT SPECIFICATIONS
Specifications for fused silica slip-casting radome material
[AD-745332] 01 p0028 N73-10219
Revised description and specification for CAMAC modular data processing system used with on-line digital computers
[EUR-4100-E-REV-1972] 01 p0032 N73-10246
Numerical procedures for designing cams with radial followers for conditions of straight line travel and flat faced followers with faces normal to direction of motion
[ESDU-66009] 01 p0060 N73-10490
Functional analysis and logical construction systematics for signal processing equipment design
02 p0140 N73-11136
Performance accuracy of precision stereoplotter for aerotriangulation with independent models
02 p0165 N73-11339
Standard requirements for ultrasonic Doppler probes of cardiovascular systems in medical monitoring functions
03 p0257 N73-12083
Design of cryogenic flow control components for Saturn 5 S-1C launch vehicle
03 p0349 N73-12850
Design of miniature tactical crystal oscillator for operation at ambient temperature
[AD-749271] 04 p0397 N73-13232
Design of radiometric emittance measurement system for use at high temperatures
[NASA-CR-123968] 04 p0420 N73-13421
Design and technical characteristics of rotary automatic devices for pressing and gauging of metal ceramic structural parts
04 p0432 N73-13524
Development of vortex fluid amplifier for throttling rocket exhaust
[NASA-CASE-LEW-10374-1] 04 p0463 N73-13773
Model specifications of pulsed plasma solid propellant microthruster for synchronous meteorological satellite
[NASA-CR-130126] 04 p0463 N73-13778
Development of design data for metallic materials, fasteners, joints, and structural elements used in aerospace vehicle design
[AD-748268] 04 p0479 N73-13917
Development of specifications for minicomputer hardware and software for NASA applications - App. A
[NASA-CR-129816] 05 p0515 N73-14189
Lunar laser reflector specifications and fabrication, noting test equipment thermal control, and lunar environment simulation
05 p0558 N73-14529
Contract end item specifications for defining hardware end items required by expendable second stage of space shuttle booster system - Vol. 8 Pt. 1
[NASA-CR-128663] 05 p0599 N73-14874
Preliminary system specification for design, operation, and performance of expendable second stage for reusable space shuttle booster - Vol. 9
[NASA-CR-128664] 05 p0599 N73-14875
Procurement specification for space shuttle orbiter windshield pane and factors influencing development
[NASA-CR-112209] 05 p0600 N73-14882
Operating characteristics of GEOS-C K band radar altimeter
06 p0663 N73-15387
NMR principle for designing propellant mass flow meter
[AD-751507] 07 p0801 N73-16507
Simplified techaique and device for producing industrial grade synthetic diamonds
[NASA-CASE-MFS-20698-2] 10 p1163 N73-19457
Design of digital filters for bandpass and low pass applications
[AD-754032] 11 p1265 N73-20266
Specifications for design of low, medium, and high power microwave hybrid microcircuits
[NASA-CR-124211] 13 p1533 N73-22419
Characteristics of signal conditioning electronics for vector velocity laser velocimeter
[NASA-CR-131475] 13 p1538 N73-22459
Design of katathermometer for measuring environmental cooling effects in simulated space flight
14 p1608 N73-23036
Design specifications for shipborne real time environmental data processing system
[AD-757458] 14 p1638 N73-23283
Operational cost and technological development aspects in design of space shuttle avionic systems
14 p1711 N73-23884
Transistorized feedback servomechanism design for cryogenic oxygen flow control
[NASA-TM-X-68234] 15 p1759 N73-24258
Electrical instrumentation development for spark source mass spectroscopy
[PB-214212] 16 p1871 N73-25147
Design of reserve master clock for controlling meteorological recording instruments in Antarctic weather stations
[NLL-M-22972-[5828.4F]] 16 p1911 N73-25459
Flapping- and squeeze-duty design criteria for full journal bearings under dynamic duty
[WTHD-45] 16 p1917 N73-25514
Design and operating characteristics of pulsed ruby laser source used in portable holocamera
16 p1920 N73-25541
Military design standard for noise producing equipment
[AD-750649] 16 p1945 N73-25735
Optimum design of insulating intersheaths between radio frequency cable braids
[RAE-TR-72151] 17 p1998 N73-26154
Design parameters and dynamic characteristics of navigational instruments
[JPRS-59254] 17 p2059 N73-26656
Analysis of errors and selection of design parameters for adjustable gyrocompasses
17 p2059 N73-26658
Astronomical research and instrument development by Professor M. G. Pereira de Barros
17 p2081 N73-26837
Development of method for predicting performance of barometric sensing systems used in determining sounding rocket altitude
[NASA-TM-X-65991] 17 p2087 N73-26881
Remote sensing methods and equipment
[NASA-TT-F-14973] 18 p2142 N73-27318
Natural environment design requirement for solar electric power stage based on radiation atmospheric conditions at orbital altitudes
[NASA-TM-X-64761] 18 p2193 N73-27708
Design and performance of lightweight cosmic radiation experiment for Pioneer Jupiter mission
18 p2210 N73-27837
Carbon dioxide laser frequency stability data for receiver design optimization
18 p2212 N73-27861
Specifications of portable magnetic video tape recorder for television signal reproduction
[JPRS-59611] 19 p2235 N73-28021
Design of low cost highly sensitive SHF microwave components
[NHK-LABS-NOTE-163] 20 p2381 N73-29129
Design, dynamic response, and operation of electric pressure difference transducer
[NLL-TRANS-2976-[9022.81]]
21 p2543 N73-30387
One- and two-dimensional analysis of particle deposition in turbulent slot flow with application to self cleaning air filter design
22 p2649 N73-31225
Requirements of telescopes for extra-atmospheric astronomical observations
[NASA-TT-F-15119] 22 p2715 N73-31732
Specifications of infrared detector for cloud cover determination
[BMVG-FBWT-73-13] 23 p2793 N73-32349
Integrated optics design principles of tunable CO2 laser
[AD-764638] 23 p2802 N73-32408
Selection criteria and characteristics of quiet, clean propulsion systems for use with short takeoff aircraft
24 p2876 N73-32967
Component design and draw tooling of Pt heat source liner bodies
[MLM-1972] 24 p2955 N73-33608
Use of InGaP to develop highly efficient LED
24 p2967 N73-33711
EQUIVALENCE
Physical equivalence of null plane quantum electrodynamics in null plane gage to conventional electrodynamics in Coulomb gage
09 p1066 N73-18700
Restricted proof that weak equivalence principle implies Einstein equivalence principle
[NASA-CR-131420] 11 p1324 N73-20745
Equivalence techniques used to define and simulate service vibration environments in testing laboratories
[AD-758414] 17 p2091 N73-26914
Maximum likelihood procedure used for classification problem involving equivalence classes and constant divergence
[REPT-23] 20 p2439 N73-29587
EQUIVALENT CIRCUITS
Equivalent resistance network for MHD generator noting losses and scale effect
[TH-72-E-30] 03 p0343 N73-12796
Development of numerical procedures for determining instantaneous values of current and voltage in nonlinear electrical circuits
[NLL-DRIC-TRANS-2145-[3623.66]]
05 p0522 N73-14241
RC equivalent network for flueric flip-flop inputs
[AD-752126] 08 p0899 N73-17280
Optimization of fluid amplifier cascades by means of electric equivalent circuit
[CRIF-EL-6] 10 p1142 N73-19304
Numerical analysis of multiple conductor transmission line with arbitrarily positioned impedances in series with each wire
[SC-R-72-2695] 12 p1386 N73-21244

Hysteretic synchronous motor equivalent circuits
[LRBA-E-603-NT-1/SIE] 15 p1738 N73-24093
Equivalent circuit with excitation coil for ion cyclotron waves
[IPPJ-160] 20 p2380 N73-29126
**ERBIUM**
Erbium laser rangefinder having germanium avalanche photodetector
[AD-748071] 04 p0430 N73-13502
Performance characteristics of erbium doped laser glass material
[AD-755683] 12 p1411 N73-21435
High purity phosphate core and cladding glasses for erbium doped laser
[AD-755687] 13 p1538 N73-22460
Performance capabilities of erbium lasers and tabulation of laser materials to show chemical composition, mode of operation, frequency and output characteristics
[PHL-1973-12] 14 p1672 N73-23565
**ERBIUM COMPOUNDS**
Synthesis and characterization of tetrahydroborates of lanthanum, neodymium, and erbium
[AD-759372] 17 p1992 N73-26110
**ERECTION**
U CONSTRUCTION
**EREP**
Application of Earth Resources Experiment Package data to development of commercial mining activities
[MCR-73-62] 13 p1518 N73-22308
Remote sensor system aboard Skylab in support of EREP oceanographic program
[AD-755715] 14 p1663 N73-23501
Skylab education program for high school students - Vol. 1
[NASA-EP-110] 24 p2980 N73-33811
Skylab education program for high school students - Vol. 2
[NASA-EP-111] 24 p2980 N73-33812
**ERGODIC PROCESS**
Sensitivity of coupled reaction rate equations to coefficient uncertainties
[AD-762420] 19 p2232 N73-27995
Fourier analysis on ergodic calculations of reaction kinetic rate coefficients in air dissociation and hydrogen oxygen combustion
[AD-762421] 19 p2232 N73-27996
**ERGOMETERS**
Manual actuator for exercise machine onboard spacecraft
[NASA-CASE-MFS-21481-1] 06 p0676 N73-15503
Ergometer to measure divers physiological hyperbaric stresses at all explorable depths
[AD-754401] 11 p1295 N73-20513
Development of restraint system for securing personnel to ergometer while exercising under weightless conditions
[NASA-CASE-MFS-21046-1] 18 p2150 N73-27377
Versatile ergometer with work load control
[NASA-CASE-MFS-21109-1] 19 p2224 N73-27941
Tilting table for testing human body in variety of positions while exercising on ergometer or other biomedical devices
[NASA-CASE-MFS-21010-1] 21 p2502 N73-30078
Pneumatic foot pedal operated fluidic exercising device
[NASA-CASE-MSC-11561-1] 23 p2751 N73-32014
**ERGONOMICS**
U HUMAN FACTORS ENGINEERING
**EROS [SATELLITES]**
Mapping techniques using imagery from ERTS and EROS programs
[PAPER-L2] 19 p2273 N73-28298
**EROSION**
NT SOIL EROSION
NT WATER EROSION
NT WIND EROSION
Development of porous electrode materials for plasma generators and effects of blowing protective gases through plasma
[AD-747369] 03 p0255 N73-12066
Experimental study of aerodynamic effects on erosion
[AD-749286] 05 p0539 N73-14388
Criteria development for recognizing and identifying slope failure forms, based on pattern, color contrast, and geometric form
[AD-750732] 06 p0672 N73-15464
Application of dual-scatter laser velocimeter to measure particle velocity distribution in hypersonic dust erosion facility
[AD-752225] 08 p0930 N73-17618
Analysis of particle erosion of solid surfaces using model of erosion pit nucleation and growth for solid spherical particles impacting on plane surface of elastic half space
[AD-752221] 08 p0935 N73-17657
Mathematical model for predicting erosion rate of graphite surface exposed to hot supersonic stream of hydrogen gas
[NASA-CR-130812] 09 p1050 N73-18564
Ground erosion on grassland and concrete by vertical takeoff of Do-31 aircraft
[BMVG-FBWT-72-26] 10 p1107 N73-19023
Utilization of ERTS-1 imagery to detect and map erosion features and changes in southern Arizona
[E73-10382] 10 p1152 N73-19377
Theoretical analysis of ballistic H powder erosion combustion in acoustic stream
14 p1700 N73-23796
Application of ERTS-1 data to locate wind erosion sites in West Texas and to determine extent and spread of wind erosion
[E73-10719] 17 p2019 N73-26326
Experimental determination of erosion rebound characteristics of high speed particles impacting stationary target for application to gas turbine engines operating in dusty environment
[AD-760578] 18 p2194 N73-27711
Missile site ground cover for prevention of soil erosion during launches
[AD-762136] 19 p2296 N73-28466
Land use, forest density, soil mapping, erosion, drainage, and salinity limitations in Greece from ERTS-1 data
[E73-10969] 22 p2657 N73-31283
Particle erosion of 2024 aluminum alloys
[AD-764267] 22 p2686 N73-31517
Analysis of physical properties of liquids on cavitation erosion to provide basis for developing modeling laws to reduce cavitation damage
24 p2904 N73-33175
Dune barrier erosion due to storms and wave activity near Mosquito Lagoon, Kennedy Space Center
[NASA-CR-135775] 24 p2922 N73-33337
**ERROR ANALYSIS**
New tables for forward pion nucleon scattering amplitude analyzing errors and total cross section data
[NOTA-INTERNA-382] 01 p0084 N73-10695
Error analysis on residual stress location for X ray diffraction analyses on crystal lattices
[AD-746488] 01 p0089 N73-10732
Errors in Doppler residuals of Mariner 6 and 7 Martian atmospheric occultation data
02 p0198 N73-11599
Error analysis on Doppler data associated with bent ray path radio occultation of planetary atmospheres
02 p0198 N73-11600
Errors in localization in measurement of distance to balloon-satellites
[NASA-TT-F-14701] 02 p0207 N73-11678
Development of computer program for estimating reliability of self-repair and fault-tolerant systems with respect to selected system and mission parameters
[NASA-CASE-NPO-13086-1] 03 p0305 N73-12495
Computer subroutines for propagating experimental numerical errors, rounding off numbers, checking validity of assumptions, and finding weak links in experiments
03 p0323 N73-12636
Systematic error in locating sounding balloon caused by influence of wind
[NASA-TT-F-14704] 03 p0326 N73-12654
Method for localizing position of balloon on earth, using interrogating satellite and correcting for electronic errors in distance measurement
[NASA-TT-F-14707] 03 p0328 N73-12678
Development of adaptive filter technique to minimize effect of noise produced errors in gyrocompasses and production of true azimuth data
[AD-747478] 03 p0329 N73-12685
Development of computer assisted troubleshooting system for maintenance of helicopters and aircraft using Univac 1108 computer
[AD-748665] 04 p0373 N73-13037
Refutation of microbial ability to reduce phosphate using thermochemical computations
[NASA-TT-F-14724] 04 p0379 N73-13081
Tracking errors associated with monopulse phased-array radar
[AD-748428] 04 p0391 N73-13175
Error analysis on two dimensional steady laminar boundary layer of incompressible wall flow
[AD-748771] 04 p0406 N73-13308
Effects of harmonics strengths on voltmeter reading accuracy
[NLL-ESB-TRANS-499-[3810.97]]
04 p0419 N73-13412
Analysis of resolvability of point sources of incoherent light by quantum detection, decisions of observers, and error probability
[NASA-CR-130129] 04 p0449 N73-13663
Error analysis of line intensity measurements on plasmas with electron temperature fluctuations
[AD-748474] 04 p0456 N73-13722
Error analysis of lunar control by orbital triangulation
04 p0468 N73-13813
Bloch law error in visual perception of capacitor discharge brightness
[AD-749452] 05 p0505 N73-14109
Analysis of digital information coding procedures with application to control of synchronization errors in data transmission on pulse code modulation systems
[NLL-TRANS-2825-[9022.81]]
05 p0507 N73-14127
PCM coding and decoding noting truncated hamming codes and analysis of error rates
[ESRO-TN-112-ESTEC] 05 p0513 N73-14173
Error performances of several digital signaling methods as function of specified signal to noise ratio
05 p0609 N73-14953
Source and form of altitude errors obtained from antenna/satellite attitude errors
06 p0664 N73-15390
Numerical comparator for indicating error in measurement transformations
[PUBL-1361] 06 p0690 N73-15615
Analysis of lateral velocity measurement errors of inertial guidance system and development of system to compensate for errors
06 p0695 N73-15665
Equations of compass motion of three axis gyrostabilizer in gyrocompass mode based on initial placement error of platform in horizontal plane
06 p0695 N73-15667
Error analyses of satellite orbital parameters based on simulations of observational variances, observation equations, and normal equations
[NASA-CR-130357] 06 p0720 N73-15878
Height error in sea-surface profile over Puerto Rican trench as determined by multi-station tracking aided by GEOS 2 satellite
[NASA-TM-X-69353] 07 p0781 N73-16347
Anomalous scattering effects of haze layer in remote sensing data on corn blight distribution
[NASA-CR-130028] 07 p0790 N73-16428
Errors in streak photography measurements caused by subject and camera misalignment
[AD-751185] 07 p0802 N73-16513
Development of matrix method for determining gimbal errors of three-axis gyrostabilized platform with constant drift rate
08 p0923 N73-17558
Development of procedure for predicting time interval of single clock and matrix equation for optimum weighting coefficients
[NBS-TN-626] 08 p0923 N73-17565
Analysis of errors recorded by modified Ligtenberg techique while measuring stress, strain, and static and dynamic loading in curved plates
[AD-752127] 08 p0926 N73-17589
Alignment control of high energy laser system and importance of external sources of alignment error
[UCRL-74050] 08 p0929 N73-17609
Reference key for error avoidance in aerial photointerpretation
[AD-752437] 09 p1037 N73-18463
Calculating error in temporal statistical structure of zonal and meridional velocity components of ground wind
09 p1060 N73-18641
Error analysis for flat earth guidance law of Europa 3 launch vehicle
[MBB-TN-RE-11-64-72-PT-2]
10 p1186 N73-19649
Numerical analysis of effects of various parameters affecting accuracy and stability of strapdown inertial navigation systems
11 p1316 N73-20685
Development and evaluation of failure detection and isolation technique for use with four gimbaled inertial measuring units
11 p1317 N73-20687
Methods employed to obtain datum position and velocity information for evaluation of inertial navigation systems and identification of error sources
11 p1320 N73-20716
Triangulation error analysis for barium ion cloud experiment
[NASA-TM-X-69222] 12 p1422 N73-21524
Dynamic error of pendulum with vibrating suspension related to finite rigidity of rod in stretching
13 p1556 N73-22612
Workload effects on operator grip pressure and neuromuscular transmission in manual tracking task error
[AD-757252] 14 p1615 N73-23089
Analog computer models of tracking system errors
14 p1683 N73-23658
Analysis of errors in wind measurements from ocean data buoys
[AD-757981] 14 p1686 N73-23685
Measurement errors and working signal structure of rubidium vapor M sub Z magnetometers and design of observatory vector magnetometer
[JPRS-58950] 15 p1786 N73-24480
Measurement errors of rubidium vapor M sub Z magnetometer
15 p1786 N73-24481
Application of Kalman-Bucy filter theory to postflight guidance error analysis
[NAL-TR-302] 15 p1808 N73-24652
Error analysis of computer calculation of magnetic field intensity and magnetic parameter
15 p1813 N73-24696
Software validation for guided missile computer
[AD-759263] 16 p1879 N73-25213
Determining mean and covariance errors in alpha-beta filter operating in Cartesian coordinates
[AD-759011] 16 p1935 N73-25656
Investigation of errors introduced into meteorological calculations through use of hypsometric equation
[AD-759489] 16 p1940 N73-25697

System modeling and performance optimization for analyzing parameters and disturbances for dynamic precision weapon delivery - Vol. 1
[AD-751505] 16 p1976 N73-25985
Error analysis on manipulator activation system using reversible self adaptive control mechanism
17 p1989 N73-26084
Error analysis for measurements of Mariner Venus Mercury 1973 gain, antenna patterns, and insertion loss of cables
[NASA-CR-133230] 17 p1997 N73-26148
Estimation of random process correlation functions, and statistical and sampling errors
17 p2026 N73-26399
Analysis of errors and selection of design parameters for adjustable gyrocompasses
17 p2059 N73-26658
Development of linear system of equations for computing errors of volume fractions or partial pressures at calculated equilibrium compositions
[NRC-TT-1665] 17 p2096 N73-26960
Analysis of ERTS-1 imagery for area measurement of land use categories in Finney County, Kansas
[E73-10764] 18 p2134 N73-27241
Error detecting algorithm for digital control computer
[AD-762241] 19 p2242 N73-28075
Compilation of diagnostic programs developed for digital computer malfunctions analysis
[AD-762237] 19 p2242 N73-28076
Control models for diagnosing malfunctions in analog computers
[AD-762220] 20 p2379 N73-29115
Errors in determining ionosphere parameters and characteristics of ionospheric inhomogeities by signals from satellite mounted radio station, Maiak
20 p2410 N73-29373
Methods for determining most probable value of recurring errors
20 p2439 N73-29594
Computerized simulation of monopulse radar antenna pointing errors due to ground reflection multipath propagation
21 p2507 N73-30114
Development of radar equation and radar calibration relationships for measuring multiple target reflectivity
21 p2568 N73-30583
Mathematical models for matching geopotential and wind fields and improving accuracy of objective analysis
21 p2573 N73-30616
Guidance and navigation error analysis for Skylab 3
[NASA-CR-133997] 21 p2576 N73-30642
Positional accuracy of aircraft radar targets as displayed in air traffic control airport surveillance radar system
[FAA-NA-72-87-PT-2] 21 p2577 N73-30650
Error model coefficients for extended Kalman filtering to dynamic calibration of inertial navigation system
[AD-763718] 21 p2577 N73-30656
Theoretical analysis of error propagation into orbital positions with emphasis on observed phenomena
[AD-763288] 21 p2599 N73-30828
Statistical error analysis of amplitude modulated radio altimeters with phase readout
22 p2629 N73-31064
Floating point system quantization errors in digital control systems
[NASA-CR-124382] 22 p2638 N73-31145
Precision theory for kinematic errors in uniaxial gyrostabilizer as angular velocity integrator
23 p2791 N73-32329

**ERROR BAND**
U ACCURACY

**ERROR CORRECTING DEVICES**
Empirical corrections for quantitative multi-element analyses using combined wavelenth- and energy-dispersive systems
[NASA-TM-X-66103] 02 p0137 N73-11113
Separation of refractivity gradient components for error elimination and inversion accuracy in occultation measurements on planetary atmospheres
02 p0198 N73-11597
Frequency sampling of target position and signal processing by linear amplitude weighting to reduce radar glint pointing errors
[AD-747348] 03 p0267 N73-12167
Flutter compensation of magnetic tape recorded data, noting single-carrier FM and frequency division multiplexed FM systems
[RAE-TR-72028] 03 p0303 N73-12474
Redundancy reduction for logic circuits by error correcting codes to improve method of increasing circuit reliability
04 p0399 N73-13249
Arithmetic error correction in redundant residue number systems
05 p0569 N73-14619
Analysis of lateral velocity measurement errors of inertial guidance system and development of system to compensate for errors
06 p0695 N73-15665
Reference key for error avoidance in aerial photointerpretation
[AD-752437] 09 p1037 N73-18463
Interpolative estimation for error reduction during video signal demodulation in noise environment
[NASA-CR-131873] 13 p1490 N73-22080
Reduction of nonuniformity of electron beam displacement on vidicon screen at raster edges
[DRIC-TRANS-2966] 13 p1500 N73-22156
Error protection techniques for data communication
[AD-759836] 17 p1999 N73-26168
Algorithm for correcting errors in linear transmission codes
[AD-760154] 17 p2000 N73-26169
Control computer for correcting ERTS video data electron beam recorder errors at ground base
18 p2211 N73-27853
Equipment certification and process verification methods for photographic processing control of ERTS images
18 p2211 N73-27854
Digital methods of television signal timing corrections
[BBC-RD-1973/15] 22 p2627 N73-31048
Automatic shot change detector for pre-programmed corrections of film reproduced by telecine
[BBC-RD-1973/10] 22 p2671 N73-31392
Guide accessories for correctly aligning paper in typewriter to correct typographical errors
[NASA-CASE-MFS-15218-1] 22 p2676 N73-31438
Self-checking multi-output combinational circuits using forced parity
[AD-765037] 23 p2769 N73-32151

**ERROR DETECTION CODES**
Automata theory for realizing reliable computer logic with fault detection
[AD-745720] 01 p0031 N73-10241
Arithmetic codes for error control in digital computation and data transmission
[AD-748201] 04 p0394 N73-13206
Performance and theory of operation of High Speed Sequential Decoder
[NASA-TM-X-62241] 11 p1260 N73-20222
Elastic matching, automatic error correction in English language words of any length
[NPL-COM-SCI-63-SUPPL] 18 p2121 N73-27144
Data smoothing and error detection based on linear interpolation
[NASA-CR-133984] 22 p2637 N73-31131

**ERROR SIGNALS**
Numerical analysis of minimum probability of error expression in digital communication system with intersymbol interference
[AD-760057] 17 p1999 N73-26167
Digital data transmission with argon laser beam through atmosphere to determine error frequency
[FTZ-44-TBR-34] 22 p2681 N73-31478
Digital error probalities of binary receivers in presence of intersymbol interference in fading channels
23 p2755 N73-32049

**ERRORS**
NT INSTRUMENT ERRORS
NT PILOT ERROR
NT POSITION ERRORS
NT RANDOM ERRORS
NT RANGE ERRORS
NT ROOT-MEAN-SQUARE ERRORS
NT TRUNCATION ERRORS
Influence of position and dimension on field errors of synchrotron bending magnet with winding cross section
[NP-19323] 03 p0345 N73-12813
Temperature effects on measurement accuracy of static deformation of semiconductor resistance strain gages
[NASA-TT-F-14616] 04 p0481 N73-13928
Boundary value equations for numerically forecasting weather in area defined by artificial boundaries
[AD-749748] 05 p0576 N73-14689
Clinical practice and problems associated with urine analysis
08 p0875 N73-17089
Error formulas and asymptotes for vocabulary size determination for one, two, and three parameter rank distribution
[NASA-CR-132023] 14 p1683 N73-23659
Superconducting magnetic suspension and balance facility data acquisition and data reduction errors
15 p1762 N73-24274
Thermoelastic response model for actively controlling primary mirror surface error of orbiting telescope
[NASA-CR-124286] 17 p2033 N73-26449
Analog models of errors in processing navigational information
17 p2059 N73-26660
Static moment and horizontal sinusoidal acceleration effects on stabilization errors in gyrovertical with mixed gyroscope correction characteristics
17 p2060 N73-26661
Effects of experimental error on stress intensity fractors from fracture testing
[NASA-TM-X-68285] 20 p2482 N73-29941
Pseudorandom 160 Mbits/s pulse generation, and digital word synchronization, for 640 Mbit/s PCM waveguide error rate measurements
[FTZ-A-442-TBR-38] 22 p2633 N73-31098
Generation and propagation of numerical error in fractional integer program
[AD-763206] 22 p2640 N73-31162
Intergrated error behavior of rawinsonde tracking system
[AD-763890] 22 p2695 N73-31585
Effect of human operater errors on reliability and effectiveness of his work
[AD-764937] 23 p2753 N73-32028
Statistical analysis of computational round-off errors associated with cutting plane solution ot linear integer programming problems
[NASA-TN-D-7457] 24 p2945 N73-33517

**ERTS**
U EARTH RESOURCES TECHNOLOGY SATELLITES

**ERTS-A**
U EARTH RESOURCES TECHNOLOGY SATELLITE 1

**ERYTHROCYTES**
Erythrocyte preservation in blood transfusion practice by cryogenic freezing with polyvinylpyrrolidone
[NASA-TT-F-14590] 04 p0378 N73-13076
Microelectrophoresis of human erthyrocytes as diagnostic tool in gynecology and obstetrics
[NASA-TT-F-14587] 04 p0378 N73-13077
Inhibiting and activating effect of mono- and biquaternary pyridioxide reactivators on bovine erythrocyte cell membrane
[BMVG-FBWT-72-9] 10 p1121 N73-19138
Effect of acute and chronic hypercapnia on Ca and inorganic P levels in guinea pig blood plasma and erythrocytes
[AD-749323] 13 p1484 N73-22035
Biophysical properties of human red blood cells exposed to hypobaric hyperoxia
[AD-755783] 14 p1612 N73-23072
Influence of transverse accelerations on electrolyte composition of plasma and erythrocytes
24 p2884 N73-33030

**ESAKI DIODES**
U TUNNEL DIODES

**ESCAPE [ABANDONMENT]**
Impact, emergency escapes, and crash survival studies
06 p0628 N73-15097

**ESCAPE CAPSULES**
Human factors characteristics and geometry of expandable structures for use as airlocks, escape capsules, and crew transfer tunnels on Skylab program
[AD-749131] 06 p0722 N73-15896
Analysis of escape systems for helicopter flight crews and passengers
[B-177166] 15 p1734 N73-24067

**ESCAPE ROCKETS**
Apollo experience report concerning general design, development, and qualification of launch escape propulsion subsystem
[NASA-TN-D-7083] 09 p1091 N73-18902

**ESCAPE SYSTEMS**
NT LAUNCH ESCAPE SYSTEMS
Modification to existing rocket catapult for reducing probability of injury to users of aircraft emergency escape systems
[AD-750318] 06 p0623 N73-15057
Dynamics and control of escape and rescue from tumbling spacecraft
[NASA-CR-130549] 08 p0964 N73-17878
Aircrew escape autogyro ejector seat/flight vehicle
09 p1089 N73-18890
Analysis of escape systems for helicopter flight crews and passengers
[B-177166] 15 p1734 N73-24067
Application of aircraft crash investigation procedures to railroad passenger train derailment
[FAA-AM-73-1] 19 p2218 N73-27896
Proceedings of symposium to determine requirements and configurations of emergency ejection systems for helicopter crews
[AGARD-AR-62] 23 p2743 N73-31954

**ESCHERICHIA**
Effects of hyperoxia on sulfhydryl concentration of Escherichia coli
[AD-746193] 02 p0134 N73-11087
Ultraviolet extraterrestrial radiation tolerances of Bacillus subtilis spores and Escherichia coli bacteriophages
15 p1740 N73-24107

**ESG [GYROSCOPES]**
U ELECTROSTATIC GYROSCOPES

**ESKERS**
U GLACIAL DRIFT

**ESRO SATELLITES**
NT AZUR SATELLITE
NT ESRO 1 SATELLITE
NT ESRO 2 SATELLITE
NT ESRO 4 SATELLITE
NT GEOS SATELLITES [ESRO]
NT HEOS A SATELLITE
NT HEOS B SATELLITE
NT HEOS SATELLITES

Planning, control, and management for European space satellite project
[ESRO-SP-70] 01 p0121 N73-10996
Scientific equipment of ionospheric ESRO-4 satellite including five experiments
[ESRO-SN-114-ESTEC] 02 p0234 N73-11906
Magnetic attitude control of ESRO 4 satellite noting magnetorquer and maneuver simulation
[ESRO-TN-108-ESTEC] 02 p0235 N73-11909
Leakage of ESRO 4 nickel cadmium batteries noting electrical and pressure measurements and KOH loss
[ESRO-CR[P]-132] 04 p0375 N73-13053
Determination of KOH loss in ESRO 4 nickel cadmium batteries by electrical measurements
[ESRO-CR[P]-132] 04 p0375 N73-13054
European scientific community as users of ESRO satellite systems
15 p1848 N73-24976
Cost estimating and price analysis in European satellite projects
15 p1849 N73-24984
Performance and growth capability of orbital test satellite for European communication satellite program
[DGLR-PAPER-73-044] 21 p2602 N73-30849

**ESRO 1 SATELLITE**
Reliability analysis of solar generator on ESRO 1 satellite
[NASA-TT-F-14498] 01 p0007 N73-10051
Calculation of direction of magnetic moments of two permanent magnets in ESRO 1 satellite
[NASA-TT-F-14499] 01 p0109 N73-10896
Attitude stability and alignment of magnetically oriented ESRO 1 satellite
[ESRO-SN-120-ESTEC] 09 p1085 N73-18854
Pitch angle distribution of 100-300 keV protons measured by ESRO 1B satellite in early morning-late afternoon local magnetic time sector
[NP-19464] 10 p1210 N73-19846
Systems engineering and project management of ESRO I satellite
15 p1847 N73-24973
ESRO 1A [Aurorae] satellite dynamic model derived from attitude sensor data using smoothing factor in spline function subroutine
[RA-SAT-3.4-C-006] 18 p2201 N73-27767

**ESRO 2 SATELLITE**
Determination of location and time of solar flare observed from HEOS A and ESRO 2 satellites
05 p0592 N73-14814

**ESRO 4 SATELLITE**
Organization and management of ESRO 4 satellite project noting planning and contractor relations
15 p1847 N73-24970
Incentive schemes as contract management tool noting use in ESRO 4 satellite project
15 p1849 N73-24989

**ESSA SATELLITES**
NT ESSA 8 SATELLITE

**ESSA 8 SATELLITE**
European climatological maps constructed from ESSA 8 satellite photographic observations during first quarter of 1972
06 p0691 N73-15630
European weather maps constructed from ESSA 8 photographs
[QR-2] 10 p1181 N73-19605
ESSA 8 photographic observations of European cloud cover for third quarter of 1972
[QR-3-PT-3] 15 p1804 N73-24623
Characteristics of NOAA 2 meteorological satellite and photographic data of weather conditions over Europe during 1972
[QR-4-PT-4] 17 p2056 N73-26627

**ESTERS**
NT CELLULOSE NITRATE
NT DIISOCYANATES
NT HYDRAZINE NITROFORM
NT ISOCYANATES
NT LACTATES
NT LEXAN [TRADEMARK]
NT NITROGLYCERIN
NT ORGANIC NITRATES
NT PETN
NT POLYCARBONATES
NT POLYESTERS
NT URETHANES
Effectiveness of polymer complex of cysteamine and sulfopropyl ester of dextran as an antiradiation drug on irradiated mice
[DRIC-TRANS-2963] 06 p0631 N73-15125
Fluorinated esters of polycarboxylic acid and lubricating compositions for use at extreme temperature
[NASA-CASE-MFS-21040-1] 21 p2505 N73-30098

**ESTIMATES**
NT COST ESTIMATES
Pilot visual threshold and perception for aircraft movement estimation during unaided visual approach control
01 p0016 N73-10125
Current distribution estimates for microwave power tube with depressed multistage collector
[NASA-TM-X-2651] 01 p0032 N73-10251
Carbonyl formation data at elevated temperatures for estimating storage life of unstabilized polyolefins
[AD-748827] 04 p0438 N73-13572
Statistical three-stage sampling model for estimating resources from remote sensor applications
[NASA-CR-130026] 07 p0800 N73-16494
Launch vehicle estimating factors for planning advanced solar system and earth orbital missions
[NHB-7100.5B] 07 p0847 N73-16866
Theoretical procedure for estimating social benefits of remote sensing
[NASA-CR-130027] 07 p0857 N73-16947
Satellite derived potential coefficients and terrestrial gravity information for estimating geopotential anomaly degree variance
[AD-754236] 11 p1290 N73-20471
Estimation of ion source yields in inhomogeneous magnetic fields using magnetohydrodynamic theory
[LYCEN-7250] 12 p1435 N73-21624
Estimation of signal-to-noise ratio in spacecraft data channel
16 p1879 N73-25207
Diffuse reflectance theory for estimating optical absorption coefficients of aerosol particles collected on filter surface
[AD-759490] 16 p1946 N73-25744
Indirect atmospheric pressure estimation from measurements of height and temperature
[AD-759920] 17 p2059 N73-26653
Estimation of parameters for nonlinearly observed dynamic systems
21 p2565 N73-30562
Argelander, Pickering, and Neyland-Blazhko methods for visually estimating variable star brightness
21 p2594 N73-30785

**ESTIMATING**
NT ORBITAL POSITION ESTIMATION
Estimating effect of inclined nut seating on fatigue strength of steel screw thread
[ESDU-67034] 01 p0060 N73-10487
Estimating fatigue strength of components subjected to constant amplitude with constant mean loading
[ESDU-71010] 01 p0111 N73-10915
Noncommuting observables in quantum detection and estimation theory, and application to analysis of coherent signal in harmonic oscillator
[NASA-CR-129694] 04 p0449 N73-13664
Prediction of fluctuating pressures acting on externally blown flap surfaces
[NASA-CR-112216] 06 p0619 N73-15026
Optimal estimation of measurement biases in Kalman-Schmidt filtering
[AD-753961] 11 p1311 N73-20641
Estimation method for correlation between two stationary random signals in noise
[AD-757459] 14 p1636 N73-23263
Feasibility of using adaptive estimation for atmospheric temperature forecasting
[AD-759346] 16 p1940 N73-25698
Estimating random signal power spectral density by filtering, fluctuating spectrum, and autocorrelation function
17 p2027 N73-26400

**ESTUARIES**
Estuarine and coastal oceanography of Block Island Sound and adjacent New York coastal waters based on ERTS-1 multispectral band scanner imagery
[E72-10171] 01 p0044 N73-10352
Interdisciplinary study of estuarine and coastal oceanography of Block Island Sound and New York Bight area using ERTS-1 imagery
[E72-10172] 01 p0044 N73-10353
One and two dimensional models of tidal propagation in St. Lawrence River
[NRC-12764] 01 p0048 N73-10382
Research report on tidal hydraulics
[AD-744784] 01 p0051 N73-10412
Estuarine coastal water dynamics controlling sediment transport and plume development in Long Island Sound
[E72-10250] 03 p0289 N73-12350
Estuary and barrier island studies using ERTS-1 imagery
[E72-10266] 03 p0291 N73-12365
ERTS-1 imagery of California nearshore processes including estuarine flushing, currents, season river discharges, and sediment dispersion
[E72-10363] 05 p0535 N73-14351
Multispectral imagery of estuarine and coastal oceanography of Block Island Sound and adjacent New York coastal waters using ERTS-1 imagery
[E73-10010] 06 p0659 N73-15346
Sedimentation levels in rivers and shoal estuarine waters based on ERTS-1 imagery
[E73-10048] 07 p0777 N73-16310
ERTS-1 imagery of estuarine and coastal water dynamics controlling sediment transport and plume development in Long Island Sound
[E73-10093] 08 p0902 N73-17305
Analysis of tidal currents, turbulent diffusion, and local shears in currents found in Trinity Bay, Texas
[NASA-CR-128734] 08 p0916 N73-17510
Estuarine and coastal water dynamics controlling sediment transport and plume development in Long Island Sound
[E73-10378] 10 p1152 N73-19373
Estuarine and coastal water dynamics controlling sediment transport and plume development in Long Island Sound
[E73-10627] 15 p1775 N73-24387
Application of ERTS-1 imagery for defining ice formations, ocean currents, beach erosion, and estuarine circulation
[E73-10780] 18 p2136 N73-27256
Color enhancement of ERTS-1 imagery of estuarine and coastal oceanography of Block Island Sound and adjacent New York coastal waters
[E73-10819] 18 p2140 N73-27294
Estuarine and coastal oceanography of Block Island Sound and adjacent New York coastal waters
[E73-10968] 21 p2533 N73-30310
Estuary and barrier island investigations utilizing ERTS-1 imagery
[E73-11041] 22 p2664 N73-31342

**ETCHING**
Small etching pits in epitaxial layer of gallium arsenide caused by accumulation of impurities
[DRIC-TRANS-2928] 06 p0709 N73-15782
Fine grinding, polishing, and graded etching techniques to eliminate surface yield on optical telescope mirrors
[NASA-CR-112217] 08 p0934 N73-17647
Development of crack propagation gases based on plating and etching processes and application to center notch, edge notch, and cleavage type specimens
[AD-754762] 11 p1295 N73-20511
Continuous measurement of residual stress in thin cylindrical pieces using deflection-etching techniques
[CRIF-MC-47] 12 p1409 N73-21418
Development of galvanic forming techniques and application to production of complex structures requiring accurate dimensions
13 p1593 N73-22918
Etch pit study of motion and generation of dislocations in electron irradiated metals and effect of point defects on mechanical properties of metals
[COO-1367-50] 15 p1799 N73-24579
Feasibility of using RF generated argon plasma for sputter etching Al and SiO2 windows and photoresist
[AD-757878] 15 p1800 N73-24588
Coordination chemistry and kinetics of preferential etching on surfaces of TiO2 [rutile]
[AD-759259] 17 p2074 N73-26780
Effects of chemical etching on magnetic and storage properties of Permalloy memory films
18 p2178 N73-27589
Variation of electrophysical parameters of epitaxial films of germanium as result of gas etching
18 p2188 N73-27665
Bibliography on etching and chemical machining techniques
[AD-763100] 21 p2554 N73-30472
Analysis of etching process in polycarbonate film when aqueous sodium hydroxide is used to develop charged particle tracks
[NASA-CR-124381] 22 p2673 N73-31415

**ETHANE**
Concentration fluctuations in critical region of binary liquid mixture 3-methylpentane-nitroethane
[AD-759740] 16 p1872 N73-25158
Laminar dispersion for measuring ethane binary diffusion coefficients in methane filled capillaries
24 p2891 N73-33079

**ETHERS**
NT POLYPHENYL ETHER
High tensile strength epoxy system for filament winding
[UCRL-73773] 07 p0812 N73-16586

**ETHIOPIA**
Geology and lithology of Afar region of Ethiopia based on ERTS-1 imagery
[E72-10261] 03 p0290 N73-12360
Mapping of major structural lineaments of Ethiopian rift using ERTS-1 imagery
[E73-10431] 11 p1281 N73-20392

**ETHYL ALCOHOL**
Blood plasma hyperosmolality and antidiuretic hormone inhibition in alcoholic intoxication
[NASA-TT-F-13910] 02 p0133 N73-11079
Guide to units and interpretation of blood alcohol measurements
[DCIEM-TM-848] 09 p0995 N73-18120
Effects of alcohol on eye movements and tracking performance during laboratory angular accelerations about yaw and pitch axes
[FAA-AM-72-34] 22 p2619 N73-30989

**ETHYL COMPOUNDS**
Conversion of 2-methyl 5-ethyl pyridine compound into 5-ethyl picoline acid by different methods
[DRIC-TRANS-2951] 06 p0638 N73-15178

**ETHYLENE**
Plasma sprayed catalyst coatings for low pressure polymerization of ethylene
[AD-750718] 05 p0568 N73-14613
Toxicity of pyrolysis products from chlorotrifluoroethylene-ethylene copolymer Halar resin
[AD-751436] 07 p0748 N73-16080

Surface structure of polymer produced by passing ethylene through radio frequency discharge
[AD-758099] 15 p1748 N73-24166
**ETHYLENE COMPOUNDS**
NT ETHYLENEDIAMINE
Development of method for determining ethylene dibromide depletion in aviation fuels
[AD-746250] 02 p0221 N73-11791
**ETHYLENE OXIDE**
Analysis of resistance of cultured and natural microbes in ethylene oxide sterilization method
[NASA-TT-F-14612] 04 p0379 N73-13078
**ETHYLENEDIAMINE**
Chemical equilibrium constants for n-ethylethylenediamine and 2-[ethylthio]-ethylamine complex reactions
[PB-213951/8] 14 p1618 N73-23104
**ETTINGSHAUSEN COOLERS**
U THERMOELECTRIC COOLING
**EUCLIDEAN GEOMETRY**
NT ANALYTIC GEOMETRY
NT ANGLES [GEOMETRY]
NT BRAGG ANGLE
NT BREWSTER ANGLE
NT CARTESIAN COORDINATES
NT CIRCLES [GEOMETRY]
NT CUBES [MATHEMATICS]
NT CYCLOIDS
NT ELLIPSES
NT HEXAGONS
NT INFLECTION POINTS
NT LINES [GEOMETRY]
NT LOCI
NT OBLATE SPHEROIDS
NT POINTS [MATHEMATICS]
NT PROJECTIVE GEOMETRY
NT RADII
NT RECTANGLES
NT TANGENTS
NT TORUSES
NT TRIANGLES
Fixed point theorems and dissipative processes in differential systems of Euclidian space
[NASA-CR-131267] 11 p1310 N73-20631
Global investigation of Einstein space of maximal mobility and Petrov Type 2
[ITF-72-140-P] 15 p1804 N73-24618
Multifold Euclidean geometry codes
[NASA-CR-133529] 20 p2439 N73-29590
**EUCLIDEAN SPACE**
U EUCLIDEAN GEOMETRY
**EULER BUCKLING**
Dynamic behavior of eccentric rotating shaft subject to linearly varying or constant tension
13 p1532 N73-22414
**EULER EQUATIONS OF MOTION**
Development of implicit finite difference method for analysis of viscous flows based on Euler and Navier-Stokes equations
[AD-746389] 01 p0043 N73-10341
Euler equations of motion of relativistic, perfect-fluid hydrodynamics, and potential application to stellar stability
07 p0840 N73-16806
Thermodynamics of light scattering from Eulerian fluid, and electron scattering by atomic hydrogen
13 p1558 N73-22627
Equations of motion for high frequency vibrations of thin crystal plates
[AD-760323] 17 p2095 N73-26948
Exact solution to nonlinear Euler equations pertaining to problem of thermally stratified compressible fluid motion on rotating sphere with gravitation
[AD-764684] 23 p2788 N73-32308
**EULER-LAGRANGE EQUATION**
Secular and long period terms of artificial satellite perturbed equation of motion noting planetary gravitational effects
01 p0105 N73-10870
Averaged Lagrangian method for obtaining equations which describe nonlinear interactions of wave components in plasma
[NASA-CR-129597] 03 p0340 N73-12777
Lagrangian method used for describing small signal wave propagation and nonlinear wave interaction in warm collisionless plasmas
[NASA-CR-129922] 05 p0583 N73-14744
Mathematical model for short period terms in satellite orbits including comparison between analytical theory and numerical integration
[GRGS-BULL-2] 05 p0596 N73-14845
Mathematical model for short period terms in satellite orbits, including comparison between analytical theory and numerical integration
05 p0596 N73-14846
Comparison of satellite orbit elements, using analytic theory and numerical integration
05 p0596 N73-14847
Numerical analysis of characteristics of rotary wing aircraft when considered as two coupled rigid bodies representing rotor and fuselage
07 p0737 N73-15994
Averaged Lagrangian method of describing small signal wave propagation and nonlinear wave interaction
17 p2066 N73-26718
**EUROPA LAUNCH VEHICLES**
NT EUROPA 1 LAUNCH VEHICLE
NT EUROPA 2 LAUNCH VEHICLE
NT EUROPA 3 LAUNCH VEHICLE
**EUROPA 1 LAUNCH VEHICLE**
Theoretical investigation of rocket steam generator with emphasis on trajectories and spectrum of injected drops and their vaporization for Europa 1 launch vehicle
[DLR-FB-71-36] 09 p1011 N73-18253
**EUROPA 2 LAUNCH VEHICLE**
Preflight tests on fluorine/ammonia propellants to be used in Europa 2 transfer stage
[BMFT-FBW-73-07] 21 p2587 N73-30731
**EUROPA 3 LAUNCH VEHICLE**
Management regulations and systems requirements for Europa 3 launch vehicle
07 p0849 N73-16885
Cryogenic upper stage requirements for Europa 3 launch vehicle analyzing performance, design, structural and test requirements
07 p0850 N73-16886
Design solutions and technologies for Europa 3 launch vehicle
07 p0850 N73-16887
Design solutions and technologies for Europa 3 launch vehicle, including second stage and propulsion system
07 p0850 N73-16888
Project planning and cost estimates for Europa 3 launch vehicle
07 p0850 N73-16889
Europa 3 launch vehicle checkout system
10 p1138 N73-19274
Comparison of flat earth guidance laws for Europa 3 launch vehicle
[MBB-TN-RE-11-93-71] 10 p1186 N73-19648
Error analysis for flat earth guidance law of Europa 3 launch vehicle
[MBB-TN-RE-11-64-72-PT-2]
10 p1186 N73-19649
Computation of aerodynamic heating for Europa 3 launch vehicle
[TN-ER/02-22/001] 10 p1224 N73-19952
Liquid propulsion transfer and injection system for Europa 3 in geostationary and interplanetary missions
[URV-47[71]] 11 p1333 N73-20822
Design configuration and operating procedures for utilizing thermonuclear propulsion for upper stage of Europa 3 launcher
[NASA-TT-F-14874] 13 p1557 N73-22623
Feasibility study for Europa 3 launch vehicle nuclear upper stage
[TR-TT-4-15/72] 15 p1811 N73-24675
Configuration of nuclear upper stage for Europa 3 launch vehicle
[TR-TK-REF-1-374/72] 15 p1811 N73-24676
Electrical equipment of nuclear upper stage for Europa 3 launch vehicle
[TR-TT-4-16/72] 15 p1811 N73-24677
Attitude control and auxiliary propulsion for nuclear upper stage of Europa 3 launch vehicle
[TR-TT-4-17/72] 15 p1811 N73-24678
Radiation shielding for thermal-nuclear stage of Europa 3 launch vehicle
[TR-TT-4-18/72] 15 p1811 N73-24679
Computation of neutrons and gamma ray distribution for radiation shielding of Europa 3 launch vehicle nuclear upper stage
[TN-3-25] 15 p1811 N73-24680
Nuclear rocket engine for Europa 3 launch vehicle
[D-1-72] 15 p1811 N73-24681
Performance of solar electric propulsion modules for out of ecliptic and cometary missions of Europa 3
15 p1826 N73-24804
Combined chemical solar electric transfer stage for inserting Europa 3 satellites into twenty-four hour orbits
[MBB-UR-V-49-71] 15 p1832 N73-24851
Apogee stage for Europa 3 launch vehicle
15 p1835 N73-24879
Feasibility study for Europa 3 launch vehicle nuclear upper stage
[TR-T/T-1.2-7/72] 15 p1836 N73-24880
**EUROPE**
Articles concerning European scientific research
[AD-742336] 02 p0245 N73-11993
European scientific research
[AD-743929] 02 p0245 N73-11994
Scientific research projects in Europe relative to aerospace technology, biology, computer development, physical sciences, and microwaves
[AD-746879] 02 p0246 N73-11996
European tracking station coordinates from GEOS B satellite data
03 p0295 N73-12400
Research on various theoretical and applied scientific disciplines and technical fields in east Europe
[JPRS-57372] 03 p0367 N73-12989
Collection of European scientific research reports
[AD-747959] 04 p0488 N73-13996
Plumb line deflection calculations for European triangulation network using astronomical observations
[MITT-122] 05 p0538 N73-14377
Investigation of thunderstorm potential in cold air cumulonimbi over northwestern Europe during winter
[AD-749493] 05 p0574 N73-14674
Research management of eastern Europe scientific affairs
[JPRS-57765] 05 p0595 N73-14838
European study of optical and signal processing problems in laser anemometry
[ET/TN/A/20] 06 p0679 N73-15526
Daily and monthly meteorological charts for Europe obtained during June, 1972 at Berlin
06 p0691 N73-15629
European climatological maps constructed from ESSA 8 satellite photographic observations during first quarter of 1972
06 p0691 N73-15630
Daily and monthly meteorological charts for Europe obtained during May, 1972 at Berlin
06 p0692 N73-15631
European research and development programs
[AD-750267] 06 p0732 N73-15972
Classification, description, and statistical treatment of European large-scale weather patterns
[NLL-M-9145-[5828.4F]] 07 p0814 N73-16600
Brief articles concerning recent developments in European Scientific Research
[AD-751630] 07 p0860 N73-16980
Western European research on open adiabatic mirror devices and radio frequency plugging - EURATOM controlled fusion report
[EUR-CEA-FC-628-AG] 08 p0948 N73-17760
Cooperation of Eastern European countries in computer and medical research
[JPRS-58063] 08 p0976 N73-17987
Accounts of scientific and technological cooperation in Eastern Europe
[JPRS-58053] 08 p0977 N73-17990
Research and development in theoretical and applied sciences in Eastern Europe
[JPRS-58121] 09 p1101 N73-18982
Daily and monthly synoptic climatological charts obtained at Berlin for August 1972
10 p1180 N73-19602
Daily and monthly synoptic climatological charts obtained at Berlin for September, 1972
10 p1181 N73-19603
European weather maps constructed from ESSA 8 photographs
[QR-2] 10 p1181 N73-19605
Existing position and future prospects of wind tunnels in European research
[AGARD-AR-60] 11 p1266 N73-20269
Articles concerning research and development in scientific disciplines and technological fields, and research management
[JPRS-58615] 11 p1352 N73-20978
Articles on European scientific research
[AD-754406] 11 p1353 N73-20985
Surface gravity and satellite derived gravimetric geoid of North America, North Atlantic, Eurasia, and Australia
[NASA-TM-X-66238] 15 p1778 N73-24413
ESSA 8 photographic observations of European cloud cover for third quarter of 1972
[QR-3-PT-3] 15 p1804 N73-24623
Effect of general atmospheric circulation of large scale and persistent weather features of Atlantic-Eurasian sector of hemisphere in 1968 to 1970
[NLL-M-22853-[5828.4F]] 16 p1936 N73-25663
Atmospheric sulfur budget for northern Europe with model for deposition variations with distance from source
[AC-17] 17 p2027 N73-26408
Characteristics of NOAA 2 meteorological satellite and photographic data of weather conditions over Europe during 1972
[QR-4-PT-4] 17 p2056 N73-26627
Worldwide airfield climatic data for Eastern Europe and USSR - Part 1
[AD-759794] 17 p2057 N73-26640
Worldwide airfield climatic data for Eastern Europe, and USSR - Part 2
[AD-759795] 17 p2057 N73-26641
Research management of East European scientific affairs
[JPRS-59273] 18 p2213 N73-27865
Winter atmospheric circulation over European sector of Northern Hemisphere in twentieth century
[NLL-M-2337-[5828.4F]] 20 p2391 N73-29205
Daily and monthly weather charts for Northern Hemisphere and Berlin, Germany for February, 1973
20 p2442 N73-29614
Inventory of European aerospace industries on satellite systems
[ESRO-SP-91] 21 p2602 N73-30852
Map of vertical crustal movements of Eastern Europe and ebb and tide studies
21 p2609 N73-30912
Measurements of atmospheric lead concentrations in European community and United Kingdom
[EUR-4982] 24 p2949 N73-33555

**EUROPEAN AIRBUS**
French aircraft development program including Concorde, Airbus, and Corvette, as well as economic study
06 p0622 N73-15045

**EUROPEAN SPACE PROGRAMS**
Analysis of alpha particle observations performed by HEOS 1 satellite and comparison with observations made by Vela 3 and Explorer 34 satellites
01 p0098 N73-10809
Management information systems for monitoring ESRO budget and program
[ESRO-PSS-02/PMC-01] 01 p0120 N73-10994
Management information systems for monitoring ESRO budget and program
[ESRO-PSS-03/PMC-02-PT-2]
01 p0121 N73-10995
Planning, control, and management for European space satellite project
[ESRO-SP-70] 01 p0121 N73-10996
Optimum design of format synchronizer for ESRO control center
[ESRO-CR[P]-127] 02 p0141 N73-11143
Magnetic test facilities at ESTEC, Netherlands, noting coils and magnetometers
[ESRO-TM-152-ESTEC] 02 p0153 N73-11238
Precision measurements of solar gravitational fields by European drag-free and twin geodetic space probes
02 p0231 N73-11879
List of scientific and technical reports published by ESRO up to Jul. 1972
[ESRO-SP-88] 02 p0245 N73-11992
ELDO computing facilities noting data links and operating procedures
[ELDO-TN-25] 05 p0518 N73-14209
Preliminary results from HEOS A satellite in electron and proton events, solar wind and interplanetary magnetic field measurement, and propagation of charged particles
[ESRO-SP-74] 05 p0592 N73-14813
CNES activities, noting French space program and international cooperation
05 p0611 N73-14971
Space activities of CNES, noting satellites, launch vehicles, sounding rockets, balloons, and ground stations
05 p0611 N73-14972
Administration, structure, personnel, and research plans of East European scientific organizations and institutions
[JPRS-57952] 07 p0857 N73-16946
Preliminary analysis of proposed European space tug
[MBB-URV-38-71-SUMMARY] 10 p1216 N73-19889
European space tug - prephase A extension
[MBB-URV-44-71] 10 p1216 N73-19890
Preliminary defination of European space tug
[HSD-TP-7227] 10 p1216 N73-19891
Study digest for European space tug
[HSD-TP-7264A] 10 p1216 N73-19892
Study logic and activities scheduling for European space tug
[HSD-TP-7227-APP-1] 10 p1216 N73-19893
Vehicle selection and economic analysis for European space tug
[HSD-TP-7227-APP-2] 10 p1216 N73-19894
Propellant control and propulsion study for European space tug
[HSD-TP-7227-APP-3] 10 p1217 N73-19895
Guidance and rendezvous sub-systems of European space tug
[HSD-TP-7227-APP-4] 10 p1217 N73-19896
Integrated electronics for European space tug
[HSD-TP-7227-APP-5] 10 p1217 N73-19897
Structure and configuration of European space tug
[HSD-TP-7227-APP-6] 10 p1217 N73-19898
Mass summary, test facilities, costs and PERT for European space tug
[HSD-TP-7227-APP-7] 10 p1217 N73-19899
European space tug study summary
[HSD-TP-7264] 10 p1217 N73-19900
European space tug alternative concepts and objectives
[HSD-TP-7264-VOL-1] 10 p1217 N73-19901
Concept definition of European space tug
[HSD-TP-7264-VOL-2] 10 p1217 N73-19902
European space tug auxiliary and main propulsion
[HSD-TP-7264-VOL-3] 10 p1217 N73-19903
European space tug guidance control rendezvous and integrated electronics
[HSD-TP-7264-VOL-4] 10 p1218 N73-19904
Structure and configuration of European space tug
[HSD-TP-7264-VOL-5] 10 p1218 N73-19905
European space tug development including analyses of performance, economics, weights, reliability, and costs
[HSD-TP-7264-VOL-6] 10 p1218 N73-19906
European space tug concepts and feasibility analyses
[HSD-TP-7316] 10 p1218 N73-19907
European space tug - Prephase A study
[MBB-URV-38-71] 10 p1218 N73-19908
Ionospheric magnetospheric, lunar and meteorite research, satellite geodesy, orbits, tracking, telemetry, and remote sensing in Finland in 1972
[S-52] 12 p1467 N73-21888
Strategies for European geosynchronous space tug mission
[VTH-171] 13 p1583 N73-22831
Mission planning for European earth resources survey aircraft
[ESRO-CR[P]-117] 14 p1661 N73-23484
Conference on project management and project control
[ESRO-SP-90] 15 p1846 N73-24962
Industrial policy of ESRO noting distribution of contracts, relations with industry, multinational consortiums, and technological research
15 p1848 N73-24975
European scientific community as users of ESRO satellite systems
15 p1848 N73-24976
Phase preparation of ground facilities for satellite missions noting procedures used at ESOC
15 p1848 N73-24979
Integrated project control for ESRO satellite management
15 p1849 N73-24985
Project management information requirements in international organization
15 p1849 N73-24990
Fokker F-27 as European earth resources survey aircraft noting design, remote sensors, and program
[ESRO-CR[P]-128] 17 p1984 N73-26035
UK-5 X ray experimental design performance
17 p2084 N73-26858
Spacelab payload analysis, shuttle interface, operational analysis, and design guidelines
[ESS/SS-399-VOL-1] 17 p2089 N73-26902
Assessment of joint NASA/ESRO Venus orbiter
[SYST/2109/MS/1V] 17 p2089 N73-26906
ESRO AEROSAT experiment using stratospheric balloon-borne transponder to relay signals from ground station to aircraft flying over sea
18 p2106 N73-27029
European space tug phase A study
[MBB-URV-53-72-VOL-2-PT-1]
18 p2200 N73-27765
Requirements of earth resources aircraft facility for remote sensing of European terrain
[ESRO-CR-97] 20 p2413 N73-29394
Inventory of European aerospace industries on satellite systems
[ESRO-SP-91] 21 p2602 N73-30852
Eastern Europe research projects involving hydrometeorology, semiconductor materials, microelectronics, and piezoelectronics
[JPRS-59617] 21 p2607 N73-30893
* Directory of European activities in remote sensing of earth resources
[ESRO/JPPC-73-20-ADD-1] 22 p2667 N73-31372
European program in multispectral scanning systems and application to earth resources surveys
[ERL/R-247-U] 23 p2787 N73-32301
European communication satellite and orbital test satellite transponders
[DGLR-PAPER-73-057] 24 p2896 N73-33116
Aims, prospects, organization, and financing of EUROSAT S.A.
24 p2994 N73-33930

**EUROPEAN SPACE RESEARCH ORGANIZATION**
**SAT**
NT AZUR SATELLITE
NT ESRO 1 SATELLITE
NT ESRO 2 SATELLITE

**EUROPIUM COMPOUNDS**
Synthesis of rare earth compounds and determination of their magnetic, optical, and semiconducting properties
[AD-747839] 03 p0348 N73-12835

**EUTECTIC ALLOYS**
Suitability of directionally solidified eutectic alloys for high temperature fasteners, material properties, and fabricating methods
[NASA-CR-123919] 02 p0177 N73-11437
Influence of interlamellar spacing on strength of Ni3Al-Ni3Cb eutectic
[AD-748658] 03 p0319 N73-12601
Improvement of high temperature eutectic alloy by compositional modification
[AD-752632] 08 p0934 N73-17644
Aluminum-copper eutectic solidification experiment to be run in M518 multipurpose electric furnace during Skylab mission
[NASA-CR-124103] 09 p1045 N73-18526
Fatigue behavior of directionally-solidified aluminum-nickel eutectic alloy under cyclic torsional loading
[AD-753689] 09 p1055 N73-18600
High temperature bonding of sapphire to sapphire by eutectic Al2O3 and ZrO2 mixture to form sapphire rubidium maser cell
[NASA-CASE-GSC-11577-1] 10 p1164 N73-19467
Abstracts on directionally grown eutectic alloy composites
[AD-754779] 11 p1309 N73-20625
Analysis of high temperature stability of reinforcing phase in eutectic composition of aluminum-nickel alloys for various rates of growth
13 p1541 N73-22487
Analysis of electrical conductivity of eutectic solutions of aluminum-nickel alloy using directional crystallization method
13 p1541 N73-22489
Directional crystallization in eutectic alloys used on casting turbine blades
[AD-759422] 16 p1931 N73-25624
Production of lamellar and fibrous composite materials from directional solidification of eutectic alloys and application to gas turbine blades and vanes
18 p2166 N73-27492
Application of directionally solidified eutectics for design and construction of gas turbine engines
18 p2166 N73-27493
Directional solidification of eutectic alloys and application to turbine blades and gas turbine engine components
18 p2166 N73-27494
Analysis of structural-eutectic transformations in liquid phase of metal-metal and metal-semiconductor systems
[NLL-M-21665-[5828.4F]] 21 p2557 N73-30496
Thermal cycling effects on structure of cobalt-niobium eutectic alloys
[AD-763706] 21 p2560 N73-30521
Creep properties of aligned silver-magnesium eutectic alloy
[AD-763375] 21 p2561 N73-30531
Effect of thermal cycling of structure and properties of directionally solidified eutectic composite
[NASA-CR-121249] 21 p2562 N73-30537
Formation of in situ composites by directional solidification
[AD-765348] 23 p2805 N73-32435

**EUTECTIC DIAGRAMS**
U PHASE DIAGRAMS

**EUTECTICS**
NT EUTECTIC ALLOYS
Crystalline structures, physical properties, chemical properties, and phase characteristics of various metal systems and alloys
[AD-746792] 02 p0189 N73-11532
Mechanical properties as function of temperature for unidirectionally solidified eutectic composites
[NASA-CR-124094] 09 p1046 N73-18527
Compilation of eutectics and melting point minima for binary combinations of metals for refractory metal brazing
[NASA-TM-X-68190] 10 p1172 N73-19537
Axial extension in directionally solidified eutectic of solid cross section during cyclic torsion
[AD-755891] 12 p1417 N73-21481

**EUTROPHICATION**
Monitoring and surveillance of state of eutrophication of inland lakes in California and Nevada
[E72-10207] 03 p0288 N73-12330
Utilization of ERTS-1 data to monitor and classify eutrophication of inland lakes
[E72-10358] 05 p0534 N73-14346
Monitoring and classifying eutrophication of inland lakes
[E73-10299] 09 p1021 N73-18331
Monitoring and classifying eutrophication of inland lakes from ERTS-1 imagery
[E73-10445] 11 p1282 N73-20405
Utilization of Skylab multispectral cameras for study of eutrophication processes in lakes important to New York State water resources
[E73-10744] 18 p2133 N73-27236
Monitoring and classifying eutrophication of inland lakes in Michigan using ERTS-1 imagery
19 p2285 N73-28375
Monitoring and classification of eutrophication of inland lakes in Michigan from ERTS-1 imagery
[E73-10898] 20 p2395 N73-29247
Interpretation techniques for Skylab monitoring of lake eutrophication in New York State
[E73-11011] 22 p2660 N73-31316

**EVACUATING [TRANSPORTATION]**
Evaporation rates and toxic plume dispersion for defining downwind evacuation areas for populations adjacent to accidental propellent spills on shipping routes
[NASA-TM-X-68188] 07 p0750 N73-16097
Computerized simulation of passenger emergency evacuation efficiency using Boeing 720 aircraft models
[FAA-AM-72-30] 08 p0879 N73-17119

**EVACUATING [VACUUM]**
Hole area for evacuating and degassing of far ultraviolet sounding rocket photometer
[MPI-PAE/EXTRATERR-68] 02 p0174 N73-11411
Vacuum displacement compression molding of tubular bodies from thermosetting plastics
[NASA-CASE-LAR-10782-2] 22 p2677 N73-31444

**EVALUATION**
Methods of evaluating electronic cockpit display devices, emphasizing control, psychology, physiology, and subjective rating
[DGLR-PAPER-72-97] 04 p0383 N73-13118

**EVAPORATION**
NT PROPELLANT EVAPORATION

NT TRANSPIRATION
Mass transfer rates at flat water surface measured during evaporation and condensation
[COO-2032-11] 03 p0263 N73-12135
Kinetics of purification of beryllium through evaporation data acquired during vacuum induction melting
[NASA-CR-123946] 04 p0431 N73-13512
Procedure for estimating changes in composition resulting from evaporation during storage of liquid oxygen
[NASA-TM-X-2686] 05 p0498 N73-14056
Evaporative segregation in binary alloys of Ni-Cr and Ni-Fe systems
[NASA-CR-123993] 05 p0561 N73-14562
Evaporation and vertical transfer of water vapor in urban areas
[NLL-M-20842-[5828.4F]] 05 p0570 N73-14625
Surface and volume mechanisms of material evaporation subject to powerful radiation fluxes
09 p0999 N73-18154
Dynamics of water drop evaporated by heating with laser pulse
[AD-752822] 09 p1001 N73-18167
Influence of defects and impurities on nucleation and growth of oriented films by evaporation
[NASA-CR-2234] 13 p1559 N73-22636
Evaporation of droplets in aerosol jets, by simulation with latex spheres
[BMVG-FBWT-73-5] 14 p1616 N73-23096
Liquid surface evaporation in rarefied gas atmosphere
[AD-765527] 24 p2893 N73-33095

**EVAPORATION RATE**
Field evaporation model for predicting tungsten surface potential in electric field
[AD-750205] 05 p0588 N73-14786
Development of differential equation for normal evaporation of nickel-aluminum alloy relating evaporating time to final solute concentration
[NASA-CR-124040] 07 p0808 N73-16558
Annual climatological measurements of evaporation in Panama Canal Zone
[AD-751782] 07 p0817 N73-16621
Instrumentation available for measuring evaporation in Canal Zone
[AD-763205] 21 p2574 N73-30629

**EVAPORATIVE COOLING**
NT FILM COOLING
NT SWEAT COOLING

**EVAPORATORS**
Laboratory prototype flash evaporator design, fabrication, and testing for space shuttle environmental control expendable heat sink
[NASA-CR-128608] 01 p0057 N73-10470

**EVECTION**
U LUNAR ORBITS
U ORBIT PERTURBATION
U SOLAR GRAVITATION

**EVENING**
Evening observations of storm-time ring current particle characteristics during beginning of magnetic storms
[NASA-TM-X-70430] 19 p2293 N73-28441

**EVENTS**
Event horizon and T-S solutions to Einstein vacuum field equation
[RIFP-177] 16 p1934 N73-25652

**EVOLUTION [DEVELOPMENT]**
NT ABIOGENESIS
NT BIOLOGICAL EVOLUTION
NT GALACTIC EVOLUTION
NT LUNAR EVOLUTION
NT PLANETARY EVOLUTION
NT STELLAR EVOLUTION
Autocorrelation analysis of velocity structure temporal evolution in solar wind
01 p0094 N73-10775
Evolution of man-machine-hybrid integration in evolving social structure
[AMRU-R-68-3] 02 p0132 N73-11069
Space technology for ground based economic support and investigating solar system origins
04 p0473 N73-13857
Genesis of free radical chemistry
08 p0881 N73-17130
Evolution of structural, cytochemical, and functional organization of gravity receptors in invertebrates and vertebrates
[NASA-TT-F-720] 11 p1247 N73-20128
Volcanic origin of mare ridges and sinuous rilles on lunar surface
12 p1454 N73-21780
Exogenetic and endogenetic origin of sinuous markings on lunar mare
12 p1455 N73-21784
Conference on annihilation reactions and gamma ray and universal evolution
[NASA-TM-X-66279] 19 p2331 N73-28753
Red shift energy distribution and black body background distortion theories of universal formation
19 p2333 N73-28770
Influence of blue green algae on crystalline calcium carbonate formation on river rocks
[NASA-TT-F-15028] 20 p2368 N73-29046
Automatic experimenter concept based on evolution strategy
24 p2908 N73-33210

**EVOLUTION [LIBERATION]**
NT GAS EVOLUTION

**EXAMINATION**
NT EYE EXAMINATIONS
Postoperational examination of externally configured test thermionic converter
[NASA-CR-131523] 12 p1426 N73-21560

**EXCAVATION**
NT TUNNELING [EXCAVATION]
Feasibility assessment of rapid excavation of hard rock by means of continuous fluid jets with pressures of 20,000 to 80,000 psi
[AD-744014] 01 p0051 N73-10416
Design and development of very high speed transportation system to include technological aspects and physical restraints
[F-4874] 04 p0488 N73-13990
Mathematical models for developing Coanda eductors for pneumatic conveying systems used in underground excavation
[AD-749088] 05 p0552 N73-14485

**EXCHANGING**
NT CHARGE EXCHANGE
NT GAS EXCHANGE
NT ION EXCHANGING
NT SPIN EXCHANGE

**EXCITATION**
NT ACOUSTIC EXCITATION
NT ATOMIC EXCITATIONS
NT HARMONIC EXCITATION
NT MOLECULAR EXCITATION
NT SELF EXCITATION
NT WAVE EXCITATION
Excitation and deexcitation of vibration in gases by oxygen and nitrogen atoms in E region of earth atmosphere
[AD-745925] 01 p0054 N73-10437
Potential barrier for neutral excitation at helium liquid-vapor interfaces
[NOTA-INTERNA-375] 01 p0083 N73-10690
Maximum root-mean-square response of square clamped aluminum plate subjected to stationary random excitation
[NASA-CR-129301] 03 p0361 N73-12939
Using microscopic models and principles for studying transfer of lattice vibrational energy into first excited state in perfect crystal
[AD-748079] 03 p0365 N73-12977
Design of transistorized oscillator for exciting gas discharge tubes
[AD-749831] 05 p0559 N73-14544
Laboratory experiments with high frequency excitation electric fields
[CONF-720705-3] 07 p0827 N73-16701
Vertical distribution of vibrationally excited molecular nitrogen in thermosphere corresponding to stable auroral red arc
[NASA-TM-X-66194] 09 p1028 N73-18390
High power output from carbon dioxide laser and effects of higher order transverse and longitudinal mode excitation
[AD-753402] 09 p1045 N73-18521
Theoretical model of optical excitation, emission, and deactivation properties of Meinel band system of nitrogen
[AD-753396] 09 p1069 N73-18722
Excitation and propagation of free flow electron waves in plasma
[IPPJ-145] 09 p1070 N73-18731
Electron and excitation temperature measurements in plasma jets stabilized by air and oxygen
[AD-752694] 09 p1071 N73-18743
Vibrationally excited carbon monoxide from reaction of oxygen with acetylene, methylacetylene, and methane
[DREV-TN-2051/72] 11 p1252 N73-20160
Electrode structures for transverse excitation produced HF lasers
[DREV-TN-2047/73] 11 p1302 N73-20565
High power tunable organic dye laser excitation of atomic fluorescence spectroscopy
12 p1409 N73-21422
Phase optimization and synthesis of antenna arrays, using variable phase and constrained amplitude excitation
13 p1499 N73-22149
Recombination electron beam-excited plasma into pulsed laser of high peak power
[AD-756681] 13 p1537 N73-22455
Plasma enhancement and diagnostic possibilities of tunable laser excitation
[AD-755373] 13 p1564 N73-22672
Electron scattering spectra of low state CO2 in energy-loss range 7 to 10 eV
[NASA-CR-132202] 17 p2064 N73-26697
Optical electron excitation cross section measurements of nitrogen at high temperatures
[AD-762257] 19 p2232 N73-28000
Semiclassical approximation to atom symmetric top rotational excitation
[NASA-CR-133849] 21 p2582 N73-30690
Calculating self-consistent propagation of intense pump beam that excites parametric decay instability for inhomogeneous plasma
[AD-763736] 21 p2584 N73-30708
Linearization method for approximate solution of rectangular plate response to excitation
[AD-763782] 22 p2727 N73-31821
Influence of excitation surface with liminary brightness on different regions of the retina
[NASA-TT-F-15124] 23 p2751 N73-32017

**EXCITED STATES**
U EXCITATION

**EXCITONS**
Interactions between rare earth ions in yttrium compound crystals
[AD-762363] 20 p2463 N73-29793

**EXECUTIVE AIRCRAFT**
U GENERAL AVIATION AIRCRAFT
U PASSENGER AIRCRAFT

**EXERCISE [PHYSIOLOGY]**
Effect of temporal uncertainty on human energy expenditure during moderate exercise
[AD-743726] 01 p0011 N73-10084
Weight, blood pressure, and intraocular pressure in young healthy males prior to and after 50-km walk
[NASA-TT-F-14557] 02 p0132 N73-11071
Effects of exercise work load on speech intelligibility at normal and increased atmospheric pressures
[AD-749321] 04 p0392 N73-13185
Manual actuator for exercise machine onboard spacecraft
[NASA-CASE-MFS-21481-1] 06 p0676 N73-15503
Physiological effects of high mountain alpinism exercises on human body
07 p0745 N73-16058
Physiological and hemodynamic adaptations to CO levels and exercise in nonsmoking normal men
[PB-213834/1] 14 p1612 N73-23073
Physiological response to prolonged muscular activity
14 p1724 N73-23990
Development of restraint system for securing personnel to ergometer while exercising under weightless conditions
[NASA-CASE-MFS-21046-1] 18 p2150 N73-27377
Exercise effects on human heart rate and oxygen uptake
20 p2365 N73-29020
Tilting table for testing human body in variety of positions while exercising on ergometer or other biomedical devices
[NASA-CASE-MFS-21010-1] 21 p2502 N73-30078
Mathematical model and digital computer simulation of cardiovascular control system response to ergometer exercise
24 p2886 N73-33049

**EXERTION**
U PHYSICAL WORK

**EXHAUST DIFFUSERS**
Flameout and ignition characteristics of jet engine fuel flame in gas turbine with exhaust diffuser
[AD-749635] 05 p0591 N73-14802
Analysis of flow characteristics of asymmetric annular diffuser with wall bleed capability and application to gas turbine combustors
[NASA-TM-X-2710] 07 p0770 N73-16251
Exhaust gas diffuser effect on test cell wall and turbofan cold-flow model engine exhaust nozzle plug and core engine cowl surface pressure
[AD-759177] 16 p1958 N73-25842

**EXHAUST FLOW SIMULATION**
NT ATMOSPHERIC ENTRY SIMULATION
NT FLIGHT SIMULATION
Jet noise suppression in turbofan engines at various exhaust flow velocities
03 p0249 N73-12016
Jet exhaust simulation in low speed wind tunnel
[DGT-8352] 13 p1507 N73-22211
Simulation of rocket plumes and reentry aerothermodynamics using oxygen/hydrogen combustion products
[NASA-CR-128955] 16 p1974 N73-25962
Reflected wave detonation of gaseous mixture in shock tube for simulating hydrogen/oxygen rocket plume
16 p1974 N73-25963

**EXHAUST GASES**
Design and evaluation of automobile thermal reactors with ceramic material construction
[NASA-TM-X-68148] 01 p0069 N73-10567
Theoretical and experimental analysis of charged metal particle detection in jet engine exhaust by cylindrical electrostatic probe
[AD-745540] 01 p0091 N73-10753
Measurement of carbonyls and noncarbonyl oxygenates in exhaust from gasoline fuels
[BM-RI-7675] 02 p0137 N73-11110
Chemical spray scrubber for cleaning toxic products from rocket exhaust gases
[AD-747023] 02 p0224 N73-11810
Portable sampling and measurement system for determining gaseous emission species in afterburn of turbojet engine at ground level
[AD-747773] 03 p0351 N73-12866

Analysis of propellant gases emitted by attitude control system to determine interference with experiments due to flow fields and plume density
[NASA-CR-114508] 03 p0363 N73-12958
Numerical prediction of exhaust products released to stratosphere during supersonic flight along definite air routes
[NASA-TT-F-14622] 04 p0371 N73-13013
Analytical procedure using gas-liquid chromatography in routine analysis of exhaust hydrocarbons from retention time data
[BM-RI-7700] 05 p0506 N73-14118
Effect of fuel front-end olefin and midrange volatility on automobile emissions
[BM-RI-7707] 05 p0506 N73-14119
Exhaust nozzle for reducing noise in gas turbines by mixing low velocity air with high velocity engine exhaust
[NASA-CASE-LEW-11569-1] 05 p0590 N73-14792
Biological effects of Viking Lander spacecraft engine fuel on extraterrestrial life during landing on planet Mars
[NASA-TM-X-2714] 06 p0630 N73-15118
Remote chemical detectors for vehicle identification by exhaust gases
[AD-751740] 07 p0753 N73-16116
Analysis of haze aerosols in rural and urban atmospheres
[PB-212609] 07 p0816 N73-16613
Tests of high pressure combustor exhaust emissions with improved air-atomizing and conventional pressure-atomizing fuel nozzle
[NASA-TN-D-7154] 07 p0855 N73-16929
Modification of jet engine fuels to reduce emissions of nitrogen oxides from jet aircraft turbine engines
[AD-752581] 08 p0953 N73-17803
Effect of fuel zoning and fuel nozzle design on exhaust pollution emissions at ground idle conditions for double-annular ram-induction combustor for turbofan engines
[NASA-CR-121094] 08 p0968 N73-17916
Performance test of internal combustion engine to determine effects of pulsed injection of secondary air on exhaust emission levels
[NASA-TM-X-2737] 08 p0969 N73-17920
Analysis of gaseous emissions from J-85 engine at various fuel-air ratios, engine speeds, and simulated altitude conditions
[NASA-TM-X-2726] 08 p0969 N73-17921
Fast computer program for prediction of nonequilibrium rocket plume properties
[AD-751984] 08 p0970 N73-17927
Thermochemical combustion effects of fuel-rich boron compound as solid rocket propellant
[AD-753105] 09 p1099 N73-18971
Analysis of air pollution caused by exhaust from military aircraft engines and development of technology for pollutant measurement to meet EPA standards
[AD-753095] 09 p1100 N73-18975
Development of techniques for reducing exhaust emissions from turbine engines
[NASA-TM-X-68192] 10 p1208 N73-19824
Development of sampling and analytical procedures for gas turbine engine exhaust using aircraft auxiliary power unit as emission source
[BM-RI-7735] 10 p1223 N73-19947
Effect of prevaporization of jet fuels on exhaust emission levels produced in turbojet combustor segment
[NASA-TM-X-68194] 10 p1224 N73-19949
Chemically reacting wave of aircraft flying at subsonic and supersonic velocity in upper troposphere and stratosphere
[AD-754918] 11 p1287 N73-20447
Stratospheric chemical reactions and perturbations caused by supersonic aircraft exhaust
[PB-213111] 11 p1290 N73-20464
Survey on aeronomic dynamics of photochemical reactions caused by supersonic aircraft exhaust
[PB-213126] 11 p1290 N73-20466
Alternate fuels to reduce aircraft exhaust pollutants
[AD-755151] 11 p1332 N73-20815
Reduction of jet engine noise due to turbulent mixing of exhaust gases with ambient atmosphere
[NASA-CASE-ARC-10712-1] 11 p1334 N73-20826
Physical and chemical characteristics, and biological activity of exhaust from beryllium-fueled motor
[AD-756531] 13 p1485 N73-22042
Detection of Combustion Improver-2 by atomic absorption spectrophotometry in smoke abatement systems
[AD-755723] 13 p1488 N73-22067
High altitude measurement of atmospheric pollution from aircraft engine exhaust gases
[NASA-TM-X-68221] 13 p1553 N73-22584
Present and predicted nature, entent, and control of air pollution related to aircraft operations in US
[REPT-72-02452] 13 p1553 N73-22586
Gas dynamic simulation of plumes from orbiter propulsion system for determining power-on aerodynamic flight characteristics of orbiter
[NASA-CR-124217] 13 p1581 N73-22814
J-57 combustor exhaust odor intensity and chemical composition considering inlet parameters, fuel types, and nozzle shapes
[NASA-CR-121159] 14 p1616 N73-23093
Endothermic decomposition in jet engine exhaust reaction
[AD-758200] 14 p1618 N73-23105
Threat of stratospheric ozone nonequilibrium by SST nitric oxide exhaust gases
[AD-757059] 14 p1719 N73-23949
Hazards of exposure to noise, fumes and vapors in military environment
14 p1723 N73-23985
Analysis of temperature and pressure parameters associated with recirculated engine exhaust from V/STOL aircraft engines exhausting normal to ground
[NASA-TT-F-14912] 15 p1768 N73-24323
Establishment of criteria for oxides of nitrogen emissions to control air pollution contribution from aircraft operating at major air terminals - Vol. I
[REPT-1162-1-VOL-1] 15 p1825 N73-24789
Development of computer program to analyze flow conditions in gas turbine compressor for application to reduction of nitrogen oxides from aircraft engine exhaust - Vol. 3
[REPT-1162-3-VOL-3] 15 p1825 N73-24791
Pollutant level measurement of exhaust gases from annular swirl can combustor
[NASA-TM-X-68247] 15 p1826 N73-24797
Pressure effects on tangential-injection film cooling in combustor exhaust stream
[NASA-TM-X-2809] 15 p1843 N73-24931
Effect of fuel vapor concentrations on combustion emissions and performance using experimental turbojet combustor segment
[NASA-TM-X-2800] 15 p1843 N73-24933
HCl acid aerosol production by space shuttle exhaust products and atmosphere
[NASA-CR-132993] 16 p1870 N73-25142
Chemical kinetics and atmospheric dynamics data base for digital modeling of climatological aircraft exhaust effects
[PB-214100/0] 16 p1908 N73-25441
Analysis of factors causing nitrogen oxides in exhaust gases of gas turbine engines and development of models of flow in gas turbine combustor
[NASA-CR-132959] 16 p1955 N73-25821
Exhaust gas diffuser effect on test cell wall and turbofan cold-flow model engine exhaust nozzle plug and core engine cowl surface pressure
[AD-759177] 16 p1958 N73-25842
Combustor research programs to gain advanced technology for reducing aircraft engine pollution
[NASA-TM-X-68256] 17 p2076 N73-26797
Condensation in rocket exhaust plumes
[AD-760039] 17 p2097 N73-26966
Wake model program for computing wake height and width
[PB-218820/9] 18 p2106 N73-27030
Kinetics of far ultraviolet chemiluminescence of exhaust plumes
[AD-760584] 18 p2114 N73-27093
Hydrocarbon chemistry and chemiluminescence in high altitude plumes
[AD-760793] 18 p2114 N73-27094
Atmospheric diffusion of carbon monoxide and lead from expressways
18 p2170 N73-27527
Testing association of automotive fuel composition with exhaust reactivity using different engines and gasolines of varied composition
[BM-RI-7756] 18 p2172 N73-27542
Performance and exhaust emission analysis of Williams research Gas Turbine Hornet automobile engine
[PB-218687/2] 18 p2173 N73-27551
Feasibility of emission control devices for motor vehicles
[PB-218942/1] 18 p2174 N73-27555
Environmental impact of highway projects as determined by vehicle emission factors
[PB-219812/5] 18 p2174 N73-27557
Contribution of automobiles to air pollution levels in Reading, England
[PB-219602/0] 18 p2175 N73-27563
Design and thermal analysis on film cooled exhaust duct for fissioning uranium plasma test reactor
[NASA-TM-X-2861] 18 p2178 N73-27585
Design of gas turbines for furnishing hot gases for turbine drives and analysis of limitations imposed by thermal stresses
[NASA-SP-8081] 18 p2193 N73-27705
Analysis of retrorocket exhaust plume of Viking Lander impinging on Martian surface and development of multiple nozzle configurtaion to reduce effects
[NASA-CR-2252] 18 p2197 N73-27737
Comparison of nitrogen oxide emissions produced by hydrogen combustion with emissions produced by jet engine fuels at simulated cruise conditions
[NASA-TM-X-68258] 18 p2206 N73-27804
Handbook on radiant emission and absorption of combustion gases for application to design of rocket combustion chambers and exhausts, turbojet engines, and industrial furnaces
[NASA-SP-3080] 18 p2206 N73-27807
Measurement of ionic conductivity and temperature in Apollo 15 plume
[AD-761484] 19 p2353 N73-28924
Analysis of aircraft emissions and recommendations for reducing impact of aircraft emissions on air pollution
[NREC-1168-1] 20 p2360 N73-28986
Analysis of jet engine test cell pollution abatement methods
[AD-763119] 20 p2450 N73-29690
Evaluation of high temperature nozzle throat materials for performance in highly oxidizing rocket exhaust environment
[AD-762533] 20 p2467 N73-29816
Development of computerized, theoretical model to predict characteristics of emissions from gas turbine engine combustors
[AD-762935] 20 p2467 N73-29819
Base region thermal environment test of scale model of Saturn S-2 stage - Vol. I
[NASA-CR-129009] 20 p2475 N73-29883
Theory and operating characteristics of equipment in laser exhaust measurement program
[PB-220429/5] 21 p2556 N73-30493
Automobile exhaust emission surveillance of light-duty vehicles
[PB-220755/3] 21 p2575 N73-30638
Exhaust emissions of 11 T56-A-15 engines
[EDR-7200] 21 p2588 N73-30736
Wind tunnel pressure signatures for scale model of Saturn 5-Apollo launch vehicle with simulated exhaust plumes
[NASA-TM-X-62129] 21 p2599 N73-30830
Capability of portable SF6 chromatograph to detect and determine behavior of plume out to 100 km
[BNL-17478] 22 p2674 N73-31417
Chemical and physical characterization of automotive exhaust particulate matter in atmosphere
[PB-221603/4] 22 p2695 N73-31589
Measurement of concentration of volatile and particulate lead compounds in atmosphere at selected road sites
[PB-221663/8] 22 p2695 N73-31592
Research projects to determine effects of exhaust products from aircraft operating in stratosphere on global and local climatic conditions
[UCRL-51336] 23 p2787 N73-32296
Sensory odor tests of exhaust from turbojet engine combustor operating at simulated idle conditions
[NASA-TM-X-71429] 23 p2829 N73-32613
Exhaust emission measurements on turbojet engine plume at simulated supersonic flight
[AD-764717] 23 p2832 N73-32632
Emission abatement in aircraft gas turbine combustor with low mass emissions
[AD-764987] 23 p2833 N73-32638
Radiative behavior of rocket exhaust plumes at high altitude
[AD-764908] 23 p2857 N73-32832
Wind tunnel tests to determine aerodynamic loads on flap systems behind engines and vibration modes of flap system
24 p2873 N73-32945
Dispersion predictions for effluents from exhaust gases from Saturn 5 and Scout-Algol 3 launch vehicles
[NASA-TM-X-2935] 24 p2921 N73-33327

**EXHAUST JETS**
U EXHAUST GASES

**EXHAUST NOZZLES**
NT CONVERGENT-DIVERGENT NOZZLES
NT PLUG NOZZLES
NT SPIKE NOZZLES

Measuring flame temperature in exhaust nozzle and combustion chamber by pyrometer
04 p0420 N73-13425
Method of characteristics for analyzing three dimensional, steady supersonic, nonequilibrium, chemically reacting flow of thermally perfect gases in exhaust nozzle
07 p0768 N73-16240
Performance of hypermixing nozzles in area ratio 23 ejector
[AD-752207] 08 p0955 N73-17821
Jet aircraft exhaust nozzle for noise reduction
[NASA-CASE-LAR-10951-1] 10 p1207 N73-19819
Shrouded divergent body attached to exhaust nozzle for jet noise suppression
[NASA-CASE-LEW-11286-1] 12 p1364 N73-21066
Analytical technique and computer program for evaluation of airbreathing propulsion exhaust nozzle performance
[AD-760541] 18 p2194 N73-27712
Flyover and static tests for determining effects of flight velocity on F-106B exhaust nozzle noise
[NASA-TM-X-2854] 19 p2329 N73-28734
Photographic recording of secondary flows at nozzle exits produced by planar nozzles with rectangular inlets from circular ducts
[AD-762743] 21 p2527 N73-30265
Assessment of jets as acoustic shields by comparison of single and multitube suppressor nozzle data
[NASA-TM-X-71450] 24 p2904 N73-33179

**EXHAUST SYSTEMS**

Design and performance of exhaust hood with protective air current outside of hood surface
08 p0872 N73-17063

Application of finite difference techniques to noise propagation in jet engine ducts
[NASA-TM-X-68261] 17 p1981 N73-26015
Base metal catalysts as platinum substitutes in petroleum refining and automobile emission devices
[NMAB-297] 18 p2113 N73-27088
Design and tests of lift fan exhaust suppression system for future VTOL aircraft noise goals
[NASA-CR-121108] 20 p2466 N73-29812
Exhaust pressure and density of pulsed thrustor systems
[NASA-TM-X-68299] 21 p2589 N73-30740
Design and characteristics of expansion chamber mufflers for reducing exhaust noise generated by helicopters
[NASA-TN-D-7309] 22 p2700 N73-31623

**EXHAUST VELOCITY**
Exhaust blast velocities and temperatures at ground level for various aircraft and wing tip vortex velocity for C-5 aircraft
[AD-764228] 22 p2616 N73-30961

**EXHAUSTION**
Various opinions on physical and mental exhaustion caused by atmospheric ion shortage
[NASA-TT-F-14646] 04 p0380 N73-13088

**EXITS [DOORS]**
U DOORS

**EXOBIOLOGY**
Supply, biosynthetic, and regenerated physicochemical systems for spacecraft life support
[NASA-TT-F-14436] 01 p0020 N73-10155
Spacecraft environment, radiation, and weightlessness effects on human biological processes in manned space flight
[JPRS-57517] 03 p0256 N73-12076
Supplement to bibliography on Aerospace Medicine and Biology, October 1972
[NASA-SP-7011[107]] 04 p0377 N73-13069
Research and development related to space biology and medicine
[JPRS-58010] 07 p0743 N73-16041
Review of papers presented at Conference on Space Biology and Aerospace Medicine
[JPRS-58345] 09 p0995 N73-18125
Medical and biological problems of manned space flight
[NASA-TT-F-719] 10 p1114 N73-19077
Detection of evolutionary organic compounds in extraterrestrial matter
10 p1118 N73-19114
Composition and effects of radioprotectors on acceleration tolerance, hypoxia toxicity, radiation protection, and dynamic space flight stress in animals
[NASA-TT-F-721] 11 p1239 N73-20054
Scientific and engineering studies for Physiology of Chimpanzees in Orbit Program
[NASA-CR-131374] 11 p1248 N73-20129
Analysis of space biology projects related to earth orbital experiment program to identify critical issues and methods of conducting experiments - Vol. 3
[NASA-CR-112327] 13 p1577 N73-22780
Data management systems, instrumentation concepts, and biotechnology laboratory for earth orbital experiment program and requirements study - Vol. 8
[NASA-CR-112332] 13 p1577 N73-22785
Research activities in exobiology and aerospace medicine
[JPRS-59015] 14 p1607 N73-23024
Microbiological experiments aboard balloons, rockets, and earth satellites - literature review
14 p1607 N73-23025
USSR conference on exobiology and aerospace medicine
14 p1609 N73-23045
Low temperature tolerance and adaptation of biological systems to space environment
[JPRS-59129] 14 p1610 N73-23055
Conference on Apollo 16 experiment for measuring microbial response to space environment
[NASA-TM-X-58103] 15 p1740 N73-24102
Cryobiological and space biological studies
[JPRS-59129] 15 p1742 N73-24120
Physical and biomedical research by earth orbiting space stations
[AD-756771] 15 p1743 N73-24126
Space biology, space medicine, and human physiology
[NASA-TT-F-14964] 16 p1867 N73-25116
Aerospace medicine and exobiology research in support of long term manned space flight
[JPRS-59702] 20 p2365 N73-29021
Effects of oxygen pressure on tissues under extreme flight factors
[NASA-TT-F-762] 21 p2500 N73-30065
Soviet research on space biology, aerospace medicine, and human factors engineering
[JPRS-59952] 22 p2618 N73-30983
Annotated bibliography and indexes on aerospace medicine and biology - September 1973
[NASA-SP-7011[119]] 24 p2882 N73-33012
Planetary quarantine requirements for automated spacecraft flights
[NASA-CR-135795] 24 p2885 N73-33040

**EXOSKELETONS**
Development and evaluation of free flying teleoperators to include semiexoskeletal master control unit, joystick-analog unit, and three dimensional television system
13 p1594 N73-22925

**EXOSPHERE**
Validity of CGL equations in solar wind problems of exosphere
[AD-756501] 13 p1575 N73-22760
Experimental determination of coupling between normal F region ionosphere and protonosphere using radar backscatter techniques at Arecibo, Puerto Rico
23 p2778 N73-32213

**EXPANDABLE STRUCTURES**
NT BALLOONS
NT BELLOWS
NT GAS BAGS
NT HIGH ALTITUDE BALLOONS
NT INFLATABLE STRUCTURES
NT METEOROLOGICAL BALLOONS
NT SKYHOOK BALLOONS
NT TETHERED BALLOONS
Human factors characteristics and geometry of expandable structures for use as airlocks, escape capsules, and crew transfer tunnels on Skylab program
[AD-749131] 06 p0722 N73-15896
Collapsible high gain antenna which can be automatically expanded to operating state
[NASA-CASE-KSC-10392] 17 p1993 N73-26117
Model tests and analysis of expandable floating bases
[AD-756048] 23 p2777 N73-32206
Expandable space frames with high expansion to collapse ratio
[NASA-CASE-ERC-10365-1] 23 p2847 N73-32749

**EXPANSION**
NT GAS EXPANSION
NT KARHUNEN-LOEVE EXPANSION
NT PRANDTL-MEYER EXPANSION
NT THERMAL EXPANSION
Elastomeric extensometer for measuring surface area changes of human body caused by body expansion and contraction
[NASA-CASE-MFS-21049-1] 02 p0173 N73-11405
Pressure changes in fluid flow along duct with sudden enlargement of area
[ESDU-72011] 04 p0403 N73-13281

**EXPANSION WAVES**
U ELASTIC WAVES

**EXPEDITIONS**
General description and scientific results of Tenth Soviet Antarctic Expedition for period 1965 to 1966
[TT70-50072] 20 p2406 N73-29339
Analysis of Tenth Soviet Antarctic Expedition to show preparations, logistic support, and operational accomplishments
20 p2406 N73-29340
Meteorological, actinometric, and aerological investigations conducted aboard ships of Tenth Soviet Antarctic Expedition
20 p2406 N73-29341
Analysis of ice conditions existing in Antarctic waters during Tenth Soviet Antarctic Expedition
20 p2407 N73-29342
Hydrological investigations conducted during Tenth Soviet Antarctic Expedition to determine temperature and salinity of ocean
20 p2407 N73-29343
Hydrographic investigations conducted aboard ships of the Tenth Soviet Antarctic Expedition
20 p2407 N73-29344
Marine geological research of submarine relief and ocean bottom sediments conducted during Tenth Soviet Antarctic Expedition
20 p2407 N73-29345
Radar analysis of ice sheets in Antarctic regions conducted during Tenth Soviet Antarctic Expedition
20 p2407 N73-29346
Clinical medicine and human factors engineering functions conducted during Tenth Soviet Antarctic Expedition
20 p2407 N73-29347
Human factors investigations and acclimatization research conducted during Tenth Soviet Antarctic Expedition
20 p2407 N73-29348
Investigation of oribatid mites found in Antarctic regions during Tenth Soviet Antarctic Expedition
20 p2407 N73-29349
Activities of meteorological section during Tenth Soviet Antarctic Expedition
20 p2408 N73-29350
Analysis of physicomechanical properties of ice conducted during Tenth Soviet Antarctic Expedition with emphasis on ice cover temperature effects
20 p2408 N73-29352
Hydrological investigations of Davis Sea conducted during Tenth Soviet Antarctic Expedition
20 p2408 N73-29353
Geophysical observations made during Tenth Soviet Antarctic Expedition with emphasis on field strength of long and short wave radio transmission
20 p2408 N73-29354
Technical and support services performed during Tenth Soviet Antarctic Expedition
20 p2408 N73-29355
Analysis of operations at ground station during Tenth Soviet Antarctic Expedition to show equipment requirements and mission accomplishments
20 p2408 N73-29356
Medical analysis of vitamin balance among personnel of Tenth Soviet Antarctic Expedition to show effects on health and acclimatization ability
20 p2408 N73-29357
Analysis of physiological effects of diet on personnel of Tenth Soviet Antarctic Expedition
20 p2409 N73-29358
Analysis of microclimate of living and service quarters during Tenth Soviet Antarctic Expedition
20 p2409 N73-29359
Operations and functions of ground station during Tenth Soviet Antarctic Expedition to obtain meteorological and geophysical data
20 p2409 N73-29360
Functions and operations of ground station during Tenth Soviet Antarctic Expedition including construction procedures and equipment installation
20 p2409 N73-29361
Analysis of ice conditions existing in Alasheyev Bight during Tenth Soviet Antarctic Expedition
20 p2409 N73-29362
Seasonal plankton collections conducted during Tenth Antarctic Expedition
20 p2409 N73-29363

**EXPERIMENTAL DESIGN**
NT FACTORIAL DESIGN
Criteria for optimal approximating functions for experimental test design
[NASA-TM-X-2663] 02 p0202 N73-11636
British Prospero satellite control noting instrumentation, equipment, and experimental performance
[RAE-TR-72088] 03 p0359 N73-12928
Corrosion control design optimizing layouts, orientation, location, and configuration
[BNWL-SA-3817-REV-1] 04 p0434 N73-13539
Free electrophoresis space experiment design for weightlessness environments
[NASA-CR-123972] 05 p0502 N73-14090
Criteria for selected response surface methodology design variants in human performance research
[AD-748236] 05 p0503 N73-14099
Biosatellite 2 experiments for determining effects of prolonged weightlessness on biological processes
[CONF-720441-1] 06 p0630 N73-15119
Advanced technology, experimental and instrument design, and mission planning for space shuttle sortie workshop - conference working group reports
[NASA-TM-X-68842] 06 p0719 N73-15867
Experimental design and scientific exploration of Mars surface by MARV
[NASA-TM-X-64719] 07 p0765 N73-16219
Production of stimulated emission in vacuum ultraviolet using molecular xenon gas excited by relativistic electron beam
[AD-753483] 09 p1045 N73-18522
Scientific space mission of small spin stabilized astronomical satellite with X ray and IR experiments
09 p1081 N73-18817
Tissue culture laboratory for first manned Skylab mission for performing experiments to detect effects of zero gravity on living human cells
09 p1088 N73-18874
Experimental design for space shuttle sortie mission payloads
[NASA-CR-112287] 11 p1343 N73-20898
NaI[T1] crystal detector for measuring proton induced activity in gamma ray spectrometer
[NASA-TM-X-66241] 15 p1787 N73-24486
Feasibility analysis of laboratory experiment on ionic excitation cross section by electron impact on laser produced plasmas
[ESRO-SN-122] 15 p1818 N73-24737
Design and performance of stable CO and CO2 lasers
[AD-758774] 16 p1924 N73-25568
Experimental design, research programs, and equipment design activities of Astronomical Space Laboratory for 1971 to 1972
[RAP-01-72] 17 p2011 N73-26261
Propagation and merging of high current relativistic electron beams in particle accelerator facility
[AD-760344] 17 p2011 N73-26266
Sensitivity of low weight CPNE for planetary composition analysis
[NASA-CR-132208] 17 p2032 N73-26448
Atlas S183 experiment for ultraviolet stellar spectrophotometry onboard Skylab manned space station
17 p2033 N73-26454
OAO-C X ray experimental design
17 p2084 N73-26857
UK-5 X ray experimental design performance
17 p2084 N73-26858
X ray Astronomical Netherlands Satellite experimental design for soft and hard source identification and spectral analysis
17 p2084 N73-26860

Corsa 1 and 2 instruments, experimental design, and data systems for X ray astronomy
17 p2084 N73-26864
OSO-J experimental design, and equipment for soft X ray sources and diffuse components in 0.01 to 2.0 keV range
17 p2085 N73-26865
HEAO-A experimental design and equipment for mapping celestial X ray sources and spectral analysis over 0.2 to 150 keV
17 p2085 N73-26866
Proposed experiments dealing with classical free turbulent flows
19 p2254 N73-28172
Skylab experiments on convection and molten metal flow and solidification under reduced gravity
[NASA-CR-124329] 19 p2343 N73-28852
Determination of variability of oblique and horizontal visibility for aircraft landing by analysis of experimental data
[NLL-M-23046-[5828.4F]] 21 p2567 N73-30576
Laboratory investigation of Coriolis acceleration effects on vestibular apparatus of cosmonauts
[NASA-TT-F-15129] 22 p2620 N73-30993
Design, fabrication, and tests of ground station hardware for ATS-F millimeter wave experiment
[NASA-CR-132802] 22 p2673 N73-31409
Enlarged and revised set of tables of two-associate-class partially balanced design
[NBS-AMS-63] 22 p2691 N73-31556
Identification, selection, and description of earth observation experiments for shuttle sortie missions in 1980's
[NASA-CR-124368] 22 p2717 N73-31751
Methodology of planning experiments under nonuniform conditions
24 p2944 N73-33513

**EXPERIMENTATION**
Generation of random experiment schedules for space station using Monte Carlo technique
[NASA-TM-X-64557] 03 p0355 N73-12894
Telemetry data processing systems for experiments flown on Injun 5 satellite, OV-3 satellite, OV-4 satellite, OV-5 satellite, OV-6 satellite, and OV-15 satellite
[AD-751508] 07 p0759 N73-16166
Abstracts of experimental studies on superconductivity
[AD-751869] 08 p0952 N73-17794
Skylab experiments to assess weightlessness effects on human nutritional metabolism and musculoskeletal function
09 p0994 N73-18115
Problems of electron accelerator scattering experiments
[CONF-710974-7] 17 p2065 N73-26708
Automated Microbial Metabolism Laboratory experimentation for detecting and elucidating extraterrestrial metabolism using labeled release experiment
[NASA-CR-135638] 23 p2770 N73-32154
Automatic experimenter concept based on evolution strategy
24 p2908 N73-33210

**EXPIRED AIR**
Toxic effects of human exhaled air on mice organisms
10 p1117 N73-19103
Calcium metabolism determination in rats by measuring argon isotope in exhaled air after neutron irradiation
[NASA-CR-128816] 10 p1120 N73-19130

**EXPLODING CONDUCTOR CIRCUITS**
U CIRCUITS
U EXPLODING WIRES

**EXPLODING CONDUCTORS**
U EXPLODING WIRES

**EXPLODING WIRES**
Exploding wire plasma accelerator simulating hypervelocity micrometeoritic damage at impact
[ISL-26/71] 07 p0821 N73-16657
Volt-ampere characteristics of explosive wires using pulse-current generator
[AD-753552] 10 p1135 N73-19251
Generation of narrow high current pulses
10 p1228 N73-19980

**EXPLOITATION**
Technical utilization of advanced equipment for oceanological exploitation by US
[JPRS-58696] 12 p1401 N73-21363

**EXPLORATION**
NT LUNAR EXPLORATION
NT MINERAL EXPLORATION
NT OIL EXPLORATION
NT SPACE EXPLORATION
General description and scientific results of Tenth Soviet Antarctic Expedition for period 1965 to 1956
[TT70-50072] 20 p2406 N73-29339
Marine ice observations during Tenth Soviet Antarctic Expedition to measure formation, growth, disintegration, and physicomechanical properties
20 p2408 N73-29351

**EXPLORER SATELLITES**
NT EXPLORER 12 SATELLITE
NT EXPLORER 18 SATELLITE
NT EXPLORER 21 SATELLITE
NT EXPLORER 24 SATELLITE
NT EXPLORER 27 SATELLITE
NT EXPLORER 31 SATELLITE
NT EXPLORER 32 SATELLITE
NT EXPLORER 33 SATELLITE
NT EXPLORER 34 SATELLITE
NT EXPLORER 35 SATELLITE
NT EXPLORER 38 SATELLITE
NT EXPLORER 40 SATELLITE
NT EXPLORER 41 SATELLITE
NT EXPLORER 49 SATELLITE
NT IMP
NT RADIO ASTRONOMY EXPLORER SATELLITE
Perigee rotation effects on orbit-integrated proton and electron fluxes for AE-C orbit
[NASA-TM-X-66059] 01 p0103 N73-10855
Atmosphere Explorer Control System for automatic control of AE spacecraft and experiments
[NASA-TM-X-66086] 02 p0232 N73-11888
Ultraviolet photometry experiment for Atmosphere Explorer C, D, and E missions to record solar irradiance
[NASA-TM-X-66130] 04 p0422 N73-13437
Explorer 44 measurement of solar X rays and ultraviolet radiation
[AD-748992] 04 p0479 N73-13919
Correlative studies of effects of solar wind and interplanetary magnetic field on bow shock and geomagnetic cavity
[NASA-CR-129924] 05 p0592 N73-14808
Fuel expulsion efficiency and service life of Arde metallic diaphragm used in Atmospheric Explorer propulsion subsystem
[NASA-TM-X-66191] 09 p1078 N73-18794
Adaptive filter for estimating atmospheric density profile during Atmospheric Explorer missions from accelerometer data
[NASA-TM-X-66202] 10 p1154 N73-19388
Effects of photoelectron emission on multiple-probe spacecraft near plasmapause
[NASA-TM-X-69313] 12 p1403 N73-21380
Satellite observations of geomagnetic disturbance reaction time in upper atmosphere
[REPT-85] 14 p1658 N73-23458
Atmosphere Explorer satellite absolute pressure measurements of upper atmosphere
[AD-757908] 15 p1782 N73-24447
Adsorption, surface reaction, and recombination of atomic oxygen related to dual air density explorer satellites
[NASA-CR-2271] 16 p1906 N73-25421
Polar motion and earth tides from Beacon Explorer C
[NASA-TM-X-70460] 22 p2664 N73-31350
Summary of attitude dynamic analysis for IMP-J S/C wire antenna spacecraft
[NASA-TM-X-70465] 22 p2720 N73-31764
Digital attitude control system for Explorer 50 satellite
[NASA-TM-X-70488] 24 p2950 N73-33567
Magnetic field data from magnetometer experiments and trajectories of Explorers 33, 35, 41, 43, and 47
[NASA-TM-X-70481] 24 p2979 N73-33809

**EXPLORER 12 SATELLITE**
MHD wave transmission and production near magnetopause studied from Explorer 12 magnetometer data
22 p2665 N73-31354

**EXPLORER 18 SATELLITE**
Probe measurements of dc electric fields from IMP 1
08 p0973 N73-17950

**EXPLORER 21 SATELLITE**
System for measuring charge spectra of solar cosmic rays on IMP-6
08 p0973 N73-17960

**EXPLORER 24 SATELLITE**
Cinetheodolite observations of Explorer 24 satellite between Nov. 1965 and Mar. 1966, using azimuth and elevation values
[ROE-STS-131] 04 p0479 N73-13916
Drag coefficients for Echo 1 and Explorer 24 spherical surfaces in atomic oxygen over energy range from 4 to 200 eV
[NASA-CR-2233] 10 p1192 N73-19697

**EXPLORER 27 SATELLITE**
Determination of earth tidal amplitude and phase from orbital perturbations of Beacon Explorer C spacecraft
[NASA-TM-X-70420] 20 p2409 N73-29365

**EXPLORER 31 SATELLITE**
Explorer 31 measurements of photoelectron escape fluxes for equatorial and midlatitude regions
[NASA-TM-X-68921] 07 p0789 N73-16416

**EXPLORER 32 SATELLITE**
Explorer 32 satellite data on atmospheric hydrogen
08 p0972 N73-17945

**EXPLORER 33 SATELLITE**
Analyses of solar wind plasma data obtained by Explorer 33 and Explorer 35
[NASA-CR-129923] 05 p0592 N73-14807
Perpendicular fast reverse shock wave found in interplanetary plasma and magnetic field data from Explorers 33 and 35
[NASA-TM-X-70451] 21 p2523 N73-30235

**EXPLORER 34 SATELLITE**
Existence of natural radio noise between electron plasma frequency and upper hybrid resonance frequency as detected by long electric antennas of IMP-6 satellite
[NASA-CR-130273] 07 p0843 N73-16832
Energetic particle flux experiments aboard Explorer 34 and 41 satellites
[NASA-CR-130172] 08 p0946 N73-17747
Analysis of data from charged particle experiment of Explorer 34 satellite and Explorer 35 satellite
[NASA-CR-130171] 08 p0976 N73-17985
Development and characteristics of solid state cosmic ray telescope for use on IMP F and G missions
[NASA-CR-132767] 16 p1912 N73-25473

**EXPLORER 35 SATELLITE**
Analyses of solar wind plasma data obtained by Explorer 33 and Explorer 35
[NASA-CR-129923] 05 p0592 N73-14807
Analysis of data from charged particle experiment of Explorer 34 satellite and Explorer 35 satellite
[NASA-CR-130171] 08 p0976 N73-17985
Solar proton anisotropies in interplanetary space as measured by Explorer 35 solid state detectors
13 p1573 N73-22744
Perpendicular fast reverse shock wave found in interplanetary plasma and magnetic field data from Explorers 33 and 35
[NASA-TM-X-70451] 21 p2523 N73-30235

**EXPLORER 38 SATELLITE**
Explorer 38 observations of solar type 3 radio bursts
19 p2339 N73-28813

**EXPLORER 40 SATELLITE**
Injun 5 observations of charged particle precipitation over auroral zone during magnetic substorm
13 p1515 N73-22272
Direct comparison between electric field measurements by Injun 5 satellite and visual aurora data
[NASA-CR-132958] 16 p1906 N73-25416
Injun 5 satellite extended mission analysis discussing experiments, data processing telemetry, and geophysical data
[BMBW-FBW-72-24] 22 p2722 N73-31786

**EXPLORER 41 SATELLITE**
Energetic particle flux experiments aboard Explorer 34 and 41 satellites
[NASA-CR-130172] 08 p0946 N73-17747
Development and characteristics of solid state cosmic ray telescope for use on IMP F and G missions
[NASA-CR-132767] 16 p1912 N73-25473

**EXPLORER 49 SATELLITE**
Seven gravity gradient dynamics experiment in lunar orbit, using RAE-B spacecraft
[NASA-TM-X-66271] 17 p2024 N73-26375

**EXPLOSIONS**
NT AERIAL EXPLOSIONS
NT CHEMICAL EXPLOSIONS
NT GAS EXPLOSIONS
NT NUCLEAR EXPLOSIONS
NT UNDERGROUND EXPLOSIONS
NT UNDERWATER EXPLOSIONS
Abstracts and bibliographies on research in laser technology, effects of explosions, geosciences, and particle beams
[AD-749488] 04 p0430 N73-13504
Excitation of Lamb atmospheric edge mode by tail of large atmospheric explosion
05 p0509 N73-14143
Noise and blast environments providing definition of units and techniques of noise measurement and giving booster-launch and spacecraft noise data
06 p0629 N73-15106
Seismological wave spectra for differentiating between earthquakes and explosions
[AD-749874] 06 p0671 N73-15457
Device for detection of combustion light preceding gaseous explosions
[NASA-CASE-LAR-10739-1] 07 p0798 N73-16484
Gas ionization and plasma generation by explosive shock wave
[AD-751152] 07 p0829 N73-16725
Laser technology, strong explosion effects, geosciences, and particle beams bibliographies
[AD-754946] 11 p1353 N73-20982
Laser technology, strong explosion effects, geosciences, and particle beams - bibliographies
[AD-754962] 11 p1353 N73-20988
Anomaly report of explosive failure of ground support equipment decontamination unit tank during postflight deactivation of Apollo 16 command module
[NASA-TM-X-69323] 17 p2088 N73-26897
Density analysis of quartz grains to determine rock damage from small charge blasting in granite
[BM-RI-7751] 18 p2144 N73-27327
Bibliography on lasers, strong explosions, geosciences, particle beams, and material sciences
[AD-759275] 18 p2215 N73-27884
Computer program for estimating peak static pressure from internal explosions in closed vessels
[AD-762402] 19 p2350 N73-28907
Abstracts and bibliographies of Soviet literature on lasers, explosion effects, particle beams, and geosciences
[AD-762376] 19 p2356 N73-28955

Propagation of shock waves following explosion of finite cylindrical charge based on finite difference numerical analysis
24 p2991 N73-33907
EXPLOSIVE DEVICES
NT BOMBS [ORDNANCE]
NT DETONATORS
NT INITIATORS [EXPLOSIVES]
NT SHAPED CHARGES
NT TORPEDOES
Apollo experience report on use of pyrotechnic devices in systems of Apollo spacecraft
[NASA-TN-D-7141] 10 p1215 N73-19878
Development and characteristics of squib actuated explosive disconnect for spacecraft release from launch vehicle
[NASA-CASE-NPO-11330] 17 p2096 N73-26958
Description of pyrotechnic systems principles with application to systems and equipment on space shuttle
[NASA-CR-2292] 21 p2600 N73-30840
Explosive magnetohydrodynamic programs
[AD-762934] 21 p2607 N73-30890
EXPLOSIVE FORMING
Explosive forming and manufacturing of titanium alloy plates
[AD-745113] 01 p0062 N73-10512
Regular forging and explosive forming effects on mechanical properties of aluminum alloy
[AD-748710] 04 p0427 N73-13484
Thermomechanical processing of nickel-base superalloys by explosive shock wave deformation
[AD-761218] 18 p2162 N73-27462
EXPLOSIVE GASES
U FLAMMABLE GASES
EXPLOSIVE WELDING
Explosive welding process for producing molybdenum wire reinforced columbium alloy composites
[NASA-CR-123937] 03 p0305 N73-12490
Explosive welding of thin metal scarf joint
[NASA-CASE-LAR-11211-1] 05 p0552 N73-14480
Fracture mechanics evaluation of effect of explosive bonding on fatigue crack growth in aluminum plates
[AD-756423] 13 p1544 N73-22511
Various applications of explosive welding
[AD-758844] 16 p1919 N73-25530
Method for eliminating noise and debris of explosive welding techniques by using complete enclosure
[NASA-CASE-LAR-10941-2] 23 p2797 N73-32371
EXPLOSIVES
NT CELLULOSE NITRATE
NT HYDRAZINE NITROFORM
NT RDX
NT TRINITROTOLUENE
Acoustic holography for imaging cylindrical plastic-bonded explosive loads
[AD-746468] 01 p0067 N73-10547
Using microscopic models and principles for studying transfer of lattice vibrational energy into first excited state in perfect crystal
[AD-748079] 03 p0365 N73-12977
Compatibility with explosives and propellants of natural, butyl and chloroprene rubbers containing Octamine or Flectol H as antioxidants
[ERDE-TN-55] 05 p0565 N73-14592
Computer program for determining influx towards center of spherical metal shell following detonation of spherical, symmetrically placed explosive
[FOA-2-C-2471-25] 06 p0653 N73-15305
Bibliography of nuclear explosion effects on explosives
[ICT-11/71] 08 p0946 N73-17749
Lateral gas expansion behind explosive detonating slab
[ISL-19/71] 09 p1016 N73-18291
Mach reflection in solids, liquids, and explosives using annular shock wave generated by explosion of cylinder coatings
[BMVG-FBWT-72-3] 09 p1016 N73-18292
Thermal dilatation coefficients of explosive monocrystals determined by extensometry
[ISL-24/71] 09 p1099 N73-18969
Manufacture, stabilization, and properties of polyvinyl nitrate explosives
[ICT-7/71] 10 p1127 N73-19178
Explosives for lunar seismic studies
[NASA-CR-128876] 11 p1348 N73-20939
Simulation of plastic bonded hexanitrostilbene/Teflon explosive for lunar seismology
[NASA-CR-131370] 11 p1349 N73-20949
Accidental initiation of encased high explosive charges through rapid closure of air gap due to accidental drop of device
[AD-758255] 15 p1844 N73-24941
Evaluation of explosive loaded material during air-drop operations
[AD-759228] 17 p2099 N73-26981
Compilation of card-gap and projectile impact sensitivity data for wide variety of explosive compositions
[BM-IC-8605] 18 p2206 N73-27802
Detonation sensitivity and shock resistance of explosives at impact
[ISL-2/73] 19 p2353 N73-28923
Fracture characteristics of small cylindrical bodies partly prefragmented by external notching subject to detonation of high explosive filling
[REPT-545-PT-1] 20 p2483 N73-29943
Development of technique and apparatus for optically detonating insensitive high explosives
[NASA-CASE-NPO-11743-1] 20 p2485 N73-29959
Physical and detonation properties of dry blended hexanitrostilbene/Teflon explosive charges used on Apollo 17 seismic experiment
[NASA-CR-133838] 21 p2606 N73-30886
Time evolution of finite power density blast waves
[AD-763834] 22 p2656 N73-31278
Reactivity of tungsten in mixture of Hexogen and aluminum in bomb calorimeter
[ICT-12/72] 22 p2730 N73-31845
Production of intermetallic compounds by effect of shock waves from explosions and compaction of powder
[NASA-CASE-MFS-20861-1] 23 p2806 N73-32437
Military treatment and disposal of high energy materials
[AD-764534] 23 p2858 N73-32835
EXPONENTIAL FUNCTIONS
Noise characteristics of functional correlators using nonlinear elements with exponential characteristics
12 p1386 N73-21241
Orthogonal and unitary transformations for asymmetrically loaded symmetric systems
[AD-761542] 20 p2440 N73-29601
EXPORTS
U INTERNATIONAL TRADE
EXPOSURE
Mechanical exposure interlock device for preventing film overexposure in oscilloscope camera
[NASA-CASE-LAR-10319-1] 23 p2790 N73-32322
EXPRESSIONS [MATHEMATICS]
U FORMULAS [MATHEMATICS]
EXPULSION BLADDERS
Fuel expulsion efficiency and service life of Arde metallic diaphragm used in Atmospheric Explorer propulsion subsystem
[NASA-TM-X-66191] 09 p1078 N73-18794
EXTENSIONS
Research and development of transpiration cooled inflatable nozzle extension
[NASA-CR-124165] 11 p1269 N73-20300
Thermal and stress analyses of interfaces for nozzles and nozzle extensions
[NASA-CR-132211] 15 p1768 N73-24324
EXTENSOMETERS
Elastomeric extensometer for measuring surface area changes of human body caused by body expansion and contraction
[NASA-CASE-MFS-21049-1] 02 p0173 N73-11405
Improved dilatometer with helium cryostat for low temperature measurements
[AD-747555] 03 p0304 N73-12484
Determination of coefficients of linear expansion for turbine parts as result of heating by Chevenard dilatometer
[AD-749735] 05 p0607 N73-14935
EXTERNAL COMBUSTION ENGINES
Fundemental aspects of regenerative cooled, upper stage rocket plane with external-burning thrust augmentation
[AD-756498] 13 p1583 N73-22832
Structural analysis of mechanical rhombic drives for machines operating on Stirling cycle
[AD-761594] 19 p2330 N73-28749
EXTERNAL STORES
NT PODS [EXTERNAL STORES]
Aerodynamic characteristics of four configurations of rounded shoulder boattail nozzles mounted on F-106B aircraft at subsonic speeds
[NASA-TM-X-2626] 02 p0124 N73-11013
Analysis of aerodynamic interference effects between aircraft and external store carried under wing based on inviscid flow characteristics
[AD-748348] 04 p0370 N73-13005
Effect of internal spinning fly wheel on air launched missile stability and resulting launch disturbance
[AD-749027] 04 p0375 N73-13047
Wind tunnel measurement of surface pressure distributions on three bodies of revolution at Mach numbers from 0.7 to 2.02
[AD-749934] 05 p0492 N73-14012
Effects of various external stores characteristics, spanwise positions, and Mach number on static longitudinal stability of several military aircraft
[AD-750120] 06 p0624 N73-15063
Aerodynamic characteristics of helicopters with sling loads in hovering and near-hovering conditions
[AD-750618] 06 p0625 N73-15073
Development of equipment for securing external stores SH-3G helicopter and analysis of failure modes
[AD-757001] 13 p1474 N73-21943
Design, fabrication, and evaluation of mechanical devices for supporting external stores on military helicopters
[AD-755532] 13 p1535 N73-22436
Wind tunnel tests to determine effect of longitudinally oriented wing-mounted pods on aerodynamic characteristics of V/STOL transport model in cruise flight mode
[NASA-TN-D-7199] 15 p1731 N73-24035
Aerodynamic forces and trajectories of external stores separated from F-4 aircraft
[AD-757932] 15 p1850 N73-24993
Wind tunnel tests to determine pressure distribution on two dimensional airfoil with pylon mounted stores at subsonic speeds using F-4 aircraft model
[AD-759582] 16 p1859 N73-25053
Aerodynamic interference between aircraft and external store mounted on elliptical wing under inviscid flow conditions
[AD-759170] 16 p1864 N73-25094
Analysis of descent trajectories to determine static and dynamic stability of free-fall stores with freely spinning stabilizer devices
[AD-760677] 18 p2102 N73-26999
Analysis of alternate space shuttle concepts to examine stage-and-one-half concept for reusable shuttle system and cost of external hydrogen tank development program
[NASA-CR-124421] 23 p2850 N73-32774
Aerodynamic characteristics of alternate space shuttle configurations and trajectory analysis with external drop tanks installed
[NASA-CR-124418] 23 p2850 N73-32775
EXTERNALLY BLOWN FLAPS
Noise sources and noise scaling laws of externally blown STOL flaps
03 p0250 N73-12024
Design of augmentor wing jet flap configuration with minimum noise generation for jet STOL transport aircraft
03 p0250 N73-12025
Pressures and temperatures on the lower surfaces of an externally blown flap system during full-scale ground tests
[NASA-TN-D-7138] 06 p0614 N73-14984
Design aspects of stall of powered-lift aircraft with externally blown flaps and methods for predicting increment in maximum lift coefficient due to power
06 p0617 N73-15011
Prediction of fluctuating pressures acting on externally blown flap surfaces
[NASA-CR-112216] 06 p0619 N73-15026
Reduction of noise generated by externally blown flaps using slot near trailing edge of flap with low velocity secondary air blown through slot
[NASA-TM-X-68172] 06 p0619 N73-15027
Screening tests of upper surface blowing on externally blown flaps configurations to obtain noise and turning effectiveness data
[NASA-TM-X-68167] 06 p0620 N73-15030
Comparison of mechanical high lift flaps with externally blown flaps for STOL aircraft
[MBB-UH-12-72-O] 07 p0739 N73-16017
Wind tunnel tests to determine acoustic properties of semispan wing with externally blown jet flap to include effects of flap size, vertical location and forward speed
[NASA-TM-X-2749] 09 p0985 N73-18041
Analysis of basic acoustic characteristics and noise reduction potential of upper surface of blown flap
[NASA-CR-112246] 11 p1234 N73-20017
Acoustic measurements of aerodynamic noise generated by externally blown flap lift augmentation system for various aerodynamic configurations
[NASA-TM-X-2776] 12 p1363 N73-21059
Wind tunnel tests to determine static longitudinal aerodynamic characteristics of jet transport wing-body with upper surface blown jet flap for lift augmentation for takeoff and landing
[NASA-TN-D-7183] 13 p1470 N73-21907
Wind tunnel tests to determine acoustic properties of externally blown jet flap and augmentor wing short takeoff aircraft concepts
[NASA-TM-X-62251] 13 p1472 N73-21924
Comparison of aerodynamic lift developed by mechanical high lift systems and lift developed by externally blown flaps on short takeoff aircraft
[NASA-TT-F-14895] 14 p1601 N73-22981
Effect of jet stream blowing downwards from lower surface of slender delta wing to obtain lift augmentation for takeoff and landing
[ARC-R/M-3288] 15 p1727 N73-24009
Simulator analysis of effect of engine response characteristics on approach and landing operations of powered lift aircraft with externally blown flaps
[NASA-TM-X-62265] 17 p1982 N73-26021
Analysis of influence of engine response characteristics on approach and landing performance of aircraft equipped with externally blown flap
[NASA-TM-X-62265[2]] 17 p1982 N73-26022
Wind tunnel tests to determine acoustic properties of jet augmented lifting flap configuration
[NASA-TT-F-14951] 17 p1983 N73-26030
Analysis of acoustic properties and aerodynamic characteristics of engine over wing configuration with flow attached and unattached on upper surface of flaps
[NASA-TM-X-71419] 21 p2494 N73-30015

Effect of wing aspect ratio and flap span on aerodynamic characteristics of short takeoff model with externally blown jet flap
[NASA-TN-D-7205] 21 p2494 N73-30020
Wind tunnel tests to determine effects of variations in Reynolds number and leading edge configurations on aerodynamic characteristics of STOL transport with externally blown flaps
[NASA-TN-D-7194] 21 p2494 N73-30021
Development of data for numerical analysis of aerodynamic performance of jet, blown, and ejector flaps
[AD-763793] 21 p2498 N73-30049
System for reducing noise generated by jet impinging on external flap using injection of secondary air from slot near trailing edge of flap
[NASA-CR-132270] 22 p2611 N73-30930
Takeoff and landing performance characteristics and field length requirements for jet short takeoff transport aircraft with full span, externally blown flaps
[NASA-TN-D-7441] 23 p2741 N73-31939
Evaluation of low speed flying qualities of short takeoff aircraft with externally blown flap wing or augmentor wing using flight simulator
[NASA-TN-D-7454] 23 p2742 N73-31951
Aerodynamic and performance characteristics of short takeoff aircraft equipped with externally blown flaps
24 p2872 N73 32935
Wind tunnel tests to determine stability and control characteristics of externally blown jet-flap configurations
24 p2872 N73-32940
Wind tunnel tests to determine aerodynamic loads on flap systems behind engines and vibration modes of flap system
24 p2873 N73-32945
Measurement of fluctuating surface pressures induced on externally blown flaps by jet impingement and relationship to sonic fatigue of airframes
24 p2873 N73-32946
Full-scale ground tests of externally blown flap system on F-111 aircraft wing to determine pressure and temperature distributions on undersurface of wing, vane, and flap
24 p2873 N73-32947
Simulations of powered-lift STOL transport aircraft with either externally blown flap configuration or augmentor wing configuration
24 p2873 N73-32948
Acoustic measurements of aerodynamic noise produced by impingement of jet exhaust on wing and flap of externally blown flap system installed on F-111 aircraft
24 p2875 N73-32964
Wind tunnel tests to determine acoustic properties of externally blown flap and augmentor wing for short takeoff aircraft configurations
24 p2875 N73-32965
Aerodynamic noise characteristics of short takeoff aircraft with externally blown flaps and engines mounted over and under wing
24 p2876 N73-32966
Method for predicting noise generated by deflecting engine exhaust for under-the-wing and over-the-wing versions of externally blown flap configuration
[NASA-TM-X-71449] 24 p2876 N73-32969
Wind tunnel tests of large scale subsonic jet transport with upper surface blowing flap system for lift augmentation
[NASA-TM-X-62296] 24 p2876 N73-32973

**EXTINCTION**
NT INTERSTELLAR EXTINCTION

**EXTINGUISHERS**
U FIRE EXTINGUISHERS

**EXTINGUISHING**
Effects of solvent composition in quenching fluorescence of Pr[3 plus] ions in aprotic solvents
[CRC-TN-657] 21 p2505 N73-30104

**EXTRACTION**
Research and development in chemical and extractive metallurgy and molecular crystals
[AD-754797] 11 p1327 N73-20770
Theory and applications of centrifugal extraction process based on numerical analysis of flow characteristics of liquid residue
[NLL-RTS-7990] 15 p1790 N73-24512

**EXTRAGALACTIC LIGHT**
U EXTRATERRESTRIAL RADIATION
U LIGHT (VISIBLE RADIATION)

**EXTRAGALACTIC MEDIA**
U INTERGALACTIC MEDIA

**EXTRAGALACTIC RADIO SOURCES**
NT RADIO GALAXIES
Relative flux density measurements and spectra of extragalactic radio sources at decimetric wavelengths
07 p0838 N73-16788
X ray astronomy and its impact on galactic and extragalactic radio source mapping
17 p2084 N73-26856
Optical variability in peculiar extragalactic radio sources
23 p2755 N73-32047

**EXTRAPOLATION**
Variational extrapolation method for wind and atmospheric temperature analysis
[AD-745354] 01 p0051 N73-10413
Optimum interpolation and extrapolation of meteorological fields
[NLL-M-22856-[5828.4F]] 11 p1313 N73-20654
Extrapolation technique to obtain estimates of mesospheric density, pressure, and temperature
[NASA-CR-2223] 12 p1401 N73-21364
Stress-rupture strength testing and principles of creep-rupture in heat resistant alloys
[JPRS-58760] 13 p1542 N73-22494
Extrapolating stress-rupture test results of heat resistant alloys
13 p1542 N73-22495
Flight plan position extrapolation in automated oceanic air traffic control system
[FAA-RD-73-72] 21 p2576 N73-30648
Headlamp research program for extrapolation/interpolation of surface values from predefined grid
[LTR-ST-602] 22 p2637 N73-31129
Extrapolation predictive displays for manual path and position control of VTOL aircraft
24 p2880 N73-33000

**EXTRASOLAR PLANETS**
Short wave radio emission measurements on giant planets during outer planets grand tour
[NASA-CR-133500] 19 p2343 N73-28844

**EXTRATERRESTRIAL ENVIRONMENTS**
NT CHROMOSPHERE
NT INTERPLANETARY SPACE
NT INTERSTELLAR SPACE
NT JUPITER ATMOSPHERE
NT LUNAR ATMOSPHERES
NT LUNAR ENVIRONMENT
NT MARS ATMOSPHERE
NT MARS ENVIRONMENT
NT PLANETARY ATMOSPHERES
NT PLANETARY ENVIRONMENTS
NT SOLAR ATMOSPHERE
NT STELLAR ATMOSPHERES
Analysis of natural environment design requirements for space tug to show orbital environmental impacts and short-period atmospheric density variation effects
[NASA-TM-X-64713] 05 p0600 N73-14881
Isotope effects for environmental monitoring and control
[ORNL-IIC-39] 06 p0703 N73-15730
Space shuttle related technology development and utilization
[NASA-CR-124260] 16 p1977 N73-25988
Extraterrestrial disposal of radioactive waste from thermoelectric propulsion
[NASA-TM-X-62272] 19 p2225 N73-27943

**EXTRATERRESTRIAL LIFE**
Extraterrestrial life detection using Automated Microbial Metabolism Laboratory
[NASA-CR-129508] 03 p0279 N73-12266
Analysis of techniques and procedures for determining existence of extraterrestrial intelligent life
[NASA-CR-114445] 09 p1082 N73-18822
Survival and reproduction of protozoa in simulated Mars environment
10 p1118 N73-19115
Procedures and instrumentation for life detection on Mars
[NASA-CR-133186] 19 p2344 N73-28854
Social, philosophical, and humanistic impacts of possible existence of extraterrestrial life
[NASA-SP-328] 21 p2596 N73-30807
Search for biological life forms on Mars and other planets
22 p2619 N73-30985
Automated Microbial Metabolism Laboratory experimentation for detecting and elucidating extraterrestrial metabolism using labeled release experiment
[NASA-CR-135638] 23 p2770 N73-32154

**EXTRATERRESTRIAL MATTER**
NT COSMIC GASES
NT COSMIC PLASMA
NT INTERSTELLAR GAS
Detection of evolutionary organic compounds in extraterrestrial matter
10 p1118 N73-19114
Terrestrial quarantine considerations for unmanned sample return missions
[NASA-CR-132071] 15 p1742 N73-24118

**EXTRATERRESTRIAL RADIATION**
NT EXTRATERRESTRIAL RADIO WAVES
NT GALACTIC RADIATION
NT GALACTIC RADIO WAVES
NT GEGENSCHEIN
NT INTERSTELLAR RADIATION
NT LUNAR RADIATION
NT PLANETARY RADIATION
NT PRIMARY COSMIC RAYS
NT RADIO BURSTS
NT SOLAR CORPUSCULAR RADIATION
NT SOLAR COSMIC RAYS
NT SOLAR ELECTRONS
NT SOLAR PROTONS
NT SOLAR RADIATION
NT SOLAR RADIO BURSTS
NT SOLAR RADIO EMISSION
NT SOLAR WIND
NT SOLAR X-RAYS
NT STELLAR RADIATION
NT SUNLIGHT
NT TYPE 2 BURSTS
NT TYPE 3 BURSTS
NT TYPE 4 BURSTS
NT TYPE 5 BURSTS
NT ZODIACAL LIGHT
Data acquisition system for spark chamber spectrometer and review of space radiation measurement techniques
[AD-741761] 01 p0059 N73-10482
Measurement of extraterrestrial Lyman alpha emission by OGO 5 satellite while outside geocorona
01 p0099 N73-10812
Development of model of scattering of solar Lyman alpha from spatial distribution of neutral hydrogen in interplanetary space
01 p0099 N73-10813
Astrophysical flow problems, planetary atmospheres, and space radiation
04 p0468 N73-13814
Electron-proton spectrometer applied to Skylab program for measurement of electrons and protons resulting from solar flares to determine radiobiological safety factors
[NASA-CR-128704] 08 p0925 N73-17577
Physical and experimental data obtained by artificial satellites for estimating extraterrestrial radiation hazard in manned space flight
[NASA-TT-F-724] 09 p0992 N73-18098
Apollo experience report to analyze radiation protection problems on earth and in space
[NASA-TN-D-7080] 09 p1090 N73-18899
Deuterium absorption line in extraterrestrial radiation from galactic center
[AD-754079] 11 p1340 N73-20873
Development of multiwire proportional chamber for high resolution spatial detector in cosmic ray investigations and analysis of operating parameters
[NASA-CR-128899] 13 p1506 N73-22210
Ultraviolet extraterrestrial radiation tolerances of Bacillus subtilis spores and Escherichia coli bacteriophages
15 p1740 N73-24107
Space flight ultraviolet irradiation effects on Bacillus thuringiensis toxin production capability
15 p1740 N73-24109
Phenotype numbers and survival rates of fungi exposed to space environment during Apollo 16 flight
15 p1740 N73-24110
Ultraviolet space irradiation effects on Aeromonas proteolytica extracellular enzyme production
15 p1741 N73-24111
High resolution film actinometric measurements of ultraviolet irradiation levels during space flight
15 p1741 N73-24112
Lithium fluoride thermoluminescent dosimeter for measuring ionizing radiation exposure during Apollo 16 flight
15 p1741 N73-24115
Characteristics of electron-proton spectrometer to measure geomagnetically trapped radiation in geostationary orbit at 6.6 earth radii in outer radiation belt
[NASA-CR-132786] 18 p2150 N73-27381
Method for predicting degradation of solar array in space radiation environment
[NASA-CR-133738] 21 p2499 N73-30055
Space shuttle rendezvous, radiation and reentry analysis code
[NASA-TM-X-64768] 21 p2595 N73-30795

**EXTRATERRESTRIAL RADIO WAVES**
NT GALACTIC RADIO WAVES
NT RADIO BURSTS
NT SOLAR RADIO BURSTS
NT SOLAR RADIO EMISSION
NT TYPE 2 BURSTS
NT TYPE 3 BURSTS
NT TYPE 4 BURSTS
NT TYPE 5 BURSTS
Spaceborne and ground-based data and atmospheric model of Venus microwave emission
[AD-743982] 01 p0100 N73-10820
Analysis of techniques and procedures for determining existence of extraterrestrial intelligent life
[NASA-CR-114445] 09 p1082 N73-18822
Search for Lambda 21 cm absorption in QSS and other sources near to spiral galaxies
[AD-754120] 11 p1339 N73-20871
Radio continuum survey of elliptical galaxies at 6 cm
[AD-754121] 11 p1339 N73-20872
Flux density measurements of extragalactic sources
13 p1490 N73-22075
Characteristics of radio astronomy radiometer to include operation, maintenance, data acquisition, and data retrieval
[NASA-CR-131830] 13 p1579 N73-22796
Radio and optical data on outburst in Cygnus constellation
[AD-756464] 15 p1833 N73-24862
Search for deuterium recombination line emission from Orion A 10
[AD-762001] 21 p2598 N73-30824

EXTRATERRESTRIAL ROVING VEHICLES
U ROVING VEHICLES
EXTRAVEHICULAR ACTIVITY
Welding experiments during flight of Soyuz 6
[AD-749745] 05 p0553 N73-14496
Extravehicular activity support systems and equipment with emphasis on physical operational and performance characteristics of major systems
[NASA-CR-2160] 06 p0718 N73-15858
Parameters requiring consideration by planners and designers when planning EVA functions for astronauts - Vol. 1
[NASA-CR-128926] 14 p1614 N73-23081
Conceptual designs of versatile EVA work-stations - Vol. 2
[NASA-CR-128927] 14 p1614 N73-23082
Model for estimating impact of manned EVA costs on future payloads - Vol. 3
[NASA-CR-128928] 14 p1614 N73-23083
Identification of requirements and systems for intravehicular activity and extravehicular activity during space shuttle missions - Vol. 1
[NASA-CR-128941] 15 p1835 N73-24875
Identification of requirements and systems for intravehicular activity during space shuttle missions - Vol. 2
[NASA-CR-128942] 15 p1835 N73-24876
Serpentine teleoperator device for simulating intravehicular and extravehicular activities in space
[NASA-TR-R-414] 16 p1879 N73-25210
Analysis of Apollo 17 flight to show extravehicular activities, lunar surface experiments, orbital science projects, and spacecraft reentry and recovery
[NASA-TM-X-69527] 17 p2083 N73-26851
Regenerable CO2 sorbent formulation and fabrication for extravehicular activity
[NASA-CR-114632] 20 p2371 N73-29054
Equipment requirements for space shuttle EVA/IVA pressure suit, life support system, mobility aids, vehicle support provisions, and emergency support
[NASA-CR-133991] 21 p2503 N73-30089
Analytical methods, thermal model, and user manual for extravehicular mobility unit routines
[NASA-CR-134005] 21 p2521 N73-30218
Analytical methods, thermal model, and user manual for extravehicular mobility unit routines
[NASA-CR-134006] 21 p2521 N73-30219
Guidelines for extravehicular and intravehicular activities during space shuttle operation with emphasis on contingency situations - Vol. 2
[NASA-CR-133992] 22 p2622 N73-31007
Pressure suit requirements and characteristics for space shuttle personnel performing EVA and IVA activities - Vol. 3
[NASA-CR-133993] 22 p2622 N73-31008
Alkali metal carbonate-bicarbonate solid gas reaction for removing CO2 from atmosphere of EVA life support system
[NASA-CR-114661] 22 p2622 N73-31013
Intra- and extravehicular life support space suite for Apollo astronauts
[NASA-CASE-MSC-12609-1] 23 p2751 N73-32012
EXTREMA
U RANGE (EXTREMES)
EXTREMELY HIGH FREQUENCIES
Operating characteristics of GEOS-C K band radar altimeter
06 p0663 N73-15387
GaAs and InP reflection amplifier noise figure and power gain at extremely high frequencies
[ESRO-CR[P]-262] 19 p2244 N73-28088
Development of procedure for measuring short-term instability of millimeter band klystron frequency
22 p2630 N73-31080
Usability of 42 and 85 GHz mm waves for terrestrial television broadcasting
[FTZ-455-TBR-37] 22 p2634 N73-31107
Nitrogen gas supply system for EHF waveguides to improve attenuation by control of water vapor and oxygen content
[FTZ-A-333-TBR-10] 22 p2642 N73-31175
EXTREMELY LOW FREQUENCIES
Sound transmission at extremely low frequency in far field radiation from turbulent wake
[AD-747238] 02 p0212 N73-11721
Procedures for producing electric fields in conductive media at extremely low frequencies
[AD-748303] 04 p0391 N73-13177
Procedures and equipment for analyzing field strengths transmitted at extremely low frequencies and measurement of radial magnetic component
[REPT-72-4-ADD] 06 p0664 N73-15401
OGO-D electromagnetic wave propagation measurements with whistler and hiss formations in plasmasphere
[NASA-CR-130351] 07 p0754 N73-16126
ELF signal propagation statistics in 40 to 70 Hz band at Norway, Saipan, and Greece during May 1972
[AD-753685] 10 p1129 N73-19199
ELF and VLF experiment on OGO-D, revealing ion whistlers and ELF hiss features
12 p1377 N73-21170
Spherical Hankel functions for approximating radio transmission in earth ionosphere
[AD-755391] 12 p1380 N73-21192
Schumann resonance frequencies and electrical conductivity of mesosphere [40 to 100 km] from ELF spectra
[AD-758775] 15 p1784 N73-24463
Review of geomagnetic micropulsation modes for possible communications application
[AD-759380] 16 p1878 N73-25203
Modes of cable vibration compared with pure flexing mode in production of motion induced noise from towed ELF H field antenna
[AD-762936] 22 p2645 N73-31199
Technique for reducing ambient electric field generated by inductive voltages in extreme low frequency magnetic field generators
[AD-764531] 23 p2768 N73-32142
EXTREMELY LOW RADIO FREQUENCIES
Statistical attenuation analysis on extremely low radio frequency propagation
[AD-747779] 03 p0267 N73-12166
Computer program for estimating interference in world extremely low frequency radio transmission
[AD-757080] 14 p1633 N73-23238
Equipment for continuous recording of natural electromagnetic noise of extremely low frequencies
[AD-757482] 14 p1634 N73-23244
Extremely low frequency radio communication in ocean environment
[PB-213904/6] 14 p1636 N73-23264
Artificial ultralow frequency generation in ionosphere and magnetosphere for global communication system
[AD-759012] 16 p1878 N73-25199
Diffusive equilibrium model for calculating characteristics of broadband ELF, VLF, and LF emissions in magnetosphere
[NASA-CR-133925] 22 p2666 N73-31363
EXTREMUM VALUES
NT MAXIMA
Applicability of various laws of statistics of extremal values for approximating empirical distributions of maximum wind velocities
04 p0442 N73-13608
Dynamic performance criteria for power actuating components of electrohydraulic actuation servosystem
[NASA-TM-X-2736] 09 p0990 N73-18079
Application of theoretical framework of governing equations and extremum principles to classical elasticity and plasticity yield-point problems
[AD-753137] 09 p1096 N73-18948
Synthesis and analysis of systems combining extreme principle of control with correlation processing of signals entering from object being controlled
14 p1644 N73-23334
Design and analysis of Type 2 correlation-extreme systems composed of control circuits and gages for measuring random functions
14 p1644 N73-23335
Divergence and necessary conditions for extremums associated with dimension reducing transformation matrix
20 p2438 N73-29577
Statistics of extreme values of meteorological parameters
[MONO-89] 21 p2566 N73-30568
EXTRUDING
Hard alloy shaping tools for extruding steels and nonferrous materials
[NLL-NEL-TT-2400-[6075.461]]
02 p0177 N73-11435
Extrusion can for extruding ceramics under heat and pressure
[NASA-CASE-NPO-10812] 04 p0425 N73-13464
Detection of C, H, and Ni in Pu metal by hot extrusion-combustion method
[FOA-VOL-6-NO-10] 05 p0506 N73-14115
Elastic properties and internal friction of hydrostatically extruded molybdenum
[AD-749539] 05 p0563 N73-14574
Effects of interstitial solute content on deformation kinetics in hot extrusion of titanium aluminum vanadium alloy
[AD-750556] 06 p0677 N73-15511
Analysis of metallurgical factors and mechanical effects during and subsequent to cold hydrostatic extrusion of magnesium and aluminum alloys
[AD-751739] 07 p0805 N73-16527
Development of extruding machine for producing parts with complicated shapes, high degree of mass, and requiring precision surfaces
[AD-751146] 07 p0805 N73-16534
Analysis of defects in metals produced by high speed extrusion
[AD-752867] 09 p1041 N73-18488
Deformation of gamma and epsilon phases in intermetallic compounds by extrusion method
[AD-754523] 11 p1307 N73-20605
Tooling workpiece interface condition effects on metal flow and product quality in extrusion
[AD-755832] 13 p1535 N73-22439
Homogenization processing of aluminum alloy ingots during extrusion for changing structure and properties of product
[AD-759245] 16 p1919 N73-25527
Temperature effects on hot extrusion of stainless steels
[AD-761538] 19 p2306 N73-28551
Comparison of normal and hydrostatic extruding processes under fluid pressure
[NLL-NEL-TT-2467-[6075.461]]
20 p2422 N73-29453
Analysis of ductile flow of metal during extrusion process with application to manufacture of cable sheathing
[NLL-M-21661-[5828.4F]] 21 p2557 N73-30498
Sintering kinetics of zirconium and titanium carbides by hot extrusion in regions of homogeneity
23 p2808 N73-32448
EYE [ANATOMY]
NT FOVEA
NT NYSTAGMUS
NT OCULOMOTOR NERVES
NT RETINA
Compilation of data concerning effects of infrared radiation on eye
[NASA-CR-128407] 01 p0008 N73-10064
Weight, blood pressure, and intraocular pressure in young healthy males prior to and after 50-km walk
[NASA-TT-F-14557] 02 p0132 N73-11071
Examination of GaAs laser radiation injuries and thresholds of ocular system during night vision exercises
[AD-750350] 05 p0559 N73-14542
Evoked compensatory reflex reactions of rabbit ocular and eyelid muscles during hypoxia
13 p1480 N73-21992
Atmospheric effects on laser propagation and impact on eye safety
[AD-755405] 13 p1485 N73-22044
Literature review on human macular pigment absorption and density spectrum of cone receptor
[IZF-1972-17] 14 p1609 N73-23046
Optical modulation transfer functions of human eye for white light
[IZF-1973-2] 14 p1609 N73-23047
Chromatic induction and spatial intraocular straylight effects in human perception of contrast colors
[IZF-1972-19] 14 p1692 N73-23730
Ultrasonic device for ophthalmic eye surgery with safe removal of macerated material
[NASA-CASE-LEW-11669-1] 18 p2110 N73-27062
Surgical liquification pump for removing macerated tissue from eye
[NASA-CASE-LEW-12051-1] 23 p2749 N73-32000
EYE DISEASES
NT ASTIGMATISM
NT CATARACTS
EYE EXAMINATIONS
Standardization of tests and classification of color perception abnormalities in military personnel
10 p1113 N73-19071
Automated visual sensitivity tester for determining visual field sensitivity and blind spot size
[NASA-CASE-ARC-10329-1] 17 p1988 N73-26072
EYE MOVEMENTS
NT NYSTAGMUS
Influence of illumination on electro-oculographic measurements of human eye potential
[AMRU-R-71-1] 02 p0131 N73-11064
Physiological factors in human oculomotor responses to space flight stress
[DR-208-VOL-1] 06 p0632 N73-15136
Anti-compensatory oculomotor response of pilot to rotational head stimuli
06 p0632 N73-15138
Upper eye lid position effects in electro-oculograhic vertical eye movement recordings
06 p0633 N73-15143
Vestibular stimulation effect in human and animal retinal image stabilization
06 p0633 N73-15144
Compensatory oculogravic response of eye movement direction during slow head rotation
06 p0634 N73-15148
Predictive control of human eye tracking movements in response to visual stimuli
06 p0634 N73-15149
Application of extra-foveal vision to predicting target acquisition in air-to-ground search
10 p1225 N73-19960
Modelling of random human visual search performance based on physical properties of eye
10 p1225 N73-19961
Control mechanism in accommodation-vergence eye movement system in human eyes and importance of central and peripheral vision in pattern perception by human beings
21 p2500 N73-30061
Measurement of control mechanism of accommodation-vergence eye movement system in human eyes using electro-optical measuring instrument
21 p2500 N73-30062
EYE PROTECTION
Transmission characteristics of commercially available, laser eye protectors with Cary 14 spectrophotometer
[AD-746293] 02 p0136 N73-11100

Plastic materials for eye protection from lasers
[AD-752594] 08 p0880 N73-17127
IR laser radiation eye protector
[AD-753080] 09 p0998 N73-18142
Optical density properties of ocular glass laser protective filters
[AD-755406] 13 p1487 N73-22057
Performance of hadron laser safety eyeshields in protecting personnel from accidental ocular exposure to common laser radiation
[AD-759921] 17 p1991 N73-26099

# F

F CENTERS
U COLOR CENTERS
F DISPLAYS
U F REGION
F LAYER
U F REGION
F REGION
NT F 1 REGION
NT F 2 REGION
Direct scatter effects from field aligned E and F layer irregularities and scatter from subauroral ionospheric clouds at 19.4 MHz
[AD-746311] 01 p0054 N73-10436
Daily summaries for vertical echo sounding of upper atmosphere over Freiburg, Germany - Aug. 1972
[REPT-314-F] 04 p0414 N73-13380
Daily summaries for vertical echo sounding of upper atmosphere over Freiburg, Germany - Sept. 1972
[REPT-315-F] 04 p0414 N73-13381
Diurnal variations in ionospheric F region tilts near magnetic equator
[WRE-TN-A-199[AP]] 04 p0414 N73-13384
F layer electron density fluctuations and disturbances following nuclear explosion at ionospheric height
05 p0513 N73-14169
Daily summaries for vertical echo sounding of upper atmosphere over Freiburg, Germany - July 1972
[REPT-313-F] 05 p0538 N73-14380
Ionospheric propagation data for E and F regions, India - Jan. 1971
[RTRC-A188] 06 p0664 N73-15397
Ionospheric propagation data for E and F regions, India - Feb. 1971
[RTRC-A189] 06 p0664 N73-15398
Ionospheric propagation data for E and F regions, India - March 1971
[RTRC-A190] 06 p0664 N73-15399
Technique for determining plasma drifts, applied to dynamic processes in topside F region
07 p0774 N73-16288
Electron heating in F region by high power radio frequency beam detected by intensity changes in atomic oxygen nightglow
07 p0775 N73-16293
Ionograms and cosmic radio noise absorption studies of anomalous behavior of F region during solar eclipse of 22 Sept. 1968
[RSD-73] 07 p0789 N73-16414
Possibility of developing theoretical models of disturbed F region, using ground based and spaceborne experiments
[RSD-77] 07 p0789 N73-16417
Intense, high frequency radiation causing F region plasma phenomena
[AD-753162] 09 p1032 N73-18426
Dependence of onset time of F-region electron density disturbance upon local time of geomagnetic storm commencement and main phase onset
[AD-753665] 09 p1033 N73-18433
Electron density irregularities and evening anomalies in midlatitude nighttime F region
13 p1514 N73-22270
Predicting regular variations in geometric parameters of N[h] profiles and h prime f characteristics of quiet and disturbed ionosphere
13 p1520 N73-22321
Predicting geometric parameters of N[h] profiles and h prime f characteristics of F region during disturbances
13 p1520 N73-22323
Long-term prognosis of midday N[h] profiles of F region
13 p1521 N73-22325
Disappearance of E region following changes in geomagnetic H component
[AER-73-04] 14 p1658 N73-23455
Daily summaries for vertical echo sounding of upper atmosphere over Freiburg Germany, January 1973
[REPT-319-F] 14 p1659 N73-23460
Daily summaries for vertical echo sounding of upper atmosphere over Freiburg, Germany, December 1972
[REPT-318-F] 14 p1659 N73-23461
Daily summaries for vertical echo sounding of upper atmosphere over Freiburg, Germany - February 1973
[REPT-320-F] 15 p1777 N73-24406
Ionospheric F-region electron recombination, heating, and electron production
17 p2017 N73-26311
Ionospheric drifts and Sq current system
[WRE-TN-680[WR/D]-PT-2] 19 p2293 N73-28438
Ionosphere D and F region high frequency ray propagation effects and design of high frequency dynamic phase metering instruments
20 p2375 N73-29083
Daily summaries for vertical echo sounding of upper atmosphere over Freiburg, Germany - April 1973
[REPT-322-F] 21 p2537 N73-30342
Daily summaries for vertical echo sounding of upper atmosphere over Freiburg, Germany - May 1973
[REPT-323-F] 21 p2537 N73-30343
Daily summaries for vertical echo sounding of upper atmosphere over Freiburg, Germany - June 1973
[REPT-324-F] 21 p2537 N73-30344
Solving equations of motion for behavior of plasma clouds in layered model ionosphere
[MPI-PAE/EXTRATERR-73] 22 p2704 N73-31658
Experimental determination of coupling between normal F region ionosphere and protonosphere using radar backscatter techniques at Arecibo, Puerto Rico
23 p2778 N73-32213
OGO-6 ion concentration irregularity studies
[NASA-CR-132814] 23 p2786 N73-32286
Computer program for modeling E and F region of ionosphere
[AD-766662] 23 p2789 N73-32312
Daily summaries for vertical echo sounding of upper atmosphere over Freiburg, Germany - July 1973
24 p2920 N73-33322
Observations of amplitude scintillations produced in F region in equatorial areas based on Applications Technology Satellite transmissions
[NASA-TM-X-70478] 24 p2921 N73-33326
F 1 REGION
Temperature and ion composition measurements of F 1 region during solar eclipse on 7 March 1970
24 p2921 N73-33329
F 2 REGION
Full wave solution for electron density perturbations caused by gravity waves in F2 region
05 p0509 N73-14145
Electron cooling in F2 region at low and midlatitudes, caused by electron-ion collisions and electron impact induced transitions
[RSD-74] 07 p0789 N73-16413
Model of equatorial F 2 region ionosphere based on known physical and chemical processes
13 p1514 N73-22268
Articles on ionospheric disturbances, and techniques for predicting condition of ionosphere for planning radio communication
[NASA-TT-F-746] 13 p1519 N73-22314
Anomalous F region ionization patterns during winter in dark ionosphere in polar regions
13 p1520 N73-22318
Using statistical distribution of F 2 layer critical frequency deviations from sliding median for planning radio communication
13 p1520 N73-22319
Prediction of F 2 region critical frequencies from spatial and temporal correlation data
13 p1520 N73-22320
Predicting daily variations in geometric parameters of N[h] profiles and h prime f characteristics of quiet and disturbed ionosphere
13 p1520 N73-22322
Influence of F 2 regional disturbances and magnetic activity on short wave radio communications
13 p1521 N73-22327
Analytical expressions for geographic distribution of midday ionization of F 2 layer in temperate latitudes
13 p1521 N73-22331
F-80 AIRCRAFT
U T-33 AIRCRAFT
F-4 AIRCRAFT
Minimum quadratic cost optimal control technology for design of F-4C aircraft manual control system
01 p0018 N73-10137
Weapon delivery accuracy of F-4 aircraft with experimental stick to rudder interconnect to minimize lateral tracking error
[AD-746000] 02 p0126 N73-11027
Weapon delivery accuracy of F-4 aircraft with high gain control augmentation system
[AD-746001] 02 p0126 N73-11028
Development of performance criteria to estimate relative proficiency of aircraft pilots during aircraft carrier qualification training with F-4 aircraft
[AD-746095] 02 p0127 N73-11030
Investigation of midair collision between commercial DC 9 aircraft and Marine Corps F-4B aircraft at Duarte, California on 6 June 1971
[NTSB-AAR-72-26] 03 p0252 N73-12037
Development and characteristics of six degree of freedom, fast time predictor model for simulation of F-4 aircraft landing on aircraft carrier
[AD-750294] 05 p0504 N73-14102
Criterion development in replacement air group, using F-4 aircraft
[AD-748195] 05 p0505 N73-14111
Evaluation of energy maneuverability procedures in aircraft flight path optimization and performance estimation
[AD-754909] 11 p1236 N73-20035
Development of computer programs for numerical analysis of spinning aircraft based on Euler integration and minimization by gradient search
[AD-757257] 14 p1602 N73-22990
Psychometric criteria for pilot performance in F-4 aircraft fleet
[AD-755184] 14 p1614 N73-23087
Aerodynamic forces and trajectories of external stores separated from F-4 aircraft
[AD-757932] 15 p1850 N73-24993
Wind tunnel tests to determine pressure distribution on two dimensional airfoil with pylon mounted stores at subsonic speeds using F-4 aircraft model
[AD-759582] 16 p1859 N73-25053
Cyclic pressure tests of F-4 aircraft forward and aft canopies to determine safe service life after delamination of acrylic sheet
[AD-759349] 16 p1862 N73-25084
Analysis of performance benefits for fighter aircraft by application of maneuver load control and relaxed static stability parameters
[AD-762299] 19 p2222 N73-27922
Logistic performance data book for F-4D aircraft fire control system to show reliability, maintainability, logistics support, and operating problems
[AD-762229] 19 p2358 N73-28969
Logistics performance data book for RF-4C aircraft landing gear system to show reliability, maintainability, logistics support, and operating problems
[AD-762231] 19 p2358 N73-28970
Logistic performance data book for F-4E flight control system to show reliability, maintainability, logistic support, and operating problems
[AD-762230] 19 p2358 N73-28973
Logistic performance data book for RF-4C photographic reconnaissance system to show reliability, maintainability, logistic support, and operating problems
[AD-762232] 19 p2358 N73-28974
Field maintenance and operational experience with various selected models of F-4 aircraft
[AD-762747] 20 p2362 N73-28995
Analysis of flight crew errors contributing to aircraft accidents on P-3 and F-4 aircraft for improved air safety
[AD-764868] 23 p2746 N73-31979
F-5 AIRCRAFT
Method for predicting flight characteristics of F-5 and A-7 aircraft during atmospheric turbulence using large amplitude flight simulator
[AD-749480] 05 p0495 N73-14030
Development of rolling maneuver fatigue load data for F-5 and F-105 aircraft based on statistical flight loads data
[AD-761491] 19 p2221 N73-27915
Acquisition of stress data and aerodynamic loads on F-5 aircraft using mechanical strain gages and oscillograph recorders for service life determination
[AD-760567] 20 p2361 N73-28991
F-8 AIRCRAFT
Flight control improvement of F-8 aircraft relative to carrier takeoff and landing
[AD-753010] 09 p0986 N73-18052
Flight tests of F-8C aircraft to determine effects of flaps on buffet characteristics and wing-rock onset at subsonic and supersonic speeds
[NASA-TM-X-2873] 19 p2220 N73-27905
Design and development of cryptosteady energy separator for use with turbojet engines on supersonic aircraft
[AD-762032] 19 p2331 N73-28752
Analysis of energy separator for application to air conditioning system of E-8 aircraft
[AD-762590] 20 p2364 N73-29014
Design and development of cryptosteady energy separator for application to F-8 aircraft air conditioning system
[AD-762579] 20 p2364 N73-29015
Transonic wind tunnel tests to determine lift, drag, and stability characteristics of F-8 aircraft model with oblique wing
[NASA-TM-X-62273] 24 p2877 N73-32974
F-110 AIRCRAFT
U F-4 AIRCRAFT
F-14 AIRCRAFT
Role of flight simulation in development of S-3 and F-14 aircraft
08 p0865 N73-17001
Performance tests of F-14 aircraft with jet blast deflector to determine effects of backflow of jet exhaust on aircraft launch operation
[AD-752018] 08 p0867 N73-17023
Analysis of infrared spectra generated by OV-1D, F-14, and UH-1 aircraft using Fourier spectroscopy
[RM-572] 13 p1529 N73-22390
Wind tunnel tests to determine low speed characteristics of large scale model of F-14A aircraft with emphasis on high lift configuration stability
[NASA-TM-X-62244] 23 p2741 N73-31940
F-15 AIRCRAFT
Analysis of F-15 contract structure and contribution to effective program management
[AD-750849] 06 p0732 N73-15975

Modifications in development of high pressure version of vibrating cylinder pressure transducer
[AD-755533] 13 p1502 N73-22173
F-27 AIRCRAFT
Fokker F-27 as European earth resources survey aircraft noting design, remote sensors, and program
[ESRO-CR[P]-128] 17 p1984 N73-26035
F-28 TRANSPORT AIRCRAFT
Development of F-28 transport aircraft wing and analysis characteristics to show effects of boundary layer fences
06 p0618 N73-15015
Fokker F-28 fellowship structure adhesive bonding processes and quality control methods
[FOK-K-67] 21 p2497 N73-30037
F-86 AIRCRAFT
Aircraft accident involving attempted takeoff of Sabre Mark 5 aircraft at Sacramento, California airport on 24 Sept. 1972
[NTSB-AAR-73-6] 14 p1602 N73-22985
F-100 AIRCRAFT
Flight tests of modified F-100 aircraft to determine effectiveness of fast-acting flaps as direct-lift-control devices to improve station keeping
[NASA-TM-X-2936] 24 p2876 N73-32970
F-102 AIRCRAFT
Flight loads data recording system for F-102 aircraft maneuver load analysis for data acquisition and application to development of structural design criteria
[AD-747016] 03 p0253 N73-12047
F-104 AIRCRAFT
Performance tests of hemispherical flow-direction sensor mounted on F-104 aircraft to develop Mach number position error calibration curve
[NASA-TN-D-7461] 23 p2743 N73-31956
F-105 AIRCRAFT
Measurement of noise levels produced by F-105 aircraft and analysis of effects on environment and land use
[AD-753113] 09 p0987 N73-18056
Development of rolling maneuver fatigue load data for F-5 and F-105 aircraft based on statistical flight loads data
[AD-761491] 19 p2221 N73-27915
F-106 AIRCRAFT
Aerodynamic characteristics of four configurations of rounded shoulder boattail nozzles mounted on F-106B aircraft at subsonic speeds
[NASA-TM-X-2626] 02 p0124 N73-11013
Flight test F-106 aircraft to determine comparative time advantages of energy optimization climb and acceleration methodology
[AD-760571] 18 p2107 N73-27041
Flyover and static tests for determining effects of flight velocity on F-106B exhaust nozzle noise
[NASA-TM-X-2854] 19 p2329 N73-28734
Flight tests of modified F-106 aircraft to determine installation effects of two aft underwing nacelles housing afterburning J-85 engines
[NASA-TM-X-71439] 23 p2743 N73-31959
F-111 AIRCRAFT
Analysis of fatigue crack propagation characteristics of steel structures in F-111 aircraft under specific flight loading spectra
[AD-746343] 02 p0127 N73-11033
Pressures and temperatures on the lower surfaces of an externally blown flap system during full-scale ground tests
[NASA-TN-D-7138] 06 p0614 N73-14984
Analysis of stall and post-stall characteristics of F-111 aircraft and development of regression techniques to obtain aerodynamic derivatives
06 p0617 N73-15013
Development of computer programs for numerical analysis of spinning aircraft based on Euler integration and minimization by gradient search
[AD-757257] 14 p1602 N73-22990
Application of boron/epoxy composite materials for airframe construction with specific development of F-111 stabilizer
18 p2164 N73-27480
Cost history of F-111 aircraft airframe system to show logistics organization, support costs, reliability and maintainability, and development problems
[AD-762213] 19 p2356 N73-28958
Logistic performance data book for bomb navigation avionics system of F-111 aircraft to show support cost, reliability, maintenance, and problems
[AD-762214] 19 p2357 N73-28959
Measurement of sound power levels, power spectra, and directivity patterns for jet exit velocities of F-111A aircraft
[NASA-TN-D-7376] 20 p2361 N73-28989
Analysis of steady-state and dynamic pressure conditions in F-111 aircraft engine to determine causes of engine compressor stalls
[NASA-TN-D-7328] 20 p2465 N73-29806
Full-scale ground tests of externally blown flap system on F-111 aircraft wing to determine pressure and temperature distributions on undersurface of wing, vane, and flap
24 p2873 N73-32947
Acoustic measurements of aerodynamic noise produced by impingement of jet exhaust on wing and flap of externally blown flap system installed on F-111 aircraft
24 p2875 N73-32964
FAB [PROGRAMMING LANGUAGE]
U FORTRAN
FABRICATION
NT SPACE MANUFACTURING
Fabrication of integrated magnetic storage devices by vapor deposition of gold on copper substrate
01 p0031 N73-10239
Fabrication processes for silicon Schottky barrier diodes
[FRNC-TH-179] 03 p0274 N73-12218
Fabrication of uranium mononitride fuel pin assembly for fast lithium cooled space power reactor
[NASA-CR-120956] 05 p0579 N73-14710
Design and fabrication of annular ring detector consisting of optical fibers terminated with photodetectors
[NASA-CR-124089] 09 p1065 N73-18683
Fabrication and encapsulation processes for multiconductor cables
[BDX-613-740] 10 p1134 N73-19245
Improved fabrication and encapsulation techniques for multiconductor cables
[BDX-613-687] 10 p1134 N73-19246
Analysis of materials, processing criteria, processing techniques, and apparatus for preparation of composite materials in space
[NASA-CR-124172] 11 p1307 N73-20609
Photoresist fabrication of printed circuit boards
[BDX-613-496] 12 p1387 N73-21245
Fabrication of updated block data composer and holographic storage array for breadboard holographic read/write memory system
[NASA-CR-124442] 23 p2801 N73-32399
Fabrication and evaluation of composite thermal engine insulation
[NASA-CR-124457] 24 p2938 N73-33458
FABRICS
NT DACRON [TRADEMARK]
NT PARACHUTE FABRICS
Tests of fabric friction on human skin for aircrew tropical clothing comfort
[RAE-TR-72037] 01 p0020 N73-10157
Correlation of wear behavior and properties of coated fabric hovercraft fingers
[RAE-TR-71210] 08 p0935 N73-17654
Procedures for improving resistance of Nomex fabric and webbing to actinic degradation
[AD-759217] 17 p2051 N73-26596
Dynamic testing of fabrics and Mylar in shock tubes
[NASA-CR-132284] 23 p2770 N73-32157
Fiber distribution and orientation of aerodynamically spun nonwoven fabrics
24 p2907 N73-33196
FABRY-PEROT INTERFEROMETERS
Frequency shift of flash lamp pumped dye laser with two Fabry-Perot interferometer wavelength selectors
01 p0064 N73-10527
Fabry-Perot laser interferometer for studying atomic collisional rate and ionization relaxation time in helium shock wave
[AD-749553] 04 p0408 N73-13326
Michelson and Fabry-Perot interferometers with light sources of Gaussian and Lorentzian spectral distribution
[KFKI-72-62] 10 p1159 N73-19432
Large aperture Fabry-Perot interferometer used to scan barium ion clouds
[AD-757563] 14 p1663 N73-23495
Fabry-Perot interferometer measurements at Ester Dome, Alaska during 1971-73
[NASA-CR-124348] 21 p2538 N73-30351
FABRY-PEROT LASERS
U LASERS
FACE [ANATOMY]
Color photographic system using grid projector and telecentric lenses for recording contours of human face for aircrew oxygen mask fitting
[RAE-TR-71184] 07 p0750 N73-16099
FACE CENTERED CUBIC LATTICES
Effects of magnetostriction and superlattice formation in ferromagnetic thin films
16 p1952 N73-25794
Thermal and electrical properties of titanium alloyed with vanadium and high temperature creep of metal with fcc lattice
[JPRS-59623] 22 p2683 N73-31490
High temperature creep of metals with face centered cubic lattice
22 p2683 N73-31492
FACILITIES
Facilities engineering for NASA space program
08 p0873 N73-17070
Technical and support services performed during Tenth Soviet Antarctic Expedition
20 p2408 N73-29355
FACSIMILE COMMUNICATION
NT AUTOMATIC PICTURE TRANSMISSION
Integration of spectrometer capability with imagery function of facsimile cameras for use on planetary landers
[NASA-CASE-LAR-11207-1] 19 p2300 N73-28496
Characteristics of direct-coupled photodetector-preamplifier for use in facsimile camera for improved sensitivity and reduced mechanical complexity
[NASA-TN-D-7338] 23 p2769 N73-32148
FACSIMILE TRANSMISSION
U FACSIMILE COMMUNICATION
FACTORIAL DESIGN
Computer program for fitting and model selection of two-level factorial replication-free experiments
[NASA-TM-X-2706] 09 p1005 N73-18201
Algorithm and computer program for generating all distinct 2[p-q] fractional factorial designs and applications to design of experiments
[NASA-TN-D-7327] 16 p1934 N73-25650
FACTORIALS
High energy density primary batteries using CuF2/LiAsF6-MF/Li electrochemical system
[NASA-CR-120857] 07 p0741 N73-16032
FACTORIES
U INDUSTRIAL PLANTS
FACULAE
Wave propagation and magnetic fields effects on velocity oscillations in solar plage regions
16 p1961 N73-25864
FADING
NT SIGNAL FADING
Behavior of alpha-beta tracker for maneuvering targets under noise, false target, and fade conditions
[AD-748993] 04 p0391 N73-13182
Volumetric factor of precipitation phase causing X ray diffraction fading in alloys
[JPRS-58761] 12 p1414 N73-21455
Nonisothermal constitutive equations and related thermodynamical aspects of simple materials with fading memory
[AD-761634] 19 p2327 N73-28720
FAIL-SAFE SYSTEMS
Fail safe latching mechanism for spacecraft docking
[NASA-CASE-MSC-12549-1] 02 p0178 N73-11443
Computer program system for automatic operation and safety backup in ground based ATC system
[FAA-EM-73-7] 15 p1808 N73-24654
Fail-safe and safe-life design of aircraft components made from Ti-alloys
[NLR-TR-72034-U] 22 p2685 N73-31510
FAILURE
NT BURNTHROUGH [FAILURE]
NT ENGINE FAILURE
NT FAILURE ANALYSIS
NT STRUCTURAL FAILURE
NT SYSTEM FAILURES
Tensile and stripping strength data in terms of failure probability for bolts, nuts, screws, and threaded rods
[ESDU-67019] 01 p0110 N73-10908
Formation and failure of chromium sesquioxide on cobalt-base alloy L-605 during oxidation at high temperatures
[NASA-TN-D-7255] 12 p1414 N73-21454
Effect of stress corrosion cracking and hydrogen embrittlement on failure of high strength spacecraft fasteners
[AD-758754] 15 p1800 N73-24591
Effect of wall thickness variations on failure during burst tests of Zircaloy tubing
[WAPD-TM-1104] 17 p2093 N73-26935
Tensor analysis of strength and failure of composite materials
[AD-761994] 19 p2313 N73-28600
FAILURE ANALYSIS
Failure analysis of Geiger counters used in nucleonic oil gauging system of USAF aircraft
[AD-746267] 01 p0059 N73-10485
Effects of axially symmetric deformation of metal on mechanical and physical properties of samples
[AD-745551] 01 p0063 N73-10513
Energy-absorbing efficiency of ply-tear webbings and discussion of warp and weft count and binder property effects
[RAE-TR-72051] 01 p0113 N73-10936
Survey of field of fault diagnosis and key algorithms and heuristics currently in use
[NASA-CR-129095] 02 p0178 N73-11440
Failure analysis and fracture modes of carbon epoxy composites
[NASA-CR-121000] 02 p0191 N73-11550
Analysis of combined vibrations of blades in axial turbomachinery using dynamic stiffness method
[NLL-RTS-7305] 02 p0236 N73-11917
On-line failure testing of synchronous sequential computers
03 p0271 N73-12197
Computerized simulation of faulty logic circuits
03 p0271 N73-12198
Computerized simulation for failure analysis of logic circuits
03 p0271 N73-12199
Logic comparison of failure diagnosis for digital systems
03 p0272 N73-12203
Automatic test generator for failure detection and localization in logic systems, LADISLAS
03 p0272 N73-12204
Universal cellular network for combinational switching functions with simple failure testing
03 p0278 N73-12252

Test procedure for failure analysis in multiple elementary gate networks using iterative test function
03 p0278 N73-12256
Failure analysis of combinational logic circuits with input reconvergent fan-out
03 p0278 N73-12257
Failure analysis of NOR gate network with parity for easy testing
03 p0278 N73-12258
Effects of free edge shear stresses on failure of fiber-reinforced angle ply laminates
[AD-747343] 03 p0322 N73-12625
Development and application of multiple system checkout procedures for use with gimbaled inertial measuring units
[NASA-CR-123953] 03 p0328 N73-12676
Failure analysis of crystals exposed to laser emissions
[AD-747730] 03 p0347 N73-12830
Plastic-strain controlled failure criteria and design parameters
[COO-2048-4] 03 p0361 N73-12941
Electron fractography of stress corrosion fracture surfaces of aircraft materials as high strength steels, Al-Zn-Mg, Al-Cu and Ti alloys
[NLR-TR-71038-U] 03 p0361 N73-12945
Analysis of multiple faults in combinational logic networks
04 p0399 N73-13247
Test generation for multiple faults in parity circuits
04 p0399 N73-13248
Redundancy reduction for logic circuits by error correcting codes to improve method of increasing circuit reliability
04 p0399 N73-13249
Automata theory of cubical complexes applied to diagnosis and algorithmic description, noting logic design of ultra LSI
[NASA-CR-130388] 05 p0517 N73-14201
Universal functional scheme for realizing any combination or sequential function for proliferation problem in LSI technology
[NASA-CR-130387] 05 p0517 N73-14204
Transformation of relay contact networks in logic gate circuits for failure analysis
05 p0522 N73-14248
Failure analysis of malfunction of Apollo 16 television camera monitor on command module
[NASA-TM-X-68930] 06 p0639 N73-15190
Failure analysis of tape recorders for spacecraft applications
[NASA-SP-307] 06 p0643 N73-15225
Conference on environmental effects on mechanical failures
[AD-750411] 06 p0677 N73-15512
Failure analysis of aluminum alloy components with history of failures in aerospace applications
[NASA-CR-2166] 06 p0684 N73-15568
Fatigue tests of aluminum alloy specimens used for aircraft structures under simulated acoustic loading conditions
[ESDU-72015] 06 p0723 N73-15899
Fatigue analysis and fatigue mode studies in bonded joints of composite materials
[AD-750134] 06 p0728 N73-15941
Analysis of aircraft fire warning system performance and procedures for eliminating false fire warning indications
[AD-751346] 07 p0740 N73-16025
Reliability engineering methods for electronic components
[FTL-A-A16-1] 07 p0803 N73-16517
Correlation between full scale fatigue test failures and actual service failures for several military aircraft
07 p0851 N73-16901
Reliability and its development in time, frequency and probability domain
[TR-72-38] 08 p0927 N73-17595
Analysis of defects in metals produced by high speed extrusion
[AD-752867] 09 p1041 N73-18488
Failure criteria in cyclic elasto-plastic deformation
10 p1219 N73-19915
Failure and diagnosis of faults in logic and combinational circuits of digital computers
[AD-754029] 11 p1265 N73-20264
Failure mechanics and compressive biaxial strength of ceramics
[AD-754826] 11 p1309 N73-20621
Analysis of acoustic properties of jet engine malfunction as means for detecting jet engine burnthrough - Vol. I
[FAA-RD-72-149-VOL-1] 11 p1334 N73-20825
Analysis of Apollo 16 reaction control system helium pressure regulator filter failure
[NASA-TM-X-69131] 11 p1334 N73-20827
Report by Apollo 16 crew that lunar roving vehicle rear steering was inoperative
[NASA-TM-X-69124] 11 p1339 N73-20864
Inflight incident involving separation of cargo compartment door on DC-10 aircraft near Windsor, Ontario, Canada on 12 June, 1972
[NTSB-AAR-73-2] 12 p1363 N73-21061
Fatigue life and wear tests of spur gears based on pitting fatigue at pitch circle to compare AISI M-50 and super nitralloy materials
[NASA-TN-D-7261] 12 p1408 N73-21411
Development of equipment for securing external stores SH-3G helicopter and analysis of failure modes
[AD-757001] 13 p1474 N73-21943
Failure analysis of components of CH-47A auxiliary power plants
[AD-756407] 13 p1478 N73-21975
Analysis of algorithms for failure detection, isolation, and correction of redundant inertial instruments in strapdown dodecahedron configuration
[NASA-CR-124234] 13 p1556 N73-22608
Experimental determination of pressure distribution in burning flaws in solid propellant grains
[AD-756912] 13 p1569 N73-22718
Sensitivity of thin-walled compression members to column axis imperfection
[VTH-172] 13 p1587 N73-22863
Failure detector for dc to ac inverter circuit
[NASA-CASE-NPO-13160-1] 14 p1667 N73-23525
High strength steel delayed failure analysis including hydrogen embrittlement
[NLR-TR-72113-U] 14 p1715 N73-23917
Failure analysis and design criteria for transducers in Apollo environmental control systems
[NASA-CR-128921] 15 p1756 N73-24231
Analysis of methods of fault diagnosis used with logic circuits and effect of procedures on structure of circuit assemblies
[NLL-PO-2913-[9022.81]] 15 p1759 N73-24255
Design of thermal protection system for 8-foot HTST combustor
[NASA-CR-112310] 15 p1760 N73-24262
Analysis of resistance of reinforced and unreinforced structural plastics to static and fatigue failure
[AD-758626] 15 p1802 N73-24608
Predictive model for failure times of adhesive bonded aluminum under constant stress
[AD-758845] 16 p1919 N73-25528
Congressional hearing to determine malfunction on Skylab 1 workshop and proposed methods for correcting malfunction
16 p1964 N73-25884
Analysis of fatigue behavior of airframe components and development of methods for predicting service life of aircraft structures
[RAE-LIB-TRANS-1678] 17 p1981 N73-26012
Electronic failure and quality control of microcircuit devices
[AD-759846] 17 p2005 N73-26215
Methods for evaluating physical properties, and causes of failure of materials
[AD-759225] 17 p2047 N73-26563
Inertial subsystem warning and coupling data unit failure indications on Apollo 16 mission
[NASA-TM-X-69199] 17 p2089 N73-26898
Thesaurus of terms for information on mechanics of structural failure modes and mechanisms for aerospace structures
[NASA-CR-121199] 17 p2091 N73-26917
Identification of sources for specialized information on failure modes and mechanisms of aerospace structures
[NASA-CR-121201] 17 p2091 N73-26919
Bibliography of citations related to problem areas in mechanics of failure in aerospace structures
[NASA-CR-121202] 17 p2091 N73-26920
Failure analysis of telemetry anomalies during Apollo 17 flight
[NASA-TM-X-69367] 18 p2117 N73-27118
Nondestructive tests and failure analysis of Vamistor resistors
[NASA-TM-X-64754] 18 p2122 N73-27154
Failure analysis of fiber reinforced composite rocket engine case using distortional energy and maximum strain theories of failure
18 p2167 N73-27500
Location of adhesive bond failure on Al surface during coupon surface treatment by radioactive tracing
[AD-761073] 18 p2168 N73-27509
Failure of fluorocarbon sulfonic acid membrane for hydrogen oxygen fuel cell
[NASA-CR-121007] 19 p2223 N73-27928
Techniques for controlling time to fatigue crack initiation in design of aircraft structures and application of residual stress analyses
20 p2481 N73-29930
Development of rational analytic theory for analyzing fatigue of airframes based on maximum stress-field parameter and maximum load excursion ratio
20 p2481 N73-29931
Application of growth rate data and analytical retardation models for predicting crack growth under variable amplitude loading
20 p2481 N73-29932
Analysis of errors in fatigue life prediction procedures and methods for improving accuracy of prediction analysis techniques
20 p2481 N73-29934
Failure analysis of synchronizing drive shaft adapter on CH-47A helicopter for improved reliability and cost reduction
[AD-763186] 21 p2497 N73-30041
Analysis of failure modes of blades on CH-47 helicopter rotary wings for improved helicopter reliability and cost reduction
[AD-763187] 21 p2497 N73-30042
Analysis of failure modes of tail rotor on OH-58 helicopter for improved reliability and cost reduction
[AD-763188] 21 p2497 N73-30043
Failure analysis of semiconductor devices by metallography
[DLR-MITT-72-20] 22 p2643 N73-31184
Method for determining time to failure of blades on aircraft gas turbine engines at steady mode and transient mode of operation
[NASA-TT-F-15113] 22 p2710 N73-31700
Apollo experience report on various phases of post-flight testing of command modules to resolve or minimize anomalies discovered during flight
[NASA-TN-D-7435] 22 p2721 N73-31773
Congressional hearing to determine causes of malfunctions of Skylab space vehicle
22 p2737 N73-31914
Thermoelastic analysis for predicting thermal stress failure in silicon solar cell array
[NASA-CR-135713] 23 p2748 N73-31993
Photosensitivity failure analysis on integrated microcircuit caused by surface inversion
[AD-764708] 23 p2766 N73-32132
Bench and thermal-vacuum testing of superconductors and heat pipe systems to determine failure characteristics
[NASA-TN-D-7395] 24 p2992 N73-33909

**FAILURE MODES**

Fatigue analysis and fatigue mode studies in bonded joints of composite materials
[AD-750134] 06 p0728 N73-15941
Environmental tests and failure modes for microelectric devices
[AD-753256] 10 p1135 N73-19253
Fire control computer program for Poseidon missile failure data processing
[AD-754426] 11 p1260 N73-20230
Development and evaluation of failure detection and isolation technique for use with four gimbaled inertial measuring units
11 p1317 N73-20687
Failure modes for isotropic and anisotropic composite materials
[AD-756889] 14 p1681 N73-23639
Mechanical properties and failure modes of glass fiber reinforced epoxy plates under high tensile loads
[AD-759153] 16 p1933 N73-25640
Heat flow failure mechanism in overstressed microelectronic circuits
[AD-761792] 19 p2244 N73-28094
Rate theory for determining failure accumulation in composite propellants
[AD-763806] 21 p2588 N73-30733
Reliability and failure modes of GaAs Gunn and impatt diodes and Si impatt diodes
[AD-763929] 22 p2644 N73-31193

**FAIRCHILD MILITARY AIRCRAFT**

U FAIRCHILD-HILLER AIRCRAFT
U MILITARY AIRCRAFT

**FAIRCHILD-HILLER AIRCRAFT**

NT XC-142 AIRCRAFT
Aircraft accident involving crash of Fairchild Hiller FH-227b aircraft near Albany County Airport, New York on 3 March 1972
[NTSB-AAR-73-8] 17 p1982 N73-26018

**FAIREY AIRCRAFT**

NT FD 2 AIRCRAFT

**FAIREY DELTA 2 AIRCRAFT**

U FD 2 AIRCRAFT

**FAIRINGS**

System for deploying and ejecting releasable clamshell fairing sections from spinning sounding rockets
[NASA-CASE-GSC-10590-1] 05 p0597 N73-14853

**FALLING SPHERES**

Measurement of upper atmospheric parameters using free-falling sphere
[AD-747037] 02 p0170 N73-11383
Triaxial accelerometer for determining upper air density, temperature, and pressure
[AD-749881] 05 p0543 N73-14422
Measurements of meteorological parameters at Woomera using falling spheres from February to June 1972
[WRE-TN-787[WR/D]] 14 p1685 N73-23670
Approximation of atmospheric density and winds from radar track of passive inflatable sphere
17 p2057 N73-26633
Woomera atmospheric parameters measured during falling sphere ejection from rocket soundings between Feb. and Jun. 1972 noting comparison with atmospheric models
[WRE-TN-787] 18 p2146 N73-27341
Falling sphere experiment for profiles of basic atmospheric parameters in Woomera, Australia
[WRE-TN-786[WR/D]] 22 p2694 N73-31579
Falling sphere measurement data on atmospheric parameters
[WRE-TN-799[WR/D]] 24 p2958 N73-33639

**FALLOUT**
Sr, Ba, and Ce fallout from nuclear explosions and weapons tests, monitored in ground-level air, in rain, and in atmosphere
[ORO-2529-30] 03 p0333 N73-12719
Emergency radiological and meteorological instrumentation criteria for reactors
[BNWL-1635] 04 p0422 N73-13443
Measurement of radioisotopes in air and rain water for areas around Helsinki and Ivalo, Finland
[REPT-11] 07 p0815 N73-16604
Atmospheric models for evaluating nuclear facility sites
[BNWL-1651-VOL-2-PT-1] 24 p2885 N73-33044

**FALLOW FIELDS**
U FARMLANDS

**FAN IN WING AIRCRAFT**
NT XV-5 AIRCRAFT
Acoustic measurements of sound pressure levels due to cross flow over face of lift fans on fan-in-wing and V/STOL model transport aircraft
[NASA-CR-114566] 13 p1473 N73-21928

**FANLIFT DEVICES**
U LIFT FANS

**FANS**
Low noise level fan and pump concept for space shuttle
[NASA-CR-128986] 17 p2037 N73-26477
Design, fabrication, and test of boron-polyimide reinforced titanium fan disks to operate at high temperatures
18 p2167 N73-27498

**FAR FIELDS**
Three-dimensional electromagnetic inverse scattering identity based on physical optics approximation for monostatic scattered far field cross section of perfect conductors
02 p0200 N73-11615
Laser illumination for stellar interferometry
[AD-752902] 09 p1068 N73-18712
Gravitational wave observations as tool for testing relativistic gravity
[NASA-CR-133411] 18 p2145 N73-27337
Far-field pattern of antenna determined from probe compensated near-field measurements over surface of right circular cylinder enclosing antenna
20 p2375 N73-29084
Relationship between distribution of outflow of acoustic energy over jet boundary and far-field intensity
[NASA-TN-D-7269] 24 p2905 N73-33181

**FAR INFRARED RADIATION**
Far infrared radiation detection with quantum photodetectors, noting application to submillimeter wave communication
[FTZ-A-14-TBR-4] 02 p0141 N73-11144
Design, fabrication, and performance evaluation of Faraday effect far infrared isolators
[AD-751319] 07 p0808 N73-16552
Bremsstrahlung for enhancing far infrared laser scattering from theta pinch plasma
[AD-753404] 09 p1073 N73-18755
Hydrostatic pressure studies of magnetic modes in far infrared
[COO-3151-12] 12 p1428 N73-21577
Enhanced far infrared radiation from theta pinch plasma
12 p1432 N73-21601
Instrumentation for far infrared spectroscopy
[AD-762313] 19 p2302 N73-28512
Collimator for analyzing spatial location of near and distant sources of radiation
[NASA-CASE-MFS-20546-2] 21 p2543 N73-30389
Far infrared and submillimeter background
[AD-763139] 21 p2598 N73-30823
Raman and far infrared spectra of crystalline fluorine obtained in solid phases
[AD-763686] 22 p2626 N73-31039

**FAR ULTRAVIOLET RADIATION**
NT LYMAN ALPHA RADIATION
NT LYMAN BETA RADIATION
Rate of solar extreme ultraviolet radiation heating in upper atmosphere
[AD-745305] 01 p0051 N73-10410
Far ultraviolet heating in upper atmosphere variations
[AD-745309] 01 p0051 N73-10411
Molecular branching ratio method for intensity calibration of optical systems in far ultraviolet
[NASA-TM-X-66070] 01 p0103 N73-10853
Measurement of ultraviolet and far ultraviolet transmission of transparent materials during high energy electron irradiation
[NASA-CR-129297] 03 p0334 N73-12726
High resolution spectral reflectance of potassium chlorides and bromides at room temperature in far ultraviolet yields new structures
[NOTA-INTERNA-402] 05 p0587 N73-14777
OSO 5 spectrophotometer design, solar EUV data acquired, and data reduction
[NASA-CR-130159] 08 p0956 N73-17828
Observation of venus far ultraviolet spectrum by sounding rockets
13 p1572 N73-22741
Problems associated with measuring VUV radiation in shock layer around hypersonic reentry vehicles
[AD-757150] 14 p1693 N73-23740
High optical resolution derivative spectrometer for measuring optical properties of solids in vacuum UV and far IR range
15 p1785 N73-24474
Xenon gas laser oscillations in vacuum ultraviolet
[AD-759069] 16 p1925 N73-25576
Kinetics of far ultraviolet chemiluminescence of exhaust plumes
[AD-760584] 18 p2114 N73-27093
Photometric aspects of interferometry in far ultraviolet
[AD-762151] 19 p2233 N73-28003

**FARADAY EFFECT**
Feasibility of using terbium-silicate glass as Faraday rotator-isolator in high power laser
[AD-749919] 05 p0559 N73-14543
Stability of laser gyro with Faraday cell
[FOA-2-C-2467-54] 06 p0696 N73-15671
Design, fabrication, and performance evaluation of Faraday effect far infrared isolators
[AD-751319] 07 p0808 N73-16552
Linear variation of magnetic field as inverse Faraday effect in plasma
[FRNC-TH-217] 08 p0948 N73-17762
Ionospheric electron content measurements by Faraday effect and dispersive Doppler effect
[BMBW-FBW-72-31] 09 p1027 N73-18380
Faraday rotation angle phi of radio signal from ATS-C
[AD-753088] 09 p1031 N73-18414
Faraday rotation and attenuation in InSb in 10.6 micron wavelength region
[AD-761213] 18 p2190 N73-27685

**FARADAY ROTATION**
U FARADAY EFFECT

**FARM CROPS**
NT ALFALFA
NT CORN
NT COTTON
NT FRUITS
NT GRAINS [FOOD]
NT WHEAT
Legal liabilities and impact of satellite meteorology on agricultural crops and economics
[NASA-CR-129994] 06 p0692 N73-15636
Case studies of meteorological satellite impact on agricultural crops and recreational activities
06 p0693 N73-15641
Development of procedure and system for uniform mapping and monitoring of earth resources and environmental complexes using ERTS-1 imagery
[E73-10350] 11 p1275 N73-20344
Evaluation and comparison of ERTS-1 measurements of major crops and soil conditions for selected areas in Central United States
[E73-10384] 11 p1275 N73-20348
ERTS-1 imagery of flood damage to farmlands in South Dakota
[NASA-CR-131641] 12 p1401 N73-21361
Climatic variability of winter wheat harvest for USSR
13 p1552 N73-22578
Use of soil-vegetation system brightness coefficients to measure vegetation quantity and crop yield
20 p2406 N73-29334
Hail protection method for reducing or eliminating farm crop damage
20 p2446 N73-29649
Application of space photography for small-scale mapping and analysis of farm lands
21 p2535 N73-30326
Utilization of ERTS data to study air pollution, insect infestation, and water transport in Minnesota
[NASA-CR-135565] 23 p2783 N73-32266
Aerial photography for detecting cereal crop insect infestation
[PAPER-8076] 23 p2783 N73-32268
Agroclimatology study of highlands of eastern Africa
[WMO-339] 24 p2886 N73-33045

**FARMLANDS**
ERTS-1 imagery of strip mining activity in Cumberland Plateau, Tennessee Test Site and agricultural areas in Alabama, Georgia, and Tennessee
[E73-10694] 16 p1902 N73-25386
Analysis of ERTS-1 imagery for crop identification and area estimates in Iowa
[E73-10699] 16 p1903 N73-25391
Digital analysis of ERTS-1 imagery for southeastern South Dakota to determine cultivated areas and to identify crops
[PAPER-A3] 19 p2259 N73-28211
Application of ERTS-1 imagery for identifying citrus groves and rice fields in Valencia region of Eastern Spain
[PAPER-A4] 19 p2260 N73-28212
Application of ERTS-1 imagery for identification of ecological analogs of natural vegetation and food crops in California, Colorado, and Louisiana
[PAPER-A6] 19 p2260 N73-28214
Quantitative evaluation of computer processed ERTS-1 MSS data classifications to identify major agricultural crops in Illinois
[PAPER-A25] 19 p2262 N73-28232
Collection and processing of ground truth crop and field data for Skylab-3
[E73-10879] 20 p2394 N73-29230
Hydrology of prehistoric farming systems in central Arizona ecotone from Skylab EREP data
[E73-11044] 23 p2779 N73-32220

**FAST FOURIER TRANSFORMATIONS**
Fast Fourier transform digital processor as spectrum analyzer and adaptive filter
01 p0025 N73-10198
Two dimensional Fourier transform and digital correlation for image processing
[BMVG-FBWT-72-1] 10 p1179 N73-19591
Algorithm for computer processing of Fourier transformations
[AD-758451] 15 p1755 N73-24222
Discrete unitary transforms with fast algorithm for encoding images for transmission
[NASA-CR-132771] 17 p2055 N73-26622

**FAST NEUTRONS**
Thin walled and solid cylinders of alumina and yttria after fast neutron irradiation
[LA-DC-72-535] 03 p0314 N73-12564
Influence of fast neutron damage to ceramic insulators on thermionic reactor design
[LA-DC-72-523] 03 p0333 N73-12716
Enhanced solar activity effects on fast neutron production at polar latitudes
04 p0465 N73-13791
Spectrometer for fast neutrons using proton recoil in stilbene crystal
[BMVG-FBWT-72-4] 09 p1036 N73-18456
Relative biological effectiveness of fast neutrons with gamma background
11 p1243 N73-20091
Flux and energy spectrum of fast neutrons and gamma rays at balloon altitudes
23 p2833 N73-32642
Measured and calculated fast neutron spectra at surface of lithium hydride and depleted uranium shielded reactors
[NASA-TM-X-2906] 24 p2953 N73-33594

**FAST NUCLEAR REACTORS**
NT FAST TEST REACTORS
Survey of aluminum-, copper-, and magnesium-alloy properties as filling materials for fast breeder fuel elements
[EUR-4857-E] 02 p0211 N73-11706
Fast reactor irradiation effects on creep behavior of annealed type 316 stainless steels
[HEDL-SA-300] 03 p0314 N73-12559
Computer program for high temperature structural design methods for LMFBR components
[ORNL-TM-3845] 03 p0333 N73-12712
Multidimensional analysis of fast spectrum material replacement measurements for systematic estimation of cross section uncertainties
[NASA-TM-X-2679] 05 p0579 N73-14709
Safety calculations for compaction and coolant voiding by airborne fast reactor
[LA-4977] 06 p0699 N73-15695
Research and development in Fast Reactor Program
[EURFNR-1034] 10 p1187 N73-19656
Fuel-oxide can compatability and reaction during fabrication of fuel elements for fast reactors
[NLL-CE-TRANS-6049-[9022.09]]
11 p1322 N73-20732
Bearings for control system of high temperature lithium or argon cooled fast nuclear reactors
[NASA-TM-X-68218] 13 p1534 N73-22429
Nuclear properties in neutron interactions with various nuclei in fast breeder reactor
[ANCR-1088] 17 p2062 N73-26677
Elastic-plastic toughness level of irradiated stainless steels used in fast reactor construction
[AD-761611] 19 p2310 N73-28580
Calculated power distribution of thermionic, beryllium oxide reflected, fast spectrum reactor
[NASA-TM-X-2838] 19 p2320 N73-28663
Evaluation of welding techniques for austenitic stainless steels for use in liquid metal fast breeder reactors
[ORNL-TM-4055] 24 p2954 N73-33601

**FAST TEST REACTORS**
Power production and fuel capability of light water cooled cavity test reactor
[NASA-TM-X-2864] 19 p2320 N73-28662

**FASTENERS**
NT BOLTS
NT LOCKS [FASTENERS]
NT NUTS [FASTENERS]
NT PINS
NT SCREWS
Suitability of directionally solidified eutectic alloys for high temperature fasteners, material properties, and fabricating methods
[NASA-CR-123919] 02 p0177 N73-11437
Design criteria for load suspension points, slings, and lifting equipment used on military helicopters
[AD-747814] 03 p0307 N73-12508

Effect of blade thickness on shear strength of fasteners
[AD-757997] 15 p1793 N73-24539
Effect of stress corrosion cracking and hydrogen embrittlement on failure of high strength spacecraft fasteners
[AD-758754] 15 p1800 N73-24591
Finite element digital procedure for stress and strain distribution in vicinity of interference fit fastners
[AD-760570] 18 p2157 N73-27425

FATIGUE [BIOLOGY]
NT FLIGHT FATIGUE
Effect of vigilance on performance of simple visual detection task
[AD-745317] 01 p0012 N73-10097
Concepts for reduction of fatigue in sustained tactical operations
[AD-746643] 02 p0134 N73-11090
Fatigue effect on human visual perception
[AD-750097] 06 p0636 N73-15171
Pressure chambers for testing effect of oxygen inspiration on fatigue during flight
[JPRS-59041] 14 p1610 N73-23051
Masking phenomenon for measuring state of fatigue and stress of nervous system
[AD-752975] 16 p1869 N73-25129
Subjective and physiological indicators of fatigue and performance during vigilance task
[AD-761503] 21 p2502 N73-30077
Effects of fatigue, age, and degree of difficulty on eye-hand coordination performance
24 p2887 N73-33051

FATIGUE [MATERIALS]
NT BENDING FATIGUE
NT METAL FATIGUE
NT THERMAL FATIGUE
Estimating effect of inclined nut seating on fatigue strength of steel screw thread
[ESDU-67034] 01 p0060 N73-10487
Fatigue tests of steel screw threads with large root radii under axial loading to determine fatigue strength and point of failure
[ESDU-67020-AMEND-A] 01 p0110 N73-10906
Fatigue strength data for thick steel and aluminum alloy cylinders under internal pressure
[ESDU-67014] 01 p0110 N73-10910
Estimating fatigue strength of components subjected to constant amplitude with constant mean loading
[ESDU-71010] 01 p0111 N73-10915
Static and fatigue strength of welded tubular joints
[AD-746894] 02 p0179 N73-11453
Vulnerability mechanism of pearlitic and austenitic steel alloys during plastic deformation
[NLL-RTS-7426] 02 p0184 N73-11493
Fatigue strength of tensile strained 45 and 40Kh steel
[NLL-SMRE-TRANS-5862-[8313.4]]
02 p0184 N73-11494
Analysis of fatigue crack growth data obtained in high strength aluminum alloys to separate metallurgical effects from other factors
[AD-745989] 02 p0187 N73-11518
Definition of basic terms, notation, and forms of presentation for fatigue data
[ESDU-70016] 02 p0237 N73-11925
Computer program to determine crack propagation characteristics of ultra high strength steel under various load cycles
[ARL/SM-NOTE-376] 02 p0237 N73-11930
Development of airframe integrity investigation procedures to determine structural deficiencies and modifications required to airframes for increased service life
[AD-746881] 03 p0253 N73-12049
References on fatigue and fracture of aircraft structures and materials to include instruments, sonic fatigue, and mechanical fasteners
[AD-748100] 03 p0254 N73-12053
Analysis of data generated by combined bending-torsion fatigue reliability research machines using probabilistic-graphically and phenomenological techniques
[NASA-CR-72839] 03 p0306 N73-12498
Statistical analysis of fatigue properties of SAE 4340 steel and description of test equipment used
[NASA-CR-72835] 03 p0313 N73-12551
Corrosion fatigue behavior of 4340 steel above K sub Iscc in distilled water
[AD-747700] 03 p0317 N73-12584
Fracture and fatigue crack propagation characteristics of annealed titanium alloy plate
[AD-748644] 03 p0319 N73-12600
Fatigue and crack propagation characteristics of aluminum alloy sheet under controlled cycle stress conditions to simulate fuel tank structural failure
[NASA-CR-128600] 03 p0360 N73-12935
Fatigue crack propagation in aluminum alloy sheets in environments of dry argon, normal air, distilled water, and aqueous sodium chloride solutions
[NLR-TR-72005-U] 04 p0431 N73-13513
Estimation procedure for fatigue failure probability of some graphites
[AECL-3958] 04 p0438 N73-13567
Fatigue behavior of hat section stringer stiffened panels compressed in post-buckling range
[AD-748855] 04 p0482 N73-13938
Exo-electron emission testing of material fatigue
[AD-748272] 05 p0549 N73-14457
Influence of thermal stresses and loads on endurance properties of heat resistant alloys used to manufacture turbine blades
[AD-749752] 05 p0591 N73-14805
Analysis of process involved in fatigue fracture of zinc alloys to show separation of zinc in front of fatigue cracks
[S-241] 05 p0602 N73-14896
Analysis of fatigue behavior of composite-reinforced, integrally stiffened metal panels and effects of temperature on adhesive substances
[NASA-CR-112148] 05 p0602 N73-14899
Effect of residual compressive stresses on fatigue strength and service life of aluminum alloy 7079 specimens
[NLR-TR-71105-U] 06 p0684 N73-15567
Application of strainrange partitioning method to high temperature fatigue
[NASA-TM-X-68171] 06 p0725 N73-15923
Analysis methods for studying fatigue in bonded joints of composite materials
[AD-750132] 06 p0728 N73-15939
Fatigue analysis and fatigue mode studies in bonded joints of composite materials
[AD-750134] 06 p0728 N73-15941
Amplitude analysis of mechanical fatigue of structures acted upon by cyclic stresses
[AD-750908] 06 p0729 N73-15947
Physical aspects of fatigue damage accumulation, including interaction and sequence effects
07 p0851 N73-16899
Fatigue crack propagation under flight simulation loading at 10, 1, and 0.1 cycles per second
07 p0851 N73-16900
Random fatigue tests on normalized carbon steel with 0.7 percent carbon
07 p0851 N73-16902
Elastic-plastic solution for calculating influence of energy dissipation on drawn wire fatigue
[AD-752017] 08 p0928 N73-17600
Measurement of fatigue crack propagation rates in heat treated steels
[PB-212208] 08 p0932 N73-17635
Statistical analysis of strength and fracture characteristics of materials with application to fiber composites using Weibull density functions
[JPL-TM-33-580] 08 p0934 N73-17650
Fatigue behavior of thin solid films induced by moving surface load
[AD-753411] 09 p1041 N73-18490
Tensile, exfoliation, fatigue, and crack growth properties of heat treated aluminum sheet alloy 7475
[AD-753709] 09 p1050 N73-18560
Interaction between creep and fatigue processes during crack growth in sheet specimens of aluminum alloy at 400 F
[AD-753688] 09 p1050 N73-18562
Time dependent mechanical behavior of boron filament reinforced aluminum composites based on static and dynamic properties
[AD-753706] 09 p1054 N73-18590
Fatigue behavior of directionally-solidified aluminum-nickel eutectic alloy under cyclic torsional loading
[AD-753689] 09 p1055 N73-18600
Thin deformable films for use as storage medium in holographic optical memory
[NASA-CR-124083] 09 p1064 N73-18681
Analysis of fatigue damage cumulation of low carbon steel specimens with transverse hole using two step rotating bending tests and block loading sequence
[TAE-164] 09 p1093 N73-18922
Development of three stage model for fatigue failure of structure with several critical regions for initial failure
[ARL/SM-NOTE-338] 09 p1093 N73-18924
Effect of strain hardening on fatigue crack resistance after single cycle peak overload in Ti-6Al-4V Ti alloy
[AD-753899] 10 p1174 N73-19553
Analysis of factors affecting fatigue failure in welded joints and significance of weld defects on fatigue strength
[NLL-RISLEY-TR-2509-[9091-9F]]
11 p1296 N73-20517
Brittle fracture and fatigue of cylindrical hollow bodies with offset seams and stiffeners
[NLL-RISLEY-TR-2527-[9001.9F]]
11 p1344 N73-20908
Development of methods for determining service life of rolling bearings based on fatigue of bearing materials
[NLL-RISLEY-TR-2524-[9091.9F]]
12 p1407 N73-21406
Effects of specimen thickness on fatigue-crack growth and fracture toughness of 7075-T6 and 7178-T6 aluminum alloy plates and sheets
[NASA-TN-D-7173] 12 p1413 N73-21453
Analysis of fracture of mixed viscous-brittle breakage of polycrystal using raster electron microscope
13 p1540 N73-22479
Extrapolating stress-rupture test results of heat resistant alloys
13 p1542 N73-22495
Fatigue damage accumulation and incompatible crack front orientation analyzed from aluminum alloys crack propagation test
[NLR-TR-72061-U] 13 p1543 N73-22504
Dislocation distribution in fatigued metals, including mean stress effects and Cu alloy single crystals
[AD-755227] 13 p1544 N73-22515
Proceedings of conference on materials and structures to include materials research, fracture control, and aerospace vehicle dynamics and control
[NASA-TM-X-69227] 13 p1585 N73-22850
Accelerated method of fatigue testing and parameters of fatigue curves
[AD-756050] 13 p1589 N73-22882
Analysis of fatigue performance of titanium alloys and steels to identify variations based on shape parameter for reliability engineering of airframes
[AD-758219] 14 p1605 N73-23008
Fatigue crack propagation and retardation experiments using polymethyl methacrylate
[AD-756490] 14 p1681 N73-23641
Performance tests to determine stress-life exponent for vacuum-processed steel ball bearing operating at 500 F
[NASA-TM-X-68240] 15 p1791 N73-24521
Analysis of resistance of reinforced and unreinforced structural plastics to static and fatigue failure
[AD-758626] 15 p1802 N73-24608
Evaluation of nondestructive testing methods for fatigue crack detection
[NASA-CR-128946] 15 p1839 N73-24901
Effects of wing structural elasticity on accumulation of fatigue damage during aircraft flight in turbulence
[AD-759634] 16 p1862 N73-25082
Fatigue mechanics of boron-aluminum composites under oscillating tensile loads
[AD-757213] 16 p1932 N73-25635
Precipitate size and distribution effects on fatigue crack initiation and propagation in high strength steel
[AD-759048] 16 p1971 N73-25940
Finite element analysis of thermoplasticity and nonlinear mechanics of fluid-saturated porous solids
[AD-758884] 16 p1972 N73-25949
Analysis of fatigue behavior of airframe components and development of methods for predicting service life of aircraft structures
[RAE-LIB-TRANS-1678] 17 p1981 N73-26012
Effect of martensitic microstructure on fatigue life and crack propagation characteristics of high strength steels
[S-253] 17 p2044 N73-26536
Fatigue strength and other mechanical properties of medium carbon steels chromed by gaseous and vapor phase methods
[DRIC-TRANS-2156] 17 p2046 N73-26550
Equivalence techniques used to define and simulate service vibration environments in testing laboratories
[AD-758414] 17 p2091 N73-26914
Thesaurus of terms for information on mechanics of structural failure modes and mechanisms for aerospace structures
[NASA-CR-121199] 17 p2091 N73-26917
Identification of sources for specialized information on failure modes and mechanisms of aerospace structures
[NASA-CR-121201] 17 p2091 N73-26919
Effect of lubricant active additives on rolling-element fatigue life using five-ball fatigue tester
[NASA-TN-D-7383] 18 p2156 N73-27417
Development of ultrasonic techniques for continuous monitoring of fatigue damage during cyclic testing of metal specimens
[AD-760787] 18 p2156 N73-27422
Effects of mechanical and metallurgical factors on crack propagation and ductile fracturing resistance of steels
[PB-218919] 18 p2161 N73-27458
Effect of stress intensity on fatigue crack growth in 5456-H117 aluminum alloys
[AD-760668] 18 p2162 N73-27465
Application of composite materials for structural purposes to show limitations and failure characteristics
18 p2164 N73-27481
Analysis of fatigue fracture under combined stress conditions for specimens of various cross sections
[NLL-RTS-7770] 18 p2202 N73-27776
Analysis of dynamic fracture in aluminum alloys using radial cylindrical wave propagation technique
18 p2202 N73-27778
Analysis of threshold of alternating range of stress intensity factor for producing extremely slow fatigue crack growth in aluminum alloys
18 p2202 N73-27779
Axial load fatigue tests on unnotched specimens of aluminum alloy extrusions following aging specimens
[ARL/SM-NOTE-386] 18 p2203 N73-27780

Numerical analysis of fatigue strength of steel specimens under symmetric loading cycles
[AD-761469] 19 p2310 N73-28581
Summaries of papers presented to AGARD conference on random load fatigue
[AGARD-AR-54] 19 p2348 N73-28884
Fatigue and creep-fatigue behavior of irradiated austenitic stainless steel used in LMFBR design
[ANCR-1096] 19 p2349 N73-28891
Fatigue failure of notched samples of titanium alloy
[AD-761588] 19 p2350 N73-28904
Development of fatigue cracks in flat plates under action of cyclic loads
[AD-761584] 19 p2351 N73-28911
Fatigue and martensitic transformations of austenitic stainless steels
20 p2427 N73-29498
Fatigue strength criteria for stressed materials
[AD-761447] 20 p2463 N73-29790
Sinusoidal simulation of material fatigue life when subjected to Gaussian narrow band random loading
20 p2477 N73-29896
Temperature characterization of below K sub Iscc corrosion fatigue behavior of HY-130 steel
20 p2477 N73-29899
Analysis of response and fatigue characteristics of light alloy integrally machined planks with emphasis on acoustic fatigue properties
20 p2479 N73-29912
Analysis of effect of damping on response of structure to acoustic excitation and experimental method for determining damping coefficients
20 p2479 N73-29917
Sonic fatigue characteristics of titanium sandwich structures and numerical analysis of natural frequencies and static stress values
20 p2480 N73-29919
Structural response and endurance tests of aircraft structural components to determine effect of critical environment on acoustic fatigue
20 p2480 N73-29920
Development of procedures for predicting fatigue life of aircraft structures based on fracture mechanics, crack propagation, and residual static strength anlaysis
[AGARD-LS-62] 20 p2480 N73-29924
Development of fatigue life prediction procedures based on measured stress-time histories and mathematical model for description of random vibrations
20 p2481 N73-29926
Techniques for controlling time to fatigue crack initiation in design of aircraft structures and application of residual stress analyses
20 p2481 N73-29930
Development of procedure for estimating fatigue life of airframes to eliminate errors caused by neglecting effect of stress redistribution after localized yielding
20 p2481 N73-29933
Effect of internal weld defects on fatigue behavior in mild structural steel butt welded connections
[PB-220896/5] 21 p2554 N73-30475
Application of fluidized bed technique for measuring relative thermal fatigue resistance of superalloys
[NASA-CR-121211] 21 p2558 N73-30507
Effect of O2-H2 atmosphere, H2, Ar, and room air on fatigue crack propagation in 4340 steel
[COO-3166-4] 21 p2559 N73-30513
Effect of stress on fatigue crack propagation in metals
[AD-763776] 21 p2560 N73-30523
Stress and corrosion effects on fatigue behavior 7075-T6 aluminum alloy
[AD-763455] 21 p2560 N73-30525
Fatigue properties of high strength high modulus graphite /glass/epoxy matrix composites
[AD-763760] 21 p2564 N73-30552
Computer program for analysis of nonlinear deformation and fatigue response of components subjected to complex load histories
[AD-763780] 21 p2604 N73-30870
Environmental fatigue crack propagation in Ti-Al-Sn
[NLR-TR-72093-U] 22 p2686 N73-31511
Fracture and fatigue properties of composite materials
[AD-764356] 22 p2689 N73-31540
Analysis of factors affecting variability in fatigue life of materials to show effects of material type, load applications, and test conditions on scatter of data
[ARL/SM-REPT-342] 23 p2853 N73-32796
Crack closure phenomenon in fatigue using Ti-6Al-4V titanium alloy
[NASA-CR-2319] 23 p2853 N73-32800
Analysis of size effects related to fatigue strength of metals under conditions of geometrical stress concentrations producing stress and strain gradients
24 p2988 N73-33876
High temperature low cycle effects on directly stressed, notched fatigue specimens
[RD/B/N-1996] 24 p2989 N73-33888

**FATIGUE DIAGRAMS**
U S-N DIAGRAMS

**FATIGUE LIFE**
General design principles for minimizing fatigue failure in structures and components
[ESDU-71009] 01 p0111 N73-10914
Fracture mechanics and prediction of fatigue life
[AD-746122] 02 p0188 N73-11521
Surface active substance effect on contact fatigue life of hardened ball bearing steel
[AD-746040] 03 p0307 N73-12506
Effect of heat treatment on fatigue life under gust loads of notched Al-Cu alloy
[ARC-CP-1221] 05 p0563 N73-14571
Effect of residual compressive stresses on fatigue strength and service life of aluminum alloy 7079 specimens
[NLR-TR-71105-U] 06 p0684 N73-15567
Measurements of positron lifetime distributions used to characterize plastic deformation in crystals
[COO-2128-2] 06 p0708 N73-15779
Random load fatigue of aircraft structures
[AGARD-CP-118] 07 p0851 N73-16896
Fatigue life assessment of aircraft structures based on random or programmed fatigue tests and loadings
07 p0851 N73-16897
Crack growth study and effects of change in spectrum severity and shape on fatigue behavior under random loading
07 p0851 N73-16898
Fatigue life prediction of military aircraft under three different load spectra
07 p0851 N73-16903
Evaluation of airframe fatigue life gage under constant and variable amplitude loading
[AD-753800] 09 p1037 N73-18464
Distributional S-N and Goodman diagrams for designing target reliabilities into rotating mechanical components
[NASA-CR-120967] 10 p1164 N73-19465
Methods for bounding life of structures subjected to constant loads and temperature within creep range
[RD/B/N-2257] 10 p1220 N73-19925
Effect of load variables on fatigue crack growth at room temperture in Ti-6Al-4V alloy
[NASA-CR-2239] 11 p1345 N73-20913
X ray and electron microscopic analysis of vacuum environment effects on 7075-T6 Al alloy fatigue life, fatigue-crack-growth behavior, and fracture toughness
[NASA-TM-X-69223] 12 p1413 N73-21450
Influence of surface conditions on Ti-6Al-4V alloy fatigue life
[AD-755385] 13 p1544 N73-22516
Secondary bending effect on aluminum alloy riveted joint fatigue strength determined by comparetive program fatigue tests
[NLR-TR-72007-U] 13 p1586 N73-22862
Statistical test of difference in fatigue life results in conventional and shot peening in aluminum-titanium alloy
[AD-758624] 15 p1794 N73-24542
Phenomenological analysis of interaction of creep and fatigue
16 p1968 N73-25922
Fatigue failure criterion for fiber reinforced laminates under stress
[AD-760146] 17 p2053 N73-26609
Fatigue damage due to seismic loads of materials with different yield strength and various ductility
[NASA-CR-133099] 17 p2091 N73-26916
Fatigue life of reactor pressure vessel steels in high temperature aqueous environment
[CONF-721104-6] 17 p2094 N73-26938
Analysis of effects of flying time on service life of wing fastening knee plates on transport aircraft
[AD-761468] 19 p2221 N73-27919
Fatigue design, below and within creep range
[AD-762619] 20 p2432 N73-29536
Sinusoidal simulation of material fatigue life when subjected to Gaussian narrow band random loading
20 p2477 N73-29896
Fatigue life and inelastic strain response under complex histories for alloy steel
20 p2478 N73-29900
Fatigue life of hybrid antifriction bearings at ultrahigh speeds
[NASA-CASE-LEW-11152-1] 23 p2795 N73-32359
Fatigue life tests of ball motion and sliding friction in arched outer race ball bearing under thrust load
[NASA-TM-X-71442] 23 p2797 N73-32375
X ray and electron microscopic studies on fatigue life of copper and copper zinc polycrystals
23 p2803 N73-32416
Fatigue life and fracture toughness of 7075-T6 Al alloy in vacuum and air environments
[NASA-TN-D-7262] 23 p2805 N73-32431
Analysis of factors affecting variability in fatigue life of materials to show effects of material type, load applications, and test conditions on scatter of data
[ARL/SM-REPT-342] 23 p2853 N73-32796
Cyclic mechanical and fatigue properties of ferroanelastic beta prime gold-cadmium
24 p2933 N73-33421

**FATIGUE TESTING MACHINES**
Automatic systems for analyzing fatigue crack propagation and for conducting constant stress intensity factor fatigue tests with servo-hydraulic machine
[RD/B/N-2013] 06 p0726 N73-15928
Fatigue test facility for space shuttle orbiters
10 p1138 N73-19273
Materials fatigue test machine for use aboard Skylab or space shuttles
[NASA-CR-132260] 16 p1913 N73-25476

**FATIGUE TESTS**
Four-phase airframe fatigue program for bending tests of aluminum alloy box beams
[AD-744673] 01 p0114 N73-10943
Fatigue tests on solid shafts with interference-fit collars
[ESDU-68005-PT-4] 02 p0177 N73-11434
Fatigue tests on unnotched steel specimens during bending and axial loading
[ESDU-FAT-F.07.04] 02 p0236 N73-11924
Time controlled creep-fatigue interaction for type 403 stainless steels at high temperature
[ORNL-4757] 03 p0315 N73-12565
Mechanisms of corrosion fatigue crack propagation in Al-Zn-Mg including effect of cyclic stress waveform
[AD-747709] 03 p0319 N73-12597
Influence of creep damage on low cycle thermal-mechanical fatigue behavior of two tantalum base alloys
[NASA-CR-121001] 04 p0431 N73-13514
Endurance of high strength steels subjected to bending
[ESDU-71027] 05 p0561 N73-14561
Fatigue properties of sintered test bars for bending and axial loads
[LBF-TM-58/71] 05 p0563 N73-14570
Determination of flat notched fatigue test specimens form numbers by stress optical method and finite element method, noting standardization
[LBF-TM-61/71] 06 p0685 N73-15573
Fatigue tests of notched and unnotched Ti6Al4V bars compared to other Ti-alloys
[LBF-TM-62/71] 06 p0685 N73-15574
Fatigue strength of notched titanium aluminum vanadium alloy between 1 million and 10 million stress cycles
[LBF-TM-63/71] 06 p0685 N73-15575
Fatigue tests to determine service life of aluminum alloy lugs with push-fit pins under tensile stress conditions
[ESDU-72020] 06 p0723 N73-15901
Fatigue behavior of corrugated panels, riveted along corrugations, subjected to cyclic compressive critical loads
[PUBL-1351] 06 p0724 N73-15915
Fatigue tests of hot pressed silicon nitride ball bearings
[NASA-TM-X-68174] 06 p0725 N73-15922
Fabrication, inspection and tests of fatigue in bonded joints of composite materials
[AD-750133] 06 p0728 N73-15940
Analysis of fatigue and fail-safe characteristics of composite-reinforced, stiffened metal panels to determine residual strength
[NASA-CR-2136] 07 p0852 N73-16909
Fatigue tests to determine service life of catapult structure on C-2 aircraft
[AD-752493] 08 p0868 N73-17028
Comparison of fatigue strength of steel joints produced by friction welding and by electrocontact welding with fusion method
[AD-753488] 09 p1049 N73-18553
Low cycle fatigue testing at high temperatures
[AGARD-R-604] 09 p1092 N73-18916
Analysis of fatigue damage cumulation of low carbon steel specimens with transverse hole using two step rotating bending tests and block loading sequence
[TAE-164] 09 p1093 N73-18922
Fatigue tests of 7075-T6 aluminum alloy under synchronous pulsating triaxial stresses
[AD-754414] 10 p1174 N73-19552
Metallurgical investigation of deformation and fatigue using high temperature tests and stress-strain diagrams on heat resistant alloys
[JPRS-58180] 10 p1219 N73-19912
Fatigue tests to determine plastic deformations in composite materials
10 p1219 N73-19913
Failure criteria in cyclic elasto-plastic deformation
10 p1219 N73-19915
Fatigue damage of helicopter rotary wing structures - bibliographies
[AD-754062] 11 p1235 N73-20027
Method of life prediction for nickel-based Udimet alloy by high temperature creep/fatigue testing
[NASA-CR-120958] 12 p1462 N73-21845
Evaluating fatigue strength of steel with nonstationary loading
[AD-756945] 13 p1545 N73-22523
Fatigue behavior of composite-reinforced, integrally stiffened metal panels
[NASA-CR-112148] 13 p1585 N73-22853
Cyclic debonding of adhesive joints
[NASA-CR-2207] 16 p1932 N73-25631

Cyclic mechanical and fatigue properties of ferroanelastic beta prime gold-cadmium alloy
[NASA-CR-131843] 16 p1969 N73-25929
Influence of gaseous atmospheres on aluminum alloy, titanium, and refractory alloy fatigue striations
[ONERA-NT-192] 17 p2045 N73-26548
Static and fatigue properties of hardened and tempered electron beam welded joints in 2.5 percent Ni-Cr-Mo steel and 18 percent Ni-Co-Mo maraging steel
[S/T-MEMO-9-71] 18 p2161 N73-27456
Mechanical properties of double melted 18 percent Ni-Co-Mo maraging steel bar or forgings
[S/T-MEMO-3-72] 18 p2161 N73-27457
Analysis of fatigue fracture under combined stress conditions for specimens of various cross sections
[NLL-RTS-7770] 18 p2202 N73-27776
Analysis of dynamic fracture in aluminum alloys using radial cylindrical wave propagation technique
18 p2202 N73-27778
Development of method for determining response of box type structures subjected to high intensity acoustic loading
20 p2479 N73-29915
Sonic fatigue characteristics of titanium sandwich structures and numerical analysis of natural frequencies and static stress values
20 p2480 N73-29919
Acoustic fatigue tests of aluminum alloy structural elements under narrow-band, random loading with zero mean stress in skin
20 p2480 N73-29921
Development of experimental program for determining response and sonic fatigue resistance of lightweight aircraft structures
20 p2480 N73-29923
Development of procedures for predicting fatigue life of aircraft structures based on fracture mechanics, crack propagation, and residual static strength anlaysis
[AGARD-LS-62] 20 p2480 N73-29924
Procedures for evaluating fatigue quality of aircraft structures based on fatigue life, crack propagation, and residual strength
20 p2480 N73-29925
Procedures for predicting fatigue life of aircraft flying under various load conditions using data obtained by counting accelerometer
20 p2481 N73-29927
Analysis of equipment and procedures for conducting sonic fatigue tests of airframes at elevated temperatures
[AD-763798] 21 p2498 N73-30052
Application of fluidized bed technique for measuring relative thermal fatigue resistance of superalloys
[NASA-CR-121211] 21 p2558 N73-30507
Fatigue tests with random loads using electrosteel test specimen
[ICAF-DOC-683] 22 p2724 N73-31801
Monitoring of fatigue damage by ultrasonic attenuation measurements
23 p2796 N73-32363
Fatigue behavior of annealed high-conductivity copper and effects of single and periodic intermediate surface layer removal
23 p2803 N73-32419
Fatigue - crack growth of Ti-6 Al-2 Cb-1 Ta-0.8 Mo alloy in air and sea water environment
[AD-765318] 23 p2805 N73-32433
Tear and fatigue crack propogation tests for determining mechanical properties of ultrafine grain alpha titanium
[AD-765329] 23 p2805 N73-32434
Definition of criteria and techniques of design, analysis, and test for using single major structural test article for performing dynamic, fatigue, and static testing
[NASA-CR-124404] 23 p2853 N73-32799
Short-term tensile and low-cycle fatigue behavior of zirconium-copper at 482C to 593C
[NASA-CR-121260] 24 p2934 N73-33430
Heat to heat variation in fatigue and creep-fatigue behavior of AISI Type 304 stainless steel, and fatigue behavior of type 308 stainless steel weld material
[ANCR-1097] 24 p2936 N73-33450

**FATTY ACIDS**
Biosynthesis of unsaturated fatty acids in yeast
[NASA-TT-F-13918] 01 p0009 N73-10068
Gas chromatography-mass spectrometry for analyzing fatty acid and sterol concentrations in plant tissue samples
[NASA-CR-128740] 10 p1120 N73-19131
Ultracentrifugation of biological materials
[NASA-CR-114673] 23 p2750 N73-32009

**FAULT MECHANICS**
U FRACTURE MECHANICS

**FAULTS**
Characterizing sequences and fault detection in sequential computers
[AD-750266] 06 p0644 N73-15233

**FBFM (MODULATION)**
U FEEDBACK FREQUENCY MODULATION

**FCC LATTICES**
U FACE CENTERED CUBIC LATTICES

**FD 2 AIRCRAFT**
Measurement of aerodynamic heating on nose of Fairey Delta aircraft at 40,000 feet and Mach numbers to 1.65 during climb and level flight
[ARC-R/M-3280] 15 p1725 N73-23996

**FEASIBILITY**
Feasibility study for laser transponder onboard SOREL space probe
[ESRO-CR[P]-123] 02 p0149 N73-11207
Feasibility of modifying supersonic drone configuration into remotely controlled research vehicle
[NASA-CR-112323] 15 p1733 N73-24057
Feasibility study to develop recombining electron beam-excited plasma into pulsed laser of exceptionally high peak power
[AD-759399] 16 p1925 N73-25579
Feasibility of electrochemical silver/silver iodide/iodine battery
[SC-RR-72-0386] 24 p2881 N73-33006

**FEASIBILITY ANALYSIS**
Feasibility of mobile nuclear reactor power plants for cargo transportation and development of remote regions on earth
[NASA-TM-X-68164] 06 p0698 N73-15693
Feasibility of developing stirred chemical reactor laser cavity based on perfectly stirred reactor concept
[AD-751299] 07 p0807 N73-16549
Feasibility of developing liquid crystal display system
[AD-751747] 07 p0833 N73-16753
Economic feasibility analysis on San Francisco rapid transit system extension to serve airport
[PB-212456] 07 p0860 N73-16978
Feasibility of effective exercise and health evaluation and enhancement program for NASA employees
08 p0875 N73-17091
Feasibility of using yttrium oxide crucible to induction melt titanium
[AD-754092] 11 p1306 N73-20597
Feasibility of using nuclear propulsion systems in spacecraft
[JPRS-58457] 11 p1323 N73-20737
Feasibility study of spaceborne plated wire memory with associated electronic circuits and components
[REPT-26/1422/EC/MB/VOL-I] 13 p1498 N73-22137
Feasibility of laser induced ablation thruster for space propulsion system
[NASA-CR-131744] 13 p1537 N73-22449
Feasibility and costs of orbiting satellite data collection systems
[NASA-CR-130232] 13 p1581 N73-22812
Feasibility analysis and design of bleachable absorber laser amplifier and detector
[AD-757361] 14 p1672 N73-23571
Cryogenic superconducting magnetic suspension and balance facility designs
15 p1761 N73-24272
Feasibility of modifying Tacan/DME system to broadcast digital data for area navigation
[FAA-RD-73-2] 15 p1808 N73-24656
Feasibility study for Europa 3 launch vehicle nuclear upper stage
[TR-TT-4-15/72] 15 p1811 N73-24675
Electrical equipment of nuclear upper stage for Europa 3 launch vehicle
[TR-TT-4-16/72] 15 p1811 N73-24677
Feasibility analysis of laboratory experiment on ionic excitation cross section by electron impact on laser produced plasmas
[ESRO-SN-122] 15 p1818 N73-24737
Feasibility study for Europa 3 launch vehicle nuclear upper stage
[TR-T/T-1.2-7/72] 15 p1836 N73-24880
Feasibility of using adaptive estimation for atmospheric temperature forecasting
[AD-759546] 16 p1940 N73-25698
Feasibility analysis for computer-based data communications and/or processing facilities at civil airport
[RAE-TR-72133] 16 p1941 N73-25711
Neutronic feasibility of fast spectrum space power reactor design concepts using boron control devices
[NASA-TM-X-2821] 16 p1943 N73-25720
Feasibility of limb controlled astronaut maneuvering scheme
18 p2110 N73-27063
Feasibility analysis and prediction performance of constant temperature heat pipe for space applications
[ESRO-CR[P]-246] 18 p2207 N73-27810
Feasibility of on-line fission gas leak detection system for 100 kW zirconium hydride reactor
[NASA-TM-X-2870] 20 p2453 N73-29717
Feasibility of ATC radar beacon system based on vehicle surveillance on airport surface in relation to vehicle time of arrival
[AD-763328] 21 p2577 N73-30655
Feasibility of using inverse rastering to irridiate large test objects by penetrating radiation beams
22 p2732 N73-31866
Feasibility of bifold nuclear power source using Pu-238 fuel
24 p2951 N73-33573

**FEATHERING**
Iterative method for analyzing feathering characteristics in airfoil whirlwinds
[DEP/PRA/NT/88/72] 14 p1600 N73-22968

**FECES**
Toxicity of gaseous urine and feces emissions on rat organism
10 p1116 N73-19097
Hydroponic cultivation of plants on clay filters from human mineralized feces
10 p1117 N73-19110

**FEDERAL BUDGETS**
Congressional hearing on 1973 fiscal budget for Department of Transportation
01 p0120 N73-10989
Congressional hearings to establish government supported projects for fire research and safety
04 p0487 N73-13981
Distribution of federal funds for research and development
[NSF-72-317-VOL-21] 09 p1100 N73-18980
Graphs, tables, and analysis of Federal R and D funding by budget function and by primary purpose
[NSF-72-313] 09 p1101 N73-18987
Congressional hearings on NASA budgetary authorizations for 1974
13 p1595 N73-22930
Planning and budgeting in lightweight fighter prototype development for military aviation
13 p1595 N73-22934
Scope of Federal funding for scientific research and development
[NSF-72-317] 15 p1846 N73-24958
Congressional hearings on appropriations for Housing and Urban Development, National Science Foundation, and Veterans organizations for 1974
16 p1976 N73-25978
Congressional committe report to identify and resolve disagreements in NASA appropriations for Fiscal Year 1974
[H-REPT-93-353] 21 p2607 N73-30892
Congressional hearings concerning appropriations for NASA operations during Fiscal Year 1974 - Part 1
21 p2608 N73-30906
Congressional hearings concerning appropriations for NASA operations during Fiscal Year 1974 - Part 3
21 p2608 N73-30907
Index of subjects presented during Congressional hearings involving NASA appropriations for Fiscal Year 1974
21 p2610 N73-30921
Economic aspects of Federal regulation of airline operations to show agencies involved and functions of government organizations
23 p2864 N73-32893

**FEDERAL REPUBLIC OF GERMANY**
U GERMANY

**FEED SYSTEMS**
Dual frequency feed systems for Cassegrainian antennas
[NASA-CASE-NPO-13091-1] 03 p0273 N73-12214
Analytical combustion model for predicting flow and pressure transients in H2-O2 RCS of rocket engine feed system
07 p0835 N73-16767
Improved injector with porous plug for bubbles of gas into feed lines of electrically conductive liquid
[NASA-CASE-NPO-11377] 18 p2154 N73-27406

**FEEDBACK**
NT NONLINEAR FEEDBACK
Acoustic feedback of subsonic and supersonic free jet impinging on obstacle, e.g. blown flap or ground, and noise reduction methods
[DGLR-PAPER-72-84] 04 p0373 N73-13031
Development of pressure transducer for satellite attitude control feeding signals back to solenoid flow control valve
[RAE-TR-72085] 05 p0548 N73-14453
Operating modes and outputs of distributed feedback side coupled waveguide lasers
[CRC-1235] 06 p0679 N73-15521
Fourier analysis of plasma deformation and feedback in stabilized rectilinear helicoid with pinch mechanism
[LRP-58/72] 10 p1196 N73-19728
Acousto-optical isolator for suppressing optical feedback generated laser instabilities
[AD-757914] 15 p1796 N73-24556

**FEEDBACK AMPLIFIERS**
Development of coupled operational amplifier circuits with emphasis on wiring for current signals and influence of errors due to coupling
[AD-743690] 01 p0033 N73-10257
Circuit with differential amplifier for synthesizing capacitance multiplier with microminiaturized feedback components
[NASA-CASE-NPO-11948-1] 06 p0647 N73-15255
Design of integrated circuit with two amplifiers and feedback stabilization for single channel gyrator
[NASA-CASE-MFS-22343-1] 09 p1008 N73-18224

**FEEDBACK CIRCUITS**
Linear shift register with feedback logic for generating pseudonoise linear recurring binary sequences
[NASA-CASE-NPO-11406] 03 p0268 N73-12175

1.2 stability in low and high frequency distributed feedback systems
[NASA-CR-129599] 03 p0277 N73-12245
Optical feedback technique to extend frequency response of solid state detector systems
[NASA-TM-X-2676] 04 p0421 N73-13430
Feedback stabilization of theta pinch plasma column by optical signal processor
[LA-DC-72-707] 05 p0584 N73-14750
Stability of two-loop dead-time feedback control systems
[DLR-FB-72-45] 22 p2646 N73-31204

**FEEDBACK CONTROL**
NT CASCADE CONTROL
Phase margin measure for determining human operator control performance in multivariable closed loop system
01 p0018 N73-10135
Analog signal to discrete time interval converter for control of dc to dc power supplies
[NASA-TM-X-68153] 02 p0128 N73-11043
Incomplete state feedback for systems with parameter uncertainty and random disturbances
[NASA-CR-129180] 02 p0150 N73-11219
Improvement in V/STOL aircraft performance with yaw control augmentation to reduce cross coupling effects
[AD-749489] 04 p0375 N73-13046
Operational control of ramjet engine with fixed nozzle diffuser geometry
[AD-748708] 04 p0465 N73-13787
Cooling systems using cold gas transfer closed loops in 15 to 80 K temperature range
[DLR-MITT-71-09] 04 p0485 N73-13964
Linear control theory for generating optimal trajectories between initial and final positions of n degree of freedom mechanical arm
[NASA-CR-123980] 05 p0551 N73-14470
Threshold circuits with feedback channels for cardiac R-wave detection in electrocardiographic heart rate monitoring
[NASA-TN-D-7152] 06 p0635 N73-15158
Design of linear feedback control system in Hilbert space
[AD-750784] 06 p0691 N73-15624
Relation between invariance conditions and characteristics of turbojet engine with afterburner multidimensional control system under variable flight conditions
[AD-749656] 06 p0714 N73-15828
Algorithm for choosing adaptive loop parameters and adjustment intervals of adaptive control systems
07 p0764 N73-16207
Design of feedback geometry for control of rotating plasma confined in magnetic mirror device
[AD-751341] 07 p0830 N73-16728
Development of adaptive control system for atmospheric reentry vehicle to meet flying quality requirements
07 p0848 N73-16871
Shift register with feedback for generating pseudorandom binary sequences
[REPT-6707] 08 p0887 N73-17183
Control theory in game problems, optimization, feedback, and probabilistic automata - conference
[JPRS-58030] 08 p0891 N73-17214
Feedback stabilization of magnetohydrodynamic turbulence in plasma column immersed in magnetic field
[AD-753102] 09 p1072 N73-18747
Following theory for feedback controls, Markov processes, and flow of automobiles and aircraft
10 p1136 N73-19259
Application of loran/inertial hybrid system and Kalman filter algorithm to fixed feedback gain
11 p1318 N73-20701
Transistorized feedback servomechanism design for cryogenic oxygen flow control
[NASA-TM-X-68234] 15 p1759 N73-24258
Analog and digital computer simulation study of pulse width modulation in feedback control systems
16 p1883 N73-25242
Contactless extremum transistorized circuit capable of cutoff, saturation, and generation
16 p1883 N73-25245
Pole and zero placement in multivariable control systems by least squares method
[NASA-CR-132962] 16 p1935 N73-25654
Mathematical models for stochastic feedback processes in optimal adaptive control systems
[AD-757900] 16 p1935 N73-25655
Analysis and design of closed loop control for slowly time-varying linear systems for space shuttle booster
[NASA-CR-128972] 16 p1966 N73-25905
Development of aerodynamic control system to control flutter over large range of oscillatory frequencies using stability augmentation techniques
[NASA-CASE-LAR-10682-1] 17 p1980 N73-26004
Remotely controlled manipulators with independent follow-up and force reproduction mechanisms
17 p1989 N73-26082
Computerized design of variable feedback system for attitude control of hypersonic vehicle
[AD-761493] 19 p2221 N73-27916
Feedback control loop stability analysis for dynamic solar array simulator, based on frequency response and using digital computer
[ESRO-CR[P]-261] 19 p2223 N73-27929
Analysis of operation of single stage, high pressure centrifugal compressor during closed loop flow of various gases
[AD-761608] 19 p2331 N73-28750
Design and tests of passive, feedback-controlled, variable conductance, gas loaded heat pipe
[NASA-TM-X-62293] 19 p2352 N73-28920
Adaptive modeling technique for synthesizing controllers to provide corrective dynamics to operator mathematical model in closed loop control system
[NASA-CR-132294] 20 p2372 N73-29060
Analysis of quantized signal dependent control of continuous process by computerized simulation
20 p2378 N73-29110
Development of feedback control in tilt rotor aircraft using swashplate cyclic and collective controls in addition to direct lift control - Vol. 7
[NASA-CR-114600] 21 p2493 N73-30011
Analytical synthesis method for feedback control of nonlinear multivariable systems
[AD-762797] 21 p2566 N73-30571
Control of 30 centimeter diameter mercury bombardment thruster
[NASA-TM-X-68297] 21 p2588 N73-30738
Stability of two-loop dead-time feedback control systems
[DLR-FB-72-45] 22 p2646 N73-31204
Feedback control for rotary wing aircraft steep approach profiles
[MBB-UFE-1021-O] 23 p2744 N73-31967
Power supply electronic tests on single jet disk type cesium thrustor with beam current feedback control
[LAAS-TNPE-73-T-17] 23 p2831 N73-32629
Riccati controlled feedback for guiding spacecraft during unpowered terminal phase of flight
23 p2847 N73-32751
Nonlinear feedback control concepts for variable stability aircraft
24 p2877 N73-32979
Sequential communication systems with information feedback
24 p2893 N73-33098

**FEEDBACK FREQUENCY MODULATION**
Characteristics of data-aided carrier tracking loop used for tracking carrier in angle modulated communications system
[NASA-CASE-NPO-11282] 07 p0764 N73-16205

**FEEDFORWARD CONTROL**
Class of multivariable, nonlinear time-varying feedback systems with instable convolution subsystem as feedforward
[NASA-CR-133183] 17 p2007 N73-26234

**FEEDING [SUPPLYING]**
Projectile loader for research gas gun
[AD-753008] 09 p1012 N73-18259

**FEEDING DEVICES**
U ANTENNA FEEDS

**FELDSPARS**
Terrestrial analogs of plagioclase feldspar and pyroxene
[RM-574J] 18 p2196 N73-27731

**FELLOWSHIP AIRCRAFT**
U F-28 TRANSPORT AIRCRAFT

**FELSITE**
U IGNEOUS ROCKS

**FEMALES**
Human factors engineering to determine maximum control forces capability of female pilots
[FAA-AM-72-27] 06 p0635 N73-15157
Anthropometry of Air Force women
[AD-743113] 13 p1484 N73-22034

**FERMENTATION**
Biodegradation of cellulose fibers and reclamation of single cell protein from refuse through fermentation process
[NASA-CR-130300] 06 p0630 N73-15115
Automatic control for absorption columns, fluidized bed processors, and continuous fermentation noting enzymatic protein production
[LAAS-PUBL-975] 24 p2892 N73-33090

**FERMI STATISTICS**
U QUANTUM STATISTICS

**FERMI SURFACES**
Effect of magnetic rupture on low frequency electroconductivity and weakly damped electromagnetic waves in metals with closed Fermi surfaces
[KHFTI-71-1] 06 p0684 N73-15569
Fermi surface changes in dilute alloys of aluminum, cadmium, and zinc
[AD-750726] 06 p0709 N73-15786
Electrical response of capacitor triggered by shock wave effect on Fermi energy level
[AD-759059] 16 p1883 N73-25239
Electron spin resonance measurements on Fermi levels in molybdenum doped rutile during hydrogen treatment
[AD-760735] 18 p2192 N73-27694
Variation of crystal Fermi energy to obtain different charge states in paramagnetic impurity ions for ESP study
[AD-760736] 20 p2464 N73-29798

**FERMI-DIRAC STATISTICS**
U QUANTUM STATISTICS

**FERMIONS**
NT BARYON RESONANCES
NT BARYONS
NT FAST NEUTRONS
NT LEPTONS
NT MESON RESONANCES
NT NEUTRONS
NT PROTONS
NT RECOIL PROTONS
NT SOLAR PROTONS
NT THERMAL NEUTRONS
Sum rule for photoproduction amplitudes in isovector Compton scattering and inconsistency of free fermion parton model in deep inelastic limit
[NUB-2169] 07 p0823 N73-16673

**FERRATES**
NT BARIUM FERRATES
Magneto-optic effects in ferrate garnet thin film waveguides
[AD-763792] 21 p2518 N73-30199

**FERRIMAGNETIC MATERIALS**
Evaluation of magnetic permeability tensors of polycrystal ferrimagnetic materials in saturated state for microwave frequencies
[REPT-9.441] 10 p1190 N73-19683
Ferrite logic device for increased reliability of digital electronic systems
[NASA-CR-132265] 19 p2248 N73-28124
Chemical vapor deposition of reproducible device quality ferrimagnetic films
[NASA-CR-132325] 24 p2891 N73-33083

**FERRITES**
Development and characteristics of reciprocal latching microwave phase shifters based on ferrimagnetic substrate
[AD-744795] 01 p0033 N73-10255
Design and fabrication of magnetic logic circuits using ferrite delay elements
[NASA-CR-112198] 03 p0277 N73-12247
Nickel zinc ferrite powders deposited on ceramic substrates by arc plasma spraying
[AD-747771] 03 p0307 N73-12509
Effects of polishing on magnetic properties of nickel-zinc ferrite toroids during annealing and procedures to restore original magnetic properties
[AD-747251] 03 p0346 N73-12822
Design and performance of digital ferrite phase shifter for phased array antenna systems
[AD-748431] 04 p0396 N73-13225
Fabrication of monolithic ferrite memory arrays
[NASA-CR-2152] 04 p0398 N73-13238
Analysis of effect of dysprosium oxide on the physical properties of nickel-zinc ferrite materials
[NLL-TRANS-746-1284-[9022.401]]
06 p0682 N73-15550
Tests to characterize crystallographic, magnetic, and optical properties of orthoferrites
[LCR-DR-1-71-97/1/R] 08 p0932 N73-17633
Sense amplifier of ferrite coincident core memory
[AD-752817] 09 p1009 N73-18235
Strip transmission line circulators using ferrites, noting new densification method for polycrystalline ferrimagnetic materials
[REPT-8.422] 12 p1384 N73-21222
Hot pressing of nickel-zinc ferrites for manufacturing read-write magnetic heads
[REPT-9.451] 13 p1500 N73-22154
Influence of titanium ions on magnetic properties of manganese-zinc ferrites
[NLL-TRANS-862-[9022.64]]
16 p1931 N73-25626
Production of screen-printed inductive components using ferrite pastes
[RAE-LIB-TRANS-1690] 17 p2072 N73-26763
Wideband SHF ferrite microelectronics
19 p2236 N73-28025
Hot pressed polycristalline garnets and ferrites of spinel type to be used at UHF
19 p2236 N73-28026
Logic and memory devices with magnetic crystals, emphasizing magnetic domains
[JPRS-59608] 20 p2461 N73-29776
Single orthoferrite crystal growth by crucibleless zone melting, including optical absorption spectra
20 p2461 N73-29777
Mossbauer spectra of ferrite catalysts used in oxidative dehydrogenation
[NASA-CR-133740] 21 p2506 N73-30108
Effect of multiword addressing with laminated ferrite arrays
[NASA-CR-124372] 21 p2512 N73-30149
Ferrite memory arrays from pre-formed metal conductors
[NASA-CASE-LAR-10994-1] 21 p2562 N73-30536
Polish research projects involving development and application of magnetically soft ferrite materials
21 p2608 N73-30902
Effect of scandium, yttrium, and lantham oxides on properties of nickel ferrite
23 p2809 N73-32460
Rare earth orthoferrites and micromagnetic interactions
[AD-764826] 23 p2827 N73-32593

**FERRITIC STAINLESS STEELS**
Development of high temperature stability in welded joints of ferritic steels by methods of constructional compensation
[NLL-RISLEY-TR-2487-[9091.9F]] 06 p0676 N73-15500

**FERROELECTRICITY**
Electrostriction in ferroelectric ceramics
[AD-745821] 01 p0089 N73-10731
Dynamics of polarization in polycrystalline ferroelectric materials
[NLL-RTS-7416] 02 p0218 N73-11762
Anomalous capacity for estimating ferroelectric phase transition in Kanzig regions
[AD-747559] 03 p0347 N73-12831
Magnetic and ferroelectric properties of rare earth compounds for signal processing devices
[AD-754775] 11 p1331 N73-20807
Two ferroelectric materials, single crystal bismuth titanate and hot pressed ceramic, lead zirconate titanate
[AD-755746] 12 p1386 N73-21237
Pyroelectric coefficient of lead zirconate titanate
[AD-755520] 13 p1567 N73-22700
Status of research on gas discharge, liquid crystal display systems, and ferroelectric ceramics in Europe
[AD-757649] 14 p1668 N73-23538

**FERROMAGNETIC FILMS**
Effects of magnetostriction and superlattice formation in ferromagnetic thin films
16 p1952 N73-25794

**FERROMAGNETIC MATERIALS**
NT FERROMAGNETIC FILMS
NT PERMALLOYS [TRADEMARK]
Lattice potential topography for 180 degree boundary in Perovskite ferroelectrics
[AD-742109] 01 p0088 N73-10724
Research of ultrasonic propagation in ferromagnetic materials
[AD-745783] 01 p0088 N73-10729
Ferromagnetic materials sensor for detecting time varying magnetic field disturbances and positional changes in ferromagnetic objects
[AD-748117] 03 p0338 N73-12757
Electromagnetic wave interactions in p type ferromagnetic semiconductors
10 p1198 N73-19751
Production of ferromagnetic MnBi thin films by optical control of vacuum deposition and annealing
[KFKI-72-70] 10 p1199 N73-19757
Ferromagnetic resonance in ferromagnetic thin films
12 p1438 N73-21651
Effects of energetic charged particle irradiation of solar system material
[NASA-CR-132045] 15 p1831 N73-24845
Magnetic and electrical properties of ferromagnetic semiconductors
[AD-762103] 19 p2327 N73-28725

**FERROMAGNETIC RESONANCE**
Ferromagnetic resonance in iron and hexagonal close packed cobalt lattices
[AD-753841] 09 p1076 N73-18783
Ferromagnetic resonance in ferromagnetic thin films
12 p1438 N73-21651
Ferromagnetic resonance measurements in Ni and Fe as function of temperature and frequency parameters
24 p2934 N73-33428

**FERROMAGNETISM**
Ising ferromagnet thermodynamic equilibrium states in low temperature regions
[NOTA-INTERNA-381] 01 p0080 N73-10660
Ising model for free spinless particles satisfying one dimensional Dirac equation
[AD-747736] 03 p0347 N73-12834
Magnetism in solids - magnetic moments, propertism of diamagnetism and paramagnetism, and coexistence of superconductivity and ferromagnetism
[ITJ-13] 04 p0449 N73-13670
Concentration dependence of high field susceptibility of Fe-Ni alloys
[NLL-LTI-746-1343-[9022.401]] 12 p1412 N73-21440
Phase diagram of decorated Ising system in nonzero magnetic field
[NUB-2175] 12 p1428 N73-21576
Far infrared laser spectroscopy of spin clusters in linear magnetic system of cobalt chloride compound
[AD-756264] 13 p1566 N73-22691
Green function technique used to calculate magnetic properties of disordered Heisenberg ferromagnets in which exchange interactions deviate randomly in strength from mean interaction
[NASA-TN-D-7208] 14 p1697 N73-23774
DOT blocking shift register and tip blocking for ferromagnetic research
[AD-763086] 20 p2365 N73-29017

**FERROUS METALS**
Electrochemical permeation technique and scanning electron microscopy used to determine hydrogen embrittlement in ferrous materials
[AD-752828] 09 p1049 N73-18557
Ferritic steels resistant to high temperature and decarburization by Na
[CEA-CONF-2118] 17 p2044 N73-26539
Frequency effect of magnetocrystalline anisotropy in nickel ferrous ferrites determined by torque measurements
18 p2159 N73-27443

**FET [TRANSISTORS]**
U FIELD EFFECT TRANSISTORS

**FEVER**
Fever generation in rabbits by intravenous injection of table salt
[NASA-TT-F-14677] 07 p0745 N73-16063

**FEYNMAN DIAGRAMS**
Null plane quantum electrodynamics
15 p1814 N73-24699

**FFT**
U FAST FOURIER TRANSFORMATIONS

**FIBER OPTICS**
Design, development, and evaluation of pressure transducer using glass fiber bundle to transmit and receive reflected light from pressure diaphragm
[AD-747521] 03 p0304 N73-12480
Development of optical data communication systems with fiber optics for military avionics
[AD-747946] 03 p0337 N73-12748
Design and fabrication of annular ring detector consisting of optical fibers terminated with photodetectors
[NASA-CR-124089] 09 p1065 N73-18683
Light communication systems using fiber optics
[AD-754566] 11 p1257 N73-20200
Analysis of ultraviolet emitting fiber optic faceplate cathode ray tubes
[AD-755509] 13 p1503 N73-22181
Feasibility of integrated optics for use in high capacity, multi-GHz telecommunications
[AD-757342] 14 p1635 N73-23254
Introduction to optical communication with lasers
[FTZ-A-465-TBR-8] 22 p2681 N73-31477
Calculation of evanescent-wave gain in TE sub Om and TM Om of optical fibers
[CRC-1247] 23 p2769 N73-32147

**FIBER ORIENTATION**
Vibrational spectral study of molecular orientation in vitreous sodium metaphosphate glass fibers
[AD-757751] 15 p1748 N73-24167
Application of directionally solidified eutectics for design and construction of gas turbine engines
18 p2166 N73-27493
Directional solidification of eutectic alloys and application to turbine blades and gas turbine engine components
18 p2166 N73-27494
Failure analysis of fiber reinforced composite rocket engine case using distortional energy and maximum strain theories of failure
18 p2167 N73-27500
Development of unidirectional fiber composite materials with emphasis on improving compressive strength
[NASA-CR-112334] 18 p2203 N73-27784
Fiber distribution and orientation of aerodynamically spun nonwoven fabrics
24 p2907 N73-33196

**FIBER STRENGTH**
Fiber properties of simple and complex S-glass/epoxy composites under biaxial loading
[UCRL-73772] 07 p0812 N73-16582
Transverse tension strength and stiffness of unidirectional carbon fiber reinforced plastic
[RAE-TR-72129] 12 p1416 N73-21477
Design of filamentary composite materials for application to construction of airframes and spacecraft structures
18 p2164 N73-27479
Controlling constituent properties for strengthening graphite fiber reinforced aluminum and magnesium composites
[AD-763211] 21 p2563 N73-30548

**FIBERGLASS**
U GLASS FIBERS

**FIBERS**
NT CARBON FIBERS
NT COTTON FIBERS
NT DACRON [TRADEMARK]
NT GLASS FIBERS
NT HAIR
NT METAL FIBERS
NT NYLON [TRADEMARK]
NT REINFORCING FIBERS
NT SYNTHETIC FIBERS
Friction reducing properties of fibers in turbulent flow of fluids in pipes
[AD-746485] 01 p0043 N73-10337
Heat transfer mechanisms in fibrous insulation materials
[PB-210117] 02 p0192 N73-11558
Effects of free edge shear stresses on failure of fiber-reinforced angle ply laminates
[AD-747343] 03 p0322 N73-12625
Bibliography on fibers and composite materials
[AD-746214] 05 p0566 N73-14595
Investigation of microstructure of mullite fibers using transmission electron microscopy
[NASA-TM-X-2750] 09 p1052 N73-18573
Properties of thermal resistant electrical insulating papers based on inorganic fibers
[NLL-RTS-7740] 10 p1175 N73-19554
Evaluation of upgraded boron fibers in epoxy-matrix composites
[NASA-CR-112266] 12 p1416 N73-21472
Performance of fibrous concrete pavement materials under cargo aircraft and roadway vehicle loads
[AD-741357] 13 p1547 N73-22537
Development of high strength composite tungsten alloy and silicon carbide filaments for high temperature applications
[AD-756867] 13 p1549 N73-22551
Investigation of fibers and composites applicable to design of high pressure gas storage vessels for satellite altitude control
[RRCM/ED/R/10] 13 p1586 N73-22856
Development of fibrous flame arrestor materials to provide explosion and fire protection for aircraft fuel tanks
[AD-759193] 16 p1863 N73-25090
Effect of filament-matrix interfaces on fatigue resistance of boron-aluminum composites
[AD-761658] 19 p2312 N73-28597
Plastic deformation of single crystal sapphire filaments
[AD-762302] 19 p2313 N73-28603
Capillary flow through partially saturated fibrous wicks in heat pipes
[AD-763427] 21 p2527 N73-30263
Maximizing impact strength of advanced graphite composites without affecting other directional strength properties
[AD-763376] 21 p2564 N73-30553
Factors affecting miniature izod impact strength of tungsten-fiber-metal-matrix composites
[NASA-TN-D-7393] 23 p2804 N73-32427
Improved flame resistance of spandex elastic elastomeric fibers
[NASA-CR-128505] 23 p2809 N73-32464
Application of protective layers of refractory oxides and carbide onto high strength fiber substrates
[NASA-CR-134466] 23 p2810 N73-32467
Microstructure of mullite composite fibers
24 p2940 N73-33474

**FIBRINOGEN**
Effect of fibrinogen concentration on viscosity of human blood
[DLR-FB-73-54] 24 p2886 N73-33046

**FIBROBLASTS**
NT COLLAGENS

**FIBROUS MATERIALS**
U FIBERS

**FIELD COILS**
Coil configuration influence on current distribution of superconducting dipoles and quadrupoles
[BNL-17168] 10 p1201 N73-19771
High quasi-stationary magnetic field production with capacitor-fed magnetic field coil
[IPF-72-7] 17 p2069 N73-26741
Technique for reducing ambient electric field generated by inductive voltages in extreme low frequency magnetic field generators
[AD-764531] 23 p2768 N73-32142
Plasma physics and field configurations
[CONF-730705-1] 24 p2964 N73-33687

**FIELD EFFECT TRANSISTORS**
Development of computer model to analyze effects of temperature variations on six basic electronic components
[AD-745189] 01 p0033 N73-10256
Large signal modeling of bipolar transistors for computer-aided circuit analysis
[AD-745772] 01 p0088 N73-10730
Performance of temperature compensated rocket-borne MOSFET electrometer amplifier for measurement of electron and ion densities in lower ionosphere
[FOA-3-C-3640-E1] 04 p0420 N73-13424
Numerical analysis of transition frequency and phase excess in double-diffused bipolar transistors
[NLL-TRANS-860-[9022.64]] 05 p0518 N73-14212
Analysis of intermodulation and cross modulation distortions in broadband balanced bridge switching state MOSFET mixer
[AD-749064] 05 p0521 N73-14234
Computer program to simulate FET transistor logic circuit performances and properties
07 p0762 N73-16191
Very high frequency Schottky barrier gate field effect transistors
[DOC-REF-3-314] 08 p0951 N73-17785
Theory and fabrication techniques for MOS field effect transistor with submicron and graded channel
12 p1382 N73-21207
Electrostatic discharge effects in JFET performance and reliability in low humidity environment
[BDX-613-815] 12 p1383 N73-21217
Effects of Jupiter high energy electron environment on gates and MOSFET performance
[AD-756215] 13 p1502 N73-22178

GaAs junction field effect transistor radiation study in fast neutron environment
[AD-756914] 13 p1503 N73-22186
Channel length effect on field effect transistor noise in hot electron regime
19 p2326 N73-28713
Flicker noise and related bulk effects in silicon junction field effect transistors
20 p2461 N73-29774
Effect of laser pulse on threshold voltage of metal oxide semiconductor field effect transistors
[CRC-1246] 21 p2585 N73-30716
Research projects involving design and technology of semiconductor devices, metal oxide semiconductor field transistors, and electron storage for memory purposes
21 p2607 N73-30895
Development of stored charge device using field effect transistor technology
[NASA-CASE-NPO-11156-2] 22 p2617 N73-30974
Performance calculation for Schottky field effect transistor on resistive substrate
22 p2641 N73-31167
Manufacturing high resolution active and passive semiconductor devices noting field effect transistors and transistor logic
[REPT-3.462] 23 p2766 N73-32126

**FIELD EMISSION**

High vacuum breakdown initiated field emission between technically pure electrodes
[AD-747586] 03 p0338 N73-12753
Measurement of magnetic field emission of spacecraft power system units at low frequencies
[ESRO-CR-57] 05 p0548 N73-14452
Influence of band structure on photofield emission from metals
[AD-749828] 05 p0589 N73-14788
Development of field emitter cathodes for electron beam devices
[AD-762322] 20 p2381 N73-29134
High field emission and capture of electrons and holes at zinc centers in N-P and P-N junctions
24 p2966 N73-33705
Enhanced electron field emission in resonant niobium superconducting cavity
[AD-765336] 24 p2970 N73-33733

**FIELD INTENSITY METERS**

Application of polyethylene materials as screens for actinometric instruments to include analysis of physical, mechanical, and optical properties
[NLL-M-22675-[5828.4F]] 01 p0069 N73-10566

**FIELD IONIZATION SOURCES**

U BRUSHES

**FIELD STRENGTH**

NT ELECTRIC FIELD STRENGTH
NT MAGNETIC FLUX

Mathematical model for calculating breakdown voltage of solid homogeneous dielectric solid during thermal breakdown
[NLL-CE-TRANS-5560-[9022.09]]
11 p1329 N73-20786
Correlation energy of quantum mechanical electron gas in intense magnetic field
[NUB-2178] 12 p1431 N73-21597

**FIELD THEORY [ALGEBRA]**

NT QUADRATIC EQUATIONS

Bjorken scaling in deep inelastic electron proton scattering and parton models
[NOTA-INTERNA-391] 03 p0340 N73-12773
Field method for linear static analysis on open branch shells of revolution under asymmetric loads
[NASA-CR-112270] 11 p1311 N73-20638

**FIELD THEORY [PHYSICS]**

Field theoretical model for critical behavor of helium 4 above critical point
[NOTA-INTERNA-374] 01 p0083 N73-10689
Invariance under Weyl scale transformations and Poincare gauge invariant matter Lagrangian
[RIFP-160] 02 p0195 N73-11578
Solution of n-dimensional scattering problem by means of k-space formulation of field equations
02 p0201 N73-11623
Fields, statistics and non-Abelian gauge groups
[NOTA-INTERNA-387] 03 p0340 N73-12771
Ising model for free spinless particles satisfying one dimensional Dirac equation
[AD-747736] 03 p0347 N73-12834
Universal repulsive component in gravity
[ORO-3992-94] 05 p0539 N73-14385
Light cone and hyperbaloid contributions to structure functions in Bjorken limit
[TR-73-076] 06 p0702 N73-15726
Noncanonically renormalized phi to 4th power theory in 4-epsilon dimensions and systematic use of Callan-Symanzik equations
[TR-73-020] 06 p0702 N73-15727
Electron positron annihilation structure functions calculated with light cone operator product expansions and Callan-Symanzik equation
[ILL-[TH]-72-12] 07 p0823 N73-16670
Field theory model for unified strong and electromagnetic interactions
09 p1066 N73-18701
Quantum electrodynamics in high magnetic fields
[AD-753042] 09 p1067 N73-18710
Solving singular axisymmetric field problem noting applications to electromagnetism and fluid mechanics
[ONERA-NT-207] 10 p1190 N73-19685
Quantization of free spin-two fields on light front
[ILL-[TH]-73-1] 11 p1326 N73-20764
Black body heat capacity and action at distance electrodynamics
[ORO-3992-97] 12 p1429 N73-21578
Stability of steady state motions of gyroscope with spring limiters on rotating platform in Newtonian central field of forces
13 p1556 N73-22611
Scalar quantum field theory in closed universe of constant curvature
15 p1813 N73-24690
Nonrenormalizable interactions as low-energy limits of renormalizable ones
15 p1813 N73-24698
Development of classical electron theory
15 p1815 N73-24710
Effects of season altitude and pitch angle on electron precipitation from OGO-D data
[NASA-TM-X-66260] 16 p1962 N73-25868
Einstein-Bonner nonsymmetric field theory of gravity and electromagnetic fields
[AD-761482] 19 p2295 N73-28460
On-line interactive computer solution of dispersion equations
22 p2636 N73-31123
Application of Boson method to quantum field theory computations and mixed state of type 2 superconductors
23 p2825 N73-32582
Off-diagonal long range crystalline order and vortex lattices in Bose system
24 p2967 N73-33708
Development of symmetric stress-energy-momentum pseudo-tensor for gravitational fields of Brans-Dicke theory and application to formation of black holes
24 p2978 N73-33800

**FIGHTER AIRCRAFT**

NT F-4 AIRCRAFT
NT F-8 AIRCRAFT
NT F-14 AIRCRAFT
NT F-15 AIRCRAFT
NT F-86 AIRCRAFT
NT F-100 AIRCRAFT
NT F-102 AIRCRAFT
NT F-104 AIRCRAFT
NT F-105 AIRCRAFT
NT F-106 AIRCRAFT
NT F-111 AIRCRAFT
NT GA-5 AIRCRAFT
NT HARRIER AIRCRAFT
NT JET PROVOST AIRCRAFT
NT MIRAGE 3 AIRCRAFT
NT P-1127 AIRCRAFT

Estimating strafing performance of unspecified foreign tactical fighter without aerodynamic stability derivatives
[AD-745997] 01 p0006 N73-10044
Effects of location of wing pivot and geometry of wing on static longitudinal aerodynamic characteristics of variable-sweep supersonic fighter aircraft model
[NASA-TM-X-2674] 03 p0247 N73-12000
Analysis of minimum time maneuvers by high thrust-to-weight aircraft using optimal control theory to determine open-loop control laws
[AD-748354] 04 p0374 N73-13039
Analysis of high subsonic and transonic characteristics of fighter aircraft and factors affecting aerodynamic boundaries for various wing design parameters
06 p0618 N73-15019
Effects of various leading edge slat devices on static aerodynamic characteristics of twin-jet, swept wing fighter model
[NASA-TN-D-6921] 07 p0736 N73-15988
Wind tunnel tests to predict full scale aircraft buffet loads during buffet boundary penetration using scale flutter model of fighter aircraft with variable sweep wings
[NASA-TN-D-7066] 07 p0851 N73-16905
Correlation between lateral-directional static stability characteristics and spin susceptibility
[AD-753905] 10 p1107 N73-19029
Combat use and combat effectiveness of fighter-interceptors
[AD-751512] 12 p1468 N73-21894
Planform shape effects on aerodynamic center location and aeroelasticity of fighter aircraft
[NASA-CR-2117] 13 p1469 N73-21896
Computer program for calculating aerodynamic stability and drag of slender aircraft at subsonic and supersonic speeds
[NASA-CR-112229] 13 p1469 N73-21897
Determination of mass distributions along elastic axes of 2-spar wings in fighter aircraft design
[NASA-CR-112233] 13 p1470 N73-21901
Planning and budgeting in lightweight fighter prototype development for military aviation
13 p1595 N73-22934
Numerical methods for determining range and radius of action performance of transport and combat aircraft and effects of various parameters on performance
15 p1732 N73-24043
Analysis of parameters affecting choice of engines for transport and combat aircraft during design process
15 p1732 N73-24048
Wind tunnel tests to determine aerodynamic characteristics of vectored thrust V/STOL fighter aircraft in transition speed range
[NASA-TN-D-7191] 16 p1858 N73-25047
Research projects for improving maneuverability and buffet characteristics of fighter aircraft in high subsonic and transonic speed ranges
[NASA-TN-D-7131] 17 p1979 N73-25999
Determination of bomb range of low drag bombs delivered by fighter aircraft
[AD-762500] 20 p2488 N73-29992
Pilot rating of fighter aircraft in precision heading task using mathematical model for predicting aircraft performance
[AD-764695] 23 p2745 N73-31973
Optimization of control and damping system for fighter aircraft with quadratic cost function
24 p2877 N73-32980
VAK 191 B V/STOL fighter aircraft nonlinear feedback flight control system for gliding flight phase
24 p2878 N73-32984

**FILAMENT WINDING**

Use of unidirectional glass plastics for wound structures of electrical machines and equipment
[AD-748737] 04 p0400 N73-13252
Development and characteristics of composite materials with emphasis on non-aerospace applications
[NASA-CR-129989] 05 p0565 N73-14587
Mechanical properties data and fabrication technology for filament wound graphite/epoxy resin pressure vessels
[NASA-CR-120951] 05 p0602 N73-14897
High tensile strength epoxy system for filament winding
[UCRL-73773] 07 p0812 N73-16586
Design, fabrication, manufacture, and verification of composite material rocket engine cases for antitank missiles - Vol. 1
[AD-760566] 18 p2202 N73-27774
Design calculations, tooling sketches, manufacturing and inspection records of composite material rocket engine cases for antitank missiles - Vol. 2
[AD-760569] 18 p2202 N73-27775
Design requirements and characteristics of toroidal, continuous wound aircraft tire
[AD-764888] 23 p2746 N73-31977
Twisted wire or tube superconductor for filament windings
[NASA-CASE-LEW-11015] 23 p2823 N73-32571

**FILAMENT WOUND CONSTRUCTION**

U FILAMENT WINDING

**FILAMENTS**

Superconductivity of multifilamentary wires consisting of vanadium silicates
[BNL-16891] 03 p0346 N73-12818
Development of process for obtaining iron whiskers and description of mechanical and physical properties
[IIS-142-VOL-22-4] 05 p0586 N73-14766
Critical velocity and patterns of stationary motion of filament
[JPRS-57813] 06 p0652 N73-15293
Filament stationary motion pattern in media of diverse viscosities, allowing for gravitational and resistance forces to longitudinal motion
06 p0652 N73-15294
Critical velocity study of stationary motion, using loop filament in viscous medium
06 p0652 N73-15295
Chemical process for producing continuous fine superconducting filaments
[AD-751545] 07 p0832 N73-16746
Stability analysis for spinning flow of cylindrical liquid polymer filament with memory function
[AD-755065] 11 p1273 N73-20332
Deformation mechanism diagrams and creep of tungsten lamp filaments
[AD-755230] 12 p1441 N73-21680
Numerical analysis of load absorption of two adjacent filaments in fiber-reinforced material
[AD-759729] 16 p1933 N73-25639
Controlled diffusion reaction process for masking substrate of twisted multifilament superconductive ribbon
[NASA-CASE-LEW-11726-1] 17 p2070 N73-26752

**FILLERS**

Survey of aluminum-, copper-, and magnesium-alloy properties as filling materials for fast breeder fuel elements
[EUR-4857-E] 02 p0211 N73-11706
Increasing phase change material thermal diffusivity by means of solid fillers
[NASA-CR-124214] 13 p1590 N73-22894
Filler effect on tensile strength characteristics of thermosetting polymers
20 p2434 N73-29552

**FILM BOILING**
Analysis of critical density heat flows during internal heating of annular channels
[AD-743681] 01 p0118 N73-10972
Vaporization mechanisms and nucleate boiling in heat pipes with thin liquid films
[AD-757280] 14 p1720 N73-23955
Extension of hydrodynamic theory of peak and minimum pool boiling heat fluxes to include influence of viscosity on instability mechanisms with application to film boiling
[NASA-CR-2270] 18 p2206 N73-27808
Viscous hydrodynamic instability theory of peak and minimum pool boiling heat fluxes
[NASA-CR-134492] 22 p2653 N73-31252
Subcooled forced convection film boiling in vertical annulus
23 p2856 N73-32819
Stability of vapor film formed on horizontal cylinders during stable film boiling using variational approach
24 p2991 N73-33906

**FILM CONDENSATION**
Relationship between laminar film condensation on inside of rotating non-capillary heat pipe and pipe heat transfer capabilities
[NASA-CR-130373] 07 p0854 N73-16926
Stability of vapor film formed on horizontal cylinders during stable film boiling using variational approach
24 p2991 N73-33906

**FILM COOLING**
Turbulent, transitional, and laminar film cooling of air breathing engine inlet at hypersonic speed noting heat transfer rate measurement
[IC-AERO-72-15] 01 p0041 N73-10323
Finite difference solution of film cooling as alternate thermal protection system for spacecraft during reentry
[NASA-CR-112192] 01 p0116 N73-10958
Analysis of laminar film condensation on inside of truncated, rotating cone and noncapillary, rotating heat pipe with distilled water as working fluid
[AD-743730] 01 p0118 N73-10973
Small scale nozzle tests using heated nitrogen for effectiveness and wall heat transfer studies with hydrogen film cooling
[NASA-CR-120926] 02 p0242 N73-11970
Evaluation of boundary cooled rocket engines for development of space storable propellant combination of oxygen difluoride/diborane
[NASA-CR-129260] 03 p0350 N73-12855
Optimization of engines for commercial Mach 0.85 transport using advanced turbine cooling methods
[NASA-TM-X-68173] 06 p0619 N73-15029
Analysis of factors affecting cooling of liners in gas turbine combustion chambers
[NAL-TR-196] 06 p0713 N73-15819
Simultaneous film and convection cooling of plate inserted in exhaust stream of gas turbine combustor
[NASA-TN-D-7156] 07 p0855 N73-16930
Adverse effect of film cooling on suction surface of turbine blade
[NASA-TM-X-68210] 12 p1444 N73-21695
Pressure effects on tangential-injection film cooling in combustor exhaust stream
[NASA-TM-X-2809] 15 p1843 N73-24931
Linear stability analysis on liquid film adjacent to compressible viscous gas stream
[AD-758982] 16 p1889 N73-25290
Three dimensional effects on slot cooling in hypersonic flight
[AD-762624] 20 p2388 N73-29189
Effects of flow turning, flow acceleration, and supersonic flow on hydrogen film cooling
[NASA-CR-121235] 22 p2729 N73-31841

**FILM THICKNESS**
Analytical method to compute squeeze film thickness, pressure, and load relations between rigid ball and rigid groove when lubricated by fluid with exponential pressure-viscosity relationship
[NASA-CR-2139] 01 p0062 N73-10506
Interferometry measurements of film thickness and traction of lubrication in point contacts
[NASA-CR-120842] 05 p0551 N73-14478
X ray device for measuring titanium tritide film thickness in presence of background radiation
[NASA-TM-X-68170] 06 p0673 N73-15475
Elastohydrodynamic traction measurements and lubricant film thickness determination for high speed rolling-sliding contacts
[AD-750752] 06 p0678 N73-15520
Temperature and thickness effects on electrical conductivity of amorphous germanium semiconducting films
[AD-753827] 09 p1076 N73-18782
Durability of metal films to rupture as thickness of film increases
[AD-756616] 14 p1679 N73-23623
Superconducting lead film thickness effect on magnetic properties
[ISS-72/6-PT-2] 17 p2073 N73-26773
Development of empirical elastohydrodynamic film thickness formula for predicting minimum film thickness occurring in heavily load contacts
[NASA-TM-X-68267] 18 p2155 N73-27411

**FILTER WHEEL INFRARED SPECTROMETERS**
Preparation of field spectroradiometer equipment and tapes for Skylab S-191 experiment
[E73-10760] 17 p2022 N73-26360
Cooled filter wheel spectrometers for short wavelength telescopic observations of faint planetary objects
[NASA-CR-133413] 18 p2197 N73-27739
Cloud physics studies using Skylab S-191 filter wheel infrared spectrometer data
[E73-10880] 20 p2394 N73-29231
Utilization of Skylab EREP S-191 infrared spectra for geological surveys
[E73-10923] 20 p2398 N73-29272
Geological studies of Nevada from Skylab S-191 infrared spectra
[E73-11003] 22 p2659 N73-31308

**FILTERING**
U FILTRATION

**FILTERS**
Measurement of gas velocities in filters
[AD-747829] 04 p0407 N73-13315
Techniques for solving for optimum filter for video signal processing
[AD-753132] 09 p1003 N73-18189
Acoustic surface wave matched filters
[AD-754283] 11 p1262 N73-20245
Analysis of Apollo 16 reaction control system helium pressure regulator filter failure
[NASA-TM-X-69131] 11 p1334 N73-20827
Holographic matched filters for correcting phase heterogeneities in aperture antennas
[JPRS-59253] 17 p2003 N73-26201
Filter for determining long wave solar spectral reflection by plane surfaces
24 p2975 N73-33772

**FILTRATION**
NT SPATIAL FILTERING
Removal of mechanical impurities from AKOR-1 additive by filtration method using perlite
[AD-751947] 10 p1167 N73-19496
Evaluation of multifiltration water reclamation subsystem to reclaim domestic clothes wash water
[NASA-TM-X-2781] 13 p1595 N73-22931
Evaporator for vacuum distillation/vapor filtration water reclamation on manned space flight
[NASA-CR-124397] 23 p2796 N73-32367

**FIN STABILIZERS**
U FINS
U STABILIZERS [FLUID DYNAMICS]

**FINANCE**
Design of interactive program to teach accounting techniques
[NASA-CR-129674] 04 p0393 N73-13192

**FINANCIAL MANAGEMENT**
Management information systems for monitoring ESRO budget and program
[ESRO-PSS-02/PMC-01] 01 p0120 N73-10994
Management information systems for monitoring ESRO budget and program
[ESRO-PSS-03/PMC-02-PT-2]
01 p0121 N73-10995
Graphs, tables, and analysis of Federal R and D funding by budget function and by primary purpose
[NSF-72-313] 09 p1101 N73-18987
Analysis of economics and finances of airport operations to determine procedures for improved management and operation
[REPT-73-01210] 16 p1884 N73-25253
Congressional hearings on appropriations for Housing and Urban Development, National Science Foundation, and Veterans organizations for 1974
16 p1976 N73-25978
Congressional hearings on cost of space shuttle program to show differences between Government Accounting Office and NASA projections
22 p2737 N73-31916
Economic factors, financial management, production and marketing for air transport industry
[NASA-CR-135634] 23 p2860 N73-32848
Financial sources and airline operations
23 p2861 N73-32859
Financial requirements of air transportation industry
23 p2861 N73-32861
Bank financing in commercial jet aircraft export
23 p2861 N73-32862
Excess capacity in airline industry and operational and financial problems
23 p2862 N73-32871
Analysis of air freight rate problems to define roles of Civil Aviation Board and domestic air carriers
23 p2863 N73-32883

**FINE STRUCTURE**
Effects of aerological fine-strength characteristics of vertical distribution of aerosols
[AD-762335] 19 p2299 N73-28485

**FINENESS RATIO**
Effect of fineness ratio on boattail drag of circular arc afterbodies having closure ratios of 0.50 with jet exhaust at Mach numbers up to 1.30
[NASA-TN-D-7192] 14 p1701 N73-23802

**FINGER LAKES**
U LAKES

**FINITE DIFFERENCE THEORY**
Transients in cooling water systems of thermal power plant discussing mathematical models, computer programs and experiments
[PUBL-101-PT-1] 01 p0041 N73-10326
Development of implicit finite difference method for analysis of viscous flows based on Euler and Navier-Stokes equations
[AD-746389] 01 p0043 N73-10341
Finite difference solution of film cooling as alternate thermal protection system for spacecraft during reentry
[NASA-CR-112192] 01 p0116 N73-10958
Implicit finite difference scheme for fully coupled solution of viscous shock layer including effects of radiation and strong blowing
[NASA-TR-R-388] 02 p0156 N73-11266
Conservative finite difference method applied to meteorological advection problems
[NASA-CR-129090] 02 p0204 N73-11633
Finite difference solutions for oscillatory lift interference in slotted wind tunnel compressible and incompressible flow
[ARC-R/M-3700-PT-1-PT-2] 03 p0284 N73-12297
Finite difference solutions for oscillatory lift interference parameters for slotted wind tunnel incompressible flow
03 p0284 N73-12298
Finite difference solutions for oscillatory lift interference parameters for slotted wind tunnel compressible flow
03 p0284 N73-12299
Finite difference theory and Monte Carlo method for heat conduction and convection problems
[KFK-1554] 03 p0364 N73-12965
Spline approximation of initial value problem and successive application of finite difference and spline interpolation operators for heat equation
[AD-748774] 04 p0441 N73-13594
Development of iterative procedure for analysis of arbitrary multi-element airfoils in viscous flow
[AD-749484] 05 p0496 N73-14042
Development of finite difference procedure to calculate steady flows over several classes of airfoils under inviscid transonic flow conditions
[NASA-CR-2186] 06 p0614 N73-14989
Finite difference method for calculating interaction between spherical shock waves from underwater explosion and ocean surface
[AD-749818] 06 p0656 N73-15325
Finite difference solution to diffusion equation in spherical coordinates
[SCL-DR-72-0017] 06 p0691 N73-15623
Finite difference solutions for laminar and turbulent boundary layer equations of perfect gases and gas mixtures in chemical equilibrium
07 p0767 N73-16236
Solution of boundary layer equations of chemically reacting flat plate flow of binary gas mixture with Hermitian finite difference method
[DLR-FB-72-58] 07 p0772 N73-16272
Development of mixed finite-difference scheme for free vibration analysis of simply supported closed noncircular cylindrical shells
[NASA-TN-D-7107] 07 p0852 N73-16908
Finite difference solution for supersonic laminar flow over two dimensional compression corner
08 p0894 N73-17241
Finite difference solution for merged layer regime of hypersonic flat plate leading edge problem
08 p0895 N73-17243
Finite difference method for calculating three dimensional, unsteady and steady, inviscid gas flows around blunt bodies
[NASA-TT-F-714] 09 p0980 N73-18009
Effects of earth surface characteristics on cumulus scale convection for stable and unstable boundary layers above relatively dry ground
[AD-752914] 09 p1031 N73-18416
Finite difference algorithm for solving quasi-linear gas dynamic systems
[AD-753097] 10 p1143 N73-19309
Finite difference procedure for computing behavior of two-dimensional boundary layers and turbulence model to predict location and extent of transition region
10 p1204 N73-19796
Finite difference technique for determining transient temperature distribution in plane slab with uniform heat sources and radiative boundary conditions
10 p1223 N73-19944
Development of computer program for solving fully compressible, two-dimensional hydrodynamics problems using flux-corrected transport algorithms
[AD-754736] 11 p1271 N73-20315
Gas bearings and fluid flow tests using finite difference approximation
[AD-754800] 11 p1299 N73-20542
Construction of discrete models of nonlinear wave phenomena in elastic rods based on finite element analysis of shock waves in hyperelastic solids
[AD-754953] 11 p1346 N73-20921

Finite difference solution of three-dimensional compressible boundary layer equations for circular cones at angle of attack
[NASA-CR-112316] 12 p1391 N73-21276
Finite difference solution of general class of three-dimensional boundary layer flows
[NASA-CR-112315] 12 p1391 N73-21277
Finite difference method for evaluating supersonic flow over sharp cone
[AD-755862] 12 p1392 N73-21290
Finite difference method applied to axisymmetric random shells of revolution for unsymmetrical loading
[DRIC-TRANS-2996] 12 p1463 N73-21855
Finite difference solution to right angle circular cone streamline swallowing phenomenon during supersonic and hypersonic flow
13 p1508 N73-22218
Use of finite difference theory to calculate nonsteady flow in linear magnetohydrodynamic generators
[AD-755203] 13 p1564 N73-22673
Finite difference method for blunt body supersonic flow computation
[DLR-FB-73-10] 14 p1650 N73-23381
Navier-Stokes equation and finite difference theory for compressible viscous flow
[AD-756242] 14 p1651 N73-23389
Finite difference model for short range weather forecasting using directed differences
[AD-756078] 14 p1685 N73-23673
Numerical solutions for laminar, compressible, three dimensional boundary layer on sharp bodies of revolution at angle of attack with moderate axial spin
[SC-CR-72-3182] 15 p1768 N73-24325
Development of finite difference method for calculating boundary value problem for nonsymmetrical deformation of random shells of revolution
[NLL-DRIC-TRANS-2996-[3623.66]]
15 p1836 N73-24884
Mathematical methods of calculating strength of thin walled elastic systems
[AD-758028] 15 p1840 N73-24911
Finite difference calculations of laminar flow past blunt-nosed cone with spherical after body injecting mass into air
[AD-758009] 15 p1844 N73-24943
Application of finite difference techniques to noise propagation in jet engine ducts
[NASA-TM-X-68261] 17 p1981 N73-26015
Finite difference solution to thermoacoustic convection of fluids in low gravity environment
[NASA-CR-2269] 17 p2014 N73-26289
CONSHOC computer program for locating shock waves and contours of flow variables in finite difference flow fields
[AD-759898] 17 p2016 N73-26301
Three dimensional potential flow problems solved by means of inverse formation and finite differences
[AD-760347] 17 p2016 N73-26302
Numerical calculation of three dimensional boundary layers by finite difference methods
20 p2384 N73-29156
Analysis of steady hypersonic flow with viscous interaction over sharp slender wedge by finite difference scheme
20 p2387 N73-29177
Application of finite-difference machine code for analyzing wake-vortex problem in quasi-cylindrical boundary layer approximation
[NASA-TM-X-69495] 20 p2387 N73-29179
Finite difference formulation for sound propagation in two-dimensional soft-walled duct with uniform flow
[NASA-TM-X-68295] 20 p2454 N73-29722
Finite difference method and equations of motion for studying nonlinear vibrations of one and two degree of freedom spring mass systems
22 p2724 N73-31796
Fourth-order, time dependent, partial differential flow equation solved by coupled pair of finite difference equations
[AD-765323] 23 p2776 N73-32201
Finite difference theory of noise propagation in turbofan engine ducts
[NASA-TN-D-7339] 24 p2972 N73-33744
Propagation of shock waves following explosion of finite cylindrical charge based on finite difference numerical analysis
24 p2991 N73-33907

FINITE ELEMENT METHOD
Finite element procedure for predicting unsteady compressible gas flow in one spatial dimension
[AD-746234] 02 p0157 N73-11276
Development of computer programs to provide finite element method solutions to problems involving elastic and inelastic structures
[AD-746175] 02 p0239 N73-11942
Approximate method for computing consistent conjugate stresses in elastic finite elements
[AD-746024] 02 p0240 N73-11954
Finite element displacement method for studying transient response and dispersive behavior of elastic structures
[AD-747283] 02 p0241 N73-11956
Finite analysis of effects of varying radii of circumferential fillets in transition of cylindrical shells
[ORNL-TM-3766] 03 p0361 N73-12943
Formulation of finite element matrix in Lagrangian variables for elastic thin shells with arbitrary geometric imperfections
[AD-747321] 03 p0361 N73-12946
Finite element solution for axisymmetric transient heat conduction and thermal stress problems
[AD-747523] 03 p0362 N73-12950
Development of computer program for generating aerodynamic forces for plane and interfering wings at supersonic speeds
[NASA-CR-112184] 04 p0404 N73-13290
Elastic stress analysis of bi-material plate with crack normal to interfaces, using finite element method
[AD-748299] 04 p0439 N73-13579
Finite element model for class 4 flextensional underwater transducer shell
[AD-748187] 04 p0482 N73-13940
Application of finite element method to nonconservative stability problems with damping
[AD-748086] 04 p0483 N73-13945
Application of finite element method to determine deformation of elastic plates, shells, and membranes
[AD-749565] 04 p0483 N73-13946
Hybrid calculations based on finite element method
[RP-106[72]] 05 p0602 N73-14893
Finite element method with continuity of slope for stress analysis on arbitrary shell
[PB-211759] 05 p0604 N73-14909
Limited survey of general purpose finite element computer programs, including structural analysis
05 p0608 N73-14944
Theoretical derivation of finite element solution algorithm for transient energy conservation equation
[NASA-CR-130149] 07 p0813 N73-16593
Development of digital computer program for evaluating vibrational characteristics of large liquid-filled rigid wall tanks of general shape
[NASA-CR-124070] 08 p0953 N73-17801
Sheba triangular thin shell element application to calculation of coding towers, toruses, and roofs
[ISD-127] 09 p1095 N73-18936
Notch stress finite element method for loaded elastic cores, applicable to compositesor welded joints
[ISD-129] 09 p1095 N73-18938
Stress analysis of uniaxial steel wire-plastic composite material, using finite element method
[ISD-131] 09 p1095 N73-18940
FORTRAN subroutines for matrix operations encountered in finite element analysis of structures, noting application to flat plates
[ARC-CP-1223] 09 p1095 N73-18941
Univac 1108 computer for three dimensional stress analysis of complex structures
[AD-753211] 09 p1096 N73-18944
Finite element method of continuum and structural analysis using computer programs - users manual
[AD-753120] 09 p1097 N73-18951
Finite element method computation of 1:5 scale model prestressed concrete high temperature nuclear reactor pressure vessel
[ISD-120] 10 p1221 N73-19927
Convergence, accuracy, and stability of finite element approximations of class of nonlinear hyperbolic equations
[AD-754948] 11 p1312 N73-20646
Finite element formulation and thermoelastoviscoplasticity theory for solving problems in nonlinear continuum mechanics
[AD-754952] 11 p1331 N73-20805
Optimization of aircraft structures by finite element modeling and automated structural optimization computer program
[AD-754915] 11 p1344 N73-20905
Application of finite element method to stress wave in plates
[NASA-CR-112294] 11 p1345 N73-20911
Derivation of perturbed equations of motion and heat conduction for thermoelastic solid using finite element method
[AD-754542] 11 p1346 N73-20919
Construction of discrete models of nonlinear wave phenomena in elastic rods based on finite element analysis of shock waves in hyperelastic solids
[AD-754953] 11 p1346 N73-20921
Finite element technique for elastic stability under nonconservative forces and internal and external damping
[AD-755101] 11 p1346 N73-20925
Analysis of vibratory characteristics of sonar transducer element using finite element three dimensional mathematical model
[AD-755177] 13 p1495 N73-22117
Steady oscillatory irrotational motion of inviscid incompressible fluid described by boundary value problem of elliptic type
[AD-755465] 13 p1512 N73-22252
Finite element analysis of reinforcement mechanisms in unidirectional metal matrix composites under transverse loads
[AD-756257] 13 p1548 N73-22541
Three-dimensional finite element analysis of stress concentration near holes in laminated composites
[AD-756454] 13 p1548 N73-22545
Three-dimensional finite element studies
[AD-755539] 13 p1571 N73-22734
Finite element methods used for characterizing linear, anisotropic elastic solids
[AD-756513] 13 p1587 N73-22869
Computer program for finite element stress wave analysis
[AD-755393] 13 p1587 N73-22871
User manual for finite element program for analysis of deformations of thin elastic membranes
[AD-755953] 13 p1588 N73-22874
Survey of optimal structural design techniques to include method of fully stressed design and linear programming problems
[REPT-10432] 14 p1714 N73-23911
Assumed stress hybrid finite element method for fracture mechanics and elastic-plastic analysis
[AD-757523] 14 p1717 N73-23931
Finite element calculation of two-dimensional heating and melting of disks and applications to laser effects
[AD-757189] 14 p1719 N73-23950
Application of finite elements of triangular shape for computing plate vibrations
15 p1838 N73-24898
Application of finite element method for analyzing stability of rectangular plates in supersonic air stream
15 p1838 N73-24899
Mathematical methods of calculating strength of thin walled elastic systems
[AD-758028] 15 p1840 N73-24911
Dual finite element and shell theory analyses of linear and nonlinear structures
[AD-758790] 16 p1970 N73-25933
Conjugate basis functions and consistent stresses for finite element stiffness method
[AD-758675] 16 p1972 N73-25948
Finite element analysis of thermoplasticity and nonlinear mechanics of fluid-saturated porous solids
[AD-758884] 16 p1972 N73-25949
Computer program for designing minimum mass wings under flutter, strength and minimum gage constraints
[NASA-TN-D-7264] 17 p2092 N73-26927
Finite element calculation of tapered double cantilever beam modulus of elasticity for sharp blunted cracks
[NLR-TR-72083-U] 17 p2094 N73-26941
Dynamic finite element analysis of nonlinear oscillations of multi-degree of freedom structural systems
[ISD-136] 17 p2094 N73-26943
Finite element calculation on transmission line characteristics for coplanar waveguide
[AD-760756] 18 p2119 N73-27135
Development of method for identifying nonlinear material behavior using finite element techniques
[PB-219090/8] 18 p2204 N73-27788
Automation of input/output routines for use with computerized data processing of finite element structural analyses
[AD-761154] 18 p2204 N73-27793
Development of doubly curved triangular finite element for use in small deformation analysis of thin shells containing cutouts and irregular boundaries
[RE-453] 19 p2347 N73-28882
Finite element analysis of tapered viscous flow
20 p2386 N73-29165
Analysis of dynamics of stiffened plates using finite element modelling of flat and curved stiffened panels
20 p2479 N73-29911
Derivation of finite element properties in terms of stress functions for structural and nonstructural applications
[AD-762947] 20 p2484 N73-29953
Finite element analysis and computer graphics visualization of unsteady flow around pitching and plunging airfoils
[NASA-CR-2249] 22 p2611 N73-30926
Finite element analysis of behavior of filamentary composite plates with cutouts
[AD-764362] 22 p2689 N73-31538
Application of nonlinear finite element analysis to planar and nonplanar plane stress problems
22 p2723 N73-31789
Proceedings of conference on structural analysis with application to ships, guns, hydrofoils, marine propellers, and radar antennas
[AD-764508] 22 p2726 N73-31818
Method for iterative reanalysis in automated structural designs using direct stiffness approach
[NASA-TN-D-7357] 23 p2853 N73-32797
Finite element method for structural plasticity problems
[AD-764574] 23 p2855 N73-32811
Application of finite element analysis techniques to determine characteristics of curved elements in thin, elastic shells
24 p2987 N73-33872
Development of finite element relations for dynamic structural analysis of linearly elastic beam and plate flexure problems
24 p2987 N73-33873

Nonlinear analysis of structures by finite element method as supplement to linear analysis
[WTHD-51] 24 p2988 N73-33881
Asymmetrical bending and vibration of conical shell finite element
[TR-73-5-2] 24 p2989 N73-33884
**FINITE-STATE MACHINES**
U TURING MACHINES
**FINLAND**
Hourly geomagnetic measurements at Nurmijaeri, Finland - tables
01 p0048 N73-10383
Number and distribution of lightning flashes in Finland during summer 1971
[REPT-41] 04 p0413 N73-13371
Geomagnetic measurements in south and east Finland 1967 through 1971 and final values reduced to 1970.0
[REPT-23] 06 p0666 N73-15416
Climatological daily observations in Finland during 1971
06 p0694 N73-15652
Relationship between vertical velocity in baroclinic model and occurrence of rain and clouds in Finland
[TR-4] 07 p0814 N73-16603
Vertical wind shear measurements at Helsinki Airport - Apr. 1967 through Mar. 1968
[TR-3] 08 p0937 N73-17676
Aeronautically oriented numerical weather prediction activities in Finland during 1970
[TR-2] 08 p0937 N73-17677
Utilization of ERTS-1 imagery for study of hydrology and limnology in Finland
[E73-10101] 09 p1020 N73-18323
Applicability of ERTS-1 imagery to forestry and timber survey and identification in Finland
[E73-10297] 09 p1021 N73-18329
Ionospheric magnetospheric, lunar and meteorite research, satellite geodesy, orbits, tracking, telemetry, and remote sensing in Finland in 1972
[S-52] 12 p1467 N73-21888
Major fracture and fault zones of Baltic Shield in Finland and relationships to mineral deposits
[E73-10682] 16 p1901 N73-25377
Lightning flash counter measurements in Finland during 1972
[REPT-43] 20 p2412 N73-29390
Application of ERTS-1 imagery to timber inventory in Finland
[E73-11068] 23 p2781 N73-32244
**FINNED BODIES**
Analysis of fin bow shock wave during high speed air flow on blunt fin to determine interaction of vortices and shock waves
[AD-752210] 08 p0898 N73-17274
Structural stability of gun launched finned projectile motor case
[AD-754378] 11 p1344 N73-20906
Wind tunnel tests to determine control of magnus instabilities with aerodynamic configurations using symmetrical fin and non-finned bodies
19 p2217 N73-27885
Effect of nose shape and tail length on static stability of fin-stabilized projectile at supersonic speeds and various angles of attack
[NASA-TM-X-2831] 19 p2217 N73-27888
**FINS**
NT COOLING FINS
Deployable flexible ventral fins providing triangular planform of flexible material for spin recovery of aircraft
[NASA-CASE-LAR-10753-1] 01 p0004 N73-10031
Flow field, pressure, and heat transfer associated with small fins of half angle cone in supersonic flow
[SCL-RR-72-0339] 10 p1142 N73-19302
Turbulent heat transfer and pressure on leading edge of fin, swept wing, or antenna
[SCL-RR-72-0308] 12 p1464 N73-21863
Pressure drop in air flow isothermally across bank of helically wound, L-type fin tubes
[PB-220315/6] 24 p2911 N73-33229
**FIORDS**
Numerical model of circulation processes of fjord estuary
[AD-755233] 14 p1664 N73-23506
**FIRE CONTROL**
Estimating strafing performance of unspecified foreign tactical fighter without aerodynamic stability derivatives
[AD-745997] 01 p0006 N73-10044
Model of pilot-aircraft system for relating pilot tracking performance to overall weapon delivery
[AD-745999] 01 p0006 N73-10045
Weapon delivery accuracy of F-4 aircraft with experimental stick to rudder interconnect to minimize lateral tracking error
[AD-746000] 02 p0126 N73-11027
Weapon delivery accuracy of F-4 aircraft with high gain control augmentation system
[AD-746001] 02 p0126 N73-11028
Operational test and evaluation of angle of attack system for displaying percentage of lift produced by wing for all flap configurations
[AD-748844] 03 p0304 N73-12485
Fire control computer program for Poseidon missile failure data processing
[AD-754426] 11 p1260 N73-20230
Description of maneuvering aircraft trajectory by second-order non-Gaussian process verified by digital simulation
[TAE-167] 14 p1683 N73-23656
Analysis of computing methods for Terrier fire control system
[AD-758499] 14 p1724 N73-23993
Radar equipment components for fire control vehicle
[AD-761534] 19 p2237 N73-28031
Logistic performance data book for F-4D aircraft fire control system to show reliability, maintainability, logistics support, and operating problems
[AD-762229] 19 p2358 N73-28969
**FIRE DAMAGE**
Identification of Nevada wildland plants, vegetation, and fire scars from ERTS-1 imagery
[E72-10253] 03 p0289 N73-12353
Assessment of range fire damage in Sand Hills Region of Nebraska based on ERTS-1 imagery
[E73-10360] 10 p1149 N73-19356
Application of ERTS-1 band six imagery to determine rate of spread of grass fires in Zambesi Basin of South Africa
[PAPER-E6] 19 p2269 N73-28270
**FIRE EXTINGUISHERS**
Development and optimization of fire extinguishers for use in passenger and crew compartments of aircraft
[AD-747496] 03 p0253 N73-12051
Performance tests with halogenated hydrocarbon-foam generating fire extinguishing system for ships
[AD-749022] 05 p0612 N73-14975
Effects of chemical fire extinguishing agents containing bromotrifluoromethane on cardiovascular and nervous systems of dogs, monkeys, and baboons
[AGARD-R-599] 08 p0877 N73-17106
Papers presented at conference on halogenated fire extinguishing agents
[AD-753218] 09 p1001 N73-18168
Reduction in auxiliary extinguishing agents and systems for aircraft ground fire suppression at military airports
[AD-753069] 09 p1011 N73-18256
Chemical flame inhibitors for examining chemical microstructure of normal CH4, O2, Ar, and Halon inhibited flames
[BM-RI-7723] 09 p1034 N73-18438
Buffered gelled water to control nitrogen tetroxide-aerozine 50-hypergolic fuel fires
[NASA-CR-2198] 10 p1203 N73-19789
Design of perforated tube uniform distribution of fire extinguishing agent into commercial air transport compartments
[FAA-NA-73-3] 11 p1233 N73-20009
Fire suppression and extinguishment techniques in oxygen enriched atmospheres
[NASA-CR-121150] 15 p1842 N73-24926
Conference on uses and toxicity of halogenated fire extinguishing agents
[PB-218448/9] 18 p2214 N73-27875
Reliability of USAF fire protection systems including portable equipment
[AD-762948] 21 p2610 N73-30925
**FIRE FIGHTING**
Congressional hearings to establish government supported projects for fire research and safety
04 p0487 N73-13981
Reliability of USAF fire protection systems including portable equipment
[AD-762948] 21 p2610 N73-30925
**FIRE PREVENTION**
Development of in-flight fire detection and automatic suppression system for use on military helicopters
[AD-746630] 02 p0127 N73-11037
Silicone rubber cover for protecting flush-deck nozzles on aircraft carriers
[AD-746841] 02 p0153 N73-11241
Congressional hearings to establish government supported projects for fire research and safety
04 p0487 N73-13981
Development, design, fabrication, and testing of a self-generating overheat detection system for USAF aircraft
[AD-749474] 05 p0495 N73-14031
Performance tests with halogenated hydrocarbon-foam generating fire extinguishing system for ships
[AD-749022] 05 p0612 N73-14975
Analysis of aircraft fire warning system performance and procedures for eliminating false fire warning indications
[AD-751346] 07 p0740 N73-16025
Method and device for verifying reliability of fire detectors
[NASA-CASE-GSC-11600-1] 09 p1034 N73-18436
Development of halogenated hydrocarbon materials for use as fire and ignition suppressants for aircraft fuel tanks subjected to incendiary ammunition
[AD-755362] 12 p1365 N73-21079
Test rig simulation of gas turbine engine to determine means for minimizing incidence of lubricant sump fires in high speed aircraft engines
[NASA-CR-121158] 13 p1590 N73-22891
Development of fibrous flame arrestor materials to provide explosion and fire protection for aircraft fuel tanks
[AD-759193] 16 p1863 N73-25090
Effectiveness of crushed and graded stone aggregate in preventing or retarding rate of flame propagation from fixed ignition source for aircraft fuels
[FAA-NA-73-13] 17 p2097 N73-26962
Application of space program fire retardant technology to housing
[NASA-TN-D-7370] 19 p2312 N73-28592
**FIREPROOFING**
Intumescent paint containing nitrile rubber for fire protection
[NASA-CASE-ARC-10196-1] 04 p0437 N73-13562
Para-benzoquinone dioxime and concentrated mineral acid processed to yield intumescent or fire resistant, heat insulating materials
[NASA-CASE-ARC-10304-1] 17 p2048 N73-26572
Process for developing flame retardant elastomeric composition textiles for use in space suits
[NASA-CASE-MSC-14331-1] 18 p2167 N73-27501
Pyrolysis products of flame retardant treated cellulose
19 p2351 N73-28913
Improved flame resistance of spandex elastic elastomeric fibers
[NASA-CR-128505] 23 p2809 N73-32464
Production of fire protective intumescent coatings to show methods of manufacture and resulting material properties
[NASA-CR-114470] 23 p2810 N73-32468
**FIRES**
NT FOREST FIRES
Investigation of aircraft accident involving Beech aircraft performing air taxi service to Boise, Idaho on 20 Feb. 1972
[NTSB-AAR-72-25] 03 p0253 N73-12050
Utilization of ERTS-1 imagery to study short-lived events such as fires, volcanism, storms, and earthquakes
[E73-10025] 06 p0660 N73-15359
Analysis of aircraft fire warning system performance and procedures for eliminating false fire warning indications
[AD-751346] 07 p0740 N73-16025
Analysis of conditions existing in rising, rotating column of hot gases containing core of reacting gases
[TR-5] 10 p1223 N73-19948
Feasibility of detecting subsurface coal fires in Wyoming and Montana from ground observation, aerial photography, and satellite imagery
13 p1528 N73-22384
Directory of workers in field of fire research and related activities
[NASA-CR-121149] 15 p1845 N73-24954
Use of spaceborne microwave radiation measurements to detect fires, subsurface water, and surface temperature
[NASA-TT-F-14975] 17 p1998 N73-26153
Effectiveness of crushed and graded stone aggregate in preventing or retarding rate of flame propagation from fixed ignition source for aircraft fuels
[FAA-NA-73-13] 17 p2097 N73-26962
Identification of fire hazards in San Pablo test site area in California using ERTS-1 data and aerial photography
[PAPER-A18] 19 p2261 N73-28225
Design and development of integrated fire and overheat detection and warning system for installation in aircraft nacelle
[AD-762919] 20 p2362 N73-28999
ERTS-1 monitoring of grass seed field burning in western Oregon
[E73-10883] 20 p2394 N73-29234
Decomposition products of polyurethane foam related to aircraft cabin flash fires
[AD-763327] 22 p2730 N73-31846
**FIREWORKS**
U PYROTECHNICS
**FIRING [IGNITING]**
NT ROCKET FIRING
NT TEST FIRING
Chemical analysis of products in combustion chamber of nitrogen tetroxide/aerozine rocket engine during preignition, ignition, and postignition conditions
[NASA-CR-128898] 13 p1590 N73-22890
Characteristics of detonable gas mixtures and analysis of cylindrically expanding flames initiated by exploding wire source
24 p2990 N73-33897
**FISH**
U FISHES
**FISHES**
Utilization of ERTS-1 remotely-acquired oceanographic information for improving harvest and management of menhaden in Gulf of Mexico
[E72-10215] 02 p0162 N73-11309

Use of remote sensing data from spacecraft and aircraft to assist technology in tropical tuna and Alaska salmon fisheries
[AD-745774] 02 p0169 N73-11370
Utilization of ERTS-1 imagery to determine availability and distribution of menhaden within Mississippi Sound and adjacent waters
[E72-10279] 03 p0292 N73-12377
Improvement of menhaden fishery prediction in Mississippi Sound through ERTS-1 imagery
[E72-10340] 05 p0532 N73-14328
Meteorological assistance to fishing fleets by meteorological services
[NLL-M-9146-[5828.4F]] 05 p0569 N73-14624
Prediction of menhaden school location and movement in Mississippi Sound from ERTS-1 imagery
[E73-10079] 08 p0900 N73-17291
Effect of sonic boom on fish and fish eggs during developmental stage
[FAA-RD-73-29] 11 p1247 N73-20121
Blind fish responses to gravitational changes as in parabolic flight
12 p1368 N73-21101
Improvement of Menhaden fishery prediction in Mississippi Sound using ERTS-1 imagery
[E73-10480] 12 p1396 N73-21317
Asymmetry of fish otolithic receptor functions and vestibular disturbances during space flight
14 p1608 N73-23031
Detection of menhaden schools in Mississippi Sound by comparing ERTS-1 imagery to selected oceanographic parameters
[E73-10580] 14 p1656 N73-23441
Detection of adult menhaden fish in Mississippi Sound from ERTS-1 imagery
[E73-10624] 15 p1775 N73-24384
Assessment and monitoring oceanic gamefish through Skylab EREP data
[E73-10658] 16 p1898 N73-25354
Application of ERTS-1 imagery for determining availability and distribution of menhaden within Mississippi Sound adjacent waters
[E73-10751] 17 p2022 N73-26354
Prediction of menhaden fish distribution in Mississippi Sound based on ERTS-1 imagery
[E73-10785] 18 p2136 N73-27261
Application of ERTS-1 imagery to harvest model of menhaden fishing industry in Mississippi Sound
[PAPER-M17] 19 p2282 N73-28355
Relationship between ERTS-1 fisheries distribution information and selected oceanographic parameters in Mississippi Sound
19 p2286 N73-28385
Application of ERTS-1 data to prediction and detection model for Menhaden fishing in Mississippi Delta
[E73-10961] 21 p2532 N73-30303
Application of infrared data from satellites for use in field of fishery oceanography in Pacific Ocean
[AD-763350] 21 p2542 N73-30380
Utilization of ERTS-1 imagery to determine availability and distribution of adult Gulf menhaden within Mississippi Sound and adjacent waters
[E73-10980] 22 p2657 N73-31287
Skylab monitoring of gamefish in coastal waters off of Florida
[E73-10997] 22 p2659 N73-31303
Remote sensing of oceanic gamefish from ERTS-1 imagery
[E73-11135] 24 p2917 N73-33290
Skylab oceanic gamefish operations in Gulf of Mexico
[E73-11157] 24 p2919 N73-33311

**FISHTAILING**
U YAW

**FISSILE MATERIALS**
U FISSIONABLE MATERIALS

**FISSION**
Multiplicity measurements for fission-emitted neutron or gamma quanta
[EUR-4829-E] 01 p0082 N73-10678
Plastic, nuclear track detectors for recording and measuring multicharged, heavy particles
[NASA-CR-123918] 02 p0213 N73-11725

**FISSION ELECTRIC CELLS**
NT SNAP 8
NT SNAP 10A

**FISSION PRODUCTS**
Analysis of space base mission and accidents/events involving nuclear hazard to general public - Vol. 3 Pt. 3
[NASA-CR-123846] 02 p0210 N73-11699
Radiac set for surveying areas contaminated with fissionable materials
[AD-747051] 02 p0211 N73-11709
Soil impact test with spherical nuclear reactor containment model for fracture strength observations
[NASA-TM-X-68180] 07 p0819 N73-16641
Fission-gas release from uranium nitride at high fission-rate density
[NASA-TN-D-7171] 08 p0942 N73-17718
Time of flight spectroscopy for X ray coincidence measurements on californium isotopic fission yield
[AD-753542] 10 p1195 N73-19722
Re-solution rates of fission gases in oxide nuclear fuels under irradiation
[GEAP-12361] 17 p2062 N73-26679
Fission gas bubble, size distributions on irradiated UO2 specimens
[GEAP-12338] 17 p2062 N73-26680
Feasibility of on-line fission gas leak detection system for 100 kW zirconium hydride reactor
[NASA-TM-X-2870] 20 p2453 N73-29717
Fission gas release rates from irradiated uranium nitride specimens
[NASA-TM-X-2890] 23 p2818 N73-32530
Model to predict fission gas releases from UN fuel pins clad with various materials
[NASA-TN-D-7401] 23 p2818 N73-32531

**FISSION WEAPONS**
Ignition of mini-atomic bomb to produce thermonuclear power with capacitor produced electron beams
24 p2907 N73-33199

**FISSIONABLE MATERIALS**
Development and evaluation of test equipment for high pressure radio frequency plasma experiments and in-reactor tests of nuclear lightbulb engine
[NASA-CR-129501] 03 p0330 N73-12694
Development of graphite-matrix fuels for booster assemblies in reactor cores
09 p1063 N73-18669

**FISSIUM**
Thermal conductivity, thermal properties, and thermal diffusivity of uranium-fissium alloy
[ANL-7889] 03 p0332 N73-12710

**FITNESS**
NT FLIGHT FITNESS
NT PHYSICAL FITNESS

**FIXED POINTS [MATHEMATICS]**
Fixed point theorems and dissipative processes in differential systems of Euclidian space
[NASA-CR-131267] 11 p1310 N73-20631
Continuous dependence of fixed points of condensing maps
[NASA-CR-132021] 14 p1684 N73-23664

**FIXED WINGS**
Effectiveness of synthetic fixed wing flight training equipment for military purposes
[AD-744447] 01 p0020 N73-10158
Numerical methods for determining effect of aerodynamic lag on bending response of aircraft wings at supersonic speeds
[NAL-TN-36] 15 p1733 N73-24056

**FIXED-WING AIRCRAFT**
U AIRCRAFT CONFIGURATIONS
U FIXED WINGS

**FLAME FRONTS**
U FLAME PROPAGATION

**FLAME HOLDERS**
Combustion tests of various integral, spray-bar and flameholder configurations to determine configuration with maximum combustion efficiency
[NASA-TM-X-2855] 19 p2352 N73-28919

**FLAME INTERACTION**
U CHEMICAL REACTIONS
U FLAME PROPAGATION

**FLAME PROPAGATION**
Analysis of laminar hydrogen, ethylene, and propylene air diffusion flames burning in weightless environment
[NASA-TN-D-7165] 07 p0855 N73-16933
Kinetics and mechanisms of gas phase combustion, flames, and flame suppression
08 p0882 N73-17143
Dynamic behavior of flames in explosive acetylene oxygen mixture
[NASA-CR-130963] 09 p1099 N73-18973
Analysis of conditions existing in rising, rotating column of hot gases containing core of reacting gases
[TR-5] 10 p1223 N73-19948
Analysis of conditions under which coupling occurs between structure of combustion front and periodic oscillations
[NLL-M-22985-[5828.4F]] 15 p1842 N73-24922
Radical species concentration profiles for methane-oxygen-argon flame
[BM-RI-7766] 18 p2206 N73-27803
Analysis of flame front propagation in porous propellant charges to show wave propagation speed and mass fraction of propellant burned during flame propagation
[AD-762063] 19 p2353 N73-28928
Analysis of low speed deflagration of initially unmixed reactants under irreversible, two-step chain reaction
[AD-762459] 19 p2353 N73-28930
Analysis of parameters involved in flow of combustion to produce stable propagation and efficient fuel consumption
[NLL-T1873/BGC/73-[9022.305]] 21 p2605 N73-30874
Characteristics of weakly turbulent flame with high activation energy and comparison with laminar flame spread
[AD-763340] 21 p2606 N73-30889
Photographic recording of dynamic behavior of flames in explosive gases caused by ignition of equimolar acetylene-oxygen mixture
[NASA-CR-135672] 23 p2856 N73-32825
Characteristics of detonable gas mixtures and analysis of cylindrically expanding flames initiated by exploding wire source
24 p2990 N73-33897

**FLAME QUENCHING**
U EXTINGUISHING
U QUENCHING [COOLING]

**FLAME STABILITY**
Performance of ignition and flame stabilization using gas generator in different ramjet combustion chamber configurations
[DLR-FB-72-47] 01 p0091 N73-10748
Tests of combustion chamber with burner device using system of transverse air streams for flame stabilization
[AD-753518] 09 p1100 N73-18977
Analysis of conditions under which coupling occurs between structure of combustion front and periodic oscillations
[NLL-M-22985-[5828.4F]] 15 p1842 N73-24922
Numerical analysis and computerized simulation of open combustion processes and flame stability
[AD-762360] 19 p2353 N73-28925
Interior ballistic properties of solid fuel ramjet engines to determine regression rate if fuel as function of chamber pressure, inlet air temperature, and air flux rate
[AD-764491] 22 p2709 N73-31691

**FLAME TEMPERATURE**
Synthesis and characterization of 4,5-dicyano oxazole, low hydrogen content fuel for satisfying flame temperature criteria for gas dynamic laser
[AD-746342] 02 p0221 N73-11790
Measuring flame temperature in exhaust nozzle and combustion chamber by pyrometer
04 p0420 N73-13425
Nonsteady combustion and extinguishment effects, including external thermal radiation effects, steady flame temperature, and L-stability limit
[AD-755860] 12 p1442 N73-21686
Laser Raman probe for temperature for nitrogen and hydrogen in hydrogen-air flames
[AD-759386] 17 p2034 N73-26465
Calculating flame temperatures at constant pressure and volume
[ARL/ME-NOTE-341] 22 p2729 N73-31838

**FLAMEOUT**
Flameout and ignition characteristics of jet engine fuel flame in gas turbine with exhaust diffuser
[AD-749635] 05 p0591 N73-14802

**FLAMES**
NT DIFFUSION FLAMES
NT PREMIXED FLAMES
Chemical reactions involved with molybdenum, tungsten, vanadium, and chromium additives in hydrogen-oxygen flames seeded with potassium
[AD-743514] 01 p0023 N73-10179
Analysis of aerodynamic characteristics of free, semibounded slipstream of straight-jet laminar gas flames
[NASA-TT-F-14688] 07 p0855 N73-16934
Models for candle-like flames produced by burning of polymers
08 p0883 N73-17146
Analyses of laminar combustion phenomena in hybrid rockets
08 p0968 N73-17909
Chemical flame inhibitors for examining chemical microstructure of normal CH4, O2, Ar, and Halon inhibited flames
[BM-RI-7723] 09 p1034 N73-18438
Excitation and sound generating effects on laminar flames, and stabilizing and noise reducing effect of sound on turbulent flames
[REPT-8/1972] 09 p1099 N73-18970
Linear stabilization of flat diffusion gas flame
[AD-754049] 11 p1350 N73-20952
Characteristics of weakly turbulent flame with high activation energy and comparison with laminar flame spread
[AD-763340] 21 p2606 N73-30889
Improved flame resistance of spandex elastic elastomeric fibers
[NASA-CR-128505] 23 p2809 N73-32464

**FLAMMABILITY**
Chemical and physical properties and thermal decomposition products of certain natural fibers and synthetic materials
[AD-751899] 08 p0935 N73-17658
Analytical model for prediction of flammability limits of combustible gas
13 p1390 N73-22889
Silicone base nonflammable hydraulic fluid to aid wear resistance in military aircraft
[AD-758361] 14 p1671 N73-23562
Flash point measurements for determining flammability hazards of hydrocarbon fuels
[AD-758643] 16 p1954 N73-25814
Effectiveness of crushed and graded stone aggregate in preventing or retarding rate of flame propagation from fixed ignition source for aircraft fuels
[FAA-NA-73-13] 17 p2097 N73-26962

Analysis of physiological and toxicological aspects of smoke produced by combustion of aircraft interior materials m Part 1
[FAA-RD-73-50-PT-1] 18 p2104 N73-27014
Physio-chemical analysis of flammability characteristics and thermal degradation of rigid and flexible urethane foams used in aircraft structures - Part 2
[FAA-RD-73-50-PT-2] 18 p2105 N73-27025
Flame retardant treatments for cotton fabrics and polypropylene fibers
19 p2230 N73-27982
Identification of fire hazards in San Pablo test site area in California using ERTS-1 data and aerial photography
[PAPER-A18] 19 p2261 N73-28225
Analysis of ignition characteristics of high velocity hydrocarbon diffusion flames and comparison with ignition properties of hydrogen
21 p2605 N73-30881
Oxygen index method for evaluating flammability of organic polymeric materials
[DSL-REPT-561] 22 p2729 N73-31836
Research and development projects concerning fire hazards in aircraft cabins and design of aircraft compartments to provide greater passenger survivability
[FAA-RD-73-146] 24 p2876 N73-32972
Flammability of engineering materials in gaseous oxygen environments and applicability to Skylab program
[NASA-TM-X-64783] 24 p2891 N73-33081

**FLAMMABLE GASES**
Analysis of laminar hydrogen, ethylene, and propylene air diffusion flames burning in weightless environment
[NASA-TN-D-7165] 07 p0855 N73-16933
Chemical flame inhibitors for examining chemical microstructure of normal CH4, O2, Ar, and Halon inhibited flames
[BM-RI-7723] 09 p1034 N73-18438
Mixing processes occurring in in-flight balloons with initially separate gases
[AD-760600] 18 p2207 N73-27812
Evacuation areas for transportation accidents involving propellant tank pressure bursts
[NASA-TM-X-68277] 20 p2488 N73-29987

**FLANGE WRINKLING**
Flanged and circular data sheet-sections, beyond limit of proportionality
[ESDU-01.06.00] 01 p0110 N73-10903

**FLANGES**
Butt welding of titanium alloy rings and flanges to improve mechanical properties
10 p1163 N73-19463
Twelve simulated bolted flanges during stress relaxation
[NASA-CR-132218] 15 p1792 N73-24527
Evaluation of structural capabilities of Marman V-band coupling and flange with Conoseal gasket for use with 75K NERVA propellant lines
[NASA-CR-132219] 15 p1792 N73-24529
Determination of elongation in flanges during H-beam rolling
[NLL-M-21639-[5828.4F]] 21 p2552 N73-30455

**FLAP CONTROL**
U AIRCRAFT CONTROL
U FLAPS [CONTROL SURFACES]

**FLAPPING HINGES**
Analysis of helicopter blade flutter for both hinged and hingeless rotor blades
[AGARD-R-607] 13 p1472 N73-21920
Flapping- and squeeze-duty design criteria for full journal bearings under dynamic duty
[WTHD-45] 16 p1917 N73-25514

**FLAPS [CONTROL SURFACES]**
NT JET FLAPS
NT LEADING EDGE SLATS
NT TRAILING-EDGE FLAPS
NT WING FLAPS
Noise tests on simulated mixer nozzles and scale models of externally blown flap, lift augmentation system
[NASA-TM-X-2638] 02 p0124 N73-11012
Comparison of surface-source solution with an exact solution for two-dimensional inviscid flow about slotted-flap airfoil
[ARC-CP-1214] 03 p0248 N73-12003
Flight tests of rotating cylinder flap on YOV-10 aircraft modified to STOL configuration
[NASA-CR-2135] 04 p0371 N73-13020
Development of procedures for quieting externally-blown-flap noise sources produced by interaction of jet exhaust flow with deployed flaps
[NASA-CR-112166] 04 p0372 N73-13022
Wind tunnel tests of longitudinal aerodynamic characteristics of aspect ratio airfoil with 0.098 chord blowing flap
[NASA-TM-X-2675] 04 p0421 N73-13431
Design aspects of stall of powered-lift aircraft with externally blown flaps and methods for predicting increment in maximum lift coefficient due to power
06 p0617 N73-15011
Wind tunnel tests to determine effects of slot spoilers on longitudinal and lateral aerodynamic characteristics of twin engine light aircraft
[NASA-TN-D-7315] 21 p2496 N73-30033
Evaluation of low speed flying qualities of short takeoff aircraft with externally blown flap wing or augmentor wing using flight simulator
[NASA-TN-D-7454] 23 p2742 N73-31951
Adjustable airfoil for reversable cowl flap inlet thrust augmentation
[NASA-CASE-ARC-10754-1] 23 p2831 N73-32624
Flight tests of modified F-100 aircraft to determine effectiveness of fast-acting flaps as direct-lift-control devices to improve station keeping
[NASA-TM-X-2936] 24 p2876 N73-32970

**FLARES**
Bibliography on pyrotechnics
[AD-752700] 09 p1100 N73-18976
Illuminance measurement of two types of airborne flares
[DREV-R-673/72] 10 p1223 N73-19942
Air-to-ground target acquisition with flare illumination
10 p1226 N73-19968
Design and performance of launcher illumination XM-183 flare package for parachutes
[AD-757731] 15 p1844 N73-24940
Possible origin of soft gamma ray bursts from stellar superflares
[NASA-TM-X-66294] 18 p2197 N73-27735

**FLASH BLINDNESS**
Response time of flash blindness recovery in human exposure to constant energy flashes
[AD-747631] 04 p0380 N73-13095

**FLASH LAMPS**
Electrical analogue model of flash tube and laser rod system to determine efficiency of laser system with respect to flash duration
[WRE-TM-657[AP]] 02 p0180 N73-11462
Bloch law error in visual perception of capacitor discharge brightness
[AD-749452] 05 p0505 N73-14109
Design and performance of flash lamps with nanosecond light pulses
[AD-750788] 06 p0701 N73-15720
Performance of translucent beryllium oxide as envelope material for high intensity flash and continuous wave lamps
[AD-751661] 07 p0813 N73-16589
Lamp design and parameters for optical pumping of lasers
[AD-754643] 11 p1304 N73-20578
Optical system for measuring passive stress conditions in xenon flash lamps for use in high power lasers
[UCRL-50022-3] 12 p1410 N73-21427
Construction of experimental incandescent lamp of Nernst glower type for laser pumping
[AD-755207] 13 p1539 N73-22465
Development of high power alkali vapor lamp for laser applications
[AD-755213] 13 p1560 N73-22646
Life tests of 10 mm bore flashlamps at high fractions of explosion energy
[AD-760707] 20 p2426 N73-29488
Lamp design and operating parameters affecting laser stability and beam divergence
[AD-763932] 22 p2682 N73-31481

**FLASH POINT**
Flash point measurements for determining flammability hazards of hydrocarbon fuels
[AD-758643] 16 p1954 N73-25814

**FLASH TUBES**
U FLASH LAMPS

**FLASHING [VAPORIZING]**
Laboratory prototype flash evaporator design, fabrication, and testing for space shuttle environmental control expendable heat sink
[NASA-CR-128608] 01 p0057 N73-10470

**FLAT CONDUCTORS**
Torque measurement of flat polyimide cable crossing hinge or satellite solar array
[ESRO-TN-114-ESTEC] 05 p0603 N73-14904
Termination of flat conductor cable to NASA/MSFC plugs
[NASA-TM-X-64728] 11 p1262 N73-20239
Development of low profile flat conductor cable connecting device and permanent splice methods for use in spacecraft component electrical systems - Vol. I
[NASA-CR-128845] 11 p1262 N73-20241
Cost comparison of flat versus round conductor cable based on spacecraft electric wiring system specifications - Vol. 3
[NASA-CR-128847] 11 p1262 N73-20243
Superconducting properties and damage susceptibility of composite wire conductors
[BNL-17222] 12 p1439 N73-21660
Research projects conducted as part of NASA programs during period May 1970 through May 1972
[NASA-TM-X-64723] 13 p1593 N73-22915
Development, characteristics, and applications of flat conductor cable to include methods and facilities for fabrication
13 p1593 N73-22916
Conference papers on flat conductor cable technology and applications
[NASA-TM-X-64716] 14 p1640 N73-23294
Design characteristics and advantage of FCC use
14 p1640 N73-23295
Survey of flat electrical cable manufacturing including patented processes
14 p1640 N73-23296
Material selection for design and manufacture of FCC
14 p1640 N73-23297
Mathematical model for thermal behavior of flat conductor cable under load
14 p1640 N73-23299
Electrical characteristics of FCC determined in context of multiple transmission lines theory
14 p1640 N73-23300
Manufacturing and quality control of FCC harnesses with design and installation requirements
14 p1641 N73-23302
Energy pulse bonding method for joining flat cables
14 p1641 N73-23303
FCC transition splices and cost comparison of FCC vs. RCC
14 p1641 N73-23304
Flat conductor cabling system for electrical/electronic interwiring
14 p1641 N73-23305
Military specifications for flat connectors and cables
14 p1641 N73-23306
Flat conductor cable connectors with individually sealed contacts
14 p1641 N73-23307
No-strip-crimp connection for flat electrical signal cables
14 p1641 N73-23308
Techniques and hardware for facilitating use of flexible flat conductor cable in commercial air transports
14 p1641 N73-23310
Advanced wiring system for aircraft and space vehicle application
14 p1642 N73-23311
Survey of source availability for FCC and/or FCC connectors
14 p1642 N73-23312
Thin pressure-sensitive FCC for low voltage uses
14 p1642 N73-23313
Application of flat conductor technology to surface mounted housewiring
14 p1642 N73-23314
Flat conductors for ALSEP
14 p1642 N73-23315
Ribbon cabling designs for AEGIS phased arrays
[RE-18-1-14] 14 p1642 N73-23316
FCC in Viking articulated boom
14 p1642 N73-23317
Military and NASA programs using FCC
14 p1642 N73-23318
Design of flat conductor cable for interconnecting harness application
[NASA-TM-X-64750] 19 p2243 N73-28085
Load-carrying and thermal characteristics of flat conductor cable
[NASA-TM-X-64767] 20 p2380 N73-29125

**FLAT LAYERS**
Turbulent convective heat transfer in horizontal liquid layers with volume heating - pt. 1
[DLR-FB-71-39-PT-1] 05 p0606 N73-14927
Turbulent convective heat transfer in horizontal liquid layers with volume heating noting turbulent convection mechanism - Pt. 2
[DLR-FB-71-40-PT-2] 05 p0606 N73-14928
Frictionless plane contact between elastic layer on elastic half space with compression loads by frictionless rigid stamp
[WB-1/72] 09 p1040 N73-18478
Stiffness of flat strips in compression under sinusiodally distributed bending couples at their edges
[ESDU-05.01.30-AMEND-A] 14 p1714 N73-23906
Nonlinear diffusion of pulsed magnetic fields in planar and cylindrical plasmas
[LA-5132-MS] 24 p2963 N73-33681

**FLAT PLATES**
Estimating local or average turbulent skin friction on flat plates from Reynolds numbers
[NASA-TN-D-6945] 01 p0040 N73-10315
Method of characteristics for analyzing supersonic flow past oscillating flat plate cascades with leading edge locus
[AD-745838] 01 p0042 N73-10332
Transverse injection of water and isopropyl alcohol from flat plate into air streams
[AD-741887] 01 p0043 N73-10339
Stress effects around holes in flat plates under various combinations of loads
[ESDU-70005] 01 p0110 N73-10902
Analysis of geometric stress concentrations caused by two equal unreinforced circular holes in infinite flat plates
[ESDU-67023-AMEND-A] 01 p0110 N73-10909
Elastic stresses in flat plates, strips, and lugs due to interference-fit pins or bushes
[ESDU-71011] 01 p0111 N73-10916
Calculation of geometric stress concentration factors in two adjacent, unreinforced circular holes in infinite flat plates
[ESDU-66035] 01 p0111 N73-10919

Elastic stresses in single lap joints under compression or tension
[ESDU-67008] 01 p0111 N73-10920
Maximum deflection and stresses for initially flat circular plates under uniform pressure
[ESDU-65003] 01 p0112 N73-10924
Damping of flat square plates vibrating in air and vacuum
[AD-746054] 01 p0115 N73-10949
Heat test program for general protuberance shapes on flat plate
[NASA-CR-128400] 01 p0116 N73-10959
Normal forces and center of pressure positions for thin flat plates
[ESDU-70015-AMEND-A] 02 p0154 N73-11250
Ionized continuum flows and collisionless plasmas in electric boundary layers on flat plates and cylindrical bodies
[AD-746094] 02 p0217 N73-11753
Creep buckling of flat plates and cylindrical shells subjected to edge wise and uniform axial compression respectively
[AD-746475] 02 p0240 N73-11952
Skin friction, heat transfer and pressure measurements in laminar, transitional and turbulent boundary layers on flat plates at high Mach numbers and Reynolds numbers
[NASA-CR-112147] 03 p0283 N73-12290
Drag reduction and diffusion accompanying thin slit injections of drag reducing polymer into water turbulent boundary layer of flat plate at high Reynolds number
[AD-747248] 03 p0285 N73-12312
Ion-current collection by flush-mounted electrostatic probes on sharp flat plate in ionized hypersonic flow
[SC-CR-72-3145] 04 p0422 N73-13440
Effect of circular inclusion on stresses around two collinear finite line cracks in plate under tension
[AD-749901] 05 p0604 N73-14910
Supersonic flow past solid cylindrical and circular jet barriers on flat plates
[AD-750522] 06 p0656 N73-15327
Dynamic frequency response of curved or flat honeycomb sandwich panels having cores of negligible flexural stiffness
[ESDU-72016] 06 p0723 N73-15898
Buckling of flat isotropic plates under uniaxial and biaxial loading
[ESDU-72019] 06 p0724 N73-15908
Mathematical model for eddy viscosity in turbulent boundary layer on flat plates
07 p0771 N73-16262
Free convection effects in laminar two dimensional wake above isothermal vertical plate cooled by natural convection
08 p0894 N73-17240
Finite difference solution for merged layer regime of hypersonic flat plate leading edge problem
08 p0895 N73-17243
Boundary layer stability on two-layer flat plates using viscous liquid currents
[AD-752696] 09 p1016 N73-18294
Method of characteristics solution of flow field on lee side of flat plate delta wing with supersonic leading edges
[AD-753389] 09 p1019 N73-18319
FORTRAN subroutines for matrix operations encountered in finite element analysis of structures, noting application to flat plates
[ARC-CP-1223] 09 p1095 N73-18941
Orifice inclination effect in pressure measurements on hypersonic rarefied flow field of flat plate
10 p1140 N73-19290
Effects of circular inclusion of different elastic material on stress stage of cracked flat plates
[AD-754211] 10 p1222 N73-19936
Fracture toughness of flat elastic cracked plate with elastic circular inclusion
[AD-754210] 10 p1222 N73-19937
Analysis of effect on laminar boundary layer resulting from superposed unsteadiness on yawed infinite flat plate in adverse pressure gradient
12 p1389 N73-21265
Vibratory stability of plate over viscous heat conducting gas layer
[AD-755288] 12 p1393 N73-21293
Effects of drag reducing polymer on turbulent boundary layer of submerged flat plates
[AD-755215] 13 p1513 N73-22260
Acoustic fatigue characteristics of flat multi-layered structural panel
[NASA-CR-124079] 13 p1546 N73-22529
Combined heat and mass transfer at wet flat plate in parallel air flow forming turbulent boundary layer
[DLR-FB-73-11] 14 p1599 N73-22960
Boundary layer separation on flat plate in high supersonic free stream as caused by normal injection of two dimensional sonic or supersonic jet
[AD-757635] 14 p1652 N73-23398
Literature survey of heat transfer characteristics of single and multiple turbulent air jets impinging on flat plates
[NASA-TM-X-2778] 15 p1842 N73-24927
Development of mathematical formula for growth of compressible, turbulent boundary layers on isothermal and adiabatic walls
[ARC-R/M-3191] 16 p1853 N73-25013
Visual study of outer region of turbulent boundary layer along flat plate
18 p2129 N73-27203
Analysis of kinematic and dynamic characteristics of wake generated behind flat plate normal to parallel unbounded fluid flow
[AD-761372] 18 p2131 N73-27220
Formation of longitudinal edge waviness and center camber on sheets as measure of sheet flatness
[NLL-M-21611-[5828.4F]] 18 p2202 N73-27777
Numerical analysis of hypersonic rarefied flow past sharp leading edge of flat plate using finite difference solution of Navier-Stokes equation
19 p2251 N73-28147
Solution of unsteady Navier-Stokes equations for flow field about impulsively started flat plate
[AD-761459] 19 p2257 N73-28193
Flat circular plates of particular mass density, representing spiral or flat elliptical galaxeis
19 p2341 N73-28830
Vortex-lattice method used in model to represent jet exhausting from flat plate into crossflowing stream
[AD-762502] 20 p2389 N73-29191
Analysis of surface pressure fluctuations from jet impingement on inclined flat plate with application to design of aircraft with externally blown flaps
20 p2479 N73-29909
Analysis of structural response to acoustic loading and preparation of data sheets for various conditions of acoustic loads
20 p2479 N73-29914
Numerical analysis of effect of boundary layer profile on dynamic response and acoustic radiation of thin, elastic, flat plates
[NASA-TM-X-69568] 21 p2523 N73-30232
Analysis of surface pressure and cold wall heating rate distributions for large, flat panel at Mach 7 in high temperature wind tunnel
[NASA-TN-D-7275] 21 p2524 N73-30243
Prediction and measurement of heat transfer rates for shock-induced unsteady laminar boundary layer on flat plate
[NASA-CR-114582] 22 p2651 N73-31241
Supersonic flow configurations at inlet and exit of infinite two dimensional straight cascade of flat plates
22 p2652 N73-31244
Flat plate collector performance evaluation using simulated sun
[NASA-TM-X-71427] 23 p2835 N73-32655
Free jet boundary and distribution of flow within planar jet and pressure distribution at flat panel
[NASA-TT-F-15151] 24 p2905 N73-33180

**FLAT SURFACES**
Application of vector space processes for algebraic analysis of affine plane surfaces
02 p0196 N73-11583
Scattering of electromagnetic waves from planar and rough oscillating surfaces
22 p2627 N73-31046
On the effects of viscous interaction for a flat delta wing at incidence
[ARC-CP-1237] 24 p2870 N73-32931
Filter for determining long wave solar spectral reflection by plane surfaces
24 p2975 N73-33772

**FLAW DETECTION**
U NONDESTRUCTIVE TESTS

**FLEET BALLISTIC MISSILES**
NT POSEIDON MISSILES

**FLEXIBILITY**
Strength, mechanical properties, and deformation analysis of flexible polyethylene balloons
[AD-746308] 02 p0127 N73-11029
Analysis of shimmy in pneumatic tires due to lateral flexibility for stationary and nonstationary conditions
[WTHD-48] 16 p1917 N73-25515

**FLEXIBLE BODIES**
Detailed design guidance for flexure-pivots with strips crossing midway along lengths and at right angles to each other
[ESDU-67021] 01 p0110 N73-10907
Analysis of response of flexible helicopter rotor blade to random loads with vertical velocity component
[AD-746627] 04 p0374 N73-13038
Evaluation of exact point speed and least squares procedures for determining balance of flexible rotating machinery
[NASA-CR-121035] 05 p0551 N73-14477
Analysis of performance potential of buoyant systems and flexible structures for use with short haul passenger transport aircraft
[NASA-TM-X-62168] 08 p0866 N73-17014
Equations of motion for calculating flexible rotor influence on two gimbaled gyroscope motion
08 p0922 N73-17554
Mathematical model and analysis of attitude stability and control of spinning flexible satellite in force-free environment
08 p0964 N73-17876
Formulation of mathematical model for predicting dynamic behavior of rotating flexible space station configurations - Vol. I
[NASA-CR-112243] 10 p1189 N73-19672
User's manual for computer program to predict dynamic behavior of rotating flexible space station configurations - Vol. 2
[NASA-CR-112244] 10 p1189 N73-19673
Development and characteristics of supporting frame to isolate payloads from multi-gravitational forces
[NASA-CASE-MFS-21680-1] 11 p1297 N73-20525
Development of mathematical model of lateral motion of flexible space shuttle vehicle during ascent
[NASA-CR-124159] 11 p1340 N73-20876
Kinematic equations for unified flexible spacecraft simulation program
[NASA-CR-124170] 11 p1340 N73-20877
Development of dynamic loads computation capability for application to unified flexible spacecraft simulation program
[NASA-CR-124168] 11 p1340 N73-20878
Analysis of thermal static bending forces on deployable interlocked booms and comparison with thermal bending of seamless tubes
[NASA-TN-D-7243] 11 p1345 N73-20915
Description of canonical set of equations which governs behavior of n-body spacecraft connected by dissipative elastic joints
[NASA-CR-132155] 15 p1835 N73-24872
Dynamic characteristics of large flexible solar arrays and interaction between spacecraft attitude dynamics and elastic degrees of freedom
[UTIAS-179] 15 p1835 N73-24878
Derivation of differential equations of motion to analyze characteristics of three degree of freedom bodies joined by elastic tether
[NASA-CR-124259] 15 p1839 N73-24903
Model parameters associated with single axis attitude dynamics of flexible vehicle
[NASA-CR-132262] 16 p1964 N73-25890
Equations of motion formulated to compute transient response of multi-mass flexible rotors
[NASA-CR-2300] 23 p2797 N73-32374
Flexible airship manufacturing
24 p2879 N73-32992
Attitude stability of spinning elastic bodies based on modal analysis and criteria for idealized spinning flexible spacecraft
24 p2950 N73-33564

**FLEXIBLE WINGS**
NT PARAWINGS
Influence of aeroelasticity on flight mechanics of flexible aircraft
08 p0864 N73-16991
Calculation of induced load effects on controllability of rigid and flexible aircraft
08 p0865 N73-17004
Elastic vibrations of aircraft wing caused by distributed load, center of gravity displacement, and rotation using electromodeling techniques
[AD-760965] 18 p2108 N73-27043

**FLEXING**
Two degree inverted flexure from single block of material
[NASA-CASE-ARC-10345-1] 03 p0305 N73-12488
Application of data processing to flexural and tensile tests on rubber
[ERDE-TR-114] 09 p1052 N73-18579

**FLEXURE**
U FLEXING

**FLIGHT**
Fatigue crack propagation under flight simulation loading at 10, 1, and 0.1 cycles per second
07 p0851 N73-16900
Discussion of speed record establishment by SA-341 helicopter to include aircraft preparation procedures and requirements for successful completion
12 p1358 N73-21018
Integrated SAVVAN, VOR, and DME system for locating and controlling high altitude aircraft
14 p1688 N73-23695
Dispersion and dilution of jet aircraft exhaust at high altitudes
[NASA-TM-X-71451] 24 p2971 N73-33743

**FLIGHT ALTITUDE**
Surface based altitude measuring system for accurately measuring altitude of airborne vehicle
[NASA-CASE-ERC-10412-1] 03 p0273 N73-12211
Tabulation of minimum enroute instrument flight rules altitudes over particular routes and intersections - November 1972
06 p0697 N73-15679
Altitude-aided algorithm for determining aircraft position from radar tracking
[AD-756655] 13 p1492 N73-22097
Effects of oxygen pressure on tissues under extreme flight factors
[NASA-TT-F-762] 21 p2500 N73-30065

**FLIGHT CHARACTERISTICS**
Evaluation of minimum aircraft flying speed by digital simulation
[AD-745861] 01 p0005 N73-10038

Method for predicting flight characteristics of F-5 and A-7 aircraft during atmospheric turbulence using large amplitude flight simulator
[AD-749480] 05 p0495 N73-14030
Mission flight performance, and data acquisition of data-90 launch vehicle and InterPlanetary Monitoring Platform-H
[NASA-TM-X-68929] 05 p0595 N73-14836
Analysis of aerodynamic buffeting and related phenomena to include development of models for oscillatory rigid-body motion
06 p0618 N73-15018
Analysis of high subsonic and transonic characteristics of fighter aircraft and factors affecting aerodynamic boundaries for various wing design parameters
06 p0618 N73-15019
Simulation of flight in Concorde for improving characteristic of flight control system
08 p0866 N73-17013
Application of computer techniques for determination of flutter characteristics of aircraft and comparison with model matching data analysis
[AGARD-R-596] 09 p0983 N73-18030
Performance tests of reentry vehicle control with base plane thrusters and fluidic control logic
[SC-DC-72-2244[RD]] 09 p0985 N73-18043
Mission objectives, flight history, and scientific experiments of OSO-7
[NASA-CR-130157] 11 p1341 N73-20879
Helicopter flight performance in tactical environment
12 p1357 N73-21009
Flight characteristics and performance of Fenestron type helicopter tail rotor
12 p1359 N73-21028
Analysis of equations of aircraft dynamics and development of analog-digital simulation capability
[AD-755868] 12 p1365 N73-21077
Engine and control problems of light aircraft
14 p1600 N73-22972
Development and application of aircraft performance prediction methods for subsonic and supersonic transport and fighter aircraft
[AGARD-LS-56] 15 p1732 N73-24042
Numerical methods for determining range and radius of action performance of transport and combat aircraft and effects of various parameters on performance
15 p1732 N73-24043
Development of methods for predicting aircraft flight maneuver and climb performance to show effects of excess power and load factor
15 p1732 N73-24045
Development of methods for presenting aircraft performance data and comparison of specific methods to show sources of discrepancies
15 p1733 N73-24050
Development of computer program for determining minimum time trajectory and comparison with gradient method of computation
15 p1733 N73-24053
Systems design of facilities for studying flight problems of VTOL aircraft
[NAL-TR-306] 15 p1760 N73-24263
Development of method for calculating spanwise loading on helicopter rotor blades in forward flight at various azimuth angles
[ARC-R/M-3318] 16 p1856 N73-25032
Mariner Mars 1971 battery design, test, and flight performance
[NASA-CR-132986] 16 p1864 N73-25095
Design and flight performance of Mariner Mars 1971 power subsystem
[NASA-CR-132992] 16 p1864 N73-25096
Aerodynamic characteristics of slender delta wings to show performance under various conditions of airspeed, angle of attack, and ground effect
[NASA-TT-F-14949] 17 p1983 N73-26031
Flight control and flight transition problems of Dassault Mirage 3 [5] aircraft
18 p2102 N73-27002
Design, development, and flight characteristics of VAK 191 B V/STOL strike/reconnaissance aircraft
18 p2103 N73-27006
Computer simulation of aircraft motions and propulsion system dynamics for YF-12 aircraft under supersonic conditions
[NASA-TM-X-62245] 20 p2361 N73-28990
Mariner 9 space probe storage subsystem for flight performance
[NASA-CR-133653] 20 p2475 N73-29884
Model 2914 series Delta launch vehicle configuration
[NASA-TM-X-70455] 21 p2599 N73-30833
Aerodynamic characteristics of low speed flight using heavily loaded ducted fans, single bladed hovering rotor, and tensioned sheets with cutouts
[AD-764264] 22 p2616 N73-30964
Flight instrumentation for academic acquisition of aircraft flight performance and characteristics
[AD-764479] 22 p2675 N73-31427

**FLIGHT CONDITIONS**
Computer program for calculating Concorde aircraft flight profiles for various flight procedures and atmospheric conditions
[RAE-TR-72102] 16 p1861 N73-25074
Time shift effects on human 17-hydroxy corticosteroid diurnal excretion noting transmeridian flights
[DLR-FB-73-58] 21 p2501 N73-30070

**FLIGHT CONTROL**
NT AUTOMATIC FLIGHT CONTROL
NT AUTOMATIC LANDING CONTROL
NT FLY BY WIRE CONTROL
NT POINTING CONTROL SYSTEMS
NT THRUST VECTOR CONTROL
Development of adaptive controller for multivariable systems and application to helicopter system with time varying parameters
[AD-746492] 01 p0002 N73-10007
Manual flight control and emergency procedure task skill degradation
[NASA-CR-128612] 01 p0020 N73-10153
Fixed base flight simulator evaluation of wing spoilers for longitudinal flight path control of Cessna aircraft during instrument landing system approach
[NASA-CR-2121] 02 p0125 N73-11015
Weapon delivery accuracy of F-4 aircraft with experimental stick to rudder interconnect to minimize lateral tracking error
[AD-746000] 02 p0126 N73-11027
Construction of pitch link in CH-47 helicopter control system using composite materials of graphite, glass, and carbon-steel
[AD-747337] 02 p0127 N73-11036
Space shuttle orbiter guidance and control software functions for horizontal flight operations
[NASA-TM-X-68857] 02 p0207 N73-11682
Atmosphere Explorer Control System for automatic control of AE spacecraft and experiments
[NASA-TM-X-66086] 02 p0232 N73-11888
Guidance system for beam-rider projectiles
04 p0447 N73-13647
Control system for rockets during combustion
[REPT-13-PT-2] 04 p0463 N73-13776
Addition of feel augmentation system to improve flight control of S-67 helicopter
[AD-749284] 05 p0494 N73-14029
Analysis of compatibility between maneuver load control, relaxed static stability, and flying qualities requirements for various aircraft configurations
[AD-749479] 05 p0495 N73-14032
Development and characteristics of automatic control system for aeroelastic aircraft using optimal gain in stabilization loops
[AD-750501] 06 p0624 N73-15061
Application of optimal control theory to take-off of heavily loaded helicopters and instrumentation requirements to improve pilot flight control
[AD-750615] 06 p0625 N73-15072
Oculogravic illusion factor in theoretical model of pilot control loss in jet aircraft
06 p0633 N73-15142
Analysis of controllability and steady-state response of parallel-redundant flight control systems
[NASA-CR-130354] 07 p0737 N73-15998
Time vector technique for determining stability and control derivatives by simultaneous analysis of two maneuvers which differ by dependent control input
[NASA-TM-X-2722] 07 p0739 N73-16010
Development of adaptive control system for atmospheric reentry vehicle to meet flying quality requirements
07 p0848 N73-16871
Simulation of flight in Concorde for improving characteristic of flight control system
08 p0866 N73-17013
Design and development of stability augmentation system to eliminate coupling effects during landing of short takeoff aircraft
[NASA-CR-130543] 08 p0867 N73-17021
Performance tests of reentry vehicle control with base plane thrusters and fluidic control logic
[SC-DC-72-2244[RD]] 09 p0985 N73-18043
Flight control improvement of F-8 aircraft relative to carrier takeoff and landing
[AD-753010] 09 p0986 N73-18052
Development of integrated control system for supersonic aircraft based on pneumatic power generation
10 p1111 N73-19056
Measurements of acceleration stress effects on pilot maneuvering ability and flight control performance
[AMRL-TR-72-3] 10 p1123 N73-19154
Characteristics of system for providing yaw control of vehicles at high supersonic and hypersonic speeds by deflecting flaps mounted on upper wing surface
[NASA-CASE-LAR-11140-1] 11 p1233 N73-20008
Proceedings of conference on manual control to show interplay between man and machine and application of control theory in medicine and psychology
[NASA-CR-131244] 11 p1235 N73-20028
Design of hydrofluidic flight control system for helicopter stabilization
[AD-754602] 11 p1236 N73-20032
Human factors engineering for flight control/display system with on-line terminal
[AD-754916] 11 p1250 N73-20148
Evaluation of high response electrohydraulic digital control valve for application to flight control systems
[NASA-CR-124178] 11 p1297 N73-20523
Contributions of quality inertial system to vehicle flight control
11 p1318 N73-20700
Digital flight director for precise aircraft control
[AD-754028] 11 p1322 N73-20726
Bibliography of supersonic transport aircraft data to include program management, systems engineering, aircraft structures, and operational considerations
[AD-755600] 12 p1365 N73-21076
Application of adaptive control algorithms to self adjusting control systems for aeroelastic aircraft, flight vehicle roll, and control during reentry
[AD-756598] 13 p1474 N73-21941
Feasibility of advanced digital flight control system using digital processor as main computational element
[AD-757271] 14 p1604 N73-23002
Flight control system using tactile displays under instrument flying conditions
[AD-757344] 14 p1669 N73-23543
Development of stability augmentation systems for decoupling response of short takeoff and landing aircraft in longitudinal and lateral-directional flight modes
15 p1732 N73-24041
Characteristics of flight control system for approach flight path control of augmentor wing on powered-lift short takeoff aircraft configuration
[NASA-CR-114574] 15 p1734 N73-24062
Development and evaluation of display and control equipment for remotely piloted vehicles
[AD-757761] 15 p1736 N73-24077
Integrated digital flight control system for space shuttle orbiter
[NASA-CR-128936] 15 p1834 N73-24871
Computer programs for design of aircraft control systems based on FORTRAN subroutines for generating aircraft transfer functions in six degrees of freedom
[AD-758781] 16 p1861 N73-25615
Development of flight simulator system to show position of joystick displacement
[NASA-CASE-NPO-11497] 16 p1878 N73-25206
Optimal design of helicopter precision hover control systems
[AD-759919] 17 p1984 N73-26039
Design of landing approach automatic flight control system using optimal feedback techniques
[AD-760125] 17 p1984 N73-26040
Flight control and flight transition problems of Dassault Mirage 3 [5] aircraft
18 p2102 N73-27002
Development and characteristics of control system for short takeoff transport aircraft for ride-smoothing effect
[NASA-CR-2276] 18 p2105 N73-27026
Development of analog hardware for flight control system design to control aircraft with uncertain parameters
[NASA-CR-133416] 19 p2220 N73-27909
Analysis of performance benefits for fighter aircraft by application of maneuver load control and relaxed static stability parameters
[AD-762299] 19 p2222 N73-27922
Logistic performance data book for F-4E flight control system to show reliability, maintainability, logistic support, and operating problems
[AD-762230] 19 p2358 N73-28973
Development of digital flight control system for performing pilot assist augmentation and pilot relief automatic pilot functions
[AD-762521] 20 p2361 N73-28992
Design, development, airworthiness test, and flight test of multiplexing components for fly by wire flight control
[AD-763111] 20 p2362 N73-28996
Analysis of aircraft stability and control derivatives in turbulent conditions subject to random state disturbance
[AD-763741] 21 p2498 N73-30046
Development of theory for adaptive control of aircraft in atmospheric turbulence using stochastic identification method
[AD-763739] 21 p2498 N73-30051
Integrated digital flight control system for rotational and translational control of space shuttle orbiters
[NASA-CR-134001] 21 p2600 N73-30835
Application of active control technology for suppression of flutter with analysis of effect on B-52 aircraft configuration
[NASA-TM-X-2909] 21 p2603 N73-30864
Development and characteristics of system for integrated control of engine power and aerodynamic configuration of aircraft during landing approach
[NASA-CASE-ARC-10456-1] 22 p2613 N73-30938
Design of aircraft lateral flight director
[DLR-FB-72-44] 22 p2614 N73-30953
Algorithm for calculating correcting signals in flight control systems with high speed digital computer
[AD-764310] 22 p2640 N73-31157

Flight test of structural mode control system installed in XB-70 aircraft to determine effectiveness of system under turbulent conditions
[NASA-TN-D-7420] 23 p2742 N73-31950
Stability and control characteristics of XB-70 aircraft at airspeeds up to Mach 3.0 and addition of lateral bobweight as auxiliary stabilization device
[NASA-TM-X-2933] 23 p2743 N73-31958
Flight control for steep approach landing
[DGLR-PAPER-73-027] 23 p2744 N73-31962
Feedback control for rotary wing aircraft steep approach profiles
[MBB-UFE-1021-O] 23 p2744 N73-31967
Design, development, and evaluation of automatic departure prevention system and stall inhibitor for A-7 aircraft
[AD-764767] 23 p2745 N73-31972
Flight control display device for producing curved approach profiles in microwave instrument landing systems
[DGLR-PAPER-73-016] 23 p2818 N73-32526
Feasibility of actively guiding sounding rockets to reduce impact dispersion at White Sands Missile Range
[NASA-TM-X-70474] 23 p2851 N73-32780
Flight simulation to determine manual control of flight path and airspeed for approach and landing of powered lift jet short takeoff aircraft
24 p2873 N73-32949
Requirements of flight control systems with regard to aircraft stability and attitude control
[DLR-MITT-72-05] 24 p2877 N73-32978
Nonlinear feedback control concepts for variable stability aircraft
24 p2877 N73-32979
Optimization of control and damping system for fighter aircraft with quadratic cost function
24 p2877 N73-32980
Airborne computer role in digital flight control systems, noting systems model, man machine interface, and integration
24 p2878 N73-32982
DO-31 aircraft integrated flight control system for vertical velocity regulation in gliding, noting signal processing requirements
24 p2878 N73-32983
VAK 191 B V/STOL fighter aircraft nonlinear feedback flight control system for gliding flight phase
24 p2878 N73-32984
Design optimization and testing of flight control systems for light helicopters, applied to BO-105 helicopter
24 p2878 N73-32985
Effect of artificial longitudinal stability on aircraft performance, based on control configured vehicle concept
24 p2878 N73-32986
Effects of artificial aircraft stability control on damping, and static stability recovery by controllers
24 p2878 N73-32987
Design of pitching axis control system for aircraft with artificial stability
24 p2878 N73-32988
Vibration tests of flight control moment gyros and bearing life test fixtures
[NASA-CR-124449] 24 p2926 N73-33365

**FLIGHT CREWS**
Method for calculating aircrew radiation dosage near atmospheric nuclear weapon detonation
[AD-745084] 01 p0010 N73-10079
Statistical analysis of occurrence of backache among Royal Air Force flight crews and ground crews to show effects of crew seats on physical comfort
[AD-745177] 01 p0013 N73-10102
Test evaluation of laser protective visors for flight crews
[AD-751470] 07 p0751 N73-16102
Noise effects on hearing conservation in aircrew and ground support personnel of aerospace operations
08 p0876 N73-17101
Aircrew escape autogyro ejector seat/flight vehicle
09 p1089 N73-18890
Influence of cockpit noise on hearing in flight crew personnel
[FAA-AM-72-32] 10 p1119 N73-19125
Combined heat, noise, and vibration effects on aircrew performance
[AMRL-TR-71-113] 10 p1122 N73-19146
AGARD conference on air-to-ground target acquisition
[AGARD-CP-100] 10 p1225 N73-19959
Effect of briefing information on target acquisition performance of observer
10 p1227 N73-19972
Use of Kelly Repertory Grid Techniques for assessing subjective estimates of important parameters for target acquisition
10 p1227 N73-19973
US civil airmen statistics
[AD-754271] 11 p1251 N73-20153
Physiological aspects of sleep induction in aircrews after prolonged flight times
12 p1369 N73-21108
Analysis of nonfatal injuries to passengers and flight attendants in airline operations during period 1968 through 1971
[NTSB-AAS-73-1] 14 p1601 N73-22983
Effect of cigarette smoking on sensory perception and performance parameters of flight crews
[AD-754421] 14 p1612 N73-23071
Analysis of escape systems for helicopter flight crews and passengers
[B-177166] 15 p1734 N73-24067
Color vision standards for flying military aircrews
[FPRC/1319] 19 p2225 N73-27942
Analysis of US Navy aviation combat casualty experiences in Southeast Asia to determine effectiveness of rescue and recovery operations under combat conditions
[AD-761636] 19 p2228 N73-27972
Analysis of flight crew errors contributing to aircraft accidents on P-3 and F-4 aircraft for improved air safety
[AD-764868] 23 p2746 N73-31979

**FLIGHT FATIGUE**
Physiological stresses and medical criteria for aircrew fatigue
06 p0634 N73-15152

**FLIGHT FITNESS**
Conference on detection, evaluation, and identification of drugs and alcohol in flying personnel and effects on flight fitness
[AGARD-CP-108] 12 p1368 N73-21102
Diagnostic physiological tests for selection and training of flying personnel
[NASA-TT-F-687] 13 p1479 N73-21981
Oxygen breathing effects on human blood circulation and flight personnel fitness test
13 p1480 N73-21993
Conditioned reflex motion sickness test of statokinetic fitness for flying personnel
13 p1480 N73-21994
Barany chair rotation for acceleration tolerance testing on flying personnel
13 p1480 N73-21995
Diurnal cardiac rhythm fluctuation for cardiovascular evaluation of flight personnel
13 p1480 N73-21997
Age limits and flight fitness of civil aviation pilots
13 p1481 N73-21999
Middle ear barotrauma effect on work capacity and flight fitness of flying personnel
13 p1481 N73-22000
Syringomyelia in central nervous system affecting flying fitness
14 p1611 N73-23061

**FLIGHT HAZARDS**
NT METEOROID HAZARDS
Inflight incident involving Boeing 747 aircraft encounter with unforecast clear air turbulence during flight from Japan to Hawaii on 12 April 1972
[NTSB-AAR-72-27] 03 p0252 N73-12038
In flight incident involving near miss of Boeing 720 aircraft and Convair 240 aircraft near Front Royal, Virginia on 26 Apr. 1972
[NTSB-AAR-72-30] 03 p0252 N73-12040
Aircraft accident and incident reports for general aviation during 1970
[NTSB-BA-72-5] 04 p0371 N73-13015
Compilation and analysis of selected US civil aviation accidents for calendar year 1971
[NTSB-BA-72-4] 04 p0371 N73-13017
Aircraft accident involving Lear jet model 25 at Victoria, Texas on 18 Jan. 1972
[PB-212484] 06 p0625 N73-15076
Crash of DC-8 aircraft during takeoff from Anchorage International Airport, Alaska on 27 Nov. 1970
[NTSB-AAR-72-12] 07 p0737 N73-15999
Bibliography of aircraft accident reports for US civil aviation operations during calendar year 1971
[NTSB-BA-72-7] 07 p0738 N73-16002
Aircraft accident involving DH-114 aircraft during attempted landing at Mercedita Airport, Puerto Rico on 24 June, 1972
[NTSB-AAR-72-34] 07 p0738 N73-16004
Aircraft accident involving DC-9 aircraft landing at Fort Lauderdale, Florida airport in marginal weather conditions on 18 May, 1972
[NTSB-AAR-72-31] 07 p0738 N73-16005
Analysis of factors affecting crashworthiness of light aircraft to show nature of damage to aircraft and hazards to flight crews
[FAA-TR-FS-70-592-120A] 09 p0984 N73-18032
Effect of high intensity laser outputs on behavior and physiology of birds to determine application for reduction of flight hazards
[AD-754269] 11 p1236 N73-20038
Analysis of aircraft accidents occurring in US Civil Aviation operations during calendar year 1972
[NTSB-APA-73-1] 14 p1601 N73-22980
Aircraft accident reports of US civil aviation accidents occurring during calendar year 1972
[NTSB-BA-73-2] 15 p1734 N73-24064
Aircraft accidents involving US civil aviation operations during calendar year 1972 - Vol. 2
[NTSB-BA-73-3] 16 p1860 N73-25064
Aircraft accidents involving US civil aviation operations in calendar year 1971
[PB-214412/9] 16 p1862 N73-25078
Reports of aircraft accidents occurring in US civil aviation operations during calendar year 1972 - Issue 3
[NTSB-BA-73-4] 17 p1982 N73-26020
Statistical analysis of aircraft accidents and incidents occurring to US civil and commercial aircraft during calender year 1971 - Supplemental Issue
[NTSB-BA-73-5] 17 p1983 N73-26028
Statistical analysis of aircraft accidents occurring in US civil aviation operations during calendar year 1972 - Issue 4
[NTSB-BA-73-6] 18 p2105 N73-27024
Analysis of flight hazards caused by bird strikes on aircraft flying in Panama Canal Zone
[AD-763112] 20 p2362 N73-28997
Analysis of meteorological parameters affecting safety of civil aviation and instructions for increased flight safety
[NASA-TT-F-15069] 21 p2495 N73-30028
Reduction of midair collision hazard with bats through tracking by radar and use of high intensity lights
[AD-764828] 23 p2746 N73-31982
Bird migration patterns using radio transmitters with application to reduction of aircraft hazards during migration in congested air routes
[AD-764830] 23 p2746 N73-31983
Analysis of random motions of vortex elements behind aircraft wing and design of vortex arrays to reduce wake-vortex to small aircraft
[NASA-TM-X-62304] 24 p2877 N73-32976

**FLIGHT INSTRUMENTS**
NT APPROACH INDICATORS
NT ATTITUDE INDICATORS
NT AUTOMATIC PILOTS
NT GYRO HORIZONS
NT HORIZON SCANNERS
NT RADIO ALTIMETERS
Analysis of pilot performance in evaluating three types of aircraft altimeters during C-135B simulator flight
[ASD-TR-72-63] 04 p0383 N73-13117
Research reports on control theory in flight systems
[AD-746296] 05 p0523 N73-14251
Design and performance tests of solid state A-6 aircraft engine instruments
[AD-760351] 17 p2035 N73-26469
Flight tests of cockpit meter instrumentation system displaying aircraft specific energy and energy rate
[AD-763450] 21 p2550 N73-30448
Flight instrumentation for academic acquisition of aircraft flight performance and characteristics
[AD-764479] 22 p2675 N73-31427
Terrain proximity warning system using downward looking radar for improved flight safety
[FAA-RD-73-134] 22 p2697 N73-31603

**FLIGHT MECHANICS**
Stability and control systems for advanced aircraft flight mechanics and safety
[AGARD-AR-48] 04 p0371 N73-13018
Aerospace sciences and flight mechanics research projects
04 p0487 N73-13975
Flight mechanics of rotary wing aircraft
[DLR-MITT-71-15] 05 p0493 N73-14021
Digital simulation language for flight dynamic tests, expemplified by Fiat G-91 and Dornier Do-31 aircraft
[BMVG-FBWT-72-21] 07 p0740 N73-16019
Influence of aeroelasticity on flight mechanics of flexible aircraft
08 p0864 N73-16991
Flight control and flight transition problems of Dassault Mirage 3 [5] aircraft
18 p2102 N73-27002
Abstracts on research projects inclusive of flight dynamics to heating of swimming pools using solar collector
[ISBN-0-85494-200-9] 21 p2609 N73-30910

**FLIGHT OPTIMIZATION**
Mathematical model for optimal control of spacecraft flight considering error and perturbation factors
10 p1178 N73-19583
Computer program for calculating Concorde aircraft flight profiles for various flight procedures and atmospheric conditions
[RAE-TR-72102] 16 p1861 N73-25074
Development of techniques for real time, on-line, optimum flight path conditions and minimum time maneuvers for supersonic aircraft
[AD-758799] 16 p1862 N73-25083

**FLIGHT PATHS**
NT GLIDE PATHS
Fixed base flight simulator evaluation of wing spoilers for longitudinal flight path control of Cessna aircraft during instrument landing system approach
[NASA-CR-2121] 02 p0125 N73-11015
Statistical analysis of normal acceleration, airspeed, altitude, and flight loads on military aircraft
[AD-747285] 02 p0127 N73-11035

Optical control theory and energy-state approximation to determine parameters for minimum time flight path of supersonic aircraft
[AD-748219] 03 p0329 N73-12689
Calculation of optimal gliding flight paths associated with space shuttle orbiter transition from entry to cruising flight
[NASA-CR-128647] 03 p0359 N73-12922
Migration corridors for ducks and geese and effects on aviation safety
[AD-748114] 04 p0382 N73-13109
Thunderstorm probability and supersonic transport safety on flight paths over southern United States during July
[AD-748798] 04 p0445 N73-13628
Carrier based air trafic control system with enroute trajectory optimization capability and computer-aided marshal reassignment procedure
[AD-748302] 04 p0447 N73-13651
Development of flight path optimization procedure to minimize flight time of aircraft returning to aircraft carrier
[AD-749326] 04 p0447 N73-13653
Compilation of Instrument Flight Rules Off-Airway Non-95 Routes for US and Alaska, November 1972
05 p0577 N73-14696
Tabulation of minimum enroute instrument flight rules altitudes over particular routes and intersections - November 1972
06 p0697 N73-15679
Flight simulator evaluations of flight control, flight path, and airspeed for approach and landing of powered lift jet short takeoff aircraft
[NASA-TM-X-62203] 07 p0739 N73-16014
Analysis of military helicopter formation flight techniques with emphasis on station keeping based on nominal point coordinate system
[AD-751459] 07 p0740 N73-16021
Evaluation of head-up display instrument for providing aircraft vertical guidance during landing approach to comply with noise abatement procedures
[NASA-TM-X-62187] 09 p0982 N73-18021
Analysis of aircraft tracking techniques to show sensitivity of tracking performance to data environment
[AD-753114] 09 p1063 N73-18667
Probability of acquiring targets by search aircraft which flies along enemy line of communication
10 p1226 N73-19971
Evaluation of energy maneuverability procedures in aircraft flight path optimization and performance estimation
[AD-754909] 11 p1236 N73-20035
Aircraft accident involving crash of Cessna 182 aircraft near Duluth, Minnesota airport on 8 Nov. 1972
[NTSB-AAR-73-10] 14 p1604 N73-23006
Characteristics of flight control system for approach flight path control of augmentor wing on powered-lift short takeoff aircraft configuration
[NASA-CR-114574] 15 p1734 N73-24062
Development of techniques for real time, on-line, optimum flight path conditions and minimum time maneuvers for supersonic aircraft
[AD-758799] 16 p1862 N73-25083
Numerical analysis of space shuttle orbiter flight path and performance during approach guidance from space mission - Document 22
[NASA-CR-128962] 16 p1941 N73-25707
Development of equations of motion for energy dissipation phase of shuttle reentry and landing approach - Document 23
[NASA-CR-128960] 16 p1941 N73-25709
Operational procedures and modes of experimental guidance system for short takeoff aircraft to provide arrival time control and automatic tracking
[NASA-TM-X-62233] 16 p1941 N73-25710
Flight evaluation of glide slope determination during landing approach by reference to diamond shaped figure painted on runway
[NASA-TM-X-2849] 18 p2105 N73-27027
Flight test F-106 aircraft to determine comparative time advantages of energy optimization climb and acceleration methodology
[AD-760571] 18 p2107 N73-27041
Analysis of factors affecting approach and landing of aircraft under visual conditions to show causes of misjudgement resulting in aircraft landing accidents
[NASA-TT-F-15054] 20 p2360 N73-28980
Development of computer program to predict aerodynamic noise levels of V/STOL aircraft at various points in flight trajectory
[PB-221140/7] 21 p2499 N73-30054
User manual for Los Angeles Basin Standard Traffic Model
[FAA-RD-73-89] 21 p2576 N73-30647
User manual for Los Angeles Standard Traffic Model computer tapes
[FAA-RD-73-88] 21 p2577 N73-30649
Statistical analysis of aircraft carrier wave-off situation based on deck motion and aircraft approach geometry
[AD-764516] 22 p2616 N73-30967
Technology for evaluating ground station sites based on effectiveness in disseminating time synchronization
[FAA-RD-73-102] 23 p2770 N73-32155
Short haul aircraft operations in terminal area with concurrent conventional aircraft operations to show methods for improved utilization of facilities
24 p2874 N73-32953
Meteorological and weather effects on aircraft landings and flights along air lanes and stratospheric wind effects on supersonic transports
[JPRS-60114] 24 p2945 N73-33522
Effect of spatial variability of wind in stratosphere on flight of supersonic transports
24 p2946 N73-33529

**FLIGHT PERFORMANCE**
U FLIGHT CHARACTERISTICS

**FLIGHT PLANS**

Optical control theory and energy-state approximation to determine parameters for minimum time flight path of supersonic aircraft
[AD-748219] 03 p0329 N73-12689
Analysis of flight plans submitted at flight service stations for IFR and VFR flight clearances during calendar year 1971
[AD-748901] 04 p0447 N73-13652
Development of flight path optimization procedure to minimize flight time of aircraft returning to aircraft carrier
[AD-749326] 04 p0447 N73-13653
Flight plan position extrapolation in automated oceanic air traffic control system
[FAA-RD-73-72] 21 p2576 N73-30648
Score, approach, and major results of study of ballistic mode Mercury orbit missions
[NASA-CR-114617] 22 p2715 N73-31733
Scope, approach, and major results of study of ballistic mode of Mercury orbit missions
[NASA-CR-114618] 22 p2715 N73-31734

**FLIGHT RULES**
NT INSTRUMENT FLIGHT RULES
NT VISUAL FLIGHT RULES

**FLIGHT SAFETY**

System safety program plan for aviation accident prevention
[AD-746995] 03 p0253 N73-12048
Aircraft accident and incident reports for general aviation during 1970
[NTSB-BA-72-5] 04 p0371 N73-13015
Compilation and analysis of selected US civil aviation accidents for calendar year 1971
[NTSB-BA-72-4] 04 p0371 N73-13017
Carrier based air trafic control system with enroute trajectory optimization capability and computer-aided marshal reassignment procedure
[AD-748302] 04 p0447 N73-13651
Identification of human factors research projects in support of civil aviation for accomplishment by NASA research centers
05 p0493 N73-14015
Characteristics of air traffic control system to include components of system and application of automation to obtain system safety
[MTR-6152-REV-1] 05 p0577 N73-14698
Development and characteristics of terminal area simulation for analysis of air traffic control requirements and improvement in flight safety conditions
[NASA-CR-112195] 05 p0577 N73-14699
Analysis of Canadian air traffic control system to include human factors aspects, automation, and environmental engineering
[DCIEM-825] 06 p0696 N73-15670
Analysis of Air Traffic Control Radar Beacon System performance and effects on several Air Route Traffic Control Centers
[ECAC-PR-72-023] 06 p0696 N73-15678
Tabulation of minimum enroute instrument flight rules altitudes over particular routes and intersections - November 1972
06 p0697 N73-15679
Demand and trade study related to development of air traffic control system based on geographical regions - Vol. 3
[PB-212180] 06 p0698 N73-15690
Electrostatic charging and discharging of helicopters in flight and personnel safety
[AD-750617] 06 p0701 N73-15718
Bibliography of aircraft accident reports for US civil aviation operations during calendar year 1971
[NTSB-BA-72-6] 07 p0738 N73-16001
Survey of Air Traffic Control Beacon System to determine occurrence of excessive interrogation signals within New York air control sector - Final Report
[ECAC-PR-72-031] 07 p0818 N73-16630
Problems of flight safety in air traffic control with increased volume of traffic
[DGLR-PAPER-72-038] 07 p0818 N73-16632
Development of digital fast-time air traffic control conflict prediction models and application to specific air route traffic control situations
[UTIAS-TN-183] 08 p0941 N73-17708
Helicopter flying in poor light and featureless terrain and color vision abnormality
10 p1113 N73-19075
Proceedings of symposium on flight operations and air traffic control to show problems affecting airports, general aviation, air traffic controllers, and governmental agencies
[DLR-MITT-72-24] 10 p1183 N73-19623
Analysis of general aviation activities in Germany and recommendations for flight control procedures to reduce aircraft accident hazards
10 p1183 N73-19626
Analysis of problems in air traffic control caused by expansion of commercial and civil aviation in Germany and proposed actions for improved safety and efficiency
10 p1183 N73-19627
Requirements for air traffic control in German air operations and recommendations for improved air traffic control procedures
10 p1183 N73-19628
Development of computer programs for design of air route networks for improved flight safety - Part 1
[FAA-RD-72-118-1-PT-1] 10 p1185 N73-19643
Development of systematic methodology and computer programs for optimal design of national grid of high altitude VHF omnirange navigation systems - Part 2
[FAA-RD-72-118-2-PT-2] 10 p1185 N73-19644
Development of gradient clearance monitor concept to ascertain glide slope clearance signal
[FAA-RD-72-147] 10 p1185 N73-19645
Analysis of effects of automation on productivity and efficiency of air traffic control and flight services
[MTR-6110] 10 p1185 N73-19646
Effect of high intensity laser outputs on behavior and physiology of birds to determine application for reduction of flight hazards
[AD-754269] 11 p1236 N73-20038
Research and development projects of Federal Aviation Administration to provide improved weather data acquisition and distribution
[FAA-ED-15-1] 11 p1314 N73-20662
Analysis of interaction of major elements of Oceanic Air Traffic Control System to determine minimum longitudinal and lateral separation distances
[FAA-RD-73-8] 11 p1321 N73-20719
Research and development projects conducted by Federal Aviation Administration to improve air traffic control and flight safety
[FAA-EM-73-2] 11 p1321 N73-20720
Functional error analysis and simulation of air traffic control system to support concepts evaluation program
[PB-213148] 11 p1322 N73-20730
Analysis of aircraft pilot capability to visually detect other aircraft in air to air situation as collision avoidance feasibility
[FAA-RD-73-40] 12 p1374 N73-21145
Performance tests to determine capability of aircraft pilots to avoid midair collisions based on visual perception of target and information from pilot warning indicator
12 p1374 N73-21146
Photographic recording of aircraft in near midair collision conditions to determine feasibility of collision avoidance based on visual perception of pilot
[CDC-JL-5] 12 p1374 N73-21147
Analysis of flight tests to determine range of visual detection of aircraft as basis for visual perception to avoid midair collisions
12 p1374 N73-21148
Development of collision avoidance warning system criterion for use with aircraft operating in high density areas
13 p1471 N73-21915
Development of wake vortex avoidance system for airports to reduce hazards caused by aircraft wakes and permit increased utilization of terminal facilities
[FAA-ED-21-1] 14 p1645 N73-23342
Proceedings of conference on air traffic control developments and procedures
[AGARD-CP-105] 14 p1687 N73-23689
Air traffic control facilities operated by U.S. military forces and developments in improved air traffic control systems
14 p1687 N73-23690
Characteristics of air traffic control system to include description of electronic components and projects for developing improved equipment
14 p1687 N73-23692
Organization, functions, and capabilities of automated air traffic control system for Rome, Italy
14 p1687 N73-23694
Analysis of North Atlantic air route structure to determine impact of inertial navigation and satellite surveillance on separation reduction
14 p1688 N73-23699
Analysis of terminal air traffic control procedures to determine impact of automation on air traffic controller personnel
14 p1688 N73-23700
Development and characteristics of air traffic management system for operation of military aircraft under instrument meteorological conditions
14 p1689 N73-23704

Development and characteristics of microwave landing system with emphasis on functional design requirements for airborne equipment
14 p1689 N73-23705
Development and characteristics of system for separation and control of aircraft to avoid midair collisions
14 p1690 N73-23712
Analysis of man-machine interfaces and system reliability for air traffic control automation systems
14 p1690 N73-23715
Conceptual analysis of improved communication, navigation, and indentification system for military applications
14 p1690 N73-23719
Analysis of factors affecting flight of multi-engine aircraft with one engine inoperative
[NASA-TT-F-734] 15 p1734 N73-24060
Proceedings of conference on operational problems of air traffic control beacon system
[FAA-NA-72-80] 16 p1940 N73-25702
Evaluation of pilot assurance value of airborne display device for monitoring air traffic in high density terminal airspace
[AD-749280] 17 p2011 N73-26267
Flight evaluation of glide slope determination during landing approach by reference to diamond shaped figure painted on runway
[NASA-TM-X-2849] 18 p2105 N73-27027
Development of mathematical model for determining replacement criteria for aircraft structural components
[AD-762226] 19 p2222 N73-27921
Analysis of pilot performance and short takeoff aircraft characteristics during landing approach
[AD-762566] 20 p2362 N73-29000
Development, characteristics, and operation of test facility for determining effectiveness of runway lighting systems under various atmospheric conditions
[FAA-RD-71-94] 20 p2382 N73-29141
Development and characteristics of radar system for improved air traffic control
[FAA-RD-73-100] 20 p2452 N73-29703
Development of computer model to simulate air traffic conditions in Los Angeles, California area in 1982
[MTR-6386] 20 p2452 N73-29706
Analysis of factors affecting feasibility of minimizing runway spacings for increased air terminal operational capacity - Vol. 2
[FAA-RD-72-58-VOL-2] 20 p2452 N73-29709
Status of civil airline implementation of all-weather landings in Europe and United Kingdom
[MTR-6211] 20 p2452 N73-29711
Objectives, scope of work, and funding requirements of research project for improvement of aircraft safety
[FAA-ED-18-1] 21 p2493 N73-30008
Simulation tests of short takeoff transport aircraft to determine airport and air space requirements under normal operating conditions
[NASA-TN-D-7300] 21 p2495 N73-30026
Analysis of meteorological parameters affecting safety of civil aviation and instructions for increased flight safety
[NASA-TT-F-15069] 21 p2495 N73-30028
Development and characteristics of electronic signalling system and data processing equipment for warning systems to avoid midair collisions between aircraft
[NASA-CASE-LAR-10717-1] 21 p2576 N73-30641
Development of discrete address beacon system for application to air traffic control operations
[FAA-RD-73-101] 21 p2577 N73-30651
Statistical analysis of air traffic conditions predicted for Los Angeles, California area in 1982 - Vol. 1
[MTR-6387-VOL-1] 21 p2577 N73-30653
Statistical analysis of air traffic conditions predicted for Los Angeles, California area in 1982 - Vol. 2
[MTR-6387-VOL-2] 21 p2577 N73-30654
National Transportation Safety Board studies in aircraft and surface transportation safety
21 p2609 N73-30909
Terrain proximity warning system using downward looking radar for improved flight safety
[FAA-RD-73-134] 22 p2697 N73-31603
Algorithms to determine potential conflicts over oceanic airspace based on vertical, lateral, and longitudinal separation criteria
[FAA-RD-73-73] 22 p2697 N73-31606
Flight paths for short takeoff aircraft landing approach consistent with pilot preference passenger comfort, and microwave landing system limitations
[NASA-TN-D-7298] 23 p2742 N73-31949
Test data and description of unsymmetrical crash analysis computer program for improved helicopter structural crashworthiness analytical and design techniques - Vol. 2
[AD-764986] 23 p2747 N73-31986
Analysis and simulation of intermittent positive control of air traffic by fully automated ground facility
23 p2816 N73-32511
Restructuring of oceanic air traffic control airspace jurisdictional boundaries in presence of satellite system
[FAA-RD-73-59] 24 p2951 N73-33570
Computer model of Los Angeles, California air traffic control situation to predict conditions expected by 1982
[AD-765153] 24 p2951 N73-33571

**FLIGHT SIMULATION**

Development of computer program for complete simulation of factors involved in aircraft takeoff and landing
[AD-741942] 01 p0006 N73-10042
Visual image generation as textured flight information resembling retinal images for airborne flight simulation
01 p0017 N73-10128
Spacecraft simulation techniques applicable to flight simulator motion systems
[NASA-CR-128653] 04 p0401 N73-13266
Error analyses of satellite orbital parameters based on simulations of observational variances, observation equations, and normal equations
[NASA-CR-130357] 06 p0720 N73-15878
Summary of conference on flight simulation
08 p0864 N73-16992
Role of flight simulation in development of S-3 and F-14 aircraft
08 p0865 N73-17001
Simulation of flight in Concorde for improving characteristic of flight control system
08 p0866 N73-17013
Measurement of pilot performance during aircraft landing simulation to determine significance of vertical acceleration cues during approach and landing maneuver
[NASA-TM-X-62236] 08 p0867 N73-17020
Comparison of validity of results obtained by flight simulation with results obtained from actual flight test of short takeoff aircraft
10 p1105 N73-19007
Software conceptual designs for space shuttle simulator requirements
[NASA-CR-128882] 11 p1266 N73-20270
Biaxial simulator imposing standardized coriolis stimuli for selection, test, and rehabilitation of motion sick pilots
12 p1368 N73-21098
Bench testing ducted fan engines under conditions close to those of flight
[AD-742376] 13 p1505 N73-22198
Analysis of minimum longitudinal stability for large delta wing transport aircraft during landing approach and touchdown using inflight simulator
[TR-5084-F-1-VOL-1] 14 p1601 N73-22984
Standardized load sequence for flight simulation tests on transport aircraft wing structures
[LBF-BERICHT-FB-106] 14 p1602 N73-22986
Simulation of satellite motion in ionospheric plasma using low energy and high current ion source in vacuum chambers
[ONERA-NT-202] 15 p1762 N73-24280
Performance of pilots under simulated conditions to determine response to anti-collision warnings
[FAA-AM-73-6] 18 p2104 N73-27015
Analysis of minimum longitudinal stability for large delta wing transport aircraft during landing approach and touchdown using in-flight simulation techniques
[AD-761120] 18 p2106 N73-27036
Simulator tests to determine short takeoff transport aircraft terminal area characteristics and longitudinal handling qualities
[MDC-J5575L] 20 p2360 N73-28983
Real time piloted simulation to investigate handling qualities and performance of tilting rotor aircraft - Vol. 9
[NASA-CR-114602] 21 p2493 N73-30012
Aircraft flutter analog simulation noting structural nonlinearity effects
[DLR-FB-73-30] 22 p2615 N73-30954
Pilot performance under simulated conditions of modified aircraft control dynamics, navigational task complexity, and induced stress
[AD-764760] 23 p2752 N73-32025
Simulations of powered-lift STOL transport aircraft with either externally blown flap configuration or augmentor wing configuration
24 p2873 N73-32948
Flight simulation to determine manual control of flight path and airspeed for approach and landing of powered lift jet short takeoff aircraft
24 p2873 N73-32949
Flight simulation to determine effectiveness of head-up display for improving glide-slope tracking performance during steep visual approach of short takeoff aircraft
24 p2874 N73-32952
Dynamic flight simulation of Symphonie satellite attitude control system
[DGLR-PAPER-73-045] 24 p2986 N73-33862

**FLIGHT SIMULATORS**

NT COCKPIT SIMULATORS

Simulated STOL aircraft flight to determine effects of cruise and terminal area maneuvers on ride quality and passenger comfort
01 p0003 N73-10016
Modeling data developed during manned simulation of large transport aircraft and comparison with training simulator results - Vol. 2
[NASA-CR-114494] 01 p0004 N73-10027
Effectiveness of synthetic fixed wing flight training equipment for military purposes
[AD-744447] 01 p0020 N73-10158
Performance characteristics of model VTOL lift-fan simulator installed in two dimensional wing
[NASA-TM-X-68788] 01 p0036 N73-10282
Fixed base flight simulator evaluation of wing spoilers for longitudinal flight path control of Cessna aircraft during instrument landing system approach
[NASA-CR-2121] 02 p0125 N73-11015
Definition of requirements for flight simulator to provide space shuttle systems and space mission analysis and performance - Vol. 1
[NASA-CR-128621] 02 p0229 N73-11860
Development of requirements for space shuttle vehicle and mission simulation - Vol. 2
[NASA-CR-128622] 02 p0230 N73-11861
Analysis of space shuttle systems and space shuttle mission requirements for development of mission simulator - Vol. 3
[NASA-CR-128623] 02 p0230 N73-11862
Test and evaluation of aural signal device to prompt students to scan for aircraft during flight simulator training
[FAA-RD-72-95] 04 p0373 N73-13030
Analysis of model helicopter rotor blade response to random excitation during simulated forward flight using electromechanical apparatus
[AD-748457] 04 p0374 N73-13040
Analysis of pilot performance in evaluating three types of aircraft altimeters during C-135B simulator flight
[ASD-TR-72-63] 04 p0383 N73-13117
Motion effects in pilot reactions to ground-based flight simulator display evaluation
[AD-749370] 04 p0384 N73-13126
Method for predicting flight characteristics of F-5 and A-7 aircraft during atmospheric turbulence using large amplitude flight simulator
[AD-749480] 05 p0495 N73-14030
Development and characteristics of six degree of freedom, fast time predictor model for simulation of F-4 aircraft landing on aircraft carrier
[AD-750294] 05 p0504 N73-14102
Flight simulator tests to define minimum acceptable levels of static longitudinal stability for aircraft landing approach following failure of stability augmentation systems
[NASA-TM-X-62200] 06 p0620 N73-15034
Validity of ground training for developing flying skill during pilot training
[AD-749621] 06 p0636 N73-15168
Operational effectiveness of jet flight training simulator
[AD-750248] 06 p0636 N73-15170
In-flight simulator [TIFS] of C-131 aircraft with capability of varying six degrees of freedom
[AD-750745] 06 p0651 N73-15286
Flight simulator evaluations of flight control, flight path, and airspeed for approach and landing of powered lift jet short takeoff aircraft
[NASA-TM-X-62203] 07 p0739 N73-16014
Design and implementation of fixed-based spin simulator, and spin test results
[AD-751644] 07 p0767 N73-16229
Feasibility of missile acceleration simulator based upon track accelerator concept
[AD-751128] 07 p0767 N73-16231
Analysis of simulated aircraft landing approach to aircraft carrier to determine display system requirements and to evalute dangerous conditions
[AD-751076] 07 p0819 N73-16635
Pilot performance during simulated standard instrument procedure turn with and without predictor display
[NASA-TM-X-62201] 08 p0879 N73-17118
Analysis of capabilities, characteristics, and effectiveness of flight simulators for developing primary aeronautical skills in single-engine, land aircraft - Vol. 1
[FAA-NA-72-102-VOL-1] 08 p0892 N73-17221
Analysis of capabilities, characteristics, and effectiveness of flight simulators for developing primary aeronautical skills in pilots of single-engine, land aircraft Vol. 2
[FAA-NA-72-102-VOL-2-ADD]
08 p0892 N73-17222
Analysis of fixed base simulator tests to determine effects of two horizontal display panel locations and three map orientations on manual piloting performance
[NASA-TM-X-62198] 08 p0892 N73-17223
Theoretical relationships among displacement, velocity, acceleration, and cue duration for single degree of freedom flight simulator system during sharp onset acceleration profile
[AD-752222] 08 p0893 N73-17230

Developments in aerodynamic test facilities to show past experience, present status, free flight techniques, and future plans
[AGARD-R-603] 09 p1011 N73-18250
Proceedings of conference on flight test technology to analyze results of flight test and comparison with data obtained using flight simulators for short takeoff aircraft
[DLR-MITT-72-18] 10 p1104 N73-19005
Procedure for developing aerodynamic parameters for use in flight simulator research projects with emphasis on wind tunnel measurements
10 p1105 N73-19008
Analysis of selected problems in formation of simulation models of V/STOL aircraft
10 p1105 N73-19009
Performance of typical V/STOL aircraft and comparison of data obtained with flight simulator against data obtained by actual flight tests
10 p1105 N73-19011
Apollo experience report on development of flight simulators for spacecrew training to show functional uses, characteristics, and problems
[NASA-TN-D-7112] 10 p1214 N73-19876
Evaluation of helicopter handling qualities based on ground-based piloted flight simulator tests
12 p1359 N73-21030
Analysis of equations of aircraft dynamics and development of analog-digital simulation capability
[AD-755868] 12 p1365 N73-21077
Design, development, and capabilities of space shuttle mission simulator to show types of training available and cost effectiveness of facility
[NASA-CR-128885] 12 p1387 N73-21251
Development and use of synthetic flight trainers based on degree and fidelity of simulation as key design considerations
[AD-754957] 12 p1388 N73-21260
Physiological stress reactions in simulated flight for pilot selection and training
13 p1481 N73-22001
Simulation of digital radar landmass simulator
[AD-756219] 14 p1634 N73-23250
Development of simulation model and computer code for evaluation of operation of short takeoff aircraft for commercial airline operations
[NASA-CR-114631] 16 p1860 N73-25062
Changes in diurnal variations of pilot performance in flight simulator compared with performance after transatlantic flights
[DLR-FB-73-25] 16 p1868 N73-25122
Development of flight simulator system to show position of joystick displacement
[NASA-CASE-NPO-11497] 16 p1878 N73-25206
Design and performance of aircraft or spacecraft differential maneuvering simulator
[NASA-TN-D-7304] 16 p1885 N73-25259
Development of multielement data reduction analysis software package for use with differential maneuvering simulator
[NASA-TM-X-2705] 17 p2001 N73-26178
Pilot ground training proficiency of flight simulators
[AD-755681] 18 p2112 N73-27081
Determination of aerodynamic parameters for use in flight simulator research
[NASA-TT-F-14994] 18 p2126 N73-27178
Three axes motion simulator for satellite attitude control systems
[ESRO-CR-61] 19 p2249 N73-28132
Guidelines for assessing acceptability of pilot ground trainer devices based on simulated aircraft maneuvers
[FAA-NA-73-15] 20 p2382 N73-29139
Design of computer controlled cathode ray tube display screen for flight simulator
[AD-764762] 23 p2767 N73-32140
Digital computer-generated contact analog landing display
[AD-764764] 23 p2771 N73-32162
Characteristics and performance of piloted simulator for application as research tool in design and development of experimental aircraft
24 p2874 N73-32955
Ground-based devices for spatial orientation training in T-38 aircraft
[AD-764740] 24 p2901 N73-33157

**FLIGHT STABILITY TESTS**
Jet aircraft flight tests for stability derivative determination comparing various measuring techniques
[BMVG-FBWT-73-12] 23 p2745 N73-31971

**FLIGHT STRESS**
Effects of environmental stresses on materials used in constructing glide reentry vehicles
14 p1676 N73-23601

**FLIGHT STRESS (BIOLOGY)**
NT SPACE FLIGHT STRESS
Analysis of acceleration forces produced during aerobatic flight and effects of acceleration forces on human body
[FAA-AM-72-28] 02 p0132 N73-11075
Flight stress effects on cardiovascular reactions of pilots with a therosclerosis
03 p0258 N73-12090
Conference on operational flight stress effects on human biodynamics and performance
[AGARD-CP-101] 10 p1122 N73-19143
Flight test program to study human factors problems and flight crew performance in military aircraft
10 p1122 N73-19145
Combined heat, noise, and vibration effects on aircrew performance
[AMRL-TR-71-113] 10 p1122 N73-19146
Measures to determine psychophysiological reactions of military flight crews to flying stress
10 p1122 N73-19148
Human stress expenditures in operational airlift mission flights
10 p1123 N73-19151
Influence of long duration flight missions on metabolic and endocrine functions of pilots and navigators
10 p1123 N73-19152
Systems analysis of physiological performance related to stresses such as those experienced in high performance aircraft
[AD-754970] 12 p1372 N73-21133
Physiological responses of flying personnel to multiple stresses
[AD-759565] 18 p2113 N73-27082
Experimental research in underwater medicine, flight stress, and pilot selection
[DLR-FB-73-15] 19 p2226 N73-27951
Inflight heart and respiratory rate recording of pilots, using nose clip transducers
19 p2226 N73-27953
Diagnosis and prognosis of pilot reaction and tolerance to psychical stress
19 p2227 N73-27962
Preflight and flight stress analysis, its relation to circadian rhythms measured in pilot physiological parameters
[DLR-FB-72-39] 21 p2501 N73-30071
Human circadian rhythms of blood circulation, respiration and catabolism under flight simulation stress
[DLR-FB-72-49] 21 p2501 N73-30073

**FLIGHT TEST VEHICLES**
Flight tests to determine buffet characteristics of four high performance aircraft during transonic maneuvers
06 p0618 N73-15017

**FLIGHT TESTS**
NT FLIGHT STABILITY TESTS
Flight test program to determine effects of low frequency vibration on passenger comfort in short haul aircraft
01 p0004 N73-10025
Jet aircraft noise of XV-5B V/STOL aircraft as determined by full scale flight test and wind tunnel model tests
[NASA-TM-X-62182] 01 p0004 N73-10029
Development of airborne flight data acquisition and data processing systems
[AGARD-LS-50] 01 p0055 N73-10450
Design of aircraft flight test instrumentation systems
01 p0055 N73-10451
Selection of dynamic data processing systems
01 p0056 N73-10454
Analysis of deterministic and random flight data
01 p0056 N73-10455
Procedure for determining noise levels in flight test measuring systems
01 p0056 N73-10456
Flight and wind tunnel tests to determine effects of Reynolds number of installed boattail drag of underwing nacelle
[NASA-TM-X-68162] 02 p0124 N73-11007
Flight tests of transponder correlation ranging equipment for use in airborne collision avoidance system
[AD-746448] 02 p0175 N73-11416
Flight performance evaluation for underwing nacelle installation of auxiliary-inlet ejector nozzle with clamshell flow diverter from Mach 0.6 to 1.3
[NASA-TM-X-2655] 02 p0222 N73-11793
State space techniques for obtaining mathematical models of flight test vehicles with nonlinear measurement variables in different moving bases
[AD-746657] 02 p0235 N73-11912
Effect of external air flowing across exhaust nozzles on jet noise produced by supersonic transport aircraft at high takeoff speeds
[NASA-TM-X-68161] 03 p0250 N73-12027
Flight loads data recording system for F-102 aircraft maneuver load analysis for data acquisition and application to development of structural design criteria
[AD-747016] 03 p0253 N73-12047
Postflight evaluation of ballistic vehicle flight test boundary layer transition data
[NASA-CR-129045] 03 p0282 N73-12287
Comparison of turbulent heating predictions by three different techniques with flight test data of several reentry vehicles
[NASA-CR-130251] 03 p0282 N73-12288
Operational tests and evaluation of optical infrared pilot warning system to determine probability of detection versus range
[NASA-CR-129525] 03 p0302 N73-12463
Performance of attitude sensors determined from Skylark 586 payload flight test
[RAE-TR-72066] 03 p0359 N73-12927
Flight tests of disk-gap band parachute behind full-scale simulator of Viking reentry vehicle over maximum range of entry conditions for landing on planet Mars-Vehicle AV-1
[NASA-CR-112176] 04 p0372 N73-13021
Flight tests of disk-gap band parachute behind full-scale simulator of Viking reentry vehicle over maximum range of entry conditions for landing on planet Mars-Vehicle AV-4
[NASA-CR-112179] 04 p0372 N73-13024
Flight tests to determine lateral-directional handling qualities and roll-sideslip coupling of jet aircraft at high speeds
[AD-748435] 04 p0374 N73-13042
Evaluation of approach lighting system for visual guidance of helicopters during instrument flight rules approach and landing operations
[FAA-RD-72-133] 04 p0401 N73-13261
Addition of feel augmentation system to improve flight control of S-67 helicopter
[AD-749284] 05 p0494 N73-14029
Flight test of 55 foot diameter disk-gap parachute trailing behind bluff body, planetary aeroshell and attached instrument payload
[NASA-TM-X-2671] 06 p0621 N73-15042
Magnetic tape playback and serial time decoder for IFF flight test instrumentation
[AD-750667] 06 p0641 N73-15204
Design, development and flight tests of Super Loki Dart Meteorological Rocket Systems
[AD-750796] 06 p0722 N73-15895
Operating principles and flight test performance of aerosol counter onboard tethered balloon
[AD-751315] 07 p0816 N73-16619
Role of theoretical studies of flight dynamics in relation to flight testing
08 p0866 N73-17011
Automatic method for determining stability and control derivatives from flight data
08 p0866 N73-17012
Measurement of surface pressure fluctuations at two locations on XB-70 aircraft at local Mach number range from 0.35 to 2.45
[NASA-TN-D-7226] 09 p0981 N73-18013
Flight tests of portable diaphragm liquid pump for astronaut cooling
09 p1089 N73-18883
Environmental and flight readiness tests of scanning mirror for infrared sensors
09 p1089 N73-18888
Proceedings of conference on flight test technology to analyze results of flight test and comparison with data obtained using flight simulators for short takeoff aircraft
[DLR-MITT-72-18] 10 p1104 N73-19005
Comparison of validity of results obtained by flight simulation with results obtained from actual flight test of short takeoff aircraft
10 p1105 N73-19007
Performance of typical V/STOL aircraft and comparison of data obtained with flight simulator against data obtained by actual flight tests
10 p1105 N73-19011
Ground and flight test program of Stokes flow parachute
[NASA-CR-112251] 10 p1106 N73-19016
Flight test program to study human factors problems and flight crew performance in military aircraft
10 p1122 N73-19145
Application of parafoil equations of motion to predict flight performance of powered parafoil flight vehicle
[AD-754907] 11 p1236 N73-20034
Scale effect on swept wings at subsonic speed on basis of pressure distribution measured in flight and on wind tunnel super VC 10 model
[ARC-R/M-3707] 12 p1355 N73-20999
Analysis of procedures and problems involved in operating helicopters from decks of ships
12 p1357 N73-21010
Improvements in military helicopter flight test techniques to provide data for safety, maintainability, and reliability
12 p1357 N73-21013
Flight tests of XH-51 helicopter to determine effects of gyroscope and control spring modifications on stability and control
12 p1358 N73-21015
Application of maximum likelihood criterion and optimal input design for analyzing flight test data to obtain aircraft stability and control derivatives
[NASA-CR-2200] 12 p1364 N73-21071
Development of pilot model parameters to provide data base for multiloop, single controller, multi-input analysis of aircraft performance
[AD-755367] 12 p1365 N73-21078
Analysis of Mariner 71 attitude control subsystem flight performance and effects of performance anomalies on subsystem operation
[NASA-CR-131522] 12 p1461 N73-21835

Flight test procedures for rotary wing aircraft with emphasis on performance and flying qualities
14 p1598 N73-22959
Influence of rain on airborne Doppler velocity sensor performance
[AD-757509] 14 p1668 N73-23541
Space flight tests for determining performance efficiency of ion engine model with surface ionization of cesium on tungsten
14 p1701 N73-23801
Eridan rocket probe performance in experimental vehicles
14 p1718 N73-23940
Flight tests of 45 degree delta cropped wing to determine dynamic lateral stability characteristics
[ARC-R/M-3243] 15 p1729 N73-24027
Flight tests to determine longitudinal aerodynamic parameters of P-1127 aircraft with vectored thrust control
[NASA-TN-D-7296] 15 p1734 N73-24066
Flight-measured base pressure coefficients for thick boundary layer flow over aft-facing step for Mach numbers from 0.4 to 2.5 using XB-70 aircraft
[NASA-TN-D-7202] 15 p1767 N73-24317
Low frequency structural response and damping characteristics of XB-70 aircraft during subsonic and supersonic flight
[NASA-TN-D-7227] 15 p1837 N73-24892
Flight test measurements of control surface hinge moments on X-24 lifting body correlation with wind tunnel data
[NASA-TM-X-2816] 16 p1858 N73-25049
Flight evaluation of composite for use in aircraft structures
[NASA-TM-X-2761] 17 p2049 N73-26579
Smoothing technique for analyzing frequency response of aircraft in flight and on ground
[RAE-LIB-TRANS-1703] 17 p2054 N73-26616
Flight test and evaluation of CL-84 tilt-wing V/STOL aircraft with application to specific military roles
18 p2103 N73-27007
Flight tests for determining handling qualities and operational characteristics of Breguet 941 STOL aircraft
18 p2103 N73-27008
Flight test F-106 aircraft to determine comparative time advantages of energy optimization climb and acceleration methodology
[AD-760571] 18 p2107 N73-27041
Flight test of multispectral image dissector camera onboard high altitude aircraft
18 p2209 N73-27835
Flight tests of F-8C aircraft to determine effects of flaps on buffet characteristics and wing-rock onset at subsonic and supersonic speeds
[NASA-TM-X-2873] 19 p2220 N73-27905
Flight tests of CH-47 helicopter to determine structural performance of boron-reinforced epoxy aft rotor blades
[AD-762199] 19 p2222 N73-27927
Flyover and static tests for determining effects of flight velocity on F-106B exhaust nozzle noise
[NASA-TM-X-2854] 19 p2329 N73-28734
Measurements on high and low gain L band aircraft aerials using transmissions from high altitude balloon
[RAE-TR-73008] 20 p2377 N73-29102
Bendix AAU 19A/A AIMS altimeters - Standard three inch, counter-drum-point altimeter
[AD-762523] 20 p2420 N73-29446
Flight tests of VHF Omnirange navigation and Tacan systems to determine bearing error curves
[FAA-RD-72-73] 20 p2452 N73-29710
Analysis of flight test procedures for evaluating strength of airframes for aircraft and helicopters
[NASA-TT-F-769] 21 p2494 N73-30019
Flight tests of various steep gradient approaches to ground level short takeoff and landing runway to determine aircraft performance and navigation aids required
[FAA-NA-72-77] 21 p2495 N73-30025
Design of real time telemetry processing system for naval aircraft flight tests
[AD-763469] 21 p2509 N73-30130
Performance and growth capability of orbital test satellite for European communication satellite program
[DGLR-PAPER-73-044] 21 p2602 N73-30849
Flight tests of hydrazine control system performance and its effects on flight behavior of reentry vehicle
[SLA-73-154] 22 p2722 N73-31785
Performance tests of hemispherical flow-direction sensor mounted on F-104 aircraft to develop Mach number position error calibration curve
[NASA-TN-D-7461] 23 p2743 N73-31956
Flight tests of cryogenically cooled hygrometer
[AD-764718] 23 p2794 N73-32354
Evaluation of approach and landing performance of inertial navigation system with Kalman filter installed in CV-340 aircraft
[NASA-TN-D-7302] 23 p2816 N73-32515
Simulated launch countdown, liftoff, and flight test to demonstrate compatibility of Skylab rescue space vehicle systems, ground support, and off-site support facilities
[NASA-TM-X-69520] 23 p2850 N73-32776
Flight tests of Boeing 727 aircraft to determine effects of modifications on reduction of aerodynamic noise
[FAA-RD-72-40-VOL-3] 24 p2876 N73-32971

**FLIGHT TIME**
Human psychomotor performance circadian rhythm variations after transmeridian flight noting time shift effect
[DLR-FB-73-52] 22 p2624 N73-31022

**FLIGHT TRAINING**
Validity of ground training for developing flying skill during pilot training
[AD-749621] 06 p0636 N73-15168
Operational effectiveness of jet flight training simulator
[AD-750248] 06 p0636 N73-15170
Analysis of capabilities, characteristics, and effectiveness of flight simulators for developing primary aeronautical skills in single-engine, land aircraft - Vol. I
[FAA-NA-72-102-VOL-1] 08 p0892 N73-17221
Analysis of capabilities, characteristics, and effectiveness of flight simulators for developing primary aeronautical skills in pilots of single-engine, land aircraft Vol. 2
[FAA-NA-72-102-VOL-2-ADD] 08 p0892 N73-17222
Evaluation of standardized angle of attack flight training system
[AD-757243] 14 p1615 N73-23090
Automative adaptive flight training, using instrument flight maneuvers
[AD-759366] 18 p2112 N73-27080

**FLIGHT VEHICLES**
Design and development of active control system for air cushion vehicle to reduce or eliminate effects of excessive vertical vibratory acceleration
[NASA-CASE-LAR-10531-1] 04 p0372 N73-13023
Aircrew escape autogyro ejector seat/flight vehicle
09 p1089 N73-18890

**FLINT**
Flint glass objective prism recommended for ESO Schmidt camera due to light transmission properties
07 p0845 N73-16847

**FLIP-FLOPS**
Comparative performance characteristics of geometrically similar vented and unvented bistable amplifiers
[AD-745770] 02 p0158 N73-11279
RC equivalent network for flueric flip-flop inputs
[AD-752126] 08 p0899 N73-17280
Design of sequential circuits using edge and level sensitive flip-flops
24 p2900 N73-33146

**FLOATING**
Buckling analysis of elastic plate floating on water and stressed uniformly along periphery of internal hole
[AD-750594] 06 p0728 N73-15943
Floating baffle for tank drain
[NASA-CASE-KSC-10639] 17 p2036 N73-26472

**FLOATING POINT ARITHMETIC**
Floating point system quantization errors in digital control systems
[NASA-CR-124382] 22 p2638 N73-31145

**FLOATS**
Apollo experience report on water landing requirement and two stable flotation attitudes for upright flotation of command module
[NASA-TN-D-7081] 09 p1090 N73-18898
Floating stable platforms for combat and civilian use
[AD-754783] 11 p1353 N73-20986

**FLOOD DAMAGE**
Flood damage in west central Iowa based on ERTS-1 imagery
[E73-10045] 07 p0777 N73-16308
ERTS-1 imagery of flood damage to farmlands in South Dakota
[NASA-CR-131641] 12 p1401 N73-21361
Assessment of flood damage in Arizona using ERTS-1 MSS imagery to show extent of inundation and sediment deposition
[PAPER-W6] 19 p2271 N73-28284

**FLOOD PLAINS**
Delineation of flood plain hazard zones by means of detailed soil surveys and by means of aerial photointerpretation
[PB-211325] 05 p0541 N73-14398

**FLOOD PREDICTIONS**
Analytical procedures and correlation of hydrological data for predicting Upper Midwest watershed
[PB-214091/1] 14 p1664 N73-23505
Comparison of extreme floods statistically predicted for highway bridge design in Pennsylvania to actual floods caused by hurricane Agnes
[PB-220888/2] 21 p2575 N73-30639
Utilization of ERTS data to study air pollution, insect infestation, and water transport in Minnesota
[NASA-CR-135565] 23 p2783 N73-32266
Application of remote sensing data to analysis of spring snowmelt floods in Minnesota and surrounding areas
23 p2784 N73-32270
Survey of snow cover to predict risk of spring flood and snow storage in areas of hydroelectric power stations in Norway
[E73-11160] 24 p2919 N73-33313

**FLOODS**
ERTS-1 imagery of plant growth and annual flooding in Niger River inland delta
[E73-10078] 07 p0780 N73-16339
Repetitive ERTS-1 imagery of surface water variability and flooding along rivers and low-lying areas in Virginia, Iowa, and California
[E73-10046] 08 p0900 N73-17289
ERTS-1 observations of plant growth and annual flooding in Inland Delta of Niger River in Mali
[E73-10436] 11 p1281 N73-20396
Survey of lake flooding in Lake Champlain basin using ERTS-1 imagery
[E73-10771] 18 p2134 N73-27247
ERTS-1 imagery of algal streaks and flooding in Lake Erie and Michigan and Ohio areas
[E73-10793] 18 p2137 N73-27269
Mapping of flood inundation areas in southwestern Iowa using ERTS-1 imagery
19 p2288 N73-28395
Detection and mapping of soil erosion and flooding in southern Arizona
[E73-10950] 21 p2531 N73-30292
Thematic mapping of wetlands, forests, open water, and Mississippi River flooding from ERTS-1 imagery
[E73-10952] 21 p2531 N73-30294
Engineering procedures, blasting, and water level regulation for flood prevention and ice jam control on Dnestr and Dubossary Reservoirs
21 p2573 N73-30620
Investigation of New England reservoirs, land use, streams, flooding, and vegetation from Skylab imagery
[E73-10993] 22 p2659 N73-31299
ERTS-1 imagery of short-lived events such as forest fires, oil spills, volcanic activity, floods, and storms
[E73-11048] 23 p2779 N73-32224

**FLORA**
U PLANTS [BOTANY]

**FLORIDA**
Mimi field test of July 1970 for underwater acoustic study in Straits of Florida
[AD-744982] 01 p0080 N73-10662
Urban and regional planning in Florida using ERTS-1 imagery
[E72-10254] 03 p0290 N73-12354
Urban and regional planning in Brevard County, Florida using ERTS-1 imagery
[E73-10083] 08 p0901 N73-17295
Data collection and relay system for monitoring hydrologic conditions in south and central Florida
[E73-10092] 08 p0902 N73-17304
Monitoring of water quality in New York Bight and Tampa Bay, Florida, using ERTS-1 imagery
[E73-10395] 11 p1276 N73-20357
Application of ERTS-1 imagery to urban and regional planning in Florida
[E73-10423] 11 p1280 N73-20384
Development of data relay network for monitoring hydrologic conditions collected for south and central Florida
[E73-10491] 12 p1397 N73-21327
Acquisition and processing ERTS-1 water resources data for south Florida
[E73-10560] 14 p1656 N73-23432
Three dimensional growth rates of seeded Florida cumulus
[UM-RSMAS-73029] 14 p1661 N73-23480
Performance of fibrous reinforced concrete overlay test slabs as runways at Tampa International Airport, Florida
[FAA-RD-72-119] 14 p1680 N73-23634
Urban planning and mapping in east central Florida using ERTS-1 imagery
[E73-10605] 15 p1773 N73-24366
Measured noise level data for proposed airport sites in Florida
[PB-214459/0] 16 p1945 N73-25737
Advantages of collecting data in south Florida using ERTS data collection platforms
[E73-10803] 18 p2138 N73-27278
Detection of turbidity plumes in Tampa Bay, Florida from ERTS-1 MSS imagery
19 p2287 N73-28388
Computer maps of land use in Titusville, Florida
[E73-10852] 20 p2391 N73-29209
Forecasting air mass thunderstorms for MacDill AFB, Florida
[AD-763099] 20 p2451 N73-29696
Skylab monitoring of gamefish in coastal waters off of Florida
[E73-10997] 22 p2659 N73-31303
Mapping dynamic hydrologic conditions of surface water changes in south Florida
[E73-11028] 22 p2662 N73-31332

Urban planning and development in east central Florida from ERTS-1 processed data
[E73-11083] 24 p2913 N73-33246
Skylab oceanic gamefish operations in Gulf of Mexico
[E73-11157] 24 p2919 N73-33311
Utilization of ERTS-1 imagery for management of wetlands in Great Dismal Swamp and Lake Okeechobee
[E73-11161] 24 p2920 N73-33314
FLOTATION
Low intensity magnetic field effects on flotation properties of water
[AD-758623] 16 p1946 N73-25746
FLOTATION SYSTEMS
U FLOATS
FLOW CHARACTERISTICS
NT BOUNDARY LAYER STABILITY
NT FLAME STABILITY
NT FLOW DISTRIBUTION
NT FLOW STABILITY
NT FLOW VELOCITY
NT MAGNETOHYDRODYNAMIC STABILITY
Flow conditions around exit and downstream of stator blades with varying trailing-edge geometries and thicknesses
[NASA-TM-X-2659] 01 p0001 N73-10003
Measured and calculated mean flow characteristics of two-dimensional, hypersonic, turbulent wakes produced by wedges
[NASA-TN-D-6927] 01 p0040 N73-10316
Effects of incomplete dissolution of graphite in molten cast iron on viscosity differences with same chemical composition
[AD-747378] 03 p0317 N73-12582
Numerical analysis of pressure drop in ducts across round-wire gauzes or screens normal to fluid flow to show effects of gauze geometry and velocity of flow
[ESDU-72009] 04 p0403 N73-13280
Numerical analysis of pressure losses due to bends in fluid flow systems and application of correction factor to relate overall losses for various conditions
[ESDU-68035] 04 p0403 N73-13283
Analysis of mean velocity profiles in three-dimensional turbulent boundary layers during incompressible flow
[REPT-71-FM-13] 04 p0404 N73-13289
Analysis of pressure loss through single bends of various geometries under conditions of full incompressible flow
[ESDU-67040-AMEND-A] 05 p0525 N73-14272
Analysis of pressure loss conditions created by turbulent flow conditions for wide range of flowmeters
[ESDU-66030-AMEND-A] 05 p0525 N73-14273
Seasonal flow patterns of coastal currents along Oregon-Northern California coast
[AD-749077] 05 p0541 N73-14403
Performance tests of single stage fan-compressor to evaluate shock-in-rotor blading for jet engine applications requiring high aerodynamic performance and stability
[NASA-CR-120991] 05 p0590 N73-14795
Flow characteristics around semi-infinite plate with sharp leading edge inserted in hypersonic uniform air stream
[NAL-TR-289T] 06 p0613 N73-14979
Numerical analysis of development of incompressible, symmetrical turbulent wake flows downstream of airfoils using integral method of momentum and energy
[NAL-TR-292] 06 p0614 N73-14986
Development of finite difference procedure to calculate steady flows over several classes of airfoils under inviscid transonic flow conditions
[NASA-CR-2186] 06 p0614 N73-14989
Aerodynamic characteristics of wing moving close to interface with annular jet flowing from wing surface and impinging on screen
[AD-750933] 06 p0615 N73-14995
Application of blockage correction factors to wind tunnel test measurements on aircraft models
06 p0617 N73-15006
Analysis of aerodynamic stall characteristics of wing sections with high lift devices in two dimensional flow
06 p0617 N73-15008
Flow characteristics of two-dimensional, tangential-slot injection into turbulent boundary layer at Mach 2.4 freestream velocity
[NASA-CR-2128] 06 p0654 N73-15313
Inherent statistical properties of bubble field in two phase flow determined by correlation functions
[EUR-4840] 06 p0655 N73-15319
Analysis of unsteady flow over moving boundaries to determine characteristics of boundary layer separation
[AD-750398] 06 p0655 N73-15322
Numerical analysis of three dimensional compressible laminar boundary layer flow characteristics of right circular cone in supersonic and hypersonic flow
[AD-750130] 06 p0656 N73-15331
Oscillographic pressure measuring system for flow structure in compressor impeller bladings
[NASA-TT-F-14647] 06 p0673 N73-15480
Effects of thickness and viscosity considerations on accuracy of aerodynamic coefficients determined for thin wings in inviscid flow conditions
[ESDU-70011-AMEND-A] 07 p0735 N73-15982
Flow model of axisymmetric hypersonic nozzle for transition from turbulent flow to laminar flow with pressure gradient controlled by nozzle shape
07 p0768 N73-16237
Stabilizing and destabilizing effects of Coriolis body force on turbulent wall layers in two dimensional channel flow
07 p0768 N73-16243
Analysis of flow characteristics of asymmetric annular diffuser with wall bleed capability and application to gas turbine combustors
[NASA-TM-X-2710] 07 p0770 N73-16251
Analysis of one dimensional flow downstream of source of radiation in constant area ducts and conical nozzles
07 p0853 N73-16920
Flow characteristics of tandem bladed compressor stators at various inlet incidence angles
[NASA-TM-X-2734] 08 p0863 N73-16986
Development of model to describe characteristics of one dimensional lunar ash flow with and without heat transfer effects
[NASA-CR-130697] 08 p0895 N73-17245
Analysis of skin friction measurement techniques for incompressible flow to show instruments required and areas of difference
[FFA-AU-726] 08 p0895 N73-17246
Analysis of uniform jet flow around airfoil with separated shock wave at low supersonic velocities of incident flow
[NASA-TT-F-14813] 08 p0896 N73-17259
Analysis of axially symmetric motions of viscous neutral stratified gas in spherical layer resulting from rotation of inner sphere
[NASA-TT-F-14661] 08 p0897 N73-17260
Analysis of turbulent diffusion in rocket combustion chamber to determine Lagrangian correlation coefficient and intensity of turbulence in chamber
08 p0967 N73-17908
Wind tunnel tests to determine flow characteristics of stalled two dimensional airfoil
[NASA-CR-130919] 09 p0982 N73-18020
Jet deflection characteristics of jet-flapped airfoil with Coanda deflection surfaces based on velocity distribution and flow angle measurements for static operation
[AD-753618] 09 p0989 N73-18074
Darcy-Weisback equation for investigating solid-liquid flow in noncircular pipes
[BM-RI-7725] 09 p1013 N73-18271
Analysis of measurable and ideal quantities of nozzle beams skimmed from parallel equilibrium gas flows
[DLR-FB-72-51] 09 p1014 N73-18275
Calculation of flow through airfoils in cascade to show pressure distribution under conditions of two dimensional incompressible flow with boundary layer separation at trailing edge
[DLR-FB-72-62] 09 p1014 N73-18276
Analysis of flow distribution around harmonically oscillating circular cylinder under two dimensional flow conditions
[DLR-FB-72-56] 09 p1014 N73-18277
Measurement of aerodynamic drag of conical bodies at zero angle of attack in free molecular and near free molecular flow regime
[DLR-FB-72-64] 09 p1014 N73-18278
Analysis of two dimensional cascade flow of double circular arc blades at transonic speed with various camber angles and pitch-chord ratios
[NAL-TR-300] 09 p1014 N73-18279
Experimental investigation of two dimensional cascade flow tests for three cascade configurations - Vol. 4
[NASA-CR-121101] 09 p1015 N73-18282
Numerical analysis of inviscid, fully developed structure of lift-generated vortices behind aircraft wings and extension to arbitrary span-loaded distributions
[NASA-TM-X-62224] 09 p1016 N73-18289
Development of method for analyzing performance of magnetohydrodynamic generator based on thermodynamic properties and flow characteristics
10 p1110 N73-19051
Analysis of design flow in open jet wind tunnel and examination of processes for starting supersonic wind tunnels
[ARL/ME-138] 10 p1137 N73-19264
Application of implicit finite-difference method for solution of compressible boundary layer equations
10 p1139 N73-19277
Analysis of eddy diffusivity of momentum for heating air in turbulent annular flow and effect of various flow parameters on eddy diffusivities ratio
10 p1139 N73-19279
Numerical analysis of pressure distribution in subsonic wind tunnel resulting from interference of air flow
10 p1140 N73-19287
Methods for determining inviscid three dimensional flow about smooth shapes at supersonic speeds
[AD-753695] 10 p1143 N73-19311
Experimental investigation of mean flow characteristics of air jets issuing from rectangular orifices
[AD-754225] 10 p1143 N73-19314
Procedures for calculating velocity potential and pressure distribution of planforms oscillating harmonically in supersonic flow
[FOK-X-440] 11 p1231 N73-19994
Development of tables of gasdynamic functions in three dimensional, axisymmetric, and plane gas flows past blunt bodies of revolution
[NASA-TT-F-715] 11 p1231 N73-19996
Development of computer programs for analyzing flow distribution in nose region of blunt body at arbitrary speed and altitude - Vol. 2
[NASA-CR-128872] 11 p1271 N73-20310
Development of computer program for solving fully compressible, two-dimensional hydrodynamics problems using flux-corrected transport algorithms
[AD-754736] 11 p1271 N73-20315
Analysis of Reynolds stress in turbulent boundary layer on smooth wall with zero pressure gradient
[AD-754758] 11 p1272 N73-20319
Development and mixing of coaxial fluid jet with axisymmetric swirling vortex flow in cylindrical chamber
[AD-754613] 11 p1272 N73-20324
Analysis of interaction of rarefied gas with surface of porous moist bodies during heat and mass transfer using visual and photographic methods
[AD-754633] 11 p1272 N73-20325
Design of airfoil sections for low Reynolds numbers based on requirement to achieve transition upstream of major adverse pressure gradient
12 p1355 N73-20995
Wind tunnel tests of rotary wing to determine retreating blade stall at several preset parameters and effect of reverse flow area
12 p1360 N73-21037
Aerodynamic characteristics of rotary wings under axial flow conditions and development of numerical analysis techniques
12 p1360 N73-21039
Numerical analysis of low Reynolds number flow perpendicular to circular cylinder with constant radial suction mass flux at surface
12 p1389 N73-21264
Analysis of effect on laminar boundary layer resulting from superposed unsteadiness on yawed infinite flat plate in adverse pressure gradient
12 p1389 N73-21265
Development of numerical procedure for solving gas dynamics of pulsating, compressible flow in propulsive duct
12 p1389 N73-21266
Analysis of mean and fluctuating flow properties of compressible turbulent boundary layer in shock wave-induced adverse pressure gradient
[NASA-TN-D-7092] 12 p1391 N73-21280
Effect of steady state circumferential total pressure distortion on loss in compressor stall pressure ratio
[NASA-CR-114577] 12 p1443 N73-21693
Wind tunnel tests to determine flow distribution within model passages of hypersonic inlets for core flow and boundary layer flow conditions
[NASA-TN-D-7150] 13 p1470 N73-21905
Wind tunnel tests to determine effect of tip vortex of forward mounted wing on engine inlet ingestion
[NASA-TM-X-68225] 13 p1473 N73-21932
Flight tests to determine characteristics of vortex and turbulent wake generated by DC-10 aircraft for development of air traffic control separation criteria
[REPT-73-00470] 13 p1474 N73-21938
Physical and chemical nature of N2O flow decay in liquid propellants
[AD-755378] 13 p1489 N73-22070
Numerical analysis of turbulence equations in orthogonal tensor form, axisymmetric flow equations, and use of mass-averaged variables
[NASA-TM-X-62248] 13 p1510 N73-22235
Research projects on hypersonic and rarefied gas flows, separated and reattached wakes, viscous flow, and laminar and turbulent boundary layers with strong blowing
[AD-755276] 13 p1512 N73-22249
Analysis of internal waves generated by passage of body through density stratified medium and effects on mean flow
[AD-755714] 13 p1512 N73-22254
Prevention of N2O4 flow decay by means of contaminant removal through distillation and filtration
[AD-755380] 13 p1569 N73-22717
Design, characteristics, and performance tests of high-tip-speed, low-loading, transonic fan stage
[NASA-CR-121095] 13 p1570 N73-22727
Development and evaluation of throat bypass bleed system to increase stable airflow range of sonic mixed-compression inlet
[NASA-TM-X-2779] 14 p1597 N73-22947
Numerical analysis of Navier-Stokes equations for steady two dimensional flow to show convergence characteristics
[ARC-R/M-3239] 15 p1725 N73-23997

Numerical analysis of Navier-Stokes equations for steady, viscous, axisymmetric flow with application to flow past pitot tube at low Reynolds numbers
[ARC-R/M-3240] 15 p1725 N73-23998
Numerical analysis of shock tunnel performance operated by reflected shock technique to determine effects of disturbance to flow at nozzle entry caused by reflected waves
[ARC-R/M-3265] 15 p1725 N73-23999
Analysis of pressure distribution and surface flow on half models of wings with curved tips and 60 degree sweepback
[ARC-R/M-3244] 15 p1726 N73-24001
Wind tunnel tests to determine characteristics of turbine rotor blades with inter-blade passages operating at supersonic speed
[ARC-R/M-3275] 15 p1728 N73-24016
Effects of wall jets in still air on flat and curved surfaces under external stream in presence and absence of pressure gradient and initial boundary layer
[ARC-R/M-3252] 15 p1729 N73-24025
Performance tests of working section of variable pressure, supersonic wind tunnel to show effects of inclination of slotted walls on Mach number accuracy
[ARC-R/M-3228] 15 p1730 N73-24032
Analysis of decomposition of liquid jet injected normal to supersonic airstream to show generation of high frequency, axially propagating waves
15 p1764 N73-24296
Analysis of turbulent boundary layer on porous plate and fluid mechanics of adverse free stream pressure gradients
15 p1765 N73-24303
Numerical method of characteristics for unsteady propagation processes considering dissipative terms in equations for supersonic mixing processes
[NASA-TT-F-14825] 15 p1767 N73-24320
Wind tunnel tests to determine effect of approaching boundary layer on separated flow behind downstream facing step
[NLR-TR-70033-U] 15 p1768 N73-24322
Cavity temperature and flow characteristics in gas-core reactor for testing fissioning uranium plasmas
[NASA-TM-X-2797] 15 p1809 N73-24662
Development of formulas for calculating gradients and ordinates of camber surfaces of sweptback wings of arbitrary planform with subsonic leading edges and specified load distribution
[ARC-R/M-3217] 16 p1852 N73-25004
Development of methods for determining local skin friction of boundary layer and calibration of instruments for analyzing turbulent shear flow
[ARC-R/M-3202] 16 p1854 N73-25016
Development of mathematical procedures for determining turbulent boundary layer in arbitrary pressure gradient
[ARC-R/M-3207] 16 p1854 N73-25017
Velocity magnitude and direction, static pressure, and skin friction of circular turbulent jet impinging normally on flat surface
[ARC-R/M-3205] 16 p1856 N73-25034
Design criteria for annular supersonic nozzles to produce uniform flow in supersonic wind tunnels without limit lines or shock waves
[ARC-R/M-3227] 16 p1856 N73-25035
Analysis of gas jets expanding out of axisymmetrical nozzles into vacuum or still air at finite pressure
[ARC-R/M-3235] 16 p1856 N73-25036
Flow characteristics of axially symmetrical, supersonic, fully-expanded jet to determine relation between static pressure distributions and jet turbulence
[ARC-R/M-3292] 16 p1857 N73-25038
Application of laminar flow solutions for heat transfer and flow friction to design of heat exchangers
16 p1886 N73-25266
Numerical analysis of maximum thrust nozzles for nonequilibrium, chemically reacting gas flows based on equations for general, multi-component reacting gas
16 p1886 N73-25269
Numerical analysis of turbulence transport equation for two dimensional jet flow and pressure-velocity derivative correlations
16 p1887 N73-25270
Numerical analysis of real gas effects in supersonic flows over sharp and spherically blunted cones
16 p1887 N73-25274
Dynamic performance of beam deflection fluid amplifiers
[AD-759211] 16 p1891 N73-25306
Analysis of nonhomogeneous flow associated with two dimensional propulsive lifting system based on flow with energy addition
[NASA-CR-2250] 17 p1979 N73-25997
Analysis of minimum run times required for instationary measurements at transonic speeds during wind tunnel tests
17 p2009 N73-26243
Numerical analysis of structure of incompressible turbulent flows in plane wake and plane jet using two eddy viscosity models
17 p2012 N73-26274
Analysis of jet penetration and mixing of multiple cold air jets into ducted subsonic heated mainstream flow
[NASA-CR-121217] 17 p2014 N73-26286
Analysis of effect of turbulence intensity on aerodynamic characteristics of bodies of various shapes to develop method for measuring initial turbulence
[AD-760264] 17 p2015 N73-26297
Mathematical representation of flow curves for metallic materials
[RAE-LIB-TRANS-1675] 17 p2043 N73-26532
Numerical analysis of steady state laminar motion of viscous, incompressible, and binary fluids for rotating flow in cylindrical geometry
18 p2129 N73-27204
Numerical analysis of two dimensional incompressible potential flow around system of arbitrary airfoils using relaxation method
[NAL-TR-309] 18 p2130 N73-27212
Proceedings of conference to develop data on free turbulent shear flows to include two dimensional shear layers and axisymmetric jets
[NASA-SP-321-VOL-2] 18 p2130 N73-27213
Analysis of kinematic and dynamic characteristics of wake generated behind flat plate normal to parallel unbounded fluid flow
[AD-761372] 18 p2131 N73-27220
Relationships between fracture strength, flow stress, and material ductility in high strength steels
[AD-761217] 18 p2162 N73-27463
Analysis of transonic aerodynamics developments to include methods for computing steady and unsteady transonic flows
[AD-761551] 19 p2218 N73-27892
Numerical analysis of stability of flows of viscoelastic fluids for three conditions
19 p2251 N73-28146
Numerical analysis of hypersonic rarefied flow past sharp leading edge of flat plate using finite difference solution of Navier-Stokes equation
19 p2251 N73-28147
Analysis of supersonic flow involving viscous and inviscid flow using unified solution technique
19 p2251 N73-28148
Development of flow visualization technique using fluorescent dye to simulate smoke lines in water
[AD-761499] 19 p2257 N73-28192
Numerical transformation of basic equation for two parameter flow
[AD-762104] 19 p2257 N73-28195
Analysis of internal noise field of two axisymmetric sonic inlet models for noise suppression of turbofan engine inlets - Vol. 3
[NASA-CR-121128] 19 p2329 N73-28733
Development of semi-empirical model for predicting fluctuating pressure distribution resulting from rocket plume- induced separated regions
[NASA-CR-124346] 19 p2352 N73-28922
Analysis of flow pattern of particles in moving bed for application to manufacturing processes
[NLL-RTS-7330] 20 p2386 N73-29167
Measurement of laminar fluid flow through orifice meters to determine discharge coefficients and head losses
[NLL-NEL-TT-2457-[6075.461]]
20 p2386 N73-29169
Analysis of shock wave strenghtening by positive density gradient in cryogenic shock tube
20 p2386 N73-29173
Analysis of steady hypersonic flow with viscous interaction over sharp slender wedge by finite difference scheme
20 p2387 N73-29177
Application of finite-difference machine code for analyzing wake-vortex problem in quasi-cylindrical boundary layer approximation
[NASA-TM-X-69495] 20 p2387 N73-29179
Wind tunnel tests to determine boundary layer characteristics of air flows using laser light source and thermoanemometer
[NASA-TT-F-14945] 20 p2387 N73-29180
Flow characteristics of radial inward choked flow of liquid nitrogen stream
[NASA-TM-X-68283] 20 p2387 N73-29181
Irrotational planar supersonic cascade ideal gas flow computation using method of characteristics
[DLR-FB-73-34] 21 p2491 N73-29998
Numerical analysis of three dimensional boundary layer for various distribution laws of suction intensity on leading edge of wing
[AD-763280] 21 p2497 N73-30038
Analysis of characteristics of initially plane, strong shock wave propagating into conical convergence using multi-crystal piezoelectric probe
21 p2522 N73-30228
Development of model for analyzing pressure excitation spectrum and acoustic impedance of sound absorbers in presence of grazing flow
[NASA-TM-X-71418] 21 p2523 N73-30231
Analysis of flow distribution of nozzle designed to produce incompressible, low Reynolds number jet flow
[NASA-TM-X-69566] 21 p2523 N73-30233
Numerical analysis of inviscid transonic flow over body with supersonic underexpanded exhaust plume and characteristics of flow near boattail sting
[RM-577] 21 p2523 N73-30234
Development of computer program for determining airfoil pressure distribution for subcritical attached viscous flow
[NAL-TR-248] 21 p2523 N73-30236
Analysis of boundary layer and turbulence characteristics inside passages of axial flow inducer and technique for predicting properties of boundary layer
[NASA-CR-121248] 21 p2524 N73-30240
Development of numerical code to calculate two dimensional flow field when supersonic flow encounters double wedge configuration
[NASA-CR-134010] 21 p2524 N73-30242
Flow characteristics behind diffusers in wind tunnels
[AD-763257] 21 p2525 N73-30251
Photographic recording of secondary flows at nozzle exits produced by planar nozzles with rectangular inlets from circular ducts
[AD-762743] 21 p2527 N73-30265
Finite element analysis and computer graphics visualization of unsteady flow around pitching and plunging airfoils
[NASA-CR-2249] 22 p2611 N73-30926
Pressure recovery performance of conical diffusers at high subsonic speeds and range of geometries
[NASA-CR-2299] 22 p2611 N73-30927
Wind tunnel tests to determine flow characteristics around sharp-edged slender delta wing at large angles of attack
[NASA-TT-F-15107] 22 p2611 N73-30928
Characteristics of secondary flows around and downstream of protuberances in laminar boundary layers and conditions for development of turbulence
22 p2649 N73-31222
Effect of return bends on downstream pressure drop and heat transfer coefficient of condensing refrigerant
[DSR-72591-75] 22 p2652 N73-31246
Computation of periods, wavelengths, and amplitudes of oscillations in equatorial flows and particle trajectories within flows by using inertial motion equations
22 p2666 N73-31361
Rotating stall in axial flow compressor stages with different types of profiling along blade height and different flow regimes past profile in cascade
[NASA-TT-F-15115] 22 p2709 N73-31698
Effects of flow turning, flow acceleration, and supersonic flow on hydrogen film cooling
[NASA-CR-121235] 22 p2729 N73-31841
Measurement of flow parameters in midspan double-circular-arc section of stator in subsonic flow and comparison with computed performance
[NASA-TN-D-7425] 23 p2740 N73-31932
Flow characteristics associated with laminar oscillating flow in horizontal tube containing mild axisymmetric constriction
23 p2772 N73-32175
Numerical analysis of boundary conditions of time dependent viscous compressible flow based on small perturbation of Navier-Stokes equation
23 p2773 N73-32176
Analytical and experimental investigation of turbulent mixing flow in pressure gradient to determine existence of equilibrium flows in streams of helium and nitrogen
23 p2774 N73-32184
Development of theoretical model for determining flow characteristics of round jet in incompressible cross-flow based on matched asymptotic expansion
[NASA-CR-132324] 23 p2775 N73-32191
Incipient boundary layer separation on axisymmetric compression surfaces of conical body at hypersonic speeds
23 p2775 N73-32195
Aerodynamic design of inlet stage for two-stage compressor and performance comparison for axial, mixed flow, and centrifugal stage configurations
[NASA-CR-120943] 23 p2829 N73-32610
Flow characteristics of multiple dilution jets mixing with primary airstream for gas turbine combustors
[NASA-TM-X-71426] 23 p2829 N73-32612
Characteristics of low speed air flow over slender, sharp edged delta wing at various angles of attack and effects on longitudinal and lateral stability
24 p2869 N73-32922
Influence of periodic oscillations of mean flow on mean and turbulent structure of fully developed air flow in smooth circular pipe
24 p2902 N73-33161
Flow characteristics of merged layer regime in hypersonic, low density flow past semi-infinite sharp cone
24 p2903 N73-33168
Characteristics of laminar and turbulent wakes of spherical bodies at hypersonic speed in nitrogen atmosphere
[DREV-R-683/72] 24 p2904 N73-33178

Effect of inlet conditions on optimal shape of diffuser based on theory of potential flow of fluid in channels
[AD-765577] 24 p2911 N73-33230
Characteristics of variable geometry high Mach inlet concepts to reduce jet engine noise on subsonic, long range commercial aircraft
[NASA-CR-134495] 24 p2972 N73-33748

**FLOW CHARTS**
Fluvial environmental charts for Arctic coastal plain in Northern Alaska
[AD-749151] 05 p0542 N73-14413
Flow charts for British standard particle-size distribution for soils
[PB-211721] 06 p0667 N73-15426
AUTOFLOW flow chart system for improved documentation and maintenance of scientific applications
10 p1130 N73-19206
BELLFLOW flow chart system for accurate automatic program documentation
10 p1130 N73-19207
Flow diagrams and listings for SAP and PLTGEN programs
[NASA-CR-128985] 17 p1997 N73-26146

**FLOW COEFFICIENTS**
NT DISCHARGE COEFFICIENT
Pressure loss coefficients for fluid flowing through orifice plates, perforated plates, and cylindrical tubes
[ESDU-72010] 04 p0403 N73-13279
Characteristics of wall mass transfer coefficient for pulsed laminar flow in pipe of Newtonian fluid containing dissoloved electrolyte
15 p1765 N73-24301
Measurement of laminar flow in pipes using differential pressure generating devices
[NLL-M-23017-[5828.4F]] 20 p2386 N73-29168
Analysis of structure dependent and temperature dependent variables affecting flow curves of metals
[BLL-RAE-LIB-TRANS-1675] 21 p2556 N73-30494
Wind tunnel testing of V/STOL aircraft models to show wind tunnel wall corrections for models with large values of downwash
[AD-764255] 22 p2616 N73-30962

**FLOW DEFLECTION**
Oscillations and pressure variations in circular jet impacting on wall
[NASA-TT-F-14630] 05 p0527 N73-14284

**FLOW DIRECTION INDICATORS**
Transient thermocouple measurement of gas flow direction velocity, and temperature near injector of liquid propellant rocket
18 p2129 N73-27201

**FLOW DISTORTION**
Influence of inlet distortions on turbojet and ingestion engine stability
[AD-745852] 01 p0092 N73-10755
Mathematical models for predicting unsteady aerodynamic effects on axial flow compressor with distorted inflow - Squid project
[AD-746457] 02 p0157 N73-11271
Far field noise measurements to determine effects of flow distortion for three different installations on noise from fan designed for turbofan engines
[NASA-TN-D-7076] 03 p0280 N73-12269
Effects of vane-induced flow rotation on diffuser flow distortion in axisymmetric mixed-compression inlet
[NASA-TM-X-2752] 09 p0981 N73-18012
Analysis of scaling parameters for flow in core region of vortex generated by rectangular wing tip and vortex generated by ogee wing tip
[NASA-CR-2180] 10 p1103 N73-18995
Boundary layer transition and heat transfer in aerodynamic and thermic wall deformation
14 p1601 N73-22982
Development of techniques for measuring oscillatory derivatives in wind tunnels and analysis of wind tunnel effects on results
[ARC-R/M-3319] 15 p1729 N73-24020
Parallel heat conducting viscous gas flow in flat channel with sine wave wall perturbation
24 p2906 N73-33189

**FLOW DISTRIBUTION**
Methods used with fluid mechanics reference data on external flow to predict forces exerted on bodies of non-streamline shape
[ESDU-FME-1] 01 p0039 N73-10304
Wind tunnel tests of space shuttle models to determine effects of body and wing geometry on hypersonic shock structure and on surface impingement of interior flow field shock waves
[NASA-CR-128587] 01 p0040 N73-10317
Development of wake vortex monitoring system using laser Doppler sensors for analyzing vortex flow field
[NASA-CR-123921] 02 p0152 N73-11229
Numerical analysis of motion of inviscid fluid flow around pointed elliptic cone at incidence using fluid flow equations in conservation law form
[NASA-CR-129178] 02 p0154 N73-11251
Wind tunnel tests to determine lee surface flow characteristics and aerodynamic heating of space shuttle orbiters at supersonic speed with large angles of attack
[NASA-TN-D-7088] 02 p0233 N73-11890
Flow field and base pressure of internal-external-expansion truncated plug nozzles for open and closed wake operations
[NASA-CR-123941] 03 p0281 N73-12282
Analysis of isothermal liquid inflow patterns in spherical container during weightless conditions
[NASA-TM-X-2670] 03 p0283 N73-12291
Calculation of drag of porous lattice plates in turbulent flow
[IC-AERO-72-20] 03 p0284 N73-12300
Analysis of flow distribution around axisymmetric bodies at extreme angles of attack and calculation of pressure distribution for asymmetric steady vortex wake
[AD-747986] 03 p0286 N73-12315
Characteristics of flow around bluff body at supersonic speed with emphasis on leading shock wave formation and changes in withdrawal value for argon and nitrogen
[AD-747407] 03 p0287 N73-12325
Analysis of flow around conical body at small angles of attack in uniform supersonic flow of ideal gas
[AD-747408] 03 p0287 N73-12326
Analysis of eddies and lift forces created on vertical circular cylinder by oscillatory flow conditions
[AD-748078] 03 p0287 N73-12329
Analysis of propellant gases emitted by attitude control system to determine interference with experiments due to flow fields and plume density
[NASA-CR-114508] 03 p0363 N73-12958
Aerodynamics structure of swirling flow in short cylindrical combustion chamber
[AD-747455] 03 p0365 N73-12975
Wind tunnel tests to determine effects of gas stream flow parallel to discharging surface on flow characteristics of wire-form porous material
[NASA-TM-X-2687] 04 p0369 N73-13000
Analysis of aerodynamic interference effects between aircraft and external store carried under wing based on inviscid flow characteristics
[AD-748348] 04 p0370 N73-13005
Vortex model for calculating blade circulation flow of helicopter rotor
[NASA-TT-F-14637] 04 p0371 N73-13014
Flow distribution of low Reynolds number, high enthalpy viscous flow of diatomic gas through conical nozzles
[DGLR-PAPER-72-110] 04 p0405 N73-13302
Development of mathematical model for viscous inviscid interaction analysis and solution of boundary layer equations by finite difference scheme
[AD-748342] 04 p0408 N73-13322
Density field map in fin-flat plate junction in three dimension, using holographic interferometry
[AD-749048] 04 p0408 N73-13324
Numerical analysis of induced velocities of wing with curved axis not perpendicular to velocity of incoming flow
[AD-749843] 05 p0497 N73-14048
Analysis of flow properties in wake of 120 and 140 degree included angle conical bodies and flow characteristics of Viking 75 entry vehicle configuration
[NASA-TN-D-7089] 05 p0527 N73-14285
Ejector-driven multiple jet wind tunnel for simulation of flows in planetary boundary layer
[AD-748903] 05 p0527 N73-14289
Meander patterns of Feather and Colorado Rivers
05 p0537 N73-14366
Subsonic numerical panel method for flow calculation applied to delta wing, lifting reentry body, body-wing configurations
[MBB-UFE-889-72-O] 06 p0615 N73-14992
Analysis of air cushion vehicle landing system operation and computation of air flow requirements
[AD-750936] 06 p0625 N73-15069
Modification of UH-1 helicopter rotor to determine effects of injecting tip vortex of rotor blade with mass of linearly directed air
[AD-750634] 06 p0625 N73-15074
Analysis of lee side vortex flow distribution about ogive-cylinderfrustum-cylinder at various angles of attack and Mach numbers - Vol. 1
[NASA-CR-123997-VOL-1] 06 p0653 N73-15307
Compilation of computed parameters resulting from analysis of lee side vortex flow distribution about ogive-cylinder-frustum-cylinder at various angles of attack and Mach numbers - Vol. 2
[NASA-CR-123997-VOL-2] 06 p0653 N73-15308
Pluviometric and statistical analyses of precipitation and watercourse patterns in Israel
06 p0665 N73-15403
Generation and stabilization of coastal wave induced circulation and longshore current patterns
[AD-750291] 06 p0671 N73-15458
Configuration and structure of turbulent boundary layer flow over lateral uneven surface roughness
[AD-749944] 06 p0694 N73-15656
Application of unsteady airfoil theory to determine pressure and lift fluctuations on rotor blades of turbomachinery
07 p0735 N73-15983
Reduction of transonic drag for high performance aircraft by injecting air in rear of aircraft to alter transonic flow distribution on aft section
[AD-751269] 07 p0736 N73-15991
Development of computer program for calculating flow field resulting from sonic boom focusing
[NASA-CR-2127] 07 p0739 N73-16013
Analysis of supersonic, three-dimensional flow characteristics to determine effects of material porosity and angle of attack on jet stretcher performance
07 p0765 N73-16215
Numerical analysis of viscous, compressible, and heat conducting fluid flow patterns in rotating nozzles
07 p0768 N73-16241
Computerized simulation of shrouded propeller low field in cross flow using vortex lattice models
[AD-751463] 07 p0773 N73-16274
Predicting total pressure loss regions existing in corner between sidewall and horizontal nozzle walls at exits with convex contour curvature
[AD-751606] 07 p0773 N73-16277
Experimental analysis of three dimensional flow fields in planar nozzles and wall jets found in bistable fluid amplifiers
[AD-751627] 07 p0774 N73-16282
Measurement of microscale turbulence and turbulent flow intensity of dilute polymer solutions about circular cylinders
[AD-751640] 07 p0774 N73-16284
Mathematical models for predicting flow fields within and external to thrust reverser deployed in flight including forces and moments induced on aircraft by flow fields
[AD-751525] 07 p0837 N73-16784
Analysis of aerodynamic drag on general convex bodies at zero angle of attack during high speed flow in rarefied air
08 p0895 N73-17242
Effect of nonuniform upstream flow conditions on shock shape and surface pressure distribution on two dimensional pointed bodies
08 p0895 N73-17244
Designs and performance predictions for high performance supersonic ejector systems
[AGARDOGRAPH-163] 08 p0895 N73-17248
Conservation equations for analyzing supersonic and mixing flow regimes of supersonic ejectors
08 p0895 N73-17249
Analysis of uniform jet flow around airfoil with separated shock wave at low supersonic velocities of incident flow
[NASA-TT-F-14813] 08 p0896 N73-17259
Flow field measurements around ogive-cylinder at angles of attack to 15 degrees and Mach numbers 3.52 and 4.07
[AD-752025] 08 p0898 N73-17268
Analysis of turbulent velocity fluctuations in confined jet to determine design parameters for fluid amplifiers
[AD-752041] 08 p0899 N73-17276
Procedure for measuring flow stresses of metals during closed die forging
[AD-752588] 08 p0928 N73-17602
Computer program for analyzing flow field generated near aircraft engine operating in reverse thrust
[NASA-CR-121147] 09 p1012 N73-18264
Calculation of outer inviscid flow about rectangular wing moving at supersonic speeds
[NASA-CR-130985] 09 p1013 N73-18269
Analysis of measurable and ideal quantities of nozzle beams skimmed from parallel equilibrium gas flows
[DLR-FB-72-51] 09 p1014 N73-18275
Analysis of flow distribution around harmonically oscillating circular cylinder under two dimensional flow conditions
[DLR-FB-72-56] 09 p1014 N73-18277
Measurement of aerodynamic drag of conical bodies at zero angle of attack in free molecular and near free molecular flow regime
[DLR-FB-72-64] 09 p1014 N73-18278
Existence and uniqueness of solutions obtained from streamline curvature method of calculating flow through turbomachines for several operating points of Rolls-Royce compressor
[ARC-CP-1234] 09 p1016 N73-18293
Analysis of turbulent mixing between two streams of different density to determine effects of density difference at low Mach number and compressibility at high Mach number
[AD-753538] 09 p1019 N73-18313
Method of characteristics solution of flow field on lee side of flat plate delta wing with supersonic leading edges
[AD-753389] 09 p1019 N73-18319
Analysis of flow field around two dimensional airfoil of arbitrary shape
[AD-753387] 09 p1019 N73-18320
Numerical calculation of flow fields produced by lifting elliptic cone, lifting three dimensional wing, and lifting delta wings
[NASA-CR-131089] 10 p1139 N73-19282
Orifice inclination effect in pressure measurements on hypersonic rarefied flow field of flat plate
10 p1140 N73-19290
Flow field, pressure, and heat transfer associated with small fins of half angle cone in supersonic flow
[SCL-RR-72-0339] 10 p1142 N73-19302

Nonstationary flow of anomalous viscous liquid having particular properties of displacement speed and viscosity
[AD-753486] 10 p1142 N73-19308
Affect of sound and vibration on convective heat transfer and flow distribution on boundary layers of cylindrical bodies
[AD-754006] 10 p1143 N73-19316
Transonic flow studies in slotted wind tunnels
[AD-753911] 10 p1144 N73-19320
Observations of kinematic and thermodynamic fields over Barbados
10 p1180 N73-19596
Effects of boundary layer flow patterns on upright cascade blade performance
10 p1205 N73-19803
Development of space shuttle scale model for thermodynamic analysis of internal and external heat flow fields
[NASA-CR-128849] 10 p1215 N73-19882
Analysis of conditions existing in rising, rotating column of hot gases containing core of reacting gases
[TR-5] 10 p1223 N73-19948
Analysis of basic acoustic characteristics and noise reduction potential of upper surface of blown flap
[NASA-CR-112246] 11 p1234 N73-20017
Flow patterns of air being aspirated into blunt thickwalled tube, and inertia effects on particle trajectories
[TR-23] 11 p1270 N73-20306
Problem formulation and numerical procedures for solving flow equations for flow distribution of viscous shock layer on nose of shuttle orbiter during reentry - Vol. 1
[NASA-CR-128871] 11 p1271 N73-20309
Development of computer programs for analyzing flow distribution in nose region of blunt body at arbitrary speed and altitude - Vol. 2
[NASA-CR-128872] 11 p1271 N73-20310
Computer program for calculating structure and supersonic combustion flow with chemical reactions and shock waves
[NASA-CR-112303] 11 p1271 N73-20311
Analysis of Reynolds stress in turbulent boundary layer on smooth wall with zero pressure gradient
[AD-754758] 11 p1272 N73-20319
Development of procedure for determining geometry and strength distribution of vortex wake generated by single-bladed hovering helicopter rotor
12 p1360 N73-21035
Three dimensional supersonic flow program for calculating flow field about cone at zero angle of attack
[NASA-CR-112301] 12 p1391 N73-21282
Nonoscillatory characteristics of Taylor vortices occurring in Couette flows based on evolution of eigenvalues and analytic continuation - Part 3
[AD-754480] 12 p1392 N73-21289
Satellite television photography of geomorphological indices for developing stream meander pattern
12 p1400 N73-21352
Laser Doppler velocimeter for simultaneously measuring orthogonal fluid velocity components without flow field perturbation
[NASA-CASE-ARC-10637-1] 12 p1405 N73-21390
Examination of lunar surface patterns created by volcanic lava flows and impact debris
12 p1454 N73-21779
Effect of heat transfer on flow and temperature fields in separation nozzle measured with free molecular pressure and temperature probes
[KFK-1634] 12 p1464 N73-21865
Wind tunnel tests to determine flow distribution within model passages of hypersonic inlets for core flow and boundary layer flow conditions
[NASA-TN-D-7150] 13 p1470 N73-21905
Model for prediction of pressure within recirculation bubble of attached jet
13 p1507 N73-22216
Nozzle and wall jet flow fields in bistable fluid amplifiers
13 p1509 N73-22230
Numerical analysis of turbulence equations in orthogonal tensor form, axisymmetric flow equations, and use of mass-averaged variables
[NASA-TM-X-62248] 13 p1510 N73-22235
Application of holographic interferometry to determination of discontinuous three-dimensional density fields
[AD-756535] 13 p1511 N73-22246
Computer program to evaluate effect of closed-jet tunnel test on force coefficents of cambered, sharp-nosed, fully cavitating, two dimensional hydrofoil section
[AD-755423] 13 p1512 N73-22250
Application of laser Doppler velocimeter for measurement of central vortex filament in wind tunnel test section
[NASA-TM-X-62243] 13 p1536 N73-22448
Development of mathematical matrix technique for calculating inviscid, rotational, compressible axisymmetric flow field through axial flow compressor
[ME/A-73-1] 13 p1570 N73-22723
Analysis of dynamic inlet distortion data for turbojets
[AD-756481] 13 p1571 N73-22731
Aerothermodynamic wind tunnel tests of space shuttle configurations performed at Mach number 8 for flow distribution and heat transfer under reentry conditions
[NASA-CR-131486] 13 p1583 N73-22834
Windward surface flow distribution on lifting reentry vehicle configurations at high angles of incidence under hypersonic perfect gas conditions
[AD-756499] 14 p1599 N73-22961
Development of computer programs to predict performance of thrust reversal and thrust vector control systems on short takeoff transport aircraft - Vol. 1
[AD-756860] 14 p1603 N73-22993
Fluid mechanics facility in aerodynamics laboratory
[AD-756512] 14 p1646 N73-23350
Visualization of flow deviation by cylindrical wall cavities
14 p1649 N73-23374
Condensible vapor supersonic nozzle flows at supersaturation collapse near condensation point
[AD-756471] 14 p1651 N73-23393
Diagnostics of flow fields using Raman scattering technique
[AD-757319] 14 p1652 N73-23400
Three dimensional particle trajectories in compressible gas flow in rotating cascade
[AD-757162] 14 p1701 N73-23807
Development of slender body theory for analyzing flow past thin, conically cambered, delta wing with exact boundary conditions
[ARC-R/M-3249] 15 p1726 N73-24002
Wind tunnel tests to determine effects of leading edge modifications on flow and forces on untapered wing with 50 degree leading edge sweep and Mach numbers from 0.60 to 1.20
[ARC-R/M-3270] 15 p1726 N73-24003
Analysis of flow pattern on tapered, sweptback wing at Mach numbers between 0.6 and 1.6 and 12 degree angle of incidence
[ARC-R/M-3271] 15 p1726 N73-24004
Analysis of flow development over plane, half-wing with cropped-delta planform using surface pressure distributions and oil flow patterns with variations in incidence and Mach number
[ARC-R/M-3286] 15 p1727 N73-24008
Narrowband noise generation by flow over perforated or ventilated transonic wind tunnel walls
[AD-758254] 15 p1763 N73-24283
Numerical analysis of base pressure distribution for supersonic flow over slender wedge or backward facing step
15 p1764 N73-24295
Thermodynamic flow characteristics of arc heater, convergent-divergent nozzle, and underexpanded jet in plasma wind tunnel
[NAL-TR-307] 15 p1766 N73-24308
Development of mathematical models for turbulent flow and application to prediction of internal flows
[TM/TN/A/18] 15 p1768 N73-24321
Analysis of supersonic, unstalled torsional flutter in cascades of compressor blades to determine position of flutter boundary and aeroelastic instability
[AD-758721] 15 p1827 N73-24809
Development of numerical relationship to provide axially symmetric analog for general three dimensional boundary layers
[ARC-R/M-3200] 16 p1853 N73-25014
Numerical analysis of incompressible laminar boundary layer on infinite swept wing with arbitrary velocity and suction distribution
[ARC-R/M-3241] 16 p1854 N73-25018
Analysis of effects of shock induced boundary layer separation in transonic flight and methods for eliminating or reducing effects
[ARC-R/M-3510] 16 p1854 N73-25019
Research projects in theoretical and practical aerodynamics - Vol. 2
16 p1854 N73-25020
Development of numerical procedures for determining velocity potential on triangular wing oscillating harmonically in supersonic flow
[ARC-R/M-3229] 16 p1854 N73-25023
Computer programs for predicting supersonic and hypersonic interference flow fields and heating
[NASA-TM-X-2725] 16 p1889 N73-25285
Three dimensional flow field modules with turbulent structure
[AD-758894] 16 p1890 N73-25292
Investigation of flow issuing from nozzle in fluid amplifier and impinging on receiver with spill port oriented at 90 degrees to flow direction
[AD-759796] 16 p1890 N73-25297
Nonuniform flow in front of axial flow compressor stage
[AD-759247] 16 p1891 N73-25303
Flow field characteristics of beam deflection fluid amplifier considering pressure differential
[AD-759210] 16 p1892 N73-25315
Internal performance of mixed compression axisymmetric inlet model at Mach 0.8 to 2.65
[NASA-TN-D-7320] 16 p1955 N73-25817
Exhaust gas diffuser effect on test cell wall and turbofan cold-flow model engine exhaust nozzle plug and core engine cowl surface pressure
[AD-759177] 16 p1958 N73-25842
Analysis of Magnus forces on high fineness ratio body of revolution with ogive forebody at varying angles of attack
[AD-759987] 17 p1980 N73-26003
Development of numerical methods for correcting wall constraints in transonic wind tunnels with ventilated walls
17 p2008 N73-26241
Analysis of interference occurring in subsonic and transonic wind tunnels caused by model support system
17 p2009 N73-26242
Numerical analysis of effect of streamwise coordinate of basic flow on stability characteristics of boundary layer flow
17 p2012 N73-26270
Experimental determination of laminar boundary layer and oscillatory suspension flows by laser anemometry
17 p2012 N73-26271
Structure of weak shock wave in vibrationally relaxing gas undergoing wall reflection
17 p2013 N73-26277
Application of holographic interferometry techniques for determining asymmetric flow distribution encountered near wing-fuselage junction at transonic speed
[AD-759967] 17 p2015 N73-26296
Analysis of profile characteristics of supersonic turbulent boundary layer in region of moderate adverse pressure gradient
[AD-759915] 17 p2015 N73-26298
Turbulent nonbuoyant or buoyant jets discharged into flowing or quiescent fluids
[AD-760028] 17 p2016 N73-26300
CONSHOC computer program for locating shock waves and contours of flow variables in finite difference flow fields
[AD-759898] 17 p2016 N73-26301
Application of holography techniques for recording three dimensional flow distribution of liquid jet injected into Mach 3 gas stream
17 p2039 N73-26498
Doppler radar investigation of flow patterns in severe thunderstorms
[AD-760106] 17 p2058 N73-26649
Analysis of flow field around 18 inch diameter flat circular parachute model using helium bubble technique
[AD-761098] 18 p2106 N73-27034
Convection and dispersion patterns associated with stationary and nonstationary fluid transport
18 p2129 N73-27205
Characteristics method for calculating supersonic flow fields
[NASA-CR-132274] 18 p2130 N73-27210
Computer program for predicting inviscid, transonic flow field about isolated nacelles
[NASA-CR-112271] 18 p2130 N73-27211
Numerical analysis of two dimensional incompressible potential flow around system of arbitrary airfoils using relaxation method
[NAL-TR-309] 18 p2130 N73-27212
Holographic visualization of flow field within transonic compressor rotor
[NASA-CR-121112] 18 p2130 N73-27215
Visualization of swirling flow in rotating tube and measurement of velocity distribution by laser-Doppler anemometry
[NASA-CR-2284] 18 p2131 N73-27216
Experimental determination of bound vortex lines and flow in vicinity of trailing edge of slender delta wing
[NASA-TT-F-15012] 18 p2131 N73-27217
Possibility of similarity solution to describe flow field at juncture of sonic line and shock in flows with high subsonic Mach numbers
[AD-760801] 18 p2132 N73-27224
Flow configurations for maximum nuclear criticality eigenvalue in gas core reactor
[NASA-CR-121191] 18 p2177 N73-27578
Wind tunnel tests of short takeoff and landing fan stage model to determine airflow conditions around rotor and stator and stage pressure ratio
[NASA-TM-X-2837] 18 p2192 N73-27701
Wind tunnel tests to determine heat transfer and flow distribution of space shuttle configuration at hypersonic speeds simulating atmospheric entry
[NASA-CR-133405] 18 p2201 N73-27772
Analysis of flow distribution over three axisymmetric bodies at various angles of attack to determine boundary layer transition point characteristics
19 p2250 N73-28145
Numerical method employing plane characteristics for calculating geometrically complex three dimensional nozzle exhaust flow fields
19 p2251 N73-28149
Numerical analysis of two dimensional turbulent wakes in constant adverse and favorable pressure gradients
[AD-761389] 19 p2256 N73-28185
Solution of unsteady Navier-Stokes equations for flow field about impulsively started flat plate
[AD-761459] 19 p2257 N73-28193

Development of performance equations for cryptosteady-flow energy separator over widest range of operating conditions for turbojet engines
[AD-762030] 19 p2330 N73-28747
Analysis of rotating stall conditions in axial flow compressors and development of control system to improve flow stability
[AD-762297] 19 p2330 N73-28748
Analysis of cryptosteady-flow energy separation in turbojet engines and application to nozzle design
[AD-762031] 19 p2331 N73-28751
Analysis of energy separator for application to air conditioning system of E-8 aircraft
[AD-762590] 20 p2364 N73-29014
Effect of ablation modes and flow field distribution on cross hatching phenomenon at supersonic speeds
[TN-85] 20 p2485 N73-29963
Two and three dimensional flow field characteristics of lower surfaces of caret wings
[AASU-327] 21 p2491 N73-29997
Calculation of pressure field induced by free jet exhausted from flat plate into stagnant medium based on solution of Neumann problem in terms of singularity distributions
[NLR-TR-72040-U] 21 p2492 N73-30000
Plane elastic wave propagation through movable wall, calculating flow distribution behind wall
[DLR-FB-72-59] 21 p2525 N73-30246
Numerical analysis of flow characteristics on upper surface of wedge moving at supersonic speed when plane shock wave is incident on wedge
[AD-763283] 21 p2527 N73-30267
System for reducing noise generated by jet impinging on external flap using injection of secondary air from slot near trailing edge of flap
[NASA-CR-132270] 22 p2611 N73-30930
Kinetic molecular flow distribution at porous wall using one dimensional steady state Boltzmann equation
[VKI-TN-79] 22 p2654 N73-31259
Ice motion and interior flow field
[PB-221714/9] 22 p2669 N73-31387
Analysis of sonic boom characteristics based on second order solutions for flow distribution around slender bodies in supersonic flow - Part 1
[NASA-CR-2339] 23 p2739 N73-31927
Analysis of inviscid flow field around rectangular wing of finite thickness in supersonic flow
23 p2771 N73-32166
Flow field solution for boundary layer interaction in confined viscous vortex
23 p2772 N73-32170
Mixing region in flow field of fluidic beam deflection amplifier
23 p2772 N73-32173
Static pressure and heat transfer rate distributions on conical bodies at hypersonic speeds laminar and turbulent flow conditions
[AD-764983] 23 p2777 N73-32204
Treatment of singularities in solution of Laplace equation by integral equation method based on Green function, applied to flow distribution and transmission lines
[NPL-NAC-31] 23 p2813 N73-32490
Method of characteristics for studying flow field produced by underexpanded jet exhausted from conical nozzle into cylindrical tube
24 p2904 N73-33173
Flow module approach to flow around three dimensional obstacles in boundary layer
24 p2908 N73-33207
Effect of inlet conditions on optimal shape of diffuser based on theory of potential flow of fluid in channels
[AD-765577] 24 p2911 N73-33230

**FLOW EQUATIONS**
NT HELMHOLTZ VORTICITY EQUATION
NT VORTICITY EQUATIONS
Numerical analysis of motion of inviscid fluid flow around pointed elliptic cone at incidence using fluid flow equations in conservation law form
[NASA-CR-129178] 02 p0154 N73-11251
Development of computer programs for analyzing and predicting properties of transonic flows around certain types of wing-body combinations
[NASA-CR-2157] 03 p0247 N73-11999
Application of modified compressibility transformation for analyzing variable property turbulent boundary layers and predicting flow properties
[NASA-CR-2147] 03 p0282 N73-12286
Numerical analysis of fluid containment near stagnation point and within self-confined stagnation region for bi-component mixture
[NASA-CR-2172] 03 p0283 N73-12292
Flow equations for water/steam reaction engine with shrouded nozzles
04 p0404 N73-13293
Numerical computation of plane jet propagating onto curved wall surface submerged in viscous fluid
[NASA-TT-F-13924] 04 p0405 N73-13296
Development of mathematical model for viscous inviscid interaction analysis and solution of boundary layer equations by finite difference scheme
[AD-748342] 04 p0408 N73-13322
Analysis of pressure loss through single bends of various geometries under conditions of full incompressible flow
[ESDU-67040-AMEND-A] 05 p0525 N73-14272
Analysis of turbulent fluid flow through rectangular conduit with large aspect ratio and development of mechanical energy-balance equations
[WTHD-27] 05 p0526 N73-14279
Development of method for numerical integration of Navier-Stokes equations based on perturbation of Poisson type equation for viscous flow
[NA-7] 05 p0526 N73-14282
Effect of space-time integral of thermodynamic pressure on thermodynamic potential for compressible, adiabatic flow
[NASA-TM-X-66139] 05 p0606 N73-14926
Development of finite difference procedure to calculate steady flows over several classes of airfoils under inviscid transonic flow conditions
[NASA-CR-2186] 06 p0614 N73-14989
Development of procedure for determining characteristics of high lift systems where viscous effects dominate
06 p0617 N73-15009
Numerical analysis of change in component energies due to three dimensional distortion in homogeneous and initially axisymmetric turbulence
[REPT-72-FM-7] 06 p0652 N73-15298
Computer program for determining influx towards center of spherical metal shell following detonation of spherical, symmetrically placed explosive
[FOA-2-C-2471-25] 06 p0653 N73-15305
Numerical analysis of one-dimensional isentropic flow of thermally perfect, calorically imperfect diatomic gas
[ESDU-S.00.01.10-AMEND-A]
07 p0767 N73-16233
Numerical analysis of oscillating wedge in supersonic perfect gas flow to evaluate trends for wedge and to analyze unsteady flows
07 p0767 N73-16235
Finite difference solutions for laminar and turbulent boundary layer equations of perfect gases and gas mixtures in chemical equilibrium
07 p0767 N73-16236
Solution of viscous shock-layer equations using implicit finite difference scheme for hyperboloid body under conditions simulating atmospheric entry
07 p0768 N73-16238
Analysis of one dimensional flow downstream of source of radiation in constant area ducts and conical nozzles
07 p0853 N73-16920
Development of model to describe characteristics of one dimensional lunar ash flow with and without heat transfer effects
[NASA-CR-130697] 08 p0895 N73-17245
Numerical analysis of flow of rarefied monatomic gas through two dimensional slot to show characteristics of transition regime
[NASA-CR-124069] 09 p1012 N73-18265
Application of splitting method for numerical analysis of heat conducting gas flows in curvilinear coordinates
[NASA-TT-F-14658] 09 p1015 N73-18288
Solution of Chaplygin equation by straight line method to describe gas flow around profile at high subsonic speed with local supersonic curved shock wave
[AD-753557] 09 p1019 N73-18318
Application of implicit finite-difference method for solution of compressible boundary layer equations
10 p1139 N73-19277
Flow equations for unsteady turbulent boundary layer flow on swept infinite cylinder to show effects of variations in frequency of oscillations
[NASA-TM-X-62242] 10 p1141 N73-19297
Physical quantities in two phase flows
[FRNC-CONF-49] 10 p1142 N73-19301
Development of method for solving three dimensional, incompressible laminar and turbulent boundary layer problems for swept infinite cylinders and small cross flow
[AD-754440] 11 p1232 N73-20004
Problem formulation and numerical procedures for solving flow equations for flow distribution of viscous shock layer on nose of shuttle orbiter during reentry - Vol. 1
[NASA-CR-128871] 11 p1271 N73-20309
Development of computer programs for analyzing flow distribution in nose region of blunt body at arbitrary speed and altitude - Vol. 2
[NASA-CR-128872] 11 p1271 N73-20310
Numerical analysis of low Reynolds number flow perpendicular to circular cylinder with constant radial suction mass flux at surface
12 p1389 N73-21264
Development of statistical equations for turbulent compressible gas with emphasis on space-time correlations in boundary layer
[AD-755889] 12 p1393 N73-21291
Numerical analysis of turbulence equations in orthogonal tensor form, axisymmetric flow equations, and use of mass-averaged variables
[NASA-TM-X-62248] 13 p1510 N73-22235
Analysis of accuracy of Preston tube calibration equations to determine local skin friction in two dimensional supersonic and low hypersonic flow conditions
[NASA-TN-D-7190] 13 p1510 N73-22239
Computer program to evaluate effect of closed-jet tunnel test on force coefficents of cambered, sharp-nosed, fully cavitating, two dimensional hydrofoil section
[AD-755423] 13 p1512 N73-22250
Development of numerical relationship to provide axially symmetric analog for general three dimensional boundary layers
[ARC-R/M-3200] 16 p1853 N73-25014
Evaluation of three approximate methods for solving three dimensional boundary layer equations
[ARC-R/M-3201] 16 p1853 N73-25015
Numerical analysis of turbulence transport equation for two dimensional jet flow and pressure-velocity derivative correlations
16 p1887 N73-25270
Numerical analysis of structure of incompressible turbulent flows in plane wake and plane jet using two eddy viscosity models
17 p2012 N73-26274
Analysis of supersonic flow involving viscous and inviscid flow using unified solution technique
19 p2251 N73-28148
Analysis of arbitrarily nonuniform, nonadiabatic, two dimensional or axisymmetric basic flows based on inviscid theory of three dimensional perturbations in uniform transonic flow
[AD-761632] 19 p2256 N73-28188
Analysis of viscous effects in low-density nozzle flows using internal laminar layer equations for two dimensional or axisymmetric flow
[AD-761489] 19 p2257 N73-28191
Numerical transformation of basic equation for two parameter flow
[AD-762104] 19 p2257 N73-28195
Numerical analysis of compressible turbulent boundary layer velocity and temperature profiles with zero pressure gradient
[AD-762152] 19 p2258 N73-28200
Numerical analysis of inviscid transonic flow over body with supersonic underexpanded exhaust plume and characteristics of flow near boattail sting
[RM-577] 21 p2523 N73-30234
Study of supersonic conical flow by solving exact conical flow equations
[ISAD-4980-VOL-38-NO-9] 22 p2651 N73-31236
Second order thermal boundary layer theory for steady, laminar, compressible flow over cambered two dimensional or rotational bodies
[DLR-FB-73-31] 22 p2653 N73-31256
Development of theoretical model for determining flow characteristics of round jet in incompressible cross-flow based on matched asymptotic expansion
[NASA-CR-132324] 23 p2775 N73-32191
Fourth-order, time dependent, partial differential flow equation solved by coupled pair of finite difference equations
[AD-765323] 23 p2776 N73-32201
On the effects of viscous interaction for a flat delta wing at incidence
[ARC-CP-1237] 24 p2870 N73-32931
Finite difference solutions for flow equations of three dimensional boundary layer on blunt body
[SLA-73-366-PT-1] 24 p2909 N73-33217
Application of second-order accurate fluid algorithm for variable spatial grid
[AD-765316] 24 p2910 N73-33225

**FLOW FIELDS**
U FLOW DISTRIBUTION

**FLOW GEOMETRY**
Development of jet noise test facility for flow and acoustic measurements of mean and turbulent velocities in jet flow
[RE-450] 13 p1505 N73-22196
Development of flow visualization techniques for determining aerodynamic characteristics of bluff bodies under unsteady flow conditions
[AD-759266] 16 p1892 N73-25311
Development of theoretical model for supersonic turbulent near wakes of planar and axisymmetric configuration in supersonic flow
20 p2384 N73-29151
Stability characteristics of stratified and unstratified air flow between two horizontal, infinite disks rotating at slightly different rotation rates
20 p2384 N73-29154
Development of computer programs for designing engine inlets for VTOL and STOL aircraft based on axisymmetric potential flow parameter
[NASA-TM-X-68278] 20 p2388 N73-29182
Wind tunnel tests to determine flow distribution at inlet locations on aircraft model for various aerodynamic configurations and airspeeds
[NASA-TN-D-7364] 23 p2739 N73-31929

**FLOW MEASUREMENT**
Equipment and procedures for measuring flow of liquids and gases to identify application of specific types of equipment
[NLL-TRANS-45-[3958.4]] 02 p0154 N73-11249

Development and characteristics of test facility for measuring three dimensional boundary layers on helicopter rotor blade under various conditions
[NASA-CR-112194] 03 p0252 N73-12042
Sphere free motion in rotating fluid noting Taylor instability existence
[DLR-FB-71-32] 03 p0285 N73-12309
Development of flow visualization and flow measurement techniques and application to flow problems of turbines, aircraft engines, and missile propulsion
[AD-747613] 03 p0287 N73-12328
Numerical analysis of pressure drop in ducts across round-wire gauzes or screens normal to fluid flow to show effects of gauze geometry and velocity of flow
[ESDU-72009] 04 p0403 N73-13280
Development of design data for cascades of flat plate guide vanes suitable for use in ninety degree elbows in ducts of circular cross section
[ESDU-AERO-00.02.09] 04 p0403 N73-13284
Instrument for measuring magnitude and direction of flow velocity in flow field
[NASA-CASE-LAR-10855-1] 04 p0419 N73-13415
Development of method for numerical integration of Navier-Stokes equations based on perturbation of Poisson type equation for viscous flow
[NA-7] 05 p0526 N73-14282
Rheological investigation of lubricating media using displacement equations for three special cases
[FOA-1-C-1408-92] 06 p0672 N73-15470
Survey of data involving design of equipment for two phase flow of cryogenic fluids based on critical flow rate
[NASA-CR-130793] 09 p1013 N73-18270
Continuous reading fluidic device for measuring component flow of binary gas mixtures
[NASA-TM-X-2741] 09 p1035 N73-18445
Application of laser Doppler velocimeter for flow measurements
[AD-753243] 09 p1044 N73-18513
Procedure for developing aerodynamic parameters for use in flight simulator research projects with emphasis on wind tunnel measurements
10 p1105 N73-19008
Analysis of design flow in open jet wind tunnel and examination of processes for starting supersonic wind tunnels
[ARL/ME-138] 10 p1137 N73-19264
Wind tunnel measurements of nearly homogeneous grid turbulence field with large amplitude temperature fluctuations
10 p1139 N73-19280
Techniques and equipment for measuring stationary and nonstationary flow in wind tunnels during pressure and flutter tests
[DLR-MITT-72-25] 10 p1139 N73-19283
Development of steel wedge probe for measurement of three dimensional wake flow in subsonic and transonic flow fields
10 p1140 N73-19285
Numerical analysis of Prandtl mixing path, criteria charcterizing pressure and velocity pulsations in turbulent flow conditions
10 p1141 N73-19294
Fundamental flow problem in designing fluidic proximity sensors
10 p1158 N73-19422
Three component wake velocity measurements of full scale OH-13 helicopter rotary wing during hovering flight
[AD-754644] 11 p1235 N73-20030
Hot-wire anemometer measurements of turbulence and shear stress in circular tube flow
[KFK-1642] 12 p1392 N73-21286
Characteristics of instrument for measuring and recording water flow and modifications for improved operation
12 p1421 N73-21518
Theoretical and experimental investigation of flux-flow noise in type 2 superconductors
12 p1437 N73-21642
Digital linearization of turbulent channel flow measurements by hot-film sensor
[REPT-2/1973] 13 p1510 N73-22234
Feasibility of radar system to measure direction of shoreline ocean waves
[AD-755241] 13 p1527 N73-22373
Local flow measurements at inlet spike tip of Mach 3 supersonic cruise aircraft
[NASA-TN-D-6987] 15 p1731 N73-24037
Analysis of spoiler plate characteristics to eliminate effects of installation disturbance when conducting flow rate measurements
[NLL-NEL-TT-2439-[6075.461]]
15 p1763 N73-24288
Development of methods for determining local skin friction of boundary layer and calibration of instruments for analyzing turbulent shear flow
[ARC-R/M-3202] 16 p1854 N73-25016
Photographic equidensitometry of two phase and low density flows
[DLR-MITT-73-02] 17 p2015 N73-26293
Visualization of swirling flow in rotating tube and measurement of velocity distribution by laser-Doppler anemometry
[NASA-CR-2284] 18 p2131 N73-27216
Hot film sensor measurement of turbulent flow of fluids in pipes
[AD-762059] 19 p2258 N73-28199
Measurement of laminar flow in pipes using differential pressure generating devices
[NLL-M-23017-[5828.4F]] 20 p2386 N73-29168
Measurement of laminar fluid flow through orifice meters to determine discharge coefficients and head losses
[NLL-NEL-TT-2457-[6075.461]]
20 p2386 N73-29169
Fluid mass flow rate measurements using cavitating Venturi tubes noting application to liquid rocket propellant
[DLR-FB-72-33] 21 p2525 N73-30245
Feasibility analysis of nonradiating flow in wind tunnels using light scattering experiments
[BMBW-FBW-72-20] 21 p2580 N73-30677
Device for welding hot-wire anemometer components following breakage due to dust particles in air stream
[AERE-R-7304] 22 p2678 N73-31451
Measurement of flow parameters in midspan double-circular-arc section of stator in subsonic flow and comparison with computed performance
[NASA-TN-D-7425] 23 p2740 N73-31932
Performance tests of hemispherical flow-direction sensor mounted on F-104 aircraft to develop Mach number position error calibration curve
[NASA-TN-D-7461] 23 p2743 N73-31956
Development of wind tunnel with self correcting apparatus based on sensors to determine flow conditions on tunnel surfaces and method for varying wall geometry
[AD-764957] 23 p2771 N73-32161
Turbulent gas-solids flow measurements using laser Doppler velocimeter
23 p2773 N73-32182

**FLOW PATTERNS**
U FLOW DISTRIBUTION

**FLOW RATE**
U FLOW VELOCITY

**FLOW REGULATORS**
Gas flow control device, including housing and input port
[NASA-CASE-NPO-11479] 04 p0425 N73-13462
Flow module approach to flow around three dimensional obstacles in boundary layer
24 p2908 N73-33207

**FLOW RESISTANCE**
NT AERODYNAMIC DRAG
NT FRICTION DRAG
Numerical analysis of pressure drop in ducts across round-wire gauzes or screens normal to fluid flow to show effects of gauze geometry and velocity of flow
[ESDU-72009] 04 p0403 N73-13280
Numerical analysis of pressure losses due to bends in fluid flow systems and application of correction factor to relate overall losses for various conditions
[ESDU-68035] 04 p0403 N73-13283
Analysis of skin friction measurement techniques for incompressible flow to show instruments required and areas of difference
[FFA-AU-726] 08 p0895 N73-17246
Calculation of hydraulic resistances in pipelines
[AD-754322] 10 p1144 N73-19319
Iterative method for calculating axial flow resistance in annular slots of impeller pumps
[NLL-NEL-TT-2422-[6075.461]]
11 p1269 N73-20299
Heat transfer and frictional resistance in pipes with cooled walls during turbulent flow of high temperature gases
[NLL-RTS-7640] 11 p1347 N73-20930
Measurement of pipe resistance to instantaneous pulsating nonstationary flow
[NASA-TT-F-14881] 12 p1391 N73-21279
Analysis of viscosity of saturated hydrocarbons at different temperatures and pressures to show test equipment and procedures
[NLL-NEL-TT-2471-[6075.461]]
20 p2434 N73-29547

**FLOW SEPARATION**
U BOUNDARY LAYER SEPARATION
U SEPARATED FLOW

**FLOW STABILITY**
NT BOUNDARY LAYER STABILITY
NT FLAME STABILITY
NT MAGNETOHYDRODYNAMIC STABILITY
Causes and mechanisms of cavitating inducer instabilities
[NASA-CR-123939] 04 p0405 N73-13299
Constant flow velocity generator for calibrating hot-wire anemometers
[NASA-CASE-MFS-21424-1] 07 p0769 N73-16248
Review of linear viscous stability theory for stably stratified parallel shear flow
[CONF-720632-1] 07 p0772 N73-16270
Flow instabilities of supersonic variable ramp inlets at Mach 2 discussing Concorde aircraft intake
[ARC-R/M-3711] 10 p1104 N73-18999
Techniques and equipment for measuring stationary and nonstationary flow in wind tunnels during pressure and flutter tests
[DLR-MITT-72-25] 10 p1139 N73-19283
Hydrodynamic instability effects on performance of electromagnetic pump under certain operating conditions
[FRNC-CONF-46] 10 p1166 N73-19485
Kelvin-Helmholtz instability analysis of bounded two phase particulate incompressible inviscid flows
[AD-754815] 11 p1272 N73-20318
Analytical and experimental examination of instability of spatial system of articulated pipes conveying fluid
[NASA-CR-131605] 13 p1510 N73-22236
Development and evaluation of throat bypass bleed system to increase stable airflow range of sonic mixed-compression inlet
[NASA-TM-X-2779] 14 p1597 N73-22947
Stability analyses of idealized atmosphere and perfect gas blowing over inviscid liquid
17 p2012 N73-26269
Numerical analysis of stability of flows of viscoelastic fluids for three conditions
19 p2251 N73-28146
Stability of laminar pipe flow with rigid rotation and small three-dimensional perturbation
[MITT-55] 19 p2256 N73-28184
Analysis of rotating stall conditions in axial flow compressors and development of control system to improve flow stability
[AD-762297] 19 p2330 N73-28748
Stability characteristics of stratified and unstratified air flow between two horizontal, infinite disks rotating at slightly different rotation rates
20 p2384 N73-29154
Hydrodynamic stability of circular magnetic fields and revolving fluids
22 p2650 N73-31234
Hydrodynamic stability of axisymmetric free shear layers
24 p2902 N73-33165

**FLOW THEORY**
NT MIXING LENGTH FLOW THEORY
Analysis of velocity and temperature distribution in unsteady thermal boundary layer by approximate integral method
[NASA-TN-D-7054] 01 p0117 N73-10967
Analysis of laminar fluid flow between two rotating coaxial disks
[ISAS-485-VOL.37-11] 02 p0155 N73-11257
Development of theories for calculating pressure on perturbed plane wall in presence of viscous boundary layer
[AD-746332] 02 p0158 N73-11278
Relationships between continuum metal plastic deformation under multiaxial stress and phenomenological dislocation theory
[AD-746187] 02 p0219 N73-11769
Application of modified compressibility transformation for analyzing variable property turbulent boundary layers and predicting flow properties
[NASA-CR-2147] 03 p0282 N73-12286
Analysis of relaxation of laminar boundary layer to test gas boundary layer over flat plate in expansion tube
[NASA-TR-R-397] 03 p0283 N73-12296
Development of design data for cascades of flat plate guide vanes suitable for use in ninety degree elbows in ducts of circular cross section
[ESDU-AERO-00.02.09] 04 p0403 N73-13284
Effect of space-time integral of thermodynamic pressure on thermodynamic potential for compressible, adiabatic flow
[NASA-TM-X-66139] 05 p0606 N73-14926
Analysis of factors involved during reversion of turbulent boundary layers to laminar flow
[REPT-72-FM-2] 06 p0652 N73-15297
Numerical analysis of change in component energies due to three dimensional distortion in homogeneous and initially axisymmetric turbulence
[REPT-72-FM-7] 06 p0652 N73-15298
Rheological investigation of lubricating media using displacement equations for three special cases
[FOA-1-C-1408-92] 06 p0672 N73-15470
Effects of thickness and viscosity considerations on accuracy of aerodynamic coefficients determined for thin wings in inviscid flow conditions
[ESDU-70011-AMEND-A] 07 p0735 N73-15982
Solution of viscous shock-layer equations using implicit finite difference scheme for hyperboloid body under conditions simulating atmospheric entry
07 p0768 N73-16238
Analysis of one dimensional flow downstream of source of radiation in constant area ducts and conical nozzles
07 p0853 N73-16920
Numerical analysis of wake propulsion parameters to show effects of drag, heating, and energy conversion
[RN-64] 08 p0894 N73-17238
Development of two dimensional theory for unsteady flow disturbances caused by aeroelastic deformation of thick wing at high subsonic speeds
[NASA-CR-112114] 08 p0896 N73-17258
Calculation of outer inviscid flow about rectangular wing moving at supersonic speeds
[NASA-CR-130985] 09 p1013 N73-18269

Analysis of measurable and ideal quantities of nozzle beams skimmed from parallel equilibrium gas flows
[DLR-FB-72-51] 09 p1014 N73-18275
Application of splitting method for numerical analysis of heat conducting gas flows in curvilinear coordinates
[NASA-TT-F-14658] 09 p1915 N73-18288
Flow theory calculation of pogo instability in inducer cascades
[NASA-CR-131415] 11 p1271 N73-20313
Application of Kelvin impulse theory for computing lift on airfoils and analysis of circulation around airfoil to produce lift
16 p1851 N73-24997
Velocity magnitude and direction, static pressure, and skin friction of circular turbulent jet impinging normally on flat surface
[ARC-R/M-3205] 16 p1856 N73-25034
Analysis of gas jets expanding out of axisymmetrical nozzles into vacuum or still air at finite pressure
[ARC-R/M-3235] 16 p1856 N73-25036
Nonlinear unsteady small-disturbance theory of inviscid transonic flows for oscillating aerodynamic configurations
[NASA-CR-2258] 16 p1858 N73-25048
Numerical analysis of turbulence transport equation for two dimensional jet flow and pressure-velocity derivative correlations
16 p1887 N73-25270
Analysis of mass diffusion process from elevated point source over wind-disturbed water surface and comparison with calculated concentration distributions for diffusion in flat plate boundary layer
16 p1887 N73-25271
Calculating shock front for terminal flow of solar wind
17 p2079 N73-26816
Analysis of structure dependent and temperature dependent variables affecting flow curves of metals
[BLL-RAE-LIB-TRANS-1675] 21 p2556 N73-30494
Inviscid, isentropic, three-dimensional flow theory for rotating thin blade row in cylindrical duct
23 p2775 N73-32193

**FLOW VELOCITY**
Recirculation flow velocities and temperatures of VTOL lift engines
[DLR-FB-72-50] 02 p0223 N73-11806
Jet noise suppression in turbofan engines at various exhaust flow velocities
03 p0249 N73-12016
Measurement of gas velocities in filters
[AD-747829] 04 p0407 N73-13315
Instrument for measuring magnitude and direction of flow velocity in flow field
[NASA-CASE-LAR-10855-1] 04 p0419 N73-13415
Influence of solid suspended particles on turbulent flow properties
06 p0652 N73-15300
Doppler shift measurement of local velocities in flowing medium
[NRC-TT-1592] 06 p0654 N73-15312
Steady state solution for accelerated interface shape between a light and a heavy fluid using velocity potential
[LA-4839] 06 p0654 N73-15316
Constant flow velocity generator for calibrating hot-wire anemometers
[NASA-CASE-MFS-21424-1] 07 p0769 N73-16248
NMR principle for designing propellant mass flow meter
[AD-751507] 07 p0801 N73-16507
Survey of data involving design of equipment for two phase flow of cryogenic fluids based on critical flow rate
[NASA-CR-130793] 09 p1013 N73-18270
Analysis of oxygen flow in steel pipelines to determine maximum permissible flow and effects of solid particles and restriction on safe flow rate to avoid ignition
[NASA-TT-F-14831] 09 p1016 N73-18290
Laser Doppler velocity measurement of turbid and bubbly flow media
[UTIAS-TN-185-PT-2] 09 p1043 N73-18506
Construction of continuous rate field in plane steady state plastic flow in bi-cylindrical system of coordinates
[NLL-M-21519-[5828.4F]] 11 p1310 N73-20630
Experimental and theoretical measurement of pulsed flow velocity and pressure in circular pipes
14 p1649 N73-23372
Sequential spark method for measuring cone wake velocity profiles
[AD-759159] 16 p1893 N73-25317
Procedure for generating uniform flow at varying velocities in wind tunnel test section
[NASA-CASE-ARC-10710-1] 18 p2125 N73-27175
Transient thermocouple measurement of gas flow direction velocity, and temperature near injector of liquid propellant rocket
18 p2129 N73-27201
Theoretical analysis of two dimensional laminar jet rate sensors
[AD-761092] 18 p2153 N73-27401
Flow velocity, GeCl4 concentration, and temperature effects on growth and morphology of autoepitaxial Ge films
18 p2189 N73-27674
Flow velocity distribution in lower plenum of pressurized water reactor vessel, and design optimization of core catching structure
[BMFT-FBK-73-03] 19 p2255 N73-28182
Fluid mass flow rate measurements using cavitating Venturi tubes noting application to liquid rocket propellant
[DLR-FB-72-33] 21 p2525 N73-30245
Sign determination of laser Doppler anemometer velocity components of two Doppler difference signal components
[REPT-1/1972] 22 p2674 N73-31422
Current density, flow velocity, and mass density in coaxial annular plasma Hall accelerator
[DLR-FB-73-45] 22 p2705 N73-31663
Surface tension effect on cylindrical gas slug velocity
23 p2771 N73-32163
Computation of kinetic fluctuation energy of turbulent shear flow from mean velocity distribution
24 p2908 N73-33211
Integral relations of velocity and thermal boundary layer for approximation purposes
24 p2909 N73-33213

**FLOW VISUALIZATION**
Operator visual perception mapping during parameter adjustment in dynamic control system
01 p0017 N73-10129
Density and flow visualization of different molecular weight gases from concentric orifices as determined by beam fluorescence technique
[ISAS-486-VOL.-37-12] 02 p0155 N73-11256
Development of flow visualization and flow measurement techniques and application to flow problems of turbines, aircraft engines, and missile propulsion
[AD-747613] 03 p0287 N73-12328
Flow visualization and analytical analysis of momentum roll up of turbulent circular jet
04 p0403 N73-13286
Dual hologram interferometry for calculating density distributions from refraction index changes
[AD-749872] 05 p0559 N73-14538
Semicircular canal model with flow visualization chamber for dynamic recording of canal fluid response to angular velocity effects
06 p0634 N73-15153
Structure and behavior of confined jet flow in rotating fluid
06 p0653 N73-15301
Visualization of longitudinal vortices in stagnation area of circular cylinder in turbulent flow with splitting plate
07 p0771 N73-16264
Smoke and helium bubble visualization studies of incompressible flow past jet flap airfoil
[AD-752012] 08 p0898 N73-17270
Heat transfer and flow visualization tests of straight wing hypersonic reentry vehicle at angles of attack from 20 to 80 deg
[NASA-TN-D-7108] 09 p0979 N73-18000
Analysis of turbulent mixing between two streams of different density to determine effects of density difference at low Mach number and compressibility at high Mach number
[AD-753538] 09 p1019 N73-18313
High speed photographic system for moisture flow visualization in steam turbines
[NASA-TM-X-2763] 12 p1404 N73-21388
Application of holographic interferometry to density field determination in transonic corner flow
[AD-756534] 13 p1511 N73-22247
Electron beam optics for measuring density and temperature of aerodynamic gas flow
[ONERA-PUBL-146] 13 p1559 N73-22635
Visualization and integral methods for studying three-dimensional supersonic flow separation on delta wing
14 p1600 N73-22970
Visualization of flow deviation by cylindrical wall cavities
14 p1649 N73-23374
Schlieren method adapted as flow visualization technique to study cavitation development on axisymmetric bodies in water tunnel
[AD-757078] 14 p1652 N73-23402
Development of flow visualization techniques for determining aerodynamic characteristics of bluff bodies under unsteady flow conditions
[AD-759266] 16 p1892 N73-25311
Aerospace application of holography through nondestructive testing and flow visualization
16 p1922 N73-25550
Holographic instrumentation for use in flow visualization, nondestructive testing procedures, and optical data processing
16 p1922 N73-25551
Infrared television system used for HF laser flow visualization with selected nozzle configurations
[AD-759803] 16 p1925 N73-25577
Application of hydraulic test tunnel flow visualization techniques to determine ground effect on flow around models of aircraft
[NASA-TT-F-14958] 17 p2015 N73-26291
Application of holographic interferometry techniques for determining asymmetric flow distribution encountered near wing-fuselage junction at transonic speed
[AD-759967] 17 p2015 N73-26296
Gas dynamic analysis in near field of supersonic nozzle banks for chemical lasers
[AD-760132] 17 p2041 N73-26513
Aerodynamic characteristics of two space shuttle concepts with delta wing configurations at hypersonic speed using helium flow visualization technique
[NASA-TN-D-7282] 18 p2102 N73-26997
Holographic visualization of flow field within transonic compressor rotor
[NASA-CR-121112] 18 p2130 N73-27215
Visualization of swirling flow in rotating tube and measurement of velocity distribution by laser-Doppler anemometry
[NASA-CR-2284] 18 p2131 N73-27216
Analysis of kinematic and dynamic characteristics of wake generated behind flat plate normal to parallel unbounded fluid flow
[AD-761372] 18 p2131 N73-27220
Experimental and analytical determination of one- and two-component flows in spherical chambers for application to open-cycle gaseous-core nuclear rocket
[NASA-CR-2282] 19 p2255 N73-28175
Development of flow visualization technique using fluorescent dye to simulate smoke lines in water
[AD-761499] 19 p2257 N73-28192
Analysis of wakes generated by hovering model propellers and rotors using schlieren photography and hot-wire anemometry
[NASA-CR-2305] 21 p2491 N73-29996
Hydrogen bubble flow visualization technique for study of aerodynamic problems in water flow facilities
[ARL/A-NOTE-338] 21 p2523 N73-30229
Use of dye flow visualization techniques in small water tunnel
[ARL/A-NOTE-339] 21 p2523 N73-30230
Photographic recording of secondary flows at nozzle exits produced by planar nozzles with rectangular inlets from circular ducts
[AD-762743] 21 p2527 N73-30265
Finite element analysis and computer graphics visualization of unsteady flow around pitching and plunging airfoils
[NASA-CR-2249] 22 p2611 N73-30926
Cavitation inception and separation on axisymmetric bodies in water tunnel
23 p2771 N73-32164
Liquid crystal infrared detectors for plasma diagnostics and flow visualization using CO2 laser impulses
[BMVG-FBWT-73-16] 23 p2823 N73-32564
Hydrodynamic simulation using flow field visualization for combustor study
23 p2831 N73-32625

**FLOWMETERS**
NT GAS METERS
NT HOT-WIRE FLOWMETERS
Equipment and procedures for measuring flow of liquids and gases to identify application of specific types of equipment
[NLL-TRANS-45-[3958.4]] 02 p0154 N73-11249
Bibliography on laser Doppler velocimeter theory and usage
[AD-746634] 02 p0176 N73-11427
Numerical and perturbation theory solutions for evaluating performance of eddy current flowmeters
[BNWL-SA-4236] 03 p0302 N73-12470
Performance evaluation of volumetric and mass cryogenic turbine flowmeters
[NBS-TN-624] 04 p0420 N73-13426
Analysis of pressure loss conditions created by turbulent flow conditions for wide range of flowmeters
[ESDU-66030-AMEND-A] 05 p0525 N73-14273
Thermal flowmeter for urine volume measurement in manned space flight environment
[NASA-CR-128726] 07 p0750 N73-16095
NMR principle for designing propellant mass flow meter
[AD-751507] 07 p0801 N73-16507
Application of laser Doppler velocimeter for flow measurements
[AD-753243] 09 p1044 N73-18513
Portable laser velocimeter for stack velocity measurements
[PB-213263] 11 p1304 N73-20579
Characteristics of signal conditioning electronics for vector velocity laser velocimeter
[NASA-CR-131475] 13 p1538 N73-22459
Particle-fluid interaction corrections for turbulent flow measurements with laser Doppler flowmeter
[NASA-CR-124254] 14 p1649 N73-23379
Ultrasonic mass flowmeter for fuel flow in gas turbine engines
[AD-758462] 14 p1669 N73-23547
Life tests of small turbine type flowmeters in liquid hydrogen
[NASA-TN-D-7323] 16 p1888 N73-25278

Measurement of laminar fluid flow through orifice meters to determine discharge coefficients and head losses
[NLL-NEL-TT-2457-[6075.461]] 20 p2386 N73-29169
Respiratory analysis system to determine gas flow rate and frequency of respiration and expiration cycles in real time
[NASA-CASE-MSC-13436-1] 23 p2751 N73-32015
Low power electromagnetic flowmeter system producing zero output signal for zero flow
[NASA-CASE-ARC-10362-1] 23 p2791 N73-32326

FLOX
Combustion efficiency of FLOX/polyethylene hybrid propellants
[DGLR-PAPER-72-86] 04 p0462 N73-13766
Fabrication and acceptance tests of FLOX/MMH engine assemblies
[NASA-CR-130288] 06 p0712 N73-15814
Performance of FLOX-70/polyethylene hybrid rocket engine with cartwheel-type propellant grain geometry
[DLR-FB-72-61] 07 p0836 N73-16780
Evaluation of materials for ball bearings intended for use in liquid fluorine and/or FLOX
[NASA-CR-120820] 16 p1917 N73-25516
Experimental high energy rocket propellant combinations with heterogeneous combustion and FLOX/polyethylene engine performance 24 p2972 N73-33751

FLUCTUATION
U VARIATIONS

FLUCTUATION THEORY
Polarization fluctuation of beam wave propagating in random atmosphere 19 p2234 N73-28014

FLUENCE
Irradiation-induced changes in graphites at high temperatures and high fluences
[GULF-GA-A-10971] 03 p0321 N73-12612

FLUERICS
Experimental analysis of three dimensional flow fields in planar nozzles and wall jets found in bistable fluid amplifiers
[AD-751627] 07 p0774 N73-16282

FLUID AMPLIFICATION
U FLUID AMPLIFIERS

FLUID AMPLIFIERS
Research and development of fluidics systems and applications to industrial processes
[NASA-SP-5112] 02 p0155 N73-11260
Comparative performance characteristics of geometrically similar vented and unvented bistable amplifiers
[AD-745770] 02 p0158 N73-11279
Dynamic response analysis of analog fluid amplifiers
[AD-746274] 02 p0179 N73-11450
Development of fluidic control system for stabilizing aircraft ejection seat in pitch plane during rocket motor burn portion of ejection sequence
[AD-747630] 03 p0254 N73-12056
Closed loop fuel control techniques using electronic circuitry to sense pressure relationships at turbine engine compressor discharge
[AD-747805] 03 p0351 N73-12865
Development of vortex fluid amplifier for throttling rocket exhaust
[NASA-CASE-LEW-10374-1] 04 p0463 N73-13773
Predicting total pressure loss regions existing in corner between sidewall and horizontal nozzle walls at exits with convex contour curvature
[AD-751606] 07 p0773 N73-16277
Design and analysis of proportional fluid amplifier
[AD-751457] 07 p0773 N73-16278
Experimental analysis of three dimensional flow fields in planar nozzles and wall jets found in bistable fluid amplifiers
[AD-751627] 07 p0774 N73-16282
Design and staging of laminar flueric proportional amplifier
[AD-751182] 07 p0774 N73-16285
Experimental study and analog simulation of steady state and dynamic response of jet interaction proportional fluid amplifier
[AD-751458] 07 p0805 N73-16532
Analysis of turbulent velocity fluctuations in confined jet to determine design parameters for fluid amplifiers
[AD-752041] 08 p0899 N73-17276
Dynamic response of fluidic circuits with blocked and orifice terminated lines
[AD-753384] 09 p1018 N73-18307
Design of hydrofluidic flight control system for helicopter stabilization
[AD-754602] 11 p1236 N73-20032
Nozzle and wall jet flow fields in bistable fluid amplifiers 13 p1509 N73-22230
Mass and momentum of control signals in switching mechanism of fluid bistable amplifiers
[AD-756583] 13 p1511 N73-22243
Investigation of flow issuing from nozzle in fluid amplifier and impinging on receiver with spill port oriented at 90 degrees to flow direction
[AD-759796] 16 p1890 N73-25297
Dynamic performance of beam deflection fluid amplifiers
[AD-759211] 16 p1891 N73-25306
Flow field characteristics of beam deflection fluid amplifier considering pressure differential
[AD-759210] 16 p1892 N73-25315
Development of electro-hydrofluidic transducer for control of turbine engines
[AD-762298] 19 p2330 N73-28745
Mixing region in flow field of fluidic beam deflection amplifier 23 p2772 N73-32173

FLUID BOUNDARIES
NT GAS-SOLID INTERFACES
NT LIQUID-LIQUID INTERFACES
NT LIQUID-SOLID INTERFACES
NT LIQUID-VAPOR INTERFACES
Steady state solution for accelerated interface shape between a light and a heavy fluid using velocity potential
[LA-4839] 06 p0654 N73-15316
Effects of particle seeding on jet exhaust noise 19 p2251 N73-28150
Numerical analysis of boundary conditions of time dependent viscous compressible flow based on small perturbation of Navier-Stokes equation 23 p2773 N73-32176

FLUID DYNAMICS
NT AERODYNAMICS
NT AEROTHERMODYNAMICS
NT ELASTOHYDRODYNAMICS
NT ELECTROHYDRODYNAMICS
NT GAS DYNAMICS
NT HYDRODYNAMICS
NT MAGNETOHYDRODYNAMICS
NT RAREFIED GAS DYNAMICS
NT ROTONS
NT ROTOR AERODYNAMICS
Equations for fully cavitating flow of fluid past flat plate hydrofoil running below free surface with consideration of transverse gravity effects
[AD-746484] 02 p0157 N73-11272
Fluid-type equations describing macroscopic behavior of matter-antimatter plasma
[IPPJ-131] 02 p0215 N73-11744
Development of method for determining response of fluids under high pressure when released to atmosphere using closed form solution and numerical analysis 03 p0282 N73-12289
Fluid model for analyzing nonlinear magnetosonic wave propagation in magnetic neutral sheet
[IPPJ-139] 04 p0388 N73-13152
Development of design data for cascades of flat plate guide vanes suitable for use in ninety degree elbows in ducts of circular cross section
[ESDU-AERO-00.02.09] 04 p0403 N73-13284
Fluid wave equation for analyzing damage by excited pressure field between two elastic plates
[AD-748340] 04 p0407 N73-13316
Bubble distributions in quiescent ocean calculated from bubble transport equation
[AD-749046] 04 p0408 N73-13329
Fluid and plasma dynamics research
[AD-749287] 04 p0457 N73-13729
Fluid dynamic and chemical processes occurring in solid propellant gas generator
[AD-749144] 05 p0589 N73-14790
Structure and behavior of confined jet flow in rotating fluid 06 p0653 N73-15301
Measurement of fluctuations in free surface flow of gas and liquids 06 p0653 N73-15303
Liquid hydrogen reorientation in fuel tanks of Centaur launch vehicle using low level accelerations with and without internal baffles
[NASA-TN-D-7168] 07 p0770 N73-16252
Rotating disk measurement of drag reduction and shear properties of various dilute polymers
[AD-751552] 07 p0773 N73-16281
System for eliminating roll rate anomalies occurring during flights of slender ballistic reentry vehicles
[SC-DC-72-2244-A] 07 p0849 N73-16883
Abstracts of selected reports on heat transfer and fluid dynamics with applicability to oxygen systems
[NASA-SP-3076-VOL-3] 07 p0855 N73-16932
Evaluation of fluid dynamics of aircraft stalling to determine effects of three dimensional flow, wing sweep back, and high lift devices
[AGARD-AR-49] 09 p0982 N73-18023
Experimental investigation of two dimensional cascade flow tests for three cascade configurations - Vol. 4
[NASA-CR-121101] 09 p1015 N73-18282
Atmospheric models for fluid dynamic and chemical impacts of supersonic aircraft on climatology
[PB-212819] 11 p1291 N73-20473
Analysis of natural vibrations on stratified fluid in rectangular vessel and computer program for solving continuous density distribution 12 p1390 N73-21275
Experimental determination of turning angle and losses of axial compressor inlet guide vanes
[AD-757250] 14 p1701 N73-23805
Theoretical study of fluid dynamic energy separation 15 p1764 N73-24292
Fluid dynamic computer programs for NERVA turbopump
[NASA-CR-132222] 15 p1810 N73-24670
Nonlinear dynamics of collective modes
[BN-695] 16 p1888 N73-25282
Rossby regimes in geophysical fluid dynamics of ocean waves
[PB-214660/3] 16 p1890 N73-25295
Nonuniform flow in front of axial flow compressor stage
[AD-759247] 16 p1891 N73-25303
Determination of ventilation characteristics of blunt-based surface piercing struts in calm water and in waves
[AD-759046] 16 p1892 N73-25314
Fluid dynamics of meteor disintegration due to aerodynamic forces in heterogeneous atmosphere 16 p1960 N73-25855
Dynamic characteristics of solid particles in particulate flow through turbine and compressor cascades 17 p2013 N73-26278
Fluid motion problems in design and operation of low speed and transonic wind tunnels
[AGARD-R-602] 17 p2013 N73-26279
Structural and gas dynamic parameters at flow separation boundary in compressor cascades
[AD-762238] 19 p2257 N73-28197
Fluid dynamic aspects of cardiovascular behavior during low frequency whole-body vibration such as encountered by astronauts during launch and reentry
[NASA-CR-133843] 21 p2501 N73-30069
Pressure differences, forces, and moments on same two wings in steady subsonic flow computed by 15 different programs
[AD-763669] 23 p2776 N73-32199
Model tests and analysis of expandable floating bases
[AD-756048] 23 p2777 N73-32206
Fluid dynamics, noting boundary layer theory
[DLR-FB-72-26] 24 p2905 N73-33186
Fluid dynamics, noting boundary layer theory
[DLR-FB-72-27-PT-2] 24 p2907 N73-33202

FLUID FILMS
Stability of liquid films interacting with high pressure supersonic airstream
[SC-DC-72-1225] 07 p0772 N73-16268
Design and evaluation of hybrid boost bearings consisting of fluid film bearing coupled with rolling element bearing
[NASA-CR-2226] 09 p1039 N73-18476
Analytical solution of Reynolds equation and application to hydrodynamic lubrication to show characteristics of lubrication film
[TAE-153] 09 p1057 N73-18618
Critical scattering of laser light by thin fluid films
[COO-2203-1] 12 p1410 N73-21428

FLUID FILTERS
NT AIR FILTERS
Design and fabrication of prototype particulate regenerative filter with backflush for spacecraft fluid system
[NASA-CR-115505] 14 p1614 N73-23084
Design and characteristics of system for regenerating fluid filter to remove trapped particles with application to space shuttle systems
[NASA-CASE-MSC-14273-1] 19 p2255 N73-28179
Bactericidal properties of sorbents in spacecraft water regeneration system 20 p2367 N73-29038
Analysis of errors in measuremeat of absorbances of liquid filters caused by instrumental and chemical uncertainties using three types of liquid filters
[PAPER-76A5-733] 21 p2545 N73-30402

FLUID FLOW
NT AIR CURRENTS
NT AIR FLOW
NT AIR JETS
NT ANNULAR FLOW
NT AXIAL FLOW
NT AXISYMMETRIC FLOW
NT BAROTROPIC FLOW
NT BASE FLOW
NT BLASIUS FLOW
NT BLOOD FLOW
NT BOUNDARY LAYER FLOW
NT BOUNDARY LAYER SEPARATION
NT CAPILLARY FLOW
NT CASCADE FLOW
NT CAVITATION FLOW
NT CHANNEL FLOW
NT COAXIAL FLOW
NT COMBUSTIBLE FLOW
NT COMPRESSIBLE FLOW
NT CONICAL FLOW
NT CONTINUUM FLOW
NT CONVECTIVE FLOW
NT CORE FLOW
NT COUETTE FLOW
NT CRITICAL FLOW
NT CROSS FLOW
NT DUCTED FLOW
NT EQUILIBRIUM FLOW

NT FREE FLOW
NT FREE MOLECULAR FLOW
NT GAS FLOW
NT HELICAL FLOW
NT HYPERSONIC FLOW
NT INCOMPRESSIBLE FLOW
NT INLET FLOW
NT INVISCID FLOW
NT ISOTHERMAL FLOW
NT JET FLOW
NT JET MIXING FLOW
NT JET STREAMS [METEOROLOGY]
NT LAMINAR FLOW
NT LIQUID FLOW
NT MAGNETOHYDRODYNAMIC FLOW
NT MASS FLOW
NT MERIDIONAL FLOW
NT MOLECULAR FLOW
NT MULTIPHASE FLOW
NT NONEQUILIBRIUM FLOW
NT NONUNIFORM FLOW
NT NOZZLE FLOW
NT ONE DIMENSIONAL FLOW
NT OPEN CHANNEL FLOW
NT ORIFICE FLOW
NT OSCILLATING FLOW
NT PARALLEL FLOW
NT PERIPHERAL JET FLOW
NT PIPE FLOW
NT PLASTIC FLOW
NT POTENTIAL FLOW
NT PROPELLANT TRANSFER
NT RADIAL FLOW
NT REATTACHED FLOW
NT RECIRCULATIVE FLUID FLOW
NT REVERSED FLOW
NT SECONDARY FLOW
NT SEPARATED FLOW
NT SHEAR FLOW
NT SLIP FLOW
NT SMALL PERTURBATION FLOW
NT SOLIDS FLOW
NT STAGNATION FLOW
NT STEADY FLOW
NT STEAM FLOW
NT STOKES FLOW
NT STRATIFIED FLOW
NT SUBCRITICAL FLOW
NT SUBSONIC FLOW
NT SUPERCAVITATING FLOW
NT SUPERCRITICAL FLOW
NT SUPERSONIC FLOW
NT SUPERSONIC JET FLOW
NT THREE DIMENSIONAL FLOW
NT TRANSITION FLOW
NT TRANSONIC FLOW
NT TURBULENT FLOW
NT TWO DIMENSIONAL FLOW
NT TWO PHASE FLOW
NT UNIFORM FLOW
NT UNSTEADY FLOW
NT VERTICAL AIR CURRENTS
NT VISCOUS FLOW
NT WALL FLOW
NT WATER FLOW
NT WEDGE FLOW

Methods used with fluid mechanics reference data on external flow to predict forces exerted on bodies of non-streamline shape
[ESDU-FME-1] 01 p0039 N73-10304

Convection and mixing of stratified fluids in rotating tank
[NASA-TR-R-392] 01 p0039 N73-10312

Influence of drag, pressure, and turbulent distribution on flow of dilute Polyox WSR-301 solutions in circular cylinders
[AD-745763] 01 p0042 N73-10334

Equations which show relationship between stress and displacement velocity in non-Newtonian fluid flows
[AD-745702] 01 p0042 N73-10335

Flow control valve for high temperature fluids
[NASA-CASE-NPO-11951-1] 01 p0061 N73-10501

Dynamic stabilization of plasma confinement and fluid systems
[LRP-53/72] 01 p0085 N73-10701

CDC computer program for solving two-dimensional, two-fluid magnetohydrodynamic equations
[AD-745854] 01 p0086 N73-10713

Thermal analysis routine with capability for performing thermal analysis of systems containing flowing fluids
[NASA-CR-128593] 01 p0117 N73-10963

Analysis of laminar fluid flow between two rotating coaxial disks
[ISAS-485-VOL.-37-11] 02 p0155 N73-11257

Vortex components and flow systems
[FOA-2-C-2480-E4] 02 p0155 N73-11258

Analysis of isothermal liquid inflow patterns in spherical container during weightless conditions
[NASA-TM-X-2670] 03 p0283 N73-12291

Numerical analysis of fluid containment near stagnation point and within self-confined stagnation region for bi-component mixture
[NASA-CR-2172] 03 p0283 N73-12292

Design and development of device for moving liquid through pipes without use of mechanical pumps
[NASA-CASE-LAR-10799-1] 03 p0283 N73-12295

Viscous drag reduction caused by polymer injection in developing turbulent boundary layer
[AD-747274] 03 p0285 N73-12310

Development of equations and computer program for determining temperature distribution in walls of three eccentric annuli
[AD-747697] 03 p0287 N73-12322

Design and development of device to prevent geysering during convective circulation of cryogenic fluids
[NASA-CASE-KSC-10615] 03 p0304 N73-12486

Numerical analysis of pressure drop in ducts across round-wire gauzes or screens normal to fluid flow to show effects of gauze geometry and velocity of flow
[ESDU-72009] 04 p0403 N73-13280

Pressure changes in fluid flow along duct with sudden enlargement of area
[ESDU-72011] 04 p0403 N73-13281

Analytical methods for calculating frictional pressure losses in fluid flow through straight pipes
[ESDU-66027] 04 p0403 N73-13282

Numerical analysis of pressure losses due to bends in fluid flow systems and application of correction factor to relate overall losses for various conditions
[ESDU-68035] 04 p0403 N73-13283

Reaction engines with shrouded nozzles, reaction engines for boats, and thermodynamics of hot air bubble cooling in liquid
[JPRS-57308] 04 p0404 N73-13292

Analysis of pressure loss through single bends of various geometries under conditions of full incompressible flow
[ESDU-67040-AMEND-A] 05 p0525 N73-14272

Analysis of pressure loss conditions created by turbulent flow conditions for wide range of flowmeters
[ESDU-66030-AMEND-A] 05 p0525 N73-14273

Analysis of turbulent fluid flow through rectangular conduit with large aspect ratio and development of mechanical energy-balance equations
[WTHD-27] 05 p0526 N73-14279

Analysis of interaction between fluid and discrete particles in turbulent flow field and development of equations of motion
[WTHD-32] 05 p0526 N73-14280

Characteristics of mixing shock in mixing tube of water jet-gas pump to determine pressure distribution
[WTHD-31] 05 p0526 N73-14281

Semicircular canal model with flow visualization chamber for dynamic recording of canal fluid response to angular velocity effects
06 p0634 N73-15153

Numerical analysis of three dimensional incompressible fluid flow near large structure surface
[LA-DC-72-711] 06 p0654 N73-15315

Steady state solution for accelerated interface shape between a light and a heavy fluid using velocity potential
[LA-4839] 06 p0654 N73-15316

Chemical surface reactions, phase transformations, and reaction kinetics in flow systems
[AD-750172] 06 p0712 N73-15808

General relaxation theory for liquid behavior under dynamic conditions
[NASA-CR-2141] 07 p0769 N73-16245

Constant flow velocity generator for calibrating hot-wire anemometers
[NASA-CASE-MFS-21424-1] 07 p0769 N73-16248

Mathematical model for turbulent boundary layer of two liquid flows
07 p0772 N73-16267

Computer program to determine compressible fluid flow with friction across face seals and through narrow solts
[NASA-TN-D-6787] 07 p0803 N73-16518

Ion currents and trajectories for fluid flow diagnostics
[AD-751785] 07 p0824 N73-16681

Viscous incompressible fluid hydraulics of magnetohydrodynamic generators
[AD-751465] 07 p0829 N73-16718

Analytical combustion model for predicting flow and pressure transients in H2-O2 RCS of rocket engine feed system
07 p0835 N73-16767

Analysis of axially symmetric motions of viscous neutral stratified gas in spherical layer resulting from rotation of inner sphere
[NASA-TT-F-14661] 08 p0897 N73-17260

Techniques for determining dynamic characteristics of hydraulic duct for predicting low frequency vibrations of liquid propellant rocket engines
[ONERA-TP-1160] 09 p1015 N73-18281

Static charge generation in hydrocarbon fuels during flow through pipes
[AD-753386] 09 p1067 N73-18706

Fluid flow analysis in mold heating and cooling control loop
[BDX-613-742] 10 p1142 N73-19303

Calculation of hydraulic resistances in pipelines
[AD-754322] 10 p1144 N73-19319

Radial distribution functions and liquid structure factors for fluids of particles interacting through repulsive potentials
[LPTHE-72/45] 10 p1191 N73-19690

Gas bearings and fluid flow tests using finite difference approximation
[AD-754800] 11 p1299 N73-20542

Development of nonisothermal theory of viscoelastic fluids with fading memory and application to viscometric flow
[AD-754802] 11 p1349 N73-20948

Numerical analysis of time dependent natural convection flow within horizontal cylinder based on quasi-compressible Navier-Stokes equations
[NASA-TM-X-69220] 12 p1391 N73-21278

Laser Doppler velocimeter for simultaneously measuring orthogonal fluid velocity components without flow field perturbation
[NASA-CASE-ARC-10637-1] 12 p1405 N73-21390

Stability of thin elastic tube of infinite length containing rotating inviscid, incompressible fluid flow
13 p1508 N73-22222

Analytical and experimental examination of instability of spatial system of articulated pipes conveying fluid
[NASA-CR-131605] 13 p1510 N73-22236

Two-phase flow of two immiscible fluids considered for motion in diverging channel
[AD-756341] 13 p1513 N73-22259

Solution of thermodynamic forces and flows in magnetic field using Gibbs equation
[AD-756901] 13 p1592 N73-22909

Laser-Doppler anemometer measurements of turbulence in drag reducing flows
[AD-757075] 14 p1669 N73-23545

Two fluid models with neglected mass rotation and overestimated electric field role
[TH-72-E-28] 14 p1695 N73-23755

Analysis of spoiler plate characteristics to eliminate effects of installation disturbance when conducting flow rate measurements
[NLL-NEL-TT-2439-[6075.461]]
15 p1763 N73-24288

Mach number effect on motion of sphere in compressible low Reynolds number flow
15 p1765 N73-24298

Design and development of thermomechanical pump for transmitting warming fluid through fluid circuit to control temperature of spacecraft instrumentation
[NASA-CASE-NPO-11417] 15 p1790 N73-24513

Analysis of conditions for equilibrium of multi-component liquid at surface of solid body with allowance for selective adsorption at interphase boundaries
[NLL-M-21577-[5828.4F]] 16 p1885 N73-25261

Gravity effects on geophysical fluid dynamics
[PB-214659/5] 16 p1890 N73-25296

Analysis of coolant flow in transpiration-cooled vanes
[NASA-TN-D-7341] 16 p1974 N73-25966

Application of hydraulic test tunnel flow visualization techniques to determine ground effect on flow around models of aircraft
[NASA-TT-F-14958] 17 p2015 N73-26291

Convection and dispersion patterns associated with stationary and nonstationary fluid transport
18 p2129 N73-27205

Analysis of characteristics of supersonic flow of helium around right circular cones at zero angle of attack and Mach numbers from 1.5 to 30.0
[NASA-SP-3078] 18 p2130 N73-27208

Analysis of kinematic and dynamic characteristics of wake generated behind flat plate normal to parallel unbounded fluid flow
[AD-761372] 18 p2131 N73-27220

OAO 3 flight test on heat pipe cooling efficiency during weightlessness
18 p2208 N73-27826

Retrevial of dispersive and convective transport phenomena in fluids using time domain analysis
[NASA-TN-D-7240] 19 p2255 N73-28178

Design and characteristics of system for regenerating fluid filter to remove trapped particles with application to space shuttle systems
[NASA-CASE-MSC-14273-1] 19 p2255 N73-28179

Mathematical model for calculating transient flow of compressible condensable fluid mixtures in open channels
[UCID-16170] 19 p2255 N73-28181

Hot film sensor measurement of turbulent flow of fluids in pipes
[AD-762059] 19 p2258 N73-28199

Measurement of laminar fluid flow through orifice meters to determine discharge coefficients and head losses
[NLL-NEL-TT-2457-[6075.461]]
20 p2386 N73-29169

Analysis of drop trajectories transition of boundary layer structure and flow regime for binary spray flow over upstream surface of isothermal cylinder
20 p2386 N73-29171

Dynamic response of pipes with fluid flowing in steady and unsteady conditions
[MERL-TN-72-2] 20 p2387 N73-29178

Flow characteristics of radial inward choked flow of liquid nitrogen stream
[NASA-TM-X-68283] 20 p2387 N73-29181
Characteristics of electrostatic discharges in liquids to show importance of transport and discharge mechanisms for boundary surface phenomena and particle discharge
[NLL-M-23041-[5828.4F]] 21 p2516 N73-30182
Flow characteristics behind diffusers in wind tunnels
[AD-763257] 21 p2525 N73-30251
Experimental observations of upstream disturbances in flow of two fluids over obstacle in channel
[AD-763759] 21 p2526 N73-30259
Experimental observations and numerical simulation of Weissenberg climbing effect
22 p2649 N73-31220
Differential solution to problem of nonlinear cavitational flow around channel plates by gravity fluid
22 p2651 N73-31239
Drag reduction in fluids by addition of polymer additives
[AD-763824] 22 p2654 N73-31263
Unidirectional periodic flow about circular cylinders
[AD-764487] 22 p2656 N73-31273
Calculation of heat exchange between rotating body and moving fluid
[AD-763941] 22 p2656 N73-31275
Analysis of equal-size droplet injection in fluid flow, noting fuel injection
[DLR-MITT-72-19] 22 p2710 N73-31703
Characteristics of flow about spherical body undergoing rectilinear, sinusoidal oscillations in viscous, incompressible fluid
23 p2773 N73-32180
Theoretical and experimental analysis of flow induced by harmonic oscillation of rods with arbitrary cross sections containing incompressible, viscous, Newtonian fluid
23 p2774 N73-32183
Characteristics of natural convection induced in cylindrical layer of fluid by uniform heating from below
24 p2902 N73-33163
Heat transfer and wavelength measurement for axisymmetric flow of fluid layer heated from below
24 p2903 N73-33167
Analysis of physical properties of liquids on cavitation erosion to provide basis for developing modeling laws to reduce cavitation damage
24 p2904 N73-33175
Interactions between fluid flow and mechanical oscillators, using vibrating steel wire and cylindrical body
[DLR-FB-73-42] 24 p2909 N73-33218
Application of second-order accurate fluid algorithm for variable spatial grid
[AD-765316] 24 p2910 N73-33225
Characteristics of constant scaling method for analyzing linear inviscid internal waves in ocean, atmosphere, and experimental tanks
[AD-764579] 24 p2910 N73-33227
Electrified kerosene and gasoline aviation fuel during passage through pipes and filters of fuel tank reservoir
[AD-764941] 24 p2971 N73-33740
Effect of friction term on equations of motion of liquid helium and measurement of temperature along axis of channel carrying supercritical heat current
24 p2990 N73-33894

**FLUID INJECTION**
NT GAS INJECTION
NT LIQUID INJECTION
NT WATER INJECTION
Vaporization rates of liquid injected into high temperature, supersonic gas flow using aviation gasoline injected by Laval nozzle into air stream
[AD-747456] 03 p0286 N73-12317
Application of secondary injection to obtain controllable roll moment solid rocket propelled launch vehicles
03 p0350 N73-12856
Explosive interaction of molten metal jet injected into tank of subcooled distilled water
[ORO-3936-7] 06 p0731 N73-15961
Analytical solution for laminar boundary layer with pressure gradient and coolant injection
23 p2771 N73-32165

**FLUID JET AMPLIFIERS**
U FLUID AMPLIFIERS

**FLUID JETS**
NT AIR JETS
NT FREE JETS
NT GAS JETS
NT HYDRAULIC JETS
Feasibility assessment of rapid excavation of hard rock by means of continuous fluid jets with pressures of 20,000 to 80,000 psi
[AD-744014] 01 p0051 N73-10416
Breakup of liquid jet injected normal to supersonic airstream
[AD-747494] 04 p0406 N73-13309
Application of holography to jet breakup in supersonic flow fields and analytical method for reducing holographic droplet data
[AD-749854] 05 p0529 N73-14302
Flow field characteristics of beam deflection fluid amplifier considering pressure differential
[AD-759210] 16 p1892 N73-25315
Theoretical analysis of two dimensional laminar jet rate sensors
[AD-761092] 18 p2153 N73-27401

**FLUID MECHANICS**
NT AERODYNAMICS
NT AEROTHERMODYNAMICS
NT ELASTOHYDRODYNAMICS
NT ELECTROHYDRODYNAMICS
NT FLUID DYNAMICS
NT GAS DYNAMICS
NT HYDRODYNAMICS
NT HYDROMECHANICS
NT HYDROSTATICS
NT MAGNETOHYDRODYNAMICS
NT PNEUMATICS
NT RAREFIED GAS DYNAMICS
NT ROTONS
NT ROTOR AERODYNAMICS
Development and evaluation of three axis fluidic airspeed sensor system for use with standard aircraft power supplies
[NASA-CR-112167] 01 p0058 N73-10472
Fluid mechanics and dynamic energy separation in steady flow, nonsteady flow, and cryptosteady flow
[AD-747316] 03 p0286 N73-12314
Research projects in flow mechanics and gas dynamics
05 p0526 N73-14278
Development and characteristics of parallel plate viscometer for determination of absolute viscosity of liquids and viscoelastic materials
[NASA-CASE-NPO-11387] 05 p0545 N73-14429
Physical principles of experimental aeromechanics using wind tunnel tests
[AD-751464] 07 p0773 N73-16280
Bibliography of Belgian research reports in fluid mechanics and plasma physics from 1957 to 1972
[NT-32-1972] 07 p0860 N73-16975
Research reports on SQUID programs related to fluid mechanics, and atomic and molecular collisions
[AD-752037] 08 p0955 N73-17820
Solving singular axisymmetric field problem noting applications to electromagnetism and fluid mechanics
[ONERA-NT-207] 10 p1190 N73-19685
Lectures on properties and characteristics of rotating and stratified fluids
[AD-754066] 11 p1272 N73-20320
Dynamic behavior of eccentric rotating shaft subject to linearly varying or constant tension
13 p1532 N73-22414
Platinum-rhodium device for stirring viscous fluids
[NBS-TN-771] 13 p1532 N73-22418
Fluid mechanics facility in aerodynamics laboratory
[AD-756512] 14 p1646 N73-23350
Application of variational methods in fluid mechanics
[AD-757266] 14 p1652 N73-23399
Conference on heat transfer and fluid mechanics
[AD-758404] 14 p1653 N73-23404
Technical problems and accomplishments during reporting period
[AD-757637] 14 p1696 N73-23762
Radial flow balance in turbomachines
[ONERA-NT-209] 15 p1768 N73-24326
Numerical analysis of fluid mechanic problems
[AD-758078] 16 p1893 N73-25318
Steady state analysis of energy transfer control and compressor concepts of remote lift fan control
[NASA-TM-X-2876] 21 p2590 N73-30753
Fluid mechanics of hole tone whistle designed as efficient producer of discrete frequency sound
24 p2903 N73-33170

**FLUID SWITCHING ELEMENTS**
Electrohydraulic directional valves with fluidic ball elements
[DLR-FB-73-35] 15 p1793 N73-24535
Miniaturization of fluidic switching elements
[BMFT-FBT-73-06] 22 p2654 N73-31257

**FLUID TRANSPIRATION**
U TRANSPIRATION

**FLUIDIC CIRCUITS**
NT FLIP-FLOPS
Development and evaluation of three axis fluidic airspeed sensor system for use with standard aircraft power supplies
[NASA-CR-112167] 01 p0058 N73-10472
Fluidic elements and hydraulic impulse techniques for information processing equipment
02 p0140 N73-11135
Research and development of fluidics systems and applications to industrial processes
[NASA-SP-5112] 02 p0155 N73-11260
Design, development, and evaluation of fluidic emergency thrusters for aircraft stabilization
[NASA-CR-114490] 03 p0252 N73-12041
Performance tests of reentry vehicle control with base plane thrusters and fluidic control logic
[SC-DC-72-2244[RD]] 09 p0985 N73-18043

**FLUIDICS**
NT FLUERICS
Research and development of fluidics systems and applications to industrial processes
[NASA-SP-5112] 02 p0155 N73-11260
Performance evaluation of iridium/rhodium integrated probe/fluidic temperature sensor up to 3000 F
[AD-745987] 02 p0175 N73-11417
Development of fluidic control system for stabilizing aircraft ejection seat in pitch plane during rocket motor burn portion of ejection sequence
[AD-747630] 03 p0254 N73-12056
Two dimensional, incompressible model for response of laminar and turbulent attached jets
[AD-747761] 03 p0309 N73-12520
Development of device for measuring angular rate based on fluidic components for inertial angular rate sensors using vortex principle
[FOA-2-C-2466-54] 06 p0696 N73-15672
Design and analysis of proportional fluid amplifier
[AD-751457] 07 p0773 N73-16278
Design and staging of laminar flueric proportional amplifier
[AD-751182] 07 p0774 N73-16285
Cranfield fluidics conference of Uppsala, Sweden
[AD-751186] 07 p0774 N73-16287
Tester controlled by fluidic logic system for testing safety functions of missile safe and arm devices
[AD-751127] 07 p0802 N73-16512
Continuous reading fluidic device for measuring component flow of binary gas mixtures
[NASA-TM-X-2741] 09 p1035 N73-18445
Design of elastically geared circular disk wave drive motor and telemanipulator
[NASA-TT-F-14803] 10 p1165 N73-19482
Development and characteristics of transducer for use with fluidic generators
[AD-755104] 11 p1273 N73-20334
Two-axis fluidic wind measuring devices
[AD-755740] 12 p1425 N73-21550
Miniaturization of fluidic switching elements
[BMFT-FBT-73-06] 22 p2654 N73-31257
Coanda effect with jet displacement over planar, concave, and convex walls
[AD-764506] 22 p2655 N73-31270
Fluidic to hydromechanical interface for application to gas turbine engine control system
[AD-764368] 22 p2675 N73-31429

**FLUIDIZED BED PROCESSORS**
Pyrolytic carbon deposition in steady state fluidized beds
[AD-748223] 03 p0323 N73-12631
Application of fluidized bed technique for measuring relative thermal fatigue resistance of superalloys
[NASA-CR-121211] 21 p2558 N73-30507
Corrosion resistance of gas turbine components of power plant fueled with shredded refuse
[PB-221095/3] 21 p2591 N73-30759
Separation of fine metallic powders using air in combination with fluidized bed
23 p2809 N73-32462
Automatic control for absorption columns, fluidized bed processors, and continuous fermentation noting enzymatic protein production
[LAAS-PUBL-975] 24 p2892 N73-33090

**FLUIDS**
Mechanical wave front propagation in fluid mixtures and isotropic solids
[AD-746617] 02 p0158 N73-11281
Detection of bacteria in biological fluids and foods
[NASA-CASE-GSC-11533-1] 04 p0421 N73-13435
DESIGN OF HEAT EXCHANGERS FOR FLUID VAPORIZATION
[CEA-CONF-2010] 06 p0731 N73-15960
Free fluid electrophoresis experiment onboard Apollo 16 flight
[NASA-TM-X-64724] 09 p1000 N73-18137
Collapse of homogeneous fluid mass immersed in vertically stratified fluid
[AD-757995] 15 p1769 N73-24330
Thermal neutron scattering theory for fluid state of matter
[SGAE-2054] 15 p1815 N73-24715
Fluid polydimethylsiloxane resin with low outgassing properties in cured state
[NASA-CASE-GSC-11358-1] 17 p1991 N73-26100
Comparison of normal and hydrostatic extruding processes under fluid pressure
[NLL-NEL-TT-2467-[6075.461]]
20 p2422 N73-29453
Variational principles for examining adiabatic motions in gaseous sphere and waves in stratified horizontal fluids
21 p2523 N73-30237
Numerical analysis of collapse of homogeneous fluid mass in stratified fluid
[AD-763657] 21 p2526 N73-30257
Prediction of aerodynamic characteristics of airfoils at transonic speeds including effects of fluid viscosity
[AD-763295] 22 p2654 N73-31260
Mathematical model formulated for mean disturbance created in linear stratified fluid by growth and collapse of localized region of turbulent mixed fluid
[AD-764050] 24 p2910 N73-33224

FLUORESCENCE
NT PHOSPHORESCENCE
NT X RAY FLUORESCENCE
Visible fluorescence of earth surface materials and potential applications in remote sensing
[PB-210621] 01 p0053 N73-10434
Analysis and Monte Carlo calculations of disc laser limitations due to effects of fluorescence amplification and parasitic oscillation
[AD-747234] 02 p0183 N73-11485
Absorption and fluorescence spectra of marine and fresh water algae using pulsed N2/Ne dye laser as excitation source
[NASA-CR-62090] 03 p0310 N73-12527
Detection of large cosmic ray showers by atmospheric fluorescence
[NYO-3038-13] 05 p0593 N73-14822
Spectroscopic studies of luminescence emitted by dyes irradiated by lasers
[AD-750377] 06 p0680 N73-15535
Application of quasistatic theory of spectral line broadening to predict values for laser radiation
[AD-750156] 06 p0681 N73-15541
Gas scintillation counter for measuring fluorescence of source of radium coated with radon
[PUBL-1410] 06 p0702 N73-15725
Supernovae monitoring experiment using ground-based photomultiplier tubes sensitive to secondary fluorescence light
08 p0974 N73-17967
Laser-induced fluorescence for gas phase oxidation of aluminum atoms
[AD-753839] 10 p1127 N73-19182
Measurement of fluorescence yield in self quenched and foreign gas quenched NO2
[NASA-CR-131296] 11 p1285 N73-20426
High power tunable organic dye laser excitation of atomic fluorescence spectroscopy
12 p1409 N73-21422
Photometric observations of in situ fluorescence and bioluminescence with Biota in New York Bight
[RM-568J] 13 p1479 N73-21978
OGO-4 ultraviolet spectrometer measurements of nitric oxide fluorescence with diffusive transport model for mesospheric and lower thermospheric nitric oxide photochemistry
13 p1515 N73-22274
Results of multijoule air shower fluorescence experiment
13 p1573 N73-22743
Infrared fluorescent low level carbon monoxide analyzer
[PB-213846/7] 15 p1747 N73-24163
Marine luminescence data for monitoring algal and pollutant concentrations
[NASA-CR-114578] 16 p1867 N73-25114
Infrared optical parametric fluorescence and parametric oscillation
16 p1944 N73-25729
Visible fluorescence and thermoluminescence of YAlO3 crystals containing Er, Eu, Nd, Tb or Yb and other optically active centers
[AD-759161] 17 p1992 N73-26112
Dynamic properties of neutral excitations in electron bombarded superfluid helium
18 p2181 N73-27606
Scanning spectrometer for fluorescence measurements, and silicon detector for alpha counting
[BARC-628] 19 p2230 N73-27984
Absolute measurements of spectral radiances from uranium oxygen mixtures
[AD-762430] 19 p2232 N73-27997
Development of flow visualization technique using fluorescent dye to simulate smoke lines in water
[AD-761499] 19 p2257 N73-28192
Electron beam flouorescence diagnostics of ternary gas mixture of nitrogen, helium, and hydrogen
[AD-762930] 20 p2374 N73-29079
Effects of solvent composition in quenching fluorescence of Pr[3 plus] ions in aprotic solvents
[CRC-TN-657] 21 p2505 N73-30104
Analysis of absolute spectrofluorometry procedures and establishment of standards for calibrating spectrofluorometers
[PAPER-76A6-741] 21 p2546 N73-30407
Application of fluorescence spectroscopy for analyzing macromolecules of proteins and nucleic acids
[PAPER-76A6-744] 21 p2546 N73-30410
Development of fluorometric methods for analysis of biological compounds based on production of fluorescence by enzymic reaction
[PAPER-76A6-745] 21 p2546 N73-30411
Absorption and fluorescence of inorganic glasses and polycrystalline discs doped by heavy metal ions
[PAPER-76A6-746] 21 p2546 N73-30412
Development of fluorescent reagent and application to automated assay of amino acids and peptides
[PAPER-76A6-747] 21 p2546 N73-30413
Analysis of various organic compounds in solution and inorganic ions in glasses as possible fluorescence standard reference materials
[PAPER-76A6-748] 21 p2547 N73-30414
Fluorometric 11-hydroxycorticosteroid determination in human blood plasma
[NASA-TT-F-15092] 22 p2619 N73-30990
FLUORESCENT EMISSION
U FLUORESCENCE
FLUORIDES
NT CADMIUM FLUORIDES
NT CHLORINE FLUORIDES
NT CRYOLITE
NT HYDROFLUORIC ACID
NT LITHIUM FLUORIDES
NT NICKEL FLUORIDES
NT OXYGEN FLUORIDES
NT SODIUM FLUORIDES
NT SULFUR FLUORIDES
NT URANIUM FLUORIDES
Preparation of thermally and chemically stable fluoropolymers
[AD-747257] 02 p0139 N73-11121
Generation spectrum of excited DF molecules obtained during chemical reactions in D2/F2/N2/O2 laser system
[NLL-DRIC-TRANS-2816-[3623.66]] 02 p0180 N73-11458
Manufacturing of holmium lithium tetrafluoroytriate laser disk bonded into glass
[AD-747968] 03 p0352 N73-12871
Dry sliding friction characteristics of iron ceramic materials using solid lubricants
04 p0432 N73-13517
Reaction kinetics of fluoride pyrolysis in liquid rocket propellant
[AD-752564] 08 p0970 N73-17931
Growth of multiply sensitized Ho YLF crystals as laser materials
[AD-755530] 13 p1538 N73-22461
Vibrational relaxation of DF behind incident shock waves
[AD-756462] 13 p1562 N73-22658
Evaluation of methods for detection of fluorine-containing missile oxidizers
[AD-756525] 13 p1569 N73-22713
Mass spectrometric measurements of high temperature gaseous tungsten fluoride compounds
[AD-757231] 14 p1617 N73-23103
Static longitudinal and transverse susceptibilities calculated for iron fluoride as function of temperature
[AD-757009] 14 p1698 N73-23781
Purification of molten lithium fluoride, sodium fluoride, and potassium fluoride salt eutectics for thermal battery electrolyte application
[AD-758001] 15 p1739 N73-24097
Polyvinylfluoride pyroelectric radiometer
[NASA-TM-X-62271] 16 p1912 N73-25472
Wear processes and compressive stress of graphite fluoride lubricated machine surfaces
[AD-759560] 17 p2038 N73-26489
Design and performance of segmented holmium doped yttrium lithium fluoride laser
[AD-760019] 17 p2042 N73-26522
Kinetic model and computerized simulation of DF-carbon dioxide chemical transfer laser
[AD-762284] 19 p2309 N73-28571
Temperature dependence of several vibrational relaxation processes in DF-CO2 mixtures
[AD-762925] 20 p2374 N73-29078
Capability of portable SF6 chromatograph to detect and determine behavior of plume out to 100 km
[BNL-17478] 22 p2674 N73-31417
Energy transfer in methyl fluoride
23 p2824 N73-32575
FLUORINATION
Monte Carlo calculations on reaction kinetics in hydrogen, deuterium, and fluoride interactions
[AD-758759] 16 p1872 N73-25153
Fluorinated esters of polycarboxylic acid and lubricating compositions for use at extreme temperature
[NASA-CASE-MFS-21040-1] 21 p2505 N73-30098
FLUORINE
Data and design criteria on dynamic compatibility of fluorine with metals
[AD-756908] 13 p1489 N73-22071
Evaluation of active and passive rupture disk designs for performance at cryogenic temperatures
[NASA-CR-121118] 14 p1670 N73-23554
Computation of thermophysical properties of gaseous and liquid fluorine using measurement data
[AD-758813] 16 p1871 N73-25146
Evaluation of materials for ball bearings intended for use in liquid fluorine and/or FLOX
[NASA-CR-120820] 16 p1917 N73-25516
Chemical kinetics of nitrogen-hydrogen-fluorine systems for advanced rocket propellant technology
[AD-760770] 18 p2192 N73-27697
Preflight tests on fluorine/ammonia propellants to be used in Europa 2 transfer stage
[BMFT-FBW-73-07] 21 p2587 N73-30731
Raman and far infrared spectra of crystalline fluorine obtained in solid phases
[AD-763686] 22 p2626 N73-31039
FLUORINE COMPOUNDS
NT CADMIUM FLUORIDES
NT CHLORINE FLUORIDES
NT CRYOLITE
NT FLUORIDES
NT FLUORINE ORGANIC COMPOUNDS
NT FLUORO COMPOUNDS
NT FLUOROCARBONS
NT FLUOROHYDROCARBONS
NT HYDROFLUORIC ACID
NT LITHIUM FLUORIDES
NT NICKEL FLUORIDES
NT OXYGEN FLUORIDES
NT POLYTETRAFLUOROETHYLENE
NT SODIUM FLUORIDES
NT SULFUR FLUORIDES
NT URANIUM FLUORIDES
Design and development of optical pumps for pulsed neodymium yag lasers with emphasis on efficiency and reproducibility of product
[AD-751212] 07 p0808 N73-16557
Systhesis, thermodynamics, and electrochemical properties of graphite fluorides
[AD-755934] 12 p1377 N73-21167
Tables and graphs of thermodynamic and transport properties of gaseous CF4 in chemical equilibrium
[NASA-TN-D-7181] 18 p2206 N73-27805
FLUORINE ORGANIC COMPOUNDS
NT FLUOROCARBONS
NT FLUOROHYDROCARBONS
NT KEL-F
Perfluorostyrene syntheses, magnetic tapes, titration cell, mill work positioner, superconducting microbridges, position display device, and numbering machine
[NBS-TN-744] 02 p0245 N73-11991
Performance of 1972 ford galaxie equipt with rankine cycle power system composed of organic based working fluid and reciprocating expander
[PB-210836] 19 p2329 N73-28739
FLUORINE-LIQUID OXYGEN
U FLOX
FLUORO COMPOUNDS
NT CRYOLITE
NT FLUORINE ORGANIC COMPOUNDS
NT FLUOROCARBONS
NT FLUOROHYDROCARBONS
NT POLYTETRAFLUOROETHYLENE
Characteristics of HALAR fluoropolymer as versatile insulation material
14 p1640 N73-23298
Polycondensation syntheses of heat resistant siloxane polymers with fluoro aromatic groups at silicon atoms
[RAE-LIB-TRANS-1669] 17 p1991 N73-26104
Preparation of fluorohydroxy ethers by reacting fluoroalkylene oxides with alkali salt of polyfluoroalkylene diol
[NASA-CASE-MFS-10507] 21 p2505 N73-30101
Preparation of fluorinated polyethers from 2-hydroperhaloisopropyl alcohols
[NASA-CASE-MFS-11492] 21 p2505 N73-30102
Chemical and elastic properties of fluorinated polyurethanes
[NASA-CASE-NPO-10767-1] 24 p2891 N73-33076
FLUOROCARBONS
Toxicology of some commercial fluorocarbons
[AD-751429] 07 p0747 N73-16079
Effects of chemical fire extinguishing agents containing bromotrifluoromethane on cardiovascular and nervous systems of dogs, monkeys, and baboons
[AGARD-R-599] 08 p0877 N73-17106
Fluorocarbon combustion and theories on fluorine supported combustion kinetics
08 p0883 N73-17145
Effects of ionizing radiation and high pressure on polymerization processes of fluoroolefins and fluorocarbon compounds
[AD-750151] 16 p1870 N73-25143
Failure of fluorocarbon sulfonic acid membrane for hydrogen oxygen fuel cell
[NASA-CR-121007] 19 p2223 N73-27928
FLUOROHYDROCARBONS
Sensory receptors irritation and cardiopulmonary toxicity from fluorocarbon propellants
[AD-751426] 07 p0749 N73-16089
Cardiac toxicity of fluoroalkane gases for propelling aerosols in industry and household applications
[AD-751425] 07 p0749 N73-16090
Cardiovascular effects of fluorocarbon exposure, emphasizing epinephrine sensitivity
[AD-751427] 07 p0749 N73-16091
FLUOROMICA
U MICA
FLUOROSCOPY
Self-scanning chromatographic-fluorographic drug detector with optical readout system
[NASA-CASE-ARC-10633-1] 13 p1486 N73-22048
Application of X ray fluoroscopy and radiography for determining presence of bombs in suspicious packages and protection measures for personnel
24 p2952 N73-33586
FLUTTER
NT PANEL FLUTTER
NT SUBSONIC FLUTTER
NT SUPERSONIC FLUTTER
NT TRANSONIC FLUTTER
Interrelation of divergence, flutter and autoparametric resonance in cantilever beams
[AD-746695] 03 p0285 N73-12311

Flutter compensation of magnetic tape recorded data, noting single-carrier FM and frequency division multiplexed FM systems
[RAE-TR-72028] 03 p0303 N73-12474
Application of active controls to suppression of flutter for supersonic aircraft
08 p0865 N73-17005
Techniques and equipment for measuring stationary and nonstationary flow in wind tunnels during pressure and flutter tests
[DLR-MITT-72-25] 10 p1139 N73-19283
Construction, installation, and calibration of wind tunnel models for measuring flutter characteristics of aerodynamic shapes
10 p1140 N73-19286
Numerical analysis of bending flutter and torsional flutter in flexible hydrofoil struts
[AD-757645] 14 p1717 N73-23935
Development of aerodynamic control system to control flutter over large range of oscillatory frequencies using stability augmentation techniques
[NASA-CASE-LAR-10682-1] 17 p1980 N73-26004
Computer program for designing minimum mass wings under flutter, strength and minimum gage constraints
[NASA-TN-D-7264] 17 p2092 N73-26927
**FLUTTER ANALYSIS**
Criteria for predicting, preventing, and evaluating panel flutter
[NASA-SP-8004] 02 p0237 N73-11932
Dynamic structural design of aeroelastic wind tunnel models using combinatorial flutter analyses
10 p1140 N73-19291
Experimental method for studying panel flutter
[PUBL-90] 10 p1218 N73-19909
Variational method for approximate solutions to elastic stability problem with dissipative forces
[AD-754532] 11 p1346 N73-20918
Analysis of helicopter blade flutter for both hinged and hingeless rotor blades
[AGARD-R-607] 13 p1472 N73-21920
Development of methods for approximating aircraft with asymmetric elevator control to calculate flutter characteristics
[ARC-R/M-3256] 15 p1728 N73-24018
Analysis of supersonic, unstalled torsional flutter in cascades of compressor blades to determine position of flutter boundary and aeroelastic instability
[AD-758721] 15 p1827 N73-24809
Numerical analysis of wing bending, wing torsion, and aileron rotation at transonic speeds to determine effects on wing-aileron flutter
[ARC-R/M-3258] 16 p1855 N73-25028
Analysis of effect of localized mass on flutter characteristics of delta wing for various spanwise and chordwise positions for the mass center of gravity
[ARC-R/M-3264] 16 p1855 N73-25030
Nonlinear unsteady small-disturbance theory of inviscid transonic flows for oscillating aerodynamic configurations
[NASA-CR-2258] 16 p1858 N73-25048
Effect of surface pressure fluctuations on response of panels underlying attached and separated turbulent boundary layers and shock waves
20 p2479 N73-29910
Application of active control technology for suppression of flutter with analysis of effect on B-52 aircraft configuration
[NASA-TM-X-2909] 21 p2603 N73-30864
Aircraft flutter analog simulation noting structural nonlinearity effects
[DLR-FB-73-30] 22 p2615 N73-30954
Occurrence and magnitude of surface effect takeoff and landing aircraft skirt flutter
[AD-764137] 22 p2616 N73-30966
Transonic wind tunnel tests to determine effects on flutter of aerodynamic interference between pairs of closely spaced delta wings
[NASA-CR-2331] 24 p2989 N73-33887
**FLUX [RATE PER UNIT AREA]**
U FLUX DENSITY
**FLUX [RATE]**
NT HEAT FLUX
NT MAGNETIC FLUX
NT SOLAR FLUX
Perigee rotation effects on orbit-integrated proton and electron fluxes for AE-C orbit
[NASA-TM-X-66059] 01 p0103 N73-10855
Calculation of neutron energy and flux distributions from D-D reactions in plasma focus and Z pinch discharges
[AD-745955] 02 p0217 N73-11755
Vehicle encountered trapped electron and proton fluxes calculated for nominal UK 5 circular equatorial orbits
[NASA-TM-X-66098] 02 p0225 N73-11816
Analysis of electron and proton fluxes encountered during nominal Tiros-N trajectories
[NASA-TM-X-66107] 03 p0357 N73-12908
Energetic particle flux experiments aboard Explorer 34 and 41 satellites
[NASA-CR-130172] 08 p0946 N73-17747
Time of flight spectroscopy for X ray coincidence measurements on californium isotopic fission yield
[AD-753542] 10 p1195 N73-19722
Experimental techniques for achieving high flux, high energy electron irradiation
[AD-749856] 13 p1561 N73-22654
Magnetic particle inspection of large or irregularly shaped parts by assuring optimum magnetic flux densities
[AD-759207] 16 p1882 N73-25236
Galilean satellite thermal radiation measurements
16 p1961 N73-25866
Integral and spectral flux calculations of long wave radiation in atmosphere, using computers
[AD-761579] 19 p2298 N73-28477
European measurements of diffuse flux and Crab pulsar NP 0532
19 p2331 N73-28758
Magnetic storm effects on cosmic ray intensity
[AD-762223] 20 p2468 N73-29826
Multiplier for estimating particle flux from Explorer 8 and 9 satellite data - Part 2
[NASA-CR-132798] 22 p2665 N73-31352
Flux and energy spectrum of fast neutrons and gamma rays at balloon altitudes
23 p2833 N73-32642
**FLUX DENSITY**
NT CURRENT DENSITY
NT ELECTRON FLUX DENSITY
NT ILLUMINANCE
NT IRRADIANCE
NT LUMINANCE
NT LUMINOUS INTENSITY
NT NEUTRON FLUX DENSITY
NT PARTICLE FLUX DENSITY
NT PHOTON DENSITY
NT PROTON FLUX DENSITY
NT RADIANCE
NT RADIANT FLUX DENSITY
NT SOLAR CONSTANT
NT SOUND INTENSITY
Power density as control parameter for electron beam welding
[LA-DC-72-581] 03 p0306 N73-12502
Relative flux density measurements and spectra of extragalactic radio sources at decimetric wavelengths
07 p0838 N73-16788
Flux density variations of seven strongest variable extragalactic radio sources
08 p0956 N73-17827
Measurements of 8000-MHz flux densities of radio galaxies
08 p0958 N73-17839
Particle flux measurements of interplanetary dust and comet orbits by microphone experiments invalidated by micrometeoroid detectors flown on Pioneer 8 and 9
08 p0975 N73-17976
Surface and volume mechanisms of material evaporation subject to powerful radiation fluxes
09 p0999 N73-18154
Ionization chamber/Cerenkov counter measurements of heavy cosmic ray flux and composition
[NASA-CR-130921] 09 p1080 N73-18811
Theoretical and experimental investigation of flux-flow noise in type 2 superconductors
12 p1437 N73-21642
Flux density measurements of extragalactic sources
13 p1490 N73-22075
Graphical method for calculating field intensity and radio wave absorption by ionosphere along radio communication paths
13 p1521 N73-22326
Relation of electrostatic oscillations in lossfree plasma to dispersion and energy equation
[IPPJ-152] 16 p1949 N73-25768
Calculated power distribution of thermionic, beryllium oxide reflected, fast spectrum reactor
[NASA-TM-X-2838] 19 p2320 N73-28663
Measurement of spectral flux density of universal diffuse X ray background between 2 and 200 KeV
19 p2331 N73-28755
Molecular flux measurement in back flow region of nozzle plume in high vacuum
[NASA-CR-133602] 20 p2388 N73-29184
Changes in cosmic ray intensity over last solar modulation cycle
[AD-760789] 20 p2468 N73-29828
Auroral bremsstrahlung flux spectra at various atmospheric depths
[NASA-SP-3081] 23 p2786 N73-32293
Monte Carlo analysis of radio source counts from Ohio Survey at 1415 MHz
24 p2978 N73-33794
**FLUX MAPPING**
U FLUX DENSITY
U MAPPING
**FLUX PUMPS**
Conference on flux pumps and ac superconducting components
[CONF-720908] 21 p2580 N73-30674
**FLUX QUANTIZATION**
Experimental and theoretical determination of intrinsic fluctuations in superconducting flux detector ring closed by Josephson junction
[AD-749101] 04 p0424 N73-13458
**FLUXMETERS**
U MAGNETIC MEASUREMENT
U MEASURING INSTRUMENTS
**FLY BY WIRE CONTROL**
Artificial stabilization to correct control deficiencies for high performance aircraft
08 p0866 N73-17009
Design and development of fixed gain control system for longitudinal axis of C-141 aircraft fly-by-wire control
[AD-760763] 18 p2107 N73-27038
Design, development, airworthiness test, and flight test of multiplexing components for fly by wire flight control
[AD-763111] 20 p2362 N73-28996
**FLYBY MISSIONS**
NT GRAND TOURS
NT MARINER VENUS-MERCURY 1973
Feasibility of flyby or rendezvous cometary mission
02 p0229 N73-11852
Characteristics of blowdown-pressurized hydrazine propulsion system for trajectory correction of spacecraft during outer planet flyby missions
[NASA-CR-129796] 04 p0464 N73-13780
Characteristics of thermoelectric outer planet spacecraft attitude propulsion subsystem
[NASA-CR-129795] 04 p0464 N73-13781
Flyby missions to outer planets
04 p0473 N73-13858
Definition of scientific objectives for outer planet flyby missions
[NASA-CR-130977] 09 p1083 N73-18830
Probe study to explore atmosphere of Saturn and Uranus
[NASA-CR-131227] 10 p1215 N73-19883
Tracking and data system support of launch, near-earth, and deep space phases of Pioneer 10 space probe flight
[NASA-CR-131373] 11 p1256 N73-20188
Specifications for Atlas/Centaur 30 Pioneer G Mission
[NASA-TM-X-69267] 16 p1964 N73-25885
Nonlinear filter estimation of interplanetary spacecraft orbits during simulated Jupiter flyby and Jupiter orbiter missions
17 p2081 N73-26834
Mission operations system implementation and standard mission flight operations for Mariner 9
[NASA-CR-133184] 17 p2082 N73-26844
**FLYING BEDSTEAD AIRCRAFT**
U FLYING PLATFORMS
**FLYING PERSONNEL**
NT AIRCRAFT PILOTS
NT ASTRONAUTS
NT COSMONAUTS
NT FLIGHT CREWS
NT PILOTS [PERSONNEL]
NT SPACECREWS
Motion sickness effects on flying personnel performance during hurricane penetrations
[AD-743928] 01 p0013 N73-10100
Anthropometric survey of US army aviators conducted in 1970
[AD-743528] 01 p0021 N73-10162
Physiological stresses and medical criteria for aircrew fatigue
06 p0634 N73-15152
Color vision requirements for flying personnel of various armed forces - conferences
[AGARD-CP-99] 10 p1112 N73-19065
Color vision testing and selection procedures for flying personnel since World War I
10 p1113 N73-19069
Color vision tests as predictive indicators of flying task performance
10 p1113 N73-19074
Color vision requirements for air crew personnel of future, including coding evaluation
[AMRL-TR-71-116] 10 p1113 N73-19076
Use of photostimulation in electroencephalographic tests of flying personnel and candidates at flight schools
11 p1245 N73-20111
Conference on detection, evaluation, and identification of drugs and alcohol in flying personnel and effects on flight fitness
[AGARD-CP-108] 12 p1368 N73-21102
Drug therapy effects on flying effectiveness and psychosomatic fitness of flying personnel
12 p1369 N73-21103
Drug screening data for civil aviation personnel obtained by urinalyses
12 p1369 N73-21104
Chemotherapy for air crews in Great Britain
12 p1369 N73-21105
Suitability of insulin dependent and oral drug dependent diabetics as navigation personnel
12 p1371 N73-21120
Opthalmological examination of antimalarial drugs effects on performance of navigation personnel
12 p1371 N73-21122
Flight safety factors in prescribing tranquilizing drugs for flying personnel
12 p1371 N73-21123
Diagnostic physiological tests for selection and training of flying personnel
[NASA-TT-F-687] 13 p1479 N73-21981

Myocardial changes in flying personnel exposed to hypoxic hypoxia
13 p1479 N73-21985
Human arterial elasticity during breathing of reduced partial oxygen atmosphere
13 p1480 N73-21987
Latent coronary insufficiency detection in flying personnel using barochamber loading
13 p1480 N73-21988
Changes in vectorcardiograms of atherosclerotic flying personnel after glucose testing
13 p1480 N73-21989
Speech and tone audiometry for testing auditory acuity of flying personnel
13 p1480 N73-21990
Arterial hypertension symptoms in flying personnel
13 p1480 N73-21991
Oxygen breathing effects on human blood circulation and flight personnel fitness test
13 p1480 N73-21993
Conditioned reflex motion sickness test of statokinetic fitness for flying personnel
13 p1480 N73-21994
Barany chair rotation for acceleration tolerance testing on flying personnel
13 p1480 N73-21995
Diurnal cardiac rhythm fluctuation for cardiovascular evaluation of flight personnel
13 p1480 N73-21997
Middle ear barotrauma effect on work capacity and flight fitness of flying personnel
13 p1481 N73-22000
Physiological stress effects of space flight on human body
[JPRS-57139] 13 p1481 N73-22002
Computation of Coriolis forces in selecting flying personnel for vestibular tolerance
14 p1609 N73-23042
Physiological responses of flying personnel to multiple stresses
[AD-759565] 18 p2113 N73-27082
Psychophysiological aspects in flight personnel visual perception of image indicator
20 p2367 N73-29035

**FLYING PLATFORM STABILITY**
U AERODYNAMIC STABILITY
U FLYING PLATFORMS

**FLYING PLATFORMS**
Feasibility study for use of YF-12 aircraft as scientific instrument platform for observing 1970 solar eclipse
[NASA-CR-135482] 23 p2845 N73-32735

**FLYING QUALITIES**
U FLIGHT CHARACTERISTICS

**FLYING SPOT SCANNERS**
Optical data processing of dielectric particle trajectory detector data using flying spot scanner on-line to computer
[BMVG-FBWT-72-34] 09 p1036 N73-18457

**FLYWHEELS**
Design, development, and evaluation of flywheel powered hoist for personnel rescue missions conducted by helicopters
[AD-751217] 07 p0741 N73-16029
Design of double gimballed flywheel for spacecraft stability
[ESRO-CR[P]-135] 17 p2090 N73-26907
Environmental tests on Symphonie model momentum flywheel
[ESRO-CR-96] 21 p2553 N73-30469

**FOAMS**
Fabrication and tests of polyphenylene oxide foam panels for application as reusable insulation with LH2 tanks
[NASA-CR-123955] 05 p0565 N73-14586
Performance tests with halogenated hydrocarbon-foam generating fire extinguishing system for ships
[AD-749022] 05 p0612 N73-14975
Chemical analysis, production, and physical properties of polyimide syntactic foam
[SC-DC-72-2297] 07 p0812 N73-16583
Characteristics of gelled liquid hydrogen polyphenylene oxide foam open cell insulation
[NASA-CR-124114] 09 p1051 N73-18568
Techniques for preparation of Pyrrone structural foams for use as honeycomb filler
[NASA-CR-2222] 09 p1052 N73-18574
Development of low density foamed epoxy adhesives
[Y-1833] 13 p1547 N73-22538
Physio-chemical analysis of flammability characteristics and thermal degradation of rigid and flexible urethane foams used in aircraft structures - Part 2
[FAA-RD-73-50-PT-2] 18 p2105 N73-27025
Development and characteristics of closed pore ceramic foam insulation material for use as heat shield on space shuttle vehicle
[NASA-CR-2254] 19 p2312 N73-28591
Dielectric constant and loss tangent of Eccofoam PT at various packing densities
[NASA-CR-133550] 19 p2312 N73-28594
Dynamic compressive stress-strain data of polymer foams obtained from uniaxial compressive tests
[AD-762490] 21 p2565 N73-30559
Glass ceramic foam materials for space shuttle heat shielding system
24 p2938 N73-33464
Design of rigid ceramic foam insulation for space shuttle surface thermal protection
24 p2942 N73-33493

**FOCUSING**
NT DEFOCUSING
NT SELF FOCUSING
Radiation patterns of linear phased array focused in near field
[AD-746997] 03 p0274 N73-12226
Design of quadrupolar focusing lenses for drift tubes of heavy ion accelerator
[LYCEN-7179] 04 p0402 N73-13270
Metallic surface effects on radiative stability and focusing effects of electron ring
[JINR-P9-6318] 04 p0452 N73-13692
Accelerated electron ring focusing by image forces in conducting cylindrical screen
[JINR-P9-6421] 05 p0580 N73-14724
Focusing and deflection of microwave acoustic bulk wave
[AD-753385] 09 p1009 N73-18233
Beam focusing optical system consisting of elliptical and parabolic mirrors
[AD-757008] 13 p1560 N73-22643
Performance characteristics of proximity focused ultraviolet to visible light image converters
[NASA-TM-X-66258] 15 p1787 N73-24488
Snowplow calculations of acceleration and compression in coaxial plasma accelerator with focusing equipment
[IFP-72-4] 17 p2069 N73-26740
Holographic interferometric analysis of thermal response in ferroelectric crystal to laser radiation
[AD-764703] 23 p2820 N73-32547

**FOG**
Dissipation of fog using helicopter downwash
[AD-744471] 01 p0076 N73-10629
Two dimensional, time dependent warm fog model by airborne wide area hygroscopic particle seeding
[AD-746807] 02 p0206 N73-11674
Nonflammable antifogging agent with low level, nonobjectionable odor and capable of being dispensed from aerosol container for in-flight visibility
[AD-746844] 03 p0321 N73-12617
Effectiveness of airborne chemical seeding techniques for airport fog dispersal
[NETL-72-005-1] 04 p0444 N73-13622
Two dimensional dynamical model for fog forecasting for periods up to eight hours on local scale
[AD-750082] 05 p0575 N73-14682
Fast and accurate technique for iterative solution of saturation adjustment problem
[AD-750083] 05 p0575 N73-14683
Microphysical and meteorological data on fog cycle in California valley
[AD-750086] 05 p0576 N73-14685
Cost effectiveness analysis of propane operated fog dispersal system and evaluation of runway visual range improvement
[FAA-RD-72-123] 06 p0649 N73-15267
Laser extension measurements of visibility during ice fog for aiding in SEV pilot system design
[AD-750114] 06 p0680 N73-15537
Use of hygroscopic materials and ionic surfactants as warm fog for dispersants
[AD-751635] 07 p0817 N73-16622
Field test of warm fog dispersal using helicopter downwash and hygroscopic seeding
[AD-752046] 08 p0939 N73-17694
Fog drop measurement at Barrow, Alaska on chloride sensitive, gelatin-coated glass
[AD-752129] 08 p0940 N73-17705
Two-dimensional numerical model for simulating formation and dissipation of advection fogs
[NASA-CR-2201] 09 p1060 N73-18648
Helicopter downwash for dispersing fogs of 500 to 600 feet in depth
[AD-753357] 09 p1062 N73-18661
Air Force heating system for fog dispersal
[AD-754900] 11 p1315 N73-20675
Airborne heated glycerine droplets for fog dispersal
[TOPR-178-3-133-PT-1] 12 p1421 N73-21521
Warm fog modification by electrostatically charged particles
[AD-754100] 12 p1423 N73-21531
Air Weather Service fog dispersal and weather modification program
[AD-755659] 12 p1423 N73-21533
Coefficient of turbulent exchange in mathematical model of radiation fog evolution
[AD-757490] 14 p1662 N73-23494
Simulation of pilot decision making process in manual landing operation during fog
14 p1713 N73-23898
Fog clearing at airports by ground based heating
[AD-757897] 15 p1806 N73-24639
Optical radar evaluation of techniques for fog dissipation at airports
[AD-758767] 16 p1938 N73-25682
Influence of electric forces in development and dissipation of clouds and fog
[AD-758925] 16 p1938 N73-25683
Field tests of electrogasdynamic fog dispersal concept in Panama Canal Zone
[FAA-RD-73-33-PT-1-PT-2] 17 p2010 N73-26254
Laser observations of dense natural fog to determine backscatter and slant range visibility for aircraft landing operations
[AD-760128] 17 p2041 N73-26511
Technology assessment of fog modification
[AD-762207] 19 p2316 N73-28631
Propane aerosol dispenser for cold fog dissipation at airfields
[AD-762292] 19 p2317 N73-28635
Tabular data from helicopter downdraft fog dispersal experiments
[AD-762189] 19 p2318 N73-28643
Evaluation of electrogasdynamic concept for dispersal of warm fog based on injection of charged water droplets into fog
[ASRC-PUBL-207] 20 p2382 N73-29140
Numerical analysis of ice fog produced by automobiles during arctic conditions
20 p2441 N73-29603
Mathematical model of radiation fog from evolution to dispersal
[NLL-M-23054-[5828.4F]] 20 p2441 N73-29610
Statistical analysis of meteorological parameters during fog at US airports
[FAA-RD-72-39] 20 p2448 N73-29673
Fog chamber low visibility landing simulation film for pilot training
[FAA-RD-73-61] 20 p2452 N73-29707
Daytime fog simulator system modifications
[FAA-RD-73-130] 22 p2647 N73-31208
Theoretical studies of growth of marine fog droplets
[AD-764597] 23 p2815 N73-32503
Determination of visibility slant range when landing aircraft in radiation fog
24 p2946 N73-33523

**FOIL BEARINGS**
Influence of external pressure on foil bearing performance
[AD-751642] 07 p0805 N73-16528
Foil bearing model for predicting head to tape separation in magnetic recording system
[NASA-CR-130536] 08 p0885 N73-17167

**FOILS [MATERIALS]**
NT METAL FOILS
Effect of foil thickness on mechanical behavior of stainless steel in tension
[AD-747698] 03 p0318 N73-12596
Dynamic behavior of externally pressurized foil bearings, including film response to step reduction in tension
[AD-751604] 07 p0805 N73-16531
Thermal cycling tests of molybdenum foil-zirconium cloth insulation system
[ALO-2832-45] 10 p1224 N73-19951
Procedure for making insulating foil for use in multilayer insulating system
[NASA-CASE-LEW-11484-1] 13 p1532 N73-22415
Spectral line features of neon beam-foil spectroscopy
16 p1947 N73-25752

**FOKKER AIRCRAFT**
NT F-27 AIRCRAFT
NT F-28 TRANSPORT AIRCRAFT

**FOKKER BOND TESTERS**
U ADHESION TESTS

**FOKKER F 27 AIRCRAFT**
U F-27 AIRCRAFT

**FOKKER F 28 AIRCRAFT**
U F-28 TRANSPORT AIRCRAFT

**FOKKER FRIENDSHIP AIRCRAFT**
U F-27 AIRCRAFT

**FOKKER-PLANCK EQUATION**
Numerical solution to Vlasov-Poisson equations and to simplified Fokker-Planck-Poisson equations
[ORO-4211-3] 03 p0324 N73-12639
Numerical integration of Fokker-Planck equation for first order phase locked loop
[AD-754355] 11 p1259 N73-20214
Stochastic processes and dynamic systems noting Markov and Ito-Markov processes
[LAAS-AS-73-I-09] 24 p2945 N73-33519
Fokker-Planck study of Coulomb collisions in plasma confined by mirror magnetic configurations
[EUR-CEA-FC-687] 24 p2964 N73-33691

**FOLDING STRUCTURES**
Dynamic and aeroelastic problems of stop-rotors of V/STOL aircraft occurring during retracting and stowing of rotary wings
[DLR-FB-72-65-PT-1] 09 p0983 N73-18027
Design, fabrication, and testing of lightweight, foldable 4.27 meter spacecraft antenna
09 p1087 N73-18870
Electrically conductive wire storage in plastic capsule that allows for unfolding
[NASA-CASE-LAR-10168-1] 13 p1499 N73-22151
Design, development, and testing of foldable beryllium copper alloy elastic tubes for hinges on satellite booms
[ESRO-CR-65] 19 p2346 N73-28874
Dynamic and aeroelastic problems of V/STOL aircraft stop-rotors occurring during retracting and stowing of rotor blades
[DLR-FB-73-19] 21 p2496 N73-30035

FOLDS [GEOLOGY]
Application of ERTS-1 imagery for lineament and photogeologic mapping of western Montana
[PAPER-G32] 19 p2268 N73-28263
FOOD
Detection of bacteria in biological fluids and foods
[NASA-CASE-GSC-11533-1] 04 p0421 N73-13435
Microbiological inspections of NASA food handling facilities
[NASA-TM-X-64734] 11 p1247 N73-20127
Storage stability of intermediate moisture foods for space shuttle
[NASA-CR-133978] 19 p2225 N73-27944
Food heating tests in different atmospheres
[NASA-CR-134040] 22 p2622 N73-31012
FOOD INTAKE
Chromatographic determination of gaseous metabolites released by man during reduced food intake
03 p0258 N73-12091
Analysis of nutrient intake and absorption during Apollo 16 flight
[NASA-TM-X-58096] 03 p0260 N73-12110
Functional relationship between food preference and frequency of repetitious eating
[AD-749079] 05 p0503 N73-14100
Food consumption and morphological indices of blood in white mice with replacement of air nitrogen by inert gases in pressurized chamber
24 p2882 N73-33020
Structural, behavioral, and EEG correlates of alimentary motivation
24 p2888 N73-33063
FORBUSH DECREASES
Analysis of two dimensional pattern of interplanetary shock waves based on solar longitude dependence of time intervals between geomagnetic storms and solar flares
[NASA-TM-X-66226] 12 p1445 N73-21704
Cosmic ray disturbances following solar flare occurrences in August 1972 recorded by neutron monitoring
12 p1446 N73-21709
FORBUSH EFFECT
U FORBUSH DECREASES
FORCE
Electromechanical actuator for producing mechanical force and/or motion in response to electrical signals
[NASA-CASE-NPO-11738-1] 21 p2516 N73-30185
FORCE DISTRIBUTION
Normal forces and center of pressure positions for thin flat plates
[ESDU-70015-AMEND-A] 02 p0154 N73-11250
Variable direction force coupler for transmitting force along selectable curve path
[NASA-CASE-MFS-20317] 04 p0425 N73-13463
Analysis of forces in electrostatic gyroscope with spherical rotor and development of equations to calculate electrical forces
06 p0695 N73-15666
Modifications to helicopter active transmission isolation system to provide method for measuring forces on rotary wing of CH-53 helicopter
[NASA-CR-112245] 09 p0982 N73-18024
Development of method for calculating spanwise loading on helicopter rotor blades in forward flight at various azimuth angles
[ARC-R/M-3318] 16 p1856 N73-25032
Numerical analysis of lift and lift distribution on aircraft wing and trailing vortex flow behind wing
[AD-759262] 16 p1863 N73-25089
Devleopment of computer program for determining ultimate optimum behavior of dynamically loaded structural-mechanical system
[NASA-CR-2268] 18 p2203 N73-27783
Numerical methods for determining unsteady aerodynamic forces on helicopter rotor blades to show lift distribution as function of velocity component normal to blades
[NASA-TT-F-15039] 20 p2360 N73-28981
Analysis of loads imposed on nose gear retraction system of T-34 aircraft to determine critical mechanical adjustments
[AD-762729] 20 p2361 N73-28994
FORCE FIELDS
U FIELD THEORY [PHYSICS]
FORCE-FREE MAGNETIC FIELDS
Models for force-free magnetic fields in plasmas with finite conductivity
[TRITA-EPP-72-24] 07 p0828 N73-16715
FORCED CONVECTION
Thermodynamic properties and heat transfer characteristics of forced-convection boiling of Freon-113 in vertical annular test section
[NASA-CR-2137] 01 p0117 N73-10968
Parameters and secondary factors governing forced convective heat transfer and turbulent flow in circular tubes
[ESDU-67016] 02 p0242 N73-11964
Forced convective heat transfer for single phase, Newtonian fluid flow in smooth, straight, constant area circular tube
[ESDU-68007-PT-3] 02 p0242 N73-11965
Forced convection heat transfer and burnout measurements with twisted tapes in tubular heat exchangers
[RT/ING-[71]9] 03 p0364 N73-12969
Experimental determination of combined forced and free convection in annular region of horizontal coaxial cylinders
[AD-754017] 10 p1144 N73-19322
Budget relations of thermal variance and kinetic energy in transition zone from forced to free convection
15 p1771 N73-24342
Model developed for opposed free and forced convection flow around heated cylinder
[AD-757993] 15 p1844 N73-24942
Perturbation solutions for multicomponent, variable-property forced convection in laminar boundary layers
[AD-764563] 23 p2776 N73-32200
Subcooled forced convection film boiling in vertical annulus
23 p2856 N73-32819
FORCED OSCILLATION
U FORCED VIBRATION
FORCED VIBRATION
Computer programs for analyses of free or forced undamped vibrations of rolling contact supported rotors
[NASA-CR-132220] 15 p1810 N73-24672
Nonlinear forced vibrations of elastic structures excited by disturbing force as harmonic function of time
[AD-758810] 16 p1970 N73-25934
Forced vibrations of disturbed elastic systems during random loading
[AD-759866] 17 p2095 N73-26950
Dynamic stability of harmonically varying forced vibrations of thin spherical shell submerged in acoustic medium medium
22 p2723 N73-31792
FORCED VIBRATORY MOTION EQUATIONS
U EQUATIONS
U FORCED VIBRATION
FOREBODIES
NT NOSE CONES
NT ROCKET NOSE CONES
FORECASTING
NT LONG RANGE WEATHER FORECASTING
NT NUMERICAL WEATHER FORECASTING
NT PERFORMANCE PREDICTION
NT PREDICTION ANALYSIS TECHNIQUES
NT STATISTICAL WEATHER FORECASTING
NT TECHNOLOGICAL FORECASTING
NT WEATHER FORECASTING
Solar flare forecasts and comparisons with rocket-borne observations for flare class greater than or equal to 2F
[NASA-CR-114511] 02 p0225 N73-11814
Forecasting solar flares of classes 1N and 1B based on solar radio temperature contour maps at 3 mm wavelength
[NASA-CR-114510] 02 p0225 N73-11815
Forecasts of military air traffic activity and effect on air traffic control facilities for 1972 through 1983
05 p0493 N73-14014
Prediting mean annual runoff from solar activity
[NLL-M-20715-[5828.4F]] 05 p0529 N73-14303
Technique for using satellite pictures to analyze and forecast tropical cyclone intensities
[NOAA-TM-NESS-45] 10 p1182 N73-19611
Scenario forecasting of likely air passenger trends to 1976 over North Atlantic routes
[REPT-72-02326] 13 p1472 N73-21918
Ecological forecasting and optimizing biosphere
[JPRS-59729] 20 p2409 N73-29364
Procedures for conducting air traffic forecasts with emphasis on socio-economic and demographic characteristics of population
23 p2863 N73-32879
Research project requirements and 1973 budget forecast for French Space Laboratory
[AD-03-72] 23 p2866 N73-32915
FORECASTS
U FORECASTING
FOREIGN POLICY
NT INTERNATIONAL COOPERATION
NT INTERNATIONAL RELATIONS
FORENSIC SCIENCES
U LAW [JURISPRUDENCE]
FOREST FIRE DAMAGE
U FIRE DAMAGE
FOREST FIRE DETECTION
Radar photography of smoke in forest area for predicting bushfire behavior
[DIV-APPL-CHEM-TP-2] 04 p0388 N73-13151
Forest fire detection using airborne infrared scanners
07 p0785 N73-16390
Detection and evaluation of worldwide short-lived events from ERTS-1 imagery
[E73-10453] 11 p1283 N73-20412
ERTS-1 detection of prescribed burn in Sam Houston National Forest and subsequent effects on vegetation
[E73-10674] 16 p1900 N73-25369
Using infrared aerial photography for detection of forest fires
[AD-762259] 19 p2302 N73-28509
Forest fire detection by airbonre infrared photography
[AD-762265] 19 p2353 N73-28931
ERTS-1 imagery of short-lived events such as forest fires, oil spills, volcanic activity, floods, and storms
[E73-11048] 23 p2779 N73-32224
FOREST FIRES
Pattern recognition and detection of short-lived events such as storms, forest fires, volcanoes, and earthquakes using ERTS-1 data
[E73-10678] 16 p1901 N73-25373
Mapping of large forest fires from infrared photography
[AD-758613] 17 p2028 N73-26414
FOREST MANAGEMENT
Design of forest inventory for in-place data provision for planning and programing timber management
[PB-210276] 01 p0121 N73-10999
Geological evaluation, regional planning, forest management, and water management in North Carolina using ERTS-1 imagery
[E72-10280] 03 p0292 N73-12378
Side-looking radar applications to forestry management, and timber inventory and identification
03 p0295 N73-12404
Utilization of ERTS-1 imagery in geological evaluation, regional planning, forest management, and water management in North Carolina
[E72-10317] 04 p0413 N73-13366
Summary of side-looking radar applications in earth resources noting basic principles of side-looking radar, radar scattering, data handling, and research and development
[ESRO-CR[P]-141] 06 p0641 N73-15200
Utilization of ERTS-1 imagery in geological evaluation, regional planning, forest and water management in North Carolina
[E73-10300] 09 p1021 N73-18332
Automatic interpretation of ERTS-1 data for forest management in Minnesota
[E73-10365] 10 p1150 N73-19361
Remote sensing techniques for evaluating vigor loss in black spruce due to eastern dwarf mistletoe
[NASA-CR-131582] 13 p1523 N73-22341
Use of digitized remote sensor data and automatic data processing techniques in preparation of forest cover mapping to aid in forest resources management
[NASA-CR-131578] 13 p1523 N73-22344
Inventory of forest and rangeland and detection of forest stress at Black Hills, South Dakota, Atlanta, Georgia, and Manitou Forest test sites using ERTS-1 data
[E73-10546] 14 p1655 N73-23421
Computerized interpretation of ERTS-1 data for forest management in Minnesota
[E73-10687] 16 p1902 N73-25381
Utilization of ERTS-1 imagery in geological evaluation, regional planning, forest and water management in North Carolina
[E73-10688] 16 p1902 N73-25382
ERTS-1 data for development of information system for timber resources and land management planning in Oregon
[E73-10696] 16 p1903 N73-25388
Application of EREP data in geological evaluation, regional planning, forest management, and water management in North Carolina
[E73-10754] 17 p2022 N73-26357
Forest management in Minnesota using automatic interpretation of ERTS-1 data
[PAPER-L25] 19 p2276 N73-28320
Application of ERTS-1 data to North Carolina forest and water resources management
[PAPER-R1] 19 p2282 N73-28359
Geological evaluation, regional planning, forest management, and water management in North Carolina using ERTS-1 imagery
[E73-10962] 21 p2532 N73-30304
Utilization of Skylab EREP data in geological evaluation, regional planning, forest management, and water management in North Carolina
[E73-10966] 21 p2533 N73-30308
ERTS-1 data applications to Minnesota forest land use classification
[E73-11017] 22 p2661 N73-31321
Timber identification and inventory and forest management in Colorado, Georgia, Black Hills, California, and Hawaii from ERTS-1 imagery
[E73-11051] 23 p2779 N73-32227
Forest and rangeland inventory and detection of forest stress at Black Hills, South Dakota, Manitou, Colorado, and Atlanta, Georgia test sites
[E73-11052] 23 p2779 N73-32228
FORESTS
Development of multistage forest sampling inventory system using ERTS-1 imagery
[E72-10186] 01 p0046 N73-10365
Investigation of forest stress in Black Hills, forest inventory at Atlanta test site, and rangeland inventory at Manitou test site using ERTS-1 imagery
[E72-10219] 02 p0162 N73-11313

Forest resources evaluation, planning, protection, and management using remotely sensed imagery
[E72-10220] 02 p0162 N73-11314
Remote sensing in forestry using aerial and satellite-borne photography and imaging techniques
[E72-10221] 02 p0162 N73-11315
Land use mapping of forest area in Southeastern US by airborne multispectral scanning
[E72-10222] 02 p0162 N73-11316
Doppler radar frequency attenuation in horizontally polarized field over forest
[AD-748104] 04 p0389 N73-13163
Detection and monitoring forest insect infestation in Sierra Nevada Mountains of California using ERTS-1 imagery
[E72-10301] 04 p0411 N73-13351
Application of airborne and spaceborne photography to determine agricultural and forestry resources
07 p0782 N73-16355
Remote detection of insect damage and stress symptoms in forests of Black Hills
07 p0785 N73-16389
Forest and rangeland inventory and forest infestation of Atlanta, Manitou, and Black Hills test sites based on ERTS-1 imagery
[E73-10084] 08 p0901 N73-17296
Remote sensing of Minnesota lakes and forests using ERTS-1
[NASA-CR-130548] 08 p0916 N73-17502
Applicability of ERTS-1 imagery to forestry and timber survey and identification in Finland
[E73-10297] 09 p1021 N73-18329
Multidisciplinary analysis of forestry, agriculture, soils, and landforms in Michigan using ERTS-1 imagery
[E73-10310] 09 p1022 N73-18342
Detection of plant and forest diseases, nutrient deficiencies, soil types, and soil moisture levels from ERTS-1 imagery of Tennessee
[E73-10311] 09 p1022 N73-18343
Detection and monitoring forest insect infestations in Sierra Nevada Mountains of California using ERTS-1 imagery
[E73-10312] 09 p1022 N73-18344
Automatic interpretation of forest species and stress identification using ERTS-1 imagery of Minnesota
[E73-10366] 10 p1150 N73-19362
Filtering and vertical sensor position effects on human speech detection in jungle evnironment
[AD-753650] 10 p1190 N73-19686
Analysis of ERTS-1 data to detect and map areas of tree mortality due to insect outbreaks using color infrared positive transparencies
[E73-10351] 11 p1275 N73-20345
Inventory of forest and rangeland and detection of insect infestation from ERTS-1 imagery of Black Hills, Atlanta, and Manitou test sites
[E73-10407] 11 p1278 N73-20369
Vegetation analysis and preparation of tectonic map overlay of Bighorn Mountains region based on ERTS-1 data
[E73-10420] 11 p1279 N73-20382
Development of multistage forest sampling inventory system using ERTS-1 imagery
[E73-10428] 11 p1280 N73-20389
ERTS-1 imagery of forest insect infestation in Sierra Nevada Mountains of California
[E73-10440] 11 p1282 N73-20400
Application of ERTS-1 imagery to analysis of agricultural crops and forests in Michigan
[E73-10470] 12 p1395 N73-21307
Application of ERTS-1 imagery to identification of agricultural crops, grasslands and forestry in Mississippi Delta Region
[E73-10476] 12 p1395 N73-21313
Application of ERTS-1 data to analysis of agricultural crops, forests, soils, landforms, and acreage estimates in Michigan
[E73-10483] 12 p1396 N73-21320
Identifying phenological changes for specific forest and crop types using ERTS-1 imagery
[E73-10498] 12 p1398 N73-21334
Development of multistage forest sampling inventory system using ERTS-1 MSS data
[E73-10508] 13 p1516 N73-22283
Development of multistage forest sampling inventory system from interpretation of ERST-1 MSS photography
[E73-10528] 13 p1517 N73-22294
Multistage forest surveys from Skylab EREP multispectral band scanner and camera imagery
[E73-10531] 13 p1517 N73-22296
Classification of forest land use and detection of forest disturbances using space and high altitude aerial photography
[NASA-CR-131584] 13 p1523 N73-22339
Application of remote sensing techniques in forestry and range disciplines for timber inventory, weather forecasting, land classification, and snowfield monitoring
[NASA-CR-131583] 13 p1523 N73-22340
Use of digitized remote sensor data and automatic data processing techniques in preparation of forest cover mapping to aid in forest resources management
[NASA-CR-131578] 13 p1523 N73-22344
Inventory of forests and rangelands, including forest stress, at Black Hills, Atlanta, Georgia, and Manitou, Colorado test sites using Skylab EREP
[E73-10587] 14 p1657 N73-23447
Usefulness of Skylab multispectral band camera and scanner imagery in multistage forest surveys
[E73-10610] 15 p1773 N73-24371
Detection and monitoring of forest insect infestation in Sierra Nevada Mountains of California
[E73-10668] 16 p1899 N73-25363
ERTS-1 detection of small ponds in forested areas of Texas
[E73-10673] 16 p1900 N73-25368
Application of ERTS-1 data for multidisciplinary analysis of Michigan resources and development of computerized procedure for map coordinates correlation
[E73-10703] 17 p2018 N73-26316
Forest sampling and timber inventory in California from ERTS-1 imagery
[E73-10743] 17 p2021 N73-26348
Application of ERTS-1 imagery for identifying and mapping rivers, agricultural areas, forest, mineral resources, and water conditions in Thailand
[E73-10746] 17 p2021 N73-26350
Inventroy of forest and rangeland resources at Atlanta, Georgia, Black Hills, South Dakota, and Manitou, Colorado test sites using Skylab EREP imagery
[E73-10749] 18 p2133 N73-27237
Analysis of ERTS-1 imagery for multi-disciplinary resource inventory of soils, vegetation, and geology in Big Summit Prairie area of oregon
[E73-10770] 18 p2134 N73-27246
Multistage forest surveys using Skylab multispectral band camera and scanner imagery
[E73-10782] 18 p2136 N73-27258
Detection and inventory of timber and rangelands and forest stresses in Georgia, Colorado, and Black Hills from ERTS-1 imagery
[E73-10805] 18 p2138 N73-27280
Energy exchange characteristics of desert, meadow, forest, and marsh sites
[PB-218825/8] 18 p2173 N73-27550
Detection of phenological event for specific forest and crop types using ERTS-1 imagery
[PAPER-A19] 19 p2261 N73-28226
Analysis of ERTS-1 data for application to forest and range mapping in Houston, Texas area
[PAPER-A20] 19 p2262 N73-28227
Application of ERTS-1 data for analysis of agricultural crops and forests in Michigan
19 p2262 N73-28228
Application of ERTS-1 band six imagery to determine rate of spread of grass fires in Zambesi Basin of South Africa
[PAPER-E6] 19 p2269 N73-28270
Environmental study of Lake Champlain and Vermont land use based on ERTS-1 imagery
[PAPER-E11] 19 p2270 N73-28275
DCP-collected absolute target reflectance measurements to assist interpretation of ERTS-1 imagery of forest stresses in Black Hills, South Dakota
19 p2283 N73-28365
ERTS-1 imagery of geology, agriculture, forestry, and hydrology in Iran
19 p2287 N73-28387
Inventories of agriculture, forestry, and rangeland resources based on ERTS-1 imagery
19 p2288 N73-28396
Application of ERTS-1 imagery to land use and resource management in State of Mississippi
19 p2289 N73-28404
Results of ERTS-1 investigations of agriculture, forestry, and range resources
19 p2289 N73-28406
ERTS-1 detection of plant diseases and nutrient deficiencies, soil types and moisture levels, forests, and crop identification in Mississippi Delta
[E73-10849] 19 p2292 N73-28427
Multispectral scanning systems applied to agriculture and forestry
19 p2295 N73-28452
Analysis of ERTS data for detection and monitoring of forest insect infestations in Sierra Nevada Mountains of California
[E73-10868] 20 p2392 N73-29219
Skylab inventory of forest and rangeland resources and forest stresses at Atlanta Georgia, Manitou, Colorado, and Black Hills test sites
[E73-10895] 20 p2395 N73-29244
Tectonic and photogeologic mapping of forested and sparsely vegetated terrain of Montana and Idaho
[E73-10900] 20 p2396 N73-29249
Identification and classification of agricultural crops and forest inventory in Iowa from ERTS-1 imagery
[E73-10927] 20 p2398 N73-29276
Biometric and radiant transfer characteristics of forest vegetation
20 p2405 N73-29328
Radiation regime of forest vegetation under plant cover and open areas under various weather conditions
20 p2405 N73-29329
Light effects on organic matter balance of oak underwood growing in forest understorey
20 p2405 N73-29330
Thematic mapping of wetlands, forests, open water, and Mississippi River flooding from ERTS-1 imagery
[E73-10952] 21 p2531 N73-30294
Land use, forest density, soil mapping, erosion, drainage, and salinity limitations in Greece from ERTS-1 data
[E73-10969] 22 p2657 N73-31283
Utilization of ERTS-1 imagery for studies of agriculture, forestry, cartography, geography, hydrology, meteorology, geology, and oceanography in Thailand
[E73-10996] 22 p2659 N73-31302
Skylab imagery of terrain surface moisture, vegetation, and forestation in Colorado and Oregon
[E73-11001] 22 p2659 N73-31306
Application of aerial photography and ERTS imagery to agricultural, forest, and water resources management in Minnesota
[NASA-CR-135483] 22 p2665 N73-31357
Inventory of forest and rangeland resources and stresses at Atlanta, Georgia, Black Hills, South Dakota, and Manitou, Colorado from Skylab EREP
[E73-11040] 23 p2778 N73-32219
Application of ERTS-1 imagery to timber inventory in Finland
[E73-11068] 23 p2781 N73-32244
Development of multistage forest sampling inventory system using ERTS-1 data for Trinity Alps in California
[E73-11092] 23 p2782 N73-32259
Multistage survey of forests in Trinity Alps of California from Skylab EREP data
[E73-11093] 23 p2783 N73-32260
Application of ERTS-1 imagery to land use, forest density, and soil investigations in Greece
[E73-10988] 24 p2913 N73-33244
Survey and inventory of forest resources in Susquehanna River Basin to determine accuracy achieved in mapping vegetation classes using ERTS-1 imagery
[E73-11110] 24 p2915 N73-33267
Identification of selected forest and vegetation cover in Colorado Mountains from Skylab EREP data
[E73-11132] 24 p2917 N73-33287
Detection and monitoring forest insect infestation in Sierra Nevada Mountains of California from ERTS-1 data
[E73-11133] 24 p2917 N73-33288
Application of ERTS-1 imagery to agriculture, forestry, meteorology, and hydrology in Thailand
[E73-11145] 24 p2918 N73-33299

**FORGING**

Influence of forging deformation degree on mechanical properties of forged parts
[AD-745432] 01 p0062 N73-10510
Automated planning systems for cold forging production processes
[NLL-NEL-TT-2393-(6075.461)]
02 p0177 N73-11436
Effective tooling designs for producing precision forging using rib and web type configurations
[AD-745991] 02 p0179 N73-11449
Foreign process for developing spiral bevel gear for CH-47 helicopter
[AD-747857] 03 p0309 N73-12522
Regular forging and explosive forming effects on mechanical properties of aluminum alloy
[AD-748710] 04 p0427 N73-13484
Temperature effects on tensile-, fracture toughness-, and crack growth-properties of aluminum alloy forgings
[AD-748257] 04 p0436 N73-13554
Production of ball bearing steel ingots with emphasis on effects of temperature, surface defects, and casting methods
[AD-751252] 07 p0805 N73-16533
Procedure for measuring flow stresses of metals during closed die forging
[AD-752588] 08 p0928 N73-17602
Improvements in welding techniques to increase productivity and quality of performance of bonded joints
[JPRS-58291] 10 p1163 N73-19460
Butt welding of titanium alloy rings and flanges to improve mechanical properties
10 p1163 N73-19463
Deformation processes in forging refractory ceramic oxides
[NASA-CR-131109] 10 p1175 N73-19558
Heat treatment and forging effects on mechanical properties of maraging steel
[AD-756422] 13 p1543 N73-22507
Effect of residual impurity element on sensitivity of low alloy steels to radiation induced embrittlement
[AD-756625] 14 p1679 N73-23622
Effect of Al-Zn-Mg-Cu alloy composition variations on fracture strength and tensile properties
[RAE-TR-72173] 17 p2046 N73-26549
Development and production of thermo-mechanically forged tool steel spur gears using high energy rate forging procedures
[NASA-CR-121227] 18 p2154 N73-27409

Different types of lubricants for working of plastics
[NLL-RTS-7852] 20 p2421 N73-29449
Hot forging of aluminum alloy structural parts
[AD-764618] 23 p2798 N73-32384
**FORM FACTORS**
Asymptotic behavior of elastic form factors and light cone expansion for matrix elements
[TR-73-039] 01 p0083 N73-10683
Determination of flat notched fatigue test specimens form numbers by stress optical method and finite element method, noting standardization
[LBF-TM-61/71] 06 p0685 N73-15573
Off-shell asymptotic behavior of electromagnetic form factors of composite particle
[TR-73-070] 06 p0703 N73-15728
**FORM PERCEPTION**
U SPACE PERCEPTION
**FORMALDEHYDE**
Interferometric observations of formaldehyde absorption in front of strong galactic sources
[AD-749772] 06 p0719 N73-15873
Chemical synthesis of formaldehyde based disinfectants without penetrating odor and eye and ear irritation properties
[NASA-CASE-NPO-12115-1] 08 p0884 N73-17153
Hyperfine formaldehyde lines in molecular dust cloud L1436
[AD-757689] 15 p1833 N73-24861
**FORMAT**
Space shuttle orbiter subsystems, formats and format trees, and coding of sample format - Vol. 3
[NASA-CR-128578] 01 p0019 N73-10147
Optimum design of format synchronizer for ESRO control center
[ESRO-CR[P]-127] 02 p0141 N73-11143
**FORMATES**
Preparation of polyurethane polymer by reacting hydroxy polyformal with organic diisocyanate
[NASA-CASE-MFS-10509] 21 p2505 N73-30103
**FORMING TECHNIQUES**
NT CASTING
NT COLD WORKING
NT ELECTROFORMING
NT EXPLOSIVE FORMING
NT EXTRUDING
NT FORGING
NT HOT WORKING
NT MAGNETIC FORMING
NT METAL DRAWING
NT METAL SPINNING
NT PRESSING [FORMING]
NT ROLL FORMING
NT SLIP CASTING
NT STAMPING
Hard alloy shaping tools for extruding steels and nonferrous materials
[NLL-NEL-TT-2400-(6075.461)] 02 p0177 N73-11435
Thermocompression wobble tool bonding of beam lead devices
[SC-DC-72-1197-A] 03 p0306 N73-12501
Design and technical characteristics of rotary automatic devices for pressing and gauging of metal ceramic structural parts 04 p0432 N73-13524
Production of ball bearing steel ingots with emphasis on effects of temperature, surface defects, and casting methods
[AD-751252] 07 p0805 N73-16533
Laser forming of sliding friction bearings for instrument construction
[AD-753490] 10 p1169 N73-19511
Forming and joining techniques and properties of thin gage TD-NiCr sheet in crystallized and unrecrystallized conditions
[NASA-CR-121224] 18 p2154 N73-27408
Application of ultrasonic inspection techniques for detecting separation of solid propellant rocket case-liner and liner-propellant interfaces
[NAL-TR-308] 18 p2193 N73-27703
Compression molding apparatus for thermosetting plastic compositions
[NASA-CASE-LAR-10489-2] 22 p2677 N73-31446
**FORMULAS**
Computational formula for reliability analysis on multiple element circuits of silver zinc storage battery
[AD-754725] 11 p1238 N73-20050
**FORMULAS (MATHEMATICS)**
Equation for calculating plastic deformation of metals under tension
[AD-751151] 07 p0810 N73-16571
Analytical expressions for geographic distribution of midday ionization of F 2 layer in temperate latitudes 13 p1521 N73-22331
Prosodic signals for parenthesis in algebraic expressions 14 p1629 N73-23207
Runge-Kutta-Nystrom formulas of eighth and lower order derived for special second order differential equations
[NASA-TR-R-410] 15 p1803 N73-24614
Development of formula for calculating heat transfer coefficient in labyrinth glands of gas turbines
[NLL-RTS-7840] 18 p2192 N73-27698
**FORTRAN**
Computation of thermochemical ablation rates of pyrolytic graphite surfaces using FORTRAN 4 computer code - Vol. 1
[AD-745440] 01 p0071 N73-10579
FORTRAN program for numerical solution of steady state matrix Riccati equation of quadratic cost optimal control problem
[AD-745862] 01 p0072 N73-10589
FORTRAN program for solving transport problem for neutrons in multilayer slab system
[EUR-4839-E] 01 p0082 N73-10681
Fortran program for axisymmetric, transient heating and material ablation
[AD-745441] 01 p0118 N73-10975
Development and application of computer program for simulation of continuous systems expressed as ordinary differential and logical equations
[EUR-4836-E] 02 p0144 N73-11169
Policy iteration subroutine package for IBM 360 computer
[FOA-P-C-8287-X9] 02 p0145 N73-11173
Analytical method for estimating chamber and throat conditions in nozzle with low radius of curvature throat
[NASA-CR-128619] 02 p0156 N73-11263
Algorithms and FORTRAN 4 data analysis programs for reflectometer diagnosis of thin boundary layer plasma sheaths - users manual
[AD-747041] 02 p0217 N73-11758
FORTRAN computer program for annular airfoil pressure distribution at subsonic speeds
[ARC-CP-1217] 03 p0248 N73-12004
FORTRAN computer program for solar simulator optimization
[DLR-FB-71-34] 03 p0281 N73-12277
Implementation of FORTRAN-extended graph algorithmic language for Univac 1108
[NASA-CR-129907] 04 p0393 N73-13198
CCAMIN, computer program for fitting time of arrival and shock peak overpressure versus slant range in gas
[AD-749332] 04 p0409 N73-13330
FORTRAN computer program for calculating radar maximum range
[AD-749686] 06 p0642 N73-15208
FORTRAN 4 subroutines for time series analysis
[FOA-3-C-3672-64[11]] 06 p0643 N73-15221
Velocity determination of shell fragments, using FORTRAN routines for evaluating film from drum camera
[FOA-2-C-2475-11[44]] 06 p0643 N73-15222
FORTRAN routines for interpolation and integration of approximation with cubic splines
[FOA-2-C-2476-11] 06 p0643 N73-15223
FORTRAN subroutine for plotting computer determined transmission line parameters on Smith chart
[AD-751019] 06 p0645 N73-15243
Computer program for determining thermodynamic and transport properties of complex mixtures to include rocket performance, shock properties, and detonation properties
[NASA-TN-D-7056] 06 p0730 N73-15954
Computer program for orbit comparison plots - users manual
[NASA-TM-X-66164] 07 p0759 N73-16165
SCEPTRE support program - revised users manual using FORTRAN
[AD-751518] 07 p0764 N73-16211
FORTRAN program for handling radiation effects circuit analysis problems
[AD-751519] 07 p0765 N73-16213
On-line dialog and testing program for control of real time FORTRAN program 08 p0887 N73-17182
Implementation of FORTRAN extended graph algorithmic language for univac 1108 computer
[NASA-CR-130966] 09 p1006 N73-18212
FORTRAN program for predicting temperature-time histories of hemispherical shells subject to aerodynamic heating
[WRE-TN-783(WR/D)] 09 p1098 N73-18961
Program analysis for documentation in FORTRAN 10 p1132 N73-19222
FORTRAN program for computing XYZ potential flow about three-dimensional bodies of arbitrary shape
[AD-754429] 10 p1143 N73-19317
FORTRAN program for solution of large, sparse unsymmetric systems of linear equations
[AD-755878] 13 p1550 N73-22563
FORTRAN-4 computer program for compiling irradiation data on UN and UC fuel pins
[NASA-TM-X-68226] 13 p1558 N73-22625
Subroutine package for FORTRAN communication with graphic video system
[R-1015-NIH] 14 p1637 N73-23274
FORTRAN code for solving time dependent neutron transport equation in three-dimensional geometry by Monte Carlo method
[AD-756290] 14 p1691 N73-23728
FORTRAN program for solution of linear or nonlinear constrained optimization problems
[NASA-TM-X-62282] 17 p2055 N73-26619
FORTRAN 4 code for calculating nuclear reactor dimensions and mass from thermal-hydraulic considerations
[NASA-TM-X-68236] 17 p2061 N73-26670
Update of input instructions for operation of FORTRAN computer code TEMOD
[NASA-CR-121225] 19 p2239 N73-28047
FORTRAN computer program for computing transmittance of atmosphere in ultraviolet to infrared spectral region
[AD-763721] 21 p2541 N73-30378
Computer code which reorganizes old FORTRAN programs so that statement numbers are added sequentially and extraneous statements are deleted
[NASA-TM-X-62286] 22 p2636 N73-31128
FORTRAN 4 routine for random number generator continuous random variables
[NASA-CR-133983] 22 p2691 N73-31553
Execution time optimization for IBM 360 FORTRAN production programs
[NASA-TM-X-70477] 23 p2760 N73-32086
FORTRAN-WATFIV compiler noting differences with FORTRAN G and H extended and usefulness in program debugging
[LAAS-NT-SIS-73-T-04] 23 p2761 N73-32095
FORTRAN program, ZIP, for time sharing in SNAP reactor parametric studies
[AI-AEC-13076-VOL-1] 24 p2954 N73-33603
Computer programs for analyzing optical properties of sea water 24 p2958 N73-33638
LUIN, code for calculation of cosmic ray propagation in atmosphere
[HASL-275] 24 p2977 N73-33784
**FORWARD SCATTERING**
New tables for forward pion nucleon scattering amplitude analyzing errors and total cross section data
[NOTA-INTERNA-382] 01 p0084 N73-10695
Light cone singularities, DGS representations, and asymptotic behavior of forward scattering amplitudes
[TR-73-059] 03 p0339 N73-12765
Forward scattered light spectrum from pulsed ruby laser in liquid medium 20 p2424 N73-29470
Measurement of light scattering at various angles using point spread function and modulation transformation function techniques 24 p2957 N73-33629
**FOSSIL METEORITE CRATERS**
U METEORITE CRATERS
**FOUNDATIONS**
NT PILE FOUNDATIONS
Development and evaluation of equipment for monitoring long term sea floor foundation settlement and tilting
[AD-750258] 06 p0669 N73-15444
**FOURIER ANALYSIS**
NT FOURIER SERIES
Serial segments method for measuring pilot manual control remnant in vicinity of sine waves 01 p0018 N73-10136
Application of fourier analysis, information theory, or curvature analysis to determine information content of curved line
[MITT-128] 05 p0538 N73-14376
Fourier and Galerkin techniques for analyzing discontinuities and coupling phenomena in microstrip lines
[AD-750737] 06 p0648 N73-15264
Diffraction technique for determining three dimensional frequency spectra of photographic images
[AD-751418] 07 p0822 N73-16663
Generalized Fourier analysis of geophysical data with data points unequally spaced in time
[AD-751908] 08 p0919 N73-17529
Fourier analysis of plasma deformation and feedback in stabilized rectilinear helicoid with pinch mechanism
[LRP-58/72] 10 p1196 N73-19728
Fourier technique for quantitatively classifying lunar rilles by planimetric shape 12 p1455 N73-21781
High resolution spectral and polarization behavior of solar Type 3 bursts at 34 MHz 13 p1489 N73-22073
Application of digital signal processing to design of phase vocoder analyzer 14 p1621 N73-23131
Fourier analysis of boundary curve for identification of three dimensional objects
[AD-758895] 16 p1877 N73-25192
Fourier coefficients and power spectral density calculating device
[IPPJ-T-13] 16 p1949 N73-25766
Sensitivity of coupled reaction rate equations to coefficient uncertainties
[AD-762420] 19 p2232 N73-27995
Fourier analysis on ergodic calculations of reaction kinetic rate coefficients in air dissociation and hydrogen oxygen combustion
[AD-762421] 19 p2232 N73-27996
Signal processing facility for underwater acoustics consisting of digital computer and Fourier analyzer
[REPT-5-72] 19 p2239 N73-28055

**FOURIER LAW**
Fourier theory of using grating to extend dynamic range of laser far field camera
[UCRL-51255] 07 p0806 N73-16542

**FOURIER SERIES**
Fourier series and fourier integral formulations for improving spectrum analysis and display computer program
[AD-752113] 08 p0886 N73-17177
Fourier coefficients of Eisenstein series of the second degree
[NASA-TT-F-14937] 16 p1934 N73-25648
Analysis on Fourier coefficients of second degree Eisenstein series
[NASA-TT-F-14936] 16 p1934 N73-25649

**FOURIER TRANSFORMATION**
NT FAST FOURIER TRANSFORMATIONS
Fast Fourier transform digital processor as spectrum analyzer and adaptive filter
01 p0025 N73-10198
Fourier pattern recognition techniques applied to titanium alloy photomicrographs
[AD-746720] 02 p0188 N73-11528
Assembler language program for Fourier transform spectroscopy with PDP 11 computer
[MSC-1743] 04 p0394 N73-13200
Computerized fast Fourier transform technique for measuring human performance in compensatory tracking task
[AD-748659] 05 p0501 N73-14078
Computer computation of spectral data for Josephson junction circuit
[NBS-TN-627] 07 p0832 N73-16740
Fourier series and fourier integral formulations for improving spectrum analysis and display computer program
[AD-752113] 08 p0886 N73-17177
Digital on-line spectrum analysis using cross correlation and fast Fourier transformation techniques
[ARC-CP-1225] 09 p1006 N73-18209
Synthesis of superconducting magnetic field suspensions with maximum lift using Fourier coefficients
10 p1159 N73-19430
Two dimensional Fourier transform and digital correlation for image processing
[BMVG-FBWT-72-1] 10 p1179 N73-19591
Continuous Fourier transform method and apparatus
[NASA-CASE-ARC-10466-1] 12 p1381 N73-21199
Construction method for radio signal correlators using Fourier transformation
13 p1497 N73-22131
Pitch-synchronous, nonharmonic analysis of speech signals by application of FFT to single pitch periods
14 p1621 N73-23135
Incorporation of high resolution Fourier transform spectrometer with astronomical telescope at Mauna Kea Observatory, Hawaii
[NASA-CR-131893] 14 p1667 N73-23530
Algorithm for computer processing of Fourier transformations
[AD-758451] 15 p1755 N73-24222
Design of fast Fourier transform digital processor
[AD-761803] 19 p2245 N73-28097
Digital simulation of multicorrelated random processes and its applications
[NASA-CR-62092] 21 p2565 N73-30563
COLFTAR real time electro-optical system for generating optical Fourier transforms of two-dimensional video signals
24 p2956 N73-33613

**FOVEA**
Application of extra-foveal vision to predicting target acquisition in air-to-ground search
10 p1225 N73-19960

**FR-1 SATELLITE**
Management, storage, and computation of FR-1 satellite very low frequency data
[GRI/NTP/101] 02 p0146 N73-11187
Management, processing, and handling of French FR-1 satellite very low frequency data
[GRI/NTP/100] 09 p1005 N73-18207
Research and development of French programs for FR-1, impedance and electrostatic probes, and very low frequency wave propagation
[GRI/NTP/103] 13 p1595 N73-22936

**FRACTIONATION**
Partial condensation and fractionation for analysis on mixture of hydrogen, methane, and ethane
[NASA-TT-F-14681] 07 p0752 N73-16109
Separation of fine metallic powders using air in combination with fluidized bed
23 p2809 N73-32462

**FRACTOGRAPHY**
Low energy fracture process in high strength aluminum alloy 2014T6
[NASA-CR-131099] 10 p1170 N73-19520
Analysis of fractures in materials using scanning electron microscopes
[AD-759287] 16 p1930 N73-25617

**FRACTURE MECHANICS**
Method of potential applied to three-dimensional elastic and thermoelastic stress problems and fracture mechanics
[SCL-DR-71-0026] 01 p0113 N73-10935
Electron fractography of cleavage in metal crystals discussing crack propagation
[NLR-TR-71047-U] 02 p0187 N73-11513
Fatigue crack propagation in 2024-T3 aluminum alloy sheet in vacuum and air
[NLR-TR-71032-U] 02 p0187 N73-11514
Fracture mechanics and prediction of fatigue life
[AD-746122] 02 p0188 N73-11521
Nonmetallic inclusion effects on crack growth rate in two alloy steels
[AD-746950] 02 p0189 N73-11530
Development of rational fracture resistance test procedures to determine fracture properties of titanium alloy sections
[AD-747230] 02 p0189 N73-11533
Failure analysis and fracture modes of carbon epoxy composites
[NASA-CR-121000] 02 p0191 N73-11550
Densification of ceramic materials and mechanical behavior of ceramic materials with emphasis on fracture energies
[AD-745909] 02 p0193 N73-11561
Atomistic approach to modeling crack tips
[AD-746711] 02 p0220 N73-11784
Correspondance between energy criterion for fracture and mathematical modeling of strain effects at tip of cracks
[AD-746010] 02 p0239 N73-11943
References on fatigue and fracture of aircraft structures and materials to include instruments, sonic fatigue, and mechanical fasteners
[AD-748100] 03 p0254 N73-12053
Scanning electron microscopy applied to surface fracture mechanics study, composite materials, and powder metallurgy
[DLR-MITT-71-32] 03 p0315 N73-12571
Effect of neutron irradiation on fatigue crack propagation in stainless steel samples at high temperatures using fracture mechanics approach
[AD-747950] 03 p0316 N73-12578
Analysis of crack tip deformation in boron-aluminum sheet and laminar steel sheet resulting from crack propagation
[AD-747760] 03 p0322 N73-12623
Analysis of crack propagation properties of solid rocket propellants based on relation between crack tip stress intensity factor and crack velocity
[AD-747531] 03 p0350 N73-12853
Mapping-collocation method for elastostatic stress analysis of orthotropic rectangular plates with centrally located traction-free cracks
[NASA-TN-D-7119] 03 p0360 N73-12933
Fracture measurement in high strength brittle ceramic materials
[AECL-3677] 03 p0361 N73-12944
Brittle fracture of polycrystalline disks of alloyed alumina
[AD-748110] 04 p0439 N73-13577
Fatigue crack propagation of aluminum metal sheets under flight simulation loads corresponding to gust spectrum
[NLR-MP-72010-U] 04 p0480 N73-13926
Evaluation of structure safety against brittle fracture based on transition temperature, fracture toughness, and crack opening displacement
[ZJE-118] 04 p0481 N73-13933
Fracture behavior of silicon nitride and silicon carbide ceramics
[NASA-CR-129671] 05 p0564 N73-14585
Analysis of process involved in fatigue fracture of zinc alloys to show separation of zinc in front of fatigue cracks
[S-241] 05 p0602 N73-14896
Analysis of fatigue behavior of composite-reinforced, integrally stiffened metal panels and effects of temperature on adhesive substances
[NASA-CR-112148] 05 p0602 N73-14899
Effect of circular inclusion on stresses around two collinear finite line cracks in plate under tension
[AD-749901] 05 p0604 N73-14910
Failure analysis of aluminum alloy components with history of failures in aerospace applications
[NASA-CR-2166] 06 p0684 N73-15568
Theory of shallow spherical shells including effect of transverse shear deformation
[AD-749966] 06 p0727 N73-15935
Analysis of relation between fracture toughness and yield strength in high strength titanium alloys
[AD-752573] 08 p0933 N73-17643
Statistical analysis of strength and fracture characteristics of materials with application to fiber composites using Weibull density functions
[JPL-TM-33-580] 08 p0934 N73-17650
Nondestructive tests of fracture behavior of ATJ-S graphite
[AD-751976] 08 p0935 N73-17655
Analysis of particle erosion of solid surfaces using model of erosion pit nucleation and growth for solid spherical particles impacting on plane surface of elastic half space
[AD-752221] 08 p0935 N73-17657
Compilation of fracture mechanics data on high strength aluminum alloys, alloy steels, stainless steels, and titanium alloys
[AD-753774] 09 p1049 N73-18554
Effect of sheet thickness on plane stress fracture resistance of high strength titanium alloys
[AD-753198] 09 p1049 N73-18555
Macroscopic and microscopic fracture criteria for steels
[AD-752446] 09 p1049 N73-18559
Tensile, exfoliation, fatigue, and crack growth properties of heat treated aluminum sheet alloy 7475
[AD-753709] 09 p1050 N73-18560
Laboratory method for thermal fracture of graphite
[AD-753392] 09 p1054 N73-18592
Crack size and grain size dependence of brittle fracture stress
[AD-753525] 09 p1076 N73-18781
Static and dynamic analyses on fracture mechanics of polyester plastic sheet
[AD-749098] 09 p1097 N73-18954
Fracture mechanics and structural fatigue of nickel alloys, aluminum alloys, and molybdenum alloys at elevated temperatures
[AD-753687] 09 p1097 N73-18958
Impurities and plastic fracture in aluminum alloys
[NASA-CR-131100] 10 p1171 N73-19521
Relationship between brittle and plastic fracture of high strength steels owing to void dynamics
[NASA-CR-131101] 10 p1171 N73-19522
Fracture mechanics and plastic deformation in high strength steels
[NASA-CR-131102] 10 p1171 N73-19523
Crack tip plasticity and fracture initiation criteria
[COO-3084-16] 10 p1221 N73-19926
Analysis of factors affecting fatigue failure in welded joints and significance of weld defects on fatigue strength
[NLL-RISLEY-TR-2509-[9091-9F]]
11 p1296 N73-20517
Fracture toughness study of heat treated titanium alloys
[AD-753919] 11 p1306 N73-20598
Shear instabilities and tensile fracture characteristics of cold worked 1080 pearlitic steel
[AD-755102] 11 p1307 N73-20604
Brittle fracture and fatigue of cylindrical hollow bodies with offset seams and stiffeners
[NLL-RISLEY-TR-2527-[9001.9F]]
11 p1344 N73-20908
Analysis of crack nucleation and crack propagation caused by formal separation of impact ductility into components
[AD-754620] 11 p1346 N73-20926
Procedure for improving strength and fracture behavior of alkali halides for use as high energy laser window material
[AD-755716] 12 p1411 N73-21437
Material selection determined from mathematical model of crack growth and failure
[NASA-TN-D-7221] 12 p1413 N73-21452
Origins of fracture patterns in Type 3 marginal premare craters
12 p1455 N73-21782
Analysis of fracture and crack growth properties of 304 stainless steel to determine suitability as material for cryogenic fluid storage pressure vessels
[NASA-CR-121025] 12 p1462 N73-21847
Analysis of fracture of mixed viscous-brittle breakage of polycrystal using raster electron microscope
13 p1540 N73-22479
Fatigue mechanics studies of fatigue crack propagation in 2024 aluminum alloy panels containing transverse slits
[ARL/SM-379] 13 p1542 N73-22491
Fracture mechanics evaluation of effect of explosive bonding on fatigue crack growth in aluminum plates
[AD-756423] 13 p1544 N73-22511
Application of crack opening stretch concept to fracture problems
13 p1585 N73-22846
Closed form solution using four harmonic functions for elastic solid with plane crack subjected to concentrated shears parallel to edge of crack
[NASA-CR-112317] 13 p1585 N73-22848
Accelerated method of fatigue testing and parameters of fatigue curves
[AD-756050] 13 p1589 N73-22882
Survey of electron fractography in field of fatigue cracking, ductile fracture, cleavage, and stress corrosion
[NLR-TR-72029-U] 14 p1715 N73-23916
Assumed stress hybrid finite element method for fracture mechanics and elastic-plastic analysis
[AD-757523] 14 p1717 N73-23931
Center cracked tension specimen for determining plane stress fracture mechanics in metal plates
[AD-757654] 14 p1717 N73-23933

Development of photoelastic stress freezing and slicing method to determine stress intensity around surface flaws
[AD-758140] 14 p1717 N73-23934
Design criteria and analysis procedures to minimize occurrence of major structural failures in airframes due to undetected damage
[AD-757870] 15 p1735 N73-24074
Asymptotic finite-deformation analysis of elastostatic field near tip of crack
[AD-757777] 15 p1840 N73-24908
Dynamic tear tests for determining fracture mechanics of high strength structural steels and aluminum and titanium alloys
[AD-759351] 16 p1930 N73-25620
Modified boundary collocation method for crack fracture mechanics analysis on cylindrical section
[AD-758849] 16 p1970 N73-25932
Statistical theory for fracture of brittle structures subjected to nonuniform polyaxial stresses
[AD-759805] 16 p1970 N73-25936
Crack initiation and fatigue fracture in overload mechanism of solid structures
[AD-760007] 17 p2048 N73-26568
Mechanical property determination and fracture mechanics of fiber reinforced composite materials
[D-MAT-178] 17 p2051 N73-26589
Fracture mechanics of polycarbonates and polyimides under dynamic loads
[AD-759917] 17 p2053 N73-26608
Fracture mechanics applied to analysis of brittle fracture of unidirectional and angle-ply composites
[AD-760361] 17 p2053 N73-26610
Viscoelastic fracture characterization of cracking rocket motor
[AD-759968] 17 p2076 N73-26792
Register of experts for information on mechanics of structural failure to support safety and technology aspects of aerospace industry
[NASA-CR-121200] 17 p2091 N73-26918
Application of principles of fracture mechanics to problem of preventing brittle fracture in sheet structures
[RAE-LIB-TRANS-1648] 17 p2092 N73-26921
Irradiation effects on fracture of heavy section pressure vessel steels
[HEDL-SA-497] 17 p2094 N73-26937
Effects of mechanical and metallurgical factors on crack propagation and ductile fracturing resistance of steels
[PB-218919] 18 p2161 N73-27458
Accelerated test technique for determination of K ISCC in steels
[PB-217215/3] 18 p2161 N73-27460
Analysis of fatigue fracture under combined stress conditions for specimens of various cross sections
[NLL-RTS-7770] 18 p2202 N73-27776
Analysis of dynamic fracture in aluminum alloys using radial cylindrical wave propagation technique
18 p2202 N73-27778
Development of modeling schemes to predict effect of coalescence on observed growth characteristics during dynamic fracture
[AD-761082] 18 p2204 N73-27790
Analysis of collocation data using approximation method and fracture mechanics
[AD-761102] 18 p2204 N73-27791
Fracture mechanics of elastic interactions between cracks and inclusions in composite materials
[NASA-CR-132292] 19 p2312 N73-28593
Fracture control method for composite tanks with load sharing liners
[NASA-CR-120918] 19 p2348 N73-28889
Fracture mechanics of cylindrical pressure vessels having weld seam flaws
[AD-761532] 19 p2349 N73-28894
Fracture mechanics for Interfacial crack between adhesively bonded dissimiliar materials
20 p2477 N73-29898
Effects of experimental error on stress intensity fractors from fracture testing
[NASA-TM-X-68285] 20 p2482 N73-29941
Fracture characteristics of small cylindrical bodies partly prefragmented by external notching subject to detonation of high explosive filling
[REPT-545-PT-1] 20 p2483 N73-29943
Rate theory for determining failure accumulation in composite propellants
[AD-763806] 21 p2588 N73-30733
Application of fracture prevention principles to airframes to reduce catastrophic failure and increase service life
[AD-764513] 22 p2617 N73-30969
Effect of phase instability during low cycle fatigue on plastic deformation in steels
[AD-763235] 22 p2686 N73-31512
High temperature deformation and fracture behavior of T-111 and ASTAR-811C over temperature range of 982 to 2205 C
[NASA-CR-72859] 22 p2688 N73-31530
Fracture and fatigue properties of composite materials
[AD-764356] 22 p2689 N73-31540
Fracture toughness of homogeneous isotropic composites
[AD-764070] 22 p2689 N73-31541
Application of reliability analysis to aircraft structures subject to fatigue crack growth and periodic structural inspection
[AD-764775] 23 p2798 N73-32383
Yield and fracture model for Ti-6Al-4V titanium and 7075-T6 aluminum alloys
23 p2804 N73-32423
Creep fracture properties of weld repaired cast titanium alloy
[AD-765185] 24 p2937 N73-33451
Extension of linear elastic fracture mechanics from homogeneous isotropic metallic alloys to heterogeneous anisotropic advanced fiber composites
[NASA-CR-132337] 24 p2937 N73-33456
Linear elastic fracture mechanics applied to graphite under multiaxial stress conditions
[CONF-730707-2] 24 p2943 N73-33507
Plastic flow and fracture mechanics of brittle cuperious oxide and gamma 2Cu-Al compounds under high pressure
24 p2967 N73-33709
Strain energy density and surface layer energy for crack-like ellipse
[NASA-CR-132338] 24 p2988 N73-33879
**FRACTURE RESISTANCE**
U FRACTURE STRENGTH
**FRACTURE STRENGTH**
Interactions between residual elements, inclusion, toughness, and stress corrosion resistance in high strength steel
[PB-209655] 02 p0187 N73-11515
Use of composite laminates with weak interfaces to increase fracture toughness of Ti-6Al-4V
[AD-746765] 02 p0189 N73-11531
Development of rational fracture resistance test procedures to determine fracture properties of titanium alloy sections
[AD-747230] 02 p0189 N73-11533
Low cycle fatigue crack propagation characteristics of high strength alloys with high levels of fracture toughness
[AD-747243] 02 p0190 N73-11538
Thermal and thermophysical processes in microstructural control in high strength steel to increase fracture toughness
[LBL-832] 04 p0434 N73-13537
Crack blunting through fiber matrix debonding in Borsic-aluminum composites
[SC-DC-71-4467] 04 p0438 N73-13568
Evaluation of structure safety against brittle fracture based on transition temperature, fracture toughness, and crack opening displacement
[ZJE-118] 04 p0481 N73-13933
Experimental determination of fracture strength and critical crack length of 7075-T7351 aluminum alloy plates
[AD-748254] 05 p0563 N73-14575
Mechanical properties and fracture strengths of glass fiber reinforced plastic composites
[AD-749948] 05 p0567 N73-14608
Fracture strength of aluminum alloys 7075-T6 and 2024-T3 with surface flaws and corner cracks at holes
[NLR-TR-71033-U] 06 p0685 N73-15576
Instrumented impact hammer used on pre-cracked Charpy V-notch specimens to determine dynamic fracture toughness
[AD-750710] 06 p0728 N73-15944
Relationship of tensile properties and fracture toughness levels to microstructure of Ti6Al2Sn4Zr6Mo
[AD-751530] 07 p0810 N73-16566
Soil impact test with spherical nuclear reactor containment model for fracture strength observations
[NASA-TM-X-68180] 07 p0819 N73-16641
Electrical resistance measurements on crack propagation in fracture toughness specimens under variety of environmental and loading conditions
[MG/54/71] 08 p0966 N73-17899
Fracture strength of uranium- and tungsten-based impacted ogive penetrators
[DREV-R-652/72] 09 p1047 N73-18538
Drop impact strength and toughness of glass and carbon fiber composite materials
[AD-753101] 09 p1054 N73-18595
Fracture toughness of fiat elastic cracked plate with elastic circular inclusion
[AD-754210] 10 p1222 N73-19937
X ray and electron microscopic analysis of vacuum environment effects on 7075-T6 Al alloy fatigue life, fatigue-crack-growth behavior, and fracture toughness
[NASA-TM-X-69223] 12 p1413 N73-21450
Effects of specimen thickness on fatigue-crack growth and fracture toughness of 7075-T6 and 7178-T6 aluminum alloy plates and sheets
[NASA-TN-D-7173] 12 p1413 N73-21453
Dynamic tear tests for determining fracture resistance properties of aluminum alloys
[AD-755436] 12 p1415 N73-21465
Fracture toughness and aqueous stress corrosion resistance of high strength commercial Ti alloy
[NLR-TR-72107-U] 13 p1542 N73-22492
Fracture toughness and strength of diboride composites treated with metallic additives
[NASA-CR-131877] 13 p1547 N73-22535
Dynamic tear tests for determining fracture safety of Hanford-N reactor coolant piping material
[AD-748590] 13 p1558 N73-22626
Investigation of cracks in radial plane of solid right circular cylinder
13 p1584 N73-22841
Graphite and epoxy plastic material strength under biaxial stress
[AD-758448] 15 p1801 N73-24600
Cantilever beam tests for determining strength of tungsten carbide-cobalt alloys
16 p1927 N73-25591
Irradiation strengthening and fracture embrittlement of A533-B steel and arc weldment metal
[HEDL-SA-323] 16 p1969 N73-25931
Effect of Al-Zn-Mg-Cu alloy composition variations on fracture strength and tensile properties
[RAE-TR-72173] 17 p2046 N73-26549
Application of principles of fracture mechanics to problem of preventing brittle fracture in sheet structures
[RAE-LIB-TRANS-1648] 17 p2092 N73-26921
Influence of microstructure on tensile deformation and fracture in high strength Al-Zn-Mg alloys
[ARL/MET-NOTE-86] 18 p2160 N73-27447
Relationships between fracture strength, flow stress, and material ductility in high strength steels
[AD-761217] 18 p2162 N73-27463
Heat treating effects on fatigue strength of SO-95 and 120 type organic class
[AD-760961] 18 p2168 N73-27511
Fracture characteristics of adhesive joints
[AD-762457] 19 p2351 N73-28910
Yielding, work hardening, and fracture behavior of ordered and disorded alloys as function of dislocation
[ORO-3935-25] 21 p2559 N73-30514
Strain fracture toughness and microstructure of heat treated high strength steels
22 p2682 N73-31486
Fracture toughness of homogeneous isotropic composites
[AD-764070] 22 p2689 N73-31541
Fatigue life and fracture toughness of 7075-T6 Al alloy in vacuum and air environments
[NASA-TN-D-7262] 23 p2805 N73-32431
**FRACTURE TOUGHNESS**
U FRACTURE STRENGTH
**FRACTURES [MATERIALS]**
Scanning electron microscope study of fracture and crack propagation in metals
[AD-746125] 02 p0187 N73-11520
Development of rational fracture resistance test procedures to determine fracture properties of titanium alloy sections
[AD-747230] 02 p0189 N73-11533
Application of acoustic emission testing to yielding, fracture, slow and fast crack growth
[AD-746261] 02 p0239 N73-11941
Macroscopic and microscopic approach to fracture and hardness of carbon steels
[COO-3084-10] 08 p0932 N73-17630
Effect of biaxial strain deformation on dynamic fracture of aluminum alloy
[AD-752832] 09 p1048 N73-18549
Analysis of fractures in materials using scanning electron microscopes
[AD-759287] 16 p1930 N73-25617
Development of statistical prediction model for determining probability of glass breakage caused by sonic boom overpressures
[FAA-RD-73-79] 18 p2104 N73-27018
Photographic equipment for recording fracture of zinc single crystals under dynamic stress
20 p2461 N73-29775
Fracture characteristics of small cylindrical bodies partly prefragmented by external notching subject to detonation of high explosive filling
[REPT-545-PT-1] 20 p2483 N73-29943
Oxidative stress cracking in nylon fibers immersed in alkaline aqueous medium saturated with molecular oxygen at elevated temperature
24 p2937 N73-33455
**FRACTURING**
Major fracture and fault zones of Baltic Shield and their relationships to mineral deposits
[E72-10297] 04 p0411 N73-13347
Weakening and fracture of glass reinforced plastics during compression under conditions of one-sided heating
[AD-748526] 04 p0439 N73-13581
Mapping of regional fracture patterns and related structural features of Wind River Mountains using ERTS-1 imagery
[E72-10349] 05 p0533 N73-14337
Tensile tests of pressure effects on plastic properties and fracturing of metals
[NLL-NEL-TT-2190-[6075.461]]
06 p0682 N73-15552
Application of ERTS-1 imagery to fracture related mine safety hazards in coal mining industry in Indiana and Illinois
[E73-10371] 10 p1151 N73-19366

ERTS-1 imagery of linear fractures in Precambrian rocks of Laramie Mountains, Wyoming
[E73-10663] 16 p1899 N73-25359
Application of ERTS-1 imagery to fracture related mine safety hazards in coal mining industry in Indiana
[E73-10776] 18 p2135 N73-27252
Application of Skylab EREP imagery to fracture-related mine safety hazards and environmental problems in mining
[E73-10802] 18 p2138 N73-27277
Quality control of welded joints
[AD-761587] 19 p2306 N73-28548
Application of ERTS-1 imagery to fracture-related mine safety hazards in Ohio coal mining industry
[E73-11034] 22 p2663 N73-31338

**FRAGMENTATION**
Velocity determination of shell fragments, using FORTRAN routines for evaluating film from drum camera
[FOA-2-C-2475-11[44]] 06 p0643 N73-15222
Influence of variation in cylinder geometry on fragmentation and mode of fracture of internally detonated carbon steel cylinders
[DSL-REPT-533] 16 p1969 N73-25930
Explosive fragmentation of heat treated martensitic microstructure steel
[DSL-REPT-532] 17 p2091 N73-26915
Simulated tank fragmentation test
[NASA-TM-X-68282] 20 p2482 N73-29942

**FRAGMENTS**
Velocity slowdown calculation for spherical and cubical fragments as function of distance
[TL-1972-16] 14 p1597 N73-22943

**FRAME PHOTOGRAPHY**
In-flight photography of projectiles using film-image synchronized, rotating-slit shuttered drum field camera
[LA-DC-72-909] 10 p1161 N73-19445

**FRAMES**
NT AIRFRAMES
Computer program for dynamic structural analyses on three dimensional framework and pipework systems
[TRG-1409-REV-1] 06 p0726 N73-15929
Calculation of dynamic response of ship structural members consisting of beams and rectangular plates
[AD-762008] 19 p2350 N73-28902
Expandable space frames with high expansion to collapse ratio
[NASA-CASE-ERC-10365-1] 23 p2847 N73-32749

**FRAMING CAMERAS**
Pan-frame system model for panoramic camera in aerial triangulation
24 p2925 N73-33363

**FRANCE**
ERTS-1 imagery of French shoreline along the Atlantic Ocean and English Channel
[E72-10211] 02 p0161 N73-11306
ERTS-1 imagery of coastal marshland, tidal flats, and littoral transport in French Atlantic waters
[E72-10251] 03 p0289 N73-12351
Dynamic behavior of coastal sedimentation in Lions Gulf
[E72-10289] 04 p0410 N73-13339
Management of earth resources in France and Spain through automatic mapping inventory
[E72-10303] 04 p0411 N73-13352
English, French, and Spanish vocabulary of aircraft aeronautical terminology
[DOC-8800-VOL-1] 06 p0616 N73-14996
Impact safety for reentry of Electre nose cones along south coast of France
[ONERA-TP-1152] 09 p1084 N73-18846
Color aptitude of dyschromatopsia French navigators and pilots
10 p1113 N73-19068
ERTS-1 imagery of marshlands and turbid waters of French Atlantic littoral
[E73-10341] 10 p1147 N73-19340
Specifications and capabilities of Franco-German telecommunications satellite - Symphonie
[NASA-TT-F-14875] 12 p1461 N73-21836
Automatic processing of French speech
[AD-752811] 13 p1491 N73-22090
ERTS-1 imagery of marshes, wetlands, and turbid waters in French Atlantic littoral
[E73-10548] 13 p1518 N73-22307
Operation of electronic telephone exchange in France
[NLL-PO-2957-[9022.81]] 15 p1749 N73-24175
Lithological and structural surveys of sedimentary basin in France from ERTS-1 MSS imagery
[E73-10656] 16 p1898 N73-25352
Structural geology of Massif Central and Parisian Basins, France from ERTS-1 imagery
[E73-10657] 16 p1898 N73-25353
Management of natural resources in France and Spain by automatic cartographic inventories from ERTS-1 data
[E73-10725] 18 p2133 N73-27234
Littoral transport of sedimention coastal region of France
[E73-10822] 18 p2140 N73-27297
Analysis of ERTS-1 MSS imagery to determine geological and structural features in sedimentary basin in France
[PAPER-G6] 19 p2263 N73-28237
ERTS-1 imagery of water pollution, sedimentation, and geology of southeastern France and western Alps
[PAPER-R6] 19 p2283 N73-28364
Resources management in France through automatic cartographic inventory
[E73-10894] 20 p2395 N73-29243
Statistical analysis of annual maximum temperatures of Paris
[MN-MONO-90] 22 p2694 N73-31580

**FRAUNHOFER LINES**
Approximate determination of optical depth in different parts of Fraunhofer line contour
20 p2472 N73-29853
Photoelectric determination of change in center-limb profiles of faint Fraunhofer lines
20 p2472 N73-29854
Asymmetry of selected Fraunhofer lines at center of solar disk and near limb
20 p2472 N73-29856

**FRAUNHOFER REGION**
U FAR FIELDS

**FREDHOLM EQUATIONS**
Fredholm equations for low frequency scattering by imperfectly conducting obstacles
[AD-746048] 01 p0082 N73-10674
Determining natural components of meteorological fields
[AD-751958] 08 p0939 N73-17692

**FREDHOLM OPERATORS**
U FREDHOLM EQUATIONS
U OPERATORS [MATHEMATICS]

**FREE ATMOSPHERE**
Radiosonde measurements of subsidence in free atmosphere over Belgian weather station
[PUBL-SER-B-69] 17 p2057 N73-26637
Contour maps of global geoid and free air gravity anomalies of GEM-4 earth gravitational model
[NASA-TM-X-66240] 23 p2783 N73-32265

**FREE BOUNDARIES**
Oscillations of earths magnetic tail studied from model of plasma cylinder with free boundary
14 p1703 N73-23820

**FREE CONVECTION**
Effects of gravity-induced free convection of melting behavior of paraffin slab for thermal control devices
[NASA-CR-123954] 04 p0385 N73-13130
Role of gravity-induced free convection upon liquefaction dynamics of cylindrical paraffin slab under normal gravity conditions
[NASA-CR-129911] 04 p0385 N73-13131
Experimental determination of combined forced and free convection in annular region of horizontal coaxial cylinders
[AD-754017] 10 p1144 N73-19322
Budget relations of thermal variance and kinetic energy in transition zone from forced to free convection
15 p1771 N73-24342
Analysis of atmospheric temperature inversion conditions and requirements for thermal convection for removal of temperature inversion effects
[NLL-M-23034-[5828.4F]] 20 p2391 N73-29204
Cellular convection parameters determined from high-altitude tower measurements and meteorological earth satellite observations
22 p2693 N73-31568

**FREE ELECTRONS**
Free electron production by Raman scattering in initial phase of laser produced plasma
[IPP-4/40] 05 p0583 N73-14745

**FREE ENERGY**
NT GIBBS FREE ENERGY
Measurement of surface, grain boundary, and coherent twin boundary free energies in 304 stainless steel at elevated temperatures using method of zero creep coupled with electron microscopy
[AD-747267] 02 p0189 N73-11535
Crystal phonon contribution to free energy of identical atom pairs adsorbed on cubic lattice surface
[AD-759035] 17 p1992 N73-26109

**FREE FALL**
Computing free fall trajectories from one point to another specified point in solar system based on numerical optimization
[NASA-CR-128644] 03 p0356 N73-12901
Results of wind tunnel measurements of normal force, pitching moment, and Magnus force and moment on M823 research store with fixed and freely spinning stabilizers
[AD-757658] 13 p1471 N73-21912
IBM 7090 computer program for determining values of error sensitivity for dive and glide bombing with free fall weapons
[AD-758420] 15 p1850 N73-24994
Analysis of descent trajectories to determine static and dynamic stability of free-fall stores with freely spinning stabilizer devices
[AD-760677] 18 p2102 N73-26999

**FREE FLIGHT**
Digital analysis of dynamic response data, aerodynamic forces and stability derivatives, of free flight models
[ARC-R/M-3699] 03 p0248 N73-12006
Heat transfer and surface pressure measurements at supersonic speeds on conical delta wings with sharp leading edges
[ARC-CP-1212] 05 p0492 N73-14008
Ballistic tube for drag measurement on firing models into oncoming supersonic flow
[AD-749839] 05 p0525 N73-14271
Role of free-flight models in aircraft research and development
08 p0865 N73-17002
Effect of ablation on aerodynamic characteristics of blunted slender cone during free flight ablating conditions
[NASA-TN-D-7196] 09 p0979 N73-18002
Design, development, and manufacture of natural shape free flight balloon to include requirements, documentation, testing, and inspection
[AD-753086] 09 p0987 N73-18055
Radar observation of disk-shaped models of proposed nuclear heat source module
[NASA-TM-X-62262] 14 p1601 N73-22978
Dynamics of sounding rockets at burnout
[SC-DC-72-1613] 16 p1967 N73-25911
Diagnostic techniques for measurement of aerodynamic noise in free field and reverberant environment of wind tunnels
[NASA-CR-114636] 21 p2579 N73-30669

**FREE FLIGHT TEST APPARATUS**
Free-flight tests on space shuttle and reentry vehicle models in hypervelocity gun tunnels
[DLR-FB-72-41] 21 p2522 N73-30224

**FREE FLOW**
Measurement of fluctuations in free surface flow of gas and liquids
06 p0653 N73-15303
Excitation and propagation of free flow electron waves in plasma
[IPPJ-145] 09 p1070 N73-18731
Effect of free stream turbulence level on turbulent boundary layer behavior
10 p1204 N73-19799
Model developed for opposed free and forced convection flow around heated cylinder
[AD-757993] 15 p1844 N73-24942
Methods for calculation of turbulent free mixing
19 p2252 N73-28155
Turbulent kinetic energy equation and free mixing
19 p2254 N73-28169
Free stream pressure gradient effects on accuracy of turbulent boundary layer calculations
22 p2648 N73-31219

**FREE JETS**
Density and flow visualization of different molecular weight gases from concentric orifices as determined by beam fluorescence technique
[ISAS-486-VOL-37-12] 02 p0155 N73-11256
Acoustic feedback of subsonic and supersonic free jet impinging on obstacle, e.g. blown flap or ground, and noise reduction methods
[DGLR-PAPER-72-84] 04 p0373 N73-13031
Properties of axisymmetric supersonic free jet including relation between jet structure and discrete noise frequencies
[ISL-29/72] 12 p1365 N73-21075
Model for prediction of pressure within recirculation bubble of attached jet
13 p1507 N73-22216
Nozzle flow free jet and Prandtl-Meyer expansion rotational relaxation equation used for relaxation time calculation
[REPT-72-5] 14 p1650 N73-23383
Mass diffusion model for turbulent mixing of free jets
19 p2253 N73-28164
Drag measurement of parallel flat plates and perpendicular disks in supersonic free molecular flow
[DLR-FB-73-17] 21 p2525 N73-30248
Effects of condensation on gas velocity in free jet expansion
[AD-762503] 21 p2527 N73-30266
Free jet boundary and distribution of flow within planar jet and pressure distribution at flat panel
[NASA-TT-F-15151] 24 p2905 N73-33180
Turbulence anisotropy effects on pressure distribution and secondary flow of boundary layers, free and wall jets, and wakes
24 p2906 N73-33191
Correlation parameters for velocity, temperature and concentration of coaxial, heterogeneous, compressible free jet cores
24 p2907 N73-33201

**FREE MOLECULAR FLOW**
Measurement of hypersonic free molecular sphere drag at varying wall temperature ratios
[AD-748618] 04 p0407 N73-13320
Free molecular flow analysis for hypersonic air inlet configurations of ion engine
[AD-756680] 13 p1571 N73-22732

Drag measurement of parallel flat plates and perpendicular disks in supersonic free molecular flow
[DLR-FB-73-17] 21 p2525 N73-30248
**FREE OSCILLATIONS**
U FREE VIBRATION
**FREE RADICALS**
Electron paramagnetic resonance and formed free radical investigation of ionizing radiation damage by sulfur-containing aliphatic compounds, pyridoxine, and proteins
[BMVG-FBWT-72-6] 07 p0753 N73-16115
Genesis of free radical chemistry
08 p0881 N73-17130
Free radical mechanisms in oxidative reactions of organic compounds
08 p0881 N73-17136
Nitroxide free radicals as spin labels in biochemical systems
[NASA-TT-F-14866] 11 p1247 N73-20125
Hydrophobic iminoxyl radicals as uncouplers of photophosphorylation in choloroplasts
[NASA-TT-F-14819] 12 p1376 N73-21160
Photochemical reaction rate constant for hydroxyl radical with ozone in stratosphere
[AD-762195] 20 p2374 N73-29076
Stability of heterogeneous chemical recombination reactions of free radicals in boundary layer flow past heat conducting wall
24 p2908 N73-33209
**FREE STREAM EFFECTS**
U FREE FLOW
**FREE STREAMS**
U FREE FLOW
**FREE VIBRATION**
Free vibrations of complex system of ring with added mass, connected to thin spherical or cylindrical shell
01 p0112 N73-10930
Rayleigh-Ritz analysis of free vibration behavior in plates with discrete elastic supports
[NASA-CR-112220] 04 p0480 N73-13924
Iterative solution for free vibrations of ring stiffened toroidal shells
[AD-747024] 04 p0482 N73-13943
Effect of transverse shear deformation on large amplitude free vibrations of plates and cylindrical panels
13 p1584 N73-22845
Computer programs for analyses of free or forced undamped vibrations of rolling contact supported rotors
[NASA-CR-132220] 15 p1810 N73-24672
Dynamic analysis of free vibrations of rectangular elastic plate with central circular hole
[AD-765361] 23 p2855 N73-32816
Approximate solution for free vibrations of rotating uniform cantilever beams
[NASA-TM-X-62299] 24 p2989 N73-33885
**FREEDOM FIGHTER AIRCRAFT**
U F-5 AIRCRAFT
**FREEZE DRYING**
Production methods for preventing deterioration of freeze-dried foods
[NASA-CR-128915] 14 p1614 N73-23085
**FREEZING**
NT VIBRATIONAL FREEZING
Equation for normal freezing for ideal ternary liquid solutions solidified into ideal solid solutions of pseudobinary type
[NASA-CR-129935] 05 p0562 N73-14563
Survey and mapping of freeze-up and break-up patterns of seasonal snow and ice covers in Alaska
[E73-10282] 08 p0914 N73-17489
Freezing effects on structure of soils and biological tissues
[CNRS/LA-PUBL-440] 09 p0999 N73-18150
Organic compounds for nucleating supercooled water
[AD-758002] 15 p1748 N73-24169
Fast freezing for producing aluminum alloys from consolidated powder
[AD-759828] 17 p2048 N73-26569
Freezing points of crystalline polymers determined as functions of pressure and temperature
[AD-759007] 17 p2051 N73-26591
Survey of freeze-up and breakup patterns of seasonal snow and ice covers in Alaska
[E73-10920] 20 p2398 N73-29269
**FREEZING POINTS**
U MELTING POINTS
**FREIGHT COSTS**
Analysis of economic factors involved in air cargo operations and air cargo market development
23 p2863 N73-32881
Analysis of factors involved in developing market for air cargo services
23 p2863 N73-32882
Analysis of air freight rate problems to define roles of Civil Aviation Board and domestic air carriers
23 p2863 N73-32883
Research project to determine factors involved in expansion of air freight traffic and prospects for future expansion
23 p2863 N73-32884
Procedures for determining rates charged by airlines to show factors involved in making determinations
23 p2864 N73-32890
**FRENCH SATELLITES**
NT EOLE SATELLITES
NT FR-1 SATELLITE
Space activities of CNES, noting satellites, launch vehicles, sounding rockets, balloons, and ground stations
05 p0611 N73-14972
**FRENCH SPACE PROGRAMS**
French space programs and benefits to mankind
04 p0474 N73-13874
French space program events during 1971
[NASA-TT-F-14721] 04 p0487 N73-13985
CNES activities, noting French space program and international cooperation
05 p0611 N73-14971
Space activities of CNES, noting satellites, launch vehicles, sounding rockets, balloons, and ground stations
05 p0611 N73-14972
Research and development of French programs for FR-1, impedance and electrostatic probes, and very low frequency wave propagation
[GRI/NTP/103] 13 p1595 N73-22936
Research project requirements and 1973 budget forecast for French Space Laboratory
[AD-03-72] 23 p2866 N73-32915
Balloon sub-system of Eole experiments in Southern Hemisphere lower stratosphere
24 p2948 N73-33547
**FREON**
Thermodynamic properties and heat transfer characteristics of forced-convection boiling of Freon-113 in vertical annular test section
[NASA-CR-2137] 01 p0117 N73-10968
Toxic effects of Freon decomposition products on activity of isoenzymes of lactate dehydrogenase in rat brains
03 p0259 N73-12097
Shock wave attenuation in foam water mixtures containing Freon and exposed to hydraulic impact
[AD-748350] 04 p0407 N73-13318
Boiling inception in trichlorotrifluoroethane during forced convection at high pressures
[NASA-CR-2170] 04 p0485 N73-13960
Cardiac toxicity of fluoroalkane gases for propelling aerosols in industry and household applications
[AD-751425] 07 p0749 N73-16090
Density of liquid Freon 11 at 200 C and 8.18 to 195.46 atm pressure
[AD-752863] 09 p1000 N73-18160
Development of method for extending low temperature strain limit of rubber-based solid propellants by induced plasticization
10 p1203 N73-19788
Void fraction in subcooled trichlorotrifluoroethane boiling at high pressures
[NASA-CR-2241] 14 p1718 N73-23938
Design and tests of breadboard cryogenic hydrogen and Freon heat exchanger for space shuttle missions
[NASA-CR-128987] 17 p2096 N73-26959
**FREQUENCIES**
NT AUDIO FREQUENCIES
NT BEAT FREQUENCIES
NT BROADBAND
NT C BAND
NT CARRIER FREQUENCIES
NT CRITICAL FREQUENCIES
NT CYCLOTRON FREQUENCY
NT EXTREMELY HIGH FREQUENCIES
NT EXTREMELY LOW FREQUENCIES
NT EXTREMELY LOW RADIO FREQUENCIES
NT HIGH FREQUENCIES
NT INFRASONIC FREQUENCIES
NT LOW FREQUENCIES
NT MICROWAVE FREQUENCIES
NT PLASMA FREQUENCIES
NT RADIO FREQUENCIES
NT RESONANT FREQUENCIES
NT SUPERHIGH FREQUENCIES
NT SWEEP FREQUENCY
NT ULTRAHIGH FREQUENCIES
NT VERY HIGH FREQUENCIES
NT VERY LOW FREQUENCIES
Theorem for specifying sufficient number of input frequencies for identification through Liapunov methods
[NASA-CR-135668] 23 p2812 N73-32482
**FREQUENCY AMPLIFIERS**
U AMPLIFIERS
**FREQUENCY ANALYZERS**
Continuous Fourier transform method and apparatus
[NASA-CASE-ARC-10466-1] 12 p1381 N73-21199
Three-dimensional output from third octave frequency analysis
14 p1631 N73-23221
Analysis of fluctuations in difference frequency in ring lasers operating in single mode
17 p2040 N73-26501
Onboard frequency analyzer for measurement and analysis of acoustic and vibration data
[NASA-CR-132305] 23 p2793 N73-32343
**FREQUENCY ASSIGNMENT**
Aural analysis of sound into bands of frequencies
[NASA-TT-F-13912] 02 p0212 N73-11715
Computer program for selection of radio frequencies used in VOR, ILS, and Tacan/DME air navigation systems
[FAA-NA-73-4] 16 p1940 N73-25700
Simulated environment interference tests on adjacent channel signal receivers for frequency assignments of instrument landing systems
[FAA-RD-73-1-VOL-1] 17 p2060 N73-26665
Statistical weather analysis for optimum picture quality design of satellite television broadcasting system
18 p2115 N73-27101
**FREQUENCY BANDS**
U FREQUENCIES
**FREQUENCY COMPRESSION DEMODULATORS**
Signal to noise ratio performance of optimum digitalized FM demodulator
01 p0025 N73-10195
**FREQUENCY CONTROL**
NT AUTOMATIC FREQUENCY CONTROL
Reduction of angle frequency deviation in antenna array by waveguide parameters
[AD-748742] 04 p0389 N73-13164
Automatic frequency control circuit for FM television transmitter
[NASA-CASE-MFS-21540-1] 09 p1002 N73-18177
Economic analysis of integrated time-frequency system for aircraft
14 p1690 N73-23717
Development of acoustical controlled distributed feedback laser with continuous frequency spectrum tuning
[NASA-CASE-NPO-13175-1] 18 p2157 N73-27431
Proceedings of international telecommunication organization on peaceful uses of outer space with emphasis frequency assignments for space communication
[REPT-12] 21 p2507 N73-30118
Development of differential equations for analyzing phase radio range finders with mutual automatic scaling frequency control in interrogator and responder
22 p2629 N73-31063
Design and performance of stacked crystal filters for frequency control and signal processing
[AD-765416] 23 p2758 N73-32074
**FREQUENCY CONVERSION**
U FREQUENCY CONVERTERS
**FREQUENCY CONVERTERS**
NT FREQUENCY DIVIDERS
NT FREQUENCY MULTIPLIERS
NT FREQUENCY SYNTHESIZERS
NT PARAMETRIC FREQUENCY CONVERTERS
Bandwidth reduction technique for loran retransmission system
[AD-746055] 02 p0208 N73-11687
Local oscillator and mixer forming Josephson frequency conversion in superconducting point contact junctions
[AD-750775] 06 p0709 N73-15784
Current-to-frequency converter as ionization chamber current quantizer for radiological environmental monitoring
[ORNL-TM-3906] 07 p0800 N73-16499
Prototype 12 GHz low noise converter with mounted planar circuit in waveguide
[NASA-TT-F-14656] 09 p1007 N73-18218
Optical properties of ultraviolet down-converter materials
[AD-753578] 09 p1068 N73-18713
Numerical analysis of voltage spectra of electric inverters with pulse width modulation
[NLL-RTS-7639] 11 p1261 N73-20235
TDMA/PSK test equipment noting modulators, demodulators, converters, and transmission system
[ESRO-CR[P]-144] 17 p1998 N73-26157
Linear plasma wave conversion at lower hybrid resonance
[MATT-979] 22 p2704 N73-31657
**FREQUENCY DISTRIBUTION**
Effect of Reynolds number and frequency on control-surface buzz at high subsonic speeds noting control of flap oscillation by air jets
[ARC-R/M-3702] 03 p0248 N73-12007
Nearly instantaneous precipitation rates measured in several locations of world to determine point frequencies of occurrence
[AD-749878] 05 p0575 N73-14681
Use of Apollo 16 photogrammetry to determine frequency distributions of lunar slopes
12 p1456 N73-21792
Relative frequency of occurrence of different normal accelerations at the center of gravity of aircraft in turbulence
[ARC-R/M-3714] 24 p2870 N73-32929
**FREQUENCY DIVIDERS**
Frequency division with binary ripple counters to provide any integral division ratio
[AD-754030] 11 p1260 N73-20229
Low phase noise frequency divider for use with deep space network communication system
[NASA-CASE-NPO-11569] 17 p2007 N73-26229

**FREQUENCY DIVISION MULTIPLEXING**
Noise immunity of optical communication lines with frequency and time multiplexing subcarriers
[JPRS-57178] 02 p0181 N73-11467
Flutter compensation of magnetic tape recorded data, noting single-carrier FM and frequency division multiplexed FM systems
[RAE-TR-72028] 03 p0303 N73-12474
System for monitoring condition responsive devices by using frequency division multiplex technique
[NASA-CASE-KSC-10521] 11 p1254 N73-20176
Frequency division multiplexer for operation in double or single sideband channel
[NASA-CR-124250] 14 p1640 N73-23293
Assessment of communication channels for maritime satellite systems using broad beam and multiple beam antennas for satellite-ship links
18 p2117 N73-27121

**FREQUENCY MEASUREMENT**
Data handling theory, telemetry, and signal frequency determination for signal reconnaissance
[FOA-3-C-3653-66] 02 p0140 N73-11134
Measurement of effective collision frequency in RF heating through decay instability in Q device plasma
[CONF-720705-2] 07 p0755 N73-16136
Real time pitch period extraction by adaptive prediction of speech waveform
14 p1622 N73-23136
Formant extraction technique using adaptive predictive coding
14 p1622 N73-23137
Automatic formant and fundamental frequency extraction from digital inverse filter formulation
14 p1622 N73-23139
Accuracy of formant parameter estimation based on method of Prony
14 p1622 N73-23140
Measurement system for physical quantity represented by or converted to variable frequency signal
[NASA-CASE-MFS-20658-1] 21 p2543 N73-30386
Characteristics of ring balanced superhigh frequency modulator for carrier suppression as function of amplitude and phase of modulating voltages
22 p2631 N73-31082

**FREQUENCY MODULATION**
NT FEEDBACK FREQUENCY MODULATION
NT FREQUENCY SHIFT KEYING
NT PULSE FREQUENCY MODULATION
Difference frequency modulation technique for signal transmission
[NLL-TRANS-2835-[9022.81]]
02 p0139 N73-11124
Intensity modulation of electrical signals recorded on film using two oscilloscopes
[FOA-3-C-3677-62] 02 p0172 N73-11392
Flutter compensation of magnetic tape recorded data, noting single-carrier FM and frequency division multiplexed FM systems
[RAE-TR-72028] 03 p0303 N73-12474
Degradation of spread spectrum modulation performance in airborne multipath communication channels
[AD-747486] 04 p0391 N73-13181
Atomic hydrogen maser with bulb temperature control by output frequency difference signal for wall shift elimination
[NASA-CASE-HQN-10654-1] 04 p0428 N73-13489
FM distortion and FASP computer program for design and analysis of linear dynamic systems
[NASA-CR-130272] 07 p0754 N73-16125
Nonlinear interaction and modulation in parametric acoustic array for spherical wave field
07 p0821 N73-16650
Statistical analyses for detecting frequency shift keyed and phase keyed signals in additive disturbance
[AD-752010] 08 p0886 N73-17173
Automatic frequency control circuit for FM television transmitter
[NASA-CASE-MFS-21540-1] 09 p1002 N73-18177
Very low frequency propagation effect on minimum shift keying communication system signal transmission
[AD-755122] 11 p1258 N73-20213
Optimization of noise immunity of analog signal transmission channels by preemphasis, exemplified for AM or FM channel
[DLR-FB-73-09] 12 p1379 N73-21188
Ku-band microminiature modulators for converting 10 mW signal at 400 MHz to 10 mW signal at 15 GHz
[NASA-CR-130230] 13 p1490 N73-22078
Measurement of bandwidth for binary FM and bitenary FM signals
[AD-757139] 14 p1633 N73-23240
Frequency modulated [chirped] optical pulses in subpicosecond to microsecond pulse length range
15 p1812 N73-24686
Frequency modulated radar systems for range finding, velocity measurement, and altimeters
16 p1873 N73-25162
Signal to noise ratio of frequency locked loop FM demodulator
16 p1874 N73-25168
Device for locating electrically nonlinear objects and determining distance to object by FM signal transmission
[NASA-CASE-KSC-10108] 16 p1911 N73-25461
Computer program to obtain power spectrum of frequency modulated signal, modulated by voice signal, digital signal, and combinations of both
[FAA-RD-73-56] 18 p2116 N73-27111
Dielectric properties of ice, snow, and water at microwave frequencies and thickness measurements of ice and snow layers with radar
[CRC-1242] 21 p2537 N73-30341
Statistical error analysis of frequency modulated radio altimeter with phase readout
22 p2629 N73-31066
Characteristics of ring balanced superhigh frequency modulator for carrier suppression as function of amplitude and phase of modulating voltages
22 p2631 N73-31082
Experimental television transmission system with vestigeal sideband amplitude/frequency modulation
[FTZ-44-TBR-33] 22 p2633 N73-31102
Radio frequency bandwidth for satellite frequency modulated television broadcasting
[BBC-RD-1973/19] 24 p2893 N73-33097
Frequency modulation method for simultaneous recording of signals reflected from ionosphere
24 p2895 N73-33111

**FREQUENCY MULTIPLIERS**
Generation and measurement of ruby laser picosecond pulses
[AD-750789] 06 p0680 N73-15538
Gallium arsenide Schottky and varactor diodes for 20 and 30 GHz
07 p0762 N73-16192
Frequency multiplier based on snapoff diode and computer program for evaluating performance
08 p0888 N73-17189
Extension of frequency spectrum and improvement of semiconductor devices and techniques in microwave spectrum
[AD-753266] 09 p1044 N73-18514
Development of techniques for frequency tripling laser radiation based on mixtures of metal vapors and inert gases
[AD-754096] 11 p1304 N73-20581
Extension of microwave devices to optical frequencies
[AD-758914] 16 p1924 N73-25569
Tunable infrared parametric oscillators and coherent spectroscopy
[AD-759408] 16 p1945 N73-25741
Electron beam, quantum electronics, and solid state devices for useful frequency extension into microwave and optical frequencies
[AD-759066] 17 p2041 N73-26510
Research on electron beam devices, quantum electronic devices, plasmas, and solid state microwave devices
[AD-760033] 17 p2041 N73-26517
Selection of step recovery diodes for microwave frequency multipliers, noting frequency conversion efficiency
[FTZ-A-46-TBR-5] 22 p2642 N73-31174

**FREQUENCY RANGES**
Effects of gamma and neutron radiation on high frequency characteristics of microwave bipolar transistors
[SC-DC-72-1233] 05 p0519 N73-14220
Human perception of musical intervals between simultaneous tones
[IZF-1972-20] 14 p1613 N73-23078
Analysis of fluctuations in difference frequency in ring lasers operating in single mode
17 p2040 N73-26501

**FREQUENCY REGULATION**
U FREQUENCY CONTROL

**FREQUENCY RESPONSE**
Sampled data frequency response method for analyzing control system performance, and compensator improvement program for designing Saturn 5/S1-C compensators
[NASA-CR-123917] 02 p0195 N73-11573
Rotor frequency response to shaft pitching and rolling oscillations, and steady response and frequency response data at high advance ratios for hingeless rotors
[NASA-CR-114519] 03 p0251 N73-12032
Functional relationship between food preference and frequency of repetitious eating
[AD-749079] 05 p0503 N73-14100
Minimax approximation to frequency responsive nonrecursive digital filter
[AD-750767] 06 p0648 N73-15263
Experimental analysis of frequency response of pneumatic tee junction
[AD-750369] 06 p0656 N73-15329
Dynamic frequency response of curved or flat honeycomb sandwich panels having cores of negligible flexural stiffness
[ESDU-72016] 06 p0723 N73-15898
Frequency selectivity and two tone inhibition in neural coding of acoustic stimuli
[IZF-1972-25] 14 p1610 N73-23050
Algorithm for determining frequency response of linear control system
[TT-7304] 14 p1683 N73-23654
Resonance tests of delta wing aircraft model to determine effect of stiffness changes of wing spars on frequencies and modes of vibration
[ARC-R/M-3268] 16 p1856 N73-25031
Frequency response of structural systems excited by transient and random loads using cross correlation and spectral analysis techniques
[ISVR-TR-57] 18 p2180 N73-27598

**FREQUENCY SCANNING**
Analysis of fluctuations in difference frequency in ring lasers operating in single mode
17 p2040 N73-26501

**FREQUENCY SHIFT**
Frequency shift of flash lamp pumped dye laser with two Fabry-Perot interferometer wavelength selectors
01 p0064 N73-10527
Frequency swinging method applied to ionospheric studies for group path difference
02 p0166 N73-11349
Frequency sampling of target position and signal processing by linear amplitude weighting to reduce radar glint pointing errors
[AD-747348] 03 p0267 N73-12167
Long term frequency drift and gain stability of laser structures
[AD-749056] 05 p0558 N73-14534
Mechanisms for X irradiation induced transient changes in elastic modulus of quartz resonators
[SC-DC-72-1240] 05 p0587 N73-14771
Orbit perturbation effects on frequency shift of electrostatic, turbulent, unmagnetized plasma
09 p1071 N73-18738
Fading frequency characteristics of Es layer
13 p1521 N73-22330
Frequency effect of magnetocrystalline anisotropy in nickel ferrous ferrites determined by torque measurements
18 p2159 N73-27443
Doppler data range change measurements for Mariner 9 celestial mechanics experiment
23 p2842 N73-32709

**FREQUENCY SHIFT KEYING**
Antenna feed networks for broadbanding very low frequency and low frequency antennas to wide frequency shift keying modulation
[AD-746119] 02 p0151 N73-11226
EHF attenuation measurements of helical waveguides, using FSK shuttle pulse method and backward wave oscillator
[FTZ-333-TBR-17] 22 p2643 N73-31182

**FREQUENCY STABILITY**
Automatic measurement of frequency stability of microwave Gunn diode oscillators at low temperatures noting graphs of power and frequency against time
[SRDE-72013] 05 p0520 N73-14226
Long term frequency drift and gain stability of laser structures
[AD-749056] 05 p0558 N73-14534
Using quartz oscillators sensitive to temperature variations for frequency stabilized thermostats
[PUBL-1366] 06 p0647 N73-15253
Transistor circuit with piezoelectric crystal for stable high frequency oscillator
[NASA-CASE-GSC-11513-1] 07 p0761 N73-16185
Development and characteristics of stable master oscillator carbon dioxide laser system
[AD-752219] 08 p0930 N73-17614
Analysis of subharmonically injection locked microwave IMPATT diode oscillators to improve frequency stability and noise characteristics
10 p1133 N73-19237
Definitions for specifying frequency stability for measurements in frequency and time domains
[NBS-TN-632] 12 p1378 N73-21174
Long term frequency stability, service life, and reproducibility of NASA hydrogen maser in relation to world standards
[NASA-TM-X-66229] 12 p1410 N73-21425
Superconducting cavity stabilized oscillator of high stability
[AD-760339] 17 p2006 N73-26221
Carbon dioxide laser frequency stability data for receiver design optimization
18 p2212 N73-27861
Development of procedure for measuring short-term instability of millimeter band klystron frequency
22 p2630 N73-31080
Characteristics of ring balanced superhigh frequency modulator for carrier suppression as function of amplitude and phase of modulating voltages
22 p2631 N73-31082
Optimal accumulation time in superlong-baseline interferometer and frequency stability of sinusoidal signal generators used as heterodynes at receiving points
23 p2838 N73-32678

**FREQUENCY STANDARDS**
Greenwich time and latitude observations for Oct. to Dec. 1971
01 p0105 N73-10874

Operational frequency stability of rubidium and cesium frequency standards
[NASA-TN-D-7063] 08 p0943 N73-17724
Concepts, physical principles, and design features of frequency standards and clocks
[NBS-TN-616] 10 p1160 N73-19435
Long term frequency stability, service life, and reproducibility of NASA hydrogen maser in relation to world standards
[NASA-TM-X-66229] 12 p1410 N73-21425
Greenwich time and latitude observations for Jan. to Mar. 1972
13 p1578 N73-22791
Frequency and time broadcasts provided by National Bureau of Standards radio stations
[NBS-SP-236] 16 p1873 N73-25164
Proceedings of international telecommunication organization on peaceful uses of outer space with emphasis frequency assignments for space communication
[REPT-12] 21 p2507 N73-30118
Time signal transfer by satellite relay systems
[AD-764716] 23 p2759 N73-32078

**FREQUENCY SYNCHRONIZATION**
Frequency discriminator for on-line measurements of entrainment and synchronization in EEG signals as related to human alertness
[NASA-CR-129173] 02 p0135 N73-11091
Correlation of signals with various frequency spacing for tropospheric propagation
[FOA-3-A-3748-60[63]] 02 p0140 N73-11132
Synchronized digital communication system
[NASA-CASE-XNP-03623] 19 p2243 N73-28084
Simplification of television synchronization signal by reducing duration
[BBC-RD-1973/20] 24 p2894 N73-33100

**FREQUENCY SYNTHESIZERS**
Phase coherent frequency synthesizer for improving digital voice and data transmission in communication systems
04 p0472 N73-13853
Pair of coherent frequency-hopped/pseudo noise frequency synthesizers
[AD-753399] 10 p1135 N73-19252
Improved spectral digital frequency synthesizer
[AD-756864] 13 p1501 N73-22164
Design of avionics digital frequency synthesizer with four phase locked loops for aircraft communication and navigational aids
[AD-759699] 16 p1883 N73-25238
Analysis of stability characteristics of single frequency laser using homogeneously broadened active material
17 p2041 N73-26514

**FREQUENCY TRANSLATION**
U FREQUENCY CONVERTERS

**FRESNEL DIFFRACTION**
Radio frequency shadow calculation for airspace obstruction of radar reception considering Fresnel diffraction
[AG-5082-E-1] 20 p2377 N73-29097

**FRESNEL REFLECTORS**
Geometrical plot of light ray through leaf cross section using Fresnel equations and Snells law
[NASA-CR-132144] 15 p1813 N73-24695

**FRESNEL REGION**
Generalized radar equations and Doppler shift in Fresnel region
18 p2115 N73-27097

**FRETTING**
Fretting damage from contact between two metal surfaces
[ESDU-67012] 01 p0111 N73-10921

**FRICTION**
NT AERODYNAMIC DRAG
NT DRY FRICTION
NT FLOW RESISTANCE
NT FRICTION DRAG
NT INTERNAL FRICTION
NT SKIN FRICTION
NT SLIDING FRICTION
Microstructural studies of adhesion, wear, friction, and lubrication using LEED, Auger emission spectroscopy analysis, and field ion microscopy
[NASA-TM-X-68152] 01 p0058 N73-10471
Formation of electric fields during friction of lubricating oil on metal surface
[AD-745433] 01 p0062 N73-10511
Influence of wind stress and bottom friction on spectral response of two layer beta plane ocean currents
[AD-746506] 02 p0168 N73-11367
External friction effects on compressibility of metal powders
[AD-747722] 03 p0317 N73-12583
Analysis of friction surfaces of porous materials based on iron after prolonged operation under self lubricating conditions
[AD-748020] 03 p0317 N73-12585
Frictional properties of rubbers in presence of greases and graphite lubricants
[AD-747447] 03 p0322 N73-12622
Cost effectiveness criteria and parametric data for friction welding of missile systems hardware
[AD-747838] 04 p0427 N73-13482
Lubrication, friction, and wear in machinery
[AD-749086] 04 p0428 N73-13485
Physicomechanical and antifriction behavior of polycaproamide and Caprolon surfaces
[NLL-RISLEY-TR-2360-[9091.9F]]
05 p0550 N73-14464
Antifriction and friction powder metallurgy materials
[AD-749637] 05 p0553 N73-14495
Effect of friction and external environment on fatigue strength of medium C steels
[AD-749749] 05 p0564 N73-14580
Analysis of wear resistance of copper alloyed, magnesium cast iron by reciprocating motion of different friction pairs
[AD-750519] 06 p0687 N73-15590
Friction, wear, and thermal stability of some organotin and organosilicon compounds
[NASA-TN-D-7175] 09 p1051 N73-18569
Friction and wear measurements of CVM M-50 steel lubricated with three C-ether formulations
[NASA-TN-D-7254] 11 p1298 N73-20532
Analysis of adhesion forces in cutting metals to determine effects of formatting and destruction of adhesive connections on wear of cutting tools
[AD-754041] 11 p1301 N73-20555
Effect of reverse abrasive friction exoelectron emission and steel corrosion
[AD-754666] 11 p1307 N73-20603
Effect of viscous lubricants on metal flow during cold reverse extrusion
[AD-743242] 13 p1533 N73-22425
Temperature speed factor, contact friction, and inertial forces on deformation
[AD-758619] 16 p1919 N73-25526
Molecular-kinetic theory of nature of polymer friction
[NLL-RISLEY-TR-2577-[9091.9F]]
16 p1931 N73-25628
Adhesion, friction, and wear behavior of glasses and ionic solids
[NASA-TM-X-68255] 16 p1932 N73-25632
Effect of friction forces on fatigue breakdown of bolted and riveted joints in airframes
[AD-761446] 19 p2305 N73-28539
Effect of friction in compont on frequency of natural vibrations
[AD-761558] 19 p2306 N73-28550
Friction and lubrication in steel wire drawing
[NLL-RTS-7851] 21 p2552 N73-30454
Reduction of friction drag in polymers
[AD-757012] 23 p2777 N73-32205
Friction forces on pneumatically drawn fibers with supersonic nozzle
24 p2906 N73-33193

**FRICTION COEFFICIENT**
U COEFFICIENT OF FRICTION

**FRICTION DRAG**
NT AERODYNAMIC DRAG
Analytical methods for calculating frictional pressure losses in fluid flow through straight pipes
[ESDU-66027] 04 p0403 N73-13282
Methods for determining air resistance to fragmented shrapnel of different shapes
[FOA-2-A-2539-44] 06 p0653 N73-15304
Effect of crud deposits on frictional pressure drop in boiling channel
[AEEW-R-767] 07 p0820 N73-16645
Friction effect on lift of airfoil section with slotted flap
[DLR-FB-73-04] 12 p1356 N73-21001
Measurement of pipe resistance to instantaneous pulsating nonstationary flow
[NASA-TT-F-14881] 12 p1391 N73-21279
Turbulent fluid friction of rotating disks in incompressible flow calculations
20 p2384 N73-29155

**FRICTION FACTOR**
Development, production, and application of friction cermet and metal plastics materials
[AD-747575] 03 p0323 N73-12630
Mathematical solution to compressive bulk formation for calibrating ring test specimens using constant interface friction factor
[AD-750885] 06 p0675 N73-15492
Equations of motion for elastic tire rolling on ground and forces exerted by tire assuming absence of slippage between tire and ground
[AD-732697] 09 p1040 N73-18482
Solution of Hertz contact problem for case involving indentation of elastic half space by rigid axisymmetric punch under monotonically applied normal force with assumed Coulomb friction
[AD-755071] 11 p1299 N73-20544
Numerical analysis of effects on bearing load carrying capacity of opposing surfaces with striated roughness on both surfaces
[AD-761169] 18 p2156 N73-27423
Friction effects on inertia compensators used for heliostat base motion isolation
[AD-764706] 23 p2821 N73-32549

**FRICTION LOSS COEFFICIENT**
U FRICTION FACTOR

**FRICTION MEASUREMENT**
Mu-meter and diagonal braked vehicle measurements of runway friction at ten airports
[PSC-107] 01 p0036 N73-10281
Numerical analysis of contact stresses between cam and follower mechanisms for combinations of materials, surface finish, and lubrication conditions
[ESDU-66002] 01 p0060 N73-10492
Numerical analysis of friction forces developed in ball bearing of pendulum support to show dynamic friction torque and arm of rolling friction
[JPRS-57257] 01 p0062 N73-10507
Determination of friction and lead during rolling by electrical contact procedure and by method of core impressions
[AD-747670] 03 p0308 N73-12517
High temperature friction and wear properties of PbO for solid lubricant applications including tests in room air, controlled atmospheres, and vacuum
[NAL-TR-285] 04 p0426 N73-13470
Bench tests of wear resistance and antifriction properties of epoxy compounds
[AD-752868] 09 p1054 N73-18588
Contact interaction and friction and wear of solid bodies
[AD-755710] 13 p1535 N73-22438
Oscillographic measurements of friction moments in gas ball bearings
[NLL-RISLEY-TR-2565-[9091.9F]]
15 p1790 N73-24507
Modification of spinning torque apparatus to measure spinning torque on cageless ball thrust bearing using oil jet lubrication or thin surface film only
[NASA-TN-D-7356] 17 p2038 N73-26484
Measurement of spinning and rolling torques in angular-contact ball bearing with and without cages under several lubrication regimes
[NASA-TM-X-68271] 18 p2155 N73-27414
Device for measuring friction moments in radial thrust ball bearings and gas-dynamic bearings of gyros
20 p2418 N73-29430

**FRICTION PRESSURE DROP**
U SKIN FRICTION

**FRICTION REDUCTION**
Friction reducing properties of fibers in turbulent flow of fluids in pipes
[AD-746485] 01 p0043 N73-10337
Antifriction and antiwear properties of medium pressure polyethylene
[AD-748912] 04 p0439 N73-13582
Process for spraying metal coatings on aluminum alloys and resulting antifriction properties
[NLL-TRANS-746-1290-[9022.401]]
05 p0550 N73-14465
Design and evaluation of hybrid boost bearings consisting of fluid film bearing coupled with rolling element bearing
[NASA-CR-2226] 09 p1039 N73-18476
Numerical analysis of oil film bearing with respect to bushing based in inertial force, viscous force of liquid, and load lifting force exerted by bearing
[AD-752688] 09 p1040 N73-18483
Limiting stabilities and thickening properties of phthalocyanine lubricants in different dispersion media
[AD-752827] 09 p1040 N73-18484
Performance of gas lubricated thrust bearing based on minimum surface damage and low value of friction coefficient
[AD-753018] 09 p1041 N73-18493
Analog simulation of free piston gasifier tests relative to combustion and friction
[ME-240] 14 p1719 N73-23947
Development of lubrication theories and application of epilame-lubricant pairs for friction reduction
[NLL-RISLEY-TR-2547-[9091.9F]]
15 p1790 N73-24510
Performance tests of gas turbine engine mainshaft roller bearings to determine stress and lubrication parameters
[AD-760563] 18 p2157 N73-27426
Design, fabrication, and performance tests of foil journal bearings for application to Brayton cycle turbo-alternator-compressor
[NASA-CR-2243] 19 p2304 N73-28529
Hollow high strength rolling elements for antifriction bearings fabricated from preformed components
[NASA-CASE-LEW-11026-1] 24 p2928 N73-33383

**FRINGE PATTERNS**
U DIFFRACTION PATTERNS

**FROGS**
Comparison of development of auditory vesicle in frog embryos under weightless and terrestrial conditions
[NASA-TT-F-14624] 01 p0009 N73-10072
Mechanisms for controlling physiological rhythms in Rana pipiens
[NASA-CR-131153] 10 p1112 N73-19064
Increased toxicity of sympathomimetic amine stimulants on spinal reflexes in irradiated frogs
11 p1240 N73-20063

**FRONTAL AREAS [METEOROLOGY]**
U FRONTS [METEOROLOGY]

**FRONTS [METEOROLOGY]**
NT WARM FRONTS

Numerical analysis of gravity wave generation in atmospheric frontal zone
[AD-751638] 07 p0796 N73-16469
Classification, description, and statistical treatment of European large-scale weather patterns
[NLL-M-9145-[5828.4F]] 07 p0814 N73-16600
Frontal zone formation in tropopause as caused by slanting phenomenon
[NLL-M-22824-[5828.4F]] 11 p1274 N73-20341

**FROST**
Wind tunnel tests to determine effect of simulated hoar frost on lift coefficient of three aircraft wing configurations
[FFA-AU-902] 01 p0001 N73-10001

**FROUDE NUMBER**
Small Froude number paradoxes and wave resistance at low speeds
[AD-746191] 01 p0043 N73-10340

**FROZEN FOODS**
Production methods for preventing deterioration of freeze-dried foods
[NASA-CR-128915] 14 p1614 N73-23085

**FROZEN LAKES**
U LAKES

**FROZEN SOILS**
U PERMAFROST

**FRUITS**
Application of ERTS-1 imagery for identifying citrus groves and rice fields in Valencia region of Eastern Spain
[PAPER-A4] 19 p2260 N73-28212

**FUEL CAPSULES**
Effects of irradiation on properties of fluoride tungsten clad uranium carbide-zirconium carbide fueled capsules
[NASA-CR-120995] 05 p0578 N73-14708
Plasma arc welding procedure for Hastelloy seams of isotopic strontium titanate fuel capsule
[CONF-720917-1] 10 p1166 N73-19489
Compatability of tantalum alloys fuel capsules and [Pu-238]O2 fuels in radioisotopic thermoelectric generators
[LA-UR-73-764] 24 p2955 N73-33610

**FUEL CELL CATALYSTS**
U ELECTROCATALYSTS

**FUEL CELLS**
NT HYDROGEN OXYGEN FUEL CELLS
NT REGENERATIVE FUEL CELLS
Thermodynamic equilibria and carbon deposition in carbon-hydrogen-oxygen system of high temperature fuel cells
[ARL/ME-NOTE-333] 01 p0006 N73-10048
Performance of hydrocarbon oxidation catalysts as adsorbed layer promoter
[AD-746258] 02 p0138 N73-11117
Fuel cell applications as power supplies for rail transportation
[AD-747512] 04 p0376 N73-13056
Development of low cost cathode catalysts for air breathing fuel cells containing phosphoric acid electrolyte
[AD-748447] 04 p0376 N73-13059
Gas phase chromatographic study of electrosorbed cyclic hydrocarbon intermediates on fuel cell electrode during oxidation
[AD-750391] 05 p0500 N73-14068
Transient thermodynamic simulation of Apollo fuel cell/radiator system for proposed Skylab mission
[NASA-CR-129824] 05 p0598 N73-14860
Method for producing asbestos matrix suitable for use in fuel cell or electrolysis cell
[NASA-CASE-MSC-12568-1] 07 p0811 N73-16577
Comparison of methods for adapting hydrazine-oxygen fuel cells to cyclic pressure effects of hydrostatic pressure environment
[AD-753802] 10 p1112 N73-19062
Apollo experience report on design philosophy and experience of Apollo spacecraft electrical power generation system
[NASA-TN-D-7142] 10 p1214 N73-19873
Analysis of optimum mass and heat transfer in electrochemical fuel cells to show effects on fuel cell output
[AD-754258] 11 p1238 N73-20051
Development of phosphoric acid fuel cells operating on hydrogen produced from thermocracking or steam reforming of hydrocarbon
[AD-755206] 13 p1477 N73-21966
Cathode degradation in platinum black fuel cell
[AD-757714] 14 p1606 N73-23019
Low cost oxygen electrode for phosphoric acid fuel cell
[AD-758179] 15 p1739 N73-24095
Electrolytes for hydrocarbon air fuel cells
[AD-758180] 15 p1739 N73-24096
Hydrocarbon oxidation by metal catalysts and adsorption layer formation on electrode in propane air fuel cell
[AD-758172] 15 p1748 N73-24168
Apollo experience report on design and function of Apollo potable water system supplied as byproduct of fuel cells
[NASA-TN-D-7291] 15 p1835 N73-24874
Construction, operation, and applications of fuel cells to show advantages and limitations
[NASA-SP-5115] 17 p1985 N73-26045
Solid polymer electrolyte regenerative fuel cells for communication satellites
[AD-762923] 20 p2365 N73-29016
Fuel cell technology using low temperature potassium hydroxide electrolyte
[NASA-CR-134002] 21 p2499 N73-30056
Portable open cycle fuel cell power plant capable of operation on military fuels
[AD-764285] 22 p2618 N73-30979
Monitoring and control of fuel cell system by digital computer
[NASA-TM-X-2923] 23 p2748 N73-31994
Carbon-oxygen fuel cell of solid carbon anode, nickel gauze cathode, and flamed electrolytes
24 p2880 N73-33001
Characteristics of hydrazine-oxygen fuel cell operating under moderate temperature conditions and various power density concentrations
[AD-764530] 24 p2881 N73-33009

**FUEL COMBUSTION**
Ignition site and ignition delay time for spherical fuel droplets
[NLL-RTS-7169] 02 p0241 N73-11959
Flameout and ignition characteristics of jet engine fuel flame in gas turbine with exhaust diffuser
[AD-749635] 05 p0591 N73-14802
Laboratory experiments and mathematical models of nitrogen oxide formation in combustion of fossil fuels
[PB-211480] 05 p0606 N73-14932
Processes leading to carbon formation in premixed laminar flames of various fuels
08 p0882 N73-17144
Mixing and ignition of hydrogen jets injected normally into supersonic two dimensional flow and effect on combustion performance of hyersonic ramjet engine
[ONERA-TP-973] 09 p1098 N73-18962
Effect on nitric oxide emissions of using premixed prevaporized fuel/air in turbojet combustors
[NASA-TM-X-68220] 12 p1464 N73-21862
Corrosion resistant materials for nozzle guide vanes and turbine blades subject to vanadium containing fuel combustion
14 p1678 N73-23613
Effect of fuel vapor concentrations on combustion emissions and performance using experimental turbojet combustor segment
[NASA-TM-X-2800] 15 p1843 N73-24933
Combustion and evaporation of liquid fuels at high pressures
[NASA-CR-121113] 15 p1843 N73-24934
Thermal response of protective fabric/human skin system to JP-4 jet fuel fire
[AD-759525] 17 p1990 N73-26095
Comparison of military and civil jet engine fuel specifications and test procedures for fuel performance and quality control
17 p2098 N73-26972
Hydrogen content as measure of combustion performance for hydrocarbon fuels
[AD-763097] 20 p2465 N73-29804
Test equipment and procedure for determining electrical conductivity of stream of hot powdered fuel during combustion process
[JPRS-59752] 20 p2485 N73-29960
Incendiary vulnerability of dry bays adjacent to jet fuel tanks under gunfire
[AD-764732] 23 p2867 N73-32920
Laminar boundary layers at continuously moving wall and behind shock wave, noting fuel combustion problem
24 p2906 N73-33192
Electrified kerosene and gasoline aviation fuel during passage through pipes and filters of fuel tank reservoir
[AD-764941] 24 p2971 N73-33740

**FUEL CONSUMPTION**
Improvement of turbojet engine performance analysis by plotting parameters of two shaft turbojet engine operation
[AD-749058] 04 p0465 N73-13789
Optimum rendezvous maneuver of space vehicles on elliptical trajectories for minimum fuel consumption
[NASA-TT-F-14644] 07 p0843 N73-16828
Interrelationships between energy, resources, and environment, conference summary
[PB-213031] 11 p1333 N73-20820
Double-gimbaled control moment gyro system for maintaining Skylab attitude control without excessive fuel consumption after failure of main gyro system
[NASA-TM-X-64746] 14 p1707 N73-23851
Fuel consumption profiles of passenger and freight transportation modes
[P-4935] 14 p1721 N73-23962
Use of energy in transportation and implications for future
[P-5025] 24 p2993 N73-33921

**FUEL CONTAMINATION**
Potential plume contamination effects from two 300 lb bipropellant engines in satellite environment and electrical power loss study
[AD-746306] 01 p0007 N73-10057
Exhaust plume and contamination characteristics of bipropellant [MMH/N2O4] RCS thruster in liquid helium cooled, environmental facility
[NASA-TM-X-68212] 11 p1348 N73-20941
Literature on vanadium and nickel trace elements in distillate fuels for motor vehicles
[AD-760462] 17 p2076 N73-26793

**FUEL CONTROL**
Design, development, and evaluation of mechanical mass flow controller for regulating fuel-oxidizer mixture ratio and controlling rocket engine thrust level
[NASA-CR-128639] 03 p0351 N73-12860
Closed loop fuel control techniques using electronic circuitry to sense pressure relationships at turbine engine compressor discharge
[AD-747805] 03 p0351 N73-12865
Performance tests of hydromechanical fuel control system for J-85 engine
[NASA-TN-D-7198] 09 p0990 N73-18082
Variable-orifice hydraulic mechanism for aircraft gas turbine engine fuel control
[NASA-CASE-LEW-11187-1] 10 p1203 N73-19793
Modifications of fuel control units in aircraft gas turbine engines for reducing production costs
[NASA-TM-X-68229] 13 p1571 N73-22729

**FUEL ELEMENTS [NUCLEAR REACTORS]**
U NUCLEAR FUEL ELEMENTS

**FUEL FLOW**
NT PROPELLANT TRANSFER

**FUEL GAGES**
Design and requirements of zero-g fuel gauging system based on absorption of gamma radiation
[AD-745566] 01 p0059 N73-10479
Zero-g gaging system based on absorption of gamma radiation
[AD-749967] 06 p0675 N73-15489
Cavity resonators for measuring cryogenic propellant content in space shuttle orbiter tanks under weightlessness
10 p1162 N73-19452

**FUEL INJECTION**
Tests of high pressure combustor exhaust emissions with improved air-atomizing and conventional pressure-atomizing fuel nozzle
[NASA-TN-D-7154] 07 p0855 N73-16929
Fuel injectors with high frequency swirl generators
[AD-751079] 09 p1080 N73-18810
Gas turbine nozzle geometry of two phase flow fuel injectors
[AD-754051] 11 p1334 N73-20831
Design of fuel injection system for ramjet engines with coaxial inlet
[AD-754852] 11 p1335 N73-20835
Effect of adjacent jets on turbulent mixing rate of coaxial helium jet in Mach 4 air stream
[NASA-CR-112292] 16 p1888 N73-25281
Improved injector with porous plug for bubbles of gas into feed lines of electrically conductive liquid
[NASA-CASE-NPO-11377] 18 p2154 N73-27406
Rocket propellant injector with porous faceplate for rocket engine combustion chamber
[NASA-CASE-LEW-11071-1] 18 p2192 N73-27695
Design of injector system for fusion reactor
[MATT-949] 19 p2324 N73-28699

**FUEL OILS**
Technologies for production and utilization of petroleum, natural gas, oil shale and coal
[BM-IC-8612] 21 p2536 N73-30335
Solar energy, thermonuclear energy, and fossile fuel energy sources
[UCRL-74697] 24 p2881 N73-33005
Congressional hearings on causes and implications of impending shortages of gasoline, heating oil, diesel fuel, jet fuel, and electricity
24 p2994 N73-33928

**FUEL PUMPS**
Childdown tests on single stage inducer test rig
[NASA-CR-132212] 15 p1762 N73-24278

**FUEL SPRAYS**
Model for liquid fuel sprayed into supersonic gaseous stream and two phase flow of dispersed liquid
[AD-753515] 09 p1019 N73-18316
Combustion tests of various integral, spray-bar and flameholder configurations to determine configuration with maximum combustion efficiency
[NASA-TM-X-2855] 19 p2352 N73-28919
Two phase detonation in fuel sprays suspended in gaseous oxidizing atmospheres
20 p2484 N73-29957

**FUEL SYSTEMS**
NT AIRCRAFT FUEL SYSTEMS
Development of hydrocarbon fuels and fuel systems for advanced air breathing engines
[AD-746334] 01 p0090 N73-10741
Development of forward area refueling equipment for servicing military helicopters
[AD-746249] 02 p0154 N73-11245
Computer program for analyzing dynamics of propellant feedlines
[NASA-CR-123913] 02 p0220 N73-11785
Chemistry of deposits and their precursors in jet turbine fuel systems
[AD-754459] 11 p1332 N73-20816

FORTRAN-4 computer program for compiling irradiation data on UN and UC fuel pins
[NASA-TM-X-68226] 13 p1558 N73-22625
Analysis of factors influencing technical feasibility of operating aircraft on liquid hydrogen fuel
[NASA-TM-X-68242] 15 p1823 N73-24777
Development of electronic circuit for measurement transducer power supply to be used for liquid level measurement in liquid propellant rocket engines
[NASA-CASE-MFS-21698-1] 17 p2003 N73-26196
Design and performance tests of solid state A-6 aircraft engine instruments
[AD-760351] 17 p2035 N73-26469
Development of computer program for space shuttle orbit injection propulsion system to generate parametric feed system pressure histories - Vol. 5 B-4
[NASA-CR-133957] 17 p2087 N73-26885
Design and development of optimized cryogenic fuel supply systems for space shuttle vehicles - Vol. 2
[NASA-CR-128993] 18 p2199 N73-27751
Analysis of cryogenic supply system for space shuttle vehicles and evaluation of candidate systems - Vol. I
[NASA-CR-128992] 18 p2199 N73-27756
Development of integrated mathematical model for optimization of cryogenic fluid storage and supply systems for spacecraft - Vol. 5A-1
[NASA-CR-133953] 18 p2199 N73-27757
Development of computer program for preliminary design of propellant feed system for space shuttle orbiter main engines - Vol. 5A-2
[NASA-CR-133954] 18 p2200 N73-27758
Analysis of parameters involved in flow of combustion to produce stable propagation and efficient fuel consumption
[NLL-T1873/BGC/73-[9022.305]] 21 p2605 N73-30874
Interior ballistic properties of solid fuel ramjet engines to determine regression rate if fuel as function of chamber pressure, inlet air temperature, and air flux rate
[AD-764491] 22 p2709 N73-31691
Application of fiber glass reinforced plastic materials for ground handling of aviation fuels and hazards of static electricity caused by plastic materials
[AD-764358] 22 p2709 N73-31693

**FUEL TANK PRESSURIZATION**
Design and development of pressurization system for reusable space shuttle multilayer insulation systems
[NASA-CR-124380] 22 p2722 N73-31782

**FUEL TANKS**
Impact tests of jet transport wing leading edge fuel tanks to evaluate effects of aborted takeoff, abnormal landing, and bird strikes
[FAA-NA-72-21] 02 p0125 N73-11017
Development and evaluation of internal insulation materials for use with liquid hydrogen tanks on space shuttle
[NASA-CR-123928] 02 p0191 N73-11547
Control system design criteria to prevent air pollution from volatile fuel storage tank emission
[AD-748009] 03 p0350 N73-12854
Fuel tanks, spinup techniques, and thruster-CG misalignment problems for synchronous orbiting satellites
[AD-746845] 03 p0360 N73-12931
Shock wave attenuation in foam water mixtures containing Freon and exposed to hydraulic impact
[AD-748350] 04 p0407 N73-13318
Liquid hydrogen reorientation in fuel tanks of Centaur launch vehicle using low level accelerations with and without internal baffles
[NASA-TN-D-7168] 07 p0770 N73-16252
Fuel-oxide can compatability and reaction during fabrication of fuel elements for fast reactors
[NLL-CE-TRANS-6049-[9022.09]] 11 p1322 N73-20732
Development of halogenated hydrocarbon materials for use as fire and ignition suppressants for aircraft fuel tanks subjected to incendiary ammunition
[AD-755362] 12 p1365 N73-21079
Feasibility of liquid nitrogen fuel tank inerting system on commercial aircraft to prevent fuel tank explosions
[FS-140-72-1] 13 p1473 N73-21934
Composite materials for use as internal LH2 tank insulation for reusable boosters
[NASA-CR-124222] 13 p1546 N73-22528
Investigation of fibers and composites applicable to the design of high pressure vessels for satellites
[MAN-NT-10/72] 13 p1586 N73-22859
Perfluoroalkylene ether polymers for high temperature fuel tank sealants
[NASA-CR-124249] 14 p1680 N73-23635
Development of fibrous flame arrestor materials to provide explosion and fire protection for aircraft fuel tanks
[AD-759193] 16 p1863 N73-25090
Development of engineering analysis and computer code for predicting space shuttle orbiter longitudinal aerodynamic characteristics during abort separation
[NASA-CR-128974] 17 p2086 N73-26877

**FUEL TESTS**
NT REACTOR STARTUP TESTS

Determination of point of ignition and ignition delay period for single drop of fuel under specified conditions of temperature and vapor
[AD-745868] 02 p0244 N73-11979
Comparison of combustion characteristics of ASTM A-1, propane, and natural gas fuels in annular turbojet combustor
[NASA-TN-D-7135] 07 p0835 N73-16771
UC-ZrC fuel elements for space power reactor system
[GULF-GA-A-11073] 12 p1428 N73-21571
Comparison of military and civil jet engine fuel specifications and test procedures for fuel performance and quality control
17 p2098 N73-26972

**FUEL VALVES**
Design, development, manufacture, and specifications of automatic fuel valves for liquid propellant rocket engines
[AD-750578] 06 p0715 N73-15832

**FUEL-AIR RATIO**
Effect on nitric oxide emissions of using premixed prevaporized fuel/air in turbojet combustors
[NASA-TM-X-68220] 12 p1464 N73-21862
Test equipment and experimental procedures for determining effects of turbulent flow on ignition properties of gasoline and air mixture
[NLL-RTS-7883] 18 p2128 N73-27194

**FUELING**
U REFUELING

**FUELS**
NT AEROZINE
NT AIRCRAFT FUELS
NT CERAMIC NUCLEAR FUELS
NT CHEMICAL FUELS
NT CRYOGENIC ROCKET PROPELLANTS
NT DOUBLE BASE ROCKET PROPELLANTS
NT FISSIUM
NT FUEL OILS
NT GASOLINE
NT HIGH ENERGY FUELS
NT HYDROCARBON FUELS
NT HYDROGEN FUELS
NT HYPERGOLIC ROCKET PROPELLANTS
NT JET ENGINE FUELS
NT JP-4 JET FUEL
NT JP-5 JET FUEL
NT LIQUID ROCKET PROPELLANTS
NT METAL FUELS
NT MONOPROPELLANTS
NT NUCLEAR FUELS
NT SLURRY PROPELLANTS
NT SOLID ROCKET PROPELLANTS
Dictionary-handbook on properties and uses of fuels, lubricating materials, and special liquids
[AD-750484] 06 p0712 N73-15810
Congressional hearings concerning critical energy needs
08 p0977 N73-17989
Calculation and design of heat transfer apparatus for viscous liquids, liquid fuel, and lubricating oils
[AD-756947] 13 p1592 N73-22908
Tabular listing of minimum and maximum temperatures for use in specifying fuel and lubricant properties needed in different geographical areas
[AD-756420] 14 p1685 N73-23675
Optimal operational temperature for thermoelectric generator using organic fuel heat
[AD-762266] 19 p2223 N73-27932
Chemical determination of organic nitrate additive in diesel engine fuel
[AD-762177] 19 p2328 N73-28730
Review of resources of fossil and nuclear fuels, solar energy and hydroelectric power
[LRP-63/73] 22 p2617 N73-30975
Portable open cycle fuel cell power plant capable of operation on military fuels
[AD-764285] 22 p2618 N73-30979
Kinetic model for nitric oxide formation from organic fuel nitrogen
[FML-PUBL-73-7] 22 p2625 N73-31032
Hydrogen and other synthetic fuels
[TID-26136] 24 p2971 N73-33738

**FULL SCALE FATIGUE TESTS**
U FATIGUE TESTS

**FUMES**
Fume component tests to determine welders safe breathing level through ventilation
[ITR-1] 09 p1038 N73-18467

**FUNCTION GENERATORS**
Design of logic counters and scalers based on continued quotients for digital function generators
03 p0278 N73-12253
Laplace transform amplitude function generator utilizing thin film semiconductor
[AD-750590] 06 p0710 N73-15792
Function generators for producing complex vibration mode patterns used to identify vibration mode data
[NASA-CASE-LAR-10310-1] 11 p1263 N73-20253
Integrated circuit tangnet function generator
[NASA-CASE-MSC-13907-1] 17 p2007 N73-26230

**FUNCTION SPACE**
NT BANACH SPACE
NT HILBERT SPACE

Solution of n-dimensional scattering problem by means of k-space formulation of field equations
02 p0201 N73-11623
Extension of theorems concerning spectrum of one-dimensional and multidimensional differential operators on vector functions
[NASA-TT-F-14960] 17 p2055 N73-26620

**FUNCTION TESTS**
U TESTS

**FUNCTIONAL ANALYSIS**
NT BANACH SPACE
NT CONVOLUTION INTEGRALS
NT FOURIER TRANSFORMATION
NT FREDHOLM EQUATIONS
NT HARMONIC ANALYSIS
NT HILBERT SPACE
NT INTEGRAL EQUATIONS
NT INTEGRAL TRANSFORMATIONS
NT LAPLACE TRANSFORMATION
NT TESSERAL HARMONICS
NT VOLTERRA EQUATIONS
NT WIENER HOPF EQUATIONS
NT ZONAL HARMONICS
Measurements of automobile driver response functions in simulated steering control task with visual field display
01 p0017 N73-10130
Double steering wheel forcing functions for estimating automobile driver manual control response
01 p0017 N73-10132
Functional analysis and logical construction systematics for signal processing equipment design
02 p0140 N73-11136
Relaxation method for inverse solution to atmospheric parameters appearing as functions in integrand of radiative transfer equation
02 p0197 N73-11590
Space shuttle orbiter guidance and control software functions for horizontal flight operations
[NASA-TM-X-68857] 02 p0207 N73-11682
Standard requirements for ultrasonic Doppler probes of cardiovascular systems in medical monitoring functions
03 p0257 N73-12083
Syntheses of logical circuits by composing common inputs and common variables
[AD-748165] 03 p0279 N73-12263
J integral relationship between elastic stress and concentration factors for inelastic fracture criterion of sharp notch
[CONF-720806-2] 05 p0569 N73-14617
Design and functional description of digital computer system
[FOA-3-C-3657-63] 06 p0643 N73-15220
Application of theoretical framework of governing equations and extremum principles to classical elasticity and plasticity yield-point problems
[AD-753137] 09 p1096 N73-18948
Tabulation of plasma dispersion function with first derivative using postive imaginary part
[AD-753986] 11 p1328 N73-20780
Tabulation of plasma dispersion function and first derivative using saddle point method
[AD-754002] 11 p1328 N73-20781

**FUNCTIONAL INTEGRATION**
Sampling function representation for applying satellite-to-ocean altitude altimeter data to geoid
06 p0662 N73-15373

**FUNCTIONALS**
Set of functionals and consistent estimators for spectral analysis of continuous nonstationary random processes
[AD-748341] 04 p0441 N73-13596
Universal functional scheme for realizing any combination or sequential function for proliferation problem in LSI technology
[NASA-CR-130387] 05 p0517 N73-14204
Estimates of differential functions for proving system stability
07 p0761 N73-16179

**FUNCTIONS [MATHEMATICS]**
NT ABEL FUNCTION
NT AIRY FUNCTION
NT ANALYTIC FUNCTIONS
NT ASYMPTOTES
NT BOOLEAN FUNCTIONS
NT CONFORMAL MAPPING
NT COORDINATE TRANSFORMATIONS
NT COSINE SERIES
NT DISCRETE FUNCTIONS
NT DISTRIBUTION FUNCTIONS
NT DISTURBING FUNCTIONS
NT ELLIPTIC FUNCTIONS
NT EXPONENTIAL FUNCTIONS
NT FOURIER TRANSFORMATION
NT GREEN FUNCTION
NT HAMILTONIAN FUNCTIONS
NT HANKEL FUNCTIONS
NT HARMONIC FUNCTIONS
NT HYPERBOLIC FUNCTIONS
NT LAPLACE TRANSFORMATION
NT LEGENDRE FUNCTIONS
NT LIAPUNOV FUNCTIONS
NT LINEAR TRANSFORMATIONS
NT LORENTZ TRANSFORMATIONS
NT MATHIEU FUNCTION

NT MAXWELL-BOLTZMANN DENSITY FUNCTION
NT NORMAL DENSITY FUNCTIONS
NT ORTHOGONAL FUNCTIONS
NT PERIODIC FUNCTIONS
NT PROBABILITY DENSITY FUNCTIONS
NT PROBABILITY DISTRIBUTION FUNCTIONS
NT RECURSIVE FUNCTIONS
NT SINE SERIES
NT SPACE-TIME FUNCTIONS
NT SPHERICAL HARMONICS
NT SPLINE FUNCTIONS
NT STRESS FUNCTIONS
NT TANGENTS
NT TRANSFER FUNCTIONS
NT TRIGONOMETRIC FUNCTIONS
NT WALSH FUNCTION
NT WEIBULL DENSITY FUNCTIONS
NT WEIGHTING FUNCTIONS

Pattern recognition and linear discriminant function
[REPT-8] 20 p2437 N73-29573

Algorithm for solving approximate problem of nonlinear function
[NASA-CR-133728] 20 p2440 N73-29599

**FUNGI**
NT SPORES
NT YEAST

Chemiotaxionomic survey of carotenoid pigments in several species and groups of Basidiomycetes
[NASA-TT-F-14858] 11 p1246 N73-20117

Chemical characteristics of mushroom pigments and mycological classifications
[NASA-TT-F-14865] 11 p1247 N73-20124

Phenotype numbers and survival rates of fungi exposed to space environment during Apollo 16 flight
15 p1740 N73-24110

Susceptibility of synthetic engine and transmission lubricants of OH-58 A helicopter to microbal attack
[AD-762176] 19 p2313 N73-28604

**FURAN RESINS**
NT POLYAMIDE RESINS

**FURFURYL ALCOHOL**

Physical and mechanical properties of carbon produced from furfural alcohol resins
[AD-763499] 23 p2810 N73-32472

**FURLABLE ANTENNAS**

Development of large furlable spacecraft antennas using conical main reflectors
[NASA-CR-132989] 16 p1880 N73-25219

**FURNACES**
NT SOLAR FURNACES
NT VACUUM FURNACES

Mathematical model for convective and radiant heat transfer for gas flow and glass tube inner wall noting partial differential equations at boundary conditions
[LAAS-NI-CMOAC-72-I-11] 02 p0243 N73-11976

Induction furnace providing controlled temperature for carbonization and graphitization processes for NERVA nozzle extension
[NASA-CR-132216] 15 p1801 N73-24599

High temperature general purpose furnace for use in space
[NASA-CR-124458] 24 p2991 N73-33905

**FUSELAGE MOUNTING**
U AIRCRAFT PRODUCTION

**FUSELAGES**

Glass fiber reinforced composite materials for developing prototype missile fuselages
[AD-746288] 02 p0193 N73-11560

Computer program for shock and blast loading characteristics high explosive projectile detonation in aircraft
[AD-759002] 16 p1975 N73-25972

Development of formula for determining ideal weight of shell-type aircraft fuselages with body of revolution cross section
[RAE-LIB-TRANS-1688] 17 p1981 N73-26009

Buried engines in rear fuselage
21 p2590 N73-30750

Aerodynamic fuselage rear part configurations for aircraft stability optimization noting pressure distribution and aerodynamic forces
[DLR-FB-72-25] 22 p2612 N73-30931

**FUSES [ORDNANCE]**

Computerized design of support structure for missile fuse using finite element structural analysis program - Part 1
[AD-743879] 01 p0115 N73-10947

**FUSIFORM SHAPES**
U CONES

**FUSION**

Laser beam fusion and plasma generation on pellet
[UCID-16222] 24 p2965 N73-33697

**FUSION [MELTING]**

Influence of steam on fusion in electron beam welding
[DRIC-TRANS-2927] 03 p0307 N73-12505

Variation of electric conductivity and thermal emf at fusion of copper chalcogenides
[AD-756088] 13 p1566 N73-22694

Preflight, inflight, and post flight operations evaluation analyses for Skylab metals melting experiment facility - Appendix F
[NASA-CR-61386-APP-F] 14 p1708 N73-23860

Spectral emissions of liquid titanium, vanadium, zirconium, molybdenum, and platinum at fusion temperatures
[BM-RI-7743] 15 p1798 N73-24575

Emissivities of metals and compounds in liquid state at fusion temperatures
[NASA-CR-133521] 19 p2309 N73-28576

Research and development in solid state lasers, gas lasers, component development, diognostics, design analysis, advanced concepts, laser plasmas and laser fusion
[UCRL-50021-72-2] 24 p2931 N73-33408

Development of plasmas for industrial applications as fusion torches
24 p2961 N73-33663

**FUSION WELDING**
NT ARC WELDING
NT BRAZING
NT ELECTRON BEAM WELDING
NT GAS TUNGSTEN ARC WELDING
NT GAS WELDING
NT PLASMA ARC WELDING

Electrical resistance butt welder for welding fine gauge tungsten/rhenium thermocouple wire
[NASA-CASE-LAR-10103-1] 05 p0550 N73-14468

Solid state and fusion resistance spot welding of TD-NiCr sheet
[NASA-TN-D-7256] 12 p1412 N73-21443

Physical and chemical processes of solidification of fusion welds and its effects on weldability
[NLL-T1780/GC/72-[9022.305]]
15 p1790 N73-24508

Fusion welding of aluminum to steels
[AD-764322] 22 p2678 N73-31454

**F4H AIRCRAFT**
U F-4 AIRCRAFT

**F8U AIRCRAFT**
U F-8 AIRCRAFT


## G


**G FORCE**
U ACCELERATION [PHYSICS]

**GA-5 AIRCRAFT**

Wind tunnel tests to determine directional and longitudinal stability of Javelin aircraft model at transonic speeds
[ARC-R/M-3403] 16 p1853 N73-25012

**GADOLINIUM**

Synthesis of rare earth compounds and determination of their magnetic, optical, and semiconducting properties
[AD-747839] 03 p0348 N73-12835

Kerr magnetooptical effect in nickel, gadolinium, and dysprosium at temperatures between 10 and 300 K in 1 to 5 eV energy range
12 p1437 N73-21644

Photon energy and polarization effects on optical absorption spectra of GMO at varying temperatures
23 p2824 N73-32574

Mass spectra of doublets in samarium and gadolinium chlorides
24 p2959 N73-33648

**GAGES**
U MEASURING INSTRUMENTS

**GAIN [AMPLIFICATION]**
U AMPLIFICATION

**GALACTIC CLUSTERS**

Applications of Schmidt telescopes to study astrometry, photometry, galactic structure, quasars, and stellar spectra
07 p0844 N73-16840

History of 48-inch Palomar Schmidt telescope noting investigation of galactic red shift and radio sources
07 p0844 N73-16841

Application of Schmidt telescopes and three color photometry to galactic clusters, star distribution in galactic disk and halo and galactic white stars.
07 p0845 N73-16842

Application of Schmidt telescopes to study of galactic clusters and evolution noting new emulsion, infrared surveys, luminosity, and quasars
07 p0845 N73-16849

Balloon measurement of gamma ray emission from region of galactic center
16 p1959 N73-25844

Morphology of rich clusters of galaxies
17 p2081 N73-26832

X ray astronomy and its impact on galactic and extragalactic radio source mapping
17 p2084 N73-26856

Gas flow and wind velocity in elliptical and cluster galaxies
24 p2978 N73-33795

**GALACTIC EVOLUTION**

Origin and evolution of stars, stellar matter, and galaxies
[AD-749734] 06 p0720 N73-15875

Application of Schmidt telescopes to study of galactic clusters and evolution noting new emulsion, infrared surveys, luminosity, and quasars
07 p0845 N73-16849

Theories on giant-loop type nebula
08 p0975 N73-17975

**GALACTIC MAGNETIC FIELDS**
U INTERSTELLAR MAGNETIC FIELDS

**GALACTIC NUCLEI**

Formation of relativistic particles into clouds in quasar and Seifert nuclei, and centimeter, submillimeter, and gamma radiation emissions
[NP-30] 06 p0717 N73-15854

Study of galactic nuclei using image tube spectrographic techniques
22 p2713 N73-31718

**GALACTIC RADIATION**
NT GALACTIC RADIO WAVES

Pioneer 10 observations of galactic cosmic ray intensity from 1.0 to 2.0 AU heliocentric radial range
[AD-748614] 05 p0593 N73-14823

Galactic and background radiation measurements by rocket-borne submillimeter detectors
07 p0840 N73-16808

Diffuse X rays from galactic disk
08 p0974 N73-17968

Measurements of galactic cosmic ray dose and geomagnetically trapped radiation from OV 1-4 satellite
[AD-756924] 13 p1575 N73-22761

Near infrared spectrophotometry of cool stars in galactic anticenter
16 p1960 N73-25852

Energy spectra analysis for heavy nuclei charge compositions in galactic cosmic rays
[NASA-TM-X-66136] 17 p2079 N73-26817

Absorbed dose rate and equivalent dose rate investigation for galactic cosmic ray protons and alpha particles in manned spacecraft shields
[ORNL-TM-4029] 17 p2089 N73-26901

Galactic background maps of nonthermal radiation obtained from RAE mapping antenna data
[NASA-TM-X-66280] 18 p2196 N73-27728

Spallation reactions of light nuclei during galactic cosmic radiation interaction with interstellar gas
[FRNC-TH-333] 21 p2597 N73-30812

Rocket-borne proportional counter observations of discrete galactic X rays from supernovae
[NASA-TM-X-70463] 22 p2711 N73-31708

Solar magnetic field effects on galactic cosmic ray spectrum
22 p2733 N73-31877

**GALACTIC RADIO WAVES**

Analysis of quasi-periodic modulation of L-bursts in decametric radiation from planet Jupiter
05 p0594 N73-14833

Measurements of isotropy of cosmic background radiation at 6 cm determined from apparent sky brightness temperature differences
07 p0838 N73-16789

Deuterium absorption line in extraterrestrial radiation from galactic center
[AD-754079] 11 p1340 N73-20873

**GALACTIC STRUCTURE**

High energy particle kinetics along boundary of matter-antimatter of universe
[LPTHE-73/5] 14 p1703 N73-23818

Balloon-borne far infrared telescope observations of galactic and Magellanic Cloud objects
22 p2735 N73-31890

**GALAXIES**
NT ANDROMEDA GALAXIES
NT ELLIPTICAL GALAXIES
NT GALACTIC CLUSTERS
NT MAFFEI GALAXIES
NT MAGELLANIC CLOUDS
NT MILKY WAY GALAXY
NT RADIO GALAXIES
NT SPIRAL GALAXIES

Tidal interactions in multiple galaxies
04 p0468 N73-13816

Interferometric observations of neutral hydrogen emission line of compact galaxy 2 Zw 40
[AD-747993] 04 p0477 N73-13896

Maps of line profile at each position of aperture of neutral hydrogen in NGC 2403 and NGC 4236
[AD-748983] 06 p0719 N73-15872

Galactic brightness distribution obtained by imaging galaxies on Schmidt plates, selecting one as photometric standard and applying microdensitometric scans
07 p0845 N73-16852

Schmidt telescopes for compilation of stellar spectra and novae maps, galactic structure, and radial velocities
07 p0846 N73-16856

Investigation of stellar density distribution and luminosity function in high galactic altitudes using Schmidt telescopes
07 p0846 N73-16857

Virial theorem for analyzing structure of clusters in galaxies
08 p0959 N73-17840

Combination nuclear emulsion/spark chamber gamma ray telescope study of galactic center region
[NASA-CR-130863] 09 p1081 N73-18819

Application of kinetic gas theory to plasma physics and dynamics of galaxies
[FRNC-TH-247] 12 p1436 N73-21634

Galactic neutral hydrogen gas velocity distribution within spiral arms in local regions
12 p1447 N73-21720
Astronomical photography of Gum Nebula, galactic clusters, and zodiacal light from Apollo 16 flight
12 p1456 N73-21793
Two arc min synthesis study of spiral galaxy M51
[AD-754078] 12 p1459 N73-21822
Confinement of ultrarelativistic cosmic rays to galactic disk as result of interactions with hydromagnetic waves
13 p1572 N73-22739
Neutral hydrogen aperture synthesis maps of IC2574 and NGC 7640 galaxies
[AD-757688] 15 p1833 N73-24856
Automatic raster scanning microdensitometer measurement of luminosity profiles and density of lenticular galaxies in Virgo Cluster
16 p1961 N73-25859
Morphology of rich clusters of galaxies
17 p2081 N73-26832
Measurement of cosmic gamma ray emission from galactic center, Crab nebula, and diffuse radiation
19 p2331 N73-28757
Measurement of luminosity distribution of Coma cluster of galaxies and comparison of mass-to-light ratio of cluster with that of individual galaxies
19 p2341 N73-28829
Physical processes associated with infrared millimeter component of spectra from nuclei of Seyfert galaxies
20 p2469 N73-29834
Comparison of color index and formation conditions of cluster and field galaxies
[NLL-RTS-8000] 21 p2593 N73-30780
Using UBUH gamma photometry and spectral classifications for 48 stars in monoceros region to study dispersed part of 1 Mon association
23 p2836 N73-32658
SAS-2 measurements of gamma rays from galactic plane
[NASA-TM-X-70486] 24 p2976 N73-33778
**GALAXY AIRCRAFT**
U C-5 AIRCRAFT
**GALERKIN METHOD**
Fourier and Galerkin techniques for analyzing discontinuities and coupling phenomena in microstrip lines
[AD-750737] 06 p0648 N73-15264
Integration of Galerkin method for solving boundary layer equation with steady incompressible flow
[AD-752203] 08 p0898 N73-17275
Analysis of leakage and pressure drop characteristics across dam of gas film seal under various flow conditions
12 p1389 N73-21267
Feasibility of using Galkerin method to control cantilevered beam subjected to nonconservative force
17 p2091 N73-26913
Application of Galerkin method in nonconservative stability problems relating to thin elastic plates and slender elastic rods
[NRC-TT-1673] 21 p2603 N73-30860
**GALLIUM**
Liquid viscosity determined for gallium by means of vibration technique
[AD-750915] 06 p0656 N73-15332
Phase equilibrium diagram of intermetallic compound of vanadium and gallium
[AD-752877] 09 p1049 N73-18551
Minority carrier lifetime optimization for gallium silicon diffusion thyristor
11 p1330 N73-20795
Two cavity spectrometer for studying microwave transmission through gallium single crystals
12 p1438 N73-21647
Neutron activation analysis of Ga concentration in Ga-Se
[CONF-721069-41] 21 p2506 N73-30110
**GALLIUM ALLOYS**
Thermodynamic properties of solid Ni-Ga alloys at temperatures between 837 and 1100 K
[AD-762337] 19 p2311 N73-28588
**GALLIUM ARSENIDE LASERS**
Examination of GaAs laser radiation injuries and thresholds of ocular system during night vision exercises
[AD-750350] 05 p0559 N73-14542
Radiation hazards of gallium arsenide diode array lasers
[AD-762277] 19 p2229 N73-27975
**GALLIUM ARSENIDES**
Sheet resistivity and Hall effect study of zinc ions implanted in chromium-doped gallium arsenide
[NASA-CR-112199] 01 p0087 N73-10716
Electrical properties of p-n junctions formed by ion implantation into GaAs and [Ga,In]As
[NASA-CR-112200] 01 p0087 N73-10717
Design optimization for gallium arsenide solar cell parameters
[NASA-CR-129214] 02 p0128 N73-11041
Performance characteristics of gallium arsenide solar cells with zinc or beryllium ion implantations
[NASA-CR-129199] 02 p0128 N73-11042
GaAs wafer development, diode construction, and resonator design
[AD-746655] 02 p0150 N73-11213
Fabricating Ga-As-phosphide mis capacitors using dielectric-growth processes and radiation studies
[AD-747663] 03 p0275 N73-12232
Defect structures of GaAs by transmission and black reflection X ray topographic analysis
[AD-746895] 03 p0337 N73-12747
Modulation of infrared laser emission using gallium arsenide crystal
[AD-749631] 04 p0430 N73-13507
Optical and back reflection properties of GaAs crystals used as IR window materials
[AD-749083] 04 p0451 N73-13684
Czochralski technique for growing GaAs and III and V semiconductor crystals
[AD-748344] 04 p0461 N73-13759
Surface damage to gallium arsenide surfaces from radiation by ruby and neodymium-glass lasers
05 p0555 N73-14507
Influence of substrate temperature on properties of epitaxial layers of GaAs during growth
[NLL-RRE-TRANS-370-[8036.625]]
05 p0585 N73-14763
Angular distribution of photoemitted electrons from activated p-type gallium arsenide surfaces
[AD-750364] 06 p0645 N73-15239
Small etching pits in epitaxial layer of gallium arsenide caused by accumulation of impurities
[DRIC-TRANS-2928] 06 p0709 N73-15782
Spectral and temperature characteristics of natural photoconductivity in p-type GaAs
[AD-750696] 06 p0709 N73-15790
Measurement of picosecond laser pulse width using two-photon conductivity in GaAs and three-photon conductivity in CdS
[AD-750414] 06 p0710 N73-15798
GaAs Schottky barrier IMPATT diodes in 20 to 30 GHz frequency range
[NHK-LABS-NOTE-156] 07 p0761 N73-16183
Gallium arsenide Schottky and varactor diodes for 20 and 30 GHz
07 p0762 N73-16192
Mathematical model for nonlinear characteristics of avalanche diode
[AD-751974] 08 p0890 N73-17207
Photodielectric recombination and trapping model for low temperature n-type epitaxial gallium arsenide
[NASA-CR-130764] 08 p0950 N73-17779
Very high frequency Schottky barrier gate field effect transistors
[DOC-REF-3-314] 08 p0951 N73-17785
High resistivity gallium arsenide window material for high power carbon dioxide lasers emitting at 10.6 micrometers
[AD-752783] 09 p1048 N73-18550
Homoepitaxial films of GaAs deposited from vapor phase
[AD-754821] 11 p1331 N73-20800
Vapor phase epitaxy of gallium arsenide
[AD-755434] 12 p1441 N73-21678
Synthesis of compound semiconducting materials and application to planar microwave acoustic equipment using gallium arsenide thin films as active layer
[AD-755947] 12 p1442 N73-21684
Aanalysis of photoelectric properties of gallium arsenide and application to construction of solar cells
[AD-756228] 13 p1477 N73-21962
GaAs junction field effect transistor radiation study in fast neutron environment
[AD-756914] 13 p1503 N73-22186
Preparation techniques and quality control of GaAs substrates for use in epitaxy
13 p1566 N73-22688
Design and performance of traveling wave gallium arsenide amplifier with Schottky barrier
[AD-757219] 14 p1642 N73-23321
New methods for growth and characterization of GaAs and mixed semiconductor crystals
[AD-756259] 14 p1698 N73-23777
Preflight, inflight, and post flight operations evaluation analyses for Skylab gallium arsenide single crystal growth facility - Appendix J
[NASA-CR-61386-APP-J] 14 p1708 N73-23863
Gallium arsenide epitaxial thin films as active elements for electrooptic modulation of carbon dioxide laser radiation
[AD-757792] 15 p1796 N73-24559
Photoelectric emission of gallium arsenide from adsorbed layers of cesium and barium oxide
[NLL-DRIC-TRANS-2293-[3623.66]]
15 p1819 N73-24746
Development of high efficiency gallium arsenide solar cells using ion implantation techniques
[NASA-CR-131842] 16 p1865 N73-25099
Graded band gap p-n junction gallium arsenide/gallium aluminum arsenide solar cell
[NASA-CASE-LAR-11174-1] 17 p1985 N73-26047
Bulk, surface, and superficial analysis of semiconductor grade silicon and gallium arsenide
[CONF-721069-36] 17 p2073 N73-26770
Thermodynamics of precipitation caused by zinc diffusion into gallium arsenide
18 p2113 N73-27085
Data tables and photographs of gaas epitaxial layer perfections as influenced by substrate disorientation
18 p2189 N73-27675
Doping profile effect on stabilization mechanisms in microwave GaAs reflection amplifiers around X band
19 p2244 N73-28089
Power gain and noise figure of indium phosphide and gallium arsenide microwave reflection amplifiers
19 p2244 N73-28090
Infrared optical reflectivity analysis for determining free carrier parameters of irradiated gallium arsenide
[AD-762273] 20 p2463 N73-29791
Characterization and growth of GaAs crystals by gradient freeze and traveling heater methods
[AD-763761] 21 p2586 N73-30722
Techniques for improving performance of gallium arsenide solar cells by ion implantation
[NASA-CR-135510] 22 p2618 N73-30977
Integrated GaAs digital circuits with Gunn diodes for pulse code modulation
[FTZ-A-62-TBR-3] 22 p2646 N73-31205
Photodielectric techniques for analyzing low temperature band structure of gallium arsenide
24 p2891 N73-33080
**GALLIUM COMPOUNDS**
NT GALLIUM ARSENIDES
NT GALLIUM PHOSPHIDES
NT GALLIUM SELENIDES
Development of gallium aluminum phosphide alloys for electroluminescent diodes
[NASA-CR-112182] 03 p0273 N73-12213
Growth of bulk gallium nitride crystals by ammonolysis of gallium monochloride
[NASA-CR-112211] 03 p0344 N73-12807
Computer program for analysis of mass spectra of GaTe and GaSe
[ISS-72/11] 10 p1199 N73-19754
Temperature-modulated reflectivity in fundamental edge region of GaTe
[ISS-72/2] 10 p1199 N73-19755
Electrical and physical properties of low temperature grown cubic gallium nitride films
[AD-755237] 13 p1567 N73-22704
Effect of various growth and doping parameters on GaN for LED applications
[NASA-CR-132263] 18 p2189 N73-27676
Chemical vapor deposition of stoichiometric niobium gallium superconducting film
[NASA-CR-2308] 20 p2455 N73-29726
Evaluation of Gallium nitride for active microwave devices
[AD-763413] 21 p2586 N73-30726
**GALLIUM PHOSPHIDES**
Display system consisting of light emitting diode arrays monolithically fabricated on single wafers of GaP
[AD-746993] 03 p0274 N73-12225
Fabricating Ga-As-phosphide mis capacitors using dielectric-growth processes and radiation studies
[AD-747663] 03 p0275 N73-12232
Fabrication of monolithic light emitting diode display system on single wafers of gallium phosphide
[AD-755204] 13 p1502 N73-22172
Wavelength modulation spectra of copper, gold, silver, gallium phosphide, and indium phosphide
[LBL-1125] 24 p2927 N73-33375
Rare earth doped gallium phosphide preparation with application to electroluminescence noting physical and chemical properties
24 p2969 N73-33729
**GALLIUM SELENIDES**
Effect of external electric field on optical absorption of GaSe and GaTe single crystals and solid solutions
[AD-749750] 05 p0589 N73-14789
Neutron activation analysis of Ga concentration in Ga-Se
[CONF-721069-41] 21 p2506 N73-30110
**GALVANIC CELLS**
U ELECTROLYTIC CELLS
**GALVANIC SKIN RESPONSE**
Design and attachment of skin electrodes in human cardiac monitoring during space flight
03 p0259 N73-12095
**GAME THEORY**
NT SADDLE POINTS [GAME THEORY]
Sub-optimal control to synthesize feedback controller for two dimensional, nonlinear intercept and pursuit-evasion problems
[AD-746005] 01 p0109 N73-10901
Constrained n-person games, using extremal [linear programming] principle
[AD-746553] 02 p0203 N73-11645
Differential game theory for optimal collision avoidance between two aircraft moving in horizontal plane
[NASA-CR-129988] 05 p0577 N73-14701
Control theory in game problems, optimization, feedback, and probabilistic automata - conference
[JPRS-58030] 08 p0891 N73-17214
Differential games, nonlinear sequential machines, hyperbolic partial differential equations, and iterative solutions
[JPRS-58069] 09 p1056 N73-18609
Definitions of linearizable objects and applications in differential games of pursuit
09 p1056 N73-18610

Differential game theory applied to military operations, such as antimissile missile problem and air warfare
[BMVG-FBWT-73-9] 19 p2314 N73-28609
GAMMA RADIATION
U GAMMA RAYS
GAMMA RAY BEAMS
Expected gamma ray emission spectra from lunar surface for range of chemical compositions
[NASA-TM-X-70453] 21 p2595 N73-30796
GAMMA RAYS
Dosimetric determination of absorbed gamma and neutron radiation on human phantom
[AD-743005] 01 p0010 N73-10077
Neutron and gamma induced transient incapacitation in conditioned Macaca mulatta
[AD-742076] 01 p0010 N73-10080
Design and requirements of zero-g fuel gauging system based on absorption of gamma radiation
[AD-745566] 01 p0059 N73-10479
Multiplicity measurements for fission-emitted neutron or gamma quanta
[EUR-4829-E] 01 p0082 N73-10678
Apollo 15 and Apollo 16 spectrometric observation of X rays, gamma rays, and alpha particle emissions on lunar surface
[NASA-TM-X-66068] 01 p0103 N73-10848
Spectrum of total diffuse and discrete cosmic gamma ray background over 0.3 to 27 MeV range
[NASA-TM-X-66104] 02 p0225 N73-11818
Neutron activation analysis using gamma ray spectroscopy for determination of trace elements and short-lived nuclides
[BMBW-FBK-72-13] 03 p0262 N73-12122
Activation analysis of prompt gamma ray emission spectra for trace element determination
03 p0262 N73-12123
Gamma spectroscopic activation analysis of scheelite deposits
03 p0262 N73-12124
Computerized evaluation of activation gamma spectra for multiple trace element determination and of automation of main constituent determination
03 p0262 N73-12125
High temperature density determinations of Li, using gamma radiation attenuation technique
[ORO-3604-7] 03 p0263 N73-12134
Detection and measurement of cosmic ray charge spectrum for nuclei heavier than iron with relation to nucleosynthesis and mechanics of supernova
[NASA-TM-X-58102] 03 p0352 N73-12872
Mathematical model for calculating scanning angle distribution of planetary albedo gamma rays above 100 MeV
[NASA-TM-X-66117] 03 p0353 N73-12874
Positive diffuse cosmic gamma ray flux measurements for energies to 100 MeV range
[NASA-TM-X-66109] 03 p0353 N73-12877
High amplitude gamma current pulse degradation of semiconductor devices
[SC-RR-72-0515] 04 p0399 N73-13245
Production of gamma rays from decay of neutral pions produced by interstellar cosmic ray interactions
[NASA-TM-X-66120] 04 p0467 N73-13803
Gamma, X ray, ultraviolet, and infrared astronomy noting instrumentation and radiative transfer
[ESRO-SP-75] 04 p0476 N73-13889
Effects of passivation processes on radiation tolerance of bipolar transistors subjected to neutron or gamma radiation
[SC-DC-72-1232] 05 p0565 N73-14589
Nondestructive neutron activation and spectrum analysis using gamma ray spectrometer coupled to PDP 9 computer
[IRI-133-71-03] 05 p0582 N73-14739
Zero-g gaging system based on absorption of gamma radiation
[AD-749967] 06 p0675 N73-15489
Extended applications and improvement of 4 pi beta-gamma coincidence method in standardization of radionuclides
[RR-730] 06 p0702 N73-15724
Formation of relativistic particles into clouds in quasar and Seifert nuclei, and centimeter, submillimeter, and gamma radiation emissions
[NP-30] 06 p0717 N73-15854
Morphological changes in testes and spermatogenesis process of dogs subjected to chronic and combined gamma irradiation
07 p0743 N73-16048
Evaluation of aerial survey on terrestrial gamma radiation environment
[EGG-1183-1559] 07 p0793 N73-16447
Aerial snow gaging, using transmitted terrain gamma radiation
[EGG-1183-1557] 07 p0800 N73-16500
Efficiencies of germanium semiconductor detectors calculated by Monte Carlo method for 100 keV to 2 MeV gamma rays
[CEA-R-4316] 07 p0832 N73-16745
Theory of gamma ray line emission from solar flares
[NASA-TM-X-66165] 07 p0839 N73-16797
Total gamma ray production rate per hydrogen atom from neutral pion decay in interstellar cosmic ray interactions, and calculation of molecular hydrogen amount
[NASA-TM-X-66167] 07 p0839 N73-16798
Combination nuclear emulsion/spark chamber gamma ray telescope study of galactic center region
[NASA-CR-130863] 09 p1081 N73-18819
Calculation of high energy electron emission from metal target irridiated by gamma flux field
[NASA-TM-X-2756] 10 p1192 N73-19698
Computer code for generating spatial-angular moments of adjoint gamma-ray flux in infinite mediums
[NBS-TN-748] 10 p1193 N73-19702
LINVILL and IBIS programs for calculating gamma radiation damage to biopolar transistors
[CEA-R-4337] 10 p1194 N73-19718
Computer programming for gamma ray spectra analysis applicable to neutron activation analysis
[IRI-133-72-09] 10 p1194 N73-19720
Antiradiation effectiveness of cysteamine in mice under various conditions of gamma radiation
11 p1240 N73-20067
Effectiveness of combined chemical protectors against mixed gamma-neutron radiation with neutron contributions to absorbed dose
11 p1240 N73-20068
Gamma radiation effects on toxic cysteamine elimination in irradiated and nonirradiated mice
11 p1240 N73-20070
Influence of head and stomach shielding on radiation sickness and animal survival from gamma-neutron irradiation
11 p1241 N73-20071
Influence of shielding head and anterior stomach on course of radiation sickness in dogs subjected to total lethal gamma irradiation
11 p1241 N73-20073
Stomach shielding effects on chromosomal aberration frequency in guinea pig and rat marrow cells after gamma radiation at doses of 50 to 200 r
11 p1241 N73-20074
GAST and GALT aminotransferases activity of dog blood serum following total exposure to gamma rays with stomach or head shielded
11 p1241 N73-20075
Characteristics of pathomorphological changes in rat internal organs subjected to gamma-neutron irradiation with head and stomach shielded
11 p1241 N73-20077
Mortality rate in antiradiation drug protected mice subjected to gamma radiation overloads
11 p1242 N73-20079
Effect of transverse overloads and gamma rays at 100 to 200 r on peripheral blood in dogs
11 p1242 N73-20083
Exposure to gamma rays from Co-60 and transverse loads and effectiveness of cysteamine and AET protection
11 p1242 N73-20086
Relative biological effectiveness of fast neutrons with gamma background
11 p1243 N73-20091
Effect of chronic irradiation of dogs by Co60 gamma rays on level of autoantibodies
11 p1244 N73-20100
Morphological changes in liver of dogs subjected to chronic gamma radiation
11 p1244 N73-20101
Proliferative activity of bone marrow in dogs exposed to three-year chronic gamma irradiation
11 p1244 N73-20102
Gamma survey of rocks and soils covered by nonactive radiation absorption layers using aerial reconnaissance and fourier analysis
[AD-755003] 11 p1289 N73-20461
Spectra of prompt gamma rays following nuclear pion absorption
[NASA-CR-131398] 11 p1326 N73-20762
Electrical conductivity of ThO2 at room and high temperatures and in high intensity gamma radiation fields
[BNWL-1671] 12 p1416 N73-21475
Balloon observation of pulsed gamma rays above 250 keV from Crab Nebula pulsar NP 0532
12 p1444 N73-21698
Gamma ray spectrometer experiment during transearth coast period of Apollo 16 flight
12 p1451 N73-21752
NaI[Tl] crystal detector for measuring proton induced activity in gamma ray spectrometer
[NASA-TM-X-66241] 15 p1787 N73-24486
Computation of neutrons and gamma ray distribution for radiation shielding of Europa 3 launch vehicle nuclear upper stage
[TN-3-25] 15 p1811 N73-24680
Balloon measurement of gamma ray emission from region of galactic center
16 p1959 N73-25844
Balloon measurements on atmospheric secondary gamma rays using digitized spark chamber
[NASA-TM-X-66278] 18 p2195 N73-27718
Possible origin of soft gamma ray bursts from stellar superflares
[NASA-TM-X-66294] 18 p2197 N73-27735
Photonuclear activation with Ge L1 detectors
[AD-761992] 19 p2231 N73-27990
Computer code for generating gamma ray moments
[AD-761839] 19 p2323 N73-28689
Conference on annihilation reactions and gamma ray and universal evolution
[NASA-TM-X-66279] 19 p2331 N73-28753
Apollo 15 measurement of cosmic gamma ray spectrum between 0.3 and 27 MeV
19 p2331 N73-28756
Measurement of cosmic gamma ray emission from galactic center, Crab nebula, and diffuse radiation
19 p2331 N73-28757
SAS-2 observation of high energy gamma radiation
19 p2331 N73-28759
Cerenkov light technique for measuring high energy gamma rays in air showers
19 p2332 N73-28760
OSO-7 observations of gamma ray emission in solar flares
19 p2332 N73-28761
Metagalactic orgin of cosmic rays and gamma ray astronomy
19 p2332 N73-28764
Production of gamma rays from explosive nucleosynthesis and low energy cosmic ray scattering
19 p2332 N73-28765
Annihilation reactions and gamma ray spectra for studying large scale cosmologic antimatter
19 p2332 N73-28769
ERS 18 measurements of gamma ray fluxes during solar flare
19 p2334 N73-28784
Gamma ray and neutron emissions during solar flares
19 p2336 N73-28795
Properties of nuclear gamma ray line emissions during solar flares
19 p2336 N73-28796
Analysis of gamma ray pulse-height spectra from lunar surface
[NASA-TM-X-70421] 19 p2340 N73-28824
Directional low energy gamma ray detector for gamma ray astronomy
[NASA-TM-X-70449] 20 p2419 N73-29442
Detection of high energy gamma rays from Crab nebula pulsar by balloon flight with gas Cerenkov telescope
20 p2467 N73-29822
Energy spectra of six cosmic gamma-ray bursts in regions of 0.1 to 1.2 MeV
[NASA-TM-X-70427] 20 p2468 N73-29824
Design of gamma ray spectrometer for measurement of intense radiation using Compton scattering effect
[NASA-CASE-MFS-21441-1] 21 p2544 N73-30392
Detection effeciencies of cylindrical detectors for gamma ray photon angular distributions
[NASA-TM-X-70445] 21 p2548 N73-30424
Measurement of positive and negative pion, and double neutral pion photoproduction cross sections for incident gamma ray energies from 600 to 900 MeV
21 p2582 N73-30691
RALPH - on-line data acquisition and analysis system for processing gamma ray and coincidence data
[NASA-TM-X-69507] 22 p2639 N73-31151
Gamma ray telescope using double Compton process and measuring extraterrestrial gamma ray fluxes in energy range 1-10 MeV
[MPI-PAE/EXTRATERR-74] 22 p2674 N73-31421
X ray and gamma ray semiconductor mercury iodide detectors
[BMFT-FBK-73-09] 22 p2707 N73-31680
Geochemical analyses on lunar gamma ray spectra obtained during Apollo orbits
22 p2735 N73-31895
Continuous low dose gamma irradiation effects on cell population kinetics of mice lymphoid tissue
[NASA-CR-135723] 23 p2749 N73-31999
Flux and energy spectrum of fast neutrons and gamma rays at balloon altitudes
23 p2833 N73-32642
SAS-2 measurements of gamma rays from galactic plane
[NASA-TM-X-70486] 24 p2976 N73-33778
Celestial diffuse gamma radiation above 30 MeV observed by SAS-2
[NASA-TM-X-70485] 24 p2976 N73-33779
Sources, absorption, and detection of cosmic gamma rays
[MPI-PAE/EXTRATERR-83] 24 p2977 N73-33789
GANGLIA
NT NERVES
NT NEURONS
GAPS
NT SPARK GAPS
Magnetic field intensity calculations for gap electrical machinery with symmetric and asymmetric windings
[JPRS-58448] 11 p1324 N73-20744
Accidental initiation of encased high explosive charges through rapid closure of air gap due to accidental drop of device
[AD-758255] 15 p1844 N73-24941
Convective heating tests on joints and gaps between surface insulation tiles
24 p2940 N73-33477

Interference heating in gaps between surface insulation tiles for space shuttle thermal protection system design
24 p2942 N73-33499
GARNETS
NT YTTRIUM-ALUMINUM GARNET
NT YTTRIUM-IRON GARNET
Magnetically uniaxial rare earth garnets grown on substrates, using liquid phase epitaxial dipping technique
[AD-745903] 02 p0220 N73-11781
Production of polycrystalline bismuth-calcium-vanadium garnet phase shifters
[AD-758919] 16 p1881 N73-25224
Magneto-optic effects in ferrate garnet thin film waveguides
[AD-763792] 21 p2518 N73-30199
GARP
U GLOBAL ATMOSPHERIC RESEARCH PROGRAM
GAS ANALYSIS
NT OZONOMETRY
Apparatus for analyzing gas samples in containers including vacuum chamber, mass spectrometer, and gas chromatography
[NASA-CASE-GSC-10903-1] 03 p0300 N73-12444
Analysis of haze aerosols in rural and urban atmospheres
[PB-212609] 07 p0816 N73-16613
Laser-probe mass spectrometric analysis of solar wind, cosmogenic, and radiogenic gases in Apollo 12, 14, and 15 samples
[NASA-CR-130029] 07 p0841 N73-16811
Analysis of gaseous emissions from J-85 engine at various fuel-air ratios, engine speeds, and simulated altitude conditions
[NASA-TM-X-2726] 08 p0969 N73-17921
Gas chromatographic and mass spectrometric determinations of trace elements in human breath samples
[AD-750141] 09 p1000 N73-18159
Design and performance of metabolic gas analyzer using mass spectrometer and digital data printout
[NASA-CR-128842] 10 p1124 N73-19160
Development of techniques for reducing exhaust emissions from turbine engines
[NASA-TM-X-68192] 10 p1208 N73-19824
Development of sampling and analytical procedures for gas turbine engine exhaust using aircraft auxiliary power unit as emission source
[BM-RI-7735] 10 p1223 N73-19947
Application of laser microprobe and magnetic mass spectrometer for determining gas contents in metals by melting and vaporizing microvolumes of samples
[NASA-TT-F-14852] 11 p1305 N73-20592
Design, development, fabrication, and testing of laboratory prototype of residual gas analyzer
[NASA-CR-124177] 12 p1404 N73-21386
Comparative infrared spectroscopic analysis of liquid oxygen
[AD-756629] 14 p1646 N73-23348
Diagnostics of flow fields using Raman scattering technique
[AD-757319] 14 p1652 N73-23400
Mass spectrometric analysis of aromatic hydrocarbons and sulfur compounds
[NLL-TRANS-1193-[9022.9]]
15 p1746 N73-24151
Infrared fluorescent low level carbon monoxide analyzer
[PB-213846/7] 15 p1747 N73-24163
Tunable diode laser for air pollution gas analysis
[PB-214240/5] 16 p1871 N73-25149
Analysis of factors causing nitrogen oxides in exhaust gases of gas turbine engines and development of models of flow in gas turbine combustor
[NASA-CR-132959] 16 p1955 N73-25821
Analysis of chlorate candle generated oxygen
[AD-762276] 19 p2231 N73-27992
Development and characteristics of device for head space analysis used with dual column gas chromatographs
[NLL-M-23025-[5828.4F]] 20 p2417 N73-29415
Matrix isolation technique used to obtain thermodynamic properties of rocket combustion products
[AD-762622] 20 p2486 N73-29966
Theory and operating characteristics of equipment in laser exhaust measurement program
[PB-220429/5] 21 p2556 N73-30493
Feasibility analysis of nonradiating flow in wind tunnels using light scattering experiments
[BMBW-FBW-72-20] 21 p2580 N73-30677
Quadrupole mass spectrometer for direct sampling of atmospheric gases and condensation products
[AD-764238] 22 p2676 N73-31433
Application of gas analysis techniques to determine combustion efficiency in turbine engines and rocket engine combustion chambers
[AGARD-AG-168] 22 p2728 N73-31830
GAS BAGS
Design, development, and manufacture of natural shape free flight balloon to include requirements, documentation, testing, and inspection
[AD-753086] 09 p0987 N73-18055
Decelerator sled simulation for testing air bag restraint system effects in passenger motor vehicle crash
[PB-212706] 11 p1251 N73-20155
GAS BEARINGS
Integral relationships in planar problem of gas lubrication including applications and approximate solutions
[AD-745833] 01 p0063 N73-10515
Methods for increasing stability of rotors with gas bearings
[AD-745858] 01 p0063 N73-10517
Increased load capacities of self-generating gas bearings with circular supply
[AD-745827] 01 p0063 N73-10518
Numerical integration and variational calculation method for approximate solution to three dimensional flow of gas dynamic bearings
[AD-747377] 03 p0308 N73-12513
Procedure for balancing high speed, light weight rotary machinery resting on gas lubricated bearings
[AD-750951] 06 p0623 N73-15055
Dynamic behavior of externally pressurized foil bearings, including film response to step reduction in tension
[AD-751604] 07 p0805 N73-16531
Influence of groove inclination angle on bearing capacity of gas dynamic thrust bearing
[AD-751068] 07 p0806 N73-16535
Performance of gas lubricated thrust bearing based on minimum surface damage and low value of friction coefficient
[AD-753018] 09 p1041 N73-18493
Evaluation of ceramic materials for application as high temperature gas bearing material
[AD-753858] 09 p1042 N73-18499
Condition of drift invariance of two-stage gyroscope with arbitrary gas-lubricated main bearings in active accelerations
10 p1184 N73-19635
Gas bearings and fluid flow tests using finite difference approximation
[AD-754800] 11 p1299 N73-20542
Development of spherical, hydrostatic, compliant bearing for directional gyroscope
11 p1318 N73-20695
Design, development, and evaluation of spherical hydrostatic gas bearing gyroscope for operation in random vibration environment
[AD-755124] 11 p1322 N73-20725
Vibration response of gas bearing rotor-supports to sinusoidal and random vibrations in Brayton rotating unit turbogenerator
[NASA-CR-2177] 13 p1534 N73-22427
Performance of gas lubricated nonconforming pivoted-pad journal bearings and flexibly mounted spiral groove thrust bearing designed for Brayton cycle rotating unit
[NASA-TM-X-2765] 15 p1738 N73-24086
Synchronizing control of drag-cup gyro motor using dynamic gas bearing
[NAL-TR-304] 15 p1756 N73-24232
Design and applications of air bearings
[Y-DA-4834] 15 p1793 N73-24534
Feasibility study of applying air lubricated bearings to gas turbine engines for military aircraft
[AD-757869] 15 p1793 N73-24537
Compliant bearing designs for directional control gyroscope
[AD-762036] 19 p2305 N73-28538
GAS CHROMATOGRAPHY
Extraction and analysis by gas-liquid chromatography of catecholamine metabolites from biological tissue
[AD-745944] 03 p0260 N73-12105
Apparatus for analyzing gas samples in containers including vacuum chamber, mass spectrometer, and gas chromatography
[NASA-CASE-GSC-10903-1] 03 p0300 N73-12444
Gas chromatographic-mass spectrometric analysis of volatile organic metabolic products in terrestrial soils
[NASA-CR-129602] 04 p0386 N73-13134
Gas chromatographic method for quantitative analysis on hydrazine and its breakdown products at catalytic activity levels
[NASA-TT-F-14722] 04 p0386 N73-13137
Analytical procedure using gas-liquid chromatography in routine analysis of exhaust hydrocarbons from retention time data
[BM-RI-7700] 05 p0506 N73-14118
Development and characteristics of coulometric detector for conducting chromatographic analyses
[NLL-TRANS-857-[9022.64]]
05 p0545 N73-14425
Research on gas chromatography with computer techniques and mass spectrometer methods
[FOA-1-C-1412-34] 06 p0672 N73-15471
Gas chromatographic analysis of beryllium in aqueous solutions and biological tissues
[AD-753112] 09 p0996 N73-18131
Gas chromatography-mass spectrometry for analyzing fatty acid and sterol concentrations in plant tissue samples
[NASA-CR-128740] 10 p1120 N73-19131
Measurement of line spectra produced by high resolution mass spectrometer and application to identifying organic compounds in samples from Apollo 11 and 12 flights
[NASA-CR-128840] 10 p1160 N73-19436
System designs for automating GC/MS analyzing system
[NLL-RTS-7572] 11 p1259 N73-20218
Pyrolysis gas chromatography method for rapid identification of organic polymers
[AD-755375] 12 p1377 N73-21168
Spectroscopic and chromatographic analysis of outgassing contaminants in potting compound and paint
[NASA-CR-124227] 13 p1488 N73-22061
Pyrolysis-molecular weight chromatography of polymers
[AD-758711] 16 p1872 N73-25154
Mass spectrometer, chromatograph, and X ray analyses for determining volatilization mechanism for V2O5
[NLL-M-21570-[5828.4F]] 16 p1926 N73-25582
Cost analysis of mass spectrometers and gas chromatographs for life support atmosphere monitoring
[NASA-CR-124306] 18 p2112 N73-27076
Gas chromatographic analysis on water interfacial energy
[AD-761655] 19 p2230 N73-27988
Development and characteristics of device for head space analysis used with dual column gas chromatographs
[NLL-M-23025-[5828.4F]] 20 p2417 N73-29415
Capability of portable SF6 chromatograph to detect and determine behavior of plume out to 100 km
[BNL-17478] 22 p2674 N73-31417
GAS COMPOSITION
NT CARBON DIOXIDE CONCENTRATION
Dual channel infrared spectroradiometric analyses of rocket engine exhaust spectra
[NASA-CR-124207] 12 p1404 N73-21387
Thermodynamic and electrical properties of gaseous fuels for magnetohydrodynamic gas generator
[JUL-874-TP-VOL-9] 15 p1818 N73-24735
Development of linear system of equations for computing errors of volume fractions or partial pressures at calculated equilibrium compositions
[NRC-TT-1665] 17 p2096 N73-26960
Development of numerical method for computing transmission functions of atmospheric gases based on exact frequency integration using structure of absorption spectrum
20 p2401 N73-29296
GAS COOLED REACTORS
NT HIGH TEMPERATURE NUCLEAR REACTORS
Pulsed ionization chamber for plasma diagnostics, and applications to MHD electrical power generation from gas cooled reactors
[AD-747681] 03 p0343 N73-12800
Convective heat transfer and heat exchange during phase transformation in chemically reacting systems
[AD-756095] 13 p1488 N73-22066
GAS COOLING
Cooling systems using cold gas transfer closed loops in 15 to 80 K temperature range
[DLR-MITT-71-09] 04 p0485 N73-13964
Condensation of gas phase of fast flowing droplet gas mixture of potassium and application to operating magnetohydrodynamic generators
[NASA-TT-F-14609] 07 p0770 N73-16254
Ozone and nonreactive gas calibration of mass spectrometer with modified helium-cooled ion sources
[BMBW-FBW-72-32] 09 p1034 N73-18440
GAS DENSITY
Problems of precise physical measurements of gas density
[EUR-4797-D] 01 p0055 N73-10448
Density and flow visualization of different molecular weight gases from concentric orifices as determined by beam fluorescence technique
[ISAS-486-VOL-37-12] 02 p0155 N73-11256
Microwave attenuation and neutral gas density profile measurements behind shock waves in air
[AD-745969] 02 p0158 N73-11282
Tables of pressure, volume, density, and temperature for liquid states of oxygen, nitrogen, argon, and parahydrogen
[NBS-TN-361-REV] 04 p0386 N73-13139
Deep diving pulmonary functions of man using different breathing gas densities
[AD-749028] 05 p0501 N73-14082
Density of liquid Freon 11 at 200 C and 8.18 to 195.46 atm pressure
[AD-752863] 09 p1000 N73-18160
Electron beam probing technique for measuring hypersonic rarefied gas density, vibration, and rotational temperature
[ONERA-P-146] 15 p1788 N73-24497
Measurement of hydrogen concentration in mass diffusing jets by laser induced Raman scattering
17 p2012 N73-26272
Electron gas behavior and density in constant electric and magnetic fields
[AD-760587] 18 p2182 N73-27617
Absolute pressure measuring device for measuring gas density level in high vacuum range
[NASA-CASE-LAR-10000] 21 p2544 N73-30394

Feasibility analysis of nonradiating flow in wind tunnels using light scattering experiments
[BMBW-FBW-72-20] 21 p2580 N73-30677
Vibrational temperature and density of molecular oxygen component in expansion tube
[NASA-TN-D-7273] 22 p2653 N73-31249
GAS DETECTORS
Detection and measurement of carbon monoxide in atmosphere
[PB-211265] 05 p0575 N73-14677
Remote chemical detectors for vehicle identification by exhaust gases
[AD-751740] 07 p0753 N73-16116
Rocket and satellite instrument for simulatenous measurements of total mass density and number density of atomic oxygen in lower thermosphere
[AD-751468] 07 p0795 N73-16464
Solid state amplifier for bridge circuit of atomic absorption mercury detector
[PB-212658] 07 p0801 N73-16506
Research in development of detectors for analysis of planetary atmospheres
[NASA-CR-130700] 08 p0959 N73-17841
Application of laser microprobe and magnetic mass spectrometer for determining gas contents in metals by melting and vaporizing microvolumes of samples
[NASA-TT-F-14852] 11 p1305 N73-20592
Piezoelectric quartz crystals used as digital transducers in completely digital detection systems for monitoring gas streams
12 p1382 N73-21208
Feasibility of on-line fission gas leak detection system for 100 kW zirconium hydride reactor
[NASA-TM-X-2870] 20 p2453 N73-29717
Detection techniques for tenuous planetary atmospheres
[NASA-CR-133430] 20 p2473 N73-29869
Toxic vapor detector for Minuteman propellant leakage
[AD-763799] 21 p2551 N73-30451
Increased optical efficiency of flame photometric detector for detection of SO2 in air
[PB-220480/8] 21 p2551 N73-30453
Gas sensor for detecting H2 in air and N2, and O2 in N2
[NASA-CR-133891] 22 p2674 N73-31416
GAS DISCHARGE COUNTERS
U COUNTERS
U GAS DISCHARGE TUBES
GAS DISCHARGE TUBES
NT THYRATRONS
Design of transistorized oscillator for exciting gas discharge tubes
[AD-749831] 05 p0559 N73-14544
Ion pulse compensation circuits for recording ions produced by laser radiation in afterglow discharge plasma
[AEC-TR-7324] 08 p0949 N73-17767
Analysis of low density plasma shock waves in expanding discharge
12 p1432 N73-21602
Barometric gravity tube discharger for liquid cooling of rocket exhaust gas and analysis of improvement with air vent
[DLR-MITT-73-10] 17 p2011 N73-26262
Thin plastic flexible gas discharge tubes for automatic particle track chamber
[NOTA-INTERNA-416] 17 p2033 N73-26455
Spectrochemical analysis of nonconducting materials using cathodes from sample in Grim glow discharge tube
[NASA-TT-F-15031] 20 p2454 N73-29723
GAS DISCHARGES
NT TOROIDAL DISCHARGE
Ion acoustic instability in helium positive column
[AD-745399] 01 p0086 N73-10709
Ion flux probe for low pressure discharge plasma in thin metal plate
[TRITA-EPP-72-20] 02 p0174 N73-11410
High pressure nitrogen gas discharge initiated by fast electron beams of 100 to 300 keV energies
[DRIC-TRANS-2857] 02 p0212 N73-11716
Effect of variable magnetic field on emission of helium-neon laser and resulting parameters of discharge plasma
[AD-747443] 03 p0311 N73-12542
One dimensional radial fluid cone for studying Z-pinch enbedded in hydrogen
[AD-748179] 04 p0455 N73-13718
Mode coupled nonlinear dispersion of irregular ionization waves in glow discharges
[AD-748468] 04 p0456 N73-13721
Dispersion characteristics of plasma instabilities in carbon monoxide plasma
[AD-748470] 04 p0456 N73-13723
Effect of surrounding gas on MHD instabilities in Z pinch
[AD-748985] 04 p0457 N73-13728
Charged particle concentrations and plasma temperatures of liquid or film electrode discharges in mercury vapor
[AD-750559] 06 p0706 N73-15759
Low frequency instabilities in hollow cathode magnetoplasma discharge
[AD-750477] 06 p0707 N73-15765
Variational analysis of laser induced gas breakdown employing simplified diffusion models for plasma generation
[AD-750874] 06 p0707 N73-15767
Optical and energy measurements of strong current discharges in air
[AD-751414] 07 p0830 N73-16729
Production of laser output by excitation of hydrogen chloride vibrational levels using electron impact
[AD-752631] 08 p0930 N73-17615
Volt-ampere characteristics of pulse discharge flow in hollow hydrogen cathode
[AD-753038] 09 p1072 N73-18749
Analysis of factors affecting quality of electrostatic printing processes and procedures to improve product
[AD-755259] 12 p1409 N73-21420
Random walk theory for studying electron avalanche formation in helium electric fields
[NASA-TN-D-7224] 12 p1433 N73-21612
Atomic oxygen hydrogen reaction with acetylene, and gas discharge shock tube design
13 p1488 N73-22060
Stability of molecular gas discharges typical of those used in high power lasers
[AD-757083] 13 p1537 N73-22456
Design, development, and characteristics of atmospheric pressure, double discharge carbon dioxide laser
[AD-756517] 13 p1539 N73-22467
Analysis of laser outputs required to initiate gas breakdown when gas contains suspended particles
[AD-757517] 14 p1674 N73-23585
Time varying ac arcs or positive columns in discharges in gas mixtures
[AD-758232] 15 p1818 N73-24738
Electrophoresis in plasmas, with dc gas discharges
[AD-757886] 15 p1818 N73-24739
Plasma ion sources research, including mass spectra, gas discharges, and ion beams
[AD-758040] 15 p1819 N73-24742
Microwave excitation of electroacoustic resonances in afterglow plasmas
[AD-759789] 17 p2070 N73-26746
Effect of atmospheric contaminants on laser induced air breakdown
[AD-760175] 17 p2070 N73-26750
Fluorescent lamp discharge parameter effects on mercury resonance lines
[AD-760958] 18 p2183 N73-27627
Alloying epitaxial layers of silicon with boron and arsenic using gas discharge
18 p2187 N73-27660
Determination of rotational temperatures in flow gas discharges containing nitrogen using sidelight spectroscopy techniques
[AD-762290] 19 p2233 N73-28002
Heating and volume recombination effects on gas discharge column equilibrium
[AD-761492] 19 p2325 N73-28704
Analysis of linear and nonlinear stage of ion-acoustic instability in low pressure discharge in helium
[AD-763590] 21 p2584 N73-30707
Electron transport in gas discharge lasers
[LA-5154-MS] 22 p2681 N73-31474
Electron beam emitting device using secondary emission from cathode in low pressure gas discharge
[AD-764952] 23 p2767 N73-32138
GAS DISSOCIATION
Dissociative character of carbon dioxide adsorption on nickel film surfaces
[NLL-TRANS-746-1341-[9022.401]]
06 p0682 N73-15549
Attenuation of nitric oxide dissociation in mesosphere and stratosphere
[PSU-IRL-SCI-407] 08 p0917 N73-17518
Dissociation of nitric oxide in mesosphere and stratosphere by attenuation
[AERONOMICA-ACTA-A-112] 09 p1027 N73-18384
Mathematical models for determining transport properties and dissociation equilibrium of N2 and O2 in high temperature air
[ESDU-00.01.07-AMEND-A] 14 p1718 N73-23937
Exact equations for five-component gas mixture transport coefficients as dissociated air model gas
[DLR-FB-72-34] 21 p2580 N73-30678
Mass flow rate of laminar dissociated equilibrium boundary layer
24 p2907 N73-33200
GAS DYNAMICS
NT AERODYNAMICS
NT AEROTHERMODYNAMICS
NT RAREFIED GAS DYNAMICS
NT ROTOR AERODYNAMICS
Abstracts of papers presented at conference on rarefied gas dynamics
[AD-745974] 02 p0159 N73-11289
Research and development in surface studies, plasma physics, and gas dynamics
[AD-747132] 03 p0368 N73-12996
Mapping electron number density distribution in nonequilibrium shock layer with kinetic and radiative processes coupled to gas dynamics
[AD-748833] 04 p0407 N73-13312
CCAMIN, computer program for fitting time of arrival and shock peak overpressure versus slant range in gas
[AD-749332] 04 p0409 N73-13330
Research projects in flow mechanics and gas dynamics
05 p0526 N73-14278
Calculation of relaxation kinetics for carbon dioxide-water-nitrogen mixture to determine gas dynamics of escape from slit nozzle
[JPRS-57906] 06 p0654 N73-15310
Combustion stability and gas dynamic research
[AD-750466] 06 p0731 N73-15964
Proofs for binary collision term in Boltzmann transport equations in kinetic theory of gas and plasma dynamics
[TRITA-EPP-72-25] 07 p0772 N73-16273
High frequency wave field pressure effect on Langmuir monochromatic plasma oscillations
[AEC-TR-7337] 07 p0827 N73-16707
Self-simulation problems of machines using gas dynamic processes
[NASA-TT-F-14832] 09 p1036 N73-18454
Gas dynamic equation for investigating thermal heating modes during laser radiation flux interaction with material
09 p1043 N73-18509
Development of algorithm for testing gas dynamic design of axial flow compressors with multiple stages
[AD-753519] 09 p1080 N73-18809
Application of gas dynamics equations to determine magnitude of pressure rise due to sonic boom in stratified atmosphere
[NASA-TN-D-7105] 11 p1233 N73-20010
Design, assembly, and operation of gaseous hydrogen system with solutions to specific problems
[SC-DR-72-0593] 12 p1388 N73-21257
Development of numerical procedure for solving gas dynamics of pulsating, compressible flow in propulsive duct
12 p1389 N73-21266
Calculation of two dimensional gas dynamic flows with detonation using Lagrange variables
[JPRS-58699] 12 p1391 N73-21281
Determination and identification of gases in powdered carbonyl nickel
[NLL-LTI-746-1353-[9022.401]]
12 p1412 N73-21439
Examples of spatially homogeneous gas motions and calculations using model kinetic equation
12 p1417 N73-21485
Galactic neutral hydrogen gas velocity distribution within spiral arms in local regions
12 p1447 N73-21720
Spacecraft pressure gage reliability studies relative to gas dynamics and metal surface testing
[NASA-CR-112320] 13 p1529 N73-22392
Atmospheric physics and gas dynamics research in Soviet Union
[JPRS-58988] 14 p1649 N73-23377
Nonlinear interaction of fast magnetogasdynamic shock with tangential discontinuity
[NASA-TM-X-69178] 14 p1695 N73-23754
Molecular contamination performance determination for space chamber tests, including molecular flow conditions and parameters
[NASA-TN-D-7250] 15 p1760 N73-24264
Effect of undissolved air on compressibility of transmitting medium in hydraulic circuits
[NLL-NEL-TT-2426-[6075.461]]
15 p1763 N73-24289
Thermodynamic and electrical properties of gaseous fuels for magnetohydrodynamic gas generator
[JUL-874-TP-VOL-9] 15 p1818 N73-24735
Measurements of density, temperature, and velocity in gas dynamics using light scattering techniques
[AD-759575] 16 p1890 N73-25299
Studies in gas dynamics and heat transfer
[AD-759240] 16 p1891 N73-25304
Field tests of electrogasdynamic fog dispersal concept in Panama Canal Zone
[FAA-RD-73-33-PT-1-PT-2] 17 p2010 N73-26254
Gas dynamic analysis in near field of supersonic nozzle banks for chemical lasers
[AD-760132] 17 p2041 N73-26513
Atomic and gas dynamical processes in astrophysical plasmas
17 p2066 N73-26719
Application of gas flow dynamics to theory of jet engines and other gas devices
[AD-762307] 19 p2257 N73-28196
Gas dynamics of plane shock wave propagation in steady state moving medium
20 p2472 N73-29860
Gas dynamics of cavities-in-series gas dynamic lasers
[AD-763255] 21 p2555 N73-30483
Boundary conditions and uniqueness in internal gas dynamic flows
23 p2775 N73-32192
Aerosol growth kinetics in flow reactor
24 p2901 N73-33159
Application of kinetic theory approach to problems in gas dynamics
24 p2903 N73-33171

GAS EVACUATING
U EVACUATING [VACUUM]
GAS EVOLUTION
Effect of charge materials, melting condition, and type of melting equipment on hydrogen gas contained in copper alloys
[AD-745845] 01 p0068 N73-10558
Development of numerical model of eddy diffusive transport of emitted gases from space shuttle wake to show chemical reactions between emitted gases and ambient atmosphere
[NASA-TM-X-66215] 11 p1287 N73-20440
GAS EXCHANGE
Mathematical model for photosynthetic gas exchanges in growing wheat and radish biopaks of life support systems
03 p0257 N73-12081
Metabolic changes and cardiac output of humans in hypokinetic bed rest study
13 p1482 N73-22013
Oxygen exchange between solid electrolyte and platinum electrode in flowing gas
22 p2617 N73-30972
Method for automatically processing indices of operator gas exchange during work in trainer using computers
24 p2884 N73-33035
GAS EXPANSION
Supersonic characteristics of sonic nozzle gas flow expansion
[AD-749764] 05 p0528 N73-14297
Fundamental problem of complete expansion into evacuated tube
[AD-751983] 08 p0897 N73-17265
Optimal performance of infrared pneumatic transducer with capacitive membrane
[ONERA-TP-1150] 09 p1007 N73-18222
Numerical analysis of nonequilibrium nozzle expansions from reservoir at high specific enthalpy
[LOG-J7197] 14 p1649 N73-23375
Analysis of gas jets expanding out of axisymmetrical nozzles into vacuum or still air at finite pressure
[ARC-R/M-3235] 16 p1856 N73-25036
Gas dynamic equations for analyzing hot gas and vapor expansion in meteor trail
17 p2023 N73-26366
Mass spectra of cluster ion reaction kinetics in free jet expansions of gas mixtures
[AD-761811] 19 p2233 N73-28004
Transition model for computing population density profiles of partially ionized argon in source flow expansion
[C-37] 22 p2652 N73-31242
Vibrational temperature and density of molecular oxygen component in expansion tube
[NASA-TN-D-7273] 22 p2653 N73-31249
Combustion and expansion of propane-air mixtures near bottom of short cylinder to generate air vortex rings for removing air from cylinder
[AD-764613] 23 p2777 N73-32207
Pilot model expansion tunnel test flow properties obtained from velocity, pressure, and probe measurements
[NASA-TN-D-7310] 24 p2905 N73-33182
GAS EXPLOSIONS
Safety devices for preventing surge tank explosions in liquid nitrogen system of hypersonic wind tunnels
[SC-DC-72-1260] 03 p0280 N73-12274
Lateral gas expansion behind explosive detonating slab
[ISL-19/71] 09 p1016 N73-18291
Dynamic behavior of flames in explosive acetylene oxygen mixture
[NASA-CR-130963] 09 p1099 N73-18973
Investigation of backfires and explosions occuring in vacuum pumps of oxygen test stands
[AD-763370] 21 p2554 N73-30474
Combustion and expansion of propane-air mixtures near bottom of short cylinder to generate air vortex rings for removing air from cylinder
[AD-764613] 23 p2777 N73-32207
Photographic recording of dynamic behavior of flames in explosive gases caused by ignition of equimolar acetylene-oxygen mixture
[NASA-CR-135672] 23 p2856 N73-32825
Characteristics of detonable gas mixtures and analysis of cylindrically expanding flames initiated by exploding wire source
24 p2990 N73-33897
GAS FLOW
NT AIR CURRENTS
NT AIR FLOW
NT CONTINUUM FLOW
NT EQUILIBRIUM FLOW
NT FREE MOLECULAR FLOW
NT JET STREAMS [METEOROLOGY]
NT MERIDIONAL FLOW
NT MOLECULAR FLOW
NT NONEQUILIBRIUM FLOW
NT SLIP FLOW
NT TRANSITION FLOW
NT VERTICAL AIR CURRENTS
Shallow flowing water channel for hydraulic analogy of gas flow in transonic to hypersonic range
[ICT-4/71] 01 p0036 N73-10286
Thin film window for gas flow radioisotope proportional counter
[AD-745579] 01 p0058 N73-10477
Application of flow field models, combustion, mixing, and nonequilibrium chemistry data to development of chemical lasers
[AD-745419] 01 p0066 N73-10536
Shallow flowing water channel for hydraulic analogy of gas flow in transonic to hypersonic range
[GRI/NTP/100] 02 p0146 N73-11186
Equipment and procedures for measuring flow of liquids and gases to identify application of specific types of equipment
[NLL-TRANS-45-[3958.4]] 02 p0154 N73-11249
Physical structure of turbulent shear flows in nonreacting gase flow
[AGARD-AR-46] 02 p0156 N73-11262
Effect of skimmer interation on properties of partially condensed molecular beams
[AD-746292] 02 p0157 N73-11269
Nomographic procedure to calculate gas flow parameters at subsonic, sonic, and supersonic velocities
[AD-745898] 02 p0157 N73-11275
Finite element procedure for predicting unsteady compressible gas flow in one spatial dimension
[AD-746234] 02 p0157 N73-11276
Analysis of relaxation of laminar boundary layer to test gas boundary layer over flat plate in expansion tube
[NASA-TR-R-397] 03 p0283 N73-12296
Measurement of heat transfer in gas flow behind shock wave
[AD-747604] 03 p0286 N73-12320
Application of continuous wave gas laser and pulsed ruby laser to analyze laminar and turbulent films of air at porous wall with carbon dioxide and helium injected into air stream
[AD-747511] 03 p0287 N73-12323
Calculation of coefficient of resistance of sphere at supersonic velocities and measurement of critical point on free flying bodies
[AD-747513] 03 p0287 N73-12324
Analysis of flow around conical body at small angles of attack in uniform supersonic flow of ideal gas
[AD-747408] 03 p0287 N73-12326
Asymptotic solution of two-dimensional flow of perfect gas past blunt body at given Mach number
[AD-747545] 03 p0287 N73-12327
Development of instrument for determining total pressure in calibration chamber and numerical analysis of operating principles
[NASA-TN-D-7058] 03 p0301 N73-12452
Ablation of graphite surfaces heated in turbulent flow of air or carbon dioxide and development of method for calculating ablation rate
[AD-747727] 03 p0365 N73-12973
Analysis of motion of chemically active gases to determine heat and mass transfer in turbulent jet system during diffusion combustion
[AD-747571] 03 p0365 N73-12976
Wind tunnel tests to determine effects of gas stream flow parallel to discharging surface on flow characteristics of wire-form porous material
[NASA-TM-X-2687] 04 p0369 N73-13000
Measurement of gas velocities in filters
[AD-747829] 04 p0407 N73-13315
Simulation of flow of compressible gas through water channel of varying cross section
[AD-749134] 04 p0408 N73-13327
Gas flow control device, including housing and input port
[NASA-CASE-NPO-11479] 04 p0425 N73-13462
Influence of dead volumes on working processes of theoretical gas refrigerator
04 p0484 N73-13954
Analysis of pressure loss through single bends of various geometries under conditions of full incompressible flow
[ESDU-67040-AMEND-A] 05 p0525 N73-14272
Analysis of nonequilibrium in excited levels of electric ARC heated potassium vapor injected into argon/helium gas flow passing through supersonic nozzle
[AD-750943] 05 p0585 N73-14759
Measurement of fluctuations in free surface flow of gas and liquids
06 p0653 N73-15303
Computer program for determining influx towards center of spherical metal shell following detonation of spherical, symmetrically placed explosive
[FOA-2-C-2471-25] 06 p0653 N73-15305
Calculation of relaxation kinetics for carbon dioxide-water-nitrogen mixture to determine gas dynamics of escape from slit nozzle
[JPRS-57906] 06 p0654 N73-15310
Output and power characteristics of CS2/O2 chemical laser with flow transverse to optical axis
[DREV-R-684/72] 06 p0679 N73-15527
Numerical analysis of oscillating wedge in supersonic perfect gas flow to evaluate trends for wedge and to analyze unsteady flows
07 p0767 N73-16235
Finite difference solutions for laminar and turbulent boundary layer equations of perfect gases and gas mixtures in chemical equilibrium
07 p0767 N73-16236
Constant flow velocity generator for calibrating hot-wire anemometers
[NASA-CASE-MFS-21424-1] 07 p0769 N73-16248
Condensation of gas phase of fast flowing droplet gas mixture of potassium and application to operating magnetohydrodynamic generators
[NASA-TT-F-14609] 07 p0770 N73-16254
Heat and mass transfer analysis of liquids and air flowing in opposite directions under various atmospheric pressures
[AD-751503] 07 p0856 N73-16938
Infrared detection of hydrogen fluoride tracer for studying turbulent mixing in inert and combustion flows
08 p0880 N73-17128
Mathematical models for gas surface interactions and calculating aerodynamic coefficients for simple geometric shapes and high Mach number flow past thin airfoils
[AD-752245] 08 p0899 N73-17278
Finite difference method for calculating three dimensional, unsteady and steady, inviscid gas flows around blunt bodies
[NASA-TT-F-714] 09 p0980 N73-18009
Numerical analysis of flow of rarefied monatomic gas through two dimensional slot to show characteristics of transition regime
[NASA-CR-124069] 09 p1012 N73-18265
Application of splitting method for numerical analysis of heat conducting gas flows in curvilinear coordinates
[NASA-TT-F-14658] 09 p1015 N73-18288
Analysis of oxygen flow in steel pipelines to determine maximum permissible flow and effects of solid particles and restriction on safe flow rate to avoid ignition
[NASA-TT-F-14831] 09 p1016 N73-18290
Nonlinear differential equations in partial derivatives for nonsteady motion of liquids and gases in pipelines
[AD-752685] 09 p1017 N73-18296
Solution of Chaplygin equation by straight line method to describe gas flow around profile at high subsonic speed with local supersonic curved shock wave
[AD-753557] 09 p1019 N73-18318
Continuous reading fluidic device for measuring component flow of binary gas mixtures
[NASA-TM-X-2741] 09 p1035 N73-18445
Volt-ampere characteristics of pulse discharge flow in hollow hydrogen cathode
[AD-753038] 09 p1072 N73-18749
Gas flow in multilayer insulation systems applied to broadside pumping
[NASA-CR-124130] 10 p1139 N73-19281
Finite difference algorithm for solving quasi-linear gas dynamic systems
[AD-753097] 10 p1143 N73-19309
Acoustic properties and sound pressure of jet flow
[AD-754422] 10 p1144 N73-19321
Experimental determination of combined forced and free convection in annular region of horizontal coaxial cylinders
[AD-754017] 10 p1144 N73-19322
Effect of cooling air discharged into air-gas flow of turbine engine to improve effeciency of gas turbine engine operation
[AD-753969] 10 p1210 N73-19840
Development of tables of gasdynamic functions in three dimensional, axisymmetric, and plane gas flows past blunt bodies of revolution
[NASA-TT-F-715] 11 p1231 N73-19996
Analysis of oscillating gas flow in open-ended pipe caused by piston operating at or near resonant frequency
[AD-754647] 11 p1272 N73-20321
Development and characteristics of supersonic nozzles with perforated edges for wind tunnel applications
[AD-754601] 11 p1272 N73-20323
Analysis of interaction of rarefied gas with surface of porous moist bodies during heat and mass transfer using visual and photographic methods
[AD-754633] 11 p1272 N73-20325
Near axial zone of flow reversal of rotating supersonic unexpanded jet and helical gas flow
[AD-754617] 11 p1272 N73-20327
Heat transfer and frictional resistance in pipes with cooled walls during turbulent flow of high temperature gases
[NLL-RTS-7640] 11 p1347 N73-20930
Linear stabilization of flat diffusion gas flame
[AD-754049] 11 p1350 N73-20952
Development of precursor waves in helium and analysis of wave speed, electron temperatures, and densities using nuclear data handling techniques
12 p1387 N73-21249
Design, assembly, and operation of gaseous hydrogen system with solutions to specific problems
[SC-DR-72-0593] 12 p1388 N73-21257

Development of numerical procedure for solving gas dynamics of pulsating, compressible flow in propulsive duct
12 p1389 N73-21266
Finite difference solution of flow and energy losses of pure gases in separation nozzle geometry
[KFK-1630] 12 p1392 N73-21285
Vibratory stability of plate over viscous heat conducting gas layer
[AD-755288] 12 p1393 N73-21293
Load factors for pressure balancing of gas film seals under various flow conditions
[NASA-TM-X-68227] 12 p1408 N73-21412
Theory of two phase gas-liquid and liquid-gas flow for bladed machines and ejectors
[AD-755713] 12 p1409 N73-21419
Effects of acceleration or retardation on electric strength of gas
[AD-755848] 12 p1429 N73-21584
Calculation of gas flow in bypass compressor
[AD-756092] 13 p1535 N73-22441
Design, development, and characteristics of atmospheric pressure, double discharge carbon dioxide laser
[AD-756517] 13 p1539 N73-22467
Numerical analysis of one dimensional isentropic flow of thermally perfect, calorically imperfect diatomic gas
[ESDU-S.00.01.10-AMEND-A]
14 p1648 N73-23364
Diagnostics of flow fields using Raman scattering technique
[AD-757319] 14 p1652 N73-23400
Energy equations to analyze radiative heat transfer from gaseous suspension flow with internal heating
14 p1718 N73-23939
Kinetics of afterburning process following injection of oxidizer into high temperature gas flow
[AD-756098] 14 p1719 N73-23951
Analysis of kinetic and transport factors governing interfacial mass transfer rates in high temperature systems
[AD-758256] 14 p1720 N73-23959
Analysis of heat transfer properties of air, helium, and carbon dioxide and effects of variations of fluid properties with temperature
[ARC-R/M-3246] 15 p1729 N73-24021
Analysis of spoiler plate characteristics to eliminate effects of installation disturbance when conducting flow rate measurements
[NLL-NEL-TT-2439-(6075.461)]
15 p1763 N73-24288
Development of mathematical models for turbulent flow and application to prediction of internal flows
[TM/TN/A/18] 15 p1768 N73-24321
Analysis of temperature and pressure parameters associated with recirculated engine exhaust from V/STOL aircraft engines exhausting normal to ground
[NASA-TT-F-14912] 15 p1768 N73-24323
Nonlinear stability of liquid adjacent to supersonic stream
[AD-758103] 15 p1769 N73-24328
Analysis of deflection forces and deflection angles generated by thrust vector control nozzle at various Mach numbers and exit pressures
[AD-758521] 15 p1827 N73-24808
Performance tests of gas turbine engine with highly loaded stages operating at high pressure ratio
[ARC-R/M-3242] 16 p1854 N73-25021
Performance tests of gas turbines with high pressure ratios per stage to determine flow characteristics of supersonic nozzles for turbines
[ARC-R/M-3273] 16 p1856 N73-25037
Numerical analysis of maximum thrust nozzles for nonequilibrium, chemically reacting gas flows based on equations for general, multi-component reacting gas
16 p1886 N73-25269
Numerical analysis of turbulence transport equation for two dimensional jet flow and pressure-velocity derivative correlations
16 p1887 N73-25270
Thermohydrodynamic stability in channel flow heat and mass transfer considering variable cross section area
[AD-758748] 16 p1889 N73-25289
Measurements of density, temperature, and velocity in gas dynamics using light scattering techniques
[AD-759575] 16 p1890 N73-25299
Transport phenomena in rarefied gas flows
[AD-759165] 16 p1891 N73-25300
Wave compression and expansion effects on laminar gas boundary flow
[AD-759768] 16 p1893 N73-25320
Numerical analysis of axisymmetrical, viscous, compressible flow around blunt bodies for ideal gases with laminar unseparated boundary layers
17 p2012 N73-26273
Analysis of heat transfer in laminar flow of gas through constant diameter cylindrical tubes at low wall to bulk temperature ratios
17 p2013 N73-26275
Probabilistic model of nonisothermal gaseous flow through fine pored homogeneous media
17 p2013 N73-26276
Numerical analysis of facilitated transport of gas through liquid membranes to show dependence on three parameters
[PUB-73-2] 17 p2014 N73-26287
Application of holography techniques for recording three dimensional flow distribution of liquid jet injected into Mach 3 gas stream
17 p2039 N73-26498
Transient thermocouple measurement of gas flow direction velocity, and temperature near injector of liquid propellant rocket
18 p2129 N73-27201
Analysis of arbitrarily nonuniform, nonadiabatic, two dimensional or axisymmetric basic flows based on inviscid theory of three dimensional perturbations in uniform transonic flow
[AD-761632] 19 p2256 N73-28188
Application of gas flow dynamics to theory of jet engines and other gas devices
[AD-762307] 19 p2257 N73-28196
Base pressure of bodies of revolution in supersonic gas flow
[AD-762243] 19 p2258 N73-28198
Interferometric studies in shock tunnel simulating nozzle flow in gasdynamic lasers
[AD-761601] 19 p2308 N73-28567
One dimensional stationary analysis of air cooled, ducted gas turbines nozzle vanes
[AD-761451] 19 p2330 N73-28744
Development of performance equations for cryptosteady-flow energy separator over widest range of operating conditions for turbojet engines
[AD-762030] 19 p2330 N73-28747
Analysis of operation of single stage, high pressure centrifugal compressor during closed loop flow of various gases
[AD-761608] 19 p2331 N73-28750
Design and development of cryptosteady energy separator for use with turbojet engines on supersonic aircraft
[AD-762032] 19 p2331 N73-28752
Analysis of low speed deflagration of initially unmixed reactants under irreversible, two-step chain reaction
[AD-762459] 19 p2353 N73-28930
Effect of shock wave interaction in parallel, two-dimensional, stratified flow of heavy and light gases
20 p2384 N73-29157
Numerical analysis of aerosol concentration and deposition flux for several flow configurations with and without electrical force deposition
20 p2386 N73-29172
Analysis of shock wave strenghtening by positive density gradient in cryogenic shock tube
20 p2386 N73-29173
Application of finite-difference machine code for analyzing wake-vortex problem in quasi-cylindrical boundary layer approximation
[NASA-TM-X-69495] 20 p2387 N73-29179
Effects of condensation on gas velocity in free jet expansion
[AD-762503] 21 p2527 N73-30266
Development of optical diagnostic techniques to determine plasma refractive index using interferometers to produce space or time resolved density data
[AD-763802] 21 p2584 N73-30706
Electric discharge in turbulent flowing gas
[AD-764468] 22 p2655 N73-31265
Development of test equipment for analyzing characteristics of plasma in gas stream of nitrogen and helium mixture
22 p2703 N73-31649
Surface tension effect on cylindrical gas slug velocity
23 p2771 N73-32163
Boundary conditions and uniqueness in internal gas dynamic flows
23 p2775 N73-32192
Development and characteristics of device for removing condensate from heat exchangers with straight through gas flow
[NASA-CASE-MSC-14143-1] 23 p2856 N73-32823
Asymptotic expansion analysis of shock supported arrhenius reactions and ignition delay
24 p2903 N73-33172
Parallel heat conducting viscous gas flow in flat channel with sine wave wall perturbation
24 p2906 N73-33189
Gas flow and wind velocity in elliptical and cluster galaxies
24 p2978 N73-33795
Thermodynamic state in cascade argon arc after initiation of step increase in electrode voltage from initial steady-state D.C. level
24 p2990 N73-33893

**GAS GENERATOR ENGINES**
U ENGINES
U GAS GENERATORS

**GAS GENERATORS**
Closed loop fuel control techniques using electronic circuitry to sense pressure relationships at turbine engine compressor discharge
[AD-747805] 03 p0351 N73-12865
Actuator operated by electrolytic drive gas generator and evacuator
[NASA-CASE-NPO-11369] 04 p0425 N73-13467
Development and operating principles of gas generator for deploying recovery parachutes from space capsules during atmospheric entry
[NASA-CASE-LAR-10549-1] 04 p0477 N73-13898
Fluid dynamic and chemical processes occurring in solid propellant gas generator
[AD-749144] 05 p0589 N73-14790
Preliminary aerodynamic and mechanical design of selected gas generators and lift unit for V/STOL aircraft
[NASA-CR-120972] 10 p1106 N73-19020
Design of pyrotechnical gas generator for gate valve control
[AD-754963] 11 p1301 N73-20556
Design and evaluation of electrochemical nitrogen-hydrogen separator for use in spacecraft nitrogen generator
[NASA-CR-114580] 13 p1534 N73-22431
Simple performance calculation method for LH2/LOX engines with different cycles
[NASA-TM-X-64749] 15 p1824 N73-24786
Design of gas turbines for furnishing hot gases for turbine drives and analysis of limitations imposed by thermal stresses
[NASA-SP-8081] 18 p2193 N73-27705
Analysis of chlorate candle generated oxygen
[AD-762276] 19 p2231 N73-27992
Static tests of cylindrical ejectors using afterburning turbojet gas generators
[NASA-TM-X-52565] 23 p2830 N73-32622

**GAS GUNS**
NT LIGHT GAS GUNS
Aerodynamic drag of series of spherically-blunted conical bodies with three classes of half-vertex angles under hypersonic flow conditions
[NAL-TR-280] 06 p0613 N73-14978
Argon ion gun for cleaning surfaces and specimens for use in electron spectrometer
[ECRC/N486] 10 p1125 N73-19165

**GAS HEATING**
Carbon dioxide laser for heating hypersonic wind tunnel flow
[AD-761506] 19 p2249 N73-28134

**GAS INJECTION**
Application of continuous wave gas laser and pulsed ruby laser to analyze laminar and turbulent films of air at porous wall with carbon dioxide and helium injected into air stream
[AD-747511] 03 p0287 N73-12323
Flow characteristics of two-dimensional, tangential-slot injection into turbulent boundary layer at Mach 2.4 freestream velocity
[NASA-CR-2128] 06 p0654 N73-15313
Performance test of internal combustion engine to determine effects of pulsed injection of secondary air on exhaust emission levels
[NASA-TM-X-2737] 08 p0969 N73-17920
Gas injection of turbulent boundary layer through porous wall
[ONERA-NT-201] 13 p1510 N73-22237
Experimental data analysis for sonic injection of hydrogen from backward facing step in parallel direction to main supersonic stream
[NASA-TM-X-2828] 22 p2728 N73-31828
Design and development of logic scheme for control of Omni-Axis Secondary Thrust Vector Control system for use on space shuttle pressure fed engine
[NASA-CR-124428] 23 p2848 N73-32761

**GAS IONIZATION**
NT ATMOSPHERIC IONIZATION
NT AURORAL IONIZATION
Drift tube mass spectrometer for measuring reaction rate of uranium atoms and ions with O2 and N2
[AD-746272] 02 p0138 N73-11115
Cross section measurements for electron impact at low energies in molecular gases
[AD-747304] 02 p0139 N73-11123
Low energy electron impact excitation and ionization rate coefficients for atmospheric nitrogen and oxygen
[AD-747244] 02 p0170 N73-11378
Corrections for sidewall waveguide slots to microwave transmission data for shock-ionized air
[AD-748075] 03 p0343 N73-12801
Fabry-Perot laser interferometer for studying atomic collisional rate and ionization relaxation time in helium shock wave
[AD-749553] 04 p0408 N73-13326
Microwave breakdown at waveguide antenna discharge into ionized gas media
[AD-748830] 04 p0455 N73-13717
Mode coupled nonlinear dispersion of irregular ionization waves in glow discharges
[AD-748468] 04 p0456 N73-13721
USSR research projects involving laser technology, effects of strong explosions, geosciences, and particle beams
[AD-749487] 04 p0489 N73-13998
Electron impact excitation and ionization cross sections of nitrogen atoms
[AD-749807] 05 p0582 N73-14742
Relation of gas kinetic particle pressure and discharge field in plasma heating by pulsed longitudinal current
[AEC-TR-7330] 07 p0826 N73-16697

Shock structure characterization of normal ionizing shock waves in argon
[AD-751394] 07 p0829 N73-16719
Theta pinch generation of ionizing shock waves in argon plasma
[AD-751659] 07 p0829 N73-16721
Ionic composition of plasmas produced in helium, hydrogen, xenon, and neon gas mixtures
[AD-751327] 07 p0830 N73-16727
Light intensity effect on photon resonance in excited atom ionization for determining Stark effect potential
[KFKI-72-68] 10 p1192 N73-19694
Influence of cosmic rays on temperature and ionization rate of interstellar gas
[MPI-PAE/EXTRATERR-72] 12 p1446 N73-21710
Analysis of laser outputs required to initiate gas breakdown when gas contains suspended particles
[AD-757517] 14 p1674 N73-23585
Laboratory astrophysics research on defense applications of gas ionization, electron scattering, plasmas, and line broadening
[AD-757721] 14 p1695 N73-23753
Corona equilibrium model for ionization state distributions in carbon, aluminum, copper, and tungsten plasmas
[AD-758357] 14 p1696 N73-23767
Air breakdown and plasma generation by carbon dioxide laser
[AD-759567] 16 p1951 N73-25785
Vaporization coefficient of graphite based on ion intensity measurements
[AD-759203] 17 p1993 N73-26113
Multiphoton ionization by laser beam
[AD-760800] 18 p2159 N73-27440
Use of electron beam for preionization in Z-pinch experiment
[AD-765313] 23 p2823 N73-32568

**GAS JETS**

Mathematical models for determining impact of supersonic gas jet on solid surfaces
[NLL-RTS-7551] 02 p0154 N73-11248
Glow from light scattering in gas jets of space vehicle microengine
04 p0466 N73-13801
Analysis of aerodynamic characteristics of free, semibounded slipstream of straight-jet laminar gas flames
[NASA-TT-F-14688] 07 p0855 N73-16934
Aluminum rods for gas cooling requirements of satellite attitude and orbit control using hydrazine as low thrust propellant
[RAE-TR-72161] 09 p0991 N73-18086
Gas jets, seeding, and thermal excitation for producing neutral molecular beams
[DLR-FB-72-52] 09 p1068 N73-18717
Development of solenoid valve failure detection system based on addition of radioactive gas to propellant of cold gas jet attitude control system
[NASA-CR-130931] 10 p1165 N73-19476
Exponential laws for temperature, velocity, and CO-concentration profiles in nitrogen hot gas jet or nitrogen-propane flame in free atmosphere, in application to supersonic combustion
[DLR-FB-73-05] 12 p1465 N73-21867

**GAS LASERS**

NT CARBON DIOXIDE LASERS
NT CARBON MONOXIDE LASERS
NT HCN LASERS
NT HELIUM-NEON LASERS
NT TEA LASERS

Analysis of reaction mechanisms involved in chemical and continuous wave lasers based on carbon disulfide/oxygen system
[DREV-R-656/72] 01 p0064 N73-10525
Computerized simulation of pulsed HF laser pumped by H2 and F2 chain reaction
[AD-745425] 01 p0065 N73-10531
Atmospheric transmittance calculations of laser beams for atmospheric models with water vapor as molecular absorber
[AD-745585] 01 p0065 N73-10532
Development of air navigation system using moving map display based on holographic storage and display techniques
[AD-745025] 01 p0065 N73-10533
Modification of uncoupled radiation analysis of diffusion-type chemical laser to determine lasing diatomics of radiatively saturated medium
[AD-745311] 01 p0065 N73-10534
Analysis of energy transfer processes in molecular lasers
[AD-745368] 01 p0066 N73-10537
Analysis of applications for infrared, carbon dioxide, and chemical laser devices with emphasis on window materials and absorption mechanics
[AD-745927] 01 p0067 N73-10546
Operating principles of gas dynamic lasers and effects of gas dynamic flow on laser system properties
02 p0181 N73-11469
Interaction of electrothermal instabilities and lasing radiation field in MHD lasers including importance of CO2 dissociation
[AD-745986] 02 p0182 N73-11475
Three laser methods of remotely mapping gaseous pollutants of atmosphere
[AD-746280] 02 p0205 N73-11664
Argon laser for spin-flip Raman scattering study in cadmium sulfide at liquid helium temperature
[AD-746219] 02 p0219 N73-11768
Synthesis and characterization of 4,5-dicyano oxazole, low hydrogen content fuel for satisfying flame temperature criteria for gas dynamic laser
[AD-746342] 02 p0221 N73-11790
Application of continuous wave gas laser and pulsed ruby laser to analyze laminar and turbulent films of air at porous wall with carbon dioxide and helium injected into air stream
[AD-747511] 03 p0287 N73-12323
Absorption and fluorescence spectra of marine and fresh water algae using pulsed N2/Ne dye laser as excitation source
[NASA-CR-62090] 03 p0310 N73-12527
Argon-ion laser used to determine ocular effects of repetitive laser pulses on rhesus monkeys
[AD-746795] 04 p0380 N73-13096
Vibrational energy transfer in gas lasers
[AD-748858] 04 p0387 N73-13143
Developments in laser technology to include chemical lasers, electric discharge lasers, high power glass lasers, and laser techniques
[AD-748178] 04 p0429 N73-13498
Long term frequency drift and gain stability of laser structures
[AD-749056] 05 p0558 N73-14534
Sources responsible for long term drift of He-Ne lasers
[AD-749055] 05 p0558 N73-14535
Laser Doppler velocimeter for measuring initial velocity of projectile
[AD-749670] 05 p0559 N73-14539
Evaluation of optical properties of high power laser window materials
[AD-749864] 05 p0559 N73-14540
Discharge compositions of gas laser emissions from mercury and copper halides
[AD-749938] 05 p0559 N73-14541
Characteristics of combined gas laser pumping based on fluctuation of gas density parallel to electric field which is assumed constant
[JPRS-57880] 06 p0679 N73-15524
Operating principles and physical mechanisms of pulsed gas discharge lasers
[SC-T-72-2524] 06 p0679 N73-15529
Development and characteristics of optical communication system based on three frequency heterodyne configuration
[AD-750321] 06 p0680 N73-15533
Laser extension measurements of visibility during ice fog for aiding in SEV pilot system design
[AD-750114] 06 p0680 N73-15537
Gas laser measurements of absorptive losses introduced by water vapor and carbon dioxide for laser emission lines in 7-6 to 10-9 vibrational bands
[AD-749823] 06 p0681 N73-15542
Analytical and experimental determination of reaction mechanisms involved in HN3 plus CO2 laser
[AD-751634] 07 p0807 N73-16546
He-Xe tunable laser measurement of infrared line shape and CO2 absorption spectra
[AD-751230] 07 p0808 N73-16556
Theory of finite aperture waveguide gas laser resonators representing external reflectors by matrices
[NASA-TM-X-66186] 08 p0929 N73-17608
Production of laser output by excitation of hydrogen chloride vibrational levels using electron impact
[AD-752631] 08 p0930 N73-17615
Evaluation of infrared laser beams using thin membrane type displays of cholestric liquid crystals
[AD-752201] 08 p0930 N73-17616
Development and characteristics of electron beam excited high pressure mercury dissociation laser
[AD-752465] 08 p0930 N73-17619
Laser frequency modulation, molecular lasers, superconducting lasers, and laser induced instabilities in fluids
[AD-752633] 08 p0931 N73-17621
Hyperfine electron density fluctuation in stabilized hydrogen arc laser
08 p0943 N73-17723
Laser lines in xenon plasma caused by self-electromagnetic pinching effect
[AD-752085] 08 p0949 N73-17771
Dispersive explanation of spectral behavior of Runge mode locked dye laser
[AD-753408] 09 p1044 N73-18516
Production of stimulated emission in vacuum ultraviolet using molecular xenon gas excited by relativistic electron beam
[AD-753483] 09 p1045 N73-18522
Computerized simulation of parallel plate pulsed transversely excited atmospheric pressure laser
[DREV-TN-2054/72] 10 p1168 N73-19503
CO2/N2 laser applied to CO2 excited state population study during supersonic nozzle expansion
[ONERA-NT-204] 10 p1169 N73-19510
Dependence of photon resonance in metastable helium atom ionization on light intensity
[KFKI-72-69] 10 p1192 N73-19695
Design and performance of transverse excited atmospheric carbon dioxide lasers
[AD-754544] 11 p1303 N73-20572
Chemical and molecular laser research
[AD-754792] 11 p1303 N73-20575
Quantum mechanics for describing operational properties of gas laser containing saturable absorber in resonator
12 p1409 N73-21421
CF3I gas laser system for high power operation
[SC-T-72-2560] 12 p1410 N73-21426
Spectrometric analysis of pulsed X ray sources and detectors
[AD-755845] 12 p1436 N73-21639
Recombination electron beam-excited plasma into pulsed laser of high peak power
[AD-756681] 13 p1537 N73-22455
Stability of molecular gas discharges typical of those used in high power lasers
[AD-757083] 13 p1537 N73-22456
Analysis of buffer gas pressure effects on kinetics of generation spectrum of photodissociation laser
[AD-756334] 13 p1539 N73-22469
Development of hollow cathode plasma electron gun for gas lasers
[AD-757086] 14 p1672 N73-23570
High efficiency ion lasers and high power carbon dioxide lasers through study of improved electrode structures
[AD-757099] 14 p1673 N73-23575
Design, development, and operation of carbon dioxide-nitrogen-helium laser to show beam characteristics and power output as function of gas mixture
[AD-757263] 14 p1674 N73-23582
Research and development with gas lasers
[AD-758405] 14 p1674 N73-23587
Formyl fluoride photochemical laser and energy content of HF photoelimination product
[AD-757743] 15 p1796 N73-24558
Time responses of radiation of iodine laser with Q-factor modulation
[AD-758625] 15 p1796 N73-24560
Xenon gas laser oscillations in vacuum ultraviolet
[AD-759069] 16 p1925 N73-25576
Infrared television system used for HF laser flow visualization with selected nozzle configurations
[AD-759803] 16 p1925 N73-25577
Feasibility study to develop recombining electron beam-excited plasma into pulsed laser of exceptionally high peak power
[AD-759399] 16 p1925 N73-25579
Direct nuclear pumping of gas laser using argon as lasing medium
[NASA-CR-133210] 17 p2040 N73-26503
Results of investigations of CO lasers
[AD-759861] 17 p2041 N73-26512
Gas dynamic analysis in near field of supersonic nozzle banks for chemical lasers
[AD-760132] 17 p2041 N73-26513
Optical gain of combustion driven gas dynamic lasers
[AD-760390] 17 p2042 N73-26523
Neon line strength measurements using coherent laser spectroscopy
[NASA-CR-133406] 18 p2114 N73-27096
Kinetic theory of optically pumped gas laser oscillator
18 p2157 N73-27428
Reaction kinetics of CF3 I flash photolysis iodine laser
[AD-760806] 18 p2158 N73-27436
Research and development on chemical and molecular lasers
[AD-760701] 18 p2158 N73-27438
Development of nitrogen-laser-pumped tunable-dye laser for application as spectroscopic light source
20 p2424 N73-29473
Application of laser radiation to control operation of spark gaps to show breakdown synchronization and time characteristics
[JPRS-59677] 20 p2425 N73-29476
Stability of amplitude characteristics of laser gyroscope in magnetic field
[AD-763260] 21 p2550 N73-30442
Vibration-rotation relaxation using mode locked and Q switch gas lasers
[AD-763292] 21 p2555 N73-30481
Gas dynamics of cavities-in-series gas dynamic lasers
[AD-763255] 21 p2555 N73-30483
Electron beam stabilized electrical discharge gas lasers
[AD-763409] 21 p2555 N73-30487
Chemical and energy transfer reactions in hydrogen fluoride chemical laser system
[AD-763715] 21 p2556 N73-30491
Simulated emission predictions and measurement of H2 pressure effects on pulsed H2-F2 laser outputs
[AD-763716] 21 p2556 N73-30492
Theory and operating characteristics of equipment in laser exhaust measurement program
[PB-220429/5] 21 p2556 N73-30493

Experimental design parameters for Raman spectroscopy of turbid suspensions and powders using ion gas laser light sources and noting S/N improvement
[NOTA-INTERNA-346] 21 p2580 N73-30676
Mixing process and performance effects of continuous H2-F2 laser
[AD-763828] 22 p2682 N73-31480
Arc-driven N2CS2 mixing gas-dynamic laser
[AD-763898] 22 p2682 N73-31483
Development and application of mathematical models for chemical and gas lasers - Part 1
[AD-763905] 22 p2682 N73-31484
Chemical transfer laser development
[AD-764814] 23 p2802 N73-32409
Design of line-tunable pulsed hydrogen fluoride/deuterium fluoride laser
[AD-764709] 23 p2802 N73-32410
Mode locking and pulse selection in atmospheric gas lasers
[AD-765350] 23 p2802 N73-32411
Pulsed HF chemical laser to excite molecules to first vibrational level
[AD-765183] 23 p2858 N73-32833
Nuclear pumping in molecular gas lasers
[JPRS-60244] 24 p2931 N73-33405
Research and development in solid state lasers, gas lasers, component development, diognostics, design analysis, advanced concepts, laser plasmas and laser fusion
[UCRL-50021-72-2] 24 p2931 N73-33408
Xenon laser terminating on dissociating level
[SLA-73-5285] 24 p2931 N73-33412

**GAS LIQUEFACTION**
U CONDENSING

**GAS LUBRICANTS**
Design procedure for hydrostatic ring thrust bearings
[NRC-13180PT-3] 17 p2037 N73-26478

**GAS LUBRICATED BEARINGS**
U GAS BEARINGS

**GAS MASERS**
Atomic hydrogen maser with bulb temperature control by output frequency difference signal for wall shift elimination
[NASA-CASE-HQN-10654-1] 04 p0428 N73-13489
Long term frequency stability, service life, and reproducibility of NASA hydrogen maser in relation to world standards
[NASA-TM-X-66229] 12 p1410 N73-21425
Electronic design of rubidium-87 maser
[NASA-CR-132770] 17 p2040 N73-26502

**GAS METERS**
Equipment and procedures for measuring flow of liquids and gases to identify application of specific types of equipment
[NLL-TRANS-45-[3958.4]] 02 p0154 N73-11249
Dynamic calibration of gas flowmeters by impedance measurement in oscillating flow
[ARC-CP-1224] 05 p0548 N73-14451

**GAS MIXTURES**
NT AIR
NT DETONABLE GAS MIXTURES
Universal humidity chart allowing humidity and energy calculations for any mixture of monatomic and diatomic gases at pressures encountered in saturation diving
[AD-746162] 02 p0207 N73-11675
Analysis of mass transfer through binary, monatomic gas mixture of arbitrary composition contained between two plane parallel surfaces
[COO-2032-10] 03 p0284 N73-12304
Transfer of mass and heat through single component diatomic gas and binary monatomic gas mixture of arbitrary composition
[COO-2032-12] 03 p0364 N73-12968
Nonstationary heat and mass transfer in stationary binary gas mixture
[AD-747562] 03 p0365 N73-12974
Theoretical model of Raman rotational spectrum of gas mixture applied to air mixture of oxygen and nitrogen to determine temperature
[NASA-TN-D-7126] 06 p0679 N73-15525
Reduction in heat exchanger size with use of gas mixtures in closed gas turbine installations
[AD-750905] 06 p0715 N73-15836
Computer program for determining thermodynamic and transport properties of complex mixtures to include rocket performance, shock properties, and detonation properties
[NASA-TN-D-7056] 06 p0730 N73-15954
Partial condensation and fractionation for analysis on mixture of hydrogen, methane, and ethane
[NASA-TT-F-14681] 07 p0752 N73-16109
Ionic composition of plasmas produced in helium, hydrogen, xenon, and neon gas mixtures
[AD-751327] 07 p0830 N73-16727
Solid ceramic electrolyte system for measuring redox conditions in high temperature gas mixing
[NASA-TM-X-58105] 08 p0892 N73-17224
Continuous reading fluidic device for measuring component flow of binary gas mixtures
[NASA-TM-X-2741] 09 p1035 N73-18445
Human ability to note changes in composition of inhaled air
10 p1115 N73-19090
Helium/oxygen breathing effects on rat gas exchange and musculoskeletal heat control
10 p1115 N73-19093
Equation of state for helium and nitrogen mixture
[AD-753964] 11 p1253 N73-20169
Formation of hydrocyanic acid from mixtures of ammonia, metane and noble gas or hydrogen subjected to UHF waves
[NASA-TT-F-14678] 12 p1376 N73-21162
Solution of Boltzmann kinetic equation for relaxation of gas mixture
12 p1418 N73-21486
Transfer phenomena in reacting gas mixtures
12 p1418 N73-21492
Perturbation of Maxwellian distribution in chemically reacting gas mixtures
12 p1418 N73-21493
Effect on nitric oxide emissions of using premixed prevaporized fuel/air in turbojet combustors
[NASA-TM-X-68220] 12 p1464 N73-21862
Effect of heat transfer on flow and temperature fields in separation nozzle measured with free molecular pressure and temperature probes
[KFK-1634] 12 p1464 N73-21865
Propagation of curved waves through nonlinear elastic gas mixtures
13 p1508 N73-22219
Analytical model for prediction of flammability limits of combustible gas
13 p1590 N73-22889
Combustion instability in gas-fired T-burner
[AD-755824] 13 p1591 N73-22903
Effects of underwater breathing of helium oxygen mixture on speech recognition
[AD-759413] 16 p1878 N73-25205
Stability of horizontal layer of binary gas mixture in porous medium with different upper and lower boundary temperatures
16 p1886 N73-25263
Possible condensation in rocket exhaust plumes, using frozen gas mixture
[AD-760040] 17 p2097 N73-26965
Convergence improvement in equilibrium calculation using Newton-Raphson method for C, H, N, F system, noting monomethylhydrazine/Fe mixture
[ICT-3/72] 18 p2192 N73-27696
Mass spectra of cluster ion reaction kinetics in free jet expansions of gas mixtures
[AD-761811] 19 p2233 N73-28004
Electron beam flouorescence diagnostics of ternary gas mixture of nitrogen, helium, and hydrogen
[AD-762930] 20 p2374 N73-29079
Two phase detonation in fuel sprays suspended in gaseous oxidizing atmospheres
20 p2484 N73-29957
Exact equations for five-component gas mixture transport coefficients as dissociated air model gas
[DLR-FB-72-34] 21 p2580 N73-30678
Intermolecular force effects on infrared spectral transparency of active gas mixtures
[DRIC-TRANS-3227] 23 p2820 N73-32545
Induced reactions in gas mixtures using carbon dioxide laser pulses and electrical discharges
24 p2930 N73-33400
Ultrasonic wave propagation in He-Ar and He-Xe mixtures
24 p2956 N73-33614
Characteristics of detonable gas mixtures and analysis of cylindrically expanding flames initiated by exploding wire source
24 p2990 N73-33897

**GAS PHASES**
U VAPOR PHASES

**GAS PIPES**
Performance of gas-loaded variable conductance heat pipe with effect of gravity
[AD-757684] 14 p1720 N73-23956

**GAS PRESSURE**
Growth of hollandite crystal membranes under inert gas pressures
[NASA-CR-121033] 03 p0345 N73-12810
Tables of pressure, volume, density, and temperature for liquid states of oxygen, nitrogen, argon, and parahydrogen
[NBS-TN-361-REV] 04 p0386 N73-13139
Permeability of fine-pored carbons as function of mean pressure temperature and gas properties
[AD-749362] 05 p0499 N73-14064
Application of gas-pressure bonding to joining components for convectively cooled turbine blades and vanes
[NASA-CR-121090] 08 p0954 N73-17808
Analysis of leakage and pressure drop characteristics across dam of gas film seal under various flow conditions
12 p1389 N73-21267
Load factors for pressure balancing of gas film seals under various flow conditions
[NASA-TM-X-68227] 12 p1408 N73-21412
Analysis of buffer gas pressure effects on kinetics of generation spectrum of photodissociation laser
[AD-756334] 13 p1539 N73-22469
Design and performance of acoustic exciter for gas volume modulation in absorption cell
[NASA-CR-124269] 16 p1913 N73-25482

**GAS REACTORS**
Flow configurations for maximum nuclear criticality eigenvalue in gas core reactor
[NASA-CR-121191] 18 p2177 N73-27578

**GAS SPECTROSCOPY**
Spectroscopic and chromatographic analysis of outgassing contaminants in potting compound and paint
[NASA-CR-124227] 13 p1488 N73-22061
Collision broadening of rotational spectrum of gases
[AD-758852] 16 p1872 N73-25155

**GAS STREAMS**
Plasma production using gas stream kinetic energy in magnetic field
[DLR-FB-71-43] 04 p0455 N73-13714
Analytical prediction of transient surface heat flux and temperature on cooled turbine blade due to gas stream inlet temperature change
[NASA-TN-D-7101] 06 p0730 N73-15955
Device for measuring stagnation pressure of supersonic gas streams
[NASA-CASE-LAR-11139-1] 11 p1292 N73-20483
Ionizing wave transport in streamer breakdown of gas
[JPRS-59474] 18 p2183 N73-27622
Effect of shock wave interaction in parallel, two-dimensional, stratified flow of heavy and light gases
20 p2384 N73-29157

**GAS TEMPERATURE**
Calculation of minimum safe inspired gas temperature limits for deep diving
[AD-748197] 05 p0504 N73-14104
Turbine inlet gas temperature measurement by ultrasonic impedance
[AD-752602] 08 p0955 N73-17822
Influence of cosmic rays on temperature and ionization rate of interstellar gas
[MPI-PAE/EXTRATERR-72] 12 p1446 N73-21710

**GAS TRANSPORT**
Cooling systems using cold gas transfer closed loops in 15 to 80 K temperature range
[DLR-MITT-71-09] 04 p0485 N73-13964
Evaporation and vertical transfer of water vapor in urban areas
[N1.L-M-20842-[5828.4F]] 05 p0570 N73-14625
Atmospheric ozone transport by atmospheric circulation and vertical air currents
20 p2443 N73-29627
Exact equations for five-component gas mixture transport coefficients as dissociated air model gas
[DLR-FB-72-34] 21 p2580 N73-30678
Fission gas release rates from irradiated uranium nitride specimens
[NASA-TM-X-2890] 23 p2818 N73-32530
Generalized equations for transport coefficients assuming intramolecular interaction potentials
24 p2908 N73-33205

**GAS TUNGSTEN ARC WELDING**
Propagation of fatigue cracks in gas-tungsten-arc welded 304 stainless steels
[HEDL-SA-329] 06 p0677 N73-15510
Analysis of welding parameters for producing metallurgically sound welds and effects of heat treatment on metallurgical and mechanical properties
[Y-1855] 12 p1414 N73-21460
Press-brake roll and weld frabrication of prototype large diameter missile cases
[AD-762612] 20 p2466 N73-29815

**GAS TURBINE ENGINES**
NT CF-700 ENGINE
NT DUCTED FAN ENGINES
NT J-52 ENGINE
NT J-57 ENGINE
NT J-65 ENGINE
NT J-75 ENGINE
NT J-85 ENGINE
NT JET ENGINES
NT PULSEJET ENGINES
NT RAMJET ENGINES
NT SUPERSONIC COMBUSTION RAMJET ENGINES
NT TURBOFAN ENGINES
NT TURBOJET ENGINES
NT TURBOPROP ENGINES
Analysis of combustion liner wall temperatures under steady-state and convective heat balance conditions and comparison with experimental values
[NASA-TM-X-2711] 06 p0730 N73-15959
Design principles of gas turbine and piston engines for commercial aircraft
[AD-751510] 07 p0837 N73-16783
Analysis of gas turbine engine requirements and performance when main propulsion system furnishes auxiliary power source
10 p1110 N73-19050
Variable-orifice hydraulic mechanism for aircraft gas turbine engine fuel control
[NASA-CASE-LEW-11187-1] 10 p1203 N73-19793
Effect of ovality of radial thrust bearing balls on axial vibration of rapidly rotating rotor of engine
[AD-754615] 11 p1300 N73-20546
Design, development, and test of two types of pivoted pad journal bearings and spiral groove thrust bearing for use with Brayton cycle power unit
[NASA-CR-121098] 12 p1408 N73-21410

Effect of inlet-air humidity on formation of oxides of nitrogen from a gas turbine combustor under various air inlet temperature conditions
[NASA-TM-X-68209] 12 p1443 N73-21691
Vibration effects on self-acting and hydrodynamic shaft seals in gas turbine engines
[NASA-TM-X-68214] 13 p1534 N73-22430
Modifications of fuel control units in aircraft gas turbine engines for reducing production costs
[NASA-TM-X-68229] 13 p1571 N73-22729
Information and guidance for type certification of aircraft engines as required by Federal Aviation Administration
[FAA-AC-33-2A] 13 p1571 N73-22730
Performance of aircraft gas turbine components in hot corrosion environments
14 p1676 N73-23599
Chemical and mechanical properties of aircraft gas turbine engine components
14 p1676 N73-23600
High strength tungsten fiber reinforced oxidation resistant niobium alloy composites for use in gas turbine engines at 2000 F
[AD-757380] 14 p1678 N73-23620
Feasibility study of applying air lubricated bearings to gas turbine engines for military aircraft
[AD-757869] 15 p1793 N73-24537
Design, fabrication, and test of electronic engine control system for small turboshaft engines
[AD-758173] 15 p1827 N73-24805
Airflow distribution control in gas turbine engines
[NASA-CASE-LEW-11593-1] 16 p1955 N73-25816
Performance tests of gas turbine engine mainshaft roller bearings to determine stress and lubrication parameters
[AD-760563] 18 p2157 N73-27426
Analysis of properties of fiber reinforced materials with plastic and metallic matrix composition and application to gas turbine engines
18 p2164 N73-27476
Application of reinforced composite materials for construction of aeronautical gas turbine engines
18 p2165 N73-27490
Directional solidification of eutectic alloys and application to turbine blades and gas turbine engine components
18 p2166 N73-27494
Performance and exhaust emission analysis of Williams research Gas Turbine Hornet automobile engine
[PB-218687/2] 18 p2173 N73-27551
Design, fabrication, and performance tests of foil journal bearings for application to Brayton cycle turbo-alternator-compressor
[NASA-CR-2243] 19 p2304 N73-28529
Design and evaluation of mini-Brayton compressor-alternator-turbine system for spacecraft power supplies
[NASA-CR-133810] 21 p2553 N73-30463
Swirl can, full-annulus combustion chambers for high performance gas turbine engines
[NASA-CASE-LEW-11326-1] 21 p2579 N73-30665
Analysis of factors affecting combustion performance requirements of gas turbine engines and methods for improving gas turbine operation
21 p2606 N73-30882
Fluidic to hydromechanical interface for application to gas turbine engine control system
[AD-764368] 22 p2675 N73-31429
Effect of inlet air humidity on exhaust gas emissions of nitrogen oxides in gas turbine combustor
[NASA-TN-D-7396] 23 p2856 N73-32822

**GAS TURBINES**

Aircraft gas turbine engines in electric and transport power plants
[AD-745832] 01 p0007 N73-10055
Influence of various types of air exhaust on cooling effectiveness of trailing edges of gas turbine blades
[AD-745834] 01 p0092 N73-10754
On-line data acquisition and instrumentation improvements for transonic turbine test rig
[AD-746727] 02 p0175 N73-11422
Refractory glass ceramics for gas turbines
[NPL-IMS-17] 02 p0192 N73-11556
Design, development, and evaluation of turbine for small, low-cost turbofan engine
[NASA-TM-X-68157] 02 p0223 N73-11803
Carbon dioxide gas turbine cycles for sodium cooled fast breeder reactor
[BMBW-FBK-72-17] 03 p0334 N73-12722
Closed loop fuel control techniques using electronic circuitry to sense pressure relationships at turbine engine compressor discharge
[AD-747805] 03 p0351 N73-12865
Calculation of heat transfer on turbine blade profiles to determine transition region coordinates in boundary layer flow through gas turbine engine
[AD-747602] 03 p0352 N73-12870
Secondary flow phenomena and associated losses in high-deflection turbine rotor cascade
[AD-750183] 05 p0528 N73-14300
Experimental study of aerodynamic effects on erosion
[AD-749286] 05 p0539 N73-14388
Exhaust nozzle for reducing noise in gas turbines by mixing low velocity air with high velocity engine exhaust
[NASA-CASE-LEW-11569-1] 05 p0590 N73-14792
Performance tests of single stage fan-compressor to evaluate shock-in-rotor blading for jet engine applications requiring high aerodynamic performance and stability
[NASA-CR-120991] 05 p0590 N73-14795
Calculating trajectories of solid particles entrained by fluid flow in turbine and compressor stators
[AD-749547] 05 p0591 N73-14799
Flameout and ignition characteristics of jet engine fuel flame in gas turbine with exhaust diffuser
[AD-749635] 05 p0591 N73-14802
Cooling efficiency of air discharge on nozzle blades with deflectors
[AD-749654] 05 p0591 N73-14803
Development and operation of test facility for high temperature gas turbine experiments
[NAL-TR-282] 06 p0649 N73-15269
Cold air experiment in two-dimensional cascade to determine aerodynamic performance of turbine stator blade with suction-surface cooling
[NASA-TM-X-2685] 06 p0713 N73-15818
Analysis of factors affecting cooling of liners in gas turbine combustion chambers
[NAL-TR-196] 06 p0713 N73-15819
Reduction in heat exchanger size with use of gas mixtures in closed gas turbine installations
[AD-750905] 06 p0715 N73-15836
Development and application of procedures for determining service life of gas turbine engines and components
[NASA-TM-X-2664] 06 p0726 N73-15925
Analysis of flow characteristics of asymmetric annular diffuser with wall bleed capability and application to gas turbine combustors
[NASA-TM-X-2710] 07 p0770 N73-16251
Influence of Na2SO4 oxidation of Ni-20Cr-2ThO2 gas turbine corrosion
[AD-751259] 07 p0810 N73-16573
Articles on experimental and theoretical studies of heat transfer and cooling problems of gas turbines
[AD-751513] 07 p0837 N73-16782
Turbulent transport models for designing compressors and gas turbines
[AD-751757] 07 p0837 N73-16786
Simultaneous film and convection cooling of plate inserted in exhaust stream of gas turbine combustor
[NASA-TN-D-7156] 07 p0855 N73-16930
Performance tests to determine effects of increased rotor blade loading on gas turbine operation by reduction of rotor blade inlet diameter
[NASA-TM-X-2730] 08 p0870 N73-17039
Approximative heat transfer in thermal boundary laer on gas turbine blade
[AD-752676] 08 p0956 N73-17825
Bearing design refinement and fluid film bearing studies of solar 10 kW turbo-altenator bearing with 6000 hr test program
[AD-752895] 09 p1042 N73-18496
Three dimensional solid particle trajectories through stationary and rotating turbine cascades
[AD-753364] 09 p1080 N73-18808
Turbulence and combustion stability in gas turbines
[AD-753062] 09 p1099 N73-18972
Computerized simulation of solution to maintenance and logistics problems of gas turbine engines
[AD-753622] 10 p1210 N73-19838
Development of sampling and analytical procedures for gas turbine engine exhaust using aircraft auxiliary power unit as emission source
[BM-RI-7735] 10 p1223 N73-19947
Design and performance of advanced auxiliary power system for fighter aircraft
[AD-754903] 11 p1238 N73-20049
Development of design criteria for maximum horsepower to be transmitted using cycloidal cam transmission and application to marine gas turbine engines
[AD-754822] 11 p1301 N73-20554
Chemistry of deposits and their precursors in jet turbine fuel systems
[AD-754459] 11 p1332 N73-20816
Design and performance of gas turbines for hydrofoils
[AD-753890] 11 p1334 N73-20830
Gas turbine nozzle geometry of two phase flow fuel injectors
[AD-754051] 11 p1334 N73-20831
Experimental determination of effect of angle of rotation of stator blades on operation of small size turbine stage
[AD-754683] 11 p1335 N73-20834
Development of standard uncertainty methology for analysis of gas turbine engine performance characteristics
[AD-755356] 13 p1571 N73-22733
Gas turbine power plants in future urban energy planning
[RE-439J] 13 p1593 N73-22912
Combined heat and mass transfer at wet flat plate in parallel air flow forming turbulent boundary layer
[DLR-FB-73-11] 14 p1599 N73-22960
Ultrasonic mass flowmeter for fuel flow in gas turbine engines
[AD-758462] 14 p1669 N73-23547
Sulfur, sodium, and chloride contaminants in gas turbines
14 p1677 N73-23610
Methods of oxidation and corrosion resistance in refractory metal alloys used in gas turbine engines
14 p1678 N73-23617
Trace element [Bi, Ag, Cd, and Pb] determination in nickel base gas turbine parts by atomic absorption spectrophotometry
[AD-757015] 14 p1678 N73-23619
Protection of titanium microstructure with intermediate nickel barrier to prevent abrasion and crack propagation on turbine compressor blades
[AD-758276] 14 p1682 N73-23651
Application of cryogenic and superconductive systems for propulsion of ships
[AD-758431] 14 p1694 N73-23746
Heat exchange between gas and turbine cascade blades of gas turbine engine
[AD-756101] 14 p1701 N73-23804
Three dimensional particle trajectories in compressible gas flow in rotating cascade
[AD-757162] 14 p1701 N73-23807
Problems associated with advanced, small, high temperature rise combustors
[AD-757173] 14 p1702 N73-23808
Calculation of aerodynamic forces of bending and torsional vibration on installed vibrating cascade blades
[ARC-R/M-3254] 15 p1728 N73-24015
Wind tunnel tests to determine characteristics of turbine rotor blades with inter-blade passages operating at supersonic speed
[ARC-R/M-3275] 15 p1728 N73-24016
Nondestructive detection of flaws in gas turbine blades using luminescence and color flaw detection techniques
[AD-758047] 15 p1793 N73-24538
High temperature testing of silicon carbide ceramics for use in gas turbine vanes
[AD-757796] 15 p1802 N73-24602
Analysis of relationship between losses in rotating turbine blade and pitch irregularity after nozzle blade
[NLL-CE-TRANS-6113-[9022.09]]
15 p1824 N73-24782
Research projects in theoretical and practical aerodynamics - Vol. 2
16 p1854 N73-25020
Performance tests of gas turbine engine with highly loaded stages operating at high pressure ratio
[ARC-R/M-3242] 16 p1854 N73-25021
Performance tests of gas turbines with high pressure ratios per stage to determine flow characteristics of supersonic nozzles for turbines
[ARC-R/M-3273] 16 p1856 N73-25037
Aerodynamic design parameters and test performance of two-stage high pressure ratio centrifugal compressor
[AD-759499] 16 p1919 N73-25533
Analysis of factors causing nitrogen oxides in exhaust gases of gas turbine engines and development of models of flow in gas turbine combustor
[NASA-CR-132959] 16 p1955 N73-25821
Miniature hydrogen fueled gas turbine engine scaled to teledyne CAE model 376
[NASA-CR-112173] 16 p1956 N73-25825
Analytical model for transpiration cooling of gas turbine blades
[AD-759190] 17 p2077 N73-26805
Survey of Soviet literature on use of silicon nitride for gas turbine applications
[AD-760329] 17 p2078 N73-26810
Gas turbine generator sets in 30 kW and 60 kW sizes and turboalternator designs
[AD-761115] 18 p2108 N73-27050
Design and development of gas-film seal using shrouded Rayleigh step lift pads at primary sealing face of gas turbine engine
[NASA-CR-121177] 18 p2155 N73-27415
Production of lamellar and fibrous composite materials from directional solidification of eutectic alloys and application to gas turbine blades and vanes
18 p2166 N73-27492
Application of glass and carbon fiber reinforced structures for gas turbine engine components to operate in high temperature environments
18 p2166 N73-27495
Application of boron/aluminum composite material for construction of turbine blades with low notch sensitivity in high cycle fatigue
18 p2166 N73-27497
Development of formula for calculating heat transfer coefficient in labyrinth glands of gas turbines
[NLL-RTS-7840] 18 p2192 N73-27698
Design of gas turbines for furnishing hot gases for turbine drives and analysis of limitations imposed by thermal stresses
[NASA-SP-8081] 18 p2193 N73-27705
Experimental determination of erosion rebound characteristics of high speed particles impacting sta-

tionary target for application to gas turbine engines operating in dusty environment
[AD-760578] 18 p2194 N73-27711
Development of methods for calculating cooling requirements for gas turbine engines with initial gas temperatures of 750 to 800 C
[AD-760964] 18 p2194 N73-27713
Critical characteristics of gas turbine powered generator
[AD-762200] 19 p2223 N73-27933
Development of improved cooling system for low-flow gas turbine rotor
[AD-761452] 19 p2330 N73-28743
One dimensional stationary analysis of air cooled, ducted gas turbines nozzle vanes
[AD-761451] 19 p2330 N73-28744
Development of electro-hydrofluidic transducer for control of turbine engines
[AD-762298] 19 p2330 N73-28745
Development and characteristics of hydrogen-oxygen power unit for application to onboard systems of space shuttle orbiter vehicle
[NASA-TM-X-68262] 20 p2363 N73-29005
Adiabatic film effectiveness and heat transfer measurements with injection of coolant air through holes in flat plate into moving mainstream.
[AD-762527] 20 p2466 N73-29814
Development of computerized, theoretical model to predict characteristics of emissions from gas turbine engine combustors
[AD-762935] 20 p2467 N73-29819
Effect of electrochemical machining on mechanical properties of gas turbine engine blades made of MA-2 alloy
[AD-762497] 20 p2483 N73-29950
Stoichiometric gas turbines using hot cascades, aerodynamic cascades, and combustor rigs
[EDR-7460] 21 p2589 N73-30746
Mathematical models for analyzing origin and distribution of combustion generated pollutants in gas turbines
[NASA-CR-121208] 21 p2590 N73-30754
Corrosion resistance of gas turbine components of power plant fueled with shredded refuse
[PB-221095/3] 21 p2591 N73-30759
Method for determining time to failure of blades on aircraft gas turbine engines at steady mode and transient mode of operation
[NASA-TT-F-15113] 22 p2710 N73-31700
Flow characteristics of multiple dilution jets mixing with primary airstream for gas turbine combustors
[NASA-TM-X-71426] 23 p2829 N73-32612
Designing axial compressor airfoils with camber lines of arbitrary shape
[AD-765165] 23 p2832 N73-32636
Thermal cycling tests of gas turbine components
[AD-764930] 23 p2833 N73-32637
Emission abatement in aircraft gas turbine combustor with low mass emissions
[AD-764987] 23 p2833 N73-32638
Turbojet and turbine engine performance optimalization by configuration variations, and auxiliary turbine engine converter problem
[DLR-MITT-73-05] 24 p2973 N73-33755
Performance calculation of arbitrarily switched gas turbines by simulation with building block system on digital computer
24 p2973 N73-33758
Effects of partly filled small gas turbine hydrodynamic converter during starting process of main engines
24 p2973 N73-33759

**GAS VALVES**
Design of anesthetic flow valve canister system for exhaust gas absorption and laminar ventilation system for operating rooms
12 p1373 N73-21141
Fast closing gas valve for wind tunnel actuated by compressed air
[REPT-5/72] 13 p1505 N73-22194
Design and development of logic scheme for control of Omni-Axis Secondary Thrust Vector Control system for use on space shuttle pressure fed engine
[NASA-CR-124428] 23 p2848 N73-32761

**GAS VISCOSITY**
Capillary viscometer procedure for determining viscosity of meta-xylene at high pressure and temperatures
[AD-745851] 01 p0023 N73-10178

**GAS WELDING**
Modified filler metal composite for reducing or eliminating underbread cracking in multipass gas tungsten arc plate welds of T-111
[NASA-CR-121198] 19 p2304 N73-28530
Technique for welding small refractory metal capsules in controlled atmosphere
[AERE-R-2544] 21 p2553 N73-30466

**GAS-ION INTERACTIONS**
Sorption and desorption of ethylene oxide and methyl bromide gases on polymeric materials during sterilization
03 p0257 N73-12082

**GAS-LIQUID INTERACTIONS**
NT AIR WATER INTERACTIONS
Equilibrium distribution of helium-4 and helium-3 between the liquid and vapor phases of deuterium 2 and hydrogen 2
[NBS-TN-621] 02 p0137 N73-11109
Critical flow study in gas-liquid flow, using numerical models for predicting critical flow rate
[AEC-TR-7309] 03 p0284 N73-12303
Stability of liquid films interacting with high pressure supersonic airstream
[SC-DC-72-1225] 07 p0772 N73-16268
Abstracts on kinetics and thermodynamics of gases interacting with liquid metals
[JPRS-58282] 09 p1098 N73-18964
Approximate solution of two-dimensional problem of non-steady state stratal flow with movable gas-liquid interface
[AD-754828] 11 p1273 N73-20328
Swirling, annular, gas liquid flow down vertical tube
24 p2902 N73-33160

**GAS-METAL INTERACTIONS**
Surface stresses and mechanical properties of scales and effects on high temperature gas-metal reactions
[CONF-720515-1] 03 p0264 N73-12137
Rare molecular gas beam scattering from single metal crystal surfaces
[AD-748938] 04 p0451 N73-13685
Point defect theory and oxidation kinetics in metal reactions with high temperature gaseous environment
[GAT-T-1868] 06 p0684 N73-15571
Saturation of zirconium iodide with nitrogen and oxygen and analysis of effects on mechanical properties, deformation, and microstructure
13 p1541 N73-22488
High temperature environmental testing of gas-metal interactions to simulate severe operating conditions
14 p1677 N73-23606
Auger analysis of chemisorption of various gases to metal surfaces and sliding friction effects on interaction
[NASA-TN-D-7340] 16 p1918 N73-25520
Influence of gaseous atmospheres on aluminum alloy, titanium, and refractory alloy fatigue striations
[ONERA-NT-192] 17 p2045 N73-26548
Laser heating effects on oxide growth rates in magnesium-oxygen interaction
[AD-760176] 17 p2047 N73-26565
Thermodynamic, structural, and magnetization phenomena during hydrogen reaction with RCo5 type systems
22 p2625 N73-31033
Reflection intensities of thermal molecular beam on metals and aluminum oxide, to determine gas-solid interaction
[DLR-FB-73-14] 23 p2805 N73-32432

**GAS-SOLID INTERFACES**
Surface properties and gas-solid interface phenomena in engineering materials
[AD-753099] 09 p1000 N73-18165
Models for interaction of rarefied gas with solid surface
12 p1418 N73-21491
Particle-fluid interaction corrections for turbulent flow measurements with laser Doppler flowmeter
[NASA-CR-124254] 14 p1649 N73-23379
Laminar chemically reacting boundary layer at solid fuel/gas interface over vaporizing surface
19 p2230 N73-27981
Adhesion criterion in gas solid interface
[NASA-CR-133618] 20 p2374 N73-29075
Turbulent flow of gas-solid suspensions about ellipsoid of revolution
20 p2385 N73-29163
Turbulent gas-solid electrohydrodynamic flow into channel
23 p2772 N73-32172
Turbulent gas-solids flow measurements using laser Doppler velocimeter
23 p2773 N73-32182
Reflection intensities of thermal molecular beam on metals and aluminum oxide, to determine gas-solid interaction
[DLR-FB-73-14] 23 p2805 N73-32432
Turbulent boundary layer flow of gas-solid suspension
24 p2906 N73-33190

**GASDYNAMIC LASERS**
Reaction rate effect on gain and power of CO2-N2 gasdynamic laser in presence of H2 and H2O
[TAE-176] 16 p1920 N73-25539
Interferometric studies in shock tunnel simulating nozzle flow in gasdynamic lasers
[AD-761601] 19 p2308 N73-28567

**GASEOUS CAVITATION**
U CAVITATION FLOW
U GAS FLOW

**GASEOUS DIFFUSION**
Isothermal diffusion calculated for hydrogen dissolved in Zircaloy-yttrium combination
[GKSS-71/E/19] 03 p0263 N73-12131
Anelastic studies of hydrogen diffusion in niobium using internal friction techniques
[COO-1198-896] 03 p0264 N73-12138
Theory for Assman psychrometer based on exact analysis of diffusion process in laminar boundary layer with thermal gradients
[NLL-M-22691-[5828.4F]] 05 p0570 N73-14627
Variational analysis of laser induced gas breakdown employing simplified diffusion models for plasma generation
[AD-750874] 06 p0707 N73-15767
Propagation of curved waves through nonlinear elastic gas mixtures
13 p1508 N73-22219
Flow coupled diffusion and velocity profiles for steady laminar flow in circular duct
13 p1509 N73-22231
Effect of dissolved hydrogen on mechanical and superconducting properties of molybdenum
13 p1565 N73-22681
Oxygen diffusion in gettered tantalum alloy heat pipes at startup
[NASA-TM-X-2793] 14 p1675 N73-23589
Cone model for oxygen diffusion in brain considering spatial tissue/capillary permeability
[RAE-LIB-TRANS-1663] 17 p1987 N73-26060
Numerical analysis of facilitated transport of gas through liquid membranes to show dependence on three parameters
[PUB-73-2] 17 p2014 N73-26287
Development of invariant models of diffusion and chemical reactions in turbulent flow systems
[NASA-CR-2295] 21 p2505 N73-30106
Hydrogen diffusion and hydrogen induced cracking of structural materials
[COO-3166-5] 21 p2604 N73-30867
Gas model of solute diffusion in liquid metals
[NASA-TR-R-417] 23 p2753 N73-32032

**GASEOUS FISSION REACTORS**
Feasibility of full-scale nuclear light bulb engine and tests of fissioning uranium plasmas in unit cell of driver reactor
[NASA-CR-129500] 03 p0331 N73-12698
Thermodynamic properties of open cycle gaseous core nuclear rocket engine
[NASA-TM-X-2784] 11 p1323 N73-20733
Cavity temperature and flow characteristics in gas-core reactor for testing fissioning uranium plasmas
[NASA-TM-X-2797] 15 p1809 N73-24662
Compressional wave spectrum analysis on fissioning vacuum plasma in gas cored nuclear reactor
[NASA-CR-133235] 17 p2061 N73-26673
Feasibility of small scale, full operating gas core reactor demonstration test
[NASA-CR-121190] 18 p2177 N73-27577
Model for dynamic analysis of gas core reactor system
[NASA-CR-121253] 18 p2177 N73-27581

**GASEOUS ROCKET PROPELLANTS**
Evaluation of cooled, flightweight gaseous hydrogen-oxygen reaction control thrusters to determine catalytic igniter operational limits and performance - Vol. 1
[NASA-CR-120869] 03 p0350 N73-12858
Demonstration of duct cooling concept with gaseous hydrogen/oxygen propellant in high pressure thruster - Vol. 2
[NASA-CR-120870] 03 p0350 N73-12859
Analysis of propellant gases emitted by attitude control system to determine interference with experiments due to flow fields and plume density
[NASA-CR-114508] 03 p0363 N73-12958
Development of description for phenomenon of intrinsic unstable combustion in gas rocket
04 p0483 N73-13948
Development and characteristics of auxiliary propulsion system for space shuttle applications - Summary
[NASA-CR-128818] 10 p1208 N73-19827
Development of computer program to predict transient and steady state performance and heat transfer characteristics of pulsing gaseous propellant rocket engine
[NASA-CR-128748] 10 p1214 N73-19871
Injector design guidelines for gas/liquid propellant systems
[NASA-CR-120968] 13 p1570 N73-22726
Design, development, and operation of water electrolysis system to provide gaseous hydrogen and oxygen for satellite propulsion system
[AD-755384] 13 p1571 N73-22735
Chemical kinetics of nitrogen-hydrogen-fluorine systems for advanced rocket propellant technology
[AD-760770] 18 p2192 N73-27697
Gaseous propellant combustion and injector/chamber design guidelines
[NASA-CR-121234] 20 p2464 N73-29799
Technique for predicting high frequency stability characteristics of gaseous-propellant rocket combustion system
[NASA-TN-D-7406] 23 p2831 N73-32627

**GASES**
NT AIR
NT ARGON
NT ARGON ISOTOPES
NT CARBON DIOXIDE
NT CARBON MONOXIDE
NT COMPRESSED GAS

NT COSMIC GASES
NT DETONABLE GAS MIXTURES
NT DEUTERIUM
NT DEUTERIUM PLASMA
NT DIATOMIC GASES
NT EXHAUST GASES
NT FLAMMABLE GASES
NT GAS MIXTURES
NT GAS STREAMS
NT GRAY GAS
NT HELIUM
NT HELIUM ATOMS
NT HELIUM FILM
NT HELIUM ISOTOPES
NT HIGH TEMPERATURE AIR
NT HIGH TEMPERATURE GASES
NT HYDROGEN
NT HYDROGEN ATOMS
NT HYDROGEN IONS
NT HYDROGEN ISOTOPES
NT HYDROGEN PLASMA
NT IDEAL GAS
NT INTERSTELLAR GAS
NT IONIZED GASES
NT LIQUEFIED GASES
NT LIQUID AMMONIA
NT LIQUID HELIUM
NT LIQUID HYDROGEN
NT LIQUID NITROGEN
NT LIQUID OXYGEN
NT MOLECULAR GASES
NT MONATOMIC GASES
NT NATURAL GAS
NT NEON
NT NITROGEN
NT OXYGEN
NT RADON
NT RARE GASES
NT RAREFIED GASES
NT REAL GASES
NT RESIDUAL GAS
NT SOLIDIFIED GASES
NT TRITIUM
NT XENON

Excitation and deexcitation of vibration in gases by oxygen and nitrogen atoms in E region of earth atmosphere
[AD-745925] 01 p0054 N73-10437

Theoretical description of thermal blooming of pulsed, focused laser beams in gases
[AD-745739] 01 p0066 N73-10539

Collisional deactivation rate constants for oxygen by minor atmospheric constituents and other gases
[DREV-TN-2010/72] 01 p0082 N73-10682

Crossed molecular beam method for measuring elastic differential scattering cross sections of potassium with gaseous media
02 p0213 N73-11729

Phase method for measuring thermal conductivity of gases at high temperature
[AD-747620] 03 p0264 N73-12142

Bibliography of arc discharges in vacuum and gaseous atmospheres
[SC-B-72-3233] 03 p0278 N73-12251

Observation window for internal gas confining chamber
[NASA-CASE-NPO-10890] 03 p0279 N73-12265

Electrostatic repulsion criteria for dc high voltage spark breakdown of gas
[ORO-4211-5] 03 p0336 N73-12742

Chemical reaction of Si, SiC, and Si-SiC mixtures in CO and N at high temperature
[AD-747718] 04 p0438 N73-13569

Effects of plasma-neutral gas interaction, finite resistivity, and viscosity on gravitational modes in permeable and impermeable plasmas
[TRITA-EPP-72-06] 04 p0455 N73-13713

Development and characteristics of test equipment for investigating thermodynamic properties of gases at high temperatures
[AD-749653] 05 p0607 N73-14936

Effects of gas bubbles in decompression pathology of humans
[AD-748229] 06 p0631 N73-15126

Estimation of traces of gases in metals and alloys by vacuum fusion techniques
[BARC-590] 06 p0638 N73-15177

Chemical reactions from combustion of unmixed gases
[NASA-TT-F-14360] 06 p0730 N73-15956

Behavior of gas occlusions in arterial heat pipes
[NASA-CR-114531] 06 p0730 N73-15958

Device for detection of combustion light preceding gaseous explosions
[NASA-CASE-LAR-10739-1] 07 p0798 N73-16484

Abradable buffered labyrinth seal for control of gas path leakage in tip-turbine driven lift fan
[NASA-CR-121131] 07 p0804 N73-16524

Measurement methods based on gas chemiluminescence, emphasizing air pollution applications
[AD-753222] 09 p1000 N73-18163

Calculation of transport and equilibrium properties of simple gases with m-6-8 potential function
[NBS-TN-628] 10 p1125 N73-19167

Low energy electron diffraction and Auger electron spectroscopy used for determination of structure of adsorbed gases on solid surfaces
[LBL-878] 10 p1193 N73-19708

Calculation of thermodynamic and transport properties for chemically reacting gases
[AD-756597] 13 p1488 N73-22064

Analysis of linear oscillating temperature distribution to determine thermal diffusivity coefficient of gases
[BER-1/73] 13 p1590 N73-22895

Tabular data on transport and thermophysical properties of selected binary mixtures in gaseous state
[AD-757528] 14 p1617 N73-23101

Deceleration and vertical motion of gas puff released into upper atmosphere
[AD-757867] 15 p1782 N73-24450

Characteristics of dilute gas-solids suspensions in drag reducing flow
[NASA-CR-2267] 16 p1888 N73-25277

Heat flow and convection in gases and liquids in weightless environments
[NASA-TM-X-64735] 18 p2205 N73-27797

Calculation of heat removed by gas refrigerators and heat engines
[AD-762261] 19 p2306 N73-28544

Design and tests of passive, feedback-controlled, variable conductance, gas loaded heat pipe
[NASA-TM-X-62293] 19 p2352 N73-28920

Variational principles for examining adiabatic motions in gaseous sphere and waves in stratified horizontal fluids
21 p2523 N73-30237

Turbulent mixing layer of different gases in pressure gradient
[AD-763487] 21 p2527 N73-30260

Technologies for production and utilization of petroleum, natural gas, oil shale and coal
[BM-IC-8612] 21 p2536 N73-30335

Mechanical effects resulting from interactions of laser beams with gases, liquids, and solids
[AD-763258] 21 p2555 N73-30482

Effect of O2-H2 atmosphere, H2, Ar, and room air on fatigue crack propagation in 4340 steel
[COO-3166-4] 21 p2559 N73-30513

FORTRAN program for calculating thermodynamic properties of complex gas molecules
[AD-762614] 22 p2626 N73-31042

Interaction of laser plasma flow with neutral gases of air
[AD-764936] 23 p2823 N73-32569

Stress corrosion cracking in gaseous and aqueous environments
24 p2933 N73-33426

GASKETS
Analysis of leakage and pressure drop characteristics across dam of gas film seal under various flow conditions
12 p1389 N73-21267

Evaluation of structural capabilities of Marman V-band coupling and flange with Conoseal gasket for use with 75K NERVA propellant lines
[NASA-CR-132219] 15 p1792 N73-24529

GASOLINE
Design and manufacturing of gasoline fueled, flame-heated thermionic diode
[AD-746255] 02 p0129 N73-11047

Vaporization rates of liquid injected into high temperature, supersonic gas flow using aviation gasoline injected by Laval nozzle into air stream
[AD-747456] 03 p0286 N73-12317

Alternate fuels to reduce aircraft exhaust pollutants
[AD-755151] 11 p1332 N73-20815

Test equipment and experimental procedures for determining effects of turbulent flow on ignition properties of gasoline and air mixture
[NLL-RTS-7883] 18 p2128 N73-27194

Electrified kerosene and gasoline aviation fuel during passage through pipes and filters of fuel tank reservoir
[AD-764941] 24 p2971 N73-33740

Congressional hearings on causes and implications of impending shortages of gasoline, heating oil, diesel fuel, jet fuel, and electricity
24 p2994 N73-33928

GASTROINTESTINAL SYSTEM
NT INTESTINES
NT RECTUM
NT STOMACH

Absorption of fructose in saline mixture used for enteritis therapy of children
[NASA-TT-F-14596] 02 p0133 N73-11078

Physiology of depressed metabolic states and gastrointestinal responses to ionizing radiation
[NASA-CR-130381] 07 p0742 N73-16038

Transverse acceleration effects on rat gastrointestinal response to drugs
10 p1114 N73-19085

Effects of radioprotective drugs on motor evacuatory functions in gastrointestinal tracts of healthy and irradiated rats
11 p1239 N73-20062

Effect of some radioprotective preparations on motor and evacuator function of gastrointestinal tract of healthy and irradiated rats
[DRIC-TRANS-2962] 12 p1372 N73-21130

Effects of gastrointestinal pressure on rabbit eye nystagmus during barotrauma
13 p1479 N73-21983

Gastrointestinal proprioceptor effects on high altitude rabbit ocular reflexes
13 p1479 N73-21984

Composition of human gastrointestinal microflora during prolonged isolation
20 p2367 N73-29037

GATES
Pulsed power burnout tests of hand gate circuits
[AD-752540] 08 p0892 N73-17219

GATES (CIRCUITS)
NT THRESHOLD GATES

Test procedure for failure analysis in multiple elementary gate networks using iterative test function
03 p0278 N73-12256

Failure analysis of NOR gate network with parity for easy testing
03 p0278 N73-12258

Transformation of relay contact networks in logic gate circuits for failure analysis
05 p0522 N73-14248

Pulsed power burnout tests of hand gate circuits
[AD-752540] 08 p0892 N73-17219

Effects of Jupiter high energy electron environment on gates and MOSFET performance
[AD-756215] 13 p1502 N73-22178

Range-gated moving target indicator for use with search radar
[AD-757259] 14 p1636 N73-23265

Reliability evaluation of radiation hardened dual nand gates
[AD-765173] 24 p2900 N73-33151

Two phase, charge coupled shift registers using polysilicon gates overlapped by aluminum gates
[NASA-CR-132304] 24 p2968 N73-33722

GAUGE INVARIANCE
Invariance under Weyl scale transformations and Poincare gauge invariant matter Lagrangian
[RIFP-160] 02 p0195 N73-11578

Gauge invariant atomic orbitals and current conservatism within quantum mechanical formalism
[NASA-CR-129246] 03 p0339 N73-12762

Fields, statistics and non-Abelian gauge groups
[NOTA-INTERNA-387] 03 p0340 N73-12771

Gauge invariance, conservation laws, and Korteweg-deVries equation for class of nonlinear partial differential equations
[IPPJ-138] 04 p0440 N73-13589

Radio frequency resonant cavity mode analysis technique for fluid mass quantity gauging of space shuttle orbiter tankage
[NASA-CR-133393] 18 p2151 N73-27390

GAUSS EQUATION
Closed form, Romberg, and Gaussian procedures for calculating transonic wave drag integral using cubic splines
[NAL-TN-35] 06 p0652 N73-15299

GAUSS FUNCTION
U GAUSS EQUATION

GAUSSIAN DISTRIBUTIONS
U NORMAL DENSITY FUNCTIONS

GAUSSIAN NOISE
U RANDOM NOISE

GAUSSMETERS
U MAGNETOMETERS

GC-130 AIRCRAFT
U C-130 AIRCRAFT

GCR (REACTORS)
U GAS COOLED REACTORS

GEAR TEETH
Backlash value selection and determining dimensions for checking tooth thickness for straight spur and helical gears
[ESDU-68028] 02 p0177 N73-11430

Development and production of thermo-mechanically forged tool steel spur gears using high energy rate forging procedures
[NASA-CR-121227] 18 p2154 N73-27409

GEARS
Ground based UH-1 helicopter sonic analyzer for evaluation of effectiveness of using sonic data to diagnose mechanical condition of army helicopter power train components
[AD-745089] 01 p0004 N73-10026

Guidance on choice of nonmetallic gear materials, and method of estimating safe load for nonmetallic spur and helical gear
[ESDU-68001] 01 p0060 N73-10488

Choice of suitable manufacturing dimensions for parallel axis straight spur and helical gears
[ESDU-66001] 01 p0060 N73-10493

Data for major dimension determination for straight spur and helical gears
[ESDU-68040-AMEND-A] 02 p0176 N73-11428

Backlash value selection and determining dimensions for checking tooth thickness for straight spur and helical gears
[ESDU-68028] 02 p0177 N73-11430

Fine pitched, rolling gear checking systems
[BDX-613-563-REV] 03 p0306 N73-12500
Evaluation of potential coatings for titanium alloy gears to be used in propeller gearbox systems
[AD-753417] 09 p1041 N73-18492
Fatigue life and wear tests of spur gears based on pitting fatigue at pitch circle to compare AISI M-50 and super nitralloy materials
[NASA-TN-D-7261] 12 p1408 N73-21411
Development and production of thermo-mechanically forged tool steel spur gears using high energy rate forging procedures
[NASA-CR-121227] 18 p2154 N73-27409
Performance tests of spur gears with and without tip relief to determine service life of M-50 and Super Nitralloy metals
[NASA-TM-X-68269] 18 p2155 N73-27413
Development and characteristics of concentric output differential gearing system
[NASA-CASE-ARC-10462-1] 20 p2423 N73-29459
High precision external spur gear inspection and computerized simulation of manufacturing-inspection process
[AD-764588] 23 p2799 N73-32389
Plastic and powder metal materials for gear production
[NASA-TM-X-71446] 24 p2928 N73-33388

**GEGENSCHEIN**
Evaluation of Skylab program experiments involving contamination measurement, photometer, and gegenschein zodiacal light
[NASA-CR-61386] 18 p2200 N73-27760

**GEIGER COUNTERS**
Failure analysis of Geiger counters used in nucleonic oil gauging system of USAF aircraft
[AD-746267] 01 p0059 N73-10485

**GEIGER-MUELLER TUBES**
U GEIGER COUNTERS

**GELATINS**
Recording of holographic visual display elements in dichromated gelation
[AD-746859] 03 p0310 N73-12532

**GELATION**
Buffered gelled water to control nitrogen tetroxide-aerozine 50-hypergolic fuel fires
[NASA-CR-2198] 10 p1203 N73-19789

**GELS**
NT DOUBLE BASE ROCKET PROPELLANTS
Effect of heat treatment on adsorption properties of titano-silica gel and interactions of adsorbed molecules with silanol groups
[NLL-RTS-7360] 01 p0069 N73-10564
Chemical synthesis of formaldehyde based disinfectants without penetrating odor and eye and ear irritation properties
[NASA-CASE-NPO-12115-1] 08 p0884 N73-17153
Characteristics of gelled liquid hydrogen polyphenylene oxide foam open cell insulation
[NASA-CR-124114] 09 p1051 N73-18568

**GEMINI FLIGHTS**
Analysis of aerodynamic characteristics of Gemini spacecraft during reentry and comparison with wind tunnel data
[NASA-TM-X-58100] 13 p1577 N73-22786

**GEMINI SPACECRAFT**
Analysis of aerodynamic characteristics of Gemini spacecraft during reentry and comparison with wind tunnel data
[NASA-TM-X-58100] 13 p1577 N73-22786

**GENERAL AVIATION AIRCRAFT**
NT BEECHCRAFT 18 AIRCRAFT
NT YAK 40 AIRCRAFT
Compilation of accident reports involving corporate executive aircraft during 1970
[PB-210247] 01 p0005 N73-10040
Aircraft accident and incident reports for general aviation during 1970
[NTSB-BA-72-5] 04 p0371 N73-13015
Analysis of US general aviation accidents caused by stalls and spins for period 1967 to 1969
[NTSB-AAS-72-8] 05 p0493 N73-14018
Investigation of aircraft accidents involving US general aviation turbine powered aircraft for 1970
[NTSB-AMM-72-6] 05 p0493 N73-14019
Compilation of selected aircraft accident reports for US Civil Aviation operations during calendar year 1970 - Issue 5
[PB-211158] 05 p0497 N73-14047
Bibliography of aircraft accident reports for US civil aviation operations during calendar year 1971
[NTSB-BA-72-6] 07 p0738 N73-16001
Bibliography of aircraft accident reports for US civil aviation operations during calendar year 1971
[NTSB-BA-72-7] 07 p0738 N73-16002
Aircraft accident involving Beechcraft Queen Air aircraft on takeoff from Albuquerque, New Mexico airport on 19 May, 1972
[NTSB-AAR-72-32] 07 p0738 N73-16003
Aircraft accident involving Beechcraft 18 aircraft on air taxi flight from Cleveland, Ohio airport on 22 June, 1972
[NTSB-AAR-72-33] 07 p0738 N73-16006
Design of simple to fly, constant attitude light general purpose aircraft
[NASA-CR-2208] 09 p0984 N73-18037
Analysis of special problems and issues involved in the long range of aviation with emphasis on t aa Vol. 2
[PB-215804] 09 p1101 N73-18984
Statistical analysis of engine failure/malfunction accidents for US fixedwing aircraft of general aviation category during 1965 to 1969
[NTSB-AAS-72-10] 10 p1106 N73-19015
Analysis of general aviation activities in Germany and recommendations for flight control procedures to reduce aircraft accident hazards
10 p1183 N73-19626
Requirements for air traffic control in German air operations and recommendations for improved air traffic control procedures
10 p1183 N73-19628
Statistical anlaysis of aircraft accidents occurring in US civil aviation during calendar year 1971
[NTSB-BA-73-1] 11 p1234 N73-20015
Noise level surveys of seventeen general aviation aircraft including jet and propeller driven types
[FAA-EQ-73-1] 12 p1363 N73-21063
Measurement and analysis of aircraft noise generated by general aviation aircraft during level flyovers
[TR-S-212] 12 p1366 N73-21081
Aircraft accident involving crash of Turbo Commander aircraft following takeoff and climbout from Greater Pittsburgh Airport, Pennsylvania on 14 Aug. 1972
[NTSB-AAR-73-5] 13 p1474 N73-21936
Aircraft accident reports of US civil aviation accidents occurring during calendar year 1972
[NTSB-BA-73-2] 15 p1734 N73-24064
Development and characteristics of inflatable airbag restraint system for use in general aviation aircraft
[FAA-RD-73-3] 16 p1868 N73-25127
Evaluation of hearing protectors for general aviation aircraft
[NASA-CR-133303] 18 p2112 N73-27078

**GENERAL DYNAMICS AIRCRAFT**
NT C-131 AIRCRAFT
NT CL-84 AIRCRAFT
NT CONVAIR 880 AIRCRAFT
NT CV-340 AIRCRAFT
NT CV-990 AIRCRAFT
NT F-102 AIRCRAFT
NT F-106 AIRCRAFT
NT F-111 AIRCRAFT

**GENERAL DYNAMICS MILITARY AIRCRAFT**
U MILITARY AIRCRAFT

**GENERATORS**
Constant flow velocity generator for calibrating hot-wire anemometers
[NASA-CASE-MFS-21424-1] 07 p0769 N73-16248
Generator designs, insulations, magnetic materials, diodes, and rotor bonding
[AD-752604] 08 p0870 N73-17044
Fuel injectors with high frequency swirl generators
[AD-751079] 09 p1080 N73-18810
Design of circular symbol and video inset generator for television display devices
[AD-757621] 14 p1634 N73-23246
High pressure compressed gas magnetic diaphragm rupture system for generating megaguss magnetic field
[JPRS-59459] 18 p2179 N73-27593

**GENETICS**
NT MUTATIONS
Biostatistics of genetical processes in human populations
[NASA-CR-131508] 12 p1372 N73-21131

**GENITOURINARY SYSTEM**
NT TESTES
Luciferase ATP assay procedure for determining bacterial infections in urinary tract
[NASA-CR-130797] 09 p0992 N73-18096

**GEOASTROPHYSICS**
U ASTROPHYSICS
U GEOPHYSICS

**GEOBOTANY**
Geobotanical mapping based on spaceborne photography
[NASA-TT-F-14976] 17 p2026 N73-26392

**GEOCHEMISTRY**
Delineation of clustered points in two dimensions by measuring perimeters of convex hulls and applicability in fields of geology and geochemistry
[BM-RI-7565] 05 p0568 N73-14616
Bibliography on use of neutron activation analysis of geochemical samples
[NASA-CR-131831] 13 p1524 N73-22352
Determining past global climate by determining past trends in surface temperature of earth
[AD-757225] 14 p1686 N73-23683
Problems of sea chemistry
[TT-70-57237] 16 p1907 N73-25427
Geological and geochemical studies in Robinson Mining District, White Pine Co., Nevada using Skylab multispectral imagery
[E73-10992] 22 p2659 N73-31298
Geochemical analyses on lunar X ray spectra obtained during Apollo orbits
22 p2735 N73-31894
Geochemical analyses on lunar gamma ray spectra obtained during Apollo orbits
22 p2735 N73-31895
Organic geochemistry of amino acids in sedimentary rocks
[NASA-TT-F-14986] 23 p2787 N73-32295
Tides as energy factor in geological activity, and petrochemical coefficients of lunar rocks
[JPRS-59895] 23 p2837 N73-32668

**GEOCHRONOLOGY**
Martian surface cratering analysis using Mariner 9 observations
23 p2839 N73-32688

**GEOCORONAL EMISSIONS**
Development of model of scattering of solar Lyman alpha from spatial distribution of neutral hydrogen in interplanetary space
01 p0099 N73-10813
Characteristics of narrow field of view, sensitive photometers and application to measuring air glow, aurora, sun corona, and barium releases
[LA-DC-72-1422] 12 p1406 N73-21399

**GEODESY**
NT CELESTIAL GEODESY
Directory of principal tracking facilities used by NASA to include Deep Space Network and several radio telescopes - Vol. I
[NASA-CR-130071] 01 p0036 N73-10279
Interpolation of vertical deflections using trigonometric leveling
[AD-743986] 01 p0052 N73-10418
Contributions of Smithsonian Astrophysical Observatory to International Satellite Geodesy program
[NASA-CR-128396] 01 p0100 N73-10825
Analysis of range and range rate tracking data from satellite to satellite for geodetic applications
[AD-741683] 01 p0106 N73-10881
Development, characteristics, and evaluation of electronic distance measuring instrument
[AD-746017] 02 p0208 N73-11690
Precision measurements of solar gravitational fields by European drag-free and twin geodetic space probes
02 p0231 N73-11879
Geometric and dynamic satellite geodesy and geometric analysis and adjustment of ground stations
[NASA-CR-129516] 03 p0355 N73-12891
Analysis of computer programs for plotting geographical and political features of world based on observations from artificial satellites
[NASA-CR-129282] 03 p0356 N73-12903
Gravity values, station locations, and terrain locations for Central Colorado, Arizona, New Mexico, and Utah
[PB-211306] 05 p0540 N73-14396
Fundamental problems of geodetic gravimetry
[AD-748527] 05 p0543 N73-14420
Laser tracking techniques used for geodetic applications in space
[GRGS-BULL-1] 05 p0557 N73-14522
Geodetic use of earth satellites
[NASA-TT-F-732] 06 p0665 N73-15408
Dynamic determination of equatorial radius of earth
[NASA-TM-X-66151] 06 p0666 N73-15411
Probability of further developments of satellite geodesy
[AD-750749] 06 p0672 N73-15466
Conical section method for determining planetary configuration from spaceborne photographic data on triangulation and horizon lines
[JPRS-58304] 09 p1085 N73-18848
Geodetic reference systems for long period studies in earth physics
[NASA-TM-X-66221] 11 p1287 N73-20441
Transformation matrices between spherical harmonics and spherical sampling functions
[AD-755486] 14 p1664 N73-23509
Methods for improving 1967 geodetic reference system
[AD-755418] 14 p1665 N73-23510
Earth dynamic filtering algorithm for earthquake prediction and Love number determination
16 p1896 N73-25333
Calibration and evaluation of Skylab altimetry for geodetic determination of geoid
[E73-10671] 16 p1900 N73-25366
Development and revisions of mathematical theory of hydrostatic equilibrium for earth
[NASA-TM-X-66261] 16 p1906 N73-25415
Determining accuracy of three dimensional geodetic nets compiled from satellite observations
[NASA-TT-F-776] 16 p1906 N73-25418
Satellite tracking camera for geometric geodesy
[PUBL-27] 16 p1913 N73-25479
Standardization of geodetic instruments in U.S.S.R. research facility
[AD-759687] 16 p1914 N73-25492
Theodolitic errors in processing time dependent geodetic data
[AD-760109] 17 p2029 N73-26421
Gravimetry and satellite altimetry for determining earth gravity field
[AD-759536] 18 p2148 N73-27365
Three-dimensional geodesy and gravity gradients
[AD-759538] 18 p2148 N73-27366
Calibration and evaluation of Skylab altimetry for geodetic determination of geoid
[E73-10872] 20 p2393 N73-29223

Extensions to short arc geodetic adjustment for reduction of Doppler operations in satellite geodesy
[AD-760791] 20 p2414 N73-29401
Calibration and evaluation of Skylab altimetry for geodetic determination of geoid
[E73-11013] 22 p2660 N73-31318
Calibration and evaluation of Skylab altimetry for geodetic determination of geoid
[E73-11120] 24 p2916 N73-33275
GEODETIC COORDINATES
European tracking station coordinates from GEOS B satellite data
03 p0295 N73-12400
Strict geometric determination of ephemeris time, positions, and apparent directions of moon against stellar background
[AD-750307] 06 p0671 N73-15460
Method for transferring spherical quasi-geographic coordinates into geographic coordinates for polar navigation
10 p1185 N73-19640
Effect of parallactic refraction correction for satellite optical observations in determination of station coordinates
[NASA-TM-X-66208] 10 p1189 N73-19674
Geodetic reference systems for long period studies in earth physics
[NASA-TM-X-66221] 11 p1287 N73-20441
Proceedings of colloquium on lunar dynamics and observational coordinate systems
[NASA-CR-131263] 11 p1337 N73-20849
Computation of geodetic coordinates of aircraft from two measured distances and height above earth surface
[AD-757541] 15 p1808 N73-24658
Parameters of geodetic reference system
[AD-759127] 18 p2147 N73-27355
Ground station S band tracking in Doppler mode for calibrating Mariner 9 in deep space
18 p2210 N73-27845
Global station coordinate solution based upon camera and laser data
[NASA-TM-X-70422] 19 p2249 N73-28130
Techniques for analysis of geodynamic effects using laser data in estimating satellite orbits
[NASA-TM-X-70459] 22 p2716 N73-31739
GEODETIC SATELLITES
NT GEOS 1 SATELLITE
NT GEOS 2 SATELLITE
NT GEOS-C SATELLITE
Two FORTRAN 4 computer programs for general combination of satellite and gravity data for position and gravity field determinations
[AD-746305] 02 p0168 N73-11364
Tables on geodetic satellite gravity observations 09.0 deg E to 37.9 deg W along equator
[AD-746465] 02 p0170 N73-11379
Performance of portable Doppler geodetic receiver in satellite tracking system
[AD-751597] 07 p0757 N73-16149
Curve fitting method for comparing refractive adjustments in laser satellite ranging
[PB-214447/5] 16 p1909 N73-25445
Geophysical data as indicators of planet properties, using geodetic satellite
[NASA-TM-X-66274] 17 p2024 N73-26377
Simultaneous satellite photographic and Doppler observations for determining space triangulation chord direction
[AD-759096] 18 p2127 N73-27188
GEODETIC SURVEYS
Directory of observation stations in NASA geodetic satellites program based on preferred major datums and Modified Mercury Datum 1968 - Vol. 2
[NASA-CR-130072] 01 p0036 N73-10280
Application of satellite tracking and precision traversing data to improve accuracy of geodetic triangulation
[NASA-CR-128402] 01 p0047 N73-10377
Magnetotelluric analysis of geological structure of various locations in Rhine River Valley, Germany
[GAMMA-20] 01 p0048 N73-10388
Aerospace engineering including materials, orbits and trajectories, power sources, satellite geodesy, and structural engineering
[NASA-CR-128329] 01 p0119 N73-10981
Laser pulses transmitted from ground stations to aircraft or satellites used for 3-D multilateration system for precision geodetic measurements with 1-cm accuracy
01 p0119 N73-10982
Geocentric orientation vector from limited astro-geodetic and gravimetric data
[NASA-TM-X-66078] 02 p0165 N73-11342
Mathematical model for geodetic survey of tracking stations using laser range finder and photographs including results of European tracking network
[GRGS-BULL-3] 03 p0294 N73-12398
Mathematical model for geodetic survey of tracking stations using laser range finder and photographs
03 p0294 N73-12399
External gravity potential on earth and gravity dependent geodetic parameters
[AD-746307] 03 p0297 N73-12422
Distance measurement using electromagnetic radiation, range finders, and related geodetic research - conference summary
[AD-748067] 04 p0418 N73-13411
Combined marine astrogravimetry and marine geodetic acoustic techniques for accurate determination of global marine geoid
06 p0662 N73-15374
Performance of portable Doppler geodetic receiver in satellite tracking system
[AD-751597] 07 p0757 N73-16149
Height error in sea-surface profile over Puerto Rican trench as determined by multi-station tracking aided by GEOS 2 satellite
[NASA-TM-X-69353] 07 p0781 N73-16347
Measurements and procedures for processing measurement data in marine geodesy
[JPRS-58824] 13 p1522 N73-22335
Computer program to compute geodetic distance and azimuth between two geodetic positions
[P-4950] 14 p1659 N73-23462
Development of accurate geoidal map based on gravimetric and satellite data for determining precise location of tracking stations
[NASA-CR-131869] 14 p1710 N73-23874
Development of satellite geodesy technique for accurate determination of three dimensional coordinates of ground stations
[NASA-CR-132251] 15 p1778 N73-24412
Analysis of Skylab and EREP coverage of Wyoming and characteristics of field photometer system for measuring object reflectances
[E73-10697] 16 p1903 N73-25389
Evaluation of digital correction techniques for ERTS-1 imagery
[E73-10705] 16 p1903 N73-25396
Evaluation of utility of ERTS-1 satellite and aircraft remotely sensed data to integrated processes of state planning and land use in Maryland
[E73-10716] 17 p2019 N73-26323
Procedures for obtaining position from surface gravity observations and application of geodetic techniques to earth and ocean physics
[NASA-TM-X-66273] 17 p2059 N73-26655
Proceedings of conference on significant results obtained from ERTS-1 - Vol. I, Parts A and B
[E73-10824] 19 p2259 N73-28207
Analysis of tectonic situation in Alps and Apennine mountains using ERTS-1 imagery of previously inaccessible areas
[PAPER-G27] 19 p2267 N73-28258
Proceedings of conference on significant results obtained by ERTS-1 - Vol. 2
[E73-10825] 19 p2287 N73-28389
Application of ERTS-1 imagery for geologic development of natural resources in Alaska
19 p2287 N73-28393
Application of ERTS-1 imagery for multidisciplinary survey to aid in management of Alaskan resources
19 p2288 N73-28394
Mapping of flood inundation areas in southwestern Iowa using ERTS-1 imagery
19 p2288 N73-28395
Geodetic control net of Mars based on Mariner 9 television pictures
[NASA-CR-133845] 21 p2596 N73-30808
GEOELECTRICITY
NT TELLURIC CURRENTS
Tables of geomagnetic and geoelectric magnetograms and tellurigrams measured at Kakioka Magnetic Observatory, Japan
[REPT-12] 07 p0788 N73-16411
Geoelectric observations made from three locations in Japan
[REPT-89] 12 p1399 N73-21344
GEOFRACTURES
U GEOLOGICAL FAULTS
GEOGRAPHIC APPLICATIONS PROGRAM
Geographic applications of ERTS-1 imagery to land use and landscape changes in Tennessee
[E72-10315] 04 p0412 N73-13364
Geographic applications of ERTS-1 imagery to rural landscape change in Tennessee
[E72-10355] 05 p0534 N73-14343
Geographic applications of ERTS-1 imagery to rural landscape changes in eastern Tennessee
[E73-10040] 07 p0776 N73-16303
Passive microwave radiometry for remote sensing of earth resources and environmental monitoring programs
[ESRO-CR-75] 19 p2295 N73-28458
Requirements of earth resources aircraft facility for remote sensing of European terrain
[ESRO-CR-97] 20 p2413 N73-29394
GEOGRAPHY
NT OROGRAPHY
Analysis and interpretation of ERTS-1 ecologic, geographic, and agricultural data for Tennessee Valley
[E72-10231] 02 p0163 N73-11324
Statistical analysis of geography and seasonal variation effects on intensification of tropical cyclones over western North Pacific Ocean
[AD-746130] 02 p0206 N73-11669
Analysis of computer programs for plotting geographical and political features of world based on observations from artificial satellites
[NASA-CR-129282] 03 p0356 N73-12903
Computer graphics for theoretical geography with spatial analysis of surface topology
[AD-749377] 05 p0543 N73-14418
Summary of side-looking radar applications in earth resources noting basic principles of side-looking radar, radar scattering, data handling, and research and development
[ESRO-CR[P]-141] 06 p0641 N73-15200
Application of remote sensing from aircraft and spacecraft to geology, hydrology, and geographical data acquisition
07 p0782 N73-16354
ERTS-1 imagery of geography, geology, and glaciology of Germany and part of Alps Mountains
[E73-10099] 09 p1020 N73-18322
ERTS-1 imagery of regional geography and geomorphology of Mankoya-Kolwezi strip in Zambia and Zaire
[E73-10293] 10 p1146 N73-19331
ERTS-1 imagery of geography and geomorphology of Ndola-Mweru Wantipa strip in Zambia and Zaire
[E73-10294] 10 p1146 N73-19332
Coding systems in geographic data maps
13 p1523 N73-22343
Geographic analysis and mapping of landscape changes in Tennessee from ERTS-1 imagery
[E73-10661] 16 p1899 N73-25357
Geographic applications of ERTS-1 data to landscape changes in eastern Tennessee
[PAPER-L10] 19 p2274 N73-28306
Aerial and space photographic methods for geographic research
[NASA-TT-F-14966] 19 p2293 N73-28440
GEOIDS
Conference on laser and radar altimeter measurement of sea surface topography from space
[NASA-CR-130293] 06 p0661 N73-15369
GEOS-C data for improving geoid and gravity field determination
06 p0661 N73-15371
Sampling function representation for applying satellite-to-ocean altitude altimeter data to geoid
06 p0662 N73-15373
Combined marine astrogravimetry and marine geodetic acoustic techniques for accurate determination of global marine geoid
06 p0662 N73-15374
Gravimetric geoid construction for Atlantic Ocean area from satellite and sea surface gravimetric measurements
06 p0664 N73-15393
Quasigeoid heights and deflections of vertical for reference field of level ellipsoid
[AD-748528] 06 p0668 N73-15434
Surface gravity and satellite derived gravimetric geoid of North America, North Atlantic, Eurasia, and Australia
[NASA-TM-X-66238] 15 p1778 N73-24413
Calibration and evaluation of Skylab altimetry for geodetic determination of geoid
[E73-10671] 16 p1900 N73-25366
Calibration and evaluation of Skylab altimetry for geodetic determination of geoid
[E73-10872] 20 p2393 N73-29223
Calibration and evaluation of Skylab altimetry for geodetic determination of geoid
[E73-11013] 22 p2660 N73-31318
Satellite and surface gravity data for computing gravimetric geoid
22 p2736 N73-31910
Contour maps of global geoid and free air gravity anomalies of GEM-4 earth gravitational model
[NASA-TM-X-66240] 23 p2783 N73-32265
Calibration and evaluation of Skylab altimetry for geodetic determination of geoid
[E73-11120] 24 p2916 N73-33275
GEOLOGICAL FAULTS
NT AFRICAN RIFT SYSTEM
Application of ERTS-1 imagery to fracture related mine safety hazards in coal mining industry in Indiana
[E72-10193] 01 p0046 N73-10372
Systematic regional stress variations in fault zones in competent rocks
[AD-743837] 01 p0052 N73-10422
Acoustic holographic signals for designing underground geological viewing system
[AD-746498] 02 p0184 N73-11490
Major fracture and fault zones of Baltic Shield and their relationships to mineral deposits
[E72-10297] 04 p0411 N73-13347
Earthquake epicenters and fault intersections in central and southern California
[E72-10304] 04 p0411 N73-13353
Mapping of seismically active faults in Alaska using ERTS-1 imagery
[E72-10352] 05 p0533 N73-14340
Utilization of ERTS-1 MSS imagery for study of faulting in alluvium of California, Nevada, and Arizona
[E73-10070] 07 p0779 N73-16332

Application of ERTS-1 imagery to fracture related mine safety hazards in coal mining industry in Indiana and Illinois
[E73-10096] 09 p1020 N73-18321
Identification and interpretation of tectonic features of Colorado, California, and Sonora, Mexico
[E73-10275] 09 p1020 N73-18324
Mapping seismically active faults in Alaska from ERTS-1 imagery
[E73-10283] 09 p1020 N73-18326
Location of earthquake epicenters and major fault zones in Nevada using ERTS-1 imagery
[E73-10338] 09 p1025 N73-18366
Mineral exploration in Utah and Nevada based on ERTS-1 imagery of structural fracture and fault trends
[E73-10510] 13 p1516 N73-22285
Mapping of seismically active faults in Alaska from ERTS-1 imagery
[E73-10616] 15 p1774 N73-24377
Major fracture and fault zones of Baltic Shield in Finland and relationships to mineral deposits
[E73-10682] 16 p1901 N73-25377
Analysis of ERTS-1 imagery to determine structural and lithological characteristics of northern coast ranges and Sacramento Valley, California
[E73-10698] 16 p1903 N73-25390
Application of ERTS-1 imagery for mapping major geological structural trends and mineralization zones in Utah and Nevada
[E73-10701] 16 p1903 N73-25393
Detection and analysis of fracture systems using ERTS-1 imagery of snow cover conditions as enhancement tool
[E73-10741] 17 p2021 N73-26346
Application of ERTS-1 imagery for seismic conditions and recent fault formations in eastern California and western and central Nevada
[E73-10769] 18 p2134 N73-27245
Identification of major fault zone along California-Nevada state line from ERTS-1 MSS imagery
[E73-10773] 18 p2135 N73-27249
EREP 463 imagery of fault tectonics and earthquake hazards in peninsular ranges of southern California
[E73-10781] 18 p2136 N73-27257
Application of ERTS-1 and EREP imagery to geologically investigations of Basin and Range-Colorado Plateau boundary in Arizona
[E73-10799] 18 p2138 N73-27275
Analysis of ERTS-1 imagery to determine enhancement of ground fracture detail produced by snow cover
[PAPER-G12] 19 p2264 N73-28243
Structural analysis of Nevada using ERTS-1 imagery to identify lineaments of surface manifestations of major fault or fracture zones
[PAPER-G20] 19 p2266 N73-28251
Application of ERTS-1 imagery to identify, locate, and map faults showing geomorphic evidence of geologically recent breakage in Southern California
[PAPER-G22] 19 p2266 N73-28253
Application of ERTS-1 imagery for delineating structural features in Alaska and discovery of active strand in Denali fault
[PAPER-G23] 19 p2266 N73-28254
ERTS-1 imagery of western portion of Nicaragua following December 1972 earthquake to determine lineaments of fault systems related to earthquake
[PAPER-G24] 19 p2266 N73-28255
Analysis of lineaments and fault traces in Adantic Coastal Plain of southern Maryland using ERTS-1 imagery
[PAPER-G29] 19 p2267 N73-28260
Identification of fifty mile wide tectonic zone across Southern California using ERTS-1 imagery
[PAPER-G33] 19 p2268 N73-28264
Analysis of ERTS-1 imagery and high altitude infrared photography to determine geological fractures in Indiana and Illinois
[PAPER-E1] 19 p2268 N73-28265
Application of ERTS-1 imagery for mineral resources, geologic structure, and landform surveys
19 p2288 N73-28398
Mapping seismically active faults in Alaska using ERTS-1 imagery
[E73-10842] 19 p2291 N73-28420
Application of Skylab imagery to analysis of fault tectonics and earthquake hazards in Peninsular Ranges of Southern California
[E73-10863] 20 p2392 N73-29214
Identification and interpretation of tectonics from ERTS-1 imagery of California, Mexico, and Baja California
[E73-10875] 20 p2393 N73-29226
Igdlorssuit geomagnetic variation anomaly in rift-fault zone of northern West Greenland
[R-35] 20 p2412 N73-29389
Mapping of fracture-lineaments in New England using snow enhancement techniques
[E73-10930] 21 p2528 N73-30273
Application of ERTS-1 imagery to study of fracture-related safety hazards in Indiana coal mining industry
[E73-10970] 21 p2533 N73-30311
Simulation of San Andreas fault for determining relative motion of plates
[NASA-TM-X-70439] 21 p2537 N73-30338
Application of Skylab imagery to analysis of fault tectonics and earthquake hazards in Peninsular Ranges of Southern California
[E73-10999] 22 p2659 N73-31304
Mineral exploration and fracture trends in Utah and Nevada from ERTS-1 imagery
[E73-11032] 22 p2663 N73-31336
Application of ERTS-1 imagery to fracture-related mine safety hazards in Ohio coal mining industry
[E73-11034] 22 p2663 N73-31338
Identification and interpretation of tectonic features from ERTS-1 imagery of Southern California and Baja California
[E73-11084] 24 p2913 N73-33247
Application of Skylab imagery to analysis of fault tectonics and earthquake hazards in Peninsular Ranges, Southern California
[E73-11134] 24 p2917 N73-33289
Application of ERTS-1 imagery to fracture related coal mine safety hazards and environmental problems in mining in Indiana
[E73-11148] 24 p2918 N73-33302
Global metallogeny and geological anomalies
[NASA-TT-F-15098] 24 p2980 N73-33816

GEOLOGICAL SURVEYS
Geology and lithology of Afar region of Ethiopia based on ERTS-1 imagery
[E72-10261] 03 p0290 N73-12360
Geological evaluation, regional planning, forest management, and water management in North Carolina using ERTS-1 imagery
[E72-10280] 03 p0292 N73-12378
Geological survey of Adirondack Mountain region using ERTS-1 multispectral scanner imagery
[E72-10291] 04 p0410 N73-13341
Automatic mapping of geologic features of Fannin County, Texas using MSS imagery from ERTS-1
[E72-10306] 04 p0412 N73-13355
Geological structural surveys of North Carolina based on ERTS-1 imagery
[E72-10325] 05 p0530 N73-14313
Application of ERTS-1 imagery for locating coal refuse deposits, analysis of geologic formations and mapping of agricultural areas in Pennsylvania
[E73-10327] 09 p1024 N73-18358
Survey and mapping Colorado geology using airborne remote sensors
[NASA-CR-130822] 09 p1025 N73-18370
Evaluation and comparison of ERTS-1 measurements of major crops and soil conditions for selected areas in Central United States
[E73-10384] 11 p1275 N73-20348
Interpretation of ERTS-1 geologic data for Nevada and evaluation of materials used in compiling photomaps
[E73-10398] 11 p1277 N73-20360
Mapping of seismically active faults in Alaska using ERTS-1 imagery to determine areas of earthquake occurrence
[E73-10405] 11 p1277 N73-20367
Identification of geologic and hydrologic features of Republic of Mali, West Africa using ERTS-1 imagery
[E73-10435] 11 p1281 N73-20395
Survey of geology, minerals, and water resources in Maryland using ERTS-1 imagery
[E73-10433] 13 p1515 N73-22276
ERTS-1 imagery of Iceland geology, geophysics, hydrology, oceanography, and agriculture
[E73-10535] 13 p1518 N73-22299
Geological survey of West Pakistan from ERTS-1 multispectral imagery
[E73-10540] 13 p1518 N73-22304
Application of Earth Resources Experiment Package data to development of commercial mining activities
[MCR-73-62] 13 p1518 N73-22308
Interpretation of geologic map of Fannin County, Texas, prepared by ADP techniques from ERTS MSS data
[NASA-CR-131574] 13 p1522 N73-22333
Geological survey and mapping of ice-free valleys of Antarctica from interpretation of ERTS-1 imagery
[E73-10564] 14 p1656 N73-23436
Geological surveys and mapping of Netherlands based on ERTS-1 imagery
[E73-10584] 14 p1657 N73-23444
Geologic mapping and mineral resource inventory in South America from ERTS-1 imagery
[E73-10648] 16 p1897 N73-25344
Analysis of ERTS-1 imagery to determine structural and lithological characteristics of northern coast ranges and Sacramento Valley, California
[E73-10698] 16 p1903 N73-25390
Application of ERTS-1 imagery for mapping major geological structural trends and mineralization zones in Utah and Nevada
[E73-10701] 16 p1903 N73-25393
ERTS-1 imagery of geological, climatological, and volcanic activities in Iceland
[E73-10713] 17 p2018 N73-26320
Analysis of time-lapse data processing for dynamic hydrologic conditions based on ERTS-1 imagery and aerial photography
[E73-10729] 17 p2020 N73-26335
Cartographic evaluation of ERTS-1 imagery for area of Bristol, England to show natural and man-made features
[E73-10739] 17 p2021 N73-26345
Application of ERTS-1 imagery for identifying and mapping rivers, agricultural areas, forest, mineral resources, and water conditions in Thailand
[E73-10746] 17 p2021 N73-26350
Geological survey of Botswana using ERTS-1 imagery
[E73-10753] 17 p2022 N73-26356
Application of EREP data in geological evaluation, regional planning, forest management, and water management in North Carolina
[E73-10754] 17 p2022 N73-26357
Application of ERTS-1 imagery for seismic conditions and recent fault formations in eastern California and western and central Nevada
[E73-10769] 18 p2134 N73-27245
Analysis of ERTS-1 imagery for multi-disciplinary resource inventory of soils, vegetation, and geology in Big Summit Prairie area of oregon
[E73-10770] 18 p2134 N73-27246
EREP 463 imagery of fault tectonics and earthquake hazards in peninsular ranges of southern California
[E73-10781] 18 p2136 N73-27257
Skylab and EREP remote sensing data for tectonic analysis of Bighorn Mountains of Wyoming and Montana
[E73-10784] 18 p2136 N73-27260
Iron-absorption band analysis for discrimination of iron rich zones using ERTS-1 imagery
[E73-10789] 18 p2137 N73-27265
Bibliography on remote sensing for agriculture and geological surveys
[PB-219103/9] 18 p2147 N73-27357
Proceedings of conference on significant results obtained from ERTS-1 - Vol. I, Parts A and B
[E73-10824] 19 p2259 N73-28207
Application of ERTS-1 imagery for vegetative and geologic mapping of western Seward Peninsula, Alaska
[PAPER-A8] 19 p2260 N73-28216
Application of ERTS-1 imagery for mapping and identification of vegetation and landforms in Great Basin
[PAPER-A9] 19 p2260 N73-28217
Application of ERTS-1 imagery for mapping and managing soil and range resources in Sand Hills region of Nebraska
[PAPER-A10] 19 p2260 N73-28218
Application of ERTS-1 imagery for delineation of major soil association in loess region of Obion County, Tennessee
[PAPER-A14] 19 p2261 N73-28222
Evaluation of ERTS-1 imagery for geological surveys and topographical analysis of various terrains in New York State
[PAPER-G1] 19 p2263 N73-28233
Combined visual and digital techniques for analyzing ERTS-1 data pertaining to geologic information on selected areas in Pennsylvania
[PAPER-G2] 19 p2263 N73-28234
ERTS-1 imagery of Utah and Nevada to show structural geology, mineral exploration, limnology, and hydrology
[PAPER-G3] 19 p2263 N73-28235
Analysis of ERTS-1 MSS imagery to determine geological and structural features in sedimentary basin in France
[PAPER-G6] 19 p2263 N73-28237
Application of ERTS-1 imagery for monitoring accelerated soil erosion in southern Arizona
[PAPER-G7] 19 p2264 N73-28238
Assessment of geological applications of ERTS-1 imagery from selected areas of Canadian Arctic
[PAPER-G11] 19 p2264 N73-28242
Analysis of ERTS-1 imagery to determine enhancement of ground fracture detail produced by snow cover
[PAPER-G12] 19 p2264 N73-28243
Application of ERTS-1 imagery for differentiating quaternary surface deposits and landforms in Illinois, Iowa, Missouri, Kansas, Nebraska, and South Dakota
[PAPER-G13] 19 p2264 N73-28244
Analysis of geologic features and ground patterns in selected areas of Missouri based on ERTS-1 data
[PAPER-G15] 19 p2265 N73-28246
Analysis of spectral ratioing technique for southern end of of Wind River Range, Wyoming based on ERTS-1 analog ratio images
[PAPER-G16] 19 p2265 N73-28247
Identification of geomorphic features related to known porphyry copper deposit in Pakistan using ERTS-1 imagery
[PAPER-G17] 19 p2265 N73-28248
Analysis of ERTS-1 imagery of Northern Coast Ranges and Sacramento Valley, California for locating mercury deposits and oil and gas fields
[PAPER-G18] 19 p2265 N73-28249
Analysis of regional structures in Verde Valley region of central Arizona based on ERTS-1 data
[PAPER-G19] 19 p2265 N73-28250

Structural analysis of Nevada using ERTS-1 imagery to identify lineaments of surface manifestations of major fault or fracture zones
[PAPER-G20] 19 p2266 N73-28251
Application of ERTS-1 imagery and ground mapping in southern basin-range province of California, Nevada, and Arizona to show tectonic control of tertiary minerlization
[PAPER-G21] 19 p2266 N73-28252
Application of ERTS-1 imagery to identify, locate, and map faults showing geomorphic evidence of geologically recent breakage in Southern California
[PAPER-G22] 19 p2266 N73-28253
Application of ERTS-1 imagery for delineating structural features in Alaska and discovery of active strand in Denali fault
[PAPER-G23] 19 p2266 N73-28254
ERTS-1 imagery of western portion of Nicaragua following December 1972 earthquake to determine lineaments of fault systems related to earthquake
[PAPER-G24] 19 p2266 N73-28255
ERTS-1 imagery applied to definition of geotectonic domains of southern African crystalline shield
[PAPER-G26] 19 p2267 N73-28257
Application of ERTS-1 imagery to determine geological evidence of mineral and hydrocarbon accumulations in Alaska, Canada, Montana, Colorado, New Mexico, and Texas
[PAPER-G30] 19 p2267 N73-28261
Analysis of geological structure in Bighorn Mountains region of Wyoming and Montana based on multispectral band imagery from ERTS-1 satellite
[PAPER-G31] 19 p2267 N73-28262
Application of ERTS-1 imagery for lineament and photogeologic mapping of western Montana
[PAPER-G32] 19 p2268 N73-28263
Geological survey of New Mexico based on ERTS-1 imagery
19 p2284 N73-28370
Proceedings of conference on significant results obtained by ERTS-1 - Vol. 2
[E73-10825] 19 p2287 N73-28389
Application of ERTS-1 imagery for geologic development of natural resources in Alaska
19 p2287 N73-28393
Application of ERTS-1 imagery for multidisciplinary survey to aid in management of Alaskan resources
19 p2288 N73-28394
Application of ERTS-1 imagery for mineral resources, geologic structure, and landform surveys
19 p2288 N73-28398
Application of ERTS-1 imagery to programs conducted by Department of Interior
19 p2289 N73-28401
Application of ERTS-1 imagery to land use and resource management in State of Mississippi
19 p2289 N73-28404
Geological surveys and mapping of New York using ERTS-1 imagery
[E73-10846] 19 p2291 N73-28424
Geological surveys of Colorado from Skylab EREP photography
[E73-10919] 20 p2398 N73-29268
Utilization of Skylab EREP S-191 infrared spectra for geological surveys
[E73-10923] 20 p2398 N73-29272
Utilization of Skylab EREP data in geological evaluation, regional planning, forest management, and water management in North Carolina
[E73-10966] 21 p2533 N73-30308
Solution of certain regional geological problems using space photography
21 p2534 N73-30320
Selection of standard sections in u.s.s.r. as test sites for geological interpretation of space photography
21 p2534 N73-30321
Tyan-shan section of USSR as test site for geological interpretation of space photography
21 p2534 N73-30322
Caucasian section of USSR as test site for geological interpretation of space photography
21 p2534 N73-30323
Ustyurt section of USSR as test site for geological interpretation of space photography
21 p2535 N73-30324
Radar aerial survey and significance in combination with high altitude and space geological research techniques
21 p2535 N73-30325
Geological-structural interpretation of photographs of Balkhash region from space and their role in geological survey of Central Kazakhstan
21 p2535 N73-30329
Geologic structure and geomorphology of Antarctic
[TT-67-59071] 21 p2541 N73-30375
Geological and geochemical studies in Robinson Mining District, White Pine Co., Nevada using Skylab multispectral imagery
[E73-10992] 22 p2659 N73-31298
Application of Skylab multispectral photography and scanner images to geological survey of Basin-and Range-Colorado Plateau boundary in north central and central Arizona
[E73-11000] 22 p2659 N73-31305
Application of Skylab MSS imagery to geological survey of Basin-and-Range-Colorado Plateau boundary in Arizona
[E73-11042] 22 p2664 N73-31343
Geophysical survey of Nevada from Skylab remote sensors
[E73-10998] 23 p2778 N73-32215
Remote sensor data, particularly photography, applied to geological mapping of Rio Grande rift zone
[NASA-CR-135636] 23 p2785 N73-32279
Application of ERTS-1 and EREP imagery to geological surveys and mapping of Basin and Range - Colorado Plateau boundary in Arizona
[E73-11131] 24 p2917 N73-33286

GEOLOGY
NT GEOCHRONOLOGY
NT GEOMORPHOLOGY
NT GLACIOLOGY
NT HYDROGEOLOGY
NT LITHOLOGY
NT LUNAR GEOLOGY
NT OROGRAPHY
NT PETROGRAPHY
NT PETROLOGY
NT PHOTOGEOLOGY
NT STRUCTURAL PROPERTIES (GEOLOGY)
NT TECTONICS
NT VOLCANOES
NT VOLCANOLOGY

Geologic mapping of Basin and Range - Colorado Plateau boundary in Arizona using ERTS-1 imagery
[E72-10157] 01 p0044 N73-10347
Geology and hydrology research summaries
[USGS-PP-800-B] 01 p0048 N73-10390
Soviet Meteor meteorological satellite system and applications in weather forecasting, geological surveys, and exploration of earth resources
[NLL-M-22683-(5828.4F)] 01 p0073 N73-10599
Inventory and management of geological, botanical, and agricultural resources in Wyoming using satellite and airborne imagery and ground control data
[E72-10229] 02 p0163 N73-11322
Identification and mapping geologic, soil, agriculture, geographic, and land use features using ERTS-1 imagery of Central US
[E72-10232] 02 p0163 N73-11325
ERTS-1 imagery of permafrost and geologic hazards in Alaska
[E72-10247] 03 p0289 N73-12347
Stratigraphy, structure, and geologic history of Sangre de Cristo Mountains of Colorado based on aerial remote sensing
[NASA-CR-129519] 03 p0293 N73-12385
Geological applications of side-looking radar, noting mineral exploration, engineering geology, and soil science
03 p0295 N73-12406
Utilization of ERTS-1 imagery in geological evaluation, regional planning, forest management, and water management in North Carolina
[E72-10317] 04 p0413 N73-13366
Compilation of geological and oceanographic data collected by research vessel VEMA
[AD-747652] 04 p0417 N73-13402
Utilization of ERTS-1 imagery of Alabama to study environmental factors, land use, and geology
[E72-10319] 05 p0530 N73-14310
Monitoring changing geologic features along Texas Gulf Coast using ERTS-1 imagery
[E72-10323] 05 p0530 N73-14311
ERTS-1 data as teaching and research tool in Department of Geology at University of Alaska
[E72-10353] 05 p0534 N73-14341
Environmental analyses of Alaskan arctic and subarctic geology and geomorphology using ERTS-1 imagery
[E72-10370] 05 p0536 N73-14358
Geology photography infrared imagery, and remote sensing evaluation of Klondike Mining District, Nevada
[NASA-CR-129934] 05 p0537 N73-14371
Delineation of clustered points in two dimensions by measuring perimeters of convex hulls and applicability in fields of geology and geochemistry
[BM-RI-7565] 05 p0568 N73-14616
Summary of side-looking radar applications in earth resources noting basic principles of side-looking radar, radar scattering, data handling, and research and development
[ESRO-CR[P]-141] 06 p0641 N73-15200
Geological analysis and evaluation of ERTS-1 imagery of New Mexico
[E73-10015] 06 p0659 N73-15351
Recent Soviet investigations in geothermy
[AD-750128] 06 p0671 N73-15454
Detailed gravimetry for exploration of underthrust structures in Northern Sakhalin
[AD-750751] 06 p0672 N73-15465
Analysis of ERTS-1 imagery for identification and discrimination of geological, hydrological, and mineral phenomena in western and central Colorado
[E73-10041] 07 p0776 N73-16304
Geologic investigation of Basin and Range-Colorado Plateau boundary in northwestern and north central Arizona using ERTS-1 and EREP imagery
[E73-10074] 07 p0780 N73-16336
Application of remote sensing from aircraft and spacecraft to geology, hydrology, and geographical data acquisition
07 p0782 N73-16354
Tectonic and paleogeologic mapping of Montana using ERTS-1 imagery
[E73-10280] 08 p0914 N73-17488
ERTS-1 imagery of geography, geology, and glaciology of Germany and part of Alps Mountains
[E73-10099] 09 p1020 N73-18322
Geologic mapping of Montana using ERTS-1 imagery
[E73-10281] 09 p1020 N73-18325
Utilization of ERTS-1 imagery in geological evaluation, regional planning, forest and water management in North Carolina
[E73-10300] 09 p1021 N73-18332
ERTS-1 imagery of geology in ice free valleys of Antarctica
[E73-10309] 09 p1022 N73-18341
ERTS-1 imagery of permafrost and geologic hazards in Alaska
[E73-10320] 09 p1023 N73-18352
Application of ERTS-1 imagery to Bureau of Reclamation studies of geology, agriculture, and urban development
[E73-10336] 10 p1147 N73-19337
Utilization of ERTS-1 imagery for mapping Quaternary deposits and landforms in Great Plains and Midwest
[E73-10381] 10 p1152 N73-19376
Utilization of ERTS-1 imagery as teaching and research tool in Department of Geology at University of Alaska
[E73-10403] 11 p1277 N73-20365
Analysis of ERTS-1 imagery for identification and discrimination of geological and hydrological phenomena in central and western Colorado
[E73-10422] 11 p1280 N73-20383
Application of ecological, geological, and oceanographic ERTS-1 imagery to coastal resources management and planning in Delaware
[E73-10426] 11 p1280 N73-20387
Physical interpretation of geology, hydrology, and glaciology revealed by ERTS-1 imagery of east central Ohio
[E73-10454] 11 p1283 N73-20413
Development of electromagnetic pulse sounding probe for detection and delineation of geological anomalies in hard rock medium
[AD-754847] 11 p1288 N73-20454
Geological investigation of future ocean bottom drilling for crude oil and other raw materials
[JPRS-58668] 12 p1401 N73-21366
Literature compilation on marine geology and geophysics for Caribbean Sea and adjacent regions
14 p1607 N73-23023
Broad scale application of ERTS-1 imagery to study and mapping of geological, hydrological, land use, rangelands, and soil cultures in Wyoming
[E73-10554] 14 p1655 N73-23426
Correlation between vegetation patterns and geologic and geomorphic units in New Mexico based on ERTS-1 imagery
[E73-10588] 14 p1657 N73-23448
Geological features of Martian surface based on Mariner 9 photographs
[NASA-TT-F-14840] 14 p1704 N73-23831
ERTS-1 imagery of permafrost and geologic hazards in Alaska
[E73-10601] 15 p1772 N73-24362
Geologic, mineral, and water resources investigations in western Colorado using ERTS-1 imagery
[E73-10608] 15 p1773 N73-24369
Geological mapping in Bolivia using ERTS-1 imagery
[E73-10614] 15 p1774 N73-24375
Application of ecological, geological, and oceanographic ERTS-1 imagery to Delaware coastal resources management and planning
[E73-10631] 15 p1776 N73-24391
Utilization of ERTS-1 data as teaching and research tool in Department of Geology at University of Alaska
[E73-10635] 15 p1776 N73-24394
Geologic mapping of Bonanza Test Site Colorado using remotely sensed data
[NASA-CR-132231] 15 p1780 N73-24433
Integrated analysis of past and present climates of Northern Cumberland and Peninsula
[AD-757270] 15 p1783 N73-24457
Utilization of ERTS-1 imagery in geological evaluation, regional planning, forest and water management in North Carolina
[E73-10688] 16 p1902 N73-25382
Commercial application of ERTS-1 imagery in structural reconnaissance for minerals and petroleum
[E73-10700] 16 p1903 N73-25392
Application of ERTS-1 imagery to geologic investigations of Basin and Range Colorado Plateau boundary in northwestern and north-central Arizona
[E73-10645] 17 p2017 N73-26312

Application of ERTS-1 data to crop identification, land use, and engineering geology
[E73-10792] 18 p2137 N73-27268
Determination of variations in spectral signatures for different geological target types and correlation with radiometric measurements from air and ground
[E73-10808] 18 p2139 N73-27283
Determination of variation in spectral signatures for different geological target types using ERTS-1 radiometric data
[E73-10809] 18 p2139 N73-27284
Variations in spectral signatures for different geological types based on ERTS-1 radiometric data
[E73-10810] 18 p2139 N73-27285
Interpretation of geologic, mineral, and water resources in western Colorado from ERTS-1 imagery
[E73-10814] 18 p2139 N73-27289
Analysis of New Mexico geology using ERTS-1 imagery
[E73-10830] 18 p2140 N73-27300
Geological landforms in central Piedmont of Virginia and North Carolina from ERTS-1 imagery
[E73-10766] 19 p2259 N73-28205
Analysis of ERTS-1 MSS imagery to determine geologic, hydrologic, oceanographic, and agricultural phenomena in Iceland
[PAPER-G10] 19 p2264 N73-28241
ERTS-1 imagery of land use, agriculture, vegetation, geology, landforms, and hydrology in Central Coastal Zone of California
[PAPER-L4] 19 p2273 N73-28300
VICAR image processing system used for enhancement of ERTS-1 images for Arizona geological experiment
[PAPER-I9] 19 p2278 N73-28330
Comparison of conventional maps of southeastern Massachusetts to ERTS-1 imagery of coastal and submarine geology and hydrology
[PAPER-M18] 19 p2282 N73-28356
ERTS-1 imagery of water pollution, sedimentation, and geology of southeastern France and western Alps
[PAPER-R6] 19 p2283 N73-28364
ERTS-1 imagery of geology, agriculture, forestry, and hydrology in Iran
19 p2287 N73-28387
ERTS-1 applications in land use, geologic interpretation, resources survey, and pollution monitoring
19 p2290 N73-28413
Identification and discrimination of geological and hydrological phenomena in central and western Colorado using ERTS-1 imagery
[E73-10837] 19 p2290 N73-28415
Utilization of ERTS-1 imagery as teaching and research tool in Department of Geology at University of Alaska
[E73-10841] 19 p2290 N73-28419
Application of ERTS-1 imagery to geologic, hydrologic, agricultural, botanical, and land use studies in Wyoming
[E73-10844] 19 p2291 N73-28422
Application of multispectral scanning to agriculture, oceanography, hydrology, and geology
[ERL/R-246] 19 p2294 N73-28450
Application of multispectral scanning to geology, noting interpretation problems
19 p2295 N73-28453
ERTS-1 imagery of Namafjall geothermal area, Iceland
[E73-10874] 20 p2393 N73-29225
Geologic, mineral, and water resources of western Colorado from Skylab EREP data
[E73-10918] 20 p2398 N73-29267
Geological, hydrological, ecological, and agricultural mapping of Botswana from ERTS-1 photography
[E73-10928] 20 p2399 N73-29277
Geology, hydrology, and ecology of Botswana from ERTS-1 MSS imagery
[E73-10929] 20 p2399 N73-29278
Discovery and geographical distribution of tektites
[NASA-TT-F-15052] 20 p2411 N73-29378
Microbiology of sediments and its geological aspects
[NASA-TT-F-15022] 20 p2411 N73-29381
Determination of seasonal, meteorological, and statistical variations in spectral signatures for geological target types from ERTS-1 data
[E73-10933] 21 p2529 N73-30275
Application of ecological, geological, and oceanographic ERTS-1 imagery to Delaware coastal resources management and planning
[E73-10934] 21 p2529 N73-30276
Geology, volcanology, and glaciology of Wrangell Mountains, Alaska from ERTS-1 imagery
[E73-10940] 21 p2529 N73-30282
Mapping of Quaternary geological and geomorphological landforms of Great Plains and Midwest from ERTS-1 imagery
[E73-10949] 21 p2530 N73-30291
Geological evaluation, regional planning, forest management, and water management in North Carolina using ERTS-1 imagery
[E73-10962] 21 p2532 N73-30304
Utilization of ERTS-1 imagery for studies of agriculture, forestry, cartography, geography, hydrology, meteorology, geology, and oceanography in Thailand
[E73-10996] 22 p2659 N73-31302
Analysis of geology, ecology, and hydrology of Colorado mountains from Skylab multispectral photography and data
[E73-11002] 22 p2659 N73-31307
Geological studies of Nevada from Skylab S-191 infrared spectra
[E73-11003] 22 p2659 N73-31308
ERTS-1 imagery of geology, botany, agriculture, hydrology, and cultural features of Wyoming
[E73-11022] 22 p2661 N73-31326
Identification and mapping landform and land use characteristics and surficial geologic materials in Great Plains and Midwest
[E73-11025] 22 p2662 N73-31329
Selected reclamation studies on geology and crop inventory using ERTS-1 imagery of lower Missouri region
[E73-11027] 22 p2662 N73-31331
General geology and potential geologic problems of proposed Deer Creek Reservoir in Converse County, Wyoming
22 p2666 N73-31358
Performances and limitations of geological remote sensing from earth resources survey aircraft and satellites
[BMBW-FBW-72-28] 22 p2667 N73-31370
Interdisciplinary analysis of Colorado Rocky Mountain environments using ADP techniques
[E73-11039] 23 p2778 N73-32218
Identification and discrimination of geological, hydrological, and mineralogical phenomena in central and western Colorado from ERTS-1 data
[E73-11047] 23 p2779 N73-32223
Tectonic analysis and mapping of Bighorn Mountains from ERTS-1 imagery
[E73-11049] 23 p2779 N73-32225
Remote sensing geophysics and geology from Skylab EREP
[E73-11072] 23 p2781 N73-32247
Geological Mars data obtained by Mariner 9 observations
23 p2838 N73-32681
Geological Mars map deduced from Mariner 9 surface photography
23 p2838 N73-32682
USSR research in solid state physics, laser technology, geosciences, and materials
[AD-763742] 23 p2866 N73-32916
Ratio scannergrammetry of geology in Wyoming and South Dakota
[E73-11096] 24 p2914 N73-33253
Correlation of ERTS-1 imagery signatures with water balance ecosystem and geology of select playa lake basins in West Texas
[E73-11102] 24 p2914 N73-33259
Utilization of ERTS-1 data and imagery as teaching and research tool in Department of Geology, University of Alaska
[E73-11128] 24 p2917 N73-33283
Geology, mineral deposits, and water resources of western Colorado from Skylab EREP data
[E73-11130] 24 p2917 N73-33285
Application of Skylab EREP data to structural geology, geomorphology, vegetation mapping, and land use studies in Wyoming
[E73-11136] 24 p2917 N73-33291

**GEOMAGNETIC ANOMALIES**
U MAGNETIC ANOMALIES

**GEOMAGNETIC CROTCHETS**
U SUDDEN IONOSPHERIC DISTURBANCES

**GEOMAGNETIC EFFECTS**
U MAGNETIC EFFECTS

**GEOMAGNETIC EQUATOR**
U MAGNETIC EQUATOR

**GEOMAGNETIC FIELD**
U GEOMAGNETISM

**GEOMAGNETIC LATITUDE**
Generalized magnetic Weber-Davis model for calculating magnetic latitude effects in solar wind
01 p0094 N73-10778
Computer analysis of quasi-sinusoidal geomagnetic variations at geomagnetic midlatitude
[AD-752229] 08 p0920 N73-17543

**GEOMAGNETIC MICROPULSATIONS**
Ground based HF sounding technique for detecting ionospheric disturbances associated with Pc 1 micropulsations
[AD-752062] 08 p0919 N73-17532
Generation of artificial geomagnetic micropulsations with large ground-based current load from MHD wave propagation in ionosphere
[AD-752061] 08 p0919 N73-17533
Computer analysis of quasi-sinusoidal geomagnetic variations at geomagnetic midlatitude
[AD-752229] 08 p0920 N73-17543
Propagation of geomagnetic micropulsations into two layer conducting earth
[AD-755428] 12 p1402 N73-21375
Longitudinal source drift measure of PC 1 geomagnetic micropulsation source by signal correlation of spaced receivers
[CEPHAG-22/72] 13 p1524 N73-22353
Review of geomagnetic micropulsation modes for possible communications application
[AD-759380] 16 p1878 N73-25203
Franco-Soviet conference on conjugate points, noting analyses of Pc 1 geomagnetic micropulsations
[CEP-AG-10/73] 17 p2026 N73-26395
Magnetospheric proton density from satellite and ground observation of type Pc3 geomagnetic micropulsations
17 p2026 N73-26396
Geomagnetic latitude distribution of stationary Pc3 micropulsation statistical properties from power spectra cross correlations
17 p2026 N73-26397
Polarization of Pc1 micropulsations observed in the same hemisphere, and in conjugate points
17 p2026 N73-26398
Evaluation of Pc1 geomagnetic micropulsations with automatic signal detectors, noting dispersion
17 p2027 N73-26401
Adapted filter for dispersion measurement of coherent wave packets produced by Pc1 micropulsations
17 p2027 N73-26402

**GEOMAGNETIC PULSATIONS**
NT GEOMAGNETIC MICROPULSATIONS
Propagation of magnetohydrodynamic waves in cold plasma inclined to ionosphere and applied to geomagnetic pulsation study
[PR-119] 10 p1156 N73-19401
Geomagnetic micropulsations during magnetic storms as observed by ATS 1
12 p1447 N73-21716

**GEOMAGNETIC STORMS**
U MAGNETIC STORMS

**GEOMAGNETIC TAIL**
Simulation of geomagnetic tail by plasma flux interaction with magnetic field of three dimensional dipole
[PR-113] 05 p0584 N73-14753
Amplitudes of natural oscillations of geomagnetic tail excited by solar wind
06 p0665 N73-15404
Influence of inhomogeneity of magnetic field on oscillations of plasma layer of magnetosphere tail
06 p0665 N73-15407
Magnetospheric plasma tail study, using thermal proton density measurements from OGO 4
08 p0972 N73-17948
Magnetohydrodynamic theory of diurnal oscillations of earth magnetic tail
09 p1029 N73-18395
Substorm thinning and thickening of magnetotail plasma sheet
[LA-DC-72-1165] 10 p1155 N73-19397
Solar proton penetration into geomagnetic tail and ionospheric polar cap
10 p1210 N73-19843
Precision radar ranging of meteor trails and possible ranging techniques
[AD-754623] 11 p1339 N73-20868
Oscillations of geomagnetic tail and magnetospheric instability from solar activity
12 p1401 N73-21365
Oscillations of earths magnetic tail studied from model of plasma cylinder with free boundary
14 p1703 N73-23820
Quasi-hydrodynamic equations for analyzing pressure anisotropy effects on magnetospheric tail oscillations
14 p1703 N73-23821
Electron acceleration mechanism during geomagnetic tail collapse associated with substorm activity
[UNH-73-04] 15 p1779 N73-24418
Parallel layer model for hydromagnetic wave absorption in magnetospheric tail plasma
15 p1779 N73-24420
Velocity and outer limits of magnetic bottles ejected by solar proton flares as observed by Pioneer 6
[NASA-TM-X-66243] 15 p1828 N73-24814
Magnetic field and current configuration with boundary conditions holding geomagnetic tail
18 p2132 N73-27230
Magnetotail neutral line and associated plasma phenomena in substorms
[ISAS-497-VOL-38-NO-8] 22 p2664 N73-31346

**GEOMAGNETICALLY TRAPPED PARTICLES**
U RADIATION BELTS

**GEOMAGNETISM**
Description of magnetic and seismic facility at Great Whale River, Canada and analysis of data acquired during calendar year 1969 - Vol. 43, No. 3
[M70-43/3] 01 p0043 N73-10343
Description of magnetic and seismic facility at Baker Lake, Canada and analysis of data acquired during calendar year 1969 - Vol. 43, No. 2
[M70-43/2] 01 p0044 N73-10345
Three component aeromagnetic survey of British Columbia and northeastern Pacific Ocean to determine magnetic anomalies - Vol. 42, No. 7
[M70-42/7] 01 p0044 N73-10346
Hourly geomagnetic measurements at Nurmijaeri, Finland - tables
01 p0048 N73-10383

Dourbes [Belgium] Geophysical Observatory data on geomagnetism, ionospheric propagation, seismology, cosmic rays, and atmospheric electricity, Nov. 1971
01 p0050 N73-10401
Dourbes [Belgium] Geophysical Observatory data on geomagnetism, ionospheric propagation, seismology, cosmic rays, and atmospheric electricity, Dec. 1971
01 p0050 N73-10405
Analyzing component measurements of geomagnetic field by Sputniks for solving geophysical problems
[NASA-TT-F-14446] 01 p0105 N73-10865
Influence of interplanetary magnetic field on geomagnetic variations in polar cap
[NASA-CR-129165] 02 p0166 N73-11351
Comparison of satellite ozone contours during 1965 geomagnetic storm and L-shell parameters
[WRE-TN-80(WR/D)] 03 p0296 N73-12412
Dourbes [Belgium] Geophysical Observatory data on geomagnetism, ionospheric propagation, seismology, cosmic rays, and atmospheric electricity, Jan. 1972
SEISMOLOGY IONOSPHERIC PROPAGATION
03 p0296 N73-12416
Development and improvement of magnetovariation station for conducting magnetotelluric soundings
[JPRS-57678] 04 p0401 N73-13262
Graphical and analytical methods for describing earth magnetic field using satellite and ground based observational data
04 p0414 N73-13382
Tables of earth magnetic field intensity measurements at Sao Jose dos Campos, Brazil
[AD-747060] 04 p0415 N73-13389
Correlation between frequency of magnetic oscillations and geomagnetic disturbances, and low frequency oscillation of earth magnetic field
[NASA-CR-127801] 05 p0537 N73-14372
Correlation between frequency of magnetic oscillations observed by ATS 1 and two indices of geomagnetic disturbance
05 p0537 N73-14373
Low frequency oscillations of earth magnetic field observed by ATS 1
05 p0537 N73-14374
Geomagnetic measurements in south and east Finland 1967 through 1971 and final values reduced to 1970.0
[REPT-23] 06 p0666 N73-15416
Standard curves for interpreting magnetic anomalies due to spheres in geomagnetic surveys
[BULL-119] 06 p0666 N73-15417
Laboratory simulation of solar wind interaction with geomagnetic field, and measurements of magnetosphere at shock wave front and of field configuration on nocturnal side
[D-15] 06 p0716 N73-15838
Relationship between polar geomagnetic variations and polarity of interplanetary magnetic sectors
[NASA-CR-130270] 07 p0780 N73-16343
Tables of geomagnetic and geoelectric magnetograms and tellurigrams measured at Kakioka Magnetic Observatory, Japan
[REPT-12] 07 p0788 N73-16411
Bathymetry, free air gravity anomaly, and magnetic field intensity data on Strait of Sicily, gathered from 1965 to 1971
[SACLANTCEN-CONF-PROC-7]8 p0915 N73-17501
Computer analysis of quasi-sinusoidal geomagnetic variations at geomagnetic midlatitude
[AD-752229] 08 p0920 N73-17543
Geomagnetic measurement using cesium Z-magnetometer aboard nonmagnetic schooner Zarya
[JPRS-58040] 08 p0925 N73-17579
Dourbes, Belgium, geophysical observatory data on geomagnetism, ionospheric propagation, seismology, cosmic rays, and atmospheric electricity, Feb. 1972
09 p1030 N73-18403
Dourbes, Belgium, geophysical observatory data on geomagnetism, ionospheric propagation, seismology, cosmic rays, and atmospheric electricity, Mar. 1972
09 p1030 N73-18404
Dourbes, Belgium, geophysical observatory data on geomagnetism, ionospheric propagation, seismology, cosmic rays, and atmospheric electricity, Apr. 1972
09 p1030 N73-18405
Dourbes, Belgium, geophysical observatory data on geomagnetism, ionospheric propagation, seismology, cosmic rays, and atmospheric electricity, May 1972
09 p1030 N73-18406
Dourbes, Belgium, geophysical observatory data on geomagnetism, ionospheric propagation, seismology, cosmic rays, and atmospheric electricity, Jun. 1972
09 p1030 N73-18407
Dourbes, Belgium, geophysical observatory data on geomagnetism, ionospheric propagation, seismology, cosmic rays, and atmospheric electricity, Jul. 1972
09 p1030 N73-18408
Attitude stability and alignment of magnetically oriented ESRO I satellite
[ESRO-SN-120-ESTEC] 09 p1085 N73-18854
Magnetic results 1969, Eskdalemuir, Hartland and Lerwick observatories, emphasizing diurnal values
[BULL-3] 10 p1145 N73-19323
Penning discharge along magnetic field in collision-free plasma to simulate geomagnetic flux tube conditions
[TRITA-EPP-72-13] 10 p1189 N73-19676
VLF magnetotelluric measurements in Sweden
[KGO-72-10] 12 p1402 N73-21369
Arizona aeromagnetic map from data of digitally recording proton precession magnetometer
13 p1514 N73-22265
Two substorm studies of relations between westward electric fields in outer plasmasphere, auroral activity, and geomagnetic perturbations
[NASA-CR-131497] 13 p1518 N73-22309
Table of hourly and daily values of geomagnetic field declination and intensity recorded at Eskdalemuir, Hartland, and Lerwick Observatories, England, in 1969
[GEOMAGNETIC-BULL-3] 13 p1525 N73-22356
Conversion of geomagnetic potential into spherical coordinates of optimally offset, inclined dipole using least squares method
[AD-756460] 13 p1526 N73-22366
Diurnal geomagnetic variations
[AD-755787] 13 p1526 N73-22369
Inferring polarity of interplanetary magnetic field from observations of diurnal variation of polar geomagnetic fields
[NASA-CR-131609] 13 p1527 N73-22379
Disappearance of E region following changes in geomagnetic H component
[AER-73-04] 14 p1658 N73-23455
Catalog of data in World Data Center C2 for Geomagnetism
14 p1658 N73-23456
Satellite observations of geomagnetic disturbance reaction time in upper atmosphere
[REPT-85] 14 p1658 N73-23458
Afternoon depression of geomagnetic H field on quiet days near magnetic equator in Indian zone
[AER-73-03] 14 p1658 N73-23459
Spherical harmonic analysis of Cosmos-321 geomagnetic survey
14 p1659 N73-23463
Geomagnetic survey of Japan and nearby areas conducted from July 1969 to November 1970
[PUB-592] 14 p1660 N73-23474
Geomagnetic observations made in Japan and surrounding areas from 1967 to 1969
[PUB-591] 14 p1660 N73-23475
Forty year statistical study of geomagnetic data
[AD-756828] 14 p1663 N73-23497
Geophysical and space data bulletin
[AD-755839] 14 p1706 N73-23849
Short geomagnetic polarity intervals in marine magnetic profile for anomalies, using Fourier transformations and linear systems
15 p1770 N73-24336
Geomagnetic annuals for Spanish observatories
15 p1777 N73-24400
Geomagnetic measurements for 1970 at Toledo
15 p1777 N73-24401
Geomagnetic data for 1970 at Almeria
15 p1777 N73-24402
Geomagnetic data for 1970 at Logrono
15 p1777 N73-24403
Geomagnetic data for 1970 at Santa Cruz, Tenerife
15 p1777 N73-24404
Geomagnetic data during 1970 for Moca
15 p1777 N73-24405
Translational-rotational magnetized satellite equations of motion in geomagnetic field
15 p1832 N73-24847
Geomagnetic field direction intensity hourly variations recorded at Roburent Observatory, Italy, for 1972
16 p1907 N73-25431
Mediterranean Sea geophysical survey
[AD-757455] 16 p1910 N73-25452
Magnetic measurements of atmosphere in 1970 at Eskdalemuir, Hartland, and Lerwick
[SBN-11-880601-7] 17 p2016 N73-26305
Harmonic analysis of low altitude disturbances in geomagnetic fields
17 p2017 N73-26308
Dourbes [Belgium] geophysical observatory data on geomagnetism, ionospheric propagation, seismology, cosmic rays, and atmospheric electricity, Aug. 1972
17 p2028 N73-26411
Dourbes [Belgium] geophysical observatory data on geomagnetism, ionospheric propagation, seismology, cosmic rays, and atmospheric electricity, Sep. 1972
17 p2028 N73-26412
Survey of earth geomagnetic field
[AD-759837] 17 p2030 N73-26427
Automated iterative analysis of aeromagnetics
17 p2062 N73-26684
Cosmic rays in earth magnetic field
[NASA-TT-F-756] 17 p2079 N73-26819
Relation between azimuth component of interplanetary magnetic field and geomagnetic field in polar caps
[NASA-CR-133273] 18 p2145 N73-27338
Application of dynamic nuclear polarization to increase sensitivity and speed of nuclear precission magnetometers
[JPRS-59393] 18 p2151 N73-27386
Rude Skov Geophysical Observatory magnetic results, 1969
[ISBN-37-7478-065-4] 20 p2412 N73-29388
Ship towed magnetometer and ocean bottom mounted magnetic variation station
[JPRS-59802] 21 p2547 N73-30417
Use of differential magnetometers with mobile carriers for earth magnetic field measurements
22 p2671 N73-31398
Analysis of daily variation of geomagnetic field for eight quiet days of IGY
23 p2777 N73-32210
Information capacity of gradient method for measuring earth magnetic field
[JPRS-60100] 23 p2786 N73-32292
FORTRAN 4 program for determining transient tangential electric field and vertical magnetic dipole for stratified earth model
[PB-221240/5] 23 p2788 N73-32304
Interpretation of aeromagnetic or gravity data by method of difference mapping for mineral exploration
24 p2912 N73-33240
Magnetic observations for 1971
[M70-44/4] 24 p2920 N73-33323
Hydromagnetic gradient waves in ionosphere
24 p2921 N73-33331
Geophysical data tables and graphs for Dourbes, Belgium
24 p2924 N73-33352
Dourbes [Belgium] geophysical observatory data on geomagnetism, ionospheric propagation, seismology, cosmic rays, and atmospheric electricity. Nov. 1972
24 p2924 N73-33353
Geophysical observatory data obtained at Dourbes, Belgium in Dec. 1972 on geomagnetism, ionospheric propagation, seismology, cosmic rays, and atmospheric electricity
24 p2924 N73-33354

**GEOMETRICAL HYDROMAGNETICS**
U MAGNETOHYDRODYNAMICS
**GEOMETRICAL OPTICS**
U OPTICS
**GEOMETRODYNAMICS**
U RELATIVITY
**GEOMETRY**
NT ANALYTIC GEOMETRY
NT ANGLES [GEOMETRY]
NT BOSE GEOMETRY
NT BRAGG ANGLE
NT BREWSTER ANGLE
NT CARTESIAN COORDINATES
NT CIRCLES [GEOMETRY]
NT CUBES [MATHEMATICS]
NT CURVATURE
NT CURVES [GEOMETRY]
NT CUSPS [MATHEMATICS]
NT CYCLOIDS
NT ELLIPSES
NT EUCLIDEAN GEOMETRY
NT FIXED POINTS [MATHEMATICS]
NT FLOW GEOMETRY
NT HEXAGONS
NT IMBEDDINGS [MATHEMATICS]
NT INFLECTION POINTS
NT LIE GROUPS
NT LINES [GEOMETRY]
NT LOCI
NT METRIC SPACE
NT NOZZLE GEOMETRY
NT OBLATE SPHEROIDS
NT POINTS [MATHEMATICS]
NT PROJECTIVE GEOMETRY
NT RADII
NT RECTANGLES
NT TANGENTS
NT TENSOR ANALYSIS
NT TOPOLOGY
NT TORUSES
NT TRIANGLES
NT VECTOR ANALYSIS
NT VORTICITY
Stereoradiography study of depth and geometrical dimensions of internal flaws in weldments
[AD-749459] 04 p0428 N73-13486
Prediction analysis method to determine influence of geometry parameters on aerodynamic characteristics of body-wing configuration
[DLR-FB-72-63] 06 p0622 N73-15050
Energy variation principle for specific inductance geometry in stable toroidal plasma generation
[NYO-1480-182] 06 p0704 N73-15741
Computer program for solving radiation-hydrodynamic problems in complex geometries
[AD-752066] 08 p0970 N73-17929
Precision geometric and radiometric correction of bulk digital ERTS-1 imagery by digital techniques
[E73-10342] 10 p1148 N73-19341
Influence of variation in cylinder geometry on fragmentation and mode of fracture of internally detonated carbon steel cylinders
[DSL-REPT-533] 16 p1969 N73-25930
Digital system for precision geometric and radiometric correction of ERTS-1 RBV and MSS images
[E73-10827] 18 p2140 N73-27299

Precision geometric and radiometric correction of bulk digital ERTS-1 imagery of Baltimore, Maryland by digital method
[E73-11019] 22 p2661 N73-31323
Geometrical interpretation of 2n-th central difference using simple recursive functions
[NASA-CR-133985] 22 p2691 N73-31554
Geometric codes for calculating space radiation transport in shielding configurations
[NASA-CR-124403] 23 p2821 N73-32551
GEOMORPHOLOGY
Relationships of vegetation distribution to geomorphic characteristics of landscape and of plant phenological patterns to vegetation identification of satellite imagery of Arizona
[E72-10228] 02 p0163 N73-11321
Geomorphology, tectonics, and structural relations between Alps and Pyrenees based on ERTS-1 imagery
[E72-10286] 04 p0410 N73-13336
Automatic mapping of geologic features of Fannin County, Texas using MSS imagery from ERTS-1
[E72-10306] 04 p0412 N73-13355
Environmental analyses of Alaskan arctic and subarctic geology and geomorphology using ERTS-1 imagery
[E72-10370] 05 p0536 N73-14358
Geophysical survey of continental shelves off African coast and mapping for oil potential
[PB-211393] 05 p0541 N73-14400
ERTS-1 imagery of regional geography and geomorphology of Mankoya-Kolwezi strip in Zambia and Zaire
[E73-10293] 10 p1146 N73-19331
ERTS-1 imagery of geography and geomorphology of Ndola-Mweru Wantipa strip in Zambia and Zaire
[E73-10294] 10 p1146 N73-19332
Utilization of ERTS-1 imagery for mapping Quaternary deposits and landforms in Great Plains and Midwest
[E73-10381] 10 p1152 N73-19376
Geological structure effect on seismic wave propagation in earth and upper mantle
[AD-753110] 10 p1156 N73-19408
Application of ERTS-1 data for identifying ethnic groups, limits of occupancy, and use of physiographic features in Republic of Mali, West Africa
[E73-10434] 11 p1281 N73-20394
Possible analogs around Orientale Basin provide reasonable alternatives to geomorphologic interpretation of volcanism in Descartes highlands - Part D
12 p1453 N73-21768
Problems of preparing geological-morphological maps of moon from telescopic pictures of lunar surface
12 p1456 N73-21797
Features of lunar furrows and ridges from telescopic and satellite photographs
12 p1457 N73-21808
Interdisciplinary analysis of Skylab EREP MSS photography of vegetative and geomorphological cover types in Colorado Mountains
[E73-10533] 13 p1517 N73-22297
Geomorphic coastal variability for Northwestern Australia
[AD-755154] 13 p1527 N73-22377
Ecology, hydrology, geomorphology, and terrain modeling of Colorado mountain environments from ERTS-2 data
[E73-10551] 14 p1655 N73-23424
Correlation between vegetation patterns and geologic and geomorphic units in New Mexico based on ERTS-1 imagery
[E73-10588] 14 p1657 N73-23448
Catalog of meteorological and geomorphological data acquired from Nimbus 2 satellite
[NASA-TM-X-69886] 14 p1707 N73-23852
Application of ERTS-1 imagery to cartography, geomorphology, agronomy, and hydrology of Bolivia
[E73-10695] 16 p1902 N73-25387
Analysis of ERTS-1 imagery to determine structural and lithological characteristics of northern coast ranges and Sacramento Valley, California
[E73-10698] 16 p1903 N73-25390
Variability of coastal processes and resulting shoreline morphology along peninsula of Baja California
[AD-756676] 16 p1907 N73-25432
ERTS-1 imagery of geological, climatological, and volcanic activities in Iceland
[E73-10713] 17 p2018 N73-26320
Detection and analysis of fracture systems using ERTS-1 imagery of snow cover conditions as enhancement tool
[E73-10741] 17 p2021 N73-26346
Geomorphological structure of earth surface from spaceborne photography
[NASA-TT-F-14968] 17 p2025 N73-26388
ERTS-1 imagery applied to definition of geotectonic domains of southern African crystalline shield
[PAPER-G26] 19 p2267 N73-28257
Assessment of ERTS-1 imagery for mapping geologic features of Gaspe Peninsula, Quebec and determination of lithologic lineaments
[PAPER-G28] 19 p2267 N73-28259
Analysis of ERTS-1 data for studies of hydrogeology, geomorphology, and paleoclimatology in Bolivia, Argentina, Chile, and Peru
[PAPER-W1] 19 p2270 N73-28281
Application of ERTS-1 data to geomorphotectonics, earthquake studies, and mineral exploration at Los Angeles, California, and New Jersey coastal plain
19 p2284 N73-28367
Field sampling taxonomic units within geomorphic-soil-vegetation mapping units in Arizona
[E73-10889] 20 p2394 N73-29238
Physiographic terrain analysis in Colorado using principles of aerial photointerpretation
20 p2416 N73-29413
Mapping of Quaternary geological and geomorphological landforms of Great Plains and Midwest from ERTS-1 imagery
[E73-10949] 21 p2530 N73-30291
Synoptic identification and mapping of Quaternary geologic and geomorphic units in Midwest-Great Plains area
[E73-10951] 21 p2531 N73-30293
Geologic structure and geomorphology of Antarctic
[TT-67-59071] 21 p2541 N73-30375
Morphology of lunar surface
21 p2594 N73-30781
Identification and mapping landform and land use characteristics and surficial geologic materials in Great Plains and Midwest
[E73-11025] 22 p2662 N73-31329
Interdisciplinary analysis of Colorado Rocky Mountain environments using ADP techniques
[E73-11039] 23 p2778 N73-32218
Electronic scanning microwave radiometer system for measurement of meteorological, geomorphological, and oceanographic parameters from Nimbus 5
[NASA-CR-132812] 23 p2793 N73-32342
Scientific Mars research by Mariner 9 space probe
[NASA-CR-135530] 23 p2838 N73-32680
Mars surface erosion and canal formation by running water
23 p2838 N73-32683
Volcanic features in Mars surface photographs
23 p2839 N73-32684
Geomorphology of troughs in Mariner 9 Mars surface observations
[CONTRIB-2265] 23 p2839 N73-32685
Geomorphology of fretted and chaotic terrains on Mars surface
[CONTRIB-2264] 23 p2839 N73-32686
Geomorphology of Martian and lunar large multi-ringed circular basins
23 p2839 N73-32687
Wind erosion features in Mariner 9 Mars surface observations
23 p2839 N73-32690
Application of Skylab EREP data to structural geology, geomorphology, vegetation mapping, and land use studies in Wyoming
[E73-11136] 24 p2917 N73-33291
GEON [TRADEMARK]
U POLYVINYL CHLORIDE
GEOPHYSICAL OBSERVATORIES
NT OGO
NT OGO-A
NT OSO-5
NT OSO-6
Detection and classification of earthquakes and nuclear explosions by Swedish observatory
[FOA-4-A-4503-TR78] 01 p0101 N73-10828
Variometer recordings at Narssarssuaq Geophysical Observatory 1968 - 1970
02 p0167 N73-11356
Polar ionospheric geophysical data recording at Kiruna, Sweden, during Apr.-Jun. 1972
06 p0667 N73-15424
Ionospheric magnetospheric, lunar and meteorite research, satellite geodesy, orbits, tracking, telemetry, and remote sensing in Finland in 1972
[S-52] 12 p1467 N73-21888
Kiruna [Sweden] polar geophysic observatory ionospheric data recorded from Jul.-Sep. 1972
13 p1525 N73-22355
Diurnal and hourly geomatnetic variations recorded at Thule Geophysical Observatory, Greenland, in 1947
13 p1525 N73-22357
Diurnal and hourly geomagnetic variations recorded at Thule Geophysical Observatory, Greenland, in 1948
13 p1525 N73-22358
Dirunal and hourly geomagnetic variations recorded at Thule Geophysical Observatory, Greenland, in 1949
13 p1525 N73-22359
Evaluation of data processing systems for Alaskan and Norwegian seismic arrays
[AD-756905] 13 p1525 N73-22360
Geophysical observations of horizontal and vertical components of earth magnetic field at Feurstenfeldbruck, Germany for 1972
14 p1660 N73-23473
Solar and geophysical data obtained by ionospheric sounding over India for April, 1972
[RRC-A202-PT-2] 16 p1907 N73-25423
Polar ionospheric geophysical data recording in Sweden, Jan-Mar. 1973
19 p2295 N73-28459
Diurnal and hourly geomagnetic variations recorded at Godhavn Geophysical Observatory during 1966
[ISBN-87-7478-066-2] 23 p2788 N73-32302
Diurnal and hourly geomagnetic variations recorded at Thule Geophysical Observatory, Greenland, in 1966
[ISBN-87-7478-069-7] 23 p2788 N73-32303
GEOPHYSICAL SATELLITES
NT EXPLORER 12 SATELLITE
NT INTERCOSMOS SATELLITES
NT OGO
NT OGO-A
NT OSO-5
NT OSO-6
NT VANGUARD 3 SATELLITE
GEOPHYSICS
Soviet bloc research in astronomy, meteorology, oceanography, geology, and space science - 3 Oct. 1972
[JPRS-57162] 01 p0104 N73-10856
Annotated bibliography of atmospheric sounding, geophysics, and plasma physics
[AD-745168] 01 p0121 N73-10997
Geological and geophysical mapping of mineral resources in Australia and New Guinea
02 p0164 N73-11328
Theory of solar and terrestrial plasma physics
[AD-747034] 03 p0297 N73-12424
Soviet Bloc research in astronomy, meteorology, oceanography, geology, and space science - 1 Nov. 1972
[JPRS-57392] 03 p0355 N73-12895
Abstracts and bibliographies on research in laser technology, effects of explosions, geosciences, and particle beams
[AD-749488] 04 p0430 N73-13504
Geophysical survey of continental shelves off African coast and mapping for oil potential
[PB-211393] 05 p0541 N73-14400
Application of scale autocorrelation coefficients to atmospheric and geospheric measurements
[AD-750476] 06 p0695 N73-15661
Soviet research on astronomy, meteorology, oceanography, and space science - 27 Dec. 1972
[JPRS-57858] 06 p0717 N73-15856
Application of remote sensing techniques and models to geophysics
07 p0787 N73-16401
Soviet research in meteorology, geophysics, space, and astronomy
[JPRS-57989] 07 p0843 N73-16829
Selected papers on hydrometeorology, oceanography, navigation
07 p0857 N73-16950
Spherical sampling functions related to spherical-harmonic functions applied to geophysics
[NASA-CR-130745] 08 p0918 N73-17519
Generalized Fourier analysis of geophysical data with data points unequally spaced in time
[AD-751908] 08 p0919 N73-17529
Soviet bloc research in astromony, meteorology, oceanography, geology, and space science - 31 Jan. 1973
[JPRS-58112] 08 p0961 N73-17860
Nomenclature for describing radiation measurements and computations in geophysics
[BMBW-FBW-72-30] 09 p1027 N73-18379
Soviet Bloc research in astronomy, meteorology, oceanography, geology, and space science - Feb. 1973
[JPRS-58218] 09 p1085 N73-18851
Soviet Bloc research in astronomy, meteorology, oceanography, geology, and space science
[JPRS-58333] 09 p1085 N73-18852
Man machine systems, control theory, nuclear geophysics, and research instrumentation
[RISO-M-1509] 10 p1137 N73-19263
Abstracts of articles on Soviet Bloc research in earth and space sciences
[JPRS-58437] 11 p1338 N73-20860
Prediction of solar activity and geophysical effects, including X ray burst data
[AD-755920] 12 p1403 N73-21379
ERTS-1 imagery of Iceland geology, geophysics, hydrology, oceanography, and agriculture
[E73-10535] 13 p1518 N73-22299
Solar-geophysical activity associated with major ground level cosmic ray event of 24 January 1971
[UAG-24-PT-1] 13 p1572 N73-22737
Solar-geophysical activity associated with major ground level solar cosmic ray event of 1 September 1971
[UAG-24-PT-2] 13 p1572 N73-22738
Research projects in geophysics, astronomy, and satellite applications
[JPRS-58885] 13 p1577 N73-22776
Literature compilation on marine geology and geophysics for Caribbean Sea and adjacent regions
14 p1607 N73-23023
Geophysical survey off Surinam coast including seismics, magnetics, and gravity
[SP-6] 14 p1660 N73-23476
Manned orbital space station for geophysical and astronomical research
[NASA-TT-F-13957] 14 p1709 N73-23868
Commercial application of ERTS-1 imagery in structural reconnaissance for minerals and petroleum
[E73-10700] 16 p1903 N73-25392

ERTS-1 imagery of Bighorn-Pryor mountains of Wyoming and Montana applied to analysis of regional tectonic relationships
[E73-10704] 16 p1903 N73-25395
Tabular ionospheric data acquired by vertical incidence sounding techniques
[RRC-A207-PT-2] 16 p1905 N73-25409
Vertical incidence sounding techniques to determine ionospheric effects of solar activity
[RRC-A208-PT-2] 16 p1905 N73-25410
Geophysical data as indicators of planet properties, using geodetic satellite
[NASA-TM-X-66274] 17 p2024 N73-26377
USSR research projects in geophysics, astronomy, and aerospace subjects - May 1973
[JPRS-59136] 17 p2024 N73-26379
Soviet research in meteorology, oceanography, upper atmosphere, astronomy, and space
[JPRS-59002] 18 p2196 N73-27729
Soviet-bloc research in geophysics, astronomy, and space
[JPRS-59490] 18 p2196 N73-27730
Soviet-bloc research in geophysics, astronomy, and space research
[JPRS-59390] 18 p2196 N73-27733
Comparison between geophysical and ERTS data processing techniques
[PAPER-I13] 19 p2278 N73-28334
Glacio-climatic and geophysical rhythms of earth and space
[NASA-TT-F-14985] 19 p2342 N73-28843
ERTS-1 imagery of Namafjall geothermal area, Iceland
[E73-10874] 20 p2393 N73-29225
Geophysical observations made during Tenth Soviet Antarctic Expedition with emphasis on field strength of long and short wave radio transmission
20 p2408 N73-29354
Operations and functions of ground station during Tenth Soviet Antarctic Expedition to obtain meteorological and geophysical data
20 p2409 N73-29360
Soviet bloc research in astronomy, meteorology, oceanography and space science Aug. 1973
[JPRS-59673] 20 p2473 N73-29861
Soviet block research in astronomy meteorology, geology, and space science Aug. 1973
[JPRS-59789] 20 p2473 N73-29863
Geophysics and space data, including magnetometer, cosmic ray, and ELF noise data - 1973
[AD-763507] 21 p2593 N73-30779
Geophysical meeting, third generation computers, and computer courses
[JPRS-59825] 21 p2609 N73-30911
Application of very long-baseline interferometry at Smithsonian Astrophysical Laboratory to geophysical measurements of earth
[NASA-CR-135493] 22 p2666 N73-31365
Soviet bloc research in astronomy, meteorology, oceanography, geology, and space science - September 1973
[JPRS-60035] 22 p2716 N73-31740
Space applications research in astronomy and earth physics
[NASA-SP-331] 22 p2732 N73-31867
Geophysical survey of Nevada from Skylab remote sensors
[E73-10998] 23 p2778 N73-32215
Remote sensing geophysics and geology from Skylab EREP
[E73-11072] 23 p2781 N73-32247
Soviet research in meteorology, oceanography, geophysics, astronomy, and space
[JPRS-60165] 23 p2846 N73-32744
Nature of solar flare emissions and geophysical disturbances
[NASA-TM-X-70479] 24 p2976 N73-33781
**GEOPOTENTIAL**
NT GEOPOTENTIAL HEIGHT
Analysis of range and range rate tracking data from satellite to satellite for geodetic applications
[AD-741683] 01 p0106 N73-10881
Computer program for calculating gravimetric deflections of the vertical in central zone
[AD-747136] 02 p0170 N73-11380
External gravity potential on earth and gravity dependent geodetic parameters
[AD-746307] 03 p0297 N73-12422
Accuracy of geopotential solutions from resonant satellites
[NASA-TM-X-66147] 06 p0665 N73-15410
Development of four-level model of baroclinic atmosphere for predicting geopotential at various isobaric surfaces for Northern Hemisphere
[AD-750496] 06 p0694 N73-15659
Short range forecasting of geopotential and wind for large territory by barotropic divergent
[AD-751422] 07 p0796 N73-16475
Satellite derived potential coefficients and terrestrial gravity information for estimating geopotential anomaly degree variance
[AD-754236] 11 p1290 N73-20471
Computation of mean gravity anomalies from potential coefficients
[AD-754245] 11 p1290 N73-20472
Transformation matrices between spherical harmonics and spherical sampling functions
[AD-755486] 14 p1664 N73-23509
Earth satellite orbit perturbation due to fluid tidal effects and temporal geopotential variations
[GRGS-BULL-7] 14 p1706 N73-23847
Eleventh order resonant terms in geopotential from orbit of Vanguard 3
[NASA-TM-X-66246] 15 p1778 N73-24415
Spherical harmonics presentation of anomalous gravity potential from satellite and terrestrial data at 9km aove sea level
[AD-759909] 18 p2147 N73-27358
Statistical properties of atmospheric circulation particularly geopotential fields on global basis
20 p2442 N73-29619
Effect of orography on climatic wind distribution and geopotential fields
20 p2444 N73-29632
Numerical forecasting of geopotential, temperature, dew point fields at 830 millibar level
20 p2446 N73-29650
Mathematical models for matching geopotential and wind fields and improving accuracy of objective analysis
21 p2573 N73-30616
Structure of global geopotential fields in connection with quasi-biannual cyclicity in equatorial stratosphere
24 p2947 N73-33533
**GEOPOTENTIAL HEIGHT**
Regression relationships between Nimbus 4 SIRS-B clear-column radiances and geopotential heights of 500 mb and 300 mb levels
[AD-743711] 01 p0075 N73-10624
Synoptic weather charts of daily and monthly heights and temperature for Northern Hemisphere from Jan. to Dec. 1968
[AD-746659] 02 p0206 N73-11673
Quasigeoid heights and deflections of vertical for reference field of level ellipsoid
[AD-748528] 06 p0668 N73-15434
Geopotential topographies and currents for sea surface off west Australia
[CSIRO-DFO-TP-32] 18 p2143 N73-27323
**GEORGIA**
Investigation of forest stress in Black Hills, forest inventory at Atlanta test site, and rangeland inventory at Manitou test site using ERTS-1 imagery
[E72-10219] 02 p0162 N73-11313
Forest and rangeland inventory and forest infestation of Atlanta, Manitou, and Black Hills test sites based on ERTS-1 imagery
[E73-10084] 08 p0901 N73-17296
ERTS-1 imagery of wetlands ecology in Maryland, Georgia, and Chesepeake Bay test sites
[E73-10288] 08 p0915 N73-17494
Mapping southeastern coastal marshlands and wetlands of South Carolina and Georgia using ERTS-1 imagery
[E73-10362] 10 p1150 N73-19358
Inventory of forest and rangeland and detection of insect infestation from ERTS-1 imagery of Black Hills, Atlanta, and Manitou test sites
[E73-10407] 11 p1278 N73-20369
Mapping wetlands ecology of Chesapeake Bay, South Carolina, and Georgia from ERTS-1 imagery
[E73-10507] 13 p1516 N73-22282
Inventory of forest and rangeland and detection of forest stress at Black Hills, South Dakota, Atlanta, Georgia, and Manitou Forest test sites using ERTS-1 data
[E73-10546] 14 p1655 N73-23421
Inventory of forests and rangelands, including forest stress, at Black Hills, Atlanta, Georgia, and Manitou, Colorado test sites using Skylab EREP
[E73-10587] 14 p1657 N73-23447
ERTS-1 imagery of strip mining activity in Cumberland Plateau, Tennessee Test Site and agricultural areas in Alabama, Georgia, and Tennessee
[E73-10694] 16 p1902 N73-25386
Evaluation of existing community facilities in Macon, Georgia, and recommendations for improvements
[PB-220030/1] 18 p2127 N73-27184
Inventroy of forest and rangeland resources at Atlanta, Georgia, Black Hills, South Dakota, and Manitou, Colorado test sites using Skylab EREP imagery
[E73-10749] 18 p2133 N73-27237
Detection and inventory of timber and rangelands and forest stresses in Georgia, Colorado, and Black Hills from ERTS-1 imagery
[E73-10805] 18 p2138 N73-27280
Mapping of Atlantic coastal marshlands of Maryland and Georgia using ERTS-1 imagery
[PAPER-E7] 19 p2269 N73-28271
Skylab inventory of forest and rangeland resources and forest stresses at Atlanta Georgia, Manitou, Colorado, and Black Hills test sites
[E73-10895] 20 p2395 N73-29244
Inventory of forest and rangeland resources and stresses at Atlanta, Georgia, Black Hills, South Dakota, and Manitou, Colorado from Skylab EREP
[E73-11040] 23 p2778 N73-32219
Timber identification and inventory and forest management in Colorado, Georgia, Black Hills, California, and Hawaii from ERTS-1 imagery
[E73-11051] 23 p2779 N73-32227
Forest and rangeland inventory and detection of forest stress at Black Hills, South Dakota, Manitou, Colorado, and Atlanta, Georgia test sites
[E73-11052] 23 p2779 N73-32228
Application of Skylab multispectral photography to mineral and land resources of South Carolina and Georgia
[E73-11140] 24 p2918 N73-33295
**GEOS SATELLITES [ESRO]**
Onboard digital correlator for spacecraft VLF radio wave studies
04 p0423 N73-13446
**GEOS 1 SATELLITE**
Laser predictions of GEOS 1 and 2 trajectories
[AD-745455] 01 p0065 N73-10529
Prediction of laser return pulse shape from corner cube retroreflectors on GEOS 1 satellite
[NASA-TM-X-66123] 04 p0428 N73-13490
Second degree Love number values from analysis of lunar-solar tidal perturbations of GEOS 1 and 2 inclinations
[NASA-TM-X-66176] 08 p0960 N73-17857
**GEOS 2 SATELLITE**
Laser predictions of GEOS 1 and 2 trajectories
[AD-745455] 01 p0065 N73-10529
European tracking station coordinates from GEOS B satellite data
03 p0295 N73-12400
Second degree Love number values from analysis of lunar-solar tidal perturbations of GEOS 1 and 2 inclinations
[NASA-TM-X-66176] 08 p0960 N73-17857
Spectral analysis of data from C band radar tracking GEOS 2 satellite and development of data compaction method
[NASA-CR-62085] 13 p1490 N73-22082
Utilization of C band instrumentation radars during GEOS 2 program
[NASA-CR-62087] 13 p1491 N73-22084
**GEOS-C SATELLITE**
Design criteria for highly accurate and reliable GEOS-C satellite altimetry system
06 p0661 N73-15370
GEOS-C data for improving geoid and gravity field determination
06 p0661 N73-15371
Use of GEOS-C satellite height for determining earth gravitational field and physical ocean surface variations
06 p0662 N73-15375
Short arc tracking procedure for determining GEOS-C satellite altitude
06 p0662 N73-15376
Global network tracking data for accurate GEOS-C orbit calculation from one revolution
06 p0662 N73-15378
Operating characteristics of GEOS-C K band radar altimeter
06 p0663 N73-15387
Study program for Geodetic Satellite applications
[NASA-CR-130180] 10 p1214 N73-19868
Topographic mapping of Caribbean Sea surface by GEOS-C satellite
[AD-759041] 18 p2147 N73-27354
**GEOSTATIONARY OPERATIONAL ENVIRON SATS**
U GOE SATELLITES
**GEOSTATIONARY SATELLITES**
U SYNCHRONOUS SATELLITES
**GEOSTROPHIC WIND**
Numerical weather forecasting methods - basic equations of dynamic processes and quasi-geostrophic approximation
[NLL-M-20352-[5828.4F]-VOL-1]
01 p0073 N73-10595
FORTRAN program for calculating geostrophic trajectories
[FOA-4-C-4469-A1] 02 p0204 N73-11656
**GEOTHERMAL RESOURCES**
NT VOLCANOES
Bibliography on geothermal prospecting in arid and semiarid lands
[PB-218830/8] 18 p2148 N73-27359
ERTS-1 imagery of Namafjall geothermal area, Iceland
[E73-10874] 20 p2393 N73-29225
**GEP TELESCOPES**
U PARTICLE TELESCOPES
**GERDIEN ARC HEATERS**
U ARC HEATING
U HEATING EQUIPMENT
**GERMANIUM**
Absorption spectra analyses on germanium films for determining band structure transformations
02 p0218 N73-11765
Tungsten-germanium whisker diode far infrared detector
[UCLA-34-P-157] 03 p0274 N73-12219
Computerized design and performance of planar germanium P-I-N thermophotovoltaic cells
[AD-748895] 04 p0376 N73-13063

Calorimetric, diffraction, and microscopic examination of evaporated amorphous germanium
[AD-749363] 04 p0461 N73-13762
Radiation and annealing studies on oxygen-doped and lithium diffused germanium
[CONF-720707-7] 06 p0699 N73-15696
Optical and electrical properties of amorphous germanium and silicon semiconductors
[AD-748856] 06 p0709 N73-15788
Autoradiograms of deformed silicon and germanium single crystal surfaces
[AD-753039] 09 p1074 N73-18765
Required doping levels for germanium and silicon infrared windows at microwave energies
[AD-753466] 09 p1075 N73-18772
Boundary scattering of phonons in germanium and silicon determined from low temperature thermal conductivity measurements
[AD-753494] 09 p1076 N73-18780
Temperature and thickness effects on electrical conductivity of amorphous germanium semiconducting films
[AD-753827] 09 p1076 N73-18782
Electrical conductivity of amorphous germanium semiconductor with pseudogap structure
[AD-753824] 09 p1076 N73-18784
Characteristics of second breakdown in germanium gold diodes
[AD-755425] 12 p1385 N73-21230
Lithium-multivalent acceptor impurity interaction in germanium
12 p1437 N73-21645
Charge carrier transport properties in p-type germanium semiconductors
[AD-757232] 14 p1698 N73-23783
Measurements of excess carriers in intrinsic germanium
[AD-758211] 15 p1822 N73-24772
Anomalous X ray transmission through single germanium crystals
16 p1952 N73-25793
Low temperature epitaxial development of Ge and Si layers by chloride method
18 p2187 N73-27656
Variation of electrophysical parameters of epitaxial films of germanium as result of gas etching
18 p2188 N73-27665
Analysis of optimal conditions of selective growth of epitaxial layers of germanium and silicon
18 p2188 N73-27669
Short-range ordering in amorphous Ge thin films studied by photoemission spectrum analysis as function of film preparation at different substrate temperatures
18 p2190 N73-27680
Correlation between Ge crystal and spectrometer properties of Ge[Li] detector made from Ge crystal
[AECL-4369] 19 p2327 N73-28718
Photoconductive effect and absorption of monochromatic sub-mm radiation in n-type germanium
[RR-737] 20 p2462 N73-29782
Analysis of structural-eutectic transformations in liquid phase of metal-metal and metal-semiconductor systems
[NLL-M-21665-[5828.4F]] 21 p2557 N73-30496
Thermal conductivity of germanium in boundary scattering regime
[AD-764122] 23 p2826 N73-32589

**GERMANIUM ALLOYS**
Design and performance of cylindrical silicon germanium thermoelectric generators
06 p0626 N73-15080
X ray diffraction analysis on microstructure defects in explosively loaded copper germanium alloy
[COO-1431-15] 10 p1173 N73-19541
Vapor phase heteroepitaxial growth of silicon germanium alloys by hydrogen reduction of tetrachlorides
20 p2460 N73-29767

**GERMANIUM COMPOUNDS**
NT GERMANIUM OXIDES
Cadmium and germanium compounds chalcopyrite semiconductor materials for infrared optics
[AD-759556] 16 p1945 N73-25742

**GERMANIUM DIODES**
Time discrimination in temporal information sampling at output of planar germanium detector in gamma ray spectrometry
[NAA-SR-MEMO-6728] 07 p0824 N73-16680
Time discrimination in temporal information sampling at output of planar germanium detector in gamma ray spectrometry
[CEA-R-4355] 09 p1069 N73-18719

**GERMANIUM OXIDES**
Waveguiding in thin silver strip vacuum deposited on bismuth germanium oxide
[AD-750612] 06 p0648 N73-15262
Piezo- and thermo-optical properties of bismuth germanium oxide single crystals
17 p2071 N73-26754

**GERMANIUM RECTIFIERS**
U GERMANIUM DIODES

**GERMANY**
NT ALPS MOUNTAINS [EUROPE]
Magnetotelluric analysis of geological structure of various locations in Rhine River Valley, Germany
[GAMMA-20] 01 p0048 N73-10388
Methods for determining atmospheric circulation from satellite pictures
02 p0204 N73-11649
Airborne measurements of optical atmospheric properties and southern Germany during spring 1970
[AD-747490] 03 p0298 N73-12429
Systems and studies for direct TV reception from satellite in Germany
[DGLR-PAPER-72-50] 04 p0389 N73-13160
German central ground station including layout and equipment
[DLR-MITT-71-05] 04 p0402 N73-13276
Proposals for application of data processing to education in Germany
[BMBW-FB-DV-72-05] 04 p0488 N73-13995
Astronomical geodetic observations for longitude, latitude, and components of deflection from vertical at West German stations
[MITT-124] 05 p0538 N73-14375
Transonic and hypersonic wind tunnels in Germany
[DLR-FB-71-86] 06 p0650 N73-15278
Design and system description of hypersonic low density wind tunnel in Germany including generation of molecular beams
[DLR-FB-71-84] 06 p0650 N73-15279
Regional airport planning in Germany, noting infrastructural, economic, safety, and noise problems
[DGLR-PAPER-72-033] 06 p0650 N73-15280
Infrastructural role of airports in Germany and planning for future traffic increase
[DGLR-PAPER-72-034] 06 p0650 N73-15281
Daily and monthly meteorological charts for Europe obtained during June, 1972 at Berlin
06 p0691 N73-15629
Daily and monthly meteorological charts for Europe obtained during May, 1972 at Berlin
06 p0692 N73-15631
Solar observation and research using rocket-borne instruments, in German programs
[BMBW-FBW-72-27] 07 p0846 N73-16862
German needs for television transmission via satellite
[DGLR-PAPER-72-051] 09 p1003 N73-18183
ERTS-1 imagery of geography, geology, and glaciology of Germany and part of Alps Mountains
[E73-10099] 09 p1020 N73-18322
Global earth resource program for Germany
[DGLR-PAPER-72-072] 09 p1101 N73-18989
Organization and management methods for space programs in Germany
[DGLR-PAPER-72-052] 09 p1101 N73-18990
Color vision requirements for German Air Force personnel
10 p1112 N73-19067
Daily and monthly synoptic climatological charts obtained at Berlin for August 1972
10 p1180 N73-19602
Daily and monthly synoptic climatological charts obtained at Berlin for September, 1972
10 p1181 N73-19603
Organization and research projects for 1971
10 p1229 N73-19988
History of German aeronautical development during the first half of the century
11 p1350 N73-20956
Technical and scientific contributions of German aeronautical societies to aerospace sciences
11 p1350 N73-20957
German cooperation with AGARD research in aerospace sciences
11 p1350 N73-20958
German cooperation in international aeronautical research
11 p1351 N73-20959
History and organization of German Society for Aerospace Research
11 p1351 N73-20961
German telecommunication research and development
12 p1379 N73-21186
Specifications and capabilities of Franco-German telecommunications satellite - Symphonie
[NASA-TT-F-14875] 12 p1461 N73-21836
Geophysical observations of horizontal and vertical components of earth magnetic field at Feurstenfeldbruck, Germany for 1972
14 p1660 N73-23473
Daily and monthly synoptic weather maps for Northern Hemisphere and Berlin vicinity, December 1972
17 p2056 N73-26628
Synoptic weathermaps for ground and 500 mb levels obtained in Berlin during January, 1973
17 p2057 N73-26634
Meteorological tables and charts on Berlin temperature
17 p2057 N73-26635
Parameters of geodetic reference system
[AD-759127] 18 p2147 N73-27355
German test facilities for environment simulation
19 p2249 N73-28133
Regional airport planning in Germany
[DGLR-PAPER-73-035] 23 p2770 N73-32159
Mission objectives of German astronomical satellite, noting X ray astronomy, IR and UV experiments
[BMBW-FB-W-72-25] 23 p2851 N73-32786
Cost analysis of large research institutes in Germany
[DLR-FB-73-64] 24 p2995 N73-33931

**GERMICIDES**
U BACTERICIDES

**GETTERS**
Getter pumps applicable to Pioneer Venus Mass Spectrometer Experiment
[NASA-CR-114594] 16 p1918 N73-25518

**GHANA**
Potassium argon age, and chemical composition of glasses from Bosumtwi crater in Ghana
[NASA-TT-F-14496] 01 p0049 N73-10398

**GHOSTS**
Ghost-free dual resonance models
[LPTHE-73/16] 20 p2456 N73-29738

**GIANT STARS**
Long period giant variable stars of Mira Ceta type, emphasizing U, B, and V photometry
[AD-747564] 04 p0476 N73-13893
Polarimetric and spectrophotometric observations of late type giant and supergiant stars
17 p2080 N73-26827
Fourier spectrometer system for studying infrared spectra of K giants
23 p2836 N73-32661

**GIBBS EQUATIONS**
Solution of thermodynamic forces and flows in magnetic field using Gibbs equation
[AD-756901] 13 p1592 N73-22909

**GIBBS FREE ENERGY**
Values for standard heats and Gibbs free energies of formation, entropies, and enthalpies for rare earth elements
[NBS-TN-270-7] 14 p1616 N73-23092

**GIMBALLESS INERTIAL NAVIGATION**
Computerized inertialess guidance system for aircraft flight control
14 p1712 N73-23895

**GIMBALS**
Development and application of multiple system checkout procedures for use with gimbaled inertial measuring units
[NASA-CR-123953] 03 p0328 N73-12676
Gyro suspension systems including axis disturbance probability factors, bearing friction, astatic gyro gimbal errors with drift, and horizontal pendulum energy dissipation
[JPRS-57504] 05 p0546 N73-14432
Determination of gimbal errors of astatic gyroscope with allowance for drift
05 p0546 N73-14435
Compass effect of gyro with forced rotation of gimbal mount when installed in horizontal plane of earth
05 p0546 N73-14439
Equations of motion for calculating flexible rotor influence on two gimbaled gyroscope motion
08 p0922 N73-17554
Evaluation of control moment gyro steering laws for use on HEAO spacecraft
[NASA-TM-X-64727] 11 p1321 N73-20718
Effects of sensor deadband and actuator breakout torque control system nonlinearities on performance of Apollo telescope mount pointing capability
[NASA-TN-D-7247] 15 p1834 N73-24868
Design of double gimballed flywheel for spacecraft stability
[ESRO-CR[P]-135] 17 p2090 N73-26907
Error reduction in two-gimbal, airborne search radar system
[AD-760551] 18 p2119 N73-27131
Selected articles on gyroscopes and gyromotors
[JPRS-59053] 20 p2417 N73-29420
Influence of orthogonal gimbal axes of electrostatic gyroscope when rotor potential is zero
20 p2417 N73-29421
Effect of elastic deformation of gimbal suspension on motion of gyroscope
20 p2418 N73-29424
Elastic deformation of gimbal suspension on gyroscope nutation, moments acting on spherical rotor in magnetic suspension, and differentiating linear accelerometer
[JPRS-59740] 21 p2547 N73-30420
Influence of elastic deformation of gimbal suspension on frequency of nutation of gyroscope
21 p2547 N73-30421
Kinematics of gyroscopes and gimbals and effects on missile stability
[AD-763147] 21 p2549 N73-30440
Three axis inertial system in Apollo gimbal for fine grain evaluation of strapdown system performance in dynamic environments
[NASA-CR-135484] 22 p2698 N73-31609
Friction effects on inertia compensators used for heliostat base motion isolation
[AD-764706] 23 p2821 N73-32549
Gimballed attitude gyros for Symphonie satellite stabilization
[DGLR-PAPER-73-058] 24 p2927 N73-33377

GLACIAL DRIFT
Mapping distribution of glaciofluvial deposits and associated glacial landforms in Maine using ERTS-1 imagery
[E72-10300] 04 p0411 N73-13350
Mapping distribution of glaciofluvial deposits and associated glacial landforms
[E73-10013] 06 p0659 N73-15349
Mapping distribution of glaciofluvial deposits and associated glacial landforms in Maine from ERTS-1 imagery
[E73-10353] 10 p1148 N73-19349
Analysis of ERTS-1 imagery using electronic satellite image analysis console to display and measure snowfield extent, glacier development, and hydrologic features
[E73-10415] 11 p1279 N73-20377
Mapping of glaciofluvial deposits and associated glacial landforms in Maine
[E73-10667] 16 p1899 N73-25362
Application of ERTS-1 imagery for mapping distribution of glaciofluvial deposits and associated glacial landforms
[E73-10745] 17 p2021 N73-26349
Application of ERTS-1 imagery for recognizing and mapping alpine glacial features in mountains of northwestern Wyoming
[PAPER-G14] 19 p2265 N73-28245
Application of ERTS data for mapping distribution of glaciofluvial deposits and associated glacial landforms
[E73-10867] 20 p2392 N73-29218
Survey of terminal moraines in western Sweden and southeastern Norway from ERTS-1 imagery
[E73-11122] 24 p2916 N73-33277

GLACIERS
Mapping and detection of snow cover changes on land and on glaciers in Alaska, British Columbia, and Washington using ERTS-1 imagery
[E72-10237] 03 p0288 N73-12337
Thermal remote sensing of infrared radiant temperatures in alpine/periglacial environments
04 p0409 N73-13332
Arctic glacier mapping, research, and effects on surroundings
[AD-747001] 06 p0667 N73-15425
Mapping and detection of changes of snow cover on land and glaciers
[E73-10063] 07 p0778 N73-16325
Mapping and detection of snow cover on land and glaciers in Cascade Range using ERTS-1 imagery
[E73-10379] 10 p1152 N73-19374
Continuous observations of structural changes in deforming polycrystalline ice
[AD-755336] 13 p1527 N73-22375
Detection and mapping changes of snow cover on land and glaciers from ERTS-1 imagery
[E73-10559] 14 p1655 N73-23431
Integrated analysis of past and present climates of Northern Cumberland and Peninsula
[AD-757270] 15 p1783 N73-24457
Application of ERTS-1 imagery for mapping distribution of glaciofluvial deposits and associated glacial landforms
[E73-10745] 17 p2021 N73-26349
Spaceborne imagery of snow cover and glaciers in mountainous regions
[NASA-TT-F-14969] 17 p2025 N73-26387

GLACIOFLUVIAL DEPOSITS
U GLACIAL DRIFT

GLACIOLOGY
Glaciology and volcanology on Wrangell Mountains, Alaska
[E72-10339] 05 p0532 N73-14327
Mapping distribution of glaciofluvial deposits and associated glacial landforms
[E73-10013] 06 p0659 N73-15349
Glaciology and volcanology studies in Wrangell Mountains, Alaska using ERTS-1 imagery
[E73-10277] 08 p0914 N73-17485
ERTS-1 imagery of geography, geology, and glaciology of Germany and part of Alps Mountains
[E73-10099] 09 p1020 N73-18322
Mapping distribution of glaciofluvial deposits and associated glacial landforms in Maine from ERTS-1 imagery
[E73-10353] 10 p1148 N73-19349
ERTS-1 imagery of glaciology and volcanology in Wrangell Mountains, Alaska
[E73-10404] 11 p1277 N73-20366
Utilization of ERTS-1 imagery for mapping extent of Pleistocene glaciation and delineation of small urban areas in Wyoming
[E73-10425] 11 p1280 N73-20386
Physical interpretation of geology, hydrology, and glaciology revealed by ERTS-1 imagery of east central Ohio
[E73-10454] 11 p1283 N73-20413
Relating glaciation cycles to cosmic rhythms
[NASA-TT-F-14827] 14 p1659 N73-23469
Glaciology and volcanology in Wrangell Mountains, Alaska based on ERTS-1 imagery
[E73-10665] 16 p1899 N73-25360
Application of ERTS data for mapping distribution of glaciofluvial deposits and associated glacial landforms
[E73-10867] 20 p2392 N73-29218
Geology, volcanology, and glaciology of Wrangell Mountains, Alaska from ERTS-1 imagery
[E73-10940] 21 p2529 N73-30282
Mapping of Quaternary geological and geomorphological landforms of Great Plains and Midwest from ERTS-1 imagery
[E73-10949] 21 p2530 N73-30291

GLANDS [ANATOMY]
NT ADRENAL GLAND
NT PITUITARY GLAND
NT TESTES
NT THYROID GLAND

GLANDS [SEALS]
Evaluation of polyimide second stage rod seals at high temperatures to determine suitability for application to aircraft systems
[NASA-CR-121124] 08 p0927 N73-17592
Analysis of leakage and pressure drop characteristics across dam of gas film seal under various flow conditions
12 p1389 N73-21267
Development of formula for calculating heat transfer coefficient in labyrinth glands of gas turbines
[NLL-RTS-7840] 18 p2192 N73-27698

GLASS
NT BOROSILICATE GLASS
NT GLASS FIBERS
NT SILICA GLASS
Potassium argon age, and chemical composition of glasses from Bosumtwi crater in Ghana
[NASA-TT-F-14496] 01 p0049 N73-10398
Equipment and procedures for measuring variation of strength of sheet specimens of glass under conditions of tension, compression, and shear
[AD-743694] 01 p0067 N73-10551
Structural characterizations and key property measurements of glassy carbons
[AD-745347] 01 p0070 N73-10574
Acoustic emission and crack propagation in single crystal MgO and glass as model ceramic materials
[AD-745000] 01 p0070 N73-10575
Refractory glass ceramics for gas turbines
[NPL-IMS-17] 02 p0192 N73-11556
Silver addition in Si-As-Te glasses to permit introduction of substantial amounts of selenium and to produce infrared transmitting glasses with increased softening ranges
[AD-747333] 02 p0193 N73-11563
Structural properties of glass, using X ray and neutron diffraction methods
[AD-747311] 02 p0194 N73-11568
Pyrolysis of glassy carbons in inert atmosphere from copolymers of furfuryl alcohol
[AD-746883] 02 p0194 N73-11570
Analysis of sonic boom data recorded on strain gages mounted on windows to record overpressures and relation to window size
[FAA-RD-72-114] 03 p0251 N73-12030
Physicochemical and optical properties of glasses of BaO-PbO-Bi2O3-TiO2 system
[AD-747371] 03 p0322 N73-12620
Production of unidirectional glass reinforced plastics with high mechanical properties
[AD-747549] 03 p0323 N73-12629
Neodymium doped Q-switched laser glass illuminator oscillator
[AD-749511] 04 p0430 N73-13506
Weakening and fracture of glass reinforced plastics during compression under conditions of one-sided heating
[AD-748526] 04 p0439 N73-13581
Hydrostatic pressure technique for improving dielectric properties of inorganic glasses used as capacitor materials
[AD-750393] 05 p0521 N73-14236
Characteristics of optical glass materials with specific resistance to effects of laser radiation
05 p0554 N73-14499
Analysis of laser induced surface damage to glass materials at Brewster angle and near normal incidence
05 p0554 N73-14503
Effect of glass laser radiation on borosilicate crown glass, fused silica, and flint glass with estimates of Kerr effect and electrostriction processes
05 p0555 N73-14510
Development and characteristics of Si-As-Te glasses containing Ag and Se as constituent of chalcogenic glasses
[AD-749958] 05 p0567 N73-14603
Isothermal compressibility of amorphous semiconductors
[AD-750397] 06 p0709 N73-15785
Optical materials and design of optical equipment
[AD-751496] 07 p0822 N73-16660
Radiation damage threshold determination for glass laser materials
[AD-752549] 08 p0931 N73-17622
Model for studying excessive specific heat that glasses exhibit at low temperatures
[AD-752471] 08 p0970 N73-17930
Viscosity and electrical resistivity of molten glass over wide temperature range
[AD-753480] 09 p1055 N73-18604
Thermal stability of amorphous arsenic compound glasses and electron diffraction analyses on semiconducting arsenic selenide films
[AD-752993] 09 p1076 N73-18778
Service life of mechanically prestressed glass used in spacecraft windows
09 p1088 N73-18880
Commercial applications of rare earth elements in ceramics, glasses, and nuclear technology
[IS-2967] 10 p1175 N73-19561
Infrared beam profile measurements for determining surface damage thresholds of glass laser materials
[AD-755134] 11 p1303 N73-20571
Summer room heating in buildings with large window glass surfaces
[NASA-TT-F-14849] 11 p1349 N73-20944
High purity phosphate core and cladding glasses for erbium doped laser
[AD-755687] 13 p1538 N73-22460
Electroionic glass strengthening process conducted at below strain point temperatures
[AD-757333] 14 p1681 N73-23646
Coated reinforced materials, glass antidiffusion films, and metal binders
[AD-758167] 14 p1682 N73-23649
Electron irradiation effect on transmission properties of ceria doped solar cell cover glass
[NASA-TN-D-7245] 15 p1737 N73-24082
Effects of polarized radiation on self-focusing thresholds of laser materials
[AD-757789] 15 p1795 N73-24554
Measurement of heat transfer coefficients of air-glass, argon-glass, and argon-aluminum suspensions
[NASA-CR-2266] 15 p1843 N73-24932
Adhesion, friction, and wear behavior of glasses and ionic solids
[NASA-TM-X-68255] 16 p1932 N73-25632
Silicon solar cell with plastic film binding to cover glass
[NASA-CASE-LEW-11065-2] 17 p1985 N73-26048
Cerium and silver containing silicate and borate systems for developing high density scintillation glass for nuclear cascade detectors
[NASA-CR-133960] 17 p2049 N73-26580
Scattered light photoelastic method for predicting stress distribution in composite epoxy glass structures
[AD-759900] 17 p2052 N73-26601
Evaluation of GRP rod and rope materials and associated end fittings
[AD-759931] 17 p2053 N73-26607
Electrical properties of semiconducting film configurations with contacts to chalcogenide glasses
[AD-760335] 17 p2074 N73-26781
Development of statistical prediction model for determining probability of glass breakage caused by sonic boom overpressures
[FAA-RD-73-79] 18 p2104 N73-27018
Heat treating effects on fatigue strength of SO-95 and 120 type organic class
[AD-760961] 18 p2168 N73-27511
Development of organic glass and plastic materials with improved mechanical and physical properties for use with aircraft canopies and protective coatings
[AD-763263] 21 p2497 N73-30039
Absorption and fluorescence of inorganic glasses and polycrystalline discs doped by heavy metal ions
[PAPER-76A6-746] 21 p2546 N73-30412
Analysis of various organic compounds in solution and inorganic ions in glasses as possible fluorescence standard reference materials
[PAPER-76A6-748] 21 p2547 N73-30414
Fatigue properties of high strength high modulus graphite /glass/epoxy matrix composites
[AD-763760] 21 p2564 N73-30552
Research on preparation, structure, and optical properties of glass
[AD-763338] 22 p2689 N73-31537
Effect of oxides on elastic properties of glasses
[AD-764080] 22 p2689 N73-31539
Principles of producing glass parts from polymethl methacrylate organic glass and tensile strength tests
[AD-763282] 22 p2690 N73-31542
Crack propagation in glass and ceramic materials
[AD-764045] 22 p2690 N73-31543
Discovery of small hollow spherules of glass containing various gases in peat bogs where Tungus meteorite fell
[NASA-TT-F-15125] 22 p2716 N73-31742
Apollo experience report on window structural design and verification for command and lunar modules
[NASA-TN-D-7439] 22 p2720 N73-31770
Interionic vibrations and glass transitions in ionic oxide metaphosphate glasses
[AD-765344] 23 p2811 N73-32478
Infrared absorption spectra of lithium and potassium silicate glasses
[AD-764891] 24 p2893 N73-33092
Conference on waste glass recovery and re-use in secondary products
[NASA-CR-135792] 24 p2938 N73-33460

Glass ceramic foam materials for space shuttle heat shielding system
24 p2938 N73-33464
Equipment for removing silver crazing on aircraft glass
[AD-764972] 24 p2944 N73-33510
Composition and structural modification of glassy carbon alloys
[AD-764918] 24 p2944 N73-33511

GLASS COATINGS
Hypervelocity projectile cratering at mirror glass coating impact
[ONERA-NT-01-14-72] 07 p0822 N73-16659
Coatings of borosilicate glasses deposited on silicon solar cells by radio frequency sputtering for enhanced protection
[ESRO-CR-68] 09 p0991 N73-18087
Fused silica coatings for flexible mat insulation of space shuttle surface
24 p2939 N73-33465
Sea salt and radiant heat effects on crystalline properties of mullite/silica composite thermal insulation for space shuttle
24 p2941 N73-33486
Convective heating effects on properties of glassy surface insulation coatings
24 p2941 N73-33488

GLASS FIBERS
Glass fiber reinforced composite materials for developing prototype missile fuselages
[AD-746288] 02 p0193 N73-11560
Fabrication of helicopter rotary wings from composite materials of stainless steel liner overwrapped with fiberglass
[NASA-CR-112191] 03 p0251 N73-12031
Development and characteristics of polyimide impregnated laminates with fiberglass cloth backing for application as printed circuit broads
[NASA-CASE-MFS-20408] 03 p0320 N73-12604
Mechanical properties and fracture strengths of glass fiber reinforced plastic composites
[AD-749948] 05 p0567 N73-14608
Application of neutron radiography for inspection of fiber glass composite structures
[AD-752457] 08 p0936 N73-17665
Optimal design of elastic bodies using fiberglass reinforced plastics or fibers with high modulus of elasticity
[AD-753040] 09 p1054 N73-18589
Drop impact strength and toughness of glass and carbon fiber composite materials
[AD-753101] 09 p1054 N73-18595
Curves and general equations for design of lightweight glass fiber reinforced metal pressure vessels for space shuttles
[NASA-CR-120917] 09 p1094 N73-18932
Punch-loading technique effects on mechanical properties of composites reinforced with glass fibers
[REPT-1042/72] 10 p1176 N73-19563
Development of design concepts for metal-lines, glass-fiber composite pressure vessels and comparison with homogeneous metal pressure vessels
[NASA-TM-X-68198] 10 p1220 N73-19922
Fabrication of L-1011 aircraft panels to compare costs and service performance characteristics of PRD-49 and fiberglass
[NASA-CR-112250] 11 p1234 N73-20018
Optimal tensile strength composition for molding compounds of epoxy resin reinforced with glass fibers
[AD-754763] 11 p1309 N73-20620
Feasibility and cost effectiveness of expendable main rotor blades on UH-1 helicopter
[AD-758464] 15 p1736 N73-24078
Vibrational spectral study of molecular orientation in vitreous sodium metaphosphate glass fibers
[AD-757751] 15 p1748 N73-24167
Properties of graphite fiber/polycarbonate and glass fiber/polycarbonate composites as influenced by heat treatment
[AD-757763] 15 p1802 N73-24605
Mechanical properties and failure modes of glass fiber reinforced epoxy plates under high tensile loads
[AD-759153] 16 p1933 N73-25640
Characteristics of glass fiber reinforced plastics using boron and carbon fibers
[RAE-LIB-TRANS-1687] 17 p2049 N73-26575
Analysis of glass fiber reinforced plastic laminated structures
[MBB-UD-79-72-O] 17 p2094 N73-26942
Application of glass composites, all carbon composites, and PRD-49 organic fiber material for airframe and spacecraft construction
18 p2164 N73-27482
Application of glass reinforced and carbon reinforced composite materials for helicopter structures and rotary wings
18 p2165 N73-27483
Construction of glider aircraft using glass fiber and carbon fiber reinforced plastic composite materials for weight reduction and increased strength
18 p2165 N73-27486
Application of glass and carbon fiber reinforced structures for gas turbine engine components to operate in high temperature environments
18 p2166 N73-27495
Comparison of glass fiber reinforced plastic and bronze submarine propellers, based on binding stress analysis and cavitation behavior
[BMVG-FBWT-73-8] 19 p2256 N73-28183
Application of reinforced fiberglass thermoplastic materials for construction of military aircraft structures
[AD-763470] 21 p2498 N73-30044
Fabrication and properties of carbon-fiber glass composites and methods for improving mechanical properties
[ARL/MET-NOTE-85] 21 p2561 N73-30533
Feasibility of coating glass optical fibers by melting process
[REPT-6803] 22 p2677 N73-31439
Application of fiber glass reinforced plastic materials for ground handling of aviation fuels and hazards of static electricity caused by plastic materials
[AD-764358] 22 p2709 N73-31693
Silica fiber materials for surface insulation of space shuttle orbiters
24 p2939 N73-33467

GLASSWARE
Frangible glass canister capable of deploying payload in space without dynamically disturbing its contents
09 p1088 N73-18875
Initiator ignition effect in laboratory glass and polythene vessel studying dummy hand injuries during simulated accidents
[ERDE-TRANS-1] 15 p1744 N73-24137

GLAUERT COEFFICIENT
U AERODYNAMIC FORCES
U MACH NUMBER

GLIDE ANGLES
U GLIDE PATHS

GLIDE PATHS
Aircraft glide path stability under speed constraint
[ARC-R/M-3705] 03 p0248 N73-12008
Design and development of microwave landing system for operation of civil and military aircraft in conventional and V/STOL configurations
[AD-749505] 05 p0578 N73-14702
Bibliography of data on aircraft landings, instrument landings, approach control, glide path systems, display devices, and terminal facilities
[AD-751800] 07 p0740 N73-16024
Analysis of control and display device testing for microwave landing system - Vol. 1
[AD-758791] 16 p1942 N73-25713
Analysis of data rate requirements for low visibility approach with scanning beam landing guidance system
[AD-758786] 16 p1942 N73-25719
Analysis of factors affecting approach and landing of aircraft under visual conditions to show causes of misjudgement resulting in aircraft landing accidents
[NASA-TT-F-15054] 20 p2360 N73-28980
Radio frequency interference tests of VHF omnirange, instrument landing systems, and glideslope indicators to determine required geographical separation for ground stations
[REPT-523-0764695-00111M-VOL-2]
20 p2453 N73-29712
Model of wind shear in lower 50 meter section of glide path from low inertia measured data
[NLL-M-23036-[5828.4F]] 21 p2528 N73-30271
Development and characteristics of system for integrated control of engine power and aerodynamic configuration of aircraft during landing approach
[NASA-CASE-ARC-10456-1] 22 p2613 N73-30938
Aircraft accident involving crash of Boeing 737 aircraft during instrument approach to Chicago-Midway Airport, Illinois on 8 December 1972
[NTSB-AAR-73-16] 22 p2614 N73-30947
Effects of snow cover and snow surface conditions on image glide path systems for aircraft approach control
[FAA-RD-72-85] 22 p2697 N73-31602
Cockpit layouts in view of new landing approach methods
[MBB-UH-07-73-O] 23 p2744 N73-31966

GLIDE SLOPES
U GLIDE PATHS

GLIDERS
NT PARAWINGS
NT X-20 AIRCRAFT
Numerical analysis of minimum flight time for sail plane performance while performing cross country flight
[ME-68] 15 p1733 N73-24055
Statistical performance test evaluation in aerodynamic development of Dart sailplane
[CRANFIELD-AERO-16] 16 p1859 N73-25059
Construction of glider aircraft using glass fiber and carbon fiber reinforced plastic composite materials for weight reduction and increased strength
18 p2165 N73-27486
Analysis of three dimensional weakly controlled soaring procedures for increased sailplane performance
19 p2218 N73-27894

GLIDING
Yaw maneuverability of helicopters in gliding flight
05 p0493 N73-14022
Analysis of three dimensional weakly controlled soaring procedures for increased sailplane performance
19 p2218 N73-27894
VAK 191 B V/STOL fighter aircraft nonlinear feedback flight control system for gliding flight phase
24 p2878 N73-32984

GLINT
Formulation of radar glint tracking error reduction using frequency agility and linear amplitude weighting
16 p1874 N73-25171

GLOBAL ATMOSPHERIC RESEARCH PROGRAM
Status and planning of GARP Atlantic Tropical Experiment
[GARP-SPEC-REPT-7] 03 p0327 N73-12667
Project planning and progress for first GARP global experiment, emphasizing satellite subsystem, data management, and oceanographic programs
[GARP-SPEC-REPT-8] 03 p0327 N73-12669
Progress on GARP, GATE, and related subprograms
03 p0327 N73-12670
Radiative heating rates measured for global atmosphere
[COO-2195-4] 04 p0415 N73-13386
Parameterization and its role in atmospheric modeling
[GARP-PUBL-8] 05 p0573 N73-14654
GARP standard data sets for studying behavior of numerical global models noting data acquisition, analysis, and storage
[GARP-PUBL-9] 09 p1061 N73-18652
Annual report of WMO noting World Weather Watch, global atmospheric research program, education, technical cooperation, environmental and oceanographic aspects
[WMO-348] 17 p2057 N73-26639
Analysis of GARP radiometersonde comparisons
[WMO-358] 23 p2813 N73-32493
Description of intercomparison of radiometersondes
23 p2814 N73-32494
Analysis of radiometersonde comparisons
23 p2814 N73-32495
Subprogram planning for global atmospheric observation and weather forecasting system
[GARP-PUBL-11] 24 p2948 N73-33545
Balloon sub-system of Eole experiments in Southern Hemisphere lower stratosphere
24 p2948 N73-33547
Data processing role of weather stations, polar and synchronous satellites in global experiments
24 p2948 N73-33549
GARP subprograms including numerical experimentation, GATE climate, and oceanography
24 p2949 N73-33557

GLOBAL TRACKING NETWORK
Global network tracking data for accurate GEOS-C orbit calculation from one revolution
06 p0662 N73-15378
Optimization of global ground data transmission network for spacecraft communications
18 p2210 N73-27843
Global station coordinate solution based upon camera and laser data
[NASA-TM-X-70422] 19 p2249 N73-28130
Characteristics of minitrack tracking function to show minitrack hardware, system calibration, and quadratic listing - Vol. 2
[NASA-TM-X-70482] 24 p2901 N73-33156

GLOMERULUS
Morphological changes in juxtaglomerular apparatus in kidneys of rats during multihour exposure to accelerations in different directions
07 p0743 N73-16045

GLOSSARIES
U DICTIONARIES

GLOSTER GA-5 AIRCRAFT
U GA-5 AIRCRAFT

GLOTRAC [TRACKING NETWORK]
U GLOBAL TRACKING NETWORK

GLOVES
Performance of prototype high pressure space suit glove
[NASA-CR-114532] 06 p0635 N73-15162
Development of prototype high pressure space suit glove assembly
[NASA-CR-114535] 08 p0879 N73-17120
Dry inert gas glove box for handling of hygroscopic and corrosive materials in spectroscopic and lasers experiments
[CRC-1244] 21 p2548 N73-30430

GLOW
U LUMINESCENCE

GLOW DISCHARGES
Mode coupled nonlinear dispersion of irregular ionization waves in glow discharges
[AD-748468] 04 p0456 N73-13721
Probe measurements of electron energy in glow discharge of nitrogen plasma and air
[AD-752871] 09 p1071 N73-18744
Classification and glow discharge with hollow cathodes
[AD-755412] 12 p1385 N73-21231

Electron density and temperature measurements on negative glow plasma
12 p1433 N73-21609
Mass spectrographic determination of ions and neutral reactions in glow discharge of helium-sulfur dioxide-carbon monoxide
[BM-RI-7747] 15 p1747 N73-24157
GLUCOSE
Mathematical model for in vivo study of glucose homeostasis in humans
[NASA-CR-129171] 02 p0130 N73-11056
Effects of monomethylhydrazine on blood and cerebrospinal fluid glucose in anesthetized monkeys
[AD-751232] 07 p0749 N73-16092
Magnetic field effect on hydrated glucose crystal growth
[AD-754618] 11 p1254 N73-20172
Effect of accelerations on active transport of glucose in small intestine of rats
24 p2883 N73-33021
GLUCOSIDES
Tricyclic nitropropene nitronate intermediates in condensation reactions of symmetric trinitrobenzene with cycloalkanones, and with phloroglucinol
[NASA-CR-131288] 11 p1252 N73-20159
GLUES
Methods for designing and developing aircraft structural components by riveting, welding, and gluing aluminum alloys parts
[AD-753513] 09 p1041 N73-18491
Gluing technology for airframe construction
[AD-761496] 19 p2221 N73-27912
GLUTAMIC ACID
Relation between hyperbaric oxygenation and functional activity of differentiated brain with respect ot glutamic acid metabolism
19 p2227 N73-27960
GLYCERINS
U GLYCEROLS
GLYCEROLS
Thermal conductivity of liquid glycols, glycerols and their aqueous solutions
[ESDU-70004] 02 p0241 N73-11961
Optical and dielectric properties of liquid glycerol, tetradecane, and heptadecane
[ORO-3861-6] 06 p0647 N73-15259
Airborne heated glycerine droplets for fog dispersal
[TOPR-178-3-133-PT-1] 12 p1421 N73-21521
GLYCINE
Pyroelectric infrared detector performances investigating strontium and barium niobates, lithium sulfate and TGS materials effects on frequency ranges and sensitivity
[ESRO-CR-67] 22 p2675 N73-31425
GLYCOLS
Thermal conductivity of liquid glycols, glycerols and their aqueous solutions
[ESDU-70004] 02 p0241 N73-11961
Apollo 16 flight anomaly report on malfunction of water/glycol temperature control circuit
[NASA-TM-X-69234] 17 p2089 N73-26900
GNOTOBIOTICS
Use of ultrafine fiber filter cloth for removing bacterial contaminants from air
[NASA-TT-F-14940] 15 p1742 N73-24123
GOAL THEORY
Mathematical models and physiological mechanisms of goal-directed behavior
[JPRS-60091] 24 p2887 N73-33053
Model of organization of goal-directed behavior
24 p2888 N73-33061
GODDARD EXPERIMENT PACKAGE TELESCOPE
U PARTICLE TELESCOPES
GOE SATELLITES
Geostationary satellite position and attitude determination using picture landmarks
[NOAA-TM-NESS-21] 04 p0474 N73-13875
GOGGLES
Physical and functional performance properties of laser safety goggles
[AD-746208] 01 p0022 N73-10170
Plastic materials for eye protection from lasers
[AD-752594] 08 p0880 N73-17127
GOLD
Coincidence rate measurements for inelastically scattered electrons and associated bremsstrahlung at intermediate bombarding energies
[NASA-CR-124007] 06 p0702 N73-15723
Influence of surface finishing on adherence of radio frequency sputtered molybdenum disulfide on silver, gold, copper, and bronze
[NASA-TN-D-7169] 07 p0804 N73-16523
Microscopic analysis of silver diffusion into gold plate on electrical connector
[AD-755123] 11 p1263 N73-20249
Characteristics of second breakdown in germanium gold diodes
[AD-755425] 12 p1385 N73-21230
Aluminum-gold interaction in thin layers
[NASA-TT-F-14919] 14 p1675 N73-23595
Effect of helium gas bubbles on grain boundary motion in vapor deposited gold foil samples
[RD/B/N-2430] 15 p1798 N73-24578
Electrical conductivity and carrier lifetimes in gold doped silicon wafer
[AD-760150] 17 p2075 N73-26789
Wavelength modulation spectra of copper, gold, silver, gallium phosphide, and indium phosphide
[LBL-1125] 24 p2927 N73-33375
K shell Compton scattering on tin and gold at 145 keV and gold at 320 keV
24 p2960 N73-33654
GOLD ALLOYS
Effects of growth speed and heat treatment on deformation of aligned Ag3 Mg-AgMg and Al-Ag2 Al eutectics at minus 196 to 300 C
[AD-747310] 02 p0190 N73-11541
Mossbauer analysis of spin arrangements in gold iron and copper iron alloys at low temperature
[AD-754140] 10 p1202 N73-19787
Cyclic mechanical and fatigue properties of ferroanelastic beta prime gold-cadmium alloy
[NASA-CR-131843] 16 p1969 N73-25929
Optical determination of elsctronic structure of Au-Cu alloys in disordered and ordered phases
[AD-763239] 21 p2586 N73-30720
Interstitial and vacancy motion in defect annealing of alpha brass and copper gold alloy by electron irradiation
22 p2683 N73-31489
Cyclic mechanical and fatigue properties of ferroanelastic beta prime gold-cadmium
24 p2933 N73-33421
GOLD COATINGS
Electrical, optical, and structural properties of RF triode-sputtered gold films
18 p2186 N73-27649
Lateral diffusion in thin [film] couples of gold and silver
23 p2825 N73-32579
GOLD PLATE
U GOLD COATINGS
GONDOLAS
System for controlling torque buildup in suspension of gondola connected to balloon by parachute shroud lines
[NASA-CASE-GSC-11077-1] 04 p0370 N73-13008
GOSS [SUPPORT SYSTEM]
U GROUND OPERATIONAL SUPPORT SYSTEM
GOVERNMENT PROCUREMENT
Development of equations and mathematical models for decision making concerning military logistics, aircraft, space parts, and support equipment
[AD-747972] 03 p0368 N73-12997
Methods of improving cost estimating techniques in NASA and DOD
12 p1466 N73-21877
Planning and budgeting in lightweight fighter prototype development for military aviation
13 p1595 N73-22934
Effects of NASA expenditures to aerospace industry as factor of industrial location
18 p2207 N73-27814
Contractual requirements for submission of electromagnetic compatibility and interference control plan for government procurement
[AD-761975] 19 p2237 N73-28033
Quality control policies of DOD and application to weapon system acquisition management
[AD-762000] 19 p2305 N73-28540
Policies and guidelines for awarding weapons systems acquisition contracts
[AD-761443] 19 p2356 N73-28949
GOVERNMENT/INDUSTRY RELATIONS
Congressional hearing to establish national science policy and priorities act of 1972
03 p0367 N73-12991
Congressional assessment of governmental role in industrial and social aspects of aerospace and related technology
11 p1292 N73-20482
Congressional study of future governmental role in scientific and technological research and development
13 p1594 N73-22927
Organization and management of ESRO 4 satellite project noting planning and contractor relations
15 p1847 N73-24970
Industrial policy of ESRO noting distribution of contracts, relations with industry, multinational consortiums, and technological research
15 p1848 N73-24975
Phased project planning and development for operational space missions referring to NASA meteorological and communication satellite programs
15 p1848 N73-24978
Project management information requirements in international organization
15 p1849 N73-24990
Shortcomings in Government organization for civil aviation
[PB-215426/8] 16 p1977 N73-25994
Development of US commercial air transport industry
23 p2860 N73-32849
Federal Government participation in development of US air transportation system
23 p2860 N73-32850
Historical and constitutional framework of industry regulation with application to airline operations
23 p2864 N73-32889
Economic aspects of Federal regulation of airline operations to show agencies involved and functions of government organizations
23 p2864 N73-32893
Characteristics of Federal regulation of airline operations and predictions for type and extent of future regulation
23 p2864 N73-32894
Actions of Civil Aviation Board with respect to monopolies and mergers of domestic airline operations
23 p2864 N73-32895
Policy of Department of Transportation with respect to evaluating proposals for airline mergers
23 p2864 N73-32896
Policy of Justice Department with respect to airline merger within context of Federal Aviation Act
23 p2864 N73-32897
Advice and assistance provided by Civil Aviation Board to State Department on matters of international air transportation policy
23 p2865 N73-32899
Federal policy establishing guidelines for US participation in international air transportation services
23 p2865 N73-32902
International air transportation policy and application of policy to scheduled and chartered airline services
23 p2865 N73-32903
GOVERNMENTS
Descriptions of Federal Government environmental research and development facilities
[PB-209751] 02 p0153 N73-11239
Inventory listing of Federal Government environmental research facilities
[PB-209752] 02 p0153 N73-11240
Relation between technology and rise of multinational corporations, and impact on nation-state
[NASA-CR-129269] 03 p0367 N73-12988
Federal policy for support and use of technology
[NASA-CR-129669] 04 p0488 N73-13987
Legal liability of US Government in handling meteorological data obtained by satellites
06 p0692 N73-15638
Conceptual framework for analysis for aiding policy analyst and policy researcher in empirical investigations into policy phenomena
[NASA-CR-130669] 08 p0976 N73-17982
Analysis of Marxist-Leninist theory based on data in cybernetics, information theory, systems analysis, and semiotics
24 p2993 N73-33918
GOVERNORS
U SPEED REGULATORS
GRABENS
U GEOLOGICAL FAULTS
GRADIENTS
NT ELECTRON DENSITY PROFILES
NT PRESSURE GRADIENTS
NT TEMPERATURE GRADIENTS
NT THERMOCLINES
Subroutines for optimization of criteria under constraints using gradient projection method and HEATHER computer program
[LAAS-NI-CH-72-03] 02 p0147 N73-11191
Effects of one dimensional yield strength gradients on plastic zones in notched aluminum specimens
[AD-747783] 04 p0435 N73-13546
Gradient methods for solving incompatible systems of linear equations of higher order in photomapping problems
10 p1178 N73-19584
Numerical analysis of projected gradient method and operator formed from any linearly independent subset of gradients
[DLR-FB-73-26] 11 p1311 N73-20636
Mesh gradient technique for numerical optimization
23 p2812 N73-32481
GRADIOMETERS
U MAGNETOMETERS
GRADUATION
U CALIBRATING
GRAIN BOUNDARIES
Measurement of surface, grain boundary, and coherent twin boundary free energies in 304 stainless steel at elevated temperatures using method of zero creep coupled with electron microscopy
[AD-747267] 02 p0189 N73-11535
Deformation of polycrystalline matter to large strains by grain-boundary sliding with diffusional accommodation
[AD-746499] 02 p0218 N73-11767
Influence of grain size and cold working on static corrosion of Incoloy 800 alloy in superheated steam
[EURFNR-965] 03 p0315 N73-12570
Influence of ingot thermal-mechanical processing on grain size and mechanical properties of 7075 wrought aluminum alloy
[AD-750390] 06 p0686 N73-15588
Corrosion behavior of grain boundary constituents in Al-Zn-Mg alloys
[AD-753273] 09 p1049 N73-18556

Intergranular hydride as a linear function of hydrogen concentration in Zircaloys
09 p1063 N73-18672
Crack size and grain size dependence of brittle fracture stress
[AD-753525] 09 p1076 N73-18781
Structural models for grain boundary dislocations and ledges in crystal defects
[COO-3158-12] 10 p1173 N73-19544
Creep tests and transmission electron microscopic observation of grain boundary structure in stainless steel bicrystals
[CEA-R-4317] 10 p1200 N73-19768
Abstracts on directionally grown eutectic alloy composites
[AD-754779] 11 p1309 N73-20625
Solutions to diffusion along grain boundaries and dislocations for finite source
[NLL-CE-TRANS-6043-[9022.09]]
11 p1329 N73-20785
Coincidence structural unit models for grain boundaries in HCP metals
[AD-756884] 13 p1545 N73-22520
Effect of helium gas bubbles on grain boundary motion in vapor deposited gold foil samples
[RD/B/N-2430] 15 p1798 N73-24578
Structural and superconducting transition temperature of evaporated aluminum films as function of grain size
[NASA-CR-133450] 19 p2326 N73-28716
Oxygen grain boundary diffusion and grain growth in pure dense MgO
[NASA-CR-135719] 23 p2810 N73-32466

**GRAINS**
Microstructural analysis of 1010 modified steel and titanium alloy grains
[AD-748101] 06 p0686 N73-15584
Mechanism of grain growth in ceramics
[NASA-CR-135673] 23 p2804 N73-32425

**GRAINS [FOOD]**
NT CORN
NT RICE
NT WHEAT
Airborne multispectral scanning of maize canopy to determine temporal characteristics, and relation of leaf area index to spectral response curves
[NASA-CR-130369] 07 p0789 N73-16421
Relationship between maize canopy density and reflected energy determined from color and color infrared photographs
[NASA-CR-130370] 07 p0790 N73-16422
Airborne multispectral scanning of maize canopy to determine density, and comparision to leaf area index
[NASA-CR-130363] 07 p0790 N73-16425
Influence of solar radiation in mountainous areas on crop capacity and grain yield of spring wheat
20 p2406 N73-29335
Aerial photography for detecting cereal crop insect infestation
[PAPER-8076] 23 p2783 N73-32268

**GRAMMARS**
Digitized grammar for signal analysis and speech recognition accuracy in command and control system
[AD-746333] 06 p0643 N73-15218

**GRAND TOURS**
Development of long range plan for solar system exploration to define space missions, equipment, and trajectories for interplanetary flight
[NASA-CR-129132] 02 p0226 N73-11823
Defining energetic particle experiment for Grand Tour missions
[NASA-CR-129182] 02 p0226 N73-11824
Activities of Meteoroid Science Team for definition phase of outer planet missions
[NASA-CR-129186] 02 p0226 N73-11825
Graphs for ballistic transfers to Jupiter, Saturn, and Uranus
[NASA-CR-129162] 02 p0226 N73-11826
Flyby missions to outer planets
04 p0473 N73-13858
Computerized simulation of approach navigation accuracy and guidance requirements for 1977 Grand Tour mission to outer planets
08 p0941 N73-17707
Optical design optimization, and sensor selection for mission definition of outer planets Grand Tours
[NASA-CR-131088] 10 p1159 N73-19427
Outer Planets Grand Tour mission planning to include magnetometer systems requirements and development of hardware elements to meet objectives
12 p1448 N73-21727
High angular resolution imaging system for outer planet Grand Tour Mission
[NASA-CR-132013] 14 p1704 N73-23823
Various imaging systems and techniques for possible use aboard Grand Tour Spacecraft
[NASA-CR-132014] 14 p1704 N73-23824
Modifications to Pioneer meteoroid detection experiment for outer planet mission applications
[NASA-CR-132310] 23 p2845 N73-32739

**GRANTS**
Guide to National Science Foundation programs and grants - information for proposals
[NSF-72-23] 07 p0857 N73-16945
Grants and awards for scientific research
[NSF-73-2] 10 p1229 N73-19987

**GRANULAR MATERIALS**
Heat exchange between cooled polydisperse granular material and transversely located cylindrical tubes arranged in staggered bundle
[NLL-M-21602-[5828.4F]] 18 p2205 N73-27795
Technique for predicting thermal conductivity of randomly packed granular materials
24 p2990 N73-33892

**GRAPHITE**
NT PYROLYTIC GRAPHITE
Performance of graphite fiber reinforced polyimide composites as journal bearing materials
[NASA-TN-D-7078] 01 p0062 N73-10505
Mechanical properties of heat resistant silicon carbide-graphite composite
[AD-745434] 01 p0070 N73-10577
Development of proton-activated recession sensor based on migration of beryllium isotope in graphite at high temperature and application to nose cone conditions during reentry
[AD-745454] 01 p0109 N73-10899
Application of strain compatibility equations to evaluate thermal stresses in unidirectional graphite composites bonded to aluminum structures
[NASA-CR-112162] 02 p0125 N73-11014
Analytical analysis of graphite interaction with carbon dioxide at high temperature
[AD-747556] 03 p0264 N73-12141
Performance of powder metallurgy bronze graphite bearings operating under hydrodynamic conditions at high slipping rates
[AD-747432] 03 p0309 N73-12523
Effects of incomplete dissolution of graphite in molten cast iron on viscosity differences with same chemical composition
[AD-747378] 03 p0317 N73-12582
Irradiation-induced changes in graphites at high temperatures and high fluences
[GULF-GA-A-10971] 03 p0321 N73-12612
Influence of creep strain on elastic modulus, crystallographic orientation, and density of POCO graphite
[LA-DC-13292] 03 p0321 N73-12614
Frictional properties of rubbers in presence of greases and graphite lubricants
[AD-747447] 03 p0322 N73-12622
Resistance to damage from impulsive loading in three dimensionally graphite reinforced phenolic composite materials
[AD-748099] 03 p0323 N73-12628
Ablation of graphite surfaces heated in turbulent flow of air or carbon dioxide and development of method for calculating ablation rate
[AD-747727] 03 p0365 N73-12973
Properties and uses of silicon graphite
04 p0433 N73-13527
Estimation procedure for fatigue failure probability of some graphites
[AECL-3958] 04 p0438 N73-13567
Development and fabrication of graphite polyimide wing box beam
[NASA-CR-123959] 04 p0480 N73-13923
Development of proton-activated sensors to measure graphite nosetip recession due to ablation during nose cone reentry
[AD-748289] 05 p0548 N73-14456
Publications of carbon and graphite research results
[NYO-1710-106] 05 p0565 N73-14590
In pile neutron irradiation damage in graphite at high temperature
[CEA-CONF-1894] 07 p0820 N73-16644
Behavior of graphite electrodes in organic electrolytes
[UCRL-TRANS-1476] 08 p0870 N73-17043
Isotopic composition of carbon in Precambrian graphitoids from various parts of the USSR
[NASA-TT-F-14682] 08 p0918 N73-17520
CMB-13 research on carbon and graphite
[NASA-CR-130539] 08 p0935 N73-17652
Nondestructive tests of fracture behavior of ATJ-S graphite
[AD-751976] 08 p0935 N73-17655
Mathematical model for predicting erosion rate of graphite surface exposed to hot supersonic stream of hydrogen gas
[NASA-CR-130812] 09 p1050 N73-18564
Laboratory method for thermal fracture of graphite
[AD-753392] 09 p1054 N73-18592
Vaporization kinetics and thermodynamics of graphite using high pressure mass spectrometer
[AD-753713] 09 p1055 N73-18601
Development of graphite-matrix fuels for booster assemblies in reactor cores
09 p1063 N73-18669
Mechanical and thermal properties and oxidation resistance of seal ring carbon graphite materials with resin impregnants
[NASA-CR-120955] 10 p1165 N73-19480
Improved carbon graphite materials for high temperature self-acting seals
[NASA-CR-121092] 10 p1165 N73-19481
Computational procedure for determining heat resistance of different graphites in broad temperature range
10 p1175 N73-19557
Physical properties and dimensional changes in graphites caused by high temperature neutron irradiation
[BNWL-1672] 10 p1193 N73-19706
Soldering process of graphite materials such as zirconium carbide with composition like stoichiometric
[AD-754050] 11 p1300 N73-20552
Development of polyphenylquinoxaline graphite fiber reinforced composites for structural materials
[NASA-CR-121109] 11 p1308 N73-20611
Vaporization kinetics and thermodynamics of graphite using high pressure mass spectrometers
[AD-755853] 12 p1376 N73-21165
Systhesis, thermodynamics, and electrochemical properties of graphite fluorides
[AD-755934] 12 p1377 N73-21167
Standards for calorimeter measurement of laser beam absorption by graphite cones
[CEA-CONF-2056] 12 p1411 N73-21432
Mass spectrometer to study kinetics and thermodynamics of graphite vaporization
[AD-755899] 12 p1465 N73-21871
Graphite oxide and fluorides as depolarizers in lithium organic electrolytic cells
[AD-755159] 13 p1477 N73-21968
Research on carbon, graphite, and phenolic resin binders
[NASA-CR-131483] 13 p1547 N73-22539
Application of ultrasonic inspection for determining effect of graphite on strength characteristics of cast iron
15 p1797 N73-24571
Analysis of polymerization mechanism and fabrication of polyimide/graphite fiber composites using A-type polyimide prepolymers as matrix
[NASA-TM-X-2798] 15 p1801 N73-24597
Graphite and epoxy plastic material strength under biaxial stress
[AD-758448] 15 p1801 N73-24600
Static tests of redesigned graphite horizontal stabilizers
[AD-758718] 15 p1803 N73-24611
Design fabrication, and nondestructive testing of six experimental cylinder assemblies of selected composite graphites for NERVA nozzle extension
[NASA-CR-132233] 15 p1810 N73-24674
Modulus of elasticity measurements on materials at elevated temperatures
[AD-759060] 16 p1971 N73-25941
Heat capacity of submonolayer helium films adsorbed on exfoliated graphite in very low temperatures
16 p1973 N73-25953
Vaporization coefficient of graphite based on ion intensity measurements
[AD-759203] 17 p1993 N73-26113
Wear processes and compressive stress of graphite fluoride lubricated machine surfaces
[AD-759560] 17 p2038 N73-26489
Constant-stress irradiation creep capsules for application of load to several graphite samples by single pneumatic bellows
[BNWL-SA-4199] 17 p2050 N73-26586
OSO-1 graphite crystal polarimeter for stellar X ray astronomy
17 p2084 N73-26862
Physical and mechanical properties of high-strength, high-modulus reinforcing fibers and organic resin composite materials
18 p2164 N73-27475
Thermal conductivity and electrical resistivity ATJS graphite
[AD-762301] 19 p2313 N73-28601
Fatigue properties of high strength high modulus graphite /glass/epoxy matrix composites
[AD-763760] 21 p2564 N73-30552
Maximizing impact strength of advanced graphite composites without affecting other directional strength properties
[AD-763376] 21 p2564 N73-30553
Effects of microstructure differences on tensile strength of graphite fibers
[AD-763687] 21 p2564 N73-30557
Normal mode laser and Q switched laser for vaporization of graphite and carbides
[SLA-73-5233] 22 p2681 N73-31473
Temperature effects on structures and mechanical properties of polysulfone and poly[216-dimethyl] phenylene oxide
22 p2688 N73-31528
Metal-loaded carbon and graphite cloth reinforced composites from polymer blends
[AD-764630] 23 p2811 N73-32474
In situ monomer polarization for polyphenylquinoxaline/graphite
[NASA-TM-X-71454] 24 p2891 N73-33084
Chemical and physical properties of graphite and carbide-graphite composites developed by powder metallurgy
[LA-5147] 24 p2936 N73-33448
Mass loss rate of carbon and graphite at high temperature
[LA-5223-PR] 24 p2943 N73-33503

Linear elastic fracture mechanics applied to graphite under multiaxial stress conditions
[CONF-730707-2] 24 p2943 N73-33507
Precursor carbons and molding of graphites
[Y-1857] 24 p2954 N73-33598

**GRAPHITIZATION**
Evaluation of stabilized precursors for high strength carbon fibers
[AD-755427] 13 p1547 N73-22540

**GRAPHS (CHARTS)**
Curves for determining maximum combined stresses in long circular cylindrical shells with flat head closure under uniform pressure only
[ESDU-66010] 01 p0117 N73-10912
Curves for determining maximum elastic stresses and deflections for initially flat circular plates of uniform thickness under uniform pressure with various edge conditions
[ESDU-65002] 01 p0112 N73-10923
Curves for determining climb performance of aircraft
[ESDU-RJ1/2-AMEND-A] 02 p0124 N73-11011
Graphs for ballistic transfers to Jupiter, Saturn, and Uranus
[NASA-CR-129162] 02 p0226 N73-11826
Acyclic color rings of planar graphs
[AD-747662] 03 p0325 N73-12652
Application of graph theory to network analysis and coding problems in communication systems
[AD-748290] 04 p0391 N73-13178
Multi-terminal network flow realizability, analysis, and synthesis
[AD-748773] 04 p0441 N73-13595
Endurance of high strength steels subjected to bending
[ESDU-71027] 05 p0561 N73-14561
Graphical summary of weather and sea conditions along California coast
[AD-749781] 05 p0576 N73-14690
Standard curves for interpreting magnetic anomalies due to spheres in geomagnetic surveys
[BULL-119] 06 p0666 N73-15417
Tables and graphs on static stability and axial force characteristics of flat faced right circular cylinders at subsonic and supersonic speed
[AD-754920] 11 p1273 N73-20330
Procedure for finding minimal and maximal Hamiltonian circuits on complete graph
[AD-754842] 11 p1312 N73-20648
Three graph models and heuristic search strategies
[NASA-CR-131992] 14 p1684 N73-23662
Application of graph theory to Air Force systems design and analysis
[AD-757235] 14 p1684 N73-23666
Graphical determination of meteor radiant point curve
17 p2024 N73-26374
Decision graphs for information processing
[AD-761877] 19 p2242 N73-28078
Device for semi-automatic digital encoding of graphic data
21 p2513 N73-30157
Solubility curves from 25 to 70 C for K2HfF-K2ZrF6-HF system
[BM-RI-7785] 21 p2558 N73-30505
Satellite data presentation by means of lists, graphs, and three dimensional plots
24 p2985 N73-33859

**GRASSES**
Light and ultraviolet albedo of grass and snow including effect of sun altitude, cloud cover, and state of underlying surface on magnitude of albedo
04 p0442 N73-13609

**GRASSLANDS**
Application of ERTS-1 imagery to identification of agricultural crops, grasslands and forestry in Mississippi Delta Region
[E73-10476] 12 p1395 N73-21313
Application of ERTS-1 band six imagery to determine rate of spread of grass fires in Zambesi Basin of South Africa
[PAPER-E6] 19 p2269 N73-28270
Evaluation of ERTS-1 imagery for determining numbers and distribution of prairie ponds and lakes in North Dakota
[PAPER-W12] 19 p2272 N73-28289
ERTS-1 monitoring of grass seed field burning in western Oregon
[E73-10883] 20 p2394 N73-29234

**GRASSMANN ALGEBRA**
U VECTOR SPACES

**GRATINGS**
Extended two color photometry of faint stars by telescope with objective grating
[BULL-172] 07 p0842 N73-16819
Michelson interferometry quality control of Schmidt plate replica by [Jouan Quetin] grating copying technique noting Kerber profile
[OPT-001-72] 23 p2794 N73-32351
Kerber profile Schmidt plates uses in optical combinations with applications to cameras
[OPT-01-72] 23 p2794 N73-32352

**GRATINGS [SPECTRA]**
Use of objective grating for extension of magnitudes and colors beyond those available photoelectrically
[ROY-OBS-BULL-172] 06 p0674 N73-15486
Fourier theory of using grating to extend dynamic range of laser far field camera
[UCRL-51255] 07 p0806 N73-16542
Effects of successive concave optical gratings in spectrograph on X ray diffraction patterns
[AD-757014] 13 p1560 N73-22640
Shadowing mounds on ruled gratings for X ray and far ultraviolet spectra
[AD-757894] 15 p1814 N73-24705
Interferometrically controlled ruling machine for manufacturing optical diffraction gratings
[AD-758898] 16 p1946 N73-25745
Production technology for diffraction gratings as laser beam sampling components
[AD-762306] 19 p2322 N73-28681
Theoretical analysis of grating coupler for application in thin film integrated optical waveguides
22 p2699 N73-31621
Optical image modulation by polarization shifting diffraction gratings
[AD-765174] 24 p2959 N73-33644

**GRAVIMETERS**
Design and fabrication of cryogenic gravity meter
[AD-754242] 10 p1162 N73-19455
Semiautomatic self-leveling lunar gravimeter for Apollo 17 mission
[NASA-CR-128948] 15 p1787 N73-24490
Lunar roving vehicle/traverse gravimeter experiment motion sensitivity test showing gravity measurements in normal and bypass modes
[NASA-TM-X-69268] 16 p1963 N73-25882
High precision quartz astatic gravimeter designated GRK-1
[JPRS-59832] 21 p2548 N73-30426
Second generation laser interferometer for absolute determination of gravity acceleration
[AD-764831] 24 p2924 N73-33359
Design criterion and laboratory test results of gyrostabilized marine gravimeter
[JPRS-60183] 24 p2926 N73-33369

**GRAVIMETRY**
Interpolation of vertical deflections using trigonometric leveling
[AD-743986] 01 p0052 N73-10418
Geocentric orientation vector from limited astro-geodetic and gravimetric data
[NASA-TM-X-66078] 02 p0165 N73-11342
Two FORTRAN 4 computer programs for general combination of satellite and gravity data for position and gravity field determinations
[AD-746305] 02 p0168 N73-11364
Computer program for calculating gravimetric deflections of the vertical in central zone
[AD-747136] 02 p0170 N73-11380
Gravimetric map of Australia
[AD-747873] 04 p0417 N73-13405
Sweeping of masses theory used to solve inverse gravimetric problem and interpretation of regional gravitational field
[AD-747874] 04 p0417 N73-13406
Gravity values, station locations, and terrain locations for Central Colorado, Arizona, New Mexico, and Utah
[PB-211306] 05 p0540 N73-14396
Fundamental problems of geodetic gravimetry
[AD-748527] 05 p0543 N73-14420
Gravimetric geoid construction for Atlantic Ocean area from satellite and sea surface gravimetric measurements
06 p0664 N73-15393
Ocean circulation effects on orbiting satellite gravimetry
06 p0664 N73-15394
Least squares method in gravimetric geodesy and photogrammetry
[AD-749873] 06 p0669 N73-15440
Detailed gravimetry for exploration of underthrust structures in Northern Sakhalin
[AD-750751] 06 p0672 N73-15465
Height error in sea-surface profile over Puerto Rican trench as determined by multi-station tracking aided by GEOS 2 satellite
[NASA-TM-X-69353] 07 p0781 N73-16347
Trigonometric leveling and gravimetric survey in Antarctic
[AD-752232] 08 p0920 N73-17540
Mologenskys solution of geodetic boundary value problems
[AD-754251] 11 p1287 N73-20444
Some results of astro-gravimetric leveling in USSR
[AD-755881] 14 p1664 N73-23503
Methods for improving 1967 geodetic reference system
[AD-755418] 14 p1665 N73-23510
Manned submersible ocean bottom sampling and gravimetric prospecting
[AD-759992] 17 p2029 N73-26425
New two-metric theory of gravity with prior geometry
[NASA-CR-133501] 19 p2294 N73-28444
Time lag test of general relativity and Earth-Mars ephemeris improvement using Mariner 9 tracking data
23 p2842 N73-32713
Second generation laser interferometer for absolute determination of gravity acceleration
[AD-764831] 24 p2924 N73-33359

**GRAVIRECEPTORS**
NT OTOLITH ORGANS
Evolution of structural, cytochemical, and functional organization of gravity receptors in invertebrates and vertebrates
[NASA-TT-F-720] 11 p1247 N73-20128

**GRAVITATION**
NT ARTIFICIAL GRAVITY
NT GRAVITY ANOMALIES
NT LUNAR GRAVITATION
NT PLANETARY GRAVITATION
NT REDUCED GRAVITY
NT SOLAR GRAVITATION
External gravity potential on earth and gravity dependent geodetic parameters
[AD-746307] 03 p0297 N73-12422
Effects of gravity-induced free convection of melting behavior of paraffin slab for thermal control devices
[NASA-CR-123954] 04 p0385 N73-13130
Absolute gravity measurements using earth tides for analyzing earth structure
[AD-748529] 05 p0544 N73-14423
Bathymetry, magnetic, and gravity data for North Pacific Ocean areas collected between 1961 and 1970 - Technical Report 50
[NOAA-TR-NOS-50] 07 p0792 N73-16444
Bathymetry, magnetic, and gravity data for North Pacific Ocean areas collected between 1961 and 1970 - Technical Report 49
[NOAA-TR-NOS-49] 07 p0793 N73-16445
Relativity shift effect of gravitational vibration frequency in earth field
[ITF-72-43-P] 07 p0793 N73-16451
Inverse method for exact analytical solutions for particle motion under central Newtonian gravitational force and atmospheric drag force
[AD-751491] 07 p0847 N73-16865
Mathematical models for reducing force of gravity values from earth relief to external surface
[AD-752235] 08 p0920 N73-17538
Construction of main fundamental solution of gravity equation
[AD-752233] 08 p0922 N73-17553
Design and fabrication of cryogenic gravity meter
[AD-754242] 10 p1162 N73-19455
Nonlinear analysis of gravity wave moving over horizontal bed into vertical shear flow
[AD-754646] 11 p1272 N73-20322
Necessity of probability conservation law in quantum theories of gravitation
12 p1393 N73-21296
Interaction of nonsaturated surface gravity ocean waves with nondispersive internal waves
[AD-754281] 12 p1403 N73-21377
Gravity current model applied to analysis of squall-line gust front
12 p1419 N73-21504
Transformation matrices between spherical harmonics and spherical sampling functions
[AD-755486] 14 p1664 N73-23509
Improved earth gravitational model from combination of satellite tracking and surface mean free-air gravity anomaly data
[AD-756177] 15 p1783 N73-24459
Gravitational wave observations as tool for testing relativistic gravity
[NASA-CR-133411] 18 p2145 N73-27337
Spherical harmonics presentation of anomalous gravity potential from satellite and terrestrial data at 9km aove sea level
[AD-759909] 18 p2147 N73-27358
Three-dimensional geodesy and gravity gradients
[AD-759538] 18 p2148 N73-27366
Computer code for calculating time series of earth tidal gravity and tilt
[AD-762275] 19 p2297 N73-28468
Numerically integrated equations of motion of N particles under mutual gravitation attraction
20 p2390 N73-29202
Gravitation and general relativity
[ITF-72-106-P] 21 p2580 N73-30675
Satellite-borne hybrid measuring system for sensing earth gravitational field
24 p2912 N73-33237
Sensitivity of gravitational detector with positive electromechanical transducers
[ITF-72-90-E] 24 p2926 N73-33374
Design of precision vertical alignment system using laser with gravitationally sensitive cavity
[NASA-CASE-ARC-10444-1] 24 p2930 N73-33397

**GRAVITATION THEORY**
Tensor theory applied to special and general relativity, noting gravitational theory
02 p0231 N73-11878
Precision measurements of solar gravitational fields by European drag-free and twin geodetic space probes
02 p0231 N73-11879

Development of relativistic theory of gravity and comparison with post-Newtonian limit
[NASA-CR-129242] 03 p0293 N73-12387
Mathematical representation of gravitational theories using four dimensional manifold defined geometries
[NASA-CR-130753] 08 p0915 N73-17499
Mathematical representation with metric form to first order of gravitationally modified Maxwell equation in Lorentz symmetric linear field theory
[NASA-CR-130754] 08 p0915 N73-17500
Solutions for space-times regarded as representing gravitational fields of spinning bound masses based on formulation on axisymmetric stationary fields
[RIFP-173] 12 p1399 N73-21343
New two-metric theory of gravity with prior geometry
[NASA-CR-133501] 19 p2294 N73-28444
Preferred frame effects on stellar stability
[NASA-CR-135517] 22 p2717 N73-31754

GRAVITATIONAL COLLAPSE
NT BLACK HOLES [ASTRONOMY]
Boundary conditions and singularities in gravitational collapse and gravitational radiation
[MATSCIENCE-72] 15 p1781 N73-24437
Spherical and nonspherical gravitational collapse and Schwarzschild black holes
15 p1829 N73-24822
Electromagnetic and gravitational wave interaction of black holes
15 p1829 N73-24824
Israel-Carter conjecture of black hole physics and baryon number
15 p1829 N73-24825

GRAVITATIONAL CONSTANT
Algorithm for computing satellite orientation and tables of gravitational constants used for computations
[NASA-TT-F-14699] 15 p1831 N73-24840

GRAVITATIONAL EFFECTS
NT STELLAR GRAVITATION
Aerospace biology research, including physical principles of gravitational biology, such as forces, weight and mass, weightlessness, and size and scale effects
[NASA-CR-128471] 01 p0009 N73-10075
Gravitational effects on electrochemical batteries
[NASA-CR-129091] 02 p0128 N73-11039
Influence of nongravitational effects on accurate prediction of comet orbits
02 p0228 N73-11849
Effects of gravitational and inertial forces on cardiovascular and respiratory dynamics
[NASA-CR-129603] 03 p0256 N73-12074
Transverse acceleration effects on dioxyribonucleic acid catabolism in rat spleen and liver
03 p0257 N73-12080
Transverse acceleration effects on human cardiovascular system
03 p0258 N73-12088
Role of gravity-induced free convection upon liquefaction dynamics of cylindrical paraffin slab under normal gravity conditions
[NASA-CR-129911] 04 p0385 N73-13131
Orbit determination for self-contained stationkeeping systems, equations of satellite motion, orbit control, gravitational effects, and synchronous satellite drift
[NAL-TR-295] 04 p0469 N73-13826
Filament stationary motion pattern in media of diverse viscosities, allowing for gravitational and resistance forces to longitudinal motion
06 p0652 N73-15294
Renal component of antigravitational function in body
07 p0743 N73-16043
Approximate analytic and numerical methods for describing encounter of star with sun-comet system and resulting gravitational perturbations of cometary orbits
07 p0840 N73-16805
Solutions for space-times regarded as representing gravitational fields of spinning bound masses based on formulation on axisymmetric stationary fields
[RIFP-173] 12 p1399 N73-21343
Effects of solar pressure and gravity gradient on attitude motions of artificial satellite near far moon side libration point
12 p1447 N73-21722
Effects of solar, lunar, and earth gravity perturbations on synchronous satellite
13 p1576 N73-22767
Performance of gas-loaded variable conductance heat pipe with effect of gravity
[AD-757684] 14 p1720 N73-23956
Instrumentation and techniques for determining effects of gravitational and inertial forces on cardiovascular and respiratory dynamics
[NASA-CR-133212] 16 p1867 N73-25119
Rossby regimes in geophysical fluid dynamics of ocean waves
[PB-214660/3] 16 p1890 N73-25295
Gravity effects on geophysical fluid dynamics
[PB-214659/5] 16 p1890 N73-25296
Gravity effects upon melt-through time of metal plate subjected to high intensity lasers
[AD-759168] 16 p1925 N73-25574
Linear stability analyses for four satellite configurations using passive elements for attitude control
16 p1964 N73-25883
Procedures for obtaining position from surface gravity observations and application of geodetic techniques to earth and ocean physics
[NASA-TM-X-66273] 17 p2059 N73-26655
Acceleration effects on mechanical impedance of human body in supine position
19 p2227 N73-27963
Fundamental data for contact binaries RZ Comae, RZ Tauri and AW UMa
[NASA-TM-X-69614] 22 p2718 N73-31755
Supersonic stationary flow around atmosphere retained by gravitational force of spherical body
24 p2905 N73-33183
Dynamic model gravity compensation method for satellite orbit determination
[AD-765551] 24 p2982 N73-33828

GRAVITATIONAL FIELDS
NT STELLAR GRAVITATION
Computation of lunar gravitational field expansion coefficients utilizing Cassini equator inclination and radial lunar density distribution values
[NASA-TT-F-14605] 01 p0104 N73-10858
Tensor analysis application to relativity theory and measurements of solar gravitational fields using European geodetic solar probes
[ESRO-SN-118-ESTEC] 02 p0231 N73-11877
Development of relativistic theory of gravity and comparison with post-Newtonian limit
[NASA-CR-129242] 03 p0293 N73-12387
Homogeneous density effects for calculating earth crust structure from gravitational anomalous masses
[AD-746018] 03 p0297 N73-12427
Calculation of particle motion in gravitational field using Schwarzschild metric
[ESRO-SR-17-ESOC] 03 p0357 N73-12910
Sweeping of masses theory used to solve inverse gravimetric problem and interpretation of regional gravitational field
[AD-747874] 04 p0417 N73-13406
Effect of joint orientation relative to gravitational field direction during electron beam welding
[JPRS-57281] 04 p0426 N73-13476
Exact solution of gravitational field of rotating mass
[RIFP-161] 04 p0449 N73-13666
Exterior gravitational field of slowly rotating deformed masses, obtained by generalizing Weyl metrics into rotating Weyl metrics
[RIFP-162] 04 p0449 N73-13667
Methods for determining figure and gravity field of moon
[AD-747875] 04 p0477 N73-13897
GEOS-C data for improving geoid and gravity field determination
06 p0661 N73-15371
Use of GEOS-C satellite height for determining earth gravitational field and physical ocean surface variations
06 p0662 N73-15375
Accuracy of geopotential solutions from resonant satellites
[NASA-TM-X-66147] 06 p0665 N73-15410
Mathematical modeling of solar gravitational fields
[ITF-71-130-P] 07 p0793 N73-16452
Mathematical representation of gravitational theories using four dimensional manifold defined geometries
[NASA-CR-130753] 08 p0915 N73-17499
Calculation of gravity anomalies
[AD-752234] 08 p0920 N73-17541
Combination of satellite and gravimetric data for analysis of terrestrial gravity field blocks
[NASA-CR-130176] 10 p1153 N73-19380
Restricted proof that weak equivalence principle implies Einstein equivalence principle
[NASA-CR-131420] 11 p1324 N73-20745
Gravitational field models for solution of satellite geopotential using optical data processing
[NASA-TM-X-66207] 11 p1341 N73-20883
Solutions for space-times regarded as representing gravitational fields of spinning bound masses based on formulation on axisymmetric stationary fields
[RIFP-173] 12 p1399 N73-21343
Empirical method for determining spherical harmonic coefficients of lunar gravity field
12 p1447 N73-21718
Motion and orbital direction of particle in Kerr gravitational field
[NASA-TR-R-403] 12 p1458 N73-21816
Effect of gravitational field on polarization
15 p1770 N73-24335
Total modelling of gravitational fields into plane space with symmetry conservation
[ITF-72-139-P] 15 p1781 N73-24434
Boundary conditions and singularities in gravitational collapse and gravitational radiation
[MATSCIENCE-72] 15 p1781 N73-24437
Gravimetry and satellite altimetry for determining earth gravity field
[AD-759536] 18 p2148 N73-27365
Einstein-Bonner nonsymmetric field theory of gravity and electromagnetic fields
[AD-761482] 19 p2295 N73-28460
Coplanar transfer orbit calculation in Newton central gravitational field noting two propulsive phases applying tangential thrust and intermediate coast phase
[DLR-FB-73-29] 21 p2597 N73-30814
Celestial mechanics analysis on Mariner 9 Doppler tracking data for determining Mars gravitational field
23 p2841 N73-32706
Mariner 9 Doppler tracking short data arcs for determining Mars gravitational field
23 p2841 N73-32707
Mariner 9 Doppler tracking data filtering method for determining Mars gravity
23 p2841 N73-32708
Range points in relativistic test of celestial mechanics in Mariner 9 Doppler tracking data analysis for Mars gravity
23 p2842 N73-32710
Interpretation of aeromagnetic or gravity data by method of difference mapping for mineral exploration
24 p2912 N73-33240
Satellite motion in gravitational field of nonspherical rotating planet
[NASA-TT-F-15073] 24 p2981 N73-33825

GRAVITATIONAL POTENTIAL
U GRAVITATIONAL FIELDS

GRAVITATIONAL RADIATION
U GRAVITATIONAL FIELDS

GRAVITATIONAL WAVES
Superconducting magnetometer as strain transducer in liquid helium cooled gravitational wave antenna
[NOTA-INTERNA-373] 01 p0058 N73-10476
Conference on acoustic gravity wave effects in atmospheric transmission of radio communication signals
[AGARD-CP-115] 05 p0508 N73-14131
Comparison of ionospheric radio wave propagation and acoustic gravity wave propagation
05 p0508 N73-14132
Effects of acoustic gravity wave diffusion on atmospheric boundaries
05 p0508 N73-14136
Acoustic gravity wave generation by transient sources in isothermal atmosphere
05 p0508 N73-14139
Nuclear source model for generating ionospheric disturbances through acoustic gravity waves
05 p0509 N73-14141
Asymptotic methods for determining propagation angles of internal gravity waves traveling at ionospheric heights
05 p0509 N73-14144
Full wave solution for electron density perturbations caused by gravity waves in F2 region
05 p0509 N73-14145
Relationship between atmospheric gravity waves and spread F conditions caused by solar activity
05 p0509 N73-14146
Ionospheric gravity wave electron amplitudes and spectra
05 p0510 N73-14149
Detection of tropospheric turbulence and gravitational waves by radar sounding
05 p0510 N73-14151
Microwave radar detection and photography of gravitational waves in troposphere
05 p0510 N73-14152
Electromagnetic cross modulation and very low frequency propagation techniques for measuring acoustic gravity waves in ionospheric D region
05 p0511 N73-14153
Radar observations of meteor trains for detecting high altitude gravity waves
05 p0511 N73-14154
High frequency radar backscattering technique for determining ionospheric structure and gravity wave disturbances
05 p0511 N73-14155
Gravity wave effects in occurrence time changes of daily traveling ionospheric disturbances
05 p0511 N73-14156
Theoretical plasma perturbation model for calculating coupling effects between acoustic gravity waves and electromagnetic waves in ionospheric disturbances
05 p0512 N73-14162
Computerized simulation of gravity wave perturbed traveling ionospheric disturbances using radio ray paths
05 p0512 N73-14163
Atmospheric gravity wave effects on ionospheric transequatorial radio wave propagation in presence of traveling ionospheric disturbances
05 p0512 N73-14164
Acoustic gravity wave effects in traveling ionospheric disturbances following nuclear explosions
05 p0513 N73-14165
Nonlinear propagation and ionospheric coupling of atmospheric waves following nuclear explosion
05 p0513 N73-14168
Value of gravitational wave observations in relativistic gravity investigations
[NASA-CR-131511] 12 p1398 N73-21340

Gravitational wave observations as tool for testing relativistic gravity
[NASA-CR-133411] 18 p2145 N73-27337
Frascati gravitational wave detector signal to noise ratio optimization
18 p2145 N73-27340

GRAVITY ANOMALIES
Tables on geodetic satellite gravity observations 09.0 deg E to 37.9 deg W along equator
[AD-746465] 02 p0170 N73-11379
Homogeneous density effects for calculating earth crust structure from gravitational anomalous masses
[AD-746018] 03 p0297 N73-12427
Gravity observations near San Juan Moutains in Colorado
[PB-211430] 05 p0540 N73-14395
Bathymetry, free air gravity anomaly, and magnetic field intensity data on Strait of Sicily, gathered from 1965 to 1971
[SACLANTCEN-CONF-PROC-7]8 p0915 N73-17501
Calculation of gravity anomalies
[AD-752234] 08 p0920 N73-17541
Combination of satellite and gravimetric data for analysis of terrestrial gravity field blocks
[NASA-CR-130176] 10 p1153 N73-19380
Satellite derived potential coefficients and terrestrial gravity information for estimating geopotential anomaly degree variance
[AD-754236] 11 p1290 N73-20471
Computation of mean gravity anomalies from potential coefficients
[AD-754245] 11 p1290 N73-20472
Partial derivative analysis using equations of motion for recovering gravity anomalies from satellite observations
[NASA-CR-130240] 14 p1661 N73-23483
Rock densities within gravitational anomalies of Ukrainian shield
[AD-757540] 15 p1783 N73-24455
Mediterranean Sea geophysical survey
[AD-757455] 16 p1910 N73-25452
Tables on harmonic coefficients of isostatic reduction potential U
[NASA-TM-X-66292] 18 p2145 N73-27334
Features of earth gravity anomalies in form expansion in spherical functions
[AD-761942] 21 p2542 N73-30384
Gravity station data for upper part of Arkansas Valley area in Colorado
[PB-220865/0] 21 p2542 N73-30385
Contour maps of global geoid and free air gravity anomalies of GEM-4 earth gravitational model
[NASA-TM-X-66240] 23 p2783 N73-32265
Iterative and nonlinear procedures for studying gravity anomaly in mountainous areas
24 p2911 N73-33232

GRAVITY GRADIENT SATELLITES
NT APPLICATIONS TECHNOLOGY SATELLITES
NT ATS 1
NT ATS 3
NT ATS 5
NT ATS 6
Application of active control for stability augmentation of passive gradient satellites based on impulses from control jet engines
[NASA-CR-130112] 03 p0356 N73-12904

GRAVITY GRADIOMETERS
Seven gravity gradient dynamics experiment in lunar orbit, using RAE-B spacecraft
[NASA-TM-X-66271] 17 p2024 N73-26375
Design and development of prototype moving base gravity gradiometers
[AD-760799] 20 p2414 N73-29400
Feasibility of using gravity measuring techniques as unattended sensors for detection and classification of military targets
[AD-763889] 22 p2738 N73-31922
Design, fabrication, and tests of breadboard model of earth orbital, rotating gradiometer
[NASA-CR-112215] 23 p2792 N73-32340

GRAVITY WAVES
NT BAROCLINIC WAVES
Numerical analysis of two-dimensional gravity wave flow on nonuniform free streams
[AD-744995] 01 p0042 N73-10329
Turbulence, billows, and gravity waves in high shear region of upper atmosphere during morning twilight, determined by rocket-released lithium cloud
[WRE-TN-670(WR/D)] 02 p0164 N73-11327
Mathematical models for analyzing internal gravity waves generated by stratified inviscid fluid flow over solid body
[AD-746137] 02 p0168 N73-11369
Ionospheric disturbances and acoustic gravity wave generation by nuclear explosions
[AD-746328] 02 p0214 N73-11737
Parameterization of gravity waves noting upper boundary conditions
05 p0573 N73-14659
Numerical analysis of gravity wave generation in atmospheric frontal zone
[AD-751638] 07 p0796 N73-16469
Distribution statistics, magnitude, and spatial structure of gravity wave and planetary wave atmospheric variations
[NASA-CR-2203] 08 p0916 N73-17504
Inertial gravity wave frequency spectrum in cylindrically confined incompressible two component liquid flow
[AD-752439] 09 p1018 N73-18312
Literature survey on polar cap ionospheric disturbance characteristics
[AD-754250] 10 p1157 N73-19416
Interaction of nonsaturated surface gravity ocean waves with nondispersive internal waves
[AD-754281] 12 p1403 N73-21377
Derivation of equations governing temporal and spatial variation for amplitudes and phase of capillary and gravity waves in case of second harmonic resonance
[AD-756218] 13 p1513 N73-22262
Nonlinear acoustic and gravity waves in earth atmosphere
[TR-48] 14 p1659 N73-23466
Numerical solution and internal gravity wave approximation of solar semidiurnal tidal mode behavior in dissipative atmospheres
[NASA-CR-132779] 17 p2025 N73-26383
Gravity wave-mean flow interactions in upper atmosphere
[NASA-CR-132776] 17 p2025 N73-26384
Relation of local pressure fluctuations to large-scale meteorology, and simulation of acoustic-gravity waves in inhomogeneous media
18 p2170 N73-27528
Transient response of internal gravity waves due to midtropospheric heating
[AD-762369] 19 p2298 N73-28482
Interaction between atmospheric internal gravity wave and mean horizontal wind with shear
22 p2692 N73-31564
Numerical solution to problem of gravitational-shear waves in flow with arbitrary temperature stratification
24 p2947 N73-33532

GRAY GAS
Effects of isotropic scattering on one dimensional propagation of small disturbances in radiating gray gas
[ISAS-494-VOL-38-NO-5] 22 p2651 N73-31237

GRAZING
Prediction of ephemeral and perennial range quantity and quality during normal grazing season using ERTS-1 imagery
[E72-10269] 03 p0291 N73-12368
Prediction of ephemeral and perennial range quality and quantity during normal grazing season based on ERTS-1 imagery
[E73-10061] 07 p0778 N73-16323
Prediction of range quantity and quality in desert areas of California and Arizona during growing and grazing seasons
[E73-10068] 07 p0779 N73-16330
Prediction of ephemeral and perennial range quantity and quality during normal grazing season in Arizona based on ERTS-1 imagery
[E73-10377] 10 p1152 N73-19372
Utilization of ERTS-1 imagery to predict ephemeral and perennial range quality and quantity during normal grazing season in Arizona and California
[E73-10541] 14 p1654 N73-23418
ERTS-1 imagery of desertification, hydrology, vegetation, forage, and water resources in Republic of Mali
[PAPER-R5] 19 p2283 N73-28363

GRAZING LANDS
U GRASSLANDS

GREASES
Frictional properties of rubbers in presence of greases and graphite lubricants
[AD-747447] 03 p0322 N73-12622
Oil base effect on lubricating performance of lithium greases and soaps containing hydrocarbons
[AD-754593] 11 p1300 N73-20549

GREAT BASIN [US]
Spectral reflectance measurements of playas in Great Basin test site
[E73-10561] 14 p1656 N73-23433
Wildland resource and vegetation monitoring in Nevada and Great Basin using ERTS-1 imagery
[E73-10606] 15 p1773 N73-24367
Mapping of wildland vegetation in Great Basin area of Nevada using ERTS-1 imagery
[E73-10813] 18 p2139 N73-27288
Application of ERTS-1 imagery for mapping and identification of vegetation and landforms in Great Basin
[PAPER-A9] 19 p2260 N73-28217
Collection of ground truth data in Great Basin for support of aerial and Skylab overflights
[E73-10884] 20 p2394 N73-29235
Synoptic identification and mapping of Quaternary geologic and geomorphic units in Midwest-Great Plains area
[E73-10951] 21 p2531 N73-30293
Skylab S-190 photography of Great Basin area
[E73-11123] 24 p2916 N73-33278

GREAT LAKES [NORTH AMERICA]
Application of ERTS-1 and EREP imagery to geological surveys and mapping of Basin and Range - Colorado Plateau boundary in Arizona
[E73-11131] 24 p2917 N73-33286

GREAT BRITAIN
Circulation pattern over British Isles and system classification from 1861 to 1971
[MET-O-845B] 02 p0204 N73-11648
Conference proceedings of British Acoustical Society, 1972
[AD-747615] 03 p0338 N73-12756
Production of carbon fibers and reinforced plastics in British installations
[FOA-2-C-2468-91] 06 p0687 N73-15594
Color vision requirements of Great Britain's Armed Forces
10 p1113 N73-19072
Magnetic results 1969, Eskdalemuir, Hartland and Lerwick observatories, emphasizing diurnal values
[BULL-3] 10 p1145 N73-19323
Chemotherapy for air crews in Great Britain
12 p1369 N73-21105
Small scale mapping of England and Scotland from ERTS-1 imagery
[E73-10817] 18 p2140 N73-27292
Contribution of automobiles to air pollution levels in Reading, England
[PB-219602/0] 18 p2175 N73-27563
Human response to vibration in Great Britain noting test facilities, equipment, experiments and publications
[ISVR-TR-60] 21 p2504 N73-30093
Measurements of atmospheric lead concentrations in European community and United Kingdom
[EUR-4982] 24 p2949 N73-33555

GREAT LAKES [NORTH AMERICA]
Evaluation of ERTS-1 imagery for hydrologic information in Sierra Nevada Mountains and Lake Ontario
[E72-10170] 01 p0044 N73-10351
Utilization of ERTS-1 imagery for water depth measurement, mapping of Yellowstone Park, atmospheric effects in Colorado, lake ice surveillance, recreational land use, IFYGL Lake Ontario, image enhancement, water quality monitoring, and oil pollution detection
[E72-10201] 02 p0144 N73-11167
Utilization of ERTS-1 imagery for water depth measurement, mapping of Yellowstone Park, atmospheric effects in Colorado, lake ice surveillance, recreational land use, IFYGL Lake Ontario, image enhancement, water quality monitoring, oil pollution detection, and mapping iron compounds
[E72-10198] 02 p0160 N73-11296
Analysis of ERTS-1 MSS data for color variations in Great Lakes and Chesapeake Bay to determine if multispectral imagery usable for locating and mapping extent of distinct water masses
[E72-10224] 02 p0163 N73-11318
ERTS-1 remotely sensed imagery to support study of Lake Ontario basin as part of International Field Year for the Great Lakes
[E72-10354] 05 p0534 N73-14342
Evaluation of ERTS-1 imagery for hydrological information in Sierra Nevada Mountains and Lake Ontario areas
[E73-10016] 06 p0659 N73-15352
Utilization of ERTS-1 imagery for oceanographic studies of Great Lakes
[E73-10017] 06 p0659 N73-15353
ERTS-1 imagery of suspended sediment plumes in Lake Ontario
[E73-10057] 07 p0778 N73-16319
Water sample analysis for identifying sources of mercury pollution of Great Lakes
08 p0876 N73-17096
ERTS-1 imagery of suspended sediment plumes in Lake Ontario
[E73-10316] 09 p1023 N73-18348
Evaluation of Great Lakes oceanography from ERTS-1 imagery
[E73-10356] 10 p1149 N73-19352
Utilization of ERTS-1 imagery in mesometeorological studies of Great Lakes
[E73-10464] 11 p1284 N73-20420
Evaluation of ERTS-1 data for hydrologic information in Sierra Nevada and Lake Ontario
[E73-10485] 12 p1396 N73-21322
Dynamics of suspended sediment plumes in Lake Ontario
[E73-10493] 12 p1397 N73-21329
IFYGL data for hydrologic analysis of Lake Ontario Basin
[E73-10571] 15 p1772 N73-24351
ERTS-1 imagery of suspended sediment plumes in Lake Ontario
[E73-10599] 15 p1772 N73-24360
Remote sensing of thermal and industrial discharges along shoreline of Lake Michigan
[PB-214503/5] 16 p1908 N73-25436
Application of ERTS-1 data for identification of ice formations in Lake Erie and snow mapping in American River basin
[E73-10750] 17 p2022 N73-26353
ERTS-1 imagery of algal streaks and flooding in Lake Erie and Michigan and Ohio areas
[E73-10793] 18 p2137 N73-27269

Skylab 4 microwave radiometry of lake and sea ice in Gulf of St. Lawrence and Lake Ontario
[E73-10820] 18 p2140 N73-27295
Great lakes mesometeorological investigations using ERTS-1 data
[E73-10835] 18 p2141 N73-27305
Water balance, micrometeorology, thermal structure, and heat content of Great Lakes as determined by remote sensors during International Field Year
[IFYGL-BULL-4] 18 p2143 N73-27322
ERTS-1 imagery and high altitude photography of Lake Ontario Basin to provide input for models of river discharge and macro-scale features of lake circulation
[PAPER-W14] 19 p2272 N73-28291
Application of ERTS-1 imagery for analysis of terrestrial water balance of Lake Ontario and drainage basin
[PAPER-W15] 19 p2272 N73-28292
Application of ERTS-1 remote sensing to determine turbidity plumes in Lake Ontario
[PAPER-W16] 19 p2272 N73-28293
Analysis of ERTS-1 imagery to determine meteorological content with emphasis on mesoscale effects of Great Lakes and air pollution dispersion
[PAPER-W17] 19 p2272 N73-28294
ERTS-1 imagery of algal blooms in Lake Erie and Utah Lake, Ohio
19 p2285 N73-28376
ERTS-1 imagery of snow cover, ice conditions, and soil moisture in Sierra Nevada Mountains and Lake Ontario Basin
[E73-10869] 20 p2393 N73-29220
ERTS-1 imagery of algal bloom in Lake Erie and upwelling in Lake Michigan
[E73-10932] 21 p2529 N73-30274
ERTS-1 imagery of suspended sediment plumes and turbidity in Lake Ontario
[E73-10956] 21 p2532 N73-30298
Air circulation patterns induced by wind and atmospheric pressure over Lake Superior
[PB-220244/8] 22 p2695 N73-31590
Microwave imagery of Great Lake ice formations
22 p2736 N73-31903
Surface water transport in western Lake Superior
23 p2783 N73-32267

**GREAT PLAINS CORRIDOR [NORTH AMERICA]**
ERTS-1 imagery of Quaternary landforms and materials in Midwest and Great Plains
[E72-10272] 04 p0409 N73-13333
Soil mapping, crop identification, and rangeland assessment in Great Plains using ERTS-1 multisensor imagery
[E72-10369] 05 p0536 N73-14357
Effectiveness of ERTS-1 imagery in monitoring vegetation conditions of direct concern to range land management and agriculture business decisions in Great Plains Corridor
[E73-10302] 09 p1021 N73-18334
ERTS-1 imagery of vernal advancement and retrogradation of natural rangeland vegetation of Great Plains Corridor
[E73-10303] 09 p1021 N73-18335
Utilization of ERTS-1 imagery to study watershed hydrology in Southern Great Plains
[E73-10359] 10 p1149 N73-19355
Utilization of ERTS-1 imagery for mapping Quaternary deposits and landforms in Great Plains and Midwest
[E73-10381] 10 p1152 N73-19376
Application of ERTS-1 multisensor data in Great Plains to map rangelands, croplands, and soil formations
[E73-10443] 11 p1282 N73-20403
Monitoring vernal advancement and retrogradation of natural rangeland vegetation in Great Plains Corridor
[E73-10643] 16 p1897 N73-25340
Identification of soil associations in Great Plains from ERTS-1 imagery
[E73-10679] 16 p1901 N73-25374
Application of ERTS-1 data for monitoring vernal advancement and retrogradation of natural vegetation in Great Plains Corridor
[E73-10693] 17 p2018 N73-26315
Comparison of Skylab/EREP imagery with television and radiometric measurements from other satellites for snow cover survey in Sierra Nevada Mountains and Great Plains
[E73-10755] 17 p2022 N73-26358
Detection of phenological event for specific forest and crop types using ERTS-1 imagery
[PAPER-A19] 19 p2261 N73-28226
Monitoring vegetation conditions of direct concern to rangeland and agriculture management in Great Plains Corridor
[E73-10891] 20 p2394 N73-29240
Mapping of Quaternary geological and geomorphological landforms of Great Plains and Midwest from ERTS-1 imagery
[E73-10949] 21 p2530 N73-30291
Identification and mapping landform and land use characteristics and surficial geologic materials in Great Plains and Midwest
[E73-11025] 22 p2662 N73-31329

**GREAT POLAR CAPS**
U POLAR CAPS

**GREECE**
Artificial radioactivity of cumulus clouds moving horizontally and touching peaks of Mt. Olympus
[AEC-TR-7308] 03 p0296 N73-12413
Land use, forest density, soil mapping, erosion, drainage, and salinity limitations in Greece from ERTS-1 data
[E73-10969] 22 p2657 N73-31283
Application of ERTS-1 imagery to land use, forest density, and soil investigations in Greece
[E73-10988] 24 p2913 N73-33244

**GREEN FUNCTION**
Effect of homogeneous dielectric sphere on electromagnetic radiation from simple sources treated as boundary value problem and solution obtained by technique of dyadic Green functions
[NASA-CR-2211] 12 p1378 N73-21178
Green function for analyzing light scattering in crystals
[AD-757070] 14 p1693 N73-23741
Green function technique used to calculate magnetic properties of disordered Heisenberg ferromagnets in which exchange interactions deviate randomly in strength from mean interaction
[NASA-TN-D-7208] 14 p1697 N73-23774
Study of electrical properties of amorphous semiconductors using Green's function
[AD-757432] 14 p1699 N73-23786
Calculating temperature distribution by applying Green function to two dimensional Laplace equation
[NAL-TR-297] 15 p1842 N73-24924
Applications of eigenfunctions for solution of boundary value problems in orbital mechanics
[BMBW-FBW-72-17] 22 p2718 N73-31758

**GREEN THEOREM**
U GREEN FUNCTION

**GREENLAND**
Acoustic noise, transmission loss, and reverberation measurements in West Greenland Sea
[AD-746839] 02 p0169 N73-11373
Mapping Arctic sea ice from ERTS-1 imagery of Hudson Bay, M'Clure Strait, Beaufort Sea, and Greenland Sea
[E73-10447] 11 p1282 N73-20407
Measurements of oceanographic temperature distribution and salinity in northern Baffin Bay during midsummer 1970
[CG-373-54] 11 p1286 N73-20434
Characteristics of thermal radiation of Greenland ice measurements by Cosmos-243
[NASA-TT-F-14953] 15 p1780 N73-24427
Automatic climatological recording system at Nord, Greenland
[ISBN-87-7478-073-5] 18 p2141 N73-27307
Thule riometer observations of polar cap absorption events 1962-1972
[AD-762279] 19 p2296 N73-28467
Igdlorssuit geomagnetic variation anomaly in rift-fault zone of northern West Greenland
[R-35] 20 p2412 N73-29389

**GRENADES**
Upper atmosphere wind and temperature measurements from Sonmiani, Pakistan, using rocket grenades - 1965 - 1967
[NASA-CR-133401] 18 p2144 N73-27331

**GRIDS**
Pressure drop measurements and drag coefficients for grid spacers of hexagonal fuel rod bundles
[NLL-RISLEY-TR-2440-[9091.9F]]
02 p0209 N73-11692
Irregularities in flow behavior of parallel air jets behind smoothing grids
[NASA-TT-F-14653] 06 p0654 N73-15311
Spatial grid method for solving hyperbolic equations for signal propagation on three wire transmission line
[UCRL-73796] 07 p0764 N73-16209
Effect of grid transparency and finite collector size on RPA ion temperature and density observations
[NASA-TM-X-66153] 07 p0799 N73-16487
Design and performance of wire grid temperature probes for flowing media
11 p1294 N73-20500
Process for fabricating matched pairs of dished screen and accelerator grids for ion thruster accelerator system
[NASA-CASE-LEW-11694-1] 13 p1570 N73-22721
Passive circuit grids for stabilization of magnetohydrodynamic generator plasma
[TH-72-E-31] 14 p1695 N73-23757
Headlamp research program for extrapolation/interpolation of surface values from predefined grid
[LTR-ST-602] 22 p2637 N73-31129

**GRINDING [COMMINUTION]**
Magnetic fluid preparation by grinding and concentrating pyrophoric antiferromagnetic iron oxide colloidals
[BM-RI-7702] 05 p0580 N73-14721
Inductive plasma pulverization for protecting mechanical and electronic components
[CEA-CONF-2111] 21 p2583 N73-30701

**GRINDING [MATERIAL REMOVAL]**
NT METAL GRINDING
Fine grinding, polishing, and graded etching techniques to eliminate surface yield on optical telescope mirrors
[NASA-CR-112217] 08 p0934 N73-17647
Effectiveness of using various lubricant cooling fluids for diamond superfinishing
[AD-753980] 11 p1299 N73-20541
Determination of optimum conditions for lubrication and cooling during grinding by abrasive discs of synthetic superhard materials
[AD-754665] 11 p1302 N73-20562

**GRINDING MACHINES**
Tool positioning holder for grinding by ball nose milling cutter
[NASA-CASE-LAR-10450-1] 01 p0061 N73-10504
Quality control and composition of grinding wheels discussing microstructure and chemistry
[CRIF-MC-45] 13 p1530 N73-22399
Grinding wheel hardness determined from modulus of elasticity calculation
[CRIF-NT-9] 13 p1530 N73-22401

**GROOVES**
Influence of groove inclination angle on bearing capacity of gas dynamic thrust bearing
[AD-751068] 07 p0806 N73-16535

**GROUND BASED CONTROL**
NT AIR TRAFFIC CONTROL
Measurement methods and error analyses by ground terminals for optimizing satellite communications link
01 p0026 N73-10203
Polar upper atmosphere data recorded at Kiruna Geophysical Observatory, Sweden, from Jan. - Mar. 1972
02 p0167 N73-11353
Design, development, and evaluation of airport lighting control panel for airport traffic control towers
[FAA-RD-72-93] 03 p0260 N73-12108
Guidance system for beam-rider projectiles
04 p0447 N73-13647
Space technology for developing ground based integrated medical laboratory
04 p0472 N73-13851
Standards and procedures for generation of operational display formats for use in Mission Control Center display control system
[NASA-CR-128843] 10 p1132 N73-19228
Analysis of general aviation activities in Germany and recommendations for flight control procedures to reduce aircraft accident hazards
10 p1183 N73-19626
Analysis of effects of automation on productivity and efficiency of air traffic control and flight services
[MTR-6110] 10 p1185 N73-19646
Polar upper atmosphere data recorded at Kiruna Geophysical Observatory, Sweden, from Oct.-Dec. 1972
17 p2028 N73-26410
Conference on technology utilization in spacecraft guidance, ground operations, communications and navigation systems, and sensor development
[NASA-SP-326] 18 p2207 N73-27816
Error drift projection for ERTS orbit maintenance calculation using ground tracking data
18 p2211 N73-27847
Attitude computer facility for unmanned satellite control from ground base
18 p2211 N73-27848
Computerized ground-air-ground information system for error estimation and alignment of spacecraft attitude sensors
18 p2211 N73-27849
Equipment certification and process verification methods for photographic processing control of ERTS images
18 p2211 N73-27854
Polar ionospheric geophysical data recording in Sweden, Jan-Mar. 1973
19 p2295 N73-28459
Statistical analysis of Civil Aviation midair collisions occurring during period January 1964 to December 1971
[MTR-6334] 22 p2614 N73-30946
Numerical analysis of curved approach paths and landing sequence for multiple aircraft using same terminal facilities to provide maximum system performance
23 p2740 N73-31935
Analysis and simulation of intermittent positive control of air traffic by fully automated ground facility
23 p2816 N73-32511
Air traffic control evaluation to determine feasibility of combining smaller aircraft into gaps on flow of normal traffic to increase effectiveness of terminal facilites
[FAA-AFS-500-1] 23 p2816 N73-32517
Short haul aircraft operations in terminal area with concurrent conventional aircraft operations to show methods for improved utilization of facilities
24 p2874 N73-32953
Development and characteristics of 4-D guidance system for traffic control of STOL aircraft operating in congested areas
24 p2874 N73-32957

Evaluation of large screen display for automated oceanic air traffic control applications
[FAA-ND-73-75] 24 p2950 N73-33568
Computer model of Los Angeles, California air traffic control situation to predict conditions expected by 1982
[AD-765153] 24 p2951 N73-33571

**GROUND CREWS**
Statistical analysis of occurrence of backache among Royal Air Force flight crews and ground crews to show effects of crew seats on physical comfort
[AD-745177] 01 p0013 N73-10102
Noise effects on hearing conservation, in aircrew and ground support personnel of aerospace operations
08 p0876 N73-17101
Drug screening data for civil aviation personnel obtained by urinalyses
12 p1369 N73-21104

**GROUND EFFECT**
Influence of split ground belt on aerodynamic characteristics of high lift STOL aircraft with blown flap
[UTIAS-TN-173] 02 p0152 N73-11230
Wind tunnel tests of scale model of orbiter 040A configuration in ground effect
[NASA-CR-120082] 02 p0233 N73-11895
Wind tunnel simulation of ground effect conditions to determine effect of three dimensional turbulent boundary layer on V/STOL aircraft configurations - Pt. 1
[NASA-CR-114495] 03 p0282 N73-12283
Wind tunnel tests to determine effects of ground proximity on lift, drag, and pitching moment of rectangular wing equipped with jet flaps
[NAL-TR-294] 06 p0621 N73-15038
Development of mathematical model for optimal takeoff performance of single rotor helicopter in ground effect with various payloads
[AD-750388] 06 p0624 N73-15066
Analysis of air cushion vehicle landing system operation and computation of air flow requirements
[AD-750936] 06 p0625 N73-15069
Application of optimal control theory to take-off of heavily loaded helicopters and instrumentation requirements to improve pilot flight control
[AD-750615] 06 p0625 N73-15072
Method for estimating changes in lift curve, drag, tail lift, and downwash from wing of aircraft due to ground effect in incompressible flow
[ESDU-72023] 07 p0736 N73-15993
Numerical analysis of pressure distribution in incompressible flow on two dimensional airfoils near ground
[ARC-R/M-3238] 15 p1726 N73-24000
Application of hydraulic test tunnel flow visualization techniques to determine ground effect on flow around models of aircraft
[NASA-TT-F-14958] 17 p2015 N73-26291
Analysis of pressure distribution on plane ground surface under aircraft flying at low altitude with subsonic velocity
[FFA-AU-634-PT-2] 18 p2129 N73-27206
Air cushion landing system effect on aerodynamic characteristics of A-4 aircraft
[AD-761621] 19 p2221 N73-27917
Development of method for calculating near field noise level of free jet and influence of ground effect on noise produced by V/STOL aircraft operation
20 p2478 N73-29907
Effect of inflated air cushion landing gear on subsonic static stability of high performance aircraft operating out of ground effect
[AD-763365] 21 p2498 N73-30048
Aerodynamic characteristics of round jet located on center line of bottom of aircraft fuselage and elongated slots for lift augmentation
[NASA-TN-D-7299] 22 p2613 N73-30939
Development and characteristics of air cushion landing system for remotely piloted vehicles
[AD-764774] 23 p2747 N73-31985
Wind tunnel tests to determine magnitude of adverse ground effects on longitudinal aerodynamic coefficients of powered-lift short takeoff aircraft
24 p2873 N73-32950

**GROUND EFFECT MACHINES**
NT CUSHIONCRAFT GROUND EFFECT MACHINE
NT WESTLAND GROUND EFFECT MACHINES
Design and development of active control system for air cushion vehicle to reduce or eliminate effects of excessive vertical vibratory acceleration
[NASA-CASE-LAR-10531-1] 04 p0372 N73-13023
Development of high speed ground rapid transit facility using tracked air-cushion vehicles
[PB-211833] 05 p0524 N73-14266
Development and characteristics of tracked air cushion research vehicle for commercial high speed ground transportation
[PB-211216] 05 p0524 N73-14267
Analysis of air cushion vehicle landing system operation and computation of air flow requirements
[AD-750936] 06 p0625 N73-15069
Laser extension measurements of visibility during ice fog for aiding in SEV pilot system design
[AD-750114] 06 p0680 N73-15537
Mathematical model for tracked air cushion vehicle and guideway to determine vertical dynamic response of vehicle and guideway system to high speed vehicle passage
07 p0737 N73-15995
Nonlinear and small perturbation linear models for one dimensional heave motion of flexible skirted, air cushion suspension
[PB-212705] 07 p0766 N73-16226
Concept of nuclear powered ground effect machine for commercial operations in Arctic regions
[NASA-TM-X-2684] 08 p0977 N73-17991
Snow accumulations on air cushion vehicle track sections
[NRC-12939] 09 p1010 N73-18247
Air-cushion tankers for transporting Alaskan North Slope oil
[NASA-TM-X-2683] 09 p1100 N73-18981
Effects of ground effect vehicle tests on ecology of arctic tundra in northern Alaska
[AD-751741] 10 p1107 N73-19026
Cold weather tests to determine application of ground effect machines for military logistic purposes in Arctic regions
[AD-753527] 10 p1107 N73-19027
Effectiveness and cost of high performance watercraft for selected missions of US Coast Guard
[AD-754917] 11 p1268 N73-20295
Control technology for air cushion passenger vehicle
11 p1352 N73-20969
Evaluation of ground effect machines under various environmental conditions to determine feasibility as rescue vehicles by Coast Guard
[AD-755409] 13 p1475 N73-21947
Environmental effects and plans for controlling urban TACV noise levels
13 p1506 N73-22209
Development of collision protection equipment for ground effect machines operating in arctic regions
[AD-758359] 14 p1604 N73-23004
Nuclear power for air cushion vehicle
[NASA-TM-X-68231] 15 p1735 N73-24069
Application of ground effect machine landing systems for recovery of remotely piloted vehicles
[AD-758789] 15 p1736 N73-24079
Numerical analysis of lift and roll stability of ram air cushion vehicle to determine equations for rolling moment coefficient
[PB-219820/8] 18 p2106 N73-27032
Development of simulation program for determining characteristics of tracked air cushion research vehicle
[PB-218368/9] 18 p2106 N73-27033
Evaluation of air cushion vehicle operations over railroad beds and secondary roads and analysis of dynamic response to geometric obstacles
[AD-762169] 19 p2221 N73-27920
Operational investigation of combined all weather capabilities of Coast Guard motor lifeboat and 70 knot surface effect rescue vehicle
[AD-761460] 19 p2229 N73-27974
Research projects involving aeroelastic stability and response, stability of thin shell structures, and suspension system concept for control of vehicle responses
[AD-762568] 20 p2359 N73-28979
Analysis of landing performance of scale model of C-8 aircraft equipped with air cushion landing system on variety of surfaces including calm and rough water
[NASA-TN-D-7295] 21 p2496 N73-30032
Occurrence and magnitude of surface effect takeoff and landing aircraft skirt flutter
[AD-764137] 22 p2616 N73-30966
Computer program to evaluate dynamic characteristics of tracked air cushion vehicle
[PB-219984/2] 22 p2617 N73-30970
Loading criteria for tracked air cushion vehicle guiderails and methods for calculating dynamic responses of double-span, beam-type guide rails
[PB-221688/5] 22 p2617 N73-30971
Thrust augmentation, lift forces, and mixing properties of two-phase flow propulsion and lift system for ground effect machines
[AD-765332] 23 p2777 N73-32208
Aerothermodynamic study of air cushion vehicles buffeting noting dynamical stability, nonlinear behavior, and similitude law
[NT-33-1973] 24 p2870 N73-32933

**GROUND HANDLING**
Technical aspects of airship manufacture and ground and loading operations
24 p2879 N73-32993

**GROUND OPERATIONAL SUPPORT SYSTEM**
Computerized simulation of tactical ground surveillance system
[AD-761805] 19 p2240 N73-28059

**GROUND RESONANCE**
U GROUND EFFECT
U RESONANCE

**GROUND RUN-UP**
U ENGINE TESTS

**GROUND SPEED**
Driving speed in relation to interactions among automobile driver, roadway variables, and vehicle control
01 p0017 N73-10131
Equipment route winds and great circle distances for helicopter air routes at 5,000, 10,000, and 18,000 feet - Vol. 1
[AD-760252] 17 p1985 N73-26043
Equipment route winds and great circle distances for helicopter air routes at 5,000, 10,000 and 18,000 feet - Vol. 2
[AD-760253] 17 p1985 N73-26044

**GROUND STATE**
Two methods for derivation of structural expansion for ground state energy of simple metal
[NASA-CR-131833] 13 p1565 N73-22687

**GROUND STATIONS**
NT DEEP SPACE INSTRUMENTATION FACILITY
NT INTEGRATED MISSION CONTROL CENTER
Directory of observation stations in NASA geodetic satellites program based on preferred major datums and Modified Mercury Datum 1968 - Vol. 2
[NASA-CR-130072] 01 p0036 N73-10280
Remote automatic multipurpose station for collecting oceanographic and meteorological data in Arctic regions
[AD-746496] 01 p0038 N73-10300
Description of equipment installed in magnetic and seismic observatory at Mould Bay, Canada and analysis of data acquired during 1969 - Vol 43, No. 4
[M70-43/4] 01 p0043 N73-10344
Laser pulses transmitted from ground stations to aircraft or satellites used for 3-D multilateration system for precision geodetic measurements with 1-cm accuracy
01 p0119 N73-10982
Geometric and dynamic satellite geodesy and geometric analysis and adjustment of ground stations
[NASA-CR-129516] 03 p0355 N73-12891
Problems in changing from ground based to space based vehicle operations for on-orbit readiness
[NASA-CR-125564] 03 p0358 N73-12919
German central ground station including layout and equipment
[DLR-MITT-71-05] 04 p0402 N73-13276
TD-1A satellite ground checkout stations noting spacecraft communication and data transmission
[ESRO-TM-140-ESTEC] 04 p0402 N73-13277
Space activities of CNES, noting satellites, launch vehicles, sounding rockets, balloons, and ground stations
05 p0611 N73-14972
Evaluation of research projects involving seismic arrays, long period arrays, seismometers, and seismic signal processing
[AD-750759] 06 p0669 N73-15439
Analysis of excessive interrogation signals from Air Traffic Control Radar Beacon System and effect on operation of Jacksonville, Florida center
[ECAC-PR-72-014] 06 p0696 N73-15675
Analysis of excessive interrogation signals from Air Traffic Control Radar Beacon System and effect on operation of Washington, D.C. center
[ECAC-PR-72-022] 06 p0696 N73-15676
Analysis of excessive interrogation signals from Air Traffic Control Radar Beacon System and effect on operation of Los Angeles, California center
[ECAC-PR-72-044] 06 p0696 N73-15677
Supernovae monitoring experiment using ground-based photomultiplier tubes sensitive to secondary fluorescence light
08 p0974 N73-17967
Temporary loss of Apollo 14 command module color television picture by ground station converter
[NASA-TM-X-69296] 15 p1751 N73-24189
Phase preparation of ground facilities for satellite missions noting procedures used at ESOC
15 p1848 N73-24979
Characteristics of low cost mass producible earth terminal antenna system for broadcast satellite
18 p2122 N73-27152
Characteristics of three station network for sensing magnetic and electric fields associated with lightning discharges
[NASA-CR-133400] 18 p2151 N73-27382
Optimization of global ground data transmission network for spacecraft communications
18 p2210 N73-27843
Ground station S band tracking in Doppler mode for calibrating Mariner 9 in deep space
18 p2210 N73-27845
Low cost highly sensitive 12 GHz low noise converter for communication between broadcast satellites and ground stations
[NHK-LABS-NOTE-161] 20 p2380 N73-29127
Analysis of operations at ground station during Tenth Soviet Antarctic Expedition to show equipment requirements and mission accomplishments
20 p2408 N73-29356

Operations and functions of ground station during Tenth Soviet Antarctic Expedition to obtain meteorological and geophysical data
20 p2409 N73-29360
Functions and operations of ground station during Tenth Soviet Antarctic Expedition including construction procedures and equipment installation
20 p2409 N73-29361
Orbit calculations for communication satellite using communications ground terminal minicomputer
[AD-762510] 20 p2474 N73-29874
Azur satellite orbit perturbation recorded from Weilheim-Lichtenau ground station
[BMBW-FBW-72-18] 21 p2597 N73-30816
Equipment for program control of satellite ground station
[DLR-MITT-72-16] 22 p2647 N73-31211
Design, fabrication, and tests of ground station hardware for ATS-F millimeter wave experiment
[NASA-CR-132802] 22 p2673 N73-31409
Technology for evaluating ground station sites based on effectiveness in disseminating time synchronization
[FAA-RD-73-102] 23 p2770 N73-32155
Central ground station and local receivers for direct TV broadcasting satellite system
[DGLR-PAPER-73-055] 24 p2895 N73-33114

**GROUND SUPPORT EQUIPMENT**
NT GROUND OPERATIONAL SUPPORT SYSTEM
Development of forward area refueling equipment for servicing military helicopters
[AD-746249] 02 p0154 N73-11245
Design of ground electronic equipment shelters in mobile systems for military ground support application
[AD-748808] 04 p0400 N73-13253
Sounding rocket launches and air and ground support equipment
[AD-750544] 05 p0515 N73-14185
Cost effectiveness analysis of propane operated fog dispersal system and evaluation of runway visual range improvement
[FAA-RD-72-123] 06 p0649 N73-15267
Performance tests of aircraft arresting gear to determine allowable operating restraints on angular displacement and off-center engagements
[NATF-R125] 06 p0649 N73-15268
Requirements, basic principles of operation, design, construction, and maintenance of thermal fog dispersal system for airport applications
[FAA-RD-72-138] 07 p0766 N73-16222
Fabrication and evaluation of engineering prototype ground signal processing systems for use with satellite television
[NASA-CR-120933] 09 p1002 N73-18178
Reliability aspects of ground support equipment at Kennedy Space Center
[NASA-CR-131362] 11 p1265 N73-20268
Simple mathematical models of mechanical systems for ground support equipment, airborne launcher, vibration isolation design
[AD-754537] 11 p1267 N73-20283
Design, functional operation, and recommended expansion and enhancements for Space Ultrareliable Modular Computer interpretive simulator
[NASA-CR-124202] 12 p1380 N73-21194
Hardware manual for Space Ultrareliable Modular Computer-Demonstration Vehicle including assembly, physical and basic electrical tests
[NASA-CR-124205] 12 p1380 N73-21195
Electrical properties and performance of satellite group terminal system
[STC-TM-332] 15 p1749 N73-24178
Computer program system for automatic operation and safety backup in ground based ATC system
[FAA-EM-73-7] 15 p1808 N73-24654
Anomaly report of explosive failure of ground support equipment decontamination unit tank during post-flight deactivation of Apollo 16 command module
[NASA-TM-X-69323] 17 p2088 N73-26897
Analysis of military aircraft refueling and rearming operations in forward areas to show organization, doctrine, and equipment - Vol. 1
[AD-760524] 18 p2108 N73-27046
Analysis of military aircraft refueling and rearming operations in forward areas to show organization and equipment required - Vol. 2
[AD-760525] 18 p2108 N73-27047
Ground terminal optimization and cost effectiveness of satellite television broadcasting
18 p2115 N73-27100
Optimal engine selection for ground support equipment
[AD-763663] 21 p2591 N73-30757
Application of fiber glass reinforced plastic materials for ground handling of aviation fuels and hazards of static electricity caused by plastic materials
[AD-764358] 22 p2709 N73-31693
Evaluation of physical and operational characteristics of missile support vehicle based on procedures for inspection, servicing, and maintenance
[AD-764772] 23 p2852 N73-32791

**GROUND SUPPORT SYSTEMS**
Evaluation of device to train forward air controllers to communicate target locations
[AD-751292] 07 p0751 N73-16103
Pioneer space probe system design and development, ground support system, tracking and communication, and data processing
[NASA-SP-279-VOL-2] 08 p0964 N73-17882
Summary of KSC program for investigating reliability of ground support activities
[NASA-CR-131361] 11 p1297 N73-20521
Laser ranging technique to determine distance from satellites to ground
[NASA-CR-2264] 16 p1906 N73-25419
Computerized support system for complex spacecraft mission scheduling
18 p2211 N73-27851
Description and capabilities of ground Operations Aerospace Language [GOAL]
[NASA-TM-X-69541] 24 p2897 N73-33128

**GROUND TESTS**
NT COLD FLOW TESTS
NT PRELAUNCH TESTS

**GROUND TRUTH**
Acquisition and analysis of California coastal ground truth data for correlation with ERTS-1 imagery
[E72-10321] 04 p0413 N73-13369
Acquisition and analysis of coastal ground data for correlation with ERTS-1 imagery of Monterey Bay and Santa Barbara Channel areas of California
[E73-10043] 07 p0776 N73-16306
Development and application of field data collection techniques for remote sensing applications
07 p0785 N73-16386
Importance of ground truth data in remote sensing
[NASA-CR-130020] 07 p0800 N73-16495
Importance of ground truth data by remote sensing
[REPT-120371] 08 p0916 N73-17508
Application of dielectric constant measurements to interpretation of radar imagery of Michigan ground truth for lake ice
[E73-10391] 11 p1276 N73-20353
Application of dielectric constant measurements to interpretation of radar imagery of ground truth
[E73-10429] 11 p1280 N73-20390
Acquisition and analysis of coastal ground truth data in pacific water off California for correlation with ERTS-1 imagery
[E73-10482] 12 p1396 N73-21319
Acquisition and analysis of coastal ground truth data of Santa Monica Bay, Santa Barbara Channel, and Monterey Bay for correlation with ERTS-1 imagery
[E73-10607] 15 p1773 N73-24368
Analysis of ERTS-1 imagery of Los Angeles, California area to determine effects of haze on accuracy of ground truth data
[E73-10691] 16 p1902 N73-25384
Application of ERTS-1 remotely sensed data and ground truth information to predict and manage water quantity and quality in river basins
[E73-10689] 17 p2018 N73-26314
Utilization of ERTS-1 imagery for crop identification and acreage measurement in South Dakota, Kansas, Missouri, and Idaho
[E73-10734] 17 p2020 N73-26340
Acquisition of ground truth and meteorological data in Michigan for Skylab-3 mission
[E73-10748] 17 p2022 N73-26352
Collection of ground truth and meteorological data for Skylab test sites in Texas and Kansas
[E73-10752] 17 p2022 N73-26355
Plans for collection of ground truth data for Skylab-2 mission
[E73-10759] 17 p2022 N73-26359
Acquisition of ground truth data in Ohio for Skylab EREP
[E73-10757] 18 p2133 N73-27239
Acquisition of weather and ground truth data for Skylab EREP experiments
[E73-10797] 18 p2137 N73-27273
Coordination of ground truth and basic altimeter data processing requirements for North Atlantic test area
[E73-10811] 18 p2139 N73-27286
Application of ERTS-1 imagery for lineament and photogeologic mapping of western Montana
[PAPER-G32] 19 p2268 N73-28263
Machine processing of ERTS-1 radiometric and ground truth data and calibration of radiometers
[E73-10855] 19 p2292 N73-28432
Correlation of coastal ground truth data from Southern California waters with ERTS imagery
[E73-10864] 20 p2392 N73-29215
Collection and processing of ground truth crop and field data for Skylab-3
[E73-10879] 20 p2394 N73-29230
Collection of ground truth data in Great Basin for support of aerial and Skylab overflights
[E73-10884] 20 p2394 N73-29235
Relation of sea truth data from Cape Cod, Massachusetts, and Charleston, South Carolina on plankton composition and chlorophyll values with ERTS-1 data
[E73-10907] 20 p2397 N73-29256
Collection of ground and water truth in Nevada for Skylab-2
[E73-10887] 20 p2417 N73-29419
Ground-based radiation thermometry mapping of volcanology in Central America
[E73-10937] 21 p2529 N73-30279
Acquisition of ground truth data and site selection for SL-3 EREP experiments in South Dakota
[E73-10945] 21 p2530 N73-30287
Acquisition of ground truth data for Skylab overflights
[E73-11012] 22 p2660 N73-31317
Acquisition of ground truth data for test site
[E73-11014] 23 p2778 N73-32216
Acquisition of ground truth and processing of Skylab EREP data
[E73-11152] 24 p2919 N73-33306

**GROUND WATER**
Aerial photography used to delineate areas of ocean ground water discharge and detect submarine springs along northwest coast of Puerto Rico
[PB-210754] 01 p0052 N73-10426
Application of aerial photography and photointerpretation to analyzing groundwater conditions under various types of landscape and morphological elements
[NASA-TT-F-681] 02 p0174 N73-11409
Simulation of flow of compressible gas through water channel of varying cross section
[AD-749134] 04 p0408 N73-13327
Detection of vegetation damage associated with highways and highway facilities with reference to stress caused by chemicals and alteration to ground water table
[E72-10288] 04 p0410 N73-13338
Survey and mapping of snow and ground water levels in Norway using ERTS-1 imagery
[E73-10324] 09 p1024 N73-18356
Development of facilities and processing for determining increase in mean seasonal runoff due to cloud seeding in San Juan Mountains, Colorado
16 p1859 N73-25056
Mineral concentration in ground and river waters of Porkhov determined from their specific electroconductivity
[NASA-TT-F-14991] 17 p1992 N73-26105
Use of spaceborne microwave radiation measurements to detect fires, subsurface water, and surface temperature
[NASA-TT-F-14975] 17 p1998 N73-26153
Photointerpretation of ERTS-1 imagery to map bodies of water in Saline County, Kansas
[E73-10684] 17 p2017 N73-26313
ERTS-1 and aircraft multispectral scanner data for mapping ponds and lakes near Woodworth, North Dakota to determine changes in continental migratory bird habitat
[E73-10714] 17 p2018 N73-26321
Application of ERTS-1 imagery for grid measurement of small water bodies
[E73-10768] 18 p2134 N73-27244
Application of ERTS-1 imagery for hydrometric and hydrographic surveys of Canada
[E73-10777] 18 p2135 N73-27253
Analysis of ERTS-1 data pertaining to Delaware River Basin observations to determine performance of data collection system
[PAPER-W10] 19 p2271 N73-28287
Evaluation of ERTS-1 imagery for determining numbers and distribution of prairie ponds and lakes in North Dakota
[PAPER-W12] 19 p2272 N73-28289
Application of ERTS-1 imagery for determining location and characteristics of lake basins Texas high plains and semi-arid areas
[PAPER-W13] 19 p2272 N73-28290
Application of ERTS-1 imagery for controlling quantity and quality of ground water resources
19 p2288 N73-28399
Analysis of albedo of reservoirs from observations of total and reflected radiation measured near floating island stations
20 p2402 N73-29301
Analysis of temperature and radiation regime above paddie surfaces as obtained by helicopter-borne radiation thermometer
20 p2405 N73-29324
Electric conductivity of water extracts from soil as measure of ionic strength
[NASA-TT-F-15044] 20 p2411 N73-29377

**GROUND WAVE PROPAGATION**
Estimating distance to thunderstorms using computerized simulation of ground wave atmospherics
13 p1551 N73-22566

**GROUND WIND**
Small perturbation theory applied to effects of irregular topography on deflection of wind blowing over industrial area and then residential area and effects on air pollution
[NASA-TM-X-2653] 01 p0074 N73-10610
Determining optimal runway orientation for minimizing frequency of crosswinds and headwind reversals at Cape Kennedy
[NASA-CR-128995] 01 p0075 N73-10617

Boundary layer approach to analysis of atmospheric motion over surface obstruction
[NASA-CR-2182] 07 p0769 N73-16244
Simulation of wind gust effects on aircraft
14 p1645 N73-23338
Comparative analysis of upper troposphere maximum wind strength maps and ground surface synoptic maps
20 p2445 N73-29642
GROUND-AIR-GROUND COMMUNICATIONS
Characteristics of air traffic control system to include description of electronic components and projects for developing improved equipment
14 p1687 N73-23692
Status and trends of civil air traffic control systems and development of automated network for increased flight safety
14 p1688 N73-23696
Discretely addressable radar beacon system with airborne transponders and ground-air-ground data link for air traffic control
[FAA-RD-73-48] 16 p1940 N73-25701
ESRO AEROSAT experiment using stratospheric balloon-borne transponder to relay signals from ground station to aircraft flying over sea
18 p2106 N73-27029
Optimization of global ground data transmission network for spacecraft communications
18 p2210 N73-27843
GROUND-TO-AIR MISSILES
U SURFACE TO AIR MISSILES
GROUP BEHAVIOR
U GROUP DYNAMICS
GROUP DYNAMICS
Production planning with group techniques for welding shops using component and blank classifications
[NLL-M-22594-[5828.4F]] 05 p0550 N73-14467
GROUP THEORY
NT HOMOMORPHISMS
Multiplicative renormalization group used to compute critical indices in d equals 4 minus sigma dimensions
[NOTA-INTERNA-384] 01 p0080 N73-10661
Group theoretical descriptions of dualities in projective planes
02 p0196 N73-11582
Transformation functions between z basis and jm basis of Lorentz group principal series
[NOTA-INTERNA-386] 03 p0324 N73-12641
Fields, statistics and non-Abelian gauge groups
[NOTA-INTERNA-387] 03 p0340 N73-12771
Group theory and general relativity, including Lorentz group
[AD-749516] 04 p0451 N73-13681
Dual multiperipheral model of hadronic production amplitudes
[NUB-2164] 07 p0823 N73-16672
Right congruences and semisimplicity for Rees matrix semigroups
[AD-754816] 11 p1312 N73-20645
Baryon spectroscopy and regularities between SU[6] and SU[3] mass breaking parameters
[LPTHE-73/21] 21 p2581 N73-30687
GROUP 7A COMPOUNDS
U HALOGEN COMPOUNDS
GROUP 3A COMPOUNDS
Infrared spectra of aluminum, gallium, and indium suboxide vapors considering frequency oscillations in group 3 suboxides and molecular constants of boron oxide
[AD-752861] 09 p1000 N73-18164
GROUP 6A COMPOUNDS
Synthesis of superconducting intercalated and intermetallic compounds
[AD-751497] 07 p0833 N73-16751
GROWTH
NT CROP GROWTH
NT CRYSTAL GROWTH
NT CZOCHRALSKI METHOD
NT EPITAXY
NT HYDROTHERMAL CRYSTAL GROWTH
NT VEGETATION GROWTH
Growth response of bacteria and yeast in high pressure helium-oxygen environment
[AD-745334] 01 p0012 N73-10096
Growth rate of liquid droplets formed in supersaturated vapors
[AD-753074] 09 p1017 N73-18301
Measurements of radiation characteristics in multistoreyed overmature oak grove
20 p2405 N73-29332
Simulation of growth and mineral uptake by plants growing in lunar soil
[NASA-CR-134036] 22 p2619 N73-30988
Theory of drop growth by condensation for cloud physics application
[AD-764258] 22 p2695 N73-31586
Film growth transient measurements for stress corrosion cracking susceptibility analyses on metals
23 p2804 N73-32421
GRUMMAN AIRCRAFT
NT A-6 AIRCRAFT
NT C-2 AIRCRAFT
NT E-2 AIRCRAFT
NT F-14 AIRCRAFT
NT F-111 AIRCRAFT
GRUMMAN MILITARY AIRCRAFT
U MILITARY AIRCRAFT
GRUNEISEN CONSTANT
Physics of Gruneisen parameter for solids analyzed from view of conceptual and physical contributions
[AD-751130] 07 p0834 N73-16761
GUATEMALA
Volcano and earthquake surveillance network in Alaska, California, Washington, Hawaii, El Salvador, Nicaragua, Iceland, and Guatemala
[E73-10337] 09 p1025 N73-18365
Updating land use and resources data in Guatemala based on ERTS-1 imagery
[E73-10609] 15 p1773 N73-24370
Prototype DCP volcano surveillance network in Washington, Nicaragua, California, Guatemala, Hawaii, El Salvador, Iceland, and Alaska
[E73-11024] 22 p2662 N73-31328
GUIDANCE [MOTION]
NT AIRCRAFT GUIDANCE
NT COMMAND GUIDANCE
NT INERTIAL GUIDANCE
NT INJECTION GUIDANCE
NT MIDCOURSE GUIDANCE
NT RENDEZVOUS GUIDANCE
NT SATELLITE GUIDANCE
NT SPACECRAFT GUIDANCE
NT STRAPDOWN INERTIAL GUIDANCE
NT TERMINAL GUIDANCE
Guidance system for beam-rider projectiles
04 p0447 N73-13647
Mathematical model for tracked air cushion vehicle and guideway to determine vertical dynamic response of vehicle and guideway system to high speed vehicle passage
07 p0737 N73-15995
Space shuttle energy management, approach, and landing analysis
[NASA-CR-128937] 15 p1830 N73-24830
Research concepts for guidance and control of tactical missiles
[AD-762593] 20 p2476 N73-29890
GUIDANCE SENSORS
Dynamic testing procedures for strapdown sensors with motion induced error torques
[NASA-CR-124126] 10 p1185 N73-19641
Computerized ground-air-ground information system for error estimation and alignment of spacecraft attitude sensors
18 p2211 N73-27849
GUIDANCE STABILITY
U CONTROL STABILITY
U GUIDANCE [MOTION]
GUIDE VANES
Corrosion resistant materials for nozzle guide vanes and turbine blades subject to vanadium containing fuel combustion
14 p1678 N73-23613
Experimental determination of turning angle and losses of axial compressor inlet guide vanes
[AD-757250] 14 p1701 N73-23805
Three dimensional particle trajectories in compressible gas flow in rotating cascade
[AD-757162] 14 p1701 N73-23807
Heat transfer between gas and turbine casing in intervane channels of stators and guide vanes
[NASA-TT-F-15051] 21 p2588 N73-30737
GUIDED MISSILES
U MISSILES
GUINEA PIGS
Mortality rate of guinea pigs after decompression treatment as function of water balance
[DLR-FB-71-20] 05 p0501 N73-14075
Guinea pigs used to determine effect of intramuscular injections of drugs on fall-out and Bekhterev nystagmus occurring after unilateral and bilateral labyrinthectomies
07 p0744 N73-16049
Pharmacologic investigations of antagonistic effects of pyridines on isolated guinea pig ileum
[BMVG-FBWT-72-14] 07 p0747 N73-16075
Bradycardia and death in guinea pigs exposed to acceleration overloads after injections of aminothiol group radioprotectors
11 p1239 N73-20057
Effect of acute and chronic hypercapnia on Ca and inorganic P levels in guinea pig blood plasma and erythrocytes
[AD-749323] 13 p1484 N73-22035
Lesion threshold in guinea pig auditory sensation areas due to sonic booms
[ISL-33/72] 19 p2228 N73-27966
GULF OF ALASKA
Surface water circulation in Prince William Sound using ERTS-1 imagery
[E73-10291] 08 p0915 N73-17496
GULF OF CALIFORNIA [MEXICO]
Study of marine environment of northern Gulf of California using ERTS-1 MSS imagery
[E72-10283] 03 p0292 N73-12381
Microdensitometer scans of ERTS-1 imagery of Gulf of California
[E72-10350] 05 p0533 N73-14338
Oceanography and marine environment of Gulf of California based on ERTS-1 imagery
[E73-10021] 08 p0900 N73-17286
ERTS-1 imagery of oceanography and marine environment of northern Gulf of California
[E73-10304] 09 p1021 N73-18336
Investigation of marine environment of northern Gulf of California using ERTS data collection platforms
[E73-10550] 14 p1655 N73-23423
Oceanographic mapping of distribution and flow of water masses in northern Gulf of California by use of ERTS-1 imagery and optical models
[PAPER-M11] 19 p2281 N73-28350
Identification of female specimen of Trichocorixa reticulata in waters of Gulf of California
[E73-10926] 20 p2398 N73-29275
Oceanography and marine environment of northern Gulf of California
[E73-10941] 21 p2529 N73-30283
GULF OF MEXICO
Utilization of ERTS-1 remotely-acquired oceanographic information for improving harvest and management of menhaden in Gulf of Mexico
[E72-10215] 02 p0162 N73-11309
Location of water current boundaries in Gulf of Mexico by sensing color change associated with cyclonic edge of zone of maximum horizontal velocity shear
[E72-10233] 02 p0163 N73-11326
Land use planning on Mississippi Gulf Coast utilizing ERTS-1 remotely sensed data
[E72-10262] 03 p0290 N73-12361
Monitoring changing geologic features along Texas Gulf Coast using ERTS-1 imagery
[E72-10323] 05 p0530 N73-14311
Improvement of menhaden fishery prediction in Mississippi Sound through ERTS-1 imagery
[E72-10340] 05 p0532 N73-14328
Location of ocean current boundaries in Gulf of Mexico by ERTS-1 sensing of water color changes
[E73-10030] 06 p0660 N73-15363
Study of propagation characteristics of normal acoustic modes in Gulf of Mexico waters
[AD-753200] 09 p1032 N73-18427
Location of ocean current boundaries in Gulf of Mexico by sensing color change associated with cyclonic edge of zone of horizontal velocity shear
[E73-10022] 10 p1146 N73-19330
Oceanographic data collection on Caribbean Sea and Gulf of Mexico environments
[AD-752494] 10 p1156 N73-19404
ERTS-1 detection of oil pollution in Gulf of Mexico and in waters off Salem, Massachusetts and Oakland, California
[E73-10396] 11 p1276 N73-20358
Application of ERTS-1 imagery to land use planning and management on Mississippi Gulf Coast
[E73-10460] 11 p1284 N73-20418
Near-surface air and sea-surface temperatures for hurricanes in Gulf of Mexico
[AD-754353] 11 p1315 N73-20677
Improvement of Menhaden fishery prediction in Mississippi Sound using ERTS-1 imagery
[E73-10480] 12 p1396 N73-21317
Marine biology literature compilation for Caribbean Sea and adjacent regions
14 p1607 N73-23022
Literature compilation on marine geology and geophysics for Caribbean Sea and adjacent regions
14 p1607 N73-23023
Detection of menhaden schools in Mississippi Sound by comparing ERTS-1 imagery to selected oceanographic parameters
[E73-10580] 14 p1656 N73-23441
Detection of current boundaries in Gulf of Mexico by sensing ocean color changes
[E73-10612] 15 p1774 N73-24373
Detailed environmental profiles for seven potential Gulf Coast deep water port sites
[AD-758455] 15 p1806 N73-24637
Application of ERTS-1 imagery for determining availability and distribution of menhaden within Mississippi Sound adjacent waters
[E73-10751] 17 p2022 N73-26354
Prediction of menhaden fish distribution in Mississippi Sound based on ERTS-1 imagery
[E73-10785] 18 p2136 N73-27261
Distribution and movement of suspended sediment in Gulf of Mexico off Texas coast
[PAPER-M10] 19 p2281 N73-28349
Detection of ocean currents in eastern Gulf of Mexico using ERTS-1 imagery
[PAPER-M13] 19 p2281 N73-28352
Application of ERTS-1 imagery to harvest model of menhaden fishing industry in Mississippi Sound
[PAPER-M17] 19 p2282 N73-28355
Land use planning and management on Mississippi Gulf Coast using ERTS-1 data
[E73-10906] 20 p2396 N73-29255
Utilization of ERTS-1 imagery to determine availability and distribution of adult Gulf menhaden within Mississippi Sound and adjacent waters
[E73-10980] 22 p2657 N73-31287

Application of ERTS-1 data to land use planning on Mississippi Gulf Coast
[E73-11055] 23 p2780 N73-32231
Skylab oceanic gamefish operations in Gulf of Mexico
[E73-11157] 24 p2919 N73-33311
GULFS
NT GULF OF ALASKA
NT GULF OF CALIFORNIA [MEXICO]
NT GULF OF MEXICO
GUM VULCANIZATES
U VULCANIZED ELASTOMERS
GUMBEL THEORY
U RANGE [EXTREMES]
GUN LAUNCHERS
Microhardness tests of refractory metal alloys
[AD-750593] 06 p0686 N73-15582
Feasibility of gun launched projectile to produce magnetic flux compression
[AD-755103] 11 p1325 N73-20750
CONSHOC computer program for locating shock waves and contours of flow variables in finite difference flow fields
[AD-759898] 17 p2016 N73-26301
Manipulation of digital computer source program for terminal ballistics of gun launched guided projectiles
[AD-764225] 22 p2640 N73-31161
Target acquisition model for gun launched guided projectiles
[AD-763909] 22 p2676 N73-31432
Strain wave propagation in metal cones with compressive pulse applied at base and application to design of gun launchers
[AD-762504] 22 p2727 N73-31822
GUNFIRE
Horizontal gunfire effects on flammability of hydrocarbon turbine fuel
[AD-755361] 12 p1443 N73-21688
Incendiary vulnerability of dry bays adjacent to jet fuel tanks under gunfire
[AD-764732] 23 p2867 N73-32920
GUNN DIODES
Design, construction, and performance of Gunn local oscillator for radio receiver applications
[SRDE-72028] 20 p2376 N73-29091
Integrated GaAs digital circuits with Gunn diodes for pulse code modulation
[FTZ-A-62-TBR-3] 22 p2646 N73-31205
GUNN EFFECT
Automatic measurement of frequency stability of microwave Gunn diode oscillators at low temperatures noting graphs of power and frequency against time
[SRDE-72013] 05 p0520 N73-14226
Microwave generator using Gunn effect for magnetic tuning
[NASA-CASE-NPO-12106] 06 p0645 N73-15235
Manufacturing of Gunn diodes with short domainless ISA mode for microwave oscillators with 100 W output
15 p1757 N73-24238
Nonlinear dynamic resistance and light emission associated with carrier generation by impact ionization in Gunn domains
15 p1794 N73-24543
Doping profile effect on stabilization mechanisms in microwave GaAs reflection amplifiers around X band
19 p2244 N73-28089
Design, construction, and performance of Gunn local oscillator for radio receiver applications
[SRDE-72028] 20 p2376 N73-29091
Planar Gunn devices in dipole domain mode for high speed logic circuits in PCM equipment, noting thermal resistances and packing density
[FTZ-A-474-TBR-3] 22 p2643 N73-31183
Reliability and failure modes of GaAs Gunn and impatt diodes and Si impatt diodes
[AD-763929] 22 p2644 N73-31193
GUNS [ORDNANCE]
NT ARTILLERY
NT RIFLES
Weapon delivery accuracy of F-4 aircraft with high gain control augmentation system
[AD-746001] 02 p0126 N73-11028
GUST ALLEVIATORS
Analysis of response of constant-attitude aircraft to atmospheric turbulence
[NASA-CR-2204] 09 p0983 N73-18025
Analysis of gust alleviation system for short takeoff aircraft for improved performance under random turbulence conditions
[NASA-TN-D-7201] 11 p1233 N73-20013
GUST LOADS
Newton-Raphson least squares percentage error method for determining atmospheric turbulence field parameters
[AD-745946] 01 p0078 N73-10641
Effect of heat treatment on fatigue life under gust loads of notched Al-Cu alloy
[ARC-CP-1221] 05 p0563 N73-14571
Development of automatic system for controlling aircraft under turbulent atmospheric conditions to provide pitch stabilization
[AD-751148] 07 p0741 N73-16028
Wind tunnel tests to predict full scale aircraft buffet loads during buffet boundary penetration using scale flutter model of fighter aircraft with variable sweep wings
[NASA-TN-D-7066] 07 p0851 N73-16905
Analysis of gust alleviation system for short takeoff aircraft for improved performance under random turbulence conditions
[NASA-TN-D-7201] 11 p1233 N73-20013
Collection and processing of gust load data obtained from counting accelerometers mounted at center of gravity of various aircraft
[AGARD-R-605] 11 p1235 N73-20023
Analysis of atmospheric turbulence characteristics to show discrete gust and spectral presentations and to determine limitations of discrete gust approach
[ARC-R/M-3216] 15 p1729 N73-24026
Effect of gust loads on wing and T-tail airworthiness requirements for short haul aircraft
[FOK-K-66] 16 p1859 N73-25058
Numerical analysis of response of aircraft in three dimensional gust field to obtain aerodynamic load data on fuselage and tail structures
[AD-762511] 20 p2359 N73-28978
Comparison of gust velocities derived from accelerations of Canberra and Vulcan aircraft noting acceleration and wing loading power spectra
[ARC-CP-1244] 22 p2615 N73-30955
Helicopter gust response to include unsteady aerodynamic stall effects under short-term, control-fixed conditions
[AD-763957] 22 p2615 N73-30958
Dynamic response of short haul aircraft to gust loads
[FOK-K66] 23 p2744 N73-31960
Relative frequency of occurrence of different normal accelerations at the center of gravity of aircraft in turbulence
[ARC-R/M-3714] 24 p2870 N73-32929
GUSTS
Vertical air gust velocities and turbulence spectral structure around and within cumulonimbus clouds
[AD-748518] 04 p0445 N73-13632
Gravity current model applied to analysis of squall-line gust front
12 p1419 N73-21504
The calculated growth of lift and pitching moment on a swept wing entering a discrete vertical gust at subsonic speeds
[ARC-CP-1241] 22 p2612 N73-30932
Trivane measured fluctuations of wind and temperature over an inland lake
22 p2694 N73-31578
GUY WIRES
Establishing standards for effective wire rope clip installation
[BM-RI-7789] 24 p2994 N73-33927
GYMNASTICS
U EXERCISE [PHYSIOLOGY]
GYNECOLOGY
Microelectrophoresis of human erthyrocytes as diagnostic tool in gynecology and obstetrics
[NASA-TT-F-14587] 04 p0378 N73-13077
GYRATION
NT AUTOROTATION
NT EARTH ROTATION
NT MOLECULAR ROTATION
NT PRECESSION
NT ROTATION
NT SATELLITE ROTATION
NT SOLAR ROTATION
NT STELLAR ROTATION
GYRATORS
NT MICROWAVE FILTERS
Design of integrated circuit with two amplifiers and feedback stabilization for single channel gyrator
[NASA-CASE-MFS-22343-1] 09 p1008 N73-18224
Gyrator circuit using MOS field effect transistors
[NASA-CASE-MFS-21433] 11 p1261 N73-20232
Integrated circuit power gyrator with Z-matrix design using parallel transistors
[NASA-CASE-MFS-22342-1] 15 p1756 N73-24236
GYRO HORIZONS
Technological modification to OSO-G launch vehicle for improved guidance and control
18 p2208 N73-27817
GYROCOMPASSES
Development of adaptive filter technique to minimize effect of noise produced errors in gyrocompasses and production of true azimuth data
[AD-747478] 03 p0329 N73-12685
Synthesis of gyroscopic heading indicator and use of gyroscope in rotating gimbal mount as gyrocompass
[JPRS-57280] 05 p0546 N73-14437
Synthesis of gyroscopic heading indicator consisting of gyrocompass and direction gyroscope
05 p0546 N73-14438
Compass effect of gyro with forced rotation of gimbal mount when installed in horizontal plane of earth
05 p0546 N73-14439
Equations of compass motion of three axis gyrostabilizer in gyrocompass mode based on initial placement error of platform in horizontal plane
06 p0695 N73-15667
Analysis of gyrocompass performance characteristics to include long term accuracy, statistical attributes, and application as geophysical instrument
[AD-750890] 06 p0697 N73-15685
Analysis of errors and selection of design parameters for adjustable gyrocompasses
17 p2059 N73-26658
Inertial navigation equation simplification and dynamic characteristics of gyrocompass
[JPRS-59776] 21 p2576 N73-30643
GYROINTERACTION
U MAGNETIC RIGIDITY
GYROPLANES
U HELICOPTERS
GYROS
U GYROSCOPES
GYROSCOPES
NT ATTITUDE GYROS
NT CONTROL MOMENT GYROSCOPES
NT ELECTROSTATIC GYROSCOPES
NT GYRO HORIZONS
NT GYROCOMPASSES
NT GYROSCOPIC PENDULUMS
NT GYROSTABILIZERS
NT ROTARY GYROSCOPES
Use of gyrotheodolites for azimuth determinations on orienting points
[AD-744684] 01 p0052 N73-10419
Spin stabilized gyroscope having spining rotor and stationary platform
[NASA-CASE-GSC-11479-1] 02 p0207 N73-11680
Analysis of factors involved in specification, design, and evaluation of gyroscopes for spaceborne sensor applications
[NASA-SP-8096] 03 p0328 N73-12680
Temperature corrected circuit for gyroscope or accelerometer of digital rebalance type
[NASA-CASE-NPO-13044-1] 04 p0421 N73-13436
Gyro suspension systems including axis disturbance probability factors, bearing friction, astatic gyro gimbal errors with drift, and horizontal pendulum energy dissipation
[JPRS-57504] 05 p0546 N73-14432
Experimental determination of probability factors of disturbances relative to principal axis of gyroscope
05 p0546 N73-14433
Influence of dry friction in suspension bearings on motion of gyroscope with forced gimbal rotation
05 p0546 N73-14434
Development of apparatus and technical procedures for measuring system inertia tensor parameters of precession nonrigid systems
05 p0547 N73-14442
Characteristics of inertial guidance systems to include minimizing of errors, forces on electrostatic gyroscope, and parameters of electromagnetic load cell
[JPRS-57746] 06 p0695 N73-15664
Characteristics of symmetrical springs for elastic field between rotor and housing of gyroscopic instruments and numerical analysis of radial stiffness
06 p0696 N73-15669
Stability of laser gyro with Faraday cell
[FOA-2-C-2467-54] 06 p0696 N73-15671
Development of device for measuring angular rate based on fluidic components for inertial angular rate sensors using vortex principle
[FOA-2-C-2466-54] 06 p0696 N73-15672
Elastic gyro rotor with stable orientation of readout axis by point mass system
07 p0817 N73-16623
Analysis of motion of compound pendulum and two-gimbal gyroscope mounted in artificial satellite with prescribed orbit and constant rate of rotation
07 p0817 N73-16625
Analysis of gyroscopic instrument performance during acceleration and method for determining position of vehicle in geopolar regions
[JPRS-57990] 08 p0923 N73-17557
Development of matrix method for determining gimbal errors of three-axis gyrostabilized platform with constant drift rate
08 p0923 N73-17558
Analysis of motion of dynamically unbalanced linear acceleration gyrointegrator
08 p0923 N73-17559
Analysis of motion of gimbal mounted gyroscope during rotor acceleration
08 p0923 N73-17560
Articles on inertial systems
[JPRS-58181] 10 p1184 N73-19632
Natural vibrations of gyroscope with flexible rotor shaft and elastic axial cardan suspension
10 p1184 N73-19633
Motion of gyroscope in cardan suspension in drift mode during platform oscillations
10 p1184 N73-19634
Condition of drift invariance of two-stage gyroscope with arbitrary gas-lubricated main bearings in active accelerations
10 p1184 N73-19635
Motion induced error in tuned, flexure-mounted strapdown gyro
[NASA-CR-124161] 11 p1316 N73-20682

Development of single-degree-of-freedom gyroscope for application to strapdown inertial guidance system
11 p1317 N73-20688
Methods for conducting acceptance tests and reliability tests of gyroscopes as part of inertial platform quality control procedures
11 p1317 N73-20689
Development of spherical, hydrostatic, compliant bearing for directional gyroscope
11 p1318 N73-20695
Mathematical models for measuring operating functions and performance of gyroscope with two degrees of freedom
11 p1318 N73-20696
Dynamically tuned gyros in strapdown systems
11 p1318 N73-20697
Parameters of single-axis floated gyroscopes when used in inertial systems requiring rapid gyrocompassing for alignment
11 p1319 N73-20709
Design, development, and evaluation of spherical hydrostatic gas bearing gyroscope for operation in random vibration environment
[AD-755124] 11 p1322 N73-20725
Analytical solutions for problems of gyroscopes in inertial navigation systems
[JPRS-58722] 13 p1556 N73-22609
Equations of motion for gyroscopic devices and analysis of effects on accuracy produced by loads and vibrations in supports of gyroscopic instruments
[AD-756337] 13 p1557 N73-22622
Manufacture of quartz gyroscopes for application to General Relativity Satellite
13 p1593 N73-22920
Gyroscope noise measurements and data analysis
[AD-756977] 14 p1691 N73-23723
Development of guidelines for selection of hardware items for use in manned spacecraft design to obtain five year maintenance-free service life - Vol. 3
[NASA-CR-128907] 14 p1707 N73-23855
Precision and reliability characteristics of combined gyroscopic and correction channel
17 p2059 N73-26659
Static moment and horizontal sinusoidal acceleration effects on stabilization errors in gyrovertical with mixed gyroscope correction characteristics
17 p2060 N73-26661
Compliant bearing designs for directional control gyroscope
[AD-762036] 19 p2305 N73-28538
Selected articles on gyroscopes and gyromotors
[JPRS-59053] 20 p2417 N73-29420
Equations for determining action and deformation of bearings when force applied to center of gravity of gyromotor rotor
20 p2417 N73-29422
Equations for determining change of axial rigidity as function of component rotor weight
20 p2417 N73-29423
Effect of elastic deformation of gimbal suspension on motion of gyroscope
20 p2418 N73-29424
Analytical description of spatial distribution of scattering of gyromotor magnetic field
20 p2418 N73-29425
Performance of various types of gyroscopes
[JPRS-59498] 20 p2418 N73-29426
Quasistationary mode of rotation of spherical rotor of free gyroscope
20 p2418 N73-29427
Gyroscopic orbit errors caused by random perturbations
20 p2418 N73-29428
Effect of random perturbations relative to main gyroscope axis on ground gyrocompass readings
20 p2418 N73-29429
Device for measuring friction moments in radial thrust ball bearings and gas-dynamic bearings of gyros
20 p2418 N73-29430
Electrostatic gyroscope deviations and imbalance
[JPRS-59651] 20 p2418 N73-29432
Electrostatic gyroscope deviations from rotor asphericity with axisymmetric surface
20 p2418 N73-29433
Rundown time and rotor imbalance of electrostatic gyroscope with spherical rigid rotor
20 p2419 N73-29434
Elastic deformation of gimbal suspension on gyroscope nutation, moments acting on spherical rotor in magnetic suspension, and differentiating linear accelerometer
[JPRS-59740] 21 p2547 N73-30420
Influence of elastic deformation of gimbal suspension on frequency of nutation of gyroscope
21 p2547 N73-30421
Kinematics of gyroscopes and gimbals and effects on missile stability
[AD-763147] 21 p2549 N73-30440
Thermal stabilization of component dimensions for gyro devices
[AD-763143] 21 p2549 N73-30441
Increased sensitivity of laser gyroscopes
[AD-763284] 21 p2550 N73-30443
Threshold of sensitivity of laser gyroscope lowered by use of Zeeman effect
[AD-763160] 21 p2550 N73-30444
Feasibility of producing constant speed drive with aid of gyroscope
[AD-763256] 21 p2550 N73-30445
Optimum transfer function applied to correcting simplest single rotor gyroscope
21 p2576 N73-30645
Design operation and performance of gyro module for SIRU
[NASA-CR-135509] 22 p2698 N73-31608
Three axis inertial system in Apollo gimbal for fine grain evaluation of strapdown system performance in dynamic environments
[NASA-CR-135484] 22 p2698 N73-31609
Stability of undisturbed motion of suspension rings of gyropendulum on moving base
23 p2791 N73-32330
Strapped down gyroscope aligned with sun and star tracker optical axis calibrating roll, yaw and pitch values
[NASA-CASE-ARC-10716-1] 23 p2851 N73-32784
Equations of motion for Lincoln Experimental Satellites with gimbaled momentum wheel and gyroscope to analyze attitude control dynamics
[AD-765548] 24 p2986 N73-33867

**GYROSCOPIC DRIFT**
U GYROSCOPES
U GYROSCOPIC STABILITY

**GYROSCOPIC PENDULUMS**
Effect of energy dissipation on drift of horizontal pendulum on vibrating base with application to gyroscopic suspension systems
05 p0546 N73-14436
Dynamic error of pendulum with vibrating suspension related to finite rigidity of rod in stretching
13 p1556 N73-22612

**GYROSCOPIC STABILITY**
Effect of internal spinning fly wheel on air launched missile stability and resulting launch disturbance
[AD-749027] 04 p0375 N73-13047
Effect of energy dissipation on drift of horizontal pendulum on vibrating base with application to gyroscopic suspension systems
05 p0546 N73-14436
Development of apparatus and technical procedures for measuring system inertia tensor parameters of precession nonrigid systems
05 p0547 N73-14442
Characteristics of symmetrical springs for elastic field between rotor and housing of gyroscopic instruments and numerical analysis of radial stiffness
06 p0696 N73-15669
Analysis of gyrocompass performance characteristics to include long term accuracy, statistical attributes, and application as geophysical instrument
[AD-750890] 06 p0697 N73-15685
Equations of motion for calculating flexible rotor influence on two gimbaled gyroscope motion
08 p0922 N73-17554
Analysis of gyroscopic instrument performance during acceleration and method for determining position of vehicle in geopolar regions
[JPRS-57990] 08 p0923 N73-17557
Analysis of motion of dynamically unbalanced linear acceleration gyrointegrator
08 p0923 N73-17559
Analysis of motion of gimbal mounted gyroscope during rotor acceleration
08 p0923 N73-17560
Three axis gyro stabilized torpedo platform
11 p1318 N73-20702
Development of strapdown electrically suspended gyroscope components for increased readout accuracy
[NASA-CR-112206] 11 p1321 N73-20721
Stability of steady state motions of gyroscope with spring limiters on rotating platform in Newtonian central field of forces
13 p1556 N73-22611
Static moment and horizontal sinusoidal acceleration effects on stabilization errors in gyrovertical with mixed gyroscope correction characteristics
17 p2060 N73-26661
Stability of amplitude characteristics of laser gyroscope in magnetic field
[AD-763260] 21 p2550 N73-30442

**GYROSTABILIZERS**
Spin stabilized gyroscope having spining rotor and stationary platform
[NASA-CASE-GSC-11479-1] 02 p0207 N73-11680
Equations of compass motion of three axis gyrostabilizer in gyrocompass mode based on initial placement error of platform in horizontal plane
06 p0695 N73-15667
Analysis of biaxial gyrostabilizer system and synthesis of spherical superconducting suspensions with maximum lift
[JPRS-58356] 10 p1159 N73-19428
Application of averaging method to biaxial gyrostabilizer analysis
10 p1159 N73-19429
Gyrostabilizers on moving base, on three stage gyroscope, and as angular velocity integrator
[JPRS-60001] 23 p2791 N73-32328
Precision theory for kinematic errors in uniaxial gyrostabilizer as angular velocity integrator
23 p2791 N73-32329
Stability of indicating gyrostabilizer in viscous suspension of forced rotation of three stage gyroscopes
23 p2791 N73-32331
Development and characteristics of servoed roll gimbal to isolate gyroscopes of stabilized platform from effects of vehicle spin
[AD-764903] 23 p2818 N73-32527
Design criterion and laboratory test results of gyrostabilized marine gravimeter
[JPRS-60183] 24 p2926 N73-33369

**GYROSTATS**
U GYROSCOPES

## H

**H ALPHA LINE**
Inference of coronal and interplanetary magnetic fields and H-alpha patterns from high resolution photography
01 p0094 N73-10771
Photographic V and R magnitudes of 130 T Tauri and H alpha emission stars in Orion I
06 p0716 N73-15847
UBV and H alpha spectra for detecting interstellar dust and distances to planetary nebulae
12 p1448 N73-21724
Optical properties of solar flare spectra
19 p2333 N73-28776
Optical X ray, H alpha, and microwave emissions during solar flares
19 p2335 N73-28790

**H BETA LINE**
Low intensity H-beta emission from interstellar medium
08 p0975 N73-17973

**H GAMMA LINE**
Balmer and H gamma line profiles for determining electron density in model B stars
[NASA-TM-X-66266] 17 p2082 N73-26840
Using UBUH gamma photometry and spectral classifications for 48 stars in monoceros region to study dispersed part of 1 Mon association
23 p2836 N73-32658

**H LINES**
NT H ALPHA LINE
NT H BETA LINE
NT H GAMMA LINE
NT K LINES
NT TELLURIC LINES
Source of electrons from molecular hydrogen in H I regions
[NASA-TM-X-66079] 02 p0229 N73-11858
Density and temperature profiles of HI lines in interstellar dust clouds
12 p1448 N73-21723
Radio recombination line emission from galactic H 1 and H 2 regions
16 p1961 N73-25863
Infrared emission from southern H 2 region H2-3 with solar luminosity between 1.65 and 25 microns
[NASA-CR-135640] 23 p2785 N73-32280

**H-13 HELICOPTER**
U OH-13 HELICOPTER

**H-51 HELICOPTER**
U XH-51 HELICOPTER

**H-53 HELICOPTER**
Modifications to helicopter active transmission isolation system to provide method for measuring forces on rotary wing of CH-53 helicopter
[NASA-CR-112245] 09 p0982 N73-18024
Avionics requirements for HH-53C helicopter engaged in search and rescue operations
[AD-752625] 09 p0986 N73-18047
Analysis of aerodynamic stall characteristics of airfoils at various angles of attack with application to control forces of H-53 helicopter
[AD-752917] 09 p0986 N73-18053

**H-126 AIRCRAFT**
Wind tunnel tests to determine aerodynamic characteristics of full scale H-126 aircraft using jet flap principle
[NASA-TN-D-7252] 12 p1355 N73-20997

**HABITABILITY**
Analyses of Skylab crew quarters and habitability - App. D
[NASA-CR-61386-APP-D] 06 p0721 N73-15880
Recorded observations of crew member activities during Tektite 2 underwater habitability study
[NASA-CR-130034] 07 p0750 N73-16094
Habitability factors during long-term space and undersea missions in confined habitats
[NASA-CR-130537] 08 p0879 N73-17123
Habitability study of shuttle orbiter
[NASA-CR-128863] 10 p1124 N73-19162
Habitability study of shuttle orbiter
[NASA-CR-128864] 10 p1124 N73-19163
Habitability study of earth orbital space stations
[NASA-CR-124276] 16 p1869 N73-25132
Solution to problem of endangered living space
[NRC-TT-1636] 20 p2371 N73-29057

Payload carrier simlation data for design of manned space shuttle missions
[NASA-CR-124430] 23 p2751 N73-32018

**HABITATS**
Changes in continental migratory bird and wildlife habitats
[E72-10235] 03 p0288 N73-12335
Management of wildlife habitat in Alaska using ERTS-1 imagery
[E72-10293] 04 p0410 N73-13343
Monitoring continental migratory bird habitats
[E73-10065] 07 p0779 N73-16327
Multispectral remote sensing techniques applied to study changes in wildlife habitats
07 p0786 N73-16396
Application of ERTS-1 imagery to study of caribou movements and winter dispersal in relation to snow cover
[E73-10285] 08 p0914 N73-17491
Study of continental migratory bird habitat changes using ERTS-1 imagery
[E73-10334] 09 p1025 N73-18364
Management of wildlife habitats in Alaska using ERTS-1 imagery
[E73-10335] 10 p1147 N73-19336
Appraisal of changes in migratory bird habitats based on ERTS-1 imagery of North Dakota
[E73-10534] 13 p1518 N73-22298
ERTS-1 imagery of caribou movements and winter habitats in Alaska in relation to prevailing snow cover
[E73-10840] 19 p2290 N73-28418
Appraising changes in continental migratory bird habitats in North Dakota using Skylab EREP system
[E73-10972] 22 p2657 N73-31284
Management of wildlife habitats in Alaska using ERTS-1 MSS data
[E73-11030] 22 p2662 N73-31334
Utilization of Skylab EREP system for appraising changes in continental migratory bird habitats
[E73-11079] 23 p2782 N73-32254
Analysis of grizzly bear habitats from ERTS-1 photography
[NASA-CR-135776] 24 p2920 N73-33319

**HABITUATION [LEARNING]**
Effects of human alertness on vestibular nystagmus habituation
[AD-749352] 05 p0505 N73-14108

**HADRONS**
NT BARYONS
NT MESONS
Light cone singularities, DGS representations, and asymptotic behavior of forward scattering amplitudes
[TR-73-059] 03 p0339 N73-12765
Light cone analysis of large momentum transfer limit of electroproduction structure function at constant missing mass and of its connection with Bjorken limit
[TR-73-066] 03 p0339 N73-12766
Bjorken scaling in deep inelastic electron proton scattering and parton models
[NOTA-INTERNA-391] 03 p0340 N73-12773
Off-shell asymptotic behavior of electromagnetic form factors of composite particle
[TR-73-070] 06 p0703 N73-15728
Dual multiperipheral model of hadronic production amplitudes
[NUB-2164] 07 p0823 N73-16672
Bilocal operator expansion to two jet structure for final states of deep inelastic scattering on hadrons
[ILL-(TH]-73-4] 12 p1430 N73-21592
Survey of theoretical models used to discuss final hadronic states produced in inelastic electron-hadron scattering
[ILL-(TH]-73-2] 12 p1430 N73-21593
Hadronic component of cosmic ray shower and relation to shower size, using calorimeter
13 p1574 N73-22757
Total cross sections for electron positron annihilation producing hadron pair
[NOTA-INTERNA-420] 18 p2181 N73-27613
Harmonic oscillator quark model of hadrons with relativistic internal velocities for quarks
[LPTHE-73/15] 20 p2456 N73-29739

**HAFNIUM**
Thermal shock resistant hafnia ceramic materials
[NASA-CASE-LAR-10894-1] 05 p0564 N73-14584
Hafnium pigmentation for mullite composite thermophysical optimization
24 p2939 N73-33469

**HAFNIUM CARBIDES**
Effects of excessive HfC on mechanical properties of W-Re-Hf-C alloys
[NASA-TN-D-7210] 11 p1305 N73-20588

**HAFNIUM COMPOUNDS**
NT HAFNIUM CARBIDES
NT HAFNIUM OXIDES
Optical and magnetic resonance spectra of uranium borohydride in hafnium borohydride
[AD-759371] 17 p2074 N73-26777
Solubility curves from 25 to 70 C for K2HfF-K2ZrF6-HF system
[BM-RI-7785] 21 p2558 N73-30505

**HAFNIUM OXIDES**
Removing nitride inclusions from heat resistant alloys and hafnium dioxide particles in precipitation-hardened nickel
[JPRS-59637] 21 p2557 N73-30501
Behavior of hafnium dioxide particles in precipitation-hardened nickel during isothermal annealing
21 p2558 N73-30503
Electrical and thermal breakdown properties of tantalum oxide and hafnium oxides capacitors
22 p2641 N73-31168

**HAIL**
Empirical procedure for predicting growth of ice crystals, graupel, and hail by diffusion
[AD-746451] 02 p0205 N73-11660
Performance of dual wavelength hail detector considering meteorological and radar parameters
[TR-25] 06 p0639 N73-15191
Methods of forecasting hail, thunderstorms, and amounts of rainfall
[NLL-M-22902-[5828.4F]] 15 p1805 N73-24626
Hail protection method for reducing or eliminating farm crop damage
20 p2446 N73-29649
Evaluation of recording instrument for in-flight determination of size and distribution of hailstones
[NASA-TM-X-2817] 21 p2549 N73-30434
Analysis of radar signatures for identifying hail-bearing clouds to show effects of geographical conditions and seasons
21 p2569 N73-30586
Design and development of meteorological radar for detecting hail-bearing clouds
21 p2572 N73-30611

**HAILSTONES**
U HAIL

**HAIR**
Evaluation of hazardous conditions created by facial hair on aircrew personnel wearing oxygen masks
[AD-754075] 12 p1375 N73-21154

**HALF CONES**
Flow field, pressure, and heat transfer associated with small fins of half angle cone in supersonic flow
[SCL-RR-72-0339] 10 p1142 N73-19302

**HALF PLANES**
Structural analysis of two bonded half planes with finite crack perpendicular to and passing through interface
[NASA-CR-2181] 07 p0852 N73-16910
Bonded half planes containing an arbitrarily oriented crack
[NASA-CR-132290] 19 p2348 N73-28888

**HALF SPACES**
Wave propagation in half space due to interior point load parallel to surface
[AD-747306] 02 p0170 N73-11381
Calculation of unsteady electric field produced by radio waves in lower half space
[AD-747731] 03 p0267 N73-12164
Forced steady state response of cylindrical shell immersed in acoustic fluid bounded by elastic half space
[AD-747705] 03 p0337 N73-12750
Analysis of particle erosion of solid surfaces using model of erosion pit nucleation and growth for solid spherical particles impacting on plane surface of elastic half space
[AD-752221] 08 p0935 N73-17657
Solution of Hertz contact problem for case involving indentation of elastic half space by rigid axisymmetric punch under monotonically applied normal force with assumed Coulomb friction
[AD-755071] 11 p1299 N73-20544

**HALIDES**
NT ALKALI HALIDES
NT BORON CHLORIDES
NT CADMIUM FLUORIDES
NT CARBON TETRACHLORIDE
NT CESIUM IODIDES
NT CHLORIDES
NT CHLORINE FLUORIDES
NT COPPER CHLORIDES
NT DIBROMIDES
NT DICHLORIDES
NT FLUORIDES
NT HYDROBROMIDES
NT HYDROCHLORIC ACID
NT HYDROFLUORIC ACID
NT HYDROGEN CHLORIDES
NT IRON CHLORIDES
NT LITHIUM CHLORIDES
NT LITHIUM FLUORIDES
NT METAL HALIDES
NT NICKEL FLUORIDES
NT OXYGEN FLUORIDES
NT POTASSIUM BROMIDES
NT POTASSIUM CHLORIDES
NT POTASSIUM IODIDES
NT SILVER CHLORIDES
NT SILVER HALIDES
NT SILVER IODIDES
NT SODIUM CHLORIDES
NT SODIUM FLUORIDES
NT SULFUR FLUORIDES
NT TETRACHLORIDES
NT TITANIUM CHLORIDES
NT URANIUM FLUORIDES
NT ZIRCONIUM IODIDES
Development and characteristics of alkali halide window for application to infrared laser systems
[AD-744998] 01 p0065 N73-10530
Process for producing polycrystalline halides for use in high power laser windows to maintain optical properties with improved mechanical properties
[AD-745350] 01 p0065 N73-10535
Discharge compositions of gas laser emissions from mercury and copper halides
[AD-749938] 05 p0559 N73-14541
High temperature deformation of polycrystalline halide microstructures by infrared lasers
[AD-751655] 08 p0944 N73-17730
Low frequency Raman spectra of ammonium halides measured by double monochromator at high temperature
[NASA-CR-132049] 15 p1747 N73-24160

**HALL COEFFICIENT**
U HALL EFFECT

**HALL CURRENTS**
U ELECTRIC CURRENT
U HALL EFFECT

**HALL EFFECT**
Relation of Hall current electrojet instability to VLF hiss in auroral zone of magnetic storms
[NASA-CR-130078] 01 p0047 N73-10378
Sheet resistivity and Hall effect study of zinc ions implanted in chromium-doped gallium arsenide
[NASA-CR-112199] 01 p0087 N73-10716
Hall resistivity and electromagnetic properties of bismuth selenide crystals for cryogenic magnetometers
[NASA-TN-D-7057] 03 p0344 N73-12809
Simultaneous donor and acceptor concentration determination, using Hall effect measurements
[ONERA-DERTS-NT-02-31] 05 p0587 N73-14776
Electrical and photoelectrical properties of trigonal selenium single crystals, including Hall mobility
[PUBL-170] 06 p0707 N73-15771
Variations in electrical properties of silicon films on sapphire using MOS Hall technique
13 p1564 N73-22679
Hall mobility measurements on single crystal silicon ribbons grown from graphite dies
[NASA-CR-131601] 13 p1565 N73-22686
Alternating current Hall mobility and electrical conductivity in amorphous threshold switching semiconductors
[AD-759004] 16 p1954 N73-25809
Hall effect magnetometer for measuring magnetic fields
[NASA-CASE-LEW-11632-2] 20 p2419 N73-29437
Current density, flow velocity, and mass density in coaxial annular plasma Hall accelerator
[DLR-FB-73-45] 22 p2705 N73-31663
Speed control system for dc motor equipped with brushless Hall effect device
[NASA-CASE-MFS-20207-1] 23 p2763 N73-32107
Transverse magneto-resistance and Hall resistivity in pure cadmium and in dilute crystal alloys of Cd-Ag and Cd-In
23 p2825 N73-32585
Linear and nonlinear theory of Hall current instability
24 p2962 N73-33667

**HALL GENERATORS**
Improved ITOS attitude control system with Hall generator brushless motor and earth-splitting technique
[NASA-TM-X-66232] 14 p1708 N73-23858

**HALO PARACHUTING**
U PARACHUTE DESCENT

**HALOGEN COMPOUNDS**
NT ALKALI HALIDES
NT ALUMINUM PERCHLORATES
NT AMMONIUM PERCHLORATES
NT BORON CHLORIDES
NT BROMINE COMPOUNDS
NT CADMIUM FLUORIDES
NT CARBON TETRACHLORIDE
NT CESIUM IODIDES
NT CHLORATES
NT CHLORIDES
NT CHLORINE COMPOUNDS
NT CHLORINE FLUORIDES
NT COPPER CHLORIDES
NT CRYOLITE
NT DIBROMIDES
NT DICHLORIDES
NT FLUORINE ORGANIC COMPOUNDS
NT FLUORO COMPOUNDS
NT FLUOROCARBONS
NT FLUOROHYDROCARBONS
NT HALIDES
NT HYDROBROMIDES
NT HYDROCHLORIC ACID
NT HYDROFLUORIC ACID
NT HYDROGEN CHLORIDES
NT IODATES
NT IODIDES
NT IODINE COMPOUNDS
NT IRON CHLORIDES
NT LITHIUM CHLORIDES
NT LITHIUM FLUORIDES

NT METAL HALIDES
NT NICKEL FLUORIDES
NT OXYGEN FLUORIDES
NT PERCHLORATES
NT POLYTETRAFLUOROETHYLENE
NT POTASSIUM BROMIDES
NT POTASSIUM CHLORIDES
NT POTASSIUM IODIDES
NT SILVER CHLORIDES
NT SILVER HALIDES
NT SILVER IODIDES
NT SODIUM CHLORIDES
NT SODIUM FLUORIDES
NT SULFUR FLUORIDES
NT TETRACHLORIDES
NT TITANIUM CHLORIDES
NT URANIUM FLUORIDES
NT ZIRCONIUM IODIDES
Development and optimization of fire extinguishers for use in passenger and crew compartments of aircraft
[AD-747496] 03 p0253 N73-12051
Human and male Charles River rat exposures to Halon 1301 under hypobaric conditions, simulating aircraft compartment
[AD-747958] 03 p0260 N73-12106
Hepatotoxic effects of dichloromethane inhalation in mice
[AD-751434] 07 p0748 N73-16081
Inorganic halogen oxidizer chemistry
[AD-760696] 18 p2114 N73-27092

**HALOGENATION**
NT FLUORINATION
Papers presented at conference on halogenated fire extinguishing agents
[AD-753218] 09 p1001 N73-18168

**HALOGENS**
NT BROMINE
NT CHLORINE
NT FLUORINE
NT IODINE
NT IODINE ISOTOPES
Development of halogenated hydrocarbon materials for use as fire and ignition suppressants for aircraft fuel tanks subjected to incendiary ammunition
[AD-755362] 12 p1365 N73-21079
Dynamic compatibility of liquid and gaseous fluorine and chlorine pentafluoride propellants with designated metals for rocket engine design criteria
[AD-756916] 13 p1569 N73-22719
Conference on uses and toxicity of halogenated fire extinguishing agents
[PB-218448/9] 18 p2214 N73-27875

**HAMBURGER AIRCRAFT**
NT C-160 AIRCRAFT
NT HFB-320 AIRCRAFT

**HAMBURGER HFB-320 AIRCRAFT**
U HFB-320 AIRCRAFT

**HAMILTON-JACOBI EQUATION**
Separation of variables in special Hamilton-Jacobi equation and application to dynamical problem of constrained on moving surface
[NASA-TR-R-405] 22 p2691 N73-31557

**HAMILTONIAN FUNCTIONS**
Time evolution of quantum lattice system Hamiltonian discussing automorphism of suitable algebra
[NOTA-INTERNA-393] 03 p0340 N73-12774
Procedure for finding minimal and maximal Hamiltonian circuits on complete graph
[AD-754842] 11 p1312 N73-20648
Effects of elasticity on lunar rotation
[NASA-CR-132046] 15 p1831 N73-24844
Temperature dependence of spin-Hamiltonian parameters for chromium doped rutile
[RR-110] 24 p2968 N73-33721

**HAMSTERS**
Correlation of respiratory distress and ultrasonic transmission with severe decompression sickness in hampsters
[AD-743475] 01 p0012 N73-10091

**HAND [ANATOMY]**
Computerized teleoperator manual control system for remote mechanical hand
01 p0019 N73-10143
Study of differences between left and right hand performance in compensatory tracking task
[RAE-TR-72117] 07 p0750 N73-16098
Initiator ignition effect in laboratory glass and polythene vessel studying dummy hand injuries during simulated accidents
[ERDE-TRANS-1] 15 p1744 N73-24137
Design of terminal pointer hand controller for teleoperator applications
[NASA-CR-124307] 18 p2156 N73-27419
Motor reaction model for hand motion in decision making manual task
[AD-761518] 19 p2229 N73-27973
Heat exchange of hand as function of local thermal conditions
[NASA-TT-F-15143] 24 p2885 N73-33043

**HANDBOOKS**
NT USER MANUALS [COMPUTER PROGRAMS]
Handbook on weather patterns over Point Mugu, California
[AD-747641] 03 p0327 N73-12672
Signal processing element users reference manual for radar, sonar, and communication systems
[AD-748592] 04 p0394 N73-13205
Instrumentation handbook for operational support systems of Space and Missile Test Centers in California, Hawaii, and Pacific Ocean area
[AD-750944] 06 p0651 N73-15285
Dictionary-handbook on properties and uses of fuels, lubricating materials, and special liquids
[AD-750484] 06 p0712 N73-15810
SCEPTRE support program - revised users manual using FORTRAN
[AD-751518] 07 p0764 N73-16211
Hand book on ionizing radiation protection policies at Kennedy Space Center
[NASA-TM-X-69410] 10 p1120 N73-19133
Handbook on defense and commercial communication systems
[AD-755917] 12 p1380 N73-21191
Handbook on structural evolution of vestibular apparatus
14 p1609 N73-23044
Users guide to help formulate requests for oceanographic data and related information
14 p1658 N73-23454
Collection generation, and analysis of MIL-HDBK-5 allowable design data for aerospacecraft
[AD-761817] 19 p2347 N73-28877
Development of data base administrator user guide for use with NASA Aerospace Safety Information System [NASIS] - Vol. 8
[NASA-CR-134462] 21 p2512 N73-30146
Development of data base administrator user guide for use with NASA Aerospace Safety Information System [NASIS] using IBM 360/370 OS MVT computer - Vol. 7
[NASA-CR-134476] 22 p2637 N73-31138
Environmental sanitation handbook for occupational medicine and health procedures at Kennedy Space Center
[NASA-TM-X-69522] 23 p2752 N73-32020
Handbook for liquid and solid lubricants in aerospace industry
[NASA-CR-130490] 23 p2796 N73-32365

**HANDEDNESS**
Handedness and adaptation to distortions of size and distance underwater
[AD-759722] 17 p1991 N73-26098

**HANDLING**
U MATERIALS HANDLING

**HANDLING EQUIPMENT**
NT CRANES
Analysis of noise pollution by military vehicles, public transportation, farm equipment, private automobiles, and construction equipment
[AD-747685] 03 p0338 N73-12754
Safe handling system for iridium isotopes used in radiation therapy
12 p1374 N73-21143
Operational handling of test equipment for microorganism exposure to space environment
15 p1740 N73-24105

**HANDLING QUALITIES**
U CONTROLLABILITY

**HANFORD REACTORS**
Dynamic tear tests for determining fracture safety of Hanford-N reactor coolant piping material
[AD-748590] 13 p1558 N73-22626

**HANGARS**
Wind tunnel measuresments of time-average pressure on external and internal surfaces of large hangar-type building
[NPL-MAR-SCI-10-72] 10 p1140 N73-19292

**HANKEL FUNCTIONS**
Hankel function for calculating radio wave diffraction around earth surface
[AD-742108] 01 p0028 N73-10221

**HARBORS**
Analysis of long-period wave phenomenon for means of forecasting and control in seaport operations
04 p0443 N73-13612
New harmonic constant computed for Adriatic Sea harbors
07 p0858 N73-16961

**HARDENING**
Boron radiation hardening for stabilizing gate threshold potential of MOS devices
[NASA-CASE-GSC-11425-2] 23 p2764 N73-32114
Service life and reliability of radiation hardened lithium doped solar cells
23 p2859 N73-32840

**HARDENING [MATERIALS]**
NT COLD HARDENING
NT HOT PRESSING
NT NITRIDING
NT PRECIPITATION HARDENING
NT PULSE HEATING
NT SHOT PEENING
NT STRAIN HARDENING
NT WORK HARDENING
Concentration of solute atoms, interaction range between solute atoms and distortion, and interaction strength of solid solution hardening
[NASA-TT-F-14711] 02 p0137 N73-11112
Hardened high strength steel for making wear resistant metal cutting tools
[AD-747711] 03 p0308 N73-12511
Relationship of stress-strain rates and loading histories on material hardening
03 p0360 N73-12936
Hardening characteristics of alkali halides selected as laser window materials
[AD-749867] 05 p0559 N73-14545
Solid solution hardening in alloys of niobium-hafnium, niobium-tungsten, and niobium-tantalum
[COO-916-25] 05 p0587 N73-14774
Oxidation kinetics for nickel and its hardened compositions
13 p1542 N73-22500
Irradiation strengthening and fracture embrittlement of A533-B steel and arc weldment metal
[HEDL-SA-323] 16 p1969 N73-25931
Process of density change in epoxy bonding agents throughout curing process
[RAE-LIB-TRANS-1686] 17 p2049 N73-26576
Dynamic spring analysis for measuring hardening reaction of polymers
[RAE-LIB-TRANS-1698] 17 p2049 N73-26577
Preterrestrial shock effects, shock hardening in iron meteorites, and parent bodies
19 p2342 N73-28840
Analysis of properties of copper, titanium, and nickel specimens following hardening by shock waves at pressures up to 1,200 kilobars
[NLL-RTS-8047] 20 p2428 N73-29500
Analysis of variations in hardness and microstructure of metals subjected to shock wave pressures
[NLL-NEL-TT-2489-[6075.461]]
20 p2429 N73-29514

**HARDENING [SYSTEMS]**
Systems analysis and evaluation of perimeter acquisition radar equipment for use with Safeguard Antiballistic Missile System - Vol. 1B
[AD-748060] 03 p0267 N73-12161
Specifications for design of P-channel MOS computers
[AD-759189] 16 p1884 N73-25249

**HARDNESS**
NT MICROHARDNESS
Hardness and physical characteristics of titanium sponge with low residual chloride concentration after vacuum separation
[JPRS-58347] 09 p1048 N73-18544
Solutioning and aging reactions and effects on microstructure and hardness of niobium-based alloys
[AD-752930] 09 p1049 N73-18558
Environment-sensitive hardness effects on drilling and machining aluminum oxides
[AD-753276] 09 p1053 N73-18586
Effect of molybdenum addition on physicomechanical properties of titanium-carbon-nickel composite alloys
[NLL-LTI-746-1422-[9022.401]]
15 p1797 N73-24565
Effects of heat treatment on Brinell hardness of Co-Be alloy system
[RFP-TRANS-122] 17 p2044 N73-26541
Structural properties of dual hardness steel armor with high hardness and high carbon frontal plates
[AD-759506] 17 p2047 N73-26561
Hard materials and material removal processes
[PB-221907/9] 22 p2690 N73-31546
Hard materials and material removal processes
[PB-221908/7] 22 p2690 N73-31547

**HARDNESS TESTS**
X ray diffraction analysis on microstructure defects in explosively loaded copper germanium alloy
[COO-1431-15] 10 p1173 N73-19541
Grinding wheel hardness determined from modulus of elasticity calculation
[CRIF-NT-9] 13 p1530 N73-22401
Hot hardness characteristics of ausformed AISI M-50, Matrix 2, WD-65, modified AISI 440-C, and Super Nitralloy
[NASA-TN-D-7244] 15 p1791 N73-24517

**HARDWARE**
Control and coordination requirements for fabrication of devices in the thermonuclear research program
[B-159687] 03 p0332 N73-12703
Hardware phase of digital capacitance measuring system
[REPT-2873-2143-116] 15 p1754 N73-24218
Hardware design, implementation, and test results of two wideband channel accommodation
[NASA-CR-124267] 16 p1875 N73-25182
Coaxial connector for standard hardware program
[AD-758649] 16 p1882 N73-25233
Qualification plan for the Apollo ultraviolet spectrometer experiment, revision
[NASA-CR-128572] 16 p1916 N73-25503

**HARDWOOD FORESTS**
U FORESTS

**HARMONIC ANALYSIS**
NT TESSERAL HARMONICS
NT ZONAL HARMONICS
Harmonic functions for determining currents and voltages in nonlinear electrical circuit
[AD-748231] 03 p0276 N73-12243

New harmonic constant computed for Adriatic Sea harbors
07 p0858 N73-16961
Harmonic analysis for predicting long term artificial satellite orbital motion
10 p1178 N73-19579
Computation of mean gravity anomalies from potential coefficients
[AD-754245] 11 p1290 N73-20472
Spherical harmonic analysis of Cosmos-321 geomagnetic survey
14 p1659 N73-23463
Micron output increase of Nd YAG laser to pump optical parametric oscillator through visible spectrum
[AD-756809] 14 p1673 N73-23577
Harmonic analysis of low altitude disturbances in geomagnetic fields
17 p2017 N73-26308
Temperature dependence of second-order elastic constants of cubic crystalline materials derived on basis of quasiharmonic anisotropic continuum model
24 p2968 N73-33717

**HARMONIC EXCITATION**
Interaction characteristics of harmonic forcing excitation and panel flutter
01 p0113 N73-10932
Calculation of harmonic vibrations of elastic rectangular plates supported at two edges and reinforced vertically with eccentric ribs
[AD-748906] 04 p0483 N73-13944
Lateral bending torsion vibrations of thin cantilever beam under parametric excitation
[AD-750546] 06 p0727 N73-15934

**HARMONIC FUNCTIONS**
Closed form solution using four harmonic functions for elastic solid with plane crack subjected to concentrated shears parallel to edge of crack
[NASA-CR-112317] 13 p1585 N73-22848
Velocity potential solution of heavy incompressible liquid wave motion
[AD-758251] 15 p1769 N73-24331
Tables on harmonic coefficients of isostatic reduction potential U
[NASA-TM-X-66292] 18 p2145 N73-27334

**HARMONIC GENERATIONS**
Direct generation of far infrared power through laser action on rotational transitions in molecular gases
[AD-745984] 02 p0182 N73-11476
Effects of harmonics strengths on voltmeter reading accuracy
[NLL-ESB-TRANS-499-[3810.97]]
04 p0419 N73-13412
Third harmonic generation by indium antimonide magnetoplasma in presence of dc magnetic field
13 p1562 N73-22659
Theory for third harmonic generation due to broad band optical pulses in picosecond time region
[AD-757211] 14 p1693 N73-23742
Harmonic generation in electromagnetic wave propagating in isotropic dielectric
[AD-758911] 16 p1877 N73-25198
Harmonic generation of high power tunable lasers
[AD-760018] 17 p2042 N73-26520

**HARMONIC GENERATORS**
Tunable parametric oscillator using infrared pumping for ultraviolet frequency generation
[AD-756910] 13 p1561 N73-22650

**HARMONIC MOTION**
Influence of various aerodynamic forces on rectangular wing performance with harmonic movement parallel to sieve flow movement
12 p1361 N73-21043

**HARMONIC OSCILLATION**
Pressure measurements on harmonically oscillating wing-tailplane configurations in incompressible speed range noting wind tunnel tests on aircraft models
[DLR-FB-71-52] 04 p0373 N73-13033
Mathematical model of unsteady pressure distribution on harmonically oscillating slender cruciform wing and cylindrical body configurations
[DLR-FB-71-87] 06 p0615 N73-14990
Measurement of unsteady pressures developed on harmonically oscillating wing planform in three dimensional compressible flow
[DLR-FB-72-55] 09 p0980 N73-18007
Procedures for calculating velocity potential and pressure distribution of planforms oscillating harmonically in supersonic flow
[FOK-X-440] 11 p1231 N73-19994
Operating characteristics of avalanche diode oscillator circuit high efficiency TRAPATT modes
[NASA-CR-131399] 11 p1264 N73-20258
Analysis of aerodynamic loading for symmetrically tapered wings describing simple harmonic pitching oscillations of low frequency in supersonic flow
[ARC-R/M-3298] 15 p1728 N73-24019
Harmonic oscillator quark model of hadrons with relativistic internal velocities for quarks
[LPTHE-73/15] 20 p2456 N73-29739
Computation of periods, wavelengths, and amplitudes of oscillations in equatorial flows and particle trajectories within flows by using inertial motion equations
22 p2666 N73-31361
Characteristics of flow about spherical body undergoing rectilinear, sinusoidal oscillations in viscous, incompressible fluid
23 p2773 N73-32180
Theoretical and experimental analysis of flow induced by harmonic oscillation of rods with arbitrary cross sections containing incompressible, viscous, Newtonian fluid
23 p2774 N73-32183

**HARMONIC OSCILLATORS**
Noncommuting observables in quantum detection and estimation theory, and application to analysis of coherent signal in harmonic oscillator
[NASA-CR-129694] 04 p0449 N73-13664
Development of numerical procedures for determining velocity potential on triangular wing oscillating harmonically in supersonic flow
[ARC-R/M-3229] 16 p1854 N73-25023

**HARMONIC RADIATION**
Propagation of axisymmetric harmonic waves across interface of two semi-infinite rods composed of different isotropic materials
[AD-746721] 02 p0239 N73-11948
Synthesis of monopulse angular coordinate meters of harmonic and noiselike radiation
20 p2419 N73-29440

**HARMONICS**
NT HARMONIC EXCITATION
NT HARMONIC GENERATIONS
NT HARMONIC OSCILLATION
NT SPHERICAL HARMONICS
NT TESSERAL HARMONICS
NT ZONAL HARMONICS
Evaluation of 15th order harmonics by analysis of orbit decay of Ariel 3, Transit 1b, Cosmos 373 and Cosmos 387 satellites
[RAE-TR-72115] 05 p0597 N73-14851
Accuracy of harmonics of diurnal density variations in thermosphere determined from satellite drag data and Jacchia empirical atmospheric model
[NASA-TM-X-66160] 07 p0790 N73-16427
Derivation of equations governing temporal and spatial variation for amplitudes and phase of capillary and gravity waves in case of second harmonic resonance
[AD-756218] 13 p1513 N73-22262

**HARNESSES**
Design, development, and evaluation of aircrew restraint system for forward-facing, nonejection seat for military aircraft
[AD-746631] 02 p0128 N73-11038
Performance tests of crash protective seat belts using energy absorbers to allow system to yield at constant force
[ARL/SM-340] 06 p0619 N73-15023

**HARRIER AIRCRAFT**
Post-stall aerodynamic characteristics of Harrier GR-1 aircraft and development of lift augmenting devices
06 p0618 N73-15014
Design concept, operational performance, and military employment of AV-8A Harrier aircraft
18 p2103 N73-27005

**HARTMANN NUMBER**
Numerical solution for magnetohydrodynamic pipe flow with laminar separation at higher Hartmann number
[AD-748766] 04 p0456 N73-13719
Streaming flow of viscous fluid past sphere in uniform magnetic field at low Hartmann numbers
[AD-755060] 11 p1329 N73-20784

**HARTREE APPROXIMATION**
Self-consistent Pauli corrections in Brueckner-Hartree-Fock calculations
[NASA-TM-X-68197] 10 p1193 N73-19704
Hartree approximation of extra conductivity in quasi-superconducting thin films considering nonlinear external field effect
[LNF-72/76] 15 p1821 N73-24758

**HARTREE-APPLETON APPROXIMATION**
U HARTREE APPROXIMATION

**HARTREE-FOCK APPROXIMATION**
U HARTREE APPROXIMATION

**HASTELLOY (TRADEMARK)**
Effects of high temperature brazing and thermal cycling on mechanical properties of Hastelloy X
[NASA-TM-X-2704] 04 p0433 N73-13529
Creep rupture tests of Hastelloy-X tubes at high temperatures and internal helium pressures to determine service life
[NASA-TM-X-2727] 08 p0932 N73-17629
Plasma arc welding procedure for Hastelloy seams of isotopic strontium titanate fuel capsule
[CONF-720917-1] 10 p1166 N73-19489
Stainless steel and Hastelloy corrosion by boron trifluoride, air, and argon mixtures
[ORNL-TM-4172] 24 p2892 N73-33087
Effect of FeF2 addition on Hastelloy N compatibility with LiF-BeF2-UF in low temperature convection loop system
[ORNL-TM-4188] 24 p2936 N73-33444

**HAWAII**
Sources and dispersal patterns of suspended sediments in nearshore surface waters of Northeast Pacific Ocean and Hawaiian Islands based on ERTS-1 imagery
[E72-10271] 03 p0291 N73-12370
Radiation parameters of VLF transmitting station NPM, Lualualei, Hawaii with antenna operating in dual or parallel east and west array configuration
[AD-748177] 04 p0390 N73-13172
Uncorrected and barometer-corrected, cosmic ray, NM-64 neutron monitor data from Kula, Hawaii, Jan.-Dec. 1971
[AECL-4161] 04 p0467 N73-13804
Diurnal electron content tables obtained at Hawaii during 1971
07 p0789 N73-16419
Dispersal patterns of suspended particles in nearshore surface waters of northeast Pacific Ocean and Hawaiian Islands
[E73-10314] 09 p1023 N73-18346
Volcano and earthquake surveillance network in Alaska, California, Washington, Hawaii, El Salvador, Nicaragua, Iceland, and Guatemala
[E73-10337] 09 p1025 N73-18365
Sources and dispersal patterns of suspended particulates in nearshore surface waters of northeastern Pacific Ocean and Hawaii
[E73-10487] 12 p1396 N73-21323
Annual, monthly, and hourly rainfall for Hilo, Hawaii
[UHMET-72-03] 12 p1422 N73-21527
Effect of magnetic induction anomaly on magnetotelluric fields in Oahu, Hawaii
[PB-214444/2] 16 p1908 N73-25440
Application of ERTS-1 data for development and operation of volcano surveillance network
[E73-10711] 17 p2018 N73-26318
Sources and dispersal patterns of suspended particles in nearshore surface waters of San Francisco Bay and Gulf of Farallones
[E73-10788] 18 p2137 N73-27264
Development of volcano surveillance and early warning system using ERTS-1 data collection system
[PAPER-G9] 19 p2264 N73-28240
Format conversion of meteorological data tapes of Hawaii
[PB-220452/7] 21 p2515 N73-30179
Prototype DCP volcano surveillance network in Washington, Nicaragua, California, Guatemala, Hawaii, El Salvador, Iceland, and Alaska
[E73-11024] 22 p2662 N73-31328
Timber identification and inventory and forest management in Colorado, Georgia, Black Hills, California, and Hawaii from ERTS-1 imagery
[E73-11051] 23 p2779 N73-32227

**HAWKER P-1127 AIRCRAFT**
U P-1127 AIRCRAFT

**HAWKER SIDDELEY AIRCRAFT**
NT COMET 4 AIRCRAFT
NT GA-5 AIRCRAFT
NT HARRIER AIRCRAFT
NT P-1127 AIRCRAFT
NT VULCAN AIRCRAFT
Operational and air transport characteristics of civil V/STOL aircraft
[NASA-TT-F-14619] 04 p0371 N73-13012

**HAWKEYE AIRCRAFT**
U E-2 AIRCRAFT

**HAZARDS**
NT AIRCRAFT HAZARDS
NT FLIGHT HAZARDS
NT METEOROID HAZARDS
NT OPERATIONAL HAZARDS
NT RADIATION HAZARDS
NT TOXIC HAZARDS
Application of ERTS-1 imagery to fracture related mine safety hazards in coal mining industry in Indiana
[E72-10193] 01 p0046 N73-10372
Analysis of potential hazards caused by carrying experimental equipment on Earth Orbit Shuttle and recommendations for eliminating or reducing hazards-Vol.2 Pt.2
[NASA-CR-129103] 02 p0231 N73-11873
Analysis of hazards involved in transporting experimental equipment on space shuttle and recommended precautionary measures - Vol. 3 Pt. 2
[NASA-CR-129100] 02 p0231 N73-11876
ERTS-1 imagery of permafrost and geologic hazards in Alaska
[E72-10247] 03 p0289 N73-12347
Orbiting propellant depot safety hazards - management summary
[NASA-CR-123385] 03 p0356 N73-12898
Orbiting propellant depot safety hazards and interactions between depot and space vehicle - technical discussion
[NASA-CR-123384] 03 p0356 N73-12899
Model for awarding hazardous pay to employees
08 p0876 N73-17095
Application of ERTS-1 imagery to fracture related mine safety hazards in coal mining industry in Indiana and Illinois
[E73-10371] 10 p1151 N73-19366
Evaluation of welding processes, and health hazards in electron beam welding of beryllium
[JPRS-58148] 10 p1171 N73-19528

Health hazards in using electron beams for welding beryllium alloys
10 p1172 N73-19531
ERTS-1 imagery of permafrost and geologic hazards in Alaska
[E73-10495] 12 p1397 N73-21331
Safety hazards related to ignition and combustion in oxygen systems
[NASA-TM-X-68223] 12 p1464 N73-21861
Hazards of exposure to noise, fumes and vapors in military environment
14 p1723 N73-23985
ERTS-1 imagery of permafrost and geologic hazards in Alaska
[E73-10601] 15 p1772 N73-24362
Application of ERTS-1 imagery to fracture related mine safety hazards in coal mining industry in Indiana
[E73-10776] 18 p2135 N73-27252
Application of Skylab EREP imagery to fracture-related mine safety hazards and environmental problems in mining
[E73-10802] 18 p2138 N73-27277
Identification of fire hazards in San Pablo test site area in California using ERTS-1 data and aerial photography
[PAPER-A18] 19 p2261 N73-28225
Application of ERTS-1 imagery to study of fracture-related safety hazards in Indiana coal mining industry
[E73-10970] 21 p2533 N73-30311
Hazard identification based on energy interrelationships and integrated control technique
[NASA-TM-X-64782] 22 p2737 N73-31918
Military treatment and disposal of high energy materials
[AD-764534] 23 p2858 N73-32835
Application of ERTS-1 imagery to fracture related coal mine safety hazards and environmental problems in mining in Indiana
[E73-11148] 24 p2918 N73-33302

**HAZE**
Results of computations pertaining to brilliance of atmospheric haze and daytime sky
[NASA-TT-F-14421] 01 p0049 N73-10397
Analysis of haze aerosols in rural and urban atmospheres
[PB-212609] 07 p0816 N73-16613
Histograms of ERTS-1 MSS observations of haze
[E73-10924] 20 p2398 N73-29273
Remote haze monitoring using ERTS-1 MSS
[E73-11029] 22 p2662 N73-31333

**HAZE DETECTION**
Optimized method of remote haze detection using ERTS-1 imagery
[E73-10344] 10 p1148 N73-19343
Computer program for analysis of ERTS-1 MSS imagery of haze in Southern California test area
[E73-10346] 10 p1148 N73-19345
Optimization of haze detection by ERTS-1 MSS imagery
[E73-10499] 12 p1398 N73-21335
Analysis of ERTS-1 imagery of Los Angeles, California area to determine effects of haze on accuracy of ground truth data
[E73-10691] 16 p1902 N73-25384

**HBNQ**
U NITROGUANIDINE

**HC-1 HELICOPTER**
U CH-47 HELICOPTER

**HCN LASERS**
HCN laser interferometer for electron density measurements on helium plasma
[NP-19595] 11 p1328 N73-20774
HCN laser study of coherent scattering from waves in plasma confinement and heating experiments
[IPP-4/39] 12 p1435 N73-21631

**HEAD [ANATOMY]**
NT CRANIUM
Biodynamic response of human head and neck to impact acceleration
[AD-747988] 04 p0382 N73-13106
Mass, volume, center of mass, and mass moment of inertia determined for head and head and neck of human body
[AD-762581] 20 p2372 N73-29065

**HEAD [FLUID MECHANICS]**
Measurement of laminar fluid flow through orifice meters to determine discharge coefficients and head losses
[NLL-NEL-TT-2457-[6075.461]]
20 p2386 N73-29169

**HEAD MOVEMENT**
Development of mathematical model for slow phase rotational nystagmus induced by head movements
[AMRU-R-71-3] 02 p0131 N73-11065
Apparent object movement due to optical distortion produced by head movement under water
[AD-749319] 05 p0502 N73-14086
Anti-compensatory oculomotor responses in human visual tracking and vestibulo-ocular mechanism during rotational head movement in flight
06 p0633 N73-15140
Visual and vestibular effects in human oculomotor response during head rotation in yaw and roll
06 p0633 N73-15147
Compensatory oculogravic response of eye movement direction during slow head rotation
06 p0634 N73-15148
Predictive control of human eye tracking movements in response to visual stimuli
06 p0634 N73-15149

**HEAD-UP DISPLAYS**
Performance evaluation of airborne audio-video recording system as training device in A-7D tactical fighter
[AD-744041] 01 p0021 N73-10161
Survey of electronic cockpit displays, noting human factors, head-up, head-down and eyeglass display, and related technology
[DLR-FB-72-43] 01 p0058 N73-10474
Evaluation of head-up display instrument for providing aircraft vertical guidance during landing approach to comply with noise abatement procedures
[NASA-TM-X-62187] 09 p0982 N73-18021
Human factors engineering for flight control/display system with on-line terminal
[AD-754916] 11 p1250 N73-20148
Development of heads-up flight data display for aircraft approach and landing during all conditions of visibility
14 p1688 N73-23702
Application of hologram optical element to pilot head-up display
[AD-758057] 15 p1744 N73-24139
Daytime fog simulator system modifications
[FAA-RD-73-130] 22 p2647 N73-31208
Flight simulation to determine effectiveness of head-up display for improving glide-slope tracking performance during steep visual approach of short takeoff aircraft
24 p2874 N73-32952

**HEADSETS**
U EARPHONES

**HEALTH**
NT HEALTH PHYSICS
NT MENTAL HEALTH
Application of remote sensing techniques to public health
[NASA-CR-129822] 05 p0500 N73-14069
Industrial model for leave and overtime taking behavior of employees exposed to peak work activity periods in relation to health, demography, and job variables
08 p0872 N73-17055
Conference on occupational and environmental medical services provided to NASA employees
[NASA-TM-X-69074] 08 p0874 N73-17078
Management of NASA employee health problems by automated medical system
08 p0874 N73-17079
Chronic disease health trends and mortality rates in employee population of NASA Goddard Space Flight Center
08 p0875 N73-17086
Feasibility of effective exercise and health evaluation and enhancement program for NASA employees
08 p0875 N73-17091
Medical services of operating environmental health program for industrial workers
08 p0876 N73-17093

**HEALTH PHYSICS**
Ionizing radiation health standards and safety measures around nuclear installations
[EUR-4800-D-F-I-E-PT-1] 01 p0082 N73-10679
Biological effects of microwave irradiation on humans - literature review
[UR-3490-29] 06 p0630 N73-15120
Remote sensing techniques for detection and prevention of Rocky Mountain spotted fever, Encephalitis, Malaria, and Red Tide environmental health problems
[NASA-CR-128727] 07 p0745 N73-16060
Abstracts on radiation and health physics
[BNWL-1651-VOL-2-PT-2] 07 p0746 N73-16069
Public health exposure limits to nitrogen oxide, hydrogen chloride, and hydrogen fluoride air pollutants
[AD-751438] 07 p0748 N73-16084
Public health exposure limits for air pollutants
[AD-751437] 07 p0749 N73-16088
Cardiac toxicity of fluoroalkane gases for propelling aerosols in industry and household applications
[AD-751425] 07 p0749 N73-16090
Multiphase health screening and medical history questionnaire for preventive/occupational physical examinations
08 p0871 N73-17052
Medical concepts and functional management in NASA Environmental Health Program
08 p0872 N73-17056
Physical exercise effects on health of NASA personnel
08 p0873 N73-17069
Industrial health measures and environmental control to insure worker productivity
08 p0874 N73-17077
Effects of chemical fire extinguishing agents containing bromotrifluoromethane on cardiovascular and nervous systems of dogs, monkeys, and baboons
[AGARD-R-599] 08 p0877 N73-17106
Survey of industrial hygiene and safety in Air Forces operations
[AD-751897] 08 p0880 N73-17126
Toxicity of long term methyl isobutyl ketone exposure in dogs, monkeys, mice, and rats
[NASA-TM-X-69100] 09 p0996 N73-18130
Annual report 1971-1972 of Interuniversitair Reactor Institute in Netherlands
10 p1195 N73-19721
Proceedings of conference on radiation safety and protection in industrial applications
[DHEW-PUBL-[FDA]73-8012] 24 p2951 N73-33574
Chronology of radiation protection methods instituted in industrial plants to show specific procedures and reasons for enforcing protective measures
24 p2952 N73-33575

**HEAO**
Large orbiting X ray telescope with high resolution mirror design
[NASA-CR-124001] 10 p1158 N73-19424
Evaluation of control moment gyro steering laws for use on HEAO spacecraft
[NASA-TM-X-64727] 11 p1321 N73-20718
Handbook on scintillation counters with emphasis on cesium iodide scintillators for HEAO experiments
[NASA-TM-X-64741] 13 p1530 N73-22398
Engineering specifications for proportional counter hodoscope to be flown on HEAO A mission
[NASA-TN-D-7317] 15 p1828 N73-24816
HEAO-A experimental design and equipment for mapping celestial X ray sources and spectral analysis over 0.2 to 150 keV
17 p2085 N73-26866
HEAO-A integrated modulation collimator experiment for determining angular sizes and celestial position of X ray sources
17 p2085 N73-26867
HEAO-B Bragg crystal spectrometer for stellar X ray spectral analysis
17 p2085 N73-26870
HEAO-B cosmic ray experiment for diffuse sky brightness determination
17 p2085 N73-26871
HEAO-C X ray focusing telescopes for spectrometric and polarization studies
17 p2085 N73-26872
HEAO-C soft X ray telescope
17 p2085 N73-26873
X ray background experiment on HEAO-A
[AD-760364] 17 p2086 N73-26875
Natural evironment criteria for high energy astronomy observatory
[NASA-TM-X-64784] 24 p2979 N73-33807

**HEARING**
NT ACOUSTIC FATIGUE
NT BINAURAL HEARING
Noise effects on hearing conservation in aircrew and ground support personnel of aerospace operations
08 p0876 N73-17101
Effects of light aircraft noise on hearing
[NASA-CR-130987] 09 p0992 N73-18095
Voice and hearing in system of acoustic orientation of animals
[NLL-DRIC-TRANS-3056-[3623.66]]
15 p1739 N73-24101
Evaluation of hearing protectors for general aviation aircraft
[NASA-CR-133303] 18 p2112 N73-27078

**HEARING LOSS**
U AUDITORY DEFECTS

**HEART**
NT CARDIAC VENTRICLES
NT MYOCARDIUM
Gaussian curve simulation of multiple-dipole model of ventricular depolarization
[TH-71-E-25] 03 p0261 N73-12116
Power sources and requirements for human artificial hearts
[COO-2155-4] 05 p0503 N73-14095
Microscopic morphological changes in dog cardiac muscle after chronic gamma irradiation
20 p2366 N73-29027

**HEART DISEASES**
Physical exercise and physical fitness program for preventing and treating human coronary heart disease
08 p0871 N73-17051
Personality, occupation, and job stress effects on physiological risk factor in human coronary heart disease
08 p0871 N73-17054
Dynamic electrocardiography in periodic health examinations for detection of cardiac abnormalities
08 p0873 N73-17065
Dynamic electrocardiographic standardization for detecting cardiac risk factor in personnel
08 p0873 N73-17066
Physical exercise effects on health of NASA personnel
08 p0873 N73-17069
Continuous monitoring of hypertension and hypercholesterolemia in NASA employees for prevention of heart disease and disability
08 p0873 N73-17072

Blood lipid diagnostic and therapeutic measures to prevent heart disease in humans
08 p0874 N73-17073
Blood pressure and cholesterol level screening for preventing heart diseases in flight crews of commercial airline
08 p0874 N73-17076
Risk scoring system for identifying subjects with high risk to coronary heart disease
08 p0874 N73-17080
Electrocardiographic stress testing for determining influence of occupational and other stresses on ischemic heart disease
08 p0875 N73-17082
Clinical analysis of relationship between VPB and mortality rate in patient with acute myocardial infractions
08 p0875 N73-17083
Precoronary care and sudden death prevention due to coronary disease in industrial workers
08 p0875 N73-17084
Latent coronary insufficiency detection in flying personnel using barochamber loading
13 p1480 N73-21988

**HEART FUNCTION**
Electronic instruments for continuous cardiovascular systems measurements
[NASA-TT-F-14492] 01 p0020 N73-10154
Changes in vectorcardiograms of atherosclerotic flying personnel after glucose testing
13 p1480 N73-21989
Development of instantaneous reading tachometer for measuring electrocardiogram signal rate
[NASA-CASE-MFS-20418] 15 p1785 N73-24473

**HEART RATE**
NT ARRHYTHMIA
NT BRADYCARDIA
Rhesus monkey heart rate during expercise using implanted ECG telemeters
[AD-744930] 01 p0011 N73-10089
Sleep stage classification analysis on heart rate data recordings
[AD-740946] 01 p0021 N73-10167
Construction of sonic boom simulators to determine effects of sonic boom on human heart reactions and analysis of human responses
[UTIAS-TN-180] 02 p0152 N73-11233
Electrocardiogram recordings on magnetic tape for computerized analysis
[AD-748105] 04 p0384 N73-13124
Threshold circuits with feedback channels for cardiac R-wave detection in electrocardiographic heart rate monitoring
[NASA-TN-D-7152] 06 p0635 N73-15158
Changes in electrocardiographs of Rhesus monkeys as function of age
[NASA-TT-F-14675] 07 p0745 N73-16062
Long term exercise effects on cardiovascular response in NASA personnel with periodic ergometric evaluation
08 p0873 N73-17067
Clinical analysis of relationship between VPB and mortality rate in patient with acute myocardial infractions
08 p0875 N73-17083
Effects of prolonged bed rest on body temperature and heart rate periodicity in man
09 p0994 N73-18113
Mental and cardiovascular acceleration stress effects on heart rate studied by beta adrenergic blockage
10 p1122 N73-19149
Cardiac systole kinematics in humans exposed to hypoxic atmosphere
13 p1479 N73-21986
Diurnal cardiac rhythm fluctuation for cardiovascular evaluation of flight personnel
13 p1480 N73-21997
Metabolic changes and cardiac output of humans in hypokinetic bed rest study
13 p1482 N73-22013
Development of instantaneous reading tachometer for measuring electrocardiogram signal rate
[NASA-CASE-MFS-20418] 15 p1785 N73-24473
Inflight heart and respiratory rate recording of pilots, using nose clip transducers
19 p2226 N73-27953
Influence of He, N2, and N2O environments on physiological parameters of rats
20 p2365 N73-29019
Exercise effects on human heart rate and oxygen uptake
20 p2365 N73-29020

**HEAT**
NT DRY HEAT
NT HEAT OF DISSOCIATION
Steady state heat and mass transfer in suction boiling
15 p1842 N73-24923
Effect of sleep deprivation and heat stress on human performance in visual and auditory tasks
[OES-8/72] 22 p2624 N73-31024

**HEAT BALANCE**
Analysis of combustion liner wall temperatures under steady-state and convective heat balance conditions and comparison with experimental values
[NASA-TM-X-2711] 06 p0730 N73-15959
Analysis of tidal currents, turbulent diffusion, and local shears in currents found in Trinity Bay, Texas
[NASA-CR-128734] 08 p0916 N73-17510
Development of space shuttle scale model for thermodynamic analysis of internal and external heat flow fields
[NASA-CR-128849] 10 p1215 N73-19882
Man induced changes in earth climate by environment pollution and heat production
[PB-213676/2] 14 p1613 N73-23074
Heat generation associated with pneumatic tire operating under various conditions
[NASA-CR-121239] 18 p2205 N73-27799
Development of numerical method for determining long wave radiation balance of atmosphere based on effective surface radiation
20 p2401 N73-29295

**HEAT BUDGET**
NT ATMOSPHERIC HEAT BUDGET
Measurement of diurnal heat budget in tropical Atlantic surface layers
07 p0857 N73-16953
Analysis of energy conservation constraints on circulation of Southern Hemisphere atmosphere and oceans based on radiant, latent, and sensible heat energy transfers
[METEOROL-STUDY-26] 09 p1027 N73-18387
Sea ice dynamics, heat and mass budget of Arctic sea ice, desalinization, thermal and mechanical stresses, bearing capacity of floating ice, and interaction of oil and ice
[AD-754118] 11 p1290 N73-20463
Direct broadcasting TV satellite solar arrays, and heat budget subsystems
[DGLR-PAPER-73-051] 24 p2986 N73-33865

**HEAT CAPACITY**
U SPECIFIC HEAT

**HEAT CONDUCTION**
U CONDUCTIVE HEAT TRANSFER

**HEAT CONTENT**
U ENTHALPY

**HEAT DISSIPATION**
U COOLING

**HEAT DISSIPATION CHILLING**
U COOLING

**HEAT EFFECTS**
U TEMPERATURE EFFECTS

**HEAT ENGINES**
U ENGINES

**HEAT EQUATIONS**
U THERMODYNAMICS

**HEAT EXCHANGERS**
NT TUBE HEAT EXCHANGERS
Development of computer program for simulating performance of space radiator to account for transient and steady state performance
[NASA-CR-128594] 01 p0108 N73-10091
Numerical analysis of simplified radiator system to predict steady state system performance and to optimize system parameters for minimum area or minimum mass
[NASA-CR-128596] 01 p0108 N73-10892
Transient heat transfer analysis of space radiator heat rejection system under conditions of aerodynamic heating, solar, albedo, and planetary radiation
[NASA-CR-128595] 01 p0117 N73-10964
Analysis of critical density heat flows during internal heating of annular channels
[AD-743681] 01 p0118 N73-10972
Analysis of laminar film condensation on inside of truncated, rotating cone and noncapillary, rotating heat pipe with distilled water as working fluid
[AD-743730] 01 p0118 N73-10973
Pressure drop in plate heat exchangers with corrugations
[NLL-RTS-7505] 02 p0241 N73-11960
Analysis of thermomechanical compressor to include principles of operation and specific applications
05 p0552 N73-14482
Preliminary design of heat exchanger and duct assembly for Brayton cycle space power system
[NASA-CR-121011] 05 p0605 N73-14923
Reduction in heat exchanger size with use of gas mixtures in closed gas turbine installations
[AD-750905] 06 p0715 N73-15836
DESIGN OF HEAT EXCHANGERS FOR FLUID VAPORIZATION
[CEA-CONF-2010] 06 p0731 N73-15960
Condensation of gas phase of fast flowing droplet gas mixture of potassium and application to operating magnetohydrodynamic generators
[NASA-TT-F-14609] 07 p0770 N73-16254
Determination of heat transfer and flow friction characteristics of fibrous metals for application to heat exchanger design
[AD-751633] 07 p0856 N73-16937
Surface cooling method for very high frequency power transistor using heat pipe techniques
[AD-752076] 08 p0889 N73-17200
Acoustic amplification in fluid circuit and reactor heat exchanger vibration
[NLL-CE-TRANS-5913-[9022.09]]
12 p1390 N73-21271
Convective heat transfer and heat exchange during phase transformation in chemically reacting systems
[AD-756095] 13 p1488 N73-22066
Calculation and design of heat transfer apparatus for viscous liquids, liquid fuel, and lubricating oils
[AD-756947] 13 p1592 N73-22908
Heat exchange between gas and turbine cascade blades of gas turbine engine
[AD-756101] 14 p1701 N73-23804
Performance of gas-loaded variable conductance heat pipe with effect of gravity
[AD-757684] 14 p1720 N73-23956
Application of laminar flow solutions for heat transfer and flow friction to design of heat exchangers
16 p1886 N73-25266
Thermal conductivity of rocket motor walls with variable heat exchange coefficients
[AD-759815] 16 p1958 N73-25836
Design and tests of breadboard cryogenic hydrogen and Freon heat exchanger for space shuttle missions
[NASA-CR-128987] 17 p2096 N73-26959
Cryogenic heat exchanger for removal of waste heat from spacecraft environmental control life support system
[NASA-CR-124301] 18 p2111 N73-27071
OAO 3 flight test on heat pipe cooling efficiency during weightlessness
18 p2208 N73-27826
Performance evaluation of model energy separators
[AD-764585] 23 p2798 N73-32381
Development and characteristics of device for removing condensate from heat exchangers with straight through gas flow
[NASA-CASE-MSC-14143-1] 23 p2856 N73-32823
Development, fabrication, and evaluation of heat pipe thermal conditioning panels for temperature control of spacecraft electronic equipment - Technical Report
[NASA-CR-124451] 24 p2991 N73-33898
Development, fabrication, and evaluation of heat pipe thermal conditioning panels for temperature control of spacecraft electronic equipment - Executive Summary
[NASA-CR-124453] 24 p2991 N73-33899

**HEAT FLOW**
U HEAT TRANSMISSION

**HEAT FLUX**
Analytical prediction of transient surface heat flux and temperature on cooled turbine blade due to gas stream inlet temperature change
[NASA-TN-D-7101] 06 p0730 N73-15955
Vertical radiation heat flux profiles and spectral distribution
09 p1059 N73-18632
Analysis of forced convection film, transition, and nucleate boiling regions for water with application to boiling water reactor cooling systems
[DSR-73645-80] 13 p1590 N73-22892
Extension of hydrodynamic theory of peak and minimum pool boiling heat fluxes to include influence of viscosity on instability mechanisms with application to film boiling
[NASA-CR-2270] 18 p2206 N73-27808
Measurements of pressure, voltage, and wall heat flux in wall-stabilized arc heater
[NASA-TM-X-69571] 20 p2420 N73-29443
Influence of nonadiabatic processes particularly radiative heat influx on numerical weather forecasting
20 p2443 N73-29624
Computational methods for determining eddy momentum, heat, and fluxes in water-adjoining layer of atmosphere
20 p2445 N73-29637
Radiation and turbulent heat flux effects on variations of isobaric surface pressure and altitude in Northern Hemisphere
20 p2446 N73-29651
Surface boundary layer temperature profiles and turbulent heat flux during onshore flow
[REPT-38] 21 p2524 N73-30239
Mean monthly values of turbulent heat and moisture fluxes over oceans
21 p2572 N73-30613
Viscous hydrodynamic instability theory of peak and minimum pool boiling heat fluxes
[NASA-CR-134492] 22 p2653 N73-31252
Heat to heat variation in fatigue and creep-fatigue behavior of AISI Type 304 stainless steel, and fatigue behavior of type 308 stainless steel weld material
[ANCR-1097] 24 p2936 N73-33450

**HEAT GAIN**
U HEATING

**HEAT GENERATION**
Handbook on radiant emission and absorption of combustion gases for application to design of rocket combustion chambers and exhausts, turbojet engines, and industrial furnaces
[NASA-SP-3080] 18 p2206 N73-27807
Extension of hydrodynamic theory of peak and minimum pool boiling heat fluxes to include influence

of viscosity on instability mechanisms with application to film boiling
[NASA-CR-2270] 18 p2206 N73-27808
HEAT MEASUREMENT
Calorimetric determination of atomic ordering effects in alloy Ni2Cr
06 p0683 N73-15558
Design and performance of heat camera using indium antimony and germanium mercury infrared detectors
[FOA-2-A-2540-52] 06 p0700 N73-15704
Proton magnetic resonance spectra and calorimetry of interactions between ions, inhibitors, and substrates with two ribonucleases
[BMVG-FBWT-72-7] 07 p0746 N73-16071
Thermodynamics of chemical species relative to aerospace technology including topics in chemical reaction kinetics and heat measurement
[AD-757518] 14 p1617 N73-23097
Calorimetric calibration method for commercial power monitor used with high power microwave generators
[PB-213970/7] 14 p1669 N73-23548
Construction and operation of calorimeters for heat of solution and low temperature heat capacitance measurements
[USGS-PP-755] 16 p1912 N73-25470
Specific heat measurements on rubidium tungsten bronze and aluminum film superconductors
18 p2184 N73-27636
Thermodynamic properties of solid Ni-Ga alloys at temperatures between 837 and 1100 K
[AD-762337] 19 p2311 N73-28588
Calorimetric measurement of laser output energy and power
[UCID-16214] 22 p2681 N73-31476
HEAT OF COMBUSTION
Optimal operational temperature for thermoelectric generator using organic fuel heat
[AD-762266] 19 p2223 N73-27932
HEAT OF DISSOCIATION
Mass spectra and dissociation energies of high temperature gaseous molecules containing aluminum
[NASA-TN-D-7123] 04 p0386 N73-13138
HEAT OF VAPORIZATION
Oscillatory combustion and fuel vaporization tests to determine thermodynamic properties of droplets under various conditions
[NASA-CR-120974] 02 p0242 N73-11971
Liquid-vapor state of aluminum during electron bombardment
[AD-754449] 11 p1253 N73-20171
HEAT PIPES
Analysis of laminar film condensation on inside of truncated, rotating cone and noncapillary, rotating heat pipe with distilled water as working fluid
[AD-743730] 01 p0118 N73-10973
Performance tests of OAO-C spacecraft heat pipes under thermal-vacuum conditions
[NASA-TM-X-66072] 02 p0242 N73-11967
Results of experiments with working model of electrodynamic heat pipe
[NASA-CR-114498] 03 p0363 N73-12960
Theoretical analysis for predicting onset of Kelvin-Helmholtz instability
[NASA-CR-114499] 03 p0363 N73-12961
Design, fabrication, and comparison of heat pipes for temperature control in meteorological satellite
[ESRO-CR-59] 05 p0606 N73-14929
Bibliography of heat pipe applications
[BIB-2-72] 06 p0729 N73-15951
Development of technology for design and application of self controlled, variable conductance heat pipes for spacecraft thermal control
[NASA-CR-114530] 06 p0730 N73-15957
Behavior of gas occlusions in arterial heat pipes
[NASA-CR-114531] 06 p0730 N73-15958
Relationship between laminar film condensation on inside of rotating non-capillary heat pipe and pipe heat transfer capabilities
[NASA-CR-130373] 07 p0854 N73-16926
Design, fabrication, and test of flight qualified heat pipe diode for Advanced Thermal Control Flight Experiment
[NASA-CR-114526] 08 p0968 N73-17915
Corrosion of heat pipes
[NASA-TT-F-14689] 08 p0969 N73-17918
Analysis of porous media of heat pipe wicks to determine effects on permeability and thermal conductivity of materials
10 p1222 N73-19938
Probabilistic design model for prediction of heat transfer rate for heat pipes
[AD-752057] 10 p1224 N73-19954
Production of iodine isotope by high energy bombardment of cesium heat pipe causing spallation reaction
[NASA-CASE-LEW-11390-2] 11 p1326 N73-20763
High power transcalent silicon semiconductor thyristor device including metallization techniques and heat pipe construction
[AD-755553] 13 p1502 N73-22174
Oxygen diffusion in gettered tantalum alloy heat pipes at startup
[NASA-TM-X-2793] 14 p1675 N73-23589
Accelerated life tests of copper/acetone heat pipe for meteorological satellite temperature control, including thermal cycling tests
14 p1719 N73-23948
Vaporization mechanisms and nucleate boiling in heat pipes with thin liquid films
[AD-757280] 14 p1720 N73-23955
Performance of gas-loaded variable conductance heat pipe with effect of gravity
[AD-757684] 14 p1720 N73-23956
Analysis of thermodynamic conditions for rapid start up of high temperature, gas loaded heat pipe
[NASA-TM-X-2840] 18 p2205 N73-27800
Feasibility analysis and prediction performance of constant temperature heat pipe for space applications
[ESRO-CR[P]-246] 18 p2207 N73-27810
Heat pipe production of high purity radioiodine for thyroid measurements
[NASA-CASE-LEW-11390-3] 19 p2248 N73-28128
Conductive heat pipes from laboratory to space
[NASA-TM-X-62290] 19 p2352 N73-28917
Design and tests of passive, feedback-controlled, variable conductance, gas loaded heat pipe
[NASA-TM-X-62293] 19 p2352 N73-28920
Comparative study of TWT and klystron amplifiers for use as power amplifiers in television broadcast satellites
[ESRO-CR[P]-269-VOL-3] 21 p2508 N73-30124
Capillary flow through partially saturated fibrous wicks in heat pipes
[AD-763427] 21 p2527 N73-30263
Methanol heat pipe using nitrogen gas for temperature control
[NASA-CR-114597] 21 p2606 N73-30884
Performance evaluation of heat transfer testing of heat pipes with thermal-vacuum and bench testing
[NASA-TN-D-7219] 22 p2728 N73-31827
Thermally assisted cavitation by localized fluctuations in capillary forces
[NASA-TM-X-70458] 22 p2728 N73-31834
Experimental and theoretical applications to electrohydrodynamic heat pipe research
[NASA-CR-114646] 22 p2729 N73-31839
Structural heat pipe for spacecraft wall thermal insulation system
[NASA-CASE-GSC-11619-1] 23 p2857 N73-32828
Collector/heat pipe cooled, externally configured thermionic diode for use in thermionic electric power source
[NASA-CR-135785] 24 p2954 N73-33600
Development, fabrication, and evaluation of heat pipe thermal conditioning panels for temperature control of spacecraft electronic equipment - Technical Report
[NASA-CR-124451] 24 p2991 N73-33898
Development, fabrication, and evaluation of heat pipe thermal conditioning panels for temperature control of spacecraft electronic equipment - Executive Summary
[NASA-CR-124453] 24 p2991 N73-33899
Cumulative bibliography of research and development projects conducted on heat pipe technology and applications
[NASA-CR-135953] 24 p2991 N73-33900
Bibliography of research projects on heat pipe, development, performance, and application - January through March, 1972
[NASA-CR-135956] 24 p2991 N73-33901
Bibliography of heat pipe research and development projects conducted during April through June 1972
[NASA-CR-135955] 24 p2991 N73-33902
Bibliography of heat pipe research and development projects conducted during July through September, 1972
[NASA-CR-135952] 24 p2991 N73-33903
Supplemental report and bibliographies of heat pipe research projects conducted during calendar year 1971
[NASA-CR-135951] 24 p2991 N73-33904
Bench and thermal-vacuum testing of superconductors and heat pipe systems to determine failure characteristics
[NASA-TN-D-7395] 24 p2992 N73-33909
HEAT PUMPS
Design and development of thermomechanical pump for transmitting warming fluid through fluid circuit to control temperature of spacecraft instrumentation
[NASA-CASE-NPO-11417] 15 p1790 N73-24513
Applications of heat pumps for recovery of unused heat in factories, air conditioned buildings, and refrigeration plants
[NLL-OA-TRANS-1264-(6196.3)]
15 p1842 N73-24921
HEAT RADIATORS
NT SPACECRAFT RADIATORS
Transient heat transfer analysis of space radiator heat rejection system under conditions of aerodynamic heating, solar, albedo, and planetary radiation
[NASA-CR-128595] 01 p0117 N73-10964
Parametric weight analysis of heat rejection systems for environmental control/life support system space shuttle orbiter
[NASA-CR-128735] 08 p0965 N73-17884
Boron-aluminum radiators for space shuttle orbiters
[NASA-CR-128805] 10 p1164 N73-19468
Spacecraft advanced radiator design system program for environmental control in long duration space flights
[NASA-CR-128913] 14 p1719 N73-23946
External heat transfer problems under space conditions
[NASA-TT-F-783] 21 p2605 N73-30879
HEAT REGULATION
U TEMPERATURE CONTROL
HEAT REJECTION DEVICES
U HEAT RADIATORS
HEAT RESISTANCE
U THERMAL RESISTANCE
HEAT RESISTANT ALLOYS
NT MOLYBDENUM ALLOYS
NT NIMONIC ALLOYS
NT NIOBIUM ALLOYS
NT OSMIUM ALLOYS
NT REFRACTORY METAL ALLOYS
NT RHENIUM ALLOYS
NT TANTALUM ALLOYS
NT TUNGSTEN ALLOYS
NT UDIMET ALLOYS
Suitability of directionally solidified eutectic alloys for high temperature fasteners, material properties, and fabricating methods
[NASA-CR-123919] 02 p0177 N73-11437
High temperature and fatigue tests to determine effects of heat resistant coatings on mechanical and physical properties of nickel-chromium-iron alloys
[NLL-TRANS-746-1236-(9022.401)]
02 p0185 N73-11500
Effect of sodium chloride on mechanical properties of superalloys at elevated temperature
[NASA-TM-X-64701] 02 p0186 N73-11510
Chromium superalloy damage and temperature effects
[NASA-TN-D-7073] 03 p0312 N73-12549
Superalloys from prealloyed powders at high temperatures
[NASA-CASE-LEW-10805-1] 04 p0425 N73-13465
Properties of refractory metals and application to construction of high temperature irradiation facilities
[EUR-4757] 04 p0434 N73-13540
Papers presented at conference on processing of superalloys
[AD-748159] 04 p0436 N73-13552
Influence of thermal stresses and loads on endurance properties of heat resistant alloys used to manufacture turbine blades
[AD-749752] 05 p0591 N73-14805
Fabrication and creep strength of precipitation hardened heat resistant alloys
[ITE-MITT-7/1972] 06 p0684 N73-15572
Kinetic and structural investigation of ST-4 titanium alloy oxidizability at 700 to 1000 C, unprotected and protected by silicon and molybdenum silicide coatings
[AD-750646] 06 p0686 N73-15585
Effects of oxidation resistant coatings on thin superalloy sections in high temperature environments
[NASA-CR-121115] 07 p0809 N73-16563
Improvement of high temperature eutectic alloy by compositional modification
[AD-752632] 08 p0934 N73-17644
Production of superalloy matrix-refrectory metal fiber composites by coextrusion of blended powders
[AD-753340] 09 p1054 N73-18593
Metallurgical investigation of deformation and fatigue using high temperature tests and stress-strain diagrams on heat resistant alloys
[JPRS-58180] 10 p1219 N73-19912
Cyclic deformation diagrams of heat resistant and austenitic steels
10 p1219 N73-19914
Refractory porcelain enamel passive thermal control coating for high temperature alloys
[NASA-CASE-MFS-22324-1] 12 p1416 N73-21471
Stress-rupture strength testing and principles of creep-rupture in heat resistant alloys
[JPRS-58760] 13 p1542 N73-22494
Extrapolating stress-rupture test results of heat resistant alloys
13 p1542 N73-22495
Investigation of creep rupture strength and plastic properties of heat resistant alloys
13 p1542 N73-22496
Sintering and heat resistance of nickel alloys
[JPRS-58779] 13 p1542 N73-22499
Oxidation kinetics for nickel and its hardened compositions
13 p1542 N73-22500
Sintering heat resistant nickel alloys
13 p1543 N73-22501
Mechanical properties and behavior of heat resistant alloys semiconductors, polymers and composite materials
[AD-755660] 13 p1549 N73-22552
Conference on high temperature corrosion of alloys for aerospace applications
[AGARD-CP-120] 14 p1675 N73-23597
High temperature corrosion scale for heat resistant alloys
14 p1676 N73-23598

Multicomponent diffusion theory as applied to oxidation, corrosion, and sulfation of complex heat resistant alloys
14 p1677 N73-23609
Comparison of cobalt alloys and nickel alloys relative to hot corrosion resistance
14 p1677 N73-23612
Methods of oxidation and corrosion resistance in refractory metal alloys used in gas turbine engines
14 p1678 N73-23617
NATO national reports on high temperature corrosion of aerospace alloys
14 p1678 N73-23618
Development of method for fabricating cermets and analysis of various compositions to show electrical and physical properties
[NASA-CASE-NPO-13120-1] 14 p1679 N73-23629
Direct casting for producing cast superalloy tungsten or columbium alloy fiber composites with high strength
[NASA-TM-X-2782] 15 p1798 N73-24572
Copper alloys with necessary heat resistance and electrical conductance for use as welding electrodes
[AD-758618] 15 p1800 N73-24590
Measurement of elastic moduli and compressive yield strength for Ni3[Al,X] alloy single crystals
16 p1927 N73-25589
X ray diffraction analysis of VIA, B-1900, 713C, and 738X alloy composition after oxidation at high temperature
[NASA-TM-X-2796] 16 p1927 N73-25596
Development of high temperature titanium alloys with improved tensile strength
[AD-759215] 16 p1930 N73-25614
Influence of phase composition on mechanical properties of heat resistant vacuum tight cast aluminum alloys
[AD-759645] 16 p1930 N73-25619
Change in fine structure of nickel-chromium heat resistant alloys during creep
[AD-759233] 16 p1971 N73-25939
Dispersion strengthened nickel alloys for use as space shuttle thermal protection systems
[NASA-CR-121164] 17 p2043 N73-26526
Methods for improving heat resistance of alloys
[AD-760273] 17 p2047 N73-26564
Thermomechanical processing of nickel-base superalloys by explosive shock wave deformation
[AD-761218] 18 p2162 N73-27462
Removing nitride inclusions from heat resistant alloys and hafnium dioxide particles in precipitation-hardened nickel
[JPRS-59637] 21 p2557 N73-30501
Application of fluidized bed technique for measuring relative thermal fatigue resistance of superalloys
[NASA-CR-121211] 21 p2558 N73-30507
Physical and mechanical properties of cermets to include methods for altering characteristics for specific industrial applications
23 p2809 N73-32459

**HEAT SHIELDING**
NT REENTRY SHIELDING
Design and fabrication of honeycomb resin-composite sandwich panels for shuttle orbiter thermal shielding
[NASA-CR-128610] 01 p0061 N73-10503
Analysis of production method for manufacturing ablative heat shield panels using press filling and curing of ablation material
[NASA-CR-112124] 02 p0243 N73-11975
Destructive and nondestructive tests of carbon-carbon reentry heat shields
[SC-R-71-3354] 03 p0364 N73-12966
Development of computational techniques for design optimization of thermal protection systems for space shuttle vehicle
[NASA-CR-128618] 04 p0484 N73-13951
Fused slurry silicide protective coatings for tantalum heat shielding
[NASA-CR-121022] 06 p0688 N73-15599
Incremental theory and numerical procedure for analyzing three dimensional thermoplastic structure used in nonmetallic thermal protection system
[NASA-CR-124005] 06 p0729 N73-15948
Relative rain erosion resistance of low-density-thermal protection materials for space shuttles at subsonic velocities
[NASA-CR-130541] 08 p0969 N73-17924
Use of Apollo heat shield window to study dynamic and physical properties of meteoroids
12 p1452 N73-21760
Stationary hyperacoustic overflow of leading point of graphite blunt body by heat conducting stream of air
[AD-755784] 12 p1466 N73-21875
Windward surface flow distribution on lifting reentry vehicle configurations at high angles of incidence under hypersonic perfect gas conditions
[AD-756499] 14 p1599 N73-22961
Analysis of relationships governing shielding through radiative heat exchange
[AD-760399] 17 p2097 N73-26967
Analysis of thermophysical properties of plasma sprayed materials for use as thermal insulation coating on rocket nozzles
[NASA-CR-121144] 19 p2311 N73-28590
Development and characteristics of closed pore ceramic foam insulation material for use as heat shield on space shuttle vehicle
[NASA-CR-2254] 19 p2312 N73-28591
Fused slurry silicide coatings for tantalum reentry heat shielding
[NASA-CR-120877] 20 p2485 N73-29964
Reusable ablative heat shielding for space shuttle orbiters
[NASA-CR-132282] 21 p2605 N73-30880
Complex permittivity measurements during high temperature recycling of space shuttle antenna window and dielectric heat shield materials
[NASA-CR-2302] 22 p2707 N73-31673
Fused slurry silicide protective coatings for niobium alloy reentry heat shields for space shuttles - Vol. I
[NASA-CR-121216] 23 p2857 N73-32826
Space environment effects on space shuttle thermal protection system design
[NASA-TM-X-2721] 24 p2941 N73-33490

**HEAT SINKS**
Laboratory prototype flash evaporator design, fabrication, and testing for space shuttle environmental control expendable heat sink
[NASA-CR-128608] 01 p0057 N73-10470
Heat sink and cooling system concepts for space shuttle baseline thermal protection systems
[NASA-CR-123912] 01 p0107 N73-10884
Current lead optimization for minimizing heat loss of superconducting magnet
[BNL-17233] 12 p1439 N73-21661
Design, development, and fabrication of liquid cooled space suit using ice pack heat sink - Vol. I
[NASA-CR-114624-VOL-1] 22 p2622 N73-31006
Operating instructions for functional model icepack heat sink subsystem for cooling system of space suit - Vol. 2
[NASA-CR-114624-VOL-2] 22 p2728 N73-31829

**HEAT SOURCES**
NT GEOTHERMAL RESOURCES
Working on advanced heat source converter design designated as multihundred watt program
[MLM-1896[OP]] 03 p0333 N73-12711
Performance of battery powered electrically heated suit for reconnaissance divers
[AD-749847] 05 p0504 N73-14101
Recent Soviet investigations in geothermy
[AD-750128] 06 p0671 N73-15454
Design of prototype thermal battery incorporating pelletized alkaline heat source
[SC-RR-69-497-A] 12 p1366 N73-21084
Radar observation of disk-shaped models of proposed nuclear heat source module
[NASA-TM-X-62262] 14 p1601 N73-22978
Deep-seated thermal processes, social-economic heat utilization, and geothermal observation improvement
[JPRS-59496] 18 p2143 N73-27324
Thermodynamic analysis of MHW space electric power generator with plutonium dioxide heat source
[LA-5202-MS] 22 p2699 N73-31616
Component design and draw tooling of Pt heat source liner bodies
[MLM-1972] 24 p2955 N73-33608

**HEAT STORAGE**
Feasibility of thermal energy storage and solar heating as means of conservation and more efficient utilization of electric power
[PB-210359] 01 p0118 N73-10976

**HEAT TESTS**
U HIGH TEMPERATURE TESTS

**HEAT TOLERANCE**
Physiological regulatory mechanisms of water and electrolyte levels in human body in high temperature environment
[NASA-TT-F-13915] 01 p0008 N73-10066
Heat regulation and adaptation of rats exposed to helium oxygen atmosphere
03 p0259 N73-12096
Human adaptation to hypoxic hypoxia for increased resistance to physical stress
10 p1116 N73-19095
High temperature tolerance of rats under normal conditions, after thermal conditioning and combined with drugs
11 p1244 N73-20099
High altitude acclimatization effects on mice and rabbit tolerances to hypoxia, acceleration, and high temperature
[NASA-TT-F-14861] 11 p1247 N73-20123
Human physiological response to heat stress in preflight operation
[AD-759173] 18 p2110 N73-27060
Cooling effects on human tolerance to work induced heat stress and collapse
[NASA-CR-134059] 23 p2750 N73-32005

**HEAT TRANSFER**
NT AERODYNAMIC HEAT TRANSFER
NT CONDUCTIVE HEAT TRANSFER
NT CONVECTIVE HEAT TRANSFER
NT HYPERSONIC HEAT TRANSFER
NT LAMINAR HEAT TRANSFER
NT RADIATIVE HEAT TRANSFER
NT TURBULENT HEAT TRANSFER
Heat transfer rate measurements in separated flow region behind series of eight axisymmetric backward facing step models
[AD-735745] 01 p0037 N73-10289
Heat transfer rate measurements on cone cylinder models and in separated regions behind axially symmetric backward facing step
[AD-735744] 01 p0037 N73-10290
Characteristics of turbulent separated flows, and calculations of momentum and heat transfer in them
[EF/TN/A/49] 01 p0039 N73-10308
Wind tunnel tests to determine convective heat distribution for space shuttle configurations based on viscous/inviscid interactions of three dimensional flow fields
[NASA-CR-128586] 01 p0040 N73-10318
Equations which show relationship between stress and displacement velocity in non-Newtonian fluid flows
[AD-745702] 01 p0042 N73-10335
Development of computer program for simulating performance of space radiator to account for transient and steady state performance
[NASA-CR-128594] 01 p0108 N73-10891
Numerical analysis of simplified radiator system to predict steady state system performance and to optimize system parameters for minimum area or minimum mass
[NASA-CR-128596] 01 p0108 N73-10892
Transient heat transfer analysis of space radiator heat rejection system under conditions of aerodynamic heating, solar, albedo, and planetary radiation
[NASA-CR-128595] 01 p0117 N73-10964
Analysis of velocity and temperature distribution in unsteady thermal boundary layer by approximate integral method
[NASA-TN-D-7054] 01 p0117 N73-10967
Thermodynamic properties and heat transfer characteristics of forced-convection boiling of Freon-113 in vertical annular test section
[NASA-CR-2137] 01 p0117 N73-10968
Mechanism of heat transfer for exothermic interaction in porous body between oxidizer and reagent
[AD-745460] 01 p0118 N73-10970
Analysis of critical density heat flows during internal heating of annular channels
[AD-743681] 01 p0118 N73-10972
Analysis of mean velocity, turbulence intensity, and wall heat transfer for conical diffuser coupled to constant diameter recovery section
[NASA-TM-X-2677] 02 p0156 N73-11267
Analysis of surface flow, pressures, and heat transfer on two conical delta wings at hypersonic speed and various angles of attack
[NASA-TM-X-2668] 02 p0156 N73-11268
Proceedings of conference to define research requirements for problems involving waste heat transfer from large thermal sources into the environment
02 p0166 N73-11348
Heat transfer mechanisms in fibrous insulation materials
[PB-210117] 02 p0192 N73-11558
Digital simulations of Joule heating and heat transfer processes in amorphous semiconductor switches
[AD-746278] 02 p0219 N73-11776
Laminar flow, and transitional flow heat transfer
[ESDU-68006-AMEND-A-PT-2] 02 p0241 N73-11963
Small scale nozzle tests using heated nitrogen for effectiveness and wall heat transfer studies with hydrogen film cooling
[NASA-CR-120926] 02 p0242 N73-11970
Mathematical model for convective and radiant heat transfer for gas flow and glass tube inner wall noting partial differential equations at boundary conditions
[LAAS-NI-CMOAC-72-I-11] 02 p0243 N73-11976
Experimental procedure for estimating rate of thermal flow and heat transfer from longitudinally swept surfaces using unstable thermal regime method
[AD-746011] 02 p0243 N73-11977
Heat transfer at critical point, jet turbulence, and vortex systems
[AD-747294] 02 p0244 N73-11981
Heat transfer and cooling of electronic components and equipment
[AD-746431] 03 p0279 N73-12259
Skin friction, heat transfer and pressure measurements in laminar, transitional and turbulent boundary layers on flat plates at high Mach numbers and Reynolds numbers
[NASA-CR-112147] 03 p0283 N73-12290
Design and development of device for moving liquid through pipes without use of mechanical pumps
[NASA-CASE-LAR-10799-1] 03 p0283 N73-12295
Application of variational principle to laminar flow and heat transfer between concentric cylinders
[REPT-5/1972] 03 p0285 N73-12307
Measurement of heat transfer in gas flow behind shock wave
[AD-747604] 03 p0286 N73-12320

Modification of Navier-Stokes equation for hypersonic compressible flow to eliminate need for specifying far field and/or boundary condition parameters
[AD-747644] 03 p0287 N73-12321
Development of equations and computer program for determining temperature distribution in walls of three eccentric annuli
[AD-747697] 03 p0287 N73-12322
Evaluation of boundary cooled rocket engines for development of space storable propellant combination of oxygen difluoride/diborane
[NASA-CR-129260] 03 p0350 N73-12855
Calculation of heat transfer on turbine blade profiles to determine transition region coordinates in boundary layer flow through gas turbine engine
[AD-747602] 03 p0352 N73-12870
Development of computer program for determining thermodynamic and transport properties of para and equilibrium hydrogen
[NASA-CR-129261] 03 p0363 N73-12959
Transfer of mass and heat through single component diatomic gas and binary monatomic gas mixture of arbitrary composition
[COO-2032-12] 03 p0364 N73-12968
Nonstationary heat and mass transfer in stationary binary gas mixture
[AD-747562] 03 p0365 N73-12974
Analysis of motion of chemically active gases to determine heat and mass transfer in turbulent jet system during diffusion combustion
[AD-747571] 03 p0365 N73-12976
Heat transfer in superconducting matrix as magnet coils
[BNL-16615] 04 p0459 N73-13743
Analysis of entropy rate admissibility criterion for solutions of hyperbolic conservation laws
[NASA-CR-129594] 04 p0484 N73-13956
Research projects conducted in USSR to determine thermophysical properties of materials at high temperatures and characteristics of high temperature processes
[JPRS-57658] 04 p0484 N73-13957
Calculation of heat transfer on shuttle type configurations including effects of variable entropy at boundary layer edge
[NASA-CR-112180] 04 p0484 N73-13958
Inversion of some Laplace transforms encountered in heat transfer problems
[AD-749329] 04 p0486 N73-13968
Heat transfer and surface pressure measurements at supersonic speeds on conical delta wings with sharp leading edges
[ARC-CP-1212] 05 p0492 N73-14008
Numerical analysis of thermal resistance of air layers in air permeable clothing
[NLL-DRIC-TRANS-2717-[3623.66]] 05 p0502 N73-14089
Numerical analysis of heat transfer conditions at point of intersection of jet impinging on obstacle at subsonic and supersonic speeds
[NLL-RTS-7617] 05 p0525 N73-14274
Compilation of titles, authors, and corporate sources on subject of heat transfer in boiling metals under natural convection conditions
[NLL-RISLEY-TR-2167-[9091.9F]] 05 p0605 N73-14920
Analysis of heat transfer characteristics of hot wire normal to incompressible air flow and influence of frequency on sensitivity and temperature distribution along wire
[WTHD-33] 05 p0605 N73-14922
Wind tunnel tests to determine heat transfer and pressure distributions of hemisphere cylinders in hypersonic flow environment
[NASA-TN-D-7104] 05 p0605 N73-14925
Examination of physical processes governing heat transfer through air-penetrable clothing in wind
[DRIC-TRANS-2921] 06 p0636 N73-15166
Wind tunnel tests to determine heat transfer of near equilibrium transpired turbulent boundary layer with adverse pressure gradient
[NASA-CR-130291] 06 p0652 N73-15291
Individual and combined effects on heat transfer properties of air jets impinging on concave side of right circular semicylinder
[NASA-TN-D-7127] 06 p0730 N73-15952
Articles on experimental and theoretical studies of heat transfer and cooling problems of gas turbines
[AD-751513] 07 p0837 N73-16782
Relationship between laminar film condensation on inside of rotating non-capillary heat pipe and pipe heat transfer capabilities
[NASA-CR-130373] 07 p0854 N73-16926
Computer program for solving problems involving transient heat conduction and convection in continua
[NASA-CR-130148] 07 p0854 N73-16927
Abstracts of selected reports on heat transfer and fluid dynamics with applicability to oxygen systems
[NASA-SP-3076-VOL-3] 07 p0855 N73-16932
Analysis of pressure drop, heat transfer, and flow characteristics for forced convection boiling in helical coils
[AEEW-R-757] 07 p0855 N73-16936
Determination of heat transfer and flow friction characteristics of fibrous metals for application to heat exchanger design
[AD-751633] 07 p0856 N73-16937
Heat and mass transfer analysis of liquids and air flowing in opposite directions under various atmospheric pressures
[AD-751503] 07 p0856 N73-16938
Approximative heat transfer in thermal boundary laer on gas turbine blade
[AD-752676] 08 p0956 N73-17825
Hydrocarbon suspeasions in slush hydrogen and heat transfer to slush hydrogen
[NASA-CR-130550] 08 p0968 N73-17912
Heat transfer to slush hydrogen at 1 atm and at triple-point pressure 08 p0968 N73-17914
Design of porous cooled medium surface to maintain specified design temperature while subjected to uniform heating from external source
[NASA-TN-D-7176] 08 p0969 N73-17919
Analysis of high temperature heat exchanger processes in tubular metallic container using bed of moving pebbles for heat storage
[FRNC-TH-231] 08 p0969 N73-17923
Heat transfer and flow visualization tests of straight wing hypersonic reentry vehicle at angles of attack from 20 to 80 deg
[NASA-TN-D-7108] 09 p0979 N73-18000
Heat exchange and drag during turbulent flow of compressible gas
[AD-753046] 09 p1017 N73-18300
Analysis of energy conservation constraints on circulation of Southern Hemisphere atmosphere and oceans based on radiant, latent, and sensible heat energy transfers
[METEOROL-STUDY-26] 09 p1027 N73-18387
Interaction of velocity and temperature fields in lubricating layer of thrust slide bearings and analysis of viscosity variation along length and thickness of lubricating layer
[AD-753044] 09 p1041 N73-18487
Gas dynamic equation for investigating thermal heating modes during laser radiation flux interaction with material 09 p1043 N73-18509
Heat transfer and aerodynamic resistance of in-line smooth walled tube arrays in transverse air flow at high Reynolds number
[NLL-RTS-7689] 09 p1098 N73-18959
Coolant side, heat transfer rates for liquid hydrogen cooled, hydrogen-oxygen rocket thrust chamber
[NASA-TN-D-7207] 09 p1099 N73-18968
Flow field, pressure, and heat transfer associated with small fins of half angle cone in supersonic flow
[SCL-RR-72-0339] 10 p1142 N73-19302
Calculation method for external heat transfer to turbine blades 10 p1205 N73-19807
Development of computer program to predict transient and steady state performance and heat transfer characteristics of pulsing gaseous propellant rocket engine
[NASA-CR-128748] 10 p1214 N73-19871
Development of space shuttle scale model for thermodynamic analysis of internal and external heat flow fields
[NASA-CR-128849] 10 p1215 N73-19882
Heat transfer from radioisotope generator, using organic fluids
[CEA-CONF-2042] 10 p1224 N73-19950
Probabilistic design model for prediction of heat transfer rate for heat pipes
[AD-752057] 10 p1224 N73-19954
Analysis of optimum mass and heat transfer in electrochemical fuel cells to show effects on fuel cell output
[AD-754258] 11 p1238 N73-20051
Analysis of interaction of rarefied gas with surface of porous moist bodies during heat and mass transfer using visual and photographic methods
[AD-754633] 11 p1272 N73-20325
Graphical method for determining soil temperature from air temperature and humidity measurements
[NLL-M-22802-[5828.4F]] 11 p1274 N73-20339
Addition of three-dimensional isoparametric elements to NASTRAN structural analysis program
[NASA-CR-112269] 11 p1345 N73-20916
Laplace transformation and Volterra integral equation for studying heat transfer in laminar flow through pipe with annular space
[NLL-RTS-7525] 11 p1347 N73-20928
Heat transfer and frictional resistance in pipes with cooled walls during turbulent flow of high temperature gases
[NLL-RTS-7640] 11 p1347 N73-20930
Techniques for measuring heat transfer in short duration and rapidly varying flows
[AGARD-AG-165] 11 p1349 N73-20945
Heat transfer equation with nonlinear boundary condition and final value problem for porous medium equation
[AD-755073] 11 p1350 N73-20951
Experimental and theoretical investigation of trajectory and growth of thermal effluents with variable discharge velocities and temperatures
[NASA-TM-X-69221] 12 p1392 N73-21284
Development of statistical equations for turbulent compressible gas with emphasis on space-time correlations in boundary layer
[AD-755889] 12 p1393 N73-21291
Wind tunnel tests to determine heat transfer properties of space shuttle orbiter, booster, and launch configurations for various angles of attack and yaw
[NASA-CR-128891] 12 p1460 N73-21830
Numerical analysis of temperature distribution of complex two-dimensional body with various boundary conditions including radiation effects
[N8110R:72-040] 12 p1464 N73-21860
Effect of heat transfer on flow and temperature fields in separation nozzle measured with free molecular pressure and temperature probes
[KFK-1634] 12 p1464 N73-21865
Solution of temperature distribution in hollow cylinder for asymptotic regime and variable heat conductivity coefficient
[AD-755251] 12 p1465 N73-21872
Heat transfer in immediate vicinity of wall by measurement of average temperature profiles
[AD-756957] 13 p1512 N73-22256
Analysis of friction welding of metal structures with information on friction theory, heat liberation, basic parameters, and recommended regimes
[AD-755753] 13 p1535 N73-22440
Hydrodynamics and heat exchange with two phase flow in elements of power equipment
[AD-756564] 13 p1591 N73-22897
Temperature field calculations on cylinder solidification in axial and radial axial heat transfer
[AD-755871] 13 p1591 N73-22901
Calculation and design of heat transfer apparatus for viscous liquids, liquid fuel, and lubricating oils
[AD-756947] 13 p1592 N73-22908
Combined heat and mass transfer at wet flat plate in parallel air flow forming turbulent boundary layer
[DLR-FB-73-11] 14 p1599 N73-22960
Boundary layer transition and heat transfer in aerodynamic and thermic wall deformation 14 p1601 N73-22982
Design of katathermometer for measuring environmental cooling effects in simulated space flight 14 p1608 N73-23036
Compressible turbulent boundary layer in zero-pressure gradient nozzle flow for zero, moderate, and severe heat transfer conditions
[AD-757330] 14 p1651 N73-23391
Conference on heat transfer and fluid mechanics
[AD-758404] 14 p1653 N73-23404
Design, development, and operation of compact, high performance, magnetohydrodynamic generators
[AD-756489] 14 p1696 N73-23765
Research projects involving boundary layer flow, heat transfer during aerodynamic heating, atmospheric turbulence effects, and airframe structural analysis - Vol. 2 15 p1727 N73-24011
Development of method for calculating characteristics of laminar boundary layer on nonadiabatic wall of constant temperature in presence of pressure gradients
[ARC-R/M-3233] 15 p1728 N73-24013
Analysis of heat transfer properties of air, helium, and carbon dioxide and effects of variations of fluid properties with temperature
[ARC-R/M-3246] 15 p1729 N73-24021
Heat and mass transfer with phase and chemical transformations in reacting boundary layer
[AD-758210] 15 p1748 N73-24165
Calculation of coupled skin friction and heat transfer in two and three dimensional turbulent boundary layers
[AD-757871] 15 p1768 N73-24327
Development of analytical and experimental techniques for determining heat transfer characteristics of solid propellant rocket engine storage container system
[AD-758515] 15 p1827 N73-24807
Applications of heat pumps for recovery of unused heat in factories, air conditioned buildings, and refrigeration plants
[NLL-OA-TRANS-1264-[6196.3]] 15 p1842 N73-24921
Literature survey of heat transfer characteristics of single and multiple turbulent air jets impinging on flat plates
[NASA-TM-X-2778] 15 p1842 N73-24927
Heat transfer characteristics of impingement-cooled turbine rotor blade
[NASA-TM-X-2791] 15 p1843 N73-24929
Temperature rise at heat transfer surfaces caused by magnetite, humus, calcium, and copper deposits
[AE-459] 15 p1844 N73-24937
Nusselt-type analysis of laminar film condensation inside truncated rotating cone, emphasizing heat transfer performance
[AD-758513] 15 p1845 N73-24945

Application of laminar flow solutions for heat transfer and flow friction to design of heat exchangers
16 p1886 N73-25266
Thermohydrodynamic stability in channel flow heat and mass transfer considering variable cross section area
[AD-758748] 16 p1889 N73-25289
Approximate calculation of heat transfer in transpired boundary layers
[AD-759353] 16 p1891 N73-25301
Studies in gas dynamics and heat transfer
[AD-759240] 16 p1891 N73-25304
Velocity and heat transfer analysis in channels with porous wall for cooling turbine blades
[AD-758782] 16 p1957 N73-25833
Aerodynamic heating analysis on sounding rocket tangent ogive nose wall
[NASA-TM-X-69896] 17 p1979 N73-26001
Design and development of electric batteries for use with thermoelectric air conditioning systems
[AD-759239] 17 p1986 N73-26051
Analysis of heat transfer in laminar flow of gas through constant diameter cylindrical tubes at low wall to bulk temperature ratios
17 p2013 N73-26275
Nonstationary heat and mass transfer developed by transverse flow around cylindrical body to determine conditions at stagnation point
[AD-760396] 17 p2016 N73-26299
Research on fluid codes and heat transfer in shock tubes
[COO-3086-17] 17 p2068 N73-26733
Analysis of space shuttle cryogenic fluid storage system to determine heat absorption capability and design of radiators for additional cooling capability - Vol. 4
[NASA-CR-133952] 17 p2088 N73-26895
Design and thermal analysis on film cooled exhaust duct for fissioning uranium plasma test reactor
[NASA-TM-X-2861] 18 p2178 N73-27585
Development of methods for calculating cooling requirements for gas turbine engines with initial gas temperatures of 750 to 800 C
[AD-760964] 18 p2194 N73-27713
Wind tunnel tests to determine heat transfer and flow distribution of space shuttle configuration at hypersonic speeds simulating atmospheric entry
[NASA-CR-133405] 18 p2201 N73-27772
Numerical analysis of temperature and stresses in cylindrical body heated with constant heat flow
[NLL-M-21601-[5828.4F]] 18 p2205 N73-27794
Heat exchange between cooled polydisperse granular material and transversely located cylindrical tubes arranged in staggered bundle
[NLL-M-21602-[5828.4F]] 18 p2205 N73-27795
Heat flow and convection in gases and liquids in weightless environments
[NASA-TM-X-64735] 18 p2205 N73-27797
Analysis of local and average heat transfer characteristics of single turbulent air jet impinging on concave surface of hemisphere
[NASA-TM-X-2859] 18 p2206 N73-27806
Heat flow failure mechanism in overstressed microelectronic circuits
[AD-761792] 19 p2244 N73-28094
Velocity and temperature development in entrance region between two rotating concentric cylinders
[AD-762049] 19 p2256 N73-28187
Heat transfer in permeable thermocouple
[AD-761556] 19 p2302 N73-28511
Calculation of heat removed by gas refrigerators and heat engines
[AD-762261] 19 p2306 N73-28544
Analysis of stagnation point on blunt body in massive ablation condition to show effects of absorption coefficient enhancement on mass loss rate
19 p2351 N73-28912
Analysis of methods for determining thermoelectric cooling and heating devices using pure resistance principle
[AD-762324] 19 p2353 N73-28926
Analysis of heat exchange between liquid and bodies on which liquid flows during catalytic chemical reactions on surface of bodies
[AD-761607] 19 p2353 N73-28927
Computation of skin friction and heat transfer on sharp cone in axisymmetric turbulent hypersonic flow
[AD-761602] 19 p2353 N73-28929
Burning rate, heat transfer, and combustion physics of aluminum in composition of heterogeneous condensed systems
[AD-761609] 19 p2354 N73-28932
Regional and time variations in heat transfer from oceanic regions to atmosphere
20 p2389 N73-29195
Development of method for determining atmospheric transmission function with allowance for divergence of thermal radiation
20 p2401 N73-29298
Adiabatic film effectiveness and heat transfer measurements with injection of coolant air through holes in flat plate into moving mainstream
[AD-762527] 20 p2466 N73-29814
Heat transfer by thermal radiation in forced convective tube flow of radiation gas
20 p2484 N73-29954
Conformal mapping technique for two-dimensional porous media and jet impingement heat transfer
[NASA-TM-X-68276] 20 p2485 N73-29961
Effect of ablation modes and flow field distribution on cross hatching phenomenon at supersonic speeds
[TN-85] 20 p2485 N73-29963
Calculation of temperature fields of solids under conditions of natural heat exchange with atmosphere
[AD-762494] 20 p2486 N73-29968
Heat transfer across interface between high speed steam jet and external coaxial cocurrent water flow
[AD-763696] 21 p2527 N73-30262
Boundary layer theory for flow and heat transfer problems in turbomachine blades
21 p2590 N73-30751
Development and characteristics of thermal control system for maintaining constant temperature within spacecraft module with wide variations of component heat transfer
[NASA-CASE-GSC-11018-1] 21 p2599 N73-30829
Development of method for calculating bubble conditions in flow of boiling liquid in vertical tubes
[NLL-WH-335-[9091.9F]] 21 p2605 N73-30875
Development of fine spectral resolution procedure for determining infrared radiant heat transfer from exhaust plume
[RM-575] 21 p2605 N73-30877
External heat transfer problems under space conditions
[NASA-TT-F-783] 21 p2605 N73-30879
Heat transfer theory in layer with regular change of liquid flow direction
[AD-762794] 21 p2606 N73-30888
Design, development, and fabrication of liquid cooled space suit using ice pack heat sink - Vol. 1
[NASA-CR-114624-VOL-1] 22 p2622 N73-31006
Thermotransport of copper in liquid Al-Cu alloys
[NASA-TR-R-415] 22 p2625 N73-31030
Prediction and measurement of heat transfer rates for shock-induced unsteady laminar boundary layer on flat plate
[NASA-CR-114582] 22 p2651 N73-31241
Effect of return bends on downstream pressure drop and heat transfer coefficient of condensing refrigerant
[DSR-72591-75] 22 p2652 N73-31246
Calculation of heat and mass transfer in turbulent boundary layer on surface with arbitrary roughness
[AD-764128] 22 p2655 N73-31266
Hypersonic, turbulent, cold-wave, skin friction, and heat transfer measurements on axisymmetric sharp cone
[AD-764059] 22 p2655 N73-31269
Calculation of heat exchange between rotating body and moving fluid
[AD-763941] 22 p2656 N73-31275
Temperature control of welding equipment by detection of discrete bands of infrared radiation from objects being heated
[NASA-CASE-MFS-20781-2] 22 p2672 N73-31401
Application of spectroscopic methods in remote sensing for determining structure of microwave spectra in earth atmosphere
22 p2692 N73-31563
Performance evaluation of heat transfer testing of heat pipes with thermal-vacuum and bench testing
[NASA-TN-D-7219] 22 p2728 N73-31827
Operating instructions for functional model icepack heat sink subsystem for cooling system of space suit - Vol. 2
[NASA-CR-114624-VOL-2] 22 p2728 N73-31829
Simplified model for heat transfer and subsequent temperature distribution in thin metal target impacted by cylindrical projectile
[AD-763152] 22 p2730 N73-31850
Heat transfer in slit-like channels
[AD-762793] 22 p2730 N73-31851
Static pressure and heat transfer rate distributions on conical bodies at hypersonic speeds laminar and turbulent flow conditions
[AD-764983] 23 p2777 N73-32204
Radiative-conductive heat transfer and circulation of lower Martian atmosphere
[NASA-CR-2318] 23 p2786 N73-32287
Evaluating reusable surface insulation for space shuttle over range of heat transfer rate and surface temperature
[NASA-TM-X-2823] 23 p2809 N73-32465
Thermal flux transfer system for maintaining thrust chamber of operative reaction motor at given temperatures
[NASA-CASE-NPO-12070-1] 23 p2828 N73-32606
Heat transfer in fissioning uranium plasma reactor cavity
[NASA-TM-X-2885] 23 p2828 N73-32607
Electrostatically controlled heat transfer system for conducting thermal energy
[NASA-CASE-NPO-11942-1] 23 p2855 N73-32818
Heat exchange of hand as function of local thermal conditions
[NASA-TT-F-15143] 24 p2885 N73-33043
Continuity and Navier-Stokes equations for analyzing viscous flow heat transfer in curved tubes
24 p2902 N73-33162
Heat transfer and wavelength measurement for axiaymmetric flow of fluid layer heated from below
24 p2903 N73-33167
Parallel heat conducting viscous gas flow in flat channel with sine wave wall perturbation
24 p2906 N73-33189
Effect of heat transfer on velocity distribution and skin friction in turbulent wall boundary layers
24 p2906 N73-33195
Interference heating in gaps between surface insulation tiles for space shuttle thermal protection system design
24 p2942 N73-33499
Heat transfer-lifetime code for SNAP reactor analysis
[AI-AEC-13076-VOL-5] 24 p2955 N73-33604
Zirconium hydride reactor core heat transfer on rod spacers to liquid metal NaK
[AI-AEC-13088] 24 p2955 N73-33607
Heat transfer characteristics of container stored rocket motor
[AD-764536] 24 p2974 N73-33760
Heat transfer from wall to fluid in laminar fluid flow in circular tube
24 p2990 N73-33895
Stability of vapor film formed on horizontal cylinders during stable film boiling using variational approach
24 p2991 N73-33906
Solution of nonlinear problems of high temperature heat transfer
[AD-765747] 24 p2993 N73-33917

**HEAT TRANSFER COEFFICIENTS**

Effect of nature, structure, temperature, volume weight, and moisture content on coefficient of heat transfer for heat insulation materials
[AD-748748] 04 p0438 N73-13573
Heat transfer coefficient between fuel and cladding as parameter for calculating fuel rod temperature
[NLL-WINDSCALE-497-[9091.9F]]
05 p0578 N73-14706
Thermal dilatation coefficients of explosive monocrystals determined by extensometry
[ISL-24/71] 09 p1099 N73-18969
Analysis of two-dimensional liquid metal slot jet impinging normally against uniformly heated flat plate
[NASA-TN-D-7260] 11 p1348 N73-20938
Heat exchange coefficient for humans in constant temperature moving water
[NASA-TT-F-14867] 11 p1349 N73-20943
Calculation of heat transfer coefficients of laminar incompressible boundary layer to corrugated wall, with application to combustion chamber liquid film cooling
[DLR-FB-73-07] 12 p1465 N73-21868
Heat exchange between gas and turbine cascade blades of gas turbine engine
[AD-756101] 14 p1701 N73-23804
Measurement of heat transfer coefficients of air-glass, argon-glass, and argon-aluminum suspensions
[NASA-CR-2266] 15 p1843 N73-24932
Development of formula for calculating heat transfer coefficient in labyrinth glands of gas turbines
[NLL-RTS-7840] 18 p2192 N73-27698
Transient thermal response of globe thermometers in relation to heat transfer parameters
[DCIEM-859] 20 p2418 N73-29431
Computer program for application of phase change technique to thin sections with heating on both sides
[NASA-TN-D-7193] 20 p2485 N73-29965

**HEAT TRANSMISSION**

NT AERODYNAMIC HEAT TRANSFER
NT CONDUCTIVE HEAT TRANSFER
NT CONVECTIVE HEAT TRANSFER
NT HEAT TRANSFER
NT HYPERSONIC HEAT TRANSFER
NT LAMINAR HEAT TRANSFER
NT RADIATIVE HEAT TRANSFER
NT TURBULENT HEAT TRANSFER
Numerical analysis of simplified radiator system to predict steady state system performance and to optimize system parameters for minimum area or minimum mass
[NASA-CR-128596] 01 p0108 N73-10892
Analysis of high temperature heat-exchanger processes in tubular metallic container using bed of moving pebbles for heat storage
[FRNC-TH-231] 08 p0969 N73-17923
Analysis of eddy diffusivity of momentum for heating air in turbulent annular flow and effect of various flow parameters on eddy diffusivities ratio
10 p1139 N73-19279
Meaning coefficients for heat flows and temperature fields of simple shaped bodies with III order boundary conditions
[NLL-M-21522-[5828.4F]] 11 p1347 N73-20929
Heat flow and convection in gases and liquids in weightless environments
[NASA-TM-X-64735] 18 p2205 N73-27797

Development of computer program for solving one dimensional heat flow problem using aerodynamic heating examples
[WRE-TN-884[WR/D]] 19 p2351 N73-28914
Utilization of two rotating vessels to model and analyze certain schemes of atmospheric circulation and heat exchange
20 p2445 N73-29638
Apollo 17 heat flow and convection experiments
[NASA-TM-X-64772] 22 p2729 N73-31840

**HEAT TREATMENT**
NT ANNEALING
NT NITRIDING
NT NORMALIZING [HEAT TREATMENT]
NT PULSE HEATING
NT STRESS RELIEVING

Effect of chemical composition, method of heat treatment, and production methods, on corrosion resistance of metal sheets
[AD-742106] 01 p0067 N73-10550
Influence of high temperature thermomechanical treatment on mechanical properties of austenitic steel
[NLL-M-21480-[5828.4F]] 02 p0186 N73-11504
Linear regression analysis used on mechanical property data obtained from experiment which maximized variability in heat treating parameters of titanium alloy
[AD-747207] 02 p0190 N73-11540
Effect of mechanical-thermal pretreatments on time-to-rupture and creep strength of nickel-chromium steels
[KFK-1535] 03 p0313 N73-12557
Effects of high-speed heating after cold plastic deformation on phase composition of titanium alloy VT 15
[AD-747516] 03 p0318 N73-12591
Effect of thermomechanical treatment on stress corrosion cracking susceptibility of Beta 3 titanium
[AD-748359] 03 p0319 N73-12602
Effects of thermomechanical treatment on mechanical, microstructural, and stress corrosion resistance properties of Al alloys
[AD-748361] 04 p0427 N73-13483
Analysis of effects of heat treatment of magnetic and physical properties of molybdenum permalloy
[NLL-RTS-7641] 04 p0431 N73-13509
Effect of heat input and post-weld heat treatment on mild and low alloy steel submerged arc weld deposits
[CRANFIELD-MAT-8] 05 p0551 N73-14475
Effect of heat treatment on fatigue life under gust loads of notched Al-Cu alloy
[ARC-CP-1221] 05 p0563 N73-14571
Volumetric analysis and dilatometric study of ferrite magnesium cast iron during heat treatment
[AD-749627] 05 p0563 N73-14572
Influence of ingot thermal-mechanical processing on grain size and mechanical properties of 7075 wrought aluminum alloy
[AD-750390] 06 p0686 N73-15588
High temperature tests to determine effect of autoclave heat treatment of mechanical properties of cobalt-base alloy HS-31 in prealloyed powder form
[NASA-TN-D-7117] 07 p0809 N73-16559
Measurement of fatigue crack propagation rates in heat treated steels
[PB-212208] 08 p0932 N73-17635
Influence of heat treatment on strength properties of EI893L alloy
[JPRS-58137] 09 p1048 N73-18543
Analysis of beta titanium alloys to show heat treatment, mechanical properties, corrosion, weldability, and processing
[AD-753439] 09 p1049 N73-18552
Tensile, exfoliation, fatigue, and crack growth properties of heat treated aluminum sheet alloy 7475
[AD-753709] 09 p1050 N73-18560
Alloying and thermal treatment for improving mechanical properties of ceramics
[AD-753124] 09 p1055 N73-18597
Influence of heat treatment on physical properties of iron- and chromium-doped rutile
[RR-107] 09 p1073 N73-18760
Effect of order of welding and heat treatment operations on mechanical properties of weld joints of N18K9M5T
10 p1171 N73-19529
Physical properties and dimensional changes in graphites caused by high temperature neutron irradiation
[BNWL-1672] 10 p1193 N73-19706
Fracture toughness study of heat treated titanium alloys
[AD-753919] 11 p1306 N73-20598
Low carbon steel for studying dissolution behavior of Fe3C particles under rapid heating and short time temperature conditions
[AD-753928] 11 p1307 N73-20602
Processing techniques for high strength aluminum alloys including ingot processing, solidification and homogenization, and thermal mechanical treatments
[AD-754571] 11 p1307 N73-20606
Analysis of welding parameters for producing metallurgically sound welds and effects of heat treatment on metallurgical and mechanical properties
[Y-1855] 12 p1414 N73-21460
Structural recrystallization of steels during fast and slow heating to show structural succession caused by different mechanisms of formation of austenite
13 p1541 N73-22481
Effect of deformation performed during heat treatment on structure and mechanical properties of EI437B alloy
13 p1541 N73-22485
Metallographic analysis of morphological features of martensite formed in alloy of iron-nickel-manganese-carbon after heat treatment
13 p1541 N73-22490
Vibration damping ability of steel compressor blades subjected to different heat treatments
[AD-743119] 13 p1543 N73-22502
Thermal processing procedures for strain hardening TRIP steels
[AD-756953] 13 p1543 N73-22505
Cyclic transformation treatments on structural and mechanical properties of austenitic steels
[AD-756240] 13 p1543 N73-22506
Heat treatment and forging effects on mechanical properties of maraging steel
[AD-756422] 13 p1543 N73-22507
Heat treatment and aging behavior of rubbers
[AD-755827] 13 p1548 N73-22548
Analysis of production and characteristics of ultrahigh strength steels based on survey of literature
[ARL/SM-NOTE-378] 14 p1675 N73-23591
Development of method for fabricating cermets and analysis of various compositions to show electrical and physical properties
[NASA-CASE-NPO-13120-1] 14 p1679 N73-23629
Analysis of effects of homogenizing annealing on ductility of high strength steel
[NLL-M-21616-[5828.4F]] 15 p1796 N73-24562
Properties of graphite fiber/polycarbonate and glass fiber/polycarbonate composites as influenced by heat treatment
[AD-757763] 15 p1802 N73-24605
Composite conductors of 19-Nb3Sn filaments in normal metal matrix, using heat treatment
[BNL-17425] 15 p1821 N73-24756
Homogenization processing of aluminum alloy ingots during extrusion for changing structure and properties of product
[AD-759245] 16 p1919 N73-25527
Characteristics and production methods of iron nickel-molybdenum carbonyl powders
[NLL-LTI-746-1418-[9022.401]]
16 p1925 N73-25580
Effect of heat treatment on structure and properties of stainless steels
[NLL-M-21566-[5828.4F]] 16 p1926 N73-25585
Effect of heat treatment on corrosion of titanium alloy
[AD-759626] 16 p1931 N73-25621
Effects of heat treatment on Brinell hardness of Co-Be alloy system
[RFP-TRANS-122] 17 p2044 N73-26541
Effect of aging heat treatments on mechanical properties of Ti-8Al-1Mo-1V alloy
[AD-760461] 17 p2048 N73-26567
Static and fatigue properties of hardened and tempered electron beam welded joints in 2.5 percent Ni-Cr-Mo steel and 18 percent Ni-Co-Mo maraging steel
[S/T-MEMO-9-71] 18 p2161 N73-27456
Mechanical properties of double melted 18 percent Ni-Co-Mo maraging steel bar or forgings
[S/T-MEMO-3-72] 18 p2161 N73-27457
Influence of heat treatment on stress corrosion susceptibility of ternary Al-Zn-Mg alloy
[AD-761207] 18 p2162 N73-27467
Heat treating effects on fatigue strength of SO-95 and 120 type organic class
[AD-760961] 18 p2168 N73-27511
Experimental analysis of disappearance phenomena of packing defects in silicon epitaxial films during thermal oxidation in wet oxygen
18 p2187 N73-27662
Thermodynamics of phase changes occurring in heat treatment of carbon and alloy steels
[AD-762361] 19 p2311 N73-28589
Proceedings of conference on rolling mills for production of work hardened, heat treated metal products
[NLL-M-21649-[5828.4F]] 20 p2421 N73-29450
Process for manufacturing synthetic iron and comparison of annealing rate of synthetic iron with conventional iron
[NLL-M-21640-[5828.4F]] 20 p2429 N73-29507
Strength and microstructure of nickel base superalloys after long term heating
[TB-86] 20 p2431 N73-29526
Numerical solution of multidimensional linear thermal conductivity problems with complex boundary conditions which occur with heating of metals
[NLL-M-21666-[5828.4F]] 21 p2557 N73-30495
Development of iron alloy with high fracture toughness at cryogenic temperatures
[LBL-1121] 21 p2559 N73-30511
Thermal cycling effects on structure of cobalt-niobium eutectic alloys
[AD-763706] 21 p2560 N73-30521
Strain fracture toughness and microstructure of heat treated high strength steels
22 p2682 N73-31486
Heat treatment of titanium alloy forgings to obtain high yield strength
[BDX-613-872] 22 p2685 N73-31503
Casting and heat treatments for fabricating ductile superconducting copper base alloys
[CALT-322-51] 22 p2707 N73-31678
Heat treatment effects on metal black surfaces, and Auger spectra during magnesium and iron oxidation
[RU-20-6] 23 p2769 N73-32146
Isothermal and athermal martensitic transformation in beta copper zinc alloys
23 p2803 N73-32417
Heat treated chromium doped rutile for L-band traveling wave masers
[RR-111] 24 p2930 N73-33402

**HEATING**
NT AERODYNAMIC HEATING
NT ARC HEATING
NT ATMOSPHERIC HEATING
NT BASE HEATING
NT GAS HEATING
NT INDUCTION HEATING
NT IONOSPHERIC HEATING
NT KINETIC HEATING
NT LASER HEATING
NT PLASMA HEATING
NT PULSE HEATING
NT RADIANT HEATING
NT RADIO FREQUENCY HEATING
NT RESISTANCE HEATING
NT SHOCK HEATING
NT SOLAR HEATING
NT SUPERHEATING
NT TRANSIENT HEATING

Heat test program for general protuberance shapes on flat plate
[NASA-CR-128400] 01 p0116 N73-10959
Thermocompression wobble tool bonding of beam lead devices
[SC-DC-72-1197-A] 03 p0306 N73-12501
Weakening and fracture of glass reinforced plastics during compression under conditions of one-sided heating
[AD-748526] 04 p0439 N73-13581
Analysis of heat supply requirements and heating availability in geographical areas of USSR
[JPRS-58114] 08 p0917 N73-17513
Summer room heating in buildings with large window glass surfaces
[NASA-TT-F-14849] 11 p1349 N73-20944
Finite element calculation of two-dimensional heating and melting of disks and applications to laser effects
[AD-757189] 14 p1719 N73-23950
Fog clearing at airports by ground based heating
[AD-757897] 15 p1806 N73-24639
Analysis for stresses and buckling of heated composite stiffened structures
[NASA-CR-112227] 15 p1838 N73-24894
Influence of isolated heating of spinal column on respiratory rate and panting in dogs
[NASA-TT-F-14998] 18 p2109 N73-27054
Food heating tests in different atmospheres
[NASA-CR-134040] 22 p2622 N73-31012

**HEATING EQUIPMENT**
NT BOILERS
NT EVAPORATORS
NT FURNACES
NT SOLAR FURNACES
NT VACUUM FURNACES
NT VAPORIZERS

Construction and properties of guarded hot plate apparatus for thermal insulation study
[PB-210118] 02 p0175 N73-11415
Tank heater for lowering viscosity of highly viscous liquids in storage tanks
[NASA-CASE-WLP-10040-1] 04 p0426 N73-13475
Requirements, basic principles of operation, design, construction, and maintenance of thermal fog dispersal system for airport applications
[FAA-RD-72-138] 07 p0766 N73-16222
Self-cycling fluid heater for heating continuous fluid stream to ultrahigh temperatures to facilitate chemical reactions
[NASA-CASE-MSC-15567-1] 07 p0853 N73-16918
Technical and economic feasibility of solar powered space heating, air conditioning, and hot water heating systems for residential applications
[NASA-CR-124063] 08 p0968 N73-17911
Air Force heating system for fog dispersal
[AD-754900] 11 p1315 N73-20675
Three day advance warning system of heating plant failure using algorithmic detection methods
[NASA-CR-131571] 13 p1505 N73-22197
Use of phenol formaldehyde plastic foam as thermal insulation for solar water heaters to improve efficiency
[AD-756591] 13 p1548 N73-22543
Integrated circuit designs for self controlling electrical heater
[NASA-TN-D-7248] 15 p1786 N73-24479

Heating device to prevent icing for windmill type anemometers
[NLL-M-29974-[5828.4F]] 16 p1936 N73-25665
Extension of hydrodynamic theory of peak and minimum pool boiling heat fluxes to include influence of viscosity on instability mechanisms with application to film boiling
[NASA-CR-2270] 18 p2206 N73-27808
Cyclically heated auxiliary chamber for heating and mixing stored fluids
[NASA-CASE-ARC-10442-1] 21 p2547 N73-30415

**HEAVY COSMIC RAY PRIMARIES**
U HEAVY NUCLEI
U PRIMARY COSMIC RAYS

**HEAVY ELEMENTS**
NT CALIFORNIUM ISOTOPES
NT CURIUM 244
NT NEPTUNIUM
NT PLUTONIUM
NT PLUTONIUM 238
NT TRANSURANIUM ELEMENTS
X ray fluorescence analysis of toxic heavy elements
[CONF-721134-1] 17 p1992 N73-26106

**HEAVY IONS**
Research on nuclear reactions of energetic heavy ions
[AD-746330] 02 p0214 N73-11736
Nuclear research, including reaction mechanisms, nuclear astrophysics, isobaric analog, and heavy ions studies
[ANU-P-542] 03 p0339 N73-12769
Relation between photometric track width and velocity of heavy ions in nuclear emulsions
[LUIP-CR-72-13] 08 p0946 N73-17750
Laser generation of heavy ion plasma
[CEA-CONF-2022] 08 p0948 N73-17761
Magnetohydrodynamic equations for heavy ion plasma confined in magnetic field and ion source discharges
[LYCEN-7208] 12 p1435 N73-21625
High frequency satellite lines in X ray spectra of heavy ions
[CONF-720404-VOL-3] 19 p2323 N73-28687
Research in heavy ion scattering reactions
[CONF-720669] 22 p2702 N73-31641
Characteristics of heavy ion plasma produced by laser interaction with matter
[NASA-TT-F-15132] 22 p2703 N73-31650
Rocket-borne mass spectrometer identification of metallic ions during Encke meteor shower
22 p2735 N73-31897
Atomic structure of stripped heavy ions and their formation and destruction by collisions
[NASA-CR-135704] 23 p2821 N73-32553

**HEAVY NUCLEI**
Plastic, nuclear track detectors for recording and measuring multicharged, heavy particles
[NASA-CR-123918] 02 p0213 N73-11725
Survival of heavy nuclei in cosmic ray source environments from Goddard balloon spectrometer experiment
08 p0974 N73-17964
Impact calculation of heavy nuclei of cosmic rays
11 p1243 N73-20089
Apollo 16 experiment using biostack to determine effects of heavy nuclei on biological organisms
12 p1452 N73-21761
BIOSTACK experiment on Apollo 16 for studying combined action of heavy high energy loss nuclei and space flight factors on resting biological systems
14 p1611 N73-23062
Energy spectra analysis for heavy nuclei charge compositions in galactic cosmic rays
[NASA-TM-X-66136] 17 p2079 N73-26817
Acceleration mechanism for heavy nuclei abundance enhancement in solar flares
19 p2337 N73-28801

**HEAVY WATER**
Analysis of density of water in forms of ice, water and steam, liquid and gaseous heavy water, and sea water
[ESDU-68010-AMEND-A] 01 p0038 N73-10302
Thermal conductivity of H20 and D2O
[ESDU-67031-AMEND-A] 01 p0115 N73-10954
Specific heat capacity at constant temperature and pressure of water substances
[ESDU-68008] 01 p0116 N73-10957

**HEAVY WATER REACTORS**
Neutronics analysis of gas core rocket concept using cavity test reactor
[NASA-TM-X-2743] 09 p1063 N73-18676
Steel technology and water reactor pressure vessel safety
[ORNL-4855] 24 p2935 N73-33440

**HEF [HIGH ENERGY FUELS]**
U HIGH ENERGY FUELS

**HEIGHT**
Shipboard antenna height effect on ultrahigh frequency surface of air communication
[AD-748203] 04 p0390 N73-13171
Correlation techniques and measurements of surface wave height statistics
[NASA-CR-2153] 04 p0405 N73-13298
Distribution losses in axial compressor over blade cross sections and effects of blade heights
[AD-750931] 06 p0657 N73-15334
Classification of meteoroids according to density and beginning height
[CONTRIB-14] 11 p1337 N73-20852
Meteoroid stream search among photographic meteors
[CONTRIB-15] 11 p1337 N73-20853
Remote barometric altimetry and estimation of meteorological field variables
[AD-759910] 17 p2058 N73-26650

**HEISENBERG THEORY**
Green function technique used to calculate magnetic properties of disordered Heisenberg ferromagnets in which exchange interactions deviate randomly in strength from mean interaction
[NASA-TN-D-7208] 14 p1697 N73-23774

**HELICAL ANTENNAS**
Analysis of some slow-wave conical log-spiral and helical antennas
[AD-757913] 15 p1757 N73-24242
Collapsible high gain antenna which can be automatically expanded to operating state
[NASA-CASE-KSC-10392] 17 p1993 N73-26117
Development of exact circular polarization in short helical antennas by conducting disk at helix end
[DLR-FB-73-46] 17 p1998 N73-26156

**HELICAL FLOW**
Analysis of pressure drop, heat transfer, and flow characteristics for forced convection boiling in helical coils
[AEEW-R-757] 07 p0855 N73-16936
Fourier analysis of plasma deformation and feedback in stabilized rectilinear helicoid with pinch mechanism
[LRP-58/72] 10 p1196 N73-19728

**HELICAL WINDINGS**
Numerical analysis of elastic stresses and deflections of helical compression springs made of round wire
[ESDU-65005] 01 p0112 N73-10926
Analysis of factors affecting choice of material and manufacturing methods for production of helical compression springs
[ESDU-65006] 01 p0112 N73-10927
Induction heating and concomitant quenching for hot winding helical springs
[AD-759906] 17 p2039 N73-26495

**HELICOPTER ATTITUDE INDICATORS**
U ATTITUDE INDICATORS
U HELICOPTERS

**HELICOPTER CONTROL**
Development of adaptive controller for multivariable systems and application to helicopter system with time varying parameters
[AD-746492] 01 p0002 N73-10007
Construction of pitch link in CH-47 helicopter control system using composite materials of graphite, glass, and carbon-steel
[AD-747337] 02 p0127 N73-11036
Evaluation of helicopter rotary wing configuration consisting of conventional pitch horn linkages inboard and aerodynamic control flap outboard for controllable twist
[AD-747808] 03 p0254 N73-12054
Design, development, and evaluation of helicopter control system using fan in fin configuration for antitorque and directional control
[AD-747806] 03 p0254 N73-12055
Yaw maneuverability of helicopters in gliding flight
05 p0493 N73-14022
Helicopter autorotation capability, noting BO-105 helicopter behavior
05 p0494 N73-14023
Addition of feel augmentation system to improve flight control of S-67 helicopter
[AD-749284] 05 p0494 N73-14029
Numerical analysis of characteristics of rotary wing aircraft when considered as two coupled rigid bodies representing rotor and fuselage
07 p0737 N73-15994
Analysis of aerodynamic stall characteristics of airfoils at various angles of attack with application to control forces of H-53 helicopter
[AD-752917] 09 p0986 N73-18053
Flight tests of XH-51 helicopter to determine effects of gyroscope and control spring modifications on stability and control
12 p1358 N73-21015
Effect of elastic flapping of rotor blades on stability and control of helicopter equipped with hingeless rotor system
12 p1358 N73-21016
Flight characteristics and performance of Fenestron type helicopter tail rotor
12 p1359 N73-21028
Evaluation of helicopter handling qualities based on ground-based piloted flight simulator tests
12 p1359 N73-21030
Effect of rotary wing airfoil modifications on performance, stability, and control of helicopters
12 p1361 N73-21045
Analysis of military helicopter control and stability characteristics to determine suitability as rocket launching platform
[AD-756436] 13 p1474 N73-21944
Development of method for calculating downwash interference and longitudinal stability of tandem rotor helicopter
[ARC-R/M-3223] 15 p1729 N73-24022
Failure analysis of synchronizing drive shaft adapter on CH-47A helicopter for improved reliability and cost reduction
[AD-763186] 21 p2497 N73-30041

**HELICOPTER DESIGN**
Application of ride-quality criteria to design of commercial helicopters with emphasis on noise and vibration considerations
01 p0003 N73-10015
Helicopter design data to include kinematic and power diagrams of basic components of helicopter structures
[AD-748751] 04 p0373 N73-13035
Proceedings of conference to analyze static and dynamic loads exerted on helicopter rotary wings and application to improved helicopter design
[AGARD-R-595] 05 p0491 N73-14000
Real time hybrid simulation of tied down helicopter for optimal stability control
05 p0494 N73-14024
Analysis of parameters affecting dynamic compatibility in helicopter propulsion systems
[AD-750387] 06 p0624 N73-15065
Proceedings of conference on rotary wing aircraft developments to include operational experience, flight tests, and evaluation of structural concepts
[AGARD-CP-121] 12 p1357 N73-21008
Flight tests of Westland Scout helicopter fitted with reduced scale version of rigid rotor to determine airworthiness and handling characteristics
12 p1358 N73-21017
Survey of problems encountered in prediction of structural design loads and aeroelastic stability margins during development of rotary wing aircraft
12 p1358 N73-21020
Aerodynamic characteristics of circulation controlled rotor and fundamental problems of stopped rotor aircraft
12 p1359 N73-21024
Wind tunnel tests to determine effects of nonrotating components on helicopter performance and application for helicopter design optimization
12 p1362 N73-21052
Analysis of aerodynamic and dynamic properties of rotary wing aircraft for application to design, development, and evaluation of helicopters
[AGARD-LS-63] 14 p1597 N73-22948
Aerodynamic characteristics of helicopters with emphasis on airloads, aeroelasticity, and mechanical instabilities
14 p1597 N73-22949
Fundamentals of rotary wing aerodynamics and application to performance considerations of helicopters
14 p1598 N73-22950
Basic dynamics of rotary wings, mechanics of helicopter flight, and aerodynamic characteristics of advanced rotary wing concepts and configurations
14 p1598 N73-22951
Test data and description of unsymmetrical crash analysis computer program for improved helicopter structural crashworthiness analytical and design techniques - Vol. 2
[AD-764986] 23 p2747 N73-31986

**HELICOPTER ENGINES**
Static, ballistic, and impact behavior of glass/graphite drive shaft sections to determine suitability for heavy lift helicopters
[AD-743938] 01 p0091 N73-10752
Analysis of parameters affecting dynamic compatibility in helicopter propulsion systems
[AD-750387] 06 p0624 N73-15065
Analysis of H-58 helicopter maintenance to determine removal rate of aircraft equipment and develop failure analysis statistics
[AD-756406] 13 p1475 N73-21945
Information and guidance for type certification of aircraft engines as required by Federal Aviation Administration
[FAA-AC-33-2A] 13 p1571 N73-22730
Development of method for estimating power output of helicopter gas turbine engines operating at full power
[AD-758461] 14 p1702 N73-23811
Effect of engine vibration, shaft whirling, and dynamic instabilities on helicopter performance and standardization of vibration limit specifications
[AD-761100] 18 p2107 N73-27039
Susceptibility of synthetic engine and transmission lubricants of OH-58 A helicopter to microbal attack
[AD-762176] 19 p2313 N73-28604
Design and characteristics of expansion chamber mufflers for reducing exhaust noise generated by helicopters
[NASA-TN-D-7309] 22 p2700 N73-31623
Bibliography of technical reports of helicopter engines and rotary wings
[AD-764900] 23 p2746 N73-31981

**HELICOPTER PERFORMANCE**
Computer program listings for analysis of main rotor free wake geometry effects on blade air loads and response for helicopters in steady maneuvers - Vol. 2
[NASA-CR-2111] 02 p0124 N73-11006
Design, development, and evaluation of helicopter control system using fan in fin configuration for anti-torque and directional control
[AD-747806] 03 p0254 N73-12055
Developments in unsteady aerodynamics of helicopter rotary wings to analyze stall flutter, transient effects of interactions, and wake induced instabilities
05 p0491 N73-14001
Analysis of stability characteristics of hingeless rotary wing on flap and lead-lag degrees of freedom of single blade
[AD-750359] 06 p0623 N73-15053
Analysis of parameters affecting dynamic compatibility in helicopter propulsion systems
[AD-750387] 06 p0624 N73-15065
Development of mathematical model for optimal takeoff performance of single rotor helicopter in ground effect with various pa' .oads
[AD-750388] 06 p0624 N73-15066
Application of optimal control theory to take-off of heavily loaded helicopters and instrumentation requirements to improve pilot flight control
[AD-750615] 06 p0625 N73-15072
Aerodynamic characteristics of helicopters with sling loads in hovering and near-hovering conditions
[AD-750618] 06 p0625 N73-15073
Application of equations of motion to investigate effects of mode shape and coning angle on stability boundaries of hingeless helicopter rotor blades
[NASA-CR-114525] 07 p0739 N73-16015
Development of dynamic helicopter performance and control model based on force and rotor aerodynamic equations
[AD-751460] 07 p0740 N73-16022
Analysis of airload and blade response of rotary wings to determine sources of rotor vibratory loads in level and maneuvering flight of NH-3A and CH-53A helicopters
[NASA-CR-2225] 10 p1103 N73-18996
Predicting loads and stresses on helicopter rotor blades
[NASA-TT-F-14845] 10 p1105 N73-19014
Helicopter flight performance in tactical environment
12 p1357 N73-21009
Analysis of procedures and problems involved in operating helicopters from decks of ships
12 p1357 N73-21010
Operational performance of helicopters in French Army
12 p1357 N73-21011
Presentation of helicopter level flight performance as power coefficient compared with tip speed or advance ratio for range of thrust coefficients
12 p1358 N73-21014
Flight tests of XH-51 helicopter to determine effects of gyroscope and control spring modifications on stability and control
12 p1358 N73-21015
Effect of elastic flapping of rotor blades on stability and control of helicopter equipped with hingeless rotor system
12 p1358 N73-21016
Discussion of speed record establishment by SA-341 helicopter to include aircraft preparation procedures and requirements for successful completion
12 p1358 N73-21018
Analysis of factors inhibiting performance of rotary wing aircraft and mathematical models of rotary wing flow characteristics
12 p1358 N73-21019
Flight characteristics and performance of Fenestron type helicopter tail rotor
12 p1359 N73-21028
Evaluation of helicopter handling qualities based on ground-based piloted flight simulator tests
12 p1359 N73-21030
Development of actuator disc theory for predicting time-averaged downwash distribution and response characteristics of helicopter rotors in forward flight
12 p1360 N73-21033
Development of procedure for determining geometry and strength distribution of vortex wake generated by single-bladed hovering helicopter rotor
12 p1360 N73-21035
Parameters for enhancing performance of helicopter rotors during stationary flight
12 p1360 N73-21036
Improvements in basic rotary wing design and tests to determine effects on helicopter performance
12 p1360 N73-21038
Analysis of unsteady aerodynamic environment of rotary wings and research projects to improve understanding of rotor unsteady airfoils
12 p1361 N73-21041
Effect of rotary wing airfoil modifications on performance, stability, and control of helicopters
12 p1361 N73-21045
Development of concept of circulation control applied to rotary wings to show effects on hover, transition, and high speed cruise performance
12 p1362 N73-21050
Analysis of helicopter performance with functioning engines, disengaged transmission, and steady autorotation of coaxial rotary wings
[AD-756592] 13 p1474 N73-21942
Evaluation of performance of H-1 helicopter, CH-54 helicopter, and OH-6 helicopter under combat conditions
[AD-755554] 13 p1475 N73-21949
Analysis of aerodynamic and dynamic properties of rotary wing aircraft for application to design, development, and evaluation of helicopters
[AGARD-LS-63] 14 p1597 N73-22948
Fundamentals of rotary wing aerodynamics and application to performance considerations of helicopters
14 p1598 N73-22950
Basic dynamics of rotary wings, mechanics of helicopter flight, and aerodynamic characteristics of advanced rotary wing concepts and configurations
14 p1598 N73-22951
Flight test procedures for rotary wing aircraft with emphasis on performance and flying qualities
14 p1598 N73-22959
Effect of engine vibration, shaft whirling, and dynamic instabilities on helicopter performance and standardization of vibration limit specifications
[AD-761100] 18 p2107 N73-27039
Measurement of vibration levels in CH-47 helicopter at pilot seat, control stick, rudder pedals, instrument panel, and human interface points
[AD-761199] 18 p2107 N73-27040
Numerical methods for determining unsteady aerodynamic forces on helicopter rotor blades to show lift distribution as function of velocity component normal to blades
[NASA-TT-F-15039] 20 p2360 N73-28981
Operational parameters for UH-1H helicopters during combat flights in Southeast Asia to determine helicopter performance and reliability
[AD-764260] 22 p2616 N73-30965
Bibliography of technical reports of helicopter engines and rotary wings
[AD-764900] 23 p2746 N73-31981
**HELICOPTER PROPELLER DRIVE**
Design, development, and evaluation of flexible drive shaft coupling used for propulsion of HH-2D helicopter
[AD-746502] 01 p0063 N73-10519
Effect of dynamic absorbers and damping on noise generated by CH-47 helicopter rotor transmission
[AD-752579] 08 p0868 N73-17031
Analytic methods for calculating blade loads and shaft-transmitted vibratory forces in stiff bladed hingeless rotors operating at various advance ratios - Vol. I
[NASA-CR-114562] 09 p0984 N73-18034
Descriptions, geometry, and technical data for three rotary wing systems used in determining vibration and loads in hingeless rotary wings - Vol. 2
[NASA-CR-114568] 09 p0984 N73-18035
Analysis of parameters and elastohydrodynamic principles affecting lubrication of transmission components with application to helicopter mechanical drive systems
[NASA-TM-X-68215] 12 p1364 N73-21069
Cost effectiveness analysis of helicopter transmission components to determine effect of extended overhaul life up to 6,000 hours
[AD-758465] 14 p1604 N73-23007
Design, fabrication, and evaluation of helicopter transmission seals using dual element split ring and circumferential seal configurations
[NASA-CR-120983] 17 p2037 N73-26481
**HELICOPTER ROTORS**
U ROTARY WINGS
**HELICOPTER WAKES**
Exact theory for helicopter rotor wake calculation
05 p0494 N73-14025
Field test of warm fog dispersal using helicopter downwash and hygroscopic seeding
[AD-752046] 08 p0939 N73-17694
Analytical and experimental techniques to define geometry of vortex field of hovering rotary wing and effect on rotor performance
12 p1359 N73-21032
Development of actuator disc theory for predicting time-averaged downwash distribution and response characteristics of helicopter rotors in forward flight
12 p1360 N73-21033
Development of procedure for determining geometry and strength distribution of vortex wake generated by single-bladed hovering helicopter rotor
12 p1360 N73-21035
Analysis of unsteady aerodynamic loading on reference section of helicopter rotor blade in axial or hovering flight under compressible flow conditions
12 p1361 N73-21044
Development of technique for rotor blade design and measurement of pressure distributions along the blade chord and across blade wake near rotor tip in flight
12 p1361 N73-21047
Analysis of aerodynamic noise produced by rotary wings and methods for noise reduction based on shed vortex wakes and blade tip modification
12 p1362 N73-21053
Proceedings of conference on rotary wings to investigate rotor wakes, aerodynamic characteristics at hover and high advance ratio, and aerodynamic noise properties
13 p1473 N73-21931
**HELICOPTERS**
NT BO-105 HELICOPTER
NT CH-3 HELICOPTER
NT CH-47 HELICOPTER
NT H-53 HELICOPTER
NT MILITARY HELICOPTERS
NT OH-6 HELICOPTER
NT OH-13 HELICOPTER
NT P-531 HELICOPTER
NT SH-3 HELICOPTER
NT TANDEM ROTOR HELICOPTERS
NT UH-1 HELICOPTER
NT UH-2 HELICOPTER
NT XH-51 HELICOPTER
Analysis of helicopter pilot and passenger reaction to vibration environment to determine effects of discrete frequencies and combinations of harmonic frequencies
01 p0003 N73-10019
Ground based UH-1 helicopter sonic analyzer for evaluation of effectiveness of using sonic data to diagnose mechanical condition of army helicopter power train components
[AD-745089] 01 p0004 N73-10026
Dissipation of fog using helicopter downwash
[AD-744471] 01 p0076 N73-10629
Development and characteristics of test facility for measuring three dimensional boundary layers on helicopter rotor blade under various conditions
[NASA-CR-112194] 03 p0252 N73-12042
Evaluation of helicopter rotary wing configuration consisting of conventional pitch horn linkages inboard and aerodynamic control flap outboard for controllable twist
[AD-747808] 03 p0254 N73-12054
Application of metal-polyfluoroethylene bearings in helicopter rotor hinges for operation with and without lubrication
[AD-747428] 03 p0308 N73-12512
Performance of high speed overriding clutch assemblies for helicopters
[AD-747807] 03 p0308 N73-12518
Analysis of limitations on helicopter approach and landing during conditions of low visibility
[AD-747732] 03 p0329 N73-12686
Effects of aerodynamic stall on helicopter rotor blade element in three dimensional rotating environment
[NASA-CR-114489] 04 p0372 N73-13028
Proceedings of symposium on helicopter noise held at Durham, North Carolina Sept. 1971
[AD-748876] 04 p0373 N73-13036
Development of computer assisted troubleshooting system for maintenance of helicopters and aircraft using Univac 1108 computer
[AD-748665] 04 p0373 N73-13037
Analysis of response of flexible helicopter rotor blade to random loads with vertical velocity component
[AD-746627] 04 p0374 N73-13038
Analysis of model helicopter rotor blade response to random excitation during simulated forward flight using electromechanical apparatus
[AD-748457] 04 p0374 N73-13040
Technology of aircraft construction
[AD-748712] 04 p0374 N73-13043
Advanced technology hoist-drive system applicable to helicopter cargo hoists with capacities ranging from 12.5 to 50 tons
[AD-746629] 04 p0377 N73-13067
Evaluation of approach lighting system for visual guidance of helicopters during instrument flight rules approach and landing operations
[FAA-RD-72-133] 04 p0401 N73-13261
Application of model helicopter rotor experiments to determining dynamic stall of rotary wings and predicting aerodynamic loads developed
05 p0491 N73-14002
Numerical analysis of unsteady aerodynamic forces on helicopter rotor blades to determine lift distribution as function of velocity component normal to blades
05 p0491 N73-14003
Application of perturbation techniques to single blade helicopter rotor dynamics
[NASA-TM-X-62163] 05 p0492 N73-14006
Development of statistical technique for determining injury reduction capability of energy absorber equipment
[AD-749333] 05 p0497 N73-14044
Helicopter performance in civilian air rescue operations
[AD-748695] 05 p0502 N73-14087
Application of optimal control theory to take-off of heavily loaded helicopters and instrumentation requirements to improve pilot flight control
[AD-750615] 06 p0625 N73-15072

Aerodynamic characteristics of helicopters with sling loads in hovering and near-hovering conditions
[AD-750618] 06 p0625 N73-15073
Electrostatic charging and discharging of helicopters in flight and personnel safety
[AD-750617] 06 p0701 N73-15718
Development of dynamic helicopter performance and control model based on force and rotor aerodynamic equations
[AD-751460] 07 p0740 N73-16022
Design, development, and evaluation of flywheel powered hoist for personnel rescue missions conducted by helicopters
[AD-751217] 07 p0741 N73-16029
Nonlinear instability in flap-lag of rotor blades in forward flight
[NASA-CR-114524] 08 p0867 N73-17017
Development of computer programs to calculate helicopter rotor tip vortex geometry in hover and forward flight to include calculation of rotor harmonic air loads
[AD-752628] 08 p0869 N73-17032
Flight test of instrument for determining low airspeeds to evaluate suitability for helicopter airspeed indicator
[AD-753343] 09 p0989 N73-18071
Analysis of aerodynamic noise generated by tips of helicopter rotary wings during acceleration to near sonic speed
[AD-752301] 09 p0989 N73-18072
Analysis of V/STOL aircraft design and operation to determine effects of noise problems and constraints with emphasis on helicopter performance
[AD-752447] 09 p0989 N73-18073
Helicopter downwash for dispersing fogs of 500 to 600 feet in depth
[AD-753357] 09 p1062 N73-18661
Helicopter flying in poor light and featureless terrain and color vision abnormality
10 p1113 N73-19075
Application of night vision technology helicopter night scouts
10 p1226 N73-19970
Improved visual capability for police helicopters
10 p1228 N73-19984
Application of equations of motion to develop analog computer simulation of helicopter rotor system
[AD-754547] 11 p1235 N73-20024
Numerical analysis of ideal and real gas equations for application to lift generated by helicopter rotors
[AD-754420] 11 p1235 N73-20026
Fatigue damage of helicopter rotary wing structures - bibliographies
[AD-754062] 11 p1235 N73-20027
Design of hydrofluidic flight control system for helicopter stabilization
[AD-754602] 11 p1236 N73-20032
Analysis of procedures and problems involved in operating helicopters from decks of ships
12 p1357 N73-21010
Reliability and operational safety of mechanical helicopter transmission boxes
12 p1357 N73-21012
Improvements in military helicopter flight test techniques to provide data for safety, maintainability, and reliability
12 p1357 N73-21013
Aerodynamic, dynamic, and aeroelastic problems in rotary wing design for helicopters and V/STOL aircraft with application to hingeless rotor systems
12 p1362 N73-21051
Analysis of helicopter internal and external noise levels for various flight conditions and timing of acoustical spectra
12 p1362 N73-21055
Analysis of electrical charge generated by helicopter rotor operating near particulate matter with seeded vortex
[AD-755282] 12 p1366 N73-21080
True airspeed sensor for V/STOL aircraft with increased accuracy below 40 knots
[AD-755374] 12 p1406 N73-21403
Failure analysis of components of CH-47A auxiliary power plants
[AD-756407] 13 p1478 N73-21975
Fundamentals of helicopter noise generation and propagation to include noise control procedures and cost effectiveness of noise reduction
14 p1598 N73-22953
Analysis of vortex shedding from airfoils with application to vortex noise generated by helicopter rotary wings
[AD-757167] 14 p1602 N73-22989
Environmental endurance testing of elastomeric pitch change bearing for use on H-1 Aircraft
[AD-758463] 14 p1671 N73-23561
Application of multipoint excitation for helicopter structural dynamic testing using impedance techniques - Vol. 1
[AD-756389] 14 p1716 N73-23921
Dynamic structural analysis of helicopter structures using single point excitation techniques - Vol. 2
[AD-756390] 14 p1716 N73-23922
Dynamic structural analysis of helicopter structures using free-body response techniques - Vol. 3
[AD-756391] 14 p1716 N73-23923
Dynamic structural analysis of helicopter subsystems based on equations for combination of mobility matrices - Vol. 4
[AD-756392] 14 p1716 N73-23924
Analysis of escape systems for helicopter flight crews and passengers
[B-177166] 15 p1734 N73-24067
Design, development, and testing of inflexible blade, hingeless rotor system with hydraulic rotor control system
[AD-758514] 15 p1736 N73-24081
Numerical analysis of bending of rotating beams with application to linear flap-lag stability of hingeless rotary wings using nonlinear equations
[NASA-TM-X-2770] 15 p1838 N73-24897
Development of method for calculating spanwise loading on helicopter rotor blades in forward flight at various azimuth angles
[ARC-R/M-3318] 16 p1856 N73-25032
Development of procedures for determining service life of helicopter airframes and rotor blades
[RAE-LIB-TRANS-1520] 17 p1981 N73-26013
Optimal design of helicopter precision hover control systems
[AD-759919] 17 p1984 N73-26039
Equipment route winds and great circle distances for helicopter air routes at 5,000, 10,000, and 18,000 feet - Vol. 1
[AD-760252] 17 p1985 N73-26043
Equipment route winds and great circle distances for helicopter air routes at 5,000, 10,000 and 18,000 feet - Vol. 2
[AD-760253] 17 p1985 N73-26044
Analysis of operational problems associated with wind tunnel testing of V/STOL aircraft and helicopters
17 p2008 N73-26240
Scaling laws, constructional problems, and optimum model size associated with wind tunnel tests of helicopters and rotary wing aircraft
17 p2009 N73-26246
Analysis of products and techniques for reducing reflections of light from helicopter windshields, rotor blades and rotor hub assembly
[AD-761127] 18 p2107 N73-27037
Application of glass reinforced and carbon reinforced composite materials for helicopter structures and rotary wings
18 p2165 N73-27483
Tabular data from helicopter downdraft fog dispersal experiments
[AD-762189] 19 p2318 N73-28643
Development of procedures for stabilizing snow to permit helicopter landings
[AD-763231] 21 p2497 N73-30040
Application of composite materials to construction of helicopter airframes and landing gear
[NASA-CR-112333] 22 p2614 N73-30948
Dynamic structural analysis of fully articulated rotor blade on helicopter rotary wing for three degrees of freedom
[AD-763934] 22 p2615 N73-30957
Helicopter gust response to include unsteady aerodynamic stall effects under short-term, control-fixed conditions
[AD-763957] 22 p2615 N73-30958
Aerodynamic characteristics of low speed flight using heavily loaded ducted fans, single bladed hovering rotor, and tensioned sheets with cutouts
[AD-764264] 22 p2616 N73-30964
Design and flight tests of helicopter airspeed indicator
[AD-764240] 22 p2675 N73-31430
Proceedings of symposium to determine requirements and configurations of emergency ejection systems for helicopter crews
[AGARD-AR-62] 23 p2743 N73-31954
Construction of helicopter airframes and landing gear to show advantages of composite material prototype over metal prototype
[NASA-CR-112333] 23 p2743 N73-31957
Computer program and mathematical model for predicting dynamic response of helicopter in accident involving vertical and lateral impact
[AD-764985] 24 p2879 N73-32996
Utilization of decision and value theory concepts by helicopter pilots to plan attacks
24 p2950 N73-33565

**HELIOCENTRIC ORBITS**
U SOLAR ORBITS

**HELIOGRAPHS**
U SPECTROHELIOGRAPHS

**HELIOGRAPHY**
U SPECTROHELIOGRAPHS

**HELIOMAGNETISM**
U SOLAR MAGNETIC FIELD

**HELIOMETERS**
NT PYROHELIOMETERS
Design details of photoheliograph thermal concepts
[NASA-CR-124255] 15 p1787 N73-24492
Pyrheliometers errors with various aperture angles associated with solar aurora effects
20 p2403 N73-29311
Bolometric pyrheliometer with balanced resistance bridge and radiation detector having copper wire spiral
20 p2403 N73-29315
CIT photoheliograph functional verification unit test in Big Bear Solar Observatory vacuum chamber
[NASA-CR-124455] 24 p2925 N73-33364

**HELIOMETRY**
U HELIOMETERS
U PYROHELIOMETERS

**HELIOS PROJECT**
Electrical and mechanical properties of vector magnetometer in HELIOS experiments for interplanetary magnetic field observations
[GAMMA-21] 01 p0048 N73-10384
Design and performance of solar array for Helios solar probe
[DGLR-PAPER-72-091] 06 p0627 N73-15084
Onboard data processing system for Helios solar probe
[DGLR-PAPER-72-092] 06 p0644 N73-15229
Design of orthotropic cylindrical shell as structural adapter for Helios solar probe
[DGLR-PAPER-72-101] 06 p0722 N73-15889
Design and development of interplanetary Helios satellite
[DGLR-PAPER-72-104] 09 p1091 N73-18905

**HELIOS SATELLITES**
Ultraviolet and charged particle irradiation of solar cell coverslide materials and conductive coatings for Helios satellites
[NASA-TM-X-65945] 09 p1051 N73-18571
Analysis of lubricating oil losses under vacuum conditions and application to antifriction bearings in antenna despin system of Helios solar probe
[NLL-RISLEY-TR-2567-[9091.9F]] 15 p1790 N73-24509

**HELIPORTS**
Wind tunnel tests to determine time-averaged aerodynamic forces on model of helicopter landing pad to be installed on top of lighthouse
[MAR-SCI-R-106] 15 p1761 N73-24269

**HELIUM**
NT HELIUM ATOMS
NT HELIUM FILM
NT HELIUM IONS
NT HELIUM ISOTOPES
NT LIQUID HELIUM
Growth response of bacteria and yeast in high pressure helium-oxygen environment
[AD-745334] 01 p0012 N73-10096
Development of fluid mechanical helium argon ion laser and analysis of improvements in efficiency and power output
[NASA-CR-128397] 01 p0064 N73-10526
Ion acoustic instability in helium positive column
[AD-745399] 01 p0086 N73-10709
Observations of solar wind helium enhancements following major solar flares and relation to flare piston plasma
01 p0098 N73-10808
Application of Doppler-shifted fourth sound techniques for analyzing current states in rotating superfluid helium contained in superleak
[AD-745316] 01 p0118 N73-10974
Equilibrium distribution of helium-4 and helium-3 between the liquid and vapor phases of deuterium 2 and hydrogen 2
[NBS-TN-621] 02 p0137 N73-11109
Nozzle wall boundary layer of helium tunnel
[NASA-TN-D-6965] 02 p0156 N73-11261
Spectral line profiles of helium triplet diffuse series and quasi-static approximation for ions and electrons
[NASA-TN-D-6934] 02 p0214 N73-11731
Thermophysical properties of helium-4 under various conditions of temperature and pressure
[NASA-CR-128445] 02 p0242 N73-11966
Heat regulation and adaptation of rats exposed to helium oxygen atmosphere
03 p0259 N73-12096
Improved dilatometer with helium cryostat for low temperature measurements
[AD-747555] 03 p0304 N73-12484
On-line and off-line bench test evaluation of helium speech unscramblers under controlled conditions
[AD-748295] 04 p0391 N73-13176
Estimating quantity of helium in Venus atmosphere from measured ionization profile
[NASA-TM-X-66128] 04 p0475 N73-13883
Sources responsible for long term drift of He-Ne lasers
[AD-749055] 05 p0558 N73-14535
Ionization and excitation cross section measurements on degenerate helium levels
[NASA-TM-X-66137] 05 p0582 N73-14738
Visual evoked responses from divers subjected to hyperbaric conditions simulating depths to 1200 feet breathing various gas mixtures
[AD-749325] 06 p0631 N73-15127
Depth effect on microphone sensitivity in underwater speech communication
[AD-750650] 06 p0642 N73-15213

Equation of state for compressibility of helium, nitrogen, and their mixtures
[JPRS-57923] 07 p0752 N73-16111
Cryogenic shock tubes for studying shock wave interactions and generating large Mach number flows
[AD-753134] 09 p1012 N73-18261
Helium/oxygen breathing effects on rat gas exchange and musculoskeletal heat control
10 p1115 N73-19093
Compression of helium to high pressures and temperatures using ballistic piston apparatus with shock tube
[NASA-CR-131230] 10 p1141 N73-19298
Charge form factor of helium and center-of-mass motion
[ISS-72/12] 10 p1191 N73-19693
Energy distributions of electrons in radiation-induced helium plasmas
[NASA-CR-130980] 10 p1195 N73-19727
Large helium systems for superconducting power applications and high energy physics
[BNL-17228] 10 p1200 N73-19764
Equation of state for helium and nitrogen mixture
[AD-753964] 11 p1253 N73-20169
Helium crystal growth in preferred orientations
[AD-754442] 11 p1330 N73-20797
Measurement of phonon scattering by isotopic impurities in helium single crystals
[AD-754475] 11 p1330 N73-20798
Analysis of Apollo 16 reaction control system helium pressure regulator filter failure
[NASA-TM-X-69131] 11 p1334 N73-20827
Investigation of He-3 impurities in He-4 for development of microscopic theory of He-3 quasiparticles
12 p1375 N73-21155
Development of precursor waves in helium and analysis of wave speed, electron temperatures, and densities using nuclear data handling techniques
12 p1387 N73-21249
Design of zero-field parametric resonance magnetometer using optically pumped helium
[AD-755256] 12 p1402 N73-21376
Variations of relative abundances of helium, carbon, nitrogen, oxygen, and iron-group nuclei in solar cosmic rays and their relationship to solar particle acceleration
[NASA-TM-X-66228] 12 p1445 N73-21706
Electronic structure in disordered amorphous materials and dense helium
[AD-755260] 13 p1567 N73-22701
HEPROP - a computer program for thermophysical properties of helium
[REPT-1046/72] 13 p1591 N73-22896
Proceedings of international workshop on helium speech processing
14 p1630 N73-23210
Proceedings of workshop on processing helium speech
[AD-757329] 14 p1635 N73-23259
Use of torsional pendulum as high pressure gage and determination of viscosity of helium gas at high pressures
[NASA-TN-D-7241] 14 p1667 N73-23528
Measured and calculated transmission losses of sound waves through helium layer
[NASA-TN-D-7230] 14 p1692 N73-23735
Mass spectrographic determination of ions and neutral reactions in glow discharge of helium-sulfur dioxide-carbon monoxide
[BM-RI-7747] 15 p1747 N73-24157
Raman spectra of Van der Waals complexes in argon, helium, and xenon
[AD-758241] 15 p1748 N73-24171
Helium embrittlement of austenitic stainless steels
[AI-AEC-13047] 15 p1799 N73-24580
Effects of underwater breathing of helium oxygen mixture on speech recognition
[AD-759413] 16 p1878 N73-25205
Helium migration in aluminum matrices under temperature gradients
16 p1926 N73-25586
Spin-orbit interactions with singlet-triplet mixing in excited states of helium
16 p1947 N73-25751
Cryogenic stability and reliability of operating Nb3Sn coils in helium gas environment
[IPP-4/100] 17 p2063 N73-26690
Elastic scattering of He on LiF crystal surfaces
[NRC-TT-1652] 17 p2072 N73-26764
Helium cooled current leads in refrigerated superconductive magnet system
[DESY-72/65] 17 p2073 N73-26769
Analysis of characteristics of supersonic flow of helium around right circular cones at zero angle of attack and Mach numbers from 1.5 to 30.0
[NASA-SP-3078] 18 p2130 N73-27208
Mass spectrum identification of trace organic impurities in gaseous helium
[NASA-TN-D-6520] 19 p2230 N73-27983
Thermospheric wind effects on global distribution of helium in upper atmosphere
[NASA-TM-X-70441] 20 p2412 N73-29391
Primordial helium abundance and population II binary stars, measurement technique
20 p2469 N73-29832
Analysis of linear and nonlinear stage of ion-acoustic instability in low pressure discharge in helium
[AD-763590] 21 p2584 N73-30707
Theory of mobility of ions in superfluid helium
22 p2701 N73-31632
Tantalum surface bounding of helium discharge plasma considering resonant ion neutralization
[AD-753520] 22 p2706 N73-31670
Differential energy spectra of cosmic ray protons and helium nuclei
23 p2833 N73-32640
Biological evaluation of influence of helium-oxygen atmosphere on culture of mammalian cells
24 p2883 N73-33024
Time resolved measurements of droplet growth in Wilson expansion cloud chamber
24 p2901 N73-33158
Pressure effects on dynamic viscosity of helium in temperature range 0.4 to 400 K
24 p2908 N73-33208
Supercritical helium cooling of superconducting magnet for use in dc beam line elements
[RHEL/R-258] 24 p2969 N73-33725
**HELIUM AFTERGLOW**
Electrical discharge metastable detector for helium afterglows
[AD-765210] 23 p2823 N73-32570
**HELIUM ATOMS**
Stark shift measurements and photon resonance perturbations in triplet metastable helium atom near ionization threshold
[KFKI-72-42] 10 p1169 N73-19507
Dependence of photon resonance in metastable helium atom ionization on light intensity
[KFKI-72-69] 10 p1192 N73-19695
Time dependent scattering theory for evaluating transition cross sections in atomic helium collision with charged particle
[NASA-CR-131265] 11 p1326 N73-20761
Differential and integral scattering cross sections for H and He atoms in hydrogen
[NASA-TT-F-14900] 13 p1561 N73-22655
Differential scattering from collision of metastable atoms of He[2 3S] with molecules of N2 and O2
[NASA-TT-F-14801] 15 p1815 N73-24712
Helium excitation and structure of quiescent solar prominences
20 p2472 N73-29859
Helium self-oscillating magnetometer with optical pumping of He-4 atoms
22 p2671 N73-31397
Heating of plasma confined in Tokamak by injecting fast helium atoms
[EUR-CEA-FC-682] 24 p2964 N73-33690
**HELIUM FILM**
Heat capacity of submonolayer helium films adsorbed on exfoliated graphite in very low temperatures
16 p1973 N73-25953
Thermodynamic state of thin helium films for precise measurements of third sound velocity and attenuation
24 p2968 N73-33720
**HELIUM IONS**
Calculation of velocity distribution of helium ion in solar wind at one astronomical unit
01 p0099 N73-10814
**HELIUM ISOTOPES**
Nuclear magnetic relaxation in He-3 impuriton gas
[NUB-2155] 01 p0083 N73-10687
Field theoretical model for critical behavor of helium 4 above critical point
[NOTA-INTERNA-374] 01 p0083 N73-10689
Tables of thermophysical properties of helium 4
[NBS-TN-631] 06 p0730 N73-15953
Physical properties of liquid He-4, characteristics of He-1 and -2, and Fontaine effect
[FRNC-CONF-48] 10 p1126 N73-19171
Analysis of hydrodynamics of helium isotopes to determine entrainment of sound in moving fluid
10 p1139 N73-19278
Phase transition and entropy behavior of solid He-3
[COO-1569-96] 12 p1439 N73-21654
Three body exchange effects on Neel temperature of solid He-3
[COO-1569-97] 12 p1439 N73-21655
Spectrometric measurements of cryogenic helium 4 scattering angle and momentum transfer
[CONF-720833-10] 12 p1440 N73-21669
Differential cross sections in photodisintegration of helium-3
16 p1947 N73-25753
Specific heat measurements of He-4 monolayers on sintered and gas monolayer coated copper
16 p1973 N73-25957
Research activities in physics
[COO-535-674] 17 p2010 N73-26259
Phase characteristics of submonolayer isotopic mixtures of helium adsorbed on Grafoil
18 p2113 N73-27084
IMP measurements on hydrogen and helium isotope accelerations in solar flares
19 p2336 N73-28797
Isotopic composition of hydrogen and helium in solar cosmic ray measurements by OGO F
19 p2336 N73-28798
Acoustic pumping used to achieve analogous ac Josephson effect in He2
20 p2385 N73-29164
Energy storage in electronically excited solid helium
[NASA-CR-135716] 23 p2820 N73-32541
Variations in solar wind He-4 ion abundance occurring primarily in lower corona
23 p2834 N73-32643
Measurement of viscosity of solution of He 3 in He 4 at superflow temperatures
[JINR-P8-7009] 24 p2892 N73-33086
Abnormalities of liquid He-3 measured below 5 m K
24 p2967 N73-33713
Thermodynamic state of thin helium films for precise measurements of third sound velocity and attenuation
24 p2968 N73-33720
Measurement of heat conductivity of He 3 and He 4 at superflow temperature
[JINR-P8-7008] 24 p2992 N73-33912
**HELIUM PLASMA**
Technique for determining influence of axial magnetic field on holdup of argon in coaxially fed argon-helium plasma generated by radio frequency induction
[ORNL-TM-3700] 03 p0341 N73-12779
HCN laser interferometer for electron density measurements on helium plasma
[NP-19595] 11 p1328 N73-20774
Enhanced far infrared radiation from theta pinch plasma
12 p1432 N73-21601
Recombination coefficients and volume decay coefficient for laser-produced helium plasmas
[CEA-CONF-2102] 15 p1817 N73-24726
One dimensional, diffusion wave transverse to magnetized helium positive column plasma
[AD-763808] 22 p2705 N73-31666
**HELIUM 2**
U HELIUM ISOTOPES
U LIQUID HELIUM
**HELIUM 3**
U HELIUM ISOTOPES
**HELIUM 4**
U HELIUM ISOTOPES
**HELIUM-NEON LASERS**
Effect of variable magnetic field on emission of helium-neon laser and resulting parameters of discharge plasma
[AD-747443] 03 p0311 N73-12542
Design and development of multichaanel laser remote control system using modulated helium-neon laser as transmitter and light collector as receiving antenna
[NASA-CASE-LAR-10311-1] 07 p0806 N73-16536
Analysis of acoustical amplitude and frequency modulation techniques of continuous wave helium-neon laser for optical communication applications
[AD-757672] 14 p1674 N73-23581
**HELIX TUBES**
U TRAVELING WAVE TUBES
**HELIXES**
U CURVES [GEOMETRY]
**HELMETS**
Biomedical problems with helmet mounted sight and visual target acquisition system
10 p1226 N73-19969
Audiometric thresholds for bare headed subjects, or wearing M1 helmet, and experimental helmet
[AD-745121] 13 p1486 N73-22053
Evaluation of helmet weight on head by military personnel
[AD-748412] 13 p1487 N73-22056
Impact resistance of crash helmets for agricultural aviation pilots
[ARL/SM-NOTE-390] 22 p2623 N73-31014
**HELMHOLTZ EQUATIONS**
Neumann boundary value problem for Helmholtz oscillation equation
[NRC-TT-1606] 06 p0690 N73-15616
Helmholtz equation for solving electromagnetic wave functions of parabolic plasma density profiles
[AD-751669] 07 p0757 N73-16151
**HELMHOLTZ VORTICITY EQUATION**
Helmholtz resonator damping device for suppressing rocket combustion instability
03 p0349 N73-12845
Kelvin-Helmholtz instability analysis of bounded two phase particulate incompressible inviscid flows
[AD-754815] 11 p1272 N73-20318
Kelvin-Helmholtz instabilities in mesoscale wind and temperature structure during clear air turbulence
[AD-763084] 20 p2413 N73-29397
**HEMATITE**
Single crystals of hematitic Fe2O3 grown from Na2B4O7 and occuring as plates, rods, hoppers, and equidimensional solid crystals
[AD-755349] 13 p1567 N73-22697
**HEMATOCRIT RATIO**
Hemoglobin and erythrocyte increase in rat adaptation to hypoxic hypoxia
13 p1481 N73-22005

**HEMATOLOGY**
Hematology of miniature pigs after rapid decompression
[DLR-FB-73-63] 24 p2886 N73-33047
**HEMATOPOIETIC SYSTEM**
Leukopenic response of dog bone marrow for evaluating hematopoietic tissue function
13 p1481 N73-22009
**HEMISPHERES**
Analysis of pressure distribution around hemisphere at supersonic speeds with emphasis on differential pressure measurements
[ARC-R/M-3237] 15 p1729 N73-24023
Single-level objective analysis of meteorological observations on hemisphere by optimal interpolation
[NLL-M-22908-[5828.4F]] 18 p2169 N73-27514
**HEMISPHERICAL SHELLS**
Free-formed, flanged, acrylic shells for service as external pressure hulls with nominal 56-ft depth
[AD-749029] 05 p0603 N73-14908
Wind tunnel tests to determine heat transfer and pressure distributions of hemisphere cylinders in hypersonic flow environment
[NASA-TN-D-7104] 05 p0605 N73-14925
Nonlinear dynamic response of thin, clamped hemispherical shell subjected to suddenly applied pressure
[AD-752795] 09 p1096 N73-18950
FORTRAN program for predicting temperature-time histories of hemispherical shells subject to aerodynamic heating
[WRE-TN-783[WR/D]] 09 p1098 N73-18961
**HEMODYNAMIC RESPONSES**
State of hemocoagulation and thrombocytes during hypokinesia after adaptation to high-mountain conditions
11 p1245 N73-20107
Long term hypokinesia effect on rats hemodynamic system
14 p1607 N73-23026
Physiological and hemodynamic adaptations to CO levels and exercise in nonsmoking normal men
[PB-213834/1] 14 p1612 N73-23073
Influence of monochromatic light on physiological processes of blood
[NASA-TT-F-14941] 16 p1866 N73-25111
Lower body decompression effects on human cardiovascular hemodynamic system
20 p2367 N73-29032
Human hemodynamic responses and vestibular tolerances to body sway tests
20 p2367 N73-29034
Variations of cell enzymes, glucose, cholesterol, and 17-hydroxycorticosteroid in blood during physical work noting physical training dependence
[DLR-FB-72-48] 21 p2501 N73-30072
**HEMODYNAMICS**
Functional changes in systemic and cerebral hemodynamics with respect to vestibular stresses accompanying low accelerations
11 p1245 N73-20108
Techniques for determining effects of prolonged weightlessness on cardiovascular system of subhuman primates
[NASA-CR-131890] 13 p1479 N73-21980
**HEMOGLOBIN**
NT CARBOXYHEMOGLOBIN
Design of electrophoretic mass screening tester for sickle cell anemia
12 p1373 N73-21140
Effects of hyperoxia on heme biosynthesis
[AD-756836] 15 p1742 N73-24125
**HEOS A SATELLITE**
Shock pair observation from HEOS 1
01 p0097 N73-10797
Analysis of alpha particle observations performed by HEOS 1 satellite and comparison with observations made by Vela 3 and Explorer 34 satellites
01 p0098 N73-10809
Preliminary results from HEOS A satellite in electron and proton events, solar wind and interplanetary magnetic field measurement, and propagation of charged particles
[ESRO-SP-74] 05 p0592 N73-14813
Determination of location and time of solar flare observed from HEOS A and ESRO 2 satellites
05 p0592 N73-14814
HEOS 1 satellite recorded data on solar proton event in 1970
05 p0593 N73-14815
Electron flux density recorded onboard HEOS 1 in 1969 and 1970, discussing solar activity effects and comparing proton flux density
05 p0593 N73-14816
Injection, propagation, and interaction characteristics of solar protons based on HEOS A satellite data
05 p0593 N73-14817
Comparison of solar cycle variation of interplanetary magnetic field strength observed by HEOS A and Explorer 18 satellite
05 p0593 N73-14819
HEOS A satellite measurement of solar wind parameters
05 p0593 N73-14820
Solar wind angular measurements and correlation with solar activity, magnetic storms, plasma flow, in magnetosheath
05 p0593 N73-14821
Definition study of X ray background experiment on HEAO A
[AD-759738] 18 p2198 N73-27742
**HEOS B SATELLITE**
HEOS A 2 experimental design for solar wind and magnetospheric low frequency wave measurement
[DSRI-73-01] 19 p2295 N73-28457
**HEOS SATELLITES**
NT HEOS A SATELLITE
NT HEOS B SATELLITE
Scientific aspect of interplanetary investigation by Helios satellite
[DGLR-PAPER-72-068] 09 p1085 N73-18853
**HERCULES AIRCRAFT**
U C-130 AIRCRAFT
**HERMETIC SEALS**
Portable device for detecting pneumatic pressure leaks in hermetically sealed housings
[NASA-CASE-MFS-21761-1] 09 p1035 N73-18444
Development of epoxy resin lubricant sealant for hermetic sealing of threaded joints on pipes
[AD-752825] 09 p1040 N73-18486
**HETEROCYCLIC COMPOUNDS**
NT ADENINES
NT ADENOSINE TRIPHOSPHATE [ATP]
NT ASCORBIC ACID
NT ATROPINE
NT AZINES
NT AZULENE
NT INDOLES
NT NICOTINIC ACID
NT OXAZOLE
NT PHTHALOCYANIN
NT PYRIDOXINE
NT PYRROLES
NT RDX
NT TETRAZOLES
NT THIAMINE
Thermal decomposition of polyhydrazide and polyoxadiazoles
[AD-749853] 05 p0568 N73-14612
Synthesis of high molecular weight benzobistriazolo phenanthroline polymers for heat resistant plastic films
[AD-753414] 10 p1127 N73-19180
Pyrolysis of heterocyclic polymer compounds
[AD-764720] 24 p2892 N73-33091
**HETERODYNING**
NT OPTICAL HETERODYNING
Construction and testing of dual 10.6 micron CO2 laser AFC heterodyne system
[AD-747947] 03 p0312 N73-12544
Development and characteristics of optical communication system based on three frequency heterodyne configuration
[AD-750321] 06 p0680 N73-15533
Systems and techniques of experiment to establish air-to-ground CO2 laser heterodyne link
[NASA-TM-X-65946] 09 p1043 N73-18507
Optimal accumulation time in superlong-baseline interferometer and frequency stability of sinusoidal signal generators used as heterodynes at receiving points
23 p2838 N73-32678
**HETEROGENEITY**
Role of solid phase heterogeneity on low pressure L-star instability of nonmetallized rocket propellants
[NASA-CR-135766] 24 p2970 N73-33735
**HEURISTIC METHODS**
Survey of field of fault diagnosis and key algorithms and heuristics currently in use
[NASA-CR-129095] 02 p0178 N73-11440
Analysis-by-synthesis models of speech perception with emphasis on efficient machine realization of model
14 p1629 N73-23204
Three graph models and heuristic search strategies
[NASA-CR-131992] 14 p1684 N73-23662
Heuristic method for scheduling aircraft maintenance
[AD-761494] 19 p2355 N73-28947
**HEXAGONAL CELLS**
X ray crystallographic methods for studying preferred orientation of hexagonal metals
[RFP-TRANS-117] 11 p1306 N73-20594
**HEXAGONS**
Crystal structure of polymorphic form of carbon similar to chaoite
[AD-747476] 03 p0347 N73-12828
**HEXANITROSTILBENE /HNST/**
Simulation of plastic bonded hexanitrostilbene/Teflon explosive for lunar seismology
[NASA-CR-131370] 11 p1349 N73-20949
Physical and detonation properties of dry blended hexanitrostilbene/Teflon explosive charges used on Apollo 17 seismic experiment
[NASA-CR-133838] 21 p2606 N73-30886
**HEXENES**
Analysis of viscosity of saturated hydrocarbons at different temperatures and pressures to show test equipment and procedures
[NLL-NEL-TT-2471-[6075.461]]
20 p2434 N73-29547
**HEXOGENES [TRADEMARK]**
Reactivity of tungsten in mixture of Hexogen and aluminum in bomb calorimeter
[ICT-12/72] 22 p2730 N73-31845
**HFB-320 AIRCRAFT**
Flight control problems of steep approach landing with direct lift control, exemplified by HFB-320 aircraft
[DGLR-PAPER-73-024] 23 p2744 N73-31965
**HHX HELICOPTER**
U H-53 HELICOPTER
**HIGH ACCELERATION**
Subjective effects of sustained acceleration, including positive, negative, forward, backward, and lateral acceleration effects
06 p0628 N73-15095
**HIGH ALTITUDE**
Simulated high altitude determination of interrelation of systematic and cellular responses to acute and chronic hypoxia
[AD-743536] 01 p0010 N73-10081
High altitude wind and temperature measurement data from meteorological sounding rockets, and radiosondes for May 1971
02 p0204 N73-11651
High altitude wind and temperature measurement data from meteorological sounding rockets and radiosonde observations - February 1971
02 p0204 N73-11652
State of hemocoagulation and thrombocytes during hypokinesia after adaptation to high-mountain conditions
11 p1245 N73-20107
Integrated SAVVAN, VOR, and DME system for locating and controlling high altitude aircraft
14 p1688 N73-23695
Brittleness determination of low density blown polyethylene film balloons to account for high altitude failure
[AD-757885] 15 p1802 N73-24603
Comparison of wind tunnel measurements of impact pressure and species number density of simulated high altitude rocket exhaust plume with computer calculated values
[AD-759838] 17 p2097 N73-26968
Hot and cold atmospheres for Vanderberg AFB, California
[NASA-TM-X-64756] 18 p2141 N73-27306
CO releases at high altitude to determine atmospheric N2 vibrational temperature
[AD-762316] 19 p2298 N73-28480
Hybrid autocorrelator for high altitude incoherent scatter observations
20 p2417 N73-29417
Radiation and turbulent heat flux effects on variations of isobaric surface pressure and altitude in Northern Hemisphere
20 p2446 N73-29651
Measurement of pulmonary extravascular water volume during exposure to simulated high altitude
[AD-763355] 22 p2621 N73-31004
Dispersion and dilution of jet aircraft exhaust at high altitudes
[NASA-TM-X-71451] 24 p2971 N73-33743
**HIGH ALTITUDE BALLOONS**
NT JIMSPHERE BALLOONS
NT SKYHOOK BALLOONS
Evaluation of fiber reinforced films used in high altitude balloons
[AD-749880] 05 p0567 N73-14609
Thermodynamic properties of high altitude balloons to show effects of ascent, sunrise, surface coating, and thermal insulation
[TAMRF-921-73/05] 11 p1234 N73-20021
ESRO AEROSAT experiment using stratospheric balloon-borne transponder to relay signals from ground station to aircraft flying over sea
18 p2106 N73-27029
Design, development, fabrication, and test of propulsion system for free balloon using electric motor and 35.4 foot propeller
[AD-760754] 18 p2107 N73-27042
Measurements on high and low gain L band aircraft aerials using transmissions from high altitude balloon
[RAE-TR-73008] 20 p2377 N73-29102
Flux and energy spectrum of fast neutrons and gamma rays at balloon altitudes
23 p2833 N73-32642
**HIGH ALTITUDE BREATHING**
Pressure chambers for testing effect of oxygen inspiration on fatigue during flight
[JPRS-59041] 14 p1610 N73-23051
Cardiopulmonary adaptations of man to moderately high altitude
[AD-755192] 14 p1613 N73-23075
Respiratory function and blood acid base equilibrium in human adaptation to high altitude environment
20 p2366 N73-29030

**HIGH ALTITUDE ENVIRONMENTS**
High altitude effects on cerebral and cardiovascular systems of monkeys
[AD-745891] 02 p0134 N73-11085
Centrineurogenic etiology for pulmonary changes of high altitude pulmonary edema
[AD-756940] 15 p1743 N73-24127
**HIGH ALTITUDE FLIGHT**
U FLIGHT
U HIGH ALTITUDE
**HIGH ALTITUDE TESTS**
Coding data of 2565 individual human altitude chamber tests
[NASA-CR-114550] 07 p0746 N73-16066
**HIGH ASPECT RATIO**
Analytical representation of auxiliary functions of theory for oscillating lifting surface with high aspect ratio at subsonic speeds
[DLR-FB-73-16] 21 p2492 N73-29999
**HIGH ASPECT RATIO WINGS**
U SLENDER WINGS
**HIGH CURRENT**
High amplitude gamma current pulse degradation of semiconductor devices
[SC-RR-72-0515] 04 p0399 N73-13245
**HIGH EFFICIENCY**
U EFFICIENCY
**HIGH ENERGY ASTRONOMY OBSERVATORIES**
U HEAO
**HIGH ENERGY ELECTRONS**
Defining energetic particle experiment for Grand Tour missions
[NASA-CR-129182] 02 p0226 N73-11824
High energy electrons and surface expansion in plasma targets heated by electromagnetic radiation
[LA-4986] 06 p0704 N73-15745
Pulsed electron accelerators with energies of 20 to 50 MeV
[JPRS-58160] 09 p1011 N73-18252
Calculation of high energy electron emission from metal target irridiated by gamma flux field
[NASA-TM-X-2756] 10 p1192 N73-19698
Properties of energetic electrons accelerated during solar flare flashes
19 p2333 N73-28777
**HIGH ENERGY FUELS**
Experimental high energy rocket propellant combinations with heterogeneous combustion and FLOX/polyethylene engine performance
24 p2972 N73-33751
**HIGH ENERGY INTERACTIONS**
Continuation from deep inelastic electron scattering to deep electron-positron annihilation
[NOTA-INTERNA-378] 01 p0084 N73-10692
Triple Regge phenomenology from finite mass sum rules in proton-proton inclusive reactions
[NOTA-INTERNA-379] 01 p0084 N73-10693
Experimental facilities for nuclear particle physics research at proton energy level of 300 GeV
[CERN-1050] 04 p0402 N73-13274
High energy density primary batteries using CuF2/LiAsF6-MF/Li electrochemical system
[NASA-CR-120857] 07 p0741 N73-16032
Surface and volume mechanisms of material evaporation subject to powerful radiation fluxes
09 p0999 N73-18154
Field theory model for unified strong and electromagnetic interactions
09 p1066 N73-18701
CF3I gas laser system for high power operation
[SC-T-72-2560] 12 p1410 N73-21426
Effects of Jupiter high energy electron environment on gates and MOSFET performance
[AD-756215] 13 p1502 N73-22178
Analysis of effects of high power lasers to include interactions with plasma, metals, dielectrics, semiconductors, and gases
[AD-755820] 14 p1674 N73-23586
Optical high energy scattering models and photoprocesses in nuclei
[CERN-72-20] 15 p1814 N73-24702
Nondiffractive models with n squared approximately 1/s
18 p2182 N73-27616
Electromagnetic and strong interactions processes for producing diffuse cosmic gamma continuum radiation
19 p2332 N73-28763
Conference on solar high energy interactions
[NASA-TM-X-66290] 19 p2333 N73-28772
OSO-H observations of solar thermal and nonthermal X ray bursts
19 p2334 N73-28783
Polarimetric measurements of high energy solar X ray emission processes
19 p2335 N73-28785
Research on solar high energy physics - conference summary
19 p2340 N73-28822
String models for theoretical study of high energy collisions involving large quantum numbers
[LPTHE-73/22] 21 p2581 N73-30688
Integrated solar-quiet interplanetary electron spectrum obtained by Explorer 41 satellite
22 p2733 N73-31874
Satellite instrumentation for determining origin and energetics of solar flares
22 p2734 N73-31881
Source and diffusion of cosmic rays greater than 4.5 GV in interstellar medium measured by proportional counter-scintillation counter stack
[TR-73-136] 23 p2835 N73-32652
**HIGH ENERGY PROPELLANTS**
Handbook on thermodynamic and thermophysical properties of high propellant combustion products
[AD-754329] 11 p1253 N73-20165
Preflight tests on fluorine/ammonia propellants to be used in Europa 2 transfer stage
[BMFT-FBW-73-07] 21 p2587 N73-30731
**HIGH EXPLOSIVES**
U EXPLOSIVES
**HIGH FIELD MAGNETS**
Large helium systems for superconducting power applications and high energy physics
[BNL-17228] 10 p1200 N73-19764
Superconducting materials for high field ac magnets with one second field risetime
[BMFT-FBT-73-03] 22 p2685 N73-31509
Superconducting magnets for use in high field synchrotrons
[LBL-1703] 22 p2707 N73-31677
**HIGH FREQUENCIES**
Survey of methods to obtain electromagnetic and acoustic high frequency scattering
[AD-747044] 02 p0143 N73-11158
Construction and production problems connected with high frequency n-channel MOS transistors
[AD-747546] 03 p0276 N73-12240
L2 stability in low and high frequency distributed feedback systems
[NASA-CR-129599] 03 p0277 N73-12245
Simulation of high frequency instabilities, using Dirac delta functions
[ORNL-TM-3447] 03 p0342 N73-12790
Analysis of problems and effects in reducing sampling frequency in 625 line television digital codes to improve transmission
[REPT-1972/36] 05 p0507 N73-14129
Design of portable HF/VHF radio set for manpack usage
[AD-749510] 05 p0514 N73-14175
Auroral effects on HF radiowave propagation traversing polar regions
[AD-749515] 05 p0540 N73-14392
High frequency plasma heating in toroidal traps
[NP-19379] 06 p0705 N73-15753
Correlation of organic substance oxidation rate parameters in low temperature plasma with high frequency power
[NASA-TT-F-14671] 07 p0753 N73-16113
High frequency and pulsed electron discharge heating of turbulent skin layer in plasma
[AEC-TR-7329] 07 p0826 N73-16695
Laboratory experiments with high frequency excitation electric fields
[CONF-720705-3] 07 p0827 N73-16701
High frequency force field effect on electromagnetic wave propagation into bounded plasma configuration
[AREAEE-124] 07 p0828 N73-16712
Ground based HF sounding technique for detecting ionospheric disturbances associated with Pc 1 micropulsations
[AD-752062] 08 p0919 N73-17532
Fuel injectors with high frequency swirl generators
[AD-751079] 09 p1080 N73-18810
R-Om experimental setup for studying interaction of high frequency magnetic fields with plasma
[AEC-TR-7388] 10 p1197 N73-19737
Definitions for specifying frequency stability for measurements in frequency and time domains
[NBS-TN-632] 12 p1378 N73-21174
Development and testing of HF/VHF radio set for manpack usage
[AD-755547] 13 p1494 N73-22113
Simple method for prediction of lowest observed frequency of high frequency propagation paths between Pacific Islands
[AD-757343] 14 p1636 N73-23266
High frequency spectrum domain of turbulent jet noise
15 p1813 N73-24697
Azimuthal and diurnal high frequency backscatter and terrestrial radio noise
[AD-758776] 16 p1876 N73-25185
Improvements in design of HF communication systems for naval aircraft
[AD-759709] 16 p1878 N73-25200
Adaptive beamforming techniques for HF antenna array systems
[AD-760137] 17 p1999 N73-26166
Analysis of time-sharing voice modulated output of several collocated transmitters and receivers using very high frequencies
[AD-758567] 18 p2120 N73-27140
High frequency transport coefficients of clean type 2 superconductor near upper critical field
18 p2185 N73-27644
Hazardous region surrounding near fields of Navy HF whip antennas
[AD-761979] 19 p2237 N73-28034
Design of high frequency radar antenna equipment for radar stations
[AD-764333] 22 p2632 N73-31093
Predicting day-to-day variability of mid-latitude ionosphere for application to HF propagation predictions
[AD-764711] 23 p2789 N73-32310
Model for prediction of horizontal ray path deviation effects in high frequency ionospheric propagation
24 p2894 N73-33105
Improved high frequency performance of mixer diodes by use of Mott barrier
[AD-765182] 24 p2899 N73-33143
**HIGH GAIN**
Measurements on high and low gain L band aircraft aerials using transmissions from high altitude balloon
[RAE-TR-73008] 20 p2377 N73-29102
**HIGH GRAVITY (ACCELERATION)**
U HIGH GRAVITY ENVIRONMENTS
**HIGH GRAVITY ENVIRONMENTS**
Design and tests of counting strain gages for high-g naval aircraft
[AD-750692] 06 p0676 N73-15498
High g Approach for cockpit design
[AD-757216] 15 p1744 N73-24138
**HIGH INTENSITY**
U INTENSITY
**HIGH LATITUDES**
U POLAR REGIONS
**HIGH LIFT DEVICES**
U LIFT DEVICES
**HIGH MELTING COMPOUNDS**
U REFRACTORY MATERIALS
**HIGH PASS FILTERS**
Application of high pass broadband filters to absorption spectrophotometry
[IRI-133-72-08] 03 p0274 N73-12223
Development of allpass, highpass, bandpass, and stopband electric filter circuits using only resistors as passive components
[REPT-1404] 05 p0522 N73-14244
Application of state variable approach for analysis of selecting digital moving target indicators filters
[AD-757611] 14 p1637 N73-23269
**HIGH POLYMERS**
Accomplishments and publications list of two year project on morphology and deformation mechanisms of high polymers
[AD-762780] 21 p2565 N73-30560
Effect of high polymer drag reducing additives on longitudinal turbulent dispersion coefficient for two dimensional open channel flow
24 p2902 N73-33164
**HIGH PRESSURE**
Capillary viscometer procedure for determining viscosity of meta-xylene at high pressure and temperatures
[AD-745851] 01 p0023 N73-10178
High pressure nitrogen gas discharge initiated by fast electron beams of 100 to 300 keV energies
[DRIC-TRANS-2857] 02 p0212 N73-11716
Development of method for determining response of fluids under high pressure when released to atmosphere using closed form solution and numerical analysis
03 p0282 N73-12289
Boiling inception in trichlorotrifluoroethane during forced convection at high pressures
[NASA-CR-2170] 04 p0485 N73-13960
Analysis of electron beam induced discharge in nitrogen at high pressure
[NLL-DRIC-TRANS-2857-[3623.66]]
05 p0579 N73-14714
Performance of prototype high pressure space suit glove
[NASA-CR-114532] 06 p0635 N73-15162
Tensile tests of pressure effects on plastic properties and fracturing of metals
[NLL-NEL-TT-2190-[6075.461]]
06 p0682 N73-15552
Gain and performance measurement of expanding CO2 laser mixtures at high pressures
[AD-751694] 07 p0807 N73-16547
Operating principles of high precision orbiting astronomical observatory manned by nonprofessional cosmonaut astronomer
[NASA-TT-F-14580] 07 p0843 N73-16830
Development of prototype high pressure space suit glove assembly
[NASA-CR-114535] 08 p0879 N73-17120
Electrodeless high frequency discharges in xenon at pressures up to 40 atmospheres
[AD-751944] 08 p0949 N73-17774
Compression of helium to high pressures and temperatures using ballistic piston apparatus with shock tube
[NASA-CR-131230] 10 p1141 N73-19298
High pressure plasma research
[AD-754020] 11 p1328 N73-20776
Performance of electromagnetic accelerators in high pressure test facilities
[AD-754024] 11 p1328 N73-20779
Void fraction in subcooled trichlorotrifluoroethane boiling at high pressures
[NASA-CR-2241] 14 p1718 N73-23938

Combustion and evaporation of liquid fuels at high pressures
[NASA-CR-121113] 15 p1843 N73-24934
Modified high pressure system with small sample vessels for conducting biological reactions
[AD-752978] 16 p1885 N73-25256
High pressure compressed gas magnetic diaphragm rupture system for generating megagauss magnetic field
[JPRS-59459] 18 p2179 N73-27593
Potential applications of high pressure technology
[AD-760714] 18 p2191 N73-27686
Fabrication and mechanical testing of high pressure ratio compressor
[NASA-CR-121193] 20 p2423 N73-29463
Performance analysis and high frequency combustion stability of high pressure rocket motor
20 p2484 N73-29956
Extrapolation of thermophysical properties data for oxygen to high pressures at low temperatures
[NASA-CR-133858] 21 p2506 N73-30109
Linear and nonlinear theory of elasticity used to determine deformation of cylinder and piston of high strength steel under influence of high pressure
[AD-763971] 22 p2687 N73-31519
Performance of turboreactor turbines during high pressure stage
22 p2709 N73-31695
Effects of high pressure hydrogen environments on mechanical properties of alloys considered as candidate materials for high performance rocket engine construction
[NASA-CR-124410] 23 p2804 N73-32428
Plastic flow and fracture mechanics of brittle cuperious oxide and gamma 2Cu-Al compounds under high pressure
24 p2967 N73-33709

**HIGH PRESSURE OXYGEN**
Growth response of bacteria and yeast in high pressure helium-oxygen environment
[AD-745334] 01 p0012 N73-10096
NASA utilization of high pressure oxygen
[NASA-TM-X-68203] 11 p1266 N73-20276

**HIGH Q**
U Q FACTORS

**HIGH RESOLUTION**
High resolution attitude sensor for sensing spacecraft attitude relative to light source
[NASA-CASE-LAR-10586-1] 02 p0174 N73-11406
High resolution study of ion mobility spectra and effect on atmospheric ionization
[AD-747687] 04 p0416 N73-13396
Camera with laser driven Kerr cell having fast time resolution
[DESY-72/14] 04 p0422 N73-13438
Analysis of resolvability of point sources of incoherent light by quantum detection, decisions of observers, and error probability
[NASA-CR-130129] 04 p0449 N73-13663
High resolution interferometric observations of Venus
[AD-747992] 04 p0476 N73-13895
Analysis of high resolution vidicon optics for electronic periscope view simulator
[AD-751023] 07 p0822 N73-16664
High resolution measures of polarization and color of selected lunar areas
[NASA-CR-130018] 07 p0841 N73-16816
Image speckling reduction using multicolor illumination in holographic microscopy
[AD-752240] 08 p0945 N73-17737
High resolution transmittance curves for spectral region 320 to 1400 wavenumbers and attenuation of CO2 laser radiation
[AD-753076] 09 p1043 N73-18511
High resolution spectra of NO2 continuum emission from production of O2[1 Delta g] and O2[1 Sigma g plus] in reaction of NO with O3
[DREV-TN-2050/72] 10 p1125 N73-19166
Large orbiting X ray telescope with high resolution mirror design
[NASA-CR-124001] 10 p1158 N73-19424
High resolution imagery of Uranus obtained by Stratoscope 2
[NASA-CR-132024] 14 p1706 N73-23846
High optical resolution derivative spectrometer for measuring optical properties of solids in vacuum UV and far IR range
15 p1785 N73-24474
Use of argon-ion laser transverse mode locking to produce high resolution scanning beam
15 p1794 N73-24546
High resolution pulse width modulated parallel channel for forward looking infrared display system
[AD-759224] 16 p1882 N73-25231
Highly accurate digital barometer
[NLL-M-22973-[5828.4F]] 16 p1910 N73-25458
High resolution solar X ray astronomy from Aerobee rockets
[NASA-CR-132984] 16 p1959 N73-25849
High resolution radar transmitting system for transmitting optical pulses to targets
[NASA-CASE-NPO-11426] 17 p1994 N73-26119
Focusing optical collimator for high resolution scanning of electromagnetic radiations, neutrons, and other particles
[NASA-CASE-MFS-20932-1] 18 p2150 N73-27380

**HIGH SENSITIVITY**
U SENSITIVITY

**HIGH SPEED**
High speed holography of high speed phase object using Q switched laser outputs
[ISL-10/71] 02 p0181 N73-11471
Performance tests of ball bearings operating at high dn values
[NAL-TR-284] 04 p0426 N73-13469
High speed mechanics research, including circular cylindrical shell buckling and hydrofoil profiles
06 p0724 N73-15910
Performance and theory of operation of High Speed Sequential Decoder
[NASA-TM-X-62241] 11 p1260 N73-20222
Discussion of speed record establishment by SA-341 helicopter to include aircraft preparation procedures and requirements for successful completion
12 p1358 N73-21018
Holographic technique to record front surface detail from high velocity target
16 p1921 N73-25547
Experimental evaluation of 150-mm bore ball bearings to 3-million DN using solid and drilled balls
[NASA-TM-X-68265] 17 p2037 N73-26480

**HIGH SPEED CAMERAS**
NT FRAMING CAMERAS
Development of compact, ultrafast streaking camera to include power requirements, electronic circuitry, and performance analysis
[UCRL-73734] 07 p0801 N73-16502
Errors in streak photography measurements caused by subject and camera misalignment
[AD-751185] 07 p0802 N73-16513
In-flight photography of projectiles using film-image synchronized, rotating-slit shuttered drum field camera
[LA-DC-72-909] 10 p1161 N73-19445
Photographic recording of dynamic behavior of flames in explosive gases caused by ignition of equimolar acetylene-oxygen mixture
[NASA-CR-135672] 23 p2856 N73-32825
Photocathode for high resolution streak camera tube
[UCID-16218] 24 p2898 N73-33137

**HIGH SPEED FLIGHT**
U FLIGHT
U HIGH SPEED

**HIGH SPEED TRANSPORTATION**
U RAPID TRANSIT SYSTEMS

**HIGH STRENGTH**
Process for making high strength beryllium by hot-pressing extrusion and forging
[RFP-1816] 06 p0684 N73-15570
Ni/ZrO2 composite material for designing high strength thermal switches
[HIT-527] 12 p1383 N73-21212

**HIGH STRENGTH ALLOYS**
NT HIGH STRENGTH STEELS
NT MARAGING STEELS
Low cycle fatigue crack propagation characteristics of high strength alloys with high levels of fracture toughness
[AD-747243] 02 p0190 N73-11538
High strength aluminum alloys by optimizing precipitate microstructure
[AD-750140] 06 p0686 N73-15586
Development of advanced high strength tantalum alloys
[NASA-CR-120818] 07 p0809 N73-16562
Low energy fracture process in high strength aluminum alloy 2014T6
[NASA-CR-131099] 10 p1170 N73-19520
Fracture toughness and aqueous stress corrosion resistance of high strength commercial Ti alloy
[NLR-TR-72107-U] 13 p1542 N73-22492
Analytical rationale for sensitivity-insensitivity of dispersion strengthened alloys
[NASA-CR-124274] 16 p1928 N73-25600
Evaluation of high strength aluminum alloy plates and forgings
[AD-759557] 16 p1930 N73-25613
Cumulative damage of high strength aluminum alloy under operational loading
[ISD-133] 17 p2046 N73-26553
Influence of microstructure on tensile deformation and fracture in high strength Al-Zn-Mg alloys
[ARL/MET-NOTE-86] 18 p2160 N73-27447
Cobalt-tungsten alloys with superior strength at elevated temperatures
[NASA-CASE-LEW-10436-1] 23 p2803 N73-32415
Effects of high pressure hydrogen environments on mechanical properties of alloys considered as candidate materials for high performance rocket engine construction
[NASA-CR-124410] 23 p2804 N73-32428

**HIGH STRENGTH STEELS**
NT MARAGING STEELS
Interactions between residual elements, inclusion, toughness, and stress corrosion resistance in high strength steel
[PB-209655] 02 p0187 N73-11515
Computer program to determine crack propagation characteristics of ultra high strength steel under various load cycles
[ARL/SM-NOTE-376] 02 p0237 N73-11930
Hardened high strength steel for making wear resistant metal cutting tools
[AD-747711] 03 p0308 N73-12511
Thermal and thermophysical processes for microstructural control in high strength steel to increase fracture toughness
[LBL-832] 04 p0434 N73-13537
Biaxial testing device for measuring yield point and plastic flow properties of high strength HY-80 steel
[AD-749021] 05 p0548 N73-14454
Effect of transition zone on mechanical properties of high strength steel after cladding with thin layer of highly ductile material
[NLL-TRANS-746-1323-[9022.401]]
05 p0560 N73-14552
Hot pressing and hot rolling procedures for producing aluminum reinforced with high strength steel strips
[NLL-TRANS-746-1355-[9022.401]]
05 p0561 N73-14554
Endurance of high strength steels subjected to bending
[ESDU-71027] 05 p0561 N73-14561
Procedures for estimating stresses in titanium and high strength steel panels and comparison of estimated and measured stresses
[ESDU-72005-AMEND-A] 07 p0850 N73-16894
Electrical resistance measurements on crack propagation in fracture toughness specimens under variety of environmental and loading conditions
[MG/54/71] 08 p0966 N73-17899
Hydrogen adsorption and diffusion, and subcritical crack growth in high strength steels and nickel alloys
[NASA-CR-130979] 09 p1046 N73-18528
Strain fields around tapered interference fit steel pins in aluminum and steel alloy plates
[ARL/SM-NOTE-377] 09 p1093 N73-18919
Relationship between brittle and plastic fracture of high strength steels owing to void dynamics
[NASA-CR-131101] 10 p1171 N73-19522
Fracture mechanics and plastic deformation in high strength steels
[NASA-CR-131102] 10 p1171 N73-19523
Effect of solidification under high isostatic pressure on high strength steels
[AD-753958] 11 p1306 N73-20596
Analysis of adhesion strength of electroless nickel plating on Type 4340 steel to determine optimum plating conditions and to certify bond strength
[Y-1838] 12 p1414 N73-21459
Analysis of production and characteristics of ultrahigh strength steels based on survey of literature
[ARL/SM-NOTE-378] 14 p1675 N73-23591
High strength steel delayed failure analysis including hydrogen embrittlement
[NLR-TR-72113-U] 14 p1715 N73-23917
Analysis of effects of homogenizing annealing on ductility of high strength steel
[NLL-M-21616-[5828.4F]] 15 p1796 N73-24562
Effect of stress corrosion cracking and hydrogen embrittlement on failure of high strength spacecraft fasteners
[AD-758754] 15 p1800 N73-24591
Oxidation and stress corrosion cracking of high strength steel in gaseous environment
[AD-758848] 16 p1929 N73-25608
Corrosion fatigue crack growth of high strength steels in hydrogen and water/water vapor environments
[AD-759088] 16 p1930 N73-25615
Dynamic tear tests for determining fracture mechanics of high strength structural steels and aluminum and titanium alloys
[AD-759351] 16 p1930 N73-25620
Precipitate size and distribution effects on fatigue crack initiation and propagation in high strength steel
[AD-759048] 16 p1971 N73-25940
Effect of martensitic microstructure on fatigue life and crack propagation characteristics of high strength steels
[S-253] 17 p2044 N73-26536
Effects of irradiation on fracture and strength properties of pressure vessel steel plate and submerged arc weld
[HEDL-SA-387] 17 p2093 N73-26936
Performance tests of spur gears with and without tip relief to determine service life of M-50 and Super Nitralloy metals
[NASA-TM-X-68269] 18 p2155 N73-27413
Static and fatigue properties of hardened and tempered electron beam welded joints in 2.5 percent Ni-Cr-Mo steel and 18 percent Ni-Co-Mo maraging steel
[S/T-MEMO-9-71] 18 p2161 N73-27456
Relationships between fracture strength, flow stress, and material ductility in high strength steels
[AD-761217] 18 p2162 N73-27463
Strain fracture toughness and microstructure of heat treated high strength steels
22 p2682 N73-31486

**HIGH TEMPERATURE**
High temperature oxidation reactions of carbon monoxide and methane in oxygen-rich atmospheres in turbulent flow reactor
[AD-746284] 02 p0138 N73-11116
High temperature oxidation of uranium alloys and morphology of oxide scales
[CONF-720523-1] 03 p0263 N73-12130
Surface stresses and mechanical properties of scales and effects on high temperature gas-metal reactions
[CONF-720515-1] 03 p0264 N73-12137
Computer program for high temperature structural design methods for LMFBR components
[ORNL-TM-3845] 03 p0333 N73-12712
Design of radiometric emittance measurement system for use at high temperatures
[NASA-CR-123968] 04 p0420 N73-13421
Superalloys from prealloyed powders at high temperatures
[NASA-CASE-LEW-10805-1] 04 p0425 N73-13465
Design of high temperature liquid metal systems
[CONF-720904-1] 05 p0562 N73-14566
Thermal conductivity of air and nitrogen at high temperatures
[AD-749842] 05 p0607 N73-14934
High temperature plastic deformation of refractory metals in vacuum during rolling
[AD-750508] 06 p0678 N73-15516
Application of strainrange partitioning method to high temperature fatigue
[NASA-TM-X-68171] 06 p0725 N73-15923
In pile neutron irradiation damage in graphite at high temperature
[CEA-CONF-1894] 07 p0820 N73-16644
Solid ceramic electrolyte system for measuring redox conditions in high temperature gas mixing
[NASA-TM-X-58105] 08 p0892 N73-17224
High temperature electric resistance wire strain gages
[NASA-CR-112241] 09 p1035 N73-18446
Development of powder metallurgy nickel-base superalloy for application at 1800 to 2000 F
[NASA-CR-121099] 09 p1047 N73-18537
Nature of power losses in RF superconducting cavities at low and high temperatures
[SLAC-PUB-963] 12 p1383 N73-21213
Thermodynamic stability diagrams of high temperature O2 corrosion reactions
14 p1676 N73-23602
Kinetics of afterburning process following injection of oxidizer into high temperature gas flow
[AD-756098] 14 p1719 N73-23951
Low frequency Raman spectra of ammonium halides measured by double monochromator at high temperature
[NASA-CR-132049] 15 p1747 N73-24160
Mechanical properties of magnesium alloys operating at elevated temperature
[AD-758617] 15 p1800 N73-24593
Pulsed holographic measurement of wave propagation in thin walled shells and vibration modes in steel rectangular plates at high temperature
16 p1921 N73-25544
High temperature heating effects on structure and ductile properties of austenitic steels
[NLL-M-21563-[5828.4F]] 16 p1926 N73-25584
X ray diffraction analysis of VIA, B-1900, 713C, and 738X alloy composition after oxidation at high temperature
[NASA-TM-X-2796] 16 p1927 N73-25596
Harper-Dorn creep and microstructure of pure aluminum and other metals at high temperature
[LBL-1158] 16 p1928 N73-25604
Ferritic steels resistant to high temperature and decarburization by Na
[CEA-CONF-2118] 17 p2044 N73-26539
Influence of zirconium additions on diffusivity and solubility of hydrogen and deuterium in niobium alloys at high temperature
[BNWL-SA-4473] 17 p2065 N73-26706
Stability of refractory compounds in liquid aluminum at high temperatures
[NLL-RTS-7975] 18 p2113 N73-27083
High temperature effects on dislocation mobility of LiF single crystals
18 p2185 N73-27642
High temperature creep of Al alloys tin, and lead at intermediate and low stresses
[LBL-1183] 21 p2559 N73-30512
Development of high temperature rolling bearings for operation in liquid sodium
[NYO-4117-9] 22 p2678 N73-31452
High temperature lubricants - bibliographies
[AD-764700] 23 p2799 N73-32387
Correlation of creep rate with microstructural changes during high temperature creep
[NASA-CR-135698] 23 p2804 N73-32426
Development of high temperature resistant elastomeric sealant
[AD-764589] 23 p2811 N73-32473
Thermal cycling tests of gas turbine components
[AD-764930] 23 p2833 N73-32637
Effect of high ambient temperature on calcium content of human bone tissue
24 p2884 N73-33033
Ferromagnetic resonance measurements in Ni and Fe as function of temperature and frequency parameters
24 p2934 N73-33428
Mass loss rate of carbon and graphite at high temperature
[LA-5223-PR] 24 p2943 N73-33503
High temperature general purpose furnace for use in space
[NASA-CR-124458] 24 p2991 N73-33905
**HIGH TEMPERATURE AIR**
Analysis of approximate transport properties of high temperature air in dissociation equilibrium
[ESDU-00.01.07-AMEND-A] 07 p0853 N73-16919
Mathematical models for determining transport properties and dissociation equilibrium of N2 and O2 in high temperature air
[ESDU-00.01.07-AMEND-A] 14 p1718 N73-23937
Apparatus and method for generating large mass flow of high temperature air at hypersonic speeds
[NASA-CASE-LAR-10612-1] 19 p2250 N73-28144
**HIGH TEMPERATURE ALLOYS**
U HEAT RESISTANT ALLOYS
**HIGH TEMPERATURE ENVIRONMENTS**
Thermodynamic equilibria and carbon deposition in carbon-hydrogen-oxygen system of high temperature fuel cells
[ARL/ME-NOTE-333] 01 p0006 N73-10048
Suitability of directionally solidified eutectic alloys for high temperature fasteners, material properties, and fabricating methods
[NASA-CR-123919] 02 p0177 N73-11437
High temperature ceramic to metal seal capable of operation at 1200 C for 3 to 5 years
[NASA-CR-120831] 05 p0552 N73-14484
Point defect theory and oxidation kinetics in metal reactions with high temperature gaseous environment
[GAT-T-1868] 06 p0684 N73-15571
Effects of oxidation resistant coatings on thin superalloy sections in high temperature environments
[NASA-CR-121115] 07 p0809 N73-16563
Solid lubricants for moderate to extremely high temperature applications
[NASA-TM-X-68201] 11 p1298 N73-20537
Conference on high temperature corrosion of alloys for aerospace applications
[AGARD-CP-120] 14 p1675 N73-23597
Designs of high temperature seals for gaps between structure and aerodynamic control surfaces of space shuttle orbiter
[NASA-CR-128951] 16 p1965 N73-25891
Fatigue life of reactor pressure vessel steels in high temperature aqueous environment
[CONF-721104-6] 17 p2094 N73-26938
Design and manufacturing of composite materials with organic matrices for use in aerospace vehicle structures subjected to high temperatures
18 p2165 N73-27489
Production and characteristics of refractory materials for high temperature applications
[NLL-RTS-7942] 20 p2433 N73-29543
Analysis of equipment and procedures for conducting sonic fatigue tests of airframes at elevated temperatures
[AD-763798] 21 p2498 N73-30052
Application of structural computer program for analysis of creep stress in thrust chamber liner - Vol.3
[D5-17266-3-VOL-3] 22 p2725 N73-31807
Techniques and associated instrumentation for high temperature emissivity measurements
[NASA-CR-124423] 23 p2792 N73-32339
**HIGH TEMPERATURE FLUIDS**
NT HIGH TEMPERATURE AIR
NT HIGH TEMPERATURE GASES
Self-cycling fluid heater for heating continuous fluid stream to ultrahigh temperatures to facilitate chemical reactions
[NASA-CASE-MSC-15567-1] 07 p0853 N73-16918
**HIGH TEMPERATURE GASES**
NT HIGH TEMPERATURE AIR
Compression of helium to high pressures and temperatures using ballistic piston apparatus with shock tube
[NASA-CR-131230] 10 p1141 N73-19298
Analysis of conditions existing in rising, rotating column of hot gases containing core of reacting gases
[TR-5] 10 p1223 N73-19948
Generation of high temperature, high mass flow, and high Reynolds number air at hypersonic speeds
[NASA-CASE-LAR-10578-1] 16 p1886 N73-25262
Thermodynamic state in cascade argon arc after initiation of step increase in electrode voltage from initial steady-state D.C. level
24 p2990 N73-33893
**HIGH TEMPERATURE MATERIALS**
U REFRACTORY MATERIALS
**HIGH TEMPERATURE NUCLEAR REACTORS**
Finite element method computation of 1:5 scale model prestressed concrete high temperature nuclear reactor pressure vessel
[ISD-120] 10 p1221 N73-19927
**HIGH TEMPERATURE PLASMAS**
Closed magnetic systems for obtaining and controlling high temperature plasmas
[AD-747111] 02 p0217 N73-11759
Photoionization of room temperature gas by radiation from hot plasma in electromagnetic T-Tubes
07 p0825 N73-16684
Model of shock wave propagation parallel to external magnetic field in hot collisionless plasma with turbulent dissipation based on garden hose instability
[MPI-PAE/EXTRATERR-69] 09 p1071 N73-18736
Mathematical model for dense rotating plasma with centrifugal expansion instability at high beta values
[TRITA-EPP-72-28] 09 p1071 N73-18740
Charged particle transport in turbulent astrophysical plasmas
12 p1432 N73-21606
Experimental analysis of high Beta, hot, dense plasma
[COO-2233-1] 15 p1817 N73-24732
Experimental determination of electron attachment in high temperature plasma
[AD-763090] 20 p2459 N73-29765
Research on nonlinear waves and shock-like phenomena in hot plasmas
[NASA-CR-132808] 21 p2582 N73-30695
Particle insertion and hot plasma containment in stellarator with superconductors
[NASA-TT-F-15111] 22 p2703 N73-31648
Time resolved spectroscopic measurements of near infrared and X ray emission from high density plasma in vacuum spark
24 p2961 N73-33661
Feasibility of RF heating for high temperature turbulent plasma production noting diagnostic techniques and CO2 laser scattering
[LRP-64/73] 24 p2966 N73-33702
**HIGH TEMPERATURE RESEARCH**
High temperature reaction of carbon with refractory compounds of groups 4, 5, and 6
[NLL-RTS-7425] 01 p0022 N73-10171
Capillary viscometer procedure for determining viscosity of meta-xylene at high pressure and temperatures
[AD-745851] 01 p0023 N73-10178
Behavior of lubricating materials under high temperature and high pressure
[AD-745001] 01 p0062 N73-10509
High temperature strength and stability of tungsten reinforced copper
[AD-745700] 01 p0071 N73-10581
Development of proton-activated recession sensor based on migration of beryllium isotope in graphite at high temperature and application to nose cone conditions during reentry
[AD-745454] 01 p0109 N73-10899
Performance evaluation of iridium/rhodium integrated probe/fluidic temperature sensor up to 3000 F
[AD-745987] 02 p0175 N73-11417
High temperature and fatigue tests to determine effects of heat resistant coatings on mechanical and physical properties of nickel-chromium-iron alloys
[NLL-TRANS-746-1236-[9022.401]]
02 p0185 N73-11500
Analysis of structural changes during heating and elongation of two-phase, high chromium content Cr-Ni-Fe alloys over ranges of temperature and concentration
[NLL-TRANS-746-1153-[9022.401]]
02 p0185 N73-11501
Aluminizing of titanium and aluminum alloys in powder form with use of electric heating methods
[NLL-M-21479-[5828.4F]] 02 p0185 N73-11503
Influence of high temperature thermomechanical treatment on mechanical properties of austenitic steel
[NLL-M-21480-[5828.4F]] 02 p0186 N73-11504
Analytical analysis of graphite interaction with carbon dioxide at high temperature
[AD-747556] 03 p0264 N73-12141
Phase method for measuring thermal conductivity of gases at high temperature
[AD-747620] 03 p0264 N73-12142
Effect of chemical vapor deposition on properties of carbon-felt carbon-matrix composites at high temperature
[SC-DC-71-4395] 03 p0320 N73-12609
Irradiation-induced changes in graphites at high temperatures and high fluences
[GULF-GA-A-10971] 03 p0321 N73-12612
Chemical reaction of Si, SiC, and Si-SiC mixtures in CO and N at high temperature
[AD-747718] 04 p0438 N73-13569
Research projects conducted in USSR to determine thermophysical properties of materials at high temperatures and characteristics of high temperature processes
[JPRS-57658] 04 p0484 N73-13957
High temperature dispersion strengthening of Fe-Al alloys by internal oxidation
[BM-RI-7686] 05 p0562 N73-14564
Plastic properties and microstructure of alpha-titanium alloys at high temperature
[AD-750964] 05 p0564 N73-14581
W/Re thermocouples and high temperature irradiation program
[KFK-1556] 06 p0649 N73-15273
Influence of volatile compounds on high temperature oxidation of Cr and Cr alloys
[TM-49] 06 p0684 N73-15566

Synthesis of high temperature clothing from hexahydrobenzodipyrrole monomers
[AD-750380] 06 p0689 N73-15609
Littles theory of high temperature superconductors
[AD-751038] 07 p0753 N73-16120
High temperature tests to determine effect of autoclave heat treatment of mechanical properties of cobalt-base alloy HS-31 in prealloyed powder form
[NASA-TN-D-7117] 07 p0809 N73-16559
Evaluation of three types of CVD tungsten to determine weldability, high temperature strength, and structural stability
[NASA-CR-120876] 07 p0809 N73-16561
Generator designs, insulations, magnetic materials, diodes, and rotor bonding
[AD-752604] 08 p0870 N73-17044
Development of high temperature high radiation silicon semiconductors
[NASA-CR-124074] 08 p0950 N73-17777
Analysis of high temperature heat exchanger processes in tubular metallic container using bed of moving pebbles for heat storage
[FRNC-TH-231] 08 p0969 N73-17923
Low cycle fatigue testing at high temperatures
[AGARD-R-604] 09 p1092 N73-18916
Dissociation of HBr behind shock waves and at temperatures from 1450 to 2300 K in pure HBr
[AD-753395] 10 p1143 N73-19310
Mechanical and microstructural behavior of Al-Zn alloy in superplastic region at high temperature
10 p1170 N73-19518
Literature review of strain rate effects on mechanical properties of metals at high temperatures
[AD-754243] 10 p1174 N73-19548
Ultrasonic methods for analyzing elastic moduli of materials at high temperatures
[AD-753844] 10 p1176 N73-19567
Analysis of short time elevated temperature properties of platinum, rhodium, and palladium alloys
[NLL-M-22799-[5828.4F]] 11 p1304 N73-20582
Calorimeter for measuring high temperature specific heat of Ti and Ti based alloys during intermetallic phase
[AD-754954] 11 p1306 N73-20599
High temperature plasma diagnostics and properties
[AD-754021] 11 p1328 N73-20777
Electrical conductivity of ThO2 at room and high temperatures and in high intensity gamma radiation fields
[BNWL-1671] 12 p1416 N73-21475
High temperature corrosion scale for heat resistant alloys
14 p1676 N73-23598
Perfluoroalkylene ether polymers for high temperature fuel tank sealants
[NASA-CR-124249] 14 p1680 N73-23635
Design of thermal protection system for 8-foot HTST combustor
[NASA-CR-112310] 15 p1760 N73-24262
Analysis of phase change occurring in molten metals, semiconductors, and alloys when heated to 700 to 900 C above melting point
[NLL-M-21614-[5828.4F]] 15 p1796 N73-24563
Chemical compatibility of materials used for lithium cooled space power reactor concept at high temperature
[NASA-TN-D-7259] 15 p1809 N73-24660
Abstracts of reports on high temperature research
16 p1974 N73-25960
Atomic oxygen reaction with nickel at elevated temperatures
[NASA-TM-X-62295] 20 p2431 N73-29524
Thermal embrittlement of 4340 steels at high temperatures
[AD-763900] 22 p2687 N73-31521
Mossbauer effect study of high temperature oxidation and breakaway in 302 stainless steel
22 p2706 N73-31671
Luminescence modulation and negative resistance modulation of semiconductors and high temperature semiconductors
[AD-763840] 22 p2708 N73-31685
High temperature research of thermophysical and electrophysical properties of matter and pilot plant with magnetohydrodynamic power generator
[JPRS-59983] 22 p2728 N73-31831
High temperature research of thermophysical and electrophysical properties of matter
22 p2728 N73-31832
High temperature electrochemical devices incorporating solid oxygen electrolytes for metallurgical processing
[AD-764769] 23 p2806 N73-32436
High temperature creep resistance of Ti alloys
[AD-765784] 24 p2937 N73-33454

**HIGH TEMPERATURE TESTS**
Basic mechanisms providing oxidation resistance in structural, titanium base alloys operating above 900 C
[AD-747002] 03 p0316 N73-12575
Resistance leval indicator used in high temperature alkali tanks
[SFB-MHD-2] 04 p0422 N73-13444
High temperature friction and wear properties of PbO for solid lubricant applications including tests in room air, controlled atmospheres, and vacuum
[NAL-TR-285] 04 p0426 N73-13470
High temperature oxidation behavior of Ni3Al with and without yttrium additions and reaction kinetics of Al2O3 layer growth
[AD-750410] 06 p0686 N73-15589
Mechanical properties of welded joints in stainless and low-alloy steels at temperatures of 900 to 1300 F
[ORNL-4781] 07 p0804 N73-16525
Reliability of high temperature strain gages while measuring extreme thermal strain
[NAL-TR-287] 07 p0854 N73-16923
Creep rupture tests of Inconel 702 tubes at high temperatures and internal helium pressures to determine service life
[NASA-TM-X-2728] 08 p0932 N73-17628
Creep rupture tests of Hastelloy-X tubes at high temperatures and internal helium pressures to determine service life
[NASA-TM-X-2727] 08 p0932 N73-17629
List of metallic melting bodies for temperature determinations from 30 to 1555 degrees Celsius
[JUL-871-RB] 08 p0932 N73-17631
Combustion tests of afterburner performance of circular and parallel V-gutters for range of inlet temperatures to 1800 F
[NASA-TN-D-7212] 09 p1099 N73-18966
Cyclic deformation diagrams of heat resistant and austenitic steels
10 p1219 N73-19914
Steady state creep rate of nickel as effected by binary alloys at increased temperatures
12 p1413 N73-21448
Method of life prediction for nickel-based Udimet alloy by high temperature creep/fatigue testing
[NASA-CR-120958] 12 p1462 N73-21845
High temperature tests to determine thermodynamic properties of nonstoichiometric vanadium nitrides
[NLL-M-21551-[5828.4F]] 12 p1464 N73-21858
Design of high temperature integrated circuit holders
[BAH/DS/AG/R-412/1] 13 p1500 N73-22158
Stress-rupture strength testing and principles of creep-rupture in heat resistant alloys
[JPRS-58760] 13 p1542 N73-22494
High temperature environmental testing of gas-metal interactions to simulate severe operating conditions
14 p1677 N73-23606
Numerical analysis of effects of heating unidimensional plate under nonlinear boundary conditions
[NLL-M-21618-[5828.4F]] 15 p1764 N73-24290
High temperature testing of silicon carbide ceramics for use in gas turbine vanes
[AD-757796] 15 p1802 N73-24602
Density and light radiation measurements of molten metals, semiconductors, and alloys
[NLL-M-21580-[5828.4F]] 16 p1951 N73-25789
Analysis of heat transfer properties and thermophysical properties of materials used for aircraft and spacecraft construction
[AGARD-R-606] 16 p1975 N73-25968
Computerized simulation of temperatures on Centaur standard shroud during heated jettison tests
[NASA-TM-X-68273] 20 p2485 N73-29962
Measurement of elastic moduli of materials at elevated temperatures
[AD-763763] 21 p2554 N73-30473
Irradiation of pyrolytic carbon sealers at high temperatures to determine effects on growth rate and service life
[CONF-730601-5] 21 p2563 N73-30543
Elastomers for service with engine lubricants and hydraulic fluids
[AD-762800] 21 p2564 N73-30554
Thermal and electrical properties of titanium alloyed with vanadium and high temperature creep of metal with fcc lattice
[JPRS-59623] 22 p2683 N73-31490
High temperature creep of metals with face centered cubic lattice
22 p2683 N73-31492
High temperature deformation and fracture behavior of T-111 and ASTAR-811C over temperature range of 982 to 2205 C
[NASA-CR-72859] 22 p2688 N73-31530
Temperature relationship of monochromatic coefficients of radiation of titanium, niobium, and zirconium monocarbides in regions of homogeneity
23 p2807 N73-32442
High temperature low cycle effects on directly stressed, notched fatigue specimens
[RD/B/N-1996] 24 p2989 N73-33888

**HIGH VACUUM**
High vacuum breakdown initiated field emission between technically pure electrodes
[AD-747586] 03 p0338 N73-12753
Creep processes in vacuum sintered copper and silver
12 p1407 N73-21407
Molecular flux measurement in back flow region of nozzle plume in high vacuum
[NASA-CR-133602] 20 p2388 N73-29184
Absolute pressure measuring device for measuring gas density level in high vacuum range
[NASA-CASE-LAR-10000] 21 p2544 N73-30394

**HIGH VOLTAGES**
Design and operation of high voltage photoelectric generator
[AD-745364] 01 p0007 N73-10053
Utilization of oil dischargers in high voltage pulse circuits
[AD-751170] 07 p0765 N73-16214
High voltage distribution fields of two component dielectrics in rotational series or parallel arrangements
08 p0888 N73-17193
Life tests of 10 mm bore flashlamps at high fractions of explosion energy
[AD-760707] 20 p2426 N73-29488
High voltage solar array for ion thruster electric propulsion system
[NASA-TM-X-71462] 24 p2880 N73-33002

**HIGHLY ECCENTRIC ORBIT SATELLITES**
U HEOS SATELLITES

**HIGHWAYS**
Experimental and analytical studies of highway cable barrier and digital simulation of vehicle redirection
[NRC-12694] 01 p0119 N73-10978
Detection of vegetation damage associated with highways and highway facilities with reference to stress caused by chemicals and alteration to ground water table
[E72-10288] 04 p0410 N73-13338
Development of land use and peak runoff classification system for highway engineering using ERTS-1 imagery of Maine
[E72-10308] 04 p0412 N73-13357
ERTS-1 detection and monitoring of vegetation damage associated with highways and highway facilities in Maine
[E72-10371] 05 p0536 N73-14359
Hydrological information from ERTS-1 imagery for design of highway drainage structure in Maine
[E73-10014] 06 p0659 N73-15350
National transportation statistics summaries for 1960 to 1970
06 p0732 N73-15969
Development of land use-peak runoff classification system for highway engineering in Maryland
[E73-10100] 08 p0902 N73-17310
Use of remote sensing for assessing impact of highway construction on land use management in Michigan
[NASA-CR-130761] 08 p0917 N73-17515
Detection and monitoring vegetation damage associated with highway facilities in Maine
[E73-10331] 09 p1024 N73-18361
Utilization of ERTS-1 imagery to develop land use-peak runoff classification system for highway engineering in Maine
[E73-10456] 11 p1283 N73-20415
Detection and monitoring of vegetation damage associated with highway facilities in Maine
[E73-10522] 13 p1517 N73-22290
Detection of vegetation stress and damage associated with highways and highway facilities in Maine
[E73-10611] 15 p1773 N73-24372
Development of land use-peak runoff classification system for highway engineering in Maine
[E73-10654] 16 p1898 N73-25350
Remote color aerial photography for soil mapping and highway engineering applications
[PB-22037/6] 18 p2148 N73-27363
Atmospheric diffusion of carbon monoxide and lead from expressways
18 p2170 N73-27527
Basic fundamentals of meteorology and their effect on pollutant concentration on highway corridor
[PB-219811/7] 18 p2174 N73-27556
Environmental impact of highway projects as determined by vehicle emission factors
[PB-219812/5] 18 p2174 N73-27557
Relationship between highway traffic parameters and air quality analysis - Vol. 3
[PB-219813/3] 18 p2175 N73-27564
Mathematical approach to estimating highway impact on air quality - Vol. 4
[PB-219814/1] 18 p2175 N73-27565
Interaction between air pollution sources and meteorological conditions and impact on air quality along highway corridor - Vol. 6
[PB-219816/6] 18 p2175 N73-27566
Current use and potential capacity of rural highway system
[PB-218453/9] 18 p2214 N73-27876
Detection and monitoring vegetation damage associated with highway facilities in Maine
[E73-10856] 19 p2292 N73-28433
Utilization of Skylab EREP data for highway engineering in Maine
[E73-10909] 20 p2397 N73-29258
Development of land use-peak runoff classification system for highway engineering in Maine
[E73-10910] 20 p2397 N73-29259
Aerial photointerpretation of impact of highway construction on rural area in Thailand
20 p2417 N73-29414

Comparison of extreme floods statistically predicted for highway bridge design in Pennsylvania to actual floods caused by hurricane Agnes
[PB-220888/2] 21 p2575 N73-30639
Measurement of concentration of volatile and particulate lead compounds in atmosphere at selected road sites
[PB-221663/8] 22 p2695 N73-31592
Impact of highway transportation control strategies on Los Angeles air pollution and quality
[PB-221301/5] 22 p2696 N73-31597
HIJACKING
U AIR PIRACY
HILBERT SPACE
NT BANACH SPACE
Application of vector space processes for algebraic analysis of affine plane surfaces
02 p0196 N73-11583
Rank one, quasi-Newton minimization for infinite-dimensional, real Hilbert spaces
[NASA-TR-R-394] 03 p0323 N73-12635
Design of linear feedback control system in Hilbert space
[AD-750784] 06 p0691 N73-15624
Presentation of algebra of projections on convex cones in Hilbert space
[AD-761867] 19 p2315 N73-28619
HILL CURVES
U HILL METHOD
HILL METHOD
Perturbation theory for developing eigenvalues and eigenfunctions in power series expansion for Hill differential equation
02 p0195 N73-11581
HILLER MILITARY AIRCRAFT
U MILITARY AIRCRAFT
HILSCH TUBES
Theoretical study of fluid dynamic energy separation
15 p1764 N73-24292
HIMALAYAS
Nimbus 3 and 4 observations of snow cover and hydrological features in Western Himalayas
07 p0787 N73-16403
HINDRANCE
U CONSTRAINTS
HINGE MOMENTS
U TORQUE
HINGED ROTOR BLADES
U HINGES
U ROTARY WINGS
HINGELESS ROTORS
U RIGID ROTORS
HINGES
NT FLAPPING HINGES
Derivation of minimum dimension sets of discrete coordinate and hybrid coordinate equations of motion for hinge connected rigid bodies assembled in tree topology
[NASA-CR-129950] 05 p0602 N73-14900
Torque measurement of flat polyimide cable crossing hinge or satellite solar array
[ESRO-TN-114-ESTEC] 05 p0603 N73-14904
HISS
OGO-D electromagnetic wave propagation measurements with whistler and hiss formations in plasmasphere
[NASA-CR-130351] 07 p0754 N73-16126
Calculation of intensities of VLF hiss generated from electrons in lower magnetosphere
[NASA-TM-X-66255] 15 p1780 N73-24428
HISTAMINES
Diurnal changes in human histamine and serotonin metabolism and effects of work-sleep cycle
03 p0258 N73-12089
HISTOGRAMS
Histograms of ERTS-1 MSS observations of haze
[E73-10924] 20 p2398 N73-29273
Spline smoothing of histograms by linear programming
[NASA-CR-133987] 22 p2691 N73-31551
HISTORIES
NT CASE HISTORIES
History of Radcliffe Observatory and its scientific research activities and personnel
02 p0152 N73-11231
History of physics with emphasis on nuclear physics and astrophysics
[NASA-TT-F-14670] 07 p0843 N73-16827
History of German aeronautical development during the first half of the century
11 p1350 N73-20956
History of Zeppelin airships to show uses for civil and military purposes
24 p2879 N73-32990
HO-6 HELICOPTER
U OH-6 HELICOPTER
HODOGRAPHS
Effect of discontinuous changes in strain rate on relationship between strain rate, strain and stress in Udimet 700 alloy at elevated temperatures
10 p1219 N73-19916
Influence of strain rate on inelastic properties of Udimet alloys at elevated temperatures and presentation in form of hodograph
10 p1219 N73-19917
HODOSCOPES
Engineering specifications for proportional counter hodoscope to be flown on HEAO A mission
[NASA-TN-D-7317] 15 p1828 N73-24816
Balloon flown hodoscopic observations of rapid variations in solar proton flux in 1972
[TR-73-134] 23 p2834 N73-32650
Hodoscope measurements of cosmic ray electron spectra
[TR-73-135] 23 p2834 N73-32651
HOHMANN TRAJECTORIES
U TRANSFER ORBITS
HOHMANN TRANSFER ORBITS
U TRANSFER ORBITS
HOLDERS
NT FLAME HOLDERS
Design of high temperature integrated circuit holders
[BAH/DS/AG/R-412/1] 13 p1500 N73-22158
HOLE DISTRIBUTION [MECHANICS]
Analysis of fatigue damage cumulation of low carbon steel specimens with transverse hole using two step rotating bending tests and block loading sequence
[TAE-164] 09 p1093 N73-18922
Adjustable hole cutter for forming circular openings
[NASA-CASE-MFS-22649-1] 23 p2797 N73-32376
HOLE MOBILITY
Effects of electron-hole scattering on mobility to carriers in silicon at high injected carrier densities
01 p0087 N73-10718
Positron annihilation center decrease through migrating anion vacancies in thermal annealing of radiation damaged sodium chloride crystals
[CONF-720530-6] 10 p1194 N73-19715
Dislocation mobilities and densities in copper, lead, and zinc crystals
[CALT-767-P-3-27] 12 p1440 N73-21666
High temperature effects on dislocation mobility of LiF single crystals
18 p2185 N73-27642
HOLES
Stress effects around holes in flat plates under various combinations of loads
[ESDU-70005] 01 p0110 N73-10902
Determining maximum shear stress at hole boundary in axially loaded bar
[ESDU-66011-AMEND-A] 01 p0111 N73-10913
Development of approximate equation for determining stress intensities for quarter circular cracks emanating from circular hole in sheet material
[AD-757550] 14 p1716 N73-23928
Optimum edge reinforcement around a circular hole in a flat elastic sheet subjected to axial tensile stress
[ARC-R/M-3723] 21 p2604 N73-30869
Dynamic analysis of free vibrations of rectangular elastic plate with central circular hole
[AD-765361] 23 p2855 N73-32816
HOLES [ELECTRON DEFICIENCIES]
Effects of electron-hole scattering on mobility to carriers in silicon at high injected carrier densities
01 p0087 N73-10718
ESR spectra of paramagnetic hole centers in CeO2 after ultraviolet irradiation
[AD-746036] 02 p0220 N73-11778
Effects of electron and hole trapping on radiation hardness of aluminum oxide MIS devices
[AD-758696] 16 p1882 N73-25229
High frequency satellite lines in X ray spectra of heavy ions
[CONF-720404-VOL-3] 19 p2323 N73-28687
Rapid flux, relativity, black holes, and pulsar, and quasar models
[NASA-TM-X-62298] 23 p2846 N73-32742
High field emission and capture of electrons and holes at zinc centers in N-P and P-N junctions
24 p2966 N73-33705
HOLLAND
U NETHERLANDS
HOLLOW CATHODES
Low frequency instabilities in hollow cathode magnetoplasma discharge
[AD-750477] 06 p0707 N73-15765
Volt-ampere characteristics of pulse discharge flow in hollow hydrogen cathode
[AD-753038] 09 p1072 N73-18749
Development of hollow cathode plasma electron gun for gas lasers
[AD-757086] 14 p1672 N73-23570
Volt-ampere characteristics of enclosed keeper hollow cathode discharge
[NASA-TM-X-2799] 15 p1825 N73-24792
Tests of mercury-fed hollow cathode in bell jar at SERT 2 neutralizer conditions
[NASA-TM-X-2785] 15 p1825 N73-24793
Properties of low frequency instability in hollow cathode discharge magnetoplasma
16 p1948 N73-25758
Hollow cathode with BaO impregnated, porous tungsten inserts and tips
[NASA-TM-X-71417] 21 p2517 N73-30189
Investigation of hollow cathode performance for 30 cm thrusters
[NASA-TM-X-68298] 21 p2588 N73-30739
SERT 2 hollow cathode multiple restarts in space
[NASA-TM-X-68292] 21 p2589 N73-30742
Hollow cathode neutralizer for 30-cm diameter bombardment thruster
[NASA-TM-X-68291] 21 p2589 N73-30743
Low frequency instabilities and plasma turbulence including steady state and time dependent characteristics of positive column and hollow cathode discharge
[NASA-CR-135669] 23 p2822 N73-32562
HOLMIUM
Manufacturing of holmium lithium tetrafluoroyttriate laser disk bonded into glass
[AD-747968] 03 p0352 N73-12871
Growth of multiply sensitized Ho Y1.F crystals as laser materials
[AD-755530] 13 p1538 N73-22461
Design and performance of segmented holmium doped yttrium lithium fluoride laser
[AD-760019] 17 p2042 N73-26522
HOLOGRAPHIC INTERFEROMETRY
Application of holographic interferometry for inspection of large aircraft structures during manufacturing and maintenance
[AD-757510] 14 p1604 N73-23000
Holographic interferograms of supersonic jet aircraft acoustic field
[PB-214112/5] 14 p1693 N73-23743
Application of holographic interferometry techniques for determining asymmetric flow distribution encountered near wing-fuselage junction at transonic speed
[AD-759967] 17 p2015 N73-26296
Double exposure interferograms of discharge region of transverse electrically-excited atmospheric pressure CO2 lasers
[UCRL-13547] 20 p2425 N73-29483
Holographic interferometric measurements of three dimensional temperature fields
22 p2680 N73-31463
Real time holographic interferometry for optical surface testing
[BMFT-FBT-73-01] 22 p2681 N73-31479
HOLOGRAPHY
NT HOLOGRAPHIC INTERFEROMETRY
Development of air navigation system using moving map display based on holographic storage and display techniques
[AD-745025] 01 p0065 N73-10533
Applications of holographic interferometry in underwater acoustics research
[AD-746134] 01 p0067 N73-10545
Acoustic holography for imaging cylindrical plastic-bonded explosive loads
[AD-746468] 01 p0067 N73-10547
High speed holography of high speed phase object using Q switched laser outputs
[ISL-10/71] 02 p0181 N73-11471
Improving divergence in ruby laser radiation by holographic transformation of light field coherence
[AD-746646] 02 p0183 N73-11486
Acoustic holographic signals for designing underground geological viewing system
[AD-746498] 02 p0184 N73-11490
Recording of holographic visual display elements in dichromated gelation
[AD-746859] 03 p0310 N73-12532
Application of alkali halides for holographic recording and recovery at room temperatures for high density data storage systems
[AD-748027] 03 p0311 N73-12537
Basic principles of holography and applications
[AD-747380] 03 p0311 N73-12538
Development of map storage and display system using volume holography using iron-doped lithium niobate
[AD-748002] 03 p0311 N73-12541
Development of holographic storage and retrieval system for aerial chart information display in cockpit environment
[AD-748648] 03 p0330 N73-12690
Density field map in fin-flat plate junction in three dimension, using holographic interferometry
[AD-749048] 04 p0408 N73-13324
International conference on acoustical holography
[AD-749337] 04 p0430 N73-13505
Application of holography to jet breakup in supersonic flow fields and analytical method for reducing holographic droplet data
[AD-749854] 05 p0529 N73-14302
Effects of stoichiometry variation, heat treatment, impurity, and color center content of electrooptic crystals and kinetics of index damage process
05 p0554 N73-14501
Dual hologram interferometry for calculating density distributions from refraction index changes
[AD-749872] 05 p0559 N73-14538
Microwave holography for imaging sea surface topography in three dimensions
06 p0664 N73-15391

Technique for extending viewing angle of hologram to three hundred and sixty degrees
[AD-750250] 06 p0681 N73-15539
Spurious image and color rendition problems in producing multicolor holograms
[AD-751560] 07 p0801 N73-16508
Optical reconstruction applied to holograms recorded at microwave, acoustic, or other suboptical frequencies producing longitudinally distorted image
[AD-751408] 07 p0801 N73-16509
Development of phase contrast enhancement techniques for seismic holography without use of spatial filters
[BM-RI-7721] 07 p0806 N73-16537
Holographic interferometry from coherent laser light to detect three dimensional displacements
[UCRL-51241] 07 p0806 N73-16540
Cis-trans isomers and doped LiNbO3 for holographic ready/write/erase memory application
[NASA-CR-112248] 08 p0928 N73-17604
Application of holography for nondestructive tests of solid propellant rocket engine to detect unbonding between liner and propellant
[NASA-CR-112225] 08 p0929 N73-17606
Sonic or ultrasonic holography in nuclear industry research
[DUN-SA-191] 08 p0929 N73-17610
Image speckling reduction using multicolor illumination in holographic microscopy
[AD-752240] 08 p0945 N73-17737
Holographic techniques for particle sizing and velocity distribution
[NASA-TR-R-404] 09 p1035 N73-18448
Research and development of lasers and laser-related equipment in the Soviet Union - bibliography
[AD-753098] 09 p1043 N73-18510
Photointerpretation techniques based on holographic stereogram three dimensional presentations
[AD-753167] 09 p1044 N73-18518
Holographic memory system using argon ion lasers and acoustooptic beam deflectors
[NASA-CR-124084] 09 p1064 N73-18680
Thin deformable films for use as storage medium in holographic optical memory
[NASA-CR-124083] 09 p1064 N73-18681
Membrane-mirror elements as light valves in optical memory systems
[NASA-CR-124085] 09 p1064 N73-18682
Characteristics of holographic logic computer
09 p1066 N73-18696
Operational requirements and optical components of pulsed holographic interferometry
[LA-5058] 10 p1161 N73-19446
Holographic starfield and landmark tracker with two reference beam, coherent optical matched filter technique
[NASA-CR-112143] 10 p1168 N73-19505
Applications of holographic system with interferometric capabilities for crystal growth analysis
[AD-754737] 11 p1294 N73-20504
Method for obtaining holographic interferograms in real time scale
[AD-754632] 11 p1303 N73-20577
Evolution of nondestructive testing techniques arising from holography and microwaves
[AD-755116] 11 p1304 N73-20580
Holography in random spatially inhomogeneous medium
[AD-755781] 12 p1406 N73-21402
Holographic interferometric testing of laminate and composite structures for internal voids and material defects
[BDX-613-812] 12 p1410 N73-21429
Application of holographic interferometry to determination of discontinuous three-dimensional density fields
[AD-756535] 13 p1511 N73-22246
Application of holographic interferometry to density field determination in transonic corner flow
[AD-756534] 13 p1511 N73-22247
Annotated bibliography on holography
[AD-756600] 13 p1531 N73-22408
Measurement of surface strain deformation in materials by holographic interferometry
[NRC-TT-1623] 13 p1536 N73-22447
Holographic and acoustical tests of vibrating underwater structures
[AD-755475] 13 p1538 N73-22463
Development of optical and digital techniques for application to synthetic holograms recorded with suboptical sources
[AD-756506] 14 p1674 N73-23583
Application of hologram optical element to pilot head-up display
[AD-758057] 15 p1744 N73-24139
Spatial filtering techniques in connection with coherent light optical data processing
[LCR-DR-1-71-253/1/R] 15 p1754 N73-24220
Holography and optical filtering techniques for structural analysis, material tests, and astronomical observation - conference
[NASA-SP-299] 16 p1920 N73-25540
Design and operating characteristics of pulsed ruby laser source used in portable holocamera
16 p1920 N73-25541
Advanced technology for improving performance parameters of ruby laser
16 p1921 N73-25542
Holographic interferometry for measuring surface deflections of statically loaded turbine blades
16 p1921 N73-25543
Pulsed holographic measurement of wave propagation in thin walled shells and vibration modes in steel rectangular plates at high temperature
16 p1921 N73-25544
Holographic interferometric measurement of prebuckling deformation in cylindrical shell structures under axial compression
16 p1921 N73-25545
Application of holographic nondestructive testing to experimental production hardware components and structural problems in aerospace engineering
16 p1921 N73-25546
Holographic technique to record front surface detail from high velocity target
16 p1921 N73-25547
System for measuring scattered flux from fine grained photographic emulsions
16 p1921 N73-25548
Small phase difference measuring technique within holographically reconstructed optical fields
16 p1922 N73-25549
Aerospace application of holography through nondestructive testing and flow visualization
16 p1922 N73-25550
Holographic instrumentation for use in flow visualization, nondestructive testing procedures, and optical data processing
16 p1922 N73-25551
Reusable photoplastic recording materials in read/write holographic memories
16 p1922 N73-25553
Holography applied to matched filtering and pattern recognition
16 p1922 N73-25555
Matched filter selectivity applied to holographic velocimetry
16 p1923 N73-25556
Real image of aperture-limited, in-line Fraunhofer hologram
16 p1923 N73-25560
Optimum holographic mounting for maximal ultrahigh speed microparticle volume restitution
[ISL-32/72] 16 p1924 N73-25565
Theoretical study and mountings for magnification and holographic image reconstruction of high speed microparticles
[ISL-1/73] 16 p1924 N73-25566
Mountings for optimum magnification and holographic image reconstruction of high speed microparticles
[ISL-3/73] 16 p1924 N73-25567
Holographic matched filters for correcting phase heterogeneities in aperture antennas
[JPRS-59253] 17 p2003 N73-26201
Four step, acoustic holographic imaging system
17 p2031 N73-26435
Application of holography techniques for recording three dimensional flow distribution of liquid jet injected into Mach 3 gas stream
17 p2039 N73-26498
Development of technique for producing holograms using propagation of surface waves within layer of photosensitive material
[NASA-CASE-MFS-22040-1] 17 p2039 N73-26500
Iron-doped lithium niobate as holographic storage medium
[AD-760343] 17 p2042 N73-26518
Holographic interferometry using pulsed ruby lasers to measure electron density in toroidal plasmas
[REPT-72-70] 17 p2069 N73-26743
Holographic visualization of flow field within transonic compressor rotor
[NASA-CR-121112] 18 p2130 N73-27215
Evaluation and characterization of possible recording materials for holographic optical elements
[AD-760561] 18 p2159 N73-27441
Aberrations and imaging properties of holographic optical elements
[NASA-CR-124334] 19 p2307 N73-28555
Holographic investigations using pulsed lasers
[AD-761977] 19 p2308 N73-28565
Microwave holography describing lateral and axial resolution, computerized wave front reconstruction, and application to moving objects
[REPT-6-72] 20 p2425 N73-29484
Geometric optical properties of holographic lens systems
[AD-762526] 20 p2426 N73-29486
Image data compression using digital holography
[AD-762931] 20 p2426 N73-29487
Study of supersonic flow in inlets using holographic interfereometry
[AD-763335] 21 p2525 N73-30250
Thin film analyzer utilizing holographic techniques
[NASA-CASE-MFS-20823-1] 21 p2554 N73-30476
Holographic system for nondestructive testing
[NASA-CASE-MFS-21704-1] 21 p2554 N73-30478
Optical holographic measurement of jet noise in supersonic air/nitrogen and helium jets at Mach numbers from 1.5 to 3.4
[PB-220641/5] 21 p2581 N73-30686
Real time three dimensional motion picture camera using holography
[NASA-TR-R-409] 22 p2673 N73-31413
Performance of computer generated binary and kinoform holograms
22 p2680 N73-31464
Correction of aberrations in long wavelength holography by direct injection in formation process and computer generation
22 p2680 N73-31466
Application of holographic interferometry for detecting dewetted zones in solid rocket propellants
[AD-764470] 22 p2708 N73-31690
Optical and digital reconstruction techniques applied to synthetic holograms recorded with suboptical sources
23 p2800 N73-32394
Evaluation of holographic-recording photopolymer to determine diffraction efficiencies and development techniques
[CRC-659] 23 p2800 N73-32395
Pulsed laser holographic interferometry of shock waves within transonic fan rotors
[NASA-TM-X-71430] 23 p2801 N73-32402
Production and performance of bleached holographic lenses
[AD-764701] 23 p2821 N73-32548

**HOLOMORPHISM**
U ANALYTIC FUNCTIONS

**HOMEOSTASIS**
Mathematical model for in vivo study of glucose homeostasis in humans
[NASA-CR-129171] 02 p0130 N73-11056

**HOMING DEVICES**
Stochastic control theory for homing guidance laws for tactical missiles
[AD-761626] 19 p2347 N73-28876
Engineering test procedures for heat seeking missiles
[AD-763324] 21 p2602 N73-30853

**HOMOGENEITY**
Preparation of solid homogeneous materials in space
04 p0473 N73-13861
Stationary phase direction in absorbent media applied to ray propagation through three successive homogeneous isotropic media
[GRI/TP/110] 06 p0639 N73-15183
Semi-infinite homogeneous response to shear and compressional line sources
[UCRL-51233] 06 p0667 N73-15420

**HOMOMORPHISMS**
Homomorphically estimated restoration filter for removing image blurs
19 p2320 N73-28668

**HONEST JOHN ROCKET VEHICLE**
Meteorological and ballistics data for launching 13401 Honest John, missile number 2632, round number 626 ROL
[AD-749434] 04 p0445 N73-13635
Meteorological and ballistics data for launching of Honest John Laser, missile flight 205, vehicle 624
[AD-749430] 04 p0446 N73-13637
Meteorological and ballistics data for launching of Honest John Missile flight 1755, vehicle 625
[AD-749431] 04 p0446 N73-13638
Meteorological and ballistics data for launching of Honest John, missile number 3116, round 686
[AD-749438] 05 p0574 N73-14671
Meteorological parameters for launching of 13401 Honest John missile number 2631, round no. 627 RUL
[AD-752094] 08 p0940 N73-17704
Meteorological data for launching Honest John missile, number 2598
[AD-755777] 12 p1424 N73-21543
Meteorological and ballistics data for launching of Honest John missile number 359, round 629,
[AD-758862] 16 p1938 N73-25684
Meteorological and ballistics data for launching of Honest John missile number 627, round 632
[AD-758868] 16 p1938 N73-25685
Meteorological and ballistics data for launching of Honest John, missile number 1002, round 630
[AD-758865] 16 p1938 N73-25686
Meteorological data for launching of Honest John, missile number 1763, round 685
[AD-762158] 19 p2317 N73-28632
Meteorological and ballistics data for launching of 13401 Honest John missile no. 2542, round no. 634 RMI
[AD-762157] 19 p2317 N73-28633
Meteorological data for launching of Honest John, missile number 305, round 633
[AD-762155] 19 p2317 N73-28636

**HONEYCOMB CORES**
Design and fabrication of honeycomb resin-composite sandwich panels for shuttle orbiter thermal shielding
[NASA-CR-128610] 01 p0061 N73-10503

Structural analysis of sandwich panels with close-packed conical shells and honeycombs as fillers
[AD-747403] 03 p0362 N73-12953
Dynamic frequency response of curved or flat honeycomb sandwich panels having cores of negligible flexural stiffness
[ESDU-72016] 06 p0723 N73-15898
Techniques for preparation of Pyrrone structural foams for use as honeycomb filler
[NASA-CR-2222] 09 p1052 N73-18574
Evaluation of sandwich structures of titanium and aluminum honeycomb in edgewise compression under static and fatigue loading
[FPL-196] 16 p1969 N73-25927

**HONEYCOMB STRUCTURES**
NT HONEYCOMB CORES
Noise attenuation characteristics of cylindrical suppressors with duct lining composed of honeycomb cells covered with perforated plate
[NASA-TM-X-2652] 01 p0005 N73-10032
Development of process for bonding resinous body in cavities of honeycomb structures
[NASA-CASE-MSC-12357] 03 p0305 N73-12489
Nuclear thermal vulnerability of honey comb sandwich radome panels
[AD-753666] 09 p1056 N73-18605
Development and testing of beryllium honeycomb sandwich composite panels
[NASA-CR-130648] 15 p1838 N73-24896
Evaluation of aluminum honeycomb core landing mat with modified hinges
[AD-758840] 18 p2127 N73-27186

**HONEYWELL COMPUTERS**
Analysis of performance of Honeywell Information System 6000 series computer
[AD-759808] 16 p1879 N73-25212

**HOPPERS**
Design and development of device to prevent clogging in hoppers containing particulate materials
[NASA-CASE-LAR-10961-1] 03 p0306 N73-12496
Design of hopping transporter for lunar exploration
[NASA-CR-130010] 07 p0765 N73-16217

**HORIZON SCANNERS**
Method and equipment for locating earth infrared horizon from space, independent of season and latitude
[NASA-CASE-LAR-10726-1] 11 p1291 N73-20475
Brushless dc torque motor in-orbit performance of ITOS with improved attitude controls and earth splitting technique
[NASA-TM-X-66267] 17 p2060 N73-26662
Aerosol physical properties from horizon inversion by satellite
[NASA-CR-112311] 18 p2144 N73-27330
Development of infrared earth horizon scanner employing thermistor bolometers providing pitch and roll data of synchronous satellites
[ESRO-CR-161] 19 p2301 N73-28503
Accurate and reliable prototype earth horizon sensor head employing logic locator concept
[NASA-CR-132267] 23 p2792 N73-32334

**HORIZON SENSING**
U HORIZON SCANNERS

**HORIZONTAL FINS**
U FINS

**HORIZONTAL STABILIZERS**
U STABILIZERS [FLUID DYNAMICS]

**HORIZONTAL TAIL SURFACES**
Static tests of redesigned graphite horizontal stabilizers
[AD-758718] 15 p1803 N73-24611
Effects of addition and position of outboard stabilizers and tail configurations on aerodynamic characteristics of low-wave-drag elliptical body at hypersonic speed
[NASA-TM-X-2747] 18 p2101 N73-26993

**HORIZONTAL TAILS**
U HORIZONTAL TAIL SURFACES
U TAIL ASSEMBLIES

**HORMONE METABOLISMS**
Statistical analysis of steroid levels in parotid secretions of humans under prolonged mental stress
[AD-747682] 04 p0381 N73-13104
Conference on human endocrine secretions and hormone metabolisms during space flight stress
[NASA-TM-X-58093] 09 p0993 N73-18104
Human adrenocorticotropin level measurements as indication of adaptation to space flight stress
09 p0993 N73-18109
Water immersion model for simulating renin, aldosterone, and natriuresis effects of prolonged weightlessness on man
09 p0993 N73-18110
Multiple immunoassay system for determining parathyroid hormone, calcitonin, and vitamin D in human blood
09 p0994 N73-18112
Prolonged bed rest effects on human blood hormone level periodicities
09 p0994 N73-18114
Human pituitary and adrenal hormone reserve in acceleration stress tolerance
10 p1123 N73-19150
Chromatographic determination of aldosterone level in urine
[RAE-LIB-TRANS-1682] 17 p1987 N73-26061
Chromatographic determination of urine corticosteroids
[RAE-LIB-TRANS-1694] 17 p1987 N73-26062

**HORMONES**
NT ALDOSTERONE
NT CORTICOSTEROIDS
NT HYDROXYCORTICOSTEROID
Radioimmunoassay of urinary antidiuretic hormone excretion in man considering water loading and dehydration effects
09 p0993 N73-18107
Measurement of antidiuretic hormone excretions in human urine as indication of neurosecretory stress response during space flight
09 p0993 N73-18108

**HORN ANTENNAS**
Characteristics of four types of horn antennas for application as S-band radiometers and modifications to improve beam efficiency
[NASA-CR-2133] 07 p0755 N73-16135
Waveguide polarizer for horizontal control of antenna radiation patterns
[AD-751449] 07 p0763 N73-16198
Electrodynamic fundamentals of antenna theory and design
[AD-755689] 13 p1502 N73-22176
Effects of surface corrugation in horn antenna power loss
[NASA-CR-2317] 23 p2756 N73-32059
Theory of electroacoustical images and relationship between geometric form of horn and sound antennas based on acoustic properties
24 p2956 N73-33617

**HOSES**
Chloride and water permeability parameters for hydraulic brake hose testing
[AD-748083] 13 p1546 N73-22530

**HOT AIR**
U HIGH TEMPERATURE AIR

**HOT CATHODES**
Rotation of ion component of hot cathode Penning discharge plasma
[NASA-TT-F-14931] 16 p1948 N73-25765

**HOT CYCLE PROPULSION SYSTEM**
U TIP DRIVEN ROTORS

**HOT ELECTRONS**
Hot electron effects in SCL diodes and MOSFETS
13 p1565 N73-22680
Channel length effect on field effect transistor noise in hot electron regime
19 p2326 N73-28713

**HOT EXTRUDING**
U EXTRUDING

**HOT FORMING**
U HOT WORKING

**HOT GAS SYSTEMS**
U HIGH TEMPERATURE GASES

**HOT GASES**
U HIGH TEMPERATURE GASES

**HOT JET EXHAUST**
U HIGH TEMPERATURE GASES
U JET EXHAUST

**HOT JETS**
U JET FLOW

**HOT PLASMAS**
U HIGH TEMPERATURE PLASMAS

**HOT PRESSING**
Process for producing polycrystalline halides for use in high power laser windows to maintain optical properties with improved mechanical properties
[AD-745350] 01 p0065 N73-10535
Feasibility of hot pressing alumina composites with potassium and barium fluorine micas
[AD-742207] 01 p0071 N73-10584
Annotated bibliography of sintered and hot pressed silicon nitride
[AD-747785] 03 p0322 N73-12624
Thermogravimetric measurements for oxidation of hot pressed silicon carbide
[AD-748351] 04 p0439 N73-13578
Hot pressing and hot rolling procedures for producing aluminum reinforced with high strength steel strips
[NLL-TRANS-746-1355-(9022.401)] 05 p0561 N73-14554
Development of process for fabricating dense boron suboxide billets by hot pressing to eliminate decomposition and cracking
[AD-751980] 08 p0936 N73-17662
Liquid hot pressing of silicon carbide whiskers for reinforcing aluminum alloy composites
[AD-752589] 08 p0936 N73-17666
Diffusion bonding of plasma sprayed boron reinforced magnesium monolayer tapes by hot pressing
[SC-DR-72-0677] 10 p1166 N73-19488
Hot pressing of nickel-zinc ferrites for manufacturing read-write magnetic heads
[REPT-9.451] 13 p1500 N73-22154
Reactive hot pressing for producing silicon nitrides
[AD-757748] 15 p1802 N73-24604
Potential of hot-isostatic pressing, hydrostatic extrusion and deformable die tube tapering processes to production of titanium tubes
[AD-759504] 16 p1919 N73-25532
Microstructure of hot pressed and press forged polycrystalline refractory oxides
[AD-760353] 17 p2053 N73-26606
Hot pressed polycristalline garnets and ferrites of spinel type to be used at UHF
19 p2236 N73-28026
Development of method for determining optimum setting of regulators on metal working machinery involved in sintering process
[NLL-M-21642-(5828.4F)] 20 p2428 N73-29505
Fabricating lamellar ceramic-based composites with controllable properties by hot pressing of gamma Al2O3/Ba-mica
[AD-762839] 20 p2436 N73-29563
Fabrication and properties of carbon-fiber glass composites and methods for improving mechanical properties
[ARL/MET-NOTE-85] 21 p2561 N73-30533
Hot forging of aluminum alloy structural parts
[AD-764618] 23 p2798 N73-32384
Application of hot pressing, hot extruding, and sintering processes for production of composite materials
[JPRS-59873] 23 p2807 N73-32441
Microstructure of molybdenum carbide samples during hot pressing and development of line intensity diagram for various conditions
23 p2808 N73-32449
Characteristics of silicon carbide samples produced by hot casting under pressure
23 p2808 N73-32450
Hot pressing behavior of SiC with Al2O3
[AD-764639] 23 p2811 N73-32475

**HOT STARS**
NT A STARS
NT B STARS
NT O STARS
NT WHITE DWARF STARS
Atlas S183 experiment for ultraviolet stellar spectrophotometry onboard Skylab manned space station
17 p2033 N73-26454
Tables listing 1970.0 ecliptic coordinates of hot stars
[COMMUN-27] 19 p2344 N73-28857
Hot star catalog listed in constellation alphabetical order
[COMMUN-31] 19 p2344 N73-28858

**HOT WORKING**
Mechanical properties of various metal alloys and operating life of dies during hot deformation of stainless and heat resistant steels and alloys
[AD-745703] 01 p0068 N73-10559
Progressive technological processes and equipment for hot shaping
[AD-747402] 03 p0309 N73-12519
Effects of various forming factors and process variables on forming of sheet metal products
05 p0551 N73-14476
Process for making high strength beryllium by hot-pressing extrusion and forging
[RFP-1816] 06 p0684 N73-15570
Influence of preliminary hot rolling on superplasticity of zinc aluminum eutectoid
09 p1046 N73-18530
Deformation properties of hot worked Type 304 austenitic stainless steel, Mangalloy, and other steel alloys
[AD-758912] 15 p1800 N73-24592
Proceedings of conference on rolling mills for production of work hardened, heat treated metal products
[NLL-M-21649-(5828.4F)] 20 p2421 N73-29450

**HOT-FILM ANEMOMETERS**
Split-film atmospheric turbulence anemometer evaluation
[NASA-CR-62093] 16 p1914 N73-25485
Hot film sensor measurement of turbulent flow of fluids in pipes
[AD-762059] 19 p2258 N73-28199

**HOT-WIRE ANEMOMETERS**
Drag measurement in wake of oscillating cylinder at low Reynolds number using hot-wire technique
[DLR-FB-71-42] 09 p0981 N73-18015
Strain gage, smoke flow photograph, and hot-wire anemometer studies for determining magnus characteristics
09 p1015 N73-18286
Transient hot-wire measurement of thermal conductivity of electrolytic solutions
[RISO-264] 10 p1126 N73-19173
Transient hot-wire determination of thermal conductivity of pure, dielectric liquids
[RISO-263] 10 p1126 N73-19174
Determining open-loop response of Reynolds number dependent process as analog of drop-vaporization burning-rate process
[NASA-CR-121167] 11 p1269 N73-20301
Hot-wire anemometer measurements of turbulence and shear stress in circular tube flow
[KFK-1642] 12 p1392 N73-21286
Design of multiple output analog computer for hot-wire anemometer signal processing
[AD-756532] 13 p1498 N73-22143

Hot-wire anemometer and pitot static probe measurement of turbulent mixing in axial pressure gradients
[AD-756543] 13 p1511 N73-22244
Analysis of wakes generated by hovering model propellers and rotors using schlieren photography and hot-wire anemometry
[NASA-CR-2305] 21 p2491 N73-29996
Oscillation hot-wire anemometer based on downstream transit time of hot gas volume
[REPT-9/1972] 22 p2674 N73-31419
Device for welding hot-wire anemometer components following breakage due to dust particles in air stream
[AERE-R-7304] 22 p2678 N73-31451
PDP 8/I data acquisition and averaging program for synchronous hot-wire measurements in mouth of flow excited cavity resonator
[AD-764851] 23 p2795 N73-32357

**HOT-WIRE FLOWMETERS**
Analysis of heat transfer characteristics of hot wire normal to incompressible air flow and influence of frequency on sensitivity and temperature distribution along wire
[WTHD-33] 05 p0605 N73-14922
Hot-wire measurement of longitudinal instability phenomena in stagnation area of circular cylinder in turbulent flow
07 p0771 N73-16265

**HOT-WIRE TURBULENCE METERS**
U HOT-WIRE FLOWMETERS

**HOURGLASS VALLEYS**
U VALLEYS

**HOUSINGS**
NT RADOMES
Procedures for determining present and predicted noise exposure at residential construction sites
[PB-210590] 01 p0081 N73-10672
Gas flow control device, including housing and input port
[NASA-CASE-NPO-11479] 04 p0425 N73-13462
Space technology for solving materials and design problems of earthbased housing
04 p0474 N73-13868

**HOVERCRAFT**
U GROUND EFFECT MACHINES

**HOVERING**
Optimal control model for predicting manual VTOL pilot performance in longitudinal hovering tasks
01 p0017 N73-10134
Aerodynamic characteristics of helicopters with sling loads in hovering and near-hovering conditions
[AD-750618] 06 p0625 N73-15073
Development of computer programs to calculate helicopter rotor tip vortex geometry in hover and forward flight to include calculation of rotor harmonic air loads
[AD-752628] 08 p0869 N73-17032
Analytical and experimental techniques to define geometry of vortex field of hovering rotary wing and effect on rotor performance
12 p1359 N73-21032
Development of procedure for determining geometry and strength distribution of vortex wake generated by single-bladed hovering helicopter rotor
12 p1360 N73-21035
Development of method for predictiong performance of heavily loaded propellers and rotors in steady hovering flight
12 p1360 N73-21040
Development of pilot model parameters to provide data base for multiloop, single controller, multi-input analysis of aircraft performance
[AD-755367] 12 p1365 N73-21078
V/STOL lift fan commercial short haul transport aircraft for 1980 to 1985 period to include aircraft design, hover control, and cruise performance
[NASA-CR-2185] 13 p1473 N73-21930
Full scale hover test of 25-foot tilt rotor
[NASA-CR-114626] 16 p1861 N73-25070

**HOVERING STABILITY**
Command and control of stability of Do-31 aircraft by landing and hovering
[BMVG-FBWT-72-25] 10 p1106 N73-19022
Optimal design of helicopter precision hover control systems
[AD-759919] 17 p1984 N73-26039
Analysis of pitch damping moment for hovering helicopter rotary wing and development of formula for calculating pitch damping derivative
[NASA-TT-F-15010] 21 p2495 N73-30027

**HSS-2 HELICOPTER**
U SH-3 HELICOPTER

**HU-1 HELICOPTER**
U UH-1 HELICOPTER

**HUBS**
Analysis of products and techniques for reducing reflections of light from helicopter windshields, rotor blades and rotor hub assembly
[AD-761127] 18 p2107 N73-27037

**HUGHES AIRCRAFT**
NT OH-6 HELICOPTER

**HUGHES MILITARY AIRCRAFT**
U MILITARY AIRCRAFT

**HUGONIOT ADIABAT**
U HUGONIOT EQUATION OF STATE

**HUGONIOT EQUATION OF STATE**
Nonlinear theory using fourth order Hugoniot curves for compression shocks in cubic crystals
01 p0087 N73-10720
Method for determining density of impacting particles by using Hugoniot curves
[NASA-CASE-LAR-11059-1] 17 p2082 N73-26838

**HULLS (STRUCTURES)**
NT SHIP HULLS
Development of computer program for optimum design of submarine hulls with frame stiffened cylindrical structures
[AD-761643] 19 p2349 N73-28893

**HUMAN BEHAVIOR**
Human operator model for man machine control behavior in biodynamic flight environment
01 p0014 N73-10105
Input adaptive behavior model of human operator in pursuit tracking task
01 p0014 N73-10108
Suboptimal sampling and control behavior of human operator in output prediction task for automatic process
01 p0015 N73-10114
Analysis of cosmonaut emotional stress as determined by physiological and behavioral responses
[NASA-TT-F-14654] 03 p0261 N73-12113
Human operator adaptive behavior in slowly changing dynamic system
[AD-748243] 05 p0503 N73-14097
Functional relationship between food preference and frequency of repetitious eating
[AD-749079] 05 p0503 N73-14100
Industrial model for leave and overtime taking behavior of employees exposed to peak work activity periods in relation to health, demography, and job variables
08 p0872 N73-17055
Probabilities models of organizational behavior and human subjective performance
[IZF-1973-3] 14 p1613 N73-23076
Analysis of complex social systems relative to information, communication, and behavior
[P-4951] 14 p1721 N73-23963
Relations between sociometric variables and criteria of ability and behavior of student pilots
19 p2226 N73-27954
Algorithm of simple inductive interaction between man and surrounding objects and events
24 p2888 N73-33058
Principles of construction for class of models of intelligent behavior
24 p2888 N73-33059
Experimental evaluation of model of motor behavior
24 p2888 N73-33060
Model of organization of goal-directed behavior
24 p2888 N73-33061

**HUMAN BEINGS**
Abstracts on microwave radiation effects on human and animal physiological functions and life expectancy
[MBL-1972-6] 01 p0008 N73-10061
Influence of illumination on electro-oculographic measurements of human eye potential
[AMRU-R-71-1] 02 p0131 N73-11064
Development of mathematical model for slow phase rotational nystagmus induced by head movements
[AMRU-R-71-3] 02 p0131 N73-11065
Analysis of development of cosmos, universe, mankind, and space exploration
04 p0470 N73-13833
Oxygen, carbon dioxide, nitrogen, and noble gases for environment suitable for humans
06 p0628 N73-15093
Biophysical mechanisms of noninvasive measurement of CVP in man
[NASA-CR-130348] 07 p0742 N73-16039
Correlation of physical activity and oxygen consumption between man and mouse
[FOA-1-B-1233-A5] 08 p0877 N73-17108
Gas chromatographic and mass spectrometric determinations of trace elements in human breath samples
[AD-750141] 09 p1000 N73-18159
Biological and toxicity effects of aluminum and other chemicals in animals
[ORNL-TIP/TIRC-72-76] 10 p1121 N73-19136
Pharmacological measures for prophylactic and restorative treatment of men and animals during space flight
11 p1239 N73-20060
Influence of cysteamine hydrochlorine and vitamin B and C prophylaxis on radiation sickness in humans
11 p1242 N73-20078
Electrophysiological sleep patterns of human and animal brains
[NASA-TT-F-740] 13 p1483 N73-22023
Interdependence of slow and rapid brain waves during sleep
13 p1483 N73-22027
Man and natural environment protection and management
[JPRS-59369] 18 p2110 N73-27064
Influence of man on biospheric balance
[JPRS-59366] 18 p2110 N73-27065
Factors affecting stereoscopic vision and depth perception in human beings
[AD-759261] 20 p2369 N73-29050
Control mechanism in accommodation-vergence eye movement system in human eyes and importance of central and peripheral vision in pattern perception by human beings
21 p2500 N73-30061
Measurement of control mechanism of accommodation-vergence eye movement system in human eyes using electro-optical measuring instrument
21 p2500 N73-30062
Influence of solar activity on biological indices and disease of living organisms in biosphere
[NRC-TT-1679] 21 p2592 N73-30771

**HUMAN BODY**
Physiological regulatory mechanisms of water and electrolyte levels in human body in high temperature environment
[NASA-TT-F-13915] 01 p0008 N73-10066
Dosimetric determination of absorbed gamma and neutron radiation on human phantom
[AD-743005] 01 p0010 N73-10077
Computer program for measuring specific radioisotopes contained in human body
[AD-745578] 01 p0010 N73-10078
Whole body, plus or minus a[z] vibration on amplitude and frequencies of postural sway in human subjects
[AD-745580] 01 p0013 N73-10098
Dynamic model for nonlinear simulation of human postural control system using sticks
01 p0015 N73-10116
Tests of fabric friction on human skin for aircrew tropical clothing comfort
[RAE-TR-72037] 01 p0020 N73-10157
Influence of 45 to 60 day space flight on physiological functions of human body
[NASA-CR-129131] 02 p0132 N73-11074
Blood plasma hyperosmolality and antidiuretic hormone inhibition in alcoholic intoxication
[NASA-TT-F-13910] 02 p0133 N73-11079
Elastomeric extensometer for measuring surface area changes of human body caused by body expansion and contraction
[NASA-CASE-MFS-21049-1] 02 p0173 N73-11405
Spacecraft environment, radiation, and weightlessness effects on human biological processes in manned space flight
[JPRS-57517] 03 p0256 N73-12076
Hypoxia effects on human gastric motor functions in pressure chamber experiments using electrogastrography
03 p0257 N73-12085
Transverse acceleration effects on human cardiovascular system
03 p0258 N73-12088
Diurnal changes in human histamine and serotonin metabolism and effects of work-sleep cycle
03 p0258 N73-12089
Power sources and requirements for human artificial hearts
[COO-2155-4] 05 p0503 N73-14095
Effects of alterations in barometric pressure on humans
06 p0628 N73-15092
Effects of prolonged weightlessness during space flight on human skeletal and hematopoietic systems
[NASA-TT-F-730] 06 p0630 N73-15116
Biological effects of microwave irradiation on humans - literature review
[UR-3490-29] 06 p0630 N73-15120
Research on laser irradiation effects, sensory psychophysiology, and human blood processing for military medicine
[AD-749440] 06 p0631 N73-15130
Radiation effects on human visual and vestibular analyzer functions
[AD-750499] 06 p0632 N73-15132
Accelerometers, electromyogram sensors, and telemetry system for measuring human body segment motions
[AD-751134] 07 p0751 N73-16104
Stabilization methods in collecting and shipping of human sera for chemical analyses
08 p0871 N73-17053
Influence of infrasound on human body functions
09 p0875 N73-17085
Conference on human endocrine secretions and hormone metabolisms during space flight stress
[NASA-TM-X-58093] 09 p0993 N73-18104
Radioimmunoassay of urinary antidiuretic hormone excretion in man considering water loading and dehydration effects
09 p0993 N73-18107
Measurement of antidiuretic hormone excretions in human urine as indication of neurosecretory stress response during space flight
09 p0993 N73-18108
Human adrenocorticotropin level measurements as indication of adaptation to space flight stress
09 p0993 N73-18109

Water immersion model for simulating renin, aldosterone, and natriuresis effects of prolonged weightlessness on man
09 p0993 N73-18110
Radioimmunoassays of plasma aldosterone and catecholamine concentrations as human vasomotor regulators
09 p0994 N73-18111
Multiple immunoassay system for determining parathyroid hormone, calcitonin, and vitamin D in human blood
09 p0994 N73-18112
Effects of prolonged bed rest on body temperature and heart rate periodicity in man
09 p0994 N73-18113
Prolonged bed rest effects on human blood hormone level periodicities
09 p0994 N73-18114
Skylab experiments to assess weightlessness effects on human nutritional metabolism and musculoskeletal function
09 p0994 N73-18115
Weightlessness and hypodynamia effects on bodily functions during space flight
10 p1114 N73-19078
Human nitrogen and water/salt metabolisms in controlled regenerative atmosphere
10 p1115 N73-19089
Influence of immersion in temperature controlled bath on circulation and water balance in human body
[NASA-TT-F-14834] 10 p1119 N73-19124
Free amino acid excretion in urine as test for early diagnosis of radiation damage in humans
11 p1243 N73-20092
Effects of physical training on human enzyme activity, carbohydrate metabolism, cholesterol level, and adrenal function
[NASA-TT-F-14826] 11 p1243 N73-20093
Urinalysis methodology for detection of abusive and therapeutic drugs in man
12 p1370 N73-21117
Chromatographic and polarographic methods for determining metabolic levels of hypnotic drugs in blood plasma and urine of man
12 p1370 N73-21118
Effects of human biorhythms on chemotherapy and drug evaluation
12 p1370 N73-21119
Cholinesterase reactivator as antidote in human organophosphate poisoning
13 p1480 N73-21998
Physiological stress effects of space flight on human body
[JPRS-57139] 13 p1481 N73-22002
Physiological effects of long term hypodynamic weightlessness simulation on humans
13 p1482 N73-22010
Human regional blood circulation changes during bed rest experiment
13 p1482 N73-22012
Lower body negative pressure for preventing body fluid shifts during weightlessness
13 p1482 N73-22017
Long term bed rest effects on human retinal blood circulation and intraocular pressure
14 p1608 N73-23038
Radiation effects on human chromosomal aberrations in peripheral blood lymphocytes
14 p1609 N73-23041
Optical modulation transfer functions of human eye for white light
[IZF-1973-2] 14 p1609 N73-23047
Thermal effects of microwave and radio frequency radiation on biological systems
[MBL-1971-7-PT-1] 14 p1609 N73-23048
Accuracy of various tracer methods for measuring body water compartments during bed rest
[NASA-TR-R-406] 15 p1744 N73-24133
Synchronization kinetics in control of movement links in human extremities
17 p1990 N73-26089
Acceleration effects on mechanical impedance of human body in supine position
19 p2227 N73-27963
Exercise effects on human heart rate and oxygen uptake
20 p2365 N73-29020
Pure oxygen and oxygen/nitrogen atmospheres for preventing decompression disease in astronauts
20 p2366 N73-29029
Human hydroxycorticosteroid and aldosterone excretions during hypodynamic space flight conditions
20 p2367 N73-29031
Lower body decompression effects on human cardiovascular hemodynamic system
20 p2367 N73-29032
Human body temperature dynamics in adaptation to changed work-sleep cycles
20 p2367 N73-29036
Composition of human gastrointestinal microflora during prolonged isolation
20 p2367 N73-29037
Response variations of microphone worn on human body
[BM-RI-7810] 20 p2371 N73-29058
Tilting table for testing human body in variety of positions while exercising on ergometer or other biomedical devices
[NASA-CASE-MFS-21010-1] 21 p2502 N73-30078
U.S., Soviet, and Polish standards for radiation levels for humans
21 p2608 N73-30905
Physiological stress effects of aerospace environment on human body and animals
[NASA-TT-F-15081] 23 p2749 N73-32001
Hypothalamus as internal heat regulator for warm-blooded animals
[NASA-TT-F-15138] 23 p2749 N73-32002
Physical fitness effects on human thermoregulation during exercise
[NASA-TT-F-15142] 23 p2749 N73-32003
Computerized simulation of anatomically correct geometrical model of human body
[NASA-CR-134043] 23 p2752 N73-32022
Treadmill running effect on human oxygen consumption
24 p2882 N73-33013

**HUMAN CENTRIFUGES**
Feasibility of multichannel rheography for studying cardiovascular system on centrifuge
03 p0259 N73-12094
Aerial combat acceleration environment testing of human performance capability using human centrifuges
[AD-759174] 16 p1869 N73-25134

**HUMAN ENGINEERING**
U HUMAN FACTORS ENGINEERING

**HUMAN FACTORS ENGINEERING**
Proceedings of conference on ride qualities of air, surface, and water vehicles with emphasis on human factors engineering for comfort in transportation
[NASA-TM-X-2620] 01 p0002 N73-10012
Analysis of current knowledge regarding ride quality factors in passenger transportation and development of criteria based on human factors engineering
01 p0002 N73-10013
Guidelines and criteria for developing ride quality in air transportation based on external and internal environment conditions
01 p0002 N73-10014
Application of ride-quality criteria to design of commercial helicopters with emphasis on noise and vibration considerations
01 p0003 N73-10015
Simulated STOL aircraft flight to determine effects of cruise and terminal area maneuvers on ride quality and passenger comfort
01 p0003 N73-10016
Analysis of airline passenger reactions to vibration environments encountered in supersonic transport and commercial jet aircraft
01 p0003 N73-10017
Evaluation of effectiveness of indices relating to effect of vehicle vibrations on passenger comfort with application to railroad travel
01 p0003 N73-10018
Analysis of helicopter pilot and passenger reaction to vibration environment to determine effects of discrete frequencies and combinations of harmonic frequencies
01 p0003 N73-10019
Analysis of vibration environment in aerospace and surface vehicles with definitions of effect on human comfort and performance
01 p0003 N73-10021
Development of mathematical model to analyze traveler acceptance factors in short haul air carrier operations
01 p0004 N73-10023
Analysis of research activities conducted to determine criteria for passenger comfort in various methods of transportation
01 p0004 N73-10024
Flight test program to determine effects of low frequency vibration on passenger comfort in short haul aircraft
01 p0004 N73-10025
Integrated information presentation and control system analysis to determine control and display requirements for contingency operation of jet aircraft - Vol. 3
[AD-740435] 01 p0006 N73-10041
Indicators and controls for validating human reliability data
[AD-744551] 01 p0011 N73-10085
Overview of literature concerning retention of learned skills with emphasis on space flight skill retention
[NASA-CR-128611] 01 p0020 N73-10152
Performance tests to determine proficiency of maintenance personnel in servicing fuel start solenoid in UH-1 helicopter
[AD-745163] 01 p0021 N73-10166
Survey of electronic cockpit displays, noting human factors, head-up, head-down and eyeglass display, and related technology
[DLR-FB-72-43] 01 p0058 N73-10474
Design, development, and evaluation of aircrew restraint system for forward-facing, nonejection seat for military aircraft
[AD-746631] 02 p0128 N73-11038
Systems engineering for incorporating human factors in design of transportation
[NASA-CR-129092] 02 p0245 N73-11989
Operational tests and evaluation of optical infrared pilot warning system to determine probability of detection versus range
[NASA-CR-129525] 03 p0302 N73-12463
Effect of mood on human performance, possibility of using skin analyzer for communication, and effect of prolonged exposure to depths of 160 m on mental functioning
[JPRS-57541] 04 p0378 N73-13072
Engineering psychology for developing practical designs of man machine systems
[AD-748237] 04 p0384 N73-13121
Identification of human factors research projects in support of civil aviation for accomplishment by NASA research centers
05 p0493 N73-14015
Development of statistical technique for determining injury reduction capability of energy absorber equipment
[AD-749333] 05 p0497 N73-14044
Anthropometric data of Japanese Air Self-Defense Force personnel
05 p0502 N73-14091
Bibliography of research reports and publications issued by Human Engineering Division for April 1946 to December 1970
[AD-749933] 05 p0504 N73-14103
Modification to existing rocket catapult for reducing probability of injury to users of aircraft emergency escape systems
[AD-750318] 06 p0623 N73-15057
Human factors engineering to determine maximum control forces capability of female pilots
[FAA-AM-72-27] 06 p0635 N73-15157
Measurement and effects of triaxial vibration on pilots in P-531 [Scout] helicopter under different flight conditions
[ISVR-TR-58] 07 p0751 N73-16100
Electronic detectors and computer software for analyzing human electroencephalographs in isolated environment
[AD-751272] 07 p0751 N73-16105
Conceptual model for pilot workload
08 p0866 N73-17010
Conference on occupational medicine support in NASA programs to prevent health and emotional problems in personnel
[NASA-TM-X-69072] 08 p0871 N73-17048
Physical exercise and physical fitness program for preventing and treating human coronary heart disease
08 p0871 N73-17051
Facilities engineering for NASA space program
08 p0873 N73-17070
Problems of environmental pollution and natural resource depletion caused by man
[JPRS-58113] 08 p0879 N73-17121
Habitability factors during long-term space and undersea missions in confined habitats
[NASA-CR-130537] 08 p0879 N73-17123
Analysis of fixed base simulator tests to determine effects of two horizontal display panel locations and three map orientations on manual piloting performance
[NASA-TM-X-62198] 08 p0892 N73-17223
Approach light properties for visual discrimination in pilot landing environment
[NASA-TT-F-14667] 08 p0941 N73-17710
Interaction of man machine systems
[JPRS-58290] 09 p0997 N73-18136
Interaction between man and electronic computer in operational planning
09 p0997 N73-18138
Bibliography on human factors in man machine interactions and systems design
[AD-752800] 09 p0997 N73-18141
Human factors guide for design of diver-operated hand and power tools
[AD-753262] 09 p1041 N73-18489
Accuracy of method of constant stimuli for studying sensory capabilities of man in relation to display systems
[AD-753009] 10 p1121 N73-19141
Flight test program to study human factors problems and flight crew performance in military aircraft
10 p1122 N73-19145
Measures to determine psychophysiological reactions of military flight crews to flying stress
10 p1122 N73-19148
Use of psychometric tests to account for subjective variations in operations performance relative to target acquisition
10 p1227 N73-19974
Comparative evaluation of cockpit displays considering human factors and aircraft control data
[NASA-TT-F-14846] 11 p1234 N73-20019
Research in space biology and medicine
[JPRS-58620] 11 p1243 N73-20094
Human factors criteria for adaptive computer aiding in man-machine control system
[AD-754835] 11 p1250 N73-20147

Human factors engineering for flight control/display system with on-line terminal
[AD-754916] 11 p1250 N73-20148
Quantitative description of mobility for human torso
[AD-754924] 11 p1251 N73-20151
Application of normal bivariate distributions and anthropometric correlations for design of workspaces in aircraft
[AD-754780] 11 p1290 N73-20468
Heat exchange coefficient for humans in constant temperature moving water
[NASA-TT-F-14867] 11 p1349 N73-20943
Photographic recording of aircraft in near midair collision conditions to determine feasibility of collision avoidance based on visual perception of pilot
[CDC-JL-5] 12 p1374 N73-21147
Psychophysiological analysis of job performance for optimizing operator production in man machine systems
[NASA-TT-F-14888] 12 p1374 N73-21150
Proceedings of conference on research and development projects conducted by US Air Force Research and Development Command
[AD-753071] 12 p1467 N73-21890
Psychological, physiological, and work hygiene problems in ergonomic technology
[JPRS-58792] 13 p1486 N73-22050
Evaluation of helmet weight on head by military personnel
[AD-748412] 13 p1487 N73-22056
Cold weather construction practices relative to men, materials, and equipment
[AD-745395] 13 p1506 N73-22206
Development of aircraft seat for high acceleration tolerance of flight crew personnel by elevating pelvis and legs forward
[AD-756630] 14 p1605 N73-23009
Workload effects on operator grip pressure and neuromuscular transmission in manual tracking task error
[AD-757252] 14 p1615 N73-23089
Analysis of human performance in synthesis on non-nazalized vowels and input resistance as function of frequency
14 p1630 N73-23213
Onboard computers for automatic control of manned aerospace systems considering human factors integration
[AGARD-CP-114] 14 p1710 N73-23881
Computerized integrated control and information management system with graphic display for manned space flight
14 p1710 N73-23882
Reliability design of manned supersonic aircraft considering safety hazards
14 p1711 N73-23883
Human factors in design of aircraft in-flight monitoring and automatic landing system for low weather operation
14 p1713 N73-23901
On-going research relevant to continuous operations
14 p1723 N73-23983
Human habitability data for zero gravity environmental architecture
[NASA-TM-X-69322] 15 p1744 N73-24135
Revised edition of human engineering guide to equipment design
[AD-758339] 15 p1744 N73-24140
Correlation between instructor rating of students and successful completion of military flight training course
[AD-757693] 15 p1745 N73-24146
Design parameters and systems analysis of crew compartment for space shuttle orbiter - Summary Report
[NASA-CR-128949] 16 p1965 N73-25893
Design parameters and systems analysis of crew compartment for space shuttle orbiter - Final Report
[NASA-CR-128950] 16 p1965 N73-25894
Design requirements for remotely controlled master-slave manipulators
17 p1989 N73-26076
Human factors in design of avionics subsystems considering training costs and performance of Air Force personnel
[AD-759583] 17 p1990 N73-26096
Human factors analysis of astronaut working conditions in space vehicles
[NASA-TT-F-750] 19 p2225 N73-27946
Design approaches to application of Boyle's law to emergency suits for fliers
[AD-761797] 19 p2228 N73-27970
Bibliography of anthropometric information for Air Force human factors engineering
[AD-762287] 19 p2229 N73-27978
Clinical medicine and human factors engineering functions conducted during Tenth Soviet Antarctic Expedition
20 p2407 N73-29347
Human factors investigations and acclimatization research conducted during Tenth Soviet Antarctic Expedition
20 p2407 N73-29348
Development of noise standard for permissible noise levels in air traffic control and navigational facilities
[FAA-RD-72-47] 20 p2452 N73-29708
Time shift effects on human 17-hydroxy corticosteroid diurnal excretion noting transmeridian flights
[DLR-FB-73-58] 21 p2501 N73-30070
Ergonomic research and design principles for automatic control and man machine systems
[NASA-TT-F-716] 21 p2502 N73-30079
Ergonomic solution to organizational problems of human living conditions and activities
21 p2502 N73-30080
Psychological conception of operator participation in ergonomic process
21 p2502 N73-30081
Ergonomic control system information models
21 p2503 N73-30082
Operational principles and functions of mnemonic diagrams in controlled system
21 p2503 N73-30083
Direct and indirect environmental factors affecting functional state of operators
21 p2503 N73-30084
Influence of emotional states on human operator performance and efficiency
21 p2503 N73-30085
Methods and procedures for ergonomic research
21 p2503 N73-30086
Military personnel management and human factors engineering
[AD-763168] 21 p2504 N73-30094
Soviet research on space biology, aerospace medicine, and human factors engineering
[JPRS-59952] 22 p2618 N73-30983
Requirements for mobility aids and restraint devices for use by personnel of space shuttle - Vol. 4
[NASA-CR-133994] 22 p2622 N73-31009
Pilot knee ejection clearances for Canadian military aircrafts
[DCIEM-936] 23 p2741 N73-31938
Analysis of flight crew errors contributing to aircraft accidents on P-3 and F-4 aircraft for improved air safety
[AD-764868] 23 p2746 N73-31979
Payload carrier simlation data for design of manned space shuttle missions
[NASA-CR-124430] 23 p2751 N73-32018
Application of skill requirement method for determining skills required of on-orbit crew personnel performing earth-orbital research
[NASA-CR-124452] 24 p2982 N73-33830

**HUMAN FACTORS LABORATORIES**
Human response to vibration in Great Britain noting test facilities, equipment, experiments and publications
[ISVR-TR-60] 21 p2504 N73-30093
Pilot performance under simulated conditions of modified aircraft control dynamics, navigational task complexity, and induced stress
[AD-764760] 23 p2752 N73-32025

**HUMAN PATHOLOGY**
Chromatographic determination of gaseous metabolites released by man during reduced food intake
03 p0258 N73-12091
Effects of gas bubbles in decompression pathology of humans
[AD-748229] 06 p0631 N73-15126
Industrial health hazard in chronic exposure to monomethylhydrazine and dose related hemolytic anemia in humans
[AD-751440] 07 p0749 N73-16087
Blood lipid diagnostic and therapeutic measures to prevent heart disease in humans
08 p0874 N73-17073
Periodic health examinations and automatic processing of medical histories for detection and prevention of human diseases
08 p0874 N73-17074
Blood pressure and cholesterol level screening for preventing heart diseases in flight crews of commercial airline
08 p0874 N73-17076
Bibliography on titanium toxicity in human and animal organisms
[ORNL-TIP/TIRC-72-65] 10 p1120 N73-19135
Validity of rapid delta-aminolevulinic acid determination in urine for lead intoxication tests on industrial workers
[NASA-TT-F-14864] 12 p1371 N73-21128
Electropolygraphic analyses of sleep patterns in humans with neurological disorders
13 p1483 N73-22024
Somnofunctional mapping of deep brain waves in neurological patients
13 p1484 N73-22029
Pathophysiological justifications for using drugs in aerospace medicine
[NASA-TT-F-736] 13 p1484 N73-22033

**HUMAN PERFORMANCE**
NT ASTRONAUT PERFORMANCE
NT BLACKOUT PREVENTION
NT OPERATOR PERFORMANCE
NT PILOT PERFORMANCE
Effect of temporal uncertainty on human energy expenditure during moderate exercise
[AD-743726] 01 p0011 N73-10084
Influence of illumination color, viewing distance, and turbidity on underwater vision
[AD-743756] 01 p0012 N73-10092
Annotated bibliography on reaction times in selected human information processing tasks
[AD-745416] 01 p0012 N73-10095
Effect of vigilance on performance of simple visual detection task
[AD-745317] 01 p0012 N73-10097
Moton sickness effects on flying personnel performance during hurricane penetrations
[AD-743928] 01 p0013 N73-10100
Nonlinear multiparameter control model for human operator as vehicle controller
01 p0014 N73-10106
Random Gaussian distribution for input noise approximation in human response tracker modeling
01 p0014 N73-10110
Matrix methods for dynamic modeling of human operator performance using Liapunov functions
01 p0014 N73-10111
Operator visual perception mapping during parameter adjustment in dynamic control system
01 p0017 N73-10129
Human physiological and psychological responses in long time exposure to simulated space station atmosphere as observed by critical tracking task
01 p0017 N73-10133
Hypoxia stress effects on human operator performance in unstable tracking task using manual control
01 p0018 N73-10138
Attention sharing effects on human operator performing simultaneously dynamic compensatory tracking control tasks
01 p0018 N73-10140
Manual flight control and emergency procedure task skill degradation
[NASA-CR-128612] 01 p0020 N73-10153
Effects of stress upon psychophysiological responses and performance following sleep deprivation
[NASA-CR-128620] 02 p0132 N73-11073
Human recognition of contrasting target in noisy environment with diversion of attention
[FOA-2-C-2482-H5] 02 p0135 N73-11092
Sonic boom effects on individuals compensatory tracking performance for unstable system
[UTIAS-TN-179] 02 p0135 N73-11098
Effects of simulated artificial gravity on human performance
[NASA-CR-2129] 03 p0260 N73-12111
Analysis of reaction time to different visual cuing methods in large displays during secondary task performance
[AD-747688] 03 p0262 N73-12120
Effect of mood on human performance, possibility of using skin analyzer for communication, and effect of prolonged exposure to depths of 160 m on mental functioning
[JPRS-57541] 04 p0378 N73-13072
Effect of mood on testing human performance
04 p0378 N73-13075
Measurement of operator workload in formation processing
[NASA-CR-2150] 04 p0379 N73-13087
Correlation of assessed maximum oxygen intake with predicted performance in running events
[AD-746867] 04 p0380 N73-13093
Human operator model performance in tracking high performance aircraft
[AD-746725] 04 p0381 N73-13101
Reinforcement effects on human attention and performance in continuous response to visual stimuli
[AD-747798] 04 p0381 N73-13103
Noise and response complexity effects on human attention and performance in visual perception task
[AD-747797] 04 p0381 N73-13105
Physiological and mental performance effects of underwater work on humans
[AD-747701] 04 p0382 N73-13107
Cognitive functioning test to measure human performance in underwater diving stress
[AD-748036] 04 p0382 N73-13108
Human attention and reaction performance as function of type and latency in response to signal stimulus
[AD-747801] 04 p0382 N73-13110
Feasibility of saliva analysis for measuring mental stress in man
[AD-747671] 04 p0382 N73-13111
Influence of time zones on physiological organs and systems and performance of athlete
[NASA-TT-F-14632] 04 p0383 N73-13116
Bibliography on effects of underwater environment on tools, equipment, and human performance
[AD-748000] 04 p0384 N73-13122
Computerized fast Fourier transform technique for measuring human performance in compensatory tracking task
[AD-748659] 05 p0501 N73-14078
Human performance measurement - bibliographies
[AD-749100] 05 p0501 N73-14080

Pupil enlargement in relation to operator stress during adaptive critical tracking task
[AD-749075] 05 p0501 N73-14081
Simulated lunar magnetic environment effects on humans, using scotopic critical flicker frequency measurements to indicate psychophysiological stress
[AD-748193] 05 p0502 N73-14088
Systems engineering methods for human performance enhancement in signal detection and flight control
[AD-748239] 05 p0503 N73-14098
Criteria for selected response surface methodology design variants in human performance research
[AD-748236] 05 p0503 N73-14099
Optimization of work-rest cycles to ensure acceptably high human performance in man machine systems
[AD-750176] 05 p0504 N73-14107
Cyclically changing temperature effects on monitoring behavior and physiological responses of man
[AD-748451] 05 p0505 N73-14110
Bioastronautics research, including stress effects, sensory perception, and human performance
[NASA-SP-3006] 06 p0627 N73-15091
Capabilities and limitations of man as element in closed loop control system under normal environmental conditions
06 p0629 N73-15107
Work, heat, and oxygen cost of various activities of man
06 p0629 N73-15109
Prolonged bed rest and positive radial acceleration effects on human visual response time
[NASA-TN-D-7161] 06 p0630 N73-15117
Human factors engineering to determine maximum control forces capability of female pilots
[FAA-AM-72-27] 06 p0635 N73-15157
Fatigue effect on human visual perception
[AD-750097] 06 p0636 N73-15171
Decision making behavior of sonar operator in target detection and reporting
[AD-750761] 06 p0637 N73-15174
Computer generation of patterns for analysis of human visual perception of form
[FOA-2-C-2473-52] 06 p0643 N73-15224
Diurnal dynamics of psychic performance during 72-hour continuous wakefulness
07 p0744 N73-16056
Study of differences between left and right hand performance in compensatory tracking task
[RAE-TR-72117] 07 p0750 N73-16098
Effects of quantized luminance levels and display contrast on sonar target recognition
[AD-751711] 07 p0757 N73-16148
Mental health services for emotional counselling in NASA facilities to insure maximum human performance
08 p0872 N73-17062
Industrial health measures and environmental control to insure worker productivity
08 p0874 N73-17077
Noise effects on hearing conservation in aircrew and ground support personnel of aerospace operations
08 p0876 N73-17101
Standardized performance battery for assessing effects of environmental stressors particularly noise on human performance
[NASA-CR-2149] 08 p0877 N73-17102
Reliability of search strategies for information retrieval by aerospace personnel
[AD-751977] 08 p0977 N73-17995
Conference on operational flight stress effects on human biodynamics and performance
[AGARD-CP-101] 10 p1122 N73-19143
Combined stress effects in human communication and motion sickness biodynamics
10 p1122 N73-19144
Flight test program to study human factors problems and flight crew performance in military aircraft
10 p1122 N73-19145
Combined heat, noise, and vibration effects on aircrew performance
[AMRL-TR-71-113] 10 p1122 N73-19146
Combined noise and vibration effects on human mental and psychomotor performance
[AMRL-TR-71-115] 10 p1122 N73-19147
Human stress expenditures in operational airlift mission flights
10 p1123 N73-19151
Human performance in sequential task training for acquisition of perceptual motor skills under flight stress
10 p1123 N73-19153
Temperature and noise irradiation effects on human energetic metabolism during vigilance task
10 p1123 N73-19155
Study to validate Non-Interference Performance Assessment
[NASA-CR-128865] 10 p1124 N73-19164
Filtering and vertical sensor position effects on human speech detection in jungle evnironment
[AD-753650] 10 p1190 N73-19686
Effect of briefing information on target acquisition performance of observer
10 p1227 N73-19972
Human performance and life support engineering for space environment conditions
[AD-754216] 11 p1252 N73-20157
Residual effects of hypnotic drugs on human nervous function and performance
12 p1369 N73-21106
Hashish smoking effects on human oxygen consumption during physical stress and safe driving ability
12 p1370 N73-21115
Spectral analysis on human biorhythmic performance to evaluate tranquilizer effects
12 p1370 N73-21116
Suitability of insulin dependent and oral drug dependent diabetics as navigation personnel
12 p1371 N73-21120
Drug effects on vision of flying personnel
12 p1371 N73-21121
Flight safety factors in prescribing tranquilizing drugs for flying personnel
12 p1371 N73-21123
Comparison of alcohol and dizepam effects on human mental and psychomotor functions
12 p1371 N73-21126
Systems analysis of physiological performance related to stresses such as those experienced in high performance aircraft
[AD-754970] 12 p1372 N73-21133
Stimulating and tranquilizing drug effects on human performance indices
13 p1483 N73-22021
Human performance in schematic concept formation as a function of socio-economic level, personality, intelligence, and race
[AD-744781] 13 p1486 N73-22052
Acceleration effects on human visual functions under hypoxic conditions
14 p1609 N73-23040
Effect of cigarette smoking on sensory perception and performance parameters of flight crews
[AD-754421] 14 p1612 N73-23071
Probabilities models of organizational behavior and human subjective performance
[IZF-1973-3] 14 p1613 N73-23076
Analysis of human performance in synthesis on non-nazalized vowels and input resistance as function of frequency
14 p1630 N73-23213
Analysis of air traffic controller responses under stress conditions to show effects of accuracy, quality, and comprehensiveness of available data
14 p1690 N73-23714
Mathematical models for human performance in manned spacecraft control
14 p1712 N73-23897
Conference on human performance under sustained work, and interdisciplinary research
[AD-744782] 14 p1723 N73-23981
Work-rest schedules for military tracking crews under prolonged vibration
14 p1723 N73-23986
Work-rest schedule for optimum performance of monitoring tasks
14 p1723 N73-23987
Effects of work-rest schedules, circadian rhythms, continuous work, and sleep loss on sustained performance
14 p1723 N73-23988
Biological effects of sleep deprivation, and effects of prolonged work on performance under combat conditions
14 p1723 N73-23989
Human visual/motor response to tracking task during long term confinement in simulated space station
[NASA-CR-2240] 15 p1744 N73-24134
Human psychomotor and cognitive performance in humid environment
[AD-756835] 15 p1745 N73-24142
Automation of decision making process in air traffic controllers terminal operations
[FAA-RD-72-63-VOL-3] 15 p1808 N73-24657
Job attitudes of air traffic controllers
[FAA-AM-73-2] 18 p2110 N73-27066
Effects of two sequential transatlantic flights on circadian rhythm of body function and performance
19 p2227 N73-27964
Effects of adverse Northern environment on human physiology and performance under military exercise conditions
[DCIEM-882] 20 p2371 N73-29056
Improved performance of visual perception of solar patrol observers monitoring sun activity
[AD-760802] 20 p2372 N73-29063
Subjective and physiological indicators of fatigue and performance during vigilance task
[AD-761503] 21 p2502 N73-30077
Effects of alcohol on eye movements and tracking performance during laboratory angular accelerations about yaw and pitch axes
[FAA-AM-72-34] 22 p2619 N73-30989
Effect of sleep deprivation and heat stress on human performance in visual and auditory tasks
[OES-8/72] 22 p2624 N73-31024
Sleep deprivation effects on accuracy and speed of response selection and execution
22 p2731 N73-31854
Scale, haze, and image motion effects on human performance in photointerpretation of aerial photography
[AD-763908] 23 p2752 N73-32024
Combat job performance and training for air cavalry aeroscout pilot and aeroscout observer
[AD-755505] 23 p2753 N73-32027
Effect of human operator errors on reliability and effectiveness of his work
[AD-764937] 23 p2753 N73-32028
Optimization of human performance in system design, training, and operation
[AD-764761] 24 p2890 N73-33075

**HUMAN REACTIONS**

Analysis of airline passenger reactions to vibration environments encountered in supersonic transport and commercial jet aircraft
01 p0003 N73-10017
Evaluation of effectiveness of indices relating to effect of vehicle vibrations on passenger comfort with application to railroad travel
01 p0003 N73-10018
Analysis of helicopter pilot and passenger reaction to vibration environment to determine effects of discrete frequencies and combinations of harmonic frequencies
01 p0003 N73-10019
Analysis of physiological mechanisms contributing to occurrence of motion sickness
01 p0003 N73-10020
Analysis of factors affecting ride quality of water vehicles and human reactions to motion caused by rough water
01 p0003 N73-10022
Direction-specific adaptation effects acquired by humans in slowly rotating room
[NASA-CR-129063] 01 p0008 N73-10062
Physiological and pathological responses of humans exposed to electricity
[NASA-CR-128422] 01 p0008 N73-10065
Noise abatement and measurement, and human response to noise
[PB-210591] 01 p0081 N73-10671
Vestibulo-ocular response of man to oscillatory rotation during sleep
[AMRU-R-70-3] 02 p0131 N73-11066
Construction of sonic boom simulators to determine effects of sonic boom on human heart reactions and analysis of human responses
[UTIAS-TN-180] 02 p0152 N73-11233
Vestibular function loss in man after unilateral section of eighth cranial nerve
[NASA-CR-129672] 04 p0379 N73-13084
Response time of flash blindness recovery in human exposure to constant energy flashes
[AD-747631] 04 p0380 N73-13095
Reinforcement effects on human attention and performance in continuous response to visual stimuli
[AD-747798] 04 p0381 N73-13103
Statistical analysis of steroid levels in parotid secretions of humans under prolonged mental stress
[AD-747682] 04 p0381 N73-13104
Human attention and reaction performance as function of type and latency in response to signal stimulus
[AD-747801] 04 p0382 N73-13110
Reaction tester for testing reaction to light stimuli
[NASA-CASE-MSC-13604-1] 04 p0383 N73-13114
Motion effects in pilot reactions to ground-based flight simulator display evaluation
[AD-749370] 04 p0384 N73-13126
Evaluation of subjective annoyance caused by noise generated by turbofan short takeoff aircraft and comparison with noise of conventional takeoff aircraft
[NASA-TN-D-7102] 06 p0621 N73-15040
Visual evoked responses from divers subjected to hyperbaric conditions simulating depths to 1200 feet breathing various gas mixtures
[AD-749325] 06 p0631 N73-15127
Physiological factors in human oculomotor responses to space flight stress
[DR-208-VOL-1] 06 p0632 N73-15136
Human semicircular canal response to rotational stimuli in yaw, pitch, and roll planes of the head
06 p0632 N73-15137
Anti-compensatory oculomotor response of pilot to rotational head stimuli
06 p0632 N73-15138
Coding data of 2565 individual human altitude chamber tests
[NASA-CR-114550] 07 p0746 N73-16066
Recorded observations of crew member activities during Tektite 2 underwater habitability study
[NASA-CR-130034] 07 p0750 N73-16094
Analysis of temperature conditions in hermetically sealed room to determine human tolerances under various climatic conditions
[FOA-1-A-1527-76] 07 p0854 N73-16924

Long term exercise effects on cardiovascular response in NASA personnel with periodic ergometric evaluation
08 p0873 N73-17067
Structural vibrations in aerospace operations and effects on man
08 p0876 N73-17099
Choice reaction tasks for discriminating individual skill potentials in information handling situations
[AD-752073] 08 p0878 N73-17115
Measurements of endocrine metabolic responses to space flight stress on Apollo 14 and Apollo 15 crewmen
09 p0993 N73-18105
Unique field-laboratory methodology for assessing human response to noise
[NASA-CR-2221] 09 p0995 N73-18124
Changes in circadian rhythm of aircraft pilot oral body temperature as result of transmeridian flights
[DLR-FB-73-01] 09 p0997 N73-18140
Cardiovascular and respiratory systems reactions in cosmonauts during space flight
10 p1114 N73-19079
Effects of space flight noise intensities on human physiological functions
10 p1114 N73-19080
Immersion effects on human physiological motor functions
10 p1114 N73-19081
Human oxygen metabolism and pulmonary functions during hypodynamic water immersion
10 p1114 N73-19082
Transverse acceleration effects on human respiratory rate and oxygen metabolism
10 p1114 N73-19084
Sound, light, and proprioceptive stimuli for inhibiting vestibular illusion in man
10 p1115 N73-19087
Human ability to note changes in composition of inhaled air
10 p1115 N73-19090
Mental and cardiovascular acceleration stress effects on heart rate studied by beta adrenergic blockage
10 p1122 N73-19149
Role of social synchronizers in adaptation process of humans to inversion of diurnal sleep and wakefulness regime
11 p1245 N73-20109
Bactericidal activity of human skin at different times of day
11 p1245 N73-20110
Conference on human visual search and perception
[AD-754327] 11 p1248 N73-20133
Literature review on human macular pigment absorption and density spectrum of cone receptor
[IZF-1972-17] 14 p1609 N73-23046
Comparison of electroencephalographic response patterns in man and monkeys to visually evoked cortical stimuli
[IZF-1972-24] 14 p1609 N73-23049
Human continuous reaction time task distribution rates for paced and selfpaced responses to visual stimuli
[IZF-1973-5] 14 p1613 N73-23077
Human perception of musical intervals between simultaneous tones
[IZF-1972-20] 14 p1613 N73-23078
Analysis of air traffic controller responses under stress conditions to show effects of accuracy, quality, and comprehensiveness of available data
14 p1690 N73-23714
Chromatic induction and spatial intraocular straylight effects in human perception of contrast colors
[IZF-1972-19] 14 p1692 N73-23730
Photometric measurements on human sensitivity to optical luminosity considering seasonal and monthly fluctuations
14 p1692 N73-23732
Performance of pilots under simulated conditions to determine response to anti-collision warnings
[FAA-AM-73-6] 18 p2104 N73-27015
Analysis of self-destructive tendencies created by psychological stress and relationship to aircraft accidents
[FAA-AM-73-5] 18 p2104 N73-27016
Electroencephalographic and behavioral responses of humans to aircraft noise during sleep
[NASA-CR-2279] 18 p2109 N73-27058
Job attitudes of air traffic controllers
[FAA-AM-73-2] 18 p2110 N73-27066
Resynchronization of circadian rhythms following transmeridian flight observed in two group of students
19 p2227 N73-27958
Diagnosis and prognosis of pilot reaction and tolerance to psychical stress
19 p2227 N73-27962
Effects of two sequential transatlantic flights on circadian rhythm of body function and performance
19 p2227 N73-27964
Interrelationship and reaction of human subjects to spacecraft cabin environment
[NASA-TT-F-15020] 20 p2368 N73-29041
Medical analysis of vitamin balance among personnel of Tenth Soviet Antarctic Expedition to show effects on health and acclimatization ability
20 p2408 N73-29357
Analysis of human reactions to short takeoff aircraft aerodynamic noise for predicting community acceptance of short haul air service operations
24 p2875 N73-32960
Effect of high ambient temperature on calcium content of human bone tissue
24 p2884 N73-33033
Human skin reactions to lotions and distilled water during hypokinesia
24 p2884 N73-33034

**HUMAN TOLERANCES**

Biological effectiveness of microwave field and human tolerance
[JPRS-57209] 01 p0009 N73-10073
Ionizing radiation health standards and safety measures around nuclear installations
[EUR-4800-D-F-I-E-PT-1] 01 p0082 N73-10679
Radiation ecological aspects of environmental pollution and control for human safety
[EUR-4800-D-F-I-E-PT-2] 01 p0082 N73-10680
Mathematical models for studying vestibuli adaptation to stimuli in humans
[AMRU-R-70-1] 02 p0131 N73-11062
Analysis of acceleration forces produced during aerobatic flight and effects of acceleration forces on human body
[FAA-AM-72-28] 02 p0132 N73-11075
Human tolerance and adaptation in long term exposure to sonar signals at elevated intensities
[AD-746103] 02 p0134 N73-11089
Hypoxia effects on human vestibular tolerance during exposure to coriolis accelerations
03 p0258 N73-12092
Psychobiological factors for predicting monotony tolerance and selecting personnel for isolated duty
[AD-747272] 04 p0381 N73-13098
Biodynamic response of human head and neck to impact acceleration
[AD-747988] 04 p0382 N73-13106
Deep diving pulmonary functions of man using different breathing gas densities
[AD-749028] 05 p0501 N73-14082
Heat and cold stress effects in humans
06 p0628 N73-15094
Impact, emergency escapes, and crash survival studies
06 p0628 N73-15097
Human tolerance to vibration
06 p0628 N73-15098
Tolerance levels, physiological effects, and performance degradation during simultaneous or sequential exposures to environmental stresses
06 p0629 N73-15110
Visual and vestibular effects in human oculomotor response during head rotation in yaw and roll
06 p0633 N73-15147
Analysis of mechanisms of human tolerance to lower body decompression
07 p0744 N73-16054
Analysis of temperature conditions in hermetically sealed room to determine human tolerances under various climatic conditions
[FOA-1-A-1527-76] 07 p0854 N73-16924
Personality, occupation, and job stress effects on physiological risk factor in human coronary heart disease
08 p0871 N73-17054
Toxicity and safety hazard of dry beryllium copper alloy machining for human operator
08 p0872 N73-17059
Structural vibration and noise effects on man in aerospace operations
[AGARDOGRAPH-151] 08 p0876 N73-17098
Structural vibrations in aerospace operations and effects on man
08 p0876 N73-17099
Airborne noise in aerospace operations and bioacoustics effects on man
08 p0876 N73-17100
Physical and experimental data obtained by artificial satellites for estimating extraterrestrial radiation hazard in manned space flight
[NASA-TT-F-724] 09 p0992 N73-18098
Radiation hazards and spacecraft shielding requirements for human safety during manned space flight
09 p0992 N73-18099
Ionization, thermoluminescence, and nuclear photographic emulsion dosimetry for monitoring radiation loads in spacecrews during manned space flight
09 p0992 N73-18100
Radiobiological effects of cosmic radiation in animals and standardization of permissible radiation levels for spacecrews
09 p0993 N73-18102
Blockage effect in external ear canal on diver auditory perception threshold
[AD-751664] 09 p0996 N73-18132
Hypodynamia effect on human transverse acceleration tolerance
10 p1114 N73-19083
Human adaptation to hypoxic hypoxia for increased resistance to physical stress
10 p1116 N73-19095
Human pituitary and adrenal hormone reserve in acceleration stress tolerance
10 p1123 N73-19130
Positive pressure breathing for increased human acceleration tolerance
10 p1123 N73-19136
Human adaptation to hypoxia and tolerance of high environmental temperatures
[NASA-TT-F-14860] 11 p1247 N73-20122
Noise pollution effects on human communities
[PB-213021] 11 p1325 N73-20756
Cardiac systole kinematics in humans exposed to hypoxic atmosphere
13 p1479 N73-21986
Low barometric pressure effects on human thermoregulation function
13 p1480 N73-21996
Human horizontal or antiorthostatic position effect in hypodynamic weightlessness test
13 p1482 N73-22011
Lower body decompression effects on cardiac cycle and human acceleration tolerance
14 p1608 N73-23037
Aerospace medicine research, including human tolerance to various stress factors - conferences
[AGARD-CP-110] 14 p1610 N73-23057
Human exposure criteria to laser energy for combat use
14 p1612 N73-23067
Italian thermal conditions affecting acceleration tolerance and psychomotor performance of flying personnel
14 p1612 N73-23068
Loudness level perception of human ear and reference level for telephone engineering
[NLL-PO-2831-[9022.81]] 15 p1812 N73-24684
Noise effects on human hearing process and central nervous system functions
[NASA-TT-F-748] 19 p2223 N73-27935
Diagnosis and prognosis of pilot reaction and tolerance to psychical stress
19 p2227 N73-27962
Respiratory function and blood acid base equilibrium in human adaptation to high altitude environment
20 p2366 N73-29030
Physical/mathematical analyses on human vestibular responses to acceleration stresses
20 p2367 N73-29033
Human hemodynamic responses and vestibular tolerances to body sway tests
20 p2367 N73-29034
Analysis of human reactions to short takeoff aircraft aerodynamic noise for predicting community acceptance of short haul air service operations
24 p2875 N73-32960

**HUMAN WASTES**

NT FECES
NT SWEAT
NT URINE
Collection and disposal of human wastes in aesthetic and reliable manner to prevent degradation of crew performance
06 p0629 N73-15111
Radiation oxidation of water impurities in moisture-containing products of human vital functions
07 p0744 N73-16051
Medical and biological problems of manned space flight
[NASA-TT-F-719] 10 p1114 N73-19077
Preservatives for human urine storage and water reclamation in spacecraft cabin
10 p1116 N73-19099
Toxic effect of indole inhalation on man, mouse, rat, and rabbit organisms
10 p1117 N73-19102
Toxic effects of human exhaled air on mice organisms
10 p1117 N73-19103
Oxidation of atmospheric impurities in space cabin and purity of reclamated water
10 p1117 N73-19104
Antimicrobial water reclamation methods for processing human urine
10 p1117 N73-19105
Stress effects on element balance in human waste for life support recycling system
10 p1117 N73-19107
Biological mineralization products of human waste for autotroph cultivation
10 p1117 N73-19109
Hydroponic cultivation of plants on clay filters from human mineralized feces
10 p1117 N73-19110
Thermal combustion requirements for burner devices of human vegetative waste products
10 p1118 N73-19111
Antimicrobial phenyl preparations for human urine conservation during space flight
10 p1118 N73-19112
Cosmonaut adaptation to dehydrated food products and effects on human waste cycle
10 p1118 N73-19113

Reduced-gravity fecal collector seat and urinal
[NASA-CASE-MFS-22102-1] 11 p1249 N73-20141
Design and test performance of space crew waste collection system
[NASA-CR-133977] 19 p2225 N73-27945

**HUMIDITY**
Correlation of total precipitable water in atmosphere with surface absolute humidity for California and Pacific Ocean islands
[AD-745954] 02 p0206 N73-11666
Universal humidity chart allowing humidity and energy calculations for any mixture of monatomic and diatomic gases at pressures encountered in saturation diving
[AD-746162] 02 p0207 N73-11675
Sterilization parameters for spacecraft
[NASA-CR-129272] 03 p0259 N73-12101
Long-wave radiation divergence measurements over water and land compared with calculated divergences from temperature and humidity profiles
[AD-748997] 04 p0418 N73-13410
Influence of humidity on thermal life determination of electrical insulation
[AD-749926] 05 p0521 N73-14238
Tabulation of relative humidity data obtained from network of weather stations in Switzerland
05 p0572 N73-14645
Specific humidity distributions over Northern Hemisphere during monsoon season in Asia at 1000, 850, and 700 mb levels for June and July 1970
[NOTE-9] 05 p0572 N73-14647
Diurnal cycles of high absolute humidity at earth surface, using dew point and temperature measurements
[AD-753078] 09 p1061 N73-18654
Electrostatic discharge effects in JFET performance and reliability in low humidity environment
[BDX-613-815] 12 p1383 N73-21217
Human psychomotor and cognitive performance in humid environment
[AD-756835] 15 p1745 N73-24142
Effect of humidity on laminar recovery temperature measurements during supersonic air flow in wind tunnels
[ARC-R/M-3215] 16 p1857 N73-25042
Radiosonde sounding data for determining vertical atmospheric temperature and humidity profiles
[AD-764949] 23 p2815 N73-32508
Effect of inlet air humidity on exhaust gas emissions of nitrogen oxides in gas turbine combustor
[NASA-TN-D-7396] 23 p2856 N73-32822

**HUMIDITY MEASUREMENT**
Residual temperature-induced humidity errors in radiosondes
[AD-762484] 20 p2450 N73-29694

**HUNGARY**
Astronomical, mathematical, and neuropathological research projects in Hungary, and scientific development policy in Poland
[JPRS-57271] 02 p0244 N73-11986
Operational activities of Hungarian National Bureau of Metrology and use of photogrammetry in city planning and modernization
[JPRS-57792] 06 p0731 N73-15965
Role and activities of Hungarian National Bureau of Metrology
06 p0731 N73-15966
Macrosynoptic tropopause formula for long range weather forecasts in Budapest
[NLL-M-22839-[5828.4F]] 16 p1894 N73-25322

**HUNTING H-126 AIRCRAFT**
U H-126 AIRCRAFT

**HUNTING P-84 AIRCRAFT**
U JET PROVOST AIRCRAFT

**HURRICANES**
Motion sickness effects on flying personnel performance during hurricane penetrations
[AD-743928] 01 p0013 N73-10100
Seeding experiment effects on hurricane Ginger, Sep. 1971, analyzed from ATS 3 photographs
[SMRP-RP-106] 03 p0326 N73-12657
Mean monthly hurricane heat potential and sea surface temperature changes associated with storm passage for North Atlantic and North Pacific Oceans
[AD-751590] 07 p0790 N73-16429
Confidence intervals for ocean wave spectra for ordinary waves and hurricane sized waves
[AD-752135] 08 p0920 N73-17542
Steady state, symmetrical, hurricane-ocean interaction model
[AD-753620] 09 p1062 N73-18659
Development of Hurricane Inez, 1966 as shown by Nimbus 2 radiometer data and ESSA-1 and 3 television photographs
[NASA-TM-X-65943] 10 p1182 N73-19616
Near-surface air and sea-surface temperatures for hurricanes in Gulf of Mexico
[AD-754353] 11 p1315 N73-20677
Numerical simulation of free-boundary shoreline under hurrican action
15 p1770 N73-24337
Simulation of asymmetric hurricane with fine mesh multiple grid primitive equation model
15 p1805 N73-24631
Variational optimization technique used as analysis scheme for application to high energy portion of hurricane
15 p1805 N73-24632
Comparison of extreme floods statistically predicted for highway bridge design in Pennsylvania to actual floods caused by hurricane Agnes
[PB-220888/2] 21 p2575 N73-30639
Satellite infrared radiometer observation of hurricane intensification
22 p2736 N73-31906
Skylab S-193 RADSCAT measurements of Hurricane Ava
[E73-11062] 23 p2781 N73-32238

**HUYGENS PRINCIPLE**
Extended Huygens-Fresnel principle for image plane illuminance distribution of extended object in turbulent atmosphere
[AD-763717] 21 p2581 N73-30683

**HU2K-1 HELICOPTER**
U UH-2 HELICOPTER

**HYBRID COMBUSTION**
U HYBRID PROPELLANT ROCKET ENGINES

**HYBRID COMPUTERS**
Design features and capabilities of quasi analog and hybrid computers
[AD-747579] 03 p0273 N73-12210
Obtaining rocket trajectories by anological-hybrid computation
04 p0470 N73-13828
Application of continued fractions to rational scale counter design
05 p0517 N73-14208
Hybrid calculations based on finite element method
[RP-106[72]] 05 p0602 N73-14893
Hybrid computer program for processing several channels of sweep frequency data simultaneously
[NASA-TM-X-2753] 09 p1005 N73-18206
Multilayer and disk type, ceramic chip capacitors for thick and thin film hybrid circuits
[ECR-28] 12 p1383 N73-21211
Synthetic speech generation and recognition under hybrid computer control, using one set of linguistic rules
13 p1496 N73-22127
Hybrid computer simulation of turbulent diffusion in atmosphere by Monte Carlo method and stochastic processes
13 p1514 N73-22266
Real time analysis of multichannel electrophysiological recording, using hybrid computers
14 p1611 N73-23064
Analog - digital near real time image processing system
17 p2031 N73-26433
Processing quantities of multispectra data gathered by scanner systems using hybrid computers
[NASA-CR-133976] 19 p2239 N73-28048
D region blunt probe data analysis using hybrid computer techniques
[NASA-CR-135646] 22 p2639 N73-31147
Hybrid computer multiplication-division modular unit for ASMODEE minicomputer noting three state gate circuits, integrated circuits, and algorithms
[LAAS-TNPE-73-I-07] 23 p2761 N73-32094

**HYBRID NAVIGATION SYSTEMS**
Development of integrated system for air navigation using radio range measurements and data from onboard inertial sensors for aircraft approach and landing
[NASA-TM-X-62199] 13 p1556 N73-22614
Air or inertial data addition to onboard navigation system for improved air traffic control
16 p1940 N73-25699

**HYBRID PROPELLANT ROCKET ENGINES**
NT LITHERGOL ROCKET ENGINES
Performance of FLOX-70/polyethylene hybrid rocket engine with cartwheel-type propellant grain geometry
[DLR-FB-72-61] 07 p0836 N73-16780
Evaluation of propellant grain configurations for use in hybrid propellant rocket engines - Vol. I
[DLR-FB-72-60-PT-1] 09 p1077 N73-18792
Binary boron/lithium system as propellant additive of hybrid rocket engines, noting enthalpy and reaction product density
[DLR-MITT-73-08] 17 p2075 N73-26791
High energy rocket engines - propellant physical chemistry, propulsion system performance, hydrogen oxygen engines, boosters, nozzles - conferences
[DLR-MITT-72-09] 24 p2972 N73-33749
Experimental high energy rocket propellant combinations with heterogeneous combustion and FLOX/polyethylene engine performance
24 p2972 N73-33751

**HYBRID PROPELLANTS**
Analysis of transient and steady-state combustion processes in hybrid rocket system based on gaseous oxidizer flowing within tube of solid fuel
[NASA-CR-112201] 02 p0242 N73-11968
Combustion efficiency of FLOX/polyethylene hybrid propellants
[DGLR-PAPER-72-86] 04 p0462 N73-13766
Analyses of laminar combustion phenomena in hybrid rockets
08 p0968 N73-17909

**HYBRID PROPULSION**
Analytical determination of mode transition in integral ramjet rocket propulsion system
[AD-753904] 10 p1224 N73-19955

**HYBRID ROCKET ENGINES**
Hybrid rocket interior ballistics and heat transfer limited model
[AD-754769] 11 p1335 N73-20833

**HYDRATES**
Vapor phase chemistry for producing hydrated ions in upper atmosphere
[AD-753940] 10 p1157 N73-19411
Magnetic susceptibilities of NiCl2.6H2O
[AD-759417] 17 p2046 N73-26555
Solubility curves from 25 to 70 C for K2HfF-K2ZrF6-HF system
[BM-RI-7785] 21 p2558 N73-30505

**HYDRATION**
Behavior of dielectric constant and loss factor of zeolite with various degrees of hydration
[AD-753512] 09 p1055 N73-18603
Water load tests for determining hydration status and adrenal and kidney functions during post flight period
[NASA-TT-F-15091] 22 p2620 N73-30998

**HYDRAULIC ACTUATORS**
U ACTUATORS
U HYDRAULIC EQUIPMENT

**HYDRAULIC ANALOGIES**
Shallow flowing water channel for hydraulic analogy of gas flow in transonic to hypersonic range
[ICT-4/71] 01 p0036 N73-10286
Shallow flowing water channel for hydraulic analogy of gas flow in transonic to hypersonic range
[GRI/NTP/100] 02 p0146 N73-11186
Research and development of fluidics systems and applications to industrial processes
[NASA-SP-5112] 02 p0155 N73-11260

**HYDRAULIC CONTROL**
Fluidic elements and hydraulic impulse techniques for information processing equipment
02 p0140 N73-11135
Effects of trapped air on operation of aircraft hydraulic systems and methods for removing air contamination
[NLL-NEL-TT-2420-[6075.461]]
11 p1232 N73-20005
Design of hydrofluidic flight control system for helicopter stabilization
[AD-754602] 11 p1236 N73-20032
Design of electrohydraulic control system for underwater manipulator with position feedback
17 p1989 N73-26085

**HYDRAULIC EQUIPMENT**
NT AIRCRAFT HYDRAULIC SYSTEMS
Textbook on hydraulic systems
[AD-746713] 02 p0158 N73-11280
Compressive instability of hydraulic jacks overlapping stiffness
[ESDU-01.01.24] 02 p0236 N73-11922
Design and development of device to prevent geysering during convective circulation of cryogenic fluids
[NASA-CASE-KSC-10615] 03 p0304 N73-12486
Redundant hydraulic control system for actuators with three main valve combination
[NASA-CASE-MFS-20944] 04 p0425 N73-13466
Design, development, manufacture, and specifications of automatic fuel valves for liquid propellant rocket engines
[AD-750578] 06 p0715 N73-15832
Conversion of electrical signals into hydraulic signals using electrostatic hydraulic converter with no moving parts
[AD-751246] 07 p0759 N73-16168
Characteristics of power generating systems and application in missiles for production of hydraulic and electric energy
10 p1110 N73-19044
Influence of adiabatic oil compression on power of hydraulic motors and pumps
10 p1111 N73-19055
Design and development of space storable isolation valves for control of flow of liquid rocket propellants
[TRW-73-4781-6-15] 10 p1165 N73-19477
Hydraulic damping of sensors of differential manometers of dynamic pressure logs
10 p1184 N73-19637
Numerical analysis of aircraft shock absorber operation to show initial charging, motion, and force parameters during static and dynamic compression of landing gear
[AD-754609] 11 p1236 N73-20031
Evaluation of high response electrohydraulic digital control valve for application to flight control systems
[NASA-CR-124178] 11 p1297 N73-20523
Design, development, and evaluation of servoactuator device to include application to optimized system configuration
[NASA-CR-124025] 11 p1297 N73-20524

Chloride and water permeability parameters for hydraulic brake hose testing
[AD-748083] 13 p1546 N73-22530
Design, development, and testing of inflexible blade, hingeless rotor system with hydraulic rotor control system
[AD-758514] 15 p1736 N73-24081
Effect of hydraulic fluid density on system performance
[NLL-NEL-TT-2427-(6075.461)] 15 p1763 N73-24287
Hydraulic system noise study, emphasizing airborne pump noise
[AD-757776] 15 p1769 N73-24333
Characteristics of turbine pump for use with nuclear engine for rocket vehicles
[NASA-CR-132232] 15 p1792 N73-24530
Electrohydraulic directional valves with fluidic ball elements
[DLR-FB-73-35] 15 p1793 N73-24535
Design of IDPF servovalve applicable for controlling hydraulic systems
[NAL-TR-303] 15 p1824 N73-24787
Development and characteristics of combined pressure regulator and shutoff valve with variable pressure response characteristics
[NASA-CASE-NPO-13201-1] 17 p2036 N73-26474
Active-standby servoactuator for failure detection of space shuttle main engine hydraulic actuation system
[NASA-CR-124299] 18 p2156 N73-27418
Rocket propellant injector with porous faceplate for rocket engine combustion chamber
[NASA-CASE-LEW-11071-1] 18 p2192 N73-27695
Design and characteristics of system for regenerating fluid filter to remove trapped particles with application to space shuttle systems
[NASA-CASE-MSC-14273-1] 19 p2255 N73-28179
Nonlinear vibrations of pipelines containing pressurized fluids with application to aircraft hydraulic systems
[AD-764154] 22 p2616 N73-30968
Wear of hydraulic turbines, axial, and centrifugal pumps from cavitation and deposit
[AD-758322] 24 p2911 N73-33228

**HYDRAULIC FLUIDS**
Textbook on hydraulic systems
[AD-746713] 02 p0158 N73-11280
Viscous incompressible fluid hydraulics of magnetohydrodynamic generators
[AD-751465] 07 p0829 N73-16718
Influence of adiabatic oil compression on power of hydraulic motors and pumps
10 p1111 N73-19055
Effects of trapped air on operation of aircraft hydraulic systems and methods for removing air contamination
[NLL-NEL-TT-2420-(6075.461)] 11 p1232 N73-20005
Silicone base nonflammable hydraulic fluid to aid wear resistance in military aircraft
[AD-758361] 14 p1671 N73-23562
Effect of hydraulic fluid density on system performance
[NLL-NEL-TT-2427-(6075.461)] 15 p1763 N73-24287
Effect of undissolved air on compressibility of transmitting medium in hydraulic circuits
[NLL-NEL-TT-2426-(6075.461)] 15 p1763 N73-24289
Computation of bulk moduli of synthetic hydrocarbon hydraulic fluid
[AD-760776] 18 p2163 N73-27471
Measurement of density distribution and patterns of stowing mixture in hydraulic installations by radiometric scanning
[ITJ-35] 21 p2549 N73-30436
Elastomers for service with engine lubricants and hydraulic fluids
[AD-762800] 21 p2564 N73-30554
Hydraulic pump-looped circuit evaluation of candidate silicone base nonflammable hydraulic fluid
[AD-764064] 22 p2679 N73-31456

**HYDRAULIC HEATING SOURCES**
U HEAT SOURCES
U HYDRAULIC EQUIPMENT

**HYDRAULIC JETS**
High speed water jets from vertically accelerated cones partially filled with water
[MT-64] 11 p1270 N73-20302
Two-dimensional submerged slot jets to diffuse thermally buoyant water jets into moving water stream
[PB-213461/7] 14 p1651 N73-23395
Water jet impingement wear tests on plexiglass, aluminum alloys, nickel, cobalt alloys, and stainless steels
[PB-215631/3] 16 p1890 N73-25294
Liquid jet impact against elastomeric materials
[PB-220972/4] 21 p2528 N73-30269

**HYDRAULIC PUMPS**
U HYDRAULIC EQUIPMENT
U PUMPS

**HYDRAULIC SYSTEMS**
U HYDRAULIC EQUIPMENT

**HYDRAULIC TEST TUNNELS**
Wet-steam tunnel facility design and program for future use
[PB-210654] 01 p0038 N73-10298
Schlieren method adapted as flow visualization technique to study cavitation development on axisymmetric bodies in water tunnel
[AD-757078] 14 p1652 N73-23402
Application of hydraulic test tunnel flow visualization techniques to determine ground effect on flow around models of aircraft
[NASA-TT-F-14958] 17 p2015 N73-26291
Hydrogen bubble flow visualization technique for study of aerodynamic problems in water flow facilities
[ARL/A-NOTE-338] 21 p2523 N73-30229
Use of dye flow visualization techniques in small water tunnel
[ARL/A-NOTE-339] 21 p2523 N73-30230

**HYDRAULIC VALVES**
U HYDRAULIC EQUIPMENT
U VALVES

**HYDRAULICS**
Research report on tidal hydraulics
[AD-744784] 01 p0051 N73-10412
Tray hydraulic research, using cyclic operation of plate columns for gas-liquid contact
[PB-211853] 05 p0507 N73-14126
Calculation of hydraulic resistances in pipelines
[AD-754322] 10 p1144 N73-19319

**HYDRAZIDES**
Thermal decomposition of polyhydrazide and polyoxadiazoles
[AD-749853] 05 p0568 N73-14612
Chemical reactions of urea with carbohydrazide in smelts and aqueous solutions
[ICT-5/72] 18 p2114 N73-27090

**HYDRAZINE ENGINES**
Characteristics of blowdown-pressurized hydrazine propulsion system for trajectory correction of spacecraft during outer planet flyby missions
[NASA-CR-129796] 04 p0464 N73-13780
Design and qualification of hydrazine attitude control engines for Aeros satellite
[DGLR-PAPER-72-79] 06 p0714 N73-15824
Pressurized gas and electrothermal hydrazine engine for European satellite attitude control
[DGLR-PAPER-72-78] 06 p0714 N73-15825
Monolithic catalyst bed for monopropellant hydrazine decomposition
[NASA-CR-132983] 16 p1914 N73-25486
Engineering model of 20 millipound thrust monopropellant hydrazine resistojet program
[NASA-CR-130762] 16 p1956 N73-25828
Tests of potential thermal degradation of ATS-F radiant cooler form contaminants generated by hydrazine thruster in simulated space
[NASA-CR-132988] 16 p1974 N73-25965
Performance tests of hydrazine catalytic thruster to determine capability for spacecraft limit-cycle attitude control with short thruster pulse durations
[NASA-CR-135489] 22 p2710 N73-31701
Hydrazine engine tests and small bipropellant engine calibration in Molsink facility
23 p2858 N73-32837

**HYDRAZINE NITROFORM**
Solid propellant containing hydrazinium nitroformate oxidizer and polymeric hydrocarbon binder
[NASA-CASE-NPO-12015] 07 p0834 N73-16764
Anhydrous ammonia for removing nitrogen dioxide from stack emission simulating hydrazine nitrogen tetroxide rocket fuel combustion exhaust
08 p0874 N73-17075

**HYDRAZINES**
NT METHYLHYDRAZINE
Effects of intraperitoneally administered hydrazine on electrophysiology, general behavior, and performance of cats
[AD-746014] 02 p0133 N73-11081
Assessment of materials compatibility data for hydrazine monopropellant propulsion systems of space shuttle vehicle in multicycle extended life applications
[NASA-CR-128491] 02 p0221 N73-11788
Gas chromatographic method for quantitative analysis on hydrazine and its breakdown products at catalytic activity levels
[NASA-TT-F-14722] 04 p0386 N73-13137
Hyperammonemia development in metabolic toxicity of hydrazine
[AD-749519] 05 p0501 N73-14077
Reaction kinetics when liquid hydrazines adsorbed on supported ruthenium catalyst
[RPE-TR-72/1-PT-5] 05 p0506 N73-14122
Long-term storability and decomposition kinetics of monopropellant formulations containing hydrazine, hydrazine azide, and ammonia
[AD-750900] 06 p0711 N73-15806
Aluminum rods for gas cooling requirements of satellite attitude and orbit control using hydrazine as low thrust propellant
[RAE-TR-72161] 09 p0991 N73-18086
Kinetics of liquid hydrazine decomposition on supported rhodium catalyst
[RPE-TR-71/16-PT-4] 10 p1126 N73-19177
Compatibility of Ti and Ni alloys, stainless steels, Al, tungsten carbide, butyl, and Ep rubbers with hydrazine noting decomposition rates and effects of carbonic acid
[ESRO-CR-85-PT-2] 13 p1569 N73-22712
Silicone additives for heat flux reduction in hydrazine rocket propellants
[AD-756913] 14 p1700 N73-23798
Physical properties, and hydrazine compatibility of rubber compounds
[NASA-CR-131836] 16 p1932 N73-25633
Electrothermal hydrazine thruster
[NASA-CR-132763] 16 p1956 N73-25827
Design and fabrication of monopropellant hydrazine thruster
[NASA-CR-132784] 18 p2193 N73-27702
Constant strain rate tensile tests to determine long-time dynamic compatibility of elastomeric materials with hydrazine
[NASA-CR-133794] 21 p2562 N73-30538
Mono propellant hydrazine tank pressurization concept based on surface tension feed of propellant to reactor catalyst bed
[AD-763803] 21 p2588 N73-30734
Survey of contaminants and impurities in propellant grade hydrazine
[AD-764365] 22 p2626 N73-31040
Equilibrium concentration and catalytic decomposition products of hydrazine at elevated temperatures and pressures
[NASA-CR-135478] 23 p2753 N73-32031
Characteristics of hydrazine-oxygen fuel cell operating under moderate temperature conditions and various power density concentrations
[AD-764530] 24 p2881 N73-33009

**HYDRAZOIC ACID**
Analytical and experimental determination of reaction mechanisms involved in HN3 plus CO2 laser
[AD-751634] 07 p0807 N73-16546

**HYDRIDES**
NT BOROHYDRIDES
NT CARBORANE
NT DIBORANE
NT LITHIUM HYDRIDES
NT METAL HYDRIDES
NT SILANES
NT ZIRCONIUM HYDRIDES
Effects of crystallization conditions on properties of autoepitaxial and heteroepitaxial layers of silicon obtained by hydride pyrolysis
18 p2188 N73-27667
Thermostability of titanium hydridonitrides
20 p2430 N73-29522

**HYDROACOUSTICS**
U UNDERWATER ACOUSTICS

**HYDROAEROMECHANICS**
U AERODYNAMICS

**HYDROBAROPHONES**
U HYDROPHONES

**HYDROBROMIDES**
Dissociation of HBr behind shock waves and at temperatures from 1450 to 2300 K in pure HBr
[AD-753395] 10 p1143 N73-19310

**HYDROCARBON COMBUSTION**
Shock tube measurements of surface oxidation rates of soot formed during combustion of hydrocarbon fuels
[FML-PUBL-72-8] 01 p0023 N73-10176

**HYDROCARBON FUELS**
NT GASOLINE
NT JET ENGINE FUELS
NT JP-4 JET FUEL
NT JP-5 JET FUEL
Development of hydrocarbon fuels and fuel systems for advanced air breathing engines
[AD-746334] 01 p0090 N73-10741
Molecular beam sampling system for measuring size; size distribution, and particle concentration of carbon particles in acetylene-oxygen flame
[AD-744920] 01 p0118 N73-10971
Conservation of fossil fuels in commercial aviation by using hydrogen
[NASA-CR-112204] 02 p0125 N73-11019
Effect of antiicing additives on flammability properties of hydrocarbon fuels used in jet aircraft
[AD-747945] 03 p0349 N73-12852
Static charge generation in hydrocarbon fuels during flow through pipes
[AD-753386] 09 p1067 N73-18706
Horizontal gunfire effects on flammability of hydrocarbon turbine fuel
[AD-755361] 12 p1443 N73-21688
Flash point measurements for determining flammability hazards of hydrocarbon fuels
[AD-758643] 16 p1954 N73-25814
Analysis of ignition characteristics of high velocity hydrocarbon diffusion flames and comparison with ignition properties of hydrogen
21 p2605 N73-30881

**HYDROCARBONS**
NT ACETYLENE
NT ALKENES
NT BENZENE
NT BUTADIENE
NT BUTENES

NT CAROTENE
NT CYCLIC HYDROCARBONS
NT CYCLOBUTANE
NT DIPHENYL COMPOUNDS
NT ETHANE
NT ETHYLENE
NT HEXENES
NT METHANE
NT METHYLENE
NT NAPHTHALENE
NT NATURAL GAS
NT PARAFFINS
NT PENTANES
NT PROPANE
NT PROPYLENE
NT TOLUENE
NT XYLENE
Analysis of thermal conductivity of liquid aliphatic hydrocarbons with saturated and unsaturated straight or branch chain carbons
[ESDU-67018] 01 p0116 N73-10955
Analysis of thermal conductivity of liquid halogenated aliphatic hydrocarbons and commercial refrigerants
[ESDU-68024-AMEND-A] 01 p0116 N73-10956
Performance of hydrocarbon oxidation catalysts as adsorbed layer promoter
[AD-746258] 02 p0138 N73-11117
Evaluation of disubstituted perylene compounds as monomers for high temperature polymers and as possible binders for carbon fibers
[AD-746626] 02 p0139 N73-11122
Measurement of pollutant levels of nitrogen oxides, unburned hydrocarbons, and carbon monoxide for annular, swirl can combustor
[NASA-TM-X-68160] 02 p0243 N73-11974
Electrical conductivity methods for measuring effects of high energy radiation on dielectric hydrocarbon liquids
[HMI-B-117] 04 p0452 N73-13693
Gas phase chromatographic study of electrosorbed cyclic hydrocarbon intermediates on fuel cell electrode during oxidation
[AD-750391] 05 p0500 N73-14068
Analytical procedure using gas-liquid chromatography in routine analysis of exhaust hydrocarbons from retention time data
[BM-RI-7700] 05 p0506 N73-14118
Optical and dielectric properties of liquid glycerol, tetradecane, and heptadecane
[ORO-3861-6] 06 p0647 N73-15259
Cryogenic research and development on slush hydrogen heat transfer and hydrocarbon suspension
[NASA-CR-130362] 06 p0729 N73-15950
Solid propellant containing hydrazinium nitroformate oxidizer and polymeric hydrocarbon binder
[NASA-CASE-NPO-12015] 07 p0834 N73-16764
Production of HCN by pyrolysis of hydrocarbons in nitrogen plasma
[NASA-TT-F-14685] 07 p0854 N73-16925
Analysis of pyrolysis mechanisms in hydrocarbons
08 p0881 N73-17132
Hydrocarbon suspensions in slush hydrogen and heat transfer to slush hydrogen
[NASA-CR-130550] 08 p0968 N73-17912
Preparation of hydrocarbon suspensions in slush hydrogen for nuclear fuel element corrosion inhibition in rocket engines
08 p0968 N73-17913
Analysis of gaseous emissions from J-85 engine at various fuel-air ratios, engine speeds, and simulated altitude conditions
[NASA-TM-X-2726] 08 p0969 N73-17921
Friction induced surface activity of some hydrocarbons with clean and oxide-covered iron
[NASA-TN-D-7233] 11 p1297 N73-20527
Oil base effect on lubricating performance of lithium greases and soaps containing hydrocarbons
[AD-754593] 11 p1300 N73-20549
Approximate thermochemical tables for some C-H and C-H-O species
[NASA-CR-2178] 11 p1347 N73-20932
Development of halogenated hydrocarbon materials for use as fire and ignition suppressants for aircraft fuel tanks subjected to incendiary ammunition
[AD-755362] 12 p1365 N73-21079
Development of phosphoric acid fuel cells operating on hydrogen produced from thermocracking or steam reforming of hydrocarbon
[AD-755206] 13 p1477 N73-21966
Acute and subacute inhalation toxicity experiments with organic solvents, rocket propellants, and various hydrocarbons in confined environments
[NASA-CR-131675] 13 p1485 N73-22043
Data tables on nonmetallic materials for offgassing CO and hydrocarbons in 5 psia O2
[NASA-TM-X-64745] 14 p1680 N73-23631
Mass spectrometric analysis of aromatic hydrocarbons and sulfur compounds
[NLL-TRANS-1193-[9022.9]]
15 p1746 N73-24151
Hydrocarbon chemistry and chemiluminescence in high altitude plumes
[AD-760793] 18 p2114 N73-27094
Computation of bulk moduli of synthetic hydrocarbon hydraulic fluid
[AD-760776] 18 p2163 N73-27471
Nationwide air pollutant trends for hydrocarbons, oxides, and particulates from 1940 to 1970
[AP-115] 18 p2171 N73-27537
Orientation of molecules of soil soluble surfactant in absorption layers on liquid-liquid interface
[NLL-M-22998-[5828.4F]] 20 p2373 N73-29068
Determination of complex Hamaker constants of molecular interactions in black hydrocarbon emulsion films
[NLL-M-2300-[5828.4F]] 20 p2373 N73-29069
Effects of properties of organic phase on thickness and intermolecular interaction of black hydrocarbon films
[NLL-M-22999-[5828.4F]] 20 p2373 N73-29070
Synthesis and properties of perchloroaromatic compounds
[AD-763125] 20 p2375 N73-29081
Analysis of viscosity of saturated hydrocarbons at different temperatures and pressures to show test equipment and procedures
[NLL-NEL-TT-2471-[6075.461]]
20 p2434 N73-29547
Hydrocarbon polymeric binder for advanced solid propellants
[NASA-CR-133615] 20 p2464 N73-29800
Determination of Hamaker complex constants in hydrocarbon emulsion films by measurement of contact angles and interfacial tension
[NLL-M-23001-[5828.4F]] 21 p2504 N73-30095
HYDROCHLORIC ACID
Corrosion kinetics of Ti-Pd alloy in HCl at room temperature determined by radioactive tracer method
[NLL-TRANS-746-1328-[9022.401]]
05 p0505 N73-14112
Critical evaluation of existing optical remote sensors for HCl vapor detection in solid rocket propellant plumes
[NASA-CR-112274] 15 p1780 N73-24431
HCl acid aerosol production by space shuttle exhaust products and atmosphere
[NASA-CR-132993] 16 p1870 N73-25142
Stimulated emission in 3 to 5 wavelength band by exciting HCl vibrational levels by electron impact
[AD-761671] 19 p2308 N73-28562
HYDROCYANIC ACID
Stabilization of aqueous prussic acid during synthesis from ammonia by carbon dioxide
[NASA-TT-F-14691] 07 p0752 N73-16110
Production of HCN by pyrolysis of hydrocarbons in nitrogen plasma
[NASA-TT-F-14685] 07 p0854 N73-16925
Homogeneous cyanoethylation of hydrogen cyanide in presence of alkaline catalysts
[NASA-TT-F-14690] 08 p0884 N73-17154
Speed of alkaline polymerization of hydrocyanic acid - Part I
[NASA-TT-F-14651] 09 p0998 N73-18145
Chemical composition of polymers formed by alkaline polymerization of hydrocyanic acid - Part 2
[NASA-TT-F-14645] 09 p0998 N73-18146
Storage instability of hydrocyanic acid mixed with stabilizing agents - Part 3
[NASA-TT-F-14652] 09 p0998 N73-18147
HYDRODYNAMIC EQUATIONS
NT HELMHOLTZ VORTICITY EQUATION
Eulerian incompressible hydrodynamic numerical model and laboratory simulations of tsunamis
[AD-745420] 01 p0053 N73-10430
Thermohydrodynamic equations of nonlinear mesometeorological processes
[NLL-M-20716-[5828.4F]] 01 p0072 N73-10590
Hydrodynamics of surface layer of atmosphere and micrometeorological processes over flat homogeneous surface
[NLL-M-22574-[5828.4F]] 01 p0072 N73-10593
Numerical weather forecasting methods - basic equations of dynamic processes and quasi-geostrophic approximation
[NLL-M-20352-[5828.4F]-VOL-1]
01 p0073 N73-10595
Hydrodynamic calculations and experimental observations of ionospheric shock front propagation following nuclear explosion
05 p0510 N73-14150
Magnetopause boundary dependence on orientation of interplanetary magnetic field and hydromagnetic properties of magnetosphere shift southwards
06 p0718 N73-15857
Euler equations of motion of relativistic, perfect-fluid hydrodynamics, and potential application to stellar stability
07 p0840 N73-16806
Numerical solution of one hydrodynamics equation
[AD-756099] 14 p1651 N73-23394
Quasi-hydrodynamic equations for analyzing pressure anisotropy effects on magnetospheric tail oscillations
14 p1703 N73-23821
Hydrodynamic models for studying pressure and wind fields in low latitudes
20 p2444 N73-29630
Methods for studying effect of sea on thermal regime of atmosphere
20 p2445 N73-29636
Numerical experiments for solving complete equations of hydrodynamics
[AD-763143] 21 p2539 N73-30359
HYDRODYNAMIC STABILITY
U FLOW STABILITY
HYDRODYNAMIC TUNNELS
U PLASMA JET WIND TUNNELS
HYDRODYNAMICS
NT ELASTOHYDRODYNAMICS
NT ELECTROHYDRODYNAMICS
NT MAGNETOHYDRODYNAMICS
Single layer, hydrodynamic numerical model for oceanography
[AD-745759] 01 p0053 N73-10432
Analysis of stream-stream interaction between slow solar wind and leading faster solar wind
01 p0097 N73-10800
Textbook on hydraulic systems
[AD-746713] 02 p0158 N73-11280
Adaptive Kalman filter approach for identifying submarine trajectory from hydrodynamic parameters
[AD-747315] 02 p0159 N73-11288
Computer program for determining influx towards center of spherical metal shell following detonation of spherical, symmetrically placed explosive
[FOA-2-C-2471-25] 06 p0653 N73-15305
Numerical analysis of structure of solitary waves using partial differential equations
[AD-750565] 06 p0655 N73-15323
Kantorovich variational method for solving isothermal problem of hydrodynamic theory of lubrication for thrust bearing with nondeformed pad
[AD-750485] 06 p0678 N73-15519
Spall calculations in one-dimensional hydrodynamics codes using aluminum and high explosives
[LA-5001] 07 p0855 N73-16935
Procedure for applying structure-fluid interactions effect to dynamic frequency response calculations for submerged structures
[AD-752484] 08 p0967 N73-17906
Computer program for solving radiation-hydrodynamic problems in complex geometries
[AD-752066] 08 p0970 N73-17929
CDC 6600 computer analysis of numerical stabilizer effects on computing time for second order accurate schemes
[AD-753165] 09 p1018 N73-18308
Design factors resulting from hydrodynamic loads induced on large underwater structures by impulsive motion
[AD-753603] 09 p1019 N73-18315
Ellipticity condition of three dimensional partial differential equation as turbulence criterion in atmospheric motion
[AD-746624] 09 p1032 N73-18424
Numerical analysis of oil film bearing with respect to bushing based in inertial force, viscous force of liquid, and load lifting force exerted by bearing
[AD-752688] 09 p1040 N73-18483
Analytical solution of Reynolds equation and application to hydrodynamic lubrication to show characteristics of lubrication film
[TAE-153] 09 p1057 N73-18618
Hydrodynamic and weight loads of self-contained buoy stations for oceanographic research in strong current areas
09 p1059 N73-18638
Hydrodynamic design of thrust slide bearings
[AD-753965] 10 p1168 N73-19501
Hydrodynamic equations of motion for studying sound interaction in transient chemical reactions
[AD-753798] 10 p1191 N73-19688
Hydrodynamic and chemical properties of stratospheric aircraft wake
[PB-213114] 11 p1290 N73-20465
Numerical analysis of hydrodynamic properties of liquid helium based on quantum statistical mechanics
12 p1390 N73-21270
Vibration effects on self-acting and hydrodynamic shaft seals in gas turbine engines
[NASA-TM-X-68214] 13 p1534 N73-22430
Multiperipherism and hydrodynamics of multiple processes
[NASA-TT-F-14896] 13 p1561 N73-22656
Hydrodynamics and heat exchange with two phase flow in elements of power equipment
[AD-756564] 13 p1591 N73-22897
High energy particle kinetics along boundary of matter-antimatter of universe
[LPTHE-73/5] 14 p1703 N73-23818
Oscillations of earths magnetic tail studied from model of plasma cylinder with free boundary
14 p1703 N73-23820
Numerical calculation of vertical water entry of finite cones
[AD-759006] 16 p1891 N73-25302
Velocity and temperature development in entrance region between two rotating concentric cylinders
[AD-762049] 19 p2256 N73-28187
Analysis of wake collapse in sea water and stratified fluids with emphasis on final stages of decay
[AD-761622] 19 p2257 N73-28189

Fundamental concepts and statistical foundation of mechanics of continuous medium
[AD-764370] 22 p2727 N73-31820
Effects on drag of injecting aqueous solutions of polyethylene oxide into turbulent boundary layer of flat plate
[AD-764896] 23 p2776 N73-32202
Two dimensional elastic-plastic hydrodynamics code for calculating dynamic response of semiconductor configuration to electron loading
[AD-763943] 23 p2826 N73-32590
Hydrodynamic simulation using flow field visualization for combustor study
23 p2831 N73-32625

HYDROELASTICITY
Development of structural dynamics model of space shuttle and evaluation of structural and hydroelastic analysis methods
[NASA-CR-112196] 04 p0478 N73-13911
Effect of undissolved air on compressibility of transmitting medium in hydraulic circuits
[NLL-NEL-TT-2426-[6075.461]]
15 p1763 N73-24289
Dynamic response of pipes with fluid flowing in steady and unsteady conditions
[MERL-TN-72-2] 20 p2387 N73-29178

HYDROELECTRIC POWER STATIONS
Survey of snow cover to predict risk of spring flood and snow storage in areas of hydroelectric power stations in Norway
[E73-11160] 24 p2919 N73-33313

HYDROFLUORIC ACID
Computerized simulation of pulsed HF laser pumped by H2 and F2 chain reaction
[AD-745425] 01 p0065 N73-10531
Laser luminescence and shock heating for hydrogen fluoride vibrational relaxation measurements in shock tube
[AD-745953] 02 p0138 N73-11119
Model of diffusion-type, HF chemical laser
[AD-745952] 02 p0183 N73-11484
Calculation of vibrational energy level distributions of hydrogen fluoride formed during atomic fluoride reaction with molecular hydrogen
[AD-748291] 04 p0387 N73-13146
Public health exposure limits to nitrogen oxide, hydrogen chloride, and hydrogen fluoride air pollutants
[AD-751438] 07 p0748 N73-16084
Infrared detection of hydrogen fluoride tracer for studying turbulent mixing in inert and combustion flows
08 p0880 N73-17128
Monte Carlo calculations of reaction rates for collisions of H atoms with vibrationally excited HF
[AD-751910] 08 p0884 N73-17157
Solid state laser induced excitation of HF second vibration rotation energy levels
15 p1794 N73-24547
Formyl fluoride photochemical laser and energy content of HF photoelimination product
[AD-757743] 15 p1796 N73-24558
Electron beam stabilized electrical discharge HF laser
[AD-763464] 21 p2556 N73-30489
Design of line-tunable pulsed hydrogen fluoride/deuterium fluoride laser
[AD-764709] 23 p2802 N73-32410
Pulsed HF chemical laser to excite molecules to first vibrational level
[AD-765183] 23 p2858 N73-32833
Photoelectron spectroscopic analysis of excited hydrogen fluoride in contaminated atmospheres
[AD-764813] 24 p2893 N73-33093

HYDROFOIL BOATS
U HYDROFOIL CRAFT

HYDROFOIL CRAFT
Design and performance of gas turbines for hydrofoils
[AD-753890] 11 p1334 N73-20830
Numerical analysis of bending flutter and torsional flutter in flexible hydrofoil struts
[AD-757645] 14 p1717 N73-23935
Parametric design analysis to determine characteristics and performance of class of high speed hydrofoil craft
[AD-760355] 17 p2016 N73-26303
Optimization of forward foil lift control for hydrofoil craft
[AD-760684] 18 p2131 N73-27221
Design criteria and materials for reducing structural weight of hydrofoil boats
[AD-761123] 18 p2132 N73-27222
Linear optimal plant and controller model for hydrofoil craft
[AD-760698] 18 p2132 N73-27226

HYDROFOILS
Singular perturbation method for predicting pressure distribution on supercavitating hydrofoils with rounded noses
[AD-745791] 01 p0063 N73-10514
Equations for fully cavitating flow of fluid past flat plate hydrofoil running below free surface with consideration of transverse gravity effects
[AD-746484] 02 p0157 N73-11272
High speed mechanics research, including circular cylindrical shell buckling and hydrofoil profiles
06 p0724 N73-15910
Supercavitating jet flapped hydrofoil with drag reduction due to combined effects of foil camber jet flap
[REPT-249] 06 p0724 N73-15912
Surface pressure distribution on hydrofoil profiles in accelerated cascades, using boundary layer calculations
[REPT-251] 06 p0724 N73-15914
Cavitation in liquid cryogens with determination of flow and thermodynamic conditions of cavitating hydrofoil
[NASA-CR-2156] 07 p0770 N73-16255
Analysis of two dimensional cascade flow of double circular arc blades at transonic speed with various camber angles and pitch-chord ratios
[NAL-TR-300] 09 p1014 N73-18279
Experimental investigation of two dimensional cascade flow tests for three cascade configurations - Vol. 4
[NASA-CR-121101] 09 p1015 N73-18282
Computer program to evaluate effect of closed-jet tunnel test on force coefficients of cambered, sharp-nosed, fully cavitating, two dimensional hydrofoil section
[AD-755423] 13 p1512 N73-22250
Applying sequential estimation technique of system identification to determination of unknown coefficients in vertical plane equation of motion of hydrofoil
[AD-755738] 13 p1512 N73-22253
Automatic motion stabilization system controlling foil lift of hydrofoil
[AD-758286] 15 p1769 N73-24332
Hydrofoil design criteria based on model for minimum control power
[AD-759286] 16 p1892 N73-25312
Determination of ventilation characteristics of blunt-based surface piercing struts in calm water and in waves
[AD-759046] 16 p1892 N73-25314
Analytical methods for evaluating high performance ship design concepts particularly hydrofoil concepts
[AD-759376] 17 p2009 N73-26251
Application of exact method for numerical computations of supercavitating hydrofoils of parabolic shape
[AD-763465] 22 p2654 N73-31261
Pressure differences, forces, and moments on same two wings in steady subsonic flow computed by 15 different programs
[AD-763669] 23 p2776 N73-32199

HYDROGEN
NT DEUTERIUM
NT DEUTERIUM PLASMA
NT HYDROGEN ATOMS
NT HYDROGEN IONS
NT HYDROGEN ISOTOPES
NT HYDROGEN PLASMA
NT LIQUID HYDROGEN
NT TRITIUM
Effect of charge materials, melting condition, and type of melting equipment on hydrogen gas contained in copper alloys
[AD-745845] 01 p0068 N73-10558
Interstellar cloud heating by collisionally de-exciting vibrationally excited molecular hydrogen
[NASA-TM-X-66064] 01 p0103 N73-10851
Spectrophotometric analysis of Orion nebula emission spectra with dust lanes in hydrogen region
[AD-745314] 01 p0104 N73-10863
Background Lyman alpha radiation and interstellar hydrogen gas taking into account radiative heat transfer
01 p0105 N73-10872
Solar wind plasma/interstellar hydrogen gas interactions
01 p0105 N73-10873
Synthesis observations of neutral hydrogen emission in two spiral galaxies NGC 6946 and IC 342
[AD-744679] 01 p0106 N73-10876
Rate coefficient data for recombination reaction hydrogen plus oxygen plus argon yields water and argon in mixtures behind incident shock waves
[NASA-TN-D-6990] 01 p0117 N73-10965
Equilibrium distribution of helium-4 and helium-3 between the liquid and vapor phases of deuterium 2 and hydrogen 2
[NBS-TN-621] 02 p0137 N73-11109
Procedure for measuring effect of hydrogen content on toughness and sustained load cracking resistance of titanium alloys including results obtained for Ti-6Al-4V
[AD-746443] 02 p0187 N73-11517
Source of electrons from molecular hydrogen in H I regions
[NASA-TM-X-66079] 02 p0229 N73-11858
Lyman and Werner molecular hydrogen bands in ultraviolet interstellar spectrum of delta Scorpii
[NASA-TM-X-66102] 02 p0230 N73-11865
Analysis of hydrogen mixing and combustion in hypersonic air stream to show hydrogen concentration and pressure distribution
[AD-746341] 02 p0243 N73-11978
Isothermal diffusion calculated for hydrogen dissolved in Zircaloy-yttrium combination
[GKSS-71/E/19] 03 p0263 N73-12131
Multistep chemical processes for water decomposition, using nuclear heat for producing hydrogen
[EUR-4776-E] 03 p0263 N73-12132
Anelastic studies of hydrogen diffusion in niobium using internal friction techniques
[COO-1198-896] 03 p0264 N73-12138
Influence of surface processes on rate of permeation of hydrogen through metals
[NASA-CR-129276] 03 p0312 N73-12548
Hydrogen embrittlement of cadmium coated steels due to paint stripping
[AD-747634] 03 p0319 N73-12599
Development of computer program for determining thermodynamic and transport properties of para and equilibrium hydrogen
[NASA-CR-129261] 03 p0363 N73-12959
Development of low cost cathode catalysts for air breathing fuel cells containing phosphoric acid electrolyte
[AD-748447] 04 p0376 N73-13059
Chemical evolution of air and hydrogen in turbulent mixing layer
[NASA-TT-F-14633] 04 p0386 N73-13141
Melting characteristics and thermophysical properties of solid hydrogen
[AD-748847] 04 p0387 N73-13144
Calculation of vibrational energy level distributions of hydrogen fluoride formed during atomic fluoride reaction with molecular hydrogen
[AD-748291] 04 p0387 N73-13146
Effect of breathing hydrogen at depths greater than 1000 feet on speech intelligibility
[AD-749320] 04 p0392 N73-13184
Effect of breathing hydrogen at 200 feet below sea level on speech intelligibility
[AD-749322] 04 p0392 N73-13186
Sintering behavior of UO2 powder compacts under hydrogen atmosphere
[CEA-R-4285] 04 p0427 N73-13477
Atomic hydrogen maser with bulb temperature control by output frequency difference signal for wall shift elimination
[NASA-CASE-HQN-10654-1] 04 p0428 N73-13489
Generation of vacuum ultraviolet xenon laser and X ray hydrogen laser
[SC-T-72-2513] 04 p0429 N73-13494
Production and current measurement of intense hydrogen-ion beams in pulsed conditions
[NP-19351] 04 p0454 N73-13705
Interferometric observations of neutral hydrogen emission line of compact galaxy 2 Zw 40
[AD-747993] 04 p0477 N73-13896
X ray apparatus for investigating hydrogen induced changes in fine crystalline structure of N1 powders and electrolyic films
[NLL-TRANS-746-1294-[9022.401]]
05 p0505 N73-14113
Electrochemical analysis of cathodic hydrogen absorption by iron and steel
[BARC-585] 05 p0506 N73-14116
Instabilities in gaseous hydrogen-liquid oxygen rocket engine noting influence of pressure and concentration
[DLR-FB-71-47] 06 p0711 N73-15805
Maps of line profile at each position of aperture of neutral hydrogen in NGC 2403 and NGC 4236
[AD-748983] 06 p0719 N73-15872
Cryogenic research and development on slush hydrogen heat transfer and hydrocarbon suspension
[NASA-CR-130362] 06 p0729 N73-15950
Energy transfer in laminar hypersonic boundary layers by hydrogen combustion
07 p0771 N73-16260
Performance evaluation of coaxial injectors for use in gaseous hydrogen-liquid oxygen rocket engines
[DLR-FB-71-56] 07 p0836 N73-16779
Total gamma ray production rate per hydrogen atom from neutral pion decay in interstellar cosmic ray interactions, and calculation of molecular hydrogen amount
[NASA-TM-X-66167] 07 p0839 N73-16798
Hyperfine electron density fluctuation in stabilized hydrogen arc laser
08 p0943 N73-17723
Temperature effects on hydrogen decomposition of wall surface coatings
[NASA-TM-X-2735] 08 p0946 N73-17748
Explorer 32 satellite data on atmospheric hydrogen
08 p0972 N73-17945
Analysis of downstream mixing of transverse hydrogen injection from single and multiple orifices in Mach 4 boundary layer over flat plate
[NASA-CR-112254] 09 p1015 N73-18285
Method for producing storage bulb for atomic hydrogen maser
[NASA-CASE-NPO-13050-1] 09 p1043 N73-18508
Hydrogen adsorption and diffusion, and subcritical crack growth in high strength steels and nickel alloys
[NASA-CR-130979] 09 p1046 N73-18528
Electrochemical permeation technique and scanning electron microscopy used to determine hydrogen embrittlement in ferrous materials
[AD-752828] 09 p1049 N73-18557

Mathematical model for predicting erosion rate of graphite surface exposed to hot supersonic stream of hydrogen gas
[NASA-CR-130812] 09 p1050 N73-18564
Observations of neutral hydrogen absorption spectrum of Cygnus X-3
[AD-752497] 09 p1085 N73-18856
Mixing and ignition of hydrogen jets injected normally into supersonic two dimensional flow and effect on combustion performance of hyersonic ramjet engine
[ONERA-TP-973] 09 p1098 N73-18962
Three body recombination and dissociation rate coefficients for reversible reactions H2 plus H yields H plus H plus H
[FML-PUBL-72-11] 10 p1126 N73-19169
Initial temperature effects on diffusion burning of hydrogen flame in closed channel with supersonic flow
[NASA-TT-F-14844] 10 p1141 N73-19295
Recombination coefficients of electrons with hydrogen and carbon monoxide ions
[NASA-CR-131107] 10 p1192 N73-19699
Electron recombination with hydrogen ions
[NASA-CR-131108] 10 p1192 N73-19700
Nuclear resonance investigation in niobium-hydrogen and niobium-deuterium systems
[JUL-853-FF] 10 p1193 N73-19707
Topler schlieren photographic study of diffusion flame structure
[NASA-TT-F-14843] 10 p1223 N73-19946
Electrode structures for transverse excitation produced HF lasers
[DREV-TN-2047/73] 11 p1302 N73-20565
Quantitative analysis of hydrogen-induced slow crack growth in low alloy steel in gaseous hydrogen and distilled water environments
[NASA-TM-X-62253] 11 p1305 N73-20589
Hydrogen lamp with lithium fluoride window for Lyman beta radiation output
[AD-754572] 11 p1325 N73-20753
Design, assembly, and operation of gaseous hydrogen system with solutions to specific problems
[SC-DR-72-0593] 12 p1388 N73-21257
Gas phase hydrogen permeation through alpha iron, 4130 steels, and 304 stainless steels from less than 100 C to near 600 C
[NASA-TN-D-7265] 12 p1412 N73-21442
Effects of hydrogen environment embrittlement of steels and alloys
[NASA-CR-2163] 12 p1412 N73-21444
Determination of diffusion coefficient of hydrogen through nickel and iron-nickel alloys
[UCRL-TRANS-10651] 12 p1415 N73-21463
Design and performance of liquid nitrogen cooled nozzle for producing pulsed cylindrical hydrogen cluster beams
[KFK-1610] 12 p1436 N73-21632
Galactic neutral hydrogen gas velocity distribution within spiral arms in local regions
12 p1447 N73-21720
Two arc min synthesis study of spiral galaxy M51
[AD-754078] 12 p1459 N73-21822
Atomic oxygen hydrogen reaction with acetylene, and gas discharge shock tube design
13 p1488 N73-22060
Design and evaluation of electrochemical nitrogen-hydrogen separator for use in spacecraft nitrogen generator
[NASA-CR-114580] 13 p1534 N73-22431
Stress corrosion cracking in 410 stainless steel due to hydrogen embrittlement
13 p1539 N73-22471
Stress corrosion cracking in high strength aluminum alloys due to hydrogen embrittlement
13 p1539 N73-22472
Effect of dissolved hydrogen on mechanical and superconducting properties of molybdenum
13 p1565 N73-22681
Design and analysis of low speed hydrogen and oxygen inducers applicable to space tugs
[NASA-CR-124233] 13 p1570 N73-22722
Development of dynamic model of solar corona based on equations for ideal, inviscid, fully ionized hydrogen gas in gravitational field
13 p1572 N73-22740
High strength steel delayed failure analysis including hydrogen embrittlement
[NLR-TR-72113-U] 14 p1715 N73-23917
Upper atmospheric neutral hydrogen distribution
15 p1779 N73-24423
Mass spectrometric measurement of hydrogen in milligram-size quantities of titanium
[NASA-TN-D-7326] 15 p1798 N73-24574
Neutral hydrogen aperture synthesis maps of IC2574 and NGC 7640 galaxies
[AD-757688] 15 p1833 N73-24856
Monte Carlo calculations on reaction kinetics in hydrogen, deuterium, and fluoride interactions
[AD-758759] 16 p1872 N73-25153
Technology utilization program relating to hydrogen effects on metal alloys and mechanical properties of recently developed alloys
[NASA-SP-5940[03]] 16 p1928 N73-25598
Density profiles of supersonic jet target of hydrogen-deuterium in vacuum
[LA-UR-73-231] 17 p2010 N73-26260
Measurement of hydrogen concentration in mass diffusing jets by laser induced Raman scattering
17 p2012 N73-26272
Analysis of embrittlement in zone refined iron and Armco iron after charging with hydrogen to determine cause of reaction
[RAE-LIB-TRANS-1666] 17 p2043 N73-26530
Electrochemical and mechanical parameters of localization hydrogen in iron and maraging steel using high resolving power autoradiography
[RAE-LIB-TRANS-1665] 17 p2044 N73-26533
Design and tests of breadboard cryogenic hydrogen and Freon heat exchanger for space shuttle missions
[NASA-CR-128987] 17 p2096 N73-26959
Distribution profiles of admixtures in epitaxial silicon layers prepared with hydrogen of high purity
18 p2187 N73-27661
Interferometer aperature synthesis in interstellar neutral hydrogen line spectra of radio sources
[AD-760013] 18 p2198 N73-27744
Equations of state for hydrogen including low temperature regions
[UCID-16095] 19 p2230 N73-27986
Radio telescope observation of low velocity interstellar neutral atomic hydrogen in direction of early type stars
19 p2342 N73-28836
Digital computer calculation of molecular hydrogen-atomic hydrogen interaction energy and electric dipole moment
[NASA-TM-X-2839] 20 p2455 N73-29733
Chemical reactivity of hydrogen, nitrogen, and oxygen below 100 K
[NASA-CR-133654] 20 p2456 N73-29742
Hydrogen content as measure of combustion performance for hydrocarbon fuels
[AD-763097] 20 p2465 N73-29804
Aperture synthesis in interstellar neutral hydrogen line
21 p2594 N73-30782
Hydrogen diffusion and hydrogen induced cracking of structural materials
[COO-3166-5] 21 p2604 N73-30867
Gas sensor for detecting H2 in air and N2, and O2 in N2
[NASA-CR-133891] 22 p2674 N73-31416
Properties of materials in high pressure hydrogen at cryogenic, room, and elevated temperatures
[NASA-CR-124394] 22 p2725 N73-31804
Experimental data analysis for sonic injection of hydrogen from backward facing step in parallel direction to main supersonic stream
[NASA-TM-X-2828] 22 p2728 N73-31828
Effects of flow turning, flow acceleration, and supersonic flow on hydrogen film cooling
[NASA-CR-121235] 22 p2729 N73-31841
Diffuse optical emissions from interstellar gas
22 p2734 N73-31887
Effects of high pressure hydrogen environments on mechanical properties of alloys considered as candidate materials for high performance rocket engine construction
[NASA-CR-124410] 23 p2804 N73-32428
Simultaneous determination of carbon, hydrogen, and nitrogen in organic compounds
[UCID-16198] 24 p2892 N73-33085
Hydrogen and other synthetic fuels
[TID-26136] 24 p2971 N73-33738
Spectrometric measurement of D/H ratio in Jupiter atmosphere
24 p2978 N73-33797

**HYDROGEN ATOMS**

Low temperature addition reactions of hydrogen and oxygen atoms with chemical compounds through creation of secondary valence
[NASA-TT-F-14643] 06 p0703 N73-15729
Monte Carlo calculations of reaction rates for collisions of H atoms with vibrationally excited HF
[AD-751910] 08 p0884 N73-17157
Lowering of ionization potentials of hydrogen and carbon atoms immersed in high temperature and high density thermal plasma
[AD-753247] 09 p1072 N73-18752
Gas phase recombination of hydrogen and deuterium atoms
[NASA-CR-131417] 11 p1252 N73-20162
Differential and integral scattering cross sections for H and He atoms in hydrogen
[NASA-TT-F-14900] 13 p1561 N73-22655
Laboratory experiments on interaction of fast protons and hydrogen atoms with earth atmosphere
[AD-757505] 14 p1663 N73-23499
Differential scattering of hydrogen and oxygen atoms in methane molecules
[NASA-TT-F-14898] 14 p1694 N73-23751
Interstellar molecular hydrogen lines in ultraviolet spectrum of delta Scorpii
22 p2734 N73-31886

**HYDROGEN CHLORIDES**

NT HYDROCHLORIC ACID

Public health exposure limits to nitrogen oxide, hydrogen chloride, and hydrogen fluoride air pollutants
[AD-751438] 07 p0748 N73-16084
Theoretical performance of HCl continuous wave chemical laser
[AD-762924] 20 p2427 N73-29493

**HYDROGEN COMPOUNDS**

NT BOROHYDRIDES
NT CARBORANE
NT DEUTERIUM COMPOUNDS
NT DIBORANE
NT HEAVY WATER
NT HYDRIDES
NT HYDROBROMIDES
NT HYDROCYANIC ACID
NT HYDROGEN PEROXIDE
NT HYDROGEN SULFIDE
NT LITHIUM HYDRIDES
NT METAL HYDRIDES
NT SILANES
NT ZIRCONIUM HYDRIDES

Determination of vibrational temperature of molecular nitrogen in high atmosphere by chemical release of hydrogen iodide from sounding rocket
[AD-757909] 15 p1782 N73-24448

**HYDROGEN CYANIDES**

U HYDROCYANIC ACID

Formation of hydrocyanic acid from mixtures of ammonia, metane and noble gas or hydrogen subjected to UHF waves
[NASA-TT-F-14678] 12 p1376 N73-21162

**HYDROGEN DEUTERIUM OXIDE**

U HEAVY WATER

**HYDROGEN EMBRITTLEMENT**

Hydrogen embrittlement of aged tantalum and niobium alloys
[NASA-TM-X-68293] 20 p2431 N73-29525
Mechanical behavior of polycrystalline nickel deformed by tension and simultaneously cathodically charged with hydrogen
[AD-759036] 20 p2432 N73-29535

**HYDROGEN FLUORIDES**

U HYDROFLUORIC ACID

**HYDROGEN FUELS**

Nuclear energy in hydrogen production by water dissociation method
[EUR-4838] 06 p0699 N73-15699
Development and characteristics of hydrogen-based mobile fuel systems and analysis of technical and economic problems in large scale application
[UCRL-51228] 07 p0834 N73-16766
Preliminary appraisal of hydrogen and methane fuel and fuel tank configuration in Mach 2.7 supersonic transport
[NASA-TM-X-68222] 13 p1568 N73-22711
Miniature hydrogen fueled gas turbine engine scaled to teledyne CAE model 376
[NASA-CR-112173] 16 p1956 N73-25825

**HYDROGEN IONS**

Systems data for initial formation of incompressible hydrogen ion beams
[NLL-DRIC-TRANS-2351-[3623.66]]
02 p0215 N73-11740
Soft X ray and hydrogen alpha structure of solar flare
22 p2734 N73-31879

**HYDROGEN ISOTOPES**

NT DEUTERIUM
NT TRITIUM

IMP measurements on hydrogen and helium isotope accelerations in solar flares
19 p2336 N73-28797
Isotopic composition of hydrogen and helium in solar cosmic ray measurements by OGO F
19 p2336 N73-28798

**HYDROGEN OXYGEN ENGINES**

NT J-2 ENGINE

Technology for developing hydrogen-oxygen thruster for space shuttle ACPS
[NASA-TM-X-68146] 01 p0090 N73-10744
Hydrogen oxygen engine for space shuttle attitude control and stationary or pulsed operation
[MBB-UR-158-72-O] 06 p0714 N73-15823
Analytical combustion model for predicting flow and pressure transients in H2-O2 RCS of rocket engine feed system
07 p0835 N73-16767
Design solutions and technologies for Europa 3 launch vehicle, including second stage and propulsion system
07 p0850 N73-16888
Analytical and experimental evaluation of high pressure thrust chamber concepts for hydrogen oxygen auxiliary propulsion for space shuttle vehicle
[NASA-CR-120895] 09 p1079 N73-18800
Design and tests of low pressure thrust chamber concepts for hydrogen oxygen auxiliary propulsion for space shuttle vehicle
[NASA-CR-120896] 09 p1079 N73-18801
Propellant control and propulsion study for European space tug
[HSD-TP-7227-APP-3] 10 p1217 N73-19895

Development and characteristics of hydrogen-oxygen power unit for application to onboard systems of space shuttle orbiter vehicle
[NASA-TM-X-68262] 20 p2363 N73-29005
High energy rocket engines - propellant physical chemistry, propulsion system performance, hydrogen oxygen engines, boosters, nozzles - conferences
[DLR-MITT-72-09] 24 p2972 N73-33749
Performance tests of hydrogen oxygen rocket engines for various propellant mixing ratios
24 p2973 N73-33752

HYDROGEN OXYGEN FUEL CELLS
Present international status of research and development of electrochemistry and fuel cells
[AD-755106] 11 p1238 N73-20048
Optimization of oxygen hydrogen fuel cell power system for advanced spacecraft
[NASA-CR-121136] 17 p1986 N73-26050
Improving resistance of chrysotile asbestos to potassium hydroxide at temperatures above 100 C
[AD-761512] 19 p2223 N73-27931
Dynamic response characteristics of aqueous electrolyte hydrogen oxygen fuel cells
22 p2617 N73-30973

HYDROGEN PEROXIDE
Mass spectrometric analysis of reactions of nitrogen oxide and nitrogen dioxide with hydrogen peroxide at 25 C
[NASA-CR-130831] 09 p0999 N73-18155
Hydrogen peroxide aerosols for decontamination of influenza atmosphere
[NASA-TT-F-15127] 23 p2750 N73-32006

HYDROGEN PLASMA
NT DEUTERIUM PLASMA
Analysis of laser induced two dimensional wave motions in hydrogen plasma
[AD-746681] 03 p0343 N73-12798
Production and current measurement of hydrogen ion beam and plasma in duoplasmatron with cusped magnetic field
[NP-19364] 05 p0583 N73-14747
Properties of dense helical microwave plasma source in intense magnetic field
[CEA-EUR-FC-652] 12 p1435 N73-21626
Observation of high-order stimulated Raman-antiStokes radiation and its role in initial phase of plasma production by lasers
[IPP-4/40] 12 p1435 N73-21629
Laser light absorption characteristics of laser produced hydrogen plasma
[AD-756524] 13 p1538 N73-22458
Shear stabilization of drift instability in hydrogen plasma
[EUR-CEA-FC-646] 15 p1818 N73-24734
Equilibrium compositions and thermodynamic properties of mixed plasmas, including argon-hydrogen plasmas at .01 to 100 atmospheres between 2,000 K and 35,000 K
16 p1948 N73-25764
Experiments on velocity distribution and critical velocity of rotating hydrogen plasma
[TRITA-EPP-73-06] 17 p2068 N73-26736
Generation of induction heated, seeded hydrogen plasmas at one atmosphere pressure
20 p2457 N73-29746
Spectrometric and photographic analysis of neodymium glass laser produced hydrogen plasma
[AD-764496] 22 p2705 N73-31667

HYDROGEN RECOMBINATIONS
Analysis of hydrogen diffusion in alpha-iron in six degree to seventy seven degrees Kelvin using magnetic after-effect technique
[COO-1198-903] 03 p0314 N73-12561
Rearrangement collision leading to formation of highly excited hydrogenlike states
[NASA-TM-X-66184] 08 p0945 N73-17743

HYDROGEN SULFIDE
Decomposition of hydrogen sulfide, in electrical discharge, to elemental sulfur
[BM-RI-7780] 21 p2505 N73-30105

HYDROGEN 2
U DEUTERIUM

HYDROGEN 3
U TRITIUM

HYDROGENATION
Cost data for modified hydrogen depolarized carbon dioxide concentrator in life support system
[NASA-CR-124462] 24 p2887 N73-33052

HYDROGEOLOGY
Data for assessing water supply changes and effects on hydrogeological management of San Joaquin Valley
12 p1400 N73-21353
Analysis of ERTS-1 data for studies of hydrogeology, geomorphology, and paleoclimatology in Bolivia, Argentina, Chile, and Peru
[PAPER-W1] 19 p2270 N73-28281

HYDROGRAPHY
Hydrographic data from Oregon waters in 1971
[AD-746515] 03 p0297 N73-12421
Analysis of tidal currents, turbulent diffusion, and local shears in currents found in Trinity Bay, Texas
[NASA-CR-128734] 08 p0916 N73-17510
Study of suspended sediment and aquatic fronts in Delaware Bay using ERTS-1 imagery
[E73-10368] 10 p1150 N73-19364
Environmental quality program, environmental forecasting program, and seabed assessment program for international decade of ocean exploration
12 p1400 N73-21359
Development of procedure for calculating ocean currents based on given density field and comparison with current techniques
12 p1421 N73-21516
Characteristics of system for obtaining continuous profiles of ocean conductivity, temperature, and sound velocity as functions of depth
[NOAA-IFS-73009] 15 p1787 N73-24489
Mediterranean Sea geophysical survey
[AD-757455] 16 p1910 N73-25452
Application of ERTS-1 imagery for grid measurement of small water bodies
[E73-10768] 18 p2134 N73-27244
Survey of lake flooding in Lake Champlain basin using ERTS-1 imagery
[E73-10771] 18 p2134 N73-27247
Application of ERTS-1 imagery for hydrometric and hydrographic surveys of Canada
[E73-10777] 18 p2135 N73-27253
Water balance, micrometeorology, thermal structure, and heat content of Great Lakes as determined by remote sensors during International Field Year
[IFYGL-BULL-4] 18 p2143 N73-27322
Hydrological investigations conducted during Tenth Soviet Antarctic Expedition to determine temperature and salinity of ocean
20 p2407 N73-29343
Hydrographic investigations conducted aboard ships of the Tenth Soviet Antarctic Expedition
20 p2407 N73-29344
Hydrological investigations of Davis Sea conducted during Tenth Soviet Antarctic Expedition
20 p2408 N73-29353

HYDROKINETICS
U HYDROMECHANICS

HYDROLOGY
NT HYDROGEOLOGY
Evaluation of ERTS-1 imagery for hydrologic information in Sierra Nevada Mountains and Lake Ontario
[E72-10170] 01 p0044 N73-10351
Data processing of hydrologic conditions using ERTS-1 time lapse imagery of Wrangell Mountains
[E72-10187] 01 p0046 N73-10366
Geology and hydrology research summaries
[USGS-FP-800-B] 01 p0048 N73-10390
Utilization of ERTS-1 imagery for water depth measurement, mapping of Yellowstone Park, atmospheric effects in Colorado, lake ice surveillance, recreational land use, IFYGL Lake Ontario, image enhancement, water quality monitoring, and oil pollution detection
[E72-10201] 02 p0144 N73-11167
Utilization of ERTS-1 imagery for water depth measurement, mapping of Yellowstone Park, atmospheric effects in Colorado, lake ice surveillance, recreational land use, IFYGL Lake Ontario, image enhancement, water quality monitoring, oil pollution detection, and mapping iron compounds
[E72-10198] 02 p0160 N73-11296
Preparation of hydrologic atlases of arid land watersheds using ERTS-1 imagery of Wyoming, Utah, Montana, and New Mexico
[E72-10240] 03 p0288 N73-12340
Hydrological applications of side-looking radar, noting soil moisture, ground water, and water loss
03 p0295 N73-12407
Soviet research and development in meteorology and hydrology
[JPRS-57127] 04 p0442 N73-13602
Review of Soviet publication on development of hydrology in USSR
04 p0443 N73-13616
USSR developments in meteorology, weather forecasting, climate control, and hydrological forecasting
[JPRS-57608] 04 p0444 N73-13623
Soviet articles on microclimatology, agricultural meteorology, hydrology, and weather modification and forecasting
[JPRS-57652] 04 p0444 N73-13624
Possibility of water on planets, and origin and development of worlds
[JPRS-57709] 04 p0475 N73-13882
Use of resource indicators and remote sensing to plan and manage hydrologic and water resource systems
05 p0536 N73-14364
Fluvial environment of Arctic coastal plain in Northern Alaska
[AD-749150] 05 p0542 N73-14412
Fluvial environmental charts for Arctic coastal plain in Northern Alaska
[AD-749151] 05 p0542 N73-14413
Energy balance equations for parameterization of hydrological processes effecting atmospheric circulation
05 p0573 N73-14663
Summary of side-looking radar applications in earth resources noting basic principles of side-looking radar, radar scattering, data handling, and research and development
[ESRO-CR[P]-141] 06 p0641 N73-15200
Hydrological information from ERTS-1 imagery for design of highway drainage structure in Maine
[E73-10014] 06 p0659 N73-15350
Evaluation of ERTS-1 imagery for hydrological information in Sierra Nevada Mountains and Lake Ontario areas
[E73-10016] 06 p0659 N73-15352
Automated thematic mapping and interpretation of hydrologic and agricultural resources using ERTS-1 imagery
[E73-10023] 06 p0660 N73-15357
Time-lapse data processing of ERTS-1 imagery for dynamic hydrologic conditions
[E73-10035] 07 p0776 N73-16299
Analysis of ERTS-1 imagery for identification and discrimination of geological, hydrological, and mineral phenomena in western and central Colorado
[E73-10041] 07 p0776 N73-16304
ERTS-1 imagery of geology, agriculture, hydrology, and ecology of Niger River Delta, Republic of Mali
[E73-10047] 07 p0777 N73-16309
Geographical, physicomathematical, and hydrological engineering treatment of river runoff in USSR
[TT-70-50058] 07 p0781 N73-16346
Application of remote sensing from aircraft and spacecraft to geology, hydrology, and geographical data acquisition
07 p0782 N73-16354
Nimbus 3 and 4 observations of snow cover and hydrological features in Western Himalayas
07 p0787 N73-16403
Analysis of hydrologic conditions based on Nimbus satellite imagery
07 p0788 N73-16405
Hydrology of Sicilian Channel recorded onboard S.S. Dectra in 1969
07 p0858 N73-16958
Data collection and relay system for monitoring hydrologic conditions in south and central Florida
[E73-10092] 08 p0902 N73-17504
Utilization of ERTS-1 imagery for study of hydrology and limnology in Finland
[E73-10101] 09 p1020 N73-18323
Preparation of hydrologic atlases of arid land watersheds using ERTS-1 imagery
[E73-10318] 09 p1023 N73-18350
Meteorological and hydrological researCh over and in oceans
[JPRS-58025] 09 p1059 N73-18631
Articles on meteorology and hydrology
[JPRS-58133] 09 p1060 N73-18646
Utilization of ERTS-1 imagery to study watershed hydrology in Southern Great Plains
[E73-10359] 10 p1149 N73-19353
Analysis of ERTS-1 imagery using electronic satellite image analysis console to display and measure snowfield extent, glacier development, and hydrologic features
[E73-10415] 11 p1279 N73-20377
Analysis of ERTS-1 imagery for identification and discrimination of geological and hydrological phenomena in central and western Colorado
[E73-10422] 11 p1280 N73-20383
Identification of geologic and hydrologic features of Republic of Mali, West Africa using ERTS-1 imagery
[E73-10435] 11 p1281 N73-20395
Physical interpretation of geology, hydrology, and glaciology revealed by ERTS-1 imagery of east central Ohio
[E73-10454] 11 p1283 N73-20413
Evaluation of ERTS-1 data for hydrologic information in Sierra Nevada and Lake Ontario
[E73-10485] 12 p1396 N73-21322
Evaluation of hydrology and vegetation in Sahelian zone of Mali, Mauritania, and Senegal during dry season/drought period based on ERTS-1 imagery
[E73-10488] 12 p1396 N73-21324
Development of data relay network for monitoring hydrologic conditions collected for south and central Florida
[E73-10491] 12 p1397 N73-21327
USSR research projects in subjects of microclimate, agricultural meteorology, weather forecasting, climate control, and hydrological forecasting
[JPRS-58483] 12 p1420 N73-21510
ERTS-1 imagery of Iceland geology, geophysics, hydrology, oceanography, and agriculture
[E73-10535] 13 p1518 N73-22299
ERTS-1 imagery of suspended matter and hydrologic interfaces in Delaware Bay
[E73-10515] 14 p1653 N73-23409
Ecology, hydrology, geomorphology, and terrain modeling of Colorado mountain environments from ERTS-2 data
[E73-10551] 14 p1655 N73-23424
Broad scale application of ERTS-1 imagery to study and mapping of geological, hydrological, land use, rangelands, and soil cultures in Wyoming
[E73-10554] 14 p1655 N73-23426

Analytical procedures and correlation of hydrological data for predicting Upper Midwest watershed
[PB-214091/1] 14 p1664 N73-23505
IFYGL data for hydrologic analysis of Lake Ontario Basin
[E73-10571] 15 p1772 N73-24351
Time-lapse data processing for dynamic hydrologic conditions at Mt. Rainier, Washington
[E73-10582] 15 p1772 N73-24356
Automated thematic mapping and change detection of hydrological and agricultural resources from ERTS-1 imagery
[E73-10644] 16 p1897 N73-25341
Hydrological investigation of drainage basin characteristics from ERTS-1 imagery for improved regression estimates of water flow
[E73-10652] 16 p1898 N73-25348
ERTS-1 measurement of surface area of water bodies in Houston and Galveston, Texas area
[E73-10675] 16 p1900 N73-25370
Development of environmental indices covering land, water, and air quality compatible with ERTS-1 imagery for two test sites in Pennsylvania
[E73-10709] 16 p1904 N73-25400
Application of ERTS-1 remotely sensed data and ground truth information to predict and manage water quantity and quality in river basins
[E73-10689] 17 p2018 N73-26314
Analysis of time-lapse data processing for dynamic hydrologic conditions based on ERTS-1 imagery and aerial photography
[E73-10729] 17 p2020 N73-26335
Bibliography of references on urban hydrology
[PB-219105/4] 18 p2146 N73-27348
ERTS-1 imagery of Utah and Nevada to show structural geology, mineral exploration, limnology, and hydrology
[PAPER-G3] 19 p2263 N73-28235
Analysis of ERTS-1 MSS imagery to determine geologic, hydrologic, oceanographic, and agricultural phenomena in Iceland
[PAPER-G10] 19 p2264 N73-28241
ERTS-1 imagery of land use, agriculture, vegetation, geology, landforms, and hydrology in Central Coastal Zone of California
[PAPER-L4] 19 p2273 N73-28300
Analysis and enhancement of ERTS-1 hydrology imagery using electronic satellite image analysis console
[PAPER-I15] 19 p2279 N73-28336
Application of ERTS-1 imagery to analysis of suspended sediments and aquatic fronts in Delaware Bay
[PAPER-M3] 19 p2280 N73-28343
Comparison of conventional maps of southeastern Massachusetts to ERTS-1 imagery of coastal and submarine geology and hydrology
[PAPER-M18] 19 p2282 N73-28356
ERTS-1 imagery of desertification, hydrology, vegetation, forage, and water resources in Republic of Mali
[PAPER-R5] 19 p2283 N73-28363
ERTS-1 imagery of geology, agriculture, forestry, and hydrology in Iran
19 p2287 N73-28387
Application of ERTS-1 imagery for controlling quantity and quality of ground water resources
19 p2288 N73-28399
Identification and discrimination of geological and hydrological phenomena in central and western Colorado using ERTS-1 imagery
[E73-10837] 19 p2290 N73-28415
Application of ERTS-1 imagery to geologic, hydrologic, agricultural, botanical, and land use studies in Wyoming
[E73-10844] 19 p2291 N73-28422
Application of multispectral scanning to agriculture, oceanography, hydrology, and geology
[ERL/R-246] 19 p2294 N73-28450
Application of multispectral scanning to hydrology and water resources, noting measurement of soil moisture, water depth, and water quality
19 p2295 N73-28454
ERTS-1 imagery of snow cover, ice conditions, and soil moisture in Sierra Nevada Mountains and Lake Ontario Basin
[E73-10869] 20 p2393 N73-29220
Acquisition of land use, soil moisture, and hydrological data of Ontario, Canada and Syracuse, New York for Skylab-3
[E73-10888] 20 p2394 N73-29237
Geological, hydrological, ecological, and agricultural mapping of Botswana from ERTS-1 photography
[E73-10928] 20 p2399 N73-29277
Geology, hydrology, and ecology of Botswana from ERTS-1 MSS imagery
[E73-10929] 20 p2399 N73-29278
Hydrological and meteorological forecasting and climate control
[JPRS-59052] 20 p2446 N73-29647
Utilization of ERTS-1 imagery for studies of agriculture, forestry, cartography, geography, hydrology, meteorology, geology, and oceanography in Thailand
[E73-10996] 22 p2659 N73-31302
Analysis of geology, ecology, and hydrology of Colorado mountains from Skylab multispectral photography and data
[E73-11002] 22 p2659 N73-31307
ERTS-1 imagery of geology, botany, agriculture, hydrology, and cultural features of Wyoming
[E73-11022] 22 p2661 N73-31326
Mapping dynamic hydrologic conditions of surface water changes in south Florida
[E73-11028] 22 p2662 N73-31332
Hydrographic, chemical, and optical observations from Legs 4 and 5, YALOC-71 in vicinity of Panama Basin
[AD-763591] 22 p2669 N73-31386
Interdisciplinary analysis of Colorado Rocky Mountain environments using ADP techniques
[E73-11039] 23 p2778 N73-32218
Hydrology of prehistoric farming systems in central Arizona ecotone from Skylab EREP data
[E73-11044] 23 p2779 N73-32220
Identification and discrimination of geological, hydrological, and mineralogical phenomena in central and western Colorado from ERTS-1 data
[E73-11047] 23 p2779 N73-32223
Time lapse processing of dynamic hydrologic conditions
[E73-11054] 23 p2780 N73-32230
Application of ERTS-1 imagery to agriculture, forestry, meteorology, and hydrology in Thailand
[E73-11145] 24 p2918 N73-33299
Conference on hydrologic research in representative and experimental basins
24 p2947 N73-33538

**HYDROLYSIS**
Amino acids, urea, guanidine, glycocyamine, and 5-amino 4-imidazole carboxamidine from hydrolysis of azulmic acids
[NASA-TT-F-14640] 04 p0380 N73-13089
Hydrolytic stability of polyurethane potting compounds in Navy aircraft
[AD-759972] 17 p2053 N73-26604

**HYDROMAGNETIC FLOW**
U MAGNETOHYDRODYNAMIC FLOW

**HYDROMAGNETIC STABILITY**
U MAGNETOHYDRODYNAMIC STABILITY

**HYDROMAGNETIC WAVES**
U MAGNETOHYDRODYNAMIC WAVES

**HYDROMAGNETICS**
U MAGNETOHYDRODYNAMICS

**HYDROMAGNETISM**
U MAGNETOHYDRODYNAMICS

**HYDROMECHANICS**
NT ELASTOHYDRODYNAMICS
NT ELECTROHYDRODYNAMICS
NT HYDRODYNAMICS
NT HYDROSTATICS
NT MAGNETOHYDRODYNAMICS
Fluidic to hydromechanical interface for application to gas turbine engine control system
[AD-764368] 22 p2675 N73-31429
Analysis of water table simulation of transpirationally cooled nozzle, and formulation of two flow models of water table boundary layer
[NASA-TM-X-2884] 22 p2710 N73-31702

**HYDROMETEOROLOGY**
NT MARINE METEOROLOGY
Hydrometeorologic study of precipitation in Viroin basin; Belgium
[IRMB-PUBL-A-70-2] 01 p0047 N73-10381
Long-term tendencies in atmospheric circulation variations for deveoping long-range hydrometeorological forecasting
[NLL-M-22333-[5828.4F]] 01 p0072 N73-10592
Review of Soviet publication on navigational hydrometeorology
04 p0443 N73-13617
Quasi-analog computer proposed for Soviet hydrometeorological service for calculating nonsteady state motion of water in river channels
04 p0443 N73-13618
Experimental control of hydrometeorological factors for solution of agrometeorological problems
[JPRS-57637] 04 p0444 N73-13619
Extremes of precipitation aloft mandatory for design of military equipment capable of operating at altitude anywhere in world
[AD-747482] 04 p0445 N73-13629
Physical and hydrometeorological characteristics of Snowy Range Observatory, including precipitation, temperature, solar radiation, and wind data
[PB-211618] 05 p0524 N73-14268
Marine climatological summaries for Mediterranean and Southern Indian Ocean, including Australian waters
06 p0693 N73-15646
Small scale interaction between ocean and atmosphere [heat flow, vapor, and momentum]
[AD-751415] 07 p0796 N73-16474
Selected papers on hydrometeorology, oceanography, navigation
07 p0857 N73-16950
Development of automated hydrometeorological service and establishment of information-computation network for data recording
12 p1421 N73-21515
Hydrometeorological study of periodic precipitation variations over Lesse Basin, Belgium
[PUBL-SER-A-76] 12 p1423 N73-21530
Measurement of extreme rainfall intensites and associated liquid water content at altitude in tropical regions
[AD-756832] 13 p1554 N73-22593
On-site digital accumulation and storage of hydrometerological data for use in data acquisition systems
[PB-214185/1] 13 p1555 N73-22604
Precipitation scatter experiment to refine coordination procedures in frequency allocations for terrestrial and space services
[NASA-TM-X-66259] 16 p1875 N73-25175
Water balance, micrometeorology, thermal structure, and heat content of Great Lakes as determined by remote sensors during International Field Year
[IFYGL-BULL-4] 18 p2143 N73-27322
Analysis of epochal variations in atmospheric circulation of Northern Hemisphere, atmosphere, and hydrosphere for making long and extra long range hydrometeorological forecasts
20 p2444 N73-29635
Research in hydrometeorology and forecasting
[JPRS-59210] 20 p2447 N73-29662
Information retrieval system for hydrometeorology applications
20 p2448 N73-29666
Hydrometeorological characteristics for weather forecasting
20 p2448 N73-29668
Statistical procedures for hydrometeorological and weather forecasting and climate control
[JPRS-59580] 21 p2572 N73-30612
Statistical structure and automated monitoring of meteorological and hydrometeorological fields
21 p2573 N73-30623
Eastern Europe research projects involving hydrometeorology, semiconductor materials, microelectronics, and piezoelectronics
[JPRS-59617] 21 p2607 N73-30893
Meteorological services and technology of USSR
[JPRS-59962] 22 p2692 N73-31565
Prospects for development and growth of USSR hydrometeorological service
22 p2692 N73-31566
Technical equipment for large scale automation of USSR hydrometeorological service
[AD-763956] 22 p2696 N73-31593
Articles on meteorology and hydrology
[JPRS-60164] 24 p2946 N73-33530
Deficiencies in development of hydrometeorological science
24 p2947 N73-33536
Transient effects in pulse radar hydrometeor detection
24 p2956 N73-33616

**HYDROPHONES**
Development and characteristics of digital beamformer for narrowband sonar systems
[AD-745302] 01 p0029 N73-10224
Hydrophone measurement of acoustic propagation and CW signals from underwater explosions in shallow Bering Sea
[AD-745735] 01 p0081 N73-10667
Feasibility of mounting geophone arrays on pack ice to provide passive sonar system with improved signal to noise ratios over hydrophone arrays
[AD-747327] 02 p0143 N73-11161
Testing hydrophone types for acceleration response
[AD-748038] 03 p0338 N73-12758
Procedure for resolving directional ambiguities of line array of hydrophones
[AD-749939] 05 p0514 N73-14180
Estimation of noise directionality spectrum directly from cross-spectral matrix of received processes at hydrophone array elements
[AD-749940] 05 p0514 N73-14181
Minicomputer for digital measuring system for hydrophone calibration
[AD-749927] 05 p0549 N73-14461
Digital filter theory for broadband beamforming and hydrophone array steering
[AD-746206] 06 p0641 N73-15201
Sensitivity testing of hydrophones using Univac 1108 computer
[AD-754099] 11 p1262 N73-20244
Analysis of underwater sound signals to show coherence, noise level, and reverberation between vertically separated hydrophones
[AD-755696] 12 p1430 N73-21591
Metrology standards of underwater reference division
[AD-761147] 18 p2180 N73-27603

**HYDROPLANING**
Performance tests to determine cornering characteristics of cantilever aircraft tire on dry, damp, and flooded runway surfaces over range of yaw angles
[NASA-TN-D-7203] 12 p1363 N73-21058

**HYDROPOWER STATIONS**
U HYDROELECTRIC POWER STATIONS

**HYDROSPHERE [EARTH]**
U EARTH HYDROSPHERE

**HYDROSTATIC PRESSURE**
Effect of hydrostatic pressure on plasticity of L-62 copper-zinc brass and LS-59-1 brass
[NLL-NEL-TT-2398-[6075.461]]
02 p0185 N73-11497
Structural behavior of glass hulls under external hydrostatic and cyclic pressure
[AD-746878] 03 p0362 N73-12947
Hydrostatic pressure technique for improving dielectric properties of inorganic glasses used as capacitor materials
[AD-750393] 05 p0521 N73-14236
Deep sea calibration of transducers at elevated hydrostatic pressure
[AD-750666] 06 p0641 N73-15203
Hydrostatic pressure effects on mechanical behavior and properties of polymers
[AD-750731] 06 p0688 N73-15605
Comparison of methods for adapting hydrazine-oxygen fuel cells to cyclic pressure effects of hydrostatic pressure environment
[AD-753802] 10 p1112 N73-19062
Hydrostatic pressure studies of magnetic modes in far infrared
[COO-3151-12] 12 p1428 N73-21577
Effects of hydrostatic water bath pressure on capillary blood pressure and connective tissue dehydration
[NASA-TT-F-14894] 14 p1610 N73-23052
Measurement of deep ocean hydrostatic pressure fluctuations
[AD-757098] 15 p1783 N73-24458
Collocation method for numerical solution of buckling of conical shells under hydrostatic pressure
[AD-758834] 16 p1971 N73-25947
Design procedure for hydrostatic ring thrust bearings
[NRC-13180PT-3] 17 p2037 N73-26478
Analysis of fracture and creep properties of metals after extension under conditions of hydrostatic pressure as function of time
[NLL-NEL-TT-2475-[6075.461]]
20 p2429 N73-29515
Effect of high hydrostatic pressure on flow stress of 18-8 stainless steel
[NLL-NEL-TT-2458-[6075.461]]
20 p2430 N73-29516
Analysis of effects of hydrostatic pressure on yield stress, flow stress, and ductility of metals
[NLL-NEL-TT-2488-[6075.461]]
20 p2478 N73-29904
Effect of surface properties on tensile properties of beryllium under hydrostatic pressure
[NEL-537] 22 p2684 N73-31502
Influence of hydrostatic pressure on ductility and fracture mechanics of bismuth and tin-bismuth alloys
[AD-764241] 22 p2686 N73-31514
Inelastic buckling of deep spherical shell subject to uniformly distributed external pressure
[AD-764085] 22 p2726 N73-31815

**HYDROSTATICS**
Design of combined hydrostatic and dynamic bearings
[AD-752821] 09 p1040 N73-18479
Nomograph for calculating optimal working characteristics of hydrostatic sliding bearings
[AD-753553] 09 p1042 N73-18501
Hydrocompression treatment to lower residual stresses in weld joints of forge-welded carbon steel vessels
10 p1163 N73-19461
Design and construction of hydrostatic azimuth thrust bearing for tracking antenna of very large size
[NASA-CR-130930] 10 p1165 N73-19478
Development and revisions of mathematical theory of hydrostatic equilibrium for earth
[NASA-TM-X-66261] 16 p1906 N73-25415
Hydrostatic equilibrium models of ionization zone instability causing planetary nebulae
19 p2341 N73-28828
Comparison of normal and hydrostatic extruding processes under fluid pressure
[NLL-NEL-TT-2467-[6075.461]]
20 p2422 N73-29453

**HYDROTHERMAL CRYSTAL GROWTH**
Hydrothermal method for growing single crystal zircon polarizers
[AD-752147] 08 p0952 N73-17793

**HYDROX ENGINES**
U HYDROGEN OXYGEN ENGINES

**HYDROXIDES**
NT LITHIUM HYDROXIDES
NT POTASSIUM HYDROXIDES
NT SODIUM HYDROXIDES
Development of nickel hydroxide electrode for use in rechargeable alkaline batteries
[AD-746335] 01 p0007 N73-10058
Optimum conditions for depositing aluminum and silicon hydroxides on titanium dioxide particles
[NLL-RTS-7638] 04 p0425 N73-13460

**HYDROXYCORTICOSTEROID**
Time shift effects on human 17-hydroxy corticosteroid diurnal excretion noting transmeridian flights
[DLR-FB-73-58] 21 p2501 N73-30070
Fluorometric 11-hydroxycorticosteroid determination in human blood plasma
[NASA-TT-F-15092] 22 p2619 N73-30990

**HYDROXYL COMPOUNDS**
NT ALCOHOLS
NT BISPHENOLS
NT ETHYL ALCOHOL
NT GLYCOLS
NT ISOPROPYL ALCOHOL
NT METHYL ALCOHOLS
NT PHENOLS
Dielectric susceptibilities of potassium chloride to lithium and hydroxyl, sodium chloride to hydroxyl, and rubidium chloride to cyanides
[COO-3151-14] 10 p1200 N73-19763
Hydroxyl terminated polybutadience polymer for solid propellant binder
[AD-760579] 18 p2168 N73-27507
Hydroxyproline determination in collagen-like plasma and urine
[NASA-TT-F-15093] 22 p2620 N73-30997

**HYDROXYL EMISSION**
Synthesis of A to X bands of OH and a to X bands of O2 for studying electronic transitions, rational branch structure, and rotational transition probabilities
[DREV-TN-2012/72] 08 p0945 N73-17742
Searches for interstellar OH and other molecular emission and recombination lines in radio frequency range
[RR-108] 09 p1084 N73-18845
Analysis of ground and airborne hydroxyl emission observations in northern polar regions
[NASA-CR-130237] 15 p1777 N73-24408
Accurate positions of OH emission sources at 1665 and 1667 MHz
[AD-756086] 15 p1833 N73-24859
Photochemical reaction rate constant for hydroxyl radical with ozone in stratosphere
[AD-762195] 20 p2374 N73-29076

**HYGIENE**
Industrial hygiene, radiological health, and spacecraft sanitation studies in NASA Environmental Health Program
08 p0872 N73-17057
Survey of industrial hygiene and safety in Air Forces operations
[AD-751897] 08 p0880 N73-17126
Dermatological testing of personal hygiene cleansing agents and laundry detergents for possible use in Skylab Program
[NASA-CR-128880] 11 p1250 N73-20143
Data analysis for predicting human personal hygienic needs during long term space flight
[NASA-CR-128929] 15 p1743 N73-24132
Analysis of microclimate of living and service quarters during Tenth Soviet Antarctic Expedition
20 p2409 N73-29359

**HYGROMETERS**
NT PSYCHROMETERS
Airborne aluminum oxide hygrometer for water vapor measurements in atmosphere
[NASA-TM-X-70475] 23 p2792 N73-32341
Flight tests of cryogenically cooled hygrometer
[AD-764718] 23 p2794 N73-32354

**HYGROSCOPICITY**
Use of hygroscopic materials and ionic surfactants as warm fog for dispersants
[AD-751635] 07 p0817 N73-16622
Dry inert gas glove box for handling of hygroscopic and corrosive materials in spectroscopic and lasers experiments
[CRC-1244] 21 p2548 N73-30430

**HYPERBARIC CHAMBERS**
Studies concerning high pressure hyperexcitability in Squirrel Monkey
[AD-745779] 02 p0134 N73-11086
Annotated bibliography with preliminary analysis on dysbaric osteonecrosis
[AD-747258] 04 p0381 N73-13100
Metabolic implications in hyperbaric oxygen systems
[AD-749381] 05 p0504 N73-14106
Behavior of enzyme activities in blood plasma after breathing hyperbaric oxygen
[DLR-FB-71-96] 06 p0635 N73-15163
Ergometer to measure divers physiological hyperbaric stresses at all explorable depths
[AD-754401] 11 p1295 N73-20513
Hyperbaric chamber used to determine influence of increased ambient pressure and gas density on cardiac rate in man
[AD-755129] 13 p1487 N73-22058
Extreme aeroembolism case and successful therapy in hyperbaric chamber
19 p2227 N73-27959
Influence of He, N2, and N2O environments on physiological parameters of rats
20 p2365 N73-29019
Muscle force transducer to detect tremors in divers under hyperbaric conditions
[AD-763343] 23 p2750 N73-32010

**HYPERBOLIC COORDINATES**
Spatial grid method for solving hyperbolic equations for signal propagation on three wire transmission line
[UCRL-73796] 07 p0764 N73-16209
Navigation with hyperbolic coordinates, and coordinate transformation to geographic and grid coordinates
[SER-C/DISS-176] 10 p1185 N73-19647

**HYPERBOLIC FUNCTIONS**
Convergence, accuracy, and stability of finite element approximations of class of nonlinear hyperbolic equations
[AD-754948] 11 p1312 N73-20646

**HYPERBOLIC NAVIGATION**
NT LORAN
NT LORAN C
NT LORAN D
Composite signals for lane identification in Omega
[AD-746503] 02 p0208 N73-11686
Development, characteristics, and evaluation of electronic distance measuring instrument
[AD-746017] 02 p0208 N73-11690
Navigation with hyperbolic coordinates, and coordinate transformation to geographic and grid coordinates
[SER-C/DISS-176] 10 p1185 N73-19647
Optimization of integrated navigation systems combining several independent navigation sensors to provide self-contained aircraft navigation capability
11 p1317 N73-20694
Proceedings of conference on precise time and time interval planaing for application to hypersonic navigation systems
[AD-758739] 16 p1942 N73-25717
Effects of polar cap absorption events on performance of Omega navigation system operating in high latitudes
[AD-759009] 16 p1942 N73-25718

**HYPERBOLIC REENTRY**
Radiative coupled viscous flow past ablating blunt body at hyperbolic entry conditions
[NASA-CR-2236] 11 p1347 N73-20934

**HYPERBOLIC SPACE**
U HYPERBOLIC COORDINATES

**HYPERBOLIC SYSTEMS**
CDC 6600 computer analysis of numerical stabilizer effects on computing time for second order accurate schemes
[AD-753165] 09 p1018 N73-18308
Development of radio locating system for monitoring geographic movement of surface vehicles in metropolitan area using unsynchronized radio broadcasting stations
[NASA-CASE-NPO-13217-1] 17 p1997 N73-26144

**HYPERBOLIC TRAJECTORIES**
Use of aerodynamic drag for transfer from hyperbolic trajectories to satellite orbits noting spacecraft guidance
[D-149] 05 p0596 N73-14849

**HYPERCAPNIA**
Effect of acute and chronic hypercapnia on Ca and inorganic P levels in guinea pig blood plasma and erythrocytes
[AD-749323] 13 p1484 N73-22035
Toxicological aspects of carbon dioxide exposure in chronic hypercapnia
[AD-763394] 22 p2621 N73-31005

**HYPERFINE STRUCTURE**
Hyperfine electron density fluctuation in stabilized hydrogen arc laser
08 p0943 N73-17723
Structures of ionized vanadium and manganese atoms with incomplete shells considering spin-orbital and spin-spin interactions
[NLL-RTS-7856] 18 p2180 N73-27604
Mossbauer absorption spectra of iron 57 in single crystal of potassium iron fluoride
[AD-764635] 23 p2827 N73-32597
Monte Carlo method for fitting iron 57 Mossbauer spectra
[AD-764634] 23 p2828 N73-32602

**HYPERGOLIC ROCKET PROPELLANTS**
Pulse performance data for small monopropellant and hypergolic bipropellant rocket engines
03 p0349 N73-12846
Asymptotic analysis of radiant and hypergolic ignition of solid propellant undergoing exothermic heterogeneous Arrphenius reaction with gaseous oxidizer
[AD-751303] 07 p0856 N73-16939
Underwater ignition of hypergolic rocket propellants as function of injection system, fuel combustions, water depth, and salinity
[DLR-MITT-73-07] 16 p1954 N73-25813
Analysis of ignition properties of hypergolic fluids under low pressure conditions to determine relations of time, temperature, and thermodynamic properties
21 p2605 N73-30878

**HYPEROXIA**
Effects of hyperoxia on sulfhydryl concentration of Escherichia coli
[AD-746193] 02 p0134 N73-11087
Hyperoxia effects on elimination of carbon monoxide, ammonia, ketones, and aldehydes by rats
03 p0256 N73-12077

Hyperoxic damage in animal cells, tissues, and organs
10 p1115 N73-19091
Hyperoxic morphological changes in connective rat tissues
10 p1115 N73-19092
Effect of hypoxia and hyperoxia on rate of blood deoxygenation, and influence of antioxidants in mice
11 p1244 N73-20096
Hyperoxic atmosphere effect on rat metabolism and elimination of gaseous wastes
13 p1481 N73-22004
Biophysical properties of human red blood cells exposed to hypobaric hyperoxia
[AD-755783] 14 p1612 N73-23072
Effects of hyperoxia on heme biosynthesis
[AD-756836] 15 p1742 N73-24125
Mechanisms of oxygen toxicity at cellular level
[AD-758725] 16 p1868 N73-25124
Epinephrine oxidation and indole production during high pressure oxygen poisoning
[AD-759405] 18 p2110 N73-27061
Effects of oxygen pressure on tissues under extreme flight factors
[NASA-TT-F-762] 21 p2500 N73-30065
Course of infectious process and functional activity of pulmonary macrophages in mice confined to atmosphere with high oxygen content
24 p2882 N73-33016
Mechanism of inert gas narcosis in human body and mice
[NASA-CR-62096] 24 p2885 N73-33038

**HYPERSONIC AIRCRAFT**
NT X-20 AIRCRAFT
Design analysis and fabrication of hypersonic wing test structure
[NASA-CR-127490] 24 p2988 N73-33883

**HYPERSONIC BOUNDARY LAYER**
Hypersonic axisymmetric turbulent boundary layer compression in adverse pressure gradient along cylindrical axisymmetric body
[NASA-CR-112247] 07 p0770 N73-16253
Mathematical model for wall cooling in laminar hypersonic boundary layer
07 p0770 N73-16258
Normal pressure gradients in hypersonic boundary layers, including systematic derivation of equations of motion and energy equations
07 p0771 N73-16259
Energy transfer in laminar hypersonic boundary layers by hydrogen combustion
07 p0771 N73-16260
Finite difference solution for merged layer regime of hypersonic flat plate leading edge problem
08 p0895 N73-17243
Wind tunnel tests to determine flow distribution within model passages of hypersonic inlets for core flow and boundary layer flow conditions
[NASA-TN-D-7150] 13 p1470 N73-21905
High enthalpy hypersonic bounary layer flow
[NASA-CR-135479] 23 p2774 N73-32187

**HYPERSONIC FLIGHT**
Wake transition of blunt cones in hypersonic flight using schlieren photography and opto-electronic laser system
[ISL-12/72] 03 p0310 N73-12531
Aerodynamic heating of supersonic models due to shock wave impingement
[AD-749946] 06 p0655 N73-15324
Finite difference calculations of laminar flow past blunt-nosed cone with spherical after body injecting mass into air
[AD-758009] 15 p1844 N73-24943
Three dimensional effects on slot cooling in hypersonic flight
[AD-762624] 20 p2388 N73-29189

**HYPERSONIC FLOW**
Wind tunnel tests of space shuttle models to determine effects of body and wing geometry on hypersonic shock structure and on surface impingement of interior flow field shock waves
[NASA-CR-128587] 01 p0040 N73-10317
Boundary layer control under hypersonic flow conditions using tangential injection of gas
[NASA-TT-F-13927] 01 p0041 N73-10320
Inverse method for calculating hypersonic flow shock layer around axisymmetrical two-dimensional blunt bodies
[ISL-42/71] 01 p0041 N73-10325
Development of finite difference techniques for computing static pressure distribution downstream of strong shock wave using navier-Stokes equation
[AD-747978] 03 p0286 N73-12318
Modification of Navier-Stokes equation for hypersonic compressible flow to eliminate need for specifying far field and/or boundary condition parameters
[AD-747644] 03 p0287 N73-12321
Contour of wave drag optimized bodies of revolution as function of Mach number in hypersonic flow
[DGLR-PAPER-72-108] 04 p0369 N73-13003
Explicit difference method for steady two dimensional or axisymmetric hypersonic flow
[DGLR-PAPER-72-66] 04 p0405 N73-13303
Mapping electron number density distribution in nonequilibrium shock layer with kinetic and radiative processes coupled to gas dynamics
[AD-748833] 04 p0407 N73-13312
Ion-current collection by flush-mounted electrostatic probes on sharp flat plate in ionized hypersonic flow
[SC-CR-72-3145] 04 p0422 N73-13440
Laminar, transitional, and turbulent heat transfer measurements on yawed blunt conical nosetip in free stream Mach 5
[AD-748292] 04 p0486 N73-13967
Aerodynamic drag of series of spherically-blunted conical bodies with three classes of half-vertex angles under hypersonic flow conditions
[NAL-TR-280] 06 p0613 N73-14978
Design and system description of hypersonic low density wind tunnel in Germany including generation of molecular beams
[DLR-FB-71-84] 06 p0650 N73-15279
Hypersonic air flow effects on aerodynamic characteristics of elliptical cones at large angles of attack
[AD-749738] 06 p0657 N73-15335
Laminar and turbulent boundary layers, including hypersonic flow, wall flow and stagnation area
[DLR-MITT-71-13] 07 p0770 N73-16256
Measured maximal laminar heat transfer on cone with spherical nose in hot hypersonic flow
07 p0771 N73-16263
Mass spectrometer for investigating hypersonic air flows in shock tube for application to reentry body problems
[BMVG-FBWT-72-20] 07 p0801 N73-16505
Analog computer study of hypersonic laminar heat transfer
[AD-752022] 08 p0898 N73-17269
Measurement of aerodynamic drag of conical bodies at zero angle of attack in free molecular and near free molecular flow regime
[DLR-FB-72-64] 09 p1014 N73-18278
Development of electrically driven shock tube for generation of high velocity shock waves and analysis of physical properties of shock waves
[AREAEE-149] 12 p1388 N73-21258
Meksyn asymptotic integration method for studying viscous interaction within hypersonic rarefied gas flow regime
12 p1389 N73-21263
Theoretical and experimental studies on microwave transmission through hypersonic air plasma generated about blunt wedge
[SC-CR-72-3164] 12 p1434 N73-21621
Wind tunnel tests to determine flow distribution within model passages of hypersonic inlets for core flow and boundary layer flow conditions
[NASA-TN-D-7150] 13 p1470 N73-21905
Finite difference solution to right angle circular cone streamline swallowing phenomenon during supersonic and hypersonic flow
13 p1508 N73-22218
Compressible laminar boundary layer on cone near plane of symmetry and stagnation point boundary layer with hydrogen injection
13 p1509 N73-22228
Analysis of accuracy of Preston tube calibration equations to determine local skin friction in two dimensional supersonic and low hypersonic flow conditions
[NASA-TN-D-7190] 13 p1510 N73-22239
Research projects on hypersonic and rarefied gas flows, separated and reattached wakes, viscous flow, and laminar and turbulent boundary layers with strong blowing
[AD-755276] 13 p1512 N73-22249
Drag and stability characteristics of hypersonic blunt nosed conical bodies in gas mixtures
[NASA-CR-131986] 14 p1599 N73-22962
Analysis of viscous hypersonic flow around slender sharp wedges and unyawed cones
[AD-757037] 14 p1650 N73-23386
Viscous shock layer in hypersonic flow of perfect gas past axisymmetric blunt nosed body
15 p1764 N73-24297
Semiempirical solution of six types of shock interference heating in hypersonic flows
[NASA-TN-D-7139] 16 p1888 N73-25283
Computer programs for predicting supersonic and hypersonic interference flow fields and heating
[NASA-TM-X-2725] 16 p1889 N73-25285
Technique for measuring hypersonic flow velocity profiles
[NASA-TN-D-7270] 17 p2032 N73-26443
Application of holography techniques for recording three dimensional flow distribution of liquid jet injected into Mach 3 gas stream
17 p2039 N73-26498
Analysis of characteristics of supersonic flow of helium around right circular cones at zero angle of attack and Mach numbers from 1.5 to 30.0
[NASA-SP-3078] 18 p2130 N73-27208
Interaction of hypersonic source flow and axisymmetric free jet with rarefied background as examined by equations of motion
[AD-761149] 18 p2131 N73-27218
Numerical analysis of hypersonic rarefied flow past sharp leading edge of flat plate using finite difference solution of Navier-Stokes equation
19 p2251 N73-28147
Analysis of steady hypersonic flow with viscous interaction over sharp slender wedge by finite difference scheme
20 p2387 N73-29177
Effect of wall cooling on shock wave laminar boundary layer interactions in hypersonic two dimensional flow
[AD-762937] 20 p2389 N73-29192
Analysis of surface pressure and cold wall heating rate distributions for large, flat panel at Mach 7 in high temperature wind tunnel
[NASA-TN-D-7275] 21 p2524 N73-30243
Experimental data analysis for sonic injection of hydrogen from backward facing step in parallel direction to main supersonic stream
[NASA-TM-X-2828] 22 p2728 N73-31828
Static pressure and heat transfer rate distributions on conical bodies at hypersonic speeds laminar and turbulent flow conditions
[AD-764983] 23 p2777 N73-32204
Flow characteristics of merged layer regime in hypersonic, low density flow past semi-infinite sharp cone
24 p2903 N73-33168

**HYPERSONIC GLIDERS**
NT X-20 AIRCRAFT

**HYPERSONIC HEAT TRANSFER**
Laminar surface heat transfer distribution about cones at hypersonic speeds
[AD-754056] 11 p1349 N73-20946

**HYPERSONIC INLETS**
Turbulent, transitional, and laminar film cooling of air breathing engine inlet at hypersonic speed noting heat transfer rate measurement
[IC-AERO-72-15] 01 p0041 N73-10323
Systems for controlling boundary layer in hypersonic air intakes
[AD-750513] 06 p0715 N73-15834

**HYPERSONIC NOZZLES**
Calibration of flow in working section of hypersonic blowdown wind tunnel to include test equipment required and techniques used
[ARA-30] 08 p0892 N73-17225

**HYPERSONIC REENTRY**
Force measurements on caret and delta wings at high incidence in hypersonic reentry conditions noting comparison with theoretical predictions
[IC-AERO-72-16] 01 p0001 N73-10004

**HYPERSONIC SHOCK**
Analysis of sonic boom pressure signatures recorded during reentry of Apollo 15 command module and correlation with wind tunnel signatures
[NASA-TM-X-62111] 04 p0371 N73-13016

**HYPERSONIC SPEED**
Accuracy of transitional boundary layer theory in low hypersonic Mach number range
[NASA-CR-2131] 01 p0041 N73-10322
Analysis of surface flow, pressures, and heat transfer on two conical delta wings at hypersonic speed and various angles of attack
[NASA-TM-X-2668] 02 p0156 N73-11268
Analysis of shock interaction and interference heating on military aerospace vehicles at hypersonic speeds
[AD-747765] 03 p0286 N73-12319
Guidance method for transition of space shuttle from hypersonic entry to subsonic cruise flight
[NASA-CR-128648] 03 p0357 N73-12905
Wind tunnel tests to determine pressure distribution on Apollo command module and Saturn launch vehicle at supersonic and hypersonic speeds
[NASA-TM-X-62117] 04 p0477 N73-13904
Wind tunnel tests to determine effects of hypersonic flow interaction on thrustor nozzle configurations and procedures to prevent excess heating
[NASA-CR-129914] 05 p0597 N73-14857
Wind tunnel tests to determine heat transfer and pressure distributions of hemisphere cylinders in hypersonic flow environment
[NASA-TN-D-7104] 05 p0605 N73-14925
Flow characteristics around semi-infinite plate with sharp leading edge inserted in hypersonic uniform air stream
[NAL-TR-289T] 06 p0613 N73-14979
Fabrication and evaluation of cooled-gas pyrometer for application in hypersonic research engine program
[NASA-TM-X-2715] 07 p0800 N73-16496
Effects of nozzle orientation and configuration on roll control and base pressure of hypersonic reentry vehicle
[SC-DC-72-1187-A] 07 p0849 N73-16884
Wind tunnel tests of space shuttle orbiter scale model to determine aerodynamic characteristics at hypersonic speed in various configurations
[NASA-CR-128754] 12 p1461 N73-21838
Generation of high temperature, high mass flow, and high Reynolds number air at hypersonic speeds
[NASA-CASE-LAR-10578-1] 16 p1886 N73-25262

Numerical analysis of nonstationary three dimensional motion of reentry vehicles entering atmosphere at hypersonic speeds
16 p1965 N73-25897
Effects of addition and position of outboard stabilizers and tail configurations on aerodynamic characteristics of low-wave-drag elliptical body at hypersonic speed
[NASA-TM-X-2747] 18 p2101 N73-26993
Aerodynamic characteristics of two space shuttle concepts with delta wing configurations at hypersonic speed using helium flow visualization technique
[NASA-TN-D-7282] 18 p2102 N73-26997
Apparatus and method for generating large mass flow of high temperature air at hypersonic speeds
[NASA-CASE-LAR-10612-1] 19 p2250 N73-28144
Procedure for evaluating relative economic value of technology factors affecting design, configuration, and operation of hypersonic cruise transport
[NASA-CR-2286] 23 p2743 N73-31953
Incipient boundary layer separation on axisymmetric compression surfaces of conical body at hypersonic speeds
23 p2775 N73-32195
Characteristics of laminar and turbulent wakes of spherical bodies at hypersonic speed in nitrogen atmosphere
[DREV-R-683/72] 24 p2904 N73-33178

**HYPERSONIC TEST APPARATUS**
Hypersonic and hyperthermic test apparatus for hypersonic vehicle aerodynamic investigations
[VTH-170] 09 p1011 N73-18255

**HYPERSONIC VEHICLES**
NT HYPERSONIC AIRCRAFT
NT LIFTING REENTRY VEHICLES
NT X-20 AIRCRAFT
Wind tunnel determination of supersonic aerodynamic characteristics of variable geometry spacecraft designed for high hypersonic performance
[NASA-TM-X-2703] 07 p0735 N73-15985
Electron density distribution in viscous flows as applied to Trailblazer 2 reentry vehicle
[AD-755397] 13 p1564 N73-22674
Ion probes used to determine structure of ionized turbulent wakes of hypersonic spheres
[AD-759157] 17 p2090 N73-26908
Computerized design of variable feedback system for attitude control of hypersonic vehicle
[AD-761493] 19 p2221 N73-27916

**HYPERSONIC WAKES**
Measured and calculated mean flow characteristics of two-dimensional, hypersonic, turbulent wakes produced by wedges
[NASA-TN-D-6927] 01 p0040 N73-10316
Reliability analysis of Abel transformation algorithm applied to mass measurement in hypersonic wakes
[ISL-21/70] 01 p0041 N73-10324
Wake transition of blunt cones in hypersonic flight using schlieren photography and opto-electronic laser system
[ISL-12/72] 03 p0310 N73-12531
Mapping velocity field in hypersonic wake by use of iron probe array
[AD-751450] 08 p0897 N73-17264
Development of numerical model of eddy diffusive transport of emitted gases from space shuttle wake to show chemical reactions between emitted gases and ambient atmosphere
[NASA-TM-X-66215] 11 p1287 N73-20440
Cooled film anemometry applied to determination of temperature and velocity distributions in wake of projectiles travelling at hypersonic speeds in free flight range
[DREV-R-648/72] 14 p1648 N73-23365
Electron density determination in thermodynamic equilibrium behind reflected shock wave in air, using microwave reflectometer in shock tube
[ISL-43/71] 16 p1889 N73-25288
Ion density measurements in wake of hypersonic sphere
[AD-759158] 17 p2090 N73-26909
Growth characteristics of hypersonic turbulent wakes with spatially resolved measurements
[DREV-R-687/73] 24 p2869 N73-32925

**HYPERSONIC WIND TUNNELS**
NT CASCADE WIND TUNNELS
NT PLASMA JET WIND TUNNELS
NT SHOCK TUNNELS
Analysis of supersaturation conditions in Mach 7.5 wind tunnel in expansion region of nozzle and technique for visualization of shock waves and shear layers
[ARL/A-139] 14 p1648 N73-23367
Hypersonic wind tunnel tests of air breathing engines
23 p2770 N73-32158

**HYPERTENSION**
Circadian rhythm change study of transmeridian flight and medication effects on mildly hypertensive subject
[AD-743300] 01 p0011 N73-10090
Arterial hypertension symptoms in flying personnel
13 p1480 N73-21991

**HYPERTHERMIA**
Change in content of gases in blood when man is exposed to high ambient temperatures
11 p1245 N73-20105

**HYPERTONIA**
U OSMOSIS

**HYPERVELOCITY ACCELERATORS**
U HYPERVELOCITY GUNS

**HYPERVELOCITY CRATERING**
U HYPERVELOCITY PROJECTILES
U PROJECTILE CRATERING

**HYPERVELOCITY GUNS**
Improved version of modified machine gun for use as combustion stability rating device with various rocket combustors
[NASA-TM-X-2792] 15 p1842 N73-24928
Free-flight tests on space shuttle and reentry vehicle models in hypervelocity gun tunnels
[DLR-FB-72-41] 21 p2522 N73-30224
Collapsible piston for hypervelocity gun
[NASA-CASE-MSC-13789-1] 23 p2769 N73-32152

**HYPERVELOCITY IMPACT**
Scaling hypervelocity impact of glass projectiles on aluminum targets
[ISL-24/70] 01 p0036 N73-10285
Multimaterial lamination as means of retarding penetration and spallation failures in plates from hypervelocity impact
[NASA-TN-D-6989] 02 p0238 N73-11934
Hypervelocity impact tests of Skylab electrical cables for simulation of micrometeoroid environment
[NASA-TN-D-7178] 07 p0761 N73-16186
Errors in streak photography measurements caused by subject and camera misalignment
[AD-751185] 07 p0802 N73-16513
Exploding wire plasma accelerator simulating hypervelocity micrometeoritic damage at impact
[ISL-26/71] 07 p0821 N73-16657
Hypervelocity projectile cratering at mirror glass coating impact
[ONERA-NT-01-14-72] 07 p0822 N73-16659
Impact damage caused by polystyrene, aluminum, or iron hypervelocity particles on glass
08 p0934 N73-17651
Hypervelocity meteoritic impact resulting in structural damage of orbital space stations
[NASA-CR-124241] 14 p1705 N73-23841
Meteoroid impact resistance of bumper protected laminated spacecraft mainwalls
[NASA-CR-2262] 14 p1714 N73-23909
Experimental determination of erosion rebound characteristics of high speed particles impacting stationary target for application to gas turbine engines operating in dusty environment
[AD-760578] 18 p2194 N73-27711
Analysis of threshold penetration of spherical projectiles impacting aluminum single wall targets at hypervelocity speeds
[NASA-TN-D-7308] 21 p2603 N73-30865

**HYPERVELOCITY LAUNCHERS**
Structural design of implosion-driven hypervelocity launchers
[AD-742993] 03 p0281 N73-12280
Techniques for reduction of damage to models caused by launching accelerations in hypervelocity launcher
[AD-752554] 08 p0893 N73-17232
Cylindrical impact technique for second-stage augmentation with explosively driven hypervelocity launcher
[NASA-CR-114589] 12 p1388 N73-21252

**HYPERVELOCITY PROJECTILES**
Performance characteristics and prediction methods for hypervelocity light gas gun
[NASA-CR-129292] 03 p0300 N73-12450
Development and test of explosively driven two-stage hypervelocity rocket launcher for use in meteoroid studies
[NASA-CR-2143] 06 p0649 N73-15272
Optical measuring instruments used at hypervelocity ballistic range facility
[AD-750866] 06 p0651 N73-15284
Hypervelocity projectile cratering at mirror glass coating impact
[ONERA-NT-01-14-72] 07 p0822 N73-16659
Techniques and equipment for field photography of artillery projectiles in flight
[LA-5030] 12 p1405 N73-21396
Amplitudes and widths of Gaussian distributions of electron density in wakes of hypervelocity projectiles flown in air and nitrogen at various pressures
[AD-759065] 16 p1893 N73-25316
Analysis of threshold penetration of spherical projectiles impacting aluminum single wall targets at hypervelocity speeds
[NASA-TN-D-7308] 21 p2603 N73-30865

**HYPERVELOCITY WIND TUNNELS**
NT CASCADE WIND TUNNELS
NT PLASMA JET WIND TUNNELS
NT SHOCK TUNNELS
Hypervelocity wind tunnel tests of aerothermal characteristics of winged space shuttle booster model
[NASA-TM-X-2642] 01 p0109 N73-10895
Calibration tests of Lewis hypersonic tunnel facility at Mach 5,6, and 7
[NASA-TN-D-7100] 02 p0153 N73-11237
Nonequilibrium effects caused by vibrational freezing in hypervelocity wind tunnel
[VKI-TN-83] 03 p0248 N73-12009
Safety devices for preventing surge tank explosions in liquid nitrogen system of hypersonic wind tunnels
[SC-DC-72-1260] 03 p0280 N73-12274
Aerodynamic design of Mach 8 contoured nozzle for hypervelocity wind tunnel
[AD-747477] 03 p0281 N73-12278
Ballistic tube for drag measurement on firing models into oncoming supersonic flow
[AD-749839] 05 p0525 N73-14271
Transonic and hypersonic wind tunnels in Germany
[DLR-FB-71-86] 06 p0650 N73-15278
Development of ceramic materials for construction of full scale, high pressure, hypersonic facility for testing aircraft and missile models
[AD-751298] 07 p0812 N73-16588
Calibration of flow in working section of hypersonic blowdown wind tunnel to include test equipment required and techniques used
[ARA-30] 08 p0892 N73-17225
Application of dual-scatter laser velocimeter to measure particle velocity distribution in hypersonic dust erosion facility
[AD-752225] 08 p0930 N73-17618
Carbon dioxide laser for heating hypersonic wind tunnel flow
[AD-761506] 19 p2249 N73-28134
Analysis of surface pressure and cold wall heating rate distributions for large, flat panel at Mach 7 in high temperature wind tunnel
[NASA-TN-D-7275] 21 p2524 N73-30243

**HYPERVOLEMIA**
Renin-angiotension system in simulated hypervolemia induced by immersion
[NASA-TT-F-14885] 13 p1484 N73-22036

**HYPOBARIC ATMOSPHERES**
Human and male Charles River rat exposures to Halon 1301 under hypobaric conditions, simulating aircraft compartment
[AD-747958] 03 p0260 N73-12106
Low barometric pressure effects on human thermoregulation function
13 p1480 N73-21996
Biophysical properties of human red blood cells exposed to hypobaric hyperoxia
[AD-755783] 14 p1612 N73-23072
Respiratory function and blood acid base equilibrium in human adaptation to high altitude environment
20 p2366 N73-29030

**HYPODYNAMIA**
Effect of prolonged hypodynamia on rat biology
07 p0744 N73-16050
Medical and biological problems of manned space flight
[NASA-TT-F-719] 10 p1114 N73-19077
Weightlessness and hypodynamia effects on bodily functions during space flight
10 p1114 N73-19078
Hypodynamia effect on human transverse acceleration tolerance
10 p1114 N73-19083
Human hydroxycorticosteroid and aldosterone excretions during hypodynamic space flight conditions
20 p2367 N73-29031

**HYPOGLYCEMIA**
Liquid retention in chlorpropamide therapy and water intoxication of patients
[NASA-TT-F-14597] 02 p0133 N73-11077

**HYPOKINESIA**
Effect of hypokinesis of varying duration on fluid-electrolyte metabolism and composition in blood and tissues of animals
11 p1244 N73-20098
State of hemocoagulation and thrombocytes during hypokinesia after adaptation to high-mountain conditions
11 p1245 N73-20107
Latent coronary insufficiency detection in flying personnel using barochamber loading
13 p1480 N73-21988
Dystrophic degeneration of suprarenal rat cortex during hypokinesia
13 p1481 N73-22003
Hypokinetic disturbances of rats after exposure to carbon monoxide
13 p1481 N73-22007
Long term hypokinesia effect on rats hemodynamic system
14 p1607 N73-23026
Long term hypokinesia effect on protein and nucleic acid content in rat tissue
14 p1607 N73-23027
Depressing effect of hypokinesia on rat skeletal muscle functions
14 p1607 N73-23028
Atrophy and metabolic changes in internal organs and skeletal muscles of rats exposed to hypokinesia
14 p1607 N73-23029

Tolerance of hypokinetic rats to carbon monoxide exposure
14 p1609 N73-23043
Blood supply to skeletal muscles of rats during hypokinesia
24 p2882 N73-33018
Fluid-electrolyte balance during 120-day bed rest
24 p2883 N73-33028
Elimination of creatinine in urine during prolonged hypokinesia
24 p2884 N73-33029
Human skin reactions to lotions and distilled water during hypokinesia
24 p2884 N73-33034
Using lower body negative pressure to prevent decrease in volume of circulating plasma during hypokinesia
24 p2885 N73-33036
Functional disturbances during hypokinesia in man
[NASA-TT-F-15148] 24 p2890 N73-33073

**HYPOTHALAMUS**
Hypothalamus as internal heat regulator for warm-blooded animals
[NASA-TT-F-15138] 23 p2749 N73-32002

**HYPOTHERMIA**
Hypothermy effects on drug actions in physiological rabbit functions
11 p1240 N73-20064
Dynamics of nitrogenous cerebral metabolites accompanying repeated hypothermia and subsequent self-heating
11 p1244 N73-20097

**HYPOXEMIA**
Analysis of arterial hypoxemia caused by pulmonary malfunctions and regulation of oxygen during exercise and rest
[AD-746979] 04 p0380 N73-13092
Human adaptation to hypoxic hypoxia for increased resistance to physical stress
10 p1116 N73-19095
Human arterial elasticity during breathing of reduced partial oxygen atmosphere
13 p1480 N73-21987

**HYPOXIA**
Simulated high altitude determination of interrelation of systematic and cellular responses to acute and chronic hypoxia
[AD-743536] 01 p0010 N73-10081
Hypoxia stress effects on human operator performance in unstable tracking task using manual control
01 p0018 N73-10138
Hypoxia effects on human gastric motor functions in pressure chamber experiments using electrogastrography
03 p0257 N73-12085
Hypoxia effects on human vestibular tolerance during exposure to coriolis accelerations
03 p0258 N73-12092
Oxygen content and hydrogen ion concentration in monkey blood after incapacitating ionizing radiation dosage
[AD-750681] 06 p0632 N73-15134
Thermoregulation reactions of rats in hypoxic atmosphere with nitrogen and helium dilution
07 p0743 N73-16046
Effects of hypoxia and acceleration stresses on enzyme activities in erythrocytes and blood plasma
[DLR-FB-72-71] 07 p0746 N73-16070
Medical and biological problems of manned space flight
[NASA-TT-F-719] 10 p1114 N73-19077
Hypoxia adaptation of rats for increased resistance to toxic atmospheric gases
10 p1116 N73-19100
Composition and effects of radioprotectors on acceleration tolerance, hypoxia toxicity, radiation protection, and dynamic space flight stress in animals
[NASA-TT-F-721] 11 p1239 N73-20054
Hypoxia and reduced acceleration tolerance of rats after injection of cysteamine radioprotector
11 p1239 N73-20058
Pathophysiological response reactions of rats to acute hypoxia after injection of cysteamine and aminothiol group radioprotector
11 p1239 N73-20059
X ray effect on animal resistance to anoxic, anemic, and histotoxic hypoxia
11 p1243 N73-20087
Effect of hypoxia and hyperoxia on rate of blood deoxygenation, and influence of antioxidants in mice
11 p1244 N73-20096
Dynamics of some characteristics of induced potential of optical region in cerebral cortex in rabbits with increasing hypoxia
11 p1244 N73-20103
Human adaptation to hypoxia and tolerance of high environmental temperatures
[NASA-TT-F-14860] 11 p1247 N73-20122
High altitude acclimatization effects on mice and rabbit tolerances to hypoxia, acceleration, and high temperature
[NASA-TT-F-14861] 11 p1247 N73-20123
Myocardial changes in flying personnel exposed to hypoxic hypoxia
13 p1479 N73-21985
Cardiac systole kinematics in humans exposed to hypoxic atmosphere
13 p1479 N73-21986
Evoked compensatory reflex reactions of rabbit ocular and eyelid muscles during hypoxia
13 p1480 N73-21992
Hemoglobin and erythrocyte increase in rat adaptation to hypoxic hypoxia
13 p1481 N73-22005
Altitude acclimatization period effects on rat resistance to hypoxia
13 p1481 N73-22006
Nutrient protein intake of rats and tolerance to acute hypoxia
14 p1608 N73-23035
Acceleration effects on human visual functions under hypoxic conditions
14 p1609 N73-23040
Cardiopulmonary adaptations of man to moderately high altitude
[AD-755192] 14 p1613 N73-23075
Hypoxia effects on release of gaseous wastes from rat vital functions
20 p2366 N73-29025
Role of respiratory enzymes on human adaptation to hypoxia
[NASA-TT-F-15058] 21 p2500 N73-30060
State of blood filling and bioelectric activity of grain in circulatory hypoxia in healthy persons and individuals with early forms of autonomic vascular dysfunction
24 p2883 N73-33027

**HYSTERESIS**
Hysteresis behavior of glass fiber reinforced plastic specimens under compressive cyclic loading
[AD-753823] 10 p1176 N73-19566
Magnetic hysteresis of lunar surface and permanent remanence in lunar samples
[NASA-TM-X-65941] 10 p1212 N73-19860
Hysteretic synchronous motor equivalent circuits
[LRBA-E-603-NT-1/SIE] 15 p1738 N73-24093
Experimental methods for determining internal damping in metal alloys and identification of factors causing internal damping
[NLL-CE-TRANS-6132-[9022.09]]
20 p2429 N73-29508
Analysis of effect of damping on response of structure to acoustic excitation and experimental method for determining damping coefficients
20 p2479 N73-29917
Packaging of precision quartz crystal resonators and effect on aging and thermal hysteresis
[AD-763215] 21 p2519 N73-30202

## I

**I BEAMS**
Mathematical model for bending of hybrid and composite hybrid beams
[CRIF-MT-79] 05 p0603 N73-14902

**IBM COMPUTERS**
NT IBM 360 COMPUTER
NT IBM 1130 COMPUTER
ELDO computing facilities noting data links and operating procedures
[ELDO-TN-25] 05 p0518 N73-14209

**IBM 360 COMPUTER**
Policy iteration subroutine package for IBM 360 computer
[FOA-P-C-8287-X9] 02 p0145 N73-11173
Users manual for network analysis program
[AD-752600] 08 p0892 N73-17218
Syntax-directed documentation for PL360
10 p1131 N73-19213
IBM 360 FORTRAN computer program for three dimensional stress analysis of structural parts
[AD-753617] 10 p1221 N73-19932
Design and construction of multifunction display man/machine interface for use with IBM 360 system - Vol. 1
[NASA-CR-128934] 15 p1754 N73-24214
Design and construction of multifunction display man/machine interface for use with IBM 360 system - Vol. 2
[NASA-CR-128935] 15 p1754 N73-24215

**IBM 1130 COMPUTER**
Subroutines for use of IBM 1627 x-y plotter associated with IBM 1130 computer
[LAAS-NT-SIS-72-T-09] 02 p0147 N73-11190
IBM 1130 computer programs for astrophysics optical data processing noting optical systems simulation and stellar density theoretical estimates
[CALC-01-72] 23 p2846 N73-32747

**ICARUS ASTEROID**
Analysis of asteroids selected for space mission objectives to show significant parameters
[NASA-CR-129248] 03 p0355 N73-12890
Photometric and polarimetric measurements of Bruderheim meteorite particles and comparison with astronomical data to determine composition of asteroids
[NASA-CR-131418] 11 p1339 N73-20865

**ICE**
NT GLACIERS
NT ICE FLOES
NT ICEBERGS
NT LAKE ICE
NT LAND ICE
NT SEA ICE
Evaluation of ice-water mixture thermocouple reference chamber discussing best operating parameter combination for high accuracy
[RAE-TR-72035] 01 p0058 N73-10475
Method for calculating intensity of scattered light from large diameter infinite ice cylinders in normal plane
[AD-747481] 03 p0338 N73-12759
Sea, ice, and surface water circulation in Alaskan Continental Shelf
[E72-10347] 05 p0533 N73-14335
High resolution FM radar at X band for measuring snow and ice thickness
[CRC-TN-646] 06 p0639 N73-15184
Ice problems in Canada, estimates of economic significance of problems, and order of priorities of research programs and management
[REPT-17] 07 p0788 N73-16412
Investigation of positron annihilation in water and ice by measuring angular correlation
07 p0859 N73-16969
Application of ERTS-1 imagery to thematic mapping of open water, ice and snow cover, vegetation, and works of man
[E73-10089] 08 p0902 N73-17301
ERTS-1 imagery of snow cover and break-up characteristics in Chena River Basin, Alaska
[E73-10292] 08 p0915 N73-17497
Thermodynamic and kinetic behavior of protons and deuterons in regular and heavy ice
[NASA-TT-F-14692] 08 p0946 N73-17744
Radar cross section measurements of snow and ice
[AD-752900] 09 p1004 N73-18192
ERTS-1 imagery of ice break-up characteristics of Chena River Basin
[E73-10400] 11 p1277 N73-20362
Electromagnetic wave scattering from snow, ice, and sea ice
[AD-758071] 15 p1783 N73-24454
Molecular mechanisms of conduction and polarization in water vapor, liquid water, and ice
[AD-762060] 19 p2231 N73-27993
Survey of freeze-up and breakup patterns of seasonal snow and ice covers in Alaska
[E73-10920] 20 p2398 N73-29269
Dielectric properties of ice, snow, and water at microwave frequencies and thickness measurements of ice and snow layers with radar
[CRC-1242] 21 p2537 N73-30341
Engineering procedures, blasting, and water level regulation for flood prevention and ice jam control on Dnestr and Dubossary Reservoirs
21 p2573 N73-30620
Creep tests of fine-grained polycrystalline ice under uniaxial and multiaxial stress conditions to predict time-dependent deformational behavior
22 p2723 N73-31791
ERTS-1 imagery of sea, ice, and surface water circulation along Alaskan continental shelf
[E73-11050] 23 p2779 N73-32226

**ICE FLOES**
ERTS-1 imagery of icebergs and sea ice in Antarctic region
[E73-10686] 16 p1902 N73-25380
Remote sensing of Arctic Sea ice motion by ERTS instrumentation
22 p2736 N73-31902

**ICE FORMATION**
NT CLOUD GLACIATION
Methodology for determining climatological probability of aircraft icing throughout Northern Hemisphere
[AD-745098] 01 p0075 N73-10623
Empirical procedure for predicting growth of ice crystals, graupel, and hail by diffusion
[AD-746451] 02 p0205 N73-11660
Lake, river, and land-fast sea ice thickness in North American Arctic and subarctic regions during 1968-1969 and 1969-1970
[AD-746256] 04 p0416 N73-13400
Solar and terrestrial radiation regimes over arctic ice packs
[AD-748214] 04 p0467 N73-13808
Winter wind and ocean conditions in Labrador fishing waters, and effects on pack ice drifting and icing hazards
[NLL-M-22670-[5828.4F]] 05 p0570 N73-14630
Ice particle formation and lifetime in space environment, affecting Skylab program
05 p0609 N73-14949
Laser extension measurements of visibility during ice fog for aiding in SEV pilot system design
[AD-750114] 06 p0680 N73-15537

Statistical evaluation of meteorological ice formation parameters: free moisture content, drop diameters, and temperature, obtained from Transall C-160 flights
[MBB-UH-11-72-O] 07 p0739 N73-16016
Instrumentation and data handling process of NAE T-33 turbulence research aircraft, stationary gas turbine icing problems, and role of plastic deformation in metal powder compaction
[DME/NAE-1972[4]] 12 p1466 N73-21882
Analysis of meteorological parameters and climatological effects leading to heavy icing of ships
[NLL-M-22981-[5828.4F]] 16 p1935 N73-25657
Application of ERTS-1 imagery for mapping distribution of glaciofluvial deposits and associated glacial landforms
[E73-10745] 17 p2021 N73-26349
Application of ERTS-1 data for identification of ice formations in Lake Erie and snow mapping in American River basin
[E73-10750] 17 p2022 N73-26353
Marine ice observations during Tenth Soviet Antarctic Expedition to measure formation, growth, disintegration, and physicomechanical properties
20 p2408 N73-29351
Analysis of physicomechanical properties of ice conducted during Tenth Soviet Antarctic Expedition with emphasis on ice cover temperature effects
20 p2408 N73-29352
Numerical analysis of ice fog produced by automobiles during arctic conditions
20 p2441 N73-29603
Formation and prevention of ice on ships
[NLL-M-23007-[5828.4F]] 21 p2528 N73-30270
Evaluation of recording instrument for in-flight determination of size and distribution of hailstones
[NASA-TM-X-2817] 21 p2549 N73-30434
Polycrystals and monocrystals of ice grown from KCl solution
[CONTRIB-1247] 22 p2646 N73-31203
Analysis and mapping sediment deposition, permafrost areas, snow cover, and icing in Arctic regions of Alaska from ERTS-1 data
[E73-11067] 23 p2781 N73-32243
Mariner 9 observations of Mars north polar region
[CONTRIB-2249] 23 p2840 N73-32694
Snow and fresh water lake ice interpretations from ERTS-1 imagery of Whitefish Bay, Michigan and Green Bay, Wisconsin
[E73-11129] 24 p2917 N73-33284
Acquisition of conditions of icing on modern civil transport aircraft from flight data
24 p2946 N73-33528

**ICE MAPPING**
Surveillance and mapping of sea ice in Arctic regions based on ERTS-1 imagery
[E72-10199] 02 p0160 N73-11297
Arctic glacier mapping, research, and effects on surroundings
[AD-747001] 06 p0667 N73-15425
Mapping Arctic sea ice from ERTS-1 MSS imagery
[E73-10278] 08 p0914 N73-17486
Alaskan arctic and subarctic sediment deposition, permafrost, snow cover, and ice mapping from ERTS-1 imagery
[E73-10279] 08 p0914 N73-17487
Survey and mapping of freeze-up and break-up patterns of seasonal snow and ice covers in Alaska
[E73-10282] 08 p0914 N73-17489
Detection and mapping Arctic sea ice using ERTS-1 imagery
[E73-10374] 10 p1151 N73-19369
Mapping Arctic sea ice from ERTS-1 imagery of Hudson Bay, M'Clure Strait, Beaufort Sea, and Greenland Sea
[E73-10447] 11 p1282 N73-20407
Detection and mapping of sea ice in Arctic regions using ERTS-1 RBV and MSS data
[E73-10595] 14 p1658 N73-23452
Application of ERTS-1 imagery for mapping distribution of glaciofluvial deposits and associated glacial landforms
[E73-10745] 17 p2021 N73-26349
Application of ERTS-1 data for identification of ice formations in Lake Erie and snow mapping in American River basin
[E73-10750] 17 p2022 N73-26353
Detection and mapping Arctic sea ice from ERTS-1 imagery
[PAPER-M14] 19 p2281 N73-28353
Analysis of ERTS data on ice formation in Bering Sea and correlation with ice observations by aerial reconnaissance
[E73-10865] 20 p2392 N73-29216
ERTS-1 imagery of snow cover, ice conditions, and soil moisture in Sierra Nevada Mountains and Lake Ontario Basin
[E73-10869] 20 p2393 N73-29220
Analysis of ice conditions existing in Antarctic waters during Tenth Soviet Antarctic Expedition
20 p2407 N73-29342
Radar analysis of ice sheets in Antarctic regions conducted during Tenth Soviet Antarctic Expedition
20 p2407 N73-29346
Marine ice observations during Tenth Soviet Antarctic Expedition to measure formation, growth, disintegration, and physicomechanical properties
20 p2408 N73-29351
Application of ERTS-1 data to detection and mapping of sea ice in Beaufort Sea and Bering Sea areas
[E73-11037] 22 p2663 N73-31341
Multispectral ERTS imagery for polar ice mapping
22 p2736 N73-31901
Microwave imagery of Great Lake ice formations
22 p2736 N73-31903
Mesoscale movement and deformation of sea ice in Beaufort Sea
[E73-11153] 24 p2919 N73-33307

**ICE NUCLEI**
Existence of icy-conglomerate cometary nucleus
02 p0227 N73-11835
Ice crystal multiplication in convective precipitation considering cloud top temperature
[PB-215626/3] 16 p1908 N73-25439

**ICE OBSERVATION**
U ICE REPORTING

**ICE PACKS**
U SEA ICE

**ICE PREVENTION**
Formation and prevention of ice on ships
[NLL-M-23007-[5828.4F]] 21 p2528 N73-30270

**ICE REPORTING**
Interpretation of meteorological satellite TV pictures of ice in Baltic Sea
[NLL-M-20841-[5828.4F]] 05 p0529 N73-14306
Aerial tracking of icebergs off Labrador coast during July 1970 and July 1971
[MC/ORB-8/71] 05 p0538 N73-14378
Application of TIROS satellite data to mapping of ice fields through development of composite minimum brightness chart
07 p0788 N73-16409
Detection and mapping Arctic sea ice using ERTS-1 imagery
[E73-10374] 10 p1151 N73-19369
Survey of seasonal snow and ice covers in Alaska using ERTS-1 imagery
[E73-10438] 11 p1281 N73-20398
Mapping permafrost areas of Alaska, correlating snowpack cover of Caribou-Poker Creek with stream runoff, and mapping and inventorying icing on Chena River
[E73-10511] 13 p1516 N73-22286
Lake ice surveillance using radar imagery
[E73-10569] 15 p1771 N73-24349
ERTS-1 imagery of ice conditions on Lake Champlain
[E73-10806] 18 p2138 N73-27281
Analysis of ERTS data on ice formation in Bering Sea and correlation with ice observations by aerial reconnaissance
[E73-10865] 20 p2392 N73-29216
Analysis of ice conditions existing in Alasheyev Bight during Tenth Soviet Antarctic Expedition
20 p2409 N73-29362
Application of ERTS-1 data to detection and mapping of sea ice in Beaufort Sea and Bering Sea areas
[E73-11037] 22 p2663 N73-31341
Remote sensing of Arctic Sea ice motion by ERTS instrumentation
22 p2736 N73-31902

**ICE SHELVES**
U LAND ICE

**ICEBERGS**
Aerial tracking of icebergs off Labrador coast during July 1970 and July 1971
[MC/ORB-8/71] 05 p0538 N73-14378
ERTS-1 imagery of icebergs and sea ice in Antarctic region
[E73-10686] 16 p1902 N73-25380
Survey of Antarctic icebergs using ERTS-1 imagery
[E73-10692] 16 p1902 N73-25385

**ICELAND**
Thermal surveillance of volcanoes of Cascade Range and Iceland using ERTS-1 imagery and data collection platforms
[E72-10246] 03 p0289 N73-12346
Thermal surveillance of volcanoes of Cascade Range and Iceland using ERTS-1 DCP systems and imagery
[E73-10317] 09 p1023 N73-18349
Volcano and earthquake surveillance network in Alaska, California, Washington, Hawaii, El Salvador, Nicaragua, Iceland, and Guatemala
[E73-10337] 09 p1025 N73-18365
ERTS-1 imagery of Iceland geology, geophysics, hydrology, oceanography, and agriculture
[E73-10535] 13 p1518 N73-22299
Thermal surveillance of active volcanoes in Washington, California, and Iceland
[E73-10556] 14 p1655 N73-23428
ERTS-1 imagery of geological, climatological, and volcanic activities in Iceland
[E73-10713] 17 p2018 N73-26320
Development of volcano surveillance and early warning system using ERTS-1 data collection system
[PAPER-G9] 19 p2264 N73-28240
Analysis of ERTS-1 MSS imagery to determine geologic, hydrologic, oceanographic, and agricultural phenomena in Iceland
[PAPER-G10] 19 p2264 N73-28241
ERTS-1 imagery of Namafjall geothermal area, Iceland
[E73-10874] 20 p2393 N73-29225
Prototype DCP volcano surveillance network in Washington, Nicaragua, California, Guatemala, Hawaii, El Salvador, Iceland, and Alaska
[E73-11024] 22 p2662 N73-31328

**ICING**
U ICE FORMATION

**IDAHO**
NT YELLOWSTONE NATIONAL PARK [ID-MT-WY]
Crop identification and acreage measurement in Idaho, Missouri, Kansas, and South Dakota using ERTS-1 imagery
[E72-10179] 01 p0045 N73-10358
Definition of characteristics and boundaries of vegetation-soil types in Southern Idaho from ERTS-1 remotely sensed imagery
[E72-10203] 02 p0161 N73-11300
Crop identification and acreage measurement in Missouri, Kansas, South Dakota, and Idaho using ERTS-1 imagery
[E72-10336] 05 p0531 N73-14324
Utilization of ERTS-1 imagery to map soils and vegetation in Idaho
[E72-10356] 05 p0534 N73-14344
Crop identification and acreage measurement in Missouri, Kansas, South Dakata, and Idaho based on ERTS-1 imagery and aerial photography
[E73-10328] 09 p1024 N73-18359
Identification of vegetation and soils in Idaho using ERTS-1 remotely sensed imagery
[E73-10512] 13 p1516 N73-22287
Application of ERTS-1 remote sensing data in study of vegetation and soils in Idaho
[E73-10708] 16 p1904 N73-25399
Utilization of ERTS-1 imagery for crop identification and acreage measurement in South Dakota, Kansas, Missouri, and Idaho
[E73-10734] 17 p2020 N73-26340
Tectonic and photogeologic mapping of forested and sparsely vegetated terrain of Montana and Idaho
[E73-10900] 20 p2396 N73-29249
Interpretation of seasonal changes in vegetation and soils in Idaho from ERTS-1 imagery
[E73-10936] 21 p2529 N73-30278
Crop identification and acreage measurement in Missouri and Idaho from ERTS-1 imagery
[E73-10982] 22 p2658 N73-31289

**IDEAL GAS**
Numerical calculation of supersonic three dimensional jet plum in perfect gas with inviscid and compressible properties
04 p0404 N73-13287
Numerical analysis of oscillating wedge in supersonic perfect gas flow to evaluate trends for wedge and to analyze unsteady flows
07 p0767 N73-16235
Method of characteristics for analyzing three dimensional, steady supersonic, nonequilibrium, chemically reacting flow of thermally perfect gases in exhaust nozzle
07 p0768 N73-16240
Shock wave structure in gas consisting of ideally elastic, rigid spherical molecules
12 p1418 N73-21488
Windward surface flow distribution on lifting reentry vehicle configurations at high angles of incidence under hypersonic perfect gas conditions
[AD-756499] 14 p1599 N73-22961
Numerical analysis of one dimensional isentropic flow of thermally perfect, calorically imperfect diatomic gas
[ESDU-S.00.01.10-AMEND-A]
14 p1648 N73-23364
Stability analyses of idealized atmosphere and perfect gas blowing over inviscid liquid
17 p2012 N73-26269
Numerical analysis of axisymmetrical, viscous, compressible flow around blunt bodies for ideal gases with laminar unseparated boundary layers
17 p2012 N73-26273
Nearly spherical constant power detonation waves driven by focused laser beam in gas
23 p2772 N73-32171

**IDENTIFYING**
NT CROP IDENTIFICATION
NT TIMBER IDENTIFICATION
SAL storage for AN/UPA-59/60 IFF [identification friend or foe] decoders for displaying aircraft targets
[AD-746445] 02 p0208 N73-11685
Magnetic tape playback and serial time decoder for IFF flight test instrumentation
[AD-750667] 06 p0641 N73-15204
Differential light scattering patterns for identifying different species of bacteria
08 p0875 N73-17090
Construction of combined identification system of individual voices under natural speech conditions
14 p1627 N73-23190

Hazard identification based on energy interrelationships and integrated control technique
[NASA-TM-X-64782] 22 p2737 N73-31918
IFR [RULES]
U INSTRUMENT FLIGHT RULES
IGNEOUS ROCKS
NT ANORTHOSITE
NT BASALT
NT PUMICE
Recognition of geologic framework for copper porphyry-type deposits on ERTS-1 imagery
[E72-10210] 02 p0161 N73-11305
IGNIMBRITE
U IGNEOUS ROCKS
IGNITERS
NT DETONATORS
NT INITIATORS [EXPLOSIVES]
Fabrication and testing of 22 sounding rockets using solid propellants
[AD-753089] 09 p1092 N73-18911
Characteristics of solid propellant rocket engine with controlled rate of thrust buildup operating in vacuum environment
[NASA-CASE-NPO-11559] 15 p1824 N73-24784
Remote fire stack igniter on vent stack with flame cage near top
[NASA-CASE-MFS-21675-1] 22 p2727 N73-31826
IGNITION
NT ELECTRIC IGNITION
NT SOLID PROPELLANT IGNITION
NT SPARK IGNITION
Ignition site and ignition delay time for spherical fuel droplets
[NLL-RTS-7169] 02 p0241 N73-11959
Ignition and combustion characteristics of high density storable fuels injected into supersonic and subsonic air streams
[AD-746063] 02 p0244 N73-11980
Using microscopic models and principles for studying transfer of lattice vibrational energy into first excited state in perfect crystal
[AD-748079] 03 p0365 N73-12977
Flameout and ignition characteristics of jet engine fuel flame in gas turbine with exhaust diffuser
[AD-749635] 05 p0591 N73-14802
Reaction between molecular hydrogen and molecular oxygen subjected to temperature and pressure pulses in shock tubes
[NASA-TM-X-2707] 07 p0854 N73-16928
Mechanisms of detonation initiation in solid rocket propellants by low amplitude stimuli
[AD-752242] 08 p0970 N73-17928
High-efficiency, self-contained, small neodymium laser for pyrotechnic ignition
10 p1228 N73-19979
Safety hazards related to ignition and combustion in oxygen systems
[NASA-TM-X-68223] 12 p1464 N73-21861
Ignition and deflagration of in nitrocellulose based solid propellants
[AD-756880] 13 p1570 N73-22720
Initiator ignition effect in laboratory glass and polythene vessel studying dummy hand injuries during simulated accidents
[ERDE-TRANS-1] 15 p1744 N73-24137
Effects of vehicle ignition noise on VHF/UHF band terminals
[STC-TM-340] 15 p1749 N73-24179
Photochemical enhancement of combustion and mixing in supersonic flows
[AD-758802] 15 p1844 N73-24944
Underwater ignition of hypergolic rocket propellants as function of injection system, fuel combustions, water depth, and salinity
[DLR-MITT-73-07] 16 p1954 N73-25813
Effects of additives on high speed ignition and combustion characteristics of slurry fuels using magnesium and lithium fluoride
[AD-762615] 20 p2465 N73-29802
Laser ignition of pyrotechnic compositions being considered as drag reducing fumers
[AD-765415] 23 p2858 N73-32834
IGNITION LIMITS
Performance of ignition and flame stabilization using gas generator in different ramjet combustion chamber configurations
[DLR-FB-72-47] 01 p0091 N73-10748
Determination of point of ignition and ignition delay period for single drop of fuel under specified conditions of temperature and vapor
[AD-745868] 02 p0244 N73-11979
Evaluation of cooled, flightweight gaseous hydrogen-oxygen reaction control thrusters to determine catalytic igniter operational limits and performance - Vol. 1
[NASA-CR-120869] 03 p0350 N73-12858
Demonstration of duct cooling concept with gaseous hydrogen/oxygen propellant in high pressure thruster - Vol. 2
[NASA-CR-120870] 03 p0350 N73-12859
Analysis of oxygen flow in steel pipelines to determine maximum permissible flow and effects of solid particles and restriction on safe flow rate to avoid ignition
[NASA-TT-F-14831] 09 p1016 N73-18290
Analytical models for ignition and complete combustion of aluminized slurry fuels in ramjet engines
[AD-754117] 10 p1203 N73-19792
Test equipment and experimental procedures for determining effects of turbulent flow on ignition properties of gasoline and air mixture
[NLL-RTS-7883] 18 p2128 N73-27194
Analysis of ignition properties of hypergolic fluids under low pressure conditions to determine relations of time, temperature, and thermodynamic properties
21 p2605 N73-30878
Analysis of ignition characteristics of high velocity hydrocarbon diffusion flames and comparison with ignition properties of hydrogen
21 p2605 N73-30881
Characteristics of detonable gas mixtures and analysis of cylindrically expanding flames initiated by exploding wire source
24 p2990 N73-33897
Ignition properties and combustion physics of beryllium to show effects of various physical parameters and composition of combustion products
24 p2992 N73-33908
Screening factor which reduces densities at which carbon ignition can occur in helium, exhausted carbon, and oxygen stellar core models
[UCRL-74669-REV-1] 24 p2992 N73-33913
IGNITION SYSTEMS
Performance of prototype monopropellant engines using electrolytic ignition system
[AD-745993] 02 p0224 N73-11808
IGNITION TEMPERATURE
NT FLASH POINT
Determination of point of ignition and ignition delay period for single drop of fuel under specified conditions of temperature and vapor
[AD-745868] 02 p0244 N73-11979
IGY [GEOPHYSICAL YEAR]
U INTERNATIONAL GEOPHYSICAL YEAR
ILLIAC COMPUTERS
NT ILLIAC 4 COMPUTER
ILLIAC 4 COMPUTER
ILLIAC 4 systems characteristics and programming manual
[NASA-CR-2159] 10 p1132 N73-19225
ILLIAC 4 and parallel assembler, Pandora
[AD-757779] 14 p1639 N73-23286
ILLINOIS
NT WABASH RIVER BASIN [IL-IN-OH]
Environmental and ecological impact of construction and operation of dam and impoundment on Sangamon River in Illinois
[E72-10216] 02 p0162 N73-11310
Effect of dam construction and staged filling of reservoirs in Illinois on environment and ecology
[E72-10217] 02 p0162 N73-11311
Environmental and ecological impact of construction and staged filling of reservoirs in Illinois
[E72-10309] 04 p0412 N73-13358
Crop identification and acreage estimation using ERTS-1 MSS imagery of northern Illinois
[E73-10039] 07 p0776 N73-16302
Environmental and ecological impact of construction and filling of reservoir on Sangamon River in Illinois
[E73-10082] 08 p0901 N73-17294
Application of ERTS-1 imagery to fracture related mine safety hazards in coal mining industry in Indiana and Illinois
[E73-10096] 09 p1020 N73-18321
Application of ERTS-1 imagery to fracture related mine safety hazards in coal mining industry in Indiana and Illinois
[E73-10371] 10 p1151 N73-19366
Environmental and ecological impact of construction and operation of Oakley Dam and Friends Creek impoundment located on Sangamon River in East Central Illinois
[E73-10484] 12 p1396 N73-21321
Environmental and ecological impact of construction and operation of Oakley Dam and Friends Creek impoundment located on Sangamon River in East Central Illinois
[E73-10555] 16 p1898 N73-25351
Quantitative evaluation of computer processed ERTS-1 MSS data classifications to identify major agricultural crops in Illinois
[PAPER-A25] 19 p2262 N73-28232
Application of ERTS-1 imagery for differentiating quaternary surface deposits and landforms in Illinois, Iowa, Missouri, Kansas, Nebraska, and South Dakota
[PAPER-G13] 19 p2264 N73-28244
Analysis of ERTS-1 imagery and high altitude infrared photography to determine geological fractures in Indiana and Illinois
[PAPER-E1] 19 p2268 N73-28265
Environmental and ecological impact of construction and operation of Oakley Dam and Friends Creek Impoundment located on Sangamon River in East central Illinois
[E73-10882] 20 p2394 N73-29233
Environmental and ecological impact of major construction of reservoirs in Illinois
[E73-10892] 20 p2395 N73-29241
Skylab monitoring of surface mining activities and reclamation in Ohio, West Virginia, Pennsylvania, Indiana, Kentucky, and Illinois
[E73-11033] 22 p2663 N73-31337
Effect of construction and staged filling of Oakley Dam and Friends Creek impoundment in Illinois on environment and ecology
[E73-11124] 24 p2916 N73-33279
ILLUMINANCE
Illuminance measurement of two types of airborne flares
[DREV-R-673/72] 10 p1223 N73-19942
ILLUMINATING
Bibliography on pyrotechnics
[AD-752700] 09 p1100 N73-18976
Contraves cinetheodolite optical system modification
[SC-DR-72-0754] 16 p1914 N73-25487
ILLUMINATION
Dark side illumination of Saturns ring by scattering
[REPT-13] 10 p1212 N73-19855
Apollo experience report on lighting requirements for Apollo command and lunar modules for internal and external lighting
[NASA-TN-D-7290] 16 p1964 N73-25887
Influence of atmosphere pathlengths on ERTS-1 MSS imagery acquired over southwestern Kansas
[E73-10763] 18 p2133 N73-27240
Application of incoherent and coherent light sources for underwater illumination and comparison of efficiency for various conditions
24 p2958 N73-33633
ILLUMINATORS
Compact sealed beam plasma arc illuminator with integral reflector
[AD-756968] 13 p1564 N73-22678
ILLUSIONS
NT OCULOGRAVIC ILLUSIONS
ILS [LANDING SYSTEMS]
U INSTRUMENT LANDING SYSTEMS
IMAGE CONTRAST
Television reviewing conditions, including contrast handling requirements of color TV display
[BBC-1972/37] 06 p0638 N73-15182
Diffraction technique for determining three dimensional frequency spectra of photographic images
[AD-751418] 07 p0822 N73-16663
Applications of Tautenburg 134-cm Schmidt telescope noting instrument efficiency and astrophysical statistics
07 p0846 N73-16860
Methods of charging/discharging in scanning electron microscopy of dielectrics to preserve resolution and contrast
[DRIC-TRANS-2970] 10 p1162 N73-19451
Use of telecamera as contrast monitor for photospheric surveys
[RR-1] 17 p2032 N73-26440
Contrast enhancement of ERTS-1 imagery by photographic techniques and methods
19 p2286 N73-28381
Relationship between intermediate medium, and transformation and contrast phenomena
[NASA-TT-F-15035] 20 p2371 N73-29055
Instrumented methods for finding variable stars on sky photographs
21 p2594 N73-30784
Generation of line-containing picture samples from gray level pictures using contrast gradient
[BMVG-FBWT-73-10] 23 p2761 N73-32092
IMAGE CONVERTERS
NT CELESCOPES
NT IMAGE TUBES
Investigating polymers for suitability of use as light valve display device called deformographic storage display tube
[AD-744689] 01 p0033 N73-10258
Analysis of gray scale image storage techniques in electroluminescent and photoconductor image conversion panels
[AD-745758] 01 p0033 N73-10261
Development of mosaic image conversion panels sensitive to ultraviolet, X ray, near infrared, and visible light
[AD-745757] 01 p0033 N73-10262
Use of TV equipment for converting color negative cinefilm into color positive image
[DRIC-TRANS-2835] 02 p0174 N73-11412
Millimeter wave image conversion panel using p-i-n diode structures for carrier injection and bulk conductivity modulation
[AD-747409] 03 p0276 N73-12241
Device for converting optical images into electron beams
[NASA-CASE-GSC-11602-1] 04 p0395 N73-13214
Development of optical equipment including image converters and infrared detectors employing coherent radiation
[AD-753275] 09 p1067 N73-18711
Millimeter wave image conversion system for optical display of objects obscured by fog or rain
13 p1489 N73-22074
Performance characteristics of proximity focused ultraviolet to visible light image converters
[NASA-TM-X-66258] 15 p1787 N73-24488

Optoelectronic shutters with opening times of 0.05 nsec for image converters
[IPF-72-5] 17 p2033 N73-26456
Infrared image converter, based on temperature sensitive liquid-solid interface, using GE-AU IR detector
[IPF-72-6] 17 p2033 N73-26457
Semiconductor image conversion panels using millimeter diodes
[AD-762116] 19 p2246 N73-28109
Image converter based on multilayer semiconductor dielectric structures
[JPRS-59636] 19 p2326 N73-28714
Photoconducting semiconductor system for converting stored optical images into video signals
[NASA-CASE-NPO-13131-1] 22 p2680 N73-31467
Nonlinear materials including univalent metal iodates for IR image upconversion
[AD-763952] 22 p2701 N73-31630
Properties of liquid crystals noting use in display devices, light modulation, image converters, and nondestructive testing
[LCR-DR-1-71-223/1/R] 23 p2765 N73-32125
Semiconductor panel modulation for millimeter image conversion
[AD-765418] 23 p2767 N73-32133

IMAGE CORRELATORS
Walsh transformation for two dimensional correlation and convolution in pattern recognition
[AD-746701] 03 p0272 N73-12207
Development of holographic storage and retrieval system for aerial chart information display in cockpit environment
[AD-748648] 03 p0330 N73-12690
Development of phase contrast enhancement techniques for seismic holography without use of spatial filters
[BM-RI-7721] 07 p0806 N73-16537
Optical and digital reconstruction techniques applied to synthetic holograms recorded with suboptical sources
23 p2800 N73-32394
Techniques for predicting effects of thermal and saline inhomogeneities on optical imaging systems with application to optical properties of sea water
24 p2957 N73-33625
Effects of resolution, signal to noise ratio, and contrast on underwater imaging systems performance
24 p2958 N73-33631

IMAGE DISSECTOR TUBES
Evaluation of image dissector sensor for Earth Resources program
[NASA-CR-130131] 05 p0547 N73-14443
Development of electrostatically focused image dissector tube for use in spacecraft attitude control star trackers
[NASA-CR-132153] 15 p1787 N73-24487
Flight test of multispectral image dissector camera onboard high altitude aircraft
18 p2209 N73-27835
EMR 549-120 image dissector test and calibration noting geometrical and photometric tube properties
[ELEC-010-72] 23 p2766 N73-32127

IMAGE ENHANCEMENT
Lunar Orbiter photographic and photometric data enhancement - frameset joining, digitization, data improvement, and statistical error analysis
[NASA-CR-128581] 01 p0057 N73-10463
Spectral resolution and image enhancement by focusing of lense optics
[TPD-1972-0-2] 01 p0079 N73-10655
Computer techniques for pseudocolor image enhancement
[P-4870] 01 p0080 N73-10657
Utilization of ERTS-1 imagery for water depth measurement, mapping of Yellowstone Park, atmospheric effects in Colorado, lake ice surveillance, recreational land use, IFYGL Lake Ontario, image enhancement, water quality monitoring, and oil pollution detection
[E72-10201] 02 p0144 N73-11167
Utilization of ERTS-1 imagery for water depth measurement, mapping of Yellowstone Park, atmospheric effects in Colorado, lake ice surveillance, recreational land use, IFYGL Lake Ontario, image enhancement, water quality monitoring, oil pollution detection, and mapping iron compounds
[E72-10198] 02 p0160 N73-11296
Optical and digital data processing and handling of SLR imagery
[ESRO-CR(P)-139-VOL-4] 03 p0297 N73-12419
Tests and evaluations of methods for recovering ground colors in aerial photographs
[AD-747340] 03 p0304 N73-12481
Subjective tests of target acquisition time using television with image enhancement possibilities
[MBB-UFE-892-72-O] 06 p0636 N73-15165
Computer technique for stereo image processing of Mariner 9 spacecraft color photographs
[NASA-CR-130305] 06 p0644 N73-15226
Snow enhancement in New England test areas based on ERTS-1 imagery
[E73-10001] 06 p0657 N73-15337
Computer processing, enhancement, and recognition of ERTS imagery of Tennessee Valley
[E73-10056] 07 p0778 N73-16318
Development of phase contrast enhancement techniques for seismic holography without use of spatial filters
[BM-RI-7721] 07 p0806 N73-16537
Utilization of ERT-1 imagery for water depth measurement, Yellowstone Park data, atmospheric effects in Colorado, lake ice surveillance, recreational land use, IFYGL, image enhancement, water quality monitoring, oil pollution detection, and mapping iron compounds
[E73-10086] 08 p0901 N73-17298
Land use mapping and image enhancement of ERTS-1 imagery of Phoenix Quadrangle
[E73-10090] 08 p0902 N73-17302
Image speckling reduction using multicolor illumination in holographic microscopy
[AD-752240] 08 p0945 N73-17737
Two dimensional Fourier transform and digital correlation for image processing
[BMVG-FBWT-72-1] 10 p1179 N73-19591
Enhancement of multispectral aircraft scanner data using scan overlap redundancy
[NASA-CR-131587] 13 p1530 N73-22395
Linear preprocessing point spread function for optimal image restoration filter
[NASA-CR-131588] 13 p1559 N73-22634
Data processing and image enhancement of ERTS-1 MSS data for Kansas
[E73-10596] 14 p1658 N73-23453
Image enhancement and information extraction techniques for ERTS-1 MSS imagery
[E73-10572] 15 p1772 N73-24352
Processing and enhancement of Earth Resources Program photography
[NASA-CR-131819] 15 p1787 N73-24491
Effectiveness of snow cover as photogeological enhancement technique for ERTS-1 imagery of western Massachusetts
[E73-10594] 16 p1896 N73-25334
Heuristic method for controlling edge sharpness of image observed through inadequate imaging system
[AD-760320] 17 p2064 N73-26694
Linear estimation technique for enhancement of black and white images
[AD-760779] 18 p2180 N73-27601
VICAR image processing system used for enhancement of ERTS-1 images for Arizona geological experiment
[PAPER-I9] 19 p2278 N73-28330
Digital enhancement of ERTS-1 MSS data for maximum image visibility
[PAPER-I10] 19 p2278 N73-28331
Enhancement of ERTS-1 images by density slicing and application to mapping of Yucca trees in Mojave Desert of Southern California and Nevada
[PAPER-I11] 19 p2278 N73-28332
Pseudocolor transformation of ERTS-1 imagery of Monterey Bay-San Francisco, California area
[PAPER-I12] 19 p2278 N73-28333
Analysis and enhancement of ERTS-1 hydrology imagery using electronic satellite image analysis console
[PAPER-I15] 19 p2279 N73-28336
Contrast enhancement of ERTS-1 imagery by photographic techniques and methods
19 p2286 N73-28381
Image acquisition and enhancement techniques for oceanographic photography using photo-optical and electronic methods
[AD-761663] 19 p2296 N73-28463
Multi-image photointerpretation system for processing several types of photographs
22 p2636 N73-31125
Application of spatial filtering and image restoration to underwater photographs of floodlit images
24 p2958 N73-33637

IMAGE FILTERS
Linear preprocessing point spread function for optimal image restoration filter
[NASA-CR-131588] 13 p1559 N73-22634
Homomorphically estimated restoration filter for removing image blurs
19 p2320 N73-28668

IMAGE INTENSIFIERS
NT IMAGE ORTHICONS
Operation of image intensifier tubes and analysis of fluctuation theory on visual contrast sensitivity with ideal image intensifiers
[IZF-1972-18] 02 p0148 N73-11202
Parametric modifications for improved image intensification of forward looking infrared imaging devices in night fire control
[AD-750374] 06 p0646 N73-15251
Image intensifier system for daytime missile tracking telescopes
[AD-753342] 09 p1068 N73-18715
Design, development, and characteristics of field ion microscope for image intensification
[ARL/INST-NOTE-78] 17 p2032 N73-26445
Photoelectronic devices for amplifying brightness image of variable stars
21 p2594 N73-30788
Optimum resolution filter for radar target enhancement and surface reconstruction
23 p2755 N73-32048

IMAGE MOTION COMPENSATION
Design and fabrication of optical system to compensate for motions of stellar field image on focal plane of large orbiting telescope based on single-axis system
[NASA-TN-D-7145] 07 p0799 N73-16488
Development of mathematical methods for calibrating lunar orbiter photography
[NASA-CR-128279] 08 p0924 N73-17572
Space-variant image motion degradation and restoration in linear incoherent optical systems
15 p1812 N73-24687
Compensation formulas for panoramic aerial photography cameras
[AD-764168] 22 p2676 N73-31431

IMAGE ORTHICONS
Equipment for simultaneous radar observations by image-orthicon and optical observations
01 p0101 N73-10833

IMAGE TRANSDUCERS
Control computer for correcting ERTS video data electron beam recorder errors at ground base
18 p2211 N73-27853
Multislot shadow transducer for maintaining solar orientation
20 p2419 N73-29439

IMAGE TUBES
Evaluation of photon imaging devices and subsystems with emphasis on television camera tubes
[AD-748005] 03 p0275 N73-12234
Assessment of luminous and spectral sensitivity and electro-optical properties of image tubes
[BARC-610] 08 p0888 N73-17194
Study of galactic nuclei using image tube spectrographic techniques
22 p2713 N73-31718
Amplification of low light level optical sigmals by preferential integration in imaging tubes
[AD-763724] 23 p2766 N73-32129

IMAGE VELOCITY SENSORS
Split-film atmospheric turbulence anemometer evaluation
[NASA-CR-62093] 16 p1914 N73-25485

IMAGERY
NT AERIAL PHOTOGRAPHY
NT ALL SKY PHOTOGRAPHY
NT ASTRONOMICAL PHOTOGRAPHY
NT AUTORADIOGRAPHY
NT BLACK AND WHITE PHOTOGRAPHY
NT CHRONOPHOTOGRAPHY
NT CINEMATOGRAPHY
NT CLOUD PHOTOGRAPHY
NT COLOR PHOTOGRAPHY
NT HOLOGRAPHY
NT INFRARED IMAGERY
NT INFRARED PHOTOGRAPHY
NT KINOFORM
NT LUNAR PHOTOGRAPHY
NT MICROWAVE IMAGERY
NT PHOTOMICROGRAPHY
NT PHOTORECONNAISSANCE
NT RADAR IMAGERY
NT RADAR PHOTOGRAPHY
NT RADIOGRAPHY
NT REPRODUCTION (COPYING)
NT SATELLITE-BORNE PHOTOGRAPHY
NT SCHLIEREN PHOTOGRAPHY
NT SHADOWGRAPH PHOTOGRAPHY
NT SPACEBORNE PHOTOGRAPHY
NT SPECTROHELIOGRAPHS
NT SPECTROPHOTOGRAPHY
NT STEREOPHOTOGRAPHY
NT ULTRAVIOLET PHOTOMETRY
Bibliography on digital image processing information
[AD-745790] 01 p0029 N73-10231
Geologic mapping of Basin and Range - Colorado Plateau boundary in Arizona using ERTS-1 imagery
[E72-10157] 01 p0044 N73-10347
Utilization of ERTS-1 imagery for state and local agency management and planning in North Carolina
[E72-10167] 01 p0044 N73-10348
Determination of boundaries of aircraft and spacecraft data within which water quality can be obtained
[E72-10168] 01 p0044 N73-10349
Sediment pattern correlations with inflow and tidal action in Chesapeake Bay based on ERTS-1 imagery
[E72-10169] 01 p0044 N73-10350
Evaluation of ERTS-1 imagery for hydrologic information in Sierra Nevada Mountains and Lake Ontario
[E72-10170] 01 p0044 N73-10351
Estuarine and coastal oceanography of Block Island Sound and adjacent New York coastal waters based on ERTS-1 multispectral band scanner imagery
[E72-10171] 01 p0044 N73-10352
Interdisciplinary study of estuarine and coastal oceanography of Block Island Sound and New York Bight area using ERTS-1 imagery
[E72-10172] 01 p0044 N73-10353
Mapping and managing soil and range resources in Sand Hills Region of Nebraska using ERTS-1 imagery
[E72-10175] 01 p0044 N73-10354
Landform-vegetation relationships in southern Arizona based on interpretation of ERTS-1 imagery
[E72-10176] 01 p0044 N73-10355

Monitoring rural landscape changes in eastern Tennessee through interpretation of ERTS-1 imagery
[E72-10177] 01 p0045 N73-10356
Application of ERTS-1 imagery data to protection and management of New Jersey coastal environment
[E72-10178] 01 p0045 N73-10357
Crop identification and acreage measurement in Idaho, Missouri, Kansas, and South Dakota using ERTS-1 imagery
[E72-10179] 01 p0045 N73-10358
Interpretation and mapping large scale structural lineaments in Precambrian shield areas and basins containing younger sediments using ERTS-1 imagery
[E72-10180] 01 p0045 N73-10359
Monitoring by ERTS-1 imagery for resource inventory, planning, land use zoning, and resource development in Oregon
[E72-10182] 01 p0045 N73-10361
Classification and pattern recognition of short lived events using ERTS-1 imagery
[E72-10183] 01 p0045 N73-10362
Inventory and monitoring of natural vegetation-landform relationships in arid regions of southern Arizona using ERTS-1 imagery
[E72-10184] 01 p0045 N73-10363
Uniform mapping and monitoring of natural ecosystems and environmental complexes from ERTS-1 imagery
[E72-10185] 01 p0046 N73-10364
Development of multistage forest sampling inventory system using ERTS-1 imagery
[E72-10186] 01 p0046 N73-10365
Land use mapping of northern megalopolis using ERTS-1 imagery
[E72-10188] 01 p0046 N73-10367
Acquisition of earth resources data for Bolivia using ERTS-1 imagery
[E72-10191] 01 p0046 N73-10370
Application of ERTS-1 imagery to fracture related mine safety hazards in coal mining industry in Indiana
[E72-10193] 01 p0046 N73-10372
Lithological and structural surveys of African rift system using ERTS-1 imagery
[E72-10194] 01 p0046 N73-10373
Mineral exploration in Arizona using ERTS-1 imagery
[E72-10197] 01 p0047 N73-10376
In situ spectroradiometric quantification of ERTS-1 imagery of Arizona and Texas
[E72-10173] 01 p0055 N73-10444
In situ spectroradiometric quantification of ERTS-1 MSS and RBV imagery
[E72-10174] 01 p0055 N73-10445
Definition of characteristics and boundaries of vegetation-soil types in Southern Idaho from ERTS-1 remotely sensed imagery
[E72-10203] 02 p0161 N73-11300
Analysis of ERTS-1 imagery for Colorado environments using automatic data processing techniques
[E72-10204] 02 p0161 N73-11301
Geological fracture mapping based on enhancement of ERTS-1 snow cover imagery of Massachusetts, Connecticut, and Feather River/Lake Tahoe area
[E72-10205] 02 p0161 N73-11302
Digital correction techniques for ERTS-1 imagery
[E72-10206] 02 p0161 N73-11303
ERTS-1 imagery of French shoreline along the Atlantic Ocean and English Channel
[E72-10211] 02 p0161 N73-11306
Evaluation of simultaneous ERTS-1 and aerial photography of Arizona
[E72-10213] 02 p0162 N73-11308
Utilization of ERTS-1 remotely-acquired oceanographic information for improving harvest and management of menhaden in Gulf of Mexico
[E72-10215] 02 p0162 N73-11309
Detection of regional tectonic structures and mineral exploration in Arizona using ERTS-1 imagery
[E72-10218] 02 p0162 N73-11312
Investigation of forest stress in Black Hills, forest inventory at Atlanta test site, and rangeland inventory at Manitou test site using ERTS-1 imagery
[E72-10219] 02 p0162 N73-11313
Spectral geological mapping of New York using ERTS-1 imagery
[E72-10223] 02 p0163 N73-11317
Evaluation of data compression technique for ERTS-1 multispectral imagery
[E72-10226] 02 p0163 N73-11319
Relationships of vegetation distribution to geomorphic characteristics of landscape and of plant phenological patterns to vegetation identification of satellite imagery of Arizona
[E72-10228] 02 p0163 N73-11321
ERTS-1 imagery of Lake Champlain and Vermont environments
[E72-10225] 03 p0288 N73-12333
Land use mapping of Phoenix quadrangle using ERTS-1 imagery
[E72-10236] 03 p0288 N73-12336
Application of ERTS-1 imagery to selected Bureau of Reclamation projects
[E72-10238] 03 p0288 N73-12338
Mapping land use and land use change in Central Atlantic Region using ERTS-1 imagery
[E72-10241] 03 p0288 N73-12341
ERTS-1 imagery of coastal marshland, tidal flats, and littoral transport in French Atlantic waters
[E72-10251] 03 p0289 N73-12351
ERTS-1 return beam vidicon imagery of Lake Champlain region and Vermont
[E72-10252] 03 p0289 N73-12352
Identification of Nevada wildland plants, vegetation, and fire scars from ERTS-1 imagery
[E72-10253] 03 p0289 N73-12353
Establishment of radiometric calibration technique to permit absolute reflectance characteristics of ground targets to be determined from ERTS-1 data
[E72-10255] 03 p0290 N73-12355
Identification of playa lakes in Texas High Plains from ERTS-1 imagery
[E72-10257] 03 p0290 N73-12357
Strip mine identification, land use assessment, smoke plume detection, and sedimentation patterns in Sandusky Bay from ERTS-1 imagery of Ohio
[E72-10259] 03 p0290 N73-12358
Geology and lithology of Afar region of Ethiopia based on ERTS-1 imagery
[E72-10261] 03 p0290 N73-12360
Monitoring plant development in California rangeland environments using ERTS-1 and supporting aircraft data
[E72-10263] 03 p0290 N73-12362
Application of ERTS-1 imagery to agriculture resource and land use evaluation in Mariposa County, Arizona and San Joaquin County, California
[E72-10264] 03 p0291 N73-12363
Vegetation, soil, and water reflectance measurements from ERTS-1 imagery of Hidalgo County, Texas
[E72-10267] 03 p0291 N73-12366
Prediction of ephemeral and perennial range quantity and quality during normal grazing season using ERTS-1 imagery
[E72-10269] 03 p0291 N73-12368
Polar region mapping using ERTS-1 return beam vidicon imagery
[E72-10273] 03 p0291 N73-12371
Photomapping of US using ERTS-1 return beam vidicon imagery
[E72-10274] 03 p0291 N73-12372
Thematic mapping using ERTS-1 return beam vidicon imagery
[E72-10275] 03 p0291 N73-12373
Overall evaluation of ERTS-1 RBV and MSS imagery for cartographic applications
[E72-10278] 03 p0292 N73-12376
Utilization of ERTS-1 imagery to determine availability and distribution of menhaden within Mississippi Sound and adjacent waters
[E72-10279] 03 p0292 N73-12377
Automated thematic mapping using multispectral and spatial pattern recognition techniques on ERTS-1 imagery
[E72-10281] 03 p0292 N73-12379
Land use mapping, limnology, wetlands, geomorphic and landform surveys, and river monitoring of Lake Champlain Basin and Vermont using ERTS-1 imagery
[E72-10282] 03 p0292 N73-12380
Study of marine environment of northern Gulf of California using ERTS-1 MSS imagery
[E72-10283] 03 p0292 N73-12381
Automatic photointerpretation for plant species and stress identification using ERTS-1 imagery
[E72-10258] 03 p0300 N73-12448
ERTS-1 imagery of Quaternary landforms and materials in Midwest and Great Plains
[E72-10272] 04 p0409 N73-13333
Natural resource inventory in Arizona using ERTS-1 imagery
[E72-10287] 04 p0410 N73-13337
Mapping, evaluation, and monitoring of coastal and saline wetlands ecology and shallow water environments using ERTS-1 imagery
[E72-10290] 04 p0410 N73-13340
Geological survey of Adirondack Mountain region using ERTS-1 multispectral scanner imagery
[E72-10291] 04 p0410 N73-13341
Digital precision processing of ERTS-1 imagery of Chesapeake Bay
[E72-10292] 04 p0410 N73-13342
Remote sensing of Thailand earth resources using ERTS-1 imagery
[E72-10298] 04 p0411 N73-13348
Application of ERTS-1 imagery to regional land use planning in Wisconsin
[E72-10299] 04 p0411 N73-13349
Environmental and resource study of Kansas using ERTS-1 imagery
[E72-10305] 04 p0412 N73-13354
Automatic identification of land uses in Milwaukee, Wisconsin using ERTS-1 imagery
[E72-10307] 04 p0412 N73-13356
Development of land use and peak runoff classification system for highway engineering using ERTS-1 imagery of Maine
[E72-10308] 04 p0412 N73-13357
Tectonic analysis of Bighorn Mountains using ERTS-1 imagery
[E72-10310] 04 p0412 N73-13359
Investigation of natural resources in remote and unexplored areas of Venezuela using ERTS-1 remotely sensed imagery
[E72-10311] 04 p0412 N73-13360
Application of ERTS-1 imagery to agricultural practices in Mississippi Delta Region
[E72-10312] 04 p0412 N73-13361
Multidisciplinary analysis of Michigan resources utilizing ERTS-1 imagery
[E72-10313] 04 p0412 N73-13362
Remote sensing of native arid plant distribution using ERTS-1
[E72-10314] 04 p0412 N73-13363
ERTS-1 imagery of California coastal nearshore processes
[E72-10316] 04 p0413 N73-13365
Utilization of ERTS-1 imagery in geological evaluation, regional planning, forest management, and water management in North Carolina
[E72-10317] 04 p0413 N73-13366
Acquisition and analysis of California coastal ground truth data for correlation with ERTS-1 imagery
[E72-10321] 04 p0413 N73-13369
Utilization of ERTS-1 imagery in national program for inspection of dams
[E72-10322] 04 p0413 N73-13370
Spectral geological mapping in diverse terranes of New York using ERTS-1 imagery
[E72-10302] 05 p0530 N73-14309
Utilization of ERTS-1 imagery of Alabama to study environmental factors, land use, and geology
[E72-10319] 05 p0530 N73-14310
Monitoring changing geologic features along Texas Gulf Coast using ERTS-1 imagery
[E72-10323] 05 p0530 N73-14311
First order land use classification in North Carolina based on ERTS-1 imagery
[E72-10324] 05 p0530 N73-14312
Radiometric calibration technique to permit absolute reflectance characteristics of ground targets to be determined from ERTS-1 data
[E72-10326] 05 p0530 N73-14314
Suitability of ERTS-1 imagery for oil exploration in Oklahoma
[E72-10327] 05 p0530 N73-14315
Resource inventory, land use, and pollution within Susquehanna River Basin based on interpretation of ERTS-1 data
[E72-10329] 05 p0531 N73-14317
Environmental indices covering land, water, and air quality compatible with ERTS-1 imagery
[E72-10330] 05 p0531 N73-14318
Utility of ERTS-1 imagery in study of geological structures and exploration for economic mineral deposits in Utah and Nevada
[E72-10332] 05 p0531 N73-14320
Sediment pattern correlation with tidal and inflow action in Chesapeake Bay using ERTS-1 data
[E72-10334] 05 p0531 N73-14322
Identification of agricultural crops and soil moisture stress in Iowa using ERTS-1 imagery
[E72-10335] 05 p0531 N73-14323
Crop identification and acreage measurement in Missouri, Kansas, South Dakota, and Idaho using ERTS-1 imagery
[E72-10336] 05 p0531 N73-14324
Tectonic analysis of Southwestern Wyoming from ERTS-1 imagery
[E72-10337] 05 p0532 N73-14325
Location of archaeological village sites in Alaska by ERTS-1 imagery
[E72-10338] 05 p0532 N73-14326
Improvement of menhaden fishery prediction in Mississippi Sound through ERTS-1 imagery
[E72-10340] 05 p0532 N73-14328
University of Alaska survey of environment using ERTS-1 imagery
[E72-10341] 05 p0532 N73-14329
Identification of phenological stages and vegetative types for land use classification based on ERTS-1 imagery
[E72-10342] 05 p0532 N73-14330
Survey of seasonal snow cover of Alaska from ERTS-1 imagery
[E72-10344] 05 p0532 N73-14332
ERTS-1 sensing of fall snow melting in Chena River Basin, Alaska
[E72-10345] 05 p0533 N73-14333
Application of ERTS-1 imagery to study of caribou movements and winter dispersal in relation to prevailing snow cover
[E72-10346] 05 p0533 N73-14334
ERTS-1 imagery of surface water circulation in Prince William Sound
[E72-10348] 05 p0533 N73-14336
Mapping of regional fracture patterns and related structural features of Wind River Mountains using ERTS-1 imagery
[E72-10349] 05 p0533 N73-14337
Microdensitometer scans of ERTS-1 imagery of Gulf of California
[E72-10350] 05 p0533 N73-14338

Identification of phenological events, rangelands, and crops using ERTS-1 imagery
[E72-10351] 05 p0533 N73-14339
ERTS-1 data as teaching and research tool in Department of Geology at University of Alaska
[E72-10353] 05 p0534 N73-14341
ERTS-1 remotely sensed imagery to support study of Lake Ontario basin as part of International Field Year for the Great Lakes
[E72-10354] 05 p0534 N73-14342
Geographic applications of ERTS-1 imagery to rural landscape change in Tennessee
[E72-10355] 05 p0534 N73-14343
Utilization of ERTS-1 imagery to map soils and vegetation in Idaho
[E72-10356] 05 p0534 N73-14344
Mapping of land use in Northern Megalopolis of Massachusetts, Connecticut, Rhode Island, and New York based on ERTS-1 imagery
[E72-10357] 05 p0534 N73-14345
Utilization of ERTS-1 data to monitor and classify eutrophication of inland lakes
[E72-10358] 05 p0534 N73-14346
Determination of aerosol optical thickness in atmosphere at Salton Sea and San Diego based on ERTS-1 data
[E72-10359] 05 p0534 N73-14347
Inventory and monitoring of natural vegetation and related resources in arid environment of Arizona using ERTS-1 imagery
[E72-10360] 05 p0534 N73-14348
Identification of mine dumps with and without vegetative cover using ERTS-1 imagery
[E72-10361] 05 p0535 N73-14349
ERTS-1 measurement of vegetation, soil, and water reflectance
[E72-10364] 05 p0535 N73-14352
Digital correction techniques for ERTS-1 imagery
[E72-10365] 05 p0535 N73-14353
Utilization of ERTS-1 imagery in air pollution and marine biology studies of lower Chesapeake Bay and continental shelf of Eastern US
[E72-10367] 05 p0535 N73-14355
Land use mapping of northern megalopolis using ERTS-1 imagery
[E72-10368] 05 p0535 N73-14356
Soil mapping, crop identification, and rangeland assessment in Great Plains using ERTS-1 multisensor imagery
[E72-10369] 05 p0536 N73-14357
Environmental analyses of Alaskan arctic and subarctic geology and geomorphology using ERTS-1 imagery
[E72-10370] 05 p0536 N73-14358
ERTS-1 detection and monitoring of vegetation damage associated with highways and highway facilities in Maine
[E72-10371] 05 p0536 N73-14359
Snow enhancement in New England test areas based on ERTS-1 imagery
[E73-10001] 06 p0657 N73-15337
Ocean water color assessment from ERTS-1 RBV and MSS imagery
[E73-10002] 06 p0658 N73-15338
Utilization of ERTS-1 imagery for mapping large scale structural lineamants in Precambrian Shield and basins containing younger sediments and for mineral and petroleum exploration
[E73-10004] 06 p0658 N73-15340
Geological structure of selected areas of East Africa based on ERTS-1 imagery
[E73-10005] 06 p0658 N73-15341
Photointerpretation and thematic mapping of ERTS-1 imagery of Brownsville, Texas area
[E73-10006] 06 p0658 N73-15342
Identification and mapping of coastal vegetation species in ERTS-1 imagery of Delaware
[E73-10007] 06 p0658 N73-15343
Resources inventory and land use management in Oregon using ERTS-1 imagery
[E73-10008] 06 p0658 N73-15344
Mapping of remote desert dune fields using ERTS-1 imagery
[E73-10009] 06 p0659 N73-15345
Evaluation of ERTS-1 imagery data compression algorithm technique
[E73-10012] 06 p0659 N73-15348
Mapping distribution of glaciofluvial deposits and associated glacial landforms
[E73-10013] 06 p0659 N73-15349
Geological analysis and evaluation of ERTS-1 imagery of New Mexico
[E73-10015] 06 p0659 N73-15351
Evaluation of ERTS-1 imagery for hydrological information in Sierra Nevada Mountains and Lake Ontario areas
[E73-10016] 06 p0659 N73-15352
Utilization of ERTS-1 imagery for oceanographic studies of Great Lakes
[E73-10017] 06 p0659 N73-15353
Photointerpretation of ERTS-1 imagery of Arizona with emphasis on porphyry copper deposits occurring at intersection of major faults and igneous intrusions
[E73-10018] 06 p0659 N73-15354
Wildland resources inventory of Nevada Great Basin using ERTS-1 imagery
[E73-10019] 06 p0659 N73-15355
Recognition of geologic framework of copper and molybdenum porphyry deposits on ERTS-1 imagery of Navada and Utah
[E73-10020] 06 p0659 N73-15356
Automated thematic mapping and interpretation of hydrologic and agricultural resources using ERTS-1 imagery
[E73-10023] 06 p0660 N73-15357
Mapping and inventories of land use and natural resources in New York based on ERTS-1 imagery
[E73-10024] 06 p0660 N73-15358
Utilization of ERTS-1 imagery to study short-lived events such as fires, volcanism, storms, and earthquakes
[E73-10025] 06 p0660 N73-15359
Mapping of major geological structures of African Rift System using ERTS-1 imagery
[E73-10026] 06 p0660 N73-15360
ERTS-1 imagery of crustal structure of area from eastern Sierra Nevada to Colorado Plateau
[E73-10028] 06 p0660 N73-15361
Location of ocean current boundaries in Gulf of Mexico by ERTS-1 sensing of water color changes
[E73-10030] 06 p0660 N73-15363
Geological mapping of New York State using ERTS-1 imagery
[E73-10031] 06 p0660 N73-15364
Resources management in Ohio utilizing ERTS-1 imagery
[E73-10032] 06 p0661 N73-15365
Interdisciplinary analysis of ERTS-1 multispectral data of Colorado mountain areas using automatic data processing techniques
[E73-10033] 06 p0661 N73-15366
Land use mapping and change detection in Central Atlantic Regional Ecological Test Site based on ERTS-1 MSS imagery
[E73-10034] 06 p0661 N73-15367
Time-lapse data processing of ERTS-1 imagery for dynamic hydrologic conditions
[E73-10035] 07 p0776 N73-16299
Application of ERTS-1 imagery to evaluation and management of Wyoming natural resources
[E73-10037] 07 p0776 N73-16300
Regional planning based on ERTS-1 MSS imagery
[E73-10038] 07 p0776 N73-16301
Crop identification and acreage estimation using ERTS-1 MSS imagery of northern Illinois
[E73-10039] 07 p0776 N73-16302
Geographic applications of ERTS-1 imagery to rural landscape changes in eastern Tennessee
[E73-10040] 07 p0776 N73-16303
Acquisition and analysis of coastal ground data for correlation with ERTS-1 imagery of Monterey Bay and Santa Barbara Channel areas of California
[E73-10043] 07 p0776 N73-16306
Flood damage in west central Iowa based on ERTS-1 imagery
[E73-10045] 07 p0777 N73-16308
ERTS-1 imagery of geology, agriculture, hydrology, and ecology of Niger River Delta, Republic of Mali
[E73-10047] 07 p0777 N73-16309
Sedimentation levels in rivers and shoal estuarine waters based on ERTS-1 imagery
[E73-10048] 07 p0777 N73-16310
Surveying and mapping earth resources over large areas utilizing ERTS-1 imagery
[E73-10049] 07 p0777 N73-16311
Application of ERTS-1 MSS imagery to coastal engineering planning and construction
[E73-10050] 07 p0777 N73-16312
Cartographic applications of ERTS-1 imagery in polar regions
[E73-10051] 07 p0777 N73-16313
Cultural interpretation and map revisions from ERTS-1 imagery
[E73-10052] 07 p0777 N73-16314
Cartographic applications of ERTS-1 MSS imagery
[E73-10053] 07 p0777 N73-16315
Digital processing of ERTS-1 imagery of Tennessee Valley
[E73-10054] 07 p0778 N73-16316
Reservoir and watershed management utilizing ERTS-1 imagery
[E73-10055] 07 p0778 N73-16317
Computer processing, enhancement, and recognition of ERTS imagery of Tennessee Valley
[E73-10056] 07 p0778 N73-16318
ERTS-1 imagery of suspended sediment plumes in Lake Ontario
[E73-10057] 07 p0778 N73-16319
Prediction of ephemeral and perennial range quality and quantity during normal grazing season based on ERTS-1 imagery
[E73-10061] 07 p0778 N73-16323
Mapping and detection of changes of snow cover on land and glaciers
[E73-10063] 07 p0778 N73-16325
Census cities experiment in urban land use and change detection using ERRS-1 imagery
[E73-10064] 07 p0778 N73-16326
Application of ERTS-1 remotely sensed imagery to selected reclamation projects
[E73-10066] 07 p0779 N73-16328
Utilization of ERTS-1 imagery for evaluation of Iranian playas as potential locations for economic and engineering development
[E73-10067] 07 p0779 N73-16329
Prediction of range quantity and quality in desert areas of California and Arizona during growing and grazing seasons
[E73-10068] 07 p0779 N73-16330
Utilization of ERTS-1 MSS imagery for study of faulting in alluvium of California, Nevada, and Arizona
[E73-10070] 07 p0779 N73-16332
Value of ERTS-1 imagery in resource evaluation on national scale in South Africa
[E73-10071] 07 p0779 N73-16333
Land use planning and management on Mississippi Gulf Coast using ERTS-1 imagery
[E73-10072] 07 p0779 N73-16334
Mapping and control of pink cotton bollworm in California
[E73-10073] 07 p0780 N73-16335
Geologic investigation of Basin and Range-Colorado Plateau boundary in northwestern and north central Arizona using ERTS-1 and EREP imagery
[E73-10074] 07 p0780 N73-16336
Applicated of ERTS-1 imagery to agriculture practices in Mississippi Delta region
[E73-10075] 07 p0780 N73-16337
ERTS-1 MSS imagery of Great Plains rangeland, croplands, and land systems
[E73-10076] 07 p0780 N73-16338
ERTS-1 imagery of plant growth and annual flooding in Niger River inland delta
[E73-10078] 07 p0780 N73-16339
Planimetric, topographic, and thematic mapping using remotely sensed imagery
07 p0786 N73-16391
Regional land use mapping and management using remotely sensed imagery
07 p0786 N73-16392
Acquisition of data concerning urban housing quality using remotely sensed imagery
07 p0786 N73-16393
Urban and regional changes based on city census and remotely sensed imagery
07 p0786 N73-16395
Detection, identification, measurement, and monitoring environmental pollution by remote sensing devices and techniques
07 p0786 N73-16397
Utilization of ERTS-1 imagery for water resources management in Delaware River Basin
07 p0787 N73-16404
Analysis of hydrologic conditions based on Nimbus satellite imagery
07 p0788 N73-16405
Earth resources surveys and management in California using ERTS-1 and supporting aircraft data
[E73-10027] 08 p0900 N73-17287
Tectonic analysis of Bighorn Mountains using ERTS-1 imagery
[E73-10036] 08 p0900 N73-17288
Repetitive ERTS-1 imagery of surface water variability and flooding along rivers and low-lying areas in Virginia, Iowa, and California
[E73-10046] 08 p0900 N73-17289
Application of ERTS-1 imagery to regional land use planning in Wisconsin
[E73-10077] 08 p0900 N73-17290
Prediction of menhaden school location and movement in Mississippi Sound from ERTS-1 imagery
[E73-10079] 08 p0900 N73-17291
Digital processing of ERTS-1 imagery
[E73-10080] 08 p0901 N73-17292
Utilization of ERTS-1 and aircraft remotely sensed data for land use inventory and planning in Maryland
[E73-10081] 08 p0901 N73-17293
Urban and regional planning in Brevard County, Florida using ERTS-1 imagery
[E73-10083] 08 p0901 N73-17295
Forest and rangeland inventory and forest infestation of Atlanta, Manitou, and Black Hills test sites based on ERTS-1 imagery
[E73-10084] 08 p0901 N73-17296
Determination of meteorological information of ERTS-1 MSS bulk data at 0.6 - 0.7 microns as function of resolution
[E73-10085] 08 p0901 N73-17297
Utilization of ERT-1 imagery for water depth measurement, Yellowstone Park data, atmospheric effects in Colorado, lake ice surveillance, recreational land use, IFYGL, image enhancement, water quality monitoring, oil pollution detection, and mapping iron compounds
[E73-10086] 08 p0901 N73-17298
Mapping snow cover in western US using ERTS-1 MSS imagery
[E73-10087] 08 p0901 N73-17299
Photomapping of US using ERTS-1 MSS and RBV imagery
[E73-10088] 08 p0902 N73-17300

Application of ERTS-1 imagery to thematic mapping of open water, ice and snow cover, vegetation, and works of man
[E73-10089] 08 p0902 N73-17301
Land use mapping and image enhancement of ERTS-1 imagery of Phoenix Quadrangle
[E73-10090] 08 p0902 N73-17302
ERTS-1 imagery of estuarine and coastal water dynamics controlling sediment transport and plume development in Long Island Sound
[E73-10093] 08 p0902 N73-17305
Distribution and density of phreatophytes and other arid land plants measured from ERTS-1 imagery
[E73-10094] 08 p0902 N73-17306
Investigation of phytoplankton populations in waters along eastern coast of US using ERTS-1 imagery and surface measurements
[E73-10097] 08 p0902 N73-17308
ERTS-1 detection of potential locust breeding sites in Saudi Arabian desert
[E73-10098] 08 p0902 N73-17309
Development of land use-peak runoff classification system for highway engineering in Maryland
[E73-10100] 08 p0902 N73-17310
ERTS-1 identification of phenological stages and vegetation types in Alaska for land use classification
[E73-10276] 08 p0914 N73-17484
Glaciology and volcanology studies in Wrangell Mountains, Alaska using ERTS-1 imagery
[E73-10277] 08 p0914 N73-17485
Mapping Arctic sea ice from ERTS-1 MSS imagery
[E73-10278] 08 p0914 N73-17486
Alaskan arctic and subarctic sediment deposition, permafrost, snow cover, and ice mapping from ERTS-1 imagery
[E73-10279] 08 p0914 N73-17487
Tectonic and paleogeologic mapping of Montana using ERTS-1 imagery
[E73-10280] 08 p0914 N73-17488
Preparation of mosaic of Alaska using ERTS-1 imagery
[E73-10284] 08 p0914 N73-17490
Application of ERTS-1 imagery to study of caribou movements and winter dispersal in relation to snow cover
[E73-10285] 08 p0914 N73-17491
Regional geologic, tectonic, and volcanic surveys of Bolivia using ERTS-1 imagery
[E73-10286] 08 p0914 N73-17492
Evaluation of data compression techniques for ERTS-1 MSS imagery
[E73-10287] 08 p0915 N73-17493
ERTS-1 imagery of wetlands ecology in Maryland, Georgia, and Chesepeake Bay test sites
[E73-10288] 08 p0915 N73-17494
Development of system for mapping and monitoring natural ecosystems and environmental complexes from ERTS-1 imagery of California, Nevada, Four Corners Area, Louisiana, and Colorado Plateau
[E73-10289] 08 p0915 N73-17495
Surface water circulation in Prince William Sound using ERTS-1 imagery
[E73-10291] 08 p0915 N73-17496
ERTS-1 imagery of snow cover and break-up characteristics in Chena River Basin, Alaska
[E73-10292] 08 p0915 N73-17497
Application of ERTS-1 imagery to fracture related mine safety hazards in coal mining industry in Indiana and Illinois
[E73-10096] 09 p1020 N73-18321
ERTS-1 imagery of geography, geology, and glaciology of Germany and part of Alps Mountains
[E73-10099] 09 p1020 N73-18322
Utilization of ERTS-1 imagery for study of hydrology and limnology in Finland
[E73-10101] 09 p1020 N73-18323
Identification and interpretation of tectonic features of Colorado, California, and Sonora, Mexico
[E73-10275] 09 p1020 N73-18324
Geologic mapping of Montana using ERTS-1 imagery
[E73-10281] 09 p1020 N73-18325
Mapping seismically active faults in Alaska from ERTS-1 imagery
[E73-10283] 09 p1020 N73-18326
Mapping of soil-vegetation groupings in Arizona using ERTS-1 imagery
[E73-10290] 09 p1020 N73-18327
Applicability of ERTS-1 imagery to forestry and timber survey and identification in Finland
[E73-10297] 09 p1021 N73-18329
Evaluation of ERTS-1 imagery for mapping geological structures in New York
[E73-10298] 09 p1021 N73-18330
Monitoring and classifying eutrophication of inland lakes
[E73-10299] 09 p1021 N73-18331
Utilization of ERTS-1 imagery in geological evaluation, regional planning, forest and water management in North Carolina
[E73-10300] 09 p1021 N73-18332
Distinguishing major lithologic types in rocks of Precambrian age in central Wyoming using multilevel sensing
[E73-10301] 09 p1021 N73-18333
Effectiveness of ERTS-1 imagery in monitoring vegetation conditions of direct concern to range land management and agriculture business decisions in Great Plains Corridor
[E73-10302] 09 p1021 N73-18334
ERTS-1 imagery of vernal advancement and retrogradation of natural rangeland vegetation of Great Plains Corridor
[E73-10303] 09 p1021 N73-18335
ERTS-1 imagery of oceanography and marine environment of northern Gulf of California
[E73-10304] 09 p1021 N73-18336
Vegetation map of western Seward Peninsula, Alaska, based on ERTS-1 imagery
[E73-10305] 09 p1022 N73-18337
Land use management and planning in Alaska using ERTS-1 imagery
[E73-10307] 09 p1022 N73-18339
Reservoir management and operation using ERTS-1 imagery
[E73-10308] 09 p1022 N73-18340
ERTS-1 imagery of geology in ice free valleys of Antarctica
[E73-10309] 09 p1022 N73-18341
Multidisciplinary analysis of forestry, agriculture, soils, and landforms in Michigan using ERTS-1 imagery
[E73-10310] 09 p1022 N73-18342
Detection of plant and forest diseases, nutrient deficiencies, soil types, and soil moisture levels from ERTS-1 imagery of Tennessee
[E73-10311] 09 p1022 N73-18343
Detection and monitoring forest insect infestations in Sierra Nevada Mountains of California using ERTS-1 imagery
[E73-10312] 09 p1022 N73-18344
Evaluation of ERTS-1 imagery for study of geological structures and features and exploration of mineral deposits in Utah and Nevada
[E73-10313] 09 p1022 N73-18345
Dispersal patterns of suspended particles in nearshore surface waters of northeast Pacific Ocean and Hawaiian Islands
[E73-10314] 09 p1023 N73-18346
ERTS-1 multispectral imagery of West Pakistan
[E73-10315] 09 p1023 N73-18347
ERTS-1 imagery of suspended sediment plumes in Lake Ontario
[E73-10316] 09 p1023 N73-18348
Thermal surveillance of volcanoes of Cascade Range and Iceland using ERTS-1 DCP systems and imagery
[E73-10317] 09 p1023 N73-18349
Preparation of hydrologic atlases of arid land watersheds using ERTS-1 imagery
[E73-10318] 09 p1023 N73-18350
Information system for ERTS-1 data on timber resources in Washington and Oregon
[E73-10319] 09 p1023 N73-18351
ERTS-1 imagery of permafrost and geologic hazards in Alaska
[E73-10320] 09 p1023 N73-18352
ERTS-1 imagery of geostructures of Alaskan continental crust and relation to mineral resources
[E73-10321] 09 p1024 N73-18353
Oil exploration in Oklahoma using ERTS-1 MSS imagery
[E73-10322] 09 p1024 N73-18354
Evaluation of ERTS-1 imagery of major crops and soil associations for selected sites in central United States
[E73-10323] 09 p1024 N73-18355
Survey and mapping of snow and ground water levels in Norway using ERTS-1 imagery
[E73-10324] 09 p1024 N73-18356
Dynamics of plankton populations in upwelling waters along Arabian Coast, Somali Coast, and Northwest Coast of Africa
[E73-10325] 09 p1024 N73-18357
Crop identification and acreage measurement in Missouri, Kansas, South Dakata, and Idaho based on ERTS-1 imagery and aerial photography
[E73-10328] 09 p1024 N73-18359
Cartographic evaluation of ERTS-1 MSS imagery
[E73-10329] 09 p1024 N73-18360
Detection and monitoring vegetation damage associated with highway facilities in Maine
[E73-10331] 09 p1024 N73-18361
Study of continental migratory bird habitat changes using ERTS-1 imagery
[E73-10334] 09 p1025 N73-18364
Location of earthquake epicenters and major fault zones in Nevada using ERTS-1 imagery
[E73-10338] 09 p1025 N73-18366
Location of ocean current boundaries in Gulf of Mexico by sensing color change associated with cyclonic edge of zone of horizontal velocity shear
[E73-10022] 10 p1146 N73-19330
ERTS-1 imagery of regional geography and geomorphology of Mankoya-Kolwezi strip in Zambia and Zaire
[E73-10293] 10 p1146 N73-19331
ERTS-1 imagery of geography and geomorphology of Ndola-Mweru Wantipa strip in Zambia and Zaire
[E73-10294] 10 p1146 N73-19332
Application of ERTS-1 imagery to protection and management of New Jersey coastal environment
[E73-10330] 10 p1147 N73-19335
Application of ERTS-1 imagery to Bureau of Reclamation studies of geology, agriculture, and urban development
[E73-10336] 10 p1147 N73-19337
Utilization of ERTS-1 imagery for evaluation of Iranian playas as potential locations for economic and engineering development
[E73-10339] 10 p1147 N73-19338
Precision geometric and radiometric correction of bulk digital ERTS-1 imagery by digital techniques
[E73-10342] 10 p1148 N73-19341
Identification and classification of Iowa crop lands using ERTS-1 imagery and aerial photography
[E73-10343] 10 p1148 N73-19342
Optimized method of remote haze detection using ERTS-1 imagery
[E73-10344] 10 p1148 N73-19343
Geologic and land use exploitation of ERTS-1 imagery of New England using snow enhancement techniques
[E73-10345] 10 p1148 N73-19344
Computer program for analysis of ERTS-1 MSS imagery of haze in Southern California test area
[E73-10346] 10 p1148 N73-19345
Development of standards for classification, mapping and scientific analysis of land use and land use change in Central Atlantic Region Ecological Test Site using ERTS-1 imagery
[E73-10347] 10 p1148 N73-19346
Interdisciplinary analysis of ERTS-1 imagery for Colorado mountain areas using ADP techniques
[E73-10348] 10 p1148 N73-19347
Evaluation of ERTS-1 imagery for mapping land use and updating Minnesota land management information system
[E73-10352] 10 p1148 N73-19348
Mapping distribution of glaciofluvial deposits and associated glacial landforms in Maine from ERTS-1 imagery
[E73-10353] 10 p1148 N73-19349
ERTS-1 imagery of crustal structure of strip from eastern Sierra Nevada to Colorado Plateau
[E73-10355] 10 p1149 N73-19351
Evaluation of Great Lakes oceanography from ERTS-1 imagery
[E73-10356] 10 p1149 N73-19352
Meteorological utility of high resolution ERTS-1 multispectral data
[E73-10357] 10 p1149 N73-19353
Evaluation of geologic applications of ERTS-1 imagery for New Mexico
[E73-10358] 10 p1149 N73-19354
Utilization of ERTS-1 imagery to study watershed hydrology in Southern Great Plains
[E73-10359] 10 p1149 N73-19355
Assessment of range fire damage in Sand Hills Region of Nebraska based on ERTS-1 imagery
[E73-10360] 10 p1149 N73-19356
Detection and mapping snow cover in Salt-Verde Watershed of Arizona using ERTS-1 imagery
[E73-10361] 10 p1149 N73-19357
Mapping northern Atlantic coastal marshlands of Maryland, Delaware, and Virginia using ERTS-1 imagery
[E73-10363] 10 p1150 N73-19359
Crop identification, soil mapping, water resources, and urban land use analysis in Wabash River Basin based on ERTS-1 imagery
[E73-10364] 10 p1150 N73-19360
Automatic interpretation of ERTS-1 data for forest management in Minnesota
[E73-10365] 10 p1150 N73-19361
Automatic interpretation of forest species and stress identification using ERTS-1 imagery of Minnesota
[E73-10366] 10 p1150 N73-19362
Identification of marsh vegetation and coastal land use in Delaware from ERTS-1 imagery
[E73-10367] 10 p1150 N73-19363
Study of suspended sediment and aquatic fronts in Delaware Bay using ERTS-1 imagery
[E73-10368] 10 p1150 N73-19364
Identification of native arid plant distribution in Avra Valley, Arizona using ERTS-1 imagery
[E73-10369] 10 p1151 N73-19365
Application of ERTS-1 imagery to fracture related mine safety hazards in coal mining industry in Indiana and Illinois
[E73-10371] 10 p1151 N73-19366
Mapping and management of soil range resources in Sand Hills Region of Nebraska using ERTS-1 imagery
[E73-10372] 10 p1151 N73-19367
Computer processing of multispectral imagery of India
[E73-10373] 10 p1151 N73-19368
Detection and mapping Arctic sea ice using ERTS-1 imagery
[E73-10374] 10 p1151 N73-19369
Measurement of coastal currents and processes and seaward extent of suspended sediment transport in waters of California
[E73-10375] 10 p1151 N73-19370

Prediction of ephemeral and perennial range quantity and quality during normal grazing season in Arizona based on ERTS-1 imagery
[E73-10377] 10 p1152 N73-19372
Mapping and detection of snow cover on land and glaciers in Cascade Range using ERTS-1 imagery
[E73-10379] 10 p1152 N73-19374
Analysis of ERTS-1 multispectral imagery of Northwest Saudi Arabia
[E73-10380] 10 p1152 N73-19375
Utilization of ERTS-1 imagery to detect and map erosion features and changes in southern Arizona
[E73-10382] 10 p1152 N73-19377
Thematic mapping and terrain analysis using diffraction patterns of ERTS-1 imagery
[E73-10385] 10 p1153 N73-19378
Automated thematic mapping and analysis of terrain in Arizona, Texas, Washington, Utah, Louisiana, and California using ERTS-1 imagery
[E73-10386] 10 p1153 N73-19379
Soil mapping of rangelands in Bennett County, South Dakota using remotely sensed imagery
[NASA-CR-131229] 10 p1155 N73-19395
Radiometric calibration technique to permit absolute reflectance characteristics of ground targets to be determined from ERTS-1 imagery
[E73-10349] 11 p1274 N73-20343
Sea ice and surface water circulation in Cook Inlet, Alaska, and along continental shelves
[E73-10370] 11 p1275 N73-20346
Catalogue of selected remote sensing data for New Jersey environment protection and management
[E73-10383] 11 p1275 N73-20347
Processing, analysis, and management of ERTS-1 data for selected disciplines and areas
[E73-10387] 11 p1275 N73-20349
Water depth measurement and mapping of shallow water features of Little Baham Bank using ERTS-1 imagery
[E73-10388] 11 p1275 N73-20350
Terrain classification mapping of Yellowstone National Park
[E73-10389] 11 p1276 N73-20351
Atmospheric effects on recognition of rice and corn in ERTS-1 imagery of Sacramento Valley
[E73-10390] 11 p1276 N73-20352
Computer mapping of Michigan recreational land use using ERTS-1 data
[E73-10392] 11 p1276 N73-20354
Processing of IFYGL data for Lake Ontario and its drainage basin
[E73-10393] 11 p1276 N73-20355
Atmospheric effects on ERTS-1 imagery and spatial resolution of MSS data
[E73-10394] 11 p1276 N73-20356
Monitoring of water quality in New York Bight and Tampa Bay, Florida, using ERTS-1 imagery
[E73-10395] 11 p1276 N73-20357
ERTS-1 detection of oil pollution in Gulf of Mexico and in waters off Salem, Massachusetts and Oakland, California
[E73-10396] 11 p1276 N73-20358
Spectral ratio mapping of iron ore deposits in Wind River Range, Wyoming, using ERTS-1 data
[E73-10397] 11 p1276 N73-20359
ERTS-1 imagery of ice bréak-up characteristics of Chena River Basin
[E73-10400] 11 p1277 N73-20362
Utilization of ERTS-1 imagery for study of caribou movements and winter dispersal in relation to prevailing Alaskan snow cover
[E73-10401] 11 p1277 N73-20363
ERTS-1 imagery of water circulation in Prince William Sound
[E73-10402] 11 p1277 N73-20364
Utilization of ERTS-1 imagery as teaching and research tool in Department of Geology at University of Alaska
[E73-10403] 11 p1277 N73-20365
ERTS-1 imagery of glaciology and volcanology in Wrangell Mountains, Alaska
[E73-10404] 11 p1277 N73-20366
Locating archaeological village sites in Alaska from remotely sensed imagery
[E73-10406] 11 p1277 N73-20368
ERTS-1 spectral reflectance measurements of vegetation, soil, and water in Rio Grande Valley, New Mexico
[E73-10408] 11 p1278 N73-20370
Search for porphyry copper deposits in Pakistani Baluchistan using ERTS-1 imagery
[E73-10410] 11 p1278 N73-20372
Timber inventory and management in Washington using ERTS-1 imagery
[E73-10411] 11 p1278 N73-20373
ERTS-1 imagery of inner shelf and coastal sedimentation environment of Beaufort Sea, Alaska
[E73-10412] 11 p1278 N73-20374
Utilization of ERTS-1 imagery in structural reconnaissance for minerals and oil in Alaska, Canada, Montana, Colorado, New Mexico, and Texas
[E73-10414] 11 p1279 N73-20376
Determination of ecosystem-vegetation boundaries from ERTS-1 imagery of Tennessee
[E73-10417] 11 p1279 N73-20379
Location of center pivot sprinkler irrigation systems in Finney County, Kansas, based on ERTS-1 interpretation
[E73-10418] 11 p1279 N73-20380
Detection of smoke pollution in Virginia by photogrammetric and densitometric analysis of ERTS-1 imagery
[E73-10419] 11 p1279 N73-20381
Analysis of ERTS-1 imagery for identification and discrimination of geological and hydrological phenomena in central and western Colorado
[E73-10422] 11 p1280 N73-20383
Application of ERTS-1 imagery to urban and regional planning in Florida
[E73-10423] 11 p1280 N73-20384
Correlation of chlorophyll and suspended sediments in Chesapeake Bay to ERTS-1 imagery
[E73-10424] 11 p1280 N73-20385
Utilization of ERTS-1 imagery for mapping extent of Pleistocene glaciation and delineation of small urban areas in Wyoming
[E73-10425] 11 p1280 N73-20386
Application of ecological, geological, and oceanographic ERTS-1 imagery to coastal resources management and planning in Delaware
[E73-10426] 11 p1280 N73-20387
Development of multistage forest sampling inventory system using ERTS-1 imagery
[E73-10428] 11 p1280 N73-20389
Ecological effects of coal strip mining in Ohio
[E73-10430] 11 p1281 N73-20391
Mapping of major structural lineaments of Ethiopian rift using ERTS-1 imagery
[E73-10431] 11 p1281 N73-20392
ERTS-1 observations of plant growth and annual flooding in Inland Delta of Niger River in Mali
[E73-10436] 11 p1281 N73-20396
Resources management in Ohio using ERTS-1 imagery
[E73-10437] 11 p1281 N73-20397
Survey of seasonal snow and ice covers in Alaska using ERTS-1 imagery
[E73-10438] 11 p1281 N73-20398
ERTS-1 imagery applied to geological and water resources investigations of Basin and Range - Colorado Plateau boundary in northwestern and north central Arizona
[E73-10441] 11 p1282 N73-20401
Natural resources management and inventory of Arizona using ERTS-1 imagery
[E73-10442] 11 p1282 N73-20402
Suitability of ERTS-1 imagery for oil exploration
[E73-10444] 11 p1282 N73-20404
Monitoring and classifying eutrophication of inland lakes from ERTS-1 imagery
[E73-10445] 11 p1282 N73-20405
Identification and interpretation of tectonic features and mercury deposited in California coast ranges and western transverse ranges
[E73-10446] 11 p1282 N73-20406
Application of ERTS-1 imagery to regional land use planning in Wisconsin
[E73-10448] 11 p1283 N73-20408
Wildland resource evaluation in Nevada using ERTS-1 imagery
[E73-10450] 11 p1283 N73-20410
Detection and evaluation of worldwide short-lived events from ERTS-1 imagery
[E73-10453] 11 p1283 N73-20412
Physical interpretation of geology, hydrology, and glaciology revealed by ERTS-1 imagery of east central Ohio
[E73-10454] 11 p1283 N73-20413
Coordination and establishment of centralized facilities and services for University of Alaska ERTS-1 survey of Alaskan environment
[E73-10459] 11 p1284 N73-20417
Utilization of ERTS-1 imagery in mesometeorological studies of Great Lakes
[E73-10464] 11 p1284 N73-20420
ERTS-1 imagery in national program for inspection of dams
[AD-754579] 11 p1288 N73-20449
Coupled modes on dielectric image waveguide
12 p1382 N73-21206
Establishment of radiometric calibration technique to permit absolute reflectance characteristics of ground targets to be determined from ERTS-1 data
[E73-10458] 12 p1394 N73-21300
Location of wet areas and detection of potential locust breeding sites using ERTS-1 imagery of Red Sea coastal plain of Saudi Arabia
[E73-10462] 12 p1394 N73-21301
Thematic and photomapping of Arizona CARETS, and polar regions from ERTS-1 imagery
[E73-10463] 12 p1394 N73-21302
Technique for processing and compressing ERTS-1 imagery of California
[E73-10465] 12 p1394 N73-21303
Characterization of wetlands and marshlands by automatic processing of ERTS-1 data
[E73-10467] 12 p1394 N73-21304
Application of ERTS-1 imagery to analysis of agricultural crops and forests in Michigan
[E73-10470] 12 p1395 N73-21307
Detection and indentification of major airports in northeastern Kansas and northwestern Missouri
[E73-10471] 12 p1395 N73-21308
Identification of corn harvesting in Finney County, Kansas from ERTS-1 imagery
[E73-10472] 12 p1395 N73-21309
Compilation of photomaps of Nevada geology from ERTS-1 imagery
[E73-10473] 12 p1395 N73-21310
Mapping of land use in agriculture area of Finney County, Kansas based on ERTS-1 imagery
[E73-10474] 12 p1395 N73-21311
Identification and mapping soil in Tennessee Valley from ERTS-1 imagery
[E73-10477] 12 p1395 N73-21314
ERTS-1 imagery of structural and lithological properties of Northern Coast Ranges and Sacramento Valley, california
[E73-10478] 12 p1396 N73-21315
Improvement of Menhaden fishery prediction in Mississippi Sound using ERTS-1 imagery
[E73-10480] 12 p1396 N73-21317
Development of techniques for evaluation of ERTS-1 imagery of natural resources in remote and unexplored areas of Venezuela
[E73-10481] 12 p1396 N73-21318
Acquisition and analysis of coastal ground truth data in pacific water off California for correlation with ERTS-1 imagery
[E73-10482] 12 p1396 N73-21319
Application of ERTS-1 data to analysis of agricultural crops, forests, soils, landforms, and acreage estimates in Michigan
[E73-10483] 12 p1396 N73-21320
Evaluation of ERTS-1 data for hydrologic information in Sierra Nevada and Lake Ontario
[E73-10485] 12 p1396 N73-21322
Evaluation of hydrology and vegetation in Sahelian zone of Mali, Mauritania, and Senegal during dry season/drought period based on ERTS-1 imagery
[E73-10488] 12 p1396 N73-21324
Utilization of ERTS-1 imagery for monitoring weather conditions for cloud seeding control
[E73-10489] 12 p1397 N73-21325
Census cities experiment in detection of urban change and land use
[E73-10490] 12 p1397 N73-21326
ERTS-1 imagery of inner shelf and coastal sedimentation environment of Beaufort Sea
[E73-10492] 12 p1397 N73-21328
ERTS-1 imagery of permafrost and geologic hazards in Alaska
[E73-10495] 12 p1397 N73-21331
Prototype regional environmental information system based on ERTS-1 imagery of Central Atlantic Regional Ecological Test Site
[E73-10497] 12 p1397 N73-21333
Identifying phenological changes for specific forest and crop types using ERTS-1 imagery
[E73-10498] 12 p1398 N73-21334
Optimization of haze detection by ERTS-1 MSS imagery
[E73-10499] 12 p1398 N73-21335
Application of ERTS-1 imagery to thematic mapping of Washington-Baltimore corridors
[E73-10500] 12 p1398 N73-21336
Photomapping of Phoenix area from ERTS-1 RBV imagery
[E73-10502] 12 p1398 N73-21338
ERTS-1 imagery of flood damage to farmlands in South Dakota
[NASA-CR-131641] 12 p1401 N73-21361
Digital correction techniques for ERTS-1 MSS imagery
[E73-10503] 13 p1515 N73-22278
Development of multistage forest sampling inventory system using ERTS-1 MSS data
[E73-10508] 13 p1516 N73-22283
Application of ERTS-1 MSS imagery to multidisciplinary investigations in Alabama
[E73-10509] 13 p1516 N73-22284
Identification of vegetation and soils in Idaho using ERTS-1 remotely sensed imagery
[E73-10512] 13 p1516 N73-22287
Crop identification and land acreage measurement in Kansas using ERTS-1 imagery
[E73-10514] 13 p1517 N73-22288
Analysis of digital microdensitometer data from ERTS-1 imagery of San Francisco, California
[E73-10521] 13 p1517 N73-22289
Determination of aerosol content in atmosphere at Salton Sea test site using ERTS-1 data
[E73-10524] 13 p1517 N73-22291
ERTS-1 imagery of California nearshore sediment transport, coastal processes, and tidal currents
[E73-10525] 13 p1517 N73-22292
ERTS-1 imagery of Iceland geology, geophysics, hydrology, oceanography, and agriculture
[E73-10535] 13 p1518 N73-22299
Application of ERTS-1 imagery to selected Bureau of Reclamation projects
[E73-10537] 13 p1518 N73-22301

Utilization of ERTS-1 imagery to evaluate Iranian playas as potential locations for economic or engineering development
[E73-10539] 13 p1518 N73-22303
Mapping distribution and density of phreatophytes and other arid land plant communities in Arizona using ERTS-1 imagery
[E73-10543] 13 p1518 N73-22306
Compilation of aerial photographs of coastal areas of United States
[AD-755508] 13 p1526 N73-22368
Utilization of ERTS-1 remotely sensed imagery for land use evaluation and planning in Power River Basin, Wyoming
14 p1653 N73-23407
ERTS-1 imagery of suspended matter and hydrologic interfaces in Delaware Bay
[E73-10515] 14 p1653 N73-23409
Determination of arid plant distribution in Arizona from ERTS-1 imagery
[E73-10520] 14 p1654 N73-23413
Uniform mapping of earth resources and environmental complexes from Skylab imagery
[E73-10532] 14 p1654 N73-23417
Preparation for multidisciplinary study of Wyoming test sites using EREP remotely sensed data from Skylab
[E73-10552] 14 p1655 N73-23425
Broad scale application of ERTS-1 imagery to study and mapping of geological, hydrological, land use, rangelands, and soil cultures in Wyoming
[E73-10554] 14 p1655 N73-23426
Land use mapping of Central Atlantic Region using ERTS-1 imagery
[E73-10557] 14 p1655 N73-23429
Uniform mapping of earth resources and environmental complexes from Skylab imagery
[E73-10562] 14 p1656 N73-23434
Evaluation of ERTS-1 imagery and automatic data processing techniques for characterization of wetlands and marshlands
[E73-10576] 14 p1656 N73-23437
Resources inventory, planning, land use zoning, and resources development in Oregon using ERTS-1 imagery
[E73-10579] 14 p1656 N73-23440
Detection of menhaden schools in Mississippi Sound by comparing ERTS-1 imagery to selected oceanographic parameters
[E73-10580] 14 p1656 N73-23441
Utilization of ERTS-1 imagery for tectonic analysis and geological mapping of Bighorn Mountains
[E73-10583] 14 p1657 N73-23443
Geological surveys and mapping of Netherlands based on ERTS-1 imagery
[E73-10584] 14 p1657 N73-23444
Evaluation of compression technique for ERTS-1 data tapes
[E73-10589] 14 p1657 N73-23449
Detection of regional tectonic structures related to mineralization in Arizona
[E73-10591] 14 p1657 N73-23450
Remote detection of oceanic eddies in Lesser Antilles using ERTS-1 imagery
[E73-10592] 14 p1657 N73-23451
High resolution imagery of Uranus obtained by Stratoscope 2
[NASA-CR-132024] 14 p1706 N73-23846
Inventory and monitoring natural vegetation and related resources in arid environments using ERTS-1 imagery
[E73-10519] 15 p1771 N73-24344
Calculation of water depth in Caribbean from ERTS-1 MSS data
[E73-10566] 15 p1771 N73-24346
Atmospheric effects on ERTS-1 imagery for land use mapping
[E73-10568] 15 p1771 N73-24348
Image enhancement and information extraction techniques for ERTS-1 MSS imagery
[E73-10572] 15 p1772 N73-24352
ERTS-1 monitoring of water quality and ocean dumping
[E73-10573] 15 p1772 N73-24353
Characterization of wetlands and marshlands from ERTS-1 imagery
[E73-10590] 15 p1772 N73-24357
Cartographic applications of ERTS-1 imagery
[E73-10600] 15 p1772 N73-24361
Acquisition and analysis of coastal ground truth data of Santa Monica Bay, Santa Barbara Channel, and Monterey Bay for correlation with ERTS-1 imagery
[E73-10607] 15 p1773 N73-24368
ERTS-1 imagery of water circulation in Prince William Sound
[E73-10617] 15 p1774 N73-24378
Data compression technique for ERTS-1 imagery of Montreal and Lake St. John, Canada, Orange County, California, San Pedro/Long Beach, California, and Chesapeake Bay
[E73-10625] 15 p1775 N73-24385
Thematic mapping of Mississippi River from ERTS-1 imagery
[E73-10628] 15 p1775 N73-24388
Land use of northern megalopolis of Massachusetts, Connecticut, and Rhode Island from ERTS-1 imagery
[E73-10630] 15 p1776 N73-24390
Processing techniques for ERTS-1 imagery of Tennessee Valley
[E73-10633] 15 p1776 N73-24392
Location of archeological village sites in Alaska from ERTS-1 imagery
[E73-10638] 15 p1776 N73-24397
Design study of optical system for annular imagery
[AD-758637] 15 p1789 N73-24505
Application of ERTS-1 data to agricultural practices in Mississippi Delta Region
[E73-10597] 16 p1896 N73-25335
Evaluation of ERTS-1 image data compression techniques
[E73-10647] 16 p1897 N73-25343
Assessment and monitoring oceanic gamefish through Skylab EREP data
[E73-10658] 16 p1898 N73-25354
Mapping phenological changes using ERTS-1 imagery
[E73-10660] 16 p1899 N73-25356
Mapping and monitoring natural ecosystems and environmental complexes and estimation of rice crop yield in California and Louisiana from ERTS-1 imagery
[E73-10669] 16 p1899 N73-25364
Image processing techniques and applications to Earth Resources Technology Satellite program
[NASA-CR-124285] 16 p1967 N73-25910
Application of ERTS-1 imagery to geologic investigations of Basin and Range Colorado Plateau boundary in northwestern and north-central Arizona
[E73-10645] 17 p2017 N73-26312
Forest sampling and timber inventory in California from ERTS-1 imagery
[E73-10743] 17 p2021 N73-26348
Geological survey of Botswana using ERTS-1 imagery
[E73-10753] 17 p2022 N73-26356
Four step, acoustic holographic imaging system
17 p2031 N73-26435
Management of natural resources in France and Spain by automatic cartographic inventories from ERTS-1 data
[E73-10725] 18 p2133 N73-27234
Soil analysis and mapping from Skylab EREP imagery
[E73-10756] 18 p2133 N73-27238
Analysis of New Mexico geology using ERTS-1 imagery
[E73-10830] 18 p2140 N73-27300
Design of two dimensional digital computer for optical image processing onboard spacecraft using liquid crystal circuits
18 p2209 N73-27827
Aberrations and imaging properties of holographic optical elements
[NASA-CR-124334] 19 p2307 N73-28555
Digital precision processing of ERTS-1 imagery of Monterey Bay, California
[E73-10948] 21 p2530 N73-30290
Investigation of land use and earth resources using Skylab EREP
[E73-10964] 21 p2533 N73-30306
Identification of conjugate, or corresponding points in multitemporal imagery for obtaining coefficients of misregistration
[NASA-CR-133640] 21 p2566 N73-30565
Design of programming language for image processing
22 p2636 N73-31124
Feature extraction process using gray level structure of imagery
22 p2636 N73-31127
Computerized photon counting technique for recording optical images
22 p2700 N73-31622
Utilization of Skylab imagery for thematic mapping
[E73-11162] 24 p2920 N73-33315

**IMAGES**
NT RETINAL IMAGES
Two dimensional, second order Markov process representation for recursive restoration of images
[USC-113P19-31] 02 p0146 N73-11182
Optical texture perception and pattern recognition imagery
[AD-746658] 02 p0212 N73-11722
Device for converting optical images into electron beams
[NASA-CASE-GSC-11602-1] 04 p0395 N73-13214
Specification for group delay variation' in upper video band of television transmission system based on chrominance pulse tests
[BBC-1972/39] 06 p0638 N73-15181
Design and performance of two dimensional sensor array system for image area measurements
[AD-750315] 06 p0675 N73-15490
Liquid crystal Fourier plane filter for real time optical image processing
[NASA-CR-130185] 10 p1188 N73-19670
Use of edges of photographic images as specifiers of image quality
[AD-753947] 11 p1295 N73-20512
Structure analysis of digital picture processing system
[AD-755699] 13 p1499 N73-22147
Signal processing of speech pattern recognition using PDP 9 Computer
[AD-757109] 14 p1635 N73-23258
Space shuttle visual simulation system design study
[NASA-CR-128940] 15 p1760 N73-24265
Modulation transfer functions for linear image formation with partially coherent light
15 p1812 N73-24689
Discrete unitary transforms with fast algorithm for encoding images for transmission
[NASA-CR-132771] 17 p2055 N73-26622
Users manual for digital image processing system
[AD-764280] 23 p2761 N73-32097
Detection and estimation of optical images by photon counting techniques
[NASA-CR-135498] 23 p2792 N73-32335
Speech and picture processing
[AD-764968] 24 p2898 N73-33131
Optical image modulation by polarization shifting diffraction gratings
[AD-765174] 24 p2959 N73-33644

**IMAGING TECHNIQUES**
NT IMAGE ENHANCEMENT
NT RADAR IMAGERY
Development of graphical method for determining chromaticity and relative luminance of test color reproduced by color television display
[BBC-1972/30] 01 p0023 N73-10182
Algorithm for reducing redundancy during image transmission
01 p0024 N73-10189
Acoustic holography for imaging cylindrical plastic-bonded explosive loads
[AD-746468] 01 p0067 N73-10547
Operation of image intensifier tubes and analysis of fluctuation theory on visual contrast sensitivity with ideal image intensifiers
[IZF-1972-18] 02 p0148 N73-11202
Geological fracture mapping based on enhancement of ERTS-1 snow cover imagery of Massachusetts, Connecticut, and Feather River/Lake Tahoe area
[E72-10205] 02 p0161 N73-11302
Remote sensing in forestry using aerial and satellite-borne photography and imaging techniques
[E72-10221] 02 p0162 N73-11315
Studies of soundings and imaging measurements from geostationary satellites
[NASA-CR-130122] 03 p0359 N73-12925
Acoustic-optical imaging techniques for detecting bubble formation in circulatory system during decompression
[AD-749087] 04 p0424 N73-13457
Phototransistor imaging system with mosaic of phototransistors on semiconductor substrate
[NASA-CASE-MFS-20809] 04 p0448 N73-13660
Computerized optical system for producing multiple images of a scene simultaneously
[NASA-CASE-MSC-12404-1] 04 p0448 N73-13661
Microwave holography for imaging sea surface topography in three dimensions
06 p0664 N73-15391
Transform coding and block quantization for remote aircraft scanner data and digitized satellite imagery compression
[NASA-CR-130365] 07 p0759 N73-16161
Effect of residual motion smear or image reproduction processes on detail of lunar surface imagery from orbiting command module
[NASA-CR-130378] 07 p0798 N73-16485
Spurious image and color rendition problems in producing multicolor holograms
[AD-751560] 07 p0801 N73-16508
Performance of scanning acoustical imaging telescope at microwave frequencies
07 p0820 N73-16648
Galactic brightness distribution obtained by imaging galaxies on Schmidt plates, selecting one as photometric standard and applying microdensitometric scans
07 p0845 N73-16852
Development of mathematical methods for calibrating lunar orbiter photography
[NASA-CR-128279] 08 p0924 N73-17572
Review of coherent optical data processing
09 p1065 N73-18685
Optical processing in incoherent light
09 p1065 N73-18686
Digital image processing for processing pictures from space vehicles
09 p1065 N73-18687
Parallel image processing including electronic, noncoherent, and coherent methods
09 p1065 N73-18691
Parallel image logical operations using cross correlation
09 p1066 N73-18695
Application of remote sensing and aerial photography to Houston metropolitan area
[NASA-CR-128746] 10 p1159 N73-19431
Optical-to-optical interface device for use in coherent optical parallel processing systems
[NASA-CR-130183] 10 p1188 N73-19671

Display device for real time display of computer generated half tone pictures
[AD-753672] 11 p1260 N73-20224
Application of electronic image analyzer to dimensional measurements from neutron radiographs of nuclear fuel elements
[NASA-TM-X-68200] 11 p1293 N73-20495
Carbon dioxide lasers, optical measurement instrumentation and imaging techniques for air pollution detection
[AD-754939] 11 p1303 N73-20574
Optical imaging system for increasing light absorption efficiency of imaging detector
[NASA-CASE-ARC-10194-1] 11 p1324 N73-20741
Effects of atmospheric aerosols on image transfer in aerial photography using polarized light
12 p1400 N73-21356
Development of techniques for solving image correlation and image sampling of multispectral data
[NASA-CR-130223] 13 p1529 N73-22389
Automatic data processing techniques for computer graphics and image processing
[AD-757530] 14 p1638 N73-23284
Technique for reproducing negative color film in telecine
[BBC-RD-1973/2] 14 p1666 N73-23517
High angular resolution imaging system for outer planet Grand Tour Mission
[NASA-CR-132013] 14 p1704 N73-23823
Various imaging systems and techniques for possible use aboard Grand Tour Spacecraft
[NASA-CR-132014] 14 p1704 N73-23824
MJS imaging and baseline TV system
[NASA-CR-132012] 14 p1704 N73-23825
Meteorological implications of airborne optical imaging through tropopause
[AD-758207] 15 p1782 N73-24449
Linear shift-invariant image preprocessing technique for multispectral scanners
[NASA-CR-132957] 15 p1787 N73-24485
Application of ultrafast laser pulses to high resolution imaging radar systems
[AD-758059] 15 p1795 N73-24551
Spin scan camera photography of Jupiter from rotating outer planet orbiters
[NASA-TM-X-62260] 15 p1830 N73-24836
Method for evaluating image errors of mapping camera locked to stellar cameras
[AD-759491] 16 p1915 N73-25497
Binocular vision models for designing image distortion compensation system
16 p1920 N73-25534
Theoretical study and mountings for magnification and holographic image reconstruction of high speed microparticles
[ISL-1/73] 16 p1924 N73-25566
Mountings for optimum magnification and holographic image reconstruction of high speed microparticles
[ISL-3/73] 16 p1924 N73-25567
Processing and displaying techniques for optical images
[AD-759038] 17 p2001 N73-26183
Evaluation of ERTS-1 image data compression technique
[E73-10717] 17 p2019 N73-26324
EREP imagery for detection of strip mines and reclamation activities in Ohio, West Virginia, and Pennsylvania
[E73-10731] 17 p2020 N73-26337
Use of telecamera as contrast monitor for photospheric surveys
[RR-1] 17 p2032 N73-26440
HEAO-C X ray focusing telescopes for spectrometric and polarization studies
17 p2085 N73-26872
Nondestructive test equipment using acousto-optical imaging techniques
[AD-760554] 18 p2152 N73-27397
Restoration of atmospherically degraded laser beam and definition of isoplanatic patch size
[AD-760548] 18 p2158 N73-27437
High resolution radiometer for visible and infrared imagery onboard meteorological satellite
18 p2209 N73-27836
Computerized acoustic imaging technique with automatic pattern recognition
[AD-761497] 19 p2240 N73-28060
Application of digital techniques to processing of ERTS-1 MSS and RBV image data
[PAPER-I7] 19 p2278 N73-28328
Analysis of ERTS-1 imagery by combining human and computer interpretation capabilities
[PAPER-I14] 19 p2279 N73-28335
Data compression and storage techniques for ERTS-1 image data
[E73-10853] 19 p2292 N73-28430
Device for displaying and recording angled views of samples to be viewed by microscope
[NASA-CASE-GSC-11690-1] 19 p2301 N73-28499
System for displaying low resolution digital grayscale images of ladar target imaging system
[DREV-TN-2075/73] 19 p2307 N73-28552
Extraction of edges from photographs of quadric bodies
[AD-762589] 20 p2420 N73-29445
Image data compression using digital holography
[AD-762931] 20 p2426 N73-29487
Data compression algorithm and techniques for ERTS-1 imagery
[E73-10959] 21 p2532 N73-30301
Processing of multispectral scanned data noting imaging techniques and user operations
[ERL/R-245] 21 p2539 N73-30356
Ritchey-Chretien telescope responsive to images located off telescope optical axis
[NASA-CASE-GSC-11487-1] 21 p2544 N73-30393
Formulation of image quality prediction criteria for Viking lander camera
[NASA-TM-X-2802] 21 p2548 N73-30425
Extended Huygens-Fresnel principle for image plane illuminance distribution of extended object in turbulent atmosphere
[AD-763717] 21 p2581 N73-30683
Radar imagery processing techniques to include binary quantized signals, radar meters, interperiod compensation systems, and radar signal detection
[JPRS-56143] 22 p2628 N73-31054
Optical data and image display recorder/processor
[NASA-CASE-GSC-11553-1] 22 p2631 N73-31089
Performances and limitations of geological remote sensing from earth resources survey aircraft and satellites
[BMBW-FBW-72-28] 22 p2667 N73-31370
Computer enhancement of radiographs using digital filtering techniques
[NASA-CR-124393] 22 p2673 N73-31414
Users manual for interactive digital image processing and graphic display system
[NASA-TM-X-70472] 23 p2760 N73-32084
Computerized image processing and graphic display system
[NASA-TM-X-70473] 23 p2760 N73-32085
Generation of line-containing picture samples from gray level pictures using contrast gradient
[BMVG-FBWT-73-10] 23 p2761 N73-32092
Amplification of low light level optical sigmals by preferential integration in imaging tubes
[AD-763724] 23 p2766 N73-32129
Detection and estimation of optical images by photon counting techniques
[NASA-CR-135498] 23 p2792 N73-32335
Techniques for predicting effects of thermal and saline inhomogeneities on optical imaging systems with application to optical properties of sea water
24 p2957 N73-33625
Effects of resolution, signal to noise ratio, and contrast on underwater imaging systems performance
24 p2958 N73-33631
Application of spatial filtering and image restoration to underwater photographs of floodlit images
24 p2958 N73-33637

**IMBEDDINGS [MATHEMATICS]**
Volterra factorization of Green matrix and imbedding of general linear boundary value problems
[TR-72-48] 02 p0202 N73-11634

**IMBLMS**
Development of procedures of identification of microorganisms on orbiting spacecraft
[NASA-CR-128747] 10 p1120 N73-19132
Site selection, program planning, cost and design studies for support of IMBLMS
[NASA-CR-133961] 17 p2088 N73-26894

**IMCC [CONTROL CENTER]**
U INTEGRATED MISSION CONTROL CENTER

**IMMERSION**
U SUBMERGING

**IMMISCIBILITY**
U SOLUBILITY

**IMMITTANCE**
U ELECTRICAL IMPEDANCE

**IMMOBILIZATION**
Materials for immobilization of electrolyte in pellet-type thermal batteries
[SC-RR-66-202-A] 22 p2618 N73-30978

**IMMUNITY**
Effect of chronic irradiation of dogs by Co60 gamma rays on level of autoantibodies
11 p1244 N73-20100
Prodromal disease - Immune responses of host macrophage system to humoral factors
[NASA-CR-133455] 19 p2224 N73-27938

**IMMUNOLOGY**
Automated procedures for Passive Immune Agglutination system
[NASA-CR-128731] 08 p0877 N73-17107
Immunological effectiveness of X ray irradiation on histocompatibility of mice skin transplants
13 p1481 N73-22008
Functional state of lymphoid cell in peripheral blood of astronauts and immunoreactivity of individual astronants after space flight
[NASA-TT-F-15089] 22 p2620 N73-30999

**IMP**
Program requirements, operational support, and systems analysis for IMP satellite to identify responsibilities of launching organizations
[NASA-CR-129268] 03 p0358 N73-12916
Operations summary and mission planning for IMP-H spacecraft
[NASA-TM-X-68880] 04 p0478 N73-13907
Mission flight performance, and data acquisition of data-90 launch vehicle and InterPlanetary Monitoring Platform-H
[NASA-TM-X-68929] 05 p0595 N73-14836
Particle entry measurements from IMP 5 of polar or dayside cusp
08 p0972 N73-17949
Flux density of low energy solar flare particles measured by IMP-7
[TR-73-137] 23 p2835 N73-32653
IMP-7 measurement of very low energy cosmic ray energy spectra and concentration during solar flares
[TR-73-138] 23 p2835 N73-32654

**IMP-A**
U EXPLORER 18 SATELLITE

**IMP-B**
U EXPLORER 21 SATELLITE

**IMP-D**
U EXPLORER 33 SATELLITE

**IMP-E**
U EXPLORER 35 SATELLITE

**IMP-F**
U EXPLORER 34 SATELLITE

**IMP-G**
U EXPLORER 41 SATELLITE

**IMP-1**
U EXPLORER 18 SATELLITE

**IMP-2**
U EXPLORER 21 SATELLITE

**IMP-4**
U EXPLORER 34 SATELLITE

**IMP-5**
U EXPLORER 41 SATELLITE

**IMPACT**
NT ELECTRON IMPACT
NT HYPERVELOCITY IMPACT
NT ION IMPACT
NT PROTON IMPACT
Identification of artificial lunar impact craters produced by Ranger 7 and 9 spacecraft and S-4B stage of Apollo 13 and 14 - Part I
12 p1453 N73-21773
Identification of Ranger 7 and 9 impact craters from Apollo 16 photography - Part J
12 p1454 N73-21774
Apollo 16 photography of V-shaped ridges associated with secondary craters - Part K
12 p1454 N73-21775
Impact of thin elastic circular shell on surface of compressible fluid
[AD-763259] 21 p2526 N73-30252
Multiplier for estimating particle flux from Explorer 8 and 9 satellite data - Part 2
[NASA-CR-132798] 22 p2665 N73-31352

**IMPACT ACCELERATION**
Biodynamic response of human head and neck to impact acceleration
[AD-747988] 04 p0382 N73-13106
Cylindrical impact technique for second-stage augmentation with explosively driven hypervelocity launcher
[NASA-CR-114589] 12 p1388 N73-21252
Impact acceleration effects on rabbit central nervous system
20 p2366 N73-29024

**IMPACT DAMAGE**
NT METEORITIC DAMAGE
NT RAIN IMPACT DAMAGE
Scaling hypervelocity impact of glass projectiles on aluminum targets
[ISL-24/70] 01 p0036 N73-10285
Fluid wave equation for analyzing damage by excited pressure field between two elastic plates
[AD-748340] 04 p0407 N73-13316
Impact damage caused by polystyrene, aluminum, or iron hypervelocity particles on glass
08 p0934 N73-17651
Reactivity change in fast spectrum space power reactor due to 328 meter/sec impact
[NASA-TM-X-2886] 23 p2818 N73-32532

**IMPACT DECELERATION**
U DECELERATION
U IMPACT ACCELERATION

**IMPACT LOADS**
Transient response of finite longitudinally-layered cylindrical membrane shell impacted by longitudinal axisymmetric loads
[TAE-154] 02 p0237 N73-11929
Estimation of impact pressures of drops against solid surface
[AD-748731] 03 p0363 N73-12956
Development of statistical technique for determining injury reduction capability of energy absorber equipment
[AD-749333] 05 p0497 N73-14044

Series expansion method for calculating longitudinal load impact on rod of rate-dependent material
[AD-751979] 08 p0967 N73-17904
Development of criteria for predicting landing impact loads for V/STOL aircraft based on data obtained by flight tests of X-22 aircraft
[AD-753852] 09 p0989 N73-18075
Techniques for casting large area polysulfone film capacitors onto thick aluminum substrates for application as meteoroid impact sensors
[NASA-CR-128862] 10 p1160 N73-19441
Elastoplastic deformation of slender rod subjected to impact loads
[AD-754241] 10 p1221 N73-19935
Analysis of crack nucleation and crack propagation caused by formal separation of impact ductility into components
[AD-754620] 11 p1346 N73-20926
Influence of axial impact loads on dynamic properties and strain wave speeds in polycarbonate Lexan
[AD-755457] 12 p1417 N73-21482
Calculation of effect of short-term impulse loads on structures with finite and infinite numbers of degrees of freedom
[AD-756959] 13 p1587 N73-22868
Wave propagation and impact in composite materials
[NASA-CR-121226] 20 p2482 N73-29935
Exhaust pressure and density of pulsed thrustor systems
[NASA-TM-X-68299] 21 p2589 N73-30740

**IMPACT PREDICTION**
Weapon delivery accuracy of F-4 aircraft with high gain control augmentation system
[AD-746001] 02 p0126 N73-11028
Application of point position radar data to determine aerodynamic drag of projectile
[AD-750564] 05 p0492 N73-14013
Impact safety for reentry of Electre nose cones along south coast of France
[ONERA-TP-1152] 09 p1084 N73-18846
Vertical wind effects in trajectory calculations and impact predictions for rockets and projectiles
[AD-753349] 09 p1092 N73-18913
Meteorological data for Lance missile number 2186, round number 169 APL
[AD-754559] 11 p1316 N73-20680
Analysis of military helicopter control and stability characteristics to determine suitability as rocket launching platform
[AD-756436] 13 p1474 N73-21944
Feasibility of actively guiding sounding rockets to reduce impact dispersion at White Sands Missile Range
[NASA-TM-X-70474] 23 p2851 N73-32780
Computerized simulation of weapon system terminal ballistics and impact effectiveness
[AD-764884] 23 p2867 N73-32921

**IMPACT PRESSURES**
U IMPACT LOADS

**IMPACT RESISTANCE**
Compressive surface layer formation on hot pressed silicon carbide and nitride to improve impact resistance
[NASA-CR-121002] 02 p0222 N73-11796
Increased heat and impact resistance of ceramics made of zirconium dioxide reinforced with mullite whiskers
[JPRS-57770] 05 p0565 N73-14588
Post impact behavior of mobile reactor core containment systems
[NASA-TM-X-68176] 07 p0819 N73-16642
Analysis of crack nucleation and crack propagation caused by formal separation of impact ductility into components
[AD-754620] 11 p1346 N73-20926
Meteoroid impact resistance of bumper protected laminated spacecraft mainwalls
[NASA-CR-2262] 14 p1714 N73-23909
Computer simulation to evaluate methods for determining threshold stimulus levels for impact sensitivity tests
[NASA-TM-X-64087] 15 p1801 N73-24598
Compilation of card-gap and projectile impact sensitivity data for wide variety of explosive compositions
[BM-IC-8605] 18 p2206 N73-27802
Impact resistance of crash helmets for agricultural aviation pilots
[ARL/SM-NOTE-390] 22 p2623 N73-31014

**IMPACT SENSITIVITY**
U IMPACT RESISTANCE

**IMPACT STRENGTH**
Fracture strength of uranium- and tungsten-based impacted ogive penetrators
[DREV-R-652/72] 09 p1047 N73-18538
Drop impact strength and toughness of glass and carbon fiber composite materials
[AD-753101] 09 p1054 N73-18595
Impact calculation of heavy nuclei of cosmic rays 11 p1243 N73-20089
Water jet impingement wear tests on plexiglass, aluminum alloys, nickel, cobalt alloys, and stainless steels
[PB-215631/3] 16 p1890 N73-25294
Maximizing impact strength of advanced graphite composites without affecting other directional strength properties
[AD-763376] 21 p2564 N73-30553
Factors affecting miniature izod impact strength of tungsten-fiber-metal-matrix composites
[NASA-TN-D-7393] 23 p2804 N73-32427
Effect of aging temperature and time on impact and tensile properties of L-605 cobalt alloy
[ORNL-TM-3734] 24 p2934 N73-33435

**IMPACT TESTING MACHINES**
Instrumented impact hammer used on pre-cracked Charpy V-notch specimens to determine dynamic fracture toughness
[AD-750710] 06 p0728 N73-15944

**IMPACT TESTS**
NT CHARPY IMPACT TEST
Impact tests of jet transport wing leading edge fuel tanks to evaluate effects of aborted takeoff, abnormal landing, and bird strikes
[FAA-NA-72-21] 02 p0125 N73-11017
Stress behavior of lithium fluoride crystals exposed to shock wave impact
[AD-748267] 04 p0460 N73-13757
Analysis of plastification effects in notched, impact-bending specimens of steel
[NLL-RISLEY-TR-2457-[9091.9F]] 05 p0601 N73-14887
Impact, emergency escapes, and crash survival studies 06 p0628 N73-15097
Firing tests to determine cratering produced by impact of flat ended, high density metal cylinders striking mild steel plate targets
[DREV-TN-2034/72] 06 p0726 N73-15927
Shock test of electron-proton spectrometer structural test unit to verify structural integrity of spectrometer design and to analyze shock response of electronic housing
[NASA-CR-128698] 08 p0924 N73-17574
Application of dual-scatter laser velocimeter to measure particle velocity distribution in hypersonic dust erosion facility
[AD-752225] 08 p0930 N73-17618
Numerical analysis of dynamic problem of axisymmetrically impacting finite-length rods
[AD-754119] 11 p1346 N73-20923
Anthropometry for protective equipment evaluation and human impact acceleration experiments 14 p1612 N73-23066
Analysis of metal transition into brittle state with determination of impact strength
[AD-758252] 14 p1679 N73-23627
Computer simulation to evaluate methods for determining threshold stimulus levels for impact sensitivity tests
[NASA-TM-X-64087] 15 p1801 N73-24598
Performance tests of L-band truss cable meteoroid shielding on Skylab space station at minus 180 degrees Fahrenheit
[NASA-TM-X-64743] 15 p1834 N73-24867
Water impact damage to radome materials
[AD-759973] 17 p2000 N73-26170
Development of method for predicting crater profiles produced in ductile materials by impact of rigid projectiles at ballistic velocities
[DREV-R-686/73] 18 p2203 N73-27782
Stress analysis of impact in composite plates
[NASA-CR-121110] 18 p2203 N73-27786
Development of modeling schemes to predict effect of coalescence on observed growth characteristics during dynamic fracture
[AD-761082] 18 p2204 N73-27790
Stress analysis of large plastic deformations in hollow sphere deformed during impact tests
[NASA-TM-X-68270] 20 p2482 N73-29940
Stress-strain diagrams and mechanical properties of metal wires as determined by tranverse impact method
[AD-764105] 22 p2687 N73-31523
Impact tests on selected polymers
[AD-764628] 23 p2811 N73-32479
Response of laminated elastic plate to planar impact loads using vibratory modes to develop transient response solution 23 p2853 N73-32795

**IMPACT TOLERANCES**
Analysis of bumper plate penetration by meteoroid and subsequent phenomena
[NASA-CR-124061] 08 p0966 N73-17894
Analysis of high velocity spacecraft crash landing on planetary surfaces for possible encapsulated microorganism release
[NASA-CR-131835] 16 p1966 N73-25904

**IMPACTORS**
Jet impactor for size separation of aerosol particles
[BMVG-FBWT-72-11] 07 p0805 N73-16526
Aerosol particle size determination and distribution with aerodynamically focused impactor, applied to coal mine dust
[BMVG-FBWT-73-1] 14 p1667 N73-23533

**IMPATT DIODES**
U AVALANCHE DIODES

**IMPEDANCE**
NT ACOUSTIC IMPEDANCE
NT CONTACT RESISTANCE
NT ELECTRICAL IMPEDANCE
NT ELECTRICAL RESISTANCE
NT MECHANICAL IMPEDANCE
NT RESPIRATORY IMPEDANCE
Dynamic calibration of gas flowmeters by impedance measurement in oscillating flow
[ARC-CP-1224] 05 p0548 N73-14451
Electromagnetic waves propagation and impedance analysis of double stream interaction in semiconductors
[NASA-CR-131293] 11 p1329 N73-20791
Microwave surface impedance of thin niobium superconducting films subjected to varying dc magnetic fields 12 p1438 N73-21649
Calculation and computer program of impedance and far field of short helix antenna above infinite groundplane
[PHL-1972-27] 14 p1619 N73-23110
Design and performance characteristics of trap loaded cylindrical antennas 21 p2516 N73-30183
Multi-impedance loading of linear antennas to improve transmitting and receiving characteristics 21 p2516 N73-30184

**IMPEDANCE MATCHING**
Computer aided broadband impedance matching technique using comparison reflectometer
[NASA-CR-129567] 04 p0398 N73-13237
Radio auroras and nighttime magnetic field disturbances
[AD-750019] 05 p0543 N73-14415
Design and performance of series power combiner for microwave solid state amplifiers
[AD-764728] 23 p2766 N73-32130
Considerations for precise measurement of amplifier noise with hot and cold noise standards and mismatch problems
[NBS-TN-640] 24 p2898 N73-33136

**IMPEDANCE MEASUREMENTS**
Impedance measurement for two planar, equiangular, printed circuit, two arm, spiral antennas
[AD-756706] 14 p1643 N73-23322
Power equation theory for defining ultrahigh frequency and microwave measurements
[NBS-TN-637] 15 p1750 N73-24182
Electronic properties of beryllium single crystals with emphasis on microwave surface impedance 18 p2185 N73-27646

**IMPEDANCE PROBES**
NT RADIO FREQUENCY IMPEDANCE PROBES
Impedance probe and counter-voltage analyzer used on Aeros satellite for plasma diagnostics experiment
[DGLR-PAPER-72-070] 09 p1036 N73-18455
Research and development of French programs for FR-1, impedance and electrostatic probes, and very low frequency wave propagation
[GRI/NTP/103] 13 p1595 N73-22936
Cosmos 381 measurement of ionospheric electron concentration using impedance probe 15 p1779 N73-24422
Characteristics of swept frequency impedance probe installed in unmanned satellite to measure impedance of space plasma
[ISAS-495-VOL-38-NO-6] 22 p2672 N73-31403

**IMPELLER BLADES**
U ROTOR BLADES [TURBOMACHINERY]

**IMPELLERS**
NT PUMP IMPELLERS
Influence of transverse force on impeller bearing rupture of centrifugal pumps 02 p0179 N73-11446
Computer programs for predicting hydrodynamic forces and vibration characteristics of rocket engine turbopump inducer - Vol. 2 Revised
[NASA-CR-72712-VOL-2-REV] 09 p1078 N73-18797
Magnus forces on center of gravity and rotational startup response of self-spinning rotor in subsonic air stream
[AD-755108] 11 p1232 N73-20001
Design and fabrication of backswept impeller vane island diffuser, and advanced-concepts compressor rig
[NASA-CR-120942] 11 p1298 N73-20531

**IMPERFECTIONS**
U DEFECTS

**IMPERIAL VALLEY (CA)**
Utilization of ERTS-1 imagery for mapping and control of pink bollworm in Imperial, Coachella, and Palo Verde Valleys of California
[E73-10858] 19 p2292 N73-28435

**IMPERMEABILITY**
U PERMEABILITY

**IMPINGEMENT**
NT JET IMPINGEMENT
Impulse base flow facility tests of space shuttle stage separation plume impingement loads
[NASA-CR-124000] 06 p0729 N73-15949
Heat transfer characteristics of impingement-cooled turbine rotor blade
[NASA-TM-X-2791] 15 p1843 N73-24929

**IMPLANTATION**
NT ION IMPLANTATION
Unified approach to biomechanics of dental implantology 10 p1227 N73-19977

Chemical and orthopedic properties of ceramic bone implants in monkeys
[AD-754982] 11 p1248 N73-20134
IMPLOSIONS
Structural design of implosion-driven hypervelocity launchers
[AD-742993] 03 p0281 N73-12280
High energy plasma generation by electromagnetic implosion of thin metal foil cylinder
[AD-759826] 16 p1951 N73-25788
IMPREGNATING
X ray fluorescence analysis of impregnating solutions for wooden communication poles containing As, Cu, Cr, F and B
[FTZ-A-518-TBR-1] 22 p2626 N73-31037
IMPROVED TIROS OPERATIONAL SATELLITES
NT ITOS 1
NT ITOS 2
NT ITOS 3
NT ITOS 4
ITOS D and Nimbus E radiometer data
08 p0972 N73-17943
Daily hemispheric mosaics by satellite for use in selection of climatological data
22 p2693 N73-31576
IMPROVEMENT
Improvement to primary standard of measurement associated with International System of Units
[NPL-QU-AR-71] 10 p1161 N73-19450
IMPULSE GENERATORS
Optimum three impulse generator with patched conic trajectory model
[NASA-CR-130244] 15 p1831 N73-24843
IMPULSE NOISE
U ELECTROMAGNETIC NOISE
IMPULSE TRANSFER ORBITS
U TRANSFER ORBITS
IMPULSES
Optical parameter effects of sea water and spatial-temporal structure of light impulses
[JPRS-57332] 03 p0335 N73-12733
Test stand for precise measurement of impulse bit and thrust vector of reaction jet thrusters in attitude control system
[NASA-TN-D-7402] 22 p2719 N73-31762
IMPURITIES
Compensating impurities in semiconductors which give majority charge carriers
[NLL-RTS-7358] 02 p0218 N73-11761
Influence of chemical composition, non-metallic impurities, and production methods on physical properties of molten high alloy steels and special alloys
[AD-747394] 03 p0316 N73-12579
Physical and chemical properties of steel surfaces exposed to deoxidation products
[AD-747828] 04 p0435 N73-13547
Excited state paramagnetic resonance interpretation of Zeeman effects in optical spectra of neodymium and erbium containing impurity ions
[AD-750343] 06 p0700 N73-15712
Electron-impurity spin interchange model for analyzing magnetic properties of diluted magnetic alloys at low temperatures
08 p0931 N73-17626
Removal of mechanical impurities from AKOR-1 additive by filtration method using perlite
[AD-751947] 10 p1167 N73-19496
Impurities and plastic fracture in aluminum alloys
[NASA-CR-131100] 10 p1171 N73-19521
Measurement of phonon scattering by isotopic impurities in helium single crystals
[AD-754475] 11 p1330 N73-20798
Dielectric properties of pure and doped insulating materials
[COO-623-182] 12 p1439 N73-21662
Iron contamination effect in liquid rocket propellant system of high density acid
[AD-755376] 14 p1700 N73-23797
Dynamics of dislocation pinning by impurity atoms during dynamic strain aging
[AD-760574] 18 p2162 N73-27466
Weight measurement of impurities during aspiration of aerosol samples from flow, using zero intake tubes
[AD-762329] 19 p2232 N73-27998
Bose model for foreign particle interaction with superfluid helium
20 p2455 N73-29732
Influence of applied stress, magnetic and electric fields, and impurity concentration on electrical conductance of n-type germanium at very low temperatures
[RR-738] 20 p2462 N73-29783
Variation of crystal Fermi energy to obtain different charge states in paramagnetic impurity ions for ESP study
[AD-760736] 20 p2464 N73-29798
Impurity resonances in dilute copper cobalt alloy, aluminum manganese alloy, and copper vanadium alloy at low temperatures
24 p2960 N73-33655
IN-FLIGHT MONITORING
In-flight data acquisition and processing systems
01 p0056 N73-10452
Verification program for Inflight Blood Collection system
[NASA-CR-128645] 03 p0261 N73-12112
In-flight tests and operational reliability of jet aircraft nullable compressor face rake
[NASA-TN-D-7162] 07 p0769 N73-16247
User manual and source listings for computer programs to solve problems in analysis of in-flight thrust reversers
[AD-751526] 07 p0837 N73-16785
Ionization, thermoluminescence, and nuclear photographic emulsion dosimetry for monitoring radiation loads in spacecrews during manned space flight
Development of quality monitoring system for water recovery cycle in weightlessness environment
09 p0992 N73-18100
[NASA-CR-112267] 11 p1250 N73-20144
Onboard computer system for in-flight monitoring of space shuttle in support of flight crew
14 p1712 N73-23893
Active-standby servoactuator for failure detection of space shuttle main engine hydraulic actuation system
[NASA-CR-124299] 18 p2156 N73-27418
Onboard control systems for spacecraft
[JPRS-60179] 23 p2847 N73-32755
Automated monitoring of reliability of onboard computers and simulation of malfunction problem using Markov processes nonuniform in time
23 p2848 N73-32757
IN-FLIGHT THRUST MEASUREMENT
U IN-FLIGHT MONITORING
U THRUST MEASUREMENT
INACTIVATION
U DEACTIVATION
INCANDESCENCE
Procedures, techniques, and equipment for calibrating luminous intensity, luminous flux, and color temperature of incandescent lamps
[NBS-TN-594-3] 02 p0174 N73-11408
INCENTIVE TECHNIQUES
Incentive schemes as contract management tool noting use in ESRO 4 satellite project
15 p1849 N73-24989
INCIDENCE
Linear and nonlinear parts of slender body of revolution aerodynamic coefficients in supersonic flow, noting influence of incidence on pressure distribution
[DLR-FB-72-42] 01 p0001 N73-10006
Numerical analysis of parameters of shock waves and dependence on angle of incidence and amplitude of shock wave
[AD-763157] 21 p2526 N73-30253
Pressure fields over hypersonic wing-body configuration at moderate incidence
[AD-763762] 21 p2526 N73-30256
INCLINATION
Influence of groove inclination angle on bearing capacity of gas dynamic thrust bearing
[AD-751068] 07 p0806 N73-16535
Optimum inclination of inclination non-sensitive satellites for shuttle retrieval
[NASA-TM-X-64780] 22 p2715 N73-31730
INCLUSIONS
Stress concentration effects due to shape discontinuity, inclusions, or local load distributions
[ESDU-65004-AMEND-A-B-C] 01 p0112 N73-10925
Nonmetallic inclusion effects on crack growth rate in two alloy steels
[AD-746950] 02 p0189 N73-11530
Effects of circular inclusion of different elastic material on stress stage of cracked flat plates
[AD-754211] 10 p1222 N73-19936
Fracture toughness of flat elastic cracked plate with elastic circular inclusion
[AD-754210] 10 p1222 N73-19937
Inclusive spectra at large transverse momentum for study of massive decay resonances
[TUETP-73-6] 14 p1694 N73-23748
Determination of temperature distributions and deformations of rectangular plates with circular elastic inclusions
[AD-756183] 14 p1717 N73-23930
Fracture mechanics of elastic interactions between cracks and inclusions in composite materials
[NASA-CR-132292] 19 p2312 N73-28593
Interaction between circular inclusion and arbitrarily oriented crack
[NASA-CR-132291] 19 p2348 N73-28886
Removing nitride inclusions from heat resistant alloys and hafnium dioxide particles in precipitation-hardened nickel
[JPRS-59637] 21 p2557 N73-30501
INCOHERENT SCATTERING
Determining ion composition of ionosphere by incoherent scattering of radio waves, and ionospheric sounding in USSR
[JPRS-57474] 04 p0413 N73-13372
Determining ion composition using high-potential radar sets with storage elements for detecting non-coherent scattered radio signals
04 p0413 N73-13373
Development and operation of matched incoherent radar systems to improve accuracy in range measurement and increase probability of target detection
07 p0755 N73-16134
Neutral atmospheric models compatible with satellite orbital decay and incoherent scatter measurements
[NASA-CR-131294] 11 p1285 N73-20427
Influence of collisions on incoherent scattering spectrum of nonequilibrium inhomogeneous absorbing plasma
[CEA-R-4351] 12 p1436 N73-21633
Dynamics of neutral atmosphere in 200 to 500 km height region at low latitudes from incoherent scattering measurements
13 p1513 N73-22263
Auroral ionospheric measurements from incoherent scatter radar facility
[AD-757358] 14 p1664 N73-23504
Hybrid autocorrelator for high altitude incoherent scatter observations
20 p2417 N73-29417
Digital decoder for processing Barker coded pulses in incoherent scatter observations of ionosphere
23 p2778 N73-32212
Maser amplification of incoherent radiation
[RR-113-PT-1] 24 p2930 N73-33401
Noncoherent model for microwave emissions and backscattering from sea surface
[NASA-CR-2326] 24 p2948 N73-33542
Backscattering from two-scale rough surface application to radar sea return
[NASA-CR-2327] 24 p2948 N73-33543
INCOMPRESSIBILITY
Stability criteria for incompressible elastic materials
[AD-753459] 10 p1221 N73-19931
INCOMPRESSIBLE BOUNDARY LAYER
Calculation of heat transfer coefficients of laminar incompressible boundary layer to corrugated wall, with application to combustion chamber liquid film cooling
[DLR-FB-73-07] 12 p1465 N73-21868
Measurements of pressure distributions, mean velocity profiles, and Reynolds stresses in thick incompressible turbulent boundary layer near tail of body of revolution
[AD-759014] 16 p1892 N73-25310
Parametric integral method for calculating laminar and turbulent incompressible flow- and temperature boundary layers
[DLR-FB-73-24] 22 p2653 N73-31255
INCOMPRESSIBLE FLOW
NT STOKES FLOW
Eulerian incompressible hydrodynamic numerical model and laboratory simulations of tsunamis
[AD-745420] 01 p0053 N73-10430
Analysis of mean velocity, turbulence intensity, and wall heat transfer for conical diffuser coupled to constant diameter recovery section
[NASA-TM-X-2677] 02 p0156 N73-11267
Limit process expansion techniques used to analyze fully developed turbulent incompressible flow in infinitely long channel with plane parallel walls
[AD-746112] 02 p0158 N73-11283
Plane turbulent gradient flow of incompressible fluid along porous surface in presence of blowing or suction
[AD-746933] 02 p0159 N73-11290
Incompressible boundary layer flow separation over moving boundaries
[AD-746869] 02 p0159 N73-11292
Two dimensional, incompressible model for response of laminar and turbulent attached jets
[AD-747761] 03 p0309 N73-12520
Analysis of mean velocity profiles in three-dimensional turbulent boundary layers during incompressible flow
[REPT-71-FM-13] 04 p0404 N73-13289
Error analysis on two dimensional steady laminar boundary layer of incompressible wall flow
[AD-748771] 04 p0406 N73-13308
Analysis of pressure loss through single bends of various geometries under conditions of full incompressible flow
[ESDU-67040-AMEND-A] 05 p0525 N73-14272
Analysis of velocity profiles in boundary layer produced by incompressible flow during takeoff
06 p0616 N73-15001
Development of momentum integral type method for solving relaxation-diffusion model for turbulent shear stress of incompressible plane turbulent wakes
[REPT-72-FM-5] 06 p0652 N73-15296
Numerical analysis of three dimensional incompressible fluid flow near large structure surface
[LA-DC-72-711] 06 p0654 N73-15315
Method for estimating changes in lift curve, drag, tail lift, and downwash from wing of aircraft due to ground effect in incompressible flow
[ESDU-72023] 07 p0736 N73-15993
Analysis of skin friction measurement techniques for incompressible flow to show instruments required and areas of difference
[FFA-AU-726] 08 p0895 N73-17246
Integration of Galerkin method for solving boundary layer equation with steady incompressible flow
[AD-752203] 08 p0898 N73-17275
Techniques for determining dynamic characteristics of hydraulic duct for predicting low frequency vibrations of liquid propellant rocket engines
[ONERA-TP-1160] 09 p1015 N73-18281

Inertial gravity wave frequency spectrum in cylindrically confined incompressible two component liquid flow
[AD-752439] 09 p1018 N73-18312

Singularity method for calculating incompressible flow through cascades with separation
10 p1205 N73-19802

Development of method for solving three dimensional, incompressible laminar and turbulent boundary layer problems for swept infinite cylinders and small cross flow
[AD-754440] 11 p1232 N73-20004

Kelvin-Helmholtz instability analysis of bounded two phase particulate incompressible inviscid flows
[AD-754815] 11 p1272 N73-20318

Mathematical theory of viscous incompressible flow and solutions to Navier-Stokes equations
[AD-754995] 11 p1350 N73-20953

Partial differential equations for studying laminar boundary layer separations
13 p1508 N73-22221

Separation of incompressible boundary layer from axisymmetric curved afterbody
13 p1509 N73-22226

Numerical analysis of Navier-Stokes equations for steady two dimensional flow to show convergence characteristics
[ARC-R/M-3239] 15 p1725 N73-23997

Numerical analysis of pressure distribution in incompressible flow on two dimensional airfoils near ground
[ARC-R/M-3238] 15 p1726 N73-24000

Application of conformal mapping procedures for designing airfoil shapes with high design lift coefficients
[AD-757813] 15 p1731 N73-24040

Velocity potential solution of heavy incompressible liquid wave motion
[AD-758251] 15 p1769 N73-24331

Numerical analysis of incompressible laminar boundary layer on infinite swept wing with arbitrary velocity and suction distribution
[ARC-R/M-3241] 16 p1854 N73-25018

Perturbation method for separated laminar incompressible flows in divergent channels
16 p1886 N73-25268

Incompressible free turbulent mixing in adverse and favorable pressure gradients
[AD-758664] 16 p1891 N73-25308

Numerical analysis of structure of incompressible turbulent flows in plane wake and plane jet using two eddy viscosity models
17 p2012 N73-26274

Differential equations for analyzing nonstationary incompressible viscous fluid flow in elastic cylindrical tube
17 p2014 N73-26290

Numerical analysis of two dimensional incompressible potential flow around system of arbitrary airfoils using relaxation method
[NAL-TR-309] 18 p2130 N73-27212

Velocity and temperature development in entrance region between two rotating concentric cylinders
[AD-762049] 19 p2256 N73-28187

Turbulent fluid friction of rotating disks in incompressible flow calculations
20 p2384 N73-29155

Numerical analysis of steady, two-dimensional, laminar, incompressible, high Reynolds number separated flow past thin airfoils
[NASA-CR-114656] 20 p2388 N73-29185

Analysis of drag and pressure measurements made in subsonic wind tunnel tests on two annular airfoils noting relation between pressure distribution in compressible flow and at high speed
[ARC-R/M-2718] 21 p2492 N73-30003

Characteristics of flow about spherical body undergoing rectilinear, sinusoidal oscillations in viscous, incompressible fluid
23 p2773 N73-32180

Development of theoretical model for determining flow characteristics of round jet in incompressible cross-flow based on matched asymptotic expansion
[NASA-CR-132324] 23 p2775 N73-32191

Asymptotic expansion analysis of jet entrainment in incompressible cross flow
24 p2902 N73-33166

Numerical solution of time-dependent Navier-Stokes equation with periodic boundary condition
[AD-764582] 24 p2910 N73-33226

**INCOMPRESSIBLE FLUIDS**

Influence of inlet deformation on characteristics of ejector jet devices operating on incompressible fluids
[AD-747079] 02 p0179 N73-11454

Uniqueness theorem for two-dimensional nonstationary wall boundary layer in incompressible fluid
[AD-748743] 04 p0407 N73-13314

Reynolds time-averaged equations adopted for fully turbulent two dimensional flow of incompressible fluid through channel with plane smooth walls
[AD-752462] 08 p0898 N73-17272

Steady oscillatory irrotational motion of inviscid incompressible fluid described by boundary value problem of elliptic type
[AD-755465] 13 p1512 N73-22252

Stalling characteristics of airfoil in laminar viscous incompressible fluid with consideration of starting vortex and separation bubble
[AD-758831] 15 p1769 N73-24334

Stability analyses of idealized atmosphere and perfect gas blowing over inviscid liquid
17 p2012 N73-26269

Implicit numerical solution for laminar and turbulent flow of incompressible fluid along axis of 90-degree corner
20 p2384 N73-29152

Transition from laminar to turbulent flow for radially inward throughflow of incompressible Newtonian fluid between closely spaced parallel corotating disks
20 p2385 N73-29159

Numerical analysis of solitary wave propagation in incompressible rotating fluids
20 p2385 N73-29160

Numerical analysis of laminar unsteady flow around airfoil in viscous, incompressible fluid
22 p2649 N73-31226

**INCONEL [TRADEMARK]**

Influence of grain size and cold working on static corrosion of Incoloy 800 alloy in superheated steam
[EURFNR-965] 03 p0315 N73-12570

Reaction of Fe-Ni-Cr alloys with oxygen-containing sodium
[IS-T-508] 04 p0433 N73-13534

Creep rupture tests of Inconel 702 tubes at high temperatures and internal helium pressures to determine service life
[NASA-TM-X-2728] 08 p0932 N73-17628

**INDENTATION**

Experimental method of measuring direction and residual stress in steel using surface displacements around indentations
[AD-756869] 13 p1546 N73-22526

**INDEPENDENT VARIABLES**

NT LATTICE PARAMETERS

Finite difference solutions for oscillatory lift interference parameters for slotted wind tunnel incompressible flow
03 p0284 N73-12298

Finite difference solutions for oscillatory lift interference parameters for slotted wind tunnel compressible flow
03 p0284 N73-12299

Summation method for computing vocabulary size for two parameter rank distribution
[NASA-CR-129806] 04 p0393 N73-13197

Signal ratio measurements for determining terminal invariant parameters in microwave system calibration
[SC-DR-72-0315] 04 p0395 N73-13216

Coefficients for estimated values of location and scale parameters from ordered statistical samples, applied to Gumbel and Weibull distributions
[FOA-P-B-8010-11] 06 p0690 N73-15619

Acceleration and compression parameters in plasma focus
[LA-TR-72-24] 07 p0826 N73-16694

Asymptotic properties of feedback systems containing uncertain parameters and subjected to stochastic perturbations
[NASA-CR-131372] 11 p1264 N73-20260

Model parameters associated with single axis attitude dynamics of flexible vehicle
[NASA-CR-132262] 16 p1964 N73-25890

Determination of parameter s for characterizing meteoric distribution from SOM-1 radar data
17 p2023 N73-26371

Measurments of monotonic and cyclic strain hardening parameters by five alloys
[AD-762610] 20 p2433 N73-29540

Theory of spline interpolation extended to case of two independent variables
21 p2512 N73-30153

Reflecting solutions of high order elliptic differential equations in two independent variables across analytic arcs
[NASA-CR-135667] 23 p2812 N73-32483

**INDEXES**

Bibliography of AGARD publications
[AGARD-INDEX-52/70-PT-1] 11 p1352 N73-20973

Subject index for AGARD publications bibliography - Part 2
[AGARD-INDEX-52/70-PT-2] 11 p1352 N73-20974

Indexes to patent abstracts bibliography
[NASA-SP-7039(2)-SECTION-2] 16 p1976 N73-25977

**INDEXES [DOCUMENTATION]**

NT KWIC INDEXES

Titles of all Data Items issued by ESDU to end of 1971
01 p0002 N73-10009

Index of information collected by Soviet weather satellites
[NASA-TT-F-14447] 01 p0075 N73-10616

Annotated bibliography and indexes on aerospace medicine and biology - Aug. 1972
[NASA-SP-7011[106]] 02 p0130 N73-11054

Index and introduction to Principles of Information Theory of Visibility in Atmosphere
[NASA-TT-F-14435] 02 p0211 N73-11712

Annotated bibliography and indexes on aerospace medicine and biology - July 1972
[NASA-SP-7011[105]] 03 p0256 N73-12073

Effect of using weighted index terms in document retrieval system with cluster analysis
[NASA-CR-129804] 04 p0393 N73-13195

Computer index on bibliographical references to microscopic neutron data
05 p0582 N73-14734

Index of bibliographies for patents and patent applications May 1969 through June 1972
[NASA-SP-7039[01]-SECTION-2] 08 p0971 N73-17932

Annotated bibliography and indexes on Aerospace Medicine and Biology - December 1972
[NASA-SP-7011[109]] 09 p0992 N73-18094

Automated computer index and retrieval system on machining of materials
[AD-752000] 09 p1053 N73-18582

Index to reports of National Conference on Weights and Measures from 1905 to 1971
[NBS-SP-377] 09 p1101 N73-18985

Annotated bibliography and indexes on aerospace medicine and biology - January 1973
[NASA-SP-7011[110]] 11 p1238 N73-20052

Annotated bibliography and indexes on aerospace medicine and biology
[NASA-SP-7011[112]] 12 p1367 N73-21087

Annotated bibliography and indexes on aerospace medicine and biology for 1961 to 1965
[NASA-TT-F-14662] 14 p1610 N73-23053

Annotated bibliography and indexes on Aerospace Medicine and Biology - February 1973
[NASA-SP-7011[113]] 15 p1739 N73-24099

Annotated bibliography and indexes on aerospace medicine and biology - January 1973
[NASA-SP-7011[111]] 15 p1739 N73-24100

Directory of workers in field of fire research and related activities
[NASA-CR-121149] 15 p1845 N73-24954

Sixth supplement to bibliography on planetary quarantine with indexes
[NASA-CR-131817] 16 p1866 N73-25112

Annotated bibliography and indexes on Aerospace Medicine and Biology - April 1973
[NASA-SP-7011[114]] 17 p1986 N73-26055

Catalogue indexes to local weather forecasts
[AD-760091] 17 p2058 N73-26648

Register of experts for information on mechanics of structural failure to support safety and technology aspects of aerospace industry
[NASA-CR-121200] 17 p2091 N73-26918

Index of international scientific rocketlaunches
[NASA-TM-X-69350] 18 p2196 N73-27732

Abstracts of 1972 NASA Tech Briefs
[NASA-SP-5021[13]] 19 p2355 N73-28941

Index of subjects presented during Congressional hearings involving NASA appropriations for Fiscal Year 1974
21 p2610 N73-30921

Space vehicles launched between January and August 1973
[TECH-MEMO-SPACE-199] 23 p2847 N73-32753

Annotated bibliography and indexes on aerospace medicine and biology - September 1973
[NASA-SP-7011[119]] 24 p2882 N73-33012

**INDEXES [RATIOS]**

NT MORPHOLOGICAL INDEXES

Development of noise index based on slow and fast noise level variation perception, and applied to aircraft noise data
[REPT-3/1973] 19 p2220 N73-27911

**INDIA**

Solar flares, magnetic storms, ionospheric disturbances, and geophysical observations recorded by weather stations in India during Feb. 1972
[RRC-A-201-PT-2] 01 p0048 N73-10386

Atomic energy and space research in India for 1971 and 1972
[NP-19407] 07 p0860 N73-16974

Computer processing of multispectral imagery of India
[E73-10373] 10 p1151 N73-19368

Technological and economical factors of satellite television network in India
[PB-213226] 11 p1258 N73-20208

**INDIAN OCEAN**

Marine climatological summaries for Mediterranean and Southern Indian Ocean, including Australian waters
06 p0693 N73-15646

Temperature and wind conditions in stratosphere and troposphere of equatorial latitudes in Indian Ocean
09 p1059 N73-18634

Frequency and tracks of depressions, storms, and hurricanes in North Indian Ocean from November 1966 to December 1970
[AD-764859] 23 p2815 N73-32505

**INDIANA**

NT WABASH RIVER BASIN [IL-IN-OH]

Application of ERTS-1 imagery to fracture related mine safety hazards in coal mining industry in Indiana
[E72-10193] 01 p0046 N73-10372

Application of multispectral remote sensing to soil survey research in Indiana
[NASA-CR-130033] 07 p0790 N73-16424
Land use classification, utilizing remote multispectral scanner data and computer analysis techniques over Lafayette, Indiana
[NASA-CR-130759] 08 p0917 N73-17516
Application of ERTS-1 imagery to fracture related mine safety hazards in coal mining industry in Indiana and Illinois
[E73-10096] 09 p1020 N73-18321
Application of ERTS-1 imagery to fracture related mine safety hazards in coal mining industry in Indiana and Illinois
[E73-10371] 10 p1151 N73-19366
Evaluation and comparison of ERTS-1 measurements of major crops and soil conditions for selected areas in Central United States
[E73-10384] 11 p1275 N73-20348
Identification and mapping land use classes in Marion County, Indiana from ERTS-1 MSS data
[E73-10680] 16 p1901 N73-25375
Application of ERTS-1 imagery to fracture related mine safety hazards in coal mining industry and identification of mine subsidence areas in Indiana
[E73-10681] 16 p1901 N73-25376
Application of ERTS-1 imagery to fracture related mine safety hazards in coal mining industry in Indiana
[E73-10776] 18 p2135 N73-27252
Application of Skylab EREP imagery to fracture-related mine safety hazards and environmental problems in mining
[E73-10802] 18 p2138 N73-27277
Analysis of ERTS-1 imagery and high altitude infrared photography to determine geological fractures in Indiana and Illinois
[PAPER-E1] 19 p2268 N73-28265
Preparation of urban land use inventories of Wisconsin and Indiana by machine-processing of ERTS-1 MSS data
[PAPER-L19] 19 p2275 N73-28314
Application of ERTS-1 imagery to study of fracture-related safety hazards in Indiana coal mining industry
[E73-10970] 21 p2533 N73-30311
Skylab monitoring of surface mining activities and reclamation in Ohio, West Virginia, Pennsylvania, Indiana, Kentucky, and Illinois
[E73-11033] 22 p2663 N73-31337
Application of ERTS-1 imagery to fracture related coal mine safety hazards and environmental problems in mining in Indiana
[E73-11148] 24 p2918 N73-33302
ERTS-1 measurements of major crops and soil associations in Indiana, North Dakota, Iowa, Nebraska, Kansas, and Texas
[E73-11155] 24 p2919 N73-33309

**INDICATING INSTRUMENTS**
NT ANEMOMETERS
NT APPROACH INDICATORS
NT ATTITUDE INDICATORS
NT CLOUD HEIGHT INDICATORS
NT FLOW DIRECTION INDICATORS
NT GYRO HORIZONS
NT GYROCOMPASSES
NT HOT-FILM ANEMOMETERS
NT HOT-WIRE ANEMOMETERS
NT MICROBALANCES
NT MICROWAVE SENSORS
NT PLAN POSITION INDICATORS
NT POSITION INDICATORS
NT RADIO DIRECTION FINDERS
NT SPACECRAFT POSITION INDICATORS
NT SPEED INDICATORS
NT STRAIN GAGE BALANCES
NT TACHOMETERS

Underwater equipment for locating and recovery of objects from ocean bottom by whales
[AD-747612] 04 p0417 N73-13403
Comparison of contact analog channel display with conventional indicators in cockpit simulator
[DGLR-PAPER-72-100] 04 p0422 N73-13445
Modifications to helicopter active transmission isolation system to provide method for measuring forces on rotary wing of CH-53 helicopter
[NASA-CR-112245] 09 p0982 N73-18024
Digital flight director for precise aircraft control
[AD-754028] 11 p1322 N73-20726
Psychophysiological aspects in flight personnel visual perception of image indicator
20 p2367 N73-29035

**INDIUM**
Intensity of EPR line spectra as affected by indium doped zinc oxide
[AD-764490] 22 p2708 N73-31684

**INDIUM ALLOYS**
Pressure effects on phonon spectrum, electron-phonon interaction strength, and electron-phonon coupling function in Pb-In superconductors using electron tunneling
07 p0831 N73-16739
Materials for ball bearings for space applications using chromium steel and silver-indium alloy
[REPT-781-4.4] 10 p1166 N73-19490

**INDIUM ANTIMONIDES**
Design and development of photoparameteric detector-amplifier using indium antimonide photovoltaic reactions
[AD-749034] 04 p0451 N73-13683
Single crystal growth of indium antimonide
05 p0608 N73-14940
Third harmonic generation by indium antimonide magnetoplasma in presence of dc magnetic field
13 p1562 N73-22659
Device fabrication and radiation effect studies of various semiconductors
[AD-756249] 13 p1566 N73-22689
Faraday rotation and attenuation in InSb in 10.6 micron wavelength region
[AD-761213] 18 p2190 N73-27685
Fabrication and radiation effects of high mobility semiconducting films
23 p2824 N73-32576

**INDIUM ARSENIDES**
Electrical properties of p-n junctions formed by ion implantation into GaAs and [Ga,In]As
[NASA-CR-112200] 01 p0087 N73-10717
Quantum efficiencies of photomultiplier range finders for detection of infrared laser light
[AD-749269] 04 p0397 N73-13230
Neutron irradiation damage in indium arsenide semiconductors and effect on electrical crystal properties
[AD-757468] 14 p1699 N73-23792

**INDIUM COMPOUNDS**
NT INDIUM ANTIMONIDES
NT INDIUM ARSENIDES
NT INDIUM PHOSPHIDES
Computer processing for calculating optical constants from reflectance data of InBi
05 p0609 N73-14952
Environmental tests of strength and durability of transparent tin oxide and indium oxide films on glass
[AD-756558] 14 p1680 N73-23637
Alloying effect on superconducting temperature La3In
[IS-M-2] 17 p2073 N73-26771
Use of InGaP to develop highly efficient LED
24 p2967 N73-33711

**INDIUM PHOSPHIDES**
Synthesis of stoichiometric crystals of InP doped with impurities for obtaining semiconductor with desired resistance
[NLL-RRE-TRANS-381-[8036.625]]
11 p1329 N73-20790
Power gain and noise figure of indium phosphide and gallium arsenide microwave reflection amplifiers
19 p2244 N73-28090
Wavelength modulation spectra of copper, gold, silver, gallium phosphide, and indium phosphide
[LBL-1125] 24 p2927 N73-33375

**INDOLES**
Toxic effect of indole inhalation on man, mouse, rat, and rabbit organisms
10 p1117 N73-19102
Stabilities of nitrogen containing heterocyclic radicals, computation of simple potential energy surfaces, and photophysical properties of indolizine
[NASA-CR-133919] 22 p2625 N73-31034

**INDUCED FLUID FLOW**
U FLUID FLOW

**INDUCERS**
U INTAKE SYSTEMS

**INDUCTANCE**
Induction furnace providing controlled temperature for carbonization and graphitization processes for NERVA nozzle extension
[NASA-CR-132216] 15 p1801 N73-24599
Inductance of cryogenic synchronous equipment with damping system
[AD-759235] 16 p1884 N73-25250
Production of screen-printed inductive components using ferrite pastes
[RAE-LIB-TRANS-1690] 17 p2072 N73-26763

**INDUCTION HEATING**
Feasibility of using yttrium oxide crucible to induction melt titanium
[AD-754092] 11 p1306 N73-20597
Induction heating and concomitant quenching for hot winding helical springs
[AD-759906] 17 p2039 N73-26495
Laser radiation and RF induction heating for production of metal vapor
[AD-762917] 20 p2374 N73-29080
Generation of induction heated, seeded hydrogen plasmas at one atmosphere pressure
20 p2457 N73-29746

**INDUCTION MOTORS**
Voltage controlled oscillator circuit for two-phase induction motor control
[NASA-CASE-MFS-21465-1] 23 p2768 N73-32145

**INDUCTION SYSTEMS**
U INTAKE SYSTEMS

**INDUCTORS**
Superconducting magnet systems, high-power turbogenerators with superconducting field windings, and synchronous generators with superconducting inductors
[JPRS-57638] 04 p0458 N73-13735
Low frequency magnetic field interference of dc/dc regulators and transformers
[ESRO-CR-58] 05 p0499 N73-14059
Computerized simulation of inductor performance constraints
[AD-749685] 06 p0646 N73-15249
Influence of combined rotary flow inductors and dry turbojets on side line noise levels of supersonic transports
[NASA-TM-X-68233] 20 p2466 N73-29809

**INDUSTRIAL AREAS**
Analysis of water pollution levels in USSR lake and measures to protect water purity under conditions of economic development in vicinity
12 p1420 N73-21512

**INDUSTRIAL MANAGEMENT**
NT ENGINEERING MANAGEMENT
NT INVENTORY MANAGEMENT
NT PERSONNEL MANAGEMENT
Technology of small computer systems for industrial automation and control
[FOA-2-C-2485-E5] 02 p0145 N73-11176
Precoronary care and sudden death prevention due to coronary disease in industrial workers
08 p0875 N73-17084
Phased development, planning, and management of new industrial products
15 p1848 N73-24980
Management concept for reliability assurance from aerospace industry experience applied to shipbuilding
[MBB-UA-60-72-O] 17 p2099 N73-26980
Environmental factors influencing Canadian industrial growth
[DRAE-34] 18 p2207 N73-27815
Textbook for engineers for planning control systems for industrial automation
[JPRS-60162] 23 p2797 N73-32373

**INDUSTRIAL PLANTS**
Maskmaking facility for microelectronic systems
[NASA-TM-X-64703] 01 p0036 N73-10284
Dissolved oxygen analyzer for measuring dissolved oxygen concentration in industrial water systems
[NOAA-IFS-73005] 01 p0057 N73-10467
Simulation of emission-dispersion of inert pollutant in lower atmosphere in industrial zones by numerical integration of conservation and pollutant flow equations
06 p0693 N73-15649
Solutions to problem of wear processes experienced by steel industry
[PB-211173] 07 p0809 N73-16565
Catalog of economic, social, and educational institutions in Houston Area Test Site
[NASA-CR-128719] 07 p0856 N73-16944
Industrial model for leave and overtime taking behavior of employees exposed to peak work activity periods in relation to health, demography, and job variables
08 p0872 N73-17055
Bibliography on applications of nuclear explosions in mines, chemistry, and gas and oil extraction
[CEA-BIB-129-ADD-1] 08 p0942 N73-17719
Simplified technique and device for producing industrial grade synthetic diamonds
[NASA-CASE-MFS-20698-2] 10 p1163 N73-19457
Mercury emission control systems for primary mercury facility and for chlor-alkali plant
[AP-118] 11 p1314 N73-20661

**INDUSTRIAL SAFETY**
Application of pneumatically controlled prosthetic arm to industrial handling problems
[NASA-TT-F-14628] 04 p0383 N73-13115
Personnel protection and emergencies handling for oxygen systems
[NASA-CR-120922-VOL-4] 05 p0580 N73-14719
Survey of industrial hygiene and safety in Air Forces operations
[AD-751897] 08 p0880 N73-17126
Occupational hazards and control measures to prevent air pollution from asbestos processing
[AP-117] 11 p1314 N73-20660
Application of ERTS-1 imagery to study of fracture-related safety hazards in Indiana coal mining industry
[E73-10970] 21 p2533 N73-30311
Proceedings of conference on radiation safety and protection in industrial applications
[DHEW-PUBL-[FDA]73-8012] 24 p2951 N73-33574
Chronology of radiation protection methods instituted in industrial plants to show specific procedures and reasons for enforcing protective measures
24 p2952 N73-33575
Characteristics and application of various radiation safety monitoring devices for application to industrial safety protection
24 p2952 N73-33576
Development, application, and characteristics of radiation measuring devices for protection of personnel performing hazardous industrial work
24 p2952 N73-33577
Industrial applications of radiation technology for conducting nondestructive tests
24 p2952 N73-33578

Safety precautions for personnel handling radioactive isotopes to prevent accidental exposure to radiation hazards
24 p2952 N73-33582
Radiation hazards produced by gages used in industrial processes and precautions to avoid exposure of personnel to radiation hazards
24 p2952 N73-33583
Provisions of Occupation Health and Safety Act to show requirements imposed on employers and employees for protection from radiation hazards
24 p2953 N73-33587
Preparation and enforcement of safety recommendations established by American National Standards Institute
24 p2953 N73-33588
Atomic Energy Commission policies and procedures for licensing and regulating industrial uses of radioisotopes
24 p2953 N73-33589
Activities of Food and Drug Administration in enforcing safety measures pertaining to industrial radiation equipment
24 p2953 N73-33590
Recommended practices for avoiding exposure of personnel to radiation hazards
24 p2953 N73-33593

INDUSTRIES
NT AEROSPACE INDUSTRY
NT AIRCRAFT INDUSTRY
NT DEFENSE INDUSTRY
Research facilities, and educational and research programs of Institute of Industrial Science, University of Tokyo
01 p0035 N73-10277
Use of remote sensing data from spacecraft and aircraft to assist technology in tropical tuna and Alaska salmon fisheries
[AD-745774] 02 p0169 N73-11370
Relation between technology and rise of multinational corporations, and impact on nation-state
[NASA-CR-129269] 03 p0367 N73-12988
Soviet industry uses of heat resistant titanium alloys
04 p0433 N73-13528
Industrial health measures and environmental control to insure worker productivity
08 p0874 N73-17077
Medical services of operating environmental health program for industrial workers
08 p0876 N73-17093
Design and operational services of small data centers to technical users
[AGARD-CP-117] 15 p1752 N73-24201
Functions of small industrial information center
15 p1752 N73-24203
Information dissemination services to industry
15 p1753 N73-24210
Effects of techno-economic and organizational factors on adoption of NASA innovations by commercial firms in US
16 p1975 N73-25975
Industrial applications of cryogenic technology
[AD-762315] 20 p2455 N73-29728
Absorptive equipment for control of air polluting industrial wastes
[PB-221138/1] 21 p2575 N73-30637
Trends in usage of tungsten including analyses of supply/demand balance and possible substitutes
[NMAB-309] 22 p2684 N73-31495
Heliothermic conversion of solar radiation for industrial use
24 p2975 N73-33767

INELASTIC BODIES
U RIGID STRUCTURES
INELASTIC COLLISIONS
Generalized vector meson dominance model derived from extended quark model with electron proton inelastic scattering
[TUEP-72-43] 07 p0823 N73-16669
Electron correlation and band structure in solids using X ray Compton effect
15 p1820 N73-24751

INELASTIC SCATTERING
Inelastic lepton-nucleon process in Bjorken limit for neutral gluon model
[ILL-(TH]-72-10] 01 p0083 N73-10684
Continuation from deep inelastic electron scattering to deep electron-positron annihilation
[NOTA-INTERNA-378] 01 p0084 N73-10692
Coincidence rate measurements for inelastically scattered electrons and associated bremsstrahlung at intermediate bombarding energies
[NASA-CR-124007] 06 p0702 N73-15723
Formula for calculating intensity of elastic and inelastic X ray scattering in crystal lattice of vanadium
[NASA-TT-F-13913] 06 p0708 N73-15775
Computing electrical conductivity of thermal plasma taking nonelastic collisions into account
[AD-753972] 10 p1198 N73-19746
Bilocal operator expansion to two jet structure for final states of deep inelastic scattering on hadrons
[ILL-(TH]-73-4] 12 p1430 N73-21592
Survey of theoretical models used to discuss final hadronic states produced in inelastic electron-hadron scattering
[ILL-(TH]-73-2] 12 p1430 N73-21593
Neutron inelastic scattering spectroscopy for studying problems in materials science
[COO-3352-4] 15 p1815 N73-24713
Inelastic atom-atom scattering within intense laser beam
[AD-761180] 18 p2159 N73-27442
Angular distributions of elastically and inelastically scattered 42 MeV alpha particles from Cu-65
[NASA-TN-D-7354] 18 p2181 N73-27611
Diffractive excitation model for evaluation of inelastic part of proton-proton unitarity equation
18 p2182 N73-27614
Production of gamma rays from explosive nucleosynthesis and low energy cosmic ray scattering
19 p2332 N73-28765
Inelastic light scattering from molecular gases with applications to remote detection of air pollutants
24 p2891 N73-33077

INELASTICITY
U ELASTIC PROPERTIES
INEQUALITIES
Distribution function inequalities in order statistics
[NASA-CR-130962] 09 p1058 N73-18627
Evaluation of algorithm for linear inequalities and its applications
[REPT-11] 20 p2437 N73-29576
Existence and representation of diophantine and mixed diophantine solutions to linear equations and inequalities
[AD-763384] 21 p2566 N73-30570
INERT ATMOSPHERE
Technique for welding small refractory metal capsules in controlled atmosphere
[AERE-R-2544] 21 p2553 N73-30466
INERT GASES
U RARE GASES
INERTIA
Lateral inertia effects on elastic-plastic wave propagation in slender rods
[AD-750102] 06 p0728 N73-15938
Flow patterns of air being aspirated into blunt thickwalled tube, and inertia effects on particle trajectories
[TR-23] 11 p1270 N73-20306
Instrumentation and techniques for determining effects of gravitational and inertial forces on cardiovascular and respiratory dynamics
[NASA-CR-133212] 16 p1867 N73-25119
Air or inertial data addition to onboard navigation system for improved air traffic control
16 p1940 N73-25699

INERTIA MOMENTS
U MOMENTS OF INERTIA
INERTIA WHEELS
U REACTION WHEELS
INERTIAL ACCELEROMETERS
U ACCELEROMETERS
INERTIAL COORDINATES
Equation of motion of sand particle under influence of aerodynamic drag developed in inertial coordinate system
[AD-757724] 14 p1653 N73-23405
INERTIAL FORCES
U INERTIA
INERTIAL GUIDANCE
NT STRAPDOWN INERTIAL GUIDANCE
Advanced guidance techniques for Pershing missile
[AD-745897] 02 p0208 N73-11689
Compensating and matching short period seismometers for laboratory inertial guidance and control
[AD-748245] 04 p0424 N73-13455
Design and performance of vibratory output gyro using asymmetrical rotor for rocket inertial attitude control
[NAL-TR-290] 04 p0447 N73-13645
Characteristics of inertial guidance systems to include minimizing of errors, forces on electrostatic gyroscope, and parameters of electromagnetic load cell
[JPRS-57746] 06 p0695 N73-15664
Analysis of lateral velocity measurement errors of inertial guidance system and development of system to compensate for errors
06 p0695 N73-15665
Development of pneumatically isolated stabilized platform to provide active control to local gravity vector
[AD-750869] 06 p0697 N73-15686
Comparison of flat earth guidance laws for Europa 3 launch vehicle
[MBB-TN-RE-11-93-71] 10 p1186 N73-19648
Error analysis for flat earth guidance law of Europa 3 launch vehicle
[MBB-TN-RE-11-64-72-PT-2]
10 p1186 N73-19649
Development and evaluation of failure detection and isolation technique for use with four gimbaled inertial measuring units
11 p1317 N73-20687
Development of low cost inertial measurement unit with navigational accuracy performance based on optimum size design of inertial instruments and platform
11 p1317 N73-20690
Design optimization of SRAM inertial navigation and guidance
11 p1319 N73-20705
Laboratory tests of accelerometers used in inertial guidance systems in French military programs
11 p1320 N73-20714
Guidance equations for present and advanced techniques
[AD-754923] 11 p1322 N73-20728
Performance of computerized inertial guidance system for Delta launch vehicle
18 p2208 N73-27819
Inertial gyro attitude reference system for pitch and yaw control of OAO spacecraft
18 p2208 N73-27821
Titan 3c guidance with carousel vehicle borne inertial guidance system
[AD-764729] 23 p2852 N73-32788
INERTIAL MEASURING UNITS
U INERTIAL PLATFORMS
INERTIAL NAVIGATION
NT GIMBALLESS INERTIAL NAVIGATION
Analysis of geometrical, analytical, and semi-analytical inertial navigation systems for application to shipbuilding industry
[JPRS-57694] 04 p0447 N73-13650
Description of Geographical Position Locator system with emphasis on means for automatically reducing position errors
[UCRL-74039] 07 p0818 N73-16631
Celestial navigation method using astronomical refraction effects
07 p0859 N73-16971
Development and evaluation of Geographic Position Locator for accurate, long-term, land based inertial navigation
[UCRL-51130-VOL-1] 08 p0941 N73-17713
Angular alignment of inertial reference by non-directional data from radio aids
[NASA-CR-128806] 10 p1185 N73-19639
Proceedings of conference on inertial navigation components and systems with emphasis on concepts and techniques involving cost and performance tradeoffs
[AGARD-CP-116] 11 p1316 N73-20684
Numerical analysis of effects of various parameters affecting accuracy and stability of strapdown inertial navigation systems
11 p1316 N73-20685
Research activities of electronic laboratory in development of inertial navigation systems to include applications for space missions and commercial aviation
11 p1316 N73-20686
Development of rapid initialization of inertial navigation system using azimuth wander mechanization
11 p1317 N73-20693
Optimization of integrated navigation systems combining several independent navigation sensors to provide self-contained aircraft navigation capability
11 p1317 N73-20694
Contributions of quality inertial system to vehicle flight control
11 p1318 N73-20700
Application of cluster rotation to improvement of existing platforms in strike aircraft
11 p1319 N73-20704
Design optimization of SRAM inertial navigation and guidance
11 p1319 N73-20705
Parameters of single-axis floated gyroscopes when used in inertial systems requiring rapid gyrocompassing for alignment
11 p1319 N73-20709
A-7 aircraft airborne, ground, and shipboard inertial navigator alignment methodology
11 p1319 N73-20710
Design of Penguin missile inertial navigation system for midcourse guidance
11 p1320 N73-20711
Fault isolation and maintenance concepts of advanced inertial navigation system
11 p1320 N73-20713
Methods employed to obtain datum position and velocity information for evaluation of inertial navigation systems and identification of error sources
11 p1320 N73-20716
Life cycle cost analysis of inertial navigation systems for aircraft and air to surface missiles
11 p1320 N73-20717
Development of navigation system design factors through computerized simulation for application to loran/inertial hybrid system
[AD-754548] 11 p1322 N73-20731
Analysis of equations of aircraft dynamics and development of analog-digital simulation capability
[AD-755868] 12 p1365 N73-21077
Algorithm for determining location of moving object by inertial navigation
12 p1419 N73-21500

Analytical solutions for problems of gyroscopes in inertial navigation systems
[JPRS-58722] 13 p1556 N73-22609
Algorithm for determining position of moving object by inertial navigation methods
13 p1556 N73-22613
Characteristics of airborne area navigation equipment and application to air traffic control functions
14 p1688 N73-23698
Analysis of North Atlantic air route structure to determine impact of inertial navigation and satellite surveillance on separation reduction
14 p1688 N73-23699
Procedure for aligning inertial reference unit of space shuttle by celestial references - Document 20
[NASA-CR-128964] 16 p1941 N73-25706
Analog models of errors in processing navigational information
17 p2059 N73-26660
Software description and program documentation for strapdown inertial reference unit system
[NASA-CR-128965] 18 p2175 N73-27567
Development and characteristics of hybrid loran and inertial navigation system as alternative to high precision navigation sensors
[AD-761027] 18 p2176 N73-27572
Determination of orientation of instrument trihedrons and applications in inertial navigation
20 p2451 N73-29701
Development of kinematic equations for analyzing performance of gimballess inertial navigation system
[JPRS-59688] 20 p2452 N73-29704
Inertial navigation equation simplification and dynamic characteristics of gyrocompass
[JPRS-59776] 21 p2576 N73-30643
Inertial navigation methods to determine coordinates of moving object in vicinity of earth
21 p2576 N73-30644
Error model coefficients for extended Kalman filtering to dynamic calibration of inertial navigation system
[AD-763718] 21 p2577 N73-30656
Evaluation of approach and landing performance of inertial navigation system with Kalman filter installed in CV-340 aircraft
[NASA-TN-D-7302] 23 p2816 N73-32515
Dynamic calibration of inertial navigation system using extended Kalman filtering and command torquing of platform gyros
24 p2950 N73-33566

**INERTIAL PLATFORMS**
Development and application of multiple system checkout procedures for use with gimbaled inertial measuring units
[NASA-CR-123953] 03 p0328 N73-12676
Analysis of propagating and non-propagating motions produced by earth tides and earth rates and effects on inertial instrument performance
[AD-748274] 03 p0330 N73-12691
Equations of compass motion of three axis gyrostabilizer in gyrocompass mode based on initial placement error of platform in horizontal plane
06 p0695 N73-15667
Characteristics of symmetrical springs for elastic field between rotor and housing of gyroscopic instruments and numerical analysis of radial stiffness
06 p0696 N73-15669
Development of device for measuring angular rate based on fluidic components for inertial angular rate sensors using vortex principle
[FOA-2-C-2466-54] 06 p0696 N73-15672
Test plan for evaluation of redundant sensor strapdown inertial measuring unit to include operating procedures and data and analysis requirements
[NASA-CR-123513] 08 p0941 N73-17711
General test plan for redundant sensor strapdown inertial measuring unit evaluation program
[NASA-CR-130722] 08 p0941 N73-17712
Methods for determining plane of meridian during initial alignment of inertial systems
10 p1184 N73-19636
Analysis of microplasticity of materials used in inertial navigation systems to show friction stress, yield stress, and rate of strain hardening in microstrain region
11 p1317 N73-20692
Development of rapid initialization of inertial navigation system using azimuth wander mechanization
11 p1317 N73-20693
Advanced procedures for self alignment and calibration of inertial platforms
11 p1319 N73-20706
Estimation procedures for in-flight vertical misalignment of platforms
11 p1319 N73-20707
Modelling error sensitivity of digital filters for alignment of inertial platforms
11 p1319 N73-20708

**INERTIAL REFERENCE SYSTEMS**
Development of apparatus and technical procedures for measuring system inertia tensor parameters of precession nonrigid systems
05 p0547 N73-14442
Development of mathematical model to represent small motions relative to inertial reference coordinate system of spacecraft in low, circular earth orbit
07 p0847 N73-16867
Articles on inertial systems
[JPRS-58181] 10 p1184 N73-19632
Procedure for aligning inertial reference unit of space shuttle by celestial references - Document 20
[NASA-CR-128964] 16 p1941 N73-25706

**INFARCTION**
NT MYOCARDIAL INFARCTION

**INFECTIONS**
U INFECTIOUS DISEASES

**INFECTIOUS DISEASES**
NT INFLUENZA
NT SYPHILIS
Research in control of infectious diseases weather forecasting, and epidemic of Q fever without pneumonia
[JPRS-57663] 04 p0475 N73-13886
Luciferase ATP assay procedure for determining bacterial infections in urinary tract
[NASA-CR-130797] 09 p0992 N73-18096
Management of asymptomatic carriers of hepatitis associated antigen in Hellenic Air Force personnel
14 p1611 N73-23060
Meteorological conditions and infection of upper respiratory tract in children
[NLL-M-22866-[5828.4F]] 16 p1866 N73-25109
Prodromal disease - Immune responses of host macrophage system to humoral factors
[NASA-CR-133455] 19 p2224 N73-27938

**INFESTATION**
Investigation of forest stress in Black Hills, forest inventory at Atlanta test site, and rangeland inventory at Manitou test site using ERTS-1 imagery
[E72-10219] 02 p0162 N73-11313
Control of pink bollworm infestation in southern California cotton fields using ERTS-1 remotely sensed imagery
[E72-10285] 04 p0409 N73-13335
Detection and monitoring forest insect infestation in Sierra Nevada Mountains of California using ERTS-1 imagery
[E72-10301] 04 p0411 N73-13351
Forest and rangeland inventory and forest infestation of Atlanta, Manitou, and Black Hills test sites based on ERTS-1 imagery
[E73-10084] 08 p0901 N73-17296
Inventory of forest and rangeland and detection of insect infestation from ERTS-1 imagery of Black Hills, Atlanta, and Manitou test sites
[E73-10407] 11 p1278 N73-20369
ERTS-1 imagery of forest insect infestation in Sierra Nevada Mountains of California
[E73-10440] 11 p1282 N73-20400
Control and mapping of pink bollworm infestations in cotton fields of California desert areas
[E73-10452] 11 p1283 N73-20411
Remote sensing techniques for evaluating vigor loss in black spruce due to eastern dwarf mistletoe
[NASA-CR-131582] 13 p1523 N73-22341
Detection and monitoring of forest insect infestation in Sierra Nevada Mountains of California
[E73-10668] 16 p1899 N73-25363
Analysis of ERTS-1 data and underflight photography for detection of insect infestation and timber resources in Sierra Nevada Mountains of California
[PAPER-A16] 19 p2261 N73-28224
Analysis of ERTS data for detection and monitoring of forest insect infestations in Sierra Nevada Mountains of California
[E73-10868] 20 p2392 N73-29219
Early detection of insect infestations and density/distribution of host citrus trees along Rio Grande River in Texas
[E73-11073] 23 p2782 N73-32248
Early detection of insect infestations and density/distribution of host citrus trees in Texas
[E73-11074] 23 p2782 N73-32249
Detection of insect infestations and density/distribution of host citrus trees in Texas
[E73-11075] 23 p2782 N73-32250
Skylab detection of insect infestations and density/distribution of host plants in Texas
[E73-11076] 23 p2782 N73-32251
Detection of insect infestations and density/distribution of host citrus trees in Texas
[E73-11077] 23 p2782 N73-32252
Utilization of ERTS data to study air pollution, insect infestation, and water transport in Minnesota
[NASA-CR-135565] 23 p2783 N73-32266
Aerial photography for detecting cereal crop insect infestation
[PAPER-8076] 23 p2783 N73-32268
Detection and monitoring forest insect infestation in Sierra Nevada Mountains of California from ERTS-1 data
[E73-11133] 24 p2917 N73-33288

**INFILTRATION**
Infiltrating porous and particulate materials with metallic alloys
[Y-1846] 12 p1414 N73-21458

**INFINITE SPAN WINGS**
Numerical analysis of incompressible laminar boundary layer on infinite swept wing with arbitrary velocity and suction distribution
[ARC-R/M-3241] 16 p1854 N73-25018
Infinum principle with nonscalar-valued performance criterion
[NASA-CR-132052] 15 p1804 N73-24617

**INFLATABLE DEVICES**
U INFLATABLE STRUCTURES

**INFLATABLE STRUCTURES**
NT BALLOONS
NT GAS BAGS
NT HIGH ALTITUDE BALLOONS
NT METEOROLOGICAL BALLOONS
NT SKYHOOK BALLOONS
NT TETHERED BALLOONS
Analysis of performance potential of buoyant systems and flexible structures for use with short haul passenger transport aircraft
[NASA-TM-X-62168] 08 p0866 N73-17014
Equations of motion for elastic tire rolling on ground and forces exerted by tire assuming absence of slippage between tire and ground
[AD-732697] 09 p1040 N73-18482
Research and development of transpiration cooled inflatable nozzle extension
[NASA-CR-124165] 11 p1269 N73-20300
Development and characteristics of inflatable airbag restraint system for use in general aviation aircraft
[FAA-RD-73-3] 16 p1868 N73-25127
Analysis of rigid airship operations for commercial cargo handling in United Kingdom
[CRANFIELD-CTS-3] 20 p2360 N73-28985
Flight tests of folding sidewall, expandable tires on C-131 aircraft to determine operation of inflation and deflation system
[AD-762730] 20 p2361 N73-28993
Analysis of landing performance of scale model of C-8 aircraft equipped with air cushion landing system on variety of surfaces including calm and rough water
[NASA-TN-D-7295] 21 p2496 N73-30032
Effect of inflated air cushion landing gear on subsonic static stability of high performance aircraft operating out of ground effect
[AD-763365] 21 p2498 N73-30048
Design requirements and characteristics of toroidal, continuous wound aircraft tire
[AD-764888] 23 p2746 N73-31977

**INFLECTION POINTS**
Graphical determination of meteor radiant point curve
17 p2024 N73-26374

**INFLUENZA**
Hydrogen peroxide aerosols for decontamination of influenza atmosphere
[NASA-TT-F-15127] 23 p2750 N73-32006

**INFORMATION DISSEMINATION**
NT SELECTIVE DISSEMINATION OF INFORMATION
Employee communication at NASA Langley Research Center
[NASA-TM-X-68854] 02 p0244 N73-11985
Quality control for rawinsonde data dissemination to ships
[NOAA-TM-NWS-NMC-52] 11 p1314 N73-20663
Data users note for dissemination of Apollo 16 lunar photographs
[NSSDC-73-01] 15 p1785 N73-24468
Technology transfer and information dissemination services provided by Technology Use Studies Center
[NASA-CR-132963] 16 p1977 N73-25991
Combined micrographic and computerized data storage and search system for information processing
[DSIS-TN-13] 23 p2760 N73-32083

**INFORMATION FLOW**
Information capacity of gradient method for measuring earth magnetic field
[JPRS-60100] 23 p2786 N73-32292

**INFORMATION MANAGEMENT**
Interactive information system with application in medical area
[NASA-TM-X-66076] 01 p0020 N73-10156
Index of information collected by Soviet weather satellites
[NASA-TT-F-14447] 01 p0075 N73-10616
Effects of computerized management of information on organizational structures and functions
[REPT-486-70] 04 p0393 N73-13191
Augmentation and improvement of information management system simulation model
[NASA-CR-128718] 07 p0765 N73-16218
Standards and procedures for generation of operational display formats for use in Mission Control Center display control system
[NASA-CR-128843] 10 p1132 N73-19228

Relationships between United States of America and Latin American telecommunication institutions
[PB-214619/9] 16 p1876 N73-25187
Annotated bibliography of literature on resource sharing computer networks
[NBS-SP-384] 22 p2638 N73-31140
Information management for Skylab earth resources experiments in oceanography and marine science
[NOAA-TM-NESS-51] 24 p2921 N73-33328
Automation of processes of gathering and primary processing of scientific information on expeditions of Arctic and Antarctic Scientific Research Institute
24 p2947 N73-33537

INFORMATION RETRIEVAL
Cost effective data security safeguards in personal information databanks
[P-4871] 02 p0145 N73-11178
Information retrieval system combining magnetic storage and microfilm reader/copier
[CRIF-EL-5] 02 p0147 N73-11188
Development of holographic storage and retrieval system for aerial chart information display in cockpit environment
[AD-748648] 03 p0330 N73-12690
Effect of using weighted index terms in document retrieval system with cluster analysis
[NASA-CR-129804] 04 p0393 N73-13195
Computer index on bibliographical references to microscopic neutron data
05 p0582 N73-14734
Reliability of search strategies for information retrieval by aerospace personnel
[AD-751977] 08 p0977 N73-17995
Computer programs for information retrieval and data analysis
[NASA-SP-5955[01]] 09 p1005 N73-18204
Automated computer index and retrieval system on machining of materials
[AD-752000] 09 p1053 N73-18582
Rate distortion theory for providing privacy transformations in data banks
[P-4952] 14 p1619 N73-23113
Survey of easy methods of developing easy computer systems useable by everyman
[P-4962] 14 p1638 N73-23278
Development of processing and information extraction techniques for Skylab multispectral band scanner data
[E73-10563] 14 p1656 N73-23435
Data collection problems for small documentary centers
15 p1753 N73-24208
Electronic computer processing of data stored in data banks
15 p1753 N73-24212
Image enhancement and information extraction techniques for ERTS-1 MSS imagery
[E73-10572] 15 p1772 N73-24352
Associative approach test model data management system
[AD-750147] 16 p1879 N73-25209
Tactical routing indicator look-up and header preparation device
[AD-759944] 17 p2002 N73-26192
Organizational subsystems of information computer center for automatic systems control
[AD-761480] 19 p2240 N73-28057
Information retrieval system for hydrometeorology applications
20 p2448 N73-29666
Data analysis, feature extraction, and pattern recognition for automatic target classification
[AD-763493] 21 p2550 N73-30449
Abstracts on research projects inclusive of flight dynamics to heating of swimming pools using solar collector
[ISBN-0-85494-200-9] 21 p2609 N73-30910
Development of processing and extraction techniques for Skylab EREP MSS data
[E73-11078] 23 p2782 N73-32253
Development of report search code for computer generated bibliographic data in machine readable form
[DSIS-TN-11] 24 p2897 N73-33125
Automatic hybrid interactive information storage and search system
[DSIS-TN-13] 24 p2897 N73-33126

INFORMATION SYSTEMS
NT MANAGEMENT INFORMATION SYSTEMS
Bibliography on digital image processing information
[AD-745790] 01 p0029 N73-10231
Proposed control tower and cockpit visibility readouts based on airport-aircraft information flow system
[AD-744718] 01 p0078 N73-10647
Classification system for indexing and retrieving documents on structural analysis
[ESDU-00.00.01] 01 p0112 N73-10928
Points of contact for scientific and technical information
[AD-746615] 02 p0246 N73-11997
Timber resource management and information system
[E72-10245] 03 p0289 N73-12345
Computerized information processing for radar system by subdivisions and multiple decision making processes
04 p0389 N73-13158
Effects of computerized management of information on organizational structures and functions
[REPT-486-70] 04 p0393 N73-13191
Solid state electronics, information systems, plasma and quantum electronics, biomedical electronics, acoustics, and radio sciences
[AD-748281] 04 p0400 N73-13256
Canadian Defence Scientific Information Service experience with microfiche and microfilm cartridges
[DSIS-TN-9] 04 p0486 N73-13972
Research progress in electronic equipment, data processing, plasma physics, and information systems
[AD-750669] 06 p0732 N73-15976
Proceedings of conference on management of information analysis centers
[COSATI-72-1] 07 p0766 N73-16224
Operational activities of mechanical properties technical information center
[AD-752499] 08 p0894 N73-17236
Information system for space law
[NASA-CR-130746] 08 p0976 N73-17986
Independent radar systems using information processing, data correlation, and telecommunication
09 p1002 N73-18179
Proceedings of conference on laser beam data transmission and development of laser information systems
[AD-753944] 10 p1169 N73-19513
Prototype regional environmental information system based on ERTS-1 imagery of Central Atlantic Regional Ecological Test Site
[E73-10497] 12 p1397 N73-21333
Management planning for California water resource information gathering system
12 p1399 N73-21349
Network data handling system, including software release and global weather data base
[AD-757686] 14 p1638 N73-23282
Space station information subsystem for automatic support of manned operations
14 p1711 N73-23887
Analysis of complex social systems relative to information, communication, and behavior
[P-4951] 14 p1721 N73-23963
Design and operational services of small data centers to technical users
[AGARD-CP-117] 15 p1752 N73-24201
Design and operation of Turkish information systems
15 p1752 N73-24202
Functions of small industrial information center
15 p1752 N73-24203
Problems of library and information services to large research center
15 p1753 N73-24204
Curriculum development and personnel training for information centers
15 p1753 N73-24205
Management methods for developing information systems
15 p1753 N73-24209
Information dissemination services of technical information service of National Research Council of Canada
15 p1753 N73-24211
ERTS-1 data for development of information system for timber resources and land management planning in Oregon
[E73-10696] 16 p1903 N73-25388
TAXIR information retrieval system for analyzing climatic conditions on east slope of Colorado front range
[PB-214341/0] 16 p1939 N73-25688
Navy research reports on electronics, optical physics, and information systems
[PB-215342/7] 16 p1977 N73-25992
Progress in plasma physics, integrated circuits, solid state, and information and digital systems
[AD-759697] 17 p2099 N73-26984
Ergonomic control system information models
21 p2503 N73-30082
Research on probabilistic information processing
[NASA-CR-133918] 22 p2738 N73-31920

INFORMATION THEORY
Estimation of magnitude-squared coherence function spectrum
[AD-743945] 01 p0029 N73-10225
Information theory criteria for electronic jaming and countermeasures for air defense
[FOA-3-C-3644-66] 02 p0140 N73-11133
Index and introduction to Principles of Information Theory of Visibility in Atmosphere
[NASA-TT-F-14435] 02 p0211 N73-11712
Research in plasma dynamics, communication and general physics
[AD-747350] 03 p0368 N73-12998
Soviet abstracts on analog and digital systems, control systems, information theory, and automata theory
[JPRS-57520] 04 p0393 N73-13190
Application of fourier analysis, information theory, or curvature analysis to determine information content of curved line
[MITT-128] 05 p0538 N73-14376
Estimation of time delays generated by random field propagating across array of noise sensors in optimal processing of multiple sensor data
[AD-751555] 07 p0756 N73-16146
Research and development in solid state physics, plasma physics, electrical engineering systems and information sciences, and mathematical biosciences and biomedical engineering
[AD-751515] 07 p0834 N73-16757
Detection scheme with threshold learning for amplitude shift keyed signals
[AD-752009] 08 p0886 N73-17171
Statistical analyses for detecting frequency shift keyed and phase keyed signals in additive disturbance
[AD-752010] 08 p0886 N73-17173
Statistical analysis on nonparametric detection of M-ary time varying signals with intersymbol interference and additive noise
[AD-752011] 08 p0886 N73-17174
Fourier series and fourier integral formulations for improving spectrum analysis and display computer program
[AD-752113] 08 p0886 N73-17177
Detection of time varying signals in amplitude shift keyed signals with additive disturbance
[AD-752008] 08 p0890 N73-17208
Research in plasma physics, communication and data processing
[AD-751213] 08 p0944 N73-17729
Detecting point radiator in presence of nongaussian interference
[AD-752712] 09 p1004 N73-18191
Numerical integration of Fokker-Planck equation for first order phase locked loop
[AD-754355] 11 p1259 N73-20214
Maximum likelihood testing algorithm for estimating monopulse radar signal amplitude in air traffic control
[AD-756844] 13 p1493 N73-22105
Nonlinear modulation of analog data with improved digital enhancement technique
[AD-755939] 13 p1494 N73-22112
Rate distortion theory for providing privacy transformations in data banks
[P-4952] 14 p1619 N73-23113
Burst random access channel for satellite computerized data transmission system
[AD-756226] 14 p1635 N73-23252
Analysis of modifications of ALOHA random access channel by considering synchronization among users
[AD-756227] 14 p1637 N73-23271
Performance of digital matched filter receiver designed to receive biphase modulated signal in presence of interference
[AD-756841] 14 p1643 N73-23326
Development of algorithms for calculating modal trajectory estimate, conditional mean state estimate, and weighted least squares trajectory estimate
[AD-757240] 14 p1684 N73-23665
Error protection techniques for data communication
[AD-759836] 17 p1999 N73-26168
Correlation loss of Gaussian signal passed through odd quantizer
[AD-760310] 17 p2006 N73-26225
Application of discrete transforms in adaptive radar detection systems and effect functional performance
[AD-761219] 18 p2120 N73-27139
Performance characteristics, except direction, of detection receivers in processing known signals
[AD-762048] 19 p2236 N73-28029
Decision graphs for information processing
[AD-761877] 19 p2242 N73-28078
Multivariate statistical analysis including divergence, probability of misclassification, information theory, and matrix analysis
[NASA-CR-128990] 20 p2438 N73-29578
Sufficient statistics for divergence and brattacharyya distance
[REPT-13] 20 p2438 N73-29579
Sufficient statistics for divergence and probability of misclassification
[REPT-14] 20 p2438 N73-29580
Rank-k maximal statistics for divergence and probability of misclassification
[REPT-21] 20 p2438 N73-29585
Development of guidelines for definition of relevant information content in data classes
[NASA-CR-124356] 20 p2488 N73-29990
Design techniques for data base oriented computer networks for information flow
[AD-763791] 22 p2640 N73-31163
Research on plasma physics, information theory, biophysics, and data processing systems
[AD-765002] 23 p2867 N73-32919
Analysis of Marxist-Leninist theory based on data in cybernetics, information theory, systems analysis, and semiotics
24 p2993 N73-33918

INFORMATION TRANSFER
U COMMUNICATING

INFORMATION TRANSMISSION
U DATA TRANSMISSION
INFRARED ASTRONOMY
Gamma, X ray, ultraviolet, and infrared astronomy noting instrumentation and radiative transfer
[ESRO-SP-75] 04 p0476 N73-13889
Sortie Lab system evaluation, future growth, and IR astronomy experiment accommodation
[ESS/SS-399-VOL-3] 17 p2089 N73-26904
INFRARED DETECTORS
Two channel infrared scanning, display, and recording system for measuring varying atmospheric effects on image transmission
[AD-747053] 02 p0176 N73-11425
Dual channel, 10.6 micron infrared scanner system
[AD-747052] 02 p0213 N73-11724
Tungsten-germanium whisker diode far infrared detector
[UCLA-34-P-157] 03 p0274 N73-12219
Corrections for airborne sea surface temperature measurements by infrared techniques
[AD-747011] 03 p0297 N73-12425
Characteristics of infrared photodetectors manufactured from semiconductor material irradiated by electron beam
[NASA-CASE-LAR-10728-1] 03 p0300 N73-12445
Laser induced infrared quantum counter upconversion experiments utilizing rare earth ions in single crystals
[AD-747415] 03 p0312 N73-12546
Quantum efficiencies of photomultiplier range finders for detection of infrared laser light
[AD-749269] 04 p0397 N73-13230
Design and development of photoparameteric detector-amplifier using indium antimonide photovoltaic reactions
[AD-749034] 04 p0451 N73-13683
Application of absorber laser amplifier and detector to wide angle low noise optical radar and communication systems
[AD-749543] 05 p0558 N73-14533
Photomultiplier tubes and laser range finders for infrared detection
[AD-749645] 06 p0646 N73-15245
Parametric modifications for improved image intensification of forward looking infrared imaging devices in night fire control
[AD-750374] 06 p0646 N73-15251
Design and performance of heat camera using indium antimony and germanium mercury infrared detectors
[FOA-2-A-2540-52] 06 p0700 N73-15704
Two satellite microwave occultation system for determining pressure levels in atmosphere using infrared sensors
07 p0775 N73-16294
Development of infrared camera for detecting wilt root disease in coconut trees
07 p0783 N73-16369
Displacement damage to infrared detectors from high energy neutrons
[AD-751340] 07 p0802 N73-16510
Measurement of cloud base temperature with infrared detector and comparison with lidar and radiosonde results
[BMVG-FBWT-72-17] 07 p0815 N73-16611
Galactic and background radiation measurements by rocket-borne submillimeter detectors
07 p0840 N73-16808
Infrared detection of hydrogen fluoride tracer for studying turbulent mixing in inert and combustion flows
08 p0880 N73-17128
Optimal performance of infrared pneumatic transducer with capacitive membrane
[ONERA-TP-1150] 09 p1007 N73-18222
Frequency stable Q switched carbon dioxide laser oscillators, free-running and injection locked pulsed lasers, and optical heterodyne measurements of frequency stability
[AD-753605] 09 p1045 N73-18523
Development of optical equipment including image converters and infrared detectors employing coherent radiation
[AD-753275] 09 p1067 N73-18711
Millimeter and submillimeter wave detection and mixing with superconducting weak links
[AD-754083] 10 p1202 N73-19783
Photon detector applications and theoretical considerations of heterojunction photo-effect
[AD-754026] 10 p1202 N73-19784
Open resonator with volumetric detector for tunable millimeter and submillimeter receiver
[AD-754829] 11 p1323 N73-20739
Design of infrared detector array using multielement heterodyne technology
[AD-754443] 11 p1325 N73-20751
Effect of charge carrier heating on volt-ampere characteristics of thermoelectric indicators of microwave emissions
[AD-756561] 13 p1531 N73-22407
Plasma diagnostic visualization with pulsed carbon dioxide TEA laser and liquid crystal infrared detector, noting spark discharges
[ISL-18/72] 13 p1563 N73-22668
Evaluation of cryogenic devices for application in surveillance, radiation detection, and communications
[AD-756175] 14 p1668 N73-23537
Feasibility analysis and design of bleachable absorber laser amplifier and detector
[AD-757361] 14 p1672 N73-23571
Analysis of relative intensity profiles of density fluctuations based on acoustic properties of subsonic and supersonic unheated jet flow
[NASA-CR-124563] 16 p1861 N73-25073
Development of 10.6 micrometer range gated upconversion imaging laser radar receiver with 150 by 150 resolution elements
[AD-759077] 16 p1915 N73-25495
Design of 10.6 micrometer detector array using 77 K, 1500 MHz photodiodes
[AD-758714] 16 p1915 N73-25496
Thin film lead and tin selenide photoconductive infrared detectors
[AD-758685] 16 p1915 N73-25499
Infrared image converter, based on temperature sensitive liquid-solid interface, using GE-AU IR detector
[IPF-72-6] 17 p2033 N73-26457
Metallurgical and electrical properties of thin film Pb[0.9]Sn[0.1]Se photoconductive infrared detectors
[AD-758519] 17 p2064 N73-26693
Application of infrared reconnaissance satellites for detecting missiles and military satellites
[AD-760951] 18 p2152 N73-27395
Threshold detection system for infrared nutating optical system
[AD-761380] 18 p2180 N73-27600
Application of infrared detectors for location and identification of asteroids during sky survey activities
[AD-760107] 18 p2198 N73-27745
Thermal and infrared testing for nondestructive evaluation of flaws
19 p2304 N73-28523
Electrical properties of MIS semiconductors and application as infrared detectors
[AD-761510] 19 p2327 N73-28719
Development of Hg Cd Te elevated temperature photovoltaic detectors
[AD-762352] 20 p2381 N73-29131
Growth of high quality, single crystalline, Pb Sn Te by vapor-phase epitaxy for infrared detectors
[AD-762344] 20 p2463 N73-29795
Various infrared detectors, including thermal detectors and photodetectors
[DRIC-TRANS-3179] 21 p2549 N73-30439
Research on ternary diamond-like semiconductors as long wavelength infrared detectors
[AD-763466] 21 p2586 N73-30725
Pyroelectric infrared detector performances investigating strontium and barium niobates, lithium sulfate and TGS materials effects on frequency ranges and sensitivity
[ESRO-CR-67] 22 p2675 N73-31425
Satellite infrared radiometer observation of hurricane intensification
22 p2736 N73-31906
Vertical temperature profile data obtained by satellite radiometer sounding
[NOAA-TR-NESS-65] 23 p2786 N73-32291
Infrared sensitive television camera for horizon and depth perception in whiteout
[DREO-TN-73-11] 23 p2791 N73-32332
Specifications of infrared detector for cloud cover determination
[BMVG-FBWT-73-13] 23 p2793 N73-32349
Infrared detection of zero pi pulses generated by mode locked CO2 lasers
[AD-764692] 23 p2802 N73-32406
Liquid crystal infrared detectors for plasma diagnostics and flow visualization using CO2 laser impulses
[BMVG-FBWT-73-16] 23 p2823 N73-32564
INFRARED FILTERS
Process for producing polycrystalline halides for use in high power laser windows to maintain optical properties with improved mechanical properties
[AD-745350] 01 p0065 N73-10535
Instrumentation for atmospheric rocket sounding by occultation including infrared interferometer, Fabry-Perot interference filter, and vacuum spectrometer
[BMBW-FBW-72-14-PT-1] 22 p2667 N73-31368
INFRARED HORIZON SCANNERS
U HORIZON SCANNERS
U INFRARED SCANNERS
INFRARED IMAGERY
Improved multibeam cathode ray tube for real time display of infrared reconnaissance data
[AD-749475] 05 p0520 N73-14228
Geology photography infrared imagery, and remote sensing evaluation of Klondike Mining District, Nevada
[NASA-CR-129934] 05 p0537 N73-14371
Investigation of 106 micron propagation phenomena
[AD-749504] 05 p0581 N73-14727
Parametric modifications for improved image intensification of forward looking infrared imaging devices in night fire control
[AD-750374] 06 p0646 N73-15251
Electromagnetic interference identification in infrared line scan imaging patterns
[DREO-TN-72-25] 07 p0821 N73-16652
Comparison of day and night infrared thermal imagery with results obtained using color photography and multispectral band sensor imagery
[AD-752217] 08 p0919 N73-17535
Electronic equipment for infrared television camera used in terrain analysis
[LCR-DR-1-71-210/1/R] 13 p1500 N73-22157
Analysis of image forming ability of infrared line scan system based on laboratory measurements and flight tests using ground test array
[DREV-TN-2053/72] 14 p1666 N73-23520
Statistical processing of Nimbus infrared data for synoptic atmospheric climatology
18 p2170 N73-27523
Feasibility of charge coupled lead-tin-telluride semiconductor for infrared imagery
[AD-761473] 19 p2245 N73-28099
Nonlinear materials including univalent metal iodates for IR image upconversion
[AD-763952] 22 p2701 N73-31630
Optimum use of infrared data as obtained from satellites for meteorological and oceanographic applications
24 p2911 N73-33233
Present status in meteorological satellites, wind observation, cloud cover, and the imagery compared with predictions made in 1962
24 p2949 N73-33552
INFRARED INSPECTION
Evaluation of several thermographic infrared techniques and their applicability to detection of unbonded areas in babbitted bearings
[AD-745730] 01 p0063 N73-10516
Cost effectiveness of infrared inspection and maintenance of ARTCC eiectrical equipment
[C-208] 04 p0447 N73-13648
INFRARED INSTRUMENTS
NT INFRARED DETECTORS
NT INFRARED SCANNERS
NT INFRARED SPECTROMETERS
NT INFRARED SPECTROPHOTOMETERS
Atmospheric transmittance from sun and sky radiance measurements with Nimbus E infrared temperature profile radiometer prototype used at Mauna Loa Observatory
[NOAA-TR-NESS-61] 01 p0048 N73-10391
Silver addition in Si-As-Te glasses to permit introduction of substantial amounts of selenium and to produce infrared transmitting glasses with increased softening ranges
[AD-747333] 02 p0193 N73-11563
Infrared polarimeter for airborne measurement of terrestrial cloud particle sizes and shapes
[NASA-CR-130119] 03 p0301 N73-12458
Environmental and flight readiness tests of scanning mirror for infrared sensors
09 p1089 N73-18888
Infrared measurement of brightness temperature of Martian surface by Mars-3 automatic interplanetary station
[NASA-TT-F-14837] 10 p1211 N73-19852
Effectiveness of infrared radiometer and digital recording equipment as clear air turbulence warning system
[AD-757501] 14 p1685 N73-23677
Infrared site monitor operations at McDonald Observatory
[NASA-CR-133394] 18 p2152 N73-27392
Engineering design handbook on infrared systems for military applications
[AD-763495] 21 p2581 N73-30684
INFRARED INTERFEROMETERS
Global distribution of total ozone as determined by Nimbus 3 satellite infrared interferometer spectrometer
16 p1895 N73-25326
Nimbus 4 IRIS spectra in 750-1250/cm atmospheric window region
[NASA-TM-X-66281] 18 p2142 N73-27315
Instrumentation for atmospheric rocket sounding by occultation including infrared interferometer, Fabry-Perot interference filter, and vacuum spectrometer
[BMBW-FBW-72-14-PT-1] 22 p2667 N73-31368
INFRARED LASERS
Development and characteristics of alkali halide window for application to infrared laser systems
[AD-744998] 01 p0065 N73-10530
Feasibility of infrared laser/sonar beam communication system between submarine and aircraft and effects of air water interaction
[AD-746106] 02 p0143 N73-11156
Window material for high power carbon dioxide infrared lasers
[AD-746500] 02 p0182 N73-11473
Design and operation of amplitude stabilized pulsed laser operating at approximately 1.06 microns in fundamental transverse mode
[AD-746512] 02 p0182 N73-11474
Ocular effects of near infrared laser radiation for safety criteria
[AD-746793] 04 p0381 N73-13097

Near infrared laser action for Kodak organic dyes using linear flash lamp for excitation
[AD-748863] 04 p0429 N73-13496
Atmospheric water vapor absorption at CO, HF, and DF laser frequencies using 1-km white absorption cell and laser sources
[AD-748437] 04 p0430 N73-13501
Modulation of infrared laser emission using gallium arsenide crystal
[AD-749631] 04 p0430 N73-13507
Pressure induced optical distortion in high power, infrared laser system windows and determination of figures of merit based on minimum thickness
05 p0556 N73-14517
Thermal lensing in infrared laser window materials
[AD-749481] 05 p0558 N73-14536
Photomultiplier tubes and laser range finders for infrared detection
[AD-749645] 06 p0646 N73-15245
Development and characteristics of optical communication system based on three frequency heterodyne configuration
[AD-750321] 06 p0680 N73-15533
Optical design approach for large array of high speed heterodyne receivers for infrared laser radiation
[AD-750402] 06 p0700 N73-15711
Mechanical properties of polycrystalline alkali halides determined for application to high power infrared laser windows
[AD-752193] 08 p0930 N73-17617
High temperature deformation of polycrystalline halide microstructures by infrared lasers
[AD-751655] 08 p0944 N73-17730
IR laser radiation eye protector
[AD-753080] 09 p0998 N73-18142
Optical absorption properties of polycrystalline zinc selenide and cadmium telluride materials for infrared laser windows
[AD-753068] 09 p1044 N73-18512
Preparation, characterization, and evaluation of materials for infrared windows
[AD-754280] 10 p1169 N73-19512
Retinal damage in monkeys exposed to near infrared gallium arsenide laser pulses
[AD-753419] 11 p1248 N73-20135
Predicted multiline continuous wave power output from perfectly stirred reactor chemical laser
[AD-755904] 12 p1411 N73-21433
Multiphonon infrared absorption by crystal inclusions of optical window materials
[AD-756080] 13 p1537 N73-22453
Atmospheric pressure gas lasers
[AD-755477] 13 p1538 N73-22462
Ultrawide-bandwidth laser communication system using high efficiency, single frequency lasers and optical modulators
[AD-755219] 13 p1539 N73-22468
Optical performance evaluation of infrared transmitting materials
[AD-756825] 14 p1673 N73-23576
Micron output increase of Nd YAG laser to pump optical parametric oscillator through visible spectrum
[AD-756809] 14 p1673 N73-23577
Development of cadmium telluride modulator for infrared laser communication system
[NASA-CR-112321] 15 p1795 N73-24549
Growth and hardening of potassium chloride single crystals for infrared laser windows
[AD-757893] 15 p1795 N73-24550
Significant population inversion in flow structure behind blast wave
[AD-757881] 15 p1795 N73-24555
Gallium arsenide epitaxial thin films as active elements for electrooptic modulation of carbon dioxide laser radiation
[AD-757792] 15 p1796 N73-24559
Cooled carbon monoxide laser for pulsed operation with pressure up to 1 atmosphere using electron beam for gas excitation
[AD-759755] 16 p1924 N73-25570
Measurement of vibrational temperatures in carbon monoxide laser
[AD-759237] 16 p1925 N73-25575
IR laser study of absorption and saturation properties of molecular gases
[NASA-CR-132769] 19 p2307 N73-28554
Research on near-infrared dye lasers
[AD-762354] 20 p2426 N73-29485
High power infrared window materials for laser applications
[AD-765354] 23 p2802 N73-32412
Absorption spectra of infrared window matrials
[AD-764904] 24 p2969 N73-33730

**INFRARED MASERS**
U INFRARED LASERS

**INFRARED PHOTOGRAPHY**
Infrared nondestructive testing techniques used to detect unbonded areas in laminated structures and incipient failures in electrical circuit boards
[AD-746233] 02 p0175 N73-11419
Application of color photography and infrared photography for determining effects of weather on coffee crop production
07 p0783 N73-16365
Detection of disease in coffee crops using color photography and infrared photography techniques
07 p0783 N73-16366
Comparison of imagery obtained with several types of remote sensors over Test Site 701, Mexico
07 p0783 N73-16367
Analysis of imagery obtained from infrared color and color photography used for highway and railroad engineering applications
07 p0783 N73-16368
Development of infrared camera for detecting wilt root disease in coconut trees
07 p0783 N73-16369
Detection of citrus tree anomalies by remote sensing with infrared color aerial photography
07 p0785 N73-16384
Application of color infrared film to measure spatial and temporal changes in vegetation
07 p0788 N73-16406
Analysis of oceanography remote sensing using black and white, color, and color infrared photographic recording
07 p0788 N73-16407
Relationship between maize canopy density and reflected energy determined from color and color infrared photographs
[NASA-CR-130370] 07 p0790 N73-16422
Infrared sky survey in Southern Hemisphere for finding late M stars
07 p0846 N73-16854
Civil engineering in Arctic regions using dual channel infrared scanner and infrared photography
[AD-753048] 09 p1037 N73-18461
Correlation and regression analysis of aerial photography and soil samples to determine principal soil limitations
[NASA-CR-131110] 10 p1154 N73-19392
Analysis of ERTS-1 data to detect and map areas of tree mortality due to insect outbreaks using color infrared positive transparencies
[E73-10351] 11 p1275 N73-20345
Analysis of ERTS-1 photographic imagery for identification, definition, and mapping, of terrestrial ecosystems in interior Alaska
[E73-10399] 11 p1277 N73-20361
Bibliography on infrared photography and infrared films
[AD-754600] 11 p1295 N73-20509
Analysis of earth based remote sensing data and infrared observations to determine nature of Apollo 16 landing site
12 p1455 N73-21787
Reflected energy of vegetative ground cover measured with multispectral band scanners and infrared photographs
[NASA-CR-131575] 13 p1524 N73-22348
Weather forecasts using satellite information
[NLL-M-22897-[5828.4F]] 15 p1804 N73-24625
Color and color infrared aerial photographic detection of Dutch elm disease
16 p1866 N73-25110
Mapping of large forest fires from infrared photography
[AD-758613] 17 p2028 N73-26414
Using infrared aerial photography for detection of forest fires
[AD-762259] 19 p2302 N73-28509
Forest fire detection by airbonre infrared photography
[AD-762265] 19 p2353 N73-28931
Aerochrome infrared aerial photography over Barro Colorado Inland, using multispectral, line scan data for tropical forests
[AD-762583] 20 p2415 N73-29410
Thermal infrared imagery of North American Arctic for different seasons
[AD-764239] 22 p2668 N73-31376
Near infrared photometry and absolute magnitudes of carbon stars, barium stars, CH stars, and hydrogen deficient carbon stars
22 p2714 N73-31722

**INFRARED RADIATION**
NT FAR INFRARED RADIATION
NT NEAR INFRARED RADIATION
Compilation of data concerning effects of infrared radiation on eye
[NASA-CR-128407] 01 p0008 N73-10064
Physical model of excitation processes and infrared radiation
[AD-745319] 01 p0051 N73-10409
Design study of infrared 10.6 micrometer, quantum noise limited, optical receiver subsystem
[NASA-CR-130091] 01 p0056 N73-10458
Detection of internal ocean waves using three-color infrared radiometer
[AD-745004] 01 p0059 N73-10484
Catalog of 383 celestial objects emitting infrared radiation near 10 microns
[AD-743891] 01 p0106 N73-10878
Direct generation of far infrared power through laser action on rotational transitions in molecular gases
[AD-745984] 02 p0182 N73-11476
Reflectivity measurements with 10.6 micrometer infrared radiation from CO2 laser
[AD-746238] 02 p0183 N73-11482
Infrared observations of comets, 1969g and 1969i
02 p0227 N73-11837
Infrared observations of comets Ikeya-Seki [1965f] and Bennett [1969i]
02 p0227 N73-11838
Thermal remote sensing of infrared radiant temperatures in alpine/periglacial environments
04 p0409 N73-13332
Physical-statistical inference model using satellite infrared data for estimating cloud distribution from empirical histographs of equivalent black body temperatures
04 p0441 N73-13597
Scattering and absorption effects in atmospheric transmission of infrared radiation
[AD-750084] 05 p0542 N73-14410
Application of infrared technology for measuring infrared radiation emitted by military aircraft
[AD-749798] 06 p0623 N73-15058
Calibration and temperature control system for airborne interferometer
[AD-749876] 06 p0667 N73-15427
He-Xe tunable laser measurement of infrared line shape and CO2 absorption spectra
[AD-751230] 07 p0808 N73-16556
Design and operation of tunable parametric oscillators with range between 1.0 and 5.0 micrometers
[AD-753347] 09 p1044 N73-18517
Required doping levels for germanium and silicon infrared windows at microwave energies
[AD-753466] 09 p1075 N73-18772
Measurement of infrared radiation from Mercury and Moon
[NASA-CR-130968] 09 p1085 N73-18849
Atmospheric aerosol particles in infrared radiation transfer process
10 p1146 N73-19325
Light and infrared radiation propagation and absorption in atmosphere
[AD-753974] 10 p1158 N73-19418
Analysis of noise sources in jet aircraft based on measurement of infrared emission
[NASA-TT-F-14851] 11 p1234 N73-20020
Astrobee rocket instrumentation for infrared radiation measurements on auroral display
[AD-755823] 12 p1402 N73-21373
Satellite solar occultation absorption measurements of pollutant concentrations and spectral properties of molecules in infrared region
[REPT-011023-1-T] 12 p1444 N73-21700
Research and development of infrared photocathodes
[AD-756239] 13 p1501 N73-22162
Analysis of infrared spectra generated by OV-1D, F-14, and UH-1 aircraft using Fourier spectroscopy
[RM-572] 13 p1529 N73-22390
Physical and spectral characteristics of infrared solid state dispersion filters
[NASA-TT-F-14838] 13 p1558 N73-22631
Infrared sensitive photoconductors
[AD-755224] 13 p1560 N73-22647
Tunable parametric oscillator using infrared pumping for ultraviolet frequency generation
[AD-756910] 13 p1561 N73-22650
Absolute cross sections for rotational Raman scattering derived for nitrogen and oxygen from near UV to infrared
[AD-756808] 13 p1566 N73-22695
Distribution of tropospheric infrared radiative fluxes and associated heating and cooling rates in Southern hemisphere
15 p1771 N73-24340
Operational exploitation of satellite infrared channel radiances in resolution of atmospheric thermal-structure variabilities
[AD-757773] 15 p1782 N73-24443
High optical resolution derivative spectrometer for measuring optical properties of solids in vacuum UV and far IR range
15 p1785 N73-24474
Attenuation of thermal radiation by transpiration of absorbing gas using porous Porolloy plate
15 p1812 N73-24685
Polarization of infrared waves due to propagation through atmosphere
16 p1895 N73-25327
Infrared optical parametric fluorescence and parametric oscillation
16 p1944 N73-25729
Tunable infrared parametric oscillators and coherent spectroscopy
[AD-759408] 16 p1945 N73-25741
Cadmium and germanium compounds chalcopyrite semiconductor materials for infrared optics
[AD-759556] 16 p1945 N73-25742
Design of prototype infrared countermeasure arc lamp
[AD-759752] 17 p2063 N73-26692
Radiative cascade limit in recombination oxygen plasma
[AD-759010] 17 p2070 N73-26747

Evaluation of radiometric computations in infrared window and water vapor absorption band regions based on 4-D atmospheric models
[NASA-CR-129007] 18 p2172 N73-27546
Handbook on radiant emission and absorption of combustion gases for application to design of rocket combustion chambers and exhausts, turbojet engines, and industrial furnaces
[NASA-SP-3080] 18 p2206 N73-27807
High resolution interferometer spectrometer measurements of auroral infrared emissions to simulate high altitude nuclear explosions
[AD-762013] 19 p2297 N73-28475
Infrared emission from chemical and radiative processes to study auroral altitudes
[AD-762318] 19 p2298 N73-28479
Predicted and measured infrared radiation data for Mercury and Moon
19 p2341 N73-28831
Development of techniques for simulating infrared emission from turbojet aircraft exhaust plumes
[AD-763123] 20 p2486 N73-29967
Materials for semiconductor radiation detectors and infrared techniques
20 p2487 N73-29978
Spectral density of infrared radiation reflected by earth atmosphere
[AD-763158] 21 p2539 N73-30361
Application of infrared data from satellites for use in field of fishery oceanography in Pacific Ocean
[AD-763350] 21 p2542 N73-30380
Infrared laboratory studies of synthetic planetary atmospheres
[NASA-CR-133855] 21 p2597 N73-30810
Engineering test procedures for heat seeking missiles
[AD-763324] 21 p2602 N73-30853
Development of fine spectral resolution procedure for determining infrared radiant heat transfer from exhaust plume
[RM-575] 21 p2605 N73-30877
Temperature control of welding equipment by detection of discrete bands of infrared radiation from objects being heated
[NASA-CASE-MFS-20781-2] 22 p2672 N73-31401
Dense plasma focus using CO2 laser scattering and infrared bremsstrahlung emission
[COO-2233-2] 22 p2703 N73-31652
Infrared emission from southern H 2 region H2-3 with solar luminosity between 1.65 and 25 microns
[NASA-CR-135640] 23 p2785 N73-32280
High power infrared window materials for laser applications
[AD-765354] 23 p2802 N73-32412
Simultaneous satellite observations of infrared and reflected energy measured to infer convective activity of tropical cloud clusters
[NOAA-TM-NESS-50] 23 p2814 N73-32498
Aerial thermal infrared surveillance of active volcanoes in northern Cascade Range
[E73-11100] 24 p2914 N73-33257
Infrared photometry of variable stars
[AD-764686] 24 p2981 N73-33827
Objectives of infrared radiometry experiment
24 p2983 N73-33838

**INFRARED SCANNERS**

Operational tests and evaluation of optical infrared pilot warning system to determine probability of detection versus range
[NASA-CR-129525] 03 p0302 N73-12463
Application of thermal infrared scanner data to agriculture
07 p0785 N73-16387
Forest fire detection using airborne infrared scanners
07 p0785 N73-16390
Automatic computer mapping of infrared scanner data of terrain classes in Yellowstone National Park
07 p0787 N73-16400
Electromagnetic interference identification in infrared line scan imaging patterns
[DREO-TN-72-25] 07 p0821 N73-16652
Photographic and infrared scanning surveys over Harper Lake, California
[AD-752226] 08 p0920 N73-17536
Digital data processing system for infrared video scan
[AD-752069] 08 p0944 N73-17731
Civil engineering in Arctic regions using dual channel infrared scanner and infrared photography
[AD-753048] 09 p1037 N73-18461
Infrared and microwave radiometric data of intertropical convergence zone acquired by Nimbus 3 satellite
[NASA-TM-X-66203] 10 p1188 N73-19669
Method and equipment for locating earth infrared horizon from space, independent of season and latitude
[NASA-CASE-LAR-10726-1] 11 p1291 N73-20475
Atmospheric observation techniques using aircraft infrared radiometers as prototypes for spacecraft remote sensing application
[NOAA-TR-NESS-64] 11 p1293 N73-20494
Analysis of image forming ability of infrared line scan system based on laboratory measurements and flight tests using ground test array
[DREV-TN-2053/72] 14 p1666 N73-23520
Evaluation of image forming ability of infrared line scan system using laboratory and flight test techniques
15 p1786 N73-24476
High resolution pulse width modulated parallel channel for forward looking infrared display system
[AD-759224] 16 p1882 N73-25231
Application of infrared detectors for location and identification of asteroids during sky survey activities
[AD-760107] 18 p2198 N73-27745
Visible infrared spin-scan radiometer system for earth and cloud cover photography by synchronous meteorological satellite
18 p2209 N73-27834
Development of infrared earth horizon scanner employing thermistor bolometers providing pitch and roll data of synchronous satellites
[ESRO-CR-161] 19 p2301 N73-28503
Computerized laser position detector and optical stereo display system
24 p2897 N73-33121

**INFRARED SPECTRA**

Threecomponent optical system with variable focal length for infrared region of spectrum
[AD-745356] 01 p0080 N73-10665
Methane mixing ratios in stratosphere deduced from balloon-observed solar infrared spectra
[AERONOMICA-ACTA-A-105] 01 p0092 N73-10757
Description of linear polyethylene standard reference material
[NBS-SP-260-42] 02 p0192 N73-11552
Formation of nitrous oxide molecules from ion-molecule reactions following sea level nuclear burst
[AD-746958] 03 p0298 N73-12428
Optical and back reflection properties of GaAs crystals used as IR window materials
[AD-749083] 04 p0451 N73-13684
Catalog of micron celestial objects
[AD-747776] 04 p0476 N73-13894
Infrared absorption bands of nitrous oxide in earth atmosphere
[AD-749879] 05 p0541 N73-14405
Infrared and NMB spectra of poly[carborane-siloxane] s containing icosahedral cages in nitrogen environment
[AD-749386] 05 p0566 N73-14599
Application of infrared technology for measuring infrared radiation emitted by military aircraft
[AD-749798] 06 p0623 N73-15058
Measurement of infrared emission spectra of liquid cyclopentane derivatives excited by carbon dioxide laser
[AD-750480] 06 p0681 N73-15544
Infrared spectra of aluminum, gallium, and indium suboxide vapors considering frequency oscillations in group 3 suboxides and molecular constants of boron oxide
[AD-752861] 09 p1000 N73-18164
Minimization technique for determining structural parameters of IR and vibrational rotational spectra of H2O
[AD-754612] 11 p1253 N73-20166
Far infrared laser spectroscopy of spin clusters in linear magnetic system of cobalt chloride compound
[AD-756264] 13 p1566 N73-22691
Infrared spectra of group 3 metal-oxides
[NASA-CR-133100] 17 p1991 N73-26102
Absolute measurements of spectral radiances from uranium oxygen mixtures
[AD-762430] 19 p2232 N73-27997
Rocket produced infrared emissions for analyzing auroral atmospheric mechanisms
[AD-762206] 19 p2298 N73-28478
Rocket infrared multicolor observations of interplanetary medium H II regions and galactic center region, using Cornell liquid helium cooled rocket telescope
19 p2342 N73-28838
Utilization of Skylab EREP S-191 infrared spectra for geological surveys
[E73-10923] 20 p2398 N73-29272
Atmospheric absorption line parameters for infrared-active molecules occurring naturally in terrestrial atmosphere
[AD-762904] 21 p2542 N73-30382
Arizona-NASA atlas of infrared solar spectrum in 13350 - 34100 A wavelength
[LPL-COMMUN-166] 21 p2591 N73-30762
Experimental and theoretical IR spectra of atmospheric hydrocarbon gases CO, CO2, and NH4 for occultation sounding
[BMBW-FBW-72-14-PT-2] 22 p2667 N73-31369
Bidirectional reflectance of zinc oxide in ultraviolet and infrared spectral bands
[NASA-CR-135494] 22 p2678 N73-31450
Nimbus 4 satellite infrared spectra for analyzing cloud spectral effects
22 p2736 N73-31907
Atmospheric infrared transmission spectral analysis discussing computed and measured data, and absorption due to atmospheric components
[BMVG-FBWT-73-11] 23 p2787 N73-32297
Intermolecular force effects on infrared spectral transparency of active gas mixtures
[DRIC-TRANS-3227] 23 p2820 N73-32545
Fourier spectrometer system for studying infrared spectra of K giants
23 p2836 N73-32661
Infrared quantitative spectral star classification system
23 p2836 N73-32665
Analysis of Mariner 9 infrared radiometric Mars surface measurements
23 p2841 N73-32701
Infrared absorption spectra of lithium and potassium silicate glasses
[AD-764891] 24 p2893 N73-33092
Infrared signatures of high performance jet aircraft and evaluation of air to air missile effectiveness
[SLA-73-5271] 24 p2994 N73-33929

**INFRARED SPECTROMETERS**

NT FILTER WHEEL INFRARED SPECTROMETERS
Fourier spectrometer for measuring absolute spectral intensity of emissions from earth and other planets
[NASA-TT-F-14425] 02 p0172 N73-11397
Infrared spectral emittance data, and infrared spectrometry studies
[NASA-CR-128646] 03 p0335 N73-12730
Atmospheric dust and circulation, carbon dioxide and water vapor transmittancies, surface pressure; and topography of Mars determined from Mariner 9 infrared spectrometers
[NASA-TM-X-66150] 06 p0718 N73-15864
Effect of cloud conditions on satellite infrared spectrometer temperature retrievals
[NOAA-TR-NESS-63] 09 p1034 N73-18435
Infrared spectrometer for use with ground based telescope
[NASA-CR-131512] 12 p1448 N73-21726
Utilization of satellite infrared spectrometer data for resolution of atmospheric variables
[AD-757774] 15 p1789 N73-24501
Global distribution of total ozone as determined by Nimbus 3 satellite infrared interferometer spectrometer
16 p1895 N73-25326
Study of recreational land and open space with Skylab imagery EREP 443
[E73-10783] 18 p2136 N73-27259
Nimbus 4 IRIS spectra in 750-1250/cm atmospheric window region
[NASA-TM-X-66281] 18 p2142 N73-27315

**INFRARED SPECTROPHOTOMETERS**

Infrared interferometer spectrophotometer for infrared spectra measurement of CO2 in atmospheres of Earth and Venus
08 p0973 N73-17954
Near infrared spectrophotometry of cool stars in galactic anticenter
16 p1960 N73-25852
Instrumentation for far infrared spectroscopy
[AD-762313] 19 p2302 N73-28512
Thin layer chromatographic identification and infrared spectrophotometric quantification of antitoxants used in manufacturing polyolefinic polymers
[REPT-6726] 22 p2625 N73-31029

**INFRARED SPECTROSCOPY**

Regression relationships between Nimbus 4 SIRS-B clear-column radiances and geopotential heights of 500 mb and 300 mb levels
[AD-743711] 01 p0075 N73-10624
Operating characteristics of far infrared spectroscopic system for analyzing plasma diagnostics
[AD-748280] 04 p0456 N73-13726
Infrared absorption spectra analysis of contaminant materials and binary mixtures to determine contamination of spacecraft by material outgassing
[NASA-CR-124072] 08 p0934 N73-17645
Intraday time scale variability of infrared, optical, and radio observations from 3C 120, BI Lac, and OJ 287
[AD-752214] 08 p0962 N73-17871
Determination of impurities in titanium tetrachloride by infrared spectroscopy, emission spectra, and chemical analysis
[NLL-RTS-7725] 09 p1045 N73-18524
Infrared spectroscopic investigation of polyimide films containing silver metal
[TR-62] 09 p1048 N73-18545
Derivation of temperature fields from Mariner 9 infrared spectroscopy and calculation of Martian atmospheric tidal pressure and wind fields
[NASA-TM-X-66230] 12 p1458 N73-21818
Analysis of infrared spectra generated by OV-1D, F-14, and UH-1 aircraft using Fourier spectroscopy
[RM-572] 13 p1529 N73-22390
Comparative infrared spectroscopic analysis of liquid oxygen
[AD-756629] 14 p1646 N73-23348
Infrared fluorescent low level carbon monoxide analyzer
[PB-213846/7] 15 p1747 N73-24163
Satellite infrared channel radiances for resolution of atmospheric thermal structure and developing weather analysis and forecasting system
[AD-758734] 15 p1807 N73-24644

Raman and far infrared spectroscopy for materials characterization
[AD-762303] 19 p2233 N73-28006
Instrumentation for far infrared spectroscopy
[AD-762313] 19 p2302 N73-28512
Exploitation of satellite observed radiances for increased resolution of atmospheric thermal structure
[AD-762752] 20 p2450 N73-29692
Report of the Astronomer Royal for Scotland for the year ending 31 March 1973
22 p2718 N73-31760
Polymer coatings for moisture protection of optical windows in infrared spectroscopy
[NASA-CASE-ARC-10749-1] 23 p2820 N73-32542
Infrared spectra of Mars atmospheric and surface properties
23 p2840 N73-32700
Overview of infrared spectroscopy experiment on Mariner 9 space probe
24 p2983 N73-33839

INFRARED STARS
Identification of infrared stars using Schmidt telescopes, infrared photometry, and slit spectra
07 p0846 N73-16855
Infrared stars with strong 1665-1667-mHz main-line OH emission
[AD-753898] 12 p1459 N73-21821
Mechanisms by which stars radiate excess infrared energy, and correlation between rapid mass loss and infrared excesses in stars
13 p1575 N73-22766
Near infrared photometry and absolute magnitudes of carbon stars, barium stars, CH stars, and hydrogen deficient carbon stars
22 p2714 N73-31722
Balloon-borne far infrared telescope observations of galactic and Magellanic Cloud objects
22 p2735 N73-31890
Infrared quantitative spectral star classification system
23 p2836 N73-32665

INFRARED TRACKING
Calibration of missile infrared track and acquisition system
[AD-754944] 11 p1295 N73-20507
Calibration of target acquisition system using infrared tracking
[AD-756845] 13 p1595 N73-22937
Threshold detection system for infrared nutating optical system
[AD-761380] 18 p2180 N73-27600

INFRASONIC FREQUENCIES
NT MICROSONICS
Infrasonic resonant tube determination of wind and temperature variabilities in lower troposphere
[AD-745912] 02 p0206 N73-11667
Auroral infrasonic sound wave generation and downward propagation into lower atmosphere
05 p0508 N73-14134
Auroral infrasonic shock wave generation by supersonic electrojet arcs
05 p0508 N73-14137
Observations of weak infrasound emission during magnetic storms caused by ionospheric auroral electrojets
05 p0508 N73-14138
Ionospheric oscillations caused by infrasonic waves propagating from thunderstorms
05 p0510 N73-14148
Infrasonic detection of propagating atmospheric shock waves caused by supersonic aircraft
05 p0512 N73-14161
Influence of infrasound on human body functions
08 p0875 N73-17085

INGESTION [BIOLOGY]
NT GRAZING
Ingestible miniaturized telemetry device for deep body temperature measurements on humans and animals
[NASA-CASE-ARC-10583-1] 05 p0503 N73-14093

INGESTION [ENGINES]
Influence of inlet distortions on turbojet and ingestion engine stability
[AD-745852] 01 p0092 N73-10755
Establishment of takeoff and landing environment criteria for V/STOL aircraft with emphasis on airborne particle concentration
[AD-749463] 05 p0495 N73-14034
Engine ingestion prevention on low wing aircraft, particularly Mercury aircraft, by jet blast
[FO-1149] 06 p0622 N73-15049
Wind tunnel tests to determine structural integrity of birds under conditions simulating ingestion of birds into inlets of high speed aircraft
[NASA-TM-X-68163] 06 p0629 N73-15114

INGOTS
Influence of ingot thermal-mechanical processing on grain size and mechanical properties of 7075 wrought aluminum alloy
[AD-750390] 06 p0686 N73-15588

INHALATION
U RESPIRATION

INHIBITION
Reaction kinetics in vibrationally excited nitrogen quenching by atomic oxygen
[AD-752542] 08 p0946 N73-17751
Bioelectrical activity differentiations in cat cortex during sleep inhibition
13 p1483 N73-22026

INHIBITORS
NT WEAR INHIBITORS
Corrosion tests of inhibitors for protection of aluminum
[AD-749705] 06 p0689 N73-15606
Chemical synthesis inhibitor of oceanic species having antibiotic properties
07 p0858 N73-16962
Phenol preservative for reducing toxic urine outgassing into air environment
10 p1116 N73-19098
Using optical interference coatings to produce bandpass filters for spectral region
[NASA-CR-135671] 23 p2819 N73-32537

INHOMOGENEITY
Methods for determining electric permittivity of inhomogeneous dielectric medium that is uniform in two dimensions and varies according to profile function in other dimension
02 p0201 N73-11622
Shortwave propagation medium with random heterogeneities in approximate Markovian random process
[AD-746714] 02 p0203 N73-11644
Radiative mass flow transfer model for inhomogeneous structure of chromosphere
04 p0466 N73-13798
Nonlinear excitation of longitudinal plasma oscillations in inhomogeneous plasma
[AREAEE-125] 07 p0828 N73-16713

INITIAL VALUE PROBLEMS
U BOUNDARY VALUE PROBLEMS

INITIATION
Accidental initiation of encased high explosive charges through rapid closure of air gap due to accidental drop of device
[AD-758255] 15 p1844 N73-24941
Detonation sensitivity and shock resistance of explosives at impact
[ISL-2/73] 19 p2353 N73-28923

INITIATORS [EXPLOSIVES]
NT DETONATORS
Precision closed bomb calorimeter for monitoring electrically or mechanically actuated flame and gas producing devices
[NASA-CR-131371] 11 p1295 N73-20510
Initiator ignition effect in laboratory glass and polythene vessel studying dummy hand injuries during simulated accidents
[ERDE-TRANS-1] 15 p1744 N73-24137

INJECTION
NT CARRIER INJECTION
NT FLUID INJECTION
NT FUEL INJECTION
NT GAS INJECTION
NT ION INJECTION
NT LIQUID INJECTION
NT SECONDARY INJECTION
NT TRANSEARTH INJECTION
NT WATER INJECTION
Precipitation of auroral and ring current particles in magnetosphere by artificial plasma injection
[AD-755352] 12 p1403 N73-21381
Boundary layer separation on flat plate in high supersonic free stream as caused by normal injection of two dimensional sonic or supersonic jet
[AD-757635] 14 p1652 N73-23398
Injection locking of positive pulse microwave magnetrons by stabilized low power source
[AD-758198] 15 p1758 N73-24248

INJECTION CARBURETORS
U FUEL INJECTION

INJECTION GUIDANCE
Model 2914 series Delta launch vehicle configuration
[NASA-TM-X-70455] 21 p2599 N73-30833

INJECTION LASERS
Waveguide and luminescent properties of thin film Pb-salt injection lasers
[AD-763757] 21 p2556 N73-30488

INJECTORS
NT VORTEX INJECTORS
Combustion stability with hydrogen-oxygen liquid rocket propellants
03 p0349 N73-12844
Performance evaluation of coaxial injectors for use in gaseous hydrogen-liquid oxygen rocket engines
[DLR-FB-71-56] 07 p0836 N73-16779
Thermocouple measurement of gas velocity and temperature near liquid rocket injector face
[NASA-CR-121100] 11 p1270 N73-20304
Injector design guidelines for gas/liquid propellant systems
[NASA-CR-120968] 13 p1570 N73-22726
Transient thermocouple measurement of gas flow direction velocity, and temperature near injector of liquid propellant rocket
18 p2129 N73-27201
Improved injector with porous plug for bubbles of gas into feed lines of electrically conductive liquid
[NASA-CASE-NPO-11377] 18 p2154 N73-27406
Gaseous propellant combustion and injector/chamber design guidelines
[NASA-CR-121234] 20 p2464 N73-29799

INJUN SATELLITES
NT INJUN 3 SATELLITE

INJUN 5 SATELLITE
U EXPLORER 40 SATELLITE

INJUN 3 SATELLITE
Satellite observations of geomagnetic disturbance reaction time in upper atmosphere
[REPT-85] 14 p1658 N73-23458

INJURIES
NT BACK INJURIES
NT BAROTRAUMA
NT BURNS [INJURIES]
NT CRASH INJURIES
NT EJECTION INJURIES
NT LESIONS
NT NOISE INJURIES
NT RADIATION INJURIES
Analysis of nonfatal injuries to passengers and flight attendants in airline operations during period 1968 through 1971
[NTSB-AAS-73-1] 14 p1601 N73-22983
Defined shock wave effects on miniature swine, describing organ injuries
19 p2227 N73-27965
ERTS-1 sensor analysis of air pollution and air pollution related injuries to plant vegetation in metropolitan Minnesota
23 p2784 N73-32269

INLET FLOW
Influence of inlet distortions on turbojet and ingestion engine stability
[AD-745852] 01 p0092 N73-10755
Turbulent boundary layers on walls of rectangular water pipe inlets
02 p0155 N73-11259
Influence of inlet deformation on characteristics of ejector jet devices operating on incompressible fluids
[AD-747079] 02 p0179 N73-11454
Analysis of radial distributions of flow conditions at inlet and outlet of high speed rotors to determine effects of blade part-span dampers on rotor performance
[NASA-TM-X-2696] 06 p0614 N73-14985
Procedure for designing axisymmetric, translating, centerbody inlet bleed system for operation at Mach 3.5
[NASA-CR-2187] 06 p0713 N73-15821
Flow characteristics of tandem bladed compressor stators at various inlet incidence angles
[NASA-TM-X-2734] 08 p0863 N73-16986
Turbine inlet gas temperature measurement by ultrasonic impedance
[AD-752602] 08 p0955 N73-17822
Analysis of internal flow conditions of inlet with centerbody retracted for short takeoff and landing aircraft takeoff and approach operations
[NASA-TN-D-7185] 09 p0980 N73-18010
Effects of vane-induced flow rotation on diffuser flow distortion in axisymmetric mixed-compression inlet
[NASA-TM-X-2752] 09 p0981 N73-18012
Vortice distribution field for calculating inlet flow of ducted propeller
[AD-754114] 10 p1144 N73-19318
Flow patterns of air being aspirated into blunt thickwalled tube, and inertia effects on particle trajectories
[TR-23] 11 p1270 N73-20306
Effect of inlet-air humidity on formation of oxides of nitrogen from a gas turbine combustor under various air inlet temperature conditions
[NASA-TM-X-68209] 12 p1443 N73-21691
Effect of steady state circumferential total pressure distortion on loss in compressor stall pressure ratio
[NASA-CR-114577] 12 p1443 N73-21693
Wind tunnel tests to determine flow distribution within model passages of hypersonic inlets for core flow and boundary layer flow conditions
[NASA-TN-D-7150] 13 p1470 N73-21905
Wind tunnel tests to determine effect of tip vortex of forward mounted wing on engine inlet ingestion
[NASA-TM-X-68225] 13 p1473 N73-21932
Development and evaluation of throat bypass bleed system to increase stable airflow range of sonic mixed-compression inlet
[NASA-TM-X-2779] 14 p1597 N73-22947
Local flow measurements at inlet spike tip of Mach 3 supersonic cruise aircraft
[NASA-TN-D-7320] 15 p1731 N73-24037
Kinetic energy transfer in multiple jet mixing flow of duct inlet
[AD-758836] 16 p1891 N73-25305
Internal performance of mixed compression axisymmetric inlet model at Mach 0.8 to 2.65
[NASA-TN-D-7320] 16 p1955 N73-25817
Performance tests of terminal shock and restart control system of two dimensional twin-duct compression inlet
[NASA-TM-X-2818] 16 p1956 N73-25824

Effects of free stream velocity and incidence angle on aerodynamic and acoustic performance of translating centerbody choked flow inlet
[NASA-TM-X-2773] 16 p1957 N73-25829
Time dependent flow field model for subsonic diffuser section of supersonic inlet
[AD-758803] 16 p1957 N73-25835
Program summary of research project for sonic inlet technology involving design concepts for aerodynamic performance and noise suppression - Vol. 1
[NASA-CR-121126] 19 p2328 N73-28731
Research project for noise suppression of sonic inlets used with turbofan engines and improvement in engine inlet flow characteristics - Vol. 2
[NASA-CR-121127] 19 p2328 N73-28732
Analysis of internal noise field of two axisymmetric sonic inlet models for noise suppression of turbofan engine inlets - Vol. 3
[NASA-CR-121128] 19 p2329 N73-28733
Development of computer programs for designing engine inlets for VTOL and STOL aircraft based on axisymmetric potential flow parameter
[NASA-TM-X-68278] 20 p2388 N73-29182
Analysis of steady-state and dynamic pressure conditions in F-111 aircraft engine to determine causes of engine compressor stalls
[NASA-TN-D-7328] 20 p2465 N73-29806
Analysis of intake duct noise of turbofan engine and effect on duct structure due to acoustic fatigue
20 p2479 N73-29916
Pressure recovery performance of conical diffusers at high subsonic speeds and range of geometries
[NASA-CR-2299] 22 p2611 N73-30927
Wind tunnel tests to determine boundary layer flow characteristics in supersonic axisymmetric inlet
[NASA-TM-X-2902] 23 p2739 N73-31926
Wind tunnel tests to determine flow distribution at inlet locations on aircraft model for various aerodynamic configurations and airspeeds
[NASA-TN-D-7364] 23 p2739 N73-31929
Flow interference between supersonic intake and airframe to show three dimensional separation of boundary layer
23 p2775 N73-32194
Aerodynamic design of inlet stage for two-stage compressor and performance comparison for axial, mixed flow, and centrifugal stage configurations
[NASA-CR-120943] 23 p2829 N73-32610
Effect of inlet conditions on optimal shape of diffuser based on theory of potential flow of fluid in channels
[AD-765577] 24 p2911 N73-33230
Characteristics of variable geometry high Mach inlet concepts to reduce jet engine noise on subsonic, long range commercial aircraft
[NASA-CR-134495] 24 p2972 N73-33748

**INLET NOZZLES**
Flight performance evaluation for underwing nacelle installation of auxiliary-inlet ejector nozzle with clamshell flow diverter from Mach 0.6 to 1.3
[NASA-TM-X-2655] 02 p0222 N73-11793
Analysis of dynamic inlet distortion data for turbojets
[AD-756481] 13 p1571 N73-22731
Analysis of temperature and pressure parameters associated with recirculated engine exhaust from V/STOL aircraft engines exhausting normal to ground
[NASA-TT-F-14912] 15 p1768 N73-24323

**INLET PRESSURE**
Analysis of radial distributions of flow conditions at inlet and outlet of high speed rotors to determine effects of blade part-span dampers on rotor performance
[NASA-TM-X-2696] 06 p0614 N73-14985
Wind tunnel tests to determine flow distribution at inlet locations on aircraft model for various aerodynamic configurations and airspeeds
[NASA-TN-D-7364] 23 p2739 N73-31929
Flow interference between supersonic intake and airframe to show three dimensional separation of boundary layer
23 p2775 N73-32194

**INLETS [DEVICES]**
U INTAKE SYSTEMS

**INLETS [TOPOGRAPHY]**
NT COOK INLET [AK]

**INOCULATION**
Automatic inoculating device for agar trays using cotton swab or loop
[NASA-CASE-LAR-11074-1] 07 p0750 N73-16096

**INORGANIC COATINGS**
NT ANODIC COATINGS
NT CERAMIC COATINGS
Composition of diffuse reflective coating containing sodium chloride in combination with diol solvent and organic wetting and drying agents
[NASA-CASE-GSC-11214-1] 04 p0385 N73-13128
Development of technique for measuring residual stresses in thin coatings based on analysis of stress induced deflections of substrate
[NASA-CR-130813] 09 p1051 N73-18566

**INORGANIC COMPOUNDS**
NT AMMONIA
NT LIQUID AMMONIA
Development of low melting fused salt electrolytes
[AD-755528] 13 p1477 N73-21965
Application of inorganic exchangers to radiochemical separations on neutron activated high purity materials
[CONF-721069-42] 17 p2050 N73-26584
Lithium anode cells operating at room temperature using electrolytic solutions in inorganic solutions
[AD-763478] 23 p2754 N73-32039

**INORGANIC MATERIALS**
Hydrostatic pressure technique for improving dielectric properties of inorganic glasses used as capacitor materials
[AD-750393] 05 p0521 N73-14236
Research in inorganic materials
[LBL-425] 06 p0732 N73-15970
Properties of thermal resistant electrical insulating papers based on inorganic fibers
[NLL-RTS-7740] 10 p1175 N73-19554
Performance tests and failure analyses on silver zinc cells with inorganic separator materials
[NASA-CR-121215] 18 p2108 N73-27049

**INORGANIC NITRATES**
NT AMMONIUM NITRATES
NT SODIUM NITRATES

**INORGANIC PEROXIDES**
NT HYDROGEN PEROXIDE

**INORGANIC SULFIDES**
NT CADMIUM SULFIDES
NT COPPER SULFIDES
NT HYDROGEN SULFIDE
NT LEAD SULFIDES
NT MOLYBDENUM DISULFIDES
NT MOLYBDENUM SULFIDES
NT ZINC SULFIDES

**INPUT**
Fitting linear multistage models to input/output data by maximum likelihood method
[AD-750139] 06 p0691 N73-15625
Description of computer program, main subroutines, input, output, and program requirements of Goddard Brouwer Orbit Bulletin
[NASA-TM-X-66141] 06 p0719 N73-15869
Theorem for specifying sufficient number of input frequencies for identification through Liapunov methods
[NASA-CR-135668] 23 p2812 N73-32482

**INPUT/OUTPUT ROUTINES**
Design of high speed, real time symbiont for analog telemetry processing
[NASA-TM-X-66090] 02 p0146 N73-11183
Identification of unknown parameters of multiple input/output, linear, constant, discrete time system from measurements made on inputs and outputs
[AD-747693] 03 p0325 N73-12653
Arithmetic and logic units in digital computer for processing of radar, sonar, and communication systems signals
[AD-750665] 06 p0646 N73-15248
Structure identification of multivariable stochastic systems
[TR-31] 17 p2054 N73-26614
Automation of input/output routines for use with computerized data processing of finite element structural analyses
[AD-761154] 18 p2204 N73-27793
Update of input instructions for operation of FORTRAN computer code TEMOD
[NASA-CR-121225] 19 p2239 N73-28047
Design of communications processor for access control to computer system
[AD-761804] 19 p2241 N73-28064
Principles of construction, technical characteristics, and functions of several checking general-purpose computers
[AD-762212] 19 p2243 N73-28082
Modification of input/output procedures to computer code for structural analysis of general shells
[AD-761806] 19 p2350 N73-28905
Digital input/output modules for binary signals
[KFK-1688] 20 p2379 N73-29114
Computer program to compute MF sky-wave interference
[BBC-RD-1973/8] 20 p2391 N73-29206
Characteristics and equipment for third generation computers
21 p2609 N73-30913

**INSECT DAMAGE**
U INFESTATION

**INSECTICIDES**
NT URETHANES

**INSECTS**
NT LARVAE
NT LOCUSTS
NT TRIBOLIA
Detection and monitoring forest insect infestation in Sierra Nevada Mountains of California using ERTS-1 imagery
[E72-10301] 04 p0411 N73-13351
Remote detection of insect damage and stress symptoms in forests of Black Hills
07 p0785 N73-16389
Detection and monitoring forest insect infestations in Sierra Nevada Mountains of California using ERTS-1 imagery
[E73-10312] 09 p1022 N73-18344
Analysis of ERTS-1 data to detect and map areas of tree mortality due to insect outbreaks using color infrared positive transparencies
[E73-10351] 11 p1275 N73-20345
Analysis of ERTS-1 photographic imagery for identification, definition, and mapping, of terrestrial ecosystems in interior Alaska
[E73-10399] 11 p1277 N73-20361
Inventory of forest and rangeland and detection of insect infestation from ERTS-1 imagery of Black Hills, Atlanta, and Manitou test sites
[E73-10407] 11 p1278 N73-20369
ERTS-1 imagery of forest insect infestation in Sierra Nevada Mountains of California
[E73-10440] 11 p1282 N73-20400
Detection of ponderosa pine tree stresses from insects or diseases using multispectral photography
[NASA-CR-131586] 13 p1522 N73-22337
Detection and monitoring of forest insect infestation in Sierra Nevada Mountains of California
[E73-10668] 16 p1899 N73-25363
Analysis of ERTS-1 data and underflight photography for detection of insect infestation and timber resources in Sierra Nevada Mountains of California
[PAPER-A16] 19 p2261 N73-28224
Investigation of oribatid mites found in Antarctic regions during Tenth Soviet Antarctic Expedition
20 p2407 N73-29349
Early detection of insect infestations and density/distribution of host citrus trees along Rio Grande River in Texas
[E73-11073] 23 p2782 N73-32248
Early detection of insect infestations and density/distribution of host citrus trees in Texas
[E73-11074] 23 p2782 N73-32249
Detection of insect infestations and density/distribution of host citrus trees in Texas
[E73-11075] 23 p2782 N73-32250
Skylab detection of insect infestations and density/distribution of host plants in Texas
[E73-11076] 23 p2782 N73-32251
Detection of insect infestations and density/distribution of host citrus trees in Texas
[E73-11077] 23 p2782 N73-32252
Detection and monitoring forest insect infestation in Sierra Nevada Mountains of California from ERTS-1 data
[E73-11133] 24 p2917 N73-33288

**INSENSITIVITY**
U SENSITIVITY

**INSEQUENT STREAMS**
U STREAMS

**INSERTION LOSS**
Magnetoelastic transmission delay lines for S band noting insertion loss reduction
[REPT-8.425] 13 p1491 N73-22087
Error analysis for measurements of Mariner Venus Mercury 1973 gain, antenna patterns, and insertion loss of cables
[NASA-CR-133230] 17 p1997 N73-26148

**INSERTS**
NT NOZZLE INSERTS

**INSHORE ZONES**
U BEACHES

**INSPECTION**
NT INFRARED INSPECTION
NT X RAY INSPECTION
Utilization of ERTS-1 imagery in national program for inspection of dams
[E72-10322] 04 p0413 N73-13370
Nondestructive inspection techniques for examining catapult and arresting gear structures on E-2 aircraft
[AD-752492] 08 p0868 N73-17027
UH-1 helicopter test bed program for evaluation of automatic inspection, diagnosis, and prognostic maintenance functions on selected subsystems - Vol. 1
[AD-752890] 09 p0987 N73-18058
Application of holographic interferometry for inspection of large aircraft structures during manufacturing and maintenance
[AD-757510] 14 p1604 N73-23000
Procedures for ultrasonic inspection of wing attachment fittings on Viscount aircraft
[TR-7211.621] 20 p2422 N73-29455

**INSTABILITY**
U STABILITY

**INSTITUTIONS**
Development of scientific centers in USSR during past 50 years and considerations for future development
[JPRS-58596] 11 p1267 N73-20281

**INSTRUCTIONS**
U EDUCATION

**INSTRUMENT APPROACH**
Rotary wing aircraft steep instrument approach limits
[MBB-UD-101-73-O] 23 p2745 N73-31969

**INSTRUMENT COMPENSATION**
NT TEMPERATURE COMPENSATION
Use of quartz and corundum monocrystals to verify dilatometric measurements in USSR
[AD-745840] 01 p0059 N73-10480

**INSTRUMENT DRIFT**
U DRIFT [INSTRUMENTATION]

**INSTRUMENT ERRORS**
Performance accuracy of precision stereoplotter for aerotriangulation with independent models
02 p0165 N73-11339
Errors in air temperature measurement resulting from instrument inertia
04 p0443 N73-13615
Influence of elastic properties of human body on arterial blood pressure measurement
05 p0500 N73-14072
Determination of gimbal errors of astatic gyroscope with allowance for drift
05 p0546 N73-14435
Astronomical techniques for spacecraft orientation and aircraft instrument errors
[JPRS-57704] 05 p0577 N73-14693
Aircraft instrument errors
05 p0577 N73-14695
Comparative assessment of three methods of measurement of pressure error corrections for aircraft pitot-static systems
[CRANFIELD-AERO-11] 08 p0924 N73-17570
Error sources in pressure measurements on turbulent supersonic flows by nonstationary microphone
10 p1140 N73-19289
Error sources in pressure measurements on turbulent supersonic flows by nonstationary microphone
10 p1184 N73-19629
Computerized simulation of instrument limited angular measurement errors in phased array radar
[AD-754922] 11 p1257 N73-20201
Transient temperature measurement errors in intrinsic thermocouples caused by heat transfer
[SC-RR-72-0719] 16 p1975 N73-25970
Theodolitic errors in processing time dependent geodetic data
[AD-760109] 17 p2029 N73-26421
Gyroscopic orbit errors caused by random perturbations
20 p2418 N73-29428
Residual temperature-induced humidity errors in radiosondes
[AD-762484] 20 p2490 N73-29694
Parameters and errors of magnetically sensitive elements of ferrosonde gradiometers
22 p2671 N73-31399

**INSTRUMENT FLIGHT RULES**
Analysis of aircraft pilot experiences during landing approaches in minimum visibility situations
[AD-747654] 03 p0329 N73-12687
Analysis of flight plans submitted at flight service stations for IFR and VFR flight clearances during calendar year 1971
[AD-748901] 04 p0447 N73-13652
Tabulation of minimum enroute instrument flight rules altitudes over particular routes and intersections - November 1972
06 p0697 N73-15679
Aircraft accident involving crash of Cessna 182 aircraft near Duluth, Minnesota airport on 8 Nov. 1972
[NTSB-AAR-73-10] 14 p1604 N73-23006
Development of mathematical and simulation models to calculate capacity of single runway under instrument flight rules conditions
[MTR-4102-REV-2] 14 p1645 N73-23345
Flight control system using tactile displays under instrument flying conditions
[AD-757344] 14 p1669 N73-23543
Air traffic control procedures for simultaneous instrument flight rules approaches to set of three parallel runways
[FAA-NA-73-23] 14 p1687 N73-23687
Analysis and recommendations concerning relaxation of spacing requirements for independent IFR parallel approaches into closely spaced runways
[MTR-6282] 19 p2249 N73-28129
Analysis of glide path parameters, approach control system precision, and separation standards for extension of runway capacity under instrument flight rule conditions
[AD-763142] 21 p2578 N73-30657

**INSTRUMENT LANDING SYSTEMS**
NT AUTOMATIC LANDING CONTROL
Fixed base flight simulator evaluation of wing spoilers for longitudinal flight path control of Cessna aircraft during instrument landing system approach
[NASA-CR-2121] 02 p0125 N73-11015
Mathematical model for radio frequency interference time history at ILS localizer radio receivers
[AASU-317] 03 p0329 N73-12682
Development and evaluation of instrument landing system with VHF and UHF capability for localizer and glide slope
[AD-747656] 03 p0329 N73-12688
Operational test and evaluation of four configurations of flight director display for instrument landings based on command heading and command flight path angle
[AD-748244] 04 p0374 N73-13041
Analysis of position determination accuracy obtainable with microwave landing guidance system
[NASA-TN-D-7116] 06 p0697 N73-15681
Bibliography of data on aircraft landings, instrument landings, approach control, glide path systems, display devices, and terminal facilities
[AD-751800] 07 p0740 N73-16024
Analysis of Microwave Landing System performance to determine signal formats and to reduce effects of multipath transmission
[AG-5011-B-1] 07 p0818 N73-16628
Alcohol induced performance degradation in pilot instrument approach landings
12 p1370 N73-21113
Airborne C band pulsed transmitter for instrument landing system
13 p1491 N73-22086
Development and characteristics of microwave landing system with emphasis on functional design requirements for airborne equipment
14 p1689 N73-23705
Development of Doppler microwave landing system and techniques for eliminating effects of multipath transmissions
14 p1689 N73-23706
Development and characteristics of instrument landing system using radioactive materials along runways for glide slope and alignment information
14 p1689 N73-23707
Human factors in design of aircraft in-flight monitoring and automatic landing system for low weather operation
14 p1713 N73-23901
Computer program for selection of radio frequencies used in VOR, ILS, and Tacan/DME air navigation systems
[FAA-NA-73-4] 16 p1940 N73-25700
Aircraft accident involving crash of Fairchild Hiller FH-227b aircraft near Albany County Airport, New York on 3 March 1972
[NTSB-AAR-73-8] 17 p1982 N73-26018
Simulated environment interference tests on adjacent channel signal receivers for frequency assignments of instrument landing systems
[FAA-RD-73-1-VOL-1] 17 p2060 N73-26665
Control and display testing for air traffic instrument landing system
[AD-759539] 17 p2060 N73-26667
Application of microwave landing system to provide operational flexibility and improved capacity in terminal area
[FAA-RD-73-143] 18 p2104 N73-27019
Performance tests of visual approach slope indicator [VASI] equipment and systems for improved terminal area effectiveness
[FAA-NA-73-64] 18 p2175 N73-27568
Radio frequency interference tests of VHF omnirange, instrument landing systems, and glideslope indicators to determine required geographical separation for ground stations
[REPT-523-0764695-00111M-VOL-2] 20 p2453 N73-29712
Design of aircraft lateral flight director
[DLR-FB-72-44] 22 p2614 N73-30953
Radio frequency interference tests of VHF omnirange system, localizer, and glideslope receiving equipment to determine geographical separation requirements - Vol. 2 Book 2
[FAA-RD-73-1-VOL-2-BK-2] 23 p2816 N73-32513
Improvement of instrument landing systems with respect to multipath propagation effects and surface reflections
[DGLR-PAPER-73-017] 23 p2817 N73-32521
New type of instrument landing systems, according to ICAO requirements
[DGLR-PAPER-73-011] 23 p2817 N73-32522
Description of sector-Tacan and DME-supported instrument landing systems
[DGLR-73-019] 23 p2817 N73-32523
Compatible ILS, using microwave frequencies, and precision ILS, using antenna arrays, as improved standard instrument landing systems
[DGLR-PAPER-73-018] 23 p2817 N73-32524
Effects of transition from conventional to quiet takeoff and landing air traffic, noting introduction of microwave ILS and area navigation
[MBB-UH-05-73-O] 23 p2817 N73-32525
Flight control display device for producing curved approach profiles in microwave instrument landing systems
[DGLR-PAPER-73-016] 23 p2818 N73-32526

**INSTRUMENT ORIENTATION**
Design and development of brushless, direct drive solar array reorientation control system for satellites
[NASA-CR-130153] 11 p1261 N73-20236
Kinematics of orientation in rotating coordinate system and determination of orientation of instrument trihedrons
[JPRS-59162] 20 p2451 N73-29700
Determination of orientation of instrument trihedrons and applications in inertial navigation
20 p2451 N73-29701

**INSTRUMENT PACKAGES**
NT APOLLO LUNAR SURFACE EXPERIMENTS PACKAGE
NT EREP
Scientific equipment of ionospheric ESRO-4 satellite including five experiments
[ESRO-SN-114-ESTEC] 02 p0234 N73-11906
Thermal control of scientific instrument package in large scale telescope
05 p0608 N73-14946
Payload guidelines for space shuttle/tug
[NASA-CR-130025] 07 p0848 N73-16872
Effect of trapped electron and proton radiation on onboard components and payloads of low thrust orbits through Van Allen belts
[NASA-TM-X-2777] 11 p1335 N73-20840
Apollo experience report on instrument calibration data to provide correct engineering data for tests and mission support
[NASA-TN-D-7144] 11 p1341 N73-20881
MASS computer models for analyzing space shuttles and space shuttle payload operations
[NASA-CR-112286] 11 p1343 N73-20897
Experimental design for space shuttle sortie mission payloads
[NASA-CR-112287] 11 p1343 N73-20898

**INSTRUMENT TRANSMITTERS**
Applications of photoelectronic and thermoelectronic instruments
[JPRS-59951] 22 p2672 N73-31404

**INSTRUMENTAL ANALYSIS**
U AUTOMATION

**INSTRUMENTATION**
U INSTRUMENTS

**INSTRUMENTS**
Minicomputer for controlling data transfer between process instrumentation and on-line computer
[HMI-B-123] 02 p0145 N73-11171
Design and characteristics of instrument for monitoring carbon monoxide content of ambient atmosphere to include operations and maintenance instructions
[NASA-CR-128602] 02 p0172 N73-11394
Modification of atmosphere contamination sensor to include carbon monoxide monitoring capability
[NASA-CR-128604] 02 p0172 N73-11395
Instrumentation handbook for operational support systems of Space and Missile Test Centers in California, Hawaii, and Pacific Ocean area
[AD-750944] 06 p0651 N73-15285
International research on aerospace instrumentation systems
[AD-750653] 06 p0675 N73-15493
Portable instrumentation kit feasibility study
[AD-751188] 07 p0802 N73-16514
Cryogenic instrumentation for present and possible future large scale systems operating at liquid hydrogen temperatures
[LA-DC-72-855] 07 p0832 N73-16743
Development and characteristics of scientific instrument package for use with Large Space Telescope - Vol. 4
[NASA-TM-X-64726-VOL-4] 09 p1036 N73-18452
Astronomical research and instrument development by Professor M. G. Pereira de Barros
17 p2081 N73-26837
Apollo experience report on command and service module instrumentation subsystem to show requirements determination and conceptual design
[NASA-TN-D-7374] 22 p2719 N73-31761
Development of instrument to measure steady and oscillatory aerodynamic forces on sting-mounted model using forced oscillation technique
[ATN-7101] 24 p2926 N73-33366

**INSULATING MATERIALS**
U INSULATION

**INSULATION**
NT ELECTRICAL INSULATION
NT MULTILAYER INSULATION
NT THERMAL INSULATION
Acoustic field of infinite circular cylindrical transducer partially covered by layer of sound-soft material
[JPRS-57367] 03 p0335 N73-12732
Automatic through-insulation welding of small-diameter solid conductor wires to facilitate production of miniature electronic assemblies
[NASA-CR-130751] 08 p0927 N73-17591
Purge and vent characteristics of GAC-9 insulation system
[NASA-CR-124052] 09 p1050 N73-18565
Characteristics of gelled liquid hydrogen polyphenylene oxide foam open cell insulation
[NASA-CR-124114] 09 p1051 N73-18568
Rotational injection moulding for designing polythene sheathed closures on large size cables
[REPT-6713] 10 p1164 N73-19474
Thermal cycling tests of molybdenum foil-zirconium cloth insulation system
[ALO-2832-45] 10 p1224 N73-19951
Design allowables for room temperature vulcanizing silicone rubber based adhesives for attaching reusable surface insulation to space shuttle structures
[NASA-CR-128887] 11 p1308 N73-20615
Insulated electrode for electrocardiographic recording without paste electrolyte
[NASA-CASE-MSC-14339-1] 12 p1374 N73-21151
Composite materials for use as internal LH2 tank insulation for reusable boosters
[NASA-CR-124222] 13 p1546 N73-22528

Liquid hydrogen booster propellant tank internal insulation system for use in reusable spacecraft
[NASA-CR-121102] 15 p1842 N73-24925

INSULATORS
Influence of fast neutron damage to ceramic insulators on thermionic reactor design
[LA-DC-72-523] 03 p0333 N73-12716
Ion implantation of amorphous insulators and switching effects in silicon oxides
[LETI/ME-773] 07 p0832 N73-16744
Dielectric properties of pure and doped insulating materials
[COO-623-182] 12 p1439 N73-21662
Optimum design of insulating intersheaths between radio frequency cable braids
[RAE-TR-72151] 17 p1998 N73-26134

INSULIN
Suitability of insulin dependent and oral drug dependent diabetics as navigation personnel
12 p1371 N73-21120

INTAKE SYSTEMS
NT AIR INTAKES
NT ENGINE INLETS
NT HYPERSONIC INLETS
NT INTERNAL COMPRESSION INLETS
NT SIDE INLETS
NT SUPERSONIC INLETS
Evaluation of bucket and intake system for measuring sea surface temperature and statistical analysis of data obtained from international ship observations
[WMO-336] 01 p0050 N73-10406
Optimal inlet parameters for magnetohydrodynamic channel using combustion products of kerosene and gaseous oxygen
[AD-748750] 04 p0376 N73-13057
Effect of two dimensional suction flows into double intakes on upper surface of Joukowski airfoil for application to vertical takeoff and landing aircraft
[AD-754208] 10 p1104 N73-19003
Computer program for three dimensional inlet and analysis of capture area, ram force, spillage force, and surface pressure force
[NASA-CR-112304] 11 p1271 N73-20312
Flow theory calculation of pogo instability in inducer cascades
[NASA-CR-131415] 11 p1271 N73-20313
Compressor face distortion dependence on test cell inlet design configurations
[AD-756540] 13 p1507 N73-22215
Design and analysis of low speed hydrogen and oxygen inducers applicable to space tugs
[NASA-CR-124233] 13 p1570 N73-22722
Blockage ring used for inlet stall problem with supersonic axial flow compressor stage having tip Mach number of 2.0
[AD-757217] 14 p1702 N73-23809
Chilldown tests on single stage inducer test rig
[NASA-CR-132212] 15 p1762 N73-24278
Modified 1964 Dodge Dart induction system
[PB-218730/0] 18 p2194 N73-27710
Study of supersonic flow in inlets using holographic interfereometry
[AD-763335] 21 p2525 N73-30250
High tip speed fan inlet noise reduction using treated inlet splitters and accelerating inlets.
[NASA-CR-121268] 21 p2589 N73-30745
Wind tunnel tests to determine effect of inlet turbulence length scale on fan discrete tone noise
[NASA-TM-X-62300] 22 p2700 N73-31625
Experimental investigation of large scale, two dimensional, mixed compression inlet system
[NASA-TN-D-7445] 23 p2739 N73-31928
Effects of blade tip clearance and leading edge sweepback of compressor rotor blades on inducer performance and blade pressure loading
[NASA-CR-72712] 23 p2739 N73-31930
Three-dimensional flow characteristics in three bladed rocket pump inducer
[NASA-CR-2290] 23 p2775 N73-32190
Stability effects of steady state circumferential distortions of inlet total temperature and pressure
[NASA-TM-X-71431] 23 p2829 N73-32614
Development of aft intake system for ramjet powered missile
23 p2851 N73-32785
Effect of inlet air humidity on exhaust gas emissions of nitrogen oxides in gas turbine combustor
[NASA-TN-D-7396] 23 p2856 N73-32822

INTEG MED AND BEHAVIORAL LAB MEASUR SYSTEM
U IMBLMS

INTEGERS
Algorithm for solving pure integer linear programming problem
[NPL-NAC-20-PT-1] 09 p1057 N73-18621
Generation and propagation of numerical error in fractional integer program
[AD-763206] 22 p2640 N73-31162

INTEGRAL CALCULUS
Integration of nonlinear differential equations describing one-dimensional steady flow across normal shock wave, considering transport, degree of freedom relaxation, and chemical reactions
[DLR-FB-72-54] 12 p1392 N73-21288
Methods for computing numerical quadrature of integrable function over finite inerval
[NASA-TM-X-66277] 18 p2169 N73-27518

INTEGRAL EQUATIONS
NT FREDHOLM EQUATIONS
NT VOLTERRA EQUATIONS
NT WIENER HOPF EQUATIONS
Methods for determining electric permittivity of inhomogeneous dielectric medium that is uniform in two dimensions and varies according to profile function in other dimension
02 p0201 N73-11622
Integral wave analysis in inhomogeneous fluid, bifurcation in regular and singular eigenvalue problems, and asymptotic expansion of integrals
[AD-747280] 02 p0203 N73-11647
J integral relationship between elastic stress and concentration factors for inelastic fracture criterion of sharp notch
[CONF-720806-2] 05 p0569 N73-14617
Neumann boundary value problem for Helmholtz oscillation equation
[NRC-TT-1606] 06 p0690 N73-15616
Spatial grid method for solving hyperbolic equations for signal propagation on three wire transmission line
[UCRL-73796] 07 p0764 N73-16209
Electron positron annihilation structure functions calculated with light cone operator product expansions and Callan-Symanzik equation
[ILL-[TH]-72-12] 07 p0823 N73-16670
Hallens integral equation for current on dipole antennas in homogeneous isotropic media
[AD-752474] 08 p0890 N73-17206
Determining natural components of meteorological fields
[AD-751958] 08 p0939 N73-17692
Integrable and nonintegrable Lie-algebra representations relative to particle physics
10 p1191 N73-19692
MIMIC programming language for solving Abel integral equations
[AD-754003] 11 p1311 N73-20642
Integral equation for calculating influence of linear channels on correlation processing of noise signals
12 p1378 N73-21180
Energy release integral equation for finite elastic and viscoelastic materials
[CONF-720930-1] 12 p1463 N73-21851
Mathematical and mechanical consideration of finite strip compressed between two rough rigid stamps
[NASA-CR-112318] 13 p1585 N73-22849
Visualization and integral methods for studying three-dimensional supersonic flow separation on delta wing
14 p1600 N73-22970
Integral equation for studying three dimensional turbulent boundary layer development
14 p1648 N73-23369
Integral calculation of three-dimensional turbulent boundary layer velocity profiles
14 p1648 N73-23370
Integral equations for calculating incompressible potential flows around profiles with suction and blowing
[NASA-TT-F-14962] 18 p2130 N73-27209
Uncorrelated jet model in proton-proton and proton-antiproton annihilation integral
18 p2182 N73-27615
Computer solution to Hallens equation on half wavelength elements of planar symmetrical antenna arrays
[AD-761471] 19 p2245 N73-28103
Integral turbulent kinetic energy analysis of free shear flows
19 p2254 N73-28170
Solution of acoustic and electromagnetic scattering problems in exterior domains using integral equations
[NPL-NAC-30] 19 p2314 N73-28608
Two-dimensional nozzle flow problem solved by method of integral relations
20 p2385 N73-29161
Integral characteristics and models of general atmospheric circulation
20 p2443 N73-29621
Parametric integral method for calculating laminar and turbulent incompressible flow- and temperature boundary layers
[DLR-FB-73-24] 22 p2653 N73-31255
Intergral equations for incident electromagnetic wave scattering by slotted spherical antenna
[AD-764880] 23 p2758 N73-32075
Integral method for analyzing two-dimensional and axisymmetric compressible and three-dimensional incompressible turbulent boundary layer
23 p2772 N73-32169
Treatment of singularities in solution of Laplace equation by integral equation method based on Green function, applied to flow distribution and transmission lines
[NPL-NAC-31] 23 p2813 N73-32490

INTEGRAL TRANSFORMATIONS
NT CONVOLUTION INTEGRALS
NT FAST FOURIER TRANSFORMATIONS
NT FOURIER TRANSFORMATION
NT LAPLACE TRANSFORMATION
Abel integral transform and ray tracing methods for radio occultation data inversion to obtain refractive index profiles of planetary atmospheres
02 p0197 N73-11596
Gradient methods for solving incompatible systems of linear equations of higher order in photomapping problems
10 p1178 N73-19584
Efficiency of numerical integration methods for differential equations
10 p1178 N73-19585
Survey on numerical integration methods for differential equations
10 p1178 N73-19586
Steady-state response of interface to disturbance moving with constant velocity
16 p1886 N73-25267
The calculated growth of lift and pitching moment on a swept wing entering a discrete vertical gust at subsonic speeds
[ARC-CP-1241] 22 p2612 N73-30932
Integral transformations for compressible laminar partial differential equations of second order boundary layer theory
24 p2907 N73-33198

INTEGRATED CIRCUITS
NT LARGE SCALE INTEGRATION
Development and application of polyimide films for hybrid and beam lead substrates
[AD-745731] 01 p0033 N73-10260
Flow behavior of integrated circuits in bipolar transistors
[CEA-CONF-1971] 01 p0087 N73-10722
Large signal modeling of bipolar transistors for computer-aided circuit analysis
[AD-745772] 01 p0088 N73-10730
Large scale integrated circuits used for designing 128 words x 72 bits/word memory
[REPT-1404] 03 p0272 N73-12205
Minimizing area required for resistor-capacitor time constants in integrated circuits
[NASA-TN-D-7110] 03 p0344 N73-12808
Monolithic display using metal oxide semiconducting circuits and liquid crystal layer
[CEA-CONF-1991] 03 p0345 N73-12814
Characteristics of ion transport in silicon dioxide, interface phenomena, and photoelectric method of storing charge in floating gate MOS memory
[AD-746999] 03 p0346 N73-12823
Ion migration in SiO2 layer of integrated circuit oxides
[AD-747435] 03 p0348 N73-12836
Ultrasonic marine biotelemetry transmitter utilizing metal oxide semiconductor integrated circuits
[AD-748605] 04 p0383 N73-13119
Design and development of integrated magnetic memories
04 p0394 N73-13203
Temperature controlled piezoelectric crystal oscillator with digital integrated circuitry for timing of pulses
[AECL-4160] 04 p0396 N73-13217
Performance of wire bound electrical connectors used in integrated and hybrid circuits and low power semiconductor devices
[AD-748788] 04 p0396 N73-13220
Fabrication and evaluation of RF sputtered barium titanate thin films for integrated circuit application
[AD-749236] 04 p0397 N73-13227
Integrated circuit operational amplifiers
[AD-749013] 04 p0397 N73-13229
Fabrication of thin film silicon integrated square wave oscillator circuit capacitors
[AD-749266] 04 p0397 N73-13231
Computation, design, and manufacture of integrated circuits for application to computer construction and operation
[JPRS-57333] 04 p0398 N73-13239
Relations between signal shaping noise and timing resolution in nuclear particle detection
[NASA-CR-129613] 04 p0452 N73-13688
Simplified model for comparative evaluation of effectiveness of integrated circuits in digital equipment
[AD-749640] 05 p0518 N73-14211
Production and costs of producing reliable semiconductor integrated circuits
[AD-749834] 05 p0521 N73-14240
Boundary test procedure for determining characteristics and design of integrated transistor-transistor logic circuits
[AD-749604] 05 p0523 N73-14253
Welding leads of integrated circuits to printed circuit boards
[AD-749838] 05 p0523 N73-14254
Approximation method for calculation of temperature distribution in microcircuit
[AD-749762] 05 p0523 N73-14255
Magnetic bubble circuits for satellite data storage
[AD-750660] 06 p0644 N73-15232
High resistivity semiconductor waveguides for device and circuit functions
[AD-750317] 06 p0645 N73-15241
Performance and reliability of large scale integrated circuits
[AD-750577] 06 p0646 N73-15250

Electrical and structural criteria for design optimization of integrated circuits
[AD-750947] 06 p0648 N73-15261
Proceedings of 1972 GOMAC conference on microcircuit applications
[AD-751316] 07 p0765 N73-16212
Research and development in advance electronics including applications to digital computers, air traffic control, and solid state physics
[AD-751308] 07 p0834 N73-16758
Development of highly accurate and reliable telemeter system utilizing integrated circuits
[AD-752481] 08 p0886 N73-17176
Quality control tests of small scale integration electronic components to determine diverging quality levels among manufacturers
[ECR-24] 08 p0891 N73-17213
Physical properties and limitations of components used in hybrid microcircuits
[AD-752216] 08 p0891 N73-17216
Research progress in functional network theory and microcircuit systems
[AD-752243] 08 p0891 N73-17217
Pulsed power burnout tests of hand gate circuits
[AD-752540] 08 p0892 N73-17219
Modification of Auburn University Model S-2 FM television transmitter through use of integrated circuits and conversion to receive telemetry signals
[NASA-CR-124082] 09 p1001 N73-18171
Design of integrated circuit with two amplifiers and feedback stabilization for single channel gyrator
[NASA-CASE-MFS-22343-1] 09 p1008 N73-18224
Simple method for developing computer models for digital and analog integrated circuits
[AD-753413] 09 p1008 N73-18232
Design of automated production facility capable of manufacturing beam-lead CMOS integrated circuits
[NASA-CR-124116] 09 p1038 N73-18465
Application of integrated circuit technology and digital computer techniques to electric control of jet engines
[NAL-TR-281] 09 p1078 N73-18799
Integrated circuit differential amplifier for magnetic probe measurements
[LRP-55/72] 10 p1134 N73-19241
Microwave UHF and SHF semiconductor oscillators and power amplifiers, noting gunn and impatt diode solutions, and integrated circuit development
[DLR-MITT-73-06] 10 p1135 N73-19248
Environmental tests and failure modes for microelectric devices
[AD-753256] 10 p1135 N73-19253
Artificial intelligence in integrated circuit control of bionic manipulators
[NASA-CR-131403] 11 p1251 N73-20156
Frequency division with binary ripple counters to provide any integral division ratio
[AD-754030] 11 p1260 N73-20229
Quantum electronics, solid state devices, and solid microelectronics
[AD-754945] 11 p1331 N73-20806
Effects of small LSI packages and modularity on development of digital filters
[AD-755657] 12 p1385 N73-21228
Integrated microcircuits and complementary four-phase logic system
[NASA-CASE-MSC-14240-1] 12 p1386 N73-21240
Failure modes and mechanisms for integrated circuits with stressed pin pair combinations
[AD-755807] 12 p1387 N73-21247
Design of high temperature integrated circuit holders
[BAH/DS/AG/R-412/1] 13 p1500 N73-22158
Characteristics of tunable bandpass filter with large range of resonant frequency
[AD-756662] 13 p1501 N73-22165
Extended life testing of complementary MOS integrated circuits
[NASA-CR-124215] 13 p1533 N73-22422
Transient radiation caused performance degradation in integrated ferrite phase shifter driven circuit
[AD-757618] 14 p1644 N73-23336
Ultrasonic torsional welding system for simultaneously bonding beam leads of hybrid integrated circuit device to suitable substrate
[AD-757561] 14 p1671 N73-23559
Integrated circuit power gyrator with Z-matrix design using parallel transistors
[NASA-CASE-MFS-22342-1] 15 p1756 N73-24236
Design analysis and integration of MOS threshold logic gates
[AD-758021] 15 p1759 N73-24260
Integrated circuit designs for self controlling electrical heater
[NASA-TN-D-7248] 15 p1786 N73-24479
Limitations in microelectronic circuits, design of power Schottky diode, and strontium titanate permittivity
16 p1880 N73-25218
Evaluation of computer program for analyzing radiation effects on complex semiconductor devices and microcircuits
[AD-758883] 16 p1882 N73-25237
Research and development progress on electronic equipment, integrated circuits, semiconductors, and digital computers
[AD-759180] 16 p1884 N73-25251
Prototype of high resolution duplicator for large scale integration circuit masks
[REPT-3424] 16 p1914 N73-25488
Multistable semiconductor devices and integrated circuits
16 p1951 N73-25791
Electronic failure and quality control of microcircuit devices
[AD-759846] 17 p2005 N73-26215
Design of stable temperature compensated crystal oscillator for voice communication system
[AD-759938] 17 p2006 N73-26220
Integrated circuit tangnet function generator
[NASA-CASE-MSC-13907-1] 17 p2007 N73-26230
Ion and electron beam techniques for fabricating integrated optics circuits
[AD-760051] 17 p2008 N73-26237
Microwave solid state devices and circuits
[AD-759833] 17 p2075 N73-26787
Progress in plasma physics, integrated circuits, solid state, and information and digital systems
[AD-759697] 17 p2099 N73-26984
Directional coupler design using coplanar waveguides for microwave integrated circuits
[AD-760533] 18 p2124 N73-27166
Heat flow failure mechanism in overstressed microelectronic circuits
[AD-761792] 19 p2244 N73-28094
Semiconductor microcircuits for recording of optical radiation, mechanical stresses, and magnetic fields
[AD-762312] 19 p2247 N73-28119
Analysis of electrical properties, structure, values of passive elements, and operating mode of hybrid neuristor lines
[AD-762311] 19 p2247 N73-28120
Integrated circuits using thin magnetic film elements
[AD-762267] 19 p2248 N73-28127
Large scale integration for users and suppliers within circuit technology, manufacturing techniques for bipolar devices and semiconductors memory arrays
[PB-221013/6] 21 p2520 N73-30212
Analysis of microelectronic industry in Poland and comparison with capabilities in United States
21 p2607 N73-30896
Status of microwave equipment development in Poland with emphasis on research projects and higher education
21 p2607 N73-30897
Integrated GaAs digital circuits with Gunn diodes for pulse code modulation
[FTZ-A-62-TBR-3] 22 p2646 N73-31205
Inverted geometry transistor for use with monolithic integrated circuit
[NASA-CASE-ARC-10330-1] 23 p2763 N73-32112
Photosensitivity failure analysis on integrated microcircuit caused by surface inversion
[AD-764708] 23 p2766 N73-32132
Economics and performance characteristics of high speed digital integrated circuits used in nuclear instrumentation
[LBL-1750] 24 p2900 N73-33150

**INTEGRATED MISSION CONTROL CENTER**
Standards and procedures for generation of operational display formats for use in Mission Control Center display control system
[NASA-CR-128843] 10 p1132 N73-19228

**INTEGRATION [REAL VARIABLES]**
U MEASURE AND INTEGRATION

**INTEGRATORS**
NT DIGITAL INTEGRATORS
Satterthwaite approximation distribution for resistance capacitance integrated Chi-squared noise
[AD-747208] 02 p0150 N73-11217
Gyrostabilizers on moving base, on three stage gyroscope, and as angular velocity integrator
[JPRS-60001] 23 p2791 N73-32328
Estimation and approximation of integrand in J for spline function study
[NASA-CR-124454] 24 p2945 N73-33516

**INTEGRODIFFERENTIAL EQUATIONS**
U DIFFERENTIAL EQUATIONS
U INTEGRAL EQUATIONS

**INTELLIGENCE**
NT ARTIFICIAL INTELLIGENCE
Human performance in schematic concept formation as a function of socio-economic level, personality, intelligence, and race
[AD-744781] 13 p1486 N73-22052
Methods for meeting terrain intelligence needs of airmobile division in tactical situation
[AD-756191] 13 p1531 N73-22411

**INTELLIGIBILITY**
NT SPEECH RECOGNITION
Speech intelligibility in naval aircraft radio communications
[AD-748202] 03 p0268 N73-12173
On-line and off-line bench test evaluation of helium speech unscramblers under controlled conditions
[AD-748295] 04 p0391 N73-13176
Effects of exercise work load on speech intelligibility at normal and increased atmospheric pressures
[AD-749321] 04 p0392 N73-13185
Underwater divers and speech communication problems
[AD-751665] 07 p0757 N73-16150
Pitch-synchronous time-compression speech sampling method for greater intelligibility
14 p1621 N73-23134
Diagnostic evaluation of intelligibility in digital vocoders
14 p1624 N73-23161
Stimulus time interval and response mode methods using signal to noise ratios to test speech intelligibility
14 p1625 N73-23164
Improvements in intelligibility testing reliability using experienced listeners
14 p1625 N73-23166
Enhancement of speech intelligibility through appropriate spectral weighting and effect of passing through optimum filter on signal to noise ratios
14 p1630 N73-23211
Experimental analysis of probability density function of instantaneous amplitude of speech and effect of filtering and compression
14 p1630 N73-23212
Effect of reverberation and interfering noise on speech intelligibility as determined from physical description of running speech
14 p1631 N73-23219

**INTELSAT SATELLITES**
Postflight analysis of Atlas/Centaur - 29 and Intelsat 4 launch and orbit establishment
[NASA-TM-X-68649] 01 p0102 N73-10845
Beacon transmissions from Intelsat 2F-1 and 2F-2
[AD-750469] 06 p0668 N73-15433

**INTENSIFICATION**
U AMPLIFICATION

**INTENSIFIER TUBES**
U IMAGE INTENSIFIERS

**INTENSIFIERS**
NT IMAGE INTENSIFIERS
NT IMAGE ORTHICONS

**INTENSITY**
Statistical correlations between maximum intensity of precipitation of different types and mean intensities for given precipitation
[NLL-M-23044-[5828.4F]] 21 p2567 N73-30574

**INTERACTIONS**
NT AIR WATER INTERACTIONS
Intensity relations and spectral satellite studies of alkali/foreign gas interactions
13 p1528 N73-22385
Mechanical effects resulting from interactions of laser beams with gases, liquids, and solids
[AD-763258] 21 p2555 N73-30482

**INTERATOMIC FORCES**
Effects of interatomic forces on diffusion mechanisms in silver cadmium alloys, silver indium alloys and silver lead alloys
[CEA-R-4292] 03 p0333 N73-12714
Radial distribution functions and liquid structure factors for fluids of particles interacting through repulsive potentials
[LPTHE-72/45] 10 p1191 N73-19690
Interactions of copper lattice atoms with holes, dislocations, and interstitial atoms
[JUL-857-FF] 10 p1194 N73-19714

**INTERCEPTION**
Sub-optimal control to synthesize feedback controller for two dimensional, nonlinear intercept and pursuit-evasion problems
[AD-746005] 01 p0109 N73-10901
Constant gain optimal tracking control laws for finite final time
[AD-761091] 18 p2214 N73-27882

**INTERCEPTOR AIRCRAFT**
U FIGHTER AIRCRAFT

**INTERCONTINENTAL BALLISTIC MISSILES**
NT MINUTEMAN ICBM

**INTERCOSMOS SATELLITES**
Equipment, data processing, and results of Intercosmos observations of cosmic rays
[JPRS-57913] 06 p0716 N73-15839
Analysis of ionospheric investigations conducted with Intercosmos satellite number two
14 p1659 N73-23464
Intercosmos satellite observation of cosmic rays
15 p1828 N73-24817

**INTERFACE STABILITY**
Sea ice dynamics, heat and mass budget of Arctic sea ice, desalinization, thermal and mechanical stresses, bearing capacity of floating ice, and interaction of oil and ice
[AD-754118] 11 p1290 N73-20463
Analysis of conditions for equilibrium of multi-component liquid at surface of solid body with allowance for selective adsorption at interphase boundaries
[NLL-M-21577-[5828.4F]] 16 p1885 N73-25261
Interface message processors for ARPA computer network
[AD-760023] 17 p2003 N73-26193

**INTERFACES**
NT FLUID BOUNDARIES
NT GAS-SOLID INTERFACES

NT LIQUID-LIQUID INTERFACES
NT LIQUID-SOLID INTERFACES
NT LIQUID-VAPOR INTERFACES
NT SOLID-SOLID INTERFACES
Reflection and transmission of large amplitude shockless waves at interface with semi-infinite medium
[AD-746642] 04 p0483 N73-13947
Development of economical ways of integrating and interfacing new storage devices and data processing programs into computer systems - App. B
[NASA-CR-129817] 05 p0515 N73-14190
Programmable computer interface for computer aided measurement and control instrumentation systems
[NASA-TN-D-7148] 09 p1005 N73-18205
Optical-to-optical interface device for use in coherent optical parallel processing systems
[NASA-CR-130183] 10 p1188 N73-19671
Interface requirements for design and development of Physiology of Chimpanzees in Orbit experiment
[NASA-CR-131397] 11 p1248 N73-20130
Reaction of nickel oxide with steel in argon and vacuum atmospheres
[AD-754776] 11 p1306 N73-20600
Engine interface control for coordinating engine and component design activities
[NASA-CR-132215] 15 p1809 N73-24665
Interface message processor for digital computer network
[AD-763734] 23 p2761 N73-32098
Sharp interface in unbounded turbulent shear flows determined by linear array of hot-wire probes
23 p2773 N73-32178

**INTERFACIAL ENERGY**
Analysis of adhesion forces in cutting metals to determine effects of formatting and destruction of adhesive connections on wear of cutting tools
[AD-754041] 11 p1301 N73-20555
Gas chromatographic analysis on water interfacial energy
[AD-761655] 19 p2230 N73-27988

**INTERFACIAL STRAIN**
U INTERFACIAL TENSION

**INTERFACIAL TENSION**
Effects of various oxide additives on volume change on melting, surface tension, and viscosity of liquid aluminum oxide
[NASA-CR-120910] 07 p0811 N73-16580
Determination of Hamaker complex constants in hydrocarbon emulsion films by measurement of contact angles and interfacial tension
[NLL-M-23001-[5828.4F]] 21 p2504 N73-30095
Method to determine surface tension of refrigerants
[NLL-NEL-TT-2480-[6075.461]] 21 p2578 N73-30663
Streaming in liquid metals due to thermal surface tension gradient
[TRITA-EPP-73-10] 22 p2700 N73-31626
Surface tension effect on cylindrical gas slug velocity
23 p2771 N73-32163

**INTERFERENCE**
Interference theory in slotted wind tunnels extended to subsonic rectangular wind tunnels with ventilated tool, longitudinal slots and perforated screens of arbitrary porosity
[ARC-R/M-3706] 05 p0492 N73-14007
Calculation of wind tunnel wall interference velocities affecting pitching moments of high lift wings
[NASA-CR-2191] 10 p1137 N73-19269
Monte Carlo method for analyzing tracking disruptions
14 p1683 N73-23657
Markov random processes for tracking disruption analyses on quasi-stationary systems
17 p1997 N73-26150
Finite element digital procedure for stress and strain distribution in vicinity of interference fit fastners
[AD-760570] 18 p2157 N73-27425

**INTERFERENCE DRAG**
Development of computer program for generating aerodynamic forces for plane and interfering wings at supersonic speeds
[NASA-CR-112184] 04 p0404 N73-13290
Results of aerodynamic jet interference tests for Do-31 aircraft and application to future VSTOL development for lift-loss calculation
[BMVG-FBWT-72-22] 09 p0985 N73-18044
Development of theory for wind tunnel boundary upwash interference on symmetrical finite wing with arbitrary lift distribution
[AD-757196] 14 p1652 N73-23397
Semiempirical solution of six types of shock interference heating in hypersonic flows
[NASA-TN-D-7139] 16 p1888 N73-25283
Effect of interference of engine jet on aerodynamic characteristics of lifting surface induced by horizontal or vertical jet
[NASA-TT-F-14956] 17 p2015 N73-26292

**INTERFERENCE LIFT**
Finite difference solutions for oscillatory lift interference in slotted wind tunnel compressible and incompressible flow
[ARC-R/M-3700-PT-1-PT-2] 03 p0284 N73-12297
Finite difference solutions for oscillatory lift interference parameters for slotted wind tunnel incompressible flow
03 p0284 N73-12298
Finite difference solutions for oscillatory lift interference parameters for slotted wind tunnel compressible flow
03 p0284 N73-12299
Pressure measurements on harmonically oscillating wing-tailplane configurations in incompressible speed range noting wind tunnel tests on aircraft models
[DLR-FB-71-52] 04 p0373 N73-13033
Development of computer program for generating aerodynamic forces for plane and interfering wings at supersonic speeds
[NASA-CR-112184] 04 p0404 N73-13290
Effect of interference of engine jet on aerodynamic characteristics of lifting surface induced by horizontal or vertical jet
[NASA-TT-F-14956] 17 p2015 N73-26292

**INTERFERENCE MONOCHROMATIZATION**
U DIFFRACTION

**INTERFEROGRAMS**
U INTERFEROMETRY

**INTERFEROMETERS**
NT FABRY-PEROT INTERFEROMETERS
NT INFRARED INTERFEROMETERS
NT MACH-ZEHNDER INTERFEROMETERS
NT MICHELSON INTERFEROMETERS
NT MICROWAVE INTERFEROMETERS
NT PHASE SWITCHING INTERFEROMETERS
NT RADIO INTERFEROMETERS
Meter wavelength observations of Crab nebula pulsar using very long base-line interferometry techniques
[NASA-TM-X-66071] 01 p0103 N73-10852
Numerical analysis of semiconductor saturable absorber and extablishment of criteria for operation of laser saturable resonator in bistable regime
[AD-746736] 02 p0183 N73-11488
Two beam interferometer-polarimeter
[NASA-CASE-NPO-11239] 03 p0300 N73-12446
Laser interferometer instrumentation techniques for study of plane stress wave propagation in solids
[SC-DC-70-5465] 03 p0310 N73-12529
Density field map in fin-flat plate junction in three dimension, using holographic interferometry
[AD-749048] 04 p0408 N73-13324
Development of scaling counter for use as laser interferometer readout system to obtain improved length measurement capabilities
[BDX-613-703] 04 p0429 N73-13492
Characteristics of cryogenic interferometric spectrometer and application to measuring low level emittance or absorption in optical elements
05 p0556 N73-14518
Measuring distribution of radiation as function of its angular coordinates by Talbot spectrometer
[AD-749875] 05 p0581 N73-14733
Calibration and temperature control system for airborne interferometer
[AD-749876] 06 p0667 N73-15427
Holographic interferometry from coherent laser light to detect three dimensional displacements
[UCRL-51241] 07 p0806 N73-16540
High resolution laser interferometer investigation of mechanical behavior of polymethyl methacrylate
[SC-DC-72-1174] 08 p0935 N73-17653
Infrared interferometer spectrophotometer for infrared spectra measurement of CO2 in atmospheres of Earth and Venus
08 p0973 N73-17954
Interferometric investigation of anisotropy in light speed
10 p1187 N73-19661
Holographic interferometric testing of laminate and composite structures for internal voids and material defects
[BDX-613-812] 12 p1410 N73-21429
Five possible supernova remnants mapped by aperture synthesis interferometry
12 p1447 N73-21721
Homodyne interferometer for measuring phase variations of laser beam wave front
[AD-756885] 14 p1668 N73-23539
Interferometer prism and control system for precisely determining direction to remote light source
[NASA-CASE-ARC-10278-1] 16 p1911 N73-25463
Numerical analysis of Josephson junction interferometers
16 p1911 N73-25464
Development of breadboard model correlation interferometer for carbon monoxide pollution experiment
[NASA-CR-112212] 16 p1913 N73-25478
Holographic interferometry for measuring surface deflections of statically loaded turbine blades
16 p1921 N73-25543
Holographic interferometric measurement of prebuckling deformation in cylindrical shell structures under axial compression
16 p1921 N73-25545
Computerized design of polarization interferometer
[AD-760564] 18 p2180 N73-27602
Interferometer aperture synthesis in interstellar neutral hydrogen line spectra of radio sources
[AD-760013] 18 p2198 N73-27744
Photometric aspects of interferometry in far ultraviolet
[AD-762151] 19 p2233 N73-28003
Aperture synthesis in interstellar neutral hydrogen line
21 p2594 N73-30782
HCN laser for interferometric measurements in Tokamak machine
[EUR-CEA-FC-670] 22 p2681 N73-31475
Application of holographic interferometry for detecting dewetted zones in solid rocket propellants
[AD-764470] 22 p2708 N73-31690
Observations of decametric radiation of Jupiter with very-long-baseline interferometer
23 p2836 N73-32659
Optimal accumulation time in superlong-baseline interferometer and frequency stability of sinusoidal signal generators used as heterodynes at receiving points
23 p2838 N73-32678
Second generation laser interferometer for absolute determination of gravity acceleration
[AD-764831] 24 p2924 N73-33339
Holographic interferometric measurement of plasma density in electron beam diode
[SLA-73-5483] 24 p2927 N73-33376
Development of high resolving power interferometer for line shape measurement applications
[AD-764719] 24 p2927 N73-33380
Behavior of macroscopic quantum interferometer composed of supercoducting tin rings containing two Josephson junctions
24 p2967 N73-33710

**INTERFEROMETRY**
NT DIFFERENTIAL INTERFEROMETRY
Application of continuous wave gas laser and pulsed ruby laser to analyze laminar and turbulent films of air at porous wall with carbon dioxide and helium injected into air stream
[AD-747511] 03 p0287 N73-12323
Advanced Figure Sensor for measuring parabolic mirror surfaces
[NASA-CR-130114] 03 p0301 N73-12454
Interferometric study of expansion of plasma created by laser
[CEA-R-4299] 04 p0454 N73-13708
High resolution interferometric observations of Venus
[AD-747992] 04 p0476 N73-13895
Interferometric observations of neutral hydrogen emission line of compact galaxy 2 Zw 40
[AD-747993] 04 p0477 N73-13896
Interferometry measurements of film thickness and traction of lubrication in point contacts
[NASA-CR-120842] 05 p0551 N73-14478
Capabilities and projected accuracy of various satellite tracking systems
06 p0662 N73-15379
Interferometric observations of formaldehyde absorption in front of strong galactic sources
[AD-749772] 06 p0719 N73-15873
Laser illumination for stellar interferometry
[AD-752902] 09 p1068 N73-18712
Operational requirements and optical components of pulsed holographic interferometry
[LA-5058] 10 p1161 N73-19446
Applications of holographic system with interferometric capabilities for crystal growth analysis
[AD-754737] 11 p1294 N73-20504
Method for obtaining holographic interferograms in real time scale
[AD-754632] 11 p1303 N73-20577
Application of holographic interferomctry to determination of discontinuous three-dimensional density fields
[AD-756535] 13 p1511 N73-22246
Application of holographic interferometry to density field determination in transonic corner flow
[AD-756534] 13 p1511 N73-22247
Measurement of surface strain deformation in materials by holographic interferometry
[NRC-TT-1623] 13 p1536 N73-22447
Small phase difference measuring technique within holographically reconstructed optical fields
16 p1922 N73-25549
Aerospace application of holography through nondestructive testing and flow visualization
16 p1922 N73-25550
Plasma diagnostics with infrared schlieren and interferometric techniques using TEA-CO2 laser, exemplified by electric spark transient response
[ISL-19/72] 16 p1950 N73-25779
Earth rotation aperture synthesis technique and polarized interferometry for determining polarized intensity distributions of Cygnus A at 8300 and 9600 MHz
16 p1961 N73-25865
Laser interferometry for plasma diagnostic measurements
[INR-1442] 17 p2040 N73-26506

Holographic interferometry using pulsed ruby lasers to measure electron density in toroidal plasmas
[REPT-72-70] 17 p2069 N73-26743
Doppler difference monochromatic baseline interferometry for tracking lunar roving vehicle
18 p2210 N73-27844
High resolution interferometer spectrometer measurements of auroral infrared emissions to simulate high altitude nuclear explosions
[AD-762013] 19 p2297 N73-28475
Interferometric studies in shock tunnel simulating nozzle flow in gasdynamic lasers
[AD-761601] 19 p2308 N73-28567
Developments in laser interferometry
[RFP-1963] 20 p2425 N73-29482
Study of supersonic flow in inlets using holographic interfereometry
[AD-763335] 21 p2525 N73-30250
Application of very long-baseline interferometry at Smithsonian Astrophysical Laboratory to geophysical measurements of earth
[NASA-CR-135493] 22 p2666 N73-31365
Analysis of interferometric characteristics of stellar figure sensor for orbiting astronomical telescope
[NASA-CR-132795] 22 p2673 N73-31408
Observation equations to utilize lunar laser ranging and very long baseline interferometry measurements for selenodetic control
[NASA-CR-135774] 24 p2931 N73-33404

**INTERGALACTIC MEDIA**

Monte Carlo calculation of cosmic isotope buildup in iron meteorites
[ORNL-TR-2620] 07 p0846 N73-16861
Interaction of ultrahigh energy cosmic rays protons with relicit radiation in extragalactic space
19 p2332 N73-28766
Characteristics of steady galactic winds created by escape of cosmic rays from galaxy
24 p2975 N73-33775

**INTERGRANULAR CORROSION**

Analysis of corrosion in metal specimens by application of X ray irradiation and measurement of secondary X ray emissions using X ray spectrometer
[NLL-TRANS-746-1218-[9022.401]]
02 p0185 N73-11502
Analysis of beta titanium alloys to show heat treatment, mechanical properties, corrosion, weldability, and processing
[AD-753439] 09 p1049 N73-18552
Effect of passivation and dissolution phenomena on structural corrosion of Cr-Ni stainless steels
[NLL-RISLEY-TR-2500-[9091.9F]]
11 p1305 N73-20586

**INTERIOR BALLISTICS**

Numerical analysis of nonlinear longitudinal combustion instability in metallized solid propellant rocket engines - Vol. 1
[AD-748415] 04 p0462 N73-13767
Numerical analysis of nonlinear longitudinal combustion instability in metallized solid propellant rocket engines - Vol. 2
[AD-748417] 04 p0462 N73-13768
Solid propellant grain design and internal ballistics
[NASA-SP-8076] 06 p0711 N73-15804
Development of model to describe flow process, energy transfer, and flame front propagation during combustion of porous propellant charges
08 p0968 N73-17910
Spectroscopic measurements of flame composition an temperature of composite solid propellants during unstable combustion
10 p1222 N73-19939
Hybrid rocket interior ballistics and heat transfer limited model
[AD-754769] 11 p1335 N73-20833
Manual of CDC 6400 computer program for predicting nozzleless rocket motor internal ballistics
[AD-759559] 16 p1958 N73-25838
Nonsteady combustion and extinguishment tests to determine acoustic instabilities of solid rocket propellants during combustion
[AD-760788] 18 p2207 N73-27813
Analysis of flame front propagation in porous propellant charges to show wave propagation speed and mass fraction of propellant burned during flame propagation
[AD-762063] 19 p2353 N73-28928
Interior ballistic properties of solid fuel ramjet engines to determine regression rate if fuel as function of chamber pressure, inlet air temperature, and air flux rate
[AD-764491] 22 p2709 N73-31691

**INTERLACING DRAINAGE**

U DRAINAGE PATTERNS

**INTERLAYERS**

NT MULTILAYER INSULATION

**INTERMEDIATE FREQUENCY AMPLIFIERS**

Thick film hybrid radio receiver module consisting of intermediate frequency amplifier and discriminator manpack
[AD-756428] 13 p1494 N73-22108

**INTERMETALLICS**

Structural-, thermal-, and magnetic-properties of various metals and intermetallic compounds
[COO-3427-7] 04 p0434 N73-13536
Magnetic properties and crystalline structures of rare earth-cobalt alloys
[AD-748270] 04 p0436 N73-13555
Neutron diffraction and single crystal X ray determination of rare earth-cobalt-iron intermetallic magnetic structure
[AD-748429] 04 p0460 N73-13754
Synthesis of superconducting intercalated and intermetallic compounds
[AD-751497] 07 p0833 N73-16751
Phase equilibrium diagram of intermetallic compound of vanadium and gallium
[AD-752877] 09 p1049 N73-18551
NMR studies in metals and metallic compounds
[AD-752912] 09 p1074 N73-18767
Deformation of gamma and epsilon phases in intermetallic compounds by extrusion method
[AD-754523] 11 p1307 N73-20605
Processing methods for rare earth cobalt compounds as permanent magnets
[AD-754951] 11 p1325 N73-20749
Low temperature optical absorption of some unusual intermetallic compounds
12 p1438 N73-21646
Controlled diffusion reaction process for masking substrate of twisted multifilament superconductive ribbon
[NASA-CASE-LEW-11726-1] 17 p2070 N73-26752
Elastic constants for calculating parallel Shockley partial dislocations in ordered alloys and intermetallic compounds
23 p2803 N73-32420
Production of intermetallic compounds by effect of shock waves from explosions and compaction of powder
[NASA-CASE-MFS-20861-1] 23 p2806 N73-32437

**INTERMODULATION**

Analysis of intermodulation and cross modulation distortions in broadband balanced bridge switching state MOSFET mixer
[AD-749064] 05 p0521 N73-14234
Tunable filter system for reducing intermodulation noise in radio transmitter
[AD-754938] 11 p1257 N73-20197
Analysis of intermodulation of weak signal with strong signal in ionosphere to determine variations as function of modulation frequency of strong signal
[BBC-RD-1973/5] 19 p2234 N73-28010

**INTERMOLECULAR FORCES**

Digital computer calculation of molecular hydrogen-atomic hydrogen interaction energy and electric dipole moment
[NASA-TM-X-2839] 20 p2455 N73-29733

**INTERMONTANE FLOORS**

U VALLEYS

**INTERNAL COMBUSTION ENGINES**

NT CF-700 ENGINE
NT DIESEL ENGINES
NT DUCTED FAN ENGINES
NT GAS TURBINE ENGINES
NT HELICOPTER ENGINES
NT J-52 ENGINE
NT J-57 ENGINE
NT J-65 ENGINE
NT J-75 ENGINE
NT J-85 ENGINE
NT JET ENGINES
NT PULSEJET ENGINES
NT RAMJET ENGINES
NT SUPERSONIC COMBUSTION RAMJET ENGINES
NT TURBOFAN ENGINES
NT TURBOJET ENGINES
NT TURBOPROP ENGINES

Application of pattern recognition to fault diagnosis of internal combustion engines
[AD-747334] 03 p0351 N73-12863
Development and characteristics of hydrogen-based mobile fuel systems and analysis of technical and economic problems in large scale application
[UCRL-51228] 07 p0834 N73-16766
Performance test of internal combustion engine to determine effects of pulsed injection of secondary air on exhaust emission levels
[NASA-TM-X-2737] 08 p0969 N73-17920
Development of method for determining zinc dialkyl diaryl dithiophosphate in lubricating oils
[AD-757605] 14 p1671 N73-23563
Analysis of factors influencing technical feasibility of operating aircraft on liquid hydrogen fuel
[NASA-TM-X-68242] 15 p1823 N73-24777

**INTERNAL COMPRESSION INLETS**

Supersonic wind tunnel tests of internal performance of rectangular variable geometry air inlets noting effect of incidence
[ARC-CP-1242] 22 p2612 N73-30933
Supersonic wind tunnel tests of internal performance of rectangular variable geometry air inlets at zero incidence
[ARC-CP-1243-PT-1] 22 p2612 N73-30934

**INTERNAL ENERGY**

Energy equations to analyze radiative heat transfer from gaseous suspension flow with internal heating
14 p1718 N73-23939

**INTERNAL FRICTION**

Recovery of elastic properties and internal friction of hydrostatically extruded molybdenum with 0 to 80 percent deformation
[AD-747515] 03 p0317 N73-12586
Elastic properties and internal friction of hydrostatically extruded molybdenum
[AD-749539] 05 p0563 N73-14574
Dislocation damping in cu single crystals of controlled substructure, and ultrasonic attenuation data
[AD-750712] 06 p0711 N73-15801
Internal friction and crystal defects of magnesium oxide crystals
09 p1063 N73-18673
Internal friction measurements on brass and aluminum alloys during plastic deformation loading
[AD-760145] 17 p2048 N73-26570
Experimental methods for determining internal damping in metal alloys and identification of factors causing internal damping
[NLL-CE-TRANS-6132-[9022.09]]
20 p2429 N73-29508
Effect of high hydrostatic pressure on flow stress of 18-8 stainless steel
[NLL-NEL-TT-2458-[6075.461]]
20 p2430 N73-29516

**INTERNAL PRESSURE**

Fatigue strength data for thick steel and aluminum alloy cylinders under internal pressure
[ESDU-67014] 01 p0110 N73-10910
Creep rupture tests of Inconel 702 tubes at high temperatures and internal helium pressures to determine service life
[NASA-TM-X-2728] 08 p0932 N73-17628
Creep rupture tests of Hastelloy-X tubes at high temperatures and internal helium pressures to determine service life
[NASA-TM-X-2727] 08 p0932 N73-17629
Temperature and internal pressure response of nuclear waste disposal container following impact on earth
[NASA-CR-121186] 16 p1943 N73-25721
Bending stresses produced by internal pressure in thin walled hollow cylinders with out-of-round cross section
[NLL-CE-TRANS-6040-[9022.09]]
20 p2478 N73-29902

**INTERNAL STRESS**

U RESIDUAL STRESS

**INTERNATIONAL COOPERATION**

Joint Soviet-US research radio astronomy and plans involving spaceborne telescope
[NLL-M-22684-[5828.4F]] 01 p0100 N73-10823
International cooperation in nuclear data field, emphasizing nuclear energy role
[INDC[NDS]-40-U] 04 p0452 N73-13691
Political, legal, and international management of space data and space programs
04 p0474 N73-13871
Use of space exploration and benefits to procure world peace
04 p0474 N73-13872
French space programs and benefits to mankind
04 p0474 N73-13874
French space program events during 1971
[NASA-TT-F-14721] 04 p0487 N73-13985
Possibilities of assessing global environmental quality in relation to future prosperity of man, for Global Environmental Monitoring System
[BULL-10] 05 p0538 N73-14379
Climate changes caused by human activities and need for international studies
[NLL-M-22770-[5828.4F]] 05 p0570 N73-14628
Speech on problem of aircraft hijacking and efforts to prevent hijackers from continuing to conduct air piracy
05 p0611 N73-14970
English, Spanish, and French definitions for international civil aviation terminology
[DOC-8800-VOL-2] 06 p0616 N73-14997
Data compiled in international comparative creep rupture program using two types of steel as test materials
[PB-211174] 06 p0685 N73-15578
Selected abstracts on boron from internaticonference held at Tbilisi
[JPRS-57879] 06 p0687 N73-15596
International aspects of Earth Resources Survey Program to include proposals for data availability and assistance to be provided by various nations
07 p0782 N73-16352
Overview of scientific and technological research in Yugoslavia on NBS grants, 1971 - 1972
[NBS-TN-753] 08 p0976 N73-17979
Cooperation of Eastern European countries in computer and medical research
[JPRS-58063] 08 p0976 N73-17987
Accounts of scientific and technological cooperation in Eastern Europe
[JPRS-58053] 08 p0977 N73-17990
Design of docking system of androgynous and peripheral type for creation of compatible system for US and Soviet spacecraft
09 p1087 N73-18869

Present international status of research and development of electrochemistry and fuel cells
[AD-755106] 11 p1238 N73-20048
German cooperation with AGARD research in aerospace sciences
11 p1350 N73-20958
German cooperation in international aeronautical research
11 p1351 N73-20959
International conference on fundamental atomic and molecular physics
[AD-757890] 15 p1816 N73-24717
NASA participation in international space programs
[NASA-TM-X-69259] 15 p1846 N73-24957
Project management in aerospace industry
15 p1847 N73-24967
Industrial policy of ESRO noting distribution of contracts, relations with industry, multinational consortiums, and technological research
15 p1848 N73-24975
Relationships between United States of America and Latin American telecommunication institutions
[PB-214619/9] 16 p1876 N73-25187
French-Soviet cooperation in space research
[AD-759106] 16 p1978 N73-25996
International cooperation in noctilucent cloud research
[NASA-TT-F-14950] 17 p2026 N73-26390
Foreign reports on environmental pollution
[PB-218839/9] 18 p2148 N73-27360
Foreign reports on environmental pollution legislative, economic, and social aspects
[PB-218858/9] 18 p2148 N73-27361
Index of international scientific rocketlaunches
[NASA-TM-X-69350] 18 p2196 N73-27732
Catalog of international rocket and satellite launching data
18 p2199 N73-27750
Administration, development, and maintenance of NASA tracking network with emphasis on Australia
[NASA-CR-133828] 21 p2521 N73-30214
Requirements for international laws of remote sensing
[NASA-TT-F-15055] 21 p2535 N73-30330
Planned 1973 AGARD meetings, and list of 1972 AGARD publications
[AGARD-BULL-73-1] 21 p2610 N73-30919
United States cooperation with the USSR and Japan in science and technology
22 p2737 N73-31917
Description of intercomparison of radiometersondes
23 p2814 N73-32494
International civil aviation organization for air traffic forecasting and airport development
23 p2861 N73-32865
Advice and assistance provided by Civil Aviation Board to State Department on matters of international air transportation policy
23 p2865 N73-32899
Lectures presented at International Conference on Chemiluminescence
[AD-765525] 24 p2893 N73-33094
Summary of COSPAR meetings and reports on news from national and international organizations about rockets and propelled vehicles
24 p2994 N73-33922
Aims, prospects, organization, and financing of EUROSAT S.A.
24 p2994 N73-33930

**INTERNATIONAL FIELD YEAR FOR GREAT LAKES**
Utilization of ERT-1 imagery for water depth measurement, Yellowstone Park data, atmospheric effects in Colorado, lake ice surveillance, recreational land use, IFYGL, image enhancement, water quality monitoring, oil pollution detection, and mapping iron compounds
[E73-10086] 08 p0901 N73-17298
Processing of IFYGL data for Lake Ontario and its drainage basin
[E73-10393] 11 p1276 N73-20355
IFYGL data for hydrologic analysis of Lake Ontario Basin
[E73-10571] 15 p1772 N73-24351

**INTERNATIONAL GEOPHYSICAL YEAR**
Water balance, micrometeorology, thermal structure, and heat content of Great Lakes as determined by remote sensors during International Field Year
[IFYGL-BULL-4] 18 p2143 N73-27322

**INTERNATIONAL LAW**
NT SPACE LAW
Juridical problems in use of stationary orbits for artificial earth satellites
[JPRS-59819] 20 p2473 N73-29862
Study of terrestrial resources by satellites, and international law
[NASA-TT-F-15094] 23 p2846 N73-32740

**INTERNATIONAL RELATIONS**
NT INTERNATIONAL COOPERATION
International aspects of Earth Resources Survey Program to include proposals for data availability and assistance to be provided by various nations
07 p0782 N73-16352

**INTERNATIONAL SATS FOR IONOSPHERIC STUDY**
U ISIS SATELLITES

**INTERNATIONAL SYSTEM OF UNITS**
Metric calibration of aerial photographic system by method of mixed ranges
[AD-748812] 04 p0423 N73-13452
Industrial conversion to metrication standards
[NASA-CR-130534] 08 p0925 N73-17584
Development of metric system design for large space telescope to show effect on production cost and time required
[NASA-CR-124133] 10 p1159 N73-19426
Improvement to primary standard of measurement associated with International System of Units
[NPL-QU-AR-71] 10 p1161 N73-19450
Tables of conversion factors and physical constants in International System of Units
[NASA-SP-7012] 17 p2098 N73-26969
Congressional hearing on national program to establish international metric system as official and standard system for United States commerce and industry
21 p2610 N73-30920
Congressional hearings on legislation for conversion to metric system of weights and meaures in United States
21 p2610 N73-30922
Coversion data for transition from english to metric system for design and fabrication of transformers
[NASA-CR-133932] 22 p2700 N73-31624

**INTERNATIONAL TRADE**
Bank financing in commercial jet aircraft export
23 p2861 N73-32862

**INTERPLANETARY DUST**
NT ZODIACAL DUST
Bessel theory for analyzing head and tail regions of dust comets
02 p0228 N73-11846
Particle flux measurements of interplanetary dust and comet orbits by microphone experiments invalidated by micrometeoroid detectors flown on Pioneer 8 and 9
08 p0975 N73-17976
UBV and H alpha spectra for detecting interstellar dust and distances to planetary nebulae
12 p1448 N73-21724

**INTERPLANETARY EXPLORER**
U EXPLORER 18 SATELLITE

**INTERPLANETARY FLIGHT**
NT GRAND TOURS
Psychological stresses and crew compatibility during interplanetary spacecraft flight
[JPRS-57878] 06 p0629 N73-15113
Effects of planetary quarantine constraints on advanced planetary mission planning
[NASA-CR-130861] 09 p0995 N73-18123
Optimum trajectory and spacecraft data for unmanned interplanetary missions from 1975 to 1990 using solar electric propulsion
[NASA-CR-132765] 16 p1966 N73-25907
Hybrid programmable attitude control electronic analog digital system for preflight and in-flight changes in planetary missions
22 p2731 N73-31859
Deep Space Network tracking support of planetary and interplanetary flight projects - Vol. 17
[NASA-CR-135708] 23 p2757 N73-32064

**INTERPLANETARY MAGNETIC FIELDS**
Conference on magnetic structure of interplanetary and solar magnetic fields and solar wind
[NASA-SP-308] 01 p0092 N73-10760
Archimedes spiral and solar wind induced structures in interplanetary magnetic field
01 p0093 N73-10766
Effect of solar wind velocity on interplanetary magnetic field properties
01 p0093 N73-10767
Observation of interplanetary and solar magnetic field sector structure from 1962 through 1968
01 p0094 N73-10770
Inference of coronal and interplanetary magnetic fields and H-alpha patterns from high resolution photography
01 p0094 N73-10771
High resolution measurements of complex microstructure of interplanetary magnetic field and plasma, including hydromagnetic waves and discontinuities
01 p0095 N73-10787
Possible noise sources in power spectra measurement of interplanetary magnetic field
01 p0096 N73-10791
Power spectra of interplanetary magnetic field near earth bow shock
01 p0096 N73-10792
Calculation of shock normals using least squares technique on combined magnetic field and plasma data from single spacecraft
01 p0097 N73-10798
Analysis of solar flare energetics based on shock velocity, ambient solar wind velocity and density, and ambient azimuthal Mach number
01 p0097 N73-10799
Effect of flow of interstellar neutral particles on loss of field angular momentum by solar wind
01 p0099 N73-10815
Influence of interplanetary magnetic field on geomagnetic variations in polar cap
[NASA-CR-129165] 02 p0166 N73-11351
Influence of interplanetary magnetic field on geomagnetism in polar regions during sunspot cycles
[DMI-GEOPHYS-PAPERS-R-29]
02 p0167 N73-11355
Interplanetary magnetic fields and magnetic disturbances induced by ionospheric
[DMI-GEOPHYS-PAPERS-R-32]
02 p0216 N73-11749
Magnetospheric convection, currents feeding polar cap ionosphere, and interplanetary magnetic fields
[NASA-CR-130124] 04 p0413 N73-13375
Preliminary results from HEOS A satellite in electron and proton events, solar wind and interplanetary magnetic field measurement, and propagation of charged particles
[ESRO-SP-74] 05 p0592 N73-14813
Injection, propagation, and interaction characteristics of solar protons based on HEOS A satellite data
05 p0593 N73-14817
Comparison of solar cycle variation of interplanetary magnetic field strength observed by HEOS A and Explorer 18 satellite
05 p0593 N73-14819
Correlation length for interplanetary magnetic field fluctuations
[NASA-TM-X-66138] 05 p0595 N73-14841
Magnetopause boundary dependence on orientation of interplanetary magnetic field and hydromagnetic properties of magnetosphere shift southwards
06 p0718 N73-15857
Calculation of interplanetary magnetic field induced asymmetries in forward stagnation region of solar-wind magnetospheric interaction
07 p0838 N73-16792
Mie scattering of interplanetary magnetic field by whole moon
[NASA-TM-X-62225] 07 p0844 N73-16833
Electromagnetic lunar conductivity measurements on dark side radial magnetic fields
[NASA-TM-X-62226] 07 p0844 N73-16834
Magnetic field around spherical moon and downstream cylindrical cavity formed by solar wind, derived for parallel and perpendicular interplanetary magnetic fields
[NASA-TM-X-62227] 08 p0960 N73-17851
Interplanetary magnetic field annihilation and resulting D-sheets
[NASA-TM-X-66187] 09 p1080 N73-18813
Charged particle and magnetic field research using ATS 1 and Mariner measurements
[NASA-CR-131269] 11 p1338 N73-20857
Influence of polarity of interplanetary magnetic field on magnetic activity at high latitudes
[GRI/NT/87] 12 p1402 N73-21371
Inferring polarity of interplanetary magnetic field from observations of diurnal variation of polar geomagnetic fields
[NASA-CR-131609] 13 p1527 N73-22379
Propagation of Alfven waves in spiral interplanetary magnetic field
[NASA-CR-131569] 13 p1563 N73-22665
Research projects for space exploration by out-of-ecliptic spacecraft
[NASA-CR-131865] 13 p1578 N73-22792
Analysis of boundaries between solar magnetic sectors and comparison with observations of stellar magnetism
[NASA-CR-131832] 13 p1579 N73-22795
Erosion rate of dayside magnetic flux based on quantitative study of dependence of polar cusp latitude on interplanetary magnetic field
[NASA-TM-X-66256] 15 p1831 N73-24837
Relation between azimuth component of interplanetary magnetic field and geomagnetic field in polar caps
[NASA-CR-133273] 18 p2145 N73-27338
Perpendicular fast reverse shock wave found in interplanetary plasma and magnetic field data from Explorers 33 and 35
[NASA-TM-X-70451] 21 p2523 N73-30235
High latitude electric fields and modulations related to interplanetary magnetic field parameters
[NASA-TM-X-70444] 21 p2535 N73-30331

**INTERPLANETARY MEDIUM**
NT INTERPLANETARY DUST
NT ZODIACAL DUST
Properties of active and helmet coronal streamers based on radio observations
01 p0093 N73-10769
Large scale structure of solar wind during fading and maximum portions of two different cycles
01 p0094 N73-10774
Theoretical models of interplanetary shock waves and solar wind disturbances with large scale characteristics
01 p0096 N73-10794
Calculation of shock normals using least squares technique on combined magnetic field and plasma data from single spacecraft
01 p0097 N73-10798
Observations of solar plasma using interplanetary scintillation techniques and radio scattering methods
01 p0097 N73-10801

Variations of interplanetary scintillation index with wavelength in accordance with smooth, power law spectrum of plasma fluctuations
01 p0097 N73-10802
Spectral form of irregularities in electron density causing interplanetary scintillation of small angular diameter radio sources
01 p0098 N73-10804
Effect of sputtering corotating source of thin solar plasma streams on electron content of solar wind
01 p0098 N73-10805
Analysis of isotopic composition of solar wind based on collecting foils and lunar material
01 p0098 N73-10807
Analysis of alpha particle observations performed by HEOS 1 satellite and comparison with observations made by Vela 3 and Explorer 34 satellites
01 p0098 N73-10809
Characteristics of solar wind and interaction with interstellar plasma and magnetic field
01 p0099 N73-10811
Effect of flow of interstellar neutral particles on loss of field angular momentum by solar wind
01 p0099 N73-10815
Differential energy spectra of cosmic ray protons and helium nuclei dominated by solar modulation of local interstellar spectra, and numerical solutions to transport equation
[NASA-CR-130298] 06 p0715 N73-15837
Cosmic ray phenomenon of quiettime electron increases
08 p0974 N73-17962
Correlation between ionospheric disturbance and solar wind velocity, density, and positive ion flux of interplanetary medium
13 p1519 N73-22316
Alfven wave refraction by interplanetary inhomogeneities from analysis of Pioneer 6 data
[NASA-TM-X-62270] 16 p1962 N73-25867
Shielding lengths in magnetospheric and interplanetary plasmas
[AD-760795] 18 p2147 N73-27352
Integrated solar-quiet interplanetary electron spectrum obtained by Explorer 41 satellite
22 p2733 N73-31874
Experimental radio and radar studies on lunar and planetary atmospheres and surfaces, interplanetary medium, and software and hardware conceptions
[NASA-CR-135670] 23 p2845 N73-32734
Sound wave, Alfven wave and heat flow effects on normal shock waves noting shock wave attenuation, Rankine-Hugoniot relation extension, and application to interplanetary shock waves
24 p2965 N73-33701

**INTERPLANETARY MONITORING PLATFORM**
U IMP

**INTERPLANETARY PROPULSION**
U INTERPLANETARY SPACECRAFT
U ROCKET ENGINES

**INTERPLANETARY SPACE**
Numerical integration procedure for determining electromagnetic structure of interplanetary space
01 p0093 N73-10768
Flare-associated interplanetary shock data of 15-16 Feb. 1967 analyzed for estimation of ecliptic plane geometry of shock surface near 1 AU
[NASA-TM-X-66115] 03 p0353 N73-12875
Doppler frequency of interplanetary radar signal from earth to another planet or to space probe determined according to general relativity
[NASA-CR-130147] 07 p0755 N73-16131
Interplanetary sector structure and heliomagnetic equator
[AD-751909] 08 p0963 N73-17874
Motion of sources for type 2 and type 4 radio bursts and flare-associated interplanetary disturbances
[NASA-TM-X-70452] 21 p2507 N73-30117
Solar flares and relativistic electron events in interplanetary space
[NASA-CR-135491] 22 p2712 N73-31715
Satellite measurements on lunar and planetary environments in solar system
22 p2735 N73-31891
Direct charge state measurements of low energy solar carbon and oxygen in interplanetary space
[TR-73-132] 23 p2834 N73-32648
Interplanetary distribution of meteors in radar observations
[NASA-CR-2316] 23 p2844 N73-32727

**INTERPLANETARY SPACECRAFT**
NT EXPLORER 18 SATELLITE
NT JUPITER PROBES
NT MARINER SPACE PROBES
NT MARINER SPACECRAFT
NT MARINER VENUS-MERCURY 1973
NT MARINER 3 SPACE PROBE
NT MARINER 7 SPACE PROBE
NT MARINER 9 SPACE PROBE
NT MARS PROBES
NT MARS 2 SPACECRAFT
NT MARS 3 SPACECRAFT
NT PIONEER SPACE PROBES
NT PIONEER 6 SPACE PROBE
NT PIONEER 8 SPACE PROBE
NT PIONEER 9 SPACE PROBE
NT PIONEER 10 SPACE PROBE
NT TOPS [SPACECRAFT]
NT VENERA SATELLITES
NT VENERA 8 SATELLITE
NT VENUS PROBES
NT VIKING LANDER SPACECRAFT
NT VIKING ORBITER SPACECRAFT
NT VIKING 75 ENTRY VEHICLE
Performance prediction for nuclear electric propulsion systems in advanced unmanned missions to outer planets and solar system
[NASA-CR-129134] 02 p0210 N73-11705
Lightweight insulation for long duration low pressure planetary orbiter-type rocket engine applications
[NASA-CR-114513] 04 p0485 N73-13959
Scientific aspect of interplanetary investigation by Helios satellite
[DGLR-PAPER-72-068] 09 p1085 N73-18853
Control equipment for sterilization facility used to thermally inactivate microbes on interplanetary space vehicle components
[NASA-CR-131103] 10 p1119 N73-19122
Actuator shaft sealing techniques for long term interplanetary spacecraft missions
[NASA-CR-130927] 10 p1165 N73-19479
Planning and source allocation for planetary quarantine measures for interplanetary automated spacecrafts
[NASA-CR-131291] 11 p1247 N73-20126
Spin scan camera photography of Jupiter from rotating outer planet orbiters
[NASA-TM-X-62260] 15 p1830 N73-24836
Dry heat inactivation of atypical Bacillus subtilis var. niger spores in and on interplanetary space vehicle components
[NASA-CR-133224] 17 p1987 N73-26059
Development of test equipment, propellants, and control equipment for interplanetary spacecraft
[NASA-CR-133863] 22 p2731 N73-31858
Cost effective measures for preventing solar proton interference with interplanetary spacecraft operation
22 p2732 N73-31863

**INTERPLANETARY TRAJECTORIES**
Computer program for determining precision interplanetary trajectories
[NASA-CR-128655] 04 p0475 N73-13884
Comparison of accuracy of patched-conic and linearization methods for predicting trajectories in sun-planet system
[AD-748345] 04 p0476 N73-13891
Problems in estimation theory with applications to orbit determinations
[AD-755802] 12 p1458 N73-21820
Application of matched asymptotic expansions to lunar and interplanetary trajectories
[NASA-CR-2255] 18 p2197 N73-27738
Derivations of second-order asymptotic boundary value solutions for lunar and interplanetary trajectories
[NASA-CR-2256] 19 p2343 N73-28845
Payloads of ballistic trajectories in Mercury orbit, and interplanetary trajectory characteristics for Venus swingbys to Mercury
[NASA-CR-2298] 23 p2846 N73-32745

**INTERPOLATION**
Interpolation of vertical deflections using trigonometric leveling
[AD-743986] 01 p0052 N73-10418
Tight binding interpolation representing transition and noble metal s, p, and d bands applied to Mo and Cu
[IS-T-515] 04 p0434 N73-13535
Optimum interpolation and extrapolation of meteorological fields
[NLL-M-22856-[5828.4F]] 11 p1313 N73-20654
Numerical smoothing and interpolation methods noting spline function method
[ONERA-NT-205] 15 p1804 N73-24619
Program for one level objective analysis of meteorological fields by optimal interpolation
[NLL-M-22883-[5828.4F]] 16 p1936 N73-25664
Single-level objective analysis of meteorological observations on hemisphere by optimal interpolation
[NLL-M-22908-[5828.4F]] 18 p2169 N73-27514
Interpolation of functions of one variable by cubic spline functions
21 p2512 N73-30152
Theory of spline interpolation extended to case of two independent variables
21 p2512 N73-30153
Approximation of curves and surfaces in three-dimensional space by smooth circular interpolation
21 p2512 N73-30154
Use of regularization method for interpolation and differentiation of experimental data
[NLL-M-21660-[5828.4F]] 21 p2565 N73-30561
Headlamp research program for extrapolation/interpolation of surface values from predefined grid
[LTR-ST-602] 22 p2637 N73-31129
Data smoothing and error detection based on linear interpolation
[NASA-CR-133984] 22 p2637 N73-31131

**INTERPRETATION**
Analysis and interpretation of ERTS-1 ecologic, geographic, and agricultural data for Tennessee Valley
[E72-10231] 02 p0163 N73-11324
Characteristics of multispectral sensors and methods for interpreting multispectral data obtained during earth resources surveys
07 p0784 N73-16378
Application of dielectric constant measurements to interpretation of radar imagery of Michigan ground truth for lake ice
[E73-10391] 11 p1276 N73-20353
Application of dielectric constant measurements to interpretation of radar imagery of ground truth
[E73-10429] 11 p1280 N73-20390
Processes, algorithms, and procedures for extraction and interpretation ERTS-1 data
19 p2290 N73-28412

**INTERSTELLAR EXTINCTION**
High dispersion Coude spectrograms of zeta Oph and Per, and molecular absorption in interstellar medium
[NASA-TM-X-66073] 02 p0224 N73-11812
Determination of wavelength dependence of interstellar reddening law and applicability to all stars
08 p0975 N73-17971
Investigation of ultraviolet interstellar extinction
[NASA-CR-131990] 14 p1706 N73-23843
Interstellar extinction in ultraviolet
[NASA-CR-133924] 22 p2717 N73-31753
Report of the Astronomer Royal for Scotland for the year ending 31 March 1973
22 p2718 N73-31760

**INTERSTELLAR GAS**
Development of model of scattering of solar Lyman alpha from spatial distribution of neutral hydrogen in interplanetary space
01 p0099 N73-10813
Interstellar cloud heating by collisionally de-exciting vibrationally excited molecular hydrogen
[NASA-TM-X-66064] 01 p0103 N73-10851
Solar wind/interstellar gas interactions and Lyman alpha background radiation
[TRITA-EPP-72-03] 01 p0105 N73-10871
Background Lyman alpha radiation and interstellar hydrogen gas taking into account radiative heat transfer
01 p0105 N73-10872
Solar wind plasma/interstellar hydrogen gas interactions
01 p0105 N73-10873
Total gamma ray production rate per hydrogen atom from neutral pion decay in interstellar cosmic ray interactions, and calculation of molecular hydrogen amount
[NASA-TM-X-66167] 07 p0839 N73-16798
Interstellar CO in ultraviolet spectrum of Zeta Ophiuchi
08 p0975 N73-17972
Low intensity H-beta emission from interstellar medium
08 p0975 N73-17973
Searches for interstellar OH and other molecular emission and recombination lines in radio frequency range
[RR-108] 09 p1084 N73-18845
Influence of cosmic rays on temperature and ionization rate of interstellar gas
[MPI-PAE/EXTRATERR-72] 12 p1446 N73-21710
Galactic neutral hydrogen gas velocity distribution within spiral arms in local regions
12 p1447 N73-21720
Radio telescope observation of low velocity interstellar neutral atomic hydrogen in direction of early type stars
19 p2342 N73-28836
Aperture synthesis in interstellar neutral hydrogen line
21 p2594 N73-30782
Spallation reactions of light nuclei during galactic cosmic radiation interaction with interstellar gas
[FRNC-TH-333] 21 p2597 N73-30812
Diffuse optical emissions from interstellar gas
22 p2734 N73-31887

**INTERSTELLAR MAGNETIC FIELDS**
Existing stochastic models of galactic magnetic field
[NASA-CR-130158] 08 p0959 N73-17847

**INTERSTELLAR MATTER**
Interferometric observations of formaldehyde absorption in front of strong galactic sources
[AD-749772] 06 p0719 N73-15873
Origin and evolution of stars, stellar matter, and galaxies
[AD-749734] 06 p0720 N73-15875
Low energy cosmic ray protons from nuclear interactions of cosmic rays with interstellar medium
[NASA-TM-X-66181] 08 p0956 N73-17829
Search for interstellar C[14]O
[AD-751912] 08 p0962 N73-17870
Model for ionized part of interstellar medium based on low frequency observations by RAE satellite
08 p0975 N73-17970
Density and temperature profiles of HI lines in interstellar dust clouds
12 p1448 N73-21723
Mapping of Perseus arm feature in spectrum of Cassiopeia A
[AD-757687] 15 p1832 N73-24854

Hyperfine formaldehyde lines in molecular dust cloud L1436
[AD-757689] 15 p1833 N73-24861
Penetration and wake formation in interstellar cloud collision
16 p1961 N73-25862
Spectroscopic observation of metastable helium line in alpha-orionis and interstellar media
17 p2081 N73-26830
Emission spectra of interstellar molecules
[NASA-TT-F-14961] 17 p2083 N73-26849
Interferometer aperature synthesis in interstellar neutral hydrogen line spectra of radio sources
[AD-760013] 18 p2198 N73-27744
Far infrared and submillimeter background
[AD-763139] 21 p2598 N73-30823
Reaction rate characteristics of interstellar matter and cosmic cloud formation
22 p2735 N73-31896

**INTERSTELLAR MICROWAVE SPECTRA**
U INTERSTELLAR RADIATION
U MICROWAVE SPECTRA

**INTERSTELLAR RADIATION**
Ultraviolet interstellar polarization measurement
22 p2735 N73-31889

**INTERSTELLAR REDDENING**
U INTERSTELLAR EXTINCTION

**INTERSTELLAR SPACE**
Tables on structure of interstellar masers and quasars
14 p1704 N73-23826
Conference on cosmic ray and solar particle diffusion and concentration in interstellar space
[NASA-CR-135528] 23 p2834 N73-32646
Source and diffusion of cosmic rays greater than 4.5 GV in interstellar medium measured by proportional counter-scintillation counter stack
[TR-73-136] 23 p2835 N73-32652

**INTERSTITIALS**
Computer simulations of split interstitial equilibrium positions and binding energies in tungsten crystals
[AD-745839] 01 p0088 N73-10728
Interstitial impurity diffusion coefficients and crystal lattice defects in cubic alloys
[AD-746949] 02 p0188 N73-11529
Effects of interstitial solute content on deformation kinetics in hot extrusion of titanium aluminum vanadium alloy
[AD-750556] 06 p0677 N73-15511
Multiphonon infrared absorption by crystal inclusions of optical window materials
[AD-756080] 13 p1537 N73-22453
Age hardening and precipation behavior of V-Ti, V-Ti-Si, V-Zr, and V-Hf alloys with reference to interstitial metalloid
[KFK-1680] 15 p1799 N73-24582
Computer simulation techniques to determine equilibrium positions and binding energies of inert gas atoms implanted in tungsten crystal
[AD-758501] 15 p1799 N73-24585

**INTERVALS**
Gravity wave effects in occurrence time changes of daily traveling ionospheric disturbances
05 p0511 N73-14156
Human perception of musical intervals between simultaneous tones
[IZF-1972-20] 14 p1613 N73-23078

**INTESTINES**
NT RECTUM
Pharmacologic investigations of antagonistic effects of pyridines on isolated guinea pig ileum
[BMVG-FBWT-72-14] 07 p0747 N73-16075
Effect of accelerations on active transport of glucose in small intestine of rats
24 p2883 N73-33021

**INTRAMOLECULAR STRUCTURES**
Potentiometric stability data analyses for nickel, lead, and zinc organic acetate complexes
[JINR-E12-6776] 24 p2935 N73-33436
Functional stability calculations for organometallic complexes of copper and cadmium
[JINR-E12-6775] 24 p2935 N73-33437
Stability constants correlation for metal-inorganic ligands in organometallic cadmium, rhodium, and lead compounds
[JINR-E12-6773] 24 p2935 N73-33438

**INTRAOCULAR PRESSURE**
Long term bed rest effects on human retinal blood circulation and intraocular pressure
14 p1608 N73-23038

**INTRAVEHICULAR ACTIVITY**
Astronaut manual performance limits in intravehicular Skylab environment
[NASA-CR-128590] 01 p0019 N73-10130
Identification of requirements and systems for intravehicular activity and extravehicular activity during space shuttle missions - Vol. 1
[NASA-CR-128941] 15 p1835 N73-24875
Identification of requirements and systems for intravehicular activity during space shuttle missions - Vol. 2
[NASA-CR-128942] 15 p1835 N73-24876
Guidelines for extravehicular and intravehicular activities during space shuttle operation with emphasis on contingency situations - Vol. 2
[NASA-CR-133992] 22 p2622 N73-31007
Requirements and equipment for space shuttle emergency intravehicular activity and effectiveness of emergency procedures - Vol. 5
[NASA-CR-133995] 22 p2622 N73-31010
Intra- and extravehicular life support space suite for Apollo astronauts
[NASA-CASE-MSC-12609-1] 23 p2751 N73-32012

**INTRUDER AIRCRAFT**
U A-6 AIRCRAFT

**INVALIDITY**
U ERRORS

**INVARIANCE**
NT GAUGE INVARIANCE
Use of cross ratio invariance for analysis and error evaluation in automatic microwave network analyzers
[NBS-TN-623] 03 p0277 N73-12246
Projective invariance of dual resonance models from spin analyticity and Lorentz invariance
[NOTA-INTERNA-388] 03 p0340 N73-12772
Condition of drift invariance of two-stage gyroscope with arbitrary gas-lubricated main bearings in active accelerations
10 p1184 N73-19635
Multifold Euclidean geometry codes
[NASA-CR-133529] 20 p2439 N73-29590

**INVENTIONS**
List of NASA inventions available for licensing in foreign countries
[NASA-SP-7038[01]] 15 p1845 N73-24947
NASA patent abstracts bibliography
[NASA-SP-7039[2]-SECTION-1]
16 p1976 N73-25976
Government-owned patent survey for technology utilization in commercial enterprises
16 p1976 N73-25981

**INVENTORIES**
NT TIMBER INVENTORY
Inventory listing of Federal Government environmental research facilities
[PB-209752] 02 p0153 N73-11240
Development of multistage forest sampling inventory system using ERTS-1 imagery
[E73-10428] 11 p1280 N73-20389
Natural resources management and inventory of Arizona using ERTS-1 imagery
[E73-10442] 11 p1282 N73-20402
Development of multistage forest sampling inventory system using ERTS-1 MSS data
[E73-10508] 13 p1516 N73-22283
Development of multistage forest sampling inventory system from interpretation of ERST-1 MSS photography
[E73-10528] 13 p1517 N73-22294
Inventory of forests and rangelands, including forest stress, at Black Hills, Atlanta, Georgia, and Manitou, Colorado test sites using Skylab EREP
[E73-10587] 14 p1657 N73-23447
Inventory of ponds, lakes, and reservoirs in selected areas of State of Massachusetts
[PB-214116/6] 14 p1665 N73-23512
Taxonomic identification and natural resource inventory using ERTS-1 data
[E73-10666] 16 p1899 N73-25361
Management of natural resources in France and Spain by automatic cartographic inventories from ERTS-1 data
[E73-10725] 18 p2133 N73-27234
Inventorying land use in New York State using ERTS-1 multispectral imagery
[E73-10772] 18 p2134 N73-27248

**INVENTORY CONTROLS**
Bayes theorem for optimal decision and stop models of production processes
13 p1497 N73-22132

**INVENTORY MANAGEMENT**
NT INVENTORY CONTROLS
Effectiveness of DOD guidelines in determining time of aircraft engine replacements
[AD-745396] 01 p0091 N73-10749

**INVERSIONS**
NT CENTRIFUGING STRESS
NT POPULATION INVERSION
NT TEMPERATURE INVERSIONS
One-dimensional and multi-dimensional inversion techniques for processing remote atmospheric and ionospheric sounding data
[NASA-TM-X-62150] 02 p0196 N73-11585
Inversion layer silicon solar cells with induced junctions
[NASA-CR-131840] 16 p1865 N73-25100
General expression for derivative of inverse of differentiable matrix
[REPT-22] 20 p2439 N73-29586

**INVERTEBRATES**
NT ARTEMIA
NT INSECTS
NT LARVAE
NT PROTOZOA
NT SPORES
NT TRIBOLIA
NT WORMS

**INVERTED CONVERTERS [DC TO AC]**
Failure detector for dc to ac inverter circuit
[NASA-CASE-NPO-13160-1] 14 p1667 N73-23525
Design and performance of solid state inverter/converter modular system with pulse width modulation
[NASA-TM-X-2795] 15 p1737 N73-24083
Construction and tests of MHD generator channel and electrical power converter
[AD-758783] 16 p1866 N73-25106
Static characteristics of electrohydrodynamic inverted converters
[AD-760966] 18 p2183 N73-27630

**INVERTERS**
NT STATIC INVERTERS
Operational performance of breadboarded silicon controlled rectifier series inverter circuitry for ion thruster power supply
[NASA-TM-X-2699] 06 p0626 N73-15082
Analysis of power consumption and switching times of micropower complementary bipolar transistor inverters
18 p2125 N73-27172

**INVESTIGATION**
NT ACCIDENT INVESTIGATION
NT AIRCRAFT ACCIDENT INVESTIGATION

**INVESTMENT**
Commercial application of ERTS-1 imagery in structural reconnaissance for minerals and petroleum
[E73-10700] 16 p1903 N73-25392

**INVISCID FLOW**
NT STAGNATION FLOW
Numerical analysis of motion of inviscid fluid flow around pointed elliptic cone at incidence using fluid flow equations in conservation law form
[NASA-CR-129178] 02 p0154 N73-11251
Numerical analysis of viscous-inviscid interaction in supersonic flow around blunt body
[AD-746891] 02 p0160 N73-11293
Mathematical models for analyzing internal gravity waves generated by stratified inviscid fluid flow over solid body
[AD-746137] 02 p0168 N73-11369
Comparison of surface-source solution with an exact solution for two-dimensional inviscid flow about slotted-flap airfoil
[ARC-CP-1214] 03 p0248 N73-12003
Analysis of aerodynamic interference effects between aircraft and external store carried under wing based on inviscid flow characteristics
[AD-748348] 04 p0370 N73-13005
Mathematical model for inviscid stream flowing over turbulent fluid that behaves as elastic jelly
[AD-746990] 04 p0407 N73-13319
Prediction of pressure gradient on delta wing between uniform and nonuniform supersonic inviscid flow
[ARC-CP-1228] 05 p0492 N73-14010
Method for estimating aerodynamic characteristics of airfoils in compressible inviscid flow based on thickness and camber line parameters
[ESDU-72024] 07 p0735 N73-15981
Effects of thickness and viscosity considerations on accuracy of aerodynamic coefficients determined for thin wings in inviscid flow conditions
[ESDU-70011-AMEND-A] 07 p0735 N73-15982
Finite difference method for calculating three dimensional, unsteady and steady, inviscid gas flows around blunt bodies
[NASA-TT-F-714] 09 p0980 N73-18009
Calculation of outer inviscid flow about rectangular wing moving at supersonic speeds
[NASA-CR-130985] 09 p1013 N73-18269
Development of tables of gasdynamic functions in three dimensional, axisymmetric, and plane gas flows past blunt bodies of revolution
[NASA-TT-F-715] 11 p1231 N73-19996
Kelvin-Helmholtz instability analysis of bounded two phase particulate incompressible inviscid flows
[AD-754815] 11 p1272 N73-20318
Application of integral relations to analyzing inviscid supercritical flow about lifting airfoils with embedded shock wave
[AD-755762] 14 p1651 N73-23390
Nonlinear unsteady small-disturbance theory of inviscid transonic flows for oscillating aerodynamic configurations
[NASA-CR-2258] 16 p1858 N73-25048
Development of alternating direction relaxation method for computing inviscid two dimensional transonic flows through cascades
17 p2012 N73-26268
Stability analyses of idealized atmosphere and perfect gas blowing over inviscid liquid
17 p2012 N73-26269
Analysis of supersonic flow involving viscous and inviscid flow using unified solution technique
19 p2251 N73-28148
Numerical analysis of inviscid transonic flow over body with supersonic underexpanded exhaust plume and characteristics of flow near boattail sting
[RM-577] 21 p2523 N73-30234
Analysis of inviscid flow field around rectangular wing of finite thickness in supersonic flow
23 p2771 N73-32166

Characteristics of constant scaling method for analyzing linear inviscid internal waves in ocean, atmosphere, and experimental tanks
[AD-764579] 24 p2910 N73-33227
**INVISIBILITY**
U VISIBILITY
**IODATES**
Laser damage in lithium iodate and proustite
[AD-748935] 04 p0451 N73-13682
**IODIDES**
NT CESIUM IODIDES
NT POTASSIUM IODIDES
NT SILVER IODIDES
NT ZIRCONIUM IODIDES
Determination of vibrational temperature of molecular nitrogen in high atmosphere by chemical release of hydrogen iodide from sounding rocket
[AD-757909] 15 p1782 N73-24448
Atmospheric pollution due to use of lead iodide in weather modification
[NLL-M-23006-[5828.4F]] 20 p2441 N73-29607
**IODINE**
NT IODINE ISOTOPES
Spectrophotometric determination of aqueous iodine complexed with potassium iodide showing free iodine optimally determined at isosbestic point for solutions
[NASA-CR-128585] 01 p0022 N73-10172
Target design for cyclotron irradiation using iodine nucleus
[NASA-TM-X-68156] 02 p0214 N73-11733
Mass spectroscopy of C state in iodine by crossing of molecular beam with pulsed laser beam and monitoring recoil photofragments
[AD-751611] 07 p0753 N73-16117
Stress-corrosion cracking of zirconium alloy fuel element sheaths subjected to tension stress in iodine vapor environment
09 p1063 N73-18671
Time responses of radiation of iodine laser with Q-factor modulation
[AD-758625] 15 p1796 N73-24560
Gain measurements of excited iodine atom decay rates in photochemical iodine laser
[UCRL-TRANS-10692] 24 p2931 N73-33409
**IODINE COMPOUNDS**
NT CESIUM IODIDES
NT IODATES
NT IODIDES
NT POTASSIUM IODIDES
NT SILVER IODIDES
NT ZIRCONIUM IODIDES
Electroconductivity of system I-Me4NI and comparison with conductivity of iodine solutions of KI and RbI
[NASA-TT-F-13911] 01 p0022 N73-10174
Reaction kinetics of CF3 I flash photolysis iodine laser
[AD-760806] 18 p2158 N73-27436
**IODINE ISOTOPES**
Production of iodine isotope by high energy bombardment of cesium heat pipe causing spallation reaction
[NASA-CASE-LEW-11390-2] 11 p1326 N73-20763
Heat pipe production of high purity radioiodine for thyroid measurements
[NASA-CASE-LEW-11390-3] 19 p2248 N73-28128
**ION ACCELERATORS**
Development and characteristics of synchrotrons with steady-state field in energy range of 35 to 300 giga electron volts
[JPRS-57489] 03 p0280 N73-12271
Design of quadrupolar focusing lenses for drift tubes of heavy ion accelerator
[LYCEN-7179] 04 p0402 N73-13270
Design and operation of 5 MeV Van de Graaff ion accelerator at Central Research Institute for Physics in Budapest, Hungary
[KFKI-71-47] 05 p0524 N73-14260
Plastic detectors used to confirm acceleration of argon nuclei to relativistic velocities at Princeton Particle Accelerator
[AD-749863] 05 p0549 N73-14458
Design and construction of 200 kV ion accelerator
[AD-754274] 11 p1268 N73-20290
Ion acceleration by electron ring in decreasing magnetic field
[AD-753968] 11 p1268 N73-20291
Collective method for developing charged ion accelerator
[AD-754624] 11 p1268 N73-20293
Laser production of plasmas and injection of pulsed ion beams
[LYCEN-7253] 12 p1411 N73-21431
**ION ACOUSTIC WAVES**
Experiment, theory, and simulation of Cerenkov ion acoustic radiation generated by pseudowaves
[ORO-4211-2] 03 p0342 N73-12791
Computerized simulation of ion acoustic wave and pseudowave generation in plasma including grid effects
[ORO-4211-1] 03 p0342 N73-12792
Collisionless ion acoustic shocks with high Mach number in plasma
[IPPJ-119] 08 p0948 N73-17765
Ion acoustic wave response to double plasma excitation impulse
[IPPJ-144] 09 p1027 N73-18386
Influence of shock-producing piston on structure of electrostatic ion acoustic laminar shocks
[NASA-CR-130994] 09 p1069 N73-18724
Plasma device for studying ion acoustic solitons
[IPPJ-149] 15 p1816 N73-24723
Korteweg-deVries equation for studying effect of Landau damping on nonlinear ion acoustic waves
[IPPJ-155] 16 p1949 N73-25775
Parametric instabilities generated by electromagnetic pump in quiescent plasma device
[AD-759543] 16 p1951 N73-25786
Damping and ion heating mechanisms in hydromagnetic waves around ion cyclotron frequency
[CEA-CONF-2138] 17 p2067 N73-26724
Stabilization of ion acoustic waves by electron trapping
[AD-761174] 18 p2183 N73-27628
Ion acoustic wave excitation in ionized plasma by radio frequency heating
[AD-760794] 18 p2184 N73-27633
Microwave probe for observing parametrically excited ion acoustic wave oscillations in argon plasma
[AD-762380] 19 p2325 N73-28705
Linear ion acoustic waves in density gradient in collisionless discharge plasma
[ORO-4338-2] 22 p2702 N73-31640
Structure of collisionless ion acoustic shocks in plasma device
[NASA-CR-135490] 22 p2703 N73-31651
Parametric ion acoustic wave excitation in ionized plasma
23 p2822 N73-32559
**ION ATOM INTERACTIONS**
Reaction kinetics in pulsed atomic beam generation by laser vaporization of metallic atoms
[AD-748278] 04 p0387 N73-13145
Atomic and molecular reaction kinetics in upper atmosphere
[AD-753246] 09 p1000 N73-18158
Interactions of copper lattice atoms with holes, dislocations, and interstitial atoms
[JUL-857-FF] 10 p1194 N73-19714
**ION BEAMS**
Systems data for initial formation of incompressible hydrogen ion beams
[NLL-DRIC-TRANS-2351-[3623.66]]
02 p0215 N73-11740
Penning ionization gage ion sources for generating heavy ion beams
[LYCEN-7207] 04 p0453 N73-13695
Production and current measurement of intense hydrogen-ion beams in pulsed conditions
[NP-19351] 04 p0454 N73-13705
Numerically controlled ion beam sputtering process for manufacturing solid optical surfaces
[AD-750347] 05 p0581 N73-14730
Electron impact excitation and ionization cross sections of nitrogen atoms
[AD-749807] 05 p0582 N73-14742
Production and current measurement of hydrogen ion beam and plasma in duoplasmatron with cusped magnetic field
[NP-19364] 05 p0583 N73-14747
Argon ion gun for cleaning surfaces and specimens for use in electron spectrometer
[ECRC/N486] 10 p1125 N73-19165
Measurement of low airspeeds with ion beam produced in positive corona discharge based on beam deflection properties
10 p1158 N73-19423
Laser production of plasmas and injection of pulsed ion beams
[LYCEN-7253] 12 p1411 N73-21431
Electromagnetic dispersion relation for two counterstreaming ion beams flowing parallel to direct current magnetic field
[NASA-CR-132953] 15 p1814 N73-24701
Ion beam dose and sputtering characteristics of ion implanted semiconductor devices
[NASA-CR-132254] 15 p1820 N73-24754
Ion optical design with applications to solar wind mass spectrometer
[NASA-CR-133053] 16 p1913 N73-25481
Spectral line features of neon beam-foil spectroscopy
16 p1947 N73-25752
Observation of laminar electrostatic shock waves in collisionless plasma generated by ion beam
[IPPJ-156] 16 p1949 N73-25771
Ion and electron beam techniques for fabricating integrated optics circuits
[AD-760051] 17 p2008 N73-26237
Radiation resistance of thin insulating films deposited with ion beam system
[AD-760118] 17 p2075 N73-26788
Measurement of performance of ion exhaust beam current flow for multiply charged ion species using time of flight techniques
[NASA-CR-131841] 17 p2076 N73-26795
Development and characteristics of improved dispensing targets for ion beam particle generators
[NASA-CASE-NPO-13112-1] 20 p2382 N73-29138
Sputtering of multicomponent materials by ion bombardment
[AD-762813] 20 p2423 N73-29466
Ion-ion hybrid resonance heating of D-T plasmas
[IPPJ-165] 20 p2459 N73-29758
Measurement of beam divergence of 30-cm dished grids
[NASA-TM-X-68286] 20 p2466 N73-29808
Design and evaluation of ion beam probe plasma diagnostic system
[COO-2229-2] 21 p2583 N73-30700
Application of Boltzmann transport theory for determining penetration of matter by heavy-ion beam
[AD-765315] 23 p2822 N73-32556
**ION CHAMBERS**
U IONIZATION CHAMBERS
**ION CHARGE**
Ion energy distribution function measurements parallel and perpendicular to magnetic Penning discharge field
[NASA-TN-D-7167] 07 p0825 N73-16690
Coaxial anode for gas radiation counter for suppressing background ionization interference
[NASA-CASE-GSC-11492-1] 19 p2301 N73-28497
Quadrupole mass spectrometer using noise spectrum for ion separation and identification
[NASA-CASE-XNP-04231] 23 p2791 N73-32325
**ION CONCENTRATION**
Design and development of mass spectrometer using quadrupole fields to stabilize ions based on mass of ions
06 p0672 N73-15468
Cosmos measurements of ion concentration in earth atmosphere
07 p0792 N73-16439
Cosmos 434 measurement of oscillations in ion concentration levels in earth ionosphere at 200 to 1300 km altitudes
09 p1028 N73-18394
Estimation of ion source yields in inhomogeneous magnetic fields using magnetohydrodynamic theory
[LYCEN-7250] 12 p1435 N73-21624
OGO-6 ion concentration irregularity studies
[NASA-CR-132814] 23 p2786 N73-32286
Determination of nitric oxide concentrations from eclipse variations of ion concentrations
24 p2994 N73-33926
**ION CURRENTS**
Characteristics of ion transport in silicon dioxide, interface phenomena, and photoelectric method of storing charge in floating gate MOS memory
[AD-746999] 03 p0346 N73-12823
Ion migration in SiO2 layer of integrated circuit oxides
[AD-747435] 03 p0348 N73-12836
Ion-current collection by flush-mounted electrostatic probes on sharp flat plate in ionized hypersonic flow
[SC-CR-72-3145] 04 p0422 N73-13440
Selection and preliminary evaluation of 2 hollandites, 1 titanate, and 1 tungstate as potential solid conductors of alkali ions
[NASA-TN-D-7157] 06 p0708 N73-15774
Ion currents and trajectories for fluid flow diagnostics
[AD-751785] 07 p0824 N73-16681
Identification and preparation of materials for use as nonporous solid ionic conductors in rechargeable high energy battery at low temperatures
[NASA-CR-120964] 09 p0990 N73-18078
Electrical screening procedure for solid ionic conductors
[NASA-TN-D-7146] 09 p1073 N73-18758
Analysis of plasma sheath ion current data measured by electric probes on third flight of Trailblazer 2
[AD-758763] 15 p1836 N73-24883
Measurement of performance of ion exhaust beam current flow for multiply charged ion species using time of flight techniques
[NASA-CR-131841] 17 p2076 N73-26795
**ION CYCLOTRON RADIATION**
Ion acoustic and ion cyclotron turbulence effects in plasma resistivity, diffusion, and heating
[NASA-CR-130177] 03 p0340 N73-12776
Theoretical and experimental determination of harmonic ion cyclotron wave propagation in hot, bounded plasma
[ORO-3778-7] 03 p0342 N73-12786
High power radio frequency ion heating effects on harmonics of ion cyclotron radiation
[ORO-3871-7] 08 p0889 N73-17197
Performance of ion cyclotron plasma generator using radio frequency coil for plasma control
[NASA-TN-D-7187] 09 p1069 N73-18725
Theoretical analysis of ion cyclotron wave dynamics in cold plasma
[IPPJ-150] 15 p1816 N73-24722
Summaries of research in plasma sources, hydromagnetic shock waves rotating plasmas, ion cyclotrons, air pollution, and laser diagnostics
[NP-19643] 15 p1817 N73-24727
Experimental determination of ion resonance heating of plasma
[COO-2194-1] 15 p1817 N73-24733

Low loss coupling method for RF heating of plasma ions by electrostatic ion cyclotron waves
[IPP-4/30] 16 p1948 N73-25763
Dispersion of electrostatic ion plasma waves near harmonics of ion cyclotron frequency
17 p2066 N73-26716
Equivalent circuit with excitation coil for ion cyclotron waves
[IPPJ-160] 20 p2380 N73-29126
Collision frequency and velocity effects on ion cyclotron resonance line shape
[NASA-CR-135724] 23 p2821 N73-32552

**ION DENSITY [CONCENTRATION]**
NT IONOSPHERIC ION DENSITY
NT MAGNETOSPHERIC PROTON DENSITY
NT PROTON DENSITY [CONCENTRATION]
Calculation of velocity distribution of helium ion in solar wind at one astronomical unit
01 p0099 N73-10814
Mid-latitude depletions in electron and total ion density by direct and indirect techniques
[NASA-TM-X-66089] 02 p0165 N73-11341
Ion flux probe for low pressure discharge plasma in thin metal plate
[TRITA-EPP-72-20] 02 p0174 N73-11410
Ionized continuum flows and collisionless plasmas in electric boundary layers on flat plates and cylindrical bodies
[AD-746094] 02 p0217 N73-11753
Analysis of ion current density at central point of charged mass spectrometer during atmospheric and ionospheric sounding
[AD-750483] 06 p0671 N73-15456
Analysis of light ion mass spectrometer data from OGO-E experiment
[NASA-CR-130156] 07 p0791 N73-16432
High latitude proton precipitation and light ion density profiles during magnetic storm initial phase
[NASA-TM-X-66166] 07 p0792 N73-16438
Effect of grid transparency and finite collector size on RPA ion temperature and density observations
[NASA-TM-X-66153] 07 p0799 N73-16487
Rocket-borne mass spectrometric measurements of atmospheric ion composition
15 p1779 N73-24421
Ion density measurements in wake of hypersonic sphere
[AD-759158] 17 p2090 N73-26909
Measurement of positive ion composition in midlatitude sporadic E layer using rocket-borne ion mass spectrometer
[NASA-TM-X-66276] 18 p2142 N73-27313
Ion concentration distribution in equatorial domain measured on Intercosmos 2
20 p2410 N73-29370
Solar energy effect in galactic cosmic ray modulation
22 p2733 N73-31875

**ION DISTRIBUTION**
Multiple ion interaction energy and metal structure distribution
01 p0087 N73-10721
Numerical analysis of ion dissipation in high Mach number bow shocks
[IPP-6/102] 04 p0405 N73-13300
Ion energy distribution function measurements parallel and perpendicular to magnetic Penning discharge field
[NASA-TN-D-7167] 07 p0825 N73-16690
Ionic composition of plasmas produced in helium, hydrogen, xenon, and neon gas mixtures
[AD-751327] 07 p0830 N73-16727
Resistivity and ion energy distribution in turbulent plasma heating
[COO-3165-3] 17 p2067 N73-26727
Ion drift measurements from Cosmos 184 during 3 Nov. 1967 magnetic storm
20 p2410 N73-29371
Collisional effects on ion distribution function and potential in Tonks-Langmuir plasma sheath problem
20 p2457 N73-29745
Monochromatic isophote determination of particle distribution in bright comet
22 p2735 N73-31898
Striation of ion cloud in Oosik barium release experiment
[LA-UR-73-677] 24 p2923 N73-33349

**ION EMISSION**
Ion energy distribution function measurements parallel and perpendicular to magnetic Penning discharge field
[NASA-TN-D-7167] 07 p0825 N73-16690

**ION ENGINES**
NT CESIUM ENGINES
Durability test of Hughes SIT-5
[NASA-TM-X-68155] 02 p0223 N73-11802
Design of high frequency mercury ion engine for application to communication satellite stationkeeping
[DGLR-PAPER-72-88] 03 p0351 N73-12861
Operational performance of breadboarded silicon controlled rectifier series inverter circuitry for ion thruster power supply
[NASA-TM-X-2699] 06 p0626 N73-15082
Design, fabrication, and testing of thrust vectorable ion optical systems with emphasis on response time and minimal power consumption
[NASA-CR-121142] 08 p0955 N73-17816
Colloid thruster producing beams with anisotropic current, specific charge, and mass flow distributions
[AD-754902] 11 p1335 N73-20836
Autocathode as gas discharge ion source for ion engines, noting field emission mechanism
[DLR-FB-72-73] 12 p1444 N73-21696
Safety procedure for testing thermionic reactor in test facility
[NASA-TM-X-68224] 13 p1558 N73-22624
Process for fabricating matched pairs of dished screen and accelerator grids for ion thruster accelerator system
[NASA-CASE-LEW-11694-1] 13 p1570 N73-22721
Free molecular flow analysis for hypersonic air inlet configurations of ion engine
[AD-756680] 13 p1571 N73-22732
Space flight tests for determining performance efficiency of ion engine model with surface ionization of cesium on tungsten
14 p1701 N73-23801
Characteristics of ion rocket engine with combination keeper electrode and electron baffle
[NASA-CASE-NPO-11880] 15 p1824 N73-24783
Fluxgate magnetometer for measuring magnetic flux density of several electron-bombardment ion thrusters
[NASA-TM-X-68239] 15 p1826 N73-24796
Dynamometer thrust measurements of electrostatic mercury electron bombardment ion engine ESKA 18 P
[DLR-FB-73-48] 17 p2077 N73-26803
Single grid accelerator system for electron bombardment type ion thrustor
[NASA-CASE-XLE-10453-2] 18 p2192 N73-27699
Operating principles and application of ion engines for spacecraft propulsion
[JPRS-59061] 18 p2192 N73-27700
Development, characteristics, and performance of ion thruster engine for attitude control and station-keeping of synchronous satellite
[NASA-CR-121183] 19 p2329 N73-28736
Design characteristics, and operation of ion thruster test facility
[RAE-TR-73061] 20 p2382 N73-29143
Measurement of beam divergence of 30-cm dished grids
[NASA-TM-X-68286] 20 p2466 N73-29808
Durability test of five cm diameter ion thruster for 9700 hours
[NASA-TM-X-68284] 21 p2589 N73-30741
Performance of 30 cm ion thrusters with dished accelerator grids
[NASA-TM-X-68294] 21 p2589 N73-30744
Eight cm electron bombardment thruster for auxiliary propulsion
[NASA-TM-X-68296] 22 p2709 N73-31694
Performance tests of geometrically different sets of dished accelerator grids on ion thruster engines
[NASA-TM-X-71420] 23 p2830 N73-32615
Design and development of thermionic reactor power system for future interplanetary exploration - Vol. 4
[GULF-GA-C-12308-VOL-4] 24 p2954 N73-33602
Use of mercury ion engines for attitude control of communication satellites
[DGLR-PAPER-73-048] 24 p2986 N73-33863

**ION EXCHANGE MEMBRANE ELECTROLYTES**
Chemical stability, electrochemical properties and wetting characteristics of polyvinyl and polyethylene membrane separators for alkaline silver zinc batteries
[NASA-CR-130154] 07 p0741 N73-16030
Failure of fluorocarbon sulfonic acid membrane for hydrogen oxygen fuel cell
[NASA-CR-121007] 19 p2223 N73-27928

**ION EXCHANGE RESINS**
Potassium exchange on sulfocation resins containing divinylbenzene for drinking water regeneration
03 p0257 N73-12078

**ION EXCHANGING**
Trace element detection by automated distillation and ion exchange in neutron activation analysis for As, Cd, Cu, Hg, Se, and Zn
[IRI-133-72-10] 07 p0753 N73-16114
Stability constants and distribution of tin IV complexes by anion exchange resin with carboxylic acids
[AREAEE-128] 07 p0824 N73-16679
Optimal molecular composition of zirconium phosphate ion exchanger for separation of radioactive actinide series elements
08 p0883 N73-17151
Electroionic glass strengthening process conducted at below strain point temperatures
[AD-757333] 14 p1681 N73-23646
Ion exchange interactions in magnetically diluted nickel fluorides
[REPT-734] 14 p1694 N73-23749
Fuel system for thermal nuclear reactor which uses inorganic ion exchanger
[NASA-CASE-LEW-11645-2] 19 p2319 N73-28660

**ION GAGES**
U IONIZATION GAGES

**ION IMPACT**
Effects of ion implantation displacement damage in silicon diodide insulator of MIS capacitor
[AD-758695] 16 p1881 N73-25228
Development and characteristics of improved dispensing targets for ion beam particle generators
[NASA-CASE-NPO-13112-1] 20 p2382 N73-29138

**ION IMPLANTATION**
Research and development on microwave oscillators, diode structures, and ion implantation and diffusion
[AD-759542] 17 p1998 N73-26161
Determining the effects of ion implantation in aluminum oxide including implanted impurities and crystal damage by electrical resistivity and photoluminescence
17 p2071 N73-26755
Feasibility determination of using ultrahigh fluences of implanted oxygen ions to create usable oxide layer on silicon for semiconductor device applications
[AD-760350] 17 p2075 N73-26785
Perturbed angular correlation measurements on attenuations caused by rare earth nuclei implantation into metals
18 p2184 N73-27638
Ion implantation damage in silicon and semiconductor devices
[AD-761486] 19 p2245 N73-28104

**ION INJECTION**
Ion concentration profiles of injected boron and phosphorus including substitution of arsenic for phosphorus
05 p0522 N73-14249
Charge trap structure of pyrolytic alumina layer in metal oxide semiconductor capacitor
[AD-751629] 07 p0762 N73-16195
Axial injection of Grenoble cyclotron for multicharged heavy ion injection
[FRNC-CONF-59] 10 p1138 N73-19270
Artificial plasma injection of lithium cloud in program to stimulate electromagnetic cyclotron instabilities in magnetosphere
[AD-760032] 17 p2029 N73-26424

**ION IRRADIATION**
NT PROTON IRRADIATION
Increase in laser damage threshold of sapphire surfaces by polishing with energetic argon ion beams
05 p0555 N73-14505
Bulk radiation effects in terrestrial minerals, meteorites, and lunar rocks, and fission track studies in Apollo 12 samples
07 p0831 N73-16736
Formation of cavities in nickel and some austenitic steels irradiated by medium energy heavy ions
[CEA-CONF-2113] 17 p2045 N73-26542
Application of Boltzmann transport theory for determining penetration of matter by heavy-ion beam
[AD-765315] 23 p2822 N73-32556

**ION MICROSCOPES**
Microstructural studies of adhesion, wear, friction, and lubrication using LEED, Auger emission spectroscopy analysis, and field ion microscopy
[NASA-TM-X-68152] 01 p0058 N73-10471
Ion microscopic measurements on divacancy and monovacancy concentrations in high purity platinum
[NYO-3504-55] 04 p0434 N73-13541
Very bright field ionization and evaporation ion sources for use in ion probes of scanning instruments
[IPP-9/6] 10 p1194 N73-19717
Design, development, and characteristics of field ion microscope for image intensification
[ARL/INST-NOTE-78] 17 p2032 N73-26445

**ION MOTION**
Ion acoustic and ion cyclotron turbulence effects in plasma resistivity, diffusion, and heating
[NASA-CR-130177] 03 p0340 N73-12776
Ion migration in SiO2 layer of integrated circuit oxides
[AD-747435] 03 p0348 N73-12836
High resolution study of ion mobility spectra and effect on atmospheric ionization
[AD-747687] 04 p0416 N73-13396
Ion mobility expression and diffusion coefficient of plasma in crossed electric and magnetic fields
[NASA-TT-F-14523] 07 p0825 N73-16689
Grid excitation and digitized probe measurements for oscilloscopic display of phase space diagram distribution functions of plasma waves
[IPPJ-147] 09 p1070 N73-18732
Oblique plasma resonance measured from quadrupolar impedance probe noting motion effect of plasma parallel to geomagnetic field
[GRI/NTP/110] 13 p1563 N73-22669
Rotation of ion component of hot cathode Penning discharge plasma
[NASA-TT-F-14931] 16 p1948 N73-25765
Ionic migration and weathering in frozen Antarctic soils
[NASA-CR-2283] 18 p2143 N73-27326
Ion motions in liquid and solid helium
[COO-2027-6] 24 p2969 N73-33728

**ION OSCILLATION**
U PLASMA OSCILLATIONS

**ION PROBES**
Ion flux probe for low pressure discharge plasma in thin metal plate
[TRITA-EPP-72-20] 02 p0174 N73-11410
Ion pulse compensation circuits for recording ions produced by laser radiation in afterglow discharge plasma
[AEC-TR-7324] 08 p0949 N73-17767
Very bright field ionization and evaporation ion sources for use in ion probes of scanning instruments
[IPP-9/6] 10 p1194 N73-19717
Ion probes used to determine structure of ionized turbulent wakes of hypersonic spheres
[AD-759157] 17 p2090 N73-26908
**ION PRODUCTION RATES**
Ion pulse compensation circuits for recording ions produced by laser radiation in afterglow discharge plasma
[AEC-TR-7324] 08 p0949 N73-17767
**ION PROPULSION**
Tests of grid-translation type beam deflection system on 5-cm diameter mercury ion thruster
[NASA-TM-X-68185] 07 p0836 N73-16777
Design, fabrication, and testing of thrust vectorable ion optical systems with emphasis on response time and minimal power consumption
[NASA-CR-121142] 08 p0955 N73-17816
Process for fabricating matched pairs of dished screen and accelerator grids for ion thruster accelerator system
[NASA-CASE-LEW-11694-1] 13 p1570 N73-22721
Measurement of performance of ion exhaust beam current flow for multiply charged ion species using time of flight techniques
[NASA-CR-131841] 17 p2076 N73-26795
Operating principles and application of ion engines for spacecraft propulsion
[JPRS-59061] 18 p2192 N73-27700
Development, characteristics, and performance of ion thruster engine for attitude control and station-keeping of synchronous satellite
[NASA-CR-121183] 19 p2329 N73-28736
Design characteristics, and operation of ion thruster test facility
[RAE-TR-73061] 20 p2382 N73-29143
Control of 30 centimeter diameter mercury bombardment thruster
[NASA-TM-X-68297] 21 p2588 N73-30738
High voltage pulse for igniting electron bombardment mercury ion thruster
[NASA-TM-X-71425] 23 p2765 N73-32119
Performance tests of geometrically different sets of dished accelerator grids on ion thruster engines
[NASA-TM-X-71420] 23 p2830 N73-32615
High voltage solar array for ion thruster electric propulsion system
[NASA-TM-X-71462] 24 p2880 N73-33002
**ION RECOMBINATION**
Low temperature addition reactions of hydrogen and oxygen atoms with chemical compounds through creation of secondary valence
[NASA-TT-F-14643] 06 p0703 N73-15729
Development of high efficiency gallium arsenide solar cells using ion implantation techniques
[NASA-CR-131842] 16 p1865 N73-25099
Ion-ion hybrid resonance dispersion relation
[IPPJ-157] 16 p1949 N73-25774
Ion recombination loss in high intensity radiation dosimetry
[REPT-736] 17 p2064 N73-26698
Techniques for improving performance of gallium arsenide solar cells by ion implantation
[NASA-CR-135510] 22 p2618 N73-30977
**ION SOURCES**
NT DUOPLASMATRONS
Analysis of ion current density at central point of charged mass spectrometer during atmospheric and ionospheric sounding
[AD-750483] 06 p0671 N73-15456
Low frequency oscillations in Penning discharge under conditions of cyclotron ion source
[NASA-TT-F-14649] 06 p0703 N73-15736
Mass spectrometer and ion source for flight experiment measurements of thermosphere number density
08 p0899 N73-17283
Determination of atmospheric density numbers by sounding rocket carrying mass spectrometer with cryo ion source
[BMBW-FBW-72-34] 09 p1027 N73-18381
Ozone and nonreactive gas calibration of mass spectrometer with modified helium-cooled ion sources
[BMBW-FBW-72-32] 09 p1034 N73-18440
Very bright field ionization and evaporation ion sources for use in ion probes of scanning instruments
[IPP-9/6] 10 p1194 N73-19717
High intensity proton sources for high energy accelerators
[BNL-17159] 10 p1194 N73-19719
Rocket-borne mass spectrometer experiment with cryo-cooled ion source to determine neutral atmosphere composition between 85 and 125 km altitude
[BMFT-FBW-73-03] 11 p1285 N73-20431
Estimation of ion source yields in inhomogeneous magnetic fields using magnetohydrodynamic theory
[LYCEN-7250] 12 p1435 N73-21624
Autocathode as gas discharge ion source for ion engines, noting field emission mechanism
[DLR-FB-72-73] 12 p1444 N73-21696
Plasma ion sources research, including mass spectra, gas discharges, and ion beams
[AD-758040] 15 p1819 N73-24742
Measurement of performance of ion exhaust beam current flow for multiply charged ion species using time of flight techniques
[NASA-CR-131841] 17 p2076 N73-26795
**ION TEMPERATURE**
Ion energy distribution functions parallel and perpendicular to modified Penning discharge with high kinetic temperatures and Maxwellian velocity distribution of ions
[NASA-TM-X-68150] 01 p0079 N73-10656
Effect of grid transparency and finite collector size on RPA ion temperature and density observations
[NASA-TM-X-66153] 07 p0799 N73-16487
Multichannel digital spectrometer for measuring ion temperature of Circe 25-kW device
[EUR-CEA-FC-641] 08 p0925 N73-17582
Spectroscopic examination of electric field intensity and ion temperature of turbulent plasma
[AEC-TR-7375] 12 p1434 N73-21623
Reactive crossed molecular beam studies using free jet sources
18 p2180 N73-27605
Ion analyzer onboard Cosmos 348 for measuring ion temperature and horizontal gradients
20 p2411 N73-29376
**ION TRAPS [INSTRUMENTATION]**
Design and development of mass spectrometer using quadrupole fields to stabilize ions based on mass of ions
06 p0672 N73-15468
**ION-GAS INTERACTIONS**
U GAS-ION INTERACTIONS
**IONIC COLLISIONS**
Research on nuclear reactions of energetic heavy ions
[AD-746330] 02 p0214 N73-11736
Turbulent collisions for interpreting excitation processes in plasma
[AEC-TR-7382] 10 p1197 N73-19740
Design, construction, and performance of crossed beams tandem mass spectrometer for study of low energy ionic collisions
[AD-762450] 19 p2231 N73-27991
Collision frequency and velocity effects on ion cyclotron resonance line shape
[NASA-CR-135724] 23 p2821 N73-32552
**IONIC CONDUCTIVITY**
U ION CURRENTS
**IONIC CRYSTALS**
Study of trivalent Y3Al5O12 ionic crystals by radiation stimulated thermoluminescence
20 p2461 N73-29781
Interactions between rare earth ions in yttrium compound crystals
[AD-762363] 20 p2463 N73-29793
**IONIC DIFFUSION**
Solutions to diffusion along grain boundaries and dislocations for finite source
[NLL-CE-TRANS-6043-[9022.09]]
11 p1329 N73-20785
Industrial application of ion implantation for doped semiconducting structures
[NLL-TRANS-861-[9022.64]]
15 p1759 N73-24257
Ionic diffusion in electron boundary layer of spotless discharge crossing nitrogen magnetohydrodynamic flow
[IPF-72-3] 17 p2069 N73-26739
**IONIC MOBILITY**
Stability constants and distribution of tin IV complexes by anion exchange resin with carboxylic acids
[AREAEE-128] 07 p0824 N73-16679
Ion mobility, electrical conductance, and decomposition reactions of ammonium nitrate and ammonium perchlorate oxidizers
[AD-762744] 22 p2626 N73-31041
Theory of mobility of ions in superfluid helium
22 p2701 N73-31632
**IONIC PROPELLANTS**
U ION ENGINES
**IONIC REACTIONS**
Experimental determination of energy loss rate of fast ions in dense plasma and comparison of results with predictions of Spitzer formula
[UCRL-51175] 03 p0342 N73-12793
Electrochemical methods for determining acidity standard, atomic weight, stoichiometric composition, and trace contaminants
[NBS-TN-583] 09 p0999 N73-18153
**IONIC WAVES**
Pseudowaves produced by grids in plasma devices and excitation of ion-acoustic pulses
[ORO-4211-6] 03 p0341 N73-12782
Collisionless shock waves in argon plasma pinch discharge
[AD-762426] 19 p2325 N73-28707
Equivalent circuit with excitation coil for ion cyclotron waves
[IPPJ-160] 20 p2380 N73-29126
Shear stabilization of collisionless drift wave instability
[IPPJ-166] 20 p2459 N73-29759
**IONIZATION**
NT ATMOSPHERIC IONIZATION
NT AURORAL IONIZATION
NT AUTOIONIZATION
NT GAS IONIZATION
NT ION PRODUCTION RATES
NT NONEQUILIBRIUM IONIZATION
NT PHOTOIONIZATION
NT SURFACE IONIZATION
Reaction rate field, emphasizing ionization and upper atmosphere processes
[AD-745370] 01 p0051 N73-10414
Reaction rate field data, emphasizing ionization and upper atmosphere processes
[AD-745371] 01 p0051 N73-10415
Total air ionization and tissue dose rate in atmosphere
[HASL-254] 03 p0353 N73-12881
Gas ionization and plasma generation by explosive shock wave
[AD-751152] 07 p0829 N73-16725
Multiphoton ionization cross section function of atomic polarization
[NASA-TM-X-66179] 09 p1068 N73-18718
Recombination coefficients of electrons with hydrogen and carbon monoxide ions
[NASA-CR-131107] 10 p1192 N73-19699
Electron recombination with hydrogen ions
[NASA-CR-131108] 10 p1192 N73-19700
Analytical expressions for geographic distribution of midday ionization of F 2 layer in temperate latitudes
13 p1521 N73-22331
Generation of laboratory spectra at photon energies from highly ionized atoms
[AD-758606] 16 p1960 N73-25851
Computer code to calculate ionization distribution for polar ionosphere
[AD-760044] 17 p2029 N73-26423
Effect of multiple ionization on fluorescence yield of Ne
[RLO-1388-189] 17 p2065 N73-26710
Structures of ionized vanadium and manganese atoms with incomplete shells considering spin-orbital and spin-spin interactions
[NLL-RTS-7856] 18 p2180 N73-27604
Optical potential approach to electron-atom impact ionization threshold problem
[NASA-TM-X-66282] 18 p2181 N73-27609
One dimensional flow of partially ionized argon in hypersonic nozzle
[AD-760967] 18 p2184 N73-27632
Low energy X ray absorption and electron ionization cross section measurements on solids
[CONF-720404-VOL-2] 19 p2322 N73-28683
Pulse radiolysis of biphenyl solutions in cyclohexane noting life distribution of biphenyl ions
[IRI-133-72-07] 19 p2323 N73-28686
Electron gun for pre-ionization of high beta toroidal pinch system
[IPPJ-164] 20 p2458 N73-29757
Electron transport in high density fully ionized liquid metals
[NASA-CR-135648] 22 p2684 N73-31497
Parachute-borne blunt probe measurement of mesospheric ionization
[NASA-CR-135637] 23 p2784 N73-32277
Ionization mechanisms in cesium
24 p2932 N73-33419
**IONIZATION CHAMBERS**
NT BUBBLE CHAMBERS
NT CLOUD CHAMBERS
NT GEIGER COUNTERS
NT PROPORTIONAL COUNTERS
NT SPARK CHAMBERS
Current-to-frequency converter as ionization chamber current quantizer for radiological environmental monitoring
[ORNL-TM-3906] 07 p0800 N73-16499
Calculation of energy deposition distributions for simple geometries
[NASA-TN-D-7195] 08 p0957 N73-17832
Ionization chamber/Cerenkov counter measurements of heavy cosmic ray flux and composition
[NASA-CR-130921] 09 p1080 N73-18811
Ion recombination loss in high intensity radiation dosimetry
[REPT-736] 17 p2064 N73-26698
Measurement of mean isotopic composition of even-charge cosmic ray elements using balloon-borne ionization chamber
[NASA-CR-135516] 22 p2711 N73-31711
Molecular transition principle for constructing liquid- and solidhydrogen particle track chambers
[JINR-P13-7067] 24 p2960 N73-33658
**IONIZATION COUNTERS**
U IONIZATION CHAMBERS
U RADIATION COUNTERS
**IONIZATION CROSS SECTIONS**
Cross section measurements for electron impact at low energies in molecular gases
[AD-747304] 02 p0139 N73-11123

Ionization and excitation cross section measurements on degenerate helium levels
[NASA-TM-X-66137] 05 p0582 N73-14738
Crossed beam method for measuring photoionization cross section on atomic barium beam
06 p0707 N73-15770
Airborne measurement of ionization cross sections suitable for assessing HF propagation conditions in Arctic ionosphere
[AD-751235] 07 p0797 N73-16480
Ionization processes in mercury plasma due to excited state interactions and electron impact
[NASA-CR-130924] 10 p1192 N73-19701
Photoionization cross section of barium and strontium, determined with atomic beam crossed with ultraviolet radiation
[MPI-PAE/EXTRATERR-75] 15 p1781 N73-24440
Feasibility analysis of laboratory experiment on ionic excitation cross section by electron impact on laser produced plasmas
[ESRO-SN-122] 15 p1818 N73-24737
Mathematical model for calculating relative molecular orbital photoionization cross sections in soft X ray region
[UUIP-753] 17 p2066 N73-26714
Cross section data for collision processes between molecular oxygen and electrons
[NASA-TT-F-15011] 19 p2354 N73-28934

**IONIZATION GAGES**
NT PENNING GAGES
Ionization gage for measuring ultrahigh vacuum levels
[NASA-CASE-XLA-05087] 21 p2544 N73-30391

**IONIZATION POTENTIALS**
Perturbation theoretical and graphical representation of vertical ionization energies and electron affinities of free molecules
08 p0916 N73-17506
Lowering of ionization potentials of hydrogen and carbon atoms immersed in high temperature and high density thermal plasma
[AD-753247] 09 p1072 N73-18752
Using single crystals to determine ionization energies of organic semiconductors
[NASA-CR-133827] 21 p2517 N73-30188
Temperature relationship of work function of silicon carbide for application to direct conversion of thermal energy to electrical energy
23 p2807 N73-32443

**IONIZED GASES**
NT CESIUM PLASMA
NT CHARGED PARTICLES
NT COLD PLASMAS
NT COLLISIONLESS PLASMAS
NT COSMIC PLASMA
NT ELECTRON PLASMA
NT PLASMA CLOUDS
NT PLASMA JETS
NT PLASMA LAYERS
NT PLASMA SHEATHS
NT PLASMA SLABS
NT RELATIVISTIC PLASMAS
NT SOLAR WIND
NT THERMAL PLASMAS
NT TOROIDAL PLASMAS
Ion-current collection by flush-mounted electrostatic probes on sharp flat plate in ionized hypersonic flow
[SC-CR-72-3145] 04 p0422 N73-13440
Absorption, reflection, and scattering of electromagnetic waves by plasma media as electronic countermeasures in radar detection
[FOA-3-C-3652-66] 06 p0639 N73-15189
Laser generation of heavy ion plasma
[CEA-CONF-2022] 08 p0948 N73-17761
Uniform plasmas of N2, He, and CO for advanced MHD generator and electric laser design
[AD-755892] 12 p1436 N73-21638
Development of dynamic model of solar corona based on equations for ideal, inviscid, fully ionized hydrogen gas in gravitational field
13 p1572 N73-22740
Perturbed Lorentzian solutions for transport properties of partially ionized argon and helium plasmas
16 p1948 N73-25761
Analysis of nonequilibrium conditions among populations of excited levels of potassium vapor passing through supersonic nozzle
18 p2128 N73-27199
Transition model for computing population density profiles of partially ionized argon in source flow expansion
[C-37] 22 p2652 N73-31242
Guidance of high voltage electrical breakdown streamers by laser induced ionization in air
[AD-763827] 22 p2705 N73-31665
Plasma and magnetic field measurements in vicinity of Venus from Venera 4 and Mariner 5 flights
[NASA-TT-F-15128] 22 p2716 N73-31743

**IONIZED PLASMAS**
U PLASMAS [PHYSICS]

**IONIZERS**
Process for fabricating matched pairs of dished screen and accelerator grids for ion thruster accelerator system
[NASA-CASE-LEW-11694-1] 13 p1570 N73-22721

**IONIZING RADIATION**
NT ALPHA PARTICLES
NT BETA PARTICLES
NT COSMIC RAY SHOWERS
NT COSMIC RAYS
NT FAR ULTRAVIOLET RADIATION
NT GAMMA RAY BEAMS
NT GAMMA RAYS
NT LYMAN ALPHA RADIATION
NT LYMAN BETA RADIATION
NT NEAR ULTRAVIOLET RADIATION
NT PRIMARY COSMIC RAYS
NT SECONDARY COSMIC RAYS
NT SOLAR COSMIC RAYS
NT SOLAR X-RAYS
NT ULTRAVIOLET RADIATION
NT X RAYS
Ionizing radiation health standards and safety measures around nuclear installations
[EUR-4800-D-F-I-E-PT-1] 01 p0082 N73-10679
Radiation ecological aspects of environmental pollution and control for human safety
[EUR-4800-D-F-I-E-PT-2] 01 p0082 N73-10680
Penetrating ionizing space radiations with diversity in energy range of both particulate and electromagnetic components
06 p0628 N73-15100
Physiology of depressed metabolic states and gastrointestinal responses to ionizing radiation
[NASA-CR-130381] 07 p0742 N73-16038
Electron paramagnetic resonance and formed free radical investigation of ionizing radiation damage by sulfur-containing aliphatic compounds, pyridoxine, and proteins
[BMVG-FBWT-72-6] 07 p0753 N73-16115
Model for ionized part of interstellar medium based on low frequency observations by RAE satellite
08 p0975 N73-17970
Effects of ionizing radiation and space flight conditions on microorganisms, plants, animals, enzymes, and immunological preparations
09 p0993 N73-18103
Hand book on ionizing radiation protection policies at Kennedy Space Center
[NASA-TM-X-69410] 10 p1120 N73-19133
Influence of light flashes from heavy ionizing particles on astronaut nervous system
[LBL-1011] 10 p1120 N73-19134
Radioresistance recovery rate with combined exposure to ionizing radiation and dynamic factors [vibration and acceleration]
11 p1242 N73-20080
Radiation sterilization with Van de Graaff accelerators
[NASA-TT-F-14821] 11 p1247 N73-20120
Lithium fluoride thermoluminescent dosimeter for measuring ionizing radiation exposure during Apollo 16 flight
15 p1741 N73-24115
Effects of ionizing radiation and high pressure on polymerization processes of fluoroolefins and fluorocarbon compounds
[AD-750151] 16 p1870 N73-25143
Thermoradiation sterilization of naturally occurring microorganisms in soil from Kennedy Space Center
[NASA-CR-132197] 16 p1904 N73-25404
Study of ionizing wave in coaxial plasma guns to explain plasma-neutral gas interaction
[TRITA-EPP-72-31] 16 p1950 N73-25778
Research in electron and ion collisions and radiation dosimetry
[ORNL-4811] 17 p2064 N73-26700
Measuring ionizing radiation in near-earth space
[NASA-TT-F-754] 19 p2340 N73-28825
Environmental and medical problems caused by nonionizing radiation
[PB-220851/0] 21 p2509 N73-30134
Second breakdown in diodes and transistors from intense ionizing radiation
[AD-763951] 22 p2644 N73-31192
Characteristics and performance of radiographic machine for conducting inspections of parcels for contraband using ionizing radiation
24 p2952 N73-33585
Function of state governments in enforcing radiation safety and protection regulations for industrial, research, and medical uses of ionizing radiation
24 p2953 N73-33591

**IONOGRAMS**
Ionogram observations supporting chemical release studies in E region
[AD-762927] 20 p2415 N73-29409
Analysis of ionograms to determine HF auroral backscatter over bistatic path
24 p2911 N73-33231

**IONOSONDES**
Ionosonde using solid state analog components and digital arrays for continuously monitoring ionosphere
[AD-745965] 02 p0167 N73-11359
Digital data processing portion of Dartmouth ionosonde network used to analyze traveling ionospheric disturbances
07 p0775 N73-16290
Observation of propagation characteristics of electromagnetic pulse-type signals at altitudes between 100 and 280 km - 30 Oct. 1971
[LA-4947] 08 p0918 N73-17521
Fixed frequency ionosonde receiver with phase swept interferometer
[KGO-726] 18 p2118 N73-27122

**IONOSPHERE**
NT D REGION
NT E REGION
NT F REGION
NT F 1 REGION
NT F 2 REGION
NT LOWER IONOSPHERE
NT SPORADIC E LAYER
NT UPPER IONOSPHERE
ATS 5 and Intelsat 1 observations of L band and VHF signals during ionospheric scintillation
[NASA-TM-X-66060] 01 p0028 N73-10216
Programs and techniques for statistical analysis and reduction of ionospheric physics data
[AD-745966] 02 p0167 N73-11360
Scientific equipment of ionospheric ESRO-4 satellite including five experiments
[ESRO-SN-114-ESTEC] 02 p0234 N73-11906
Structure and variation of topside ionosphere at mid-latitudes during sunrise period based on Alouette 1 electron density measurements
[AD-748430] 03 p0299 N73-12443
Diurnal variations in ionospheric F region tilts near magnetic equator
[WRE-TN-A-199[AP]] 04 p0414 N73-13384
Energization of electrons in ionosphere and magnetoplasma by wave particle interaction
[AD-747093] 04 p0415 N73-13391
Papers on Arctic ionospheric modeling
[AD-748796] 04 p0416 N73-13398
Design of ionospheric plasma simulator for analyzing and modeling high altitude plasma phenomena
[AD-748311] 04 p0417 N73-13401
Diurnal variations in ionospheric tilt near magnetic dip equator due to gravity waves
05 p0512 N73-14160
Geophysics and space data bulletin
[AD-749815] 05 p0597 N73-14852
Computer program for tracing paths of high frequency electromagnetic rays through two-dimensional models of ionosphere
[AWRE-O-34/72] 06 p0644 N73-15228
Cosmos measurements of ion concentration in earth atmosphere
07 p0792 N73-16439
Airborne measurement of ionization cross sections suitable for assessing HF propagation conditions in Arctic ionosphere
[AD-751235] 07 p0797 N73-16480
Ionospheric irregularities by low-frequency electrostatic gradient-driven instabilities and their nonlinear evolution in equatorial electrojet plasma
08 p0900 N73-17284
Derivation of empirical global thermosphere model for magnetically quiet conditions from longitudinally averaged gas densities using expansion in spherical harmonics
[NASA-TM-X-66183] 08 p0917 N73-17512
Generation of artificial geomagnetic micropulsations with large ground-based current load from MHD wave propagation in ionosphere
[AD-752061] 08 p0919 N73-17533
Rocket-borne instrument for ionospheric electric field measurements
[AD-751926] 08 p0920 N73-17537
Stokes parameters for calculating polarization of radio waves reflected from inhomogeneous ionosphere
[NASA-TT-F-14676] 09 p1002 N73-18174
Cosmos 434 measurement of oscillations in ion concentration levels in earth ionosphere at 200 to 1300 km altitudes
09 p1028 N73-18394
Steady illumination photolysis of ionospheric ozone in near ultraviolet
[NASA-CR-130830] 09 p1029 N73-18399
Evaluation of worldwide empirical ionospheric model to assist in design of satellite navigational system - Vol. 1
[AD-753081] 09 p1031 N73-18419
Evaluation of worldwide empirical ionospheric model to assist in design of satellite navigational system - Vol. 2
[AD-753082] 09 p1031 N73-18420
Evaluation of worldwide empirical ionospheric model to assist in design of satellite navigational system - Vol. 3
[AD-753083] 09 p1032 N73-18421
Energy spectra of ionospheric photoelectrons measured in 30 to 150 eV range from Cosmos 348 satellite in summer 1970
[PR-107] 10 p1155 N73-19400

Solar proton penetration into geomagnetic tail and ionospheric polar cap
10 p1210 N73-19843
Mid-latitude ionospheric and neutral atmospheric models
[NASA-CR-131547] 12 p1399 N73-21342
Comparison of charged particle conductivities measured in very low ionosphere with atmospheric parameters and high frequency radio wave absorption measurements
[NASA-CR-131604] 13 p1519 N73-22313
Total electron content of ionosphere with emphasis on North Atlantic region
[AGARD-AG-166] 13 p1524 N73-22350
Photoelectron transport energy for calculating electron and ion temperatures of ionospheric models
[AD-756241] 13 p1525 N73-22362
Solar photoionization rate constants for nitrogen, oxygen, nitrogen oxides and ultraviolet intensities
[AD-756480] 13 p1574 N73-22759
Analysis and modeling of ionospheric data collected worldwide
[AD-757480] 14 p1662 N73-23491
Geophysical and space data bulletin
[AD-755839] 14 p1706 N73-23849
Laboratory simulation of behavior of artificial plasma clouds in ionosphere
[AD-758064] 15 p1782 N73-24442
Model of stationary, adiabatic plasma flow in magnetosphere interacting with ionosphere
[TRITA-EPP-72-22-PT-1] 17 p2027 N73-26404
Computer code to calculate ionization distribution for polar ionosphere
[AD-760044] 17 p2029 N73-26423
Launching Radio Exploration Satellite using Mu-4S-4 rocket for studying ionosphere and magnetosphere
17 p2088 N73-26888
Plasma and neutral atmospheric motion in earths polar ionosphere
18 p2132 N73-27229
Plasma modification associated with electromagnetic waves and parametric instabilities within ionosphere - Parts 1 and 2
[AD-760809] 18 p2147 N73-27351
Analog model for arctic ionosphere
[AD-762280] 19 p2299 N73-28484
Errors in determining ionosphere parameters and characteristics of ionospheric inhomogeities by signals from satellite mounted radio station, Maiak
20 p2410 N73-29373
Total electron content studies of radio waves of ionosphere
[AD-762481] 20 p2414 N73-29403
Digital decoder for processing Barker coded pulses in incoherent scatter observations of ionosphere
23 p2778 N73-32212
Electron collision processes in ionosphere
[UILU-ENG-73-2504] 23 p2784 N73-32276
Debris particle distribution in ionosphere escaping fireball through charge exchange collisions
[AD-764955] 23 p2819 N73-32535
Hydromagnetic gradient waves in ionosphere
24 p2921 N73-33331

**IONOSPHERIC ABSORPTION**
U ELECTROMAGNETIC ABSORPTION
U IONOSPHERIC PROPAGATION

**IONOSPHERIC BLACKOUT**
U BLACKOUT [PROPAGATION]

**IONOSPHERIC COMPOSITION**
Development of mathematical processes for deriving ionospheric electron density as function of altitude and frequency measurements obtained by vertical incidence ionospheric sounders
02 p0198 N73-11602
Development of procedure for converting topside ionograms into topside electron density profiles using modified lamination method
02 p0198 N73-11603
Development of methods for solving group height equation based on data contained in single ionogram trace
02 p0198 N73-11604
Analysis of requirements for numerical inversion method to calculate ionospheric electron density from ionograms
02 p0199 N73-11605
Automatic data selection and profile inversion to obtain ionospheric electron density profiles from digitized radio soundings
02 p0199 N73-11606
Application of oblique-to-vertical transformation and direct inversion of oblique incidence ionogram techniques for deriving true height profiles
02 p0199 N73-11607
Determining ion composition of ionosphere by incoherent scattering of radio waves, and ionospheric sounding in USSR
[JPRS-57474] 04 p0413 N73-13372
Numerical analysis of ionospheric and plasma sheet particle densities, fluxes, and bulk velocities along auroral magnetic field for ion-exosphere model
[A-N-109-1972] 06 p0664 N73-15400
Analysis of ionospheric storm research with emphasis on ionospheric parameters available for study and observational techniques employed
[PSU-IRL-SCI-404] 06 p0666 N73-15413
Analysis of ionospheric investigations conducted with Intercosmos satellite number two
14 p1659 N73-23464
Analysis of ionospheric response to solar eclipse of 7 March 1970 by Thomson scatter radar technique at Millstone Hill Ionospheric Observatory
24 p2912 N73-33239

**IONOSPHERIC CONDUCTIVITY**
Ionospheric transfer impedance of rocket-borne quadrupole probe near lower hybrid resonance
[NRC-TT-1614] 06 p0666 N73-15414
Effect of ionospheric conductivity on barium ion cloud dynamics
[NASA-CR-131533] 12 p1433 N73-21610
Measurement of auroral electrojet magnetic activity indices for calendar year 1970
[UAG-22] 18 p2133 N73-27231

**IONOSPHERIC CURRENTS**
NT AURORAL ELECTROJETS
NT ELECTROJETS
NT EQUATORIAL ELECTROJET
Interplanetary magnetic fields and magnetic disturbances induced by ionospheric
[DMI-GEOPHYS-PAPERS-R-32]
02 p0216 N73-11749
Numerical analysis of ionospheric and plasma sheet particle densities, fluxes, and bulk velocities along auroral magnetic field for ion-exosphere model
[A-N-109-1972] 06 p0664 N73-15400
Evaluation of field aligned ionospheric currents produced by azimuthal and radial magnetospheric disturbances
[PR-122] 10 p1156 N73-19402
Ionospheric electric field and current distributions, assuming certain time variable convection field profiles at 1250 km
[TRITA-EPP-73-03] 16 p1907 N73-25429

**IONOSPHERIC DISTURBANCES**
NT IONOSPHERIC STORMS
NT SUDDEN IONOSPHERIC DISTURBANCES
NT TRAVELING IONOSPHERIC DISTURBANCES
Atmospheric and man made disturbances, resulting in noise pulses of random amplitude affecting delay lines in HF communication
[AD-745184] 01 p0029 N73-10223
Solar flares, magnetic storms, ionospheric disturbances, and geophysical observations recorded by weather stations in India during Feb. 1972
[RRC-A-201-PT-2] 01 p0048 N73-10386
Analysis of chromospheric patterns produced by changes in interplanetary and geomagnetic fields
[AD-745100] 01 p0106 N73-10877
Numerical analysis of effects of lower ionosphere on propagation of radio waves at low frequencies for conditions of quiet day, night, and disturbed night
[FOA-3-C-3673-60] 02 p0140 N73-11131
Frequency swinging method applied to ionospheric studies for group path difference
02 p0166 N73-11349
Analysis of all-sky photographs and ionograms taken during flights and ground magnetic records from auroral zone stations
[AD-746283] 02 p0205 N73-11663
Ionospheric disturbances and acoustic gravity wave generation by nuclear explosions
[AD-746328] 02 p0214 N73-11737
Numerical code for studying double resonance production of ionospheric irregularities
[AD-747495] 03 p0299 N73-12440
Nuclear source model for generating ionospheric disturbances through acoustic gravity waves
05 p0509 N73-14141
Full wave solution for electron density perturbations caused by gravity waves in F2 region
05 p0509 N73-14145
Ionospheric oscillations caused by infrasonic waves propagating from thunderstorms
05 p0510 N73-14148
Ionospheric gravity wave electron amplitudes and spectra
05 p0510 N73-14149
Hydrodynamic calculations and experimental observations of ionospheric shock front propagation following nuclear explosion
05 p0510 N73-14150
High frequency radar backscattering technique for determining ionospheric structure and gravity wave disturbances
05 p0511 N73-14155
Continuous wave Doppler radar observations of ionospheric disturbances generated by Saturn-Apollo launchings
05 p0511 N73-14157
Ionospheric disturbance effects on sky wave bearing measurement
05 p0511 N73-14159
Infrasonic detection of propagating atmospheric shock waves caused by supersonic aircraft
05 p0512 N73-14161
Theoretical plasma perturbation model for calculating coupling effects between acoustic gravity waves and electromagnetic waves in ionospheric disturbances
05 p0512 N73-14162
Nonlinear propagation and ionospheric coupling of atmospheric waves following nuclear explosion
05 p0513 N73-14168
F layer electron density fluctuations and disturbances following nuclear explosion at ionospheric height
05 p0513 N73-14169
Auroral substorm model for predicting high frequency radio absorption
[AD-749859] 05 p0542 N73-14408
Magnetic storm effects on topside ionospheric electron density profiles in low and equatorial latitudes
[PSU-IRL-SCI-399] 06 p0666 N73-15412
Solar eclipse prediction, ionospheric reflection, ionospheric data reduction, and microwave acoustics
[AD-749882] 06 p0668 N73-15432
D region ionization during polar cap absorption determined from parachuteborne blunt probe measurements of charged particle conductivity
[AD-750570] 06 p0670 N73-15448
Ionograms and cosmic radio noise absorption studies of anomalous behavior of F region during solar eclipse of 22 Sept. 1968
[RSD-73] 07 p0789 N73-16414
Electrical and meteorological experimentation in upper atmosphere of polar regions - bibliography
[AD-751336] 07 p0796 N73-16472
Bibliography and abstracts on upper atmospheric phenomena in inner region of polar caps
[AD-751335] 07 p0796 N73-16473
Tables on ionospheric data measured by vertical echo sounding
[REPT-316-F] 08 p0916 N73-17507
Ground based HF sounding technique for detecting ionospheric disturbances associated with Pc 1 micropulsations
[AD-752062] 08 p0919 N73-17532
Forecasting magnitude of solar proton and polar cap absorption events using semi-integrated flux density
[AD-751925] 08 p0957 N73-17835
Intense, high frequency radiation causing F region plasma phenomena
[AD-753162] 09 p1032 N73-18426
Dependence of onset time of F-region electron density disturbance upon local time of geomagnetic storm commencement and main phase onset
[AD-753665] 09 p1033 N73-18433
Radio telescope and satellite studies of atmosphere, ionosphere, and magnetosphere under disturbed conditions produced by enhanced solar activity
[AD-754252] 10 p1157 N73-19410
Atmospheric sounding and ionospheric disturbance measurements by rocket-borne instruments
[AD-754244] 10 p1157 N73-19412
Digital photometer for recording measurements of ionospheric disturbances
[AD-754436] 10 p1157 N73-19415
Literature survey on polar cap ionospheric disturbance characteristics
[AD-754250] 10 p1157 N73-19416
Articles on ionospheric disturbances, and techniques for predicting condition of ionosphere for planning radio communication
[NASA-TT-F-746] 13 p1519 N73-22314
Principles governing ionospheric disturbances
13 p1519 N73-22315
Correlation between ionospheric disturbance and solar wind velocity, density, and positive ion flux of interplanetary medium
13 p1519 N73-22316
Ionospheric disturbance and geophysical effects caused by proton burst on X/28/1963 at 0135 UT
13 p1519 N73-22317
Predicting geometric parameters of N[h] profiles and h prime f characteristics of F region during disturbances
13 p1520 N73-22323
Predicting arrival angle and skip distance variations of quiet and disturbed ionosphere on basis of N[h] profiles and h prime f characteristics
13 p1520 N73-22324
Influence of F 2 regional disturbances and magnetic activity on short wave radio communications
13 p1521 N73-22327
Disappearance of E region following changes in geomagnetic H component
[AER-73-04] 14 p1658 N73-23455
ATS-3 satellite measurement of ionospheric effects during partial solar eclipses of July 10, 1972
[AD-758855] 15 p1784 N73-24461
Ionospheric disturbances produced by severe thunderstorms
[NOAA-PP-6] 16 p1905 N73-25406
Lower ionospheric disturbances in polar region
[NDRE-62] 16 p1905 N73-25407
Temporal variations in atmospheric electric fields noting propagation and disturbances
[TRITA-EPP-73-02] 17 p2027 N73-26405

Radio wave propagation prediction using D region model accounting for quiet and disturbed VLF propagation
[AD-760685] 18 p2118 N73-27130
High latitude ionospheric patterns during magnetospheric substorms
18 p2133 N73-27232
Photometric measurements of airglow and auroral intensity and ionsopheric disturbances by Goose Ionospheric Observatory
[AD-762081] 19 p2297 N73-28471
Auroral clutter mapping with Homer backscattering radar to study reaction of upper atmosphere to nuclear explosions
[AD-762012] 19 p2297 N73-28474
Ionospheric disturbances and fading of radio waves in polar regions
[AD-762282] 19 p2299 N73-28483
Nonequilbrium ionospheric disturbances in lower ionosphere
20 p2390 N73-29196
Theoretical calculation of heavy particle induced ionization rates during PCA events
[AD-763089] 20 p2415 N73-29407
Proceedings of conference on solar proton event of Nov. 1969
[AD-763081] 20 p2468 N73-29830
Frequency modulation method for simultaneous recording of signals reflected from ionosphere
24 p2895 N73-33111
Analysis of data on ionospheric parameters gathered by multi-probe rockets
[AD-764781] 24 p2924 N73-33356
Effects of polar cap absorption events on phase deviations in Omega navigation system
[AD-764521] 24 p2951 N73-33572

**IONOSPHERIC DRIFT**

Cosmos-187 measurement of ion drift velocity in upper ionosphere during magnetic storms
17 p2024 N73-26381

**IONOSPHERIC ELECTRON DENSITY**

Development of mathematical processes for deriving ionospheric electron density as function of altitude and frequency measurements obtained by vertical incidence ionospheric sounders
02 p0198 N73-11602
Development of procedure for converting topside ionograms into topside electron density profiles using modified lamination method
02 p0198 N73-11603
Analysis of requirements for numerical inversion method to calculate ionospheric electron density from ionograms
02 p0199 N73-11605
Automatic data selection and profile inversion to obtain ionospheric electron density profiles from digitized radio soundings
02 p0199 N73-11606
Application of oblique-to-vertical transformation and direct inversion of oblique incidence ionogram techniques for deriving true height profiles
02 p0199 N73-11607
Inversion of VLF-LF sounder data to obtain D region electron density distributions
02 p0201 N73-11626
Ionospheric electron content and satellite signal scintillation
[AD-747507] 03 p0298 N73-12430
Daytime ionospheric attenuation of very low frequency signal transmission over Greenland ice
[AD-746636] 04 p0389 N73-13161
Ionospheric gravity wave electron amplitudes and spectra
05 p0510 N73-14149
F layer electron density fluctuations and disturbances following nuclear explosion at ionospheric height
05 p0513 N73-14169
Effects of acoustic gravity waves following nuclear explosion on ionospheric electron density and high frequency communications
05 p0513 N73-14170
Latitude-time variations of ionospheric electron densities at high latitudes during periods of solar activity
07 p0791 N73-16431
Isotropic models for determining effect of velocity distribution on electron temperature in ionospheric plasma
[NASA-TM-X-66157] 07 p0791 N73-16433
Plasma wave generation in ionosphere by rocket-borne electron beam accelerator
08 p0947 N73-17753
Ionospheric electron content measurements by Faraday effect and dispersive Doppler effect
[BMBW-FBW-72-31] 09 p1027 N73-18380
Dependence of onset time of F-region electron density disturbance upon local time of geomagnetic storm commencement and main phase onset
[AD-753665] 09 p1033 N73-18433
Atmospheric model for predicting seasonal and diurnal behavior of D region electron density
[AD-755447] 12 p1403 N73-21383
Computer techniques for fitting electron density profiles to oblique path VLF propagation data
[AD-757341] 13 p1492 N73-22098
Long-term prognosis of midday N[h] profiles of F region
13 p1521 N73-22325
Phenomenological model of global ionospheric electron density in E, F 1, and F 2 region
[AD-757507] 14 p1663 N73-23498
Cosmos 381 measurement of ionospheric electron concentration using impedance probe
15 p1779 N73-24422
Ionospheric total electron content during magnetic storm, 14-17 Dec. 1971
[KGO-728] 18 p2146 N73-27344
Ionospheric electron content from satellite beacon measurements
[NASA-CR-133475] 19 p2294 N73-28446
Analysis of ionospheric response to fluctuations of solar radiation based on sensitivity and delay of electron content
[NASA-CR-133474] 19 p2294 N73-28447
Low energy electron measurement onboard meteorological rockets in polar region
20 p2411 N73-29375
Distribution of vibrationally excited molecular nitrogen in auroral red arc and effect on ionospheric electron densities
24 p2912 N73-33241

**IONOSPHERIC F-SCATTER PROPAGATION**

Solar radio interferometry for traveling ionospheric disturbance detection
05 p0511 N73-14158
Power spectrum of satellite radio signal phase modulation caused by F region diffraction
[NASA-CR-131280] 11 p1254 N73-20178
Space time laws governing F-scattering at various latitudes
13 p1521 N73-22328

**IONOSPHERIC HEATING**

Experimental data obtained with high frequency radio heating of ionosphere
[AD-748222] 04 p0416 N73-13394
Electron heating in F region by high power radio frequency beam detected by intensity changes in atomic oxygen nightglow
07 p0775 N73-16293
Ionospheric modification experiments showing enhanced plasma line temperature of approximately 4000 K due to ion-acoustic parametric instability excitation
[AD-752060] 08 p0921 N73-17547
High frequency plasma line fluctuation for ionospheric heating analysis
[AD-758779] 16 p1907 N73-25433

**IONOSPHERIC ION DENSITY**

Development of methods for solving group height equation based on data contained in single ionogram trace
02 p0198 N73-11604
Determining ion composition using high-potential radar sets with storage elements for detecting noncoherent scattered radio signals
04 p0413 N73-13373
Analysis of ionospheric storm research with emphasis on ionospheric parameters available for study and observational techniques employed
[PSU-IRL-SCI-404] 06 p0666 N73-15413
Computerized simulation of ion collection by ionospheric probe
[AD-757481] 14 p1662 N73-23492
Measurement of positive ion composition in midlatitude sporadic E layer using rocket-borne ion mass spectrometer
[NASA-TM-X-66276] 18 p2142 N73-27313
Analysis of ionospheric response to fluctuations of solar radiation based on sensitivity and delay of electron content
[NASA-CR-133474] 19 p2294 N73-28447

**IONOSPHERIC NOISE**

NT WHISTLERS

**IONOSPHERIC PROPAGATION**

NT IONOSPHERIC F-SCATTER PROPAGATION
Dourbes [Belgium] Geophysical Observatory data on geomagnetism, ionospheric propagation, seismology, cosmic rays, and atmospheric electricity, Nov. 1971
01 p0050 N73-10401
Polarization of wave propagating in ionosphere noting signal fading recorded at Garchy
[GRI/NT/84] 01 p0050 N73-10403
Dourbes [Belgium] Geophysical Observatory data on geomagnetism, ionsopheric propagation, seismology, cosmic rays, and atmospheric electricity, Dec. 1971
01 p0050 N73-10405
Numerical analysis of effects of lower ionosphere on propagation of radio waves at low frequencies for conditions of quiet day, night, and disturbed night
[FOA-3-C-3673-60] 02 p0140 N73-11131
Analysis of instabilities resulting from interaction of electromagnetic waves with active medium or system
[AD-746893] 02 p0143 N73-11159
Electromagnetic wave transmission in space-time varying dielectrics and plasmas
[AD-746676] 02 p0144 N73-11165
Ionospheric refractivity influence on electromagnetic wave propagation errors discussing electron density profiles
[DLR-MITT-71-31] 03 p0266 N73-12154
Analysis of backscatter from radar transmission and effect of field aligned laminae in both E and F layers of ionosphere
[AD-747027] 03 p0297 N73-12426
Numerical code for studying double resonance production of ionospheric irregularities
[AD-747495] 03 p0299 N73-12440
Daily summaries for vertical echo sounding of upper atmosphere over Freiburg, Germany - Aug. 1972
[REPT-314-F] 04 p0414 N73-13380
Daily summaries for vertical echo sounding of upper atmosphere over Freiburg, Germany - Sept. 1972
[REPT-315-F] 04 p0414 N73-13381
Observations of weak infrasound emission during magnetic storms caused by ionospheric auroral electrojets
05 p0508 N73-14138
Electromagnetic cross modulation and very low frequency propagation techniques for measuring acoustic gravity waves in ionospheric D region
05 p0511 N73-14153
Atmospheric gravity wave effects on ionospheric transequatorial radio wave propagation in presence of traveling ionospheric disturbances
05 p0512 N73-14164
Daily summaries for vertical echo sounding of upper atmosphere over Freiburg, Germany - July 1972
[REPT-313-F] 05 p0538 N73-14380
Algorithms for predicting ionospheric effects on pseudo-ranging from synchronous satellite navigation system
[AD-749486] 05 p0539 N73-14391
Auroral effects on HF radiowave propagation traversing polar regions
[AD-749515] 05 p0540 N73-14392
Ionospheric propagation data for E and F regions, India - Jan. 1971
[RTRC-A188] 06 p0664 N73-15397
Ionospheric propagation data for E and F regions, India - Feb. 1971
[RTRC-A189] 06 p0664 N73-15398
Ionospheric propagation data for E and F regions, India - March 1971
[RTRC-A190] 06 p0664 N73-15399
Procedures and equipment for analyzing field strengths transmitted at extremely low frequencies and measurement of radial magnetic component
[REPT-72-4-ADD] 06 p0664 N73-15401
Solar eclipse prediction, ionospheric reflection, ionospheric data reduction, and microwave acoustics
[AD-749882] 06 p0668 N73-15432
Beacon transmissions from Intelsat 2F-1 and 2F-2
[AD-750469] 06 p0668 N73-15433
Ionospheric modification of electromagnetic pulse from nuclear explosions
[SC-RR-72-0400] 06 p0699 N73-15697
Ionospheric range error given by expansion expression in terms of elevation angle and moment of refractivity distribution
[NASA-TM-X-66159] 07 p0790 N73-16426
Solar X-ray spectra for predicting ionospheric radio wave propagation during solar activity
[AD-751575] 07 p0794 N73-16459
Mathematical models of midlatitude bottomside electron density profiles
[AD-751267] 07 p0796 N73-16477
Observation of propagation characteristics of electromagnetic pulse-type signals at altitudes between 100 and 280 km - 30 Oct. 1971
[LA-4947] 08 p0918 N73-17521
Dourbes, Belgium, geophysical observatory data on geomagnetism, ionospheric propagation, seismology, cosmic rays, and atmospheric electricity, Feb. 1972
09 p1030 N73-18403
Dourbes, Belgium, geophysical observatory data on geomagnetism, ionospheric propagation, seismology, cosmic rays, and atmospheric electricity, Mar. 1972
09 p1030 N73-18404
Dourbes, Belgium, geophysical observatory data on geomagnetism, ionospheric propagation, seismology, cosmic rays, and atmospheric electricity, Apr. 1972
09 p1030 N73-18405
Dourbes, Belgium, geophysical observatory data on geomagnetism, ionospheric propagation, seismology, cosmic rays, and atmospheric electricity, May 1972
09 p1030 N73-18406
Dourbes, Belgium, geophysical observatory data on geomagnetism, ionospheric propagation, seismology, cosmic rays, and atmospheric electricity, Jun. 1972
09 p1030 N73-18407
Dourbes, Belgium, geophysical observatory data on geomagnetism, ionospheric propagation, seismology, cosmic rays, and atmospheric electricity, Jul. 1972
09 p1030 N73-18408
Faraday rotation angle phi of radio signal from ATS-C
[AD-753088] 09 p1031 N73-18414

Propagation of magnetohydrodynamic waves in cold plasma inclined to ionosphere and applied to geomagnetic pulsation study
[PR-119] 10 p1156 N73-19401
Antenna design and transionospheric propagation relative to space communication - conference
[AD-754061] 11 p1256 N73-20193
Calculation of very low frequency radio wave propagation characteristics of earth-ionosphere waveguide
[AD-754033] 11 p1256 N73-20194
Spherical Hankel functions for approximating radio transmission in earth ionosphere
[AD-755391] 12 p1380 N73-21192
Computer techniques for fitting electron density profiles to oblique path VLF propagation data
[AD-757341] 13 p1492 N73-22098
Research projects on wake turbulence and atmospheric boundary layers, turbulent mixing and shear flows, and high temperature gas dynamics
[AD-755273] 13 p1512 N73-22251
Graphical method for calculating field intensity and radio wave absorption by ionosphere along radio communication paths
13 p1521 N73-22326
Ionospheric radio wave propagation in presence of tropospheric duct
[AD-757198] 14 p1634 N73-23248
Daily summaries for vertical echo sounding of upper atmosphere over Freiburg Germany, January 1973
[REPT-319-F] 14 p1659 N73-23460
Daily summaries for vertical echo sounding of upper atmosphere over Freiburg, Germany, December 1972
[REPT-318-F] 14 p1659 N73-23461
Ionosonde virtual height observations based on first order, electron density profile from incoherent scatter
[UILU-ENG-73-2503] 14 p1661 N73-23482
Satellite ionospheric research, including ray tracing program
[AD-757498] 14 p1662 N73-23487
Daily summaries for vertical echo sounding of upper atmosphere over Freiburg, Germany - February 1973
[REPT-320-F] 15 p1777 N73-24406
Artificial ultralow frequency generation in ionosphere and magnetosphere for global communication system
[AD-759012] 16 p1878 N73-25199
Determination of D region electron density distributions from radio propagation data
[AD-759018] 16 p1909 N73-25449
Scintillation and polarimeter measurements of ionospheric column using ATS 1
[AD-759533] 16 p1910 N73-25451
Temporal variations in atmospheric electric fields noting propagation and disturbances
[TRITA-EPP-73-02] 17 p2027 N73-26405
Dourbes [Belgium] geophysical observatory data on geomagnetism, ionospheric propagation, seismology, cosmic rays, and atmospheric electricity, Aug. 1972
17 p2028 N73-26411
Dourbes [Belgium] geophysical observatory data on geomagnetism, ionospheric propagation, seismology, cosmic rays, and atmospheric electricity, Sep. 1972
17 p2028 N73-26412
Polarization fading effect in angle of rotation measurements on ionospheric radio signal scattering
18 p2115 N73-27105
Digitally recorded sferics waveforms providing ELF attenuation rates for day and night propagation
[AD-760686] 18 p2119 N73-27132
Analysis of intermodulation of weak signal with strong signal in ionosphere to determine variations as function of modulation frequency of strong signal
[BBC-RD-1973/5] 19 p2234 N73-28010
Ionosphere D and F region high frequency ray propagation effects and design of high frequency dynamic phase metering instruments
20 p2375 N73-29083
Winter anomalous radio wave absorption days at 32 N, and prevalent solar radiation
[AD-762191] 20 p2378 N73-29105
Experimental system for conducting ionospheric scintillation measurements using ATS geostationary satellites at 136 and 1550 MHz
[PB-220564/9] 21 p2509 N73-30133
Daily summaries for vertical echo sounding of upper atmosphere over Freiburg, Germany - April 1973
[REPT-322-F] 21 p2537 N73-30342
Daily summaries for vertical echo sounding of upper atmosphere over Freiburg, Germany - May 1973
[REPT-323-F] 21 p2537 N73-30343
Daily summaries for vertical echo sounding of upper atmosphere over Freiburg, Germany - June 1973
[REPT-324-F] 21 p2537 N73-30344
Backscatter spectrum comparisons, including ionospheric inhomogeneity effects
[NASA-CR-133809] 21 p2538 N73-30349
Analysis of meteorological nature and characteristics of anomalous radio echoes received during vertical sounding of troposphere
21 p2571 N73-30602
Medium frequency wave ionospheric propagation loss in earth reflected paths
[BBC-RD-1973/17] 22 p2627 N73-31050
Loss estimation in predicting ionospheric medium frequency sky wave propagation
[BBC-RD-1973/13] 22 p2627 N73-31051
Propagation of electromagnetic signals through ionized media
[AD-764281] 22 p2635 N73-31114
Predicting day-to-day variability of mid-latitude ionosphere for application to HF propagation predictions
[AD-764711] 23 p2789 N73-32310
Model for prediction of horizontal ray path deviation effects in high frequency ionospheric propagation
24 p2894 N73-33105
Daily summaries for vertical echo sounding of upper atmosphere over Freiburg, Germany - July 1973
24 p2920 N73-33322
Dourbes [Belgium] geophysical observatory data on geomagnetism, ionospheric propagation, seismology, cosmic rays, and atmospheric electricity. Nov. 1972
24 p2924 N73-33353
Geophysical observatory data obtained at Dourbes, Belgium in Dec. 1972 on geomagnetism, ionospheric propagation, seismology, cosmic rays, and atmospheric electricity
24 p2924 N73-33354

**IONOSPHERIC REFLECTION**
U IONOSPHERIC PROPAGATION
**IONOSPHERIC SOUNDING**

Ionospheric sounding and cosmic ray neutron flux density tables, Dourbes, Belgium, Feb. 1972
01 p0050 N73-10402
Ionospheric sounding and cosmic ray neutron flux density tables, Dourbes, Belgium, Mar. 1972
02 p0166 N73-11352
Ionosonde using solid state analog components and digital arrays for continuously monitoring ionosphere
[AD-745965] 02 p0167 N73-11359
One-dimensional and multi-dimensional inversion techniques for processing remote atmospheric and ionospheric sounding data
[NASA-TM-X-62150] 02 p0196 N73-11585
Development of mathematical processes for deriving ionospheric electron density as function of altitude and frequency measurements obtained by vertical incidence ionospheric sounders
02 p0198 N73-11602
Development of procedure for converting topside ionograms into topside electron density profiles using modified lamination method
02 p0198 N73-11603
Development of methods for solving group height equation based on data contained in single ionogram trace
02 p0198 N73-11604
Analysis of requirements for numerical inversion method to calculate ionospheric electron density from ionograms
02 p0199 N73-11605
Automatic data selection and profile inversion to obtain ionospheric electron density profiles from digitized radio soundings
02 p0199 N73-11606
Application of oblique-to-vertical transformation and direct inversion of oblique incidence ionogram techniques for deriving true height profiles
02 p0199 N73-11607
Inversion of VLF-LF sounder data to obtain D region electron density distributions
02 p0201 N73-11626
Ionospheric sounding and cosmic ray neutron flux density tables, Dourbes, Belgium, Apr. 1972
03 p0297 N73-12420
Analysis of backscatter from radar transmission and effect of field aligned laminae in both E and F layers of ionosphere
[AD-747027] 03 p0297 N73-12426
Determining ion composition of ionosphere by incoherent scattering of radio waves, and ionospheric sounding in USSR
[JPRS-57474] 04 p0413 N73-13372
Ionospheric soundings in USSR for IQSY
04 p0413 N73-13374
Ionospheric sounding and cosmic ray neutron flux density tables, Dourbes, Belgium, May 1972
05 p0539 N73-14387
Aircraft measurements of microscale motions and atmospheric structure associated with thin echo layers in stable stratified zones
[AD-749512] 05 p0540 N73-14393
Electron beam-induced luminescence studies of thermospheric temperatures and particle densities, using two Aerobee 150 rockets
[AD-749877] 05 p0541 N73-14406
Data analysis on reflected oblique soundings of ionosphere using short pulses
[AD-749766] 05 p0543 N73-14417
Aircraft measurement of long wave radiation brightness and angular distribution
[AD-750945] 05 p0544 N73-14424
Multiring ionospheric plasma probe, including plasma parameter and current study
05 p0610 N73-14960
Radio frequency impedance probe measurement of ionspheric electron density profiles using Veronique rocket for sounding
06 p0667 N73-15423
Polar ionospheric geophysical data recording at Kiruna, Sweden, during Apr.-Jun. 1972
06 p0667 N73-15424
Using simultaneous measurements of ozone profile and solar extinction to obtain absorption coefficient for calculating ozone distribution
[AD-750404] 06 p0668 N73-15429
Analysis of ion current density at central point of charged mass spectrometer during atmospheric and ionospheric sounding
[AD-750483] 06 p0671 N73-15456
Tables on ionospheric data measured by vertical echo sounding
[REPT-316-F] 08 p0916 N73-17507
Ionospheric sounding and cosmic ray neutron flux density tables, Dourbes, Belgium, Jun. 1972
08 p0918 N73-17524
Ground based HF sounding technique for detecting ionospheric disturbances associated with Pc 1 micropulsations
[AD-752062] 08 p0919 N73-17532
Solar eclipse effects on atmosphere, measured by three pitot probe rocket soundings
08 p0972 N73-17944
Ionospheric sounding and cosmic ray neutron flux density tables, Dourbes, Belgium, Jul. 1972
09 p1030 N73-18409
Atmospheric sounding and ionospheric disturbance measurements by rocket-borne instruments
[AD-754244] 10 p1157 N73-19412
Electron, positive ion, and proton flux measurements by small rocket instrumentation over polar cap
[AD-754897] 11 p1289 N73-20457
Ionospheric sounding and cosmic ray neutron flux density tables, Dourbes, Belgium, Aug. 1972
13 p1524 N73-22354
Kiruna [Sweden] polar geophysic observatory ionospheric data recorded from Jul.-Sep. 1972
13 p1525 N73-22355
High altitude plasma physics and experiments simulating release of artificial plasma clouds in ionosphere
[AD-756684] 13 p1525 N73-22364
High resolution optical measurements of high altitude barium releases at Elgin AFB during January 1971
[AD-756938] 13 p1528 N73-22382
Analysis of ionospheric investigations conducted with Intercosmos satellite number two
14 p1659 N73-23464
Ionospheric sounding by scientific satellites
[AD-756483] 14 p1662 N73-23490
Computerized simulation of ion collection by ionospheric probe
[AD-757481] 14 p1662 N73-23492
Auroral ionospheric measurements from incoherent scatter radar facility
[AD-757358] 14 p1664 N73-23504
Analysis of magnetospheric data obtained by satellite sounding
[AD-755390] 14 p1665 N73-23516
Ionospheric sounding and cosmic ray neutron flux density tables from Dourbes, Belgium for Oct. 1972
15 p1781 N73-24438
Striations in large barium ion clouds in two stage process
[AD-757916] 15 p1807 N73-24643
Tabular ionospheric data acquired by vertical incidence sounding techniques
[RRC-A207-PT-2] 16 p1905 N73-25409
Vertical incidence sounding techniques to determine ionospheric effects of solar activity
[RRC-A208-PT-2] 16 p1905 N73-25410
Solar and geophysical data obtained by ionospheric sounding over India for April, 1972
[RRC-A202-PT-2] 16 p1907 N73-25423
Tables on solar and magnetic activity
[RRC-A210-PT-2] 16 p1907 N73-25424
Tables on solar and magnetic activity
[RRC-A203-PT-2] 16 p1907 N73-25425
Ionospheric sounding and cosmic ray neutron flux density tables, Dourbes, Belgium, Sep. 1972
16 p1907 N73-25428
Ionospheric sounding data from Monte Capellino Observatory, Italy, 1972
16 p1907 N73-25430
VHF radars to probe ion columns left by meteors
[AD-758765] 16 p1908 N73-25434
Weather forecasting and measurement of air pollution by laser sounding of atmosphere
[NASA-TT-F-14948] 17 p2026 N73-26391
Ionospheric sounding and cosmic ray neutron flux density tables, Dourbes, Belgium, Dec. 1972
18 p2146 N73-27342
Ionospheric sounding and cosmic ray neutron flux density tables, Dourbes, Belgium, Nov. 1972
18 p2146 N73-27343
Ionospheric drifts and Sq current system
[WRE-TN-680[WR/D]-PT-2] 19 p2293 N73-28438
Polar ionospheric geophysical data recording in Sweden, Jan-Mar. 1973
19 p2295 N73-28459

Numerical analysis of barium cloud growth and striation in conducting background
[AD-761828] 19 p2317 N73-28637
Using upper air soundings to compute refractive-index gradients in lower atmosphere
[AD-762501] 20 p2414 N73-29404
Digital data generation and processing in airborne ionospheric research
[AD-763088] 20 p2414 N73-29406
Ionogram observations supporting chemical release studies in E region
[AD-762927] 20 p2415 N73-29409
International comparisons of sample-type radiosondes from U.S.S.R., Finland, and Japan
20 p2448 N73-29670
Exploitation of satellite observed radiances for increased resolution of atmospheric thermal structure
[AD-762752] 20 p2450 N73-29692
Ionospheric sounding and cosmic ray neutron flux density tables, Dourbes, Belgium, Mar. 1973
21 p2539 N73-30354
Ionospheric sounding and cosmic ray neutron flux density tables, Dourbes, Belgium, Apr. 1973
21 p2539 N73-30355
Rocket sounding of zonal wind field structure in stratosphere and lower mesosphere of tropical zone during equinoxes
21 p2573 N73-30617
Profile inversion technique for determination of electron density from wave interaction data
[AD-764297] 22 p2668 N73-31378
Ionospheric sounding and cosmic ray neutron flux density tables, Dourbes, Belgium Jan. 1973
24 p2923 N73-33350
Ionospheric sounding and cosmic ray neutron flux density tables, Dourbes, Belgium, Feb. 1973
24 p2923 N73-33351
Analysis of data on ionospheric parameters gathered by multi-probe rockets
[AD-764781] 24 p2924 N73-33356

**IONOSPHERIC STORMS**
NT SUDDEN IONOSPHERIC DISTURBANCES
Very low frequency radio signal transmission during three polar substorms in 1969
[KGO-PREPRINT-72-303] 01 p0050 N73-10404
Relationship between atmospheric gravity waves and spread F conditions caused by solar activity
05 p0509 N73-14146
Analysis of ionospheric storm research with emphasis on ionospheric parameters available for study and observational techniques employed
[PSU-IRL-SCI-404] 06 p0666 N73-15413

**IONOSPHERICS**
NT DAWN CHORUS
NT HISS
Ionospheric investigation of auroral activity using rocket-borne spectrophotometric techniques
[NASA-CR-131484] 13 p1519 N73-22311
Operational characteristics of sky noise measuring instruments and analysis of discrepancies in data acquired by each instrument
[NASA-CR-133415] 18 p2151 N73-27383

**IONS**
NT ANTIPROTONS
NT CESIUM ION
NT DEUTERONS
NT HEAVY IONS
NT HELIUM IONS
NT HYDROGEN IONS
NT METAL IONS
NT MOLECULAR IONS
NT NITROGEN IONS
NT PROTONS
NT SOLAR PROTONS
NT TRITONS
Relation between momentum transfer and capture, and total scattering cross sections for ion-dipole collisions
[NASA-TM-X-68151] 01 p0083 N73-10685
Ion drag and winds aloft in high latitudes
[NASA-TM-X-66083] 02 p0165 N73-11340
Spectral line profiles of helium triplet diffuse series and quasi-static approximation for ions and electrons
[NASA-TN-D-6954] 02 p0214 N73-11731
Application of X ray spectrometry to study of multicharged ions in plasmas
[EUR-CEA-FC-629] 04 p0452 N73-13694
Secondary ionic emission procedure for studying semiconductor properties
[CEA-CONF-1969] 04 p0459 N73-13745
Association, switching, and rearrangement for positively charged cluster ions at 80 km in upper atmosphere
[AD-751140] 07 p0797 N73-16478
Effect of chloride ion additions on dissolution behavior of Fe-Ni alloys in sulfuric acid
[AD-751258] 07 p0811 N73-16574
Ion clusters and atmospheric composition of Venus ultraviolet haze layer
08 p0973 N73-17952
Measurement and analysis of fast ions and neutral particles in Penning discharge with ring anode in magnetic field
[TRITA-EPP-72-12] 09 p1071 N73-18739
Electron density, electron and ion temperature, and ion composition values obtained during eclipse on 7 Mar. 1970
[UILU-ENG-73-2501] 10 p1154 N73-19390
Micrometeoroid analyzer using arrays of interconnected capacitors and ion detector
[NASA-CASE-ARC-10443-1] 11 p1291 N73-20477
Numerical calculation of current-voltage characteristics for ionized plasma containing negative ions with unequal electron and ion temperatures
[LOG-J7146] 13 p1563 N73-22667
Mass spectrographic determination of ions and neutral reactions in glow discharge of helium-sulfur dioxide-carbon monoxide
[BM-RI-7747] 15 p1747 N73-24157
Mass spectra of cluster ion reaction kinetics in free jet expansions of gas mixtures
[AD-761811] 19 p2233 N73-28004
PH influence on hexachloroiridite and hexachloroiridate ions in aqueous solutions
[IRI-133-73-02-PT-2] 21 p2506 N73-30111
OV1-18 mass spectrometer detection of heavy ions in magnetosphere
[AD-763436] 21 p2542 N73-30379
Nighttime composition measurements at geomagnetic equator
[NASA-TM-X-70476] 23 p2785 N73-32283
Cross sections for reactions of atmospheric ions with atomic oxygen
[AD-765333] 23 p2789 N73-32316

**IOWA**
Identification of agricultural crops and soil moisture stress in Iowa using ERTS-1 imagery
[E72-10335] 05 p0531 N73-14323
Flood damage in west central Iowa based on ERTS-1 imagery
[E73-10045] 07 p0777 N73-16308
Repetitive ERTS-1 imagery of surface water variability and flooding along rivers and low-lying areas in Virginia, Iowa, and California
[E73-10046] 08 p0900 N73-17289
Identification and classification of Iowa crop lands using ERTS-1 imagery and aerial photography
[E73-10343] 10 p1148 N73-19342
Analysis of ERTS-1 imagery for crop identification and area estimates in Iowa
[E73-10699] 16 p1903 N73-25391
Photointerpretation of ERTS-1 imagery and airborne photography to determine vegetation growth in Iowa
[E73-10715] 17 p2018 N73-26322
State airport system plan for Iowa - Volume 1
[PB-217531/3] 18 p2127 N73-27192
State airport system plan for Iowa - Volume 2
[PB-217532/1] 18 p2128 N73-27193
Mapping of flood inundation areas in southwestern Iowa using ERTS-1 imagery
19 p2288 N73-28395
Identification and classification of agricultural crops and forest inventory in Iowa from ERTS-1 imagery
[E73-10927] 20 p2398 N73-29276
Comparison of ERTS-1 spectral reflectance measurements of major crops and soil associations for selected sites in Iowa, Kansas, North Dakota, and Texas
[E73-10981] 22 p2657 N73-31288
ERTS-1 measurements of major crops and soil associations in Indiana, North Dakota, Iowa, Nebraska, Kansas, and Texas
[E73-11155] 24 p2919 N73-33309

**IP (IMPACT PREDICTION)**
U COMPUTERIZED SIMULATION

**IRAN**
Utilization of ERTS-1 multispectral photography in evaluating Iranian playas as potential locations for economic and engineering development
[E72-10270] 03 p0291 N73-12369
Utilization of ERTS-1 imagery for evaluation of Iranian playas as potential locations for economic and engineering development
[E73-10067] 07 p0779 N73-16329
Utilization of ERTS-1 imagery for evaluation of Iranian playas as potential locations for economic and engineering development
[E73-10339] 10 p1147 N73-19338
Utilization of ERTS-1 imagery to evaluate Iranian playas as potential locations for economic or engineering development
[E73-10539] 13 p1518 N73-22303
ERTS-1 imagery of geology, agriculture, forestry, and hydrology in Iran
19 p2287 N73-28387
Evaluation of Iranian playas as potential locations for economic and engineering development
[E73-11026] 22 p2662 N73-31330

**IRASERS**
U INFRARED LASERS

**IRIDESCENCE**
Iridescence and selective reflection of cholesteric liquid crystals according to various models
[BMVG-FBWT-72-27] 10 p1190 N73-19684

**IRIDIUM**
Cladding materials research, including Pt-Rh-W alloy and Ir properties and Ir purification
[ORNL-TM-3865] 04 p0453 N73-13696
Thermodynamic properties of iridium sulfides at equilibrium pressures
[AD-753897] 11 p1253 N73-20168
Growth of single crystals of rhenium and iridium dioxides
[NASA-CR-133213] 17 p2072 N73-26768
PH influence on hexachloroiridite and hexachloroiridate ions in aqueous solutions
[IRI-133-73-02-PT-2] 21 p2506 N73-30111

**IRON**
NT IRON 57
X ray fluorescence analysis of trace elements in high purity irons
[NPL-CHEM-17-PT-2] 03 p0264 N73-12139
Determination of oxygen, silicon, phosphorus, and copper in iron and steel by 14-MeV neutron activation analysis
[EURISOTOP-57] 03 p0313 N73-12556
Analysis of friction surfaces of porous materials based on iron after prolonged operation under self lubricating conditions
[AD-748020] 03 p0317 N73-12585
Detection and measurement of cosmic ray charge spectrum for nuclei heavier than iron with relation to nucleosynthesis and mechanics of supernova
[NASA-TM-X-58102] 03 p0352 N73-12872
Electrochemical analysis of cathodic hydrogen absorption by iron and steel
[BARC-585] 05 p0506 N73-14116
Kinetics of Fe and Al atom oxidation reactions at high temperatures
[AD-749380] 05 p0507 N73-14125
Production of metal powders with emphasis on iron powder
[NLL-TRANS-746-1262-[9022.401]]
05 p0561 N73-14557
Evidence for one source mechanism for primary cosmic rays and another mechanism for iron nuclei, based on balloon-borne ionization spectrometer
[NASA-TM-X-66149] 06 p0716 N73-15841
Impact damage caused by polystyrene, aluminum, or iron hypervelocity particles on glass
08 p0934 N73-17651
Influence of heat treatment on physical properties of iron- and chromium-doped rutile
[RR-107] 09 p1073 N73-18760
Ferromagnetic resonance in iron and hexagonal close packed cobalt lattices
[AD-753841] 09 p1076 N73-18783
X ray attenuation coefficients in absorption spectra of titanium, iron, cobalt, nickel, copper, and zinc
[UCRL-73923] 10 p1189 N73-19675
Friction induced surface activity of some hydrocarbons with clean and oxide-covered iron
[NASA-TN-D-7233] 11 p1297 N73-20527
Rocket-borne instrument detection of X ray flux from iron line of Cassiopeia A
[NASA-TM-X-66216] 11 p1336 N73-20843
Gas phase hydrogen permeation through alpha iron, 4130 steels, and 304 stainless steels from less than 100 C to near 600 C
[NASA-TN-D-7265] 12 p1412 N73-21442
Nitrogen exchange between furnace atmosphere and argon plasma arc when melting pure iron
12 p1413 N73-21447
Measurements of Mossbauer absorption spectra to investigate diffusion mechanism of iron in beta-titanium
12 p1413 N73-21449
Effects of carbon and copper on magnetic properties of iron and iron-silicon alloys
[NASA-TT-F-14857] 12 p1428 N73-21574
Variations of relative abundances of helium, carbon, nitrogen, oxygen, and iron-group nuclei in solar cosmic rays and their relationship to solar particle acceleration
[NASA-TM-X-66228] 12 p1445 N73-21706
Relationship of geological structures to iron-rich zones in Nevada based on ERTS-1 imagery
[E73-10555] 14 p1655 N73-23427
Auger spectroscopy of oxygen and sulfur interactions with clean iron surface and rubbing contact effect on interactions
[NASA-TN-D-7283] 14 p1670 N73-23555
Analysis of effects of alternating current on corrosion of iron in aqueous solutions of acidic and neutral salts
[REPT-733] 14 p1675 N73-23590
Growth of iron whiskers by hydrogen reduction of iron halide salts
[AD-757588] 14 p1699 N73-23788
Feasibility of using iron magnetic support to extend cold magnetic balance wind tunnel system to subsonic flow regimes and continuous spinning aircraft configurations
15 p1762 N73-24275
Kinetic study of copper cementation on iron
[BM-RI-7761] 15 p1791 N73-24519
Application of ultrasonic inspection for determining effect of graphite on strength characteristics of cast iron
15 p1797 N73-24571
Mass spectrometric analyses on laser induced vaporization of iron and zirconium hydride
[LBL-1177] 17 p1992 N73-26108

Electrochemical and mechanical parameters of localization hydrogen in iron and maraging steel using high resolving power autoradiography
[RAE-LIB-TRANS-1665] 17 p2044 N73-26533
Strip rolling mill for high speed rolling of iron and titanium powders
[AD-759241] 17 p2047 N73-26556
Calculated iron abundance in moon from magnetometer measurements
[NASA-TM-X-62279] 17 p2082 N73-26841
Bibliography of test equipment and procedures for determining physical and mechanical properties of iron and steel products
[PB-219047] 18 p2161 N73-27459
Analysis of X ray data obtained during solar flares
[NASA-CR-133341] 18 p2195 N73-27721
Process for manufacturing synthetic iron and comparison of annealing rate of synthetic iron with conventional iron
[NLL-M-21640-[5828.4F]] 20 p2429 N73-29507
Development of procedures for determining molybdenum in iron and steel with emphasis on factors affecting stablity and temperature dependence
[TN-303] 20 p2431 N73-29529
Shock wave effects in porous iron
[AD-763796] 21 p2540 N73-30368
Thermodynamic stability diagrams for iron, nickel, and chromium in fused sodium hydroxide
22 p2625 N73-31028
Measurements of Fe, Mn, Fn, Cu, Ni, and Pb in aerosols and precipitation in clean tropospheric air
[NOAA-TR-ERL-248-APCL-24]
22 p2664 N73-31349
Precipitation hardening of copper alloys and iron
[AD-764150] 22 p2686 N73-31516
Ferromagnetic resonance measurements in Ni and Fe as function of temperature and frequency parameters
24 p2934 N73-33428

**IRON ALLOYS**
NT AUSTENITIC STAINLESS STEELS
NT CARBON STEELS
NT CHROMIUM STEELS
NT FERRITIC STAINLESS STEELS
NT HIGH STRENGTH STEELS
NT MARAGING STEELS
NT MARTENSITIC STAINLESS STEELS
NT NICKEL STEELS
NT STAINLESS STEELS
NT STEELS
High temperature and fatigue tests to determine effects of heat resistant coatings on mechanical and physical properties of nickel-chromium-iron alloys
[NLL-TRANS-746-1236-[9022.401]]
02 p0185 N73-11500
Preparation and homogeneity characteristics of austenitic iron-chromium-nickel alloy at micrometer level of spatial resolution to establish standard reference material
[NBS-SP-260-43] 02 p0186 N73-11511
Effects of incomplete dissolution of graphite in molten cast iron on viscosity differences with same chemical composition
[AD-747378] 03 p0317 N73-12582
Quantitative examination of ordering effects in nickel-iron alloy system
[NLL-RTS-7547] 04 p0431 N73-13510
Effects of atomic ordering in ternary solid solutions containing alloys of nickel and iron and relation of Youngs modulus with temperature
[NLL-RTS-7654] 04 p0431 N73-13511
Orthorhombic chromium carbide for increased strength of sintered iron ceramic structural material
04 p0432 N73-13516
Dry sliding friction characteristics of iron ceramic materials using solid lubricants
04 p0432 N73-13517
Sintering temperature and tungsten content effects on volumetric shrinkage of ferrotungsten alloy briquets
04 p0432 N73-13518
Cold plastic deformation process for manufacturing molds and stamps from sintered metal powder ceramic blanks
04 p0432 N73-13519
Magnetic properties and phase composition of finely-dispersed nondeformed powders from highly-anisotropic gamma-phase Fe-Pd alloys
[NLL-TRANS-746-1389-[9022.401]]
05 p0560 N73-14553
Evaporative segregation in binary alloys of Ni-Cr and Ni-Fe systems
[NASA-CR-123993] 05 p0561 N73-14562
High temperature dispersion strengthening of Fe-Al alloys by internal oxidation
[BM-RI-7686] 05 p0562 N73-14564
Volumetric analysis and dilatometric study of ferrite magnesium cast iron during heat treatment
[AD-749627] 05 p0563 N73-14572
Analysis of volume changes in composite wrought iron associated with fiber buckling
[AD-749711] 05 p0567 N73-14606
Development of process for obtaining iron whiskers and description of mechanical and physical properties
[IIS-142-VOL-22-4] 05 p0586 N73-14766
Analysis of wear resistance of copper alloyed, magnesium cast iron by reciprocating motion of different friction pairs
[AD-750519] 06 p0687 N73-15590
Effects of prior deformation and transformations on microstructure of iron nickel alloy
[AD-750716] 06 p0687 N73-15591
Effect of chloride ion additions on dissolution behavior of Fe-Ni alloys in sulfuric acid
[AD-751258] 07 p0811 N73-16574
Magnetic measurements of superconducting iron-shielded dipoles
[BNL-17190] 08 p0893 N73-17227
Ultrasonic measurements of elastic constants of polycrystalline alloys of iron in vanadium
[AD-753615] 10 p1174 N73-19547
Concentration dependence of high field susceptibility of Fe-Ni alloys
[NLL-LTI-746-1343-[9022.401]]
12 p1412 N73-21440
Determination of diffusion coefficient of hydrogen through nickel and iron-nickel alloys
[UCRL-TRANS-10651] 12 p1415 N73-21463
Effects of carbon and copper on magnetic properties of iron and iron-silicon alloys
[NASA-TT-F-14857] 12 p1428 N73-21574
Effect of substrate topography on magnetic properties of cylindrical Ni-Fe thin films
[NLL-LTI-746-1370-[9022.401]]
12 p1437 N73-21641
Application of nuclear gamma resonance for changing structural state of crystal lattice of alloys to improve strength properties
13 p1541 N73-22486
Metallographic analysis of morphological features of martensite formed in alloy of iron-nickel-manganese-carbon after heat treatment
13 p1541 N73-22490
Magnetic properties of highly dispersed iron-cobalt-nickel alloy powders
[NLL-LTI-746-1419-[9022.401]]
15 p1797 N73-24566
Cyclic furnace tests of nickel-, cobalt-, and iron-base alloys oxidation resistance considering scale spalling
[NASA-TM-X-68252] 16 p1870 N73-25144
Analysis of iron-nickel alloys to determine nature of Mossbauer effect at high pressures and low temperatures
16 p1927 N73-25592
Analysis of embrittlement in zone refined iron and Armco iron after charging with hydrogen to determine cause of reaction
[RAE-LIB-TRANS-1666] 17 p2043 N73-26530
Development of iron alloy with high fracture toughness at cryogenic temperatures
[LBL-1121] 21 p2559 N73-30511
Thermodynamic properties of solid alloys of chromium with nickel and iron
[COO-1791-4] 21 p2559 N73-30516
Strain rate sensitivity and yield stress of Fe-Mo, Fe-Ti, and Fe-Re solid solutions
21 p2602 N73-30855
Application of divergent beam X ray microdiffraction technique for measuring residual and impressed stresses and strains in iron-silicon alloy transformer sheet
[NBS-MONOGRAPH-130] 22 p2672 N73-31407
Thermodynamic property measurements of solid chromium sesquioxide and chromium in solid alloys with iron and nickel
[TID-26322] 24 p2934 N73-33433

**IRON CHLORIDES**
Magnetic phase transition in FeCl3
[AD-764982] 23 p2827 N73-32595

**IRON COMPOUNDS**
NT BARIUM FERRATES
NT FERRATES
NT FERRITES
NT HEMATITE
NT IRON CHLORIDES
NT IRON OXIDES
Mapping iron compounds in Wind River Range using ERTS-1 multispectral scanner imagery
[E72-10181] 01 p0045 N73-10360
Analysis of hydrogen diffusion in alpha-iron in six degree to seventy seven degrees Kelvin using magnetic after-effect technique
[COO-1198-903] 03 p0314 N73-12561
Crystal growth and magnetic properties of transition metal chalcogenides
[AD-748864] 04 p0459 N73-13748
Utilization of ERT-1 imagery for water depth measurement, Yellowstone Park data, atmospheric effects in Colorado, lake ice surveillance, recreational land use, IFYGL, image enhancement, water quality monitoring, oil pollution detection, and mapping iron compounds
[E73-10086] 08 p0901 N73-17298
Growth of FeS[x] and NbO2 single crystals
[AD-753270] 09 p1074 N73-18768
Low carbon steel for studying dissolution behavior of Fe3C particles under rapid heating and short time temperature conditions
[AD-753928] 11 p1307 N73-20602
Single crystals of hematitic Fe2O3 grown from Na2B4O7 and occuring as plates, rods, hoppers, and equidimensional solid crystals
[AD-755349] 13 p1567 N73-22697
Static longitudinal and transverse susceptibilities calculated for iron fluoride as function of temperature
[AD-757009] 14 p1698 N73-23781
Mapping exposed silicate rock types and exposed ferric and ferrous compounds from Skylab
[E73-10877] 20 p2393 N73-29228
Evaluation of stripe domain light deflector using iron compounds
[AD-762475] 20 p2426 N73-29490
Multidisciplinary research on water depth measurement, Yellowstone Park, atmospheric effects, lake ice surveillance, recreational land use, IFYGL, image enhancement, water quality, oil pollution detection, and mapping iron compounds from ERTS-1 data
[E73-11119] 23 p2783 N73-32264

**IRON ISOTOPES**
NT IRON 57

**IRON METEORITES**
Monte Carlo calculation of cosmic isotope buildup in iron meteorites
[ORNL-TR-2620] 07 p0846 N73-16861

**IRON ORES**
NT HEMATITE
Iron absorption band analysis for discrimination of iron-rich zones in California and Nevada
[E72-10294] 04 p0410 N73-13344
Spectral ratio mapping of iron ore deposits in Wind River Range, Wyoming, using ERTS-1 data
[E73-10397] 11 p1276 N73-20359
Ratio mapping iron ore deposits in Atlantic City District, Wyoming
[E73-10575] 15 p1772 N73-24355
Effect of neutron irradiation on remanent magnetization in Apollo 11 and 12 lunar samples of iron and kamacite
15 p1813 N73-24692
Iron-absorption band analysis for discrimination of iron rich zones using ERTS-1 imagery
[E73-10789] 18 p2137 N73-27265
Role of microorganisms during iron-manganese ore formation in lakes and seas
[NASA-TT-F-15023] 21 p2537 N73-30346
Structural and spectral analysis of lineaments and circular features for discrimination of iron-rich zones in Nevada
[E73-11020] 22 p2661 N73-31324
Hypothesis for enormous accumulation and exclusive occurrence of ferruginous quartzite in Precambrian rock
[NASA-TT-F-15121] 23 p2786 N73-32290

**IRON OXIDES**
NT HEMATITE
Magnetic fluid preparation by grinding and concentrating pyrophoric antiferromagnetic iron oxide colloidals
[BM-RI-7702] 05 p0580 N73-14721
Magnetic properties of iron oxides in boron oxides
[AD-754104] 10 p1202 N73-19780
Acetone decomposition by austenitic stainless steel, iron oxide, and chromium oxide
[AERE-R-7408] 24 p2892 N73-33089

**IRON 57**
Mossbauer absorption spectra of iron 57 in single crystal of potassium iron fluoride
[AD-764635] 23 p2827 N73-32597
Monte Carlo method for fitting iron 57 Mossbauer spectra
[AD-764634] 23 p2828 N73-32602

**IROQUOIS HELICOPTER**
U UH-1 HELICOPTER

**IRRADIANCE**
NT ILLUMINANCE
NT SOLAR CONSTANT
Mean irradiance distribution of finite cross section laser beam propagating in sea water
[AD-745956] 02 p0183 N73-11483
Ultraviolet photometry experiment for Atmosphere Explorer C, D, and E missions to record solar irradiance
[NASA-TM-X-66130] 04 p0422 N73-13437
Atmospheric radiative transfer model for predicting solar and daytime sky irradiance of ground target
[AD-757149] 14 p1693 N73-23739
Digital computer model to predict spectral irradiance on ground target from sun and sky
[AD-758877] 16 p1945 N73-25739

**IRRADIATION**
NT ELECTRON IRRADIATION
NT ION IRRADIATION
NT NEUTRON IRRADIATION
NT PROTON IRRADIATION
NT X RAY IRRADIATION
Research on biological effects of microwave radiation
[MBL-1972-5] 01 p0008 N73-10060
Irradiation-induced changes in graphites at high temperatures and high fluences
[GULF-GA-A-10971] 03 p0321 N73-12612
Properties of refractory metals and application to construction of high temperature irradiation facilities
[EUR-4757] 04 p0434 N73-13540

Mechanical properties of types 304 and 304 plus 0.15 percent Ti stainless steel after irradiation at temperatures in range of 400 to 820 C
[ORNL-TM-3733] 05 p0562 N73-14569
Radiation oxidation of water impurities in moisture-containing products of human vital functions
07 p0744 N73-16051
Mechanism of peroxidation of polymers under irradiation conditions
08 p0881 N73-17137
Mathematical model of thermodynamic damage to metals irradiated by laser beams
[DREV-R-672/72] 09 p1043 N73-18503
Results of uranium dioxide-tungsten irradiation test and post-test examination
[NASA-TM-X-2709] 09 p1063 N73-18677
Effect of chronic irradiation of dogs by Co60 gamma rays on level of autoantibodies
11 p1244 N73-20100
Degradation rate of thermal control coatings exposed to solar ultraviolet irradiation
[NASA-CR-124149] 11 p1307 N73-20608
FORTRAN-4 computer program for compiling irradiation data on UN and UC fuel pins
[NASA-TM-X-68226] 13 p1558 N73-22625
Coefficient of turbulent exchange in mathematical model of radiation fog evolution
[AD-757490] 14 p1662 N73-23494
Effects of energetic charged particle irradiation of solar system material
[NASA-CR-132045] 15 p1831 N73-24845
Influence of monochromatic light on physiological processes of blood
[NASA-TT-F-14941] 16 p1866 N73-25111
Constant-stress irradiation creep capsules for application of load to several graphite samples by single pneumatic bellows
[BNWL-SA-4199] 17 p2050 N73-26586
Irradiation tests on tungsten clad uranium carbide/zirconium carbide thermionic emitter fuel configurations
[NASA-TM-X-2834] 18 p2178 N73-27587
Irradiation of TZM-Uranium dioxide fuel pin at 1700 K
[NASA-TM-X-2755] 18 p2178 N73-27588
Effect of irradiation on absolute thermal EMF of alloys, metals, and thermocouple materials
[NASA-TT-F-15015] 19 p2309 N73-28574
Elastic-plastic toughness level of irradiated stainless steels used in fast reactor construction
[AD-761611] 19 p2310 N73-28580
Fatigue and creep-fatigue behavior of irradiated austenitic stainless steel used in LMFBR design
[ANCR-1096] 19 p2349 N73-28891
Computer program for modeling UO2 cladding strain resulting from irradiation
[NASA-TM-X-68281] 20 p2453 N73-29715
Unrestrained swelling of uranium nitride fuel irradiated at temperatures ranging from 1100 to 1400 K
[NASA-TM-X-2907] 21 p2578 N73-30659
Design and operation of tantalum alloy clad uranium mononitride irradiated fuel pins
[NASA-TM-X-2878] 22 p2698 N73-31614

**IRREGULARITIES**
Ionospheric irregularities by low-frequency electrostatic gradient-driven instabilities and their nonlinear evolution in equatorial electrojet plasma
08 p0900 N73-17284
Postflight analysis of Apollo 14 translunar docking anomaly
09 p1089 N73-18884

**IRRIGATION**
Location of center pivot sprinkler irrigation systems in Finney County, Kansas, based on ERTS-1 interpretation
[E73-10418] 11 p1279 N73-20380
Identification of winter wheat on irrigated land in southern Finney County, Kansas
[E73-10475] 12 p1395 N73-21312

**IRRITATION**
NT TOXICITY AND SAFETY HAZARD

**IRROTATIONAL FLOW**
U POTENTIAL FLOW

**ISCHEMIA**
Relationship between peaks of cosmic radiation and ischemic heart disease
[NASA-TT-F-14992] 17 p1987 N73-26065

**ISENTROPIC PROCESSES**
Numerical analysis of one-dimensional isentropic flow of thermally perfect, calorically imperfect diatomic gas
[ESDU-S.00.01.10-AMEND-A]
07 p0767 N73-16233
Numerical analysis of one dimensional isentropic flow of thermally perfect, calorically imperfect diatomic gas
[ESDU-S.00.01.10-AMEND-A]
14 p1648 N73-23364
Isentropic frictionless equilibrium flow of evaporating two phase mixtures with low vapor content in convergent-divergent nozzles
[SFB-MHD-5] 22 p2653 N73-31254

**ISING MODEL**
U FERROMAGNETISM
U MATHEMATICAL MODELS

**ISIS SATELLITES**
NT ALOUETTE 2 SATELLITE
NT ISIS-A
Indications of dayside midlatitude plasma trough by ISIS-1 electrostatic probe measurements of electron density and temperature in photonosphere
[NASA-TM-X-70436] 21 p2595 N73-30797

**ISIS-A**
Low energy particle measurements by soft particle spectrometer on ISIS-1 orbiting satellite and relation to production of auroral particles
10 p1146 N73-19329
Telemetry data from data processing system for spherical electrostatic analyzer experiment onboard ISIS-A satellite
[AD-760148] 17 p2001 N73-26179
ISIS-A electro static probe measurements of electron concentration and temperature of plasmapause at mid-latitudes
[NASA-TM-X-70429] 19 p2293 N73-28442

**ISLANDS**
NT BARBADOS
NT BERMUDA
NT GREAT BRITAIN
NT GREENLAND
NT ICELAND
NT JAPAN
NT LONG ISLAND [NY]
NT MARTINIQUE
NT NEW GUINEA [ISLAND]
NT PACIFIC ISLANDS
NT PHILIPPINES
NT PUERTO RICO
NT WALLOPS ISLAND
NT WEST INDIES
Estuary and barrier island studies using ERTS-1 imagery
[E72-10266] 03 p0291 N73-12365
Regional seismic reflection survey of Strait of Sicily, using multichannel digital techniques
[SACLANTCEN-CONF-PROC-7] 07 p0789 N73-16418
ERTS A spectrophotographic measurement of water pollution in Charlotte Amalie harbor, St. Thomas
[NASA-CR-130008] 07 p0792 N73-16437
Development of mathematical model for wind-driven circulation in ocean basin containing island formation
[AD-754354] 11 p1290 N73-20469
Aeromagnetic survey of Amchitka Island, Alaska and adjacent insular shelf for studying tertiary volcanic rocks
[USGS-PP-707] 14 p1661 N73-23481
Seismic reflection, refraction, and near bottom observations in Aleutian trench near 173 deg W
[AD-755455] 14 p1664 N73-23508
ERTS-1 I2S imagery of Virgin Islands
[E73-10767] 18 p2134 N73-27243
ERTS-1 multispectral imagery of topography of Assateague Island
[E73-10848] 19 p2292 N73-28426
Estuary and barrier island investigations utilizing ERTS-1 imagery
[E73-11041] 22 p2664 N73-31342

**ISOBARS (PRESSURE)**
Meteorological ground level maps of Northern Hemisphere for fourth quarter in 1971
[QR-4-PT-4] 06 p0691 N73-15628
Temperatures of various adiabatic and isobaric mixtures of humid atmospheric air with water or ice
[PUBL-SER-B-68] 12 p1465 N73-21866
Radiation and turbulent heat flux effects on variations of isobaric surface pressure and altitude in Northern Hemisphere
20 p2446 N73-29651
Dependence of clear air turbulence on evolution of baric field and effect on synoptic forecasting
24 p2946 N73-33526

**ISOBUTYLENE**
U BUTENES

**ISOCYANATES**
NT DIISOCYANATES
Isocyanide spin label for studying conformational transitions in cytochrome c, emphasizing heme group
[NASA-TT-F-14623] 03 p0259 N73-12099

**ISOLATION**
NT SOCIAL ISOLATION

**ISOLATORS**
NT VIBRATION ISOLATORS
Feasibility of using terbium-silicate glass as Faraday rotator-isolator in high power laser
[AD-749919] 05 p0559 N73-14543
Design, fabrication, and performance evaluation of Faraday effect far infrared isolators
[AD-751319] 07 p0808 N73-16552
Development and characteristics of supporting frame to isolate payloads from multi-gravitational forces
[NASA-CASE-MFS-21680-1] 11 p1297 N73-20525
Acousto-optical isolator for suppressing optical feedback generated laser instabilities
[AD-757914] 15 p1796 N73-24556
Mercury thruster isolator lifetime tests
[NASA-TM-X-71422] 23 p2830 N73-32617

**ISOMERS**
Cis-trans isomers and doped LiNbO3 for holographic ready/write/erase memory application
[NASA-CR-112248] 08 p0928 N73-17604

**ISOPHOTES**
Dust tail of comet Seki-Lines mapped isophotometrically for relative intensities
23 p2836 N73-32662

**ISOPLETHS**
U NOMOGRAPHS

**ISOPROPYL ALCOHOL**
Transverse injection of water and isopropyl alcohol from flat plate into air streams
[AD-741887] 01 p0043 N73-10339
Preparation of fluorinated polyethers from 2-hydroperhaloisopropyl alcohols
[NASA-CASE-MFS-11492] 21 p2505 N73-30102

**ISOSTASY**
Tables on harmonic coefficients of isostatic reduction potential U
[NASA-TM-X-66292] 18 p2145 N73-27334

**ISOSTATIC PRESSURE**
Effect of solidification under high isostatic pressure on high strength steels
[AD-753958] 11 p1306 N73-20596

**ISOTHERMAL FLOW**
Analysis of isothermal liquid inflow patterns in spherical container during weightless conditions
[NASA-TM-X-2670] 03 p0283 N73-12291
Damping of accelerated isothermal superfluid helium flow by roton polarization
[NOTA-INTERNA-395] 03 p0336 N73-12743

**ISOTHERMAL PROCESSES**
Analysis of lattice spacings and changes in platinum metals as function of temperature and applied pressure
[NLL-TRANS-746-1316-[9022.401]]
05 p0561 N73-14558
Development of nonisothermal theory of viscoelastic fluids with fading memory and application to viscometric flow
[AD-754802] 11 p1349 N73-20948
Physical and chemical properties of nickel alloys following cyclic and isothermal oxidation
[NASA-TN-D-7267] 14 p1675 N73-23594
Role of isothermal stresses generated during oxidation and modes of stress relaxation
14 p1676 N73-23605
Probabilistic model of nonisothermal gaseous flow through fine pored homogeneous media
17 p2013 N73-26276
Prediction of yeld strength on isothermal aging of precipitation-hardening alloy Nimonic PE16
[TRG-REPORT-2267] 24 p2935 N73-33442

**ISOTHERMS**
Determination of values for roughness parameters of isotherms in Pacific thermocline using thermistor chain
07 p0858 N73-16954

**ISOTOPE EFFECT**
Isotope effects for environmental monitoring and control
[ORNL-IIC-39] 06 p0703 N73-15730
Alpha particle beam spalling production of aluminum, oxygen, carbon, and beryllium isotopes, and cosmic ray transport theory
13 p1561 N73-22651

**ISOTOPE SEPARATION**
Laser excitation for isotope separation
[WRE-TM-494[WR/D]] 04 p0453 N73-13701
Molecular diffusion in mixing binary flow and separation of uranium isotopes by fixed wall centrifugation
06 p0653 N73-15302
Dissipative losses in separation nozzle flow determined for uranium isotope separation conditions from Pitot tube measurements
[KFK-1562] 07 p0772 N73-16271
Optimal molecular composition of zirconium phosphate ion exchanger for separation of radioactive actinide series elements
08 p0883 N73-17151
Nuclear chemistry and geochemistry research projects including isotope separations, meteorite and tektite compositions, and solid gamma spectrometer development
[COO-3236-3] 08 p0884 N73-17156
General equations for describing molecular diffusion in vortex flow and possible application to isotopic separation by fixed wall centrifugation
[FRNC-TH-213] 08 p0897 N73-17262
Separation of short half life O-15 and N-13 isotopes from alkali metals, steels, copper, and indium by gamma activation analysis
[CONF-721069-24] 18 p2160 N73-27453
Isotope separation in rare gases caused by centrifugal force in plasmas
[TRITA-EPP-72-27] 19 p2325 N73-28701

**ISOTOPE SHIFT**
U ISOTOPE EFFECT

**ISOTOPES**
NT ARGON ISOTOPES
NT CALCIUM ISOTOPES
NT CALIFORNIUM ISOTOPES
NT CARBON ISOTOPES

NT COBALT 60
NT COPPER ISOTOPES
NT CURIUM 244
NT DEUTERIUM
NT HELIUM ISOTOPES
NT HYDROGEN ISOTOPES
NT IODINE ISOTOPES
NT IRON 57
NT LITHIUM ISOTOPES
NT NEPTUNIUM
NT NICKEL ISOTOPES
NT NITROGEN ISOTOPES
NT OXYGEN ISOTOPES
NT PLUTONIUM
NT PLUTONIUM 238
NT RADIOACTIVE ISOTOPES
NT RADIUM 226
NT RUBIDIUM ISOTOPES
NT TANTALUM ISOTOPES
NT TELLURIUM
NT TRANSURANIUM ELEMENTS
NT TRITIUM
NT URANIUM 233
NT VANADIUM ISOTOPES
Organic fluid capsule test and thermoelectric module test in isotope kilowatt program
[ORNL-TM-3805] 04 p0448 N73-13657
Isotope chemistry studies, including bulk density and vapor pressure measurements
[COO-3498-2] 05 p0506 N73-14121
Production of isotopic fuel pellets by vacuum hot pressing
[ORNL-4796] 05 p0579 N73-14711
Abundance and isotopic composition of noble gases release from lunar fines
[NASA-CR-130327] 07 p0841 N73-16812
Neutron capture and total cross sections for isotopes of reactor materials
[COO-3058-27] 17 p2065 N73-26702
Isotopic composition of chemical elements in solar atmosphere
[AD-758769] 18 p2198 N73-27748
Portable nuclear radiation spectrometer for field measurement of mixed isotopic contaminants
[LA-5203-MS] 22 p2674 N73-31418
Measurement of mean isotopic composition of even-charge cosmic ray elements using balloon-borne ionization chamber
[NASA-CR-135516] 22 p2711 N73-31711
Analysis of isotopic composition of chemical elements in solar structure using photospheric and sunspot spectra
[NP-19727] 24 p2981 N73-33826
**ISOTOPIC LABELING**
Corrosion kinetics of Ti-Pd alloy in HCl at room temperature determined by radioactive tracer method
[NLL-TRANS-746-1328-[9022.401]] 05 p0505 N73-14112
Radionuclide measurements on plasma and red cell mass volume losses in Apollo spacecrews 09 p0993 N73-18106
Isotopic composition of carbon in carbonaceous rocks from oil field of Belorussia as indication of their origin
[NASA-TT-F-14938] 15 p1780 N73-24426
Radioactive isotope measurements and neutron activation analyses for identifying contaminants in space environment simulator
[NASA-CR-128931] 15 p1815 N73-24709
Kinetic deuterium isotope effect in aqueous reaction of methyl radicals with deuterated alpha-alanine and glycine
[NASA-TT-F-15123] 23 p2753 N73-32033
**ISOTROPIC MEDIA**
Mechanical wave front propagation in fluid mixtures and isotropic solids
[AD-746617] 02 p0158 N73-11281
Propagation of axisymmetric harmonic waves across interface of two semi-infinite rods composed of different isotropic materials
[AD-746721] 02 p0239 N73-11948
Correlation functions for displacements in semiboundless isotropic elastic media
[ITF-72-78-P] 12 p1429 N73-21579
Distribution of current in coupled dipole antennas in homogeneous isotropic media
[AD-761167] 18 p2124 N73-27169
Inequalities satisfied by strain energy functions for isotopic elastic material
[AD-761624] 19 p2315 N73-28616
**ISOTROPIC TURBULENCE**
Numerical analysis of Langmuir wave spectra development in turbulent plasma
[JINR-P9-6432] 04 p0455 N73-13712
Effects of isotropic scattering on one dimensional propagation of small disturbances in radiating gray gas
[ISAS-494-VOL-38-NO-5] 22 p2651 N73-31237
Experimental analysis of nearly isotropic turbulence behind jet grid 24 p2904 N73-33174
**ISOTROPISM**
Failure modes for isotropic and anisotropic composite materials
[AD-756889] 14 p1681 N73-23639
**ISOTROPY**
NT ISOTROPIC MEDIA
Stationary phase direction in absorbent media applied to ray propagation through three successive homogeneous isotropic media
[GRI/TP/110] 06 p0639 N73-15183
Fracture toughness of homogeneous isotropic composites
[AD-764070] 22 p2689 N73-31541
**ISRAEL**
Israeli use of ERTS-1 imagery to detect and map oil slicks in Gulf of Suez
[E73-10800] 19 p2259 N73-28206
**ITALY**
NT ALPS MOUNTAINS (EUROPE)
Bora observations from Yugoslavia and Italy
[CLIMATOL-NOTES-10] 05 p0571 N73-14636
Bora-day chronology at Ajdovscina and Trieste with 10 m/s peak gust 05 p0571 N73-14641
Regional seismic reflection survey of Strait of Sicily, using multichannel digital techniques
[SACLANTCEN-CONF-PROC-7] 07 p0789 N73-16418
Remote sensing of areas in Italy using infrared scanners for thermal radiation map 07 p0859 N73-16968
Bathymetry, free air gravity anomaly, and magnetic field intensity data on Strait of Sicily, gathered from 1965 to 1971
[SACLANTCEN-CONF-PROC-7] 08 p0915 N73-17501
Effect of perturbation on frequency and intensity of thunderstorms in Italy 10 p1181 N73-19608
Italian thermal conditions affecting acceleration tolerance and psychomotor performance of flying personnel 14 p1612 N73-23068
Ionospheric sounding data from Monte Capellino Observatory, Italy, 1972 16 p1907 N73-25430
ERTS-1 surveillance of volcanic areas of Southern Italy 19 p2284 N73-28368
Atmospheric model of artificial night sky illumination in Italy 21 p2538 N73-30348
Annual variations of Garda Lake surface temperature using airborne bolometric equipment and earth based infrared video equipment
[IFA-STR-23] 23 p2787 N73-32298
Bibliography of Italian climatology
[IFA-STR-22] 23 p2814 N73-32499
**ITERATION**
NT ITERATIVE SOLUTION
Iterative methods and relaxation algorithm for calculating vertical atmospheric structure from noise contaminated infrared spectral measurements 02 p0196 N73-11588
Comparison of statistical and iteration methods for obtaining vertical temperature profiles from multispectral radiation measurements 02 p0196 N73-11589
Adaptive equalization of pulse amplitude modulated signal with noise interference by successive iterative methods
[NASA-TR-R-402] 10 p1128 N73-19190
Cellular arrays as iterative logical and memory structures
[NASA-CR-130936] 10 p1132 N73-19227
Iterative method for calculating axial flow resistance in annular slots of impeller pumps
[NLL-NEL-TT-2422-[6075.461]] 11 p1269 N73-20299
**ITERATIVE NETWORKS**
Development of numerical procedures for determining instantaneous values of current and voltage in nonlinear electrical circuits
[NLL-DRIC-TRANS-2145-[3623.66]] 05 p0522 N73-14241
Construction method for radio signal correlators using Fourier transformation 13 p1497 N73-22131
**ITERATIVE SOLUTION**
Iterative algorithm for determining thermal instabilities in viscoelastic rod under cyclic loads
[AD-746470] 02 p0240 N73-11953
Iterative solution for characteristic exponents of linear differential equations with periodic coefficients
[ARC-CP-1218] 03 p0324 N73-12642
Iterative solution for free vibrations of ring stiffened toroidal shells
[AD-747024] 04 p0482 N73-13943
Numerical technique for obtaining solutions to governing equations for gas flowing in axially symmetric constricted-arc heaters
[NASA-TM-X-2700] 07 p0769 N73-16246
Mesh gradient technique for numerical optimization of descent trajectories
[NASA-TM-X-68181] 08 p0937 N73-17670
Differential games, nonlinear sequential machines, hyperbolic partial differential equations, and iterative solutions
[JPRS-58069] 09 p1056 N73-18609
Iterative method for refining diagnostic procedures, and applications to geological surveys 09 p1056 N73-18613
Algorithms for iterative solution of unconstrained optimization problems
[NPL-NAC-25] 09 p1058 N73-18625
Iterative directional analysis of ocean waves
[AD-753825] 11 p1289 N73-20460
Solution of relaxation problem for Boltzmann equation by integral iteration method 12 p1418 N73-21489
Thermodynamics of light scattering from Eulerian fluid, and electron scattering by atomic hydrogen 13 p1558 N73-22627
Iterative method for analyzing feathering characteristics in airfoil whirlwinds
[DEP/PRA/NT/88/72] 14 p1600 N73-22968
Automated iterative analysis of aeromagnetics 17 p2062 N73-26684
Iterative technique for solving nonlinear integral equation for radiative transfer
[NASA-TN-D-7292] 19 p2352 N73-28916
Differential correction schemes in nonlinear regression
[REPT-3] 20 p2437 N73-29568
Algorithm for solving approximate problem of nonlinear function
[NASA-CR-133728] 20 p2440 N73-29599
Iterative search for resonance frequencies of multibranched coastal inlets with tsunami amplification 23 p2784 N73-32274
Iterative and nonlinear procedures for studying gravity anomaly in mountainous areas 24 p2911 N73-33232
**ITOS 1**
ITOS system and design of TIROS M spacecraft
[NASA-CR-130163] 07 p0849 N73-16880
Secondary subsystems of ITOS 1
[NASA-CR-130164] 07 p0849 N73-16881
Brushless dc torque motor in-orbit performance of ITOS with improved attitude controls and earth splitting technique
[NASA-TM-X-66267] 17 p2060 N73-26662
Structure of dust storms determined from ITOS-1 television pictures
[NLL-M-23033-[5828.4F]] 21 p2528 N73-30272
Operational processing of solar proton monitor data from ITOS
[NOAA-TM-NESS-49] 21 p2592 N73-30772
**ITOS 2**
Improved ITOS attitude control system with Hall generator brushless motor and earth-splitting technique
[NASA-TM-X-66232] 14 p1708 N73-23858
**ITOS 3**
Cloud cover mosaics developed from environmental satellite imagery for April, 1973 18 p2171 N73-27534
**ITOS 4**
Research on remote sensing applications and satellite observation data - conferences
[NASA-SP-312] 08 p0971 N73-17934
ITOS D and Nimbus E radiometer data 08 p0972 N73-17943
**IZSAK ELLIPSOID**
U ELLIPSOIDS
U GEODESY
**I2S CAMERAS**
ERTS-1 I2S imagery of Virgin Islands
[E73-10767] 18 p2134 N73-27243
Correlation of sediment patterns with inflow and tidal action using MSS and I2S imagery
[E73-10794] 18 p2137 N73-27270

## J

**J-2 ENGINE**
Rocket nozzle redesign for improving Saturn launch vehicle J-2 engine performance and reliability 03 p0349 N73-12849
**J-52 ENGINE**
Performance tests on J-52 turbojet engines to determine acceptable compressor stall margin
[AD-755152] 11 p1334 N73-20832
**J-57 ENGINE**
Analysis of thermal failures in combustion chambers of J-57 jet engine and system for detecting burnthrough prior to engine case rupture
[FAA-NA-72-92] 07 p0835 N73-16772
J-57 combustor exhaust odor intensity and chemical composition considering inlet parameters, fuel types, and nozzle shapes
[NASA-CR-121159] 14 p1616 N73-23093
**J-58 ENGINE**
Analysis of data obtained in evaluation tests of circumferential airflow uniformity entering combustors from two advanced engine compressors
[NASA-CR-121009] 05 p0526 N73-14276
**J-65 ENGINE**
Effect of sound absorbing exhaust duct on rear quadrant noise of J-65 engine and contributions of internal and jet components
[NASA-TM-X-2718] 07 p0739 N73-16011

J-75 ENGINE
Adverse effect of film cooling on suction surface of turbine blade
[NASA-TM-X-68210] 12 p1444 N73-21695
J-85 ENGINE
Analysis of gaseous emissions from J-85 engine at various fuel-air ratios, engine speeds, and simulated altitude conditions
[NASA-TM-X-2726] 08 p0969 N73-17921
Performance tests of hydromechanical fuel control system for J-85 engine
[NASA-TN-D-7198] 09 p0990 N73-18082
Flight tests of modified F-106 aircraft to determine installation effects of two aft underwing nacelles housing afterburning J-85 engines
[NASA-TM-X-71439] 23 p2743 N73-31959
JACKING EQUIPMENT
U JACKS [LIFTS]
JACKS [ELECTRICAL]
U ELECTRIC CONNECTORS
JACKS [LIFTS]
Compressive instability of hydraulic jacks overlapping stiffness
[ESDU-01.01.24] 02 p0236 N73-11922
JAMMING
Kalman filtering algorithm for detecting continuous wave interference signals in digital telecommunications
01 p0027 N73-10210
Information theory criteria for electronic jaming and countermeasures for air defense
[FOA-3-C-3644-66] 02 p0140 N73-11133
Jamming of surveillance radar station by airborne electronic countermeasures
[FOA-3-C-3645-66] 06 p0639 N73-15187
Telecommunication jamming of robot aircraft control system by pulse amplitude modulation or pulse time modulation
[FOA-3-C-3649-66] 06 p0639 N73-15188
Mathematical and computer analysis of multiple channel sidelobe canceller
[AD-753571] 09 p1004 N73-18198
JAPAN
Aerological data from balloon and rocket flights for Japan and its vicinity - tables for Oct. 1971
01 p0073 N73-10601
Aerological data from balloon and rocket flights for Japan and its vicinity, tables for Dec. 1971, and ozone data, tables for Jan. - Dec. 1971
01 p0073 N73-10603
Aerological data from balloon and rocket flights for Japan and its vicinity-tables for Nov. 1971
01 p0073 N73-10604
Aerological data from balloon and rocket flights for Japan and its vicinity for period from 1966 to 1970
01 p0074 N73-10605
Typhoon associated tornadoes in Japan and suction vortices in Omiya tornado
[SMRP-RP-101] 03 p0326 N73-12659
Anthropometric data of Japanese Air Self-Defense Force personnel
05 p0502 N73-14091
Meteorological parameters of upper atmosphere over Japan during March 1972
05 p0572 N73-14648
High concentration sulfur dioxide pollution over Osaka, Japan during summer
[NLL-M-20713-[5828.4F]] 06 p0692 N73-15634
Aerological data from balloon and rocket flights for Japan and vicinity - Jan. 72
06 p0693 N73-15647
Upper atmospheric data of Japan and vicinity Feb. 1972
06 p0693 N73-15648
Quantitative analysis and identification of chemical properties of minerals in Japanese placer platinoids
[NASA-TT-F-14625] 09 p1048 N73-18547
Tables of synoptic meteorological observations for Okinawa, Sakishima Islands, and southern East China Sea
[AD-753216] 09 p1061 N73-18656
Aerological data from balloon and rocket flights for Japan and vicinity - May 1972
10 p1182 N73-19612
Aerological data from radiosonde observations for Japan and vicinity during 1969 and 1970
10 p1182 N73-19613
Aerological data from flights for Japan - June 1972
10 p1182 N73-19614
Aerological data from balloon and rocket flights for Japan and vicinity - Apr. 1972
10 p1182 N73-19615
Tables of synoptic meteorological observations for Japanese and Korean coastal marine areas
[AD-753468] 10 p1182 N73-19619
Tables of synoptic meteorological observations of Japan coastal marine areas
[AD-754773] 11 p1314 N73-20668
Tables on geomagnetic observations made by Kakioka Magnetic Observatory
[REPT-86] 12 p1399 N73-21345
Tables on geomagnetic observations made by Kanoya Magnetic Observatory
[REPT-88] 12 p1399 N73-21346
Tables on geomagnetic observations made by Memambetsu Magnetic Observatory
[REPT-87] 12 p1400 N73-21358
Generative model for prosody of connected speech in Japanese
14 p1624 N73-23154
Geomagnetic survey of Japan and nearby areas conducted from July 1969 to November 1970
[PUB-592] 14 p1660 N73-23474
Geomagnetic observations made in Japan and surrounding areas from 1967 to 1969
[PUB-591] 14 p1660 N73-23475
Modification of Japan climate by environmental pollution
[AD-757487] 14 p1686 N73-23678
Aerological data from balloon and rocket flights for Japan and vicinity
15 p1777 N73-24407
Effects of wind shaped trees on macro- and microclimatological conditions in Japan
[CLIMATOL-NOTES-12] 18 p2171 N73-27530
Aerological data from balloon and rocket flights for Japan and vicinity - September 1972
18 p2172 N73-27539
Aerological data from balloon and rocket flights for Japan and vicinity - Aug. 1972
18 p2172 N73-27540
Aerological data from balloon and rocket flights for Japan and vicinity - Oct. 1972
18 p2172 N73-27541
Analysis of erosion along Niigata Beach, and development of improved methods of erosion control based on ERTS-1 imagery
[PAPER-E14A] 19 p2270 N73-28278
Analysis of ERTS-1 multispectral scanner imagery to determine polluted and turbid water masses in Osaka Bay, Japan
[PAPER-E14C] 19 p2270 N73-28280
Aerological data from balloon and rocket flights for Japan and vicinity - December 1972
24 p2921 N73-33325
Aerological data from balloon and rocket flights for Japan and vicinity - Nov. 1972
24 p2947 N73-33540
Aerological data from balloon and rocket flights for Japan and vicinity - Jan. 1973
24 p2947 N73-33541
JARRING
U MECHANICAL SHOCK
JAVELIN AIRCRAFT
U GA-5 AIRCRAFT
JC-130 AIRCRAFT
U C-130 AIRCRAFT
JEEPS
U AUTOMOBILES
JET AIRCRAFT
NT A-4 AIRCRAFT
NT A-6 AIRCRAFT
NT A-7 AIRCRAFT
NT AN-24 AIRCRAFT
NT B-52 AIRCRAFT
NT B-57 AIRCRAFT
NT B-70 AIRCRAFT
NT BOEING 707 AIRCRAFT
NT BOEING 720 AIRCRAFT
NT BOEING 727 AIRCRAFT
NT BOEING 737 AIRCRAFT
NT BOEING 747 AIRCRAFT
NT BREGUET 941 AIRCRAFT
NT BREGUET 1150 AIRCRAFT
NT C-2 AIRCRAFT
NT C-5 AIRCRAFT
NT C-135 AIRCRAFT
NT C-141 AIRCRAFT
NT C-160 AIRCRAFT
NT CANBERRA AIRCRAFT
NT CL-84 AIRCRAFT
NT COMET 4 AIRCRAFT
NT CONCORDE AIRCRAFT
NT CONVAIR 880 AIRCRAFT
NT CV-990 AIRCRAFT
NT DC 8 AIRCRAFT
NT DC 9 AIRCRAFT
NT DC 10 AIRCRAFT
NT DO-31 AIRCRAFT
NT F-4 AIRCRAFT
NT F-5 AIRCRAFT
NT F-8 AIRCRAFT
NT F-14 AIRCRAFT
NT F-15 AIRCRAFT
NT F-27 AIRCRAFT
NT F-28 TRANSPORT AIRCRAFT
NT F-86 AIRCRAFT
NT F-100 AIRCRAFT
NT F-102 AIRCRAFT
NT F-104 AIRCRAFT
NT F-105 AIRCRAFT
NT F-106 AIRCRAFT
NT F-111 AIRCRAFT
NT FD 2 AIRCRAFT
NT GA-5 AIRCRAFT
NT H-126 AIRCRAFT
NT HFB-320 AIRCRAFT
NT JET PROVOST AIRCRAFT
NT L-1011 AIRCRAFT
NT LEAR JET AIRCRAFT
NT MIRAGE 3 AIRCRAFT
NT OV-10 AIRCRAFT
NT P-3 AIRCRAFT
NT P-1127 AIRCRAFT
NT T-33 AIRCRAFT
NT T-38 AIRCRAFT
NT TU-144 AIRCRAFT
NT TURBOPROP AIRCRAFT
NT U-2 AIRCRAFT
NT VISCOUNT AIRCRAFT
NT VULCAN AIRCRAFT
NT X-14 AIRCRAFT
NT XC-142 AIRCRAFT
NT XV-5 AIRCRAFT
NT YAK 40 AIRCRAFT
Integrated information presentation and control system analysis to determine control and display requirements for contingency operation of jet aircraft - Vol. 3
[AD-740435] 01 p0006 N73-10041
Impact tests of jet transport wing leading edge fuel tanks to evaluate effects of aborted takeoff, abnormal landing, and bird strikes
[FAA-NA-72-21] 02 p0125 N73-11017
Wind tunnel tests to determine aerodynamic characteristics of V/STOL aircraft configurations using blowing flapped wing and direct jet lift systems
[NASA-CR-114496] 03 p0282 N73-12284
Operational test and evaluation of angle of attack system for displaying percentage of lift produced by wing for all flap configurations
[AD-748844] 03 p0304 N73-12485
Flight tests to determine lateral-directional handling qualities and roll-sideslip coupling of jet aircraft at high speeds
[AD-748435] 04 p0374 N73-13042
In-flight tests and operational reliability of jet aircraft nullable compressor face rake
[NASA-TN-D-7162] 07 p0769 N73-16247
Mathematical models for predicting flow fields within and external to thrust reverser deployed in flight including forces and moments induced on aircraft by flow fields
[AD-751525] 07 p0837 N73-16764
User manual and source listings for computer programs to solve problems in analysis of in-flight thrust reversers
[AD-751526] 07 p0837 N73-16785
Combustion efficiency of annular turbojet combustor using heated natural gas as fuel
[NASA-TM-X-2742] 09 p1098 N73-18960
Criteria on jet blast velocities and effects during operation of commercial aircraft and recommended procedures to reduce adverse impact
[AC-150/5325-6A] 11 p1266 N73-20271
Flight investigation to determine velocity and persistence characteristics of trailing vortices generated by jumbo jet transport
[NASA-TN-D-7172] 12 p1364 N73-21068
Dynamic stability information for space shuttles, high performance military aircraft, and short takeoff aircraft at high angles of attack
[NASA-CR-114583] 13 p1505 N73-22201
Fatigue tests on Comet aircraft pressure cabin to determine effects of pressure cycles on structural stability of cabin windows
[ARC-R/M-3248] 15 p1728 N73-24017
Methods for evaluating and predicting airfield performance of turbojet and turbofan aircraft operating in conventional and short takeoff modes
15 p1732 N73-24044
Development of two methods for optimizing design of subsonic, swept wing jet transport aircraft
15 p1733 N73-24054
Flight tests of cockpit meter instrumentation system displaying aircraft specific energy and energy rate
[AD-763450] 21 p2550 N73-30448
Aerodynamic characteristics and aircraft performance of jet aircraft during takeoff run
[AD-764314] 22 p2615 N73-30959
Performance decrement and response time of current and noncurrent jet Naval pilots
[AD-761463] 22 p2624 N73-31025
Jet aircraft flight tests for stability derivative determination comparing various measuring techniques
[BMVG-FBWT-73-12] 23 p2745 N73-31971
Mathematical model for predicting pilot rating of aircraft in pitch tracking under gust conditions
[AD-764698] 23 p2746 N73-31976
Performance evaluation of model energy separators
[AD-764585] 23 p2798 N73-32381
Feasibility study for use of YF-12 aircraft as scientific instrument platform for observing 1970 solar eclipse
[NASA-CR-135482] 23 p2845 N73-32735
Bank financing in commercial jet aircraft export
23 p2861 N73-32862
Dispersion and dilution of jet aircraft exhaust at high altitudes
[NASA-TM-X-71451] 24 p2971 N73-33743
Infrared signatures of high performance jet aircraft and evaluation of air to air missile effectiveness
[SLA-73-5271] 24 p2994 N73-33929

**JET AIRCRAFT NOISE**
Jet aircraft noise of XV-5B V/STOL aircraft as determined by full scale flight test and wind tunnel model tests
[NASA-TM-X-62182] 01 p0004 N73-10029
Noise caused by jet exhaust and wing for STOL engine-over-wing configuration
[NASA-TM-X-68159] 02 p0125 N73-11018
Effect of external air flowing across exhaust nozzles on jet noise produced by supersonic transport aircraft at high takeoff speeds
[NASA-TM-X-68161] 03 p0250 N73-12027
Calculation of acoustic field generated by circular jet in presence of low speed crossflow
[NASA-CR-2169] 03 p0252 N73-12036
Aerodynamic analytical model for reducing supersonic jet exhaust noise
[AD-747774] 03 p0337 N73-12752
Acoustic feedback of subsonic and supersonic free jet impinging on obstacle, e.g. blown flap or ground, and noise reduction methods
[DGLR-PAPER-72-84] 04 p0373 N73-13031
Proceedings of symposium on helicopter noise held at Durham, North Carolina Sept. 1971
[AD-748876] 04 p0373 N73-13036
Research project to analyze and evaluate supersonic jet noise generation and radiation - Vol. 1
[AD-749428] 05 p0495 N73-14035
Definition of supersonic aircraft jet noise generation and methods for reducing noise intensity - Vol. 2
[AD-749137] 05 p0495 N73-14036
Development of unified theory of jet engine noise based on fluctuating motions in fluids - Vol. 3
[AD-749138] 05 p0496 N73-14037
Development of theory for jet noise generated by turbulence, noise radiation from upstream sources, and combustion noise - Vol. 4
[AD-749139] 05 p0496 N73-14038
Analysis of noise sources associated with supersonic jet noise and establishment of effects of refraction on radiated field of sources - Vol. 5 App. 1
[AD-749141] 05 p0496 N73-14039
Development of remote sensing devices to measure jet exhaust fluctuating density gradients, mean and turbulent velocity, and mean temperature Vol. 6
[AD-749143] 05 p0496 N73-14041
Acoustic properties of supersonic jet noise and refraction effects on noise field
[AD-749140] 05 p0581 N73-14728
Analysis of jet noise produced by supersonic transport aircraft with augmentor wing and four duct burning turbofan engines
[NASA-TM-X-68177] 06 p0619 N73-15028
Mission performance analysis of three supersonic transport configurations and effects of limitations on allowable engine noise
[NASA-TM-X-68178] 06 p0620 N73-15032
Analysis of jet aircraft noise propagation near airports and methods for reducing noise intensity
[NASA-TT-F-14655] 06 p0700 N73-15707
Computerized prediction of noise levels for jet aircraft with or without noise suppression devices
[NASA-CR-114517] 06 p0700 N73-15708
Measurement of noise levels produced by Boeing 737 aircraft and correlation with local meteorological parameters including wind force and direction, temperature, and atmospheric pressure
[FAA-RD-72-145] 07 p0821 N73-16651
Development of theory of aerodynamic noise to analyze jet noise directivity and shear-noise contribution to overall jet noise
[NASA-TN-D-7158] 07 p0821 N73-16654
Evaluation of head-up display instrument for providing aircraft vertical guidance during landing approach to comply with noise abatement procedures
[NASA-TM-X-62187] 09 p0982 N73-18021
Far and near sound fields of Do-31 aircraft, and noise reduction for future VSTOL aircraft
[BMVG-FBWT-72-23] 09 p0985 N73-18045
Measurement of noise levels produced by F-105 aircraft and analysis of effects on environment and land use
[AD-753113] 09 p0987 N73-18056
Development of techniques for reduction of aircraft noise generated by short takeoff aircraft
[NASA-TM-X-68195] 10 p1106 N73-19021
Model of jet aircraft shock cell noise generation and reduction
[NRC-12923] 10 p1188 N73-19666
Jet aircraft exhaust nozzle for noise reduction
[NASA-CASE-LAR-10951-1] 10 p1207 N73-19819
Analysis of noise sources in jet aircraft based on measurement of infrared emission
[NASA-TT-F-14851] 11 p1234 N73-20020
Research facility for studying noise generated by bluff body flow interaction inside ducted fuel combustion system
[AD-754094] 11 p1268 N73-20286
Reduction of jet engine noise due to turbulent mixing of exhaust gases with ambient atmosphere
[NASA-CASE-ARC-10712-1] 11 p1334 N73-20826
Analysis of common aircraft noise measures in terms of selected human response for jet transport aircraft
[FAA-RD-71-112] 12 p1365 N73-21074
Research in aircraft noise and sonic booms reduction, remote sensing of water pollution, and earth surface changes
[DLR-MITT-72-15] 12 p1375 N73-21153
Development of jet noise test facility for flow and acoustic measurements of mean and turbulent velocities in jet flow
[RE-450] 13 p1505 N73-22196
Jet aircraft noise and sonic boom measuring device which converts sound pressure into electric current
[NASA-CASE-LAR-11173-1] 13 p1529 N73-22387
Development of annular acoustically porous elements for installation in exhaust and inlet ducts of turbofan engine to reduce aircraft engine noise intensity
[NASA-CASE-LAR-11141-1] 14 p1600 N73-22975
Acoustic feedback of subsonic and supersonic jet impinging on obstacle
[DLR-FB-72-72] 14 p1602 N73-22987
High frequency spectrum domain of turbulent jet noise
15 p1813 N73-24697
Evaluation of courses of action and costs to reduce aircraft noise levels in vicinity of airports
[PB-215611/5] 16 p1862 N73-25080
Acoustic shielding baffle for determining jet noise source location
[NASA-TN-D-7229] 16 p1944 N73-25734
Afterburner instability vortex shedding model for air breathing turbojet combustion
[AD-758890] 16 p1957 N73-25834
Development of aircraft configuration for reduction of jet aircraft noise by exhausting engine gases over upper surface of wing
[NASA-CASE-LAR-11087-1] 17 p1980 N73-26008
Cold flow tests of factors affecting noise suppression and thrust loss of divergent lobe supersonic jet noise suppressor
[NASA-TM-X-2820] 18 p2101 N73-26992
Performance data for three turbofan engine configurations with noise reduction features tested over range of flight conditions
[NASA-CR-121258] 18 p2193 N73-27707
Modifications of turbojet engine with ejector to reduce jet engine exhaust noise
[NASA-TM-X-2841] 19 p2217 N73-27887
Analysis of supersonic jet aircraft noise using fluctuating jet pressures to characterize the sources
[AD-762296] 19 p2222 N73-27923
Effects of particle seeding on jet exhaust noise
19 p2251 N73-28150
Structure of axisymmetric jet in near field for jet noise and impingement schemes
[NASA-CR-121257] 19 p2255 N73-28177
Flyover and static tests for determining effects of flight velocity on F-106B exhaust nozzle noise
[NASA-TM-X-2854] 19 p2329 N73-28734
Flyover and static tests of noise and thrust performance of two spoke, suppressor plug nozzles and basic plug nozzle
[NASA-TM-X-2856] 19 p2329 N73-28735
Velocity decay and acoustic characteristics of various nozzle geometries with forward velocity
[NASA-TM-X-68259] 20 p2388 N73-29183
Analysis of noise problems created by supersonic transport aircraft, conventional aircraft, and short takeoff aircraft to show methods for jet exhaust noise reduction
21 p2495 N73-30024
Development of computer programs to analyze sound power and peak noise levels for turbojet exhaust noise at various velocities
21 p2496 N73-30029
Optical holographic measurement of jet noise in supersonic air/nitrogen and helium jets at Mach numbers from 1.5 to 3.4
[PB-220641/5] 21 p2581 N73-30686
Analysis of aircraft engine noise sources and characteristics of engine noise produced by turbofan engines
21 p2588 N73-30735
Reduction of aircraft noise by installing acoustically absorbent material
[NASA-CR-2261] 22 p2613 N73-30941
Method and apparatus for improving operating efficiency and reducing low speed noise for turbine aircraft engines
[NASA-CASE-LAR-11310-1] 22 p2710 N73-31699
Automatic control system for in-duct cancellation of spinning modes of sound
[NASA-CR-132317] 23 p2819 N73-32540
Jet noise emission and reduction by secondary cold annular flow for SST and military aircraft
23 p2820 N73-32543
Analysis of human reactions to short takeoff aircraft aerodynamic noise for predicting community acceptance of short haul air service operations
24 p2875 N73-32960
Characteristics of aerodynamic noise generated by interaction of airstream with flap surface to show location and control of noise sources
24 p2875 N73-32963
Forward velocity effects on jet noise with dominant internal noise source
[NASA-TM-X-71438] 24 p2876 N73-32968
Relationship between distribution of outflow of acoustic energy over jet boundary and far-field intensity
[NASA-TN-D-7269] 24 p2905 N73-33181
Nozzle geometry and forward velocity effects on noise for CTOL engine-over-wing concept
[NASA-TM-X-71453] 24 p2971 N73-33742
Characteristics of variable geometry high Mach inlet concepts to reduce jet engine noise on subsonic, long range commercial aircraft
[NASA-CR-134495] 24 p2972 N73-33748

**JET AIRSTREAMS**
U JET STREAMS [METEOROLOGY]

**JET AUGMENTED WING FLAPS**
U JET FLAPS
U WING FLAPS

**JET BLAST EFFECTS**
Engine ingestion prevention on low wing aircraft, particularly Mercury aircraft, by jet blast
[FO-1149] 06 p0622 N73-15049
Criteria on jet blast velocities and effects during operation of commercial aircraft and recommended procedures to reduce adverse impact
[AC-150/5325-6A] 11 p1266 N73-20271

**JET CONDENSERS**
Development of model to predict formation and detection of molecular cluster size distribution for various materials in supersonic free jet
15 p1765 N73-24300

**JET CONTROL**
Application of active control for stability augmentation of passive gradient satellites based on impulses from control jet engines
[NASA-CR-130112] 03 p0356 N73-12904
Development of solenoid valve failure detection system based on addition of radioactive gas to propellant of cold gas jet attitude control system
[NASA-CR-130931] 10 p1165 N73-19476

**JET DAMPING**
U DAMPING
U SPIN REDUCTION

**JET DRIVE**
U JET PROPULSION

**JET ENGINE FUELS**
NT JP-4 JET FUEL
NT JP-5 JET FUEL
Ignition and combustion characteristics of high density storable fuels injected into supersonic and subsonic air streams
[AD-746063] 02 p0244 N73-11980
Effect of antiicing additives on flammability properties of hydrocarbon fuels used in jet aircraft
[AD-747945] 03 p0349 N73-12852
Modification of jet engine fuels to reduce emissions of nitrogen oxides from jet aircraft turbine engines
[AD-752581] 08 p0953 N73-17803
Effect of prevaporization of jet fuels on exhaust emission levels produced in turbojet combustor segment
[NASA-TM-X-68194] 10 p1224 N73-19949
Chemistry of deposits and their precursors in jet turbine fuel systems
[AD-754459] 11 p1332 N73-20816
Preliminary appraisal of hydrogen and methane fuel and fuel tank configuration in Mach 2.7 supersonic transport
[NASA-TM-X-68222] 13 p1568 N73-22711
Anomalous rheological characteristics of high-internal-phase-ratio emulsions containing 97 to 98 percent liquid fuel as dispersed phase
[AD-758908] 15 p1823 N73-24779
Research projects conducted by organizations of National Research Council of Canada on structural analysis, jet fuels, air pollution, and very low frequency navigation
[DME/NAE-1973[1]] 17 p2098 N73-26970
Comparison of military and civil jet engine fuel specifications and test procedures for fuel performance and quality control
17 p2098 N73-26972
Comparison of nitrogen oxide emissions produced by hydrogen combustion with emissions produced by jet engine fuels at simulated cruise conditions
[NASA-TM-X-68258] 18 p2206 N73-27804
Effects of additives on high speed ignition and combustion characteristics of slurry fuels using magnesium and lithium fluoride
[AD-762615] 20 p2465 N73-29802
Hydrogen content as measure of combustion performance for hydrocarbon fuels
[AD-763097] 20 p2465 N73-29804
Interior ballistic properties of solid fuel ramjet engines to determine regression rate if fuel as function of chamber pressure, inlet air temperature, and air flux rate
[AD-764491] 22 p2709 N73-31691
Application of fiber glass reinforced plastic materials for ground handling of aviation fuels and hazards of static electricity caused by plastic materials
[AD-764358] 22 p2709 N73-31693
Incendiary vulnerability of dry bays adjacent to jet fuel tanks under gunfire
[AD-764732] 23 p2867 N73-32920

Congressional hearings on causes and implications of impending shortages of gasoline, heating oil, diesel fuel, jet fuel, and electricity
24 p2994 N73-33928

**JET ENGINES**
NT CF-700 ENGINE
NT DUCTED FAN ENGINES
NT J-52 ENGINE
NT J-57 ENGINE
NT J-58 ENGINE
NT J-65 ENGINE
NT J-75 ENGINE
NT J-85 ENGINE
NT PULSEJET ENGINES
NT RAMJET ENGINES
NT SUPERSONIC COMBUSTION RAMJET ENGINES
NT TURBOFAN ENGINES
NT TURBOJET ENGINES
NT TURBOPROP ENGINES

Theoretical and experimental analysis of charged metal particle detection in jet engine exhaust by cylindrical electrostatic probe
[AD-745540] 01 p0091 N73-10753

Inflight incident involving number two engine failure on DC 10 aircraft near Tucson International Airport, Arizona on 2 May, 1972
[NTSB-AAR-72-29] 03 p0251 N73-12035

Theory and operation of various jet aircraft engines
[AD-747406] 03 p0352 N73-12868

Fabrication and performance of real-time jet engine simulator for development of jet engine components and control systems
[NAL-TR-283] 06 p0713 N73-15820

Application of integrated circuit technology and digital computer techniques to electric control of jet engines
[NAL-TR-281] 09 p1078 N73-18799

Aerodynamic performance of core-engine turbine stator vane tested in two-dimensional cascade of 10 vanes and in single-vane tunnel
[NASA-TM-X-2766] 11 p1333 N73-20823

Analysis of acoustic properties of jet engine malfunction as means for detecting jet engine burnthrough - Vol. I
[FAA-RD-72-149-VOL-1] 11 p1334 N73-20825

Analysis formation of carbon deposits on jet engines and effect on reliability, efficiency, and service life
[AD-754607] 11 p1335 N73-20837

Information and guidance for type certification of aircraft engines as required by Federal Aviation Administration
[FAA-AC-33-2A] 13 p1571 N73-22730

Endothermic decomposition in jet engine exhaust reaction
[AD-758200] 14 p1618 N73-23105

Analysis of techniques and equipment required to conduct test of jet aircraft engine models in wind tunnels
17 p2009 N73-26245

Test parameters and methods used in Soviet Union for jet engines
[AD-760963] 18 p2194 N73-27714

Modifications of turbojet engine with ejector to reduce jet engine exhaust noise
[NASA-TM-X-2841] 19 p2217 N73-27887

Application of gas flow dynamics to theory of jet engines and other gas devices
[AD-762307] 19 p2257 N73-28196

Process for welding compressor and turbine blades to rotors and discs of jet engines
[NASA-CASE-LEW-10533-1] 19 p2303 N73-28515

Method to increase full-scale inlet/engine system testing capability of AEDC 16-ft transonic wind tunnel
[AD-762912] 20 p2383 N73-29146

Analysis of jet engine test cell pollution abatement methods
[AD-763119] 20 p2450 N73-29690

Model scale air jets for sound study of coaxial circular jets
[FAA-RD-71-101-VOL-1] 20 p2454 N73-29721

Display device for integrated jet engine instrument system program
[AD-763440] 21 p2550 N73-30450

Scaling laws to predict supersonic jet noise generated by rectangular and axisymmetric nozzles
[PB-221855/0] 22 p2700 N73-31629

**JET EXHAUST**

Numerical prediction of exhaust products released to stratosphere during supersonic flight along definite air routes
[NASA-TT-F-14622] 04 p0371 N73-13013

Performance tests of F-14 aircraft with jet blast deflector to determine effects of backflow of jet exhaust on aircraft launch operation
[AD-752018] 08 p0867 N73-17023

Effect of prevaporization of jet fuels on exhaust emission levels produced in turbojet combustor segment
[NASA-TM-X-68194] 10 p1224 N73-19949

Criteria on jet blast velocities and effects during operation of commercial aircraft and recommended procedures to reduce adverse impact
[AC-150/5325-6A] 11 p1266 N73-20271

Jet exhaust simulation in low speed wind tunnel
[DGT-8352] 13 p1507 N73-22211

Effect of fineness ratio on boattail drag of circular arc afterbodies having closure ratios of 0.50 with jet exhaust at Mach numbers up to 1.30
[NASA-TN-D-7192] 14 p1701 N73-23802

Analysis of temperature and pressure parameters associated with recirculated engine exhaust from V/STOL aircraft engines exhausting normal to ground
[NASA-TT-F-14912] 15 p1768 N73-24323

Effects of variations in fineness ratio and closure ratio on boattail drag of circular arc afterbody models at static conditions and at Mach number of 1.30
[NASA-TN-D-7163] 16 p1957 N73-25830

Development of aircraft configuration for reduction of jet aircraft noise by exhausting engine gases over upper surface of wing
[NASA-CASE-LAR-11087-1] 17 p1980 N73-26008

Development of transmissometer for measuring optical transmission through aircraft jet engine exhausts
[AD-760050] 17 p2035 N73-26467

Modifications of turbojet engine with ejector to reduce jet engine exhaust noise
[NASA-TM-X-2841] 19 p2217 N73-27887

Model for estimation of turbojet engine exhaust dispersion into atmosphere
[NASA-TN-D-7382] 19 p2254 N73-28174

Measurement of sound power levels, power spectra, and directivity patterns for jet exit velocities of F-111A aircraft
[NASA-TN-D-7376] 20 p2361 N73-28989

Development of computerized, theoretical model to predict characteristics of emissions from gas turbine engine combustors
[AD-762935] 20 p2467 N73-29819

Development of techniques for simulating infrared emission from turbojet aircraft exhaust plumes
[AD-763123] 20 p2486 N73-29967

Development of computer programs to analyze sound power and peak noise levels for turbojet exhaust noise at various velocities
21 p2496 N73-30029

Exhaust blast velocities and temperatures at ground level for various aircraft and wing tip vortex velocity for C-5 aircraft
[AD-764228] 22 p2616 N73-30961

Acoustic measurements of aerodynamic noise produced by impingement of jet exhaust on wing and flap of externally blown flap system installed on F-111 aircraft
24 p2875 N73-32964

Method of characteristics for studying flow field produced by underexpanded jet exhausted from conical nozzle into cylindrical tube
24 p2904 N73-33173

Assessment of jets as acoustic shields by comparison of single and multitube suppressor nozzle data
[NASA-TM-X-71450] 24 p2904 N73-33179

Dispersion and dilution of jet aircraft exhaust at high altitudes
[NASA-TM-X-71451] 24 p2971 N73-33743

**JET FLAMES**
U FLAMES
U JET FLOW

**JET FLAPS**
NT EXTERNALLY BLOWN FLAPS

Influence of split ground belt on aerodynamic characteristics of high lift STOL aircraft with blown flap
[UTIAS-TN-173] 02 p0152 N73-11230

Wind tunnel tests to determine effects of ground proximity on lift, drag, and pitching moment of rectangular wing equipped with jet flaps
[NAL-TR-294] 06 p0621 N73-15038

Development of nonlinearized solution for aerodynamic characteristics of jet flap lifting surface with span-wise slot near trailing edge
[NASA-CR-2190] 07 p0736 N73-15986

Air foils based on utilization of jet flap principle
[AD-751075] 07 p0774 N73-16283

Development of analytical technique for computing performance of arbitrary jet-flapped wing with compensations for variations in wing geometry
[NASA-CR-2179] 08 p0863 N73-16982

Smoke and helium bubble visualization studies of incompressible flow past jet flap airfoil
[AD-752012] 08 p0898 N73-17270

Numerical analysis of aerodynamic characteristics of unsteady, two-dimensional, jet-flapped wing
[AD-752928] 09 p0986 N73-18051

Jet deflection characteristics of jet-flapped airfoil with Coanda deflection surfaces based on velocity distribution and flow angle measurements for static operation
[AD-753618] 09 p0989 N73-18074

Wind tunnel tests to determine aerodynamic characteristics of full scale H-126 aircraft using jet flap principle
[NASA-TN-D-7252] 12 p1355 N73-20997

Development of jet-flap rotor and application to heavy helicopter and stoppable rotor designs
12 p1359 N73-21025

Wind tunnel tests to determine static longitudinal aerodynamic characteristics of jet transport wing-body with upper surface blown jet flap for lift augmentation
[NASA-TN-D-7183] 13 p1470 N73-21907

Development of high performance, low volume thrust augmentation using combined Coanda inlet and jet flap diffusion techniques
[AD-756895] 13 p1476 N73-21954

Theoretical investigation of longitudinal stability, control, and response characteristics of jet flap aircraft
[ARC-R/M-3272] 15 p1730 N73-24028

Performance tests of negative hub reaction turbine with jet flap stator and jet flap rotor
[NASA-CR-2244] 15 p1731 N73-24036

Application of cold thrust augmentation techniques for improved performance of short takeoff aircraft performance
[AD-758202] 15 p1735 N73-24073

Wind tunnel tests to determine effect of interference on performance of full span jet flap mounted on trailing edge of high aspect ratio unswept wing
[ARC-R/M-3219] 16 p1852 N73-25005

Development of data for numerical analysis of aerodynamic performance of jet, blown, and ejector flaps
[AD-763793] 21 p2498 N73-30049

Aerodynamic noise and flow field characteristics of internal flow, jet augmented flap configurations
22 p2612 N73-30937

Wind tunnel tests to determine aerodynamic characteristics of upper surface blown jet-flap concept incorporating high-bypass-ratio turbofan engines
24 p2872 N73-32943

Wind tunnel tests to determine aerodynamic loads on flap systems behind engines and vibration modes of flap system
24 p2873 N73-32945

Characteristics of aerodynamic noise generated by interaction of airstream with flap surface to show location and control of noise sources
24 p2875 N73-32963

**JET FLIGHT**
U JET AIRCRAFT

**JET FLOW**
NT AIR JETS
NT PERIPHERAL JET FLOW
NT SUPERSONIC JET FLOW

Acoustic measurements of aerodynamic noise generated by air jet impinging on large flat board for variable impingement angles, jet velocities, and distances from board
[NASA-TN-D-7075] 04 p0372 N73-13026

Numerical computation of plane jet propagating onto curved wall surface submerged in viscous fluid
[NASA-TT-F-13924] 04 p0405 N73-13296

Parametric relations for ordinary and confluent turbulent wall jet flows with external stream velocity and arbitrary pressure distribution
04 p0405 N73-13297

Numerical analysis of heat transfer conditions at point of intersection of jet impinging on obstacle at subsonic and supersonic speeds
[NLL-RTS-7617] 05 p0525 N73-14274

Oscillations and pressure variations in circular jet impacting on wall
[NASA-TT-F-14630] 05 p0527 N73-14284

Structure and behavior of confined jet flow in rotating fluid
06 p0653 N73-15301

Individual and combined effects on heat transfer properties of air jets impinging on concave side of right circular semicylinder
[NASA-TN-D-7127] 06 p0730 N73-15952

Acoustic properties and sound pressure of jet flow
[AD-754422] 10 p1144 N73-19321

Fundamental flow problem in designing fluidic proximity sensors
10 p1158 N73-19422

Flow and acoustic characteristics determined for subsonic and supersonic jets and supersonic suppressors
[NASA-CR-131297] 11 p1233 N73-20006

Analysis of two-dimensional liquid metal slot jet impinging normally against uniformly heated flat plate
[NASA-TN-D-7260] 11 p1348 N73-20938

Analysis of transition region of subsonic turbulent jets to determine noise producing potential based on far field acoustic density
[NASA-TN-D-7242] 12 p1428 N73-21573

Development of jet noise test facility for flow and acoustic measurements of mean and turbulent velocities in jet flow
[RE-450] 13 p1505 N73-22196

Analysis of aerodynamic interference resulting from jet issuing normal to chordal plane of two dimensional wing in crossflow conditions
13 p1508 N73-22223

Computer program to evaluate effect of closed-jet tunnel test on force coefficents of cambered, sharp-nosed, fully cavitating, two dimensional hydrofoil section
[AD-755423] 13 p1512 N73-22250

Development of model to predict formation and detection of molecular cluster size distribution for various materials in supersonic free jet
15 p1765 N73-24300
Velocity magnitude and direction, static pressure, and skin friction of circular turbulent jet impinging normally on flat surface
[ARC-R/M-3205] 16 p1856 N73-25034
Analysis of gas jets expanding out of axisymmetrical nozzles into vacuum or still air at finite pressure
[ARC-R/M-3235] 16 p1856 N73-25036
Flow characteristics of axially symmetrical, supersonic, fully-expanded jet to determine relation between static pressure distributions and jet turbulence
[ARC-R/M-3292] 16 p1857 N73-25038
Analysis of relative intensity profiles of density fluctuations based on acoustic properties of subsonic and supersonic unheated jet flow
[NASA-CR-124563] 16 p1861 N73-25073
Effect of interference of engine jet on aerodynamic characteristics of lifting surface induced by horizontal or vertical jet
[NASA-TT-F-14956] 17 p2015 N73-26292
Analysis of amplitude modulation of ultrasonic sound beam impinging at right angles to turbulent water jet
[RAE-LIB-TRANS-1671] 17 p2063 N73-26686
Literature survey on jet propagation and interference in lifting surface aerodynamics
[NASA-TT-F-14957] 19 p2217 N73-27886
Calculation of pressure field induced by free jet exhausted from flat plate into stagnant medium based on solution of Neumann problem in terms of singularity distributions
[NLR-TR-72040-U] 21 p2492 N73-30000
Development of model for analyzing pressure excitation spectrum and acoustic impedance of sound absorbers in presence of grazing flow
[NASA-TM-X-71418] 21 p2523 N73-30231
Analysis of flow distribution of nozzle designed to produce incompressible, low Reynolds number jet flow
[NASA-TM-X-69566] 21 p2523 N73-30233
Numerical analysis of inviscid transonic flow over body with supersonic underexpanded exhaust plume and characteristics of flow near boattail sting
[RM-577] 21 p2523 N73-30234
Analysis of fluctuating density with high temperature subsonic jet and characteristics of noise radiated to surroundings
[NASA-CR-133789] 21 p2524 N73-30241
Transition model for computing population density profiles of partially ionized argon in source flow expansion
[C-37] 22 p2652 N73-31242
Development of theoretical model for determining flow characteristics of round jet in incompressible cross-flow based on matched asymptotic expansion
[NASA-CR-132324] 23 p2775 N73-32191
Asymptotic expansion analysis of jet entrainment in incompressible cross flow
24 p2902 N73-33166
Experimental analysis of nearly isotropic turbulence behind jet grid
24 p2904 N73-33174
Relationship between distribution of outflow of acoustic energy over jet boundary and far-field intensity
[NASA-TN-D-7269] 24 p2905 N73-33181
Incompressible turbulent plane jets exhausting downstream into external flow having favorable longitudinal pressure gradient
[ARC-CP-1236] 24 p2909 N73-33219
Subsonic jet noise measurements by means of directional microphone system
24 p2956 N73-33612

**JET FUELS**
U JET ENGINE FUELS

**JET IMPINGEMENT**
Numerical solutions for jets impinging on curved surfaces
[NASA-CR-129136] 02 p0154 N73-11252
Acoustic measurements of aerodynamic noise generated by air jet impinging on large flat board for variable impingement angles, jet velocities, and distances from board
[NASA-TN-D-7075] 04 p0372 N73-13026
Acoustic feedback of subsonic and supersonic free jet impinging on obstacle, e.g. blown flap or ground, and noise reduction methods
[DGLR-PAPER-72-84] 04 p0373 N73-13031
Measurement of sound generated by impingement of turbulent jet on elastic plates
[DGLR-PAPER-72-85] 04 p0373 N73-13032
Numerical analysis of heat transfer conditions at point of intersection of jet impinging on obstacle at subsonic and supersonic speeds
[NLL-RTS-7617] 05 p0525 N73-14274
Aerodynamic characteristics of wing moving close to interface with annular jet flowing from wing surface and impinging on screen
[AD-750933] 06 p0615 N73-14995
Individual and combined effects on heat transfer properties of air jets impinging on concave side of right circular semicylinder
[NASA-TN-D-7127] 06 p0730 N73-15952
Analysis of two-dimensional liquid metal slot jet impinging normally against uniformly heated flat plate
[NASA-TN-D-7260] 11 p1348 N73-20938
Acoustic feedback of subsonic and supersonic jet impinging on obstacle
[DLR-FB-72-72] 14 p1602 N73-22987
Literature survey of heat transfer characteristics of single and multiple turbulent air jets impinging on flat plates
[NASA-TM-X-2778] 15 p1842 N73-24927
Velocity magnitude and direction, static pressure, and skin friction of circular turbulent jet impinging normally on flat surface
[ARC-R/M-3205] 16 p1856 N73-25034
Computer programs for predicting supersonic and hypersonic interference flow fields and heating
[NASA-TM-X-2725] 16 p1889 N73-25285
Effect of interference of engine jet on aerodynamic characteristics of lifting surface induced by horizontal or vertical jet
[NASA-TT-F-14956] 17 p2015 N73-26292
Analysis of retrorocket exhaust plume of Viking Lander impinging on Martian surface and development of multiple nozzle configurtaion to reduce effects
[NASA-CR-2252] 18 p2197 N73-27737
Analysis of local and average heat transfer characteristics of single turbulent air jet impinging on concave surface of hemisphere
[NASA-TM-X-2859] 18 p2206 N73-27806
Numerical analysis of disturbance pressure due to impinging of plane shock wave of arbitrary strength on moving slender body
19 p2251 N73-28151
Analysis of surface pressure fluctuations from jet impingement on inclined flat plate with application to design of aircraft with externally blown flaps
20 p2479 N73-29909
Conformal mapping technique for two-dimensional porous media and jet impingement heat transfer
[NASA-TM-X-68276] 20 p2485 N73-29961
Liquid jet impact against elastomeric materials
[PB-220972/4] 21 p2528 N73-30269
Effects of accelerating gas flow on atomization characteristics of liquid sprays produced by impinging two liquid jets - Part 1
[NASA-CR-134478] 22 p2652 N73-31247
Secondary atomization produced by accelerating gas flow to show effects on liquid sprays produced by impinging two liquid jets - Part 2
[NASA-CR-134479] 22 p2652 N73-31248
Measurement of fluctuating surface pressures induced on externally blown flaps by jet impingement and relationship to sonic fatigue of airframes
24 p2873 N73-32946

**JET LIFT**
Results of aerodynamic jet interference tests for Do-31 aircraft and application to future VSTOL development for lift-loss calculation
[BMVG-FBWT-72-22] 09 p0985 N73-18044

**JET MIXING FLOW**
Boundary layer control under hypersonic flow conditions using tangential injection of gas
[NASA-TT-F-13927] 01 p0041 N73-10320
Noise tests on simulated mixer nozzles and scale models of externally blown flap, lift augmentation system
[NASA-TM-X-2638] 02 p0124 N73-11012
Vaporization rates of liquid injected into high temperature, supersonic gas flow using aviation gasoline injected by Laval nozzle into air stream
[AD-747456] 03 p0286 N73-12317
Analysis of motion of chemically active gases to determine heat and mass transfer in turbulent jet system during diffusion combustion
[AD-747571] 03 p0365 N73-12976
Theoretical and experimental determination of interaction of semi-confined, subsonic, turbulent jets
[AD-749023] 04 p0408 N73-13325
Characteristics of mixing shock in mixing tube of water jet-gas pump to determine pressure distribution
[WTHD-31] 05 p0526 N73-14281
Analysis of swirling jet of gas injected into vacuum and effect of centrifugal force on separation of constituents
[ISAS-487-VOL-37-NO-13] 05 p0526 N73-14283
Navier-Stokes equations governing flow of subsonic or supersonic jets mixing with surrounding atmosphere
[AD-750185] 05 p0528 N73-14296
Analysis of nonequilibrium in excited levels of electric ARC heated potassium vapor injected into argon/helium gas flow passing through supersonic nozzle
[AD-750943] 05 p0585 N73-14759
Aerodynamic characteristics of wing moving close to interface with annular jet flowing from wing surface and impinging on screen
[AD-750933] 06 p0615 N73-14995
Molecular diffusion in mixing binary flow and separation of uranium isotopes by fixed wall centrifugation
06 p0653 N73-15302
Irregularities in flow behavior of parallel air jets behind smoothing grids
[NASA-TT-F-14653] 06 p0654 N73-15311
Flow characteristics of two-dimensional, tangential-slot injection into turbulent boundary layer at Mach 2.4 freestream velocity
[NASA-CR-2128] 06 p0654 N73-15313
Analysis of critical conditions of gas ejectors at large pressure drops within framework of ideal-gas dynamics
[AD-750536] 06 p0656 N73-15328
Provisional analysis of two dimensional turbulent mixing with variable density
[AD-751541] 07 p0773 N73-16275
Semiempirical theory on bending and development of round turbulent jet in subsonic crosswind
[AD-751093] 07 p0774 N73-16286
Experimental study and analog simulation of steady state and dynamic response of jet interaction proportional fluid amplifier
[AD-751458] 07 p0805 N73-16532
Conservation equations for analyzing supersonic and mixing flow regimes of supersonic ejectors
08 p0895 N73-17249
One- and two-D core theories for analyzing ducted mixing and burning of coaxial streams
08 p0896 N73-17253
Analysis of turbulent velocity fluctuations in confined jet to determine design parameters for fluid amplifiers
[AD-752041] 08 p0899 N73-17276
Performance of hypermixing nozzles in area ratio 23 ejector
[AD-752207] 08 p0955 N73-17821
Analysis of downstream mixing of transverse hydrogen injection from single and multiple orifices in Mach 4 boundary layer over flat plate
[NASA-CR-112254] 09 p1015 N73-18285
Analysis of turbulent mixing between two streams of different density to determine effects of density difference at low Mach number and compressibility at high Mach number
[AD-753538] 09 p1019 N73-18313
Mixing and ignition of hydrogen jets injected normally into supersonic two dimensional flow and effect on combustion performance of hypersonic ramjet engine
[ONERA-TP-973] 09 p1098 N73-18962
Semiempirical model for development of round turbulent jet in cross flow using asymptotic solution for jet excess velocity
[NLR-TR-71107-U] 10 p1142 N73-19307
Boundary layer control for mixing region in three dimensional laminar elliptical jet for thrust augmentation
[AD-754227] 10 p1143 N73-19313
Development and mixing of coaxial fluid jet with axisymmetric swirling vortex flow in cylindrical chamber
[AD-754613] 11 p1272 N73-20324
Computations of turbulent mixing and combustion of swirling jets in coaxial stream
[NASA-CR-2231] 11 p1348 N73-20935
Numerical analysis of nonlinear elliptic-hyperbolic mixing about wing profiles at Mach 1
14 p1597 N73-22944
Performance evaluation of two-dimensional slot nozzle ejector with variable area mixing sections
[NASA-CR-2251] 15 p1730 N73-24034
Analysis of breakup length and breakup pattern for jets of liquids of different viscosity and surface tension ejected vertically downward into atmosphere
[NLL-RTS-8049] 15 p1764 N73-24291
Analysis of decomposition of liquid jet injected normal to supersonic airstream to show generation of high frequency, axially propagating waves
15 p1764 N73-24296
Kinetic energy transfer in multiple jet mixing flow of duct inlet
[AD-758836] 16 p1891 N73-25305
Analysis of jet penetration and mixing of multiple cold air jets into ducted subsonic heated mainstream flow
[NASA-CR-121217] 17 p2014 N73-26286
Fluctuating pressure characteristics for far field acoustic radiation in mixing region of perturbed and unperturbed round free jet
[AD-759377] 17 p2015 N73-26294
Turbulent nonbuoyant or buoyant jets discharged into flowing or quiescent fluids
[AD-760028] 17 p2016 N73-26300
Application of holography techniques for recording three dimensional flow distribution of liquid jet injected into Mach 3 gas stream
17 p2039 N73-26498
Analysis of submerged, turbulent, two-dimensional, heated slot jet flowing into moving stream
18 p2128 N73-27197
Interaction of hypersonic source flow and axisymmetric free jet with rarefied background as examined by equations of motion
[AD-761149] 18 p2131 N73-27218

Vortex-lattice method used in model to represent jet exhausting from flat plate into crossflowing stream
[AD-762502] 20 p2389 N73-29191
Heat transfer across interface between high speed steam jet and external coaxial cocurrent water flow
[AD-763696] 21 p2527 N73-30262
System for reducing noise generated by jet impinging on external flap using injection of secondary air from slot near trailing edge of flap
[NASA-CR-132270] 22 p2611 N73-30930
Effects of accelerating gas flow on atomization characteristics of liquid sprays produced by impinging two liquid jets - Part 1
[NASA-CR-134478] 22 p2652 N73-31247
Secondary atomization produced by accelerating gas flow to show effects on liquid sprays produced by impinging two liquid jets - Part 2
[NASA-CR-134479] 22 p2652 N73-31248
Mixing process and performance effects of continuous H2-F2 laser
[AD-763828] 22 p2682 N73-31480
Flow characteristics of multiple dilution jets mixing with primary airstream for gas turbine combustors
[NASA-TM-X-71426] 23 p2829 N73-32612

**JET NOISE**
U JET AIRCRAFT NOISE

**JET PILOTS**
U AIRCRAFT PILOTS

**JET PLUMES**
U PLUMES

**JET PROPULSION**
Development and characteristics of tracked air cushion research vehicle for commercial high speed ground transportation
[PB-211216] 05 p0524 N73-14267
Research reports on SQUID programs related to fluid mechanics, and atomic and molecular collisions
[AD-752037] 08 p0955 N73-17820

**JET PROVOST AIRCRAFT**
Modifications of Jet Provost and Strikemaster trainer aircraft to provide adequate stall warning without excessive penalty on maximum lift at low speed
06 p0617 N73-15012

**JET PUMPS**
Influence of inlet deformation on characteristics of ejector jet devices operating on incompressible fluids
[AD-747079] 02 p0179 N73-11454
Characteristics of mixing shock in mixing tube of water jet-gas pump to determine pressure distribution
[WTHD-31] 05 p0526 N73-14281
Theory of two phase gas-liquid and liquid-gas flow for bladed machines and ejectors
[AD-755713] 12 p1409 N73-21419

**JET STREAMS [METEOROLOGY]**
Short-period comets and meteor stream genetic origin discussing formation processes
[TRITA-EPP-72-18] 02 p0231 N73-11880
Traveling ionospheric disturbance generation by tropopause jet stream
05 p0510 N73-14147
Stratospheric turbulence as an effect of jet streams, vorticity, temperature gradients, and temperature distribution
[NLL-M-22823-[5828.4F]] 11 p1274 N73-20338
Instability of internal waves in stratified nonviscous jet stream
[AD-761373] 18 p2149 N73-27368
Application of ERTS-1 multispectral scanner data for detecting thin cirrus and clear air turbulence
[PAPER-E14B] 19 p2270 N73-28279
Jet streams for studying kinetics of atmospheric circulation
20 p2444 N73-29628
Orgin of jet streams in earth atmosphere
20 p2446 N73-29652
Study of low level boundary layer jet streams for predicting dangerous atmospheric conditions
21 p2573 N73-30622

**JET THRUST**
Analysis of optimum nozzle thrust deflection angles in cruising flight
[ARC-CP-1222] 05 p0590 N73-14796
Method for calculating transient thrust and flowrate levels for Mariner type attitude control nitrogen gas jets
[NASA-CR-132987] 16 p1888 N73-25279
Transonic wind tunnel tests of thrust effects on missile aerodynamics
[AD-762576] 20 p2476 N73-29889

**JETAVATORS**
U GUIDE VANES

**JETS**
Supersonic flow past solid cylindrical and circular jet barriers on flat plates
[AD-750522] 06 p0656 N73-15327
Acoustic feedback of subsonic and supersonic jet impinging on obstacle
[DLR-FB-72-72] 14 p1602 N73-22987

**JETTIES**
U BREAKWATERS

**JETTISON SYSTEMS**
System for deploying and ejecting releasable clamshell fairing sections from spinning sounding rockets
[NASA-CASE-GSC-10590-1] 05 p0597 N73-14853
Computerized simulation of temperatures on Centaur standard shroud during heated jettison tests
[NASA-TM-X-68273] 20 p2485 N73-29962
Effects of ascent trajectory mode and tank disposal method on shuttle payload accommodation
[NASA-TM-X-64773] 21 p2599 N73-30831

**JIMSPHERE BALLOONS**
Jimsphere tracking for determining accuracy of meteorological radars
[AD-757624] 14 p1634 N73-23251

**JITTER**
U VIBRATION

**JOINING**
Significant advances in welding, bonding, and joining techniques since 1960
[AD-754262] 10 p1168 N73-19502

**JOINTS [ANATOMY]**
Nonlinear model relating neural input to force and muscle contraction in human ankle joint
01 p0015 N73-10117
Synchronization kinetics in control of movement links in human extremities
17 p1990 N73-26089

**JOINTS [JUNCTIONS]**
NT BEAM LEADS
NT BUTT JOINTS
NT LAP JOINTS
NT METAL JOINTS
NT RIVETED JOINTS
NT SEAMS [JOINTS]
NT SOLDERED JOINTS
NT SPOT WELDS
NT WELDED JOINTS
Reduction of peak shear stress in bonded joint
[NASA-CASE-LAR-10900-1] 01 p0061 N73-10499
Ultrasonic scanner for inspection and evaluation of in-place brazed tube joints
[NASA-TM-X-64702] 02 p0178 N73-11445
Stress-rupture strength of turbine blade root joints at elevated temperature and prolonged stress loads
[AD-749589] 04 p0465 N73-13788
Explosive welding of thin metal scarf joint
[NASA-CASE-LAR-11211-1] 05 p0552 N73-14480
Prototype elbow joint for remote control of heavy duty cargo boom
[AD-749520] 05 p0553 N73-14487
Development of epoxy resin lubricant sealant for hermetic sealing of threaded joints on pipes
[AD-752825] 09 p1040 N73-18486
Reliability and failure time prediction for titanium adhesive bonds using multiple regression analysis
[AD-754526] 11 p1301 N73-20560
Analysis of aircraft construction methods to compare riveting, welded joints, and bonded joints for structural stability
[AD-755754] 13 p1475 N73-21948
Improved latching device for joining structural components in motionless relationship
[NASA-CASE-MFS-21606-1] 13 p1532 N73-22417
Analysis of structural reliability of large scale bonded joints for advanced composite wing to determine service life of boron epoxy to titanium scarf joint
[AD-756893] 14 p1603 N73-22995
Metallurgical and mechanical properties of joints treated by weld-braze joining process
[NASA-TN-D-7281] 15 p1798 N73-24573
Design of expansion joint unit for coolant piping loop of reactor thermoelectric system - SNAP program
[NASA-CR-121209] 15 p1809 N73-24663
Performance of airfield pavement construction joints under heavy aircraft loads
[FAA-RD-72-106] 16 p1969 N73-25926
Aging tests of light alloys bonded with various adhesives and development of new aging test criteria
[RAE-LIB-TRANS-1662] 17 p2043 N73-26528
Life durability tests of bounded microcircuit joints subjected to prestressing
[AD-762333] 19 p2246 N73-28107
Equations for creep and stress relaxation in nickel-based alloy bolted joints subjected to vibration
[AD-761455] 19 p2349 N73-28897
Fracture characteristics of adhesive joints
[AD-762457] 19 p2351 N73-28910
Shielding analysis of joints and connectors in coaxial cables
[AD-761825] 21 p2518 N73-30201
Zero leakage separable and semipermanent ducting joints for space flight vehicles
[NASA-CR-124386] 22 p2722 N73-31780
Convective heating tests on joints and gaps between surface insulation tiles
24 p2940 N73-33477

**JORDAN FORM**
Algorithm for calculating Jordan canonical form of matrix
[NASA-CR-131654] 13 p1550 N73-22557

**JOSEPHSON JUNCTIONS**
Weak-link apparatus for superconducting instrumentation
[LNF-72/4] 04 p0422 N73-13439
Experimental and theoretical determination of intrinsic fluctuations in superconducting flux detector ring closed by Josephson junction
[AD-749101] 04 p0424 N73-13458
Josephson junctions and superconducting quantum interference devices
[NBS-TN-630] 06 p0707 N73-15772
Use of Josephson devices to measure low frequency magnetic fields and voltages
[LBL-845] 06 p0708 N73-15777
Local oscillator and mixer forming Josephson frequency conversion in superconducting point contact junctions
[AD-750775] 06 p0709 N73-15784
Use of very high Q superconducting microwave cavities to obtain strong coupling between electromagnetic field and Josephson junction
[AD-749986] 06 p0710 N73-15795
Properties of evaporated Josephson junctions coupled to high q superconducting microwave cavities
[AD-749981] 06 p0710 N73-15796
Computer computation of spectral data for Josephson junction circuit
[NBS-TN-627] 07 p0832 N73-16740
Perturbation method for calculating voltage and impedance response of Josephson point contacts to external HF currents
[AD-751911] 08 p0951 N73-17786
Response of self-driven, weakly connected superconducting ring incorporating small voltage-biased Josephson junction
[AD-752213] 08 p0951 N73-17788
Shunted junction model applied to point contact Josephson junctions, using dc characteristics as function of temperature, contact pressure, and RF power
[AD-754082] 11 p1331 N73-20801
Quasi-particle pair interference current in superconducting weak links of Josephson junctions
[AD-754081] 11 p1331 N73-20803
Coherent behavior of Josephson junction arrays
[BNL-17232] 12 p1441 N73-21671
Application of electron tunneling process to superconductor technology
[AD-756081] 13 p1566 N73-22692
Design and operation of superconducting quantum point contact interference device
[PB-214758/5] 15 p1823 N73-24775
Numerical analysis of Josephson junction interferometers
16 p1911 N73-25464
Liquid helium experiments on ac Josephson effect in superfluid helium and superfluid critical velocities
16 p1944 N73-25728
Design and performance of superconducting quantum interference devices
[PB-214757/7] 16 p1954 N73-25810
Characteristics of antenna arrays of superconducting point contact Josephson junctions
17 p1994 N73-26120
Polymeric monolayer barrier for thin film Josephson junctions
[NASA-CR-121270] 19 p2326 N73-28715
Behavior of macroscopic quantum interferometer composed of superconducting tin rings containing two Josephson junctions
24 p2967 N73-33710

**JOULE HEATING**
U OHMIC DISSIPATION
U RESISTANCE HEATING

**JOULE-THOMSON EFFECT**
Design of Joule-Thomson cascade for refrigeration cooling using liquid helium
[CEA-CONF-2044] 10 p1199 N73-19761

**JOURNAL BEARINGS**
Early stage design and choice of journal bearings
[ESDU-65007] 01 p0061 N73-10495
Performance of graphite fiber reinforced polyimide composites as journal bearing materials
[NASA-TN-D-7078] 01 p0062 N73-10505
Evaluation of several thermographic infrared techniques and their applicability to detection of unbonded areas in babbitted bearings
[AD-745730] 01 p0063 N73-10516
Design of steadily loaded, pressure fed, 360 degree, hydrodynamic journal bearings
[ESDU-66023] 02 p0177 N73-11431
Data sheet for prediction of loaded hydrodynamic journal bearing performance
[ESDU-69002-AMEND-A] 02 p0177 N73-11432
Performance characteristics of self lubricating sintered sulfur-iron material used for bushings in naval aircraft
[AD-748175] 03 p0319 N73-12603
MoS2 and MoS2/PTFE composite layers for dry lubrication of journal bearings in atmosphere or vacuum
[DLR-FB-72-69] 09 p1038 N73-18470
Analytical solution of Reynolds equation and application to hydrodynamic lubrication to show characteristics of lubrication film
[TAE-153] 09 p1057 N73-18618
Bearing sectors for controlling self excited instability of journal bearing shafts rotating at high speeds in low viscosity lubricants
[NASA-CASE-LEW-11076-2] 11 p1298 N73-20533
Design, development, and test of two types of pivoted pad journal bearings and spiral groove thrust bearing for use with Brayton cycle power unit
[NASA-CR-121098] 12 p1408 N73-21410

Investigation of wear behavior and load capacity of journal bearings in transition range from full to boundary lubrication using radioisotopes
[KFK-1569] 15 p1793 N73-24533
Flapping- and squeeze-duty design criteria for full journal bearings under dynamic duty
[WTHD-45] 16 p1917 N73-25514
Design, fabrication, and performance tests of foil journal bearings for application to Brayton cycle turbo-alternator-compressor
[NASA-CR-2243] 19 p2304 N73-28529
Optical radar angle tracking mount
[AD-765213] 23 p2759 N73-32077

JOURNALS (DOCUMENTS)
U PERIODICALS

JOURNALS (SHAFTS)
U SHAFTS (MACHINE ELEMENTS)

JP-4 JET FUEL
Burning rate of JP-4 and air propellant in closed combustion chamber
[AD-757634] 14 p1720 N73-23954
Physical and chemical properties of JP-4 jet fuel for 1972
[AD-764690] 23 p2828 N73-32605

JP-5 JET FUEL
Effectiveness of relaxation chamber and static charge reducer in dissipating electrostatic charge during JP-5 refueler loading
[AD-748995] 04 p0462 N73-13772

JUDGMENTS
Effect of simulated sonic booms and overpressure on EEG waveform patterns and disturbance judgments
[FAA-RD-73-115] 21 p2500 N73-30066

JUNCTION DIODES
Tungsten-germanium whisker diode far infrared detector
[UCLA-34-P-157] 03 p0274 N73-12219
Millimeter wave image conversion panel using p-i-n diode structures for carrier injection and bulk conductivity modulation
[AD-747409] 03 p0276 N73-12241
Computer program for p-n junction diode simulation
08 p0887 N73-17186
Deep trap model for predicting capacitance voltage characteristics of irradiated silicon diodes and resistors
08 p0888 N73-17188
Phototransistor with base collector junction diode for integration into photo sensor arrays
[NASA-CASE-MFS-20407] 10 p1133 N73-19235
Characteristics of second breakdown in germanium gold diodes
[AD-755425] 12 p1385 N73-21230
Manufacturing of Gunn diodes with short domainless ISA mode for microwave oscillators with 100 W output
15 p1757 N73-24238
Study of heterojunction Pb 1-x Sn X Te diodes
[AD-761767] 19 p2244 N73-28093
Junction capacitance techniques to characterize radiation damage in silicon
[AD-762482] 20 p2464 N73-29796
Selection of step recovery diodes for microwave frequency multipliers, noting frequency conversion efficiency
[FTZ-A-46-TBR-5] 22 p2642 N73-31174

JUNCTION TRANSISTORS
Analog model for minority charge carrier diffusion to base contact of bipolar transistor with current amplification
[NLL-TRANS-2861-[9022.81]]
02 p0148 N73-11201
Electrical properties of MOS field effect transistors and Schottky barrier photodiode
[AD-748862] 04 p0459 N73-13746
Surface cooling method for very high frequency power transistor using heat pipe techniques
[AD-752076] 08 p0889 N73-17200
Electrostatic discharge effects in JFET performance and reliability in low humidity environment
[BDX-613-815] 12 p1383 N73-21217
Flicker noise and related bulk effects in silicon junction field effect transistors
20 p2461 N73-29774

JUNCTIONS
Experimental analysis of frequency response of pneumatic tee junction
[AD-750369] 06 p0656 N73-15329
Dynamic plastic behavior of metal shell intersection
[AD-760012] 17 p2095 N73-26952

JUPITER (PLANET)
Calculation of all occultations by planet Jupiter of stars brighter than magnitude 6.55 for period 1951 to 2000
[NASA-TT-F-14626] 01 p0104 N73-10862
Inhomogeneous models of Jovian atmosphere with two cloud layers
04 p0468 N73-13817
Instrumentation for spectrum analysis of short bursts and pulses of Jovian decametric radio emission recorded on magnetic tape
05 p0547 N73-14440
Analysis of quasi-periodic modulation of L-bursts in decametric radiation from planet Jupiter
05 p0594 N73-14833
Observations of Jovian satellite eclipse
[NASA-CR-130292] 06 p0717 N73-15849
Spectrophotometric observations of planet Jupiter to determine ultraviolet absorption for different regions of disk
09 p1083 N73-18835
Photoelectric measurements of solar phase brightness relationship of planet Jupiter Galilean satellites to show porous nature of surface layers of satellites
09 p1083 N73-18838
Tracking and data system support of launch, near-earth, and deep space phases of Pioneer 10 space probe flight
[NASA-CR-131373] 11 p1256 N73-20188
Pioneer F and G missions to Jupiter
[NASA-TM-X-69125] 11 p1338 N73-20859
Spacecraft microbial burden reduction for Jupiter due to atmospheric entry heating
[NASA-CR-132072] 15 p1741 N73-24117
Spin scan camera photography of Jupiter from rotating outer planet orbiters
[NASA-TM-X-62260] 15 p1830 N73-24836
Galilean satellite thermal radiation measurements
16 p1961 N73-25866
Observations of atmospheric limb darkening in visual continuium and multiple scattering analysis of jupiter and saturns atmospheres
22 p2713 N73-31719
Observations of decametric radiation of Jupiter with very-long-baseline interferometer
23 p2836 N73-32659
Theory of radial diffusion applied to electron and proton radiation belts of Jupiter
23 p2836 N73-32663

JUPITER ATMOSPHERE
Visual and photographic observations of Beta Scorpii occultation by Jupiter
[NASA-CR-129990] 05 p0594 N73-14832
Composition, temperature, and optical properties of Jupiter and Saturn atmospheres
[NLL-M-20702-[5828.4F]] 06 p0716 N73-15845
Space vehicle descent into Mars, Jupiter, and Venus atmospheres
[NASA-TT-F-768] 07 p0844 N73-16838
Jovian radiation belts investigation, including particle and field studies
08 p0973 N73-17956
Jovian emission spectrum analysis for temperature and ammonia profiles, and Martian infrared limb profile analysis for atmospheric temperature and water vapor
[NASA-CR-131266] 11 p1337 N73-20847
Spectrophotometric analyses of Jovian and Saturnian limb darkenings
[NASA-CR-131891] 13 p1576 N73-22772
Jovian magnetosphere model with thermal plasma and superimposed radiation belts
[NASA-CR-132960] 16 p1963 N73-25878
Methane spectral line formation in Jovian atmosphere
17 p2080 N73-26826
Spectrometric measurement of D/H ratio in Jupiter atmosphere
24 p2978 N73-33797

JUPITER PROBES
Effects of Jupiter high energy electron environment on gates and MOSFET performance
[AD-756215] 13 p1502 N73-22178
Nonlinear filter estimation of interplanetary spacecraft orbits during simulated Jupiter flyby and Jupiter orbiter missions
17 p2081 N73-26834
Pioneer 11 high field fluxgate magnetometer experiment
[NASA-TM-X-70467] 22 p2672 N73-31405
Thermoelectric generator for Pioneer interplanetary Jupiter flyby mission
[IESD-2873-172] 23 p2818 N73-32529


## K


K BAND
U EXTREMELY HIGH FREQUENCIES

K LINES
X ray attenuation coefficients in absorption spectra of titanium, iron, cobalt, nickel, copper, and zinc
[UCRL-73923] 10 p1189 N73-19675
Solar X ray based calculations of K alpha line emission from sulfur, argon, calcium, and iron
[NASA-TM-X-66210] 11 p1335 N73-20839

KA BAND
U EXTREMELY HIGH FREQUENCIES

KALMAN FILTERS
Kalman filtering algorithm for detecting continuous wave interference signals in digital telecommunications
01 p0027 N73-10210
Optimal emitter location algorithm using Kalman filtering for computerized airborne direction finding
[AD-745888] 02 p0208 N73-11688
Missile trajectory smoothed by Kalman method using data from several cameras, radars, and Doppler receivers
[WRE-TN-705[T]] 02 p0227 N73-11831
Theory of Kalman filtering and applications to real time tracking systems for air traffic control, satellite observation, and aircraft navigation
[AD-751485] 07 p0818 N73-16634
Kalman filter theory for estimating sonobuoy reference system in antisubmarine warfare
[AD-753608] 10 p1129 N73-19201
Fault detection possibilities in integrated navigation system employing Kalman filtering
11 p1320 N73-20712
Application of Kalman-Bucy filter theory to post-flight guidance error analysis
[NAL-TR-302] 15 p1808 N73-24652
Using extended Kalman filter and weighted least square error filtering techniques to estimate orbital parameters of near earth satellite
[AD-757880] 15 p1832 N73-24852
Earth dynamic filtering algorithm for earthquake prediction and Love number determination
16 p1896 N73-25333
Design of extended Kalman filter for detection and ranging of ground radar from aircraft
[AD-760764] 18 p2123 N73-27158
Evaluation of approach and landing performance of inertial navigation system with Kalman filter installed in CV-340 aircraft
[NASA-TN-D-7302] 23 p2816 N73-32515
Dynamic calibration of inertial navigation system using extended Kalman filtering and command torquing of platform gyros
24 p2950 N73-33566

KALMAN-SCHMIDT FILTERING
Kalman filter equations for calculating quadratic forms for turn detector
[AD-744582] 01 p0028 N73-10220
Target maneuvers and sensor noise effects on proportional navigation systems noting Kalman filtering
[AASU-316] 03 p0329 N73-12681
Applying Kalman filtering to radar track-while-scan problem
[AD-747696] 04 p0390 N73-13173
Kalman filtering applied to surface and air navigation using celestial body coordinates
07 p0860 N73-16973
Optimal estimation of measurement biases in Kalman-Schmidt filtering
[AD-753961] 11 p1311 N73-20641
Application of loran/inertial hybrid system and Kalman filter algorithm to fixed feedback gain
11 p1318 N73-20701
Error model coefficients for extended Kalman filtering to dynamic calibration of inertial navigation system
[AD-763718] 21 p2577 N73-30656

KAMACITE
Effect of neutron irradiation on remanent magnetization in Apollo 11 and 12 lunar samples of iron and kamacite
15 p1813 N73-24692

KAMAN AIRCRAFT
NT UH-2 HELICOPTER

KAMAN UH-2A HELICOPTER
U UH-2 HELICOPTER

KAME
U GLACIAL DRIFT

KANSAS
Crop identification and acreage measurement in Idaho, Missouri, Kansas, and South Dakota using ERTS-1 imagery
[E72-10179] 01 p0045 N73-10358
Environmental and resource study of Kansas using ERTS-1 imagery
[E72-10305] 04 p0412 N73-13354
Crop identification and acreage measurement in Missouri, Kansas, South Dakota, and Idaho using ERTS-1 imagery
[E72-10336] 05 p0531 N73-14324
Crop identification and acreage measurement in Missouri, Kansas, South Dakata, and Idaho based on ERTS-1 imagery and aerial photography
[E73-10328] 09 p1024 N73-18359
Location of center pivot sprinkler irrigation systems in Finney County, Kansas, based on ERTS-1 interpretation
[E73-10418] 11 p1279 N73-20380
Detection and indentification of major airports in northeastern Kansas and northwestern Missouri
[E73-10471] 12 p1395 N73-21308
Identification of corn harvesting in Finney County, Kansas from ERTS-1 imagery
[E73-10472] 12 p1395 N73-21309
Mapping of land use in agriculture area of Finney County, Kansas based on ERTS-1 imagery
[E73-10474] 12 p1395 N73-21311
Identification of winter wheat on irrigated land in southern Finney County, Kansas
[E73-10475] 12 p1395 N73-21312
Crop identification and land acreage measurement in Kansas using ERTS-1 imagery
[E73-10514] 13 p1517 N73-22288

Identification and mapping of land use classes in Kansas City area by machine processing of ERTS-1 data
[E73-10578] 14 p1656 N73-23439
Data processing and image enhancement of ERTS-1 MSS data for Kansas
[E73-10596] 14 p1658 N73-23453
Photointerpretation of ERTS-1 imagery to map bodies of water in Saline County, Kansas
[E73-10684] 17 p2017 N73-26313
Utilization of ERTS-1 imagery for crop identification and acreage measurement in South Dakota, Kansas, Missouri, and Idaho
[E73-10734] 17 p2020 N73-26340
Collection of ground truth and meteorological data for Skylab test sites in Texas and Kansas
[E73-10752] 17 p2022 N73-26355
Influence of atmosphere pathlengths on ERTS-1 MSS imagery acquired over southwestern Kansas
[E73-10763] 18 p2133 N73-27240
Analysis of ERTS-1 imagery for area measurement of land use categories in Finney County, Kansas
[E73-10764] 18 p2134 N73-27241
Interpretation of ERTS-1 data to determine acreage of winter wheat in Kansas based on multispectral band scanner data
[PAPER-A1] 19 p2259 N73-28209
Application of ERTS-1 imagery for differentiating quaternary surface deposits and landforms in Illinois, Iowa, Missouri, Kansas, Nebraska, and South Dakota
[PAPER-G13] 19 p2264 N73-28244
Analysis of water turbidity in two federal reservoirs in Kansas using ERTS-1 multispectral band scanners
[PAPER-E12] 19 p2270 N73-28276
Detection and monitoring of water quality parameters in reservoirs and lakes in Kansas from Skylab imagery
[E73-10938] 21 p2529 N73-30280
Detection and monitoring water quality in Kansas reservoirs from Skylab data
[E73-10939] 21 p2529 N73-30281
Soil moisture and vegetation surveys of Kansas and Texas for Skylab investigations
[E73-10944] 21 p2530 N73-30286
Influence of image position on urban place detection in ERTS-1 imagery of Kansas and Missouri
[E73-10971] 21 p2533 N73-30312
ERTS-1 imagery of surface water aera in Quivera National Wildlife Refuge, Kansas
[E73-10974] 21 p2533 N73-30313
Detection of precipitation pattern in west central Kansas from ERTS-1 MSS imagery
[E73-10975] 21 p2533 N73-30314
Detection of urban street patterns in ERTS-1 imagery of Lincoln, Nebraska
[E73-10976] 21 p2534 N73-30315
Comparison of ERTS-1 spectral reflectance measurements of major crops and soil associations for selected sites in Iowa, Kansas, North Dakota, and Texas
[E73-10981] 22 p2657 N73-31288
Interpretation of land use and stream drainage in Pawnee River Basin, Kansas
[E73-11005] 22 p2660 N73-31310
ERTS-1 measurements of major crops and soil associations in Indiana, North Dakota, Iowa, Nebraska, Kansas, and Texas
[E73-11155] 24 p2919 N73-33309

**KAPITZA RESISTANCE**
Theory for thermal boundary, kapitza, resistance to include effects of phonon attenuation near interface
24 p2968 N73-33719

**KAPTON [TRADEMARK]**
Kapton covered cadmium sulfide solar cell performance tests in aerospace and earth atmosphere environments
[ONERA-DERTS-NT-02-32] 03 p0255 N73-12062

**KARHUNEN-LOEVE EXPANSION**
Three day advance warning system of heating plant failure using algorithmic detection methods
[NASA-CR-131571] 13 p1505 N73-22197
Unique approach to feature selection based on Karhunen-Loeve expansion
[TR-29] 20 p2440 N73-29598

**KC-130 AIRCRAFT**
U C-130 AIRCRAFT

**KC-135 AIRCRAFT**
U C-135 AIRCRAFT

**KEL-F**
Method of testing materials based on teflon and Kel-F for friction at low temperatures by using X18H9T steel in helium medium for different slip rates and loads
22 p2688 N73-31531

**KENTUCKY**
NT TENNESSEE VALLEY [AL-KY-TN]
ERTS-1 imagery of landscape changes in Tennessee and Kentucky due to strip mining
[E72-10265] 03 p0291 N73-12364
Detection of plant diseases and nutrient deficiencies, soil types, and moisture levels from ERTS-1 imagery of Tennessee and Kentucky
[E73-10468] 12 p1395 N73-21305
Skylab monitoring of surface mining activities and reclamation in Ohio, West Virginia, Pennsylvania, Indiana, Kentucky, and Illinois
[E73-11033] 22 p2663 N73-31337

**KEROSENE**
Electrified kerosene and gasoline aviation fuel during passage through pipes and filters of fuel tank reservoir
[AD-764941] 24 p2971 N73-33740

**KERR CELLS**
High speed photography of electro-optical fringe patterns for measuring pulsed electric field between Kerr cell electrodes
[SC-DC-72-1375] 04 p0399 N73-13243
Camera with laser driven Kerr cell having fast time resolution
[DESY-72/14] 04 p0422 N73-13438

**KERR MAGNETOOPTICAL EFFECT**
Kerr magnetooptical effect in nickel, gadolinium, and dysprosium at temperatures between 10 and 300 K in 1 to 5 eV energy range
12 p1437 N73-21644
Magnetooptical measurements of demagnetizing fields in cylindrical magnetic films
[JPRS-59624] 19 p2321 N73-28670

**KESTREL AIRCRAFT**
U P-1127 AIRCRAFT

**KETONES**
NT ACETONE
NT PENTANONE
Methylisobutylketone causing lesions in first and second sections of proximal convoluted tubule of nephron of kidney
[AD-751444] 07 p0748 N73-16083
Electronic spectra of benzophenone crystals and low temperature spectra of ketones
[AD-753380] 10 p1201 N73-19775
Spectroscopic analyses of molecular energy levels in crystals
[AD-753382] 10 p1201 N73-19776
Tricyclic nitropropene nitronate intermediates in condensation reactions of symmetric trinitrobenzene with cycloalkanones, and with phloroglucinol
[NASA-CR-131288] 11 p1252 N73-20159
Validity of rapid delta-aminolevulinic acid determination in urine for lead intoxication tests on industrial workers
[NASA-TT-F-14864] 12 p1371 N73-21128

**KEYING**
NT FREQUENCY SHIFT KEYING
NT PHASE SHIFT KEYING

**KIDNEY DISEASES**
Methylisobutylketone causing lesions in first and second sections of proximal convoluted tubule of nephron of kidney
[AD-751444] 07 p0748 N73-16083

**KIDNEYS**
Morphological changes in juxtaglomerular apparatus in kidneys of rats during multihour exposure to accelerations in different directions
07 p0743 N73-16045
Morphological changes in rat kidneys exposed to different accelerations
20 p2366 N73-29023
Water load tests for determining hydration status and adrenal and kidney functions during post flight period
[NASA-TT-F-15091] 22 p2620 N73-30998

**KIMBERLITE**
U BIOTITE

**KINEMATIC EQUATIONS**
Kinematic equations for unified flexible spacecraft simulation program
[NASA-CR-124170] 11 p1340 N73-20877

**KINEMATICS**
NT BODY KINEMATICS
Observations of kinematic and thermodynamic fields over Barbados
10 p1180 N73-19596
Kinematic method in vertical motion and atmospheric energy computations
12 p1394 N73-21298
Cardiac systole kinematics in humans exposed to hypoxic atmosphere
13 p1479 N73-21986
Kinematics of noctilucent clouds and wind discontinuities at mesopause
[NASA-TT-F-14928] 14 p1660 N73-23471
Computer program for analyzing kinematical responses of structures caused by excitations for use in NERVA program
[NASA-CR-132214] 15 p1810 N73-24671
Volumetric kinematic analysis on servomechansim of remote handling manipulator
17 p1989 N73-26075
Matrix method for analyzing kinematics of spatial mechanisms for manipulators
17 p1989 N73-26077
Manipulator kinematics in selecting geometrical shapes of containers and chambers
17 p1990 N73-26087
Screw calculus in kinematic and power analyses on spatial positions of manipulator link mechanisms
17 p1990 N73-26092
Kinematics of orientation in rotating coordinate system and determination of orientation of instrument trihedrons
[JPRS-59162] 20 p2451 N73-29700
Kinematics of stability of orientation in rotating coordinate system signal processing
20 p2451 N73-29702
One dimensional elastic collision problem in which two approaching masses are separated by elastic particle
[AD-764514] 22 p2726 N73-31814
Precision theory for kinematic errors in uniaxial gyrostabilizer as angular velocity integrator
23 p2791 N73-32329
Kinematic properties of carbon stars
24 p2977 N73-33791

**KINETIC ENERGY**
Dissipation of kinetic and thermal energy in mixed surface layer of ocean from measurements made in Barbados oceanographic and meteorological experiment
[AD-745343] 01 p0053 N73-10431
Conversion of magnetic field energy into kinetic energy in solar wind as function of heliocentric distance
01 p0095 N73-10780
Analysis of vibration characteristics of laminated plates and modifications of plate theory to produce results consistent with continuum theory
[AD-746951] 02 p0240 N73-11949
Momentum, energy, and mass budgets of stratosphere
[COO-2195-2] 04 p0415 N73-13385
Plasma production using gas stream kinetic energy in magnetic field
[DLR-FB-71-43] 04 p0455 N73-13714
Kinetic energy of abrasive particles knocked from metal surface during impact
[AD-750500] 06 p0655 N73-15321
Particle production and energy dissipation in stationary fusion plasma
[FOA-4-C-4465-25] 06 p0703 N73-15734
Relation of gas kinetic particle pressure and discharge field in plasma heating by pulsed longitudinal current
[AEC-TR-7330] 07 p0826 N73-16697
Mass spectrometer to study kinetics and thermodynamics of graphite vaporization
[AD-755899] 12 p1465 N73-21871
High energy particle kinetics along boundary of matter-antimatter of universe
[LPTHE-73/5] 14 p1703 N73-23818
Prediction of free turbulent mixing using turbulent kinetic energy method
19 p2253 N73-28167
Turbulent kinetic energy equation and free mixing
19 p2254 N73-28169
Integral turbulent kinetic energy analysis of free shear flows
19 p2254 N73-28170
Numerical procedure for determining relationship between shear stress and turbulent kinetic energy in two dimensional flow
22 p2649 N73-31221
Computation of kinetic fluctuation energy of turbulent shear flow from mean velocity distribution
24 p2908 N73-33211

**KINETIC EQUATIONS**
NT HELMHOLTZ VORTICITY EQUATION
NT HYDRODYNAMIC EQUATIONS
NT KINEMATIC EQUATIONS
Breakdown of quasi-linear derivation of kinetic equation describing cosmic ray distribution function in random magnetic field
[NASA-TM-X-65949] 09 p1081 N73-18815
Examples of spatially homogeneous gas motions and calculations using model kinetic equation
12 p1417 N73-21485
N-particle kinetic equation for classical gas with central force interactions
20 p2456 N73-29735

**KINETIC FRICTION**
NT SLIDING FRICTION

**KINETIC HEATING**
NT AERODYNAMIC HEATING
NT SHOCK HEATING
High frequency wave field pressure effect on Langmuir monochromatic plasma oscillations
[AEC-TR-7337] 07 p0827 N73-16707
Kinetic energy and X ray conversion in plasma heated by laser
[AD-751048] 07 p0830 N73-16733
Development of plasmas for industrial applications as fusion torches
24 p2961 N73-33663

**KINETIC THEORY**
NT MIXING LENGTH FLOW THEORY
NT TRANSPORT THEORY
Molecular-kinetic theory for determining temperature dependence of simple liquid viscosity
[AD-747089] 02 p0159 N73-11286
Steady-state solutions for discrete-velocity Boltzmann systems in restricted flow region
[AD-748182] 04 p0406 N73-13311

Research in analytical methods in nonrelativistic field theory and singular perturbation theory in kinetic theory
[AD-750482] 06 p0702 N73-15721
Proofs for binary collision term in Boltzmann transport equations in kinetic theory of gas and plasma dynamics
[TRITA-EPP-72-25] 07 p0772 N73-16273
Statistical mechanics and kinetic theory for two dimensional plasma in uniform magnetic field
07 p0825 N73-16685
Thermodynamic and kinetic behavior of protons and deuterons in regular and heavy ice
[NASA-TT-F-14692] 08 p0946 N73-17744
Singular limits of Boltzmann equation solutions for describing qualitative and quantitative properties of rarefied gas
[AD-753691] 10 p1143 N73-19312
Kinetic theory of stress-strain relations and temperature induced dislocation in crystal lattices
[AD-753576] 10 p1201 N73-19777
Lectures on properties and characteristics of rotating and stratified fluids
[AD-754066] 11 p1272 N73-20320
Solution of Boltzmann kinetic equation for relaxation of gas mixture
12 p1418 N73-21486
Application of kinetic gas theory to plasma physics and dynamics of galaxies
[FRNC-TH-247] 12 p1436 N73-21634
Kinetics of decomposition of adsorbed sarin determined microcalorimetrically
[REPT-1972-18] 14 p1616 N73-23091
Application of kinetic theory to collisionless regions of polar and solar winds
[AERONOMICA-ACTA-A-N-115-1973]
14 p1702 N73-23812
Kinetic theory of completely ionized plasma
[AD-758612] 15 p1819 N73-24744
Molecular-kinetic theory of nature of polymer friction
[NLL-RISLEY-TR-2577-[9091.9F]]
16 p1931 N73-25628
Kinetic theory for input impedance of cylindrical dipole antenna in anisotropic plasma
17 p2067 N73-26720
Kinetic theory of optically pumped gas laser oscillator
18 p2157 N73-27428
Plasma kinetic theory and plasma dynamics
[NASA-CR-132785] 18 p2183 N73-27623
Kinetic model for nitric oxide formation from organic fuel nitrogen
[FML-PUBL-73-7] 22 p2625 N73-31032
Application of kinetic theory approach to problems in gas dynamics
24 p2903 N73-33171

**KINETICS**
NT KINETIC ENERGY
NT REACTION KINETICS
Kinetics of purification of beryllium through evaporation data acquired during vacuum induction melting
[NASA-CR-123946] 04 p0431 N73-13512
Micrometeoroid analyzer using arrays of interconnected capacitors and ion detector
[NASA-CASE-ARC-10443-1] 11 p1291 N73-20477
Kinetics and thermodynamics of oxygen conversion from gas to metal phase in tungsten and molybdenum
12 p1412 N73-21446
Model of pulsed CO/N2 molecular laser system with emphasis on mixture components and temperature variation
[AD-755197] 14 p1673 N73-23573
Kinetic study of copper cementation on iron
[BM-RI-7761] 15 p1791 N73-24519
Synchronization kinetics in control of movement links in human extremities
17 p1990 N73-26089
Topology and kinetics of grain growth
[AD-760580] 18 p2162 N73-27468
Kinetics of chemically pumped CO2 and CH2N2-CO2 photolysis laser systems
20 p2424 N73-29469
Excitation and relaxation processes in H2O discharges and lasers
20 p2424 N73-29471
Jet streams for studying kinetics of atmospheric circulation
20 p2444 N73-29628

**KINOFORM**
Performance of computer generated binary and kinoform holograms
22 p2680 N73-31464

**KIRCHHOFF LAW**
Examination of dynamic laws in Kirchoff and Lagrange schemes
10 p1187 N73-19663

**KIRCHHOFF LAW OF RADIATION**
Kirchhoff approximation correction for application to electromagnetic wave scattering by rough surfaces
[NASA-CR-112263] 16 p1875 N73-25180
Curvature corrected Kirchhoff formulation for radar sea-return from near vertical
22 p2628 N73-31053

**KIRCHHOFF-HELMHOLTZ FLOW**
U PIPE FLOW

**KIRCHHOFF-HUYGENS PRINCIPLE**
U DIFFRACTION
U WAVE PROPAGATION

**KITE BALLOONS**
U TETHERED BALLOONS

**KLEIN-GORDON EQUATION**
Solution to Klein-Gordon and Dirac equations for charged particles in two noncollinear electromagnetic waves
[AD-754307] 11 p1327 N73-20769

**KLYSTRONS**
Refocusing of spent axisymmetric beam in klystron tubes for optimal entry into multistage depressed potential collector
[NASA-CR-121114] 05 p0519 N73-14217
Electron bunching in drift area of two cavity klystrons via one dimensional approximation, using electron beam disk model
[AD-751073] 07 p0763 N73-16204
Design of klystron microwave amplifier tube for troposcatter communication system
[AD-752075] 08 p0890 N73-17204
Phase locking of reflex klystron with stable microwave source
[AD-758677] 16 p1882 N73-25235
Klystron 100 megawatt amplifier with 400 MHz bandwidth
[AD-762929] 20 p2381 N73-29133
Comparative study of TWT and klystron amplifiers for use as power amplifiers in television broadcast satellites
[ESRO-CR[P]-267-VOL-1] 21 p2508 N73-30122
Comparative study of TWT and klystron amplifiers for use as power amplifiers in television broadcast satellites
[ESRO-CR[P]-268] 21 p2508 N73-30123
Comparative study of TWT and klystron amplifiers for use as power amplifiers in television broadcast satellites
[ESRO-CR[P]-269-VOL-3] 21 p2508 N73-30124
Development of procedure for measuring short-term instability of millimeter band klystron frequency
22 p2630 N73-31080
Comparative study of TWT and klystron for use as power amplifier in TV broadcast satellites
[ESRO-CR[P]-271] 22 p2634 N73-31109
Comparative study of TWT and klystron for use as power amplifier in TV broadcast satellites
[ESRO-CR[P]-272] 22 p2634 N73-31110
Low ripple klystron power supply for experimental array radar transmitter
[AD-765515] 24 p2881 N73-33010

**KNOWLEDGE**
NT PHILOSOPHY

**KOREA**
Tables of synoptic meteorological observations for Japanese and Korean coastal marine areas
[AD-753468] 10 p1182 N73-19619
Transfer of technology developed for aerospace program to specific industrial problems of developing nation [Korea]
[NASA-CR-133358] 19 p2355 N73-28943

**KRYPTON**
Chemical analysis of krypton and xenon isotopes in three meteorites and for melt extractions on samples of five terrestrial sedimentary rocks
08 p0958 N73-17836

**KU BAND**
U SUPERHIGH FREQUENCIES

**KUTTA-JOUKOWSKI CONDITION**
Analysis of Kutta-Joukowsky condition in three dimensional flow with application to vortex sheet attachment to wing surface
[NASA-TT-F-14918] 15 p1767 N73-24319
Kutta-Joukowski condition for describing three dimensional flow over arbitrary wing
[RAE-LIB-TRANS-1709] 24 p2905 N73-33185

**KWIC INDEXES**
KWIC index on oceanography
[NOAA-TM-EDS-ESIC-5] 18 p2213 N73-27867

# L

**L BAND**
U ULTRAHIGH FREQUENCIES

**L-1011 AIRCRAFT**
Investigation of crash of L-1011 aircraft near Miami, Florida on 29 Dec. 1972
06 p0619 N73-15024
Fabrication of L-1011 aircraft panels to compare costs and service performance characteristics of PRD-49 and fiberglass
[NASA-CR-112250] 11 p1234 N73-20018
Aircraft accident involving L-1011 aircraft crash near Miami, Florida on 29 Dec. 1972 during examination of suspected nose gear malfunction
[NTSB-AAR-73-14] 20 p2360 N73-28984

**LABELING [MARKING]**
U MARKING

**LABOR**
Model for estimating cost of unmanned lunar and planetary exploration programs
[NASA-CR-131897] 14 p1705 N73-23840

**LABORATORIES**
NT ENGINE TESTING LABORATORIES
NT ENVIRONMENTAL LABORATORIES
NT HUMAN FACTORS LABORATORIES
NT LUNAR RECEIVING LABORATORY
NT MANNED ORBITAL LABORATORIES
NT MANNED ORBITAL RESEARCH LABORATORIES
NT SPACE LABORATORIES
Environmental pollution monitoring for radioactive isotope laboratory
[MLM-1922] 03 p0340 N73-12770
Organization and functions of research facility for conducting projects involving low temperature effects
04 p0487 N73-13976
Operational descriptions of some electronics and nuclear laboratories in Poland
[AD-752772] 09 p1011 N73-18257
Laboratory experiments on interaction of fast protons and hydrogen atoms with earth atmosphere
[AD-757505] 14 p1663 N73-23499

**LABORATORY EQUIPMENT**
Analysis of laser applications in medicine, biology, research, chemical processing, initiation of thermonuclear reactions, and weapon systems
[AD-743098] 01 p0066 N73-10541
Laboratory restraint chair for squirrel monkeys
[AD-746661] 02 p0154 N73-11246
Operating characteristics of far infrared spectroscopic system for analyzing plasma diagnostics
[AD-748280] 04 p0456 N73-13726
Simulator research at Netherlands National Aerospace Laboratory
[AD-750589] 06 p0650 N73-15283
Operating principles of force measuring and generating equipment in NBS research facilities
[NBS-SP-370] 09 p1010 N73-18243
Apparatus for mixing two or more liquids under zero gravity conditions
[NASA-CASE-LAR-10195-1] 10 p1163 N73-19458
Conceptual design of space shuttle comm/nav research laboratory and identification of major laboratory equipment - Vol. 3
[NASA-CR-124138] 11 p1266 N73-20275
Design, development, fabrication, and testing of laboratory prototype of residual gas analyzer
[NASA-CR-124177] 12 p1404 N73-21386
Self-scanning chromatographic-fluorographic drug detector with optical readout system
[NASA-CASE-ARC-10633-1] 13 p1486 N73-22048

**LABRADOR**
Aerial tracking of icebergs off Labrador coast during July 1970 and July 1971
[MC/ORB-8/71] 05 p0538 N73-14378
Winter wind and ocean conditions in Labrador fishing waters, and effects on pack ice drifting and icing hazards
[NLL-M-22670-[5828.4F]] 05 p0570 N73-14630

**LABYRINTH**
NT COCHLEA
NT VESTIBULES
Comparison of development of auditory vesicle in frog embryos under weightless and terrestrial conditions
[NASA-TT-F-14624] 01 p0009 N73-10072
Analysis of electronystagmograms for healthy persons in labyrinthal calorization tests
24 p2883 N73-33026

**LABYRINTHECTOMY**
Guinea pigs used to determine effect of intramuscular injections of drugs on fall-out and Bekhterev nystagmus occurring after unilateral and bilateral labyrinthectomies
07 p0744 N73-16049

**LACTATES**
Complete activity of lactate dehydrogenase and isoenzymes in plasma and myeloid cells
[NASA-TT-F-14586] 01 p0009 N73-10070
Use of Ringers lactate solution in pre- and postoperative fluid therapy
[NASA-TT-F-14600] 01 p0009 N73-10071

**LADDERS**
Multiperipherism and hydrodynamics of multiple processes
[NASA-TT-F-14896] 13 p1561 N73-22656

**LAGOONS**
Lagrangian computer program for predicting movement and dispersion of pollutant in tidal embayment, and application to Bolinas Lagoon, California
[USGS-582-B] 01 p0048 N73-10389
Dune barrier erosion due to storms and wave activity near Mosquito Lagoon, Kennedy Space Center
[NASA-CR-135775] 24 p2922 N73-33337

**LAGRANGE COORDINATES**
Lagrangian theory of internal ocean wave interaction
[AD-746149] 02 p0169 N73-11371
Formulation of finite element matrix in Lagrangian variables for elastic thin shells with arbitrary geometric imperfections
[AD-747321] 03 p0361 N73-12946

Examination of dynamic laws in Kirchoff and Lagrange schemes
10 p1187 N73-19663
LAGRANGE EQUATIONS OF MOTION
U EULER-LAGRANGE EQUATION
LAKE BEDS
U BEDS [GEOLOGY]
LAKE CHAMPLAIN BASIN [NY-VT]
ERTS-1 imagery of Lake Champlain and Vermont environments
[E72-10225] 03 p0288 N73-12333
ERTS-1 return beam vidicon imagery of Lake Champlain region and Vermont
[E72-10252] 03 p0289 N73-12352
Water pollution detection and monitoring in Lake Champlain and Vermont using ERTS-1 imagery
[E72-10268] 03 p0291 N73-12367
Land use mapping, limnology, wetlands, geomorphic and landform surveys, and river monitoring of Lake Champlain Basin and Vermont using ERTS-1 imagery
[E72-10282] 03 p0292 N73-12380
Analysis of ERTS-1 imagery for land use and lake turbidity mapping of Lake Champlain Basin and Vermont
[E73-10432] 11 p1281 N73-20393
ERTS-1 imagery of land use, lake ice, and water pollution, Lake Champlain Basin and Vermont
[E73-10690] 16 p1902 N73-25383
Monitoring water pollution plume in Lake Champlain using ERTS-1 imagery
[E73-10742] 17 p2021 N73-26347
Survey of lake flooding in Lake Champlain basin using ERTS-1 imagery
[E73-10771] 18 p2134 N73-27247
ERTS-1 imagery of ice conditions on Lake Champlain
[E73-10806] 18 p2138 N73-27281
Environmental study of Lake Champlain and Vermont land use based on ERTS-1 imagery
[PAPER-E11] 19 p2270 N73-28275
LAKE ICE
NT ICE FLOES
Utilization of ERTS-1 imagery for water depth measurement, mapping of Yellowstone Park, atmospheric effects in Colorado, lake ice surveillance, recreational land use, IFYGL Lake Ontario, image enhancement, water quality monitoring, and oil pollution detection
[E72-10201] 02 p0144 N73-11167
Utilization of ERTS-1 imagery for water depth measurement, mapping of Yellowstone Park, atmospheric effects in Colorado, lake ice surveillance, recreational land use, IFYGL Lake Ontario, image enhancement, water quality monitoring, oil pollution detection, and mapping iron compounds
[E72-10198] 02 p0160 N73-11296
Interdependence of lake ice and climate in central North America
[E72-10362] 05 p0535 N73-14350
Utilization of ERT-1 imagery for water depth measurement, Yellowstone Park data, atmospheric effects in Colorado, lake ice surveillance, recreational land use, IFYGL, image enhancement, water quality monitoring, oil pollution detection, and mapping iron compounds
[E73-10086] 08 p0901 N73-17298
Application of dielectric constant measurements to interpretation of radar imagery of Michigan ground truth for lake ice
[E73-10391] 11 p1276 N73-20353
Lake ice surveillance using radar imagery
[E73-10569] 15 p1771 N73-24349
ERTS-1 imagery of land use, lake ice, and water pollution, Lake Champlain Basin and Vermont
[E73-10690] 16 p1902 N73-25383
Application of ERTS-1 data for identification of ice formations in Lake Erie and snow mapping in American River basin
[E73-10750] 17 p2022 N73-26353
ERTS-1 imagery of ice conditions on Lake Champlain
[E73-10806] 18 p2138 N73-27281
Skylab 4 microwave radiometry of lake and sea ice in Gulf of St. Lawrence and Lake Ontario
[E73-10820] 18 p2140 N73-27295
Multidisciplinary research on water depth measurement, Yellowstone Park, atmospheric effects, lake ice surveillance, recreational land use, IFYGL, image enhancement, water quality, oil pollution detection, and mapping iron compounds from ERTS-1 data
[E73-11119] 23 p2783 N73-32264
LAKE PONTCHARTRAIN [LA]
ERTS-1 identification of duckweeds in Lake Pontchartrain, Louisiana
[E73-10613] 15 p1774 N73-24374
Seasonal variations of vegetation, circulation patterns in Lake Pontchartrain, and urban neighborhood quality in Louisiana from ERTS-1 imagery
[E73-10838] 19 p2290 N73-28416
LAKES
NT GREAT LAKES [NORTH AMERICA]
NT LAKE PONTCHARTRAIN [LA]
Monitoring and surveillance of state of eutrophication of inland lakes in California and Nevada
[E72-10207] 03 p0288 N73-12330
Identification of playa lakes in Texas High Plains from ERTS-1 imagery
[E72-10257] 03 p0290 N73-12357
Water pollution detection and monitoring in Lake Champlain and Vermont using ERTS-1 imagery
[E72-10268] 03 p0291 N73-12367
Utilization of ERTS-1 data to monitor and classify eutrophication of inland lakes
[E72-10358] 05 p0534 N73-14346
Dynamics of playa lakes in Texas High Plains
[E73-10042] 07 p0776 N73-16305
Remote sensing of Minnesota lakes and forests using ERTS-1
[NASA-CR-130548] 08 p0916 N73-17502
Monitoring and classifying eutrophication of inland lakes
[E73-10299] 09 p1021 N73-18331
Monitoring and classifying eutrophication of inland lakes from ERTS-1 imagery
[E73-10445] 11 p1282 N73-20405
Regional wet census of playa lakes on Southern High Plains area of Texas and New Mexico from ERTS-1 MSS imagery
[E73-10455] 11 p1283 N73-20414
Effect of bottom topography, eddy diffusivity, and wind variation on circulation in two-layer stratified lake
[NASA-TN-D-7235] 11 p1286 N73-20433
Analysis of water pollution levels in USSR lake and measures to protect water purity under conditions of economic development in vicinity
12 p1420 N73-21512
Inventory of ponds, lakes, and reservoirs in selected areas of State of Massachusetts
[PB-214116/6] 14 p1665 N73-23512
Dynamics of playa lakes in Texas High Plains analyzed from ERTS-1 imagery
[E73-10598] 15 p1772 N73-24359
Delineation of lakes and water turbidity identification in ERTS-1 imagery of Houston, Texas area
[E73-10672] 16 p1900 N73-25367
Aerial reconnaissance of thermal discharges along shoreline of Lake Michigan
[PB-214407/9] 16 p1908 N73-25437
Photointerpretation of ERTS-1 imagery to map bodies of water in Saline County, Kansas
[E73-10684] 17 p2017 N73-26313
Utilization of Skylab multispectral cameras for study of eutrophication processes in lakes important to New York State water resources
[E73-10744] 18 p2133 N73-27236
Application of ERTS-1 imagery for hydrometric and hydrographic surveys of Canada
[E73-10777] 18 p2135 N73-27253
Dynamics of playa lakes in Texas high plains
[E73-10832] 18 p2141 N73-27302
Evaluation of ERTS-1 imagery for determining numbers and distribution of prairie ponds and lakes in North Dakota
[PAPER-W12] 19 p2272 N73-28289
Application of ERTS-1 imagery for determining location and characteristics of lake basins Texas high plains and semi-arid areas
[PAPER-W13] 19 p2272 N73-28290
Processing and interpretation of ERTS-1 MSS data for Lake Livingston, Texas
[PAPER-I8] 19 p2278 N73-28329
Monitoring and classifying eutrophication of inland lakes in Michigan using ERTS-1 imagery
19 p2285 N73-28375
Monitoring and classification of eutrophication of inland lakes in Michigan from ERTS-1 imagery
[E73-10898] 20 p2395 N73-29247
Tributaries of Lake Baykal
20 p2447 N73-29657
Detection and monitoring of water quality parameters in reservoirs and lakes in Kansas from Skylab imagery
[E73-10938] 21 p2529 N73-30280
Skylab monitoring of temperatures of lakes and playas and soil moisture in Nevada
[E73-11004] 22 p2660 N73-31309
Interpretation techniques for Skylab monitoring of lake eutrophication in New York State
[E73-11011] 22 p2660 N73-31316
Dynamics of wind driven lake currents and application of vertical cross-section models
23 p2777 N73-32211
Annual variations of Garda Lake surface temperature using airborne bolometric equipment and earth based infrared video equipment
[IFA-STR-23] 23 p2787 N73-32298
Snow and fresh water lake ice interpretations from ERTS-1 imagery of Whitefish Bay, Michigan and Green Bay, Wisconsin
[E73-11129] 24 p2917 N73-33284
LAMB WAVES
Excitation of Lamb atmospheric edge mode by tail of large atmospheric explosion
05 p0509 N73-14143
Lamb dip in millimeter-wave molecular spectroscopy
20 p2454 N73-29719
LAMINAR BOUNDARY LAYER
Stability of laminar boundary layers
[NASA-CR-128532] 01 p0039 N73-10311
Turbulent and laminar boundary layer behind blast waves generated in shock tubes
[ISL-5/72] 04 p0406 N73-13306
Error analysis on two dimensional steady laminar boundary layer of incompressible wall flow
[AD-748771] 04 p0406 N73-13308
Three dimensional laminar boundary layer flow over bodies of revolution
[AD-748282] 04 p0408 N73-13323
Theory for Assman psychrometer based on exact analysis of diffusion process in laminar boundary layer with thermal gradients
[NLL-M-22691-[5828.4F]] 05 p0570 N73-14627
Laminar and turbulent boundary layers, including hypersonic flow, wall flow and stagnation area
[DLR-MITT-71-13] 07 p0770 N73-16256
Mathematical model for energy losses and velocity distribution in laminar boundary layers, using quadrature formulas
07 p0770 N73-16257
Mathematical model for wall cooling in laminar hypersonic boundary layer
07 p0770 N73-16258
Energy transfer in laminar hypersonic boundary layers by hydrogen combustion
07 p0771 N73-16260
Magnus effect in supersonic laminar boundary layer on spinning body of revolution
[SC-DC-72-1173] 07 p0772 N73-16269
Analytical solution of nonsimilar laminar boundary layer with pressure gradient, variable wall temperature, and continuous mass injection
[AD-751804] 07 p0773 N73-16279
Laminar heat transfer problem on spheres and cylinders solved by laminar boundary layer theory
[VKI-TN-84] 10 p1142 N73-19306
Optimization method for turbomachine blade design based on boundary layer concepts
10 p1204 N73-19801
Orr-Sommerfeld equation for studying laminar boundary layer stability on elastic surface
[NASA-TT-F-14855] 11 p1270 N73-20307
Analysis of effect on laminar boundary layer resulting from superposed unsteadiness on yawed infinite flat plate in adverse pressure gradient
12 p1389 N73-21265
Pitot pressure survey of laminar boundary layer on supersonic spinning ogive cylinder
[AD-755694] 12 p1393 N73-21294
Calculation of heat transfer coefficients of laminar incompressible boundary layer to corrugated wall, with application to combustion chamber liquid film cooling
[DLR-FB-73-07] 12 p1465 N73-21868
Finite difference solution to right angle circular cone streamline swallowing phenomenon during supersonic and hypersonic flow
13 p1508 N73-22218
Compressible laminar boundary layer on cone near plane of symmetry and stagnation point boundary layer with hydrogen injection
13 p1509 N73-22228
Invariant-group properties of equations for boundary layer of electrically conductive liquid in magnetic field
[AD-756956] 13 p1513 N73-22257
Development of method for calculating characteristics of laminar boundary layer on nonadiabatic wall of constant temperature in presence of pressure gradients
[ARC-R/M-3233] 15 p1728 N73-24013
Effect of small amplitude wall waviness upon stability of laminar boundary layer with respect to two dimensional disturbances
15 p1764 N73-24293
Numerical analysis of incompressible laminar boundary layer on infinite swept wing with arbitrary velocity and suction distribution
[ARC-R/M-3241] 16 p1854 N73-25018
Wave compression and expansion effects on laminar gas boundary flow
[AD-759768] 16 p1893 N73-25320
Force measurements and pressure distributions on three Gottinger airfoil profiles during transition from laminar to turbulent boundary layer flow
[NASA-TT-F-14959] 17 p1979 N73-26000
Experimental determination of laminar boundary layer and oscillatory suspension flows by laser anemometry
17 p2012 N73-26271
Effect of wall cooling on shock wave laminar boundary layer interactions in hypersonic two dimensional flow
[AD-762937] 20 p2389 N73-29192
Numerical analysis of laminar boundary layer on slipping wing
[AD-763285] 21 p2526 N73-30255
Prediction and measurement of heat transfer rates for shock-induced unsteady laminar boundary layer on flat plate
[NASA-CR-114582] 22 p2651 N73-31241

Parametric integral method for calculating laminar and turbulent incompressible flow- and temperature boundary layers
[DLR-FB-73-24] 22 p2653 N73-31255
General methods for calculating three dimensional laminar boundary layers over inclined blunt bodies
[AD-763831] 22 p2656 N73-31274
Analytical solution for laminar boundary layer with pressure gradient and coolant injection
23 p2771 N73-32165
Perturbation solutions for multicomponent, variable-property forced convection in laminar boundary layers
[AD-764563] 23 p2776 N73-32200
Laminar boundary layers at continuously moving wall and behind shock wave, noting fuel combustion problem
24 p2906 N73-33192
Viscous laminar flow through laval nozzles
24 p2907 N73-33197
Integral transformations for compressible laminar partial differential equations of second order boundary layer theory
24 p2907 N73-33198
Mass flow rate of laminar dissociated equilibrium boundary layer
24 p2907 N73-33200
Theory for small perturbation laminar boundary layer stability at longitudinally curved walls
24 p2909 N73-33212

**LAMINAR BOUNDARY LAYER SEPARATION**
U BOUNDARY LAYER SEPARATION
U LAMINAR BOUNDARY LAYER

**LAMINAR FLAMES**
U FLAMES
U LAMINAR FLOW

**LAMINAR FLOW**
NT BLASIUS FLOW
NT STRATIFIED FLOW
Calculating laminar viscous, compressible flows
[NASA-TN-D-6998] 01 p0040 N73-10313
Laminar flow, and transitional flow heat transfer
[ESDU-68006-AMEND-A-PT-2]
02 p0241 N73-11963
Skin friction, heat transfer and pressure measurements in laminar, transitional and turbulent boundary layers on flat plates at high Mach numbers and Reynolds numbers
[NASA-CR-112147] 03 p0283 N73-12290
Assessing laminar flow on conical vehicles during hyperbolic entry by studying boundary layer transition on ablating cones
[NASA-TM-X-68867] 03 p0283 N73-12293
Analysis of relaxation of laminar boundary layer to test gas boundary layer over flat plate in expansion tube
[NASA-TR-R-397] 03 p0283 N73-12296
Application of variational principle to laminar flow and heat transfer between concentric cylinders
[REPT-5/1972] 03 p0285 N73-12307
Development of equations and computer program for determining temperature distribution in walls of three eccentric annuli
[AD-747697] 03 p0287 N73-12322
Numerical solution for magnetohydrodynamic pipe flow with laminar separation at higher Hartmann number
[AD-748766] 04 p0456 N73-13719
Development of iterative procedure for analysis of arbitrary multi-element airfoils in viscous flow
[AD-749484] 05 p0496 N73-14042
Calculation of compressible flow in three dimensional cascade of turbomachine blades using stream line curvature technique
[ARC-R/M-3704] 05 p0527 N73-14287
Analysis of laminar part of separation bubbles in two dimensional incompressible flow for various shaped objects
06 p0616 N73-15000
Application of functional analysis to obtain exact semianalytical solutions of boundary layer flows under turbulent and laminar conditions
06 p0616 N73-15003
Design characteristics and performance of airfoils with high lift at low and medium subsonic speeds and various angles of attack
06 p0616 N73-15004
Analysis of factors involved during reversion of turbulent boundary layers to laminar flow
[REPT-72-FM-2] 06 p0652 N73-15297
Numerical analysis of three dimensional compressible laminar boundary layer flow characteristics of right circular cone in supersonic and hypersonic flow
[AD-750130] 06 p0656 N73-15331
Flow model of axisymmetric hypersonic nozzle for transition from turbulent flow to laminar flow with pressure gradient controlled by nozzle shape
07 p0768 N73-16237
Computer program to determine compressible fluid flow with friction across face seals and through narrow solts
[NASA-TN-D-6787] 07 p0803 N73-16518
Analysis of aerodynamic characteristics of free, semibounded slipstream of straight-jet laminar gas flames
[NASA-TT-F-14688] 07 p0855 N73-16934
Analog computer study of hypersonic laminar heat transfer
[AD-752022] 08 p0898 N73-17269
Supersonic laminar flow reattachment and redevelopment behind two-dimensional rearward facing step
[AD-753358] 09 p1018 N73-18306
Laplace transformation and Volterra integral equation for studying heat transfer in laminar flow through pipe with annular space
[NLL-RTS-7525] 11 p1347 N73-20928
Laminar surface heat transfer distribution about cones at hypersonic speeds
[AD-754056] 11 p1349 N73-20946
Numerical analysis of time dependent natural convection flow within horizontal cylinder based on quasi-compressible Navier-Stokes equations
[NASA-TM-X-69220] 12 p1391 N73-21278
Transition Poiseuille flow through long cylindrical capillary
13 p1508 N73-22224
Equations of motion for studying convection transport processes in strongly curved tubes
13 p1509 N73-22227
Flow coupled diffusion and velocity profiles for steady laminar flow in circular duct
13 p1509 N73-22231
Numerical analysis of base pressure distribution for supersonic flow over slender wedge or backward facing step
15 p1764 N73-24295
Characteristics of wall mass transfer coefficient for pulsed laminar flow in pipe of Newtonian fluid containing dissoloved electrolyte
15 p1765 N73-24301
Numerical solutions for laminar, compressible, three dimensional boundary layer on sharp bodies of revolution at angle of attack with moderate axial spin
[SC-CR-72-3182] 15 p1768 N73-24325
Stalling characteristics of airfoil in laminar viscous incompressible fluid with consideration of starting vortex and separation bubble
[AD-758831] 15 p1769 N73-24334
Analysis of motion of laminar and turbulent viscous vortex rings produced in air by pneumatic actuated piston vortex generator
16 p1886 N73-25265
Application of laminar flow solutions for heat transfer and flow friction to design of heat exchangers
16 p1886 N73-25266
Perturbation method for separated laminar incompressible flows in divergent channels
16 p1886 N73-25268
Analysis of heat transfer in laminar flow of gas through constant diameter cylindrical tubes at low wall to bulk temperature ratios
17 p2013 N73-26275
Theoretical analysis of two dimensional laminar jet rate sensors
[AD-761092] 18 p2153 N73-27401
Stability of laminar pipe flow with rigid rotation and small three-dimensional perturbation
[MITT-55] 19 p2256 N73-28184
Implicit numerical solution for laminar and turbulent flow of incompressible fluid along axis of 90-degree corner
20 p2384 N73-29152
Analysis of boundary value problem associated with laminar fluid flow
20 p2385 N73-29158
Theoretical analysis of flow recompression, reattachment, and redevelopment associated with supersonic laminar flow past rearward facing step
20 p2385 N73-29162
Measurement of laminar flow in pipes using differential pressure generating devices
[NLL-M-23017-[5828.4F]] 20 p2386 N73-29168
Measurement of laminar fluid flow through orifice meters to determine discharge coefficients and head losses
[NLL-NEL-TT-2457-[6075.461]]
20 p2386 N73-29169
Characteristics of electrostatic discharges in liquids to show importance of transport and discharge mechanisms for boundary surface phenomena and particle discharge
[NLL-M-23041-[5828.4F]] 21 p2516 N73-30182
Numerical analysis of laminar unsteady flow around airfoil in viscous, incompressible fluid
22 p2649 N73-31226
Steady laminar flow of viscous fluid in circular tube entrance
22 p2650 N73-31232
Second order thermal boundary layer theory for steady, laminar, compressible flow over cambered two dimensional or rotational bodies
[DLR-FB-73-31] 22 p2653 N73-31256
Laminar secondary Taylor-Goertler vortex flow in rectangular cross section channel
[AD-764503] 22 p2655 N73-31268
Unidirectional periodic flow about circular cylinders
[AD-764487] 22 p2656 N73-31273
Rheological and optical properties of deformable particles in laminar shear flows
24 p2959 N73-33647
Heat transfer from wall to fluid in laminar fluid flow in circular tube
24 p2990 N73-33895

**LAMINAR FLOW CONTROL**
U BOUNDARY LAYER CONTROL
U LAMINAR BOUNDARY LAYER

**LAMINAR HEAT TRANSFER**
Laminar, transitional, and turbulent heat transfer measurements on yawed blunt conical nosetip in free stream Mach 5
[AD-748292] 04 p0486 N73-13967
Measured maximal laminar heat transfer on cone with spherical nose in hot hypersonic flow
07 p0771 N73-16263
Analog computer study of hypersonic laminar heat transfer
[AD-752022] 08 p0898 N73-17269
Laminar heat transfer problem on spheres and cylinders solved by laminar boundary layer theory
[VKI-TN-84] 10 p1142 N73-19306

**LAMINAR JETS**
U JET FLOW
U LAMINAR FLOW

**LAMINAR MIXING**
Mixing region in flow field of fluidic beam deflection amplifier
23 p2772 N73-32173

**LAMINAR WAKES**
Numerical analysis of wake propulsion parameters to show effects of drag, heating, and energy conversion
[RN-64] 08 p0894 N73-17238
Free convection effects in laminar two dimensional wake above isothermal vertical plate cooled by natural convection
08 p0894 N73-17240
Characteristics of laminar and turbulent wakes of spherical bodies at hypersonic speed in nitrogen atmosphere
[DREV-R-683/72] 24 p2904 N73-33178

**LAMINATED MATERIALS**
U LAMINATES

**LAMINATES**
Equipment and procedures for measuring variation of strength of sheet specimens of glass under conditions of tension, compression, and shear
[AD-743694] 01 p0067 N73-10551
Mechanical properties of boron carbide reinforced titanium laminates
[AD-745002] 01 p0070 N73-10570
Structural dynamic behavior of laminated plates and shells composed of bonded elastic orthotropic layers
[AD-745336] 01 p0114 N73-10944
Infrared nondestructive testing techniques used to detect unbonded areas in laminated structures and incipient failures in electrical circuit boards
[AD-746233] 02 p0175 N73-11419
Use of composite laminates with weak interfaces to increase fracture toughness of Ti-6Al-4V
[AD-746765] 02 p0189 N73-11531
Polyphenylquinoxaline resin systems for high temperature composite materials
[AD-746273] 02 p0193 N73-11559
Multimaterial lamination as means of retarding penetration and spallation failures in plates from hypervelocity impact
[NASA-TN-D-6989] 02 p0238 N73-11934
Development of mathematical relationships to define the behavior of multilayer, thin shell structures under various conditions of shear and bending
02 p0238 N73-11936
Analysis of vibration characteristics of laminated plates and modifications of plate theory to produce results consistent with continuum theory
[AD-746951] 02 p0240 N73-11949
Development and characteristics of polyimide impregnated laminates with fiberglass cloth backing for application as printed circuit broads
[NASA-CASE-MFS-20408] 03 p0320 N73-12604
Effects of free edge shear stresses on failure of fiber-reinforced angle ply laminates
[AD-747343] 03 p0322 N73-12625
Development and characteristics of composite materials with emphasis on non-aerospace applications
[NASA-CR-129989] 05 p0565 N73-14587
Flexural deformation of laminated beams subjected to initial stresses
[AD-750574] 05 p0604 N73-14912
Optimization of transparent ethylene terpolymer and compilation of engineering data for use as adhesive in polycarbonate composite aircraft transparencies
[AD-750814] 06 p0689 N73-15611
Numerical analysis of stress in face plates of sandwich panel structures subjected to random acoustic loading
[ESDU-72017] 06 p0723 N73-15900

Processes for developing high quality multilayer printed wiring boards
[BDX-613-382-REV] 07 p0762 N73-16189
Mechanical properties of monolithic transparent polycarboaate plastic sheet
[AD-751551] 07 p0813 N73-16590
Analysis of environmental effects on physical, mechanical, and thermodynamic properties of various multilayer insulation materials - Vol. 1
[NASA-CR-120978] 08 p0934 N73-17648
Analysis of environmental effects on physical, mechanical, and thermodynamic properties of various multilayer insulation materials - Vol. 2
[NASA-CR-120979] 08 p0934 N73-17649
Improvement in interlaminar shear strength of organic matrix composites using plasma deposited coupling agents
[AD-753857] 09 p1055 N73-18599
Static, vibration, and thermal stress analyses of laminated plates and shells by hybrid-stress finite element method including transverse shear deformation effects
[AD-753651] 09 p1097 N73-18955
Structural analysis of laminated aluminum alloy sheets to determine flaw growth behavior in roll diffusion bonded and adhesive bonded structures
[NASA-CR-128844] 10 p1220 N73-19921
Analysis of linear elastic wave propagation normal to laminations of periodically laminated porous composite
[AD-753900] 10 p1221 N73-19934
Theoretical and experimental determination of nonlinear behavior of angleplied boron/aluminum composites
[NASA-TM-X-68205] 11 p1309 N73-20617
Modulus theories for determining microstructure elasticity of laminated plates
[AD-754528] 11 p1309 N73-20619
Development of composite structures for spacecraft to serve as anti-meteoroid device
[NASA-CASE-LAR-10788-1] 11 p1341 N73-20880
Mechanical strength of multilayer thin metal films
[AD-756582] 13 p1543 N73-22508
Notch sensitivity and static strength of laminated steels
[AD-756556] 13 p1545 N73-22524
Three-dimensional finite element analysis of stress concentration near holes in laminated composites
[AD-756454] 13 p1548 N73-22545
Meteoroid impact resistance of bumper protected laminated spacecraft mainwalls
[NASA-CR-2262] 14 p1714 N73-23909
Simple thickness modes for couple stress theory for laminated media
[AD-759133] 16 p1933 N73-25642
Analysis of optimal configurations for thin walled, axisymmetric, laminated shells based on shell configuration, loading, fiber alignment, and material properties of composite structure
16 p1969 N73-25924
Structural properties and stability of solid materials and structures with different geometric configurations
[AD-759558] 16 p1971 N73-25942
Development and evaluation of polyimide laminates for printed wiring board applications
[NASA-TM-X-64760] 17 p2050 N73-26581
Compressive strength and modulus of unidirectional carbon fiber reinforced plastic laminates
[RAE-TR-72096] 17 p2050 N73-26587
Fatigue failure criterion for fiber reinforced laminates under stress
[AD-760146] 17 p2053 N73-26609
Analysis of glass fiber reinforced plastic laminated structures
[MBB-UD-79-72-O] 17 p2094 N73-26942
Response of general laminated plates to applied loads with coupling between bending and extensional modes of deformation
18 p2165 N73-27488
Preparation and testing of pyrolytic graphite film polymeric matrix laminates
[AD-761124] 18 p2168 N73-27510
Utilization of sandwich method to obtain epitaxial layers of Si, GaAs, and heteroepitaxial GaAs-Ge
18 p2186 N73-27654
Ultrasonic inspection and control for laminated steel disc
[TR-73-2-640] 20 p2423 N73-29461
Vibration stability contact and interfacial crack propagation for partially delaminated layered circular cylindrical shells
20 p2476 N73-29891
Interaction between parallel cracks in layered composites
[NASA-CR-132287] 20 p2482 N73-29936
Application of reinforced fiberglass thermoplastic materials for construction of military aircraft structures
[AD-763470] 21 p2498 N73-30044
Effect of multiword addressing with laminated ferrite arrays
[NASA-CR-124372] 21 p2512 N73-30149
Outdoor weathering influence on polyester and epoxy glasscloth reinforced laminate flexural strength and surface appearance
[FOK-R-1627] 21 p2563 N73-30546
Development of linear analysis method for predicting buckling of composite structures with arbitrary uniform cross section
[NASA-CR-2216] 21 p2603 N73-30863
Computerized design of multilayer thin film filters
[WRE-TN-903(AP)] 23 p2759 N73-32082
Thermophysical properties of synthetic resin-base materials with fillers to show errors in development of mathematical relationships
23 p2807 N73-32446
Extension of linear elastic fracture mechanics from homogeneous isotropic metallic alloys to heterogeneous anisotropic advanced fiber composites
[NASA-CR-132337] 24 p2937 N73-33456
Structural analysis of unsymmetrically laminated anisotropic plates using linear plate theory and strain-displacement relations
24 p2987 N73-33875

**LAMINATIONS**
U LAMINATES

**LAMPS**
U LUMINAIRES

**LANCE MISSILE**
Meteorological and ballistics data for launching of Lance Missile 2143, vehicle 159
[AD-749429] 04 p0445 N73-13636
Meteorological and ballistics data for launching of Lance Missile 2168, vehicle 160
[AD-749432] 04 p0446 N73-13639
Meteorological and ballistics data for launching of Lance Missile 2159, vehicle 161
[AD-749433] 04 p0446 N73-13640
Meteorological data for launching 11601 Lance, missile 2138, round number 165
[AD-752093] 08 p0939 N73-17689
Meteorological and ballistics data for launching of 11601 Lance Missile number 2154, round number 163 RBL
[AD-752088] 08 p0939 N73-17690
Meteorological and ballistics data for launching of 11602 Lance Missile number 5175, round number 164 ESL
[AD-752090] 08 p0940 N73-17695
Meteorological and ballistics data for launching of Lance missile, number 2183, round no. 167 APT
[AD-752098] 08 p0940 N73-17700
Meteorological data for launching of 12801 Lance missile numbers 2216/2310, round no. 166 EET
[AD-752097] 08 p0940 N73-17703
Meteorological data from 14802 Lance missile, 17 Nov. 1972
[AD-754555] 11 p1314 N73-20664
Meteorological data of upper atmosphere from sounding rockets for Lance missile launch
[AD-754554] 11 p1314 N73-20666
Meteorological and ballistics data for launching of 14801 Lance missile no. 2184, round no. 168 APT 9
[AD-754556] 11 p1315 N73-20669
Meteorological data for launching of Lance missile probe of upper atmosphere
[AD-754565] 11 p1315 N73-20672
Meteorological data for launching Lance missile probe of upper atmosphere
[AD-754564] 11 p1315 N73-20673
Meteorological and ballistics data for launching of 12802 Lance missile no. 2150, round no. 174 ESL
[AD-754563] 11 p1316 N73-20678
Meteorological data for Lance missile number 2186, round number 169 APL
[AD-754559] 11 p1316 N73-20680
Meteorological and ballistics data for launching of 11602 Lance missile, number 2174, round 181
[AD-755773] 12 p1424 N73-21539
Meteorological and ballistics data for launching of 12893 Lance missile, number 2354, round 182
[AD-755774] 12 p1424 N73-21540
Meteorological data for launching Lance missile, number 2170
[AD-755768] 12 p1424 N73-21544
Meteorological data for launching Lance missile, number 2352
[AD-755769] 12 p1424 N73-21545
Meteorological data for launching Lance missile, number 2148
[AD-755770] 12 p1424 N73-21546
Meteorological data for launching Lance missile, number 2176
[AD-755778] 12 p1425 N73-21548
Meteorological data for launching Lance missile, number 2351
[AD-755771] 12 p1425 N73-21549
Meteorological and ballistics data for launching of Lance missile, number 2149, round 180
[AD-755772] 13 p1555 N73-22599
Meteorological data from Lance missile no. 2355, round no. 184 EST [29 Jan. 1973]
[AD-758860] 15 p1807 N73-24648
Meteorological and ballistics data for launching of Lance missile, number 2237, round 185
[AD-758864] 16 p1939 N73-25687
Shielding effectiveness of exterior shield and connector assemblies on Lance umbilical cables
[AD-761078] 18 p2201 N73-27771
Meteorological data for launching of Lance missile, number 2238, round 187
[AD-762162] 19 p2317 N73-28638
Meteorological data gathered for launching 11604 Lance missile
[AD-762156] 19 p2317 N73-28642

**LAND**
NT FARMLANDS
NT GRASSLANDS
NT RANGELANDS
Mapping and detection of snow cover changes on land and on glaciers in Alaska, British Columbia, and Washington using ERTS-1 imagery
[E72-10237] 03 p0288 N73-12337
Environmental indices covering land, water, and air quality compatible with ERTS-1 imagery
[E72-10330] 05 p0531 N73-14318
Mapping and detection of changes of snow cover on land and glaciers
[E73-10063] 07 p0778 N73-16325
Mapping and detection of snow cover on land and glaciers in Cascade Range using ERTS-1 imagery
[E73-10379] 10 p1152 N73-19374
Detection and mapping changes of snow cover on land and glaciers from ERTS-1 imagery
[E73-10559] 14 p1655 N73-23431
Application of Skylab multispectral photography to mineral and land resources of South Carolina
[E73-10831] 18 p2141 N73-27301
Cosmos 243 measurements of radioemission properties of land surfaces
[NASA-TT-F-14978] 18 p2143 N73-27320
Environmental factors in production and use of energy and effects on air, water, and land
[R-992-RF] 21 p2537 N73-30340
Application of Skylab multispectral photography to mineral and land resources of South Carolina and Georgia
[E73-11140] 24 p2918 N73-33295

**LAND ICE**
Characteristics of thermal radiation of Greenland ice measurements by Cosmos-243
[NASA-TT-F-14953] 15 p1780 N73-24427
Application of ERTS-1 imagery for mapping distribution of glaciofluvial deposits and associated glacial landforms
[E73-10745] 17 p2021 N73-26349

**LAND MANAGEMENT**
Updating and adding detail to Minnesota Land Management Information Systems utilizing ERTS-1 imagery
[E72-10195] 01 p0047 N73-10374
Automatic photointerpretation for land use management in Minnesota
[E72-10227] 02 p0163 N73-11320
Application of ERTS-1 imagery to selected Bureau of Reclamation projects
[E72-10238] 03 p0288 N73-12338
Resources inventory and land use management in Oregon using ERTS-1 imagery
[E73-10008] 06 p0658 N73-15344
Application of ERTS-1 imagery to Minnesota Land Management Information System and analysis of land use classes
[E73-10029] 06 p0660 N73-15362
Land use planning and management on Mississippi Gulf Coast using ERTS-1 imagery
[E73-10072] 07 p0779 N73-16334
Regional land use mapping and management using remotely sensed imagery
07 p0786 N73-16392
Land use management and planning in Alaska using ERTS-1 imagery
[E73-10307] 09 p1022 N73-18339
Environmental factors and cost problems of selecting optimum sanitary landfill site for solid waste disposal
[NASA-CR-128744] 10 p1124 N73-19157
Evaluation of ERTS-1 imagery for mapping land use and updating Minnesota land management information system
[E73-10352] 10 p1148 N73-19348
Application of ERTS-1 imagery to land use planning and management on Mississippi Gulf Coast
[E73-10460] 11 p1284 N73-20418
Resources inventory, planning, land use zoning, and resources development in Oregon using ERTS-1 imagery
[E73-10579] 14 p1656 N73-23440
Land use management in Minnesota using ERTS-1 imagery
[E73-10581] 14 p1657 N73-23442
Land use management and mapping for Phoenix Quadrangle from ERTS-1 imagery
[E73-10650] 16 p1897 N73-25346
Land use management and planning on Mississippi Gulf Coast using ERTS-1 imagery
[E73-10653] 16 p1898 N73-25349
Land management planning and timber resources management in Washington and Oregon from ERTS-1 imagery
[E73-10804] 18 p2138 N73-27279

Application of ERTS-1 imagery to land management information system in Minnesota
[E73-10821] 18 p2140 N73-27296
Utilization of ERTS-1 imagery and data for land use mapping and management in Minnesota
[PAPER-L14] 19 p2275 N73-28310
Utilization of ERTS-1 data for inventory of critical land resources for regional land use planning in Wisconsin
[PAPER-L16] 19 p2275 N73-28311
Utilization of ERTS-1 data for land use and resources survey in Michigan
[PAPER-L26] 19 p2276 N73-28321
Resources and land use management and planning in Oregon using ERTS-1 data
[PAPER-R2] 19 p2282 N73-28360
Land use management in Minnesota by automatic interpretation of ERTS-1 MSS data
19 p2285 N73-28379
Resectioning programs developed to provide precision annotation of predetermined primary land sampling units on ERTS-1 MSS imagery
19 p2286 N73-28382
Application of ERTS-1 imagery to land use inventory and management and mapping techniques
19 p2289 N73-28407
Land use planning and management on Mississippi Gulf Coast using ERTS-1 data
[E73-10906] 20 p2396 N73-29255
ERTS-1 applications for land use management in Minnesota
[E73-10965] 21 p2533 N73-30307
Regional land use planning and management in Tri-State area from ERTS-1 MSS photography
[E73-10986] 22 p2658 N73-31293
Automatic photointerpretation for land use management in Minnesota
[E73-11046] 23 p2779 N73-32222
Application of ERTS-1 data to land use planning on Mississippi Gulf Coast
[E73-11055] 23 p2780 N73-32231
Automatic photointerpretation of ERTS-1 imagery for land use management in Minnesota
[E73-11058] 23 p2780 N73-32234
Automatic photointerpretation of ERTS-1 imagery for land use management in Minnesota
[E73-11059] 23 p2780 N73-32235
Automatic photointerpretation and mapping for land use management in Minnesota
[E73-11060] 23 p2780 N73-32236
Automatic photointerpretation of ERTS-1 imagery for land use management in Minnesota
[E73-11061] 23 p2780 N73-32237
Utilization of ERTS-1 imagery for management of wetlands in Great Dismal Swamp and Lake Okeechobee
[E73-11161] 24 p2920 N73-33314

**LAND USE**

Crop identification and acreage measurement in Idaho, Missouri, Kansas, and South Dakota using ERTS-1 imagery
[E72-10179] 01 p0045 N73-10358
Monitoring by ERTS-1 imagery for resource inventory, planning, land use zoning, and resource development in Oregon
[E72-10182] 01 p0045 N73-10361
Land use mapping of northern megalopolis using ERTS-1 imagery
[E72-10188] 01 p0046 N73-10367
Updating and adding detail to Minnesota Land Management Information Systems utilizing ERTS-1 imagery
[E72-10195] 01 p0047 N73-10374
Utilization of ERTS-1 imagery for water depth measurement, mapping of Yellowstone Park, atmospheric effects in Colorado, lake ice surveillance, recreational land use, IFYGL Lake Ontario, image enhancement, water quality monitoring, and oil pollution detection
[E72-10201] 02 p0144 N73-11167
Utilization of ERTS-1 imagery for water depth measurement, mapping of Yellowstone Park, atmospheric effects in Colorado, lake ice surveillance, recreational land use, IFYGL Lake Ontario, image enhancement, water quality monitoring, oil pollution detection, and mapping iron compounds
[E72-10198] 02 p0160 N73-11296
Land use mapping of forest area in Southeastern US by airborne multispectral scanning
[E72-10222] 02 p0162 N73-11316
Automatic photointerpretation for land use management in Minnesota
[E72-10227] 02 p0163 N73-11320
Identification and mapping geologic, soil, agriculture, geographic, and land use features using ERTS-1 imagery of Central US
[E72-10232] 02 p0163 N73-11325
Crop identification, acreage estimation, urban land use, soil mapping, and earth resources identification in Wabash River Basin using ERTS-1 imagery
[E72-10208] 03 p0288 N73-12331
Land use mapping of Phoenix quadrangle using ERTS-1 imagery
[E72-10236] 03 p0288 N73-12336
Mapping land use and land use change in Central Atlantic Region using ERTS-1 imagery
[E72-10241] 03 p0288 N73-12341
Automatic pattern recognition of urban land use and land use change
[E72-10244] 03 p0289 N73-12344
Strip mine identification, land use assessment, smoke plume detection, and sedimentation patterns in Sandusky Bay from ERTS-1 imagery of Ohio
[E72-10259] 03 p0290 N73-12358
Land use planning on Mississippi Gulf Coast utilizing ERTS-1 remotely sensed data
[E72-10262] 03 p0290 N73-12361
Application of ERTS-1 imagery to agriculture resource and land use evaluation in Mariposa County, Arizona and San Joaquin County, California
[E72-10264] 03 p0291 N73-12363
Land use mapping, limnology, wetlands, geomorphic and landform surveys, and river monitoring of Lake Champlain Basin and Vermont using ERTS-1 imagery
[E72-10282] 03 p0292 N73-12380
Community/airport economic development model for assisting land use planning near metropolitan airports
[FAA-EQ-72-3-VOL-1] 04 p0400 N73-13259
Data concerning airport development including land use, noise level compatibility, and zoning
[FAA-EQ-72-3-VOL-2] 04 p0401 N73-13267
Application of ERTS-1 imagery to regional land use planning in Wisconsin
[E72-10299] 04 p0411 N73-13349
Automatic identification of land uses in Milwaukee, Wisconsin using ERTS-1 imagery
[E72-10307] 04 p0412 N73-13356
Development of land use and peak runoff classification system for highway engineering using ERTS-1 imagery of Maine
[E72-10308] 04 p0412 N73-13357
Geographic applications of ERTS-1 imagery to land use and landscape changes in Tennessee
[E72-10315] 04 p0412 N73-13364
Utilization of ERTS-1 imagery of Alabama to study environmental factors, land use, and geology
[E72-10319] 05 p0530 N73-14310
First order land use classification in North Carolina based on ERTS-1 imagery
[E72-10324] 05 p0530 N73-14312
Resource inventory, land use, and pollution within Susquehanna River Basin based on interpretation of ERTS-1 data
[E72-10329] 05 p0531 N73-14317
Crop identification and acreage measurement in Missouri, Kansas, South Dakota, and Idaho using ERTS-1 imagery
[E72-10336] 05 p0531 N73-14324
Identification of phenological stages and vegetative types for land use classification based on ERTS-1 imagery
[E72-10342] 05 p0532 N73-14330
Mapping of land use in Northern Megalopolis of Massachusetts, Connecticut, Rhode Island, and New York based on ERTS-1 imagery
[E72-10357] 05 p0534 N73-14345
Land use mapping of northern megalopolis using ERTS-1 imagery
[E72-10368] 05 p0535 N73-14356
Remote sensing data for determining land use potential of northern California coastal zone
05 p0536 N73-14365
Use of remote sensing data to analyze impact of California State Water Project on regional planning and land use of west side of San Joaquin Valley
05 p0537 N73-14367
Resources inventory and land use management in Oregon using ERTS-1 imagery
[E73-10008] 06 p0658 N73-15344
Mapping and inventories of land use and natural resources in New York based on ERTS-1 imagery
[E73-10024] 06 p0660 N73-15358
Application of ERTS-1 imagery to Minnesota Land Management Information System and analysis of land use classes
[E73-10029] 06 p0660 N73-15362
Land use mapping and change detection in Central Atlantic Regional Ecological Test Site based on ERTS-1 MSS imagery
[E73-10034] 06 p0661 N73-15367
Discrimination and mapping land use categories in Puerto Rico using various types of multispectral remote sensor imagery
07 p0776 N73-16298
Remote sensing of selected Bureau of Reclamation land projects
[E73-10062] 07 p0778 N73-16324
Census cities experiment in urban land use and change detection using ERRS-1 imagery
[E73-10064] 07 p0778 N73-16326
Land use planning and management on Mississippi Gulf Coast using ERTS-1 imagery
[E73-10072] 07 p0779 N73-16334
ERTS-1 MSS imagery of Great Plains rangeland, croplands, and land systems
[E73-10076] 07 p0780 N73-16338
Regional land use mapping and management using remotely sensed imagery
07 p0786 N73-16392
Automatic processing of remote sensed data to aid in land use mapping and agricultural conservation
[NASA-CR-130372] 07 p0790 N73-16423
Application of ERTS-1 imagery to regional land use planning in Wisconsin
[E73-10077] 08 p0900 N73-17290
Utilization of ERTS-1 and aircraft remotely sensed data for land use inventory and planning in Maryland
[E73-10081] 08 p0901 N73-17293
Utilization of ERT-1 imagery for water depth measurement, Yellowstone Park data, atmospheric effects in Colorado, lake ice surveillance, recreational land use, IFYGL, image enhancement, water quality monitoring, oil pollution detection, and mapping iron compounds
[E73-10086] 08 p0901 N73-17298
Land use mapping and image enhancement of ERTS-1 imagery of Phoenix Quadrangle
[E73-10090] 08 p0902 N73-17302
Development of land use-peak runoff classification system for highway engineering in Maryland
[E73-10100] 08 p0902 N73-17310
ERTS-1 identification of phenological stages and vegetation types in Alaska for land use classification
[E73-10276] 08 p0914 N73-17484
Earth resource survey using remote sensing techniques to improve land use and management in Michigan
[NASA-CR-130758] 08 p0917 N73-17514
Use of remote sensing for assessing impact of highway construction on land use management in Michigan
[NASA-CR-130761] 08 p0917 N73-17515
Land use classification, utilizing remote multispectral scanner data and computer analysis techniques over Lafayette, Indiana
[NASA-CR-130759] 08 p0917 N73-17516
Classification of landforms for land use and regional planning using aerial photographic interpretation
[PB-212774] 08 p0918 N73-17525
Comparison of day and night infrared thermal imagery with results obtained using color photography and multispectral band sensor imagery
[AD-752217] 08 p0919 N73-17535
Land use management and planning in Alaska using ERTS-1 imagery
[E73-10307] 09 p1022 N73-18339
Application of ERTS-1 imagery for locating coal refuse deposits, analysis of geologic formations and mapping of agricultural areas in Pennsylvania
[E73-10327] 09 p1024 N73-18358
Crop identification and acreage measurement in Missouri, Kansas, South Dakata, and Idaho based on ERTS-1 imagery and aerial photography
[E73-10328] 09 p1024 N73-18359
Ross Barnett Reservoir remote sensing project to determine water sediment, investigate erosion, and improve land use
[NASA-CR-130960] 09 p1029 N73-18396
Operational system for employment of remote sensing and automated information in urban land management
[NASA-CR-130969] 09 p1030 N73-18410
Environmental factors and cost problems of selecting optimum sanitary landfill site for solid waste disposal
[NASA-CR-128744] 10 p1124 N73-19157
Water reclamation and waste disposal technology applied to land use and aerospace engineering
[NASA-CR-128857] 10 p1124 N73-19158
Waste disposal and water reclamation technology for land use and aerospace engineering application
[NASA-CR-128858] 10 p1124 N73-19159
Agricultural and urban land use mapping of Phoenix Quadrangle based on ERTS-1 imagery
[E73-10340] 10 p1147 N73-19339
Identification and classification of Iowa crop lands using ERTS-1 imagery and aerial photography
[E73-10343] 10 p1148 N73-19342
Geologic and land use exploitation of ERTS-1 imagery of New England using snow enhancement techniques
[E73-10345] 10 p1148 N73-19344
Development of standards for classification, mapping and scientific analysis of land use and land use change in Central Atlantic Region Ecological Test Site using ERTS-1 imagery
[E73-10347] 10 p1148 N73-19346
Evaluation of ERTS-1 imagery for mapping land use and updating Minnesota land management information system
[E73-10352] 10 p1148 N73-19348
Crop identification, soil mapping, water resources, and urban land use analysis in Wabash River Basin based on ERTS-1 imagery
[E73-10364] 10 p1150 N73-19360
Identification of marsh vegetation and coastal land use in Delaware from ERTS-1 imagery
[E73-10367] 10 p1150 N73-19363
Land use, water quality, and air quality indices useful to environmental resources managers and data processing equipment and techniques for production of indices
[E73-10376] 10 p1151 N73-19371

Analysis of factors involved in selection of suitable sites for sanitary land fills with emphasis on economic and social problems
[NASA-CR-128745] 10 p1229 N73-19989
Analysis of technical and economic feasibility of constructing offshore airport in New York Metropolitan area
[FAA-RD-73-45] 11 p1267 N73-20280
Development of procedure and system for uniform mapping and monitoring of earth resources and environmental complexes using ERTS-1 imagery
[E73-10350] 11 p1275 N73-20344
Evaluation and comparison of ERTS-1 measurements of major crops and soil conditions for selected areas in Central United States
[E73-10384] 11 p1275 N73-20348
Computer mapping of Michigan recreational land use using ERTS-1 data
[E73-10392] 11 p1276 N73-20354
Application of ERTS-1 imagery for mapping coverage of megalopolitan New England to show land use
[E73-10427] 11 p1280 N73-20388
Analysis of ERTS-1 imagery for land use and lake turbidity mapping of Lake Champlain Basin and Vermont
[E73-10432] 11 p1281 N73-20393
Application of ERTS-1 data for identifying ethnic groups, limits of occupancy, and use of physiographic features in Republic of Mali, West Africa
[E73-10434] 11 p1281 N73-20394
Identification of phenological stages and vegetative types from ERTS-1 imagery for land use classification in Alaska
[E73-10439] 11 p1281 N73-20399
Application of ERTS-1 imagery to regional land use planning in Wisconsin
[E73-10448] 11 p1283 N73-20408
Utilization of ERTS-1 imagery to develop land use-peak runoff classification system for highway engineering in Maine
[E73-10456] 11 p1283 N73-20415
Application of ERTS-1 imagery to land use planning and management on Mississippi Gulf Coast
[E73-10460] 11 p1284 N73-20418
Classification of land use in California using textural information in ERTS-1 MSS imagery
[E73-10461] 11 p1284 N73-20419
Mapping of land use in agriculture area of Finney County, Kansas based on ERTS-1 imagery
[E73-10474] 12 p1395 N73-21311
Census cities experiment in detection of urban change and land use
[E73-10490] 12 p1397 N73-21326
Data for assessing water supply changes and effects on hydrogeological management of San Joaquin Valley
12 p1400 N73-21353
Effects of water management on land use in southern California valley and river basin
12 p1400 N73-21354
Remote sensing techniques for water management and land use classification in California coastal zone considering river deltas
12 p1400 N73-21357
Research and applications of remote sensing to local and state governments
[NASA-CR-131643] 12 p1400 N73-21360
Land use, urban development, and regional planning for Los Angeles County based on photointerpretation of MSS imagery and multispectral information extraction
[E73-10486] 13 p1515 N73-22277
Development of environmental indices covering land, water, and air quality in Pennsylvania compatible with ERTS-1 imagery
[E73-10505] 13 p1516 N73-22280
Land use in northern megalopolis of Massachusetts, Connecticut, and Rhode Island
[E73-10506] 13 p1516 N73-22281
Crop identification and land acreage measurement in Kansas using ERTS-1 imagery
[E73-10514] 13 p1517 N73-22288
Census cities experiment in detection of urban development and land use from ERTS-1 imagery
[E73-10538] 13 p1518 N73-22302
Urban land use mapping of San Francisco Bay area by machine processing of ERTS-1 multispectral data
[NASA-CR-131589] 13 p1522 N73-22334
Classification of forest land use and detection of forest disturbances using space and high altitude aerial photography
[NASA-CR-131584] 13 p1523 N73-22339
Application of remote sensing techniques in forestry and range disciplines for timber inventory, weather forecasting, land classification, and snowfield monitoring
[NASA-CR-131583] 13 p1523 N73-22340
Application of spaceborne photography and aerial photography to ecological resource inventory and analysis of naturally vegetated areas in Arizona
[NASA-CR-131581] 13 p1523 N73-22342
Preparation of urban land use inventories by automated processing of ERTS MSS data
[NASA-CR-131576] 13 p1524 N73-22347
Effective land use of airport-incompatible areas through conversion planning from residential to compatible zones
[FAA-EQ-72-1] 13 p1594 N73-22926
Utilization of ERTS-1 remotely sensed imagery for land use evaluation and planning in Power River Basin, Wyoming
14 p1653 N73-23407
Identification of marshland vegetation and coastal land use in Delaware from ERTS-1 imagery
[E73-10516] 14 p1655 N73-23410
Utilization of ERTS-1 data for crop identification and acreage estimation, soil mapping, urban land use, water resources, atmospheric modeling, and earth surface feature identification in Wabash River Basin
[E73-10549] 14 p1655 N73-23422
Broad scale application of ERTS-1 imagery to study and mapping of geological, hydrological, land use, rangelands, and soil cultures in Wyoming
[E73-10554] 14 p1655 N73-23426
Land use mapping of Central Atlantic Region using ERTS-1 imagery
[E73-10557] 14 p1655 N73-23429
Identification and mapping of land use classes in Kansas City area by machine processing of ERTS-1 data
[E73-10578] 14 p1656 N73-23439
Resources inventory, planning, land use zoning, and resources development in Oregon using ERTS-1 imagery
[E73-10579] 14 p1656 N73-23440
Land use management in Minnesota using ERTS-1 imagery
[E73-10581] 14 p1657 N73-23442
ERTS-1 applications in water depth calculation, terrain classification, land use mapping, water pollution, and mineral exploration
[E73-10565] 15 p1771 N73-24345
Atmospheric effects on ERTS-1 imagery for land use mapping
[E73-10568] 15 p1771 N73-24348
Digital recreational land use mapping in Oakland County, Michigan
[E73-10570] 15 p1772 N73-24350
Updating land use and resources data in Guatemala based on ERTS-1 imagery
[E73-10609] 15 p1773 N73-24370
Identification of phenological stages and vegetative types in Alaska for land use classification
[E73-10618] 15 p1774 N73-24379
Relevance of ERTS-1 imagery to land use, resources, and environment management in Ohio
[E73-10621] 15 p1775 N73-24382
Land use of northern megalopolis of Massachusetts, Connecticut, and Rhode Island from ERTS-1 imagery
[E73-10630] 15 p1776 N73-24390
Land use management and mapping for Phoenix Quadrangle from ERTS-1 imagery
[E73-10650] 16 p1897 N73-25346
Land use management and planning on Mississippi Gulf Coast using ERTS-1 imagery
[E73-10653] 16 p1898 N73-25349
Development of land use-peak runoff classification system for highway engineering in Maine
[E73-10654] 16 p1898 N73-25350
Identification and mapping land use classes in Marion County, Indiana from ERTS-1 MSS data
[E73-10680] 16 p1901 N73-25375
ERTS-1 imagery of land use, lake ice, and water pollution, Lake Champlain Basin and Vermont
[E73-10690] 16 p1902 N73-25383
ERTS-1 data for development of information system for timber resources and land management planning in Oregon
[E73-10696] 16 p1903 N73-25388
Analysis of ERTS-1 imagery for crop identification and area estimates in Iowa
[E73-10699] 16 p1903 N73-25391
Application of ERTS-1 remote sensing data in study of vegetation and soils in Idaho
[E73-10708] 16 p1904 N73-25399
Development of environmental indices covering land, water, and air quality compatible with ERTS-1 imagery for two test sites in Pennsylvania
[E73-10709] 16 p1904 N73-25400
Urban impact on areas of maximum environmental quality in Washington Metropolitan Area, 1971
[PB-214544/9] 16 p1977 N73-25993
Evaluation of utility of ERTS-1 satellite and aircraft remotely sensed data to integrated processes of state planning and land use in Maryland
[E73-10716] 17 p2019 N73-26323
Application of ERTS-1 imagery to determine land use in Massachusetts, Connecticut, and Rhode Island
[E73-10723] 17 p2019 N73-26330
Study of recreational land and open spaces using Skylab multispectral band cameras and scanners
[E73-10724] 17 p2019 N73-26331
Land use management and planning in Maryland based on ERTS-1 data
[E73-10732] 17 p2020 N73-26338
Application of EREP data in geological evaluation, regional planning, forest management, and water management in North Carolina
[E73-10734] 17 p2022 N73-26357
Spaceborne photography of vegetation, soils, and agricultural land use
[NASA-TT-F-14967] 17 p2026 N73-26393
Land use models for Houston area
[NASA-CR-128991] 17 p2098 N73-26975
Guide for airport planning and development to identify and resolve environmental problems caused by air pollution, water pollution, and aircraft noise
[PB-219957/8] 18 p2127 N73-27187
Analysis of ERTS-1 imagery for area measurement of land use categories in Finney County, Kansas
[E73-10764] 18 p2134 N73-27241
Inventorying land use in New York State using ERTS-1 multispectral imagery
[E73-10772] 18 p2134 N73-27248
Resources management, land use mapping, and water quality management in Ohio based on ERTS-1 imagery
[E73-10775] 18 p2135 N73-27251
Study of recreational land and open space with Skylab imagery EREP 443
[E73-10783] 18 p2136 N73-27259
Application of ERTS-1 data to crop identification, land use, and engineering geology
[E73-10792] 18 p2137 N73-27268
Automatic land use classification based on optical density and shapes from ERTS-1 imagery
[E73-10816] 18 p2140 N73-27291
Sampling strategies in thematic land use mapping of Maryland, Virginia, and District of Columbia using Skylab EREP data
[E73-10823] 18 p2140 N73-27298
Detection and identification of crops in Imperial Valley, California using ERTS-1 sequential imagery and remote sensing techniques
[PAPER-A2] 19 p2259 N73-28210
Digital analysis of ERTS-1 imagery for southeastern South Dakota to determine cultivated areas and to identify crops
[PAPER-A3] 19 p2259 N73-28211
Application of ERTS-1 imagery for identifying citrus groves and rice fields in Valencia region of Eastern Spain
[PAPER-A4] 19 p2260 N73-28212
Application of ERTS-1 imagery for determining rice growing areas in Philippines and assessment of crop condition
[PAPER-A5] 19 p2260 N73-28213
Application of ERTS-1 imagery for mapping and managing soil and range resources in Sand Hills region of Nebraska
[PAPER-A10] 19 p2260 N73-28218
Application of ERTS-1 imagery and aerial photography for monitoring forage crop resources in California
[PAPER-A11] 19 p2260 N73-28219
Mapping of cotton fields in Southern California using ERTS-1 data for control of pink bollworm growth
[PAPER-A15] 19 p2261 N73-28223
Application of ERTS-1 data for analysis of agricultural crops and forests in Michigan
19 p2262 N73-28228
Preparation of recognition map to determine crop species and mensuration accuracy in Sacramento Valley, California
[PAPER-A22] 19 p2262 N73-28229
Agricultural analysis of ERTS-1 multispectral band scanner data for Monterey Bay, California
[PAPER-A23] 19 p2262 N73-28230
Evaluation of ERTS-1 data for production of land use stratifications and crop inventory process in San Joaquin County, California
[PAPER-A24] 19 p2262 N73-28231
Quantitative evaluation of computer processed ERTS-1 MSS data classifications to identify major agricultural crops in Illinois
[PAPER-A25] 19 p2262 N73-28232
Environmental study of Lake Champlain and Vermont land use based on ERTS-1 imagery
[PAPER-E11] 19 p2270 N73-28275
Analysis of ERTS-1 imagery of southern Arizona plant communities using electronic satellite image analysis console
[PAPER-W7] 19 p2271 N73-28285
Land use mapping of Phoenix Quadrangle, Arizona from ERTS-1 Photography
[PAPER-L3] 19 p2273 N73-28299
ERTS-1 imagery of land use, agriculture, vegetation, geology, landforms, and hydrology in Central Coastal Zone of California
[PAPER-L4] 19 p2273 N73-28300
Utilization of ERTS-1 imagery for monitoring land use change and regional planning in Coachella Valley, California
[PAPER-L5] 19 p2273 N73-28301
Land use change and classification using ERTS-1 imagery of Central Atlantic Regional Ecological Test Site
[PAPER-L6] 19 p2274 N73-28302
Linking land use and environmental processes in Central Atlantic Region using ERTS-1 data
[PAPER-L7] 19 p2274 N73-28303

Land cover and land use mapping of Central Atlantic Region shoreline zone using ERTS-1 imagery
[PAPER-L8] 19 p2274 N73-28304
Timber inventory and land use in Province of Huelva-Spain based on ERTS-1 imagery
[PAPER-L9] 19 p2274 N73-28305
Mapping and digitization of land use in northern megalopolis of Masssachusetts, Connecticut, and Rhode Island using ERTS-1 data
[PAPER-L12] 19 p2274 N73-28308
Land use inventory and mapping in Wyoming from ERTS-1 data
[PAPER-L13] 19 p2274 N73-28309
Utilization of ERTS-1 imagery and data for land use mapping and management in Minnesota
[PAPER-L14] 19 p2275 N73-28310
Utilization of ERTS-1 data for inventory of critical land resources for regional land use planning in Wisconsin
[PAPER-L16] 19 p2275 N73-28311
Application of ERTS-1 and U-2 photography to study of urban land use in Pennsylvania
[PAPER-L17] 19 p2275 N73-28312
Preparation of urban land use inventories of Wisconsin and Indiana by machine-processing of ERTS-1 MSS data
[PAPER-L19] 19 p2275 N73-28314
Land use mapping and inventory of Houston, Texas using ERTS-1 and high altitude photography
[PAPER-L20] 19 p2276 N73-28315
Digital land use mapping in Oakland Country, Michigan using ERTS-1 data
[PAPER-L21] 19 p2276 N73-28316
Mapping of agricultural land use in Lancaster and Lebandon Counties, Pennsylvania from ERTS-1 digital data
[PAPER-L22] 19 p2276 N73-28317
Utilization of ERTS-1 data for land use and resources survey in Michigan
[PAPER-L26] 19 p2276 N73-28321
Algorithm for classifying land use categories of ERTS-1 data by textural features
[PAPER-I16] 19 p2279 N73-28337
Resources and land use management and planning in Oregon using ERTS-1 data
[PAPER-R2] 19 p2282 N73-28360
Utilization of ERTS-1 imagery and data for land use, regional planning, and urban development in Metropolitan Washington area
19 p2285 N73-28377
Mapping land use and detecting land use change in Montgomery County, Alabama using ERTS-1 data
19 p2285 N73-28378
Land use management in Minnesota by automatic interpretation of ERTS-1 MSS data
19 p2285 N73-28379
Development of land management programs based on ERTS-1 imagery and computer compatible tapes for machine processing of data
19 p2288 N73-28397
Application of ERTS-1 imagery for mineral resources, geologic structure, and landform surveys
19 p2288 N73-28398
Application of ERTS-1 imagery to land use inventory and management and mapping techniques
19 p2289 N73-28407
ERTS-1 applications in land use, geologic interpretation, resources survey, and pollution monitoring
19 p2290 N73-28413
Utilization of Skylab imagery as information service for investigating land use and natural resources in New York State
[E73-10829] 19 p2290 N73-28414
Application of ERTS-1 imagery to geologic, hydrologic, agricultural, botanical, and land use studies in Wyoming
[E73-10844] 19 p2291 N73-28422
Computer maps of land use in Titusville, Florida
[E73-10852] 20 p2391 N73-29209
Utilization of ERTS-1 imagery for soil mapping, land use, and urban mapping in Wabash River Basin
[E73-10862] 20 p2392 N73-29213
Application of ERTS-1 imagery to land use inventory, land capability evaluation, and land use suitability in Maryland
[E73-10873] 20 p2393 N73-29224
ERTS-1 monitoring of grass seed field burning in western Oregon
[E73-10883] 20 p2394 N73-29234
Acquisition of land use, soil moisture, and hydrological data of Ontario, Canada and Syracuse, New York for Skylab-3
[E73-10888] 20 p2394 N73-29237
ERTS-1 identification of phenological stages and vegetatine types for land use classification in Alaska
[E73-10905] 20 p2396 N73-29254
Land use planning and management on Mississippi Gulf Coast using ERTS-1 data
[E73-10906] 20 p2396 N73-29255
Development of land use-peak runoff classification system for highway engineering in Maine
[E73-10910] 20 p2397 N73-29259
Computer processing of Skylab MSS data for land use mapping of Baltimore, Maryland-Washington, D.C. area
[E73-10913] 20 p2397 N73-29262
Study of recreation land and open space in Oakland County, Michigan using Skylab MSS data
[E73-10915] 20 p2397 N73-29264
Analysis of Milwaukee county, Wisconsin land use by machine processing of ERTS-1 remotely sensed data
[NASA-CR-133643] 20 p2412 N73-29385
Utilization of Skylab EREP imagery for land use and regional planning
[E73-10886] 20 p2417 N73-29418
Improved water and air quality and land use in Poland
20 p2487 N73-29977
Land use mapping and modelling for Phoenix Quadrangle using ERTS-1 imagery
[E73-10955] 21 p2531 N73-30297
Investigation of land use and earth resources using Skylab EREP
[E73-10964] 21 p2533 N73-30306
ERTS-1 applications for land use management in Minnesota
[E73-10965] 21 p2533 N73-30307
Land use, forest density, soil mapping, erosion, drainage, and salinity limitations in Greece from ERTS-1 data
[E73-10969] 22 p2657 N73-31283
Skylab imagery of recreational land and open space in Oakland County, Michigan
[E73-10973] 22 p2657 N73-31285
Crop identification and acreage measurement in Missouri and Idaho from ERTS-1 imagery
[E73-10982] 22 p2658 N73-31289
Regional land use planning and management in Tri-State area from ERTS-1 MSS photography
[E73-10986] 22 p2658 N73-31293
Land use in northern megalopolis of New England
[E73-10991] 22 p2659 N73-31297
Investigation of New England reservoirs, land use, streams, flooding, and vegetation from Skylab imagery
[E73-10993] 22 p2659 N73-31299
Interpretation of land use and stream drainage in Pawnee River Basin, Kansas
[E73-11005] 22 p2660 N73-31310
ERTS-1 data applications to Minnesota forest land use classification
[E73-11017] 22 p2661 N73-31321
Sampling strategies for automatic thematic land use mapping of Washington D.C., Maryland counties, and Alice Springs, Australia using Skylab multispectral photography
[E73-11018] 22 p2661 N73-31322
Identification and mapping landform and land use characteristics and surficial geologic materials in Great Plains and Midwest
[E73-11025] 22 p2662 N73-31329
Land use change and environmental quality in urban areas, emphasizing flood plains and wetlands
[PB-220742/1] 22 p2669 N73-31382
Automatic photointerpretation for land use management in Minnesota
[E73-11046] 23 p2779 N73-32222
Application of ERTS-1 data to land use planning on Mississippi Gulf Coast
[E73-11055] 23 p2780 N73-32231
Automatic photointerpretation of ERTS-1 imagery for land use management in Minnesota
[E73-11058] 23 p2780 N73-32234
Automatic photointerpretation of ERTS-1 imagery for land use management in Minnesota
[E73-11059] 23 p2780 N73-32235
Automatic photointerpretation and mapping for land use management in Minnesota
[E73-11060] 23 p2780 N73-32236
Automatic photointerpretation of ERTS-1 imagery for land use management in Minnesota
[E73-11061] 23 p2780 N73-32237
Identification of phenological stages and vegetative types for land use classification in Alaska
[E73-11066] 23 p2781 N73-32242
Multidisciplinary research on water depth measurement, Yellowstone Park, atmospheric effects, lake ice surveillance, recreational land use, IFYGL, image enhancement, water quality, oil pollution detection, and mapping iron compounds from ERTS-1 data
[E73-11119] 23 p2783 N73-32264
Application of ERTS-1 imagery to land use, forest density, and soil investigations in Greece
[E73-10988] 24 p2913 N73-33244
Delineation of major terrain features, land uses, and crop species in Tennessee Valley through computerized analysis
[E73-11089] 24 p2913 N73-33251
Regional and local land use planning and mapping of Ohio from Skylab EREP data
[E73-11090] 24 p2914 N73-33252
Land use mapping and modelling for Phoenix Quadrangle
[E73-11098] 24 p2914 N73-33255
Photointerpretation and digital data mapping of land use in Pennsylvania
[E73-11106] 24 p2915 N73-33263
Thematic mapping of land use near Harrisburg, Pennsylvania from ERTS-1 digital data
[E73-11109] 24 p2915 N73-33266
Utilization of Skylab imagery as information service for investigating land use and natural resources in New York
[E73-11113] 24 p2915 N73-33270
Application of Skylab EREP data to structural geology, geomorphology, vegetation mapping, and land use studies in Wyoming
[E73-11136] 24 p2917 N73-33291
Sampling strategies in land use mapping using Skylab EREP multispectral photography
[E73-11139] 24 p2918 N73-33294
Development of land use, water quality, and air quality indices from ERTS-1 imagery for environmental resources management in Susquehanna River Basin and Quantico, Virginia test areas
[E73-11143] 24 p2918 N73-33298
Mapping coastal vegetation and wetlands use for Delaware from ERTS-1 imagery
[E73-11146] 24 p2918 N73-33300
Skylab photography of recreational land and urban resources in Oakland County, Michigan
[E73-11150] 24 p2919 N73-33304
Resource inventory, land use, and pollution of Susquehanna River Basin from ERTS-1 data
[E73-11156] 24 p2919 N73-33310
Agricultural crop identification and land use patterns from Skylab data of California
[E73-11163] 24 p2920 N73-33316

**LANDAU DAMPING**
Korteweg-deVries equation for studying effect of Landau damping on nonlinear ion acoustic waves
[IPPJ-155] 16 p1949 N73-25775

**LANDAU-GINZBURG EQUATIONS**
Transition properties of type 1 and magnetic properties of type 2 semiconductors with small Ginzburg-Landau parameters
[JUL-854-FF] 10 p1200 N73-19762

**LANDFORMS**
NT BARRIERS [LANDFORMS]
NT BEDS [GEOLOGY]
NT DELTAS
NT DUNES
NT FIORDS
NT GREAT BASIN [US]
NT ISLANDS
NT LAGOONS
NT MOUNTAINS
NT PIEDMONTS
NT PLAYAS
NT RIDGES
NT STEPPES
NT STRUCTURAL BASINS
NT VOLCANOES
Landform-vegetation relationships in southern Arizona based on interpretation of ERTS-1 imagery
[E72-10176] 01 p0044 N73-10355
Inventory and monitoring of natural vegetation-landform relationships in arid regions of southern Arizona using ERTS-1 imagery
[E72-10184] 01 p0045 N73-10363
ERTS-1 imagery of landscape changes in Tennessee and Kentucky due to strip mining
[E72-10265] 03 p0291 N73-12364
Land use mapping, limnology, wetlands, geomorphic and landform surveys, and river monitoring of Lake Champlain Basin and Vermont using ERTS-1 imagery
[E72-10282] 03 p0292 N73-12380
Side-looking radar applications to studies of terrain topography and landforms
03 p0295 N73-12405
ERTS-1 imagery of Quaternary landforms and materials in Midwest and Great Plains
[E72-10272] 04 p0409 N73-13333
Mapping distribution of glaciofluvial deposits and associated glacial landforms in Maine using ERTS-1 imagery
[E72-10300] 04 p0411 N73-13350
Geographic applications of ERTS-1 imagery to land use and landscape changes in Tennessee
[E72-10315] 04 p0412 N73-13364
Geographic applications of ERTS-1 imagery to rural landscape change in Tennessee
[E72-10355] 05 p0534 N73-14343
Mapping distribution of glaciofluvial deposits and associated glacial landforms
[E73-10013] 06 p0659 N73-15349
Classification of landforms for land use and regional planning using aerial photographic interpretation
[PB-212774] 08 p0918 N73-17525
Multidisciplinary analysis of forestry, agriculture, soils, and landforms in Michigan using ERTS-1 imagery
[E73-10310] 09 p1022 N73-18342
Mapping distribution of glaciofluvial deposits and associated glacial landforms in Maine from ERTS-1 imagery
[E73-10353] 10 p1148 N73-19349

Utilization of ERTS-1 imagery for mapping Quaternary deposits and landforms in Great Plains and Midwest
[E73-10381] 10 p1152 N73-19376
Application of ERTS-1 data to analysis of agricultural crops, forests, soils, landforms, and acreage estimates in Michigan
[E73-10483] 12 p1396 N73-21320
Structural aspects of distinctive landforms collectively referred to as Imbrium sculpture - Part G
12 p1453 N73-21771
Discovery of previously unknown structural basin and crater on Apollo 16 photography of far side highlands near eastern limb of moon - Part H
12 p1453 N73-21772
Geographic analysis and mapping of landscape changes in Tennessee from ERTS-1 imagery
[E73-10661] 16 p1899 N73-25357
Mapping of glaciofluvial deposits and associated glacial landforms in Maine
[E73-10667] 16 p1899 N73-25362
Classification of landscapes into taxonomic groups on basis of optical properties
[NASA-TT-F-14970] 17 p2025 N73-26386
Geological landforms in central Piedmont of Virginia and North Carolina from ERTS-1 imagery
[E73-10766] 19 p2259 N73-28205
Application of ERTS-1 imagery for differentiating quaternary surface deposits and landforms in Illinois, Iowa, Missouri, Kansas, Nebraska, and South Dakota
[PAPER-G13] 19 p2264 N73-28244
ERTS-1 imagery of land use, agriculture, vegetation, geology, landforms, and hydrology in Central Coastal Zone of California
[PAPER-L4] 19 p2273 N73-28300
Geographic applications of ERTS-1 data to landscape changes in eastern Tennessee
[PAPER-L10] 19 p2274 N73-28306
Mineral resources, geological structures, and landform surveys from ERTS-1 imagery
19 p2289 N73-28408
ERTS-1 imagery of landscape changes, strip mines, timber, agriculture, and water resources in eastern Tennessee
[E73-10843] 19 p2291 N73-28421
Mapping of Quaternary geological and geomorphological landforms of Great Plains and Midwest from ERTS-1 imagery
[E73-10949] 21 p2530 N73-30291
Identification and mapping landform and land use characteristics and surficial geologic materials in Great Plains and Midwest
[E73-11025] 22 p2662 N73-31329

**LANDING**
NT AIRCRAFT LANDING
NT CRASH LANDING
NT LUNAR LANDING
NT MARS LANDING
NT PLANETARY LANDING
NT SOFT LANDING
NT SPACECRAFT LANDING
NT TOUCHDOWN
NT VERTICAL LANDING
NT WATER LANDING

**LANDING AIDS**
NT AIRPORT BEACONS
NT AIRPORT LIGHTS
NT APPROACH INDICATORS
NT ARRESTING GEAR
NT AUTOMATIC LANDING CONTROL
NT INSTRUMENT LANDING SYSTEMS
NT LANDING INSTRUMENTS
NT RUNWAY LIGHTS
Incident involving collision of Boeing 727 aircraft with landing light system at Atlanta International Airport, Georgia on 21 Dec. 1971
[NTSB-AAR-72-22] 07 p0737 N73-16000
Bibliography of data on aircraft landings, instrument landings, approach control, glide path systems, display devices, and terminal facilities
[AD-751800] 07 p0740 N73-16024
Analysis of Microwave Landing System performance to determine signal formats and to reduce effects of multipath transmission
[AG-5011-B-1] 07 p0818 N73-16628
Characteristics and functions of various types of aircraft landing fields in Germany and development of airfields for improved air safety
10 p1183 N73-19624
Analysis of electromagnetic compatibility of microwave landing guidance system and candidate interim systems
[ECAC-PR-72-069] 12 p1425 N73-21554
Development of heads-up flight data display for aircraft approach and landing during all conditions of visibility
14 p1688 N73-23702
Development of control and display testing requirements for evaluation of microwave landing system - Vol. 2
[AD-758792] 16 p1942 N73-25714
Performance tests of visual approach slope indicator [VASI] equipment and systems for improved terminal area effectiveness
[FAA-NA-73-64] 18 p2175 N73-27568
Development, characteristics, and operation of test facility for determining effectiveness of runway lighting systems under various atmospheric conditions
[FAA-RD-71-94] 20 p2382 N73-29141
Statistical analysis of aircraft carrier wave-off situation based on deck motion and aircraft approach geometry
[AD-764516] 22 p2616 N73-30967
Effects of snow cover and snow surface conditions on image glide path systems for aircraft approach control
[FAA-RD-72-85] 22 p2697 N73-31602
Air traffic control evaluation to determine feasibility of combining smaller aircraft into gaps on flow of normal traffic to increase effectiveness of terminal facilites
[FAA-AFS-500-1] 23 p2816 N73-32517

**LANDING GEAR**
Analysis of dynamic aircraft landing loads, and a proposal for rational design landing load requirements
01 p0002 N73-10010
Development and evaluation of space shuttle main landing gear door constructed of boron/epoxy composite material ribs on titanium panel
[NASA-CR-112172] 02 p0233 N73-11889
Development of statistical technique for determining injury reduction capability of energy absorber equipment
[AD-749333] 05 p0497 N73-14044
Active control in landing gear of aircraft for reducing fatigue damage from ground induced vibration during taxiing
[AD-750137] 06 p0678 N73-15515
Development of criteria for predicting landing impact loads for V/STOL aircraft based on data obtained by flight tests of X-22 aircraft
[AD-753852] 09 p0989 N73-18075
Development problems and flight performance evaluation of Apollo lunar module landing gear
09 p1088 N73-18878
Numerical analysis of aircraft shock absorber operation to show initial charging, motion, and force parameters during static and dynamic compression of landing gear
[AD-754609] 11 p1236 N73-20031
Performance tests to determine cornering characteristics of cantilever aircraft tire on dry, damp, and flooded runway surfaces over range of yaw angles
[NASA-TN-D-7203] 12 p1363 N73-21058
Development of method for determining optimal lunar landing gear design parameter values for front-foot touchdown mode
13 p1579 N73-22798
Development of boron composite materials for construction of aircraft landing gear for A-37 aircraft - Vol. 1
[AD-756922] 14 p1603 N73-22996
Design, fabrication, and test of boron composite material landing gear for use as main landing gear on A-37 aircraft - Vol. 2
[AD-756923] 14 p1603 N73-22997
Air cushion landing system effect on aerodynamic characteristics of A-4 aircraft
[AD-761621] 19 p2221 N73-27917
Loading force diagrams and structural properties of landing gear
[AD-761644] 19 p2221 N73-27918
Logistic performance data book for C-5A aircraft landing gear to show system reliability, maintainability, logistic support cost, and performance data
[AD-762248] 19 p2357 N73-28963
Logistics performance data book for RF-4C aircraft landing gear system to show reliability, maintainability, logistics support, and operating problems
[AD-762231] 19 p2358 N73-28970
Flight tests of folding sidewall, expandable tires on C-131 aircraft to determine operation of inflation and deflation system
[AD-762730] 20 p2361 N73-28993
Analysis of loads imposed on nose gear retraction system of T-34 aircraft to determine critical mechanical adjustments
[AD-762729] 20 p2361 N73-28994
Effect of inflated air cushion landing gear on subsonic static stability of high performance aircraft operating out of ground effect
[AD-763365] 21 p2498 N73-30048
Application of composite materials to construction of helicopter airframes and landing gear
[NASA-CR-112333] 22 p2614 N73-30948
Design requirements and characteristics of toroidal, continuous wound aircraft tire
[AD-764888] 23 p2746 N73-31977
Development and characteristics of air cushion landing system for remotely piloted vehicles
[AD-764774] 23 p2747 N73-31985

**LANDING INSTRUMENTS**
NT APPROACH INDICATORS
Flight control improvement of F-8 aircraft relative to carrier takeoff and landing
[AD-753010] 09 p0986 N73-18052

**LANDING LOADS**
Analysis of dynamic aircraft landing loads, and a proposal for rational design landing load requirements
01 p0002 N73-10010
Landing loads of Do-31 aircraft in vertical landing, noting undercarriage reactions and sinking speed
[BMVG-FBWT-72-24] 09 p0986 N73-18046
Development of criteria for predicting landing impact loads for V/STOL aircraft based on data obtained by flight tests of X-22 aircraft
[AD-753852] 09 p0989 N73-18075

**LANDING MODULES**
NT LUNAR LANDING MODULES
NT LUNAR MODULE

**LANDING SIMULATION**
Magnetic data tapes containing measurements of pilot scanning behavior, control response and vehicle response during simulated instrument landing approaches
01 p0016 N73-10124
Simulation of pilot decision making process in manual landing operation during fog
14 p1713 N73-23898
Simulator analysis of effect of engine response characteristics on approach and landing operations of powered lift aircraft with externally blown flaps
[NASA-TM-X-62265] 17 p1982 N73-26021
Fog chamber low visibility landing simulation film for pilot training
[FAA-RD-73-61] 20 p2452 N73-29707

**LANDING SITES**
NT LUNAR LANDING SITES
Development of fiberglass reinforced polyester for expedient airfield pavement system
[AD-743958] 01 p0114 N73-10941
Performance tests of Andover C short takeoff transport aircraft on grass, concrete and soil landing sites
[ARC-CP-1220] 04 p0373 N73-13034
Design, construction, and maintenance of landing fields and runways
[AD-751400] 09 p1012 N73-18263
Ground erosion on grassland and concrete by vertical takeoff of Do-31 aircraft
[BMVG-FBWT-72-26] 10 p1107 N73-19023
Landing site selections for Viking Mars probes
[NASA-NEWS-RELEASE-73-91]
13 p1576 N73-22768
Performance of aircraft taxiing on dirt surfaces
[AD-756588] 16 p1861 N73-25077
Analysis of dual lane runway operations at high density airport terminals using computerized simulation techniques
[ATC-17] 16 p1885 N73-25254
Evaluation of aluminum honeycomb core landing mat with modified hinges
[AD-758840] 18 p2127 N73-27186
Development of procedures for stabilizing snow to permit helicopter landings
[AD-763231] 21 p2497 N73-30040

**LANDING SYSTEMS**
U LANDING AIDS

**LANDMARKS**
Stellar-inertial measurement system trade study on spacecraft orbital ephemeris and attitude errors for landmark location
[NASA-CR-134042] 24 p2984 N73-33845

**LANDSCAPE**
U TERRAIN
U TOPOGRAPHY

**LANGMUIR PROBES**
U ELECTROSTATIC PROBES

**LANGUAGES**
NT ALGOL
NT ASSEMBLY LANGUAGE
NT ENGLISH LANGUAGE
NT FORTRAN
NT MACHINE ORIENTED LANGUAGES
NT PL/1
NT PROGRAMMING LANGUAGES
NT SENTENCES
NT SYLLABLES
NT WORDS [LANGUAGE]

**LANTHANIDE SERIES METALS**
U RARE EARTH ELEMENTS

**LANTHANUM**
Thermodynamics of oxygen solubility in lanthanum uranium oxide measured on solid state electrolytic cell
[KFK-1649] 12 p1376 N73-21163

**LANTHANUM COMPOUNDS**
Synthesis and characterization of tetrahydroborates of lanthanum, neodymium, and erbium
[AD-759372] 17 p1992 N73-26110
Optical spectra and crystal field parameters of neodymium in lanthanum aluminate
17 p2071 N73-26757
Alloying effect on superconducting temperature La3In
[IS-M-2] 17 p2073 N73-26771

**LAP JOINTS**
Static and fatigue loading tests of bonded lap joints to determine crack length leading to failure of joint
[NASA-CR-112219] 08 p0966 N73-17896
Stress analysis on lap joint subjected to loads
[AD-753469] 10 p1221 N73-19929
Joint strength, adhesive ductility of adhesively bonded joints of epoxy resins bonded to aluminum and titanium alloys
[DLR-FB-73-22] 14 p1680 N73-23636

Stress analysis of adhesive lap joint subjected to tension, shear force, and bending moments for various material properties and thickness of adherents
24 p2988 N73-33877

LAPLACE EQUATION
Interactive graphics solution, PDQ 3, to Laplace and Poisson equations
[AD-749252] 05 p0569 N73-14621
Velocity potential solution of heavy incompressible liquid wave motion
[AD-758251] 15 p1769 N73-24331
Calculating temperature distribution by applying Green function to two dimensional Laplace equation
[NAL-TR-297] 15 p1842 N73-24924
Treatment of singularities in solution of Laplace equation by integral equation method based on Green function, applied to flow distribution and transmission lines
[NPL-NAC-31] 23 p2813 N73-32490

LAPLACE OPERATORS
U LAPLACE TRANSFORMATION

LAPLACE TRANSFORMATION
Inversion of some Laplace transforms encountered in heat transfer problems
[AD-749329] 04 p0486 N73-13968
Laplace transform amplitude function generator utilizing thin film semiconductor
[AD-750590] 06 p0710 N73-15792
Multidimensional Laplace-Galois transform for nonlinear sequential machines
09 p1056 N73-18611
Power series solution to partial differential equation in thermal conductivity analysis on body of variable density
[AD-754256] 10 p1225 N73-19957
Solution of inverse problem of transient heat conduction using Laplace transformation
16 p1973 N73-25954

LAPSE RATE
Mean temperature lapse rates within lower 300 meters
[NLL-M-22838-[5828.4F]] 12 p1419 N73-21503

LARGE APERTURE SEISMIC ARRAY
Performance of equipment and software of SAAC [LASA] system
[AD-745874] 02 p0169 N73-11375
Operations summary of Seismic Array Analysis Center for period Apr. - June 1972
[AD-750779] 06 p0668 N73-15435

LARGE SCALE INTEGRATION
Large scale integration techniques for computer multiprocessing system
[NASA-CR-128395] 01 p0030 N73-10234
Automata theory of cubical complexes applied to diagnosis and algorithmic description, noting logic design of ultra LSI
[NASA-CR-130388] 05 p0517 N73-14201
Universal functional scheme for realizing any combination or sequential function for proliferation problem in LSI technology
[NASA-CR-130387] 05 p0517 N73-14204
Performance and reliability of large scale integrated circuits
[AD-750577] 06 p0646 N73-15250
Effects of small LSI packages and modularity on development of digital filters
[AD-755657] 12 p1385 N73-21228
Prototype of high resolution duplicator for large scale integration circuit masks
[REPT-3424] 16 p1914 N73-25488
XY translational device controlled by differential interferometer for large scale integration microelectronics
[LCR-71-213/1/R] 18 p2152 N73-27394
Large scale integration for users and suppliers within circuit technology, manufacturing techniques for bipolar devices and semiconductors memory arrays
[PB-221013/6] 21 p2520 N73-30212

LARGE SPACE TELESCOPE
Design technique for control systems of large space telescope mirrors
[NASA-TN-D-7090] 05 p0522 N73-14247
Design and fabrication of optical system to compensate for motions of stellar field image on focal plane of large orbiting telescope based on single-axis system
[NASA-TN-D-7145] 07 p0799 N73-16488
Development of Large Space Telescope for conducting astronomical observations from unmanned satellites and analysis of constraints and tradeoffs during design phase - Vol. 1
[NASA-TM-X-64726-VOL-1] 09 p1035 N73-18449
Mission description and system design for Large Space Telescope used on unmanned satellites - Vol. 2
[NASA-TM-X-64726-VOL-2] 09 p1036 N73-18450
Development and characteristics of optical telescope assembly system for Large Space Telescope based on mission-related and optical parameters - Vol. 3
[NASA-TM-X-64726-VOL-3] 09 p1036 N73-18451
Development and characteristics of scientific instrument package for use with Large Space Telescope - Vol. 4
[NASA-TM-X-64726-VOL-4] 09 p1036 N73-18452
Development and characteristics of support systems module for use with Large Space Telescope - Vol. 5
[NASA-TM-X-64726-VOL-5] 09 p1036 N73-18453
Development of metric system design for large space telescope to show effect on production cost and time required
[NASA-CR-124133] 10 p1159 N73-19426
Active optics simulation system for designing mirror control system for large space telescope
[NASA-CR-112259] 10 p1159 N73-19433
Design, development, and operation of remote control system for Large Space Telescope
[NASA-TM-X-64740] 12 p1405 N73-21394
Scientific instrument package for large space telescope
[NASA-CR-130214] 13 p1529 N73-22394
Literature survey of articles dealing with all aspects of predicting, measuring, and controlling unwanted scattered light in large space telescopes
[NASA-CR-124240] 14 p1667 N73-23531
Large space telescope engineering scale model optical design
[NASA-CR-124561] 16 p1913 N73-25484
Design and performance of optically stabilized telescope pointing system using digital star tracker
[NASA-TN-D-7204] 18 p2125 N73-27173
Manufacturing of large structural mirror supports for space telescopes using titanium alloys
18 p2209 N73-27828
Design of optical instrument package for large space telescope
18 p2210 N73-27839

LARVAE
Physiological responses of parasitic worms and their larvae to solar ultraviolet irradiation and space flight stress
15 p1740 N73-24106

LARYNX
Functional reactions of human otorhinolaryngolic organs during hypokinesia
13 p1482 N73-22015

LASER ALTIMETERS
Development and characteristics of laser altimeter for use with Apollo Lunar Orbital Experiments Mission
[NASA-CR-128738] 08 p0924 N73-17567
Use of laser altimetry in Apollo 16 flight to aid in spacecraft position determination and lunar geological investigation
12 p1455 N73-21790
Estimates of moon geometry using lunar orbiter imagery and Apollo laser altimeter data
[NASA-TR-R-407] 23 p2846 N73-32743

LASER BEAM DEFOCUSING
U THERMAL BLOOMING

LASER COMMUNICATION
U OPTICAL COMMUNICATION

LASER HEATING
Measurement of electron density in carbon plasma created by heating solid target with laser radiation
[AD-746221] 01 p0086 N73-10715
Effect of purification of transparent dielectrics from dust on breakdown threshold under action of laser irradiation
[AD-748230] 03 p0338 N73-12760
Analysis of laser induced two dimensional wave motions in hydrogen plasma
[AD-746681] 03 p0343 N73-12798
Reaction kinetics in pulsed atomic beam generation by laser vaporization of metallic atoms
[AD-748278] 04 p0387 N73-13145
Laser optics and diagnostic methods for vaporization and heating of confined spherical overdense plasmas
[AD-748260] 04 p0456 N73-13720
Interferometric determination for distribution of electron density of two colliding laser plasmas
[AD-749618] 05 p0584 N73-14754
Plasma generation within magnetic containment field by laser irradiation of solid particle
[COO-3547-2] 06 p0704 N73-15740
Variational analysis of laser induced gas breakdown employing simplified diffusion models for plasma generation
[AD-750874] 06 p0707 N73-15767
Gas dynamic equation for investigating thermal heating modes during laser radiation flux interaction with material
09 p1043 N73-18509
Photoionization cross section measurements on excited cesium maser by light beams
[AD-756217] 13 p1564 N73-22677
CO2 laser-plasma heating and diagnostic scattering experiments
[LA-5167-MS] 17 p2040 N73-26509
Time prediction for laser melting and vaporization of metal sheet
[AD-760113] 17 p2042 N73-26521
Laser heating effects on oxide growth rates in magnesium-oxygen interaction
[AD-760176] 17 p2047 N73-26565
Effect of laser pulse on threshold voltage of metal oxide semiconductor field effect transistors
[CRC-1246] 21 p2585 N73-30716
Laser vaporization of aluminum wire and heating to thermonuclear temperatures
23 p2800 N73-32392

LASER MATERIALS
CO2 laser radiation damage to surface of infrared laser optical material
[DREV-TN-2013/72] 01 p0064 N73-10524
Analysis of reaction mechanisms involved in chemical and continuous wave lasers based on carbon disulfide/oxygen system
[DREV-R-656/72] 01 p0064 N73-10525
Development of fluid mechanical helium argon ion laser and analysis of improvements in efficiency and power output
[NASA-CR-128397] 01 p0064 N73-10526
Application of Nernst glower metal oxide conductors to laser pumping to produce spectral energy within pumping band of laser material
[AD-745796] 01 p0066 N73-10538
Development of yttrium aluminate material for optically pumped lasers and measurement of optical absorption and emission spectra
[AD-746032] 01 p0066 N73-10540
Analysis of laser applications in medicine, biology, research, chemical processing, initiation of thermonuclear reactions, and weapon systems
[AD-743098] 01 p0066 N73-10541
Construction of carbon dioxide transversely excited atmospheric laser and application to absorption studies of laser induced plasmas
[AD-745842] 01 p0066 N73-10542
Analysis of applications for infrared, carbon dioxide, and chemical laser devices with emphasis on window materials and absorption mechanics
[AD-745927] 01 p0067 N73-10546
Operating principles of gas dynamic lasers and effects of gas dynamic flow on laser system properties
02 p0181 N73-11469
Development of efficient high power NDY ceramic laser material
[AD-746521] 02 p0184 N73-11491
Defect structures of GaAs by transmission and black reflection X ray topographic analysis
[AD-746895] 03 p0337 N73-12747
Developments in laser technology to include chemical lasers, electric discharge lasers, high power glass lasers, and laser techniques
[AD-748178] 04 p0429 N73-13498
USSR research projects involving laser technology, effects of strong explosions, geosciences, and particle beams
[AD-749487] 04 p0489 N73-13998
Development of interaction gradient concept and application to laser radiation damage to quartz crystals, fused quartz, and laser glass samples
05 p0554 N73-14500
Measurement of physical and chemical properties of well characterized surfaces for application to optical elements in high power laser development
05 p0555 N73-14508
Evaluation of optical properties of high power laser window materials
[AD-749864] 05 p0559 N73-14540
Hardening characteristics of alkali halides selected as laser window materials
[AD-749867] 05 p0559 N73-14545
Growth of single crystal CdTe materials for use in infrared electro-optic devices
[AD-749368] 05 p0588 N73-14783
Excited state paramagnetic resonance interpretation of Zeeman effects in optical spectra of neodymium and erbium containing impurity ions
[AD-750343] 06 p0700 N73-15712
Proceedings of conference to determine research projects for development of lasers for optical communications applications
[PB-212692] 07 p0807 N73-16543
Design, fabrication, and performance evaluation of Faraday effect far infrared isolators
[AD-751319] 07 p0808 N73-16552
Analysis of thermal lensing in high power laser window materials
[AD-751266] 07 p0808 N73-16554
Development and characteristics of stable master oscillator carbon dioxide laser system
[AD-752219] 08 p0930 N73-17614
Laser frequency modulation, molecular lasers, superconducting lasers, and laser induced instabilities in fluids
[AD-752633] 08 p0931 N73-17621
Radiation damage threshold determination for glass laser materials
[AD-752549] 08 p0931 N73-17622
Development of electronically tunable dye laser with capability for producing two randomly accessible and simultaneous frequencies
[AD-752053] 08 p0933 N73-17641
Mechanism for formation of inverse population of oscillatory levels in gas discharge carbon monoxide laser
[AD-753559] 09 p1045 N73-18520
Production of stimulated emission in vacuum ultraviolet using molecular xenon gas excited by relativistic electron beam
[AD-753483] 09 p1045 N73-18522

Optical properties of ultraviolet down-converter materials
[AD-753578] 09 p1068 N73-18713
Measurement of stimulated emission cross section of neodymium laser based on laser threshold gain and inverted population
[AD-753901] 10 p1170 N73-19514
Evaluation of cold cathode materials for sealed off carbon dioxide lasers to show power output and service life
[NASA-CR-130202] 11 p1302 N73-20564
Development of techniques for frequency tripling laser radiation based on mixtures of metal vapors and inert gases
[AD-754096] 11 p1304 N73-20581
Melt stoichiometry and growth of yttrium vanadate polarizer material
[AD-754650] 11 p1332 N73-20809
Performance characteristics of erbium doped laser glass material
[AD-755683] 12 p1411 N73-21435
Procedure for improving strength and fracture behavior of alkali halides for use as high energy laser window material
[AD-755716] 12 p1411 N73-21437
High purity phosphate core and cladding glasses for erbium doped laser
[AD-755687] 13 p1538 N73-22460
Design, development, and characteristics of continuous wave laser using organic dyes
[AD-756514] 13 p1539 N73-22466
Design, development, and characteristics of atmospheric pressure, double discharge carbon dioxide laser
[AD-756517] 13 p1539 N73-22467
Analysis of buffer gas pressure effects on kinetics of generation spectrum of photodissociation laser
[AD-756334] 13 p1539 N73-22469
Research reports on amorphous, laser window, composite, and gradient materials
[AD-755585] 13 p1545 N73-22521
Characteristics of dye lasers with emphasis on lasing mechanism of dyes
[PHL-1973-2] 14 p1672 N73-23566
Analysis of atmospheric transmission properties of 1.06 microns radiation using neodymium laser
[AD-757249] 14 p1672 N73-23572
Analysis of elementary, exothermic, atom-molecule reactions for application as laser materials for chemical lasers
[AD-756686] 14 p1673 N73-23578
Spectroscopic analysis of energy transfer in rare earth compounds to determine effect of transfer phenomena on lasing efficiency
[AD-757520] 14 p1673 N73-23579
Design, development, and operation of carbon dioxide-nitrogen-helium laser to show beam characteristics and power output as function of gas mixture
[AD-757263] 14 p1674 N73-23582
Performance tests of copper vapor laser and analysis of relaxation of metastable lower levels
15 p1794 N73-24544
Effects of polarized radiation on self-focusing thresholds of laser materials
[AD-757789] 15 p1795 N73-24554
Development of laser head for simultaneous optical pumping of several dye lasers
[NASA-CASE-LAR-11341-1] 16 p1923 N73-25564
Development of technique for producing holograms using propagation of surface waves within layer of photosensitive material
[NASA-CASE-MFS-22040-1] 17 p2039 N73-26500
Surface damage induced in optical materials by laser
[AD-760131] 17 p2042 N73-26519
Laser induced damage and avalanche breakdown in transparent insulators
[AD-761168] 18 p2158 N73-27439
Cold cathode materials for constructing sealed off CO2 lasers
[NASA-TN-D-7307] 20 p2425 N73-29480
Analysis of dynamic Stark effect in laser-atom interactions to show distortion of atomic structure in high intensity laser fields
[CEA-CONF-2135] 20 p2425 N73-29481
Characteritics of carbon dioxide lasers and application for transmission of data
21 p2554 N73-30479
Research and development of laser materials, semiconductor materials, and magnetic materials
[AD-763709] 21 p2555 N73-30486
Dynamic processes for laser emission in pulsed pumping of transversely excited atmospheric carbon dioxide laser
[DREV-TN-2036/73] 23 p2800 N73-32396
Bibliography of chemical laser publications with tables showing chemical systems exhibiting laser action
[DREV-TN-2080/73] 23 p2801 N73-32403

**LASER MODE LOCKING**

Stable mode-locking and pulse coupling of longitudinal discharge carbon dioxide laser with single electro-optical element
[AD-744996] 01 p0064 N73-10528
Oscilloscopic measurement of mode locked ultrashort laser pulses produced by linear and nonlinear photoelectric effects
[KFKI-72-41] 07 p0806 N73-16539
LLL studies of various lasers and analysis of laser produced plasmas
[UCRL-50022-1] 07 p0806 N73-16541
Design of Brewster angle acousto-optic modulator for high power mode locked C02 laser
[AD-751680] 07 p0807 N73-16544
Pockels cell for splitting light pulses from NdYAG mode locked pulsed laser
[AD-751532] 07 p0807 N73-16550
Operating principles and performance tests results for optical modulator system with mode locked Nd-YAG laser
[NASA-CR-130195] 11 p1302 N73-20569
Use of argon-ion laser transverse mode locking to produce high resolution scanning beam
15 p1794 N73-24546
Procedure and device for effecting dual mode locking in pulsed Nd-YAG lasers
[NASA-CASE-GSC-11746-1] 23 p2800 N73-32398
Infrared detection of zero pi pulses generated by mode locked CO2 lasers
[AD-764692] 23 p2802 N73-32406
Mode locking and pulse selection in atmospheric gas lasers
[AD-765350] 23 p2802 N73-32411

**LASER MODES**

Frequency shift of flash lamp pumped dye laser with two Fabry-Perot interferometer wavelength selectors
01 p0064 N73-10527
Atmospheric effects on laser beam propagation
[AD-746053] 01 p0066 N73-10544
Method for analyzing dominant TEM mode of complex laser cavities
[AD-746215] 02 p0183 N73-11481
Developments in laser technology to include chemical lasers, electric discharge lasers, high power glass lasers, and laser techniques
[AD-748178] 04 p0429 N73-13498
Measurements of laser induced surface damage processes at ruby and neodymium YAG laser wavelengths to determine laser damage at different wavelengths to transparent media
05 p0555 N73-14506
Operating modes and outputs of distributed feedback side coupled waveguide lasers
[CRC-1235] 06 p0679 N73-15521
Laser-plasma coupling and laser absorption by solid deuterium
[UCRL-50022-2] 10 p1169 N73-19506
Quantum mechanics for describing operational properties of gas laser containing saturable absorber in resonator
12 p1409 N73-21421
Laser generation of plasma and plasma diagnostics, and laser fusion research
[UCRL-50021-72-1] 12 p1410 N73-21430
Light source and geometrical requirements for optimization of optical anemometry signals
[ET/TN/A/18] 13 p1537 N73-22451
Theoretical model developed for carbon dioxide laser operating in short pumping time, gain switched, mode-locked mode of operation
[AD-756456] 13 p1537 N73-22452
Pulse position modulation laser communication system for voice transmission
[AD-757258] 14 p1633 N73-23237
Development of acoustical controlled distributed feedback laser with continuous frequency spectrum tuning
[NASA-CASE-NPO-13175-1] 18 p2157 N73-27431
Wind tunnel tests to determine boundary layer characteristics of air flows using laser light source and thermoanemometer
[NASA-TT-F-14945] 20 p2387 N73-29180
Development of laser amplifier using disks of neodymium glass and measurement of beam amplification for laser beams
[EP-RR-35] 20 p2425 N73-29478

**LASER OUTPUTS**

Analysis of reaction mechanisms involved in chemical and continuous wave lasers based on carbon disulfide/oxygen system
[DREV-R-656/72] 01 p0064 N73-10525
Development of fluid mechanical helium argon ion laser and analysis of improvements in efficiency and power output
[NASA-CR-128397] 01 p0064 N73-10526
Analysis of energy transfer processes in molecular lasers
[AD-745368] 01 p0066 N73-10537
Theoretical description of thermal blooming of pulsed, focused laser beams in gases
[AD-745739] 01 p0066 N73-10539
Development of yttrium aluminate material for optically pumped lasers and measurement of optical absorption and emission spectra
[AD-746032] 01 p0066 N73-10540
Analysis of laser applications in medicine, biology, research, chemical processing, initiation of thermonuclear reactions, and weapon systems
[AD-743098] 01 p0066 N73-10541
Construction of carbon dioxide transversely excited atmospheric laser and application to absorption studies of laser induced plasmas
[AD-745842] 01 p0066 N73-10542
Analysis of applications for infrared, carbon dioxide, and chemical laser devices with emphasis on window materials and absorption mechanics
[AD-745927] 01 p0067 N73-10546
Laser pulses transmitted from ground stations to aircraft or satellites used for 3-D multilateration system for precision geodetic measurements with 1-cm accuracy
01 p0119 N73-10982
Analysis of dependence of refractive index of gas discharge medium in carbon dioxide laser on amplitude of discharge current
[NLL-DRIC-TRANS-2815-[3623.66]]
02 p0180 N73-11459
Electrical analogue model of flash tube and laser rod system to determine efficiency of laser system with respect to flash duration
[WRE-TM-657[AP]] 02 p0180 N73-11462
Analysis of conditions created by intense laser beam focused on plasma with application as plasma diagnostic technique
[DREV-R-676/72] 02 p0181 N73-11463
Attenuation of carbon dioxide laser beams in atmosphere at various frequencies and method for calculating absorption coefficients from measured data
[FOA-2-A-2542-E3/E4/E6] 02 p0181 N73-11465
Operating principles of gas dynamic lasers and effects of gas dynamic flow on laser system properties
02 p0181 N73-11469
Analysis of dispersion, correlation and structural functions in amplitude and phase of laser being propagated into turbulent atmosphere
02 p0181 N73-11470
High speed holography of high speed phase object using Q switched laser outputs
[ISL-10/71] 02 p0181 N73-11471
Numerical analysis of semiconductor saturable absorber and extablishment of criteria for operation of laser saturable resonator in bistable regime
[AD-746736] 02 p0183 N73-11488
Influence of intense laser radiation on plasma generation of large magnetic fields
[AD-746098] 02 p0216 N73-11752
Model for behavior of solid deuterium slab under laser irradiation
[LA-DC-72-415] 03 p0310 N73-12530
Design, development, and performance tests of long pulse liquid laser oscillator and circulatory subsystem
[AD-747964] 03 p0311 N73-12536
Monopulse laser emission study of moving objects during shadow photography
[AD-747607] 03 p0311 N73-12539
Effect of variable magnetic field on emission of helium-neon laser and resulting parameters of discharge plasma
[AD-747443] 03 p0311 N73-12542
Frequency stability characteristics of single frequency neodymium YAG laser system with coherent ultrashort pulses for high resolution imaging
[AD-747967] 03 p0312 N73-12543
Scintillation reductions in multiwavelength laser propagation by near field transmitter apertures
[AD-747640] 03 p0337 N73-12751
Analysis of laser light scattered from marginally stable hydrogen plasma
[INR-P-1377] 04 p0429 N73-13491
Transient, two dimensional temperature field of laser pulse in solid
[SC-DR-72-0393] 04 p0429 N73-13495
Computer program for propagation and thermal blooming of pulsed, focused laser beams
[AD-748991] 04 p0430 N73-13503
Second order coherence function discriminating between thermal and laser radiation
[ONERA-NT-196] 04 p0450 N73-13675
Laser damage in lithium iodate and proustite
[AD-748935] 04 p0451 N73-13682
Laser excitation for isotope separation
[WRE-TM-494[WR/D]] 04 p0453 N73-13701
Scattering and absorption effects in atmospheric transmission of infrared radiation
[AD-750084] 05 p0542 N73-14410
Procedures and equipment for measuring angular distribution of laser beam scattering by evolving water vapor
[NLL-M-22457-[5828.4F]] 05 p0554 N73-14497
Proceedings of symposium on laser radiation damage to transparent dielectrics, plasma formation at dielectric surfaces, and damage morphology of thin film coatings
[NBS-SP-372] 05 p0554 N73-14498
Characteristics of optical glass materials with specific resistance to effects of laser radiation
05 p0554 N73-14499
Development of interaction gradient concept and application to laser radiation damage to quartz crystals, fused quartz, and laser glass samples
05 p0554 N73-14500
Effects of stoichiometry variation, heat treatment, impurity, and color center content of electrooptic crystals and kinetics of index damage process
05 p0554 N73-14501
Analysis of laser bulk damage in alkali-halides with no self-focusing and measurement of damaging fields

considering effects of inclusions on bulk optical strength
05 p0554 N73-14502
Analysis of laser induced surface damage to glass materials at Brewster angle and near normal incidence
05 p0554 N73-14503
Analysis of entrance and exit surface laser induced radiation damage on sapphire crystal samples as function of beam size and divergence at surfaces
05 p0555 N73-14504
Measurements of laser induced surface damage processes at ruby and neodymium YAG laser wavelengths to determine laser damage at different wavelengths to transparent media
05 p0555 N73-14506
Surface damage to gallium arsenide surfaces from radiation by ruby and neodymium-glass lasers
05 p0555 N73-14507
Analysis of time dependent, self focusing optical beams with elliptical constant intensity contours
05 p0555 N73-14509
Effect of glass laser radiation on borosilicate crown glass, fused silica, and flint glass with estimates of Kerr effect and electrostriction processes
05 p0555 N73-14510
Analysis of self focusing damage in laser rods with subnanosecond pulse
05 p0555 N73-14511
Analysis of damage to thin films and substrate surfaces during irradiation by Q switched ruby laser
05 p0556 N73-14512
Measurement of damage thresholds for multiple layer dielectric mirrors for laser pulses of twenty nanoseconds and twenty picoseconds duration
05 p0556 N73-14513
Analysis of laser damage to thin film coatings caused by radiation from Q switched ruby laser
05 p0556 N73-14514
Analysis of damage threshold and damage mode from laser radiation for multilayer and periodic inhomogeneous film systems
05 p0556 N73-14515
Analysis of fundamental absorption properties of laser window materials and limitations imposed by uncontrolled impurities
05 p0556 N73-14516
Analysis of surface damage mechanisms to mirrors and mirror coatings resulting from irradiation by pulsed carbon dioxide lasers
05 p0556 N73-14519
Analysis of conditions required to obtain laser action based on chemical reactions
[DREV-TN-2004/72] 05 p0557 N73-14520
Laser tracking techniques used for geodetic applications in space
[GRGS-BULL-1] 05 p0557 N73-14522
Laser telemetry discussing equipment specifications, errors, and noise reduction
05 p0557 N73-14524
Aberration due to high velocity satellites for laser telemetry
05 p0557 N73-14526
Efficiency of laser telemetry tracking for satellites carrying reflectors
05 p0557 N73-14527
Efficiency of laser telemetry tracking for satellite carrying laser reflector sphere
05 p0557 N73-14528
Effects of spacecraft stabilization on laser tracking efficiency
05 p0558 N73-14531
Laser heating of dense plasma through excitation of parametric instabilities
[AD-749970] 05 p0584 N73-14756
Spectral deficits in visual acuity due to laser irradiation
[AD-750394] 06 p0637 N73-15173
Operating modes and outputs of distributed feedback side coupled waveguide lasers
[CRC-1235] 06 p0679 N73-15521
Vibrational energy distribution of positive Cs ions in output from Cs2O2 chemical laser
[DREV-TN-2019/72] 06 p0679 N73-15522
Mathematical model of thermally induced nonlinear propagation of laser beam in absorbing fluid medium
[DREV-TN-2049/72] 06 p0679 N73-15523
Characteristics of combined gas laser pumping based on fluctuation of gas density parallel to electric field which is assumed constant
[JPRS-57880] 06 p0679 N73-15524
Output and power characteristics of CS2/O2 chemical laser with flow transverse to optical axis
[DREV-R-684/72] 06 p0679 N73-15527
Operating principles and physical mechanisms of pulsed gas discharge lasers
[SC-T-72-2524] 06 p0679 N73-15529
Structural effects of various optical coatings on single shot laser induced damage threshold using pulsed neodymium glass laser
[AD-749852] 06 p0680 N73-15531
Development and characteristics of optical communication system based on three frequency heterodyne configuration
[AD-750321] 06 p0680 N73-15533
Application of quasistatic theory of spectral line broadening to predict values for laser radiation
[AD-750156] 06 p0681 N73-15541
Absorption of carbon dioxide laser radiation by gaseous sulfur hexafluorine in air boundary layers
[AD-751016] 06 p0681 N73-15546
Stability of laser gyro with Faraday cell
[FOA-2-C-2467-54] 06 p0696 N73-15671
Design and development of multichannel laser remote control system using modulated helium-neon laser as transmitter and light collector as receiving antenna
[NASA-CASE-LAR-10311-1] 07 p0806 N73-16536
Proceedings of conference to determine research projects for development of lasers for optical communications applications
[PB-212692] 07 p0807 N73-16543
Power spectrum computation for phototube current of laser Doppler velocimeter
[NASA-TM-X-68184] 07 p0824 N73-16675
Development and characteristics of stable master oscillator carbon dioxide laser system
[AD-752219] 08 p0930 N73-17614
Evaluation of infrared laser beams using thin membrane type displays of cholestric liquid crystals
[AD-752201] 08 p0930 N73-17616
Analysis of laser beam scintillation due to atmospheric turbulence
[AD-752565] 08 p0930 N73-17620
Laser frequency modulation, molecular lasers, superconducting lasers, and laser induced instabilities in fluids
[AD-752633] 08 p0931 N73-17621
Development of electronically tunable dye laser with capability for producing two randomly accessible and simultaneous frequencies
[AD-752053] 08 p0933 N73-17641
Analysis of plasmas produced by high power laser beam irradiation of beryllium, carbon, and polyethylene targets
[IPPJ-142] 08 p0947 N73-17754
Laser generation of heavy ion plasma
[CEA-CONF-2022] 08 p0948 N73-17761
Ion pulse compensation circuits for recording ions produced by laser radiation in afterglow discharge plasma
[AEC-TR-7324] 08 p0949 N73-17767
Technique for determining atmospheric transmittance of coherent light between two points in terrestrial atmosphere for selected laser frequencies
[AD-753075] 09 p1030 N73-18412
Application of laser Doppler velocimeter for flow measurements
[AD-753243] 09 p1044 N73-18513
Effects of turbulence instabilities on laser propagation
[AD-753401] 09 p1044 N73-18515
Mechanism for formation of inverse population of oscillatory levels in gas discharge carbon monoxide laser
[AD-753559] 09 p1045 N73-18520
High power output from carbon dioxide laser and effects of higher order transverse and longitudinal mode excitation
[AD-753402] 09 p1045 N73-18521
Laser illumination for stellar interferometry
[AD-752902] 09 p1068 N73-18712
Laser-Doppler velocity measurement of large particles in two-phase gas-solid nozzle flow
[VKI-TN-81] 10 p1142 N73-19305
Characteristics of carbon dioxide laser for use as interferometric and light scattering plasma diagnostic radiation source
[LRP-54/72] 10 p1168 N73-19504
Effects of heavy particle external ionization source on carbon dioxide laser efficiency
[COO-2007-24] 10 p1169 N73-19509
Laser forming of sliding friction bearings for instrument construction
[AD-753490] 10 p1169 N73-19511
Proceedings of conference on laser beam data transmission and development of laser information systems
[AD-753944] 10 p1169 N73-19513
Measurement of stimulated emission cross section of neodymium laser based on laser threshold gain and inverted population
[AD-753901] 10 p1170 N73-19514
Variation of laser radiation intensity along axis of unstable optical cavity with partially transmitting mirrors or gratings
[AD-753902] 10 p1170 N73-19515
Design of particle accelerator using pulsed laser beam
[RLO-2041-71] 10 p1193 N73-19705
Laser heating of pinched plasma in cavity
[LA-5010] 10 p1196 N73-19730
Effect of high intensity laser outputs on behavior and physiology of birds to determine application for reduction of flight hazards
[AD-754269] 11 p1236 N73-20038
Retinal damage in monkeys exposed to near infrared gallium arsenide laser pulses
[AD-753419] 11 p1248 N73-20135
Laser technology and utilization
[NASA-TT-F-14871] 11 p1302 N73-20568
Development of techniques for frequency tripling laser radiation based on mixtures of metal vapors and inert gases
[AD-754096] 11 p1304 N73-20581
Analysis of inversion medium of quasi-stationary carbon dioxide laser to show molecules in vibrational and rotational states
12 p1410 N73-21424
Predicted multiline continuous wave power output from perfectly stirred reactor chemical laser
[AD-755904] 12 p1411 N73-21433
Interpretation of signals from cylindrical Langmuir probe for diagnosis of properties of streaming laser-produced plasma
12 p1431 N73-21600
Atmospheric effects on laser propagation and impact on eye safety
[AD-755405] 13 p1485 N73-22044
Characteristics of carbon dioxide laser operating at atmospheric pressure
[TM-50] 13 p1536 N73-22446
Theoretical model developed for carbon dioxide laser operating in short pumping time, gain switched, mode-locked mode of operation
[AD-756456] 13 p1537 N73-22452
Principles and techniques of Bragg diffraction laser beam probing of ultrasonic field
[AD-756521] 13 p1537 N73-22454
Device for measuring angle of arrival of laser beams and predictions of expected results for input apertures and turbulence
[AD-755404] 13 p1538 N73-22464
Design, development, and characteristics of continuous wave laser using organic dyes
[AD-756514] 13 p1539 N73-22466
Analysis of buffer gas pressure effects on kinetics of generation spectrum of photodissociation laser
[AD-756334] 13 p1539 N73-22469
Dispersion of light intensity logarithm along axis of laser beam propagating in atmosphere
[AD-756094] 13 p1539 N73-22470
Human exposure criteria to laser energy for combat use
14 p1612 N73-23067
Performance capabilities of erbium lasers and tabulation of laser materials to show chemical composition, mode of operation, frequency and output characteristics
[PHL-1973-12] 14 p1672 N73-23565
Analysis of atmospheric transmission properties of 1.06 microns radiation using neodymium laser
[AD-757249] 14 p1672 N73-23572
Laser beam propagation in turbulent air
[AD-757221] 14 p1673 N73-23574
Laser beam scintillation caused by atmospheric turbulence
[AD-757562] 14 p1674 N73-23580
Design, development, and operation of carbon dioxide-nitrogen-helium laser to show beam characteristics and power output as function of gas mixture
[AD-757263] 14 p1674 N73-23582
Analysis of laser outputs required to initiate gas breakdown when gas contains suspended particles
[AD-757517] 14 p1674 N73-23585
Analysis of effects of high power lasers to include interactions with plasma, metals, dielectrics, semiconductors, and gases
[AD-755820] 14 p1674 N73-23586
Development of satellite geodesy technique for accurate determination of three dimensional coordinates of ground stations
[NASA-CR-132251] 15 p1778 N73-24412
Performance tests of copper vapor laser and analysis of relaxation of metastable lower levels
15 p1794 N73-24544
Modulation of electron beam by laser beam in thin film with production of light
15 p1795 N73-24548
Application of ultrafast laser pulses to high resolution imaging radar systems
[AD-758059] 15 p1795 N73-24551
Multiple line output from tunable CW dye lasers
[AD-757772] 15 p1796 N73-24557
Recombination coefficients and volume decay coefficient for laser-produced helium plasmas
[CEA-CONF-2102] 15 p1817 N73-24726
Feasibility analysis of laboratory experiment on ionic excitation cross section by electron impact on laser produced plasmas
[ESRO-SN-122] 15 p1818 N73-24737
Performance of CO2 laser excited by H-3 [neutron, proton] reaction
16 p1920 N73-25536
Influence on output power of coupling orifice of CO2 gas laser cavity operating in mode of excitation by microsecond pulses
16 p1923 N73-25563
Development of laser head for simultaneous optical pumping of several dye lasers
[NASA-CASE-LAR-11341-1] 16 p1923 N73-25564
General expression for short term average optical beam spread of initially coherent beam wave propagating in turbulent medium
[AD-759804] 16 p1925 N73-25573

Alternating direction implicit magnetohydrodynamic code for simulating laser plasmas
[SC-DR-72-0733] 16 p1949 N73-25776
Laser interferometric equipment for vibration and distance to surface measurement of mass memory magnetic disk floating heads
[LCR-71-216/1/R] 17 p2034 N73-26461
Application of matched filtering techniques for detection of mode locked laser signals
17 p2039 N73-26496
Development of technique for producing holograms using propagation of surface waves within layer of photosensitive material
[NASA-CASE-MFS-22040-1] 17 p2039 N73-26500
Analysis of fluctuations in difference frequency in ring lasers operating in single mode
17 p2040 N73-26501
Computation of laser gain as function of time in CO2 gas lasers
[LA-5151] 17 p2040 N73-26508
Analysis of stability characteristics of single frequency laser using homogeneously broadened active material
17 p2041 N73-26514
Development and characteristics of instrument to measure back reflection of laser radiation
17 p2041 N73-26515
Analysis of changes in amplitudes and frequencies of laser oscillations due to effect of weak reflected signal
17 p2041 N73-26516
Properties of laser generated plasma trapped in stellarator
[NP-19656] 17 p2067 N73-26725
Numerical analysis of stationary internal structure of plasma in homogeneous carbon dioxide laser discharge
[DREV-TN-2061/73] 18 p2157 N73-27430
Development of acoustical controlled distributed feedback laser with continuous frequency spectrum tuning
[NASA-CASE-NPO-13175-1] 18 p2157 N73-27431
Development of laser model for analyzing pulsed excitation of molecules in discharge and nonequilibrium discharge of supersonic flow in vacuum
[JPRS-59040] 18 p2158 N73-27432
Absolute calorimeter for high power TEA-CO2 infrared laser output power measurement, consisting of plastic covered copper plate and thermocouple
[LRP-59/73] 18 p2158 N73-27433
Inelastic atom-atom scattering within intense laser beam
[AD-761180] 18 p2159 N73-27442
Theoretical treatment of Schwarz-Hora effect in which electron beam passing through crystal is monulated by laser light and reproduces it on striking nonluminescent target
18 p2185 N73-27643
Stimulated emission in 3 to 5 wavelength band by exciting HCl vibrational levels by electron impact
[AD-761671] 19 p2308 N73-28562
Production technology for diffraction gratings as laser beam sampling components
[AD-762306] 19 p2322 N73-28681
Effect of transverse pumping distribution on energetics and profiles of thermo-optical distortions of laser in solution of rhodamine dye
[NLL-M-23052-[5828.4F]] 20 p2424 N73-29472
Development of nitrogen-laser-pumped tunable-dye laser for application as spectroscopic light source
20 p2424 N73-29473
Measurement of resonant second harmonic generation in exciton of copper chloride and zinc oxide using Q-switched ruby laser
20 p2424 N73-29474
Design of high power continuous wave HF chemical laser
[DREV-TN-2060/73] 20 p2425 N73-29475
Application of laser radiation to control operation of spark gaps to show breakdown synchronization and time characteristics
[JPRS-59677] 20 p2425 N73-29476
Development of laser amplifier using disks of neodymium glass and measurement of beam amplification for laser beams
[EP-RR-35] 20 p2425 N73-29478
Analysis of dynamic Stark effect in laser-atom interactions to show distortion of atomic structure in high intensity laser fields
[CEA-CONF-2135] 20 p2425 N73-29481
Evaluation of stripe domain light deflector using iron compounds
[AD-762475] 20 p2426 N73-29490
Effect of atmospheric turbulence on stability of laser radiation propagation
[AD-763109] 20 p2427 N73-29494
Development of technique and apparatus for optically detonating insensitive high explosives
[NASA-CASE-NPO-11743-1] 20 p2485 N73-29959
Measurement of quantum yields using chemistry, laser technology, photodetector instrumentation, and calorimetry
[PAPER-76A6-742] 21 p2546 N73-30408
Characterictics of carbon dioxide lasers and application for transmission of data
21 p2554 N73-30479
Molecular population inversion by Laval nozzle expansion in N2/He/carbon dioxide laser
[DLR-FB-72-21] 21 p2554 N73-30480
Using simple numerical model of CW chemical laser to study output power
[AD-763169] 21 p2555 N73-30485
Simulated emission predictions and measurement of H2 pressure effects on pulsed H2-F2 laser outputs
[AD-763716] 21 p2556 N73-30492
Airborne laser profilometer for evaluating surface roughness of landing sites
[AD-763180] 22 p2648 N73-31218
Picosecond laser beam study of four photon effects and temporal behavior of optical phonons
22 p2680 N73-31465
Calorimetric measurement of laser output energy and power
[UCID-16214] 22 p2681 N73-31476
Characteristics of heavy ion plasma produced by laser interaction with matter
[NASA-TT-F-15132] 22 p2703 N73-31650
Nearly spherical constant power detonation waves driven by focused laser beam in gas
23 p2772 N73-32171
Performance of ac power supply developed for CO2 laser system
[NASA-CASE-GSC-11222-1] 23 p2800 N73-32391
Dynamic processes for laser emission in pulsed pumping of transversely excited atmospheric carbon dioxide laser
[DREV-TN-2036/73] 23 p2800 N73-32396
Operation of Laflamme double-discharge laser structure up to pressures of several atmospheres
[DREV-TN-2092/73] 23 p2800 N73-32397
Procedure and device for effecting dual mode locking in pulsed Nd-YAG lasers
[NASA-CASE-GSC-11746-1] 23 p2800 N73-32398
Infrared detection of zero pi pulses generated by mode locked CO2 lasers
[AD-764692] 23 p2802 N73-32406
Holographic interferometric analysis of thermal response in ferroelectric crystal to laser radiation
[AD-764703] 23 p2820 N73-32547
Computerized laser position detector and optical stereo display system
24 p2897 N73-33121
Application of laser energy to induce homogeneous exchange reaction of hydrogen and deuterium
24 p2930 N73-33399
Variations in beam characteristics of ruby laser used in lidar system
[SLA-73-347] 24 p2931 N73-33407
Self focusing of laser beams
[AD-763541] 24 p2932 N73-33416
Application of incoherent and coherent light sources for underwater illumination and comparison of efficiency for various conditions
24 p2958 N73-33633
Instabilities of laser beam interactions with plasmas
[UCID-16272] 24 p2963 N73-33683
Laser generation of fusion plasmas
[UCRL-74628] 24 p2964 N73-33685
Bibliography on plasma generation by lasers
[LS-255] 24 p2964 N73-33688
Theoretical analysis of laser-created plasmas confined by external magnetic field
[CEA-R-4410] 24 p2965 N73-33695
Laser beam fusion and plasma generation on pellet
[UCID-16222] 24 p2965 N73-33697

**LASER PLASMAS**
Interaction of laser plasma flow with neutral gases of air
[AD-764936] 23 p2823 N73-32569

**LASER RADAR**
U OPTICAL RADAR

**LASER RANGE FINDERS**
Application of laser rangefinder on autonomous Martian roving vehicle for navigation and mid-range path selection
[NASA-CR-128398] 01 p0064 N73-10523
Mathematical model for geodetic survey of tracking stations using laser range finder and photographs including results of European tracking network
[GRGS-BULL-3] 03 p0294 N73-12398
Mathematical model for geodetic survey of tracking stations using laser range finder and photographs
03 p0294 N73-12399
Quantum efficiencies of photomultiplier range finders for detection of infrared laser light
[AD-749269] 04 p0397 N73-13230
Laser range finding for satellite angular coordinate determination using echo recorded by Schmidt telescope
05 p0557 N73-14523
Laser ranging techniques applied to ground base line measurements between French South Coast and Corsica
05 p0558 N73-14532
Photomultiplier tubes and laser range finders for infrared detection
[AD-749645] 06 p0646 N73-15245
Conference on laser and radar altimeter measurement of sea surface topography from space
[NASA-CR-130293] 06 p0661 N73-15369
Spaceborne laser ranging system for accurately mapping ocean surface
06 p0662 N73-15377
Designing light weight Q switch laser transmitter for rangefinders
[AD-750383] 06 p0680 N73-15536
Filtered lunar ranging data, and unfiltered photon detections
[NASA-CR-131498] 13 p1576 N73-22771
Analysis of electromagnetic noise in photodetection system consisting of germanium avalanche photodiode with application to laser range finders
[PHL-1972-24] 14 p1672 N73-23568
Laser ranging technique to determine distance from satellites to ground
[NASA-CR-2264] 16 p1906 N73-25419
Atmospheric effects on light distance finder measurements
[AD-763505] 21 p2581 N73-30682
Filtered and unfiltered photon detections obtained during laser ranging operations between McDonald Observatory and Apollo 11, 14, and 15 reflectors
[NASA-CR-133927] 22 p2681 N73-31472
Observation equations to utilize lunar laser ranging and very long baseline interferometry measurements for selenodetic control
[NASA-CR-135774] 24 p2931 N73-33404

**LASER RANGER/TRACKER**
Laser ranging techniques applied to ground base line measurements between French South Coast and Corsica
05 p0558 N73-14532
Techniques for analysis of geodynamic effects using laser data in estimating satellite orbits
[NASA-TM-X-70459] 22 p2716 N73-31739
Laser tracking of satellite for measuring polar motion and solid earth tide
22 p2737 N73-31911

**LASERS**
NT ARGON LASERS
NT CARBON DIOXIDE LASERS
NT CARBON MONOXIDE LASERS
NT CHEMICAL LASERS
NT CONTINUOUS WAVE LASERS
NT GALLIUM ARSENIDE LASERS
NT GAS LASERS
NT GASDYNAMIC LASERS
NT HCN LASERS
NT HELIUM-NEON LASERS
NT INFRARED LASERS
NT INJECTION LASERS
NT LIQUID LASERS
NT ORGANIC LASERS
NT PULSED LASERS
NT Q SWITCHED LASERS
NT RAMAN LASERS
NT RING LASERS
NT RUBY LASERS
NT SEMICONDUCTOR LASERS
NT SOLID STATE LASERS
NT TEA LASERS
NT YAG LASERS
Physical and functional performance properties of laser safety goggles
[AD-746208] 01 p0022 N73-10170
Laser predictions of GEOS 1 and 2 trajectories
[AD-745455] 01 p0065 N73-10529
Process for producing polycrystalline halides for use in high power laser windows to maintain optical properties with improved mechanical properties
[AD-745350] 01 p0065 N73-10535
Application of Nernst glower metal oxide conductors to laser pumping to produce spectral energy within pumping band of laser material
[AD-745796] 01 p0066 N73-10538
Analysis of laser applications in medicine, biology, research, chemical processing, initiation of thermonuclear reactions, and weapon systems
[AD-743098] 01 p0066 N73-10541
Transmission characteristics of commercially available, laser eye protectors with Cary 14 spectrophotometer
[AD-746293] 02 p0136 N73-11100
Development of wake vortex monitoring system using laser Doppler sensors for analyzing vortex flow field
[NASA-CR-123921] 02 p0152 N73-11229
Bibliography on laser Doppler velocimeter theory and usage
[AD-746634] 02 p0176 N73-11427
Electrical analogue model of flash tube and laser rod system to determine efficiency of laser system with respect to flash duration
[WRE-TM-657[AP]] 02 p0180 N73-11462
Analysis of dispersion, correlation and structural functions in amplitude and phase of laser being propagated into turbulent atmosphere
02 p0181 N73-11470
Bibliography of Soviet laser research and development
[AD-746339] 02 p0183 N73-11480

Mean irradiance distribution of finite cross section laser beam propagating in sea water
[AD-745956] 02 p0183 N73-11483
Analysis and Monte Carlo calculations of disc laser limitations due to effects of fluorescence amplification and parasitic oscillation
[AD-747234] 02 p0183 N73-11485
Numerical analysis of semiconductor saturable absorber and extablishment of criteria for operation of laser saturable resonator in bistable regime
[AD-746736] 02 p0183 N73-11488
Relationship between damage in materials exposed to high intensity laser radiation and self focusing thresholds
[AD-747290] 02 p0184 N73-11489
Procedures for operating and modulating beam of laser locating devices
[AD-747003] 02 p0184 N73-11492
Feasibility of using photovoltaic cells to convert laser energy into electrical energy
[LA-DC-72-468] 03 p0255 N73-12061
Development of procedure for measuring sinusoidal vibration displacement amplitude using laser homodyne system
[RM-560J] 03 p0310 N73-12526
Laser interferometer instrumentation techniques for study of plane stress wave propagation in solids
[SC-DC-70-5465] 03 p0310 N73-12529
Development of frequency modulated diode laser transmitter for point-to-point voice communication system
[AD-747524] 03 p0311 N73-12540
Frequency stability characteristics of single frequency neodymium YAG laser system with coherent ultrashort pulses for high resolution imaging
[AD-747967] 03 p0312 N73-12543
Flexural strength of aluminum oxide substrates separated by lasers and diamond sawing
[SC-DC-71-4496] 03 p0321 N73-12613
Dynamics of laser triggered spark discharge channel with nanosecond pulse formation
[AD-747510] 03 p0343 N73-12799
Failure analysis of crystals exposed to laser emissions
[AD-747730] 03 p0347 N73-12830
Manufacturing of holmium lithium tetrafluoroytriate laser disk bonded into glass
[AD-747968] 03 p0352 N73-12871
Remote recording of speed with laser Doppler anemometry
[RISO-M-1489] 04 p0422 N73-13442
Prediction of laser return pulse shape from corner cube retroreflectors on GEOS 1 satellite
[NASA-TM-X-66123] 04 p0428 N73-13490
Development of scaling counter for use as laser interferometer readout system to obtain improved length measurement capabilities
[BDX-613-703] 04 p0429 N73-13492
Lead lanthanum zirconate titanate ceramics as intracavity tuning elements in rhodamine 6G dye laser
[SC-RR-72-0273] 04 p0429 N73-13493
Generation of vacuum ultraviolet xenon laser and X ray hydrogen laser
[SC-T-72-2513] 04 p0429 N73-13494
Bibliography on laser development in Soviet Union
[AD-748258] 04 p0430 N73-13499
Erbium laser rangefinder having germanium avalanche photodetector
[AD-748071] 04 p0430 N73-13502
Abstracts and bibliographies on research in laser technology, effects of explosions, geosciences, and particle beams
[AD-749488] 04 p0430 N73-13504
Thermal blooming of laser beams in viscous and thermally conductive fluids
[AD-748994] 04 p0431 N73-13508
Interferometric study of expansion of plasma created by laser
[CEA-R-4299] 04 p0454 N73-13708
Feasibility of using terbium-silicate glass as Faraday rotator-isolator in high power laser
[AD-749919] 05 p0559 N73-14543
Study of relative condensabilities of radioactive vapors in nuclear debris by use of high-powered lasers
[AD-750263] 05 p0579 N73-14713
Diagnostic techniques for characterizing near surface of solids
[UCRL-73925] 05 p0587 N73-14773
Capabilities and projected accuracy of various satellite tracking systems
06 p0662 N73-15379
European study of optical and signal processing problems in laser anemometry
[ET/TN/A/20] 06 p0679 N73-15526
Design and operation of picosecond neodymium glass laser in terawatt range
[UCRL-TRANS-10633] 06 p0679 N73-15528
Feasibility of electron beam excited, high pressure recombination laser
[AD-750777] 06 p0680 N73-15530
Alternate methods for soft X ray pulse generation by light flux available with high pulse energy lasers
[AD-750375] 06 p0680 N73-15534
Spectroscopic studies of luminescence emitted by dyes irradiated by lasers
[AD-750377] 06 p0680 N73-15535
Photon-echo generation and behavior
[AD-750155] 06 p0681 N73-15540
Study of optical masers
[AD-750711] 06 p0681 N73-15543
Application of light emitting diodes to pumping of solid-state laser rods
[AD-750576] 06 p0681 N73-15545
Theoretical model for laser flux absorption by plasma instability mechanism
[LA-4984] 06 p0704 N73-15739
Measurement of picosecond laser pulse width using two-photon conductivity in GaAs and three-photon conductivity in CdS
[AD-750414] 06 p0710 N73-15798
Test evaluation of laser protective visors for flight crews
[AD-751470] 07 p0751 N73-16102
Tracking performance and quality of colocated laser tracking stations
[NASA-TM-X-66158] 07 p0765 N73-16220
Boltzmann equations for kinetic modeling of supersonically flowing electrically excited laser system
[NASA-TM-X-62196] 07 p0806 N73-16538
Fourier theory of using grating to extend dynamic range of laser far field camera
[UCRL-51255] 07 p0806 N73-16542
Analysis of video transmission range in water by laser beam
[AD-751445] 07 p0807 N73-16548
Damage thresholds of multilayered dielectric reflecting mirrors subjected to nanosecond laser pulses
[AD-751265] 07 p0808 N73-16553
Plastic materials for eye protection from lasers
[AD-752594] 08 p0880 N73-17127
Laser scattering from curved aluminum and titanium aircraft surfaces in clear atmosphere
08 p0884 N73-17159
Computer programs for calculating transfer functions of retroreflector laser arrays carried by orbiting satellites
[NASA-CR-130696] 08 p0888 N73-17190
Laser modulation mechanisms and optical communication technology
08 p0928 N73-17603
Investigation for attenuation and extinction in interaction between laser beams and flowing particulate clouds
[RM-567] 08 p0929 N73-17605
Alignment control of high energy laser system and importance of external sources of alignment error
[UCRL-74050] 08 p0929 N73-17609
Bibliography of laser communication systems
[AD-751900] 08 p0929 N73-17612
High resolution laser interferometer investigation of mechanical behavior of polymethyl methacrylate
[SC-DC-72-1174] 08 p0935 N73-17653
Electronically tunable acousto-optical filter for laser applications
[AD-752052] 08 p0944 N73-17733
Ultrasonic radiation and microwave research projects
[AD-752055] 08 p0944 N73-17736
Laser-produced plasma as radiation source in 1000 to 20 A range, and detection with double-grating spectrometer
[FRNC-TH-216] 08 p0948 N73-17763
Ionization hydrodynamics of laser produced plasma
[AD-751880] 08 p0949 N73-17773
Dynamics of water drop evaporated by heating with laser pulse
[AD-752822] 09 p1001 N73-18167
Laser method for measuring axial solute dispersion in turbulent pipe flow
[AD-753801] 09 p1019 N73-18314
Mathematical model of thermodynamic damage to metals irradiated by laser beams
[DREV-R-672/72] 09 p1043 N73-18503
Laser Doppler velocity measurement of turbid and bubbly flow media
[UTIAS-TN-185-PT-2] 09 p1043 N73-18506
Research and development of lasers and laser-related equipment in the Soviet Union - bibliography
[AD-753098] 09 p1043 N73-18510
Effects of high energy radiations in laser materials of calcium tungstates
[AD-753534] 09 p1044 N73-18519
Using lasers to study properties of atmosphere
[JPRS-58346] 09 p1060 N73-18647
Generation of magnetic field energy from radiation pressure in laser-produced plasma thermal energy
[AD-748180] 09 p1071 N73-18742
Frequency spectrum of laser scattering from dense plasma focus
[AD-753705] 09 p1073 N73-18754
Bremsstrahlung for enhancing far infrared laser scattering from theta pinch plasma
[AD-753404] 09 p1073 N73-18755
Research activities in solid state physics
[AD-753255] 09 p1075 N73-18770
Phonon emission by laser beams and thermal conductivity of optical crystals
[AD-753698] 09 p1077 N73-18791
Laser-induced fluorescence for gas phase oxidation of aluminum atoms
[AD-753839] 10 p1127 N73-19182
Exposure of 0.29 micron Ni-Fe films to continuous laser light in infrared spectra
[AD-753962] 10 p1129 N73-19202
Laser Doppler anemometer for measuring steam and water velocities in two phase flow
[UTIAS-TN-184-PT-1] 10 p1141 N73-19293
Laser operation in vacuum and active scattering particle spectrometers
[NASA-CR-124111] 10 p1159 N73-19425
Radiation effects in semiconducting laser materials
[AD-754217] 10 p1170 N73-19516
Turbulence-induced beam spread of optical beam propagating through random medium
[AD-754204] 10 p1191 N73-19689
Conference on semiconductors, lasers, and photodiodes
[AD-754237] 10 p1202 N73-19782
Electrode structures for transverse excitation produced HF lasers
[DREV-TN-2047/73] 11 p1302 N73-20565
Operating principles and performance tests results for optical modulator system with mode locked Nd-YAG laser
[NASA-CR-130195] 11 p1302 N73-20569
Laser mirror technology
[AD-754101] 11 p1303 N73-20570
Infrared beam profile measurements for determining surface damage thresholds of glass laser materials
[AD-755134] 11 p1303 N73-20571
Research in high energy laser technology
[AD-754410] 11 p1303 N73-20573
Lamp design and parameters for optical pumping of lasers
[AD-754643] 11 p1304 N73-20578
Portable laser velocimeter for stack velocity measurements
[PB-213263] 11 p1304 N73-20579
Application of laser microprobe and magnetic mass spectrometer for determining gas contents in metals by melting and vaporizing microvolumes of samples
[NASA-TT-F-14852] 11 p1305 N73-20592
Laser technology, strong explosion effects, geosciences, and particle beams bibliographies
[AD-754946] 11 p1353 N73-20982
Laser technology, strong explosion effects, geosciences, and particle beams - bibliographies
[AD-754962] 11 p1353 N73-20988
Critical scattering of laser light by thin fluid films
[COO-2203-1] 12 p1410 N73-21428
Laser production of plasmas and injection of pulsed ion beams
[LYCEN-7253] 12 p1411 N73-21431
Standards for calorimeter measurement of laser beam absorption by graphite cones
[CEA-CONF-2056] 12 p1411 N73-21432
Laser beam study of proton production cross sections determined for stable and radioactive rare gases
[TID-26183] 12 p1427 N73-21566
Observation of high-order stimulated Raman-antiStokes radiation and its role in initial phase of plasma production by lasers
[IPP-4/40] 12 p1435 N73-21629
Uniform plasmas of N2, He, and CO for advanced MHD generator and electric laser design
[AD-755892] 12 p1436 N73-21638
Proceedings of conference on research and development projects conducted by US Air Force Research and Development Command
[AD-753071] 12 p1467 N73-21890
Optical density properties of ocular glass laser protective filters
[AD-755406] 13 p1487 N73-22057
Time base stability and intermachine compatibility in wideband laser recording systems
13 p1536 N73-22444
Light emitting diode pumped Nd/YAG lasers
[NASA-CR-124225] 13 p1536 N73-22445
Feasibility of laser induced ablation thruster for space propulsion system
[NASA-CR-131744] 13 p1537 N73-22449
Laser light absorption characteristics of laser produced hydrogen plasma
[AD-756524] 13 p1538 N73-22458
Characteristics of signal conditioning electronics for vector velocity laser velocimeter
[NASA-CR-131475] 13 p1538 N73-22459
Growth of multiply sensitized Ho YLF crystals as laser materials
[AD-755530] 13 p1538 N73-22461
Construction of experimental incandescent lamp of Nernst glower type for laser pumping
[AD-755207] 13 p1539 N73-22465
Development of high power alkali vapor lamp for laser applications
[AD-755213] 13 p1560 N73-22646
Homodyne interferometer for measuring phase variations of laser beam wave front
[AD-756885] 14 p1668 N73-23539

Quality testing of neodymium yttrium-aluminum garnet lasers
[PHL-1972-22] 14 p1672 N73-23567
Spectroscopic analysis of energy transfer in rare earth compounds to determine effect of transfer phenomena on lasing efficiency
[AD-757520] 14 p1673 N73-23579
Theory for third harmonic generation due to broad band optical pulses in picosecond time region
[AD-757211] 14 p1693 N73-23742
Spontaneous generation of magnetic fields associated with laser produced plasmas
[AD-757247] 14 p1695 N73-23759
Research in solid state physics including semiconductor lasers and laser spectroscopy
[AD-757559] 14 p1698 N73-23779
Finite element calculation of two-dimensional heating and melting of disks and applications to laser effects
[AD-757189] 14 p1719 N73-23950
Creation shape and flow of tridimensional spark by focused radiation
[NASA-CR-2230] 15 p1766 N73-24311
Neodymium-glass laser system production of plasmas for research on controlled thermonuclear fusion
15 p1794 N73-24545
Bibliography of Soviet research and development of lasers
[AD-758259] 15 p1795 N73-24552
Phase difference temporal spectra measurements of laser beams
[AD-757915] 15 p1795 N73-24553
Acousto-optical isolator for suppressing optical feedback generated laser instabilities
[AD-757914] 15 p1796 N73-24556
Airborne laser remote sensing of coastal waters
[AD-759781] 16 p1910 N73-25454
Periodic functional analysis of ultra-short pulse generation and propagation in laser systems
16 p1920 N73-25535
Gravity effects upon melt-through time of metal plate subjected to high intensity lasers
[AD-759168] 16 p1925 N73-25574
Performance of hadron laser safety eyeshields in protecting personnel from accidental ocular exposure to common laser radiation
[AD-759921] 17 p1991 N73-26099
Designing laser drill to correct beam wandering during drilling
[AD-759966] 17 p2006 N73-26224
Measurement of hydrogen concentration in mass diffusing jets by laser induced Raman scattering
17 p2012 N73-26272
Weather forecasting and measurement of air pollution by laser sounding of atmosphere
[NASA-TT-F-14948] 17 p2026 N73-26391
Optical laser triggering of high voltage spark gap
[IPP-4/102] 17 p2040 N73-26504
Laser interferometry for plasma diagnostic measurements
[INR-1442] 17 p2040 N73-26506
Electric modulator circuit for controlling output power of commercial laser
[LA-5166-MS] 17 p2040 N73-26507
Analysis of stability characteristics of single frequency laser using homogeneously broadened active material
17 p2041 N73-26514
Surface damage induced in optical materials by laser
[AD-760131] 17 p2042 N73-26519
Design and performance of segmented holmium doped yttrium lithium fluoride laser
[AD-760019] 17 p2042 N73-26522
Uniform distribution of illumination at output of high power amplifier
[UCRL-TRANS-10663] 17 p2063 N73-26691
Development of portable transmissometer calibrating unit using laser as projector source
[AD-757282] 18 p2153 N73-27403
Polarization effects in photon echoes and in anisotropic mirror laser cavities
18 p2157 N73-27429
Development of acoustical controlled distributed feedback laser with continuous frequency spectrum tuning
[NASA-CASE-NPO-13175-1] 18 p2157 N73-27431
Techniques for producing laser pulses of nanosecond duration
[AD-760752] 18 p2158 N73-27435
Multiphoton ionization by laser beam
[AD-760800] 18 p2159 N73-27440
Coherent laser light measurement of ceramic material surface roughness
[AD-761198] 18 p2168 N73-27512
Research in plasma physics and laser diagnostics
[NP-19681] 18 p2183 N73-27625
Photoconductivity of gallium arsenide-, Cadmium sulfide-, and cadmium selenide-semiconductors correlated to laser pulse width
[AD-760560] 18 p2190 N73-27682
Balloon measurements of stellar scintillation for predicting fading on space to ground laser propagation path
18 p2212 N73-27858
Performance of neodymium-yag optical data transmission system and development of channel simulator
18 p2212 N73-27859
Bibliography on lasers, strong explosions, geosciences, particle beams, and material sciences
[AD-759275] 18 p2215 N73-27884
Study of heterojunction Pb 1-x Sn X Te diodes
[AD-761767] 19 p2244 N73-28093
Autonomous Martian roving vehicle determination of terrain gradients from laser measurements
[NASA-CR-133498] 19 p2307 N73-28556
Research on lasers and laser produced plasmas
[UCRL-50021-71-REV-1] 19 p2307 N73-28557
Dye laser bibliography from 1966 to 1972
19 p2307 N73-28559
Molecular absorption coefficients for H20-N2 mixtures as measured by Co laser
[AD-760140] 19 p2308 N73-28561
Comparison of photographic digital recording systems using laser technology
[AD-761521] 19 p2308 N73-28563
Laser technology and propagation, optical measurements, and optical equipment
[AD-762320] 19 p2308 N73-28566
Ultrashort optical pulse propagation through resonant media
[AD-762209] 19 p2309 N73-28569
Abstracts and bibliographies of Soviet literature on lasers, explosion effects, particle beams, and geosciences
[AD-762376] 19 p2356 N73-28955
Laser radiation and RF induction heating for production of metal vapor
[AD-762917] 20 p2374 N73-29080
Excitation and relaxation processes in H2O discharges and lasers
20 p2424 N73-29471
Developments in laser interferometry
[RFP-1963] 20 p2425 N73-29482
Propagation of multiwavelength laser radiation through atmospheric turbulence
[AD-762516] 20 p2426 N73-29491
Bibliography of Soviet laser developments. Jan. - Mar. 1973
[AD-762569] 20 p2427 N73-29492
Measurement capabilities of one dimensional laser Doppler velocimeter system
[NASA-TM-X-64774] 21 p2548 N73-30427
Dry inert gas glove box for handling of hygroscopic and corrosive materials in spectroscopic and lasers experiments
[CRC-1244] 21 p2548 N73-30430
Increased sensitivity of laser gyroscopes
[AD-763284] 21 p2550 N73-30443
Threshold of sensitivity of laser gyroscope lowered by use of Zeeman effect
[AD-763160] 21 p2550 N73-30444
Laser motivated studies of chemiluminescence in metal oxides and nitrides
21 p2554 N73-30477
Mechanical effects resulting from interactions of laser beams with gases, liquids, and solids
[AD-763258] 21 p2555 N73-30482
Electron beam stabilized electrical discharge HF laser
[AD-763464] 21 p2556 N73-30489
Comparison of laser Doppler measurements of wind velocities and turbulence with measurements by anemometers
[NASA-CR-124355] 21 p2574 N73-30627
Absorption spectra of laser excited Ba2NaNb5O15 crystal
21 p2585 N73-30714
System for maintaining intensity of laser beam constant in thermomagnetic recording and magneto-optic playback system
[NASA-CASE-NPO-11317-2] 22 p2680 N73-31468
Electron transport in gas discharge lasers
[LA-5154-MS] 22 p2681 N73-31474
Introduction to optical communication with lasers
[FTZ-A-465-TBR-8] 22 p2681 N73-31477
LASNEX equations for self-generated magnetic fields and nonthermal electrons in laser produced plasmas
[UCRL-74110] 22 p2703 N73-31653
Guidance of high voltage electrical breakdown streamers by laser induced ionization in air
[AD-763827] 22 p2705 N73-31665
Spectrometric and photographic analysis of neodymium glass laser produced hydrogen plasma
[AD-764496] 22 p2705 N73-31667
Turbulent gas-solids flow measurements using laser Doppler velocimeter
23 p2773 N73-32182
Pulsed laser holographic interferometry of shock waves within transonic fan rotors
[NASA-TM-X-71430] 23 p2801 N73-32402
Development of X ray laser and experimental investigation of possible applications
[AD-764691] 23 p2801 N73-32405
Synthesis of polycrystalline oxide ceramic laser rods
[AD-765345] 23 p2802 N73-32413
USSR research in solid state physics, laser technology, geosciences, and materials
[AD-763742] 23 p2866 N73-32916
USSR research in solid state physics, plasma physics, atmospheric physics, and seismology
[AD-763743] 23 p2866 N73-32918
Wing tip vortex measurements with laser Doppler velocimeter
[NASA-CR-124444] 24 p2869 N73-32924
Applications of mathematics to design and development of electronic equipment, microelectronic devices, and lasers
24 p2900 N73-33147
Analyzing behavior of instantaneous point source as it disperses in thick, neutrally stratified, turbulent shear layer by laser light scattering technique
24 p2904 N73-33176
Second generation laser interferometer for absolute determination of gravity acceleration
[AD-764831] 24 p2924 N73-33359
Design of precision vertical alignment system using laser with gravitationally sensitive cavity
[NASA-CASE-ARC-10444-1] 24 p2930 N73-33397
Laser development and applications to plasma physics
[UCRL-50022-4] 24 p2931 N73-33410
Stability theory of laser beam self focusing
[LA-UR-73-671] 24 p2932 N73-33414

**LASV**
U F-111 AIRCRAFT

**LATCHES**
Fail safe latching mechanism for spacecraft docking
[NASA-CASE-MSC-12549-1] 02 p0178 N73-11443
Improved latching device for joining structural components in motionless relationship
[NASA-CASE-MFS-21606-1] 13 p1532 N73-22417

**LATE STARS**
Applications of Schmidt telescopes to study astrometry, photometry, galactic structure, quasars, and stellar spectra
07 p0844 N73-16840

**LATENCY**
U REACTION TIME

**LATERAL CONTROL**
Linear differential equations describing aircraft lateral motion in presence of atmospheric turbulence
[AASU-311] 03 p0253 N73-12045
Optimal adaptive control of aircraft lateral dynamics in gust presence using Pontryagin principle and cost function
[AASU-314] 03 p0253 N73-12046
System for eliminating roll rate anomalies occurring during flights of slender ballistic reentry vehicles
[SC-DC-72-2244-A] 07 p0849 N73-16883
Effects of nozzle orientation and configuration on roll control and base pressure of hypersonic reentry vehicle
[SC-DC-72-1187-A] 07 p0849 N73-16884
Influence of load and wing load distribution on lateral and longitudinal maneuverability of aircraft
08 p0865 N73-16998
Design of aircraft lateral flight director
[DLR-FB-72-44] 22 p2614 N73-30953

**LATERAL OSCILLATION**
Longitudinal and lateral data, lateral oscillatory derivatives, and aileron and rudder powers for BAC 221 aircraft
[ARC-CP-1230] 05 p0494 N73-14027

**LATERAL STABILITY**
Comparison of longitudinal and lateral stability and control characteristics of Phase B Grumman H-33 space shuttle orbiter
[NASA-CR-120080] 01 p0108 N73-10889
Comparison of longitudinal and lateral stability and control characteristics of baseline 040A space shuttle orbiter
[NASA-CR-120081] 01 p0109 N73-10894
Prediction of lateral directional aerodynamic characteristics for twin engine propeller driven airplane
[NASA-TN-D-6946] 02 p0125 N73-11016
Development of procedure for determining characteristics of aircraft roll coupling moment caused by flow induced by deflected wings and cross flow
[ISAS-488-VOL-37-NO-14] 14 p1597 N73-22945
Flight tests of 45 degree delta cropped wing to determine dynamic lateral stability characteristics
[ARC-R/M-3243] 15 p1729 N73-24027
Strapped down gyroscope aligned with sun and star tracker optical axis calibrating roll, yaw and pitch values
[NASA-CASE-ARC-10716-1] 23 p2851 N73-32784
Characteristics of low speed air flow over slender, sharp edged delta wing at various angles of attack and effects on longitudinal and lateral stability
24 p2869 N73-32922

**LATERALITY**
U LATERAL STABILITY

**LATERALIZATION**
U LATERAL CONTROL

**LATEX**
Determination of aerodynamic diameter of latex spheres and asbestos fibers using aerosol spiral centrifuge
[BMWG-FBWT-72-10] 07 p0812 N73-16585

**LATITUDE**
NT GEOMAGNETIC LATITUDE

Longitude, latitude, and azimuth determinations using transit instrument
[MITT-99] 01 p0101 N73-10826
Greenwich time and latitude observations for Oct. to Dec. 1971
01 p0105 N73-10874
Greenwich time and latitude observations - Oct. through Dec. 1971
02 p0244 N73-11983
Latitude-time variations of ionospheric electron densities at high latitudes during periods of solar activity
07 p0791 N73-16431
Space time laws governing F-scattering at various latitudes
13 p1521 N73-22328
Greenwich time and latitude observations for Jan. to Mar. 1972
13 p1578 N73-22791
Greenwich time and latitude observations for Apr. to Jun. 1972
18 p2197 N73-27740
Hydrodynamic models for studying pressure and wind fields in low latitudes
20 p2444 N73-29630
Greenwich time and latitude observations, Jul. through Sep. 1972
21 p2598 N73-30820

**LATITUDE MEASUREMENT**
Generalized magnetic Weber-Davis model for calculating magnetic latitude effects in solar wind
01 p0094 N73-10778
Astronomical geodetic observations for longitude, latitude, and components of deflection from vertical at West German stations
[MITT-124] 05 p0538 N73-14375
Tables of Greenwich time and latitude observations
19 p2293 N73-28437
Tables on time and latitude observations made by Greenwich Time and Latitude service
22 p2664 N73-31345

**LATTICE DRAINAGE PATTERNS**
U DRAINAGE PATTERNS

**LATTICE IMPERFECTIONS**
U CRYSTAL DEFECTS

**LATTICE PARAMETERS**
Off-diagonal long range crystalline order and vortex lattices in Bose system
24 p2967 N73-33708

**LATTICE VIBRATIONS**
Defect structure of semiconducting III-V compounds and determination of vibrational properties of imperfect systems
[AD-751052] 07 p0834 N73-16762
Microscopic dipole model for lattice dynamics in transition metals
08 p0950 N73-17782
Shell model for phonon dispersion anomalies and lattice instabilities in hard metalcarbides-nitrides and transition metals
08 p0951 N73-17783
Lattice dynamics of crystals surfaces
[AD-764644] 23 p2827 N73-32600

**LATTICES [MATHEMATICS]**
NT BOOLEAN ALGEBRA
NT BOOLEAN FUNCTIONS
Mesh gradient technique for numerical optimization
23 p2812 N73-32481

**LAUNCH COMPLEXES**
U LAUNCHING BASES

**LAUNCH ESCAPE SYSTEMS**
Apollo experience report concerning general design, development, and qualification of launch escape propulsion subsystem
[NASA-TN-D-7083] 09 p1091 N73-18902

**LAUNCH VEHICLE CONFIGURATIONS**
Configuration of nuclear upper stage for Europa 3 launch vehicle
[TR-TK-REF-1-374/72] 15 p1811 N73-24676
Delta vehicle configuration changes and performance increases considering cost effectiveness
18 p2208 N73-27818
Test objectives and mission planning for extended long tank Delta Launch Vehicle
[NASA-CR-133644] 20 p2475 N73-29886
Model 2914 series Delta launch vehicle configuration
[NASA-TM-X-70455] 21 p2599 N73-30833
Cryogenic tanking and partial jettison tests of Centaur launch vehicle and Centaur standard shroud to develop insulation, purge, and vent systems
[NASA-TM-X-71455] 24 p2984 N73-33850

**LAUNCH VEHICLES**
NT ATLAS CENTAUR LAUNCH VEHICLE
NT ATLAS LAUNCH VEHICLES
NT CENTAUR LAUNCH VEHICLE
NT DELTA LAUNCH VEHICLE
NT EUROPA 1 LAUNCH VEHICLE
NT EUROPA 2 LAUNCH VEHICLE
NT EUROPA 3 LAUNCH VEHICLE
NT RECOVERABLE LAUNCH VEHICLES
NT REUSABLE LAUNCH VEHICLES
NT SATURN LAUNCH VEHICLES
NT SATURN 1B LAUNCH VEHICLES
NT SATURN 5 LAUNCH VEHICLES
NT SCOUT LAUNCH VEHICLE
NT TITAN LAUNCH VEHICLES
NT TITAN 3 LAUNCH VEHICLE
Space activities of CNES, noting satellites, launch vehicles, sounding rockets, balloons, and ground stations
05 p0611 N73-14972
Launch vehicle estimating factors for planning advanced solar system and earth orbital missions
[NHB-7100.5B] 07 p0847 N73-16866
Criteria for designing launch vehicle structural reliability
[NT-D3-71.040] 07 p0850 N73-16890
Squib actuated disconnect for spacecraft coupling to launch vehicle
[NASA-CASE-NPO-13172-1] 08 p0969 N73-17917
Characteristics of Performance Analysis and Design Synthesis computer program for determining size of launch vehicles for optimal trajectories - Vol. 2, Pt. 1
[NASA-CR-128678] 09 p1083 N73-18831
Description of QL module Performance Analysis and Design Synthesis computer program for determining optimal trajectory of launch vehicles - Vol. 2, Pt. 2
[NASA-CR-128657] 09 p1083 N73-18832
Parametric studies of space shuttle booster, orbiter and launch vehicle concepts
[NASA-CR-124090] 09 p1086 N73-18862
Linear programming for design of large flexible launch vehicle autopilots
[NASA-CR-124124] 10 p1183 N73-19621
Users manual for COEBRA program for design of launch vehicle autopilots
[NASA-CR-124125] 10 p1183 N73-19622
Development of computer program to size launch vehicles for optimal trajectories and application for general purpose branched trajectory optimization
[NASA-CR-128725] 10 p1214 N73-19869
Possible space destinations and launch vehicles for space disposal of radioactive waste
[NASA-TM-X-68211] 12 p1427 N73-21563
Wind tunnel tests to determine pressure distribution of space shuttle launch configuration for various combinations of geometric components and Mach number
[NASA-CR-120058] 14 p1709 N73-23872
Traffic model data for 1973 expendable launch vehicle
[NASA-TM-X-64752] 17 p2083 N73-26846
Launching Radio Exploration Satellite using Mu-4S-4 rocket for studying ionosphere and magnetosphere
17 p2088 N73-26888
Evaluation of physical and operational characteristics of missile support vehicle based on procedures for inspection, servicing, and maintenance
[AD-764772] 23 p2852 N73-32791

**LAUNCHERS**
NT AIRCRAFT LAUNCHING DEVICES
NT GUN LAUNCHERS
NT HYPERVELOCITY LAUNCHERS
NT MISSILE LAUNCHERS
Design and performance of launcher illumination XM-183 flare package for parachutes
[AD-757731] 15 p1844 N73-24940

**LAUNCHING**
NT AIR LAUNCHING
NT ROCKET LAUNCHING
NT SPACECRAFT LAUNCHING
Simulation for use in dynamics and control analysis during boost from liftoff to orbit insertion
[NASA-CR-128592] 01 p0108 N73-10890

**LAUNCHING BASES**
NT CAPE KENNEDY LAUNCH COMPLEX
Status of space shuttle and Skylab programs and shuttle facilities
10 p1215 N73-19880

**LAUNCHING DEVICES**
U LAUNCHERS

**LAUNCHING SITES**
Installations and support equipment for launching guided missiles
[AD-756083] 13 p1507 N73-22214
Missile site ground cover for prevention of soil erosion during launches
[AD-762136] 19 p2296 N73-28466

**LAVA**
Examination of lunar surface patterns created by volcanic lava flows and impact debris
12 p1454 N73-21779
Volcanic activity on moon
12 p1457 N73-21804

**LAW [JURISPRUDENCE]**
NT INTERNATIONAL LAW
NT LEGAL LIABILITY
NT SPACE LAW
Role of law in technology assessment
[NASA-CR-129270] 03 p0367 N73-12987
Legal and administrative measures adopted by U.S.S.R. for protection of environment
[JPRS-59436] 20 p2486 N73-29971
System of legal protection for environment of U.S.S.R.
20 p2486 N73-29972
Normative acts relating to legal protection of natural areas in U.S.S.R.
20 p2487 N73-29973
Supervision of use and protection of natural resources according to Soviet legislation
20 p2487 N73-29975
Cable television, emphasizing juridical and economical aspects in various nations
23 p2757 N73-32067
Historical and constitutional framework of industry regulation with application to airline operations
23 p2864 N73-32889
Actions of Civil Aviation Board with respect to monopolies and mergers of domestic airline operations
23 p2864 N73-32895
Provisions of Occupation Health and Safety Act to show requirements imposed on employers and employees for protection from radiation hazards
24 p2953 N73-33587
Function of state governments in enforcing radiation safety and protection regulations for industrial, research, and medical uses of ionizing radiation
24 p2953 N73-33591

**LAWS**
NT CONSERVATION LAWS
NT FOURIER LAW
NT KIRCHHOFF LAW OF RADIATION
NT RADIATION LAWS
NT SCALING LAWS
NT SIMILITUDE LAW
NT SNELLS LAW
Relationship between law and scientific and technical progress in socialist systems
[JPRS-57318] 03 p0367 N73-12992

**LAYERS**
Crystal chemistry of anhydrous and hydrous layer silicates
[NRC-TT-1479] 04 p0458 N73-13734

**LAYOUTS**
Layout of scientific experiments in Aeros satellite, including description and function of satellite-borne instruments
[DGLR-PAPER-72-069] 09 p1091 N73-18906

**LC CIRCUITS**
Loss reduction in high voltage LC oscillator circuits by applying cryogenic temperatures
[BMBW-FBK-72-31] 22 p2704 N73-31659

**LCRE REACTOR**
U LITHIUM COOLED REACTOR EXPERIMENT

**LEACHING**
Desilification in alumina and cement production by sintering disintegration method
[NLL-LIB-TRANS-1725-[5205.9]]
15 p1746 N73-24150

**LEAD [METAL]**
Influence of shock compression pressure on critical shear in aluminum, copper, and lead
[AD-745365] 01 p0068 N73-10555
X ray fluorescence analysis for determining lead content of paint on pencils in Goddard supply system
08 p0876 N73-17097
Langmuir measurements of thermodynamic lead vapor properties
[IS-2871] 10 p1173 N73-19542
Electrical strength of pressed lead azide
10 p1199 N73-19753
Electromagnetic response of Pb superconducting film as function of magnetic field in microwave range
[ISS-72/5] 10 p1199 N73-19756
Influence of reversible reaction transition superconducting to normal on plastic properties of transition and lead metal and alloy single crystals
[ANL-7903] 10 p1200 N73-19766
Atmospheric diffusion of carbon monoxide and lead from expressways
18 p2170 N73-27527
Nucleocosmochrometers for short lived Pb-205 s-process nucleosynthesis study
[AD-760535] 18 p2182 N73-27618
Development of lead/lead oxide solid electrolyte cell and evaluation of electrical properties in terms of equivalent circuit for cell
20 p2363 N73-29003
High temperature creep of Al alloys tin, and lead at intermediate and low stresses
[LBL-1183] 21 p2559 N73-30512
Charge characteristics of sealed nickel cadmium and lead acid batteries
[PB-221475/7] 22 p2618 N73-30981
Measurements of Fe, Mn, Fn, Cu, Ni, and Pb in aerosols and precipitation in clean tropospheric air
[NOAA-TR-ERL-248-APCL-24]
22 p2664 N73-31349
Bonding methods of aluminum beam leaded devices on microcircuit ceramic substrates
[NASA-CR-124434] 23 p2797 N73-32369
Application of diffusion bonding to electronic interconnection of flatpack leads
[NASA-CR-124460] 24 p2934 N73-33429
Measurements of atmospheric lead concentrations in European community and United Kingdom
[EUR-4982] 24 p2949 N73-33555

**LEAD ALLOYS**
Mechanical properties, machinability, and corrosion characteristics of 80-10-10 high leaded tin bronze alloy
[PB-211945] 05 p0363 N73-14576

Pressure effects on phonon spectrum, electron-phonon interaction strength, and electron-phonon coupling function in Pb-In superconductors using electron tunneling
07 p0831 N73-16739

LEAD COMPOUNDS
NT LEAD OXIDES
NT LEAD SELENIDES
NT LEAD SULFIDES
NT LEAD TELLURIDES
NT LEAD TITANATES
NT LEAD TUNGSTATES
Semiconductor radiation detectors with lead and mercury compounds
[BMBW-FBK-72-19] 09 p1036 N73-18458
Intrinsic and extrinsic nonstoichiometry in lead zirconate titanate system
[LBL-880] 10 p1126 N73-19172
Pyroelectric coefficient of lead zirconate titanate
[AD-755520] 13 p1567 N73-22700
Properties of piezoelectric lead zirconate titanate ceramic resonator material produced by adding lead niobates to material
[AD-757617] 14 p1681 N73-23644
Atmospheric pollution due to use of lead iodide in weather modification
[NLL-M-23006-[5828.4F]] 20 p2441 N73-29607
Measurement of concentration of volatile and particulate lead compounds in atmosphere at selected road sites
[PB-221663/8] 22 p2695 N73-31592

LEAD OXIDES
High temperature friction and wear properties of PbO for solid lubricant applications including tests in room air, controlled atmospheres, and vacuum
[NAL-TR-285] 04 p0426 N73-13470
Development of lead/lead oxide solid electrolyte cell and evaluation of electrical properties in terms of equivalent circuit for cell
20 p2363 N73-29003

LEAD POISONING
Validity of rapid delta-aminolevulinic acid determination in urine for lead intoxication tests on industrial workers
[NASA-TT-F-14864] 12 p1371 N73-21128

LEAD SELENIDES
Thin film lead and tin selenide photoconductive infrared detectors
[AD-758685] 16 p1915 N73-25499

LEAD SULFIDES
Hall coefficient, resistivity, and charge carrier mobility of epitaxial films of n-type and p-type PbS before and after neutron irradiation
[AD-749689] 06 p0710 N73-15791
Refracted electron beam temperature as indication of lead sulfide purity
[AD-753556] 09 p1077 N73-18787

LEAD TELLURIDES
Absorption coefficient and index of refraction data for Pb[1-x]S n[x] Te thin films
[AD-751650] 07 p0832 N73-16747

LEAD TITANATES
Testing point dipole electro-optic model by application to lead titanate
[AD-753467] 09 p1075 N73-18773
Two ferroelectric materials, single crystal bismuth titanate and hot pressed ceramic, lead zirconate titanate
[AD-755746] 12 p1386 N73-21237

LEAD TUNGSTATES
Fabrication and testing of thin walled cylinders made from tungsten lead composite
[LA-511] 17 p2038 N73-26485

LEADING EDGE SLATS
Computer program for designing leading edge slats for producing specified pressure distribution on main airfoil
[AD-749485] 05 p0496 N73-14043
Design aspects of stall of powered-lift aircraft with externally blown flaps and methods for predicting increment in maximum lift coefficient due to power
06 p0617 N73-15011
Effects of various leading edge slat devices on static aerodynamic characteristics of twin-jet, swept wing fighter model
[NASA-TN-D-6921] 07 p0736 N73-15988
Wind tunnel tests of two dimensional wing model with leading edge slat and trailing edge flap
[FAA-AU-862] 08 p0863 N73-16984
Rotor noise reduction by serrated brass strip attachment to blade leading edges
[NASA-TN-D-7371] 19 p2219 N73-27898
Aerodynamic forces, pressure distribution, and wakes of wing profile with trailing edge flaps and leading edge slats
24 p2906 N73-33187

LEADING EDGES
NT SHARP LEADING EDGES
Method of characteristics for analyzing supersonic flow past oscillating flat plate cascades with leading edge locus
[AD-745838] 01 p0042 N73-10332
Impact tests of jet transport wing leading edge fuel tanks to evaluate effects of aborted takeoff, abnormal landing, and bird strikes
[FAA-NA-72-21] 02 p0125 N73-11017
Development of method for calculating small separation zones near leading edge of airfoil at incidence
06 p0616 N73-15002
Finite difference solution for merged layer regime of hypersonic flat plate leading edge problem
08 p0895 N73-17243
Angles of attack for shock wave detachment from sharp leading edge of five delta wing models with flat compression surfaces
[AD-752206] 08 p0898 N73-17271
Vortex sheet and increased lift caused by blowing from leading edges of slender delta wing
[ARC-R/M-3692] 09 p0981 N73-18016
Turbulent heat transfer and pressure on leading edge of fin, swept wing, or antenna
[SCL-RR-72-0308] 12 p1464 N73-21863
Application of modified slender wing theory to analyze aerodynamic characteristics of slender, lifting, wings with curved leading edges at supersonic speeds
[ARC-R/M-3278] 15 p1727 N73-24006
Analysis of wing leading edge buckling due to aerodynamic heating to show effect of shear modulus of material and geometry of leading edge on buckling onset
[ARC-R/M-3197] 16 p1851 N73-25000
Aerodynamic characteristics and noise attenuation effects of leading edge serrations on rotary wings
[AD-759028] 16 p1863 N73-25088

LEAKAGE
Leakage of ESRO 4 nickel cadmium batteries noting electrical and pressure measurements and KOH loss
[ESRO-CR[P]-132] 04 p0375 N73-13053
Design and fabrication of flight weight ultrasonic contact sensor leak detection system
[NASA-TM-X-68909] 05 p0546 N73-14431
Abradable buffered labyrinth seal for control of gas path leakage in tip-turbine driven lift fan
[NASA-CR-121131] 07 p0804 N73-16524
Portable device for detecting pneumatic pressure leaks in hermetically sealed housings
[NASA-CASE-MFS-21761-1] 09 p1035 N73-18444
Leak-testing methods for gas and liquid systems
19 p2304 N73-28526
Nitrogen and hydrazine leakage of monopropellant ACS valves
[AD-762943] 20 p2423 N73-29465
Leak detector with high vacuum seals
[NASA-CASE-LAR-11237-1] 23 p2793 N73-32344

LEAR JET AIRCRAFT
Aircraft accident involving Lear jet model 25 at Victoria, Texas on 18 Jan. 1972
[PB-212484] 06 p0625 N73-15076
Aircraft accident involving Lear jet aircraft following takeoff from Atlanta, Georgia Airport on 26 Feb. 1973
[NTSB-AAR-73-12] 17 p1984 N73-26036
Shuttle sortie simulation using lear jet aircraft
[NASA-TM-X-62283] 20 p2473 N73-29868

LEARNING
NT ASTRONAUT TRAINING
NT CONDITIONING [LEARNING]
NT HABITUATION [LEARNING]
NT TRANSFER OF TRAINING
Effects of direct auditory feedback of electromyogram on learning to control single unit
[AD-745107] 01 p0021 N73-10165

LEARNING MACHINES
Feasibility of using computer system for echo detection and identification of moving targets
[AD-758266] 15 p1751 N73-24191

LEARNING THEORY
Development and application of computer programs as instructional methods for physics laboratory experiments
05 p0516 N73-14198
Themis Project results on adaptive learning control systems and pattern recognition
[AD-756424] 13 p1550 N73-22562

LEAST SQUARES METHOD
Newton-Raphson least squares percentage error method for determining atmospheric turbulence field parameters
[AD-745946] 01 p0078 N73-10641
Least squares polynomial approximation for computer generation of differentiable functions
[USC-113P19-27] 02 p0146 N73-11180
Least squares curve fitting method for smoothing pressure distribution data for various cross sections of circular cylinder
[WRE-TN-688[WR/D]] 02 p0195 N73-11577
Applications of least squares method to analysis of parameters and confidence region determination
[LAAS-NT-SIS-72-T-08] 04 p0441 N73-13593
Least squares method in gravimetric geodesy and photogrammetry
[AD-749873] 06 p0669 N73-15440
Application of least square point matching for stress analysis of shallow, perforated, cylindrical shell subjected to tension, edge moment, or transverse shear
[AD-750942] 06 p0728 N73-15942
Least squares representatiion for charge distribution on monopole antenna immersed in dissipative medium
[AD-753092] 09 p1008 N73-18230
Least squares adjustment of geometrical global satellite network data
[NASA-CR-131535] 12 p1459 N73-21823
Conversion of geomagnetic potential into spherical coordinates of optimally offset, inclined dipole using least squares method
[AD-756460] 13 p1526 N73-22366
Least squares and cross correlation procedure for determining absolute timing of pulsars
13 p1575 N73-22765
Using extended Kalman filter and weighted least square error filtering techniques to estimate orbital parameters of near earth satellite
[AD-757880] 15 p1832 N73-24852
Pole and zero placement in multivariable control systems by least squares method
[NASA-CR-132962] 16 p1935 N73-25654
Least squares method for constructing meteorological fields from measurement data
[AD-759872] 17 p2058 N73-26645
Optimal methods for processing observations
20 p2439 N73-29593
Nondestructive determination of radionuclides in lunar samples using large low-background gamma ray spectrometer and application of least squares fitting
[NASA-TM-X-69581] 22 p2718 N73-31756
Least squares fitting of bicubic spline surfaces to general data at arbitrary points noting householder orthogonal transformation, solution stability, and ranking
[NPL-NAC-22] 23 p2813 N73-32489
Multidimensional linear system parameter estimation computer program using least squares method evaluating mathematical model stability, observability and real time operation
[LAAS-AS-73-I-06] 23 p2813 N73-32491

LEAVES
Remote detection of water content and spectral properties of leaves in different soybean crop species
04 p0378 N73-13070
Reflectance, transmittance and absorbance spectra of normal and six types of maize leaves
[NASA-CR-130032] 07 p0745 N73-16065
Spectral characteristics of normal and nutrient-deficient maize leaves
[NASA-CR-132145] 15 p1742 N73-24119
Scattering of polarized light by rough and smooth leaf surfaces
20 p2405 N73-29333

LEBESGUE THEOREM
Steklov-Lebesgue norm used in stress analysis of solid rocket propellants to determine viscoelastic response with aging
[AD-748943] 04 p0462 N73-13771

LED [DIODES]
U LIGHT EMITTING DIODES

LEDGES
Structural models for grain boundary dislocations and ledges in crystal defects
[COO-3158-12] 10 p1173 N73-19544

LEE WAVES
Mathematical models for analyzing internal gravity waves generated by stratified inviscid fluid flow over solid body
[AD-746137] 02 p0168 N73-11369

LEGAL LIABILITY
Legal restraints on dissemination of instructional materials by educational communications systems
[NASA-CR-129271] 03 p0366 N73-12983
Political, legal, and international management of space data and space programs
04 p0474 N73-13871
Legal liabilities and impact of satellite meteorology on agricultural crops and economics
[NASA-CR-129994] 06 p0692 N73-15636
Legal liability of US Government in handling meteorological data obtained by satellites
06 p0692 N73-15638
Legal considerations of satellite communications system for teleconferencing applications
[NASA-CR-133592] 20 p2377 N73-29099
Selected bibliography of articles on product liability
[NASA-TM-X-69493] 20 p2488 N73-29985

LEGENDRE CODE
U COMPUTER PROGRAMMING
U NEUTRON SCATTERING

LEGENDRE FUNCTIONS
Higher order theories and solution techniques for moderately thick shells of revolution using Reissner Theory and Legendre functions
13 p1584 N73-22842

LEGENDRE POLYNOMIALS
U LEGENDRE FUNCTIONS

LEGENDRE TRANSFORMATION
U LEGENDRE FUNCTIONS

LEGIBILITY
Legibility and recognition by test groups of displayed signals differing by brightness or color
[DLR-FB-71-57] 06 p0674 N73-15484
LEM [LUNAR MODULE]
U LUNAR MODULE
LEMMAS
U THEOREMS
LENNARD-JONES GAS
Transport properties and time correlation functions of Lennard-Jones liquid near its triple point
[LPTHE-72/22] 10 p1141 N73-19296
LENS ANTENNAS
Electrodynamic fundamentals of antenna theory and design
[AD-755689] 13 p1502 N73-22176
LENS DESIGN
Optical design and performance evaluation of athermal solid and liquid acoustic lenses
[AD-745734] 01 p0081 N73-10668
Design of Schmidt telescope with possibility of converting to Cassegrain configuration and noting achromatic corrector and angular resolution
07 p0846 N73-16858
Parameters and components of ESO Schmidt telescope
07 p0846 N73-16859
Design and fabrication of two dimensional dielectric lens contained in parallel plate waveguide system in multibeam antenna study
[NASA-CR-132793] 22 p2641 N73-31171
Production and performance of bleached holographic lenses
[AD-764701] 23 p2821 N73-32548
LENSES
NT MAGNETIC LENSES
NT WIDE ANGLE LENSES
Optical transfer function measurements on lenses and lens systems
[TPD-1972-0-1] 01 p0079 N73-10654
Spectral resolution and image enhancement by focusing of lense optics
[TPD-1972-0-2] 01 p0079 N73-10655
Threecomponent optical system with variable focal length for infrared region of spectrum
[AD-745356] 01 p0080 N73-10665
Method and data reduction tables for determining resolving power of photographic and other optical systems under typical field conditions
[AD-747265] 03 p0303 N73-12475
Effects of camera lense photosensitivity on signal loss in vidicon tubes
[AD-750530] 05 p0549 N73-14459
Thermal lensing in infrared laser window materials
[AD-749481] 05 p0558 N73-14536
Wave scattering by lenses and microsound elastic waveguides
[AD-750766] 06 p0701 N73-15717
Analysis of thermal lensing in high power laser window materials
[AD-751266] 07 p0808 N73-16554
Optical materials and design of optical equipment
[AD-751496] 07 p0822 N73-16660
Plural beam antenna with parabolic reflectors
[NASA-CASE-GSC-11013-1] 10 p1133 N73-19234
Development of method for determining resolving power of photographic lenses
[NBS-SP-374] 18 p2151 N73-27387
Geometric optical properties of holographic lens systems
[AD-762526] 20 p2426 N73-29486
Characteristics of lenses and ports for underwater imaging systems to compare depth of field and relative aperture for several lens port combinations
24 p2958 N73-33635
LEPTONS
NT ELECTRONS
NT MUONS
NT NEUTRINOS
NT POSITRONS
Inelastic lepton-nucleon process in Bjorken limit for neutral gluon model
[ILL-(TH)-72-10] 01 p0083 N73-10684
Finiteness of radiative corrections to semileptonic decays in unified gauge theories
[TR-74-021] 22 p2701 N73-31637
LES
U LINCOLN EXPERIMENTAL SATELLITES
LES [ESCAPE SYSTEMS]
U LAUNCH ESCAPE SYSTEMS
LESIONS
Lesions of nervous system and vascular embolisms in decompression sickness
[AD-743330] 01 p0010 N73-10076
Methylisobutylketone causing lesions in first and second sections of proximal convoluted tubule of nephron of kidney
[AD-751444] 07 p0748 N73-16083
LETHALITY
Daylight and disinfectant effects on bacteria survival times on plastic surfaces
[NASA-TT-F-13923] 01 p0009 N73-10069
Energy comparisons for lethal doses of gamma radiation and visible light with energy of basal cell metabolism
[AD-746750] 04 p0381 N73-13102
Influence of shielding head and anterior stomach on course of radiation sickness in dogs subjected to total lethal gamma irradiation
11 p1241 N73-20073
LETTERS [SYMBOLS]
U SYMBOLS
LEUKOCYTES
NT LYMPHOCYTES
LEUKOPENIA
Leukopenic response of dog bone marrow for evaluating hematopoietic tissue function
13 p1481 N73-22009
LEVEL [QUANTITY]
NT ATOMIC ENERGY LEVELS
NT EFFECTIVE PERCEIVED NOISE LEVELS
NT ELECTRON STATES
NT ENERGY LEVELS
NT GROUND STATE
NT INTERMOLECULAR FORCES
NT MOLECULAR ENERGY LEVELS
LEVELING
Automatically operable self-leveling load table with plurality of solenoid valves
[NASA-CASE-MFS-22039-1] 21 p2548 N73-30428
LEVITATION
Cryogenics applications for development of superconducting levitated system of high speed ground transportation
[NBS-TN-635] 14 p1645 N73-23344
LEXAN [TRADEMARK]
Influence of axial impact loads on dynamic properties and strain wave speeds in polycarbonate Lexan
[AD-755457] 12 p1417 N73-21482
LIABILITIES
NT LEGAL LIABILITY
LIAPUNOV FUNCTIONS
Matrix methods for dynamic modeling of human operator performance using Liapunov functions
01 p0014 N73-10111
Synthesis of adaptive control tracking systems using Liapunov second method
[NASA-CR-129175] 02 p0150 N73-11220
Liapunov functions for analyzing stability properties of various large scale electrical power systems - conferences
07 p0760 N73-16169
Liapunov direct method for studying transient stability of multimachine power system
07 p0760 N73-16171
Stability margins for electrical power systems with perturbations in its multiareas
07 p0760 N73-16173
Liapunov type methods for checking dynamic security in power system stability theory
07 p0760 N73-16174
Principle and vector Liapunov functions for studying stability in large scale dynamic systems
07 p0760 N73-16176
Algebraic criteria for connective stability of large scale dynamic systems subjected to structural perturbations
07 p0760 N73-16177
Analysis of satellite stability of motion using Liapunov system as applied to flexible bodies
07 p0848 N73-16869
Liapunov solutions to linear differential equations with periodic coefficients
[NASA-TT-F-14835] 10 p1179 N73-19588
Application of Liapunov function for analysis of finite stability of complex system in limited range of parameters
[NASA-TT-F-14869] 11 p1311 N73-20640
Modal analysis for Liapunov stability of rotating elastic bodies
[NASA-CR-124258] 15 p1839 N73-24904
LIBRARIES
Computerized file management system for library reference searches
[UCRL-73355-REV-1] 03 p0271 N73-12193
Problems of library and information services to large research center
15 p1753 N73-24204
Pennsylvania State University library catalogue for remotely sensed digital data tapes
[E73-11115] 24 p2916 N73-33272
LIBRATION
Apollo 16 photography of Gegenschein-Moulton region for libration point determination of Sun-Earth system
12 p1451 N73-21750
LIBRATIONAL MOTION
Solutions for motion about libration points of elliptic restricted three-body problem
15 p1829 N73-24826
LIDAR
U OPTICAL RADAR
LIE GROUPS
Integrable and nonintegrable Lie-algebra representations relative to particle physics
10 p1191 N73-19692
LIFE [BIOLOGY]
U LIFE SCIENCES
LIFE [DURABILITY]
NT FATIGUE LIFE
NT SATELLITE LIFETIME
NT SERVICE LIFE
NT STORAGE STABILITY
Demountable electro-optical system tests for improving pattern threshold recognition device
[AD-745915] 02 p0147 N73-11194
Minority carrier lifetime optimization for gallium silicon diffusion thyristor
11 p1330 N73-20795
Method of life prediction for nickel-based Udimet alloy by high temperature creep/fatigue testing
[NASA-CR-120958] 12 p1462 N73-21845
Extended life testing of complementary MOS integrated circuits
[NASA-CR-124215] 13 p1533 N73-22422
Aging stability of samarium cobalt magnets
[AD-758806] 16 p1881 N73-25222
Life tests of small turbine type flowmeters in liquid hydrogen
[NASA-TN-D-7323] 16 p1888 N73-25278
Design of vertical multijunction silicon solar cells with prolonged lifetimes
[AD-760172] 17 p1986 N73-26052
Proof testing of ceramic materials for component lifetimes
[AD-759373] 17 p2051 N73-26590
Life durability tests of bounded microcircuit joints subjected to prestressing
[AD-762333] 19 p2246 N73-28107
X ray inspection and quality control of AEG cathode life-tests tubes after 44,000/hr life for prediction of communication satellite traveling wave tube durability
[ESRO-TM-148-ESTEC] 19 p2305 N73-28536
Pulse radiolysis of biphenyl solutions in cyclohexane noting life distribution of biphenyl ions
[IRI-133-72-07] 19 p2323 N73-28686
Life tests of 10 mm bore flashlamps at high fractions of explosion energy
[AD-760707] 20 p2426 N73-29488
Minority carrier lifetime control in n-type base regions of gallium diffused silicon power thyristors and diodes
[BMPT-FB-T-73-05] 23 p2765 N73-32123
LIFE DETECTORS
Extraterrestrial life detection using Automated Microbial Metabolism Laboratory
[NASA-CR-129508] 03 p0279 N73-12266
LIFE RAFTS
Inflatable stabilizing system for use on life raft to reduce rocking and preclude capsizing
[NASA-CASE-MSC-12393-1] 17 p1980 N73-26006
LIFE SCIENCES
Conservational and rational use of natural resources and wildlife to preserve biosphere environment
[JPRS-58429] 11 p1250 N73-20145
State and prospects of biogeocenological research
[JPRS-59395] 18 p2109 N73-27053
Life sciences payload definition and integration study to show design of space laboratory for space shuttle and cost analysis of project - Vol. 2
[NASA-CR-124412] 23 p2849 N73-32766
Research equipment requirements for space laboratory concepts involved in conducting life sciences experiments in space - Vol. 3
[NASA-CR-124414] 23 p2849 N73-32767
Specification catalog to identify test equipment for use in conducting life sciences experiments aboard space laboratory - Vol. 4
[NASA-CR-124413] 23 p2849 N73-32768
LIFE SPAN
Abstracts on microwave radiation effects on human and animal physiological functions and life expectancy
[MBL-1972-6] 01 p0008 N73-10061
LIFE SUPPORT SYSTEMS
NT BIOPAKS
NT CLOSED ECOLOGICAL SYSTEMS
NT EMERGENCY LIFE SUSTAINING SYSTEMS
NT UNDERWATER BREATHING APPARATUS
Supply, biosynthetic, and regenerated physicochemical systems for spacecraft life support
[NASA-TT-F-14436] 01 p0020 N73-10155
Long-term testing of water electrolysis systems for regenerative life support system in manned space stations
[NASA-CR-128629] 02 p0135 N73-11095
Device for removing air from water for use in life support systems in manned space flight
[NASA-CASE-XLA-8914] 03 p0305 N73-12492
Analytical assessment of potential methods for replenishing auxiliary propulsion onboard orbiting space stations
[NASA-CR-123947] 04 p0461 N73-13764
New knowledge gain from crew life support aspect of manned space program and applicability to earth-based problems
[NASA-CR-129514] 04 p0486 N73-13970
Factors relevant to respiratory support and equipment design
06 p0628 N73-15102

Extravehicular activity support systems and equipment with emphasis on physical operational and performance characteristics of major systems
[NASA-CR-2160] 06 p0718 N73-15858
Development of computer program to optimize space shuttle environmental and thermal control life support system
[NASA-CR-128736] 08 p0964 N73-17883
Cost effectiveness of water reclamation subsystem in advanced aerospace life support systems
[NASA-CR-124098] 09 p0997 N73-18134
Medical and biological problems of manned space flight
[NASA-TT-F-719] 10 p1114 N73-19077
Preservatives for human urine storage and water reclamation in spacecraft cabin
10 p1116 N73-19099
Human performance and life support engineering for space environment conditions
[AD-754216] 11 p1252 N73-20157
Cost analysis of oxygen supply equipment and recovery systems for orbital space stations
[NASA-CR-124175] 12 p1373 N73-21137
Evaluation of hazardous conditions created by facial hair on aircrew personnel wearing oxygen masks
[AD-754075] 12 p1375 N73-21154
Proceedings of conference on research and development projects conducted by US Air Force Research and Development Command
[AD-753071] 12 p1467 N73-21890
Hydrogen depolarized cell for removing CO2 in spacecraft life support systems
[NASA-CR-131868] 13 p1486 N73-22047
Effectiveness of phased dilution compared to current demand diluter oxygen delivery system
14 p1611 N73-23065
Temperature and humidity control in air quality modeling for optimal life support system of spacecraft cabin
15 p1743 N73-24131
Apollo experience report on design and function of Apollo potable water system supplied as byproduct of fuel cells
[NASA-TN-D-7291] 15 p1835 N73-24874
Identification of requirements and systems for intravehicular activity and extravehicular activity during space shuttle missions - Vol. 1
[NASA-CR-128941] 15 p1835 N73-24875
Identification of requirements and systems for intravehicular activity during space shuttle missions - Vol. 2
[NASA-CR-128942] 15 p1835 N73-24876
Water recovery system for three man crew aboard spacecraft
[NASA-CR-128983] 17 p1990 N73-26094
Spacelab configurations noting thermal control, life support, electrical power, communication, and altitude control subsystems
[ESS/SS-399-VOL-2] 17 p2089 N73-26903
Biological development of human living environment
[NASA-TT-F-15005] 18 p2111 N73-27067
Cryogenic heat exchanger for removal of waste heat from spacecraft environmental control life support system
[NASA-CR-124301] 18 p2111 N73-27071
Cost estimating method for life support systems of manned earth orbital programs
[NASA-CR-124305] 18 p2111 N73-27072
Cost analysis of oxygen recovery subsystems for life support systems
[NASA-CR-124304] 18 p2112 N73-27075
Cost analysis of mass spectrometers and gas chromatographs for life support atmosphere monitoring
[NASA-CR-124306] 18 p2112 N73-27076
Personnel life support clothing for protection against environmental hazards
[AD-762428] 19 p2229 N73-27976
Aerospace medicine and exobiology research in support of long term manned space flight
[JPRS-59702] 20 p2365 N73-29021
Equipment requirements for space shuttle EVA/IVA pressure suit, life support system, mobility aids, vehicle support provisions, and emergency support
[NASA-CR-133991] 21 p2503 N73-30089
Space shuttle environmental and thermal control/life support system
[NASA-CR-134009] 21 p2504 N73-30091
Requirements for mobility aids and restraint devices for use by personnel of space shuttle - Vol. 4
[NASA-CR-133994] 22 p2622 N73-31009
Requirements and equipment for space shuttle emergency intravehicular activity and effectiveness of emergency procedures - Vol. 5
[NASA-CR-133995] 22 p2622 N73-31010
Alkali metal carbonate-bicarbonate solid gas reaction for removing CO2 from atmosphere of EVA life support system
[NASA-CR-114661] 22 p2622 N73-31013
Intra- and extravehicular life support space suite for Apollo astronauts
[NASA-CASE-MSC-12609-1] 23 p2751 N73-32012
Electrochemical system with solid electrolyte for regenerating oxygen from CO2 and H2O
24 p2882 N73-33015
Light and carbon dioxide effects on algal life support systems in space flight
[NASA-CR-135796] 24 p2885 N73-33039

LIFEBOATS
Operational investigation of combined all weather capabilities of Coast Guard motor lifeboat and 70 knot surface effect rescue vehicle
[AD-761460] 19 p2229 N73-27974

LIFETIME [DURABILITY]
U LIFE [DURABILITY]

LIFT
NT INTERFERENCE LIFT
NT JET LIFT
NT ZERO LIFT
Wind tunnel tests to determine effect of simulated hoar frost on lift coefficient of three aircraft wing configurations
[FFA-AU-902] 01 p0001 N73-10001
ALGOL program for lift distribution determination on thin wing in subsonic flow
[NLR-TR-70088-U] 03 p0274 N73-12224
Wind tunnel tests to determine aerodynamic characteristics of V/STOL aircraft configurations using blowing flapped wing and direct jet lift systems
[NASA-CR-114496] 03 p0282 N73-12284
Operational test and evaluation of angle of attack system for displaying percentage of lift produced by wing for all flap configurations
[AD-748844] 03 p0304 N73-12485
Development of numerical analysis techniques for determining lifting surface characteristics of circular wings and parabolic wing tips
[AD-748433] 04 p0370 N73-13006
Numerical analysis of pressure distribution at parabolic wing tips on circular wing model based on occurrence of logarithmic sets
[AD-748432] 04 p0370 N73-13007
Low speed wind tunnel tests on slender variable sweep wing of lift, drag, and pitching moments
[ARC-CP-1227] 05 p0492 N73-14009
Numerical analysis of ideal and real gas equations for application to lift generated by helicopter rotors
[AD-754420] 11 p1235 N73-20026
Analysis of optimum pressure distribution on multi-element airfoils to obtain conditions for maximum lift coefficient
12 p1355 N73-20996
Friction effect on lift of airfoil section with slotted flap
[DLR-FB-73-04] 12 p1356 N73-21001
Application of modified slender wing theory to analyze aerodynamic characteristics of slender, lifting, wings with curved leading edges at supersonic speeds
[ARC-R/M-3278] 15 p1727 N73-24006
Application of Kelvin impulse theory for computing lift on airfoils and analysis of circulation around airfoil to produce lift
16 p1851 N73-24997
Evaluation of double integral equation for calculation of wave drag due to volume and aerodynamic lift of slender wings
[ARC-R/M-3221] 16 p1852 N73-25006
Design criteria for slender warped wings with unswept trailing edge with zero load along leading edge and near planar vortex sheet at trailing edge for design lift coefficient
[ARC-R/M-3406] 16 p1852 N73-25008
Numerical analysis of lift and lift distribution on aircraft wing and trailing vortex flow behind wing
[AD-759262] 16 p1863 N73-25089
Analysis of nonhomogeneous flow associated with two dimensional propulsive lifting system based on flow with energy addition
[NASA-CR-2250] 17 p1979 N73-25997
Equivalence rule and transonic flows involving lift around thin smooth configuration with swept leading edge
[AD-760349] 17 p1985 N73-26042
Optimization of forward foil lift control for hydrofoil craft
[AD-760684] 18 p2131 N73-27221
Numerical methods for determining unsteady aerodynamic forces on helicopter rotor blades to show lift distribution as function of velocity component normal to blades
[NASA-TT-F-15039] 20 p2360 N73-28981
Measurement of drag, lift and pitching moments on slender winged low aspect ratio gothic planforms at subsonic speed
[ARC-R/M-3720] 21 p2492 N73-30005
Wind tunnel tests to determine two dimensional characteristics of airfoil optimized for maximum lift coefficient at various angles of attack
[NASA-TN-D-7071] 22 p2611 N73-30929
The calculated growth of lift and pitching moment on a swept wing entering a discrete vertical gust at subsonic speeds
[ARC-CP-1241] 22 p2612 N73-30932
The lift and stalling characteristics of a 35 deg sweptback wing designed to have identical chordwise pressure distributions at all spanwise stations when near maximum lift
[ARC-R/M-3721] 22 p2612 N73-30935

LIFT AUGMENTATION
Numerical determination of augmented lift due to wing-slipstream interaction for application to V/STOL aircraft
[AD-743257] 01 p0005 N73-10035
Noise tests on simulated mixer nozzles and scale models of externally blown flap, lift augmentation system
[NASA-TM-X-2638] 02 p0124 N73-11012
Development of nonlinearized solution for aerodynamic characteristics of jet flap lifting surface with span-wise slot near trailing edge
[NASA-CR-2190] 07 p0736 N73-15986
Short takeoff aircraft lift augmentation and prevention of airflow separation on cambered elliptical airfoil section using circulation control
[AD-751045] 07 p0736 N73-15992
Development of analytical technique for computing performance of arbitrary jet-flapped wing with compensations for variations in wing geometry
[NASA-CR-2179] 08 p0863 N73-16982
Wind tunnel tests to determine aerodynamic characteristics of full scale H-126 aircraft using jet flap principle
[NASA-TN-D-7252] 12 p1355 N73-20997
Wind tunnel tests to determine static longitudinal aerodynamic characteristics of jet transport wingbody with upper surface blown jet flap for lift augmentation
[NASA-TN-D-7183] 13 p1470 N73-21907
Development of high performance, low volume thrust augmentation using combined Coanda inlet and jet flap diffusion techniques
[AD-756895] 13 p1476 N73-21954
Comparison of aerodynamic lift developed by mechanical high lift systems and lift developed by externally blown flaps on short takeoff aircraft
[NASA-TT-F-14895] 14 p1601 N73-22981
Effect of jet stream blowing downwards from lower surface of slender delta wing to obtain lift augmentation for takeoff and landing
[ARC-R/M-3288] 15 p1727 N73-24009
Theoretical investigation of longitudinal stability, control, and response characteristics of jet flap aircraft
[ARC-R/M-3272] 15 p1730 N73-24028
Noise tests on large scale model of externally blown flap lift augmentation system using mixer nozzle
[NASA-TN-D-7236] 15 p1733 N73-24059
Characteristics of flight control system for approach flight path control of augmentor wing on powered-lift short takeoff aircraft configuration
[NASA-CR-114574] 15 p1734 N73-24062
Simulator analysis of effect of engine response characteristics on approach and landing operations of powered lift aircraft with externally blown flaps
[NASA-TM-X-62265] 17 p1982 N73-26021
Wind tunnel tests to determine acoustic properties of jet augmented lifting flap configuration
[NASA-TT-F-14951] 17 p1983 N73-26030
Propulsive-lift technology program for development of short takeoff aircraft propulsion systems and lift augmentation devices
18 p2103 N73-27009
Design, development, and evaluation of Buffalo/Spey Augmentor-Wing research aircraft using internally blown flap for lift augmentation
18 p2103 N73-27010
Design and characteristics of augmentor wing cruise blowing valveless system for STOL passenger aircraft to define requirements for test facilities - Vol. 2
[NASA-CR-114570] 19 p2220 N73-27907
Development and characteristics of experimental aircraft for demonstrating augmentor wing jet short takeoff concept using modified C-8A aircraft - Vol. 1
[NASA-CR-114503] 21 p2494 N73-30016
Flight tests of modified C-8A aircraft to demonstrate augmentor wing, short takeoff concept - Vol. 2
[NASA-CR-114504] 21 p2494 N73-30017
Aerodynamic characteristics of round jet located on center line of bottom of aircraft fuselage and elongated slots for lift augmentation
[NASA-TN-D-7299] 22 p2613 N73-30939
Evaluation of low speed flying qualities of short takeoff aircraft with externally blown flap wing or augmentor wing using flight simulator
[NASA-TN-D-7454] 23 p2742 N73-31951
Thrust augmentation, lift forces, and mixing properties of two-phase flow propulsion and lift system for ground effect machines
[AD-765332] 23 p2777 N73-32208
Aerodynamic and performance characteristics of short takeoff aircraft equipped with externally blown flaps
24 p2872 N73-32939
Wind tunnel tests to determine basic performance of swept augmentor wing configuration and effect on longitudinal characteristics of aircraft
24 p2872 N73-32941
Aerodynamic characteristics of augmentor wings and analysis of augmentation and entrainment in defining a net thrust coefficient
24 p2872 N73-32942

Wind tunnel tests to determine aerodynamic characteristics of upper surface blown jet-flap concept incorporating highlbypass-ratio turbofan engines
24 p2872 N73-32943
Simulations of powered-lift STOL transport aircraft with either externally blown flap configuration or augmentor wing configuration
24 p2873 N73-32948
Flight tests of augmentor-wing jet STOL research aircraft to compare wind tunnel data with flight data for dynamic characteristics and limitations
24 p2874 N73-32954
Wind tunnel tests of large scale subsonic jet transport with upper surface blowing flap system for lift augmentation
[NASA-TM-X-62296] 24 p2876 N73-32973

**LIFT COEFFICIENTS**
U AERODYNAMIC COEFFICIENTS
U LIFT

**LIFT DEVICES**
Development of auxiliary lifting system to provide ferry capability for entry vehicles
[NASA-CASE-LAR-10574-1] 04 p0400 N73-13257
Development of two experimental approaches for analyzing two dimensional flow on high lift devices
06 p0617 N73-15005
Comparison of mechanical high lift flaps with externally blown flaps for STOL aircraft
[MBB-UH-12-72-O] 07 p0739 N73-16017
Literature survey on jet propagation and interference in lifting surface aerodynamics
[NASA-TT-F-14957] 19 p2217 N73-27886
Load near apex of lifting swept wing in linearized subsonic flow
[ARC-R/M-3716] 21 p2492 N73-30001
Flight tests of modified F-100 aircraft to determine effectiveness of fast-acting flaps as direct-lift-control devices to improve station keeping
[NASA-TM-X-2936] 24 p2876 N73-32970

**LIFT DISTRIBUTION**
U FORCE DISTRIBUTION
U LIFT

**LIFT FANS**
Performance characteristics of model VTOL lift-fan simulator installed in two dimensional wing
[NASA-TM-X-68788] 01 p0036 N73-10282
Wind tunnel tests of VTOL lift fan stages to determine changes in thrust characteristics with varations in back pressure imposed on stages by cross flow
[NASA-TM-X-68169] 06 p0620 N73-15031
Dynamics and control analysis of turbofan lift engines
[NASA-TM-X-68175] 06 p0713 N73-15815
Hybrid computer simulation used for analysis of integral lift-fan engine being considered for VTOL applications
[NASA-TM-X-2691] 06 p0713 N73-15817
Abradable buffered labyrinth seal for control of gas path leakage in tip-turbine driven lift fan
[NASA-CR-121131] 07 p0804 N73-16524
Preliminary aerodynamic and mechanical design of selected gas generators and lift unit for V/STOL aircraft
[NASA-CR-120972] 10 p1106 N73-19020
Wind tunnel tests to determine low speed aerodynamic characteristics of large scale V/STOL transport models with lift fan lift-cruise fan propulsion system
[NASA-TM-X-62231] 11 p1233 N73-20014
Design of V/STOL research transport aircraft to achieve low fan noise with high thrust/weight capability of high pressure ratio lift fan system
[NASA-CR-121146] 12 p1364 N73-21065
Acoustic measurements of sound pressure levels due to cross flow over face of lift fans on fan-in-wing and V/STOL model transport aircraft
[NASA-CR-114566] 13 p1473 N73-21928
Wind tunnel tests to determine effect of cross flow velocity on jet noise power level using V/STOL model transport
[NASA-CR-114571] 13 p1473 N73-21929
Analysis of reverberant-field noise produced by three lift fan models operating at various rotor tip speeds
[NASA-TM-X-68243] 17 p1981 N73-26014
Preliminary design analysis of quiet integral fan lift engines for VTOL transport applications in next decade
[NASA-CR-120969] 17 p2076 N73-26796
Four VTOL propulsion concepts compared parametrically for subsonic applications with three types of aircrafts
[NASA-TM-X-68279] 20 p2466 N73-29810
Design and tests of lift fan exhaust suppression system for future VTOL aircraft noise goals
[NASA-CR-121108] 20 p2466 N73-29812
Energy transfer control and compressor bleed concepts of remote lift fan control
[NASA-TM-X-2863] 21 p2590 N73-30749
Steady state analysis of energy transfer control and compressor concepts of remote lift fan control
[NASA-TM-X-2876] 21 p2590 N73-30753
Wind tunnel tests to determine effect of inlet turbulence length scale on fan discrete tone noise
[NASA-TM-X-62300] 22 p2700 N73-31625
Wind tunnel tests to determine acoustic properties of large scale lift fan transport aircraft model
[NASA-TM-X-62284] 24 p2877 N73-32975

**LIFT FORCES**
U LIFT

**LIFTING BODIES**
NT LIFTING REENTRY VEHICLES
NT X-20 AIRCRAFT
NT X-24 AIRCRAFT
Computer program for subsonic lifting surface analysis with static aeroelastic effects
[AD-745894] 02 p0157 N73-11273
Static force balancing system attached to lifting body
[NASA-CASE-LAR-10348-1] 03 p0279 N73-12264
Improving method of numerical calculation of aerodynamic coefficients for subsonic lifting surface
[REPT-32] 05 p0491 N73-14004
Gust field generation in wind tunnel for determining transfer function of lifting surface
12 p1387 N73-21248
ALGOL procedures for calculating velocity and pressure distribution on rectangular and triangular planforms oscillating harmonically in supersonic flow - Part 1
[FOK-X-449-PT-1] 13 p1471 N73-21909
ALGOL procedures for calculating velocity and pressure distribution on rectangular and triangular planforms oscillating harmonically in supersonic flow - Part 2
[FOK-X-449-PT-2] 13 p1471 N73-21910
Computer graphics for solving three dimensional lifting body potential flow nonlinear equations to determine aerodynamic loads
[DGT-7510] 13 p1474 N73-21939
Forced oscillation test equipment for measuring dynamic stability of roll velocity on lifting bodies
[AD-762258] 19 p2250 N73-28139
Analytical representation of auxiliary functions of theory for oscillating lifting surface with high aspect ratio at subsonic speeds
[DLR-FB-73-16] 21 p2492 N73-29999

**LIFTING REENTRY VEHICLES**
NT X-20 AIRCRAFT
NT X-24 AIRCRAFT
User manual for computer program of potential flow calculation about three-dimensional lifting bodies
[AD-755933] 12 p1393 N73-21292
Development of method for calculating potential flow about arbitrary lifting three dimensional bodies with emphasis on bound vorticity and application of Kutta condition
[AD-755480] 13 p1471 N73-21914
Heat transfer tests for simple delta wings at Mach numbers 8 and 10.5
[NASA-CR-131485] 13 p1591 N73-22900
Windward surface flow distribution on lifting reentry vehicle configurations at high angles of incidence under hypersonic perfect gas conditions
[AD-756499] 14 p1599 N73-22961
Development and characteristics of pitch/yaw dynamic stability, forced-oscillation test mechanism for measuring stability derivatives of lifting reentry vehicles
[AD-762286] 19 p2250 N73-28143

**LIFTING ROTORS**
Wind tunnel tests of VTOL lift fan stages to determine changes in thrust characteristics with varations in back pressure imposed on stages by cross flow
[NASA-TM-X-68169] 06 p0620 N73-15031
Numerical calculation of flow fields produced by lifting elliptic cone, lifting three dimensional wing, and lifting delta wings
[NASA-CR-131089] 10 p1139 N73-19282
Application of momentum theory to determine performance limits of propellers, and lifting rotors with axes parallel to undisturbed flow
[AD-754072] 11 p1235 N73-20025
Transonic perturbation equation for studying steady compressible flow past lifting and nonlifting wings at high subsonic Mach numbers
[NASA-CR-2246] 15 p1766 N73-24312
Actuator disk approximation for calculating lifting rotor velocity distribution in forward flight
[FFA-123] 16 p1858 N73-25051
Aerodynamic characteristics and noise attenuation effects of leading edge serrations on rotary wings
[AD-759028] 16 p1863 N73-25088

**LIFTING SURFACES**
U LIFT DEVICES
U LIFTING BODIES
U SURFACES

**LIGANDS**
Potentiometric stability data analyses for nickel, lead, and zinc organic acetate complexes
[JINR-E12-6776] 24 p2935 N73-33436

**LIGHT [VISIBLE RADIATION]**
NT AIRGLOW
NT COHERENT LIGHT
NT DAYGLOW
NT GEGENSCHEIN
NT GEOCORONAL EMISSIONS
NT LIGHT BEAMS
NT NIGHTGLOW
NT POLARIZED LIGHT
NT SKY RADIATION
NT SUNLIGHT
NT TWILIGHT GLOW
NT ZODIACAL LIGHT
Daylight and disinfectant effects on bacteria survival times on plastic surfaces
[NASA-TT-F-13923] 01 p0009 N73-10069
Diffraction of light by ultrasonic waves and intensity of diffraction spectrum
[NASA-TT-F-13926] 02 p0212 N73-11714
Using simultaneous measurements of ozone profile and solar extinction to obtain absorption coefficient for calculating ozone distribution
[AD-750404] 06 p0668 N73-15429
Device for detection of combustion light preceding gaseous explosions
[NASA-CASE-LAR-10739-1] 07 p0798 N73-16484
Assessment of luminous and spectral sensitivity and electro-optical properties of image tubes
[BARC-610] 08 p0888 N73-17194
Scattered solar radiation distribution in cloud absence by sky zones in entire spectrum, including visible and ultraviolet sections
09 p1059 N73-18637
Investigation of light flash phenomenon observed by Apollo crews
[NASA-CR-128866] 10 p1213 N73-19867
Dynamics of some characteristics of induced potential of optical region in cerebral cortex in rabbits with increasing hypoxia
11 p1244 N73-20103
Light flash observation experiments conducted by Apollo 16 astronauts - Part C
12 p1452 N73-21763
Interpretation of Apollo 16 photography of Orientale Basin deposits under earthshine illumination conditions - Part E
12 p1453 N73-21769
Micron output increase of Nd YAG laser to pump optical parametric oscillator through visible spectrum
[AD-756809] 14 p1673 N73-23577
Analysis of products and techniques for reducing reflections of light from helicopter windshields, rotor blades and rotor hub assembly
[AD-761127] 18 p2107 N73-27037
Light effects on organic matter balance of oak underwood growing in forest understorey
20 p2405 N73-29330

**LIGHT ABSORPTION**
U ELECTROMAGNETIC ABSORPTION

**LIGHT ADAPTATION**
Influence of illumination on electro-oculographic measurements of human eye potential
[AMRU-R-71-1] 02 p0131 N73-11064
Response time of flash blindness recovery in human exposure to constant energy flashes
[AD-747631] 04 p0380 N73-13095

**LIGHT AIRCRAFT**
NT BEECHCRAFT 18 AIRCRAFT
NT OH-6 HELICOPTER
NT YAK 40 AIRCRAFT
Prediction of lateral directional aerodynamic characteristics for twin engine propeller driven airplane
[NASA-TN-D-6946] 02 p0125 N73-11016
Binaural processing of speech intelligibility in light aircraft
[FAA-AM-72-31] 05 p0503 N73-14094
Design modifications to improve static performance and lateral-directional dynamic stability of light aircraft
07 p0737 N73-15996
Wind tunnel tests of full scale model of light aircraft to determine effects of configuration changes on aerodynamic characteristics
[NASA-TN-D-6896] 07 p0739 N73-16012
Analysis of response of constant-attitude aircraft to atmospheric turbulence
[NASA-CR-2204] 09 p0983 N73-18025
Analysis of factors affecting crashworthiness of light aircraft to show nature of damage to aircraft and hazards to flight crews
[FAA-TR-FS-70-592-120A] 09 p0984 N73-18032
Design of simple to fly, constant attitude light general purpose aircraft
[NASA-CR-2208] 09 p0984 N73-18037
Effects of light aircraft noise on hearing
[NASA-CR-130987] 09 p0992 N73-18095
Analysis of structural response of light aircraft to crash loadings based on dynamic buckling of discretely stiffened shells
10 p1219 N73-19910
Engine and control problems of light aircraft
14 p1600 N73-22972
Development of techniques for predicting point and path performance of light aircraft
[NASA-CR-2272] 18 p2105 N73-27022
Flight tests of light aircraft to determine detection by terminal radar observer for various conditions of flight
[FAA-NA-73-50] 20 p2452 N73-29705
Wind tunnel tests to determine effects of slot spoilers on longitudinal and lateral aerodynamic characteristics of twin engine light aircraft
[NASA-TN-D-7315] 21 p2496 N73-30033

Wind tunnel tests to determine static longitudinal, lateral, and directional characteristics of twin-engine light aircraft scale model
[NASA-TN-D-7109] 22 p2614 N73-30951
Air traffic control evaluation to determine feasibility of combining smaller aircraft into gaps on flow of normal traffic to increase effectiveness of terminal facilites
[FAA-AFS-500-1] 23 p2816 N73-32517
LIGHT ALLOYS
NT ALUMINUM ALLOYS
NT BERYLLIUM ALLOYS
NT MAGNESIUM ALLOYS
Development of experimental program for determining response and sonic fatigue resistance of lightweight aircraft structures
20 p2480 N73-29923
LIGHT AMPLIFIERS
Operation of image intensifier tubes and analysis of fluctuation theory on visual contrast sensitivity with ideal image intensifiers
[IZF-1972-18] 02 p0148 N73-11202
Design and performance of carbon dioxide laser amplifier with double discharge electrode geometry
[DREV-TN-2022/72] 10 p1134 N73-19240
Uniform distribution of illumination at output of high power amplifier
[UCRL-TRANS-10663] 17 p2063 N73-26691
LIGHT BEAMS
Atmospheric effects on laser beam propagation
[AD-746053] 01 p0066 N73-10544
Computer program for evaluating effects of conical light beams through interference filters, tilting filter, and energy distribution variations across beam
[WRE-TN-710(AP)] 04 p0449 N73-13665
Analysis of time dependent, self focusing optical beams with elliptical constant intensity contours
05 p0555 N73-14509
Birefringence properties of total reflection of light beam at separation plane
[LPTHE-72/39] 10 p1188 N73-19668
Turbulence-induced beam spread of optical beam propagating through random medium
[AD-754204] 10 p1191 N73-19689
Geometrical plot of light ray through leaf cross section using Fresnel equations and Snells law
[NASA-CR-132144] 15 p1813 N73-24695
Light beam attenuation in suspensions of algae
20 p2405 N73-29325
LIGHT BULBS
U LUMINAIRES
LIGHT COMMUNICATION
U OPTICAL COMMUNICATION
LIGHT DURATION
U PULSE DURATION
LIGHT ELEMENTS
IMP 6 measurements of light element composition of solar cosmic rays during flares of Apr. and Sept. 1971
[NASA-TM-X-65947] 09 p1080 N73-18814
LIGHT EMISSION
NT BIOLUMINESCENCE
NT CHEMILUMINESCENCE
NT ELECTROLUMINESCENCE
NT FLUORESCENCE
NT INCANDESCENCE
NT LUMINESCENCE
NT OPTICAL RESONANCE
NT PHOSPHORESCENCE
NT PHOTOLUMINESCENCE
NT THERMOLUMINESCENCE
NT X RAY FLUORESCENCE
Influence of light flashes from heavy ionizing particles on astronaut nervous system
[LBL-1011] 10 p1120 N73-19134
Fabrication of monolithic light emitting diode display system on single wafers of gallium phosphide
[AD-755204] 13 p1502 N73-22172
Nonlinear dynamic resistance and light emission associated with carrier generation by impact ionization in Gunn domains
15 p1794 N73-24543
Monolithic light emitting diode display devices
[AD-758853] 16 p1882 N73-25232
Real time measurement of three-dimensional position of light emitting diodes
[AD-762028] 19 p2241 N73-28070
Development of numerical procedures for computing true brightness of radiant energy measurements from smoothed brightness
20 p2400 N73-29289
Development and characteristics of radar receiver for detecting coherent and incoherent optical signals against background of noise
22 p2630 N73-31075
Diffuse optical emissions from interstellar gas
22 p2734 N73-31887
Aurora data from Michigan airglow payload and stellar occultation data
[NASA-CR-135718] 23 p2785 N73-32281
Light curve computations from astrophysical models of W Ursae Majoris systems
23 p2836 N73-32664
LIGHT EMITTING DIODES
Use of InGaP to develop highly efficient LED
24 p2967 N73-33711
LIGHT GAS GUNS
Scaling hypervelocity impact of glass projectiles on aluminum targets
[ISL-24/70] 01 p0036 N73-10285
Performance characteristics and prediction methods for hypervelocity light gas gun
[NASA-CR-129292] 03 p0300 N73-12450
Light gas gun generating high intensity shock waves
[ISL-6/72] 05 p0527 N73-14288
Development and test of explosively driven two-stage hypervelocity rocket launcher for use in meteoroid studies
[NASA-CR-2143] 06 p0649 N73-15272
Projectile loader for research gas gun
[AD-753008] 09 p1012 N73-18259
LIGHT INTENSITY
U LUMINOUS INTENSITY
LIGHT MODULATION
NT ULTRASONIC LIGHT MODULATION
Procedures for operating and modulating beam of laser locating devices
[AD-747003] 02 p0184 N73-11492
Half wave voltage for optimum orientation for barium sodium niobate transverse light modulator
[CRC-1229] 04 p0457 N73-13733
Projectile rotation measurement by polarized light modulation
[BMVG-FBWT-72-18] 07 p0766 N73-16225
Laser modulation mechanisms and optical communication technology
08 p0928 N73-17603
Design of light modulator for generation of periodic visual stimuli
[AD-754562] 11 p1250 N73-20149
Ultrashort pulse generation from mode locked carbon dioxide laser by resonant acoustic loss modulator
[DREV-TN-2024/72] 11 p1302 N73-20566
Operating principles and performance tests results for optical modulator system with mode locked Nd-YAG laser
[NASA-CR-130195] 11 p1302 N73-20569
Ultrawide-bandwidth laser communication system using high efficiency, single frequency lasers and optical modulators
[AD-755219] 13 p1539 N73-22468
Evaluation of image forming ability of infrared line scan system using laboratory and flight test techniques
15 p1786 N73-24476
Theoretical treatment of Schwarz-Hora effect in which electron beam passing through crystal is modulated by laser light and reproduces it on striking nonluminescent target
18 p2185 N73-27643
Properties of liquid crystals noting use in display devices, light modulation, image converters, and nondestructive testing
[LCR-DR-1-71-223/1/R] 23 p2765 N73-32125
Optical image modulation by polarization shifting diffraction gratings
[AD-765174] 24 p2959 N73-33644
LIGHT PRESSURE
U ILLUMINANCE
LIGHT PROBES
U LIGHT BEAMS
LIGHT SCATTERING
Mathematical inversion of light scattering data to obtain atmospheric ozone profile
02 p0196 N73-11586
Method for calculating intensity of scattered light from large diameter infinite ice cylinders in normal plane
[AD-747481] 03 p0338 N73-12759
Analysis of laser light scattered from marginally stable hydrogen plasma
[INR-P-1377] 04 p0429 N73-13491
Glow from light scattering in gas jets of space vehicle microengine
04 p0466 N73-13801
Light scattering technique for studying Brownian particles
[AD-750110] 06 p0701 N73-15716
Differential light scattering patterns for identifying different species of bacteria
08 p0875 N73-17090
Laser scattering from curved aluminum and titanium aircraft surfaces in clear atmosphere
08 p0884 N73-17159
Nephelometer design and data on total light scatter and backscatter component of extinction of light due to aerosols
08 p0899 N73-17281
Matrix solution for one dimensional model of radiation field arising from multiple scattered photons in planetary atmosphere
[NASA-CR-130755] 08 p0943 N73-17722
Frequency spectrum of laser scattering from dense plasma focus
[AD-753705] 09 p1073 N73-18754
Bremsstrahlung for enhancing far infrared laser scattering from theta pinch plasma
[AD-753404] 09 p1073 N73-18755
Transmission of light through randomly scattering medium
[AD-754074] 11 p1325 N73-20752
Critical scattering of laser light by thin fluid films
[COO-2203-1] 12 p1410 N73-21428
Thermodynamics of light scattering from Eulerian fluid, and electron scattering by atomic hydrogen
13 p1558 N73-22627
Stimulated and spontaneous scattering of electromagnetic radiation
[AD-757082] 13 p1559 N73-22639
Literature survey of articles dealing with all aspects of predicting, measuring, and controlling unwanted scattered light in large space telescopes
[NASA-CR-124240] 14 p1667 N73-23531
Green function for analyzing light scattering in crystals
[AD-757070] 14 p1693 N73-23741
Mesospheric diffuse skylight measurement onboard Centaure sounding rockets launched from Kiruna during August 1969
[ISL-16/72-PT-1] 15 p1781 N73-24439
Measurements of density, temperature, and velocity in gas dynamics using light scattering techniques
[AD-759575] 16 p1890 N73-25299
Multispectral remote sensing techniques for measuring light absorption, scattering, and particle concentrations in water
[AD-759668] 16 p1914 N73-25491
System for measuring scattered flux from fine grained photographic emulsions
16 p1921 N73-25548
Mesospheric scattered sunlight measured during twilight from ESRO Centaur rocket photoelectric polarimeters
[AP-8] 18 p2172 N73-27547
Scattering of polarized light by rough and smooth leaf surfaces
20 p2405 N73-29333
Feasibility analysis of nonradiating flow in wind tunnels using light scattering experiments
[BMBW-FBW-72-20] 21 p2580 N73-30677
Laser anemometer self aligning reference beam method for measurement of three flow velocity components, with reference beam produced by scattering
[REPT-3/1972] 22 p2674 N73-31423
Ultrasound and light scattering in diffusing and chemical reacting binary mixture of fluids
23 p2774 N73-32185
Carbon dioxide laser scattering by Alfvenic disturbance in helium plasma
23 p2822 N73-32560
Inelastic light scattering from molecular gases with applications to remote detection of air pollutants
24 p2891 N73-33077
Analyzing behavior of instantaneous point source as it disperses in thick, neutrally stratified, turbulent shear layer by laser light scattering technique
24 p2904 N73-33176
Scattering of ruby laser beam by plasma focus of coaxial gun
[CEA-R-4430] 24 p2931 N73-33411
Effect of ocean depth on light scattering and attenuation parameters to include optical properties influenced by concentration, size, and shape of particulate matter
24 p2957 N73-33626
Mathematical theories for determining light propagation by sea water
24 p2957 N73-33627
Light scattering by particles in sea water based on volume scattering function and point spread function
24 p2957 N73-33628
Measurement of light scattering at various angles using point spread function and modulation transformation function techniques
24 p2957 N73-33629
Effect of various parameters on long range underwater vision for narrow and broad beam illumination
24 p2958 N73-33630
Application of Fourier techniques to calculate spread of scattered light for circular spot, Gaussian profile, and linear stripe cases
24 p2958 N73-33632
Measurement of turbulence in collisionless oblique plasma shock by scattered ruby laser light
24 p2961 N73-33665
Correction of observed penumbral intensities for scattered light
[NP-19732] 24 p2977 N73-33787
LIGHT SOURCES
NT ILLUMINATORS
High resolution attitude sensor for sensing spacecraft attitude relative to light source
[NASA-CASE-LAR-10586-1] 02 p0174 N73-11406
Analysis of resolvability of point sources of incoherent light by quantum detection, decisions of observers, and error probability
[NASA-CR-130129] 04 p0449 N73-13663
Computer program for calculating constant dose range in air transport of neutron and photon radiation from point source in atmosphere
[LA-DC-13293] 04 p0453 N73-13700

Development of temperature compensated light source with components and circuitry for maintaining luminous intensity independent of temperature variations
[NASA-CASE-ARC-10467-1] 05 p0518 N73-14214
Michelson and Fabry-Perot interferometers with light sources of Gaussian and Lorentzian spectral distribution
[KFKI-72-62] 10 p1159 N73-19432
Interferometer prism and control system for precisely determining direction to remote light source
[NASA-CASE-ARC-10278-1] 16 p1911 N73-25463
Design of high intensity atomic emission line sources in vacuum ultraviolet region for atmospheric gas trace detection
[AP-11] 17 p2034 N73-26459
Glacing incidence telescope for evaluating polarization of light source
18 p2210 N73-27840
Xenon lamp light sources for plant growth research
20 p2403 N73-29314
Development of nitrogen-laser-pumped tunable-dye laser for application as spectroscopic light source
20 p2424 N73-29473
Utilization of solar rays as internal light sources in architectural designs
24 p2975 N73-33771

**LIGHT SPEED**
Interferometric investigation of anisotropy in light speed
10 p1187 N73-19661

**LIGHT TRANSMISSION**
NT LIGHT SCATTERING
Transmission characteristics of commercially available, laser eye protectors with Cary 14 spectrophotometer
[AD-746293] 02 p0136 N73-11100
Two channel infrared scanning, display, and recording system for measuring varying atmospheric effects on image transmission
[AD-747053] 02 p0176 N73-11425
Shortwave propagation medium with random heterogeneities in approximate Markovian random process
[AD-746714] 02 p0203 N73-11644
Dual channel, 10.6 micron infrared scanner system
[AD-747052] 02 p0213 N73-11724
Scintillation reductions in multiwavelength laser propagation by near field transmitter apertures
[AD-747640] 03 p0337 N73-12751
Effects of turbulence instabilities on laser propagation
[AD-748809] 04 p0450 N73-13677
Modulation transfer function of atmospheric medium as function of light wavelength
[AD-751641] 07 p0796 N73-16471
Flint glass objective prism recommended for ESO Schmidt camera due to light transmission properties
07 p0845 N73-16847
Optical transmission measurements of single crystal and polycrystal CsI
[NASA-TM-X-66178] 08 p0951 N73-17784
Technique for determining atmospheric transmittance of coherent light between two points in terrestrial atmosphere for selected laser frequencies
[AD-753075] 09 p1030 N73-18412
High resolution transmittance curves for spectral region 320 to 1400 wavenumbers and attenuation of CO2 laser radiation
[AD-753076] 09 p1043 N73-18511
Transport equations for studying radiative transport through dense plasma
[AD-753245] 09 p1072 N73-18753
Penetration and transmission of light in sea water
[AD-753029] 10 p1156 N73-19409
Light and infrared radiation propagation and absorption in atmosphere
[AD-753974] 10 p1158 N73-19418
Measurement of stimulated emission cross section of neodymium laser based on laser threshold gain and inverted population
[AD-753901] 10 p1170 N73-19514
Variation of laser radiation intensity along axis of unstable optical cavity with partially transmitting mirrors or gratings
[AD-753902] 10 p1170 N73-19515
Turbulence-induced beam spread of optical beam propagating through random medium
[AD-754204] 10 p1191 N73-19689
Transmission of light through randomly scattering medium
[AD-754074] 11 p1325 N73-20752
Low temperature optical absorption of some unusual intermetallic compounds
12 p1438 N73-21646
Dispersion of light intensity logarithm along axis of laser beam propagating in atmosphere
[AD-756094] 13 p1539 N73-22470
Monte Carlo studies of light transport through natural atmospheres
[AD-757494] 14 p1661 N73-23486
Laser beam propagation in turbulent air
[AD-757221] 14 p1673 N73-23574
Analysis of acoustical amplitude and frequency modulation techniques of continuous wave helium-neon laser for optical communication applications
[AD-757672] 14 p1674 N73-23581
Green function for analyzing light scattering in crystals
[AD-757070] 14 p1693 N73-23741
Phase difference temporal spectra measurements of laser beams
[AD-757915] 15 p1795 N73-24553
Development of Mach-Zehnder interferometer theory based on time history of wave front produced by element of extended light source
[ARC-R/M-3173] 16 p1856 N73-25033
Approximate methods for solving spherical transfer equation in spherical case
[AD-759392] 16 p1910 N73-25453
Diffuse reflectance theory for estimating optical absorption coefficients of aerosol particles collected on filter surface
[AD-759490] 16 p1946 N73-25744
Ultrashort optical pulse propagation through resonant media
[AD-762209] 19 p2309 N73-28569
Proceedings of conference on actinometry and atmospheric optics to include effects of solar radiation and atmospheric light on photosynthesis
[TT-70-50159] 20 p2399 N73-29280
Effect of transverse pumping distribution on energetics and profiles of thermo-optical distortions of laser in solution of rhodamine dye
[NLL-M-23052-[5828.4F]] 20 p2424 N73-29472
Effect of atmospheric turbulence on stability of laser radiation propagation
[AD-763109] 20 p2427 N73-29494
Atmospheric infrared transmission spectral analysis discussing computed and measured data, and absorption due to atmospheric components
[BMVG-FBWT-73-11] 23 p2787 N73-32297
Monte Carlo calculations of polarization of radiation in earth atmosphere and ocean
[AD-764622] 23 p2789 N73-32313
Salinity effects on extinction coefficient of sea ice
[AD-763882] 24 p2924 N73-33355
Proceedings of conference on electromagnetic and optical properties of sea water for application to surveillance, mapping, communications, and visibility
[AGARD-LS-61] 24 p2956 N73-33619
Radiance distribution as function of depth in upper layers of ocean and numerical analysis of inherent and apparent optical properties
24 p2957 N73-33621
Optical properties of pure and turbulent sea water
24 p2957 N73-33624
Effect of ocean depth on light scattering and attenuation parameters to include optical properties influenced by concentration, size, and shape of particulate matter
24 p2957 N73-33626
Light scattering by particles in sea water based on volume scattering function and point spread function
24 p2957 N73-33628
Effect of various parameters on long range underwater vision for narrow and broad beam illumination
24 p2958 N73-33630
Application of Fourier techniques to calculate spread of scattered light for circular spot, Gaussian profile, and linear stripe cases
24 p2958 N73-33632
Application of incoherent and coherent light sources for underwater illumination and comparison of efficiency for various conditions
24 p2958 N73-33633

**LIGHTHILL METHOD**
Application of conformal mapping procedures for designing airfoil shapes with high design lift coefficients
[AD-757813] 15 p1731 N73-24040

**LIGHTING**
U ILLUMINATING

**LIGHTING EQUIPMENT**
NT AIRPORT LIGHTS
NT ARC LAMPS
NT FLASH LAMPS
NT ILLUMINATORS
NT LUMINAIRES
NT MERCURY LAMPS
NT QUARTZ LAMPS
NT RUNWAY LIGHTS
NT XENON LAMPS
Design, development, and evaluation of airport lighting control panel for airport traffic control towers
[FAA-RD-72-93] 03 p0260 N73-12108
Illuminance measurement of two types of airborne flares
[DREV-R-673/72] 10 p1223 N73-19942
Flashlight adaptation of ultraviolet source for illuminating fluorescent map
[AD-755435] 12 p1429 N73-21585
Apollo experience report on lighting requirements for Apollo command and lunar modules for internal and external lighting
[NASA-TN-D-7290] 16 p1964 N73-25887

**LIGHTNING**
NT BALL LIGHTNING
Small rocket wire deployment for simulating electrical properties of large rocket engine to study lightning triggering or diversion
[AD-746309] 01 p0078 N73-10644
Measuring electric field intensities of lightning strokes for determining lightning channel currents
[NASA-CR-2161] 02 p0205 N73-11658
Number and distribution of lightning flashes in Finland during summer 1971
[REPT-41] 04 p0413 N73-13371
Papers presented at conference on lightning and static electricity
[AD-752551] 08 p0922 N73-17552
Performance of lightning and surge suppressors for digital transmission equipment
[AD-752448] 09 p1004 N73-18195
Apparatus for determining distance to lighting strokes from single station by magnetic and electric field sensing antennas
[NASA-CASE-KSC-10698] 11 p1254 N73-20175
Probability of aircraft being struck by lightning
[NLL-M-22800-[5828.4F]] 11 p1313 N73-20656
Characteristics of three station network for sensing magnetic and electric fields associated with lightning discharges
[NASA-CR-133400] 18 p2151 N73-27382
Lightning flash counter measurements in Finland during 1972
[REPT-43] 20 p2412 N73-29390
Bibliography of lighting theory, instrumentation, and protection
[AD-763667] 21 p2540 N73-30366
Systems for protection of low altitude tethered balloons from effects of atmospheric electricity
[AD-764651] 23 p2746 N73-31978
System for locating lightning strokes by coordination of directional antenna signals
[NASA-CASE-KSC-10729-1] 23 p2763 N73-32110
Sources of energy for ball lightning
[NASA-TT-F-15097] 23 p2786 N73-32289
Monitoring and recording lightning strokes in predetermined area
[NASA-CASE-KSC-10728-1] 23 p2790 N73-32319

**LIGHTS**
U LUMINAIRES

**LIMB DARKENING**
Spectrophotometric analyses of Jovian and Saturnian limb darkenings
[NASA-CR-131891] 13 p1576 N73-22772
Observations of atmospheric limb darkening in visual continuium and multiple scattering analysis of jupiter and saturns atmospheres
22 p2713 N73-31719

**LIMBS [ANATOMY]**
NT HAND [ANATOMY]
Feasibility of limb controlled astronaut maneuvering scheme
18 p2110 N73-27063

**LIME**
U CALCIUM OXIDES

**LIMITATIONS**
U CONSTRAINTS

**LIMITER AMPLIFIERS**
Frequency limited amplifier for proportional counter pulse shape and pulse height control
[NLL-WH-TRANS-343-[9091.9F]]
15 p1755 N73-24227
Performance of prototype broadband selective ferrite limiters
[AD-759951] 17 p2005 N73-26219

**LIMITER CIRCUITS**
Operating theory and measured results of yttrium-iron garnet frequency selective limiter under varying signal environments
[AD-760817] 18 p2124 N73-27165
Design and performance of semiconductor limiters for microwave isolation
[AD-762168] 20 p2463 N73-29794
Signal to noise ratios in coherent bandpass limiters
[NASA-CR-135781] 23 p2765 N73-32122

**LIMNOLOGY**
ERTS-1 imagery of structures and lithology of Northern California Coast Ranges and Sacramento Valley, California
[E72-10214] 03 p0288 N73-12332
Land use mapping, limnology, wetlands, geomorphic and landform surveys, and river monitoring of Lake Champlain Basin and Vermont using ERTS-1 imagery
[E72-10282] 03 p0292 N73-12380
Utilization of ERTS-1 imagery for study of hydrology and limnology in Finland
[E73-10101] 09 p1020 N73-18323
ERTS-1 imagery of Utah and Nevada to show structural geology, mineral exploration, limnology, and hydrology
[PAPER-G3] 19 p2263 N73-28235

**LINCOLN EXPERIMENTAL SATELLITES**
Design of solar ephemeris synthesizer for LES-8/9 stationkeeping system
[AD-752250] 08 p0965 N73-17891

Equations of motion for Lincoln Experimental Satellites with gimbaled momentum wheel and gyroscope to analyze attitude control dynamics
[AD-765548] 24 p2986 N73-33867

LINE SPECTRA
NT BALMER SERIES
NT D LINES
NT ELECTRONIC SPECTRA
NT FRAUNHOFER LINES
NT H ALPHA LINE
NT H BETA LINE
NT H GAMMA LINES
NT H LINES
NT K LINES
NT TELLURIC LINES

Absorptive losses in carbon monoxide laser emission lines
[AD-746170] 02 p0182 N73-11479

Atomic line shapes, shifts, and broadening - bibliography for 1889 through Mar. 1972
[NBS-SP-366] 02 p0214 N73-11732

Error analysis of line intensity measurements on plasmas with electron temperature fluctuations
[AD-748474] 04 p0456 N73-13722

Line spectra analysis for temperature distribution in stellar atmosphere
04 p0466 N73-13793

Ground based line spectra analyses for determining stellar chromospheres
04 p0466 N73-13795

Spaceborne ultraviolet emission lines in stellar sources as chromospheric indicators
04 p0466 N73-13796

Electron paramagnetic resonance spectra of trivalent titanium ions in used silica
[NLL-RTS-7523] 05 p0564 N73-14583

Line spectra and spectral energy distribution of early type stars
05 p0594 N73-14829

Computer programs for curve-of-growth analysis using dimensions of stellar lines as input
[ROY-OBS-BULL-171] 06 p0644 N73-15230

Gas laser measurements of absorptive losses introduced by water vapor and carbon dioxide for laser emission lines in 7-6 to 10-9 vibrational bands
[AD-749823] 06 p0681 N73-15542

Spectral line thickness and temperature distribution in inhomogeneous sodium plasma confined between parallel mirrors
[INR-1388] 06 p0705 N73-15751

Chemical composition and abundance of alpha Centauri visual binary determined from spectral lines
[ROY-OBS-BULL-173] 06 p0719 N73-15870

He-Xe tunable laser measurement of infrared line shape and CO2 absorption spectra
[AD-751230] 07 p0808 N73-16556

Aerobee-borne spectrometer/monochromator for advanced studies of solar X-ray line emissions and preliminary results
[NASA-CR-130359] 07 p0838 N73-16793

Theory of gamma ray line emission from solar flares
[NASA-TM-X-66165] 07 p0839 N73-16797

Chemical composition of line spectra for binary alpha Centauri and determination of abundances
[BULL-173] 07 p0842 N73-16820

Hyperfine electron density fluctuation in stabilized hydrogen arc laser
08 p0943 N73-17723

Electron spin overlap model for quantitative analyses on magnetic spectra of coordination compounds with unpaired electrons
08 p0945 N73-17740

Aerobee rocket observation of ultraviolet line spectra of Delta Scorpii and Zeta Ophiuchi
08 p0958 N73-17838

Line source beneath free surface of semi-infinite fluid
[AD-753140] 09 p1018 N73-18311

Dispersive explanation of spectral behavior of Runge mode locked dye laser
[AD-753408] 09 p1044 N73-18516

Time development of line radiation emitted from plasma produced by Q switched ruby laser onto magnesium target
[AD-755119] 11 p1328 N73-20775

Solar X ray based calculations of K alpha line emission from sulfur, argon, calcium, and iron
[NASA-TM-X-66210] 11 p1335 N73-20839

Rocket-borne instrument detection of X ray flux from iron line of Cassiopeia A
[NASA-TM-X-66216] 11 p1336 N73-20843

Infrared stars with strong 1665-1667-mHz main-line OH emission
[AD-753898] 12 p1459 N73-21821

Hyperfine formaldehyde lines in molecular dust cloud L1436
[AD-757689] 15 p1833 N73-24861

High frequency plasma line fluctuation for ionospheric heating analysis
[AD-758779] 16 p1907 N73-25433

Spectral line features of neon beam-foil spectroscopy
16 p1947 N73-25752

Balloon measurement of gamma ray emission from region of galactic center
16 p1959 N73-25844

Radio recombination line emission from galactic H 1 and H 2 regions
16 p1961 N73-25863

Design of high intensity atomic emission line sources in vacuum ultraviolet region for atmospheric gas trace detection
[AP-11] 17 p2034 N73-26459

Spectroscopic observation of Nova Delphini 1967 in gamma gamma 4,000 to 9,000 region
17 p2080 N73-26825

Methane spectral line formation in Jovian atmosphere
17 p2080 N73-26826

Spectroscopic observation of metastable helium line in alpha-orionis and interstellar media
17 p2081 N73-26830

Fluorescent lamp discharge parameter effects on mercury resonance lines
[AD-760958] 18 p2183 N73-27627

Chromium concentration effect on duration and width of luminescent lines in ruby spectrum
[AD-761374] 18 p2191 N73-27692

Analysis of X ray data obtained during solar flares
[NASA-CR-133341] 18 p2195 N73-27721

Mathematical formulation of physically correct contribution function for spectral lines
[AD-758770] 18 p2198 N73-27749

Molecular absorption coefficients for H20-N2 mixtures as measured by Co laser
[AD-760140] 19 p2308 N73-28561

Atmospheric absorption line parameters for infrared-active molecules occurring naturally in terrestrial atmosphere
[AD-762904] 21 p2542 N73-30382

Computer program for determining rotational line intensity of diatomic molecules -users manual
[NASA-TN-D-7268] 21 p2582 N73-30689

Aperture synthesis in interstellar neutral hydrogen line
21 p2594 N73-30782

Line strengths in spectra of seven double-lined Am binary stars
[BULL-177] 21 p2596 N73-30803

Observations of recombination line emission in direction of supernova remnants
[AD-762002] 21 p2598 N73-30825

Water vapor absorption by highly attenuated CO laser lines
[AD-764376] 22 p2682 N73-31485

Intensity of EPR line spectra as affected by indium doped zinc oxide
[AD-764490] 22 p2708 N73-31684

Sulfur line density in spectrographic scan of Orion nebula
22 p2734 N73-31888

Atomic oxygen emission line in high resolution spectra of zenith day airglow
23 p2778 N73-32214

Structural and spectral studies of sunspots
[NASA-CR-135787] 24 p2975 N73-33776

LINEAMENT
U STRUCTURAL PROPERTIES [GEOLOGY]

LINEAR ACCELERATORS
Beam current monitoring system and performance for linear accelerator
[AD-745841] 01 p0038 N73-10299

PDP 8 computer control of linac system used in photonuclear experiments
[CEA-N-1527] 03 p0302 N73-12466

Problems involved with construction of Silund high current induction linear accelerator of nanosecond range
[AD-749613] 05 p0524 N73-14265

Measurement of accelerator tube and waveguide system parameters for improving linear accelerator performance
[RISO-M-1518] 07 p0766 N73-16223

Computerized positron scintillation camera data acquisition and display system for linear accelerator facility
[UCRL-51288] 10 p1161 N73-19447

LINEAR AMPLIFIERS
Scattering characterization inputs in computerized design of wideband linear amplifiers for pulse operation
[LBL-772] 07 p0762 N73-16188

Computer-controlled fine attenuators for fine gain adjustments of linear amplifiers
[KFK-1707] 20 p2381 N73-29130

LINEAR ARRAYS
Measured element factor of linear array for various waveguide radiating elements
[PHL-1973-1] 14 p1639 N73-23287

Influence of flare shapes on element factors and gain as function of scan angle of 40 element linear array at superhigh frequencies
[PHL-1973-10] 14 p1639 N73-23288

Approximative gain calculations for linear and rectangular arrays using vertically directed noise model
[AD-760690] 18 p2119 N73-27133

LINEAR EQUATIONS
Library of numerical linear algebra programs
[AD-745430] 01 p0072 N73-10588

Volterra factorization of Green matrix and imbedding of general linear boundary value problems
[TR-72-48] 02 p0202 N73-11634

Iterative solution for characteristic exponents of linear differential equations with periodic coefficients
[ARC-CP-1218] 03 p0324 N73-12642

Computer programs for solution of systems of linear algebraic equations
[NASA-CR-2173] 08 p0887 N73-17181

Numerical solution of linear differential equations describing dynamic response of vehicles
[TT-7212-PT-1] 08 p0937 N73-17669

Linear differential equations for analyzing viscoelastic properties and mechanical behavior of high polymers
08 p0966 N73-17898

Definitions of linearizable objects and applications in differential games of pursuit
09 p1056 N73-18610

Gradient methods for solving incompatible systems of linear equations of higher order in photomapping problems
10 p1178 N73-19584

Liapunov solutions to linear differential equations with periodic coefficients
[NASA-TT-F-14835] 10 p1179 N73-19588

FORTRAN program for solution of large, sparse unsymmetric systems of linear equations
[AD-755878] 13 p1550 N73-22563

Existence and representation of diophantine and mixed diophantine solutions to linear equations and inequalities
[AD-763384] 21 p2566 N73-30570

The prediction of instabilities of linear differential equations with periodic coefficients
[ARC-R/M-3713] 24 p2945 N73-33518

LINEAR FILTERS
NT KALMAN FILTERS

Linear filtration effect on correlation properties of phase manipulated signals
12 p1378 N73-21175

Integral equation for calculating influence of linear channels on correlation processing of noise signals
12 p1378 N73-21180

Mathematics of linear predictive filtering and application to speech analysis and synthesis
[AD-765176] 24 p2896 N73-33117

LINEAR PREDICTION
Predictive display with continuous parameter tracking for quasi-linear model of human pilot transfer function in closed loop system
01 p0015 N73-10120

Description of maneuvering aircraft trajectory by second-order non-Gaussian process verified by digital simulation
[TAE-167] 14 p1683 N73-23656

Linear estimation technique for enhancement of black and white images
[AD-760779] 18 p2180 N73-27601

LINEAR PROGRAMMING
Heuristic algorithm for mixed integer linear programming problems
[NPL-NAC-18] 02 p0202 N73-11637

Simplex method for linear programming problem solving with explanation of terminology
[NPL-NAC-19] 02 p0202 N73-11638

Constrained n-person games, using extremal [linear programming] principle
[AD-746553] 02 p0203 N73-11645

Multi-terminal network flow realizability, analysis, and synthesis
[AD-748773] 04 p0441 N73-13595

Minimax approximation to frequency responsive nonrecursive digital filter
[AD-750767] 06 p0648 N73-15263

Algorithm for solving pure integer linear programming problem
[NPL-NAC-20-PT-1] 09 p1057 N73-18621

Linear programming for design of large flexible launch vehicle autopilots
[NASA-CR-124124] 10 p1183 N73-19621

Users manual for COEBRA program for design of launch vehicle autopilots
[NASA-CR-124125] 10 p1183 N73-19622

Linear programming and its application to pattern recognition problems
[REPT-9] 20 p2437 N73-29574

Generation and propagation of numerical error in fractional integer program
[AD-763206] 22 p2640 N73-31162

Spline smoothing of histograms by linear programming
[NASA-CR-133987] 22 p2691 N73-31551

Application of mathematics to general job-shop scheduling noting criteria, procedures, and linear programming
[LAAS-OD-73-I-21] 23 p2813 N73-32488

Statistical analysis of computational round-off errors associated with cutting plane solution ot linear integer programming problems
[NASA-TN-D-7457] 24 p2945 N73-33517

**LINEAR SYSTEMS**
Adaptive control of linear, noisy systems using two controllers
[AD-746679] 02 p0151 N73-11227
Discrete control of linear distributed systems with specific application to primary mirror for orbiting astronomical observatory
[NASA-TM-X-68855] 02 p0173 N73-11400
Full order adaptive observer for single-input single-output continuous differential system with unknown parameters
[NASA-CR-129172] 02 p0195 N73-11574
Full order adaptive observer for single input, single output, stable, linear differential systems
[NASA-CR-129193] 02 p0195 N73-11575
Application of stochastic inverse theory for solutions to linear system of integral equations representing reduced gross earth data
02 p0201 N73-11621
Bang-bang controller operating in chatter mode for disturbance regulation in linear system
[AD-745896] 02 p0203 N73-11643
Identification of unknown parameters of multiple input/output, linear, constant, discrete time system from measurements made on inputs and outputs
[AD-747693] 03 p0325 N73-12653
Subroutines for estimating linear system parameters by matrix methods
[LAAS-AS-72-I-14] 04 p0394 N73-13204
FM distortion and FASP computer program for design and analysis of linear dynamic systems
[NASA-CR-130272] 07 p0754 N73-16125
Singular perturbation approach to stability analysis of linear time varying systems
07 p0761 N73-16180
Oscillation and nonoscillation in solutions of standard linear sets of differential equations
[NASA-TT-F-14809] 08 p0937 N73-17672
Computation of optimal output-feedback compensators for linear time-invariant systems
[NASA-CR-130988] 09 p1056 N73-18607
Algorithm for adjusting linear and nonlinear classifiers
[BMVG-FBWT-72-5] 09 p1057 N73-18623
Family of m-ary linear feedback shift register with binary logic
[NASA-CASE-NPO-11868] 11 p1264 N73-20254
Abstract algebraic techniques to determine synchronization properties of binary, linear, and maximal length sequences
[AD-744101] 13 p1550 N73-22560
Algorithm for determining frequency response of linear control system
[TT-7304] 14 p1683 N73-23654
Application of multipoint excitation for helicopter structural dynamic testing using impedance techniques - Vol. I
[AD-756389] 14 p1716 N73-23921
Linear shift-invariant image preprocessing technique for multispectral scanners
[NASA-CR-132957] 15 p1787 N73-24485
Space-variant image motion degradation and restoration in linear incoherent optical systems
15 p1812 N73-24687
Analysis and design of closed loop control for slowly time-varying linear systems for space shuttle booster
[NASA-CR-128972] 16 p1966 N73-25905
Dual finite element and shell theory analyses of linear and nonlinear structures
[AD-758790] 16 p1970 N73-25933
Adaptive control for multivariable systems using reduced dynamic ordering
[NASA-CR-133429] 19 p2314 N73-28607
Parameter plane methods for linear systems with time delay
[AD-761761] 19 p2314 N73-28611
Optimal compensation of linear multivariable systems with structurally constrained dynamic compensators
22 p2690 N73-31548
Formulation of system and sensor configuration control problem for class of linear stochastic systems corrupted by Gaussian noise
22 p2690 N73-31549
Development of procedures for simultaneous structure and parameter identification of linear dynamical systems
[TAE-173] 23 p2854 N73-32808
Analysis of linear systems to show characteristics and to evaluate distortion on basis of quadratic criteria
24 p2944 N73-33515

**LINEAR TRANSFORMATIONS**
Linear vector space theory used to develop general representation of random vectors and data sets
[NASA-TR-R-398] 09 p1057 N73-18620
Correlation processing of phase modulated signals
14 p1619 N73-23115
Structure identification of multivariable stochastic systems
[TR-31] 17 p2054 N73-26614

**LINEARITY**
Symplectic matrices and structures of sets of unstable canonical systems with periodic coefficients
[NASA-TT-F-14810] 11 p1311 N73-20639
Linear stabilization of flat diffusion gas flame
[AD-754049] 11 p1350 N73-20952
Infinum principle with nonscalar-valued performance criterion
[NASA-CR-132052] 15 p1804 N73-24617

**LINEARIZATION**
Definitions of linearizable objects and applications in differential games of pursuit
09 p1056 N73-18610
Method and application of linearizing characteristics of thermistor element
[NLL-M-22863-(5828.4F)] 11 p1291 N73-20479
Application of computerized series manipulation system to planetary theory using recursive linearization
12 p1447 N73-21715
Digital linearization of turbulent channel flow measurements by hot-film sensor
[REPT-2/1973] 13 p1510 N73-22234
Linear preprocessing point spread function for optimal image restoration filter
[NASA-CR-131588] 13 p1559 N73-22634
Modulation transfer functions for linear image formation with partially coherent light
15 p1812 N73-24689
Parametric linearization for approximating dynamic and thermal boundary layers for nonNewtonian fluids with arbitrary pressure and surface temperature gradients
[AD-764170] 22 p2655 N73-31271
Linear and nonlinear theory of Hall current instability
24 p2962 N73-33667

**LINES [GEOMETRY]**
Computer subroutine for drawing networks of latitude and longitude lines by plotter
[EDFB-IBP-72-7-PT-2] 06 p0667 N73-15421

**LING-TEMCO-VOUGHT AIRCRAFT**
NT A-7 AIRCRAFT
NT F-8 AIRCRAFT
NT XC-142 AIRCRAFT

**LING-TEMCO-VOUGHT MILITARY AIRCRAFT**
U MILITARY AIRCRAFT

**LINGUISTICS**
NT MACHINE TRANSLATION
NT PHONEMES
NT PHONEMICS
NT SENTENCES
NT SYLLABLES
NT SYNTAX
NT WORDS [LANGUAGE]
System of morphemic decomposition for improvement in Braille transcription
14 p1621 N73-23128
Automatic speech recognition program to provide segmentation, acoustical parameters, and phonetic feature classifications in speech
14 p1623 N73-23146
Model of speech production mechanism based on anatomical structures and physiological natures of articulatory organs
14 p1624 N73-23153
Generative model for prosody of connected speech in Japanese
14 p1624 N73-23154
Principles for regulation of timing in speech
14 p1624 N73-23155
Linguistic and perceptual role of syntactic hypotheses in speech recognition systems
14 p1625 N73-23168
Segmentation and classification of speech using low Q single-tuned filters
14 p1631 N73-23220
Advantages and disadvantages of using computers in engineering linguistics
[JPRS-59397] 18 p2213 N73-27870
Nature, investigative instrumentation, and practical application of speech and linguistics
[AD-762373] 19 p2237 N73-28036

**LININGS**
NT ROCKET LININGS
Performance prediction for acoustically lined engine nacelle design
03 p0250 N73-12019
Installation of stainless steel lining to stop water leakage from 2MV HOR swimming pool reactors
[IRI-131-72-01] 03 p0334 N73-12723
Shock wave attenuation in foam water mixtures containing Freon and exposed to hydraulic impact
[AD-748330] 04 p0407 N73-13318
Plastic coatings for lining hydrostatic bearings
[AD-750525] 06 p0690 N73-15614
Analysis of combustion liner wall temperatures under steady-state and convective heat balance conditions and comparison with experimental values
[NASA-TM-X-2711] 06 p0730 N73-15959
Fracture control method for composite tanks with load sharing liners
[NASA-CR-120918] 19 p2348 N73-28889
Component design and draw tooling of Pt heat source liner bodies
[MLM-1972] 24 p2955 N73-33608

**LINKAGES**
Screw calculus in kinematic and power analyses on spatial positions of manipulator link mechanisms
17 p1990 N73-26092
Development of mechanical linkage for lifting pin-supported electronic packages from electronic circuit boards without damage to connector pins
[NASA-CASE-NPO-13157-1] 17 p2036 N73-26475

**LINKING**
U JOINING

**LIP READING**
Lipreading aid indicating voice/voiceless feature, using visual or tactile sense
14 p1626 N73-23179
Improved indication of stops, using transposer as lip reading aid
14 p1626 N73-23180

**LIPIDS**
NT LIPOPROTEINS
Effects of Apollo 12 lunar materials on lipid levels, including fatty acids and sterols, of tobacco tissue and slash pine cultures
[NASA-CR-128606] 01 p0008 N73-10063
Blood lipid diagnostic and therapeutic measures to prevent heart disease in humans
08 p0874 N73-17073
Absorption of bile acids and cholesterol by polymers
10 p1227 N73-19976

**LIPOPROTEINS**
Blood lipid diagnostic and therapeutic measures to prevent heart disease in humans
08 p0874 N73-17073

**LIQUEFACTION**
Role of gravity-induced free convection upon liquefaction dynamics of cylindrical paraffin slab under normal gravity conditions
[NASA-CR-129911] 04 p0385 N73-13131

**LIQUEFIED GASES**
NT LIQUID AMMONIA
NT LIQUID HELIUM
NT LIQUID HYDROGEN
NT LIQUID NITROGEN
NT LIQUID OXYGEN
Tables of pressure, volume, density, and temperature for liquid states of oxygen, nitrogen, argon, and parahydrogen
[NBS-TN-361-REV] 04 p0386 N73-13139
Design, development, and tests of liquid diborane
[NASA-CR-130303] 06 p0676 N73-15502
Density of liquid Freon 11 at 200 C and 8.18 to 195.46 atm pressure
[AD-752863] 09 p1000 N73-18160
Physical properties of liquid He-4, characteristics of He-1 and -2, and Fontaine effect
[FRNC-CONF-48] 10 p1126 N73-19171
Specific impulse of auxiliary rocket thrusters using liquefied gases
[NASA-TT-F-14878] 12 p1444 N73-21694
Calculation of heat of evaporation of liquid chlorine into calorimeter for rocket propulsion
[AD-755894] 12 p1466 N73-21874
Evaluation of materials for ball bearings intended for use in liquid fluorine and/or FLOX
[NASA-CR-120820] 16 p1917 N73-25516

**LIQUID AIR**
Low temperature addition reactions of hydrogen and oxygen atoms with chemical compounds through creation of secondary valence
[NASA-TT-F-14643] 06 p0703 N73-15729

**LIQUID ALLOYS**
Thermotransport in liquid alkali metal alloys as function of composition
[COO-841-29] 24 p2992 N73-33915

**LIQUID AMMONIA**
Removal of lithium from 1040 C aged tantalum alloy by liquid ammonia and vacuum distillation techniques
[NASA-TM-X-2775] 11 p1305 N73-20590
Stress corrosion cracking of steels in liquid ammonia environments
24 p2932 N73-33420

**LIQUID BEARINGS**
Design and evaluation of hybrid boost bearings consisting of fluid film bearing coupled with rolling element bearing
[NASA-CR-2226] 09 p1039 N73-18476
Development of spherical, hydrostatic, compliant bearing for directional gyroscope
11 p1318 N73-20695
Fatigue life of hybrid antifriction bearings at ultrahigh speeds
[NASA-CASE-LEW-11152-1] 23 p2795 N73-32359

**LIQUID BREATHING**
Design and performance of demand regulated liquid breathing systems for mammalian respiration
13 p1478 N73-21976

**LIQUID COOLED REACTORS**
NT ADVANCED SODIUM COOLED REACTOR
NT BOILING WATER REACTORS
NT HEAVY WATER REACTORS
NT LIQUID METAL COOLED REACTORS
NT LITHIUM COOLED REACTOR EXPERIMENT
NT PRESSURIZED WATER REACTORS
NT WATER COOLED REACTORS

**LIQUID COOLING**
NT FILM COOLING
Effectiveness of using various lubricant cooling fluids for diamond superfinishing
[AD-753980] 11 p1299 N73-20541

Automatic temperature controller for liquid cooled garment based on total evaporative water loss during exercise
[NASA-TN-D-7311] 16 p1868 N73-25126
Rocket nozzle coolant channel thermal analysis program
[NASA-CR-132185] 16 p1957 N73-25832
Automatic temperature control for liquid cooled space suit
[NASA-CASE-ARC-10599-1] 17 p1988 N73-26071
Cooling effects on human tolerance to work induced heat stress and collapse
[NASA-CR-134059] 23 p2750 N73-32005

**LIQUID CRYSTALS**
Procedures for using liquid crystal tape for thermographic testing of bonded structures for aircraft
[NASA-CR-123932] 03 p0300 N73-12451
Monolithic display using metal oxide semiconducting circuits and liquid crystal layer
[CEA-CONF-1991] 03 p0345 N73-12814
EPR study of molecular ordering in smectic-A liquid crystals without nematic phases
[NASA-TN-D-7124] 04 p0437 N73-13563
Electron paramagnetic resonance studies of viscous nematic liquid crystal using vanadyl acetyl acetonate and nitroxides as paramagnetic probes
[NASA-TN-D-7122] 04 p0437 N73-13564
Feasibility determination of using nematic liquid crystals for aircraft displays
[AD-751667] 07 p0832 N73-16748
Feasibility of developing liquid crystal display system
[AD-751747] 07 p0833 N73-16753
Use of liquid crystals in integrated optical circuits as waveguides
[AD-751537] 07 p0833 N73-16755
Evaluation of infrared laser beams using thin membrane type displays of cholestric liquid crystals
[AD-752201] 08 p0930 N73-17616
Photoactivated liquid crystal light valve
09 p1065 N73-18692
Liquid crystal Fourier plane filter for real time optical image processing
[NASA-CR-130185] 10 p1188 N73-19670
Iridescence and selective reflection of cholesteric liquid crystals according to various models
[BMVG-FBWT-72-27] 10 p1190 N73-19684
Plasma diagnostic visualization with pulsed carbon dioxide TEA laser and liquid crystal infrared detector, noting spark discharges
[ISL-18/72] 13 p1563 N73-22668
Liquid crystal applications as electronic, electro-optic, and diagnostic materials
[AD-755831] 13 p1567 N73-22703
Status of research on gas discharge, liquid crystal display systems, and ferroelectric ceramics in Europe
[AD-757649] 14 p1668 N73-23538
Magnetic bubble material and magnetic properties of Mott transition
[AD-757435] 14 p1699 N73-23787
Conference on liquid crystals
[AD-757224] 14 p1699 N73-23789
Papers on crystallography and liquid and solid structures
[NASA-CR-132048] 15 p1820 N73-24752
Design of two dimensional digital computer for optical image processing onboard spacecraft using liquid crystal circuits
18 p2209 N73-27827
Luminescent diode and liquid crystal display devices for telephony, using COS/MOS and TTL logic
[FTZ-421-TBR-4] 22 p2633 N73-31105
Effective x-y addressed, liquid crystal display panel
[AD-763927] 22 p2646 N73-31206
Properties of liquid crystals noting use in display devices, light modulation, image converters, and nondestructive testing
[LCR-DR-1-71-223/1/R] 23 p2765 N73-32125
Liquid crystal infrared detectors for plasma diagnostics and flow visualization using CO2 laser impulses
[BMVG-FBWT-73-16] 23 p2823 N73-32564

**LIQUID DROPS**
U DROPS [LIQUIDS]

**LIQUID DYNAMICS**
U FLUID DYNAMICS
U LIQUID FLOW

**LIQUID FILLED SHELLS**
Influence of cavity radius on energy dissipation rate in liquid filled spherical cavities
01 p0040 N73-10319
Development of digital computer program for evaluating vibrational characteristics of large liquid-filled rigid wall tanks of general shape
[NASA-CR-124070] 08 p0953 N73-17801
Performance of baffles as energy dissipation suppressors in liquid filled precessing cavities
16 p1888 N73-25280
Development of statistical methods for determining vibration and acoustic radiation of fluid loaded cylindrical shells
20 p2477 N73-29895

**LIQUID FLOW**
NT OPEN CHANNEL FLOW
NT WATER FLOW
Viscosity of liquids and classification of lubricating oils
[ESDU-68036] 02 p0154 N73-11247
Equipment and procedures for measuring flow of liquids and gases to identify application of specific types of equipment
[NLL-TRANS-45-[3958.4]] 02 p0154 N73-11249
Nonisothermal stationary flow of viscoplastic liquid between two concentric cylinders
[AD-748908] 04 p0408 N73-13321
Simulating liquid propellant motion in partially filled containers during docking maneuver in orbit
[NASA-CR-124055] 09 p1013 N73-18268
Darcy-Weisback equation for investigating solid-liquid flow in noncircular pipes
[BM-RI-7725] 09 p1013 N73-18271
Theory of two phase gas-liquid and liquid-gas flow for bladed machines and ejectors
[AD-755713] 12 p1409 N73-21419
Flow characteristics in earth liquid core
[NRC-TT-1635] 16 p1904 N73-25402
Equilibrium limits of molten zirconium nitride flow over nickel-cobalt solid coating
[NLL-M-21572-[5828.4F]] 16 p1926 N73-25583
Carrier liquid system containing bodies of ablative material
[NASA-CASE-LEW-10359-2] 16 p1972 N73-25952
Zero gravity liquid transfer device, using spiral shaped screen
[NASA-CASE-KSC-10626] 18 p2150 N73-27378
Heat transfer theory in layer with regular change of liquid flow direction
[AD-762794] 21 p2606 N73-30888

**LIQUID HELIUM**
Potential barrier for neutral excitation at helium liquid-vapor interfaces
[NOTA-INTERNA-375] 01 p0083 N73-10690
Damping of accelerated isothermal superfluid helium flow by roton polarization
[NOTA-INTERNA-395] 03 p0336 N73-12743
Elementary excitation spectrum of superfluid helium
10 p1198 N73-19750
Design of Joule-Thomson cascade for refrigeration cooling using liquid helium
[CEA-CONF-2044] 10 p1199 N73-19761
Numerical analysis of hydrodynamic properties of liquid helium based on quantum statistical mechanics
12 p1390 N73-21270
Epoxy resins for use in superconducting magnets at liquid helium temperatures
[RHEL/R-251] 12 p1416 N73-21476
Interferometric measurement of hypersonic sound wave attenuation in liquid helium transition region
13 p1558 N73-22629
Quantum physics of liquid helium
[MATSCIENCE-73] 15 p1814 N73-24704
Liquid helium experiments on ac Josephson effect in superfluid helium and superfluid critical velocities
16 p1944 N73-25728
Phonon dispersions and three particle correlations in liquid helium, and adsorbed helium monolayers
16 p1944 N73-25730
Low temperature energy spectrum near roton minimum region in superfluid helium
17 p2064 N73-26696
Metal cryostat for studying superconductors in liquid helium
[IPP-4/95] 17 p2072 N73-26766
Dynamic properties of neutral excitations in electron bombarded superfluid helium
18 p2181 N73-27606
Bose model for foreign particle interaction with superfluid helium
20 p2455 N73-29732
Digital detector for measuring liquid helium level
[PB-221313] 22 p2676 N73-31436
Thermodynamics of lambda transition in liquid helium and phase transformations
23 p2856 N73-32820
Abnormalities of liquid He-3 measured below 5 m K
24 p2967 N73-33713
Ion motions in liquid and solid helium
[COO-2027-6] 24 p2969 N73-33728
Effect of friction term on equations of motion of liquid helium and measurement of temperature along axis of channel carrying supercritical heat current
24 p2990 N73-33894
Cooling of 60 to 400 cm length circular tubes with superfluid helium
[KFK-1786] 24 p2992 N73-33910

**LIQUID HYDROGEN**
Ball bearing performance in liquid hydrogen at 30,000 rpm under thrust load of 1780 N
[NASA-TN-D-6981] 02 p0178 N73-11441
Development and evaluation of internal insulation materials for use with liquid hydrogen tanks on space shuttle
[NASA-CR-123928] 02 p0191 N73-11547
Liquid hydrogen reorientation in fuel tanks of Centaur launch vehicle using low level accelerations with and without internal baffles
[NASA-TN-D-7168] 07 p0770 N73-16252
Cryogenic instrumentation for present and possible future large scale systems operating at liquid hydrogen temperatures
[I.A-DC-72-855] 07 p0832 N73-16743
Hydrocarbon suspensions in slush hydrogen and heat transfer to slush hydrogen
[NASA-CR-130550] 08 p0968 N73-17912
Preparation of hydrocarbon suspensions in slush hydrogen for nuclear fuel element corrosion inhibition in rocket engines
08 p0968 N73-17913
Heat transfer to slush hydrogen at 1 atm and at triple-point pressure
08 p0968 N73-17914
Characteristics of gelled liquid hydrogen polyphenylene oxide foam open cell insulation
[NASA-CR-124114] 09 p1051 N73-18568
Coolant side, heat transfer rates for liquid hydrogen cooled, hydrogen-oxygen rocket thrust chamber
[NASA-TN-D-7207] 09 p1099 N73-18968
Rapid vaporization of liquid hydrogen in noninsulated reservoir placed in water
[CEA-CONF-2082] 12 p1429 N73-21582
Chilldown tests on single stage inducer test rig
[NASA-CR-132212] 15 p1762 N73-24278
Increased service life of rolling element radial bearings in nuclear engine for rocket vehicles by liquid hydrogen cooling and bearing modifications
[NASA-CR-132229] 15 p1792 N73-24531
Liquid hydrogen cold neutron moderator for use in channel H5 EL 3 reactor
[CEA-N-1571] 15 p1815 N73-24714
Analysis of factors influencing technical feasibility of operating aircraft on liquid hydrogen fuel
[NASA-TM-X-68242] 15 p1823 N73-24777
Simple performance calculation method for LH2/LOX engines with different cycles
[NASA-TM-X-64749] 15 p1824 N73-24786
Liquid hydrogen booster propellant tank internal insulation system for use in reusable spacecraft
[NASA-CR-121102] 15 p1842 N73-24925
Life tests of small turbine type flowmeters in liquid hydrogen
[NASA-TN-D-7323] 16 p1888 N73-25278
Liquid hydrogen turbopump rapid start program with coated and uncoated system tests
[NASA-CR-124262] 16 p1918 N73-25522
Revisions to LH2 and LO2 turbopump assemblies program test plan
[NASA-CR-124194] 17 p2036 N73-26476
Thermodynamic behavior of liquid hydrogen and nitrogen cavitation in ogives
[NASA-CR-2242] 19 p2251 N73-28153
Development and application of self evacuating multilayer insulation system for application to space shuttle orbiter liquid hydrogen tanks
[NASA-CR-121166] 21 p2606 N73-30883
Advanced material composites for use as insulations for space shuttle LH2 tanks
[NASA-CR-124388] 22 p2688 N73-31532
Pulsing liquid hydrogen/liquid oxygen attitude control propulsion system at cryogenic inlet conditions
[NASA-TM-X-71444] 23 p2830 N73-32621
Molecular transition principle for constructing liquid- and solidhydrogen particle track chambers
[JINR-P13-7067] 24 p2960 N73-33658
Feasibility of thermodynamic vent and screen baffle integration for orbital storage and transfer of liquid hydrogen
[NASA-CR-134482] 24 p2970 N73-33737

**LIQUID INJECTION**
NT WATER INJECTION
Breakup of liquid jet injected normal to supersonic airstream
[AD-747494] 04 p0406 N73-13309
Analysis of equal-size droplet injection in fluid flow, noting fuel injection
[DLR-MITT-72-19] 22 p2710 N73-31703

**LIQUID LASERS**
Design, development, and performance tests of long pulse liquid laser oscillator and circulatory subsystem
[AD-747964] 03 p0311 N73-12536
Construction of liquid laser designed for operation as oscillator-amplifier in high brightness mode
[AD-757072] 13 p1538 N73-22457
HCN laser for interferometric measurements in Tokamak machine
[EUR-CEA-FC-670] 22 p2681 N73-31475

**LIQUID LEVELS**
Digital detector for measuring liquid helium level
[PB-221313] 22 p2676 N73-31436

**LIQUID MERCURY**
U MERCURY [METAL]

**LIQUID METAL COOLED REACTORS**
NT ADVANCED SODIUM COOLED REACTOR
NT LITHIUM COOLED REACTOR EXPERIMENT
Design of high temperature liquid metal systems
[CONF-720904-1] 05 p0562 N73-14566
Mixed convection in reactor channel utilizing sodium as working fluid
[CEA-CONF-2001] 06 p0654 N73-15317
Triple wall tube exchanger/steam generator for sodium cooled fast breeder reactor
[BMBW-FBK-72-28] 22 p2699 N73-31619

Computer code for thermal/hydraulic stress analysis on liquid metal zirconium hydride reactor core
[AI-AEC-13065] 24 p2954 N73-33596
Evaluation of welding techniques for austenitic stainless steels for use in liquid metal fast breeder reactors
[ORNL-TM-4055] 24 p2954 N73-33601

LIQUID METALS
NT LIQUID SODIUM
NT MERCURY [METAL]
NT MERCURY VAPOR

Acoustic measurements and sound velocity calculations for molten rubidium at high pressures
[AD-746838] 02 p0138 N73-11120
Wetting of alumina, magnesia, zirconia, and carbides and borides of vanadium, titanium, and zirconium by palladium melts
[NLL-RTS-7321] 02 p0190 N73-11544
Emission and absorption spectra for mixtures of liquid uranium and uranium oxide using carbon tube furnace facility
[AD-746687] 02 p0194 N73-11571
Research on fuel cycle technology, sodium technology, fast reactor materials properties, liquid metal and molten salt chemistry, and reactor safety
[ANL-7850] 03 p0263 N73-12136
U shaped heated tube for distillation and purification of liquid metals
[NASA-CASE-XNP-08124-2] 04 p0385 N73-13129
Resistance leval indicator used in high temperature alkali tanks
[SFB-MHD-2] 04 p0422 N73-13444
Unsteady liquid metal flow in conduction MHD devices with constant magnetic field
[AD-748745] 04 p0455 N73-13715
Microstructure and mechanical properties of rapidly quenched liquid and powder metal alloys
[AD-749679] 05 p0564 N73-14578
Compilation of titles, authors, and corporate sources on subject of heat transfer in boiling metals under natural convection conditions
[NLL-RISLEY-TR-2167-[9091.9F]] 05 p0605 N73-14920
Liquid viscosity determined for gallium by means of vibration technique
[AD-750915] 06 p0656 N73-15332
Thermodynamic efficiencies of accelerators for liquid metal magnetohydrodynamic converter considering vapor liquefying effect on flow characteristics
[JPRS-57915] 06 p0703 N73-15735
Explosive interaction of molten metal jet injected into tank of subcooled distilled water
[ORO-3936-7] 06 p0731 N73-15961
Design and calibration of liquid metal calorimeter for high temperature operation
[AD-752443] 09 p1037 N73-18462
Abstracts on kinetics and thermodynamics of gases interacting with liquid metals
[JPRS-58282] 09 p1098 N73-18964
Development of superconducting homopolar machines with multiple discs and superconducting field winding using liquid metals for armature sliding contacts 10 p1109 N73-19037
Magnetohydrodynamic systems of liquid metals
[LM-MHD-1] 10 p1172 N73-19534
Analysis of two-dimensional liquid metal slot jet impinging normally against uniformly heated flat plate
[NASA-TN-D-7260] 11 p1348 N73-20938
Analysis of liquid metal magnetohydrodynamic energy conversion systems to determine performance limits and identify system parameters
[AD-757065] 14 p1606 N73-23013
Design and tests of liquid metal slip ring/solar orientation mechanism
[NASA-CR-120885] 14 p1640 N73-23292
Billet processing from rapidly quenched liquid metals
[AD-757677] 14 p1678 N73-23621
NaK loop testing of thermoelectric converter modules for SNAP program
[NASA-CR-121192] 14 p1691 N73-23727
Spectral emissions of liquid titanium, vanadium, zirconium, molybdenum, and platinum at fusion temperatures
[BM-RI-7743] 15 p1798 N73-24575
Equilibrium limits of molten zirconium nitride flow over nickel-cobalt solid coating
[NLL-M-21572-[5828.4F]] 16 p1926 N73-25583
Ziman theory for calculating electrical conductivity of liquid aluminum
[UCRL-51322] 16 p1929 N73-25605
Stability of refractory compounds in liquid aluminum at high temperatures
[NLL-RTS-7975] 18 p2113 N73-27083
Ultrasonic absorption in liquid metals and in liquid selenium 18 p2178 N73-27590
Emissivities of metals and compounds in liquid state at fusion temperatures
[NASA-CR-133521] 19 p2309 N73-28576
Skylab experiments on convection and molten metal flow and solidification under reduced gravity
[NASA-CR-124329] 19 p2343 N73-28852
Thermodynamic effects on liquid metal magnetohydrodynamic converter flow
[AD-761548] 20 p2459 N73-29762
Traveling wave of magnetic field having variable phase velocity and amplitude during movement of liquid metal in expanding channel
[AD-763159] 21 p2583 N73-30702
Thermotransport of copper in liquid Al-Cu alloys
[NASA-TR-R-415] 22 p2625 N73-31030
Electron transport in high density fully ionized liquid metals
[NASA-CR-135648] 22 p2684 N73-31497
Universal diagram representing changes in viscosity of liquid metals as function of temperature
[FRNC-CONF-45] 22 p2684 N73-31501
Determiniig thermodynamic properties of liquid copper-magnesium alloys by magnesium vapor pressure
[BARC-613] 22 p2685 N73-31504
Streaming in liquid metals due to thermal surface tension gradient
[TRITA-EPP-73-10] 22 p2700 N73-31626
Gas model of solute diffusion in liquid metals
[NASA-TR-R-417] 23 p2753 N73-32032
Self diffusion in liquid metals conducted over wide temperature intervals
[COO-841-30] 24 p2934 N73-33434
Heat capacity of liquid metals and stainless steels
[ORO-3291-17] 24 p2992 N73-33914

LIQUID NITROGEN
Galvanomagnetic and thermoelectric properties of monocrystalline alloys of bismuth and antimony at liquid nitrogen temperature
[AD-745865] 01 p0089 N73-10734
Feasibility of liquid nitrogen fuel tank inerting system on commercial aircraft to prevent fuel tank explosions
[FS-140-72-1] 13 p1473 N73-21934
Thermodynamic behavior of liquid hydrogen and nitrogen cavitation in ogives
[NASA-CR-2242] 19 p2251 N73-28153
Flow characteristics of radial inward choked flow of liquid nitrogen stream
[NASA-TM-X-68283] 20 p2387 N73-29181

LIQUID OXIDIZERS
Reaction kinetics of fluoride pyrolysis in liquid rocket propellant
[AD-752564] 08 p0970 N73-17931

LIQUID OXYGEN
Handbook of thermophysical properties of liquid and gaseous oxygen
[NASA-SP-3071] 04 p0484 N73-13952
Procedure for estimating changes in composition resulting from evaporation during storage of liquid oxygen
[NASA-TM-X-2686] 05 p0498 N73-14056
Instabilities in gaseous hydrogen-liquid oxygen rocket engine noting influence of pressure and concentration
[DLR-FB-71-47] 06 p0711 N73-15805
Performance evaluation of coaxial injectors for use in gaseous hydrogen-liquid oxygen rocket engines
[DLR-FB-71-56] 07 p0836 N73-16779
Abstracts of selected reports on heat transfer and fluid dynamics with applicability to oxygen systems
[NASA-SP-3076-VOL-3] 07 p0855 N73-16932
Influence of liquid oxygen on chromate coated aluminum tubing of breathing apparatus
[AD-752030] 08 p0936 N73-17661
Comparative infrared spectroscopic analysis of liquid oxygen
[AD-756629] 14 p1646 N73-23348
Simple performance calculation method for LH2/LOX engines with different cycles
[NASA-TM-X-64749] 15 p1824 N73-24786
Revisions to LH2 and LO2 turbopump assemblies program test plan
[NASA-CR-124194] 17 p2036 N73-26476
Cryogenic insulation of liquid oxygen dewars for aircraft pilot breathing masks
[AD-763325] 22 p2624 N73-31026
Pulsing liquid hydrogen/liquid oxygen attitude control propulsion system at cryogenic inlet conditions
[NASA-TM-X-71444] 23 p2830 N73-32621
Experimental analysis of two phase liquid oxygen pumping
[NASA-TN-D-7451] 24 p2972 N73-33747

LIQUID PHASES
Elementary chemical processes involved in degradation of polymers in melts 08 p0881 N73-17133
Binary and ternary system epitaxial crystal growth from liquid phase to obtain high purity, electroluminescent, and infrared detector materials 12 p1441 N73-21674

LIQUID PROPELLANT ROCKET ENGINES
NT AJ-10 ENGINE
NT HYDRAZINE ENGINES
NT HYDROGEN OXYGEN ENGINES
NT J-2 ENGINE
Theoretical analysis of rotating two phase detonation in liquid propellant rocket engine 04 p0461 N73-13763
Instabilities in gaseous hydrogen-liquid oxygen rocket engine noting influence of pressure and concentration
[DLR-FB-71-47] 06 p0711 N73-15805
Design, development, manufacture, and specifications of automatic fuel valves for liquid propellant rocket engines
[AD-750578] 06 p0715 N73-15832
Performance evaluation of coaxial injectors for use in gaseous hydrogen-liquid oxygen rocket engines
[DLR-FB-71-56] 07 p0836 N73-16779
Design solutions and technologies for Europa 3 launch vehicle 07 p0850 N73-16887
Development of computer model to simulate pulse mode performance operation of liquid bipropellant attitude control engines
[AD-752610] 08 p0955 N73-17819
Cost analysis of single stage space tug operations with several types of liquid propellant rocket engine propulsion systems - Vol. 3
[NASA-CR-124147] 11 p1344 N73-20903
Simplified procedures for correlation of experimentally measured and predicted thrust chamber performance
[NASA-CR-131519] 12 p1442 N73-21685
Mathematical techniques for studying high frequency nonlinear longitudinal combustion instability in liquid propellant rocket engines 12 p1443 N73-21689
Longitudinal vibration of rockets with liquid fuel engines
[AD-756076] 13 p1572 N73-22736
Chemical analysis of products in combustion chamber of nitrogen tetroxide/aerozine rocket engine during preignition, ignition, and postignition conditions
[NASA-CR-128898] 13 p1590 N73-22890
Analysis of tangential mode, nonlinear wave motion in liquid propellant rocket engine using two phase detonation wave as reaction model
[NASA-CR-121194] 14 p1718 N73-23944
History and future of Titan/Centaur launch vehicle
[NASA-TM-X-68249] 15 p1835 N73-24877
Theory and design of feed units of liquid propellant rocket engines
[AD-760265] 17 p2078 N73-26808
Rocket propellant injector with porous faceplate for rocket engine combustion chamber
[NASA-CASE-LEW-11071-1] 18 p2192 N73-27695
Development of three dimensional nozzle admittance theory for various liquid rocket engine nozzles subjected to three dimensional oscillations 20 p2387 N73-29174
Analysis of earth storable bimodal engine using earth storable propellants and operating in either monopropellant or bipropellant mode
[BELL-8706-933005] 20 p2466 N73-29811
Computation of coolant and wall temperatures of regeneratively cooled liquid propellant rocket engines
[DLR-FB-72-29] 21 p2591 N73-30755
Monograph for design and development of combustion chambers for liquid propellant rocket engines
[NASA-SP-8087] 22 p2709 N73-31697
Rocket motor chamber pressure and orifice effects in hydraulic flip
[AD-764730] 23 p2832 N73-32630
Hydrazine engine tests and small bipropellant engine calibration in Molsink facility 23 p2858 N73-32837
Basic problems of liquid fueled rocket engines
[JPRS-60208] 24 p2972 N73-33745

LIQUID ROCKET PROPELLANTS
NT AEROZINE
NT CRYOGENIC ROCKET PROPELLANTS
NT HYPERGOLIC ROCKET PROPELLANTS
NT MONOPROPELLANTS
NT SLURRY PROPELLANTS
Combustion stability with hydrogen-oxygen liquid rocket propellants 03 p0349 N73-12844
Evaluation of boundary cooled rocket engines for development of space storable propellant combination of oxygen difluoride/diborane
[NASA-CR-129260] 03 p0350 N73-12855
Design, development, and evaluation of mechanical mass flow controller for regulating fuel-oxidizer mixture ratio and controlling rocket engine thrust level
[NASA-CR-128639] 03 p0351 N73-12860
Initiation and propagation of low-velocity detonation in confined energetic liquids
[AD-748438] 04 p0485 N73-13966
Corrosion tests of candidate rocket engine materials exposed to standard high density acids for liquid propellant compatibility determination
[AD-749965] 06 p0712 N73-15807
Advanced measurement techniques for determining compatibility of materials with propellants
[NASA-CR-130546] 08 p0953 N73-17800
Prediction of three-dimensional liquid-propellant rocket nozzle admittances
[NASA-CR-121129] 08 p0954 N73-17807
Simulating liquid propellant motion in partially filled containers during docking maneuver in orbit
[NASA-CR-124055] 09 p1013 N73-18268

Techniques for determining dynamic characteristics of hydraulic duct for predicting low frequency vibrations of liquid propellant rocket engines
[ONERA-TP-1160] 09 p1015 N73-18281
Design and development of space storable isolation valves for control of flow of liquid rocket propellants
[TRW-73-4781-6-15] 10 p1165 N73-19477
NO2 and UDMH absorbing properties of rocket propellant gas mask canisters
[AD-752538] 10 p1203 N73-19791
Thermocouple measurement of gas velocity and temperature near liquid rocket injector face
[NASA-CR-121100] 11 p1270 N73-20304
Apollo 16 flight anomaly report to determine cause of burn holes in main parachute canopy
[NASA-TM-X-69127] 11 p1338 N73-20863
Energy addition from propellant spray combustion to liquid fuel efficiency
[AD-755879] 12 p1443 N73-21687
Physical and chemical nature of N2O flow decay in liquid propellants
[AD-755378] 13 p1489 N73-22070
Performance of storable liquid system components and tankage under severe conditions of humidity and temperature
[AD-755383] 13 p1569 N73-22716
Prevention of N2O4 flow decay by means of contaminant removal through distillation and filtration
[AD-755380] 13 p1569 N73-22717
Dynamic compatibility of liquid and gaseous fluorine and chlorine pentafluoride propellants with designated metals for rocket engine design criteria
[AD-756916] 13 p1569 N73-22719
Injector design guidelines for gas/liquid propellant systems
[NASA-CR-120968] 13 p1570 N73-22726
Iron contamination effect in liquid rocket propellant system of high density acid
[AD-755376] 14 p1700 N73-23797
Silicone additives for heat flux reduction in hydrazine rocket propellants
[AD-756913] 14 p1700 N73-23798
Development of electronic circuit for measurement transducer power supply to be used for liquid level measurement in liquid propellant rocket engines
[NASA-CASE-MFS-21698-1] 17 p2003 N73-26196
Results of Resonant Infrasonic Gauging System development
[NASA-CR-124314] 19 p2301 N73-28500
Analytical model and computer program for studying disturbances of liquid propellants in feedline systems
[NASA-CR-124308] 20 p2388 N73-29188
Toxic vapor detector for Minuteman propellant leakage
[AD-763799] 21 p2551 N73-30451
Survey of contaminants and impurities in propellant grade hydrazine
[AD-764365] 22 p2626 N73-31040
Design of detonating propellant propulsion system for exploring planets with hot dense atmospheres
22 p2732 N73-31864
Determination of vapor pressure, viscosity, and thermal conductivity of several liquid rocket propellants
24 p2972 N73-33750

**LIQUID ROTATION**
U ROTATING LIQUIDS

**LIQUID SLOSHING**
Damping of liquid oscillations using flexible ring baffles
[NASA-TM-X-64730] 12 p1390 N73-21273
Effects of low Bond number sloshing on thermal stratification of cryogenic liquids
12 p1391 N73-21283
Propellant oscillation modes and frequencies for tanks of any shape, fill level, or orientation
[NASA-CR-124277] 16 p1889 N73-25287
Slosh testing of spherical mercury propellant tank with positive expulsion diaphragm
[NASA-CR-133790] 21 p2600 N73-30838

**LIQUID SODIUM**
Mixed convection in reactor channel utilizing sodium as working fluid
[CEA-CONF-2001] 06 p0654 N73-15317
Design of hydrostatic shaft guide bearings for sodium pumps
[CEA-CONF-2045] 10 p1166 N73-19486
Electromotive force measurements for determining oxygen concentration in liquid sodium
[NLL-CE-TRANS-6073-[9022.09]]
15 p1746 N73-24148
Development of high temperature rolling bearings for operation in liquid sodium
[NYO-4117-9] 22 p2678 N73-31452
Thermodynamic and transport properties of saturated liquid sodium
[RD/B/M-2479] 22 p2730 N73-31844

**LIQUID SURFACES**
Liquid surface evaporation in rarefied gas atmosphere
[AD-765527] 24 p2893 N73-33095
Resonance stabilization of air cushion between liquid and oscillation source
[IPP-2/209] 24 p2963 N73-33674

**LIQUID-GAS MIXTURES**
NT AEROSOLS
NT FOG
Supersonic two phase air-water flows, noting expansion, acoustic velocity and X ray density measurements, and nozzle flow tests
[BMVG-FBWT-73-4] 14 p1650 N73-23380
Analysis of ERTS-1 data to determine aerosol content in atmosphere and comparison with data obtained by sun photometer at Salton Sea, California
[E73-10702] 16 p1903 N73-25394
Characteristics of zero aerosol sampling tube for aspiration of samples from gas flow with minimum changes in isokinetic coefficient
[AD-759868] 17 p2035 N73-26470
Performance tests of hydrogen oxygen rocket engines for various propellant mixing ratios
24 p2973 N73-33752

**LIQUID-LIQUID INTERFACES**
Steady state solution for accelerated interface shape between a light and a heavy fluid using velocity potential
[LA-4839] 06 p0654 N73-15316
Mathematical model for turbulent boundary layer of two liquid flows
07 p0772 N73-16267
Orientation of molecules of soil soluble surfactant in absorption layers on liquid-liquid interface
[NLL-M-22998-[5828.4F]] 20 p2373 N73-29068

**LIQUID-SOLID INTERFACES**
Steady state response of semi-infinite fluid-solid interface subjected to subsonic and intersonic load velocities
[AD-747253] 02 p0159 N73-11287
Dynamic response of fluid-solid interface to supersonic disturbance
[AD-750253] 05 p0604 N73-14917
Analysis of conditions for equilibrium of multi-component liquid at surface of solid body with allowance for selective adsorption at interphase boundaries
[NLL-M-21577-[5828.4F]] 16 p1885 N73-25261
Steady-state response of interface to disturbance moving with constant velocity
16 p1886 N73-25267
Infrared image converter, based on temperature sensitive liquid-solid interface, using GE-AU IR detector
[IPF-72-6] 17 p2033 N73-26457
TOPAL computer program for investigating metal-liquid thermal interactions under shock tube conditions
[GRO/44/91/26-PT-1] 18 p2125 N73-27174

**LIQUID-VAPOR EQUILIBRIUM**
Equilibrium distribution of helium-4 and helium-3 between the liquid and vapor phases of deuterium 2 and hydrogen 2
[NBS-TN-621] 02 p0137 N73-11109

**LIQUID-VAPOR INTERFACES**
Potential barrier for neutral excitation at helium liquid-vapor interfaces
[NOTA-INTERNA-375] 01 p0083 N73-10690
Regularity in phase transitions of magnetic and liquid-gas systems
[COO-1112-63] 03 p0364 N73-12967
Thermodynamic efficiencies of accelerators for liquid metal magnetohydrodynamic converter considering vapor liquefying effect on flow characteristics
[JPRS-57915] 06 p0703 N73-15735
Analysis of energy conservation constraints on circulation of Southern Hemisphere atmosphere and oceans based on radiant, latent, and sensible heat energy transfers
[METEOROL-STUDY-26] 09 p1027 N73-18387
Nonlinear stability of liquid adjacent to supersonic stream
[AD-758103] 15 p1769 N73-24328
Effect of fuel vapor concentrations on combustion emissions and performance using experimental turbojet combustor segment
[NASA-TM-X-2800] 15 p1843 N73-24933

**LIQUIDS**
NT AEROZINE
NT CRYOGENIC FLUIDS
NT CRYOGENIC ROCKET PROPELLANTS
NT FLOX
NT HYDRAULIC FLUIDS
NT HYPERGOLIC ROCKET PROPELLANTS
NT LIQUEFIED GASES
NT LIQUID AMMONIA
NT LIQUID HELIUM
NT LIQUID HYDROGEN
NT LIQUID METALS
NT LIQUID NITROGEN
NT LIQUID OXIDIZERS
NT LIQUID OXYGEN
NT LIQUID ROCKET PROPELLANTS
NT LIQUID SODIUM
NT MERCURY [METAL]
NT MERCURY VAPOR
NT MONOPROPELLANTS
NT ORGANIC LIQUIDS
NT ROTATING LIQUIDS
NT SLURRY PROPELLANTS
Viscosity variation with temperature at atmospheric or saturation pressure for liquids
[ESDU-66024] 01 p0039 N73-10305
Molecular-kinetic theory for determining temperature dependence of simple liquid viscosity
[AD-747089] 02 p0159 N73-11286
Measurement of momentum of two-phase liquid-vapor flow from pipe of circular cross-section
[EUR-4785-I] 03 p0284 N73-12302
Electrical conductivity methods for measuring effects of high energy radiation on dielectric hydrocarbon liquids
[HMI-B-117] 04 p0452 N73-13693
Equation for normal freezing for ideal ternary liquid solutions solidified into ideal solid solutions of pseudobinary type
[NASA-CR-129935] 05 p0562 N73-14563
Acoustic signal recorders and electroacoustic measurements in liquids
[JPRS-57778] 05 p0580 N73-14720
Measurement of infrared emission spectra of liquid cyclopentane derivatives excited by carbon dioxide laser
[AD-750480] 06 p0681 N73-15544
Dictionary-handbook on properties and uses of fuels, lubricating materials, and special liquids
[AD-750484] 06 p0712 N73-15810
Critical transport properties in binary liquid phase transition
[AD-752473] 08 p0884 N73-17158
Automatic liquid collection and disposal system
[NASA-CASE-LAR-11071-1] 09 p1039 N73-18474
Test data on liquid dielectric breakdown mechanisms
[AD-752819] 09 p1053 N73-18585
Apparatus for mixing two or more liquids under zero gravity conditions
[NASA-CASE-LAR-10195-1] 10 p1163 N73-19458
Radial distribution functions and liquid structure factors for fluids of particles interacting through repulsive potentials
[LPTHE-72/45] 10 p1191 N73-19690
Surface instability of liquid layer subjected to perpendicular motion
[NASA-TT-F-14880] 12 p1390 N73-21274
Electric strength breakdown in insulating dielectric liquids
[AD-755756] 13 p1548 N73-22546
Use of radiation for preparative chemistry in liquid solutions
[NASA-TN-D-7285] 15 p1747 N73-24156
Combustion and evaporation of liquid fuels at high pressures
[NASA-CR-121113] 15 p1843 N73-24934
Instrumentation and techniques for measuring viscosity of liquids by vibration method
[AD-759389] 17 p2034 N73-26464
Heat flow and convection in gases and liquids in weightless environments
[NASA-TM-X-64735] 18 p2205 N73-27797
Perturbation theory of dynamic structure factors in high frequency liquids
[AD-761659] 19 p2230 N73-27987
Influence of atmospheric pressure and temperature on viscosity and density of mineral oil and siloxane liquids
[AD-761590] 19 p2232 N73-27999
Forward scattered light spectrum from pulsed ruby laser in liquid medium
20 p2424 N73-29470
Liquid jet impact against elastomeric materials
[PB-220972/4] 21 p2528 N73-30269
Mechanical effects resulting from interactions of laser beams with gases, liquids, and solids
[AD-763258] 21 p2555 N73-30482
Equations describing dynamical motions of small cavitation bubbles in liquids
[AD-764075] 22 p2656 N73-31277
Sensitivity and comparison evaluation of liquid penetrants used in Saturn 5 vehicle hardware to detect surface cracks
[NASA-TM-X-64769] 22 p2688 N73-31529
Handbook for liquid and solid lubricants in aerospace industry
[NASA-CR-130490] 23 p2796 N73-32365
Thermodynamics of low and high molecular weight liquids
23 p2859 N73-32841

**LISTS**
Computer program for producing and updating wiring lists for use in development and production of electronic equipment
[ECR-31] 12 p1386 N73-21239
Flow diagrams and listings for SAP and PLTGEN programs
[NASA-CR-128985] 17 p1997 N73-26146
Catalog on standard reference materials, their properties, compositions, and characterizations
[NBS-SP-260] 17 p2049 N73-26573
Tables listing 1970.0 ecliptic coordinates of hot stars
[COMMUN-27] 19 p2344 N73-28857
Satellite data presentation by means of lists, graphs, and three dimensional plots
24 p2985 N73-33859

**LITERATURE**
NT DOCUMENTATION
NT PROCEEDINGS
Literature survey on polar cap ionospheric disturbance characteristics
[AD-754250] 10 p1157 N73-19416
Literature review of strain rate effects on mechanical properties of metals at high temperatures
[AD-754243] 10 p1174 N73-19548
Literature on thermodynamics of electrostatic waves and ionized plasmas
[AD-754014] 10 p1198 N73-19745
Marine biology literature compilation for Caribbean Sea and adjacent regions
14 p1607 N73-23022
Literature compilation on marine geology and geophysics for Caribbean Sea and adjacent regions
14 p1607 N73-23023
Microbiological experiments aboard balloons, rockets, and earth satellites - literature review
14 p1607 N73-23025
Literature review on human macular pigment absorption and density spectrum of cone receptor
[IZF-1972-17] 14 p1609 N73-23046
Bibliography of literature on phase locked loops
[NASA-CR-133225] 17 p2004 N73-26202
Literature survey on jet propagation and interference in lifting surface aerodynamics
[NASA-TT-F-14957] 19 p2217 N73-27886
**LITHERGOL ROCKET ENGINES**
Theoretic performance of simple lithium compounds in lithergol rocket engines
[DLR-FB-73-23] 15 p1823 N73-24778
**LITHERGOLIC PROPELLANTS**
U HYBRID PROPELLANTS
**LITHIUM**
NT LITHIUM ISOTOPES
Radiation damage recovery characteristics of lithium doped solar silicon cells
[NASA-CR-129183] 02 p0128 N73-11044
High temperature density determinations of Li, using gamma radiation attenuation technique
[ORO-3604-7] 03 p0263 N73-12134
Anodic efficiency of lithium in electrolytic cells
[AD-749009] 04 p0387 N73-13147
Radiation and annealing studies on oxygen-doped and lithium diffused germanium
[CONF-720707-7] 06 p0699 N73-15696
Development of processing techniques for fabrication of lithium doped solar cells noting behavior during electron irradiation and annealing
[ESRO-CR-94] 09 p0991 N73-18088
Dielectric susceptibilities of potassium chloride to lithium and hydroxyl, sodium chloride to hydroxyl, and rubidium chloride to cyanides
[COO-3151-14] 10 p1200 N73-19763
Removal of lithium from 1040 C aged tantalum alloy by liquid ammonia and vacuum distillation techniques
[NASA-TM-X-2775] 11 p1305 N73-20590
Lithium-multivalent acceptor impurity interaction in germanium
12 p1437 N73-21645
Bearings for control system of high temperature lithium or argon cooled fast nuclear reactors
[NASA-TM-X-68218] 13 p1534 N73-22429
Laser interaction with high density lithium plasma
15 p1816 N73-24718
Effect of oxygen on corrosion of niobium and tantalum by liquid lithium at 600 C
[ORNL-TM-4069] 17 p2045 N73-26547
Position sensitive detector with lithium diffused layer as uniform resistive layer
[NASA-CR-133408] 18 p2152 N73-27391
Development of lithium-doped silicon solar cells with increased stability, efficiency, and radiation resistance
[AD-762941] 20 p2364 N73-29011
Use of lithium/sulfur batteries as load-leveling devices in electrical utility networks
[ANL-7958] 21 p2499 N73-30058
Lithium anode cells operating at room temperature using electrolytic solutions in inorganic solutions
[AD-763478] 23 p2754 N73-32039
**LITHIUM ALLOYS**
Preliminary evaluation of lithium aluminum electrode for thermal batteries
[AD-757007] 13 p1477 N73-21964
Elastic and mechanical properties of Al-Li alloy
[AD-759423] 16 p1931 N73-25625
Structure and properties of magnesium-lithium alloys
[JPRS-59738] 20 p2430 N73-29523
**LITHIUM CHLORIDES**
Development and characteristics of electric storage battery using lithium-silver chloride couple
[SC-DC-72-2298] 07 p0742 N73-16033
Performance of prototype lithium-inorganic electrolyte battery
[AD-758856] 16 p1865 N73-25101
**LITHIUM COMPOUNDS**
NT LITHIUM CHLORIDES
NT LITHIUM FLUORIDES
NT LITHIUM HYDRIDES
NT LITHIUM HYDROXIDES
NT LITHIUM NIOBATES
NT LITHIUM OXIDES
Performance of lithium battery with inorganic electrolyte
[AD-746633] 02 p0129 N73-11052
Manufacturing of holmium lithium tetrafluoroytriate laser disk bonded into glass
[AD-747968] 03 p0352 N73-12871
Laser damage in lithium iodate and proustite
[AD-748935] 04 p0451 N73-13682
Beryllium and beryllium-lithium complexes in single crystal silicon with acceptor levels 191 and 145 MeV
[NASA-TR-R-395] 04 p0458 N73-13736
Development of lithium-nickel sulfide electric storage battery for operation at high discharge rates and low temperatures
[AD-749861] 05 p0500 N73-14067
Effect of proton bombardment on photoelectric characteristics of n-p junctions alloyed with n-type silicon and lithium admixture
[AD-750977] 06 p0709 N73-15783
Design and development of optical pumps for pulsed neodymium yag lasers with emphasis on efficiency and reproducibility of product
[AD-751212] 07 p0808 N73-16557
Cis-trans isomers and doped LiNbO3 for holographic ready/write/erase memory application
[NASA-CR-112248] 08 p0928 N73-17604
Oil base effect on lubricating performance of lithium greases and soaps containing hydrocarbons
[AD-754593] 11 p1300 N73-20549
Growth of multiply sensitized Ho YLF crystals as laser materials
[AD-755530] 13 p1538 N73-22461
Spectroscopic analysis of energy transfer in rare earth compounds to determine effect of transfer phenomena on lasing efficiency
[AD-757520] 14 p1673 N73-23579
Theoretic performance of simple lithium compounds in lithergol rocket engines
[DLR-FB-73-23] 15 p1823 N73-24778
Design and performance of segmented holmium doped yttrium lithium fluoride laser
[AD-760019] 17 p2042 N73-26522
Utilization of lithium p-lithiphenoxide to prepare star polymers
[NASA-CASE-NPO-10998-1] 23 p2753 N73-32029
Infrared absorption spectra of lithium and potassium silicate glasses
[AD-764891] 24 p2893 N73-33092
**LITHIUM COOLED REACTOR EXPERIMENT**
Fabrication of cermet bearings for control system of high temperature lithium cooled nuclear reactors
[NASA-TM-X-2892] 24 p2953 N73-33595
**LITHIUM FLUORIDES**
Stress behavior of lithium fluoride crystals exposed to shock wave impact
[AD-748267] 04 p0460 N73-13757
Hydrogen lamp with lithium fluoride window for Lyman beta radiation output
[AD-754572] 11 p1325 N73-20753
Lithium fluoride thermoluminescent dosimeter for measuring ionizing radiation exposure during Apollo 16 flight
15 p1741 N73-24115
Elastic scattering of He on LiF crystal surfaces
[NRC-TT-1652] 17 p2072 N73-26764
High temperature effects on dislocation mobility of LiF single crystals
18 p2185 N73-27642
Electrical and luminescence phenomena in pure and dope lithium Floride
[ORNL-4850] 19 p2230 N73-27985
Theoretical analysis of plastic flow and diffusion during sintering of Life, Ag, and Ni systems
20 p2428 N73-29499
Temperature effects and effect of addition of lithium fluoride on conductivity of magnesium oxide
[NLL-M-23040-[5828.4F]] 21 p2585 N73-30711
**LITHIUM HYDRIDES**
Lithium hydride and depleted uranium shield materials for space power nuclear reactor
[NASA-TM-X-2835] 18 p2177 N73-27580
Measured and calculated fast neutron spectra at surface of lithium hydride and depleted uranium shielded reactors
[NASA-TM-X-2906] 24 p2953 N73-33594
**LITHIUM HYDROXIDES**
Bibliography on carbon dioxide removal from gases by lithium hydroxide
[CL-1971-15] 04 p0386 N73-13136
Preparation of lithium oxide, [Li3O2] by decomposition of anhydrous lithium hydroxide
[NASA-TM-X-2888] 21 p2506 N73-30107
**LITHIUM ISOTOPES**
Proton spallation of neon and lithium production in stellar flares
22 p2701 N73-31631
**LITHIUM NIOBATES**
Iron-doped lithium niobate as holographic storage medium
[AD-760343] 17 p2042 N73-26518
**LITHIUM OXIDES**
Preparation of lithium oxide, [Li3O2] by decomposition of anhydrous lithium hydroxide
[NASA-TM-X-2888] 21 p2506 N73-30107
**LITHIUM 4**
U LITHIUM ISOTOPES
**LITHIUM 6**
U LITHIUM ISOTOPES
**LITHOLOGY**
Lithological and structural surveys of African rift system using ERTS-1 imagery
[E72-10194] 01 p0046 N73-10373
Geology and lithology of Afar region of Ethiopia based on ERTS-1 imagery
[E72-10261] 03 p0290 N73-12360
ERTS-1 imagery of structure and lithology of Northern California Coast Ranges and Sacramento Valley
[E72-10333] 05 p0531 N73-14321
Distinguishing major lithologic types in rocks of Precambrian age in central Wyoming using multilevel sensing
[E73-10301] 09 p1021 N73-18333
ERTS-1 imagery of structural and lithological properties of Northern Coast Ranges and Sacramento Valley, california
[E73-10478] 12 p1396 N73-21315
Automatic processing of ERTS-1 data for physiography and geologic mapping of San Juan Basin, Colorado
[NASA-CR-131577] 13 p1524 N73-22346
Structural and lithological investigation of Northern Coast Ranges and Sacramento Valley, California
[E73-10577] 14 p1656 N73-23438
Lithological and structural surveys of sedimentary basin in France from ERTS-1 MSS imagery
[E73-10656] 16 p1898 N73-25352
Collection of ground truth data in Great Basin for support of aerial and Skylab overflights
[E73-10884] 20 p2394 N73-29235
Structural and lightological systems of Sierra Nevada Mountains and Sacramento Valley of California from ERTS-1 imagery
[E73-10942] 21 p2530 N73-30284
Oil exploration using ERTS-1 imagery of lithology and geological structures
[E73-11053] 23 p2780 N73-32229
Mapping lineaments, structures, and lithological formations of African Rift System in Africa and Yemen from ERTS-1 imagery
[E73-11126] 24 p2916 N73-33281
**LITHOSPHERE**
NT EARTH CORE
NT EARTH CRUST
NT EARTH MANTLE
NT EARTH SURFACE
Regionalization of lithosphere and asthenosphere of Pacific Ocean from Rayleigh wave phase velocity dispersion curves
20 p2390 N73-29197
**LITTLE JOHN ROCKET VEHICLE**
Meteorological and ballistics data for launching 13901 Little John, missile number 2172, round number 684 AM
[AD-749435] 04 p0445 N73-13634
Meteorological and ballistics data for launching of Little John, missile number 3175, round 687 RO
[AD-749439] 05 p0574 N73-14669
Meteorological and ballistics data for launching of Little John, missile number 2253, round 683 RO
[AD-749437] 05 p0574 N73-14670
Meteorological data for launching 13801 Little John, missiles 3086 and 3166
[AD-752089] 08 p0939 N73-17688
Meteorological and ballistics data for launching of 13901 Little John Missile number 1463, round number 692 RG
[AD-752091] 08 p0940 N73-17696
Meteorological and ballistics data for launching of 14101 Little John RIP missile number 12751
[AD-752092] 08 p0940 N73-17697
Meteorological and ballistics data for launching of 13801 Little John ARM-P Ripple, missile numbers 3102, 3142 and 3257, round numbers 693, 694 and 695 RO
[AD-752095] 08 p0940 N73-17698
Meteorological data for launching of 13801 Little John Missile number 3070, round number 696 RO
[AD-752096] 08 p0940 N73-17702
Meteorological and ballistics data for launching of 15001 Little John missile no. 1508, round no. 697 RG
[AD-754558] 11 p1314 N73-20665
Meteorological data for launch of Little John probe of upper atmosphere
[AD-754561] 11 p1315 N73-20671
Meteorological data gathered for Little John launching 14101
[AD-754560] 11 p1316 N73-20679
Meteorological data from 3901 Little John missile no. 2192, round no. 693 RM, [24 Jan. 1973]
[AD-758859] 15 p1807 N73-24649
Meteorological and ballistics data for launching of 03702 Honest John missile number 1003, round number 631 AML
[AD-758869] 15 p1807 N73-24650
Meteorological data gathered for launching 15001 Little John
[AD-762161] 19 p2317 N73-28641

LITTORAL CURRENTS
U COASTAL CURRENTS
LITTORAL DRIFT
ERTS-1 imagery of littoral drift and sedimentation patterns of beach and nearshore areas of Maryland section of Chesapeake Bay
[PAPER-M2] 19 p2280 N73-28342
LITTORAL TRANSPORT
ERTS-1 imagery of coastal marshland, tidal flats, and littoral transport in French Atlantic waters
[E72-10251] 03 p0289 N73-12351
ERTS-1 imagery of marshes, wetlands, and turbid waters in French Atlantic littoral
[E73-10548] 13 p1518 N73-22307
Littoral transport of sedimention coastal region of France
[E73-10822] 18 p2140 N73-27297
Seasonal changes of littoral transport and beach width of Maryland portion of Chesapeake Bay and resultant effect on protective structures
[PAPER-M1] 19 p2280 N73-28341
LIVER
Transverse acceleration effects on dioxyribonucleic acid catabolism in rat spleen and liver
03 p0257 N73-12080
Hepatotoxic effects of dichloromethane inhalation in mice
[AD-751434] 07 p0748 N73-16081
Toxic effects of chronic exposure to dichloromethane in liver microsomal cytochromes
[NASA-TM-X-69101] 09 p0996 N73-18128
Transverse acceleration effects on rat hepatocytic structures
10 p1115 N73-19086
Morphological changes in liver of dogs subjected to chronic gamma radiation
11 p1244 N73-20101
Management of asymptomatic carriers of hepatitis associated antigen in Hellenic Air Force personnel
14 p1611 N73-23060
Incidence of abnormal liver function tests in drug addicts without history of jaundice
[NASA-TT-F-15041] 20 p2368 N73-29044
LLANOS ORIENTALES [COLOMBIA]
Analysis of ERTS-1 imagery for extrapolating existing soil maps into unmapped areas of Llanos Orientales of Colombia, South America
[PAPER-A13] 19 p2261 N73-28221
LMCR [REACTORS]
U LIQUID METAL COOLED REACTORS
LOAD DISTRIBUTION [FORCES]
Acoustic emission and discontinuous yielding of dead weight in Portevin-Le Chatelier effect
[COO-2204-1] 10 p1190 N73-19680
Analysis of Michell framework for uniform load between fixed supports
[REPT-1054/73] 13 p1586 N73-22861
Fracture control method for composite tanks with load sharing liners
[NASA-CR-120918] 19 p2348 N73-28889
LOAD FACTORS
U LOADS [FORCES]
LOAD TESTING MACHINES
Load cell for combined axial load and torque with good sensitivity reliability and low cross talk
[AD-746471] 02 p0175 N73-11420
LOAD TESTS
Shock tests on rectangular steel beams, relation of tension-compression properties to moment-curvature equation, and viscoelastic cantilever beam response to shock
[AD-748656] 04 p0482 N73-13941
Structural design and load tests on carbon fiber reinforced plastic VC-10 aileron control strut
[ARC-CP-1229] 05 p0603 N73-14903
Punch-loading technique effects on mechanical properties of composites reinforced with glass fibers
[REPT-1042/72] 10 p1176 N73-19563
LOADING FORCES
U LOADS [FORCES]
LOADING OPERATIONS
Technical aspects of airship manufacture and ground and loading operations
24 p2879 N73-32993
LOADING RATE
Effect of strain hardening on fatigue crack resistance after single cycle peak overload in Ti-6Al-4V Ti alloy
[AD-753899] 10 p1174 N73-19553
LOADING WAVES
U ELASTIC WAVES
U LOADS [FORCES]
LOADS [FORCES]
NT AERODYNAMIC LOADS
NT AXIAL COMPRESSION LOADS
NT AXIAL LOADS
NT BLAST LOADS
NT COMPRESSION LOADS
NT CRITICAL LOADING
NT CYCLIC LOADS
NT DYNAMIC LOADS
NT EDGE LOADING
NT GUST LOADS
NT IMPACT LOADS
NT LANDING LOADS
NT RANDOM LOADS
NT ROLLING CONTACT LOADS
NT SHOCK LOADS
NT STATIC LOADS
NT THRUST LOADS
NT TRANSIENT LOADS
NT VIBRATORY LOADS
NT WING LOADING
Guidance on choice of nonmetallic gear materials, and method of estimating safe load for nonmetallic spur and helical gear
[ESDU-68001] 01 p0060 N73-10488
Analysis of factors affecting design of interference-fit collars on rotating shafts
[ESDU-68002] 01 p0061 N73-10496
Numerical analysis of nominal interface pressures and stresses for shafts with interference fit collars
[ESDU-68003-AMEND-A] 01 p0061 N73-10497
Increased load capacities of self-generating gas bearings with circular supply
[AD-745827] 01 p0063 N73-10518
Stress effects around holes in flat plates under various combinations of loads
[ESDU-70005] 01 p0110 N73-10902
Flanged and circular data sheet-sections, beyond limit of proportionality
[ESDU-01.06.00] 01 p0110 N73-10903
Estimating fatigue strength of components subjected to constant amplitude with constant mean loading
[ESDU-71010] 01 p0111 N73-10915
Curves for determining maximum elastic stresses and deflections for initially flat circular plates of uniform thickness under uniform pressure with various edge conditions
[ESDU-65002] 01 p0112 N73-10923
Stress concentration effects due to shape discontinuity, inclusions, or local load distributions
[ESDU-65004-AMEND-A-B-C] 01 p0112 N73-10925
Steady state response of semi-infinite fluid-solid interface subjected to subsonic and intersonic load velocities
[AD-747253] 02 p0159 N73-11287
Effects of pavement surface condition on cornering forces developed by automobile tires of different tread design
[NASA-TN-D-6964] 02 p0192 N73-11551
Criteria and guidelines for combining loads during ascent phase of space flight
[NASA-SP-8099] 02 p0234 N73-11897
Graphical solution to bending moment of curved strut subjected to end loads
[ESDU-01.01.14] 02 p0236 N73-11919
Influence of end loads and moments on bending moment of straight strut
[ESDU-01.01.15] 02 p0236 N73-11920
Bending moments at ends of strut due to end load and triangularly distributed side load
[ESDU-01.01.25] 02 p0236 N73-11923
Safe carrying loads of external pressure for cylindrical shells
02 p0238 N73-11935
Characteristics of yield surfaces for hardening body as function of preliminary loading path
02 p0238 N73-11937
Linear and nonlinear analysis of static equilibrium stability, and vibrations of shell of revolution subjected to unsymmetric loadings
[AD-745967] 02 p0238 N73-11939
Analysis of forces imposed on aircraft wing from landing gear impact in relation to weight of wing, damping, and frequency of periodic load
[AD-747381] 03 p0254 N73-12052
Resistance to damage from impulsive loading in three dimensionally graphite reinforced phenolic composite materials
[AD-748099] 03 p0323 N73-12628
Relationship of stress-strain rates and loading histories on material hardening
03 p0360 N73-12936
Wave forces on horizontal circular cylinder subjected to train of gravity waves
[AD-747532] 03 p0362 N73-12951
Variable direction force coupler for transmitting force along selectable curve path
[NASA-CASE-MFS-20317] 04 p0425 N73-13463
Moving point force on solid-solid interface
[AD-750252] 05 p0604 N73-14916
Application of Ritz-Galerkin method and complementary energy to problems in theory of nonconservative elastic stability
[AD-750575] 06 p0729 N73-15945
Prediction of horizontal wave forces acting on vertical pile structures of floating ocean platforms
[AD-751574] 07 p0794 N73-16460
Velocity diagram and design of highly loaded four and one half stage fan turbine
[NASA-CR-2140] 07 p0835 N73-16770
Procedures for determining shell stability under various types of dynamic loads
07 p0852 N73-16906
Theory of plates and shields to include response of structurally loaded shells of cylindrical and spherical configurations
[AD-751502] 07 p0852 N73-16913
Measurement of parachute cord loads using lightweight transmitting load cell
[AD-751913] 08 p0867 N73-17022
Analysis of errors recorded by modified Ligtenberg techique while measuring stress, strain, and static and dynamic loading in curved plates
[AD-752127] 08 p0926 N73-17589
Design factors resulting from hydrodynamic loads induced on large underwater structures by impulsive motion
[AD-753603] 09 p1019 N73-18315
Methods for bounding life of structures subjected to constant loads and temperature within creep range
[RD/B/N-2257] 10 p1220 N73-19925
Stress analysis on lap joint subjected to loads
[AD-753469] 10 p1221 N73-19929
Current-voltage, load, and spectral characteristics of p- and n-type GaAs
[NASA-TT-F-14859] 11 p1330 N73-20793
Effect of load variables on fatigue crack growth at room temperture in Ti-6Al-4V alloy
[NASA-CR-2239] 11 p1345 N73-20913
Load factors for pressure balancing of gas film seals under various flow conditions
[NASA-TM-X-68227] 12 p1408 N73-21412
Plastic instability in stainless steels and effects on load bearing capacity of structural components
[COO-2048-8] 12 p1463 N73-21850
Design study of despin mechanism noting alignment accuracy, lubrication system, load carrying capacity and bearings
[ESRO-CR[P]-227-APP] 13 p1535 N73-22433
Buckling of stiffened cylindrical shells subjected to combined axial compression, normal pressure, bending, and shear loads
13 p1585 N73-22847
Effect of biaxial loading on flaw growth rate of aluminum alloys used in space shuttle cryogenic tankage
[NASA-CR-128904] 13 p1586 N73-22855
Maximum and minimum possible values of dynamic load factors for damped and undamped simple oscillators
[AD-755168] 13 p1588 N73-22875
Behavior of cantilevered beam of elastic foundation subjected to following force
[NASA-CR-131608] 13 p1588 N73-22877
Inelastic buckling of eccentrically loaded simply supported columns of rectangular and circular cross sections
[AD-756186] 13 p1589 N73-22887
Standardized load sequence for flight simulation tests on transport aircraft wing structures
[LBF-BERICHT-FB-106] 14 p1602 N73-22986
Turnbuckle device for tensile stress load measurements
[NASA-CASE-MFS-21488-1] 14 p1667 N73-23526
Structural stability testing of aerospace components under pyrotechnic loading conditions using subscale plastic models
[NASA-CR-128911] 14 p1715 N73-23914
Stability of cylindrical shell stiffened by frames and loaded with external pressure
[AD-757726] 14 p1717 N73-23929
Investigation of wear behavior and load capacity of journal bearings in transition range from full to boundary lubrication using radioisotopes
[KFK-1569] 15 p1793 N73-24533
Finite deformation of annealed metals including loading and unloading constitutive and second order transitions
[AD-758261] 15 p1799 N73-24586
Stability of cylindrical shells with consideration of initial imperfections
[AD-757728] 15 p1840 N73-24909
Effect of arrangement of stiffening ribs for cylindrical shell on critical load value
[AD-758029] 15 p1840 N73-24912
Stability of loaded equilibrium configuration of elastic bodies
[AD-757856] 15 p1841 N73-24917
Numerical analysis of load absorption of two adjacent filaments in fiber-reinforced material
[AD-759729] 16 p1933 N73-25639
Stability of various equilibrium states in cubed incompressible neo-Hookean material subjected to pure homogeneous deformation
[AD-758700] 16 p1970 N73-25937
Thermodynamic analysis of high speed tapered roller bearings operating with fluid lubrication under combined loads
[NASA-CR-121207] 17 p2037 N73-26482
Buckling and structural response of two magnesium ring stiffened conical shells subjected to uniform external pressure
[NASA-TN-D-7303] 17 p2092 N73-26926
Performance tests of high speed ball bearings with lead and lead alloy plated retainers operating in liquid hydrogen at 30,000 rpm and 400 pound thrust load
[NASA-TM-X-68268] 18 p2155 N73-27412
Response of general laminated plates to applied loads with coupling between bending and extensional modes of deformation
18 p2165 N73-27488

Statistical analysis of load-carrying capacity of smooth cylindrical shells
[AD-760946] 18 p2204 N73-27787
Loading force diagrams and structural properties of landing gear
[AD-761644] 19 p2221 N73-27918
Versatile ergometer with work load control
[NASA-CASE-MFS-21109-1] 19 p2224 N73-27941
Summaries of papers presented to AGARD conference on random load fatigue
[AGARD-AR-54] 19 p2348 N73-28884
Effect of imperfections on behavior of thin elastic shells subject to loads
[AD-761448] 19 p2349 N73-28899
Stability of deep beam subjected to concentrated, transverse follower force applied at center of beam
[AD-762124] 19 p2350 N73-28900
Stability of cylindrical shell under nonuniform radial loads
[AD-762242] 19 p2351 N73-28909
Analysis of loads imposed on nose gear retraction system of T-34 aircraft to determine critical mechanical adjustments
[AD-762729] 20 p2361 N73-28994
Load absorption and interaction of two elastic filaments in fiber reinforced composite material
20 p2433 N73-29542
Dynamical response of cylindrical shells due to moving excitations
20 p2476 N73-29892
Three-axis, adjustable loading structure for testing soundness of aircraft skin by applying pressure
[NASA-CASE-FRC-10051-1] 21 p2547 N73-30416
Development of linear analysis method for predicting buckling of composite structures with arbitrary uniform cross section
[NASA-CR-2216] 21 p2603 N73-30863
Solutions to problems involving helical springs under load
[AD-762776] 21 p2604 N73-30871
Test fixture design for boron-aluminum and beryllium test panels
[NASA-CR-124401] 23 p2792 N73-32337

**LOCALIZATION**
U POSITION [LOCATION]

**LOCATES SYSTEM**
System for locating lightning strokes by coordination of directional antenna signals
[NASA-CASE-KSC-10729-1] 23 p2763 N73-32110

**LOCATION OF AIR TRAFFIC SATELLITES**
U LOCATES SYSTEM

**LOCI**
Algorithms for developing equations yielding root locus diagram
[TT-7303] 14 p1683 N73-23653

**LOCKHEED AIRCRAFT**
NT C-5 AIRCRAFT
NT C-130 AIRCRAFT
NT C-141 AIRCRAFT
NT F-104 AIRCRAFT
NT L-1011 AIRCRAFT
NT P-3 AIRCRAFT
NT T-33 AIRCRAFT
NT U-2 AIRCRAFT
NT XH-51 HELICOPTER

**LOCKHEED C-5 AIRCRAFT**
U C-5 AIRCRAFT

**LOCKHEED CL-595 HELICOPTER**
U XH-51 HELICOPTER

**LOCKHEED MILITARY AIRCRAFT**
U MILITARY AIRCRAFT

**LOCKHEED U-2 AIRCRAFT**
U U-2 AIRCRAFT

**LOCKHEED 186 HELICOPTER**
U XH-51 HELICOPTER

**LOCKING**
NT LASER MODE LOCKING

**LOCKS [FASTENERS]**
Establishing standards for effective wire rope clip installation
[BM-RI-7789] 24 p2994 N73-33927

**LOCOMOTION**
NT ASTRONAUT LOCOMOTION
Accelerometers, electromyogram sensors, and telemetry system for measuring human body segment motions
[AD-751134] 07 p0751 N73-16104

**LOCUST DAMAGE**
U INFESTATION

**LOCUST SWARMS**
U LOCUSTS

**LOCUSTS**
ERTS-1 detection of potential locust breeding sites in Saudi Arabian desert
[E73-10098] 08 p0902 N73-17309
Location of wet areas and detection of potential locust breeding sites using ERTS-1 imagery of Red Sea coastal plain of Saudi Arabia
[E73-10462] 12 p1394 N73-21301

**LOG PERIODIC ANTENNAS**
Gain pattern measurements for delta antenna and log periodic antenna configurations
[AD-757619] 14 p1633 N73-23239
VHF broadband directional log periodic antenna study, including pattern and impedance data
[AD-755199] 14 p1643 N73-23323

**LOGARITHMIC RECEIVERS**
Design and performance of transistorized broadband logarithmic amplifier using hybrid thick film technology
[ECR-32] 12 p1382 N73-21210

**LOGIC CIRCUITS**
NT THRESHOLD GATES
Automata theory for realizing reliable computer logic with fault detection
[AD-745720] 01 p0031 N73-10241
Development of coupled operational amplifier circuits with emphasis on wiring for current signals and influence of errors due to coupling
[AD-743690] 01 p0033 N73-10257
Synthesis of delay-free asynchronous sequential switching circuits
[AD-746392] 01 p0035 N73-10273
PERT planning run time reduction with special purpose cellular logic computer
03 p0271 N73-12195
Computerized simulation of faulty logic circuits
03 p0271 N73-12198
Computerized simulation for failure analysis of logic circuits
03 p0271 N73-12199
Asynchronous control circuits for digital systems representation and modular design
03 p0272 N73-12202
Logic comparison of failure diagnosis for digital systems
03 p0272 N73-12203
Automatic test generator for failure detection and localization in logic systems, LADISLAS
03 p0272 N73-12204
Synthesis of digital unit of variable structure in all purpose digital selection system
[AD-747726] 03 p0272 N73-12208
Design and fabrication of magnetic logic circuits using ferrite delay elements
[NASA-CR-112198] 03 p0277 N73-12247
Universal cellular network for combinational switching functions with simple failure testing
03 p0278 N73-12252
Design of logic counters and scalers based on continued quotients for digital function generators
03 p0278 N73-12253
Test procedure for failure analysis in multiple elementary gate networks using iterative test function
03 p0278 N73-12256
Failure analysis of combinational logic circuits with input reconvergent fan-out
03 p0278 N73-12257
Failure analysis of NOR gate network with parity for easy testing
03 p0278 N73-12258
Syntheses of logical circuits by composing common inputs and common variables
[AD-748165] 03 p0279 N73-12263
Logical function and circuit generator
[NASA-CASE-XLA-05099] 04 p0395 N73-13209
Analysis of multiple faults in combinational logic networks
04 p0399 N73-13247
Test generation for multiple faults in parity circuits
04 p0399 N73-13248
Redundancy reduction for logic circuits by error correcting codes to improve method of increasing circuit reliability
04 p0399 N73-13249
Redundant cells to improve reliability of asynchronous automata
04 p0399 N73-13250
Asynchronous sequential circuit model with input delays and feedback
04 p0400 N73-13251
Design and operation of programmable logic tester for high speed static testing of circuit boards
[REPT-6570] 04 p0420 N73-13422
Statistical and deterministic tests for failure analysis of sequential computer storage devices
05 p0517 N73-14203
Review of macrocellular research for digital computers, noting parallel computers
05 p0517 N73-14205
Ordering theories of variables for realization procedures of multithreshold logic circuits
05 p0522 N73-14242
Transformation of relay contact networks in logic gate circuits for failure analysis
05 p0522 N73-14248
Boundary test procedure for determining characteristics and design of integrated transistor-transistor logic circuits
[AD-749604] 05 p0523 N73-14253
Characterizing sequences and fault detection in sequential computers
[AD-750266] 06 p0644 N73-15233
Circuit with differential amplifier for synthesizing capacitance multiplier with microminiaturized feedback components
[NASA-CASE-NPO-11948-1] 06 p0647 N73-15255
Computer program to simulate FET transistor logic circuit performances and properties
07 p0762 N73-16191
Monte Carlo simulation of complex reliability systems using logic circuit analysis programs linked to statistics programs
[TR-72-39] 08 p0927 N73-17596
Synthesis of combination adder with group carry circuits
[AD-752816] 09 p1007 N73-18216
Cellular arrays as iterative logical and memory structures
[NASA-CR-130936] 10 p1132 N73-19227
Program for logic design of digital counters or sequential circuits
[NASA-CR-2212] 10 p1132 N73-19230
Simulation of logical functions for construction of computerized control system for onboard spacecraft instrumentation
10 p1177 N73-19573
Simulation of program sequencing functions in design of computerized digital control system for onboard spacecraft instrumentation
10 p1177 N73-19574
Failure and diagnosis of faults in logic and combinational circuits of digital computers
[AD-754029] 11 p1265 N73-20264
Integrated microcircuits and complementary four-phase logic system
[NASA-CASE-MSC-14240-1] 12 p1386 N73-21240
Computer design of sequential synchronous circuits and multiple output logical networks
[CEA-R-4294] 12 p1387 N73-21246
Development of hermetically sealed nickel cadmium battery and associated control logic and charger circuit for aircraft applications
[AD-757535] 14 p1606 N73-23017
Detection and measurement of radio frequency interference and methods of logic circuit protection
[NLL-PO-2928-[9022.81]] 15 p1759 N73-24254
Analysis of methods of fault diagnosis used with logic circuits and effect of procedures on structure of circuit assemblies
[NLL-PO-2913-[9022.81]] 15 p1759 N73-24255
Simulation of complex microelectronic module functions in Delta Sigma Speech Coder containing analogue and digital elements
[AD-761206] 18 p2119 N73-27136
Fault detection test methods in combinational digital logic networks
[AD-760543] 18 p2121 N73-27146
Principles of construction, technical characteristics, and functions of several checking general-purpose computers
[AD-762212] 19 p2243 N73-28082
Ferrite logic device for increased reliability of digital electronic systems
[NASA-CR-132265] 19 p2248 N73-28124
Diagnostics of malfunctions in logic circuits and switching circuits
[AD-762234] 20 p2379 N73-29116
Electronic digital data synchronizing and instrumentation amplification techniques
[AD-763797] 21 p2509 N73-30131
Planar Gunn devices in dipole domain mode for high speed logic circuits in PCM equipment, noting thermal resistances and packing density
[FTZ-A-474-TBR-3] 22 p2643 N73-31183
Bibliography on computer-aided logical processes
[AD-764400] 23 p2762 N73-32099
Three level Boolean digital simulation program for logic circuits noting topological matrix circuit representation and simplified temporal simulation
[LAAS-SL-73-I-08] 23 p2769 N73-32149
Self-checking multi-output combinational circuits using forced parity
[AD-765037] 23 p2769 N73-32151
Design of sequential circuits using edge and level sensitive flip-flops
24 p2900 N73-33146

**LOGIC DESIGN**
Automata theory for realizing reliable computer logic with fault detection
[AD-745720] 01 p0031 N73-10241
Program for logic design of digital counters or sequential circuits
[NASA-CR-2212] 10 p1132 N73-19230
Computer design of sequential synchronous circuits and multiple output logical networks
[CEA-R-4294] 12 p1387 N73-21246
Proceedings of conference on multiple-valued logic
[AD-762123] 19 p2240 N73-28063
Reliability improvement by redundancy in electronic systems
[RAE-TR-72200] 21 p2520 N73-30208

**LOGIC NETWORKS**
U LOGIC CIRCUITS

**LOGICAL ELEMENTS**
Large scale integration techniques for computer multiprocessing system
[NASA-CR-128395] 01 p0030 N73-10234
Design and fabrication of magnetic logic circuits using ferrite delay elements
[NASA-CR-112198] 03 p0277 N73-12247

Simulation of logical functions for construction of computerized control system for onboard spacecraft instrumentation
10 p1177 N73-19573

LOGISTICS
NT SPACE LOGISTICS
Development of usage rate system to determine logistics requirements for military aircraft support
[AD-746482] 02 p0127 N73-11034
Development of equations and mathematical models for decision making concerning military logistics, aircraft, space parts, and support equipment
[AD-747972] 03 p0368 N73-12997
Development of concepts and procedures for preparation of loads for airdrop to reduce time required and increase reliability of operation
[AD-750705] 05 p0612 N73-14976
Interrelation of logistics cost in managing nickel cadmium batteries
[AD-750907] 06 p0733 N73-15977
Development and characteristics of dual cargo hook system for use on military transport helicopters
12 p1358 N73-21022
Computerized simulation of containership loading and unloading of heavy lift helicopters for military logistic applications
[AD-756865] 13 p1475 N73-21946
Stationary point processes and applications to communications and logistic systems
[AD-758281] 15 p1804 N73-24621
Analysis of military aircraft refueling and rearming operations in forward areas to show organization, doctrine, and equipment - Vol. 1
[AD-760524] 18 p2108 N73-27046
Analysis of military aircraft refueling and rearming operations in forward areas to show organization and equipment required - Vol. 2
[AD-760525] 18 p2108 N73-27047
Ship to shore transportation of military cargo using tethered balloons
[AD-765352] 23 p2747 N73-31987
Logistics of orbital vehicle servicing computer specification to improve utilization of space shuttle and tug
[NASA-CR-135709] 23 p2845 N73-32736
Logistics support for launches of sounding rockets
[AD-765231] 23 p2852 N73-32789

LOGISTICS MANAGEMENT
NT INVENTORY MANAGEMENT
Computerized simulation of solution to maintenance and logistics problems of gas turbine engines
[AD-753622] 10 p1210 N73-19838
Cost history of F-111 aircraft airframe system to show logistics organization, support costs, reliability and maintainability, and development problems
[AD-762213] 19 p2356 N73-28958
Logistic performance data book for bomb navigation avionics system of F-111 aircraft to show support cost, reliability, maintenance, and problems
[AD-762214] 19 p2357 N73-28959
Logistics performance data book on bombing and navigation system for A-7D aircraft to show reliability, maintainability, cost, and problems
[AD-762215] 19 p2357 N73-28960
Logistic performance data book for electronic countermeasures system of B-52G aircraft to show reliability, maintenance, costs, and problems
[AD-762216] 19 p2357 N73-28961
Logistic performance data book on propulsion system for KC-135 aircraft to show reliability, maintenance, costs, and problems
[AD-762217] 19 p2357 N73-28962
Logistic performance data book for C-5A aircraft landing gear to show system reliability, maintainability, logistic support cost, and performance data
[AD-762248] 19 p2357 N73-28963
Logistic performance data book for C-130E aircraft propulsion system to show reliability, maintainability, logistic support costs, and operational problems
[AD-762249] 19 p2357 N73-28964
Logistic performance data book for UH-1F helicopter airframe to show reliability, maintainability, logistic costs, and operational problems
[AD-762251] 19 p2357 N73-28965
Development of system for predicting system failure rate and determination of optimal economic replacement interval
[AD-762417] 19 p2357 N73-28966
Logistic performance data book for C-5A airframe to show reliability, maintainability, logistics support, and operating problems
[AD-762233] 19 p2358 N73-28968
Logistic performance data book for F-4D aircraft fire control system to show reliability, maintanability, logistics support, and operating problems
[AD-762229] 19 p2358 N73-28969
Logistics performance data book for RF-4C aircraft landing gear system to show reliability, maintainability, logistics support, and operating problems
[AD-762231] 19 p2358 N73-28970
Logistic performance data book for C-141A aircraft radio navigation system to show reliability, maintainability, logistics support, and operating problems
[AD-762250] 19 p2358 N73-28971
Logistic performance data book for KC-135 aircraft electrical power system to show reliability, maintainability, logistics support, and operating problems
[AD-762225] 19 p2358 N73-28972
Logistic performance data book for F-4E flight control system to show reliability, maintainability, logistic support, and operating problems
[AD-762230] 19 p2358 N73-28973
Logistic performance data book for RF-4C photographic reconnaissance system to show reliability, maintainability, logistic support, and operating problems
[AD-762232] 19 p2358 N73-28974
Field maintenance and operational experience with various selected models of F-4 aircraft
[AD-762747] 20 p2362 N73-28995
Computer simulated loading of Army Brigade and equipment into several medium short takeoff transport aircraft configurations
[AD-762916] 20 p2362 N73-29002
Analysis of Tenth Soviet Antarctic Expedition to show preparations, logistic support, and operational accomplishments
20 p2406 N73-29340
Technical and support services performed during Tenth Soviet Antarctic Expedition
20 p2408 N73-29355

LOH HELICOPTER
U OH-6 HELICOPTER

LOKI ROCKET VEHICLE
Design, development and flight tests of Super Loki Dart Meteorological Rocket Systems
[AD-750796] 06 p0722 N73-15895

LONG ISLAND [NY]
Estuarine coastal water dynamics controlling sediment transport and plume development in Long Island Sound
[E72-10250] 03 p0289 N73-12350
ERTS-1 imagery of estuarine and coastal water dynamics controlling sediment transport and plume development in Long Island Sound
[E73-10093] 08 p0902 N73-17305
Estuarine and coastal water dynamics controlling sediment transport and plume development in Long Island Sound
[E73-10378] 10 p1152 N73-19373
Analysis of technical and economic feasibility of constructing offshore airport in New York Metropolitan area
[FAA-RD-73-45] 11 p1267 N73-20280
Analysis of ERTS-1 imagery using electronic satellite image analysis console to display and measure snowfield extent, glacier development, and hydrologic features
[E73-10415] 11 p1279 N73-20377
Estuarine and coastal water dynamics controlling sediment transport and plume development in Long Island Sound
[E73-10627] 15 p1775 N73-24387
ERTS-1 imagery of plume development where Connecticut River flows into Long Island Sound
[PAPER-M5] 19 p2280 N73-28345

LONG RANGE NAVIGATION
U LORAN
U LORAN D

LONG RANGE WEATHER FORECASTING
Long-term tendencies in atmospheric circulation variations for deveoping long-range hydrometeorological forecasting
[NLL-M-22333-[5828.4F]] 01 p0072 N73-10592
Comprehension and use of weather forecasts by Wisconsin agricultural groups
06 p0692 N73-15639
Impact of accurate long range weather forecasts on Wisconsin pea production
06 p0693 N73-15640
Case studies of meteorological satellite impact on agricultural crops and recreational activities
06 p0693 N73-15641
Synoptic-climatological method for long range forecast of heavy rain for European USSR
[NLL-M-22865-[5828.4F]] 11 p1313 N73-20653
Forecasting monthly mean air temperature anomalies by analogs
[NLL-M-22859-[5828.4F]] 11 p1313 N73-20655
Selection of statistically significant relationships for predictors in long range weather forecasting
[NLL-M-22803-[5828.4F]] 11 p1313 N73-20657
Long range forecast by means of spectral nonlinear baroclinic model of atmosphere
[AD-754682] 11 p1315 N73-20670
Optimum utilization of long range forecasts and climatology in making economic decisions
13 p1552 N73-22573
Preparation of long range weather forecasts using principle of analogy of the fields of the meteorological elements
[NLL-M-22852-[5828.4F]] 15 p1805 N73-24628
Macrosynoptic tropopause formula for long range weather forecasts in Budapest
[NLL-M-22839-[5828.4F]] 16 p1894 N73-25322
Long-term cyclic fluctuations of atmospheric precipitation in USSR
[NLL-M-22891-[5828.4F]] 16 p1935 N73-25659
Analysis of long term weather variations, climate changes, and atmospheric circulation
20 p2444 N73-29634
Analysis of epochal variations in atmospheric circulation of Northern Hemisphere, atmosphere, and hydrosphere for making long and extra long range hydrometeorological forecasts
20 p2444 N73-29635
Atmospheric circulation for long range weather forecasts
20 p2445 N73-29641
Sorting analogs to composite-kinematic maps of natural synoptic periods
21 p2573 N73-30618

LONG TERM EFFECTS
Human physiological and psychological responses in long time exposure to simulated space station atmosphere as observed by critical tracking task
01 p0017 N73-10133
Numerical integration of artificial satellite orbit perturbation due to planetary gravitational effects, including long period and secular terms
[GRGS-BULL-5] 01 p0105 N73-10868
Secular and long period terms of artificial satellite perturbed equation of motion noting planetary gravitational effects
01 p0105 N73-10870
Influence of 45 to 60 day space flight on physiological functions of human body
[NASA-CR-129131] 02 p0132 N73-11074
Mathematical model for short period terms in satellite orbits including comparison between analytical theory and numerical integration
[GRGS-BULL-2] 05 p0596 N73-14845
Mathematical model for short period terms in satellite orbits, including comparison between analytical theory and numerical integration
05 p0596 N73-14846
Comparison of satellite orbit elements, using analytic theory and numerical integration
05 p0596 N73-14847
Effects of prolonged weightlessness during space flight on human skeletal and hematopoietic systems
[NASA-TT-F-730] 06 p0630 N73-15116
Evolution of neural messages in human adaptation to prolonged zero gravity flight
06 p0634 N73-15154
Analysis of pole tide fluctuations in earth atmosphere and ocean
[NLL-M-20647-[5828.4F]] 06 p0657 N73-15336
Residual effects of hypnotic drugs on human nervous function and performance
12 p1369 N73-21106
Pilot performance and sleep patterns in long duration flights and control of hypnotic drug and alcohol use
12 p1369 N73-21107
Physiological aspects of sleep induction in aircrews after prolonged flight times
12 p1369 N73-21108
Effects of isoniazid treatment on pilot performance
12 p1369 N73-21111
Altitude acclimatization period effects on rat resistance to hypoxia
13 p1481 N73-22006
Human pulmonary volume decrease during long term bed rest
13 p1482 N73-22016
Mathematical procedure for calculating tectonic plate movement and the secular shift of the mean pole
[NASA-TM-X-66272] 17 p2024 N73-26376
Aerospace medicine and exobiology research in support of long term manned space flight
[JPRS-59702] 20 p2365 N73-29021
Constant strain rate tensile tests to determine long-time dynamic compatibility of elastomeric materials with hydrazine
[NASA-CR-133794] 21 p2562 N73-30538

LONG WAVE RADIATION
Vertical profiles of long wave components of total radiation damage in daytime
[AD-749641] 05 p0542 N73-14409
Aircraft measurement of long wave radiation brightness and angular distribution
[AD-750945] 05 p0544 N73-14424
Integral and spectral flux calculations of long wave radiation in atmosphere, using computers
[AD-761579] 19 p2298 N73-28477
Zonal, hemispherical, and global averages for satellite measurements of albedo and outgoing long wave radiation
[NOAA-TM-NESS-48] 19 p2340 N73-28823
Development of numerical method for determining long wave radiation balance of atmosphere based on effective surface radiation
20 p2401 N73-29295
Development and characteristics of radiometer for airborne measurement of outgoing long wave radiation from earth surface between 8 and 12 microns
20 p2402 N73-29302
Performance tests of radiation thermoelements to determine stability of detectors and feasibility of daytime measurement of long wave radiation
20 p2403 N73-29309

Correction of aberrations in long wavelength holography by direct injection in formation process and computer generation
22 p2680 N73-31466

**LONGITUDE**
Longitude, latitude, and azimuth determinations using transit instrument
[MITT-99] 01 p0101 N73-10826
Determination of longitudinal cross section in inelastic electron proton scattering in Delta[1236] resonance region
02 p0213 N73-11728
Hot star catalog listed in constellation alphabetical order
[COMMUN-31] 19 p2344 N73-28858

**LONGITUDE MEASUREMENT**
Astronomical geodetic observations for longitude, latitude, and components of deflection from vertical at West German stations
[MITT-124] 05 p0538 N73-14375

**LONGITUDINAL CONTROL**
Longitudinal and lateral data, lateral oscillatory derivatives, and aileron and rudder powers for BAC 221 aircraft
[ARC-CP-1230] 05 p0494 N73-14027
Influence of load and wing load distribution on lateral and longitudinal maneuverability of aircraft
08 p0865 N73-16998
Equations of motion and response curve fitting method for determining transfer function coefficients of longitudinal aircraft motion
[DLR-FB-73-39] 17 p1984 N73-26034
Design and development of fixed gain control system for longitudinal axis of C-141 aircraft fly-by-wire control
[AD-760763] 18 p2107 N73-27038
Linear optimal plant and controller model for hydrofoil craft
[AD-760698] 18 p2132 N73-27226

**LONGITUDINAL STABILITY**
Digital computer program for solution of aircraft longitudinal stability characteristics at or near stall point
[AD-745557] 01 p0005 N73-10037
Comparison of longitudinal and lateral stability and control characteristics of Phase B Grumman H-33 space shuttle orbiter
[NASA-CR-120080] 01 p0108 N73-10889
Comparison of longitudinal and lateral stability and control characteristics of baseline 040A space shuttle orbiter
[NASA-CR-120081] 01 p0109 N73-10894
Definitions of aircraft longitudinal stability to account for effects of aircraft structure distortion and compressibility effects
[ESDU-00.00.03] 02 p0124 N73-11010
Low speed wind tunnel tests on siender variable sweep wing of lift, drag, and pitching moments
[ARC-CP-1227] 05 p0492 N73-14009
Flight simulator tests to define minimum acceptable levels of static longitudinal stability for aircraft landing approach following failure of stability augmentation systems
[NASA-TM-X-62200] 06 p0620 N73-15034
Effects of various external stores characteristics, spanwise positions, and Mach number on static longitudinal stability of several military aircraft
[AD-750120] 06 p0624 N73-15063
Development of automatic system for controlling aircraft under turbulent atmospheric conditions to provide pitch stabilization
[AD-751148] 07 p0741 N73-16028
Hot-wire measurement of longitudinal instability phenomena in stagnation area of circular cylinder in turbulent flow
07 p0771 N73-16265
Effects of thrust characteristics on longitudinal stability in supersonic flight
08 p0865 N73-16997
Series expansion method for calculating longitudinal load impact on rod of rate-dependent material
[AD-751979] 08 p0967 N73-17904
Flight test of X-22 aircraft to determine longitudinal stability requirements of short takeoff aircraft during terminal area operations
[AD-754840] 11 p1235 N73-20029
Wind tunnel tests to determine oscillatory longitudinal derivatives of thin delta wing with 0.8 aspect ratio over range of incidences
[ATN-7105] 13 p1470 N73-21903
Wind tunnel tests to determine static longitudinal aerodynamic characteristics of jet transport wing-body with upper surface blown jet flap for lift augmentation
[NASA-TN-D-7183] 13 p1470 N73-21907
Longitudinal vibration of rockets with liquid fuel engines
[AD-756076] 13 p1572 N73-22736
Development of method for calculating downwash interference and longitudinal stability of tandem rotor helicopter
[ARC-R/M-3223] 15 p1729 N73-24022
Theoretical investigation of longitudinal stability, control, and response characteristics of jet flap aircraft
[ARC-R/M-3272] 15 p1730 N73-24028
Flight tests to determine longitudinal aerodynamic parameters of P-1127 aircraft with vectored thrust control
[NASA-TN-D-7296] 15 p1734 N73-24066
Wind tunnel tests to determine directional and longitudinal stability of Javelin aircraft model at transonic speeds
[ARC-R/M-3403] 16 p1853 N73-25012
Longitudinal stability derivatives from flight data by model with automatic parameter adjustment
[DLR-FB-73-13] 17 p1984 N73-26033
Analysis of minimum longitudinal stability for large delta wing transport aircraft during landing approach and touchdown using in-flight simulation techniques
[AD-761120] 18 p2106 N73-27036
Longitudinal stability of Boeing 707 aircraft during steep approach, for noise reduction
[DGLR-PAPER-73-023] 23 p2744 N73-31963
Characteristics of low speed air flow over slender, sharp edged delta wing at various angles of attack and effects on longitudinal and lateral stability
24 p2869 N73-32922
Wind tunnel tests to determine basic performance of swept augmentor wing configuration and effect on longitudinal characteristics of aircraft
24 p2872 N73-32941
Wind tunnel tests to determine magnitude of adverse ground effects on longitudinal aerodynamic coefficients of powered-lift short takeoff aircraft
24 p2873 N73-32950
Effect of artificial longitudinal stability on aircraft performance, based on control configured vehicle concept
24 p2878 N73-32986

**LONGITUDINAL WAVES**
NT PLANE WAVES
Effect of longitudinal slot in circular waveguide
[PB-208160] 01 p0034 N73-10267
Filament stationary motion pattern in media of diverse viscosities, allowing for gravitational and resistance forces to longitudinal motion
06 p0652 N73-15294
Nonlinear excitation of longitudinal plasma oscillations in inhomogeneous plasma
[AREAEE-125] 07 p0828 N73-16713
Excitation of longitudinal waves in collisionless and cold plasma in presence of uniform magnetic field
[AD-756477] 14 p1696 N73-23764
Longitudinal electroacoustic wave attenuation in plasma
[AD-762272] 19 p2325 N73-28706
Complex variable theory used in representation of electric field of longitudinal waves in plasma
[AD-762905] 20 p2459 N73-29763
Dynamics of field-aligned longitudinal currents in magnetosphere
[NASA-TT-F-15075] 23 p2787 N73-32294

**LONGSHORE CURRENTS**
U COASTAL CURRENTS

**LOOK ANGLES**
U AZIMUTH
U ELEVATION ANGLE

**LOOP ANTENNAS**
Wooded terrain effects on radiation patterns of circular and directional antennas
[FOA-3-A-3747-60] 11 p1255 N73-20179
Lossy earth effects on very high frequency antenna patterns near ground level
[AD-754637] 11 p1257 N73-20204
Fourier solution for determining radiation patterns of dielectric coated loop antenna
[AD-762041] 19 p2245 N73-28100
Automatic carrier acquisition system for phase locked loop receiver
[NASA-CASE-NPO-11628-1] 21 p2506 N73-30113

**LOOPS**
Filter for third order phase locked loops in signal receivers
[NASA-CASE-NPO-11941-1] 18 p2125 N73-27171

**LOR [RENDEZVOUS]**
U LUNAR ORBITAL RENDEZVOUS

**LORAN**
Bandwidth reduction technique for loran retransmission system
[AD-746055] 02 p0208 N73-11687
Accuracy/resolution relationship of NAVAID systems Loran/Omega for measuring vertical wind profile
[AD-748275] 03 p0328 N73-12675
Application of loran/inertial hybrid system and Kalman filter algorithm to fixed feedback gain
11 p1318 N73-20701
Development of navigation system design factors through computerized simulation for application to loran/inertial hybrid system
[AD-754548] 11 p1322 N73-20731
Characteristics of airborne area navigation equipment and application to air traffic control functions
14 p1688 N73-23698
Development and characteristics of hybrid loran and inertial navigation system as alternative to high precision navigation sensors
[AD-761027] 18 p2176 N73-27572

**LORAN C**
Development, characteristics, and applications of Loran C navigation system for air navigation and microsecond clock synchronization
[NBS-MONO-129] 05 p0577 N73-14700
Coastline induced Loran C anomalies
[AD-757142] 14 p1691 N73-23724
Analysis of Loran C signal processing techniques using hybrid simulation procedure
[AD-757586] 14 p1691 N73-23725

**LORAN D**
Application of propagation theory to analyze development and effectiveness of loran navigation system in Germany
[AD-750006] 06 p0697 N73-15682
Evaluation of loran antenna modification to determine effect of increased height on radiated power and system performance
[AD-751978] 08 p0942 N73-17714

**LORENTZ FORCE**
Mathematical representation with metric form to first order of gravitationally modified Maxwell equation in Lorentz symmetric linear field theory
[NASA-CR-130754] 08 p0915 N73-17500
Transient behavior of currents and forces in coil system of stellarator during operational disturbances
[NASA-TT-F-15014] 18 p2126 N73-27182

**LORENTZ TRANSFORMATIONS**
Transformation functions between z basis and jm basis of Lorentz group principal series
[NOTA-INTERNA-386] 03 p0324 N73-12641

**LOS ALAMOS TURRET REACTOR**
U HIGH TEMPERATURE NUCLEAR REACTORS

**LOSSES**
Equivalent resistance network for MHD generator noting losses and scale effect
[TH-72-E-30] 03 p0343 N73-12796
Determination of KOH loss in ESRO 4 nickel cadmium batteries by electrical measurements
[ESRO-CR[P]-132] 04 p0375 N73-13054
Azimuthal distribution losses of protons at synchrophasotron ejection determined by scintillation counters
[JINR-P16-6433] 04 p0453 N73-13699
Influence of light conditions and understorey tree death on organic matter loss balance in oak underwood
20 p2405 N73-29331

**LOUDNESS**
Mathematical models for deriving loudness function from physical evidence without human judgment
[NASA-TN-D-7297] 15 p1742 N73-24121

**LOUISIANA**
NT MISSISSIPPI DELTA [LA]
Visual inspection of runway conditions at Fort Polk Army Airfield, Louisiana
[AD-743858] 01 p0037 N73-10292
Development of system for mapping and monitoring natural ecosystems and environmental complexes from ERTS-1 imagery of California, Nevada, Four Corners Area, Louisiana, and Colorado Plateau
[E73-10289] 08 p0915 N73-17495
Automated thematic mapping and analysis of terrain in Arizona, Texas, Washington, Utah, Louisiana, and California using ERTS-1 imagery
[E73-10386] 10 p1153 N73-19379
Mapping and monitoring natural ecosystems and environmental complexes and estimation of rice crop yield in California and Louisiana from ERTS-1 imagery
[E73-10669] 16 p1899 N73-25364
Application of ERTS-1 imagery for identification of ecological analogs of natural vegetation and food crops in California, Colorado, and Louisiana
[PAPER-A6] 19 p2260 N73-28214
Seasonal variations of vegetation, circulation patterns in Lake Pontchartrain, and urban neighborhood quality in Louisiana from ERTS-1 imagery
[E73-10838] 19 p2290 N73-28416
Uniform mapping and monitoring of natural ecosystems and environments in California, Louisiana, and Colorado from ERTS-2 imagery
[E73-10839] 19 p2290 N73-28417
Mapping rice crops of California and Louisiana and natural vegetation of Colorado Plateau from Skylab photography
[E73-10885] 20 p2394 N73-29236
Photomapping of rice crops and natural vegetation in Louisiana and California from Skylab EREP imagery
[E73-10916] 20 p2397 N73-29265
Uniform mapping of rice crops in Louisiana and California and desert vegetation in southwestern Colorado from Skylab imagery
[E73-10979] 22 p2657 N73-31286
Computer interpretation of multispectral data of Chesapeake Bay, Lake Pontchartrain, Louisiana, and lower Mississippi Valley
[E73-11007] 22 p2660 N73-31312

Uniform mapping and monitoring of natural ecosystems and environmental complexes of Colorado Plateau and Sierra-Lahontan areas and estimation of rice crop yields in California and Louisiana
[E73-11070] 23 p2781 N73-32246
Uniform mapping of vegetation and rice in Colorado Plateau, Sierra-Lahontan, California, and Louisiana coastal plain from Skylab multispectral photography
[E73-11149] 24 p2919 N73-33303

**LOUVERS**
Research and development of high performance satellite thermal control louver array actuator including single blade and multiple blade actuation system
[ESRO-CR[P]-247] 18 p2201 N73-27766

**LOVE WAVES**
Tidal effects in motion of earth satellites and Love parameters of earth
[NASA-TM-X-66173] 08 p0961 N73-17858
Earth dynamic filtering algorithm for earthquake prediction and Love number determination
16 p1896 N73-25333

**LOW ALLOY STEELS**
U HIGH STRENGTH STEELS

**LOW ALTITUDE**
Limitations on pilot visual perception of target from low flying aircraft
[AD-759651] 16 p1869 N73-25136
Harmonic analysis of low altitude disturbances in geomagnetic fields
17 p2017 N73-26308
Analysis of pressure distribution on plane ground surface under aircraft flying at low altitude with subsonic velocity
[FFA-AU-634-PT-2] 18 p2129 N73-27206

**LOW ALTITUDE SUPERSONIC VEHICLES**
U F-111 AIRCRAFT

**LOW ASPECT RATIO**
Performance tests on low hub-tip ratio supersonic axial flow compressor
[AD-752585] 09 p1079 N73-18805

**LOW ASPECT RATIO WINGS**
NT DELTA WINGS
Wind tunnel tests of scale model of orbiter 040A configuration in ground effect
[NASA-CR-120082] 02 p0233 N73-11895
Force and pressure distribution measurements on wing-body combination with wing of low aspect ratio in compressible flow
[DLR-FB-72-08] 09 p0980 N73-18008
Mass distribution analyses for design of low aspect ratio aerodynamic stable fighter wings
[NASA-CR-112232] 13 p1469 N73-21900
Determination of mass distributions along elastic axes of 2-spar wings in fighter aircraft design
[NASA-CR-112233] 13 p1470 N73-21901

**LOW COST**
Low cost efficient thermionic converter for use in nuclear reactors
[NASA-CASE-NPO-13121-1] 03 p0332 N73-12702
Low cost arc welding technique for thick sections of HY-150 steels
[NASA-CR-120994] 09 p1039 N73-18472
Resonator design for low cost microwave bandpass filter
[NHK-LABS-NOTE-162] 20 p2381 N73-29128
Design of low cost highly sensitive SHF microwave components
[NHK-LABS-NOTE-163] 20 p2381 N73-29129

**LOW DENSITY FLOW**
Investigation of low density hypersonic flow by controlled boundary layer removal from nozzle wall
[AD-754276] 11 p1271 N73-20316
Photographic equidensitometry of two phase and low density flows
[DLR-MITT-73-02] 17 p2015 N73-26293
Drag measurement of parallel flat plates and perpendicular disks in supersonic free molecular flow
[DLR-FB-73-17] 21 p2525 N73-30248

**LOW DENSITY GASES**
U RAREFIED GASES

**LOW DENSITY MATERIALS**
Chemical analysis, production, and physical properties of polyimide syntactic foam
[SC-DC-72-2297] 07 p0812 N73-16583
Development of method and equipment for detecting cracks in materials with porous subsurface matrix covered by impervious coating
[NASA-CASE-MSC-14187-1] 08 p0923 N73-17564
Development of low density foamed epoxy adhesives
[Y-1833] 13 p1547 N73-22538
Aging tests of light alloys bonded with various adhesives and development of new aging test criteria
[RAE-LIB-TRANS-1662] 17 p2043 N73-26528
Development and characteristics of closed pore ceramic foam insulation material for use as heat shield on space shuttle vehicle
[NASA-CR-2254] 19 p2312 N73-28591

**LOW DENSITY WIND TUNNELS**
Design and system description of hypersonic low density wind tunnel in Germany including generation of molecular beams
[DLR-FB-71-84] 06 p0650 N73-15279

**LOW FINENESS RATIO**
U FINENESS RATIO

**LOW FREQUENCIES**
NT VERY LOW FREQUENCIES
Thermal and atmospheric noise effects on optimization of underwater low frequency communications
[FOA-3-C-3671-60] 02 p0139 N73-11129
Numerical analysis of effects of lower ionosphere on propagation of radio waves at low frequencies for conditions of quiet day, night, and disturbed night
[FOA-3-C-3673-60] 02 p0140 N73-11131
Antenna feed networks for broadbanding very low frequency and low frequency antennas to wide frequency shift keying modulation
[AD-746119] 02 p0151 N73-11226
Computerized simulation of instability response of magnetized two ion species plasma to low frequency electric field oscillations
[AD-746109] 02 p0217 N73-11757
L2 stability in low and high frequency distributed feedback systems
[NASA-CR-129599] 03 p0277 N73-12245
Low-frequency quasi-static instabilities in fully ionized plasma
[NASA-CR-129517] 03 p0341 N73-12778
Effects of low frequency background noise on electrical properties of semiconductor materials and components
05 p0519 N73-14222
Low frequency oscillations of earth magnetic field observed by ATS 1
05 p0537 N73-14374
Low frequency radio continuum arising in inner magnetosphere from trapped and untrapped electrons
07 p0775 N73-16291
Analysis of improved signal processing techniques for low frequency, one-way ranging for aircraft radio navigation
[AD-754031] 11 p1322 N73-20727
Nonlinear detection of low frequency plane wave by directional circular piston beam
[AD-755167] 12 p1430 N73-21588
Design and performance of low frequency/very low frequency omnidirectional antenna model
[AD-757556] 14 p1643 N73-23324
Fluid dynamic aspects of cardiovascular behavior during low frequency whole-body vibration such as encountered by astronauts during launch and reentry
[NASA-CR-133843] 21 p2501 N73-30069
Diffusive equilibrium model for calculating characteristics of broadband ELF, VLF, and LF emissions in magnetosphere
[NASA-CR-133925] 22 p2666 N73-31363

**LOW FREQUENCY BANDS**
NT VERY LOW FREQUENCIES

**LOW GRAVITY**
U REDUCED GRAVITY

**LOW GRAVITY MANUFACTURING**
Development of manufacturing in space processes for Skylab program to include operating sequence description and results obtained
13 p1594 N73-22922

**LOW LATITUDES**
U TROPICAL REGIONS

**LOW LEVEL TURBULENCE**
Comparison of gust velocities derived from accelerations of Canberra and Vulcan aircraft noting acceleration and wing loading power spectra
[ARC-CP-1244] 22 p2615 N73-30955

**LOW MOLECULAR WEIGHTS**
Thermodynamics of low and high molecular weight liquids
23 p2859 N73-32841

**LOW NOISE**
Application of absorber laser amplifier and detector to wide angle low noise optical radar and communication systems
[AD-749543] 05 p0558 N73-14533
Low phase noise frequency divider for use with deep space network communication system
[NASA-CASE-NPO-11569] 17 p2007 N73-26229
Termination resistance as standard for calibrating low noise temperature in electronic equipment
[NASA-TT-F-15016] 19 p2243 N73-28086

**LOW PASS FILTERS**
Design of digital filters for bandpass and low pass applications
[AD-754032] 11 p1265 N73-20266
Comparative study of TWT and klystron amplifiers for use as power amplifiers in television broadcast satellites
[ESRO-CR[P]-269-VOL-3] 21 p2508 N73-30124

**LOW PRESSURE**
Ion flux probe for low pressure discharge plasma in thin metal plate
[TRITA-EPP-72-20] 02 p0174 N73-11410
Low pressure air-water annular flow in horizontal tube
[AERE-R-6687] 06 p0655 N73-15320
Effects of various gases on conductivity of four organic semiconductors at very low pressures
[REPT-1972-19] 14 p1697 N73-23772
Static dielectric constant of solid methane at low temperatures and high pressures
15 p1745 N73-24147
Detection of low pressure center by viewing cloud pattern and wind direction in ERTS-1 photography
[E73-10978] 24 p2913 N73-33243

**LOW PRESSURE CHAMBERS**
U VACUUM CHAMBERS

**LOW SPEED**
Small Froude number paradoxes and wave resistance at low speeds
[AD-746191] 01 p0043 N73-10340
Low speed pull-up maneuvers for slender wing transport aircraft with stability and control augmentation
[ARC-CP-1231] 04 p0369 N73-13004
Initiation and propagation of low-velocity detonation in confined energetic liquids
[AD-748438] 04 p0485 N73-13966

**LOW SPEED HANDLING**
U CONTROLLABILITY
U LOW SPEED

**LOW SPEED STABILITY**
Analysis of parameters affecting aircraft stall and post stall gyrations to include aerodynamic configurations and pilot performance
06 p0616 N73-14999
Aerodynamic characteristics of low speed flight using heavily loaded ducted fans, single bladed hovering rotor, and tensioned sheets with cutouts
[AD-764264] 22 p2616 N73-30964

**LOW SPEED WIND TUNNELS**
NT SUBSONIC WIND TUNNELS
Wind tunnel tests of blowing on circular cylinders applied to aircraft control and braking at low speeds
[ARC-CP-1232] 10 p1104 N73-19000
Wind tunnel tests to determine low speed aerodynamic characteristics of large scale V/STOL transport models with lift fan lift-cruise fan propulsion system
[NASA-TM-X-62231] 11 p1233 N73-20014
Jet exhaust simulation in low speed wind tunnel
[DGT-8352] 13 p1507 N73-22211
Objectives of dynamic tests in low speed wind tunnels and techniques for measuring oscillatory derivatives and transient motion effects
17 p2009 N73-26244
Fluid motion problems in design and operation of low speed and transonic wind tunnels
[AGARD-R-602] 17 p2013 N73-26279

**LOW TEMPERATURE**
Ising ferromagnet thermodynamic equilibrium states in low temperature regions
[NOTA-INTERNA-381] 01 p0080 N73-10660
Thermionic emission from oxide-coated cathodes at low temperatures
[AD-747319] 02 p0150 N73-11218
Analysis of low temperature proton irradiation induced defects in metals
[COO-3431-1] 04 p0434 N73-13542
Determination of activation parameters and microcreep in niobium single crystals at low temperature
[COO-1198-909] 04 p0458 N73-13742
Thermal conductivity measurements of electron and phonon scattering behavior in low temperature solids
[COO-1629-31] 04 p0485 N73-13961
Cooling systems using cold gas transfer closed loops in 15 to 80 K temperature range
[DLR-MITT-71-09] 04 p0485 N73-13964
Automatic measurement of frequency stability of microwave Gunn diode oscillators at low temperatures noting graphs of power and frequency against time
[SRDE-72013] 05 p0520 N73-14226
Low temperature bonding of solar panel materials
[AD-746684] 05 p0553 N73-14493
Correlation of organic substance oxidation rate parameters in low temperature plasma with high frequency power
[NASA-TT-F-14671] 07 p0753 N73-16113
Low temperature resistivity of high purity copper wire in high magnetic fields
[U-235] 08 p0943 N73-17725
Model for studying excessive specific heat that glasses exhibit at low temperatures
[AD-752471] 08 p0970 N73-17930
Identification and preparation of materials for use as nonporous solid ionic conductors in rechargeable high energy battery at low temperatures
[NASA-CR-120964] 09 p0990 N73-18078
Low temperature chemical vapor deposition process and potential applications
10 p1164 N73-19475
Nature of power losses in RF superconducting cavities at low and high temperatures
[SLAC-PUB-963] 12 p1383 N73-21213
Development of low melting fused salt electrolytes
[AD-755528] 13 p1477 N73-21965
Electrical and physical properties of low temperature grown cubic gallium nitride films
[AD-755237] 13 p1567 N73-22704
Low temperature performance of air electrodes for use in zinc-air and metal-air battery systems
[AD-758171] 14 p1607 N73-23021
Measurements and techniques of low temperature acoustic thermometry
[NBS-TN-765] 14 p1666 N73-23518
Constitutive equations for determining elastic deformation twinning in body centered cubic lattice metals at low temperatures
[AD-757042] 14 p1679 N73-23624

Static dielectric constant of solid methane at low temperatures and high pressures
15 p1745 N73-24147
Pulse-echo technique for measuring ultrasonic attenuation in Bi12GeO20 single crystals at low temperature
16 p1952 N73-25798
Personnel and laboratory listing in low temperature research
[AD-757651] 16 p1953 N73-25805
Specific heat measurements of He-4 monolayers on sintered and gas monolayer coated copper
16 p1973 N73-25957
Square sectioned single crystals of Cu-Al alloys at low temperature
17 p2043 N73-26525
Low temperature measurement of heat pulse and ultrasonic wave interaction with stress-split acceptor states in semiconductors
18 p2186 N73-27647
Low temperature epitaxial development of Ge and Si layers by chloride method
18 p2187 N73-27656
Equations of state for hydrogen including low temperature regions
[UCID-16095] 19 p2230 N73-27986
Spin energy transfer processes at low temperatures
[AD-762618] 20 p2455 N73-29731
Chemical reactivity of hydrogen, nitrogen, and oxygen below 100 K
[NASA-CR-133654] 20 p2456 N73-29742
Influence of applied stress, magnetic and electric fields, and impurity concentration on electrical conductance of n-type germanium at very low temperatures
[RR-738] 20 p2462 N73-29783
Fuel cell technology using low temperature potassium hydroxide electrolyte
[NASA-CR-134002] 21 p2499 N73-30056
Extrapolation of thermophysical properties data for oxygen to high pressures at low temperatures
[NASA-CR-133858] 21 p2506 N73-30109
Low temperature properties and specific heat of plutonium and neptunium
[AERE-R-7172] 24 p2934 N73-33432
Effect of FeF2 addition on Hastelloy N compatibility with LiF-BeF2-UF in low temperature convection loop system
[ORNL-TM-4188] 24 p2936 N73-33444
Spectrographic study of rare earth crystal absorption spectra in magnetic fields at liquid helium temperature
[NASA-TT-F-14732] 24 p2958 N73-33640
Abnormalities of liquid He-3 measured below 5 m K
24 p2967 N73-33713

**LOW TEMPERATURE ENVIRONMENTS**
Organization and functions of research facility for conducting projects involving low temperature effects
04 p0487 N73-13976
Development of iron alloy with high fracture toughness at cryogenic temperatures
[LBL-1121] 21 p2559 N73-30511
Climatized electrical equipment for tropical and cold climates
[AD-764393] 23 p2766 N73-32128

**LOW TEMPERATURE PHYSICS**
Analysis of conditions required to produce superconductivity in materials under high pressure
[NLL-NEL-TT-2402-[6075.461]]
02 p0186 N73-11505
Organization and functions of research facility for conducting projects involving low temperature effects
04 p0487 N73-13976
Epoxy resins for use in superconducting magnets at liquid helium temperatures
[RHEL/R-251] 12 p1416 N73-21476
Research projects in solid state physics, low temperature physics, superconducting films, and quantum liquids and crystals
[COO-1569-93] 12 p1439 N73-21657
Calibration of liquid helium-cooled germanium bolometers to determine responsitivity at different chopper frequencies and cryostat temperatures
[BMFT-FBW-73-05] 14 p1666 N73-23524
Research and development conducted at Spanish universities on solid state and low temperature physics
[AD-757991] 14 p1700 N73-23795
Low temperature superconductivity research at Danish universities
[AD-760317] 17 p2075 N73-26786

**LOW TEMPERATURE PLASMAS**
U COLD PLASMAS

**LOW TEMPERATURE TESTS**
Apparatus for low temperature cavitation testing of materials at increased static pressure
[AD-748108] 03 p0304 N73-12482
Electrochemical effects of low temperature operation on zinc air battery performance
[AD-749270] 04 p0377 N73-13068
Use of low temperature quenching techniques to retain simple vacancy defects in magnesium
[NLL-CE-TRANS-5944-[9022.09]]
05 p0561 N73-14559
Electronic spectra of benzophenone crystals and low temperature spectra of ketones
[AD-753380] 10 p1201 N73-19775
Low temperature optical absorption of some unusual intermetallic compounds
12 p1438 N73-21646
Heat capacity of submonolayer helium films adsorbed on exfoliated graphite in very low temperatures
16 p1973 N73-25953
Low temperature tests of elastomeric bearing rotors on OH-58 helicopter
[AD-759957] 17 p2038 N73-26490
Low temperature thermal magnetoresistance of potassium
[COO-3150-12] 22 p2625 N73-31036
Method of testing materials based on teflon and Kel-F for friction at low temperatures by using X18H9T steel in helium medium for different slip rates and loads
22 p2688 N73-31531

**LOW THRUST**
NT MICROTHRUST
Logical flow and guidelines for constructing low thrust orbit determination computer program
[NASA-CR-112256] 08 p0961 N73-17862
Comparison of several first and second order deterministic low-thrust guidance methods
08 p0963 N73-17875
Guidance strategies and analysis for low thrust navigation
[NASA-CR-130862] 09 p1062 N73-18663
Effect of trapped electron and proton radiation on onboard components and payloads of low thrust orbits through Van Allen belts
[NASA-TM-X-2777] 11 p1335 N73-20840

**LOW THRUST PROPULSION**
NT ELECTROMAGNETIC PROPULSION
NT ELECTROSTATIC PROPULSION
NT ION PROPULSION
NT PLASMA PROPULSION
NT SOLAR PROPULSION
Solar electric propulsion system integration technology study to show spacecraft and mission applications - Vol. 2
[NASA-CR-130702] 08 p0954 N73-17812
Solar electric propulsion system integration technology study to show spacecraft and mission applications - Vol. 3
[NASA-CR-130703] 08 p0954 N73-17813
Optimal control, guidance, and trajectory for low thrust acceleration spacecraft
15 p1829 N73-24827

**LOW VELOCITY**
U LOW SPEED

**LOW VISIBILITY**
Analysis of limitations on helicopter approach and landing during conditions of low visibility
[AD-747732] 03 p0329 N73-12686
Cost effectiveness analysis of propane operated fog dispersal system and evaluation of runway visual range improvement
[FAA-RD-72-123] 06 p0649 N73-15267
Effect of low visibility on performance of vehicle operators
[AD-749248] 13 p1486 N73-22051
Laser observations of dense natural fog to determine backscatter and slant range visibility for aircraft landing operations
[AD-760128] 17 p2041 N73-26511
Fog chamber low visibility landing simulation film for pilot training
[FAA-RD-73-61] 20 p2452 N73-29707
Determination of variability of oblique and horizontal visibility for aircraft landing by analysis of experimental data
[NLL-M-23046-[5828.4F]] 21 p2567 N73-30576
Aircraft landing problems under low visibility weather conditions
[DGLR-PAPER-73-015] 23 p2817 N73-32520

**LOW VOLTAGE**
Low voltage pellet type thermal batteries
[SC-DC-71-4102] 03 p0254 N73-12059
Thin pressure-sensitive FCC for low voltage uses
14 p1642 N73-23313

**LOW WING AIRCRAFT**
Engine ingestion prevention on low wing aircraft, particularly Mercury aircraft, by jet blast
[FO-1149] 06 p0622 N73-15049

**LOWER ATMOSPHERE**
NT OZONOSPHERE
NT TROPOSPHERE
Monthly mean climatological statistics for surface to 5 mb pressure level over Australia - Dec. 1971
01 p0074 N73-10606
Monthly mean climatological statistics for surface to 5 mb pressure level over Australia - Aug. 1971
01 p0074 N73-10607
Monthly mean climatological statistics from surface to 5 mb level over Australia - January 1972
02 p0204 N73-11654
Influence of atmospheric sulfur budget on biosphere
[BNL-16906] 04 p0415 N73-13387
Meteorological rocket and radiosonde data on lower and upper atmospheres - Mar. 1971
06 p0692 N73-15633
Aerological data from balloon and rocket flights for Japan and vicinity - Jan. 72
06 p0693 N73-15647
Upper atmospheric data of Japan and vicinity Feb. 1972
06 p0693 N73-15648
FM CW radar data of lower atmosphere, including observations on atmospheric turbulence, wave motions, and rain
[AD-752034] 08 p0921 N73-17546
Interaction between radiative transfer and turbulent exchange in lower layers of atmosphere
[NASA-TT-F-14518] 09 p1026 N73-18378
Meteorological rocket and radiosonde data on lower and upper atmospheres - Apr. 1971
10 p1180 N73-19600
Aerological data from balloon and rocket flights for Japan and vicinity - May 1972
10 p1182 N73-19612
Aerological data from balloon and rocket flights for Japan and vicinity - Apr. 1972
10 p1182 N73-19615
Mean temperature lapse rates within lower 300 meters
[NLL-M-22838-[5828.4F]] 12 p1419 N73-21503
CSTR system for measuring ozone reactions in lower atmosphere
13 p1514 N73-22269
Role of biosphere in regulating chemical processes in atmosphere
[AERONOMICA-ACTA-A-116] 13 p1551 N73-22569
Solid phase trace element aerosol concentrations in lowest 34 meters of atmosphere
15 p1771 N73-24343
Aerological data from balloon and rocket flights for Japan and vicinity
15 p1777 N73-24407
Air pollution of biosphere
[NLL-M-22885-[5828.4F]] 16 p1936 N73-25669
Meteorological rocket and radiosonde data on lower and upper atmospheres - July 1971
16 p1937 N73-25671
Meteorological rocket and radiosonde data on lower and upper atmospheres - August 1971
16 p1937 N73-25672
Meteorological rocket and radiosonde data on lower and upper atmosphere - September 1971
16 p1937 N73-25673
Proving solar activity effect on biosphere by correlation between activity indices with biological indices
[NASA-TT-F-14984] 17 p2079 N73-26821
Influence of man on biospheric balance
[JPRS-59366] 18 p2110 N73-27065
Aerological data from balloon and rocket flights for Japan and vicinity - September 1972
18 p2172 N73-27539
Aerological data from balloon and rocket flights for Japan and vicinity - Aug. 1972
18 p2172 N73-27540
Aerological data from balloon and rocket flights for Japan and vicinity - Oct. 1972
18 p2172 N73-27541
Proceedings of conference on actinometry and atmospheric optics to include effects of solar radiation and atmospheric light on photosynthesis
[TT-70-50159] 20 p2399 N73-29280
Ecological forecasting and optimizing biosphere
[JPRS-59729] 20 p2409 N73-29364
Monthly mean climatological statistics for surface to 5 mb pressure level over Australia - October 1972
20 p2449 N73-29678
Monthly mean climatological statistics for surface to 5 mb pressure level over Australia - Dec. 1972
20 p2449 N73-29679
Monthly mean climatological statistics for surface to 5 mb pressure level over Australia - September 1972
20 p2449 N73-29680
Monthly mean climatological statistics for surface to 5 mb pressure level over Australia - November 1972
20 p2449 N73-29681
Aerological data from balloon and rocket flights for Japan and vicinity - December 1972
24 p2921 N73-33325
Measurement of atmospheric radiation levels at low altitude in vincinity of Vienna, Austria during 1972
[NP-19751] 24 p2922 N73-33340
Aerological data from balloon and rocket flights for Japan and vicinity - Nov. 1972
24 p2947 N73-33540
Aerological data from balloon and rocket flights for Japan and vicinity - Jan. 1973
24 p2947 N73-33541

**LOWER BODY NEGATIVE PRESSURE [LBNP]**
U ACCELERATION STRESSES [PHYSIOLOGY]

**LOWER IONOSPHERE**
NT D REGION
Nonequilbrium ionospheric disturbances in lower ionosphere
20 p2390 N73-29196

**LOX [OXYGEN]**
U LIQUID OXYGEN

**LOX-HYDROGEN ENGINES**
U HYDROGEN OXYGEN ENGINES

LRV [VEHICLE]
U LUNAR ROVING VEHICLES
LSI
U LARGE SCALE INTEGRATION
LST
U LARGE SPACE TELESCOPE
LUBRICANT TESTS
Analysis of lubricating oil losses under vacuum conditions and application to antifriction bearings in antenna despin system of Helios solar probe
[NLL-RISLEY-TR-2567-[9091.9F]] 15 p1790 N73-24509
LUBRICANTS
NT GAS LUBRICANTS
NT LUBRICATING OILS
NT SOLID LUBRICANTS
Analytical method to compute squeeze film thickness, pressure, and load relations between rigid ball and rigid groove when lubricated by fluid with exponential pressure-viscosity relationship
[NASA-CR-2139] 01 p0062 N73-10506
Electrical resistance of lubricating film in friction of various metals
[AD-747451] 03 p0308 N73-12515
Performance of powder metallurgy bronze graphite bearings operating under hydrodynamic conditions at high slipping rates
[AD-747432] 03 p0309 N73-12523
Frictional properties of rubbers in presence of greases and graphite lubricants
[AD-747447] 03 p0322 N73-12622
Wide Temperature range, nonpolymeric, large molecular weight lubricants based on combination of siloxane and aromatic groups, for equipment near spacecraft nuclear reactors
[NASA-CR-123966] 04 p0447 N73-13654
Lubricant supply for mechanical antenna bearings
[NLL-RISLEY-TR-2308-[9091.9F]] 05 p0550 N73-14463
Influence of chemical composition and molecular structure of liquid lubricant on its performance
[NASA-TM-X-68183] 07 p0804 N73-16521
Limiting stabilities and thickening properties of phthalocyanine lubricants in different dispersion media
[AD-752827] 09 p1040 N73-18484
Development of epoxy resin lubricant sealant for hermetic sealing of threaded joints on pipes
[AD-752825] 09 p1040 N73-18486
Removal of mechanical impurities from AKOR-1 additive by filtration method using perlite
[AD-751947] 10 p1167 N73-19496
Friction and wear measurements of CVM M-50 steel lubricated with three C-ether formulations
[NASA-TN-D-7254] 11 p1298 N73-20532
Bearing sectors for controlling self excited instability of journal bearing shafts rotating at high speeds in low viscosity lubricants
[NASA-CASE-LEW-11076-2] 11 p1298 N73-20533
High-speed oscillating and thermal resistance tests of 25 self-lubricating composites
[AD-755112] 11 p1299 N73-20539
Effectiveness of using various lubricant cooling fluids for diamond superfinishing
[AD-753980] 11 p1299 N73-20541
Influence of zinc diamyldithiocarbamate on stability of mineral oil inhibited with 2,6 diterciarybutyl-p-cresol
[AD-754664] 11 p1300 N73-20548
Determination of optimum conditions for lubrication and cooling during grinding by abrasive discs of synthetic superhard materials
[AD-754665] 11 p1302 N73-20562
Rheological behavior of lubricant in rolling and sliding elastohydrodynamic lubricated contact
[NASA-CR-2206] 12 p1408 N73-21413
Effect of viscous lubricants on metal flow during cold reverse extrusion
[AD-743242] 13 p1533 N73-22425
Test rig simulation of gas turbine engine to determine means for minimizing incidence of lubricant sump fires in high speed aircraft engines
[NASA-CR-121158] 13 p1590 N73-22891
Tabular listing of minimum and maximum temperatures for use in specifying fuel and lubricant properties needed in different geographical areas
[AD-756420] 14 p1685 N73-23675
Development of lubrication theories and application of epilame-lubricant pairs for friction reduction
[NLL-RISLEY-TR-2547-[9091.9F]] 15 p1790 N73-24510
Surface potential and wear measurements on carbamate, amine, and phosphorothioate lubricant additives
[AD-759126] 17 p2051 N73-26595
Utilization of thiophenyl ether disiloxane and trisiloxane as lubricant fluids in severe environment including space
[NASA-CASE-MFS-22411-1] 19 p2304 N73-28532
Susceptibility of synthetic engine and transmission lubricants of OH-58 A helicopter to microbal attack
[AD-762176] 19 p2313 N73-28604
Different types of lubricants for working of plastics
[NLL-RTS-7852] 20 p2421 N73-29449
Fluorinated esters of polycarboxylic acid and lubricating compositions for use at extreme temperature
[NASA-CASE-MFS-21040-1] 21 p2505 N73-30098
Lubricants for use in space environment at high and low temperature and zero gravity - bibliographies
[AD-765300] 23 p2799 N73-32385
High temperature lubricants - bibliographies
[AD-764700] 23 p2799 N73-32387
Roller bearings technology - material, design, and lubricants
[NASA-TM-X-71441] 24 p2929 N73-33389
LUBRICATING OILS
Formation of electric fields during friction of lubricating oil on metal surface
[AD-745433] 01 p0062 N73-10511
Viscosity of liquids and classification of lubricating oils
[ESDU-68036] 02 p0154 N73-11247
Tank design for forced circulation oil lubricating systems
[ESDU-68039] 02 p0177 N73-11429
Test equipment and procedures for determining foaming and aeration characteristics of aircraft engine lubricants
[AD-747804] 03 p0321 N73-12618
Elastohydrodynamic traction measurements and lubricant film thickness determination for high speed rolling-sliding contacts
[AD-750752] 06 p0678 N73-15520
Dictionary-handbook on properties and uses of fuels, lubricating materials, and special liquids
[AD-750484] 06 p0712 N73-15810
Organometallic and physical property standards for diluent oil calibration
[NBS-TN-751] 08 p0883 N73-17150
Nucleonic sensor for detecting metal in recirculating lubricating oil systems
[AD-752580] 08 p0926 N73-17588
Interaction of velocity and temperature fields in lubricating layer of thrust slide bearings and analysis of viscosity variation along length and thickness of lubricating layer
[AD-753044] 09 p1041 N73-18487
Oil base effect on lubricating performance of lithium greases and soaps containing hydrocarbons
[AD-754593] 11 p1300 N73-20549
Emulsifying capacity of oils and wearability of additives during contact with water
[AD-754622] 11 p1302 N73-20561
Spectroscopic, photometric, and electron microscope analyses of metal wear particles in JT3D turbojet engine oil
[DLR-FB-73-06] 12 p1409 N73-21417
Calculation and design of heat transfer apparatus for viscous liquids, liquid fuel, and lubricating oils
[AD-756947] 13 p1592 N73-22908
Development of method for determining zinc dialkyl diaryl dithiophosphate in lubricating oils
[AD-757605] 14 p1671 N73-23563
Wear inhibiting effect of automotive oils containing polymethacrylate
[NLL-TRANS-1190-[9022.9]] 15 p1746 N73-24149
Analysis of lubricating oil losses under vacuum conditions and application to antifriction bearings in antenna despin system of Helios solar probe
[NLL-RISLEY-TR-2567-[9091.9F]] 15 p1790 N73-24509
Wear inhibition of carboxylic acids in synthetic lubricating oils on ester basis
[DLR-FB-73-43] 15 p1793 N73-24536
Preventive maintenance of internal combustion engines and transmissions using spectrochemical oil analysis techniques
[PB-216168/5] 16 p1919 N73-25525
Effect of lubricating oils on life and reliability of machine parts
[AD-760945] 18 p2156 N73-27424
Frictional processes, electric contact resistance, and wear of pin on disk friction pair
[NASA-TT-F-15049] 24 p2929 N73-33391
LUBRICATION
NT BOUNDARY LUBRICATION
Microstructural studies of adhesion, wear, friction, and lubrication using LEED, Auger emission spectroscopy analysis, and field ion microscopy
[NASA-TM-X-68152] 01 p0058 N73-10471
Integral relationships in planar problem of gas lubrication including applications and approximate solutions
[AD-745833] 01 p0063 N73-10515
Effects of striated roughness and grooving on load carrying capacity of lubricating films
[AD-747307] 02 p0180 N73-11457
Vacuum life tests on lubricated bearings and slip rings
[ESRO-CR-91] 03 p0307 N73-12504
Lubrication, friction, and wear in machinery
[AD-749086] 04 p0428 N73-13485
Interferometry measurements of film thickness and traction of lubrication in point contacts
[NASA-CR-120842] 05 p0551 N73-14478
Rheological investigation of lubricating media using displacement equations for three special cases
[FOA-1-C-1408-92] 06 p0672 N73-15470
Elastohydrodynamic analysis using power law pressure-viscosity relation
[NASA-TN-D-7121] 06 p0677 N73-15507
Analysis of electrical contact occurrences between rolling surfaces with application to elastohydrodynamic lubrication
[NASA-TN-D-7134] 06 p0690 N73-15620
Surface roughness effects on elastohydrodynamic lubrication
[NASA-CR-2195] 07 p0804 N73-16522
MoS2 and MoS2/PTFE composite layers for dry lubrication of journal bearings in atmosphere or vacuum
[DLR-FB-72-69] 09 p1038 N73-18470
Numerical analysis of oil film bearing with respect to bushing based in inertial force, viscous force of liquid, and load lifting force exerted by bearing
[AD-752688] 09 p1040 N73-18483
Analytical solution of Reynolds equation and application to hydrodynamic lubrication to show characteristics of lubrication film
[TAE-153] 09 p1057 N73-18618
Reversible sliding and lubrication effects in internal stress friction on thin plate
[AD-751723] 09 p1097 N73-18957
Solid lubricants for moderate to extremely high temperature applications
[NASA-TM-X-68201] 11 p1298 N73-20537
Analysis of parameters and elastohydrodynamic principles affecting lubrication of transmission components with application to helicopter mechanical drive systems
[NASA-TM-X-68215] 12 p1364 N73-21069
Variable resistance tension and lubrication device, using oil-saturated leather wiper
[NASA-CASE-KSC-10723-1] 14 p1670 N73-23553
Feasibility study of applying air lubricated bearings to gas turbine engines for military aircraft
[AD-757869] 15 p1793 N73-24537
Endurance and performance tests of bore ball bearings lubrication thrust loaded 120-mm to 3 million DN
[NASA-TM-X-68264] 17 p2037 N73-26479
Modification of spinning torque apparatus to measure spinning torque on cageless ball thrust bearing using oil jet lubrication or thin surface film only
[NASA-TN-D-7356] 17 p2038 N73-26484
Development of empirical elastohydrodynamic film thickness formula for predicting minimum film thickness occurring in heavily load contacts
[NASA-TM-X-68267] 18 p2155 N73-27411
Performance tests of high speed ball bearings with lead and lead alloy plated retainers operating in liquid hydrogen at 30,000 rpm and 400 pound thrust load
[NASA-TM-X-68268] 18 p2155 N73-27412
Measurement of spinning and rolling torques in angular-contact ball bearing with and without cages under several lubrication regimes
[NASA-TM-X-68271] 18 p2155 N73-27414
Effect of lubricant active additives on rolling-element fatigue life using five-ball fatigue tester
[NASA-TN-D-7383] 18 p2156 N73-27417
Numerical analysis of effects on bearing load carrying capacity of opposing surfaces with striated roughness on both surfaces
[AD-761169] 18 p2156 N73-27423
Performance tests of gas turbine engine mainshaft roller bearings to determine stress and lubrication parameters
[AD-760563] 18 p2157 N73-27426
Friction and lubrication in steel wire drawing
[NLL-RTS-7851] 21 p2552 N73-30454
Hollow high strength rolling elements for antifriction bearings fabricated from preformed components
[NASA-CASE-LEW-11026-1] 24 p2928 N73-33383
LUBRICATION SYSTEMS
Tank design for forced circulation oil lubricating systems
[ESDU-68039] 02 p0177 N73-11429
Nucleonic sensor for detecting metal in recirculating lubricating oil systems
[AD-752580] 08 p0926 N73-17588
Development of lubrication theories and application of epilame-lubricant pairs for friction reduction
[NLL-RISLEY-TR-2547-[9091.9F]] 15 p1790 N73-24510
LUCITE [TRADEMARK]
U POLYMETHYL METHACRYLATE
LUDER BANDS
U PLASTIC DEFORMATION
U YIELD POINT
LUMBERING AREAS
U FORESTS
LUMINAIRES
NT AIRPORT LIGHTS
NT ARC LAMPS
NT FLASH LAMPS
NT MERCURY LAMPS
NT QUARTZ LAMPS
NT RUNWAY LIGHTS
NT XENON LAMPS

Procedures, techniques, and equipment for calibrating luminous intensity, luminous flux, and color temperature of incandescent lamps
[NBS-TN-594-3] 02 p0174 N73-11408
Push button power supply for measuring light output performance of switchboard lamps
[REPT-6688] 04 p0395 N73-13211
Hydrogen lamp with lithium fluoride window for Lyman beta radiation output
[AD-754572] 11 p1325 N73-20753
Electrodeless lamp circuit driven by induction
[NASA-CASE-MFS-21214-1] 21 p2516 N73-30181
Headlamp research program for extrapolation/interpolation of surface values from predefined grid
[LTR-ST-602] 22 p2637 N73-31129

**LUMINANCE**
Development of system for eliminating constant luminance failure in color television systems by modifying coding process
[BBC-1972/29] 01 p0023 N73-10180

**LUMINESCENCE**
NT BIOLUMINESCENCE
NT CHEMILUMINESCENCE
NT ELECTROLUMINESCENCE
NT FLUORESCENCE
NT OPTICAL RESONANCE
NT PHOSPHORESCENCE
NT PHOTOLUMINESCENCE
NT THERMOLUMINESCENCE
NT X RAY FLUORESCENCE
Spectral analysis of nonconducting siliceous materials by luminescent discharge
[CEA-CONF-2060] 12 p1405 N73-21397
Luminescence of normal and deformed single crystals of AgCl of different thickness measured at minus 180 C
[AD-755430] 12 p1441 N73-21677
Simazine influence on green algae photosynthetic pigments noting chlorophyll luminescence spectra
[DRIC-TRANS-2992] 13 p1485 N73-22040
Night sky luminescence in upper atmosphere during IQSY
[NASA-TT-F-14927] 14 p1660 N73-23478
Thermal quenching of luminescence and conformational transformations in macromolecules of some polymers
[NRC-TT-1631] 15 p1815 N73-24711
Rare earth oxysulfide luminescent films for use in CRT screens
[AD-758760] 16 p1954 N73-25808
Nondestructive tests for luminescent and color flaw detection, using magnetic particles and dye penetration
[AD-759253] 17 p2038 N73-26488
Electrical and luminescence phenomena in pure and dope lithium Floride
[ORNL-4850] 19 p2230 N73-27985
Proceedings of conference on accuracy in spectrophotometry and luminescence measurements
[NBS-SP-378] 21 p2544 N73-30396
Measurements of illumination in atmosphere and on surface of planet Venus obtained by automatic interplanetary station Venera-8
[JPRS-59963] 21 p2595 N73-30794
Influence of electronic states, electronic transport, and radiative transitions on luminescent defects in pure and doped single crystal compound semiconductors
[AD-764278] 22 p2708 N73-31683
Luminescence modulation and negative resistance modulation of semiconductors and high temperature semiconductors
[AD-763840] 22 p2708 N73-31685
Influence of excitation surface with liminary brightness on different regions of the retina
[NASA-TT-F-15124] 23 p2751 N73-32017

**LUMINESCENT INTENSITY**
U LUMINOUS INTENSITY

**LUMINOSITY**
NT STELLAR LUMINOSITY
Underluminosity and magnetic fields in Beta Lyrae
[NASA-TM-X-68895] 06 p0717 N73-15848
Derivation of closed formula for relation between luminosity and red shift in expanding Friedman universe
07 p0840 N73-16802
Mass-luminosity relationship of Hyades and other stars
[BULL-175] 10 p1212 N73-19857
Luminosity function of quasars based on comparison of data on optically selected quasars and quasars in radio catalog
[NASA-CR-131111] 10 p1213 N73-19864
Automatic raster scanning microdensitometer measurement of luminosity profiles and density of lenticular galaxies in Virgo Cluster
16 p1961 N73-25859
Measurement of luminosity distribution of Coma cluster of galaxies and comparison of mass-to-light ratio of cluster with that of individual galaxies
19 p2341 N73-28829
Relationship between intermediate medium, and transformation and contrast phenomena
[NASA-TT-F-15035] 20 p2371 N73-29055
Infrared emission from southern H 2 region H2-3 with solar luminosity between 1.65 and 25 microns
[NASA-CR-135640] 23 p2785 N73-32280

**LUMINOUS FLUX DENSITY**
U LUMINOUS INTENSITY

**LUMINOUS INTENSITY**
NT ILLUMINANCE
NT LUMINANCE
Procedures, techniques, and equipment for calibrating luminous intensity, luminous flux, and color temperature of incandescent lamps
[NBS-TN-594-3] 02 p0174 N73-11408
Organic dyes for improving light intensity of Nd YAG laser pump system
[AD-747401] 03 p0312 N73-12545
Push button power supply for measuring light output performance of switchboard lamps
[REPT-6688] 04 p0395 N73-13211
Light intensity effect on photon resonance in excited atom ionization for determining Stark effect potential
[KFKI-72-68] 10 p1192 N73-19694
Dependence of photon resonance in metastable helium atom ionization on light intensity
[KFKI-72-69] 10 p1192 N73-19695
Radiative light transfer model for aerosol radiance loss in atmospheric photometry
13 p1558 N73-22628
Chromium concentration effect on duration and width of luminescent lines in ruby spectrum
[AD-761374] 18 p2191 N73-27692
Use of soil-vegetation system brightness coefficients to measure vegetation quantity and crop yield
20 p2406 N73-29334
Dust tail of comet Seki-Lines mapped isophotometrically for relative intensities
23 p2836 N73-32662
Blue to violet intensity distributions in S, C-S, and C stars
23 p2837 N73-32666
Literature concerning retinal adaptation to varying light intensities
[NASA-TT-F-15036] 24 p2890 N73-33074

**LUMPING**
Design of continuous lumped parameter linear filters
[AD-757545] 16 p1881 N73-25226

**LUNAR ATMOSPHERES**
Apollo 17 far ultraviolet scanning spectrometer experiment for lunar atmosphere measurements
[NASA-CR-128835] 10 p1160 N73-19440
Construction of far ultraviolet Ebert spectrometer for use on Apollo 17 flight to observe lunar atmosphere
[NASA-CR-128889] 11 p1293 N73-20491
Properties of lunar atmosphere and ionosphere
13 p1575 N73-22763
Historical account of data and theories pertaining to lunar atmosphere prior to Apollo
[NASA-CR-128548] 15 p1833 N73-24863

**LUNAR BASES**
Systems engineering study for proposed lunar colony
[NASA-CR-129164] 02 p0152 N73-11236

**LUNAR CINEMATOGRAPHY**
U LUNAR PHOTOGRAPHY

**LUNAR COMPOSITION**
NT LUNAR CORE
Analysis of selected features of Mercury, Venus, and Mars and seismic propagation on Moon
07 p0840 N73-16807
Evidence on composition and mineralogy of lunar highlands
08 p0975 N73-17977
Apollo 15 X ray fluorescence experiment
08 p0975 N73-17978
Accomplishments of Apollo project and objectives of post-Apollo lunar scientific investigations
[LC-72-93379] 12 p1446 N73-21714
Analysis of metallic compounds produced by reduction of material of simulated lunar composition as basis for origin of metallic mounds on lunar glasses
[NASA-CR-131870] 13 p1576 N73-22769
Characteristics of Hertzian dipole antenna radiation patterns and application to lunar surface and subsurface electrical properties investigation - Vol. 2
[NASA-CR-128919] 14 p1705 N73-23836
Calculated iron abundance in moon from magnetometer measurements
[NASA-TM-X-62279] 17 p2082 N73-26841
Measurement of Rb-87 and Sr-87 in lunar material obtained by Lunar 20 to determine soil composition
[NASA-TT-F-14981] 17 p2083 N73-26847
Evolution of earth and moon tectonic elements
[NASA-TT-F-14947] 17 p2083 N73-26848
Explaining differences in composition of terrestrial planets and moon by accretion during condensation
[NASA-CR-132209] 17 p2083 N73-26854

**LUNAR CORE**
Particles and fields subsatellite magnetometer experiment to calculate lunar interior electrical conductivity
12 p1451 N73-21757

**LUNAR CRATERS**
Proceedings of colloquium on lunar dynamics and observational coordinate systems
[NASA-CR-131263] 11 p1337 N73-20849
Small scale analogs of Cayley Formation and Descartes Mountains in impact crater-associated deposits - Part C
12 p1453 N73-21767
Identification of artificial lunar impact craters produced by Ranger 7 and 9 spacecraft and S-4B stage of Apollo 13 and 14 - Part I
12 p1453 N73-21773
Identification of Ranger 7 and 9 impact craters from Apollo 16 photography - Part J
12 p1454 N73-21774
Apollo 16 photography of V-shaped ridges associated with secondary craters - Part K
12 p1454 N73-21775
Morphometric analysis of Apollo 16 photography of lunar craters - Part L
12 p1454 N73-21776
Apollo 16 orbital photography of King Crater and surrounding environment - Part M
12 p1454 N73-21777
Interpretation of ejecta blanket deposition from King Crater photographs
12 p1454 N73-21778
Origins of fracture patterns in Type 3 marginal premare craters
12 p1455 N73-21782
Near terminator photography of low relief features and mare units of Descartes Region
12 p1455 N73-21785
Explanatory notes for geological-morphological maps of southern part of Mare Imbrium, crater Copernicus and its vicinity
12 p1456 N73-21799
Geology and physical properties of region of Crater Archimedes and Apennine and Haemus Mountains
12 p1457 N73-21802
Some features of small craters on moon
12 p1457 N73-21805
Distribution of lunar craters as a function of their diameter
12 p1457 N73-21806
Cayley formation, emphasizing secondary lunar craters
[NASA-TM-X-62302] 21 p2596 N73-30804
Interpretation of data on crater distribution on surface of moon
[NASA-TT-F-15122] 24 p2979 N73-33808

**LUNAR CRUST**
Thickness of procellarum complex
12 p1456 N73-21798
Analysis of metallic compounds produced by reduction of material of simulated lunar composition as basis for origin of metallic mounds on lunar glasses
[NASA-CR-131870] 13 p1576 N73-22769
Dating of ocean floor rocks and investigation of kinetic processes in lunar regolith
17 p2017 N73-26307
Analysis of gamma ray pulse-height spectra from lunar surface
[NASA-TM-X-70421] 19 p2340 N73-28824
Geochemical analyses on lunar X ray spectra obtained during Apollo orbits
22 p2735 N73-31894
Geochemical analyses on lunar gamma ray spectra obtained during Apollo orbits
22 p2735 N73-31895

**LUNAR DUST**
Analysis of lunar material to determine presence of magnetic monopoles with description of equipment used
[NASA-CR-128642] 03 p0356 N73-12902
Far ultraviolet diffuse reflectivity of lunar dust samples
[NASA-CR-128546] 15 p1834 N73-24864

**LUNAR ECHOES**
NT LUNAR RADAR ECHOES

**LUNAR EFFECTS**
NT LUNAR TIDES
Formulation of disturbing function for computing lunisolar perturbations in satellite motion
[NASA-CR-130743] 08 p0941 N73-17709
Observations of lunar behavior in stellar occulation
[PUBL-25] 17 p2081 N73-26836

**LUNAR ENVIRONMENT**
NT LUNAR ATMOSPHERES
Progress in multidisciplinary research leading to utilization of extraterrestrial resources
[NASA-CR-129109] 02 p0226 N73-11827
Simulated lunar magnetic environment effects on humans, using scotopic critical flicker frequency measurements to indicate psychophysiological stress
[AD-748193] 05 p0502 N73-14088
Lunar laser reflector specifications and fabrication, noting test equipment thermal control, and lunar environment simulation
05 p0558 N73-14529

**LUNAR EVOLUTION**
Evolution of earth and moon tectonic elements
[NASA-TT-F-14947] 17 p2083 N73-26848
Rock composition of lunar samples
22 p2735 N73-31893

Distribution pattern of chemical components, and petrochemical coefficients of lunar rocks
23 p2837 N73-32669
LUNAR EXPLORATION
Familiarization course for Apollo 17 flight Lunar Surface Experiments package
[NASA-CR-128636] 03 p0301 N73-12459
Error analysis of lunar control by orbital triangulation
04 p0468 N73-13813
Time and motion study of lunar surface activity on Apollo 15
[NASA-CR-128695] 07 p0842 N73-16823
Analysis of test films to assess readiness of Apollo 17 radar equipment with emphasis on lunar sounder equipment
[NASA-CR-128883] 11 p1338 N73-20858
Accomplishments of Apollo project and objectives of post-Apollo lunar scientific investigations
[LC-72-93179] 12 p1446 N73-21714
Preliminary results of Apollo 16 investigations
[NASA-SP-315] 12 p1448 N73-21729
LUNAR FAR SIDE
Electromagnetic lunar conductivity measurements on dark side radial magnetic fields
[NASA-TM-X-62226] 07 p0844 N73-16834
Evaluation of Halo and Hummingbird satellites for lunar libration point satellite to provide tracking and communications link with far side of moon
[NASA-CR-130135] 07 p0844 N73-16836
LUNAR FLYING VEHICLES
Design, development, and configuration of reusable lunar shuttlecraft
[NASA-CR-135794] 24 p2984 N73-33849
LUNAR GEOLOGY
NT LUNAR CORE
Familiarization course for Apollo 17 flight Lunar Surface Experiments package
[NASA-CR-128636] 03 p0301 N73-12459
Stratigraphy of Apollo 15 drill core
[NASA-TM-X-58101] 05 p0595 N73-14839
Attenuation of surface elastic waves as related to mass defects and applied to lunar geology
08 p0958 N73-17837
Preliminary results of Apollo 16 lunar experiments
12 p1449 N73-21733
Apollo 16 visual observations of surface geology from lunar orbit
12 p1452 N73-21764
Analysis of earth based remote sensing data and infrared observations to determine nature of Apollo 16 landing site
12 p1455 N73-21787
Physical and geological aspects of heiligenschein measurements made from Apollo 16 Flight
12 p1455 N73-21789
Use of laser altimetry in Apollo 16 flight to aid in spacecraft position determination and lunar geological investigation
12 p1455 N73-21790
Geological structure of moon based on lunar photography
[NASA-TT-F-689] 12 p1456 N73-21795
Problems which could be solved by comparative geological study of planets of solar system
12 p1456 N73-21796
Thickness of procellarum complex
12 p1456 N73-21798
Explanatory notes for geological-morphological maps of southern part of Mare Imbrium, crater Copernicus and its vicinity
12 p1456 N73-21799
Lunar features and geology of northern part of Mare Nubium
12 p1456 N73-21800
Geological features of region of Cirques Theophilus and Ptolemaeus
12 p1457 N73-21801
Geology and physical properties of region of Crater Archimedes and Apennine and Haemus Mountains
12 p1457 N73-21802
Extent, origin and features of ancient seas over moon
12 p1457 N73-21803
Volcanic activity on moon
12 p1457 N73-21804
Some features of small craters on moon
12 p1457 N73-21805
Processes leading to formation of lunar features
12 p1457 N73-21809
Geological comparison of moon and earth
12 p1457 N73-21810
Geologic mapping of moon from pictures by Ranger 7, 8, and 9
[NASA-CR-133090] 17 p2082 N73-26839
Identification and source of lunar rocks, lunar interior and, lunar magmas
[NASA-CR-133457] 19 p2344 N73-28853
Morphology of lunar surface
21 p2594 N73-30781
Tides as energy factor in geological activity, and petrochemical coefficients of lunar rocks
[JPRS-59895] 23 p2837 N73-32668
Distribution pattern of chemical components, and petrochemical coefficients of lunar rocks
23 p2837 N73-32669
Tides as energy factor in geological activity of moon
23 p2837 N73-32670
LUNAR GRAVITATION
Computation of lunar gravitational field expansion coefficients utilizing Cassini equator inclination and radial lunar density distribution values
[NASA-TT-F-14605] 01 p0104 N73-10858
Methods for determining figure and gravity field of moon
[AD-747875] 04 p0477 N73-13897
Empirical method for determining spherical harmonic coefficients of lunar gravity field
12 p1447 N73-21718
Use of superhigh frequency transponder on Apollo 16 subsatellite to measure lunar gravitational field as preliminary investigation of lunar mass
12 p1451 N73-21758
Semiautomatic self-leveling lunar gravimeter for Apollo 17 mission
[NASA-CR-128948] 15 p1787 N73-24490
LUNAR IONOSPHERE
U LUNAR ATMOSPHERES
LUNAR LANDING
Development of method for determining optimal lunar landing gear design parameter values for front-foot touchdown mode
13 p1579 N73-22798
Operational and engineering aspects of Apollo 17 lunar landing mission
[NASA-TM-X-69292] 14 p1706 N73-23844
Apollo experience report on development of Apollo digital autopilots for primary attitude control during all phases of lunar landing mission
[NASA-TN-D-7289] 16 p1964 N73-25888
Analysis of Apollo 17 flight to show extravehicular activities, lunar surface experiments, orbital science projects, and spacecraft reentry and recovery
[NASA-TM-X-69527] 17 p2083 N73-26851
Apollo experience report on evolution of rendezvous maneuver plan for lunar landing missions
[NASA-TN-D-7388] 20 p2475 N73-29882
LUNAR LANDING MODULES
NT LUNAR MODULE
Design, development, and configuration of reusable lunar shuttlecraft
[NASA-CR-135794] 24 p2984 N73-33849
LUNAR LANDING SITES
High resolution measures of polarization and color of selected lunar areas
[NASA-CR-130018] 07 p0841 N73-16816
Selection of lunar landing site for Apollo 16
12 p1448 N73-21730
Topographic mapping of Apollo 16 landing from high resolution photographs by lunar orbiter
12 p1448 N73-21732
Preliminary results of Apollo 16 lunar experiments
12 p1449 N73-21733
Analysis of earth based remote sensing data and infrared observations to determine nature of Apollo 16 landing site
12 p1455 N73-21787
LUNAR LIMB
Improving selenodetic control on lunar limb using Apollo 15 transearth photography
[NASA-CR-131264] 11 p1336 N73-20846
LUNAR MAGNETIC FIELDS
Total and induced magnetic fields line structure within Moon and diamagnetic cavity based on asymmetric theory of lunar induction
[NASA-CR-114543] 06 p0718 N73-15860
Development of theory for time dependent magnetic fields inside Moon and diamagnetic cavity caused by interplanetary eletromagnetic field fluctuation
[NASA-CR-114546] 06 p0718 N73-15861
Electromagnetic lunar conductivity measurements on dark side radial magnetic fields
[NASA-TM-X-62226] 07 p0844 N73-16834
Magnetic field around spherical moon and downstream cylindrical cavity formed by solar wind, derived for parallel and perpendicular interplanetary magnetic fields
[NASA-TM-X-62227] 08 p0960 N73-17851
Particles and fields subsatellite magnetometer experiment to calculate lunar interior electrical conductivity
12 p1451 N73-21757
Internal lunar properties calculated from surface magnetometer experiments data
[NASA-TM-X-62278] 17 p2082 N73-26842
LUNAR MAPS
Near terminator photography of low relief features and mare units of Descartes Region
12 p1455 N73-21785
Problems of preparing geological-morphological maps of moon from telescopic pictures of lunar surface
12 p1456 N73-21797
Explanatory notes for geological-morphological maps of southern part of Mare Imbrium, crater Copernicus and its vicinity
12 p1456 N73-21799
Lunar features and geology of northern part of Mare Nubium
12 p1456 N73-21800
Geological features of region of Cirques Theophilus and Ptolemaeus
12 p1457 N73-21801
Geology and physical properties of region of Crater Archimedes and Apennine and Haemus Mountains
12 p1457 N73-21802
Geological comparison of moon and earth
12 p1457 N73-21810
Apollo 16 lunar maps
[NASA-CR-132066] 15 p1785 N73-24469
LUNAR MARIA
Dynamic mass modeling and geophysical analysis of lunar maria based on Apollo tracking data
[NASA-TM-X-65940] 11 p1338 N73-20854
Origins of fracture patterns in Type 3 marginal premare craters
12 p1455 N73-21782
Stereoscopic photographs for studying low relief mare features of lunar surface
12 p1455 N73-21783
Exogenetic and endogenetic origin of sinuous markings on lunar mare
12 p1455 N73-21784
Near terminator photography of low relief features and mare units of Descartes Region
12 p1455 N73-21785
Distribution of color variations in Mare Nubium and Southern Oceanus Procellarum lunar regions
12 p1455 N73-21786
Explanatory notes for geological-morphological maps of southern part of Mare Imbrium, crater Copernicus and its vicinity
12 p1456 N73-21799
Lunar features and geology of northern part of Mare Nubium
12 p1456 N73-21800
Extent, origin and features of ancient seas over moon
12 p1457 N73-21803
LUNAR MODULE
Erasable-memory programs for guidance computers in command and lunar modules
[NASA-CR-128689] 07 p0817 N73-16626
Development problems and flight performance evaluation of Apollo lunar module landing gear
09 p1088 N73-18878
Apollo experience report on lunar module ascent propulsion subsystem to identify significant technical problems encountered during all phases of program
[NASA-TN-D-7082] 09 p1090 N73-18900
Apollo experience report of structural subsystem, structural configuration, and design verification of lunar module spacecraft
[NASA-TN-D-7084] 09 p1091 N73-18901
Performance of LM-11 Descent propulsion System during Apollo 16 Mission
[NASA-CR-128826] 10 p1213 N73-19865
Apollo experience report on propulsion system for descent stage of lunar module with emphasis on throttling capability and cryogenic helium pressurization system
[NASA-TN-D-7143] 10 p1215 N73-19877
Development of method for determining optimal lunar landing gear design parameter values for front-foot touchdown mode
13 p1579 N73-22798
Apollo experience report on lighting requirements for Apollo command and lunar modules for internal and external lighting
[NASA-TN-D-7290] 16 p1964 N73-25887
Performance of Apollo 14 lunar module descent propulsion system
[NASA-TM-X-69491] 20 p2466 N73-29813
Apollo experience report on window structural design and verification for command and lunar modules
[NASA-TN-D-7439] 22 p2720 N73-31770
LUNAR MODULE ASCENT STAGE
Postflight analysis of Apollo 15 LM APS
[NASA-TM-X-68932] 06 p0712 N73-15813
LUNAR OCCULTATION
NT SOLAR ECLIPSES
HELOS lunar occultation experiment on X ray galactic and extragalactic source position and angular size determination
17 p2085 N73-26868
HELOS spacecraft subsystems for attitude control, tracking, telecommand, and X ray source detection
17 p2085 N73-26869
LUNAR ORBITAL RENDEZVOUS
Apollo experience report on evolution of rendezvous maneuver plan for lunar landing missions
[NASA-TN-D-7388] 20 p2475 N73-29882
LUNAR ORBITER
Analysis of management procedures applied to Surveyor and Lunar Orbiter projects
[NASA-SP-4901] 04 p0486 N73-13973
Topographic mapping of Apollo 16 landing from high resolution photographs by lunar orbiter
12 p1448 N73-21732
Estimates of moon geometry using lunar orbiter imagery and Apollo laser altimeter data
[NASA-TR-R-407] 23 p2846 N73-32743

**LUNAR ORBITS**
Atlas of reconstructed lunar photographs taken by Lunar Orbiters during 1966 and 1967
[NASA-SP-206] 04 p0475 N73-13879
Development and characteristics of laser altimeter for use with Apollo Lunar Orbital Experiments Mission
[NASA-CR-128738] 08 p0924 N73-17567
Orbital evolution and stability analysis for earth and lunar orbiter trajectories
[AD-754738] 11 p1339 N73-20869
Apollo 16 visual observations of surface geology from lunar orbit
12 p1452 N73-21764
Photographic observations of solar corona by Apollo 16 command module from lunar orbit
12 p1456 N73-21794
Numerical integration techniques for solution of orbital elements of moon and planets
[AD-755164] 14 p1707 N73-23850
Solutions for motion about libration points of elliptic restricted three-body problem
15 p1829 N73-24826
Calculating position of moon as function of time using numerical techniques
[AD-761651] 21 p2598 N73-30821
**LUNAR PERTURBATION**
U LUNAR EFFECTS
**LUNAR PHOTOGRAPHS**
Lunar Orbiter photographic and photometric data enhancement - framelet joining, digitization, data improvement, and statistical error analysis
[NASA-CR-128581] 01 p0057 N73-10463
Atlas of reconstructed lunar photographs taken by Lunar Orbiters during 1966 and 1967
[NASA-SP-206] 04 p0475 N73-13879
Development of mathematical methods for calibrating lunar orbiter photography
[NASA-CR-128279] 08 p0924 N73-17572
Methods for obtaining statistical morphological characteristics of lunar surface using photographic imagery
09 p1084 N73-18840
Stereoscopic photographs for studying low relief mare features of lunar surface
12 p1455 N73-21783
Apollo 17 mission at Taurus Littrow with color illustration and summaries
[NASA-EP-102] 24 p2979 N73-33804
**LUNAR PHOTOGRAPHY**
Apoll 15 photography of lunar surface
[NASA-TM-X-68910] 05 p0595 N73-14834
Autocorrelation evaluation for texture indicator for lunar ground photos
05 p0609 N73-14955
Effect of residual motion smear or image reproduction processes on detail of lunar surface imagery from orbiting command module
[NASA-CR-130378] 07 p0798 N73-16485
Improving selenodetic control on lunar limb using Apollo 15 transearth photography
[NASA-CR-131264] 11 p1336 N73-20846
Topographic mapping of Apollo 16 landing from high resolution photographs by lunar orbiter
12 p1448 N73-21732
Photographic summary for Apollo 16 flight
12 p1449 N73-21734
Interpretation of Apollo 16 photography of Orientale Basin deposits under earthshine illumination conditions - Part E
12 p1453 N73-21769
Photogeologic analysis of Apollo 16 metric photography of northern Nectaris Basin - Part F
12 p1453 N73-21770
Discovery of previously unknown structural basin and crater on Apollo 16 photography of far side highlands near eastern limb of moon - Part H
12 p1453 N73-21772
Apollo 16 orbital photography of King Crater and surrounding environment - Part M
12 p1454 N73-21777
Near terminator photography of low relief features and mare units of Descartes Region
12 p1455 N73-21785
Geological structure of moon based on lunar photography
[NASA-TT-F-689] 12 p1456 N73-21795
Problems of preparing geological-morphological maps of moon from telescopic pictures of lunar surface
12 p1456 N73-21797
Features of lunar furrows and ridges from telescopic and satellite photographs
12 p1457 N73-21808
Data users note for dissemination of Apollo 16 lunar photographs
[NSSDC-73-01] 15 p1785 N73-24468
Geologic mapping of moon from pictures by Ranger 7, 8, and 9
[NASA-CR-133090] 17 p2082 N73-26839
**LUNAR PROBES**
NT LUNIK 16 LUNAR PROBE
NT LUNIK 20 LUNAR PROBE
NT RANGER LUNAR PROBES
NT RANGER 7 LUNAR PROBE
NT RANGER 9 LUNAR PROBE
NT SURVEYOR LUNAR PROBES
NT SURVEYOR 3 LUNAR PROBE
Preliminary data on lunar soil collected by Luna-20 automatic station
[NASA-TT-F-14615] 04 p0476 N73-13888
Spaceflights by Soviet devices to the moon and results of lunar surface research
[NASA-TT-F-14983] 21 p2596 N73-30801
**LUNAR PROGRAMS**
NT APOLLO PROJECT
NT SURVEYOR PROJECT
**LUNAR RADAR ECHOES**
Radar methods of investigating moon and planets
[NASA-TT-F-729] 09 p1084 N73-18847
**LUNAR RADIATION**
Measurement of infrared radiation from Mercury and Moon
[NASA-CR-130968] 09 p1085 N73-18849
Analysis of gamma ray pulse-height spectra from lunar surface
[NASA-TM-X-70421] 19 p2340 N73-28824
Expected gamma ray emission spectra from lunar surface for range of chemical compositions
[NASA-TM-X-70453] 21 p2595 N73-30796
**LUNAR RANGEFINDING**
Strict geometric determination of ephemeris time, positions, and apparent directions of moon against stellar background
[AD-750307] 06 p0671 N73-15460
Filtered lunar ranging data, and unfiltered photon detections
[NASA-CR-131498] 13 p1576 N73-22771
Filtered and unfiltered photon detections obtained during laser ranging operations between McDonald Observatory and Apollo 11, 14, and 15 reflectors
[NASA-CR-133927] 22 p2681 N73-31472
Observation equations to utilize lunar laser ranging and very long baseline interferometry measurements for selenodetic control
[NASA-CR-135774] 24 p2931 N73-33404
**LUNAR RAYS**
Exogenetic and endogenetic origin of sinuous markings on lunar mare
12 p1455 N73-21784
**LUNAR RECEIVING LABORATORY**
Occupational medicine procedures for personnel in lunar receiving laboratory for Apollo 11 crew members
08 p0871 N73-17049
Development of germ-free plants and tissues
[NASA-CR-128947] 15 p1742 N73-24122
**LUNAR ROCKS**
Progress in multidisciplinary research leading to utilization of extraterrestrial resources
[NASA-CR-129109] 02 p0226 N73-11827
Analysis of radioactivity in lunar samples returned by Apollo 16 flight and relationship to occurrence of solar flares
[NASA-CR-129291] 03 p0354 N73-12886
Bulk radiation effects in terrestrial minerals, meteorites, and lunar rocks, and fission track studies in Apollo 12 samples
07 p0831 N73-16736
Laser-probe mass spectrometric analysis of solar wind, cosmogenic, and radiogenic gases in Apollo 12, 14, and 15 samples
[NASA-CR-130029] 07 p0841 N73-16811
Rare gas abundances in Apollo 11 rocks 10017 and 10071, and rock age determinations
07 p0842 N73-16818
Mineral analysis of lunar samples of crystalline rocks from Apollo 12 flight
[NASA-SP-306] 07 p0844 N73-16837
Evidence on composition and mineralogy of lunar highlands
08 p0975 N73-17977
Magnetic hysteresis of lunar surface and permanent remanence in lunar samples
[NASA-TM-X-65941] 10 p1212 N73-19860
Preliminary results of examining lunar rock samples from Apollo 16 flight
12 p1449 N73-21736
Chemical, petrographic, and textural characteristics of Apollo 16 rock and soil samples
12 p1449 N73-21737
Special samples which were collected on Apollo 16 for specific investigations
12 p1449 N73-21738
Unstable component of magnetization found in lunar samples
12 p1449 N73-21739
Effect of neutron irradiation on remanent magnetization in Apollo 11 and 12 lunar samples of iron and kamacite
15 p1813 N73-24692
Effects of energetic charged particle irradiation of solar system material
[NASA-CR-132045] 15 p1831 N73-24845
Depth profiles of galactic cosmic ray produced radionuclides in lunar samples
17 p2079 N73-26814
Cooling histories of lunar rocks
[NASA-CR-133333] 19 p2343 N73-28851
Apollo lunar sample return containers for storing and protecting lunar samples
[Y-1867] 21 p2553 N73-30465
Analysis of concept to mine, refine, and transport lunar minerals to earth for terrestrial industries - Vol.1
[NASA-TM-X-62267] 21 p2595 N73-30798
Analysis of technologies and systems required for establishing mining base, mining, refining, and transporting lunar minerals for earth use - Vol.2
[NASA-TM-X-62268] 21 p2595 N73-30799
Particle track research and lunar rock studies
[NASA-CR-134023] 21 p2596 N73-30806
Mass spectrometric determination of rare earth concentration in basaltic rocks and luna sample 14305
[FRNC-TH-335] 21 p2597 N73-30813
Rock composition of lunar samples
22 p2735 N73-31893
Distribution pattern of chemical components, and petrochemical coefficients of lunar rocks
23 p2837 N73-32669
**LUNAR ROTATION**
Effects of elasticity on lunar rotation
[NASA-CR-132046] 15 p1831 N73-24844
**LUNAR ROVING VEHICLES**
NT MANNED LUNAR SURFACE VEHICLES
Performance tests of scale model of lunar roving vehicle used on Apollo 15 mission to determine vehicle mobility
[NASA-CR-129176] 02 p0152 N73-11234
Tests of lunar roving vehicle wheels in simulated lunar soil to determine effects of wheel speed, wheel load, presence of fender, travel direction, and soil strength
[NASA-CR-129612] 04 p0401 N73-13263
Performance of lunar roving vehicle during Apollo 15 mission
[NASA-TR-R-401] 07 p0841 N73-16817
Design and evalution of lunar roving vehicle deployment mechanism
09 p1088 N73-18876
Lunar cart for carrying experimental payloads between Apollo 11 and lunar roving vehicle
09 p1088 N73-18882
Analysis of off-scale low indications of voltmeters for batteries at initial powerup for Apollo 16 lunar roving vehicle
[NASA-TM-X-69123] 11 p1266 N73-20272
Report by Apollo 16 crew that lunar roving vehicle rear steering was inoperative
[NASA-TM-X-69124] 11 p1339 N73-20864
Lunar roving vehicle/traverse gravimeter experiment motion sensitivity test showing gravity measurements in normal and bypass modes
[NASA-TM-X-69268] 16 p1963 N73-25882
Inoperative conditions of rear steering system of lunar roving vehicle on Apollo 16 flight
[NASA-TM-X-69198] 17 p2010 N73-26256
Doppler difference monochromatic baseline interferometry for tracking lunar roving vehicle
18 p2210 N73-27844
Postflight analysis of Apollo 15 flight to determine performance of launch vehicle, spacecraft, and lunar roving vehicle and to analyze malfunctions
[NASA-TM-X-69539] 24 p2981 N73-33819
Postflight analysis of Apollo 16 flight to show spacecraft performance, launch vehicle performance, and malfunctions occuring during flight
[NASA-TM-X-69535] 24 p2981 N73-33823
**LUNAR SATELLITES**
NT EXPLORER 18 SATELLITE
NT IMP
NT LUNAR ORBITER
Estimation of unmodeled forces on lunar satellite
[AD-765151] 23 p2846 N73-32748
**LUNAR SCATTERING**
U DIFFUSE RADIATION
U LUNAR RADAR ECHOES
**LUNAR SEISMOGRAPHS**
Analysis of selected features of Mercury, Venus, and Mars and seismic propagation on Moon
07 p0840 N73-16807
Attenuation of surface elastic waves as related to mass defects and applied to lunar geology
08 p0958 N73-17837
Passive seismic experiment at Descartes landing site of Apollo 16 mission
12 p1449 N73-21741
Active seismic experiment deployed to provide data concerning near-surface structure at Apollo 16 landing site
12 p1450 N73-21742
**LUNAR SOIL**
NT LUNAR DUST
Effects of Apollo 12 lunar materials on lipid levels, including fatty acids and sterols, of tobacco tissue and slash pine cultures
[NASA-CR-128606] 01 p0008 N73-10063
Determination of oxygen content of lunar samples obtained from Luna 16 flight by 14-MeV neutron activation analysis
[KFKI-72-25] 03 p0263 N73-12133
Analysis of radioactivity in lunar samples returned by Apollo 16 flight and relationship to occurrence of solar flares
[NASA-CR-129291] 03 p0354 N73-12886

Thermophysical properties of lunar fines
[NASA-CR-129293] 03 p0354 N73-12888
Analysis of lunar material to determine presence of magnetic monopoles with description of equipment used
[NASA-CR-128642] 03 p0356 N73-12902
Tests of lunar roving vehicle wheels in simulated lunar soil to determine effects of wheel speed, wheel load, presence of fender, travel direction, and soil strength
[NASA-CR-129612] 04 p0401 N73-13263
Preliminary data on lunar soil collected by Luna-20 automatic station
[NASA-TT-F-14615] 04 p0476 N73-13888
Abundance and isotopic composition of noble gases release from lunar fines
[NASA-CR-130327] 07 p0841 N73-16812
Simulated micrometeoroid impact cratering in lunar materials using electrostatically accelerated microparticles impacting in oligoclase single crystals
[NASA-CR-130356] 07 p0841 N73-16813
Development of model to describe characteristics of one dimensional lunar ash flow with and without heat transfer effects
[NASA-CR-130697] 08 p0895 N73-17245
Portable penetrometer for analyzing soil characteristics
[NASA-CASE-MFS-20774] 10 p1158 N73-19420
Measurement of line spectra produced by high resolution mass spectrometer and application to identifying organic compounds in samples from Apollo 11 and 12 flights
[NASA-CR-128840] 10 p1160 N73-19436
Soil mechanics for lunar soils near landing site for Apollo 16 mission
12 p1449 N73-21740
Analysis of metallic compounds produced by reduction of material of simulated lunar composition as basis for origin of metallic mounds on lunar glasses
[NASA-CR-131870] 13 p1576 N73-22769
Cytological changes in pine tissues treated with lunar materials collected on Apollo 12 quarantine mission
[NASA-CR-128914] 14 p1610 N73-23054
Evolution of conceptual design of flight hardware for surface electrical Properties experiment - Vol. 1
[NASA-CR-128918] 14 p1705 N73-23835
Characteristics of Hertzian dipole antenna radiation patterns and application to lunar surface and subsurface electrical properties investigation - Vol. 2
[NASA-CR-128919] 14 p1705 N73-23836
Measurement of Rb-87 and Sr-87 in lunar material obtained by Lunar 20 to determine soil composition
[NASA-TT-F-14981] 17 p2083 N73-26847
Analysis of concept to mine, refine, and transport lunar minerals to earth for terrestrial industries - Vol.1
[NASA-TM-X-62267] 21 p2595 N73-30798
Analysis of technologies and systems required for establishing mining base, mining, refining, and transporting lunar minerals for earth use - Vol.2
[NASA-TM-X-62268] 21 p2595 N73-30799
Simulation of growth and mineral uptake by plants growing in lunar soil
[NASA-CR-134036] 22 p2619 N73-30988
Chemical composition of lunar soil samples obtained by Lunik 20 lunar probe
[NASA-TT-F-15100] 22 p2716 N73-31744
Nondestructive determination of radionuclides in lunar samples using large low-background gamma ray spectrometer and application of least squares fitting
[NASA-TM-X-69581] 22 p2718 N73-31756
Rock composition of lunar samples
22 p2735 N73-31893
Mass spectrometric analysis of rare earth elements contained in lunar samples
[CONF-730402-[P1-2]] 24 p2923 N73-33344
Natural exoelectron emission of anorthosite rocks from Luna-20
[NASA-TT-F-15116] 24 p2980 N73-33817

**LUNAR SPACECRAFT**
NT APOLLO SPACECRAFT
NT LUNAR LANDING MODULES
NT LUNAR MODULE
NT LUNAR ORBITER
NT LUNAR PROBES
NT LUNAR SATELLITES
NT LUNIK 16 LUNAR PROBE
NT LUNIK 20 LUNAR PROBE
NT RANGER LUNAR PROBES
NT RANGER 7 LUNAR PROBE
NT RANGER 9 LUNAR PROBE
NT SURVEYOR LUNAR PROBES
NT SURVEYOR 3 LUNAR PROBE
Measurement of Rb-87 and Sr-87 in lunar material obtained by Lunar 20 to determine soil composition
[NASA-TT-F-14981] 17 p2083 N73-26847

**LUNAR SURFACE**
U LUNAR TOPOGRAPHY

**LUNAR SURFACE VEHICLES**
NT LUNAR ROVING VEHICLES
NT MANNED LUNAR SURFACE VEHICLES
Design of hopping transporter for lunar exploration
[NASA-CR-130010] 07 p0765 N73-16217

**LUNAR TIDES**
Second degree Love number values from analysis of lunar-solar tidal perturbations of GEOS 1 and 2 inclinations
[NASA-TM-X-66176] 08 p0960 N73-17857
Tidal and lunar data for Point Mugu, San Nicholas Island, and Barking Sands areas for 1973
[AD-752892] 10 p1156 N73-19407
Tides as energy factor in geological activity, and petrochemical coefficients of lunar rocks
[JPRS-59895] 23 p2837 N73-32668
Tides as energy factor in geological activity of moon
23 p2837 N73-32670

**LUNAR TOPOGRAPHY**
Apollo 15 and Apollo 16 spectrometric observation of X rays, gamma rays, and alpha particle emissions on lunar surface
[NASA-TM-X-66068] 01 p0103 N73-10848
Computer aided photogrammetric analysis of lunar topography
[AD-744867] 02 p0232 N73-11881
Determining optimal selenodetic control network on moon
04 p0469 N73-13822
Atlas of reconstructed lunar photographs taken by Lunar Orbiters during 1966 and 1967
[NASA-SP-206] 04 p0475 N73-13879
Apoll 15 photography of lunar surface
[NASA-TM-X-68910] 05 p0595 N73-14834
Lunar surface layer density from radar measurements by satellites and automatic stations
[D-17] 06 p0639 N73-15185
High resolution measures of polarization and color of selected lunar areas
[NASA-CR-130018] 07 p0841 N73-16816
Methods for obtaining statistical morphological characteristics of lunar surface using photographic imagery
09 p1084 N73-18840
Magnetic hysteresis of lunar surface and permanent remanence in lunar samples
[NASA-TM-X-65941] 10 p1212 N73-19860
Proceedings of colloquium on lunar dynamics and observational coordinate systems
[NASA-CR-131263] 11 p1337 N73-20849
Explosives for lunar seismic studies
[NASA-CR-128876] 11 p1348 N73-20939
Bistatic radar investigation of lunar electromagnetic and surface properties from Apollo 16 command and service module
12 p1451 N73-21759
Apollo 16 visual observations of surface geology from lunar orbit
12 p1452 N73-21764
Relative ages of near side and far side terra plains based on interpretation of Apollo 16 photogeology - Part A
12 p1452 N73-21765
Possible analogs around Orientale Basin provide reasonable alternatives to geomorphologic interpretation of volcanism in Descartes highlands - Part D
12 p1453 N73-21768
Examination of lunar surface patterns created by volcanic lava flows and impact debris
12 p1454 N73-21779
Fourier technique for quantitatively classifying lunar rilles by planimetric shape
12 p1455 N73-21781
Stereoscopic photographs for studying low relief mare features of lunar surface
12 p1455 N73-21783
Distribution of color variations in Mare Nubium and Southern Oceanus Procellarum lunar regions
12 p1455 N73-21786
Apollo 16 radar echo data for predicting blockiness of lunar surface
12 p1455 N73-21788
Photogrammetric techniques from Apollo 15 and 16 flights to provide accurate measurement of lunar topography
12 p1456 N73-21791
Use of Apollo 16 photogrammetry to determine frequency distributions of lunar slopes
12 p1456 N73-21792
Problems of preparing geological-morphological maps of moon from telescopic pictures of lunar surface
12 p1456 N73-21797
Comparison of forms of lunar relief with terrestrial volcanic formations
12 p1457 N73-21807
Processes leading to formation of lunar features
12 p1457 N73-21809
Geologic mapping of moon from pictures by Ranger 7, 8, and 9
[NASA-CR-133090] 17 p2082 N73-26839
USSR automatic stations on mars and venus, lunar continental region samples, and 24 hour satellite earth watching
[NASA-TT-F-14929] 19 p2342 N73-28841
Identification and source of lunar rocks, lunar interior and, lunar magmas
[NASA-CR-133457] 19 p2344 N73-28853
Apollo 16 lunar surface cosmic ray experiment S-152
[NASA-CR-134019] 21 p2592 N73-30770
Spaceflights by Soviet devices to the moon and results of lunar surface research
[NASA-TT-F-14983] 21 p2596 N73-30801
Apollo 17 mission at Taurus Littrow with color illustration and summaries
[NASA-EP-102] 24 p2979 N73-33804
Interpretation of data on crater distribution on surface of moon
[NASA-TT-F-15122] 24 p2979 N73-33808

**LUNAR TRAJECTORIES**
Postflight trajectory for Apollo/Saturn V AS-511 spent S-4B/IU stage from CSM separation to lunar impact
[NASA-CR-123975] 05 p0594 N73-14826
Application of matched asymptotic expansions to lunar and interplanetary trajectories
[NASA-CR-2253] 18 p2197 N73-27738
Derivations of second-order asymptotic boundary value solutions for lunar and interplanetary trajectories
[NASA-CR-2256] 19 p2343 N73-28845
Estimation of unmodeled forces on lunar satellite
[AD-765151] 23 p2846 N73-32748

**LUNGS**
Measurement of pulmonary extravascular water volume during exposure to simulated high altitude
[AD-763355] 22 p2621 N73-31004

**LUNIK LUNAR PROBES**
NT LUNIK 16 LUNAR PROBE
NT LUNIK 20 LUNAR PROBE

**LUNIK 16 LUNAR PROBE**
Determination of oxygen content of lunar samples obtained from Luna 16 flight by 14-MeV neutron activation analysis
[KFKI-72-25] 03 p0263 N73-12133

**LUNIK 20 LUNAR PROBE**
Chemical composition of lunar soil samples obtained by Lunik 20 lunar probe
[NASA-TT-F-15100] 22 p2716 N73-31744

**LYAPUNOV FUNCTIONS**
U LIAPUNOV FUNCTIONS

**LYMAN ALPHA RADIATION**
Measurement of extraterrestrial Lyman alpha emission by OGO 5 satellite while outside geocorona
01 p0099 N73-10812
Development of model of scattering of solar Lyman alpha from spatial distribution of neutral hydrogen in interplanetary space
01 p0099 N73-10813
Solar wind/interstellar gas interactions and Lyman alpha background radiation
[TRITA-EPP-72-03] 01 p0105 N73-10871
Background Lyman alpha radiation and interstellar hydrogen gas taking into account radiative heat transfer
01 p0105 N73-10872
L alpha photometry of Comet Bennett
02 p0228 N73-11841
Research data on cometary structure and characteristics particularly Lyman alpha emission
02 p0229 N73-11853
Monte Carlo technique using Stokes vectors of Lyman alpha radiation
24 p2975 N73-33774

**LYMAN BETA RADIATION**
Hydrogen lamp with lithium fluoride window for Lyman beta radiation output
[AD-754572] 11 p1325 N73-20753

**LYMPH**
NT LYMPHOCYTES

**LYMPHOCYTES**
Observation of circulating lymphocytoid cell in monkey after exposure to radio waves
[AD-749583] 06 p0631 N73-15128
Radiation effects on human chromosomal aberrations in peripheral blood lymphocytes
14 p1609 N73-23041
Functional state of lymphoid cell in peripheral blood of astronauts and immunoreactivity of individual astronants after space flight
[NASA-TT-F-15089] 22 p2620 N73-30999
Continuous low dose gamma irradiation effects on cell population kinetics of mice lymphoid tissue
[NASA-CR-135723] 23 p2749 N73-31999

**LYOPHILS**
U COLLOIDS

**LYRAE CONSTELLATION**
Underluminosity and magnetic fields in Beta Lyrae
[NASA-TM-X-68895] 06 p0717 N73-15848
UBV observations of HD 176387
[BULL-174] 10 p1212 N73-19856
UBV observations of RR Lyrae variable HD 176387
[ROY-OBS-BULL-174] 13 p1578 N73-22787
Study of known RR Lyrae type variable stars in Messier 3
[REPT-63] 23 p2846 N73-32746

# M

M WINGS
U VARIABLE SWEEP WINGS
MACH NUMBER
Nonlinear partial differential equations for studying viscous compressible corner flow at subsonic and supersonic Mach numbers
15 p1764 N73-24294
Mach number effect on motion of sphere in compressible low Reynolds number flow
15 p1765 N73-24298
MACH-ZEHNDER INTERFEROMETERS
Mach-Zehnder interferometric determination of nitrogen and oxygen atom specific refractivities during atmospheric entry
[AD-745132] 02 p0138 N73-11114
Development of Mach-Zehnder interferometer theory based on time history of wave front produced by element of extended light source
[ARC-R/M-3173] 16 p1856 N73-25033
MACHINE LEARNING
U LEARNING MACHINES
MACHINE LIFE
U SERVICE LIFE
MACHINE ORIENTED LANGUAGES
Total machine language conception for sequential automaton from modular evolution
04 p0394 N73-13201
Extended computer language for real time simulation of process control in large systems
14 p1712 N73-23892
Concept of comments in programming languages
[NPL-NAC-34] 22 p2639 N73-31154
MACHINE RECOGNITION
U ARTIFICIAL INTELLIGENCE
MACHINE STORAGE
U COMPUTER STORAGE DEVICES
U CORE STORAGE
MACHINE TOOLS
NT GRINDING MACHINES
NT MILLING MACHINES
Hardened high strength steel for making wear resistant metal cutting tools
[AD-747711] 03 p0308 N73-12511
Efficiency of computer for numerically controlled machine tools
[CRIF-MC-44] 04 p0427 N73-13478
Investigation of high performance variable speed 10 hp machine tool spindle drive system
[E/C-3] 06 p0677 N73-15505
Development of extruding machine for producing parts with complicated shapes, high degree of mass, and requiring precision surfaces
[AD-751146] 07 p0805 N73-16534
Bibliography of techniques, procedures, manufacturing methods, time studies, and shop layout in machine shop practice
[AD-765400] 23 p2799 N73-32388
Two component force dynamometer and tool control system for dynamic machine tool research
[NASA-TM-X-64786] 24 p2926 N73-33371
MACHINE TRANSLATION
Automatic processing of French speech
[AD-752811] 13 p1491 N73-22090
MACHINERY
Lubrication, friction, and wear in machinery
[AD-749086] 04 p0428 N73-13485
Self-simulation problems of machines using gas dynamic processes
[NASA-TT-F-14832] 09 p1036 N73-18454
Effect of lubricating oils on life and reliability of machine parts
[AD-760945] 18 p2156 N73-27424
Development and characteristics of concentric output differential gearing system
[NASA-CASE-ARC-10462-1] 20 p2423 N73-29459
Apparatus for manufacturing polyester drive belts
[NASA-CASE-NPO-13205-1] 22 p2677 N73-31442
MACHINING
NT CHEMICAL MACHINING
NT ELECTROCHEMICAL MACHINING
NT MILLING [MACHINING]
NT SPARK MACHINING
Toxicity and safety hazard of dry beryllium copper alloy machining for human operator
08 p0872 N73-17059
Plastic deformation of brittle materials by machining
[AD-753027] 09 p1041 N73-18494
Automated computer index and retrieval system on machining of materials
[AD-752000] 09 p1053 N73-18582
Environment-sensitive hardness effects on drilling and machining aluminum oxides
[AD-753276] 09 p1053 N73-18586
Residual stresses and plastic deformations of machined magnesium oxide crystals
[AD-759411] 17 p2073 N73-26776
Digital system for programmed control of maching process for turbine blade foil
[AD-759682] 17 p2077 N73-26804
MACROCLIMATE
U CLIMATE
MACROMOLECULES
U MOLECULES
MACROPHAGES
Prodromal disease - Immune responses of host macrophage system to humoral factors
[NASA-CR-133455] 19 p2224 N73-27938
MACULAR VISION
U VISION
MAFFEI GALAXIES
Astronomical mapping of rotating spiral Maffei galaxy
[AD-752042] 08 p0962 N73-17873
MAGELLANIC CLOUDS
Development of photoelectric and photographic standards for Magellanic clouds and analysis of differences in stellar population of regions
02 p0227 N73-11832
Schmidt telescopes in Southern Hemisphere survey noting possible sites and study of Magellanic clouds
07 p0846 N73-16853
Balloon-borne far infrared telescope observations of galactic and Magellanic Cloud objects
22 p2735 N73-31890
MAGNESIUM
Use of low temperature quenching techniques to retain simple vacancy defects in magnesium
[NLL-CE-TRANS-5944-[9022.09]]
05 p0561 N73-14559
Influence of small magnesium additives on effect of superplasticity in aluminum-zinc eutectoid as function of temperature and velocity of deformation
09 p1046 N73-18532
Role of titanium in fabricating magnesium-graphite fiber composites with improved strength and stiffness
[AD-754570] 11 p1310 N73-20627
Time development of line radiation emitted from plasma produced by Q switched ruby laser onto magnesium target
[AD-755119] 11 p1328 N73-20775
Buckling and structural response of two magnesium ring stiffened conical shells subjected to uniform external pressure
[NASA-TN-D-7303] 17 p2092 N73-26926
Chemical spot test for identifying magnesium or magnesium alloys used in aerospace applications
[NASA-CASE-LAR-10953-1] 18 p2160 N73-27446
Controlling constituent properties for strengthening graphite fiber reinforced aluminum and magnesium composites
[AD-763211] 21 p2563 N73-30548
Nuclear spin-lattice relaxation in magnesium metal
24 p2960 N73-33651
MAGNESIUM ALLOYS
Ternary phase diagram of magnesium yttrium zinc in magnesium alloy
[AD-746724] 02 p0188 N73-11526
Effects of growth speed and heat treatment on deformation of aligned Ag3 Mg-AgMg and Al-Ag2 Al eutectics at minus 196 to 300 C
[AD-747310] 02 p0190 N73-11541
Physical properties of intermetallic magnesium tin compound
[AD-745942] 02 p0219 N73-11773
Analysis of wear resistance of copper alloyed, magnesium cast iron by reciprocating motion of different friction pairs
[AD-750519] 06 p0687 N73-15590
Analysis of metallurgical factors and mechanical effects during and subsequent to cold hydrostatic extrusion of magnesium and aluminum alloys
[AD-751739] 07 p0805 N73-16527
Preparation of magnesium-yttrium alloys by electroduction of yttrium oxide dissolved in yttrium fluoride-lithium fluoride bath
[BM-RI-7722] 07 p0809 N73-16560
Seven year tropical exposure test to evaluate corrosion resistance effectiveness of finishing systems for aluminum and magnesium
[AD-752907] 09 p1042 N73-18498
Corrosion behavior of grain boundary constituents in Al-Zn-Mg alloys
[AD-753273] 09 p1049 N73-18556
Mechanical properties of magnesium alloys operating at elevated temperature
[AD-758617] 15 p1800 N73-24593
Chemical spot test for identifying magnesium or magnesium alloys used in aerospace applications
[NASA-CASE-LAR-10953-1] 18 p2160 N73-27446
Structure and properties of magnesium-lithium alloys
[JPRS-59738] 20 p2430 N73-29523
Effect of electrochemical machining on mechanical properties of gas turbine engine blades made of MA-2 alloy
[AD-762497] 20 p2483 N73-29950
Creep properties of aligned silver-magnesium eutectic alloy
[AD-763375] 21 p2561 N73-30531
Determining thermodynamic properties of liquid copper-magnesium alloys by magnesium vapor pressure
[BARC-613] 22 p2685 N73-31504
MAGNESIUM CELLS
Structure and composition of anodic coatings formed on magnesium dry cell
[AD-764253] 22 p2618 N73-30980
MAGNESIUM COMPOUNDS
NT CHLOROPHYLLS
NT MAGNESIUM OXIDES
Magnesium thermal reduction method for interaction mechanism of titanium chloride with magnesium
06 p0683 N73-15561
MAGNESIUM OXIDES
Acoustic emission and crack propagation in single crystal MgO and glass as model ceramic materials
[AD-745000] 01 p0070 N73-10575
Internal friction and crystal defects of magnesium oxide crystals
09 p1063 N73-18673
Laser heating effects on oxide growth rates in magnesium-oxygen interaction
[AD-760176] 17 p2047 N73-26565
Residual stresses and plastic deformations of machined magnesium oxide crystals
[AD-759411] 17 p2073 N73-26776
Temperature effects and effect of addition of lithium fluoride on conductivity of magnesium oxide
[NLL-M-23040-[5828.4F]] 21 p2585 N73-30711
Oxygen grain boundary diffusion and grain growth in pure dense MgO
[NASA-CR-135719] 23 p2810 N73-32466
MAGNESYN [TRADEMARK]
U SERVOMOTORS
MAGNET COILS
NT FIELD COILS
Heat transfer in superconducting matrix as magnet coils
[BNL-16615] 04 p0459 N73-13743
Electromagnetic superconducting force producing coil for positioning models in wind tunnel
15 p1762 N73-24276
Transient behavior of currents and forces in coil system of stellarator during operational disturbances
[NASA-TT-F-15014] 18 p2126 N73-27182
MAGNETIC ABSORPTION
U ELECTROMAGNETIC ABSORPTION
MAGNETIC ANOMALIES
Description of magnetic and seismic facility at Great Whale River, Canada and analysis of data acquired during calendar year 1969 - Vol. 43, No. 3
[M70-43/3] 01 p0043 N73-10343
Description of equipment installed in magnetic and seismic observatory at Mould Bay, Canada and analysis of data acquired during 1969 - Vol 43, No. 4
[M70-43/4] 01 p0043 N73-10344
Description of magnetic and seismic facility at Baker Lake, Canada and analysis of data acquired during calendar year 1969 - Vol. 43, No. 2
[M70-43/2] 01 p0044 N73-10345
Three component aeromagnetic survey of British Columbia and northeastern Pacific Ocean to determine magnetic anomalies - Vol. 42, No. 7
[M70-42/7] 01 p0044 N73-10346
Standard curves for interpreting magnetic anomalies due to spheres in geomagnetic surveys
[BULL-119] 06 p0666 N73-15417
Detection of intermediate size magnetic anomalies in Cosmos-49 and OGO-2, 4, and 6 data
[NASA-TM-X-66225] 12 p1401 N73-21368
Electron density irregularities and evening anomalies in midlatitude nighttime F region
13 p1514 N73-22270
Satellite observations of geomagnetic disturbance reaction time in upper atmosphere
[REPT-85] 14 p1658 N73-23458
Short geomagnetic polarity intervals in marine magnetic profile for anomalies, using Fourier transformations and linear systems
15 p1770 N73-24336
Effect of magnetic induction anomaly on magnetotelluric fields in Oahu, Hawaii
[PB-214444/2] 16 p1908 N73-25440
Igdlorssuit geomagnetic variation anomaly in rift-fault zone of northern West Greenland
[R-35] 20 p2412 N73-29389
Method for calculating ocean bottom magnetic anomalies
[AD-762532] 22 p2668 N73-31380
MAGNETIC CIRCUITS
Evaluation of magnetic cards with cylindrical domains for application to magnetic circuits, noting domain propagation
[LCR-71-232/1/R] 16 p1945 N73-25736
MAGNETIC COILS
NT FIELD COILS
Magnetic test facilities at ESTEC, Netherlands, noting coils and magnetometers
[ESRO-TM-152-ESTEC] 02 p0153 N73-11238
MHD parameter optimization procedure for determining optimum coil geometry for 10 MW level superconducting magnet system
[AD-745322] 02 p0212 N73-11717
Closed magnetic systems for obtaining and controlling high temperature plasmas
[AD-747111] 02 p0217 N73-11759

Cost analysis and design of possible fusion reactor coil systems
[UCRL-73187] 03 p0336 N73-12741
Design of coils and switches for superconducting magnetic energy storage and transfer
[LA-DC-72-470] 03 p0345 N73-12816
Toroidal magnetic field spectrometer for experimentation with high energy beams
[LNF-72/59] 11 p1294 N73-20501
Elliptical integral expressions for magnetic field due to current loop
[ORNL-TM-4023] 12 p1429 N73-21581
Magnetic coil design and physical phenomena responsible for ac losses in superconductivity
15 p1761 N73-24273
Apparatus for measuring magnetization curve of superconducting coil
[EUR-CEA-FC-661] 15 p1821 N73-24760
Production and confinement of hot plasma and electron thermalization in superconducting ring device
[UCRL-74337] 16 p1950 N73-25777

MAGNETIC CONTROL
Closed magnetic systems for obtaining and controlling high temperature plasmas
[AD-747111] 02 p0217 N73-11759
Magnetic attitude control of ESRO 4 satellite noting magnetorquer and maneuver simulation
[ESRO-TN-108-ESTEC] 02 p0235 N73-11909
Production and current measurement of hydrogen ion beam and plasma in duoplasmatron with cusped magnetic field
[NP-19364] 05 p0583 N73-14747
Vibration tests of magnetic control assembly for Nimbus and ERTS satellites
[NASA-CR-130143] 06 p0673 N73-15478
Design and performance of segmented magnetic torque converter for mechanical drives
[AD-753541] 10 p1167 N73-19498

MAGNETIC CORES
Analysis of magnetic device with longitudinal field for experimentation with Adone reactor
[LNF-71/90] 04 p0448 N73-13659
Sense amplifier of ferrite coincident core memory
[AD-752817] 09 p1009 N73-18235
Evaluation of stability derivatives obtained from dynamic tests of model in cold magnetic balance wind tunnel facility
[NASA-CR-112305] 11 p1267 N73-20279
Method and device for providing banded transformer cores for use in spacecraft power systems
[NASA-CASE-NPO-11966] 13 p1499 N73-22150
Effect of multiword addressing with laminated ferrite arrays
[NASA-CR-124372] 21 p2512 N73-30149
Polish research projects involving development and application of magnetically soft ferrite materials
21 p2608 N73-30902
Performance data and characteristics of magnetic antennas
[AD-765364] 24 p2899 N73-33141

MAGNETIC DIFFUSION
Nonlinear diffusion of pulsed magnetic fields in planar and cylindrical plasmas
[LA-5132-MS] 24 p2963 N73-33681

MAGNETIC DIPOLES
Simulation of geomagnetic tail by plasma flux interaction with magnetic field of three dimensional dipole
[PR-113] 05 p0584 N73-14753
Comparing properties of open magnetosphere and its electric field to simple model of dipole in constant field
[NASA-TM-X-66132] 05 p0595 N73-14842
Approximate second invariant for charged particle trapped in field of magnetic dipole
[AD-750860] 06 p0701 N73-15715
Magnetic measurements of superconducting iron-shielded dipoles
[BNL-17190] 08 p0893 N73-17227
Coil configuration influence on current distribution of superconducting dipoles and quadrupoles
[BNL-17168] 10 p1201 N73-19771
Conversion of geomagnetic potential into spherical coordinates of optimally offset, inclined dipole using least squares method
[AD-756460] 13 p1526 N73-22366
Core polarization and mesonic exchange current modifications of nuclear magnetic dipole operator
[COO-3001-32] 17 p2064 N73-26701
Tilted image dipole model of magnetosphere replacing earth dipole by full internal field expansion
22 p2657 N73-31281

MAGNETIC DISKS
Laser interferometric equipment for vibration and distance to surface measurement of mass memory magnetic disk floating heads
[LCR-71-216/1/R] 17 p2034 N73-26461

MAGNETIC DISTURBANCES
NT MAGNETIC STORMS
Behavior of large scale positive polarity magnetic fields and geomagnetic disturbances
01 p0094 N73-10772
Interplanetary magnetic fields and magnetic disturbances induced by ionospheric
[DMI-GEOPHYS-PAPERS-R-32]
02 p0216 N73-11749
Ferromagnetic materials sensor for detecting time varying magnetic field disturbances and positional changes in ferromagnetic objects
[AD-748117] 03 p0338 N73-12757
Correlation between frequency of magnetic oscillations and geomagnetic disturbances, and low frequency oscillation of earth magnetic field
[NASA-CR-127801] 05 p0537 N73-14372
Correlation between frequency of magnetic oscillations observed by ATS 1 and two indices of geomagnetic disturbance
05 p0537 N73-14373
Evaluation of solar wind data obtained from Pioneer 6, Mariner 5, and Explorer 35 for velocity variations, magnetopause motion, and geomagnetic disturbances
[NASA-CR-129880] 05 p0591 N73-14806
Evaluation of field aligned ionospheric currents produced by azimuthal and radial magnetospheric disturbances
[PR-122] 10 p1156 N73-19402
Plasma convection patterns in polar upper ionosphere obtained from Cosmos 184 satellite measurements during magnetic disturbance of 4 Nov. 1967
[PR-130] 10 p1156 N73-19403
Charged particle and magnetic field research using ATS 1 and Mariner measurements
[NASA-CR-131269] 11 p1338 N73-20857
Tables on geomagnetic observations made by Kakioka Magnetic Observatory
[REPT-86] 12 p1399 N73-21345
Tables on geomagnetic observations made by Kanoya Magnetic Observatory
[REPT-88] 12 p1399 N73-21346
Tables on geomagnetic observations made by Memambetsu Magnetic Observatory
[REPT-87] 12 p1400 N73-21358
Analysis of two dimensional pattern of interplanetary shock waves based on solar longitude dependence of time intervals between geomagnetic storms and solar flares
[NASA-TM-X-66226] 12 p1445 N73-21704
Propagation pattern of shock waves emitted by solar flares occurring in active region of McMath No. 9740 from 23 Oct. - 4 Nov. 1968
[NASA-TM-X-66227] 12 p1445 N73-21705
Cosmic ray disturbances following solar flare occurrences in August 1972 recorded by neutron monitoring
12 p1446 N73-21709
Influence of F 2 regional disturbances and magnetic activity on short wave radio communications
13 p1521 N73-22327
Convection velocity measurements in polar upper ionsphere made by Cosmos 184 Satellite during moderate magnetic disturbance
15 p1780 N73-24430
Dichotomy in geomagnetic disturbance and its solar origin
[AD-759791] 16 p1909 N73-25447
Harmonic analysis of low altitude disturbances in geomagnetic fields
17 p2017 N73-26308
Interpretation of OGO 2, 4, and 6 measurements of near earth magnetic field disturbances in total field at high latitudes
[NASA-TM-X-70443] 21 p2536 N73-30332
OGO 2, 4, and 6 measurements of near earth magnetic field disturbances in total field at high latitudes
[NASA-TM-X-70442] 21 p2536 N73-30333

MAGNETIC DOMAINS
Evaluation of magnetic cards with cylindrical domains for application to magnetic circuits, noting domain propagation
[LCR-71-232/1/R] 16 p1945 N73-25736
Logic and memory devices with magnetic crystals, emphasizing magnetic domains
[JPRS-59608] 20 p2461 N73-29776
Magnetostatic trap generation for control of cylindrical magnetic domain
20 p2461 N73-29778
Propagation schemes and domain distribution in magnetic shift registers for domain memory devices
20 p2461 N73-29779
Boolean functions for logic and mathematic operations in magnetic domain devices
20 p2461 N73-29780

MAGNETIC DRUMS
Performance estimates for airborne magnetic drum memories
[AD-754933] 11 p1260 N73-20226

MAGNETIC EFFECTS
NT MAGNETIC RIGIDITY
Literature survey for action of applied magnetic field on conducting liquid in circular cylindrical container
[AE-447] 04 p0450 N73-13674
Production and research applications of magnetic bremsstrahlung
[BNL-TR-480] 04 p0452 N73-13689
Correlative studies of effects of solar wind and interplanetary magnetic field on bow shock and geomagnetic cavity
[NASA-CR-129924] 05 p0592 N73-14808
Influence of absorption magnetic thermal RF breakdown in superconducting cavities
[KFK-EXT-3/72-2] 06 p0708 N73-15780
Magnetic field effect on hydrated glucose crystal growth
[AD-754618] 11 p1254 N73-20172
Muon production altitude in cosmic ray air showers from lateral and angular muon separation from shower core, and geomagnetic effects on muon charge ratio
13 p1574 N73-22754
Application of magnetic perturbation technique to nondestructively detect subsurface nonmetallic inclusions in inner races of deep groove ball bearings
[NASA-TM-X-68260] 18 p2155 N73-27410
Liquid-solid transition for materials processing in space
[NASA-CR-124294] 18 p2179 N73-27596
Analytical description of spatial distribution of scattering of gyromotor magnetic field
20 p2418 N73-29425

MAGNETIC EQUATOR
Computation of lunar gravitational field expansion coefficients utilizing Cassini equator inclination and radial lunar density distribution values
[NASA-TT-F-14605] 01 p0104 N73-10858
Diurnal variations in ionospheric tilt near magnetic dip equator due to gravity waves
05 p0512 N73-14160
Simultaneous ultrahigh and very high frequency ionospheric effects from ATS 5 at the magnetic equator
[NASA-TM-X-65948] 12 p1378 N73-21173
Afternoon depression of geomagnetic H field on quiet days near magnetic equator in Indian zone
[AER-73-03] 14 p1658 N73-23459
Nighttime composition measurements at geomagnetic equator
[NASA-TM-X-70476] 23 p2785 N73-32283

MAGNETIC FIELD COILS
U FIELD COILS

MAGNETIC FIELD CONFIGURATIONS
Plasma physics and field configurations
[CONF-730705-1] 24 p2964 N73-33687

MAGNETIC FIELD INTENSITY
U MAGNETIC FLUX

MAGNETIC FIELDS
NT FORCE-FREE MAGNETIC FIELDS
NT GEOMAGNETISM
NT INTERPLANETARY MAGNETIC FIELDS
NT INTERSTELLAR MAGNETIC FIELDS
NT LUNAR MAGNETIC FIELDS
NT NONUNIFORM MAGNETIC FIELDS
NT PALEOMAGNETISM
NT PLANETARY MAGNETIC FIELDS
NT SOLAR MAGNETIC FIELD
NT STELLAR MAGNETIC FIELDS
Collisional aspects of 45 mtorr Avco experiment with and without applied magnetic field
[AD-745374] 01 p0084 N73-10698
Conversion of magnetic field energy into kinetic energy in solar wind as function of heliocentric distance
01 p0095 N73-10780
Magnetic field merging in solar wind in terms of steady state merging
01 p0096 N73-10790
Pitch angle diffusion coefficient for cosmic rays in static random magnetic field
[NASA-TM-X-66077] 01 p0100 N73-10819
Analysis of chromospheric patterns produced by changes in interplanetary and geomagnetic fields
[AD-745100] 01 p0106 N73-10877
Seasonal, altitude, and universal time differences in field-aligned electrons
[NASA-TM-X-66099] 02 p0166 N73-11345
Anisotropic instability of plasma without permanent magnetic field
02 p0166 N73-11350
Statistical mechanics of 2 and 3 dimensional plasmas in strong dc magnetic field
[NASA-CR-129177] 02 p0215 N73-11741
Characteristic oscillations of plasma in point cusp
[IPPJ-133] 02 p0215 N73-11743
Anomalous resistivity in turbulent plasma confined in strong magnetic field considering low and high electric field regimes
02 p0216 N73-11748
Influence of intense laser radiation on plasma generation of large magnetic fields
[AD-746098] 02 p0216 N73-11752
Impulsive plasma acceleration in inductive device
[AD-746044] 02 p0217 N73-11754
Greenstadt binary index criterion for distinguishing between laminar and pulsating bow shock crossings expressed as critical angle between shock normal and magnetic field
[NASA-TM-X-66105] 02 p0225 N73-11817
On variational relationships between solar wind parameters, magnetospheric magnetic activity, and magnetospheric storm electrons
02 p0225 N73-11820
Equivalent circuit of electromechanical or magnetohydrodynamic converter with traveling magnetic field
[AD-747611] 03 p0256 N73-12072
Effect of variable magnetic field on emission of helium-neon laser and resulting parameters of discharge plasma
[AD-747443] 03 p0311 N73-12542

Some six block coil configurations for cosine bending magnet
[BNL-16787] 03 p0336 N73-12740
Approximation of diffusion coefficients for charged particles in random magnetic field
[NASA-CR-129523] 03 p0339 N73-12767
Technique for determining influence of axial magnetic field on holdup of argon in coaxially fed argon-helium plasma generated by radio frequency induction
[ORNL-TM-3700] 03 p0341 N73-12779
Analysis of magnetogasdynamic shock fronts caused by solar winds and development of theoretical concepts and models for phenomenon
[NASA-TM-X-66106] 03 p0353 N73-12876
Analysis of magnetic field near planet Mars from data obtained by Mars 2 and Mars 3 spacecraft
[NASA-TM-X-66116] 03 p0357 N73-12907
Static magnetic fields inside idealized structures resembling missile cells
[AD-748409] 03 p0360 N73-12932
Integrated magnetic suspension and propulsion system characteristics
[BNL-16909] 04 p0402 N73-13271
Graphical and analytical methods for describing earth magnetic field using satellite and ground based observational data
04 p0414 N73-13382
Asymmetric magnetic yoke for shaping uniform field in electromagnets
[NP-19359] 04 p0450 N73-13673
Literature survey for action of applied magnetic field on conducting liquid in circular cylindrical container
[AE-447] 04 p0450 N73-13674
Production and current measurement of intense hydrogen-ion beams in pulsed conditions
[NP-19351] 04 p0454 N73-13705
Nonhomogeneity effects of magnetic field on plasma heating by electron beam in mirror trap of probkotron type
[SFTI-1] 04 p0454 N73-13710
Plasma production using gas stream kinetic energy in magnetic field
[DLR-FB-71-43] 04 p0455 N73-13714
Unsteady liquid metal flow in conduction MHD devices with constant magnetic field
[AD-748745] 04 p0455 N73-13715
One dimensional radial fluid cone for studying Z-pinch enbedded in hydrogen
[AD-748179] 04 p0455 N73-13718
Low frequency magnetic field interference of dc/dc regulators and transformers
[ESRO-CR-58] 05 p0499 N73-14059
Conference on biological effects of magnetic fields
[NRC-TT-1545] 05 p0500 N73-14070
OGO 5 fluxgate magnetometer measurements of large field depressions in magnetosphere
[NASA-TM-X-66133] 05 p0539 N73-14382
Radio auroras and nighttime magnetic field disturbances
[AD-750019] 05 p0543 N73-14415
Pump for cryogenic liquids using magnetocaloric material
[NASA-CASE-LEW-11672-1] 05 p0551 N73-14479
Computer program for calculating forces and energy in magnet systems
[ANL-TKK/RJL-2] 05 p0580 N73-14722
Simulation of geomagnetic tail by plasma flux interaction with magnetic field of three dimensional dipole
[PR-113] 05 p0584 N73-14753
Procedures and equipment for analyzing field strengths transmitted at extremely low frequencies and measurement of radial magnetic component
[REPT-72-4-ADD] 06 p0664 N73-15401
Effect of magnetic rupture on low frequency electroconductivity and weakly damped electromagnetic waves in metals with closed Fermi surfaces
[KHFTI-71-1] 06 p0684 N73-15569
Analysis of forces in electrostatic gyroscope with spherical rotor and development of equations to calculate electrical forces
06 p0695 N73-15666
Effect of displacements of suspended mass on accuracy of electromagnetic load cell and selection of parameters for increased accuracy
06 p0696 N73-15668
Approximate dispersion relationship of hydrodynamic waves in thin rotating spherical shells of incompressible fluid pervaded by uniform magnetic field
[MET-O-857] 06 p0699 N73-15702
Apparatus and program for turbulent torus experiment
[ORO-4087-8] 06 p0704 N73-15737
Plasma generation within magnetic containment field by laser irradiation of solid particle
[COO-3547-2] 06 p0704 N73-15740
Energy variation principle for specific inductance geometry in stable toroidal plasma generation
[NYO-1480-182] 06 p0704 N73-15741
Microwave measurements of magnetic field local shearing in confined plasma
[EUR-CEA-FC-632] 06 p0705 N73-15749
Pulsed magnetic field apparatus, and microstructure influence on critical current density of superconducting Nb3Sn strips in pulsed fields
[LBL-448] 06 p0708 N73-15778
Underluminosity and magnetic fields in Beta Lyrae
[NASA-TM-X-68895] 06 p0717 N73-15848
Magnetospheric field model incorporating OGO B and E magnetic field measurements
[NASA-TM-X-66172] 07 p0792 N73-16442
Relativity shift effect of gravitational vibration frequency in earth field
[ITF-72-43-P] 07 p0793 N73-16451
Secular magnetic variation and inner zone of energetic fields of earth
[AD-751284] 07 p0795 N73-16463
Interaction of intense relativistic electron beam with axial and convergent magnetic guide fields
07 p0820 N73-16647
Magnetic field measurements of Lewis Research Center cyclotron using Hall effect magnetic field transducer
[NASA-TM-X-2692] 07 p0824 N73-16677
Statistical mechanics and kinetic theory for two dimensional plasma in uniform magnetic field
07 p0825 N73-16685
Hot electron plasma control in superconducting toroids
[UCRL-73806] 07 p0826 N73-16699
Low temperature resistivity of high purity copper wire in high magnetic fields
[U-235] 08 p0943 N73-17725
Slowly changing, large magnetic induction in plasma core of rotating magnetic field pinch
[LRP-56/72] 08 p0947 N73-17756
Linear variation of magnetic field as inverse Faraday effect in plasma
[FRNC-TH-217] 08 p0948 N73-17762
Equilibrium plasma produced by theta pinch gun firing into magnetic field
[AD-752498] 08 p0949 N73-17772
Quantum electrodynamics in high magnetic fields
[AD-753042] 09 p1067 N73-18710
Linearized theory for MPD duct flows with exterior magnetic fields and Hall effect
[DLR-FB-72-67] 09 p1069 N73-18726
Measurement and analysis of fast ions and neutral particles in Penning discharge with ring anode in magnetic field
[TRITA-EPP-72-12] 09 p1071 N73-18739
Generation of magnetic field energy from radiation pressure in laser-produced plasma thermal energy
[AD-748180] 09 p1071 N73-18742
Solar wind propagation in low pressure gas and plasma containment in magnetic fields
[AD-753087] 09 p1072 N73-18750
Breakdown of quasi-linear derivation of kinetic equation describing cosmic ray distribution function in random magnetic field
[NASA-TM-X-65949] 09 p1081 N73-18815
Analysis of effect of mass on operation of airborne superconductor magnetic system with aluminum stabilized conductor
10 p1108 N73-19034
Development of high magnetic fields using superconductors with high current densities and application to power-conversion and energy storage
10 p1108 N73-19035
Application of superconducting coils for energy storage and determination of optimizing parameters for inductive energy storage
10 p1109 N73-19042
Method for calculating magnetic field map of magnetic suspension in ultracentrifuge
[LNF-72/49] 10 p1138 N73-19272
Development of method for determining conductivity of surface layer of sea by recording field of remote transmitters operating in superlong wavelength range
10 p1153 N73-19382
Evaluation of field aligned ionospheric currents produced by azimuthal and radial magnetospheric disturbances
[PR-122] 10 p1156 N73-19402
Fabrication and calibration of Tomahawk sounding rocket payload for magnetic field measurements in ionosphere
[AD-754246] 10 p1157 N73-19413
Penning discharge along magnetic field in collision-free plasma to simulate geomagnetic flux tube conditions
[TRITA-EPP-72-13] 10 p1189 N73-19676
Adiabatic processes in spiral magnetic field
[UCRL-TRANS-1487] 10 p1189 N73-19679
Influence of magnetoacoustic oscillations on electromagnetic excitation of shear acoustic waves
[COO-3150-4] 10 p1190 N73-19681
Alignment and field distribution of coil currents in storage accelerators using superconducting magnets
[BNL-17272] 10 p1194 N73-19712
Mechanism of plasma heating by large amplitude oscillating electric field
[UCB-34-P-128-X-2] 10 p1196 N73-19731
Microwave discharge plasma in magnetic fields greater than cyclotron
[AEC-TR-7372] 10 p1196 N73-19735
R-Om experimental setup for studying interaction of high frequency magnetic fields with plasma
[AEC-TR-7388] 10 p1197 N73-19737
Electromagnetic response of Pb superconducting film as function of magnetic field in microwave range
[ISS-72/5] 10 p1199 N73-19756
Apparatus for determining distance to lighting strokes from single station by magnetic and electric field sensing antennas
[NASA-CASE-KSC-10698] 11 p1254 N73-20175
Ion acceleration by electron ring in decreasing magnetic field
[AD-753968] 11 p1268 N73-20291
Slow toroidal oscillations of thin spherical shell of conducting fluid in magnetic field
[AD-755059] 11 p1273 N73-20331
OGO-5 fluxgate magnetometer for measuring magnetic field over range of OGO-5 orbit
[NASA-CR-130205] 11 p1294 N73-20498
Effects of propagation parallel to magnetic field on type I irregularity instability
[NASA-CR-131359] 11 p1327 N73-20771
Deviation from rotational symmetry of electric arcs in transverse magnetic fields
[AD-754022] 11 p1328 N73-20778
OGO D and F magnetic field results and surface data comparison
[NASA-TM-X-66218] 11 p1339 N73-20866
Binary code signals produced by electron beam deflection in magnetic fields
12 p1378 N73-21176
Oscillations of geomagnetic tail and magnetospheric instability from solar activity
12 p1401 N73-21365
Phase diagram of decorated Ising system in nonzero magnetic field
[NUB-2175] 12 p1428 N73-21576
Elliptical integral expressions for magnetic field due to current loop
[ORNL-TM-4023] 12 p1429 N73-21581
Diamagnetic measurements of electrically driven shock tube to determine general conditions of moving plasma in longitudinal magnetic field interactions
[AREAEE-145] 12 p1429 N73-21583
Correlation energy of quantum mechanical electron gas in intense magnetic field
[NUB-2178] 12 p1431 N73-21597
Wave interactions between plasma-electron beam system in magnetic fields
[AEC-TR-7355] 12 p1434 N73-21616
Interaction of plasma streams with stationary, axisymmetric magnetic fields
[AEC-TR-7354] 12 p1434 N73-21620
Transient processes due to interaction of shock produced plasma flows with magnetic fields
[IPP-4/41] 12 p1435 N73-21628
Microwave surface impedance of thin niobium superconducting films subjected to varying dc magnetic fields
12 p1438 N73-21649
Analysis of conditions leading to generation of cosmic rays by acceleration of charged particles caused by electromagnetic field of pulsars
[PPG-144] 12 p1445 N73-21703
Apollo 16 particles and fields subsatellite for measuring vector magnetic fields and plasma and energetic particle fluxes
12 p1451 N73-21756
Invariant-group properties of equations for boundary layer of electrically conductive liquid in magnetic field
[AD-756956] 13 p1513 N73-22257
Development of procedure for controlling crystallization of metal in molten pools and effect of electromagnetic treatment during welding
[AD-756335] 13 p1536 N73-22443
Electromagnetic properties of plane slab of finite thickness immersed in uniform magnetic field
[VTH-169] 13 p1559 N73-22637
Oblique plasma resonance measured from quadrupolar impedance probe noting motion effect of plasma parallel to geomagnetic field
[GRI/NTP/110] 13 p1563 N73-22669
Low frequency transverse waves in two-fluid solar wind having radial magnetic field and streaming velocity
[NASA-CR-131570] 13 p1573 N73-22745
Correlation of solar magnetograms with interplanetary magnetic field
[NASA-CR-131607] 13 p1577 N73-22775
Solution of thermodynamic forces and flows in magnetic field using Gibbs equation
[AD-756901] 13 p1592 N73-22909
Controlled magnetic and electric excitation of airframe of LOH-6A helicopter and measurement of impedance, radiation patterns, and bandwidths
[AD-757143] 14 p1602 N73-22992
Physiological regeneration of corneal epithelial mice cells exposed to strong magnetic fields
14 p1608 N73-23034
Geophysical observations of horizontal and vertical components of earth magnetic field at Feurstenfeldbruck, Germany for 1972
14 p1660 N73-23473

Spontaneous generation of magnetic fields associated with laser produced plasmas
[AD-757247] 14 p1695 N73-23759
Excitation of longitudinal waves in collisionless and cold plasma in presence of uniform magnetic field
[AD-756477] 14 p1696 N73-23764
Design, development, and operation of compact, high performance, magnetohydrodynamic generators
[AD-756489] 14 p1696 N73-23765
Magnetic field effects in cathode mechanism of electric arc initiation and travel between copper electrodes
[NLL-CE-TRANS-6108-[9022.09]] 15 p1755 N73-24226
Electromagnetic dispersion relation for two counterstreaming ion beams flowing parallel to direct current magnetic field
[NASA-CR-132953] 15 p1814 N73-24701
Dispersion relations for electromagnetic waves propagating in partially ionized gases immersed in dc magnetic field
[AD-757865] 15 p1819 N73-24743
Physical processes occurring in vortex stabilized arcs with and without applied axial magnetic fields
[AD-759187] 16 p1892 N73-25313
Low intensity magnetic field effects on flotation properties of water
[AD-758623] 16 p1946 N73-25746
Coupling of magnetic pulse to initially magnetized collisionless plasma 16 p1948 N73-25759
Impulsive plasma accelerator study of plasma acceleration by magnetic field annihilation
[AD-758880] 16 p1950 N73-25780
Equations of motion for plasma drift, deformation, and diffusion in magnetic field
[AD-759742] 16 p1950 N73-25782
Unique approach for deriving cosmic ray diffusion equation for charged particles in static, random magnetic field
[NASA-TM-X-66263] 16 p1959 N73-25848
Wave propagation and magnetic fields effects on velocity oscillations in solar plage regions 16 p1961 N73-25864
Meissner effects and magnetization curves for superconductors - conference
[LA-5115] 17 p2010 N73-26257
Quantitative modeling of electric fields induced in magetosphere by changes in magnetospheric magnetic field
[AD-760058] 17 p2029 N73-26418
Effects of electric and magnetic fields on nucleation and growth of metallic thin films
[USC-113-P-22-3] 17 p2045 N73-26546
Experimental determination of width of near anode region in knudsen mode of thermionic converter having variable interelectrode gap filled by Ba plus Cs mixture
[AD-760394] 17 p2062 N73-26682
Low frequency instabilities in plasmas with magnetic shear 17 p2066 N73-26717
Reverse deflection and contraction of plasma beam entering a curved magnetic field
[TRITA-EPP-72-32] 17 p2068 N73-26735
Hypersonic, shock tube generated, plasma flow interaction with strong magnetic fields, studied by interferometric, pressure, and light emission measurements
[IPF-72-2] 17 p2069 N73-26738
High quasi-stationary magnetic field production with capacitor-fed magnetic field coil
[IPF-72-7] 17 p2069 N73-26741
Dynamic and adiabatic approximation applied to polarons in uniform magnetic field 17 p2071 N73-26753
Measurement of electromagnetic wave diffraction by finite plane-parallel waveguide system 18 p2117 N73-27116
Magnetic field and current configuration with boundary conditions holding geomagnetic tail 18 p2132 N73-27230
Measurement of auroral electrojet magnetic activity indices for calendar year 1970
[UAG-22] 18 p2133 N73-27231
Characteristics of three station network for sensing magnetic and electric fields associated with lightning discharges
[NASA-CR-133400] 18 p2151 N73-27382
Measurement of electromagnetically excited acoustic standing-wave resonance 18 p2159 N73-27444
High pressure compressed gas magnetic diaphragm rupture system for generating megaguss magnetic field
[JPRS-59459] 18 p2179 N73-27593
Numerical analysis of transient currents and forces in toroidal coils for stellarators and effects of sudden disturbance of normal operation
[NASA-TT-F-15013] 18 p2179 N73-27595
Relativistic particle motion in electromagnetic wave traveling in direction of uniform static magnetic field
[NASA-CR-132781] 18 p2181 N73-27610
Electron gas behavior and density in constant electric and magnetic fields
[AD-760587] 18 p2182 N73-27617
Metastable states of superconductors in presence of magnetic fields 18 p2185 N73-27645
Solar wind plasma and magnetic field measurements from Pioneers 9 and 10 flights
[NASA-TM-X-62291] 18 p2195 N73-27719
Magnetic field interference of transformers for dc/dc converters for spacecraft power supplies
[ESRO-CR-84] 19 p2225 N73-27930
Kinetics of change in electrical resistance of thin films annealed in magnetic field at high temperature
[JPRS-59625] 19 p2309 N73-28575
Finite element analysis on cylindrical and toroidal plasma stabilities contained in magnetic field
[JAERI-M-4890] 19 p2324 N73-28700
Finite plasma stream adiabatic motion in inhomogeneous, transverse magnetic field
[TRITA-EPP-73-08] 19 p2325 N73-28702
Superconducting magnetic field trapping device for producing magnetic field in air
[NASA-CASE-XNP-01185] 19 p2326 N73-28710
Analytical description of spatial distribution of scattering of gyromotor magnetic field 20 p2418 N73-29425
Hall effect magnetometer for measuring magnetic fields
[NASA-CASE-LEW-11632-2] 20 p2419 N73-29437
Channeling of supersonic free jet of plasma by axisymmetric magnetic field 20 p2457 N73-29744
Stability of microwaves generated by intense relativistic electron beam in rippled magnetic field
[AD-763337] 21 p2508 N73-30126
Interpretation of OGO 2, 4, and 6 measurements of near earth magnetic field disturbances in total field at high latitudes
[NASA-TM-X-70443] 21 p2536 N73-30332
OGO 2, 4, and 6 measurements of near earth magnetic field disturbances in total field at high latitudes
[NASA-TM-X-70442] 21 p2536 N73-30333
Ship towed magnetometer for direct measurement of horizontal component of earth magnetic field 21 p2547 N73-30418
Stability of amplitude characteristics of laser gyroscope in magnetic field
[AD-763260] 21 p2550 N73-30442
Scattering by charged particle density fluctuations of plasma for zero magnetic field
[NASA-CR-133808] 21 p2582 N73-30694
Development of optical diagnostic techniques to determine plasma refractive index using interferometers to produce space or time resolved density data
[AD-763802] 21 p2584 N73-30706
Hydrodynamic stability of circular magnetic fields and revolving fluids 22 p2650 N73-31234
Pioneer 11 high field fluxgate magnetometer experiment
[NASA-TM-X-70467] 22 p2672 N73-31405
Design, construction, and performance of large superconducting magnetic shield
[NASA-CR-135486] 22 p2700 N73-31627
Coherent charged particle propagation in magnetic fields
[NASA-CR-135492] 22 p2702 N73-31639
LASNEX equations for self-generated magnetic fields and nonthermal electrons in laser produced plasmas
[UCRL-74110] 22 p2703 N73-31653
One dimensional, diffusion wave transverse to magnetized helium positive column plasma
[AD-763808] 22 p2705 N73-31666
Analysis of steady state flow of solar wind and effect on magnetic field of dipole
[NASA-TT-F-15071] 22 p2711 N73-31709
Magnetic field effects on burning rate of solid rocket propellants
[AD-763894] 22 p2730 N73-31847
Physical theory of coherent cosmic ray propagation in random magnetic fields
[TR-73-133] 23 p2834 N73-32649
Spectrographic study of rare earth crystal absorption spectra in magnetic fields at liquid helium temperature
[NASA-TT-F-14732] 24 p2958 N73-33640
Analytical solutions to plasma generation near neutral point in magnetic field
[EUR-CEA-FC-685] 24 p2963 N73-33678
Nonlinear diffusion of pulsed magnetic fields in planar and cylindrical plasmas
[LA-5132-MS] 24 p2963 N73-33681
Theoretical analysis of laser-created plasmas confined by external magnetic field
[CEA-R-4410] 24 p2965 N73-33695
Magnetic field data from magnetometer experiments and trajectories of Explorers 33, 35, 41, 43, and 47
[NASA-TM-X-70481] 24 p2979 N73-33809
Thermodynamic properties of electron gas in magnetic fields of varying strengths to include magnetic susceptibility, internal energy, and specific heat 24 p2990 N73-33896

**MAGNETIC FILMS**
Magnetic bubble circuits for satellite data storage
[AD-750660] 06 p0644 N73-15232
Magnetostatic and magnetoelastic surface wave interactions in magnetized yttrium-iron garnet film
[AD-754106] 11 p1331 N73-20802
Plated thin magnetic film wire element for high speed main memories
[REPT-732] 14 p1619 N73-23112
Effects of chemical etching on magnetic and storage properties of Permalloy memory films
Integrated circuits using thin magnetic film elements
[AD-762267] 19 p2248 N73-28127
Electrodeposition of cylindrical magnetic films
[JPRS-59626] 19 p2305 N73-28534
Magnetooptical measurements of demagnetizing fields in cylindrical magnetic films
[JPRS-59624] 19 p2321 N73-28670
Design and construction of thin magnetic film shift register
[NHK-LABS-NOTE-164] 20 p2379 N73-29112
Magneto-optic phase change for detecting magnetization reversal in magnetic films
[AD-764549] 24 p2959 N73-33645

**MAGNETIC FLUX**
Review of solar rotation and solar magnetic fields 01 p0092 N73-10761
Tables of earth magnetic field intensity measurements at Sao Jose dos Campos, Brazil
[AD-747060] 04 p0415 N73-13389
Fast radial motion of toroidal plasma column in transverse magnetic field resulting in controlled displacement of plasma column
[NP-19401] 06 p0705 N73-15734
Interplanetary magnetic field annihilation and resulting D-sheets
[NASA-TM-X-66187] 09 p1080 N73-18813
Method for calculating magnetic field map of magnetic suspension in ultracentrifuge
[LNF-72/49] 10 p1138 N73-19272
Penning discharge along magnetic field in collision-free plasma to simulate geomagnetic flux tube conditions
[TRITA-EPP-72-13] 10 p1189 N73-19676
Magnetic field intensity calculations for gap electrical machinery with symmetric and asymmetric windings
[JPRS-58448] 11 p1324 N73-20744
Feasibility of gun launched projectile to produce magnetic flux compression
[AD-755103] 11 p1325 N73-20750
Comparison of simultaneous particle detector and search coil magnetometer measurements of precipitating particles and field aligned currents from OGO-D
[NASA-TM-X-66224] 12 p1401 N73-21367
Error analysis of computer calculation of magnetic field intensity and magnetic parameter 15 p1813 N73-24696
Fluxgate magnetometer for measuring magnetic flux density of several electron-bombardment ion thrusters
[NASA-TM-X-68239] 15 p1826 N73-24796
Erosion rate of dayside magnetic flux based on quantitative study of dependence of polar cusp latitude on interplanetary magnetic field
[NASA-TM-X-66256] 15 p1831 N73-24837
Magnetic particle inspection of large or irregularly shaped parts by assuring optimum magnetic flux densities
[AD-759207] 16 p1882 N73-25236
Automated iterative analysis of aeromagnetics 17 p2062 N73-26684
Magnetic flux pump for changing intensity of magnetic fields
[NASA-CASE-XNP-01187] 19 p2303 N73-28516
Method for increasing intensity of magnetic field by transferring flux
[NASA-CASE-XNP-01188] 23 p2795 N73-32361
Fluxon coupling force measurements on superconducting dc transformers noting film thickness and silicon monoxide layer 24 p2898 N73-33135

**MAGNETIC FORMING**
Refining in-house magnetic forming capability, using 18,000 joule high energy capacitor
[AD-762844] 20 p2424 N73-29468

**MAGNETIC INDUCTION**
Estimation of radio frequency power required to induce direct current in strong magnetic field of thermonuclear fusion device
[IPPJ-135] 02 p0216 N73-11746
Microwave generator using Gunn effect for magnetic tuning
[NASA-CASE-NPO-12106] 06 p0645 N73-15235
Electromechanical response of induction triphase motor to voltage perturbation in feeder network
[PUBL-1362] 06 p0647 N73-15254
Slowly changing, large magnetic induction in plasma core of rotating magnetic field pinch
[LRP-56/72] 08 p0947 N73-17756
Experimental determination of compressive behavior of linear induction motor reaction rail
[NASA-TM-X-69276] 17 p2011 N73-26263
Inductive reactances of direct sequence of synchronous machine with ferromagnetic screen
[AD-759879] 17 p2039 N73-26494

**MAGNETIC INDUCTION PROBES**
U MAGNETIC PROBES

**MAGNETIC LENSES**
Design of quadrupolar focusing lenses for drift tubes of heavy ion accelerator
[LYCEN-7179] 04 p0402 N73-13270
Analysis of performance of pulsed coaxial guns based on snowplow model allowing for variable initial mass-loading distribution
10 p1111 N73-19057
Development of procedure for aligning pole piece system of magnetic electron microscope
[NLL-M-23011-[5828.4F]] 20 p2417 N73-29416
Quadrupole mass spectrometer using noise spectrum for ion separation and identification
[NASA-CASE-XNP-04231] 23 p2791 N73-32325
**MAGNETIC MATERIALS**
NT FERRIMAGNETIC MATERIALS
NT FERROMAGNETIC FILMS
NT FERROMAGNETIC MATERIALS
NT PERMALLOYS [TRADEMARK]
Analysis of lunar material to determine presence of magnetic monopoles with description of equipment used
[NASA-CR-128642] 03 p0356 N73-12902
Rare earth-cobalt permanent magnet materials processing
[AD-748264] 04 p0451 N73-13679
Superconductor interactions and properties, and amorphous semiconducting and magnetic materials
[NASA-CR-129524] 04 p0457 N73-13731
Reliable source of high quality magnetic bubble materials
[AD-749806] 05 p0589 N73-14787
Development of solid state magnetic digital temperature transducer - Vol. I
[NASA-CR-133832] 08 p0923 N73-17556
Production and evaluation of magnetic and electrical materials capable of operating in 800 to 1600 F temperature range for advanced space electric power systems
[NASA-CR-2224] 09 p0990 N73-18084
Technology of high performance transition metal, rare earth permanent magnets for critical applications
[AD-754959] 11 p1306 N73-20601
Processing methods for rare earth cobalt compounds as permanent magnets
[AD-754951] 11 p1325 N73-20749
Effect of electron-phonon interaction on temperature dependence of paramagnetic susceptibility in metals
[AD-753984] 11 p1331 N73-20804
Hydrostatic pressure studies of magnetic modes in far infrared
[COO-3151-12] 12 p1428 N73-21577
Dynamic interface effects on electromagnetic response of magnetic semiconductors
[AD-755861] 12 p1442 N73-21681
Development of virtually zero magnetic bearing for application to electric motor construction
[NASA-CR-130225] 13 p1499 N73-22152
Magnetic bubble garnet materials for thin film storage devices
[AD-755546] 13 p1568 N73-22705
Ion exchange interactions in magnetically diluted nickel fluorides
[REPT-734] 14 p1694 N73-23749
Neutron scattering, computerized simulation, and magnetic resonance techniques for studying phase transitions in magnetic materials
[AD-757223] 14 p1698 N73-23782
Magnetic bubble material and magnetic properties of Mott transition
[AD-757435] 14 p1699 N73-23787
Magnetic couplings and magnetomechanical transmissions for airtight manipulator design
17 p1989 N73-26086
Electron paramagnetic resonance of dilute magnetic alloys including Mg-Gd, and noble metal-rare earth
17 p2071 N73-26756
Materials processing method for optimization of rare earth cobalt compounds as permanent magnets
[AD-760777] 18 p2180 N73-27599
Research and development of rare earth-transition metal alloys as permanent magnet materials
[AD-762304] 20 p2432 N73-29534
Research and development of laser materials, semiconductor materials, and magnetic materials
[AD-763709] 21 p2555 N73-30486
Polish research projects involving development and application of magnetically soft ferrite materials
21 p2608 N73-30902
Magnetic materials selection for spacecraft transformers used in static inverters, converters, and transformer-rectifier supplies
[NASA-CR-135642] 23 p2764 N73-32118
Transport coefficient anomalies in antiferromagnetic metals in vicinity of Neel temperature
24 p2933 N73-33424
Affect of antiferromagnetic ordering onset at Neel temperature on transport properties of CeAl, AuHo, and ErCu systems
24 p2933 N73-33425
Thermal and magnetic properties of magnetic crystals
[COO-3574-95] 24 p2969 N73-33727

**MAGNETIC MEASUREMENT**
Hourly geomagnetic measurements at Nurmijaeri, Finland - tables
01 p0048 N73-10383
Equatorial electrojet measurement made by Cosmos 321 and magnetic observatories
04 p0414 N73-13377
Graphical and analytical methods for describing earth magnetic field using satellite and ground based observational data
04 p0414 N73-13382
Magnetic tests of UK 4 spacecraft to determine magnetic characteristics and to provide desirable magnetic conditions
[NASA-TM-X-66125] 04 p0478 N73-13912
Low frequency magnetic field interference of dc/dc regulators and transformers
[ESRO-CR-58] 05 p0499 N73-14059
Measurement of magnetic field emission of spacecraft power system units at low frequencies
[ESRO-CR-57] 05 p0548 N73-14452
Computer program for calculating forces and energy in magnet systems
[ANL-TKK/RJL-2] 05 p0580 N73-14722
Geomagnetic measurements in south and east Finland 1967 through 1971 and final values reduced to 1970.0
[REPT-23] 06 p0666 N73-15416
Use of Josephson devices to measure low frequency magnetic fields and voltages
[LBL-845] 06 p0708 N73-15777
Bathymetry, magnetic, and gravity data for North Pacific Ocean areas collected between 1961 and 1970 - Technical Report 50
[NOAA-TR-NOS-50] 07 p0792 N73-16444
Bathymetry, magnetic, and gravity data for North Pacific Ocean areas collected between 1961 and 1970 - Technical Report 49
[NOAA-TR-NOS-49] 07 p0793 N73-16445
Magnetic field measurements of Lewis Research Center cyclotron using Hall effect magnetic field transducer
[NASA-TM-X-2692] 07 p0824 N73-16677
Electromagnetic lunar conductivity measurements on dark side radial magnetic fields
[NASA-TM-X-62226] 07 p0844 N73-16834
Wear process and colloidal particle production test on sliding metal surfaces using magnetic measurements
[AD-753251] 09 p1040 N73-18481
VLF magnetotelluric measurements in Sweden
[KGO-72-10] 12 p1402 N73-21369
Geomagnetic annuals for Spanish observatories
15 p1777 N73-24400
Geomagnetic measurements for 1970 at Toledo
15 p1777 N73-24401
Geomagnetic data for 1970 at Almeria
15 p1777 N73-24402
Geomagnetic data for 1970 at Logrono
15 p1777 N73-24403
Geomagnetic data for 1970 at Santa Cruz, Tenerife
15 p1777 N73-24404
Geomagnetic data during 1970 for Moca
15 p1777 N73-24405
Apparatus for measuring magnetization curve of superconducting coil
[EUR-CEA-FC-661] 15 p1821 N73-24760
Magnetic measurements of atmosphere in 1970 at Eskdalemuir, Hartland, and Lerwick
[SBN-11-880601-7] 17 p2016 N73-26305
Application of dynamic nuclear polarization to increase sensitiviy and speed of nuclear precission magnetometers
[JPRS-59393] 18 p2151 N73-27386
Solar wind plasma and magnetic field measurements from Pioneers 9 and 10 flights
[NASA-TM-X-62291] 18 p2195 N73-27719
Magnetic and transport properties of dilute magnetic alloys
[AD-763710] 21 p2586 N73-30721
Magnetic observations for 1971
[M70-44/4] 24 p2920 N73-33323
**MAGNETIC MEMORIES**
U MAGNETIC STORAGE
**MAGNETIC METALS**
U MAGNETIC MATERIALS
U METALS
**MAGNETIC MIRRORS**
Influence of Coulomb collisions on plasma ion relaxation in confined circular stabilized magnetic mirror
[EUR-CEA-FC-640] 03 p0341 N73-12783
Anomalous radial plasma losses in Q machine with mirror magnetic fields
[UCRL-51207] 03 p0343 N73-12794
Anisotropy and angular distribution of bremsstrahlung radiation emitted by electrons confined in magnetic mirrors
[ORNL-TM-3821] 04 p0453 N73-13698
Behavior of plasma column in high voltage theta pinch with and without magnetic mirrors
[LA-DC-72-703] 05 p0584 N73-14751
Particle motion in magnetic mirror with high frequency electric field
[COO-2181-7] 06 p0703 N73-15731
Design of feedback geometry for control of rotating plasma confined in magnetic mirror device
[AD-751341] 07 p0830 N73-16728
Containment of deuterium plasma in magnetic mirror well
[UCRL-74087] 08 p0949 N73-17769
Steady-state characteristics of four plasma sources developed for mirror machine
[AD-754233] 10 p1197 N73-19742
Low frequency instabilities in plasma confined by magnetic mirror system
[AD-754004] 10 p1197 N73-19743
Parallel magnetic multipole confinement of magnetic field-free plasma
12 p1432 N73-21603
Radio frequency heating in THM-2 mirror machine
[LPS-95] 17 p2068 N73-26729
Magnetic mirrors for controlled nuclear fusion
[IAEA/SM-170/49] 19 p2320 N73-28665
Fokker-Planck study of Coulomb collisions in plasma confined by mirror magnetic configurations
[EUR-CEA-FC-687] 24 p2964 N73-33691
**MAGNETIC MOMENTS**
Calculation of direction of magnetic moments of two permanent magnets in ESRO I satellite
[NASA-TT-F-14499] 01 p0109 N73-10896
Magnetism in solids - magnetic moments, propertism of diamagnetism and paramagnetism, and coexistence of superconductivity and ferromagnetism
[ITJ-13] 04 p0449 N73-13670
Magnetic tests of UK 4 spacecraft to determine magnetic characteristics and to provide desirable magnetic conditions
[NASA-TM-X-66125] 04 p0478 N73-13912
Fabrication and tests of magnetic control assembly designed as add-on unit for components of Nimbus and ERTS attitude control system
[NASA-CR-130142] 06 p0673 N73-15479
Mossbauer analysis of spin arrangements in gold iron and copper iron alloys at low temperature
[AD-754140] 10 p1202 N73-19787
Core polarization and mesonic exchange current modifications of nuclear magnetic dipole operator
[COO-3001-32] 17 p2064 N73-26701
**MAGNETIC PERMEABILITY**
Susceptibility of model polymer with diagonal viscosity and weak interaction
[COO-3161-2] 04 p0387 N73-13142
Evaluation of magnetic permeability tensors of polycrystal ferrimagnetic materials in saturated state for microwave frequencies
[REPT-9.441] 10 p1190 N73-19683
Effect of electron-phonon interaction on temperature dependence of paramagnetic susceptibility in metals
[AD-753984] 11 p1331 N73-20804
Concentration dependence of high field susceptibility of Fe-Ni alloys
[NLL-LTI-746-1343-[9022.401]]
12 p1412 N73-21440
Static longitudinal and transverse susceptibilities calculated for iron fluoride as function of temperature
[AD-757009] 14 p1698 N73-23781
Magnetic susceptibilities of NiCl2.6H2O
[AD-759417] 17 p2046 N73-26555
**MAGNETIC PISTONS**
Equilibrium structure of boundary layer between plane magnetic piston and low density plasma
[JUL-890-PP] 22 p2704 N73-31655
**MAGNETIC PROBES**
Ferromagnetic materials sensor for detecting time varying magnetic field disturbances and positional changes in ferromagnetic objects
[AD-748117] 03 p0338 N73-12757
Magnetic probes and instrumentation of capacitive discharges
[AD-748610] 04 p0423 N73-13450
Integrated circuit differential amplifier for magnetic probe measurements
[LRP-55/72] 10 p1134 N73-19241
Underwater devices for target detection on sea bottom
[JPRS-58916] 14 p1667 N73-23529
Fourier coefficients and power spectral density calculating device
[IPPJ-T-13] 16 p1949 N73-25766
Application of dynamic nuclear polarization to increase sensitivity and speed of nuclear precission magnetometers
[JPRS-59393] 18 p2151 N73-27386
**MAGNETIC PROPERTIES**
NT ANTIFERROMAGNETISM
NT DIAMAGNETISM
NT FERROMAGNETISM
NT GEOMAGNETISM
NT MAGNETIC EFFECTS
NT MAGNETIC INDUCTION
NT MAGNETIC MOMENTS
NT MAGNETIC PERMEABILITY
NT MAGNETIC RIGIDITY
NT MAGNETIC SUSPENSION
NT MAGNETOACTIVITY
NT MAGNETORESISTIVITY
NT MAGNETOSTRICTION
NT PALEOMAGNETISM
NT PARAMAGNETISM

NT POLARIZATION CHARACTERISTICS
NT REMANENCE
NT SPIN-LATTICE RELAXATION
Conference on magnetic structure of interplanetary and solar magnetic fields and solar wind
[NASA-SP-308] 01 p0092 N73-10760
Effect of solar wind velocity on interplanetary magnetic field properties
01 p0093 N73-10767
Observation of interplanetary and solar magnetic field sector structure from 1962 through 1968
01 p0094 N73-10770
Behavior of large scale positive polarity magnetic fields and geomagnetic disturbances
01 p0094 N73-10772
Large scale structure of solar wind during fading and maximum portions of two different cycles
01 p0094 N73-10774
Analysis of cobalt alloys containing samarium additives to determine effects on saturation magnetization, residual magnetization, and coercive forces
[NLL-M-21478-[5828.4F]] 02 p0185 N73-11499
Electrical-, thermal-, and magnetic-properties of zirconium and niobium carbide solid solutions
[AD-746217] 02 p0219 N73-11772
Analysis of hydrogen diffusion in alpha-iron in six degree to seventy seven degrees Kelvin using magnetic after-effect technique
[COO-1198-903] 03 p0314 N73-12561
Magnetic properties of transition metals
[BNL-16679-PT-1-PT-2] 03 p0336 N73-12738
Optical and magnetic properties of actinide and rare earth ions in insulators and semiconductors
[RLO-2221-T-6-14] 03 p0345 N73-12815
Effects of polishing on magnetic properties of nickel-zinc ferrite toroids during annealing and procedures to restore original magnetic properties
[AD-747251] 03 p0346 N73-12822
Analysis of lunar material to determine presence of magnetic monopoles with description of equipment used
[NASA-CR-128642] 03 p0356 N73-12902
Analysis of effects of heat treatment of magnetic and physical properties of molybdenum permalloy
[NLL-RTS-7641] 04 p0431 N73-13509
Magnetic properties and crystalline structures of rare earth-cobalt alloys
[AD-748270] 04 p0436 N73-13555
Crystal growth and magnetic properties of transition metal chalcogenides
[AD-748864] 04 p0459 N73-13748
Effect of structural changes on electrical and magnetic properties of amorphous semiconducting material
[AD-748661] 04 p0460 N73-13751
Magnetic, optical, and transport properties of semiconductors
[AD-747692] 04 p0460 N73-13752
Neutron diffraction and single crystal X ray determination of rare earth-cobalt-iron intermetallic magnetic structure
[AD-748429] 04 p0460 N73-13754
Magnetic properties and phase composition of finely-dispersed nondeformed powders from highly-anisotropic gamma-phase Fe-Pd alloys
[NLL-TRANS-746-1389-[9022.401]]
05 p0560 N73-14553
Magnetic properties of single crystal nickel powers
[NLL-TRANS-746-1390-[9022.401]]
05 p0585 N73-14762
Physics research on solid state materials - radiation damage, electronic structure, and magnetic, electrical, surface, low temperature, and lattice properties
[ORNL-4779] 06 p0708 N73-15776
Electron-impurity spin interchange model for analyzing magnetic properties of diluted magnetic alloys at low temperatures
08 p0931 N73-17626
Electron spin overlap model for quantitative analyses on magnetic spectra of coordination compounds with unpaired electrons
08 p0945 N73-17740
Micromagnetic interactions of rare earth orthoferrites and Mossbauer spectroscopy
[AD-751995] 08 p0951 N73-17789
Electrical properties of reinforced dielectrics, magnetic permeabilities of multicomponent materials, and electromagnetic waves in fibrous dielectrics
[AD-752693] 09 p1053 N73-18583
Effects of electromagnetic forces, energy radiation, and discharge losses on design of superconducting coils for energy storage elements
10 p1109 N73-19043
Dependence of magnetic effective length and fringe field correction constant on central field flux density for beam transport systems
[LA-DC-72-1121] 10 p1190 N73-19682
Magnetic properties of superconducting films
[ISS-72/6] 10 p1199 N73-19758
Transition properties of type 1 and magnetic properties of type 2 semiconductors with small Ginzburg-Landau parameters
[JUL-854-FF] 10 p1200 N73-19762
Magnetic properties of iron oxides in boron oxides
[AD-754104] 10 p1202 N73-19780
Mossbauer analysis of spin arrangements in gold iron and copper iron alloys at low temperature
[AD-754140] 10 p1202 N73-19787
Magnetic and ferroelectric properties of rare earth compounds for signal processing devices
[AD-754775] 11 p1331 N73-20807
Magnetic, optical, and semiconducting properties of rare earth compounds
[AD-755925] 12 p1376 N73-21164
Effects of carbon and copper on magnetic properties of iron and iron-silicon alloys
[NASA-TT-F-14857] 12 p1428 N73-21574
Magnetic properties of powdered samples of Dy2Ti2O7
[NASA-TM-X-68219] 12 p1428 N73-21575
Computer simulation of collisionless plasma with self-electric and magnetic interactions
[COO-2200-1] 12 p1434 N73-21619
Effect of substrate topography on magnetic properties of cylindrical Ni-Fe thin films
[NLL-LTI-746-1370-[9022.401]]
12 p1437 N73-21641
Magnetic instabilities in Type-2 superconductors
[CEA-N-1552] 12 p1440 N73-21667
Magnetic bubble material and magnetic properties of Mott transition
[AD-757435] 14 p1699 N73-23787
Magnetic properties of highly dispersed iron-cobalt-nickel alloy powders
[NLL-LTI-746-1419-[9022.401]]
15 p1797 N73-24566
Powder neutron diffraction and susceptibility measuring techniques to study magnetic properties of RbMnBr3
[BNL-17519] 15 p1814 N73-24703
Influence of titanium ions on magnetic properties of manganese-zinc ferrites
[NLL-TRANS-862-[9022.64]]
16 p1931 N73-25626
Itinerant electron magnetism in ZrZn2 phase
[REPT-735] 16 p1944 N73-25733
Magnetic properties of cobalt rare earth thin films
16 p1951 N73-25790
Magnetic phenomena in solid state physics
[COO-3150-10] 16 p1953 N73-25803
Nondestructive tests for luminescent and color flaw detection, using magnetic particles and dye penetration
[AD-759253] 17 p2038 N73-26488
Superconducting lead film thickness effect on magnetic properties
[ISS-72/6-PT-2] 17 p2073 N73-26773
Effects of chemical etching on magnetic and storage properties of Permalloy memory films
18 p2178 N73-27589
Magnetic techniques for nondestructive evaluation of defects in materials
19 p2304 N73-28525
Analysis of physical and mechanical properties of nonmagnetic steels and suitability for producing tubes and forgings
[NLL-M-21647-[5828.4F]] 20 p2422 N73-29451
Magnetic interactions and spin wave dispersion in rare earth metals
[CONF-730402-10] 20 p2455 N73-29727
Magnetic and transport properties of dilute magnetic alloys
[AD-763710] 21 p2586 N73-30721
Electrical, magnetic, and thermal properties of dilute and concentrated magnetic alloys
[AD-763820] 22 p2707 N73-31682
Rare earth orthoferrites and micromagnetic interactions
[AD-764826] 23 p2827 N73-32593
Magnetic phase transition in FeCl3
[AD-764982] 23 p2827 N73-32595
One-dimensional analysis of electric fields and electric potential near photo emitting plate emmersed in solar wind plasma
23 p2858 N73-32839
Magnetic observations for 1971
[M70-44/4] 24 p2920 N73-33323
Magnetic and specific heat measurements of carbides, nitrides, and uranium and thorium sulfides
[CEA-R-4453] 24 p2943 N73-33506
Thermal and magnetic properties of magnetic crystals
[COO-3574-95] 24 p2969 N73-33727
Electromagnetic characteristics of single crystal niobium, niobium alloy, and molybdenum alloy superconductors
[AD-765368] 24 p2970 N73-33731
Thermodynamic properties of electron gas in magnetic fields of varying strengths to include magnetic susceptibility, internal energy, and specific heat
24 p2990 N73-33896

**MAGNETIC PUMPING**
Superhigh frequency emission of collisionless magnetized plasma on its interaction with pumping wave in microwave range
[AEC-TR-7373] 10 p1197 N73-19736
Plasma heating by magnetic pulse in theta pinch and nuclear fusion
[AD-757043] 13 p1563 N73-22671
Magnetic flux pump for changing intensity of magnetic fields
[NASA-CASE-XNP-01187] 19 p2303 N73-28516
Method for increasing intensity of magnetic field by transferring flux
[NASA-CASE-XNP-01188] 23 p2795 N73-32361

**MAGNETIC RECORDING**
Electrocardiogram recordings on magnetic tape for computerized analysis
[AD-748105] 04 p0384 N73-13124
Instrumentation for spectrum analysis of short bursts and pulses of Jovian decametric radio emission recorded on magnetic tape
05 p0547 N73-14440
Characteristics of video tape recording film and procedures for controlling magnetic properties during production
[NHK-LABS-NOTE-155] 07 p0754 N73-16122
Production of narrow-track video recording head to include characteristics of recording tape and tetrode sputtering equipment
[NHK-LABS-NOTE-154] 07 p0754 N73-16124
Foil bearing model for predicting head to tape separation in magnetic recording system
[NASA-CR-130536] 08 p0885 N73-17167
High speed digital recording system for VLF and ELF sferic waveforms
[AD-757427] 14 p1669 N73-23544
Thermomagnetic recording of analog signals on CrO2 magnetic tape
[NHK-LABS-NOTE-157] 18 p2116 N73-27112
Comparison of film and video as the recording medium in high voltage electron microscopy
[NPL-IMS-20] 21 p2549 N73-30438
System for maintaining intensity of laser beam constant in thermomagnetic recording and magneto-optic playback system
[NASA-CASE-NPO-11317-2] 22 p2680 N73-31468
Video cassette recording techniques and commercial aspects
23 p2757 N73-32066
Azur satellite telemetry, noting real time and tape telemetry systems
24 p2985 N73-33853

**MAGNETIC RELAXATION**
NT SPIN-LATTICE RELAXATION

**MAGNETIC RESONANCE**
NT ELECTRON PARAMAGNETIC RESONANCE
NT FERROMAGNETIC RESONANCE
NT NUCLEAR MAGNETIC RESONANCE
NT PARAMAGNETIC RESONANCE
NT PROTON MAGNETIC RESONANCE
Development and characteristics of transducer for use with fluidic generators
[AD-755104] 11 p1273 N73-20334
Optical excitation of atomic levels for orientation of nuclei, polarized electron production, and magnetic resonance experiments
[NASA-TT-F-14862] 11 p1326 N73-20765
Neutron scattering, computerized simulation, and magnetic resonance techniques for studying phase transitions in magnetic materials
[AD-757223] 14 p1698 N73-23782
Experimental analysis of rutile properties including crystal growth, hydrogen diffusion, and magnetic resonance determination of defects
[AD-760667] 18 p2190 N73-27684
Magnetic resonance phenomena in domain of radio frequencies
[NASA-TT-F-14733] 22 p2632 N73-31091

**MAGNETIC RIGIDITY**
Calculations of cosmic ray effective cut-off rigidities in real magnetic field
[AD-763124] 20 p2468 N73-29829

**MAGNETIC SHIELDING**
Design, construction, and performance of large superconducting magnetic shield
[NASA-CR-135486] 22 p2700 N73-31627

**MAGNETIC SIGNATURES**
Tables of geomagnetic and geoelectric magnetograms and tellurigrams measured at Kakioka Magnetic Observatory, Japan
[REPT-12] 07 p0788 N73-16411

**MAGNETIC SPECTROSCOPY**
Differential equation for trajectories in exact form
[LNF-71/81] 04 p0450 N73-13671
Recalibration of magnetic spectrometer designed to measure 0.1 to 1.0 MeV electron flux in space environment
[AD-755790] 12 p1406 N73-21404

**MAGNETIC STORAGE**
NT CORE STORAGE
NT MAGNETIC DISKS
NT MAGNETIC DRUMS
Fabrication of integrated magnetic storage devices by vapor deposition of gold on copper substrate
01 p0031 N73-10239
Information retrieval system combining magnetic storage and microfilm reader/copier
[CRIF-EL-5] 02 p0147 N73-11188
Large scale integrated circuits used for designing 128 words x 72 bits/word memory
[REPT-1404] 03 p0272 N73-12205

Design and development of integrated magnetic memories
04 p0394 N73-13203
Fabrication of monolithic ferrite memory arrays
[NASA-CR-2152] 04 p0398 N73-13238
Momentum wheel design for spacecraft attitude control and magnetic drum and head system for data storage
[NASA-CASE-NPO-11481] 04 p0446 N73-13644
Shock heating of plasmas based on superposed superconducting circuits and magnetic energy storage
[TRITA-EPP-72-29] 07 p0829 N73-16717
Production of integrated toroidal magnetic memories of 500 bits/sq cm, including electric and magnetic testing
[REPT-1541] 10 p1133 N73-19232

MAGNETIC STORMS
Relation of Hall current electrojet instability to VLF hiss in auroral zone of magnetic storms
[NASA-CR-130078] 01 p0047 N73-10378
Sunspot, solar flare, magnetic storm, and SID data, Delhi - Dec. 1971
[RRC-A-199-PT-2] 01 p0048 N73-10385
Solar flares, magnetic storms, ionospheric disturbances, and geophysical observations recorded by weather stations in India during Feb. 1972
[RRC-A-201-PT-2] 01 p0048 N73-10386
Sunspot, solar flare, magnetic storm, and SID data, Delhi Jan. 1972
[RRC-A-200-PT-2] 01 p0048 N73-10387
Low energy electron precipitation observed as function of substorm phase by polar satellites
[NASA-TM-X-66063] 01 p0049 N73-10393
Correlation between geomagnetic field increases or storm commencements with variations in electron content of solar wind
01 p0098 N73-10810
On variational relationships between solar wind parameters, magnetospheric magnetic activity, and magnetospheric storm electrons
02 p0225 N73-11820
Electric field noise phenomena observed by S3-A spacecraft near plasmapause during magnetic storm
[NASA-CR-129243] 03 p0293 N73-12388
Three-dimensional, two-constituent model for composition characteristics, temperature and mass density of magnetic storm
[NASA-TM-X-66112] 03 p0294 N73-12394
Comparison of satellite ozone contours during 1965 geomagnetic storm and L-shell parameters
[WRE-TN-80[WR/D]] 03 p0296 N73-12412
Observations of weak infrasound emission during magnetic storms caused by ionospheric auroral electrojets
05 p0508 N73-14138
Enchancement of 0.24-0.96 MeV trapped protons during 25 May 1967 magnetic storm, measured from OV 1-9 polar orbiting satellite
[AD-749866] 05 p0543 N73-14421
Magnetic storm effects on topside ionospheric electron density profiles in low and equatorial latitudes
[PSU-IRL-SCI-399] 06 p0666 N73-15412
High latitude proton precipitation and light ion density profiles during magnetic storm initial phase
[NASA-TM-X-66166] 07 p0792 N73-16438
Radar sounding of magnetospheric instability and atmospheric density using barium release clouds
[AD-751567] 07 p0795 N73-16461
Tables of Dst hourly variations for July, August, and September 1972
[NASA-TM-X-66156] 07 p0842 N73-16822
MHD equations for calculating joule heating and winds from geomagnetic storms in thermosphere
[NASA-CR-124071] 08 p0915 N73-17498
Equatorial magnetic storm-time variation data from Hermanus, Kakioka, Honolulu, and San Juan
[NASA-TM-X-66174] 08 p0917 N73-17511
Meridional wind effects on advection heating in thermosphere during geomagnetic storms
[AD-751921] 08 p0919 N73-17528
Magnetospheric convection theory for substorm growth and expansion
[NASA-CR-130499] 09 p1032 N73-18423
Dependence of onset time of F-region electron density disturbance upon local time of geomagnetic storm commencement and main phase onset
[AD-753665] 09 p1033 N73-18433
Substorm thinning and thickening of magnetotail plasma sheet
[I.A-DC-72-1165] 10 p1155 N73-19397
Synchronous satellite observations on magnetospheric substorms in relation to plasma sheath structure
[RLO-2229-T-5-2] 10 p1155 N73-19398
Geomagnetic micropulsations during magnetic storms as observed by ATS I
12 p1447 N73-21716
VHF/UHF technique for determination of columnar electron contents of plasmasphere and of protonosphere using geostationary satellite transmissions of magnetic storm observations
15 p1770 N73-24338
Electron acceleration mechanism during geomagnetic tail collapse associated with substorm activity
[UNH-73-04] 15 p1779 N73-24418
Tables on solar and magnetic activity
[RRC-A210-PT-2] 16 p1907 N73-25424
Tables on solar and magnetic activity
[RRC-A203-PT-2] 16 p1907 N73-25425
Cosmos-187 measurement of ion drift velocity in upper ionosphere during magnetic storms
17 p2024 N73-26381
Programs for comparing experimental data with mathematical models with respect to magnetic activity
[AD-760117] 17 p2029 N73-26422
High latitude ionospheric patterns during magnetospheric substorms
18 p2133 N73-27232
Ionospheric total electron content during magnetic storm, 14-17 Dec. 1971
[KGO-728] 18 p2146 N73-27344
Evening observations of storm-time ring current particle characteristics during beginning of magnetic storms
[NASA-TM-X-70430] 19 p2293 N73-28441
Ion drift measurements from Cosmos 184 during 3 Nov. 1967 magnetic storm
20 p2410 N73-29371
Magnetic storm effects on cosmic ray intensity
[AD-762223] 20 p2468 N73-29826
Magnetotail neutral line and associated plasma phenomena in substorms
[IAS-497-VOL-38-NO-8] 22 p2664 N73-31346
Plasma sheet behavior during magnetospheric substorms
[RLO-2229-T-5-3] 24 p2923 N73-33346

MAGNETIC SUBSTORMS
U MAGNETIC STORMS

MAGNETIC SURVEYS
Three component aeromagnetic survey of British Columbia and northeastern Pacific Ocean to determine magnetic anomalies - Vol. 42, No. 7
[M70-42/7] 01 p0044 N73-10346
Development and improvement of magnetovariation station for conducting magnetotelluric soundings
[JPRS-57678] 04 p0401 N73-13262
Geomagnetic survey of Japan and nearby areas conducted from July 1969 to November 1970
[PUB-592] 14 p1660 N73-23474
Geomagnetic observations made in Japan and surrounding areas from 1967 to 1969
[PUB-591] 14 p1660 N73-23475

MAGNETIC SUSCEPTIBILITY
U MAGNETIC PERMEABILITY

MAGNETIC SUSPENSION
Fourier analysis for characterizing force field of superconducting suspension for spacecraft elements
03 p0335 N73-12731
Integrated magnetic suspension and propulsion system characteristics
[BNL-16909] 04 p0402 N73-13271
Magnetic fluid preparation by grinding and concentrating pyrophoric antiferromagnetic iron oxide colloidals
[BM-RI-7702] 05 p0580 N73-14721
Electronic circuits for synchronous rotation of rotors suspended in magnetic field
[SRARI-P-120] 06 p0647 N73-15257
Effect of displacements of suspended mass on accuracy of electromagnetic load cell and selection of parameters for increased accuracy
06 p0696 N73-15668
Method for calculating magnetic field map of magnetic suspension in ultracentrifuge
[LNF-72/49] 10 p1138 N73-19272
Analysis of biaxial gyrostabilizer system and synthesis of spherical superconducting suspensions with maximum lift
[JPRS-58356] 10 p1159 N73-19428
Synthesis of superconducting magnetic field suspensions with maximum lift using Fourier coefficients
10 p1159 N73-19430
Developing facility on Skylab mission for electromagnetic suspension of small molten spheres in space
[NASA-CR-124134] 11 p1297 N73-20522
Development of virtually zero magnetic bearing for application to electric motor construction
[NASA-CR-130225] 13 p1499 N73-22152
Superconducting electromagnetic suspension and balance and supersonic wind tunnel facility for dynamic stability studies
[NASA-CR-132255] 15 p1761 N73-24271
Cryogenic superconducting magnetic suspension and balance facility designs
15 p1761 N73-24272
Superconducting magnetic suspension and balance facility data acquisition and data reduction errors
15 p1762 N73-24274
Feasibility of using iron magnetic support to extend cold magnetic balance wind tunnel system to subsonic flow regimes and continuous spinning aircraft configurations
15 p1762 N73-24275
System failure and safety features of superconducting magnetic suspension systems
15 p1762 N73-24277
Design and performance of momentum wheel suspended by magnetic bearings for rotor operation in space environment
18 p2209 N73-27829
Dependences between braking and precession moments acting on spherical rotor in magnetic suspension
21 p2547 N73-30422

MAGNETIC SWITCHING
Analysis of magnon contribution to total heat current and magneto-elastic coupling in antiferromagnetic materials
16 p1932 N73-25630

MAGNETIC TAPE RECORDERS
U MAGNETIC RECORDING
U TAPE RECORDERS

MAGNETIC TAPE TRANSPORTS
Foil bearing model for predicting head to tape separation in magnetic recording system
[NASA-CR-130536] 08 p0885 N73-17167

MAGNETIC TAPES
Signal dropout detection and counting tester for magnetic tape measurements
[NBS-TN-739] 01 p0030 N73-10236
Perfluorostyrene syntheses, magnetic tapes, titration cell, mill work positioner, superconducting microbridges, position display device, and numbering machine
[NBS-TN-744] 02 p0245 N73-11991
Flutter compensation of magnetic tape recorded data, noting single-carrier FM and frequency division multiplexed FM systems
[RAE-TR-72028] 03 p0303 N73-12474
Electrocardiogram recordings on magnetic tape for computerized analysis
[AD-748105] 04 p0384 N73-13124
Magnetic tape playback and serial time decoder for IFF flight test instrumentation
[AD-750667] 06 p0641 N73-15204
Characteristics of video tape recording film and procedures for controlling magnetic properties during production
[NHK-LABS-NOTE-155] 07 p0754 N73-16122
Production of narrow-track video recording head to include characteristics of recording tape and tetrode sputtering equipment
[NHK-LABS-NOTE-154] 07 p0754 N73-16124
Procedure for repairing and recovering voice data from heat damaged magnetic tapes
[NASA-CASE-MSC-14219-1] 07 p0755 N73-16132
On-line computer graphics for display of magnetic tape data from digital computer
[IPPJ-T-10] 08 p0887 N73-17179
Magnetic tape transport unit for ERTS recording instruments - Vol. I
[NASA-CR-130186] 10 p1129 N73-19194
Magnetic tape version of substance-property index and bibliographies
[NBS-TN-760] 11 p1260 N73-20223
Low cost magnetic tape recording system for test instrumentation use
[AD-757011] 13 p1493 N73-22102
Evaluation of compression technique for ERTS-1 data tapes
[E73-10589] 14 p1657 N73-23449
Evaluation of ERTS-1 image data compression techniques to show four ERTS MSS tapes recorded on single compressed tape
[E73-10730] 17 p2020 N73-26336
Preparation of field spectroradiometer equipment and tapes for Skylab S-191 experiment
[E73-10760] 17 p2022 N73-26360
Thermomagnetic recording of analog signals on CrO2 magnetic tape
[NHK-LABS-NOTE-157] 18 p2116 N73-27112
Digital reproducing amplifiers for magnetically recording data from airborne processor
[ARL/ME-337] 20 p2376 N73-29090
Generation and physical characteristics of ERTS MSS system corrected computer compatible tapes
[NASA-TM-X-70426] 20 p2410 N73-29366
Format conversion of meteorological data tapes of Hawaii
[PB-220452/7] 21 p2515 N73-30179
User manual for Los Angeles Standard Traffic Model computer tapes
[FAA-RD-73-88] 21 p2577 N73-30649
Operational system for processing both imagery and computer compatible tapes of ERTS-1 and aerial data of Pennsylvania
[E73-11105] 24 p2915 N73-33262
Pennsylvania State University library catalogue for remotely sensed digital data tapes
[E73-11115] 24 p2916 N73-33272
Preprocessing of Azur satellite telemetry data to provide several output tape formats
24 p2985 N73-33854

MAGNETIC TRAPS
U PLASMA CONTROL

MAGNETIC VARIATIONS
NT GEOMAGNETIC MICROPULSATIONS
NT GEOMAGNETIC PULSATIONS
Influence of interplanetary magnetic field on geomagnetic variations in polar cap
[NASA-CR-129165] 02 p0166 N73-11351

Electrical conductivity of ocean basement determined from measurements of geomagnetic time variations on sea floor off Southern California
[AD-749931] 06 p0668 N73-15431

Relationship between polar geomagnetic variations and polarity of interplanetary magnetic sectors
[NASA-CR-130270] 07 p0780 N73-16343

Equatorial Dst tables for Nov. and Dec. 1972
[NASA-TM-X-66197] 10 p1212 N73-19861

Influence of polarity of interplanetary magnetic field on magnetic activity at high latitudes
[GRI/NT/87] 12 p1402 N73-21371

Table of hourly and daily values of geomagnetic field declination and intensity recorded at Eskdalemuir, Hartland, and Lerwick Observatories, England, in 1969
[GEOMAGNETIC-BULL-3] 13 p1525 N73-22356

Diurnal and hourly geomatnetic variations recorded at Thule Geophysical Observatory, Greenland, in 1947
13 p1525 N73-22357

Diurnal and hourly geomagnetic variations recorded at Thule Geophysical Observatory, Greenland, in 1948
13 p1525 N73-22358

Dirunal and hourly geomagnetic variations recorded at Thule Geophysical Observatory, Greenland, in 1949
13 p1525 N73-22359

Diurnal geomagnetic variations
[AD-755787] 13 p1526 N73-22369

Geophysical observations of horizontal and vertical components of earth magnetic field at Feurstenfeldbruck, Germany for 1972
14 p1660 N73-23473

Paleomagnetic study of Mano Lake, California to determine secular variations during past 30,000 years
16 p1895 N73-25325

Ionospheric total electron content during magnetic storm, 14-17 Dec. 1971
[KGO-728] 18 p2146 N73-27344

Diurnal and hourly geomagnetic variations recorded at Godhavn Geophysical Observatory during 1966
[ISBN-87-7478-066-2] 23 p2788 N73-32302

Diurnal and hourly geomagnetic variations recorded at Thule Geophysical Observatory, Greenland, in 1966
[ISBN-87-7478-069-7] 23 p2788 N73-32303

**MAGNETICALLY TRAPPED PARTICLES**
NT OUTER RADIATION BELT
NT PROTON BELTS
NT RADIATION BELTS

Fast electron production by protons trapped in sunspot magnetic field as energy source for solar flares
19 p2333 N73-28774

Quasi-linear equations for stochastic plasma diffusion processes of trapped particles in magnetosphere using two selected plasma resonances
[TRITA-EPP-73-09] 21 p2593 N73-30777

**MAGNETIZATION**

Magneto-optical effects of YIG in presence of homogeneous and inhomogeneous magnetization
03 p0336 N73-12744

Magnetization experiments to simulate cusp coil tests
[ORNL-TM-3887] 04 p0459 N73-13744

Modified GRACY magnet program for computing magnetization effects in superconducting magnets
[BNL-17219] 10 p1201 N73-19772

Quantum mechanical Racah and Stevens operators used in magnetism theory
[RISO-259] 12 p1429 N73-21580

Unstable component of magnetization found in lunar samples
12 p1449 N73-21739

Studies of electron mirror microscopy and its application to superconductivity and magnetism
16 p1952 N73-25797

Theoretical and experimental investigations of superconductivity, and amorphous semiconductors, superconductivity and magnetism
[NASA-CR-133234] 17 p2072 N73-26767

Thermodynamic, structural, and magnetization phenomena during hydrogen reaction with RCo5 type systems
22 p2625 N73-31033

**MAGNETO-OPTICS**

Magneto-optical effects of YIG in presence of homogeneous and inhomogeneous magnetization
03 p0336 N73-12744

Technology assessment for thin film development of magneto-optical manganese bismuth memory
04 p0394 N73-13202

Magneto-optical and electro-optical approaches for meeting time memory demands
09 p1065 N73-18688

Growth of single barium ferrite crystals for magnetic optical devices
[AD-758926] 16 p1953 N73-25807

Faraday rotation and attenuation in InSb in 10.6 micron wavelength region
[AD-761213] 18 p2190 N73-27685

Magneto-optic effects in ferrate garnet thin film waveguides
[AD-763792] 21 p2518 N73-30199

System for maintaining intensity of laser beam constant in thermomagnetic recording and magneto-optic playback system
[NASA-CASE-NPO-11317-2] 22 p2680 N73-31468

Magneto-optic phase change for detecting magnetization reversal in magnetic films
[AD-764549] 24 p2959 N73-33645

**MAGNETOACOUSTIC WAVES**

Experiments on magnetoacoustic oscillations in rotating hydrogen and deuterium plasmas with superimposed high frequency heating
[TRITA-EPP-72-34] 12 p1436 N73-21635

**MAGNETOACTIVITY**
NT MAGNETORESISTIVITY

High frequency pressure effect on wave propagation along layer of magnetoactive plasma
[AEC-TR-7336] 07 p0826 N73-16698

**MAGNETOELASTIC VIBRATIONS**
U MAGNETOELASTIC WAVES

**MAGNETOELASTIC WAVES**
NT MAGNETOACOUSTIC WAVES

Fluid model for analyzing nonlinear magnetosonic wave propagation in magnetic neutral sheet
[IPPJ-139] 04 p0388 N73-13152

S band magnetoelastic transmission-type delay line design using YIG birefringent device
[REPT-8.445] 12 p1384 N73-21220

Magnetoelastic transmission delay lines for S band noting insertion loss reduction
[REPT-8.425] 13 p1491 N73-22087

**MAGNETOELASTICITY**
U MAGNETOSTRICTION

**MAGNETOGASDYNAMICS**
U MAGNETOHYDRODYNAMICS

**MAGNETOGRAMS**
U MAGNETIC SIGNATURES

**MAGNETOGRAPHS**
U MAGNETOMETERS
U RECORDING INSTRUMENTS

**MAGNETOHYDRODYNAMIC ACCELERATION**
U PLASMA ACCELERATION

**MAGNETOHYDRODYNAMIC FLOW**

Numerical solution for magnetohydrodynamic pipe flow with laminar separation at higher Hartmann number
[AD-748766] 04 p0456 N73-13719

Ionizing flow in solar wind passage through cometary coma
[TRITA-EPP-71-33] 06 p0716 N73-15842

Test facility for combustion flow in open cycle magnetohydrodynamic generator
[AD-751251] 07 p0742 N73-16036

Numerical technique for obtaining solutions to governing equations for gas flowing in axially symmetric constricted-arc heaters
[NASA-TM-X-2700] 07 p0769 N73-16246

Plasma flow effects on axisymmetric equilibria in toroidal geometry
[IPP-6/107] 07 p0828 N73-16708

Temperature and electrical conductivity of nonequilibrium ionizing gas-particle flow through convergent-divergent nozzle geometry
08 p0947 N73-17752

Magnetohydrodynamic wall flow with laminar separation
[AD-753149] 09 p1072 N73-18751

Streaming flow of viscous fluid past sphere in uniform magnetic field at low Hartmann numbers
[AD-755060] 11 p1329 N73-20784

Turbulence spectra of magnetic pulsating nonisothermal plasma
[AEC-TR-7379] 12 p1434 N73-21622

Steady state dynamics of compressible plasma flows across inhomogeneous magnetic fields in ducts with inclined walls
[AD-755944] 14 p1696 N73-23761

Numerical calculation of several two dimensional magnetohydrodynamic flows in channels
[AD-759424] 16 p1893 N73-25319

Improving preformance of magnetoplasmadynamic arc rocket engine
[NASA-CASE-LEW-11180-1] 16 p1948 N73-25760

Model of stationary, adiabatic plasma flow in magnetosphere interacting with ionosphere
[TRITA-EPP-72-22-PT-1] 17 p2027 N73-26404

Resistive instabilities in plasmas with shear flow
[IPP-6/114] 17 p2068 N73-26731

Reverse deflection and contraction of plasma beam entering a curved magnetic field
[TRITA-EPP-72-32] 17 p2068 N73-26735

Ionic diffusion in electron boundary layer of spotless discharge crossing nitrogen magnetohydrodynamic flow
[IPF-72-3] 17 p2069 N73-26739

Nonequilibrium phenomena in flowing plasmas
[AD-760792] 18 p2184 N73-27634

Thermodynamic effects on liquid metal magnetohydrodynamic converter flow
[AD-761548] 20 p2459 N73-29762

Interaction of laser plasma flow with neutral gases of air
[AD-764936] 23 p2823 N73-32569

Magnetospheric plasma flow and magnetospheric boundary layer observations by Vela satellite
[LA-UR-73-732] 24 p2964 N73-33686

**MAGNETOHYDRODYNAMIC GENERATORS**

Development of superconducting magnet system for magnetohydrodynamic power generation
[AD-745321] 01 p0032 N73-10247

Operation of plasma accelerator in quasi-steady mode to determine ratio of energy deposition into kinetic and thermal modes
[NASA-CR-128408] 01 p0035 N73-10275

MHD parameter optimization procedure for determining optimum coil geometry for 10 MW level superconducting magnet system
[AD-745322] 02 p0212 N73-11717

MHD power systems with potential high efficiencies of constant liquid velocity, two phase, liquid metal dc MHD generator
[AD-747323] 03 p0255 N73-12064

Development of porous electrode materials for plasma generators and effects of blowing protective gases through plasma
[AD-747369] 03 p0255 N73-12066

Performance of closed cycle MHD generators
[AD-747661] 03 p0255 N73-12068

Equivalent circuit of electromechanical or magnetohydrodynamic converter with traveling magnetic field
[AD-747611] 03 p0256 N73-12072

Research on closed cycle MHD power generation for converting heat into electricity
[RT/ING-[71]20] 03 p0341 N73-12784

Equivalent resistance network for MHD generator noting losses and scale effect
[TH-72-E-30] 03 p0343 N73-12796

Pulsed ionization chamber for plasma diagnostics, and applications to MHD electrical power generation from gas cooled reactors
[AD-747681] 03 p0343 N73-12800

Optimal inlet parameters for magnetohydrodynamic channel using combustion products of kerosene and gaseous oxygen
[AD-748750] 04 p0376 N73-13057

Basic physical processes in thermionic and magnetohydrodynamic converters of thermal energy into electrical energy
[AD-748707] 04 p0376 N73-13061

Aerospace MHD large scale power generation
04 p0473 N73-13865

Experimental investigations of two-dimensional flow problems and electric power generation in open cycle vortex MHD generator
[BM-RI-7699] 05 p0583 N73-14746

Thermodynamic efficiencies of accelerators for liquid metal magnetohydrodynamic converter considering vapor liquefying effect on flow characteristics
[JPRS-57915] 06 p0703 N73-15735

Theoretical and parametric study of inductive magnetohydrodynamic converters including design of cryogenic experimental 4 kW converter
[DLR-FB-71-74] 06 p0706 N73-15757

Test facility for combustion flow in open cycle magnetohydrodynamic generator
[AD-751251] 07 p0742 N73-16036

Principles of magnetohydrodynamic energy generation to include flows in magnetohydrodynamic generator, physical processes, diagnostics, and required equipment - Part 1
[JPRS-57940-1-PT-1] 07 p0825 N73-16687

Principles of magnetohydrodynamic energy generation to include open and closed cycle magnetohydrodynamic generators, liquid-metal plants, and materials for generators -Part 2
[JPRS-57940-2-PT-2] 07 p0825 N73-16688

Viscous incompressible fluid hydraulics of magnetohydrodynamic generators
[AD-751465] 07 p0829 N73-16718

Nonlinear time dependent phenomena in JxB devices applicable to MHD power generators and electric propulsion engines
[AD-751943] 08 p0956 N73-17826

Mathematical model for thermodynamic efficiency of combined power plants incorporating magnetohydrodynamic generators
[AD-753031] 09 p0991 N73-18090

Characteristics of large, lightweight, saddle-coil, superconducting dipole magnet for airborne magnetohydrodynamic generators
10 p1109 N73-19038

Development of method for analyzing performance of magnetohydrodynamic generator based on thermodynamic properties and flow characteristics
10 p1110 N73-19051

Uniform plasmas of N2, He, and CO for advanced MHD generator and electric laser design
[AD-755892] 12 p1436 N73-21638

Redesign of Argas 2 facility for using superconducting magnet
[NASA-TT-F-14876] 13 p1562 N73-22662

Use of finite difference theory to calculate nonsteady flow in linear magnetohydrodynamic generators
[AD-755203] 13 p1564 N73-22673

Superconductors in marine technology, including coils, solenoids, and magnetic systems
[AD-755711] 13 p1567 N73-22702

Design, development, and operation of compact, high performance, magnetohydrodynamic generators
[AD-756489] 14 p1696 N73-23765

Thermodynamic and electrical properties of gaseous fuels for magnetohydrodynamic gas generator
[JUL-874-TP-VOL-9] 15 p1818 N73-24735

Experiments in shock tunnel driven MHD generator designed for high enthalpy extraction
[AD-757771] 15 p1819 N73-24741
Feasibility of potassium-cesium mixture for seeding magnetohydrodynamic combustion plasma
[PB-214314/7] 16 p1865 N73-25102
Construction and tests of MHD generator channel and electrical power converter
[AD-758783] 16 p1866 N73-25106
Closed cycle nuclear MHD power plants
19 p2319 N73-28654
MHD generator performance limitation from electrical properties, including conductivity and Hall parameter
19 p2319 N73-28655
Three thermodynamic cycles of advanced nuclear MHD power plant systems
19 p2319 N73-28657
Design of MHD generators with fuel gas and air turbine
[JUL-892-TP-VOL-11] 21 p2583 N73-30699
Explosive magnetohydrodynamic programs
[AD-762934] 21 p2607 N73-30890
Stability of nonequilibrium inert gas plasma for use in MHD power generators
22 p2702 N73-31642
Uncompensated dc MHD generator, with longitudinal end effect
[SFB-MHD-6] 22 p2704 N73-31661
Analysis of longitudinal end effects on constant and traveling wave MHD generators by electrodynamics
[SFB-MHD-7] 22 p2705 N73-31662
High temperature research of thermophysical and electrophysical properties of matter and pilot plant with magnetohydrodynamic power generator
[JPRS-59983] 22 p2728 N73-31831
U-25 pilot plant with open cycle MHD generator operating on natural gas
22 p2728 N73-31833
Design of high temperature combustor for use as solid fuel MHD generator and thermodynamic analysis of combustion conditions
[AD-764153] 22 p2730 N73-31848
Magnetohydrodynamic generator for combined magnetohydrodynamic electric power plant with first generation open cycle
[AD-764925] 23 p2748 N73-31996
High melting oxide and carbide materials in electrode walls of magnetohydrodynamic generators
[AD-764969] 24 p2944 N73-33508

MAGNETOHYDRODYNAMIC STABILITY
Dynamic stabilization of plasma confinement and fluid systems
[LRP-53/72] 01 p0085 N73-10701
Influence of axial current on stability of plasma column
[LRP-52/72] 01 p0085 N73-10702
Plasma instability at initial stage of electrode plasma discharge in rarefied plasma
[AD-745458] 01 p0085 N73-10707
Magnetohydrodynamic instabilities in ELMAX plasma device
[AD-744818] 01 p0086 N73-10711
Anisotropic instability of plasma without permanent magnetic field
02 p0166 N73-11350
Influence of inhomogeneity on structure of collisionless turbulent shock wave in high beta infinite plasma
[AD-746467] 02 p0217 N73-11756
Low-frequency quasi-static instabilities in fully ionized plasma
[NASA-CR-129517] 03 p0341 N73-12778
Computerized simulation of nonlinear evolution of high frequency, flute-like plasma microinstabilities
[ORNL-TM-3812] 03 p0341 N73-12781
Analysis of linear and nonlinear properties of density gradient driven drift waves instability using single-ended Q-machine
[AD-747852] 03 p0344 N73-12803
Computerized simulation of whistler instabilities in anisotropic collisionless plasmas
[AD-748176] 03 p0344 N73-12805
Effects of plasma-neutral gas interaction, finite resistivity, and viscosity on gravitational modes in permeable and impermeable plasmas
[TRITA-EPP-72-06] 04 p0455 N73-13713
Dispersion characteristics of plasma instabilities in carbon monoxide plasma
[AD-748470] 04 p0456 N73-13723
Effect of surrounding gas on MHD instabilities in Z pinch
[AD-748985] 04 p0457 N73-13728
Increased plasma stability in shock heated toroidal z-pinch using preionization
[LA-DC-72-726] 05 p0583 N73-14749
Analysis of nonequilibrium in excited levels of electric ARC heated potassium vapor injected into argon/helium gas flow passing through supersonic nozzle
[AD-750943] 05 p0585 N73-14759
Theoretical model for laser flux absorption by plasma instability mechanism
[LA-4984] 06 p0704 N73-15739
Research on microinstabilities of finite mirror-confined plasmas
[COO-2168-3] 06 p0704 N73-15747
Screw pinch device with improved torus for stabilization of toroidal plasma
[NP-19381] 06 p0705 N73-15748
Low frequency instabilities in hollow cathode magnetoplasma discharge
[AD-750477] 06 p0707 N73-15765
Research on impermeable plasmas in poloidal magnetic fields for nuclear fusion reactors
[TRITA-EPP-72-21] 07 p0828 N73-16714
Plasma instability saturation by resonant mode coupling of shock waves
[AD-751538] 07 p0829 N73-16722
Classification of plasma instability including stable and unstable disturbances
[TRITA-EPP-72-23] 09 p1070 N73-18734
Model of shock wave propagation parallel to external magnetic field in hot collisionless plasma with turbulent dissipation based on garden hose instability
[MPI-PAE/EXTRATERR-69] 09 p1071 N73-18736
Mathematical model for dense rotating plasma with centrifugal expansion instability at high beta values
[TRITA-EPP-72-28] 09 p1071 N73-18740
Experiments on rotating plasmas for determining magnetohydrodynamic stability at high beta values
[TRITA-EPP-72-33] 09 p1071 N73-18741
Feedback stabilization of magnetohydrodynamic turbulence in plasma column immersed in magnetic field
[AD-753102] 09 p1072 N73-18747
Linear and nonlinear plasma response to impulse electric field
10 p1195 N73-19725
Stability of plasma located in field of self-consistent Alven wave
[AEC-TR-7384] 10 p1197 N73-19738
Dispersion relations and drift instability in ionized magnetoplasma
[AD-754005] 10 p1198 N73-19744
Theoretical research on plasma instabilities
[AD-754019] 10 p1198 N73-19747
Instability of rotating plasmas at beta value before reaching critical velocity
[TRITA-EPP-73-01] 12 p1436 N73-21636
Quenching of beam plasma instability by mode mixing at density discontinuity
[AD-755658] 12 p1436 N73-21637
Passive circuit grids for stabilization of magnetohydrodynamic generator plasma
[TH-72-E-31] 14 p1695 N73-23757
Instabilities of homogeneous plasmas caused by particle velocity distributions
[AD-755688] 14 p1696 N73-23760
Magnetohydrodynamic analysis of instability due to discontinuity in conductivity and solitary waves of finite amplitude in conducting fluid
15 p1816 N73-24721
Research on Tokamak reactors and microinstabilities in inhomogeneous plasma
[COO-1478-13] 15 p1817 N73-24729
Shear stabilization of drift instability in hydrogen plasma
[EUR-CEA-FC-646] 15 p1818 N73-24734
Vlasov equation for studying anisotropy produced instabilities in confined hot electron plasma
[EUR-CEA-FC-664] 15 p1818 N73-24736
Diffused boundary model for magnetohydrodynamic equilibrium in straight and toroidal plasmas
[IPPJ-159] 16 p1949 N73-25769
Equilibrium pattern and control of plasma current distribution in diffuse pinch configuration
[IPPJ-158] 16 p1949 N73-25770
Double layers and two-stream instability in solar flares, noting evacuating mechanism in solar atmosphere
[TRITA-EPP-73-05] 16 p1959 N73-25850
Low frequency instabilities in plasmas with magnetic shear
17 p2066 N73-26717
Explosive instabilities of waves in plasmas relating to dissipation and phase effects
[ITF-72-159-E] 17 p2068 N73-26730
Resistive instabilities in plasmas with shear flow
[IPP-6/114] 17 p2068 N73-26731
Spectroscopic methods used for analysis of beam-plasma instability
[LBL-1531] 17 p2068 N73-26732
Equilibrium of weakly toroidal plasma column surrounded by Tokamak field
[REPT-72-71] 17 p2069 N73-26744
Spatial growth properties of parametric and backscattering plasma instabilities
[AD-761173] 18 p2184 N73-27631
Literature abstracts for plasma instability research
[UNICP-SR95-PT-2] 19 p2324 N73-28696
Finite element analysis on cylindrical and toroidal plasma stabilities contained in magnetic field
[JAERI-M-4890] 19 p2324 N73-28700
Longitudinal electroacoustic wave attenuation in plasma
[AD-762272] 19 p2325 N73-28706
Correlation of potential and density fluctuations of plasma resulting from rotational instability of hot cathode Penning discharge
[NASA-TT-F-15026] 20 p2458 N73-29751
Rate effects on instabilities in slightly ionized plasmas
[NASA-CR-133599] 20 p2458 N73-29753
Shear stabilization of collisionless drift wave instability
[IPPJ-166] 20 p2459 N73-29759
Two dimensional analysis of electron-ion streaming instabilities using computerized simulation
[AD-763336] 21 p2583 N73-30703
Turbulent heating of plasmas by streaming instabilities
[AD-763777] 21 p2584 N73-30705
Parametric instabilities of damped modes in inhomogeneous plasmas
[AD-763737] 21 p2584 N73-30709
Generation of MHD plasma turbulence in magnetospheric domains
22 p2657 N73-31282
Stability of nonequilibrium inert gas plasma for use in MHD power generators
22 p2702 N73-31642
Pressure distribution and stability of a magnetized plasma with neutral gas blanket
[TRITA-EPP-73-12] 22 p2705 N73-31664
Nonlinear small-amplitude behavior of collisionless plasma
23 p2822 N73-32561
Low frequency instabilities and plasma turbulence including steady state and time dependent characteristics of positive column and hollow cathode discharge
[NASA-CR-135669] 23 p2822 N73-32562
Parametric instabilities of electromagnetic waves in plasmas
[AD-764610] 23 p2823 N73-32565
Absolute Raman scattering instabilities in inhomogeneous plasma
[AD-764611] 23 p2823 N73-32566
Linear and nonlinear theory of Hall current instability
24 p2962 N73-33667
Electromagnetic wave interaction and plasma attenuation
[KHFTI-72-24] 24 p2962 N73-33673
Vlasov equations for analyzing plasma equilibrium stability
[IPP-6/117] 24 p2963 N73-33675
Plasma transport properties and confinement
[COO-2168-5] 24 p2965 N73-33696
Plasma excitation and instabilities
[ORO-3405-37] 24 p2965 N73-33698

MAGNETOHYDRODYNAMIC TURBULENCE
NT PLASMA TURBULENCE
Magnetohydrodynamic equilibrium perturbations in toroidal fields with circular cross sections
[CEA-CONF-2014] 06 p0705 N73-15755

MAGNETOHYDRODYNAMIC WAVES
NT ELECTROSTATIC WAVES
NT PLASMA WAVES
Calculation of hydromagnetic wave induced energy transfer in solar wind
01 p0094 N73-10777
Coronal Alfven waves in solar wind at 1 AU
01 p0096 N73-10793
Approximate dispersion relationship of hydrodynamic waves in thin rotating spherical shells of incompressible fluid pervaded by uniform magnetic field
[MET-O-857] 06 p0699 N73-15702
Effects of Alfven waves in solar wind on angular momentum, wave pressure, and Poynting flux
[MPI-PAE/EXTRATERR-70] 07 p0839 N73-16799
Generation of artificial geomagnetic micropulsations with large ground-based current load from MHD wave propagation in ionosphere
[AD-752061] 08 p0919 N73-17533
Propagation of magnetohydrodynamic waves in cold plasma inclined to ionosphere and applied to geomagnetic pulsation study
[PR-119] 10 p1156 N73-19401
Stability of plasma located in field of self-consistent Alven wave
[AEC-TR-7384] 10 p1197 N73-19738
Structure of large amplitude stationary hydromagnetic disturbance in collisionless plasma
12 p1432 N73-21604
Propagation of Alfven waves in spiral interplanetary magnetic field
[NASA-CR-131569] 13 p1563 N73-22665
Confinement of ultrarelativistic cosmic rays to galactic disk as result of interactions with hydromagnetic waves
13 p1572 N73-22739
Extension of drift instability theory to plasmas of arbitrary beta
[NASA-CR-131880] 14 p1695 N73-23758
Oscillations of earths magnetic tail studied from model of plasma cylinder with free boundary
14 p1703 N73-23820

Parallel layer model for hydromagnetic wave absorption in magnetospheric tail plasma
15 p1779 N73-24420
Magnetohydrodynamic analysis of instability due to discontinuity in conductivity and solitary waves of finite amplitude in conducting fluid
15 p1816 N73-24721
Summaries of research in plasma sources, hydromagnetic shock waves rotating plasmas, ion cyclotrons, air pollution, and laser diagnostics
[NP-19643] 15 p1817 N73-24727
Alfven wave refraction by interplanetary inhomogeneities from analysis of Pioneer 6 data
[NASA-TM-X-62270] 16 p1962 N73-25867
Flare induced magnetohydrodynamic disturbance propagation in solar corona considering Moreton surface waves and type 2 shocks
19 p2339 N73-28816
MHD wave transmission and production near magnetopause studied from Explorer 12 magnetometer data
22 p2665 N73-31354
Forces and torques on satellites moving through rarefied plasmas
23 p2847 N73-32752
Hydromagnetic gradient waves in ionosphere
24 p2921 N73-33331
Characteristics of steady galactic winds created by escape of cosmic rays from galaxy
24 p2975 N73-33775

**MAGNETOHYDRODYNAMICS**
CDC computer program for solving two-dimensional, two-fluid magnetohydrodynamic equations
[AD-745854] 01 p0086 N73-10713
Physical model for determining structure of neutral sheets in solar corona
01 p0093 N73-10765
Interaction of electrothermal instabilities and lasing radiation field in MHD lasers including importance of CO2 dissociation
[AD-745986] 02 p0182 N73-11475
Analysis of magnetogasdynamic shock fronts caused by solar winds and development of theoretical concepts and models for phenomenon
[NASA-TM-X-66106] 03 p0353 N73-12876
Closed cycle magnetohydrodynamics - conference paper abstracts
[TH-72-E-29] 04 p0453 N73-13703
Unsteady liquid metal flow in conduction MHD devices with constant magnetic field
[AD-748745] 04 p0455 N73-13715
Approximation of behavior of matter in plasma focus
[UCRL-73932] 06 p0704 N73-15746
MHD equations for calculating joule heating and winds from geomagnetic storms in thermosphere
[NASA-CR-124071] 08 p0915 N73-17498
Slowly changing, large magnetic induction in plasma core of rotating magnetic field pinch
[LRP-56/72] 08 p0947 N73-17756
Ionization hydrodynamics of laser produced plasma
[AD-751880] 08 p0949 N73-17773
Magnetohydrodynamic theory of diurnal oscillations of earth magnetic tail
09 p1029 N73-18395
Magnetohydrodynamic equilibrium in axisymmetric torus
[IPPJ-141] 09 p1070 N73-18727
Magnetohydrodynamic systems of liquid metals
[LM-MHD-1] 10 p1172 N73-19534
Magnetohydrodynamic frequency-wavelength relation in isothermal atmosphere
[BBSO-0127] 11 p1324 N73-20743
Magnetohydrodynamic equations for heavy ion plasma confined in magnetic field and ion source discharges
[LYCEN-7208] 12 p1435 N73-21625
Equations of motion in wave solutions for cold collisional plasma
[AD-755388] 12 p1437 N73-21640
Time dependent correlation functions between magnetohydrodynamics and space transport coefficients
13 p1562 N73-22660
Relativistic principles of magnetohydrodynamics
13 p1562 N73-22661
Analysis of liquid metal magnetohydrodynamic energy conversion systems to determine performance limits and identify system parameters
[AD-757065] 14 p1606 N73-23013
Nonlinear interaction of fast magnetogasdynamic shock with tangential discontinuity
[NASA-TM-X-69178] 14 p1695 N73-23754
Design, development, and operation of compact, high performance, magnetohydrodynamic generators
[AD-756489] 14 p1696 N73-23765
Steady state solution of hydromagnetic mode of initial value problem of micropulsations
[AD-757866] 15 p1783 N73-24451
Description and operating experience of experimental MHD facility
[JUL-883-TP-VOL-10] 17 p2068 N73-26734
Comparison of toroidal screw pinch experiments with one-dimensional MHD computer calculations
[REPT-72-72] 17 p2070 N73-26745
Computerized simulation of belt pinch experiments including plasma external circuit interactions
[LRP-61/73] 18 p2183 N73-27626
Mechanical analogue for hydromagnetic propagation in magnetosphere
[AD-764712] 23 p2788 N73-32307
Analytical solutions to plasma generation near neutral point in magnetic field
[EUR-CEA-FC-685] 24 p2963 N73-33678

**MAGNETOIONIC PLASMA**
U PLASMAS [PHYSICS]

**MAGNETOMETERS**
NT VARIOMETERS
Electrical and mechanical properties of vector magnetometer in HELIOS experiments for interplanetary magnetic field observations
[GAMMA-21] 01 p0048 N73-10384
Superconducting magnetometer as strain transducer in liquid helium cooled gravitational wave antenna
[NOTA-INTERNA-373] 01 p0058 N73-10476
Magnetic test facilities at ESTEC, Netherlands, noting coils and magnetometers
[ESRO-TM-152-ESTEC] 02 p0153 N73-11238
Hall resistivity and electromagnetic properties of bismuth selenide crystals for cryogenic magnetometers
[NASA-TN-D-7057] 03 p0344 N73-12809
OGO 5 fluxgate magnetometer measurements of large field depressions in magnetosphere
[NASA-TM-X-66133] 05 p0539 N73-14382
Comparison of solar cycle variation of interplanetary magnetic field strength observed by HEOS A and Explorer 18 satellite
05 p0593 N73-14819
Magnetic attitude acquisition and control system for automatic despinning of satellite
[NASA-CR-130145] 06 p0673 N73-15477
Geomagnetic measurement using cesium Z-magnetometer aboard nonmagnetic schooner Zarya
[JPRS-58040] 08 p0925 N73-17579
Design and development of prototype moving base gravity gradiometer
[AD-752231] 08 p0926 N73-17587
Development of two cell cesium optically pumped gradient magnetometer
[AD-753060] 09 p1037 N73-18460
Analysis of effect of mass on operation of airborne superconductor magnetic system with aluminum stabilized conductor
10 p1108 N73-19034
OGO-5 fluxgate magnetometer for measuring magnetic field over range of OGO-5 orbit
[NASA-CR-130205] 11 p1294 N73-20498
Comparison of simultaneous particle detector and search coil magnetometer measurements of precipitating particles and field aligned currents from OGO-D
[NASA-TM-X-66224] 12 p1401 N73-21367
Design of zero-field parametric resonance magnetometer using optically pumped helium
[AD-755256] 12 p1402 N73-21376
Outer Planets Grand Tour mission planning to include magnetometer systems requirements and development of hardware elements to meet objectives
12 p1448 N73-21727
Apollo 16 lunar surface magnetometer providing measurements of global response of moon to large-scale solar and terrestrial magnetic fields
12 p1450 N73-21743
Permanent magnetic field on lunar surface measured by Apollo 16 lunar portable magnetometer experiment
12 p1450 N73-21744
Particles and fields subsatellite magnetometer experiment to calculate lunar interior electrical conductivity
12 p1451 N73-21757
Development of system for collection and processing of telemetered magnetometer data received from artificial satellite
[GAMMA-17-167S] 14 p1658 N73-23457
Spherical harmonic analysis of Cosmos-321 geomagnetic survey
14 p1659 N73-23463
Geomagnetic survey of Japan and nearby areas conducted from July 1969 to November 1970
[PUB-592] 14 p1660 N73-23474
Geomagnetic observations made in Japan and surrounding areas from 1967 to 1969
[PUB-591] 14 p1660 N73-23475
Evaluation of cryogenic devices for application in surveillance, radiation detection, and communications
[AD-756175] 14 p1668 N73-23537
Measurement errors and working signal structure of rubidium vapor M sub Z magnetometers and design of observatory vector magnetometer
[JPRS-58950] 15 p1786 N73-24480
Measurement errors of rubidium vapor M sub Z magnetometer
15 p1786 N73-24481
Structure of working signal of rubidium vapor M sub Z magnetometer
15 p1786 N73-24482
Design and operation of observatory vector magnetometer
15 p1786 N73-24483
Fluxgate magnetometer for measuring magnetic flux density of several electron-bombardment ion thrusters
[NASA-TM-X-68239] 15 p1826 N73-24796
Data base of electron and proton spectrometer, Orbiting Geophysical Observatory, and fluxgate magnetometer experiments
[UCRL-51314] 17 p2033 N73-26453
Calculated iron abundance in moon from magnetometer measurements
[NASA-TM-X-62279] 17 p2082 N73-26841
Internal lunar properties calculated from surface magnetometer experiments data
[NASA-TM-X-62278] 17 p2082 N73-26842
Application of dynamic nuclear polarization to increase sensitivity and speed of nuclear precission magnetometers
[JPRS-59393] 18 p2151 N73-27386
Modifications and testing of portable ultra-sensitive superconducting magnetometer
[AD-759735] 18 p2153 N73-27400
Hall effect magnetometer for measuring magnetic fields
[NASA-CASE-LEW-11632-2] 20 p2419 N73-29437
Ship towed magnetometer and ocean bottom mounted magnetic variation station
[JPRS-59802] 21 p2547 N73-30417
Ship towed magnetometer for direct measurement of horizontal component of earth magnetic field
21 p2547 N73-30418
SQUID magnetometer measurement of fluctuation diamagnetism of Al and Al alloys above superconducting transition temperature
[COO-3156-56] 21 p2559 N73-30515
MHD wave transmission and production near magnetopause studied from Explorer 12 magnetometer data
22 p2665 N73-31354
Technology related to design and operation of magnetometers
[JPRS-59674] 22 p2671 N73-31396
Helium self-oscillating magnetometer with optical pumping of He-4 atoms
22 p2671 N73-31397
Use of differential magnetometers with mobile carriers for earth magnetic field measurements
22 p2671 N73-31398
Parameters and errors of magnetically sensitive elements of ferrosonde gradiometers
22 p2671 N73-31399
Compensation of static fields for ferrosonde magnetometer mounted on mobile carrier
22 p2672 N73-31400
Pioneer 11 high field fluxgate magnetometer experiment
[NASA-TM-X-70467] 22 p2672 N73-31405
Magnetograph for recording magnetic fields in solar active region
[AD-762485] 22 p2712 N73-31713
Information capacity of gradient method for measuring earth magnetic field
[JPRS-60100] 23 p2786 N73-32292
Satellite-borne hybrid measuring system for sensing earth gravitational field
24 p2912 N73-33237
Magnetic field data from magnetometer experiments and trajectories of Explorers 33, 35, 41, 43, and 47
[NASA-TM-X-70481] 24 p2979 N73-33809

**MAGNETOMETRY**
U MAGNETIC MEASUREMENT

**MAGNETOPAUSE**
Hydromagnetic waves and trapped particle discontinuities in magnetopause
[NASA-TM-X-66146] 06 p0665 N73-15405
Calculation of shape of earth magnetopause for various orientations of solar wind stream with respect to earth dipole axis
16 p1895 N73-25328
MHD wave transmission and production near magnetopause studied from Explorer 12 magnetometer data
22 p2665 N73-31354

**MAGNETOPLASMADYNAMICS**
U MAGNETOHYDRODYNAMICS

**MAGNETOPLASMAS**
U PLASMAS [PHYSICS]

**MAGNETORESISTANCE**
U MAGNETORESISTIVITY

**MAGNETORESISTIVITY**
Magnetic field intensity calculations for gap electrical machinery with symmetric and asymmetric windings
[JPRS-58448] 11 p1324 N73-20744
Low temperature thermal magnetoresistance of potassium
[COO-3150-12] 22 p2625 N73-31036
Transverse magneto-resistance and Hall resistivity in pure cadmium and in dilute crystal alloys of Cd-Ag and Cd-In
23 p2825 N73-32585

**MAGNETOSPHERE**
NT GEOMAGNETIC TAIL
NT MAGNETOPAUSE

On variational relationships between solar wind parameters, magnetospheric magnetic activity, and magnetospheric storm electrons
02 p0225 N73-11820
Magnetospheric and upper atmospheric physics data obtained during 1971
[AD-746326] 02 p0232 N73-11882
Position of satellite with respect to earth magnetosphere
[AD-746469] 02 p0232 N73-11883
Scientific equipment of ionospheric ESRO-4 satellite including five experiments
[ESRO-SN-114-ESTEC] 02 p0234 N73-11906
Magnetospheric convection, currents feeding polar cap ionosphere, and interplanetary magnetic fields
[NASA-CR-130124] 04 p0413 N73-13375
Analysis of heating of electron component of magnetoplasma due to localized time varying magnetic field perturbations
[AD-747094] 04 p0415 N73-13390
Barium release measurements in support of OOSIK experiment
[AD-749016] 04 p0417 N73-13409
OGO 5 fluxgate magnetometer measurements of large field depressions in magnetosphere
[NASA-TM-X-66133] 05 p0539 N73-14382
Solar wind angular measurements and correlation with solar activity, magnetic storms, plasma flow, in magnetosheath
05 p0593 N73-14821
Comparing properties of open magnetosphere and its electric field to simple model of dipole in constant field
[NASA-TM-X-66132] 05 p0595 N73-14842
Radial diffusion of charged particles and splitting of drift shells surrounding earth
[AD-750741] 06 p0668 N73-15437
Radial diffusion calculations of ionized helium and protons as probe for magnetospheric dynamics
[AD-750861] 06 p0670 N73-15449
Approximate second invariant for charged particle trapped in field of magnetic dipole
[AD-750860] 06 p0701 N73-15715
Laboratory simulation of solar wind interaction with geomagnetic field, and measurements of magnetosphere at shock wave front and of field configuration on nocturnal side
[D-15] 06 p0716 N73-15838
Magnetopause boundary dependence on orientation of interplanetary magnetic field and hydromagnetic properties of magnetosphere shift southwards
06 p0718 N73-15857
Review of material presented at conference on magnetospheric wave-particle interaction
[AD-751568] 07 p0756 N73-16145
Low frequency radio continuum arising in inner magnetosphere from trapped and untrapped electrons
07 p0775 N73-16291
Observation of magnetospherically reflected whistlers made by OGO-A and OGO-C
[NASA-CR-130352] 07 p0781 N73-16344
Determination of path latitude and electron concentration along path of whistlers in magnetosphere
[NASA-CR-130353] 07 p0781 N73-16345
Magnetospheric field model incorporating OGO B and E magnetic field measurements
[NASA-TM-X-66172] 07 p0792 N73-16442
Radar sounding of magnetospheric instability and atmospheric density using barium release clouds
[AD-751567] 07 p0795 N73-16461
Calculation of interplanetary magnetic field induced asymmetries in forward stagnation region of solar-wind magnetospheric interaction
07 p0838 N73-16792
Magnetic field around spherical moon and downstream cylindrical cavity formed by solar wind, derived for parallel and perpendicular interplanetary magnetic fields
[NASA-TM-X-62227] 08 p0960 N73-17851
Theoretical study of sunspots and electrical and thermal conductivities of solar magnetoplasma
[AD-752230] 08 p0962 N73-17872
OGO 3 and 5 observations of inner magnetosphere and ring currents
08 p0972 N73-17947
Temporal behavior of trapped protons alpha particles and ions in magnetosphere
[NASA-CR-130860] 09 p1029 N73-18397
Computer simulation of whistler turbulence and velocity space diffusion in magnetospheric type plasma
[AD-753196] 09 p1031 N73-18415
Magnetospheric convection theory for substorm growth and expansion
[NASA-CR-130499] 09 p1032 N73-18423
Solar proton intensities in magnetosphere over polar regions and comparison to interplanetary intensities
[AD-753679] 09 p1081 N73-18821
Substorm thinning and thickening of magnetotail plasma sheet
[LA-DC-72-1165] 10 p1155 N73-19397
Radio telescope and satellite studies of atmosphere, ionosphere, and magnetosphere under disturbed conditions produced by enhanced solar activity
[AD-754252] 10 p1157 N73-19410
Satellite-borne electric field measurement in magnetosphere
[NASA-CR-131419] 11 p1287 N73-20442
Precipitation of auroral and ring current particles in magnetosphere by artificial plasma injection
[AD-755352] 12 p1403 N73-21381
Magnetospheric radio frequencies attenuations by plasma clouds and energetic particles
[AD-757085] 13 p1493 N73-22106
Study of effects of solar activity on geophysical phenomena using numerical techniques
13 p1514 N73-22264
Temporal behavior of trapped protons, alpha particles, and ions in outer zone of magnetosphere
13 p1515 N73-22273
Theoretical analysis of wave particle interactions in magnetosphere and solar wind
[NASA-CR-131573] 13 p1573 N73-22746
Analysis of magnetospheric data obtained by satellite sounding
[AD-755390] 14 p1665 N73-23516
VHF/UHF technique for determination of columnar electron contents of plasmasphere and of protonosphere using geostationary satellite transmissions of magnetic storm observations
15 p1770 N73-24338
Calculation of intensities of VLF hiss generated from electrons in lower magnetosphere
[NASA-TM-X-66255] 15 p1780 N73-24428
Upper atmosphere, magnetosphere, and solar physics and solar-terrestrial interactions
[AD-757874] 15 p1782 N73-24444
Low energy particle experiment in earth magnetoplasma
[AD-758101] 15 p1782 N73-24446
Artificial ultralow frequency generation in ionosphere and magnetosphere for global communication system
[AD-759012] 16 p1878 N73-25199
Sounding rocket injection of controlled beam of energetic electrons into trapping region of magnetosphere
16 p1895 N73-25329
Conference on wave-particle interactions in magnetosphere and wave amplification for communications
[AD-759071] 16 p1909 N73-25450
Tensor viral method for modeling and studying pulsars in rapidly rotating magnetosphere
16 p1960 N73-25858
Model of stationary, adiabatic plasma flow in magnetosphere interacting with ionosphere
[TRITA-EPP-72-22-PT-1] 17 p2027 N73-26404
Quantitative modeling of electric fields induced in magetosphere by changes in magnetospheric magnetic field
[AD-760058] 17 p2029 N73-26418
Artificial plasma injection of lithium cloud in program to stimulate electromagnetic cyclotron instabilities in magnetosphere
[AD-760032] 17 p2029 N73-26424
Launching Radio Exploration Satellite using Mu-4S-4 rocket for studying ionosphere and magnetosphere
17 p2088 N73-26888
Magnetosphere diagnostics using naturally occurring ELF and VLF waves
[R-34] 18 p2141 N73-27309
Shielding lengths in magnetospheric and interplanetary plasmas
[AD-760795] 18 p2147 N73-27352
Sounding rocket instrument for measuring polar electrojet position and current parameters
[AD-760767] 18 p2152 N73-27396
Design and development of radio sounding satellite for measuring composition of plasmapause during entry and exit phases of orbit
[NOAA-TR-ERL-242-AL-8] 18 p2200 N73-27762
HEOS A 2 experimental design for solar wind and magnetospheric low frequency wave measurement
[DSRI-73-01] 19 p2295 N73-28457
Pitch angle diffusion of relativistic electrons in plasmasphere
[AD-762952] 20 p2414 N73-29405
Electromagnetic radiation trapped in magnetosphere above plasma frequency
[NASA-CR-133837] 21 p2540 N73-30367
OV1-18 mass spectrometer detection of heavy ions in magnetosphere
[AD-763436] 21 p2542 N73-30379
Quasi-linear equations for stochastic plasma diffusion processes of trapped particles in magnetosphere using two selected plasma resonances
[TRITA-EPP-73-09] 21 p2593 N73-30777
Boundary between open and closed magnetospheres of pulsar atmosphere
[AD-761883] 21 p2598 N73-30822
Tilted image dipole model of magnetosphere replacing earth dipole by full internal field expansion
22 p2657 N73-31281
Generation of MHD plasma turbulence in magnetospheric domains
22 p2657 N73-31282
Diffusive equilibrium model for calculating characteristics of broadband ELF, VLF, and LF emissions in magnetosphere
[NASA-CR-133925] 22 p2666 N73-31363
Dynamics of field-aligned longitudinal currents in magnetosphere
[NASA-TT-F-15075] 23 p2787 N73-32294
Mechanical analogue for hydromagnetic propagation in magnetosphere
[AD-764712] 23 p2788 N73-32307
Pulsar magnetospheric model where radiation is produced near surface of neutron star
[NASA-CR-135587] 23 p2844 N73-32731
Selection of similarity criteria for stream of plasma flying into magnetic dipole by mathematical model
[NASA-TT-F-15057] 24 p2962 N73-33670
Magnetospheric plasma flow and magnetospheric boundary layer observations by Vela satellite
[LA-UR-73-732] 24 p2964 N73-33686

**MAGNETOSPHERIC ELECTRON DENSITY**
Azur satellite proton and electron telescope measurements in radiation belt, and conclusions regarding magnetospheric processes
[MPI-PAE/EXTRATERR-66] 02 p0226 N73-11821
Existence of natural radio noise between electron plasma frequency and upper hybrid resonance frequency as detected by long electric antennas of IMP-6 satellite
[NASA-CR-130273] 07 p0843 N73-16832

**MAGNETOSPHERIC INSTABILITY**
Evaluation of solar wind data obtained from Pioneer 6, Mariner 5, and Explorer 35 for velocity variations, magnetopause motion, and geomagnetic disturbances
[NASA-CR-129880] 05 p0591 N73-14806
Synchronous satellite observations on magnetospheric substorms in relation to plasma sheath structure
[RLO-2229-T-5-2] 10 p1155 N73-19398
Oscillations of geomagnetic tail and magnetospheric instability from solar activity
12 p1401 N73-21365
Two substorm studies of relations between westward electric fields in outer plasmasphere, auroral activity, and geomagnetic perturbations
[NASA-CR-131497] 13 p1518 N73-22309
Spontaneous intensification of magnetospheric very low frequency ducts due to coupling between magnetosphere and ionosphere
[AD-756461] 14 p1662 N73-23488
Plasma sheet behavior during magnetospheric substorms
[RLO-2229-T-5-3] 24 p2923 N73-33346

**MAGNETOSPHERIC ION DENSITY**
NT MAGNETOSPHERIC PROTON DENSITY

**MAGNETOSPHERIC PROTON DENSITY**
Azur satellite proton and electron telescope measurements in radiation belt, and conclusions regarding magnetospheric processes
[MPI-PAE/EXTRATERR-66] 02 p0226 N73-11821
Magnetospheric proton density from satellite and ground observation of type Pc3 geomagnetic micropulsations
17 p2026 N73-26396

**MAGNETOSTRICTION**
Effects of magnetostriction and superlattice formation in ferromagnetic thin films
16 p1952 N73-25794

**MAGNETOTELLURIC PROFILING**
U GEOMAGNETISM
U MAGNETIC SURVEYS

**MAGNETOVARIOGRAPHS**
U VARIOMETERS

**MAGNETRONS**
Injection locking of positive pulse microwave magnetrons by stabilized low power source
[AD-758198] 15 p1758 N73-24248

**MAGNETS**
NT CRYOGENIC MAGNETS
NT ELECTROMAGNETS
NT HIGH FIELD MAGNETS
NT SUPERCONDUCTING MAGNETS
Calculation of direction of magnetic moments of two permanent magnets in ESRO 1 satellite
[NASA-TT-F-14499] 01 p0109 N73-10896
Multifilamentary niobium-titanium superconductors for winding pulsed magnets
[BNL-16764] 03 p0345 N73-12817
Magnetic intermetallic cobalt-rare earth compounds for electromechanical energy converters
[AD-750338] 06 p0645 N73-15242
Detailed design study for synchrotron booster magnets and associated power supplies and orbit calculations
[DNPL/R-13[VOL-2]] 06 p0649 N73-15274
Thermomagnetic analysis of rare earth transition metal alloys as permanent magnet materials
[AD-750746] 06 p0686 N73-15587
Mineral insulated conductors for inorganic magnet coils for withstanding high radiation dosage
[LA-DC-72-1106] 10 p1189 N73-19677
Physical property changes of rare earth cobalt magnet materials in temperature range up to 1000 C
[AD-753572] 10 p1201 N73-19778
Technology of high performance transition metal, rare earth permanent magnets for critical applications
[AD-754959] 11 p1306 N73-20601
Electromechanical energy conversion devices using both conventional and rare-earth cobalt permanent magnet materials
[AD-756433] 13 p1501 N73-22168

Design of ironless armature torque motor using samarium cobalt permanent magnets
[NASA-CR-130224] 13 p1532 N73-22416
X ray diffraction analysis of Al based rare earth alloys with potential permanent properties
[AD-756245] 14 p1698 N73-23776
Aging stability of samarium cobalt magnets
[AD-758806] 16 p1881 N73-25222
Technological development of high performance transition metal-rare earth magnets for critical applications
[AD-760178] 17 p2048 N73-26566
Method for fabricating samarium cobalt permanent magnets
[BM-RI-7784] 21 p2580 N73-30679

MAGNITUDE
Derivation of closed formula for relation between luminosity and red shift in expanding Friedman universe
07 p0840 N73-16802
Computation of optical sensor output relative to known star magnitudes for attitude control of spacecraft
[NASA-CR-130926] 10 p1212 N73-19859
Determination of magnitude and brightness of variable stars by photographic photometry
21 p2594 N73-30786

MAGNONS
Far infrared laser spectroscopy of spin clusters in linear magnetic system of cobalt chloride compound
[AD-756264] 13 p1566 N73-22691
Analysis of magnon contribution to total heat current and magneto-elastic coupling in antiferromagnetic materials
16 p1932 N73-25630
Magnetic interactions and spin wave dispersion in rare earth metals
[CONF-730402-10] 20 p2455 N73-29727

MAGNUS EFFECT
Calculation of Magnus forces on axisymmetric bodies at small angles of attack with incompressible turbulent boundary layers
[AD-746449] 02 p0157 N73-11270
Calculation of Magnus sideforce developed by spinning cylinder at angle of attack considering effects of boundary layer and shed vorticity in crossflow
03 p0247 N73-11998
Analysis of Magnus sideforce developed by spinning cylinder at angle of attack based on boundary layer and shed vorticity in cross flow
07 p0768 N73-16239
Magnus effect in supersonic laminar boundary layer on spinning body of revolution
[SC-DC-72-1173] 07 p0772 N73-16269
Strain gage, smoke flow photograph, and hot-wire anemometer studies for determining magnus characteristics
09 p1015 N73-18286
Magnus forces on center of gravity and rotational startup response of self-spinning rotor in subsonic air stream
[AD-755108] 11 p1232 N73-20001
Development of base bleed techniques to reduce Magnus moment on long spinning bodies and improved drag characteristics
[AD-754755] 11 p1232 N73-20002
Results of wind tunnel measurements of normal force, pitching moment, and Magnus force and moment on M823 research store with fixed and freely spinning stabilizers
[AD-757658] 13 p1471 N73-21912
Prediction of Magnus force and moment coefficients for bodies of revolution
[SC-RR-72-0537] 15 p1731 N73-24039
Analysis of Magnus forces on high fineness ratio body of revolution with ogive forebody at varying angles of attack
[AD-759987] 17 p1980 N73-26003
Wind tunnel tests to determine control of magnus instabilities with aerodynamic configurations using symmetrical fin and non-finned bodies
19 p2217 N73-27885

MAIN SEQUENCE STARS
Evolutionary sequences for high-mass stars from zero-age main sequence to end of core helium burning, computed with Ledoux criterion for convective instability
[NASA-TM-X-68914] 07 p0841 N73-16814
Infrared sky survey in Southern Hemisphere for finding late M stars
07 p0846 N73-16854
Application of line-blanketed model stellar atmospheres to Sirius
19 p2342 N73-28837

MAINE
Mapping distribution of glaciofluvial deposits and associated glacial landforms in Maine using ERTS-1 imagery
[E72-10300] 04 p0411 N73-13350
Development of land use and peak runoff classification system for highway engineering using ERTS-1 imagery of Maine
[E72-10308] 04 p0412 N73-13357
ERTS-1 detection and monitoring of vegetation damage associated with highways and highway facilities in Maine
[E72-10371] 05 p0536 N73-14359
Hydrological information from ERTS-1 imagery for design of highway drainage structure in Maine
[E73-10014] 06 p0659 N73-15350
Detection and monitoring vegetation damage associated with highway facilities in Maine
[E73-10331] 09 p1024 N73-18361
Mapping distribution of glaciofluvial deposits and associated glacial landforms in Maine from ERTS-1 imagery
[E73-10353] 10 p1148 N73-19349
Utilization of ERTS-1 imagery to develop land use-peak runoff classification system for highway engineering in Maine
[E73-10456] 11 p1283 N73-20415
Detection and monitoring of vegetation damage associated with highway facilities in Maine
[E73-10522] 13 p1517 N73-22290
Tabular and graphical data for moderate and heavy snow for Loring AFB, Maine
[AD-756881] 13 p1555 N73-22605
Reservoir and water management in Maine using ERTS-1 data collection platforms and imagery
[E73-10585] 14 p1657 N73-23445
Detection of vegetation stress and damage associated with highways and highway facilities in Maine
[E73-10611] 15 p1773 N73-24372
Development of land use-peak runoff classification system for highway engineering in Maine
[E73-10654] 16 p1898 N73-25350
Mapping of glaciofluvial deposits and associated glacial landforms in Maine
[E73-10667] 16 p1899 N73-25362
Evaluation of ERTS-1 image data compression technique
[E73-10717] 17 p2019 N73-26324
Detection and monitoring vegetation damage associated with highway facilities in Maine
[E73-10856] 19 p2292 N73-28433
Utilization of Skylab EREP data for highway engineering in Maine
[E73-10909] 20 p2397 N73-29258
Development of land use-peak runoff classification system for highway engineering in Maine
[E73-10910] 20 p2397 N73-29259

MAINTENANCE
NT AIRCRAFT MAINTENANCE
NT SPACE MAINTENANCE
Mass spectrometer system for monitoring atmospheric constituents and pollutants -operation and maintenance manual
[NASA-CR-128603] 01 p0057 N73-10469
Deformation and repair of artificial runway surfaces using new structural materials
[AD-746718] 02 p0153 N73-11242
Development of process for bonding resinous body in cavities of honeycomb structures
[NASA-CASE-MSC-12357] 03 p0305 N73-12489
Development of equations and mathematical models for decision making concerning military logistics, aircraft, space parts, and support equipment
[AD-747972] 03 p0368 N73-12997
Tasks analyses to determine technical personnel requirements for maintenance of Navy microelectronic shipboard equipment
[AD-748040] 04 p0384 N73-13123
Development of troubleshooting skills to isolate causes of malfunctions in complex electronic assemblies
[BDX-613-337-REV] 04 p0398 N73-13241
Cost effectiveness of infrared inspection and maintenance of ARTCC electrical equipment
[C-208] 04 p0447 N73-13648
Organizational and decision processes for determining essential scheduled maintenance requirements for space shuttle orbiter
[NASA-TM-X-69004] 04 p0478 N73-13908
Maintenance programs for oxygen systems to prevent accidents
[NASA-CR-120922-VOL-3] 05 p0580 N73-14718
Operation and maintenance of shipboard meteorological systems
[AD-751691] 07 p0816 N73-16617
Computerized simulation of solution to maintenance and logistics problems of gas turbine engines
[AD-753622] 10 p1210 N73-19838
Fault isolation and maintenance concepts of advanced inertial navigation system
11 p1320 N73-20713
Three day advance warning system of heating plant failure using algorithmic detection methods
[NASA-CR-131571] 13 p1505 N73-22197
Analysis of methods of fault diagnosis used with logic circuits and effect of procedures on structure of circuit assemblies
[NLL-PO-2913-[9022.81]] 15 p1759 N73-24255
Development of procedures for repairing damaged runway pavements
[AD-756806] 15 p1763 N73-24286
Preventive maintenance of internal combustion engines and transmissions using spectrochemical oil analysis techniques
[PB-216168/5] 16 p1919 N73-25525
Design and feasibility analysis of field-replaceable rotor blade pocket
[AD-759956] 17 p1984 N73-26038
Development of method for determining cost functions involving aircraft rework and engine repair programs at military installation
[AD-761475] 19 p2249 N73-28135
All-weather permanent street patching material for flexible and rigid pavements
[NASA-CR-133549] 19 p2312 N73-28595
Field maintenance and operational experience with various selected models of F-4 aircraft
[AD-762747] 20 p2362 N73-28995
Technical and support services performed during Tenth Soviet Antarctic Expedition
20 p2408 N73-29355

MAJORITY CARRIERS
Compensating impurities in semiconductors which give majority charge carriers
[NLL-RTS-7358] 02 p0218 N73-11761
Diagnostic technique for determining excess free carrier lifetime and ambipolar diffusion coefficient in localized regions within semiconductors
24 p2966 N73-33706

MALFUNCTIONS
Application of pattern recognition to fault diagnosis of internal combustion engines
[AD-747334] 03 p0351 N73-12863
Development of troubleshooting skills to isolate causes of malfunctions in complex electronic assemblies
[BDX-613-337-REV] 04 p0398 N73-13241
Thermal vacuum testing of spacecraft performance using flight models to determine malfunctions
[NASA-TM-X-66188] 09 p1090 N73-18895
Analysis of acoustic properties of jet engine malfunction as means for detecting jet engine burnthrough - Vol. 1
[FAA-RD-72-149-VOL-1] 11 p1334 N73-20825
Apollo 16 flight anomaly report to determine cause of burn holes in main parachute canopy
[NASA-TM-X-69127] 11 p1338 N73-20863
Congressional hearing to determine malfunction on Skylab 1 workshop and proposed methods for correcting malfunction
16 p1964 N73-25884
Postflight analysis of Apollo 11 glycol temperature control valve failure
[NASA-TM-X-69200] 17 p2088 N73-26896
Anomaly report of explosive failure of ground support equipment decontamination unit tank during postflight deactivation of Apollo 16 command module
[NASA-TM-X-69323] 17 p2088 N73-26897
Postflight analysis of Apollo 16 scanning telescope system to determine cause of uneven drive rates
[NASA-TM-X-69233] 17 p2089 N73-26899
Analysis of electronic digital computer inaccuracies
[AD-762235] 19 p2241 N73-28068
Statistical prediction of malfunction in digital computer
[AD-762263] 19 p2242 N73-28079
Determination of diagnostic nucleus of digital computer
[AD-762264] 19 p2242 N73-28080
Control models for diagnosing malfunctions in analog computers
[AD-762220] 20 p2379 N73-29115
Diagnostics of malfunctions in logic circuits and switching circuits
[AD-762234] 20 p2379 N73-29116
Congressional hearing on Skylab 1 solar array system failure
23 p2866 N73-32912

MALI
ERTS-1 imagery of geology, agriculture, hydrology, and ecology of Niger River Delta, Republic of Mali
[E73-10047] 07 p0777 N73-16309
ERTS-1 imagery of plant growth and annual flooding in Niger River inland delta
[E73-10078] 07 p0780 N73-16339
Application of ERTS-1 data for identifying ethnic groups, limits of occupancy, and use of physiographic features in Republic of Mali, West Africa
[E73-10434] 11 p1281 N73-20394
Identification of geologic and hydrologic features of Republic of Mali, West Africa using ERTS-1 imagery
[E73-10435] 11 p1281 N73-20395
ERTS-1 observations of plant growth and annual flooding in Inland Delta of Niger River in Mali
[E73-10436] 11 p1281 N73-20396
Evaluation of hydrology and vegetation in Sahelian zone of Mali, Mauritania, and Senegal during dry season/drought period based on ERTS-1 imagery
[E73-10488] 12 p1396 N73-21324
ERTS-1 imagery of desertification, hydrology, vegetation, forage, and water resources in Republic of Mali
[PAPER-R5] 19 p2283 N73-28363

MAMMALS
NT BATS
NT CALVES

NT CARIBOUS
NT CATS
NT CHIMPANZEES
NT DOGS
NT DOLPHINS
NT GUINEA PIGS
NT HAMSTERS
NT HUMAN BEINGS
NT MICE
NT MONKEYS
NT PRIMATES
NT RABBITS
NT RATS
NT SEALS [ANIMALS]
NT SWINE
NT WHALES

Effects of real or simulated sonic booms of six pounds per square foot over-pressure on reproduction in farm-raised mink
[FAA-EQ-72-2] 03 p0251 N73-12028

Receiver operating characteristics for underwater signal detection performance of sea lions
[AD-746520] 04 p0382 N73-13113

Telemetry experiments with hibernating bear
[NASA-CR-133926] 22 p2620 N73-31000

MAN
U HUMAN BEINGS

MAN MACHINE SYSTEMS

Conference on manual control systems for human operator modeling and display systems in man machine environments
[NASA-SP-281] 01 p0013 N73-10104

Human operator model for man machine control behavior in biodynamic flight environment
01 p0014 N73-10105

Nonlinear multiparameter control model for human operator as vehicle controller
01 p0014 N73-10106

Manual control model structure for industrial management of man machine systems
01 p0015 N73-10115

Utilization of simplified man machine interface concept to manage and control complex space system involving multiple redundant computers that control multiple redundant systems - Vol. I
[NASA-CR-128576] 01 p0019 N73-10145

Methods for implementation of man machine interface of digital data links for air traffic control
[AD-744721] 01 p0079 N73-10648

Evolution of man-machine-hybrid integration in evolving social structure
[AMRU-R-68-3] 02 p0132 N73-11069

Capability of training human to control and/or interact with complex electronic or mechanical systems
[AD-746179] 02 p0136 N73-11101

Screen touching device for computer graphic display operation
[RHEL/R-248] 03 p0271 N73-12194

Methods of evaluating electronic cockpit display devices, emphasizing control, psychology, physiology, and subjective rating
[DGLR-PAPER-72-97] 04 p0383 N73-13118

Engineering psychology for developing practical designs of man machine systems
[AD-748237] 04 p0384 N73-13121

Man machine communication techniques for improving problem solving capability
[AD-748240] 04 p0394 N73-13207

Optimization of work-rest cycles to ensure acceptably high human performance in man machine systems
[AD-750176] 05 p0504 N73-14107

Avionics requirements for multimission, fixed wing, twin engine aircraft designed for search and rescue operations
[AD-750463] 06 p0624 N73-15064

Problems of cockpit environment
08 p0864 N73-16990

Interaction of man machine systems
[JPRS-58290] 09 p0997 N73-18136

Role of cosmonaut in spacecraft control
09 p0997 N73-18137

Interaction between man and electronic computer in operational planning
09 p0997 N73-18138

Bibliography on human factors in man machine interactions and systems design
[AD-752800] 09 p0997 N73-18141

Man machine systems, control theory, nuclear geophysics, and research instrumentation
[RISO-M-1509] 10 p1137 N73-19263

Proceedings of conference on manual control to show interplay between man and machine and application of control theory in medicine and psychology
[NASA-CR-131244] 11 p1235 N73-20028

Human factors criteria for adaptive computer aiding in man-machine control system
[AD-754835] 11 p1250 N73-20147

Pilot error analysis for airborne navigation procedures
[AD-754214] 11 p1251 N73-20150

Graphical computers and computing techniques for real time aid in human problem solving tests
[AD-754282] 11 p1260 N73-20227

Role of cosmonaut in man-spacecraft system, and psychological aspects in training cosmonauts as operators
[NASA-TT-F-727] 12 p1372 N73-21129

Cybernetic integration of experiments into CVT system
[NASA-CR-124150] 12 p1373 N73-21136

Psychophysiological analysis of job performance for optimizing operator production in man machine systems
[NASA-TT-F-14888] 12 p1374 N73-21150

Development and evaluation of free flying teleoperators to include semiexoskeletal master control unit, joystick-analog unit, and three dimensional television system
13 p1594 N73-22925

Analysis of man-machine interfaces and system reliability for air traffic control automation systems
14 p1690 N73-23715

Analysis of interface between controller and computer in automated air traffic control system
14 p1690 N73-23716

Design of airborne flight data transmission system for automatic acquisition and tracking
14 p1711 N73-23885

Computerized multistage decision process for radar operator aid in collision avoidance trajectory control
14 p1711 N73-23886

Space station information subsystem for automatic support of manned operations
14 p1711 N73-23887

Onboard computer system for in-flight monitoring of space shuttle in support of flight crew
14 p1712 N73-23893

Mathematical models for human performance in manned spacecraft control
14 p1712 N73-23897

Computerized teleoperator applications in manned aerospace systems
14 p1713 N73-23904

Computerized design of fighter aircraft cockpit electronic control system considering man machine interaction
14 p1714 N73-23905

Revised edition of human engineering guide to equipment design
[AD-758339] 15 p1744 N73-24140

Design of manipulator mechanisms with manual, bioelectric, and automatic control systems
[NASA-TT-F-14336] 17 p1989 N73-26073

Quantitative evaluations of adaptive physical operator/manipulator control systems
17 p1990 N73-26090

Interaction concept for improving efficiency of man machine systems
[JPRS-59149] 18 p2111 N73-27070

Experimental design formulated for alternative modes of man-computer dialogue
[AD-760010] 18 p2118 N73-27129

Analysis of ERTS-1 imagery by combining human and computer interpretation capabilities
[PAPER-I14] 19 p2279 N73-28335

Adaptive modeling technique for synthesizing controllers to provide corrective dynamics to operator mathematical model in closed loop control system
[NASA-CR-132294] 20 p2372 N73-29060

Ergonomic research and design principles for automatic control and man machine systems
[NASA-TT-F-716] 21 p2502 N73-30079

Examination of man machine systems efficiency in relation to cost criteria
21 p2503 N73-30087

Effect of human operator errors on reliability and effectiveness of his work
[AD-764937] 23 p2753 N73-32028

Airborne computer role in digital flight control systems, noting systems model, man machine interface, and integration
24 p2878 N73-32982

MANAGEMENT
NT CONFIGURATION MANAGEMENT
NT CONTRACT MANAGEMENT
NT DATA MANAGEMENT
NT ENGINEERING MANAGEMENT
NT ENVIRONMENT MANAGEMENT
NT FINANCIAL MANAGEMENT
NT FOREST MANAGEMENT
NT INDUSTRIAL MANAGEMENT
NT INFORMATION MANAGEMENT
NT INVENTORY MANAGEMENT
NT LOGISTICS MANAGEMENT
NT PERSONNEL MANAGEMENT
NT PROCUREMENT MANAGEMENT
NT PRODUCTION MANAGEMENT
NT PROJECT MANAGEMENT
NT RESEARCH MANAGEMENT
NT RESOURCES MANAGEMENT
NT SAFETY MANAGEMENT
NT SYSTEMS MANAGEMENT
NT WATER MANAGEMENT

Scheduling management, and costs of St. Louis air pollution facility
[PB-210020] 01 p0077 N73-10639

Pilot program for transfer of aerospace technology to city management
[NASA-CR-131918] 14 p1724 N73-23992

Aims, prospects, organization, and financing of EUROSAT S.A.
24 p2994 N73-33930

MANAGEMENT ANALYSIS

Analysis of management procedures applied to Surveyor and Lunar Orbiter projects
[NASA-SP-4901] 04 p0486 N73-13973

Model for awarding hazardous pay to employees
08 p0876 N73-17095

Relation between top managers in Federal agencies and operations research/management science groups
[NASA-CR-130668] 08 p0976 N73-17980

Impact on political and organizational policy and decision making of operations research/management science
[NASA-CR-130667] 08 p0976 N73-17981

Project system requirements [planning, communication, analysis] and impediments to implementation
15 p1850 N73-24992

MANAGEMENT INFORMATION SYSTEMS

Management information systems for monitoring ESRO budget and program
[ESRO-PSS-02/PMC-01] 01 p0120 N73-10994

Management information systems for monitoring ESRO budget and program
[ESRO-PSS-03/PMC-02-PT-2]
01 p0121 N73-10995

Planning process, objectives of program areas, and index of plans for air traffic control system improvements
[AD-750224] 05 p0578 N73-14705

Application of ERTS-1 imagery to Minnesota Land Management Information System and analysis of land use classes
[E73-10029] 06 p0660 N73-15362

Integration of system specifications and program coding as basis for final system documentation
10 p1130 N73-19209

Automatic editing of manuals for computer program documentation
10 p1130 N73-19211

Integrated state-wide information management system for water quality control for California
10 p1228 N73-19982

Annotated bibliography of reports, articles, and documents introduced into NASA scientific and technical information system in 1972
[NASA-SP-7500[07]] 15 p1845 N73-24946

Analysis of performance of Honeywell Information System 6000 series computer
[AD-759808] 16 p1879 N73-25212

Bibliography of management planning and information systems
[AD-758900] 17 p2099 N73-26986

Application of ERTS-1 imagery to land management information system in Minnesota
[E73-10821] 18 p2140 N73-27296

Utilization of Skylab imagery as information service for investigating land use and natural resources in New York State
[E73-10829] 19 p2290 N73-28414

Indicators for describing state of science in US for setting priorities in allocating resources
[NSB73-1] 19 p2354 N73-28939

Objectives and performance indicators for aircraft maintenance organizations
[AD-762270] 19 p2356 N73-28951

Data base management information systems and selected Air Force applications
[AD-765203] 23 p2762 N73-32103

Development of resources management information system for resources data from Potomac River Basin
[E73-11069] 23 p2781 N73-32245

MANAGEMENT METHODS

Impact of cybernetics on management of business organizations
[NASA-CR-129728] 04 p0488 N73-13993

Advanced NASA and DOD technology management techniques, and application to NATO programs for defense and civil needs
06 p0732 N73-15968

Development of decision models for choosing techniques and procedures to obtain information for investment decisions in natural resources programs
07 p0783 N73-16363

Accounts of scientific and technological cooperation in Eastern Europe
[JPRS-58053] 08 p0977 N73-17990

Accomplishments during evaluation of automatic inspection, diagnostic, and prognostic maintenance system using UH-1 helicopter as test bed - Vol. 2
[AD-752891] 09 p0987 N73-18059

Development of automatic inspection diagnostic and prognostic systems for maintenance of military helicopters - Vol. 1
[AD-752893] 09 p0987 N73-18060

Development of automatic inspection diagnostic and prognostic systems for maintenance of military helicopters - Vol. 2
[AD-752894] 09 p0987 N73-18061

Formulation of automatic inspection, diagnostic, and prognostic system for maintenance of army aircraft r Vol. 1
[AD-752882] 09 p0988 N73-18062
Design and tradeoff studies applied to automatic inspection, diagnostic, and prognostic maintenance system for military aircraft - Vol. 2
[AD-752883] 09 p0988 N73-18063
Technical proposal and development plan for automatic inspection, diagnostic, and prognostic maintenance system for military aircraft - Vol. 3
[AD-752884] 09 p0988 N73-18064
General specification for automatic inspection, diagnostic, and prognostic maintenance system for military aircraft - Vol. 4
[AD-752885] 09 p0988 N73-18065
Computer output data for automatic inspection, diagnostic, and prognostic system for maintenance of military aircraft - Appendix D
[AD-752887] 09 p0988 N73-18067
Maintenance data tabulations for automatic inspection, diagnostic, and prognostic systems for military aircraft maintenance - Appendix E
[AD-752888] 09 p0988 N73-18068
Cost effectiveness of automatic inspection, diagnostic, and prognostic maintenance system for military aircraft - Appendix F
[AD-752889] 09 p0988 N73-18069
Air Force research and development programs in aircraft electrical power systems to show planning process for developing specific classes of technology
10 p1111 N73-19052
Proceedings of seminar on organization of NASA to show areas of responsibility, resource allocation, and program management
[NASA-CR-131087] 10 p1225 N73-19958
Management methods for Skylab program to include mission operations support, environmental and thermal design criteria, optical contamination, and materials science
[NASA-TM-X-64725] 11 p1342 N73-20886
Management and organization in aerospace science and technology research
11 p1350 N73-20955
Functional characteristics and test methodology for DMS
[AD-748811] 13 p1497 N73-22136
Management methods for developing information systems
15 p1753 N73-24209
Project management system and application of management method
15 p1847 N73-24968
Organization and management of CERN/ISR project
15 p1847 N73-24969
Comparison of management, planning and control for Nimrod avionics system and hospital projects
15 p1847 N73-24971
Requirements, functions, and tasks of project control teams within European space program
15 p1848 N73-24982
Application of program evaluation and review technique for planning and management of air transport operations
[NASA-TT-F-742] 16 p1860 N73-25067
Hazard control and safety management role of project manager
[NASA-TM-X-64764] 19 p2354 N73-28937
Application of NASA management techniques to problems of community violence
[NASA-CR-133830] 21 p2609 N73-30915
Regulatory policies of Civil Aviation Board for controlling operations of commercial airlines
23 p2864 N73-32891
Analysis of airline mergers to show effects on management, personnel, and overall airline operations
23 p2865 N73-32898
Analysis of factors affecting operation of domestic airline to overseas areas
23 p2865 N73-32901
Methodology of planning experiments under nonuniform conditions
24 p2944 N73-33513

MANAGEMENT PLANNING
NT PRODUCTION PLANNING
NT PROJECT PLANNING
Utilization of ERTS-1 imagery for state and local agency management and planning in North Carolina
[E72-10167] 01 p0044 N73-10348
Application of ERTS-1 imagery data to protection and management of New Jersey coastal environment
[E72-10178] 01 p0045 N73-10357
Monitoring by ERTS-1 imagery for resource inventory, planning, land use zoning, and resource development in Oregon
[E72-10182] 01 p0045 N73-10361
Development of usage rate system to determine logistics requirements for military aircraft support
[AD-746482] 02 p0127 N73-11034
Forest resources evaluation, planning, protection, and management using remotely sensed imagery
[E72-10220] 02 p0162 N73-11314
Qualitative identification of steps required to assure incorporation of radiological system safety principles into all phases of manned space base program - Vol. 6
[DOC-72SD4201-6-VOL-6] 02 p0210 N73-11703
Analysis of space tug operating techniques and requirements to include engineering support, off-site facility requirements, and checkout procedures
[NASA-CR-129163] 02 p0232 N73-11887
Guide for coding Dynamic Operational Requirements and Cost Analysis Program to show subroutines and flow charts - Vol. 2
[NASA-CR-129264] 03 p0270 N73-12184
Program listing for Dynamic Operational Requirements and Cost Analysis Program to provide space mission planning and project management capability - Vol. 3
[NASA-CR-129265] 03 p0270 N73-12185
Program listing for Dynamic Operational Requirements and Cost Analysis Program to provide space mission planning and project management capability - Vol. 3
[NASA-CR-123380] 03 p0270 N73-12190
PERT planning run time reduction with special purpose cellular logic computer
03 p0271 N73-12195
Effects of computerized management of information on organizational structures and functions
[REPT-486-70] 04 p0393 N73-13191
Semilinear, topological, spaces and applications to social and economic equilibrium analysis and optimization
[NASA-CR-129591] 04 p0441 N73-13591
Application of Apollo Project managerial practices to solution of problems encountered in modern civilization
04 p0470 N73-13834
Organizational and decision processes for determining essential scheduled maintenance requirements for space shuttle orbiter
[NASA-TM-X-69004] 04 p0478 N73-13908
Analysis of management procedures applied to Surveyor and Lunar Orbiter projects
[NASA-SP-4901] 04 p0486 N73-13973
Management planning models for decision making under conditions of uncertainty
[NASA-CR-129592] 04 p0487 N73-13986
Use of resource indicators and remote sensing to plan and manage hydrologic and water resource systems
05 p0536 N73-14364
Planning process, objectives of program areas, and index of plans for air traffic control system improvements
[AD-750224] 05 p0578 N73-14705
Preliminary design of selected Research and Applications Module [RAM] concepts, operations, and missions
[NASA-CR-129828] 05 p0597 N73-14856
Analysis of operations and resources required to support expendable second stage reusable space shuttle booster - Vol. 5
[NASA-CR-128660] 05 p0599 N73-14871
Technical and economic feasibility of V/STOL lift-fan commercial aircraft for short haul transport applications
[NASA-CR-2184] 06 p0621 N73-15041
Application of aerial and spaceborne photography to urban, regional, and management planning
[NASA-CR-130290] 06 p0673 N73-15473
Development and characteristics of air traffic control system to show system performance tradeoffs and technonogical alternatives - Vol. 1
[PB-212178] 06 p0698 N73-15688
Analysis of technological alternatives involved in development of air traffic control systems - Vol. 2
[PB-212179] 06 p0698 N73-15689
Demand and trade study related to development of air traffic control system based on geographical regions - Vol. 3
[PB-212180] 06 p0698 N73-15690
Air traffic control system development to show factors involved in system selection - Vol. 4
[PB-212181] 06 p0698 N73-15691
Research and development involved in design and implementation of air traffic control system - Vol. 5
[PB-212182] 06 p0698 N73-15692
User manual for computer programs applied to community/airport economic development model - Vol. 3
[FAA-EQ-72-3-VOL-3] 06 p0732 N73-15971
Analysis of earth resources based on mapping, human needs, minerals, water, and food and contributions made by remote sensing satellites
07 p0781 N73-16350
International aspects of Earth Resources Survey Program to include proposals for data availability and assistance to be provided by various nations
07 p0782 N73-16352
Analysis of political, institutional, and economic factors to determine feasibility of conducting earth resources surveys in developing nations
07 p0783 N73-16362
Analysis of remote sensing of earth resources program conducted by Brazil
07 p0783 N73-16364
Accomplishments of United Nations in providing earth resources data to developing nations
07 p0783 N73-16370
Organization, planning, and development of remote sensor programs for Canada
07 p0784 N73-16371
Utilization of ERTS-1 and aircraft remotely sensed data for land use inventory and planning in Maryland
[E73-10081] 08 p0901 N73-17293
Urban and regional planning in Brevard County, Florida using ERTS-1 imagery
[E73-10083] 08 p0901 N73-17295
Research and development in theoretical and applied sciences in Eastern Europe
[JPRS-58121] 09 p1101 N73-18982
Proceedings of seminar on organization of NASA to show areas of responsibility, resource allocation, and program management
[NASA-CR-131087] 10 p1225 N73-19958
Research and development projects conducted by Federal Aviation Administration to improve air traffic control and flight safety
[FAA-EM-73-2] 11 p1321 N73-20720
Management of technological progress and effects on society
11 p1351 N73-20966
Research management for technical applications
11 p1351 N73-20967
Management models for large research institute considering aerospace sciences
11 p1351 N73-20968
Management planning for California water resource information gathering system
12 p1399 N73-21349
Methods of improving cost estimating techniques in NASA and DOD
12 p1466 N73-21877
Analysis of NASA programs during post-Apollo period to show organization of field centers, planning activities, operational activities, and resources utilization
[NASA-CR-131931] 12 p1466 N73-21879
Development of computerized training aid for research and development managers based or spacecraft design operations
[NASA-TN-D-7238] 12 p1466 N73-21880
Analysis of manned space flight capability development for support of earth orbital experiment program and requirements - Vol. 2
[NASA-CR-112326] 13 p1577 N73-22779
Present status and future alternatives of transportation in US
[REPT-72-02328] 13 p1592 N73-22911
Effect of scientific and technical progress on economic control parameters in USSR
[JPRS-58976] 15 p1845 N73-24952
Motivation, planning, and management of research and development programs using controlled thermonuclear fusion as examples
15 p1846 N73-24964
Organization and management of ESRO 4 satellite project noting planning and contractor relations
15 p1847 N73-24970
Application of program evaluation and review technique for planning and management of air transport operations
[NASA-TT-F-742] 16 p1860 N73-25067
Problems of air transport economics and efficiency of air transport utilization in USSR
[NASA-TT-F-741] 16 p1860 N73-25069
Analysis of economics and finances of airport operations to determine procedures for improved management and operation
[REPT-73-01210] 16 p1884 N73-25253
Land use management and planning on Mississippi Gulf Coast using ERTS-1 imagery
[E73-10653] 16 p1898 N73-25349
Planning of short haul air transportation system based on computer simulation of various concepts
[FAA-QS-73-2] 17 p1983 N73-26026
Review and analysis of air carrier/reliever airport grant allocations and technological forecast of airport demands
[FAA-AV-72-4] 17 p2010 N73-26253
Land use management and planning in Maryland based on ERTS-1 data
[E73-10732] 17 p2020 N73-26338
Bibliography of management planning and information systems
[AD-758900] 17 p2099 N73-26986
Tables of data for airline economic impact computer model - Vol. 2
[AD-749491] 17 p2100 N73-26989
Land management planning and timber resources management in Washington and Oregon from ERTS-1 imagery
[E73-10804] 18 p2138 N73-27279
State of Delaware and New York City using space age management for social problems
[NASA-TM-X-66296] 18 p2213 N73-27873
Contractual requirements for submission of electromagnetic compatibility and interference control plan for government procurement
[AD-761975] 19 p2237 N73-28033

Organizational subsystems of information computer center for automatic systems control
[AD-761480] 19 p2240 N73-28057
Analysis of erosion along Niigata Beach, and development of improved methods of erosion control based on ERTS-1 imagery
[PAPER-E14A] 19 p2270 N73-28278
Development of land management programs based on ERTS-1 imagery and computer compatible tapes for machine processing of data
19 p2288 N73-28397
Application of ERTS-1 imagery to programs conducted by Department of Interior
19 p2289 N73-28401
Application of ERTS-1 imagery to land use and resource management in State of Mississippi
19 p2289 N73-28404
Statistical analysis of naval experience in fixed-price incentive contract management for aircraft and missile procurement
[AD-761396] 19 p2355 N73-28946
Technology planning objectives and supporting technical goals for Air Force Flight Dynamics Laboratory during Fiscal Year 1974
[AD-762300] 19 p2356 N73-28950
Application of ERTS-1 imagery to land use inventory, land capability evaluation, and land use suitability in Maryland
[E73-10873] 20 p2393 N73-29224
Land use planning and management on Mississippi Gulf Coast using ERTS-1 data
[E73-10906] 20 p2396 N73-29255
Analysis of technologies and systems required for establishing mining base, mining, refining, and transporting lunar minerals for earth use - Vol.2
[NASA-TM-X-62268] 21 p2595 N73-30799
Application of ERTS-1 imagery to resources management and planning in Ohio
[E73-10987] 22 p2658 N73-31294
Analysis of regional aviation system for Southern California with extension to system of global airports to cope with future requirements
22 p2697 N73-31607
Application of ERTS-1 data to land use planning on Mississippi Gulf Coast
[E73-11055] 23 p2780 N73-32231
Development and characteristics of advanced technology laboratory for use with space shuttle concept
[NASA-TM-X-2813] 23 p2851 N73-32781
Economics, traffic demand, and community acceptance of short haul air transportation system in California Corridor - Vol. I
[NASA-CR-114634] 23 p2859 N73-32842
Procedures for conducting air traffic forecasts with emphasis on socio-economic and demographic characteristics of population
23 p2863 N73-32879
Analysis of airline mergers to show effects on management, personnel, and overall airline operations
23 p2865 N73-32898

**MANAGEMENT SYSTEMS**
NT MANAGEMENT INFORMATION SYSTEMS
Impact of cybernetics on management of business organizations
[NASA-CR-129728] 04 p0488 N73-13993
Development of economical ways of integrating and interfacing new storage devices and data processing programs into computer systems - App. B
[NASA-CR-129817] 05 p0515 N73-14190
Proceedings of conference on management of information analysis centers
[COSATI-72-1] 07 p0766 N73-16224
Quarterly report of JPL research and development
[NASA-CR-131152] 10 p1227 N73-19975
Computer-based pupil/tracking monitoring system for Mesa Public Schools, Mesa Arizona
10 p1228 N73-19985
Application of systems analysis techniques to improve management controls within biomedical research programs
[NBS-TN-761] 13 p1478 N73-21977
Design of compatible modular data management systems
[AD-749910] 13 p1497 N73-22133
Conference on project management and project control
[ESRO-SP-90] 15 p1846 N73-24962
Methods, procedures, and means for comprehensive project management system
15 p1847 N73-24966
Project control at ESTEC, noting network analysis, phased project planning, cost control, and contract management
15 p1848 N73-24981
Data processing in project control illustrated by cost and network analysis and resource allocation modules
15 p1848 N73-24983
Integrated project control for ESRO satellite management
15 p1849 N73-24985
Management system for functional support demands in multiproject institution
15 p1850 N73-24991

**MANEUVERABILITY**
Low speed pull-up maneuvers for slender wing transport aircraft with stability and control augmentation
[ARC-CP-1231] 04 p0369 N73-13004
Yaw maneuverability of helicopters in gliding flight
05 p0493 N73-14022
Relationship between mission requirements of piloted aircraft stability and maneuverability
08 p0864 N73-16995
Influence of load and wing load distribution on lateral and longitudinal maneuverability of aircraft
08 p0865 N73-16998
Influence of powered controls on stability and maneuverability
08 p0866 N73-17008
Maneuverable reentry body trajectory calculation using optimizing and nonoptimizing programs
[BMBW-FBW-72-15] 21 p2597 N73-30815
Technical conditions for airship development, noting weight reduction, propulsion system performance, and maneuverability improvement
24 p2879 N73-32995

**MANEUVERABLE REENTRY BODIES**
Maneuverable reentry body trajectory calculation using optimizing and nonoptimizing programs
[BMBW-FBW-72-15] 21 p2597 N73-30815

**MANEUVERABLE SATELLITES**
U SATELLITES

**MANEUVERABLE SPACECRAFT**
NT AEROSPACEPLANES
NT APOLLO SPACECRAFT
NT LIFTING REENTRY VEHICLES
NT RENDEZVOUS SPACECRAFT
NT X-20 AIRCRAFT

**MANEUVERS**
NT LUNAR ORBITAL RENDEZVOUS
NT ORBITAL RENDEZVOUS
NT SIDESLIP
NT SPACECRAFT DOCKING
NT SPACECRAFT MANEUVERS

**MANGANESE**
X ray fluorescence analysis of manganese and trace elements in mild steels
[NPL-CHEM-16-PT-1] 03 p0264 N73-12140
Elucidation of satellite lines of manganese-doped zinc selenide single crystals in electron paramagnetic resonance spectrum
[AD-753507] 09 p1077 N73-18788
Effect of warm rolling on mechanical properties of unstable chromium-manganese austenitic steels
10 p1171 N73-19526
Structures of ionized vanadium and manganese atoms with incomplete shells considering spin-orbital and spin-spin interactions
[NLL-RTS-7856] 18 p2180 N73-27604

**MANGANESE ALLOYS**
NT MANGANIN [TRADEMARK]
Metallographic analysis of morphological features of martensite formed in alloy of iron-nickel-manganese-carbon after heat treatment
13 p1541 N73-22490
Thermal conductivity of Kondo superconductor Zn-Mn
13 p1565 N73-22682
Deformation properties of hot worked Type 304 austenitic stainless steel, Mangalloy, and other steel alloys
[AD-758912] 15 p1800 N73-24592

**MANGANESE COMPOUNDS**
NT MANGANESE OXIDES
Production of ferromagnetic MnBi thin films by optical control of vacuum deposition and annealing
[KFKI-72-70] 10 p1199 N73-19757
Role of microorganisms during iron-manganese ore formation in lakes and seas
[NASA-TT-F-15023] 21 p2537 N73-30346

**MANGANESE OXIDES**
Operational characteristics of carbon manganese dioxide electrode for metal air battery
[AD-751693] 09 p0991 N73-18089
Hygienic importance and toxicity of manganese oxides, and clinical medicine of chronic manganese exposure
[NASA-TT-F-15000] 21 p2501 N73-30067

**MANGANIN [TRADEMARK]**
Microwire casting development and technology in USSR
[JPRS-57655] 04 p0426 N73-13473

**MANIFOLDS**
High Q active filter channel for UHF active filter manifolds
[AD-747012] 02 p0150 N73-11216

**MANIFOLDS [MATHEMATICS]**
Mathematical representation of gravitational theories using four dimensional manifold defined geometries
[NASA-CR-130753] 08 p0915 N73-17499

**MANIPULATION**
U MANIPULATORS

**MANIPULATORS**
Experiments and simulations to determine effect of compliance and force feedback on manipulator performance
[NASA-CR-128605] 01 p0019 N73-10151
Linear control theory for generating optimal trajectories between initial and final positions of n degree of freedom mechanical arm
[NASA-CR-123980] 05 p0551 N73-14470
Remote control manipulator for space maintenance
[DGLR-PAPER-72-098] 06 p0722 N73-15888
Sophisticated maintenance of orbital space vehicles with application of remotely controlled telemanipulation concept
[NASA-TT-F-14804] 08 p0965 N73-17885
Analysis of control and simulation methods for space shuttle manipulator
09 p1089 N73-18889
Design of elastically geared circular disk wave drive motor and telemanipulator
[NASA-TT-F-14803] 10 p1165 N73-19482
Vibration considerations in design of flexible manipulators
[NASA-CR-124189] 11 p1249 N73-20138
Experiments in video camera positioning with regard to remote manipulators
[NASA-CR-124190] 11 p1249 N73-20139
Construction of remote controlled mechanical manipulators using biodynamic principles
[NASA-TT-F-14889] 12 p1374 N73-21152
Comparison of computed torque method and conventional position servo computer controlled manipulator
[NASA-CR-131521] 12 p1381 N73-21198
Long range objectives of design and control study of remote manipulators
[NASA-CR-124191] 13 p1486 N73-22046
Design of automatic controlled remote arm mechanism incorporating feedback information
[NASA-CR-2238] 13 p1487 N73-22055
Development and evaluation of free flying teleoperators to include semiexoskeletal master control unit, joystick-analog unit, and three dimensional television system
13 p1594 N73-22925
Design of manipulator mechanisms with manual, bioelectric, and automatic control systems
[NASA-TT-F-14336] 17 p1989 N73-26073
Conference on manipulator design considering basic elements
17 p1989 N73-26074
Volumetric kinematic analysis on servomechansim of remote handling manipulator
17 p1989 N73-26075
Design requirements for remotely controlled master-slave manipulators
17 p1989 N73-26076
Matrix method for analyzing kinematics of spatial mechanisms for manipulators
17 p1989 N73-26077
Remote control of underwater manipulator using cables and automatic servomechanics
17 p1989 N73-26078
Structural design of computer controlled manipulator for remote handling
17 p1989 N73-26079
Construction of reversible self synchronous control system for manipulator
17 p1989 N73-26080
Systems engineering for design of two dimensional automatic manipulator control system using reversible follow-up
17 p1989 N73-26081
Remotely controlled manipulators with independent follow-up and force reproduction mechanisms
17 p1989 N73-26082
Design analysis for reversible, self adaptive manipulator control system
17 p1989 N73-26083
Error analysis on manipulator activation system using reversible self adaptive control mechanism
17 p1989 N73-26084
Design of electrohydraulic control system for underwater manipulator with position feedback
17 p1989 N73-26085
Magnetic couplings and magnetomechanical transmissions for airtight manipulator design
17 p1989 N73-26086
Manipulator kinematics in selecting geometrical shapes of containers and chambers
17 p1990 N73-26087
Bioelectric control system design for reversible slave mechanism manipulator using single muscle input
17 p1990 N73-26088
Motor function modeling of human arm by manipulator using myoelectric control pulses
17 p1990 N73-26091
Screw calculus in kinematic and power analyses on spatial positions of manipulator link mechanisms
17 p1990 N73-26092
Attached manipulator system for simulating and demonstrating shuttle manipulator cargo handling operations under weightless conditions
[NASA-CR-133964] 18 p2126 N73-27176
Identification of feasible and practical applications of space teleoperator technology for problems of handicapped
[NASA-CR-133357] 19 p2225 N73-27949

Automation of computer controlled robot manipulators
[JPRS-59717] 20 p2371 N73-29051
Development and characteristics of variable ratio, mixed-mode, bilateral master-slave control system for space shuttle remote manipulator system
[NASA-CASE-MSC-14245-1] 21 p2599 N73-30832
MANNED LUNAR SURFACE VEHICLES
Performance of lunar roving vehicle during Apollo 15 mission
[NASA-TR-R-401] 07 p0841 N73-16817
MANNED ORBITAL LABORATORIES
NT MANNED ORBITAL RESEARCH LABORATORIES
Conceptual designs for manned, space shuttle sortie mission laboratory for communications and navigation experiments - Vol. 1 - Exec. Summary
[NASA-CR-124136] 11 p1266 N73-20273
Selection and definition of candidate experiments and associated instrumentation requirements for space shuttle communication/navigation experiments laboratory - Vol. 2
[NASA-CR-124137] 11 p1266 N73-20274
Conceptual design of space shuttle comm/nav research laboratory and identification of major laboratory equipment - Vol. 3
[NASA-CR-124138] 11 p1266 N73-20275
MANNED ORBITAL RESEARCH LABORATORIES
Mission definition and analysis for manned earth observatory based on projected technology for 1980 time period - Vol. 2
[NASA-CR-124340] 19 p2343 N73-28847
Conceptual design of earth observation facility to include sensor payload, crew functions and accomodations, and common core equipment - Vol. 3
[NASA-CR-124338] 19 p2343 N73-28848
Schedules, costs, requirements, and equipment for manned earth observatory missions - Vol 4
[NASA-CR-124339] 19 p2343 N73-28849
Development of flight experiment work performance and workstation interface requirements for Sortie Lab
[NASA-CR-124409] 23 p2845 N73-32733
MANNED ORBITAL SPACE STATIONS
U ORBITAL SPACE STATIONS
MANNED ORBITAL TELESCOPES
NT APOLLO TELESCOPE MOUNT
MANNED SPACE FLIGHT
NT APOLLO FLIGHTS
NT APOLLO 9 FLIGHT
NT APOLLO 11 FLIGHT
NT APOLLO 12 FLIGHT
NT APOLLO 13 FLIGHT
NT APOLLO 14 FLIGHT
NT APOLLO 15 FLIGHT
NT APOLLO 16 FLIGHT
NT APOLLO 17 FLIGHT
NT GEMINI FLIGHTS
NT MERCURY FLIGHTS
Aerogenic microbial contamination of manned pressurized cabin atmosphere at reduced temperature and high humidity
03 p0259 N73-12098
Physiological responses to environmental factors related to space flight
[NASA-CR-129518] 03 p0260 N73-12107
Device for removing air from water for use in life support systems in manned space flight
[NASA-CASE-XLA-8914] 03 p0305 N73-12492
Impact of space program on efforts to improve standards of living and to reduce harmful pollution of environment
04 p0471 N73-13836
Contributions of astronomy to understanding solar system and initiating manned space flight and exploration
04 p0471 N73-13837
Analysis of photographic data obtained during manned and unmanned space flight and application to oceanography, hydrology, geography, and geology
04 p0471 N73-13843
New knowledge gain from crew life support aspect of manned space program and applicability to earth-based problems
[NASA-CR-129514] 04 p0486 N73-13970
Effects of prolonged weightlessness during space flight on human skeletal and hematopoietic systems
[NASA-TT-F-730] 06 p0630 N73-15116
Physiological factors in human oculomotor responses to space flight stress
[DR-208-VOL-1] 06 p0632 N73-15136
Evolution of neural messages in human adaptation to prolonged zero gravity flight
06 p0634 N73-15154
History of USSR space program to include design of manned spacecraft, solution of space flight problems, and chronology of manned USSR space flights
[NLL-M-22222-[5828.4F]] 06 p0720 N73-15876
History and future of solar system observation, exploration and exploitation
[NASA-TT-F-767] 07 p0844 N73-16839
Findings and data products developed during crew interface specification study for inflight maintenance and stowage functions in future manned space flights
[NASA-CR-128685] 07 p0849 N73-16878
Indices of emotional stress in cosmonauts during Voskhod 2 and Soyuz flights
[JPRS-58039] 08 p0877 N73-17104
Habitability factors during long-term space and undersea missions in confined habitats
[NASA-CR-130537] 08 p0879 N73-17123
Electron-proton spectrometer applied to Skylab program for measurement of electrons and protons resulting from solar flares to determine radiobiological safety factors
[NASA-CR-128704] 08 p0925 N73-17577
Analysis of visual observation data gathered by Soviet manned spacecraft
[JPRS-58055-2-PT-2] 08 p0960 N73-17853
Physical and experimental data obtained by artificial satellites for estimating extraterrestrial radiation hazard in manned space flight
[NASA-TT-F-724] 09 p0992 N73-18098
Radiation hazards and spacecraft shielding requirements for human safety during manned space flight
09 p0992 N73-18099
Mission analysis for manned flight experiments
[NASA-CR-130989] 09 p1082 N73-18828
Compilation of mishaps in manned space flight activity
[NASA-CR-120998] 09 p1090 N73-18896
Compilation of mishaps in manned space flight program for 1970 to 1971
[NASA-CR-120999] 09 p1090 N73-18897
Medical and biological problems of manned space flight
[NASA-TT-F-719] 10 p1114 N73-19077
Cardiovascular and respiratory systems reactions in cosmonauts during space flight
10 p1114 N73-19079
Physiological research in support of manned space flight
[NASA-CR-128741] 10 p1120 N73-19129
Study to validate Non-Interference Performance Assessment
[NASA-CR-128865] 10 p1124 N73-19164
Research in space biology and medicine
[JPRS-58620] 11 p1243 N73-20094
Morphological composition of peripheral blood of crew members of Soyuz-9 and Salyut-1
11 p1245 N73-20104
Microdosimetric pattern of galactic heavy primaries dissipation in tissues during space flight
[NASA-CR-131467] 12 p1372 N73-21132
Synopsis of past, present, and future progress in aerospace engineering and manned space exploration
[UTIAS-REV-37] 16 p1976 N73-25979
Mission events for Skylab 2 flight
[NASA-TM-X-69197] 17 p2088 N73-26893
Crew safety for in-flight spacecraft emergencies
[NASA-TT-F-14997] 18 p2111 N73-27068
Development of design information for molecular sieve sorbants regenerative CO2-removal systems for manned spacecraft
[NASA-CR-2277] 19 p2225 N73-27948
Comments on plasma propulsion, manned spaceflight, and evolution of solar system
[TRITA-EPP-72-08] 19 p2355 N73-28944
Aerospace medicine and exobiology research in support of long term manned space flight
[JPRS-59702] 20 p2365 N73-29021
Effects of weightlessness and acceleration on human body during space flight
20 p2365 N73-29022
Physical monitoring and aftereffects of two manned space flights
[NASA-TT-F-15076] 22 p2620 N73-30992
Steam reactor system for manned spacecraft waste processing
[NASA-CR-134048] 23 p2752 N73-32021
Evaporator for vacuum distillation/vapor filtration water reclamation on manned space flight
[NASA-CR-124397] 23 p2796 N73-32367
Problems involved in achieving harmony in life and work of small groups applied to prolonged space flights
24 p2884 N73-33032
Light and carbon dioxide effects on algal life support systems in space flight
[NASA-CR-135796] 24 p2885 N73-33039
MANNED SPACECRAFT
NT AEROSPACEPLANES
NT APOLLO SPACECRAFT
NT GEMINI SPACECRAFT
NT LUNAR MODULE
NT MANNED ORBITAL LABORATORIES
NT MANNED ORBITAL RESEARCH LABORATORIES
NT ORBITAL SPACE STATIONS
NT ORBITAL WORKSHOPS
NT SALYUT SPACE STATION
NT SKYLAB I
NT SOYUZ SPACECRAFT
NT SPACE SHUTTLES
NT SPACE STATIONS
NT VOSTOK SPACECRAFT
Systems analyses on external and internal radio frequency communication and tracking assemblies for manned space station
[NASA-CR-128561] 03 p0265 N73-12147
Solid polymer for water electrolysis system to generate oxygen and hydrogen in manned space station
[NASA-CR-112183] 04 p0375 N73-13052
Design and performance of prototype nitrogen/oxygen supply unit using water/hydrazine electrolysis to provide cabin leakage makeup in manned spacecraft
[NASA-CR-128688] 06 p0635 N73-15159
Results of OFO-A vestibular experiment and requirements of artificial gravity onboard manned spacecraft
[NASA-TT-F-14836] 08 p0961 N73-17861
Spectrophotometric observation of earth atmosphere and underlying surfaces near twilight horizon from manned spacecraft
09 p1026 N73-18375
Analysis of manned space flight capability development for support of earth orbital experiment program and requirements - Vol. 2
[NASA-CR-112326] 13 p1577 N73-22779
Analysis of major problems in early stages of manned spaceflight, Vostok and Mercury flights, and Mars exploration
[NASA-TT-F-14916] 14 p1709 N73-23867
Manned orbital space station for geophysical and astronomical research
[NASA-TT-F-13957] 14 p1709 N73-23868
Performance characteristics of vehicles traveling in near-earth orbits at super-satellite velocities
[AD-757522] 14 p1710 N73-23878
Cost estimating method for life support systems of manned earth orbital programs
[NASA-CR-124305] 18 p2111 N73-27072
Human factors analysis of astronaut working conditions in space vehicles
[NASA-TT-F-750] 19 p2225 N73-27946
Design, development, and application of 10,000 watt solar array panel for application to three possible space missions and review of solar cell technology
[NASA-CR-133616] 20 p2363 N73-29006
Decomposition of compounds adsorbed in charcoal of manned spacecraft breathing system
[NASA-CR-134013] 21 p2504 N73-30092
Optimal detumbling of large manned spacecraft using internal moving mass
[NASA-CR-135515] 22 p2722 N73-31783
Spacecraft with artificial gravity and earthlike atmosphere
[NASA-CASE-LEW-11101-1] 23 p2847 N73-32750
MANOMETERS
Piston manometer as absolute standard for vacuum gage calibration in 2 to 500 millitorr range
[NASA-TN-D-7059] 02 p0173 N73-11402
Hydraulic damping of sensors of differential manometers of dynamic pressure logs
10 p1184 N73-19637
Absolute pressure measuring device for measuring gas density level in high vacuum range
[NASA-CASE-LAR-10000] 21 p2544 N73-30394
MANPOWER
Transfer of unemployed aerospace professionals to small businesses
[NASA-CR-129504] 03 p0366 N73-12979
Analysis of inflow of professional and technical personnel to US from foreign countries
[NSF-72-312] 05 p0611 N73-14969
Utilization of scientific and technical personnel by urban governments
[PB-212762] 07 p0860 N73-16979
Summary of national patterns of R and D funding and manpower allocations
[NSF-73-303] 15 p1846 N73-24960
Manpower requirements for aircraft maintenance operations of USAF
[AD-760082] 17 p1991 N73-26097
Graduate science students and manpower resources
[NSF-73-304] 21 p2609 N73-30908
MANTLE [EARTH STRUCTURE]
U EARTH MANTLE
MANUAL CONTROL
NT CONTROL STICKS
NT VISUAL CONTROL
Conference on manual control systems for human operator modeling and display systems in man machine environments
[NASA-SP-281] 01 p0013 N73-10104
Nonlinear multiparameter control model for human operator as vehicle controller
01 p0014 N73-10106
Input adaptive behavior model of human operator in pursuit tracking task
01 p0014 N73-10108
Runway separation standards according to reaction time of pilot manual control response to air traffic controller communication
01 p0015 N73-10113
Manual control model structure for industrial management of man machine systems
01 p0015 N73-10115
Dynamic model for nonlinear simulation of human postural control system using sticks
01 p0015 N73-10116

Predictive display with continuous parameter tracking for quasi-linear model of human pilot transfer function in closed loop system
01 p0015 N73-10120
Optimal control model for predicting display requirements in pilot landing performance
01 p0016 N73-10121
Improved pilot performance using simulated pictorial landing display with symbols
01 p0016 N73-10122
Visual display format effects on pilot describing functions in manual tracking performance
01 p0016 N73-10123
Magnetic data tapes containing measurements of pilot scanning behavior, control response and vehicle response during simulated instrument landing approaches
01 p0016 N73-10124
Effect of automatic landing system display on pilot information requirements
01 p0016 N73-10126
Measurements of automobile driver response functions in simulated steering control task with visual field display
01 p0017 N73-10130
Driving speed in relation to interactions among automobile driver, roadway variables, and vehicle control
01 p0017 N73-10131
Double steering wheel forcing functions for estimating automobile driver manual control response
01 p0017 N73-10132
Human physiological and psychological responses in long time exposure to simulated space station atmosphere as observed by critical tracking task
01 p0017 N73-10133
Optimal control model for predicting manual VTOL pilot performance in longitudinal hovering tasks
01 p0017 N73-10134
Phase margin measure for determining human operator control performance in multivariable closed loop system
01 p0018 N73-10135
Serial segments method for measuring pilot manual control remnant in vicinity of sine waves
01 p0018 N73-10136
Minimum quadratic cost optimal control technology for design of F-4C aircraft manual control system
01 p0018 N73-10137
Hypoxia stress effects on human operator performance in unstable tracking task using manual control
01 p0018 N73-10138
Effect of concurrent audio tasks on human operator compensatory tracking performance using manual control system
01 p0018 N73-10139
Attention sharing effects on human operator performing simultaneously dynamic compensatory tracking control tasks
01 p0018 N73-10140
Motion cue effects on pilot manual control tracking task
01 p0018 N73-10141
Dynamic model for pilot manual control ability using aural compensatory tracking
01 p0018 N73-10142
Computerized teleoperator manual control system for remote mechanical hand
01 p0019 N73-10143
SMAC with two manual methods and one computer program with queueing simulation up to five parallel servers or up to three series servers
05 p0610 N73-14956
Criteria for designing manual control system for military transport aircraft
08 p0866 N73-17007
Workload effects on operator grip pressure and neuromuscular transmission in manual tracking task error [AD-757252] 14 p1615 N73-23089
Analysis of manual control theory of vertical situation displays for short takeoff aircraft [NASA-CR-114620] 15 p1734 N73-24061
Development of flight simulator system to show position of joystick displacement [NASA-CASE-NPO-11497] 16 p1878 N73-25206
Motor reaction model for hand motion in decision making manual task [AD-761518] 19 p2229 N73-27973
System controls description for 36 zone thermal simulation system for operation and maintenance [NASA-CR-124436] 24 p2901 N73-33154

**MANUALS**
NT USER MANUALS (COMPUTER PROGRAMS)
Mass spectrometer system for monitoring atmospheric constituents and pollutants -operation and maintenance manual [NASA-CR-128603] 01 p0057 N73-10469
Numerical simulation of one-dimensional collisionless plasma phenomena - users manual [AD-745423] 01 p0085 N73-10706
Stress and strength guide for engineering design [ESDU-SS1] 01 p0111 N73-10917
Users information and computer program for hydrodynamic-numerical model for oceanographic analyses [AD-745760] 02 p0167 N73-11358
Users manual for interpretive computer program implementation on large computer [NBS-TN-552] 04 p0393 N73-13193
Sample output for community/aircraft economic development model - programmers manual [FAA-EQ-72-3-VOL-4] 04 p0401 N73-13260
Computer program for determining aerodynamic influence coefficients on interferring wings in unsteady supersonic conditions - programmers manual [NASA-CR-112185] 04 p0404 N73-13291
Manual of chemical processes related to spacecraft development technology [NASA-TM-X-2635] 05 p0506 N73-14117
Hardware and software requirements, and program operations and descriptions for cartographic data base program - manual [AD-749498] 05 p0540 N73-14394
Finite element method of continuum and structural analysis using computer programs - users manual [AD-753120] 09 p1097 N73-18951
Users manual for COEBRA program for design of launch vehicle autopilots [NASA-CR-124125] 10 p1183 N73-19622
Electromagnetic compatibility of avionic weapon system [AD-754412] 11 p1265 N73-20262
Manual on electromagnetic compatibility and interference between aircraft weapon systems [AD-754411] 11 p1265 N73-20263
Statistical analysis and computer techniques [NBS-TN-756] 11 p1311 N73-20635
GUERAP computer code for accurately measuring off axis rejection characteristics of optical system - users manual [AD-755353] 13 p1560 N73-22645
Nimbus 4 satellite users guide detailing instrumentation, configuration, and experimentation [NASA-TM-X-69887] 13 p1580 N73-22803
Manual for FORTRAN program designed to plot output graphs using IBM 1130 computer [NASA-TM-X-64744] 15 p1753 N73-24213
Manual for 70mm hand held photography from Skylab [NASA-TM-X-66262] 16 p1912 N73-25475
Manual of CDC 6400 computer program for predicting nozzleless rocket motor internal ballistics [AD-759559] 16 p1958 N73-25838
Flow diagrams and listings for SAP and PLTGEN programs [NASA-CR-128985] 17 p1997 N73-26146
Computer manual for transpiration cooling analysis on gas turbine blades [AD-759192] 17 p2078 N73-26807
System controls description for 36 zone thermal simulation system for operation and maintenance [NASA-CR-124436] 24 p2901 N73-33154

**MANUFACTURING**
NT LOW GRAVITY MANUFACTURING
NT SPACE MANUFACTURING
Survey on materials and manufacturing processes for solid state electronic devices [AD-745745] 01 p0034 N73-10266
Choice of suitable manufacturing dimensions for parallel axis straight spur and helical gears [ESDU-66001] 01 p0060 N73-10493
Solid states physics and manufacturing methods for microwave generation, amplification, and control devices [AD-749500] 04 p0397 N73-13234
Development of high power diode microcircuits [SC-CR-72-3142] 05 p0519 N73-14219
Numerically controlled ion beam sputtering process for manufacturing solid optical surfaces [AD-750347] 05 p0581 N73-14730
Fabrication of Nb-Ti and Al composite for use in superconducting rod [COO-3311-1] 05 p0587 N73-14775
Printed circuit boards for microminiaturized electronic manufacturing [AD-750918] 06 p0648 N73-15265
University course on dimensioning, construction, and manufacturing of nonmetallic structural sandwich elements [FOA-4-C-4467-61] 06 p0677 N73-15506
Copper brass bimetal cladding layers on steel strips for manufacturing elastic current conducting springs [NLL-M-21498-[5828.4F]] 06 p0682 N73-15554
Production of carbon fibers and reinforced plastics in British installations [FOA-2-C-2468-91] 06 p0687 N73-15594
Production and applications of transuranic elements [FOA-4-C-4463-22[13]] 07 p0819 N73-16637
Manufacturing of superconducting cylindrical films of niobium and niobium nitride by sputter etch techniques [AD-752593] 08 p0952 N73-17799
Survey of heavy duty composite materials, development, manufacturing, costs, and applications 09 p1352 N73-18577
Design and fabrication of prototype particulate regenerative filter with backflush for spacecraft fluid system [NASA-CR-115505] 14 p1614 N73-23084
Survey of flat electrical cable manufacturing including patented processes 14 p1640 N73-23296
Manufacturing of Gunn diodes with short domainless ISA mode for microwave oscillators with 100 W output 15 p1757 N73-24238
Manufacturing processes for aircraft engine parts [AD-759577] 16 p1958 N73-25837
Technological development of high performance transition metal-rare earth magnets for critical applications [AD-760178] 17 p2048 N73-26566
Chemical machining of steels, iron, nickel, cobalt, copper, and light alloys 18 p2161 N73-27454
Electron beam imaging for manufacturting high rfequency surface acoustic wave transducers [AD-761625] 19 p2245 N73-28101
Design, fabrication, and performance evaluation of CO laser [AD-762334] 19 p2308 N73-28568
Transfer of technology developed for aerospace program to specific industrial problems of developing nation [Korea] [NASA-CR-133358] 19 p2355 N73-28943
Methods for manufacturing computer systems elements and programming methods [TT-71-50054/1] 21 p2516 N73-30180
Apparatus for manufacturing polyester drive belts [NASA-CASE-NPO-13205-1] 22 p2677 N73-31442
Properties of dielectric layers of negative electrosensitive resin noting masking capability and application to MOS circuit manufacturing [REPT-5.497] 23 p2765 N73-32124
Manufacturing high resolution active and passive semiconductor devices noting field effect transistors and transistor logic [REPT-3.462] 23 p2766 N73-32126
Bibliography of techniques, procedures, manufacturing methods, time studies, and shop layout in machine shop practice [AD-765400] 23 p2799 N73-32388
Flexible airship manufacturing 24 p2879 N73-32992
Technical aspects of airship manufacture and ground and loading operations 24 p2879 N73-32993
Electroforming used for manufacture of hollow wind tunnel models and nozzles [DLR-FB-73-40] 24 p2929 N73-33395
Bibliography of manufacturing methods of composite materials [AD-764600] 24 p2944 N73-33512

**MANY BODY PROBLEM**
One boson exchange nucleon-nucleon potential in two nucleon and many nucleon problems [NOTA-INTERNA-380] 01 p0084 N73-10694
Application of many body theory to superconductivity and superfluidity [AD-754961] 11 p1331 N73-20808
Many body theory of aerodynamic forces 16 p1851 N73-24995
Derivations of second-order asymptotic boundary value solutions for lunar and interplanetary trajectories [NASA-CR-2256] 19 p2343 N73-28845

**MANY PARTICLE THEORY**
U MANY BODY PROBLEM

**MAPPING**
NT CADASTRAL MAPPING
NT ICE MAPPING
NT PHOTOMAPPING
NT SOIL MAPPING
NT THEMATIC MAPPING
Mapping iron compounds in Wind River Range using ERTS-1 multispectral scanner imagery [E72-10181] 01 p0045 N73-10360
Uniform mapping and monitoring of natural ecosystems and environmental complexes from ERTS-1 imagery [E72-10185] 01 p0046 N73-10364
Land use mapping of northern megalopolis using ERTS-1 imagery [E72-10188] 01 p0046 N73-10367
Application of satellite tracking and precision traversing data to improve accuracy of geodetic triangulation [NASA-CR-128402] 01 p0047 N73-10377
Utilization of ERTS-1 imagery for water depth measurement, mapping of Yellowstone Park, atmospheric effects in Colorado, lake ice surveillance, recreational land use, IFYGL Lake Ontario, image enhancement, water quality monitoring, and oil pollution detection [E72-10201] 02 p0144 N73-11167
Utilization of ERTS-1 imagery for water depth measurement, mapping of Yellowstone Park, atmospheric effects in Colorado, lake ice surveillance, recreational land use, IFYGL Lake Ontario, image enhancement,

water quality monitoring, oil pollution detection, and mapping iron compounds
[E72-10198] 02 p0160 N73-11296
Detection and mapping snow cover from ERTS-1 remotely sensed imagery of western US and Arctic
[E72-10202] 02 p0160 N73-11299
Land use mapping of forest area in Southeastern US by airborne multispectral scanning
[E72-10222] 02 p0162 N73-11316
Spectral geological mapping of New York using ERTS-1 imagery
[E72-10223] 02 p0163 N73-11317
Assessment of cartographers role in automatic cartography system
[AD-746019] 02 p0169 N73-11376
Computer program for mapping satellite-borne narrow beam antenna footprints on earth
[NASA-CR-129283] 03 p0265 N73-12149
Land use mapping of Phoenix quadrangle using ERTS-1 imagery
[E72-10236] 03 p0288 N73-12336
Mapping and detection of snow cover changes on land and on glaciers in Alaska, British Columbia, and Washington using ERTS-1 imagery
[E72-10237] 03 p0288 N73-12337
Mapping land use and land use change in Central Atlantic Region using ERTS-1 imagery
[E72-10241] 03 p0288 N73-12341
Mapping ecological effects of coal strip mining in Ohio
[E72-10256] 03 p0290 N73-12356
Polar region mapping using ERTS-1 return beam vidicon imagery
[E72-10273] 03 p0291 N73-12371
Cultural resources interpretation and map revision from ERTS-1 RBV and MSS imagery of Washington state
[E72-10276] 03 p0291 N73-12374
Cartographic evaluation of ERTS-1 orbit and attitude data
[E72-10277] 03 p0292 N73-12375
Overall evaluation of ERTS-1 RBV and MSS imagery for cartographic applications
[E72-10278] 03 p0292 N73-12376
Comparison of mapping accuracies obtained by analytic system of aerotriangulation with accuracies obtained using conventional first-order plotting instruments
03 p0294 N73-12391
Mapping distribution of glaciofluvial deposits and associated glacial landforms in Maine using ERTS-1 imagery
[E72-10300] 04 p0411 N73-13350
Management of earth resources in France and Spain through automatic mapping inventory
[E72-10303] 04 p0411 N73-13352
Automatic mapping of geologic features of Fannin County, Texas using MSS imagery from ERTS-1
[E72-10306] 04 p0412 N73-13355
Theory and practice of aerial photography to include aerial triangulation, stereometric methods of photointerpretation, and production of maps
[AD-748871] 04 p0423 N73-13449
Analysis of problems in mapping Venus surface with radar from orbiting spacecraft
[NASA-CR-129821] 04 p0477 N73-13900
Spectral geological mapping in diverse terranes of New York using ERTS-1 imagery
[E72-10302] 05 p0530 N73-14309
Identification, definition, and mapping of terrestrial ecosystems in interior Alaska
[E72-10343] 05 p0532 N73-14331
Mapping of regional fracture patterns and related structural features of Wind River Mountains using ERTS-1 imagery
[E72-10349] 05 p0533 N73-14337
Hardware and software requirements, and program operations and descriptions for cartographic data base program - manual
[AD-749498] 05 p0540 N73-14394
Mapping of remote desert dune fields using ERTS-1 imagery
[E73-10009] 06 p0659 N73-15345
Mapping distribution of glaciofluvial deposits and associated glacial landforms
[E73-10013] 06 p0659 N73-15349
Mapping and inventories of land use and natural resources in New York based on ERTS-1 imagery
[E73-10024] 06 p0660 N73-15358
Mapping of major geological structures of African Rift System using ERTS-1 imagery
[E73-10026] 06 p0660 N73-15360
Geological mapping of New York State using ERTS-1 imagery
[E73-10031] 06 p0660 N73-15364
Land use mapping and change detection in Central Atlantic Regional Ecological Test Site based on ERTS-1 MSS imagery
[E73-10034] 06 p0661 N73-15367
Mathematical and computer methods of cartography
[BUL.-56] 06 p0666 N73-15415
Discrimination and mapping land use categories in Puerto Rico using various types of multispectral remote sensor imagery
07 p0776 N73-16298
Multispectral band survey and mapping of earth in 18 days
[E73-10044] 07 p0777 N73-16307
Surveying and mapping earth resources over large areas utilizing ERTS-1 imagery
[E73-10049] 07 p0777 N73-16311
Cartographic applications of ERTS-1 imagery in polar regions
[E73-10051] 07 p0777 N73-16313
Cultural interpretation and map revisions from ERTS-1 imagery
[E73-10052] 07 p0777 N73-16314
Cartographic applications of ERTS-1 MSS imagery
[E73-10053] 07 p0777 N73-16315
Mapping and detection of changes of snow cover on land and glaciers
[E73-10063] 07 p0778 N73-16325
Mapping and control of pink cotton bollworm in California
[E73-10073] 07 p0780 N73-16335
Forests and range resources inventory and mapping using remote sensors
07 p0785 N73-16388
Regional land use mapping and management using remotely sensed imagery
07 p0786 N73-16392
Control and mapping of water pollution using remote sensors
07 p0787 N73-16398
Automatic computer mapping of infrared scanner data of terrain classes in Yellowstone National Park
07 p0787 N73-16400
Utilization of ERT-1 imagery for water depth measurement, Yellowstone Park data, atmospheric effects in Colorado, lake ice surveillance, recreational land use, IFYGL, image enhancement, water quality monitoring, oil pollution detection, and mapping iron compounds
[E73-10086] 08 p0901 N73-17298
Mapping snow cover in western US using ERTS-1 MSS imagery
[E73-10087] 08 p0901 N73-17299
Land use mapping and image enhancement of ERTS-1 imagery of Phoenix Quadrangle
[E73-10090] 08 p0902 N73-17302
Tectonic and paleogeologic mapping of Montana using ERTS-1 imagery
[E73-10280] 08 p0914 N73-17488
Development of system for mapping and monitoring natural ecosystems and environmental complexes from ERTS-1 imagery of California, Nevada, Four Corners Area, Louisiana, and Colorado Plateau
[E73-10289] 08 p0915 N73-17495
Research and development in topographic mapping
[NASA-CR-130540] 08 p0918 N73-17527
Geologic mapping of Montana using ERTS-1 imagery
[E73-10281] 09 p1020 N73-18325
Mapping seismically active faults in Alaska from ERTS-1 imagery
[E73-10283] 09 p1020 N73-18326
Vegetation map of western Seward Peninsula, Alaska, based on ERTS-1 imagery
[E73-10305] 09 p1022 N73-18337
Identification, analysis, and mapping of terrestrial ecosystems and vegetation types in Alaska based on ERTS-1 imagery
[E73-10306] 09 p1022 N73-18338
Survey and mapping of snow and ground water levels in Norway using ERTS-1 imagery
[E73-10324] 09 p1024 N73-18356
Cartographic evaluation of ERTS-1 MSS imagery
[E73-10329] 09 p1024 N73-18360
Survey and mapping Colorado geology using airborne remote sensors
[NASA-CR-130822] 09 p1025 N73-18370
Utilization of artificial satellites and spacecraft for surveying and mapping earth resources
[NASA-TT-F-739] 09 p1026 N73-18377
Agricultural and urban land use mapping of Phoenix Quadrangle based on ERTS-1 imagery
[E73-10340] 10 p1147 N73-19339
Development of standards for classification, mapping and scientific analysis of land use and land use change in Central Atlantic Region Ecological Test Site using ERTS-1 imagery
[E73-10347] 10 p1148 N73-19346
Evaluation of ERTS-1 imagery for mapping land use and updating Minnesota land management information system
[E73-10352] 10 p1148 N73-19348
Mapping distribution of glaciofluvial deposits and associated glacial landforms in Maine from ERTS-1 imagery
[E73-10353] 10 p1148 N73-19349
Detection and mapping snow cover in Salt-Verde Watershed of Arizona using ERTS-1 imagery
[E73-10361] 10 p1149 N73-19357
Mapping southeastern coastal marshlands and wetlands of South Carolina and Georgia using ERTS-1 imagery
[E73-10362] 10 p1150 N73-19358
Mapping northern Atlantic coastal marshlands of Maryland, Delaware, and Virginia using ERTS-1 imagery
[E73-10363] 10 p1150 N73-19359
Mapping and detection of snow cover on land and glaciers in Cascade Range using ERTS-1 imagery
[E73-10379] 10 p1152 N73-19374
Utilization of ERTS-1 imagery for mapping Quaternary deposits and landforms in Great Plains and Midwest
[E73-10381] 10 p1152 N73-19376
Utilization of ERTS-1 imagery to detect and map erosion features and changes in southern Arizona
[E73-10382] 10 p1152 N73-19377
Design of towed sonar transducer array for bathymetric mapping of ocean bottom topography
[AD-755113] 11 p1259 N73-20216
Development of procedure and system for uniform mapping and monitoring of earth resources and environmental complexes using ERTS-1 imagery
[E73-10350] 11 p1275 N73-20344
Water depth measurement and mapping of shallow water features of Little Baham Bank using ERTS-1 imagery
[E73-10388] 11 p1275 N73-20350
Computer mapping of Michigan recreational land use using ERTS-1 data
[E73-10392] 11 p1276 N73-20354
Spectral ratio mapping of iron ore deposits in Wind River Range, Wyoming, using ERTS-1 data
[E73-10397] 11 p1276 N73-20359
Interpretation of ERTS-1 geologic data for Nevada and evaluation of materials used in compiling photomaps
[E73-10398] 11 p1277 N73-20360
Utilization of ERTS-1 imagery for mapping extent of Pleistocene glaciation and delineation of small urban areas in Wyoming
[E73-10425] 11 p1280 N73-20386
Application of ERTS-1 imagery for mapping coverage of megalopolitan New England to show land use
[E73-10427] 11 p1280 N73-20388
Mapping of major structural lineaments of Ethiopian rift using ERTS-1 imagery
[E73-10431] 11 p1281 N73-20392
Analysis of ERTS-1 imagery for land use and lake turbidity mapping of Lake Champlain Basin and Vermont
[E73-10432] 11 p1281 N73-20393
Application of ERTS-1 data for identifying ethnic groups, limits of occupancy, and use of physiographic features in Republic of Mali, West Africa
[E73-10434] 11 p1281 N73-20394
Construction of cartographic scanner/plotter for computer aided mapping
[AD-754648] 11 p1288 N73-20452
Detection of surface specific points by local parallel processing of discrete terrain elevation data
[AD-753701] 11 p1289 N73-20459
Mapping of land use in agriculture area of Finney County, Kansas based on ERTS-1 imagery
[E73-10474] 12 p1395 N73-21311
Mapping of polar regions using ERTS-1 multispectral photography
[E73-10501] 12 p1398 N73-21337
Processing digital radar data base to create simulated mapping-radar scope images
[AD-755722] 13 p1495 N73-22118
Color coding scheme for hierarchically representing cartographic symbology
[AD-740606] 13 p1497 N73-22134
Mapping of coastal sedimentation and related processes in Cook Inlet, Alaska and distribution and environmental interrelationships of permafrost terrain
[E73-10421] 13 p1515 N73-22275
Mapping wetlands ecology of Chesapeake Bay, South Carolina, and Georgia from ERTS-1 imagery
[E73-10507] 13 p1516 N73-22282
Interpretation of ERTS-1 imagery of man made culture and revision of small-scale maps
[E73-10536] 13 p1518 N73-22300
Application of remote sensing techniques in forestry and range disciplines for timber inventory, weather forecasting, land classification, and snowfield monitoring
[NASA-CR-131583] 13 p1523 N73-22340
Coding systems in geographic data maps
13 p1523 N73-22343
Use of digitized remote sensor data and automatic data processing techniques in preparation of forest cover mapping to aid in forest resources management
[NASA-CR-131578] 13 p1523 N73-22344
Sonar mapping of underside of sea ice
[AD-755243] 13 p1527 N73-22374
Uniform mapping of earth resources and environmental complexes from Skylab imagery
[E73-10532] 14 p1654 N73-23417
Cartographic evaluation of ERTS-1 orbit and attitude data
[E73-10544] 14 p1654 N73-23419

Land use mapping of Central Atlantic Region using ERTS-1 imagery
[E73-10557] 14 p1655 N73-23429
Detection and mapping changes of snow cover on land and glaciers from ERTS-1 imagery
[E73-10559] 14 p1655 N73-23431
Uniform mapping of earth resources and environmental complexes from Skylab imagery
[E73-10562] 14 p1656 N73-23434
Geological survey and mapping of ice-free valleys of Antarctica from interpretation of ERTS-1 imagery
[E73-10564] 14 p1656 N73-23436
Geological surveys and mapping of Netherlands based on ERTS-1 imagery
[E73-10584] 14 p1657 N73-23444
Development of accurate geoidal map based on gravimetric and satellite data for determining precise location of tracking stations
[NASA-CR-131869] 14 p1710 N73-23874
ERTS-1 applications in water depth calculation, terrain classification, land use mapping, water pollution, and mineral exploration
[E73-10565] 15 p1771 N73-24345
Terrain classification mapping of Yellowstone Park from ERTS-1 imagery
[E73-10567] 15 p1771 N73-24347
Atmospheric effects on ERTS-1 imagery for land use mapping
[E73-10568] 15 p1771 N73-24348
Digital recreational land use mapping in Oakland County, Michigan
[E73-10570] 15 p1772 N73-24350
Ratio mapping iron ore deposits in Atlantic City District, Wyoming
[E73-10575] 15 p1772 N73-24355
Cartographic applications of ERTS-1 imagery
[E73-10600] 15 p1772 N73-24361
Urban planning and mapping in east central Florida using ERTS-1 imagery
[E73-10605] 15 p1773 N73-24366
Geological mapping in Bolivia using ERTS-1 imagery
[E73-10614] 15 p1774 N73-24375
Identification, definition, and mapping of terrestrial ecosystems in interior Alaska from ERTS-1 imagery
[E73-10634] 15 p1776 N73-24393
Geologic mapping of Bonanza Test Site Colorado using remotely sensed data
[NASA-CR-132231] 15 p1780 N73-24433
Research on geodesy, topography, cartography, photography, astronomy, and chemistry
[AD-758290] 15 p1788 N73-24500
Mapping of Perseus arm feature in spectrum of Cassiopeia A
[AD-757687] 15 p1832 N73-24854
Detection, monitoring, and mapping coal strip mining and reclamation in Ohio from ERTS-1 imagery
[E73-10641] 16 p1896 N73-25338
Geologic mapping and mineral resource inventory in South America from ERTS-1 imagery
[E73-10648] 16 p1897 N73-25344
Land use management and mapping for Phoenix Quadrangle from ERTS-1 imagery
[E73-10650] 16 p1897 N73-25346
Cartographic applications of ERTS-1 RBV imagery of Arctic and Antarctic regions
[E73-10651] 16 p1898 N73-25347
Mapping phenological changes using ERTS-1 imagery
[E73-10660] 16 p1899 N73-25356
Geographic analysis and mapping of landscape changes in Tennessee from ERTS-1 imagery
[E73-10661] 16 p1899 N73-25357
Mapping of glaciofluvial deposits and associated glacial landforms in Maine
[E73-10667] 16 p1899 N73-25362
Mapping and monitoring natural ecosystems and environmental complexes and estimation of rice crop yield in California and Louisiana from ERTS-1 imagery
[E73-10669] 16 p1899 N73-25364
Identification and mapping land use classes in Marion County, Indiana from ERTS-1 MSS data
[E73-10680] 16 p1901 N73-25375
Tectonic and structural mapping in Alaska using ERTS-1 imagery
[E73-10685] 16 p1901 N73-25379
Application of ERTS-1 imagery to cartography, geomorphology, agronomy, and hydrology of Bolivia
[E73-10695] 16 p1902 N73-25387
Application of Skylab and EREP imagery for uniform mapping of earth resources and environmental complexes
[E73-10706] 16 p1904 N73-25397
Urban mapping activities assisted by aerial photography and ground surveying in connection with urban planning and community development
[PB-214305/5] 16 p1915 N73-25494
Method for evaluating image errors of mapping camera locked to stellar cameras
[AD-759491] 16 p1915 N73-25497
Erratic operation of mapping camera extension mechanism on Apollo spacecraft
[NASA-TM-X-69269] 16 p1967 N73-25909
Photointerpretation of ERTS-1 imagery to map bodies of water in Saline County, Kansas
[E73-10684] 17 p2017 N73-26313
Analysis of time-lapse data processing for dynamic hydrologic conditions based on ERTS-1 imagery and aerial photography
[E73-10729] 17 p2020 N73-26335
Cartographic evaluation of ERTS-1 imagery for area of Bristol, England to show natural and man-made features
[E73-10739] 17 p2021 N73-26345
Geobotanical mapping based on spaceborne photography
[NASA-TT-F-14976] 17 p2026 N73-26392
Mapping of large forest fires from infrared photography
[AD-758613] 17 p2028 N73-26414
Management of natural resources in France and Spain by automatic cartographic inventories from ERTS-1 data
[E73-10725] 18 p2133 N73-27234
Application of ERTS-1 imagery for grid measurement of small water bodies
[E73-10768] 18 p2134 N73-27244
Resources management, land use mapping, and water quality management in Ohio based on ERTS-1 imagery
[E73-10775] 18 p2135 N73-27251
Mapping of wildland vegetation in Great Basin area of Nevada using ERTS-1 imagery
[E73-10813] 18 p2139 N73-27288
Small scale mapping of England and Scotland from ERTS-1 imagery
[E73-10817] 18 p2140 N73-27292
Sampling strategies in thematic land use mapping of Maryland, Virginia, and District of Columbia using Skylab EREP data
[E73-10823] 18 p2140 N73-27298
Mapping snow cover in central Arizona mountains and southern Sierra Nevada of California from ERTS-1 imagery
[E73-10833] 18 p2141 N73-27303
Algorithm for automatic classification and mapping of earth resources satellite data
[NASA-TM-X-64762] 18 p2144 N73-27332
Topographic mapping of Caribbean Sea surface by GEOS-C satellite
[AD-759041] 18 p2147 N73-27354
Application of image sensing arrays to metrology, mapping, and optical data acquisition
[AD-761121] 18 p2149 N73-27370
Israeli use of ERTS-1 imagery to detect and map oil slicks in Gulf of Suez
[E73-10800] 19 p2259 N73-28206
Application of ERTS-1 imagery for vegetative and geologic mapping of western Seward Peninsula, Alaska
[PAPER-A8] 19 p2260 N73-28216
Application of ERTS-1 imagery for mapping and identification of vegetation and landforms in Great Basin
[PAPER-A9] 19 p2260 N73-28217
Application of ERTS-1 imagery for mapping and managing soil and range resources in Sand Hills region of Nebraska
[PAPER-A10] 19 p2260 N73-28218
Analysis of ERTS-1 imagery for extrapolating existing soil maps into unmapped areas of Llanos Orientales of Colombia, South America
[PAPER-A13] 19 p2261 N73-28221
Analysis of ERTS-1 data for application to forest and range mapping in Houston, Texas area
[PAPER-A20] 19 p2262 N73-28227
Evaluation of ERTS-1 data for production of land use stratifications and crop inventory process in San Joaquin County, California
[PAPER-A24] 19 p2262 N73-28231
Quantitative evaluation of computer processed ERTS-1 MSS data classifications to identify major agricultural crops in Illinois
[PAPER-A25] 19 p2262 N73-28232
Evaluation of ERTS-1 imagery for geological surveys and topographical analysis of various terrains in New York State
[PAPER-G1] 19 p2263 N73-28233
Construction of mosaic map of Morocco, North Africa using ERTS-1 data and comparison with data obtained from Gemini 5 flight
[PAPER-G5] 19 p2263 N73-28236
Assessment of geological applications of ERTS-1 imagery from selected areas of Canadian Arctic
[PAPER-G11] 19 p2264 N73-28242
Application of ERTS-1 imagery for recognizing and mapping alpine glacial features in mountains of northwestern Wyoming
[PAPER-G14] 19 p2265 N73-28245
Analysis of geologic features and ground patterns in selected areas of Missouri based on ERTS-1 data
[PAPER-G15] 19 p2265 N73-28246
Analysis of spectral ratioing technique for southern end of of Wind River Range, Wyoming based on ERTS-1 analog ratio images
[PAPER-G16] 19 p2265 N73-28247
Identification of geomorphic features related to known porphyry copper deposit in Pakistan using ERTS-1 imagery
[PAPER-G17] 19 p2265 N73-28248
Analysis of regional structures in Verde Valley region of central Arizona based on ERTS-1 data
[PAPER-G19] 19 p2265 N73-28250
Structural analysis of Nevada using ERTS-1 imagery to identify lineaments of surface manifestations of major fault or fracture zones
[PAPER-G20] 19 p2266 N73-28251
Application of ERTS-1 imagery and ground mapping in southern basin-range province of California, Nevada, and Arizona to show tectonic control of tertiary minerlization
[PAPER-G21] 19 p2266 N73-28252
Application of ERTS-1 imagery for delineating structural features in Alaska and discovery of active strand in Denali fault
[PAPER-G23] 19 p2266 N73-28254
Analysis of ERTS-1 multispectral data by automatic pattern recognition procedures for geological mapping of San Juan Basin, Colorado
[PAPER-G25] 19 p2267 N73-28256
Assessment of ERTS-1 imagery for mapping geologic features of Gaspe Peninsula, Quebec and determination of lithologic lineaments
[PAPER-G28] 19 p2267 N73-28259
Analysis of geological structure in Bighorn Mountains region of Wyoming and Montana based on multispectral band imagery from ERTS-1 satellite
[PAPER-G31] 19 p2267 N73-28262
Application of ERTS-1 imagery for lineament and photogeologic mapping of western Montana
[PAPER-G32] 19 p2268 N73-28263
Analysis of ERTS-1 imagery and high altitude infrared photography to determine geological fractures in Indiana and Illinois
[PAPER-E1] 19 p2268 N73-28265
Digital processing of ERTS-1 data for identification of strip mining areas in west branch area of Susquehanna River and mine drainage in Pennsylvania
[PAPER-E3] 19 p2268 N73-28267
Application of ERTS-1 band six imagery to determine rate of spread of grass fires in Zambesi Basin of South Africa
[PAPER-E6] 19 p2269 N73-28270
Mapping of Atlantic coastal marshlands of Maryland and Georgia using ERTS-1 imagery
[PAPER-E7] 19 p2269 N73-28271
Environmental study of Lake Champlain and Vermont land use based on ERTS-1 imagery
[PAPER-E11] 19 p2270 N73-28275
Application or ERTS-1 imagery for determining course of Ebro River in northeast Spain
[PAPER-W2] 19 p2271 N73-28282
Application of ERTS-1 multispectral imagery to water resources development in lower Mekong River basin in southeast Asia
[PAPER-W3] 19 p2271 N73-28283
Analysis of ERTS-1 imagery of southern Arizona plant communities using electronic satellite image analysis console
[PAPER-W7] 19 p2271 N73-28285
Mapping of snow cover in western areas of US based on ERTS-1 data
[PAPER-W18] 19 p2272 N73-28295
Measurement of percentage of snow cover area on specific drainage basins in Cascade Mountains in Washington state using ERTS-1 imagery
[PAPER-W19] 19 p2273 N73-28296
Cartographic quality of ERTS-1 RBV and MSS imagery
[PAPER-L1] 19 p2273 N73-28297
Mapping techniques using imagery from ERTS and EROS programs
[PAPER-L2] 19 p2273 N73-28298
Land use mapping of Phoenix Quadrangle, Arizona from ERTS-1 Photography
[PAPER-L3] 19 p2273 N73-28299
Linking land use and environmental processes in Central Atlantic Region using ERTS-1 data
[PAPER-L7] 19 p2274 N73-28303
Land cover and land use mapping of Central Atlantic Region shoreline zone using ERTS-1 imagery
[PAPER-L8] 19 p2274 N73-28304
Mapping and digitization of land use in northern megalopolis of Masssachusetts, Connecticut, and Rhode Island using ERTS-1 data
[PAPER-L12] 19 p2274 N73-28308
Land use inventory and mapping in Wyoming from ERTS-1 data
[PAPER-L13] 19 p2274 N73-28309
Utilization of ERTS-1 imagery and data for land use mapping and management in Minnesota
[PAPER-L14] 19 p2275 N73-28310
Land use mapping and inventory of Houston, Texas using ERTS-1 and high altitude photography
[PAPER-L20] 19 p2276 N73-28315
Mapping of agricultural land use in Lancaster and Lebandon Counties, Pennsylvania from ERTS-1 digital data
[PAPER-L22] 19 p2276 N73-28317

Use of temporal dimension in classifying and mapping central Pennsylvania area from ERTS-1 MSS data
[PAPER-L23] 19 p2276 N73-28318
Identification and mapping of coal refuse banks in Pennsylvania anthracite coal fields from ERTS-1 data
[PAPER-L24] 19 p2276 N73-28319
Terrain classification maps of Yellowstone Park from ERTS-1 imagery
[PAPER-L27] 19 p2277 N73-28322
Enhancement of ERTS-1 images by density slicing and application to mapping of Yucca trees in Mojave Desert of Southern California and Nevada
[PAPER-I11] 19 p2278 N73-28332
Calculation of water depth off Little Bahama Bank from ERTS-1 data for use in upgrading and mapping world navigation charts of shallow waters
[PAPER-M20] 19 p2282 N73-28358
Application of ERTS-1 TV imagery to map-making 19 p2283 N73-28366
Mapping land use and detecting land use change in Montgomery County, Alabama using ERTS-1 data 19 p2285 N73-28378
Resectioning programs developed to provide precision annotation of predetermined primary land sampling units on ERTS-1 MSS imagery 19 p2286 N73-28382
Application of ERTS-1 for mapping California, identifying natural resources, and developing programs for environmental improvement 19 p2287 N73-28390
Mapping of flood inundation areas in southwestern Iowa using ERTS-1 imagery 19 p2288 N73-28395
Inventories of agriculture, forestry, and rangeland resources based on ERTS-1 imagery 19 p2288 N73-28396
Development of land management programs based on ERTS-1 imagery and computer compatible tapes for machine processing of data 19 p2288 N73-28397
Application of ERTS-1 imagery for mineral resources, geologic structure, and landform surveys 19 p2288 N73-28398
Application of ERTS-1 imagery for controlling quantity and quality of ground water resources 19 p2288 N73-28399
Application of ERTS-1 imagery to programs conducted by Department of Interior 19 p2289 N73-28401
Application of ERTS-1 imagery to land use inventory and management and mapping techniques 19 p2289 N73-28407
Uniform mapping and monitoring of natural ecosystems and environments in California, Louisiana, and Colorado from ERTS-2 imagery
[E73-10839] 19 p2290 N73-28417
Utilization of ERTS-1 imagery for mapping and control of pink bollworm in Imperial, Coachella, and Palo Verde Valleys of California
[E73-10858] 19 p2292 N73-28435
Homomorphically estimated restoration filter for removing image blurs 19 p2320 N73-28668
Computer maps of land use in Titusville, Florida
[E73-10852] 20 p2391 N73-29209
Application of ERTS data for mapping distribution of glaciofluvial deposits and associated glacial landforms
[E73-10867] 20 p2392 N73-29218
Mapping exposed silicate rock types and exposed ferric and ferrous compounds from Skylab
[E73-10877] 20 p2393 N73-29228
Field sampling taxonomic units within geomorphic-soil-vegetation mapping units in Arizona
[E73-10889] 20 p2394 N73-29238
Resources management in France through automatic cartographic inventory
[E73-10894] 20 p2395 N73-29243
Computer processing of Skylab MSS data for land use mapping of Baltimore, Maryland-Washington, D.C. area
[E73-10913] 20 p2397 N73-29262
Identification, definition, and mapping vegetation and terrestrial ecosystems in interior Alaska using ERTS-1 imagery
[E73-10921] 20 p2398 N73-29270
Geological, hydrological, ecological, and agricultural mapping of Botswana from ERTS-1 photography
[E73-10928] 20 p2399 N73-29277
Interpretation of space photographs of dry piedmont steppe region for hydrologic mapping
[NASA-TT-F-14974] 20 p2411 N73-29382
Water, agriculture, and soil resource management and planning in California using ERTS-1 imagery
[E73-10935] 21 p2529 N73-30277
Ground-based radiation thermometry mapping of volcanology in Central America
[E73-10937] 21 p2529 N73-30279
Detection and mapping of soil erosion and flooding in southern Arizona
[E73-10950] 21 p2531 N73-30292
Cartographic applications of ERTS-1 RBV imagery in polar regions
[E73-10953] 21 p2531 N73-30295
Land use mapping and modelling for Phoenix Quadrangle using ERTS-1 imagery
[E73-10955] 21 p2531 N73-30297
User manual for Los Angeles Basin Standard Traffic Model
[FAA-RD-73-89] 21 p2576 N73-30647
User manual for Los Angeles Standard Traffic Model computer tapes
[FAA-RD-73-88] 21 p2577 N73-30649
Galactic nucleus map at ten microns with few arc second resolutions
[LPL-COMMUN-169] 21 p2592 N73-30765
Uniform mapping of rice crops in Louisiana and California and desert vegetation in southwestern Colorado from Skylab imagery
[E73-10979] 22 p2657 N73-31286
Utilization of ERTS-1 imagery for studies of agriculture, forestry, cartography, geography, hydrology, meteorology, geology, and oceanography in Thailand
[E73-10996] 22 p2659 N73-31302
Identification and mapping landform and land use characteristics and surficial geologic materials in Great Plains and Midwest
[E73-11025] 22 p2662 N73-31329
Snow cover surveys of Sierra Nevada, Cascades, and Wasatch mountains using Skylab EREP data
[E73-11036] 22 p2663 N73-31340
Research and development in topographic mapping, field surveys, photogrammetry, orthophotomapping, and space technology
[PB-221469] 22 p2669 N73-31384
Star mapper using solid-state detectors discussing dioptric and mirror objectives, and star recognition algorithms
[ESRO-CR-82] 22 p2698 N73-31610
Star mapper breadboard model for satellite attitude control using either photomultipliers or Si photodiodes
[ESRO-CR-162] 22 p2698 N73-31611
Detection and mapping snow cover in Arizona and California from ERTS-1 imagery
[E73-11038] 23 p2778 N73-32217
Identification, definition, and mapping of terrestrial ecosystems in interior Alaska
[E73-11065] 23 p2781 N73-32241
Multidisciplinary research on water depth measurement, Yellowstone Park, atmospheric effects, lake ice surveillance, recreational land use, IFYGL, image enhancement, water quality, oil pollution detection, and mapping iron compounds from ERTS-1 data
[E73-11119] 23 p2783 N73-32264
Image maps of point targets applied to hard limited, synthetic aperture radar application
[AD-763660] 23 p2788 N73-32306
Metric cartographic potential of geostationary/geosynchronous satellite camera 24 p2912 N73-33238
Interpretation of aeromagnetic or gravity data by method of difference mapping for mineral exploration 24 p2912 N73-33240
Regional and local land use planning and mapping of Ohio from Skylab EREP data
[E73-11090] 24 p2914 N73-33252
Land use mapping and modelling for Phoenix Quadrangle
[E73-11098] 24 p2914 N73-33255
Photointerpretation and digital data mapping of land use in Pennsylvania
[E73-11106] 24 p2915 N73-33263
Mapping of anthracite wastes from mining in Pennsylvania
[E73-11107] 24 p2915 N73-33264
Sampling strategies in land use mapping using Skylab EREP multispectral photography
[E73-11139] 24 p2918 N73-33294
Uniform mapping of vegetation and rice in Colorado Plateau, Sierra-Lahontan, California, and Louisiana coastal plain from Skylab multispectral photography
[E73-11149] 24 p2919 N73-33303

**MAPS**
NT ASTRONOMICAL MAPS
NT LUNAR MAPS
NT METEOROLOGICAL CHARTS
NT PHOTOMAPS
NT RADAR CLUTTER MAPS
NT RADAR MAPS
NT RELIEF MAPS

Preparation of hydrologic atlases of arid land watersheds using ERTS-1 imagery of Wyoming, Utah, Montana, and New Mexico
[E72-10240] 03 p0288 N73-12340
Development of holographic storage and retrieval system for aerial chart information display in cockpit environment
[AD-748648] 03 p0330 N73-12690
Digitizing of topographic maps for electronic data processing
[MITT-130] 04 p0414 N73-13379
Gravimetric map of Australia
[AD-747873] 04 p0417 N73-13405
Stratospheric daily altitude maps and monthly mean maps of Northern Hemisphere 05 p0570 N73-14633
Stratospheric daily altitude maps and monthly mean maps of Northern Hemisphere 05 p0571 N73-14634
Technical evaluation of cartography for use in civil air navigation map displays to determine information elements required to operate in 1975 to 1980 airspace - Vol. 1
[FAA-RD-72-129-VOL-1] 10 p1155 N73-19393
Evaluation of cartographic information for use in civil air navigation map displays to determine information elements required to operate in 1975 to 1980 airspace - Vol. 2
[FAA-RD-72-129-VOL-2] 10 p1155 N73-19394
Arizona aeromagnetic map from data of digitally recording proton precession magnetometer 13 p1514 N73-22265
Terrain factor analysis and automatic color coded mapping using image processing methods in estimation of construction time relative to prospective military airfields
[AD-755531] 13 p1526 N73-22367
Continuous dependence of fixed points of condensing maps
[NASA-CR-132021] 14 p1684 N73-23664
Neutral hydrogen aperture synthesis maps of IC2574 and NGC 7640 galaxies
[AD-757688] 15 p1833 N73-24856
Geological Mars map deduced from Mariner 9 surface photography 23 p2838 N73-32682

**MARAGING STEELS**
Heat treatment and forging effects on mechanical properties of maraging steel
[AD-756422] 13 p1543 N73-22507
Billet processing from rapidly quenched liquid metals
[AD-757677] 14 p1678 N73-23621
Rotating electrode process for processing 18Ni maraging steel by powder metallurgy
[AD-758439] 15 p1800 N73-24589
Electrochemical and mechanical parameters of localization hydrogen in iron and maraging steel using high resolving power autoradiography
[RAE-LIB-TRANS-1665] 17 p2044 N73-26533
Mechanical properties of double melted 18 percent Ni-Co-Mo maraging steel bar or forgings
[S/T-MEMO-3-72] 18 p2161 N73-27457

**MARIA**
NT LUNAR MARIA

**MARINE BIOLOGY**
Ultrasonic marine biotelemetry transmitter utilizing metal oxide semiconductor integrated circuits
[AD-748605] 04 p0383 N73-13119
Development and characteristics of self-contained, portable data acquisition system for conducting marine and ecological research 04 p0471 N73-13842
Utilization of ERTS-1 imagery in air pollution and marine biology studies of lower Chesapeake Bay and continental shelf of Eastern US
[E72-10367] 05 p0535 N73-14355
Investigation of phytoplankton populations in waters along eastern coast of US using ERTS-1 imagery and surface measurements
[E73-10097] 08 p0902 N73-17308
Research in protecting equipment from tropical environment and seas 10 p1228 N73-19986
Effect of sonic boom on fish and fish eggs during developmental stage
[FAA-RD-73-29] 11 p1247 N73-20121
Marine biology literature compilation for Caribbean Sea and adjacent regions 14 p1607 N73-23022
Relation of chlorophyll and suspended sediment content in lower Chesapeake Bay to ERTS-1 imagery and application of marine station data to study of productivity along eastern shelf waters of US
[E73-10593] 15 p1772 N73-24358
Marine luminescence data for monitoring algal and pollutant concentrations
[NASA-CR-114578] 16 p1867 N73-25114
Application of ERTS-1 data to develop and implement utilization of living marine resources in Mississippi Sound
[E73-10707] 16 p1904 N73-25398
Establishment of data management system for ERTS-1 data by National Marine Fisheries Service Engineering Laboratory
[E73-10720] 17 p2019 N73-26327
Analysis of ERTS-1 data for interdisciplinary study of estuarine and coastal oceanography of Block Island Sound and adjacent New York coastal waters
[E73-10735] 17 p2020 N73-26341
Analysis of ERTS-1 data for interdisciplinary study of estuarine and coastal oceanography of Block Island Sound and adjacent New York coastal waters
[E73-10736] 17 p2020 N73-26342
Application of ERTS-1 imagery for determining availability and distribution of menhaden within Mississippi Sound adjacent waters
[E73-10751] 17 p2022 N73-26354
Biological oceanography by airborne spectrophotometer
[NASA-CR-133325] 18 p2147 N73-27353
Analysis of coastal vegetation species in Delaware Bay, Delaware based on ERTS-1 imagery and high altitude photography
[PAPER-E8] 19 p2269 N73-28272

ERTS-1 imagery for monitoring dumping of municipal and industrial wastes in New York Bight
[PAPER-E10] 19 p2269 N73-28274
Analysis of ERTS-1 multispectral scanner imagery to determine polluted and turbid water masses in Osaka Bay, Japan
[PAPER-E14C] 19 p2270 N73-28280
ERTS-1 imagery of biomass in upwelling waters along northwest coast of Africa
[PAPER-M15] 19 p2281 N73-28354
Assessment of ERTS-1 imagery for identification of marine resources to include sources of pollution, beach erosion, and navigation in ice-filled waterways
19 p2289 N73-28402
Application of multispectral scanning to sea surface temperature, coastal topography and water sediment load, marine biology, sea ice, and oil slicks
19 p2295 N73-28455
Identification of female specimen of Trichocorixa reticulata in waters of Gulf of California
[E73-10926] 20 p2398 N73-29275
Seasonal plankton collections conducted during Tenth Antarctic Expedition
20 p2409 N73-29363
Collection of phytoplankton and chlorophyll samples from waters of Chesapeake Bay
[E73-11154] 24 p2919 N73-33308

**MARINE ENVIRONMENTS**
Environmental studies of sedimentation and nearshore marine processes in Cook Inlet, Alaska, and regional study of permafrost regimes in Alaska using ERTS-1 imagery
[E72-10209] 02 p0161 N73-11304
Utilization of ERTS-1 imagery to determine availability and distribution of menhaden within Mississippi Sound and adjacent waters
[E72-10279] 03 p0292 N73-12377
Study of marine environment of northern Gulf of California using ERTS-1 MSS imagery
[E72-10283] 03 p0292 N73-12381
Oceanography and marine environment of Gulf of California based on ERTS-1 imagery
[E73-10021] 08 p0900 N73-17286
ERTS-1 imagery of oceanography and marine environment of northern Gulf of California
[E73-10304] 09 p1021 N73-18336
Military technology for marine radar design
[AD-754408] 11 p1259 N73-20215
ERTS-1 imagery of inner shelf and coastal sedimentation environment of Beaufort Sea, Alaska
[E73-10412] 11 p1278 N73-20374
ERTS-1 imagery of inner shelf and coastal sedimentation environment of Beaufort Sea
[E73-10492] 12 p1397 N73-21328
Extremely low frequency radio communication in ocean environment
[PB-213904/6] 14 p1636 N73-23264
Investigation of marine environment of northern Gulf of California using ERTS data collection platforms
[E73-10550] 14 p1655 N73-23423
Detection of adult menhaden fish in Mississippi Sound from ERTS-1 imagery
[E73-10624] 15 p1775 N73-24384
Detailed environmental profiles for seven potential Gulf Coast deep water port sites
[AD-758455] 15 p1806 N73-24637
Marine science newsletters - 1973 annotated bibliography
[NOAA-TM-EDS-NODC-3] 16 p1906 N73-25417
Survey of atmospheric aerosol concentrations over seas
[PB-214170/3] 16 p1909 N73-25442
Design technology of aeronautical satellite communication system for air traffic control over Atlantic Ocean
[FAA-ED-17-1] 18 p2115 N73-27104
Position reporting and cmmunications systems of aviation and marine rescue operations
[AD-761756] 19 p2228 N73-27967
Influence of sea ice on coastal marine environment of Beaufort Sea, Alaska
[PAPER-M7] 19 p2280 N73-28346
Application of classification algorithms to ERTS-1 MSS imagery of Texas land and water coastal features
19 p2286 N73-28383
Application of ERTS-1 imagery to study of coastal areas and processes
19 p2286 N73-28386
Assessment of ERTS-1 imagery for identification of marine resources to include sources of pollution, beach erosion, and navigation in ice-filled waterways
19 p2289 N73-28402
Significant results from marine resources and ocean surveys of discipline overall ERTS program
19 p2290 N73-28411
Utilization of ERTS-1 data for regulation, protection, and management of New Jersey coastal environment
[E73-10845] 19 p2291 N73-28423
Solar radiation effects on photosynthesis of submerged aquatic plants
20 p2405 N73-29327
Classification of coastal environments along Americas and Africa
[AD-761193] 20 p2415 N73-29412
Oceanography and marine environment of northern Gulf of California
[E73-10941] 21 p2529 N73-30283
Utilization of ERTS-1 imagery to determine availability and distribution of adult Gulf menhaden within Mississippi Sound and adjacent waters
[E73-10980] 22 p2657 N73-31287
Skylab oceanic gamefish operations in Gulf of Mexico
[E73-11157] 24 p2919 N73-33311

**MARINE METEOROLOGY**
First-order analyses of wind and current time series from Totem buoy off Oregon coast during 1970
[AD-746832] 02 p0206 N73-11668
Analysis of oceanographic/meteorological sensors for ocean data stations
[AD-755755] 12 p1425 N73-21552
Tables of synoptic meteorological observations for Japanese and Korean coastal marine areas
[AD-757107] 14 p1685 N73-23674
Numerical advection model for simulating maritime fog
[AD-757328] 14 p1685 N73-23676
Analysis of errors in wind measurements from ocean data buoys
[AD-757981] 14 p1686 N73-23685
Computerized simulation of maritime cumulus clouds considering meteorological parameters and cloud seeding
[AD-759368] 16 p1939 N73-25693
Synoptic marine meteorological observations of Chinese and Taiwan coastal areas - Vol. 2
[AD-760333] 17 p2058 N73-26647
Random errors of marine meteorological observations by ships in tropical Atlantic Ocean
20 p2447 N73-29659
Synoptic meteorological data for Philippine coastal marine surfaces
[AD-762424] 20 p2450 N73-29688
Synoptic meteorological data for Philippine and Vietnam coastal marine surfaces
[AD-762425] 20 p2450 N73-29689
Statistical procedures for hydrometeorological and weather forecasting and climate control
[JPRS-59580] 21 p2572 N73-30612
Mean monthly values of turbulent heat and moisture fluxes over oceans
21 p2572 N73-30613
Environmental conditions of offshore east and west coasts of US and in Gulf of Mexico
23 p2786 N73-32288
Theoretical studies of growth of marine fog droplets
[AD-764597] 23 p2815 N73-32503

**MARINE NAVIGATION**
U SURFACE NAVIGATION

**MARINE PROPULSION**
NT UNDERWATER PROPULSION
Reaction engines with shrouded nozzles, reaction engines for boats, and thermodynamics of hot air bubble cooling in liquid
[JPRS-57308] 04 p0404 N73-13292
Direct reaction engines for water surface vessels, using admixture of air and outboard water
04 p0404 N73-13295
Vortice distribution field for calculating inlet flow of ducted propeller
[AD-754114] 10 p1144 N73-19318
Development of design criteria for maximum horsepower to be transmitted using cycloidal cam transmission and application to marine gas turbine engines
[AD-754822] 11 p1301 N73-20554
Application of cryogenic and superconductive systems for propulsion of ships
[AD-758431] 14 p1694 N73-23746

**MARINE TECHNOLOGY**
Development and characteristics of self-contained, portable data acquisition system for conducting marine and ecological research
04 p0471 N73-13842
Oceanographic equipment and ocean bottom data resulting from Pacific cruise of Iguana
[AD-750679] 06 p0671 N73-15459
Technical utilization of advanced equipment for oceanological exploitation by US
[JPRS-58696] 12 p1401 N73-21363
Measurements and procedures for processing measurement data in marine geodesy
[JPRS-58824] 13 p1522 N73-22335
Synthesis of fire resistant phosphonitrilic plastics and elastomers for marine applications
[AD-755188] 13 p1548 N73-22547
Manned submerzible ocean bottom sampling and gravimetric prospecting
[AD-759992] 17 p2029 N73-26425
Environmental conditions of offshore east and west coasts of US and in Gulf of Mexico
23 p2786 N73-32288

**MARINER PROGRAM**
NT MARINER VENUS-MERCURY 1973
Saturn satellite encounter opportunities for Mariner Jupiter-Saturn 1977 project
23 p2838 N73-32838

**MARINER SPACE PROBES**
NT MARINER VENUS-MERCURY 1973
NT MARINER 3 SPACE PROBE
NT MARINER 6 SPACE PROBE
NT MARINER 7 SPACE PROBE
NT MARINER 9 SPACE PROBE
Errors in Doppler residuals of Mariner 6 and 7 Martian atmospheric occultation data
02 p0196 N73-11599
Tracking and data system report for Mariner Mars 1971 mission
[NASA-CR-132955] 15 p1761 N73-24270
Design and flight performance of Mariner Mars 1971 power subsystem
[NASA-CR-132992] 16 p1864 N73-25096
Mariner Mars 1971 sun sensor model development and simulation
[NASA-CR-132990] 16 p1912 N73-25468
Mariner 9 solar array design, manufacture, and performance
[NASA-CR-132991] 16 p1912 N73-25469

**MARINER SPACECRAFT**
Design operation, testing, and calibration of Mariner Mars 1971 ultra violet spectrometer
[NASA-CR-128493] 02 p0172 N73-11396
Mariner Mars 1971 radio frequency subsystem to provide communication link between spacecraft and Deep Space Instrumentation Facility
[NASA-CR-130866] 08 p0885 N73-17164
Method for calculating transient thrust and flowrate levels for Mariner type attitude control nitrogen gas jets
[NASA-CR-132987] 16 p1888 N73-25279
Numerical analysis of space navigation parameters for interplanetary Mars spacecraft based on equations of motion of spacecraft
[NASA-TT-F-14897] 16 p1940 N73-25704
Analysis and simulation of Mariner Mars 1971 scan platform, and spacecraft dynamic interaction
[NASA-CR-133793] 21 p2600 N73-30837
Silicon vidicon camera for slow scan operation onboard Mariner spacecraft
22 p2732 N73-31862

**MARINER VENUS-MERCURY 1973**
Error analysis for measurements of Mariner Venus Mercury 1973 gain, antenna patterns, and insertion loss of cables
[NASA-CR-133230] 17 p1997 N73-26148
Score, approach, and major results of study of ballistic mode Mercury orbit missions
[NASA-CR-114617] 22 p2715 N73-31733
Scope, approach, and major results of study of ballistic mode of Mercury orbit missions
[NASA-CR-114618] 22 p2715 N73-31734

**MARINER 3 SPACE PROBE**
Water content of Mars atmospheres as measured by Mars 3 automatic space station
[JPRS-59231] 15 p1830 N73-24833

**MARINER 6 SPACE PROBE**
Mariner 6 and 7 television photographs of Mars
[NASA-SP-263] 04 p0475 N73-13878
Using Mariner 6 and 7 photographs to investigate nature of linear trends on Mars
[NASA-TM-X-62264] 14 p1703 N73-23817

**MARINER 7 SPACE PROBE**
Mariner 6 and 7 television photographs of Mars
[NASA-SP-263] 04 p0475 N73-13878
Using Mariner 6 and 7 photographs to investigate nature of linear trends on Mars
[NASA-TM-X-62264] 14 p1703 N73-23817

**MARINER 9 SPACE PROBE**
Design and in-flight performance of Mariner 9 spacecraft propulsion system
[NASA-CR-129097] 02 p0222 N73-11795
Atmospheric dust and circulation, carbon dioxide and water vapor transmittancies, surface pressure; and topography of Mars determined from Mariner 9 infrared spectrometers
[NASA-TM-X-66150] 06 p0718 N73-15864
Solar radiation pressure on Mariner 9 Mars Orbiter
[NASA-CR-130724] 08 p0957 N73-17831
Mariner 9 photographs of Martian shield volcanoes
[NASA-TM-X-62222] 09 p1084 N73-18841
Mariner 9 space probe microfiche library
[NASA-CR-130925] 10 p1128 N73-19193
Collection of data relating to Mariner 9 TV pictures
[NASA-CR-131416] 11 p1337 N73-20850
Mariner Mars 1971 development through launch and trajectory correction maneuver
[NASA-CR-131268] 11 p1338 N73-20855
Derivation of temperature fields from Mariner 9 infrared spectroscopy and calculation of Martian atmospheric tidal pressure and wind fields
[NASA-TM-X-66230] 12 p1458 N73-21818
Availability of Mariner 9 TV picture data
[NASA-TM-X-69216] 14 p1704 N73-23822
Geological features of Martian surface based on Mariner 9 photographs
[NASA-TT-F-14840] 14 p1704 N73-23831
Mission operations system implementation and standard mission flight operations for Mariner 9
[NASA-CR-133184] 17 p2082 N73-26844
Mariner 9 spectroscopic evidence for H2O ice clouds in Martian atmosphere
[NASA-TM-X-66289] 18 p2142 N73-27312
Sequence design and picture coverage catalog for Mariner Mars 1971 television pictures
[NASA-CR-133614] 20 p2473 N73-29864

Mariner 9 space probe storage subsystem for flight performance
[NASA-CR-133653] 20 p2475 N73-29884
Geodetic control net of Mars based on Mariner 9 television pictures
[NASA-CR-133845] 21 p2596 N73-30808
Wind tunnel studies of Martian aeolian processes
[NASA-TM-X-62297] 22 p2716 N73-31746
Mariner 9 observations on Mars atmosphere and surface
22 p2735 N73-31892
User guide to Mariner 9 television reduced data record
[NASA-CR-135712] 23 p2793 N73-32347
Scientific Mars research by Mariner 9 space probe
[NASA-CR-135530] 23 p2838 N73-32680
Geological Mars data obtained by Mariner 9 observations
23 p2838 N73-32681
Geological Mars map deduced from Mariner 9 surface photography
23 p2838 N73-32682
Mariner 9 range and Doppler data analyses for relativistic time delay effects
23 p2842 N73-32711
Planetary ephemerides for Mariner 9 based on radar range data using normal points
23 p2842 N73-32714
Performance of Mariner 9 television cameras
23 p2843 N73-32718
Mariner 9 missions operations summary
23 p2844 N73-32725
Objectives of experiments on Mariner 9 space probe
[NASA-CR-135726] 24 p2983 N73-33834
Project objectives and mission profile for Mariner Mars 1971
24 p2983 N73-33835
Celestial mechanics for Mariner 9 space probe
24 p2983 N73-33836
Summary of S band occultation experiment
24 p2983 N73-33837
Objectives of infrared radiometry experiment
24 p2983 N73-33838
Overview of infrared spectroscopy experiment on Mariner 9 space probe
24 p2983 N73-33839
Ultraviolet spectrometer experiment on Mariner 9 space probe
24 p2983 N73-33840
Television experiment on Mariner 9
24 p2983 N73-33841
Atmospheric processes on Mars based on atmospheric observations from Mariner 9
24 p2984 N73-33844

**MARKET RESEARCH**
Market research, economic analysis, and technology of conventional STOL aircraft in Europe
[DGLR-PAPER-72-54] 06 p0622 N73-15046
Trends in usage of tungsten including analyses of supply/demand balance and possible substitutes
[NMAB-309] 22 p2684 N73-31495
Concepts of expanding airline marketing strategies
23 p2862 N73-32874

**MARKETING**
Economic factors, financial management, production and marketing for air transport industry
[NASA-CR-135634] 23 p2860 N73-32848
Marketing and cost effectiveness in air transportation economics
23 p2860 N73-32855
Economic efficiency in pricing of air transport services
23 p2860 N73-32856
Differential pricing policy in airline operations
23 p2861 N73-32857
Demand factors in air transportation marketing
23 p2861 N73-32863
Economic risk analysis for propeller STOL transport market
23 p2861 N73-32866
Economic market structure of airline industry
23 p2862 N73-32869
Consumer marketing for airline industry
23 p2862 N73-32873

**MARKING**
NT ISOTOPIC LABELING
Exogenetic and endogenetic origin of sinuous markings on lunar mare
12 p1455 N73-21784
Comparative evaluation of point marking devices and their suitability for photogrammetric problems
13 p1528 N73-22383

**MARKOV CHAINS**
Markov chain model for classifying stochastic automation
02 p0195 N73-11579
Following theory for feedback controls, Markov processes, and flow of automobiles and aircraft
10 p1136 N73-19259
Dispersion of angular coordinate estimate during digital processing of radar data based on application of discrete Markov chains
22 p2628 N73-31058
Application of Monte Carlo method and Markov random walks to determine molecular diffusion through rarefied gas
[NASA-TN-D-7405] 23 p2776 N73-32197
Application of random walks for search optimization and function space
24 p2944 N73-33514

**MARKOV PROCESSES**
NT MARKOV CHAINS
Two dimensional, second order Markov process representation for recursive restoration of images
[USC-113P19-31] 02 p0146 N73-11182
Shortwave propagation medium with random heterogeneities in approximate Markovian random process
[AD-746714] 02 p0203 N73-11644
Model for analyzing Markovian decision processes with unobservable states and costs
[P-4917] 12 p1419 N73-21495
Markovian decision processes with limited state observability and unobservable costs
[P-4925] 12 p1419 N73-21496
Markov model for analyzing tracking disruption in automatic radio operation
14 p1619 N73-23116
Markov random processes for tracking disruption analyses on quasi-stationary systems
17 p1997 N73-26150
Theory and application of random Markov processes to analysis of tracking disruption
18 p2169 N73-27520
Statistical analysis on Markovian plasma turbulence using perturbed particle propagator
22 p2702 N73-31644
Stochastic processes and dynamic systems noting Markov and Ito-Markov processes
[LAAS-AS-73-1-09] 24 p2945 N73-33519

**MARROW**
Stomach shielding effects on chromosomal aberration frequency in guinea pig and rat marrow cells after gamma radiation at doses of 50 to 200 r
11 p1241 N73-20074

**MARS [PLANET]**
Application of laser rangefinder on autonomous Martian roving vehicle for navigation and mid-range path selection
[NASA-CR-128398] 01 p0064 N73-10523
Analysis of magnetic field near planet Mars from data obtained by Mars 2 and Mars 3 spacecraft
[NASA-TM-X-66116] 03 p0357 N73-12907
Biological effects of Viking Lander spacecraft engine fuel on extraterrestrial life during landing on planet Mars
[NASA-TM-X-2714] 06 p0630 N73-15118
Characteristics and requirements of instruments for advanced Viking seismic experiments on Mars
[NASA-CR-130358] 06 p0717 N73-15850
Analysis of selected features of Mercury, Venus, and Mars and seismic propagation on Moon
07 p0840 N73-16807
Buckling modes of four optimized Mars entry aeroshell configurations at angle of attack loadings based on experimental pressure distributions
[NASA-CR-2087] 07 p0852 N73-16907
Simulation and evaluation of proposed path selection systems for autonomous Martian Roving vehicle
[NASA-CR-130978] 09 p1010 N73-18242
Photometric analysis of violet clouds on planet Mars and determination of monochromatic albedo
09 p1083 N73-18834
Photoelectric measurements of brightness distribution and brightness phase dependence of spheres with different colors and roughness to find optical properties of Mars surface
09 p1083 N73-18837
Derivation of temperature fields from Mariner 9 infrared spectroscopy and calculation of Martian atmospheric tidal pressure and wind fields
[NASA-TM-X-66230] 12 p1458 N73-21818
Mars bibliography, including topography and atmosphere
[AD-759291] 18 p2198 N73-27743
Procedures and instrumentation for life detection on Mars
[NASA-CR-133186] 19 p2344 N73-28854
Sequence design and picture coverage catalog for Mariner Mars 1971 television pictures
[NASA-CR-133614] 20 p2473 N73-29864
Geodetic control net of Mars based on Mariner 9 television pictures
[NASA-CR-133845] 21 p2596 N73-30808
Search for biological life forms on Mars and other planets
22 p2619 N73-30985
Mariner 9 television observations of Martian planets Phobos and Deimos
23 p2841 N73-32705
Celestial mechanics analysis on Mariner 9 Doppler tracking data for determining Mars gravitational field
23 p2841 N73-32706
Mariner 9 Doppler tracking short data arcs for determining Mars gravitational field
23 p2841 N73-32707
Mariner 9 Doppler tracking data filtering method for determining Mars gravity
23 p2841 N73-32708
Range points in relativistic test of celestial mechanics in Mariner 9 Doppler tracking data analysis for Mars gravity
23 p2842 N73-32710
Subsurface characteristics of Mercury and Mars determined by analysis of thermal microwave emission
24 p2979 N73-33801

**MARS ATMOSPHERE**
Errors in Doppler residuals of Mariner 6 and 7 Martian atmospheric occultation data
02 p0198 N73-11599
Photodissociative excitation of carbon dioxide as source of atomic oxygen in Martian atmosphere
[NASA-TM-X-66088] 02 p0229 N73-11856
Possibilities of obtaining temperature profiles for Mars atmosphere by thermal sounding
[NASA-TT-F-14715] 02 p0229 N73-11859
Directions of strong Martian winds inferred from Mariner 6 and 7 photographs and relation to dust storms and topographic wind funneling
[NASA-CR-129520] 03 p0354 N73-12885
Atmospheric dust and circulation, carbon dioxide and water vapor transmittancies, surface pressure; and topography of Mars determined from Mariner 9 infrared spectrometers
[NASA-TM-X-66150] 06 p0718 N73-15864
Microphotometer analysis of absorption spectra, physical and chemical properties of NO2 system in Martian atmosphere
07 p0752 N73-16107
Space vehicle descent into Mars, Jupiter, and Venus atmospheres
[NASA-TT-F-768] 07 p0844 N73-16838
Investigation of physical characteristics of Mars atmosphere and surface as reported by Mars 2 and Mars 3 orbital spacecraft
[NASA-TT-F-14814] 08 p0961 N73-17863
Measurement of water content of Martian atmosphere by Mars 3 spacecraft
[NASA-TT-F-14815] 08 p0961 N73-17864
Analysis of Martian atmosphere data obtained from Mars 2 spacecraft
[NASA-TT-F-14817] 08 p0961 N73-17865
Mariner 6 and 7 flybys measuring hot CO on Mars with ultraviolet scanning spectrometers
08 p0973 N73-17955
Chemical dynamic model of moist Martian atmosphere
[NASA-CR-130799] 09 p1082 N73-18825
Survival and reproduction of protozoa in simulated Mars environment
10 p1118 N73-19115
Microorganism survival in simulated Mars environment
10 p1118 N73-19116
Jovian emission spectrum analysis for temperature and ammonia profiles, and Martian infrared limb profile analysis for atmospheric temperature and water vapor
[NASA-CR-131266] 11 p1337 N73-20847
Derivation of temperature fields from Mariner 9 infrared spectroscopy and calculation of Martian atmospheric tidal pressure and wind fields
[NASA-TM-X-66230] 12 p1458 N73-21818
Results of Mars 2 and Mars 3 space probes
[NASA-TT-F-14914] 14 p1709 N73-23869
Onboard, on-line parameter updating for Mars stratosphere and troposphere, using maximum likelihood estimation
15 p1829 N73-24821
Water content of Mars atmospheres as measured by Mars 3 automatic space station
[JPRS-59231] 15 p1830 N73-24833
Mariner 9 spectroscopic evidence for H2O ice clouds in Martian atmosphere
[NASA-TM-X-66289] 18 p2142 N73-27312
Mariner 9 observations on Mars atmosphere and surface
22 p2735 N73-31892
Radiative-conductive heat transfer and circulation of lower Martian atmosphere
[NASA-CR-2318] 23 p2786 N73-32287
Scientific Mars research by Mariner 9 space probe
[NASA-CR-135530] 23 p2838 N73-32680
Mariner 9 television observations of Mars atmosphere variations
23 p2840 N73-32699
Infrared spectra of Mars atmospheric and surface properties
23 p2840 N73-32700
Ultraviolet evening terminator observations in Martian atmosphere by Mariner 9 space probe
23 p2841 N73-32702
Ultraviolet spectrometer data on Mars atomic oxygen emission and distribution
23 p2841 N73-32703
Seasonal ozone variations in ultraviolet spectra of Mars atmosphere
23 p2841 N73-32704

Mariner 9 S band radio occultation measurements of Mars polar and intermediate latitude atmosphere and topography
23 p2843 N73-32716
Mariner 9 radio occultation approximations of Mars surface and atmosphere
23 p2843 N73-32717
Physical behavior of water and carbon dioxide on Mars
24 p2984 N73-33843
Atmospheric processes on Mars based on atmospheric observations from Mariner 9
24 p2984 N73-33844

**MARS ENVIRONMENT**
NT MARS ATMOSPHERE
Survival and reproduction of protozoa in simulated Mars environment
10 p1118 N73-19115
Design and performance of photostat for simulating Mars environment
10 p1118 N73-19117
Derivation of temperature fields from Mariner 9 infrared spectroscopy and calculation of Martian atmospheric tidal pressure and wind fields
[NASA-TM-X-66230] 12 p1458 N73-21818
Photographic determinations of Mars satellites orbital parameters
16 p1961 N73-25860

**MARS LANDING**
Analysis and design of capsule landing system and surface vehicle control system for Mars exploration
[NASA-CR-131515] 12 p1459 N73-21825
Unmanned roving vehicle design for surface exploration of Mars
16 p1884 N73-25252
Analysis of requirements for unmanned spacecraft mission to planet Mars and characteristics of lander vehicles for planetary exploration - Vol. 3
[NASA-CR-132258] 16 p1962 N73-25875
Thermal stress and mechanical shock effects on release of bacterial spores from stainless steel surfaces with application to Mars landing
[NASA-CR-133868] 22 p2619 N73-30987

**MARS PROBES**
NT MARINER 3 SPACE PROBE
NT MARINER 6 SPACE PROBE
NT MARINER 7 SPACE PROBE
NT MARS 2 SPACECRAFT
NT MARS 3 SPACECRAFT
NT VIKING LANDER SPACECRAFT
NT VIKING MARS PROGRAM
NT VIKING ORBITER SPACECRAFT
NT VIKING 75 ENTRY VEHICLE
Analysis of Martian atmosphere data obtained from Mars 2 spacecraft
[NASA-TT-F-14817] 08 p0961 N73-17865
Analysis of Mariner 71 attitude control subsystem flight performance and effects of performance anomalies on subsystem operation
[NASA-CR-131522] 12 p1461 N73-21835
Results of Mars 2 and Mars 3 space probes
[NASA-TT-F-14914] 14 p1709 N73-23869

**MARS SPACECRAFT**
U MARINER SPACECRAFT

**MARS SURFACE**
Procedure for assaying enzyme activity in soils and application to presumptive life tests in Martian soil
[NASA-CR-128399] 01 p0008 N73-10059
Application of laser rangefinder on autonomous Martian roving vehicle for navigation and mid-range path selection
[NASA-CR-128398] 01 p0064 N73-10523
Mariner 6 and 7 television photographs of Mars
[NASA-SP-263] 04 p0475 N73-13878
Atmospheric dust and circulation, carbon dioxide and water vapor transmittancies, surface pressure; and topography of Mars determined from Mariner 9 infrared spectrometers
[NASA-TM-X-66150] 06 p0718 N73-15864
Experimental design and scientific exploration of Mars surface by MARV
[NASA-TM-X-64719] 07 p0765 N73-16219
Investigation of physical characteristics of Mars atmosphere and surface as reported by Mars 2 and Mars 3 orbital spacecraft
[NASA-TT-F-14814] 08 p0961 N73-17863
Photometric profiles of dust particle size and dust cloud origins during dust storms on Mars as reported by Mars 3 Automatic Interplanetary Station
[NASA-TT-F-14818] 08 p0962 N73-17866
Interpretation of Mariner 6 and 7 Martian photometry for sediment geomorphology
[NASA-CR-2194] 08 p0962 N73-17869
Mariner 9 photographs of Martian shield volcanoes
[NASA-TM-X-62222] 09 p1084 N73-18841
Analysis of correlation between Martian surface temperature deviations and theory of nitrogen oxides on Mars
10 p1211 N73-19849
Infrared measurement of brightness temperature of Martian surface by Mars-3 automatic interplanetary station
[NASA-TT-F-14837] 10 p1211 N73-19852
Nature of blue clearings on Martian photographs in short wave region
[NASA-TT-F-14820] 11 p1338 N73-20856
Landing site selections for Viking Mars probes
[NASA-NEWS-RELEASE-73-91] 13 p1576 N73-22768
Using Mariner 6 and 7 photographs to investigate nature of linear trends on Mars
[NASA-TM-X-62264] 14 p1703 N73-23817
Geological features of Martian surface based on Mariner 9 photographs
[NASA-TT-F-14840] 14 p1704 N73-23831
Autonomous Martian roving vehicle determination of terrain gradients from laser measurements
[NASA-CR-133498] 19 p2307 N73-28556
Robot computer problem solving system which represents robot exploration vehicle in simulated Mars environment
[NASA-CR-133942] 22 p2638 N73-31146
Wind tunnel studies of Martian aeolian processes
[NASA-TM-X-62297] 22 p2716 N73-31746
Mariner 9 observations on Mars atmosphere and surface
22 p2735 N73-31892
Scene analysis and computer perception with breadboard Mars robot operating in laboratory environment containing rocks of various sizes
[NASA-CR-135711] 23 p2770 N73-32156
User guide to Mariner 9 television reduced data record
[NASA-CR-135712] 23 p2793 N73-32347
Scientific Mars research by Mariner 9 space probe
[NASA-CR-135530] 23 p2838 N73-32680
Geological Mars data obtained by Mariner 9 observations
23 p2838 N73-32681
Geological Mars map deduced from Mariner 9 surface photography
23 p2838 N73-32682
Mars surface erosion and canal formation by running water
23 p2838 N73-32683
Volcanic features in Mars surface photographs
23 p2839 N73-32684
Geomorphology of troughs in Mariner 9 Mars surface observations
[CONTRIB-2265] 23 p2839 N73-32685
Geomorphology of fretted and chaotic terrains on Mars surface
[CONTRIB-2264] 23 p2839 N73-32686
Geomorphology of Martian and lunar large multiringed circular basins
23 p2839 N73-32687
Martian surface cratering analysis using Mariner 9 observations
23 p2839 N73-32688
Erosional latitudinal debris distribution on Mars surface
23 p2839 N73-32689
Wind erosion features in Mariner 9 Mars surface observations
23 p2839 N73-32690
Wind erosion and dune formations in Mars surface topography
[CONTRIB-2353] 23 p2839 N73-32691
Wind erosion and sandstorm effects on Mars surface topography
23 p2839 N73-32692
Mariner 9 mapping of Mars surface albedo variations
23 p2840 N73-32693
Mariner 9 observations of Mars north polar region
[CONTRIB-2249] 23 p2840 N73-32694
Wind erosion effects in Martian polar regions
23 p2840 N73-32695
Topographic depressions in Mars south polar terrain
[CONTRIB-2266] 23 p2840 N73-32696
Geomorphology of layered deposits in Mariner 9 observations of Martian polar regions
23 p2840 N73-32697
Liquid carbon dioxide in Martian polar laminated surface layers
23 p2840 N73-32698
Infrared spectra of Mars atmospheric and surface properties
23 p2840 N73-32700
Analysis of Mariner 9 infrared radiometric Mars surface measurements
23 p2841 N73-32701
Mariner 9 S band radio occultation measurements of Mars polar and intermediate latitude atmosphere and topography
23 p2843 N73-32716
Mariner 9 radio occultation approximations of Mars surface and atmosphere
23 p2843 N73-32717
Photogrammetric determination of Martian surface coordinates using Mariner 9 photos
23 p2843 N73-32719
Mars surface mapping with Mariner 9 aerographic coordinate system
23 p2843 N73-32720
Photogrammetric evaluation of Mariner 9 Mars surface pictures
23 p2843 N73-32721
Analytical stereophotogrammetric evaluation of Martian topography using Mariner 9 photographs
[CONTRIB-2250] 23 p2843 N73-32722
Cartographic mapping of Martian surface by Mariner 9 digital picture data evaluation
23 p2843 N73-32723
Stereographic albedo map of Mars south polar region using Mariner 9 video data
23 p2844 N73-32724
Methods for primary and secondary triangulation of Martian surface
[NASA-CR-135586] 23 p2845 N73-32732
Objectives of experiments on Mariner 9 space probe
[NASA-CR-135726] 24 p2983 N73-33834
Mars surface properties working group
24 p2984 N73-33842

**MARS 2 SPACECRAFT**
Analysis of Martian atmosphere data obtained from Mars 2 spacecraft
[NASA-TT-F-14817] 08 p0961 N73-17865

**MARS 3 SPACECRAFT**
Analysis of magnetic field near planet Mars from data obtained by Mars 2 and Mars 3 spacecraft
[NASA-TM-X-66116] 03 p0357 N73-12907
Investigation of physical characteristics of Mars atmosphere and surface as reported by Mars 2 and Mars 3 orbital spacecraft
[NASA-TT-F-14814] 08 p0961 N73-17863
Measurement of water content of Martian atmosphere by Mars 3 spacecraft
[NASA-TT-F-14815] 08 p0961 N73-17864
Photometric profiles of dust particle size and dust cloud origins during dust storms on Mars as reported by Mars 3 Automatic Interplanetary Station
[NASA-TT-F-14818] 08 p0962 N73-17866

**MARS 69 PROJECT**
Directions of strong Martian winds inferred from Mariner 6 and 7 photographs and relation to dust storms and topographic wind funneling
[NASA-CR-129520] 03 p0354 N73-12885

**MARS 71 PROJECT**
Mariner Mars 1971 radio frequency subsystem to provide communication link between spacecraft and Deep Space Instrumentation Facility
[NASA-CR-130866] 08 p0885 N73-17164
Analysis of Mariner 71 attitude control subsystem flight performance and effects of performance anomalies on subsystem operation
[NASA-CR-131522] 12 p1461 N73-21835
Tracking and data system report for Mariner Mars 1971 mission
[NASA-CR-132955] 15 p1761 N73-24270
Mariner Mars 1971 battery design, test, and flight performance
[NASA-CR-132986] 16 p1864 N73-25095

**MARSHES**
U MARSHLANDS

**MARSHLANDS**
ERTS-1 imagery of coastal marshland, tidal flats, and littoral transport in French Atlantic waters
[E72-10251] 03 p0289 N73-12351
ERTS-1 imagery of marshlands and turbid waters of French Atlantic littoral
[E73-10341] 10 p1147 N73-19340
Mapping southeastern coastal marshlands and wetlands of South Carolina and Georgia using ERTS-1 imagery
[E73-10362] 10 p1150 N73-19358
Mapping northern Atlantic coastal marshlands of Maryland, Delaware, and Virginia using ERTS-1 imagery
[E73-10363] 10 p1150 N73-19359
Identification of marsh vegetation and coastal land use in Delaware from ERTS-1 imagery
[E73-10367] 10 p1150 N73-19363
Characterization of wetlands and marshlands by automatic processing of ERTS-1 data
[E73-10467] 12 p1394 N73-21304
ERTS-1 imagery of marshes, wetlands, and turbid waters in French Atlantic littoral
[E73-10548] 13 p1518 N73-22307
Identification of marshland vegetation and coastal land use in Delaware from ERTS-1 imagery
[E73-10516] 14 p1653 N73-23410
Evaluation of ERTS-1 imagery and automatic data processing techniques for characterization of wetlands and marshlands
[E73-10576] 14 p1656 N73-23437
Characterization of wetlands and marshlands from ERTS-1 imagery
[E73-10590] 15 p1772 N73-24357
ERTS-1 detection and measurement of coastal marshes in Houston area test site
[E73-10676] 16 p1900 N73-25371
Aerial photography and multispectral analysis for mapping of Delaware coastal marshes
16 p1905 N73-25414
Evaluation of satellite remote sensing and automatic data techniques for analysis of wetlands and marshlands using ERTS-1 imagery
[E73-10740] 18 p2133 N73-27235
Application of ERTS-1 imagery for grid measurement of small water bodies
[E73-10768] 18 p2134 N73-27244

Energy exchange characteristics of desert, meadow, forest, and marsh sites
[PB-218825/8] 18 p2173 N73-27550
Mapping of Atlantic coastal marshlands of Maryland and Georgia using ERTS-1 imagery
[PAPER-E7] 19 p2269 N73-28271
Analysis of coastal vegetation species in Delaware Bay, Delaware based on ERTS-1 imagery and high altitude photography
[PAPER-E8] 19 p2269 N73-28272
Discovery of small hollow spherules of glass containing various gases in peat bogs where Tungus meteorite fell
[NASA-TT-F-15125] 22 p2716 N73-31742

**MARTENSITE**
Interrelation of martensitic conversion during deformation and structural properties of trip steel
10 p1171 N73-19527
Metallographic analysis of morphological features of martensite formed in alloy of iron-nickel-manganese-carbon after heat treatment
13 p1541 N73-22490
Effect of martensitic microstructure on fatigue life and crack propagation characteristics of high strength steels
[S-253] 17 p2044 N73-26536
Acoustic emission from ferrous martensites as function of thermomechanical history
[AD-761220] 18 p2163 N73-27472

**MARTENSITIC STAINLESS STEELS**
Directional martensite transformations in steel and alloy development
[AD-748408] 04 p0436 N73-13553
Microstructural analysis of high-chromium martensitic semiferritic and ferritic steel phase transformations and thermal expansion coefficient determination
[AD-749522] 04 p0436 N73-13559
Explosive fragmentation of heat treated martensitic microstructure steel
[DSL-REPT-532] 17 p2091 N73-26915
Fatigue and martensitic transformations of austenitic stainless steels
20 p2427 N73-29498
Thermoplastic strengthening of martensite steels and titanium alloys
[AD-760953] 21 p2560 N73-30520

**MARTIN AIRCRAFT**
NT B-57 AIRCRAFT

**MARTIN MILITARY AIRCRAFT**
U MILITARY AIRCRAFT

**MARTINIQUE**
Martinique climate variations noting wind circulation, cyclones and tropical storms recorded from various weather stations and meteorological satellites
[MONO-86] 07 p0815 N73-16610

**MARYLAND**
NT CHESAPEAKE BAY (US)
NT POTOMAC RIVER VALLEY (MD-VA-WV)
NT SUSQUEHANNA RIVER BASIN (MD-NY-PA)
Resource inventory, land use, and pollution within Susquehanna River Basin based on interpretation of ERTS-1 data
[E72-10329] 05 p0531 N73-14317
Utilization of ERTS-1 and aircraft remotely sensed data for land use inventory and planning in Maryland
[E73-10081] 08 p0901 N73-17293
Development of land use-peak runoff classification system for highway engineering in Maryland
[E73-10100] 08 p0902 N73-17310
ERTS-1 imagery of wetlands ecology in Maryland, Georgia, and Chesepeake Bay test sites
[E73-10288] 08 p0915 N73-17494
Mapping northern Atlantic coastal marshlands of Maryland, Delaware, and Virginia using ERTS-1 imagery
[E73-10363] 10 p1150 N73-19359
Application of ERTS-1 imagery to thematic mapping of Washington-Baltimore corridors
[E73-10500] 12 p1398 N73-21336
Survey of geology, minerals, and water resources in Maryland using ERTS-1 imagery
[E73-10433] 13 p1515 N73-22276
Differentiation of serpentinitic from nonserpentinitic ultramafic rocks in Maryland Piedmont using ERTS-1 MSS imagery
[E73-10632] 16 p1896 N73-25337
Evaluation of utility of ERTS-1 satellite and aircraft remotely sensed data to integrated processes of state planning and land use in Maryland
[E73-10716] 17 p2019 N73-26323
Land use management and planning in Maryland based on ERTS-1 data
[E73-10732] 17 p2020 N73-26338
Sampling strategies in thematic land use mapping of Maryland, Virginia, and District of Columbia using Skylab EREP data
[E73-10823] 18 p2140 N73-27298
Analysis of lineaments and fault traces in Atlantic Coastal Plain of southern Maryland using ERTS-1 imagery
[PAPER-G29] 19 p2267 N73-28260
Mapping of Atlantic coastal marshlands of Maryland and Georgia using ERTS-1 imagery
[PAPER-E7] 19 p2269 N73-28271
Digital analysis of ERTS-1 data to determine sedimentation levels in Potomac and Anacostia Rivers confluence and strip mining in Allegheny County, Maryland
[PAPER-E13] 19 p2270 N73-28277
Seasonal changes of littoral transport and beach width of Maryland portion of Chesapeake Bay and resultant effect on protective structures
[PAPER-M1] 19 p2280 N73-28341
ERTS-1 imagery of littoral drift and sedimentation patterns of beach and nearshore areas of Maryland section of Chesapeake Bay
[PAPER-M2] 19 p2280 N73-28342
Utilization of ERTS-1 imagery and data for land use, regional planning, and urban development in Metropolitan Washington area
19 p2285 N73-28377
ERTS-1 multispectral imagery of topography of Assateague Island
[E73-10848] 19 p2292 N73-28426
Application of ERTS-1 imagery to land use inventory, land capability evaluation, and land use suitability in Maryland
[E73-10873] 20 p2393 N73-29224
Computer processing of Skylab MSS data for land use mapping of Baltimore, Maryland-Washington, D.C. area
[E73-10913] 20 p2397 N73-29262
Digital correction techniques for ERTS-1 imagery of Baltimore, Maryland
[E73-10963] 21 p2533 N73-30305
Sampling strategies for automatic thematic land use mapping of Washington D.C., Maryland counties, and Alice Springs, Australia using Skylab multispectral photography
[E73-11018] 22 p2661 N73-31322
Precision geometric and radiometric correction of bulk digital ERTS-1 imagery of Baltimore, Maryland by digital method
[E73-11019] 22 p2661 N73-31323

**MASER RESONATORS**
U MASERS

**MASERS**
NT GAS MASERS
NT TRAVELING WAVE MASERS
Method for producing storage bulb for atomic hydrogen maser
[NASA-CASE-NPO-13050-1] 09 p1043 N73-18508
High temperature bonding of sapphire to sapphire by eutectic Al2O3 and ZrO2 mixture to form sapphire rubidium maser cell
[NASA-CASE-GSC-11577-1] 10 p1164 N73-19467
Maser amplification of incoherent radiation
[RR-113-PT-1] 24 p2930 N73-33401

**MASKING**
Maskmaking facility for microelectronic systems
[NASA-TM-X-64703] 01 p0036 N73-10284
Masking phenomenon for measuring state of fatigue and stress of nervous system
[AD-752975] 16 p1869 N73-25129
Masking of ERTS-1 RBV images to reduce stationary residual inaccuracies in radiometric shading corrections
[PAPER-I4] 19 p2277 N73-28326
Properties of dielectric layers of negative electrosensitive resin noting masking capability and application to MOS circuit manufacturing
[REPT-5.497] 23 p2765 N73-32124

**MASKS**
NT OXYGEN MASKS
NO2 and UDMH absorbing properties of rocket propellant gas mask canisters
[AD-752538] 10 p1203 N73-19791
Prototype of high resolution duplicator for large scale integration circuit masks
[REPT-3424] 16 p1914 N73-25488

**MASONRY**
NT BRICKS

**MASS**
NT ELECTRON MASS
NT PARTICLE MASS
NT STELLAR MASS
Measurement of missing mass spectrum from pion [minus] plus proton reaction
[NUB-2160] 01 p0083 N73-10686
Light cone analysis of large momentum transfer limit of electroproduction structure function at constant missing mass and of its connection with Bjorken limit
[TR-73-066] 03 p0339 N73-12766
Sweeping of masses theory used to solve inverse gravimetric problem and interpretation of regional gravitational field
[AD-747874] 04 p0417 N73-13406
Attitude dynamics of nearly spherical dual spin satellite with asymmetrical bodies, orbital results for OSO 7, and critical mass properties
07 p0848 N73-16877
Mass and momentum of control signals in switching mechanism of fluid bistable amplifiers
[AD-756583] 13 p1511 N73-22243
Mass formula calculations on baryonic resonances using radial excited symmetric quark model
[TR-74-018] 22 p2701 N73-31636

**MASS BALANCE**
Momentum, energy, and mass budgets of stratosphere
[COO-2195-2] 04 p0415 N73-13385
Evaluation of exact point speed and least squares procedures for determining balance of flexible rotating machinery
[NASA-CR-121035] 05 p0551 N73-14477
Analysis of mass properties of reusable space shuttle booster and expendable second stage for three specified payloads - Vol. 4
[NASA-CR-128659] 05 p0599 N73-14870
Elastic gyro rotor with stable orientation of readout axis by point mass system
07 p0817 N73-16623

**MASS DISTRIBUTION**
Analysis of mass properties of reusable space shuttle booster and expendable second stage for three specified payloads - Vol. 4
[NASA-CR-128659] 05 p0599 N73-14870
Dynamic mass modeling and geophysical analysis of lunar maria based on Apollo tracking data
[NASA-TM-X-65940] 11 p1338 N73-20854
Mass distribution analyses for design of low aspect ratio aerodynamic stable fighter wings
[NASA-CR-112232] 13 p1469 N73-21900
Determination of mass distributions along elastic axes of 2-spar wings in fighter aircraft design
[NASA-CR-112233] 13 p1470 N73-21901
Aerodynamic size and mass distribution of aerosol particles determined with spiral centrifuge compared to other precipitators
[BMVG-FBWT-73-3] 14 p1668 N73-23535
Mass properties and related data for solid propellant rocket engine used with space shuttle vehicle - Vol. 2, Book 4
[NASA-CR-124237] 15 p1826 N73-24800
Analysis of effect of localized mass on flutter characteristics of delta wing for various spanwise and chordwise positions for the mass center of gravity
[ARC-R/M-3264] 16 p1855 N73-25030
Optimization of mass distribution of solid beams and panels for structural design of airframes and panels
[AD-759169] 16 p1859 N73-25054
Effects of particle seeding on jet exhaust noise
19 p2251 N73-28150
Current density, flow velocity, and mass density in coaxial annular plasma Hall accelerator
[DLR-FB-73-45] 22 p2705 N73-31663

**MASS FILTERS**
U FLUID FILTERS

**MASS FLOW**
Comparison of turbine annulus mass flow calculations when computed by one- and two-dimensional analysis
[NASA-TM-X-2661] 02 p0156 N73-11264
Radiative mass flow transfer model for inhomogeneous structure of chromosphere
04 p0466 N73-13798
Remote sensing of rapid mass wastage, mudflow, and debris slide
[NASA-CR-130379] 07 p0792 N73-16443
Analytical approach for loss and deflection behavior of cascades in transonic flow including axial mass flow variation
10 p1204 N73-19800
Colloid thruster producing beams with anisotropic current, specific charge, and mass flow distributions
[AD-754902] 11 p1335 N73-20836
Ultrasonic mass flowmeter for fuel flow in gas turbine engines
[AD-758462] 14 p1669 N73-23547
Generation of high temperature, high mass flow, and high Reynolds number air at hypersonic speeds
[NASA-CASE-LAR-10578-1] 16 p1886 N73-25262
Radio frequency resonant cavity mode analysis technique for fluid mass quantity gauging of space shuttle orbiter tankage
[NASA-CR-133393] 18 p2151 N73-27390
Dynamic particle mass flow model for solar flares
19 p2333 N73-28773

**MASS FLOW FACTORS**
Design, development, and evaluation of mechanical mass flow controller for regulating fuel-oxidizer mixture ratio and controlling rocket engine thrust level
[NASA-CR-128639] 03 p0351 N73-12860
Two fluid models with neglected mass rotation and overestimated electric field role
[TH-72-E-28] 14 p1695 N73-23755

**MASS FLOW RATE**
Design, development, and evaluation of mechanical mass flow controller for regulating fuel-oxidizer mixture ratio and controlling rocket engine thrust level
[NASA-CR-128639] 03 p0351 N73-12860
Calculation of mass flow rate of methane and natural gas through nozzles
[NASA-SP-3074] 06 p0653 N73-15309
Analytical solution of nonsimilar laminar boundary layer with pressure gradient, variable wall temperature, and continuous mass injection
[AD-751804] 07 p0773 N73-16279
Mass flow rate of laminar dissociated equilibrium boundary layer
24 p2907 N73-33200

**MASS RATIOS**
Mathematical models of aircraft mass and performance
15 p1732 N73-24047

**MASS SPECTRA**
Measurement of missing mass spectrum from pion [minus] plus proton reaction
[NUB-2160] 01 p0083 N73-10686
Mass spectra and dissociation energies of high temperature gaseous molecules containing aluminum
[NASA-TN-D-7123] 04 p0386 N73-13138
Mass spectroscopy of C state in iodine by crossing of molecular beam with pulsed laser beam and monitoring recoil photofragments
[AD-751611] 07 p0753 N73-16117
Analysis of light ion mass spectrometer data from OGO-E experiment
[NASA-CR-130156] 07 p0791 N73-16432
Meson resonance production in missing mass spectra using quark model for negative pion proton yields proton negative x diffraction calculation
[TUEP-72-41] 07 p0823 N73-16667
Missing mass spectrum structures for meson resonances in S, T, U, region
[NUB-2167] 07 p0823 N73-16671
Diagnostic spectroscopy of plasmas produced in molecular gases
[AD-751938] 08 p0950 N73-17776
Computer program for analysis of mass spectra of GaTe and GaSe
[ISS-72/11] 10 p1199 N73-19754
Mass spectra of electrochemical propane oxidation
[AD-755254] 12 p1376 N73-21166
Comsic ray air shower muon momentum spectra, noting dependence on shower primary energy, zenith angle, and arrival directions
13 p1574 N73-22755
Plasma ion sources research, including mass spectra, gas discharges, and ion beams
[AD-758040] 15 p1819 N73-24742
Mass spectrometric analyses on laser induced vaporization of iron and zirconium hydride
[LBL-1177] 17 p1992 N73-26108
Mass spectrum identification of trace organic impurities in gaseous helium
[NASA-TN-D-6520] 19 p2230 N73-27983
Mass spectra of cluster ion reaction kinetics in free jet expansions of gas mixtures
[AD-761811] 19 p2233 N73-28004
Mass spectra of doublets in samarium and gadolinium chlorides
24 p2959 N73-33648

**MASS SPECTROMETERS**
Mass spectrometer system for monitoring atmospheric constituents and pollutants -operation and maintenance manual
[NASA-CR-128603] 01 p0057 N73-10469
Mass spectrometer identification of positive metal ions in Comet Encke beta Taurids meteor shower
[NASA-TM-X-66084] 02 p0229 N73-11855
Apparatus for analyzing gas samples in containers including vacuum chamber, mass spectrometer, and gas chromatography
[NASA-CASE-GSC-10903-1] 03 p0300 N73-12444
Design and development of mass spectrometer using quadrupole fields to stabilize ions based on mass of ions
06 p0672 N73-15468
Research on gas chromatography with computer techniques and mass spectrometer methods
[FOA-1-C-1412-34] 06 p0672 N73-15471
Mass spectrometer for investigating hypersonic air flows in shock tube for application to reentry body problems
[BMVG-FBWT-72-20] 07 p0801 N73-16505
Laser-probe mass spectrometric analysis of solar wind, cosmogenic, and radiogenic gases in Apollo 12, 14, and 15 samples
[NASA-CR-130029] 07 p0841 N73-16811
Mass spectrometer and ion source for flight experiment measurements of thermosphere number density
08 p0899 N73-17283
Derivation of empirical global thermosphere model for magnetically quiet conditions from longitudinally averaged gas densities using expansion in spherical harmonics
[NASA-TM-X-66183] 08 p0917 N73-17512
Thermospheric composition and density, measured by neutral mass spectrometer onboard OGO-6 satellite
08 p0972 N73-17946
Mass spectrometric analysis of reactions of nitrogen oxide and nitrogen dioxide with hydrogen peroxide at 25 C
[NASA-CR-130831] 09 p0999 N73-18155
Determination of atmospheric density numbers by sounding rocket carrying mass spectrometer with cryo ion source
[BMBW-FBW-72-34] 09 p1027 N73-18381
Ozone and nonreactive gas calibration of mass spectrometer with modified helium-cooled ion sources
[BMBW-FBW-72-32] 09 p1034 N73-18440
Design and performance of metabolic gas analyzer using mass spectrometer and digital data printout
[NASA-CR-128842] 10 p1124 N73-19160
Development and characteristics of molecular beam mass spectrometer system for sampling rocket engine combustion chambers
[NASA-CR-130933] 10 p1137 N73-19267
Measurement of line spectra produced by high resolution mass spectrometer and application to identifying organic compounds in samples from Apollo 11 and 12 flights
[NASA-CR-128840] 10 p1160 N73-19436
Application of nuclear and X ray techniques for analysis of enviromental pollution samples
[CONF-721002-1] 10 p1161 N73-19443
System designs for automating GC/MS analyzing system
[NLL-RTS-7572] 11 p1259 N73-20218
Rocket-borne mass spectrometer experiment with cryo-cooled ion source to determine neutral atmosphere composition between 85 and 125 km altitude
[BMFT-FBW-73-03] 11 p1285 N73-20431
Role of gas-surface interactions in reduction of OGO 6 neutral-particle mass spectrometer data
[NASA-TN-D-7239] 11 p1286 N73-20432
Application of laser microprobe and magnetic mass spectrometer for determining gas contents in metals by melting and vaporizing microvolumes of samples
[NASA-TT-F-14852] 11 p1305 N73-20592
Vaporization kinetics and thermodynamics of graphite using high pressure mass spectrometers
[AD-755853] 12 p1376 N73-21165
Lunar orbital mass spectrometer for lunar atmosphere detection and lunar volcanism search
12 p1451 N73-21755
Mass spectrometer to study kinetics and thermodynamics of graphite vaporization
[AD-755899] 12 p1465 N73-21871
Feasibility of mechanical pumps for use with Pioneer-Venus probe mass spectrometer inlet system
[NASA-CR-114581] 14 p1670 N73-23551
Mass spectrometric measurement of hydrogen in milligram-size quantities of titanium
[NASA-TN-D-7326] 15 p1798 N73-24574
Ion optical design with applications to solar wind mass spectrometer
[NASA-CR-133053] 16 p1913 N73-25481
Valve testing for application in inlet system of Pioneer Venus Probe mass spectrometer
[NASA-CR-114627] 16 p1918 N73-25517
Getter pumps applicable to Pioneer Venus Mass Spectrometer Experiment
[NASA-CR-114594] 16 p1918 N73-25518
Design of chemical pumps for Venus Pioneer mass spectrometer used to determine atmospheric composition of Venus
[NASA-CR-114604] 16 p1918 N73-25519
Mass spectrometer, chromatograph, and X ray analyses for determining volatilization mechanism for V2O5
[NLL-M-21570-[5828.4F]] 16 p1926 N73-25582
Instrumentation for determining composition of Venus clouds
[NASA-CR-132766] 16 p1963 N73-25876
Cost analysis of mass spectrometers and gas chromatographs for life support atmosphere monitoring
[NASA-CR-124306] 18 p2112 N73-27076
Program for reducing data from high resolution mass spectrometer
[NASA-TM-X-2847] 18 p2113 N73-27089
Measurement of positive ion composition in midlatitude sporadic E layer using rocket-borne ion mass spectrometer
[NASA-TM-X-66276] 18 p2142 N73-27313
Global characteristics in diurnal compoeents of OGO-6 neutral mass spectrometer measurements of thermosphere
[NASA-TM-X-66295] 18 p2145 N73-27335
Design, construction, and performance of crossed beams tandem mass spectrometer for study of low energy ionic collisions
[AD-762450] 19 p2231 N73-27991
Propane oxidation using electrochemical mass spectrometry
[AD-762356] 20 p2374 N73-29077
OV1-18 mass spectrometer detection of heavy ions in magnetosphere
[AD-763436] 21 p2542 N73-30379
Modified quadrupole mass spectrometer for in situ space simulation thermal vacuum testing of sophisticated payloads
[NASA-TM-X-64775] 21 p2549 N73-30435
Design and construction of vacuum system and safety interlocks for photoionization mass spectrometer
[AD-763685] 21 p2550 N73-30447
Altitude test of rocket-borne mass spectrometer cooled by liquid helium in arc heated plasma jet wind tunnel
[DLR-MITT-72-23] 22 p2675 N73-31424
Test performance of pump for Pioneer Venus probe mass spectrometer inlet
[NASA-CR-114660] 22 p2678 N73-31448
Quadrupole mass spectrometer using noise spectrum for ion separation and identification
[NASA-CASE-XNP-04231] 23 p2791 N73-32325

**MASS SPECTROMETRY**
U MASS SPECTROSCOPY

**MASS SPECTROSCOPY**
Gas chromatographic-mass spectrometric analysis of volatile organic metabolic products in terrestrial soils
[NASA-CR-129602] 04 p0386 N73-13134
Ion sensitive emulsion detection system for use in cycloidal focusing mass spectrometer for measuring atomic species of solar plasma
[NASA-CR-130134] 05 p0592 N73-14810
Vaporization kinetics and thermodynamics of graphite using high pressure mass spectrometer
[AD-753713] 09 p1055 N73-18601
Gas chromatography-mass spectrometry for analyzing fatty acid and sterol concentrations in plant tissue samples
[NASA-CR-128740] 10 p1120 N73-19131
Mass fragmentography-computer for identification and quantitation of amino acids in soil
[NASA-CR-131507] 12 p1376 N73-21159
Mass spectrometric analysis of aromatic hydrocarbons and sulfur compounds
[NLL-TRANS-1193-[9022.9]]
15 p1746 N73-24151
Electrical instrumentation development for spark source mass spectroscopy
[PB-214212] 16 p1871 N73-25147
Proceedings of conference on mass spectrometry of metal containing compounds
20 p2431 N73-29527
Mass spectrometric determination of rare earth concentration in basaltic rocks and luna sample 14305
[FRNC-TH-335] 21 p2597 N73-30813
Quadrupole mass spectrometer for direct sampling of atmospheric gases and condensation products
[AD-764238] 22 p2676 N73-31433
Mass spectrometric analysis of rare earth elements contained in lunar samples
[CONF-730402-[P1-2]] 24 p2923 N73-33344

**MASS TRANSFER**
Mass transfer rates at flat water surface measured during evaporation and condensation
[COO-2032-11] 03 p0263 N73-12135
Analysis of mass transfer through binary, monatomic gas mixture of arbitrary composition contained between two plane parallel surfaces
[COO-2032-10] 03 p0284 N73-12304
Transfer of mass and heat through single component diatomic gas and binary monatomic gas mixture of arbitrary composition
[COO-2032-12] 03 p0364 N73-12968
Nonstationary heat and mass transfer in stationary binary gas mixture
[AD-747562] 03 p0365 N73-12974
Radiative mass flow transfer model for inhomogeneous structure of chromosphere
04 p0466 N73-13798
Research projects conducted in USSR to determine thermophysical properties of materials at high temperatures and characteristics of high temperature processes
[JPRS-57658] 04 p0484 N73-13957
One dimensional flow and mass transfer between two fixed parallel walls at different temperatures by moment method
[NASA-CR-130744] 08 p0897 N73-17261
Long lived, alpha radioisotopes applied to transfer mechanism of air masses in tropopause
09 p1060 N73-18642
Analysis of optimum mass and heat transfer in electrochemical fuel cells to show effects on fuel cell output
[AD-754258] 11 p1238 N73-20051
Analysis of interaction of rarefied gas with surface of porous moist bodies during heat and mass transfer using visual and photographic methods
[AD-754633] 11 p1272 N73-20325
Combined heat and mass transfer at wet flat plate in parallel air flow forming turbulent boundary layer
[DLR-FB-73-11] 14 p1599 N73-22960
Mass transfer rates of swirling and pulsating flow through axisymmetric duct
[AD-756546] 14 p1652 N73-23396
Research on atmospheric eddy transport
[AD-757692] 14 p1663 N73-23496
Heat and mass transfer with phase and chemical transformations in reacting boundary layer
[AD-758210] 15 p1748 N73-24165
Characteristics of wall mass transfer coefficient for pulsed laminar flow in pipe of Newtonian fluid containing dissoloved electrolyte
15 p1765 N73-24301
Steady state heat and mass transfer in suction boiling
15 p1842 N73-24923
Vectored injection into non-adiabatic boundary layer flows including incipient separation
[VPI-AERO-003] 19 p2255 N73-28176
Numerical analysis of horizontal diffusion in ocean water to determine lifetime and spatial extent of submarine wakes in various turbulent media
[AD-762046] 19 p2256 N73-28186
Analysis of stagnation point on blunt body in massive ablation condition to show effects of absorption coefficient enhancement on mass loss rate
19 p2351 N73-28912

Numerical model to simulate vertical mass transfer and stratification in layer of buoyant convection
20 p2391 N73-29208
Development of method for calculating bubble conditions in flow of boiling liquid in vertical tubes
[NLL-WH-335-[9091.9F]] 21 p2605 N73-30875
Calculation of heat and mass transfer in turbulent boundary layer on surface with arbitrary roughness
[AD-764128] 22 p2655 N73-31266
Mass loss rate of carbon and graphite at high temperature
[LA-5223-PR] 24 p2943 N73-33503

**MASSACHUSETTS**
Geological fracture mapping based on enhancement of ERTS-1 snow cover imagery of Massachusetts, Connecticut, and Feather River/Lake Tahoe area
[E72-10205] 02 p0161 N73-11302
ERTS-1 detection of oil pollution in Gulf of Mexico and in waters off Salem, Massachusetts and Oakland, California
[E73-10396] 11 p1276 N73-20358
Land use in northern megalopolis of Massachusetts, Connecticut, and Rhode Island
[E73-10506] 13 p1516 N73-22281
Inventory of ponds, lakes, and reservoirs in selected areas of State of Massachusetts
[PB-214116/6] 14 p1665 N73-23512
Land use of northern megalopolis of Massachusetts, Connecticut, and Rhode Island from ERTS-1 imagery
[E73-10630] 15 p1776 N73-24390
Effectiveness of snow cover as photogeological enhancement technique for ERTS-1 imagery of western Massachusetts
[E73-10594] 16 p1896 N73-25334
Application of ERTS-1 imagery to determine land use in Massachusetts, Connecticut, and Rhode Island
[E73-10723] 17 p2019 N73-26330
Mapping and digitization of land use in northern megalopolis of Masssachusetts, Connecticut, and Rhode Island using ERTS-1 data
[PAPER-L12] 19 p2274 N73-28308
Comparison of conventional maps of southeastern Massachusetts to ERTS-1 imagery of coastal and submarine geology and hydrology
[PAPER-M18] 19 p2282 N73-28356
Relation of sea truth data from Cape Cod, Massachusetts, and Charleston, South Carolina on plankton composition and chlorophyll values with ERTS-1 data
[E73-10907] 20 p2397 N73-29256

**MATCHING**
Elastic matching, automatic error correction in English language words of any length
[NPL-COM-SCI-63-SUPPL] 18 p2121 N73-27144

**MATERIAL BALANCE**
NT WATER BALANCE
Two-reservoir exchange model for Baltic Sea material balance
[GH-4] 17 p2027 N73-26407

**MATERIAL REMOVAL (MACHINING)**
U MACHINING

**MATERIALS**
Research in solid state physics, materials, and physical chemistry
[AD-746866] 03 p0347 N73-12826
Space manufacturing of biological and electronic materials
04 p0473 N73-13862
Preparation of pure materials, radiation chemistry, and solid state studies
[BARC-599] 05 p0506 N73-14120
Recovery of barium oxide reagent from residue from preparing lubricant additives in centrifuge
[AD-751945] 09 p1042 N73-18500
Gas dynamic equation for investigating thermal heating modes during laser radiation flux interaction with material
09 p1043 N73-18509
Stability criteria for incompressible elastic materials
[AD-753459] 10 p1221 N73-19931
Computer radiation interaction program for calculating material response to X ray and electron beam impact
[AD-755147] 11 p1327 N73-20767
Material selection determined from mathematical model of crack growth and failure
[NASA-TN-D-7221] 12 p1413 N73-21452
Technical development and future use of materials in aerospace systems
[AD-755371] 12 p1415 N73-21466
Measurement of surface strain deformation in materials by holographic interferometry
[NRC-TT-1623] 13 p1536 N73-22447
Tables of thermophysical properties of materials
[AD-758175] 15 p1747 N73-24164
Solid state physics, physical chemistry, and materials research
[AD-758374] 15 p1821 N73-24764
Catalog on standard reference materials, their properties, compositions, and characterizations
[NBS-SP-260] 17 p2049 N73-26573
Atomic materials research in Canada
[AECL-4353] 17 p2065 N73-26711
Superconductive materials for military rotating electrical machinery
[AD-760330] 17 p2074 N73-26782
Compilation of outgassing data for spacecraft materials
[NASA-TN-D-7362] 23 p2810 N73-32469
Flammability of engineering materials in gaseous oxygen environments and applicability to Skylab program
[NASA-TM-X-64783] 24 p2891 N73-33081
Absorption spectra of infrared window matrials
[AD-764904] 24 p2969 N73-33730

**MATERIALS EROSION**
U EROSION

**MATERIALS HANDLING**
NT GROUND HANDLING
NT PROPELLANT TRANSFER
NT REMOTE HANDLING
Air lock mechanism for inserting and removing specimens from vacuum furnace
[NASA-CASE-LAR-10841-1] 03 p0305 N73-12494
Design and development of device to prevent clogging in hoppers containing particulate materials
[NASA-CASE-LAR-10961-1] 03 p0306 N73-12496
Design criteria for load suspension points, slings, and lifting equipment used on military helicopters
[AD-747814] 03 p0307 N73-12508
Advanced technology hoist-drive system applicable to helicopter cargo hoists with capacities ranging from 12.5 to 50 tons
[AD-746629] 04 p0377 N73-13067
Application of pneumatically controlled prosthetic arm to industrial handling problems
[NASA-TT-F-14628] 04 p0383 N73-13115
NASA MS/MS program for manufacturing materials during space shuttle missions
04 p0473 N73-13860
Compatibility and safety of materials for liquid and gaseous oxygen systems
[NASA-CR-120922-VOL-1] 05 p0579 N73-14716
Operational hazards and safety regulations for liquid and gaseous oxygen system handling
[NASA-CR-120922-VOL-2] 05 p0580 N73-14717
Development of concepts and procedures for preparation of loads for airdrop to reduce time required and increase reliability of operation
[AD-750705] 05 p0612 N73-14976
Stabilization methods in collecting and shipping of human sera for chemical analyses
08 p0871 N73-17053
Computer based automation for performing material handling, assembly, and quality control tasks
[AD-752464] 08 p0928 N73-17601
Analysis of factors involved in selection of suitable sites for sanitary land fills with emphasis on economic and social problems
[NASA-CR-128745] 10 p1229 N73-19989
Microbiological inspections of NASA food handling facilities
[NASA-TM-X-64734] 11 p1247 N73-20127
Development of ultrasonic radiation equipment for removing material from host surface and vacuum apparatus for recovery of material
[NASA-CASE-NPO-11213] 11 p1296 N73-20514
Instruction manual for safe and efficient use of 200-pound diborane shipping container
[NASA-CR-131290] 11 p1296 N73-20519
Development and characteristics of dual cargo hook system for use on military transport helicopters
12 p1358 N73-21022
Computerized simulation of containership loading and unloading of heavy lift helicopters for military logistic applications
[AD-756865] 13 p1475 N73-21946
Stochastic network to model materials handling operations at air cargo terminals
[AD-757629] 14 p1647 N73-23356
Preflight, inflight, and post flight operations evaluation analyses for Skylab materials processing facility - Appendix E
[NASA-CR-61386-APP-E] 14 p1708 N73-23859
Development and characteristics of system for skin packaging articles using thermoplastic film heating and vacuum operated equipment
[NASA-CASE-MFS-20855] 18 p2154 N73-27405
Army materiel susceptability to high intensity electromagnetic radiation in radio frequency spectrum
[AD-763141] 21 p2508 N73-30125
Hard materials and material removal processes
[PB-221907/9] 22 p2690 N73-31546
Hard materials and material removal processes
[PB-221908/7] 22 p2690 N73-31547
Ship to shore transportation of military cargo using tethered balloons
[AD-765352] 23 p2747 N73-31987
Flexible airship manufacturing
24 p2879 N73-32992
Combined parachute and retrorocket system for low altitude aerial delivery of military cargo
[AD-765422] 24 p2880 N73-32997
Safety precautions for personnel handling radioactive isotopes to prevent accidental exposure to radiation hazards
24 p2952 N73-33582

**MATERIALS RECOVERY**
NT WATER RECLAMATION
Underwater equipment for locating and recovery of objects from ocean bottom by whales
[AD-747612] 04 p0417 N73-13403
Hardness and physical characteristics of titanium sponge with low residual chloride concentration after vacuum separation
[JPRS-58347] 09 p1048 N73-18544
Removal of mechanical impurities from AKOR-1 additive by filtration method using perlite
[AD-751947] 10 p1167 N73-19496
Proceedings of Congressional committee on use of recycled materials in NASA programs and requirement for recycling legislation for environmental and economy improvement
11 p1308 N73-20614
Theory and applications of centrifugal extraction process based on numerical analysis of flow characteristics of liquid residue
[NLL-RTS-7990] 15 p1790 N73-24512
Extraction-Photometric methods for determining impurities in beryllium
[JAERI-1222] 17 p2044 N73-26537

**MATERIALS SCIENCE**
Expanded research program in materials sciences
[AD-749068] 05 p0588 N73-14785
Interdisciplinary research on materials science
[AD-749383] 05 p0612 N73-14974
Solid state physics, materials, and semiconductor research
[AD-752063] 09 p1053 N73-18581
University program accomplishments in materials science and engineering research
[AD-753845] 09 p1077 N73-18789
Scientific and technological applications of rare earth materials
[IS-2965] 10 p1166 N73-19484
Modification of Ber and Friedman mathematical theory of elasticity
10 p1172 N73-19536
Commercial applications of rare earth elements in ceramics, glasses, and nuclear technology
[IS-2967] 10 p1175 N73-19561
Research reports on amorphous, laser window, composite, and gradient materials
[AD-755585] 13 p1545 N73-22521
Research reports for various engineering sciences and materials and metallurgy
14 p1721 N73-23961
Conference on materials research
[AD-758571] 15 p1802 N73-24609
Statistical mechanics for relating material properties to their atomic and molecular structures
[AD-758257] 15 p1814 N73-24708
Neutron inelastic scattering spectroscopy for studying problems in materials science
[COO-3352-4] 15 p1815 N73-24713
Research projects in solid state chemistry and materials science
[AECL-4351] 16 p1871 N73-25145
Materials research covering properties, structure, and synthesis
[AD-760021] 17 p2100 N73-26988
Raman and far infrared spectroscopy for materials characterization
[AD-762303] 19 p2233 N73-28006
Device for measuring thermoelectric properties of materials under high pressure
[NASA-CASE-NPO-11749] 19 p2299 N73-28486
Fatigue strength criteria for stressed materials
[AD-761447] 20 p2463 N73-29790
Research and development progress in solid state physics, chemistry, electronics, and materials science
[AD-763501] 21 p2610 N73-30924
Summaries of materials research projects
[AD-764819] 23 p2828 N73-32601
USSR research in solid state physics, laser technology, geosciences, and materials
[AD-763742] 23 p2866 N73-32916

**MATERIALS TESTING REACTORS**
U NUCLEAR RESEARCH AND TEST REACTORS

**MATERIALS TESTS**
Characteristics of dry rubbing bearings with guide to design and material selection based on specific applications
[ESDU-68018] 01 p0060 N73-10491
Behavior of lubricating materials under high temperature and high pressure
[AD-745001] 01 p0062 N73-10509
Equipment and procedures for measuring variation of strength of sheet specimens of glass under conditions of tension, compression, and shear
[AD-743694] 01 p0067 N73-10551
Design, development, and characteristics of radioisotope shielding systems for use with spacecraft electric propulsion system - Vol. 2
[NASA-CR-114506] 01 p0091 N73-10746
Design and analysis of radioisotope shield for thermionic power supply used in spacecraft electric propulsion systems - Vol. 3
[NASA-CR-114507] 01 p0091 N73-10747

Calculation of geometric stress concentration factors in two adjacent, unreinforced circular holes in infinite flat plates
[ESDU-66035] 01 p0111 N73-10919
Numerical analysis of elastic stresses and deflections of helical compression springs made of round wire
[ESDU-65005] 01 p0112 N73-10926
Analysis of factors affecting choice of material and manufacturing methods for production of helical compression springs
[ESDU-65006] 01 p0112 N73-10927
Development of methods for determining relationships between shapes of creep curves and changes in structure of metal specimens by exponential function of real order
[NLL-NEL-TT-2404-(6075.461)] 02 p0185 N73-11498
Analysis of conditions required to produce superconductivity in materials under high pressure
[NLL-NEL-TT-2402-(6075.461)] 02 p0186 N73-11505
Analysis of metallurgical, physical, and mechanical properties of uranium alloys to determine breakdown strain, elongation, and high density characteristics
[FOA-4-C-4471-D4] 02 p0186 N73-11508
Densification of ceramic materials and mechanical behavior of ceramic materials with emphasis on fracture energies
[AD-745909] 02 p0193 N73-11561
Development of nondestructive test procedures for determining properties of multidirectional fiber reinforced resin matrix composites
[AD-746592] 02 p0193 N73-11562
Development of direct method for determining complex modulus of linear viscoelastic materials as function of frequency
[UTIAS-159] 02 p0237 N73-11928
Characteristics of yield surfaces for hardening body as function of preliminary loading path 02 p0238 N73-11937
Analysis of production method for manufacturing ablative heat shield panels using press filling and curing of ablation material
[NASA-CR-112124] 02 p0243 N73-11975
Statistical analysis of fatigue properties of SAE 4340 steel and description of test equipment used
[NASA-CR-72835] 03 p0313 N73-12551
Problems of using metallurgical and chemical materials in direct conversion systems
[UCRL-73560] 03 p0333 N73-12718
Sonar equipment research project to include determination of temperature and heat dissipation characteristics of ceramics used in high frequency projectors
[AD-749960] 05 p0515 N73-14187
Development of procedures for determining contamination characteristics of materials which become volatile in space environment
[NASA-CR-130132] 05 p0600 N73-14878
Analysis of fatigue behavior of composite-reinforced, integrally stiffened metal panels and effects of temperature on adhesive substances
[NASA-CR-112148] 05 p0602 N73-14899
Analysis of heat dissipation and frictional properties of materials used in aircraft brakes
[NASA-CR-121116] 06 p0687 N73-15595
Development and testing of primary structural elements of windshield system for space shuttle orbiter
[NASA-CR-112234] 06 p0720 N73-15879
Compressive stress-strain properties of aircraft materials
[ESDU-00.01.01-AMEND-A] 06 p0723 N73-15902
Evaluation of three types of CVD tungsten to determine weldability, high temperature strength, and structural stability
[NASA-CR-120876] 07 p0809 N73-16561
Development of ceramic materials for construction of full scale, high pressure, hypersonic facility for testing aircraft and missile models
[AD-751298] 07 p0812 N73-16588
Design and development of ultrasonic instrumentation to facilitate quantitative nondestructive evaluation of defects in materials
[NASA-CR-124021] 08 p0923 N73-17562
Tests to characterize crystallographic, magnetic, and optical properties of orthoferrites
[LCR-DR-1-71-97/1/R] 08 p0932 N73-17633
Evaluation of aluminum strain hardenable alloys for suitability as materials for cartridge cases
[AD-749508] 08 p0933 N73-17640
Evaluation of ceramic materials for application as high temperature gas bearing material
[AD-753858] 09 p1042 N73-18499
Effect of sheet thickness on plane stress fracture resistance of high strength titanium alloys
[AD-753198] 09 p1049 N73-18555
Numerical analysis of stress and deformation at crack tip for case where finite plastic zone exists along crack line
[NAL-TR-293] 09 p1092 N73-18918
Analysis of fatigue damage cumulation of low carbon steel specimens with transverse hole using two step rotating bending tests and block loading sequence
[TAE-164] 09 p1093 N73-18922
Multiaxes vibration device for making vibration tests along orthogonal axes of test specimen
[NASA-CASE-MFS-20242] 10 p1158 N73-19421
Design and development of space storable isolation valves for control of flow of liquid rocket propellants
[TRW-73-4781-6-15] 10 p1165 N73-19477
Preparation, characterization, and evaluation of materials for infrared windows
[AD-754280] 10 p1169 N73-19512
Thermal vacuum environment tests of materials used in space technology to determine effect of ultraviolet radiation on contaminative properties
[NASA-CR-122374] 10 p1175 N73-19556
Analysis of porous media of heat pipe wicks to determine effects on permeability and thermal conductivity of materials 10 p1222 N73-19938
Material testing system with load sensor for applying and measuring cyclic tensile and compressive loads to test specimens
[NASA-CASE-MFS-20673] 11 p1291 N73-20476
Evaluation of cold cathode materials for sealed off carbon dioxide lasers to show power output and service life
[NASA-CR-130202] 11 p1302 N73-20564
Analysis of microplasticity of materials used in inertial navigation systems to show friction stress, yield stress, and rate of strain hardening in microstrain region 11 p1317 N73-20692
Fatigue life and wear tests of spur gears based on pitting fatigue at pitch circle to compare AISI M-50 and super nitralloy materials
[NASA-TN-D-7261] 12 p1408 N73-21411
Strengthening of zirconium alloys in creep through interaction of mobile dislocations and gas bubbles
[AECL-4252] 12 p1415 N73-21464
X ray Mossbauer study of strengthening properties of laves phases in austenitic steels
[JPRS-58852] 13 p1543 N73-22503
Performance of fibrous concrete pavement materials under cargo aircraft and roadway vehicle loads
[AD-741357] 13 p1547 N73-22537
Compatibility of Ti and Ni alloys, stainless steels, Al, tungsten carbide, butyl, and Ep rubbers with hydrazine noting decomposition rates and effects of carbonic acid
[ESRO-CR-85-PT-2] 13 p1569 N73-22712
Proceedings of conference on materials and structures to include materials research, fracture control, and aerospace vehicle dynamics and control
[NASA-TM-X-69227] 13 p1585 N73-22850
Chemistry and physics of thin liquid films in contact with solid substrates and application to boundary lubrication of propulsion systems
[AD-757061] 14 p1670 N73-23556
Degradation and reuse of radiative-thermal protection materials for space shuttle
[NASA-CR-123587] 14 p1709 N73-23866
Development of lubrication theories and application of epilame-lubricant pairs for friction reduction
[NLL-RISLEY-TR-2547-(9091.9F)] 15 p1790 N73-24510
Development and testing of beryllium honeycomb sandwich composite panels
[NASA-CR-130648] 15 p1838 N73-24896
Water jet impingement wear tests on plexiglass, aluminum alloys, nickel, cobalt alloys, and stainless steels
[PB-215631/3] 16 p1890 N73-25294
Holography and optical filtering techniques for structural analysis, material tests, and astronomical observation - conference
[NASA-SP-299] 16 p1920 N73-25540
Stability of various equilibrium states in cubed incompressible neo-Hookean material subjected to pure homogeneous deformation
[AD-758700] 16 p1970 N73-25937
Analysis of heat transfer properties and thermophysical properties of materials used for aircraft and spacecraft construction
[AGARD-R-606] 16 p1975 N73-25968
Development of test equipment for random and constant amplitude loading on resonant and electrohydraulic fatigue machines
[RAE-TR-72226] 17 p2009 N73-26250
Analysis of embrittlement in zone refined iron and Armco iron after charging with hydrogen to determine cause of reaction
[RAE-LIB-TRANS-1666] 17 p2043 N73-26530
Standards for metallic specimens to include methods of mechanical and technological testing
[JPRS-59280] 17 p2044 N73-26538
Characteristics of glass fiber reinforced plastics using boron and carbon fibers
[RAE-LIB-TRANS-1687] 17 p2049 N73-26575
Analysis of aluminum oxide to determine material characterization, particle size distribution, and specific surface area 17 p2050 N73-26582
Application of principles of fracture mechanics to problem of preventing brittle fracture in sheet structures
[RAE-LIB-TRANS-1648] 17 p2092 N73-26921
Effects of irradiation on fracture and strength properties of pressure vessel steel plate and submerged arc weld
[HEDL-SA-387] 17 p2093 N73-26936
Performance tests of spur gears with and without tip relief to determine service life of M-50 and Super Nitralloy metals
[NASA-TM-X-68269] 18 p2155 N73-27413
Proceedings of conference on nondestructive testing and materials characterization with emphasis on development of new techniques for materials testing
[AD-760174] 18 p2157 N73-27427
Effects of mechanical and metallurgical factors on crack propagation and ductile fracturing resistance of steels
[PB-218919] 18 p2161 N73-27458
Bibliography of test equipment and procedures for determining physical and mechanical properties of iron and steel products
[PB-219047] 18 p2161 N73-27459
Axial load fatigue tests on unnotched specimens of aluminum alloy extrusions following aging specimens
[ARL/SM-NOTE-386] 18 p2203 N73-27780
Development of method for identifying nonlinear material behavior using finite element techniques
[PB-219090/8] 18 p2204 N73-27788
Thermal conductivity measurements of particulate materials in vacuum using basalt and soda lime glass beads of various size ranges as samples
[NASA-TM-X-64759] 18 p2205 N73-27801
Statistical analysis of crack growth in various materials resulting from variable loads
[AD-761445] 19 p2349 N73-28895
Development and characteristics of spectrophotometer for measuring transmittance of solid and liquid materials
[PAPER-76A5-729] 21 p2545 N73-30398
Procedures for accurate measurement of molar absorptivities to show sources of determinant error and methods for elimination of errors
[PAPER-76A5-734] 21 p2545 N73-30403
Materials technology programs in support of mercury rankine space power system
[NASA-TN-D-7355] 21 p2558 N73-30508
Research projects to develop and evaluate ceramic materials in areas of refractory structural ceramics and solid electrolyte ceramics
[NASA-CR-133741] 21 p2562 N73-30540
Research projects involving development and application of semiconductor materials and process for measuring properties of semiconductors at high pressures 21 p2607 N73-30894
Mathematical models for determining dynamic response of strain sensitive materials and structure to dynamic loads 22 p2724 N73-31797
Nondestructive tests of metallic and nonmetallic materials
[AD-764200] 23 p2798 N73-32378
Method for determining heat capacity of ceramic materials by measuring heat transfer during condensation process 23 p2807 N73-32445
Characteristics of silicon carbide samples produced by hot casting under pressure 23 p2808 N73-32450
Production of fire protective intumescent coatings to show methods of manufacture and resulting material properties
[NASA-CR-114470] 23 p2810 N73-32468
Analysis of factors affecting variability in fatigue life of materials to show effects of material type, load applications, and test conditions on scatter of data
[ARL/SM-REPT-342] 23 p2853 N73-32796
Definition of criteria and techniques of design, analysis, and test for using single major structural test article for performing dynamic, fatigue, and static testing
[NASA-CR-124404] 23 p2853 N73-32799
Stress analysis of adhesive lap joint subjected to tension, shear force, and bending moments for various material properties and thickness of adherents 24 p2988 N73-33877

**MATHEMATICAL ANALYSIS**
U APPLICATIONS OF MATHEMATICS

**MATHEMATICAL LOGIC**
NT ALGORITHMS
NT BOOLEAN ALGEBRA
NT BOOLEAN FUNCTIONS
NT EQUIVALENCE
NT FORMULAS [MATHEMATICS]
NT LATTICES [MATHEMATICS]
NT SET THEORY
NT THRESHOLD LOGIC

Synthesis of delay-free asynchronous sequential switching circuits
[AD-746392] 01 p0035 N73-10273
Logical function and circuit generator
[NASA-CASE-XLA-05099] 04 p0395 N73-13209
Algorithm for choosing adaptive loop parameters and adjustment intervals of adaptive control systems 07 p0764 N73-16207
Elements of numerical calculus
[ISS-72/13-PT-1] 10 p1179 N73-19590

Representations of language recognition problem for theorem prover in first order logic
[NASA-CR-131402] 11 p1310 N73-20632
Power of programming features in computer languages
[NASA-CR-131895] 14 p1638 N73-23280
Notes on problem involving permutations as subsequences
[NASA-CR-133103] 17 p2055 N73-26624
MATHEMATICAL MODELS
NT ANALOG SIMULATION
NT DIGITAL SIMULATION
Neural model as pulse interval processor
[AD-746007] 01 p0022 N73-10169
Mathematical model to simulate sphere-centered thin dipole antenna
[AD-745285] 01 p0034 N73-10264
Turbulent flow calculation and models
[NASA-CR-128372] 01 p0039 N73-10309
Solution of Navier-Stokes equation for sea water pressure determination
[NOTA-INTERNA-377] 01 p0042 N73-10328
One and two dimensional models of tidal propagation in St. Lawrence River
[NRC-12764] 01 p0048 N73-10382
Numerical analysis of stability and convergence conditions based on mathematical model of Arctic Ocean
[AD-745182] 01 p0053 N73-10429
Single layer, hydrodynamic numerical model for oceanography
[AD-745759] 01 p0053 N73-10432
Numerical weather forecasting methods - atmospheric and weather forcasting models
[NLL-M-20352-[5828.4F]-VOL-2] 01 p0073 N73-10596
Field theoretical model for critical behavor of helium 4 above critical point
[NOTA-INTERNA-374] 01 p0083 N73-10689
Mathematical models for studying coronal magnetic fields and solar wind 01 p0092 N73-10762
Current sheet magnetic field model for computing three dimensional currents flowing in solar corona 01 p0093 N73-10764
Physical model for determining structure of neutral sheets in solar corona 01 p0093 N73-10765
Generalized magnetic Weber-Davis model for calculating magnetic latitude effects in solar wind 01 p0094 N73-10778
Nonalgorithmic methods for determination of strength, oscillations and static and dynamic stability of deformable systems
[AD-745426] 01 p0114 N73-10939
Mathematical model for in vivo study of glucose homeostasis in humans
[NASA-CR-129171] 02 p0130 N73-11056
Mathematical models for studying vestibuli adaptation to stimuli in humans
[AMRU-R-70-1] 02 p0131 N73-11062
Development of mathematical model for slow phase rotational nystagmus induced by head movements
[AMRU-R-71-3] 02 p0131 N73-11065
Mathematical models for determining impact of supersonic gas jet on solid surfaces
[NLL-RTS-7551] 02 p0154 N73-11248
Mathematical models for predicting unsteady aerodynamic effects on axial flow compressor with distorted inflow - Squid project
[AD-746457] 02 p0157 N73-11271
Nonlinear interactions among standing surface and internal gravity waves
[AD-746138] 02 p0168 N73-11368
Mathematical models for analyzing internal gravity waves generated by stratified inviscid fluid flow over solid body
[AD-746137] 02 p0168 N73-11369
Procedures for studying reliability characteristics of systems with standbys - Themis project
[AD-745911] 02 p0179 N73-11451
Model of diffusion-type, HF chemical laser
[AD-745952] 02 p0183 N73-11484
Application of Backus-Gilbert theory for geophysical inverse problems to seismic body wave travel-time problem 02 p0200 N73-11618
Application of Backus-Gilbert method to electrical conductivity problem 02 p0200 N73-11619
Culling of redundant earth data for geophysical model fitting 02 p0200 N73-11620
Transmission line inversion problem applied to speech communication process 02 p0201 N73-11625
Comparative evolution of inverse problems and various mathematical methods used 02 p0201 N73-11629
Empirical procedure for predicting growth of ice crystals, grauple, and hail by diffusion
[AD-746451] 02 p0205 N73-11660
Attitude stability of dual spin spacecraft with mathematical model covering fuel sloshing, nutation dampers, and flexible bearings
[ESRO-CR-56] 02 p0235 N73-11908
State space techniques for obtaining mathematical models of flight test vehicles with nonlinear measurement variables in different moving bases
[AD-746657] 02 p0235 N73-11912
Mathematical model for convective and radiant heat transfer for gas flow and glass tube inner wall noting partial differential equations at boundary conditions
[LAAS-NI-CMOAC-72-I-11] 02 p0243 N73-11976
Computer model for determining economic impact of aircraft retrofit on airlines
[FAA-EQ-72-4-VOL-1] 02 p0245 N73-11988
Analytical model for parallel flow-induced vibrations experimentally checked on single rod test facility in water loop
[EUR-4771] 03 p0284 N73-12301
Critical flow study in gas-liquid flow, using numerical models for predicting critical flow rate
[AEC-TR-7309] 03 p0284 N73-12303
Mathematical model for geodetic survey of tracking stations using laser range finder and photographs including results of European tracking network
[GRGS-BULL-3] 03 p0294 N73-12398
Mathematical model for geodetic survey of tracking stations using laser range finder and photographs 03 p0294 N73-12399
Model for behavior of solid deuterium slab under laser irradiation
[LA-DC-72-415] 03 p0310 N73-12530
Aerodynamic analytical model for reducing supersonic jet exhaust noise
[AD-747774] 03 p0337 N73-12752
Bjorken scaling in deep inelastic electron proton scattering and parton models
[NOTA-INTERNA-391] 03 p0340 N73-12773
Analytical procedure for determining aerospike nozzle performance particularly performance around base area 03 p0349 N73-12848
Mathematical model for calculating scanning angle distribution of planetary albedo gamma rays above 100 MeV
[NASA-TM-X-66117] 03 p0353 N73-12874
Analysis of arterial hypoxemia caused by pulmonary malfunctions and regulation of oxygen during exercise and rest
[AD-746979] 04 p0380 N73-13092
Human operator model performance in tracking high performance aircraft
[AD-746725] 04 p0381 N73-13101
Mathematical model for phase change solidification in thermal control devices, including natural convection effects and transient, two dimensional, finite difference solution
[NASA-CR-129910] 04 p0385 N73-13132
Mathematical model and experimental evaluation of performance of phase change thermal control devices containing high thermal conductivity metal matrices
[NASA-CR-129909] 04 p0385 N73-13133
Procedures for constructing and analyzing combat models for planning and executing naval combat operations
[JPRS-57404] 04 p0393 N73-13194
Mathematical model of atmospheric drag distortion of long spinning, flexible antennas
[CRC-1232] 04 p0395 N73-13210
Asynchronous sequential circuit model with input delays and feedback 04 p0400 N73-13251
Analysis procedure for three dimensional, subsonic, duct flow
[AD-748649] 04 p0407 N73-13313
Mathematical model for inviscid stream flowing over turbulent fluid that behaves as elastic jelly
[AD-746990] 04 p0407 N73-13319
Model for stationary motion of atmosphere in equatorial latitudes based on nonlinear system of equations of hydrothermodynamics 04 p0442 N73-13604
Model for U-shaped solar bursts based on one single group of moderately relativistic electrons radiating in cold magnetoplasma
[AD-747033] 04 p0468 N73-13812
Extended theory of imperfect modeling with error approximation for application to thermal modeling of spacecrafts 04 p0483 N73-13949
Two stochastic models for petroleum exploration
[NASA-CR-129611] 04 p0488 N73-13992
Mathematical model for energy distribution in waveguide bifurcations
[DLR-FB-71-17] 05 p0520 N73-14224
Synthesis of gyroscopic heading indicator and use of gyroscope in rotating gimbal mount as gyrocompass
[JPRS-57280] 05 p0546 N73-14437
Synthesis of gyroscopic heading indicator consisting of gyrocompass and direction gyroscope 05 p0546 N73-14438
Mathematical models for developing Coanda eductors for pneumatic conveying systems used in underground excavation
[AD-749088] 05 p0552 N73-14485
Mathematical model of deformed state of metal strips during upsetting
[NLL-M-21511-[5828.4F]] 05 p0561 N73-14560
Theoretical statistical distribution model representing worldwide cloud cover
[NASA-TM-X-64714] 05 p0573 N73-14653
Parameterization of clouds in numerical circulation model 05 p0573 N73-14657
Mathematical model for short period terms in satellite orbits including comparison between analytical theory and numerical integration
[GRGS-BULL-2] 05 p0596 N73-14845
Mathematical model for short period terms in satellite orbits, including comparison between analytical theory and numerical integration 05 p0596 N73-14846
Comparison of satellite orbit elements, using analytic theory and numerical integration 05 p0596 N73-14847
Mathematical model for bending of hybrid and composite hybrid beams
[CRIF-MT-79] 05 p0603 N73-14902
Mathematical model of unsteady pressure distribution on harmonically oscillating slender cruciform wing and cylindrical body configurations
[DLR-FB-71-87] 06 p0615 N73-14990
Approximative parameters and probabilistic sequential subsets for modeling linear and renewal sources in communication theory 06 p0639 N73-15186
Computer calculations of two-phase flow transients in once-through steam generators
[CEA-CONF-2009] 06 p0655 N73-15318
Performance of mathematical snowmelt models and statistical analysis of avalanche forecasts 06 p0665 N73-15402
Computer program models for reliability prediction of electronic and electromechanical components
[NLL-RISLEY-TR-2329-[9091.9F]] 06 p0676 N73-15501
Mathematical model of thermally induced nonlinear propagation of laser beam in absorbing fluid medium
[DREV-TN-2049/72] 06 p0679 N73-15523
Theoretical model of Raman rotational spectrum of gas mixture applied to air mixture of oxygen and nitrogen to determine temperature
[NASA-TN-D-7126] 06 p0679 N73-15525
CO2 laser model study of electron beam
[AD-750314] 06 p0680 N73-15532
Fitting linear multistage models to input/output data by maximum likelihood method
[AD-750139] 06 p0691 N73-15625
Off-shell asymptotic behavior of electromagnetic form factors of composite particle
[TR-73-070] 06 p0703 N73-15728
Plasma diagnostics by means of collision dominated spherical electrostatic probes including mathematical model
[DLR-FB-71-41] 06 p0705 N73-15756
Pogo stability model considering time lag, magnitude of feedback, and loss of mass
[NASA-TN-D-7091] 06 p0726 N73-15924
Mathematical model for resonant vibration of cylindrical shells using the Rayleigh-Ritz method
[DLR-FB-71-92] 06 p0727 N73-15931
Mathematical model for unsteady one dimensional reaction waves during combustion of gas mixtures including application to air-propane mixture
[DLR-FB-71-66] 06 p0731 N73-15962
Mathematical models for analyzing synchronous functions of multimachine electrical power systems 07 p0760 N73-16175
Mathematical models for predicting microwave breakdown in fringing field of rectangular slot antenna
[AD-751320] 07 p0763 N73-16202
Augmentation and improvement of information management system simulation model
[NASA-CR-128718] 07 p0765 N73-16218
Mathematical model for energy losses and velocity distribution in laminar boundary layers, using quadrature formulas 07 p0770 N73-16257
Mathematical model for turbulent boundary layer of two liquid flows 07 p0772 N73-16267
Application of remote sensing techniques and models to geophysics 07 p0787 N73-16401
Magnetospheric field model incorporating OGO B and E magnetic field measurements
[NASA-TM-X-66172] 07 p0792 N73-16442
Mathematical modeling of solar gravitational fields
[ITF-71-130-P] 07 p0793 N73-16452
Mathematical model for reflection of shock waves
[REPT-9/71] 07 p0794 N73-16453
Mathematical models of midlatitude bottomside electron density profiles
[AD-751267] 07 p0796 N73-16477
Boltzmann equations for kinetic modeling of supersonically flowing electrically excited laser system
[NASA-TM-X-62196] 07 p0806 N73-16538
Models for force-free magnetic fields in plasmas with finite conductivity
[TRITA-EPP-72-24] 07 p0828 N73-16715

Mathematical models for predicting flow fields within and external to thrust reverser deployed in flight including forces and moments induced on aircraft by flow fields
[AD-751525] 07 p0837 N73-16784
Turbulent transport models for designing compressors and gas turbines
[AD-751757] 07 p0837 N73-16786
Zonal and tesseral harmonics of gravitational fields of major planets and constraints placed on models of planet interiors
[NASA-CR-130346] 07 p0841 N73-16810
Analytical methods for estimating circumferential and longitudinal temperature distributions in large space telescope
[NASA-TN-D-7174] 07 p0855 N73-16931
Models for candle-like flames produced by burning of polymers
08 p0883 N73-17146
Ejector flow model for predicting performance characteristics of supersonic ejector systems
08 p0896 N73-17251
One- and two-D core theories for analyzing ducted mixing and burning of coaxial streams
08 p0896 N73-17253
Mathematical models for gas surface interactions and calculating aerodynamic coefficients for simple geometric shapes and high Mach number flow past thin airfoils
[AD-752245] 08 p0899 N73-17278
Derivation of empirical global thermosphere model for magnetically quiet conditions from longitudinally averaged gas densities using expansion in spherical harmonics
[NASA-TM-X-66183] 08 p0917 N73-17512
Mathematical models for reducing force of gravity values from earth relief to external surface
[AD-752235] 08 p0920 N73-17538
Investigation of urban heat island phenomena in Austin, Texas, using two-dimensional, time-dependent, earth atmosphere mathematical model
[REPT-32] 08 p0938 N73-17681
Mathematical model and analysis of attitude stability and control of spinning flexible satellite in force-free environment
08 p0964 N73-17876
Computer models for application to automatic inspection, diagnostic, and prognostic system for maintenance of military aircraft - Appendix C
[AD-752886] 09 p0988 N73-18066
Development of mathematical models for C-130 aircraft to predict general trends and probable values for stability derivatives and mode parameters over flight envelope
[AD-753388] 09 p0989 N73-18076
Mathematical modeling of communication systems transponders and receivers at circuit detail and block levels
[NASA-CR-124097] 09 p1001 N73-18172
Simple method for developing computer models for digital and analog integrated circuits
[AD-753413] 09 p1008 N73-18232
Mathematical modeling of turbulent mixing
[NASA-CR-124086] 09 p1013 N73-18267
Darcy-Weisback equation for investigating solid-liquid flow in noncircular pipes
[BM-RI-7725] 09 p1013 N73-18271
Mathematical model of thermodynamic damage to metals irradiated by laser beams
[DREV-R-672/72] 09 p1043 N73-18503
Mathematical model for predicting erosion rate of graphite surface exposed to hot supersonic stream of hydrogen gas
[NASA-CR-130812] 09 p1050 N73-18564
Numerical calculation of quantitative characteristics of observation systems
[NAL-TR-301] 09 p1057 N73-18616
Two-dimensional numerical model for simulating formation and dissipation of advection fogs
[NASA-CR-2201] 09 p1060 N73-18648
Mathematical models for measuring stellar orientation of spacecraft
[JPRS-58389] 09 p1062 N73-18665
Mathematical model to predict scattering of plane acoustic wave from elastic spherical shell with different fluid media inside and out
[AD-752760] 09 p1067 N73-18708
Development of three stage model for fatigue failure of structure with several critical regions for initial failure
[ARL/SM-NOTE-338] 09 p1093 N73-18924
Mathematical model of force coefficient and pitching moment by wing-body configuration
[BMVG-FBWT-72-28] 10 p1103 N73-18997
Mathematical model of transition flight and application to Do-31 aircraft
[BMVG-FBWT-72-30] 10 p1107 N73-19025
Method of moments for approximating current distribution in antenna array with arbitrarily located parallel center fed dipoles with terminals in common plane
10 p1133 N73-19236
Computer simulation of space station computer-steered high gain antenna
[NASA-CR-128749] 10 p1134 N73-19239
Feasibility determination for application of principle of corresponding states to two phase choked flow
[NASA-TM-X-68193] 10 p1141 N73-19299
Semiempirical model for development of round turbulent jet in cross flow using asymptotic solution for jet excess velocity
[NLR-TR-71107-U] 10 p1142 N73-19307
Time dependent two dimensional numerical model for studying structure of squall line thunderstorm
10 p1180 N73-19597
Finite difference procedure for computing behavior of two-dimensional boundary layers and turbulence model to predict location and extent of transition region
10 p1204 N73-19796
Analytical approach for loss and deflection behavior of cascades in transonic flow including axial mass flow variation
10 p1204 N73-19800
Calculation method for external heat transfer to turbine blades
10 p1205 N73-19807
Method for prediction of turbulent boundary layer flow in vaneless radial diffuser and experimental validation
10 p1206 N73-19809
Mathematical model for prediction of axial compressor performance including effect of annulus wall boundary layers
10 p1206 N73-19812
Model for inherent contrast conditions in full-form objects
10 p1226 N73-19966
Statistical models of electromagnetic scattering from radar targets
[AD-753936] 11 p1256 N73-20192
Simple mathematical models of mechanical systems for ground support equipment, airborne launcher, vibration isolation design
[AD-754537] 11 p1267 N73-20283
Approximate solution of two-dimensional problem of non-steady state stratal flow with movable gas-liquid interface
[AD-754828] 11 p1273 N73-20328
Geometrical shock wave transmission model used to determine water surface peak spall velocities above single charge cratering detonations in medium overlain with water
[AD-755099] 11 p1273 N73-20329
Inclusion problem for monadic recursion schemes
[NASA-CR-131292] 11 p1311 N73-20634
Air pollution models, and problem areas in air pollution dispersion modeling
[NASA-SP-322] 11 p1313 N73-20658
Mathematical models for measuring inertial qualities of spherical gyroscope rotors with electric suspension
11 p1317 N73-20691
Mathematical models for measuring operating functions and performance of gyroscope with two degrees of freedom
11 p1318 N73-20696
Estimation procedures for in-flight vertical misalignment of platforms
11 p1319 N73-20707
Modelling error sensitivity of digital filters for alignment of inertial platforms
11 p1319 N73-20708
Differential method for evaluating performance of nonlinear accelerometers
11 p1320 N73-20715
Mathematical model for calculating breakdown voltage of solid homogeneous dielectric solid during thermal breakdown
[NLL-CE-TRANS-5560-[9022.09]]
11 p1329 N73-20786
Reliability model and associated computer code developed to compute reliability of monopropellant hydrazine spacecraft auxiliary propulsion system as function of time
[NASA-CR-131400] 11 p1333 N73-20821
MASS computer models for analyzing space shuttles and space shuttle payload operations
[NASA-CR-112286] 11 p1343 N73-20897
Cartesian and curvilinear coordinates for studying axial symmetrical deformation of rotatory bodies
[NLL-M-22827-[5828.4F]] 11 p1344 N73-20907
Laplace transformation and Volterra integral equation for studying heat transfer in laminar flow through pipe with annular space
[NLL-RTS-7525] 11 p1347 N73-20928
Comparisons between analog and numerical methods for studying response of an aircraft
[PUBL-97] 12 p1357 N73-21007
Computer modification of MOS transistor mathematical models
[CEA-R-4332] 12 p1383 N73-21218
Analytical models of viscoseal performance with rarefied gas sealant
[NASA-CR-121089] 12 p1408 N73-21409
Material selection determined from mathematical model of crack growth and failure
[NASA-TN-D-7221] 12 p1413 N73-21452
Numerical methods in theory of rarefied gases with application of Boltzmann equation
[NASA-TT-F-638] 12 p1417 N73-21483
Review of numerical methods used in solving Boltzmann equation
12 p1417 N73-21484
Asymptotic properties of full information estimators in dynamic autoregressive simultaneous equations
[P-4924] 12 p1418 N73-21494
Model for analyzing Markovian decision processes with unobservable states and costs
[P-4917] 12 p1419 N73-21495
Mathematical models for educational planning and personnel selection in Soviet Union
[JPRS-58793] 12 p1419 N73-21497
Mathematical models on various modes of functioning in linear dynamic programming
[NASA-TT-F-685] 12 p1419 N73-21499
Phase diagram of decorated Ising system in nonzero magnetic field
[NUB-2175] 12 p1428 N73-21576
Theory of amorphous semiconductors with electronic states in undulatory-graded band-gap model
12 p1438 N73-21650
Mathematical techniques for studying high frequency nonlinear longitudinal combustion instability in liquid propellant rocket engines
12 p1443 N73-21689
Analysis of vibratory characteristics of sonar transducer element using finite element three dimensional mathematical model
[AD-755177] 13 p1495 N73-22117
Analytic model to make comprehensive transition run-out calculations for compressible boundary layer with wall cooling
[AD-756890] 13 p1513 N73-22258
Statistical models for smoothing environmental economics and communications data
13 p1549 N73-22554
Mathematical model for development of first-order secular solutions to rotational motions of triaxial rigid body - Part 2
[NASA-CR-131878] 13 p1549 N73-22555
Two flux radiative transfer model for measuring absorption and scattering coefficients for nonhomogeneous minerals
[RE-451J] 13 p1558 N73-22632
Analytical model for prediction of flammability limits of combustible gas
13 p1590 N73-22889
Analysis of linear oscillating temperature distribution to determine thermal diffusivity coefficient of gases
[BER-1/73] 13 p1590 N73-22895
Mathematical model for thermal behavior of flat conductor cable under load
14 p1640 N73-23299
Analytical prediction of crosstalk in multi-wire digital data transmission
14 p1641 N73-23301
Step adaptation algorithms and application of stochastic graphs for analysis of discrete automatic systems
14 p1644 N73-23332
Stochastic network to model materials handling operations at air cargo terminals
[AD-757629] 14 p1647 N73-23356
Activity network to model cargo flow through air cargo terminal
[AD-757628] 14 p1647 N73-23357
Three-dimensional representation of hypersustentation during separated flow
[REF-8467] 14 p1648 N73-23371
Experimental and theoretical measurement of pulsed flow velocity and pressure in circular pipes
14 p1649 N73-23372
Mathematical models for calculating subcritical and supercritical compressible flow about blade cascades
14 p1649 N73-23378
Coefficient of turbulent exchange in mathematical model of radiation fog evolution
[AD-757490] 14 p1662 N73-23494
Analog computer models of tracking system errors
14 p1683 N73-23658
Numerical advection model for simulating maritime fog
[AD-757328] 14 p1685 N73-23676
Real forecast verification data for testing Hatter terminal weather forecast models
[AD-757489] 14 p1686 N73-23679
Mathematical model for Andromeda galaxy
[NASA-TT-F-14839] 14 p1704 N73-23830
Mathematical models for determining transport properties and dissociation equilibrium of N2 and O2 in high temperature air
[ESDU-00.01.07-AMEND-A] 14 p1718 N73-23937
Mathematical models of aircraft mass and performance
15 p1732 N73-24047
Mathematical models for deriving loudness function from physical evidence without human judgment
[NASA-TN-D-7297] 15 p1742 N73-24121
Mathematical models and computer simulation for predicting spectral parameters of radar echoes from rain clouds
[STC-TM-308] 15 p1750 N73-24180
Numerical simulation of free-boundary shoreline under hurrican action
15 p1770 N73-24337

Total modelling of gravitational fields into plane space with symmetry conservation
[ITF-72-139-P] 15 p1781 N73-24434
Position errors in airspeed calibration methods
[NAL-TR-298] 15 p1786 N73-24477
Mathematical models for surface ablation of silica-reinforced composites
15 p1801 N73-24596
Circulation model for feasibility of modifying earth surface climate at middle and high northern latitudes
[AD-757795] 15 p1807 N73-24641
Statistical reliability model and analysis of 5-kwe reactor thermoelectric system
[NASA-CR-121205] 15 p1809 N73-24661
Computerized simulation of plasmas in controlled thermonuclear fusion devices
[SU-799-X-1] 15 p1817 N73-24730
Model developed for opposed free and forced convection flow around heated cylinder
[AD-757993] 15 p1844 N73-24942
Associative approach test model data management system
[AD-750147] 16 p1879 N73-25209
Effectiveness of eddy viscosity models for coaxial and two-dimensional jets with and without coflowing stream
[AD-759576] 16 p1890 N73-25298
Compressible turbulent boundary layer solutions using eddy viscosity models
[AD-759164] 16 p1891 N73-25307
Development and revisions of mathematical theory of hydrostatic equilibrium for earth
[NASA-TM-X-66261] 16 p1906 N73-25415
Mathematical model for calculating time required for continuous wave CO2 laser to perforate thin metal sheets
[REPT-534] 16 p1923 N73-25562
Ziman theory for calculating electrical conductivity of liquid aluminum
[UCRL-51322] 16 p1929 N73-25605
Mathematical programming used in computer-aided-compensator design for control system
[NASA-CR-2248] 16 p1934 N73-25651
Feasibility of using adaptive estimation for atmospheric temperature forecasting
[AD-759546] 16 p1940 N73-25698
Digital computer model to predict spectral irradiance on ground target from sun and sky
[AD-758877] 16 p1945 N73-25739
Probabilistic model of nonisothermal gaseous flow through fine pored homogeneous media
17 p2013 N73-26276
Gas dynamic equations for analyzing hot gas and vapor expansion in meteor trail
17 p2023 N73-26366
Mathematical models for analyzing resonance effects on wave absorption and scattering in meteor trails
17 p2023 N73-26372
Mathematical models for studying atmospheric heating by ozone absorption of sunlight
[NASA-CR-132778] 17 p2024 N73-26382
Models for radiative heating and cooling and ozone photochemistry in stratosphere
[NASA-CR-132777] 17 p2025 N73-26385
Two-reservoir exchange model for Baltic Sea material balance
[GH-4] 17 p2027 N73-26407
Programs for comparing experimental data with mathematical models with respect to magnetic activity
[AD-760117] 17 p2029 N73-26422
Thermoelastic response model for actively controlling primary mirror surface error of orbiting telescope
[NASA-CR-124286] 17 p2033 N73-26449
Mathematical representation of flow curves for metallic materials
[RAE-LIB-TRANS-1675] 17 p2043 N73-26532
Numerical model of dry and wet cumulus convection
17 p2056 N73-26630
Method for calculating ground level concentration of pollutants emitted from high stack based on plume aerodynamics and atmospheric mixing
[PUB-73-3] 17 p2057 N73-26636
Statistical error model for solar electric propulsion thrust subsystem
[NASA-CR-133232] 17 p2077 N73-26799
Exponential equation for power law strain hardening behavior during tensile tests of structural alloys
[RAE-LIB-TRANS-1689] 17 p2092 N73-26922
Analytical method for determination of large signal characteristics of impatt amplifiers
18 p2122 N73-27151
Development of mathematical models for processing Skylab EREP altimeter data
[E73-10801] 18 p2138 N73-27276
Mathematical models for processing Skylab S-193 radar altimeter data
[E73-10812] 18 p2139 N73-27287
Instability model for stress corrosion and fatigue crack propagation in 4340 steel
[AD-761148] 18 p2162 N73-27461
Numerical time dependent model for simulating life-cycle of cumuli under different environmental conditions
18 p2170 N73-27525
Mathematical approach to estimating highway impact on air quality - Vol. 4
[PB-219814/1] 18 p2175 N73-27565
Diffractive excitation model for evaluation of inelastic part of proton-proton unitarity equation
18 p2182 N73-27614
Uncorrelated jet model in proton-proton and proton-antiproton annihilation integral
18 p2182 N73-27615
Nondiffractive models with n squared approximately 1/s
18 p2182 N73-27616
Computerized simulation of belt pinch experiments including plasma external circuit interactions
[LRP-61/73] 18 p2183 N73-27626
ESRO 1A [Aurorae] satellite dynamic model derived from attitude sensor data using smoothing factor in spline function subroutine
[RA-SAT-3.4-C-006] 18 p2201 N73-27767
Analysis of electronic digital computer inaccuracies
[AD-762235] 19 p2241 N73-28068
Proceedings of conference on free turbulent shear flows - Vol. 1
[NASA-SP-321-VOL-1] 19 p2252 N73-28154
Methods for calculation of turbulent free mixing
19 p2252 N73-28155
Application of statistical turbulence theory for validity determination of turbulence phenomenology
19 p2252 N73-28157
Kinematic eddy viscosity model which accounts for influence of density variations and preturbulence
19 p2252 N73-28159
Relationship between eddy-transport and second-order closure models for stratified media and for vortices
19 p2253 N73-28161
Model for free turbulent mixing in coflowing stream
19 p2253 N73-28162
Predictions of axisymmetric free turbulent shear flows using generalized eddy viscosity approach
19 p2253 N73-28163
Mass diffusion model for turbulent mixing of free jets
19 p2253 N73-28164
Comparison of six different turbulence models for prediction of free shear flows
19 p2253 N73-28165
Prediction of free turbulent mixing using turbulent kinetic energy method
19 p2253 N73-28167
General classification of approaches used for prediction of turbulent shear flows
19 p2254 N73-28173
Mathematical model for calculating transient flow of compressible condensable fluid mixtures in open channels
[UCID-16170] 19 p2255 N73-28181
Static penetration resistance of soils
[NASA-CR-133460] 19 p2294 N73-28445
Theoretical model of Sparton Model 601 M horizontal velocity gage
[AD-762268] 19 p2302 N73-28508
Mathematical technique for optimal control problems with initial conditions
[AD-762253] 19 p2315 N73-28620
Adaptive modeling technique for synthesizing controllers to provide corrective dynamics to operator mathematical model in closed loop control system
[NASA-CR-132294] 20 p2372 N73-29060
Modelling, analysis, and applications of class of all digital phase locked loops
20 p2375 N73-29082
Physical models of radio outbursts in extragalactic radio sources
20 p2375 N73-29087
Modelling, experimentation, and estimation for multipath signals between ground terminal and aerospace vehicle
20 p2376 N73-29089
Analytical model and computer program for studying disturbances of liquid propellants in feedline systems
[NASA-CR-124308] 20 p2388 N73-29188
Vortex-lattice method used in model to represent jet exhausting from flat plate into crossflowing stream
[AD-762502] 20 p2389 N73-29191
Mathematical model for shaping aerosol spectrum in troposphere
20 p2389 N73-29194
Acquisition of quick look data from SL-2, SL-3 planning, and development of mathematical models to process S-193 radar altimeter data
[E73-10917] 20 p2398 N73-29266
Mathematical model of radiation fog from evolution to dispersal
[NLL-M-23054-[5828.4F]] 20 p2441 N73-29610
Theoretical model for studying circulation and climate of atmosphere
20 p2442 N73-29616
Mathematical models for studying beta effect on meridional velocity of disturbed flow in ocean
20 p2447 N73-29655
Improved numerical models of mesoscale and small scale effects of atmospheric motion which influence global weather
[AD-762584] 20 p2451 N73-29698
Ghost-free dual resonance models
[LPTHE-73/16] 20 p2456 N73-29738
Ignition model for predicting ignition delay times of boron particle clouds in oxidizing atmosphere
20 p2484 N73-29955
Ergonomic control system information models
21 p2503 N73-30082
Application of computer systems for effective investigation of mathematical models in mechanical engineering
21 p2513 N73-30155
Static parameters of mechanical model of thin film electrostatic relay
21 p2514 N73-30171
Modeling flow cavitation in water
[PB-220531/8] 21 p2528 N73-30268
Application of ERTS-1 data to prediction and detection model for Menhaden fishing in Mississippi Delta
[E73-10961] 21 p2532 N73-30303
Reliability analysis and characterization model of adhesive bonds
[AD-763707] 21 p2563 N73-30549
Analytical synthesis method for feedback control of nonlinear multivariable systems
[AD-762797] 21 p2566 N73-30571
Mathematical models for matching geopotential and wind fields and improving accuracy of objective analysis
21 p2573 N73-30616
Mathematical models for analyzing origin and distribution of combustion generated pollutants in gas turbines
[NASA-CR-121208] 21 p2590 N73-30754
Model for energetic solar proton fluxes with applications to earth spacecraft
[NASA-TM-X-70433] 21 p2592 N73-30769
Extended automatic avionics interference prediction model
[ECAC-PR-73-002] 22 p2631 N73-31086
Finite element model of jointed concrete pavement on nonlinear viscous subgrade dynamic interaction of aircraft-pavement systems
[AD-764243] 22 p2647 N73-31213
Transition model for computing population density profiles of partially ionized argon in source flow expansion
[C-37] 22 p2652 N73-31242
General methods for calculating three dimensional laminar boundary layers over inclined blunt bodies
[AD-763831] 22 p2656 N73-31274
Diffusive equilibrium model for calculating characteristics of broadband ELF, VLF, and LF emissions in magnetosphere
[NASA-CR-133925] 22 p2666 N73-31363
Method for calculating ocean bottom magnetic anomalies
[AD-762532] 22 p2668 N73-31380
Target acquisition model for gun launched guided projectiles
[AD-763909] 22 p2676 N73-31432
Development and application of mathematical models for chemical and gas lasers - Part I
[AD-763905] 22 p2682 N73-31484
Mathematical model for identification of crops from directional reflectance
[NASA-CR-133989] 22 p2691 N73-31555
Enlarged and revised set of tables of two-associate-class partially balanced design
[NBS-AMS-63] 22 p2691 N73-31556
Solving equations of motion for behavior of plasma clouds in layered model ionosphere
[MPI-PAE/EXTRATERR-73] 22 p2704 N73-31658
Mathematical model for steady state wind-moon interaction
[COO-3577-2] 22 p2711 N73-31712
Mathematical models for determining dynamic response of strain sensitive materials and structure to dynamic loads
22 p2724 N73-31797
Mathematical model for real time simulation of tilt rotor aircraft to evaluate aircraft performance and handling qualities
[NASA-CR-114601] 23 p2742 N73-31947
Kalman filter estimation of aircraft pilot performance
[AD-764694] 23 p2752 N73-32026
Statistical model of turbulence based on elementary solutions of linearized Navier-Stokes equations
23 p2773 N73-32177
Stochastic modeling of turbulent heat and mass transport in anisotropic shear flow
23 p2773 N73-32181
Dynamics of wind driven lake currents and application of vertical cross-section models
23 p2777 N73-32211
Contour maps of global geoid and free air gravity anomalies of GEM-4 earth gravitational model
[NASA-TM-X-66240] 23 p2783 N73-32265

Construction of reliability cost-model
[NASA-TM-X-64777] 23 p2797 N73-32372
Multi-criteria resource allocation decision aid
23 p2812 N73-32480
Model to predict fission gas releases from UN fuel pins clad with various materials
[NASA-TN-D-7401] 23 p2818 N73-32531
Geometric codes for calculating space radiation transport in shielding configurations
[NASA-CR-124403] 23 p2821 N73-32551
Electron network model of solid interfaces, surface defects, planar defects, and thin films
23 p2825 N73-32584
One-dimensional time dependent diffusion convection model analysis of cosmic ray modulation during solar maximum
[TR-73-131] 23 p2834 N73-32647
Mathematical model of VHF ranging system to analyze performance of Apollo Soyuz test project
[NASA-CR-134063] 23 p2846 N73-32741
Modification of world dynamics model to account for pollution abatement
[NASA-TM-X-2832] 23 p2866 N73-32910
Airborne computer role in digital flight control systems, noting systems model, man machine interface, and integration
24 p2878 N73-32982
Mathematical model and digital computer simulation of cardiovascular control system response to ergometer exercise
24 p2886 N73-33049
Mathematical models and physiological mechanisms of goal-directed behavior
[JPRS-60091] 24 p2887 N73-33053
Theory of systems for effective behavior predictions
24 p2887 N73-33054
Approach to construction of formal model of behavior
24 p2887 N73-33055
One class of adaptive systems and results of computer modeling of their self instruction
24 p2887 N73-33056
Expedient functioning of automata with normal and disturbed behavior in experiments on reinforcement selection
24 p2887 N73-33057
Principles of construction for class of models of intelligent behavior
24 p2888 N73-33059
Experimental evaluation of model of motor behavior
24 p2888 N73-33060
Model of organization of goal-directed behavior
24 p2888 N73-33061
Statistical modeling of electromagnetic scattering from radar targets
24 p2893 N73-33099
Mathematical voice model for a priori digital speech analysis
24 p2894 N73-33104
Model for prediction of horizontal ray path deviation effects in high frequency ionospheric propagation
24 p2894 N73-33105
Mathematics of linear predictive filtering and application to speech analysis and synthesis
[AD-765176] 24 p2896 N73-33117
Shock wave propagation at interface between two rectilinear ducts noting oblique shock waves and mathematical models
[PUBL-137] 24 p2910 N73-33223
Mathematical model formulated for mean disturbance created in linear stratified fluid by growth and collapse of localized region of turbulent mixed fluid
[AD-764050] 24 p2910 N73-33224
Two dimensional time dependent numerical simulation of atmospheric flow over urban area
24 p2911 N73-33235
Snowmelt model for Chena River Basin
[E73-11085] 24 p2913 N73-33248
Land use mapping and modelling for Phoenix Quadrangle
[E73-11098] 24 p2914 N73-33255
Mathematical model for Northern Hemisphere atmospheric circulation during cold season
[AD-765544] 24 p2950 N73-33562
Mathematical theories for determining light propagation by sea water
24 p2957 N73-33627
Selection of similarity criteria for stream of plasma flying into magnetic dipole by mathematical model
[NASA-TT-F-15057] 24 p2962 N73-33670
Mathematical model for noncollisional plasma
[FRNC-TH-329] 24 p2963 N73-33679
Simulation procedures in plasma physics
[JUL-CONF-7] 24 p2963 N73-33680

**MATHEMATICAL STATISTICS**
U STATISTICAL ANALYSIS

**MATHEMATICS**
Summaries of research in mathematics, physics, chemistry, biophysics-biochemistry, and biology, and related reports - Weizmann Institute of Science
01 p0119 N73-10977
Soviet scientific abstracts on physics and mathematics
[JPRS-57242] 03 p0366 N73-12984

**MATHIEU EQUATION**
U MATHIEU FUNCTION

**MATHIEU FUNCTION**
Computer program for calculating individual characteristic values and associated solutions of Mathieu equation
[VUB-STR-1] 14 p1683 N73-23655

**MATRICES [CIRCUITS]**
Three axis addressing techniques for matrix display panels
[AD-751666] 07 p0833 N73-16749

**MATRICES [MATHEMATICS]**
NT ADJOINTS
NT CANONICAL FORMS
NT EIGENVALUES
NT EIGENVECTORS
NT JORDAN FORM
Continuation from deep inelastic electron scattering to deep electron-positron annihilation
[NOTA-INTERNA-378] 01 p0084 N73-10692
Algorithm for synthesizing mass and stiffness matrices from experimental vibration modes
01 p0119 N73-10983
Application of vector space processes for algebraic analysis of affine plane surfaces
02 p0196 N73-11583
Formulation of finite element matrix in Lagrangian variables for elastic thin shells with arbitrary geometric imperfections
[AD-747321] 03 p0361 N73-12946
Subroutines for estimating linear system parameters by matrix methods
[LAAS-AS-72-I-14] 04 p0394 N73-13204
Matrix method for computing radar scattering cross sections of airplanes
[AD-750486] 06 p0643 N73-15217
Law of formation of determinants of maximum value
[NRC-TT-1605] 06 p0690 N73-15617
Statistics of parallel dimers on mxn lattice
[NUB-2166] 07 p0813 N73-16594
Development of matrix method for determining gimbal errors of three-axis gyrostabilized platform with constant drift rate
08 p0923 N73-17558
Matrix solution for one dimensional model of radiation field arising from multiple scattered photons in planetary atmosphere
[NASA-CR-130755] 08 p0943 N73-17722
Hypermatrix core storage problem solved by triangularization method
[ISD-112] 09 p1058 N73-18624
Precision State and Filter Weighting Matrix Extrapolation routine for space shuttle guidance navigation
[NASA-CR-128803] 10 p1184 N73-19631
Arguments on symplectic matrices group of canonical differential equations
[NASA-TT-F-14806] 11 p1311 N73-20637
Symplectic matrices and structures of sets of unstable canonical systems with periodic coefficients
[NASA-TT-F-14810] 11 p1311 N73-20639
Right congruences and semisimplicity for Rees matrix semigroups
[AD-754816] 11 p1312 N73-20645
Development of mathematical matrix technique for calculating inviscid, rotational, compressible axisymmetric flow field through axial flow compressor
[ME/A-73-1] 13 p1570 N73-22723
Transfer matrix techniques for vibration analysis of curved skin-stringer structures with tuned elastomeric dampers
[AD-758220] 14 p1605 N73-23010
Semiempirical calculations of gf values, LS transition arrays, and spin-orbit matrices
[SAO-SPECIAL-REPT-351] 16 p1904 N73-25405
Fourier coefficients of Eisenstein series of the second degree
[NASA-TT-F-14937] 16 p1934 N73-25648
Analysis on Fourier coefficients of second degree Eisenstein series
[NASA-TT-F-14936] 16 p1934 N73-25649
Matrix equation for finite planar antenna arrays
[AD-759008] 17 p2004 N73-26209
High percentage of zero elements of sparse matrix methods based on orthogonality and conjugacy
[NASA-CR-133231] 17 p2054 N73-26617
Synthetic verification matrices of subjective weather forecasting
[AD-761485] 19 p2316 N73-28630
Matrix methods for determining nature of eigencurrents and eigenfields in conducting bodies
[AD-761456] 19 p2321 N73-28675
Divergence and necessary conditions for extremums associated with dimension reducing transformation matrix
20 p2438 N73-29577
Multivariate statistical analysis including divergence, probability of misclassification, information theory, and matrix analysis
[NASA-CR-128990] 20 p2438 N73-29578
Subroutines SYMAT and COVAR for use as test procedures in matrix calculations
[REPT-17] 20 p2438 N73-29581
Computational forms for transformed covariance matrix of multivariate normal populations
[REPT-19] 20 p2438 N73-29583
Perturbation and sensitivity inequalities in divergence calculations
[REPT-20] 20 p2438 N73-29584
General expression for derivative of inverse of differentiable matrix
[REPT-22] 20 p2439 N73-29586
Expression for transformed covariance matrix of multivariate normal populations
[REPT-24] 20 p2439 N73-29588
Orthogonal and unitary transformations for asymmetrically loaded symmetric systems
[AD-761542] 20 p2440 N73-29601
Matrix equations of radiation diffusion
20 p2472 N73-29857
Variability of eigenvectors and eigenvalues using autocorrelation matrices of vertical temperature profiles on regional latitudes
[AD-763145] 21 p2539 N73-30360
Baryon spectroscopy and regularities between SU[6] and SU[3] mass breaking parameters
[LPTHE-73/21] 21 p2581 N73-30687
Matrix perturbation techniques in structural dynamics
[NASA-CR-133795] 21 p2603 N73-30862
Three level Boolean digital simulation program for logic circuits noting topological matrix circuit representation and simplified temporal simulation
[LAAS-SL-73-I-08] 23 p2769 N73-32149

**MATRIX ALGEBRA**
U MATRICES [MATHEMATICS]

**MATRIX ANALYSIS**
U MATRICES [MATHEMATICS]

**MATRIX METHODS**
Matrix methods for dynamic modeling of human operator performance using Liapunov functions
01 p0014 N73-10111
Matrix method for calculating adaptive pre-whitening filter for radar echo signal processing
01 p0025 N73-10197
Analysis and design by matrix methods of circular antenna arrays consisting of identical parallel dipoles
12 p1382 N73-21205
Structural influence coefficient matrix for computer simulation of aerodynamic aircraft stability
[NASA-CR-112230] 13 p1469 N73-21898
Aerodynamic influence coefficient matrix for nonplanar wing-body-tail configurations
[NASA-CR-112231] 13 p1469 N73-21899
Matrix method for analyzing kinematics of spatial mechanisms for manipulators
17 p1989 N73-26077
Matrix displacement analysis of shells using curved SHEBA elements to approximate surface geometry
[ISD-134] 20 p2483 N73-29947
FORTRAN matrix abstraction program for structural analysis of aerospace structures, Vol. 2 - Digital computer program description
[AD-764360] 22 p2640 N73-31158
FORTRAN matrix abstraction program for structural analysis of aerospace structures, Vol. 5 - Engineering user and technical report
[AD-763812] 22 p2640 N73-31159
FORTRAN matrix abstraction program for structural analysis of aerospace structures, Vol. 6 - Digital computer program Phase I description
[AD-764366] 22 p2640 N73-31160
Computer programs for three dimensional civil engineering lattice structures noting matrix methods, computerized design, and repetitive lattices
[CRIF-MT-82] 24 p2989 N73-33889

**MATRIX STRESS CALCULATION**
U MATRIX METHODS

**MATRIX THEORY**
Asymptotic behavior of elastic form factors and light cone expansion for matrix elements
[TR-73-039] 01 p0083 N73-10683
Sum of two scattering matrices connected together by two hybrid circuits
[NLL-M-22701-[5828.4F]] 05 p0568 N73-14614

**MATTER [PHYSICS]**
Matter in neutron stars and relevance to pulsar observation
[NASA-TM-X-66067] 01 p0103 N73-10849
Continuous wave dye laser for studying interaction of electromagnetic radiation with matter
[AD-762370] 19 p2309 N73-28572
Annihilation processes as origin of matter-antimatter in universe
19 p2332 N73-28767

**MATURE STREAMS**
U STREAMS

**MATURE VEGETATION**
U VEGETATION

**MAURITANIA**
Evaluation of hydrology and vegetation in Sahelian zone of Mali, Mauritania, and Senegal during dry season/drought period based on ERTS-1 imagery
[E73-10488] 12 p1396 N73-21324

**MAXIMA**
Law of formation of determinants of maximum value
[NRC-TT-1605] 06 p0690 N73-15617
**MAXIMUM LIKELIHOOD ESTIMATES**
Computerized simulation of maximum likelihood decoding algorithm
[NASA-TR-R-396] 02 p0141 N73-11141
Maximum likelihood fit of straight line to pairs of seismological magnitudes having variations and measurement errors
[FOA-4-C-4474-A1] 04 p0440 N73-13588
Fitting linear multistage models to input/output data by maximum likelihood method
[AD-750139] 06 p0691 N73-15625
Application of maximum likelihood criterion and optimal input design for analyzing flight test data to obtain aircraft stability and control derivatives
[NASA-CR-2200] 12 p1364 N73-21071
Altitude-aided algorithm for determining aircraft position from radar tracking
[AD-756655] 13 p1492 N73-22097
Maximum likelihood testing algorithm for estimating monopulse radar signal amplitude in air traffic control
[AD-756844] 13 p1493 N73-22105
Onboard, on-line parameter updating for Mars stratosphere and troposphere, using maximum likelihood estimation
15 p1829 N73-24821
Comparisons of maximum likelihood estimator, Bayesian estimator, and known failure rate
[NASA-CR-133227] 17 p2004 N73-26203
Maximum likelihood efficiency estimation procedures for statistical reliability analyses
[AD-760152] 17 p2039 N73-26493
Measurement subsystem parameter optimization to enhance estimates
[AD-759175] 17 p2055 N73-26625
Maximum likelihood determination of electron tracks in propane, propane-Freon, and hydrogen-neon bubble chambers
[JINR-P10-6868] 17 p2066 N73-26712
Maximum likelihood estimate of parameters of Gaussian random processes
18 p2170 N73-27522
Rank-k maximal statistics for divergence and probability of misclassification
[REPT-21] 20 p2438 N73-29585
Maximum likelihood procedure used for classification problem involving equivalence classes and constant divergence
[REPT-23] 20 p2439 N73-29587
Maximum likelihood receiver for pulse communication systems
[AD-764641] 23 p2758 N73-32072
**MAXIMUM PRINCIPLE**
Maximum principle for determining necessary conditions for optimality when delay depends on state, control, and time
[AD-753675] 10 p1179 N73-19592
**MAXWELL EQUATION**
Propagation properties of ion density perturbations and waves in collisionless plasmas with Maxwellian velocity distribution functions
[RISO-257] 03 p0343 N73-12795
Mathematical representation with metric form to first order of gravitationally modified Maxwell equation in Lorentz symmetric linear field theory
[NASA-CR-130754] 08 p0915 N73-17500
Description of linear wave propagation in hot collisionless plasmas using Vlasov and Maxwell equations
[NASA-CR-131496] 13 p1562 N73-22663
Numerical calculation of several two dimensional magnetohydrodynamic flows in channels
[AD-759424] 16 p1893 N73-25319
Four moment method for studying thermal conductivity in rarefied gas confined in concentric cylinders
16 p1973 N73-25955
Maxwell equation and approximation theory for examining attenuation behavior of coaxial cables with woven outer conductors
[RAE-LIB-TRANS-1642] 17 p1997 N73-26147
**MAXWELL-BOLTZMANN DENSITY FUNCTION**
Ion energy distribution functions parallel and perpendicular to modified Penning discharge with high kinetic temperatures and Maxwellian velocity distribution of ions
[NASA-TM-X-68150] 01 p0079 N73-10656
Perturbation of Maxwellian distribution in chemically reacting gas mixtures
12 p1418 N73-21493
**MAXWELLIAN DISTRIBUTION (DENSITY)**
U MAXWELL-BOLTZMANN DENSITY FUNCTION
**MCDONNELL AIRCRAFT**
NT DC 10 AIRCRAFT
NT F-4 AIRCRAFT
**MCDONNELL MILITARY AIRCRAFT**
U MILITARY AIRCRAFT
**MEAN**
Mean monthly values of turbulent heat and moisture fluxes over oceans
21 p2572 N73-30613
**MEAN TIME BETWEEN FAILURES**
U MTBF
**MEANDERS**
Meander patterns of Feather and Colorado Rivers
05 p0537 N73-14366
**MEASURANDS**
U MEASUREMENT
**MEASURE AND INTEGRATION**
NT BINARY INTEGRATION
NT FUNCTIONAL INTEGRATION
NT INTEGRAL CALCULUS
NT LEBESGUE THEOREM
NT NUMERICAL INTEGRATION
NT RUNGE-KUTTA METHOD
NT WEIGHTING FUNCTIONS
Automatic analog to digital assembly for measuring electronic equipment characteristics
[CEA-CONF-1966] 03 p0302 N73-12468
Computerized on-line measurement processor for quality control of electronic materials
[CEA-CONF-1967] 03 p0302 N73-12469
**MEASURE THEORY**
U MEASURE AND INTEGRATION
**MEASUREMENT**
Absolute gravity measurements using earth tides for analyzing earth structure
[AD-748529] 05 p0544 N73-14423
Dynamic calibration of gas flowmeters by impedance measurement in oscillating flow
[ARC-CP-1224] 05 p0548 N73-14451
**MEASURES**
Index to reports of National Conference on Weights and Measures from 1905 to 1971
[NBS-SP-377] 09 p1101 N73-18985
**MEASURING**
U MEASUREMENT
**MEASURING APPARATUS**
U MEASURING INSTRUMENTS
**MEASURING INSTRUMENTS**
NT ACCELEROMETERS
NT ACTINOMETERS
NT ALTIMETERS
NT AMMETERS
NT ANALYZERS
NT ANEMOMETERS
NT APPROACH INDICATORS
NT ATOMIC CLOCKS
NT ATTITUDE INDICATORS
NT BAROMETERS
NT BATHYMETERS
NT BOLOMETERS
NT BOMB CALORIMETERS
NT CALORIMETERS
NT CERENKOV COUNTERS
NT CHRONOMETERS
NT CINETHEODOLITES
NT CLOCKS
NT CLOUD HEIGHT INDICATORS
NT COMPARATORS
NT COULOMETERS
NT COUNTERS
NT DEFORMETERS
NT DENSITOMETERS
NT DIFFRACTOMETERS
NT DISTANCE MEASURING EQUIPMENT
NT DOSIMETERS
NT DROPSONDES
NT DYNAMOMETERS
NT EBERT SPECTROMETERS
NT ELECTRICAL CONDUCTIVITY METERS
NT ELECTROMETERS
NT ELECTRON COUNTERS
NT ELECTRON PROBES
NT ELECTROPHOTOMETERS
NT ELECTROSTATIC PROBES
NT ELLIPSOMETERS
NT ERGOMETERS
NT EXTENSOMETERS
NT FABRY-PEROT INTERFEROMETERS
NT FIELD INTENSITY METERS
NT FILTER WHEEL INFRARED SPECTROMETERS
NT FLOW DIRECTION INDICATORS
NT FLOWMETERS
NT FUEL GAGES
NT GAS METERS
NT GEIGER COUNTERS
NT GRAVIMETERS
NT GRAVITY GRADIOMETERS
NT GYRO HORIZONS
NT GYROCOMPASSES
NT HELIOMETERS
NT HODOSCOPES
NT HOT-FILM ANEMOMETERS
NT HOT-WIRE ANEMOMETERS
NT HOT-WIRE FLOWMETERS
NT HYGROMETERS
NT IMPEDANCE PROBES
NT INDICATING INSTRUMENTS
NT INFRARED DETECTORS
NT INFRARED INSTRUMENTS
NT INFRARED INTERFEROMETERS
NT INFRARED SCANNERS
NT INFRARED SPECTROMETERS
NT INFRARED SPECTROPHOTOMETERS
NT INTERFEROMETERS
NT ION PROBES
NT ION TRAPS [INSTRUMENTATION]
NT IONIZATION GAGES
NT IONOSONDES
NT LASER ALTIMETERS
NT LASER RANGE FINDERS
NT LUNAR SEISMOGRAPHS
NT MACH-ZEHNDER INTERFEROMETERS
NT MAGNETIC PROBES
NT MAGNETOMETERS
NT MANOMETERS
NT MASS SPECTROMETERS
NT METEOROLOGICAL INSTRUMENTS
NT MICHELSON INTERFEROMETERS
NT MICROBALANCES
NT MICRODENSITOMETERS
NT MICROWAVE INTERFEROMETERS
NT MICROWAVE PLASMA PROBES
NT MICROWAVE PROBES
NT MICROWAVE RADIOMETERS
NT MICROWAVE REFLECTOMETERS
NT MICROWAVE SENSORS
NT MONOCHROMATORS
NT NEPHELOMETERS
NT NEUTRON COUNTERS
NT NEUTRON SPECTROMETERS
NT NOISE METERS
NT OCULOMETERS
NT OMEGA NAVIGATION SYSTEM
NT OPTICAL MEASURING INSTRUMENTS
NT OPTICAL RANGE FINDERS
NT OPTICAL SCANNERS
NT OSCILLOGRAPHS
NT OXYGEN ANALYZERS
NT PARTICLE TELESCOPES
NT PASSIVE L-BAND RADIOMETERS
NT PENETROMETERS
NT PENNING GAGES
NT PHASE SWITCHING INTERFEROMETERS
NT PHOTOMETERS
NT PIEZOELECTRIC GAGES
NT PLAN POSITION INDICATORS
NT PLASMA PROBES
NT POLARIMETERS
NT POSITION INDICATORS
NT POTENTIOMETERS [INSTRUMENTS]
NT PRESSURE GAGES
NT PROFILOMETERS
NT PROPORTIONAL COUNTERS
NT PSYCHROMETERS
NT PYRANOMETERS
NT PYROHELIOMETERS
NT PYROMETERS
NT QUANTUM COUNTERS
NT RADIATION COUNTERS
NT RADIATION DETECTORS
NT RADIATION MEASURING INSTRUMENTS
NT RADIATION PYROMETERS
NT RADIO ALTIMETERS
NT RADIO DIRECTION FINDERS
NT RADIO FREQUENCY IMPEDANCE PROBES
NT RADIO INTERFEROMETERS
NT RADIOMETERS
NT RADIOSONDES
NT RAIN GAGES
NT RANGE FINDERS
NT RAWINSONDES
NT REFLECTOMETERS
NT RESISTANCE THERMOMETERS
NT RESONANCE PROBES
NT RESPIROMETERS
NT RIOMETERS
NT SATELLITE-BORNE INSTRUMENTS
NT SCATTEROMETERS
NT SCINTILLATION COUNTERS
NT SEISMOGRAPHS
NT SHOCK MEASURING INSTRUMENTS
NT SIGNAL ANALYZERS
NT SILICON RADIATION DETECTORS
NT SOLAR SPECTROMETERS
NT SPACECRAFT POSITION INDICATORS
NT SPARK CHAMBERS
NT SPECTROHELIOGRAPHS
NT SPECTROMETERS
NT SPECTROPHOTOMETERS
NT SPECTRORADIOMETERS
NT SPEED INDICATORS
NT STRAIN GAGE BALANCES
NT STRAIN GAGES
NT TACHOMETERS
NT TEMPERATURE MEASURING INSTRUMENTS
NT TEMPERATURE PROBES
NT TENSOMETERS
NT THEODOLITES
NT THERMAL CONDUCTIVITY GAGES
NT THERMOMETERS
NT THRESHOLD DETECTORS [DOSIMETERS]
NT TIMING DEVICES
NT TRANSMISSOMETERS
NT ULTRAVIOLET SPECTROMETERS
NT ULTRAVIOLET SPECTROPHOTOMETERS
NT VACUUM GAGES
NT VARIOMETERS

NT VIBRATION METERS
NT VISCOMETERS
NT VOLTMETERS
NT WEATHER DATA RECORDERS
Electronic instruments for continuous cardiovascular systems measurements
[NASA-TT-F-14492] 01 p0020 N73-10154
Cross flexure sting designed for measuring dynamic stability of slender bodies of revolution with delta wings in supersonic wind tunnel tests
[FFA-AU-637] 01 p0035 N73-10278
Procedure for determining noise levels in flight test measuring systems
01 p0056 N73-10456
Instrumentation for photometry, and amplifier and circuit design
[NBS-TN-594-2] 01 p0056 N73-10459
Failure analysis of Geiger counters used in nucleonic oil gauging system of USAF aircraft
[AD-746267] 01 p0059 N73-10485
Nuclear and instrumentation research
[AECL-4129] 01 p0079 N73-10651
Laser pulses transmitted from ground stations to aircraft or satellites used for 3-D multilateration system for precision geodetic measurements with 1-cm accuracy
01 p0119 N73-10982
Technique and instrument for measuring adhesive force
[NLL-TRANS-2863-[9022.81]]
02 p0171 N73-11384
Comet probe for analyzing properties of solar wind and direction of type 1 comet tails
02 p0228 N73-11845
Surface based altitude measuring system for accurately measuring altitude of airborne vehicle
[NASA-CASE-ERC-10412-1] 03 p0273 N73-12211
Computerized on-line measurement processor for quality control of electronic materials
[CEA-CONF-1967] 03 p0302 N73-12469
Computer system for control of electronics measuring devices and numerical information processing of measurements
[CEA-CONF-1968] 03 p0333 N73-12713
Portable sampling and measurement system for determining gaseous emission species in afterburn of turbojet engine at ground level
[AD-747773] 03 p0351 N73-12866
Instrument for measuring magnitude and direction of flow velocity in flow field
[NASA-CASE-LAR-10855-1] 04 p0419 N73-13415
Errors in air temperature measurement resulting from instrument inertia
04 p0443 N73-13615
Radiant power measuring instrument for measurement of downwelling and reflected radiance within ERTS multispectral scanner bands
[E72-10366] 05 p0535 N73-14354
Automatic device for measuring human metabolic oxygen rate and breathing dynamics
[NASA-CASE-MFS-21415-1] 06 p0635 N73-15156
Device for recording locations of measurements made by hand-held noncontacting probe
[NASA-CASE-LAR-10806-1] 06 p0673 N73-15474
X ray device for measuring titanium tritide film thickness in presence of background radiation
[NASA-TM-X-68170] 06 p0673 N73-15475
Design and performance of two dimensional sensor array system for image area measurements
[AD-750315] 06 p0675 N73-15490
Performance of sensing system having inverse function amplifier
[RD/B/M-2306] 08 p0889 N73-17196
Microwave gauge for measuring thickness of hot steel product during production
[PB-212210] 08 p0925 N73-17583
Operating principles of force measuring and generating equipment in NBS research facilities
[NBS-SP-370] 09 p1010 N73-18243
Man machine systems, control theory, nuclear geophysics, and research instrumentation
[RISO-M-1509] 10 p1137 N73-19263
Multiaxes vibration device for making vibration tests along orthogonal axes of test specimen
[NASA-CASE-MFS-20242] 10 p1158 N73-19421
Material testing system with load sensor for applying and measuring cyclic tensile and compressive loads to test specimens
[NASA-CASE-MFS-20673] 11 p1291 N73-20476
Development of droplet monitoring probe for use in analysis of droplet propagation in mixed-phase fluid stream
[NASA-CASE-NPO-10985] 11 p1291 N73-20478
Remotely controlled device for detection of mass changes in selected specimens
[NASA-CASE-MFS-21556-1] 11 p1292 N73-20487
Development of crack propagation gases based on plating and etching processes and application to center notch, edge notch, and cleavage type specimens
[AD-754762] 11 p1295 N73-20511
NBS activities in developing measuring methods for semiconductors
[NASA-CR-131275] 11 p1330 N73-20792
Reliability and performance of landbased and shipboard Air Force instrumentation systems
[AD-755916] 12 p1389 N73-21262
Characteristics of noise-resistant receiver for wireless electrical communication circuit for drill speed measurement
[AD-756090] 13 p1495 N73-22122
Jet aircraft noise and sonic boom measuring device which converts sound pressure into electric current
[NASA-CASE-LAR-11173-1] 13 p1529 N73-22387
Spacecraft pressure gage reliability studies relative to gas dynamics and metal surface testing
[NASA-CR-112320] 13 p1529 N73-22392
Determination of corrosion resistance of coatings on low alloy steel and susceptibility to exfoliation of 7178 aluminum alloy using Lawrence corrosion detection gauge
[AD-755163] 13 p1531 N73-22405
Device for measuring angle of arrival of laser beams and predictions of expected results for input apertures and turbulence
[AD-755404] 13 p1538 N73-22464
Design and analysis of Type 2 correlation-extreme systems composed of control circuits and gages for measuring random functions
14 p1644 N73-23335
Instrumentation improvement program for Pacific Missile Range during 1971 - 1972
[AD-757815] 14 p1647 N73-23360
Instrumentation and techniques for determining effects of gravitational and inertial forces on cardiovascular and respiratory dynamics
[NASA-CR-133212] 16 p1867 N73-25119
Preparation of equipment and procedures for program to perform broadband noise measurements at sea
[AD-759033] 16 p1877 N73-25195
Improvement of system for measuring intensity of radio echoes from meteorological radar
[AD-759759] 16 p1878 N73-25201
Device for measuring tensile forces applied to tension members
[NASA-CASE-MFS-21728-1] 16 p1912 N73-25467
Standardization of geodetic instruments in U.S.S.R. research facility
[AD-759687] 16 p1914 N73-25492
Improvement in methods of measurement for semiconductor materials, process control, and devices
[NASA-CR-133030] 16 p1953 N73-25800
Design and operation of sonic velometer using transit times of ultrasonic pulses in air to measure air velocity
17 p2031 N73-26434
Characteristics and operational problems of overflow snow gage
[NLL-M-22982-[5828.4F]] 18 p2150 N73-27375
Operational characteristics of sky noise measuring instruments and analysis of discrepancies in data acquired by each instrument
[NASA-CR-133415] 18 p2151 N73-27383
Device for measuring thermoelectric properties of materials under high pressure
[NASA-CASE-NPO-11749] 19 p2299 N73-28486
Ionosphere D and F region high frequency ray propagation effects and design of high frequency dynamic phase metering instruments
20 p2375 N73-29083
Profiles of atmospheric temperature and optical refractive index structure measured over land and ocean to 3 km above surface
[AD-762460] 20 p2450 N73-29687
Determination of orientation of instrument trihedrons and applications in inertial navigation
20 p2451 N73-29701
Primordial helium abundance and population II binary stars, measurement technique
20 p2469 N73-29832
Measurement of control mechanism of accommodation-vergence eye movement system in human eyes using electro-optical measuring instrument
21 p2500 N73-30062
Radio frequency source resistance measuring instruments of varied design
[NASA-CASE-NPO-11291-1] 21 p2543 N73-30388
Absolute pressure measuring device for measuring gas density level in high vacuum range
[NASA-CASE-LAR-10000] 21 p2544 N73-30394
Three-axis, adjustable loading structure for testing soundness of aircraft skin by applying pressure
[NASA-CASE-FRC-10051-1] 21 p2547 N73-30416
Thin film analyzer utilizing holographic techniques
[NASA-CASE-MFS-20823-1] 21 p2554 N73-30476
Electrophotometry, photoelectronic images, converters, and television equipment for studying variable stars
[NASA-TT-F-797] 21 p2594 N73-30783
Digital detector for measuring liquid helium level
[FB-221313] 22 p2676 N73-31436
Techniques and associated instrumentation for high temperature emissivity measurements
[NASA-CR-124423] 23 p2792 N73-32339
Prototype automatic sleep analyzer for clinical applications
[NASA-CR-134049] 23 p2793 N73-32346
Radiation hazards produced by gages used in industrial processes and precautions to avoid exposure of personnel to radiation hazards
24 p2952 N73-33583

MECHANICAL DEVICES
Design, development, and characteristics of industrial robot machinery to show load capacity, positioning accuracy, power actuators, and method of controls
01 p0060 N73-10486
Numerical procedures for designing cams with radial followers for conditions of straight line travel and flat faced followers with faces normal to direction of motion
[ESDU-66009] 01 p0060 N73-10490
Characteristics of dry rubbing bearings with guide to design and material selection based on specific applications
[ESDU-68018] 01 p0060 N73-10491
Numerical analysis of contact stresses between cam and follower mechanisms for combinations of materials, surface finish, and lubrication conditions
[ESDU-66002] 01 p0060 N73-10492
Numerical analysis of performance of sinusoidal acceleration cams using radial followers and no opening or closing ramps
[ESDU-66026-AMEND-A] 01 p0060 N73-10494
Design, development, and evaluation of flexible drive shaft coupling used for propulsion of HH-2D helicopter
[AD-746502] 01 p0063 N73-10519
Development of design data for metallic materials, fasteners, joints, and structural elements used in aerospace vehicle design
[AD-748268] 04 p0479 N73-13917
Linear control theory for generating optimal trajectories between initial and final positions of n degree of freedom mechanical arm
[NASA-CR-123980] 05 p0551 N73-14470
Development and characteristics of rotary actuator for use on spacecraft to deploy and support pivotal structures such as solar panels
[NASA-CASE-NPO-10680] 05 p0597 N73-14855
Design, development, and evaluation of flywheel powered hoist for personnel rescue missions conducted by helicopters
[AD-751217] 07 p0741 N73-16029
Automatic inoculating device for agar trays using cotton swab or loop
[NASA-CASE-LAR-11074-1] 07 p0750 N73-16096
Papers presented at 7th Aerospace Mechanisms Symposium
[NASA-TM-X-58106] 09 p1087 N73-18866
Mechanical component screening for multispectral scanner mirror mechanism used on Earth Resources Technology Satellite
09 p1087 N73-18872
Design, fabrication, and evaluation of mechanical devices for supporting external stores on military helicopters
[AD-755532] 13 p1535 N73-22436
Development of guidelines for selection of hardware items for use in manned spacecraft design to obtain five year maintenance-free service life - Vol. 3
[NASA-CR-128907] 14 p1707 N73-23855
Development of guidelines for selection of manned spacecraft equipment and recommendations for performance and quality control tests
[NASA-CR-128909] 14 p1708 N73-23857
Collapsible support for antenna reflector applied to installation of spacecraft antennas
[NASA-CASE-NPO-11751] 15 p1749 N73-24176
Development of mechanical linkage for lifting pin-supported electronic packages from electronic circuit boards without damage to connector pins
[NASA-CASE-NPO-13157-1] 17 p2036 N73-26475
Analysis of dynamics of free-piston expander-compressor machinery
18 p2156 N73-27416
Inductive plasma pulverization for protecting mechanical and electronic components
[CEA-CONF-2111] 21 p2583 N73-30701
Pneumatic foot pedal operated fluidic exercising device
[NASA-CASE-MSC-11561-1] 23 p2751 N73-32014
Mechanical exposure interlock device for preventing film overexposure in oscilloscope camera
[NASA-CASE-LAR-10319-1] 23 p2790 N73-32322
Development of mechanical equipment reliability prediction techniques
[AD-765367] 23 p2799 N73-32390

MECHANICAL DRAWINGS
U ENGINEERING DRAWINGS

MECHANICAL DRIVES
NT HELICOPTER PROPELLER DRIVE
NT MAGNETIC TAPE TRANSPORTS
Analysis of factors affecting design of interference-fit collars on rotating shafts
[ESDU-68002] 01 p0061 N73-10496
Numerical analysis of nominal interface pressures and stresses for shafts with interference fit collars
[ESDU-68003-AMEND-A] 01 p0061 N73-10497
State of stress and strain in rectangular belt pulled over cylindrical pulley
[AD-747318] 03 p0307 N73-12507
Foreign process for developing spiral bevel gear for CH-47 helicopter
[AD-747857] 03 p0309 N73-12522

Advanced technology hoist-drive system applicable to helicopter cargo hoists with capacities ranging from 12.5 to 50 tons
[AD-746629] 04 p0377 N73-13067
Design and technical characteristics of rotary automatic devices for pressing and gauging of metal ceramic structural parts
04 p0432 N73-13524
Evaluation of exact point speed and least squares procedures for determining balance of flexible rotating machinery
[NASA-CR-121035] 05 p0551 N73-14477
Development and characteristics of rotary actuator for use on spacecraft to deploy and support pivotal structures such as solar panels
[NASA-CASE-NPO-10680] 05 p0597 N73-14855
Investigation of high performance variable speed 10 hp machine tool spindle drive system
[E/C-3] 06 p0677 N73-15505
Effect of dynamic absorbers and damping on noise generated by CH-47 helicopter rotor transmission
[AD-752579] 08 p0868 N73-17031
Design and performance of segmented magnetic torque converter for mechanical drives
[AD-753541] 10 p1167 N73-19498
Development of design criteria for maximum horsepower to be transmitted using cycloidal cam transmission and application to marine gas turbine engines
[AD-754822] 11 p1301 N73-20554
Reliability and operational safety of mechanical helicopter transmission boxes
12 p1357 N73-21012
Analysis of parameters and elastohydrodynamic principles affecting lubrication of transmission components with application to helicopter mechanical drive systems
[NASA-TM-X-68215] 12 p1364 N73-21069
Fatigue life and wear tests of spur gears based on pitting fatigue at pitch circle to compare AISI M-50 and super nitralloy materials
[NASA-TN-D-7261] 12 p1408 N73-21411
Cost effectiveness analysis of helicopter transmission components to determine effect of extended overhaul life up to 6,000 hours
[AD-758465] 14 p1604 N73-23007
Mechanical drives of electrical motors
[AD-756705] 14 p1642 N73-23319
Basic principles of variable speed drives including torque, speed ratio, and power
[NASA-TM-X-68244] 15 p1791 N73-24522
Magnetic couplings and magnetomechanical transmissions for airtight manipulator design
17 p1989 N73-26086
Development of turbine engine accessory drive techniques to establish potential systems for lightweight low profile package
[AD-761527] 19 p2330 N73-28741
Structural analysis of mechanical rhombic drives for machines operating on Stirling cycle
[AD-761594] 19 p2330 N73-28749
Development and characteristics of concentric output differential gearing system
[NASA-CASE-ARC-10462-1] 20 p2423 N73-29459
Failure analysis of synchronizing drive shaft adapter on CH-47A helicopter for improved reliability and cost reduction
[AD-763186] 21 p2497 N73-30041
Feasibility of producing constant speed drive with aid of gyroscope
[AD-763256] 21 p2550 N73-30445
Prototype mechanical drive for boiling water reactor in-core out-core neutron flux detectors
[BMBW-FBK-72-25] 22 p2699 N73-31617
Mechanical drives for communication satellite antennas and solar arrays
[DGLR-PAPER-73-050] 24 p2986 N73-33864

**MECHANICAL ENGINEERING**
Research reports for various engineering sciences and materials and metallurgy
14 p1721 N73-23961
Dynamic and rotary machinery, design and reliability
[AD-762440] 19 p2305 N73-28542
Application of computer systems in solution of complex problems of planning in mechanical engineering
21 p2512 N73-30151
Application of computer systems for effective investigation of mathematical models in mechanical engineering
21 p2513 N73-30155

**MECHANICAL IMPEDANCE**
Application of multipoint excitation for helicopter structural dynamic testing using impedance techniques - Vol. I
[AD-756389] 14 p1716 N73-23921
Dynamic structural analysis of helicopter structures using single point excitation techniques - Vol. 2
[AD-756390] 14 p1716 N73-23922
Acceleration effects on mechanical impedance of human body in supine position
19 p2227 N73-27963

**MECHANICAL MEASUREMENT**
NT DISPLACEMENT MEASUREMENT
NT DRAG MEASUREMENT
NT FLOW MEASUREMENT
NT FRICTION MEASUREMENT
NT PRESSURE MEASUREMENTS
NT STRESS MEASUREMENT
NT THRUST MEASUREMENT
NT VELOCITY MEASUREMENT
NT VIBRATION MEASUREMENT
NT WIND MEASUREMENT
NT WIND VELOCITY MEASUREMENT
Data processing in reducing effort of mechanical testing polymers for flexural deformation and displacement
[ERDE-TR-111] 09 p1052 N73-18578
Development of strain gage mounting assembly for amplifying measurable deformation applied to strain gage
[NASA-CASE-NPO-13170-1] 19 p2300 N73-28495

**MECHANICAL OSCILLATORS**
NT GYROSCOPIC PENDULUMS
NT PENDULUMS
Interactions between fluid flow and mechanical oscillators, using vibrating steel wire and cylindrical body
[DLR-FB-73-42] 24 p2909 N73-33218

**MECHANICAL PROPERTIES**
NT ABRASION RESISTANCE
NT AEROELASTICITY
NT ANELASTICITY
NT BRITTLENESS
NT BULK MODULUS
NT COMPRESSIBILITY
NT COMPRESSIVE STRENGTH
NT CREEP PROPERTIES
NT CREEP RUPTURE STRENGTH
NT CREEP STRENGTH
NT DUCTILITY
NT DYNAMIC MODULUS OF ELASTICITY
NT ELASTIC PROPERTIES
NT ELASTOPLASTICITY
NT ELECTROSTRICTION
NT FATIGUE LIFE
NT FIBER STRENGTH
NT FLEXIBILITY
NT FRACTURE STRENGTH
NT HARDNESS
NT HIGH STRENGTH
NT HYDROELASTICITY
NT IMPACT STRENGTH
NT MAGNETOSTRICTION
NT MICROHARDNESS
NT MODULUS OF ELASTICITY
NT NOTCH SENSITIVITY
NT NOTCH STRENGTH
NT PHOTOELASTICITY
NT PHOTOPLASTICITY
NT PIEZOELECTRICITY
NT PLASTIC PROPERTIES
NT PROPORTIONAL LIMIT
NT SHEAR PROPERTIES
NT SHEAR STRENGTH
NT SHELL STABILITY
NT STIFFNESS
NT STRESS CYCLES
NT STRESS RELAXATION
NT STRUCTURAL STABILITY
NT TENSILE CREEP
NT TENSILE PROPERTIES
NT TENSILE STRENGTH
NT THERMAL RESISTANCE
NT THERMOELASTICITY
NT THERMOPLASTICITY
NT THERMOVISCOELASTICITY
NT TOUGHNESS
NT VISCOELASTICITY
NT VISCOPLASTICITY
NT WELD STRENGTH
NT YIELD POINT
NT YIELD STRENGTH
Electrical and mechanical properties of vector magnetometer in HELIOS experiments for interplanetary magnetic field observations
[GAMMA-21] 01 p0048 N73-10384
Numerical analysis of performance of sinusoidal acceleration cams using radial followers and no opening or closing ramps
[ESDU-66026-AMEND-A] 01 p0060 N73-10494
Influence of forging deformation degree on mechanical properties of forged parts
[AD-745432] 01 p0062 N73-10510
Analysis of sensitivity of elevated temperature deformation of nickel alloy to grain size and shape under tension and creep conditions
[NASA-CR-128403] 01 p0067 N73-10549
Mechanical properties of various metal alloys and operating life of dies during hot deformation of stainless and heat resistant steels and alloys
[AD-745703] 01 p0068 N73-10559
Mechanical properties of boron carbide reinforced titanium laminates
[AD-745002] 01 p0070 N73-10570
Structural characterizations and key property measurements of glassy carbons
[AD-745347] 01 p0070 N73-10574
Mechanical properties of heat resistant silicon carbide-graphite composite
[AD-745434] 01 p0070 N73-10577
High temperature strength and stability of tungsten reinforced copper
[AD-745700] 01 p0071 N73-10581
Stress and strength guide for engineering design
[ESDU-SS1] 01 p0111 N73-10917
Ultrasonic method for detecting onset of fatigue damage in metal specimens
[AD-745978] 02 p0175 N73-11418
Influence of high temperature thermomechanical treatment on mechanical properties of austenitic steel
[NLL-M-21480-[5828.4F]] 02 p0186 N73-11504
Mechanical property and stress corrosion evaluation of Custom 455 stainless steel alloy at cryogenic temperatures
[NASA-TM-X-64682] 02 p0186 N73-11509
Effect of sodium chloride on mechanical properties of superalloys at elevated temperature
[NASA-TM-X-64701] 02 p0186 N73-11510
Linear regression analysis used on mechanical property data obtained from experiment which maximized variability in heat treating parameters of titanium alloy
[AD-747207] 02 p0190 N73-11540
Formation mechanism and strength of adhesive bond between polyvinyl acetate and steel
[NLL-RTS-7520] 02 p0190 N73-11543
Effect of heat transfer level on mechanical properties of elastomeric ablative material used on spherically blunted cones
[NASA-TM-X-2612] 02 p0191 N73-11548
Densification of ceramic materials and mechanical behavior of ceramic materials with emphasis on fracture energies
[AD-745909] 02 p0193 N73-11561
Low temperature investigation of polyethylene balloon film mechanical properties and structural factors affecting such properties
[AD-746678] 02 p0194 N73-11572
Surface stresses and mechanical properties of scales and effects on high temperature gas-metal reactions
[CONF-720515-1] 03 p0264 N73-12137
Correlation of substructure with mechanical properties of 304 and 316 stainless steel plastically deformed at elevated temperatures
03 p0313 N73-12554
Effects of annealing on microstructure and room temperature mechanical properties of 0.100 inch thick ingot-source beryllium sheet
[RFP-1831] 03 p0314 N73-12562
Correlation of substructure with mechanical properties of 304 and 316 stainless steel plastically deformed at elevate temperatures
[COO-2107-5] 03 p0315 N73-12568
Effect of nitriding on mechanical properties of niobium
[AD-747450] 03 p0318 N73-12593
Effect of foil thickness on mechanical behavior of stainless steel in tension
[AD-747698] 03 p0318 N73-12596
Effect of chemical vapor deposition on properties of carbon-felt carbon-matrix composites at high temperature
[SC-DC-71-4395] 03 p0320 N73-12609
Flexural strength of aluminum oxide substrates separated by lasers and diamond sawing
[SC-DC-71-4496] 03 p0321 N73-12613
Effect of bubble inclusions on mechanical properties of cast polymethyl methacrylate
[AD-746862] 03 p0321 N73-12616
Production of unidirectional glass reinforced plastics with high mechanical properties
[AD-747549] 03 p0323 N73-12629
Technology for determining mechanical properties of single crystal and polycrystals at low temperature
[AD-748744] 03 p0348 N73-12838
Residual stresses and mechanical properties in circumferentially wrapped composite cylinders
[SC-DC-72-1291] 03 p0361 N73-12942
Regular forging and explosive forming effects on mechanical properties of aluminum alloy
[AD-748710] 04 p0427 N73-13484
Orthorhombic chromium carbide for increased strength of sintered iron ceramic structural material
04 p0432 N73-13516
Fabrication and properties of structural materials based on ceramic titanium powders alloyed with molybdenum and aluminum
04 p0432 N73-13520
Effects of high temperature brazing and thermal cycling on mechanical properties of Hastelloy X
[NASA-TM-X-2704] 04 p0433 N73-13529
Temperature effects on tensile-, fracture toughness-, and crack growth-properties of aluminum alloy forgings
[AD-748257] 04 p0436 N73-13554
Physicomechanical and antifriction behavior of polycaproamide and Caprolon surfaces
[NLL-RISLEY-TR-2360-[9091.9F]] 05 p0550 N73-14464
Mechanical properties of uranium alloys containing additions of aluminum, iron, molybdenum, silicon, and chromium over temperature range from 20 to 640 C
[UJV-2802-M] 05 p0562 N73-14567

Mechanical properties of types 304 and 304 plus 0.15 percent Ti stainless steel after irradiation at temperatures in range of 400 to 820 C
[ORNL-TM-3733] 05 p0562 N73-14569
Improved mechanical properties of aluminum alloys cast at ambient temperature
[AD-750532] 05 p0563 N73-14577
Microstructure and mechanical properties of rapidly quenched liquid and powder metal alloys
[AD-749679] 05 p0564 N73-14578
Mechanical properties of thin films of Ni-SiO
[NLL-TRANS-746-1329-[9022.401]] 05 p0564 N73-14582
Data processing and recording applications in tensile testing of thermoplastics
[ERDE-TR-99] 05 p0565 N73-14593
Thermomechanical behavior and structure of poly[carborane-siloxane]s containing icosahedral cages in nitrogen environment
[AD-749364] 05 p0566 N73-14598
Diffusion coating and residual stress effects on steel product strength
[AD-749089] 05 p0566 N73-14600
Mechanical properties and fracture strengths of glass fiber reinforced plastic composites
[AD-749948] 05 p0567 N73-14608
Evaluation of fiber reinforced films used in high altitude balloons
[AD-749880] 05 p0567 N73-14609
Mathematical characterization of mechanical behavior of porous frictional granular media
[NASA-CR-124006] 06 p0661 N73-15368
Correlation of mechanical properties to microstructure of titanium alloys
[AD-749932] 06 p0685 N73-15581
Influence of ingot thermal-mechanical processing on grain size and mechanical properties of 7075 wrought aluminum alloy
[AD-750390] 06 p0686 N73-15588
Selection of resin matrices for composites with improved unidirectional strength
[NASA-TM-X-68166] 06 p0687 N73-15597
Electrical, mechanical, and thermal properties of transparent optical adhesives
[AD-750571] 06 p0688 N73-15602
Hydrostatic pressure effects on mechanical behavior and properties of polymers
[AD-750731] 06 p0688 N73-15605
Mechanical properties of elastic rectangular plates with linear variations of thicknesses
[PB-211229] 06 p0727 N73-15932
Mechanical properties of welded joints in stainless and low-alloy steels at temperatures of 900 to 1300 F
[ORNL-4781] 07 p0804 N73-16525
Preparation and properties of polytetrafluoroethylene impregnated with rhenium oxides
[NASA-TN-D-7166] 07 p0811 N73-16579
Effects of rebinders on strength of polyethylene and polymethyl methacrylate
[AD-751615] 07 p0812 N73-16587
Mechanical properties of monolithic transparent polycarbonate plastic sheet
[AD-751551] 07 p0813 N73-16590
Operational activities of mechanical properties technical information center
[AD-752499] 08 p0894 N73-17236
Mechanical properties of polycrystalline alkali halides determined for application to high power infrared laser windows
[AD-752193] 08 p0930 N73-17617
Effect of metallurgical conditions on mechanical properties of ASTAR-811C sheet
[NASA-CR-121096] 08 p0931 N73-17625
Forming and subsequent mechanical properties of high strength work hardened sheet materials
[PB-212207] 08 p0932 N73-17634
High resolution laser interferometer investigation of mechanical behavior of polymethyl methacrylate
[SC-DC-72-1174] 08 p0935 N73-17653
Plasticization of polyvinyl chloride with various reagents and effect on physicomechanical properties of systems
[AD-751875] 08 p0935 N73-17656
Correlation of mechanical properties for stored and carton sampled solid rocket propellants
[AD-752612] 08 p0953 N73-17804
Linear differential equations for analyzing viscoelastic properties and mechanical behavior of high polymers 08 p0966 N73-17898
Dynamic testing and structural modeling of aircraft tire properties
[NASA-CR-2219] 09 p0985 N73-18042
Mechanical properties as function of temperature for unidirectionally solidified eutectic composites
[NASA-CR-124094] 09 p1046 N73-18527
Influence of microdoping with cerium on quality of fractures in structural steels 09 p1047 N73-18535
Influence of heat treatment on strength properties of EI893L alloy
[JPRS-58137] 09 p1048 N73-18543
Tin alloying effects on plastic deformation, mechanical, and stress-rupture properties of Ni-Cr alloys
[JPRS-58159] 09 p1048 N73-18546
Mechanical properties of unidirectionally solidified, in-situ grown composites
[ONERA-TP-1147] 09 p1051 N73-18570
Alloying and thermal treatment for improving mechanical properties of ceramics
[AD-753124] 09 p1055 N73-18597
Telemetric monitor for in-situ transmission of solid propellant mechanical property data
[AD-754253] 10 p1162 N73-19454
Fabrication and properties of prealloyed steel powders
[AD-753325] 10 p1167 N73-19497
Mechanical and microstructural behavior of Al-Zn alloy in superplastic region at high temperature 10 p1170 N73-19518
Effect of warm rolling on mechanical properties of unstable chromium-manganese austenitic steels 10 p1171 N73-19526
Interrelation of martensitic conversion during deformation and structural properties of trip steel 10 p1171 N73-19527
Effect of order of welding and heat treatment operations on mechanical properties of weld joints of N18K9M5T 10 p1171 N73-19529
Literature review of strain rate effects on mechanical properties of metals at high temperatures
[AD-754243] 10 p1174 N73-19548
Microstructure and mechanical properties of precipitation hardened-dispersion strengthened aluminum and titanium alloys and refractory materials
[AD-753910] 10 p1174 N73-19550
Effect of fabrication conditions on mechanical properties of Be-Al monolayer tape and composite specimens
[SC-DR-72-0731] 10 p1175 N73-19559
Electric resistance spot welding and brazing for producing metal bonds with superior mechanical and structural characteristics
[NASA-CASE-LAR-11072-1] 11 p1298 N73-20535
Effects of excessive HfC on mechanical properties of W-Re-Hf-C alloys
[NASA-TN-D-7210] 11 p1305 N73-20588
Theoretical and experimental determination of nonlinear behavior of angleplied boron/aluminum composites
[NASA-TM-X-68205] 11 p1309 N73-20617
Mechanical and physical properties of discontinuous thermoset carbon fiber reinforced plastic composites
[AD-754034] 11 p1309 N73-20622
Crystal structure and mechanical and physical properties of polymide S-6 - Nylon
[AD-753967] 11 p1309 N73-20624
Effect of flaws on chemical, electrical, mechanical, and masking properties of Si3N4 films
[NLL-DRIC-TRANS-2902-[3623.66]] 11 p1329 N73-20789
Computerized simulation of heat transfer and elasticity in bars
[PB-213060] 11 p1347 N73-20927
Technique for determining mechanical properties of full-size aircraft tires from tests conducted with small-scale model tires
[NASA-CR-2220] 12 p1357 N73-21006
Procedure for improving strength and fracture behavior of alkali halides for use as high energy laser window material
[AD-755716] 12 p1411 N73-21437
Mechanical properties and stress corrosion cracking of 431 stainless steel alloy at low temperatures
[NASA-TM-X-64729] 12 p1412 N73-21441
Metal thin films with extremely high mechanical strength
[AD-755924] 12 p1417 N73-21480
Creation of discontinuities in high strength steels to evaluate effects on mechanical properties of welds
[AD-755524] 13 p1535 N73-22437
Effect of deformation performed during heat treatment on structure and mechanical properties of EI437B alloy 13 p1541 N73-22485
Analysis of high temperature stability of reinforcing phase in eutectic composition of aluminum-nickel alloys for various rates of growth 13 p1541 N73-22487
X ray Mossbauer study of strengthening properties of laves phases in austenitic steels
[JPRS-58852] 13 p1543 N73-22503
Cyclic transformation treatments on structural and mechanical properties of austenitic steels
[AD-756240] 13 p1543 N73-22506
Heat treatment and forging effects on mechanical properties of maraging steel
[AD-756422] 13 p1543 N73-22507
Mechanical strength of multilayer thin metal films
[AD-756582] 13 p1543 N73-22508
Vacuum effects on mechanical behavior of filled elastomeric spacecraft materials 13 p1546 N73-22527
Mechanical properties of aluminum stainless steel composites and associated interface microstructures
[AD-756673] 13 p1548 N73-22542
Mechanical properties and behavior of heat resistant alloys semiconductors, polymers and composite materials
[AD-755660] 13 p1549 N73-22552
Effect of dissolved hydrogen on mechanical and superconducting properties of molybdenum 13 p1565 N73-22681
Automated processing system for mechanical property test data of composite solid propellants and binders
[AD-755515] 13 p1569 N73-22714
Analysis of fatigue performance of titanium alloys and steels to identify variations based on shape parameter for reliability engineering of airframes
[AD-758219] 14 p1605 N73-23008
Chemical and mechanical properties of aircraft gas turbine engine components 14 p1676 N73-23600
Performance of fibrous reinforced concrete overlay test slabs as runways at Tampa International Airport, Florida
[FAA-RD-72-119] 14 p1680 N73-23634
Effects of environmental variables on physical, thermal, and mechanical properties of resin matrix and metal matrix composite materials
[AD-757524] 14 p1681 N73-23640
Electroionic glass strengthening process conducted at below strain point temperatures
[AD-757333] 14 p1681 N73-23646
Direct casting for producing cast superalloy tungsten or columbium alloy fiber composites with high strength
[NASA-TM-X-2782] 15 p1798 N73-24572
Metallurgical and mechanical properties of joints treated by weld-braze joining process
[NASA-TN-D-7281] 15 p1798 N73-24573
Effects of O2 on mechanical properties, elastic limit, and tension resistance of nonferrous metals
[EURISOTOP-59] 15 p1798 N73-24577
Etch pit study of motion and generation of dislocations in electron irradiated metals and effect of point defects on mechanical properties of metals
[COO-1367-50] 15 p1799 N73-24579
Mechanical properties of magnesium alloys operating at elevated temperature
[AD-758617] 15 p1800 N73-24593
Vacuum effects on mechanical properties of composite heat ablator and solid problem material 15 p1801 N73-24594
Influence of plastic deformation on structure and mechanical behavior of glassy amorphous polymers 15 p1801 N73-24595
Physical and mechanical properties of glassy carbons
[AD-757765] 15 p1802 N73-24606
Thermophysical and mechanical properties of closed pore insulation
[NASA-CR-112295] 15 p1843 N73-24930
Production and performance of strain gage embedded in boron/epoxy materials
[AD-759548] 16 p1915 N73-25493
Effect of heat treatment on structure and properties of stainless steels
[NLL-M-21566-[5828.4F]] 16 p1926 N73-25585
Technology utilization program relating to hydrogen effects on metal alloys and mechanical properties of recently developed alloys
[NASA-SP-5940[03]] 16 p1928 N73-25598
Evaluation of high strength aluminum alloy plates and forgings
[AD-759557] 16 p1930 N73-25613
Influence of phase composition on mechanical properties of heat resistant vacuum tight cast aluminum alloys
[AD-759645] 16 p1930 N73-25619
Corrosion resistant properties of titanium alloys
[AD-759621] 16 p1931 N73-25622
Elastic and mechanical properties of Al-Li alloy
[AD-759423] 16 p1931 N73-25625
Radiation damage in epoxy materials of reduced viscosity
[RHEL/R-249] 16 p1932 N73-25634
Mechanical properties and failure modes of glass fiber reinforced epoxy plates under high tensile loads
[AD-759153] 16 p1933 N73-25640
Effect of interface in aluminum, boron, and silicon carbide coated boron on mechanical properties
[AD-759204] 16 p1933 N73-25641
Cyclic mechanical and fatigue properties of ferroanelastic beta prime gold-cadmium alloy
[NASA-CR-131843] 16 p1969 N73-25929
Computer programs for solving metal working equations by considering mechanical properties
[AD-759830] 17 p2038 N73-26491
Standards for metallic specimens to include methods of mechanical and technological testing
[JPRS-59280] 17 p2044 N73-26538
Relationship between microstructure and properties of austenitic stainless steels
[ORO-4044-3] 17 p2045 N73-26545

Fatigue strength and other mechanical properties of medium carbon steels chromed by gaseous and vapor phase methods
[DRIC-TRANS-2156] 17 p2046 N73-26550
Effect of aging heat treatments on mechanical properties of Ti-8Al-1Mo-1V alloy
[AD-760461] 17 p2048 N73-26567
Mechanical properties of alloys on aluminum beryllium base with magnesium
[AD-759876] 17 p2048 N73-26571
Torsional braid analysis of polymers
[AD-759412] 17 p2051 N73-26593
Strength of randomly oriented short fiber composite laminates
[AD-759827] 17 p2051 N73-26594
Evaluation of GRP rod and rope materials and associated end fittings
[AD-759931] 17 p2053 N73-26607
Mechanical properties of amorphous semiconductors at high pressures
[AD-759849] 17 p2075 N73-26784
Vibrational characteristics, mechanical properties, and stress analysis of thin shell structures of various cross sections
[NASA-SP-288] 17 p2092 N73-26924
Materials research covering properties, structure, and synthesis
[AD-760021] 17 p2100 N73-26988
Mechanical properties of double melted 18 percent Ni-Co-Mo maraging steel bar or forgings
[S/T-MEMO-3-72] 18 p2161 N73-27457
Microstructure and mechanical properties of thermal barrier materials produced by arc plasma spraying
[AD-762045] 19 p2312 N73-28598
Tensor analysis of strength and failure of composite materials
[AD-761994] 19 p2313 N73-28600
Analysis of physicomechanical properties of ice conducted during Tenth Soviet Antarctic Expedition with emphasis on ice cover temperature effects
20 p2408 N73-29352
Structure and properties of magnesium-lithium alloys
[JPRS-59738] 20 p2430 N73-29523
Strength and microstructure of nickel base superalloys after long term heating
[TB-86] 20 p2431 N73-29526
Mechanical behavior of polycrystalline nickel deformed by tension and simultaneously cathodically charged with hydrogen
[AD-759036] 20 p2432 N73-29535
Strength of brittle matrix materials reinforced with steel fibers or whiskers
[NLL-CE-TRANS-6145-[9022.09]]
20 p2434 N73-29545
Mechanical properties and crack growth in thick welded plates of aluminum at room and cryogenic temperature
[NASA-TN-D-7377] 20 p2483 N73-29946
Effect of copper and silicon on selected mechanical properties of hot rolled medium carbon steels
[BM-RI-7777] 21 p2558 N73-30504
Effect of aluminum on fundamental mechanical properties of titanium
[AD-763785] 21 p2560 N73-30524
Outdoor weathering influence on polyester and epoxy glasscloth reinforced laminate flexural strength and surface appearance
[FOK-R-1627] 21 p2563 N73-30546
Controlling constituent properties for strengthening graphite fiber reinforced aluminum and magnesium composites
[AD-763211] 21 p2563 N73-30548
Determining mechanical properties of composite materials using computers
[AD-763708] 21 p2563 N73-30550
Effects of microstructure differences on tensile strength of graphite fibers
[AD-763687] 21 p2564 N73-30557
Dynamic compressive stress-strain data of polymer foams obtained from uniaxial compressive tests
[AD-762490] 21 p2565 N73-30559
Mathematical structure and stress constitutive problem of materials with permanent memory particularly filled propellants
[AD-763753] 21 p2587 N73-30732
Peel, shear, and tensile strength measurements of transistor header lead welds
[BDX-613-871] 22 p2642 N73-31173
Mechanical and physical property tests of TD-NiCr [Ni-20Cr-2ThO2] alloy sheet
[NASA-CR-121221] 22 p2683 N73-31493
Determining mechanical properties of high conductivity metals and alloys
[NASA-CR-133890] 22 p2684 N73-31498
Influence of hydrostatic pressure on ductility and fracture mechanics of bismuth and tin-bismuth alloys
[AD-764241] 22 p2686 N73-31514
Stress-strain diagrams and mechanical properties of metal wires as determined by tranverse impact method
[AD-764105] 22 p2687 N73-31523
Sintering kinetics and mechanical properties of high purity mullite
22 p2688 N73-31527
Temperature effects on structures and mechanical properties of polysulfone and poly[216-dimethyl] phenylene oxide
22 p2688 N73-31528
Influence of epoxy resins on mechanical properties of superconducting windings
[RHEL/R-265-PT-2] 22 p2689 N73-31534
Thermal stress ratcheting of structures subjected to mechanical and cyclic thermal stresses
22 p2723 N73-31790
Properties of materials in high pressure hydrogen at cryogenic, room, and elevated temperatures
[NASA-CR-124394] 22 p2725 N73-31804
Effects of high pressure hydrogen environments on mechanical properties of alloys considered as candidate materials for high performance rocket engine construction
[NASA-CR-124410] 23 p2804 N73-32428
Tear and fatigue crack propogation tests for determining mechanical properties of ultrafine grain alpha titanium
[AD-765329] 23 p2805 N73-32434
Effect of scandium, yttrium, and lantham oxides on properties of nickel ferrite
23 p2809 N73-32460
Thermal and mechanical properties of low density elastomeric ablation material
[NASA-CR-132281] 23 p2809 N73-32463
Physical and mechanical properties of carbon produced from furfural alcohol resins
[AD-763499] 23 p2810 N73-32472
Research in dynamics of thin films polymer chemistry mechanical and chemical properties of materials
[NASA-CR-135697] 23 p2865 N73-32906
Influence of alloy additives on strength of nickel base alloys at temperatures from 25 to 650 C
[ORNL-TM-4173] 24 p2936 N73-33446
Mechanical and thermophysical characteristics of nonmetallic insulation materials for space shuttle orbiter surface
24 p2939 N73-33471
Mechanical and thermophysical properties of composite materials
[LA-5173] 24 p2943 N73-33505
Application of tension stress relaxation measurements to determine physical and mechanical properties of rubber networks during chemical reactions
[RR-204] 24 p2987 N73-33868

**MECHANICAL RESONANCE**
U RESONANT VIBRATION

**MECHANICAL SHOCK**
Preterrestrial shock effects, shock hardening in iron meteorites, and parent bodies
19 p2342 N73-28840
Thermal stress and mechanical shock effects on release of bacterial spores from stainless steel surfaces with application to Mars landing
[NASA-CR-133868] 22 p2619 N73-30987

**MECHANICAL TWINNING**
Constitutive equations for determining elastic deformation twinning in body centered cubic lattice metals at low temperatures
[AD-757042] 14 p1679 N73-23624

**MECHANICS [PHYSICS]**
Brief summaries of 13th International Congress of Theoretical and Applied Mechanics
[NASA-CR-132236] 15 p1846 N73-24955

**MECHANIZATION**
Design, development, and characteristics of industrial robot machinery to show load capacity, positioning accuracy, power actuators, and method of controls
01 p0060 N73-10486
Automatic experimenter concept based on evolution strategy
24 p2908 N73-33210

**MEDIA**
NT ANISOTROPIC MEDIA
NT ELASTIC MEDIA
NT INTERGALACTIC MEDIA
NT INTERPLANETARY DUST
NT INTERPLANETARY MEDIUM
NT ZODIACAL DUST

**MEDIAN [STATISTICS]**
Distribution-free confidence intervals and significance tests for population median of random sample
[NASA-CR-131989] 14 p1683 N73-23660

**MEDICAL ELECTRONICS**
Biomedical electronics and solid state and quantum electronics research
[AD-745968] 02 p0151 N73-11225
Design and development of biomedical prosthetic and electronic devices
[NASA-CR-130022] 07 p0750 N73-16093
Initial systole and dicrotic notch detecting circuitry for monitoring arterial pressure pulse
[NASA-CASE-LEW-11581-1] 09 p0997 N73-18139
Development of electrocardiogram protection circuits to prevent accidental electrocution and digital cardiotachometer system to display heart rate
13 p1594 N73-22924

**MEDICAL EQUIPMENT**
NT ARTIFICIAL EARS
NT ARTIFICIAL HEART VALVES
NT CARDIOTACHOMETERS
NT PROSTHETIC DEVICES
NT SURGICAL INSTRUMENTS
Biomedical electronics and solid state and quantum electronics research
[AD-745968] 02 p0151 N73-11225
Use of space technology to solve medical problems and improve medical equipment
04 p0472 N73-13848
Biophysical mechanisms of noninvasive measurement of CVP in man
[NASA-CR-130348] 07 p0742 N73-16039
Management of NASA employee health problems by automated medical system
08 p0874 N73-17079
Utilization of aerospace technology in biomedical field - Southwest Research Institute report for Jan. 1973
[NASA-CR-130984] 09 p0992 N73-18097
Design of hemoglobin tester, flow ventilation systems, blood viscometer, isotope handling equipment, and blood pressure measuring device
[NASA-TM-X-66214] 12 p1373 N73-21139
Design of anesthetic flow valve canister system for exhaust gas absorption and laminar ventilation system for operating rooms
12 p1373 N73-21141
Multichannel medical monitoring system to measure physiological parameters from display device at remote control station
[NASA-CASE-MSC-14180-1] 13 p1486 N73-22045
Research projects conducted as part of NASA programs during period May 1970 through May 1972
[NASA-TM-X-64723] 13 p1593 N73-22915
Development of electrocardiogram protection circuits to prevent accidental electrocution and digital cardiotachometer system to display heart rate
13 p1594 N73-22924
Equipment for implanting electrodes in subcortical structures of cat brain
[NASA-TT-F-15001] 19 p2225 N73-27947
Tilting table for testing human body in variety of positions while exercising on ergometer or other biomedical devices
[NASA-CASE-MFS-21010-1] 21 p2502 N73-30078
NASA bioinstrumentation list for public utilization
[NASA-SP-5958[01]] 23 p2750 N73-32007
Automatic device for assaying urine on bacterial adenosine triphosphate content
[NASA-CASE-GSC-11169-2] 23 p2750 N73-32011

**MEDICAL PERSONNEL**
NT PHYSICIANS
Medical examinations and protection procedures for NASA employees working in radiologically controlled areas
08 p0871 N73-17050
Clinical medicine and human factors engineering functions conducted during Tenth Soviet Antarctic Expedition
20 p2407 N73-29347

**MEDICAL PHENOMENA**
Experimental research in underwater medicine, flight stress, and pilot selection
[DLR-FB-73-15] 19 p2226 N73-27951

**MEDICAL SCIENCE**
NT DENTISTRY
NT GYNECOLOGY
NT IMMUNOLOGY
NT NEUROLOGY
NT NEUROPSYCHIATRY
NT PATHOLOGY
NT RADIOBIOLOGY
NT RADIOLOGY
Research and development in Army aviation medical science and problems
[AD-749456] 06 p0631 N73-15129
Development of PDP 8 computer programs for medical biological laboratory in Netherlands
[MBL-1972-4] 14 p1637 N73-23275
Applications of aerospace technology in biology and medicine
[NASA-CR-133226] 17 p1988 N73-26067
Application of aerospace medicine research in science and technology
[JPRS-59803] 20 p2368 N73-29040
Aerospace Medical Research Laboratory handbook to medical monitoring and treatment of environmental stresses
[AD-760813] 20 p2372 N73-29061
Medical analysis of vitamin balance among personnel of Tenth Soviet Antarctic Expedition to show effects on health and acclimatization ability
20 p2408 N73-29357
Medical evaluation of pilots using onboard flight recorders
22 p2619 N73-30986
Articles concerning development of scientific disciplines and technical fields in Eastern Europe
[JPRS-60063] 23 p2865 N73-32904

**MEDICAL SERVICES**
Space technology for developing ground based integrated medical laboratory
04 p0472 N73-13851
Conference on occupational medicine support in NASA programs to prevent health and emotional problems in personnel
[NASA-TM-X-69072] 08 p0871 N73-17048

Occupational medicine procedures for personnel in lunar receiving laboratory for Apollo 11 crew members
08 p0871 N73-17049
Multiphase health screening and medical history questionnaire for preventive/occupational physical examinations
08 p0871 N73-17052
Automated medical history questionnaire for screening industrial personnel and scheduling physical examinations
08 p0872 N73-17060
Routine proctosigmoidoscopic examinations of asymptotic NASA personnel for cancer prevention
08 p0872 N73-17061
Industrial health measures and environmental control to insure worker productivity
08 p0874 N73-17077
Conference on occupational and environmental medical services provided to NASA employees
[NASA-TM-X-69074] 08 p0874 N73-17078
Influence of repeated test and dietary counseling on hypercholesterolemia control in NASA employees
08 p0875 N73-17081
Precoronary care and sudden death prevention due to coronary disease in industrial workers
08 p0875 N73-17084
Automated medical record system for identifying and managing medical problems for Navy
08 p0875 N73-17087
Medical services of operating environmental health program for industrial workers
08 p0876 N73-17093
Clinical medicine and human factors engineering functions conducted during Tenth Soviet Antarctic Expedition
20 p2407 N73-29347
Analysis of physiological effects of diet on personnel of Tenth Soviet Antarctic Expedition
20 p2409 N73-29358
Spectrophotometric procedures applied to medical services in clinical chemistry laboratories and analysis of sources of error in diagnoses
[PAPER-76A5-736] 21 p2545 N73-30405

**MEDICINE**
Cooperation of Eastern European countries in computer and medical research
[JPRS-58063] 08 p0976 N73-17987
Sports medicine - parameters necessary for maintaining competitive form
12 p1370 N73-21114

**MEDITERRANEAN SEA**
Bora on Adriatic and Black Sea coasts - bibliographies
05 p0571 N73-14637
Marine climatological summaries for Mediterranean and Southern Indian Ocean, including Australian waters
06 p0693 N73-15646
Influence of bottom topography and earth rotation of wind-driven circulation in Mediterranean Sea
07 p0858 N73-16956
Temperature-salinity profiles of Tyrrhenian Sea
[CONTRIB-2725] 07 p0858 N73-16957
Hydrology of Sicilian Channel recorded onboard S.S. Dectra in 1969
07 p0858 N73-16958
Measurement of sound transmission and attenuation in Tyrrhenian Sea discussing experimental design and results
07 p0858 N73-16959
New harmonic constant computed for Adriatic Sea harbors
07 p0858 N73-16961
Influence of solar flares on thunderstorms and meteorological phenomena over Mediterranean Sea
07 p0859 N73-16965
Measurement of Mediterranean Sea temperature profiles using free drifting, self-recording drogues equipped with thermistor chains
[AD-753442] 12 p1402 N73-21372
Mediterranean Sea geophysical survey
[AD-757455] 16 p1910 N73-25452
Conference on use of solar energy in Mediterranean
[BULL-22] 24 p2974 N73-33762

**MEETINGS**
U CONFERENCES

**MEGALOPOLISES**
Land use mapping of northern megalopolis using ERTS-1 imagery
[E72-10188] 01 p0046 N73-10367
Mapping of land use in Northern Megalopolis of Massachusetts, Connecticut, Rhode Island, and New York based on ERTS-1 imagery
[E72-10357] 05 p0534 N73-14345
Land use mapping of northern megalopolis using ERTS-1 imagery
[E72-10368] 05 p0535 N73-14356
Application of ERTS-1 imagery for mapping coverage of megalopolitan New England to show land use
[E73-10427] 11 p1280 N73-20388
Land use in northern megalopolis of Massachusetts, Connecticut, and Rhode Island
[E73-10506] 13 p1516 N73-22281
Land use of northern megalopolis of Massachusetts, Connecticut, and Rhode Island from ERTS-1 imagery
[E73-10630] 15 p1776 N73-24390
Application of ERTS-1 imagery to determine land use in Massachusetts, Connecticut, and Rhode Island
[E73-10723] 17 p2019 N73-26330
Mapping and digitization of land use in northern megalopolis of Masssachusetts, Connecticut, and Rhode Island using ERTS-1 data
[PAPER-L12] 19 p2274 N73-28308
Land use in northern megalopolis of New England
[E73-10991] 22 p2659 N73-31297

**MEISSNER EFFECT**
U DIAMAGNETISM
U SUPERCONDUCTIVITY

**MELTING**
NT ARC MELTING
NT FUSION [MELTING]
NT VACUUM MELTING
Effects of gravity-induced free convection of melting behavior of paraffin slab for thermal control devices
[NASA-CR-123954] 04 p0385 N73-13130
Melting characteristics and thermophysical properties of solid hydrogen
[AD-748847] 04 p0387 N73-13144
ERTS-1 sensing of fall snow melting in Chena River Basin, Alaska
[E72-10345] 05 p0533 N73-14333
Performance of mathematical snowmelt models and statistical analysis of avalanche forecasts
06 p0665 N73-15402
Survey and mapping of freeze-up and break-up patterns of seasonal snow and ice covers in Alaska
[E73-10282] 08 p0914 N73-17489
ERTS-1 imagery of snow cover and break-up characteristics in Chena River Basin, Alaska
[E73-10292] 08 p0915 N73-17497
List of metallic melting bodies for temperature determinations from 30 to 1555 degrees Celsius
[JUL-871-RB] 08 p0932 N73-17631
Radial distribution functions and liquid structure factors for fluids of particles interacting through repulsive potentials
[LPTHE-72/45] 10 p1191 N73-19690
ERTS-1 imagery of ice break-up characteristics of Chena River Basin
[E73-10400] 11 p1277 N73-20362
Development of low melting fused salt electrolytes
[AD-755528] 13 p1477 N73-21965
Finite element calculation of two-dimensional heating and melting of disks and applications to laser effects
[AD-757189] 14 p1719 N73-23950
Electrical resistance measurement for determining electron state densities in molten germanium-silver and germanium-copper systems
[NLL-M-21613-[5828.4F]] 15 p1746 N73-24153
Short range order effect on interatomic reaction and heat of displacement in molten nickel and silicon alloys
[NLL-M-21597-[5828.4F]] 15 p1797 N73-24568
Gravity effects upon melt-through time of metal plate subjected to high intensity lasers
[AD-759168] 16 p1925 N73-25574
Time prediction for laser melting and vaporization of metal sheet
[AD-760113] 17 p2042 N73-26521
Electroslag melting method in casting of aluminum alloy ingot
[AD-759758] 17 p2047 N73-26558
Development of manufacturing method for elimination of nitride inclusions from titanium alloys during melting and ingot consolidation
[AD-748261] 18 p2163 N73-27473
ERTS-1 imagery of snow melt in Chena River Basin of Alaska
[E73-10903] 20 p2396 N73-29252
Survey of freeze-up and breakup patterns of seasonal snow and ice covers in Alaska
[E73-10920] 20 p2398 N73-29269
Performance of study plan for proposed Skylab experiments concerning metals melting and sphere forming
[NASA-CR-124396] 23 p2796 N73-32368
Snowmelt model for Chena River Basin
[E73-11085] 24 p2913 N73-33248

**MELTING POINTS**
Effects of various oxide additives on volume change on melting, surface tension, and viscosity of liquid aluminum oxide
[NASA-CR-120910] 07 p0811 N73-16580
Compilation of eutectics and melting point minima for binary combinations of metals for refractory metal brazing
[NASA-TM-X-68190] 10 p1172 N73-19537
Density and light radiation measurements of molten metals, semiconductors, and alloys
[NLL-M-21580-[5828.4F]] 16 p1951 N73-25789
Emissivities of metals and compounds in liquid state at fusion temperatures
[NASA-CR-133521] 19 p2309 N73-28576

**MEMBRANE ANALOGY**
U MEMBRANE STRUCTURES
U STRUCTURAL ANALYSIS

**MEMBRANE STRUCTURES**
NT SKIN [STRUCTURAL MEMBER]
Growth of hollandite crystal membranes under inert gas pressures
[NASA-CR-121033] 03 p0345 N73-12810
Application of finite element method to determine deformation of elastic plates, shells, and membranes
[AD-749565] 04 p0483 N73-13946
Numerical analysis of facilitated transport of gas through liquid membranes to show dependence on three parameters
[PUB-73-2] 17 p2014 N73-26287

**MEMBRANE THEORY**
U MEMBRANE STRUCTURES
U STRUCTURAL ANALYSIS

**MEMBRANES**
NT ION EXCHANGE MEMBRANE ELECTROLYTES
NT MEMBRANE STRUCTURES
NT SKIN [STRUCTURAL MEMBER]
Photosynthetic energy conversion in membranes, tissues, and reaction centers of bacteria and viruses
[COO-3162-9] 04 p0380 N73-13091
Membrane-mirror elements as light valves in optical memory systems
[NASA-CR-124085] 09 p1064 N73-18682
User manual for finite element program for analysis of deformations of thin elastic membranes
[AD-755953] 13 p1588 N73-22874
Suitability determination of redesigned XW18 membrane as expedient surfacing for waterproofing and dustproofing hastily prepared airfields for operations of C-130 aircraft
[AD-761089] 18 p2127 N73-27190

**MEMORY**
Short-term memory results from connected speech experiments using adult listeners
14 p1625 N73-23169
Ferrite memory arrays from pre-formed metal conductors
[NASA-CASE-LAR-10994-1] 21 p2562 N73-30536

**MEMORY STORAGE UNITS**
U COMPUTER STORAGE DEVICES
U CORE STORAGE

**MENTAL HEALTH**
Mental health services for emotional counselling in NASA facilities to insure maximum human performance
08 p0872 N73-17062
Conference on preventive medical and environmental control measures for NASA and aviation industry personnel management
[NASA-TM-X-69073] 08 p0873 N73-17064

**MENTAL PERFORMANCE**
Annotated bibliography on reaction times in selected human information processing tasks
[AD-745416] 01 p0012 N73-10095
Frequency discriminator for on-line measurements of entrainment and synchronization in EEG signals as related to human alertness
[NASA-CR-129173] 02 p0135 N73-11091
Effect of mood on human performance, possibility of using skin analyzer for communication, and effect of prolonged exposure to depths of 160 m on mental functioning
[JPRS-57541] 04 p0378 N73-13072
Mental functions of aquanauts during and after exposure to depths up to 160 m
04 p0378 N73-13073
Physiological and mental performance effects of underwater work on humans
[AD-747701] 04 p0382 N73-13107
Feasibility of saliva analysis for measuring mental stress in man
[AD-747671] 04 p0382 N73-13111
Differences in speed of mentally processing displays containing information about right and left
[AD-759723] 17 p1988 N73-26070
Analysis of self-destructive tendencies created by psychological stress and relationship to aircraft accidents
[FAA-AM-73-5] 18 p2104 N73-27016

**MENTAL STRESS**
U STRESS [PSYCHOLOGY]

**MERCAPTAN**
U THIOLS

**MERCAPTO COMPOUNDS**
U THIOLS

**MERCURE AIRCRAFT**
Engine ingestion prevention on low wing aircraft, particularly Mercury aircraft, by jet blast
[FO-1149] 06 p0622 N73-15049

**MERCURY [METAL]**
NT MERCURY VAPOR
Durability test of Hughes SIT-5
[NASA-TM-X-68155] 02 p0223 N73-11802
Effects and prevention of possible mercury pollution from failure of solar electric propulsion spacecraft using mercury propellant
[NASA-CR-130286] 06 p0717 N73-15855
Water sample analysis for identifying sources of mercury pollution of Great Lakes
08 p0876 N73-17096
Development and characteristics of electron beam excited high pressure mercury dissociation laser
[AD-752465] 08 p0930 N73-17619

Ionization processes in mercury plasma due to excited state interactions and electron impact
[NASA-CR-130924] 10 p1192 N73-19701
Identification and interpretation of tectonic features and mercury deposited in California coast ranges and western transverse ranges
[E73-10446] 11 p1282 N73-20406
Magnetic filtering technique for treating water containing low concentrations of mercury
[NASA-TM-X-2764] 11 p1352 N73-20972
Tests of mercury-fed hollow cathode in bell jar at SERT 2 neutralizer conditions
[NASA-TM-X-2785] 15 p1825 N73-24793
Fluorescent lamp discharge parameter effects on mercury resonance lines
[AD-760958] 18 p2183 N73-27627
Analysis of ERTS-1 imagery of Northern Coast Ranges and Sacramento Valley, California for locating mercury deposits and oil and gas fields
[PAPER-G18] 19 p2265 N73-28249
Control of 30 centimeter diameter mercury bombardment thruster
[NASA-TM-X-68297] 21 p2588 N73-30738
Slosh testing of spherical mercury propellant tank with positive expulsion diaphragm
[NASA-CR-133790] 21 p2600 N73-30838
Sputter erosion and deposition in discharge chamber of small mercury ion thruster
[NASA-TM-X-71424] 23 p2829 N73-32611
Mercury thruster isolator lifetime tests
[NASA-TM-X-71422] 23 p2830 N73-32617

**MERCURY [PLANET]**
Analysis of selected features of Mercury, Venus, and Mars and seismic propagation on Moon
07 p0840 N73-16807
Determination of parameters related to interior of Mercury
[NASA-CR-130981] 09 p1082 N73-18823
Measurement of infrared radiation from Mercury and Moon
[NASA-CR-130968] 09 p1085 N73-18849
Finite series expansion study on motion of Mercury perihelion
[PB-213059] 11 p1339 N73-20870
Predicted and measured infrared radiation data for Mercury and Moon
19 p2341 N73-28831
Modification of JPL space simulator for simulating solar intensities at Mercury
[NASA-CR-133791] 21 p2521 N73-30217
Subsurface characteristics of Mercury and Mars determined by analysis of thermal microwave emission
24 p2979 N73-33801

**MERCURY COMPOUNDS**
NT MERCURY TELLURIDES
Discharge compositions of gas laser emissions from mercury and copper halides
[AD-749938] 05 p0559 N73-14541
Semiconductor radiation detectors with lead and mercury compounds
[BMBW-FBK-72-19] 09 p1036 N73-18458

**MERCURY FLIGHTS**
Score, approach, and major results of study of ballistic mode Mercury orbit missions
[NASA-CR-114617] 22 p2715 N73-31733
Scope, approach, and major results of study of ballistic mode of Mercury orbit missions
[NASA-CR-114618] 22 p2715 N73-31734

**MERCURY LAMPS**
Flashlight adaptation of ultraviolet source for illuminating fluorescent map
[AD-755435] 12 p1429 N73-21585

**MERCURY TELLURIDES**
Temperature dependence of mercury telluride band gap
15 p1820 N73-24749
Mercury cadmium telluride 10.6-micron photodiode
[AD-762167] 19 p2248 N73-28122

**MERCURY VAPOR**
Charged particle concentrations and plasma temperatures of liquid or film electrode discharges in mercury vapor
[AD-750559] 06 p0706 N73-15759
Solid state amplifier for bridge circuit of atomic absorption mercury detector
[PB-212658] 07 p0801 N73-16506
Mercury emission control systems for primary mercury facility and for chlor-alkali plant
[AP-118] 11 p1314 N73-20661
Ionizational relaxation in shock-heated mercury vapor
15 p1816 N73-24719
High voltage pulse for igniting electron bombardment mercury ion thruster
[NASA-TM-X-71425] 23 p2765 N73-32119

**MERIDIANS**
U LATITUDE
U LONGITUDE

**MERIDIONAL FLOW**
Meridional wind effects on advection heating in thermosphere during geomagnetic storms
[AD-751921] 08 p0919 N73-17528
Solar meridional circulation and latitudinal sunspot drift analysis
[AD-751268] 09 p1081 N73-18820
Effect of general atmospheric circulation of large scale and persistent weather features of Atlantic-Eurasian sector of hemisphere in 1968 to 1970
[NLL-M-22853-[5828.4F]] 16 p1936 N73-25663
Nature of zonal and meridional circulation components of troposphere and stratosphere of Northern Hemisphere
20 p2443 N73-29626
Mathematical models for studying beta effect on meridional velocity of disturbed flow in ocean
20 p2447 N73-29655

**MEROMORPHIC FUNCTIONS**
NT ELLIPTIC FUNCTIONS

**MESOMETEOROLOGY**
Thermohydrodynamic equations of nonlinear mesometeorological processes
[NLL-M-20716-[5828.4F]] 01 p0072 N73-10590
Mesoscale processes in circulation models noting parameterization
05 p0573 N73-14660
Parameterization of near surface mesoscale circulation
05 p0574 N73-14665
Utilization of ERTS-1 imagery in mesometeorological studies of Great Lakes
[E73-10464] 11 p1284 N73-20420
Great lakes mesometeorological investigations using ERTS-1 data
[E73-10835] 18 p2141 N73-27305
Cellular convection parameters determined from high-altitude tower measurements and meteorological earth satellite observations
22 p2693 N73-31568
Design for development of network in Moscow and vicinity for mesometeorological observations
22 p2693 N73-31573

**MESON RESONANCES**
Dual resonance model for predicting density matrix elements of vector mesons produced in inclusive reactions
[ILL-[TH]-72-11] 05 p0582 N73-14735
Meson resonance production in missing mass spectra using quark model for negative pion proton yields proton negative x diffraction calculation
[TUEP-72-41] 07 p0823 N73-16667
Missing mass spectrum structures for meson resonances in S, T, U, region
[NUB-2167] 07 p0823 N73-16671
Dual resonance type model for quasi two body reactions in subprocesses of pion nucleon yields pion omega meson nucleon
22 p2701 N73-31635

**MESON-NUCLEON INTERACTIONS**
Theoretical model of Regge phenomena in medium x region for kaon proton interactions
[TUEP-72-46] 07 p0823 N73-16668

**MESONS**
NT MESON RESONANCES
NT MUONS
NT OMEGA-MESONS
NT PIONS
NT VECTOR MESONS
Origins and history of Los Alamos meson physics facility
[LA-5000] 05 p0524 N73-14261
Generalized vector meson dominance model derived from extended quark model with electron proton inelastic scattering
[TUEP-72-43] 07 p0823 N73-16669

**MESOPAUSE**
Disposition of scattering layers over polar-regions as observed by OGO-6 airglow photometer
[NASA-CR-130271] 07 p0791 N73-16436
Seasonal transitions in spring and autumn in mesopause region for Northern Hemisphere
[NASA-TT-F-14924] 14 p1685 N73-23672

**MESOSPHERE**
Mesospheric circulation and noctilucent clouds
[NASA-TT-F-14712] 01 p0105 N73-10866
Meteorological rocket sounding data on stratospheric and mesospheric structures and circulations
[NASA-TR-R-391] 02 p0205 N73-11657
Attenuation of nitric oxide dissociation in mesosphere and stratosphere
[PSU-IRL-SCI-407] 08 p0917 N73-17518
Development and use of three payloads for studying mesospheric parameters, using Arcas rockets
[AD-752241] 08 p0921 N73-17545
Photodissociation and formation of nitric acid in mesosphere and stratosphere
[AERONOMICA-ACTA-A-113] 09 p1027 N73-18382
Dissociation of nitric oxide in mesosphere and stratosphere by attenuation
[AERONOMICA-ACTA-A-112] 09 p1027 N73-18384
Extrapolation technique to obtain estimates of mesospheric density, pressure, and temperature
[NASA-CR-2223] 12 p1401 N73-21364
Direct measurement of mesosphere and stratosphere electrical conductivity and relaxation time
15 p1779 N73-24419
Mesospheric diffuse skylight measurement onboard Centaure sounding rockets launched from Kiruna during August 1969
[ISL-16/72-PT-1] 15 p1781 N73-24439
Schumann resonance frequencies and electrical conductivity of mesosphere [40 to 100 km] from ELF spectra
[AD-758775] 15 p1784 N73-24463
ESRO sounding rocket experiment R-175 in presence of noctilucent clouds on polar summer upper atmosphere structure, composition, and ionization
[AP-7] 17 p2027 N73-26406
Mesospheric scattered sunlight measured during twilight from ESRO Centaur rocket photoelectric polarimeters
[AP-8] 18 p2172 N73-27547
Parachute-borne blunt probe measurement of mesospheric ionization
[NASA-CR-135637] 23 p2784 N73-32277
Photochemical ozone theory and microwave spectroscopy using microwave radiometry for remotely verifying mesospheric ozone diurnal variations
[AD-764705] 23 p2789 N73-32314

**MESSAGES**
Adaptive routing techniques for message switching computer-communication networks
[AD-749678] 06 p0646 N73-15246

**METABOLIC WASTES**
NT FECES
NT HUMAN WASTES
NT URINE
Hyperoxia effects on elimination of carbon monoxide, ammonia, ketones, and aldehydes by rats
03 p0256 N73-12077
Chromatographic determination of gaseous metabolites released by man during reduced food intake
03 p0258 N73-12091
Toxic effects of metabolic waste gases on rat organisms
10 p1116 N73-19101
Hyperoxic atmosphere effect on rat metabolism and elimination of gaseous wastes
13 p1481 N73-22004
Feasibility demonstration of biowaste propellant resistojet engines for space station attitude control system
[NASA-CR-132269] 18 p2193 N73-27706
Hypoxia effects on release of gaseous wastes from rat vital functions
20 p2366 N73-29025

**METABOLISM**
NT ADRENAL METABOLISM
NT CALCIUM METABOLISM
NT CARBOHYDRATE METABOLISM
NT CATABOLISM
NT ELECTROLYTE METABOLISM
NT ENZYME ACTIVITY
NT FERMENTATION
NT HORMONE METABOLISMS
NT HYPOGLYCEMIA
NT OXYGEN METABOLISM
NT PHOSPHORUS METABOLISM
NT PROTEIN METABOLISM
Extraterrestrial life detection using Automated Microbial Metabolism Laboratory
[NASA-CR-129508] 03 p0279 N73-12266
Design and performance of breathing metabolic simulator
04 p0472 N73-13850
Hyperammonemia development in metabolic toxicity of hydrazine
[AD-749519] 05 p0501 N73-14077
Physiology of depressed metabolic states and gastrointestinal responses to ionizing radiation
[NASA-CR-130381] 07 p0742 N73-16038
Effect of accelerations on thiamine S-35 distribution in organs, tissues, and subcellular structures of white mice
07 p0743 N73-16044
Skylab experiments to assess weightlessness effects on human nutritional metabolism and musculoskeletal function
09 p0994 N73-18115
Metabolism and propagation of microbes in outer planets
[NASA-CR-131091] 10 p1120 N73-19127
Influence of long duration flight missions on metabolic and endocrine functions of pilots and navigators
10 p1123 N73-19152
Dynamics of nitrogenous cerebral metabolites accompanying repeated hypothermia and subsequent self-heating
11 p1244 N73-20097
Effect of hypokinesis of varying duration on fluid-electrolyte metabolism and composition in blood and tissues of animals
11 p1244 N73-20098
In vitro metabolism of antipyrine in rats
[NASA-TT-F-14868] 11 p1246 N73-20116
Exercise and muscle stimulation for preventing metabolism changes during bed rest
13 p1483 N73-22019
Atrophy and metabolic changes in internal organs and skeletal muscles of rats exposed to hypokinesia
14 p1607 N73-23029

Effects of atmospheric oxygen concentration on Chlorella photosynthesis
14 p1608 N73-23032
Mechanism of inert gas influence on metabolism
[NASA-CR-133214] 16 p1867 N73-25120
Relation between hyperbaric oxygenation and functional activity of differentiated brain with respect ot glutamic acid metabolism
19 p2227 N73-27960
Metabolism and propagation of microbial contamination in planetary atmospheres
[NASA-CR-133638] 20 p2369 N73-29049
Automated Microbial Metabolism Laboratory experimentation for detecting and elucidating extraterrestrial metabolism using labeled release experiment
[NASA-CR-135638] 23 p2770 N73-32154

**METAGALAXY**
U UNIVERSE

**METAL AIR BATTERIES**
NT ZINC-OXYGEN BATTERIES
Operational characteristics of carbon manganese dioxide electrode for metal air battery
[AD-751693] 09 p0991 N73-18089
Design and tests of mechanically rechargable zinc air batteries
[AD-753361] 09 p0991 N73-18091
Low temperature performance of air electrodes for use in zinc-air and metal-air battery systems
[AD-758171] 14 p1607 N73-23021

**METAL ALLOYS**
U ALLOYS

**METAL BONDING**
NT METAL-METAL BONDING
Development of process for bonding resinous body in cavities of honeycomb structures
[NASA-CASE-MSC-12357] 03 p0305 N73-12489
Explosive welding process for producing molybdenum wire reinforced columbium alloy composites
[NASA-CR-123937] 03 p0305 N73-12490
Electric arc bonding of aluminum bronze onto clean steel surface
[AD-747768] 03 p0307 N73-12510
Improvements in welding techniques to increase productivity and quality of performance of bonded joints
[JPRS-58291] 10 p1163 N73-19460
Production of ceramic-metal compounds by contact-reactive brazing for increasing mechanical strength
10 p1163 N73-19462
Electron probe microanalysis of ductile metal bond to Ti alloy disc
[AECL-4251] 10 p1172 N73-19535
Electric resistance spot welding and brazing for producing metal bonds with superior mechanical and structural characteristics
[NASA-CASE-LAR-11072-1] 11 p1298 N73-20535
Developments in vacuum diffusion welding methods and metallurgical applications of solar energy
[NLL-M-22830-[5828.4F]] 11 p1304 N73-20584
Energy pulse bonding method for joining flat cables
14 p1641 N73-23303
Causes of defects in silver-brazed steel joints
[AD-762120] 19 p2305 N73-28541
Ceramic to metal bonding, noting improvement of Mo-Mn silicate method, and use of interfacially active metals
[BMFT-FB-T-73/07] 23 p2798 N73-32377

**METAL CARBIDES**
U CARBIDES

**METAL COATINGS**
NT ALUMINUM COATINGS
NT GOLD COATINGS
NT NICKEL COATINGS
Metallic alloy and aluminide coating for metallic base system
[NASA-CASE-LEW-11696-1] 01 p0061 N73-10502
Effective thermal conductivities of four metal-ceramic composite coatings in hydrogen-oxygen rocket firings
[NASA-TN-D-7055] 01 p0116 N73-10961
Factors affecting orientation of chemical vapor deposited molybdenum coatings precipitated from gaseous phase
[AD-747082] 02 p0194 N73-11566
Physicomechanical and antifriction behavior of polycaproamide and Caprolon surfaces
[NLL-RISLEY-TR-2360-[9091.9F]]
05 p0550 N73-14464
Process for spraying metal coatings on aluminum alloys and resulting antifriction properties
[NLL-TRANS-746-1290-[9022.401]]
05 p0550 N73-14465
Effect of galvanic and thermodiffusive coatings on wear resistance of shafts and hinged joints
[AD-750533] 05 p0553 N73-14494
Effect of transition zone on mechanical properties of high strength steel after cladding with thin layer of highly ductile material
[NLL-TRANS-746-1323-[9022.401]]
05 p0560 N73-14552
Diffusion coating and residual stress effects on steel product strength
[AD-749089] 05 p0566 N73-14600
Abrasive wear resistance of vapor plated chrome coatings
[AD-749769] 05 p0567 N73-14605
Characteristics of molybdenum disulfide films radio frequency sputtered on aluminum and nickel surfaces at elevated, ambient, and liquid nitrogen temperatures
[NASA-TN-D-7170] 08 p0927 N73-17593
Conductive, lusterless coatings for light metals with improved corrosion durability
[AD-753360] 09 p1054 N73-18594
Boiler surface coating effects on water heated by solar energy
[NASA-TT-F-14850] 11 p1237 N73-20043
Bronze coating of alloys in argon atmosphere
[AD-753985] 11 p1309 N73-20623
Copper coating of welded aluminum spacecraft structures to resist oxidation and aid detection of incomplete penetration
[NASA-CR-124251] 15 p1791 N73-24515
Equilibrium limits of molten zirconium nitride flow over nickel-cobalt solid coating
[NLL-M-21572-[5828.4F]] 16 p1926 N73-25583
Silicon carbide backward diode with coated lead attachment
[NASA-CASE-ERC-10224-2] 18 p2122 N73-27150
Life tests of niobium coatings used on alkali metal arc lamps
[AD-761204] 18 p2168 N73-27508
Sputtering of multicomponent materials by ion bombardment
[AD-762813] 20 p2423 N73-29466
Bibliography on refractory coatings in industrial processes
[AD-763150] 21 p2563 N73-30547
Electrolytic and other methods for applying protective titanium coatings
[AD-764318] 22 p2690 N73-31544

**METAL COMPOUNDS**
Application of laser microprobe and magnetic mass spectrometer for determining gas contents in metals by melting and vaporizing microvolumes of samples
[NASA-TT-F-14852] 11 p1305 N73-20592
Acetone decomposition by stainless steel and other metal compounds
[AERE-R-7407] 24 p2892 N73-33088

**METAL CORROSION**
U CORROSION

**METAL CRYSTALS**
Electron fractography of cleavage in metal crystals discussing crack propagation
[NLR-TR-71047-U] 02 p0187 N73-11513
Dislocation mobilities and densities in copper, lead, and zinc crystals
[CALT-767-P-3-27] 12 p1440 N73-21666
Development of procedure for controlling crystallization of metal in molten pools and effect of electromagnetic treatment during welding
[AD-756335] 13 p1536 N73-22443
Analysis of metals and alloys to include superelasticity properties, plastic growth in cracks, strain aging, and strengthening by nuclear gamma resonance
[JPRS-58611] 13 p1540 N73-22477
Analysis of fracture of mixed viscous-brittle breakage of polycrystal using raster electron microscope
13 p1540 N73-22479
Attenuation and thermal release dislocations by interstitial impurities in bcc lattice metals
[NASA-TT-F-14920] 14 p1675 N73-23596
Effect of helium gas bubbles on grain boundary motion in vapor deposited gold foil samples
[RD/B/N-2430] 15 p1798 N73-24578
Measurement of work functions of copper and copper-nickel single crystals at low pressures and determination of thermionic emission constant
16 p1927 N73-25593
Analysis of unidirectionally solidified aluminum alloys to determine properties of random polycrystals, columnar crystals, and growth twin crystals
16 p1927 N73-25594
Characteristics of single crystals of metals with melting points and effects of crystal growth under zero-gravity conditions
[NASA-CR-124354] 20 p2432 N73-29532
Point, line, and planar defects in metal crystals
[COO-3158-17] 24 p2968 N73-33723

**METAL CUTTING**
Analysis of adhesion forces in cutting metals to determine effects of formatting and destruction of adhesive connections on wear of cutting tools
[AD-754041] 11 p1301 N73-20555
Determination of optimum conditions for lubrication and cooling during grinding by abrasive discs of synthetic superhard materials
[AD-754665] 11 p1302 N73-20562
Metal shearing energy absorber
[NASA-CASE-HQN-10638-1] 21 p2552 N73-30460

**METAL DRAWING**
Characteristics of metal drawing processes based on hypotheses of plane cross sections and deformation zone equilibrium conditions
[NLL-M-21553-[5828.4F]] 11 p1296 N73-20518
Friction and lubrication in steel wire drawing
[NLL-RTS-7851] 21 p2552 N73-30454

**METAL FATIGUE**
Fatigue strength curves for large steel screw threads under axial loading
[ESDU-68045] 01 p0110 N73-10905
Ultrasonic method for detecting onset of fatigue damage in metal specimens
[AD-745978] 02 p0175 N73-11418
Four basic types of metal fatigue with distinctive modes of crack initiation and growth
[AD-746121] 02 p0187 N73-11519
Development of general theory for studying large plastic deformation of metals
[AD-746689] 02 p0190 N73-11542
Effect of heat treatment on fatigue life under gust loads of notched Al-Cu alloy
[ARC-CP-1221] 05 p0563 N73-14571
Boron filament splitting in boron aluminum composites caused by water vapor effects
[AD-749971] 05 p0566 N73-14602
Macroscopic and microscopic approach to fracture and hardness of carbon steels
[COO-3084-10] 08 p0932 N73-17630
Irradiation effects on fatigue and creep-fatigue properties of stainless steels
[ANCR-1078] 10 p1173 N73-19539
Constitutive equations for studying finite elastic-plastic deformation of ductile metals
[AD-761635] 19 p2310 N73-28578
Nondestructive evaluation of metal fatigue
[AD-762608] 20 p2433 N73-29541
Fatigue crack tip deformation and fatigue crack propagation
21 p2602 N73-30854
Analytical investigation of hexagonal metal deformation with particular application to Ti and Be
[AD-763835] 22 p2686 N73-31518
Short-term tensile and low-cycle fatigue behavior of zirconium-copper at 482C to 593C
[NASA-CR-121260] 24 p2934 N73-33430
Analysis of size effects related to fatigue strength of metals under conditions of geometrical stress concentrations producing stress and strain gradients
24 p2988 N73-33876

**METAL FIBERS**
Kalman filtering applied to surface and air navigation using celestial body coordinates
07 p0860 N73-16973
Direct casting for producing cast superalloy tungsten or columbium alloy fiber composites with high strength
[NASA-TM-X-2782] 15 p1798 N73-24572

**METAL FILMS**
Analysis of oxidation of high purity tantalum single crystals and large-grained tantalum sheets
[AD-745341] 01 p0068 N73-10554
Effect of transition zone on mechanical properties of high strength steel after cladding with thin layer of highly ductile material
[NLL-TRANS-746-1323-[9022.401]]
05 p0560 N73-14552
Dissociative character of carbon dioxide adsorption on nickel film surfaces
[NLL-TRANS-746-1341-[9022.401]]
06 p0682 N73-15549
Friction, wear, and transfer of carbon and graphite to copper, chromium, and aluminum metal surfaces in vacuum
[NASA-TN-D-7206] 09 p1039 N73-18475
Exposure of 0.29 micron Ni-Fe films to continuous laser light in infrared spectra
[AD-753962] 10 p1129 N73-19202
Development of crack propagation gases based on plating and etching processes and application to center notch, edge notch, and cleavage type specimens
[AD-754762] 11 p1295 N73-20511
Optical properties of films based on tin dioxide and cobalt oxides
[AD-755250] 12 p1417 N73-21479
Metal thin films with extremely high mechanical strength
[AD-755924] 12 p1417 N73-21480
Superconducting properties of crystalline films of aluminum on silicon, considering fluctuating critical temperatures
[BNL-17240] 12 p1441 N73-21672
Porous structure and surface energy of evaporated metal thin films
13 p1565 N73-22683
Aluminum-gold interaction in thin layers
[NASA-TT-F-14919] 14 p1675 N73-23595
Durability of metal films to rupture as thickness of film increases
[AD-756616] 14 p1679 N73-23623
Tensile strength testing of multilayer thin metal film structures
[AD-757723] 14 p1681 N73-23645
Structural and superconducting transition temperature of evaporated aluminum films as function of grain size
[NASA-CR-133450] 19 p2326 N73-28716
Ellipsometric measurements on passive film prior to initiation of breakdown in aluminum
[NASA-CR-132301] 20 p2432 N73-29533
Development of technique and apparatus for optically detonating insensitive high explosives
[NASA-CASE-NPO-11743-1] 20 p2485 N73-29959

Bibliography of reports on sputtering in industrial processes for applying coatings
[AD-763600] 23 p2798 N73-32379
METAL FINISHING
NT ELECTROPOLISHING
NT SHOT PEENING
Refractory porcelain enamel passive thermal control coating for high temperature alloys
[NASA-CASE-MFS-22324-1] 12 p1416 N73-21471
METAL FOILS
Proficiency of X ray fluorescence spectrospectory and wet chemical techniques in measuring trace copper impurities in beryllium foils
[SC-RR-72-0722] 10 p1126 N73-19175
Development of technique for production of beryllium foil with high surface finish
[RFP-1842] 10 p1166 N73-19483
Radio frequency induced sidebands in Mossbauer and Rayleigh scattering radiation from nickel foils
23 p2755 N73-32050
METAL FORGING
U FORGING
METAL FORMING
U FORMING TECHNIQUES
U METAL WORKING
METAL FUELS
Bibliography on metallic fuels for pyrotechnic compositions
[AD-759761] 17 p2097 N73-26963
METAL GRINDING
Standardization values for grinding forces and surface roughness in cylindrical grinding, noting steels
[CRIF-MC-46] 10 p1167 N73-19491
METAL HALIDES
NT ALKALI HALIDES
NT CADMIUM FLUORIDES
NT CESIUM IODIDES
NT COPPER CHLORIDES
NT IRON CHLORIDES
NT LITHIUM CHLORIDES
NT LITHIUM FLUORIDES
NT NICKEL FLUORIDES
NT POTASSIUM BROMIDES
NT POTASSIUM CHLORIDES
NT POTASSIUM IODIDES
NT SILVER CHLORIDES
NT SILVER HALIDES
NT SILVER IODIDES
NT SODIUM CHLORIDES
NT SODIUM FLUORIDES
NT TITANIUM CHLORIDES
NT URANIUM FLUORIDES
NT ZIRCONIUM IODIDES
Evaluation of semiconductive metal halides as cathode material for high energy-density batteries
[AD-757883] 15 p1739 N73-24094
METAL HARDENING
U HARDENING [MATERIALS]
METAL HYDRIDES
NT LITHIUM HYDRIDES
Preparation and structure of complex metal hydrides for high energy solid rocket propellants
[AD-760346] 17 p2076 N73-26794
METAL INSULATOR SEMICONDUCTORS
U MIS [SEMICONDUCTORS]
METAL IONS
Mass spectrometer identification of positive metal ions in Comet Encke beta Taurids meteor shower
[NASA-TM-X-66084] 02 p0229 N73-11855
METAL JOINTS
NT SOLDERED JOINTS
NT SPOT WELDS
NT WELDED JOINTS
Effect of galvanic and thermodiffusive coatings on wear resistance of shafts and hinged joints
[AD-750533] 05 p0553 N73-14494
Relaxation tests on high temperature bolted metal joints
[NLL-ESB-TRANS-503-[3810.97]]
06 p0683 N73-15555
Evaluation of tantalum/316 stainless steel transition joints
[NASA-CR-121111] 07 p0804 N73-16519
Plasma arc welding procedure for Hastelloy seams of isotopic strontium titanate fuel capsule
[CONF-720917-1] 10 p1166 N73-19489
Joint strength, adhesive ductility of adhesively bonded joints of epoxy resins bonded to aluminum and titanium alloys
[DLR-FB-73-22] 14 p1680 N73-23636
Causes of defects in silver-brazed steel joints
[AD-762120] 19 p2305 N73-28541
METAL MATRIX COMPOSITES
Oxidation rate and compatibility of tungsten filament copper matrix composites
[AD-745324] 01 p0069 N73-10569
Effects of molybdenum and tungsten fiber reinforcements on nickel chromium aluminum matrix alloys
[NLL-TRANS-746-1193-[9022.401]]
02 p0191 N73-11546
Physical, technological, and wear resistant properties of naturally alloyed metal ceramic material developed from iron powder
[AD-747626] 03 p0322 N73-12626
Mathematical model and experimental evaluation of performance of phase change thermal control devices containing high thermal conductivity metal matrices
[NASA-CR-129909] 04 p0385 N73-13133
Hot pressing of chromium carbide alloy matrice tools for cold drawing of pipes
04 p0432 N73-13522
Technology assessment of silicon carbide reinforced composites with aluminum or nickel matrix discussing mechanical resistance at high temperatures
04 p0434 N73-13543
Electrolytic procedure for manufacturing aluminum whisker and pure nickel matrix composites with reinforced fibers
04 p0435 N73-13544
Development, characteristics, and applications of composite materials containing inorganic fiber or metal fiber reinforcement
[NLL-RTS-7657] 04 p0437 N73-13561
Crack blunting through fiber matrix debonding in Borsic-aluminum composites
[SC-DC-71-4467] 04 p0438 N73-13568
Fabrication and nondestructive tests of beryllium reinforced metal matrix composites
[AD-750764] 06 p0686 N73-15583
Liquid hot pressing of silicon carbide whiskers for reinforcing aluminum alloy composites
[AD-752589] 08 p0936 N73-17666
Optimal design of elastic bodies using fiberglass reinforced plastics or fibers with high modulus of elasticity
[AD-753040] 09 p1054 N73-18589
Production of superalloy matrix-refrectory metal fiber composites by coextrusion of blended powders
[AD-753340] 09 p1054 N73-18593
Diffusion bonding of plasma sprayed boron reinforced magnesium monolayer tapes by hot pressing
[SC-DR-72-0677] 10 p1166 N73-19488
Mechanical properties of silicon carbide and aluminum oxide sapphire filaments for design of metal matrix composites
[AD-753711] 10 p1176 N73-19568
Modified lamination process for developing boron carbide ribbon reinforced titanium matrix composites
[AD-754478] 11 p1309 N73-20618
Role of titanium in fabricating magnesium-graphite fiber composites with improved strength and stiffness
[AD-754570] 11 p1310 N73-20627
Finite element analysis of reinforcement mechanisms in unidirectional metal matrix composites under transverse loads
[AD-756257] 13 p1548 N73-22541
Analysis of melting, mixing, and solidification of metal matrix composite materials in weightless environment
13 p1594 N73-22921
Role of microstructure on acoustic emission in deformation of Al-CuAl2 composites
[AD-758378] 14 p1679 N73-23628
Effects of environmental variables on physical, thermal, and mechanical properties of resin matrix and metal matrix composite materials
[AD-757524] 14 p1681 N73-23640
Helium migration in aluminum matrices under temperature gradients
16 p1926 N73-25586
Analysis of properties of fiber reinforced materials with plastic and metallic matrix composition and application to gas turbine engines
18 p2164 N73-27476
Production of fibrous metal composites by rolling of powder with strong reinforcing wires and application to aerospace vehicle structures
18 p2164 N73-27478
Application of composite materials to reinforce metallic structures for low cost improvement in structural stability of airframes
18 p2165 N73-27485
Development of fiber reinforced composite materials for application to air breathing engines, aeronautical vehicles, and spacecraft components
18 p2166 N73-27491
Modified filler metal composite for reducing or eliminating underbread cracking in multipass gas tungsten arc plate welds of T-111
[NASA-CR-121198] 19 p2304 N73-28530
Effect of filament-matrix interfaces on fatigue resistance of boron-aluminum composites
[AD-761658] 19 p2312 N73-28597
Mechanical processes for developing metal matrix composite Al/B tubes
[NASA-CR-124407] 23 p2797 N73-32370
Metal matrix composites with Ni and NiCr20 matrix materials, and Al2O3, SiC, W, and Mo reinforcing fibers
[BMFT-FB-T-73-08] 23 p2810 N73-32471
METAL OXIDE SEMICONDUCTORS
Application of Nernst glower metal oxide conductors to laser pumping to produce spectral energy within pumping band of laser material
[AD-745796] 01 p0066 N73-10538
Construction and production problems connected with high frequency n-channel MOS transistors
[AD-747546] 03 p0276 N73-12240
Monolithic display using metal oxide semiconducting circuits and liquid crystal layer
[CEA-CONF-1991] 03 p0345 N73-12814
Annealing phase and space charge decay following pulsed irradiation of MOS structures
[AD-748007] 03 p0347 N73-12833
Ultrasonic marine biotelemetry transmitter utilizing metal oxide semiconductor integrated circuits
[AD-748605] 04 p0383 N73-13119
Performance of temperature compensated rocketborne MOSFET electrometer amplifier for measurement of electron and ion densities in lower ionosphere
[FOA-3-C-3640-E1] 04 p0420 N73-13424
Design of low power high performance MOS random access memory unit
[NASA-CR-123943] 04 p0457 N73-13732
Electrical properties of MOS field effect transistors and Schottky barrier photodiode
[AD-748862] 04 p0459 N73-13746
Charge trap structure of pyrolytic alumina layer in metal oxide semiconductor capacitor
[AD-751629] 07 p0762 N73-16195
Design of automated production facility capable of manufacturing beam-lead CMOS integrated circuits
[NASA-CR-124116] 09 p1038 N73-18465
Design and performance of metal oxide semiconductor analog shift register as image sensor and reading aid for blind persons
[AD-753259] 09 p1075 N73-18776
Gyrator circuit using MOS field effect transistors
[NASA-CASE-MFS-21433] 11 p1261 N73-20232
Theory and fabrication techniques for MOS field effect transistor with submicron and graded channel
12 p1382 N73-21207
Computer modification of MOS transistor mathematical models
[CEA-R-4332] 12 p1383 N73-21218
MOS photodetector mosaics for application to readout of optical memories with charge storage
13 p1500 N73-22155
Extended life testing of complementary MOS integrated circuits
[NASA-CR-124215] 13 p1533 N73-22422
Transient radiation caused performance degradation in integrated ferrite phase shifter driven circuit
[AD-757618] 14 p1644 N73-23336
Design analysis and integration of MOS threshold logic gates
[AD-758021] 15 p1759 N73-24260
Electrical properties of thin sputtered aluminum-silica capacitors
[NASA-CR-121165] 16 p1880 N73-25220
Specifications for design of P-channel MOS computers
[AD-759189] 16 p1884 N73-25249
Plasma anodization and oxidation of thin metal film semiconductors
[AD-760171] 17 p2052 N73-26600
Noise in metal nitride oxide semiconductor devices
[AD-760544] 18 p2124 N73-27163
Design of MOS floating gate transistor amplifier
[AD-761660] 19 p2244 N73-28092
Effect of laser pulse on threshold voltage of metal oxide semiconductor field effect transistors
[CRC-1246] 21 p2585 N73-30716
Research projects involving design and technology of semiconductor devices, metal oxide semiconductor field transistors, and electron storage for memory purposes
21 p2607 N73-30895
Boron radiation hardening for stabilizing gate threshold potential of MOS devices
[NASA-CASE-GSC-11425-2] 23 p2764 N73-32114
Properties of dielectric layers of negative electrosensitive resin noting masking capability and application to MOS circuit manufacturing
[REPT-5.497] 23 p2765 N73-32124
Theoretical calculation of surface mobility in MOS surface inversion layers at room temperature
23 p2825 N73-32578
Properties of silicon-silicon dioxide interface properties in thin oxide metal oxide semiconductor structures
24 p2968 N73-33718
METAL OXIDES
NT ALUMINUM OXIDES
NT BARIUM OXIDES
NT BERYLLIUM OXIDES
NT BISMUTH OXIDES
NT CALCIUM OXIDES
NT CERIUM OXIDES
NT CHROMIUM OXIDES
NT COBALT OXIDES
NT HAFNIUM OXIDES
NT HEMATITE
NT IRON OXIDES
NT LEAD OXIDES
NT LITHIUM OXIDES
NT MAGNESIUM OXIDES
NT MANGANESE OXIDES
NT NICKEL OXIDES
NT NIOBIUM OXIDES
NT PLUTONIUM OXIDES
NT RUTILE
NT SAPPHIRE

NT SCHEELITE
NT TANTALUM OXIDES
NT THORIUM OXIDES
NT TIN OXIDES
NT TITANIUM OXIDES
NT URANIUM OXIDES
NT VANADIUM OXIDES
NT YTTRIUM OXIDES
NT ZINC OXIDES
NT ZIRCONIUM OXIDES
Polarization and thermionic emission effects on resistivity measurements for metal oxide electrical insulators at high temperatures
[HEDL-TME-72-73] 12 p1386 N73-21243
Preparation of metal-oxide-hydroxide protective layers under controlled pO2-pH2O-T conditions
[AD-755729] 13 p1544 N73-22514
Structural, electrical, and magnetic properties of transition metal oxide phosphate glasses
[AD-758373] 14 p1699 N73-23790
Infrared spectra of group 3 metal-oxides
[NASA-CR-133100] 17 p1991 N73-26102
Vapor condensation of Ni-Fe phases and paleomagnetic records in carbonaceous chondrites
17 p2017 N73-26310
Melt-grown, oxide-metal composites for high field electron emission testing
[AD-759507] 17 p2051 N73-26592
Laser motivated studies of chemiluminescence in metal oxides and nitrides
21 p2554 N73-30477

**METAL PARTICLES**
NT METAL POWDER
NT PLATINUM BLACK
Spectroscopic, photometric, and electron microscope analyses of metal wear particles in JT3D turbojet engine oil
[DLR-FB-73-06] 12 p1409 N73-21417
Effect of metal additives on combustion rate of solid rocket propellants
[AD-764155] 22 p2730 N73-31849

**METAL PLATES**
Explosive forming and manufacturing of titanium alloy plates
[AD-745113] 01 p0062 N73-10512
Damping of flat square plates vibrating in air and vacuum
[AD-746054] 01 p0115 N73-10949
Numerical analysis of stress field in semi-infinite elastic-plastic medium under generalized plane deformation
[AD-746046] 01 p0115 N73-10951
Application of strain compatibility equations to evaluate thermal stresses in unidirectional graphite composites bonded to aluminum structures
[NASA-CR-112162] 02 p0125 N73-11014
Multimaterial lamination as means of retarding penetration and spallation failures in plates from hypervelocity impact
[NASA-TN-D-6989] 02 p0238 N73-11934
Stress freezing and slicing techniques of photoelasticity to analyze local stresses near deep surface flaws under cylindrical bending fields
[AD-746976] 02 p0240 N73-11950
Development of formula for calculating natural frequencies of cantilever plate in fluid medium
[AD-747206] 02 p0241 N73-11958
Maximum root-mean-square response of square clamped aluminum plate subjected to stationary random excitation
[NASA-CR-129301] 03 p0361 N73-12939
Fluid wave equation for analyzing damage by excited pressure field between two elastic plates
[AD-748340] 04 p0407 N73-13316
Anisotropic nature of toughness due to texture in titanium and titanium alloy plate
[AD-748390] 04 p0435 N73-13549
Fatigue crack propagation of aluminum metal sheets under flight simulation loads corresponding to gust spectrum
[NLR-MP-72010-U] 04 p0480 N73-13926
Preparation of porous metal samples for quantitative metallographic analysis and effects of procedure on accuracy of results obtained
[NLL-TRANS-746-1255-[9022.401]]
05 p0561 N73-14555
Experimental determination of fracture strength and critical crack length of 7075-T7351 aluminum alloy plates
[AD-748254] 05 p0563 N73-14575
Numerical analysis of stress in face plates of sandwich panel structures subjected to random acoustic loading
[ESDU-72017] 06 p0723 N73-15900
Subcritical crack propagation in pressure vessel plates due to cyclic loads and stresses
[NASA-CR-120834] 06 p0725 N73-15920
Firing tests to determine cratering produced by impact of flat ended, high density metal cylinders striking mild steel plate targets
[DREV-TN-2034/72] 06 p0726 N73-15927
Procedures for estimating stresses in titanium and high strength steel panels and comparison of estimated and measured stresses
[ESDU-72005-AMEND-A] 07 p0850 N73-16894
Analysis of response of structure to acoustic excitation to include vibration of structure, natural frequencies and damping, and noise field characteristics
[ESDU-72001-AMEND-A] 07 p0850 N73-16895
Analysis of fatigue and fail-safe characteristics of composite-reinforced, stiffened metal panels to determine residual strength
[NASA-CR-2136] 07 p0852 N73-16909
Microwave gauge for measuring thickness of hot steel product during production
[PB-212210] 08 p0925 N73-17583
Analysis of structural properties produced by selective reinforcement of aluminum compression panels with unidirectional boron epoxy composite materials
[NASA-CR-2145] 08 p0966 N73-17895
Penetration of truncated cones into ductile targets
[DREV-R-655/72] 09 p1093 N73-18926
Calculation of bifurcation stress in elastic/plastic plate under uniaxial compression
[AD-753136] 09 p1096 N73-18949
Application of correlation equations to evaluate structural strength and reliability of various materials
[AD-753497] 09 p1097 N73-18956
Fatigue behavior of composite-reinforced, integrally stiffened metal panels
[NASA-CR-112148] 13 p1585 N73-22853
Neutron irradiation effects on pair defect accumulation in thin rectangular isotropic metal plates
14 p1675 N73-23593
Stress analysis of plates with part circular and flat bottomed cracks and various flaw depths using stress intensity factors from photoelastic data
[NASA-CR-132015] 14 p1715 N73-23915
Development of approximate equation for determining stress intensities for quarter circular cracks emanating from circular hole in sheet material
[AD-757550] 14 p1716 N73-23928
Center cracked tension specimen for determining plane stress fracture mechanics in metal plates
[AD-757654] 14 p1717 N73-23933
Gravity effects upon melt-through time of metal plate subjected to high intensity lasers
[AD-759168] 16 p1925 N73-25574
Finite element digital procedure for stress and strain distribution in vicinity of interference fit fastners
[AD-760570] 18 p2157 N73-27425
Response of thick rectangular plate of incompressible, isotropic elastic material to tensile forces applied to opposite faces
[AD-761941] 19 p2350 N73-28903
Effect of air resistance on vibration damping in metal plates
[AD-761591] 19 p2350 N73-28906
Elastic stress analysis of aluminum-epoxy plate with crack normal to interfaces
20 p2478 N73-29901
Analysis of response and fatigue characteristics of light alloy integrally machined planks with emphasis on acoustic fatigue properties
20 p2479 N73-29912
Application of Galerkin method in nonconservative stability problems relating to thin elastic plates and slender elastic rods
[NRC-TT-1673] 21 p2603 N73-30860
Analysis of threshold penetration of spherical projectiles impacting aluminum single wall targets at hypervelocity speeds
[NASA-TN-D-7308] 21 p2603 N73-30865
Computer program for analysis of nonlinear deformation and fatigue response of components subjected to complex load histories
[AD-763780] 21 p2604 N73-30870
Stress and strain distribution along round, circular cavity in infinite space
[AD-764104] 22 p2726 N73-31819
Simplified model for heat transfer and subsequent temperature distribution in thin metal target impacted by cylindrical projectile
[AD-763152] 22 p2730 N73-31850
Tungsten-coated tungsten-uranium dioxide nuclear fuel plates
[NASA-CASE-XLE-00209] 23 p2818 N73-32528
Variational method for numerical analysis of bending and supercritical behavior of heterogeneous slightly curved plates
[AD-765543] 24 p2990 N73-33891

**METAL POLISHING**
NT ELECTROPOLISHING
Preparation of porous metal samples for quantitative metallographic analysis and effects of procedure on accuracy of results obtained
[NLL-TRANS-746-1255-[9022.401]]
05 p0561 N73-14555
Relationship between temperature and surface layer quality of two row roller bearings polished with abrasive cloth
[AD-754678] 11 p1301 N73-20559

**METAL POWDER**
NT PLATINUM BLACK
B4C-alkali metal carbonates for boronizing steel surfaces
[NLL-RTS-7197] 01 p0069 N73-10562
External friction effects on compressibility of metal powders
[AD-747722] 03 p0317 N73-12583
Sintering behavior of UO2 powder compacts under hydrogen atmosphere
[CEA-R-4285] 04 p0427 N73-13477
Production engineering methods for metal ceramic structural materials and parts
[JPRS-57487] 04 p0431 N73-13515
Compactibility, shrinkage, and microhardness of electrolytic titanium powders obtained at low temperatures from melts
04 p0432 N73-13521
Pressure sintering of beryllium oxide powder blended with aluminum oxide powder
[AD-748389] 04 p0439 N73-13576
X ray apparatus for investigating hydrogen induced changes in fine crystalline structure of Ni powders and electrolytic films
[NLL-TRANS-746-1294-[9022.401]]
05 p0505 N73-14113
Magnetic properties and phase composition of finely-dispersed nondeformed powders from highly-anisotropic gamma-phase Fe-Pd alloys
[NLL-TRANS-746-1389-[9022.401]]
05 p0560 N73-14553
Production of metal powders with emphasis on iron powder
[NLL-TRANS-746-1262-[9022.401]]
05 p0561 N73-14557
Microstructure and mechanical properties of rapidly quenched liquid and powder metal alloys
[AD-749679] 05 p0564 N73-14578
Magnetic properties of single crystal nickel powers
[NLL-TRANS-746-1390-[9022.401]]
05 p0585 N73-14762
High temperature tests to determine effect of autoclave heat treatment of mechanical properties of cobalt-base alloy HS-31 in prealloyed powder form
[NASA-TN-D-7117] 07 p0809 N73-16559
Production of superalloy matrix-refrectory metal fiber composites by coextrusion of blended powders
[AD-753340] 09 p1054 N73-18593
Characteristics and production methods of iron nickel-molybdenum carbonyl powders
[NLL-LTI-746-1418-[9022.401]]
16 p1925 N73-25580
Bibliography on metallic fuels for pyrotechnic compositions
[AD-759761] 17 p2097 N73-26963
Metal plating process employing spraying of metallic power/peening particle mixture
[NASA-CASE-GSC-11163-1] 23 p2795 N73-32360
Process for removing plasticizer from hard metal alloy extruded samples during low temperature sintering
23 p2808 N73-32454
Separation of fine metallic powders using air in combination with fluidized bed
23 p2809 N73-32462
Plastic and powder metal materials for gear production
[NASA-TM-X-71446] 24 p2928 N73-33388

**METAL SHEETS**
Effect of chemical composition, method of heat treatment, and production methods, on corrosion resistance of metal sheets
[AD-742106] 01 p0067 N73-10550
Wedge procedure for determining stress corrosion cracking susceptibility of 5000 series aluminum alloy sheets
[AD-747944] 03 p0316 N73-12577
Fatigue and crack propagation characteristics of aluminum alloy sheet under controlled cycle stress conditions to simulate fuel tank structural failure
[NASA-CR-128600] 03 p0360 N73-12935
Fatigue crack propagation in aluminum alloy sheets in environments of dry argon, normal air, distilled water, and aqueous sodium chloride solutions
[NLR-TR-72005-U] 04 p0431 N73-13513
Effects of various forming factors and process variables on forming of sheet metal products
05 p0551 N73-14476
Explosive welding of thin metal scarf joint
[NASA-CASE-LAR-11211-1] 05 p0552 N73-14480
Environmental fatigue crack propagation in titanium sheet alloys in atmospheres of argon, normal air, distilled water, and salt solution
[NLR-TR-72019-U] 05 p0602 N73-14894
Effect of metallurgical conditions on mechanical properties of ASTAR-811C sheet
[NASA-CR-121096] 08 p0931 N73-17625
Forming and subsequent mechanical properties of high strength work hardened sheet materials
[PB-212207] 08 p0932 N73-17634
Effect of sheet thickness on plane stress fracture resistance of high strength titanium alloys
[AD-753198] 09 p1049 N73-18555
Pulsed electron beam heating for optimal penetration and forming of welds
[AD-754684] 11 p1301 N73-20557
Aluminum alloy sheet bonding with steel sheets to form high strength composites
[TN-279] 13 p1533 N73-22421
Buckling and vibration behavior of tensioned sheets with elliptical openings
13 p1584 N73-22840

Visual and microscopic studies on corrosion resistance of anodized aluminum sheets
[M72-09-96-REI/BLA/PUT] 14 p1675 N73-23592
Mathematical model for calculating time required for continuous wave CO2 laser to perforate thin metal sheets
[REPT-534] 16 p1923 N73-25562
Time prediction for laser melting and vaporization of metal sheet
[AD-760113] 17 p2042 N73-26521
Measurement of electromagnetically excited acoustic standing-wave resonance
18 p2159 N73-27444
Formation of longitudinal edge waviness and center camber on sheets as measure of sheet flatness
[NLL-M-21611-[5828.4F]] 18 p2202 N73-27777
Development of workable high strength metastable beta titanium sheet alloy
[AD-761515] 19 p2310 N73-28577
Analysis of size effects related to fatigue strength of metals under conditions of geometrical stress concentrations producing stress and strain gradients
24 p2988 N73-33876

**METAL SHELLS**
Fabrication of plastic encapsulated metal containers by rotational molding process
[AD-753344] 10 p1168 N73-19499

**METAL SPINNING**
Fabrication and hydrotests of shear spun rocket engine cases
[AD-761129] 18 p2201 N73-27770

**METAL STRIPS**
Mathematical model of deformed state of metal strips during upsetting
[NLL-M-21511-[5828.4F]] 05 p0561 N73-14560
Stiffness of flat strips in compression under sinusoidally distributed bending couples at their edges
[ESDU-02.01.30-AMEND-A] 06 p0723 N73-15905

**METAL SURFACES**
Intermodulation interference effects of metal surface transmitters and receivers in near field locations of transmission system
01 p0027 N73-10212
Formation of electric fields during friction of lubricating oil on metal surface
[AD-745433] 01 p0062 N73-10511
Fretting damage from contact between two metal surfaces
[ESDU-67012] 01 p0111 N73-10921
Bibliographic survey on yield behavior of metal surfaces
[AD-746473] 02 p0188 N73-11524
Influence of surface processes on rate of permeation of hydrogen through metals
[NASA-CR-129276] 03 p0312 N73-12548
Bidirectional reflectance of metallic surfaces as function of wavelength and surface roughness
[UILU-ENG-72-4001] 03 p0335 N73-12728
Compatibility of protective coatings for niobium alloy gas turbine blades
[AD-748837] 04 p0439 N73-13575
Metallic surface effects on radiative stability and focusing effects of electron ring
[JINR-P9-6318] 04 p0452 N73-13692
Kinetic energy of abrasive particles knocked from metal surface during impact
[AD-750500] 06 p0655 N73-15321
X ray analysis to determine occurrence of metal surface texturing as result of sliding friction
[NASA-TN-D-7136] 06 p0677 N73-15508
Determination of surface structure of metal crystals by chemisorption method
[NLL-TRANS-746-1340-[9022.401]]
06 p0682 N73-15548
Effect of magnetic rupture on low frequency electroconductivity and weakly damped electromagnetic waves in metals with closed Fermi surfaces
[KHFTI-71-1] 06 p0684 N73-15569
Suitibility of Nb surfaces in superconducting RF cavities
[KFK-EXT-3/72-3] 06 p0709 N73-15781
Laser scattering from curved aluminum and titanium aircraft surfaces in clear atmosphere
08 p0884 N73-17159
Wear process and colloidal particle production test on sliding metal surfaces using magnetic measurements
[AD-753251] 09 p1040 N73-18481
Spacecraft pressure gage reliability studies relative to gas dynamics and metal surface testing
[NASA-CR-112320] 13 p1529 N73-22392
Influence of surface preparation, surface texture, and initial oxidation on metal surface crystallization
14 p1676 N73-23603
Theory of electron density distribution inouced at metal surface by small static external charge distribution
[AD-758380] 15 p1814 N73-24707
Corrosion and protective properties of organic complex-forming agents which produce insoluble chelate compounds with various metal surfaces
[DRIC-TRANS-3079] 17 p2046 N73-26551
Metal-ceramic bonding detailing dry soldering method
[FTZ-A-97-TBR-2] 22 p2678 N73-31453
Heat treatment effects on metal black surfaces, and Auger spectra during magnesium and iron oxidation
[RU-20-6] 23 p2769 N73-32146
Film growth transient measurements for stress corrosion cracking susceptibility analyses on metals
23 p2804 N73-32421
Chemical bonding of solid polymers to metal surfaces and formation of organometallics
[NASA-TM-X-71452] 24 p2929 N73-33390
Characteristics of bulk and surface modes in simple metals using modified self-consistent linear response theory
24 p2933 N73-33427
Surface roughness effects on bidirectional reflectance of metallic surfaces
24 p2955 N73-33611

**METAL VAPORS**
NT MERCURY VAPOR
NT SODIUM VAPOR
Release technique for creating large dense vapor clouds in upper atmosphere using thermite formulation of barium metal and barium nitrate
[AD-745980] 01 p0054 N73-10438
Derivation of formulas for calculating interfacial thermal resistance and condensation coefficient during condensation of metal vapors
[AD-748048] 03 p0365 N73-12972
Stress corrosion cracking of titanium and titanium alloys in organic liquids and vapors
[AD-751528] 07 p0810 N73-16572
Langmuir measurements of thermodynamic lead vapor properties
[IS-2871] 10 p1173 N73-19542
Joule heating model for cathode surface structure effect on metal evaporation in vacuum discharge
[TH-73-E-33] 14 p1643 N73-23329
Analysis of phase change occurring in molten metals, semiconductors, and alloys when heated to 700 to 900 C above melting point
[NLL-M-21614-[5828.4F]] 15 p1796 N73-24563
Laser radiation and RF induction heating for production of metal vapor
[AD-762917] 20 p2374 N73-29080

**METAL WHISKER REINFORCEMENT**
U WHISKER COMPOSITES

**METAL WORKING**
NT CLADDING
NT EXPLOSIVE FORMING
NT FORGING
NT MAGNETIC FORMING
NT METAL DRAWING
NT METAL SPINNING
Effects of axially symmetric deformation of metal on mechanical and physical properties of samples
[AD-745551] 01 p0063 N73-10513
Development of method for classifying stresses in isotropic work hardening media using polarized light
[NLL-M-21475-[5828.4F]] 02 p0236 N73-11918
Analysis of stress formation and changes in physical properties of pipes during rotary swaging using explosion or pulsed magnetic field energy
[AD-747454] 03 p0308 N73-12516
Thermal and thermophysical processes for microstructural control in high strength steel to increase fracture toughness
[LBL-832] 04 p0434 N73-13537
Characteristics of high performance metal castings and procedures for improving reliability
[AD-748462] 04 p0436 N73-13557
Effects of various forming factors and process variables on forming of sheet metal products
05 p0551 N73-14476
Analysis of metallurgical factors and mechanical effects during and subsequent to cold hydrostatic extrusion of magnesium and aluminum alloys
[AD-751739] 07 p0805 N73-16527
Production of ball bearing steel ingots with emphasis on effects of temperature, surface defects, and casting methods
[AD-751252] 07 p0805 N73-16533
Development of extruding machine for producing parts with complicated shapes, high degree of mass, and requiring precision surfaces
[AD-751146] 07 p0805 N73-16534
Analysis of defects in metals produced by high speed extrusion
[AD-752867] 09 p1041 N73-18488
Analysis of beta titanium alloys to show heat treatment, mechanical properties, corrosion, weldability, and processing
[AD-753439] 09 p1049 N73-18552
Effect of fabrication conditions on mechanical properties of Be-Al monolayer tape and composite specimens
[SC-DR-72-0731] 10 p1175 N73-19559
Properties of zinc-copper-titanium alloys to include microstructure composition, mechanical properties, and effects of hot and cold deformation
[NLL-M-22842-[5828.4F]] 11 p1304 N73-20583
Effect of viscous lubricants on metal flow during cold reverse extrusion
[AD-743242] 13 p1533 N73-22425
Analysis of melting, mixing, and solidification of metal matrix composite materials in weightless environment
13 p1594 N73-22921
Analysis of production and characteristics of ultrahigh strength steels based on survey of literature
[ARL/SM-NOTE-378] 14 p1675 N73-23591
Characteristics of photoelectric pyrometer for measuring temperature of thin wire during rolling process
[NLL-M-21634-[5828.4F]] 15 p1785 N73-24471
Analysis of effects of homogenizing annealing on ductility of high strength steel
[NLL-M-21616-[5828.4F]] 15 p1796 N73-24562
Evaluation of low cost techniques for forming boron-reinforced aluminum structural shapes from diffusion-bonded flat sheet and plate
[NASA-CR-124279] 16 p1918 N73-25523
Materials response to welding and forming
[PB-214213] 16 p1918 N73-25524
Processing condition effects on microstructures of sheets, wire and bars made from nickel chromium iron alloy 718
[WAPD-TM-1077] 16 p1928 N73-25603
Computer programs for solving metal working equations by considering mechanical properties
[AD-759830] 17 p2038 N73-26491
Mathematical representation of flow curves for metallic materials
[RAE-LIB-TRANS-1675] 17 p2043 N73-26532
Development and production of thermo-mechanically forged tool steel spur gears using high energy rate forging procedures
[NASA-CR-121227] 18 p2154 N73-27409
Development of manufacturing method for elimination of nitride inclusions from titanium alloys during melting and ingot consolidation
[AD-748261] 18 p2163 N73-27473
Pressure shaping of steels and alloys
[AD-762308] 19 p2306 N73-28549
Development of workable high strength metastable beta titanium sheet alloy
[AD-761515] 19 p2310 N73-28577
Plastic deformation of cold worked metals
[AD-762468] 19 p2310 N73-28583
Proceedings of conference on rolling mills for production of work hardened, heat treated metal products
[NLL-M-21649-[5828.4F]] 20 p2421 N73-29450
Analysis of physical and mechanical properties of nonmagnetic steels and suitability for producing tubes and forgings
[NLL-M-21647-[5828.4F]] 20 p2422 N73-29451
Processes of metal working in Themis project
[AD-763122] 20 p2423 N73-29464
Analysis of properties of copper, titanium, and nickel specimens following hardening by shock waves at pressures up to 1,200 kilobars
[NLL-RTS-8047] 20 p2428 N73-29500
Development of method for analyzing stress deformation state of metal during process of lengthwise rolling of tubes
[NLL-M-21655-[5828.4F]] 20 p2428 N73-29501
Analysis of stress-strain state in metal and contact stresses developed during continuous rolling on long mandrel for reducing and drawing metal tubes
[NLL-M-21688-[5828.4F]] 20 p2428 N73-29502
Development of method for determining optimum setting of regulators on metal working machinery involved in sintering process
[NLL-M-21642-[5828.4F]] 20 p2428 N73-29505
Process for manufacturing synthetic iron and comparison of annealing rate of synthetic iron with conventional iron
[NLL-M-21640-[5828.4F]] 20 p2429 N73-29507
Analysis of variations in hardness and microstructure of metals subjected to shock wave pressures
[NLL-NEL-TT-2489-[6075.461]]
20 p2429 N73-29514
Development of computer method for solving axisymmetric variational problems of theory of treatment of metals by pressure
[NLL-M-21659-[5828.4F]] 20 p2430 N73-29517
Analysis of effects of hydrostatic pressure on yield stress, flow stress, and ductility of metals
[NLL-NEL-TT-2488-[6075.461]]
20 p2478 N73-29904
Determination of elongation in flanges during H-beam rolling
[NLL-M-21639-[5828.4F]] 21 p2552 N73-30455
Analysis of structure dependent and temperature dependent variables affecting flow curves of metals
[BLL-RAE-LIB-TRANS-1675] 21 p2556 N73-30494
Discrete method for variational problems in treatment of metals by pressure
[NLL-M-21663-[5828.4F]] 21 p2557 N73-30497
Analysis of ductile flow of metal during extrusion process with application to manufacture of cable sheathing
[NLL-M-21661-[5828.4F]] 21 p2557 N73-30498
Effect of copper and silicon on selected mechanical properties of hot rolled medium carbon steels
[BM-RI-7777] 21 p2558 N73-30504
Analysis of melt segregation effects on solidification of metals under weightless conditions
[NASA-CR-124358] 21 p2559 N73-30510
Development of iron alloy with high fracture toughness at cryogenic temperatures
[LBL-1121] 21 p2559 N73-30511

Application of hot pressing, hot extruding, and sintering processes for production of composite materials
[JPRS-59873] 23 p2807 N73-32441
**METAL-GAS SYSTEMS**
Point defect theory and oxidation kinetics in metal reactions with high temperature gaseous environment
[GAT-T-1868] 06 p0684 N73-15571
**METAL-METAL BONDING**
Pack rolling effects on bond strength between Nb and Cu
[AD-750511] 06 p0678 N73-15517
Structural analysis of laminated aluminum alloy sheets to determine flaw growth behavior in roll diffusion bonded and adhesive bonded structures
[NASA-CR-128844] 10 p1220 N73-19921
Analysis of adhesion strength of electroless nickel plating on Type 4340 steel to determine optimum plating conditions and to certify bond strength
[Y-1838] 12 p1414 N73-21459
Aluminum alloy sheet bonding with steel sheets to form high strength composites
[TN-279] 13 p1533 N73-22421
Metallic chain compounds and organometallic complexes for high temperature superconductor materials
[AD-759767] 17 p2074 N73-26778
**METALLIC PLASMAS**
NT CESIUM PLASMA
NT URANIUM PLASMAS
Ionization processes in mercury plasma due to excited state interactions and electron impact
[NASA-CR-130924] 10 p1192 N73-19701
Corona equilibrium model for ionization state distributions in carbon, aluminum, copper, and tungsten plasmas
[AD-758357] 14 p1696 N73-23767
**METALLIZING**
Diffusion metallizing and service life of gas turbine engine blades
[NASA-TT-F-13914] 02 p0223 N73-11801
**METALLOGRAPHY**
Analysis of metallurgical, physical, and mechanical properties of uranium alloys to determine breakdown strain, elongation, and high density characteristics
[FOA-4-C-4471-D4] 02 p0186 N73-11508
Aluminum metallographic method to obtain dislocation etchings and microstructural details
[AD-747086] 02 p0189 N73-11537
Quantitative examination of ordering effects in nickel-iron alloy system
[NLL-RTS-7547] 04 p0431 N73-13510
Bibliography on capabilities and limitations of chemical milling techniques
[AD-752050] 08 p0928 N73-17597
Effect of metallurgical conditions on mechanical properties of ASTAR-811C sheet
[NASA-CR-121096] 08 p0931 N73-17625
Compilation of metallurgical processes for variety of metals and alloys
[NASA-SP-5953[01]] 11 p1306 N73-20593
Research and development in chemical and extractive metallurgy and molecular crystals
[AD-754797] 11 p1327 N73-20770
Review and compilation of technical data on Lorenz ratio of metals and alloys to include electrical resistivity and thermal conductivity
[NBS-TN-634] 12 p1413 N73-21451
Analysis of metals and alloys to include superelasticity properties, plastic growth in cracks, strain aging, and strengthening by nuclear gamma resonance
[JPRS-58611] 13 p1540 N73-22477
Analysis of phase change occurring in molten metals, semiconductors, and alloys when heated to 700 to 900 C above melting point
[NLL-M-21614-[5828.4F]] 15 p1796 N73-24563
Etch pit study of motion and generation of dislocations in electron irradiated metals and effect of point defects on mechanical properties of metals
[COO-1367-50] 15 p1799 N73-24579
Metallographic and X ray analysis of metastable alloys of titanium
[AD-759387] 16 p1931 N73-25623
Influence of titanium ions on magnetic properties of manganese-zinc ferrites
[NLL-TRANS-862-[9022.64]] 16 p1931 N73-25626
Characteristics and production of silicon nitride-alumina sintered materials
[NLL-RTS-7988] 16 p1931 N73-25627
Density and light radiation measurements of molten metals, semiconductors, and alloys
[NLL-M-21580-[5828.4F]] 16 p1951 N73-25789
Mathematical representation of flow curves for metallic materials
[RAE-LIB-TRANS-1675] 17 p2043 N73-26532
Standards for metallic specimens to include methods of mechanical and technological testing
[JPRS-59280] 17 p2044 N73-26538
Development of nondestructive inspection procedures for determining quality of welded joints in aluminum spacecraft structures
[NASA-CR-124332] 18 p2156 N73-27420
Principles of nondestructive testing and organization of Soviet metallography laboratories at industries
[JPRS-59424] 18 p2160 N73-27449
Bibliography of test equipment and procedures for determining physical and mechanical properties of iron and steel products
[PB-219047] 18 p2161 N73-27459
Development of manufacturing method for elimination of nitride inclusions from titanium alloys during melting and ingot consolidation
[AD-748261] 18 p2163 N73-27473
Development of method for calculating molar volume and density of molten binary alloys with strongly interacting dissimilar atoms
[NLL-M-21695-[5828.4F]] 20 p2429 N73-29512
Flourescent X ray spectrography of low alloy steel specimens to determine presence of eight elements
[BM-RI-7773] 20 p2433 N73-29539
Failure analysis of semiconductor devices by metallography
[DLR-MITT-72-20] 22 p2643 N73-31184
**METALLOIDS**
NT ANTIMONY
NT ARSENIC
NT BORON
NT GERMANIUM
NT SILICON
NT TELLURIUM
Age hardening and precipation behavior of V-Ti, V-Ti-Si, V-Zr, and V-Hf alloys with reference to interstitial metalloid
[KFK-1680] 15 p1799 N73-24582
Precipitation and age hardening phenomena in vanadium alloys with reference to metalloid additives
[EURFNR-1060] 24 p2935 N73-33439
**METALLORGANIC COMPOUNDS**
U ORGANOMETALLIC COMPOUNDS
**METALLURGY**
Problems of using metallurgical and chemical materials in direct conversion systems
[UCRL-73560] 03 p0333 N73-12718
Reports on electrical and mechanical properties of beryllium, chromium-manganese austenitic steels, and martensitic conversion during deformation
[JPRS-58357] 10 p1171 N73-19524
High, medium, and low energy physics, mathematics and computers, chemistry, and metallurgy and materials research
[IS-2800] 10 p1189 N73-19678
Metallurgical investigation of deformation and fatigue using high temperature tests and stress-strain diagrams on heat resistant alloys
[JPRS-58180] 10 p1219 N73-19912
Procedure for fabricating element with cavity closed by thin wall with precisely shaped slit
[NASA-CASE-LAR-10409-1] 11 p1297 N73-20526
Metallurgical reports on plasma jets, creep properties of nickel alloys, oxygen and nitrogen interactions with metals, and Mossbauer effect as applied to diffusion mechanisms
[JPRS-58508] 12 p1412 N73-21445
Preflight, inflight, and post flight operations evaluation analyses for Skylab metals melting experiment facility - Appendix F
[NASA-CR-61386-APP-F] 14 p1708 N73-23860
Research reports for various engineering sciences and materials and metallurgy
14 p1721 N73-23961
Metallurgical and mechanical properties of joints treated by weld-braze joining process
[NASA-TN-D-7281] 15 p1798 N73-24573
Technology utilization program relating to hydrogen effects on metal alloys and mechanical properties of recently developed alloys
[NASA-SP-5940[03]] 16 p1928 N73-25598
Published articles on mining and metallurgy
[TT-70-56005/4] 21 p2561 N73-30527
Reserach and development in metallurgical thermodynamics
[TT-71-56066] 21 p2561 N73-30528
High temperature electrochemical devices incorporating solid oxygen electrolytes for metallurgical processing
[AD-764769] 23 p2806 N73-32436
Global metallogeny and geological anomalies
[NASA-TT-F-15098] 24 p2980 N73-33816
**METALS**
NT ALKALI METALS
NT ALUMINUM
NT ALUMINUM COATINGS
NT ANTIMONY
NT BARIUM
NT BERYLLIUM
NT BISMUTH
NT CADMIUM
NT CALCIUM
NT CALCIUM ISOTOPES
NT CALIFORNIUM ISOTOPES
NT CERIUM
NT CESIUM
NT CHROMIUM
NT COBALT
NT COBALT 60
NT COPPER ISOTOPES
NT CURIUM 244
NT DYSPROSIUM
NT ERBIUM
NT FERROUS METALS
NT GADOLINIUM
NT GALLIUM
NT GOLD
NT GOLD COATINGS
NT HAFNIUM
NT HOLMIUM
NT INDIUM
NT IRIDIUM
NT IRON
NT IRON 57
NT LANTHANUM
NT LEAD [METAL]
NT LIQUID METALS
NT LIQUID SODIUM
NT LITHIUM
NT LITHIUM ISOTOPES
NT MAGNESIUM
NT MANGANESE
NT MERCURY [METAL]
NT MERCURY VAPOR
NT METAL COATINGS
NT METAL CRYSTALS
NT METAL FILMS
NT METAL FOILS
NT METAL MATRIX COMPOSITES
NT METAL POWDER
NT METAL VAPORS
NT MOLYBDENUM
NT NEODYMIUM
NT NEPTUNIUM
NT NICKEL
NT NICKEL COATINGS
NT NICKEL ISOTOPES
NT NIOBIUM
NT NOBLE METALS
NT NONFERROUS METALS
NT OSMIUM
NT PALLADIUM
NT PLATINUM
NT PLATINUM BLACK
NT PLUTONIUM
NT PLUTONIUM 238
NT POTASSIUM
NT PRASEODYMIUM
NT RADIUM 226
NT RARE EARTH ELEMENTS
NT REFRACTORY METALS
NT RHENIUM
NT RHODIUM
NT RUBIDIUM
NT RUBIDIUM ISOTOPES
NT RUTHENIUM
NT SAMARIUM
NT SILVER
NT SODIUM
NT SODIUM VAPOR
NT STRONTIUM
NT TANTALUM
NT THALLIUM
NT THULIUM
NT TIN
NT TITANIUM
NT TRANSITION METALS
NT TRANSURANIUM ELEMENTS
NT TUNGSTEN
NT ULTRAPURE METALS
NT URANIUM
NT URANIUM 233
NT VANADIUM
NT YTTERBIUM
NT ZIRCONIUM
Differential scanning calorimeter for solid state reaction analysis in pure metals and alloys
[EUR-4802-D] 01 p0055 N73-10449
Electronic and thermodynamic properties of dense plasma interacting with metallic and nonmetallic materials
[CEA-R-4268] 01 p0085 N73-10705
Multiple ion interaction energy and metal structure distribution
01 p0087 N73-10721
Using specific heat method to study vacancies
[AD-743695] 01 p0088 N73-10725
Influence of thermal cycles on weld properties of all weld metal heat affected zone and base metal
[AD-746886] 02 p0179 N73-11452
Creep measurements on metals for calculating stress-strain-time relaxation curves
02 p0186 N73-11507
Scanning electron microscope study of fracture and crack propagation in metals
[AD-746125] 02 p0187 N73-11520
Electron bombardment and energy losses in beryllium, aluminum, copper, tin, gadolinium, and lead
[AD-747077] 02 p0215 N73-11739
Relationships between continuum metal plastic deformation under multiaxial stress and phenomenological dislocation theory
[AD-746187] 02 p0219 N73-11769
Assessment of materials compatibility data for hydrazine monopropellant propulsion systems of space shuttle vehicle in multicycle extended life applications
[NASA-CR-128491] 02 p0221 N73-11788
Time dependent inelastic behavior of metals and metal structures
[AD-746340] 02 p0240 N73-11951

Reaction kinetics in pulsed atomic beam generation by laser vaporization of metallic atoms
[AD-748278] 04 p0387 N73-13145
Antifriction interaction between metals and steels on polyamide surfaces
[NLL-RTS-7378] 04 p0425 N73-13461
Pseudopotential analysis of interaction between conduction electrons and metal lattice field
[ITJ-16] 04 p0433 N73-13532
Structural-, thermal-, and magnetic-properties of various metals and intermetallic compounds
[COO-3427-7] 04 p0434 N73-13536
Analysis of low temperature proton irradiation induced defects in metals
[COO-3431-1] 04 p0434 N73-13542
Electrical resistivity of space electric power insulating materials
[LA-4978] 05 p0498 N73-14058
Weldability and properties of materials undergoing electron beam welding
[CRANFIELD-MAT-7] 05 p0551 N73-14474
Research on neutron irradiation induced voids in metals
[CONF-710601] 05 p0562 N73-14568
Numerical calculation of physical and electronic properties of metals
[AD-749546] 05 p0588 N73-14782
Influence of band structure on photofield emission from metals
[AD-749828] 05 p0589 N73-14788
Estimation of traces of gases in metals and alloys by vacuum fusion techniques
[BARC-590] 06 p0638 N73-15177
Tensile tests of pressure effects on plastic properties and fracturing of metals
[NLL-NEL-TT-2190-[6075.461]] 06 p0682 N73-15552
Corrosion tests of candidate rocket engine materials exposed to standard high density acids for liquid propellant compatibility determination
[AD-749965] 06 p0712 N73-15807
Equation for calculating plastic deformation of metals under tension
[AD-751151] 07 p0810 N73-16571
List of metallic melting bodies for temperature determinations from 30 to 1555 degrees Celsius
[JUL-871-RB] 08 p0932 N73-17631
Transport properties of anodic oxides in metals 09 p1063 N73-18674
Magnetic impurities and boundary effects in metals and superfluids
[AD-753100] 09 p1074 N73-18763
NMR studies in metals and metallic compounds
[AD-752912] 09 p1074 N73-18767
Electrons in metal ammonia solutions - abstracts of conference papers
[AD-752915] 10 p1127 N73-19179
Anneal hardening of irradiated molybdenum metals and alloys
[ORO-3612-9] 10 p1173 N73-19545
Literature review of strain rate effects on mechanical properties of metals at high temperatures
[AD-754243] 10 p1174 N73-19548
Compilation of metallurgical processes for variety of metals and alloys
[NASA-SP-5953[01]] 11 p1306 N73-20593
X ray crystallographic methods for studying preferred orientation of hexagonal metals
[RFP-TRANS-117] 11 p1306 N73-20594
Research projects in metals and ceramics
[ORNL-4820] 11 p1330 N73-20796
Data and design criteria on dynamic compatibility of fluorine with metals
[AD-756908] 13 p1489 N73-22071
Exoelectronic emission and relationship with various surface properties of metals and alloys
[AD-756943] 13 p1543 N73-22509
Engineering data on aerospace structural materials - Vol. I
[AD-755407] 13 p1544 N73-22517
Engineering data on aerospace structural materials - Vol. 2
[AD-755408] 13 p1545 N73-22518
Two methods for derivation of structural expansion for ground state energy of simple metal
[NASA-CR-131833] 13 p1565 N73-22687
Instruments for recording force deflection from Charpy impact tests on metals
[REPT-527] 13 p1585 N73-22852
Analysis of metal transition into brittle state with determination of impact strength
[AD-758252] 14 p1679 N73-23627
Thin layer chromatography for qualitative analyses on steelwork materials
[PB-214232/1] 16 p1871 N73-25148
Theoretical prediction of thermal stress waves in metal conductors induced by relativistic electron beam 16 p1926 N73-25587
Absolute electron yields and spectral characteristics of X ray induced photoemission from metals
[AD-750875] 16 p1928 N73-25599
Temperature dependence of strain hardening in metals
[RAE-LIB-TRANS-1672] 17 p2043 N73-26531
Mechanical properties and crystal structures of polymorphous metals and alloys
[AD-759753] 17 p2074 N73-26779
Perturbed angular correlation measurements on attenuations caused by rare earth nuclei implantation into metals 18 p2184 N73-27638
Analysis of tunneling in metal semiconductor junctions 18 p2185 N73-27640
Effect of irradiation on absolute thermal EMF of alloys, metals, and thermocouple materials
[NASA-TT-F-15015] 19 p2309 N73-28574
Effect of high speed volumetric deformation on ductility of metals and alloys
[AD-762246] 19 p2310 N73-28582
Analysis of fracture and creep properties of metals after extension under conditions of hydrostatic pressure as function of time
[NLL-NEL-TT-2475-[6075.461]] 20 p2429 N73-29515
Bimetallic fluid displacement apparatus for stirring and heating stored gases and liquids
[NASA-CASE-ARC-10441-1] 21 p2552 N73-30461
Numerical solution of multidimensional linear thermal conductivity problems with complex boundary conditions which occur with heating of metals
[NLL-M-21666-[5828.4F]] 21 p2557 N73-30495
Combustibility and toxicity of metals and alloys
[AD-764287] 22 p2621 N73-31003
Utilization of live trees and inanimate metal structures as efficient HF radio antennas
[AD-763887] 22 p2645 N73-31195
Stress-strain diagrams and mechanical properties of metal wires as determined by tranverse impact method
[AD-764105] 22 p2687 N73-31523
Metal plating process employing spraying of metallic powder/peening particle mixture
[NASA-CASE-GSC-11163-1] 23 p2795 N73-32360
Performance of study plan for proposed Skylab experiments concerning metals melting and sphere forming
[NASA-CR-124396] 23 p2796 N73-32368
Plastic response of metals under dynamic loading
[AD-765522] 24 p2937 N73-33452
Analysis of isotopic composition of chemical elements in solar structure using photospheric and sunspot spectra
[NP-19727] 24 p2981 N73-33826

**METASTABILITY**
U METASTABLE STATE

**METASTABLE ATOMS**
Shock deactivation cross sections of metastable barium and thallium atoms in shock tube
[MPI-PAE/EXTRATERR-65] 02 p0214 N73-11734
Role of metastable atoms [D] in thermospheric heating
[NASA-TT-F-14901] 14 p1705 N73-23832
Differential scattering from collision of metastable atoms of He[2 3S] with molecules of N2 and O2
[NASA-TT-F-14801] 15 p1815 N73-24712

**METASTABLE STATE**
Development of powder metallurgy nickel-base superalloy for application at 1800 to 2000 F
[NASA-CR-121099] 09 p1047 N73-18537
Metallographic and X ray analysis of metastable alloys of titanium
[AD-759387] 16 p1931 N73-25623
Metastable states of superconductors in presence of magnetic fields 18 p2185 N73-27645
Atomic structure of stripped heavy ions and their formation and destruction by collisions
[NASA-CR-135704] 23 p2821 N73-32553
Electrical discharge metastable detector for helium afterglows
[AD-765210] 23 p2823 N73-32570

**METAZOA**
U ANIMALS

**METEOR BURSTS**
U METEOROID SHOWERS

**METEOR CRATERS**
U CRATERS

**METEOR HAZARDS**
U METEOROID HAZARDS

**METEOR TRAILS**
Analysis procedure for radar observations 01 p0102 N73-10835
Radar equipment for tracking meteor trails
[AD-745959] 02 p0169 N73-11372
Radar observations of meteor trains for detecting high altitude gravity waves 05 p0511 N73-14154
High resolution radar system for measuring wind velocity and height of meteor trails
[NASA-CR-131644] 12 p1377 N73-21172
Dynamics of lower thermosphere through comparison of optical observations of motions of vapor trails with radar observations of ionized meteor trails
[NASA-CR-131645] 12 p1420 N73-21509
Low light level television system for coherent optical matched filtering for meteor trail detection 16 p1922 N73-25554
Radar measurement of air mass circulation and meteor trail drift in upper atmosphere during IQSY
[NASA-TT-F-744] 17 p2023 N73-26363
Two spaced radar measurement of wind characteristics in meteor zones 17 p2023 N73-26365
Gas dynamic equations for analyzing hot gas and vapor expansion in meteor trail 17 p2023 N73-26366
SOM-3 radar design for measuring meteor trail physics and upper atmosphere physical properties 17 p2023 N73-26368
Sector radio measurements of meteor trail drifts by low frequency radar transmissions 17 p2023 N73-26369
SOM-1 radar measurement of diffusion in meteor zones 17 p2023 N73-26370
Mathematical models for analyzing resonance effects on wave absorption and scattering in meteor trails 17 p2023 N73-26372
Graphical determination of meteor radiant point curve 17 p2024 N73-26374

**METEORITE COLLISIONS**
Studying collisions of heavy particles to understand collision of meteoroids with upper atmosphere 01 p0102 N73-10842
Pressurized panel meteoroid detector
[NASA-CASE-XLA-08916-2] 19 p2299 N73-28487
Modifications to Pioneer meteoroid detection experiment for outer planet mission applications
[NASA-CR-132310] 23 p2845 N73-32739

**METEORITE COMPRESSION TESTS**
U COMPRESSION TESTS
U MECHANICAL PROPERTIES
U METEORITES

**METEORITE CRATERS**
Small scale analogs of Cayley Formation and Descartes Mountains in impact crater-associated deposits - Part C 12 p1453 N73-21767
Composition and physical characteristics of meteorites and meteoritic craters
[SAO-909-42] 14 p1704 N73-23827
Discovery of small hollow spherules of glass containing various gases in peat bogs where Tungus meteorite fell
[NASA-TT-F-15125] 22 p2716 N73-31742

**METEORITES**
NT BRUDERHEIM METEORITE
NT CARBONACEOUS METEORITES
NT CHONDRITES
NT IRON METEORITES
NT TEKTITES
NT TUNGUSK METEORITE
Element abundances in meteoritic chondrules by neutron activation analysis 12 p1446 N73-21713
Laboratory simulation of meteors and meteoroid impact
[NASA-CR-131468] 12 p1448 N73-21725
Chemical analyses of orthopyroxene and clinopyroxene composition of chondrites
[NASA-TM-X-62259] 15 p1830 N73-24835
Preterrestrial shock effects, shock hardening in iron meteorites, and parent bodies 19 p2342 N73-28840
Clarification concerning fall of Borodino meteorite
[NASA-TT-F-15126] 22 p2717 N73-31749

**METEORITIC COMPOSITION**
Nature and origin of cometary heads 02 p0228 N73-11839
Bulk radiation effects in terrestrial minerals, meteorites, and lunar rocks, and fission track studies in Apollo 12 samples 07 p0831 N73-16736
Nuclear chemistry and geochemistry research projects including isotope separations, meteorite and tektite compositions, and solid gamma spectrometer development
[COO-3236-3] 08 p0884 N73-17156
Chemical analysis of krypton and xenon isotopes in three meteorites and for melt extractions on samples of five terrestrial sedimentary rocks 08 p0958 N73-17836
Composition and physical characteristics of meteorites and meteoritic craters
[SAO-909-42] 14 p1704 N73-23827
Fission and spallation by protons, meteorite composition, and radiation detection
[COO-1167-22] 16 p1947 N73-25754

**METEORITIC DAMAGE**
Exploding wire plasma accelerator simulating hypervelocity micrometeoritic damage at impact
[ISL-26/71] 07 p0821 N73-16657
Laboratory simulation of meteors and meteoroid impact
[NASA-CR-131468] 12 p1448 N73-21725
Hypervelocity meteoritic impact resulting in structural damage of orbital space stations
[NASA-CR-124241] 14 p1705 N73-23841

Meteoroid impact simulation tests on bonded fiber/aluminum skin panels for space shuttle insulation
24 p2941 N73-33485

METEORITIC DUST
U MICROMETEOROIDS

METEORITIC IONIZATION
U ATMOSPHERIC IONIZATION
U METEOR TRAILS

METEORITIC MICROSTRUCTURES
Gas proportional counting of chlorine-36 in iron and iron meteorites
23 p2835 N73-32656

METEOROID CONCENTRATION
Mass-dependent influx of meteors to earth for calculating meteoroid hazards
01 p0102 N73-10839
Determination of parameter s for characterizing meteoric distribution from SOM-1 radar data
17 p2023 N73-26371

METEOROID CRATERS
U METEORITE CRATERS

METEOROID DUST CLOUDS
NT ZODIACAL DUST

METEOROID HAZARDS
Mass-dependent influx of meteors to earth for calculating meteoroid hazards
01 p0102 N73-10839
Contrast color coating for meteoroid impact position locator for space vehicles
[NASA-CASE-LAR-10629-1] 23 p2793 N73-32348

METEOROID PROTECTION
Analysis of bumper plate penetration by meteoroid and subsequent phenomena
[NASA-CR-124061] 08 p0966 N73-17894
Development of composite structures for spacecraft to serve as anti-meteoroid device
[NASA-CASE-LAR-10788-1] 11 p1341 N73-20880
Integrated thermal protection and structural meteoroid protection system in space vehicles - Vol. 1
[NASA-CR-121103] 15 p1834 N73-24865
Space vehicle integrated thermal protection/structural meteoroid protection system - Vol. 2
[NASA-CR-121104] 15 p1834 N73-24866
Performance tests of L-band truss cable meteoroid shielding on Skylab space station at minus 180 degrees Fahrenheit
[NASA-TM-X-64743] 15 p1834 N73-24867

METEOROID SHOWERS
NT TAURID METEOROIDS
Statistical analysis of stream meteor composition
02 p0229 N73-11851
Rocket-borne mass spectrometer identification of metallic ions during Encke meteor shower
22 p2735 N73-31897

METEOROIDS
NT MICROMETEOROIDS
NT RADIO METEORS
NT TAURID METEOROIDS
NT ZODIACAL DUST
Measurement of meteor winds based on radar tracking
[AD-745971] 01 p0054 N73-10440
Statistics from synoptic year sample of 20,000 radar meteor observations using eight station radar network
[NASA-CR-2109] 01 p0101 N73-10830
Results of Meteor Research Program
01 p0101 N73-10831
Description of eight-station radar at Havana, Illinois
01 p0101 N73-10832
Equipment for simultaneous radar observations by image-orthicon and optical observations
01 p0101 N73-10833
Antenna pattern calibration for Havana radar systems
01 p0101 N73-10834
Analysis procedure for television observations and simultaneous observations
01 p0102 N73-10836
Results from synoptic year
01 p0102 N73-10837
Results from simultaneous radar-television observations
01 p0102 N73-10838
List of active meteor streams
01 p0102 N73-10844
Short-period comets and meteor stream genetic origin discussing formation processes
[TRITA-EPP-72-18] 02 p0231 N73-11880
Cameras for photographing meteors in selected sky area
[NASA-CASE-LAR-10226-1] 10 p1158 N73-19419
Techniques for casting large area polysulfone film capacitors onto thick aluminum substrates for application as meteoroid impact sensors
[NASA-CR-128862] 10 p1160 N73-19441
Classification of meteoroids according to density and beginning height, and meteor stream search
[NASA-CR-131177] 11 p1337 N73-20851
Classification of meteoroids according to density and beginning height
[CONTRIB-14] 11 p1337 N73-20852
Meteoroid stream search among photographic meteors
[CONTRIB-15] 11 p1337 N73-20853
Precision radar ranging of meteor trails and possible ranging techniques
[AD-754623] 11 p1339 N73-20868
Use of Apollo heat shield window to study dynamic and physical properties of meteoroids
12 p1452 N73-21760
Equipment and mission of Astrophysics Institute in Tadzhikistan relative to radar tracking and wind velocity measurement
[AD-756100] 14 p1706 N73-23848
Meteoroid impact resistance of bumper protected laminated spacecraft mainwalls
[NASA-CR-2262] 14 p1714 N73-23909
VHF radars to probe ion columns left by meteors
[AD-758765] 16 p1908 N73-25434
Influence of mountain barriers on radio wave propagation by meteors
17 p2023 N73-26373
Interplanetary distribution of meteors in radar observations
[NASA-CR-2316] 23 p2844 N73-32727

METEOROLOGICAL BALLOONS
NT JIMSPHERE BALLOONS
EOLE satellite tracking of meteorological balloons released in Southern Hemisphere to trace horizontal motion of air masses
[NASA-TM-X-66152] 06 p0694 N73-15651
Characteristics of polyurethane film for fabrication of expandable envelopes subjected to solar heating at high altitudes
[AD-762803] 20 p2362 N73-29001
Intergrated error behavior of rawinsonde tracking system
[AD-763890] 22 p2695 N73-31585
Balloon sub-system of Eole experiments in Southern Hemisphere lower stratosphere
24 p2948 N73-33547
Wind determination in tropics by balloon carrying dropsondes using Omega navigation system
24 p2948 N73-33548

METEOROLOGICAL CHARTS
Meteorological charts and tables on wind altitude over French Polynesia
[MN-MONO-85] 01 p0073 N73-10602
Meteorological rocket sounding data on stratospheric and mesospheric structures and circulations
[NASA-TR-R-391] 02 p0205 N73-11657
Synoptic weather charts of daily and monthly heights and temperature for Northern Hemisphere from Jan. to Dec. 1968
[AD-746659] 02 p0206 N73-11673
Universal humidity chart allowing humidity and energy calculations for any mixture of monatomic and diatomic gases at pressures encountered in saturation diving
[AD-746162] 02 p0207 N73-11675
Two methods of analyzing persistence of weather map types, using January MSL presure data for Colorado map typing window
[AD-749130] 04 p0446 N73-13641
Cloud cover maps for North America and western North Atlantic for August, 1972
[AD-749128] 05 p0575 N73-14678
Meteorological ground level maps of Northern Hemisphere for fourth quarter in 1971
[QR-4-PT-4] 06 p0691 N73-15628
Daily and monthly meteorological charts for Europe obtained during June, 1972 at Berlin
06 p0691 N73-15629
Daily and monthly meteorological charts for Europe obtained during May, 1972 at Berlin
06 p0692 N73-15631
Northern hemisphere monthly mean 500-mb and 1000-500-mb thickness charts
[MET-O-845C] 06 p0692 N73-15632
Synoptic meteorological weather charts for Northern Hemisphere obtained at ground level, 500 mb, and 850 mb during July, 1972, at Berlin
06 p0692 N73-15635
Development of four-level model of baroclinic atmosphere for predicting geopotential at various isobaric surfaces for Northern Hemisphere
[AD-750496] 06 p0694 N73-15659
Tables and charts of meteorological data gathered at Oarai site for 1970
[JAERI-M-4657] 08 p0939 N73-17685
Survey of climatological conditions in Martinique
[MN-MONO-86] 09 p1060 N73-18644
Daily and monthly synoptic climatological charts obtained at Berlin for August 1972
10 p1180 N73-19602
Daily and monthly synoptic climatological charts obtained at Berlin for September, 1972
10 p1181 N73-19603
Meteorological charts of upper atmosphere of Northern Hemisphere
[QR-4-PT-4] 10 p1181 N73-19604
European weather maps constructed from ESSA 8 photographs
[QR-2] 10 p1181 N73-19605
Daily meteorological ground level charts for Northern Hemisphere, January through June, 1971
[SAR-1-PT-1] 10 p1181 N73-19606



Meteorological ground level charts for Northern Hemisphere, April through June, 1971
[QR-2-PT-2] 10 p1181 N73-19607
Synoptic weather maps of Northern Hemisphere for October 1972 obtained in Berlin
13 p1551 N73-22564
Stratospheric weather maps for Northern Hemisphere
[QTSR-1] 13 p1551 N73-22570
Composite maps from 950 mb to 150 mb of relative wind field, mixing ratio R
[AD-755485] 13 p1555 N73-22600
Tabular and graphical data for moderate and heavy snow for Loring AFB, Maine
[AD-756881] 13 p1555 N73-22605
Daily and monthly meteorological charts for Northern Hemisphere obtained during November, 1972 at Berlin
14 p1684 N73-23668
ESSA 8 photographic observations of European cloud cover for third quarter of 1972
[QR-3-PT-3] 15 p1804 N73-24623
Northern Hemisphere ground weather maps for July through December, 1972
[QR-2-PT-2] 15 p1804 N73-24624
Synoptic weather maps and data tables on daily and monthly Northern Hemisphere stratospheric height and temperature
[QTSR-3] 17 p2056 N73-26626
Daily and monthly synoptic weather maps for Northern Hemisphere and Berlin vicinity, December 1972
17 p2056 N73-26628
Synoptic weathermaps for ground and 500 mb levels obtained in Berlin during January, 1973
17 p2057 N73-26634
Meteorological tables and charts on Berlin temperature
17 p2057 N73-26635
Least squares method for constructing meteorological fields from measurement data
[AD-759872] 17 p2058 N73-26645
Daily summaries for vertical echo sounding of upper atmosphere over Freiburg, Germany during March, 1973
[REPT-321F] 18 p2141 N73-27308
Technical evaluation of weather clutter feasibility model to provide air traffic controllers with weather display of air traffic and contour depiction of weather detected by radar
[FAA-NA-73-48] 20 p2376 N73-29094
Synoptic charts for 50mb in Northern Hemisphere from January to June, 1972
[QR-1/2-PT-1/2] 20 p2442 N73-29613
Daily and monthly weather charts for Northern Hemisphere and Berlin, Germany for February, 1973
20 p2442 N73-29614
Comparative analysis of upper troposphere maximum wind strength maps and ground surface synoptic maps
20 p2445 N73-29642
Sorting analogs to composite-kinematic maps of natural synoptic periods
21 p2573 N73-30618
Atlas presenting oceanographic data collected during Barbados oceanograpic and meteorological experiment
22 p2666 N73-31362

METEOROLOGICAL FLIGHT
Skyhook balloon flight operations
[AD-761657] 19 p2221 N73-27913
Analysis of aircraft measurements of long-wave radiation fluxes, water content, and temperature in presence of stratified and stratocumulus clouds
22 p2693 N73-31574

METEOROLOGICAL INSTRUMENTS
NT BAROMETERS
NT CLOUD HEIGHT INDICATORS
NT DROPSONDES
NT IONOSONDES
NT RADIOSONDES
NT RAIN GAGES
NT RAWINSONDES
NT WEATHER DATA RECORDERS
Design, development, and specifications of thermohygrometer for measuring fluctuations in temperature due to clouds and precipitation
[NLL-M-20703-[5828.4F]] 01 p0055 N73-10442
Radioisotope snow cover gage
[NLL-M-22676-[5828.4F]] 01 p0055 N73-10443
Development of system to correct upper atmosphere temperature readings to ambient air temperature
[AD-747973] 03 p0298 N73-12433
Emergency radiological and meteorological instrumentation criteria for reactors
[BNWL-1635] 04 p0422 N73-13443
Observation, measurement, and automatic calculation of runway visibilities
[NLL-M-20785-[5828.4F]] 07 p0814 N73-16597
Observation and measurement of visibility at ground
07 p0814 N73-16598

Automatic calculation of runway visual range on airdromes
07 p0814 N73-16599
Operation and maintenance of shipboard meteorological systems
[AD-751691] 07 p0816 N73-16617
Tables on airborne and ground based measurements of optical atmospheric properties in central New Mexico
[AD-751936] 08 p0919 N73-17534
Self contained, air-droppable, expendable, remote-operating weather station
[AD-751924] 08 p0939 N73-17691
R/V Knorr cruise in Oct. 1970 to deploy and recover instrumented deep sea moorings
[AD-754796] 11 p1288 N73-20455
Analysis of oceanographic/meteorological sensors for ocean data stations
[AD-755755] 12 p1425 N73-21552
Meteorological instruments to measure atmospheric electricity aboard modified B-57 aircraft
[AD-755400] 13 p1526 N73-22372
Solid state laser multiwavelength identification and display system for detection and spectrum analysis of air pollutants
[AD-755161] 13 p1554 N73-22598
Instrumentation to aid radar investigations of cloud and precipitation physics
[AD-755401] 13 p1555 N73-22606
Nimbus 4 satellite catalog of observations for period 1 July through 31 August, 1970 - Vol. 3
[NASA-TM-X-69890] 13 p1580 N73-22806
Catalog of Nimbus 4 satellite observations for 1 November through 31 December, 1970 - Vol. 5
[NASA-TM-X-69892] 13 p1580 N73-22808
Effectiveness of infrared radiometer and digital recording equipment as clear air turbulence warning system
[AD-757501] 14 p1685 N73-23677
Highly accurate digital barometer
[NLL-M-22973-[5828.4F]] 16 p1910 N73-25458
Design of reserve master clock for controlling meteorological recording instruments in Antarctic weather stations
[NLL-M-22972-[5828.4F]] 16 p1911 N73-25459
Coherence statistics of horizontal wind speed as measured by micrometeorological mast array
16 p1937 N73-25675
Development and characteristics of self-contained digital integrator for recording daily solar irradiance
[AD-760318] 17 p2035 N73-25468
Automatic climatological recording system at Nord, Greenland
[ISBN-87-7478-073-5] 18 p2141 N73-27307
Characteristics and operational problems of overflow snow gage
[NLL-M-22982-[5828.4F]] 18 p2150 N73-27375
Meteorological conditions and instruments analysis by Soviet aerometeorological service
[JPRS-59581] 18 p2171 N73-27533
Application of radar techniques for measuring precipitation and comparison with measurements obtained from conventional meteorological instruments
21 p2568 N73-30582
Statistical structure and automated monitoring of meteorological and hydrometeorological fields
21 p2573 N73-30623
Instrumentation available for measuring evaporation in Canal Zone
[AD-763205] 21 p2574 N73-30629
Technical equipment for large scale automation of USSR hydrometeorological service
[AD-763956] 22 p2696 N73-31593

**METEOROLOGICAL PARAMETERS**

Meteorological parameters of stratosphere from rocket sounding data
[NLL-M-22213-[5828.4F]] 01 p0073 N73-10594
Equations and nomograms depicting probabilities of rare meteorological phenomena
[NLL-M-22672-[5828.4F]] 01 p0073 N73-10598
Aerological data from balloon and rocket flights for Japan and its vicinity - tables for Oct. 1971
01 p0073 N73-10601
Aerological data from balloon and rocket flights for Japan and its vicinity, tables for Dec. 1971, and ozone data, tables for Jan. - Dec. 1971
01 p0073 N73-10603
Aerological data from balloon and rocket flights for Japan and its vicinity-tables for Nov. 1971
01 p0073 N73-10604
Aerological data from balloon and rocket flights for Japan and its vicinity for period from 1966 to 1970
01 p0074 N73-10605
Monthly mean climatological statistics for surface to 5 mb pressure level over Australia - Dec. 1971
01 p0074 N73-10606
Monthly mean climatological statistics for surface to 5 mb pressure level over Australia - Aug. 1971
01 p0074 N73-10607
Radiosonde height and temperature data for updating asynoptic meteorological measurements
[NOAA-TM-NWS-NMC-51] 01 p0074 N73-10613
Meteorological parameter table for Belgian weather stations, June 1972
01 p0075 N73-10618
Night cloud cover and meteorological parameter variations determined at La Silla, Chile, in 1970
[ESO-BULL-9] 01 p0075 N73-10620
Global distributions of mean January surface wind stress, diabatic heating rate, and rate of moisture addition as simulated in 30-day integration with atmospheric general circulation model
[AD-745752] 01 p0077 N73-10640
Measurement of upper atmospheric parameters using free-falling sphere
[AD-747037] 02 p0170 N73-11383
Maximum probability and minimum variance methods for interpreting remote soundings on meteorological structure of atmosphere
02 p0196 N73-11587
Meteorological data from radiosondes at Berlin
02 p0204 N73-11650
Monthly mean climatological statistics from surface to 5 mb level over Australia - January 1972
02 p0204 N73-11654
Meteorological upper air statistics in Australian region
02 p0204 N73-11655
Simulation of alternate expressions for meteorological phenomena of atmospheric boundary layer - tables
[AD-746247] 02 p0205 N73-11665
Method for computing effects of meteorological conditions on sound in vicinity of subsonic aircraft
[SC-DC-72-1007] 03 p0253 N73-12044
Methods for acquiring meteorological parameter data and procedures for analyzing wind data
[AD-747480] 03 p0298 N73-12432
Meteorological parameter tables for Belgian weather stations, Aug. 1972
03 p0327 N73-12664
Meteorological parameter tables for Belgian weather stations, Sep. 1972
03 p0327 N73-12668
Analysis of standard radiosonde system for accurate measurement of meteorological parameters which affect artillery fire
[AD-747759] 03 p0327 N73-12671
Analysis of limitations on helicopter approach and landing during conditions of low visibility
[AD-747732] 03 p0329 N73-12686
Studies of soundings and imaging measurements from geostationary satellites
[NASA-CR-130122] 03 p0359 N73-12925
Airborne and seaborne observations of radar scattering by sea water surfaces
[JPRS-57409] 04 p0388 N73-13156
Meteorological and ballistics data for launching of Athena rocket flight 134, vehicle H-004J
[AD-749436] 04 p0445 N73-13633
Meteorological and ballistics data for launching 13901 Little John, missile number 2172, round number 684 AM
[AD-749435] 04 p0445 N73-13634
Meteorological and ballistics data for launching 13401 Honest John, missile number 2632, round number 626 ROL
[AD-749434] 04 p0445 N73-13635
Meteorological and ballistics data for launching of Lance Missile 2143, vehicle 159
[AD-749429] 04 p0445 N73-13636
Meteorological and ballistics data for launching of Honest John Laser, missile flight 205, vehicle 624
[AD-749430] 04 p0446 N73-13637
Meteorological and ballistics data for launching of Honest John Missile flight 1755, vehicle 625
[AD-749431] 04 p0446 N73-13638
Meteorological and ballistics data for launching of Lance Missile 2168, vehicle 160
[AD-749432] 04 p0446 N73-13639
Meteorological and ballistics data for launching of Lance Missile 2159, vehicle 161
[AD-749433] 04 p0446 N73-13640
Algorithm for calculating distribution functions of meteorological parameters by computer technique
[AD-749588] 04 p0446 N73-13642
Hourly rates corrected for atmospheric temperature and pressure from four cosmic ray stations in Canada
[AECL-4077] 04 p0467 N73-13805
Establishment of radar information transmission network for dissemination of meteorological data
[NLL-M-22692-[5828.4F]] 05 p0507 N73-14128
Meteorology and climatology of Northern Hemisphere during calendar year 1972 - Vol. 128 No. 4
05 p0570 N73-14631
Bibliography on meteorological phenomena in Switzerland
[REPT-71-II] 05 p0571 N73-14643
Bibliography on meteorological phenomena in Switzerland
[REPT-72-I] 05 p0571 N73-14644
Tabulation of relative humidity data obtained from network of weather stations in Switzerland
05 p0572 N73-14645
Annual report of meteorological observations conducted by weather stations in Switzerland during calendar year 1970
05 p0572 N73-14646
Meteorological parameters of upper atmosphere over Japan during March 1972
05 p0572 N73-14648
Meteorological and ballistics data for launching of Little John, missile number 3175, round 687 RO
[AD-749439] 05 p0574 N73-14669
Meteorological and ballistics data for launching of Little John, missile number 2253, round 683 RO
[AD-749437] 05 p0574 N73-14670
Meteorological and ballistics data for launching of Honest John, missile number 3116, round 686
[AD-749438] 05 p0574 N73-14671
Analysis of cloud console devices used in displaying meteorological satellite imagery
[AD-750085] 05 p0575 N73-14684
Microphysical and meteorological data on fog cycle in California valley
[AD-750086] 05 p0576 N73-14685
Data from marine surface observations in Southeast Asian coastal marine areas
[AD-749936] 05 p0576 N73-14686
Meteorological rocket and radiosonde data on lower and upper atmospheres - Mar. 1971
06 p0692 N73-15633
Aerological data from balloon and rocket flights for Japan and vicinity - Jan. 72
06 p0693 N73-15647
Climatological daily observations in Finland during 1971
06 p0694 N73-15652
Meteorological parameter tables for Belgian weather stations, Oct. 1972
06 p0694 N73-15654
Tables of synoptic meteorological observations for Southeast Asian coastal marine areas
[AD-750159] 06 p0694 N73-15658
Development of four-level model of baroclinic atmosphere for predicting geopotential at various isobaric surfaces for Northern Hemisphere
[AD-750496] 06 p0694 N73-15659
Application of scale autocorrelation coefficients to atmospheric and geophysical measurements
[AD-750476] 06 p0695 N73-15661
Design, development and flight tests of Super Loki Dart Meteorological Rocket Systems
[AD-750796] 06 p0722 N73-15895
Monitoring weather conditions for cloud seeding control
[E73-10059] 07 p0778 N73-16321
Extension of US standard atmosphere to region from 80 to 200 km
[NASA-TM-X-66171] 07 p0792 N73-16441
Development of mathematical meteorological models for objective forecasting
[AD-751744] 07 p0816 N73-16614
Measurement of noise levels produced by Boeing 737 aircraft and correlation with local meteorological parameters including wind force and direction, temperature, and atmospheric pressure
[FAA-RD-72-145] 07 p0821 N73-16651
Distribution statistics, magnitude, and spatial structure of gravity wave and planetary wave atmospheric variations
[NASA-CR-2203] 08 p0916 N73-17504
Tables and charts of meteorological data gathered at Oarai site for 1970
[JAERI-M-4657] 08 p0939 N73-17685
Meteorological parameter tables for Belgian weather stations, Nov. 1972
08 p0939 N73-17687
Meteorological data for launching 13801 Little John, missiles 3086 and 3166
[AD-752089] 08 p0939 N73-17688
Meteorological data for launching 11601 Lance, missile 2138, round number 165
[AD-752093] 08 p0939 N73-17689
Meteorological and ballistics data for launching of 11601 Lance Missile number 2154, round number 163 RBI.
[AD-752088] 08 p0939 N73-17690
Meteorological and ballistics data for launching of 11602 Lance Missile number 5175, round number 164 ESI.
[AD-752090] 08 p0940 N73-17695
Meteorological and ballistics data for launching of 13901 Little John Missile number 1463, round number 692 RG
[AD-752091] 08 p0940 N73-17696
Meteorological and ballistics data for launching of 14101 Little John RIP missile number 12751
[AD-752092] 08 p0940 N73-17697
Meteorological and ballistics data for launching of 13801 Little John ARM-P Ripple, missile numbers 3102, 3142 and 3257, round numbers 693, 694 and 695 RO
[AD-752095] 08 p0940 N73-17698
Meteorological and ballistics data for launching of Lance missile, number 2183, round no. 167 APT
[AD-752098] 08 p0940 N73-17700
Meteorological data for launching of 13801 Little John Missile number 3070, round number 696 RO
[AD-752096] 08 p0940 N73-17702
Meteorological data for launching of 12801 Lance missile numbers 2216/2310, round no. 166 EET
[AD-752097] 08 p0940 N73-17703
Meteorological parameters for launching of 13401 Honest John missile number 2631, round no. 627 RUI.
[AD-752094] 08 p0940 N73-17704

Lidar anemometry for quick determination of aerological data above launching site prior to rocket firing
[ONERA-TP-1151] 09 p1027 N73-18385
Characteristics of wind, pressure, cloud, and precipitation fields in intratropical zone of convergence
09 p1059 N73-18633
Meteorological parameter tables for Belgian weather stations, Dec. 1972
09 p1061 N73-18651
GARP standard data sets for studying behavior of numerical global models noting data acquisition, analysis, and storage
[GARP-PUBL-9] 09 p1061 N73-18652
Tables of synoptic meteorological observations for Okinawa, Sakishima Islands, and southern East China Sea
[AD-753216] 09 p1061 N73-18656
Meteorological rocket and radiosonde data on lower and upper atmospheres - Apr. 1971
10 p1180 N73-19600
Aerological data from balloon and rocket flights for Japan and vicinity - May 1972
10 p1182 N73-19612
Aerological data from radiosonde observations for Japan and vicinity during 1969 and 1970
10 p1182 N73-19613
Aerological data from flights for Japan - June 1972
10 p1182 N73-19614
Aerological data from balloon and rocket flights for Japan and vicinity - Apr. 1972
10 p1182 N73-19615
Engineering analysis of tornado structures and occurrence climatology
[SC-M-72-0688] 10 p1182 N73-19617
Tables of synoptic meteorological observations for Japanese and Korean coastal marine areas
[AD-753468] 10 p1182 N73-19619
Influence on volcanic eruption exerted by particular weather and climatic situations
[NLL-M-22864-[5828.4F]] 11 p1313 N73-20652
Optimum interpolation and extrapolation of meteorological fields
[NLL-M-22856-[5828.4F]] 11 p1313 N73-20654
Meteorological data from 14802 Lance missile, 17 Nov. 1972
[AD-754555] 11 p1314 N73-20664
Meteorological and ballistics data for launching of 15001 Little John missile no. 1508, round no. 697 RG
[AD-754558] 11 p1314 N73-20665
Meteorological data of upper atmosphere from sounding rockets for Lance missile launch
[AD-754554] 11 p1314 N73-20666
Meteorological data gathered for launching of Athena flight 135
[AD-754557] 11 p1314 N73-20667
Tables of synoptic meteorological observations of Japan coastal marine areas
[AD-754773] 11 p1314 N73-20668
Meteorological and ballistics data for launching of 14801 Lance missile no. 2184, round no. 168 APT 9
[AD-754556] 11 p1315 N73-20669
Meteorological data for launch of Little John probe of upper atmosphere
[AD-754561] 11 p1315 N73-20671
Meteorological data for launching of Lance missile probe of upper atmosphere
[AD-754565] 11 p1315 N73-20672
Meteorological data for launching Lance missile probe of upper atmosphere
[AD-754564] 11 p1315 N73-20673
Meteorological and ballistics data for launching of 12802 Lance missile no. 2150, round no. 174 ESL
[AD-754563] 11 p1316 N73-20678
Meteorological data gathered for Little John launching 14101
[AD-754560] 11 p1316 N73-20679
Meteorological data for Lance missile number 2186, round number 169 APL
[AD-754559] 11 p1316 N73-20680
Simulation of atmospheric vortex based on boundary conditions and parameter values of strong atmospheric tornadoes and waterspouts
12 p1390 N73-21269
Geoelectric observations made from three locations in Japan
[REPT-89] 12 p1399 N73-21344
Ground-based continuous measurements of upper atmosphere
[DATA-SUMMARY-72/7-9] 12 p1401 N73-21362
Meteorological investigation of stratospheric turbulence using radiosonde data
[NLL-M-22819-[5828.4F]] 12 p1419 N73-21502
Development of automated hydrometeorological service and establishment of information-computation network for data recording
12 p1421 N73-21515
Analysis of atmospheric pollution parameters to show sources, physiological effects, biological effects, and meteorological effects
12 p1421 N73-21519
Visibility range in presence of various meteorological phenomena
[NASA-TT-F-14886] 12 p1422 N73-21525
Meteorological and ballistics data for launching of 11602 Lance missile, number 2174, round 181
[AD-755773] 12 p1424 N73-21539
Meteorological and ballistics data for launching of 12893 Lance missile, number 2354, round 182
[AD-755774] 12 p1424 N73-21540
Meteorological and ballistics data for launching of 14101 RIP missile, numbers 12723/12720, rounds 3/4
[AD-755775] 12 p1424 N73-21541
Meteorological and ballistics data for launching of Athena rocket vehicle, flight 137, vehicle H-005
[AD-755776] 12 p1424 N73-21542
Meteorological data for launching Honest John missile, number 2598
[AD-755777] 12 p1424 N73-21543
Meteorological data for launching Lance missile, number 2170
[AD-755768] 12 p1424 N73-21544
Meteorological data for launching Lance missile, number 2352
[AD-755769] 12 p1424 N73-21545
Meteorological data for launching Lance missile, number 2148
[AD-755770] 12 p1424 N73-21546
Meteorological and ballistics data for launching of Athena rocket vehicle, flight 136, vehicle H-009
[AD-755779] 12 p1424 N73-21547
Meteorological data for launching Lance missile, number 2176
[AD-755778] 12 p1425 N73-21548
Meteorological data for launching Lance missile, number 2351
[AD-755771] 12 p1425 N73-21549
Long term climatological study of meteorological parameters for Northern Hemisphere
13 p1551 N73-22565
Method for calculating turbulent fluxes by measuring meteorological parameters at two meter height
13 p1552 N73-22576
Climatic variability of winter wheat harvest for USSR
13 p1552 N73-22578
Meteorological parameter tables for Belgian weather stations, Jan. 1973
13 p1553 N73-22591
Meteorological and ballistics data for launching of Lance missile, number 2149, round 180
[AD-755772] 13 p1555 N73-22599
Catalog of data acquired from Nimbus 4 meteorological satellite from 18 Apr. through 22 May 1970
[NASA-TM-X-69888] 13 p1580 N73-22804
Daily and monthly meteorological charts for Northern Hemisphere obtained during November, 1972 at Berlin
14 p1684 N73-23668
Measurements of meteorological parameters at Woomera using falling spheres from February to June 1972
[WRE-TN-787[WR/D]] 14 p1685 N73-23670
Tables of synoptic meteorological observations for Japanese and Korean coastal marine areas
[AD-757107] 14 p1685 N73-23674
Computer programs for numerical approximation of selected meteorological parameters related to cloud physics
[AD-757623] 14 p1686 N73-23680
Aerological data from balloon and rocket flights for Japan and vicinity
15 p1777 N73-24407
Measurement of atmospheric transport properties in stratosphere
[AD-757927] 15 p1782 N73-24445
Utilization of satellite infrared spectrometer data for resolution of atmospheric variables
[AD-757774] 15 p1789 N73-24501
Preparation of long range weather forecasts using principle of analogy of the fields of the meteorological elements
[NLL-M-22852-[5828.4F]] 15 p1805 N73-24628
Variational optimization technique used as analysis scheme for application to high energy portion of hurricane
15 p1805 N73-24632
Meteorological parameter tables for Belgian weather stations, Feb. 1973
15 p1806 N73-24636
Detailed environmental profiles for seven potential Gulf Coast deep water port sites
[AD-758455] 15 p1806 N73-24637
Meteorological and ballistics data for launching of Athena rocket flight 138, vehicle H-008
[AD-758866] 15 p1807 N73-24645
Meteorological and ballistics data for launching Athena rocket flight 139, vehicle H-006
[AD-758867] 15 p1807 N73-24646
Meteorological and ballistics data for launching of 14101 RIP missile nos. 9623/9034, round nos. 5/6
[AD-758861] 15 p1807 N73-24647
Meteorological data from Lance missile no. 2355, round no. 184 EST [29 Jan. 1973]
[AD-758860] 15 p1807 N73-24648
Meteorological data from 3901 Little John missile no. 2192, round no. 693 RM, [24 Jan. 1973]
[AD-758859] 15 p1807 N73-24649
Meteorological and ballistics data for launching of 03702 Honest John missile number 1003, round number 631 AMI.
[AD-758869] 15 p1807 N73-24650
Meteorological data for launching of RIP 14101, missile numbers 12712 and 12716
[AD-758863] 15 p1808 N73-24651
Meteorological measurements from geosynchronous satellites
[NASA-CR-130246] 15 p1834 N73-24870
Meteorological conditions and infection of upper respiratory tract in children
[NLL-M-22866-[5828.4F]] 16 p1866 N73-25109
Analysis of meteorological parameters and climatological effects leading to heavy icing of ships
[NLL-M-22981-[5828.4F]] 16 p1935 N73-25657
Analysis of convective cumulus cloud development and numerical relationships of hydrodynamic and thermodynamic concepts of cloud formation
[NLL-M-22840-[5828.4F]] 16 p1936 N73-25666
Meteorological rocket and radiosonde data on lower and upper atmospheres - July 1971
16 p1937 N73-25671
Meteorological rocket and radiosonde data on lower and upper atmospheres - August 1971
16 p1937 N73-25672
Meteorological rocket and radiosonde data on lower and upper atmosphere - September 1971
16 p1937 N73-25673
Computer programs for ceiling and visibility forecasting using air terminal weather data
[FAA-RD-73-13] 16 p1937 N73-25677
Meteorological and ballistics data for launching of Honest John missile number 359, round 629,
[AD-758862] 16 p1938 N73-25684
Meteorological and ballistics data for launching of Honest John missile number 627, round 632
[AD-758868] 16 p1938 N73-25685
Meteorological and ballistics data for launching of Honest John, missile number 1002, round 630
[AD-758865] 16 p1938 N73-25686
Meteorological and ballistics data for launching of Lance missile, number 2237, round 185
[AD-758864] 16 p1939 N73-25687
Investigation of errors introduced into meteorological calculations through use of hypsometric equation
[AD-759489] 16 p1940 N73-25697
Acquisition of ground truth and meteorological data in Michigan for Skylab-3 mission
[E73-10748] 17 p2022 N73-26352
Collection of ground truth and meteorological data for Skylab test sites in Texas and Kansas
[E73-10752] 17 p2022 N73-26355
Characteristics of NOAA 2 meteorological satellite and photographic data of weather conditions over Europe during 1972
[QR-4-PT-4] 17 p2056 N73-26627
Parameterization of meteorological factors for unusual atmospheric circulation in Northern Hemisphere in January 1963
17 p2056 N73-26631
Meteorological parameter tables for Belgian weather stations, Mar. 1973
17 p2057 N73-26638
Simulation research to develop objective meteorological prediction capability - Volume I
[AD-759928] 17 p2058 N73-26642
Simulation research to develop objective meteorological prediction capability - Volume 2
[AD-759929] 17 p2058 N73-26643
Least squares method for constructing meteorological fields from measurement data
[AD-759872] 17 p2058 N73-26645
Correlation of ERTS-1 data with ground data for determining characteristics of air pollution in Norfolk, Virginia area
[E73-10779] 18 p2135 N73-27255
Acquisition of weather and ground truth data for Skylab EREP experiments
[E73-10797] 18 p2137 N73-27273
Great lakes mesometeorological investigations using ERTS-1 data
[E73-10835] 18 p2141 N73-27305
Woomera atmospheric parameters measured during falling sphere ejection from rocket soundings between Feb. and Jun. 1972 noting comparison with atmospheric models
[WRE-TN-787] 18 p2146 N73-27341
Influence of ocean waves and meteorological variables on beach erosion at Plum Island, Massachusetts
[AD-759513] 18 p2148 N73-27364
Single-level objective analysis of meteorological observations on hemisphere by optimal interpolation
[NLL-M-22908-[5828.4F]] 18 p2169 N73-27514
Meteorological conditions and instruments analysis by Soviet aerometeorological service
[JPRS-59581] 18 p2171 N73-27533
Aerological data from balloon and rocket flights for Japan and vicinity - September 1972
18 p2172 N73-27539
Aerological data from balloon and rocket flights for Japan and vicinity - Aug. 1972
18 p2172 N73-27540
Aerological data from balloon and rocket flights for Japan and vicinity - Oct. 1972
18 p2172 N73-27541

High altitude meteorological data measured at Sonmiani, Pakistan 1964-1970
[W-119] 18 p2172 N73-27543
Analysis of wind profiles in thunderstorm gusts and method for predicting velocity of winds at altitude
[NASA-CR-2289] 18 p2172 N73-27544
Interaction between air pollution sources and meteorological conditions and impact on air quality along highway corridor - Vol. 6
[PB-219816/6] 18 p2175 N73-27566
Analysis of ERTS-1 imagery to determine meteorological content with emphasis on mesoscale effects of Great Lakes and air pollution dispersion
[PAPER-W17] 19 p2272 N73-28294
Analog scheme for analyzing meteorological parameters to determine their predictive value for forecasting intensity changes in western North Pacific tropical cyclones
[AD-761726] 19 p2316 N73-28625
Meteorological data for launching of Honest John, missile number 1763, round 685
[AD-762158] 19 p2317 N73-28632
Meteorological and ballistics data for launching of 13401 Honest John missile no. 2542, round no. 634 RMI
[AD-762157] 19 p2317 N73-28633
Meteorological data for launching of Honest John, missile number 305, round 633
[AD-762155] 19 p2317 N73-28636
Meteorological data for launching of Lance missile, number 2238, round 187
[AD-762162] 19 p2317 N73-28638
Meteorological and ballistic data gathered for launching Athena flight 140
[AD-762160] 19 p2317 N73-28639
Meteorological data gathered for launching 150601 Little John
[AD-762161] 19 p2317 N73-28641
Meteorological data gathered for launching 11604 Lance missile
[AD-762156] 19 p2317 N73-28642
Development, characteristics, and operation of test facility for determining effectiveness of runway lighting systems under various atmospheric conditions
[FAA-RD-71-94] 20 p2382 N73-29141
Effects of solar activity on present day changes of climate
[N.I.L.-M-23005-[5828.4F]] 20 p2442 N73-29612
Spectral analysis of variations in meteorological elements for periods ranging from several years to several tens of years
20 p2443 N73-29620
Procedures for determining variations of meteorological parameters from satellite radiation measurements
20 p2443 N73-29625
Geoisochronous satellites for obtaining and transmitting meteorological data
20 p2447 N73-29658
Four dimensional processing of a synchronously arriving meteorological data based on dynamic statistical approach
20 p2447 N73-29664
Statistical analysis of meteorological parameters during fog at US airports
[FAA-RD-72-39] 20 p2448 N73-29673
Surface climatological data for Australia - October 1972
20 p2449 N73-29676
Surface climatological data for Australia - September 1972
20 p2449 N73-29677
Monthly mean climatological statistics for surface to 5 mb pressure level over Australia - October 1972
20 p2449 N73-29678
Monthly mean climatological statistics for surface to 5 mb pressure level over Australia - Dec. 1972
20 p2449 N73-29679
Monthly mean climatological statistics for surface to 5 mb pressure level over Australia - September 1972
20 p2449 N73-29680
Monthly mean climatological statistics for surface to 5 mb pressure level over Australia - November 1972
20 p2449 N73-29681
Surface climatological data for Australia - November 1972
20 p2449 N73-29682
Yearbook of meteorological parameters measured for Denmark and Faroe Islands - 1968
20 p2449 N73-29683
Surface climatological data for Australia Dec. 1972
20 p2449 N73-29684
Surface climatological data for Australia - Jan. 1973
20 p2449 N73-29685
Analysis of meteorological parameters affecting safety of civil aviation and instructions for increased flight safety
[NASA-TT-F-15069] 21 p2495 N73-30028
Statistics of extreme values of meteorological parameters
[MONO-89] 21 p2566 N73-30568
Predicted weather conditions for USSR during winter of December 1971 through March 1972
[N.I.L.-M-23035-[5828.4F]] 21 p2568 N73-30578
Proceedings of conference on application of radar techniques to meteorological observations and weather forecasting
[TT-70-50120] 21 p2568 N73-30580
Synchronous observations of precipitation microstructure by radar and ground-level instruments to determine accuracy of radar measurements
21 p2568 N73-30584
Development and application of meteorological radar for detecting zones of cloudiness, precipitation, and storms for synoptic weather analysis
21 p2571 N73-30604
Equipment and procedures for obtaining meteorological radar information on clouds, cloud systems, and dangerous meteorological formations
21 p2571 N73-30605
Development of equipment and methods for obtaining and processing meteorological radar data
21 p2571 N73-30606
Characteristics and development of receiving device for automatic conversion of meteorological radar data
21 p2572 N73-30608
Development of system for quantitative evaluation of radio echo intensities received during measurement of atmospheric formations
21 p2572 N73-30609
Statistical structure and automated monitoring of meteorological and hydrometeorological fields
21 p2573 N73-30623
Surface climatological data for Australia - August 1972
21 p2574 N73-30626
Meteorological parameter tables for Belgian weather stations, May 1973
21 p2574 N73-30628
Falling sphere experiment for profiles of basic atmospheric parameters in Woomera, Australia
[WRE-TN-786[WR/D]] 22 p2694 N73-31579
Simulation studies and design of GARP Global Experiment
[NASA-TM-X-69613] 22 p2694 N73-31582
Characteristics of three meteorological radar systems to include principles of operation, circuit description, and fuctions of subsystems
[AD-765363] 23 p2759 N73-32076
Electronic scanning microwave radiometer system for measurement of meteorological, geomorphological, and oceanographic parameters from Nimbus 5
[NASA-CR-132812] 23 p2793 N73-32342
Numerical weather prediction activities of National Meteorological Center for first half of 1973
23 p2814 N73-32497
Aerological data from balloon and rocket flights for Japan and vicinity - December 1972
24 p2921 N73-33325
Meteorological and weather effects on aircraft landings and flights along air lanes and stratospheric wind effects on supersonic transports
[JPRS-60114] 24 p2945 N73-33522
Nonlinear methods for evaluating informativeness of meteorological parameters and classifying meteorological phenomena
24 p2947 N73-33534
Aerological data from balloon and rocket flights for Japan and vicinity - Nov. 1972
24 p2947 N73-33540
Aerological data from balloon and rocket flights for Japan and vicinity - Jan. 1973
24 p2947 N73-33541
Subprogram planning for global atmospheric observation and weather forecasting system
[GARP-PUBL-11] 24 p2948 N73-33545
Methods for measuring and elaborating atmospheric phenomena and meteorological yearbook
[EUR-4943] 24 p2949 N73-33554
Meteorological parameter tables for Belgian weather stations, Apr. 1973
24 p2950 N73-33561
Handbook on monthly weather forecasts
[AD-765607] 24 p2950 N73-33563

**METEOROLOGICAL RADAR**

Canadian research on atmospheric precipation in antarctic regions and meteorological radar systems
[AD-746604] 04 p0444 N73-13627
X-band pulsed-Doppler radar measurement of radial velocity spectra in Arizona light showers
[PB-211388] 05 p0574 N73-14675
Performance of dual wavelength hail detector considering meteorological and radar parameters
[TR-25] 06 p0639 N73-15191
Real time meteorological radar data for predicting rainfall effects on satellite communication system
[AD-751742] 07 p0757 N73-16147
Remote sensing with meteorological radar equipment
[AD-753813] 09 p1004 N73-18197
Analysis of mesoscale weather systems in tropics from radar data of south Florida
[AD-753611] 09 p1062 N73-18660
Accuracy and reliability engineering of precipitation measurement by radar
[N.I.L.-M-22841-[5828.4F]] 12 p1420 N73-21505
Estimation of random error variance from simultaneous radar measurements
[AD-755402] 13 p1494 N73-22114
Weather forecasting and atmospheric activity detection using meteorological radar and remote sensing equipment
[AD-755438] 13 p1554 N73-22597
Instrumentation to aid radar investigations of cloud and precipitation physics
[AD-755401] 13 p1555 N73-22606
Jimsphere tracking for determining accuracy of meteorological radars
[AD-757624] 14 p1634 N73-23251
Radar/radiometer system for measuring temporal and spatial precipitation characteristics particularly thunderstorm activity
[NASA-CR-130235] 14 p1667 N73-23532
Evaluation of improved quantizer detector modification to production common digitizer
[FAA-RD-73-54] 15 p1750 N73-24181
Improvement of system for measuring intensity of radio echoes from meteorological radar
[AD-759759] 16 p1878 N73-25201
Meteorological processes and FM-CW radar soundings in boundary layer
[AD-759019] 16 p1939 N73-25695
Ultrahigh frequency precipitation attenuation measurements by ATS 5 weather radar and radiometer
17 p1996 N73-26142
Radar measurement of air mass circulation and meteor trail drift in upper atmosphere during IQSY
[NASA-TT-F-744] 17 p2023 N73-26363
Radar observation of air mass circulation in upper atmosphere during IQSY
17 p2023 N73-26364
Two spaced radar measurement of wind characteristics in meteor zones
17 p2023 N73-26365
SOM-3 radar design for measuring meteor trail physics and upper atmosphere physical properties
17 p2023 N73-26368
SOM-1 radar measurement of diffusion in meteor zones
17 p2023 N73-26370
Determination of parameter s for characterizing meteoric distribution from SOM-1 radar data
17 p2023 N73-26371
Budrio meteorological radar station
[IFA-CP-289] 19 p2293 N73-28436
Analysis of radar measurements of precipitation and comparison with ground level observations
21 p2568 N73-30581
Application of radar techniques for measuring precipitation and comparison with measurements obtained from conventional meteorological instruments
21 p2568 N73-30582
Development of radar equation and radar calibration relationships for measuring multiple target reflectivity
21 p2568 N73-30583
Synchronous observations of precipitation microstructure by radar and ground-level instruments to determine accuracy of radar measurements
21 p2568 N73-30584
Analysis of radar methods for measuring intensity of precipitation and development of mathematical models for radar reflectivity and microwave attenuation
21 p2569 N73-30585
Analysis of radar signatures for identifying hail-bearing clouds to show effects of geographical conditions and seasons
21 p2569 N73-30586
Analysis of radar data for time variability of cumulonimbus clouds in shower and thunderstorm stages
21 p2569 N73-30587
Application of polarized radar signals for analyzing structure of cumulonimbus clouds
21 p2569 N73-30588
Application of radio wave propagation and radar signatures for analyzing structure of clouds
21 p2569 N73-30589
Application of radar direction finding observations to determine extent and severity of storm centers
21 p2569 N73-30590
Application of radar techniques for determining microstructure parameters of cumulonimbus clouds
21 p2569 N73-30591
Application of polarized electromagnetic radiation for analyzing parameters of atmospheric formations
21 p2569 N73-30592
Application of radio astronomy methods for analyzing microwave absorption spectrum and properties of atmospheric cloud formations
21 p2570 N73-30593
Analysis of atmospheric attenuation of circularly polarized electromagnetic radiation from meteorological radar
21 p2570 N73-30595
Application of meteorological radar measurements of atmospheric turbulence using velocities of reflectors located in scattering volume of radar set
21 p2570 N73-30596
Application of radar signatures for analyzing the turbulent flow structure of earth adjacent layers of subfrontal clouds and precipitation
21 p2570 N73-30597

Development of methods for conducting radar measurements of parameters of atmospheric turbulence
21 p2570 N73-30598
Characteristics of electromagnetic radiation reflected from invisible objects in troposphere to show effects of electromagnetic radiation polarization
21 p2571 N73-30599
Development of backscattering diagrams for sources of reflections from clear sky based on signatures from meteorological radar
21 p2571 N73-30600
Application of pulsed Doppler radar for analyzing motion of sources of reflection from clear skies to show effect of wind
21 p2571 N73-30601
Analysis of radar data to determine characteristics of precipitation belts resulting from weather modification practices
21 p2571 N73-30603
Development and application of meteorological radar for detecting zones of cloudiness, precipitation, and storms for synoptic weather analysis
21 p2571 N73-30604
Equipment and procedures for obtaining meteorological radar information on clouds, cloud systems, and dangerous meteorological formations
21 p2571 N73-30605
Development of equipment and methods for obtaining and processing meteorological radar data
21 p2571 N73-30606
Characteristics of meteorological radar operating in millimeter wavelength range and methods for improving radar performance
21 p2572 N73-30607
Characteristics and development of receiving device for automatic conversion of meteorological radar data
21 p2572 N73-30608
Procedure for determining lower cloud boundaries using dual range meteorological radar operating in vertical sounding mode
21 p2572 N73-30610
Design and development of meteorological radar for detecting hail-bearing clouds
21 p2572 N73-30611
Meteorological radar analysis of convective cloud evolution
22 p2693 N73-31570
Characteristics of three meteorological radar systems to include principles of operation, circuit description, and fuctions of subsystems
[AD-765363] 23 p2759 N73-32076
Meteorological radar observations of clouds and precipitation
[AD-764934] 23 p2815 N73-32510

**METEOROLOGICAL ROCKETS**
U SOUNDING ROCKETS

**METEOROLOGICAL SATELLITES**
NT AEROS SATELLITE
NT EOLE SATELLITES
NT ESSA 8 SATELLITE
NT METEOSAT SATELLITE
NT NIMBUS SATELLITES
NT NIMBUS 2 SATELLITE
NT NIMBUS 3 SATELLITE
NT NIMBUS 4 SATELLITE
NT NIMBUS 5 SATELLITE
NT SAN MARCO 3 SATELLITE
NT SYNCHRONOUS METEOROLOGICAL SATELLITE
NT TIROS SATELLITES

Soviet Meteor meteorological satellite system and applications in weather forecasting, geological surveys, and exploration of earth resources
[NLL-M-22683-[5828.4F]] 01 p0073 N73-10599
Index of information collected by Soviet weather satellites
[NASA-TT-F-14447] 01 p0075 N73-10616
Using satellite observations for enhancing accuracy and detail of numerical analysis in sparse-data areas
[AD-745173] 01 p0077 N73-10633
Structural design, subsystem analysis and mechanical integration of synchronous meteorological satellite - Vol. 3
[NASA-TM-X-68839] 02 p0234 N73-11900
Studies of soundings and imaging measurements from geostationary satellites
[NASA-CR-130122] 03 p0359 N73-12925
Actinometric equipment on Soviet meteorological satellites for thermal radiation measurements of earth atmosphere
[AD-749622] 04 p0479 N73-13920
Interpretation of meteorological satellite TV pictures of ice in Baltic Sea
[NLL-M-20841-[5828.4F]] 05 p0529 N73-14306
Numerical analysis through proportional differences for analyzing meteorological satellite data and predicting synoptic weather patterns
[AD-749072] 05 p0574 N73-14672
Analysis of cloud console devices used in displaying meteorological satellite imagery
[AD-750085] 05 p0575 N73-14684
Legal liabilities and impact of satellite meteorology on agricultural crops and economics
[NASA-CR-129994] 06 p0692 N73-15636
Microanalytic analysis of satellite meteorology on resource utilization, commerce, and agriculture
06 p0692 N73-15637
Legal liability of US Government in handling meteorological data obtained by satellites
06 p0692 N73-15638
Case studies of meteorological satellite impact on agricultural crops and recreational activities
06 p0693 N73-15641
Management and use meteorological satellite data to detect severe storms and crop disease
[NASA-CR-130000] 06 p0693 N73-15642
Analysis of weather satellite program management and organization systems
06 p0693 N73-15643
Utilization of meteorological satellite data to forecast severe thunderstorms and tornadoes
06 p0693 N73-15644
Meteorological satellites for detecting and aiding southern corn leaf blight disease
06 p0693 N73-15645
Energy exchange between earth and space from meteorological satellite measurements of infrared radiant emittance and reflected and scattered solar radiation
[NASA-CR-130152] 07 p0780 N73-16341
Application of remote sensors for determining meteorological and environmental parameters with emphasis on data obtained by satellite infrared sensors
07 p0782 N73-16357
Revision of tropical cyclone climatology by satellite data for northern Pacific Ocean
[AD-753584] 09 p1061 N73-18658
Configuration and functions of ITOS D and E system of meteorological satellites to expand basic capability of TIROS M/ITOS system
[NASA-CR-130160] 09 p1086 N73-18863
Design characteristics of data handling equipment for ITOS D and E meteorological satellites - Vol. 2
[NASA-CR-130161] 09 p1087 N73-18864
Stress analysis of ITOS D and E structural members - Vol. 3
[NASA-CR-130162] 09 p1087 N73-18865
Quantitative analysis of radiation measurements from polar and geosynchronous satellites
[NASA-CR-130194] 13 p1551 N73-22568
Appraisal of meteorological satellite data as aid in weather modification programs
[NASA-CR-131876] 13 p1553 N73-22583
Model of symmetric large scale whirl using equations of motion as applied to satellite data
[AD-756096] 13 p1554 N73-22596
Operational exploitation of satellite infrared channel radiances in resolution of atmospheric thermal-structure variabilities
[AD-757773] 15 p1782 N73-24443
Satellite infrared channel radiances for resolution of atmospheric thermal structure and developing weather analysis and forecasting system
[AD-758734] 15 p1807 N73-24644
Phased project planning and development for operational space missions referring to NASA meteorological and communication satellite programs
15 p1848 N73-24978
Exploration of natural landscape using TV pictures from meteorological satellites
[NASA-TT-F-14965] 17 p2025 N73-26389
Techniques for improving accuracy of numerical 24-hour cloud cover forecasts in sparse data areas using satellite data
[AD-759986] 17 p2058 N73-26644
Application of meteorological satellite data in analysis and forecasting
[ESSA-TR-NESC-51-SUPPL-2]
18 p2171 N73-27532
High resolution radiometer for visible and infrared imagery onboard meteorological satellite
18 p2209 N73-27836
Calculation of cloud cover from vertical velocity data supplied by meteorological satellites
[AD-761545] 19 p2317 N73-28634
Satellite activities of NOAA
19 p2346 N73-28871
Procedures for determining variations of meteorological parameters from satellite radiation measurements
20 p2443 N73-29625
Development of satellite equipment for solving inverse problems of meteorological satellites
20 p2447 N73-29661
Exploitation of satellite observed radiances for increased resolution of atmospheric thermal structure
[AD-762752] 20 p2450 N73-29692
Comparison of surface cloud cover observations and cloud cover estimates determined by satellite measurements for Southeast Asia
[AD-763098] 20 p2451 N73-29695
Characteristics of vertical distribution of atmospheric moisture using satellite measurements
[AD-763286] 21 p2540 N73-30364
Cellular convection parameters determined from high-altitude tower measurements and meteorological earth satellite observations
22 p2693 N73-31568
Effect of television camera and radiometer resolution on accuracy of cloud quantity determinations from satellites
22 p2693 N73-31569
Meteorological services, satellites, and numerical weather forecasting
[WMO-342] 24 p2948 N73-33550
Origin, development and prospects of World Weather Watch noting role to be played by meteorological satellites and GARP
24 p2949 N73-33551
Present status in meteorological satellites, wind observation, cloud cover, and the imagery compared with predictions made in 1962
24 p2949 N73-33552
Meteorological satellite technology and operation
[PUBL-SER-B-70] 24 p2949 N73-33558

**METEOROLOGICAL SERVICES**
Automatic data processing in meteorological services
[NLL-M-20789-[5828.4F]] 01 p0072 N73-10591
Advances in educational communication and meteorology as derived from satellite technology
04 p0474 N73-13869
Meteorological assistance to fishing fleets by meteorological services
[NLL-M-9146-[5828.4F]] 05 p0569 N73-14624
Marine weather program for providing weather and river advisories to public sector
06 p0663 N73-15382
Research and development projects of Federal Aviation Administration to provide improved weather data acquisition and distribution
[FAA-ED-15-1] 11 p1314 N73-20662
Development of automated hydrometeorological service and establishment of information-computation network for data recording
12 p1421 N73-21515
Development of agrometeorological forecasts with emphasis on optimal decisions on taking preventive measures for frost control
12 p1421 N73-21517
Annual report of WMO noting World Weather Watch, global atmospheric research program, education, technical cooperation, environmental and oceanographic aspects
[WMO-348] 17 p2057 N73-26639
Activities of meteorological section during Tenth Soviet Antarctic Expedition
20 p2408 N73-29350
Procedures and equipment for automatic reception and processing of meteorological data
[NLL-M-23015-[5828.4F]] 20 p2441 N73-29609
Meteorological services and technology of USSR
[JPRS-59962] 22 p2692 N73-31565
Prospects for development and growth of USSR hydrometeorological service
22 p2692 N73-31566
Optimum use of infrared data as obtained from satellites for meteorological and oceanographic applications
24 p2911 N73-33233
Meteorological services, satellites, and numerical weather forecasting
[WMO-342] 24 p2948 N73-33550
Origin, development and prospects of World Weather Watch noting role to be played by meteorological satellites and GARP
24 p2949 N73-33551

**METEOROLOGICAL STATIONS**
U WEATHER STATIONS

**METEOROLOGY**
NT AEROLOGY
NT HYDROMETEOROLOGY
NT LONG RANGE WEATHER FORECASTING
NT MARINE METEOROLOGY
NT MESOMETEOROLOGY
NT MICROMETEOROLOGY
NT NUMERICAL WEATHER FORECASTING
NT RADIO METEOROLOGY
NT STATISTICAL WEATHER FORECASTING
NT SYNOPTIC METEOROLOGY
NT TROPICAL METEOROLOGY
NT WEATHER FORECASTING

Meteorological data from ERTS-1 high resolution multispectral photography
[E72-10189] 01 p0046 N73-10368
Influence of meteorological conditions on air pollution
[PB-210381] 01 p0077 N73-10634
USSR space program accomplishments in fields of geophysics, astronomy, meteorology, oceanography, upper atmosphere, and space sciences
[JPRS-57229] 01 p0104 N73-10864
Project planning and progress for first GARP global experiment, emphasizing satellite subsystem, data management, and oceanographic programs
[GARP-SPEC-REPT-8] 03 p0327 N73-12669
USSR research projects in geosphysics, astronomy, and space - No. 288
[JPRS-57505] 03 p0357 N73-12906
Soviet research and development in meteorology and hydrology
[JPRS-57127] 04 p0442 N73-13602

USSR developments in meteorology, weather forecasting, climate control, and hydrological forecasting
[JPRS-57608] 04 p0444 N73-13623
Soviet research on meteorology, oceanography, upper atmosphere, and astronomy
[JPRS-57630] 04 p0474 N73-13876
USSR research projects involving meteorology, oceanography, upper atmosphere, space research, and terrestrial geophysics
[JPRS-57777] 05 p0596 N73-14844
Application of remote sensors for determining meteorological and environmental parameters with emphasis on data obtained by satellite infrared sensors
07 p0782 N73-16357
Soviet research in meteorology, geophysics, space, and astronomy
[JPRS-57989] 07 p0843 N73-16829
Determination of meteorological information of ERTS-1 MSS bulk data at 0.6 - 0.7 microns as function of resolution
[E73-10085] 08 p0901 N73-17297
Role of mathematics in meteorology
08 p0938 N73-17678
Meteorological and hydrological researCh over and in oceans
[JPRS-58025] 09 p1059 N73-18631
Meteorological utility of high resolution ERTS-1 multispectral data
[E73-10357] 10 p1149 N73-19353
Meteorological and climatological radiosonde observations
10 p1180 N73-19601
Abstracts of articles on Soviet Bloc research in earth and space sciences
[JPRS-58437] 11 p1338 N73-20860
Calculation of expected anomaly criteria for some meteorological fields using statistical analysis methods
[NI.L-M-22804-[5828.4F]] 12 p1420 N73-21507
USSR research projects in subjects of microclimate, agricultural meteorology, weather forecasting, climate control, and hydrological forecasting
[JPRS-58483] 12 p1420 N73-21510
USSR research projects in meteorology, oceanography, geophysics, upper atmosphere, and extraterrestrial radiation - No. 298
[JPRS-58734] 12 p1458 N73-21817
Research projects conducted by Australian atmospheric physics laboratory to analyze atmospheric radiation, micrometeorology, ozone, airglow, and cloud physics
14 p1659 N73-23465
Meteorological implications of airborne optical imaging through tropopause
[AD-758207] 15 p1782 N73-24449
Air pollution modeling and meteorology for California particularly San Francisco Bay Area
[UCRL-74335] 15 p1806 N73-24635
Meteorological measurements from geosynchronous satellites
[NASA-CR-130246] 15 p1834 N73-24870
Estimates of meteorological autocorrelation and cross-correlation functions
[NI.L-M-22887-[5828.4F]] 16 p1934 N73-25646
Program for one level objective analysis of meteorological fields by optimal interpolation
[NI.L-M-22883-[5828.4F]] 16 p1936 N73-25664
Approximation methods for solving hyperbolic partial differential equations of meteorology and oceanography
[GARP-PUBL-10] 16 p1938 N73-25680
Collection of ground truth data in Great Basin for support of aerial and Skylab overflights
[E73-10884] 20 p2394 N73-29235
General description and scientific results of Tenth Soviet Antarctic Expedition for period 1965 to 1966
[TT70-50072] 20 p2406 N73-29339
Meteorological, actinometric, and aerological investigations conducted aboard ships of Tenth Soviet Antarctic Expedition
20 p2406 N73-29341
Operations and functions of ground station during Tenth Soviet Antarctic Expedition to obtain meteorological and geophysical data
20 p2409 N73-29360
Procedures and equipment for automatic reception and processing of meteorological data
[NI.L-M-23015-[5828.4F]] 20 p2441 N73-29609
Photographic recordings and meteorological data obtained by Environmental Research Satellite during January 1973
20 p2475 N73-29879
Photographic recordings and meteorological data obtained by Environmental Research Satellite During June 1973
20 p2475 N73-29880
Format conversion of meteorological data tapes of Hawaii
[PB-220452/7] 21 p2515 N73-30179
Determination of seasonal, meteorological, and statistical variations in spectral signatures for geological target types from ERTS-1 data
[E73-10933] 21 p2529 N73-30275
Utilization of ERTS-1 imagery for studies of agriculture, forestry, cartography, geography, hydrology, meteorology, geology, and oceanography in Thailand
[E73-10996] 22 p2659 N73-31302
Soviet research in meteorology, oceanography, geophysics, astronomy, and space
[JPRS-60165] 23 p2846 N73-32744
Agroclimatology study of highlands of eastern Africa
[WMO-339] 24 p2886 N73-33045
Application of ERTS-1 imagery to agriculture, forestry, meteorology, and hydrology in Thailand
[E73-11145] 24 p2918 N73-33299
Fort Lauderdale Workshop on chemistry and meteorology
[WASH-1217] 24 p2923 N73-33342

**METEORS**
U METEOROIDS

**METEOSAT SATELLITE**
Objective and mission of Meteosat satellite
[DGLR-PAPER-72-82] 06 p0721 N73-15887

**METERS**
U MEASURING INSTRUMENTS

**METHACRYLATE RESINS**
U ACRYLIC RESINS

**METHANE**
Methane mixing ratios in stratosphere deduced from balloon-observed solar infrared spectra
[AERONOMICA-ACTA-A-105] 01 p0092 N73-10757
Toxic effects of continuous exposure to dichloromethane vapor on dogs, monkeys, rats, and mice
[AD-746295] 02 p0134 N73-11088
Preparation of tetraperchlorate of methane by displacement of halogen from carbon tetrahalides using halogan perchlorates
[NASA-CR-129168] 02 p0137 N73-11106
High temperature oxidation reactions of carbon monoxide and methane in oxygen-rich atmospheres in turbulent flow reactor
[AD-746284] 02 p0138 N73-11116
Vertical distribution and dissociation of methane in stratosphere and CO production
[A-N-103-1972] 02 p0164 N73-11329
Calculation of mass flow rate of methane and natural gas through nozzles
[NASA-SP-3074] 06 p0653 N73-15309
Hepatotoxic effects of dichloromethane inhalation in mice
[AD-751434] 07 p0748 N73-16081
Effects of chemical fire extinguishing agents containing bromotrifluoromethane on cardiovascular and nervous systems of dogs, monkeys, and baboons
[AGARD-R-599] 08 p0877 N73-17106
Toxic effects of chronic exposure to dichloromethane in liver microsomal cytochromes
[NASA-TM-X-69101] 09 p0996 N73-18128
Analysis of stage-by-stage combustion process of methane in air
[AD-752862] 09 p1100 N73-18974
Vibrationally excited carbon monoxide from reaction of oxygen with acetylene, methylacetylene, and methane
[DREV-TN-2051/72] 11 p1252 N73-20160
Formation of hydrocyanic acid from mixtures of ammonia, metane and noble gas or hydrogen subjected to UHF waves
[NASA-TT-F-14678] 12 p1376 N73-21162
Molecular orbital energies in spectra of tervalent titanium chlorocomplexes
13 p1542 N73-22493
Preliminary appraisal of hydrogen and methane fuel and fuel tank configuration in Mach 2.7 supersonic transport
[NASA-TM-X-68222] 13 p1568 N73-22711
Differential scattering of hydrogen and oxygen atoms in methane molecules
[NASA-TT-F-14898] 14 p1694 N73-23751
Static dielectric constant of solid methane at low temperatures and high pressures
15 p1745 N73-24147
Methane spectral line formation in Jovian atmosphere
17 p2080 N73-26826
Radical species concentration profiles for methane-oxygen-argon flame
[BM-RI-7766] 18 p2206 N73-27803
Tables and graphs of thermodynamic and transport properties of gaseous CF4 in chemical equilibrium
[NASA-TN-D-7181] 18 p2206 N73-27805
Stratospheric and tropospheric composition and chemical reactions
[AP-12] 21 p2539 N73-30357
Laminar dispersion for measuring ethane binary diffusion coefficients in methane filled capillaries
24 p2891 N73-33079

**METHOD OF CHARACTERISTICS**
Method of characteristics for analyzing supersonic flow past oscillating flat plate cascades with leading edge locus
[AD-745838] 01 p0042 N73-10332
Shock wave generation and attenuation in tunnel noting computer programming based on characteristics method
[ISL-36/71] 04 p0406 N73-13305
Shock wave propagation and attenuation in tunnels noting computer programming based on method of characteristics
[ISL-11/72] 04 p0406 N73-13307
Method of characteristics for analyzing three dimensional, steady supersonic, nonequilibrium, chemically reacting flow of thermally perfect gases in exhaust nozzle
07 p0768 N73-16240
Method of characteristics solution of flow field on lee side of flat plate delta wing with supersonic leading edges
[AD-753389] 09 p1019 N73-18319
Characteristics method for calculating supersonic flow fields
[NASA-CR-132274] 18 p2130 N73-27210
Irrotational planar supersonic cascade ideal gas flow computation using method of characteristics
[DLR-FB-73-34] 21 p2491 N73-29998
Steady, supersonic, three dimensional flow in rotating and stationary annular cascades treated by method of characteristics in three independent variables
[DLR-FB-73-12] 21 p2525 N73-30247
Method of characteristics laser and mixing program for examining chemical laser flows and reactants in axial and lateral pressure gradients
[AD-763906] 22 p2682 N73-31482
Numerical method of characteristics for unsteady flow with dissipation
[DLR-FB-72-23] 23 p2776 N73-32198
Method of characteristics for studying flow field produced by underexpanded jet exhausted from conical nozzle into cylindrical tube
24 p2904 N73-33173

**METHODOLOGY**
Mathematical basis for operational availability, and its relation to performance effectiveness
[NASA-CR-61382] 02 p0245 N73-11987
Articles on methodology and historical importance of scientific research in creativity
[TT-70-57147-2] 21 p2502 N73-30075
Methods and procedures for ergonomic research
21 p2503 N73-30086
Individual nondestructive evaluation techniques
[NASA-SP-3079] 22 p2677 N73-31441

**METHODS**
U METHODOLOGY

**METHYL ALCOHOLS**
Methanol heat pipe using nitrogen gas for temperature control
[NASA-CR-114597] 21 p2606 N73-30884

**METHYL CHLORIDE**
Effects of continuous methylene chloride exposure on spontaneous activity of mice for two weeks
[AD-751435] 07 p0748 N73-16082

**METHYL COMPOUNDS**
NT METHYL NITRATE
Conversion of 2-methyl 5-ethyl pyridine compound into 5-ethyl picoline acid by different methods
[DRIC-TRANS-2951] 06 p0638 N73-15178
Toxicity of long term methyl isobutyl ketone exposure in dogs, monkeys, mice, and rats
[NASA-TM-X-69100] 09 p0996 N73-18130
Concentration fluctuations in critical region of binary liquid mixture 3-methylpentane-nitroethane
[AD-759740] 16 p1872 N73-25158
Energy transfer in methyl fluoride
23 p2824 N73-32575

**METHYL NITRATE**
Photolysis of CH3ONO
[NASA-CR-131355] 11 p1285 N73-20425

**METHYLENE**
Toxicity of atmospheric dichloromethane levels in simulated space cabin atmosphere on dogs, rats, mice, and monkeys
[NASA-TM-X-69099] 09 p0996 N73-18129

**METHYLHYDRAZINE**
Animal species susceptibility to toxic effects of long term exposure to environmental monomethylhydrazine
[AD-751441] 07 p0748 N73-16086
Industrial health hazard in chronic exposure to monomethylhydrazine and dose related hemolytic anemia in humans
[AD-751440] 07 p0749 N73-16087
Effects of monomethylhydrazine on blood and cerebrospinal fluid glucose in anesthetized monkeys
[AD-751232] 07 p0749 N73-16092
Convergence improvement in equilibrium calculation using Newton-Raphson method for C, H, N, F system, noting monomethylhydrazine/Fe mixture
[ICT-3/72] 18 p2192 N73-27696

**METRIC SPACE**
NT HILBERT SPACE
Mathematical representation with metric form to first order of gravitationally modified Maxwell equation in Lorentz symmetric linear field theory
[NASA-CR-130754] 08 p0915 N73-17500
Event horizon and T-S solutions to Einstein vacuum field equation
[RIFP-177] 16 p1934 N73-25652

METRIC SYSTEM
U INTERNATIONAL SYSTEM OF UNITS
METROLOGY
Soviet research in field of photographic metrology
[NASA-TT-F-13921] 01 p0075 N73-10615
Development of scaling counter for use as laser interferometer readout system to obtain improved length measurement capabilities
[BDX-613-703] 04 p0429 N73-13492
Research and development related to maintaining national standards of measurement of physical quantities in Australia
[NP-19392] 06 p0650 N73-15276
Operational activities of Hungarian National Bureau of Metrology and use of photogrammetry in city planning and modernization
[JPRS-57792] 06 p0731 N73-15965
Role and activities of Hungarian National Bureau of Metrology
06 p0731 N73-15966
Development of metric system design for large space telescope to show effect on production cost and time required
[NASA-CR-124133] 10 p1159 N73-19426
Application of image sensing arrays to metrology, mapping, and optical data acquisition
[AD-761121] 18 p2149 N73-27370
Metrology standards of underwater reference division
[AD-761147] 18 p2180 N73-27603
Systems theory in analysis and system of analytical quantity ranges
[NASA-TT-F-15029] 20 p2423 N73-29460
Congressional hearing on national program to establish international metric system as official and standard system for United States commerce and industry
21 p2610 N73-30920
Congressional hearings on legislation for conversion to metric system of weights and meaures in United States
21 p2610 N73-30922
METROPOLITAN AREAS
U CITIES
MEXICO
Evaluation of three types of aerial photographs used in coastal studies of Baja California
[AD-744310] 01 p0052 N73-10421
Identification and interpretation of tectonic features of Colorado, California, and Sonora, Mexico
[E73-10275] 09 p1020 N73-18324
Variability of coastal processes and resulting shoreline morphology along peninsula of Baja California
[AD-756676] 16 p1907 N73-25432
Identification and interpretation of tectonics from ERTS-1 imagery of California, Mexico, and Baja California
[E73-10875] 20 p2393 N73-29226
Identification and interpretation of tectonic features from ERTS-1 imagery of Southern California and Baja California
[E73-11084] 24 p2913 N73-33247
MICA
NT BIOTITE
Feasibility of hot pressing alumina composites with potassium and barium fluorine micas
[AD-742207] 01 p0071 N73-10584
Fabricating lamellar ceramic-based composites with synthetic fluorine mica
[AD-750353] 06 p0688 N73-15601
Effects of beta radiation on electrical resistivity of mica
[NLL-RTS-7926] 18 p2184 N73-27635
MICE
Effectiveness of pharmacochemical protective substances on irradiated mice as neutron component increases
[DRIC-TRANS-2961] 06 p0631 N73-15124
Effect of accelerations on thiamine S-35 distribution in organs, tissues, and subcellular structures of white mice
07 p0743 N73-16044
Mortality and blood cell count variation in mice after irradiation with fast neutrons and X rays
[BMVG-FBWT-72-16] 07 p0747 N73-16077
Hepatotoxic effects of dichloromethane inhalation in mice
[AD-751434] 07 p0748 N73-16081
Effects of continuous methylene chloride exposure on spontaneous activity of mice for two weeks
[AD-751435] 07 p0748 N73-16082
Correlation of physical activity and oxygen consumption between man and mouse
[FOA-1-B-1233-A5] 08 p0877 N73-17108
Toxic effects of human exhaled air on mice organisms
10 p1117 N73-19103
Resistance of mice to acceleration overloads after injection of aminothiol group radioprotector
11 p1239 N73-20056
Transverse acceleration overload effects on mice sensitivity to toxic doses of cysteamine and aminothiol group antiradiation drugs
11 p1239 N73-20061
Antiradiation effectiveness of cysteamine in mice under various conditions of gamma radiation
11 p1240 N73-20067
Gamma radiation effects on toxic cysteamine elimination in irradiated and nonirradiated mice
11 p1240 N73-20070
Mortality rate in antiradiation drug protected mice subjected to gamma radiation overloads
11 p1242 N73-20079
High altitude acclimatization effects on mice and rabbit tolerances to hypoxia, acceleration, and high temperature
[NASA-TT-F-14861] 11 p1247 N73-20123
Physiological regeneration of corneal epithelial mice cells exposed to strong magnetic fields
14 p1608 N73-23034
Continuous low dose gamma irradiation effects on cell population kinetics of mice lymphoid tissue
[NASA-CR-135723] 23 p2749 N73-31999
Course of infectious process and functional activity of pulmonary macrophages in mice confined to atmosphere with high oxygen content
24 p2882 N73-33016
Food consumption and morphological indices of blood in white mice with replacement of air nitrogen by inert gases in pressurized chamber
24 p2882 N73-33020
MICHELL THEOREM
Analysis of Michell framework for uniform load between fixed supports
[REPT-1054/73] 13 p1586 N73-22861
MICHELSON INTERFEROMETERS
Computerized optical system for producing multiple images of a scene simultaneously
[NASA-CASE-MSC-12404-1] 04 p0448 N73-13661
Michelson interferometry quality control of Schmidt plate replica by [Jouan Quetin] grating copying technique noting Kerber profile
[OPT-001-72] 23 p2794 N73-32351
MICHIGAN
Multidisciplinary analysis of Michigan resources utilizing ERTS-1 imagery
[E72-10313] 04 p0412 N73-13362
Use of remote sensing for assessing impact of highway construction on land use management in Michigan
[NASA-CR-130761] 08 p0917 N73-17515
Multidisciplinary analysis of forestry, agriculture, soils, and landforms in Michigan using ERTS-1 imagery
[E73-10310] 09 p1022 N73-18342
Application of dielectric constant measurements to interpretation of radar imagery of Michigan ground truth for lake ice
[E73-10391] 11 p1276 N73-20353
Computer mapping of Michigan recreational land use using ERTS-1 data
[E73-10392] 11 p1276 N73-20354
Application of ERTS-1 imagery to analysis of agricultural crops and forests in Michigan
[E73-10470] 12 p1395 N73-21307
Application of ERTS-1 data to analysis of agricultural crops, forests, soils, landforms, and acreage estimates in Michigan
[E73-10483] 12 p1396 N73-21320
Digital recreational land use mapping in Oakland County, Michigan
[E73-10570] 15 p1772 N73-24350
Application of ERTS-1 data for multidisciplinary analysis of Michigan resources and development of computerized procedure for map coordinates correlation
[E73-10703] 17 p2018 N73-26316
Acquisition of ground truth and meteorological data in Michigan for Skylab-3 mission
[E73-10748] 17 p2022 N73-26352
Study of recreational land and open space with Skylab imagery EREP 443
[E73-10783] 18 p2136 N73-27259
Application of ERTS-1 data for analysis of agricultural crops and forests in Michigan
19 p2262 N73-28228
Digital land use mapping in Oakland Country, Michigan using ERTS-1 data
[PAPER-1.21] 19 p2276 N73-28316
Utilization of ERTS-1 data for land use and resources survey in Michigan
[PAPER-1.26] 19 p2276 N73-28321
Monitoring and classifying eutrophication of inland lakes in Michigan using ERTS-1 imagery
19 p2285 N73-28375
Monitoring and classification of eutrophication of inland lakes in Michigan from ERTS-1 imagery
[E73-10898] 20 p2395 N73-29247
Study of recreation land and open space in Oakland County, Michigan using Skylab MSS data
[E73-10915] 20 p2397 N73-29264
Skylab imagery of recreational land and open space in Oakland County, Michigan
[E73-10973] 22 p2657 N73-31285
Atmospheric effects on Skylab MSS data for Williamston, Michigan
[E73-11043] 22 p2664 N73-31344
Remote sensing techniques in Michigan for resource management and environmental protection in both public and private interests
[NASA-CR-135639] 23 p2785 N73-32282
Snow and fresh water lake ice interpretations from ERTS-1 imagery of Whitefish Bay, Michigan and Green Bay, Wisconsin
[E73-11129] 24 p2917 N73-33284
Skylab photography of recreational land and urban resources in Oakland County, Michigan
[E73-11150] 24 p2919 N73-33304
MICROANALYSIS
Design and development of mass spectrometer using quadrupole fields to stabilize ions based on mass of ions
06 p0672 N73-15468
Electron probe microanalysis of ductile metal bond to Ti alloy disc
[AECL-4251] 10 p1172 N73-19535
Data reduction procedure for quantitative electron probe microanalysis
[NBS-TN-769] 21 p2549 N73-30433
MICROBALANCES
Contamination tests of Vacuum Chamber A and cryogenic/vacuum study of quartz crystal microbalance
[NASA-TM-X-64776] 21 p2521 N73-30220
MICROBE
U MICROORGANISMS
MICROBIOLOGY
NT BACTERIOLOGY
Characteristics of photogenic bacteria - Micrococcus pierantonii
[NASA-TT-F-14439] 02 p0132 N73-11072
Aerogenic microbial contamination of manned pressurized cabin atmosphere at reduced temperature and high humidity
03 p0259 N73-12098
Extraterrestrial life detection using Automated Microbial Metabolism Laboratory
[NASA-CR-129508] 03 p0279 N73-12266
Analysis of resistance of cultured and natural microbes in ethylene oxide sterilization method
[NASA-TT-F-14612] 04 p0379 N73-13078
Microbial analysis of Apollo 14 astronauts
[NASA-TM-X-58094] 05 p0500 N73-14073
Automatic swabbing apparatus for sampling of microbiological surfaces
[NASA-CASE-LAR-11069-1] 07 p0745 N73-16061
Automatic inoculating device for agar trays using cotton swab or loop
[NASA-CASE-LAR-11074-1] 07 p0750 N73-16096
Analysis of standards and precedures for planetary quarantine with emphasis on determination of mission specifications
[NASA-CR-130558] 08 p0877 N73-17103
Microbiological assay procedures for spacecraft cabling, antennas, solar panels, and thermal blankets
[NASA-CR-130383] 08 p0877 N73-17109
Antimicrobial water reclamation methods for processing human urine
10 p1117 N73-19105
Microbiological investigation of neutral buoyancy simulator for weightless space environment testing
[NASA-TM-X-64736] 12 p1371 N73-21127
Apollo 16 microbiological experiment on microbial response to aerospace environments - Part B
12 p1452 N73-21762
Microbiological experiments aboard balloons, rockets, and earth satellites - literature review
14 p1607 N73-23025
Use of ultrafine fiber filter cloth for removing bacterial contaminants from air
[NASA-TT-F-14940] 15 p1742 N73-24123
Microbiology of sediments and its geological aspects
[NASA-TT-F-15022] 20 p2411 N73-29381
MICROCALORIMETERS
U CALORIMETERS
MICROCIRCUITS
U MICROELECTRONICS
MICROCLIMATOLOGY
Soviet articles on microclimatology, argricultural meteorology, hydrology, and weather modification and forecasting
[JPRS-57652] 04 p0444 N73-13624
Effects of wind shaped trees on macro- and microclimatological conditions in Japan
[CLIMATOL-NOTES-12] 18 p2171 N73-27530
Analysis of microclimate of living and service quarters during Tenth Soviet Antarctic Expedition
20 p2409 N73-29359
MICROCRACKS
Ultrasonic testing of closures for rocket HEAT 66 mm I.IA2
[TM-52] 20 p2423 N73-29462
Interaction of advancing crack with pre-existing diffusion bonded microcracks in Ti-AlV alloy composites
[AD-765166] 23 p2811 N73-32476
MICRODENSITOMETERS
Radiographic analysis using isodensitometer techniques
[AD-746954] 03 p0303 N73-12477

Microdensitometer scans of ERTS-1 imagery of Gulf of California
[E72-10350] 05 p0533 N73-14338
Analysis of digital microdensitometer data from ERTS-1 imagery of San Francisco, California
[E73-10521] 13 p1517 N73-22289
MICROELECTRONICS
NT LARGE SCALE INTEGRATION
Maskmaking facility for microelectronic systems
[NASA-TM-X-64703] 01 p0036 N73-10284
Elec..ical characterization of complex microcircuits for amplifiers, comparators, and regulators
[AD-748242] 04 p0400 N73-13255
Glow from light scattering in gas jets of space vehicle microengine
04 p0466 N73-13801
Development of high power diode microcircuits
[SC-CR-72-3142] 05 p0519 N73-14219
Approximation method for calculation of temperature distribution in microcircuit
[AD-749762] 05 p0523 N73-14255
Reliability data for hybrid microcircuit discrete components
[NASA-TM-X-64686] 07 p0764 N73-16208
Irradiation of three low power microcircuits by Co-60 gamma radiation, low and high energy electrons, and neutrons
[NASA-CR-130750] 08 p0891 N73-17215
Automatic through-insulation welding of small-diameter solid conductor wires to facilitate production of miniature electronic assemblies
[NASA-CR-130751] 08 p0927 N73-17591
Environmental tests and failure modes for microelectric devices
[AD-753256] 10 p1135 N73-19253
Development of method for calculating characteristics of coupled microstrip lines and directional couplers
[REPT-6731] 10 p1136 N73-19261
Organic amine and nitroaromatic mixed compound for heat change detection in microelectronic components
[NASA-CASE-NPO-10764-2] 11 p1264 N73-20259
Quantum electronics, solid state devices, and solid microelectronics
[AD-754945] 11 p1331 N73-20806
Specifications for design of low, medium, and high power microwave hybrid microcircuits
[NASA-CR-124211] 13 p1533 N73-22419
Design and tests of hybrid microelectronics solid state relay for 2500 volts isolation and minus 120 C to 80 C thermal cycling range
[NASA-TM-X-68248] 15 p1756 N73-24235
Aluminum ribbon wire for ultrasonic bonding of semiconductor microelectronic interconnections
[AD-758981] 16 p1881 N73-25223
Electronic failure and quality control of microcircuit devices
[AD-759846] 17 p2005 N73-26215
Research on solid state devices and microelectronics
[AD-760815] 18 p2190 N73-27683
Life durability tests of bounded microcircuit joints subjected to prestressing
[AD-762333] 19 p2246 N73-28107
Tabulation of environmental tests on microelectronic devices
[AD-761951] 19 p2247 N73-28113
Semiconductor microcircuits for recording of optical radiation, mechanical stresses, and magnetic fields
[AD-762312] 19 p2247 N73-28119
Microcircuit reliability bibliography
[AD-763764] 21 p2518 N73-30194
Scanning electron microscope examination of wire bonds from high reliability microelectronic devices
[NBS-TN-785] 21 p2549 N73-30432
Analysis of microelectronic industry in Poland and comparison with capabilities in United States
21 p2607 N73-30896
Applications of mathematics to design and development of electronic equipment, microelectronic devices, and lasers
24 p2900 N73-33147
MICROFILMS
Information retrieval system combining magnetic storage and microfilm reader/copier
[CRIF-FI.-5] 02 p0147 N73-11188
Canadian Defence Scientific Information Service experience with microfiche and microfilm cartridges
[DSIS-TN-9] 04 p0486 N73-13972
Mariner 9 space probe microfiche library
[NASA-CR-130925] 10 p1128 N73-19193
Microfilm system and update for acquisition, storage, and retrieval of solid propellant mechanical behavior data
[AD-757245] 14 p1700 N73-23799
Integrated microform-machine processing system and costs of using such systems
15 p1753 N73-24206
User guide to microfilm records of data obtained in energetic particle experiment with OGO-5
[UCRL-51307] 22 p2639 N73-31150
MICROGRAPHY
U PHOTOMICROGRAPHY
MICROHARDNESS
Compactibility, shrinkage, and microhardness of electrolytic titanium powders obtained at low temperatures from melts
04 p0432 N73-13521
Microhardness tests of refractory metal alloys
[AD-750593] 06 p0686 N73-15582
Microhardness and corrosion resistance of Zr-Nb alloy prepared by reaction of ZrC with Nb2O5
[BARC-612] 15 p1799 N73-24583
Relationship determination between strain and microhardness, using viscoelasticity on surface or within specimen
[AD-759197] 17 p2047 N73-26562
MICROINDENTATION
U MICROHARDNESS
MICROMANOMETERS
U MANOMETERS
MICROMETEOROIDS
NT ZODIACAL DUST
Simulated micrometeoroid impact cratering in lunar materials using electrostatically accelerated microparticles impacting in oligoclase single crystals
[NASA-CR-130356] 07 p0841 N73-16813
Micrometeoroid analyzer using arrays of interconnected capacitors and ion detector
[NASA-CASE-ARC-10443-1] 11 p1291 N73-20477
Cold cathode discharge tube with pressurized gas cell for meteoroid detection in space
[NASA-CASE-LAR-10483-1] 23 p2791 N73-32327
MICROMETEOROLOGY
Hydrodynamics of surface layer of atmosphere and micrometeorological processes over flat homogeneous surface
[NLL-M-22574-[5828.4F]] 01 p0072 N73-10593
Vertical wind shear measurements at Helsinki Airport - Apr. 1967 through Mar. 1968
[TR-3] 08 p0937 N73-17676
Solid phase trace element aerosol concentrations in lowest 34 meters of atmosphere
15 p1771 N73-24343
Coherence statistics of horizontal wind speed as measured by micrometeorological mast array
16 p1937 N73-25675
MICROMETEORS
U MICROMETEOROIDS
MICROMINIATURIZATION
NT LARGE SCALE INTEGRATION
Development and application of polyimide films for hybrid and beam lead substrates
[AD-745731] 01 p0033 N73-10260
Microminiaturization and reliability of electronic radio equipment
[AD-745828] 01 p0034 N73-10265
Proceedings of 1972 GOMAC conference on microcircuit applications
[AD-751316] 07 p0765 N73-16212
Methods for chip mounting and establishing electrical connections in miniaturized printed circuits and thick and thin film hybrid circuits
[ECR-27] 08 p0891 N73-17212
Physical properties and limitations of components used in hybrid microcircuits
[AD-752216] 08 p0891 N73-17216
Annotated bibliography on microminiaturization electronics
[AD-764800] 23 p2767 N73-32136
MICROMINIATURIZED ELECTRONIC DEVICES
Minicomputer for digital measuring system for hydrophone calibration
[AD-749927] 05 p0549 N73-14461
Printed circuit boards for microminiaturized electronic manufacturing
[AD-750918] 06 p0648 N73-15265
Research in solid state physics including semiconductor lasers and laser spectroscopy
[AD-757559] 14 p1698 N73-23779
Analysis of microelectronic industry in Poland and comparison with capabilities in United States
21 p2607 N73-30896
MICROORGANISMS
NT AEROBES
NT BACILLUS
NT BACTERIA
NT ESCHERICHIA
NT PROTOZOA
NT PSEUDOMONAS
NT PSYCHROPHILES
NT SPORES
NT STAPHYLOCOCCUS
NT STREPTOCOCCUS
NT VIRUSES
Analysis of resistance of cultured and natural microbes in ethylene oxide sterilization method
[NASA-TT-F-14612] 04 p0379 N73-13078
Refutation of microbial ability to reduce phosphate using thermochemical computations
[NASA-TT-F-14724] 04 p0379 N73-13081
Gas chromatographic-mass spectrometric analysis of volatile organic metabolic products in terrestrial soils
[NASA-CR-129602] 04 p0386 N73-13134
Soil sampling and microorganism analysis in planetary spacecraft assembly area for prevention of Mars contamination
[NASA-CR-130009] 07 p0745 N73-16059
Automatic swabbing apparatus for sampling of microbiological surfaces
[NASA-CASE-LAR-11069-1] 07 p0745 N73-16061
Microorganism survival in simulated Mars environment
10 p1118 N73-19116
Evolutionary adaptation and resistance of unicellular organisms to solar radiation
10 p1118 N73-19118
Control equipment for sterilization facility used to thermally inactivate microbes on interplanetary space vehicle components
[NASA-CR-131103] 10 p1119 N73-19122
Microbial contamination studies for spacecraft assemblies
[NASA-CR-131086] 10 p1119 N73-19123
Metabolism and propagation of microbes in outer planets
[NASA-CR-131091] 10 p1120 N73-19127
Development of procedures of identification of microorganisms on orbiting spacecraft
[NASA-CR-128747] 10 p1120 N73-19132
Apollo 16 microbiological experiment on microbial response to aerospace environments - Part B
12 p1452 N73-21762
Ability of organism to maintain normal physiological activities in bioregenerative system
[NASA-CR-130807] 13 p1479 N73-21979
Microbiological studies of Apollo 17 command module preflight and postflight samples
[NASA-CR-132022] 14 p1610 N73-23056
Conference on Apollo 16 experiment for measuring microbial response to space environment
[NASA-TM-X-58103] 15 p1740 N73-24102
Design of microbial test system for Apollo 16 mission
15 p1740 N73-24103
Device for extravehicular microbe exposures to space environment during Apollo 16 flight
15 p1740 N73-24104
Operational handling of test equipment for microorganism exposure to space environment
15 p1740 N73-24105
Thermoradiation sterilization of naturally occurring microorganisms in soil from Kennedy Space Center
[NASA-CR-132197] 16 p1904 N73-25404
Analysis of high velocity spacecraft crash landing on planetary surfaces for possible encapsulated microorganism release
[NASA-CR-131835] 16 p1966 N73-25904
Metabolism and propagation of microbial contamination in planetary atmospheres
[NASA-CR-133638] 20 p2369 N73-29049
Biodetection grinder for sampling aerospace materials for microorganisms
[NASA-TM-X-64765] 20 p2372 N73-29059
Effects of microflora on rock weathering and edaphic factor
[NASA-TT-F-15033] 20 p2411 N73-29380
Role of microorganisms during iron-manganese ore formation in lakes and seas
[NASA-TT-F-15023] 21 p2537 N73-30346
Portable vacuum probe surface sampler for sampling large surface areas with relatively light loading densities of microorganisms
[NASA-CASE-LAR-10623-1] 21 p2544 N73-30395
MICROPARTICLES
Simulated micrometeoroid impact cratering in lunar materials using electrostatically accelerated microparticles impacting in oligoclase single crystals
[NASA-CR-130356] 07 p0841 N73-16813
Optimum holographic mounting for maximal ultrahigh speed microparticle volume restitution
[ISL-32/72] 16 p1924 N73-25565
Theoretical study and mountings for magnification and holographic image reconstruction of high speed microparticles
[ISL-1/73] 16 p1924 N73-25566
Mountings for optimum magnification and holographic image reconstruction of high speed microparticles
[ISL-3/73] 16 p1924 N73-25567
MICROPHONES
Design and evaluation of inertial microphone headset system
[AD-745088] 01 p0032 N73-10254
Design and development of underwater breathing apparatus with microphone for underwater communication
[AD-746105] 02 p0142 N73-11154
Depth effect on microphone sensitivity in underwater speech communication
[AD-750650] 06 p0642 N73-15213
Error sources in pressure measurements on turbulent supersonic flows by nonstationary microphone
10 p1140 N73-19289
Error sources in pressure measurements on turbulent supersonic flows by nonstationary microphone
10 p1184 N73-19629

Porous surface microphones for acoustic measurements in subsonic flow in wind tunnels
[NASA-CR-114593] 14 p1639 N73-23289
Optimization of microphone propagation in television studio
[BBC-RD-1973/3] 15 p1749 N73-24173
Response variations of microphone worn on human body
[BM-RI-7810] 20 p2371 N73-29058
MICROPHOTOMETERS
U PHOTOMETERS
MICROPROGRAMMING
Signal processing digital computer for microprogramming all applications computer
[AD-761610] 19 p2242 N73-28081
MICROPULSATIONS
NT GEOMAGNETIC MICROPULSATIONS
Correlation between frequency of magnetic oscillations and geomagnetic disturbances, and low frequency oscillation of earth magnetic field
[NASA-CR-127801] 05 p0537 N73-14372
Correlation between frequency of magnetic oscillations observed by ATS 1 and two indices of geomagnetic disturbance
05 p0537 N73-14373
Steady state solution of hydromagnetic mode of initial value problem of micropulsations
[AD-757866] 15 p1783 N73-24451
Cataloging of Pc4 and Pc5 micropulsations at ATS-1
[NASA-CR-133847] 21 p2583 N73-30698
MICROSCALES
U MICROBALANCES
MICROSCOPES
NT ELECTRON MICROSCOPES
NT ION MICROSCOPES
First-order geometrical optics analysis of quasi-microscope planetary landers
[NASA-TN-D-7129] 07 p0800 N73-16498
Hand-held, lightweight, portable photomicroscope
[NASA-CASE-ARC-10468-1] 24 p2925 N73-33361
MICROSCOPY
Analysis of microstructure of radio frequency-sputtered, thin lead-dielectric cermet films using transmission electron microscopy
[NASA-TR-R-393] 03 p0345 N73-12811
Macroscopic and microscopic approach to fracture and hardness of carbon steels
[COO-3084-10] 08 p0932 N73-17630
Image speckling reduction using multicolor illumination in holographic microscopy
[AD-752240] 08 p0945 N73-17737
MICROSONICS
Solar eclipse prediction, ionospheric reflection, ionospheric data reduction, and microwave acoustics
[AD-749882] 06 p0668 N73-15432
MICROSTRUCTURE
NT METEORITIC MICROSTRUCTURES
Analysis of sensitivity of elevated temperature deformation of nickel alloy to grain size and shape under tension and creep conditions
[NASA-CR-128403] 01 p0067 N73-10549
High resolution measurements of complex microstructure of interplanetary magnetic field and plasma, including hydromagnetic waves and discontinuities
01 p0095 N73-10787
Influence of thermal cycles on weld properties of all weld metal heat affected zone and base metal
[AD-746886] 02 p0179 N73-11452
Analysis of structural changes during heating and elongation of two-phase, high chromium content Cr-Ni-Fe alloys over ranges of temperature and concentration
[NLL-TRANS-746-1153-[9022.401]]
02 p0185 N73-11501
Aluminizing of titanium and aluminum alloys in powder form with use of electric heating methods
[NLL-M-21479-[5828.4F]] 02 p0185 N73-11503
Preparation and homogenicity characteristics of austenitic iron-chromium-nickel alloy at micrometer level of spatial resolution to establish standard reference material
[NBS-SP-260-43] 02 p0186 N73-11511
Microstructure of thick film resistors
[AD-747980] 03 p0276 N73-12238
Effects of irradiation microstructure and creep rupture properties of annealed and cold worked type 316 stainless steel
[CONF-720604-4] 03 p0314 N73-12560
Effects of annealing on microstructure and room temperature mechanical properties of 0.100 inch thick ingot-source beryllium sheet
[RFP-1831] 03 p0314 N73-12562
Proceedings of conference on microstructure of titanium, uranium, and zirconium body centered cubic lattices
[AD-748035] 03 p0319 N73-12598
Research on zirconium microstructure and uranium carbide as nuclear fuel
[AECL-4159] 03 p0332 N73-12708
Analysis of microstructure of radio frequency-sputtered, thin lead-dielectric cermet films using transmission electron microscopy
[NASA-TR-R-393] 03 p0345 N73-12811
Computer technique for automatic analysis of planar characteristics of chromosome patterns in microscopic observations
[JPRS-57418] 04 p0379 N73-13085
Sintering behavior of UO2 powder compacts under hydrogen atmosphere
[CEA-R-4285] 04 p0427 N73-13477
Thermal and thermophysical processes for microstructural control in high strength steel to increase fracture toughness
[LBL-832] 04 p0434 N73-13537
Improved oxidation resistance of dispersion strengthened nickel-chromium alloys and thermomechanical procedure to produce course grain microstructure
[AD-748266] 04 p0436 N73-13556
Microstructural analysis of high-chromium martensitic semiferritic and ferritic steel phase transformations and thermal expansion coefficient determination
[AD-749522] 04 p0436 N73-13559
Weldability and properties of materials undergoing electron beam welding
[CRANFIELD-MAT-7] 05 p0551 N73-14474
Structure and phase composition of electrodeposited iron-nickel-chromium alloys analyzed by X ray spectroscopy and electron microscopy
[NLL-TRANS-746-1327-[9022.401]]
05 p0560 N73-14551
Analysis of lattice spacings and changes in platinum metals as function of temperature and applied pressure
[NLL-TRANS-746-1316-[9022.401]]
05 p0561 N73-14558
Microstructure and mechanical properties of rapidly quenched liquid and powder metal alloys
[AD-749679] 05 p0564 N73-14578
Plastic properties and microstructure of alpha-titanium alloys at high temperature
[AD-750964] 05 p0564 N73-14581
Analysis of volume changes in composite wrought iron associated with fiber buckling
[AD-749711] 05 p0567 N73-14606
Microwave properties and microstructure of polycrystalline UHF garnets
[AD-749509] 05 p0588 N73-14781
Analysis of effect of dysprosium oxide on the physical properties of nickel-zinc ferrite materials
[NLL-TRANS-746-1284-[9022.401]]
06 p0682 N73-15550
Microstructural features of deformation analyzed in two-phase titanium alloys to determine beta phase effect on ductility
06 p0683 N73-15557
Correlation of mechanical properties to microstructure of titanium alloys
[AD-749932] 06 p0685 N73-15581
Microstructural analysis of 1010 modified steel and titanium alloy grains
[AD-748101] 06 p0686 N73-15584
Kinetic and structural investigation of ST-4 titanium alloy oxidizability at 700 to 1000 C, unprotected and protected by silicon and molybdenum silicide coatings
[AD-750646] 06 p0686 N73-15585
High strength aluminum alloys by optimizing precipitate microstructure
[AD-750140] 06 p0686 N73-15586
Effects of prior deformation and transformations on microstructure of iron nickel alloy
[AD-750716] 06 p0687 N73-15591
Statistical characteristics of physical structure for various types of precipitation
[NLL-M-20844-[5828.4F]] 06 p0691 N73-15627
Relationship of tensile properties and fracture toughness levels to microstructure of Ti6Al2Sn4Zr6Mo
[AD-751530] 07 p0810 N73-16566
Significance of grain boundary microstructure and pH in chloride ion solution as stress corrosives in 7075 aluminum alloys
[RM-564J] 08 p0931 N73-17624
Development of process for fabricating dense boron suboxide billets by hot pressing to eliminate decomposition and cracking
[AD-751980] 08 p0936 N73-17662
Freezing effects on structure of soils and biological tissues
[CNRS/LA-PUBL-440] 09 p0999 N73-18150
Chemical flame inhibitors for examining chemical microstructure of normal CH4, O2, Ar, and Halon inhibited flames
[BM-RI-7723] 09 p1034 N73-18438
Microstructural analysis of nickel-base alloy WAZ-20 using qualitative and quantitative electron optical techniques
[NASA-TM-D-7209] 09 p1047 N73-18541
Solutioning and aging reactions and effects on microstructure and hardness of niobium-based alloys
[AD-752930] 09 p1049 N73-18558
Investigation of microstructure of mullite fibers using transmission electron microscopy
[NASA-TM-X-2750] 09 p1052 N73-18573
Mechanical and microstructural behavior of Al-Zn alloy in superplastic region at high temperature
10 p1170 N73-19518
X ray diffraction analysis on microstructure defects in explosively loaded copper germanium alloy
[COO-1431-15] 10 p1173 N73-19541
Topographic interpretation of uranium alloy X ray diffraction patterns
[SC-T-72-2467] 10 p1173 N73-19543
Microstructure and mechanical properties of precipitation hardened-dispersion strengthened aluminum and titanium alloys and refractory materials
[AD-753910] 10 p1174 N73-19550
Analysis of microstructure and optical properties of thin lead dielectric cermet films
10 p1175 N73-19555
Influence of ammonia perchlorate binder and surface microstructure on combustion velocity development in solid composite propellants
[ONERA-TP-1167] 10 p1222 N73-19941
Microscopic analysis of silver diffusion into gold plate on electrical connector
[AD-755123] 11 p1263 N73-20249
Properties of zinc-copper-titanium alloys to include microstructure composition, mechanical properties, and effects of hot and cold deformation
[NLL-M-22842-[5828.4F]] 11 p1304 N73-20583
Analysis of microplasticity of materials used in inertial navigation systems to show friction stress, yield stress, and rate of strain hardening in microstrain region
11 p1317 N73-20692
Development of procedure for controlling crystallization of metal in molten pools and effect of electromagnetic treatment during welding
[AD-756335] 13 p1536 N73-22443
Analysis of metals and alloys to include superelasticity properties, plastic growth in cracks, strain aging, and strengthening by nuclear gamma resonance
[JPRS-58611] 13 p1540 N73-22477
Development of model for conditions of superplasticity related to maximum interphase surface of fluctuation nuclei of phase transformation
13 p1540 N73-22478
Structural recrystallization of steels during fast and slow heating to show structural succession caused by different mechanisms of formation of austenite
13 p1541 N73-22481
Analysis of alpha to gamma transformation in steel to determine effect of initial state nonequilibrium on starting temperature
13 p1541 N73-22482
Analysis of strain aging process in high carbon quenched steels caused by plastic deformation of martensite and migration of carbon to crystal defects in microstructure
13 p1541 N73-22484
Effect of deformation performed during heat treatment on structure and mechanical properties of E1437B alloy
13 p1541 N73-22485
Saturation of zirconium iodide with nitrogen and oxygen and analysis of effects on mechanical properties, deformation, and microstructure
13 p1541 N73-22488
Metallographic analysis of morphological features of martensite formed in alloy of iron-nickel-manganese-carbon after heat treatment
13 p1541 N73-22490
Microstructure of recrystallized heat resistant steel
[JPRS-58840] 13 p1542 N73-22498
Mechanical properties of aluminum stainless steel composites and associated interface microstructures
[AD-756673] 13 p1548 N73-22542
Surface wave interaction and thermal microstructure of sea water
[AD-757425] 14 p1664 N73-23502
Phase transformations in titanium alloy TiAl6V4
[DLR-FB-73-38] 15 p1799 N73-24584
Nondestructive tests for predicting effect of copper and aluminum microstructure on acoustic emission
[AD-758216] 15 p1800 N73-24587
Coherent optical correlation techniques for detection of microstructural surface alterations during cyclic stressing
16 p1923 N73-25558
High temperature heating effects on structure and ductile properties of austenitic steels
[NLL-M-21563-[5828.4F]] 16 p1926 N73-25584
Processing condition effects on microstructures of sheets, wire and bars made from nickel chromium iron alloy 718
[WAPD-TM-1077] 16 p1928 N73-25603
Harper-Dorn creep and microstructure of pure aluminum and other metals at high temperature
[LBL-1158] 16 p1928 N73-25604
Effect of microstructure on elastic limit of low carbon alloy and low carbon steels
[RAE-LIB-TRANS-1700] 17 p2044 N73-26534
Effect of martensitic microstructure on fatigue life and crack propagation characteristics of high strength steels
[S-253] 17 p2044 N73-26536
Relationship between microstructure and properties of austenitic stainless steels
[ORO-4044-3] 17 p2045 N73-26545

Analysis of aluminum oxide to determine material characterization, particle size distribution, and specific surface area
17 p2050 N73-26582
Microstructure of hot pressed and press forged polycrystalline refractory oxides
[AD-760353] 17 p2053 N73-26606
Influence of prior microstructure on neutron irradiation damage in 316 stainless steel foils
[HEDL-SA-407] 17 p2065 N73-26707
Explosive fragmentation of heat treated martensitic microstructure steel
[DSL-REPT-532] 17 p2091 N73-26915
Application of magnetic perturbation technique to nondestructively detect subsurface nonmetallic inclusions in inner races of deep groove ball bearings
[NASA-TM-X-68260] 18 p2155 N73-27410
Development of nondestructive inspection procedures for determining quality of welded joints in aluminum spacecraft structures
[NASA-CR-124332] 18 p2156 N73-27420
Influence of microstructure on tensile deformation and fracture in high strength Al-Zn-Mg alloys
[ARL/MET-NOTE-86] 18 p2160 N73-27447
Structure and segragation in cast alloys
[AD-761202] 18 p2163 N73-27470
Electrical, optical, and structural properties of RF triode-sputtered gold films
18 p2186 N73-27649
Microstructure and mechanical properties of thermal barrier materials produced by arc plasma spraying
[AD-762045] 19 p2312 N73-28598
Analysis of physical and mechanical properties of nonmagnetic steels and suitability for producing tubes and forgings
[NLL-M-21647-[5828.4F]] 20 p2422 N73-29451
Analysis of effects of plastic deformation on internal structure of austenitic steels as shown by anomalies in tensile stress-strain curves
[NLL-M-23029-[5828.4F]] 20 p2428 N73-29504
Evaluation and characterization of superplastic properties of aluminum, zinc, and titanium alloys in various microstructural conditions
20 p2429 N73-29509
Development of method for calculating molar volume and density of molten binary alloys with strongly interacting dissimilar atoms
[NLL-M-21695-[5828.4F]] 20 p2429 N73-29512
Strength and microstructure of nickel base superalloys after long term heating
[TB-86] 20 p2431 N73-29526
Analysis of structure dependent and temperature dependent variables affecting flow curves of metals
[BLL-RAE-LIB-TRANS-1675] 21 p2556 N73-30494
Microstructural determination of bonding strength of steel bimetal produced by pressure working
[NLL-M-21699-[5828.4F]] 21 p2557 N73-30499
Carbon fiber/cobalt/chromium system tensile and high temperature strength noting different solidification modes
[DLR-FB-73-37] 21 p2560 N73-30519
Effect of thermal cycling of structure and properties of directionally solidified eutectic composite
[NASA-CR-121249] 21 p2562 N73-30537
Effects of microstructure differences on tensile strength of graphite fibers
[AD-763687] 21 p2564 N73-30557
Effects of inclusions and voids in welding electrodes and welding materials on quality of welded joints
22 p2678 N73-31447
Strain fracture toughness and microstructure of heat treated high strength steels
22 p2682 N73-31486
X ray and electron microscopic studies on fatigue life of copper and copper zinc polycrystals
23 p2803 N73-32416
Stress analysis of vacuum deposited nickel films to determine correlation between microstructure and measured stress
23 p2804 N73-32424
Correlation of creep rate with microstructural changes during high temperature creep
[NASA-CR-135698] 23 p2804 N73-32426
Tear and fatigue crack propogation tests for determining mechanical properties of ultrafine grain alpha titanium
[AD-765329] 23 p2805 N73-32434
Development of continuum theory with microstructure for wave propagation in composite materials
23 p2806 N73-32438
Microstructure of molybdenum carbide samples during hot pressing and development of line intensity diagram for various conditions
23 p2808 N73-32449
Effect of addition of transition metals on cast zirconium to show changes in microstructure, macrostructure, microhardness, and electrical resistance
23 p2809 N73-32457
Effect of rare earth metals on macrostructure, microstructure, strength, and ductility of cast titanium samples
23 p2809 N73-32458
Microstructure of mullite composite fibers
24 p2940 N73-33474

**MICROTHRUST**
Fabrication and tests of flight prototype pulsed plasma microthruster propulsion system for Synchronous Meteorological Satellite
[NASA-CR-130133] 05 p0590 N73-14794
Fabrication and tests of 2.5-centimeter Kaufman electron bombardment microthruster
[NASA-TM-X-2708] 07 p0836 N73-16774
**MICROTOPOGRAPHY**
U TERRAIN
**MICROWAVE AMPLIFIERS**
Design and development of wideband TRAPATT amplifier in microstrip configuration for use in phased-array radar modules in S-band
[AD-747050] 02 p0150 N73-11215
Investigation of nonlinearities in X band IMPATT reflection amplifiers
[AD-747796] 03 p0275 N73-12231
Design and construction of broadband combinable amplifier using stripline techniques for UHF amplification
[AD-747404] 04 p0396 N73-13218
Transferred electron and avalanche diodes and solid state materials, for solid state microwave oscillators and amplifiers
[AD-748241] 04 p0460 N73-13755
Fabrication and tests of L band, RF pulse amplifier
[AD-749791] 05 p0514 N73-14182
Design and tests of one kilowatt L band solid state power amplifier
[AD-751279] 07 p0758 N73-16155
Development of broadband S band hybrid traveling wave tube
[AD-751262] 07 p0763 N73-16200
Design of klystron microwave amplifier tube for troposcatter communication system
[AD-752075] 08 p0890 N73-17204
Development and characteristics of traveling wave maser amplifier for use in radio astronomy and deep space communication experiments
[REPT-107] 09 p1043 N73-18504
Microwave UHF and SHF semiconductor oscillators and power amplifiers, noting gunn and impatt diode solutions, and integrated circuit development
[DLR-MITT-73-06] 10 p1135 N73-19248
Phase shift variations of platinotron microwave amplifier oscillator for pulse radar and steerable antennas
[DLR-MITT-73-03] 12 p1379 N73-21187
Microwave amplifier circuit for testing avalanche diode
[AD-756520] 13 p1503 N73-22180
Technical study of tunnel diode and its microwave amplification and oscillation
[AD-756932] 13 p1503 N73-22183
Interaction between drifting streams of electrons with transverse cyclotron motions and electromagnetic fields
[NASA-CR-130208] 13 p1504 N73-22188
Electron beam semiconductor S-band amplifier
[AD-759948] 17 p2005 N73-26212
Analytical method for determination of large signal characteristics of impatt amplifiers
18 p2122 N73-27151
Design of broadband continuous wave amplifier for phased array
[AD-760545] 18 p2124 N73-27167
GaAs and InP reflection amplifier noise figure and power gain at extremely high frequencies
[ESRO-CR[P]-262] 19 p2244 N73-28088
Doping profile effect on stabilization mechanisms in microwave GaAs reflection amplifiers around X band
19 p2244 N73-28089
Power gain and noise figure of indium phosphide and gallium arsenide microwave reflection amplifiers
19 p2244 N73-28090
Klystron 100 megawatt amplifier with 400 MHz bandwidth
[AD-762929] 20 p2381 N73-29133
Theoretical and developmental work on high efficiency avalanche diode sources and amplifiers
[FAA-RD-73-93] 21 p2517 N73-30186
Electron beam semiconductor S-band amplifier
[AD-763223] 21 p2518 N73-30200
Theoretical and experimental analysis of transferred electron amplifiers
22 p2641 N73-31169
Solid state avalanche diodes for use as microwave amplifiers and oscillators
[NASA-CR-132300] 22 p2642 N73-31172
Noise in microwave semiconductor oscillators and amplifiers
[AD-764259] 22 p2644 N73-31188
Design and performance of series power combiner for microwave solid state amplifiers
[AD-764728] 23 p2766 N73-32130
**MICROWAVE ANTENNAS**
NT HORN ANTENNAS
NT LENS ANTENNAS
NT SLOT ANTENNAS
Microwave breakdown at waveguide antenna discharge into ionized gas media
[AD-748830] 04 p0455 N73-13717
Characteristics of microwave antenna with conical reflectors to generate plane wave front
[NASA-CASE-NPO-11661] 05 p0507 N73-14130
Computer program for shape of microwave reflector antenna
[REPT-53199] 10 p1135 N73-19247
Radar microwave link antenna pattern measurements
[FAA-RD-73-118] 22 p2631 N73-31087
Electromagnetic absorber reflectance and anechoic chamber design for microwave antenna measurements
[FTZ-A-454-TBR-13] 22 p2642 N73-31176
**MICROWAVE ATTENUATION**
Microwave attenuation and neutral gas density profile measurements behind shock waves in air
[AD-745969] 02 p0158 N73-11282
Electric field amplitude within superhigh frequency wave absorption by plasma using Stark effect analysis
[FTI-413] 06 p0705 N73-15750
Real time meteorological radar data for predicting rainfall effects on satellite communication system
[AD-751742] 07 p0757 N73-16147
Water evaporation interference in phase measurements by transhorizontal microwave propagation over sea surface
17 p1994 N73-26125
Attenuation and phase dispersion of radio wave in atmosphere due to oxygen microwave spectrum
17 p1994 N73-26126
Rain depolarization of linearly and circularly polarized microwaves
17 p1995 N73-26127
Use of differential phase and gain for predicting performance of ultrahigh frequency telecommunication system
17 p1995 N73-26132
Rain attenuation and multipath fading in ultrahigh frequency radio relay systems
17 p1995 N73-26134
Rain attenuation statistics for ultrahigh frequency microwave link using meteorological data
17 p1996 N73-26135
**MICROWAVE CIRCUITS**
Microwave network synthesis including grating transducer technology and channel-dropping-filter geometry
[AD-751746] 07 p0764 N73-16210
Computerized design optimization program for microwave circuits
[AD-756875] 13 p1504 N73-22191
Specifications for design of low, medium, and high power microwave hybrid microcircuits
[NASA-CR-124211] 13 p1533 N73-22419
Status of microwave equipment development in Poland with emphasis on research projects and higher education
21 p2607 N73-30897
Polish institutes involved in research and development of microwave tubes and recommendations for new research projects
21 p2608 N73-30900
**MICROWAVE COUPLING**
NT COUPLING CIRCUITS
Standard coupler effects on EHF attenuation in waveguides with bending moments
[FTZ-A-333-TBR-18] 22 p2632 N73-31096
**MICROWAVE EMISSION**
Spaceborne and ground-based data and atmospheric model of Venus microwave emission
[AD-743982] 01 p0100 N73-10820
Four channel radiometer for remote sensing of microwave emission from atmospheric oxygen and water vapor
[AD-759535] 16 p1939 N73-25696
Theory of microwave and X ray emission mechanisms in solar flares considering nonthermal electrons
19 p2335 N73-28786
Gyrosynchrotron and magnetoactive absorption processes in solar microwave emission
19 p2335 N73-28787
Research projects involving design and technology of semiconductor devices, metal oxide semiconductor field transistors, and electron storage for memory purposes
21 p2607 N73-30895
Noncoherent model for microwave emissions and backscattering from sea surface
[NASA-CR-2326] 24 p2948 N73-33542
Subsurface characteristics of Mercury and Mars determined by analysis of thermal microwave emission
24 p2979 N73-33881
**MICROWAVE EQUIPMENT**
NT BACKWARD WAVE TUBES
NT CATHODE RAY TUBES
NT CELESCOPES
NT GYRATORS
NT HORN ANTENNAS
NT IMAGE ORTHICONS
NT IMAGE TUBES
NT KLYSTRONS
NT LENS ANTENNAS
NT MAGNETRONS
NT MICROWAVE AMPLIFIERS
NT MICROWAVE ANTENNAS
NT MICROWAVE FILTERS
NT MICROWAVE INTERFEROMETERS

NT MICROWAVE OSCILLATORS
NT MICROWAVE PLASMA PROBES
NT MICROWAVE PROBES
NT MICROWAVE RADIOMETERS
NT MICROWAVE TUBES
NT PHOTOMULTIPLIER TUBES
NT SLOT ANTENNAS
NT THERMIONIC DIODES
NT THYRATRONS
NT TRAVELING WAVE TUBES
NT VIDICONS

Radar and microwave equipment and materials, and related research and development
[RRE-11] 01 p0023 N73-10181

Development and characteristics of reciprocal latching microwave phase shifters based on ferrimagnetic substrate
[AD-744795] 01 p0033 N73-10255

Comparison of European and United States of America reproduced broadband microwave components
[FOA-3-A-3750-E6] 02 p0148 N73-11204

Numerical techniques for analysis of microstrip transmission line configurations
[AD-746059] 02 p0151 N73-11223

Growths and applications of compound semiconductor materials and devices
[AD-746882] 02 p0220 N73-11783

Dual frequency feed systems for Cassegrainian antennas
[NASA-CASE-NPO-13091-1] 03 p0273 N73-12214

Use of cross ratio invariance for analysis and error evaluation in automatic microwave network analyzers
[NBS-TN-623] 03 p0277 N73-12246

Solid states physics and manufacturing methods for microwave generation, amplification, and control devices
[AD-749500] 04 p0397 N73-13234

Microwave radar detection and photography of gravitational waves in troposphere
05 p0510 N73-14152

Research and development in slot line construction techniques
[AD-749070] 05 p0520 N73-14230

Design of microwave power transistor for providing power amplification in 1350 to 1850 MHz
[AD-749789] 05 p0521 N73-14237

Design and development of microwave landing system for operation of civil and military aircraft in conventional and V/STOL configurations
[AD-749505] 05 p0578 N73-14702

Microwave properties and microstructure of polycrystalline UHF garnets
[AD-749509] 05 p0588 N73-14781

Microwave holography for imaging sea surface topography in three dimensions
06 p0664 N73-15391

Analysis of position determination accuracy obtainable with microwave landing guidance system
[NASA-TN-D-7116] 06 p0697 N73-15681

Microwave measurements of magnetic field local shearing in confined plasma
[EUR-CEA-FC-632] 06 p0705 N73-15749

Characteristics of radar equipment and microwave radiometers to show application to earth resources surveys
07 p0784 N73-16377

Analysis of Microwave Landing System performance to determine signal formats and to reduce effects of multipath transmission
[AG-5011-B-1] 07 p0818 N73-16628

Microwave gauge for measuring thickness of hot steel product during production
[PB-212210] 08 p0925 N73-17583

Ultrasonic radiation and microwave research projects
[AD-752055] 08 p0944 N73-17736

Design of microwave signal processing devices for broadband operation
[AD-753168] 09 p1075 N73-18775

Microwave discharge plasma in magnetic fields greater than cyclotron
[AEC-TR-7372] 10 p1196 N73-19735

Design and fabrication of microwave acoustic surface wave delay lines
[AD-754896] 11 p1263 N73-20252

Magnetic and ferroelectric properties of rare earth compounds for signal processing devices
[AD-754775] 11 p1331 N73-20807

Analysis of electromagnetic compatibility of microwave landing guidance system and candidate interim systems
[ECAC-PR-72-069] 12 p1425 N73-21554

Synthesis of compound semiconducting materials and application to planar microwave acoustic equipment using gallium arsenide thin films as active layer
[AD-755947] 12 p1442 N73-21684

Technical study of tunnel diode and its microwave amplification and oscillation
[AD-756932] 13 p1503 N73-22183

Computerized analysis of noise quality on microwave equipment
[AD-756862] 13 p1504 N73-22192

Microwave Doppler shift technique for measuring dynamic bulk modulus of dielectric materials including solid propellants
[NASA-CR-131743] 13 p1546 N73-22532

Calorimetric calibration method for commercial power monitor used with high power microwave generators
[PB-213970/7] 14 p1669 N73-23548

Development and characteristics of microwave landing system with emphasis on functional design requirements for airborne equipment
14 p1689 N73-23705

Development of Doppler microwave landing system and techniques for eliminating effects of multipath transmissions
14 p1689 N73-23706

Extension of microwave devices to optical frequencies
[AD-758914] 16 p1924 N73-25569

Analysis of control and display device testing for microwave landing system - Vol. 1
[AD-758791] 16 p1942 N73-25713

Development of control and display testing requirements for evaluation of microwave landing system - Vol. 2
[AD-758792] 16 p1942 N73-25714

Design and testing of high power microwave components for communications satellites
[NASA-CR-120927] 17 p1998 N73-26152

Papers presented at conference on microwave transistors
[AD-760315] 17 p2005 N73-26213

Synthesis of microwave network having surface acoustic wave transducer
[AD-759934] 17 p2008 N73-26236

Microwave solid state devices and circuits
[AD-759833] 17 p2075 N73-26787

Application of microwave landing system to provide operational flexibility and improved capacity in terminal area
[FAA-RD-73-143] 18 p2104 N73-27019

Directional coupler design using coplanar waveguides for microwave integrated circuits
[AD-760533] 18 p2124 N73-27166

Wideband SHF ferrite microelectronics
19 p2236 N73-28025

Applications of inverse Fourier transform method of producing high peak power for use with solid state radio beacon - Vol. 2
[AD-761526] 19 p2247 N73-28116

Analysis of power loss for coupled transmission and reaction resonator circuits
[AD-762252] 19 p2248 N73-28126

Design of low cost highly sensitive SHF microwave components
[NHK-LABS-NOTE-163] 20 p2381 N73-29129

Design and performance of semiconductor limiters for microwave isolation
[AD-762168] 20 p2463 N73-29794

Status of microwave equipment development in Poland with emphasis on research projects and higher education
21 p2607 N73-30897

Minority carrier lifetime and switching time of step recovery diode for pulse generators in microwave equipment
[FTZ-A-651-TBF-3] 22 p2643 N73-31180

Optimized sensitivity of computer controlled microwave spectrometer for trace element detection
[BMVG-FBWT-73-18] 23 p2754 N73-32037

MICROWAVE FILTERS
Selective bandpass resonators using bandstop resonator pairs for microwave frequency operation
[NASA-CASE-GSC-10990-1] 17 p2003 N73-26195

Resonator design for low cost microwave bandpass filter
[NHK-LABS-NOTE-162] 20 p2381 N73-29128

MICROWAVE FREQUENCIES
NT C BAND
NT EXTREMELY HIGH FREQUENCIES
NT SUPERHIGH FREQUENCIES

Biological effectiveness of microwave field and human tolerance
[JPRS-57209] 01 p0009 N73-10073

Combined radar-radiometer for remote sensing at microwave performance
[NASA-CR-128492] 03 p0265 N73-12145

Computer simulation of ion heating by pulsed microwaves
[CONF-720705-1] 03 p0336 N73-12739

Procedures for measuring radar cross section areas of extremely small objects in superhigh frequency ranges
[AD-749788] 05 p0515 N73-14186

Performance of scanning acoustical imaging telescope at microwave frequencies
07 p0820 N73-16648

Curves for solving low angle radar transmission problems at microwave frequencies over ocean surface
[TR-72-31] 08 p0885 N73-17165

Diversity techniques for airborne communications in presence of ground reflection multipath
[AD-752249] 08 p0887 N73-17178

Ultrasonic radiation and microwave research projects
[AD-752055] 08 p0944 N73-17736

Analysis of electron cyclotron heating characteristics and generation of hot electron plasma in magnetic mirror trap by microwaves
[IPPJ-140] 08 p0947 N73-17755

Microwave frequency reflection characteristics of quasi-tapered anechoic chamber for radar echo tests
[AD-754203] 10 p1138 N73-19275

Evaluation of magnetic permeability tensors of polycrystal ferrimagnetic materials in saturated state for microwave frequencies
[REPT-9.441] 10 p1190 N73-19683

Microwave emissivity and sea brightness temperatures of surface waves
[AD-753533] 11 p1287 N73-20443

Type 4 solar radio bursts and their relation to expanding magnetic bottles
[NASA-TM-X-66217] 11 p1336 N73-20844

Microwave surface resistance of niobium tantalum - and lead indium-superconducting alloys considering thermodynamic vortices
[AD-757875] 15 p1822 N73-24770

Elimination of principal source of energy loss in microwave acoustic transducers
16 p1880 N73-25216

Multimode antenna feed system for microwave and broadband communication
[NASA-CASE-GSC-11046-1] 19 p2234 N73-28013

Dielectric properties of ice, snow, and water at microwave frequencies and thickness measurements of ice and snow layers with radar
[CRC-1242] 21 p2537 N73-30341

Application of microwave radar for monitoring tropopause level to determine dynamic instability and turbulence generation in clear atmosphere
[NOAA-TR-ERL-243-WPL-21] 22 p2665 N73-31353

Microwave heating of electron plasma
[CONF-720705-8] 24 p2959 N73-33642

MICROWAVE IMAGERY
Earth resources laboratory data system for analyzing and processing multispectral, radiometric, photographic, and passive microwave imagery data
[NASA-CR-128693] 07 p0758 N73-16160

Equipment certification and process verification methods for photographic processing control of ERTS images
18 p2211 N73-27854

Microwave holography describing lateral and axial resolution, computerized wave front reconstruction, and application to moving objects
[REPT-6-72] 20 p2425 N73-29484

Microwave imagery of Great Lake ice formations
22 p2736 N73-31903

MICROWAVE INTERFEROMETERS
Radio astronomy observation of planet Saturn using interferometer at 21.1 centimeters wavelength
[AD-760014] 18 p2198 N73-27746

MICROWAVE OSCILLATORS
NT BACKWARD WAVE TUBES

Transferred electron and avalanche diodes and solid state materials, for solid state microwave oscillators and amplifiers
[AD-748241] 04 p0460 N73-13755

Trends in microwave solid state power generation
[AD-749503] 05 p0499 N73-14063

Automatic measurement of frequency stability of microwave Gunn diode oscillators at low temperatures noting graphs of power and frequency against time
[SRDE-72013] 05 p0520 N73-14226

Microwave generator using Gunn effect for magnetic tuning
[NASA-CASE-NPO-12106] 06 p0645 N73-15235

Use of very high Q superconducting microwave cavities to obtain strong coupling between electromagnetic field and Josephson junction
[AD-749986] 06 p0710 N73-15795

Properties of evaporated Josephson junctions coupled to high q superconducting microwave cavities
[AD-749981] 06 p0710 N73-15796

Analysis of subharmonically injection locked microwave IMPATT diode oscillators to improve frequency stability and noise characteristics
10 p1133 N73-19237

Microwave UHF and SHF semiconductor oscillators and power amplifiers, noting gunn and impatt diode solutions, and integrated circuit development
[DLR-MITT-73-06] 10 p1135 N73-19248

Phase shift variations of platinotron microwave amplifier oscillator for pulse radar and steerable antennas
[DLR-MITT-73-03] 12 p1379 N73-21187

Technical study of tunnel diode and its microwave amplification and oscillation
[AD-756932] 13 p1503 N73-22183

Manufacturing of Gunn diodes with short domainless ISA mode for microwave oscillators with 100 W output
15 p1757 N73-24238

Research and development progress on solid state microwave oscillator and amplifier
[AD-758244] 15 p1757 N73-24241

Phase locking of reflex klystron with stable microwave source
[AD-758677] 16 p1882 N73-25235

Research and development on microwave oscillators, diode structures, and ion implantation and diffusion
[AD-759542] 17 p1998 N73-26161
Characteristics of subharmonically injection locked microwave diode oscillators
[AD-759540] 17 p2004 N73-26208
Superconducting cavity stabilized oscillator of high stability
[AD-760339] 17 p2006 N73-26221
Nonlinear and parametric effects on synchronization and mixing of electron transfer microwave oscillators
18 p2123 N73-27155
Design, construction, and performance of Gunn local oscillator for radio receiver applications
[SRDE-72028] 20 p2376 N73-29091
Frequency domain analysis on noise in avalanche diode microwave oscillator
22 p2641 N73-31166
Solid state avalanche diodes for use as microwave amplifiers and oscillators
[NASA-CR-132300] 22 p2642 N73-31172
Selection of step recovery diodes for microwave frequency multipliers, noting frequency conversion efficiency
[FTZ-A-46-TBR-5] 22 p2642 N73-31174
Dynamic characteristics of microwave synchronized oscillators
22 p2643 N73-31185
Noise in microwave semiconductor oscillators and amplifiers
[AD-764259] 22 p2644 N73-31188

**MICROWAVE PLASMA PROBES**
Microwave signal interaction with plasma medium
[AD-746677] 02 p0144 N73-11164
Microwave reflection from electron density ramps produced behind shock waves in nitrogen oxygen mixtures
07 p0824 N73-16682
Microwave measurements of electron density profiles in mirror contained plasma
[UCRL-51348] 19 p2323 N73-28685

**MICROWAVE PROBES**
NT MICROWAVE PLASMA PROBES
Materials and devices for generation, amplification, and millimeter wave energies
[NASA-CR-130113] 03 p0334 N73-12724
Microwave probe studies on chemical additives behavior in nitrogen oxygen plasma
[AD-748469] 04 p0456 N73-13724
Microwave measurements and Skylab S193 analysis of wind field over ocean
[CONTRIB-118] 06 p0663 N73-15384

**MICROWAVE RADIATION**
U MICROWAVES

**MICROWAVE RADIOMETERS**
Airborne and satellite-borne, microwave radiometer, remote sensing systems
[CRC-1231] 02 p0172 N73-11387
Microwave radiometer technique for detecting and identifying man-made objects and discriminating them from natural objects
[DREO-R-661] 04 p0449 N73-13669
Infrared and microwave radiometric data of intertropical convergence zone acquired by Nimbus 3 satellite
[NASA-TM-X-66203] 10 p1188 N73-19669
Airborne electrical scanning microwave radiometric measurements of soil moisture in Texas, California, and Arizona
[NASA-CR-130204] 11 p1284 N73-20423
Passive microwave radiometry and its application to earth resources surveys
[ESRO-CR-116] 13 p1530 N73-22402
Calibration and operational characteristics of highly sensitive microwave radiometers
[AD-756563] 13 p1531 N73-22406
Application of airborne microwave radiometers for remote monitoring of soil moisture in selected areas of Texas and Oklahoma
[NASA-CR-133102] 17 p2031 N73-26438
Application of airborne microwave radiometry for remote sensing of soil moisture in southwest US
[NASA-TM-X-66265] 17 p2032 N73-26444
Skylab 4 microwave radiometry of lake and sea ice in Gulf of St. Lawrence and Lake Ontario
[E73-10820] 18 p2140 N73-27295
Determination of sea surface conditions using Skylab L-band and Radscat passive microwave radiometers
[E73-10847] 19 p2291 N73-28425
Atmospheric effects on radiometric measurements using EREP of Skylab
[E73-10857] 19 p2292 N73-28434
Passive microwave radiometry for remote sensing of earth resources and environmental monitoring programs
[ESRO-CR-75] 19 p2295 N73-28458
Determination of sea surface conditions using Skylab passive L-band and Radscat microwave radiometers
[E73-10911] 20 p2397 N73-29260
Meteorological interpretations of images from Nimbus 5 with electrically scanned microwave radiometer
[NASA-TM-X-70424] 20 p2448 N73-29671
Description of Breguet 1150 to be used as European earth resources survey aircraft noting sensor payload
21 p2538 N73-30353
Characteristics of microwave radiometer scatterometer system for Skylab program
22 p2671 N73-31394
Skylab S-193 RADSCAT measurements of Hurricane Ava
[E73-11062] 23 p2781 N73-32238
Photochemical ozone theory and microwave spectroscopy using microwave radiometry for remotely verifying mesospheric ozone diurnal variations
[AD-764705] 23 p2789 N73-32314
Electronic scanning microwave radiometer system for measurement of meteorological, geomorphological, and oceanographic parameters from Nimbus 5
[NASA-CR-132812] 23 p2793 N73-32342

**MICROWAVE REFLECTOMETERS**
Electron density determination in thermodynamic equilibrium behind reflected shock wave in air, using microwave reflectometer in shock tube
[ISL-43/71] 16 p1889 N73-25288

**MICROWAVE RESONANCE**
Application of microwave-optical double resonance spectroscopy to analyze structural properties of phosphorescent triplet states of organic molecules
[COO-3435-6] 12 p1405 N73-21398
Magnetic phenomena in solid state physics
[COO-3150-10] 16 p1953 N73-25803
Continuous wave dye laser for studying interaction of electromagnetic radiation with matter
[AD-762370] 19 p2309 N73-28572

**MICROWAVE SCATTERING**
Microwave breakdown at waveguide antenna discharge into ionized gas media
[AD-748830] 04 p0455 N73-13717
Microwave scattering from plasma turbulence
[AD-752149] 08 p0886 N73-17175
Scattering in transhorizon ultrahigh frequency radio link due to rain
17 p1995 N73-26133
Calculation of Mie differential scattering cross section of spherical particles with complex refractivity, for mm wave propagation through precipitation
[FTZ-A-455-TBR-35] 22 p2633 N73-31100

**MICROWAVE SENSORS**
Signal ratio measurements for determining terminal invariant parameters in microwave system calibration
[SC-DR-72-0315] 04 p0395 N73-13216
Status of microwave equipment development in Poland with emphasis on research projects and higher education
21 p2607 N73-30897
Contamination of sensors installed in spacecraft and recommendations for eliminating or correcting
[NASA-TM-X-70487] 24 p2926 N73-33367

**MICROWAVE SPECTRA**
Extension of frequency spectrum and improvement of semiconductor devices and techniques in microwave spectrum
[AD-753266] 09 p1044 N73-18514
Absolute polarization and microwave optical photoselection spectroscopy of zerofield transitions of triplet state
[AD-759996] 17 p1993 N73-26115
Iron-absorption band analysis for discrimination of iron rich zones using ERTS-1 imagery
[E73-10789] 18 p2137 N73-27265
Statistical analysis on flux density spectra of solar microwave bursts
19 p2334 N73-28779
Application of spectroscopic methods in remote sensing for determining structure of microwave spectra in earth atmosphere
22 p2692 N73-31563
Photochemical ozone theory and microwave spectroscopy using microwave radiometry for remotely verifying mesospheric ozone diurnal variations
[AD-764705] 23 p2789 N73-32314

**MICROWAVE SWITCHING**
Design and fabrication of microwave reciprocal latching ferrite phase shifters
[AD-763216] 21 p2519 N73-30204

**MICROWAVE TRANSMISSION**
Measurement of accelerator tube and waveguide system parameters for improving linear accelerator performance
[RISO-M-1518] 07 p0766 N73-16223
Theoretical and experimental studies on microwave transmission through hypersonic air plasma generated about blunt wedge
[SC-CR-72-3164] 12 p1434 N73-21621
Finite element calculation on transmission line characteristics for coplanar waveguide
[AD-760756] 18 p2119 N73-27135
Diversity and selection effects for improving microwave relay link performance
[AD-756605] 18 p2120 N73-27141

**MICROWAVE TUBES**
NT BACKWARD WAVE TUBES
NT CATHODE RAY TUBES
NT CELESCOPES
NT IMAGE ORTHICONS
NT IMAGE TUBES
NT KLYSTRONS
NT MAGNETRONS
NT MICROWAVE OSCILLATORS
NT PHOTOMULTIPLIER TUBES
NT THERMIONIC DIODES
NT THYRATRONS
NT TRAVELING WAVE TUBES
Current distribution estimates for microwave power tube with depressed multistage collector
[NASA-TM-X-2651] 01 p0032 N73-10251
Electrostatic charged particle collector containing stacked electrodes for microwave tube
[NASA-CASE-LEW-11192-1] 04 p0395 N73-13208
Very high stability microwave oscillator with Q superconducting cavity
[AD-763684] 21 p2518 N73-30196
Polish institutes involved in research and development of microwave tubes and recommendations for new research projects
21 p2608 N73-30900

**MICROWAVES**
NT MICROWAVE EMISSION
NT MILLIMETER WAVES
Research on biological effects of microwave radiation
[MBL-1972-5] 01 p0008 N73-10060
Abstracts on microwave radiation effects on human and animal physiological functions and life expectancy
[MBL-1972-6] 01 p0008 N73-10061
Techniques for generation and processing microwave signals using elastic, electromagnetic and carrier space charge waves in solid media
[AD-747047] 02 p0220 N73-11782
Mathematical analysis and curve plotting for microwave physics
[AD-747035] 03 p0337 N73-12746
Corrections for sidewall waveguide slots to microwave transmission data for shock-ionized air
[AD-748075] 03 p0343 N73-12801
Microwave coupled stripline, surface crack detector, using pair of conductors over ground to support propagation in two orthogonal TEM modes
[AD-749799] 05 p0549 N73-14462
Biological effects of microwave irradiation on humans - literature review
[UR-3490-29] 06 p0630 N73-15120
Response of pituitary-thyroid axis to microwave radiation
[VR-3490-149] 06 p0630 N73-15122
Literature review of experimental studies to assess relationship of exposure to microwaves and subsequent development of cataracts
[UR-3490-103] 06 p0631 N73-15123
Mathematical models for predicting microwave breakdown in fringing field of rectangular slot antenna
[AD-751320] 07 p0763 N73-16202
Microwave acoustic signal processing with time-variant distributed networks using surface amplifiers
07 p0820 N73-16649
Observations and characteristics of 1.35-cm emissions of water vapor in galactic sources
07 p0837 N73-16787
Augmentation of signal transmission using microwave radio relay systems
[JPRS-58044] 08 p0885 N73-17162
Focusing and deflection of microwave acoustic bulk wave
[AD-753385] 09 p1009 N73-18233
Short-duration solar microwave bursts and associated soft X ray emission
[NASA-CR-130859] 09 p1081 N73-18816
Research progress in electro-optics, plasma physics, microwaves, wave propagation, telecommunication, data processing
[AD-753710] 09 p1102 N73-18993
Superhigh frequency emission of collisionless magnetized plasma on its interaction with pumping wave in microwave range
[AEC-TR-7373] 10 p1197 N73-19736
Electromagnetic response of Pb superconducting film as function of magnetic field in microwave range
[ISS-72/5] 10 p1199 N73-19756
Remote sensing equipment to ensure efficiency in microwave electric power transmission to remote receiving stations
[NASA-CASE-MFS-21470-1] 11 p1264 N73-20257
Evolution of nondestructive testing techniques arising from holography and microwaves
[AD-755116] 11 p1304 N73-20580
Definitions for specifying frequency stability for measurements in frequency and time domains
[NBS-TN-632] 12 p1378 N73-21174
Quenching of beam plasma instability by mode mixing at density discontinuity
[AD-755658] 12 p1436 N73-21637
Two cavity spectrometer for studying microwave transmission through gallium single crystals
12 p1438 N73-21647
Infrared stars with strong 1665-1667-mHz main-line OH emission
[AD-753898] 12 p1459 N73-21821
Thermal effects of microwave and radio frequency radiation on biological systems
[MBL-1971-7-PT-1] 14 p1609 N73-23048
Measurements and predictions of loss and multipath variations for microwave troposcatter communication link
[AD-757553] 14 p1635 N73-23256

Generation and processing of microwave signals using elastic, electro-magnetic, and carrier space charge waves in solid media
[AD-757555] 14 p1699 N73-23784
Power equation theory for defining ultrahigh frequency and microwave measurements
[NBS-TN-637] 15 p1750 N73-24182
Analysis of electron number density and collision frequency levels behind reflected shock waves and shock wave interactions in argon
16 p1887 N73-25275
Agricultural study using microwave radiation from Cosmos 243 satellite over European USSR
[NASA-TT-F-14952] 16 p1944 N73-25732
Use of spaceborne microwave radiation measurements to detect fires, subsurface water, and surface temperature
[NASA-TT-F-14975] 17 p1998 N73-26153
Power spectral analysis of solar 2 cm microwave intensity data
[NASA-CR-133228] 17 p2079 N73-26820
Microwave techniques for nondestructive evaluation of flaws in materials
19 p2304 N73-28524
Stability of microwaves generated by intense relativistic electron beam in rippled magnetic field
[AD-763337] 21 p2508 N73-30126
Microwave radiation effects on rat tissues and length of survival
21 p2608 N73-30904
Perturbation technique for determining microwave interactions in magnetized waveguide plasma
22 p2702 N73-31643

**MICROWEIGHING**
U WEIGHT MEASUREMENT

**MICTURITION**
U URINATION

**MIDAIR COLLISIONS**
Development of statistical-probabilistic method of collision probability calculation and application to arbitrary flight paths and vehicle shapes
[AD-744722] 01 p0006 N73-10046
Investigation of midair collision between commercial DC 9 aircraft and Marine Corps F-4B aircraft at Duarte, California on 6 June 1971
[NTSB-AAR-72-26] 03 p0252 N73-12037
Differential game theory for optimal collision avoidance between two aircraft moving in horizontal plane
[NASA-CR-129988] 05 p0577 N73-14701
Analysis of aeromedical factors leading to midair collisions and recommended actions to avoid collisions
[AD-758189] 14 p1604 N73-23005
Aircraft accident involving midair collision of Convair 340 and DHC-6 near Appleton, Wisconsin on 29 June 1972
[NTSB-AAR-73-9] 17 p1981 N73-26016
Performance of pilots under simulated conditions to determine response to anti-collision warnings
[FAA-AM-73-6] 18 p2104 N73-27015
Development and characteristics of electronic signalling system and data processing equipment for warning systems to avoid midair collisions between aircraft
[NASA-CASE-LAR-10717-1] 21 p2576 N73-30641
Statistical analysis of Civil Aviation midair collisions occurring during period January 1964 to December 1971
[MTR-6334] 22 p2614 N73-30946
Reduction of midair collision hazard with bats through tracking by radar and use of high intensity lights
[AD-764828] 23 p2746 N73-31982
Bird migration patterns using radio transmitters with application to reduction of aircraft hazards during migration in congested air routes
[AD-764830] 23 p2746 N73-31983

**MIDCOURSE GUIDANCE**
Design of Penguin missile inertial navigation system for midcourse guidance
11 p1320 N73-20711

**MIDCOURSE TRAJECTORIES**
Aerospace engineering including materials, orbits and trajectories, power sources, satellite geodesy, and structural engineering
[NASA-CR-128329] 01 p0119 N73-10981
Summary of Pioneer 10 mission objectives and midcourse maneuver strategies
01 p0120 N73-10987

**MIDDLE EAR**
Middle ear barotrauma effect on work capacity and flight fitness of flying personnel
13 p1481 N73-22000
Middle ear muscle reflex thresholds to various aircraft noises
[AD-764739] 24 p2886 N73-33048

**MIDLATITUDE ATMOSPHERE**
Mathematical models of midlatitude bottomside electron density profiles
[AD-751267] 07 p0796 N73-16477
Electron density irregularities and evening anomalies in midlatitude nighttime F region
13 p1514 N73-22270

**MIDLATITUDES**
U TEMPERATE REGIONS

**MIE SCATTERING**
NT RAYLEIGH SCATTERING
Mie scattering of interplanetary magnetic field by whole moon
[NASA-TM-X-62225] 07 p0844 N73-16833
Laser operation in vacuum and active scattering particle spectrometers
[NASA-CR-124111] 10 p1159 N73-19425
Calculation of Mie differential scattering cross section of spherical particles with complex refractivity, for mm wave propagation through precipitation
[FTZ-A-455-TBR-35] 22 p2633 N73-31100

**MIE THEORY**
U MIE SCATTERING

**MIGRATION**
Changes in continental migratory bird and wildlife habitats
[E72-10235] 03 p0288 N73-12335
Migration corridors for ducks and geese and effects on aviation safety
[AD-748114] 04 p0382 N73-13109
Monitoring continental migratory bird habitats
[E73-10065] 07 p0779 N73-16327
Study of continental migratory bird habitat changes using ERTS-1 imagery
[E73-10334] 09 p1025 N73-18364
Appraisal of changes in migratory bird habitats based on ERTS-1 imagery of North Dakota
[E73-10534] 13 p1518 N73-22298
Helium migration in aluminum matrices under temperature gradients
16 p1926 N73-25586
ERTS-1 and aircraft multispectral scanner data for mapping ponds and lakes near Woodworth, North Dakota to determine changes in continental migratory bird habitat
[E73-10714] 17 p2018 N73-26321
Appraising changes in continental migratory bird habitats in North Dakota using Skylab EREP system
[E73-10972] 22 p2657 N73-31284
Utilization of Skylab EREP system for appraising changes in continental migratory bird habitats
[E73-11079] 23 p2782 N73-32254

**MILITARY AIR FACILITIES**
Visual investigation of runway and taxiway pavements at Campbell Army Airfield, Fort Campbell, Kentucky
[AD-743462] 01 p0037 N73-10291
Visual inspection of runway conditions at Fort Polk Army Airfield, Louisiana
[AD-743858] 01 p0037 N73-10292
Visual inspection of runway conditions at Butts Army Airfield, Fort Carson, Colorado
[AD-743859] 01 p0037 N73-10293
Visual inspection of runway pavement conditions at Forney Army Airfield, Fort Leonard Wood, Missouri
[AD-743856] 01 p0037 N73-10294
Visual inspection of runway conditions at Redstone Army Airfield, Huntsville, Ala.
[AD-743857] 01 p0037 N73-10295
Visual survey of runway and taxiway conditions at Davison Army Airfield, Fort Belvoir, Virginia
[AD-743463] 01 p0038 N73-10296
Structural evaluation of cellular plastic as base course material for military expedient pavement to withstand limited number of aircraft coverages
[AD-747048] 02 p0153 N73-11244
Automatic controlled pressure system for onshore fueling of navy aircraft
[AD-748211] 04 p0489 N73-13997
Evaluation of aluminum 1 by 12 ft extruded light-duty landing mat with symmetrical butt-type end connectors
[AD-752079] 08 p0893 N73-17233
Terrain factor analysis and automatic color coded mapping using image processing methods in estimation of construction time relative to prospective military airfields
[AD-755531] 13 p1526 N73-22367
Emplacement and maintenance of dust control materials for military aircraft and helicopter landing facilities
[AD-756179] 14 p1647 N73-23359
Air traffic control facilities operated by U.S. military forces and developments in improved air traffic control systems
14 p1687 N73-23690
Catalogue indexes to local weather forecasts
[AD-760091] 17 p2058 N73-26648
Guidelines for evaluation and maintenance of expedient-surfaced airfield facilities
[AD-762126] 19 p2249 N73-28137
Installation of XM19 airfield landing mat and ancillary items
[AD-762137] 20 p2383 N73-29148
Preliminary analysis of possible factors associated with asphaltic concrete airfield pavement defects
[AD-762404] 20 p2383 N73-29150
Short-range terminal weather forecasting techniques in AWS
[AD-762938] 20 p2451 N73-29699

**MILITARY AIRCRAFT**
Effectiveness of DOD guidelines in determining time of aircraft engine replacements
[AD-745396] 01 p0091 N73-10749
Development of usage rate system to determine logistics requirements for military aircraft support
[AD-746482] 02 p0127 N73-11034
Statistical analysis of normal acceleration, airspeed, altitude, and flight loads on military aircraft
[AD-747285] 02 p0127 N73-11035
Design, development, and evaluation of aircrew restraint system for forward-facing, nonejection seat for military aircraft
[AD-746631] 02 p0128 N73-11038
Development of airframe integrity investigation procedures to determine structural deficiencies and modifications required to airframes for increased service life
[AD-746881] 03 p0253 N73-12049
Performance characteristics of self lubricating sintered sulfur-iron material used for bushings in naval aircraft
[AD-748175] 03 p0319 N73-12603
Development of optical data communication systems with fiber optics for military avionics
[AD-747946] 03 p0337 N73-12748
Development of equations and mathematical models for decision making concerning military logistics, aircraft, space parts, and support equipment
[AD-747972] 03 p0368 N73-12997
Development of flight path optimization procedure to minimize flight time of aircraft returning to aircraft carrier
[AD-749326] 04 p0447 N73-13653
Forecasts of military air traffic activity and effect on air traffic control facilities for 1972 through 1983
05 p0493 N73-14014
Proceedings of conference on fluid dynamics of aircraft stalling to include stall and post-stall aerodynamic characteristics of various military aircraft
[AGARD-CP-102] 06 p0616 N73-14998
Aerodynamic design, engineering development, and flight testing of naval aircraft for operation at high angles of attack
06 p0618 N73-15020
Application of infrared technology for measuring infrared radiation emitted by military aircraft
[AD-749798] 06 p0623 N73-15058
Effects of various external stores characteristics, spanwise positions, and Mach number on static longitudinal stability of several military aircraft
[AD-750120] 06 p0624 N73-15063
Portable instrumentation kit feasibility study
[AD-751188] 07 p0802 N73-16514
Correlation between full scale fatigue test failures and actual service failures for several military aircraft
07 p0851 N73-16901
Fatigue life prediction of military aircraft under three different load spectra
07 p0851 N73-16903
Relation between measured C.G. vertical accelerations and loads at T-tail of military aircraft
07 p0851 N73-16904
Design criteria for satisfactory stability and control of military aircraft
08 p0865 N73-16996
Performance of auxiliary power systems for advanced Army rotary wing aircraft
[AD-751854] 08 p0870 N73-17046
Formulation of automatic inspection, diagnostic, and prognostic system for maintenance of army aircraft - Vol. 1
[AD-752882] 09 p0988 N73-18062
Design and tradeoff studies applied to automatic inspection, diagnostic, and prognostic maintenance system for military aircraft - Vol. 2
[AD-752883] 09 p0988 N73-18063
Technical proposal and development plan for automatic inspection, diagnostic, and prognostic maintenance system for military aircraft - Vol. 3
[AD-752884] 09 p0988 N73-18064
General specification for automatic inspection, diagnostic, and prognostic maintenance system for military aircraft - Vol. 4
[AD-752885] 09 p0988 N73-18065
Computer models for application to automatic inspection, diagnostic, and prognostic system for maintenance of military aircraft - Appendix C
[AD-752886] 09 p0988 N73-18066
Computer output data for automatic inspection, diagnostic, and prognostic system for maintenance of military aircraft - Appendix D
[AD-752887] 09 p0988 N73-18067
Maintenance data tabulations for automatic inspection, diagnostic, and prognostic systems for military aircraft maintenance - Appendix E
[AD-752888] 09 p0988 N73-18068
Cost effectiveness of automatic inspection, diagnostic, and prognostic maintenance system for military aircraft - Appendix F
[AD-752889] 09 p0988 N73-18069
Analysis of air pollution caused by exhaust from military aircraft engines and development of technology for pollutant measurement to meet EPA standards
[AD-753095] 09 p1100 N73-18975
Application of loran/inertial hybrid system and Kalman filter algorithm to fixed feedback gain
11 p1318 N73-20701

Development of navigation system design factors through computerized simulation for application to loran/inertial hybrid system
[AD-754548] 11 p1322 N73-20731
Methods for meeting terrain intelligence needs of airmobile division in tactical situation
[AD-756191] 13 p1531 N73-22411
Silicone base nonflammable hydraulic fluid to aid wear resistance in military aircraft
[AD-758361] 14 p1671 N73-23562
Development and characteristics of air traffic management system for operation of military aircraft under instrument meteorological conditions
14 p1689 N73-23704
Development and characteristics of forward area homing and landing guidance for military aircraft operations
14 p1689 N73-23708
Tactical integrated electronic systems for Swedish military aircraft
14 p1711 N73-23889
Feasibility study of applying air lubricated bearings to gas turbine engines for military aircraft
[AD-757869] 15 p1793 N73-24537
Statistical analysis of counting accelerometer data obtained on Navy and Marine fleet aircraft from 1 Jan. 1962 to 1 Jan. 1972
[AD-760321] 17 p1985 N73-26041
Hydrolytic stability of polyurethane potting compounds in Navy aircraft
[AD-759972] 17 p2053 N73-26604
Simultaneous equation production functions for decisions pertaining to sea-based tactical air resources
17 p2054 N73-26612
Proceedings of conference on military applications of V/STOL aircraft to include current and proposed research projects to meet military requirements
[AGARD-CP-126-VOL-1] 18 p2102 N73-27000
Review of V/STOL aircraft research and development programs to increase effectiveness of aircraft and develop mission improvements
18 p2102 N73-27001
Design concept, operational performance, and military employment of AV-8A Harrier aircraft
18 p2103 N73-27005
Design, development, and flight characteristics of VAK 191 B V/STOL strike/reconnaissance aircraft
18 p2103 N73-27006
Design, development, and requirements for short takeoff transport aircraft for military applications using civil aircraft production procedures
18 p2103 N73-27011
Development of digital computing system for synthesis and optimization of military flight vehicle preliminary designs
[AD-760568] 18 p2108 N73-27045
Analysis of military aircraft refueling and rearming operations in forward areas to show organization, doctrine, and equipment - Vol. 1
[AD-760524] 18 p2108 N73-27046
Analysis of military aircraft refueling and rearming operations in forward areas to show organization and equipment required - Vol. 2
[AD-760525] 18 p2108 N73-27047
Analysis of US Navy aviation combat casualty experiences in Southeast Asia to determine effectiveness of rescue and recovery operations under combat conditions
[AD-761636] 19 p2228 N73-27972
Development of method for determining cost functions involving aircraft rework and engine repair programs at military installation
[AD-761475] 19 p2249 N73-28135
Computer simulation of aircraft motions and propulsion system dynamics for YF-12 aircraft under supersonic conditions
[NASA-TM-X-62245] 20 p2361 N73-28990
Analysis of voice command systems for application to military aircraft operation to show manufacturers, specifications, and research projects
[AD-762922] 20 p2362 N73-28998
Ground vibration tests of YF-12 aircraft to determine frequency response data, measured node lines, and elastic mode shapes for aircraft components
[NASA-TM-X-2880] 20 p2483 N73-29944
Application of reinforced fiberglass thermoplastic materials for construction of military aircraft structures
[AD-763470] 21 p2498 N73-30044
Effect of inflated air cushion landing gear on subsonic static stability of high performance aircraft operating out of ground effect
[AD-763365] 21 p2498 N73-30048
Pilot knee ejection clearances for Canadian military aircrafts
[DCIEM-936] 23 p2741 N73-31938

**MILITARY AVIATION**
Chemistry research program for Air Force
[AD-749544] 05 p0507 N73-14124
Safety standards for Air Force nuclear weapons systems
[AD-759574] 17 p2062 N73-26681
Color vision standards for flying military aircrews
[FPRC/1319] 19 p2225 N73-27942
Bibliography of anthropometric information for Air Force human factors engineering
[AD-762287] 19 p2229 N73-27978

**MILITARY HELICOPTERS**
NT CH-3 HELICOPTER
NT CH-47 HELICOPTER
NT H-53 HELICOPTER
NT OH-6 HELICOPTER
NT OH-13 HELICOPTER
NT S-67 HELICOPTER
NT UH-1 HELICOPTER
NT UH-2 HELICOPTER
Development of in-flight fire detection and automatic suppression system for use on military helicopters
[AD-746630] 02 p0127 N73-11037
Development of forward area refueling equipment for servicing military helicopters
[AD-746249] 02 p0154 N73-11245
Design criteria for load suspension points, slings, and lifting equipment used on military helicopters
[AD-747814] 03 p0307 N73-12508
Analysis of military helicopter formation flight techniques with emphasis on station keeping based on nominal point coordinate system
[AD-751459] 07 p0740 N73-16021
Development of automatic inspection diagnostic and prognostic systems for maintenance of military helicopters - Vol. 1
[AD-752893] 09 p0987 N73-18060
Development of automatic inspection diagnostic and prognostic systems for maintenance of military helicopters - Vol. 2
[AD-752894] 09 p0987 N73-18061
Development and characteristics of dual cargo hook system for use on military transport helicopters
12 p1358 N73-21022
Analysis of military helicopter control and stability characteristics to determine suitability as rocket launching platform
[AD-756436] 13 p1474 N73-21944
Analysis of H-58 helicopter maintenance to determine removal rate of aircraft equipment and develop failure analysis statistics
[AD-756406] 13 p1475 N73-21945
Computerized simulation of containership loading and unloading of heavy lift helicopters for military logistic applications
[AD-756865] 13 p1475 N73-21946
Evaluation of performance of H-1 helicopter, CH-54 helicopter, and OH-6 helicopter under combat conditions
[AD-755554] 13 p1475 N73-21949
Design, fabrication, and evaluation of mechanical devices for supporting external stores on military helicopters
[AD-755532] 13 p1535 N73-22436
Controlled magnetic and electric excitation of airframe of LOH-6A helicopter and measurement of impedance, radiation patterns, and bandwidths
[AD-757143] 14 p1602 N73-22992
Low temperature tests of elastomeric bearing rotors on OH-58 helicopter
[AD-759957] 17 p2038 N73-26490
Analysis of military aircraft refueling and rearming operations in forward areas to show organization, doctrine, and equipment - Vol. 1
[AD-760524] 18 p2108 N73-27046
Analysis of military aircraft refueling and rearming operations in forward areas to show organization and equipment required - Vol. 2
[AD-760525] 18 p2108 N73-27047
Development of analytic models for describing differential models of attack helicopters supporting a battalion task force - Vol. 1
[AD-762432] 19 p2356 N73-28956
Numerical analysis of military helicopters and air defense weapons to define operations in support of battalion task force combat - Vol. 2
[AD-762433] 19 p2356 N73-28957
Analysis of failure modes of tail rotor on OH-58 helicopter for improved reliability and cost reduction
[AD-763188] 21 p2497 N73-30043
Test data and description of unsymmetrical crash analysis computer program for improved helicopter structural crashworthiness analytical and design techniques - Vol. 2
[AD-764986] 23 p2747 N73-31986
Systems analysis of avionics and aircraft equipment for search and rescue helicopters to determine cost effective improvements - Vol. 7
[AD-764914] 24 p2927 N73-33381

**MILITARY PSYCHIATRY**
U MILITARY PSYCHOLOGY

**MILITARY PSYCHOLOGY**
Time-span of discretion as measure of military work and responsibility
[DRAE-M45] 13 p1486 N73-22049

**MILITARY SPACECRAFT**
NT RECONNAISSANCE SPACECRAFT
NT VELA SATELLITES

**MILITARY TECHNOLOGY**
Real time computerized message switching and data transmission systems for military communications network
01 p0026 N73-10206
Automated technical control system for military communications facility
01 p0027 N73-10207
Development of equations and mathematical models for decision making concerning military logistics, aircraft, space parts, and support equipment
[AD-747972] 03 p0368 N73-12997
Procedures for constructing and analyzing combat models for planning and executing naval combat operations
[JPRS-57404] 04 p0393 N73-13194
Military applications of single gun color cathode ray tubes in display devices
[AD-748385] 04 p0396 N73-13222
Extremes of precipitation aloft mandatory for design of military equipment capable of operating at altitude anywhere in world
[AD-747482] 04 p0445 N73-13629
Contributions of military technology, research, and development to civil aviation programs - Vol. 1
[NASA-CR-129572] 04 p0487 N73-13982
Military technology, research, and development contributions to civil aviation programs - Vol. 2
[NASA-CR-129573] 04 p0487 N73-13983
Military technology, research, and development contributions to US aviation advances since 1925 - Exec. Summary
[NASA-CR-129574] 04 p0487 N73-13984
Analysis of factors involved in transfer of technology from Department of Defense developments to solution of problems in civilian community
[B-175132] 04 p0488 N73-13994
Research and development projects conducted to improve weapon systems and to conduct ionospheric and upper atmosphere experiments in Australia
05 p0611 N73-14965
Research and development in Army aviation medical science and problems
[AD-749456] 06 p0631 N73-15129
Research and development projects compiled at Army science conference
[AD-750300] 06 p0732 N73-15973
Performance of auxiliary power systems for advanced Army rotary wing aircraft
[AD-751854] 08 p0870 N73-17046
Radio navigation system for providing all-weather short baseline navigation capability for Army aeronautical missions
[AD-752466] 08 p0942 N73-17715
Bibliography of armed forces research and development bibliographies - Vol. 1
[AD-752150] 08 p0978 N73-17997
Annotated bibliography of military research and development bibliographies - Vol. 2
[AD-752160] 08 p0978 N73-17998
Aircrew escape autogyro ejector seat/flight vehicle
09 p1089 N73-18890
Calculation of ephemeris for Navy navigation satellites
[AD-753807] 09 p1092 N73-18914
Military technology for marine radar design
[AD-754408] 11 p1259 N73-20215
Naval research in aerodynamics, ballistics, mathematics, and physics
[AD-754397] 11 p1268 N73-20292
Air Force heating system for fog dispersal
[AD-754900] 11 p1315 N73-20675
Laboratory tests of accelerometers used in inertial guidance systems in French military programs
11 p1320 N73-20714
Reliability and performance of landbased and shipboard Air Force instrumentation systems
[AD-755916] 12 p1389 N73-21262
Atmospheric density extremes up to 15,000 feet for design of military aircraft
[AD-755791] 12 p1403 N73-21382
Air Weather Service fog dispersal and weather modification program
[AD-755659] 12 p1423 N73-21533
Computerized simulation of containership loading and unloading of heavy lift helicopters for military logistic applications
[AD-756865] 13 p1475 N73-21946
Evaluation of performance of H-1 helicopter, CH-54 helicopter, and OH-6 helicopter under combat conditions
[AD-755554] 13 p1475 N73-21949
Evaluation of helmet weight on head by military personnel
[AD-748412] 13 p1487 N73-22056
Service life and operation of military equipment in subzero Siberian environments
[AD-756478] 13 p1554 N73-22595
Air defense articles written by Soviet military personnel
[AD-755679] 13 p1596 N73-22942
Military and NASA programs using FCC
14 p1642 N73-23318

Laboratory astrophysics research on defense applications of gas ionization, electron scattering, plasmas, and line broadening
[AD-757721] 14 p1695 N73-23753
Conference on human performance under sustained work, and interdisciplinary research
[AD-744782] 14 p1723 N73-23981
Factors for determining army requirements for research
14 p1723 N73-23982
Manufacture of military hardware using powder metallurgy
[DREV-TN-2035/72] 15 p1797 N73-24570
Conference on military research and numerical analysis
[AD-758145] 15 p1804 N73-24620
Military design standard for noise producing equipment
[AD-750649] 16 p1945 N73-25735
Navy research reports on electronics, optical physics, and information systems
[PB-215342/7] 16 p1977 N73-25992
Manpower requirements for aircraft maintenance operations of USAF
[AD-760082] 17 p1991 N73-26097
Safety standards for Air Force nuclear weapons systems
[AD-759574] 17 p2062 N73-26681
Superconductive materials for military rotating electrical machinery
[AD-760330] 17 p2074 N73-26782
Analysis of air space control problems associated with military operations and development of doctrine for improved command and control
[AD-761034] 18 p2176 N73-27573
Research activities for DREV during 1972
[DREV-692/73] 19 p2307 N73-28553
Differential game theory applied to military operations, such as antimissile missile problem and air warfare
[BMVG-FBWT-73-9] 19 p2314 N73-28609
Research projects in environmental and electromagnetic technologies
[AD-761483] 19 p2355 N73-28948
Technology planning objectives and supporting technical goals for Air Force Flight Dynamics Laboratory during Fiscal Year 1974
[AD-762300] 19 p2356 N73-28950
Development of analytic models for describing differential models of attack helicopters supporting a battalion task force - Vol. 1
[AD-762432] 19 p2356 N73-28956
Numerical analysis of military helicopters and air defense weapons to define operations in support of battalion task force combat - Vol. 2
[AD-762433] 19 p2356 N73-28957
Air Force research and technology accomplishments during calendar year 1971
[AD-762269] 19 p2357 N73-28967
Field maintenance and operational experience with various selected models of F-4 aircraft
[AD-762747] 20 p2362 N73-28995
Computer simulated loading of Army Brigade and equipment into several medium short takeoff transport aircraft configurations
[AD-762916] 20 p2362 N73-29002
Military personnel management and human factors engineering
[AD-763168] 21 p2504 N73-30094
Engineering design handbook on infrared systems for military applications
[AD-763495] 21 p2581 N73-30684
Reliability of USAF fire protection systems including portable equipment
[AD-762948] 21 p2610 N73-30925
Ship to shore transportation of military cargo using tethered balloons
[AD-765352] 23 p2747 N73-31987
Combat job performance and training for air cavalry aeroscout pilot and aeroscout observer
[AD-755505] 23 p2753 N73-32027
Military treatment and disposal of high energy materials
[AD-764534] 23 p2858 N73-32835
Advances in technology and armament in USSR
[AD-763323] 23 p2866 N73-32917
Utilization of decision and value theory concepts by helicopter pilots to plan attacks
24 p2950 N73-33565

**MILITARY VEHICLES**

Apparatus for measuring velocity and acceleration of military vehicles
[PHL-1972-5] 01 p0055 N73-10446
Analysis of noise pollution by military vehicles, public transportation, farm equipment, private automobiles, and construction equipment
[AD-747685] 03 p0338 N73-12754
Vibrational effects on visual acuity of human operator seated in military tracked vehicle
[AD-750345] 06 p0636 N73-15172
Method for evaluating physical characteristics of material
[AD-755626] 12 p1467 N73-21892
Cold weather tests on military equipment
[AD-761105] 18 p2214 N73-27881

**MILKY WAY GALAXY**

X ray sources in galactic center and comparison of Aerobee data with Uhuru data
[NASA-TM-X-66114] 03 p0353 N73-12873
Star cluster data used to obtain absorption values for different galactic longitudes in northern part of Milky Way
20 p2471 N73-29842
Fifty-two variable stars in Cepheus-Lacerta field of Milky Way processed on Castel Gandolfo plates
21 p2596 N73-30802

**MILLIMETER WAVES**

Measurement and analysis of depolarization and differential attenuation during propagation of millimeter wave signals through rain
[NASA-CR-130107] 01 p0028 N73-10217
Absorption of 4 to 6 mm wavelength band in atmosphere from zenith attenuation measurements
[AD-745951] 02 p0168 N73-11363
Characteristics of diversity satellite-to-ground communication link measured using ATS 5 15.3 GHz downlink
[NASA-CR-130118] 03 p0265 N73-12144
Characteristics of millimeter attenuation and reflection coefficient measurement system and specifications for waveguide standards fabrication
[NBS-TN-619] 03 p0302 N73-12462
Millimeter and submillimeter wave detection and mixing with superconducting weak links
[AD-754083] 10 p1202 N73-19783
Open resonator with volumetric detector for tunable millimeter and submillimeter receiver
[AD-754829] 11 p1323 N73-20739
Millimeter wave image conversion system for optical display of objects obscured by fog or rain
13 p1489 N73-22074
Utilization of millimeter wave radiation from atmospheric oxygen to provide vertical sensing information to satellite-borne radiometer
[NASA-CR-2229] 13 p1530 N73-22396
Third harmonic generation by indium antimonide magnetoplasma in presence of dc magnetic field
13 p1562 N73-22659
Reduction of probability of simultaneous rainfall on millimeter wave earth satellite space communication terminals
[AD-757506] 14 p1633 N73-23242
Attenuation and fading characteristics of ATS 5 15 and 32 GHz millimeter ground-space links
18 p2212 N73-27856
Semiconductor image conversion panels using millimeter diodes
[AD-762116] 19 p2246 N73-28109
Solar burst observations at millimeter wavelengths
19 p2334 N73-28781
Laboratory model of distributed pin diode millimeter wave phase shifter
[AD-762572] 20 p2381 N73-29136
Lamb dip in millimeter-wave molecular spectroscopy
20 p2454 N73-29719
Physical processes associated with infrared millimeter component of spectra from nuclei of Seyfert galaxies
20 p2469 N73-29834
Development of procedure for measuring short-term instability of millimeter band klystron frequency
22 p2630 N73-31080
Design, fabrication, and tests of ground station hardware for ATS-F millimeter wave experiment
[NASA-CR-132802] 22 p2673 N73-31409
Semiconductor panel modulation for millimeter image conversion
[AD-765418] 23 p2767 N73-32133
Millimeter wave polarimeters and Cotton-Mouton effect in plasmas
[EUR-CEA-FC-675] 24 p2965 N73-33694

**MILLING [MACHINING]**

Analysis of adhesion forces in cutting metals to determine effects of formatting and destruction of adhesive connections on wear of cutting tools
[AD-754041] 11 p1301 N73-20555
Tangent milling and spline approximation techniques for wings
[NAL-TN-33] 15 p1792 N73-24524

**MILLING MACHINES**

Tool positioning holder for grinding by ball nose milling cutter
[NASA-CASE-LAR-10450-1] 01 p0061 N73-10504

**MINE DETECTORS**

Underwater devices for target detection on sea bottom
[JPRS-58916] 14 p1667 N73-23529

**MINERAL DEPOSITS**

Recognition of geologic framework for copper porphyry-type deposits on ERTS-1 imagery
[E72-10210] 02 p0161 N73-11305
Geological and geophysical mapping of mineral resources in Australia and New Guinea
02 p0164 N73-11328
Identification of continental crust geostructures and their relation to mineral resources based on ERTS-1 imagery
[E72-10296] 04 p0410 N73-13346
Major fracture and fault zones of Baltic Shield and their relationships to mineral deposits
[E72-10297] 04 p0411 N73-13347
Recognition of geologic framework of copper and molybdenum porphyry deposits on ERTS-1 imagery of Navada and Utah
[E73-10020] 06 p0659 N73-15356
ERTS-1 imagery of geostructures of Alaskan continental crust and relation to mineral resources
[E73-10321] 09 p1024 N73-18353
Spectral ratio mapping of iron ore deposits in Wind River Range, Wyoming, using ERTS-1 data
[E73-10397] 11 p1276 N73-20359
Search for porphyry copper deposits in Pakistani Baluchistan using ERTS-1 imagery
[E73-10410] 11 p1278 N73-20372
Identification and interpretation of tectonic features and mercury deposited in California coast ranges and western transverse ranges
[E73-10446] 11 p1282 N73-20406
Mineral prospecting in tropical areas by application of geochemical, botanical, geophysical, and remote sensing techniques
[PB-213230] 11 p1289 N73-20456
Identification of geostructures of continental crust and relation to mineral resources
[E73-10496] 12 p1397 N73-21332
Geological investigation of future ocean bottom drilling for crude oil and other raw materials
[JPRS-58668] 12 p1401 N73-21366
Recognition of characteristic geological structures associated with mineral deposits of copper molybdenum porphyry type
[E73-10526] 13 p1517 N73-22293
Application of Earth Resources Experiment Package data to development of commercial mining activities
[MCR-73-62] 13 p1518 N73-22308
Ratio mapping iron ore deposits in Atlantic City District, Wyoming
[E73-10575] 15 p1772 N73-24355
Major fracture and fault zones of Baltic Shield in Finland and relationships to mineral deposits
[E73-10682] 16 p1901 N73-25377
Application of ERTS-1 imagery for mapping major geological structural trends and mineralization zones in Utah and Nevada
[E73-10701] 16 p1903 N73-25393
Mineral yearbook containing domestic industry data
[PB-214329/5] 16 p1905 N73-25411
Identification of copper/molybdenum porphyry mineral deposits in characteristic geologic setting in Nevada, Arizona, Colorado, Australia, Alaska, and New Guinea
[E73-10762] 17 p2023 N73-26362
Identification of geostructures of continental crust and relation to mineral resources
[E73-10787] 18 p2136 N73-27263
Interpretation of geologic, mineral, and water resources in western Colorado from ERTS-1 imagery
[E73-10814] 18 p2139 N73-27289
Application of Skylab multispectral photography to mineral and land resources of South Carolina
[E73-10831] 18 p2141 N73-27301
Mineral resources, geological structures, and landform surveys from ERTS-1 imagery
19 p2289 N73-28408
Recognition of geologic framework for ERTS-1 identification of mineral deposits of copper/molybdenum prophyry type in Colorado, Nevada, Arizona, and Australia
[E73-10960] 21 p2532 N73-30302
Analysis of concept to mine, refine, and transport lunar minerals to earth for terrestrial industries - Vol.1
[NASA-TM-X-62267] 21 p2595 N73-30798
Analysis of technologies and systems required for establishing mining base, mining, refining, and transporting lunar minerals for earth use - Vol.2
[NASA-TM-X-62268] 21 p2595 N73-30799
Photointerpretation of Skylab MSS photography of mineral deposits in Nevada
[E73-10983] 22 p2658 N73-31290
Identification of geostructures of continental crust from ERTS-1 imagery and relationship to mineral resources in Alaska
[E73-11023] 22 p2662 N73-31327
Inventories of mineral deposits and geologic structures in Susquehanna River Basin from Skylab EREP data
[E73-11056] 23 p2780 N73-32232
Geology, mineral deposits, and water resources of western Colorado from Skylab EREP data
[E73-11130] 24 p2917 N73-33285

**MINERAL EXPLORATION**

Mineral exploration in Arizona using ERTS-1 imagery
[E72-10197] 01 p0047 N73-10376
Detection of regional tectonic structures and mineral exploration in Arizona using ERTS-1 imagery
[E72-10218] 02 p0162 N73-11312
Geological and geophysical mapping of mineral resources in Australia and New Guinea
02 p0164 N73-11328

Utility of ERTS-1 imagery in study of geological structures and exploration for economic mineral deposits in Utah and Nevada
[E72-10332] 05 p0531 N73-14320
Utilization of ERTS-1 imagery for mapping large scale structural lineamants in Precambrian Shield and basins containing younger sediments and for mineral and petroleum exploration
[E73-10004] 06 p0658 N73-15340
Photointerpretation of ERTS-1 imagery of Arizona with emphasis on porphyry copper deposits occurring at intersection of major faults and igneous intrusions
[E73-10018] 06 p0659 N73-15354
Evaluation of ERTS-1 imagery for study of geological structures and features and exploration of mineral deposits in Utah and Nevada
[E73-10313] 09 p1022 N73-18345
Utilization of ERTS-1 imagery in structural reconnaissance for minerals and oil in Alaska, Canada, Montana, Colorado, New Mexico, and Texas
[E73-10414] 11 p1279 N73-20376
Mineral exploration in Utah and Nevada based on ERTS-1 imagery of structural fracture and fault trends
[E73-10510] 13 p1516 N73-22285
Relationship of geological structures to iron-rich zones in Nevada based on ERTS-1 imagery
[E73-10555] 14 p1655 N73-23427
Detection of regional tectonic structures related to mineralization in Arizona
[E73-10591] 14 p1657 N73-23450
ERTS-1 applications in water depth calculation, terrain classification, land use mapping, water pollution, and mineral exploration
[E73-10565] 15 p1771 N73-24345
Geologic, mineral, and water resources investigations in western Colorado using ERTS-1 imagery
[E73-10608] 15 p1773 N73-24369
Geologic mapping and mineral resource inventory in South America from ERTS-1 imagery
[E73-10648] 16 p1897 N73-25344
Application of ERTS-1 imagery to determine geological evidence of mineral and hydrocarbon accumulations in Alaska, Canada, Montana, Colorado, New Mexico, and Texas
[PAPER-G30] 19 p2267 N73-28261
Application of ERTS-1 data to geomorphotectonics, earthquake studies, and mineral exploration at Los Angeles, California, and New Jersey coastal plain
19 p2284 N73-28367
Exploration for copper porphyry deposits in West Pakistan using ERTS-1 imagery
[E73-10954] 21 p2531 N73-30296
Structural and spectral analysis of lineaments and circular features for discrimination of iron-rich zones in Nevada
[E73-11020] 22 p2661 N73-31324
Mineral exploration and fracture trends in Utah and Nevada from ERTS-1 imagery
[E73-11032] 22 p2663 N73-31336
Identification of geostructures of continental crust in Alaska and relation to mineral resources and exploration
[E73-11035] 22 p2663 N73-31339
Activities of Australian Bureau of Mineral Resources
24 p2921 N73-33324

**MINERAL OILS**
Influence of zinc diamyldithiocarbamate on stability of mineral oil inhibited with 2,6 diterciarybutyl-p-cresol
[AD-754664] 11 p1300 N73-20548
Influence of atmospheric pressure and temperature on viscosity and density of mineral oil and siloxane liquids
[AD-761590] 19 p2232 N73-27999

**MINERALOGY**
Mineral analysis of lunar samples of crystalline rocks from Apollo 12 flight
[NASA-SP-306] 07 p0844 N73-16837
Plagioclase mineralogy of olivine alkaline basalt in Potrillo volcanic field
[NASA-CR-130918] 09 p1025 N73-18368
Commercial application of ERTS-1 imagery in structural reconnaissance for minerals and petroleum
[E73-10700] 16 p1903 N73-25392
Geologic, mineral, and water resources of western Colorado from Skylab EREP data
[E73-10918] 20 p2398 N73-29267
Geologic and mineral and water resources of western Colorado from Skylab multispectral photography
[E73-11010] 22 p2660 N73-31315
Identification and discrimination of geological, hydrological, and mineralogical phenomena in central and western Colorado from ERTS-1 data
[E73-11047] 23 p2779 N73-32223
Global metallogeny and geological anomalies
[NASA-TT-F-15098] 24 p2980 N73-33816

**MINERALS**
NT AMPHIBOLES
NT ASBESTOS
NT BIOTITE
NT CRYOLITE
NT FELDSPARS
NT GARNETS
NT GRAPHITE
NT HEMATITE
NT IRON ORES
NT KAMACITE
NT MICA
NT NEPHELITE
NT PEROVSKITES
NT PROUSTITE
NT PYROXENES
NT QUARTZ
NT SCHEELITE
NT SPINEL
Elastic modulus and coefficient of linear thermal expansion of perlite-containing porcelain mixes
[AD-747393] 03 p0322 N73-12627
Theory of spectral reflectance or emittance of particulate minerals
[NASA-CR-128638] 03 p0335 N73-12729
Growth of hollandite crystal membranes under inert gas pressures
[NASA-CR-121033] 03 p0345 N73-12810
Therapeutic value of mineral water diets especially Karlsbad Muhlbrunn water
[NASA-TT-F-14620] 04 p0379 N73-13079
Extraterrestrial space for supplying earth with vanishing minerals, materials, and needed electric power
04 p0473 N73-13863
Analysis of ERTS-1 imagery for identification and discrimination of geological, hydrological, and mineral phenomena in western and central Colorado
[E73-10041] 07 p0776 N73-16304
Bulk radiation effects in terrestrial minerals, meteorites, and lunar rocks, and fission track studies in Apollo 12 samples
07 p0831 N73-16736
Satellite vs aircraft imagery of Saudi Arabia for mineral exploration
08 p0971 N73-17936
Biological mineralization products of human waste for autotroph cultivation
10 p1117 N73-19109
Survey of geology, minerals, and water resources in Maryland using ERTS-1 imagery
[E73-10433] 13 p1515 N73-22276
Two flux radiative transfer model for measuring absorption and scattering coefficients for nonhomogeneous minerals
[RE-451] 13 p1558 N73-22632
Commercial utility of ERTS-1 imagery in structural reconnaissance of Precambrian Shield for minerals and petroleum
[E73-10523] 14 p1654 N73-23414
Mineral concentration in ground and river waters of Porkhov determined from their specific electroconductivity
[NASA-TT-F-14991] 17 p1992 N73-26105
Significance of biological factors in weathering of rocks and minerals
[NASA-TT-F-14892] 18 p2142 N73-27316
Identification of geomorphic features related to known porphyry copper deposit in Pakistan using ERTS-1 imagery
[PAPER-G17] 19 p2265 N73-28248
Application of ERTS-1 imagery for mineral resources, geologic structure, and landform surveys
19 p2288 N73-28398
Simulation of growth and mineral uptake by plants growing in lunar soil
[NASA-CR-134036] 22 p2619 N73-30988
Application of Skylab multispectral photography to mineral and land resources of South Carolina and Georgia
[E73-11140] 24 p2918 N73-33295

**MINES [EXCAVATIONS]**
Application of ERTS-1 imagery to fracture related mine safety hazards in coal mining industry in Indiana
[E72-10193] 01 p0046 N73-10372
Portable radon alpha decay detectors for use in fluorspar mines
[BMBW-FBK-72-14] 03 p0303 N73-12473
Identification of mine dumps with and without vegetative cover using ERTS-1 imagery
[E72-10361] 05 p0535 N73-14349
Performance of piezoelectric transducer for seismic communication in mine environment
[AD-752218] 08 p0885 N73-17169
Bibliography on applications of nuclear explosions in mines, chemistry, and gas and oil extraction
[CEA-BIB-129-ADD-1] 08 p0942 N73-17719
Application of ERTS-1 imagery to fracture related mine safety hazards in coal mining industry in Indiana and Illinois
[E73-10096] 09 p1020 N73-18321
Application of ERTS-1 imagery for locating coal refuse deposits, analysis of geologic formations and mapping of agricultural areas in Pennsylvania
[E73-10327] 09 p1024 N73-18358
Differentiation between mine dumps in South Africa having varying degrees of vegetative cover based on ERTS-1 imagery
[E73-10326] 10 p1147 N73-19334
Application of ERTS-1 imagery to fracture related mine safety hazards in coal mining industry in Indiana and Illinois
[E73-10371] 10 p1151 N73-19366
Feasibility of detecting subsurface coal fires in Wyoming and Montana from ground observation, aerial photography, and satellite imagery
13 p1528 N73-22384
Aerosol particle size determination and distribution with aerodynamically focused impactor, applied to coal mine dust
[BMVG-FBWT-73-1] 14 p1667 N73-23533
Identification of mine dumps in South Africa by growth and decline of vegetation
[E73-10642] 16 p1896 N73-25339
Application of ERTS-1 imagery to fracture related mine safety hazards in coal mining industry and identification of mine subsidence areas in Indiana
[E73-10681] 16 p1901 N73-25376
Application of ERTS-1 imagery to fracture related mine safety hazards in coal mining industry in Indiana
[E73-10776] 18 p2135 N73-27252
Application of Skylab EREP imagery to fracture-related mine safety hazards and environmental problems in mining
[E73-10802] 18 p2138 N73-27277
ERTS-1 imagery analysis to determine varying degrees of vegetation on mine dumps in South Africa
[PAPER-4E] 19 p2268 N73-28268
Application of ERTS-1 imagery to study of fracture-related safety hazards in Indiana coal mining industry
[E73-10970] 21 p2533 N73-30311
Published articles on mining and metallurgy
[TT-70-56005/4] 21 p2561 N73-30527
Geological and geochemical studies in Robinson Mining District, White Pine Co., Nevada using Skylab multispectral imagery
[E73-10992] 22 p2659 N73-31298
Application of ERTS-1 imagery to fracture-related mine safety hazards in Ohio coal mining industry
[E73-11034] 22 p2663 N73-31338
Interpretation of aeromagnetic or gravity data by method of difference mapping for mineral exploration
24 p2912 N73-33240
Mapping of anthracite wastes from mining in Pennsylvania
[E73-11107] 24 p2915 N73-33264
Application of ERTS-1 imagery to fracture related coal mine safety hazards and environmental problems in mining in Indiana
[E73-11148] 24 p2918 N73-33302

**MINES [ORDNANCE]**
Pyroelectric temperature sensors for ignition mechanism of anti-vehicle mines
[LCR-DR-1-71-266/1/R] 12 p1465 N73-21870

**MINIATURE ELECTRONIC EQUIPMENT**
Design of miniature tactical crystal oscillator for operation at ambient temperature
[AD-749271] 04 p0397 N73-13232
Ingestible miniaturized telemetry device for deep body temperature measurements on humans and animals
[NASA-CASE-ARC-10583-1] 05 p0503 N73-14093
Development of method for calculating characteristics of coupled microstrip lines and directional couplers
[REPT-6731] 10 p1136 N73-19261
Development of miniature electronic trimmable thin film resistor chips having precision responses
[BDX-613-728] 12 p1383 N73-21216
Design of miniaturized 37 GHz low noise receiver
[AD-763402] 21 p2509 N73-30129

**MINIATURIZATION**
NT MICROMINIATURIZATION
Radio electronics, printed circuitry, miniaturization, microminiaturization, data processing, and radio equipment
[AD-746715] 02 p0151 N73-11224
Fabricating miniature fluidic elements using photochemical engraving
04 p0426 N73-13472
Miniature hydrogen fueled gas turbine engine scaled to teledyne CAE model 376
[NASA-CR-112173] 16 p1956 N73-25825
Tactical miniature crystal oscillators
[AD-759484] 17 p2004 N73-26207
Miniaturization of fluidic switching elements
[BMFT-FBT-73-06] 22 p2654 N73-31257

**MINICOMPUTERS**
Development of specifications for minicomputer hardware and software for NASA applications - App. A
[NASA-CR-129816] 05 p0515 N73-14189
Data 620 minicomputer system performance in acquiring and processing data
[AD-751636] 07 p0759 N73-16167
Interfacing and programming of minicomputer for Doppler spectrum analysis
[NOAA-TR-ERL-241-AL-7] 14 p1692 N73-23733
Relocatable assembler and loader systems for Minuteman guidance computer
[AD-760758] 18 p2121 N73-27148
Orbit calculations for communication satellite using communications ground terminal minicomputer
[AD-762510] 20 p2474 N73-29874
Hybrid computer multiplication-division modular unit for ASMODEE minicomputer noting three state gate circuits, integrated circuits, and algorithms
[LAAS-TNPE-73-1-07] 23 p2761 N73-32094

**MINIMAX TECHNIQUE**
Gradient procedures for solving dual optimal control and max-min problems
[AD-753129] 09 p1058 N73-18628

**MINIMIZATION**
U OPTIMIZATION

**MINIMUM DRAG**
Contour of wave drag optimized bodies of revolution as function of Mach number in hypersonic flow
[DGLR-PAPER-72-108] 04 p0369 N73-13003

**MINIMUM VARIANCE ORBIT DETERMINATION**
Adaptive filter using minimum variance criteria to estimate state noise covariance
[NASA-TM-X-66080] 01 p0032 N73-10252
Computer algorithm for calculating orbital trajectories by optimization of equation of motion parameters
18 p2211 N73-27846
Error drift projection for ERTS orbit maintenance calculation using ground tracking data
18 p2211 N73-27847

**MINING**
Mineral yearbook containing domestic industry data
[PB-214329/5] 16 p1905 N73-25411
Peculiarities of common deep point composite tapes
[JPRS-59754] 20 p2439 N73-29591
Analysis of concept to mine, refine, and transport lunar minerals to earth for terrestrial industries - Vol.1
[NASA-TM-X-62267] 21 p2595 N73-30798
Analysis of technologies and systems required for establishing mining base, mining, refining, and transporting lunar minerals for earth use - Vol.2
[NASA-TM-X-62268] 21 p2595 N73-30799

**MINITRACK OPTICAL TRACKING SYSTEM**
U MINITRACK SYSTEM

**MINITRACK SYSTEM**
Minitrack tracking function description - Vol. 1
[NASA-TM-X-66213] 15 p1762 N73-24279
Simultaneous observation solutions for NASA-MOTS and SPEOPT station positions on North American Datum
[NASA-TM-X-66297] 18 p2145 N73-27336
Characteristics of minitrack tracking function to show minitrack hardware, system calibration, and quadratic listing - Vol. 2
[NASA-TM-X-70482] 24 p2901 N73-33156

**MINIVAR ORBIT DETERMINATION**
U MINIMUM VARIANCE ORBIT DETERMINATION

**MINKOWSKI SPACE**
Chain geometry theorem for Minkowski space
02 p0203 N73-11641

**MINNESOTA**
Updating and adding detail to Minnesota Land Management Information Systems utilizing ERTS-1 imagery
[E72-10195] 01 p0047 N73-10374
Automatic photointerpretation for land use management in Minnesota
[E72-10227] 02 p0163 N73-11320
Application of ERTS-1 imagery to Minnesota Land Management Information System and analysis of land use classes
[E73-10029] 06 p0660 N73-15362
Remote sensing of Minnesota lakes and forests using ERTS-1
[NASA-CR-130548] 08 p0916 N73-17502
Evaluation of ERTS-1 imagery for mapping land use and updating Minnesota land management information system
[E73-10352] 10 p1148 N73-19348
Automatic interpretation of ERTS-1 data for forest management in Minnesota
[E73-10365] 10 p1150 N73-19361
Automatic interpretation of forest species and stress identification using ERTS-1 imagery of Minnesota
[E73-10366] 10 p1150 N73-19362
Land use management in Minnesota using ERTS-1 imagery
[E73-10581] 14 p1657 N73-23442
Algorithm for automatic photointerpretation of plant species and stresses in Minnesota imagery
[E73-10639] 15 p1776 N73-24398
Computerized interpretation of ERTS-1 data for forest management in Minnesota
[E73-10687] 16 p1902 N73-25381
Application of ERTS-1 imagery to land management information system in Minnesota
[E73-10821] 18 p2140 N73-27296
Utilization of ERTS-1 imagery and data for land use mapping and management in Minnesota
[PAPER-L14] 19 p2275 N73-28310
Forest management in Minnesota using automatic interpretation of ERTS-1 data
[PAPER-L25] 19 p2276 N73-28320
Land use management in Minnesota by automatic interpretation of ERTS-1 MSS data
19 p2285 N73-28379
ERTS-1 applications for land use management in Minnesota
[E73-10965] 21 p2533 N73-30307
ERTS-1 data applications to Minnesota forest land use classification
[E73-11017] 22 p2661 N73-31321
Application of aerial photography and ERTS imagery to agricultural, forest, and water resources management in Minnesota
[NASA-CR-135483] 22 p2665 N73-31357
Automatic photointerpretation for land use management in Minnesota
[E73-11046] 23 p2779 N73-32222
Automatic photointerpretation of ERTS-1 imagery for land use management in Minnesota
[E73-11058] 23 p2780 N73-32234
Automatic photointerpretation of ERTS-1 imagery for land use management in Minnesota
[E73-11059] 23 p2780 N73-32235
Automatic photointerpretation and mapping for land use management in Minnesota
[E73-11060] 23 p2780 N73-32236
Automatic photointerpretation of ERTS-1 imagery for land use management in Minnesota
[E73-11061] 23 p2780 N73-32237
Automatic photointerpretation for plant species and stress identification in Minnesota
[E73-11063] 23 p2781 N73-32239
Utilization of ERTS data to study air pollution, insect infestation, and water transport in Minnesota
[NASA-CR-135565] 23 p2783 N73-32266
Application of remote sensing data to analysis of spring snowmelt floods in Minnesota and surrounding areas
23 p2784 N73-32270
ERTS analysis of geological relationships of Precambrian Greenstone belts and Troctolite series rocks of Minnesota
23 p2784 N73-32271

**MINORITY CARRIERS**
Analog model for minority charge carrier diffusion to base contact of bipolar transistor with current amplification
[NLL-TRANS-2861-[9022.81]]
02 p0148 N73-11201
Minority carrier lifetime optimization for gallium silicon diffusion thyristor
11 p1330 N73-20795
Minority carrier lifetime and switching time of step recovery diode for pulse generators in microwave equipment
[FTZ-A-651-TBF-3] 22 p2643 N73-31180
Minority carrier lifetime control in n-type base regions of gallium diffused silicon power thyristors and diodes
[BMFT-FB-T-73-05] 23 p2765 N73-32123

**MINUTEMAN ICBM**
Digital mimicomputer, D-17B, for NSQ-10 Minuteman I missile guidance system
[AD-746008] 02 p0147 N73-11193
Modification of Minuteman digital computer system to provide for single channel autoanalyzer waveform analysis
[AD-746264] 02 p0147 N73-11197
Software requirements and testing for Minuteman 3 missile system
[AD-757212] 13 p1583 N73-22833
Software validation for guided missile computer
[AD-759263] 16 p1879 N73-25213
Relocatable assembler and loader systems for Minuteman guidance computer
[AD-760758] 18 p2121 N73-27148
Assembly and operation of direct-drive pulser used in minuteman in-place electromagnetic pulse test program
[AD-763114] 20 p2476 N73-29887
Design, operation, and maintence of digital recording CW system for Minuteman 2 missiles
[AD-763115] 20 p2488 N73-29991
Toxic vapor detector for Minuteman propellant leakage
[AD-763799] 21 p2551 N73-30451

**MINUTEMAN MISSILES**
U MINUTEMAN ICBM

**MIRAGE 3 AIRCRAFT**
Prediction of sonic boom effect on avalanches to prepare mirage 3 flight over Lavey Valley
[ISL-13/72] 13 p1474 N73-21940
Performance of Mirage 3 sigma 4 after body
14 p1597 N73-22946
Flight control and flight transition problems of Dassault Mirage 3 [5] aircraft
18 p2102 N73-27002

**MIRRORS**
NT CELESCOPES
NT FRESNEL REFLECTORS
NT MAGNETIC MIRRORS
NT PARABOLOID MIRRORS
Discrete control of linear distributed systems with specific application to primary mirror for orbiting astronomical observatory
[NASA-TM-X-68855] 02 p0173 N73-11400
Design technique for control systems of large space telescope mirrors
[NASA-TN-D-7090] 05 p0522 N73-14247
Measurement of damage thresholds for multiple layer dielectric mirrors for laser pulses of twenty nanoseconds and twenty picoseconds duration
05 p0556 N73-14513
Analysis of surface damage mechanisms to mirrors and mirror coatings resulting from irradiation by pulsed carbon dioxide lasers
05 p0556 N73-14519
Correction of axisymmetric deformations in space telescope mirrors by thermally induced elastic strains
[NASA-TM-X-2673] 06 p0672 N73-15472
Determination of optical/mechanical properties of low expansion glass ceramic material for use as lightweight substrate for primary mirror on large spaceborne telescope
[NASA-CR-130141] 06 p0674 N73-15481
Particle loss rate from mirror machines, and radiation coupling in dense plasmas
[COO-2181-9] 06 p0704 N73-15744
Damage thresholds of multilayered dielectric reflecting mirrors subjected to nanosecond laser pulses
[AD-751265] 07 p0808 N73-16553
Surveyor 3 lunar probe television mirror pit X ray analysis and scanning electron microscopy for micrometeoroid impact study
[ONERA-NT-01-15] 07 p0847 N73-16864
Development of strain gage ambiguity sensor for measuring alignment of optical mirror segments
[NASA-CASE-MFS-20506-1] 08 p0923 N73-17563
Fine grinding, polishing, and graded etching techniques to eliminate surface yield on optical telescope mirrors
[NASA-CR-112217] 08 p0934 N73-17647
Western European research on open adiabatic mirror devices and radio frequency plugging - EURATOM controlled fusion report
[EUR-CEA-FC-628-AG] 08 p0948 N73-17760
Environmental and flight readiness tests of scanning mirror for infrared sensors
09 p1089 N73-18888
Active optics simulation system for designing mirror control system for large space telescope
[NASA-CR-112259] 10 p1159 N73-19433
Laser mirror technology
[AD-754101] 11 p1303 N73-20570
N wave focusing on principal axis of spherical mirror
[AD-757035] 14 p1692 N73-23736
Design technique to reduce absorption in multilayer dielectric mirrors using optical interference coatings
15 p1812 N73-24688
Exit slit mirrors for Ebert ultraviolet spectrometer Apollo experiment
[NASA-CR-128549] 16 p1916 N73-25504
Thermoelastic response model for actively controlling primary mirror surface error of orbiting telescope
[NASA-CR-124286] 17 p2033 N73-26449
Analysis of dynamics of thin primary mirrors for large astronomical telescopes
[NASA-TM-X-2790] 17 p2090 N73-26911
Operation of reflectometer and correct procedure for measuring mirror reflectivity
[AD-760589] 18 p2152 N73-27398
Manufacturing of large structural mirror supports for space telescopes using titanium alloys
18 p2209 N73-27828
Development of mirror material for carbon monoxide and carbon dioxide lasers
[AD-763795] 21 p2556 N73-30490
Active cleaning technique for removing contaminants from optical surfaces in space
[NASA-CR-124374] 21 p2583 N73-30697
Real time holographic interferometry for optical surface testing
[BMFT-FBT-73-01] 22 p2681 N73-31479

**MIS [SEMICONDUCTORS]**
Luminescence of ZnSe and ZnS crystals compared to electroluminescence of MS and MIS structures, preparation of heterojunction structures, and solution growth of wafers
[AD-749135] 05 p0588 N73-14784
Fabrication and analysis of metal insulator semiconductor capacitors for radiation vulnerability studies
16 p1880 N73-25217
Effects of ion implantation displacement damage in silicon diodide insulator of MIS capacitor
[AD-758695] 16 p1881 N73-25228
Effects of electron and hole trapping on radiation hardness of aluminum oxide MIS devices
[AD-758696] 16 p1882 N73-25229
Manufacturing of metal insulator semiconductor capacitors on single crystal silicon substrates
[AD-760009] 17 p2005 N73-26214
Radiation resistance of thin insulating films deposited with ion beam system
[AD-760118] 17 p2075 N73-26788
Feasibility of charge coupled lead-tin-telluride semiconductor for infrared imagery
[AD-761473] 19 p2245 N73-28099
Electrical properties of MIS semiconductors and application as infrared detectors
[AD-761510] 19 p2327 N73-28719

**MISALIGNMENT**
Estimation procedures for in-flight vertical misalignment of platforms
11 p1319 N73-20707

**MISCIBILITY**
U SOLUBILITY
**MISFIRES**
U FAILURE
U FIRING [IGNITING]
**MISMATCH**
U IMPEDANCE MATCHING
**MISORIENTATION**
U MISALIGNMENT
**MISS DISTANCE**
Miss distance radar for air defense weapons testing
[AD-750323] 06 p0642 N73-15210
**MISSILE ANTENNAS**
Calculation of lower bounds of blackout of plasma-covered antennas
[AD-759790] 16 p1881 N73-25227
**MISSILE BODIES**
Coning motion, autorotation and vortex system of slender missiles
[BMVG-FBWT-72-31] 10 p1103 N73-18998
**MISSILE CASES**
U MISSILE BODIES
**MISSILE COMPONENTS**
NT MISSILE ANTENNAS
NT MISSILE BODIES
Development of specifications for design of avionics subsystems to improve reliability
[AD-746029] 01 p0006 N73-10043
Research and development of ceramic systems for use as structural components in hypersonic missile applications
[AD-745744] 01 p0071 N73-10580
Computerized design of support structure for missile fuse using finite element structural analysis program - Part I
[AD-743879] 01 p0115 N73-10947
Glass fiber reinforced composite materials for developing prototype missile fuselages
[AD-746288] 02 p0193 N73-11560
Static magnetic fields inside idealized structures resembling missile cells
[AD-748409] 03 p0360 N73-12932
Feasibility of missile acceleration simulator based upon track accelerator concept
[AD-751128] 07 p0767 N73-16231
Proceedings of conference on application of superconductivity techniques to auxiliary power systems for aircraft and missiles
[AGARD-CP-104] 10 p1108 N73-19030
Characteristics of power generating systems and application in missiles for production of hydraulic and electric energy
10 p1110 N73-19044
Survey of USSR missile defense system
[AD-754629] 11 p1353 N73-20983
**MISSILE CONFIGURATIONS**
SOS - computer program for calculating weight, center of gavity, and inertias of asymmetrical missiles
[AD-749251] 05 p0601 N73-14885
Aerodynamic characteristics of two-stage, flexible, variable-mass missile with internal flow, discrete masses, and aerodynamic forces in powered flight
07 p0848 N73-16870
Development of computer program to predict lift, drag, and center of pressure on bodies of revolution at subsonic, transonic, and supersonic speeds
[AD-754098] 13 p1471 N73-21913
Wind tunnel determination of effect of fin planform on aerodynamic characteristics of wingless missile with aft cruciform controls at Mach 1.60, 2.36, and 2.86
[NASA-TM-X-2774] 18 p2101 N73-26995
Ballistic design of solid propellant missiles to include analysis of physical properties and determination of reliability
[JPRS-59060] 18 p2200 N73-27759
Wind tunnel tests to determine aerodynamic characteristics of two missile configurations with common body at transonic and supersonic speeds
[NASA-TM-X-2780] 19 p2218 N73-27891
Application of oscillation theory and mathematical statistics to problems of aircraft structures and aerodynamic loads on aircraft and missiles
[NASA-TT-F-753] 19 p2220 N73-27908
Analysis of methods for determining mass, geometric, and thrust characteristics of missiles to provide given interval of ranges
[JPRS-59565] 20 p2474 N73-29877
Development of principles for design, development, and evaluation of ballistic missiles and support systems
[JPRS-51810] 20 p2475 N73-29881
**MISSILE CONTROL**
Solving problems of long-range ballistic missiles - launching, trajectory and flight characteristics, and firing data
[AD-743687] 01 p0109 N73-10898
Turnstile slot antenna system for spacecraft or missile telemetry and command control
[NASA-CASE-GSC-11428-1] 02 p0149 N73-11206
Analysis of propagating and non-propagating motions produced by earth tides and earth rates and effects on inertial instrument performance
[AD-748274] 03 p0330 N73-12691
Effect of internal spinning fly wheel on air launched missile stability and resulting launch disturbance
[AD-749027] 04 p0375 N73-13047
Application of on-board digital computers for stabilization of missile and rocket control systems
[JPRS-57893] 06 p0721 N73-15881
Control concept utilizing interaction of injected fluid with airstream surrounding missile
[AD-750306] 06 p0722 N73-15894
Aerodynamic characteristics of two-stage, flexible, variable-mass missile with internal flow, discrete masses, and aerodynamic forces in powered flight
07 p0848 N73-16870
Analysis of guidance systems used with guided missiles
[AD-751089] 07 p0850 N73-16892
Wind tunnel determination of effect of fin planform on aerodynamic characteristics of wingless missile with aft cruciform controls at Mach 1.60, 2.36, and 2.86
[NASA-TM-X-2774] 18 p2101 N73-26995
Transformation of guided missile computer input/output routine for general purpose applications
[AD-760761] 18 p2121 N73-27147
Analysis of methods for determining mass, geometric, and thrust characteristics of missiles to provide given interval of ranges
[JPRS-59565] 20 p2474 N73-29877
Kinematics of gyroscopes and gimbals and effects on missile stability
[AD-763147] 21 p2549 N73-30440
Engineering test procedures for heat seeking missiles
[AD-763324] 21 p2602 N73-30853
**MISSILE DEFENSE SYSTEMS**
U MISSILE SYSTEMS
**MISSILE DESIGN**
Ballistic design of solid propellant missiles to include analysis of physical properties and determination of reliability
[JPRS-59060] 18 p2200 N73-27759
Analysis of methods for determining mass, geometric, and thrust characteristics of missiles to provide given interval of ranges
[JPRS-59565] 20 p2474 N73-29877
Development of principles for design, development, and evaluation of ballistic missiles and support systems
[JPRS-51810] 20 p2475 N73-29881
**MISSILE DETECTION**
NT RADAR DETECTION
Application of infrared reconnaissance satellites for detecting missiles and military satellites
[AD-760951] 18 p2152 N73-27395
**MISSILE ENGINE CASES**
U ROCKET ENGINE CASES
**MISSILE GUIDANCE**
U MISSILE CONTROL
**MISSILE LAUNCHERS**
Solving problems of long-range ballistic missiles - launching, trajectory and flight characteristics, and firing data
[AD-743687] 01 p0109 N73-10898
Development and test of explosively driven two-stage hypervelocity rocket launcher for use in meteoroid studies
[NASA-CR-2143] 06 p0649 N73-15272
Feasibility of missile acceleration simulator based upon track accelerator concept
[AD-751128] 07 p0767 N73-16231
Installations and support equipment for launching guided missiles
[AD-756083] 13 p1507 N73-22214
Missile site ground cover for prevention of soil erosion during launches
[AD-762136] 19 p2296 N73-28466
Evaluation of physical and operational characteristics of missile support vehicle based on procedures for inspection, servicing, and maintenance
[AD-764772] 23 p2852 N73-32791
**MISSILE RANGES**
Instrumentation handbook for operational support systems of Space and Missile Test Centers in California, Hawaii, and Pacific Ocean area
[AD-750944] 06 p0651 N73-15285
Instrumentation improvement program for Pacific Missile Range during 1971 - 1972
[AD-757815] 14 p1647 N73-23360
Feasibility of actively guiding sounding rockets to reduce impact dispersion at White Sands Missile Range
[NASA-TM-X-70474] 23 p2851 N73-32780
**MISSILE ROLL CONTROL**
U LATERAL CONTROL
U MISSILE CONTROL
**MISSILE SILOS**
Ground-silo-missile mount transmissibility characteristics
[AD-753079] 09 p1097 N73-18953
Shock absorbing systems used by US guided missile silos
[AD-761577] 19 p2356 N73-28954
**MISSILE SIMULATION [MATH MODELS]**
U MATHEMATICAL MODELS
U MISSILES
**MISSILE SIMULATORS [TRAINING]**
U MISSILES
U TRAINING SIMULATORS
**MISSILE STABILIZATION**
U MISSILE CONTROL
U STABILIZATION
**MISSILE STAGING**
U MISSILES
U STAGE SEPARATION
**MISSILE SYSTEMS**
NT SAFEGUARD SYSTEM
Survey of USSR missile defense system
[AD-754629] 11 p1353 N73-20983
Frequency and duration of extreme surface temperatures and effects on missile systems development in hot-dry climates
[AD-759899] 17 p2059 N73-26652
Tests and evaluation of seal for movable rocket nozzle systems
[AD-762944] 20 p2423 N73-29467
Development of principles for design, development, and evaluation of ballistic missiles and support systems
[JPRS-51810] 20 p2475 N73-29881
**MISSILE TEST LABORATORIES**
U LABORATORIES
U MISSILE TESTS
**MISSILE TEST RANGES**
U MISSILE RANGES
**MISSILE TESTS**
Feasibility of porous jet stretcher nozzle for angle of attack testing of missiles in supersonic wind tunnel
[AD-750867] 06 p0651 N73-15288
Assembly and operation of direct-drive pulser used in minuteman in-place electromagnetic pulse test program
[AD-763114] 20 p2476 N73-29887
**MISSILE TRACKING**
Nonlinear transformation relating rectangular coordinates to range instrumentation coordinates in guided missile tracking system
[AD-746637] 02 p0144 N73-11163
Performance tests of strapdown air to air tracking system for short range weapons control system
[AD-751654] 07 p0818 N73-16633
Image intensifier system for daytime missile tracking telescopes
[AD-753342] 09 p1068 N73-18715
Calibration of missile infrared track and acquisition system
[AD-754944] 11 p1295 N73-20507
Survey of USSR missile defense system
[AD-754629] 11 p1353 N73-20983
Reliability and performance of landbased and shipboard Air Force instrumentation systems
[AD-755916] 12 p1389 N73-21262
**MISSILE TRAJECTORIES**
Solving problems of long-range ballistic missiles - launching, trajectory and flight characteristics, and firing data
[AD-743687] 01 p0109 N73-10898
Missile trajectory smoothed by Kalman method using data from several cameras, radars, and Doppler receivers
[WRE-TN-705[T]] 02 p0227 N73-11831
Computer program for optimal design of advanced thrust vector control of missile trajectory
[AD-749126] 05 p0590 N73-14797
Computer program manual for optimal design of advanced thrust vector control for missile trajectory
[AD-749127] 05 p0590 N73-14798
Subharmonic angular motion response in asymmetric missile trajectory analysis
[AD-749787] 06 p0722 N73-15893
Application of control theory to determine time history of thrust profile to achieve optimal maneuvers of aerospace lifting vehicles
[AD-751281] 07 p0850 N73-16891
Techniques for determining attitude of rocket axis for vehicle AH 7.886
[AD-751937] 08 p0965 N73-17890
Influence of wind speed and directional variability on trajectory of unguided missile at WSMR, New Mexico
[AD-753348] 09 p1062 N73-18662
Vertical wind effects in trajectory calculations and impact predictions for rockets and projectiles
[AD-753349] 09 p1092 N73-18913
Computerized simulation of terminal homing missile trajectory
[AD-754543] 11 p1344 N73-20904
Development of computer program to predict lift, drag, and center of pressure on bodies of revolution at subsonic, transonic, and supersonic speeds
[AD-754098] 13 p1471 N73-21913
Feedback control techniques for proportional target interception and acceleration
[AD-755795] 13 p1578 N73-22794
Analysis of development of rocket dynamics
[AD-756962] 13 p1583 N73-22835
Point defense missile simulation program
[AD-759969] 17 p2099 N73-26985
Mathematical methods for development of improved rocket trajectories from radar tracking data
[AD-762203] 19 p2347 N73-28878

MISSILE WINGS
U LOW ASPECT RATIO WINGS
MISSILES
NT AIR TO AIR MISSILES
NT AIR TO SURFACE MISSILES
NT ANTIAIRCRAFT MISSILES
NT ANTIMISSILE MISSILES
NT ANTITANK MISSILES
NT BALLISTIC MISSILES
NT CRUISE MISSILES
NT LANCE MISSILE
NT MINUTEMAN ICBM
NT NIKE MISSILES
NT NIKE-AJAX MISSILE
NT NIKE-HERCULES MISSILE
NT PERSHING MISSILE
NT POSEIDON MISSILES
NT RAMJET MISSILES
NT SHORT RANGE BALLISTIC MISSILES
NT SURFACE TO AIR MISSILES
NT SURFACE TO SURFACE MISSILES
NT TERRIER MISSILE
Acceptance criteria specification for slip-cast fused silica radomes
[AD-745743] 01 p0029 N73-10230
Adaptation of lidar to aircraft and missile rangefinding
[NASA-TT-F-14716] 02 p0181 N73-11466
Determining parameters of rocket capable of 8 km/sec using simplified equations of motion
[REPT-13] 04 p0463 N73-13775
Control system for rockets during combustion
[REPT-13-PT-2] 04 p0463 N73-13776
Tester controlled by fluidic logic system for testing safety functions of missile safe and arm devices
[AD-751127] 07 p0802 N73-16512
General trends in guided missile development since World War 2
[AD-753510] 09 p1092 N73-18912
Ground-silo-missile mount transmissibility characteristics
[AD-753079] 09 p1097 N73-18953
Meteorological and ballistics data for launching of 14101 RIP missile, numbers 12723/12720, rounds 3/4
[AD-755775] 12 p1424 N73-21541
Destruction capabilities and nuclear radiation potential of rockets with nuclear warheads
[AD-756565] 13 p1595 N73-22938
Simulation studies of missile and rocket systems using digital, analog, and hybrid computers
[AD-759226] 16 p1967 N73-25914
Stochastic control theory for homing guidance laws for tactical missiles
[AD-761626] 19 p2347 N73-28876
Thrust magnitude control for strategic and tactical missiles
[AD-762915] 20 p2476 N73-29888
Transonic wind tunnel tests of thrust effects on missile aerodynamics
[AD-762576] 20 p2476 N73-29889
Research concepts for guidance and control of tactical missiles
[AD-762593] 20 p2476 N73-29890
MISSILRY
U MISSILES
MISSION PLANNING
Solar sonde in earth-sun orbit with 0.26 AU perihelion
[NASA-TT-F-14700] 01 p0104 N73-10860
Summary of Pioneer 10 mission objectives and midcourse maneuver strategies
01 p0120 N73-10987
Development of abort sequence trees for reference zirconium hydride reactor power module for each phase of space base program mission - Vol. 3 Pt. 2A
[NASA-CR-123845] 02 p0209 N73-11698
Development of long range plan for solar system exploration to define space missions, equipment, and trajectories for interplanetary flight
[NASA-CR-129132] 02 p0226 N73-11823
Activities of Meteoroid Science Team for definition phase of outer planet missions
[NASA-CR-129186] 02 p0226 N73-11825
NASA plans and priorities thru 1985
02 p0227 N73-11834
Feasibility of flyby or rendezvous cometary mission
02 p0229 N73-11852
Definition of requirements for flight simulator to provide space shuttle systems and space mission analysis and performance - Vol. 1
[NASA-CR-128621] 02 p0229 N73-11860
Development of requirements for space shuttle vehicle and mission simulation - Vol. 2
[NASA-CR-128622] 02 p0230 N73-11861
Analysis of space shuttle systems and space shuttle mission requirements for development of mission simulator - Vol. 3
[NASA-CR-128623] 02 p0230 N73-11862
Analysis of external interfaces, crew procedures, visual cues, and aural cues for space shuttle vehicle and mission simulation - Vol. 4
[NASA-CR-128624] 02 p0230 N73-11863
Analysis of emergency crew transfer operations using Earth Orbit Shuttle to determine mission effectiveness and cost requirements - Vol. 2 Pt. 3
[NASA-CR-129102] 02 p0231 N73-11874
Analysis of space shuttle rescue capability based on mission, shuttle configuration and performance, and ground launched ascent and rendezvous time -Vol. 3 Pt. 1
[NASA-CR-129101] 02 p0231 N73-11875
Eole and support operations planning
[NASA-TT-F-14709] 03 p0249 N73-12011
Capabilities of Dynamic Operational Requirements and Cost Analysis Program for space mission planning - Vol. 1
[NASA-CR-129263] 03 p0269 N73-12183
Guide for coding Dynamic Operational Requirements and Cost Analysis Program to show subroutines and flow charts - Vol. 2
[NASA-CR-129264] 03 p0270 N73-12184
Program listing for Dynamic Operational Requirements and Cost Analysis Program to provide space mission planning and project management capability - Vol. 3
[NASA-CR-129265] 03 p0270 N73-12185
Description of functions and capabilities of Dynamic Operational Requirements and Cost Analysis Program - Vol. 4
[NASA-CR-129266] 03 p0270 N73-12186
User guide for Dynamic Operational Requirements and Cost Analysis Program for space mission planning and project management - Vol. 1
[NASA-CR-123378] 03 p0270 N73-12188
Programmer manual for Dynamic Operational Requirements and Cost Analysis Program for space mission planning and project management - Vol. 2
[NASA-CR-123379] 03 p0270 N73-12189
Program listing for Dynamic Operational Requirements and Cost Analysis Program to provide space mission planning and project management capability - Vol. 3
[NASA-CR-123380] 03 p0270 N73-12190
Development of payload for mission planning for missions to outer planets as function of flight time for various launch years, launch vehicles, and orbit sizes
[NASA-CR-129244] 03 p0354 N73-12887
Assessment of present state of knowledge of asteroids for identifying mission and target priorities
[NASA-CR-129247] 03 p0354 N73-12889
Analysis of space program costs and launch vehicle traffic based on either expendable, partially reusable, or fully reusable launch vehicle fleet
[NASA-CR-125847] 03 p0355 N73-12896
Analysis of costs and effectiveness of space missions, aerospace vehicles, and propulsion systems
[NASA-CR-129258] 03 p0358 N73-12917
Four periodic comets [Encke, dArrest, Kopff, and Halley] for comet rendezvous mission study
[NASA-CR-129820] 04 p0469 N73-13823
Feasibility of atmospheric entry probe missions to Uranus and Neptune
[NASA-CR-129815] 04 p0469 N73-13824
Analysis of Skylab program to show construction of spacecraft, test facilities, personnel accomodations, and research projects
04 p0470 N73-13831
Impact of space shuttle operations on national economy, technological superiority, and development of future space activities
04 p0470 N73-13832
Operations summary and mission planning for IMP-H spacecraft
[NASA-TM-X-68880] 04 p0478 N73-13907
Projected space missions and space transportation system with payload and cost analysis for space shuttle system - Vol. 2
[NASA-CR-129571] 04 p0487 N73-13978
Economic analysis of space transportation system for use during 1980 time period based on various configurations of space shuttle and space tug - Executive Summary
[NASA-CR-129570] 04 p0487 N73-13980
Preliminary design of selected Research and Applications Module [RAM] concepts, operations, and missions
[NASA-CR-129828] 05 p0597 N73-14856
Analysis of payloads for space shuttle based on space missions, planetary exploration, and international rendezvous and docking - Vol. 2
[NASA-CR-129844] 05 p0598 N73-14862
Pioneer space probe project to show history, design, development, flight operations, and results accomplished
[NASA-SP-278] 05 p0598 N73-14864
Analysis of operations and resources required to support expendable second stage reusable space shuttle booster - Vol. 5
[NASA-CR-128660] 05 p0599 N73-14871
Evaluation of scientific and technical experiments for space missions
05 p0610 N73-14963
Proceedings of Space Shuttle Sortie Workshop
[NASA-TM-X-68841] 06 p0719 N73-15866
Advanced technology, experimental and instrument design, and mission planning for space shuttle sortie workshop - conference working group reports
[NASA-TM-X-68842] 06 p0719 N73-15867
Objective and mission of Meteosat satellite
[DGLR-PAPER-72-82] 06 p0721 N73-15887
Effect of Apollo project accomplishments on earth resources surveys and conduct of earth resources investigations in future space missions
07 p0781 N73-16349
Objectives of NASA Earth Resources Survey Program to include types of sensors used and data acquired by aircraft, spacecraft, and ground observations
07 p0782 N73-16351
Launch vehicle estimating factors for planning advanced solar system and earth orbital missions
[NHB-7100.5B] 07 p0847 N73-16866
ITOS system and design of TIROS M spacecraft
[NASA-CR-130163] 07 p0849 N73-16880
Relationship between mission requirements of piloted aircraft stability and maneuverability
08 p0864 N73-16995
Investigation of solar electric propulsion as method for exploring space beyond reach of ballistic missions - Vol. 1
[NASA-CR-130701] 08 p0954 N73-17811
Effects of planetary quarantine constraints on advanced planetary mission planning
[NASA-CR-130861] 09 p0995 N73-18123
Earth resources requirements for Skylab missions - Appendix B
[NASA-TM-X-69137] 09 p1029 N73-18402
Mission description and system design for Large Space Telescope used on unmanned satellites - Vol. 2
[NASA-TM-X-64726-VOL-2] 09 p1036 N73-18450
Cost effectiveness and mission value comparisons of three propulsion systems for delivery of advanced probe spacecraft
[NASA-TM-X-2751] 09 p1079 N73-18802
Research in support of definition phase of Outer Planets Mission
[NASA-CR-130917] 09 p1082 N73-18826
Mission analysis for manned flight experiments
[NASA-CR-130989] 09 p1082 N73-18828
Baseline astronomy sortie mission concept for space shuttle
[NASA-CR-124043] 09 p1084 N73-18842
Automated documentation for mission analysis and trajectory simulation program
10 p1131 N73-19220
Optical design optimization, and sensor selection for mission definition of outer planets Grand Tours
[NASA-CR-131088] 10 p1159 N73-19427
Mission analysis of VTOL passenger transport aircraft to determine optimum engine cycle for minimum direct operating cost
[NASA-TM-X-68186] 10 p1208 N73-19826
Feasibility determination of astronomy sortie missions concept including definitions of support hardware, mission profiles, and interfaces with space shuttle and sortie lab
[NASA-CR-124042] 10 p1211 N73-19851
Planning and source allocation for planetary quarantine measures for interplanetary automated spacecrafts
[NASA-CR-131291] 11 p1247 N73-20126
Mission objectives, flight history, and scientific experiments of OSO-7
[NASA-CR-130157] 11 p1341 N73-20879
Management methods for Skylab program to include mission operations support, environmental and thermal design criteria, optical contamination, and materials science
[NASA-TM-X-64725] 11 p1342 N73-20886
Summary of advanced mission planning for solar system exploration
[NASA-CR-131395] 11 p135u N73-20954
Presidential report on progress and activities of various aerospace programs in 1972 and comments on future mission planning
11 p1352 N73-20975
Development of computerized multistage failure process simulation to evaluate risk in solar electric space mission
[NASA-CR-131518] 12 p1457 N73-21813
Analysis of NASA programs for 1970 to 1980 period with application to earth orbital experiment program and requirements - Vol. 1
[NASA-CR-112325] 13 p1577 N73-22778
Analysis of manned space flight capability development for support of earth orbital experiment program and requirements - Vol. 2
[NASA-CR-112326] 13 p1577 N73-22779
Analysis of space biology projects related to earth orbital experiment program to identify critical issues and methods of conducting experiments - Vol. 3
[NASA-CR-112327] 13 p1577 N73-22780
Development of space astronomy projects identified during orbital experiment program and requirements study - Vol. 4
[NASA-CR-112328] 13 p1577 N73-22781

Development of space communications and navigation projects involved in earth orbital experiment program and requirements study - Vol. 5
[NASA-CR-112329] 13 p1577 N73-22782
Earth observation experiments identified during earth orbital experiment program and requirements study - Vol. 6
[NASA-CR-112330] 13 p1577 N73-22783
Definition of supporting technology development requirements for earth orbital experiment program and requirements study - Vol. 7
[NASA-CR-112331] 13 p1577 N73-22784
Data management systems, instrumentation concepts, and biotechnology laboratory for earth orbital experiment program and requirements study - Vol. 8
[NASA-CR-112332] 13 p1577 N73-22785
Research projects for space exploration by out-of-ecliptic spacecraft
[NASA-CR-131865] 13 p1578 N73-22792
Strategies for European geosynchronous space tug mission
[VTH-171] 13 p1583 N73-22831
Parameters requiring consideration by planners and designers when planning EVA functions for astronauts - Vol. 1
[NASA-CR-128926] 14 p1614 N73-23081
Model for estimating impact of manned EVA costs on future payloads - Vol. 3
[NASA-CR-128928] 14 p1614 N73-23083
Mission planning for European earth resources survey aircraft
[ESRO-CR[P]-117] 14 p1661 N73-23484
Achievements in space exploration to include spacecraft design, planetary composition, lunar missions, and predicted space accomplishments
[NASA-TT-F-737] 15 p1830 N73-24829
European scientific community as users of ESRO satellite systems
15 p1848 N73-24976
Phase preparation of ground facilities for satellite missions noting procedures used at ESOC
15 p1848 N73-24979
Apollo 17 flight plan for prelaunch checkout support and continuous support to be provided during mission - Revision A
[NASA-TM-X-69530] 17 p2083 N73-26853
Space shuttle traffic and payload data developed from 1971 mission model
[NASA-TM-X-64731] 17 p2086 N73-26878
Sortie Lab system evaluation, future growth, and IR astronomy experiment accommodation
[ESS/SS-399-VOL-3] 17 p2089 N73-26904
Development and employment of orbital space stations to conduct earth resources surveys and provide space manufacturing facilities
[JPRS-59650] 18 p2199 N73-27754
Input usage guide for mission planning program
[AD-760796] 18 p2201 N73-27769
Computerized support system for complex spacecraft mission scheduling
18 p2211 N73-27851
Real time computer technique for mission control and schedule planning
18 p2211 N73-27852
Mission definition and analysis for manned earth observatory based on projected technology for 1980 time period - Vol. 2
[NASA-CR-124340] 19 p2343 N73-28847
Conceptual design of earth observation facility to include sensor payload, crew functions and accomodations, and common core equipment - Vol. 3
[NASA-CR-124338] 19 p2343 N73-28848
Schedules, costs, requirements, and equipment for manned earth observatory missions - Vol 4
[NASA-CR-124339] 19 p2343 N73-28849
Acquisition of quick look data from SL-2, SL-3 planning, and development of mathematical models to process S-193 radar altimeter data
[E73-10917] 20 p2398 N73-29266
Design analysis and tradeoff studies for defining Astronomy Sortie Mission based on mission requirements and payload limitations - Vol. 3 Bk. 1
[NASA-CR-124047] 20 p2473 N73-29870
Design analysis and trade studies to support candidate configurations and payloads for Astronomy Sortie Missions - Vol. 3 Bk. 2
[NASA-CR-124044] 20 p2474 N73-29871
Program development requirements for selected Astronomy Sortie Missions concept to show rationale and explanations of guidelines and assumptions - Vol. 4
[NASA-CR-124046] 20 p2474 N73-29872
Systems analysis of Radio Astronomy Satellite - B to show mission objective, spacecraft configuration, and launch operations
[NASA-TM-X-69490] 20 p2475 N73-29878
Schedule of NASA space missions through 1991
[NASA-TM-X-64739] 20 p2488 N73-29984
Space shuttle rendezvous, radiation and reentry analysis code
[NASA-TM-X-64768] 21 p2595 N73-30795
Mission planning for Pioneer Saturn/Uranus atmospheric probe missions
[NASA-TM-X-2824] 21 p2595 N73-30800
Airborne research management and shuttle sortie planning
[NASA-TM-X-62287] 22 p2715 N73-31729
Identification, selection, and description of earth observation experiments for shuttle sortie missions in 1980's
[NASA-CR-124368] 22 p2717 N73-31751
Apollo experience report on process of crew procedures development for systems procedures and flight procedures
[NASA-TN-D-7436] 22 p2721 N73-31772
Congressional hearings on cost of space shuttle program to show differences between Government Accounting Office and NASA projections
22 p2737 N73-31916
Payload definition and integration study to establish planning concepts for life sciences spacecraft laboratories - Vol. 1
[NASA-CR-124411] 23 p2849 N73-32765
Life sciences payload definition and integration study to show design of space laboratory for space shuttle and cost analysis of project - Vol. 2
[NASA-CR-124412] 23 p2849 N73-32766
Research equipment requirements for space laboratory concepts involved in conducting life sciences experiments in space - Vol. 3
[NASA-CR-124414] 23 p2849 N73-32767
Representative shuttle mission applications
[NASA-CR-124431] 23 p2850 N73-32771
Mission objectives of German astronomical satellite, noting X ray astronomy, IR and UV experiments
[BMBW-FB-W-72-25] 23 p2851 N73-32786
Application of aerospace engineering to planetary exploration and spacecraft shielding problems
[NASA-CR-135529] 23 p2858 N73-32836
Saturn satellite encounter opportunities for Mariner Jupiter-Saturn 1977 project
23 p2858 N73-32838
Satellite quarantine constraints in outer planet mission planning
[NASA-CR-135791] 24 p2885 N73-33041
Mission project management, and description of Symphonie communication satellite
[DGLR-PAPER-73-043] 24 p2895 N73-33113
History, development, and description of Skylab program
[NASA-EP-107] 24 p2979 N73-33803
Spacecraft mass properties data for use in mission planning for Apollo/Soyuz Test Project
[NASA-TM-X-69502] 24 p2980 N73-33813
Objectives of experiments on Mariner 9 space probe
[NASA-CR-135726] 24 p2983 N73-33834
Project objectives and mission profile for Mariner Mars 1971
24 p2983 N73-33835
Relationships between performance, safety, cost, and schedule parameters to generate program models for total space program
[NASA-CR-135903] 24 p2993 N73-33919
Relationships between performance, safety, cost, and schedule parameters to generate program models for total space program
[NASA-CR-135902] 24 p2993 N73-33920

**MISSIONS**
Analysis of costs and effectiveness of space missions, aerospace vehicles, and propulsion systems
[NASA-CR-129258] 03 p0358 N73-12917

**MISSISSIPPI**
Land use planning on Mississippi Gulf Coast utilizing ERTS-1 remotely sensed data
[E72-10262] 03 p0290 N73-12361
Utilization of ERTS-1 imagery to determine availability and distribution of menhaden within Mississippi Sound and adjacent waters
[E72-10279] 03 p0292 N73-12377
Land use planning and management on Mississippi Gulf Coast using ERTS-1 imagery
[E73-10072] 07 p0779 N73-16334
Ross Barnett Reservoir remote sensing project to determine water sediment, investigate erosion, and improve land use
[NASA-CR-130960] 09 p1029 N73-18396
Application of ERTS-1 imagery to land use planning and management on Mississippi Gulf Coast
[E73-10460] 11 p1284 N73-20418
Thematic mapping of Mississippi River from ERTS-1 imagery
[E73-10628] 15 p1775 N73-24388
Land use management and planning on Mississippi Gulf Coast using ERTS-1 imagery
[E73-10653] 16 p1898 N73-25349
Application of ERTS-1 data to develop and implement utilization of living marine resources in Mississippi Sound
[E73-10707] 16 p1904 N73-25398
Application of ERTS-1 imagery for determining availability and distribution of menhaden within Mississippi Sound adjacent waters
[E73-10751] 17 p2022 N73-26354
Prediction of menhaden fish distribution in Mississippi Sound based on ERTS-1 imagery
[E73-10785] 18 p2136 N73-27261
Detection of phenological event for specific forest and crop types using ERTS-1 imagery
[PAPER-A19] 19 p2261 N73-28226
Application of ERTS-1 imagery to land use and resource management in State of Mississippi
19 p2289 N73-28404
Agricultural and crop identification decisions in Mississippi Delta region of Mississippi using Skylab EREP data
[E73-10870] 20 p2393 N73-29221
Investigation of agricultural practices in Mississippi Delta region of Mississippi using ERTS-1 imagery
[E73-10881] 20 p2394 N73-29232
Land use planning and management on Mississippi Gulf Coast using ERTS-1 data
[E73-10906] 20 p2396 N73-29255
Thematic mapping of wetlands, forests, open water, and Mississippi River flooding from ERTS-1 imagery
[E73-10952] 21 p2531 N73-30294
Computer interpretation of multispectral data of Chesapeake Bay, Lake Pontchartrain, Louisiana, and lower Mississippi Valley
[E73-11007] 22 p2660 N73-31312
Application of ERTS-1 data to land use planning on Mississippi Gulf Coast
[E73-11055] 23 p2780 N73-32231

**MISSISSIPPI DELTA [LA]**
Application of ERTS-1 imagery to agricultural practices in Mississippi Delta Region
[E72-10312] 04 p0412 N73-13361
Improvement of menhaden fishery prediction in Mississippi Sound through ERTS-1 imagery
[E72-10340] 05 p0532 N73-14328
Applicated of ERTS-1 imagery to agriculture practices in Mississippi Delta region
[E73-10075] 07 p0780 N73-16337
Prediction of menhaden school location and movement in Mississippi Sound from ERTS-1 imagery
[E73-10079] 08 p0900 N73-17291
Application of ERTS-1 imagery to identification of agricultural crops, grasslands and forestry in Mississippi Delta Region
[E73-10476] 12 p1395 N73-21313
Improvement of Menhaden fishery prediction in Mississippi Sound using ERTS-1 imagery
[E73-10480] 12 p1396 N73-21317
Detection of menhaden schools in Mississippi Sound by comparing ERTS-1 imagery to selected oceanographic parameters
[E73-10580] 14 p1656 N73-23441
Detection of adult menhaden fish in Mississippi Sound from ERTS-1 imagery
[E73-10624] 15 p1775 N73-24384
Application of ERTS-1 data to agricultural practices in Mississippi Delta Region
[E73-10597] 16 p1896 N73-25335
Application of ERTS-1 imagery to harvest model of menhaden fishing industry in Mississippi Sound
[PAPER-M17] 19 p2282 N73-28355
Relationship between ERTS-1 fisheries distribution information and selected oceanographic parameters in Mississippi Sound
19 p2286 N73-28385
ERTS-1 detection of plant diseases and nutrient deficiencies, soil types and moisture levels, forests, and crop identification in Mississippi Delta
[E73-10849] 19 p2292 N73-28427
Agricultural and crop identification decisions in Mississippi Delta region of Mississippi using Skylab EREP data
[E73-10870] 20 p2393 N73-29221
Investigation of agricultural practices in Mississippi Delta region of Mississippi using ERTS-1 imagery
[E73-10881] 20 p2394 N73-29232
Application of ERTS-1 data to prediction and detection model for Menhaden fishing in Mississippi Delta
[E73-10961] 21 p2532 N73-30303
Utilization of ERTS-1 imagery to determine availability and distribution of adult Gulf menhaden within Mississippi Sound and adjacent waters
[E73-10980] 22 p2657 N73-31287
Identification of agricultural crops in Mississippi Delta from ERTS-1 imagery
[E73-11094] 23 p2783 N73-32261
Utilization of Skylab EREP data in making agriculturally oriented decisions in Mississippi Delta alluvial plain region
[E73-11125] 24 p2916 N73-33280

**MISSOURI**
Visual inspection of runway pavement conditions at Forney Army Airfield, Fort Leonard Wood, Missouri
[AD-743856] 01 p0037 N73-10294
Crop identification and acreage measurement in Idaho, Missouri, Kansas, and South Dakota using ERTS-1 imagery
[E72-10179] 01 p0045 N73-10358
Laboratory facility for regional air pollution study at St. Louis, Missouri
[PB-210019] 01 p0077 N73-10638
Scheduling management, and costs of St. Louis air pollution facility
[PB-210020] 01 p0077 N73-10639
Crop identification and acreage measurement in Missouri, Kansas, South Dakota, and Idaho using ERTS-1 imagery
[E72-10336] 05 p0531 N73-14324
Weekend effect in CCN spectra and St. Louis urban heat island
[TN-45] 07 p0815 N73-16606

Crop identification and acreage measurement in Missouri, Kansas, South Dakata, and Idaho based on ERTS-1 imagery and aerial photography
[E73-10328] 09 p1024 N73-18359
Detection and indentification of major airports in northeastern Kansas and northwestern Missouri
[E73-10471] 12 p1395 N73-21308
Identification and mapping of land use classes in Kansas City area by machine processing of ERTS-1 data
[E73-10578] 14 p1656 N73-23439
Utilization of ERTS-1 imagery for crop identification and acreage measurement in South Dakota, Kansas, Missouri, and Idaho
[E73-10734] 17 p2020 N73-26340
Inadvertent modification of cloud formation and weather by St. Louis area - Project Metromex 1
[PB-218678/1] 18 p2173 N73-27549
Application of ERTS-1 imagery for differentiating quaternary surface deposits and landforms in Illinois, Iowa, Missouri, Kansas, Nebraska, and South Dakota
[PAPER-G13] 19 p2264 N73-28244
Analysis of geologic features and ground patterns in selected areas of Missouri based on ERTS-1 data
[PAPER-G15] 19 p2265 N73-28246
Influence of image position on urban place detection in ERTS-1 imagery of Kansas and Missouri
[E73-10971] 21 p2533 N73-30312
Crop identification and acreage measurement in Missouri and Idaho from ERTS-1 imagery
[E73-10982] 22 p2658 N73-31289
Selected reclamation studies on geology and crop inventory using ERTS-1 imagery of lower Missouri region
[E73-11027] 22 p2662 N73-31331

**MIXED FLOW**
U MULTIPHASE FLOW

**MIXERS**
Millimeter wave mixer with small metallic wafer embedded with diodes
[NASA-CR-124060] 08 p0925 N73-17581
Design of dc brushless motor driven mixer unit for use in cryogenic fluids
[NASA-CR-120963] 22 p2647 N73-31209

**MIXING**
NT DISSOLVING
NT LAMINAR MIXING
NT SUSPENDING [MIXING]
NT TURBULENT MIXING
Convection and mixing of stratified fluids in rotating tank
[NASA-TR-R-392] 01 p0039 N73-10312

**MIXING CIRCUITS**
Design and performance of wideband down-converter for satellite ground terminal
[NASA-CR-128394] 01 p0032 N73-10249
Analysis of intermodulation and cross modulation distortions in broadband balanced bridge switching state MOSFET mixer
[AD-749064] 05 p0521 N73-14234
Nonlinear and parametric effects on synchronization and mixing of electron transfer microwave oscillators
18 p2123 N73-27155

**MIXING LENGTH FLOW THEORY**
Mixing length theory used to determine influence of pressure gradients on wall region of turbulent boundary layer
[AD-749371] 05 p0527 N73-14290
Rational approach to use of Prandtl mixing length model in free turbulent shear flow calculations
19 p2252 N73-28158

**MIXTURES**
NT ADMIXTURES
NT AEROSOLS
NT AQUEOUS SOLUTIONS
NT BINARY FLUIDS
NT BINARY MIXTURES
NT COLLOIDAL PROPELLANTS
NT COLLOIDS
NT DETONABLE GAS MIXTURES
NT DISPERSIONS
NT EMULSIONS
NT EUTECTIC ALLOYS
NT EUTECTICS
NT FOG
NT GAS MIXTURES
NT LIQUID-GAS MIXTURES
NT METAL MATRIX COMPOSITES
NT NUCLEAR EMULSIONS
NT PHOTOGRAPHIC EMULSIONS
NT SMOKE
NT SOLID SOLUTIONS
NT SOLID SUSPENSIONS
NT SOLUTIONS

**MNEMONICS**
Operational principles and functions of mnemonic diagrams in controlled system
21 p2503 N73-30083

**MOBILITY**
NT ELECTRON MOBILITY
NT HOLE MOBILITY
NT IONIC MOBILITY

**MODAL RESPONSE**
Modal analysis for Liapunov stability of rotating elastic bodies
[NASA-CR-124258] 15 p1839 N73-24904

**MODE OF VIBRATION**
U VIBRATION MODE

**MODE SHAPES**
U MODAL RESPONSE

**MODELS**
NT AIRCRAFT MODELS
NT ANALOG SIMULATION
NT ASTRONOMICAL MODELS
NT ATMOSPHERIC MODELS
NT BREADBOARD MODELS
NT DIGITAL SIMULATION
NT DYNAMIC MODELS
NT MATHEMATICAL MODELS
NT NUCLEAR MODELS
NT OCEAN MODELS
NT REFERENCE ATMOSPHERES
NT SCALE MODELS
NT SEMISPAN MODELS
NT SPACECRAFT MODELS
NT VECTOR DOMINANCE MODEL
NT WIND TUNNEL MODELS
Macroscopic models of quasi-chemical reactions, dielectric relaxation, and deformation energy
01 p0087 N73-10719
Computerized aerotriangulation with independent models and planimetric point adjustments
02 p0164 N73-11332
Computer program for strip triangulation by independent models in aerial photogrammetry
02 p0164 N73-11334
Model for operating partly resistive superconducting point contact, quantum interference device
[FOA-2-B-2035-E1] 02 p0218 N73-11764
Solar phenomenon, based on dynamo model
[PUBL-5] 05 p0592 N73-14809
Model medium concept in geometric optics for electromagnetic wave propagation in absorbing media
[MPI-PAE/EXTRATERR-60] 08 p0943 N73-17727
Theoretical model of optical excitation, emission, and deactivation properties of Meinel band system of nitrogen
[AD-753396] 09 p1069 N73-18722
Modeling atomic clock performance and detection of abnormal clock behavior
[NBS-TN-636] 12 p1427 N73-21565
Model for prediction of pressure within recirculation bubble of attached jet
13 p1507 N73-22216
Model of speech processing with perceptual asymmetry
14 p1626 N73-23173
Laboratory demonstration model of active cleaning technique device
[NASA-CR-124335] 21 p2582 N73-30696
VFR flight operations in 1972 Los Angeles Basin air traffic model
[FAA-NA-73-51] 22 p2697 N73-31605
Field measurements and earth model of polar motion
[NASA-TT-F-15066] 24 p2922 N73-33334

**MODEMS**
Performance analysis and conceptual design of waveform and modem to provide jamming-resistant command and control data link for ground station control of drone aircraft
[AD-756933] 13 p1496 N73-22125
Wideband communication command and control modem
[AD-762281] 19 p2238 N73-28042

**MODERATION [ENERGY ABSORPTION]**
NT THERMALIZATION [ENERGY ABSORPTION]

**MODERATORS**
Liquid hydrogen cold neutron moderator for use in channel H5 EL 3 reactor
[CEA-N-1571] 15 p1815 N73-24714

**MODES**
NT COUPLED MODES
NT LASER MODES
NT PROPAGATION MODES
NT VIBRATION MODE

**MODIFICATION**
U REVISIONS

**MODIFIERS**
U ADDITIVES

**MODULATION**
NT AMPLITUDE MODULATION
NT DELTA MODULATION
NT FEEDBACK FREQUENCY MODULATION
NT FREQUENCY MODULATION
NT FREQUENCY SHIFT KEYING
NT INTERMODULATION
NT LIGHT MODULATION
NT PHASE MODULATION
NT PHASE SHIFT KEYING
NT PULSE AMPLITUDE MODULATION
NT PULSE CODE MODULATION
NT PULSE DURATION MODULATION
NT PULSE FREQUENCY MODULATION
NT PULSE MODULATION
NT PULSE POSITION MODULATION
NT TRAVELING WAVE MODULATION
NT ULTRASONIC LIGHT MODULATION
NT VELOCITY MODULATION
Multimode transponders for tracking and data relay satellites
[NASA-CR-130170] 08 p0888 N73-17191
Digital coding and modulation processes in radio transmission
[NLL-PO-2832-[9022.81]] 11 p1254 N73-20177
Radar cross section modulation power spectrum in periodic motion of scattering object
[AD-756488] 13 p1494 N73-22109
Nonlinear modulation of analog data with improved digital enhancement technique
[AD-755939] 13 p1494 N73-22112
Design and performance of acoustic exciter for gas volume modulation in absorption cell
[NASA-CR-124269] 16 p1913 N73-25482
Spread spectrum modulation technique for use in airborne relay communication link
[AD-761522] 19 p2236 N73-28027
Cosmic ray modulation in solar envelope
19 p2337 N73-28803

**MODULATORS**
Growth of single crystal CdTe materials for use in infrared electro-optic devices
[AD-749368] 05 p0588 N73-14783
Coherent optical processing of phased array radar data, using electron beam addressed, potassium dideuterium phosphate modulator
05 p0610 N73-14957
Design of Brewster angle acousto-optic modulator for high power mode locked C02 laser
[AD-751680] 07 p0807 N73-16544
Modulator/demodulator for probing and analyzing forward scatter path at 15 GHz to clear air turbulence
[AD-753090] 09 p1030 N73-18413
Optical rotating intensity modulator for measuring positions and magnitudes of stars
10 p1211 N73-19848
Development of cadmium telluride modulator for infrared laser communication system
[NASA-CR-112321] 15 p1795 N73-24549
CO2 waveguide laser as master oscillator for high resolution optical radar application
[AD-758706] 15 p1796 N73-24561
Real time thermoplastic modulator for coherent optical processing
[AD-762920] 20 p2379 N73-29119

**MODULATORS-DEMODULATORS**

**MODULES**
NT COMMAND MODULES
NT COMMAND SERVICE MODULES
NT ELECTRONIC MODULES
NT LUNAR LANDING MODULES
NT LUNAR MODULE
NT SERVICE MODULES
NT SPACECRAFT MODULES
Design of compatible modular data management systems
[AD-749910] 13 p1497 N73-22133
Flow module approach to flow around three dimensional obstacles in boundary layer
24 p2908 N73-33207

**MODULUS OF ELASTICITY**
NT DYNAMIC MODULUS OF ELASTICITY
Development of direct method for determining complex modulus of linear viscoelastic materials as function of frequency
[UTIAS-159] 02 p0237 N73-11928
Influence of creep strain on elastic modulus, crystallographic orientation, and density of POCO graphite
[LA-DC-13292] 03 p0321 N73-12614
Elastic modulus and coefficient of linear thermal expansion of perlite-containing porcelain mixes
[AD-747393] 03 p0322 N73-12627
Effects of atomic ordering in ternary solid solutions containing alloys of nickel and iron and relation of Youngs modulus with temperature
[NLL-RTS-7654] 04 p0431 N73-13511
Elastic stress analysis of bi-material plate with crack normal to interfaces, using finite element method
[AD-748299] 04 p0439 N73-13579
Nondestructive measurement of modulus of elasticity of carbon fibers
[AD-749011] 04 p0440 N73-13585
Elastic modulus of composite polyblends and polymers having phase inversion
[AD-749973] 05 p0566 N73-14601
Mechanical properties of elastic rectangular plates with linear variations of thicknesses
[PB-211229] 06 p0727 N73-15932
Extended natural mode method for calculating flapwise bending, edgewise bending, and torsional vibration modes and frequencies of helicopter rotor blades
[DLR-FB-71-108] 09 p0983 N73-18026
Ultrasonic methods for analyzing elastic moduli of materials at high temperatures
[AD-753844] 10 p1176 N73-19567
Modulus theories for determining microstructure elasticity of laminated plates
[AD-754528] 11 p1309 N73-20619
Grinding wheel hardness determined from modulus of elasticity calculation
[CRIF-NT-9] 13 p1530 N73-22401

Analysis of elastic properties of Invar and Elinvar alloys at various temperatures
13 p1540 N73-22480
Techniques for determining complex Young and shear modulus of linear viscoelastic materials
[AD-755718] 13 p1588 N73-22873
Measurement of elastic moduli and compressive yield strength for Ni3[Al,X] alloy single crystals
16 p1927 N73-25589
Modulus of elasticity measurements on materials at elevated temperatures
[AD-759060] 16 p1971 N73-25941
Mechanical property determination and fracture mechanics of fiber reinforced composite materials
[D-MAT-178] 17 p2051 N73-26589
Finite element calculation of tapered double cantilever beam modulus of elasticity for sharp blunted cracks
[NLR-TR-72083-U] 17 p2094 N73-26941
Statistical elasticity theory for initial stresses in reinforced and filled polymers
20 p2434 N73-29551
Measurement of elastic moduli of materials at elevated temperatures
[AD-763763] 21 p2554 N73-30473
Single crystal elastic moduli of V3Si for measuring hydrostatic pressures
24 p2967 N73-33714

**MOHR CIRCLES**
U FRACTURE MECHANICS

**MOIRE EFFECTS**
Moire patterns in circular carrier frequency photography for observing phase objects
[NASA-CR-130198] 11 p1292 N73-20481
Formation of longitudinal edge waviness and center camber on sheets as measure of sheet flatness
[NLL-M-21611-[5828.4F]] 18 p2202 N73-27777

**MOISTURE**
NT SOIL MOISTURE
High speed photographic system for moisture flow visualization in steam turbines
[NASA-TM-X-2763] 12 p1404 N73-21388

**MOISTURE CONTENT**
NT ATMOSPHERIC MOISTURE
Hydrological applications of side-looking radar, noting soil moisture, ground water, and water loss
03 p0295 N73-12407
Remote detection of water content and spectral properties of leaves in different soybean crop species
04 p0378 N73-13070
Detection of plant diseases and nutrient deficiencies, soil types, and moisture levels in Tennessee using ERTS-1 imagery
[E72-10320] 04 p0413 N73-13368
Measurements of thermal conductivity in boulder clay and effects of soil moisture conductivity
[NASA-TT-F-14664] 07 p0793 N73-16446
Soil moisture measurements for microwave radiometers onboard Convair 990 aircraft
08 p0971 N73-17935
Remote sensing of fallow soil moisture, using visible and infrared scanners
13 p1514 N73-22267
Use of remote airborne photopolarimeters to measure soil moisture content in southwestern United States
[NASA-CR-130211] 13 p1522 N73-22332
Utilization of ERTS-1 imagery to detect plant diseases, nutrient deficiencies, soil types, and moisture levels in Tennessee
[E73-10640] 15 p1776 N73-24399
Water content of Mars atmospheres as measured by Mars 3 automatic space station
[JPRS-59231] 15 p1830 N73-24833
Application of airborne microwave radiometers for remote monitoring of soil moisture in selected areas of Texas and Oklahoma
[NASA-CR-133102] 17 p2031 N73-26438
Application of airborne microwave radiometry for remote sensing of soil moisture in southwest US
[NASA-TM-X-66265] 17 p2032 N73-26444
Aircraft gamma surveys of moisture content in soil detention layer
20 p2448 N73-29667
Skylab imagery of terrain surface moisture, vegetation, and forestation in Colorado and Oregon
[E73-11001] 22 p2659 N73-31306

**MOISTURE METERS**
NT HYGROMETERS
NT PSYCHROMETERS

**MOL [ORBITAL LABORATORIES]**
U MANNED ORBITAL LABORATORIES

**MOLDING MATERIALS**
Optimal tensile strength composition for molding compounds of epoxy resin reinforced with glass fibers
[AD-754763] 11 p1309 N73-20620
Mathematical structure and stress constitutive problem of materials with permanent memory particularly filled propellants
[AD-763753] 21 p2587 N73-30732
Precursor carbons and molding of graphites
[Y-1857] 24 p2954 N73-33598

**MOLDS**
Vacuum displacement compression molding of tubular bodies from thermosetting plastics
[NASA-CASE-LAR-10782-2] 22 p2677 N73-31444
Compression molding apparatus for thermosetting plastic compositions
[NASA-CASE-LAR-10489-2] 22 p2677 N73-31446

**MOLECULAR ABSORPTION**
High dispersion Coude spectrograms of zeta Oph and Per, and molecular absorption in interstellar medium
[NASA-TM-X-66073] 02 p0224 N73-11812
Absorption cross sections of Schumann-Runge bands of molecular oxygen
[A-107-1972] 04 p0385 N73-13127
Molecular absorption coefficients for H20-N2 mixtures as measured by Co laser
[AD-760140] 19 p2308 N73-28561

**MOLECULAR BEAMS**
Effect of skimmer interation on properties of partially condensed molecular beams
[AD-746292] 02 p0157 N73-11269
Rare molecular gas beam scattering from single metal crystal surfaces
[AD-748938] 04 p0451 N73-13685
Design and system description of hypersonic low density wind tunnel in Germany including generation of molecular beams
[DLR-FB-71-84] 06 p0650 N73-15279
Mass spectroscopy of C state in iodine by crossing of molecular beam with pulsed laser beam and monitoring recoil photofragments
[AD-751611] 07 p0753 N73-16117
Design of time of flight chemical accelerator for low center-of-mass energy spreads and measurement of electron affinity of N02
[AD-753133] 09 p1012 N73-18258
Gas jets, seeding, and thermal excitation for producing neutral molecular beams
[DLR-FB-72-52] 09 p1068 N73-18717
Development and characteristics of molecular beam mass spectrometer system for sampling rocket engine combustion chambers
[NASA-CR-130933] 10 p1137 N73-19267
Reactive crossed molecular beam studies using free jet sources
18 p2180 N73-27605

**MOLECULAR BONDS**
U CHEMICAL BONDS

**MOLECULAR CHAINS**
Ultraviolet radiation, X rays, freezing, and thawing effects on ribonuclease
10 p1119 N73-19120

**MOLECULAR COLLISIONS**
Crossed molecular beam method for measuring elastic differential scattering cross sections of potassium with gaseous media
02 p0213 N73-11729
Vibrational energy transfer in gas lasers
[AD-748858] 04 p0387 N73-13143
Research reports on SQUID programs related to fluid mechanics, and atomic and molecular collisions
[AD-752037] 08 p0955 N73-17820
Theoretical analysis of effects of outgassing and waste dumping on contamination of orbiting spacecraft
[NASA-CR-124131] 11 p1340 N73-20875
Equations of motion for calculating collision dynamics of diatomic molecules
[NASA-CR-131527] 12 p1431 N73-21594
Cross section data for collision processes between molecular oxygen and electrons
[NASA-TT-F-15011] 19 p2354 N73-28934
Semiclassical approximation to atom symmetric top rotational excitation
[NASA-CR-133849] 21 p2582 N73-30690

**MOLECULAR DIFFUSION**
Molecular diffusion in mixing binary flow and separation of uranium isotopes by fixed wall centrifugation
06 p0653 N73-15302
General equations for describing molecular diffusion in vortex flow and possible application to isotopic separation by fixed wall centrifugation
[FRNC-TH-213] 08 p0897 N73-17262
Diffision in niobium of beryllium and aluminum from solid phase at 900 to 1300 deg
[NLL-CE-TRANS-5121-[9022.09]]
20 p2429 N73-29513
Effects of diffusion on aluminum depletion and degradation of NiAl coatings on superalloys
[NASA-TM-X-68274] 20 p2435 N73-29555
Application of Monte Carlo method and Markov random walks to determine molecular diffusion through rarefied gas
[NASA-TN-D-7405] 23 p2776 N73-32197

**MOLECULAR DISSOCIATION**
U DISSOCIATION

**MOLECULAR ELECTRONICS**
NT LARGE SCALE INTEGRATION

**MOLECULAR ENERGY LEVELS**
NT INTERMOLECULAR FORCES
Analysis of energy transfer processes in molecular lasers
[AD-745368] 01 p0066 N73-10537
Molecular branching ratio method for intensity calibration of optical systems in far ultraviolet
[NASA-TM-X-66070] 01 p0103 N73-10853
Calculation of vibrational energy level distributions of hydrogen fluoride formed during atomic fluoride reaction with molecular hydrogen
[AD-748291] 04 p0387 N73-13146
Mass spectroscopy of C state in iodine by crossing of molecular beam with pulsed laser beam and monitoring recoil photofragments
[AD-751611] 07 p0753 N73-16117
Perturbation theoretical and graphical representation of vertical ionization energies and electron affinities of free molecules
08 p0916 N73-17506
Production of laser output by excitation of hydrogen chloride vibrational levels using electron impact
[AD-752631] 08 p0930 N73-17615
Synthesis of A to X bands of OH and a to X bands of O2 for studying electronic transitions, rational branch structure, and rotational transition probabilities
[DREV-TN-2012/72] 08 p0945 N73-17742
Analysis of wave propagation and amplification properties of molecular electronic plasma to show energy transfer effects
[PSU-IRL-SCI-403] 08 p0948 N73-17759
Infrared spectra of aluminum, gallium, and indium suboxide vapors considering frequency oscillations in group 3 suboxides and molecular constants of boron oxide
[AD-752861] 09 p1000 N73-18164
Analyses of vibrational levels by least squares method for determining transition moment probabilities in nitrogen band
[AD-753394] 09 p1075 N73-18774
CO2/N2 laser applied to CO2 excited state population study during supersonic nozzle expansion
[ONERA-NT-204] 10 p1169 N73-19510
Spectroscopic analyses of molecular energy levels in crystals
[AD-753382] 10 p1201 N73-19776
Chemical and molecular laser research
[AD-754792] 11 p1303 N73-20575
Excitation and deexcitation of vibration in gases by nitrogen and oxygen atoms in upper atmosphere
[AD-757050] 14 p1617 N73-23099
Model of pulsed CO/N2 molecular laser system with emphasis on mixture components and temperature variation
[AD-755197] 14 p1673 N73-23573
Analysis of elementary, exothermic, atom-molecule reactions for application as laser materials for chemical lasers
[AD-756686] 14 p1673 N73-23578
Electron beam analysis of molecular and atomic oxygen properties
[AD-759196] 16 p1872 N73-25159
Molecular laser model for pulsed carbon monoxide/nitrogen system
[AD-759509] 16 p1924 N73-25571
Oscillation relaxation time of CO2 molecular energy levels in temperature intervals 300 to 600 K.
[AD-762436] 19 p2323 N73-28688
Vibrational cross section resonances of excited state in nitrogen and carbon monoxide
[AD-764596] 23 p2754 N73-32042
Photoelectron spectroscopic analysis of excited hydrogen fluoride in contaminated atmospheres
[AD-764813] 24 p2893 N73-33093

**MOLECULAR EXCITATION**
Interstellar cloud heating by collisionally de-exciting vibrationally excited molecular hydrogen
[NASA-TM-X-66064] 01 p0103 N73-10851
Generation spectrum of excited DF molecules obtained during chemical reactions in D2/F2/N2/O2 laser system
[NLL-DRIC-TRANS-2816-[3623.66]]
02 p0180 N73-11458
Analysis of inversion medium of quasi-stationary carbon dioxide laser to show molecules in vibrational and rotational states
12 p1410 N73-21424
Distribution of vibrationally excited molecular nitrogen in auroral red arc and effect on ionospheric electron densities
24 p2912 N73-33241

**MOLECULAR FLOW**
NT SLIP FLOW
NT TRANSITION FLOW
Measurement of aerodynamic drag of conical bodies at zero angle of attack in free molecular and near free molecular flow regime
[DLR-FB-72-64] 09 p1014 N73-18278
Gas jets, seeding, and thermal excitation for producing neutral molecular beams
[DLR-FB-72-52] 09 p1068 N73-18717
Kinetic molecular flow distribution at porous wall using one dimensional steady state Boltzmann equation
[VKI-TN-79] 22 p2654 N73-31259

**MOLECULAR GASES**
NT DIATOMIC GASES
Cross section measurements for electron impact at low energies in molecular gases
[AD-747304] 02 p0139 N73-11123

Direct generation of far infrared power through laser action on rotational transitions in molecular gases
[AD-745984] 02 p0182 N73-11476
Electrically excited, high power, molecular gas lasers
[AD-746148] 02 p0182 N73-11478
Reaction between molecular hydrogen and molecular oxygen subjected to temperature and pressure pulses in shock tubes
[NASA-TM-X-2707] 07 p0854 N73-16928
Diagnostic spectroscopy of plasmas produced in molecular gases
[AD-751938] 08 p0950 N73-17776
Stability of molecular gas discharges typical of those used in high power lasers
[AD-757083] 13 p1537 N73-22456
Differential scattering from collision of metastable atoms of He[2 3S] with molecules of N2 and O2
[NASA-TT-F-14801] 15 p1815 N73-24712
IR laser study of absorption and saturation properties of molecular gases
[NASA-CR-132769] 19 p2307 N73-28554
Vibrational temperature and density of molecular oxygen component in expansion tube
[NASA-TN-D-7273] 22 p2653 N73-31249
Inelastic light scattering from molecular gases with applications to remote detection of air pollutants
24 p2891 N73-33077

**MOLECULAR INTERACTIONS**
NT MOLECULAR COLLISIONS
EPR study of molecular ordering in smectic-A liquid crystals without nematic phases
[NASA-TN-D-7124] 04 p0437 N73-13563
Atomic and molecular reaction kinetics in upper atmosphere
[AD-753246] 09 p1000 N73-18158
Vapor phase chemistry for producing hydrated ions in upper atmosphere
[AD-753940] 10 p1157 N73-19411
Models for interaction of rarefied gas with solid surface
12 p1418 N73-21491
Thermoelectric converter and 5-kwe reactor system integration
[NASA-CR-121230] 16 p1943 N73-25726
Determination of complex Hamaker constants of molecular interactions in black hydrocarbon emulsion films
[NLL-M-2300-[5828.4F]] 20 p2373 N73-29069
Adhesion criterion in gas solid interface
[NASA-CR-133618] 20 p2374 N73-29075
Intermolecular force effects on infrared spectral transparency of active gas mixtures
[DRIC-TRANS-3227] 23 p2820 N73-32545
Generalized equations for transport coefficients assuming intramolecular interaction potentials
24 p2908 N73-33205

**MOLECULAR IONS**
Mass spectra and dissociation energies of high temperature gaseous molecules containing aluminum
[NASA-TN-D-7123] 04 p0386 N73-13138
Molecular mechanisms of conduction and polarization in water vapor, liquid water, and ice
[AD-762060] 19 p2231 N73-27993

**MOLECULAR ORBITALS**
Mathematical model for calculating relative molecular orbital photoionization cross sections in soft X ray region
[UUIP-753] 17 p2066 N73-26714

**MOLECULAR OSCILLATIONS**
Laser luminescence and shock heating for hydrogen fluoride vibrational relaxation measurements in shock tube
[AD-745953] 02 p0138 N73-11119
Operating principles of gas dynamic lasers and effects of gas dynamic flow on laser system properties
02 p0181 N73-11469

**MOLECULAR PHYSICS**
Summary of experimental programs performed using NBS reactor during 1971 and 1972
[NBS-TN-758] 12 p1426 N73-21559

**MOLECULAR RELAXATION**
Nuclear magnetic relaxation in He-3 impuriton gas
[NUB-2155] 01 p0083 N73-10687
Acoustic properties of air and sound absorption anomalies due to molecular relaxation
[AD-750220] 05 p0581 N73-14732
General relaxation theory for liquid behavior under dynamic conditions
[NASA-CR-2141] 07 p0769 N73-16245
Measurement of volume relaxation and crystal defects associated with interstitial ion in X irradiated KBr during isothermal annealing
07 p0831 N73-16735
Solution of Boltzmann kinetic equation for relaxation of gas mixture
12 p1418 N73-21486
Solution of relaxation problem for Boltzmann equation by integral iteration method
12 p1418 N73-21489
Vibrational relaxation of DF behind incident shock waves
[AD-756462] 13 p1562 N73-22658
Electron beam probing technique for measuring hypersonic rarefied gas density, vibration, and rotational temperature
[ONERA-P-146] 15 p1788 N73-24497
Structure of weak shock wave in vibrationally relaxing gas undergoing wall reflection
17 p2013 N73-26277
Electric discharges in supersonic high pressure gas flow to improve carbon dioxide laser power
[ISL-20/72] 19 p2307 N73-28560
Vibration-rotation relaxation using mode locked and Q switch gas lasers
[AD-763292] 21 p2555 N73-30481

**MOLECULAR ROTATION**
Nuclear magnetic resonance spectroscopy to measure order parameter in diatomic molecule rotational ordering transitions
[NOTA-INTERNA-376] 01 p0083 N73-10691
Nozzle flow free jet and Prandtl-Meyer expansion rotational relaxation equation used for relaxation time calculation
[REPT-72-5] 14 p1650 N73-23383
Electron beam probing technique for measuring hypersonic rarefied gas density, vibration, and rotational temperature
[ONERA-P-146] 15 p1788 N73-24497
Solid state laser induced excitation of HF second vibration rotation energy levels
15 p1794 N73-24547

**MOLECULAR SIEVES**
U ABSORBENTS

**MOLECULAR SPECTRA**
NT ELECTRONIC SPECTRA
NT RAMAN SPECTRA
NT VIBRATIONAL SPECTRA
Spontaneous and stimulating scattering and molecular spectra
[AD-746497] 02 p0212 N73-11718
Atomic and molecular spectra of SC stars
04 p0469 N73-13821
Rotational temperature measurement in nitrogen using unresolved rotational spectra
[DLR-FB-72-15] 09 p0998 N73-18148
Monochromatic absorption coefficient in narrow regions of oscillatory-rotational spectrum of H2O
[AD-759238] 16 p1946 N73-25743
Emission spectra of interstellar molecules
[NASA-TT-F-14961] 17 p2083 N73-26849
Interstellar molecular hydrogen lines in ultraviolet spectrum of delta Scorpii
22 p2734 N73-31886

**MOLECULAR SPECTROSCOPY**
NT RAMAN SPECTROSCOPY
Valence electron model for calculating ionization energies and excited levels in photoelectron- and absorption-spectra
08 p0945 N73-17741
Application of microwave-optical double resonance spectroscopy to analyze structural properties of phosphorescent triplet states of organic molecules
[COO-3435-6] 12 p1405 N73-21398
Research projects in atomic and molecular spectroscopy
[NASA-CR-131829] 13 p1495 N73-22119
Intensity relations and spectral satellite studies of alkali/foreign gas interactions
13 p1528 N73-22385
Collision broadening of rotational spectrum of gases
[AD-758852] 16 p1872 N73-25155
Absolute polarization and microwave optical photoselection spectroscopy of zerofield transitions of triplet state
[AD-759996] 17 p1993 N73-26115
Analysis of electron spectroscopy considering line widths, resolution, X ray emission, and quantum mechanics
[UUIP-752] 17 p2034 N73-26460
Lamb dip in millimeter-wave molecular spectroscopy
20 p2454 N73-29719
Optimized sensitivity of computer controlled microwave spectrometer for trace element detection
[BMVG-FBWT-73-18] 23 p2754 N73-32037
Development of high resolving power interferometer for line shape measurement applications
[AD-764719] 24 p2927 N73-33380

**MOLECULAR STRUCTURE**
Isocyanide spin label for studying conformational transitions in cytochrome c, emphasizing heme group
[NASA-TT-F-14623] 03 p0259 N73-12099
Effect of structural changes on electrical and magnetic properties of amorphous semiconducting material
[AD-748661] 04 p0460 N73-13751
Thermomechanical behavior and structure of poly(carborane-siloxane)s containing icosahedral cages in nitrogen environment
[AD-749364] 05 p0566 N73-14598
Relationship of molecular structure to thermo-oxidative stability of carborane-siloxane polymers with icosohedral CB10H10C cages
[AD-749820] 05 p0567 N73-14610
Influence of chemical composition and molecular structure of liquid lubricant on its performance
[NASA-TM-X-68183] 07 p0804 N73-16521
Valence electron model for calculating ionization energies and excited levels in photoelectron- and absorption-spectra
08 p0945 N73-17741
Electronic spectra of benzophenone crystals and low temperature spectra of ketones
[AD-753380] 10 p1201 N73-19775
Minimization technique for determining structural parameters of IR and vibrational rotational spectra of H2O
[AD-754612] 11 p1253 N73-20166
Research and development in chemical and extractive metallurgy and molecular crystals
[AD-754797] 11 p1327 N73-20770
Molecular structures and optical properties of polymer chain materials
[AD-758837] 16 p1872 N73-25156
Phonon dispersions and three particle correlations in liquid helium, and adsorbed helium monolayers
16 p1944 N73-25730
Nuclear magnetic resonance spectrum analysis for rings inversion rate in benzodiazepine derivatives
[RAE-LIB-TRANS-1628] 17 p1991 N73-26103
Molecular structure studied by electron spectroscopy emphasizing X ray induced spectra
[UUIP-754] 17 p2066 N73-26715
Optical and magnetic resonance spectra of uranium borohydride in hafnium borohydride
[AD-759371] 17 p2074 N73-26777
Materials research covering properties, structure, and synthesis
[AD-760021] 17 p2100 N73-26988
Perturbation theory of dynamic structure factors in high frequency liquids
[AD-761659] 19 p2230 N73-27987
Molecular organization of active center of microsomal cytochrome P-450
[NASA-TT-F-15042] 20 p2368 N73-29042
Chemical analysis of structure and strength of polymeric glasses, elastomers, fibers, and solid polymeric systems with high degree of crosslinking
[AD-763398] 21 p2564 N73-30555
Computer program for determining rotational line intensity of diatomic molecules -users manual
[NASA-TN-D-7268] 21 p2582 N73-30689

**MOLECULAR THEORY**
Molecular-kinetic theory for determining temperature dependence of simple liquid viscosity
[AD-747089] 02 p0159 N73-11286
International conference on fundamental atomic and molecular physics
[AD-757890] 15 p1816 N73-24717
Molecular-kinetic theory of nature of polymer friction
[NLL-RISLEY-TR-2577-[9091.9F]] 16 p1931 N73-25628

**MOLECULAR WEIGHT**
NT LOW MOLECULAR WEIGHTS
Density and flow visualization of different molecular weight gases from concentric orifices as determined by beam fluorescence technique
[ISAS-486-VOL-37-12] 02 p0155 N73-11256
Photolysis of perfluorodienes and diacyl fluorides to produce high molecular weight perfluorocarbon polyether gums
[NASA-CR-130552] 08 p0883 N73-17149
Quadratic programming with regularization for analyzing polymer molecular weight distribution
[AD-761818] 19 p2234 N73-28009

**MOLECULES**
NT DIATOMIC MOLECULES
Molecular contamination performance determination for space chamber tests, including molecular flow conditions and parameters
[NASA-TN-D-7250] 15 p1760 N73-24264
Thermal quenching of luminescence and conformational transformations in macromolecules of some polymers
[NRC-TT-1631] 15 p1815 N73-24711
Orientation of molecules of soil soluble surfactant in absorption layers on liquid-liquid interface
[NLL-M-2298-[5828.4F]] 20 p2373 N73-29068

**MOLIERE FORMULA**
U COSMIC RAY SHOWERS
U SECONDARY COSMIC RAYS
U SPATIAL DISTRIBUTION

**MOLNIYA SATELLITES**
Orientation system for Molniya-1 communications satellite
23 p2848 N73-32756

**MOLTEN SALT ELECTROLYTES**
Ultrasonic velocity measurements for determining adiabatic compressibilities of ionic solutions and molten salts
[AD-749353] 04 p0451 N73-13686
Thermodynamics of molten mixtures of lithium chloride-potassium chloride at 640 C
[AD-752087] 08 p0970 N73-17925
Purification of molten lithium fluoride, sodium fluoride, and potassium fluoride salt eutectics for thermal battery electrolyte application
[AD-758001] 15 p1739 N73-24097

**MOLYBDATES**
Chemical reactions involved with molybdenum, tungsten, vanadium, and chromium additives in hydrogen-oxygen flames seeded with potassium
[AD-743514] 01 p0023 N73-10179
Photon energy and polarization effects on optical absorption spectra of GMO at varying temperatures
23 p2824 N73-32574

**MOLYBDENUM**
Factors affecting orientation of chemical vapor deposited molybdenum coatings precipitated from gaseous phase
[AD-747082] 02 p0194 N73-11566
Explosive welding process for producing molybdenum wire reinforced columbium alloy composites
[NASA-CR-123937] 03 p0305 N73-12490
Recrystallization of hydrostatically extruded molybdenum, and plastic deformation of extruded samples
[AD-747400] 03 p0317 N73-12581
Recovery of elastic properties and internal friction of hydrostatically extruded molybdenum with 0 to 80 percent deformation
[AD-747515] 03 p0317 N73-12586
PUO2-Mo cermet spheres for use as isotopic power fuels
[MCM-1887] 03 p0333 N73-12715
Fabrication and properties of structural materials based on ceramic titanium powders alloyed with molybdenum and aluminum
04 p0432 N73-13520
Tight binding interpolation representing transition and noble metal s, p, and d bands applied to Mo and Cu
[IS-T-515] 04 p0434 N73-13535
Elastic properties and internal friction of hydrostatically extruded molybdenum
[AD-749539] 05 p0563 N73-14574
Recognition of geologic framework of copper and molybdenum porphyry deposits on ERTS-1 imagery of Navada and Utah
[E73-10020] 06 p0659 N73-15356
Characteristic property data for plutonia molybdenum radioisotopic cermet fuel
[LA-4976] 06 p0698 N73-15694
Development of plutonium dioxide molybdenum cermet nuclear fuels
[MLM-1905] 07 p0820 N73-16643
Kinetics and thermodynamics of oxygen conversion from gas to metal phase in tungsten and molybdenum
12 p1412 N73-21446
Recognition of characteristic geological structures associated with mineral deposits of copper molybdenum porphyry type
[E73-10526] 13 p1517 N73-22293
Effect of dissolved hydrogen on mechanical and superconducting properties of molybdenum
13 p1565 N73-22681
Identification of copper/molybdenum porphyry mineral deposits in characteristic geologic setting in Nevada, Arizona, Colorado, Australia, Alaska, and New Guinea
[E73-10762] 17 p2023 N73-26362
Electron spin resonance measurements on Fermi levels in molybdenum doped rutile during hydrogen treatment
[AD-760735] 18 p2192 N73-27694
Development of procedures for determining molybdenum in iron and steel with emphasis on factors affecting stablity and temperature dependence
[TN-303] 20 p2431 N73-29529
Recognition of geologic framework for ERTS-1 identification of mineral deposits of copper/molybdenum prophyry type in Colorado, Nevada, Arizona, and Australia
[E73-10960] 21 p2532 N73-30302
Reaction kinetics and solid solubility of oxygen in molybdenum
22 p2624 N73-31027
Adsorption kinetics of CO on [100] face of molybdenum single crystal
[CEA-CONF-2194] 22 p2684 N73-31499
Molybdenum reflector reactivity and space power reactor control
[NASA-TM-X-2922] 23 p2819 N73-32533
Ultrasonic attenuation of longitudial sound waves in superconducting molybdenum single crystals
23 p2825 N73-32581
Annealing effects on room temperature ductility of molybdenum
[CEA-CONF-2236] 24 p2935 N73-33443

**MOLYBDENUM ALLOYS**
Effects of molybdenum and tungsten fiber reinforcements on nickel chromium aluminum matrix alloys
[NLL-TRANS-746-1193-[9022.401]]
02 p0191 N73-11546
Analysis of effects of heat treatment of magnetic and physical properties of molybdenum permalloy
[NLL-RTS-7641] 04 p0431 N73-13509
Effect of molybdenum addition on physicomechanical properties of titanium-carbon-nickel composite alloys
[NLL-LTI-746-1422-[9022.401]]
15 p1797 N73-24565
Interfacial wear reactions in nickel and molybdenum alloy mechanical face seals
[AD-762076] 19 p2306 N73-28546
Homogeneity regions of superconducting phases in molybdenum - platinum system
[NASA-TT-F-15139] 22 p2706 N73-31674

**MOLYBDENUM CARBIDES**
Microstructure of molybdenum carbide samples during hot pressing and development of line intensity diagram for various conditions
23 p2808 N73-32449
Interaction of powders of carbides of zirconium, niobium, and molybdenum with silicon using X ray and chemical analysis to determine reaction products
23 p2809 N73-32461

**MOLYBDENUM COMPOUNDS**
NT MOLYBDATES
NT MOLYBDENUM DISULFIDES
Thermal cycling tests of molybdenum foil-zirconium cloth insulation system
[ALO-2832-45] 10 p1224 N73-19951
Thermodynamics of chemical species relative to aerospace technology including topics in chemical reaction kinetics and heat measurement
[AD-757518] 14 p1617 N73-23097
Production and characteristics of sintered titanium diboride-molybdenum compacts
23 p2808 N73-32453

**MOLYBDENUM DISULFIDES**
Properties and applications of solid lubricant coatings using molybdenum disulfide base
[AD-750998] 06 p0678 N73-15518
Influence of surface finishing on adherence of radio frequency sputtered molybdenum disulfide on silver, gold, copper, and bronze
[NASA-TN-D-7169] 07 p0804 N73-16523
Characteristics of molybdenum disulfide films radio frequency sputtered on aluminum and nickel surfaces at elevated, ambient, and liquid nitrogen temperatures
[NASA-TN-D-7170] 08 p0927 N73-17593
High field superconductivity in alkali metal [Na, K, Rb, and Cs] intercalates of MoS2
[NASA-TM-X-68206] 11 p1330 N73-20794

**MOLYBDENUM SULFIDES**
NT MOLYBDENUM DISULFIDES
MoS2 and MoS2/PTFE composite layers for dry lubrication of journal bearings in atmosphere or vacuum
[DLR-FB-72-69] 09 p1038 N73-18470

**MOMENT DISTRIBUTION**
Prediction of Magnus force and moment coefficients for bodies of revolution
[SC-RR-72-0537] 15 p1731 N73-24039
Four moment method for studying thermal conductivity in rarefied gas confined in concentric cylinders
16 p1973 N73-25955

**MOMENTS**
NT BENDING MOMENTS
NT DIPOLE MOMENTS
NT DISTRIBUTION MOMENTS
NT ELECTRIC MOMENTS
NT MAGNETIC MOMENTS
NT MEAN
NT MOMENTS OF INERTIA
NT PITCHING MOMENTS
NT ROLLING MOMENTS
NT STABILITY DERIVATIVES
NT TORQUE
NT VARIANCE [STATISTICS]
NT YAWING MOMENTS
Computer code for generating spatial-angular moments of adjoint gamma-ray flux in infinite mediums
[NBS-TN-748] 10 p1193 N73-19702
Dependences between braking and precession moments acting on spherical rotor in magnetic suspension
21 p2547 N73-30422

**MOMENTS OF INERTIA**
Errors in air temperature measurement resulting from instrument inertia
04 p0443 N73-13615
SOS - computer program for calculating weight, center of gavity, and inertias of asymmetrical missiles
[AD-749251] 05 p0601 N73-14885
Inertially coupled equations of motion for analyzing pitching and yawing motions of nonrolling wind tunnel model
[AD-752208] 08 p0926 N73-17586
Moments and products measurement of inertia of aircraft weighing up to 300,000 lbs
[AD-758398] 14 p1669 N73-23546

**MOMENTUM**
NT ANGULAR MOMENTUM
Measurement of momentum of two-phase liquid-vapor flow from pipe of circular cross-section
[EUR-4785-I] 03 p0284 N73-12302
Mass and momentum of control signals in switching mechanism of fluid bistable amplifiers
[AD-756583] 13 p1511 N73-22243
Design and performance of momentum wheel suspended by magnetic bearings for rotor operation in space environment
18 p2209 N73-27829

**MOMENTUM ENERGY**
U KINETIC ENERGY

**MOMENTUM PRECESSION**
U PRECESSION

**MOMENTUM TRANSFER**
Characteristics of turbulent separated flows, and calculations of momentum and heat transfer in them
[EF/TN/A/49] 01 p0039 N73-10308
Relation between momentum transfer and capture, and total scattering cross sections for ion-dipole collisions
[NASA-TM-X-68151] 01 p0083 N73-10685
Light cone analysis of large momentum transfer limit of electroproduction structure function at constant missing mass and of its connection with Bjorken limit
[TR-73-066] 03 p0339 N73-12766
Spectrometric measurements of cryogenic helium 4 scattering angle and momentum transfer
[CONF-720833-10] 12 p1440 N73-21669
Generalized momentum transfer hypothesis for non-Newtonian power-law fluids
23 p2771 N73-32168

**MONATOMIC GASES**
Analysis of mass transfer through binary, monatomic gas mixture of arbitrary composition contained between two plane parallel surfaces
[COO-2032-10] 03 p0284 N73-12304
Numerical analysis of flow of rarefied monatomic gas through two dimensional slot to show characteristics of transition regime
[NASA-CR-124069] 09 p1012 N73-18265
Scattering kernel analysis on monatomic gas interaction with solid surface
[AD-755838] 13 p1489 N73-22069
Transition Poiseuille flow through long cylindrical capillary
13 p1508 N73-22224

**MONITORS**
Beam current monitoring system and performance for linear accelerator
[AD-745841] 01 p0038 N73-10299
Voltage sensor counter as three-phase power disturbance monitor
[AD-746169] 02 p0129 N73-11049
Design and characteristics of instrument for monitoring carbon monoxide content of ambient atmosphere to include operations and maintenance instructions
[NASA-CR-128602] 02 p0172 N73-11394
Modification of atmosphere contamination sensor to include carbon monoxide monitoring capability
[NASA-CR-128604] 02 p0172 N73-11395
Failure analysis of malfunction of Apollo 16 television camera monitor on command module
[NASA-TM-X-68930] 06 p0639 N73-15190
List of facilities and environmental measurements to be monitored in support of Skylab 2 at Launch Complex 39
[NASA-TM-X-68916] 07 p0849 N73-16879
Opposed electrode, parallel gap, and percussive arc monitoring systems
[BDX-613-544] 10 p1134 N73-19244
Telemetric monitor for in-situ transmission of solid propellant mechanical property data
[AD-754253] 10 p1162 N73-19454
Development of droplet monitoring probe for use in analysis of droplet propagation in mixed-phase fluid stream
[NASA-CASE-NPO-10985] 11 p1291 N73-20478
Program debugging and monitoring facilities for improving diagnostic capability of compiler
[NBS-TN-763] 12 p1381 N73-21197
Multichannel medical monitoring system to measure physiological parameters from display device at remote control station
[NASA-CASE-MSC-14180-1] 13 p1486 N73-22045
CSTR system for measuring ozone reactions in lower atmosphere
13 p1514 N73-22269
Calorimetric calibration method for commercial power monitor used with high power microwave generators
[PB-213970/7] 14 p1669 N73-23548
Cost analyses on mass spectrometric and gas chromatographic atmospheric monitoring systems
[NASA-CR-124331] 19 p2315 N73-28622
Sample-and-hold circuit for monitoring system calibration
[AD-764242] 22 p2676 N73-31434
Pilot display for monitoring of automatic steep approach
[DGLR-PAPER-73-031] 23 p2744 N73-31964
Monitoring and control of fuel cell system by digital computer
[NASA-TM-X-2923] 23 p2748 N73-31994
Monitoring and recording lightning strokes in predetermined area
[NASA-CASE-KSC-10728-1] 23 p2790 N73-32319

**MONKEYS**
Neutron and gamma induced transient incapacitation in conditioned Macaca mulatta
[AD-742076] 01 p0010 N73-10080
Rhesus monkey heart rate during expercise using implanted ECG telemeters
[AD-744930] 01 p0011 N73-10089

High altitude effects on cerebral and cardiovascular systems of monkeys
[AD-745891] 02 p0134 N73-11085
Laboratory restraint chair for squirrel monkeys
[AD-746661] 02 p0154 N73-11246
Observation of circulating lymphocytoid cell in monkey after exposure to radio waves
[AD-749583] 06 p0631 N73-15128
Oxygen content and hydrogen ion concentration in monkey blood after incapacitating ionizing radiation dosage
[AD-750681] 06 p0632 N73-15134
Changes in electrocardiographs of Rhesus monkeys as function of age
[NASA-TT-F-14675] 07 p0745 N73-16062
Chemical and orthopedic properties of ceramic bone implants in monkeys
[AD-754982] 11 p1248 N73-20134
Retinal damage in monkeys exposed to near infrared gallium arsenide laser pulses
[AD-753419] 11 p1248 N73-20135
Circadian phase relationships of physiological functions of isolated monkeys subjected to varying photoperiod phases
12 p1367 N73-21088
Operant behavior of rhesus monkeys in presence of extremely low frequency, low intensity magnetic and electric fields
[AD-754058] 12 p1372 N73-21134
Comparison of electroencephalographic response patterns in man and monkeys to visually evoked cortical stimuli
[IZF-1972-24] 14 p1609 N73-23049
Advantages of breeding Rhesus monkeys in compounds for biomedical research
14 p1611 N73-23063
Temporary blindness of monkeys caused by combined effects of phosdrin and atropine exposure
[FAA-AM-73-4] 18 p2109 N73-27055

**MONOCHROMATIC RADIATION**
Influence of monochromatic light on physiological processes of blood
[NASA-TT-F-14941] 16 p1866 N73-25111
Monochromatic absorption coefficient in narrow regions of oscillatory-rotational spectrum of H2O
[AD-759238] 16 p1946 N73-25743
Upconversion method for monochromatic radiation
[NASA-TM-X-2877] 20 p2425 N73-29479
Photoconductive effect and absorption of monochromatic sub-mm radiation in n-type germanium
[RR-737] 20 p2462 N73-29782

**MONOCHROMATORS**
Aerobee-borne spectrometer/monochromator for advanced studies of solar X-ray line emissions and preliminary results
[NASA-CR-130359] 07 p0838 N73-16793
Low frequency Raman spectra of ammonium halides measured by double monochromator at high temperature
[NASA-CR-132049] 15 p1747 N73-24160

**MONOCLINAL VALLEYS**
U VALLEYS

**MONOCOQUE CYLINDERS**
U CYLINDRICAL SHELLS

**MONOCRYSTALS**
U SINGLE CRYSTALS

**MONOCULAR VISION**
Psycho-visual problems associated with monocular, bi-ocular, and binocular visual systems
[AD-749450] 05 p0502 N73-14085

**MONOLITHIC CIRCUITS**
U INTEGRATED CIRCUITS

**MONOMERS**
Evaluation of disubstituted perylene compounds as monomers for high temperature polymers and as possible binders for carbon fibers
[AD-746626] 02 p0139 N73-11122
Radiation induced grafting of fluorinated monomers on polyamide films
[AD-757376] 14 p1617 N73-23100
Monomer polymerization by plasma discharge as thin film for water purification membrane
[NASA-CASE-ARC-10643-1] 20 p2374 N73-29074

**MONOMOLECULAR FILMS**
Phase characteristics of submonolayer isotopic mixtures of helium adsorbed on Grafoil
18 p2113 N73-27084

**MONOPLANES**
NT A-4 AIRCRAFT
NT A-6 AIRCRAFT
NT A-7 AIRCRAFT
NT A-37 AIRCRAFT
NT AN-24 AIRCRAFT
NT B-52 AIRCRAFT
NT B-57 AIRCRAFT
NT B-70 AIRCRAFT
NT BEECHCRAFT 18 AIRCRAFT
NT BOEING 707 AIRCRAFT
NT BOEING 720 AIRCRAFT
NT BOEING 737 AIRCRAFT
NT BREGUET 941 AIRCRAFT
NT BREGUET 1150 AIRCRAFT
NT C-2 AIRCRAFT
NT C-130 AIRCRAFT
NT C-131 AIRCRAFT
NT C-135 AIRCRAFT
NT C-141 AIRCRAFT
NT C-160 AIRCRAFT
NT CANBERRA AIRCRAFT
NT COMET 4 AIRCRAFT
NT CONVAIR 880 AIRCRAFT
NT CV-340 AIRCRAFT
NT CV-990 AIRCRAFT
NT DC 3 AIRCRAFT
NT DC 8 AIRCRAFT
NT DO-31 AIRCRAFT
NT F-5 AIRCRAFT
NT F-8 AIRCRAFT
NT F-27 AIRCRAFT
NT F-28 TRANSPORT AIRCRAFT
NT F-86 AIRCRAFT
NT F-100 AIRCRAFT
NT F-102 AIRCRAFT
NT F-104 AIRCRAFT
NT F-105 AIRCRAFT
NT F-106 AIRCRAFT
NT FD 2 AIRCRAFT
NT GA-5 AIRCRAFT
NT H-126 AIRCRAFT
NT HFB-320 AIRCRAFT
NT JET PROVOST AIRCRAFT
NT MIRAGE 3 AIRCRAFT
NT OV-10 AIRCRAFT
NT P-3 AIRCRAFT
NT P-1127 AIRCRAFT
NT S-2 AIRCRAFT
NT T-33 AIRCRAFT
NT T-38 AIRCRAFT
NT U-2 AIRCRAFT
NT VISCOUNT AIRCRAFT
NT X-14 AIRCRAFT
NT XC-142 AIRCRAFT
NT XV-5 AIRCRAFT

**MONOPOLE ANTENNAS**
NT WHIP ANTENNAS
First order expressions for low angle radiation fields of monopole antenna over irregular ground surface
[AD-756911] 13 p1503 N73-22185

**MONOPROPELLANTS**
NT AEROZINE
Pulse performance data for small monopropellant and hypergolic bipropellant rocket engines
03 p0349 N73-12846
Long-term storability and decomposition kinetics of monopropellant formulations containing hydrazine, hydrazine azide, and ammonia
[AD-750900] 06 p0711 N73-15806
Variable energy blast wave theory applied to two phase detonation and liquid monopropellant ignition by shock wave
[AD-754525] 11 p1333 N73-20818
Reliability model and associated computer code developed to compute reliability of monopropellant hydrazine spacecraft auxiliary propulsion system as function of time
[NASA-CR-131400] 11 p1333 N73-20821
Monolithic catalyst bed for monopropellant hydrazine decomposition
[NASA-CR-132983] 16 p1914 N73-25486
Design and fabrication of monopropellant hydrazine thruster
[NASA-CR-132784] 18 p2193 N73-27702
Mono propellant hydrazine tank pressurization concept based on surface tension feed of propellant to reactor catalyst bed
[AD-763803] 21 p2588 N73-30734

**MONOPULSE RADAR**
Tracking errors associated with monopulse phased-array radar
[AD-748428] 04 p0391 N73-13175
Development of algorithm for multiple hypothesis testing with application to amplitude comparison monopulse radar system in air traffic control operations
[TN-1973-7] 09 p1002 N73-18173
Experimental array radar ear test bed
[AD-758139] 14 p1636 N73-23261
Solid state, superheterodyne monopulse receiver for experimental array radar
[AD-757610] 14 p1637 N73-23268
Development plan for experimental array radar for antimissile defense
[AD-763171] 21 p2509 N73-30132
Comparative efficiency of monopulse radar direction finding systems
[AD-765545] 24 p2896 N73-33118

**MONOSACCHARIDES**
NT RIBOSE
Absorption of fructose in saline mixture used for enteritis therapy of children
[NASA-TT-F-14596] 02 p0133 N73-11078

**MONOTONY**
Self-estimates of distractibility as related to performance decrement on task requiring sustained attention
[FAA-AM-72-25] 02 p0135 N73-11096
Psychobiological factors for predicting monotony tolerance and selecting personnel for isolated duty
[AD-747272] 04 p0381 N73-13098

**MONSOONS**
Time series analysis of summer monsoon data from Southeast Asia for 1967 and 1968
[AD-759788] 16 p1939 N73-25691
Bibliography of articles concerning water balance of monsoon Asia
[CLIMATOL-NOTES-11] 18 p2171 N73-27531
Somali current and southwest monsoon arising from ocean atmosphere instability associated with Coriolis force
[NASA-TM-X-70471] 23 p2786 N73-32285

**MONTANA**
NT BIGHORN MOUNTAINS [MT-WY]
NT YELLOWSTONE NATIONAL PARK [ID-MT-WY]
Preparation of hydrologic atlases of arid land watersheds using ERTS-1 imagery of Wyoming, Utah, Montana, and New Mexico
[E72-10240] 03 p0288 N73-12340
Tectonic and paleogeologic mapping of Montana using ERTS-1 imagery
[E73-10280] 08 p0914 N73-17488
Geologic mapping of Montana using ERTS-1 imagery
[E73-10281] 09 p1020 N73-18325
Utilization of ERTS-1 imagery in structural reconnaissance for minerals and oil in Alaska, Canada, Montana, Colorado, New Mexico, and Texas
[E73-10414] 11 p1279 N73-20376
ERTS-1 imagery of Bighorn-Pryor mountains of Wyoming and Montana applied to analysis of regional tectonic relationships
[E73-10704] 16 p1903 N73-25395
Application of ERTS-1 imagery to determine geological evidence of mineral and hydrocarbon accumulations in Alaska, Canada, Montana, Colorado, New Mexico, and Texas
[PAPER-G30] 19 p2267 N73-28261
Application of ERTS-1 imagery for lineament and photogeologic mapping of western Montana
[PAPER-G32] 19 p2268 N73-28263
Tectonic and photogeologic mapping of forested and sparsely vegetated terrain of Montana and Idaho
[E73-10900] 20 p2396 N73-29249
Research in development and utilization of atmospheric water resources in Montana
[PB-222004/4] 22 p2695 N73-31591

**MONTE CARLO METHOD**
Monte Carlo simulation model for radiation induced plasmas with nonlinear properties
[NASA-CR-128405] 01 p0084 N73-10700
Application of Monte Carlo inversion to seismic data
02 p0200 N73-11617
Monte Carlo method for computer simulation of copper crystal surface dynamics
[AD-745872] 02 p0220 N73-11780
REPRI program using Monte Carlo techniques for support compatibility studies for space station
[NASA-CR-123948] 03 p0268 N73-12174
Monte Carlo method applied to elementary processes in plasma arc discharge
[LYCEN-7205] 03 p0339 N73-12768
Generation of random experiment schedules for space station using Monte Carlo technique
[NASA-TM-X-64557] 03 p0355 N73-12894
Finite difference theory and Monte Carlo method for heat conduction and convection problems
[KFK-1554] 03 p0364 N73-12965
Efficiencies of germanium semiconductor detectors calculated by Monte Carlo method for 100 keV to 2 MeV gamma rays
[CEA-R-4316] 07 p0832 N73-16745
Monte Carlo calculation of cosmic isotope buildup in iron meteorites
[ORNL-TR-2620] 07 p0846 N73-16861
Monte Carlo simulation of complex reliability systems using logic circuit analysis programs linked to statistics programs
[TR-72-39] 08 p0927 N73-17596
Monte Carlo use in Rover nuclear rocket engine development program
[LA-DC-72-1078] 08 p0937 N73-17673
Monte Carlo radiation transport computer codes for calculating dose distributions and cell survival probabilities
[NASA-CR-130965] 09 p0996 N73-18127
One dimensional search directions from sequential Monte Carlo optimization of unconstrained stochastic systems
[AD-754413] 11 p1312 N73-20649
Monte Carlo transport routine for standard atmosphere to altitude of 90 km
[LA-5089] 12 p1422 N73-21529
Hybrid computer simulation of turbulent diffusion in atmosphere by Monte Carlo method and stochastic processes
13 p1514 N73-22266
Monte Carlo studies of light transport through natural atmospheres
[AD-757494] 14 p1661 N73-23486
Monte Carlo method for analyzing tracking disruptions
14 p1683 N73-23657

FORTRAN code for solving time dependent neutron transport equation in three-dimensional geometry by Monte Carlo method
[AD-756290] 14 p1691 N73-23728
Monte Carlo simulation for man machine task sequencing considering pilot performance degradation
14 p1713 N73-23899
Rate constants for vibrational relaxation using Monte Carlo calculations
[AD-758753] 16 p1871 N73-25152
Computer program which uses Monte Carlo technique to compute geometrical factor, and spatial and angular distributions of simulated particles
[NASA-TM-X-70428] 19 p2301 N73-28498
Stochastic model of atmosphere between 30 and 90 km was developed for use in Monte Carlo space shuttle entry studies
[NASA-TM-X-69567] 21 p2536 N73-30337
JERK Monte Carlo program for studying crystal defects in irridiated metals
[CEA-N-1567] 21 p2585 N73-30718
Monte Carlo simulation of nuclear-electromagnetic cascade development and energy response of ionization of spectrometers
[NASA-CR-133999] 22 p2672 N73-31406
Monte Carlo simulation of self bit synchronizer for binary overlapping signals
23 p2755 N73-32046
Application of Monte Carlo method and Markov random walks to determine molecular diffusion through rarefied gas
[NASA-TN-D-7405] 23 p2776 N73-32197
Monte Carlo calculations of polarization of radiation in earth atmosphere and ocean
[AD-764622] 23 p2789 N73-32313
General Monte Carlo simulation model for estimating large scale system reliability and availability
24 p2928 N73-33385
Monte Carlo technique for determining transient radiation fields or completely bounded media
24 p2956 N73-33615
Monte Carlo technique using Stokes vectors of Lyman alpha radiation
24 p2975 N73-33774
Monte Carlo analysis of radio source counts from Ohio Survey at 1415 MHz
24 p2978 N73-33794

**MONTEREY BAY [CA]**
GEK measurements of surface currents for five portions of Monteray Bay during period Nov. to Dec. 1971
[AD-749042] 05 p0541 N73-14404
Determination of coastal water types around Monterey Bay, California by analysis of ERTS-1 MSS data
[E73-10677] 16 p1901 N73-25372
Agricultural analysis of ERTS-1 multispectral band scanner data for Monterey Bay, California
[PAPER-A23] 19 p2262 N73-28230
Pseudocolor transformation of ERTS-1 imagery of Monterey Bay-San Francisco, California area
[PAPER-I12] 19 p2278 N73-28333
Digital precision processing of ERTS-1 imagery of Monterey Bay, California
[E73-10948] 21 p2530 N73-30290

**MOODS**
Effect of mood on testing human performance
04 p0378 N73-13075

**MOON**
Total and induced magnetic fields line structure within Moon and diamagnetic cavity based on asymmetric theory of lunar induction
[NASA-CR-114545] 06 p0718 N73-15860
Development of theory for time dependent magnetic fields inside Moon and diamagnetic cavity caused by interplanetary eletromagnetic field fluctuation
[NASA-CR-114546] 06 p0718 N73-15861
Mie scattering of interplanetary magnetic field by whole moon
[NASA-TM-X-62225] 07 p0844 N73-16833
Utility of Goddard Trajectory Determination System Solar/Lunar/Planetary ephemeris files
[NASA-TM-X-66185] 08 p0976 N73-17983
Radar methods of investigating moon and planets
[NASA-TT-F-729] 09 p1084 N73-18847
Description and operation guide for DSAS illumination and moon conflict programs
[NASA-TM-X-66200] 10 p1213 N73-19863
Tables on occulation of stars by moon
[PUBL-28] 17 p2081 N73-26835
Predicted and measured infrared radiation data for Mercury and Moon
19 p2341 N73-28831
Mathematical model for steady state wind-moon interaction
[COO-3577-2] 22 p2711 N73-31712

**MOONMOBILES**
U LUNAR SURFACE VEHICLES
U MANNED LUNAR SURFACE VEHICLES

**MORAINAL DELTAS**
U DELTAS

**MORAINAL LAKES**
U LAKES

**MORAINES**
U GLACIAL DRIFT

**MORALE**
Study to validate Non-Interference Performance Assessment
[NASA-CR-128865] 10 p1124 N73-19164

**MORL**
U MANNED ORBITAL RESEARCH LABORATORIES

**MOROCCO**
Construction of mosaic map of Morocco, North Africa using ERTS-1 data and comparison with data obtained from Gemini 5 flight
[PAPER-G5] 19 p2263 N73-28236

**MORPHOLOGICAL INDEXES**
Hyperoxic damage in animal cells, tissues, and organs
10 p1115 N73-19091

**MORPHOLOGY**
NT GEOMORPHOLOGY
NT POLYMORPHISM
Morphology, provenance, and movement of desert sand seas in Africa, Asia, and Australia
[E72-10249] 03 p0289 N73-12349
Morphology, provenance, and movement of desert sand seas in Africa, Asia, and Australia
[E73-10058] 07 p0778 N73-16320
Morphology, provenance, and desert sand sea movements in Asia, Australia, and Africa
[E73-10060] 07 p0778 N73-16322
Functional morphology of various organs and tissues subjected to space flight
[NASA-TT-F-738] 10 p1119 N73-19126
Morphological changes in liver of dogs subjected to chronic gamma radiation
11 p1244 N73-20101
ERTS-1 imagery of morphology, provenance, and movement of desert sand seas in Africa, Asia, and Australia
[E73-10409] 11 p1278 N73-20371
Morphometric analysis of Apollo 16 photography of lunar craters - Part L
12 p1454 N73-21776
Morphology, provenance, and movement of desert sand seas in Africa, Asia, and Australia
[E73-10542] 13 p1518 N73-22305
Classification of landscapes into taxonomic groups on basis of optical properties
[NASA-TT-F-14970] 17 p2025 N73-26386
ERTS-1 imagery of morphology, provenance, and movement of desert sand seas in Africa, Asia, and Australia
[E73-10786] 18 p2136 N73-27262
Morphology, provenance, and movement of desert sand seas in Africa, Asia, and Australia using ERTS-1 data
[PAPER-G8] 19 p2264 N73-28239
Morphological changes in rat kidneys exposed to different accelerations
20 p2366 N73-29023
Accomplishments and publications list of two year project on morphology and deformation mechanisms of high polymers
[AD-762780] 21 p2565 N73-30560
Survey of literature and morphological studies of vestibular nerve
[NASA-CR-135746] 24 p2885 N73-33042
Convective heating effects on properties of glassy surface insulation coatings
24 p2941 N73-33488

**MORTALITY**
Mortality rate of guinea pigs after decompression treatment as function of water balance
[DLR-FB-71-20] 05 p0501 N73-14075
Clinical analysis of relationship between VPB and mortality rate in patient with acute myocardial infractions
08 p0875 N73-17083
Precoronary care and sudden death prevention due to coronary disease in industrial workers
08 p0875 N73-17084
Chronic disease health trends and mortality rates in employee population of NASA Goddard Space Flight Center
08 p0875 N73-17086
Mortality rate in antiradiation drug protected mice subjected to gamma radiation overloads
11 p1242 N73-20079

**MOS [SEMICONDUCTORS]**
U METAL OXIDE SEMICONDUCTORS

**MOSAICS**
Preparation of mosaic of Alaska using ERTS-1 imagery
[E73-10284] 08 p0914 N73-17490
Construction of mosaic map of Morocco, North Africa using ERTS-1 data and comparison with data obtained from Gemini 5 flight
[PAPER-G5] 19 p2263 N73-28236

**MOSFET**
U FIELD EFFECT TRANSISTORS

**MOSS [SPACE STATIONS]**
U ORBITAL SPACE STATIONS

**MOSSBAUER EFFECT**
Mossbauer spectrometer with high efficiencies in both transmission and backscattering techniques
[NASA-CASE-LAR-11155-1] 04 p0421 N73-13433
Micromagnetic interactions of rare earth orthoferrites and Mossbauer spectroscopy
[AD-751995] 08 p0951 N73-17789
Mossbauer spectroscopic analysis of order-disorder transitions in vacuum deposited Te films
[AD-753272] 09 p1074 N73-18769
Annual report 1971-1972 of Interuniversitair Reactor Institute in Netherlands
10 p1195 N73-19721
Mossbauer analysis of spin arrangements in gold iron and copper iron alloys at low temperature
[AD-754140] 10 p1202 N73-19787
Measurements of Mossbauer absorption spectra to investigate diffusion mechanism of iron in beta-titanium
12 p1413 N73-21449
Using transition from Ni-61 to obtain Mossbauer absorption spectra with Ni-Pd alloy
[TID-26197] 12 p1414 N73-21461
X ray Mossbauer study of strengthening properties of laves phases in austenitic steels
[JPRS-58852] 13 p1543 N73-22503
Mossbauer spectroscopy studies of passivation and corrosion inhibition of metals
[AD-757705] 14 p1679 N73-23626
Analysis of iron-nickel alloys to determine nature of Mossbauer effect at high pressures and low temperatures
16 p1927 N73-25592
Ni-61 transition for obtaining Mossbauer absorption spectra with Ni-Pd alloys
18 p2185 N73-27641
Mossbauer spectra of ferrite catalysts used in oxidative dehydrogenation
[NASA-CR-133740] 21 p2506 N73-30108
Observation of amorphous to crystalline transition in vacuum deposited tellurium films using Mossbauer spectroscopy
[AD-763408] 21 p2586 N73-30724
Mossbauer effect study of high temperature oxidation and breakaway in 302 stainless steel
22 p2706 N73-31671
Radio frequency induced sidebands in Mossbauer and Rayleigh scattering radiation from nickel foils
23 p2755 N73-32050
Mossbauer absorption spectra of iron 57 in single crystal of potassium iron fluoride
[AD-764635] 23 p2827 N73-32597
Monte Carlo method for fitting iron 57 Mossbauer spectra
[AD-764634] 23 p2828 N73-32602

**MOTILITY**
U LOCOMOTION

**MOTION**
Motion cue effects on pilot manual control tracking task
01 p0018 N73-10141
Comparison of rawinsonde data with baroclinic cloud motion pictures
[NOAA-TM-NESS-43] 01 p0074 N73-10611
Iterative method for real time actuator extension transformation analysis on motion simulator
[NASA-TN-D-7067] 03 p0269 N73-12182
Motion effects in pilot reactions to ground-based flight simulator display evaluation
[AD-749370] 04 p0384 N73-13126

**MOTION EQUATIONS**
U EQUATIONS OF MOTION

**MOTION PERCEPTION**
U SPACE PERCEPTION

**MOTION PICTURES**
Motion picture study to provide combustion mechanism observations of ammonium perchlorate composite propellants
12 p1463 N73-21857
K. E. Tsiolkovskiy as film consultant
[NASA-TT-F-14890] 14 p1708 N73-23865
Stop-motion cinefluorography system for biomedical research
[AD-762412] 19 p2302 N73-28513
Real time three dimensional motion picture camera using holography
[NASA-TR-R-409] 22 p2673 N73-31413

**MOTION SICKNESS**
Analysis of physiological mechanisms contributing to occurrence of motion sickness
01 p0003 N73-10020
Moton sickness effects on flying personnel performance during hurricane penetrations
[AD-743928] 01 p0013 N73-10100
Guinea pigs used to determine effect of intramuscular injections of drugs on fall-out and Bekhterev nystagmus occurring after unilateral and bilateral labyrinthectomies
07 p0744 N73-16049
Motion sickness in fixed-base car simulator with moving visual display
[FPRC-1310] 09 p0995 N73-18119
Combined stress effects in human communication and motion sickness biodynamics
10 p1122 N73-19144
Predictability of motion sickness in pilot selection - conferences
[AGARD-CP-109] 12 p1367 N73-21092

Three different bases for susceptibility prediction to motion sickness
12 p1367 N73-21093
Clinical procedures for selecting pilot personnel based on predisposition to motion sickness
12 p1367 N73-21094
Adaptability and receptivity factors affecting motion sickness susceptibility in pilots
12 p1367 N73-21095
Reaction assessment of vestibular disorientation stress for aircrew selection, using visual displays and tasks
12 p1368 N73-21096
Motion sickness questionnaire and field independence scores as predictors of success in Naval aviation training
12 p1368 N73-21097
Biaxial simulator imposing standardized coriolis stimuli for selection, test, and rehabilitation of motion sick pilots
12 p1368 N73-21098
Physiological method for selecting and observing student pilots in Belgian Air Force for motion sickness
12 p1368 N73-21099
Metixenum and Meclocin under double blind comparison test conditions against motion sickness
12 p1368 N73-21100

**MOTION SICKNESS DRUGS**
Effects of antimotion sickness drugs, placebos, and secobarbital on postural equilibrium functions at sea level and at simulated altitudes of 12,000 feet
[AD-748192] 05 p0504 N73-14105
Effectiveness of sodium hydrocarbonate as means for treating and preventing motion sickness
07 p0745 N73-16057

**MOTION STABILITY**
NT AERODYNAMIC STABILITY
NT AIRCRAFT STABILITY
NT ATTITUDE STABILITY
NT BOUNDARY LAYER STABILITY
NT DIRECTIONAL STABILITY
NT FLAME STABILITY
NT FLOW STABILITY
NT GYROSCOPIC STABILITY
NT HOVERING STABILITY
NT LATERAL STABILITY
NT LONGITUDINAL STABILITY
NT LOW SPEED STABILITY
NT MAGNETOHYDRODYNAMIC STABILITY
NT ROTARY STABILITY
NT SPACECRAFT STABILITY

**MOTIVATION**
Motivational patterns underlying devolunteering by submarine graduate school personnel
[AD-749324] 13 p1487 N73-22054
Theoretical analysis of motivation stimulation
24 p2888 N73-33062
Structural, behavioral, and EEG correlates of alimentary motivation
24 p2888 N73-33063
Use of motivational relations to find acceptor of action with conditioned stimuli
24 p2888 N73-33064

**MOTOR SYSTEMS [BIOLOGY]**
U EFFERENT NERVOUS SYSTEMS

**MOTORS**
NT ELECTRIC MOTORS
NT SERVOMOTORS
NT SYNCHRONOUS MOTORS
NT TORQUE MOTORS
Differential equations for studying dynamic characteristics of motor with separate excitation regulated by negative resistance feed
[PUBL-1368] 06 p0645 N73-15237

**MOTS [TRACKING SYSTEM]**
U MINITRACK SYSTEM

**MOUNTAINS**
NT ALPS MOUNTAINS [EUROPE]
NT BIGHORN MOUNTAINS [MT-WY]
NT BLACK HILLS [SD-WY]
NT CASCADE RANGE [CA-OR-WA]
NT HIMALAYAS
NT PYRENEES MOUNTAINS [EUROPE]
NT ROCKY MOUNTAINS [NORTH AMERICA]
NT SIERRA NEVADA MOUNTAINS [CA]
NT WIND RIVER RANGE [WY]
NT WRANGELL MOUNTAINS [AK]
Analysis of ERTS-1 imagery for Colorado environments using automatic data processing techniques
[E72-10204] 02 p0161 N73-11301
ERTS-1 imagery of structures and lithology of Northern California Coast Ranges and Sacramento Valley, California
[E72-10214] 03 p0288 N73-12332
Mapping and detection of snow cover changes on land and on glaciers in Alaska, British Columbia, and Washington using ERTS-1 imagery
[E72-10237] 03 p0288 N73-12337
Thermal remote sensing of infrared radiant temperatures in alpine/periglacial environments
04 p0409 N73-13332
Physical and hydrometeorological characteristics of Snowy Range Observatory, including precipitation, temperature, solar radiation, and wind data
[PB-211618] 05 p0524 N73-14268
Interdisciplinary analysis of ERTS-1 multispectral data of Colorado mountain areas using automatic data processing techniques
[E73-10033] 06 p0661 N73-15366
Physiological effects of high mountain alpinism exercises on human body
07 p0745 N73-16058
Analysis of troposcatter data obtained by radar transmitter as signal source to determine index of refraction fluctuations
08 p0900 N73-17285
Atherosclerosis and hypertonia under high mountain conditions and seasonal effects
[NASA-TT-F-745] 09 p0995 N73-18121
ERTS-1 imagery of structural geology and volcanology in Central High Plateau of Bolivian Andes
[E73-10296] 10 p1146 N73-19333
Interdisciplinary analysis of ERTS-1 imagery for Colorado mountain areas using ADP techniques
[E73-10348] 10 p1148 N73-19347
Crustal structure from high resolution seismic refraction profile across transition zone from Basin and Range provinces into Middle Rocky Mountains
[AD-753850] 11 p1289 N73-20462
ERTS-1 imagery of structural and lithological properties of Northern Coast Ranges and Sacramento Valley, California
[E73-10478] 12 p1396 N73-21315
Interdisciplinary analysis of Skylab EREP MSS photography of vegetative and geomorphological cover types in Colorado Mountains
[E73-10533] 13 p1517 N73-22297
Ecology, hydrology, geomorphology, and terrain modeling of Colorado mountain environments from ERTS-2 data
[E73-10551] 14 p1655 N73-23424
Structural and lithological investigation of Northern Coast Ranges and Sacramento Valley, California
[E73-10577] 14 p1656 N73-23438
ERTS-1 imagery of linear fractures in Precambrian rocks of Laramie Mountains, Wyoming
[E73-10663] 16 p1899 N73-25359
TAXIR information retrieval system for analyzing climatic conditions on east slope of Colorado front range
[PB-214341/0] 16 p1939 N73-25688
Survey of snow cover and vegetation growth in high mountains of Swiss Alps based on ERTS-1 imagery
[E73-10733] 17 p2020 N73-26339
Influence of mountain barriers on radio wave propagation by meteors
17 p2023 N73-26373
Spaceborne imagery of snow cover and glaciers in mountainous regions
[NASA-TT-F-14969] 17 p2025 N73-26387
Ground based silver iodide cloud seeding for modifying snowfall in northern Rockies near Montana
[PB-2180512] 18 p2173 N73-27548
Application of ERTS-1 imagery for recognizing and mapping alpine glacial features in mountains of northwestern Wyoming
[PAPER-G14] 19 p2265 N73-28245
Measurement of percentage of snow cover area on specific drainage basins in Cascade Mountains in Washington state using ERTS-1 imagery
[PAPER-W19] 19 p2273 N73-28296
Skylab multispectral data for selected cover types in Colorado Mountains
[E73-10878] 20 p2393 N73-29229
Skylab MSS imagery of selected cover types in Colorado Mountains
[E73-10914] 20 p2397 N73-29263
Influence of solar radiation in mountainous areas on crop capacity and grain yield of spring wheat
20 p2406 N73-29335
Spectral energy distribution of Pamir plants at different altitudes above sea level in relation to mountain plant characteristics
20 p2406 N73-29336
Optical seeing tests on Mt. Lemmon, using Polaris telescope from Lick Observatory
[LPL-COMMUN-170] 21 p2592 N73-30766
Iterative and nonlinear procedures for studying gravity anomaly in mountainous areas
24 p2911 N73-33232
Survey of seasonal snow cover of North Slope and Alaska Range from ERTS-1 data
[E73-11086] 24 p2913 N73-33249
Identification of selected forest and vegetation cover in Colorado Mountains from Skylab EREP data
[E73-11132] 24 p2917 N73-33287
Application of Skylab imagery to analysis of fault tectonics and earthquake hazards in Peninsular Ranges, Southern California
[E73-11134] 24 p2917 N73-33289
Atmospheric turbulence near tropopause over mountainous terrain
24 p2946 N73-33525

**MOUNTING**
Techniques for packaging and mounting printed circuit boards
[NASA-CASE-MFS-21919-1] 16 p1883 N73-25243

**MOUNTS**
U SUPPORTS

**MOVEMENT**
U MOTION

**MOVING TARGET INDICATORS**
Development and characteristics of vehicle detection system with all active elements carried by moving vehicle
[NASA-CASE-NPO-11850-1] 01 p0032 N73-10248
Extracting tracks of moving targets from sensor detection
[AD-746513] 02 p0142 N73-11149
Optimal moving target indicator for long range air traffic control surveillance radars
[AD-750747] 06 p0642 N73-15209
Receiver synthesis for air traffic moving target indicator with digital signal processing
[AD-751923] 08 p0885 N73-17170
Radar arithmetic signal processing element with digital filter and Fourier transformation for moving target indication
[AD-754060] 11 p1258 N73-20206
Direction sensitive radar moving target indication
13 p1489 N73-22072
Range-gated moving target indicator for use with search radar
[AD-757259] 14 p1636 N73-23265
Application of state variable approach for analysis of selecting digital moving target indicators filters
[AD-757611] 14 p1637 N73-23269
Feasibility of using computer system for echo detection and identification of moving targets
[AD-758266] 15 p1751 N73-24191
Ultrahigh frequency coherent radar as moving target indicator
[AD-757565] 16 p1877 N73-25191
Recursive digital filters in moving target indicator of phased array radars
[AD-759901] 18 p2118 N73-27128
Systems for selecting moving targets when using interperiod compensation devices
22 p2629 N73-31067
Numerical analysis of amplitude difference and phase difference for radar signal and correlated noise in interperiod compensation system of moving target indicator
22 p2629 N73-31068
Analysis of signal and correlated noise for interperiod compensation systems of moving target selection procedures
22 p2629 N73-31069
Probability distribution function of phase difference of sum of signal and noise to determine efficiency of phase interperiod compensation systems
22 p2629 N73-31070
Tracking of reentry vehicles in strong wake echoes using moving target indicators
[AD-763944] 22 p2635 N73-31120

**MTBF**
Development and application of multiple system checkout procedures for use with gimbaled inertial measuring units
[NASA-CR-123953] 03 p0328 N73-12676

**MTI RADAR**
U MOVING TARGET INDICATORS

**MUBIS [SCANNERS]**
U MULTIPLE BEAM INTERVAL SCANNERS

**MUFFLERS**
Design and characteristics of expansion chamber mufflers for reducing exhaust noise generated by helicopters
[NASA-TN-D-7309] 22 p2700 N73-31623

**MULLITES**
Improvement and evaluation of mullite reusable surface insulation material for thermal protection system of space shuttle
[NASA-CR-124053] 08 p0934 N73-17646
Investigation of microstructure of mullite fibers using transmission electron microscopy
[NASA-TM-X-2750] 09 p1052 N73-18573
Sintering kinetics and mechanical properties of high purity mullite
22 p2688 N73-31527
Production of silica, mullite, and alumino silicate reusable surface insulation materials for space shuttle orbiters
[NASA-TM-X-2719] 24 p2938 N73-33461
Production of rigidized mullite composite materials for external insulation of shuttle orbiter
24 p2938 N73-33463
Hafnium pigmentation for mullite composite thermophysical optimization
24 p2939 N73-33469
Mechanical and thermophysical characteristics of nonmetallic insulation materials for space shuttle orbiter surface
24 p2939 N73-33471
Porosity analysis on silica and mullite composite surface insulation tiles
24 p2939 N73-33472
Microstructure of mullite composite fibers
24 p2940 N73-33474
Thermal response of glassy fibrous mullite insulation to entry environment simulation
24 p2940 N73-33478
Acoustic, reentry, and structural load environment tests on mullite insulation for space shuttle
24 p2941 N73-33483

Thermal cycling effects on properties of silica, mullite, and alumino-silicate insulation coatings
24 p2941 N73-33487
Ceramic reinforced mullite thermal protection system design for space shuttle surface
24 p2942 N73-33495
Thermostructural evaluation of mullite and silica composite materials for space shuttle surface insulation system design
24 p2942 N73-33498
MULTICHANNEL COMMUNICATION
Design and performance of multiple channel analog multiplexer for airborne data acquisition system
[ARL/F-NOTE-49] 02 p0145 N73-11172
Beat frequency detector algorithm for multichannel signal analysis
[AD-746682] 03 p0266 N73-12157
Multichannel medical monitoring system to measure physiological parameters from display device at remote control station
[NASA-CASE-MSC-14180-1] 13 p1486 N73-22045
Feedback queueing model with interference caused retransmission for space to surface data transmission
[AD-756568] 13 p1492 N73-22093
Operational principles and applications of address code communication systems
14 p1619 N73-23114
Slow speed, multiple channel, analog to digital, logging system
[NASA-CR-132954] 15 p1754 N73-24219
Statistical properties of filtered pseudorandom digital sequences used in multichannel communications system evaluation, coding theory, and modulation format design
[NASA-TM-X-64758] 18 p2169 N73-27516
Improved phase lock loop for receiver in multichannel telemetry system with suppressed carrier
[NASA-CASE-NPO-11593-1] 19 p2234 N73-28012
Technical facilities for data links in teleautomatic queueing system
[JPRS-59662] 19 p2235 N73-28022
MULTICHANNEL RECEIVERS
U MULTICHANNEL COMMUNICATION
U RECEIVERS
MULTICHANNEL TRANSMITTERS
U MULTICHANNEL COMMUNICATION
U TRANSMITTERS
MULTIENGINE VEHICLES
Analysis of factors affecting flight of multi-engine aircraft with one engine inoperative
[NASA-TT-F-734] 15 p1734 N73-24060
MULTILAYER INSULATION
Analysis of environmental effects on physical, mechanical, and thermodynamic properties of various multilayer insulation materials - Vol. 1
[NASA-CR-120978] 08 p0934 N73-17648
Analysis of environmental effects on physical, mechanical, and thermodynamic properties of various multilayer insulation materials - Vol. 2
[NASA-CR-120979] 08 p0934 N73-17649
Techniques and instrumentation for nondestructive testing of high performance multilayer thermal insulation for space shuttle orbiters
[NASA-CR-124106] 09 p1051 N73-18567
Gas flow in multilayer insulation systems applied to broadside pumping
[NASA-CR-124130] 10 p1139 N73-19281
Procedure for making insulating foil for use in multilayer insulating system
[NASA-CASE-LEW-11484-1] 13 p1532 N73-22415
Lightweight evacuated multilayer insulation systems for space shuttle vehicle
[NASA-CR-121105] 16 p1966 N73-25902
Printed wire routing on multilayer circuit boards
20 p2380 N73-29122
Development and application of self evacuating multilayer insulation system for application to space shuttle orbiter liquid hydrogen tanks
[NASA-CR-121166] 21 p2606 N73-30883
Design and development of pressurization system for reusable space shuttle multilayer insulation systems
[NASA-CR-124380] 22 p2722 N73-31782
Design, fabrication, and performance of multilayer insulation system for modular nuclear vehicle LH2 propellant tank
[NASA-CR-124400] 23 p2856 N73-32824
Cryogenic tanking and partial jettison tests of Centaur launch vehicle and Centaur standard shroud to develop insulation, purge, and vent systems
[NASA-TM-X-71455] 24 p2984 N73-33850
MULTILAYER STRUCTURES
U LAMINATES
MULTILOOP SYSTEMS
U CASCADE CONTROL
MULTIMODE RESONATORS
Multimode coaxial feeds for parabolic antennas with large aperture reflectors
[FTZ-A-454-TBR-14] 22 p2642 N73-31177
MULTIPACTOR DISCHARGES
Secondary electron densities in two-electrode interspace in ac current present during multipactor discharge
[REPT-73-74] 19 p2244 N73-28091
MULTIPATH TRANSMISSION
Multipath propagation between aeronautical relay satellite in synchronous earth orbit and aircraft flying over ocean
[NASA-TM-X-66094] 02 p0141 N73-11140
Digital simulation and angle tracking accuracy of tactical radar with multipath propagation
[AD-748384] 03 p0268 N73-12172
Degradation of spread spectrum modulation performance in airborne multipath communication channels
[AD-747486] 04 p0391 N73-13181
Definition of experiments for collection of RFI and multipath data for application to synchronous relay satellite
[NASA-CR-128717] 07 p0754 N73-16128
Spatial grid method for solving hyperbolic equations for signal propagation on three wire transmission line
[UCRL-73796] 07 p0764 N73-16209
Diversity techniques for airborne communications in presence of ground reflection multipath
[AD-752249] 08 p0887 N73-17178
Channel measurement techniques, modeling multipath structure of line-of-sight tropospheric paths, and prediction of spread spectrum modem performance as function of multipath conditions
[AD-755922] 13 p1494 N73-22115
Measurements and predictions of loss and multipath variations for microwave troposcatter communication link
[AD-757553] 14 p1635 N73-23256
Development of Doppler microwave landing system and techniques for eliminating effects of multipath transmissions
14 p1689 N73-23706
Earth surface scattering model for multiphase prediction of radiowave communication between earth satellites
[NASA-CR-132791] 18 p2116 N73-27109
Modelling, experimentation, and estimation for multipath signals between ground terminal and aerospace vehicle
20 p2376 N73-29089
Computerized simulation of monopulse radar antenna pointing errors due to ground reflection multipath propagation
21 p2507 N73-30114
Adaptive learning receiver for time varying multipath channel transmission
23 p2756 N73-32052
Improvement of instrument landing systems with respect to multipath propagation effects and surface reflections
[DGLR-PAPER-73-017] 23 p2817 N73-32521
Characterization of multipath and Doppler fading in earth scatter communication, navigation, and radar links
24 p2894 N73-33102
MULTIPHASE FLOW
NT TWO PHASE FLOW
Influence of coriolis effect on energy transfer in mixed flow rotor cascades
[ARC-R/M-3703] 03 p0285 N73-12306
MULTIPLE BEAM INTERVAL SCANNERS
Multiple beam interval scanners with dual-antennas and circular artificial dielectric lenses to provide spot beam coverage of contiguous 48 states
[NASA-CR-130168] 08 p0888 N73-17192
Design and fabrication of two dimensional dielectric lens contained in parallel plate waveguide system in multibeam antenna study
[NASA-CR-132793] 22 p2641 N73-31171
MULTIPLE DEGREES OF FREEDOM
U DEGREES OF FREEDOM
MULTIPLE OUTPUT PROGRAMS
Design of multiple output analog computer for hot-wire anemometer signal processing
[AD-756532] 13 p1498 N73-22143
Implementation and development of multiple user on amtran on datacraft dc 6024
[NASA-CR-124330] 19 p2239 N73-28052
Adaptive control for multivariable systems using reduced dynamic ordering
[NASA-CR-133429] 19 p2314 N73-28607
MULTIPLETS
U FINE STRUCTURE
MULTIPLEX TRANSMISSION
U MULTIPLEXING
MULTIPLEXERS
U MULTIPLEXING
MULTIPLEXING
NT FREQUENCY DIVISION MULTIPLEXING
NT TIME DIVISION MULTIPLEXING
Analog to digital converter with teleprinter for multiple printout of projectile ballistic measurements
[PHL-1972-4] 01 p0032 N73-10245
Design and performance of multiple channel analog multiplexer for airborne data acquisition system
[ARL/F-NOTE-49] 02 p0145 N73-11172
Coherent multiplexing and radio relay array systems for satellite communication with small terminals
[AD-747488] 03 p0268 N73-12171
Throughput, multiplex systems, and free spectral range in spectrometers
[AD-749858] 05 p0553 N73-14492
Analysis of Microwave Landing System performance to determine signal formats and to reduce effects of multipath transmission
[AG-5011-B-1] 07 p0818 N73-16628
Technology base for multiplexed data bus subsystem design for space shuttles
[NASA-CR-124030] 07 p0848 N73-16874
Digit-error-protection technique for use in multiplex pulse code modulation systems for high quality sound-signal distribution
[BBC-1972/40] 09 p1001 N73-18170
Software module for teletypes connected to HP ALOHA SYSTEM multiplexer
[NASA-CR-130492] 09 p1006 N73-18213
Analysis of effects of nonlinear electronic devices on bandpass signals consisting of modulated sine waves
[CRC-1234] 10 p1128 N73-19189
Design of prototype quad redundant data terminal and associated multiplexer/demultiplexer units
[NASA-CR-124127] 10 p1130 N73-19203
Fault tolerant data transmission and multiplexing system using digital system
[AD-756485] 13 p1493 N73-22100
Phase detector with time correlation integrator for frequency multiplexed signals
[NASA-CASE-GSC-11744-1] 14 p1640 N73-23291
Telemetry and transmission system with programmed sampling and multiplexing
[NASA-CASE-GSC-11388-1] 15 p1750 N73-24187
Associative communication multiplexer for voice data compression
[AD-758246] 15 p1754 N73-24221
Hardware design, implementation, and test results of two wideband channel accommodation
[NASA-CR-124267] 16 p1875 N73-25182
Multispectral scanner system for Earth Resources Technology Satellites
[NASA-CR-132758] 16 p1912 N73-25474
Multichannel pulse sampling system with pulse anemometers and current meters on oceanographic buoy
[AD-760336] 17 p2030 N73-26426
Television multiplexing system, using single crystal controlled clock for signal synchronization
[NASA-CASE-KSC-10654-1] 21 p2507 N73-30115
Digital circuit optimization by time multiplexing component devices
22 p2646 N73-31200
MULTIPLIER PHOTOTUBES
U PHOTOMULTIPLIER TUBES
MULTIPLIERS
NT CHANNEL MULTIPLIERS
Bifurcations, for second order recurrence, related to passing through critical case such as real multiplier having modulus equal to one
[LAAS-PUBL-934] 02 p0203 N73-11639
Circuit with differential amplifier for synthesizing capacitance multiplier with microminiaturized feedback components
[NASA-CASE-NPO-11948-1] 06 p0647 N73-15255
MULTIPOLAR FIELDS
Multipole production in superconducting dipole and quadrupole synchrotron magnets
[NP-19692] 20 p2462 N73-29785
MULTIPROCESSING (COMPUTERS)
Techniques for designing balanced, extensible computer systems
[AD-763117] 20 p2380 N73-29120
MULTIPROGRAMMING
Functional design criteria for multiprocessor computer system to provide computational capability for space station
[NASA-CR-128601] 01 p0030 N73-10235
Multiprogram structure of HRS 101 digital computer and program package for statistical measured data selection and real time presentation
[JPRS-57696] 05 p0516 N73-14192
Multiprogram structure of HRS-101 digital computer
05 p0516 N73-14194
Results of multiprocessor systems design review
[NASA-CR-124026] 07 p0848 N73-16873
Problems of multiprogramming for special purpose computers
[JPRS-58571] 12 p1381 N73-21201
Multiprogramming for scheduling parallel processable tasks for uniprocessor
[AD-760143] 17 p2002 N73-26188
Computer programming procedure for linking independent CDC 6000 series computers
[NASA-CR-2296] 23 p2760 N73-32090
MULTIPROPELLANTS
U ROCKET PROPELLANTS
MULTISPECTRAL BAND CAMERAS
Usefulness of Skylab multispectral band camera and scanner imagery in multistage forest surveys
[E73-10610] 15 p1773 N73-24371
Study of recreational land and open spaces using Skylab multispectral band cameras and scanners
[E73-10724] 17 p2019 N73-26331
Utilization of Skylab multispectral cameras for study of eutrophication processes in lakes important to New York State water resources
[E73-10744] 18 p2133 N73-27236

Multistage forest surveys using Skylab multispectral band camera and scanner imagery
[E73-10782] 18 p2136 N73-27258
Study of recreational land and open space with Skylab imagery EREP 443
[E73-10783] 18 p2136 N73-27259
Flight test of multispectral image dissector camera onboard high altitude aircraft
18 p2209 N73-27835
Usefulness of Skylab EREP multispectral band scanner and camera imagery for multistage timber inventories and surveys
[E73-10861] 20 p2392 N73-29212
SL-2 MSS photography of soils, water, and vegetation in Texas
[E73-10943] 21 p2530 N73-30285
Analysis of geology, ecology, and hydrology of Colorado mountains from Skylab multispectral photography and data
[E73-11002] 22 p2659 N73-31307
Skylab S-190 photography of Great Basin area
[E73-11123] 24 p2916 N73-33278

MULTISPECTRAL BAND SCANNERS
Estuarine and coastal oceanography of Block Island Sound and adjacent New York coastal waters based on ERTS-1 multispectral band scanner imagery
[E72-10171] 01 p0044 N73-10352
Mapping iron compounds in Wind River Range using ERTS-1 multispectral scanner imagery
[E72-10181] 01 p0045 N73-10360
Ocean water color assessment of Monterey Bay, California, from ERTS-1 RBV and MSS imagery
[E72-10190] 01 p0046 N73-10369
Determination of in-flight optical transfer functions of orbital earth resources multispectral sensors
[E72-10212] 02 p0162 N73-11307
Land use mapping of forest area in Southeastern US by airborne multispectral scanning
[E72-10222] 02 p0162 N73-11316
Evaluation of data compression technique for ERTS-1 multispectral imagery
[E72-10226] 02 p0163 N73-11319
Overall evaluation of ERTS-1 RBV and MSS imagery for cartographic applications
[E72-10278] 03 p0292 N73-12376
Study of marine environment of northern Gulf of California using ERTS-1 MSS imagery
[E72-10283] 03 p0292 N73-12381
Geological survey of Adirondack Mountain region using ERTS-1 multispectral scanner imagery
[E72-10291] 04 p0410 N73-13341
ERTS-1 multispectral data of northwest Saudi Arabia
[E72-10295] 04 p0410 N73-13345
Spectral geological mapping in diverse terranes of New York using ERTS-1 imagery
[E72-10302] 05 p0530 N73-14309
Radiant power measuring instrument for measurement of downwelling and reflected radiance within ERTS multispectral scanner bands
[E72-10366] 05 p0535 N73-14354
Four band multispectral scanner system for ERTS
[NASA-CR-130111] 05 p0546 N73-14430
Ocean water color assessment from ERTS-1 RBV and MSS imagery
[E73-10002] 06 p0658 N73-15338
Computerized simulation of data compression using ERTS-1 MSS digital tapes
[E73-10011] 06 p0659 N73-15347
Interdisciplinary analysis of ERTS-1 multispectral data of Colorado mountain areas using automatic data processing techniques
[E73-10033] 06 p0661 N73-15366
Regional planning based on ERTS-1 MSS imagery
[E73-10038] 07 p0776 N73-16301
Multispectral band survey and mapping of earth in 18 days
[E73-10044] 07 p0777 N73-16307
Application of ERTS-1 MSS imagery to coastal engineering planning and construction
[E73-10050] 07 p0777 N73-16312
Cartographic applications of ERTS-1 MSS imagery
[E73-10053] 07 p0777 N73-16315
ERTS-1 MSS imagery of Great Plains rangeland, croplands, and land systems
[E73-10076] 07 p0780 N73-16338
Characteristics and capabilities of remote sensor systems to collect and analyze earth resource data
07 p0783 N73-16361
Characteristics of multispectral sensors and methods for interpreting multispectral data obtained during earth resources surveys
07 p0784 N73-16378
Proceedings of conference on earth resources survey systems - Vol. 2
[NASA-TM-X-68912] 07 p0785 N73-16382
Airborne multispectral scanning of maize canopy to determine temporal characteristics, and relation of leaf area index to spectral response curves
[NASA-CR-130369] 07 p0789 N73-16421
Application of multispectral remote sensing to soil survey research in Indiana
[NASA-CR-130033] 07 p0790 N73-16424
Airborne multispectral scanning of maize canopy to determine density, and comparision to leaf area index
[NASA-CR-130363] 07 p0790 N73-16425
Application of pattern recognition oriented algorithms for multispectral data analysis software system
[NASA-CR-130757] 08 p0887 N73-17184
Determination of meteorological information of ERTS-1 MSS bulk data at 0.6 - 0.7 microns as function of resolution
[E73-10085] 08 p0901 N73-17297
Photomapping of US using ERTS-1 MSS and RBV imagery
[E73-10088] 08 p0902 N73-17300
Mapping Arctic sea ice from ERTS-1 MSS imagery
[E73-10278] 08 p0914 N73-17486
Evaluation of data compression techniques for ERTS-1 MSS imagery
[E73-10287] 08 p0915 N73-17493
Land use classification, utilizing remote multispectral scanner data and computer analysis techniques over Lafayette, Indiana
[NASA-CR-130759] 08 p0917 N73-17516
Comparison of day and night infrared thermal imagery with results obtained using color photography and multispectral band sensor imagery
[AD-752217] 08 p0919 N73-17535
Cartographic evaluation of ERTS-1 MSS imagery
[E73-10329] 09 p1024 N73-18360
Multiband airborne remote sensor devices for collecting data on reflective and emissive terrain properties
[AD-752420] 09 p1033 N73-18430
Mechanical component screening for multispectral scanner mirror mechanism used on Earth Resources Technology Satellite
09 p1087 N73-18872
Design and development of two long wavelength, focal plane, and cooler assemblies for use in multispectral scanner installed in earth observations aircraft
[NASA-CR-128743] 10 p1137 N73-19262
Utilization of ERTS-1 imagery to study watershed hydrology in Southern Great Plains
[E73-10359] 10 p1149 N73-19355
Analysis of ERTS-1 multispectral imagery of Northwest Saudi Arabia
[E73-10380] 10 p1152 N73-19375
Atmospheric effects on ERTS-1 imagery and spatial resolution of MSS data
[E73-10394] 11 p1276 N73-20356
Optimization of haze detection by ERTS-1 MSS imagery
[E73-10499] 12 p1398 N73-21335
Development of multistage forest sampling inventory system using ERTS-1 MSS data
[E73-10508] 13 p1516 N73-22283
Application of ERTS-1 MSS imagery to multidisciplinary investigations in Alabama
[E73-10509] 13 p1516 N73-22284
Interpretation of geologic map of Fannin County, Texas, prepared by ADP techniques from ERTS MSS data
[NASA-CR-131574] 13 p1522 N73-22333
Urban land use mapping of San Francisco Bay area by machine processing of ERTS-1 multispectral data
[NASA-CR-131589] 13 p1522 N73-22334
Preparation of urban land use inventories by automated processing of ERTS MSS data
[NASA-CR-131576] 13 p1524 N73-22347
Reflected energy of vegetative ground cover measured with multispectral band scanners and infrared photographs
[NASA-CR-131575] 13 p1524 N73-22348
Earth resources remote sensing project using multispectral band scanners to detect and measure thermal radiation from ground vegetation
[NASA-CR-124219] 13 p1529 N73-22393
Enhancement of multispectral aircraft scanner data using scan overlap redundancy
[NASA-CR-131587] 13 p1530 N73-22395
Multispectral scanning systems and potential application to earth resources, noting radiation sources, atmospheric effects, and sensor techniques
[ERL/R-243-U] 13 p1531 N73-22403
Multispectral scanning systems and potential application to earth resources noting spectral properties of common earth materials
[ERL/R-244-U] 13 p1531 N73-22404
Development of processing and information extraction techniques for Skylab multispectral band scanner data
[E73-10563] 14 p1656 N73-23435
Detection and mapping of sea ice in Arctic regions using ERTS-1 RBV and MSS data
[E73-10595] 14 p1658 N73-23452
Data processing and image enhancement of ERTS-1 MSS data for Kansas
[E73-10596] 14 p1658 N73-23453
Image enhancement and information extraction techniques for ERTS-1 MSS imagery
[E73-10572] 15 p1772 N73-24352
Usefulness of Skylab multispectral band camera and scanner imagery in multistage forest surveys
[E73-10610] 15 p1773 N73-24371
Multispectral band scanner data of Oregon coast gathered during summer of 1969
15 p1779 N73-24424
Linear shift-invariant image preprocessing technique for multispectral scanners
[NASA-CR-132957] 15 p1787 N73-24485
Evaluation of ERTS-1 image data compression techniques
[E73-10647] 16 p1897 N73-25343
Determination of coastal water types around Monterey Bay, California by analysis of ERTS-1 MSS data
[E73-10677] 16 p1901 N73-25372
Multispectral scanner system for Earth Resources Technology Satellites
[NASA-CR-132758] 16 p1912 N73-25474
Evaluation of ERTS-1 image data compression technique
[E73-10717] 17 p2019 N73-26324
Study of recreational land and open spaces using Skylab multispectral band cameras and scanners
[E73-10724] 17 p2019 N73-26331
Analysis of ERTS-1 multispectral band scanner imagery to determine cause of anomalous dark patches occurring in photographs of calm ocean surfaces
[E73-10747] 17 p2021 N73-26351
C-130 aircraft flights to obtain simulated operation of Skylab multispectral scanner, thermal scanner, and cameras
[E73-10761] 17 p2023 N73-26361
Development of techniques for processing Skylab multispectral scanner data and comparison with ERTS-1 and aircraft scanner data processed by same technique
[E73-10758] 17 p2036 N73-26473
Influence of atmosphere pathlengths on ERTS-1 MSS imagery acquired over southwestern Kansas
[E73-10763] 18 p2133 N73-27240
Development of programming technique for processing Skylab MSS data
[E73-10765] 18 p2134 N73-27242
Identification of major fault zone along California-Nevada state line from ERTS-1 MSS imagery
[E73-10773] 18 p2135 N73-27249
Multistage forest surveys using Skylab multispectral band camera and scanner imagery
[E73-10782] 18 p2136 N73-27258
Correlation of sediment patterns with inflow and tidal action using MSS and I2S imagery
[E73-10794] 18 p2137 N73-27270
Detection and monitoring oil pollution using Skylab EREP MSS imagery
[E73-10796] 18 p2137 N73-27272
Digital system for precision geometric and radiometric correction of ERTS-1 RBV and MSS images
[E73-10827] 18 p2140 N73-27299
Multispectral band scanner for Earth Resources Technology Satellite A imagery
18 p2209 N73-27831
Processing quantities of multispectra data gathered by scanner systems using hybrid computers
[NASA-CR-133976] 19 p2239 N73-28048
Interpretation of ERTS-1 data to determine acreage of winter wheat in Kansas based on multispectral band scanner data
[PAPER-A1] 19 p2259 N73-28209
Agricultural analysis of ERTS-1 multispectral band scanner data for Monterey Bay, California
[PAPER-A23] 19 p2262 N73-28230
Analysis of ERTS-1 MSS imagery to determine geologic, hydrologic, oceanographic, and agricultural phenomena in Iceland
[PAPER-G10] 19 p2264 N73-28241
Assessment of geological applications of ERTS-1 imagery from selected areas of Canadian Arctic
[PAPER-G11] 19 p2264 N73-28242
Assessment of ERTS-1 imagery for mapping geologic features of Gaspe Peninsula, Quebec and determination of lithologic lineaments
[PAPER-G28] 19 p2267 N73-28259
Analysis of geological structure in Bighorn Mountains region of Wyomieg and Montana based on multispectral band imagery from ERTS-1 satellite
[PAPER-G31] 19 p2267 N73-28262
Analysis of water turbidity in two federal reservoirs in Kansas using ERTS-1 multispectral band scanners
[PAPER-E12] 19 p2270 N73-28276
Application of ERTS-1 multispectral scanner data for detecting thin cirrus and clear air turbulence
[PAPER-E14B] 19 p2270 N73-28279
Analysis of ERTS-1 imagery of southern Arizona plant communities using electronic satellite image analysis console
[PAPER-W7] 19 p2271 N73-28285
Preparation of urban land use inventories of Wisconsin and Indiana by machine-processing of ERTS-1 MSS data
[PAPER-L19] 19 p2275 N73-28314
Use of temporal dimension in classifying and mapping central Pennsylvania area from ERTS-1 MSS data
[PAPER-L23] 19 p2276 N73-28318
Atmospheric effects on ERTS-1 data and advanced data extraction techniques
[PAPER-I1] 19 p2277 N73-28323

Application of digital techniques to processing of ERTS-1 MSS and RBV image data
[PAPER-I7] 19 p2278 N73-28328
Processing and interpretation of ERTS-1 MSS data for Lake Livingston, Texas
[PAPER-I8] 19 p2278 N73-28329
Digital enhancement of ERTS-1 MSS data for maximum image visibility
[PAPER-I10] 19 p2278 N73-28331
Classification of ERTS-1 MSS data by canonical analysis
[PAPER-I18] 19 p2279 N73-28339
Thermal surveillance of Cascade range volcanoes using ERTS-1 MSS data, aircraft imaging systems, and ground based DCP
19 p2284 N73-28369
Comparison between ground based atmospheric turbidity network measurements and ERTS-1 MSS channel 4 scene grayness measurements
19 p2284 N73-28373
Application of classification algorithms to ERTS-1 MSS imagery of Texas land and water coastal features
19 p2286 N73-28383
Mapping of flood inundation areas in southwestern Iowa using ERTS-1 imagery
19 p2288 N73-28395
Conference on significant results obtained from ERTS-1 MSS and RBV data - Vol. 3
[E73-10826] 19 p2289 N73-28405
Application of multispectral scanning to agriculture, oceanography, hydrology, and geology
[ERL/R-246] 19 p2294 N73-28450
Data acquisition of multispectral scanning noting geology, hydrology, soil sceince, and mapping applications
19 p2295 N73-28451
Multispectral scanning systems applied to agriculture and forestry
19 p2295 N73-28452
Application of multispectral scanning to geology, noting interpretation problems
19 p2295 N73-28453
Application of multispectral scanning to hydrology and water resources, noting measurement of soil moisture, water depth, and water quality
19 p2295 N73-28454
Application of multispectral scanning to sea surface temperature, coastal topography and water sediment load, marine biology, sea ice, and oil slicks
19 p2295 N73-28455
Aim, methodology, technological requirements, and flexibility of future multispectral scanning programs
19 p2295 N73-28456
Data processing and extraction techniques for Skylab S-192 MSS data
[E73-10859] 20 p2391 N73-29210
Development of extraction and processing techniques for Skylab S-192 MSS data
[E73-10860] 20 p2391 N73-29211
Usefulness of Skylab EREP multispectral band scanner and camera imagery for multistage timber inventories and surveys
[E73-10861] 20 p2392 N73-29212
Skylab multispectral data for selected cover types in Colorado Mountains
[E73-10878] 20 p2393 N73-29229
Solution of earth resources and environmental quality problems using ERT-1 MSS data
[E73-10899] 20 p2395 N73-29248
Skylab MSS imagery of selected cover types in Colorado Mountains
[E73-10914] 20 p2397 N73-29263
Histograms of ERTS-1 MSS observations of haze
[E73-10924] 20 p2398 N73-29273
Generation and physical characteristics of ERTS MSS system corrected computer compatible tapes
[NASA-TM-X-70426] 20 p2410 N73-29366
Geometric aspects in digital analysis of multispectral scanner data
[NASA-CR-133641] 21 p2511 N73-30137
Mapping and mosaic applications of ERTS-1 MSS imagery
[E73-10957] 21 p2532 N73-30299
Description of Breguet 1150 to be used as European earth resources survey aircraft noting sensor payload
21 p2538 N73-30353
Processing of multispectral scanned data noting imaging techniques and user operations
[ERL/R-245] 21 p2539 N73-30356
Minimum distance classification based on multispectral scanner data using density estimators and Kullback-Leibler numbers as distance measures
[NASA-CR-133796] 21 p2566 N73-30569
Indepth comparative analysis of multispectral remote sensing techniques applied to salinity and drainage problems in Columbia Basin, Washington
22 p2656 N73-31280
Application of Skylab multispectral photography and scanner images to geological survey of Basin-and Range-Colorado Plateau boundary in north central and central Arizona
[E73-11000] 22 p2659 N73-31305
Assessment of water color in Caribbean from ERTS-1 RBV and MSS imagery.
[E73-11006] 22 p2660 N73-31311
Precision geometric and radiometric correction of bulk digital ERTS-1 imagery of Baltimore, Maryland by digital method
[E73-11019] 22 p2661 N73-31323
Remote haze monitoring using ERTS-1 MSS
[E73-11029] 22 p2662 N73-31333
Atmospheric effects on Skylab MSS data for Williamston, Michigan
[E73-11043] 22 p2664 N73-31344
Estimating crop acreage from space-simulated multispectral scanner data
[NASA-CR-134029] 22 p2666 N73-31359
Differentiation of ocean multispectral data obtained by satellite for chlorophyll content
22 p2736 N73-31904
Development of processing and extraction techniques for Skylab EREP MSS data
[E73-11078] 23 p2782 N73-32253
Atmospheric effects in Skylab EREP MSS data
[E73-11118] 23 p2783 N73-32263
Multispectral scanning systems and potential application to earth resources surveys - bibliography
[ERL/R-249-U] 23 p2787 N73-32299
European program in multispectral scanning systems and application to earth resources surveys
[ERL/R-247-U] 23 p2787 N73-32301
Multispectral band scanner reconnaissance of Pacific Ocean off Oregon coast
[AD-763428] 23 p2789 N73-32311
Minimizing probability of incorrectory classifying spectral observations from multispectral band scanners
[NASA-CR-134058] 23 p2812 N73-32486
Ratio scannergrammetry of geology in Wyoming and South Dakota
[E73-11096] 24 p2914 N73-33253
Comparison of preprocessing and classification techniques for pattern recognition applications to MSS data
[E73-11103] 24 p2915 N73-33260
Canonical analysis applied to processing and interpreting MSS data with digital computers
[E73-11104] 24 p2915 N73-33261
Correction of banding in ERTS-1 MSS digital data
[E73-11108] 24 p2915 N73-33265
Computer programs for processing multispectral scanner data of Susquehanna River Basin
[E73-11114] 24 p2915 N73-33271
Multidisciplinary investigations using ERTS-1 data for Alabama
[E73-11137] 24 p2917 N73-33292
Data processing and information extraction techniques for Skylab S-192 data
[E73-11142] 24 p2918 N73-33297
Processing ERTS-1 MSS digital data of Susquehanna River Basin
[E73-11165] 24 p2920 N73-33318

**MULTISPECTRAL PHOTOGRAPHY**
NT INFRARED PHOTOGRAPHY
NT RADAR PHOTOGRAPHY
Meteorological data from ERTS-1 high resolution multispectral photography
[E72-10189] 01 p0046 N73-10368
Analysis of ERTS-1 MSS data for color variations in Great Lakes and Chesapeake Bay to determine if multispectral imagery usable for locating and mapping extent of distinct water masses
[E72-10224] 02 p0163 N73-11318
Interpretation of ERTS-1 multispectral data from area in West Pakistan
[E72-10234] 03 p0288 N73-12334
Utilization of ERTS-1 multispectral photography in evaluating Iranian playas as potential locations for economic and engineering development
[E72-10270] 03 p0291 N73-12369
Cultural resources interpretation and map revision from ERTS-1 RBV and MSS imagery of Washington state
[E72-10276] 03 p0291 N73-12374
Computerized optical system for producing multiple images of a scene simultaneously
[NASA-CASE-MSC-12404-1] 04 p0448 N73-13661
Application of remotely sensed data to determination of resources and conditions in Susquehanna River Basin
04 p0471 N73-13844
Feasibility of multispectral signal encoding on black and white film
[AD-749495] 05 p0548 N73-14455
Multispectral imagery of estuarine and coastal oceanography of Block Island Sound and adjacent New York coastal waters using ERTS-1 imagery
[E73-10010] 06 p0659 N73-15346
Land use mapping and change detection in Central Atlantic Regional Ecological Test Site based on ERTS-1 MSS imagery
[E73-10034] 06 p0661 N73-15367
Multispectral remote sensing techniques for identification of corn blight disease
[NASA-TM-X-69055] 07 p0745 N73-16064
Earth resources laboratory data system for analyzing and processing multispectral, radiometric, photographic, and passive microwave imagery data
[NASA-CR-128693] 07 p0758 N73-16160
Discrimination and mapping land use categories in Puerto Rico using various types of multispectral remote sensor imagery
07 p0776 N73-16298
Crop identification and acreage estimation using ERTS-1 MSS imagery of northern Illinois
[E73-10039] 07 p0776 N73-16302
Application of multispectral data processing to Delaware coastal wetlands vegetation mapping
[E73-10069] 07 p0779 N73-16331
Crop identification through interpretation of multiband and multidate photography
07 p0785 N73-16385
Multispectral remote sensing techniques applied to study changes in wildlife habitats
07 p0786 N73-16396
Multispectral data and computer processing technique for mapping soil patterns and multispectral radiation changes from corn crop canopy
[NASA-CR-130035] 07 p0789 N73-16420
Automatic processing of remote sensed data to aid in land use mapping and agricultural conservation
[NASA-CR-130372] 07 p0790 N73-16423
Procedure for defining spectrally separable classes for soil survey research
[NASA-CR-130031] 07 p0791 N73-16434
ERTS-1 multispectral imagery of West Pakistan
[E73-10315] 09 p1023 N73-18347
Multiband airborne remote sensor devices for collecting data on reflective and emissive terrain properties
[AD-752420] 09 p1033 N73-18430
Utilization of ERTS-1 imagery for evaluation of Iranian playas as potential locations for economic and engineering development
[E73-10339] 10 p1147 N73-19338
Meteorological utility of high resolution ERTS-1 multispectral data
[E73-10357] 10 p1149 N73-19353
Detection and mapping snow cover in Salt-Verde Watershed of Arizona using ERTS-1 imagery
[E73-10361] 10 p1149 N73-19357
Computer processing of multispectral imagery of India
[E73-10373] 10 p1151 N73-19368
Interpretation of ERTS-1 geologic data for Nevada and evaluation of materials used in compiling photomaps
[E73-10398] 11 p1277 N73-20360
Coherent optical system for display of spatial resolution of ERTS-1 MSS photography
[E73-10449] 11 p1283 N73-20409
Regional wet census of playa lakes on Southern High Plains area of Texas and New Mexico from ERTS-1 MSS imagery
[E73-10455] 11 p1283 N73-20414
Classification of land use in California using textural information in ERTS-1 MSS imagery
[E73-10461] 11 p1284 N73-20419
Mapping of polar regions using ERTS-1 multispectral photography
[E73-10501] 12 p1398 N73-21337
Applications of multicolor dye tracers and multispectral photography to coastal water mapping
[AD-754437] 12 p1403 N73-21378
Land use, urban development, and regional planning for Los Angeles County based on photointerpretation of MSS imagery and multispectral information extraction
[E73-10486] 13 p1515 N73-22277
Digital correction techniques for ERTS-1 MSS imagery
[E73-10503] 13 p1515 N73-22278
Development of multistage forest sampling inventory system from interpretation of ERST-1 MSS photography
[E73-10528] 13 p1517 N73-22294
Multistage forest surveys from Skylab EREP multispectral band scanner and camera imagery
[E73-10531] 13 p1517 N73-22296
Interdisciplinary analysis of Skylab EREP MSS photography of vegetative and geomorphological cover types in Colorado Mountains
[E73-10533] 13 p1517 N73-22297
Geological survey of West Pakistan from ERTS-1 multispectral imagery
[E73-10540] 13 p1518 N73-22304
Detection of ponderosa pine tree stresses from insects or diseases using multispectral photography
[NASA-CR-131586] 13 p1522 N73-22337
Development of techniques for solving image correlation and image sampling of multispectral data
[NASA-CR-130223] 13 p1529 N73-22389
Effectiveness of ERTS-1 MSS photography in characterizing watershed runoff in Texas
[E73-10513] 14 p1653 N73-23408
Use of ERTS multispectral data to solve development and management problems of agricultural resources in Lyna County, Texas
[NASA-CR-132956] 15 p1778 N73-24411
Application of ERTS-1 imagery to fracture related mine safety hazards in coal mining industry and identification of mine subsidence areas in Indiana
[E73-10681] 16 p1901 N73-25376

ERTS-1 imagery of strip mining activity in Cumberland Plateau, Tennessee Test Site and agricultural areas in Alabama, Georgia, and Tennessee
[E73-10694] 16 p1902 N73-25386
Application of ERTS-1 imagery to cartography, geomorphology, agronomy, and hydrology of Bolivia
[E73-10695] 16 p1902 N73-25387
Analysis of Skylab and EREP coverage of Wyoming and characteristics of field photometer system for measuring object reflectances
[E73-10697] 16 p1903 N73-25389
ERTS-1 imagery of Bighorn-Pryor mountains of Wyoming and Montana applied to analysis of regional tectonic relationships
[E73-10704] 16 p1903 N73-25395
Multispectral remote sensing techniques for measuring light absorption, scattering, and particle concentrations in water
[AD-759668] 16 p1914 N73-25491
Application of ERTS-1 data for monitoring vernal advancement and retrogradation of natural vegetation in Great Plains Corridor
[E73-10693] 17 p2018 N73-26315
ERTS-1 and aircraft multispectral scanner data for mapping ponds and lakes near Woodworth, North Dakota to determine changes in continental migratory bird habitat
[E73-10714] 17 p2018 N73-26321
Photointerpretation of ERTS-1 imagery and airborne photography to determine vegetation growth in Iowa
[E73-10715] 17 p2018 N73-26322
Application of ERTS-1 data to locate wind erosion sites in West Texas and to determine extent and spread of wind erosion
[E73-10719] 17 p2019 N73-26326
Evaluation of ERTS-1 image sensor spatial resolution in photographic form
[E73-10721] 17 p2019 N73-26328
Application of ERTS-1 return beam vidicon and multispectral scanner imagery for ocean water color assessment in Caribbean Sea
[E73-10726] 17 p2019 N73-26332
Evaluation of ERTS-1 image data compression techniques to show four ERTS MSS tapes recorded on single compressed tape
[E73-10730] 17 p2020 N73-26336
In situ spectroradiometric quantification of ERTS-1 data and multispectral photo analysis of Willcox Playa
[E73-10737] 17 p2020 N73-26343
In situ spectroradiometric quantification of ERTS-1 data based on Arizona test site and Willcox Playa
[E73-10738] 17 p2021 N73-26344
Detection and analysis of fracture systems using ERTS-1 imagery of snow cover conditions as enhancement tool
[E73-10741] 17 p2021 N73-26346
Application of ERTS-1 data for identification of ice formations in Lake Erie and snow mapping in American River basin
[E73-10750] 17 p2022 N73-26353
Development of techniques for processing Skylab multispectral scanner data and comparison with ERTS-1 and aircraft scanner data processed by same technique
[E73-10758] 17 p2036 N73-26473
Evaluation of satellite remote sensing and automatic data techniques for analysis of wetlands and marshlands using ERTS-1 imagery
[E73-10740] 18 p2133 N73-27235
Analysis of ERTS-1 imagery for area measurement of land use categories in Finney County, Kansas
[E73-10764] 18 p2134 N73-27241
Inventorying land use in New York State using ERTS-1 multispectral imagery
[E73-10772] 18 p2134 N73-27248
Application of Skylab multispectral photography to mineral and land resources of South Carolina
[E73-10831] 18 p2141 N73-27301
Performance of return beam vidicon multispectral camera system for remote ERTS imagery
18 p2209 N73-27832
Rectification of ERTS-1 multispectral imagery using digital techniques
[PAPER-I6] 19 p2277 N73-28327
Automatic recognition of terrain types from ERTS-1 MSS imagery
[PAPER-I17] 19 p2279 N73-28338
Correlation of ERTS-1 multispectral imagery with suspended matter and chlorophyll in lower Chesapeake Bay
[PAPER-M4] 19 p2280 N73-28344
Resectioning programs developed to provide precision annotation of predetermined primary land sampling units on ERTS-1 MSS imagery
19 p2286 N73-28382
Detection of turbidity plumes in Tampa Bay, Florida from ERTS-1 MSS imagery
19 p2287 N73-28388
ERTS-1 multispectral imagery of topography of Assateague Island
[E73-10848] 19 p2292 N73-28426
ERTS-1 multispectral photography of wetlands vegetation and plant species
[E73-10850] 19 p2292 N73-28428
Interpretation of ERTS-1 MSS imagery of Tennessee Valley
[E73-10854] 19 p2292 N73-28431
Computer processing of Skylab MSS data for land use mapping of Baltimore, Maryland-Washington, D.C. area
[E73-10913] 20 p2397 N73-29262
Geology, hydrology, and ecology of Botswana from ERTS-1 MSS imagery
[E73-10929] 20 p2399 N73-29278
Water penetration properties of multispectral photography
[UCS/72/13] 20 p2412 N73-29387
SL-2 MSS photography of soils, water, and vegetation in Texas
[E73-10943] 21 p2530 N73-30285
Influence of image position on urban place detection in ERTS-1 imagery of Kansas and Missouri
[E73-10971] 21 p2533 N73-30312
ERTS-1 imagery of surface water aera in Quivera National Wildlife Refuge, Kansas
[E73-10974] 21 p2533 N73-30313
Detection of precipitation pattern in west central Kansas from ERTS-1 MSS imagery
[E73-10975] 21 p2533 N73-30314
Photointerpretation of Skylab MSS photography of mineral deposits in Nevada
[E73-10983] 22 p2658 N73-31290
Regional land use planning and management in Tri-State area from ERTS-1 MSS photography
[E73-10986] 22 p2658 N73-31293
Urban development and regional planning in Los Angeles County using ERTS-1 MSS photography
[E73-10989] 22 p2658 N73-31295
Geological and geochemical studies in Robinson Mining District, White Pine Co., Nevada using Skylab multispectral imagery
[E73-10992] 22 p2659 N73-31298
Application of Skylab multispectral photography and scanner images to geological survey of Basin-and Range-Colorado Plateau boundary in north central and central Arizona
[E73-11000] 22 p2659 N73-31305
Computer interpretation of multispectral data of Chesapeake Bay, Lake Pontchartrain, Louisiana, and lower Mississippi Valley
[E73-11007] 22 p2660 N73-31312
Geologic and mineral and water resources of western Colorado from Skylab multispectral photography
[E73-11010] 22 p2660 N73-31315
Interpretation techniques for Skylab monitoring of lake eutrophication in New York State
[E73-11011] 22 p2660 N73-31316
Sampling strategies for automatic thematic land use mapping of Washington D.C., Maryland counties, and Alice Springs, Australia using Skylab multispectral photography
[E73-11018] 22 p2661 N73-31322
Application of Skylab MSS imagery to geological survey of Basin-and-Range-Colorado Plateau boundary in Arizona
[E73-11042] 22 p2664 N73-31343
Multispectral ERTS imagery for polar ice mapping
22 p2736 N73-31901
Analysis of ERTS-1 MSS data for West Pakistan
[E73-11097] 24 p2914 N73-33254
Aerotriangulation with very small scale photography from Skylab
[E73-11117] 24 p2916 N73-33274
Multidisciplinary investigations using ERTS-1 data for Alabama
[E73-11137] 24 p2917 N73-33292
Sampling strategies in land use mapping using Skylab EREP multispectral photography
[E73-11139] 24 p2918 N73-33294
Application of Skylab multispectral photography to mineral and land resources of South Carolina and Georgia
[E73-11140] 24 p2918 N73-33295
Water depth determination off Puerto Rico from Skylab multispectral imagery
[E73-11141] 24 p2918 N73-33296
Skylab photography of recreational land and urban resources in Oakland County, Michigan
[E73-11150] 24 p2919 N73-33304
Tectonic analysis of Bighorn Mountains of Montana and Wyoming and Black Hills of South Dakota and Wyoming from Skylab imagery
[E73-11151] 24 p2919 N73-33305

**MULTISTAGE COMPRESSORS**
U TURBOCOMPRESSORS

**MULTISTAGE ROCKET VEHICLES**
NT ASTROBEE ROCKET VEHICLES
NT ATHENA ROCKET VEHICLE
NT ATLAS CENTAUR LAUNCH VEHICLE
NT ATLAS LAUNCH VEHICLES
NT NIKE ROCKET VEHICLES
NT NIKE-TOMAHAWK ROCKET VEHICLE
NT SATURN LAUNCH VEHICLES
NT SATURN 1B LAUNCH VEHICLES
NT SATURN 5 LAUNCH VEHICLES
NT SCOUT LAUNCH VEHICLE
NT SKYLARK ROCKET VEHICLE
NT TITAN LAUNCH VEHICLES
NT TITAN 3 LAUNCH VEHICLE
Literature review on design and performance of multistage rockets
[AD-752815] 08 p0956 N73-17824

**MULTIVARIATE STATISTICAL ANALYSIS**
NT COVARIANCE
NT DISCRETE FUNCTIONS
NT REGRESSION ANALYSIS
Optimal linear combination of observable parameters for maximizing correlation between index and criterion variates for sampling classification and personnel selection
[AD-751257] 07 p0813 N73-16596
Multivariate limits for describing cockpit related anthropometric features of aviation personnel
[AD-752032] 08 p0880 N73-17124
Multivariate analysis on data used in n-station solution tracking technique
[AD-759975] 17 p2000 N73-26172
Multivariate statistical analysis including divergence, probability of misclassification, information theory, and matrix analysis
[NASA-CR-128990] 20 p2438 N73-29578
Computational forms for transformed covariance matrix of multivariate normal populations
[REPT-19] 20 p2438 N73-29583
Perturbation and sensitivity inequalities in divergence calculations
[REPT-20] 20 p2438 N73-29584
Rank-k maximal statistics for divergence and probability of misclassification
[REPT-21] 20 p2438 N73-29585
Expression for transformed covariance matrix of multivariate normal populations
[REPT-24] 20 p2439 N73-29588
Minimal probability of misclassification in feature selection problem of classifying n-dimensional observation vector into one of m-distinct classes
[REPT-26] 20 p2439 N73-29589
Statistical analysis of NASA multivariate spectrum analysis program performance after modifications
[NASA-CR-134011] 22 p2620 N73-30995
Multidimensional linear system parameter estimation computer program using least squares method evaluating mathematical model stability, observability and real time operation
[LAAS-AS-73-I-06] 23 p2813 N73-32491

**MULTIVIBRATORS**
NT FLIP-FLOPS

**MUONS**
Muon proton interactions and elastic scattering for neutron beam generation in accelerator
[BNL-17314] 10 p1193 N73-19710
Muon production altitude in cosmic ray air showers from lateral and angular muon separation from shower core, and geomagnetic effects on muon charge ratio
13 p1574 N73-22754
Comsic ray air shower muon momentum spectra, noting dependence on shower primary energy, zenith angle, and arrival directions
13 p1574 N73-22755
Results from Nottingham cosmic ray air shower muon detector
13 p1574 N73-22756
Polarization measurements of cosmic ray muons arriving at sea level with different energies and from different zenith angles
17 p2079 N73-26815

**MUSCLES**
Adenin-nucleotides NAD[plus] and NADN in skeletal muscles during intensive work and at rest
[NASA-TT-F-14856] 11 p1246 N73-20118
Atrophy and metabolic changes in internal organs and skeletal muscles of rats exposed to hypokinesia
14 p1607 N73-23029
Recording human electroencephalogram under influence of muscle noise
24 p2883 N73-33025

**MUSCULAR FUNCTION**
Nonlinear model relating neural input to force and muscle contraction in human ankle joint
01 p0015 N73-10117
Tracking tests as quantitative measurements of neuromuscular functions in clinical applications
01 p0015 N73-10118
Hypoxia effects on human gastric motor functions in pressure chamber experiments using electrogastrography
03 p0257 N73-12085
Skylab experiments to assess weightlessness effects on human nutritional metabolism and musculoskeletal function
09 p0994 N73-18115
Exercise and muscle stimulation for preventing metabolism changes during bed rest
13 p1483 N73-22019
Depressing effect of hypokinesia on rat skeletal muscle functions
14 p1607 N73-23028
Functional disturbances during hypokinesia in man
[NASA-TT-F-15148] 24 p2890 N73-33073

**MUSCULAR STRENGTH**
Human factors engineering to determine maximum control forces capability of female pilots
[FAA-AM-72-27] 06 p0635 N73-15157

MUSCULAR TONUS
Evoked compensatory reflex reactions of rabbit ocular and eyelid muscles during hypoxia
13 p1480 N73-21992
Basic causal mechanisms responsible for loss of vascular tone during alterations in shifts to zero gravity
[NASA-CR-128897] 14 p1612 N73-23069
MUSCULOSKELETAL SYSTEM
NT BONES
NT CEREBRUM
NT COLLAGENS
NT CRANIUM
NT JOINTS [ANATOMY]
NT MARROW
NT VERTEBRAL COLUMN
Quantitative description of mobility for human torso
[AD-754924] 11 p1251 N73-20151
Blood supply to skeletal muscles of rats during hypokinesia
24 p2882 N73-33018
MUSEUMS
Report to House Committee on Science and Astronautics on aerospace museum in Western United States
07 p0857 N73-16949
MUSIC
Dependence of timbre on location in diffuse sound fields
[IZF-1972-15] 02 p0211 N73-11711
Investigation of vocal cord regulatory mechanism of register, pitch, and intensity of voice during singing
14 p1632 N73-23225
MUTATIONS
Observation of circulating lymphocytoid cell in monkey after exposure to radio waves
[AD-749583] 06 p0631 N73-15128
Biostatistics of genetical processes in human populations
[NASA-CR-131508] 12 p1372 N73-21131
Ability of organism to maintain normal physiological activities in bioregenerative system
[NASA-CR-130807] 13 p1479 N73-21979
Ultraviolet extraterrestrial radiation tolerances of Bacillus subtilis spores and Escherichia coli bacteriophages
15 p1740 N73-24107
MYLAR [TRADEMARK]
Dynamic testing of fabrics and Mylar in shock tubes
[NASA-CR-132284] 23 p2770 N73-32157
MYOCARDIAL INFARCTION
Electrocardiographic stress testing for determining influence of occupational and other stresses on ischemic heart disease
08 p0875 N73-17082
Clinical analysis of relationship between VPB and mortality rate in patient with acute myocardial infractions
08 p0875 N73-17083
Myocardial changes in flying personnel exposed to hypoxic hypoxia
13 p1479 N73-21985
Microscopic morphological changes in dog cardiac muscle after chronic gamma irradiation
20 p2366 N73-29027
MYOCARDIUM
Alterations in myocardial contractility induced by bed rest
[NASA-CR-128968] 17 p1986 N73-26056
MYOELECTRIC POTENTIALS
Bioelectric control system design for reversible slave mechanism manipulator using single muscle input
17 p1990 N73-26088
Motor function modeling of human arm by manipulator using myoelectric control pulses
17 p1990 N73-26091
MYOELECTRICITY
NT MYOELECTRIC POTENTIALS


# N


N-P JUNCTIONS
U P-N JUNCTIONS
N-P-N JUNCTIONS
Two-dimensional numerical analysis of integrated silicon N-P-N bipolar transistors
22 p2706 N73-31672
N-TYPE SEMICONDUCTORS
Noise measurements on n-junction gold silicon and aluminum silicon diodes at avalanche potential considering leakage current
[FRNC-CONF-29] 05 p0519 N73-14221
Radiation and annealing studies on oxygen-doped and lithium diffused germanium
[CONF-720707-7] 06 p0699 N73-15696
Current-voltage, load, and spectral characteristics of p- and n-type GaAs
[NASA-TT-F-14859] 11 p1330 N73-20793
Effects of proton bombardment on p- and n-type PbSnTe thin films
[AD-756542] 13 p1567 N73-22696
Influence of applied stress, magnetic and electric fields, and impurity concentration on electrical conductance of n-type germanium at very low temperatures
[RR-738] 20 p2462 N73-29783
N-156 AIRCRAFT
U F-5 AIRCRAFT
NA-300 AIRCRAFT
U OV-10 AIRCRAFT
NACELLES
Flight and wind tunnel tests to determine effects of Reynolds number of installed boattail drag of underwing nacelle
[NASA-TM-X-68162] 02 p0124 N73-11007
Flight performance evaluation for underwing nacelle installation of auxiliary-inlet ejector nozzle with clamshell flow diverter from Mach 0.6 to 1.3
[NASA-TM-X-2655] 02 p0222 N73-11793
Performance prediction for acoustically lined engine nacelle design
03 p0250 N73-12019
Noise output of turbofan engine with acoustically treated nacelle
03 p0250 N73-12020
Noise output from quiet engine during simulated takeoff and approach tests
03 p0250 N73-12021
User manual for Streamtube Curvature Analysis program to predict pressure distribution about nacelle at transonic speeds - Vol. 1
[NASA-CR-112239-1] 15 p1767 N73-24313
User manual for Streamtube Curvature Analysis program to predict pressure distribution about nacelle at transonic speeds - Vol. 2
[NASA-CR-112239-2] 15 p1767 N73-24314
User manual for Streamtube Curvature Analysis program to predict pressure distribution about nacelle at transonic speeds - appendix
[NASA-CR-112239-3] 15 p1767 N73-24315
Wind tunnel tests to determine effect on cruise performance of installing long duct refan-engine nacelle on DC 8 aircraft
[NASA-CR-121218] 17 p1982 N73-26023
DC 9 refanned engine nacelle effects on cruise drag considering lateral spacing
[NASA-CR-121219] 17 p1982 N73-26024
Computer program for predicting inviscid, transonic flow field about isolated nacelles
[NASA-CR-112271] 18 p2130 N73-27211
Formulation and development of computer analysis for calculating streamlines and pressure distributions around two-dimensional isolated nacelles at transonic speeds
[NASA-CR-2217] 19 p2217 N73-27890
Design and development of integrated fire and overheat detection and warning system for installation in aircraft nacelle
[AD-762919] 20 p2362 N73-28999
Flight tests of modified F-106 aircraft to determine installation effects of two aft underwing nacelles housing afterburning J-85 engines
[NASA-TM-X-71439] 23 p2743 N73-31959
NAPHTHALENE
Removal and separation of particles by crystallization in carbon-naphthalene system
[AD-753056] 09 p1076 N73-18777
Synthesis of high molecular weight benzobistriazolo phenanthroline polymers for heat resistant plastic films
[AD-753414] 10 p1127 N73-19180
NAPPES
U FOLDS [GEOLOGY]
NARCOSIS
Mechanism of inert gas narcosis in human body and mice
[NASA-CR-62096] 24 p2885 N73-33038
NARCOTICS
Chromatographic and polarographic methods for determining metabolic levels of hypnotic drugs in blood plasma and urine of man
12 p1370 N73-21118
Incidence of abnormal liver function tests in drug addicts without history of jaundice
[NASA-TT-F-15041] 20 p2368 N73-29044
NASA PROGRAMS
NT APOLLO PROJECT
NT EARTH RESOURCES PROGRAM
NT EARTH RESOURCES SURVEY PROGRAM
NT ECHO PROJECT
NT GLOBAL ATMOSPHERIC RESEARCH PROGRAM
NT HELIOS PROJECT
NT MARINER PROGRAM
NT MARS 69 PROJECT
NT MARS 71 PROJECT
NT NIMBUS PROJECT
NT QUIET ENGINE PROGRAM
NT ROVER PROJECT
NT SKYLAB PROGRAM
NT SURVEYOR PROJECT
NT TEKTITE PROJECT
NT TILT ROTOR RESEARCH AIRCRAFT PROGRAM
NT VIKING MARS PROGRAM
Directory of observation stations in NASA geodetic satellites program based on preferred major datums and Modified Mercury Datum 1968 - Vol. 2
[NASA-CR-130072] 01 p0036 N73-10280
NASA plans and priorities thru 1985
02 p0227 N73-11834
Abstracts of Research and Technology Operating Plans used for management review and control of research for NASA programs
[NASA-TM-X-68856] 03 p0366 N73-12978
Impact of space program on efforts to improve standards of living and to reduce harmful pollution of environment
04 p0471 N73-13836
Alternatives in complement and structure of NASA teleprocessing resources for years 1975 through 1985 including options of minicomputers, mass storage devices, and software development
[NASA-CR-129825] 05 p0515 N73-14188
Development of specifications for minicomputer hardware and software for NASA applications - App. A
[NASA-CR-129816] 05 p0515 N73-14189
Production of software in NASA within predictable schedule and budget constraints and reasonable tolerances - App. C
[NASA-CR-129818] 05 p0516 N73-14191
Bibliography of publications from OGO E plasma wave investigation
[NASA-CR-130140] 06 p0644 N73-15227
Annotated bibliography of technical characteristics of remote sensors and technological experiments developed under NASA programs for earth observation
[NASA-TM-X-66144] 06 p0674 N73-15482
Advanced NASA and DOD technology management techniques, and application to NATO programs for defense and civil needs
06 p0732 N73-15968
Effect of Apollo project accomplishments on earth resources surveys and conduct of earth resources investigations in future space missions
07 p0781 N73-16349
Objectives of NASA Earth Resources Survey Program to include types of sensors used and data acquired by aircraft, spacecraft, and ground observations
07 p0782 N73-16351
International aspects of Earth Resources Survey Program to include proposals for data availability and assistance to be provided by various nations
07 p0782 N73-16352
Conference on occupational medicine support in NASA programs to prevent health and emotional problems in personnel
[NASA-TM-X-69072] 08 p0871 N73-17048
Medical concepts and functional management in NASA Environmental Health Program
08 p0872 N73-17056
Industrial hygiene, radiological health, and spacecraft sanitation studies in NASA Environmental Health Program
08 p0872 N73-17057
Environmental health measures to prevent cabin atmosphere toxicity and provide drinking water standards in manned space flight applications
08 p0872 N73-17058
Routine proctosigmoidoscopic examinations of asymptotic NASA personnel for cancer prevention
08 p0872 N73-17061
Mental health services for emotional counselling in NASA facilities to insure maximum human performance
08 p0872 N73-17062
Conference on preventive medical and environmental control measures for NASA and aviation industry personnel management
[NASA-TM-X-69073] 08 p0873 N73-17064
Long term exercise effects on cardiovascular response in NASA personnel with periodic ergometric evaluation
08 p0873 N73-17067
Computerized multivariate scheduling of physical examinations for NASA personnel in clinical intervention program
08 p0873 N73-17068
Physical exercise effects on health of NASA personnel
08 p0873 N73-17069
Facilities engineering for NASA space program
08 p0873 N73-17070
Continuous monitoring of hypertension and hypercholesterolemia in NASA employees for prevention of heart disease and disability
08 p0873 N73-17072
Conference on occupational and environmental medical services provided to NASA employees
[NASA-TM-X-69074] 08 p0874 N73-17078
Influence of repeated test and dietary counseling on hypercholesterolemia control in NASA employees
08 p0875 N73-17081
Feasibility of effective exercise and health evaluation and enhancement program for NASA employees
08 p0875 N73-17091

Influence of NASA stress lab program on physical education in US colleges
08 p0876 N73-17092
Application of NASA developed techniques, photographic film, and photographic equipment to ecological problems
[NASA-SP-5099] 09 p1034 N73-18437
Proceedings of seminar on organization of NASA to show areas of responsibility, resource allocation, and program management
[NASA-CR-131087] 10 p1225 N73-19958
NASA utilization of high pressure oxygen
[NASA-TM-X-68203] 11 p1266 N73-20276
Proceedings of Congressional committee on use of recycled materials in NASA programs and requirement for recycling legislation for environmental and economy improvement
11 p1308 N73-20614
Presidential report on progress and activities of various aerospace programs in 1972 and comments on future mission planning
11 p1352 N73-20975
Analysis of NASA programs during post-Apollo period to show organization of field centers, planning activities, operational activities, and resources utilization
[NASA-CR-131931] 12 p1466 N73-21879
Surveys of electroplating methods and techniques generated from NASA programs
[NASA-SP-5114] 13 p1533 N73-22426
Analysis of NASA programs for 1970 to 1980 period with application to earth orbital experiment program and requirements - Vol. 1
[NASA-CR-112325] 13 p1577 N73-22778
Analysis of manned space flight capability development for support of earth orbital experiment program and requirements - Vol. 2
[NASA-CR-112326] 13 p1577 N73-22779
Analysis of space biology projects related to earth orbital experiment program to identify critical issues and methods of conducting experiments - Vol. 3
[NASA-CR-112327] 13 p1577 N73-22780
Development of space astronomy projects identified during orbital experiment program and requirements study - Vol. 4
[NASA-CR-112328] 13 p1577 N73-22781
Development of space communications and navigation projects involved in earth orbital experiment program and requirements study - Vol. 5
[NASA-CR-112329] 13 p1577 N73-22782
Earth observation experiments identified during earth orbital experiment program and requirements study - Vol. 6
[NASA-CR-112330] 13 p1577 N73-22783
Definition of supporting technology development requirements for earth orbital experiment program and requirements study - Vol. 7
[NASA-CR-112331] 13 p1577 N73-22784
Data management systems, instrumentation concepts, and biotechnology laboratory for earth orbital experiment program and requirements study - Vol. 8
[NASA-CR-112332] 13 p1577 N73-22785
Research projects conducted as part of NASA programs during period May 1970 through May 1972
[NASA-TM-X-64723] 13 p1593 N73-22915
Development, characteristics, and applications of flat conductor cable to include methods and facilities for fabrication
13 p1593 N73-22916
Development and application of composite materials for weight reduction of space shuttle structural hardware
13 p1593 N73-22917
Development of galvanic forming techniques and application to production of complex structures requiring accurate dimensions
13 p1593 N73-22918
Development of electron beam welding techniques and application to welding various metal structures
13 p1593 N73-22919
Manufacture of quartz gyroscopes for application to General Relativity Satellite
13 p1593 N73-22920
Analysis of melting, mixing, and solidification of metal matrix composite materials in weightless environment
13 p1594 N73-22921
Development of manufacturing in space processes for Skylab program to include operating sequence description and results obtained
13 p1594 N73-22922
Development and characteristics of neutral buoyancy simulator for duplicating weightless conditions encountered during space missions
13 p1594 N73-22923
Development of electrocardiogram protection circuits to prevent accidental electrocution and digital cardiotachometer system to display heart rate
13 p1594 N73-22924
Development and evaluation of free flying teleoperators to include semiexoskeletal master control unit, joystick-analog unit, and three dimensional television system
13 p1594 N73-22925
NASA appropriations for FY 1974
[H-REPT-93-171] 13 p1595 N73-22929
Congressional hearings on NASA budgetary authorizations for 1974
13 p1595 N73-22930
NASA programs on life science research in aerospace environments, emphasizing cardiovascular system
14 p1611 N73-23058
Military and NASA programs using FCC
14 p1642 N73-23318
Hearings concerning NASA appropriations for FY 1974
14 p1721 N73-23960
Congressional hearings on NASA technology applications program budget
14 p1721 N73-23966
Some effects of space research on society
[NASA-TM-X-66233] 14 p1721 N73-23968
NASA authorization for fiscal year 1974
[S-REPT-93-179] 15 p1845 N73-24950
Application of NASA type management approach to other fields
[NASA-TM-X-66251] 15 p1846 N73-24956
NASA participation in international space programs
[NASA-TM-X-69259] 15 p1846 N73-24957
Phased project planning and development for operational space missions referring to NASA meteorological and communication satellite programs
15 p1848 N73-24978
Role of NASA programs and technologies in developing better communication links among people
[NASA-CR-133052] 16 p1876 N73-25183
Role of NASA in area of environmental quality
[NASA-CR-133049] 16 p1907 N73-25426
Government-owned patent survey for technology utilization in commercial enterprises
16 p1976 N73-25981
Role of NASA programs and activities in national attempt to upgrade quality of transportation services
[NASA-CR-133050] 16 p1977 N73-25990
Assessment of joint NASA/ESRO Venus orbiter
[SYST/2109/MS/1V] 17 p2089 N73-26906
Effects of NASA expenditures to aerospace industry as factor of industrial location
18 p2207 N73-27814
History of NASA
[NASA-NEWS-RELEASE-73-134]
18 p2213 N73-27868
Congressional appropriations to National Aeronautics and Space Adminstration
[PUB-LAW-91-556] 18 p2213 N73-27872
NASA supported research in photobiology and photochemistry from 1966 to 1973
[NASA-CR-133459] 19 p2224 N73-27937
Schedule of NASA space missions through 1991
[NASA-TM-X-64739] 20 p2488 N73-29984
Administration, development, and maintenance of NASA tracking network with emphasis on Australia
[NASA-CR-133828] 21 p2521 N73-30214
Congressional committe report to identify and resolve disagreements in NASA appropriations for Fiscal Year 1974
[H-REPT-93-353] 21 p2607 N73-30892
Congressional hearings concerning appropriations for NASA operations during Fiscal Year 1974 - Part 1
21 p2608 N73-30906
Congressional hearings concerning appropriations for NASA operations during Fiscal Year 1974 - Part 3
21 p2608 N73-30907
Application of NASA management techniques to problems of community violence
[NASA-CR-133830] 21 p2609 N73-30915
Congressional hearings to review NASA program accomplishments and to predict advantages to accrue from space programs
21 p2609 N73-30916
Index of subjects presented during Congressional hearings involving NASA appropriations for Fiscal Year 1974
21 p2610 N73-30921
Medically related NASA technology applications and transfer activities
[NASA-CR-135527] 22 p2621 N73-31001
Congressional hearings on cost of space shuttle program to show differences between Government Accounting Office and NASA projections
22 p2737 N73-31916
Analysis of current operations concepts of NASA and DoD to improve utilization of resources
[NASA-CR-135705] 23 p2844 N73-32729
Industrial utilization of NASA generated aerospace technology
[NASA-TM-X-71435] 24 p2994 N73-33923

**NATIONAL AIRSPACE UTILIZATION SYSTEM**
Objectives, goals, and program structure of project to improve performance of air traffic and control and navigation facilities within National Airspace System
[FAA-ED-21-2] 16 p1940 N73-25703
Proceedings of conference to develop area navigation system design concept for application to national airspace system for improved air traffic control
17 p2060 N73-26664
Performance and environmental tests of National Air Space Enroute Stage air traffic control system
[FAA-NA-73-55] 23 p2817 N73-32518

**NATIONAL AVIATION SYSTEM**
Forecasts of military air traffic activity and effect on air traffic control facilities for 1972 through 1983
05 p0493 N73-14014
Development of computer programs for design of air route networks for improved flight safety - Part 1
[FAA-RD-72-118-1-PT-1] 10 p1185 N73-19643
Development of systematic methodology and computer programs for optimal design of national grid of high altitude VHF omnirange navigation systems - Part 2
[FAA-RD-72-118-2-PT-2] 10 p1185 N73-19644
Definition and evaluation of three basic alternative national aviation systems based on forecasted increases in aviation demands
[PB-215533/1] 16 p1862 N73-25081
Organization, responsibilities, and functions of Civil Aeronautics Board in determining award of air routes to air lines
23 p2863 N73-32880

**NATIONAL SEVERE STORMS PROJECT**
Utilization of meteorological satellite data to forecast severe thunderstorms and tornadoes
06 p0693 N73-15644

**NATIONS**
Analysis of political, institutional, and economic factors to determine feasibility of conducting earth resources surveys in developing nations
07 p0783 N73-16362
Development of remote sensing activities in countries with limited resources
[PB-214861/7] 16 p1909 N73-25446
Cable television, emphasizing juridical and economical aspects in various nations
23 p2757 N73-32067

**NATURAL FREQUENCIES**
U RESONANT FREQUENCIES

**NATURAL GAS**
Calculation of mass flow rate of methane and natural gas through nozzles
[NASA-SP-3074] 06 p0653 N73-15309
Combustion efficiency of annular turbojet combustor using heated natural gas as fuel
[NASA-TM-X-2742] 09 p1098 N73-18960
U-25 pilot plant with open cycle MHD generator operating on natural gas
22 p2728 N73-31833

**NATURAL SATELLITES**
NT MOON
Observations of Jovian satellite eclipse
[NASA-CR-130292] 06 p0717 N73-15849
Photoelectric measurements of solar phase brightness relationship of planet Jupiter Galilean satellites to show porous nature of surface layers of satellites
09 p1083 N73-18838
Quarantine constraints as applied to satellites
[NASA-CR-132073] 15 p1741 N73-24116
Photographic determinations of Mars satellites orbital parameters
16 p1961 N73-25860
Galilean satellite thermal radiation measurements
16 p1961 N73-25866
Mariner 9 television observations of Martian planets Phobos and Deimos
23 p2841 N73-32705

**NAUSEA**
Analysis of physiological mechanisms contributing to occurrence of motion sickness
01 p0003 N73-10020

**NAVIER-STOKES EQUATION**
Statistical analysis of turbulent motion using Navier-Stokes equations - Part 1
[NASA-TT-F-14560] 01 p0039 N73-10310
Solution of Navier-Stokes equation for sea water pressure determination
[NOTA-INTERNA-377] 01 p0042 N73-10328
Development of implicit finite difference method for analysis of viscous flows based on Euler and Navier-Stokes equations
[AD-746389] 01 p0043 N73-10341
Development of finite difference techniques for computing static pressure distribution downstream of strong shock wave using navier-Stokes equation
[AD-747978] 03 p0286 N73-12318
Modification of Navier-Stokes equation for hypersonic compressible flow to eliminate need for specifying far field and/or boundary condition parameters
[AD-747644] 03 p0287 N73-12321
Development of method for numerical integration of Navier-Stokes equations based on perturbation of Poisson type equation for viscous flow
[NA-7] 05 p0526 N73-14282
Navier-Stokes equations governing flow of subsonic or supersonic jets mixing with surrounding atmosphere
[AD-750185] 05 p0528 N73-14296
Numerical method for solving time dependent Navier-Stokes equation in two dimensions
[AD-751628] 07 p0773 N73-16276

Navier-Stokes equations for generating and maintaining straight oblique shock wave in steady supersonic flow and computing inviscid flow field downstream of shock wave
[AD-754095] 11 p1271 N73-20317
Mathematical theory of viscous incompressible flow and solutions to Navier-Stokes equations
[AD-754995] 11 p1350 N73-20953
Two procedures for solving Navier-Stokes equations for steady, three dimensional flows with circulation
[EF/TN/A/47] 13 p1510 N73-22238
Navier-Stokes equation and finite difference theory for compressible viscous flow
[AD-756242] 14 p1651 N73-23389
Numerical analysis of Navier-Stokes equations for steady two dimensional flow to show convergence characteristics
[ARC-R/M-3239] 15 p1725 N73-23997
Numerical analysis of Navier-Stokes equations for steady, viscous, axisymmetric flow with application to flow past pitot tube at low Reynolds numbers
[ARC-R/M-3240] 15 p1725 N73-23998
Numerical analysis of hypersonic rarefied flow past sharp leading edge of flat plate using finite difference solution of Navier-Stokes equation
19 p2251 N73-28147
Velocity and temperature development in entrance region between two rotating concentric cylinders
[AD-762049] 19 p2256 N73-28187
Solution of unsteady Navier-Stokes equations for flow field about impulsively started flat plate
[AD-761459] 19 p2257 N73-28193
Applications of Wiener-Hermite expansion to theories of hydrodynamical turbulence
23 p2771 N73-32167
Statistical model of turbulence based on elementary solutions of linearized Navier-Stokes equations
23 p2773 N73-32177
Continuity and Navier-Stokes equations for analyzing viscous flow heat transfer in curved tubes
24 p2902 N73-33162
Flow characteristics of merged layer regime in hypersonic, low density flow past semi-infinite sharp cone
24 p2903 N73-33168
Numerical solution of time-dependent Navier-Stokes equation with periodic boundary condition
[AD-764582] 24 p2910 N73-33226

NAVIGATION
NT AIR NAVIGATION
NT ALL-WEATHER AIR NAVIGATION
NT ASTRONAVIGATION
NT CELESTIAL NAVIGATION
NT DOPPLER NAVIGATION
NT GIMBALLESS INERTIAL NAVIGATION
NT HYBRID NAVIGATION SYSTEMS
NT HYPERBOLIC NAVIGATION
NT INERTIAL NAVIGATION
NT LORAN
NT LORAN C
NT LORAN D
NT OMEGA NAVIGATION SYSTEM
NT POLAR NAVIGATION
NT RADAR NAVIGATION
NT RADIO NAVIGATION
NT SPACE NAVIGATION
NT SURFACE NAVIGATION
NT TACAN
NT VHF OMNIRANGE NAVIGATION
Satellites for mobile aircraft and ship communications
04 p0472 N73-13852
Selected papers on hydrometeorology, oceanography, navigation
07 p0857 N73-16950
Optimization and estimation theory applied to design of automatic navigation system
[AD-751942] 08 p0942 N73-17716
Programmatics of space shuttle supported research facilities for telecommunication and navigation - Vol. 4
[NASA-CR-124139] 10 p1137 N73-19268
Development of simulator for training personnel in underwater terrain navigation and reconnaissance
[AD-754091] 11 p1322 N73-20729

NAVIGATION AIDS
NT AIRPORT BEACONS
NT BEACONS
NT GYROCOMPASSES
NT LASER ALTIMETERS
NT NAVIGATION INSTRUMENTS
NT RADAR BEACONS
NT RADIO BEACONS
NT RADIO DIRECTION FINDERS
Application of time frequency techniques to improve navigation of ships and reduce risk of collision
[NASA-TT-F-14718] 02 p0207 N73-11679
Target maneuvers and sensor noise effects on proportional navigation systems noting Kalman filtering
[AASU-316] 03 p0329 N73-12681
Analysis of geometrical, analytical, and semi-analytical inertial navigation systems for application to shipbuilding industry
[JPRS-57694] 04 p0447 N73-13650
Development, characteristics, and applications of Loran C navigation system for air navigation and microsecond clock synchronization
[NBS-MONO-129] 05 p0577 N73-14700
Research projects involving all weather landing systems to include electronic and visual guidance, airborne systems, and data collection
[FAA-ED-07-3] 06 p0697 N73-15680
Application of propagation theory to analyze development and effectiveness of loran navigation system in Germany
[AD-750006] 06 p0697 N73-15682
Handbook of operating instructions for air navigation systems to include international air routes, Doppler radar, and great circle navigation
[AD-750493] 06 p0697 N73-15684
Operation and maintenance of shipboard meteorological systems
[AD-751691] 07 p0816 N73-16617
Description of Geographical Position Locator system with emphasis on means for automatically reducing position errors
[UCRL-74039] 07 p0818 N73-16631
Radio navigation system for providing all-weather short baseline navigation capability for Army aeronautical missions
[AD-752466] 08 p0942 N73-17715
Technical evaluation of cartography for use in civil air navigation map displays to determine information elements required to operate in 1975 to 1980 airspace - Vol. 1
[FAA-RD-72-129-VOL-1] 10 p1155 N73-19393
Evaluation of cartographic information for use in civil air navigation map displays to determine information elements required to operate in 1975 to 1980 airspace - Vol. 2
[FAA-RD-72-129-VOL-2] 10 p1155 N73-19394
Analysis of biaxial gyrostabilizer system and synthesis of spherical superconducting suspensions with maximum lift
[JPRS-58356] 10 p1159 N73-19428
Digital flight director for precise aircraft control
[AD-754028] 11 p1322 N73-20726
Development of integrated system for air navigation using radio range measurements and data from onboard inertial sensors for aircraft approach and landing
[NASA-TM-X-62199] 13 p1556 N73-22614
Evaluation of VORTAC navigation system accuracies required to support present and anticipated operational uses of system
13 p1557 N73-22616
Integrated SAVVAN, VOR, and DME system for locating and controlling high altitude aircraft
14 p1688 N73-23695
Comparison of cost, complexity, and cockpit workload for seven area navigation system configurations
14 p1688 N73-23697
Computerized automated avionics system with electronic display for Comet 4 aircraft navigation
14 p1712 N73-23896
Design of avionics digital frequency synthesizer with four phase locked loops for aircraft communication and navigational aids
[AD-759699] 16 p1883 N73-25238
Air or inertial data addition to onboard navigation system for improved air traffic control
16 p1940 N73-25699
Objectives, goals, and program structure of project to improve performance of air traffic and control and navigation facilities within National Airspace System
[FAA-ED-21-2] 16 p1940 N73-25703
Precision and reliability characteristics of combined gyroscopic and correction channel
17 p2059 N73-26659
Design, development, and test of NASA-GFSC Position Location and Aircraft Communications Equipment [PLACE]
[NASA-TM-X-66287] 18 p2117 N73-27115
Development and characteristics of hybrid loran and inertial navigation system as alternative to high precision navigation sensors
[AD-761027] 18 p2176 N73-27572
Calculation of water depth off Little Bahama Bank from ERTS-1 data for use in upgrading and mapping world navigation charts of shallow waters
[PAPER-M20] 19 p2282 N73-28358
Radio frequency interference tests of VHF omnirange, instrument landing systems, and glideslope indicators to determine required geographical separation for ground stations
[REPT-523-0764695-00111M-VOL-2] 20 p2453 N73-29712
Priority basis for satellite applications to communications, navigation, and surveillance for aircraft over contiguous US
[NASA-CR-132794] 22 p2722 N73-31784
Technology for evaluating ground station sites based on effectiveness in disseminating time synchronization
[FAA-RD-73-102] 23 p2770 N73-32155
Advanced marine technology, including submerged navigation, transfer at sea, and bottom reconnaissance
[AD-763372] 23 p2788 N73-32305

NAVIGATION INSTRUMENTS
NT ATTITUDE INDICATORS
NT GYRO HORIZONS
NT GYROCOMPASSES
NT RADIO ALTIMETERS
NT RADIO DIRECTION FINDERS
Development of air navigation system using moving map display based on holographic storage and display techniques
[AD-745025] 01 p0065 N73-10533
Space shuttle orbiter guidance and control software functions for horizontal flight operations
[NASA-TM-X-68857] 02 p0207 N73-11682
Manual space navigation research projects conducted by US Air Force in support of Skylab project
[AD-747479] 03 p0329 N73-12683
Aircraft accident investigation of Boeing 727 crash near Juneau, Alaska, 4 Sept. 71
[NTSB-AAR-72-28] 05 p0493 N73-14017
Analysis of methods for obtaining improved accuracy of aircraft position determination in Discrete Address Beacon system of air navigation
[TN-1972-38] 05 p0577 N73-14697
Handbook of operating instructions for air navigation systems to include international air routes, Doppler radar, and great circle navigation
[AD-750493] 06 p0697 N73-15684
Reliability analysis of digital computer used in system for ship navigation
[AD-750990] 06 p0697 N73-15687
Analysis of gyroscopic instrument performance during acceleration and method for determining position of vehicle in geopolar regions
[JPRS-57990] 08 p0923 N73-17557
Test plan for evaluation of redundant sensor strapdown inertial measuring unit to include operating procedures and data and analysis requirements
[NASA-CR-123513] 08 p0941 N73-17711
General test plan for redundant sensor strapdown inertial measuring unit evaluation program
[NASA-CR-130722] 08 p0941 N73-17712
Development and evaluation of Geographic Position Locator for accurate, long-term, land based inertial navigation
[UCRL-51130-VOL-1] 08 p0941 N73-17713
Development and evaluation of discrete address beacon system for air traffic control applications
[FAA-RD-73-12] 11 p1255 N73-20184
Development of low cost inertial measurement unit with navigational accuracy performance based on optimum size design of inertial instruments and platform
11 p1317 N73-20690
Development of rapid initialization of inertial navigation system using azimuth wander mechanization
11 p1317 N73-20693
Optimization of integrated navigation systems combining several independent navigation sensors to provide self-contained aircraft navigation capability
11 p1317 N73-20694
Development of integrated system for air navigation using radio range measurements and data from onboard inertial sensors for aircraft approach and landing
[NASA-TM-X-62199] 13 p1556 N73-22614
Characteristics of airborne area navigation equipment and application to air traffic control functions
14 p1688 N73-23698
Performance tests of four flight-director/attitude indicator displays under three conditions of simulator motion and comparison with flight test results
[AD-760049] 17 p2011 N73-26264
Design parameters and dynamic characteristics of navigational instruments
[JPRS-59254] 17 p2059 N73-26656
Logistics performance data book on bombing and navigation system for A-7D aircraft to show reliability, maintainability, cost, and problems
[AD-762215] 19 p2357 N73-28960
Development of kinematic equations for analyzing performance of gimballess inertial navigation system
[JPRS-59688] 20 p2452 N73-29704

NAVIGATION SATELLITES
NT TRANSIT SATELLITES
Application of unmanned spacecraft for research purposes to show benefits from Communication and Navigation satellites and Earth Observation satellites
04 p0470 N73-13830
Algorithms for predicting ionospheric effects on pseudo-ranging from synchronous satellite navigation system
[AD-749486] 05 p0539 N73-14391
Calculation of ephemeris for Navy navigation satellites
[AD-753807] 09 p1092 N73-18914
Characteristics of navigation satellite system and analysis of operation of translocation subsystem
[AD-754173] 10 p1186 N73-19650
Design and development of radio receiver for navigation satellite - Vol. 1
[AD-755149] 11 p1321 N73-20723
Design and development of low cost radio receiver for navigation satellite - Vol. 2
[AD-755150] 11 p1321 N73-20724
Analysis of North Atlantic air route structure to determine impact of inertial navigation and satellite surveillance on separation reduction
14 p1688 N73-23699

Observational errors and algorithms in determining position of ships
[JPRS-59638] 20 p2439 N73-29592
Restructuring of oceanic air traffic control airspace jurisdictional boundaries in presence of satellite system
[FAA-RD-73-59] 24 p2951 N73-33570

**NAVIGATORS**
Color aptitude of dyschromatopsia French navigators and pilots
10 p1113 N73-19068
Influence of long duration flight missions on metabolic and endocrine functions of pilots and navigators
10 p1123 N73-19152

**NAVY**
Procedures for constructing and analyzing combat models for planning and executing naval combat operations
[JPRS-57404] 04 p0393 N73-13194
Catalog of batteries for Navy weapon systems
[AD-751018] 06 p0627 N73-15087

**NC-130 AIRCRAFT**
U C-130 AIRCRAFT

**NEAR INFRARED RADIATION**
Near infrared, electron microscopic, ESR, and magnetic susceptibility measurements
[ORO-4049-3] 17 p2065 N73-26705
Collimator for analyzing spatial location of near and distant sources of radiation
[NASA-CASE-MFS-20546-2] 21 p2543 N73-30389
Optical properties of atmospheric aerosols in near infrared region of spectrum
[AD-764135] 22 p2668 N73-31374
Time resolved spectroscopic measurements of near infrared and X ray emission from high density plasma in vacuum spark
24 p2961 N73-33661

**NEAR ULTRAVIOLET RADIATION**
Steady illumination photolysis of ionospheric ozone in near ultraviolet
[NASA-CR-130830] 09 p1029 N73-18399
Absolute cross sections for rotational Raman scattering derived for nitrogen and oxygen from near UV to infrared
[AD-756808] 13 p1566 N73-22695

**NEARSHORE WATER**
NT COASTAL WATER
ERTS-1 imagery of littoral drift and sedimentation patterns of beach and nearshore areas of Maryland section of Chesapeake Bay
[PAPER-M2] 19 p2280 N73-28342
Application of ERTS-1 imagery to study of coastal areas and processes
19 p2286 N73-28386

**NEBRASKA**
NT SAND HILLS REGION [NE]
Application of ERTS-1 imagery for differentiating quaternary surface deposits and landforms in Illinois, Iowa, Missouri, Kansas, Nebraska, and South Dakota
[PAPER-G13] 19 p2264 N73-28244
ERTS-1 measurements of major crops and soil associations in Indiana, North Dakota, Iowa, Nebraska, Kansas, and Texas
[E73-11155] 24 p2919 N73-33309

**NEBULAE**
NT CASSIOPEIA A
NT CRAB NEBULA
NT PLANETARY NEBULAE
Ultraviolet continuum of O6f star HD 148937 and peculiarities of surrounding nebulae
[NASA-CR-128404] 01 p0100 N73-10824
Spectrophotometric analysis of Orion nebula emission spectra with dust lanes in hydrogen region
[AD-745314] 01 p0104 N73-10863
Theories on giant-loop type nebula
08 p0975 N73-17975
Balloon-borne telescopic observations of X ray pulsars in Gum and Crab nebulae
13 p1575 N73-22764
Search for deuterium recombination line emission from Orion A 10
[AD-762001] 21 p2598 N73-30824
Symposium on Gum Nebula and related topics
[NASA-SP-332] 22 p2715 N73-31731
Surface brightness of reflection nebulae
24 p2978 N73-33796

**NECK [ANATOMY]**
Biodynamic response of human head and neck to impact acceleration
[AD-747988] 04 p0382 N73-13106
Mass, volume, center of mass, and mass moment of inertia determined for head and head and neck of human body
[AD-762581] 20 p2372 N73-29065

**NEEL TEMPERATURE**
Three body exchange effects on Neel temperature of solid He-3
[COO-1569-97] 12 p1439 N73-21655
Transport coefficient anomalies in antiferromagnetic metals in vicinity of Neel temperature
24 p2933 N73-33424
Affect of antiferromagnetic ordering onset at Neel temperature on transport properties of CeAl, AuHo, and ErCu systems
24 p2933 N73-33425

**NEGATIVE CONDUCTANCE**
Luminescence modulation and negative resistance modulation of semiconductors and high temperature semiconductors
[AD-763840] 22 p2708 N73-31685

**NEGATIVE RESISTANCE CIRCUITS**
Multistable semiconductor devices and integrated circuits
16 p1951 N73-25791

**NEGATIVE RESISTANCE DEVICES**
Differential equations for studying dynamic characteristics of motor with separate excitation regulated by negative resistance feed
[PUBL-1368] 06 p0645 N73-15237

**NEODYMIUM**
Laser transitions in pulsed neodymium yttrium-aluminum garnet emission
[AD-746218] 02 p0181 N73-11472
Development of efficient high power NDY ceramic laser material
[AD-746521] 02 p0184 N73-11491
Neodymium doped Q-switched laser glass illuminator oscillator
[AD-749511] 04 p0430 N73-13506
Design and operation of picosecond neodymium glass laser in terawatt range
[UCRL-TRANS-10633] 06 p0679 N73-15528
High-efficiency, self-contained, small neodymium laser for pyrotechnic ignition
10 p1228 N73-19979
Ultrawide-bandwidth laser communication system using high efficiency, single frequency lasers and optical modulators
[AD-755219] 13 p1539 N73-22468
Quality testing of neodymium yttrium-aluminum garnet lasers
[PHL-1972-22] 14 p1672 N73-23567
Analysis of atmospheric transmission properties of 1.06 microns radiation using neodymium laser
[AD-757249] 14 p1672 N73-23572
Micron output increase of Nd YAG laser to pump optical parametric oscillator through visible spectrum
[AD-756809] 14 p1673 N73-23577
Optical spectra and crystal field parameters of neodymium in lanthanum aluminate
17 p2071 N73-26757

**NEODYMIUM ALLOYS**
Surface damage to gallium arsenide surfaces from radiation by ruby and neodymium-glass lasers
05 p0555 N73-14507
Thermal and electrical conductivity of Nd-Y alloy system at room temperature
[AD-756595] 13 p1566 N73-22693

**NEODYMIUM COMPOUNDS**
Synthesis and characterization of tetrahydroborates of lanthanum, neodymium, and erbium
[AD-759372] 17 p1992 N73-26110

**NEON**
Sources responsible for long term drift of He-Ne lasers
[AD-749055] 05 p0558 N73-14535
Interactions of energetic neon with emulsion nuclei
[AD-754247] 11 p1327 N73-20768
Effect of multiple ionization on fluorescence yield of Ne
[RLO-1388-189] 17 p2065 N73-26710
Neon line strength measurements using coherent laser spectroscopy
[NASA-CR-133406] 18 p2114 N73-27096
Proton spallation of neon and lithium production in stellar flares
22 p2701 N73-31631

**NEOPLASMS**
NT CANCER

**NEOPRENES**
U CHLOROPRENE RESINS

**NEPHANALYSIS**
Meteorological radar analysis of convective cloud evolution
22 p2693 N73-31570

**NEPHELITE**
Temperature effects on quantitative biotite and nepheline decomposition by weather
[NASA-TT-F-15135] 23 p2754 N73-32035

**NEPHELOMETERS**
Nephelometer design and data on total light scatter and backscatter component of extinction of light due to aerosols
08 p0899 N73-17281

**NEPTUNE [PLANET]**
Feasibility of atmospheric entry probe missions to Uranus and Neptune
[NASA-CR-129815] 04 p0469 N73-13824
Characteristics and capabilities of solar electric propulsion for orbiter missions of Uranus and Neptune
[NASA-CR-129857] 05 p0594 N73-14827

**NEPTUNIUM**
Low temperature properties and specific heat of plutonium and neptunium
[AERE-R-7172] 24 p2934 N73-33432

**NERVA [ENGINE]**
U NUCLEAR ENGINE FOR ROCKET VEHICLES

**NERVES**
Neural model as pulse interval processor
[AD-746007] 01 p0022 N73-10169
Vestibular function loss in man after unilateral section of eighth cranial nerve
[NASA-CR-129672] 04 p0379 N73-13084

**NERVOUS SYSTEM**
NT BRAIN
NT CENTRAL NERVOUS SYSTEM
NT CEREBRAL CORTEX
NT CEREBRUM
NT EFFERENT NERVOUS SYSTEMS
NT NERVES
NT NEURONS
NT PERIPHERAL NERVOUS SYSTEM
NT SPINAL CORD
NT THALAMUS
Neuroelectric oscillation in two parallel, single-unit pathways feeding back on single primary cell
[R-984-RC] 04 p0379 N73-13083
Nervous system functional changes due to forces of acceleration and weightlessness
[NASA-TT-F-733] 08 p0877 N73-17105
Radioimmunoassays of plasma aldosterone and catecholamine concentrations as human vasomotor regulators
09 p0994 N73-18111
Influence of light flashes from heavy ionizing particles on astronaut nervous system
[LBL-1011] 10 p1120 N73-19134
Masking phenomenon for measuring state of fatigue and stress of nervous system
[AD-752975] 16 p1869 N73-25129

**NETHERLANDS**
Organization, management, and research activities at National Institute for Aerospace Research of the Netherlands
11 p1351 N73-20960
Geological surveys and mapping of Netherlands based on ERTS-1 imagery
[E73-10584] 14 p1657 N73-23444

**NETS**
Performance of radio distance finding net using polygonometric grid
[AD-748866] 06 p0697 N73-15683

**NETWORK ANALYSIS**
NT CRITICAL PATH METHOD
Fast periodic steady state analysis of nonlinear large signal electronic circuits
[AD-745639] 01 p0034 N73-10271
Comparison of quasi-Newton methods for dc analysis of electronic circuits
[AD-746391] 01 p0035 N73-10274
Network synthesis and analysis of thermoelectric generators to show relation between physical properties and elements of internal structure
[AD-747617] 03 p0256 N73-12071
Use of cross ratio invariance for analysis and error evaluation in automatic microwave network analyzers
[NBS-TN-623] 03 p0277 N73-12246
Stripline n-input, n-output cascade network analysis
03 p0278 N73-12254
Application of graph theory to network analysis and coding problems in communication systems
[AD-748290] 04 p0391 N73-13178
Resource sharing computer communication networks and some aspects of distributed computation
[AD-749378] 05 p0518 N73-14210
Development of allpass, highpass, bandpass, and stopband electric filter circuits using only resistors as passive components
[REPT-1404] 05 p0522 N73-14244
Plumb line deflection calculations for European triangulation network using astronomical observations
[MITT-122] 05 p0538 N73-14377
FORTRAN program for handling radiation effects circuit analysis problems
[AD-751519] 07 p0765 N73-16213
Users manual for network analysis program
[AD-752600] 08 p0892 N73-17218
Node voltage method for analyzing nonlinear electric networks with lumped parameters
[NLL-TRANS-2865-[9022.81]]
11 p1264 N73-20255
Procedure for finding minimal and maximal Hamiltonian circuits on complete graph
[AD-754842] 11 p1312 N73-20648
Network analysis of transmission line analogs for stacked piezoelectric crystal vibrators
[AD-754545] 11 p1330 N73-20799
Numerical analysis of multiple conductor transmission line with arbitrarily positioned impedances in series with each wire
[SC-R-72-2695] 12 p1386 N73-21244
Analysis of directional antenna transmission line networks
[AD-756567] 13 p1501 N73-22163
Utilizing Out-of-Kilter Algorithm to evaluate efficiency of passenger capacity of selected air carriers between twenty cities in US
13 p1592 N73-22910
Relationship between power distribution and tolerance sensitivity in linear, two-terminal electric network
[NLL-PO-2895-[9022.81]] 15 p1759 N73-24253

Performance of algorithms for calculating shortest path trees in networks
[NBS-TN-772] 15 p1803 N73-24615
Mathematical design of electric filters using linear differential equations
[AD-757544] 16 p1881 N73-25225
Design of continuous lumped parameter linear filters
[AD-757545] 16 p1881 N73-25226
Analysis of packet switching network by computerized simulation
[NPL-COM-SCI-64] 19 p2239 N73-28053
Methods of circuit optimization and analysis of advantages and disadvantages of circuit optimization by computer
[AD-763766] 21 p2520 N73-30211
Computer simulation of multipacket-switched data communication network operating with revised link and node protocol
[NPL-COM-68] 22 p2634 N73-31112
Wave digital filter design using ladder networks
24 p2899 N73-33145

**NETWORK SYNTHESIS**
Numerical optimization techniques for computer-aided design of distributed, lumped, active networks
[AD-745640] 01 p0035 N73-10272
Narrow band equivalent circuit for two-port network using cascaded, lossless transmission lines and lossless shunt elements
[APS-EL-30] 02 p0150 N73-11221
Network synthesis and analysis of thermoelectric generators to show relation between physical properties and elements of internal structure
[AD-747617] 03 p0256 N73-12071
Equivalent circuit of electromechanical or magnetohydrodynamic converter with traveling magnetic field
[AD-747611] 03 p0256 N73-12072
Digital computer for variable active attenuation equalizer and associated impedance simulating network for unloaded cables
[REPT-6650] 04 p0398 N73-13236
Algorithms for construction of minimum cost communication networks
[PB-211233] 05 p0514 N73-14178
Circuit theory research in Europe
[AD-749346] 05 p0523 N73-14252
Microwave network synthesis including grating transducer technology and channel-dropping-filter geometry
[AD-751746] 07 p0764 N73-16210
Equivalent circuit network synthesis for branch guide directional couplers
[PB-212651] 08 p0889 N73-17198
Research progress in functional network theory and microcircuit systems
[AD-752243] 08 p0891 N73-17217
RC equivalent network for flueric flip-flop inputs
[AD-752126] 08 p0899 N73-17280
Recursive plane analysis for phase locking in pulse modulation sampling technique
[AD-756918] 13 p1492 N73-22092
Computation oriented communications network using computer resources
[AD-758098] 15 p1752 N73-24197
Accuracy estimates for syntheses of filters by optimizing mutual uncertainty function in minimax criterion
17 p1997 N73-26151
Synthesis of microwave network having surface acoustic wave transducer
[AD-759934] 17 p2008 N73-26236
Determining necessary number of channels in maritime communications satellite network
20 p2440 N73-29597
Methods of circuit optimization and analysis of advantages and disadvantages of circuit optimization by computer
[AD-763766] 21 p2520 N73-30211
Transmitter network synthesis by calculating coverage parameters of broadcast
[BBC-RD-1973/11] 22 p2626 N73-31044
Design techniques for data base oriented computer networks for information flow
[AD-763791] 22 p2640 N73-31163

**NETWORKS**
Operational performance and transmission measurements on worldwide Defense Communications System network
01 p0027 N73-10208
Feasibility of all-digital implementation of worldwide analog communications systems
01 p0027 N73-10209
Data processing systems and computer networks
[AD-746509] 01 p0031 N73-10244
Packaging techniques for miniaturized thick film networks
[BDX-613-363-REV] 03 p0277 N73-12250
Establishment of radar information transmission network for dissemination of meteorological data
[NLL-M-22692-[5828.4F]] 05 p0507 N73-14128
Interface data processing system for telecommunication computer network
[AD-754441] 11 p1260 N73-20228
Relationship between power distribution and tolerance sensitivity in linear, two-terminal electric network
[NLL-PO-2895-[9022.81]] 15 p1759 N73-24253
Simultaneous satellite photographic and Doppler observations for determining space triangulation chord direction
[AD-759096] 18 p2127 N73-27188
Interface message processor for digital computer network
[AD-763734] 23 p2761 N73-32098

**NEUMANN PROBLEM**
Neumann boundary value problem for Helmholtz oscillation equation
[NRC-TT-1606] 06 p0690 N73-15616
Calculation of pressure field induced by free jet exhausted from flat plate into stagnant medium based on solution of Neumann problem in terms of singularity distributions
[NLR-TR-72040-U] 21 p2492 N73-30000
Optimal control of parabolic systems with boundary conditions involving time delays and with application to plasma confinement
[AD-763738] 21 p2584 N73-30704

**NEURISTORS**
Analysis of electrical properties, structure, values of passive elements, and operating mode of hybrid neuristor lines
[AD-762311] 19 p2247 N73-28120

**NEUROLOGY**
Studies concerning high pressure hyperexcitability in Squirrel Monkey
[AD-745779] 02 p0134 N73-11086

**NEUROMUSCULAR TRANSMISSION**
Nonlinear model relating neural input to force and muscle contraction in human ankle joint
01 p0015 N73-10117
Tracking tests as quantitative measurements of neuromuscular functions in clinical applications
01 p0015 N73-10118
Respiratory impedance effects on electrical activities of bulbar respiratory neurons, respiratory muscles, and pulmonary ventilation in anesthesized cats
03 p0257 N73-12084
Hypoxia effects on human gastric motor functions in pressure chamber experiments using electrogastrography
03 p0257 N73-12085
Workload effects on operator grip pressure and neuromuscular transmission in manual tracking task error
[AD-757252] 14 p1615 N73-23089

**NEURON TRANSMISSION**
U BIOELECTRICITY

**NEURONS**
Dynamic response of vestibular nuclei neurons of decerebrated cats subjected to sinusoidal rotation
[AMRU-R-70-2] 02 p0130 N73-11059
Asymmetric response of cat semicircular canal neurons to symmetric sinusoidal rotation
[AMRU-R-69-2] 02 p0130 N73-11060
Respiratory impedance effects on electrical activities of bulbar respiratory neurons, respiratory muscles, and pulmonary ventilation in anesthesized cats
03 p0257 N73-12084
Evolution of neural messages in human adaptation to prolonged zero gravity flight
06 p0634 N73-15154
Neuronal changes in cortical motor region cells during pharmacological induced sleep
13 p1483 N73-22028
Frequency selectivity and two tone inhibition in neural coding of acoustic stimuli
[IZF-1972-25] 14 p1610 N73-23050
Mathematical simulation study of neuron response to vestibular analyzer exposed to periodically varying acceleration
[NASA-TT-F-15130] 22 p2623 N73-31015
Change in impulse activity of neurons in respiratory center during electric stimulation of vestibular nerve and dorsal roots in spinal cord
24 p2882 N73-33017

**NEUROPHYSIOLOGY**
Neurophysiology and dynamic response of vestibular system to angular and linear acceleration
[DR-215] 02 p0130 N73-11057
Clinical neurological and neurophysiological aspects of vestibulo-ocular reflex
06 p0633 N73-15145
Electropolygraphic analyses of sleep patterns in humans with neurological disorders
13 p1483 N73-22024
Model of speech production mechanism based on anatomical structures and physiological natures of articulatory organs
14 p1624 N73-23153

**NEUROPSYCHIATRY**
Psychoneurological problems in adaptation by man to modified diurnal regimes
24 p2884 N73-33031

**NEUROSCIENCE**
U NEUROLOGY

**NEUTRAL BEAMS**
NT MOLECULAR BEAMS
NT NEUTRON BEAMS

**NEUTRAL PARTICLES**
NT FAST NEUTRONS
NT NEUTRONS
NT THERMAL NEUTRONS
Measurement and analysis of fast ions and neutral particles in Penning discharge with ring anode in magnetic field
[TRITA-EPP-72-12] 09 p1071 N73-18739
Continuum methods for studying solar wind interaction with interstellar neutral particles
18 p2194 N73-27717
ESRO rocketborne spectrometric data on neutral particles and temperature of winter lower thermosphere at polar latitudes
[BMBW-FBW-72-29] 22 p2667 N73-31371

**NEUTRALIZERS**
Tests of mercury-fed hollow cathode in bell jar at SERT 2 neutralizer conditions
[NASA-TM-X-2785] 15 p1825 N73-24793
Hollow cathode neutralizer for 30-cm diameter bombardment thruster
[NASA-TM-X-68291] 21 p2589 N73-30743

**NEUTRINOS**
Solar neutrinos and influences of opacity, thermal instability, additional sources, and central black hole on solar models
[NASA-TM-X-68847] 08 p0959 N73-17844
Experiment observing solar neutrinos by neutrino capture reaction, using Ar-37
[BNL-16937] 12 p1445 N73-21707
Explanation of low counting rates for solar neutrinos
[BNL-TR-538] 24 p2977 N73-33786

**NEUTRON ABSORBERS**
Liquid hydrogen cold neutron moderator for use in channel H5 EL 3 reactor
[CEA-N-1571] 15 p1815 N73-24714
Neutron capture and total cross sections for isotopes of reactor materials
[COO-3058-27] 17 p2065 N73-26702

**NEUTRON ACTIVATION ANALYSIS**
Neutron activation analysis using gamma ray spectroscopy for determination of trace elements and short-lived nuclides
[BMBW-FBK-72-13] 03 p0262 N73-12122
Activation analysis of prompt gamma ray emission spectra for trace element determination
03 p0262 N73-12123
Gamma spectroscopic activation analysis of scheelite deposits
03 p0262 N73-12124
Computerized evaluation of activation gamma spectra for multiple trace element determination and of automation of main constituent determination
03 p0262 N73-12125
Activation analysis applied to industry, agriculture, and geology, including Br determination in vegetables and inactive marking of insects
03 p0262 N73-12126
Activation analysis using short-lived nuclides of boron, oxygen, fluorine, yttrium, and lead isotopes based on gamma spectra and pneumatic tube
03 p0263 N73-12127
Californium-252 isotope as neutron source for activation analysis
03 p0263 N73-12128
Determination of oxygen, silicon, phosphorus, and copper in iron and steel by 14-MeV neutron activation analysis
[EURISOTOP-57] 03 p0313 N73-12556
Nondestructive neutron activation and spectrum analysis using gamma ray spectrometer coupled to PDP 9 computer
[IRI-133-71-03] 05 p0582 N73-14739
Trace element detection by automated distillation and ion exchange in neutron activation analysis for As, Cd, Cu, Hg, Se, and Zn
[IRI-133-72-10] 07 p0753 N73-16114
Neutron activation analysis applied to determine bismuth content of meteorites and standard rocks
07 p0840 N73-16809
Neutronics analysis of gas core rocket concept using cavity test reactor
[NASA-TM-X-2743] 09 p1063 N73-18676
Computer programming for gamma ray spectra analysis applicable to neutron activation analysis
[IRI-133-72-09] 10 p1194 N73-19720
Trace element analysis of coal by neutron activation
[NASA-TM-X-68208] 12 p1431 N73-21596
Element abundances in meteoritic chondrules by neutron activation analysis
12 p1446 N73-21713
Bibliography on use of neutron activation analysis of geochemical samples
[NASA-CR-131831] 13 p1524 N73-22352
Neutron activation analysis of cosmic radiation doses in Apollo 14, 15, and 16 astronauts
[NASA-CR-131984] 14 p1612 N73-23070
Activation analysis using charged particles and gamma photons for determining oxygen in nonferrous metals
[EURISOTOP-74] 17 p2065 N73-26704
Neutron activation analyses of trace elements in germanium, silicon, and selenium semiconductors
[CONF-721069-29] 20 p2462 N73-29786

Neutron activation analysis of Ga concentration in Ga-Se
[CONF-721069-41] 21 p2506 N73-30110
Quantitative neutron activation analysis of stable elements in air pollution particulates
[AD-764715] 23 p2755 N73-32043

NEUTRON BEAMS
Muon proton interactions and elastic scattering for neutron beam generation in accelerator
[BNL-17314] 10 p1193 N73-19710
Application of Boltzmann transport theory for determining penetration of matter by heavy-ion beam
[AD-765315] 23 p2822 N73-32556

NEUTRON COUNTERS
NT NEUTRON SPECTROMETERS
Theoretical response of neutron monitor to anisotropic flux of solar cosmic rays
[AD-751275] 07 p0802 N73-16511
Spark counter for neutron and radon dosimetry discussing use and reproducibility
[BMVG-FBWT-72-33] 10 p1161 N73-19448
Neutron measurements on OGO-6 spacecraft
[NASA-CR-130181] 10 p1210 N73-19841
Cosmic ray disturbances following solar flare occurrences in August 1972 recorded by neutron monitoring
12 p1446 N73-21709
Cosmic ray neutron monitor data for Sanae Antarctica
[S-6] 15 p1827 N73-24811
Cosmic ray neutron monitor data for Potchefstroom
[P-2] 15 p1828 N73-24812
Cosmic ray neutron monitor data at Pochefstroom during period from May 1971 to December 1971
[P-1] 15 p1828 N73-24813
Cerium and silver containing silicate and borate systems for developing high density scintillation glass for nuclear cascade detectors
[NASA-CR-133960] 17 p2049 N73-26580

NEUTRON CROSS SECTIONS
Computer index on bibliographical references to microscopic neutron data
05 p0582 N73-14734
FORTRAN code for solving time dependent neutron transport equation in three-dimensional geometry by Monte Carlo method
[AD-756290] 14 p1691 N73-23728
Neutron capture and total cross sections for isotopes of reactor materials
[COO-3058-27] 17 p2065 N73-26702
Library of 28-group neutron cross sections designed for SNAP reactor analysis
[AI-AEC-13076-VOL-4] 24 p2955 N73-33605

NEUTRON DECAY
Identification of solar neutron events by satellite detection of proton flux increase in outer edge of trapped proton belt
07 p0838 N73-16790
Nuclear properties in neutron interactions with various nuclei in fast breeder reactor
[ANCR-1088] 17 p2062 N73-26677
Deuterium abundance for proving neutron loss before nucleosynthesis
19 p2332 N73-28768
Earth albedo neutrons and cosmic ray neutron decay from 10 to 100 MeV
[NASA-CR-135645] 23 p2789 N73-32315

NEUTRON DETECTORS
U NEUTRON COUNTERS

NEUTRON DIFFRACTION
Quantitative examination of ordering effects in nickel-iron alloy system
[NLL-RTS-7547] 04 p0431 N73-13510
Neutron diffraction and single crystal X ray determination of rare earth-cobalt-iron intermetallic magnetic structure
[AD-748429] 04 p0460 N73-13754
Powder neutron diffraction and susceptibility measuring techniques to study magnetic properties of RbMnBr3
[BNL-17519] 15 p1814 N73-24703

NEUTRON DISTRIBUTION
Balloon measurements on neutron energy and angular distributions in earth albedo
[NASA-CR-130019] 07 p0823 N73-16666
OSO-6 measurements on albedo neutron flux distribution and density
23 p2834 N73-32644
Collision probability method for calculating neutron transport in multidimensional systems
24 p2960 N73-33653

NEUTRON EMISSION
Neutron emission rate from plutonium dioxide nuclear fuel
[NASA-CR-129098] 02 p0211 N73-11707
Effects of heavy particle external ionization source on carbon dioxide laser efficiency
[COO-2007-24] 10 p1169 N73-19509
Gamma ray and neutron emissions during solar flares
19 p2336 N73-28795
Neutron emission spectra from protons impinging on spacecraft structural materials
[NASA-TN-D-7386] 20 p2468 N73-29825

NEUTRON FLUX
U FLUX [RATE]

NEUTRON FLUX DENSITY
Ionospheric sounding and cosmic ray neutron flux density tables, Dourbes, Belgium, Feb. 1972
01 p0050 N73-10402
Ionospheric sounding and cosmic ray neutron flux density tables, Dourbes, Belgium, Mar. 1972
02 p0166 N73-11352
Ionospheric sounding and cosmic ray neutron flux density tables, Dourbes, Belgium, Apr. 1972
03 p0297 N73-12420
Ionospheric sounding and cosmic ray neutron flux density tables, Dourbes, Belgium, May 1972
05 p0539 N73-14387
Balloon measurements on neutron energy and angular distributions in earth albedo
[NASA-CR-130019] 07 p0823 N73-16666
Ionospheric sounding and cosmic ray neutron flux density tables, Dourbes, Belgium, Jun. 1972
08 p0918 N73-17524
Ionospheric sounding and cosmic ray neutron flux density tables, Dourbes, Belgium, Jul. 1972
09 p1030 N73-18409
Ionospheric sounding and cosmic ray neutron flux density tables, Dourbes, Belgium, Aug. 1972
13 p1524 N73-22354
Ionospheric sounding and cosmic ray neutron flux density tables from Dourbes, Belgium for Oct. 1972
15 p1781 N73-24438
Ionospheric sounding and cosmic ray neutron flux density tables, Dourbes, Belgium, Sep. 1972
16 p1907 N73-25428
Ionospheric sounding and cosmic ray neutron flux density tables, Dourbes, Belgium, Dec. 1972
18 p2146 N73-27342
Ionospheric sounding and cosmic ray neutron flux density tables, Dourbes, Belgium, Nov. 1972
18 p2146 N73-27343
Ionospheric sounding and cosmic ray neutron flux density tables, Dourbes, Belgium, Mar. 1973
21 p2539 N73-30354
Ionospheric sounding and cosmic ray neutron flux density tables, Dourbes, Belgium, Apr. 1973
21 p2539 N73-30355
Prototype mechanical drive for boiling water reactor in-core out-core neutron flux detectors
[BMBW-FBK-72-25] 22 p2699 N73-31617
OSO-6 measurements on albedo neutron flux distribution and density
23 p2834 N73-32644
Ionospheric sounding and cosmic ray neutron flux density tables, Dourbes, Belgium Jan. 1973
24 p2923 N73-33350
Ionospheric sounding and cosmic ray neutron flux density tables, Dourbes, Belgium Feb. 1973
24 p2923 N73-33351
Collision probability method for calculating neutron transport in multidimensional systems
24 p2960 N73-33653

NEUTRON IRRADIATION
Dosimetric determination of absorbed gamma and neutron radiation on human phantom
[AD-743005] 01 p0010 N73-10077
Neutron and gamma induced transient incapacitation in conditioned Macaca mulatta
[AD-742076] 01 p0010 N73-10080
Changes in brittle-ductile transition temperature of pressure vessel steel following neutron irradiation
[AD-745299] 01 p0067 N73-10552
Neutron irradiation damage in precipitation hardened aluminum alloy component from High Flux Isotope Reactor
[CONF-720604-1] 03 p0313 N73-12555
Influence of neutron irradiation on physical and chemical properties of vanadium
[IS-2833] 03 p0314 N73-12558
Computer calculations of growth rates of voids in stainless steel during neutron irradiation
[HEDL-TME-72-35] 03 p0316 N73-12576
Effect of neutron irradiation on fatigue crack propagation in stainless steel samples at high temperatures using fracture mechanics approach
[AD-747950] 03 p0316 N73-12578
Influence of neutron irradiation on damage to fuel cladding and reactor structural materials
[HEDL-SA-317] 03 p0332 N73-12709
Fast flux neutron source for cyclotron simulation of reactor core
[AERE-R-6626] 04 p0402 N73-13269
Lowered ductility and crack initiation in neutron irradiated steels after tensile testing
[STU-70-419/U-350-A] 04 p0433 N73-13533
Mechanisms for increases in saturation voltage as result of neutron radiation
[SC-DR-72-0418] 04 p0467 N73-13806
Research on neutron irradiation induced voids in metals
[CONF-710601] 05 p0562 N73-14568
Effects of passivation processes on radiation tolerance of bipolar transistors subjected to neutron or gamma radiation
[SC-DC-72-1232] 05 p0565 N73-14589
Effectiveness of pharmacochemical protective substances on irradiated mice as neutron component increases
[DRIC-TRANS-2961] 06 p0631 N73-15124
Hall coefficient, resistivity, and charge carrier mobility of epitaxial films of n-type and p-type PbS before and after neutron irradiation
[AD-749689] 06 p0710 N73-15791
Mortality and blood cell count variation in mice after irradiation with fast neutrons and X rays
[BMVG-FBWT-72-16] 07 p0747 N73-16077
Sensitivity of microwave transistor amplifiers to neutron damage in low noise and high power applications
[SC-R-72-2845] 07 p0762 N73-16190
In pile neutron irradiation damage in graphite at high temperature
[CEA-CONF-1894] 07 p0820 N73-16644
Calcium metabolism determination in rats by measuring argon isotope in exhaled air after neutron irradiation
[NASA-CR-128816] 10 p1120 N73-19130
Physical properties and dimensional changes in graphites caused by high temperature neutron irradiation
[BNWL-1672] 10 p1193 N73-19706
Effectiveness of combined chemical protectors against mixed gamma-neutron radiation with neutron contributions to absorbed dose
11 p1240 N73-20068
Influence of head and stomach shielding on radiation sickness and animal survival from gamma-neutron irradiation
11 p1241 N73-20071
Characteristics of pathomorphological changes in rat internal organs subjected to gamma-neutron irradiation with head and stomach shielded
11 p1241 N73-20077
Neutron irradiation effects on pair defect accumulation in thin rectangular isotropic metal plates
14 p1675 N73-23593
Utilization of semiconductor in systematic analysis of Al after subjected to neutron irradiation
[FRNC-CONF-75] 15 p1788 N73-24495
Effect of neutron irradiation on remanent magnetization in Apollo 11 and 12 lunar samples of iron and kamacite
15 p1813 N73-24692
Neutron inelastic scattering spectroscopy for studying problems in materials science
[COO-3352-4] 15 p1815 N73-24713
Influence of prior microstructure on neutron irradiation damage in 316 stainless steel foils
[HEDL-SA-407] 17 p2065 N73-26707
Theoretical treatment of neutron irradiation caused crystal lattice defects in ceramic materials
[AECL-4375] 20 p2462 N73-29788

NEUTRON PHYSICS
Annual report 1971-19. of Interuniversitair Reactor Institute in Netherlands
10 p1195 N73-19721
Solar diurnal and semidiurnal variations in cosmic ray neutron monitor data
[NP-19650] 15 p1828 N73-24819

NEUTRON SCATTERING
Analysis of temperature-dependent neutron transmission and self-indication measurements on tantalum in unresolved region
[NASA-TN-D-7214] 09 p1064 N73-18678
Spectrometric measurements of cryogenic helium 4 scattering angle and momentum transfer
[CONF-720833-10] 12 p1440 N73-21669
Neutron scattering, computerized simulation, and magnetic resonance techniques for studying phase transitions in magnetic materials
[AD-757223] 14 p1698 N73-23782
Thermal neutron scattering theory for fluid state of matter
[SGAE-2054] 15 p1815 N73-24715
Low temperature energy spectrum near roton minimum region in superfluid helium
17 p2064 N73-26696

NEUTRON SOURCES
Californium-252 isotope as neutron source for activation analysis
03 p0263 N73-12128
Fast flux neutron source for cyclotron simulation of reactor core
[AERE-R-6626] 04 p0402 N73-13269
Design of intense neutron source for studying materials damage in fusion power reactor
[LA-4863] 04 p0402 N73-13272
Vacuum pump system for 150 kV neutron generator to reduce tritium hazards
[NASA-TM-X-2650] 09 p1038 N73-18468
Toroidal vortex annihilation and neutron production in pinched plasma
[AD-753107] 09 p1072 N73-18748
Fabrication method for plutonium-beryllium neutron sources
[BARC-629] 15 p1815 N73-24716

NEUTRON SPECTRA
Calculation of neutron energy and flux distributions from D-D reactions in plasma focus and Z pinch discharges
[AD-745955] 02 p0217 N73-11755
Comparison of neutron spectra measured with three sizes of organic liquid scintillators using differentiation analysis
[NASA-TM-X-2646] 03 p0331 N73-12699

Neutron flux spectra induced in the earth atmosphere by galactic cosmic rays
[NASA-CR-131158] 10 p1210 N73-19844
Neutron spectral measured proton recoil proportional counters
[KFK-1623] 12 p1431 N73-21598
Measured and calculated fast neutron spectra at surface of lithium hydride and depleted uranium shielded reactors
[NASA-TM-X-2906] 24 p2953 N73-33594
Measurement of neutron energy spectrum at 9 g/sq cm residual atmospheric
[ORNL-TM-3877] 24 p2976 N73-33783
NEUTRON SPECTROMETERS
Transistorized control unit for neutron spectrometers or diffractometers
[BARC-591] 05 p0547 N73-14447
Measurement of neutron energy spectrum at 9 g/sq cm residual atmospheric
[ORNL-TM-3877] 24 p2976 N73-33783
NEUTRON STARS
NT PULSARS
Gravitationally red-shifted positron annihilation radiation produced at surfaces of old neutron stars
[NASA-TM-X-66062] 01 p0100 N73-10818
Matter in neutron stars and relevance to pulsar observation
[NASA-TM-X-66067] 01 p0103 N73-10849
Astronomical techniques for determining physical parameters and energy balance of neutron stars based on pulsar observations
[NASA-TM-X-66066] 01 p0103 N73-10850
Cooling rates of neutron stars with maximum and zero superfluidity
[NASA-TM-X-66101] 02 p0230 N73-11866
Analysis of post-Newtonian effects on instability of white dwarf stars, neutron stars, and supermassive stars
[NASA-CR-129241] 03 p0355 N73-12893
Computation of neutron star mass based on crystal arrangement of particles
08 p0974 N73-17965
Calculations of equations of state for zero-temperature white dwarf and neutron stars
12 p1447 N73-21719
Radiative processes in intense magnetic fields of white dwarfs and neutron stars
16 p1961 N73-25861
Positron annihilation radiation model for neutron star density in galactic disk
22 p2733 N73-31869
Pulsar magnetospheric model where radiation is produced near surface of neutron star
[NASA-CR-135587] 23 p2844 N73-32731
NEUTRON TRANSMUTATION
U NUCLEAR REACTIONS
NEUTRONS
NT FAST NEUTRONS
NT THERMAL NEUTRONS
Multiplicity measurements for fission-emitted neutron or gamma quanta
[EUR-4829-E] 01 p0082 N73-10678
FORTRAN program for solving transport problem for neutrons in multilayer slab system
[EUR-4839-E] 01 p0082 N73-10681
Uncorrected and barometer-corrected hourly rate data on cosmic ray neutrons at Deep River, Ontario - 1960
[AECL-4209] 01 p0092 N73-10758
Uncorrected and barometer-corrected cosmic neutron data for Deep River, Canada - Jan. to Dec. 1959
[AECL-4149] 03 p0353 N73-12878
Uncorrected and barometer-corrected cosmic neutron data taken at Canadian stations - Sept. to Dec. 1971
[AECL-4148] 03 p0353 N73-12879
Computation of neutrons and gamma ray distribution for radiation shielding of Europa 3 launch vehicle nuclear upper stage
[TN-3-25] 15 p1811 N73-24680
Solar particle contributions to diurnal variations of neutron intensity in upper atmosphere
[AD-760950] 18 p2146 N73-27350
Focusing optical collimator for high resolution scanning of electromagnetic radiations, neutrons, and other particles
[NASA-CASE-MFS-20932-1] 18 p2150 N73-27380
Balloon observations of solar neutrons by scintillation counter
[NASA-CR-135496] 22 p2712 N73-31714
OGO-6 measurements of solar neutrons
23 p2833 N73-32639
NEVADA
NT GREAT BASIN [US]
Monitoring and surveillance of state of eutrophication of inland lakes in California and Nevada
[E72-10207] 03 p0288 N73-12330
Identification of Nevada wildland plants, vegetation, and fire scars from ERTS-1 imagery
[E72-10253] 03 p0289 N73-12353
Iron absorption band analysis for discrimination of iron-rich zones in California and Nevada
[E72-10294] 04 p0410 N73-13344
Utility of ERTS-1 imagery in study of geological structures and exploration for economic mineral deposits in Utah and Nevada
[E72-10332] 05 p0531 N73-14320
Geology photography infrared imagery, and remote sensing evaluation of Klondike Mining District, Nevada
[NASA-CR-129934] 05 p0537 N73-14371
Wildland resources inventory of Nevada Great Basin using ERTS-1 imagery
[E73-10019] 06 p0659 N73-15355
Utilization of ERTS-1 MSS imagery for study of faulting in alluvium of California, Nevada, and Arizona
[E73-10070] 07 p0779 N73-16332
Development of system for mapping and monitoring natural ecosystems and environmental complexes from ERTS-1 imagery of California, Nevada, Four Corners Area, Louisiana, and Colorado Plateau
[E73-10289] 08 p0915 N73-17495
Evaluation of ERTS-1 imagery for study of geological structures and features and exploration of mineral deposits in Utah and Nevada
[E73-10313] 09 p1022 N73-18345
Location of earthquake epicenters and major fault zones in Nevada using ERTS-1 imagery
[E73-10338] 09 p1025 N73-18366
Interpretation of ERTS-1 geologic data for Nevada and evaluation of materials used in compiling photomaps
[E73-10398] 11 p1277 N73-20360
Wildland resource evaluation in Nevada using ERTS-1 imagery
[E73-10450] 11 p1283 N73-20410
Compilation of photomaps of Nevada geology from ERTS-1 imagery
[E73-10473] 12 p1395 N73-21310
Mineral exploration in Utah and Nevada based on ERTS-1 imagery of structural fracture and fault trends
[E73-10510] 13 p1516 N73-22285
Relationship of geological structures to iron-rich zones in Nevada based on ERTS-1 imagery
[E73-10555] 14 p1655 N73-23427
Wildland resource and vegetation monitoring in Nevada and Great Basin using ERTS-1 imagery
[E73-10606] 15 p1773 N73-24367
Application of ERTS-1 imagery for mapping major geological structural trends and mineralization zones in Utah and Nevada
[E73-10701] 16 p1903 N73-25393
Identification of copper/molybdenum porphyry mineral deposits in characteristic geologic setting in Nevada, Arizona, Colorado, Australia, Alaska, and New Guinea
[E73-10762] 17 p2023 N73-26362
Application of ERTS-1 imagery for seismic conditions and recent fault formations in eastern California and western and central Nevada
[E73-10769] 18 p2134 N73-27245
Identification of major fault zone along California-Nevada state line from ERTS-1 MSS imagery
[E73-10773] 18 p2135 N73-27249
Iron-absorption band analysis for discrimination of iron rich zones using ERTS-1 imagery
[E73-10789] 18 p2137 N73-27265
Mapping of wildland vegetation in Great Basin area of Nevada using ERTS-1 imagery
[E73-10813] 18 p2139 N73-27288
ERTS-1 imagery of Utah and Nevada to show structural geology, mineral exploration, limnology, and hydrology
[PAPER-G3] 19 p2263 N73-28235
Structural analysis of Nevada using ERTS-1 imagery to identify lineaments of surface manifestations of major fault or fracture zones
[PAPER-G20] 19 p2266 N73-28251
Application of ERTS-1 imagery and ground mapping in southern basin-range province of California, Nevada, and Arizona to show tectonic control of tertiary minerlization
[PAPER-G21] 19 p2266 N73-28252
Enhancement of ERTS-1 images by density slicing and application to mapping of Yucca trees in Mojave Desert of Southern California and Nevada
[PAPER-I11] 19 p2278 N73-28332
Collection of ground and water truth in Nevada for Skylab-2
[E73-10887] 20 p2417 N73-29419
Recognition of geologic framework for ERTS-1 identification of mineral deposits of copper/molybdenum prophyry type in Colorado, Nevada, Arizona, and Australia
[E73-10960] 21 p2532 N73-30302
Methods of augmenting precipitation for winter storms of Sierra, Nevada
[PB-220674/6] 21 p2575 N73-30633
Photointerpretation of Skylab MSS photography of mineral deposits in Nevada
[E73-10983] 22 p2658 N73-31290
Geological and geochemical studies in Robinson Mining District, White Pine Co., Nevada using Skylab multispectral imagery
[E73-10992] 22 p2659 N73-31298
Geological studies of Nevada from Skylab S-191 infrared spectra
[E73-11003] 22 p2659 N73-31308
Skylab monitoring of temperatures of lakes and playas and soil moisture in Nevada
[E73-11004] 22 p2660 N73-31309
Structural and spectral analysis of lineaments and circular features for discrimination of iron-rich zones in Nevada
[E73-11020] 22 p2661 N73-31324
Mineral exploration and fracture trends in Utah and Nevada from ERTS-1 imagery
[E73-11032] 22 p2663 N73-31336
Geophysical survey of Nevada from Skylab remote sensors
[E73-10998] 23 p2778 N73-32215
Models for predicting wind fields over mountains, and potential radiological fields over Nevada test site
[NOAA-ARLV-351-28] 24 p2949 N73-33556
NEW ENGLAND [US]
Coastal geology bibliography of New England with punch card reference system
[AD-744001] 01 p0052 N73-10424
Land use mapping of northern megalopolis using ERTS-1 imagery
[E72-10368] 05 p0535 N73-14356
Snow enhancement in New England test areas based on ERTS-1 imagery
[E73-10001] 06 p0657 N73-15337
Geologic and land use exploitation of ERTS-1 imagery of New England using snow enhancement techniques
[E73-10345] 10 p1148 N73-19344
Application of ERTS-1 imagery for mapping coverage of megalopolitan New England to show land use
[E73-10427] 11 p1280 N73-20388
Detection and analysis of fracture systems using ERTS-1 imagery of snow cover conditions as enhancement tool
[E73-10741] 17 p2021 N73-26346
Analysis of ERTS-1 imagery to determine enhancement of ground fracture detail produced by snow cover
[PAPER-G12] 19 p2264 N73-28243
Mapping of fracture-lineaments in New England using snow enhancement techniques
[E73-10930] 21 p2528 N73-30273
Land use in northern megalopolis of New England
[E73-10991] 22 p2659 N73-31297
Investigation of New England reservoirs, land use, streams, flooding, and vegetation from Skylab imagery
[E73-10993] 22 p2659 N73-31299
NEW GUINEA [ISLAND]
Geological and geophysical mapping of mineral resources in Australia and New Guinea
02 p0164 N73-11328
Identification of copper/molybdenum porphyry mineral deposits in characteristic geologic setting in Nevada, Arizona, Colorado, Australia, Alaska, and New Guinea
[E73-10762] 17 p2023 N73-26362
NEW JERSEY
NT DELAWARE RIVER BASIN [US]
Application of ERTS-1 imagery data to protection and management of New Jersey coastal environment
[E72-10178] 01 p0045 N73-10357
Application of ERTS-1 imagery to protection and management of New Jersey coastal environment
[E73-10330] 10 p1147 N73-19335
Study of suspended sediment and aquatic fronts in Delaware Bay using ERTS-1 imagery
[E73-10368] 10 p1150 N73-19364
Catalogue of selected remote sensing data for New Jersey environment protection and management
[E73-10383] 11 p1275 N73-20347
Application of ERTS-1 data to management and protection of New Jersey coastal environment
[E73-10527] 14 p1654 N73-23415
Analysis of ERTS-1 imagery of New Jersey coastal resources to assist in resource management and allocation of funds for environmental control
[PAPER-E9] 19 p2269 N73-28273
Application of ERTS-1 data to geomorphotectonics, earthquake studies, and mineral exploration at Los Angeles, California, and New Jersey coastal plain
19 p2284 N73-28367
Utilization of ERTS-1 data for regulation, protection, and management of New Jersey coastal environment
[E73-10845] 19 p2291 N73-28423
Regional land use planning and management in Tri-State area from ERTS-1 MSS photography
[E73-10986] 22 p2658 N73-31293
Application of ERTS-1 data to protection and management of New Jersey coastal environment
[E73-11031] 22 p2662 N73-31335
NEW MEXICO
NT COLORADO PLATEAU [US]
Preparation of hydrologic atlases of arid land watersheds using ERTS-1 imagery of Wyoming, Utah, Montana, and New Mexico
[E72-10240] 03 p0288 N73-12340

Geological analysis and evaluation of ERTS-1 imagery of New Mexico
[E73-10015] 06 p0659 N73-15351
Tables on airborne and ground based measurements of optical atmospheric properties in central New Mexico
[AD-751936] 08 p0919 N73-17534
Plagioclase mineralogy of olivine alkaline basalt in Potrillo volcanic field
[NASA-CR-130918] 09 p1025 N73-18368
Evaluation of geologic applications of ERTS-1 imagery for New Mexico
[E73-10358] 10 p1149 N73-19354
ERTS-1 spectral reflectance measurements of vegetation, soil, and water in Rio Grande Valley, New Mexico
[E73-10408] 11 p1278 N73-20370
Utilization of ERTS-1 imagery in structural reconnaissance for minerals and oil in Alaska, Canada, Montana, Colorado, New Mexico, and Texas
[E73-10414] 11 p1279 N73-20376
Regional wet census of playa lakes on Southern High Plains area of Texas and New Mexico from ERTS-1 MSS imagery
[E73-10455] 11 p1283 N73-20414
Correlation between vegetation patterns and geologic and geomorphic units in New Mexico based on ERTS-1 imagery
[E73-10588] 14 p1657 N73-23448
Ozone and point discharge measurements under thunderclouds in New Mexico
[AD-758130] 14 p1665 N73-23515
Commercial application of ERTS-1 imagery in structural reconnaissance for minerals and petroleum
[E73-10700] 16 p1903 N73-25392
ERTS-1 imagery of morphology, provenance, and movement of desert sand areas in Africa, Asia, and Australia
[E73-10710] 17 p2018 N73-26317
Analysis of New Mexico geology using ERTS-1 imagery
[E73-10830] 18 p2140 N73-27300
Application of ERTS-1 imagery to determine geological evidence of mineral and hydrocarbon accumulations in Alaska, Canada, Montana, Colorado, New Mexico, and Texas
[PAPER-G30] 19 p2267 N73-28261
Geological survey of New Mexico based on ERTS-1 imagery
19 p2284 N73-28370
Statistical analysis of surface and upper air rawinsonde for White Sands Missile Range, New Mexico
[AD-762159] 19 p2297 N73-28472
Determination of earth aerosol albedo using Skylab data from White Sands, New Mexico
[E73-11080] 23 p2782 N73-32255

**NEW YORK**
NT DELAWARE RIVER BASIN [US]
NT LAKE CHAMPLAIN BASIN [NY-VT]
NT LONG ISLAND [NY]
NT SUSQUEHANNA RIVER BASIN [MD-NY-PA]
Estuarine and coastal oceanography of Block Island Sound and adjacent New York coastal waters based on ERTS-1 multispectral band scanner imagery
[E72-10171] 01 p0044 N73-10352
Interdisciplinary study of estuarine and coastal oceanography of Block Island Sound and New York Bight area using ERTS-1 imagery
[E72-10172] 01 p0044 N73-10353
Spectral geological mapping of New York using ERTS-1 imagery
[E72-10223] 02 p0163 N73-11317
Geological survey of Adirondack Mountain region using ERTS-1 multispectral scanner imagery
[E72-10291] 04 p0410 N73-13341
Spectral geological mapping in diverse terranes of New York using ERTS-1 imagery
[E72-10302] 05 p0530 N73-14309
Resource inventory, land use, and pollution within Susquehanna River Basin based on interpretation of ERTS-1 data
[E72-10329] 05 p0531 N73-14317
Multispectral imagery of estuarine and coastal oceanography of Block Island Sound and adjacent New York coastal waters using ERTS-1 imagery
[E73-10010] 06 p0659 N73-15346
Mapping and inventories of land use and natural resources in New York based on ERTS-1 imagery
[E73-10024] 06 p0660 N73-15358
Geological mapping of New York State using ERTS-1 imagery
[E73-10031] 06 p0660 N73-15364
Evaluation of ERTS-1 imagery for mapping geological structures in New York
[E73-10298] 09 p1021 N73-18330
Monitoring of water quality in New York Bight and Tampa Bay, Florida, using ERTS-1 imagery
[E73-10395] 11 p1276 N73-20357
ERTS-1 imagery of geological structures and terrains of New York
[E73-10457] 11 p1284 N73-20416
Analysis of ERTS-1 data for interdisciplinary study of estuarine and coastal oceanography of Block Island Sound and adjacent New York coastal waters
[E73-10735] 17 p2020 N73-26341
Analysis of ERTS-1 data for interdisciplinary study of estuarine and coastal oceanography of Block Island Sound and adjacent New York coastal waters
[E73-10736] 17 p2020 N73-26342
Utilization of Skylab multispectral cameras for study of eutrophication processes in lakes important to New York State water resources
[E73-10744] 18 p2133 N73-27236
Inventorying land use in New York State using ERTS-1 multispectral imagery
[E73-10772] 18 p2134 N73-27248
Color enhancement of ERTS-1 imagery of estuarine and coastal oceanography of Block Island Sound and adjacent New York coastal waters
[E73-10819] 18 p2140 N73-27294
State of Delaware and New York City using space age management for social problems
[NASA-TM-X-66296] 18 p2213 N73-27873
Evaluation of ERTS-1 imagery for geological surveys and topographical analysis of various terrains in New York State
[PAPER-G1] 19 p2263 N73-28233
ERTS-1 imagery for monitoring dumping of municipal and industrial wastes in New York Bight
[PAPER-E10] 19 p2269 N73-28274
Utilization of Skylab imagery as information service for investigating land use and natural resources in New York State
[E73-10829] 19 p2290 N73-28414
Geological surveys and mapping of New York using ERTS-1 imagery
[E73-10846] 19 p2291 N73-28424
Acquisition of land use, soil moisture, and hydrological data of Ontario, Canada and Syracuse, New York for Skylab-3
[E73-10888] 20 p2394 N73-29237
Estuarine and coastal oceanography of Block Island Sound and adjacent New York coastal waters
[E73-10968] 21 p2533 N73-30310
Regional land use planning and management in Tri-State area from ERTS-1 MSS photography
[E73-10986] 22 p2658 N73-31293
Interpretation techniques for Skylab monitoring of lake eutrophication in New York State
[E73-11011] 22 p2660 N73-31316
Spectroradiometric calibration of EREP imagery and oceanography of Block Island Sound
[E73-11015] 22 p2660 N73-31319
Utilization of Skylab imagery as information service for investigating land use and natural resources in New York
[E73-11113] 24 p2915 N73-33270

**NEWTON-RAPHSON METHOD**
Computation of steady conical flow past a yawed slender delta wing with leading edge separation using vortex sheet model and Newton-Raphson iteration
[IC-AERO-72-17] 01 p0001 N73-10005
Newton-Raphson techniques for analyzing reentry trajectories for heat minimization and terminal range maximization
[AD-745998] 01 p0106 N73-10882
ALGOL 60 subroutine for implementation of modified Newton algorithms for problem solving
[NPL-NAC-24] 09 p1057 N73-18622
Convergence improvement in equilibrium calculation using Newton-Raphson method for C, H, N, F system, noting monomethylhydrazine/Fe mixture
[ICT-3/72] 18 p2192 N73-27696
Revised algorithm for constrained optimization using quasi Newton-Raphson method based on recurring factorization of approximation to Hessian matrices
[NPL-NAC-32] 22 p2692 N73-31560

**NEWTONIAN FLUIDS**
Convective heat transfer for Newtonian fluid cross flow over circular cylinder
[ESDU-69004-AMEND-A] 02 p0241 N73-11962
Forced convective heat transfer for single phase, Newtonian fluid flow in smooth, straight, constant area circular tube
[ESDU-68007-PT-3] 02 p0242 N73-11965
Magnetic fluid preparation by grinding and concentrating pyrophoric antiferromagnetic iron oxide colloidals
[BM-RI-7702] 05 p0580 N73-14721
Stochastic derivation of equations of motion for deformable particles immersed in Newtonian fluids
[WTHD-46] 12 p1431 N73-21595
Characteristics of wall mass transfer coefficient for pulsed laminar flow in pipe of Newtonian fluid containing dissoloved electrolyte
15 p1765 N73-24301
Solution of laminar natural convection flows of Newtonian fluid in rectangular enclosures by asymptotic expansion
18 p2128 N73-27198
Experimental observations and numerical simulation of Weissenberg climbing effect
22 p2649 N73-31220
Theoretical and experimental analysis of flow induced by harmonic oscillation of rods with arbitrary cross sections containing incompressible, viscous, Newtonian fluid
23 p2774 N73-32183
Free surface secondary flow of Newtonian liquid between rotating concentric cylinders
24 p2906 N73-33188

**NICARAGUA**
Volcano and earthquake surveillance network in Alaska, California, Washington, Hawaii, El Salvador, Nicaragua, Iceland, and Guatemala
[E73-10337] 09 p1025 N73-18365
ERTS-1 imagery of western portion of Nicaragua following December 1972 earthquake to determine lineaments of fault systems related to earthquake
[PAPER-G24] 19 p2266 N73-28255
Prototype DCP volcano surveillance network in Washington, Nicaragua, California, Guatemala, Hawaii, El Salvador, Iceland, and Alaska
[E73-11024] 22 p2662 N73-31328

**NICHROME [TRADEMARK]**
Analytical rationale for sensitivity-insensitivity of dispersion strengthened alloys
[NASA-CR-124274] 16 p1928 N73-25600

**NICKEL**
NT NICKEL ISOTOPES
Development of nickel hydroxide electrode for use in rechargeable alkaline batteries
[AD-746335] 01 p0007 N73-10058
Changes in porous structure of nickel electrode substrates due to changes in manufacturing processes
[AD-748109] 03 p0255 N73-12067
Technology assessment of silicon carbide reinforced composites with aluminum or nickel matrix discussing mechanical resistance at high temperatures
04 p0434 N73-13543
Electrolytic procedure for manufacturing aluminum whisker and pure nickel matrix composites with reinforced fibers
04 p0435 N73-13544
Periodic passivation of nickel electrode and changes in properties of cathodic deposits during electrodeposition of nickel using reversible current
[NLL-TRANS-746-1317-[9022.401]]
05 p0560 N73-14549
Research trends in steels with reduced nickel content for cryogenic applications
[NLL-TRANS-746-1266-[9022.401]]
05 p0561 N73-14556
Mechanical properties of thin films of Ni-SiO
[NLL-TRANS-746-1329-[9022.401]]
05 p0564 N73-14582
Magnetic properties of single crystal nickel powers
[NLL-TRANS-746-1390-[9022.401]]
05 p0585 N73-14762
Characteristics of molybdenum disulfide films radio frequency sputtered on aluminum and nickel surfaces at elevated, ambient, and liquid nitrogen temperatures
[NASA-TN-D-7170] 08 p0927 N73-17593
Influence of tensile velocity on plasticity of cold deformed technically pure nickel
09 p1046 N73-18533
Charge composition of cosmic rays for elements silicon to nickel
[LUIP-CR-72-16] 09 p1069 N73-18721
X ray attenuation coefficients in absorption spectra of titanium, iron, cobalt, nickel, copper, and zinc
[UCRL-73923] 10 p1189 N73-19675
Kerr magnetooptical effect in nickel, gadolinium, and dysprosium at temperatures between 10 and 300 K in 1 to 5 eV energy range
12 p1437 N73-21644
Correlation between microstructure and measured stress of vacuum deposited nickel films
[COO-623-183] 12 p1439 N73-21659
Hot pressing of nickel-zinc ferrites for manufacturing read-write magnetic heads
[REPT-9.451] 13 p1500 N73-22154
Oxidation kinetics for nickel and its hardened compositions
13 p1542 N73-22500
Vapor deposition techniques for preparation of nickel foil and various ceramic materials
[AD-758389] 14 p1679 N73-23625
Measurement of gas permeability of high porosity nickel powder metallurgy parts
[NLL-LTI-746-1404-[9022.401]]
15 p1797 N73-24564
Creep test measurement of stresses generated during high temperature oxidation of copper and nickel
16 p1926 N73-25588
Service life extension of cyclically loaded copper specimens by application of electroplated layers of nickel
16 p1927 N73-25595
Temperature effects on swelling of nickel irradiated by medium energy heavy ions
[CEA-CONF-2052] 17 p2044 N73-26540
Formation of cavities in nickel and some austenitic steels irradiated by medium energy heavy ions
[CEA-CONF-2113] 17 p2045 N73-26542

Frequency effect of magnetocrystalline anisotropy in nickel ferrous ferrites determined by torque measurements
18 p2159 N73-27443
Theoretical analysis of plastic flow and diffusion during sintering of Life, Ag, and Ni systems
20 p2428 N73-29499
Atomic oxygen reaction with nickel at elevated temperatures
[NASA-TM-X-62295] 20 p2431 N73-29524
Mechanical behavior of polycrystalline nickel deformed by tension and simultaneously cathodically charged with hydrogen
[AD-759036] 20 p2432 N73-29535
Analysis of structural-eutectic transformations in liquid phase of metal-metal and metal-semiconductor systems
[NLL-M-21665-[5828.4F]] 21 p2557 N73-30496
Thermodynamic stability diagrams for iron, nickel, and chromium in fused sodium hydroxide
22 p2625 N73-31028
Measurements of Fe, Mn, Fn, Cu, Ni, and Pb in aerosols and precipitation in clean tropospheric air
[NOAA-TR-ERL-248-APCL-24]
22 p2664 N73-31349
Stress analysis of vacuum deposited nickel films to determine correlation between microstructure and measured stress
23 p2804 N73-32424
Carbon-oxygen fuel cell of solid carbon anode, nickel gauze cathode, and flamed electrolytes
24 p2880 N73-33001
Ferromagnetic resonance measurements in Ni and Fe as function of temperature and frequency parameters
24 p2934 N73-33428

**NICKEL ALLOYS**
NT HASTELLOY [TRADEMARK]
NT INCONEL [TRADEMARK]
NT KAMACITE
NT NICHROME [TRADEMARK]
NT NITINOL ALLOYS
NT UDIMET ALLOYS
Analysis of sensitivity of elevated temperature deformation of nickel alloy to grain size and shape under tension and creep conditions
[NASA-CR-128403] 01 p0067 N73-10549
Development of procedure for removing oxygen from nickel alloys by blowing hydrogen on bath surface and evacuating gases
[NLL-TRANS-746-1347-[9022.401]]
02 p0184 N73-11495
High temperature and fatigue tests to determine effects of heat resistant coatings on mechanical and physical properties of nickel-chromium-iron alloys
[NLL-TRANS-746-1236-[9022.401]]
02 p0185 N73-11500
Preparation and homogeneity characteristics of austenitic iron-chromium-nickel alloy at micrometer level of spatial resolution to establish standard reference material
[NBS-SP-260-43] 02 p0186 N73-11511
TD nickel chromium, dispersion-strengthened alloy for thermal protection system of space shuttle
[NASA-CR-120796] 02 p0187 N73-11512
Effects of molybdenum and tungsten fiber reinforcements on nickel chromium aluminum matrix alloys
[NLL-TRANS-746-1193-[9022.401]]
02 p0191 N73-11546
Effect of mechanical-thermal pretreatments on time-to-rupture and creep strength of nickel-chromium steels
[KFK-1535] 03 p0313 N73-12557
Recrystallization processes of sheet nichrome containing zirconium dioxide inclusions
[AD-747603] 03 p0318 N73-12589
Influence of interlamellar spacing on strength of Ni3Al-Ni3Cb eutectic
[AD-748658] 03 p0319 N73-12601
Quantitative examination of ordering effects in nickel-iron alloy system
[NLL-RTS-7547] 04 p0431 N73-13510
Effects of atomic ordering in ternary solid solutions containing alloys of nickel and iron and relation of Youngs modulus with temperature
[NLL-RTS-7654] 04 p0431 N73-13511
Hot pressing of chromium carbide alloy matrice tools for cold drawing of pipes
04 p0432 N73-13522
Dispersion hardening of complex chromium nickel alloy by zirconium dioxide
04 p0432 N73-13523
Diffusion creep and creep degradation in precipitation hardened TD-NiCr alloy
[NASA-TN-D-7079] 04 p0433 N73-13530
Effects of sodium salts on hot corrosion mechanism in Ni-8Cr-6Al
[AD-748349] 04 p0435 N73-13551
Improved oxidation resistance of dispersion strengthened nickel-chromium alloys and thermomechanical procedure to produce course grain microstructure
[AD-748266] 04 p0436 N73-13556
Electric field effects on oxidation mechanisms of metals and alloys
[AD-748297] 04 p0436 N73-13558
Creep and stress relaxation tests on Cr-Ni austenitic steel at 700 C
[STU-70-419/U-350-B] 04 p0481 N73-13932
Development of lithium-nickel sulfide electric storage battery for operation at high discharge rates and low temperatures
[AD-749861] 05 p0500 N73-14067
Structure and phase composition of electrodeposited iron-nickel-chromium alloys analyzed by X ray spectroscopy and electron microscopy
[NLL-TRANS-746-1327-[9022.401]]
05 p0560 N73-14551
Evaporative segregation in binary alloys of Ni-Cr and Ni-Fe systems
[NASA-CR-123993] 05 p0561 N73-14562
Analysis of effect of dysprosium oxide on the physical properties of nickel-zinc ferrite materials
[NLL-TRANS-746-1284-[9022.401]]
06 p0682 N73-15550
Physical properties of porous nickel strips used as electrodes in electro-vacuum equipment and methods for controlling expansion during production
[NLL-TRANS-746-1342-[9022.401]]
06 p0682 N73-15551
Beta-phase effect on ductility of two-phase titanium alloys and calorimetric determination of atomic ordering effects in Ni2Cr alloy
[JPRS-57578] 06 p0683 N73-15556
Calorimetric determination of atomic ordering effects in alloy Ni2Cr
06 p0683 N73-15558
High temperature oxidation behavior of Ni3Al with and without yttrium additions and reaction kinetics of Al2O3 layer growth
[AD-750410] 06 p0686 N73-15589
Effects of prior deformation and transformations on microstructure of iron nickel alloy
[AD-750716] 06 p0687 N73-15591
Time dependent edge-notch sensitivity of oxide and gamma dispersion strengthened nickel alloy sheets
[NASA-CR-121123] 06 p0725 N73-15919
Development of differential equation for normal evaporation of nickel-aluminum alloy relating evaporating time to final solute concentration
[NASA-CR-124040] 07 p0808 N73-16558
Reduction of oxidation attack of nickel-base superalloy B-1900 by addition of one percent silicon
[NASA-TM-X-68191] 07 p0809 N73-16564
Influence of Na2SO4 oxidation of Ni-20Cr-2ThO2 gas turbine corrosion
[AD-751259] 07 p0810 N73-16573
Effect of chloride ion additions on dissolution behavior of Fe-Ni alloys in sulfuric acid
[AD-751258] 07 p0811 N73-16574
Improvement of high temperature eutectic alloy by compositional modification
[AD-752632] 08 p0934 N73-17644
Hydrogen adsorption and diffusion, and subcritical crack growth in high strength steels and nickel alloys
[NASA-CR-130979] 09 p1046 N73-18528
Development of powder metallurgy nickel-base superalloy for application at 1800 to 2000 F
[NASA-CR-121099] 09 p1047 N73-18537
Microstructural analysis of nickel-base alloy WAZ-20 using qualitative and quantitative electron optical techniques
[NASA-TN-D-7209] 09 p1047 N73-18541
Tin alloying effects on plastic deformation, mechanical, and stress-rupture properties of Ni-Cr alloys
[JPRS-58159] 09 p1048 N73-18546
Fatigue behavior of directionally-solidified aluminum-nickel eutectic alloy under cyclic torsional loading
[AD-753689] 09 p1055 N73-18600
Procedure for fabricating element with cavity closed by thin wall with precisely shaped slit
[NASA-CASE-LAR-10409-1] 11 p1297 N73-20526
Dispersion effects of heat resistant metal oxides
[AD-754760] 11 p1306 N73-20595
Concentration dependence of high field susceptibility of Fe-Ni alloys
[NLL-LTI-746-1343-[9022.401]]
12 p1412 N73-21440
Solid state and fusion resistance spot welding of TD-NiCr sheet
[NASA-TN-D-7256] 12 p1412 N73-21443
Effects of hydrogen environment embrittlement of steels and alloys
[NASA-CR-2163] 12 p1412 N73-21444
Metallurgical reports on plasma jets, creep properties of nickel alloys, oxygen and nitrogen interactions with metals, and Mossbauer effect as applied to diffusion mechanisms
[JPRS-58508] 12 p1412 N73-21445
Steady state creep rate of nickel as effected by binary alloys at increased temperatures
12 p1413 N73-21448
Phase structure of crystallizing nickel tin alloy melt during cooling
[JPRS-58681] 12 p1414 N73-21456
Using transition from Ni-61 to obtain Mossbauer absorption spectra with Ni-Pd alloy
[TID-26197] 12 p1414 N73-21461
Determination of diffusion coefficient of hydrogen through nickel and iron-nickel alloys
[UCRL-TRANS-10651] 12 p1415 N73-21463
Effect of substrate topography on magnetic properties of cylindrical Ni-Fe thin films
[NLL-LTI-746-1370-[9022.401]]
12 p1437 N73-21641
Method of life prediction for nickel-based Udimet alloy by high temperature creep/fatigue testing
[NASA-CR-120958] 12 p1462 N73-21845
Analysis of elastic properties of Invar and Elinvar alloys at various temperatures
13 p1540 N73-22480
Analysis of high temperature stability of reinforcing phase in eutectic composition of aluminum-nickel alloys for various rates of growth
13 p1541 N73-22487
Analysis of electrical conductivity of eutectic solutions of aluminum-nickel alloy using directional crystallization method
13 p1541 N73-22489
Metallographic analysis of morphological features of martensite formed in alloy of iron-nickel-manganese-carbon after heat treatment
13 p1541 N73-22490
Effect of yttrium, lanthanum, and cerium additives on oxidation kinetics of nickel-chromium based alloys
[JPRS-58777] 13 p1542 N73-22497
Sintering and heat resistance of nickel alloys
[JPRS-58779] 13 p1542 N73-22499
Sintering heat resistant nickel alloys
13 p1543 N73-22501
Physical and chemical properties of nickel alloys following cyclic and isothermal oxidation
[NASA-TN-D-7267] 14 p1675 N73-23594
Addition of chromium or aluminum to improve oxidation resistance of nickel and cobalt alloys
14 p1677 N73-23611
Comparison of cobalt alloys and nickel alloys relative to hot corrosion resistance
14 p1677 N73-23612
Trace element [Bi, Ag, Cd, and Pb] determination in nickel base gas turbine parts by atomic absorption spectrophotometry
[AD-757015] 14 p1678 N73-23619
Effect of molybdenum addition on physicomechanical properties of titanium-carbon-nickel composite alloys
[NLL-LTI-746-1422-[9022.401]]
15 p1797 N73-24565
Magnetic properties of highly dispersed iron-cobalt-nickel alloy powders
[NLL-LTI-746-1419-[9022.401]]
15 p1797 N73-24566
Short range order effect on interatomic reaction and heat of displacement in molten nickel and silicon alloys
[NLL-M-21597-[5828.4F]] 15 p1797 N73-24568
Dispersion strengthened nickel-yttria sheet alloy produced from comminuted powders
[NASA-TM-X-68245] 15 p1798 N73-24576
Rotating electrode process for processing 18Ni maraging steel by powder metallurgy
[AD-758439] 15 p1800 N73-24589
Cyclic furnace tests of nickel-, cobalt-, and iron-base alloys oxidation resistance considering scale spalling
[NASA-TM-X-68252] 16 p1870 N73-25144
Measurement of elastic moduli and compressive yield strength for Ni3[Al,X] alloy single crystals
16 p1927 N73-25589
Analysis of iron-nickel alloys to determine nature of Mossbauer effect at high pressures and low temperatures
16 p1927 N73-25592
Measurement of work functions of copper and copper-nickel single crystals at low pressures and determination of thermionic emission constant
16 p1927 N73-25593
Analytical rationale for sensitivity-insensitivity of dispersion strengthened alloys
[NASA-CR-124274] 16 p1928 N73-25600
Processing condition effects on microstructures of sheets, wire and bars made from nickel chromium iron alloy 718
[WAPD-TM-1077] 16 p1928 N73-25603
Change in fine structure of nickel-chromium heat resistant alloys during creep
[AD-759233] 16 p1971 N73-25939
Dispersion strengthened nickel alloys for use as space shuttle thermal protection systems
[NASA-CR-121164] 17 p2043 N73-26526
Kinetics of phase layer growth during diffusion coating of nickel with aluminum
[AD-760365] 17 p2054 N73-26611
Forming and joining techniques and properties of thin gage TD-NiCr sheet in crystallized and unrecrystallized conditions
[NASA-CR-121224] 18 p2154 N73-27408
Thermomechanical processing of nickel-base superalloys by explosive shock wave deformation
[AD-761218] 18 p2162 N73-27462

Ni-61 transition for obtaining Mossbauer absorption spectra with Ni-Pd alloys
18 p2185 N73-27641
Interfacial wear reactions in nickel and molybdenum alloy mechanical face seals
[AD-762076] 19 p2306 N73-28546
Thermodynamic properties of solid Ni-Ga alloys at temperatures between 837 and 1100 K
[AD-762337] 19 p2311 N73-28588
Equations for creep and stress relaxation in nickel-based alloy bolted joints subjected to vibration
[AD-761455] 19 p2349 N73-28897
Interaction of nickel base ternary matrix system with tungsten reinforcing fibers
20 p2430 N73-29521
Strength and microstructure of nickel base superalloys after long term heating
[TB-86] 20 p2431 N73-29526
Effects of diffusion on aluminum depletion and degradation of NiAl coatings on superalloys
[NASA-TM-X-68274] 20 p2435 N73-29555
Enriched aluminide coatings for dispersion strengthened nickel compounds
[NASA-CR-121250] 21 p2558 N73-30506
Thermodynamic properties of solid alloys of chromium with nickel and iron
[COO-1791-4] 21 p2559 N73-30516
Carbon fiber/cobalt/chromium system tensile and high temperature strength noting different solidification modes
[DLR-FB-73-37] 21 p2560 N73-30519
Use of nickel steels for cryogenic tanks
[AD-763947] 22 p2679 N73-31457
Mechanical and physical property tests of TD-NiCr [Ni-20Cr-2ThO2] alloy sheet
[NASA-CR-121221] 22 p2683 N73-31493
Correlation of X ray and electron microscope data for fatigue in nickel and cobalt alloys
[AD-764282] 22 p2686 N73-31513
Spectrophotometric determination of B, Cu, and Ta in Ni base alloys
[JAERI-M-5094] 24 p2934 N73-33431
Thermodynamic property measurements of solid chromium sesquioxide and chromium in solid alloys with iron and nickel
[TID-26322] 24 p2934 N73-33433
Influence of alloy additives on strength of nickel base alloys at temperatures from 25 to 650 C
[ORNL-TM-4173] 24 p2936 N73-33446

**NICKEL CADMIUM BATTERIES**

Results of testing and characterization of battery plates for nickel cadmium cells
[NASA-CR-130094] 01 p0006 N73-10050
Performance of sealed nickel cadmium storage cells at very low ampere/hour percent recharge for OAO
[NASA-TM-X-66093] 02 p0128 N73-11040
Leakage of ESRO 4 nickel cadmium batteries noting electrical and pressure measurements and KOH loss
[ESRO-CR[P]-132] 04 p0375 N73-13053
Determination of KOH loss in ESRO 4 nickel cadmium batteries by electrical measurements
[ESRO-CR[P]-132] 04 p0375 N73-13054
Nickel cadmium storage battery for portable power supply of man-pack equipment
[AD-748454] 04 p0376 N73-13055
Rate of discharge of accelerated life tests of nickel cadmium cells
[AD-748253] 04 p0377 N73-13065
Temperature and temperature gradients for accelerated life tests of nickel cadmium cells
[AD-748252] 04 p0377 N73-13066
Valid tests with temperature gradients and/or rates of discharge as primary variables for accelerated life testing sealed nickel cadmium batteries
[AD-749129] 05 p0499 N73-14061
Performance data reduction for cadmium spacecraft cells from simulated orbital life tests
[AD-748251] 06 p0627 N73-15088
Interrelation of logistics cost in managing nickel cadmium batteries
[AD-750907] 06 p0733 N73-15977
Plastic compression type seals for long life Ni-Cd batteries
[NASA-CR-130867] 08 p0870 N73-17040
Performance data analysis for OAO sealed nickel cadmium cells and batteries
[NASA-CR-130233] 11 p1237 N73-20045
Proceedings of NASA/Goddard Battery Workshop, first day
[NASA-TM-X-69240] 13 p1476 N73-21956
Proceedings of NASA/Goddard Battery Work Shop, second day
[NASA-TM-X-69239] 13 p1476 N73-21957
Development of hermetically sealed nickel cadmium battery and associated control logic and charger circuit for aircraft applications
[AD-757535] 14 p1606 N73-23017
Mariner Mars 1971 battery design, test, and flight performance
[NASA-CR-132986] 16 p1864 N73-25095
Performance tests of nickel cadmium and silver cadmium electric batteries to determine service life and reliability
[NASA-CR-132801] 17 p1985 N73-26046
Charge characteristics of sealed nickel cadmium and lead acid batteries
[PB-221475/7] 22 p2618 N73-30981

**NICKEL COATINGS**

Development of nickel-iron plated wires for computer memories
[ME-72-6] 13 p1498 N73-22139
X ray reflection efficiency of nickel coated quartz optical flats
[NASA-TM-X-64747] 15 p1813 N73-24694
Intermetallic chromium containing nickel aluminide for high temperature corrosion protection of stainless steels
[NASA-CASE-LEW-11267-1] 23 p2803 N73-32414

**NICKEL COMPOUNDS**

NT NICKEL FLUORIDES
NT NICKEL OXIDES
Development of hard TiC-Ni alloys for use as cutting tools
[NLL-TRANS-746-1226-[9022.401]]
02 p0185 N73-11496
Effects of polishing on magnetic properties of nickel-zinc ferrite toroids during annealing and procedures to restore original magnetic properties
[AD-747251] 03 p0346 N73-12822
Production of fibers, plaques, and highly porous sintered nickel materials
[NLL-TRANS-746-1381-[9022.401]]
06 p0687 N73-15592
Determination and identification of gases in powdered carbonyl nickel
[NLL-LTI-746-1353-[9022.401]]
12 p1412 N73-21439
Magnetic susceptibilities of NiCl2.6H2O
[AD-759417] 17 p2046 N73-26555
Literature on vanadium and nickel trace elements in distillate fuels for motor vehicles
[AD-760462] 17 p2076 N73-26793
Effect of scandium, yttrium, and lantham oxides on properties of nickel ferrite
23 p2809 N73-32460

**NICKEL FLUORIDES**

Ion exchange interactions in magnetically diluted nickel fluorides
[REPT-734] 14 p1694 N73-23749

**NICKEL ISOTOPES**

Ni-61 transition for obtaining Mossbauer absorption spectra with Ni-Pd alloys
18 p2185 N73-27641

**NICKEL OXIDES**

Development of procedure for removing oxygen from nickel alloys by blowing hydrogen on bath surface and evacuating gases
[NLL-TRANS-746-1347-[9022.401]]
02 p0184 N73-11495
Thermogravimetric analysis of reduction of oxides of nickel and chromium
[NASA-TM-X-2688] 06 p0684 N73-15565
Reaction of nickel oxide with steel in argon and vacuum atmospheres
[AD-754776] 11 p1306 N73-20600
Oxidation kinetics for nickel and its hardened compositions
13 p1542 N73-22500

**NICKEL PLATE**

Hull cell investigation of throwing powers of various nickel plating baths
[NLL-RTS-7294] 01 p0067 N73-10548
Nickel ion absorption on alumina and titania electrolyte interfaces
[AD-754540] 11 p1253 N73-20167
Analysis of adhesion strength of electroless nickel plating on Type 4340 steel to determine optimum plating conditions and to certify bond strength
[Y-1838] 12 p1414 N73-21459

**NICKEL STEELS**

Development of diffusion welding technique for TD-NiCr metal sheet and effect on creep-rupture shear strength
[NASA-TN-D-7153] 07 p0804 N73-16520

**NICKEL ZINC BATTERIES**

Reliability analysis of nickel zinc rechargeable batteries
[AD-748896] 04 p0376 N73-13062
Characteristics of nickel-zinc electric battery and application to propulsion of hybrid electric surface vehicles
[AD-756431] 13 p1477 N73-21963
Construction and performance of sealed nickel zinc batteries
[AD-755550] 13 p1477 N73-21967

**NICOTINIC ACID**

Conversion of 2-methyl 5-ethyl pyridine compound into 5-ethyl picoline acid by different methods
[DRIC-TRANS-2951] 06 p0638 N73-15178

**NIGER**

ERTS-1 imagery of villages and cultivation sites in Niger and Upper Volta
[E73-10893] 20 p2395 N73-29242

**NIGHT**

Night cloud cover and meteorological parameter variations determined at La Silla, Chile, in 1970
[ESO-BULL-9] 01 p0075 N73-10620
Air-to-ground target acquisition with flare illumination
10 p1226 N73-19968
Nighttime composition measurements at geomagnetic equator
[NASA-TM-X-70476] 23 p2785 N73-32283

**NIGHT AIRGLOW**

U AIRGLOW
U NIGHT SKY

**NIGHT E LAYER**

U E REGION
U NIGHT SKY

**NIGHT F LAYER**

U F REGION
U NIGHT SKY

**NIGHT SKY**

Night sky spectral radiant sterance at ground level and variation with latitude and nighttime conditions, using Fourier spectroradiometer
[AD-750609] 06 p0669 N73-15442
Atmospheric model of artificial night sky illumination in Italy
21 p2538 N73-30348
Measurement of night-sky brightness in visible and ultraviolet spectral regions using photometers on Cosmos-51 and Cosmos-213 satellites
[NASA-TT-F-15154] 24 p2980 N73-33814
Measurement of night-sky brightness in visible and ultraviolet spectral regions using photometers on Cosmos-51 satellite
[NASA-TT-F-15153] 24 p2980 N73-33815

**NIGHT VISION**

Parametric modifications for improved image intensification of forward looking infrared imaging devices in night fire control
[AD-750374] 06 p0646 N73-15251
Analysis of atmospheric optical properties with application to night vision, infrared radiation, astrogeophysics, and electro-optical physics
[AD-750610] 06 p0669 N73-15443
Application of night vision technology helicopter night scouts
10 p1226 N73-19970
Research and development of electronic equipment for night combat surveillance
[AD-762351] 19 p2302 N73-28507
Systems analysis of avionics and aircraft equipment for search and rescue helicopters to determine cost effective improvements - Vol. 7
[AD-764914] 24 p2927 N73-33381

**NIGHTGLOW**

Electron density irregularities and evening anomalies in midlatitude nighttime F region
13 p1514 N73-22270

**NIKE MISSILES**

NT NIKE-AJAX MISSILE
NT NIKE-HERCULES MISSILE
Analysis of pressure fluctuations in Nike rocket case and relationship to structural vibrations of rocket case
[NASA-TN-D-6931] 01 p0113 N73-10933
PLRACTA interfaced with site acquisition radar at Nike base in Lincoln, Mass.
[AD-754231] 10 p1229 N73-19991

**NIKE ROCKET VEHICLES**

NT NIKE-TOMAHAWK ROCKET VEHICLE
Technical engineering services in support of Nike-Tomahawk sounding rocket vehicles
[NASA-CR-130123] 04 p0478 N73-13906

**NIKE-AJAX MISSILE**

Instrumentation for Nike-Ajax radar to perform real time cross section measurements on airborne targets
[AD-756538] 13 p1493 N73-22103

**NIKE-HERCULES MISSILE**

Proposed transfer of mission responsibility Army Nike-Hercules Air Defense sites to Army National Guard
[AD-760483] 18 p2214 N73-27883

**NIKE-TOMAHAWK ROCKET VEHICLE**

Electrostatic analyzer and energy spectrum determination methodology used with primary electron spectrometer on Nike-Tomahawk sounding rocket
[NASA-CR-133409] 18 p2151 N73-27389

**NIMBUS PROJECT**

History of Nimbus satellite project and selected photography
[NASA-CR-130144] 06 p0720 N73-15877

**NIMBUS SATELLITES**

NT NIMBUS 2 SATELLITE
NT NIMBUS 3 SATELLITE
NT NIMBUS 4 SATELLITE
NT NIMBUS 5 SATELLITE
Vibration tests of magnetic control assembly for Nimbus and ERTS satellites
[NASA-CR-130143] 06 p0673 N73-15478
Degradation of ultraviolet photometry systems on Nimbus 3 and 4 satellites
[NASA-TM-X-66148] 06 p0721 N73-15883
Nimbus 3 and 4 observations of snow cover and hydrological features in Western Himalayas
07 p0787 N73-16403
Analysis of hydrologic conditions based on Nimbus satellite imagery
07 p0788 N73-16405

ERTS/Nimbus satellite observations of electron flux levels as function of solar cycle
[NASA-TM-X-66236] 14 p1703 N73-23814
Statistical processing of Nimbus infrared data for synoptic atmospheric climatology
18 p2170 N73-27523

NIMBUS 2 SATELLITE
Multispectral method of determining sea surface temperatures, using Nimbus 2 infrared radiometer
08 p0971 N73-17938
Catalog of meteorological and geomorphological data acquired from Nimbus 2 satellite
[NASA-TM-X-69886] 14 p1707 N73-23852

NIMBUS 3 SATELLITE
Infrared and microwave radiometric data of intertropical convergence zone acquired by Nimbus 3 satellite
[NASA-TM-X-66203] 10 p1188 N73-19669
Annual global average earth-atmospheric system radiation balance determined from Nimbus 3 radiation measurements
[NASA-TN-D-7249] 12 p1445 N73-21702
Global distribution of total ozone as determined by Nimbus 3 satellite infrared interferometer spectrometer
16 p1895 N73-25326
Satellite infrared radiometer observation of hurricane intensification
22 p2736 N73-31906

NIMBUS 4 SATELLITE
Regression relationships between Nimbus 4 SIRS-B clear-column radiances and geopotential heights of 500 mb and 300 mb levels
[AD-743711] 01 p0075 N73-10624
Inferred ozone profiles from ultraviolet earth radiance data from Nimbus 4
[NASA-TM-X-66108] 03 p0294 N73-12397
Data catalog for Nimbus 4 from 1 March to 30 April 1971
[NASA-TM-X-68840] 03 p0326 N73-12658
Processing techniques for deducing cloud motion vectors from overlapped portions of pairs of satellite
[NASA-CR-130115] 03 p0326 N73-12660
Analysis of cloud formations, ozone distribution, and meteorological data from Nimbus 4 satellite observations
[NASA-TM-X-66190] 09 p1028 N73-18392
Analysis of backscatter ultraviolet experiment conducted with double monochromator instrument on Nimbus 4 satellite
[NASA-TM-X-66204] 10 p1153 N73-19385
Development and characteristics of rate measuring package for stabilization of Nimbus D satellite
[NASA-CR-130182] 10 p1216 N73-19888
Nimbus 4 satellite users guide detailing instrumentation, configuration, and experimentation
[NASA-TM-X-69887] 13 p1580 N73-22803
Catalog of data acquired from Nimbus 4 meteorological satellite from 18 Apr. through 22 May 1970
[NASA-TM-X-69888] 13 p1580 N73-22804
Data catalog of Nimbus 4 satellite performance capacity, experimentation, and instrumentation - Vol. 2
[NASA-TM-X-69889] 13 p1580 N73-22805
Nimbus 4 satellite catalog of observations for period 1 July through 31 August, 1970 - Vol. 3
[NASA-TM-X-69890] 13 p1580 N73-22806
Data catalog tables and pictorial montages from Nimbus 4 satellite observation
[NASA-TM-X-69891] 13 p1580 N73-22807
Catalog of Nimbus 4 satellite observations for 1 November through 31 December, 1970 - Vol. 5
[NASA-TM-X-69892] 13 p1580 N73-22808
Data catalog of Nimbus 4 satellite performance capacity, experimentation, and instrumentation - Vol. 6
[NASA-TM-X-69893] 13 p1580 N73-22809
Tables of cataloged data collected by Nimbus 4 satellite
[NASA-TM-X-69894] 13 p1580 N73-22810
Nimbus 4 data catalog for 1 May 1971 to 30 Apr. 1972, including IDCS, THIR, IRIS, AND SIRS
[NASA-TM-X-69895] 13 p1580 N73-22811
Comparison of Nimbus interferometer spectrometer observations and theoretical radiances between 425 to 1450/cm
[NASA-TM-X-66275] 18 p2142 N73-27314
Nimbus 4 IRIS spectra in 750-1250/cm atmospheric window region
[NASA-TM-X-66281] 18 p2142 N73-27315
Nimbus 4 satellite infrared spectra for analyzing cloud spectral effects
22 p2736 N73-31907

NIMBUS 5 SATELLITE
ITOS D and Nimbus E radiometer data
08 p0972 N73-17943
Design and operation of radiometer deployment subsystem for Nimbus E spacecraft
09 p1088 N73-18877
Two channel output, high resolution surface composition mapping radiometer, and thermal channels of MSDS scanner studies onboard Nimbus 5
[NASA-CR-132764] 17 p2031 N73-26437
Meteorological interpretations of images from Nimbus 5 with electrically scanned microwave radiometer
[NASA-TM-X-70424] 20 p2448 N73-29671
Electronic scanning microwave radiometer system for measurement of meteorological, geomorphological, and oceanographic parameters from Nimbus 5
[NASA-CR-132812] 23 p2793 N73-32342

NIMONIC ALLOYS
Prediction of yeld strength on isothermal aging of precipitation-hardening alloy Nimonic PE16
[TRG-REPORT-2267] 24 p2935 N73-33442

NIMPHE [ENGINE]
U HYDRAZINE ENGINES

NIOBATES
NT LITHIUM NIOBATES
Chemical diffusion coefficient of oxygen in mixed niobates to determine feasibility of modifying oxide defect structures to enhance oxidation protection of elevated temperature materials
[AD-746834] 03 p0316 N73-12574
Half wave voltage for optimum orientation for barium sodium niobate transverse light modulator
[CRC-1229] 04 p0457 N73-13733
Cis-trans isomers and doped LiNbO3 for holographic ready/write/erase memory application
[NASA-CR-112248] 08 p0928 N73-17604
Growths of barium and strontium niobate laser materials for electro-optical Q-switching of visible and near infrared radiation
[AD-752445] 09 p1076 N73-18779
Strontium barium niobate for layered optical memory material
[NASA-CR-112261] 11 p1308 N73-20612
Properties of piezoelectric lead zirconate titanate ceramic resonator material produced by adding lead niobates to material
[AD-757617] 14 p1681 N73-23644
Barium sodium niobate as nonlinear optical material
[AD-758221] 14 p1682 N73-23650
Potential use of strontium barium metaniobate crystals for electro-optics
[AD-762740] 22 p2687 N73-31520

NIOBIUM
Anelastic studies of hydrogen diffusion in niobium using internal friction techniques
[COO-1198-896] 03 p0264 N73-12138
Effect of nitriding on mechanical properties of niobium
[AD-747450] 03 p0318 N73-12593
Determination of activation parameters and microcreep in niobium single crystals at low temperature
[COO-1198-909] 04 p0458 N73-13742
Pack rolling effects on bond strength between Nb and Cu
[AD-750511] 06 p0678 N73-15517
Suitibility of Nb surfaces in superconducting RF cavities
[KFK-EXT-3/72-3] 06 p0709 N73-15781
Nuclear resonance investigation in niobium-hydrogen and niobium-deuterium systems
[JUL-853-FF] 10 p1193 N73-19707
Microwave surface impedance of thin niobium superconducting films subjected to varying dc magnetic fields
12 p1438 N73-21649
Theoretical model for current flux motion and pinning in superconducting niobium crystal lattice
[COO-3169-11] 12 p1440 N73-21663
Flux line lattice effect on critical current in plastically deformed single niobium crystal
[COO-3169-14] 12 p1440 N73-21665
Volt-ampere characteristics of deformed niobium semiconductor memory switch
[COO-3169-12] 12 p1441 N73-21673
Design and operation of superconducting quantum point contact interference device
[PB-214758/5] 15 p1823 N73-24775
Design and performance of superconducting quantum interference devices
[PB-214757/7] 16 p1954 N73-25810
Effect of oxygen on corrosion of niobium and tantalum by liquid lithium at 600 C
[ORNL-TM-4069] 17 p2045 N73-26547
Fabrication of niobium thin film superconductive tunnel junctions using semiconductor barrier
17 p2072 N73-26761
Life tests of niobium coatings used on alkali metal arc lamps
[AD-761204] 18 p2168 N73-27508
Methods for repairing coated columbian thermal protection system
[NASA-CR-124295] 18 p2206 N73-27809
Diffision in niobium of beryllium and aluminum from solid phase at 900 to 1300 deg
[NLL-CE-TRANS-5121-[9022.09]] 20 p2429 N73-29513
Assessment of technological readiness for coated columbium thermal projection systems
[NASA-TM-X-2858] 20 p2431 N73-29530
Electromicroscopic analysis of Nb3Sn bands to determine effect of carbon doping on current carrying capacity
[NLL-M 23057-[5828.4F]] 20 p2434 N73-29544
Superconductivity of copper containing small amounts of niobium
[CALT-822-50] 22 p2707 N73-31679
Absence of S band energy gap in single crystal niobium
[AD-764906] 23 p2827 N73-32594

NIOBIUM ALLOYS
Explosive welding process for producing molybdenum wire reinforced columbium alloy composites
[NASA-CR-123937] 03 p0305 N73-12490
Temperature and concentration dependence of Debye-Waller factor for superconducting Nb-Zr alloy system
[BNL-TR-483] 03 p0315 N73-12569
Diffusion interaction of components during calorization of niobium alloys with 5 to 50 wt. percent titanium
[AD-747429] 03 p0318 N73-12588
Multifilamentary niobium-titanium superconductors for winding pulsed magnets
[BNL-16764] 03 p0345 N73-12817
Ac measurements of cold worked superconducting niobium-titanium alloy
[CONF-720513-4] 03 p0346 N73-12819
Compatibility of protective coatings for niobium alloy gas turbine blades
[AD-748837] 04 p0439 N73-13575
Solid solution hardening in alloys of niobium-hafnium, niobium-tungsten, and niobium-tantalum
[COO-916-25] 05 p0587 N73-14774
Current voltage characteristics of vapor deposited tungsten niobium planar thermionic converter
[NASA-TM-X-2716] 07 p0819 N73-16639
Solutioning and aging reactions and effects on microstructure and hardness of niobium-based alloys
[AD-752930] 09 p1049 N73-18558
Superconducting properties of niobium titanium multifilamentary magnet material
[BNL-17193] 12 p1388 N73-21255
Performance prediction model and scaling laws for flux pinning in superconducting niobium zirconium and niobium titanium alloys
[COO-3169-13] 12 p1440 N73-21664
Short range structure of Ti and Zr body centered cubic lattice solid solutions containing omega phase
[AD-755454] 13 p1567 N73-22698
High strength tungsten fiber reinforced oxidation resistant niobium alloy composites for use in gas turbine engines at 2000 F
[AD-757380] 14 p1678 N73-23620
Degradation and reuse of radiative-thermal protection materials for space shuttle
[NASA-CR-123587] 14 p1709 N73-23866
Microhardness and corrosion resistance of Zr-Nb alloy prepared by reaction of ZrC with Nb2O5
[BARC-612] 15 p1799 N73-24583
Influence of zirconium additions on diffusivity and solubility of hydrogen and deuterium in niobium alloys at high temperature
[BNWL-SA-4473] 17 p2065 N73-26706
Kinetic of interstital contamination and defect growth in fused slurry silicide coated columbium alloys
[NASA-TN-D-7324] 18 p2160 N73-27448
Computer analysis of binary and ternary titanium and niobium alloys
[AD-761814] 19 p2311 N73-28585
Hydrogen embrittlement of aged tantalum and niobium alloys
[NASA-TM-X-68293] 20 p2431 N73-29525
Thermal cycling effects on structure of cobalt-niobium eutectic alloys
[AD-763706] 21 p2560 N73-30521
Fused slurry silicide protective coatings for niobium alloy reentry heat shields for space shuttles - Vol. 1
[NASA-CR-121216] 23 p2857 N73-32826
Experimental and coating processes for fused slurry silicides on niobium alloy heat shields for space shuttles - Vol. 2
[NASA-CR-134483] 23 p2857 N73-32827
Susceptibility of Zircaloy 4 and niobium base alloy to hydrogen embrittlement at elevated temperature
[LA-5169] 24 p2936 N73-33447

NIOBIUM CARBIDES
Gas phase precipitation method for preparing pure zirconium and niobium carbides
[NLL-RTS-7315] 01 p0069 N73-10563
Producing niobium carbide coatings on carbon steels and hard composite alloys
[NLL-TRANS-746-1314-[9022.40]1] 05 p0560 N73-14547
Temperature relationship of monochromatic coefficients of radiation of titanium, niobium, and zirconium monocarbides in regions of homogeneity
23 p2807 N73-32442
Interaction of powders of carbides of zirconium, niobium, and molybdenum with silicon using X ray and chemical analysis to determine reaction products
23 p2809 N73-32461

NIOBIUM COMPOUNDS
NT NIOBATES
NT NIOBIUM CARBIDES
NT NIOBIUM OXIDES
NT NIOBIUM STANNIDES

Electrical-, thermal-, and magnetic-properties of zirconium and niobium carbide solid solutions
[AD-746217] 02 p0219 N73-11772
Pulsed magnetic field apparatus, and microstructure influence on critical current density of superconducting Nb3Sn strips in pulsed fields
[LBL-448] 06 p0708 N73-15778
Manufacturing of superconducting cylindrical films of niobium and niobium nitride by sputter etch techniques
[AD-752593] 08 p0952 N73-17799
Modification and control of oxide structures on refractory metal alloys and compounds
[AD-761215] 18 p2162 N73-27464
Chemical vapor deposition of stoichiometric niobium gallium superconducting film
[NASA-CR-2308] 20 p2455 N73-29726

NIOBIUM OXIDES
Growth of FeS[x] and NbO2 single crystals
[AD-753270] 09 p1074 N73-18768

NIOBIUM STANNIDES
Magnetization experiments to simulate cusp coil tests
[ORNL-TM-3887] 04 p0459 N73-13744
Cryogenic stability and reliability of operating Nb3Sn coils in helium gas environment
[IPP-4/100] 17 p2063 N73-26690

NITINOL ALLOYS
Experimental and theoretical analysis of martensitic transition of TiNi [Nitinol]
[AD-742767] 02 p0187 N73-11516
Evaluation of nitinol fittings for joining titanium piping for shipboard application
[AD-760322] 17 p2038 N73-26492

NITRATES
NT AMMONIUM NITRATES
NT CELLULOSE NITRATE
NT HYDRAZINE NITROFORM
NT METHYL NITRATE
NT NITROGLYCERIN
NT ORGANIC NITRATES
NT PETN
NT SODIUM NITRATES
Release technique for creating large dense vapor clouds in upper atmosphere using thermite formulation of barium metal and barium nitrate
[AD-745980] 01 p0054 N73-10438
Ammonifying ability of denitrifying bacteria of species pseudomonas fluorescens
[NASA-TT-F-15086] 21 p2501 N73-30068
Synthesis and analysis of poly[vinyl-CO-vinylene]nitrate with 7 to 70 mol percent of vinylene constituents
[ICT-7/72] 22 p2626 N73-31038

NITRIC ACID
Reaction of azotetrazole anion and nitric, sulfuric and hydrochloric acid noting giving of 5-hydrazinotetrazole and 5-azidotetrazole
[ERDE-TN-44] 05 p0507 N73-14123
Photodissociation and formation of nitric acid in mesosphere and stratosphere
[AERONOMICA-ACTA-A-113] 09 p1027 N73-18382
Iron contamination effect in liquid rocket propellant system of high density acid
[AD-755376] 14 p1700 N73-23797
Measurement of absorption cross section values of nitric acid vapor in stratosphere at different wavelengths
[A-117-1973] 16 p1905 N73-25408

NITRIC OXIDE
Infrared absorption bands of nitrous oxide in earth atmosphere
[AD-749879] 05 p0541 N73-14405
Stratospheric nitric oxide production from past nuclear explosions and its relevance to projected SST pollution
[AD-751295] 07 p0795 N73-16466
Attenuation of nitric oxide dissociation in mesosphere and stratosphere
[PSU-IRL-SCI-407] 08 p0917 N73-17518
Dissociation of nitric oxide in mesosphere and stratosphere by attenuation
[AERONOMICA-ACTA-A-112] 09 p1027 N73-18384
Effect on nitric oxide emissions of using premixed prevaporized fuel/air in turbojet combustors
[NASA-TM-X-68220] 12 p1464 N73-21862
OGO-4 ultraviolet spectrometer measurements of nitric oxide fluorescence with diffusive transport model for mesospheric and lower thermospheric nitric oxide photochemistry
13 p1515 N73-22274
Threat of stratospheric ozone nonequilibrium by SST nitric oxide exhaust gases
[AD-757059] 14 p1719 N73-23949
Emission rate constant for infrared chemiluminescent reaction of oxygen with nitric oxide
[NASA-CR-132157] 15 p1747 N73-24158
Difficulty and reliability of simultaneous measurement of ozone and nitric oxide
18 p2132 N73-27228
Kinetic model for nitric oxide formation from organic fuel nitrogen
[FML-PUBL-73-7] 22 p2625 N73-31032
Formation of nitric oxide in steady laminar diffusion flame
22 p2727 N73-31825
Nitric oxide spectral line width for stratospheric aeronomical analysis
[A-114-1973] 23 p2819 N73-32536
Determination of nitric oxide concentrations from eclipse variations of ion concentrations
24 p2994 N73-33926

NITRIDES
NT SILICON NITRIDES
NT TITANIUM NITRIDES
NT ZIRCONIUM NITRIDES
Fabrication of uranium mononitride fuel pin assembly for fast lithium cooled space power reactor
[NASA-CR-120956] 05 p0579 N73-14710
Fission-gas release from uranium nitride at high fission-rate density
[NASA-TN-D-7171] 08 p0942 N73-17718
Manufacturing of superconducting cylindrical films of niobium and niobium nitride by sputter etch techniques
[AD-752593] 08 p0952 N73-17799
Evaluation of uranium nitride for in-core thermionic applications in electrically heated thermal gradient tests and in flat plate thermionic converters
[NASA-CR-131520] 12 p1416 N73-21470
High temperature tests to determine thermodynamic properties of nonstoichiometric vanadium nitrides
[NLL-M-21551-[5828.4F]] 12 p1464 N73-21858
Borides, carbides, and nitrides of silicon oxidation resistant refractory compounds for use in gas turbines and reentry vehicles
14 p1678 N73-23616
Noise in metal nitride oxide semiconductor devices
[AD-760544] 18 p2124 N73-27163
Development of manufacturing method for elimination of nitride inclusions from titanium alloys during melting and ingot consolidation
[AD-748261] 18 p2163 N73-27473
Effect of various growth and doping parameters on GaN for LED applications
[NASA-CR-132263] 18 p2189 N73-27676
Laser motivated studies of chemiluminescence in metal oxides and nitrides
21 p2554 N73-30477
Fission gas release rates from irradiated uranium nitride specimens
[NASA-TM-X-2890] 23 p2818 N73-32530
Magnetic and specific heat measurements of carbides, nitrides, and uranium and thorium sulfides
[CEA-R-4453] 24 p2943 N73-33506

NITRIDING
Effect of nitriding on mechanical properties of niobium
[AD-747450] 03 p0318 N73-12593

NITRILES
NT ACRYLONITRILES
NT PHOSPHONITRILES
Intumescent paint containing nitrile rubber for fire protection
[NASA-CASE-ARC-10196-1] 04 p0437 N73-13562
Molecular orbital energies in spectra of tervalent titanium chlorocomplexes
13 p1542 N73-22493

NITRITES
Photolysis of CH3ONO
[NASA-CR-131355] 11 p1285 N73-20425

NITRO COMPOUNDS
NT NITROGLYCERIN
NT NITROGUANIDINE
NT NITROMETHANE
NT TRINITRO COMPOUNDS
NT TRINITROTOLUENE
Polystyrene energy transfer studies using nitrostyrene compounds
[TN-257] 09 p0999 N73-18149
Concentration fluctuations in critical region of binary liquid mixture 3-methylpentane-nitroethane
[AD-759740] 16 p1872 N73-25158

NITROBENZENES
NT TRINITROTOLUENE

NITROCELLULOSE
U CELLULOSE NITRATE

NITROFORMS
NT HYDRAZINE NITROFORM

NITROGEN
NT LIQUID NITROGEN
NT NITROGEN ATOMS
NT NITROGEN IONS
NT NITROGEN ISOTOPES
Excitation and deexcitation of vibration in gases by oxygen and nitrogen atoms in E region of earth atmosphere
[AD-745925] 01 p0054 N73-10437
Drift tube mass spectrometer for measuring reaction rate of uranium atoms and ions with O2 and N2
[AD-746272] 02 p0138 N73-11115
Temperature measurements on vibrational excited microwave discharged nitrogen
[AD-746327] 02 p0138 N73-11118
Low energy electron impact excitation and ionization rate coefficients for atmospheric nitrogen and oxygen
[AD-747244] 02 p0170 N73-11378
High pressure nitrogen gas discharge initiated by fast electron beams of 100 to 300 keV energies
[DRIC-TRANS-2857] 02 p0212 N73-11716
Excitation of N I ultraviolet multiplets by electron impact on atomic nitrogen
[NASA-CR-129087] 02 p0214 N73-11730
Time of flight measurement of N2 plus meinel lifetimes
[AD-746157] 02 p0214 N73-11735
Vibration-translation and vibration-vibration relaxation rates in rapid expansions of N2 and CO2 in argon
[AD-746068] 02 p0216 N73-11751
Small scale nozzle tests using heated nitrogen for effectiveness and wall heat transfer studies with hydrogen film cooling
[NASA-CR-120926] 02 p0242 N73-11970
Photoelectron effect on second positive system of nitrogen bands in daytime glow of atmosphere from Cosmos 224 data
05 p0536 N73-14360
Intergranular corrosion resistance of matching and dissimilar welds in nitrogen-bearing and nitrogen-free austenitic steels
[NLL-TRANS-746-1313-[9022.401]]
05 p0560 N73-14546
Analysis of electron beam induced discharge in nitrogen at high pressure
[NLL-DRIC-TRANS-2857-[3623.66]]
05 p0579 N73-14714
Thermal conductivity of air and nitrogen at high temperatures
[AD-749842] 05 p0607 N73-14934
Theoretical model of Raman rotational spectrum of gas mixture applied to air mixture of oxygen and nitrogen to determine temperature
[NASA-TN-D-7126] 06 p0679 N73-15525
Microphotometer analysis of absorption spectra, physical and chemical properties of NO2 system in Martian atmosphere
07 p0752 N73-16107
Equation of state for compressibility of helium, nitrogen, and their mixtures
[JPRS-57923] 07 p0752 N73-16111
Electronic and ionic reactions in atmospheric gases
[AD-752582] 08 p0921 N73-17550
Absolute intensity, polarization, and relative line intensities of rotational Raman scattering spectra from nitrogen, oxygen, and carbon dioxide
[NASA-CR-121091] 08 p0946 N73-17746
Reaction kinetics in vibrationally excited nitrogen quenching by atomic oxygen
[AD-752542] 08 p0946 N73-17751
Rotational temperature measurement in nitrogen using unresolved rotational spectra
[DLR-FB-72-15] 09 p0998 N73-18148
Vertical distribution of vibrationally excited molecular nitrogen in thermosphere corresponding to stable auroral red arc
[NASA-TM-X-66194] 09 p1028 N73-18390
Theoretical model of optical excitation, emission, and deactivation properties of Meinel band system of nitrogen
[AD-753396] 09 p1069 N73-18722
Analyses of vibrational levels by least squares method for determining transition moment probabilities in nitrogen band
[AD-753394] 09 p1075 N73-18774
Equation of state for helium and nitrogen mixture
[AD-753964] 11 p1253 N73-20169
Controlled nitrogen additions on mechanical properties of tantalum tubing in nuclear reactors
[NASA-TN-D-6999] 11 p1305 N73-20587
Metallurgical reports on plasma jets, creep properties of nickel alloys, oxygen and nitrogen interactions with metals, and Mossbauer effect as applied to diffusion mechanisms
[JPRS-58508] 12 p1412 N73-21445
Nitrogen exchange between furnace atmosphere and argon plasma arc when melting pure iron
12 p1413 N73-21447
Variations of relative abundances of helium, carbon, nitrogen, oxygen, and iron-group nuclei in solar cosmic rays and their relationship to solar particle acceleration
[NASA-TM-X-66228] 12 p1445 N73-21706
Design and evaluation of electrochemical nitrogen-hydrogen separator for use in spacecraft nitrogen generator
[NASA-CR-114580] 13 p1534 N73-22431
Absolute cross sections for rotational Raman scattering derived for nitrogen and oxygen from near UV to infrared
[AD-756808] 13 p1566 N73-22695
Bibliography of kinetic data in gas phase reactions of nitrogen, oxygen, and nitrogen oxides
[NBS-SP-371] 14 p1616 N73-23094
Experimental facility for measuring rotational Raman scattering cross sections of nitrogen and oxygen at 10.6 microns
[AD-757111] 14 p1617 N73-23098
Nuclear magnetic resonance method for chemical shifts of amino acids and hybrid state of nitrogen atom
[NASA-TT-F-14893] 14 p1694 N73-23750

Mathematical models for determining transport properties and dissociation equilibrium of N2 and O2 in high temperature air
[FSDU-00.01.07-AMEND-A] 14 p1718 N73-23937
Determination of vibrational temperature of molecular nitrogen in high atmosphere by chemical release of hydrogen iodide from sounding rocket
[AD-757909] 15 p1782 N73-24448
Effects of aluminum oxide on Raman scattering from nitrogen and oxygen
[AD-758913] 15 p1824 N73-24781
Optical and microwave measurements of reaction kinetics behind shock waves
[AD-757230] 16 p1890 N73-25293
Ultrahigh vacuum techniques for diffusivity and solubility of N2 in Mo and N2 trapping by C in Mo
[UCRL-51182] 17 p2045 N73-26544
Optical electron excitation cross section measurements of nitrogen at high temperatures
[AD-762257] 19 p2232 N73-28000
Determination of rotational temperatures in flow gas discharges containing nitrogen using sidelight spectroscopy techniques
[AD-762290] 19 p2233 N73-28002
CO releases at high altitude to determine atmospheric N2 vibrational temperature
[AD-762316] 19 p2298 N73-28480
Electron microscopic study of stress corrosion cracking behavior of austenitic stainless steel having increased nitrogen content in boiling MgC42
20 p2427 N73-29495
Chemical reactivity of hydrogen, nitrogen, and oxygen below 100 K
[NASA-CR-133654] 20 p2456 N73-29742
Nitrogen and ozone kinetics in stratosphere
[AERONOMICA-ACTA-A-118] 21 p2537 N73-30345
Oxidation of nitrogen and ball lightning
[AD-763146] 21 p2539 N73-30358
Determination of vibrational energy of nitrogen in upper atmosphere
[AD-763749] 21 p2541 N73-30377
Methanol heat pipe using nitrogen gas for temperature control
[NASA-CR-114597] 21 p2606 N73-30884
Kinetic model for nitric oxide formation from organic fuel nitrogen
[FML-PUBL-73-7] 22 p2625 N73-31032
Stabilities of nitrogen containing heterocyclic radicals, computation of simple potential energy surfaces, and photophysical properties of indolizine
[NASA-CR-133919] 22 p2625 N73-31034
Gas sensor for detecting H2 in air and N2, and O2 in N2
[NASA-CR-133891] 22 p2674 N73-31416
Vibrational cross section resonances of excited state in nitrogen and carbon monoxide
[AD-764596] 23 p2754 N73-32042
Simultaneous determination of carbon, hydrogen, and nitrogen in organic compounds
[UCID-16198] 24 p2892 N73-33085
Distribution of vibrationally excited molecular nitrogen in auroral red arc and effect on ionospheric electron densities
24 p2912 N73-33241

**NITROGEN ATOMS**
Mach-Zehnder interferometric determination of nitrogen and oxygen atom specific refractivities during atmospheric entry
[AD-745132] 02 p0138 N73-11114
Electron impact excitation and ionization cross sections of nitrogen atoms
[AD-749807] 05 p0582 N73-14742
Nuclear reactions in hydrogen exhausted zone of star during supernova explosion and nuclei syntheses through nitrogen conversion
13 p1575 N73-22762
Excitation and deexcitation of vibration in gases by nitrogen and oxygen atoms in upper atmosphere
[AD-757050] 14 p1617 N73-23099

**NITROGEN COMPOUNDS**
NT AMMONIA
NT AMMONIUM NITRATES
NT ATROPINE
NT AZIDES [INORGANIC]
NT AZO COMPOUNDS
NT CARBAMIDES
NT CELLULOSE NITRATE
NT CYANO COMPOUNDS
NT DIISOCYANATES
NT HYDRAZINE NITROFORM
NT HYDRAZOIC ACID
NT HYDROCYANIC ACID
NT ISOCYANATES
NT LIQUID AMMONIA
NT METHYL NITRATE
NT NITRATES
NT NITRIC ACID
NT NITRIC OXIDE
NT NITRIDES
NT NITRITES
NT NITRO COMPOUNDS
NT NITROGEN DIOXIDE
NT NITROGEN OXIDES
NT NITROGEN TETROXIDE
NT NITROGLYCERIN
NT NITROGUANIDINE
NT NITROMETHANE
NT NITROUS OXIDES
NT ORGANIC NITRATES
NT PETN
NT PHOSPHONITRILES
NT POLYIMIDES
NT RDX
NT SILICON NITRIDES
NT SODIUM NITRATES
NT TITANIUM NITRIDES
NT TRINITRO COMPOUNDS
NT TRINITROTOLUENE
NT UREAS
NT ZIRCONIUM NITRIDES
Dynamics of nitrogenous cerebral metabolites accompanying repeated hypothermia and subsequent self-heating
11 p1244 N73-20097
Investigation of electrical properties of vanadium nitrides as effected by nitrogen content
13 p1540 N73-22473
Distribution of odd nitrogen in lower stratosphere and perturbations caused by stratospheric air transport
[NASA-CR-2314] 21 p2536 N73-30336

**NITROGEN DIOXIDE**
Infrared absorption spectra of stratospheric nitrogen dioxide
02 p0164 N73-11330
Reaction kinetics of nitroguanidine-nitrogen dioxide mixture
[TDCK-60180] 02 p0221 N73-11787
Chemiluminescence of O plus NO2 in afterglow
[NASA-CR-130263] 05 p0539 N73-14383
Dual gas correlation spectrometer measurements of sulfur dioxide and nitrogen dioxide in industrial area of southern California
[PB-210717] 05 p0575 N73-14676
Polymer gas reactions in air pollutants such as NO2 and SO2 as function of pressure, UV light, temperature, and morphology
08 p0882 N73-17140
Design of time of flight chemical accelerator for low center-of-mass energy spreads and measurement of electron affinity of N02
[AD-753133] 09 p1012 N73-18258

**NITROGEN IONS**
Cosmos 224 observations of N2 ions during medium solar activity
03 p0293 N73-12389

**NITROGEN ISOTOPES**
Separation of short half life O-15 and N-13 isotopes from alkali metals, steels, copper, and indium by gamma activation analysis
[CONF-721069-24] 18 p2160 N73-27453

**NITROGEN OXIDES**
NT NITRIC OXIDE
NT NITROGEN DIOXIDE
NT NITROGEN TETROXIDE
NT NITROUS OXIDES
Three laser methods of remotely mapping gaseous pollutants of atmosphere
[AD-746280] 02 p0205 N73-11664
Measurement of pollutant levels of nitrogen oxides, unburned hydrocarbons, and carbon monoxide for annular, swirl can combustor
[NASA-TM-X-68160] 02 p0243 N73-11974
Laboratory experiments and mathematical models of nitrogen oxide formation in combustion of fossil fuels
[PB-211480] 05 p0606 N73-14932
Public health exposure limits to nitrogen oxide, hydrogen chloride, and hydrogen fluoride air pollutants
[AD-751438] 07 p0748 N73-16084
Modification of jet engine fuels to reduce emissions of nitrogen oxides from jet aircraft turbine engines
[AD-752581] 08 p0953 N73-17803
Nitrogen oxide and ammonia removal from spacecabin atmosphere by catalytic oxidation with ruthenium and adsorption on silica gel
[NASA-CR-2132] 09 p0999 N73-18151
Mass spectrometric analysis of reactions of nitrogen oxide and nitrogen dioxide with hydrogen peroxide at 25 C
[NASA-CR-130831] 09 p0999 N73-18155
Relative importance of processes determining vertical distribution of nitrogen oxides in stratosphere
[AERONOMICA-ACTA-A-110] 09 p1027 N73-18383
Photolysis of ozone at 3130 A in presence of excess of nitrogen oxide
[NASA-CR-130794] 09 p1028 N73-18388
N2O photolyzed at 2139 A producing O[1 D] atoms in H2O and CO
[NASA-CR-130976] 09 p1029 N73-18398
High resolution spectra of NO2 continuum emission from production of O2[1 Delta g] and O2[1 Sigma g plus] in reaction of NO with O3
[DREV-TN-2050/72] 10 p1125 N73-19166
Analysis of correlation between Martian surface temperature deviations and theory of nitrogen oxides on Mars
10 p1211 N73-19849
Nitroxide free radicals as spin labels in biochemical systems
[NASA-TT-F-14866] 11 p1247 N73-20125
Measurement of fluorescence yield in self quenched and foreign gas quenched NO2
[NASA-CR-131296] 11 p1285 N73-20426
Effect of inlet-air humidity on formation of oxides of nitrogen from a gas turbine combustor under various air inlet temperature conditions
[NASA-TM-X-68209] 12 p1443 N73-21691
Physical and chemical nature of N2O flow decay in liquid propellants
[AD-755378] 13 p1489 N73-22070
Prevention of N2O4 flow decay by means of contaminant removal through distillation and filtration
[AD-755380] 13 p1569 N73-22717
Bibliography of kinetic data in gas phase reactions of nitrogen, oxygen, and nitrogen oxides
[NBS-SP-371] 14 p1616 N73-23094
Electron collision processes in atmospheric gases of oxygen, carbon monoxide, and nitrogen oxide
[AD-757841] 15 p1748 N73-24170
Establishment of criteria for oxides of nitrogen emissions to control air pollution contribution from aircraft operating at major air terminals - Vol. 1
[REPT-1162-1-VOL-1] 15 p1825 N73-24789
Numerical analysis of process for nitrogen oxide formation in aircraft engine exhaust products and development of computer program for application of theory - Vol. 2
[REPT-1162-2-VOL-2] 15 p1825 N73-24790
Development of computer program to analyze flow conditions in gas turbine compressor for application to reduction of nitrogen oxides from aircraft engine exhaust - Vol. 3
[REPT-1162-3-VOL-3] 15 p1825 N73-24791
Analysis of factors causing nitrogen oxides in exhaust gases of gas turbine engines and development of models of flow in gas turbine combustor
[NASA-CR-132959] 16 p1955 N73-25821
Nitrogen oxides from supersonic transports affecting stratospheric ozone depletion on solar ultraviolet radiation
[AD-761179] 18 p2195 N73-27722
Effect of inlet air humidity on exhaust gas emissions of nitrogen oxides in gas turbine combustor
[NASA-TN-D-7396] 23 p2856 N73-32822

**NITROGEN PLASMA**
Microwave probe studies on chemical additives behavior in nitrogen oxygen plasma
[AD-748469] 04 p0456 N73-13724
Production of HCN by pyrolysis of hydrocarbons in nitrogen plasma
[NASA-TT-F-14685] 07 p0854 N73-16925
Probe measurements of electron energy in glow discharge of nitrogen plasma and air
[AD-752871] 09 p1071 N73-18744
Composition calculation of nitrogen plasma in local thermodynamic equilibrium for determining electrical conductivity and continuum radiation
[DLR-FB-73-51] 23 p2822 N73-32563

**NITROGEN TETROXIDE**
Buffered gelled water to control nitrogen tetroxide-aerozine 50-hypergolic fuel fires
[NASA-CR-2198] 10 p1203 N73-19789

**NITROGLYCERIN**
Sonic boom nitroglycerin resistance noting shock simulation and sonic boom effect on detonation
[ISL-14/72] 07 p0822 N73-16658

**NITROGUANIDINE**
Reaction kinetics of nitroguanidine-nitrogen dioxide mixture
[TDCK-60180] 02 p0221 N73-11787

**NITROMETHANE**
Shock initiation of reaction in RDX/TNT, nitromethane explosives, and double base propellants
[ERDE-TR-103] 05 p0606 N73-14930

**NITROUS OXIDES**
Formation of nitrous oxide molecules from ion-molecule reactions following sea level nuclear burst
[AD-746958] 03 p0298 N73-12428

**NOBLE GASES**
U RARE GASES

**NOBLE METALS**
NT GOLD
NT RUTHENIUM
NT SILVER
Characteristics of noble metal thermocouples under prescribed temperature ranges and environmental conditions to determine effects on accuracy and stability of temperature measurements
[NASA-CR-120990] 08 p0925 N73-17578

**NOCTILUCENCE**
U LUMINESCENCE

**NOCTILUCENT CLOUDS**
Mesospheric circulation and noctilucent clouds
[NASA-TT-F-14712] 01 p0105 N73-10866
Kinematics of noctilucent clouds and wind discontinuities at mesopause
[NASA-TT-F-14928] 14 p1660 N73-23471
International cooperation in noctilucent cloud research
[NASA-TT-F-14950] 17 p2026 N73-26390

Polarization photometers in payload of sounding rocket for noctilucent cloud particle sampling
[AD-760149] 17 p2028 N73-26415
NOISE
Similarity law analysis on flow noise due to cavity resonator
[AD-749673] 05 p0581 N73-14731
NOISE (SOUND)
NT AERODYNAMIC NOISE
NT AIRCRAFT NOISE
NT ENGINE NOISE
NT JET AIRCRAFT NOISE
NT SONIC BOOMS
Behavior of alpha-beta tracker for maneuvering targets under noise, false target, and fade conditions
[AD-748993] 04 p0391 N73-13182
Noise and blast environments providing definition of units and techniques of noise measurement and giving booster-launch and spacecraft noise data
06 p0629 N73-15106
Estimates of LC stress response in aircraft skin panels to random acoustic loads
[ESDU-67028-AMEND-A] 06 p0723 N73-15904
Hydraulic system noise study, emphasizing airborne pump noise
[AD-757776] 15 p1769 N73-24333
Speech discrimination by personnel with hearing loss at 3 kHz in noise
[AD-752974] 16 p1867 N73-25118
Model scale air jets for sound study of coaxial circular jets
[FAA-RD-71-101-VOL-1] 20 p2454 N73-29721
Noise standards for habitable houses, rest homes, hospitals, camps, public facilities, and streets in residential areas
[NASA-TT-F-15065] 21 p2503 N73-30088
NOISE ATTENUATION
U NOISE REDUCTION
NOISE ELIMINATION
U NOISE REDUCTION
NOISE GENERATORS
Noise sources and noise scaling laws of externally blown STOL flaps
03 p0250 N73-12024
Measurement of sound generated by impingement of turbulent jet on elastic plates
[DGLR-PAPER-72-85] 04 p0373 N73-13032
Design of noise source for simulating supersonic spinning modes in duct acoustics
[NASA-CR-2260] 12 p1364 N73-21067
Computerized analysis of noise quality on microwave equipment
[AD-756862] 13 p1504 N73-22192
Narrowband noise generation by flow over perforated or ventilated transonic wind tunnel walls
[AD-758254] 15 p1763 N73-24283
Turbomachinery noise generation and control
[NASA-TM-X-68253] 16 p1957 N73-25831
Application of cross-spectral analysis to measurement of contribution of noise sources
[ISAS-493] 18 p2179 N73-27591
Far field sound propagation calculation for ducted fan rotor-stator interaction
[NRC-13260] 18 p2179 N73-27592
Diagnostic techniques for measurement of aerodynamic noise in free field and reverberant environment of wind tunnels
[NASA-CR-114636] 21 p2579 N73-30669
NOISE HAZARDS
U HAZARDS
U NOISE (SOUND)
NOISE INJURIES
Structural vibration and noise effects on man in aerospace operations
[AGARDOGRAPH-151] 08 p0876 N73-17098
Airborne noise in aerospace operations and bioacoustics effects on man
08 p0876 N73-17100
Interchangeability of earmuff cushions with respect to sound attenuation, including noise-pressure measurements
[IZF-1973-1] 14 p1692 N73-23729
Hazards of exposure to noise, fumes and vapors in military environment
14 p1723 N73-23985
Noise effects on human hearing process and central nervous system functions
[NASA-TT-F-748] 19 p2223 N73-27935
NOISE INTENSITY
Procedure for determining noise levels in flight test measuring systems
01 p0056 N73-10456
Human tolerance and adaptation in long term exposure to sonar signals at elevated intensities
[AD-746103] 02 p0134 N73-11089
Analysis of effective perceived noise level method for determining airport noise and comparison with actual noise measurements taken during aircraft landings
[UCLA-PAPER-ENG-0872] 03 p0249 N73-12010
Noise output of turbofan engine with acoustically treated nacelle
03 p0250 N73-12020
Noise output from quiet engine during simulated takeoff and approach tests
03 p0250 N73-12021
Definition of supersonic aircraft jet noise generation and methods for reducing noise intensity - Vol. 2
[AD-749137] 05 p0495 N73-14036
Evaluation of subjective annoyance caused by noise generated by turbofan short takeoff aircraft and comparison with noise of conventional takeoff aircraft
[NASA-TN-D-7102] 06 p0621 N73-15040
Depth effect on underwater ambient noise intensity in Caribbean Sea
[AD-750693] 06 p0670 N73-15447
Computerized prediction of noise levels for jet aircraft with or without noise suppression devices
[NASA-CR-114517] 06 p0700 N73-15708
Airborne noise in aerospace operations and bioacoustics effects on man
08 p0876 N73-17100
Standardized performance battery for assessing effects of environmental stressors particularly noise on human performance
[NASA-CR-2149] 08 p0877 N73-17102
Unique field-laboratory methodology for assessing human response to noise
[NASA-CR-2221] 09 p0995 N73-18124
Noise intensities of rectangular and circular supersonic nozzle geometries
[NASA-CR-130964] 09 p1067 N73-18704
Analysis of aircraft noise environment for land areas in vicinity of military air bases
[AD-754111] 10 p1107 N73-19028
Analysis of helicopter internal and external noise levels for various flight conditions and timing of acoustical spectra
12 p1362 N73-21055
Analysis of common aircraft noise measures in terms of selected human response for jet transport aircraft
[FAA-RD-71-112] 12 p1365 N73-21074
Measurement and analysis of aircraft noise generated by general aviation aircraft during level flyovers
[TR-S-212] 12 p1366 N73-21081
Noise characteristics of functional correlators using nonlinear elements with exponential characteristics
12 p1386 N73-21241
Analysis of effects of aircraft noise in residential communities near London, England airport
[TT-7302] 14 p1599 N73-22966
Noise properties and circuits to cancel noise in gas parametric amplifiers
15 p1756 N73-24230
Evaluation of courses of action and costs to reduce aircraft noise levels in vicinity of airports
[PB-215611/5] 16 p1862 N73-25080
Military design standard for noise producing equipment
[AD-750649] 16 p1945 N73-25735
Measured noise level data for proposed airport sites in Florida
[PB-214459/0] 16 p1945 N73-25737
Analysis of reverberant-field noise produced by three lift fan models operating at various rotor tip speeds
[NASA-TM-X-68243] 17 p1981 N73-26014
Development of noise index based on slow and fast noise level variation perception, and applied to aircraft noise data
[REPT-3/1973] 19 p2220 N73-27911
GaAs and InP reflection amplifier noise figure and power gain at extremely high frequencies
[ESRO-CR(P)-262] 19 p2244 N73-28088
Power gain and noise figure of indium phosphide and gallium arsenide microwave reflection amplifiers
19 p2244 N73-28090
Measurement of sound power levels, power spectra, and directivity patterns for jet exit velocities of F-111A aircraft
[NASA-TN-D-7376] 20 p2361 N73-28989
High intensity noise effects on urinary K-Na ratios in rats
20 p2365 N73-29018
Development of noise standard for permissible noise levels in air traffic control and navigational facilities
[FAA-RD-72-47] 20 p2452 N73-29708
Influence of combined rotary flow inductors and dry turbojets on side line noise levels of supersonic transports
[NASA-TM-X-68233] 20 p2466 N73-29809
Development of computer program to predict aerodynamic noise levels of V/STOL aircraft at various points in flight trajectory
[PB-221140/7] 21 p2499 N73-30054
Calculation procedures for predicting noise-time histories and noise contours for various types of aircraft
[NASA-CR-114649] 23 p2741 N73-31945
Analysis of jet engine noise to show sources of noise, noise spectra, and use of laminates and composite materials for noise reduction
24 p2875 N73-32962
NOISE MEASUREMENT
U ACOUSTIC MEASUREMENTS
NOISE METERS
Jet aircraft noise and sonic boom measuring device which converts sound pressure into electric current
[NASA-CASE-LAR-11173-1] 13 p1529 N73-22387
Electrotactile sound detector for deaf to detect and localize sounds
14 p1627 N73-23188
NOISE POLLUTION
Economic analysis of reducing and controlling environmental noise
[PB-206726] 01 p0081 N73-10666
Noise abatement and measurement, and human response to noise
[PB-210591] 01 p0081 N73-10671
Procedures for determining present and predicted noise exposure at residential construction sites
[PB-210590] 01 p0081 N73-10672
Analysis of noise pollution by military vehicles, public transportation, farm equipment, private automobiles, and construction equipment
[AD-747685] 03 p0338 N73-12754
Propagation model for V/STOL aircraft noise in urban area
[PB-211953] 05 p0581 N73-14729
Bibliography of USAF reports on air, water, noise, and radiation pollution
[AD-751898] 08 p0940 N73-17699
Suppression of turbine engine inlet noise
[AD-753000] 09 p1079 N73-18806
Noise measurements and frequency analysis for noise pollution control
[TR-7209.602] 10 p1164 N73-19473
Noise pollution effects on human communities
[PB-213021] 11 p1325 N73-20756
Acoustic measurement methods for evaluating aircraft noise pollution in urban areas
[PB-212875] 11 p1326 N73-20757
Control of transportation noise pollution
[PB-213007] 11 p1326 N73-20758
Guidelines for urban control of aircraft noise pollution
[PB-213020] 11 p1326 N73-20759
Environmental effects and plans for controlling urban TACV noise levels
13 p1506 N73-22209
Environmental impact of noise produced by transonic wind tunnel at Arnold Engineering Development Center
[AD-757552] 14 p1646 N73-23351
Bibliography of documents on noise pollution
[NASA-CR-131988] 14 p1692 N73-23734
Narrowband noise generation by flow over perforated or ventilated transonic wind tunnel walls
[AD-758254] 15 p1763 N73-24283
Combination of noise from separate time varying sources
[PB-214250/3] 16 p1945 N73-25738
Effect of finite source size on power statistics in reverberant room for pure tone excitation
[NASA-CR-132279] 18 p2179 N73-27594
Optical holographic measurement of jet noise in supersonic air/nitrogen and helium jets at Mach numbers from 1.5 to 3.4
[PB-220641/5] 21 p2581 N73-30686
Daytime noise environment in Tucson, Arizona
[EE-SER-40] 24 p2921 N73-33332
Abstracts of reports concerning noise pollution
[NASA-CR-135954] 24 p2956 N73-33618
NOISE PROPAGATION
Development of unified theory of jet engine noise based on fluctuating motions in fluids - Vol. 3
[AD-749138] 05 p0496 N73-14037
Analysis of noise sources associated with supersonic jet noise and establishment of effects of refraction on radiated field of sources - Vol. 5 App. 1
[AD-749141] 05 p0496 N73-14039
Development of remote sensing devices to measure jet exhaust fluctuating density gradients, mean and turbulent velocity, and mean temperature Vol. 6
[AD-749143] 05 p0496 N73-14041
Analysis of jet aircraft noise propagation near airports and methods for reducing noise intensity
[NASA-TT-F-14655] 06 p0700 N73-15707
Application of finite difference techniques to noise propagation in jet engine ducts
[NASA-TM-X-68261] 17 p1981 N73-26015
Design of ventilated walls for transonic wind tunnels with analysis of parameters affecting noise generation
17 p2014 N73-26285
Finite difference theory of noise propagation in turbofan engine ducts
[NASA-TN-D-7339] 24 p2972 N73-33744
NOISE REDUCTION
Noise attenuation characteristics of cylindrical suppressors with duct lining composed of honeycomb cells covered with perforated plate
[NASA-TM-X-2652] 01 p0005 N73-10032
Economic analysis of reducing and controlling environmental noise
[PB-206726] 01 p0081 N73-10666
Noise abatement and measurement, and human response to noise
[PB-210591] 01 p0081 N73-10671
Aerodynamic component test results of Fan C, high-bypass-ratio, low-aerodynamic loading, single stage fan
[NASA-CR-120981] 02 p0222 N73-11799

Conference on reduction and suppression of aircraft engine noise
[NASA-SP-311] 03 p0249 N73-12012
Quiet Engine Program technology application to low noise aircraft development
03 p0249 N73-12013
Turbofan design parameters for optimal acoustic and aerodynamic performance
03 p0249 N73-12014
Design and performance of suppressors for acoustic noise reduction in turbofan engines
03 p0249 N73-12015
Jet noise suppression in turbofan engines at various exhaust flow velocities
03 p0249 N73-12016
Structural changes in high bypass ratio engines for fan noise reduction to jet noise level
03 p0249 N73-12017
Performance of shrouded and unshrouded fans in low noise turbofan engines
03 p0249 N73-12018
Performance prediction for acoustically lined engine nacelle design
03 p0250 N73-12019
Estimates of reduced noise levels for turbofan engines with sound suppressors
03 p0250 N73-12022
Suppression of fan noise and effects on short takeoff aircraft systems design
03 p0250 N73-12023
Noise sources and noise scaling laws of externally blown STOL flaps
03 p0250 N73-12024
Design of augmentor wing jet flap configuration with minimum noise generation for jet STOL transport aircraft
03 p0250 N73-12025
Suppression of turbofan engine sonic inlet noise in STOL propulsion by use of acoustic nozzle insert
03 p0250 N73-12026
Audio equipment for removing impulse noise from audio signals
[NASA-CASE-NPO-11631] 03 p0277 N73-12244
Aerodynamic analytical model for reducing supersonic jet exhaust noise
[AD-747774] 03 p0337 N73-12752
Development of procedures for quieting externally-blown-flap noise sources produced by interaction of jet exhaust flow with deployed flaps
[NASA-CR-112166] 04 p0372 N73-13022
Acoustic feedback of subsonic and supersonic free jet impinging on obstacle, e.g. blown flap or ground, and noise reduction methods
[DGLR-PAPER-72-84] 04 p0373 N73-13031
Noise reduction and control in FAA air traffic control, navigational, and service facilities
[J-6250] 04 p0401 N73-13264
Definition of supersonic aircraft jet noise generation and methods for reducing noise intensity - Vol. 2
[AD-749137] 05 p0495 N73-14036
Noise exposure model MOD-5 - Vol 1
[PB-211979] 05 p0497 N73-14049
Noise exposure model MOD-5 - Vol 2
[PB-211976] 05 p0497 N73-14050
Exhaust nozzle for reducing noise in gas turbines by mixing low velocity air with high velocity engine exhaust
[NASA-CASE-LEW-11569-1] 05 p0590 N73-14792
Acoustic properties of supersonic fan
[NASA-TN-D-7096] 06 p0619 N73-15025
Reduction of noise generated by externally blown flaps using slot near trailing edge of flap with low velocity secondary air blown through slot
[NASA-TM-X-68172] 06 p0619 N73-15027
Computerized prediction of noise levels for jet aircraft with or without noise suppression devices
[NASA-CR-114517] 06 p0700 N73-15708
Effect of nozzle inlet shape, lip thickness, and exit shape and size on subsonic jet noise
[NASA-TM-X-68182] 07 p0821 N73-16655
Effect of dynamic absorbers and damping on noise generated by CH-47 helicopter rotor transmission
[AD-752579] 08 p0868 N73-17031
Evaluation of head-up display instrument for providing aircraft vertical guidance during landing approach to comply with noise abatement procedures
[NASA-TM-X-62187] 09 p0982 N73-18021
Far and near sound fields of Do-31 aircraft, and noise reduction for future VSTOL aircraft
[BMVG-FBWT-72-23] 09 p0985 N73-18045
Application of sound suppression techniques to OH-6 helicopter and measurement of resultant noise reduction
[AD-753646] 09 p0989 N73-18077
Suppression of turbine engine inlet noise
[AD-753000] 09 p1079 N73-18806
Electrothermal acoustics model for predicting and suppressing combustion instability in rocket motors
[AD-753111] 09 p1079 N73-18807
Analysis of special problems and issues involved in the long range of aviation with emphasis on 1 aa Vol. 2
[PB-215804] 09 p1101 N73-18984
Concepts for achieving low noise levels for V/STOL aircraft
[NASA-CR-120970-VOL-1] 10 p1106 N73-19018
Development of techniques for reduction of aircraft noise generated by short takeoff aircraft
[NASA-TM-X-68195] 10 p1106 N73-19021
Adaptive equalization of pulse amplitude modulated signal with noise interference by successive iterative methods
[NASA-TR-R-402] 10 p1128 N73-19190
Model of jet aircraft shock cell noise generation and reduction
[NRC-12923] 10 p1188 N73-19666
Jet aircraft exhaust nozzle for noise reduction
[NASA-CASE-LAR-10951-1] 10 p1207 N73-19819
Analysis of basic acoustic characteristics and noise reduction potential of upper surface of blown flap
[NASA-CR-112246] 11 p1234 N73-20017
Interference rejection by adaptive antenna array in spread spectrum communication system
[AD-754444] 11 p1258 N73-20211
Control of transportation noise pollution
[PB-213007] 11 p1326 N73-20758
Reduction of jet engine noise due to turbulent mixing of exhaust gases with ambient atmosphere
[NASA-CASE-ARC-10712-1] 11 p1334 N73-20826
Analysis of aerodynamic noise produced by rotary wings and methods for noise reduction based on shed vortex wakes and blade tip modification
12 p1362 N73-21053
Shrouded divergent body attached to exhaust nozzle for jet noise suppression
[NASA-CASE-LEW-11286-1] 12 p1364 N73-21066
Design and aerodynamic performance of low speed fan stage for low noise turboengine
[NASA-CR-121148] 12 p1364 N73-21070
Research in aircraft noise and sonic booms reduction, remote sensing of water pollution, and earth surface changes
[DLR-MITT-72-15] 12 p1375 N73-21153
Optimization of noise immunity of analog signal transmission channels by preemphasis, exemplified for AM or FM channel
[DLR-FB-73-09] 12 p1379 N73-21188
Performance and noise reducing properties of thrust augmentors
[NASA-TM-X-62250] 13 p1472 N73-21921
Environmental effects and plans for controlling urban TACV noise levels
13 p1506 N73-22209
Development of annular acoustically porous elements for installation in exhaust and inlet ducts of turbofan engine to reduce aircraft engine noise intensity
[NASA-CASE-LAR-11141-1] 14 p1600 N73-22975
Sonic boom minimization design for supersonic transport aircraft
[NASA-TN-D-7218] 15 p1734 N73-24065
Noise properties and circuits to cancel noise in gas parametric amplifiers
15 p1756 N73-24230
Evaluation of courses of action and costs to reduce aircraft noise levels in vicinity of airports
[PB-215611/5] 16 p1862 N73-25080
Turbomachinery noise generation and control
[NASA-TM-X-68253] 16 p1957 N73-25831
Development of aircraft configuration for reduction of jet aircraft noise by exhausting engine gases over upper surface of wing
[NASA-CASE-LAR-11087-1] 17 p1980 N73-26008
Subsonic intrinsic noise reduction of sound pressure transducers in air flow
[RAE-LIB-TRANS-1660] 17 p2063 N73-26687
Annular duct liner curvature for aircraft noise reduction
[NASA-TN-D-7277] 17 p2063 N73-26688
Cold flow tests of factors affecting noise suppression and thrust loss of divergent lobe supersonic jet noise suppressor
[NASA-TM-X-2820] 18 p2101 N73-26992
Design, development, and evaluation of Boeing 727 aircraft nacelle to conform to upper noise reduction goals
[FAA-RD-72-40-VOL-2] 18 p2104 N73-27017
Design, fabrication, and flight test of Boeing 727 aircraft nacelle modification to reduce aerodynamic noise levels
[AD-756040] 18 p2108 N73-27048
Performance data for three turbofan engine configurations with noise reduction features tested over range of flight conditions
[NASA-CR-121258] 18 p2193 N73-27707
Modifications of turbojet engine with ejector to reduce jet engine exhaust noise
[NASA-TM-X-2841] 19 p2217 N73-27887
Rotor noise reduction by serrated brass strip attachment to blade leading edges
[NASA-TN-D-7371] 19 p2219 N73-27898
Program summary of research project for sonic inlet technology involving design concepts for aerodynamic performance and noise suppression - Vol. 1
[NASA-CR-121126] 19 p2328 N73-28731
Research project for noise suppression of sonic inlets used with turbofan engines and improvement in engine inlet flow characteristics - Vol. 2
[NASA-CR-121127] 19 p2328 N73-28732
Analysis of internal noise field of two axisymmetric sonic inlet models for noise suppression of turbofan engine inlets - Vol. 3
[NASA-CR-121128] 19 p2329 N73-28733
Velocity decay and acoustic characteristics of various nozzle geometries with forward velocity
[NASA-TM-X-68259] 20 p2388 N73-29183
Finite difference formulation for sound propagation in two-dimensional soft-walled duct with uniform flow
[NASA-TM-X-68295] 20 p2454 N73-29722
Design and tests of lift fan exhaust suppression system for future VTOL aircraft noise goals
[NASA-CR-121108] 20 p2466 N73-29812
Data base for abatement and control of aircraft noise and sonic boom for rule making criteria
[FAA-ED-20-2] 21 p2495 N73-30022
Analysis of noise problems created by supersonic transport aircraft, conventional aircraft, and short takeoff aircraft to show methods for jet exhaust noise reduction
21 p2495 N73-30024
Measurements of aerodynamic noise produced by modified and standard OH-6A helicopter configurations to determine noise reduction effectiveness
[NASA-TN-D-7216] 21 p2496 N73-30031
Procedures for the measurement and evaluation of noise, noise reduction and control, and current data on noise analysis and control
[EA-7301] 21 p2579 N73-30664
High tip speed fan inlet noise reduction using treated inlet splitters and accelerating inlets.
[NASA-CR-121268] 21 p2589 N73-30745
System for reducing noise generated by jet impinging on external flap using injection of secondary air from slot near trailing edge of flap
[NASA-CR-132270] 22 p2611 N73-30930
Reduction of aircraft noise by installing acoustically absorbent material
[NASA-CR-2261] 22 p2613 N73-30941
Directional equipment for suppressing noise of Concorde propellers during high speed flight
22 p2613 N73-30942
Design and characteristics of expansion chamber mufflers for reducing exhaust noise generated by helicopters
[NASA-TN-D-7309] 22 p2700 N73-31623
Wind tunnel tests to determine effect of inlet turbulence length scale on fan discrete tone noise
[NASA-TM-X-62300] 22 p2700 N73-31625
Method and apparatus for improving operating efficiency and reducing low speed noise for turbine aircraft engines
[NASA-CASE-LAR-11310-1] 22 p2710 N73-31699
Far field noise reduction of tilting rotor aircraft based on performance and weight tradeoffs to improve acoustic signatures
[NASA-CR-114648] 23 p2740 N73-31937
Theory for predicting sonic boom intensity and techniques for sonic boom suppression
[FAA-RD-73-4] 23 p2741 N73-31944
Longitudinal stability of Boeing 707 aircraft during steep approach, for noise reduction
[DGLR-PAPER-73-023] 23 p2744 N73-31963
Noise reducing approach and takeoff profiles for short takeoff aircraft
[MBB-UH-06-73-O] 23 p2744 N73-31968
Method for eliminating noise and debris of explosive welding techniques by using complete enclosure
[NASA-CASE-LAR-10941-2] 23 p2797 N73-32371
Automatic control system for in-duct cancellation of spinning modes of sound
[NASA-CR-132317] 23 p2819 N73-32540
Jet noise emission and reduction by secondary cold annular flow for SST and military aircraft
23 p2820 N73-32543
Acoustic tests of supersonic tip speed fan with acoustic treatment and rotor casing slots and its performance in reducing engine noise
[NASA-CR-134501] 23 p2828 N73-32608
Effect of noise constraints on engine cycle optimization for long-haul transports
[NASA-TM-X-71447] 23 p2830 N73-32620
Analysis of jet engine noise to show sources of noise, noise spectra, and use of laminates and composite materials for noise reduction
24 p2875 N73-32962
Flight tests of Boeing 727 aircraft to determine effects of modifications on reduction of aerodynamic noise
[FAA-RD-72-40-VOL-3] 24 p2876 N73-32971
Recording human electroencephalogram under influence of muscle noise
24 p2883 N73-33025
Assessment of jets as acoustic shields by comparison of single and multitube suppressor nozzle data
[NASA-TM-X-71450] 24 p2904 N73-33179
Fan and core engine noise suppression for STOL aircraft
[NASA-TM-X-71448] 24 p2971 N73-33741

**NOISE SPECTRA**

Aural analysis of sound into bands of frequencies
[NASA-TT-F-13912] 02 p0212 N73-11715
Estimation of noise directionality spectrum directly from cross-spectral matrix of received processes at hydrophone array elements
[AD-749940] 05 p0514 N73-14181
Effects of low frequency background noise on electrical properties of semiconductor materials and components
05 p0519 N73-14222

Double probe measurements of electromagnetic noise spectra due to thermodynamic plasma density fluctuations for plasma diagnostics
06 p0706 N73-15758
Speech tests and typical naval noise spectra for use in evaluating voice communication equipment
[AD-753207] 09 p1003 N73-18185
Analysis of helicopter internal and external noise levels for various flight conditions and timing of acoustical spectra
12 p1362 N73-21055
Noise spectrum characteristics and directivity patterns for rotary wings as function of blade tip speed, total rotor thrust, and angle of rotor disc plane
12 p1362 N73-21056
Properties of axisymmetric supersonic free jet including relation between jet structure and discrete noise frequencies
[ISL-29/72] 12 p1365 N73-21075
Analysis of acoustic factors involved in wind tunnel tests to show contributions from various sources
17 p2009 N73-26247
Application of cross-spectral analysis to measurement of contribution of noise sources
[ISAS-493] 18 p2179 N73-27591
Measurement of sound power levels, power spectra, and directivity patterns for jet exit velocities of F-111A aircraft
[NASA-TN-D-7376] 20 p2361 N73-28989
Development of method for calculating near field noise level of free jet and influence of ground effect on noise produced by V/STOL aircraft operation
20 p2478 N73-29907

**NOISE SUPPRESSORS**
U NOISE REDUCTION

**NOISE TEMPERATURE**
Methods for predicting parametric amplifier input noise temperature degradation for pump AM noise levels undergoing signal interference
[AD-751652] 07 p0763 N73-16197
Considerations for precise measurement of amplifier noise with hot and cold noise standards and mismatch problems
[NBS-TN-640] 24 p2898 N73-33136

**NOISE THRESHOLD**
Speech and tone audiometry for testing auditory acuity of flying personnel
13 p1480 N73-21990

**NOISE TOLERANCE**
Human tolerance and adaptation in long term exposure to sonar signals at elevated intensities
[AD-746103] 02 p0134 N73-11089
Effects of space flight noise intensities on human physiological functions
10 p1114 N73-19080
Noise tolerant radio telegraphy, using orthogonal carrier modulation
[FTZ-455-TBR-39] 22 p2634 N73-31108

**NOMENCLATURES**
Nomenclature for describing radiation measurements and computations in geophysics
[BMBW-FBW-72-30] 09 p1027 N73-18379

**NOMINAL VALUES**
U APPROXIMATION

**NOMOGRAPHS**
Equations and nomograms depicting probabilities of rare meteorological phenomena
[NLL-M-22672-[5828.4F]] 01 p0073 N73-10598
Nomograph for calculating optimal working characteristics of hydrostatic sliding bearings
[AD-753553] 09 p1042 N73-18501
Nomographs for predicting aerodynamic performance of air launched stores
[AD-754428] 11 p1353 N73-20981

**NONADIABATIC CONDITIONS**
U ADIABATIC CONDITIONS

**NONAXISYMMETRY**
U ASYMMETRY

**NONCONDUCTORS**
U ELECTRICAL INSULATION

**NONCONSERVATIVE FORCES**
Feasibility of using Galkerin method to control cantilevered beam subjected to nonconservative force
17 p2091 N73-26913

**NONDESTRUCTIVE TESTS**
NT PRELAUNCH TESTS
Automated nondestructive testing - bibliography with abstracts
[CE-BIB-227] 01 p0061 N73-10498
Evaluation of several thermographic infrared techniques and their applicability to detection of unbonded areas in babbitted bearings
[AD-745730] 01 p0063 N73-10516
Applications of holographic interferometry in underwater acoustics research
[AD-746134] 01 p0067 N73-10545
Nondestructive analysis techniques for detection of defects in rigidized surface insulation for space shuttle thermal protection
[NASA-CR-128607] 01 p0108 N73-10893
Facility monitoring of stress wave emission as nondestructive testing method
[AD-745729] 01 p0114 N73-10945
Numerical analysis of stress field in semi-infinite elastic-plastic medium under generalized plane deformation
[AD-746046] 01 p0115 N73-10951
Infrared nondestructive testing techniques used to detect unbonded areas in laminated structures and incipient failures in electrical circuit boards
[AD-746233] 02 p0175 N73-11419
Stress wave emission nondestructive inspection technique for detecting flaw criticality in structural parts
[AD-747225] 02 p0176 N73-11426
Development of nondestructive test procedures for determining properties of multidirectional fiber reinforced resin matrix composites
[AD-746592] 02 p0193 N73-11562
Application of acoustic emission testing to yielding, fracture, slow and fast crack growth
[AD-746261] 02 p0239 N73-11941
Acoustic emission testing to broaden nondestructive testing capability
[LA-4724] 03 p0302 N73-12464
Survey of nondestructive technology
[NASA-CR-129245] 03 p0305 N73-12491
Nondestructive ultrasonic testing of aircraft tires
[AD-747633] 03 p0309 N73-12521
Destructive and nondestructive tests of carbon-carbon reentry heat shields
[SC-R-71-3354] 03 p0364 N73-12966
Analogous specimen-coil-arrangements in eddy current testing
[ARL/MET-REPT-88] 04 p0420 N73-13423
Nondestructive measurement of modulus of elasticity of carbon fibers
[AD-749011] 04 p0440 N73-13585
Nondestructive evaluation of stability of shells and development of mechanical device for crash simulator
04 p0480 N73-13922
Exo-electron emission testing of material fatigue
[AD-748272] 05 p0549 N73-14457
Microwave coupled stripline, surface crack detector, using pair of conductors over ground to support propagation in two orthogonal TEM modes
[AD-749799] 05 p0549 N73-14462
Capabilities and limitations for quantitative nondestructive testing of aerospace structures
[NASA-TM-X-64706] 05 p0552 N73-14483
Bibliography of literature on radiographic techniques for nondestructive tests
[AD-749258] 05 p0553 N73-14488
Nondestructive neutron activation and spectrum analysis using gamma ray spectrometer coupled to PDP 9 computer
[IRI-133-71-03] 05 p0582 N73-14739
Focused one joule pulse and Q switched ruby laser for optical production and detection of ultrasonic waves in metals for nondestructive tests
05 p0609 N73-14954
Nondestructive tests of welds in regenerative chambers
[NASA-CR-120980-APP] 06 p0677 N73-15509
Fabrication and nondestructive tests of beryllium reinforced metal matrix composites
[AD-750764] 06 p0686 N73-15583
Ultrasonic nondestructive tests of sound waves emitted from stress corrosion cracking - Part 2
[AD-751529] 07 p0810 N73-16570
Application of acoustic emission analysis to nondestructive testing on crack formation
[RFP-TRANS-101] 07 p0821 N73-16656
Evaluation of fringe multiplication technique applied to frozen stress approach of three dimensional stress analysis in three dimensions
[AD-751172] 07 p0853 N73-16917
Technology transfer in nondestructive testing and visual displays
[NASA-CR-130302] 07 p0856 N73-16941
Nondestructive inspection techniques for examining catapult and arresting gear structures on E-2 aircraft
[AD-752492] 08 p0868 N73-17027
Design and development of ultrasonic instrumentation to facilitate quantitative nondestructive evaluation of defects in materials
[NASA-CR-124021] 08 p0923 N73-17562
Analysis of errors recorded by modified Ligtenberg technique while measuring stress, strain, and static and dynamic loading in curved plates
[AD-752127] 08 p0926 N73-17589
Application of holography for nondestructive tests of solid propellant rocket engine to detect unbonding between liner and propellant
[NASA-CR-112225] 08 p0929 N73-17606
Nondestructive tests of fracture behavior of ATJ-S graphite
[AD-751976] 08 p0935 N73-17655
Space shuttle design recommendations based on aircraft maintenance experience
[NASA-TM-X-68646] 08 p0965 N73-17888
Techniques and instrumentation for nondestructive testing of high performance multilayer thermal insulation for space shuttle orbiters
[NASA-CR-124106] 09 p1051 N73-18567
Process for automatically contacting, testing, and handling beam lead semiconductor devices
[BDX-613-779] 10 p1166 N73-19487
Potentiostatic polarization method for stress corrosion tests on cracking susceptibility of materials
[AD-754205] 10 p1174 N73-19549
Development of electromagnetic pulse sounding probe for detection and delineation of geological anomalies in hard rock medium
[AD-754847] 11 p1288 N73-20454
Test equipment and methods for nondestructive inspection of welded, brazed, and composite structures
[NASA-SP-5952[02]] 11 p1297 N73-20528
Evolution of nondestructive testing techniques arising from holography and microwaves
[AD-755116] 11 p1304 N73-20580
Holographic interferometric testing of laminate and composite structures for internal voids and material defects
[BDX-613-812] 12 p1410 N73-21429
Detection and application of stress waves to nondestructive testing
[RFP-TRANS-114] 12 p1463 N73-21853
Nondestructive replica techniques for studying roadstone surface polishing by electron microscopy
[PB-212720] 13 p1531 N73-22409
Holographic and acoustical tests of vibrating underwater structures
[AD-755475] 13 p1538 N73-22463
Ultrasonic inspection and control of laminated steel blocks prior to machining
[TR-7212.620] 14 p1670 N73-23550
Automatic scanning and display eddy current system for nondestructive testing of printed circuit boards
[ARL/MET-NOTE-84] 15 p1786 N73-24478
Characteristics of emitting-receiving ultrasonic probe including beam configuration and determination of electric equivalent circuit of transducer
[EUR-4774] 15 p1788 N73-24494
Nondestructive detection of flaws in gas turbine blades using luminescence and color flaw detection techniques
[AD-758047] 15 p1793 N73-24538
Nondestructive tests for predicting effect of copper and aluminum microstructure on acoustic emission
[AD-758216] 15 p1800 N73-24587
Design fabrication, and nondestructive testing of six experimental cylinder assemblies of selected composite graphites for NERVA nozzle extension
[NASA-CR-132233] 15 p1810 N73-24674
Evaluation of nondestructive testing methods for fatigue crack detection
[NASA-CR-128946] 15 p1839 N73-24901
Magnetic particle inspection of large or irregularly shaped parts by assuring optimum magnetic flux densities
[AD-759207] 16 p1882 N73-25236
Application of holographic nondestructive testing to experimental production hardware components and structural problems in aerospace engineering
16 p1921 N73-25546
Aerospace application of holography through nondestructive testing and flow visualization
16 p1922 N73-25550
Holographic instrumentation for use in flow visualization, nondestructive testing procedures, and optical data processing
16 p1922 N73-25551
Modulus of elasticity measurements on materials at elevated temperatures
[AD-759060] 16 p1971 N73-25941
Nondestructive testing of welded silicon solar cell silver interconnections
[ESS/SS-397] 17 p2038 N73-26487
Nondestructive tests for luminescent and color flaw detection, using magnetic particles and dye penetration
[AD-759253] 17 p2038 N73-26488
Evaluation of nondestructive testing techniques for diffusion-bonded titanium alloy aircraft structures using ultrasonic radiation
[AD-760673] 18 p2106 N73-27035
Nondestructive tests and failure analysis of Vamistor resistors
[NASA-TM-X-64754] 18 p2122 N73-27154
Nondestructive test equipment using acousto-optical imaging techniques
[AD-760554] 18 p2152 N73-27397
Application of magnetic perturbation technique to nondestructively detect subsurface nonmetallic inclusions in inner races of deep groove ball bearings
[NASA-TM-X-68260] 18 p2155 N73-27410
Development of nondestructive inspection procedures for determining quality of welded joints in aluminum spacecraft structures
[NASA-CR-124332] 18 p2156 N73-27420
Proceedings of conference on nondestructive testing and materials characterization with emphasis on development of new techniques for materials testing
[AD-760174] 18 p2157 N73-27427
Principles of nondestructive testing and organization of Soviet metallography laboratories at industries
[JPRS-59424] 18 p2160 N73-27449
Application of ultrasonic inspection techniques for detecting separation of solid propellant rocket case-liner and liner-propellant interfaces
[NAL-TR-308] 18 p2193 N73-27703

Application of stress wave emission method to nondestructive testing of pressure vessels
[ISAS-492] 18 p2203 N73-27781
Principles and applications of nondestructive tests
[NASA-SP-5113] 19 p2303 N73-28517
Comparison of nondestructive evaluation methods 19 p2303 N73-28518
Liquid-penetrant inspection for surface defects 19 p2303 N73-28519
Ultrasonic testing for nondestructive evaluation of subsurface flaws 19 p2303 N73-28520
Radiography for nondestructive evaluation of internal flaws 19 p2303 N73-28521
Eddy-current inspection for locating subsurface flaws in electrical conductors 19 p2303 N73-28522
Thermal and infrared testing for nondestructive evaluation of flaws 19 p2304 N73-28523
Microwave techniques for nondestructive evaluation of flaws in materials 19 p2304 N73-28524
Magnetic techniques for nondestructive evaluation of defects in materials 19 p2304 N73-28525
Leak-testing methods for gas and liquid systems 19 p2304 N73-28526
Generally used practical methods of strain sensing 19 p2304 N73-28527
Nondestructive evaluation methods recently introduced 19 p2304 N73-28528
Nondestructive measurement of dielectric properties of slab-type materials
[AD-762359] 19 p2312 N73-28599
Nondestructive evaluation of metal fatigue
[AD-762608] 20 p2433 N73-29541
Measurement of elastic moduli of materials at elevated temperatures
[AD-763763] 21 p2554 N73-30473
Holographic system for nondestructive testing
[NASA-CASE-MFS-21704-1] 21 p2554 N73-30478
Application of fracture prevention principles to airframes to reduce catastrophic failure and increase service life
[AD-764513] 22 p2617 N73-30969
Individual nondestructive evaluation techniques
[NASA-SP-3079] 22 p2677 N73-31441
Application of holographic interferometry for detecting dewetted zones in solid rocket propellants
[AD-764470] 22 p2708 N73-31690
Nondestructive determination of radionuclides in lunar samples using large low-background gamma ray spectrometer and application of least squares fitting
[NASA-TM-X-69581] 22 p2718 N73-31756
Properties of liquid crystals noting use in display devices, light modulation, image converters, and nondestructive testing
[LCR-DR-1-71-223/1/R] 23 p2765 N73-32125
Nondestructive tests of metallic and nonmetallic materials
[AD-764200] 23 p2798 N73-32378
Test results and evaluation procedure for nondestructive tests of airfield pavements
[AD-764787] 23 p2798 N73-32382
High precision external spur gear inspection and computerized simulation of manufacturing-inspection process
[AD-764588] 23 p2799 N73-32389
Nondestructive tests of brittle ceramic materials
[AD-764795] 23 p2811 N73-32477
Industrial applications of radiation technology for conducting nondestructive tests 24 p2952 N73-33578
Application of radiation technology and equipment for nondestructive analysis of commercial aircraft structures during aircraft maintenance periods 24 p2952 N73-33579
Safety precautions to be followed during radiographic inspection of pressure vessels 24 p2952 N73-33580
Radiation hazards involved in conducting radiographic inspections of tires and protective measures for industrial personnel 24 p2952 N73-33584
Characteristics and performance of radiographic machine for conducting inspections of parcels for contraband using ionizing radiation 24 p2952 N73-33585

**NONEQUILIBRIUM CONDITIONS**
Nonequilibrium effects caused by vibrational freezing in hypervelocity wind tunnel
[VKI-TN-83] 03 p0248 N73-12009
Numerical analysis of relation between thermal fluctuations in nonequilibrium systems and nonlinear properties of systems 03 p0364 N73-12963
Formulation of second law of thermodynamics for system in thermal nonequilibrium by assumption of relationship between entropy and temperature
[AD-759970] 17 p2097 N73-26964
Rate-controlled method of constrained equilibrium applied to chemically reactive open systems
[FML-PUBL-73-6] 22 p2625 N73-31031

**NONEQUILIBRIUM DRAG**
U FRICTION DRAG

**NONEQUILIBRIUM FLOW**
Effect of nonequilibrium conditions on performance of combustors employing supersonic flows
[NASA-CR-120932] 02 p0242 N73-11969
Characterization of nonequilibrium flow and coupled chemistry associated with rocket exhaust effluent interactions in upper atmosphere
[AD-750878] 06 p0670 N73-15450

**NONEQUILIBRIUM IONIZATION**
Temperature and electrical conductivity of nonequilibrium ionizing gas-particle flow through convergent-divergent nozzle geometry 08 p0947 N73-17752

**NONEQUILIBRIUM PLASMAS**
Nonequilibrium plasma generation by strong shock waves produced in diaphragm shock tube
[BMBW-FBK-72-5] 04 p0405 N73-13301
Nonequilibrium phenomena in flowing plasmas
[AD-760792] 18 p2184 N73-27634

**NONFERROUS METALS**
Hard alloy shaping tools for extruding steels and nonferrous materials
[NLL-NEL-TT-2400-(6075.461)] 02 p0177 N73-11435
Temperature measurement of heavy nonferrous metals and alloys, steels, titanium, and other metals in plastic zone
[NLL-RTS-6867] 10 p1163 N73-19456
Effects of O2 on mechanical properties, elastic limit, and tension resistance of nonferrous metals
[EURISOTOP-59] 15 p1798 N73-24577
Activation analysis using charged particles and gamma photons for determining oxygen in nonferrous metals
[EURISOTOP-74] 17 p2065 N73-26704

**NONFLAMMABLE MATERIALS**
Intumescent paint containing nitrile rubber for fire protection
[NASA-CASE-ARC-10196-1] 04 p0437 N73-13562
Process for developing flame retardant elastomeric composition textiles for use in space suits
[NASA-CASE-MSC-14331-1] 18 p2167 N73-27501

**NONHOMOGENEITY**
U INHOMOGENEITY

**NONISOTHERMAL PROCESSES**
U ISOTHERMAL PROCESSES

**NONISOTROPIC PLATES**
U ANISOTROPIC PLATES

**NONISOTROPY**
U ANISOTROPY

**NONLINEAR EQUATIONS**
NT QUADRATIC EQUATIONS
Solution of Navier-Stokes equation for sea water pressure determination
[NOTA-INTERNA-377] 01 p0042 N73-10328
Gauge invariance, conservation laws, and Korteweg-deVries equation for class of nonlinear partial differential equations
[IPPJ-138] 04 p0440 N73-13589
Derivation of nonlinear Schroedinger equation for electron plasma waves
[IPPJ-137] 04 p0441 N73-13590
Nonlinear electroelastic equations for small fields superposed on bias
[AD-751624] 07 p0853 N73-16914
Theory for nonlinear collapse analysis of shells with general shape
[AD-751702] 07 p0853 N73-16916
Correlation properties of Gaussian random processes under nonlinear transformations 09 p1057 N73-18619
Oscillatory and nonoscillatory solutions to equations on nonlinear saturation of convective heat transfer
[AD-754228] 10 p1179 N73-19594
Convergence, accuracy, and stability of finite element approximations of class of nonlinear hyperbolic equations
[AD-754948] 11 p1312 N73-20646
Systems of nonlinear equations connecting capacity and potential at node-points of electrical network
[NLL-PO-2922-(9022.81)] 15 p1759 N73-24256
Nonlinear temperature and vorticity equations for studying convective motions of 4-day zonal circulation of upper Venus atmosphere 17 p2080 N73-26828
Iterative technique for solving nonlinear integral equation for radiative transfer
[NASA-TN-D-7292] 19 p2352 N73-28916
Iterative and nonlinear procedures for studying gravity anomaly in mountainous areas 24 p2911 N73-33232
Asymptotic solutions for nonlinear equations of oscillating plasma layers
[FEI-359] 24 p2962 N73-33671
Solution of nonlinear problems of high temperature heat transfer
[AD-765747] 24 p2993 N73-33917

**NONLINEAR FEEDBACK**
Output stability analysis on nonlinear feedback and transient power systems 07 p0760 N73-16172
Design of nonlinear feedback system with significant plant ignorance for prescribed time domain tolerances
[NASA-CR-127489] 10 p1136 N73-19260
Design of nonlinear coherence receiver with feedback signal selection for carrier tracking in telecommunications
[NASA-CASE-NPO-11921-1] 14 p1620 N73-23118
Class of multivariable, nonlinear time-varying feedback systems with instable convolution subsystem as feedforward
[NASA-CR-133183] 17 p2007 N73-26234
Nonlinear feedback control concepts for variable stability aircraft 24 p2877 N73-32979

**NONLINEAR FILTERS**
Nonlinear filter estimation of interplanetary spacecraft orbits during simulated Jupiter flyby and Jupiter orbiter missions 17 p2081 N73-26834

**NONLINEAR PROGRAMMING**
Nonlinear programming of multifilter phase-lock loops at low signal-to-noise environments
[NASA-CR-131237] 10 p1127 N73-19184
Nonlinear programming algorithms for variable design of structural cylindrical shell
[AD-761645] 19 p2240 N73-28062
Aerospace applications of stochastic continuous-time nonlinear programming
[AD-763805] 21 p2515 N73-30178

**NONLINEAR SYSTEMS**
Fast periodic steady state analysis of nonlinear large signal electronic circuits
[AD-745639] 01 p0034 N73-10271
Thermohydrodynamic equations of nonlinear mesometeorological processes
[NLL-M-20716-(5828.4F)] 01 p0072 N73-10590
Nonlinear theory using fourth order Hugoniot curves for compression shocks in cubic crystals 01 p0087 N73-10720
Nonalgorithmic methods for determination of strength, oscillations and static and dynamic stability of deformable systems
[AD-745426] 01 p0114 N73-10939
Subroutines for optimization of criteria under constraints using gradient projection method and HEATHER computer program
[LAAS-NI-CH-72-03] 02 p0147 N73-11191
Development of general mixed finite element models of nonlinear thermomechanical response of dissipative media
[AD-745994] 02 p0239 N73-11944
Optimum switching of large number of low voltage power generating elements with nonlinear volt-ampere characteristics
[AD-747560] 03 p0275 N73-12233
Numerical analysis of relation between thermal fluctuations in nonequilibrium systems and nonlinear properties of systems 03 p0364 N73-12963
Sliding friction and natural vibration of solid with rigid connection moving over dry surface
[AD-749521] 04 p0428 N73-13488
Development of numerical procedures for determining instantaneous values of current and voltage in nonlinear electrical circuits
[NLL-DRIC-TRANS-2145-(3623.66)] 05 p0522 N73-14241
Particle loss rate from mirror machines, and radiation coupling in dense plasmas
[COO-2181-9] 06 p0704 N73-15744
Output stability analysis on nonlinear feedback and transient power systems 07 p0760 N73-16172
Stabilization of nonlinear systems with dither control
[TAE-150] 09 p1009 N73-18239
Multidimensional Laplace-Galois transform for nonlinear sequential machines 09 p1056 N73-18611
Algorithm for adjusting linear and nonlinear classifiers
[BMVG-FBWT-72-5] 09 p1057 N73-18623
Node voltage method for analyzing nonlinear electric networks with lumped parameters
[NLL-TRANS-2865-(9022.81)] 11 p1264 N73-20255
Finite element formulation and thermoelastoviscoplasticity theory for solving problems in nonlinear continuum mechanics
[AD-754952] 11 p1331 N73-20805
Calculation of nonlinear evolution of disturbance in unbounded viscous fluid with uniform shear using Navier-Stokes equations
[NASA-TN-D-7284] 14 p1648 N73-23363
N wave focusing on principal axis of spherical mirror
[AD-757035] 14 p1692 N73-23736

Effects of sensor deadband and actuator breakout torque control system nonlinearities on performance of Apollo telescope mount pointing capability
[NASA-TN-D-7247] 15 p1834 N73-24868
Dual finite element and shell theory analyses of linear and nonlinear structures
[AD-758790] 16 p1970 N73-25933
Solutions of macroscopic Maxwell equations for nonlinear dispersive waves in nonlinear optics
17 p2062 N73-26683
Numerical analysis of nonlinear resonance phenomena in systems of solids having rotating and vibrating parts
17 p2092 N73-26928
Dynamic finite element analysis of nonlinear oscillations of multi-degree of freedom structural systems
[ISD-136] 17 p2094 N73-26943
Quasi-optimum digital phase locked loops derived by nonlinear estimation theory
20 p2380 N73-29121
Solutions to quasisteady problems of dynamic weather forecasting
20 p2442 N73-29618
Nonlinear Schrodinger equation for studying nonlinear wave modulation in magnetized collisionless plasma
[IPPJ-162] 20 p2458 N73-29755
Application of quadratic programming to optimize parameters of dynamic systems
21 p2515 N73-30172
Estimation of parameters for nonlinearly observed dynamic systems
21 p2565 N73-30562
Analytical synthesis method for feedback control of nonlinear multivariable systems
[AD-762797] 21 p2566 N73-30571
Anomalous nonlinear dissipation of high frequency radio waves in plasma
[JPRS-59883] 22 p2631 N73-31083
Statistical study of nonlinear energy transfer interactions in turbulence models
22 p2649 N73-31224
Stability of multiple loop nonlinear time varying systems
[AD-764631] 23 p2813 N73-32492
Aerothermodynamic study of air cushion vehicles buffeting noting dynamical stability, nonlinear behavior, and similitude law
[NT-33-1973] 24 p2870 N73-32933
Nonlinear methods for evaluating informativeness of meteorological parameters and classifying meteorological phenomena
24 p2947 N73-33534
Nonlinear optical susceptibilities of atoms, molecules, and condensed matter
[AD-764889] 24 p2959 N73-33643

**NONLINEARITY**
Monte Carlo simulation model for radiation induced plasmas with nonlinear properties
[NASA-CR-128405] 01 p0084 N73-10700
Observation of nonlinear waves near lower hybrid resonance frequency
[CONF-720804-3] 07 p0756 N73-16137
Mathematical model for nonlinear characteristics of avalanche diode
[AD-751974] 08 p0890 N73-17207
Finite difference algorithm for solving quasi-linear gas dynamic systems
[AD-753097] 10 p1143 N73-19309
Noise characteristics of functional correlators using nonlinear elements with exponential characteristics
12 p1386 N73-21241
Nonlinear acoustic and gravity waves in earth atmosphere
[TR-48] 14 p1659 N73-23466
Nonlinear dynamics of collective modes
[BN-695] 16 p1888 N73-25282
Algorithm for optimal control problems with bounded state
[AD-761790] 19 p2314 N73-28610
Modified quasilinearization algorithm for optimal control problems with bounded state variables - Part 2
[AD-761791] 19 p2315 N73-28615
Algorithm for solving approximate problem of nonlinear function
[NASA-CR-133728] 20 p2440 N73-29599
Linear and nonlinear theory of Hall current instability
24 p2962 N73-33667

**NONNEWTONIAN FLUIDS**
Equations which show relationship between stress and displacement velocity in non-Newtonian fluid flows
[AD-745702] 01 p0042 N73-10335
Rheological model - for behavior of nonNewtonian fluid
[WTHD-42] 06 p0699 N73-15701
Parametric linearization for approximating dynamic and thermal boundary layers for nonNewtonian fluids with arbitrary pressure and surface temperature gradients
[AD-764170] 22 p2655 N73-31271
Generalized momentum transfer hypothesis for non-Newtonian power-law fluids
23 p2771 N73-32168

**NONPARAMETRIC STATISTICS**
Nonparametric method of pattern recognition using computer simulation
[NASA-CR-130824] 09 p1005 N73-18203

**NONREFLECTION**
U ENERGY ABSORPTION

**NONRIGIDITY**
U FLEXIBILITY

**NONSYNCHRONIZATION**
Graphical method for solving interference problem in asynchronous circuit
[CEA-CONF-1961] 03 p0277 N73-12249
Data transmission interference after television field synchronizing signal
[BBC-RD-1973/12] 22 p2627 N73-31049
Air traffic control radar beacon system interference in terminal areas
[MTR-6239] 23 p2816 N73-32512

**NONUNIFORM FLOW**
Prediction of pressure gradient on delta wing between uniform and nonuniform supersonic inviscid flow
[ARC-CP-1228] 05 p0492 N73-14010
Effect of nonuniform upstream flow conditions on shock shape and surface pressure distribution on two dimensional pointed bodies
08 p0895 N73-17244
Temperature and electrical conductivity of nonequilibrium ionizing gas-particle flow through convergent-divergent nozzle geometry
08 p0947 N73-17752

**NONUNIFORM MAGNETIC FIELDS**
Estimation of ion source yields in inhomogeneous magnetic fields using magnetohydrodynamic theory
[LYCEN-7250] 12 p1435 N73-21624

**NONUNIFORM PLASMAS**
Spectral line thickness and temperature distribution in inhomogeneous sodium plasma confined between parallel mirrors
[INR-1388] 06 p0705 N73-15751
Wave transformation in plasma with nonmonotonic longitudinal distribution under action of superhigh frequency power
[AEC-TR-7338] 07 p0827 N73-16705
Research on Tokamak reactors and microinstabilities in inhomogeneous plasma
[COO-1478-13] 15 p1817 N73-24729
Parametric instabilities of damped modes in inhomogeneous plasmas
[AD-763737] 21 p2584 N73-30709

**NONUNIFORMITY**
Relativistic particle motion in nonuniform electromagnetic waves
[NASA-CR-133888] 22 p2632 N73-31092

**NONVISCOUS FLOW**
U TURBULENT FLOW

**NORD AIRCRAFT**
NT C-160 AIRCRAFT

**NORMAL DENSITY FUNCTIONS**
Extreme values of irregularity factor of bandpass filters for realizing steady Gauss processes with one-peak power density spectrum
[LBF-TM-64/72] 05 p0523 N73-14250
Signal to noise ratios for short term detection of narrowband Gaussian process in Gaussian noise
[AD-751573] 07 p0756 N73-16144
Correlation properties of Gaussian random processes under nonlinear transformations
09 p1057 N73-18619
Number of surge series of turbulent velocity pulsations with Gaussian distribution
09 p1059 N73-18635
Normal probabilities for Cape Kennedy wind components - monthly reference periods for all flight azimuths for altitudes from 0 to 70 kilometers
[NASA-TM-X-64771] 21 p2574 N73-30625

**NORMAL DISTRIBUTIONS**
U NORMAL DENSITY FUNCTIONS

**NORMAL FORCE DISTRIBUTION**
U FORCE DISTRIBUTION

**NORMAL SHOCK WAVES**
Calculation of shock normals using least squares technique on combined magnetic field and plasma data from single spacecraft
01 p0097 N73-10798
Performance comparison of three normal-shock position sensors for supersonic mixed compression inlets
[NASA-TM-X-2739] 08 p0955 N73-17817
Analysis of structure of collisionless shock waves using oblique shock apparatus and calculation of effects of various dissipative mechanisms
12 p1390 N73-21268

**NORMALIZING (HEAT TREATMENT)**
Anneal hardening of irradiated molybdenum metals and alloys
[ORO-3612-9] 10 p1173 N73-19545
Positron annihilation center decrease through migrating anion vacancies in thermal annealing of radiation damaged sodium chloride crystals
[CONF-720530-6] 10 p1194 N73-19715

**NORMALIZING (STATISTICS)**
Multiplicative renormalization group used to compute critical indices in d equals 4 minus sigma dimensions
[NOTA-INTERNA-384] 01 p0080 N73-10661
Analysis of sampling mechanism and operation of automatic normalization of character patterns
[REPT-726] 05 p0516 N73-14195

**NORTH AMERICA**
Interdependence of lake ice and climate in central North America
[E72-10362] 05 p0535 N73-14350
Cloud cover maps for North America and western North Atlantic for August, 1972
[AD-749128] 05 p0575 N73-14678
Surface gravity and satellite derived gravimetric geoid of North America, North Atlantic, Eurasia, and Australia
[NASA-TM-X-66238] 15 p1778 N73-24413
Daily tidal current tables for stations along Atlantic coast of North America - 1973
16 p1904 N73-25403
Simultaneous observation solutions for NASA-MOTS and SPEOPT station positions on North American Datum
[NASA-TM-X-66297] 18 p2145 N73-27336
Classification of coastal environments along Americas and Africa
[AD-761193] 20 p2415 N73-29412

**NORTH AMERICAN AIRCRAFT**
NT B-1 AIRCRAFT
NT B-70 AIRCRAFT
NT F-86 AIRCRAFT
NT F-100 AIRCRAFT
NT OV-10 AIRCRAFT
NT X-15 AIRCRAFT

**NORTH AMERICAN MILITARY AIRCRAFT**
U MILITARY AIRCRAFT

**NORTH ATLANTIC TREATY ORGANIZATION (NATO)**
Advanced NASA and DOD technology management techniques, and application to NATO programs for defense and civil needs
06 p0732 N73-15968
Planned 1973 AGARD meetings, and list of 1972 AGARD publications
[AGARD-BUL-73-1] 21 p2610 N73-30919

**NORTH CAROLINA**
Utilization of ERTS-1 imagery for state and local agency management and planning in North Carolina
[E72-10167] 01 p0044 N73-10348
Geological evaluation, regional planning, forest management, and water management in North Carolina using ERTS-1 imagery
[E72-10280] 03 p0292 N73-12378
Utilization of ERTS-1 imagery in geological evaluation, regional planning, forest management, and water management in North Carolina
[E72-10317] 04 p0413 N73-13366
First order land use classification in North Carolina based on ERTS-1 imagery
[E72-10324] 05 p0530 N73-14312
Geological structural surveys of North Carolina based on ERTS-1 imagery
[E72-10325] 05 p0530 N73-14313
Diurnal variations of precipitation and surface wind for North Carolina
[PB-211614] 05 p0576 N73-14688
Utilization of ERTS-1 imagery in geological evaluation, regional planning, forest and water management in North Carolina
[E73-10300] 09 p1021 N73-18332
Utilization of ERTS-1 imagery in geological evaluation, regional planning, forest and water management in North Carolina
[E73-10688] 16 p1902 N73-25382
Application of EREP data in geological evaluation, regional planning, forest management, and water management in North Carolina
[E73-10754] 17 p2022 N73-26357
Geological landforms in central Piedmont of Virginia and North Carolina from ERTS-1 imagery
[E73-10766] 19 p2259 N73-28205
Application of ERTS-1 data to North Carolina forest and water resources management
[PAPER-R1] 19 p2282 N73-28359
Geological evaluation, regional planning, forest management, and water management in North Carolina using ERTS-1 imagery
[E73-10962] 21 p2532 N73-30304
Utilization of Skylab EREP data in geological evaluation, regional planning, forest management, and water management in North Carolina
[E73-10966] 21 p2533 N73-30308
Utilization of ERTS-1 imagery for management of wetlands in Great Dismal Swamp and Lake Okeechobee
[E73-11161] 24 p2920 N73-33314

**NORTH DAKOTA**
Appraisal of changes in migratory bird habitats based on ERTS-1 imagery of North Dakota
[E73-10534] 13 p1518 N73-22298
ERTS-1 and aircraft multispectral scanner data for mapping ponds and lakes near Woodworth, North Dakota to determine changes in continental migratory bird habitat
[E73-10714] 17 p2018 N73-26321
Evaluation of ERTS-1 imagery for determining numbers and distribution of prairie ponds and lakes in North Dakota
[PAPER-W12] 19 p2272 N73-28289

Signal transmission in visible and infrared portions of electromagnetic spectrum of cloud free, lines of sight through atmosphere at Grand Forks, Fargo, and Minot, North Dakota
[AD-763083] 20 p2415 N73-29408
Appraising changes in continental migratory bird habitats in North Dakota using Skylab EREP system
[E73-10972] 22 p2657 N73-31284
Comparison of ERTS-1 spectral reflectance measurements of major crops and soil associations for selected sites in Iowa, Kansas, North Dakota, and Texas
[E73-10981] 22 p2657 N73-31288
ERTS-1 measurements of major crops and soil associations in Indiana, North Dakota, Iowa, Nebraska, Kansas, and Texas
[E73-11155] 24 p2919 N73-33309
**NORTHERN HEMISPHERE**
NT ARCTIC REGIONS
Aperiodic processes and formation of seasonal temperature and wind fields in stratosphere in Northern Hemisphere, and tropospheric influences
[NLL-M-20086-[5828.4F]] 01 p0043 N73-10342
Methodology for determining climatological probability of aircraft icing throughout Northern Hemisphere
[AD-745098] 01 p0075 N73-10623
Synoptic weather charts of daily and monthly heights and temperature for Northern Hemisphere from Jan. to Dec. 1968
[AD-746659] 02 p0206 N73-11673
Correlation coefficient between D region HF radio wave absorption and 10mb level winds and temperature in Northern Hemisphere
[COO-2195-5] 05 p0539 N73-14384
Meteorology and climatology of Northern Hemisphere during calendar year 1972 - Vol. 128 No. 4
05 p0570 N73-14631
Stratospheric weather maps for Northern Hemisphere based on rawinsonde and rocketsonde observations - Vol. 24, No. 3
05 p0570 N73-14632
Specific humidity distributions over Northern Hemisphere during monsoon season in Asia at 1000, 850, and 700 mb levels for June and July 1970
[NOTE-9] 05 p0572 N73-14647
Meteorological ground level maps of Northern Hemisphere for fourth quarter in 1971
[QR-4-PT-4] 06 p0691 N73-15628
Northern hemisphere monthly mean 500-mb and 1000-500-mb thickness charts
[MET-O-845C] 06 p0692 N73-15632
Synoptic meteorological weather charts for Northern Hemisphere obtained at ground level, 500 mb, and 850 mb during July, 1972, at Berlin
06 p0692 N73-15635
Monitoring Northern Hemisphere transmissions in Antarctica and some oblique sounding systems
[JPRS-58205] 10 p1128 N73-19186
Peculiarities of short wave propagation over long distance radio links connecting Antarctia with Northern Hemisphere
10 p1128 N73-19187
Meteorological charts of upper atmosphere of Northern Hemisphere
[QR-4-PT-4] 10 p1181 N73-19604
Daily meteorological ground level charts for Northern Hemisphere, January through June, 1971
[SAR-1-PT-1] 10 p1181 N73-19606
Meteorological ground level charts for Northern Hemisphere, April through June, 1971
[QR-2-PT-2] 10 p1181 N73-19607
Fluctuations of zonal atmospheric circulation in Northern Hemisphere in first half of century
[NLL-M-22855-[5828.4F]] 11 p1274 N73-20337
Relationship between solar activity and atmospheric pressure of Northern Hemisphere
[NLL-M-22858-[5828.4F]] 11 p1313 N73-20651
Synoptic weather maps of Northern Hemisphere for October 1972 obtained in Berlin
13 p1551 N73-22564
Long term climatological study of meteorological parameters for Northern Hemisphere
13 p1551 N73-22565
Stratospheric weather maps for Northern Hemisphere
[QTSR-1] 13 p1551 N73-22570
Daily and monthly meteorological charts for Northern Hemisphere obtained during November, 1972 at Berlin
14 p1684 N73-23668
Seasonal transitions in spring and autumn in mesopause region for Northern Hemisphere
[NASA-TT-F-14924] 14 p1685 N73-23672
Wind calculations of stratosphere in Northern Hemisphere at 100, 50, 30 and 10 mb
15 p1804 N73-24622
Northern Hemisphere ground weather maps for July through December, 1972
[QR-2-PT-2] 15 p1804 N73-24624
Polarization of Pc1 micropulsations observed in the same hemisphere, and in conjugate points
17 p2026 N73-26398
Seasonal variations in tropospheric and stratospheric carbon dioxide concentration determined from commercial aircraft sampling within Northern Hemisphere
[AC-24-PT-3] 17 p2028 N73-26409
Synoptic weather maps and data tables on daily and monthly Northern Hemisphere stratospheric height and temperature
[QTSR-3] 17 p2056 N73-26626
Daily and monthly synoptic weather maps for Northern Hemisphere and Berlin vicinity, December 1972
17 p2056 N73-26628
Parameterization of meteorological factors for unusual atmospheric circulation in Northern Hemisphere in January 1963
17 p2056 N73-26631
Synoptic weathermaps for ground and 500 mb levels obtained in Berlin during January, 1973
17 p2057 N73-26634
Cloud cover mosaics developed from environmental satellite imagery for April, 1973
18 p2171 N73-27534
Scanning radiometer imagery of Northern Hemisphere cloud cover obtained during May, 1973 by enivornmental satellite
18 p2171 N73-27535
Winter atmospheric circulation over European sector of Northern Hemisphere in twentieth century
[NLL-M-2337-[5828.4F]] 20 p2391 N73-29205
Synoptic charts for 50mb in Northern Hemisphere from January to June, 1972
[QR-1/2-PT-1/2] 20 p2442 N73-29613
Nature of zonal and meridional circulation components of troposphere and stratosphere of Northern Hemisphere
20 p2443 N73-29626
Atmospheric circulation effects on precipitation and temperature regimes of USSR and Northern Hemisphere
20 p2444 N73-29633
Analysis of epochal variations in atmospheric circulation of Northern Hemisphere, atmosphere, and hydrosphere for making long and extra long range hydrometeorological forecasts
20 p2444 N73-29635
Radiation and turbulent heat flux effects on variations of isobaric surface pressure and altitude in Northern Hemisphere
20 p2446 N73-29651
Mathematical model for Northern Hemisphere atmospheric circulation during cold season
[AD-765544] 24 p2950 N73-33562
**NORTHROP AIRCRAFT**
NT F-5 AIRCRAFT
NT T-38 AIRCRAFT
**NORTHROP MILITARY AIRCRAFT**
U MILITARY AIRCRAFT
**NORWAY**
Preliminary evaluation of Norwegian long period seismic array
[AD-746009] 02 p0167 N73-11361
Survey and mapping of snow and ground water levels in Norway using ERTS-1 imagery
[E73-10324] 09 p1024 N73-18356
Survey of terminal moraines in western Sweden and southeastern Norway from ERTS-1 imagery
[E73-11122] 24 p2916 N73-33277
Survey of snow cover to predict risk of spring flood and snow storage in areas of hydroelectric power stations in Norway
[E73-11160] 24 p2919 N73-33313
**NOSE CAPS**
U NOSE CONES
**NOSE CONES**
NT ROCKET NOSE CONES
Numerical analysis of supersonic, inviscid, steady flow past blunt-nosed cone at yaw
[AD-745782] 01 p0042 N73-10333
Laminar, transitional, and turbulent heat transfer measurements on yawed blunt conical nosetip in free stream Mach 5
[AD-748292] 04 p0486 N73-13967
Development of proton-activated sensors to measure graphite nosetip recession due to ablation during nose cone reentry
[AD-748289] 05 p0548 N73-14456
Measured maximal laminar heat transfer on cone with spherical nose in hot hypersonic flow
07 p0771 N73-16263
Radar echo cross sections from pyramidal shape of reentry vehicle
[AD-753684] 09 p1005 N73-18200
Problem formulation and numerical procedures for solving flow equations for flow distribution of viscous shock layer on nose of shuttle orbiter during reentry - Vol. I
[NASA-CR-128871] 11 p1271 N73-20309
Development of computer programs for analyzing flow distribution in nose region of blunt body at arbitrary speed and altitude - Vol. 2
[NASA-CR-128872] 11 p1271 N73-20310
Effect of nose geometry on aerothermodynamic environment of shuttle entry configurations
[NASA-CR-128873] 11 p1348 N73-20937
Laminar surface heat transfer distribution about cones at hypersonic speeds
[AD-754056] 11 p1349 N73-20946
Effects of nose bluntness on natural and induced boundary layer transition on axisymmetric bodies in supersonic flow
[AD-755843] 12 p1393 N73-21295
Numerical calculation of vertical water entry of finite cones
[AD-759006] 16 p1891 N73-25302
Computation of skin friction and heat transfer on sharp cone in axisymmetric turbulent hypersonic flow
[AD-761602] 19 p2353 N73-28929
Shadowgraph photography of boundary layer transition of spinning cones
[AD-762564] 22 p2656 N73-31276
Convective heat transfer determination for nose region of space shuttle entry configurations, using three dimensional flow field study
[NASA-CR-134057] 23 p2851 N73-32782
**NOSE WHEELS**
Bi-normal coordinates in discrete systems with application to aircraft shimmy problem
[AD-752548] 08 p0868 N73-17030
Analysis of loads imposed on nose gear retraction system of T-34 aircraft to determine critical mechanical adjustments
[AD-762729] 20 p2361 N73-28994
**NOSES [FOREBODIES]**
NT NOSE CONES
NT ROCKET NOSE CONES
**NOTATION**
U CODING
**NOTCH SENSITIVITY**
Time dependent edge-notch sensitivity of oxide and gamma dispersion strengthened nickel alloy sheets
[NASA-CR-121123] 06 p0725 N73-15919
Notch sensitivity and static strength of laminated steels
[AD-756556] 13 p1545 N73-22524
Low energy blow technique to determine dimensional changes and development of cracking in Charpy V-notch impact test
[CRANFIELD-MAT-10] 24 p2988 N73-33880
**NOTCH STRENGTH**
J integral relationship between elastic stress and concentration factors for inelastic fracture criterion of sharp notch
[CONF-720806-2] 05 p0569 N73-14617
Notch stress finite element method for loaded elastic cores, applicable to compositesor welded joints
[ISD-129] 09 p1095 N73-18938
Finite element analysis of behavior of filamentary composite plates with cutouts
[AD-764362] 22 p2689 N73-31538
Analysis of size effects related to fatigue strength of metals under conditions of geometrical stress concentrations producing stress and strain gradients
24 p2988 N73-33876
Low energy blow technique to determine dimensional changes and development of cracking in Charpy V-notch impact test
[CRANFIELD-MAT-10] 24 p2988 N73-33880
**NOTCH TESTS**
NT CHARPY IMPACT TEST
Analysis of plastification effects in notched, impact-bending specimens of steel
[NLL-RISLEY-TR-2457-[9091.9F]]
05 p0601 N73-14887
Application of cumulative damage theory to internal stress caused by cyclic loading in notched bars
[LBF-FB-100/72] 06 p0726 N73-15930
Fatigue failure of notched samples of titanium alloy
[AD-761588] 19 p2350 N73-28904
High temperature low cycle effects on directly stressed, notched fatigue specimens
[RD/B/N-1996] 24 p2989 N73-33888
**NOTCHED METALS**
U NOTCH TESTS
**NOTCHED STEEL**
U NOTCH TESTS
U STEELS
**NOTCHES**
Numerical analysis of elasto-plastic bending of plates with V-notch on one edge and subjected to pure bending
[NASA-CR-132225] 15 p1839 N73-24900
**NOVAE**
Spectroscopy and photography of novae and supernovae
[AD-743955] 01 p0106 N73-10875
Spectroscopic observation of Nova Delphini 1967 in gamma gamma 4,000 to 9,000 region
17 p2080 N73-26825
Simultaneous electrophotometric and spectral observations of N Del in 1967
20 p2471 N73-29848
Ultraviolet spectrophotometry of Nova Serpentis 1970 by OAO-A2 flight
23 p2836 N73-32660
**NOXIOUS MATERIALS**
U CONTAMINANTS
**NOZZLE COEFFICIENT**
U NOZZLE FLOW

**NOZZLE DESIGN**
Wind tunnel tests of twin jet afterbody models to determine thrust minus total drag and afterbody drag at Mach numbers to 2.2 and zero degree angle of attack
[NASA-TM-X-2601] 02 p0123 N73-11004
Effects of fuel nozzle design on performance of annular combustor using natural gas fuel
[NASA-TN-D-7072] 02 p0223 N73-11805
Rocket nozzle redesign for improving Saturn launch vehicle J-2 engine performance and reliability
03 p0349 N73-12849
Analysis of subsonic and supersonic burning in ram-jet combustors to determine effects of nozzle configurations
[AD-747030] 03 p0351 N73-12862
Optimum configuration of supersonic propelling nozzle for air driven two stage ejector stage with conical mixing chamber
[AD-747584] 03 p0352 N73-12869
Performance tests of wedge nozzle with cold primary and secondary flows for supersonic cruise and takeoff configurations to analyze noise suppression effects
[NASA-TM-X-2689] 06 p0714 N73-15822
Flow model of axisymmetric hypersonic nozzle for transition from turbulent flow to laminar flow with pressure gradient controlled by nozzle shape
07 p0768 N73-16237
Effect of fuel zoning and fuel nozzle design on exhaust pollution emissions at ground idle conditions for double-annular ram-induction combustor for turbofan engines
[NASA-CR-121094] 08 p0968 N73-17916
Development and characteristics of supersonic nozzles with perforated edges for wind tunnel applications
[AD-754601] 11 p1272 N73-20323
Factors affecting tangential fuel injector design and their effect on efficiency of supersonic combustion processes
[NASA-CR-112302] 11 p1334 N73-20829
Injector design guidelines for gas/liquid propellant systems
[NASA-CR-120968] 13 p1570 N73-22726
Development of galvanic forming techniques and application to production of complex structures requiring accurate dimensions
13 p1593 N73-22918
Thermal and stress analyses of interfaces for nozzles and nozzle extensions
[NASA-CR-132211] 15 p1768 N73-24324
Design analysis of NERVA nozzle including structural elements of nozzle jacket and various aspects of coolant passages
[NASA-CR-132223] 15 p1810 N73-24669
Design fabrication, and nondestructive testing of six experimental cylinder assemblies of selected composite graphites for NERVA nozzle extension
[NASA-CR-132233] 15 p1810 N73-24674
Design criteria for annular supersonic nozzles to produce uniform flow in supersonic wind tunnels without limit lines or shock waves
[ARC-R/M-3227] 16 p1856 N73-25035
Performance tests of gas turbines with high pressure ratios per stage to determine flow characteristics of supersonic nozzles for turbines
[ARC-R/M-3273] 16 p1856 N73-25037
Numerical analysis of maximum thrust nozzles for nonequilibrium, chemically reacting gas flows based on equations for general, multi-component reacting gas
16 p1886 N73-25269
Rocket nozzle coolant channel thermal analysis program
[NASA-CR-132185] 16 p1957 N73-25832
Development of performance equations for cryptosteady-flow energy separator over widest range of operating conditions for turbojet engines
[AD-762030] 19 p2330 N73-28747
Analysis of cryptosteady-flow energy separation in turbojet engines and application to nozzle design
[AD-762031] 19 p2331 N73-28751
Design and development of cryptosteady energy separator for use with turbojet engines on supersonic aircraft
[AD-762032] 19 p2331 N73-28752
Velocity decay and acoustic characteristics of various nozzle geometries with forward velocity
[NASA-TM-X-68259] 20 p2388 N73-29183
Wind tunnel tests to determine performance of lobed-display mixer nozzle with convergent nozzle at subsonic speeds
[NASA-TM-X-2806] 21 p2491 N73-29995
Analysis of flow distribution of nozzle designed to produce incompressible, low Reynolds number jet flow
[NASA-TM-X-69566] 21 p2523 N73-30233

**NOZZLE EFFICIENCY**
Tests of high pressure combustor exhaust emissions with improved air-atomizing and conventional pressure-atomizing fuel nozzle
[NASA-TN-D-7154] 07 p0855 N73-16929
Performance of hypermixing nozzles in area ratio 23 ejector
[AD-752207] 08 p0955 N73-17821
Performance evaluation of two-dimensional slot nozzle ejector with variable area mixing sections
[NASA-CR-2251] 15 p1730 N73-24034
Analytical technique and computer program for evaluation of airbreathing propulsion exhaust nozzle performance
[AD-760541] 18 p2194 N73-27712
Development of three dimensional nozzle admittance theory for various liquid rocket engine nozzles subjected to three dimensional oscillations
20 p2387 N73-29174

**NOZZLE EXPANSION**
U GAS EXPANSION
U NOZZLE FLOW

**NOZZLE FLOW**
Application of flow field models, combustion, mixing, and nonequilibrium chemistry data to development of chemical lasers
[AD-745419] 01 p0066 N73-10536
Flow field and base pressure of internal-external-expansion truncated plug nozzles for open and closed wake operations
[NASA-CR-123941] 03 p0281 N73-12282
Application of continuous wave gas laser and pulsed ruby laser to analyze laminar and turbulent films of air at porous wall with carbon dioxide and helium injected into air stream
[AD-747511] 03 p0287 N73-12323
Optimum configuration of supersonic propelling nozzle for air driven two stage ejector stage with conical mixing chamber
[AD-747584] 03 p0352 N73-12869
Flow distribution of low Reynolds number, high enthalpy viscous flow of diatomic gas through conical nozzles
[DGLR-PAPER-72-110] 04 p0405 N73-13302
Improvement of turbojet engine performance analysis by plotting parameters of two shaft turbojet engine operation
[AD-749058] 04 p0465 N73-13789
Supersonic characteristics of sonic nozzle gas flow expansion
[AD-749764] 05 p0528 N73-14297
Analysis of nonequilibrium in excited levels of electric ARC heated potassium vapor injected into argon/helium gas flow passing through supersonic nozzle
[AD-750943] 05 p0585 N73-14759
Numerical method for determining mass flow rates in two phase gas-solid rocket nozzle flow
[AD-750038] 05 p0591 N73-14804
Calculation of mass flow rate of methane and natural gas through nozzles
[NASA-SP-3074] 06 p0653 N73-15309
Calculation of relaxation kinetics for carbon dioxide-water-nitrogen mixture to determine gas dynamics of escape from slit nozzle
[JPRS-57906] 06 p0654 N73-15310
Performance tests of wedge nozzle with cold primary and secondary flows for supersonic cruise and takeoff configurations to analyze noise suppression effects
[NASA-TM-X-2689] 06 p0714 N73-15822
Individual and combined effects on heat transfer properties of air jets impinging on concave side of right circular semicylinder
[NASA-TN-D-7127] 06 p0730 N73-15952
Flow model of axisymmetric hypersonic nozzle for transition from turbulent flow to laminar flow with pressure gradient controlled by nozzle shape
07 p0768 N73-16237
Dissipative losses in separation nozzle flow determined for uranium isotope separation conditions from Pitot tube measurements
[KFK-1562] 07 p0772 N73-16271
Effects of nozzle orientation and configuration on roll control and base pressure of hypersonic reentry vehicle
[SC-DC-72-1187-A] 07 p0849 N73-16884
Calibration of flow in working section of hypersonic blowdown wind tunnel to include test equipment required and techniques used
[ARA-30] 08 p0892 N73-17225
Analysis of measurable and ideal quantities of nozzle beams skimmed from parallel equilibrium gas flows
[DLR-FB-72-51] 09 p1014 N73-18275
Effects of rocket motor nozzle geometry on jet plume characteristics and base pressure
[NASA-CR-130967] 09 p1017 N73-18303
Orifice inclination effect in pressure measurements on hypersonic rarefied flow field of flat plate
10 p1140 N73-19290
Wind tunnel tests to determine effects of nozzle geometry and upper surface blowing on aerodynamic characteristics of 14 percent thick airfoil
[NASA-CR-114560] 11 p1231 N73-19998
Calculation of flows in subsonic and transonic portions of circular nozzles
[NASA-TT-F-14847] 11 p1270 N73-20308
Development and characteristics of supersonic nozzles with perforated edges for wind tunnel applications
[AD-754601] 11 p1272 N73-20323
Finite difference solution of flow and energy losses of pure gases in separation nozzle geometry
[KFK-1630] 12 p1392 N73-21285
Effect of heat transfer on flow and temperature fields in separation nozzle measured with free molecular pressure and temperature probes
[KFK-1634] 12 p1464 N73-21865
Nozzle and wall jet flow fields in bistable fluid amplifiers
13 p1509 N73-22230
Computerized simulation of plume shapes produced by axially symmetric nozzle geometry
[AD-756380] 13 p1511 N73-22241
Shock heated argon expansion through nozzle and spherical shock wave front
[AD-756455] 13 p1511 N73-22245
Analysis of supersaturation conditions in Mach 7.5 wind tunnel in expansion region of nozzle and technique for visualization of shock waves and shear layers
[ARL/A-139] 14 p1648 N73-23367
Numerical analysis of nonequilibrium nozzle expansions from reservoir at high specific enthalpy
[LOG-J7197] 14 p1649 N73-23375
Supersonic two phase air-water flows, noting expansion, acoustic velocity and X ray density measurements, and nozzle flow tests
[BMVG-FBWT-73-4] 14 p1650 N73-23380
Nozzle flow free jet and Prandtl-Meyer expansion rotational relaxation equation used for relaxation time calculation
[REPT-72-5] 14 p1650 N73-23383
Compressible turbulent boundary layer in zero-pressure gradient nozzle flow for zero, moderate, and severe heat transfer conditions
[AD-757330] 14 p1651 N73-23391
Condensible vapor supersonic nozzle flows at supersaturation collapse near condensation point
[AD-756471] 14 p1651 N73-23393
Numerical analysis of shock tunnel performance operated by reflected shock technique to determine effects of disturbance to flow at nozzle entry caused by reflected waves
[ARC-R/M-3265] 15 p1725 N73-23999
Analysis of breakup length and breakup pattern for jets of liquids of different viscosity and surface tension ejected vertically downward into atmosphere
[NLL-RTS-8049] 15 p1764 N73-24291
Analysis of relationship between losses in rotating turbine blade and pitch irregularity after nozzle blade
[NLL-CE-TRANS-6113-[9022.09]]
15 p1824 N73-24782
Analysis of deflection forces and deflection angles generated by thrust vector control nozzle at various Mach numbers and exit pressures
[AD-758521] 15 p1827 N73-24808
Design criteria for annular supersonic nozzles to produce uniform flow in supersonic wind tunnels without limit lines or shock waves
[ARC-R/M-3227] 16 p1856 N73-25035
Analysis of gas jets expanding out of axisymmetrical nozzles into vacuum or still air at finite pressure
[ARC-R/M-3235] 16 p1856 N73-25036
Performance tests of gas turbines with high pressure ratios per stage to determine flow characteristics of supersonic nozzles for turbines
[ARC-R/M-3273] 16 p1856 N73-25037
Application of digital computer for aerodynamic design and automatic control of wind tunnel with flexible walls
[ARC-R/M-3187] 16 p1857 N73-25041
High enthalpy arc-heated helium shock tunnel for gas dynamic research
[NASA-TM-X-2814] 16 p1885 N73-25258
Numerical analysis of maximum thrust nozzles for nonequilibrium, chemically reacting gas flows based on equations for general, multi-component reacting gas
16 p1886 N73-25269
Investigation of flow issuing from nozzle in fluid amplifier and impinging on receiver with spill port oriented at 90 degrees to flow direction
[AD-759796] 16 p1890 N73-25297
Gas dynamic analysis in near field of supersonic nozzle banks for chemical lasers
[AD-760132] 17 p2041 N73-26513
Optical gain of combustion driven gas dynamic lasers
[AD-760390] 17 p2042 N73-26523
Analysis of condensation effects in supersonic nozzle flows for homogeneous and heterogeneous nucleation conditions
18 p2128 N73-27195
Analysis of nonequilibrium conditions among populations of excited levels of potassium vapor passing through supersonic nozzle
18 p2128 N73-27199
One dimensional flow of partially ionized argon in hypersonic nozzle
[AD-760967] 18 p2184 N73-27632
Aerodynamic noise of STOL engine-over-wing configuration using nozzle deflector
[NASA-TM-X-2871] 19 p2219 N73-27897
Numerical method employing plane characteristics for calculating geometrically complex three dimensional nozzle exhaust flow fields
19 p2251 N73-28149

Analysis of viscous effects in low-density nozzle flows using internal laminar layer equations for two dimensional or axisymmetric flow
[AD-761489] 19 p2257 N73-28191
Interferometric studies in shock tunnel simulating nozzle flow in gasdynamic lasers
[AD-761601] 19 p2308 N73-28567
One dimensional stationary analysis of air cooled, ducted gas turbines nozzle vanes
[AD-761451] 19 p2330 N73-28744
Development of performance equations for cryptosteady-flow energy separator over widest range of operating conditions for turbojet engines
[AD-762030] 19 p2330 N73-28747
Analysis of cryptosteady-flow energy separation in turbojet engines and application to nozzle design
[AD-762031] 19 p2331 N73-28751
Design and development of cryptosteady energy separator for use with turbojet engines on supersonic aircraft
[AD-762032] 19 p2331 N73-28752
Two-dimensional nozzle flow problem solved by method of integral relations
20 p2385 N73-29161
Development of three dimensional nozzle admittance theory for various liquid rocket engine nozzles subjected to three dimensional oscillations
20 p2387 N73-29174
Wind tunnel tests to determine performance of lobed-display mixer nozzle with convergent nozzle at subsonic speeds
[NASA-TM-X-2806] 21 p2491 N73-29995
Analysis of flow distribution of nozzle designed to produce incompressible, low Reynolds number jet flow
[NASA-TM-X-69566] 21 p2523 N73-30233
Photographic recording of secondary flows at nozzle exits produced by planar nozzles with rectangular inlets from circular ducts
[AD-762743] 21 p2527 N73-30265
Aerodynamic characteristics of round jet located on center line of bottom of aircraft fuselage and elongated slots for lift augmentation
[NASA-TN-D-7299] 22 p2613 N73-30939
Integral solution to internal separated flow problems in nozzles and orifices
23 p2772 N73-32174
Viscous laminar flow through laval nozzles
24 p2907 N73-33197
Flow through supersonic Laval nozzle with several contractions
24 p2909 N73-33216

**NOZZLE GEOMETRY**
Analytical method for estimating chamber and throat conditions in nozzle with low radius of curvature throat
[NASA-CR-128619] 02 p0156 N73-11263
Optimum configuration of supersonic propelling nozzle for air driven two stage ejector stage with conical mixing chamber
[AD-747584] 03 p0352 N73-12869
Operational control of ramjet engine with fixed nozzle diffuser geometry
[AD-748708] 04 p0465 N73-13787
Effect of nozzle inlet shape, lip thickness, and exit shape and size on subsonic jet noise
[NASA-TM-X-68182] 07 p0821 N73-16655
Effects of rocket motor nozzle geometry on jet plume characteristics and base pressure
[NASA-CR-130967] 09 p1017 N73-18303
Gas turbine nozzle geometry of two phase flow fuel injectors
[AD-754051] 11 p1334 N73-20831
Finite difference solution of flow and energy losses of pure gases in separation nozzle geometry
[KFK-1630] 12 p1392 N73-21285
Design and performance of liquid nitrogen cooled nozzle for producing pulsed cylindrical hydrogen cluster beams
[KFK-1610] 12 p1436 N73-21632
Shock heated argon expansion through nozzle and spherical shock wave front
[AD-756455] 13 p1511 N73-22245
Effects of nozzle geometry and diaphragm location on starting process in Ludwieg tubes
[AD-755357] 13 p1511 N73-22248
Analysis of dynamic inlet distortion data for turbojets
[AD-756481] 13 p1571 N73-22731
Factors affecting base flow and jet structure behind cylindrical afterbody with central nozzle at mach 2.0 and turbulent boundary layer conditions
[ARC-R/M-3224] 16 p1851 N73-25001
Nozzle geometry and forward velocity effects on noise for CTOL engine-over-wing concept
[NASA-TM-X-71453] 24 p2971 N73-33742

**NOZZLE INSERTS**
Design of augmentor wing jet flap configuration with minimum noise generation for jet STOL transport aircraft
03 p0250 N73-12025
Suppression of turbofan engine sonic inlet noise in STOL propulsion by use of acoustic nozzle insert
03 p0250 N73-12026
Cooling efficiency of air discharge on nozzle blades with deflectors
[AD-749654] 05 p0591 N73-14803

**NOZZLE THRUST COEFFICIENTS**
Analysis of optimum nozzle thrust deflection angles in cruising flight
[ARC-CP-1222] 05 p0590 N73-14796

**NOZZLE WALLS**
Nozzle wall boundary layer of helium tunnel
[NASA-TN-D-6965] 02 p0156 N73-11261
Predicting total pressure loss regions existing in corner between sidewall and horizontal nozzle walls at exits with convex contour curvature
[AD-751606] 07 p0773 N73-16277

**NOZZLES**
Silicone rubber cover for protecting flush-deck nozzles on aircraft carriers
[AD-746841] 02 p0153 N73-11241
Small scale nozzle tests using heated nitrogen for effectiveness and wall heat transfer studies with hydrogen film cooling
[NASA-CR-120926] 02 p0242 N73-11970
Prediction of three-dimensional liquid-propellant rocket nozzle admittances
[NASA-CR-121129] 08 p0954 N73-17807
Noise tests on large scale model of externally blown flap lift augmentation system using mixer nozzle
[NASA-TN-D-7236] 15 p1733 N73-24059
Elastic stresses due to axial loads on nozzle intersecting cylindrical shell
[AD-758075] 15 p1841 N73-24916
Evaluation of high temperature nozzle throat materials for performance in highly oxidizing rocket exhaust environment
[AD-762533] 20 p2467 N73-29816

**NRX-A REACTOR**
U NUCLEAR ENGINE FOR ROCKET VEHICLES

**NUCLEAR AUXILIARY POWER UNITS**
NT SNAP
NT SNAP 8
NT SNAP 10A
NT SNAP 19
NT SNAP 23
NT SPACE POWER REACTORS
NT SPACE POWER UNIT REACTORS
Control circuit for nuclear thermionic converter power source for spacecraft
[NASA-CASE-NPO-13114-1] 04 p0448 N73-13656
Feasibility of bifold nuclear power source using Pu-238 fuel
24 p2951 N73-33573
Entry and impact behavior of isotope heat source for space nuclear power following flight abort to provide safe dispersion
[LA-UR-73-741] 24 p2986 N73-33861

**NUCLEAR BINDING ENERGY**
Four particle correlations in nuclear alpha structure
[HMI-B-125] 02 p0213 N73-11727

**NUCLEAR CAPTURE**
NT ELECTRON CAPTURE

**NUCLEAR CHEMISTRY**
Annual report of German institute for inorganic and nuclear chemistry, 1971
[BMBW-FBK-72-15] 04 p0453 N73-13702

**NUCLEAR ELECTRIC POWER GENERATION**
NT NUCLEAR AUXILIARY POWER UNITS
NT NUCLEAR POWER PLANTS
NT NUCLEAR POWER REACTORS
NT SNAP
NT SNAP 8
NT SNAP 10A
NT SNAP 19
NT SNAP 23
NT SPACE POWER REACTORS
NT SPACE POWER UNIT REACTORS
NT THERMONUCLEAR POWER GENERATION
Pulsed ionization chamber for plasma diagnostics, and applications to MHD electrical power generation from gas cooled reactors
[AD-747681] 03 p0343 N73-12800
Conference on environmental, social, economic, and ecological effects of nuclear electric power generation
[TID-25857] 07 p0793 N73-16450
Safety measures for nuclear space power and propulsion systems
[LA-DC-72-1480] 17 p2061 N73-26676

**NUCLEAR ELECTRIC PROPULSION**
Performance prediction for nuclear electric propulsion systems in advanced unmanned missions to outer planets and solar system
[NASA-CR-129134] 02 p0210 N73-11705
Performance potential evaluation of unmanned nuclear electric propulsion spacecraft for single-thrust-period missions to Uranus
[NASA-TN-D-7125] 06 p0718 N73-15859
Cost effectiveness and mission value comparisons of three propulsion systems for delivery of advanced probe spacecraft
[NASA-TM-X-2751] 09 p1079 N73-18802
Nuclear electric propulsion reliability analysis
[NASA-CR-133233] 17 p2061 N73-26671

**NUCLEAR EMULSIONS**
Relation between photometric track width and velocity of heavy ions in nuclear emulsions
[LUIP-CR-72-13] 08 p0946 N73-17750
Charge composition of cosmic rays for elements silicon to nickel
[LUIP-CR-72-16] 09 p1069 N73-18721
Preparation and processing of nuclear emulsions for radiation measurement systems
[AD-756826] 13 p1562 N73-22657
Nuclear track dosimetry for monitoring cosmic ray exposure of Apollo 16 astronauts
15 p1741 N73-24114
Identifying heavy primary cosmic ray particles at energies higher than 1 GeV/nucleon by nuclear emulsion balloonborne photometry
[LUIP-CR-73-02] 21 p2593 N73-30778

**NUCLEAR ENERGY**
Annotated bibliography on nuclear energy research in Philippines
[PAEC[A]-7116-SUPPL-4] 06 p0699 N73-15698
Design and performance analysis of ZrH reactor thermoelectric nuclear power system
[AI-AEC-13039] 12 p1427 N73-21567
Application of surface barrier detectors for time measurement of nuclear energy events and comparison of two methods used for timing procedures
22 p2671 N73-31393
Atomic Energy Commission policies and procedures for licensing and regulating industrial uses of radioisotopes
24 p2953 N73-33589

**NUCLEAR ENERGY LABORATORIES**
U LABORATORIES
U NUCLEAR RESEARCH

**NUCLEAR ENGINE FOR ROCKET VEHICLES**
Monte Carlo use in Rover nuclear rocket engine development program
[LA-DC-72-1078] 08 p0937 N73-17673
Characteristics and applications of computer codes for determining weight, center of gravity, and inertia of nuclear engine for rocket vehicles
[TID-26022] 10 p1186 N73-19652
On-line digital computer control of NERVA
12 p1426 N73-21558
Design, development, and reliability analysis of bearings for turbine pump on nuclear engine for rocket vehicles
[NASA-CR-132227] 15 p1792 N73-24525
Operating characteristics and service life tests of bypass control valve seal and bearing for nuclear engine for rocket vehicles
[NASA-CR-132226] 15 p1792 N73-24526
Characteristics of turbine pump for use with nuclear engine for rocket vehicles
[NASA-CR-132232] 15 p1792 N73-24530
Increased service life of rolling element radial bearings in nuclear engine for rocket vehicles by liquid hydrogen cooling and bearing modifications
[NASA-CR-132229] 15 p1792 N73-24531
Induction furnace providing controlled temperature for carbonization and graphitization processes for NERVA nozzle extension
[NASA-CR-132216] 15 p1801 N73-24599
Natural frequencies and dynamic response of NERVA engine thrust train
[NASA-CR-132224] 15 p1809 N73-24664
Computer programs for weight, center of gravity, and mass moment of inertia calculations and documentation for NERVA
[NASA-CR-132221] 15 p1810 N73-24666
Summary of engine design and analytical studies to mature 1137400E engine baseline
[NASA-CR-132230] 15 p1810 N73-24667
Mathematical model for radiation analysis and shielding for 1137400E NERVA engine
[NASA-CR-132228] 15 p1810 N73-24668
Design analysis of NERVA nozzle including structural elements of nozzle jacket and various aspects of coolant passages
[NASA-CR-132223] 15 p1810 N73-24669
Fluid dynamic computer programs for NERVA turbopump
[NASA-CR-132222] 15 p1810 N73-24670
Computer program for analyzing kinematical responses of structures caused by excitations for use in NERVA program
[NASA-CR-132214] 15 p1810 N73-24671
Photoelastic stress analysis of NERVA structures
[NASA-CR-132213] 15 p1810 N73-24673
Design fabrication, and nondestructive testing of six experimental cylinder assemblies of selected composite graphites for NERVA nozzle extension
[NASA-CR-132233] 15 p1810 N73-24674
Research and development program for NERVA fuel elements
[Y-1868] 20 p2453 N73-29718
Thermal and nucleonic behavior of NERVA reactor during startup transient investigation
[AD-764231] 22 p2699 N73-31620

**NUCLEAR EXPLOSION EFFECT**
Development of computer code for determining survivability of aircraft following exposure to radiation from aerial nuclear explosion
[AD-746015] 02 p0215 N73-11738

Atmospheric effects on thermal radiation from tropospheric nuclear explosion to ground target
[AD-745884] 05 p0539 N73-14389
Bibliography of nuclear explosion effects on explosives
[ICT-11/71] 08 p0946 N73-17749

NUCLEAR EXPLOSIONS
Method for calculating aircrew radiation dosage near atmospheric nuclear weapon detonation
[AD-745084] 01 p0010 N73-10079
Computer analysis of temperature distributions in circular and rectangular bodies exposed to thermal radiation from nuclear weapon explosions
[AD-745727] 01 p0084 N73-10699
Detection and classification of earthquakes and nuclear explosions by Swedish observatory
[FOA-4-A-4503-TR78] 01 p0101 N73-10828
Principles of nuclear reactions and different types of nuclear explosions
[AD-745857] 01 p0121 N73-10998
Methods for predicting initial radiation exposure at ground surface resulting from nuclear explosions
[AD-745906] 02 p0133 N73-11084
Ionospheric disturbances and acoustic gravity wave generation by nuclear explosions
[AD-746328] 02 p0214 N73-11737
Photographic aerial survey over underground nuclear test at Amchitka to record changes in bioenvironment
[BMI-171-146] 03 p0296 N73-12411
Formation of nitrous oxide molecules from ion-molecule reactions following sea level nuclear burst
[AD-746958] 03 p0298 N73-12428
Sr, Ba, and Ce fallout from nuclear explosions and weapons tests, monitored in ground-level air, in rain, and in atmosphere
[ORO-2529-30] 03 p0333 N73-12719
Acoustic gravity wave propagation modes in ionosphere and neutral atmosphere following nuclear explosion
[CONTRIB-1799] 05 p0509 N73-14140
Nuclear source model for generating ionospheric disturbances through acoustic gravity waves
05 p0509 N73-14141
Infrasonic wave generation and atmospheric propagation of gravity acoustic waves
05 p0509 N73-14142
Hydrodynamic calculations and experimental observations of ionospheric shock front propagation following nuclear explosion
05 p0510 N73-14150
Acoustic gravity wave effects in traveling ionospheric disturbances following nuclear explosions
05 p0513 N73-14166
Effects of traveling ionospheric disturbances following nuclear explosion on high frequency band propagation
05 p0513 N73-14167
Nonlinear propagation and ionospheric coupling of atmospheric waves following nuclear explosion
05 p0513 N73-14168
F layer electron density fluctuations and disturbances following nuclear explosion at ionospheric height
05 p0513 N73-14169
Effects of acoustic gravity waves following nuclear explosion on ionospheric electron density and high frequency communications
05 p0513 N73-14170
Analytic model for behavior of neutral and ion chemistry in D region following nuclear burst
[AD-750395] 05 p0543 N73-14416
Study of relative condensabilities of radioactive vapors in nuclear debris by use of high-powered lasers
[AD-750263] 05 p0579 N73-14713
Lost data channels of acceleration measurements in underground nuclear tests
[UCRL-73665] 05 p0580 N73-14725
Evaluation of research projects involving seismic arrays, long period arrays, seismometers, and seismic signal processing
[AD-750759] 06 p0669 N73-15439
Ionospheric modification of electromagnetic pulse from nuclear explosions
[SC-RR-72-0400] 06 p0699 N73-15697
Stratospheric nitric oxide production from past nuclear explosions and its relevance to projected SST pollution
[AD-751295] 07 p0795 N73-16466
Simulation of thermal radiation-airblast interaction effects in conical shock tube
[AD-752023] 08 p0893 N73-17229
Seismic detection of nuclear explosions and earthquakes
[AD-751243] 08 p0918 N73-17526
Bibliography on applications of nuclear explosions in mines, chemistry, and gas and oil extraction
[CEA-BIB-129-ADD-1] 08 p0942 N73-17719
Nuclear thermal vulnerability of honey comb sandwich radome panels
[AD-753666] 09 p1056 N73-18605
Ground-silo-missile mount transmissibility characteristics
[AD-753079] 09 p1097 N73-18953
Possible uses of pulsed lasers for controlled fusion, plasma heating, and creation of controlled nuclear microexplosions
[UCRL-73931] 10 p1186 N73-19654
Dynamic functions of air blast parameters in detonation of spherical trinitrotoluene charge
[AD-753805] 10 p1187 N73-19659
Model of electrons artificially injected into inner radiation belt by Starfish nuclear explosion
[NASA-TM-X-66211] 11 p1336 N73-20842
Reaction rate data for atmospheric chemistry, metal atom oxidation, and nuclear fireball
[AD-756674] 13 p1488 N73-22063
Electromagnetic shielding and hardening of radio communication systems against atmospheric nuclear burst effects
[AD-758403] 15 p1751 N73-24196
Piezoelectric device for measuring the size and concentration of particles in clouds generated by underground nuclear explosion
[FRNC-TH-298] 17 p2065 N73-26709
Computerized design of hollow dipole antennas for measuring nuclear electromagnetic pulse
[AD-761801] 19 p2244 N73-28096
Auroral clutter mapping with Homer backscattering radar to study reaction of upper atmosphere to nuclear explosions
[AD-762012] 19 p2297 N73-28474
High resolution interferometer spectrometer measurements of auroral infrared emissions to simulate high altitude nuclear explosions
[AD-762013] 19 p2297 N73-28475
Reaction kinetics in upper atmosphere chemistry and nuclear fireball studies
[AD-764892] 23 p2754 N73-32041
Debris particle distribution in ionosphere escaping fireball through charge exchange collisions
[AD-764955] 23 p2819 N73-32535
Turbulence effects on fireball dynamics
[LA-UR-73-713] 24 p2923 N73-33347

NUCLEAR FISSION
Direct nuclear pumping of gas laser using argon as lasing medium
[NASA-CR-133210] 17 p2040 N73-26503

NUCLEAR FORCES
U NUCLEAR BINDING ENERGY

NUCLEAR FUEL BURNUP
Low cost efficient thermionic converter for use in nuclear reactors
[NASA-CASE-NPO-13121-1] 03 p0332 N73-12702
Hydrogen embrittlement of tantalum alloy cladding for uranium mononitride nuclear fuel pins at high temperatures
[NASA-TM-X-2732] 09 p1063 N73-18675
Irradiation of TZM-Uranium dioxide fuel pin at 1700 K
[NASA-TM-X-2755] 18 p2178 N73-27588

NUCLEAR FUEL ELEMENTS
Pressure drop measurements and drag coefficients for grid spacers of hexagonal fuel rod bundles
[NLL-RISLEY-TR-2440-[9091.9F]]
02 p0209 N73-11692
Survey of aluminum-, copper-, and magnesium-alloy properties as filling materials for fast breeder fuel elements
[EUR-4857-F] 02 p0211 N73-11706
Neutron emission rate from plutonium dioxide nuclear fuel
[NASA-CR-129098] 02 p0211 N73-11707
PUO2-Mo cermet spheres for use as isotopic power fuels
[MCM-1887] 03 p0333 N73-12715
Heat transfer coefficient between fuel and cladding as parameter for calculating fuel rod temperature
[NLL-WINDSCALE-497-[9091.9F]]
05 p0578 N73-14706
Thermohydraulic test facility for design of fuel elements for water and sodium cooled reactors
[NT-31-1972] 05 p0579 N73-14712
Relations between fuel swelling and clad strain for cylindrical uranium dioxide pins with niobium zirconium cladding
[NASA-TM-X-2717] 07 p0819 N73-16638
Development of plutonium dioxide molybdenum cermet nuclear fuels
[MLM-1905] 07 p0820 N73-16643
Preparation of hydrocarbon suspensions in slush hydrogen for nuclear fuel element corrosion inhibition in rocket engines
08 p0968 N73-17913
Stress-corrosion cracking of zirconium alloy fuel element sheaths subjected to tension stress in iodine vapor environment
09 p1063 N73-18671
Intergranular hydride as a linear function of hydrogen concentration in Zircaloys
09 p1063 N73-18672
Irradiation damage to tungsten rhenium and tungsten rhenium hafnium claddings of unranium nitride fuel pins
[ORNL-TM-3895] 10 p1186 N73-19653
Application of electronic image analyzer to dimensional measurements from neutron radiographs of nuclear fuel elements
[NASA-TM-X-68200] 11 p1293 N73-20495
Fuel-oxide can compatability and reaction during fabrication of fuel elements for fast reactors
[NLL-CE-TRANS-6049-[9022.09]]
11 p1322 N73-20732
Power distribution in fast spectrum thermionic reactor fuel element at core/BeO reflector boundary
[NASA-TM-X-68207] 11 p1323 N73-20735
UC-ZrC fuel elements for space power reactor system
[GULF-GA-A-11073] 12 p1428 N73-21571
Effects of thermal cycling at high temperature on rates of distortion of UO2/clad fuel elements
[NASA-CR-133236] 17 p2061 N73-26672
Properties and processing of plutonium fuel for isotopic power source
[MLM-1983] 17 p2061 N73-26674
Evaluation of fuel pin design concepts for fast spectrum lithium cooled compact space power reactor
[NASA-CR-121181] 18 p2178 N73-27584
Irradiation of TZM-Uranium dioxide fuel pin at 1700 K
[NASA-TM-X-2755] 18 p2178 N73-27588
Calculated power distribution of thermionic, beryllium oxide reflected, fast spectrum reactor
[NASA-TM-X-2838] 19 p2320 N73-28663
Analysis of maximum fuel pin temperature during nominal operation of advanced power reactor to show possible variations in maximum temperature
[NASA-TM-X-68217] 20 p2453 N73-29716
Research and development program for NERVA fuel elements
[Y-1868] 20 p2453 N73-29718
Design and characteristics of capsule assembly to evaluate tungsten emitter and carbide fuel combinations for thermionic fuel elements
[NASA-TM-X-2887] 21 p2578 N73-30658
Design and operation of tantalum alloy clad uranium mononitride irradiated fuel pins
[NASA-TM-X-2878] 22 p2698 N73-31614
Tungsten-coated tungsten-uranium dioxide nuclear fuel plates
[NASA-CASE-XLE-00209] 23 p2818 N73-32528

NUCLEAR FUELS
NT CERAMIC NUCLEAR FUELS
NT FISSIUM
NT NUCLEAR FUEL BURNUP
Pu-238 grade fuels for supplying power to artificial heart and circulatory assist devices
[LA-DC-72-473] 03 p0261 N73-12115
Research on zirconium microstructure and uranium carbide as nuclear fuel
[AECL-4159] 03 p0332 N73-12708
Use of Cm-244 as radioisotope power fuel in electric power conversion systems
[CONF-720519-1] 03 p0333 N73-12717
Effects of irradiation on properties of fluoride tungsten clad uranium carbide-zirconium carbide fueled capsules
[NASA-CR-120995] 05 p0578 N73-14708
Fabrication of uranium mononitride fuel pin assembly for fast lithium cooled space power reactor
[NASA-CR-120956] 05 p0579 N73-14710
Production of isotopic fuel pellets by vacuum hot pressing
[ORNL-4796] 05 p0579 N73-14711
High speed ballistic injection of solid spherical pellet of deuterium into thermonuclear reactor plasma to analyze dynamics of pellet evaporation
[AD-751294] 07 p0830 N73-16726
Environmental tests of crystallographic and stress corrosive properties of reactor related metal alloys
[AECL-4353] 09 p1063 N73-18668
Development of graphite-matrix fuels for booster assemblies in reactor cores
09 p1063 N73-18669
Thermal simulation of oxide fuel rod by heated rods of different geometry
[EURFNR-1026] 10 p1187 N73-19655
Role of cesium in fuel-cladding interaction of austenitic stainless steels mixed with oxide fuels
[EUR-4893] 10 p1187 N73-19657
Cm-244 development as isotopic power fuels
[ORNL-TM-4035] 10 p1187 N73-19658
Onboard spacecraft propulsion using nuclear fuels and solar energy - pt. 1
[JPRS-58612-1-PT-1] 10 p1209 N73-19833
Isotopic fuel technologies
[MLM-2014] 17 p2061 N73-26675
Re-solution rates of fission gases in oxide nuclear fuels under irradiation
[GEAP-12361] 17 p2062 N73-26679
Power production and fuel capability of light water cooled cavity test reactor
[NASA-TM-X-2864] 19 p2320 N73-28662
Unrestrained swelling of uranium nitride fuel irradiated at temperatures ranging from 1100 to 1400 K
[NASA-TM-X-2907] 21 p2578 N73-30659
Performance of pure plutonium oxide fuel under operational conditions
[LA-5160-MS] 21 p2578 N73-30660
Model to predict fission gas releases from UN fuel pins clad with various materials
[NASA-TN-D-7401] 23 p2818 N73-32531

Screening factor which reduces densities at which carbon ignition can occur in helium, exhausted carbon, and oxygen stellar core models
[UCRL-74669-REV-1] 24 p2992 N73-33913
NUCLEAR FUSION
NT CONTROLLED FUSION
State of fusion reactor technology at end of 1971
[EUR-4873-E] 01 p0079 N73-10649
Method for technical evaluation of controlled nuclear fusion for energy production
[NP-19152] 03 p0332 N73-12707
Conference on research in nonchemical energy sources in nuclear fusion and plasma physics
[AD-748265] 04 p0456 N73-13725
Tritium mass transfer, isotopic separation, and permeation in fusion reactors
[UCRL-74057] 08 p0942 N73-17721
Western European research on open adiabatic mirror devices and radio frequency plugging - EURATOM controlled fusion report
[EUR-CEA-FC-628-AG] 08 p0948 N73-17760
Plasma heating by magnetic pulse in theta pinch and nuclear fusion
[AD-757043] 13 p1563 N73-22671
Concept of nuclear fusion chain reactions for supernovae and controlled fusion reactors
[SM-170/49] 17 p2062 N73-26678
Nucleocosmochrometers for short lived Pb-205 s-process nucleosynthesis study
[AD-760535] 18 p2182 N73-27618
Magnetic mirrors for controlled nuclear fusion
[IAEA/SM-170/49] 19 p2320 N73-28665
Design of injector system for fusion reactor
[MATT-949] 19 p2324 N73-28699
Production of gamma rays from explosive nucleosynthesis and low energy cosmic ray scattering
19 p2332 N73-28765
Deuterium abundance for proving neutron loss before nucleosynthesis
19 p2332 N73-28768
Consistence of cosmic ray source compulsion with explosive nucleosynthesis
[NASA-TM-X-70448] 21 p2592 N73-30768
Fundamental requirements of fusion feasibility experiment based on flux compression by collapsing liner
[AD-765314] 23 p2819 N73-32534
Laser fusion and parameteric instabilities
[COO-3227-18] 24 p2932 N73-33413
NUCLEAR INTERACTIONS
NT ELECTRON CAPTURE
NT SPIN-ORBIT INTERACTIONS
Low energy cosmic ray protons from nuclear interactions of cosmic rays with interstellar medium
[NASA-TM-X-66181] 08 p0956 N73-17829
Monte Carlo simulation of nuclear-electromagnetic cascade development and energy response of ionization of spectrometers
[NASA-CR-133999] 22 p2672 N73-31406
Cosmic ray charged particle interactions with matter
[AD-764833] 23 p2821 N73-32555
NUCLEAR LIGHTBULB ENGINES
Development of test equipment and procedures to simulate thermal environment and fuel region of small models of nuclear lightbulb engine configurations
[NASA-CR-129299] 03 p0330 N73-12692
Simulating radiant heating of propellant stream of nuclear light bulb engine
[NASA-CR-129499] 03 p0330 N73-12693
Development and evaluation of test equipment for high pressure radio frequency plasma experiments and in-reactor tests of nuclear lightbulb engine
[NASA-CR-129501] 03 p0330 N73-12694
Development of closed cycle, vortex stabilized nuclear lightbulb engine to show basic design concepts and operating principles
[NASA-CR-129298] 03 p0330 N73-12695
Analysis of heat balance characteristics of nuclear lightbulb engine to determine effects on engine performance, space radiator requirements, and cooling sequence
[NASA-CR-129295] 03 p0331 N73-12696
Design and performance characteristics of small scale model of nuclear lightbulb engine for testing in nuclear furnace reactor
[NASA-CR-129296] 03 p0331 N73-12697
Feasibility of full-scale nuclear light bulb engine and tests of fissioning uranium plasmas in unit cell of driver reactor
[NASA-CR-129500] 03 p0331 N73-12698
NUCLEAR MAGNETIC RESONANCE
NT PROTON MAGNETIC RESONANCE
Nuclear magnetic relaxation in He-3 impuriton gas
[NUB-2155] 01 p0083 N73-10687
Nuclear magnetic resonance spectroscopy to measure order parameter in diatomic molecule rotational ordering transitions
[NOTA-INTERNA-376] 01 p0083 N73-10691
Infrared and NMR spectra of poly[carborane-siloxane] s containing icosahedral cages in nitrogen environment
[AD-749386] 05 p0566 N73-14599
NMR principle for designing propellant mass flow meter
[AD-751507] 07 p0801 N73-16507
Nuclear magnetic resonance technique to obtain calibrations of charged defects in semiconducting compounds
[NASA-CR-112224] 08 p0950 N73-17781
NMR studies in metals and metallic compounds
[AD-752912] 09 p1074 N73-18767
Nuclear resonance investigation in niobium-hydrogen and niobium-deuterium systems
[JUL-853-FF] 10 p1193 N73-19707
Computerized control and recording system for magnetic spectrometer
[FRNC-TH-268] 11 p1294 N73-20502
Nuclear magnetic resonance method for chemical shifts of amino acids and hybrid state of nitrogen atom
[NASA-TT-F-14893] 14 p1694 N73-23750
Measurement of electromagnetically excited acoustic standing-wave resonance
18 p2159 N73-27444
Impurity resonances in dilute copper cobalt alloy, aluminum manganese alloy, and copper vanadium alloy at low temperatures
24 p2960 N73-33655
NUCLEAR MODELS
Scaling relations for critical exponents of modified F model
[NUB-2172] 12 p1438 N73-21653
Nuclear interaction models for cosmic ray air showers to determine lateral distribution of particles and fluctuations in particle densities
13 p1574 N73-22752
String models for theoretical study of high energy collisions involving large quantum numbers
[LPTHE-73/22] 21 p2581 N73-30688
Dual resonance model with spin for reaction pion nucleon yields omega meson nucleon
[ILL-(TH)-73-12] 22 p2701 N73-31634
Dual resonance type model for quasi two body reactions in subprocesses of pion nucleon yields pion omega meson nucleon
22 p2701 N73-31635
Mass formula calculations on baryonic resonances using radial excited symmetric quark model
[TR-74-018] 22 p2701 N73-31636
NUCLEAR PARTICLES
NT ALPHA PARTICLES
NT ANTINUCLEONS
NT ANTIPROTONS
NT BETA PARTICLES
NT BOSONS
NT MESON RESONANCES
NT MESONS
NT NUCLEONS
NT PHOTOELECTRONS
NT PHOTONS
NT PIONS
NT POSITRONS
Experimental facilities for nuclear particle physics research at proton energy level of 300 GeV
[CERN-1050] 04 p0402 N73-13274
Relations between signal shaping noise and timing resolution in nuclear particle detection
[NASA-CR-129613] 04 p0452 N73-13688
NUCLEAR PHYSICS
NT FIELD THEORY [PHYSICS]
NT PLASMA PHYSICS
NT QUANTUM THEORY
NT REACTOR PHYSICS
Research activities in nuclear physics, solid state detectors and theoretical physics
[AECL-4257] 02 p0213 N73-11726
Research in nuclear physics
[AEC-TR-7223/5-6] 03 p0332 N73-12704
Abstracts on physics and mathematics, including aerohydrodynamics, magnetohydrodynamics, thermodynamics, and physics of crystals and semiconductors
[JPRS-57312] 03 p0366 N73-12985
Papers on research conducted at Riso in nuclear physics
[RISO-256] 03 p0367 N73-12993
International cooperation in nuclear data field, emphasizing nuclear energy role
[INDC(NDS)-40-U] 04 p0452 N73-13691
History of physics with emphasis on nuclear physics and astrophysics
[NASA-TT-F-14670] 07 p0843 N73-16827
Annual report for 1971 of university institute in field of nuclear, elementary particle, and solid state physics
[BMBW-FBK-72-21] 09 p1069 N73-18720
Research progress in accelerator and ion source development, detection and computer systems, and various nuclear physics projects
09 p1101 N73-18986
Atomic science and engineering developments in USSR
[AD-754040] 11 p1327 N73-20766
Research progress in astronomy, space, radio, engineering, and nuclear physics
[NP-19468] 11 p1352 N73-20979
Significant population inversion in flow structure behind blast wave
[AD-757881] 15 p1795 N73-24555
Abstracts of studies in nuclear physics, solid state physics, and plasma physics
[AD-759252] 16 p1947 N73-25756
Research and development at Belgium nuclear center
[BLG-467] 17 p2099 N73-26979
Lists on research activities in medium energy nuclear physics
[NASA-CR-132280] 18 p2181 N73-27612
Accuracy improvement of angular momentum projection
[NASA-TM-X-2875] 20 p2440 N73-29600
Research in heavy ion scattering reactions
[CONF-720669] 22 p2702 N73-31641
NUCLEAR POTENTIAL
Nuclear power for air cushion vehicle
[NASA-TM-X-68231] 15 p1735 N73-24069
NUCLEAR POWER
U NUCLEAR ENERGY
NUCLEAR POWER GENERATION
U NUCLEAR ELECTRIC POWER GENERATION
NUCLEAR POWER PLANTS
Nuclear power plants for mobile applications
[NASA-TM-X-68154] 02 p0211 N73-11708
Aerial surveillance techniques for measuring gaseous environmental pollution from nuclear power plant
[WERLV-1] 03 p0334 N73-12721
Feasibility of mobile nuclear reactor power plants for cargo transportation and development of remote regions on earth
[NASA-TM-X-68164] 06 p0698 N73-15693
Development progress of small turbine-generator units using isotope power sources for undersea power plant with 2 to 10 kW[e]
[ORNL-TM-3586] 08 p0870 N73-17041
Engineering problems of controlled thermonuclear reactor power plants
[BNWL-1685] 15 p1811 N73-24682
Satellite nuclear power station, transmitting power safely to ground by microwave beam
[NASA-CR-121254] 19 p2319 N73-28653
Closed cycle nuclear MHD power plants
19 p2319 N73-28654
Three thermodynamic cycles of advanced nuclear MHD power plant systems
19 p2319 N73-28657
Cost and applications for satellite nuclear power station
19 p2319 N73-28658
Probability of aircraft crashing into Boardman nuclear power plant
[PB-220715/7] 21 p2578 N73-30662
Entry and impact behavior of isotope heat source for space nuclear power following flight abort to provide safe dispersion
[LA-UR-73-741] 24 p2986 N73-33861
NUCLEAR POWER REACTORS
NT SNAP 8
NT SNAP 10A
NT SPACE POWER REACTORS
NT SPACE POWER UNIT REACTORS
Design and performance tests of small transportable nuclear reactors
[AD-745362] 01 p0079 N73-10652
Design of intense neutron source for studying materials damage in fusion power reactor
[LA-4863] 04 p0402 N73-13272
Analysis of maximum fuel pin temperature during nominal operation of advanced power reactor to show possible variations in maximum temperature
[NASA-TM-X-68217] 20 p2453 N73-29716
Synthesis of optimal control system for nuclear power plant and power supplies onboard spacecraft
23 p2848 N73-32758
Feasibility of bifold nuclear power source using Pu-238 fuel
24 p2951 N73-33573
NUCLEAR PROPELLED AIRCRAFT
Design of valves for reactor coolant system of nuclear powered aircraft
[SLA-73-221] 24 p2929 N73-33393
NUCLEAR PROPULSION
NT NUCLEAR ELECTRIC PROPULSION
Advanced nuclear rocket propulsion system based on chain of exploding thermonuclear micro-bombs ignited before concave magnetic reflector
[AD-746027] 01 p0079 N73-10653
Radiological safety aspects of manned space missions employing nuclear reactors for electric power and involving extended stay times in low earth orbit - Vol I
[NASA-CR-123842] 02 p0209 N73-11694
Design, construction, and operation of combined principles simulator of gas core nuclear engine
[NASA-CR-2155] 07 p0826 N73-16691
Concept of nuclear powered ground effect machine for commercial operations in Arctic regions
[NASA-TM-X-2684] 08 p0977 N73-17991
Cost effectiveness and mission value comparisons of three propulsion systems for delivery of advanced probe spacecraft
[NASA-TM-X-2751] 09 p1079 N73-18802
Feasibility of using nuclear propulsion systems in spacecraft
[JPRS-58457] 11 p1323 N73-20737

Design configuration and operating procedures for utilizing thermonuclear propulsion for upper stage of Europa 3 launcher
[NASA-TT-F-14874] 13 p1557 N73-22623
Feasibility and cost benefits of nuclear-powered standardized spacecraft
[NASA-CR-133743] 21 p2601 N73-30846

NUCLEAR RADIATION
NT BETA PARTICLES
NT FAST NEUTRONS
NT GAMMA RAY BEAMS
NT GAMMA RAYS
NT NEUTRON BEAMS
NT SPALLATION
NT THERMAL NEUTRONS
Radiological safety aspects of manned space missions employing nuclear reactors for electric power and involving extended stay times in low earth orbit - Vol I
[NASA-CR-123842] 02 p0209 N73-11694
Identification of potential and inherent radiological hazards of spacecraft with nuclear reactors for electric power generation and elimination or reduction of hazards - Vol. 2 Pt. 1
[NASA-CR-123838] 02 p0209 N73-11695
Reference design document for power module systems, facilities, launch vehicle, and mission operations of nuclear reactor for space base programs - Vol. 3 pt. 1
[NASA-CR-123844] 02 p0209 N73-11696
Analysis of terrestrial nuclear hazards involving zirconium hydride reactor-Brayton power module for all phases of space base program - Vol. 3 Pt. 2
[NASA-CR-123839] 02 p0209 N73-11697
Analysis of space base mission and accidents/events involving nuclear hazard to general public - Vol. 3 Pt. 3
[NASA-CR-123846] 02 p0210 N73-11699
Guidelines and requirements of space base nuclear system safety applied to nuclear hardware, ground support equipment, and range safety and facilities - Vol. 5 Pt. 1
[NASA-CR-123848] 02 p0210 N73-11701
Qualitative identification of steps required to assure incorporation of radiological system safety principles into all phases of manned space base program - Vol. 6
[DOC-72SD4201-6-VOL-6] 02 p0210 N73-11703
Performance tests on cryogenic insulation materials for nuclear radiation shielding
[NASA-CR-2162] 05 p0578 N73-14707
Airborne radiological measuring system for use in nuclear safety programs and routine surveillance of areas around nuclear facilities
[EGG-1183-1558] 07 p0800 N73-16501
Summary of experimental programs performed using NBS reactor during 1971 and 1972
[NBS-TN-758] 12 p1426 N73-21559
Destruction capabilities and nuclear radiation potential of rockets with nuclear warheads
[AD-756565] 13 p1595 N73-22938
Nuclear waste disposal into space, using space shuttle and nonexpendable and expendable orbital stages
[NASA-TM-X-68235] 15 p1830 N73-24834
Semiconductor detectors of nuclear radiation
[JPRS-59634] 20 p2487 N73-29979
Portable nuclear radiation spectrometer for field measurement of mixed isotopic contaminants
[LA-5203-MS] 22 p2674 N73-31418
Feasibility of using inverse rastering to irridiate large test objects by penetrating radiation beams
22 p2732 N73-31866
Effects of nuclear radiation on reverse bias electrical characteristics of silicon power diodes
[NASA-TN-D-7423] 23 p2821 N73-32554

NUCLEAR REACTIONS
NT ALPHA DECAY
NT ANNIHILATION REACTIONS
NT CONTROLLED FUSION
NT ELECTRON CAPTURE
NT ELECTRON SCATTERING
NT HIGH ENERGY INTERACTIONS
NT NEUTRON EMISSION
NT NEUTRON SCATTERING
NT NUCLEAR FISSION
NT NUCLEAR FUSION
NT NUCLEAR INTERACTIONS
NT NUCLEAR SCATTERING
NT PHOTONUCLEAR REACTIONS
NT PHOTOPRODUCTION
NT POSITRON ANNIHILATION
NT PROTON SCATTERING
NT PROTON-PROTON REACTIONS
NT RADIOACTIVE DECAY
NT RESONANCE SCATTERING
NT SPALLATION
NT SPIN-ORBIT INTERACTIONS
NT THERMONUCLEAR REACTIONS
Research on nuclear reactions of energetic heavy ions
[AD-746330] 02 p0214 N73-11736
Calculation of neutron energy and flux distributions from D-D reactions in plasma focus and Z pinch discharges
[AD-745955] 02 p0217 N73-11755
Nuclear research, including reaction mechanisms, nuclear astrophysics, isobaric analog, and heavy ions studies
[ANU-P-542] 03 p0339 N73-12769
Preliminary studies of reaction yielding triton pion from proton deuteron interaction
[NASA-TM-X-68187] 07 p0823 N73-16674
Interactions of energetic neon with emulsion nuclei
[AD-754247] 11 p1327 N73-20768
Bevatron for astrophysical and superheavy element studies with nuclear tracks in solids
[UCB-34-P-189-X-3] 12 p1445 N73-21708
Performance of CO2 laser excited by H-3 [neutron, proton] reaction
16 p1920 N73-25536
Research activities in physics
[COO-535-674] 17 p2010 N73-26259
Measurement of positive and negative pion, and double neutral pion photoproduction cross sections for incident gamma ray energies from 600 to 900 MeV
21 p2582 N73-30691
Application of surface barrier detectors for time measurement of nuclear energy events and comparison of two methods used for timing procedures
22 p2671 N73-31393
Nuclear pumping in molecular gas lasers
[JPRS-60244] 24 p2931 N73-33405

NUCLEAR REACTOR CONTROL
Three channel analog electronic warning system for control of nuclear plant
[NLL-WH-334-[9091.9F]] 02 p0144 N73-11166
Control and coordination requirements for fabrication of devices in the thermonuclear research program
[B-159687] 03 p0332 N73-12703
Feasibility of on-line fission gas leak detection system for 100 kW zirconium hydride reactor
[NASA-TM-X-2870] 20 p2453 N73-29717

NUCLEAR REACTOR MATERIALS
U REACTOR MATERIALS

NUCLEAR REACTORS
NT ADVANCED SODIUM COOLED REACTOR
NT BOILING WATER REACTORS
NT BREEDER REACTORS
NT FAST NUCLEAR REACTORS
NT FAST TEST REACTORS
NT GAS COOLED REACTORS
NT GASEOUS FISSION REACTORS
NT HANFORD REACTORS
NT HEAVY WATER REACTORS
NT HIGH TEMPERATURE NUCLEAR REACTORS
NT LIQUID METAL COOLED REACTORS
NT LITHIUM COOLED REACTOR EXPERIMENT
NT NUCLEAR POWER REACTORS
NT NUCLEAR RESEARCH AND TEST REACTORS
NT PRESSURIZED WATER REACTORS
NT SNAP 8
NT SNAP 10A
NT SPACE POWER REACTORS
NT SPACE POWER UNIT REACTORS
NT SWIMMING POOL REACTORS
NT THERMAL REACTORS
NT TOKAMAK FUSION REACTORS
NT WATER COOLED REACTORS
Identification of potential and inherent radiological hazards of spacecraft with nuclear reactors for electric power generation and elimination or reduction of hazards - Vol. 2 Pt. 1
[NASA-CR-123838] 02 p0209 N73-11695
Reference design document for power module systems, facilities, launch vehicle, and mission operations of nuclear reactor for space base programs - Vol. 3 pt. 1
[NASA-CR-123844] 02 p0209 N73-11696
Analysis of terrestrial nuclear hazards involving zirconium hydride reactor-Brayton power module for all phases of space base program - Vol. 3 Pt. 2
[NASA-CR-123839] 02 p0209 N73-11697
Development of abort sequence trees for reference zirconium hydride reactor power module for each phase of space base program mission - Vol. 3 Pt. 2A
[NASA-CR-123845] 02 p0209 N73-11698
Analysis of space base mission and accidents/events involving nuclear hazard to general public - Vol. 3 Pt. 3
[NASA-CR-123846] 02 p0210 N73-11699
Guidelines and requirements of space base nuclear system safety applied to nuclear hardware, ground support equipment, and range safety and facilities - Vol. 5 Pt. 1
[NASA-CR-123848] 02 p0210 N73-11701
Analysis of technical documents and literature for conducting manned space flight nuclear system safety study - Vol. 7 Pt. 1
[NASA-CR-123850] 02 p0210 N73-11704
Research on fuel cycle technology, sodium technology, fast reactor materials properties, liquid metal and molten salt chemistry, and reactor safety
[ANL-7850] 03 p0263 N73-12136
Perturbation theory formulas derived and applied to determine changes in neutron and gamma ray doses due to changes in various radiation shield layers for fixed sources
[NASA-TN-D-7093] 03 p0331 N73-12700
Analysis of boron carbide drum-controlled critical reactor experiment
[NASA-TM-X-2680] 03 p0331 N73-12701
Low cost efficient thermionic converter for use in nuclear reactors
[NASA-CASE-NPO-13121-1] 03 p0332 N73-12702
Cost analysis and design of possible fusion reactor coil systems
[UCRL-73187] 03 p0336 N73-12741
Development of method for determining critical stress intensity for crack propagation and application to reactor components
[RD/B/N-2143] 04 p0481 N73-13934
Soil impact test with spherical nuclear reactor containment model for fracture strength observations
[NASA-TM-X-68180] 07 p0819 N73-16641
Design, construction, and operation of combined principles simulator of gas core nuclear engine
[NASA-CR-2155] 07 p0826 N73-16691
Research on impermeable plasmas in poloidal magnetic fields for nuclear fusion reactors
[TRITA-EPP-72-21] 07 p0828 N73-16714
Tritium mass transfer, isotopic separation, and permeation in fusion reactors
[UCRL-74057] 08 p0942 N73-17721
Stress-corrosion cracking of zirconium alloys in nuclear reactor environment
09 p1063 N73-18670
Neutronics analysis of gas core rocket concept using cavity test reactor
[NASA-TM-X-2743] 09 p1063 N73-18676
Radiation effects on current density of superconducting magnets in fusion reactor
[CLM-R-120] 10 p1199 N73-19760
Controlled nitrogen additions on mechanical properties of tantalum tubing in nuclear reactors
[NASA-TN-D-6999] 11 p1305 N73-20587
Acoustic amplification in fluid circuit and reactor heat exchanger vibration
[NLL-CE-TRANS-5913-[9022.09]]
12 p1390 N73-21271
Summary of experimental programs performed using NBS reactor during 1971 and 1972
[NBS-TN-758] 12 p1426 N73-21559
Liquid hydrogen cold neutron moderator for use in channel H5 EL 3 reactor
[CEA-N-1571] 15 p1815 N73-24714
Dual throat thermoelectric NaK development pump for use on reactor thermoelectric system
[NASA-CR-121231] 16 p1918 N73-25521
FORTRAN 4 code for calculating nuclear reactor dimensions and mass from thermal-hydraulic considerations
[NASA-TM-X-68236] 17 p2061 N73-26670
Concept of nuclear fusion chain reactions for supernovae and controlled fusion reactors
[SM-170/49] 17 p2062 N73-26678
Design and thermal analysis on film cooled exhaust duct for fissioning uranium plasma test reactor
[NASA-TM-X-2861] 18 p2178 N73-27585
Irradiation of TZM-Uranium dioxide fuel pin at 1700 K
[NASA-TM-X-2755] 18 p2178 N73-27588
Thermodynamic analysis of Si film growth rate in vertical reactor
18 p2186 N73-27651
Design of injector system for fusion reactor
[MATT-949] 19 p2324 N73-28699
Feasibility of on-line fission gas leak detection system for 100 kW zirconium hydride reactor
[NASA-TM-X-2870] 20 p2453 N73-29717
Design and characteristics of capsule assembly to evaluate tungsten emitter and carbide fuel combinations for thermionic fuel elements
[NASA-TM-X-2887] 21 p2578 N73-30658
Atmospheric models for evaluating nuclear facility sites
[BNWL-1651-VOL-2-PT-1] 24 p2885 N73-33044
Measured and calculated fast neutron spectra at surface of lithium hydride and depleted uranium shielded reactors
[NASA-TM-X-2906] 24 p2953 N73-33594
Radiation shielding for zirconium hydride reactor systems
[AI-AEC-13081] 24 p2955 N73-33609

NUCLEAR RESEARCH
Nuclear and instrumentation research
[AECL-4129] 01 p0079 N73-10651
Nuclear research projects with fast electron accelerator and theoretical physics of neutron decay reactions
04 p0452 N73-13687
Sonic or ultrasonic holography in nuclear industry research
[DUN-SA-191] 08 p0929 N73-17610
Bibliography of Nuclear Science Abstracts from 1964 to 1970
[AED-C-21-10] 08 p0942 N73-17720
Operational descriptions of some electronics and nuclear laboratories in Poland
[AD-752772] 09 p1011 N73-18257
Summary of experimental programs performed using NBS reactor during 1971 and 1972
[NBS-TN-758] 12 p1426 N73-21559
Atomic materials research in Canada
[AECL-4353] 17 p2065 N73-26711

Nuclear research and neutron radiotherapy at Navy laboratory
[PB-221982/2] 22 p2738 N73-31924
NUCLEAR RESEARCH AND TEST REACTORS
NT HIGH TEMPERATURE NUCLEAR REACTORS
Neutronics analysis of gas core rocket concept using cavity test reactor
[NASA-TM-X-2743] 09 p1063 N73-18676
NUCLEAR ROCKET ENGINES
NT NUCLEAR LIGHTBULB ENGINES
Development of test equipment and procedures to simulate thermal environment and fuel region of small models of nuclear lightbulb engine configurations
[NASA-CR-129299] 03 p0330 N73-12692
Development of closed cycle, vortex stabilized nuclear lightbulb engine to show basic design concepts and operating principles
[NASA-CR-129298] 03 p0330 N73-12695
Analysis of heat balance characteristics of nuclear lightbulb engine to determine effects on engine performance, space radiator requirements, and cooling sequence
[NASA-CR-129295] 03 p0331 N73-12696
Design and performance characteristics of small scale model of nuclear lightbulb engine for testing in nuclear furnace reactor
[NASA-CR-129296] 03 p0331 N73-12697
Wide Temperature range, nonpolymeric, large molecular weight lubricants based on combination of siloxane and aromatic groups, for equipment near spacecraft nuclear reactors
[NASA-CR-123966] 04 p0447 N73-13654
Thermodynamic properties of open cycle gaseous core nuclear rocket engine
[NASA-TM-X-2784] 11 p1323 N73-20733
Design and performance of nuclear rocket engine
[LA-5057] 12 p1428 N73-21570
Safety procedure for testing thermionic reactor in test facility
[NASA-TM-X-68224] 13 p1558 N73-22624
Thermionic reactor development program
[LA-5113] 15 p1738 N73-24092
Feasibility study for Europa 3 launch vehicle nuclear upper stage
[TR-TT-4-15/72] 15 p1811 N73-24675
Configuration of nuclear upper stage for Europa 3 launch vehicle
[TR-TK-REF-1-374/72] 15 p1811 N73-24676
Radiation shielding for thermal-nuclear stage of Europa 3 launch vehicle
[TR-TT-4-18/72] 15 p1811 N73-24679
Nuclear rocket engine for Europa 3 launch vehicle
[D-1-72] 15 p1811 N73-24681
Feasibility study for Europa 3 launch vehicle nuclear upper stage
[TR-T/T-1.2-7/72] 15 p1836 N73-24880
Pilot level decision analysis of thermionic reactor development strategy for nuclear electric propulsion
[NASA-CR-133035] 16 p1943 N73-25725
Design and sizing of gas core nuclear rocket engine system components
[NASA-TM-X-2772] 18 p2176 N73-27575
Experimental and analytical determination of one- and two-component flows in spherical chambers for application to open-cycle gaseous-core nuclear rocket
[NASA-CR-2282] 19 p2255 N73-28175
International system of units for reporting Nuclear Rocket Engine Program
[LA-5285-MS] 24 p2929 N73-33394
Design and development of thermionic reactor power system for future interplanetary exploration - Vol. 4
[GULF-GA-C-12308-VOL-4] 24 p2954 N73-33602
NUCLEAR SCATTERING
NT NEUTRON SCATTERING
NT RESONANCE SCATTERING
Light cone singularities, DGS representations, and asymptotic behavior of forward scattering amplitudes
[TR-73-059] 03 p0339 N73-12765
NUCLEAR SHIELDING
U RADIATION SHIELDING
NUCLEAR STRUCTURE
Four particle correlations in nuclear alpha structure
[HMI-B-125] 02 p0213 N73-11727
Experimental and theoretical studies of nuclear structure and pion reaction mechanisms at intermediate energies
[ORO-3948-4] 04 p0453 N73-13697
Scaling relations for critical exponents of modified F model
[NUB-2172] 12 p1438 N73-21653
Analysis of nuclear matter under assumption that nucleons are arranged in lattice
24 p2960 N73-33656
NUCLEAR SUBMARINES
U SUBMARINES
NUCLEAR TEST REACTORS
U NUCLEAR RESEARCH AND TEST REACTORS
NUCLEAR WARHEADS
Destruction capabilities and nuclear radiation potential of rockets with nuclear warheads
[AD-756565] 13 p1595 N73-22938
NUCLEAR WEAPONS
NT FISSION WEAPONS
Sr, Ba, and Ce fallout from nuclear explosions and weapons tests, monitored in ground-level air, in rain, and in atmosphere
[ORO-2529-30] 03 p0333 N73-12719
Environmental pollution monitoring for radioactive isotope laboratory
[MLM-1922] 03 p0340 N73-12770
Safety standards for Air Force nuclear weapons systems
[AD-759574] 17 p2062 N73-26681
NUCLEAR-ELECTRIC MOMENTS
U ELECTRIC MOMENTS
NUCLEASE
Proton magnetic resonance spectra and calorimetry of interactions between ions, inhibitors, and substrates with two ribonucleases
[BMVG-FBWT-72-7] 07 p0746 N73-16071
Enthalpy values for reaction of retarding mononucleotides with ribonuclease and thermodynamic parameters for enzyme inhibitor interactions
[FMVG-FBWT-72-12] 07 p0747 N73-16073
Proton magnetic resonance spectra of ribonuclease A inhibitor complexes, noting effect on catalytic activity
[BMVG-FBWT-72-13] 07 p0747 N73-16074
NUCLEATE BOILING
Compilation of titles, authors, and corporate sources on subject of heat transfer in boiling metals under natural convection conditions
[NLL-RISLEY-TR-2167-[9091.9F]] 05 p0605 N73-14920
Analysis of forced convection film, transition, and nucleate boiling regions for water with application to boiling water reactor cooling systems
[DSR-73645-80] 13 p1590 N73-22892
Vaporization mechanisms and nucleate boiling in heat pipes with thin liquid films
[AD-757280] 14 p1720 N73-23955
NUCLEATION
NT CLOUD SEEDING
Nucleation and film growth mechanisms in heteroepitaxial semiconductor
[AD-748424] 04 p0460 N73-13753
Condensation nuclei measurements noting counters and importance to cloud physics
07 p0859 N73-16964
High temperature contact nucleation of supercooled water by organic chemicals for fog and cloud seeding
[AD-753465] 10 p1127 N73-19181
Electron microscopic analysis of epitaxial growth and nucleation in condensed gas crystals
[AD-753108] 10 p1201 N73-19773
Influence of defects and impurities on nucleation and growth of oriented films by evaporation
[NASA-CR-2234] 13 p1559 N73-22636
Nucleation and film growth mechanisms in heteroepitaxial semiconductor thin films
[AD-755529] 13 p1568 N73-22706
Condensible vapor supersonic nozzle flows at supersaturation collapse near condensation point
[AD-756471] 14 p1651 N73-23393
Development of model to predict formation and detection of molecular cluster size distribution for various materials in supersonic free jet
15 p1765 N73-24300
Influence of supersaturation on nucleation behavior in continuous agitated cooling crystallizers
[WTHD-44] 16 p1953 N73-25799
Vapor condensation by homogeneous nucleation in supersonic nozzle flows
17 p1991 N73-26101
Theoretical determination of heterogeneous nucleation rate of supercooled water droplets from thermally generated AgI particles
[AD-758858] 18 p2114 N73-27095
Analysis of condensation effects in supersonic nozzle flows for homogeneous and heterogeneous nucleation conditions
18 p2128 N73-27195
NUCLEI
Structure of cometary nucleus
02 p0227 N73-11836
NUCLEI [NUCLEAR PHYSICS]
NT ALPHA PARTICLES
NT DEUTERONS
NT HEAVY NUCLEI
NT TRITONS
Detection and measurement of cosmic ray charge spectrum for nuclei heavier than iron with relation to nucleosynthesis and mechanics of supernova
[NASA-TM-X-58102] 03 p0352 N73-12872
Evidence for one source mechanism for primary cosmic rays and another mechanism for iron nuclei, based on balloon-borne ionization spectrometer
[NASA-TM-X-66149] 06 p0716 N73-15841
Preliminary studies of reaction yielding triton pion from proton deuteron interaction
[NASA-TM-X-68187] 07 p0823 N73-16674
Self-consistent Pauli corrections in Brueckner-Hartree-Fock calculations
[NASA-TM-X-68197] 10 p1193 N73-19704
Interactions of energetic neon with emulsion nuclei
[AD-754247] 11 p1327 N73-20768
Photonuclear giant resonance data summary
[NBS-SP-380] 12 p1427 N73-21564
Nuclear reactions in hydrogen exhausted zone of star during supernova explosion and nuclei syntheses through nitrogen conversion
13 p1575 N73-22762
Nuclear properties in neutron interactions with various nuclei in fast breeder reactor
[ANCR-1088] 17 p2062 N73-26677
Spallation reactions of light nuclei during galactic cosmic radiation interaction with interstellar gas
[FRNC-TH-333] 21 p2597 N73-30812
Primary and secondary nuclei production in cosmic rays
22 p2733 N73-31872
Explosive carbon burning effects of observed nuclei in solar system and constraints on supernova explosions
[LA-UR-73-489] 24 p2992 N73-33911
NUCLEIC ACIDS
NT RIBONUCLEIC ACIDS
Long term hypokinesia effect on protein and nucleic acid content in rat tissue
14 p1607 N73-23027
Application of fluorescence spectroscopy for analyzing macromolecules of proteins and nucleic acids
[PAPER-76A6-744] 21 p2546 N73-30410
Ultracentrifugation of biological materials
[NASA-CR-114673] 23 p2750 N73-32009
NUCLEON POTENTIAL
One boson exchange nucleon-nucleon potential in two nucleon and many nucleon problems
[NOTA-INTERNA-380] 01 p0084 N73-10694
NUCLEON-NUCLEON INTERACTIONS
One boson exchange nucleon-nucleon potential in two nucleon and many nucleon problems
[NOTA-INTERNA-380] 01 p0084 N73-10694
NUCLEONICS
Thermal and nucleonic behavior of NERVA reactor during startup transient investigation
[AD-764231] 22 p2699 N73-31620
NUCLEONS
Inelastic lepton-nucleon process in Bjorken limit for neutral gluon model
[ILL-[TH]-72-10] 01 p0083 N73-10684
New tables for forward pion nucleon scattering amplitude analyzing errors and total cross section data
[NOTA-INTERNA-382] 01 p0084 N73-10695
Off-shell asymptotic behavior of electromagnetic form factors of composite particle
[TR-73-070] 06 p0703 N73-15728
Analysis of nuclear matter under assumption that nucleons are arranged in lattice
24 p2960 N73-33656
NUCLEOSIDES
NT ADENINES
NT ADENOSINE TRIPHOSPHATE [ATP]
NUCLEOSYNTHESIS
U NUCLEAR FUSION
NUCLEOTIDES
NT ADENINES
NT ADENOSINE TRIPHOSPHATE [ATP]
Analysis of carbonaceous Migei chondrite for content of polynucleotide
[NASA-TT-F-14683] 08 p0962 N73-17868
NUCLIDES
NT ARGON ISOTOPES
NT CALCIUM ISOTOPES
NT CALIFORNIUM ISOTOPES
NT CARBON ISOTOPES
NT COBALT 60
NT CURIUM 244
NT DEUTERIUM
NT HELIUM ISOTOPES
NT HYDROGEN ISOTOPES
NT IODINE ISOTOPES
NT IRON 57
NT ISOTOPES
NT LITHIUM ISOTOPES
NT NEPTUNIUM
NT NICKEL ISOTOPES
NT NITROGEN ISOTOPES
NT OXYGEN ISOTOPES
NT PLUTONIUM
NT PLUTONIUM 238
NT RADIOACTIVE ISOTOPES
NT RADIUM 226
NT RUBIDIUM ISOTOPES
NT TELLURIUM
NT TRANSURANIUM ELEMENTS
NT TRITIUM
NT URANIUM 233
Activation analysis using short-lived nuclides of boron, oxygen, fluorine, yttrium, and lead isotopes based on gamma spectra and pneumatic tube
03 p0263 N73-12127
Extended applications and improvement of 4 pi beta-gamma coincidence method in standardization of radionuclides
[RR-730] 06 p0702 N73-15724
Energy tables for alpha emitting nuclides
[AAEC/TM-631] 17 p2065 N73-26703
NULL REFERENCE GLIDE PATH
U GLIDE PATHS

NULL ZONES
Physical equivalence of null plane quantum electrodynamics in null plane gage to conventional electrodynamics in Coulomb gage
09 p1066 N73-18700

NUMBER THEORY
NT CONGRUENCES
NT INTEGERS
Capacity of geometric codes and increased effectiveness of semiconductor storage units using number block structures
[JPRS-57251] 02 p0145 N73-11177
Arithmetic error correction in redundant residue number systems
05 p0569 N73-14619
Digital filtering techniques
[NASA-CR-124166] 11 p1264 N73-20256
Quasi-subcycle properties in congruential pseudorandom number generators
[NASA-TM-X-62275] 17 p2054 N73-26618

NUMERICAL ANALYSIS
NT APPROXIMATION
NT CHEBYSHEV APPROXIMATION
NT DIFFERENCE EQUATIONS
NT ERROR ANALYSIS
NT FINITE DIFFERENCE THEORY
NT HARTREE APPROXIMATION
NT INTERPOLATION
NT ITERATION
NT ITERATIVE SOLUTION
NT LEAST SQUARES METHOD
NT MONTE CARLO METHOD
NT NEWTON-RAPHSON METHOD
NT NOMOGRAPHS
NT NUMERICAL INTEGRATION
NT RAYLEIGH-RITZ METHOD
NT RELAXATION METHOD [MATHEMATICS]
NT RITZ AVERAGING METHOD
NT RUNGE-KUTTA METHOD
NT SOMMERFELD APPROXIMATION
NT TRUNCATION ERRORS
Two dimensional numerical analysis based on nonlinear partial difference equations of cross sections of long alternators
[AD-744985] 01 p0007 N73-10052
Numerical analysis of finite-strength, isentropic pressure waves transverse to axis of circular cylinder
[NASA-CR-2138] 01 p0041 N73-10321
Numerical analysis of two-dimensional gravity wave flow on nonuniform free streams
[AD-744995] 01 p0042 N73-10329
Numerical solution of steady state cavitation flows
[AD-745346] 01 p0042 N73-10331
Numerical analysis of supersonic, inviscid, steady flow past blunt-nosed cone at yaw
[AD-745782] 01 p0042 N73-10333
Eulerian incompressible hydrodynamic numerical model and laboratory simulations of tsunamis
[AD-745420] 01 p0053 N73-10430
Gas-embedded z-pinch and numerical simulation of lithium liner for collapsing theta pinch
[AD-745016] 01 p0086 N73-10708
Large signal modeling of bipolar transistors for computer-aided circuit analysis
[AD-745772] 01 p0088 N73-10730
Numerical analysis of thermal problems in presence of radiation and temperature-dependent thermal conductivities
[EUR-4809-F] 01 p0116 N73-10960
Numerical solutions for small cone angles of modified dipole antennas
[AD-745979] 02 p0149 N73-11211
Numerical techniques for analysis of microstrip transmission line configurations
[AD-746059] 02 p0151 N73-11223
Numerical solutions for jets impinging on curved surfaces
[NASA-CR-129136] 02 p0154 N73-11252
Numerical analysis of viscous-inviscid interaction in supersonic flow around blunt body
[AD-746891] 02 p0160 N73-11293
Limb radiance inversion using weighting functions and iterative convergence for nonlinear kernel
02 p0197 N73-11591
Digital analysis of dynamic response data, aerodynamic forces and stability derivatives, of free flight models
[ARC-R/M-3699] 03 p0248 N73-12006
Numerical analysis to obtain error estimate for thermal resistance measurements on uncoated silicon microwave transistors as result of temperature gradients
[AD-748073] 03 p0276 N73-12235
Numerical and perturbation theory solutions for evaluating performance of eddy current flowmeters
[BNWL-SA-4236] 03 p0302 N73-12470
Bearing flexibility effect on triple-spin satellite attitude stability
[ESRO-SN-121] 03 p0359 N73-12926
Numerical analysis of terrain echo spectrum from moving radar altimeter
[SC-DR-72-0261] 04 p0389 N73-13159
Numerical calculation of supersonic three dimensional jet plum in perfect gas with inviscid and compressible properties
04 p0404 N73-13287
Numerical analysis of ion dissipation in high Mach number bow shocks
[IPP-6/102] 04 p0405 N73-13300
Numerical analysis of Pacific Ocean bottom signal reflection losses using underwater explosive sound sources and multilayered acoustic absorption model
[AD-748199] 04 p0450 N73-13676
One dimensional radial fluid cone for studying Z-pinch enbedded in hydrogen
[AD-748179] 04 p0455 N73-13718
Improving method of numerical calculation of aerodynamic coefficients for subsonic lifting surface
[REPT-32] 05 p0491 N73-14004
Numerical simulation and study of collisional plasmas and shock tube phenomena
[COO-3086-15] 05 p0583 N73-14748
Numerical calculation of physical and electronic properties of metals
[AD-749546] 05 p0588 N73-14782
Lectures on partial differential equations and numerical analysis presented at International Congress on Mathematics
[FOA-2-C-2470-11] 06 p0690 N73-15618
Theoretical and numerical analysis of pulsed plasmoid accelerator
[AD-750524] 06 p0707 N73-15764
Equations and graphs on electromagnetic field parameters
[UCRL-51245] 07 p0756 N73-16140
Numerical analysis of viscous, compressible, and heat conducting fluid flow patterns in rotating nozzles
07 p0768 N73-16241
Numerical method for solving time dependent Navier-Stokes equation in two dimensions
[AD-751628] 07 p0773 N73-16276
Analytical solution of nonsimilar laminar boundary layer with pressure gradient, variable wall temperature, and continuous mass injection
[AD-751804] 07 p0773 N73-16279
Curriculum of training course on basics and state-of-the-art of remote sensing and developments in parameter optimization
[NASA-CR-128713] 07 p0848 N73-16876
High voltage distribution fields of two component dielectrics in rotational series or parallel arrangements
08 p0888 N73-17193
Mathematical and computer analysis of multiple channel sidelobe canceller
[AD-753571] 09 p1004 N73-18198
Numerical solution to transonic airfoil problems
[AD-753390] 09 p1018 N73-18304
Numerical calculation of quantitative characteristics of observation systems
[NAL-TR-301] 09 p1057 N73-18616
Algorithms for numerical solution of problems in calculus of variations
[NPL-NAC-28] 09 p1058 N73-18626
Numerical calculation of flow fields produced by lifting elliptic cone, lifting three dimensional wing, and lifting delta wings
[NASA-CR-131089] 10 p1139 N73-19282
Combination of satellite and gravimetric data for analysis of terrestrial gravity field blocks
[NASA-CR-130176] 10 p1153 N73-19380
Development of technique for inferring atmospheric ozone information from satellite nadir measurements
[NASA-TR-R-399] 10 p1154 N73-19386
Computational procedure for determining heat resistance of different graphites in broad temperature range
10 p1175 N73-19557
Numerical solutions for variational control functions of flight dynamics in circular orbits
10 p1178 N73-19582
Elements of numerical calculus
[ISS-72/13-PT-1] 10 p1179 N73-19590
Numerical calculation of ultrahigh energy photon spectrum
[NASA-TM-X-66198] 10 p1193 N73-19703
Numerical analysis of finite deformation of elastoplastic solids
[NASA-CR-2199] 10 p1220 N73-19924
Numerical analysis of dynamic problem of axisymmetrically impacting finite-length rods
[AD-754119] 11 p1346 N73-20923
Application of mathematical procedures for determining correlation properties of radio transmissions and signal processing
12 p1379 N73-21181
Theory of two phase gas-liquid and liquid-gas flow for bladed machines and ejectors
[AD-755713] 12 p1409 N73-21419
Numerical analysis of aerodynamic load distribution on swept back wing mounted on infinite circular cylinder fuselage at zero angle of attack
[AD-756075] 13 p1475 N73-21952
Millimeter wave image conversion system for optical display of objects obscured by fog or rain
13 p1489 N73-22074
Computer analysis and design of special antenna configurations and characteristics
[AD-756470] 13 p1501 N73-22169
Study of effects of solar activity on geophysical phenomena using numerical techniques
13 p1514 N73-22264
Calculation of gas flow in bypass compressor
[AD-756092] 13 p1535 N73-22441
Analysis of algorithms for failure detection, isolation, and correction of redundant inertial instruments in strapdown dodecahedron configuration
[NASA-CR-124234] 13 p1556 N73-22608
Numerical calculation of current-voltage characteristics for ionized plasma containing negative ions with unequal electron and ion temperatures
[LOG-J7146] 13 p1563 N73-22667
Numerical analysis of nonlinear elliptic-hyperbolic mixing about wing profiles at Mach 1
14 p1597 N73-22944
Analysis of clipped speed characteristics and zero crossing-related speech phenomena
14 p1632 N73-23233
Design of sonar array using standard amplitude shading technique
[AD-755481] 14 p1633 N73-23241
Three-term solution for integral equation of current along thin cylindrical dipole antenna
[AD-758192] 14 p1643 N73-23327
Numerical analysis of gas flow ahead of supersonic cascade
[AD-756079] 14 p1650 N73-23385
Numerical solution of one hydrodynamics equation
[AD-756099] 14 p1651 N73-23394
Application of graph theory to Air Force systems design and analysis
[AD-757235] 14 p1684 N73-23666
Computer programs for numerical approximation of selected meteorological parameters related to cloud physics
[AD-757623] 14 p1686 N73-23680
Numerical analysis of resonance interactions in dynamic stability of elastic shells under compression
[AD-756237] 14 p1715 N73-23918
Numerical analysis of bending flutter and torsional flutter in flexible hydrofoil struts
[AD-757645] 14 p1717 N73-23935
Numerical smoothing and interpolation methods noting spline function method
[ONERA-NT-205] 15 p1804 N73-24619
Conference on military research and numerical analysis
[AD-758145] 15 p1804 N73-24620
Analysis of improved numerical solutions to stochastic collection equation for cloud droplets
15 p1805 N73-24629
Numerical solution of viscous fluid flow in finite tube with deformable walls in presence of valves for application to blood circulation process
16 p1867 N73-25117
Nonlinear dynamics of collective modes
[BN-695] 16 p1888 N73-25282
Numerical analysis of fluid mechanic problems
[AD-758078] 16 p1893 N73-25318
Numerical calculation of several two dimensional magnetohydrodynamic flows in channels
[AD-759424] 16 p1893 N73-25319
Numerical analysis of Josephson junction interferometers
16 p1911 N73-25464
Numerical analysis of load absorption of two adjacent filaments in fiber-reinforced material
[AD-759729] 16 p1933 N73-25639
Correspondence principle for vibration analyses on viscoelastic bodies with loss tangents
[AD-759260] 16 p1971 N73-25943
Computer program and numerical technique for calculating chemical composition of stirred reactor
[AD-751462] 16 p1974 N73-25967
Numerical analysis of minimum probability of error expression in digital communication system with intersymbol interference
[AD-760057] 17 p1999 N73-26167
Numerical solution and internal gravity wave approximation of solar semidiurnal tidal mode behavior in dissipative atmospheres
[NASA-CR-132779] 17 p2025 N73-26383
Numerical technique for determining thermo-elastic deformations in segment of hollow cylinder subjected to varying forces
[AECL-4308] 17 p2094 N73-26939
Computer program for predicting inviscid, transonic flow field about isolated nacelles
[NASA-CR-112271] 18 p2130 N73-27211
Mathematical formulation of physically correct contribution function for spectral lines
[AD-758770] 18 p2198 N73-27749
Mathematical procedure for determining exact slew reorientation of spacecraft about nonorthogonal axes
18 p2211 N73-27850
Quadratic programming with regularization for analyzing polymer molecular weight distribution
[AD-761818] 19 p2234 N73-28009
Critical review of experimental data for developed free turbulent shear layers
19 p2252 N73-28156

Numerical solution of optimal control problems with differential constraints
[AD-761787] 19 p2315 N73-28617
Numerical analysis of barium cloud growth and striation in conducting background
[AD-761828] 19 p2317 N73-28637
Numerical calculation of electric potential resulting from charged parallel plates of equal width - Part I
[AD-761866] 19 p2321 N73-28676
Detailed calculations of natural vibrations of single cylindrically curved open shells
[NASA-TT-F-14979] 19 p2347 N73-28880
Numerical technique for calculating thermal spreading resistance
[NASA-CR-12412] 19 p2352 N73-28921
Numerical analysis and computerized simulation of open combustion processes and flame stability
[AD-762360] 19 p2353 N73-28925
Numerical analysis of solitary wave propagation in incompressible rotating fluids
20 p2385 N73-29160
Numerical analysis of ice fog produced by automobiles during arctic conditions
20 p2441 N73-29603
Numerical approach to study of convective and semi-convective stability
20 p2470 N73-29836
Space vehicle design criteria based on interplanetary charged particle environments
[NASA-CR-124341] 20 p2474 N73-29876
Numerical analysis of laminar boundary layer on slipping wing
[AD-763285] 21 p2526 N73-30255
Numerical analysis of collapse of homogeneous fluid mass in stratified fluid
[AD-763657] 21 p2526 N73-30257
Numerical experiments for solving complete equations of hydrodynamics
[AD-763143] 21 p2539 N73-30359
Computer solutions of cylindrical antennas in anisotropic media
22 p2627 N73-31045
Dispersion of angular coordinate estimate during digital processing of radar data based on application of discrete Markov chains
22 p2628 N73-31058
Algorithms to determine potential conflicts over oceanic airspace based on vertical, lateral, and longitudinal separation criteria
[FAA-RD-73-73] 22 p2697 N73-31606
Two-dimensional numerical analysis of integrated silicon N-P-N bipolar transistors
22 p2706 N73-31672
Numerical method of characteristics for unsteady flow with dissipation
[DLR-FB-72-23] 23 p2776 N73-32198
Numerical solution of corner flow problem using alternating direction implicit method
[AD-765209] 23 p2776 N73-32203
Application of second-order accurate fluid algorithm for variable spatial grid
[AD-765316] 24 p2910 N73-33225
Numerical solution to problem of gravitational-shear waves in flow with arbitrary temperature stratification
24 p2947 N73-33532

**NUMERICAL CONTROL**
Numerical control of delta modulated vocal signals in air navigation telecommunication system
01 p0025 N73-10194
Manufacture and testing silver parabolic mirror cut directly with diamond tool in numerically-controlled lathe
[UCRL-51213] 03 p0335 N73-12734
Efficiency of computer for numerically controlled machine tools
[CRIF-MC-44] 04 p0427 N73-13478
Application of small digital computer to improve operation of electronic maintenance system
[Y-1837] 06 p0647 N73-15258
Comparison of computed torque method and conventional position servo computer controlled manipulator
[NASA-CR-131521] 12 p1381 N73-21198
On-line digital computer control of NERVA
12 p1426 N73-21558
Development of automated drafting and digitizing system for preparing concept, experimental, prototype, and production mechanical drawings
[AD-755502] 14 p1671 N73-23558
Application of Minuteman guidance computer for numerical processing control
[AD-760757] 18 p2121 N73-27145
Automation of computer controlled robot manipulators
[JPRS-59717] 20 p2371 N73-29051
Computer-controlled fine attenuators for fine gain adjustments of linear amplifiers
[KFK-1707] 20 p2381 N73-29130
Use of computer-controlled two-dimensional film densitometer for analysis of photographs of chemical releases at high altitudes
[AD-763082] 20 p2413 N73-29398
Simultaneous determination of carbon, hydrogen, and nitrogen in organic compounds
[UCID-16198] 24 p2892 N73-33085

**NUMERICAL INTEGRATION**
NT RUNGE-KUTTA METHOD
Numerical integration procedure for determining electromagnetic structure of interplanetary space
01 p0093 N73-10768
Applications of orbital mechanics to aerospace systems and ballistic trajectories
[AD-746706] 02 p0232 N73-11885
Numerical integration and variational calculation method for approximate solution to three dimensional flow of gas dynamic bearings
[AD-747377] 03 p0308 N73-12513
Numerical integration computer program based on integrating only perturbations in cartesian coordinates
[AD-747588] 04 p0476 N73-13890
Integration of unsteady aerodynamic forces and pressure distributions in aeroelastic analysis
[NLR-MP-71013-U] 05 p0492 N73-14011
Closed form, Romberg, and Gaussian procedures for calculating transonic wave drag integral using cubic splines
[NAL-TN-35] 06 p0652 N73-15299
Simulation of emission-dispersion of inert pollutant in lower atmosphere in industrial zones by numerical integration of conservation and pollutant flow equations
06 p0693 N73-15649
Binary concatenated coding system to measure, count, and record numerical information using minimized number of digits
[NASA-CASE-MSC-14082-1] 07 p0759 N73-16163
Theoretical derivation of finite element solution algorithm for transient energy conservation equation
[NASA-CR-130149] 07 p0813 N73-16593
Integration of Galerkin method for solving boundary layer equation with steady incompressible flow
[AD-752203] 08 p0898 N73-17275
Numerical solution of linear differential equations describing dynamic response of vehicles
[TT-7212-PT-1] 08 p0937 N73-17669
Efficiency of numerical integration methods for differential equations
10 p1178 N73-19585
Survey on numerical integration methods for differential equations
10 p1178 N73-19586
Meksyn asymptotic integration method for studying viscous interaction within hypersonic rarefied gas flow regime
12 p1389 N73-21263
Method for direct numerical integration of Boltzmann equation
12 p1418 N73-21487
Special perturbation methods for improved computational efficiency in numerical integration of artificial satellite orbits
12 p1447 N73-21717
Application of Runge-Kutta process to circular geostationary orbit equations of motion
[RAE-TR-72118] 13 p1578 N73-22790
Numerical integration technique used to re-compute influence coefficients used for development of design curves for rigid airfield runway pavements
[AD-755526] 14 p1646 N73-23353
Numerical integration techniques for solution of orbital elements of moon and planets
[AD-755164] 14 p1707 N73-23850
Methods for computing numerical quadrature of integrable function over finite inerval
[NASA-TM-X-66277] 18 p2169 N73-27518
Influence of CISK process on mass convergence in tropical planetary boundary layer
18 p2171 N73-27529
Analysis of free turbulent shear flows by numerical methods
19 p2252 N73-28160
Numerical integration techniques for shock discontinuity in one dimensional unsteady channel flow
[PUBL-138] 22 p2654 N73-31258
Numerical integration subroutines built into NASA-JSC computer
[NASA-CR-134021] 22 p2714 N73-31725
Differential approximation and numerical integration methods for analyzing behavior of wall stabilized electric arcs with radiative transport
[AD-765207] 23 p2857 N73-32831

**NUMERICAL WEATHER FORECASTING**
Numerical weather forecasting methods - basic equations of dynamic processes and quasi-geostrophic approximation
[NLL-M-20352-[5828.4F]-VOL-1]
01 p0073 N73-10595
Numerical weather forecasting methods - atmospheric and weather forcasting models
[NLL-M-20352-[5828.4F]-VOL-2]
01 p0073 N73-10596
Regression analysis used for numerical-statistical prediction of visibility at sea
[AD-743733] 01 p0076 N73-10625
Barotropic primitive equation model for numerical weather forecasting for tropics
[AD-743729] 01 p0076 N73-10626
Using satellite observations for enhancing accuracy and detail of numerical analysis in sparse-data areas
[AD-745173] 01 p0077 N73-10633
Numerical analysis through proportional differences for analyzing meteorological satellite data and predicting synoptic weather patterns
[AD-749072] 05 p0574 N73-14672
Two dimensional dynamical model for fog forecasting for periods up to eight hours on local scale
[AD-750082] 05 p0575 N73-14682
Fast and accurate technique for iterative solution of saturation adjustment problem
[AD-750083] 05 p0575 N73-14683
Boundary value equations for numerically forecasting weather in area defined by artificial boundaries
[AD-749748] 05 p0576 N73-14689
Introducing cloud seeding in model for predicting precipitation patterns over synoptic scale
[AD-750730] 05 p0576 N73-14691
Relationship between vertical velocity in baroclinic model and occurrence of rain and clouds in Finland
[TR-4] 07 p0814 N73-16603
Feasibility determination of Sutcliffe-Peterssen development theory to predict development of cyclones and anticyclones at sea level
[NASA-CR-2192] 07 p0815 N73-16605
Use of vector spherical harmonics for numerical weather forecasting
[AD-752569] 08 p0921 N73-17548
Aeronautically oriented numerical weather prediction activities in Finland during 1970
[TR-2] 08 p0937 N73-17677
Role of mathematics in meteorology
08 p0938 N73-17678
Estimation of average daily rainfall from satellite photographs
[NOAA-TM-NESS-44] 09 p1060 N73-18645
Multilayer numerical weather prediction model for studying tropical weather systems, including winds, vorticity, and divergence
[AD-752929] 09 p1061 N73-18653
Variable directions method for solving numerical weather forecasting problems
[AD-752336] 10 p1182 N73-19620
Long range forecast by means of spectral nonlinear baroclinic model of atmosphere
[AD-754682] 11 p1315 N73-20670
Numerical forecasts of barometric fields in stratosphere using quasi-geopotential model
13 p1552 N73-22574
Numerical weather prediction activities of NMC
13 p1553 N73-22582
Finite difference model for short range weather forecasting using directed differences
[AD-756078] 14 p1685 N73-23673
Real forecast verification data for testing Hatter terminal weather forecast models
[AD-757489] 14 p1686 N73-23679
Preparation of long range weather forecasts using principle of analogy of the fields of the meteorological elements
[NLL-M-22852-[5828.4F]] 15 p1805 N73-24628
Simulation of asymmetric hurricane with fine mesh multiple grid primitive equation model
15 p1805 N73-24631
Comparison of cumulus parameterization techniques in numerical integration of easterly wave
16 p1937 N73-25674
Computer programs for ceiling and visibility forecasting using air terminal weather data
[FAA-RD-73-13] 16 p1937 N73-25677
Multilevel atmospheric prediction model based on primtiive equations of moiton
[DM-8] 16 p1938 N73-25681
Nonadiabatic atmospheric model for short term weather forecasts
[AD-759631] 16 p1939 N73-25690
Difference equations for numerical weather forecasting
[AD-759620] 16 p1939 N73-25692
Simulation research to develop objective meteorological prediction capability - Volume I
[AD-759928] 17 p2058 N73-26642
Simulation research to develop objective meteorological prediction capability - Volume 2
[AD-759929] 17 p2058 N73-26643
Techniques for improving accuracy of numerical 24-hour cloud cover forecasts in sparse data areas using satellite data
[AD-759986] 17 p2058 N73-26644
Semi-implicit version of numerical weather prediction model developed by Shuman and Hovermale
[NOAA-TM-NWS-NMC-53] 18 p2172 N73-27545
Numerical boundary conditions in baroclinic and barotropic models for forecasting
[DM-9] 19 p2316 N73-28623
Analog scheme for analyzing meteorological parameters to determine their predictive value for forecasting intensity changes in western North Pacific tropical cyclones
[AD-761726] 19 p2316 N73-28625
Operational equations model forecasting extratropical cyclogenesis in evaluating the fleet numerical weather center
[AD-761727] 19 p2316 N73-28626
Calculation of cloud cover from vertical velocity data supplied by meteorological satellites
[AD-761545] 19 p2317 N73-28634

Numerical solution to boundary value problems of hydrodynamic forecasting and atmospheric circulation
[AD-761574] 19 p2317 N73-28640
Computerized optimal ship routing considering ocean meteorological charts
[AD-761620] 19 p2319 N73-28652
Synopticostatistical, numerical, and laboratory procedures for studying dynamics of atmospheric circulation in planetary atmospheres including earth
[TT-70-50052] 20 p2442 N73-29615
Influence of nonadiabatic processes particularly radiative heat influx on numerical weather forecasting
20 p2443 N73-29624
Numerical forecasting of geopotential, temperature, dew point fields at 850 millibar level
20 p2446 N73-29630
Upper air numerical forecast model designed to predict tropical macro-scale features
[AD-763102] 20 p2451 N73-29697
Numerical weather prediction activities of National Meteorological Center for first half of 1973
23 p2814 N73-32497
Atmospheric circulation and turbulence forecasting
[AD-764919] 23 p2815 N73-32507
Atmospheric field decomposition by systems of orthogonal functions
[AD-764942] 23 p2815 N73-32509
Forecasting of spring flow runoff and snow data collection network design
24 p2922 N73-33338
Time coordinate transformation for processing asynoptic meteorological data
24 p2945 N73-33521
Meteorological services, satellites, and numerical weather forecasting
[WMO-342] 24 p2948 N73-33550
Numerical weather forecasting noting atmospheric models and circulation
24 p2949 N73-33553

**NUSSELT NUMBER**
Nusselt-type analysis of laminar film condensation inside truncated rotating cone, emphasizing heat transfer performance
[AD-758513] 15 p1845 N73-24945

**NUTATION**
Attitude stability criteria and nutation decay times of dual-spin satellite with large flexible solar array
[AD-743258] 01 p0109 N73-10897
Nutation and damping theory of Dial satellite after last stage separation
[DLR-FB-72-74] 12 p1461 N73-21842
Nutation damper for use on spinning body
[NASA-CASE-GSC-11205-1] 16 p1917 N73-25513
Threshold detection system for infrared nutating optical system
[AD-761380] 18 p2180 N73-27600

**NUTATION DAMPERS**
Experimental in-orbit verification of mathematical model for RAE spacecraft gravity gradient dynamics
18 p2208 N73-27825

**NUTATIONAL OSCILLATION**
U NUTATION

**NUTRIENTS**
Detection of plant diseases and nutrient deficiencies, soil types, and moisture levels in Tennessee using ERTS-1 imagery
[E72-10320] 04 p0413 N73-13368
Spectral characteristics of normal and nutrient-deficient maize leaves
[NASA-CR-132145] 15 p1742 N73-24119
Utilization of ERTS-1 imagery to detect plant diseases, nutrient deficiencies, soil types, and moisture levels in Tennessee
[E73-10640] 15 p1776 N73-24399

**NUTRITIONAL REQUIREMENTS**
Time periods for nutrient solution exchange in optimal biomass yield on porous aggregate
10 p1117 N73-19106

**NUTS [FASTENERS]**
Estimating effect of inclined nut seating on fatigue strength of steel screw thread
[ESDU-67034] 01 p0060 N73-10487
Tensile and stripping strength data in terms of failure probability for bolts, nuts, screws, and threaded rods
[ESDU-67019] 01 p0110 N73-10908
Numerical analysis of stresses produced in bolt or similar threaded object from application of known tightening torque to bolt head or engaged nut
[ESDU-72022] 05 p0601 N73-14888
Improving screwability of titanium bolts with nuts of various materials
[AD-758037] 15 p1794 N73-24541
Device for securing together structural members with axially stretched bolt and nut
[NASA-CASE-GSC-11149-1] 21 p2552 N73-30457
Specifications for threaded fasteners
[NASA-CR-124415] 23 p2849 N73-32764

**NYLON [TRADEMARK]**
Crystal structure and mechanical and physical properties of polymide S-6 - Nylon
[AD-753967] 11 p1309 N73-20624
Performance tests of commercial nylon double braided rope for extraction lines
[AD-757209] 14 p1681 N73-23643
Stagnation-line analysis of radiative heating of phenolic-nylon ablator
[NASA-CR-112306] 15 p1766 N73-24309
Oxidative stress cracking in nylon fibers immersed in alkaline aqueous medium saturated with molecular oxygen at elevated temperature
24 p2937 N73-33455

**NYLON RESINS**
U POLYAMIDE RESINS

**NYQUIST DIAGRAM**
Nyquist criterion for control loops, using linear functional differential equations and transfer functions
[NRC-TT-1612] 06 p0690 N73-15622

**NYSTAGMUS**
Development of mathematical model for slow phase rotational nystagmus induced by head movements
[AMRU-R-71-3] 02 p0131 N73-11065
Effects of human alertness on vestibular nystagmus habituation
[AD-749352] 05 p0505 N73-14108
Visual and vestibular effects in human oculomotor response during head rotation in yaw and roll
06 p0633 N73-15147
Guinea pigs used to determine effect of intramuscular injections of drugs on fall-out and Bekhterev nystagmus occurring after unilateral and bilateral labyrinthectomies
07 p0744 N73-16049
Sound, light, and proprioceptive stimuli for inhibiting vestibular illusion in man
10 p1115 N73-19087
Effects of gastrointestinal pressure on rabbit eye nystagmus during barotrauma
13 p1479 N73-21983
Effects of alcohol on eye movements and tracking performance during laboratory angular accelerations about yaw and pitch axes
[FAA-AM-72-34] 22 p2619 N73-30989


## O


**O RING SEALS**
Actuator shaft sealing techniques for long term interplanetary spacecraft missions
[NASA-CR-130927] 10 p1165 N73-19479
Mechanical and thermal properties and oxidation resistance of seal ring carbon graphite materials with resin impregnants
[NASA-CR-120955] 10 p1165 N73-19480

**O STARS**
Ultraviolet continuum of O6f star HD 148937 and peculiarities of surrounding nebulae
[NASA-CR-128404] 01 p0100 N73-10824

**OAO**
NT OAO 2
NT OAO 3
Performance of sealed nickel cadmium storage cells at very low ampere/hour percent recharge for OAO
[NASA-TM-X-66093] 02 p0128 N73-11040
Discrete control of linear distributed systems with specific application to primary mirror for orbiting astronomical observatory
[NASA-TM-X-68855] 02 p0173 N73-11400
OAO-A2 observations of Be stars, continuous Balmer emission, and interstellar polarization
[NASA-CR-129166] 02 p0226 N73-11828
Performance tests of OAO-C spacecraft heat pipes under thermal-vacuum conditions
[NASA-TM-X-66072] 02 p0242 N73-11967
Environmental factors affecting OAO and related computer programs for data processing and scheduling observations
[NASA-TM-X-66145] 06 p0721 N73-15882
Dayglow measurements of upper atmosphere by Orbiting Astronomical Observatory A-2
[AD-752228] 08 p0920 N73-17539
Large orbiting X ray telescope with high resolution mirror design
[NASA-CR-124001] 10 p1158 N73-19424
Inertial gyro attitude reference system for pitch and yaw control of OAO spacecraft
18 p2208 N73-27821

**OAO 2**
OAO 2 observations of LY Aur
[NASA-TM-X-66131] 04 p0475 N73-13880
Filter photometric data from OAO 2 on blue Ap, band a dwarfs, and giants
[NASA-TM-X-66163] 07 p0843 N73-16826
OAO 2 observations used to determine relationship between visual and ultraviolet variations in C-4 155-nm line in Beta Cephei
08 p0975 N73-17974
Performance data analysis for OAO sealed nickel cadmium cells and batteries
[NASA-CR-130233] 11 p1237 N73-20045
Investigation of ultraviolet interstellar extinction
[NASA-CR-131990] 14 p1706 N73-23843
Catalog of ultraviolet stellar observations using celescope on OAO 2
[NASA-CR-133259] 17 p2088 N73-26889
Ultraviolet spectrophotometry of Nova Serpentis 1970 by OAO-A2 flight
23 p2836 N73-32660

**OAO 3**
Performance data analysis for OAO sealed nickel cadmium cells and batteries
[NASA-CR-130233] 11 p1237 N73-20045
OAO-C X ray experimental design
17 p2084 N73-26857
Pointing error sensor in star tracker system for OAO 3 attitude control
18 p2208 N73-27822
Onboard OAO 3 computer for commanding and data processing
18 p2208 N73-27824

**OAO-A2**
U OAO 2

**OAO-C**
U OAO 3

**OBLATE SPHEROIDS**
Investigation of causes of perturbations in Saturns rings
[REPT-14] 10 p1212 N73-19854

**OBLIQUE SHOCK WAVES**
Navier-Stokes equations for generating and maintaining straight oblique shock wave in steady supersonic flow and computing inviscid flow field downstream of shock wave
[AD-754095] 11 p1271 N73-20317
Effects of heating within oblique shock wave on its aerothermodynamic and geometric properties
[DLR-FB-73-21] 16 p1858 N73-25050
Shock wave propagation at interface between two rectilinear ducts noting oblique shock waves and mathematical models
[PUBL-137] 24 p2910 N73-33223
Measurement of turbulence in collisionless oblique plasma shock by scattered ruby laser light
24 p2961 N73-33665

**OBSCURATION**
U OCCULTATION

**OBSERVATION**
NT SATELLITE OBSERVATION
NT VISUAL OBSERVATION
Numerical calculation of quantitative characteristics of observation systems
[NAL-TR-301] 09 p1057 N73-18616

**OBSERVATION AIRCRAFT**
NT BREGUET 1150 AIRCRAFT
NT CL-84 AIRCRAFT
NT E-2 AIRCRAFT
NT F-5 AIRCRAFT
NT MIRAGE 3 AIRCRAFT
NT OH-6 HELICOPTER
NT OV-10 AIRCRAFT
NT P-1127 AIRCRAFT
NT U-2 AIRCRAFT

**OBSERVATORIES**
NT ASTRONOMICAL OBSERVATORIES
NT GEOPHYSICAL OBSERVATORIES
NT HEAO
NT OAO
NT OGO
NT OGO-A
NT OSO
NT OSO-3
NT OSO-i
NT OSO-5
NT OSO-6
NT OSO-7
NT SOLAR OBSERVATORIES
Infrared site monitor operations at McDonald Observatory
[NASA-CR-133394] 18 p2152 N73-27392

**OBSTRUCTING**
U BLOCKING

**OCCLUDED FRONTS**
U FRONTS [METEOROLOGY]

**OCCULTATION**
NT LUNAR OCCULTATION
NT RADIO OCCULTATION
NT SOLAR ECLIPSES
NT STELLAR OCCULTATION
Two satellite microwave occultation system for determining pressure levels in atmosphere using infrared sensors
07 p0775 N73-16294
Instrumentation for atmospheric rocket sounding by occultation including infrared interferometer, Fabry-Perot interference filter, and vacuum spectrometer
[BMBW-FBW-72-14-PT-1] 22 p2667 N73-31368
Experimental and theoretical IR spectra of atmospheric hydrocarbon gases CO, CO2, and NH4 for occultation sounding
[BMBW-FBW-72-14-PT-2] 22 p2667 N73-31369
Summary of S band occultation experiment
24 p2983 N73-33837

**OCEAN BOTTOM**
Analysis of thermal fluctuations in San Diego Bay, California and factors which affect thermodynamic properties
[AD-744921] 01 p0052 N73-10420

Analysis of subbottom acoustic reflection profiles along track line from Monrovia, Liberia to Lesser Antilles
[PB-209872] 01 p0053 N73-10427
Development of finite difference scheme for numerical analysis of time dependent seiche oscillating across shallow, infinite channel and transients associated with bottom spiral
[AD-745194] 01 p0053 N73-10428
Sound wave reflection from sea bed, acoustic properties of sedimentary layer, and application to Baltic Sea
[FOA-3-C-3680-E1] 02 p0164 N73-11331
Steady state response of semi-infinite solid with overlying semi-infinite fluid subjected to moving point load at supersonic speed
[AD-747252] 03 p0286 N73-12313
Sea bottom classifier device designed for use with towed underwater vehicle
[AD-748611] 04 p0415 N73-13392
Underwater equipment for locating and recovery of objects from ocean bottom by whales
[AD-747612] 04 p0417 N73-13403
Scripps Institute research on oceanographic instruments, stabilized floating platforms, ocean bottom accelerometers, and surface waves
[AD-748024] 04 p0417 N73-13407
Bottom topography effects on ocean currents
[AD-748008] 04 p0417 N73-13408
Numerical analysis of Pacific Ocean bottom signal reflection losses using underwater explosive sound sources and multilayered acoustic absorption model
[AD-748199] 04 p0450 N73-13676
Geophysical survey of continental shelves off African coast and mapping for oil potential
[PB-211393] 05 p0541 N73-14400
Electrical conductivity of ocean basement determined from measurements of geomagnetic time variations on sea floor off Southern California
[AD-749931] 06 p0668 N73-15431
Geothermal data from deep water and bottom sediment measurements in Atlantic and Pacific Oceans
[AD-749983] 06 p0669 N73-15441
Development and evaluation of equipment for monitoring long term sea floor foundation settlement and tilting
[AD-750258] 06 p0669 N73-15444
Oceanographic equipment and ocean bottom data resulting from Pacific cruise of Iguana
[AD-750679] 06 p0671 N73-15459
Digital signal processing applied to ocean bottom seismic reflection data
[PB-212155] 07 p0794 N73-16456
Influence of bottom topography and earth rotation of wind-driven circulation in Mediterranean Sea
07 p0858 N73-16956
Deploying airborne laser transmitter/receiver to measure water depth in turbid water
[AD-752486] 08 p0921 N73-17551
Acoustic properties of ocean bottom and relevance to sonar performance
[AD-753265] 09 p1032 N73-18429
Design of towed sonar transducer array for bathymetric mapping of ocean bottom topography
[AD-755113] 11 p1259 N73-20216
Marine technology developments to include submerged navigation, submersible instrumentation, geological mapping, magnetic studies, and ocean biology
[AD-754445] 11 p1288 N73-20453
Environmental quality program, environmental forecasting program, and seabed assessment program for international decade of ocean exploration
12 p1400 N73-21359
Geological investigation of future ocean bottom drilling for crude oil and other raw materials
[JPRS-58668] 12 p1401 N73-21366
Seismic reflection, refraction, and near bottom observations in Aleutian trench near 173 deg W
[AD-755455] 14 p1664 N73-23508
Dating of ocean floor rocks and investigation of kinetic processes in lunar regolith
17 p2017 N73-26307
Manned submersible ocean bottom sampling and gravimetric prospecting
[AD-759992] 17 p2029 N73-26425
Development of semi-automatic system for digitizing bathymetry charts for showing ocean bottom contour information
[AD-761647] 19 p2296 N73-28464
Marine geological research of submarine relief and ocean bottom sediments conducted during Tenth Soviet Antarctic Expedition
20 p2407 N73-29345
Influence of ocean bottom relief on genesis and intensity of typhoons
20 p2446 N73-29646
Ship towed magnetometer and ocean bottom mounted magnetic variation station
[JPRS-59802] 21 p2547 N73-30417
Method for calculating ocean bottom magnetic anomalies
[AD-762532] 22 p2668 N73-31380

Advanced marine technology, including submerged navigation, transfer at sea, and bottom reconnaissance
[AD-763372] 23 p2788 N73-32305

**OCEAN CURRENTS**
**NT COASTAL CURRENTS**
Measuring absolute surface current velocity
[AD-743706] 01 p0050 N73-10408
Analysis of thermal fluctuations in San Diego Bay, California and factors which affect thermodynamic properties
[AD-744921] 01 p0052 N73-10420
Development of finite difference scheme for numerical analysis of time dependent seiche oscillating across shallow, infinite channel and transients associated with bottom spiral
[AD-745194] 01 p0053 N73-10428
Numerical analysis of stability and convergence conditions based on mathematical model of Arctic Ocean
[AD-745182] 01 p0053 N73-10429
Influence of wind stress and bottom friction on spectral response of two layer beta plane ocean currents
[AD-746506] 02 p0168 N73-11367
Nonlinear interactions among standing surface and internal gravity waves
[AD-746138] 02 p0168 N73-11368
Integral wave analysis in inhomogeneous fluid, bifurcation in regular and singular eigenvalue problems, and asymptotic expansion of integrals
[AD-747280] 02 p0203 N73-11647
First-order analyses of wind and current time series from Totem buoy off Oregon coast during 1970
[AD-746832] 02 p0206 N73-11668
Side-looking radar applied to oceanography noting sensing of sea states, pollution, and waves
03 p0295 N73-12408
Bottom topography effects on ocean currents
[AD-748008] 04 p0417 N73-13408
Effects of vertical jet breakwaters on wind generated deep water waves
[AD-748190] 05 p0528 N73-14293
Effects of changes in ocean currents and motion on climatology
[NLL-M-22797-[5828.4F]] 05 p0529 N73-14307
Seasonal flow patterns of coastal currents along Oregon-Northern California coast
[AD-749077] 05 p0541 N73-14403
GEK measurements of surface currents for five portions of Monteray Bay during period Nov. to Dec. 1971
[AD-749042] 05 p0541 N73-14404
Location of ocean current boundaries in Gulf of Mexico by ERTS-1 sensing of water color changes
[E73-10030] 06 p0660 N73-15363
Generation and stabilization of coastal wave induced circulation and longshore current patterns
[AD-750291] 06 p0671 N73-15458
Analysis of photography from Apollo 9 flight to determine origin, movement, and dissipation of masses of discolored water near shores of North and South Carolina
07 p0788 N73-16408
Numerical analysis of ocean circulation effects on transients in atmospheric circulation
[AD-751637] 07 p0796 N73-16470
Synoptic analysis of ocean surface currents in Northern Hemisphere
07 p0858 N73-16955
Influence of bottom topography and earth rotation of wind-driven circulation in Mediterranean Sea
07 p0858 N73-16956
Analysis of tidal currents, turbulent diffusion, and local shears in currents found in Trinity Bay, Texas
[NASA-CR-128734] 08 p0916 N73-17510
Temporal propagation and numerical generated wave patterns for internal waves in stratified fluid of variable altitude or depth
[AD-753126] 09 p1031 N73-18417
Wind-driven currents and surges with bottom slipping in shallow water
09 p1059 N73-18639
Location of ocean current boundaries in Gulf of Mexico by sensing color change associated with cyclonic edge of zone of horizontal velocity shear
[E73-10022] 10 p1146 N73-19330
Water waves generated and propagated in turbulent flow field
[AD-754645] 11 p1288 N73-20451
Development of mathematical model for wind-driven circulation in ocean basin containing island formation
[AD-754354] 11 p1290 N73-20469
Environmental quality program, environmental forecasting program, and seabed assessment program for international decade of ocean exploration
12 p1400 N73-21359
Interaction of nonsaturated surface gravity ocean waves with nondispersive internal waves
[AD-754281] 12 p1403 N73-21377
Development of procedure for calculating ocean currents based on given density field and comparison with current techniques
12 p1421 N73-21516

Detection of current boundaries in Gulf of Mexico by sensing ocean color changes
[E73-10612] 15 p1774 N73-24373
Rossby regimes in geophysical fluid dynamics of ocean waves
[PB-214660/3] 16 p1890 N73-25295
Analysis of ERTS-1 imagery to interpret three seasonal nearshore processes along California coast
[E73-10727] 17 p2020 N73-26333
Multichannel pulse sampling system with pulse anemometers and current meters on oceanographic buoy
[AD-760336] 17 p2030 N73-26426
Periodic spectral solutions of combined system of equations of planetary dynamics of atmosphere and hydrosphere
[AD-759857] 17 p2058 N73-26646
Application of ERTS-1 imagery for defining ice formations, ocean currents, beach erosion, and estuarine circulation
[E73-10780] 18 p2136 N73-27256
Geopotential topographies and currents for sea surface off west Australia
[CSIRO-DFO-TP-32] 18 p2143 N73-27323
Semi-analytical solution of oceanic tidal perturbations in motion of artificial satellites
[NASA-TM-X-66298] 18 p2200 N73-27763
Detection of ocean currents in eastern Gulf of Mexico using ERTS-1 imagery
[PAPER-M13] 19 p2281 N73-28352
Determination of earth tidal amplitude and phase from orbital perturbations of Beacon Explorer C spacecraft
[NASA-TM-X-70420] 20 p2409 N73-29365
Physical oceanography problems
[AD-760704] 20 p2413 N73-29395
Oceanographic survey of eastern tropical Pacific Ocean to determine oxygen content, salinity, temperature distribution, and acceleration potential
[NOAA-NMFS-CIRC-330] 22 p2656 N73-31279
Computation of periods, wavelengths, and amplitudes of oscillations in equatorial flows and particle trajectories within flows by using inertial motion equations
22 p2666 N73-31361
Turbulent, surface, and internal motions of ocean
[AD-763804] 22 p2670 N73-31390
Test facility for generating and analyzing internal waves
[AD-763444] 22 p2670 N73-31391
Remote sensing of ocean current boundary layer in Caribbean Sea from Skylab EREP
[E73-11095] 23 p2783 N73-32262
Somali current and southwest monsoon arising from ocean atmosphere instability associated with Coriolis force
[NASA-TM-X-70471] 23 p2786 N73-32285
Degradation, dispersion and movement of oil slicks by wind and ocean as factors influencing applicability of countermeasures
[WMO-359] 23 p2787 N73-32300
Identification of suspended sediment, current circulation, water mass boundaries, and waste disposal plumes in Delaware Bay using ERTS-1 imagery
[E73-11164] 24 p2920 N73-33317

**OCEAN MODELS**
Influence of ocean on atmospheric circulation noting role of heat, momentum, and water vapor transfer
05 p0573 N73-14662
Free oscillation model for ocean basin considering earth rotation and sphericity
[PB-214445/9] 16 p1909 N73-25444
Oceanographic mapping of distribution and flow of water masses in northern Gulf of California by use of ERTS-1 imagery and optical models
[PAPER-M11] 19 p2281 N73-28350
Model for calculating thickness of quasiuniform layer of ocean
22 p2693 N73-31572

**OCEAN SURFACE**
Evaluation of bucket and intake system for measuring sea surface temperature and statistical analysis of data obtained from international ship observations
[WMO-336] 01 p0050 N73-10406
Measuring absolute surface current velocity
[AD-743706] 01 p0050 N73-10408
Macroscale fluctuations in atmospheric and oceanic variables
[AD-744976] 01 p0075 N73-10621
Upward and downward radiance calculations for numerous detector locations in atmosphere and ocean
[AD-745282] 01 p0076 N73-10627
Side-looking radar scattering from terrain and ocean surfaces
[ESRO-CR[P]-137] 03 p0266 N73-12153
Analysis of refraction of gravity water waves based on group velocity and phase velocity relationships
[AD-747982] 03 p0286 N73-12316
Sources and dispersal patterns of suspended sediments in nearshore surface waters of Northeast Pacific Ocean and Hawaiian Islands based on ERTS-1 imagery
[E72-10271] 03 p0291 N73-12370

Corrections for airborne sea surface temperature measurements by infrared techniques
[AD-747011] 03 p0297 N73-12425
Airborne and seaborne observations of radar scattering by sea water surfaces
[JPRS-57409] 04 p0388 N73-13156
ERTS-1 imagery of surface water circulation in Prince William Sound
[E72-10348] 05 p0533 N73-14336
Influence of ocean on atmospheric circulation noting role of heat, momentum, and water vapor transfer
05 p0573 N73-14662
Finite difference method for calculating interaction between spherical shock waves from underwater explosion and ocean surface
[AD-749818] 06 p0656 N73-15325
Conference on laser and radar altimeter measurement of sea surface topography from space
[NASA-CR-130293] 06 p0661 N73-15369
Use of GEOS-C satellite height for determining earth gravitational field and physical ocean surface variations
06 p0662 N73-15375
Spaceborne laser ranging system for accurately mapping ocean surface
06 p0662 N73-15377
Effect of ocean surface structure on narrow radar pulse shape
06 p0662 N73-15380
Composite scattering model for explaining rough sea surface scattering cross sections
06 p0663 N73-15383
Microwave measurements and Skylab S193 analysis of wind field over ocean
[CONTRIB-118] 06 p0663 N73-15384
Compression of satellite altimeter radar pulses and high resolution sea reflectivity
06 p0663 N73-15389
Microwave holography for imaging sea surface topography in three dimensions
06 p0664 N73-15391
Conference on dynamic wave effects on satellite-borne sea surface measurements
[NASA-CR-129993] 06 p0664 N73-15392
Gravimetric geoid construction for Atlantic Ocean area from satellite and sea surface gravimetric measurements
06 p0664 N73-15393
Ocean circulation effects on orbiting satellite gravimetry
06 p0664 N73-15394
Effect of wind wave energy balance on remote microwave sensing of sea surface
06 p0664 N73-15395
Computations of seasonal variations in internal waves and tidal phenomena in northern Atlantic Ocean
[AD-750842] 06 p0670 N73-15452
Shock wave reflection from water surface
07 p0769 N73-16250
Height error in sea-surface profile over Puerto Rican trench as determined by multi-station tracking aided by GEOS 2 satellite
[NASA-TM-X-69353] 07 p0781 N73-16347
Development of method for determining sea surface temperature using remote sensors in earth orbiting satellites
07 p0788 N73-16410
Synoptic analysis of ocean surface currents in Northern Hemisphere
07 p0858 N73-16955
Determination of mean sea level by dividing ocean into regions according to depth
07 p0858 N73-16960
Curves for solving low angle radar transmission problems at microwave frequencies over ocean surface
[TR-72-31] 08 p0885 N73-17165
Confidence intervals for ocean wave spectra for ordinary waves and hurricane sized waves
[AD-752135] 08 p0920 N73-17542
Low frequency underwater sound surface-scattering experiments in Pacific
[AD-752065] 08 p0945 N73-17739
Multispectral method of determining sea surface temperatures, using Nimbus 2 infrared radiometer
08 p0971 N73-17938
Dispersal patterns of suspended particles in nearshore surface waters of northeast Pacific Ocean and Hawaiian Islands
[E73-10314] 09 p1023 N73-18346
Analysis of energy conservation constraints on circulation of Southern Hemisphere atmosphere and oceans based on radiant, latent, and sensible heat energy transfers
[METEOROL-STUDY-26] 09 p1027 N73-18387
Relationship between wave parameters and spatial spectrum of aerial photographs of sea surface and electromagnetic method for measuring conductivity of sea surface
[JPRS-58370] 10 p1153 N73-19381
Derivation of algorithms correlating spectra of ocean wave conditions with two dimensional spectra of aerial photographs and radar imagery
10 p1153 N73-19383
Microwave emissivity and sea brightness temperatures of surface waves
[AD-753533] 11 p1287 N73-20443
Iterative directional analysis of ocean waves
[AD-753825] 11 p1289 N73-20460
Development of mathematical model for wind-driven circulation in ocean basin containing island formation
[AD-754354] 11 p1290 N73-20469
Analysis of interrelation of ocean and atmosphere based on temperature of surface layer of water in Atlantic and Pacific Oceans
12 p1421 N73-21514
Radio propagation loss over ocean surface paths
[AD-755511] 13 p1492 N73-22091
Correlation of ocean surface parameters with radar backscatter data
[E73-10530] 13 p1517 N73-22295
Characteristics of deep water waves reaching Port Phillip Heads, Australia to show effects of refraction, shoaling, and friction
13 p1524 N73-22351
Feasibility of radar system to measure direction of shoreline ocean waves
[AD-755241] 13 p1527 N73-22373
Ray tracing method for calculating underwater acoustic reflection patterns of surface originated signals from objects of arbitrary shape
[AD-757110] 14 p1694 N73-23744
Sea surface temperature measurements from Skylab EREP radiometer data
[E73-10604] 15 p1773 N73-24365
Physical properties and suspended matter of surface waters in southeastern Atlantic Ocean
[PB-214813/8] 15 p1784 N73-24467
Interactions between radio brightness and surface conditions of oceans based on Cosmos 243 data
[NASA-TT-F-14954] 16 p1904 N73-25401
Application of sea photo analysis techniques to obtain surface truth descriptors of open ocean from aerial photography
[FAA-RD-72-110] 16 p1905 N73-25412
Application of ERTS-1 RBV and multispectral scanner imagery for assessment of ocean water color
[E73-10718] 17 p2019 N73-26325
Application of ERTS-1 return beam vidicon and multispectral scanner imagery for ocean water color assessment in Caribbean Sea
[E73-10726] 17 p2019 N73-26332
Analysis of ERTS-1 imagery to interpret three seasonal nearshore processes along California coast
[E73-10727] 17 p2020 N73-26333
Analysis of ERTS-1 multispectral band scanner imagery to determine cause of anomalous dark patches occurring in photographs of calm ocean surfaces
[E73-10747] 17 p2021 N73-26351
Geopotential topographies and currents for sea surface off west Australia
[CSIRO-DFO-TP-32] 18 p2143 N73-27323
Multichannel ocean color data analysis to produce color maps
[TRW-21123-6001-RU-00] 18 p2144 N73-27328
Topographic mapping of Caribbean Sea surface by GEOS-C satellite
[AD-759041] 18 p2147 N73-27354
Laboratory investigations of whitecaps, spray and capillary waves
[AD-759407] 18 p2149 N73-27369
Mathematical models for studying energy spectra and nonlinear surface waves of ocean
[AD-759541] 18 p2149 N73-27371
Determination of sea surface conditions using Skylab L-band and Radscat passive microwave radiometers
[E73-10847] 19 p2291 N73-28425
Application of multispectral scanning to sea surface temperature, coastal topography and water sediment load, marine biology, sea ice, and oil slicks
19 p2295 N73-28455
Wave-related velocity fluctuations over ocean waves as measured from floating instrument platform during BOMEX
[AD-761768] 19 p2296 N73-28461
Image acquisition and enhancement techniques for oceanographic photography using photo-optical and electronic methods
[AD-761663] 19 p2296 N73-28463
Determination of sea surface conditions using Skylab passive L-band and Radscat microwave radiometers
[E73-10911] 20 p2397 N73-29260
Wavelength profilometer based on phase-ranging with VHF - modulated C02 laser
[AD-762453] 20 p2415 N73-29411
Oceanographic survey of eastern tropical Pacific Ocean to determine oxygen content, salinity, temperature distribution, and acceleration potential
[NOAA-NMFS-CIRC-330] 22 p2656 N73-31279
Satellite applications for earth and ocean dynamic studies
22 p2736 N73-31909
Identification of suspended sediment, current circulation, water mass boundaries, and waste disposal plumes in Delaware Bay using ERTS-1 imagery
[E73-11164] 24 p2920 N73-33317
Influence of wind drift and capillarity on blockage of short surface waves
[AD-764559] 24 p2924 N73-33358
Sea photo analysis for ocean surface truth descriptors from aircraft
[AD-764858] 24 p2924 N73-33360
Noncoherent model for microwave emissions and backscattering from sea surface
[NASA-CR-2326] 24 p2948 N73-33542
Backscattering from two-scale rough surface application to radar sea return
[NASA-CR-2327] 24 p2948 N73-33543
Proceedings of conference on electromagnetic and optical properties of sea water for application to surveillance, mapping, communications, and visibility
[AGARD-LS-61] 24 p2956 N73-33619

**OCEANOGRAPHY**

Estuarine and coastal oceanography of Block Island Sound and adjacent New York coastal waters based on ERTS-1 multispectral band scanner imagery
[E72-10171] 01 p0044 N73-10352
Interdisciplinary study of estuarine and coastal oceanography of Block Island Sound and New York Bight area using ERTS-1 imagery
[E72-10172] 01 p0044 N73-10353
Geological charts of Ontong Java Plateau including bathymetric, sedimentary isochron, and structural contour
[AD-743900] 01 p0052 N73-10423
Coastal geology bibliography of New England with punch card reference system
[AD-744001] 01 p0052 N73-10424
Geologic structure of Ontong Java Plateau determined from continuous reflection profiles taken between 1966 and 1971
[AD-743899] 01 p0052 N73-10425
Dissipation of kinetic and thermal energy in mixed surface layer of ocean from measurements made in Barbados oceanographic and meteorological experiment
[AD-745343] 01 p0053 N73-10431
Single layer, hydrodynamic numerical model for oceanography
[AD-745759] 01 p0053 N73-10432
Detection of internal ocean waves using three-color infrared radiometer
[AD-745004] 01 p0059 N73-10484
USSR space program accomplishments in fields of geophysics, astronomy, meteorology, oceanography, upper atmosphere, and space sciences
[JPRS-57229] 01 p0104 N73-10864
Utilization of ERTS-1 remotely-acquired oceanographic information for improving harvest and management of menhaden in Gulf of Mexico
[E72-10215] 02 p0162 N73-11309
Analysis of ERTS-1 MSS data for color variations in Great Lakes and Chesapeake Bay to determine if multispectral imagery usable for locating and mapping extent of distinct water masses
[E72-10224] 02 p0163 N73-11318
Users information and computer program for hydrodynamic-numerical model for oceanographic analyses
[AD-745760] 02 p0167 N73-11358
Side-looking radar applied to oceanography noting sensing of sea states, pollution, and waves
03 p0295 N73-12408
Hydrographic data from Oregon waters in 1971
[AD-746515] 03 p0297 N73-12421
USSR research projects in geosphysics, astronomy, and space - No. 288
[JPRS-57505] 03 p0357 N73-12906
Dynamic behavior of coastal sedimentation in Lions Gulf
[E72-10289] 04 p0410 N73-13339
ERTS-1 imagery of California coastal nearshore processes
[E72-10316] 04 p0413 N73-13365
Compilation of geological and oceanographic data collected by research vessel VEMA
[AD-747652] 04 p0417 N73-13402
Hydrographic survey data for Southern Pacific Ocean between Australia and Antarctica
[AD-747792] 04 p0417 N73-13404
Scripps Institute research on oceanographic instruments, stabilized floating platforms, ocean bottom accelerometers, and surface waves
[AD-748024] 04 p0417 N73-13407
Development and characteristics of self-contained, portable data acquisition system for conducting marine and ecological research
04 p0471 N73-13842
Soviet research on meteorology, oceanography, upper atmosphere, and astronomy
[JPRS-57630] 04 p0474 N73-13876
Prediction of long-term temperature fluctuations, July temperature, and annual average temperature of Barents Sea in surface to 200 m layer
[NLL-M-20600-[5828.4F]] 05 p0529 N73-14304
USSR research projects involving meteorology, oceanography, upper atmosphere, space research, and terrestrial geophysics
[JPRS-57777] 05 p0596 N73-14844
High energy density storage system with encapsulated silver zinc cells for deep ocean applications
[AD-750719] 06 p0627 N73-15085

Summary of side-looking radar applications in earth resources noting basic principles of side-looking radar, radar scattering, data handling, and research and development
[ESRO-CR[P]-141] 06 p0641 N73-15200
Analysis of pole tide fluctuations in earth atmosphere and ocean
[NLL-M-20647-[5828.4F]] 06 p0657 N73-15336
Multispectral imagery of estuarine and coastal oceanography of Block Island Sound and adjacent New York coastal waters using ERTS-1 imagery
[E73-10010] 06 p0659 N73-15346
Utilization of ERTS-1 imagery for oceanographic studies of Great Lakes
[E73-10017] 06 p0659 N73-15353
Combined marine astrogravimetry and marine geodetic acoustic techniques for accurate determination of global marine geoid
06 p0662 N73-15374
Marine weather program for providing weather and river advisories to public sector
06 p0663 N73-15382
Oceanographic equipment and ocean bottom data resulting from Pacific cruise of Iguana
[AD-750679] 06 p0671 N73-15459
Proceedings of conference on earth resources survey systems to show applications of remote sensing to agriculture, forestry, oceanography, and urban development - Vol. I
[NASA-SP-283-VOL-I] 07 p0781 N73-16348
Application of electromagnetic sensors for remote sensing of oceanographic processes to determine available resources
07 p0782 N73-16356
Analysis of oceanography remote sensing using black and white, color, and color infrared photographic recording
07 p0788 N73-16407
Analysis of photography from Apollo 9 flight to determine origin, movement, and dissipation of masses of discolored water near shores of North and South Carolina
07 p0788 N73-16408
Selected papers on hydrometeorology, oceanography, navigation
07 p0857 N73-16950
Measurement of diurnal heat budget in tropical Atlantic surface layers
07 p0857 N73-16953
Temperature-salinity profiles of Tyrrhenian Sea
[CONTRIB-2725] 07 p0858 N73-16957
Determination of mean sea level by dividing ocean into regions according to depth
07 p0858 N73-16960
Oceanography and marine environment of Gulf of California based on ERTS-1 imagery
[E73-10021] 08 p0900 N73-17286
ERTS-1 imagery of oceanography and marine environment of northern Gulf of California
[E73-10304] 09 p1021 N73-18336
Bathymetry, magnetic, and gravity data collected between 1961 and 1969 in North Central Pacific
[NOAA-TR-NOS-51] 09 p1029 N73-18401
Bathymetric survey of Pacific Ocean area for oceanographic data to support underwater acoustic experiment
[AD-752840] 09 p1032 N73-18428
Hydrodynamic and weight loads of self-contained buoy stations for oceanographic research in strong current areas
09 p1059 N73-18638
Evaluation of Great Lakes oceanography from ERTS-1 imagery
[E73-10356] 10 p1149 N73-19352
Oceanographic data collection on Caribbean Sea and Gulf of Mexico environments
[AD-752494] 10 p1156 N73-19404
Review of underwater acoustical measurements revealing layered regions at various ocean depths
[AD-753445] 10 p1156 N73-19405
Instrumented dolphins for surveying oceanographic parameters and relaying information to tracking aircraft
[AD-754761] 11 p1256 N73-20191
Application of ecological, geological, and oceanographic ERTS-1 imagery to coastal resources management and planning in Delaware
[E73-10426] 11 p1280 N73-20387
Measurements of oceanographic temperature distribution and salinity in northern Baffin Bay during midsummer 1970
[CG-373-54] 11 p1286 N73-20434
R/V Knorr cruise in Oct. 1970 to deploy and recover instrumented deep sea moorings
[AD-754796] 11 p1288 N73-20455
Abstracts of articles on Soviet Bloc research in earth and space sciences
[JPRS-58437] 11 p1338 N73-20860
USSR research projects in meteorology, oceanography, upper atmosphere and space astronomy, and terrestrial geophysics
[JPRS-58609] 11 p1339 N73-20867
Technical utilization of advanced equipment for oceanological exploitation by US
[JPRS-58696] 12 p1401 N73-21363
Measurement of Mediterranean Sea temperature profiles using free drifting, self-recording drogues equipped with thermistor chains
[AD-753442] 12 p1402 N73-21372
Analysis of oceanographic/meteorological sensors for ocean data stations
[AD-755755] 12 p1425 N73-21552
USSR research projects in meteorology, oceanography, geophysics, upper atmosphere, and extraterrestrial radiation - No. 298
[JPRS-58734] 12 p1458 N73-21817
ERTS-1 imagery of Iceland geology, geophysics, hydrology, oceanography, and agriculture
[E73-10535] 13 p1518 N73-22299
Measurements and procedures for processing measurement data in marine geodesy
[JPRS-58824] 13 p1522 N73-22335
Literature compilation on marine geology and geophysics for Caribbean Sea and adjacent regions
14 p1607 N73-23023
Detection of menhaden schools in Mississippi Sound by comparing ERTS-1 imagery to selected oceanographic parameters
[E73-10580] 14 p1636 N73-23441
Users guide to help formulate requests for oceanographic data and related information
14 p1638 N73-23454
Remote sensor system aboard Skylab in support of EREP oceanographic program
[AD-755715] 14 p1663 N73-23501
Surface wave interaction and thermal microstructure of sea water
[AD-757425] 14 p1664 N73-23502
Application of ecological, geological, and oceanographic ERTS-1 imagery to Delaware coastal resources management and planning
[E73-10631] 15 p1776 N73-24391
Multispectral band scanner data of Oregon coast gathered during summer of 1969
15 p1779 N73-24424
Computer printouts of oceanographic data collected in North Pacific between 1961 and 1970
[NOAA-TR-NOS-47] 15 p1780 N73-24429
Measurement of deep ocean hydrostatic pressure fluctuations
[AD-757098] 15 p1783 N73-24458
Application of ERTS-1 data to develop and implement utilization of living marine resources in Mississippi Sound
[E73-10707] 16 p1904 N73-25398
Approximation methods for solving hyperbolic partial differential equations of meteorology and oceanography
[GARP-PUBL-10] 16 p1938 N73-25680
Application of ERTS-1 RBV and multispectral scanner imagery for assessment of ocean water color
[E73-10718] 17 p2019 N73-26325
Research and development in coastal engineering
[AD-759283] 17 p2028 N73-26413
Procedures for obtaining position from surface gravity observations and application of geodetic techniques to earth and ocean physics
[NASA-TM-X-66273] 17 p2059 N73-26655
Application of ERTS-1 imagery for defining ice formations, ocean currents, beach erosion, and estuarine circulation
[E73-10780] 18 p2136 N73-27256
Color enhancement of ERTS-1 imagery of estuarine and coastal oceanography of Block Island Sound and adjacent New York coastal waters
[E73-10819] 18 p2140 N73-27294
Biological oceanography by airborne spectrophotometer
[NASA-CR-133325] 18 p2147 N73-27353
Development and characteristics of electronic data recording equipment for shipboard oceanography data acquisition and processing
[IFS-73010] 18 p2151 N73-27384
KWIC index on oceanography
[NOAA-TM-EDS-ESIC-5] 18 p2213 N73-27867
Numerical analysis of turbulent diffusion in stratified fluid to show variations in diffusion coefficient with changes in ocean water depth
[AD-761653] 19 p2257 N73-28190
Bubble transport theory applied to upper ocean
[AD-761999] 19 p2257 N73-28194
Analysis of ERTS-1 MSS imagery to determine geologic, hydrologic, oceanographic, and agricultural phenomena in Iceland
[PAPER-G10] 19 p2264 N73-28241
Oceanographic mapping of distribution and flow of water masses in northern Gulf of California by use of ERTS-1 imagery and optical models
[PAPER-M11] 19 p2281 N73-28350
Oceanographic features in the lee of the windward and leeward islands: ERTS and ship data
[PAPER-M12] 19 p2281 N73-28351
Utilization of ERTS-1 imagery for coastal oceanography in British Columbia
19 p2286 N73-28384
Relationship between ERTS-1 fisheries distribution information and selected oceanographic parameters in Mississippi Sound
19 p2286 N73-28385
Assessment of ERTS-1 imagery for identification of marine resources to include sources of pollution, beach erosion, and navigation in ice-filled waterways
19 p2289 N73-28402
Significant results from marine resources and ocean surveys of discipline overall ERTS program
19 p2290 N73-28411
Application of multispectral scanning to agriculture, oceanography, hydrology, and geology
[ERL/R-246] 19 p2294 N73-28450
Application of multispectral scanning to sea surface temperature, coastal topography and water sediment load, marine biology, sea ice, and oil slicks
19 p2295 N73-28455
Development of semi-automatic system for digitizing bathymetry charts for showing ocean bottom contour information
[AD-761647] 19 p2296 N73-28464
Computer program for generation of random bathymetric profiles from oceanographic data
[AD-762070] 19 p2298 N73-28476
General description and scientific results of Tenth Soviet Antarctic Expedition for period 1965 to 1966
[TT70-50072] 20 p2406 N73-29339
Hydrological investigations conducted during Tenth Soviet Antarctic Expedition to determine temperature and salinity of ocean
20 p2407 N73-29343
Hydrographic investigations conducted aboard ships of the Tenth Soviet Antarctic Expedition
20 p2407 N73-29344
Marine geological research of submarine relief and ocean bottom sediments conducted during Tenth Soviet Antarctic Expedition
20 p2407 N73-29345
Marine ice observations during Tenth Soviet Antarctic Expedition to measure formation, growth, disintegration, and physicomechanical properties
20 p2408 N73-29351
Hydrological investigations of Davis Sea conducted during Tenth Soviet Antarctic Expedition
20 p2408 N73-29353
Oceanographical observations from Danish light vessels and coastal stations - 1972
[ISBN-87-7478-080-6] 20 p2412 N73-29386
Physical oceanography problems
[AD-760704] 20 p2413 N73-29395
Sequential photography for coastal oceanography
[AD-760713] 20 p2413 N73-29399
Methodological principles of economy of ocean
[JPRS-59741] 20 p2487 N73-29980
Application of ecological, geological, and oceanographic ERTS-1 imagery to Delaware coastal resources management and planning
[E73-10934] 21 p2529 N73-30276
Oceanography and marine environment of northern Gulf of California
[E73-10941] 21 p2529 N73-30283
Estuarine and coastal oceanography of Block Island Sound and adjacent New York coastal waters
[E73-10968] 21 p2533 N73-30310
Application of infrared data from satellites for use in field of fishery oceanography in Pacific Ocean
[AD-763350] 21 p2542 N73-30380
Utilization of ERTS-1 imagery for studies of agriculture, forestry, cartography, geography, hydrology, meteorology, geology, and oceanography in Thailand
[E73-10996] 22 p2659 N73-31302
Spectroradiometric calibration of EREP imagery and oceanography of Block Island Sound
[E73-11015] 22 p2660 N73-31319
Research needs in ocean color data analysis
[NASA-TM-X-70466] 22 p2665 N73-31355
Atlas presenting oceanographic data collected during Barbados oceanograpic and meteorological experiment
22 p2666 N73-31362
Differentiation of ocean multispectral data obtained by satellite for chlorophyll content
22 p2736 N73-31904
Electronic scanning microwave radiometer system for measurement of meteorological, geomorphological, and oceanographic parameters from Nimbus 5
[NASA-CR-132812] 23 p2793 N73-32342
Soviet research in meteorology, oceanography, geophysics, astronomy, and space
[JPRS-60165] 23 p2846 N73-32744
Optimum use of infrared data as obtained from satellites for meteorological and oceanographic applications
24 p2911 N73-33233
Information management for Skylab earth resources experiments in oceanography and marine science
[NOAA-TM-NESS-51] 24 p2921 N73-33328
GARP subprograms including numerical experimentation, GATE climate, and oceanography
24 p2949 N73-33557

**OCEANS**
- NT ARCTIC OCEAN
- NT ATLANTIC OCEAN
- NT INDIAN OCEAN
- NT PACIFIC OCEAN

ERTS-1 remote sensing of chlorophyll measurements in upwelling areas of oceans
[E72-10196] 01 p0047 N73-10375
Numerical solution of parabolic partial differential equations with reference to eddy heat conduction in ocean
[AD-746205] 02 p0167 N73-11362
Temperature measurement of air layer directly over ocean surface
[NLL-M-20745-[5828.4F]] 05 p0529 N73-14308
Relationship between radar scattering coefficient and ocean wind speed and direction
07 p0774 N73-16289
Prediction of horizontal wave forces acting on vertical pile structures of floating ocean platforms
[AD-751574] 07 p0794 N73-16460
Phytoplankton density determination from ocean color measurements
08 p0972 N73-17939
Meteorological and hydrological researCh over and in oceans
[JPRS-58025] 09 p1059 N73-18631
Steady state, symmetrical, hurricane-ocean interaction model
[AD-753620] 09 p1062 N73-18659
Spectral analysis of turbulent fluctuations over ocean waves
[AD-753624] 10 p1156 N73-19406
Environmental engineering for conservation of ocean resources
[PB-212634] 11 p1290 N73-20467
Analysis of interactions between marine water and freshwater at river mouth for understanding dissemination of sediment
[AD-755158] 14 p1664 N73-23507
ERTS-1 monitoring of water quality and ocean dumping
[E73-10573] 15 p1772 N73-24353
Assessment and monitoring oceanic gamefish through Skylab EREP data
[E73-10658] 16 p1898 N73-25354
Spectral and cospectral analyses of turbulence data obtained over natural ocean waves
[AD-761504] 19 p2316 N73-28624
Mathematical models for studying beta effect on meridional velocity of disturbed flow in ocean
20 p2447 N73-29655
Flight plan position extrapolation in automated oceanic air traffic control system
[FAA-RD-73-72] 21 p2576 N73-30648
Remote sensing of oceanic gamefish from ERTS-1 imagery
[E73-11135] 24 p2917 N73-33290

**OCTAHEDRAL RESEARCH SATELLITES**
U ENVIRONMENTAL RESEARCH SATELLITES

**OCTAHEDRITE**
U MINERALS

**OCULOGRAVIC ILLUSIONS**
Oculogravic illusion factor in theoretical model of pilot control loss in jet aircraft
06 p0633 N73-15142
Compensatory oculogravic response of eye movement direction during slow head rotation
06 p0634 N73-15148

**OCULOMETERS**
Influence of illumination on electro-oculographic measurements of human eye potential
[AMRU-R-71-1] 02 p0131 N73-11064
Pupillometry using advanced design oculometer
[AD-752121] 08 p0878 N73-17116

**OCULOMOTOR NERVES**
Vestibulo-ocular response of man to oscillatory rotation during sleep
[AMRU-R-70-3] 02 p0131 N73-11066
Response characteristics of vestibulo-ocular reflex arc
[AMRU-R-71-2] 02 p0132 N73-11067
Theoretical model of utricular otolith and associated neural connections to oculomotor system and their response to angular motion with respect to acceleration in shear
[FPRC-1315] 02 p0132 N73-11070
Physiological factors in human oculomotor responses to space flight stress
[DR-208-VOL-1] 06 p0632 N73-15136
Anti-compensatory oculomotor response of pilot to rotational head stimuli
06 p0632 N73-15138
Anti-compensatory oculomotor responses in human visual tracking and vestibulo-ocular mechanism during rotational head movement in flight
06 p0633 N73-15140
Physiological control system for stabilization of retinal image in humans
06 p0633 N73-15141
Clinical neurological and neurophysiological aspects of vestibulo-ocular reflex
06 p0633 N73-15145
Visual and vestibular effects in human oculomotor response during head rotation in yaw and roll
06 p0633 N73-15147
Vestibular neuron response to rotational stimuli in space flight environment
06 p0634 N73-15150
Semicircular canal plugging response in cats to rotary stimulation
06 p0634 N73-15151
Gastrointestinal proprioceptor effects on high altitude rabbit ocular reflexes
13 p1479 N73-21984

**ODORS**
J-57 combustor exhaust odor intensity and chemical composition considering inlet parameters, fuel types, and nozzle shapes
[NASA-CR-121159] 14 p1616 N73-23093
Sensory odor tests of exhaust from turbojet engine combustor operating at simulated idle conditions
[NASA-TM-X-71429] 23 p2829 N73-32613

**OFF-ON CONTROL**
Bang-bang controller operating in chatter mode for disturbance regulation in linear system
[AD-745896] 02 p0203 N73-11643

**OGEE WINGS**
U VARIABLE SWEEP WINGS

**OGIVES**
Computerized stability derivative calculations for oscillating parabolic ogives and circular cones in transonic flow field using iterative procedure
[NASA-CR-124033] 07 p0769 N73-16249
Magnus effect in supersonic laminar boundary layer on spinning body of revolution
[SC-DC-72-1173] 07 p0772 N73-16269
Flow field measurements around ogive-cylinder at angles of attack to 15 degrees and Mach numbers 3.52 and 4.07
[AD-752025] 08 p0898 N73-17268
Fracture strength of uranium- and tungsten-based impacted ogive penetrators
[DREV-R-652/72] 09 p1047 N73-18538
Base pressure measurements on axially symmetric wind tunnel models in subsonic, transonic and supersonic speeds at high Reynolds numbers
[TAE-134] 16 p1857 N73-25044
Thermodynamic behavior of liquid hydrogen and nitrogen cavitation in ogives
[NASA-CR-2242] 19 p2251 N73-28153

**OGO**
NT OGO-A
Electric field oscillations in upstream solar wind, using OGO-5 observations
01 p0096 N73-10789
Simultaneous observations of plasma waves from electric field instruments on Pioneer 9 and OGO 5 to illustrate difference between near-earth and deep space conditions
01 p0096 N73-10795
Detection of intermediate size magnetic anomalies in Cosmos-49 and OGO-2, 4, and 6 data
[NASA-TM-X-66225] 12 p1401 N73-21368
Interpretation of OGO 2, 4, and 6 measurements of near earth magnetic field disturbances in total field at high latitudes
[NASA-TM-X-70443] 21 p2536 N73-30332
OGO 2, 4, and 6 measurements of near earth magnetic field disturbances in total field at high latitudes
[NASA-TM-X-70442] 21 p2536 N73-30333

**OGO-A**
Observation of magnetospherically reflected whistlers made by OGO-A and OGO-C
[NASA-CR-130352] 07 p0781 N73-16344

**OGO-B**
Observation of magnetospherically reflected whistlers made by OGO-A and OGO-C
[NASA-CR-130352] 07 p0781 N73-16344
Magnetospheric field model incorporating OGO B and E magnetic field measurements
[NASA-TM-X-66172] 07 p0792 N73-16442
OGO 3 and 5 observations of inner magnetosphere and ring currents
08 p0972 N73-17947

**OGO-D**
F-02 experiment onboard OGO-6, and computer program for analysis of raw data
[NASA-CR-130128] 04 p0414 N73-13376
OGO-D electromagnetic wave propagation measurements with whistler and hiss formations in plasmasphere
[NASA-CR-130351] 07 p0754 N73-16126
Magnetospheric field model incorporating OGO B and E magnetic field measurements
[NASA-TM-X-66172] 07 p0792 N73-16442
Magnetospheric plasma tail study, using thermal proton density measurements from OGO 4
08 p0972 N73-17948
Plasmapause, magnetic recovery, grounded whistler reception, and OGO 4 and 5 data
[NASA-CR-131394] 11 p1284 N73-20422
OGO D and F magnetic field results and surface data comparison
[NASA-TM-X-66218] 11 p1339 N73-20866
ELF and VLF experiment on OGO-D, revealing ion whistlers and ELF hiss features
12 p1377 N73-21170
Comparison of simultaneous particle detector and search coil magnetometer measurements of precipitating particles and field aligned currents from OGO-D
[NASA-TM-X-66224] 12 p1401 N73-21367
OGO-4 observation of banded whistlers using broadband VLF instrumentation
[NASA-CR-131495] 13 p1490 N73-22079
OGO-4 ultraviolet spectrometer measurements of nitric oxide fluorescence with diffusive transport model for mesospheric and lower thermospheric nitric oxide photochemistry
13 p1515 N73-22274
Effects of season altitude and pitch angle on electron precipitation from OGO-D data
[NASA-TM-X-66260] 16 p1962 N73-25868

**OGO-E**
Measurement of extraterrestrial Lyman alpha emission by OGO 5 satellite while outside geocorona
01 p0099 N73-10812
OGO 5 fluxgate magnetometer measurements of large field depressions in magnetosphere
[NASA-TM-X-66133] 05 p0539 N73-14382
Bibliography of publications from OGO E plasma wave investigation
[NASA-CR-130140] 06 p0644 N73-15227
Analysis of light ion mass spectrometer data from OGO-E experiment
[NASA-CR-130156] 07 p0791 N73-16432
OGO 3 and 5 observations of inner magnetosphere and ring currents
08 p0972 N73-17947
Plasmapause, magnetic recovery, grounded whistler reception, and OGO 4 and 5 data
[NASA-CR-131394] 11 p1284 N73-20422
OGO-5 fluxgate magnetometer for measuring magnetic field over range of OGO-5 orbit
[NASA-CR-130205] 11 p1294 N73-20498
Data processing and analysis of charged particle experiment on OGO-5 spacecraft
[NASA-CR-132761] 16 p1962 N73-25870
Data base of electron and proton spectrometer, Orbiting Geophysical Observatory, and fluxgate magnetometer experiments
[UCRL-51314] 17 p2033 N73-26453

**OGO-F**
Reduction and analysis of trapped and precipitating electron data from OGO 6 spectrometer experiment F-16
[NASA-CR-130137] 06 p0718 N73-15863
Disposition of scattering layers over polar-regions as observed by OGO-6 airglow photometer
[NASA-CR-130271] 07 p0791 N73-16436
Instrumentation and measurement data of OGO-F solar cosmic ray experiment
[NASA-CR-130155] 07 p0839 N73-16795
Thermospheric composition and density, measured by neutral mass spectrometer onboard OGO-6 satellite
08 p0972 N73-17946
Neutron measurements on OGO-6 spacecraft
[NASA-CR-130181] 10 p1210 N73-19841
Role of gas-surface interactions in reduction of OGO 6 neutral-particle mass spectrometer data
[NASA-TN-D-7239] 11 p1286 N73-20432
OGO D and F magnetic field results and surface data comparison
[NASA-TM-X-66218] 11 p1339 N73-20866
Global characteristics in diurnal components of OGO-6 neutral mass spectrometer measurements of thermosphere
[NASA-TM-X-66295] 18 p2145 N73-27335

**OGO-5**
User guide to microfilm records of data obtained in energetic particle experiment with OGO-5
[UCRL-51307] 22 p2639 N73-31150

**OGO-6**
OGO-6 ion concentration irregularity studies
[NASA-CR-132814] 23 p2786 N73-32286
OGO-6 measurements of solar neutrons
23 p2833 N73-32639
OGO-6 neutral atmospheric composition experiment
24 p2920 N73-33320

**OH-6 HELICOPTER**
Application of sound suppression techniques to OH-6 helicopter and measurement of resultant noise reduction
[AD-753646] 09 p0989 N73-18077
Measurements of aerodynamic noise produced by modified and standard OH-6A helicopter configurations to determine noise reduction effectiveness
[NASA-TN-D-7216] 21 p2496 N73-30031

**OH-13 HELICOPTER**
Three component wake velocity measurements of full scale OH-13 helicopter rotary wing during hovering flight
[AD-754644] 11 p1235 N73-20030

**OHIO**
NT WABASH RIVER BASIN [IL-IN-OH]
Mapping ecological effects of coal strip mining in Ohio
[E72-10256] 03 p0290 N73-12356
Strip mine identification, land use assessment, smoke plume detection, and sedimentation patterns in Sandusky Bay from ERTS-1 imagery of Ohio
[E72-10259] 03 p0290 N73-12358
Detection and monitoring area strip mining and reclamation in Ohio using ERTS-1 imagery
[E72-10284] 04 p0409 N73-13334
Earth resource surveys for management and development of resources in Ohio
04 p0472 N73-13845

Environmental and ecological effects of coal strip mining in Ohio
[E73-10003] 06 p0658 N73-15339
Resources management in Ohio utilizing ERTS-1 imagery
[E73-10032] 06 p0661 N73-15365
Ecological effects of coal strip mining in Ohio
[E73-10430] 11 p1281 N73-20391
Resources management in Ohio using ERTS-1 imagery
[E73-10437] 11 p1281 N73-20397
Physical interpretation of geology, hydrology, and glaciology revealed by ERTS-1 imagery of east central Ohio
[E73-10454] 11 p1283 N73-20413
Relevance of ERTS-1 imagery to land use, resources, and environment management in Ohio
[E73-10621] 15 p1775 N73-24382
Detection, monitoring, and mapping coal strip mining and reclamation in Ohio from ERTS-1 imagery
[E73-10641] 16 p1896 N73-25338
EREP imagery for detection of strip mines and reclamation activities in Ohio, West Virginia, and Pennsylvania
[E73-10731] 17 p2020 N73-26337
Acquisition of ground truth data in Ohio for Skylab EREP
[E73-10757] 18 p2133 N73-27239
Resources management, land use mapping, and water quality management in Ohio based on ERTS-1 imagery
[E73-10775] 18 p2135 N73-27251
Application of ERTS-1 imagery to determine ecological effects of strip mining in eastern Ohio
[PAPER-E2] 19 p2268 N73-28266
Application of ERTS-1 imagery to resource management in Ohio
[PAPER-R3] 19 p2283 N73-28361
Mapping of strip mine areas in southeastern Ohio from ERTS-1 imagery
19 p2284 N73-28372
ERTS-1 imagery of algal blooms in Lake Erie and Utah Lake, Ohio
19 p2285 N73-28376
Application of ERTS-1 imagery to resources management and planning in Ohio
[E73-10987] 22 p2658 N73-31294
Skylab monitoring of surface mining activities and reclamation in Ohio, West Virginia, Pennsylvania, Indiana, Kentucky, and Illinois
[E73-11033] 22 p2663 N73-31337
Application of ERTS-1 imagery to fracture-related mine safety hazards in Ohio coal mining industry
[E73-11034] 22 p2663 N73-31338
Regional and local land use planning and mapping of Ohio from Skylab EREP data
[E73-11090] 24 p2914 N73-33252

**OHMIC DISSIPATION**
Thermospheric heating due to EUV absorption and Joule dissipation
[AD-758758] 15 p1784 N73-24464

**OIL ADDITIVES**
Wear inhibiting effect of automotive oils containing polymethacrylate
[NLL-TRANS-1190-[9022.9]] 15 p1746 N73-24149

**OIL EXPLORATION**
Set of variables crucial to economic outcome of petroleum exploration
[NASA-CR-129595] 04 p0488 N73-13991
Two stochastic models for petroleum exploration
[NASA-CR-129611] 04 p0488 N73-13992
Suitability of ERTS-1 imagery for oil exploration in Oklahoma
[E72-10327] 05 p0530 N73-14315
Utilization of ERTS-1 imagery for mapping large scale structural lineamants in Precambrian Shield and basins containing younger sediments and for mineral and petroleum exploration
[E73-10004] 06 p0658 N73-15340
Oil exploration in Oklahoma using ERTS-1 MSS imagery
[E73-10322] 09 p1024 N73-18354
Utilization of ERTS-1 imagery in structural reconnaissance for minerals and oil in Alaska, Canada, Montana, Colorado, New Mexico, and Texas
[E73-10414] 11 p1279 N73-20376
Suitability of ERTS-1 imagery for oil exploration
[E73-10444] 11 p1282 N73-20404
Oil exploration in large intercratonic sedimentary basins in Oklahoma using ERTS-1 imagery
[E73-10646] 16 p1897 N73-25342
Oil exploration using ERTS-1 imagery of lithology and geological structures
[E73-11053] 23 p2780 N73-32229

**OIL SLICKS**
Pollution hazards from petroleum industries and shipping in Delaware Bay
07 p0857 N73-16948
ERTS-1 detection of oil pollution in Gulf of Mexico and in waters off Salem, Massachusetts and Oakland, California
[E73-10396] 11 p1276 N73-20358
Detection and evaluation of worldwide short-lived events from ERTS-1 imagery
[E73-10453] 11 p1283 N73-20412
Detection of oil pollution from ERTS-1 imagery
[E73-10574] 15 p1772 N73-24354
Detection and monitoring oil pollution using Skylab EREP MSS imagery
[E73-10796] 18 p2137 N73-27272
Visual detection of oil films on water surface
[PB-219825/7] 18 p2148 N73-27362
Israeli use of ERTS-1 imagery to detect and map oil slicks in Gulf of Suez
[E73-10800] 19 p2259 N73-28206
Detection and monitoring of oil pollution from Skylab EREP sensors
[E73-11016] 22 p2661 N73-31320
Aerial surveillance system for remote detection of real and potential oil spills threatening inland waterways
[PB-221484/9] 22 p2669 N73-31385
ERTS-1 imagery of short-lived events such as forest fires, oil spills, volcanic activity, floods, and storms
[E73-11048] 23 p2779 N73-32224
Multidisciplinary research on water depth measurement, Yellowstone Park, atmospheric effects, lake ice surveillance, recreational land use, IFYGL, image enhancement, water quality, oil pollution detection, and mapping iron compounds from ERTS-1 data
[E73-11119] 23 p2783 N73-32264
Degradation, dispersion and movement of oil slicks by wind and ocean as factors influencing applicability of countermeasures
[WMO-359] 23 p2787 N73-32300

**OILS**
NT CRUDE OIL
NT FUEL OILS
NT LUBRICATING OILS
NT MINERAL OILS
Failure analysis of Geiger counters used in nucleonic oil gauging system of USAF aircraft
[AD-746267] 01 p0059 N73-10485
Utilization of oil dischargers in high voltage pulse circuits
[AD-751170] 07 p0765 N73-16214
Utilization of ERT-1 imagery for water depth measurement, Yellowstone Park data, atmospheric effects in Colorado, lake ice surveillance, recreational land use, IFYGL, image enhancement, water quality monitoring, oil pollution detection, and mapping iron compounds
[E73-10086] 08 p0901 N73-17298
Orientation of molecules of soil soluble surfactant in absorption layers on liquid-liquid interface
[NLL-M-22998-[5828.4F]] 20 p2373 N73-29068
Regional environmental impact from oil shale development on private and public lands in Wyoming, Colorado, and Utah - Vol. 1
[EIS-AA-72-5242-D-1-VOL-1] 20 p2410 N73-29367
Energy alternatives to prototype oil shale leasing program for Wyoming, Colorado, and Utah - Vol. 2
[EIS-AA-72-5242-D-2-VOL-2] 20 p2410 N73-29368
Description of proposed leases for oil-shale program in Wyoming, Utah, and Colorado, and potential environmental impacts - Vol. 3
[EIS-AA-72-5242-D-3-VOL-3] 20 p2410 N73-29369

**OKLAHOMA**
Suitability of ERTS-1 imagery for oil exploration in Oklahoma
[E72-10327] 05 p0530 N73-14315
Oil exploration in Oklahoma using ERTS-1 MSS imagery
[E73-10322] 09 p1024 N73-18354
Study of severe local storm of 22 Apr. 71, near Norman, Oklahoma
[AD-756571] 13 p1554 N73-22592
Oil exploration in large intercratonic sedimentary basins in Oklahoma using ERTS-1 imagery
[E73-10646] 16 p1897 N73-25342
Assessment of vehicular air pollution for Tulsa, Oklahoma
20 p2441 N73-29606

**OMEGA NAVIGATION SYSTEM**
Composite signals for lane identification in Omega
[AD-746503] 02 p0208 N73-11686
Development and application of correction information to improve accuracy of differential Omega navigation system
[AD-745878] 02 p0208 N73-11691
Development of on-board navigation system based on Applications Technology Satellites, Omega navigation systems, and aircraft terminal facilities
[NASA-CR-130213] 13 p1556 N73-22615
Statistical analysis of phase data on three Omega navigation stations to determine positioning accuracies - Vol. 1
[AD-756024] 13 p1557 N73-22617
Program listings and output data summaries for differential Omega navigation system monitoring and analysis - Vol. 2
[AD-756025] 13 p1557 N73-22618
Analog charts developed during monitoring and analysis of differential Omega navigation system - Vol. 3
[AD-756026] 13 p1557 N73-22619
Characteristics of airborne area navigation equipment and application to air traffic control functions
14 p1688 N73-23698
Proceedings of conference on precise time and time interval planning for application to hypersonic navigation systems
[AD-758739] 16 p1942 N73-25717
Effects of polar cap absorption events on performance of Omega navigation system operating in high latitudes
[AD-759009] 16 p1942 N73-25718
Very low frequency timing techniques for Omega navigation system to include operational considerations, path selection, and adjustment procedure
[NASA-CR-133185] 17 p2061 N73-26669
Effects of polar cap absorption events on phase deviations in Omega navigation system
[AD-764521] 24 p2951 N73-33572

**OMEGA-MESONS**
Dual resonance type model for quasi two body reactions in subprocesses of pion nucleon yields pion omega meson nucleon
22 p2701 N73-31635

**OMNIDIRECTIONAL ANTENNAS**
NT MONOPOLE ANTENNAS
NT TURNSTILE ANTENNAS
Development of system for encoding outputs from several omnidirectional antennas and processing into modified signal to provide angle of arrival data for direction finding
[AD-747501] 03 p0329 N73-12684
VHF omnidirectional antenna developed as printed current panel from flat plate dipole with low aspect ratio
[TR-72-34] 07 p0756 N73-16142
Design and performance of low frequency/very low frequency omnidirectional antenna model
[AD-757556] 14 p1643 N73-23324
Design of omnidirectional ultrahigh frequency communication antenna fitted around pole
[AD-760201] 17 p2005 N73-26217
Omnidirectional polygon reflector antenna with cosecant radiation pattern for TV transmission in SHF range
[FTZ-A-454-TBR-16] 22 p2643 N73-31179

**OMNIRANGE NAVIGATION**
U VHF OMNIRANGE NAVIGATION

**ON-LINE PROGRAMMING**
On-line computer technique for evaluating reconnaissance image compression algorithms
01 p0024 N73-10191
Bibliography of on-line computers in nuclear and thermal power stations from 1960 to June 1972
[CE-BIB-226] 01 p0030 N73-10233
Amplitude analog signals for use with CAMAC on-line operation
[EUR-5100-E] 01 p0055 N73-10447
Evaluating video graphic performance before and after implementation
[P-4830] 01 p0080 N73-10658
Minicomputer for controlling data transfer between process instrumentation and on-line computer
[HMI-B-123] 02 p0145 N73-11171
On-line failure testing of synchronous sequential computers
03 p0271 N73-12197
RAF operating procedures for ICL 7020 Remote computer terminal
[RAE-TR-72086] 06 p0644 N73-15231
On-line dialog and testing program for control of real time FORTRAN program
08 p0887 N73-17182
Digital on-line spectrum analysis using cross correlation and fast Fourier transformation techniques
[ARC-CP-1225] 09 p1006 N73-18209
Optical data processing of dielectric particle trajectory detector data using flying spot scanner on-line to computer
[BMVG-FBWT-72-34] 09 p1036 N73-18457
On-line programming to measure correlations in plasma using fast buffer memory and digital analysis
[IPPJ-T-12] 09 p1070 N73-18729
Integrated documentation approach using on-line programming
10 p1131 N73-19218
On-line laboratory station connected to real time/time-sharing EMR 6130 computer for semiconductor radiation effects studies
[SC-DR-72-0525] 10 p1161 N73-19442
Onboard, on-line parameter updating for Mars stratosphere and troposphere, using maximum likelihood estimation
15 p1829 N73-24821
On-line interactive computer solution of dispersion equations
22 p2636 N73-31123
RALPH - on-line data acquisition and analysis system for processing gamma ray and coincidence data
[NASA-TM-X-69507] 22 p2639 N73-31151

**ONBOARD COMPUTERS**
U AIRBORNE/SPACEBORNE COMPUTERS
**ONBOARD EQUIPMENT**
NT AIRBORNE EQUIPMENT
NT AIRBORNE/SPACEBORNE COMPUTERS
NT AIRCRAFT EQUIPMENT
NT SPACECRAFT ELECTRONIC EQUIPMENT
Design of computerized airborne traffic display device with alphanumerical control for aircraft pilots
01 p0014 N73-10112
Scientific equipment of ionospheric ESRO-4 satellite including five experiments
[ESRO-SN-114-ESTEC] 02 p0234 N73-11906
Performance of attitude sensors determined from Skylark 586 payload flight test
[RAE-TR-72066] 03 p0359 N73-12927
British Prospero satellite control noting instrumentation, equipment, and experimental performance
[RAE-TR-72088] 03 p0359 N73-12928
Onboard digital correlator for spacecraft VLF radio wave studies
04 p0423 N73-13446
Onboard data processing system for Helios solar probe
[DGLR-PAPER-72-092] 06 p0644 N73-15229
Manual actuator for exercise machine onboard spacecraft
[NASA-CASE-MFS-21481-1] 06 p0676 N73-15503
Application of on-board digital computers for stabilization of missile and rocket control systems
[JPRS-57893] 06 p0721 N73-15881
Design concepts for on-board coherent optical image processor
09 p1066 N73-18694
Onboard spacecraft propulsion using nuclear fuels and solar energy - pt. 1
[JPRS-58612-1-PT-1] 10 p1209 N73-19833
Onboard spacecraft thermoelectric and chemical propulsion systems - Pt. 2
[JPRS-58612-2-PT-2] 10 p1209 N73-19834
Delayed simultaneous appendage release mechanism for use on spacecraft equipped with despin mechanisms and releasable components
[NASA-CASE-GSC-10814-1] 11 p1237 N73-20039
Effect of trapped electron and proton radiation on onboard components and payloads of low thrust orbits through Van Allen belts
[NASA-TM-X-2777] 11 p1335 N73-20840
High angular resolution imaging system for outer planet Grand Tour Mission
[NASA-CR-132013] 14 p1704 N73-23823
Fundamental characteristics of onboard digital computers and converters
16 p1879 N73-25208
Development of artificial intelligence for onboard decision making capability of unmanned spacecraft during solar system exploration - Vol. 2
[NASA-CR-132257] 16 p1962 N73-25874
Electronic strain level counter on in-flight aircraft
[NASA-CASE-LAR-10756-1] 17 p2090 N73-26910
Onboard processing for data collection satellite systems
[NASA-CR-132792] 19 p2239 N73-28049
Medical evaluation of pilots using onboard flight recorders
22 p2619 N73-30986
Apollo experience report on equipment storage and stowage arrangement in spacecraft for maximum operational performance
[NASA-TN-D-7434] 22 p2720 N73-31771
Silicon vidicon camera for slow scan operation onboard Mariner spacecraft
22 p2732 N73-31862
Onboard frequency analyzer for measurement and analysis of acoustic and vibration data
[NASA-CR-132305] 23 p2793 N73-32343
Time allocation in Azur satellite telemetry data, noting onboard clock and world time deviations on tapes
24 p2985 N73-33855
**ONBOARD NAVIGATION**
U NAVIGATION
**ONE DIMENSIONAL FLOW**
Finite element procedure for predicting unsteady compressible gas flow in one spatial dimension
[AD-746234] 02 p0157 N73-11276
Steady-state one dimensional motion of uniformly dense suspensions
[AD-750924] 06 p0656 N73-15333
Numerical analysis of one-dimensional isentropic flow of thermally perfect, calorically imperfect diatomic gas
[ESDU-S.00.01.10-AMEND-A]
07 p0767 N73-16233
Analysis of one dimensional flow downstream of source of radiation in constant area ducts and conical nozzles
07 p0853 N73-16920
One dimensional flow and mass transfer between two fixed parallel walls at different temperatures by moment method
[NASA-CR-130744] 08 p0897 N73-17261
Numerical analysis of one dimensional isentropic flow of thermally perfect, calorically imperfect diatomic gas
[ESDU-S.00.01.10-AMEND-A]
14 p1648 N73-23364
Methods for computing shock flows including one dimensional unsteady flow
[AD-760015] 18 p2131 N73-27219
One dimensional flow of partially ionized argon in hypersonic nozzle
[AD-760967] 18 p2184 N73-27632
Method for direct calculation of localization parameters for wave functions in one demensional disordered potential chains
[RE-461J] 21 p2566 N73-30566
Numerical integration techniques for shock discontinuity in one dimensional unsteady channel flow
[PUBL-138] 22 p2634 N73-31258
**ONISOTROPY**
U ANISOTROPY
**OPACITY**
Computer program for calculating equations of state, thermodynamic functions, and opacities of plasmas
[AD-751608] 07 p0829 N73-16724
Solar neutrinos and influences of opacity, thermal instability, additional sources, and central black hole on solar models
[NASA-TM-X-68847] 08 p0959 N73-17844
**OPEN CHANNEL FLOW**
Shallow flowing water channel for hydraulic analogy of gas flow in transonic to hypersonic range
[ICT-4/71] 01 p0036 N73-10286
Turbulent burst and non-turbulent durations in turbulent boundary layer of open channel
[ARL/SM-NOTE-374] 01 p0039 N73-10307
Shallow flowing water channel for hydraulic analogy of gas flow in transonic to hypersonic range
[GRI/NTP/100] 02 p0146 N73-11186
Mathematical model for calculating transient flow of compressible condensable fluid mixtures in open channels
[UCID-16170] 19 p2255 N73-28181
**OPEN PIT MINES**
U MINES [EXCAVATIONS]
**OPENINGS**
NT APERTURES
NT SLITS
**OPERATING SYSTEMS [COMPUTERS]**
RAF operating procedures for ICL 7020 Remote computer terminal
[RAE-TR-72086] 06 p0644 N73-15231
**OPERATIONAL HAZARDS**
Hazards related to use of jet thrust power
[PB-211593] 05 p0497 N73-14046
Operational hazards and safety regulations for liquid and gaseous oxygen system handling
[NASA-CR-120922-VOL-2] 05 p0580 N73-14717
Maintenance programs for oxygen systems to prevent accidents
[NASA-CR-120922-VOL-3] 05 p0580 N73-14718
Avian hazards to Air Force rocket sled test tract at Holloman AFB, New Mexico
[AD-755833] 12 p1389 N73-21261
NASA/MSFC multilayer diffusion models and computer program for operational prediction of toxic fuel hazards
[NASA-CR-129006] 19 p2239 N73-28050
Behavior of hazard rate function of two component parallel systems
19 p2305 N73-28537
**OPERATIONAL PROBLEMS**
Performance evaluation and operating characteristics of different dissolved oxygen analyzers
[RN-1007] 02 p0171 N73-11385
Operational and air transport characteristics of civil V/STOL aircraft
[NASA-TT-F-14619] 04 p0371 N73-13012
Design and operation of computer for installation onboard satellite
[RAE-LIB-TRANS-1647] 04 p0392 N73-13188
Operating principles and physical mechanisms of pulsed gas discharge lasers
[SC-T-72-2524] 06 p0679 N73-15529
Operational problems and scientific research activities at cyclotron
[AD-751539] 07 p0767 N73-16230
Operating principles of high precision orbiting astronomical observatory manned by nonprofessional cosmonaut astronomer
[NASA-TT-F-14580] 07 p0843 N73-16830
Problems of multiprogramming for special purpose computers
[JPRS-58571] 12 p1381 N73-21201
Problems of library and information services to large research center
15 p1753 N73-24204
Shortcomings in Government organization for civil aviation
[PB-215426/8] 16 p1977 N73-25994
Operational principles and functions of mnemonic diagrams in controlled system
21 p2503 N73-30083
Design, dynamic response, and operation of electric pressure difference transducer
[NLL-TRANS-2976-[9022.81]]
21 p2543 N73-30387
Performance of pure plutonium oxide fuel under operational conditions
[LA-5160-MS] 21 p2578 N73-30660
Meteorological satellite technology and operation
[PUBL-SER-B-70] 24 p2949 N73-33558
**OPERATIONS**
Characteristics and operation of educational satellite networks
[NASA-CR-129257] 03 p0265 N73-12148
**OPERATIONS RESEARCH**
Planning, control, and management for European space satellite project
[ESRO-SP-70] 01 p0121 N73-10996
Analysis of costs and effectiveness of space missions, aerospace vehicles, and propulsion systems
[NASA-CR-129258] 03 p0358 N73-12917
Analysis of criteria for establishing air transportation curricula in community college based on manpower requirements and industrial needs
04 p0486 N73-13969
Economic analysis of space shuttle transportation system based on tradeoffs, alternatives, and variations in spacecraft design - Vol. I
[NASA-CR-129568] 04 p0487 N73-13977
Analysis of operations and resources required to support expendable second stage reusable space shuttle booster - Vol. 5
[NASA-CR-128660] 05 p0599 N73-14871
Relation between top managers in Federal agencies and operations research/management science groups
[NASA-CR-130668] 08 p0976 N73-17980
Impact on political and organizational policy and decision making of operations research/management science
[NASA-CR-130667] 08 p0976 N73-17981
Development of statistical methods for estimating annual operations at non-tower airports and establishment of standardized estimation procedure
[SCI-2-040] 11 p1267 N73-20278
Procedure for finding minimal and maximal Hamiltonian circuits on complete graph
[AD-754842] 11 p1312 N73-20648
Development of procedures for accurately estimating annual air traffic levels at airports without tower control
[SCI-2-2040] 11 p1321 N73-20722
MASS computer models for analyzing space shuttles and space shuttle payload operations
[NASA-CR-112286] 11 p1343 N73-20897
Analysis of NASA programs during post-Apollo period to show organization of field centers, planning activities, operational activities, and resources utilization
[NASA-CR-131931] 12 p1466 N73-21879
Evaluation of performance of H-1 helicopter, CH-54 helicopter, and OH-6 helicopter under combat conditions
[AD-755554] 13 p1475 N73-21949
Utilizing Out-of-Kilter Algorithm to evaluate efficiency of passenger capacity of selected air carriers between twenty cities in US
13 p1592 N73-22910
On-going research relevant to continuous operations
14 p1723 N73-23983
Research strategy and precise definition of continuous operations
14 p1724 N73-23991
Systems analysis and operations analysis of solid propellant rocket engine configurations for use with space shuttles - Vol. 3
[NASA-CR-123728] 15 p1826 N73-24799
Proceedings of conference on operational problems of air traffic control beacon system
[FAA-NA-72-80] 16 p1940 N73-25702
Very low frequency timing techniques for Omega navigation system to include operational considerations, path selection, and adjustment procedure
[NASA-CR-133185] 17 p2061 N73-26669
Tables of data for airline economic impact computer model - Vol. 2
[AD-749491] 17 p2100 N73-26989
Design concept, operational performance, and military employment of AV-8A Harrier aircraft
18 p2103 N73-27005
Development of procedures for determining capacity of airports and causes of airport delays - Vol. 1
[FAA-RD-73-11-VOL-1] 18 p2126 N73-27180
Analysis of air space control problems associated with military operations and development of doctrine for improved command and control
[AD-761034] 18 p2176 N73-27573
Analysis of rigid airship operations for commercial cargo handling in United Kingdom
[CRANFIELD-CTS-3] 20 p2360 N73-28985
Operations research problem of meteorological station distribution in bounded region
20 p2446 N73-29653
Operational parameters for UH-1H helicopters during combat flights in Southeast Asia to determine helicopter performance and reliability
[AD-764260] 22 p2616 N73-30965
Functional models for airline operations
23 p2862 N73-32870
Research project to determine factors involved in expansion of air freight traffic and prospects for future expansion
23 p2863 N73-32884

Analysis of commuter air transportation services to define problems and identify methods for improvements in cost effective operations
23 p2863 N73-32885

Evaluation of new forms of air transport service for improving short haul air travel market
23 p2863 N73-32887

Actions by Civil Aviation Board to regulate and improve commuter air transportation services
23 p2864 N73-32888

Analysis of airline mergers to show effects on management, personnel, and overall airline operations
23 p2865 N73-32898

Analysis of factors affecting operation of domestic airline to overseas areas
23 p2865 N73-32901

Methodology of planning experiments under nonuniform conditions
24 p2944 N73-33513

**OPERATOR PERFORMANCE**

Conference on manual control systems for human operator modeling and display systems in man machine environments
[NASA-SP-281] 01 p0013 N73-10104

Hybrid computer identification program for visual display of adaptive control state to human operator
01 p0014 N73-10109

Measurements of automobile driver response functions in simulated steering control task with visual field display
01 p0017 N73-10130

Driving speed in relation to interactions among automobile driver, roadway variables, and vehicle control
01 p0017 N73-10131

Double steering wheel forcing functions for estimating automobile driver manual control response
01 p0017 N73-10132

Phase margin measure for determining human operator control performance in multivariable closed loop system
01 p0018 N73-10135

Effect of concurrent audio tasks on human operator compensatory tracking performance using manual control system
01 p0018 N73-10139

Optical measurements of thin slots milled in edges of aluminum alloy test blocks to determine accuracy of measurement and detectability by operators using high frequency probes
[ARL/MET-NOTE-82-PT-1] 02 p0186 N73-11506

Effects of antimotion sickness drugs, placebos, and secobarbital on postural equilibrium functions at sea level and at simulated altitudes of 12,000 feet
[AD-748192] 05 p0504 N73-14105

Development of aircraft control systems based on operator performance, adaptive displays, and coupling of manual with automatic control
[AD-751306] 07 p0741 N73-16026

Psychophysiological analysis of job performance for optimizing operator production in man machine systems
[NASA-TT-F-14888] 12 p1374 N73-21150

Effect of low visibility on performance of vehicle operators
[AD-749248] 13 p1486 N73-22051

Operator performance in interpreting side-looking airborne radar real-time imagery
[AD-759495] 16 p1878 N73-25204

Training program for improving performance of operators in locating targets in side-looking airborne radar
[AD-762342] 19 p2229 N73-27979

Psychological conception of operator participation in ergonomic process
21 p2502 N73-30081

Direct and indirect environmental factors affecting functional state of operators
21 p2503 N73-30084

Influence of emotional states on human operator performance and efficiency
21 p2503 N73-30085

Effects of fatigue, age, and degree of difficulty on eye-hand coordination performance
24 p2887 N73-33051

Application of skill requirement method for determining skills required of on-orbit crew personnel performing earth-orbital research
[NASA-CR-124452] 24 p2982 N73-33830

**OPERATORS [MATHEMATICS]**

Numerical analysis of projected gradient method and operator formed from any linearly independent subset of gradients
[DLR-FB-73-26] 11 p1311 N73-20636

Quantum mechanical Racah and Stevens operators used in magnetism theory
[RISO-259] 12 p1429 N73-21580

Extension of theorems concerning spectrum of one-dimensional and multidimensional differential operators on vector functions
[NASA-TT-F-14960] 17 p2055 N73-26620

Operator theory of n-th order modular forms
[NASA-TT-F-15006] 19 p2313 N73-28605

Boundary value problems involving T-T operators
[AD-763837] 22 p2692 N73-31562

**OPERATORS [PERSONNEL]**

NT AIRCRAFT PILOTS
NT PILOTS [PERSONNEL]

Measurement of operator workload in formation processing
[NASA-CR-2150] 04 p0379 N73-13087

Human operator model performance in tracking high performance aircraft
[AD-746725] 04 p0381 N73-13101

Human operator adaptive behavior in slowly changing dynamic system
[AD-748243] 05 p0503 N73-14097

Personnel protection and emergencies handling for oxygen systems
[NASA-CR-120922-VOL-4] 05 p0580 N73-14719

Vibrational effects on visual acuity of human operator seated in military tracked vehicle
[AD-750345] 06 p0636 N73-15172

Toxicity and safety hazard of dry beryllium copper alloy machining for human operator
08 p0872 N73-17059

Linear rating scale for selecting tracking task parameters by subjective operator
[AD-752036] 08 p0880 N73-17125

Users guide to help formulate requests for oceanographic data and related information
14 p1658 N73-23454

Computer courses for professional training of programmers and operators
21 p2609 N73-30914

Effect of human operator errors on reliability and effectiveness of his work
[AD-764937] 23 p2753 N73-32028

Method for automatically processing indices of operator gas exchange during work in trainer using computers
24 p2884 N73-33035

**OPHTHALMOLOGY**

NT EYE EXAMINATIONS

Opthalmological examination of antimalarial drugs effects on performance of navigation personnel
12 p1371 N73-21122

Ultrasonic device for ophthalmic eye surgery with safe removal of macerated material
[NASA-CASE-LEW-11669-1] 18 p2110 N73-27062

**OPTICAL ABSORPTION**

U ELECTROMAGNETIC ABSORPTION
U LIGHT TRANSMISSION

**OPTICAL ACTIVITY**

Optical variability in peculiar extragalactic radio sources
23 p2755 N73-32047

**OPTICAL AMPLIFIERS**

U LIGHT AMPLIFIERS

**OPTICAL COMMUNICATION**

Modulation and detection of signals on optical carriers
[NASA-CR-129181] 02 p0180 N73-11460

Noise immunity of optical communication lines with frequency and time multiplexing subcarriers
[JPRS-57178] 02 p0181 N73-11467

Synchronization using pulsed edge tracking in optical PPM communication systems
[NASA-CR-130117] 03 p0265 N73-12143

Development of frequency modulated diode laser transmitter for point-to-point voice communication system
[AD-747524] 03 p0311 N73-12540

Development of optical data communication systems with fiber optics for military avionics
[AD-747946] 03 p0337 N73-12748

Performance of 10-micron mercury-cadmium-telluride and lead-tin-telluride photodiodes in laser heterodyne communication systems
[NASA-TM-X-66135] 05 p0557 N73-14521

Laser telemetry discussing equipment specifications, errors, and noise reduction
05 p0557 N73-14524

Application of absorber laser amplifier and detector to wide angle low noise optical radar and communication systems
[AD-749543] 05 p0558 N73-14533

Development and characteristics of optical communication system based on three frequency heterodyne configuration
[AD-750321] 06 p0680 N73-15533

Proceedings of conference to determine research projects for development of lasers for optical communications applications
[PB-212692] 07 p0807 N73-16543

Laser modulation mechanisms and optical communication technology
08 p0928 N73-17603

Bibliography of laser communication systems
[AD-751900] 08 p0929 N73-17612

Frequency stable Q switched carbon dioxide laser oscillators, free-running and injection locked pulsed lasers, and optical heterodyne measurements of frequency stability
[AD-753605] 09 p1045 N73-18523

Proceedings of conference on laser beam data transmission and development of laser information systems
[AD-753944] 10 p1169 N73-19513

Light communication systems using fiber optics
[AD-754566] 11 p1257 N73-20200

Expressions for generalized signal to noise ratio at output of optimal detector of optical signal
12 p1378 N73-21179

CO2 laser communications for army tactical applications
[AD-756866] 13 p1496 N73-22124

Ultrawide-bandwidth laser communication system using high efficiency, single frequency lasers and optical modulators
[AD-755219] 13 p1539 N73-22468

Pulse position modulation laser communication system for voice transmission
[AD-757258] 14 p1633 N73-23237

Optical heterodyne signal power obtained from finite sized sources of radiation
[AD-756463] 14 p1633 N73-23243

Feasibility of integrated optics for use in high capacity, multi-GHz telecommunications
[AD-757342] 14 p1635 N73-23254

Feasibility analysis and design of bleachable absorber laser amplifier and detector
[AD-757361] 14 p1672 N73-23571

Analysis of acoustical amplitude and frequency modulation techniques of continuous wave helium-neon laser for optical communication applications
[AD-757672] 14 p1674 N73-23581

Summaries of papers presented at conference on optical communication systems
[PB-214778/3] 15 p1752 N73-24199

Development of cadmium telluride modulator for infrared laser communication system
[NASA-CR-112321] 15 p1795 N73-24549

Design and performance of carbon dioxide laser communication system
[AD-759483] 16 p1924 N73-25572

High resolution radar transmitting system for transmitting optical pulses to targets
[NASA-CASE-NPO-11426] 17 p1994 N73-26119

Design, development, and evaluation of optical detectors used in high speed digital laser communication links
[NASA-CR-132772] 17 p2032 N73-26446

Balloon measurements of stellar scintillation for predicting fading on space to ground laser propagation path
18 p2212 N73-27858

Performance of neodymium-yag optical data transmission system and development of channel simulator
18 p2212 N73-27859

Design of tunable waveguide carbon dioxide laser for optical heterodyne communication system between satellites
18 p2212 N73-27860

Transmitter and receiver antenna gain analysis for optical radar and communication systems
[NASA-TM-X-70423] 19 p2235 N73-28023

Development and characteristics of radar receiver for detecting coherent and incoherent optical signals against background of noise
22 p2630 N73-31075

Quantum detection and estimation in optical communication systems
22 p2679 N73-31460

Application of laser systems to space communication using carbon dioxide laser for two way communication with ATS-F satellite - Vol. 1 Pt. 1
[NASA-CR-132803] 22 p2680 N73-31469

Application of carbon dioxide laser for space communication to include ground equipment, data acquisition, and data processing - Vol. 1 Pt. 2
[NASA-CR-132804] 22 p2681 N73-31470

Requirements for design, fabrication, performance, and testing of optical heterodyne receiver subsystem for use in laser communication system - Vol. 1 Pt. 3
[NASA-CR-132805] 22 p2681 N73-31471

Introduction to optical communication with lasers
[FTZ-A-465-TBR-8] 22 p2681 N73-31477

Digital data transmission with argon laser beam through atmosphere to determine error frequency
[FTZ-44-TBR-34] 22 p2681 N73-31478

Design, development and operation of laser communication system developed for potential space shuttle application
[NASA-CR-124440] 23 p2801 N73-32400

Time synchronization in optical communication as problem of estimating arrival time of known transmitted field
[NASA-CR-132813] 23 p2801 N73-32401

Atmospheric attenuation of CO2 laser radiation measured by pyroelectric detection noting fog absorption and optical communication application
[LCR-DR-1-72-67/1/R] 23 p2801 N73-32404

Optimum receiver for detection of pulsed angle modulated optical communication system, using maximum posteriori
24 p2931 N73-33406

**OPTICAL CORRECTION PROCEDURE**

Design of Schmidt telescope with possibility of converting to Cassegrain configuration and noting achromatic corrector and angular resolution
07 p0846 N73-16858

OSUGOP computer program for adjusting geometrical or optical satellite observations
[NASA-CR-131532] 12 p1448 N73-21728

Correction of aberrations in long wavelength holography by direct injection in formation process and computer generation
22 p2680 N73-31466
Kerber profile Schmidt plates uses in optical combinations with applications to cameras
[OPT-01-72] 23 p2794 N73-32352
OPTICAL COUPLING
Radiometer quadrature control and measuring system using optical coupling circuitry
[NASA-CASE-MFS-21660-1] 04 p0421 N73-13434
Theoretical analysis of grating coupler for application in thin film integrated optical waveguides
22 p2699 N73-31621
Coupling efficiency of GaAlAs diode pumped Nd-YAG laser
24 p2930 N73-33398
OPTICAL DATA PROCESSING
Optical and digital data processing and handling of SLR imagery
[ESRO-CR[P]-139-VOL-4] 03 p0297 N73-12419
Conference on parallel image processing for earth observation systems
[NASA-TM-X-66175] 09 p1065 N73-18684
Review of coherent optical data processing
09 p1065 N73-18685
Optical processing in incoherent light
09 p1065 N73-18686
Data processing requirements for ERTS
09 p1065 N73-18689
Parallel optical data processing for earth resources satellite mission
09 p1065 N73-18690
Parallel image processing including electronic, noncoherent, and coherent methods
09 p1065 N73-18691
Synthesis of complex spatial filters for coherent optical data processing
09 p1065 N73-18693
Design concepts for on-board coherent optical image processor
09 p1066 N73-18694
Parallel image logical operations using cross correlation
09 p1066 N73-18695
Characteristics of holographic logic computer
09 p1066 N73-18696
Gravitational field models for solution of satellite geopotential using optical data processing
[NASA-TM-X-66207] 11 p1341 N73-20883
Development of techniques for solving image correlation and image sampling of multispectral data
[NASA-CR-130223] 13 p1529 N73-22389
Method for quantitative print quality evaluation of large amount of data with determination based on requirements of optical character readers
[REPT-731] 14 p1637 N73-23276
Spatial filtering techniques in connection with coherent light optical data processing
[LCR-DR-1-71-253/1/R] 15 p1754 N73-24220
Interactive digital processing of optical data in investigations of pattern recognition techniques
[AD-758517] 15 p1755 N73-24223
Research in optical computing systems
[PB-214573/8] 15 p1755 N73-24224
Holographic instrumentation for use in flow visualization, nondestructive testing procedures, and optical data processing
16 p1922 N73-25551
Hybrid optical processing system
16 p1922 N73-25552
Off-axis parabolic mirror segments in onboard optical data processing for spacecraft
16 p1923 N73-25557
Application of image sensing arrays to metrology, mapping, and optical data acquisition
[AD-761121] 18 p2149 N73-27370
Design of two dimensional digital computer for optical image processing onboard spacecraft using liquid crystal circuits
18 p2209 N73-27827
Optical data processing system using paraboloidal reflecting surfaces
[NASA-CASE-GSC-11296-1] 21 p2579 N73-30666
Optical data and image display recorder/processor
[NASA-CASE-GSC-11553-1] 22 p2631 N73-31089
Algorithm for assembling continuous boundaries and contours from black and white picture for computer processing and photointerpretation
[NPL-COM-66] 22 p2675 N73-31426
Computerized image processing and graphic display system
[NASA-TM-X-70473] 23 p2760 N73-32085
IBM 1130 computer programs for astrophysics optical data processing noting optical systems simulation and stellar density theoretical estimates
[CALC-01-72] 23 p2846 N73-32747
OPTICAL DENSITY
Spectral line thickness and temperature distribution in inhomogeneous sodium plasma confined between parallel mirrors
[INR-1388] 06 p0705 N73-15751
Optical density properties of ocular glass laser protective filters
[AD-755406] 13 p1487 N73-22057
Cerium and silver containing silicate and borate systems for developing high density scintillation glass for nuclear cascade detectors
[NASA-CR-133960] 17 p2049 N73-26580
Automatic land use classification based on optical density and shapes from ERTS-1 imagery
[E73-10816] 18 p2140 N73-27291
Development and characteristics of spectrophotometer for measuring transmittance of solid and liquid materials
[PAPER-76A5-729] 21 p2545 N73-30398
Photographic film for simplified production of equidensities in normal processing operation
[NASA-TT-F-15112] 22 p2673 N73-31410
OPTICAL EMISSION
U LIGHT EMISSION
OPTICAL EMISSION SPECTROSCOPY
Color film spectroscopy for quantitative optical radiation detection
[EGG-1183-5015] 06 p0674 N73-15483
Optical wavelength - modulation spectroscopy of solids
[LBL-1402] 21 p2549 N73-30437
OPTICAL EQUIPMENT
NT ASTRONOMICAL TELESCOPES
NT CAMERAS
NT CELESCOPES
NT CINETHEODOLITES
NT COLLIMATORS
NT DIFFRACTOMETERS
NT EBERT SPECTROMETERS
NT ELECTROPHOTOMETERS
NT ELLIPSOMETERS
NT FILTER WHEEL INFRARED SPECTROMETERS
NT FRAMING CAMERAS
NT HELIOMETERS
NT HIGH SPEED CAMERAS
NT IMAGE CONVERTERS
NT IMAGE TUBES
NT INFRARED SPECTROMETERS
NT INFRARED SPECTROPHOTOMETERS
NT MICRODENSITOMETERS
NT MICROWAVE REFLECTOMETERS
NT MULTISPECTRAL BAND CAMERAS
NT MULTISPECTRAL BAND SCANNERS
NT NEPHELOMETERS
NT OPTICAL MEASURING INSTRUMENTS
NT OPTICAL RADAR
NT OPTICAL RANGE FINDERS
NT OPTICAL SCANNERS
NT PANORAMIC CAMERAS
NT PERISCOPES
NT PHOTOMETERS
NT POLARIMETERS
NT PRISMATIC BARS
NT PRISMS
NT PYROHELIOMETERS
NT REFLECTOMETERS
NT SCHMIDT CAMERAS
NT SPECTROHELIOGRAPHS
NT SPECTROPHOTOMETERS
NT SPECTROSCOPIC TELESCOPES
NT STRATOSCOPE TELESCOPES
NT TELEVISION CAMERAS
NT THEODOLITES
NT TRANSMISSOMETERS
NT ULTRAVIOLET SPECTROMETERS
NT ULTRAVIOLET SPECTROPHOTOMETERS
NT WIDE ANGLE LENSES
NT X RAY TELESCOPES
Design study of infrared 10.6 micrometer, quantum noise limited, optical receiver subsystem
[NASA-CR-130091] 01 p0056 N73-10458
Development and characteristics of alkali halide window for application to infrared laser systems
[AD-744998] 01 p0065 N73-10530
Optical design and performance evaluation of athermal solid and liquid acoustic lenses
[AD-745734] 01 p0081 N73-10668
Molecular branching ratio method for intensity calibration of optical systems in far ultraviolet
[NASA-TM-X-66070] 01 p0103 N73-10853
Numerical analysis of semiconductor saturable absorber and establishment of criteria for operation of laser saturable resonator in bistable regime
[AD-746736] 02 p0183 N73-11488
FORTRAN computer program for solar simulator optimization
[DLR-FB-71-34] 03 p0281 N73-12277
Development of method for automatically scanning bubble chamber films based on optical system for detecting information points as vertices
[CEA-R-4329] 03 p0302 N73-12465
Feasibility of monitoring global air pollution using optical sensors installed in orbiting satellites
04 p0471 N73-13840
Development and characteristics of cyclically operable, optical shutter for use as focal plane shutter for transmitting single radiation pulses
[NASA-CASE-NPO-10758] 05 p0545 N73-14427
Numerically controlled ion beam sputtering process for manufacturing solid optical surfaces
[AD-750347] 05 p0581 N73-14730
Structural effects of various optical coatings on single shot laser induced damage threshold using pulsed neodymium glass laser
[AD-749852] 06 p0680 N73-15531
Characteristics of various types of remote sensors and identification of specific areas of application
07 p0784 N73-16373
Design and fabrication of optical system to compensate for motions of stellar field image on focal plane of large orbiting telescope based on single-axis system
[NASA-TN-D-7145] 07 p0799 N73-16488
Optical materials and design of optical equipment
[AD-751496] 07 p0822 N73-16660
Configuration and requirements for general purpose optical research facility to investigate earth atmosphere from space shuttle orbiter vehicle
[NASA-CR-128732] 08 p0893 N73-17226
Development of strain gage ambiguity sensor for measuring alignment of optical mirror segments
[NASA-CASE-MFS-20506-1] 08 p0923 N73-17563
Shock test of electron-proton spectrometer structural test unit to verify structural integrity of spectrometer design and to analyze shock response of electronic housing
[NASA-CR-128698] 08 p0924 N73-17574
Compilation of analyses generated during development of electron-proton spectrometer for Skylab program to insure reliability and quality control
[NASA-CR-128705] 08 p0925 N73-17576
Qualification tests of electron-proton spectrometer to determine suitability for use in Skylab program
[NASA-CR-128703] 08 p0925 N73-17580
Design modules for optical equipment
[AD-751964] 08 p0944 N73-17732
Development and characteristics of optical telescope assembly system for Large Space Telescope based on mission-related and optical parameters - Vol. 3
[NASA-TM-X-64726-VOL-3] 09 p1036 N73-18451
Frequency stable Q switched carbon dioxide laser oscillators, free-running and injection locked pulsed lasers, and optical heterodyne measurements of frequency stability
[AD-753605] 09 p1045 N73-18523
Development of optical equipment including image converters and infrared detectors employing coherent radiation
[AD-753275] 09 p1067 N73-18711
Operational requirements and optical components of pulsed holographic interferometry
[LA-5058] 10 p1161 N73-19446
Variation of laser radiation intensity along axis of unstable optical cavity with partially transmitting mirrors or gratings
[AD-753902] 10 p1170 N73-19515
Method for producing reticles for use in outer space
[NASA-CASE-GSC-11188-2] 10 p1184 N73-19630
Coherent optical system for display of spatial resolution of ERTS-1 MSS photography
[E73-10449] 11 p1283 N73-20409
Method and equipment for locating earth infrared horizon from space, independent of season and latitude
[NASA-CASE-LAR-10726-1] 11 p1291 N73-20475
Feasibility of producing large plastic components for optical systems
[AD-754818] 11 p1299 N73-20543
Operating principles and performance tests results for optical modulator system with mode locked Nd-YAG laser
[NASA-CR-130195] 11 p1302 N73-20569
Carbon dioxide lasers, optical measurement instrumentation and imaging techniques for air pollution detection
[AD-754939] 11 p1303 N73-20574
Optical imaging system for increasing light absorption efficiency of imaging detector
[NASA-CASE-ARC-10194-1] 11 p1324 N73-20741
Changes in optical properties of various materials due to exposure to exhaust plume of bipropellant rocket
[NASA-TM-X-68204] 11 p1349 N73-20942
Characteristics of photomultiplier tubes and application to optics, biophysics, radiometry, and astronomy for detecting weak light flows
[AD-755874] 12 p1384 N73-21226
Reliability and performance of landbased and shipboard Air Force instrumentation systems
[AD-755916] 12 p1389 N73-21262
Design, development, and operation of remote control system for Large Space Telescope
[NASA-TM-X-64740] 12 p1405 N73-21394
Optical system for measuring passive stress conditions in xenon flash lamps for use in high power lasers
[UCRL-50022-3] 12 p1410 N73-21427
Outer Planets Grand Tour mission planning to include magnetometer systems requirements and development of hardware elements to meet objectives
12 p1448 N73-21727
Beam focusing optical system consisting of elliptical and parabolic mirrors
[AD-757008] 13 p1560 N73-22643
Degradation of cold optical systems on orbiting spacecraft by cryodeposition
[AD-756772] 13 p1560 N73-22644

GUERAP computer code for accurately measuring off axis rejection characteristics of optical system - users manual
[AD-755353] 13 p1560 N73-22645
Large space bandwidth signal analysis by means of two-dimensional optical processor and synthesis of near real time optical sound-spectrograph
14 p1631 N73-23223
Analysis of image forming ability of infrared line scan system based on laboratory measurements and flight tests using ground test array
[DREV-TN-2053/72] 14 p1666 N73-23520
Research in optical computing systems
[PB-214573/8] 15 p1755 N73-24224
Meteorological implications of airborne optical imaging through tropopause
[AD-758207] 15 p1782 N73-24449
Evaluation of image forming ability of infrared line scan system using laboratory and flight test techniques
15 p1786 N73-24476
Space-variant image motion degradation and restoration in linear incoherent optical systems
15 p1812 N73-24687
High density optical memory
[AD-759032] 17 p2002 N73-26184
Design, development, and characteristics of field ion microscope for image intensification
[ARL/INST-NOTE-78] 17 p2032 N73-26445
Design, development, and evaluation of optical detectors used in high speed digital laser communication links
[NASA-CR-132772] 17 p2032 N73-26446
Observability of high altitude aerosol and atmospheric scattering layers by satellite-borne optical detector
[NASA-CR-112309] 18 p2144 N73-27329
Development of method for determining resolving power of photographic lenses
[NBS-SP-374] 18 p2151 N73-27387
Development of optical system for detecting defective components in rotating machinery with emphasis on bearing assemblies
[NASA-CASE-KSC-10752-1] 18 p2154 N73-27407
Threshold detection system for infrared nutating optical system
[AD-761380] 18 p2180 N73-27600
Linear estimation technique for enhancement of black and white images
[AD-760779] 18 p2180 N73-27601
Development, construction, and operation of polarization fourier spectrometer for conducting astronomical observations
19 p2300 N73-28492
Laser technology and propagation, optical measurements, and optical equipment
[AD-762320] 19 p2308 N73-28566
Development, characteristics, and operation of compensated thermoelectric net radiometer to show advantage over standard radiometers
20 p2402 N73-29305
Development and characteristics of single reflector interference spectrometer and associated drive system
[NASA-CASE-NPO-11932-1] 20 p2419 N73-29438
High density optical memory and electron spin dependent trapping and tunneling processes in KCl and KCl-NaCl
20 p2460 N73-29768
Development of technique and apparatus for optically detonating insensitive high explosives
[NASA-CASE-NPO-11743-1] 20 p2485 N73-29959
Development and evaluation of on-line spatial light modulator for application as input transducer for real-time optical data processing system
[NASA-CR-124375] 21 p2508 N73-30121
Techniques and equipment for achieving high accuracy spectrophotometric measurements
[PAPER-76A5-728] 21 p2544 N73-30397
Development of semiconductor electro-optical devices in Poland with emphasis on management planning and research projects to establish capability
21 p2608 N73-30898
Detection and estimation of optical images by photon counting techniques
[NASA-CR-135498] 23 p2792 N73-32335
Method for comparing photo-electronic and photographic detectors based on product of signal to noise ratio times spatial bandwidth
24 p2958 N73-33634
Characteristics of lenses and ports for underwater imaging systems to compare depth of field and relative aperture for several lens port combinations
24 p2958 N73-33635
Techniques for long range vision underwater using range-gating and dual-scan with parallax techniques
24 p2958 N73-33636

**OPTICAL FILTERS**
NT INFRARED FILTERS
Encoding action of pair of dichroic gratings suitable for single tube color television camera
[BBC-1972/32] 04 p0419 N73-13414
Computer program for evaluating effects of conical light beams through interference filters, tilting filter, and energy distribution variations across beam
[WRE-TN-710[AP]] 04 p0449 N73-13665
Filter photometric data from OAO 2 on blue Ap, band a dwarfs, and giants
[NASA-TM-X-66163] 07 p0843 N73-16826
Electronically tunable acousto-optical filter for laser applications
[AD-752052] 08 p0944 N73-17733
Holographic starfield and landmark tracker with two reference beam, coherent optical matched filter technique
[NASA-CR-112143] 10 p1168 N73-19505
Optimization of optical filtering for tracking faint stars
[NASA-CR-130199] 11 p1293 N73-20496
Optical density properties of ocular glass laser protective filters
[AD-755406] 13 p1487 N73-22057
X ray reflection efficiency of nickel coated quartz optical flats
[NASA-TM-X-64747] 15 p1813 N73-24694
Holography and optical filtering techniques for structural analysis, material tests, and astronomical observation - conference
[NASA-SP-299] 16 p1920 N73-25540
Low light level television system for coherent optical matched filtering for meteor trail detection
16 p1922 N73-25554
Holography applied to matched filtering and pattern recognition
16 p1922 N73-25555
Matched filter selectivity applied to holographic velocimetry
16 p1923 N73-25556
Adapted filter for dispersion measurement of coherent wave packets produced by Pc1 micropulsations
17 p2027 N73-26402
Computerized simulation of optical pattern recognition and image processing system
[AD-761882] 19 p2241 N73-28065
Computerized design of multilayer thin film filters
[WRE-TN-903[AP]] 23 p2759 N73-32082

**OPTICAL GENERATORS**
U LASERS

**OPTICAL HETERODYNING**
Computerized optical system for producing multiple images of a scene simultaneously
[NASA-CASE-MSC-12404-1] 04 p0448 N73-13661
Optical design approach for large array of high speed heterodyne receivers for infrared laser radiation
[AD-750402] 06 p0700 N73-15711

**OPTICAL MASER MODULATION**
U LIGHT MODULATION

**OPTICAL MASERS**
U LASERS

**OPTICAL MEASUREMENT**
NT ASTRONOMICAL PHOTOMETRY
NT COLORIMETRY
NT ELECTROPHOTOMETRY
NT PHOTOMETRY
NT POLARIMETRY
NT SPECTROPHOTOMETRY
NT STELLAR SPECTROPHOTOMETRY
NT TELEPHOTOMETRY
NT ULTRAVIOLET PHOTOMETRY
NT VISUAL PHOTOMETRY
Optical transfer function measurements on lenses and lens systems
[TPD-1972-0-1] 01 p0079 N73-10654
Horizontal standard visibility determined by natural object contrast measurements, noting visual field observation
[DLR-FB-71-22] 03 p0261 N73-12118
Characteristics of cryogenic interferometric spectrometer and application to measuring low level emittance or absorption in optical elements
05 p0556 N73-14518
Rocket-borne auroral optical measurement of proton and electron precipitation
[SC-RR-72-0543] 07 p0793 N73-16448
Optical and energy measurements of strong current discharges in air
[AD-751414] 07 p0830 N73-16729
Optical measurement of RDX and PETN monocrystal detonation velocity along different crystallographic axes
[ISL-28/71-PT-1] 09 p1052 N73-18575
Electron beam optics for measuring density and temperature of aerodynamic gas flow
[ONERA*PUBL-146] 13 p1559 N73-22635
Data obtained in Bahama channels and Northwestern Atlantic ocean during Deep Ocean Optical Measurement program
[AD-757332] 14 p1665 N73-23511
Laser technology and propagation, optical measurements, and optical equipment
[AD-762320] 19 p2308 N73-28566
Computerized data processing system for sampling, labeling, and digital recording of optical measurements
[AD-762332] 19 p2322 N73-28678
Development and characteristics of single reflector interference spectrometer and associated drive system
[NASA-CASE-NPO-11932-1] 20 p2419 N73-29438
Development of optical diagnostic techniques to determine plasma refractive index using interferometers to produce space or time resolved density data
[AD-763802] 21 p2584 N73-30706
Optical and ultraviolet methods in astronomy
22 p2734 N73-31882
Optical modeling of radiation pattern of variable profile antenna operating in Hartman diaphragm mode
23 p2837 N73-32674

**OPTICAL MEASURING INSTRUMENTS**
NT CINETHEODOLITES
NT DIFFRACTOMETERS
NT EBERT SPECTROMETERS
NT ELECTROPHOTOMETERS
NT ELLIPSOMETERS
NT FILTER WHEEL INFRARED SPECTROMETERS
NT INFRARED SPECTROMETERS
NT INFRARED SPECTROPHOTOMETERS
NT MICRODENSITOMETERS
NT MICROWAVE REFLECTOMETERS
NT NEPHELOMETERS
NT OCULOMETERS
NT OPTICAL RANGE FINDERS
NT OPTICAL SCANNERS
NT PHOTOMETERS
NT POLARIMETERS
NT REFLECTOMETERS
NT SPECTROPHOTOMETERS
NT THEODOLITES
NT TRANSMISSOMETERS
NT ULTRAVIOLET SPECTROMETERS
NT ULTRAVIOLET SPECTROPHOTOMETERS
Advanced Figure Sensor for measuring parabolic mirror surfaces
[NASA-CR-130114] 03 p0301 N73-12454
Installation, operation, and maintenance procedures for optical figure sensor and associated electronic controls
[NASA-CR-130125] 04 p0421 N73-13429
Feedback stabilization of theta pinch plasma column by optical signal processor
[LA-DC-72-707] 05 p0584 N73-14750
Optical measuring instruments used at hypervelocity ballistic range facility
[AD-750866] 06 p0651 N73-15284
Local quantities in two phase flow measured with anemometer, electrical probe, microthermocouple, and optical sensor techniques
[CEA-CONF-2033] 08 p0897 N73-17263
Optical design optimization, and sensor selection for mission definition of outer planets Grand Tours
[NASA-CR-131088] 10 p1159 N73-19427
Computation of optical sensor output relative to known star magnitudes for attitude control of spacecraft
[NASA-CR-130926] 10 p1212 N73-19859
Optical apparatus to determine effect of turbulence on modulation transfer function of atmosphere
[AD-757256] 14 p1661 N73-23485
Development of Mach-Zehnder interferometer theory based on time history of wave front produced by element of extended light source
[ARC-R/M-3173] 16 p1856 N73-25033
Application of image sensing arrays to metrology, mapping, and optical data acquisition
[AD-761121] 18 p2149 N73-27370
Design of optical instrument package for large space telescope
18 p2210 N73-27839
Development of multimode optical sensor
[NASA-CR-133980] 19 p2300 N73-28493
Analysis of physical parameters involved in spectrophotometry with high accuracy to show effects of stray light and interference
[PAPER-76A5-732] 21 p2545 N73-30401
Analysis of errors in measurement of absorbances of liquid filters caused by instrumental and chemical uncertainties using three types of liquid filters
[PAPER-76A5-733] 21 p2545 N73-30402
Procedures for accurate measurement of molar absorptivities to show sources of determinant error and methods for elimination of errors
[PAPER-76A5-734] 21 p2545 N73-30403
Analysis of parameters involved in establishing spectrophotometric standards
[PAPER-76A5-737] 21 p2546 N73-30406
Analysis of absolute spectrofluorometry procedures and establishment of standards for calibrating spectrofluorometers
[PAPER-76A6-741] 21 p2546 N73-30407
Design and performance of remote sensing system for optical sensing of emissions
[PB-221073/0] 22 p2696 N73-31599

**OPTICAL MEMORY [DATA STORAGE]**
Holographic memory system using argon ion lasers and acoustooptic beam deflectors
[NASA-CR-124084] 09 p1064 N73-18680
Thin deformable films for use as storage medium in holographic optical memory
[NASA-CR-124083] 09 p1064 N73-18681
Membrane-mirror elements as light valves in optical memory systems
[NASA-CR-124085] 09 p1064 N73-18682

Magneto-optical and electro-optical approaches for meeting time memory demands
09 p1065 N73-18688
MOS photodetector mosaics for application to readout of optical memories with charge storage
13 p1500 N73-22155
Development of photoplastic materials for optical memory storage applications
[AD-764822] 23 p2794 N73-32356

**OPTICAL METHODS**
U OPTICS

**OPTICAL MODULATION**
U LIGHT MODULATION

**OPTICAL PATHS**
Inversion of radio occultation data for planetary atmospheres by bent ray path technique
02 p0198 N73-11598
Light source and geometrical requirements for optimization of optical anemometry signals
[ET/TN/A/18] 13 p1537 N73-22451
Modulation transfer functions for linear image formation with partially coherent light
15 p1812 N73-24689

**OPTICAL PROPERTIES**
NT ABSORPTANCE
NT ABSORPTIVITY
NT BIREFRINGENCE
NT BRIGHTNESS
NT COLOR
NT DICHROISM
NT IRIDESCENCE
NT LUMINOSITY
NT OPACITY
NT OPTICAL REFLECTION
NT PHOSPHORESCENCE
NT PHOTOCONDUCTIVITY
NT PHOTOELECTRIC EFFECT
NT PHOTOELECTRIC EMISSION
NT PHOTOIONIZATION
NT PHOTOVOLTAIC EFFECT
NT RADIANCE
NT REFLECTANCE
NT REFRACTIVITY
NT SKY BRIGHTNESS
NT SPECTRAL REFLECTANCE
NT STELLAR LUMINOSITY
NT TRANSLUCENCE
NT TRANSMISSIVITY
NT TRANSMITTANCE
NT TRANSPARENCE
NT TURBIDITY
Analysis of gray scale image storage techniques in electroluminescent and photoconductor image conversion panels
[AD-745758] 01 p0033 N73-10261
Process for producing polycrystalline halides for use in high power laser windows to maintain optical properties with improved mechanical properties
[AD-745350] 01 p0065 N73-10535
Optical transfer function measurements on lenses and lens systems
[TPD-1972-0-1] 01 p0079 N73-10654
Spectral resolution and image enhancement by focusing of lense optics
[TPD-1972-0-2] 01 p0079 N73-10655
Optical properties and band structure of solids studied with electroreflectance and other optical modulation
[AD-746271] 01 p0089 N73-10736
Spectrophotometric analysis of Orion nebula emission spectra with dust lanes in hydrogen region
[AD-745314] 01 p0104 N73-10863
Determination of in-flight optical transfer functions of orbital earth resources multispectral sensors
[E72-10212] 02 p0162 N73-11307
Mathematical analysis of optical refractive index fluctuations due to salinity and temperature microstructure
[AD-746120] 02 p0168 N73-11366
Optical properties of laser resonators with spinning prism Q switch
[WRE-TN-658[AP]] 02 p0180 N73-11461
Method for analyzing dominant TEM mode of complex laser cavities
[AD-746215] 02 p0183 N73-11481
Three-dimensional electromagnetic inverse scattering identity based on physical optics approximation for monostatic scattered far field cross section of perfect conductors
02 p0200 N73-11615
Airborne measurements of optical atmospheric properties and southern Germany during spring 1970
[AD-747490] 03 p0298 N73-12429
Design, development, and evaluation of pressure transducer using glass fiber bundle to transmit and receive reflected light from pressure diaphragm
[AD-747521] 03 p0304 N73-12480
Physicochemical and optical properties of glasses of BaO-PbO-Bi2O3-TiO2 system
[AD-747371] 03 p0322 N73-12620
Maximum detection probability of optical image by photoelectric surface with unit quantum efficiency
[NASA-CR-130121] 03 p0334 N73-12725
Measurement of ultraviolet and far ultraviolet transmission of transparent materials during high energy electron irradiation
[NASA-CR-129297] 03 p0334 N73-12726
Optical parameter effects of sea water and spatial-temporal structure of light impulses
[JPRS-57332] 03 p0335 N73-12733
Optical properties of thin film deposited by electron bombardment
[NPL-OP-MET-13] 03 p0340 N73-12775
Optical and magnetic properties of actinide and rare earth ions in insulators and semiconductors
[RLO-2221-T-6-14] 03 p0345 N73-12815
Analysis of propellant gases emitted by attitude control system to determine interference with experiments due to flow fields and plume density
[NASA-CR-114508] 03 p0363 N73-12958
Device and method for determining X ray reflection efficiency, scattering properties, and surface finish of optical surfaces
[NASA-CASE-MFS-20243] 04 p0449 N73-13662
Optical and back reflection properties of GaAs crystals used as IR window materials
[AD-749083] 04 p0451 N73-13684
Magnetic, optical, and transport properties of semiconductors
[AD-747692] 04 p0460 N73-13752
Analysis of laser bulk damage in alkali-halides with no self-focusing and measurement of damaging fields considering effects of inclusions on bulk optical strength
05 p0554 N73-14502
Measurement of physical and chemical properties of well characterized surfaces for application to optical elements in high power laser development
05 p0555 N73-14508
Analysis of fundamental absorption properties of laser window materials and limitations imposed by uncontrolled impurities
05 p0556 N73-14516
Evaluation of optical properties of high power laser window materials
[AD-749864] 05 p0559 N73-14540
Optical and dielectric properties of liquid glycerol, tetradecane, and heptadecane
[ORO-3861-6] 06 p0647 N73-15259
European study of optical and signal processing problems in laser anemometry
[ET/TN/A/20] 06 p0679 N73-15526
Electrical, mechanical, and thermal properties of transparent optical adhesives
[AD-750571] 06 p0688 N73-15602
Optical properties and constants of water and aqueous solutions
[NASA-CR-130136] 06 p0699 N73-15700
Optical and electrical properties of amorphous germanium and silicon semiconductors
[AD-748856] 06 p0709 N73-15788
Rutile crystal growth, and hydrogen kinetics, electronic, and optical properties
[AD-748298] 06 p0709 N73-15789
Properties of amorphous semiconductors
[AD-750163] 06 p0710 N73-15797
Composition, temperature, and optical properties of Jupiter and Saturn atmospheres
[NLL-M-20702-[5828.4F]] 06 p0716 N73-15845
Optical materials and design of optical equipment
[AD-751496] 07 p0822 N73-16660
Analysis of high resolution vidicon optics for electronic periscope view simulator
[AD-751023] 07 p0822 N73-16664
Structural, optical, and electrical properties of amorphous semiconductors
[AD-751084] 07 p0834 N73-16760
Parameters and components of ESO Schmidt telescope
07 p0846 N73-16859
Tables on airborne and ground based measurements of optical atmospheric properties in central New Mexico
[AD-751936] 08 p0919 N73-17534
Design modules for optical equipment
[AD-751964] 08 p0944 N73-17732
Diagnostic spectroscopy of plasmas produced in molecular gases
[AD-751938] 08 p0950 N73-17776
Properties of thin dielectric TiO2 films produced by chemical vapor deposition
[NASA-CR-130763] 08 p0950 N73-17780
Intraday time scale variability of infrared, optical, and radio observations from 3C 120, BI Lac, and OJ 287
[AD-752214] 08 p0962 N73-17871
Optical absorption properties of polycrystalline zinc selenide and cadmium telluride materials for infrared laser windows
[AD-753068] 09 p1044 N73-18512
Optical properties of ultraviolet down-converter materials
[AD-753578] 09 p1068 N73-18713
Photoelectric measurements of brightness distribution and brightness phase dependence of spheres with different colors and roughness to find optical properties of Mars surface
09 p1083 N73-18837
Derivation of formula for calculating diffuse radiation from limb side of spherical planetary atmosphere
09 p1084 N73-18839
Penetration and transmission of light in sea water
[AD-753029] 10 p1156 N73-19409
Analysis of microstructure and optical properties of thin lead dielectric cermet films
10 p1175 N73-19555
Spectroscopic studies of electrical and optical properties of amorphous semiconductors
[AD-753903] 10 p1202 N73-19779
Optical atmospheric data in daytime, using airborne instrument measurements
[AD-754898] 11 p1289 N73-20458
Optical properties of sea water in Atlantic, Pacific, and Caribbean
[AD-753474] 11 p1290 N73-20470
Infrared beam profile measurements for determining surface damage thresholds of glass laser materials
[AD-755134] 11 p1303 N73-20571
Changes in optical properties of various materials due to exposure to exhaust plume of bipropellant rocket
[NASA-TM-X-68204] 11 p1349 N73-20942
Magnetic, optical, and semiconducting properties of rare earth compounds
[AD-755925] 12 p1376 N73-21164
Characteristics of ellipsometer and techniques for measuring thin films including computer program for determination of optical constants and thickness of film
[NASA-TM-X-64742] 12 p1405 N73-21392
Optical properties of films based on tin dioxide and cobalt oxides
[AD-755250] 12 p1417 N73-21479
Optical properties and electronic structure of metal alloys
[AD-755847] 12 p1441 N73-21675
Investigation of optical properties of natural objects and their aerial photographic imaging characteristics
[AD-756603] 13 p1532 N73-22413
Physical and spectral characteristics of infrared solid state dispersion filters
[NASA-TT-F-14838] 13 p1558 N73-22631
GUERAP computer code for accurately measuring off axis rejection characteristics of optical system - users manual
[AD-755353] 13 p1560 N73-22645
Structures and optical absorption spectra of mercury telluride/cadmium telluride thin films
[AD-756093] 13 p1568 N73-22709
Optical performance evaluation of infrared transmitting materials
[AD-756825] 14 p1673 N73-23576
Barium sodium niobate as nonlinear optical material
[AD-758221] 14 p1682 N73-23650
Optical and electronic properties of single crystal Cu2S-CdS photovoltaic cells
[NASA-CR-121228] 15 p1738 N73-24091
High optical resolution derivative spectrometer for measuring optical properties of solids in vacuum UV and far IR range
15 p1785 N73-24474
Molecular structures and optical properties of polymer chain materials
[AD-758837] 16 p1872 N73-25156
Design and construction of 3.5 m telescope in Italy
16 p1911 N73-25466
Large space telescope engineering scale model optical design
[NASA-CR-124561] 16 p1913 N73-25484
Small phase difference measuring technique within holographically reconstructed optical fields
16 p1922 N73-25549
Extension of microwave devices to optical frequencies
[AD-758914] 16 p1924 N73-25569
Cadmium and germanium compounds chalcopyrite semiconductor materials for infrared optics
[AD-759556] 16 p1945 N73-25742
Diffuse reflectance theory for estimating optical absorption coefficients of aerosol particles collected on filter surface
[AD-759490] 16 p1946 N73-25744
Classification of landscapes into taxonomic groups on basis of optical properties
[NASA-TT-F-14970] 17 p2025 N73-26386
Development of transmissometer for measuring optical transmission through aircraft jet engine exhausts
[AD-760050] 17 p2035 N73-26467
Design and performance of segmented holmium doped yttrium lithium fluoride laser
[AD-760019] 17 p2042 N73-26522
Piezo- and thermo-optical properties of bismuth germanium oxide single crystals
17 p2071 N73-26754
Nonlinear optical susceptibilities for electromagnetic wave coupling of semiconductors
17 p2071 N73-26758
Electrical, optical, and structural properties of RF triode-sputtered gold films
18 p2186 N73-27649
Electrical and optical properties of amorphous silicon and germanium semiconductors
[AD-760595] 18 p2191 N73-27690

Electrical and optical properties of irradiated mercury cadmium telluride semiconductors
[AD-761488] 19 p2327 N73-28721
Electronic structure of solid surfaces
[AD-762372] 19 p2328 N73-28727
Optical properties of solar flare spectra
19 p2333 N73-28776
Development of procedure for aligning pole piece system of magnetic electron microscope
[NLL-M-23011-[5828.4F]] 20 p2417 N73-29416
Geometric optical properties of holographic lens systems
[AD-762526] 20 p2426 N73-29486
Optical transitions between energy states of solute organic dye
[AD-762607] 20 p2426 N73-29489
Sensitivity and optoelectronic properties of semiconductor heterojunctions
20 p2460 N73-29770
Properties of optical radiation of variables and quasers
20 p2471 N73-29847
Approximate determination of optical depth in different parts of Fraunhofer line contour
20 p2472 N73-29853
Development of organic glass and plastic materials with improved mechanical and physical properties for use with aircraft canopies and protective coatings
[AD-763263] 21 p2497 N73-30039
Optical properties of atmospheric aerosols in near infrared region of spectrum
[AD-764135] 22 p2668 N73-31374
Feasibility of coating glass optical fibers by melting process
[REPT-6803] 22 p2677 N73-31439
Research on preparation, structure, and optical properties of glass
[AD-763338] 22 p2689 N73-31537
Optical and electrical properties of amorphous Si and their dependence on thermal history
23 p2807 N73-32440
Optical, photoelectric, and structural properties of amorphous B1-Ge thin films
23 p2824 N73-32572
Optical property effect in thermal design for insulation coating attachments
24 p2942 N73-33492
Proceedings of conference on electromagnetic and optical properties of sea water for application to surveillance, mapping, communications, and visibility
[AGARD-LS-61] 24 p2956 N73-33619
Radiance distribution as function of depth in upper layers of ocean and numerical analysis of inherent and apparent optical properties
24 p2957 N73-33621
Optical properties of pure and turbulent sea water
24 p2957 N73-33624
Techniques for predicting effects of thermal and saline inhomogeneities on optical imaging systems with application to optical properties of sea water
24 p2957 N73-33625
Effect of ocean depth on light scattering and attenuation parameters to include optical properties influenced by concentration, size, and shape of particulate matter
24 p2957 N73-33626
Light scattering by particles in sea water based on volume scattering function and point spread function
24 p2957 N73-33628
Effect of various parameters on long range underwater vision for narrow and broad beam illumination
24 p2958 N73-33630
Effects of resolution, signal to noise ratio, and contrast on underwater imaging systems performance
24 p2958 N73-33631
Application of Fourier techniques to calculate spread of scattered light for circular spot, Gaussian profile, and linear stripe cases
24 p2958 N73-33632
Characteristics of lenses and ports for underwater imaging systems to compare depth of field and relative aperture for several lens port combinations
24 p2958 N73-33635
Computer programs for analyzing optical properties of sea water
24 p2958 N73-33638
Nonlinear optical susceptibilities of atoms, molecules, and condensed matter
[AD-764889] 24 p2959 N73-33643
Rheological and optical properties of deformable particles in laminar shear flows
24 p2959 N73-33647

**OPTICAL PUMPING**
Application of Nernst glower metal oxide conductors to laser pumping to produce spectral energy within pumping band of laser material
[AD-745796] 01 p0066 N73-10538
Development of yttrium aluminate material for optically pumped lasers and measurement of optical absorption and emission spectra
[AD-746032] 01 p0066 N73-10540
Generation, measurement, and properties of picosecond laser pulses produced by mode locked lasers
[AD-746310] 01 p0066 N73-10543
Electrical analogue model of flash tube and laser rod system to determine efficiency of laser system with respect to flash duration
[WRE-TM-657[AP]] 02 p0180 N73-11462
Organic dyes for improving light intensity of Nd YAG laser pump system
[AD-747401] 03 p0312 N73-12545
Near infrared laser action for Kodak organic dyes using linear flash lamp for excitation
[AD-748863] 04 p0429 N73-13496
Characteristics of combined gas laser pumping based on fluctuation of gas density parallel to electric field which is assumed constant
[JPRS-57880] 06 p0679 N73-15524
Application of light emitting diodes to pumping of solid-state laser rods
[AD-750576] 06 p0681 N73-15545
Design and development of optical pumps for pulsed neodymium yag lasers with emphasis on efficiency and reproducibility of product
[AD-751212] 07 p0808 N73-16557
Development and characteristics of electron beam excited high pressure mercury dissociation laser
[AD-752465] 08 p0930 N73-17619
Development of two cell cesium optically pumped gradient magnetometer
[AD-753060] 09 p1037 N73-18460
Design and operation of tunable parametric oscillators with range between 1.0 and 5.0 micrometers
[AD-753347] 09 p1044 N73-18517
Measurement of stimulated emission cross section of neodymium laser based on laser threshold gain and inverted population
[AD-753901] 10 p1170 N73-19514
Lamp design and parameters for optical pumping of lasers
[AD-754643] 11 p1304 N73-20578
Optical excitation of atomic levels for orientation of nuclei, polarized electron production, and magnetic resonance experiments
[NASA-TT-F-14862] 11 p1326 N73-20765
Design of zero-field parametric resonance magnetometer using optically pumped helium
[AD-755256] 12 p1402 N73-21376
Light emitting diode pumped Nd/YAG lasers
[NASA-CR-124225] 13 p1536 N73-22445
Construction of experimental incandescent lamp of Nernst glower type for laser pumping
[AD-755207] 13 p1539 N73-22465
Design, development, and characteristics of continuous wave laser using organic dyes
[AD-756514] 13 p1539 N73-22466
Characteristics of dye lasers with emphasis on lasing mechanism of dyes
[PHL-1973-2] 14 p1672 N73-23566
Development of laser head for simultaneous optical pumping of several dye lasers
[NASA-CASE-LAR-11341-1] 16 p1923 N73-25564
Infrared optical parametric fluorescence and parametric oscillation
16 p1944 N73-25729
Direct nuclear pumping of gas laser using argon as lasing medium
[NASA-CR-133210] 17 p2040 N73-26503
Kinetic theory of optically pumped gas laser oscillator
18 p2157 N73-27428
Kinetics of chemically pumped CO2 and CH2N2-CO2 photolysis laser systems
20 p2424 N73-29469
Effect of transverse pumping distribution on energetics and profiles of thermo-optical distortions of laser in solution of rhodamine dye
[NLL-M-23052-[5828.4F]] 20 p2424 N73-29472
Helium self-oscillating magnetometer with optical pumping of He-4 atoms
22 p2671 N73-31397
Lamp design and operating parameters affecting laser stability and beam divergence
[AD-763932] 22 p2682 N73-31481
Mode locking and pulse selection in atmospheric gas lasers
[AD-765350] 23 p2802 N73-32411
Nuclear pumping in molecular gas lasers
[JPRS-60244] 24 p2931 N73-33405

**OPTICAL RADAR**
Adaptation of lidar to aircraft and missile rangefinding
[NASA-TT-F-14716] 02 p0181 N73-11466
Optical radar data for probing atmospheric composition and air pollution particulates
02 p0197 N73-11595
Frequency stability characteristics of single frequency neodymium YAG laser system with coherent ultrashort pulses for high resolution imaging
[AD-747967] 03 p0312 N73-12543
Measurement of spatial distribution of aerosols and water vapor in earth mixing layer using optical radar, particle counters, and rawinsonde
[NASA-TN-D-7103] 04 p0444 N73-13621
Application of absorber laser amplifier and detector to wide angle low noise optical radar and communication systems
[AD-749543] 05 p0558 N73-14533
Digital optical hybrid correlator for processing pulse Doppler and wideband radar signals
[AD-751695] 07 p0756 N73-16143
Optical radar system for determining tropospheric water vapor content, based on absorption line shift
[DLR-MITT-72-26] 07 p0815 N73-16608
Remote sensing with meteorological radar equipment
[AD-753813] 09 p1004 N73-18197
CO2 waveguide laser as master oscillator for high resolution optical radar application
[AD-758706] 15 p1796 N73-24561
Development, manufacture, and testing of optical beam steerer for use in spaceborne optical radar systems
[NASA-CR-124283] 16 p1884 N73-25246
Improving optical compatibility of lidar transmitter-receiver
[NASA-TM-X-64753] 16 p1923 N73-25561
Optical radar evaluation of techniques for fog dissipation at airports
[AD-758767] 16 p1938 N73-25682
Transfer equation for calculation of doubly scattered lidar returns
17 p2039 N73-26497
Laser observations of dense natural fog to determine backscatter and slant range visibility for aircraft landing operations
[AD-760128] 17 p2041 N73-26511
Transmitter and receiver antenna gain analysis for optical radar and communication systems
[NASA-TM-X-70423] 19 p2235 N73-28023
Optical radar angle tracking mount
[AD-765213] 23 p2759 N73-32077
Variations in beam characteristics of ruby laser used in lidar system
[SLA-73-347] 24 p2931 N73-33407

**OPTICAL RANGE FINDERS**
NT LASER RANGE FINDERS
Instrument for sensing errors in telescope wavefronts using coarse range sensors and fine range sensors
23 p2792 N73-32336

**OPTICAL REFLECTION**
Composition of diffuse reflective coating containing sodium chloride in combination with diol solvent and organic wetting and drying agents
[NASA-CASE-GSC-11214-1] 04 p0385 N73-13128
Reflectometer for measuring compositional modulation of copper based alloys at room temperature
23 p2803 N73-32418

**OPTICAL RESONANCE**
Design and development of optical pumps for pulsed neodymium yag lasers with emphasis on efficiency and reproducibility of product
[AD-751212] 07 p0808 N73-16557
Stark shift measurements and photon resonance perturbations in triplet metastable helium atom near ionization threshold
[KFKI-72-42] 10 p1169 N73-19507
Application of microwave-optical double resonance spectroscopy to analyze structural properties of phosphorescent triplet states of organic molecules
[COO-3435-6] 12 p1405 N73-21398

**OPTICAL SCANNERS**
NT FLYING SPOT SCANNERS
NT MULTISPECTRAL BAND SCANNERS
Wide field reflective optical scanning system for use in satellite based earth surveillance activities
[NASA-CASE-MSC-14096-1] 13 p1529 N73-22388
Heuristic method for controlling edge sharpness of image observed through inadequate imaging system
[AD-760320] 17 p2064 N73-26694
Focusing optical collimator for high resolution scanning of electromagnetic radiations, neutrons, and other particles
[NASA-CASE-MFS-20932-1] 18 p2150 N73-27380
Development of multimode optical sensor
[NASA-CR-133980] 19 p2300 N73-28493
Spacecraft attitude sensing system design with narrow field of view sensor rotating about spacecraft x-y axis
[NASA-CASE-GSC-10890-1] 21 p2575 N73-30640
Manually and automatically operable video switching system
[NASA-CASE-KSC-10782-1] 23 p2757 N73-32063

**OPTICAL SENSORS**
U OPTICAL MEASURING INSTRUMENTS

**OPTICAL SIGNALS**
U OPTICAL COMMUNICATION

**OPTICAL SLANT RANGE**
Errors in localization in measurement of distance to balloon-satellites
[NASA-TT-F-14701] 02 p0207 N73-11678

**OPTICAL SPECTRUM**
U LIGHT [VISIBLE RADIATION]
U SPECTRA

**OPTICAL THICKNESS**
Determination of optical thickness of aerosols in atmosphere around Salton Sea desert area using ERTS-1 imagery
[E72-10200] 02 p0160 N73-11298
Determination of aerosol optical thickness in atmosphere at Salton Sea and San Diego based on ERTS-1 data
[E72-10359] 05 p0534 N73-14347

**OPTICAL TRACKING**
Equipment for simultaneous radar observations by image-orthicon and optical observations
01 p0101 N73-10833
Analysis procedure for television observations and simultaneous observations
01 p0102 N73-10836
Design of precision sensors for optical tracking systems
[AD-746742] 02 p0176 N73-11424
Procedures for operating and modulating beam of laser locating devices
[AD-747003] 02 p0184 N73-11492
Laser tracking techniques used for geodetic applications in space
[GRGS-BULL-1] 05 p0557 N73-14522
Laser range finding for satellite angular coordinate determination using echo recorded by Schmidt telescope
05 p0557 N73-14523
Efficiency of laser telemetry tracking for satellites carrying reflectors
05 p0557 N73-14527
Efficiency of laser telemetry tracking for satellite carrying laser reflector sphere
05 p0557 N73-14528
Effects of spacecraft stabilization on laser tracking efficiency
05 p0558 N73-14531
Laser ranging techniques applied to ground base line measurements between French South Coast and Corsica
05 p0558 N73-14532
Optical satellite tracking of Cosmos and other artificial satellites, Edinburgh, Aug. 1972
[ROE-STS-129] 05 p0601 N73-14883
Optical satellite tracking of Cosmos and other artificial satellites, Edinburgh, Sep. 1972
[ROE-STS-130] 05 p0601 N73-14884
Upper eye lid position effects in electro-oculograhic vertical eye movement recordings
06 p0633 N73-15143
Predictive control of human eye tracking movements in response to visual stimuli
06 p0634 N73-15149
Optical satellite tracking of Cosmos and other artificial satellites, Edinburgh, Oct. 1972
[ROE-STS-133] 06 p0722 N73-15891
Control system for automatic orientation and tracking operation of Orion orbital observatory
[NASA-TT-F-14583] 07 p0799 N73-16490
Performance tests of strapdown air to air tracking system for short range weapons control system
[AD-751654] 07 p0818 N73-16633
Optical satellite tracking of Cosmos and other artificial satellites, Edinburgh, Nov. 1972
[ROE-STS-135] 09 p1091 N73-18908
Effect of parallactic refraction correction for satellite optical observations in determination of station coordinates
[NASA-TM-X-66208] 10 p1189 N73-19674
High resolution optical measurements of high altitude barium releases at Elgin AFB during January 1971
[AD-756938] 13 p1528 N73-22382
Optical satellite tracking of Cosmos and other artificial satellites, Edinburgh, Dec. 1972
[ROE-STS-138] 13 p1582 N73-22824
Optical tracking of artificial satellites between Oct. and Dec. 1972
[ROE-STS-139] 13 p1582 N73-22825
Digital command and simulation of automatic tracking device carrying pulsed laser and receiving telescope
[ONERA-NT-198] 15 p1751 N73-24190
Artificial satellite equations of motion approximations for photographic and laser tracking optimization
15 p1832 N73-24848
Optical satellite tracking of Cosmos and other artificial satellites, Edinburgh, Feb. 1973
[ROE-STS-147] 15 p1836 N73-24881
Curve fitting method for comparing refractive adjustments in laser satellite ranging
[PB-214447/5] 16 p1909 N73-25445
Satellite tracking camera for geometric geodesy
[PUBL-27] 16 p1913 N73-25479
Optical satellite tracking of Cosmos and other artificial satellites, Edinburgh, Jan. 1973
[ROE-STS-141] 16 p1967 N73-25912
Zvenigorod Experimental Station optical observations of artificial satellites
[JPRS-59567] 18 p2126 N73-27181
Stability of two coordinate angle tracking optical automatic tracking systems
[AD-762106] 19 p2250 N73-28138
Optical satellite tracking of Cosmos and other artificial satellites, Edinburgh, Jan. 1973
[ROE-STS-151] 19 p2346 N73-28872
Optical satellite tracking of Cosmos and other artificial satellites, Edinburgh, Apr. 1973
[ROE-STS-152] 19 p2346 N73-28873
Optical satellite tracking of Cosmos and other artificial satellites, Edinburgh, May 1973
[ROE-STS-154] 21 p2602 N73-30851
Friction effects on inertia compensators used for heliostat base motion isolation
[AD-764706] 23 p2821 N73-32549
Characteristics of minitrack tracking function to show minitrack hardware, system calibration, and quadratic listing - Vol. 2
[NASA-TM-X-70482] 24 p2901 N73-33156

**OPTICAL WAVEGUIDES**
Ion and electron beam techniques for fabricating integrated optics circuits
[AD-760051] 17 p2008 N73-26237
Design of tunable waveguide carbon dioxide laser for optical heterodyne communication system between satellites
18 p2212 N73-27860

**OPTICS**
Electron heating in F region by high power radio frequency beam detected by intensity changes in atomic oxygen nightglow
07 p0775 N73-16293
Analysis of dual reflector antenna system using physical optics and digital computers
[NASA-TM-X-66223] 12 p1379 N73-21183
Solutions of macroscopic Maxwell equations for nonlinear dispersive waves in nonlinear optics
17 p2062 N73-26683
Optical models for electron scattering from atoms and molecules
18 p2181 N73-27608
Integrated optics design principles of tunable CO2 laser
[AD-764638] 23 p2802 N73-32408
Investigating instantaneous structure of wall pressure under turbulent boundary layer flow in air
[REPT-9/1973] 24 p2904 N73-33177
Light coupling, light modulation, and integrated optics - bibliography
[NASA-TM-X-64787] 24 p2959 N73-33641

**OPTIMAL CONTROL**
NT TIME OPTIMAL CONTROL
Optimal control model for predicting manual VTOL pilot performance in longitudinal hovering tasks
01 p0017 N73-10134
Minimum quadratic cost optimal control technology for design of F-4C aircraft manual control system
01 p0018 N73-10137
FORTRAN program for numerical solution of steady state matrix Riccati equation of quadratic cost optimal control problem
[AD-745862] 01 p0072 N73-10589
Closed-form solutions for motion of rocket-powered vehicle during atmospheric ascent and unpowered atmospheric reentry
[NASA-TM-X-64694] 02 p0207 N73-11677
Optimal adaptive control of aircraft lateral dynamics in gust presence using Pontryagin principle and cost function
[AASU-314] 03 p0253 N73-12046
Real time hybrid simulation of tied down helicopter for optimal stability control
05 p0494 N73-14024
Application of modern control theory to design of optimum aircraft controllers
[NASA-TM-X-62208] 08 p0867 N73-17016
Control theory in game problems, optimization, feedback, and probabilistic automata - conference
[JPRS-58030] 08 p0891 N73-17214
Computation of optimal output-feedback compensators for linear time-invariant systems
[NASA-CR-130988] 09 p1056 N73-18607
Variational problems in optimization and control for hyperbolic partial differential equations
09 p1056 N73-18612
Algorithms for numerical solution of problems in calculus of variations
[NPL-NAC-28] 09 p1058 N73-18626
Gradient procedures for solving dual optimal control and max-min problems
[AD-753129] 09 p1058 N73-18628
Application of optimal control theory to design of control system for supersonic inlet of turbojet engine
[NASA-TN-D-7188] 09 p1079 N73-18803
Numerical method for determining optimal satellite control system with discontinuous links
10 p1178 N73-19581
Mathematical model for optimal control of spacecraft flight considering error and perturbation factors
10 p1178 N73-19583
Application of optimal control theory to design of constant gain filters to minimize weighted average of filtered variances
[AD-755798] 12 p1380 N73-21190
Application of optimal control technology to design of controller for space shuttle descent
[NASA-CR-124183] 12 p1459 N73-21824
Optimal control, guidance, and trajectory for low thrust acceleration spacecraft
15 p1829 N73-24827
Algorithm for optimal control problems with bounded state
[AD-761790] 19 p2314 N73-28610
Theory of modified quasilinearization algorithm for optimal control problems with bounded state variables - Part 1
[AD-761786] 19 p2315 N73-28614
Modified quasilinearization algorithm for optimal control problems with bounded state variables - Part 2
[AD-761791] 19 p2315 N73-28615
Numerical solution of optimal control problems with differential constraints
[AD-761787] 19 p2315 N73-28617
Mathematical technique for optimal control problems with initial conditions
[AD-762253] 19 p2315 N73-28620
Optimal control of shuttle system consisting of single infinite capacity carrier transporting passengers between two terminals
[P-4979] 19 p2355 N73-28940
Stochastic optimal controller for n-body spacecraft
[NASA-CR-133788] 21 p2600 N73-30839
Formulation of system and sensor configuration control problem for class of linear stochastic systems corrupted by Gaussian noise
22 p2690 N73-31549
Onboard control systems for spacecraft
[JPRS-60179] 23 p2847 N73-32755
Synthesis of optimal control system for nuclear power plant and power supplies onboard spacecraft
23 p2848 N73-32758
Computer aided design of optimal control systems
24 p2896 N73-33119

**OPTIMIZATION**
NT FLIGHT OPTIMIZATION
NT OPTIMAL CONTROL
NT TIME OPTIMAL CONTROL
NT TRAJECTORY OPTIMIZATION
Optimal control model for predicting display requirements in pilot landing performance
01 p0016 N73-10121
Measurement methods and error analyses by ground terminals for optimizing satellite communications link
01 p0026 N73-10203
Optimization of propulsion stage selection for space-based transportation
[AD-744979] 01 p0109 N73-10900
Optimum design of format synchronizer for ESRO control center
[ESRO-CR[P]-127] 02 p0141 N73-11143
Criteria for optimal approximating functions for experimental test design
[NASA-TM-X-2663] 02 p0202 N73-11636
Transport characteristics for calculating plasma diode design parameters
[TEE-3056-1] 03 p0274 N73-12221
FORTRAN computer program for solar simulator optimization
[DLR-FB-71-34] 03 p0281 N73-12277
Rank one, quasi-Newton minimization for infinite-dimensional, real Hilbert spaces
[NASA-TR-R-394] 03 p0323 N73-12635
Computing free fall trajectories from one point to another specified point in solar system based on numerical optimization
[NASA-CR-128644] 03 p0356 N73-12901
Optimal inlet parameters for magnetohydrodynamic channel using combustion products of kerosene and gaseous oxygen
[AD-748750] 04 p0376 N73-13057
Optimum conditions for depositing aluminum and silicon hydroxides on titanium dioxide particles
[NLL-RTS-7638] 04 p0425 N73-13460
Theory of preference and theory of optimization treated from order and topology vantage point, and application to social analysis
[NASA-CR-129593] 04 p0441 N73-13592
Optimization and cost factors for cryogenic and superconducting magnets in plasma physics
[IPP-4/96] 04 p0458 N73-13740
Optimization of propellant tank size delivering apogee impulses when positioning synchronous satellites
[ONERA-NT-2/1895-SY] 04 p0479 N73-13915
Development of computational techniques for design optimization of thermal protection systems for space shuttle vehicle
[NASA-CR-128618] 04 p0484 N73-13951
Computer program for design optimization of subsonic swept wing jet transport aircraft
[RAE-TM-AERO-1448] 05 p0494 N73-14026
Optimization of work-rest cycles to ensure acceptably high human performance in man machine systems
[AD-750176] 05 p0504 N73-14107
Optimization of stochastic systems including introduction to self adaptive systems
05 p0569 N73-14618
Computational techniques for design optimization of thermal protection for space shuttle
[NASA-CR-128658] 05 p0598 N73-14863

Application of optimality criteria to automation of structural design with emphasis on aerospace applications
[NASA-TN-D-7115] 05 p0603 N73-14901
Aircraft performance optimization by including flight control system in design
[MBB-UFE-895-72-O] 06 p0622 N73-15048
Application of optimal control theory to take-off of heavily loaded helicopters and instrumentation requirements to improve pilot flight control
[AD-750615] 06 p0625 N73-15072
Electrical and structural criteria for design optimization of integrated circuits
[AD-750947] 06 p0648 N73-15261
Computerized design of betatron electromagnet having optimal parameters
[AD-750523] 06 p0651 N73-15289
Theorems for optimization of Riccati equation in singular discrete time filtering and control problems
[NASA-CR-130360] 06 p0690 N73-15621
Optimal linear combination of observable parameters for maximizing correlation between index and criterion variates for sampling classification and personnel selection
[AD-751257] 07 p0813 N73-16596
Optimization of specific power highly efficient radioisotope thermoelectric generator
07 p0819 N73-16636
Curriculum of training course on basics and state-of-the-art of remote sensing and developments in parameter optimization
[NASA-CR-128713] 07 p0848 N73-16876
Parametric design optimization for multiple element short backfire antenna array
[AD-751918] 08 p0889 N73-17199
Nomograph for calculating optimal working characteristics of hydrostatic sliding bearings
[AD-753553] 09 p1042 N73-18501
Variational problems in optimization and control for hyperbolic partial differential equations
09 p1056 N73-18612
Optimum allocation of redundancy in system of serially connected subsystems
[NASA-TN-D-7164] 09 p1056 N73-18614
Algorithms for iterative solution of unconstrained optimization problems
[NPL-NAC-25] 09 p1058 N73-18625
Optimization of working conditions in plasma wind tunnel by pressure distribution control in acceleration section
[DLR-FB-72-70] 09 p1070 N73-18735
Optimization of fluid amplifier cascades by means of electric equivalent circuit
[CRIF-EL-6] 10 p1142 N73-19304
Optimized method of remote haze detection using ERTS-1 imagery
[E73-10344] 10 p1148 N73-19343
Gradient-secant algorithm for unconstrained optimization
[NASA-CR-131396] 11 p1310 N73-20633
Optimization of noise immunity of analog signal transmission channels by preemphasis, exemplified for AM or FM channel
[DLR-FB-73-09] 12 p1379 N73-21188
Optical design of radar antenna configurations with desired scattering patterns
[AD-755914] 12 p1380 N73-21193
Current lead optimization for minimizing heat loss of superconducting magnet
[BNL-17233] 12 p1439 N73-21661
Bayes theorem for optimal decision and stop models of production processes
13 p1497 N73-22132
Computerized design optimization program for microwave circuits
[AD-756875] 13 p1504 N73-22191
Optimization of basic ceramic insulation for space shuttle orbiters - Part 2
[NASA-CR-112257] 13 p1546 N73-22531
Optimized construction of thermoelectric cooling batteries
[AD-757467] 14 p1606 N73-23016
Computer program for spectral unfolding, using optimization function
[AD-755190] 14 p1638 N73-23281
Conferences on optimizing adaptive automatic systems
[JPRS-58809] 14 p1644 N73-23330
Search and optimization capabilities of collective of independent automatic devices
14 p1644 N73-23331
Random search in problems of optimization, identification, and teaching of automatic systems
14 p1644 N73-23333
Optimization of microphone propagation in television studio
[BBC-RD-1973/3] 15 p1749 N73-24173
Design of mathematical filters with finite precision
16 p1934 N73-25647
FORTRAN program for solution of linear or nonlinear constrained optimization problems
[NASA-TM-X-62282] 17 p2055 N73-26619
Frascati gravitational wave detector signal to noise ratio optimization
18 p2145 N73-27340
DOPEX-1D2C steepest descent and one-dimensional two constraint radiation shield optimization code
[NASA-TM-X-2836] 18 p2177 N73-27579
Noise model for optimal signal to noise ratio in sonar detector design
19 p2235 N73-28015
Compiler optimization techniques
[NASA-TM-X-69499] 21 p2512 N73-30148
Optimized electric welding technique for silicon solar cell arrays
[LCR-DR-1-72-52/1/R] 21 p2553 N73-30470
Optimization method for minimum weight design of structures made from fiber reinforced composites
[AD-763732] 21 p2565 N73-30558
Concept of comments in programming languages
[NPL-NAC-34] 22 p2639 N73-31154
Digital circuit optimization by time multiplexing component devices
22 p2646 N73-31200
Optimized design for vehicle suspension systems
[PB-220553/2] 22 p2648 N73-31216
Analysis and optimization of cyclic methods in orbit calculation
[NASA-CR-132806] 22 p2691 N73-31559
Revised algorithm for constrained optimization using quasi Newton-Raphson method based on recurring factorization of approximation to Hessian matrices
[NPL-NAC-32] 22 p2692 N73-31560
Physiological motor function measurements for determining optimal bed rest periods
[NASA-TT-F-15144] 23 p2749 N73-32004
Execution time optimization for IBM 360 FORTRAN production programs
[NASA-TM-X-70477] 23 p2760 N73-32086
Mesh gradient technique for numerical optimization
23 p2812 N73-32481
Similitude theory for design optimization of automatic control systems for aircraft gas turbine engines
[AD-764683] 23 p2832 N73-32631
Optimization of control and damping system for fighter aircraft with quadratic cost function
24 p2877 N73-32980
Design optimization and testing of flight control systems for light helicopters, applied to BO-105 helicopter
24 p2878 N73-32985

**OPTIMUM CONTROL**
U OPTIMAL CONTROL
**OPTIMUM THRUST PROGRAMMING**
U THRUST PROGRAMMING
**OR-GATES**
U GATES (CIRCUITS)
**ORBIT CALCULATION**
NT MINIMUM VARIANCE ORBIT DETERMINATION
Influence of nongravitational effects on accurate prediction of comet orbits
02 p0228 N73-11849
Tracking and orbit calculation of Cosmos 316 to determine upper atmospheric wind
[RAE-TR-72062] 02 p0235 N73-11910
Effects of tracking system errors of satellite orbit when single station provides satellite tracking in immediate area of altimeter evaluations
[NASA-TM-X-69352] 03 p0301 N73-12457
Problems in estimation theory with applications to orbit determination
04 p0469 N73-13820
Accuracy of atmospheric density predictions for satellite orbit determination
[D-151] 05 p0596 N73-14850
Global network tracking data for accurate GEOS-C orbit calculation from one revolution
06 p0662 N73-15378
Computer program for orbit comparison plots - users manual
[NASA-TM-X-66164] 07 p0759 N73-16165
Logical flow and guidelines for constructing low thrust orbit determination computer program
[NASA-CR-112256] 08 p0961 N73-17862
Mathematical and numerical methods for solving spacecraft control problems and mapping of celestial bodies
[NASA-TT-F-731] 10 p1177 N73-19572
Orbital evolution and stability analysis for earth and lunar orbiter trajectories
[AD-754738] 11 p1339 N73-20869
Earth-based orbit determination for SEP spacecraft in multistation tracking
[NASA-CR-132154] 15 p1830 N73-24832
Design and development of radio sounding satellite for measuring composition of plasmapause during entry and exit phases of orbit
[NOAA-TR-ERL-242-AL-8] 18 p2200 N73-27762
Computer programs for aircraft position and stationary satellite orbit determination from radar range and rate measurements
[ESRO-CR-81] 19 p2318 N73-28650
Orbit calculations for communication satellite using communications ground terminal minicomputer
[AD-762510] 20 p2474 N73-29874
Coplanar transfer orbit calculation in Newton central gravitational field noting two propulsive phases applying tangential thrust and intermediate coast phase
[DLR-FB-73-29] 21 p2597 N73-30814
Analysis and optimization of cyclic methods in orbit calculation
[NASA-CR-132806] 22 p2691 N73-31559
Analysis of tethered body problems and determination of relative molton orbit - Parts 1 and 2
[NASA-CR-132780] 22 p2714 N73-31723
Earth satellite orbit calculation with integration program
[BMBW-FBW-72-16] 22 p2718 N73-31757
Initial value problems solution on satellite geodesy and orbital mechanics using Hammerstein method for boundary value problem
[BMBW-FBW-72-23] 22 p2718 N73-31759
**ORBIT DECAY**
Air density at 200 km heights analyzed from Cosmos 286 rocket orbit decay, emphasizing annual variations and geomagnetic disturbances
[RAE-TR-72071] 03 p0296 N73-12417
Evaluation of 15th order harmonics by analysis of orbit decay of Ariel 3, Transit 1b, Cosmos 373 and Cosmos 387 satellites
[RAE-TR-72115] 05 p0597 N73-14851
Neutral atmospheric models compatible with satellite orbital decay and incoherent scatter measurements
[NASA-CR-131294] 11 p1285 N73-20427
Fifteenth order resonance on decaying orbit of TETR-3
[NASA-TM-X-70484] 24 p2979 N73-33805
**ORBIT EQUATIONS**
U ORBITAL MECHANICS
**ORBIT PERTURBATION**
NT SATELLITE PERTURBATION
Approximate analytic and numerical methods for describing encounter of star with sun-comet system and resulting gravitational perturbations of cometary orbits
07 p0840 N73-16805
Resonance capture of Toro asteroid perturbed orbit by earth
[TRITA-EPP-72-19] 07 p0846 N73-16863
Orbit perturbation effects on frequency shift of electrostatic, turbulent, unmagnetized plasma
09 p1071 N73-18738
Harmonic analysis for predicting long term artificial satellite orbital motion
10 p1178 N73-19579
Parametric design of aerodynamic control system for compensating artificial satellite orbit perturbations
10 p1178 N73-19580
Solar probe orbit perturbation calculation assuming circular gravitating asteroid ring with center at sun
[ESRO-SR-19] 19 p2344 N73-28856
Gyroscopic orbit errors caused by random perturbations
20 p2418 N73-29428
Azur satellite orbit perturbation recorded from Weilheim-Lichtenau ground station
[BMBW-FBW-72-18] 21 p2597 N73-30816
Investigation of evolution of orbit-orbit resonances
[NASA-CR-135674] 23 p2844 N73-32728
**ORBITAL ELEMENTS**
Problems in changing from ground based to space based vehicle operations for on-orbit readiness
[NASA-CR-125564] 03 p0358 N73-12919
Determining preliminary orbital elements of earth satellite from angle-only observations
[AD-755399] 13 p1578 N73-22793
Using extended Kalman filter and weighted least square error filtering techniques to estimate orbital parameters of near earth satellite
[AD-757880] 15 p1832 N73-24852
**ORBITAL MECHANICS**
NT MINIMUM VARIANCE ORBIT DETERMINATION
Applications of orbital mechanics to aerospace systems and ballistic trajectories
[AD-746706] 02 p0232 N73-11885
Appendices to support findings of Orbiting Propellant Depot Safety study - Vol. 3
[NASA-CR-123383] 03 p0254 N73-12058
Design and development of zero-gravity atmospheric cloud physics experiment laboratory for installation in orbiting spacecraft
[NASA-CR-128998] 03 p0280 N73-12270
Design and development of space shuttle system for delivering payload to earth orbit or celestial orbit
[NASA-CASE-MSC-12391] 03 p0354 N73-12884
Numerical integration computer program based on integrating only perturbations in cartesian coordinates
[AD-747588] 04 p0476 N73-13890
Development of concept of space shuttle orbiter/tug orbital insertion and application to specific space missions
[NASA-TM-X-64715] 06 p0718 N73-15862
History of USSR space program to include design of manned spacecraft, solution of space flight problems, and chronology of manned USSR space flights
[NLL-M-22222-[5828.4F]] 06 p0720 N73-15876
Error analyses of satellite orbital parameters based on simulations of observational variances, observation equations, and normal equations
[NASA-CR-130357] 06 p0720 N73-15878

Series expansion of functions using eigenfunctions and applications to initial and boundary value problems of orbital mechanics
[BMBW-FBW-72-33] 09 p1084 N73-18844
Optimal plotting of elliptical transfer orbit employing complete revolutions in equatorial plane of axisymmetric planet
[AD-753517] 09 p1085 N73-18857
Development of technique for inferring atmospheric ozone information from satellite nadir measurements
[NASA-TR-R-399] 10 p1154 N73-19386
European space tug - Prephase A study
[MBB-URV-38-71] 10 p1218 N73-19908
Computerized simulation of orbital assembly dynamics and interactions with geometrical appendages
[NASA-CR-124169] 11 p1259 N73-20220
Time variations of instantaneous orbital parameters and topocentric range and range rate of spacecraft moving in gravitational field of oblate large body
[JPL-TM-33-594] 12 p1458 N73-21814
Motion and orbital direction of particle in Kerr gravitational field
[NASA-TR-R-403] 12 p1458 N73-21816
Application of variational equations for analysis of rapidly spinning triaxial body moving in elliptical orbit
[NASA-CR-131871] 13 p1581 N73-22813
Orbital mechanics involved in rendezvous between space shuttle and Soyuz spacecraft
[NASA-TT-F-13955] 14 p1705 N73-23838
Numerical integration techniques for solution of orbital elements of moon and planets
[AD-755164] 14 p1707 N73-23850
Optimum three impulse generator with patched conic trajectory model
[NASA-130244] 15 p1831 N73-24843
Consolidation of navigation and guidance for space shuttle vehicles for all phases of space mission - Document 21
[NASA-CR-128961] 16 p1941 N73-25708
Development of autonomous stationkeeping system for controlling longitude of synchronous satellite by onboard navigation aids
[AD-759806] 16 p1942 N73-25716
Linear stability analyses for four satellite configurations using passive elements for attitude control
16 p1964 N73-25883
Early orbit capability of Goddard Trajectory Determination System for earth satellites
[NASA-TM-X-66286] 18 p2197 N73-27734
Planning for Venus radar mapping orbiter mission and spacecraft to determine technology requirements and cost effectiveness of alternative approaches-Vol. 1
[NASA-CR-114640] 22 p2715 N73-31735
Parametric studies and subsystem comparisons for orbital radar mapping mission to planet Venus - Vol. 3
[NASA-CR-114642] 22 p2715 N73-31737
Applications of eigenfunctions for solution of boundary value problems in orbital mechanics
[BMBW-FBW-72-17] 22 p2718 N73-31758
Initial value problems solution on satellite geodesy and orbital mechanics using Hammerstein method for boundary value problem
[BMBW-FBW-72-23] 22 p2718 N73-31759

**ORBITAL MOTION**
U ORBITS

**ORBITAL POSITION ESTIMATION**
Adaptive filter using minimum variance criteria to estimate state noise covariance
[NASA-TM-X-66080] 01 p0032 N73-10252
Problems in estimation theory with applications to orbit determination
04 p0469 N73-13820
Design criteria for SOREL drag-free space probe discussing attitude control and orbital position estimation
[S-3-1949-VOL-1/2] 09 p1091 N73-18904
Dynamic model gravity compensation method for satellite orbit determination
[AD-765551] 24 p2982 N73-33828

**ORBITAL RENDEZVOUS**
NT LUNAR ORBITAL RENDEZVOUS
Rendezvous and docking radar for space shuttle
10 p1129 N73-19198
Orbital mechanics involved in rendezvous between space shuttle and Soyuz spacecraft
[NASA-TT-F-13955] 14 p1705 N73-23838

**ORBITAL SIMULATORS**
U SPACE SIMULATORS

**ORBITAL SPACE STATIONS**
NT ORBITAL WORKSHOPS
NT SALYUT SPACE STATION
NT SKYLAB 1
Reliability probability analysis on ergatic process in spacecraft control during approach and docking with orbital station
03 p0258 N73-12087
Design and operation of Orion orbital astrophysical observatory
[NASA-TT-F-14581] 07 p0766 N73-16221
Control system for automatic orientation and tracking operation of Orien orbital observatory
[NASA-TT-F-14583] 07 p0799 N73-16490
Photographic characteristics of UFSh-4 film used in Orion orbital observatory
[NASA-TT-F-14585] 07 p0799 N73-16492
Cost analysis of oxygen supply equipment and recovery systems for orbital space stations
[NASA-CR-124175] 12 p1373 N73-21137
Hypervelocity meteoritic impact resulting in structural damage of orbital space stations
[NASA-CR-124241] 14 p1705 N73-23841
Manned orbital space station for geophysical and astronomical research
[NASA-TT-F-13957] 14 p1709 N73-23868
Development and employment of orbital space stations to conduct earth resources surveys and provide space manufacturing facilities
[JPRS-59650] 18 p2199 N73-27754
Cosmonaut activities onboard orbiting space stations
[NASA-TT-F-15152] 23 p2850 N73-32778

**ORBITAL TRANSFER**
U TRANSFER ORBITS

**ORBITAL WORKSHOPS**
Tests of Skylab Orbital Workshop ventilation concepts
[NASA-TM-X-64700] 07 p0848 N73-16875
Preflight, inflight, and post flight operations evaluation analyses for Skylab materials processing facility - Appendix E
[NASA-CR-61386-APP-E] 14 p1708 N73-23859
Preflight, inflight, and post flight operations evaluation analyses for Skylab metals melting experiment facility - Appendix F
[NASA-CR-61386-APP-F] 14 p1708 N73-23860
Preflight, inflight, and post flight operations evaluation analyses for Skylab exothermic brazing experiment facility - Appendix G
[NASA-CR-61386-APP-G] 14 p1708 N73-23861
Preflight, inflight, and post flight operations evaluation analyses for Skylab sphere forming experiment facility - Appendix H
[NASA-CR-61386-APP-H] 14 p1708 N73-23862
Preflight, inflight, and post flight operations evaluation analyses for Skylab gallium arsenide single crystal growth facility - Appendix J
[NASA-CR-61386-APP-J] 14 p1708 N73-23863
Preflight, inflight, and post flight operations evaluation analyses for Skylab contamination measurement sample array - Appendix S
[NASA-CR-61386-APP-S] 14 p1708 N73-23864
Congressional hearing to determine malfunction on Skylab 1 workshop and proposed methods for correcting malfunction
16 p1964 N73-25884
Congressional hearing to determine causes of malfunctions of Skylab space vehicle
22 p2737 N73-31914

**ORBITALS**
NT ELECTRON ORBITALS
NT MOLECULAR ORBITALS

**ORBITING ASTRONOMICAL OBSERVATORY**
U OAO

**ORBITING FROG OTOLITH**
Results of OFO-A vestibular experiment and requirements of artificial gravity onboard manned spacecraft
[NASA-TT-F-14836] 08 p0961 N73-17861

**ORBITING GEOPHYSICAL OBSERVATORY**
U OGO

**ORBITING SATELLITES**
U ARTIFICIAL SATELLITES

**ORBITING SOLAR OBSERVATORY**
U OSO

**ORBITS**
NT APOGEES
NT CIRCULAR ORBITS
NT EARTH ORBITS
NT LUNAR ORBITS
NT PERIGEES
NT PERIHELIONS
NT PLANETARY ORBITS
NT POLAR ORBITS
NT SATELLITE ORBITS
NT SOLAR ORBITS
NT SPACECRAFT ORBITS
NT STATIONARY ORBITS
NT TRANSFER ORBITS
NT TWENTY-FOUR HOUR ORBITS
Photographic observation of Type 1 and Type 2 tail motion in Comet Bennett
02 p0229 N73-11854

**ORDER-DISORDER TRANSFORMATIONS**
Nuclear magnetic resonance spectroscopy to measure order parameter in diatomic molecule rotational ordering transitions
[NOTA-INTERNA-376] 01 p0083 N73-10691
Beta-phase effect on ductility of two-phase titanium alloys and calorimetric determination of atomic ordering effects in Ni2Cr alloy
[JPRS-57578] 06 p0683 N73-15556
Calorimetric determination of atomic ordering effects in alloy Ni2Cr
06 p0683 N73-15558
Mossbauer spectroscopic analysis of order-disorder transitions in vacuum deposited Te films
[AD-753272] 09 p1074 N73-18769
Green function technique used to calculate magnetic properties of disordered Heisenberg ferromagnets in which exchange interactions deviate randomly in strength from mean interaction
[NASA-TN-D-7208] 14 p1697 N73-23774
Short range order effect on interatomic reaction and heat of displacement in molten nickel and silicon alloys
[NLL-M-21597-[5828.4F]] 15 p1797 N73-24568
High temperature strength and deformation properties of Ti-Al-Si alloy aged by alpha phase precipitate particles
[NASA-TN-D-7325] 16 p1928 N73-25597
Yielding, work hardening, and fracture behavior of ordered and disordered alloys as function of dislocation
[ORO-3935-25] 21 p2559 N73-30514
Optical determination of electronic structure of Au-Cu alloys in disordered and ordered phases
[AD-763239] 21 p2586 N73-30720
Affect of antiferromagnetic ordering onset at Neel temperature on transport properties of CeAl, AuHo, and ErCu systems
24 p2933 N73-33425

**ORDINATES**
U COORDINATES

**ORDNANCE**
Vacuum brazing-gas quenching process for joining chemical and ordnance munitions materials
[AD-759117] 16 p1919 N73-25531

**OREGON**
NT CASCADE RANGE [CA-OR-WA]
Monitoring by ERTS-1 imagery for resource inventory, planning, land use zoning, and resource development in Oregon
[E72-10182] 01 p0045 N73-10361
Seasonal flow patterns of coastal currents along Oregon-Northern California coast
[AD-749077] 05 p0541 N73-14403
Resources inventory and land use management in Oregon using ERTS-1 imagery
[E73-10008] 06 p0658 N73-15344
Information system for ERTS-1 data on timber resources in Washington and Oregon
[E73-10319] 09 p1023 N73-18351
Resources inventory, planning, land use zoning, and resources development in Oregon using ERTS-1 imagery
[E73-10579] 14 p1656 N73-23440
Multispectral band scanner data of Oregon coast gathered during summer of 1969
15 p1779 N73-24424
ERTS-1 data for development of information system for timber resources and land management planning in Oregon
[E73-10696] 16 p1903 N73-25388
Application of remote sensing techniques of ERTS and other sources for solution of environmental problems in Oregon
[NASA-CR-133034] 16 p1906 N73-25420
Analysis of ERTS-1 imagery for multi-disciplinary resource inventory of soils, vegetation, and geology in Big Summit Prairie area of oregon
[E73-10770] 18 p2134 N73-27246
Land management planning and timber resources management in Washington and Oregon from ERTS-1 imagery
[E73-10804] 18 p2138 N73-27279
Resources and land use management and planning in Oregon using ERTS-1 data
[PAPER-R2] 19 p2282 N73-28360
Skylab imagery of terrain surface moisture, vegetation, and forestation in Colorado and Oregon
[E73-11001] 22 p2659 N73-31306
Multispectral band scanner reconnaissance of Pacific Ocean off Oregon coast
[AD-763428] 23 p2789 N73-32311

**ORGANIC CHEMISTRY**
Development of fluorometric methods for analysis of biological compounds based on production of fluorescence by enzymic reaction
[PAPER-76A6-745] 21 p2546 N73-30411
Organic geochemistry of amino acids in sedimentary rocks
[NASA-TT-F-14986] 23 p2787 N73-32295

**ORGANIC COMPOUNDS**
NT ADENINES
NT ADENOSINE TRIPHOSPHATE [ATP]
NT AMINO ACIDS
NT FATTY ACIDS
NT FLUORINE ORGANIC COMPOUNDS
NT FLUOROCARBONS
NT FLUOROHYDROCARBONS
NT GLUTAMIC ACID
NT GLYCINE
NT NUCLEASE
NT NUCLEOTIDES
NT ORGANIC LIQUIDS
NT PENTANONE
NT PEPTIDES
NT SEROTONIN
Electrical and transport properties in polycyclic semiconductor compounds
[AD-745988] 02 p0219 N73-11771

Composition of diffuse reflective coating containing sodium chloride in combination with diol solvent and organic wetting and drying agents
[NASA-CASE-GSC-11214-1] 04 p0385 N73-13128
Near infrared laser action for Kodak organic dyes using linear flash lamp for excitation
[AD-748863] 04 p0429 N73-13496
Papers presented at conference on mechanisms of pyrolysis, oxidation, and burning of organic materials
[NBS-SP-357] 08 p0880 N73-17129
Pyrolysis of organic compounds in gas phase
08 p0881 N73-17131
Free radical mechanisms in oxidative reactions of organic compounds
08 p0881 N73-17136
Oxidative degradation of polymers and organic compounds via unimolecular decomposition of peroxy radicals
08 p0882 N73-17138
Controlled gaseous oxidations of organic compounds
08 p0882 N73-17141
Detection of evolutionary organic compounds in extraterrestrial matter
10 p1118 N73-19114
Organic amine and nitroaromatic mixed compound for heat change detection in microelectronic components
[NASA-CASE-NPO-10764-2] 11 p1264 N73-20259
Development of low melting fused salt electrolytes
[AD-755528] 13 p1477 N73-21965
Acute and subacute inhalation toxicity experiments with organic solvents, rocket propellants, and various hydrocarbons in confined environments
[NASA-CR-131675] 13 p1485 N73-22043
Effects of various gases on conductivity of four organic semiconductors at very low pressures
[REPT-1972-19] 14 p1697 N73-23772
Organic compounds for nucleating supercooled water
[AD-758002] 15 p1748 N73-24169
Light effects on organic matter balance of oak underwood growing in forest understorey
20 p2405 N73-29330
Influence of light conditions and understorey tree death on organic matter loss balance in oak underwood
20 p2405 N73-29331
Analysis of various organic compounds in solution and inorganic ions in glasses as possible fluorescence standard reference materials
[PAPER-76A6-748] 21 p2547 N73-30414
Principles of producing glass parts from polymethl methacrylate organic glass and tensile strength tests
[AD-763282] 22 p2690 N73-31542
Simultaneous determination of carbon, hydrogen, and nitrogen in organic compounds
[UCID-16198] 24 p2892 N73-33085

**ORGANIC FLUORINE COMPOUNDS**
U FLUORINE ORGANIC COMPOUNDS

**ORGANIC LASERS**
NT DYE LASERS
Organic dye pulsed laser for detecting individual atomic species concentration in upper atmosphere
[AD-747335] 02 p0169 N73-11377
Laser induced infrared quantum counter upconversion experiments utilizing rare earth ions in single crystals
[AD-747415] 03 p0312 N73-12546
Development of electronically tunable dye laser with capability for producing two randomly accessible and simultaneous frequencies
[AD-752053] 08 p0933 N73-17641
Intensity stabilization and development of turnable ultranarrowband dye laser
[AD-754112] 10 p1170 N73-19517
High power tunable organic dye laser excitation of atomic fluorescence spectroscopy
12 p1409 N73-21422
Design, development, and characteristics of continuous wave laser using organic dyes
[AD-756514] 13 p1539 N73-22466
Harmonic generation of high power tunable lasers
[AD-760018] 17 p2042 N73-26520

**ORGANIC LIQUIDS**
Organic dyes for improving light intensity of Nd YAG laser pump system
[AD-747401] 03 p0312 N73-12545
Correlation of organic substance oxidation rate parameters in low temperature plasma with high frequency power
[NASA-TT-F-14671] 07 p0753 N73-16113
Stress corrosion cracking of titanium and titanium alloys in organic liquids and vapors
[AD-751528] 07 p0810 N73-16572
Effect of constant applied stress in crack initiation of aluminum and titanium alloys exposed to salt solution and organic fluids
[NASA-CR-124110] 09 p1045 N73-18525
Heat transfer from radioisotope generator, using organic fluids
[CEA-CONF-2042] 10 p1224 N73-19950
Pulse radiolysis of biphenyl solutions in cyclohexane noting life distribution of biphenyl ions
[IRI-133-72-07] 19 p2323 N73-28686

**ORGANIC MATERIALS**
Influence of temperature on creep and strength characteristics of organic PRD49 fiber/epoxy composites
[NASA-TN-D-7120] 03 p0320 N73-12607
Application of glass composites, all carbon composites, and PRD-49 organic fiber material for airframe and spacecraft construction
18 p2164 N73-27482
Optimal operational temperature for thermoelectric generator using organic fuel heat
[AD-762266] 19 p2223 N73-27932
Development and characteristics of organic polymers for application to production of heat resistant plastics
[NLL-RISLEY-TR-2615-[9091.9F]]
20 p2434 N73-29546
Oxygen index method for evaluating flammability of organic polymeric materials
[DSL-REPT-561] 22 p2729 N73-31836
Smoke generation data on organic polymeric materials
[DSL-REPT-560] 22 p2729 N73-31837

**ORGANIC NITRATES**
NT CELLULOSE NITRATE
NT HYDRAZINE NITROFORM
NT NITROGLYCERIN
NT PETN
Chemical determination of organic nitrate additive in diesel engine fuel
[AD-762177] 19 p2328 N73-28730

**ORGANIC PHOSPHORUS COMPOUNDS**
NT PHOSPHONITRILES
Cholinesterase reactivator as antidote in human organophosphate poisoning
13 p1480 N73-21998
Temporary blindness of monkeys caused by combined effects of phosdrin and atropine exposure
[FAA-AM-73-4] 18 p2109 N73-27055
Effects of phosdrin on electrical brain potentials in squirrel monkeys
[FAA-AM-73-3] 18 p2109 N73-27056

**ORGANIC SEMICONDUCTORS**
Electronic switching phenomena in organic thin films
[AD-755267] 12 p1442 N73-21682
Using single crystals to determine ionization energies of organic semiconductors
[NASA-CR-133827] 21 p2517 N73-30188

**ORGANIC TIN COMPOUNDS**
Stability constants and distribution of tin IV complexes by anion exchange resin with carboxylic acids
[AREAEE-128] 07 p0824 N73-16679

**ORGANISMS**
Elimination of toxic cysteamine in organisms and method for prolonging its radioprotective effect
11 p1240 N73-20069

**ORGANIZATIONS**
NT NORTH ATLANTIC TREATY ORGANIZATION [NATO]
Effects of computerized management of information on organizational structures and functions
[REPT-486-70] 04 p0393 N73-13191
Organization and management of aerospace research institute
11 p1351 N73-20962
Scope of technology assessment
[NASA-CR-135783] 23 p2866 N73-32913

**ORGANOMETALLIC COMPOUNDS**
NT CARBOXYHEMOGLOBIN
NT CHLOROPHYLLS
NT HEMOGLOBIN
NT ORGANIC TIN COMPOUNDS
Metallic chain compounds and organometallic complexes for high temperature superconductor materials
[AD-759767] 17 p2074 N73-26778
Literature on vanadium and nickel trace elements in distillate fuels for motor vehicles
[AD-760462] 17 p2076 N73-26793
Chemiluminescent emissions from trimethylaluminium, iron pentacarbonyl, and lead tetraethyl upon reaction with oxygen
[AD-762317] 19 p2233 N73-28007
Proceedings of conference on mass spectrometry of metal containing compounds
20 p2431 N73-29527
Potentiometric stability data analyses for nickel, lead, and zinc organic acetate complexes
[JINR-E12-6776] 24 p2935 N73-33436
Functional stability calculations for organometallic complexes of copper and cadmium
[JINR-E12-6775] 24 p2935 N73-33437
Stability constants correlation for metal-inorganic ligands in organometallic cadmium, rhodium, and lead compounds
[JINR-E12-6773] 24 p2935 N73-33438

**ORGANS**
NT KIDNEYS
NT LIVER
NT LUNGS
NT PITUITARY GLAND
NT SPLEEN
NT STOMACH
NT TESTES
Functional morphology of various organs and tissues subjected to space flight
[NASA-TT-F-738] 10 p1119 N73-19126
Pathomorphological changes in internal organs of white rats following 120 MeV proton irradiation and effect of partial shielding on attenuation of damage
11 p1241 N73-20076
Characteristics of pathomorphological changes in rat internal organs subjected to gamma-neutron irradiation with head and stomach shielded
11 p1241 N73-20077
Atrophy and metabolic changes in internal organs and skeletal muscles of rats exposed to hypokinesia
14 p1607 N73-23029
Defined shock wave effects on miniature swine, describing organ injuries
19 p2227 N73-27965

**ORIENTATION**
X ray crystallographic methods for studying preferred orientation of hexagonal metals
[RFP-TRANS-117] 11 p1306 N73-20594
Determination of ships orientation from accelerometer signals
11 p1319 N73-20703

**ORIFICE FLOW**
Analysis of spoiler plate characteristics to eliminate effects of installation disturbance when conducting flow rate measurements
[NLL-NEL-TT-2439-[6075.461]]
15 p1763 N73-24288
Measurement of laminar fluid flow through orifice meters to determine discharge coefficients and head losses
[NLL-NEL-TT-2457-[6075.461]]
20 p2386 N73-29169
Integral solution to internal separated flow problems in nozzles and orifices
23 p2772 N73-32174
Rocket motor chamber pressure and orifice effects in hydraulic flip
[AD-764730] 23 p2832 N73-32630

**ORIFICES**
Buckling analysis of elastic plate floating on water and stressed uniformly along periphery of internal hole
[AD-750594] 06 p0728 N73-15943
Dynamic response of fluidic circuits with blocked and orifice terminated lines
[AD-753384] 09 p1018 N73-18307
Distribution and concentration profiles of stress adjacent to orifices in glass fiber-reinforced plastic plates and shells
[AD-753041] 09 p1096 N73-18945
Experimental investigation of mean flow characteristics of air jets issuing from rectangular orifices
[AD-754225] 10 p1143 N73-19314
Influence on output power of coupling orifice of CO2 gas laser cavity operating in mode of excitation by microsecond pulses
16 p1923 N73-25563
Stress distribution in infinite micropolar plate with elliptic hole
[AD-759964] 17 p2095 N73-26949

**ORION AIRCRAFT**
U P-3 AIRCRAFT

**ORION CONSTELLATION**
Photographic magnetudes of T Tauri and normal stars in Orion I
06 p0716 N73-15846
Photographic V and R magnitudes of 130 T Tauri and H alpha emission stars in Orion I
06 p0716 N73-15847
Spectroscopic observation of metastable helium line in alpha-orionis and interstellar media
17 p2081 N73-26830
Sulfur line density in spectrographic scan of Orion nebula
22 p2734 N73-31888

**ORNITHOPTER AIRCRAFT**
U RESEARCH AIRCRAFT

**OROGRAPHY**
Effect of orography on climatic wind distribution and geopotential fields
20 p2444 N73-29632

**ORRERIES**
U ASTRONOMICAL MODELS

**ORTHICONS**
NT IMAGE ORTHICONS

**ORTHOGONAL FUNCTIONS**
NT WALSH FUNCTION
High percentage of zero elements of sparse matrix methods based on orthogonality and conjugacy
[NASA-CR-133231] 17 p2054 N73-26617
Orthogonal functional analysis of unsteadiness in atmospheric circulation
20 p2442 N73-29617
Least squares fitting of bicubic spline surfaces to general data at arbitrary points noting householder orthogonal transformation, solution stability, and ranking
[NPL-NAC-22] 23 p2813 N73-32489
Atmospheric field decomposition by systems of orthogonal functions
[AD-764942] 23 p2815 N73-32509

**ORTHOSTATIC TOLERANCE**
Effect of atmosphere with increased oxygen and carbon dioxide content on human orthostatic tolerance following 10 days of bedrest
07 p0744 N73-16055
Role of extracardial innervation in compensation of orthostatic load
24 p2883 N73-33023

**ORTHOTROPIC CYLINDERS**
Design of orthotropic cylindrical shell as structural adapter for Helios solar probe
[DGLR-PAPER-72-101] 06 p0722 N73-15889
Torsion of an orthotropic, inhomogeneous bar with cylindrical anisotropy including solution by Saint Venant principle
[DRIC-TRANS-2995] 12 p1463 N73-21856
Analysis of dynamic stability of elastic orthotropic cylindrical shell to determine shell parameters, shear moduli, and buckling mode
17 p2093 N73-26930
Buckling behavior of composite cylinders to compressive loads
[NASA-CR-132264] 20 p2483 N73-29945
Numerical analysis of buckling characteristics of ring-stiffened, oval, orthotropic, cylindrical shells
[AD-763369] 21 p2604 N73-30872

**ORTHOTROPIC PLATES**
Structural dynamic behavior of laminated plates and shells composed of bonded elastic orthotropic layers
[AD-745336] 01 p0114 N73-10944
Mapping-collocation method for elastostatic stress analysis of orthotropic rectangular plates with centrally located traction-free cracks
[NASA-TN-D-7119] 03 p0360 N73-12933
Thermal stress vibrations in prebuckled region of orthotropic trapezoidal plates with two parallel opposite sides and various boundary conditions
[NASA-CR-2174] 09 p1094 N73-18928
Principal relationships of theory of elastic orthotropic plates of variable rigidity with consideration of transverse shear
[AD-752708] 09 p1095 N73-18942
Equations for structural stability of orthotropic plates and cylindrical shells
[AD-758327] 15 p1840 N73-24914
Steady state creep in orthotropic materials
22 p2724 N73-31795

**ORTHOTROPIC SHELLS**
Structural dynamic behavior of laminated plates and shells composed of bonded elastic orthotropic layers
[AD-745336] 01 p0114 N73-10944
Equilibrium stability of orthotropic cylindrical shell
[AD-747724] 03 p0362 N73-12948
Solution of axisymmetric finite deformation equations for arbitrary shallow orthotropic shell of revolution subjected to uniform pressure and edge loading
13 p1584 N73-22844
Analysis of static, buckling, and vibration characteristics of orthotropic, inhomogeneous shells of revolution
15 p1837 N73-24889

**ORTHOTROPISM**
Determination of flutter characteristics for arbitrary yaw angles with two types of corrugation-stiffened panels
[NASA-CR-2265] 14 p1714 N73-23910
Orthotropic effects in cracked cylindrical shell
[NASA-CR-132295] 19 p2348 N73-28887

**OSCILLATING CYLINDERS**
Drag measurement in wake of oscillating cylinder at low Reynolds number using hot-wire technique
[DLR-FB-71-42] 09 p0981 N73-18015
Analysis of flow distribution around harmonically oscillating circular cylinder under two dimensional flow conditions
[DLR-FB-72-56] 09 p1014 N73-18277

**OSCILLATING FLOW**
Dynamic calibration of gas flowmeters by impedance measurement in oscillating flow
[ARC-CP-1224] 05 p0548 N73-14451
Flow equations for unsteady turbulent boundary layer flow on swept infinite cylinder to show effects of variations in frequency of oscillations
[NASA-TM-X-62242] 10 p1141 N73-19297
Analysis of oscillating gas flow in open-ended pipe caused by piston operating at or near resonant frequency
[AD-754647] 11 p1272 N73-20321
Development of techniques for measuring oscillatory derivatives in wind tunnels and analysis of wind tunnel effects on results
[ARC-R/M-3319] 15 p1729 N73-24020
Velocity potential solution of heavy incompressible liquid wave motion
[AD-758251] 15 p1769 N73-24331
Experimental determination of laminar boundary layer and oscillatory suspension flows by laser anemometry
17 p2012 N73-26271
Flow characteristics associated with laminar oscillating flow in horizontal tube containing mild axisymmetric constriction
23 p2772 N73-32175
Resonance stabilization of air cushion between liquid and oscillation source
[IPP-2/209] 24 p2963 N73-33674

**OSCILLATION DAMPERS**
Analysis of radial distributions of flow conditions at inlet and outlet of high speed rotors to determine effects of blade part-span dampers on rotor performance
[NASA-TM-X-2696] 06 p0614 N73-14985
Analysis of aerodynamically induced oscillations of bundled power conductors resulting from effect of wind on transmission power lines
17 p2098 N73-26971

**OSCILLATIONS**
NT ELECTRON OSCILLATIONS
NT HARMONIC OSCILLATION
NT MOLECULAR OSCILLATIONS
NT PLASMA OSCILLATIONS
NT PRESSURE OSCILLATIONS
NT TRANSVERSE OSCILLATION
NT UNDAMPED OSCILLATIONS
NT WING OSCILLATIONS
Analysis and Monte Carlo calculations of disc laser limitations due to effects of fluorescence amplification and parasitic oscillation
[AD-747234] 02 p0183 N73-11485
Stability of small amplitude oscillations in combustion chambers for one and three dimensional problems
[AD-746132] 02 p0224 N73-11807
Application of small rate theory to resonant acoustic oscillations with damping
[AD-746981] 03 p0337 N73-12745
Low frequency oscillations of earth magnetic field observed by ATS 1
05 p0537 N73-14374
Amplitudes of natural oscillations of geomagnetic tail excited by solar wind
06 p0665 N73-15404
Influence of inhomogeneity of magnetic field on oscillations of plasma layer of magnetosphere tail
06 p0665 N73-15407
Oscillation and nonoscillation in solutions of standard linear sets of differential equations
[NASA-TT-F-14809] 08 p0937 N73-17672
Cosmos 434 measurement of oscillations in ion concentration levels in earth ionosphere at 200 to 1300 km altitudes
09 p1028 N73-18394
Magnetohydrodynamic theory of diurnal oscillations of earth magnetic tail
09 p1029 N73-18395
Theorems regarding oscillation and nonoscillation conditions for canonic linear sets of differential equations
[NASA-TT-F-14816] 09 p1057 N73-18615
Motion of gyroscope in cardan suspension in drift mode during platform oscillations
10 p1184 N73-19634
High-speed oscillating and thermal resistance tests of 25 self-lubricating composites
[AD-755112] 11 p1299 N73-20539
Theoretical calculation of generalized forces and load distribution on wings oscillating at general frequency in subsonic stream
[ARC-R/M-3710] 13 p1470 N73-21908
Influence of small periodic oscillations on viscous shock waves structure and sonic boom rise time caused by supersonic transport vibrations
13 p1507 N73-22217
Analysis of linear oscillating temperature distribution to determine thermal diffusivity coefficient of gases
[BER-1/73] 13 p1590 N73-22895
Oscillating bodies (cone, wedge, and flat plate) in supersonic flow
[AD-757254] 14 p1650 N73-23387
Oscillations of earths magnetic tail studied from model of plasma cylinder with free boundary
14 p1703 N73-23820
Propellant oscillation modes and frequencies for tanks of any shape, fill level, or orientation
[NASA-CR-124277] 16 p1889 N73-25287
Free oscillation model for ocean basin considering earth rotation and sphericity
[PB-214445/9] 16 p1909 N73-25444
Xenon gas laser oscillations in vacuum ultraviolet
[AD-759069] 16 p1925 N73-25576
Wave propagation and magnetic fields effects on velocity oscillations in solar plage regions
16 p1961 N73-25864
Axisymmetric oscillation of partially liquid-filled cylindrical shell container having hemispherical bulkheads
[NASA-TN-D-7318] 16 p1969 N73-25925
Development of electrical circuit for suppressing oscillations across inductor operating in resonant mode
[NASA-CASE-ERC-10403-1] 17 p2007 N73-26228
Objectives of dynamic tests in low speed wind tunnels and techniques for measuring oscillatory derivatives and transient motion effects
17 p2009 N73-26244
Stablity of plasma rotating in crossed electrical and magnetic fields
[NASA-TT-F-15021] 20 p2453 N73-29752
Dynamics of field-aligned longitudinal currents in magnetosphere
[NASA-TT-F-15075] 23 p2787 N73-32294
Influence of periodic oscillations of mean flow on mean and turbulent structure of fully developed air flow in smooth circular pipe
24 p2902 N73-33161

**OSCILLATORS**
NT CRYSTAL OSCILLATORS
NT GYROSCOPIC PENDULUMS
NT HARMONIC OSCILLATORS
NT MAGNETRONS
NT MECHANICAL OSCILLATORS
NT MICROWAVE OSCILLATORS
NT MICROWAVE TUBES
NT PENDULUMS
NT SYNCHRONIZED OSCILLATORS
Neodymium doped Q-switched laser glass illuminator oscillator
[AD-749511] 04 p0430 N73-13506
Design of transistorized oscillator for exciting gas discharge tubes
[AD-749831] 05 p0559 N73-14544
Transistor circuit with piezoelectric crystal for stable high frequency oscillator
[NASA-CASE-GSC-11513-1] 07 p0761 N73-16185
Development and characteristics of stable master oscillator carbon dioxide laser system
[AD-752219] 08 p0930 N73-17614
Construction of liquid laser designed for operation as oscillator-amplifier in high brightness mode
[AD-757072] 13 p1538 N73-22457
Maximum and minimum possible values of dynamic load factors for damped and undamped simple oscillators
[AD-755168] 13 p1588 N73-22875
Kinetic theory of optically pumped gas laser oscillator
18 p2157 N73-27428
Very high stability microwave oscillator with Q superconducting cavity
[AD-763684] 21 p2518 N73-30196
Loss reduction in high voltage LC oscillator circuits by applying cryogenic temperatures
[BMBW-FBK-72-31] 22 p2704 N73-31659
Electric switches for closing high voltage, high Q LC circuits, determining breakdown voltage and open and closed contact resistance
[BMBW-FBK-72-32] 22 p2704 N73-31660
Alphanumeric character display device for oscilloscopes
[NASA-CASE-GSC-11582-1] 23 p2765 N73-32120

**OSCILLOGRAMS**
U OSCILLOGRAPHS

**OSCILLOGRAPHS**
Oscillographic pressure measuring system for flow structure in compressor impeller bladings
[NASA-TT-F-14647] 06 p0673 N73-15480
Oscillographic measurements of friction moments in gas ball bearings
[NLL-RISLEY-TR-2565-[9091.9F]] 15 p1790 N73-24507
Development of electronic computer process for analyzing contact stress oscillograms
[NLL-M-21662-[5828.4F]] 21 p2511 N73-30136

**OSCILLOSCOPES**
Intensity modulation of electrical signals recorded on film using two oscilloscopes
[FOA-3-C-3677-62] 02 p0172 N73-11392
Development of delay cable to display simultaneous signals in nanosecond region in single trace on oscilloscope
[IPPJ-T-9] 04 p0395 N73-13212
Pulse radar sounding of sea ice thickness with video display
[JPRS-57841] 06 p0665 N73-15406
Oscilloscopic measurement of mode locked ultrashort laser pulses produced by linear and nonlinear photoelectric effects
[KFKI-72-41] 07 p0806 N73-16539
Mechanical exposure interlock device for preventing film overexposure in oscilloscope camera
[NASA-CASE-LAR-10319-1] 23 p2790 N73-32322

**OSCULATORY INTERPOLATION**
U ORBIT CALCULATION
U ORBIT PERTURBATION

**OSMIUM**
Measurements of work function of [110] and [111] faces of crystal from solid solution of osmium in tungsten
[NLL-TRANS-746-1315-[9022.401]] 05 p0585 N73-14760

**OSMIUM ALLOYS**
Phase diagram of Ti-Os system
[NLL-TRANS-746-1302-[9022.401]] 05 p0560 N73-14548

**OSMOSIS**
Blood plasma hyperosmolality and antidiuretic hormone inhibition in alcoholic intoxication
[NASA-TT-F-13910] 02 p0133 N73-11079
Atherosclerosis and hypertonia under high mountain conditions and seasonal effects
[NASA-TT-F-745] 09 p0995 N73-18121
Effects of hydrostatic water bath pressure on capillary blood pressure and connective tissue dehydration
[NASA-TT-F-14894] 14 p1610 N73-23052

Monomer polymerization by plasma discharge as thin film for water purification membrane
[NASA-CASE-ARC-10643-1] 20 p2374 N73-29074
OSMOTIC PRESSURE
U OSMOSIS
OSO
NT OSO-J
NT OSO-1
NT OSO-5
NT OSO-6
NT OSO-7
Attitude dynamics of nearly spherical dual spin satellite with asymmetrical bodies, orbital results for OSO 7, and critical mass properties
07 p0848 N73-16877
Mission objectives, flight history, and scientific experiments of OSO-7
[NASA-CR-130157] 11 p1341 N73-20879
Solar gamma ray and neutron observations from OSO-7 during 2B and 3B flares
[NASA-CR-131866] 13 p1574 N73-22758
Computer program to analyze solar observational data
[AD-755921] 14 p1703 N73-23815
OSO-5 X ray detector measurement of diffuse cosmic ray energy spectrum from 14 to 200 keV
[NASA-TM-X-66252] 15 p1828 N73-24815
Projected radiation environment profiles of OSO missions from 1974 to 1978
[NASA-TM-X-66264] 16 p1962 N73-25872
OSO-1 graphite crystal polarimeter for stellar X ray astronomy
17 p2084 N73-26862
OSO-7 observations of gamma ray emission in solar flares
19 p2332 N73-28761
OSO-F
U OSO-5
OSO-G
U OSO-6
OSO-J
OSO-J experimental design, and equipment for soft X ray sources and diffuse components in 0.01 to 2.0 keV range
17 p2085 N73-26865
OSO-1
Radiation monitor for cosmic X ray experiment on OSO-1
[NASA-CR-130206] 13 p1573 N73-22747
OSO-1 experimental design for cosmic X ray sources identification and diffusion background radiation spectroscopy
17 p2084 N73-26861
OSO-1 Bragg crystal spectrometer for solar and stellar X ray source analysis
17 p2084 N73-26863
OSO-5
OSO 5 spectrophotometer design, solar EUV data acquired, and data reduction
[NASA-CR-130159] 08 p0956 N73-17828
OSO-6
Technological modification to OSO-G launch vehicle for improved guidance and control
18 p2208 N73-27817
OSO-6 measurements on albedo neutron flux distribution and density
23 p2834 N73-32644
OSO-7
Attitude dynamics of nearly spherical dual spin satellite with asymmetrical bodies, orbital results for OSO 7, and critical mass properties
07 p0848 N73-16877
Evolution of solar active region and solar flare from observations of OSO-7 spectroheliograph
08 p0973 N73-17957
Performance of OSO-7 spacecraft during twelve months after launch and description of satellite components and subsystems
[NASA-CR-130184] 10 p1215 N73-19885
Analysis on OSO-H observations of solar X ray burst spectra
[NASA-CR-131245] 11 p1336 N73-20841
OSO-H observations of solar thermal and nonthermal X ray bursts
19 p2334 N73-28783
OTOLITH ORGANS
Mechanical response of otolith-dependent units of cats to sinusoidal linear rotation
[AMRU-R-69-3] 02 p0132 N73-11068
Theoretical model of utricular otolith and associated neural connections to oculomotor system and their response to angular motion with respect to acceleration in shear
[FPRC-1315] 02 p0132 N73-11070
Vestibular neuron response to rotational stimuli in space flight environment
06 p0634 N73-15150
Asymmetry of fish otolithic receptor functions and vestibular disturbances during space flight
14 p1608 N73-23031
OUTCROPS
Determination of paleotectonic principal stress orientation and spacings of joints in outcrops, and development of optical diffraction analysis method
[BM-RI-7706] 06 p0665 N73-15409
OUTER PLANET MISSIONS
U GRAND TOURS
OUTER PLANET SPACECRAFT
U OUTER PLANETS EXPLORERS
OUTER PLANETS EXPLORERS
Feasibility analysis for use of xenon-filled silicon germanium thermoelectric generators in outer planetary exploration
01 p0119 N73-10984
Performance prediction for nuclear electric propulsion systems in advanced unmanned missions to outer planets and solar system
[NASA-CR-129134] 02 p0210 N73-11705
Prelaunch mission operations for space storable propellant module for retro propulsion on unmanned outer planet orbiters
[NASA-CR-129521] 03 p0358 N73-12915
Gravity-assisted exploration of outer planets of solar system in 1980s
[AERO-72/3] 04 p0470 N73-13827
Computerized simulation of approach navigation accuracy and guidance requirements for 1977 Grand Tour mission to outer planets
08 p0941 N73-17707
Definition of scientific objectives for outer planet flyby missions
[NASA-CR-130977] 09 p1083 N73-18830
Thermoelectric outer planets spececraft advanced systems technology project
[NASA-CR-131451] 12 p1426 N73-21561
Outer Planets Grand Tour mission planning to include magnetometer systems requirements and development of hardware elements to meet objectives
12 p1448 N73-21727
Integration of spectrometer capability with imagery function of facsimile cameras for use on planetary landers
[NASA-CASE-LAR-11207-1] 19 p2300 N73-28496
Short wave radio emission measurements on giant planets during outer planets grand tour
[NASA-CR-133500] 19 p2343 N73-28844
Satellite quarantine constraints in outer planet mission planning
[NASA-CR-135791] 24 p2885 N73-33041
OUTER RADIATION BELT
Identification of solar neutron events by satellite detection of proton flux increase in outer edge of trapped proton belt
07 p0838 N73-16790
OUTGASSING
Toxicity of gaseous urine and feces emissions on rat organism
10 p1116 N73-19097
Phenol preservative for reducing toxic urine outgassing into air environment
10 p1116 N73-19098
Toxic effects of metabolic waste gases on rat organisms
10 p1116 N73-19101
Thermal vacuum environment tests of materials used in space technology to determine effect of ultraviolet radiation on contaminative properties
[NASA-CR-122374] 10 p1175 N73-19556
Theoretical analysis of effects of outgassing and waste dumping on contamination of orbiting spacecraft
[NASA-CR-124131] 11 p1340 N73-20875
Spectroscopic and chromatographic analysis of outgassing contaminants in potting compound and paint
[NASA-CR-124227] 13 p1488 N73-22061
Fluid polydimethylsiloxane resin with low outgassing properties in cured state
[NASA-CASE-GSC-11358-1] 17 p1991 N73-26100
Solid amine filter material for humidity control and carbon dioxide removal in space shuttle
[NASA-CR-133963] 18 p2113 N73-27087
Compilation of outgassing data for spacecraft materials
[NASA-TN-D-7362] 23 p2810 N73-32469
OUTLETS (GEOLOGY)
U ESTUARIES
OUTPUT
NT LASER OUTPUTS
Sample output for community/aircraft economic development model - programmers manual
[FAA-EQ-72-3-VOL-4] 04 p0401 N73-13260
Fitting linear multistage models to input/output data by maximum likelihood method
[AD-750139] 06 p0691 N73-15625
Description of computer program, main subroutines, input, output, and program requirements of Goddard Brouwer Orbit Bulletin
[NASA-TM-X-66141] 06 p0719 N73-15869
Digital address thin display tube to meet Army requirements for computer-output display
[AD-763933] 23 p2762 N73-32100
OUTWASH PLAINS
U GLACIAL DRIFT
OV-1 SATELLITES
OV1-17 satellite, polar cap measurements of solar flare protons with energies down to 12.4 keV
[AD-751467] 07 p0839 N73-16800
Atmospheric data from OV1-15 satellite
[AD-753680] 09 p1033 N73-18432
Low energy particles on front detector in coincidence in electron spectrometer on OV1-13 satellite
[AD-755789] 12 p1406 N73-21401
Atmospheric density data derived from SPADES satellite ultrasensitive triaxial accelerometer system
[AD-756831] 13 p1525 N73-22363
Profiles of neutral atmospheric density at high and middle latitudes in Southern Hemisphere from OV1-15
[AD-755396] 13 p1526 N73-22370
Measurements of galactic cosmic ray dose and geomagnetically trapped radiation from OV 1-4 satellite
[AD-756924] 13 p1575 N73-22761
OV-10 AIRCRAFT
Flight tests of rotating cylinder flap on YOV-10 aircraft modified to STOL configuration
[NASA-CR-2135] 04 p0371 N73-13020
Analysis of infrared spectra generated by OV-1D, F-14, and UH-1 aircraft using Fourier spectroscopy
[RM-572] 13 p1529 N73-22390
OVERCAST
U CLOUD COVER
OVERESTIMATION
U ERRORS
U ESTIMATING
OVEREXPOSURE
U RADIATION DOSAGE
OVERPRESSURE
Effect of simulated sonic booms and overpressure on EEG waveform patterns and disturbance judgments
[FAA-RD-73-115] 21 p2500 N73-30066
OVERTONES
U HARMONICS
OVERVOLTAGE
Overvoltage protection network for electrical equipment
[NASA-CASE-ARC-10197-1] 20 p2380 N73-29124
OXALATES
Oxide formations in thermal vacuum decomposition of rare earth oxalates
[BARC-631] 15 p1747 N73-24162
OXAZOLE
Thermal decomposition of polyhydrazide and polyoxadiazoles
[AD-749853] 05 p0568 N73-14612
OXIDATION
NT ELECTROCHEMICAL OXIDATION
Shock tube measurements of surface oxidation rates of soot formed during combustion of hydrocarbon fuels
[FML-PUBL-72-8] 01 p0023 N73-10176
Analysis of oxidation of high purity tantalum single crystals and large-grained tantalum sheets
[AD-745341] 01 p0068 N73-10554
Oxidation rate and compatibility of tungsten filament copper matrix composites
[AD-745324] 01 p0069 N73-10569
Preparation of tetraperchlorate of methane by displacement of halogen from carbon tetrahalides using halogan perchlorates
[NASA-CR-129168] 02 p0137 N73-11106
High temperature oxidation of uranium alloys and morphology of oxide scales
[CONF-720523-1] 03 p0263 N73-12130
Electric field effects on oxidation mechanisms of metals and alloys
[AD-748297] 04 p0436 N73-13558
Thermogravimetric measurements for oxidation of hot pressed silicon carbide
[AD-748351] 04 p0439 N73-13578
Kinetics of Fe and Al atom oxidation reactions at high temperatures
[AD-749380] 05 p0507 N73-14125
High temperature dispersion strengthening of Fe-Al alloys by internal oxidation
[BM-RI-7686] 05 p0562 N73-14564
Relationship of molecular structure to thermo-oxidative stability of carborane-siloxane polymers with icosohedral CB10H10C cages
[AD-749820] 05 p0567 N73-14610
Influence of volatile compounds on high temperature oxidation of Cr and Cr alloys
[TM-49] 06 p0684 N73-15566
High temperature oxidation behavior of Ni3Al with and without yttrium additions and reaction kinetics of Al2O3 layer growth
[AD-750410] 06 p0686 N73-15589
Radiation oxidation of water impurities in moisture-containing products of human vital functions
07 p0744 N73-16051
Correlation of organic substance oxidation rate parameters in low temperature plasma with high frequency power
[NASA-TT-F-14671] 07 p0753 N73-16113
Reduction of oxidation attack of nickel-base superalloy B-1900 by addition of one percent silicon
[NASA-TM-X-68191] 07 p0809 N73-16564
Papers presented at conference on mechanisms of pyrolysis, oxidation, and burning of organic materials
[NBS-SP-357] 08 p0880 N73-17129
Free radical mechanisms in oxidative reactions of organic compounds
08 p0881 N73-17136

Mechanism of peroxidation of polymers under irradiation conditions
08 p0881 N73-17137
Oxidative degradation of polymers and organic compounds via unimolecular decomposition of peroxy radicals
08 p0882 N73-17138
Mechanisms of oxidation of polyolefins below 150 C
08 p0882 N73-17139
Controlled gaseous oxidations of organic compounds
08 p0882 N73-17141
Quantitative inconsistencies in low temperature and high temperature oxidation kinetics
08 p0882 N73-17142
Oxidation of atmospheric impurities in space cabin and purity of reclamated water
10 p1117 N73-19104
Laser-induced fluorescence for gas phase oxidation of aluminum atoms
[AD-753839] 10 p1127 N73-19182
Development of semi-empirical expression for specific surface oxidation rate of soot for application to design of combustion chambers
10 p1223 N73-19943
Dispersion effects of heat resistant metal oxides
[AD-754760] 11 p1306 N73-20595
Mass spectra of electrochemical propane oxidation
[AD-755254] 12 p1376 N73-21166
Reaction rate data for atmospheric chemistry, metal atom oxidation, and nuclear fireball
[AD-756674] 13 p1488 N73-22063
Effect of yttrium, lanthanum, and cerium additives on oxidation kinetics of nickel-chromium based alloys
[JPRS-58777] 13 p1542 N73-22497
Physical and chemical properties of nickel alloys following cyclic and isothermal oxidation
[NASA-TN-D-7267] 14 p1675 N73-23594
Influence of surface preparation, surface texture, and initial oxidation on metal surface crystallization
14 p1676 N73-23603
Role of isothermal stresses generated during oxidation and modes of stress relaxation
14 p1676 N73-23605
High temperature environmental testing of gas-metal interactions to simulate severe operating conditions
14 p1677 N73-23606
Effects of oxide dispersions and rare earth elements on oxidation of Cr and Al containing alloys
14 p1677 N73-23608
Multicomponent diffusion theory as applied to oxidation, corrosion, and sulfation of complex heat resistant alloys
14 p1677 N73-23609
Hydrocarbon oxidation by metal catalysts and adsorption layer formation on electrode in propane air fuel cell
[AD-758172] 15 p1748 N73-24168
Electrode metal loss by volatilization in gas-shielded arc welding
[NLL-DRIC-TRANS-3005-[3623.66]]
15 p1790 N73-24511
Development of procedure for estimating solid phase occurrence during oxidation of heavy metal sulfides
[NLL-M-22913-[5828.4F]] 16 p1926 N73-25581
Creep test measurement of stresses generated during high temperature oxidation of copper and nickel
16 p1926 N73-25588
X ray diffraction analysis of VIA, B-1900, 713C, and 738X alloy composition after oxidation at high temperature
[NASA-TM-X-2796] 16 p1927 N73-25596
Oxidation and stress corrosion cracking of high strength steel in gaseous environment
[AD-758848] 16 p1929 N73-25608
Internal oxidation of dilute Cu-Ti alloys at 700 to 900 C
[AD-759382] 17 p2047 N73-26557
Experimental analysis of disappearance phenomena of packing defects in silicon epitaxial films during thermal oxidation in wet oxygen
18 p2187 N73-27662
Effect of applied electric field on oxidation/hot corrosion of metals and alloys in molten salt
[AD-762074] 19 p2311 N73-28584
Analysis of chemical and electrochemical processes occurring on titanium sheet metal surfaces during oxidation at room temperature by electron-diffraction method
[NLL-RTS-7888] 20 p2428 N73-29503
Atomic oxygen reaction with nickel at elevated temperatures
[NASA-TM-X-62295] 20 p2431 N73-29524
Evaluation of high temperature nozzle throat materials for performance in highly oxidizing rocket exhaust environment
[AD-762533] 20 p2467 N73-29816
Thin layer chromatographic identification and infrared spectrophotometric quantification of antioxidants used in manufacturing polyolefinic polymers
[REPT-6726] 22 p2625 N73-31029
Anodic oxidation of titanium and its alloys
[LS-254] 22 p2685 N73-31505
Mossbauer effect study of high temperature oxidation and breakaway in 302 stainless steel
22 p2706 N73-31671
Film growth transient measurements for stress corrosion cracking susceptibility analyses on metals
23 p2804 N73-32421

**OXIDATION RESISTANCE**
Basic mechanisms providing oxidation resistance in structural, titanium base alloys operating above 900 C
[AD-747002] 03 p0316 N73-12575
Oxidation resistance of capsule materials for cobalt 60 power and heat source
[DP-1300] 05 p0498 N73-14057
Comparison of oxygen transport in polymonomethylsiloxane with properties of polydimethylsiloxane to determine degradation mechanisms in pigmented coatings
[AD-753410] 10 p1176 N73-19565
Transport properties of oxide scales formed on oxidation resistant alloys
14 p1676 N73-23604
Addition of chromium or aluminum to improve oxidation resistance of nickel and cobalt alloys
14 p1677 N73-23611
Oxidation resistant refractory metal alloys for use in high temperature environments
14 p1678 N73-23615
Borides, carbides, and nitrides of silicon oxidation resistant refractory compounds for use in gas turbines and reentry vehicles
14 p1678 N73-23616
Methods of oxidation and corrosion resistance in refractory metal alloys used in gas turbine engines
14 p1678 N73-23617
NATO national reports on high temperature corrosion of aerospace alloys
14 p1678 N73-23618
High strength tungsten fiber reinforced oxidation resistant niobium alloy composites for use in gas turbine engines at 2000 F
[AD-757380] 14 p1678 N73-23620
Copper coating of welded aluminum spacecraft structures to resist oxidation and aid detection of incomplete penetration
[NASA-CR-124251] 15 p1791 N73-24515
Cyclic furnace tests of nickel-, cobalt-, and iron-base alloys oxidation resistance considering scale spalling
[NASA-TM-X-68252] 16 p1870 N73-25144
Oxidation resistance of selected mechanical carbons at 650 C in dry flowing air
[NASA-TN-D-7381] 21 p2562 N73-30539

**OXIDES**
NT ALUMINUM OXIDES
NT ANHYDRIDES
NT BARIUM OXIDES
NT BERYLLIUM OXIDES
NT BISMUTH OXIDES
NT BORON OXIDES
NT CALCIUM OXIDES
NT CARBON DIOXIDE
NT CARBON MONOXIDE
NT CERIUM OXIDES
NT CHROMIUM OXIDES
NT COBALT OXIDES
NT DIOXIDES
NT FLINT
NT GERMANIUM OXIDES
NT HAFNIUM OXIDES
NT HEAVY WATER
NT HEMATITE
NT HYDROGEN PEROXIDE
NT IRON OXIDES
NT LEAD OXIDES
NT LITHIUM OXIDES
NT MAGNESIUM OXIDES
NT MANGANESE OXIDES
NT METAL OXIDES
NT NEPHELITE
NT NICKEL OXIDES
NT NIOBATES
NT NIOBIUM OXIDES
NT NITRIC OXIDE
NT NITROGEN DIOXIDE
NT NITROGEN OXIDES
NT NITROGEN TETROXIDE
NT NITROUS OXIDES
NT PEROXIDES
NT PLUTONIUM OXIDES
NT PYROXENES
NT QUARTZ
NT RUTILE
NT SAPPHIRE
NT SCHEELITE
NT SILICON DIOXIDE
NT SILICON OXIDES
NT SULFUR OXIDES
NT TANTALUM OXIDES
NT THORIUM OXIDES
NT TIN OXIDES
NT TITANIUM OXIDES
NT URANIUM OXIDES
NT VANADIUM OXIDES
NT YTTRIUM OXIDES
NT ZINC OXIDES
NT ZIRCONIUM OXIDES
Fabrication and tests of polyphenylene oxide foam panels for application as reusable insulation with LH2 tanks
[NASA-CR-123955] 05 p0565 N73-14586
Time dependent edge-notch sensitivity of oxide and gamma dispersion strengthened nickel alloy sheets
[NASA-CR-121123] 06 p0725 N73-15919
Infrared spectra of aluminum, gallium, and indium suboxide vapors considering frequency oscillations in group 3 suboxides and molecular constants of boron oxide
[AD-752861] 09 p1000 N73-18164
Characteristics of gelled liquid hydrogen polyphenylene oxide foam open cell insulation
[NASA-CR-124114] 09 p1051 N73-18568
Transport properties of anodic oxides in metals
09 p1063 N73-18674
Magnetic properties of powdered samples of Dy2Ti2O7
[NASA-TM-X-68219] 12 p1428 N73-21575
Transport properties of oxide scales formed on oxidation resistant alloys
14 p1676 N73-23604
Environmental tests of strength and durability of transparent tin oxide and indium oxide films on glass
[AD-756558] 14 p1680 N73-23637
Growth of single crystals of rhenium and iridium dioxides
[NASA-CR-133213] 17 p2072 N73-26768
Modification and control of oxide structures on refractory metal alloys and compounds
[AD-761215] 18 p2162 N73-27464
Nationwide air pollutant trends for hydrocarbons, oxides, and particulates from 1940 to 1970
[AP-115] 18 p2171 N73-27537
Elastic properties of oxides and application for temperature compensated materials with large piezoelectric moduli
[AD-760766] 18 p2190 N73-27681
Handbook of phase diagrams of silicate and similar systems comprising oxides and fluorides - Vol. I
[TT-71-50040] 21 p2564 N73-30556
Effect of oxides on elastic properties of glasses
[AD-764080] 22 p2689 N73-31539
Utilization of lithium p-lithiphenoxide to prepare star polymers
[NASA-CASE-NPO-10998-1] 23 p2753 N73-32029
Synthesis of polycrystalline oxide ceramic laser rods
[AD-765345] 23 p2802 N73-32413
Application of protective layers of refractory oxides and carbide onto high strength fiber substrates
[NASA-CR-134466] 23 p2810 N73-32467
Interionic vibrations and glass transitions in ionic oxide metaphosphate glasses
[AD-765344] 23 p2811 N73-32478
Alumina silicate based composite materials for space shuttle heat shielding system
24 p2939 N73-33466
Refractory metal carbide/metal oxide composites for thermal insulation
[LA-5136] 24 p2943 N73-33504
Evaluation of process for burnable poison deposition on zirconium hydride fuel
[AI-AEC-13085] 24 p2955 N73-33606

**OXIDIZERS**
NT FLOX
NT LIQUID OXIDIZERS
NT LIQUID OXYGEN
NT ROCKET OXIDIZERS
Method of measuring amount of carbon monoxide by oxidizing agents to yield carbon dioxide for air pollution control
[NLL-RTS-7573] 11 p1274 N73-20340
Kinetics of afterburning process following injection of oxidizer into high temperature gas flow
[AD-756098] 14 p1719 N73-23951
Inorganic halogen oxidizer chemistry
[AD-760696] 18 p2114 N73-27092

**OXYGEN**
NT HIGH PRESSURE OXYGEN
NT LIQUID OXYGEN
NT OXYGEN ATOMS
NT OXYGEN ISOTOPES
NT OZONE
Excitation and deexcitation of vibration in gases by oxygen and nitrogen atoms in E region of earth atmosphere
[AD-745925] 01 p0054 N73-10437
Collisional deactivation rate constants for oxygen by minor atmospheric constituents and other gases
[DREV-TN-2010/72] 01 p0082 N73-10682
Rate coefficient data for recombination reaction hydrogen plus oxygen plus argon yields water and argon in mixtures behind incident shock waves
[NASA-TN-D-6990] 01 p0117 N73-10965
Distillation method for quantitative determination of oxygen solubility in sodium
[NLL-RISLEY-TR-2424-[9091.9F]]
02 p0136 N73-11105
Drift tube mass spectrometer for measuring reaction rate of uranium atoms and ions with O2 and N2
[AD-746272] 02 p0138 N73-11115

Low energy electron impact excitation and ionization rate coefficients for atmospheric nitrogen and oxygen
[AD-747244] 02 p0170 N73-11378

Heat regulation and adaptation of rats exposed to helium oxygen atmosphere
03 p0259 N73-12096

Determination of oxygen content of lunar samples obtained from Luna 16 flight by 14-MeV neutron activation analysis
[KFKI-72-25] 03 p0263 N73-12133

Chemical diffusion coefficient of oxygen in mixed niobates to determine feasibility of modifying oxide defect structures to enhance oxidation protection of elevated temperature materials
[AD-746834] 03 p0316 N73-12574

Absorption cross sections of Schumann-Runge bands of molecular oxygen
[A-107-1972] 04 p0385 N73-13127

Reaction of Fe-Ni-Cr alloys with oxygen-containing sodium
[IS-T-508] 04 p0433 N73-13534

Microwave probe studies on chemical additives behavior in nitrogen oxygen plasma
[AD-748469] 04 p0456 N73-13724

Solar flux effects on upper atmosphere oxygen photodissociation and heating rates
[AD-747777] 04 p0467 N73-13807

Tables on molecular oxygen absorption in schumann-runge band
[AERONOMICA-ACTA-A-107-PT-2]
05 p0506 N73-14114

Chemiluminescence of O plus NO2 in afterglow
[NASA-CR-130263] 05 p0539 N73-14383

Oxygen, carbon dioxide, nitrogen, and noble gases for environment suitable for humans
06 p0628 N73-15093

Oxygen, carbon monoxide, and fuel toxicity
06 p0628 N73-15101

Visual evoked responses from divers subjected to hyperbaric conditions simulating depths to 1200 feet breathing various gas mixtures
[AD-749325] 06 p0631 N73-15127

Oxygen content and hydrogen ion concentration in monkey blood after incapacitating ionizing radiation dosage
[AD-750681] 06 p0632 N73-15134

Behavior of enzyme activities in blood plasma after breathing hyperbaric oxygen
[DLR-FB-71-96] 06 p0635 N73-15163

Theoretical model of Raman rotational spectrum of gas mixture applied to air mixture of oxygen and nitrogen to determine temperature
[NASA-TN-D-7126] 06 p0679 N73-15525

Radiation and annealing studies on oxygen-doped and lithium diffused germanium
[CONF-720707-7] 06 p0699 N73-15696

Method for detecting oxygen in gas by thermoluminescence
[NASA-CASE-LAR-10668-1] 07 p0752 N73-16106

Tables of O2 absorption cross sections in Schumann-Runge band
[A-N-107-1972] 07 p0752 N73-16108

Oxygen concentration on boundary lubricating characteristics of unformulated C-ether using ball-on-disk sliding friction apparatus
[NASA-TN-D-7155] 07 p0811 N73-16578

Solid ceramic electrolyte system for measuring redox conditions in high temperature gas mixing
[NASA-TM-X-58105] 08 p0892 N73-17224

Electronic and ionic reactions in atmospheric gases
[AD-752582] 08 p0921 N73-17550

Effect of oxygen concentration on deformation of Ti-V alloys and on critical resolved shear stress of Ti-40V
[AD-752082] 08 p0933 N73-17642

Measurement of total oxidants in atmosphere using potassium iodide absorbing solutions
[LR140[AP]] 08 p0937 N73-17674

Cesium oxide/cesium solutions as sources of oxygen and cesium for improved thermionic converter performance
[NASA-CR-121119] 08 p0942 N73-17717

Synthesis of A to X bands of OH and a to X bands of O2 for studying electronic transitions, rational branch structure, and rotational transition probabilities
[DREV-TN-2012/72] 08 p0945 N73-17742

Absolute intensity, polarization, and relative line intensities of rotational Raman scattering spectra from nitrogen, oxygen, and carbon dioxide
[NASA-CR-121091] 08 p0946 N73-17746

Analysis of oxygen flow in steel pipelines to determine maximum permissible flow and effects of solid particles and restriction on safe flow rate to avoid ignition
[NASA-TT-F-14831] 09 p1016 N73-18290

Drag coefficients for Echo 1 and Explorer 24 spherical surfaces in atomic oxygen over energy range from 4 to 200 eV
[NASA-CR-2233] 10 p1192 N73-19697

Change in content of gases in blood when man is exposed to high ambient temperatures
11 p1245 N73-20105

Tables of absorption cross sections of molecular oxygen in Schumann-Runge bands
[AERONOMICA-ACTA-A-107-1972-V-1]
12 p1375 N73-21157

Tables of absorption cross sections of molecular oxygen in Schumann-Runge bands
[AERONOMICA-ACTA-A-107-1972-V-2]
12 p1375 N73-21158

Thermodynamics of oxygen solubility in lanthanum uranium oxide measured on solid state electrolytic cell
[KFK-1649] 12 p1376 N73-21163

Metallurgical reports on plasma jets, creep properties of nickel alloys, oxygen and nitrogen interactions with metals, and Mossbauer effect as applied to diffusion mechanisms
[JPRS-58508] 12 p1412 N73-21445

Kinetics and thermodynamics of oxygen conversion from gas to metal phase in tungsten and molybdenum
12 p1412 N73-21446

Variations of relative abundances of helium, carbon, nitrogen, oxygen, and iron-group nuclei in solar cosmic rays and their relationship to solar particle acceleration
[NASA-TM-X-66228] 12 p1445 N73-21706

Atomic oxygen hydrogen reaction with acetylene, and gas discharge shock tube design
13 p1488 N73-22060

Utilization of millimeter wave radiation from atmospheric oxygen to provide vertical sensing information to satellite-borne radiometer
[NASA-CR-2229] 13 p1530 N73-22396

Absolute cross sections for rotational Raman scattering derived for nitrogen and oxygen from near UV to infrared
[AD-756808] 13 p1566 N73-22695

Design and analysis of low speed hydrogen and oxygen inducers applicable to space tugs
[NASA-CR-124233] 13 p1570 N73-22722

Effectiveness of phased dilution compared to current demand diluter oxygen delivery system
14 p1611 N73-23065

Bibliography of kinetic data in gas phase reactions of nitrogen, oxygen, and nitrogen oxides
[NBS-SP-371] 14 p1616 N73-23094

Experimental facility for measuring rotational Raman scattering cross sections of nitrogen and oxygen at 10.6 microns
[AD-757111] 14 p1617 N73-23098

Auger spectroscopy of oxygen and sulfur interactions with clean iron surface and rubbing contact effect on interactions
[NASA-TN-D-7283] 14 p1670 N73-23555

Oxygen diffusion in gettered tantalum alloy heat pipes at startup
[NASA-TM-X-2793] 14 p1675 N73-23589

Thermodynamic stability diagrams of high temperature O2 corrosion reactions
14 p1676 N73-23602

Data tables on nonmetallic materials for offgassing CO and hydrocarbons in 5 psia O2
[NASA-TM-X-64745] 14 p1680 N73-23631

Role of metastable atoms [D] in thermospheric heating
[NASA-TT-F-14901] 14 p1705 N73-23832

Mathematical models for determining transport properties and dissociation equilibrium of N2 and O2 in high temperature air
[ESDU-00.01.07-AMEND-A] 14 p1718 N73-23937

Oxygen gas production during stand and discharge in silver zinc batteries
[NASA-CR-128933] 15 p1738 N73-24087

Low cost oxygen electrode for phosphoric acid fuel cell
[AD-758179] 15 p1739 N73-24095

Emission rate constant for infrared chemiluminescent reaction of oxygen with nitric oxide
[NASA-CR-132157] 15 p1747 N73-24158

Electron collision processes in atmospheric gases of oxygen, carbon monoxide, and nitrogen oxide
[AD-757841] 15 p1748 N73-24170

Effects of O2 on mechanical properties, elastic limit, and tension resistance of nonferrous metals
[EURISOTOP-59] 15 p1798 N73-24577

Fire suppression and extinguishment techniques in oxygen enriched atmospheres
[NASA-CR-121150] 15 p1842 N73-24926

Electron beam analysis of molecular and atomic oxygen properties
[AD-759196] 16 p1872 N73-25159

Optical and microwave measurements of reaction kinetics behind shock waves
[AD-757230] 16 p1890 N73-25293

Two rocket measurements of atmospheric oxygen concentration during twilight
16 p1895 N73-25331

Adsorption, surface reaction, and recombination of atomic oxygen related to dual air density explorer satellites
[NASA-CR-2271] 16 p1906 N73-25421

Four channel radiometer for remote sensing of microwave emission from atmospheric oxygen and water vapor
[AD-759535] 16 p1939 N73-25696

Effect of oxygen on corrosion of niobium and tantalum by liquid lithium at 600 C
[ORNL-TM-4069] 17 p2045 N73-26547

Radical species concentration profiles for methane-oxygen-argon flame
[BM-RI-7766] 18 p2206 N73-27803

Cross section data for collision processes between molecular oxygen and electrons
[NASA-TT-F-15011] 19 p2354 N73-28934

Chemical reactivity of hydrogen, nitrogen, and oxygen below 100 K
[NASA-CR-133654] 20 p2456 N73-29742

Extrapolation of thermophysical properties data for oxygen to high pressures at low temperatures
[NASA-CR-133858] 21 p2506 N73-30109

Observation of oxide particles below apparent oxygen solubility limit in tantalum
[NASA-TM-X-2889] 21 p2558 N73-30509

Oxygen exchange between solid electrolyte and platinum electrode in flowing gas
22 p2617 N73-30972

Interaction of titanium nitrides with oxygen and carbon dioxide
[NASA-TT-F-15108] 22 p2625 N73-31035

Vibrational temperature and density of molecular oxygen component in expansion tube
[NASA-TN-D-7273] 22 p2653 N73-31249

Gas sensor for detecting H2 in air and N2, and O2 in N2
[NASA-CR-133891] 22 p2674 N73-31416

Oxygen index method for evaluating flammability of organic polymeric materials
[DSL-REPT-561] 22 p2729 N73-31836

Cross sections for reactions of atmospheric ions with atomic oxygen
[AD-765333] 23 p2789 N73-32316

Oxygen grain boundary diffusion and grain growth in pure dense MgO
[NASA-CR-135719] 23 p2810 N73-32466

Cross section for collision processes between molecular oxygen and electron with collision energy below 100 eV
[NASA-TT-F-15048] 23 p2821 N73-32550

Direct charge state measurements of low energy solar carbon and oxygen in interplanetary space
[TR-73-132] 23 p2834 N73-32648

Photographic recording of dynamic behavior of flames in explosive gases caused by ignition of equimolar acetylene-oxygen mixture
[NASA-CR-135672] 23 p2856 N73-32825

Carbon-oxygen fuel cell of solid carbon anode, nickel gauze cathode, and flamed electrolytes
24 p2880 N73-33001

Biological evaluation of influence of helium-oxygen atmosphere on culture of mammalian cells
24 p2883 N73-33024

Flammability of engineering materials in gaseous oxygen environments and applicability to Skylab program
[NASA-TM-X-64783] 24 p2891 N73-33081

OXYGEN ANALYZERS

Model 735 dissolved oxygen analyzer for continuous measurement of dissolved oxygen concentration in shallow fresh water
[NOAA-IFS-73003] 01 p0057 N73-10465

MINOS DOM oxygen monitor for measuring dissolved oxygen in sea water to depths of 3000 meters
[NOAA-IFS-73004] 01 p0057 N73-10466

Dissolved oxygen analyzer for measuring dissolved oxygen concentration in industrial water systems
[NOAA-IFS-73005] 01 p0057 N73-10467

Performance evaluation and operating characteristics of different dissolved oxygen analyzers
[RN-1007] 02 p0171 N73-11385

OXYGEN ATOMS

Mach-Zehnder interferometric determination of nitrogen and oxygen atom specific refractivities during atmospheric entry
[AD-745132] 02 p0138 N73-11114

Low temperature addition reactions of hydrogen and oxygen atoms with chemical compounds through creation of secondary valence
[NASA-TT-F-14643] 06 p0703 N73-15729

Rocket and satellite instrument for simulatenous measurements of total mass density and number density of atomic oxygen in lower thermosphere
[AD-751468] 07 p0795 N73-16464

Reaction kinetics in vibrationally excited nitrogen quenching by atomic oxygen
[AD-752542] 08 p0946 N73-17751

Vibrationally excited carbon monoxide from reaction of oxygen with acetylene, methylacetylene, and methane
[DREV-TN-2051/72] 11 p1252 N73-20160

Excitation and deexcitation of vibration in gases by nitrogen and oxygen atoms in upper atmosphere
[AD-757050] 14 p1617 N73-23099

Differential scattering of hydrogen and oxygen atoms in methane molecules
[NASA-TT-F-14898] 14 p1694 N73-23751

Electron beam analysis of molecular and atomic oxygen properties
[AD-759196] 16 p1872 N73-25159

Atomic oxygen emission line in high resolution spectra of zenith day airglow
23 p2778 N73-32214
Ultraviolet spectrometer data on Mars atomic oxygen emission and distribution
23 p2841 N73-32703
OXYGEN BREATHING
Evaluation of hazardous conditions created by facial hair on aircrew personnel wearing oxygen masks
[AD-754075] 12 p1375 N73-21154
Oxygen breathing effects on human blood circulation and flight personnel fitness test
13 p1480 N73-21993
Oxygen breathing in decompression sickness and remedial recompression of human beings
[DRIC-TRANS-3095] 17 p1988 N73-26069
Relation between hyperbaric oxygenation and functional activity of differentiated brain with respect ot glutamic acid metabolism
19 p2227 N73-27960
Pure oxygen and oxygen/nitrogen atmospheres for preventing decompression disease in astronauts
20 p2366 N73-29029
OXYGEN COMPOUNDS
Measurement of carbonyls and noncarbonyl oxygenates in exhaust from gasoline fuels
[BM-RI-7675] 02 p0137 N73-11110
OXYGEN CONSUMPTION
Effects of hyperoxia on sulfhydryl concentration of Escherichia coli
[AD-746193] 02 p0134 N73-11087
Correlation of assessed maximum oxygen intake with predicted performance in running events
[AD-746867] 04 p0380 N73-13093
Work, heat, and oxygen cost of various activities of man
06 p0629 N73-15109
Correlation of physical activity and oxygen consumption between man and mouse
[FOA-1-B-1233-A5] 08 p0877 N73-17108
Changes in oxygen consumption in rats after inoculation with polymer combustion products
10 p1116 N73-19096
Hashish smoking effects on human oxygen consumption during physical stress and safe driving ability
12 p1370 N73-21115
Exercise effects on human heart rate and oxygen uptake
20 p2365 N73-29020
Treadmill running effect on human oxygen consumption
24 p2882 N73-33013
OXYGEN DEFICIENCY
U HYPOXIA
OXYGEN DETECTORS
U OXYGEN ANALYZERS
OXYGEN FLUORIDES
Evaluation of boundary cooled rocket engines for development of space storable propellant combination of oxygen difluoride/diborane
[NASA-CR-129260] 03 p0350 N73-12855
OXYGEN ISOTOPES
Separation of short half life O-15 and N-13 isotopes from alkali metals, steels, copper, and indium by gamma activation analysis
[CONF-721069-24] 18 p2160 N73-27453
OXYGEN MASKS
Color photographic system using grid projector and telecentric lenses for recording contours of human face for aircrew oxygen mask fitting
[RAE-TR-71184] 07 p0750 N73-16099
Evaluation of hazardous conditions created by facial hair on aircrew personnel wearing oxygen masks
[AD-754075] 12 p1375 N73-21154
OXYGEN METABOLISM
Oxygen redox processes in blood coagulation mechanism
03 p0257 N73-12079
Metabolic implications in hyperbaric oxygen systems
[AD-749381] 05 p0504 N73-14106
Automatic device for measuring human metabolic oxygen rate and breathing dynamics
[NASA-CASE-MFS-21415-1] 06 p0635 N73-15156
Human oxygen metabolism and pulmonary functions during hypodynamic water immersion
10 p1114 N73-19082
Transverse acceleration effects on human respiratory rate and oxygen metabolism
10 p1114 N73-19084
Human nitrogen and water/salt metabolisms in controlled regenerative atmosphere
10 p1115 N73-19089
Helium/oxygen breathing effects on rat gas exchange and musculoskeletal heat control
10 p1115 N73-19093
Physiological effects of argon/oxygen breathing on rats noting carbon dioxide level
10 p1116 N73-19094
Design and performance of metabolic gas analyzer using mass spectrometer and digital data printout
[NASA-CR-128842] 10 p1124 N73-19160
Pressure chambers for testing effect of oxygen inspiration on fatigue during flight
[JPRS-59041] 14 p1610 N73-23051
OXYGEN PRODUCTION
Photodissociative excitation of carbon dioxide as source of atomic oxygen in Martian atmosphere
[NASA-TM-X-66088] 02 p0229 N73-11856
Long term performance test on electrolytic oxygen generator for manned test chamber
[NASA-CR-128687] 06 p0635 N73-15160
Effect of toxic substances on algae by observing photosynthesis determined by oxygen production of algae
[DRIC-TRANS-2991] 10 p1121 N73-19139
Electrochemical system with solid electrolyte for regenerating oxygen from CO2 and H2O
24 p2882 N73-33015
OXYGEN RECOMBINATION
Radiative cascade limit in recombination oxygen plasma
[AD-759010] 17 p2070 N73-26747
OXYGEN REGULATORS
Transistorized feedback servomechanism design for cryogenic oxygen flow control
[NASA-TM-X-68234] 15 p1759 N73-24258
OXYGEN SENSORS
U OXYGEN ANALYZERS
OXYGEN SPECTRA
Attenuation and phase dispersion of radio wave in atmosphere due to oxygen microwave spectrum
17 p1994 N73-26126
OXYGEN SUPPLY EQUIPMENT
NT OXYGEN MASKS
Solid polymer for water electrolysis system to generate oxygen and hydrogen in manned space station
[NASA-CR-112183] 04 p0375 N73-13052
Compatibility and safety of materials for liquid and gaseous oxygen systems
[NASA-CR-120922-VOL-1] 05 p0579 N73-14716
Operational hazards and safety regulations for liquid and gaseous oxygen system handling
[NASA-CR-120922-VOL-2] 05 p0580 N73-14717
Maintenance programs for oxygen systems to prevent accidents
[NASA-CR-120922-VOL-3] 05 p0580 N73-14718
Personnel protection and emergencies handling for oxygen systems
[NASA-CR-120922-VOL-4] 05 p0580 N73-14719
Cleaning processes and postcleaning inspection procedures for meeting oxygen system cleaning requirements
[NASA-SP-3072] 06 p0634 N73-15155
Design and performance of prototype nitrogen/oxygen supply unit using water/hydrazine electrolysis to provide cabin leakage makeup in manned spacecraft
[NASA-CR-128688] 06 p0635 N73-15159
Long term performance test on electrolytic oxygen generator for manned test chamber
[NASA-CR-128687] 06 p0635 N73-15160
Cost analysis of oxygen supply equipment and recovery systems for orbital space stations
[NASA-CR-124175] 12 p1373 N73-21137
Safety hazards related to ignition and combustion in oxygen systems
[NASA-TM-X-68223] 12 p1464 N73-21861
Breathing apparatus for parachutists
[AD-756554] 15 p1745 N73-24141
Electrochemical process for recovery of oxygen from atmospheres of manned space capsules
[NASA-CR-114573] 16 p1869 N73-25130
Cost analysis of oxygen recovery subsystems for life support systems
[NASA-CR-124304] 18 p2112 N73-27075
Investigation of backfires and explosions occuring in vacuum pumps of oxygen test stands
[AD-763370] 21 p2554 N73-30474
Cryogenic insulation of liquid oxygen dewars for aircraft pilot breathing masks
[AD-763325] 22 p2624 N73-31026
OXYGEN SYSTEMS
U OXYGEN SUPPLY EQUIPMENT
OXYGEN TENSION
NT HYPOXEMIA
Effects of atmospheric oxygen concentration on Chlorella photosynthesis
14 p1608 N73-23032
Cone model for oxygen diffusion in brain considering spatial tissue/capillary permeability
[RAE-LIB-TRANS-1663] 17 p1987 N73-26060
OXYGEN TOXICITY
U HYPEROXIA
OXYGENATION
Electromotive force measurements for determining oxygen concentration in liquid sodium
[NLL-CE-TRANS-6073-[9022.09]]
15 p1746 N73-24148
Cone model for oxygen diffusion in brain considering spatial tissue/capillary permeability
[RAE-LIB-TRANS-1663] 17 p1987 N73-26060
Activation analysis using charged particles and gamma photons for determining oxygen in nonferrous metals
[EURISOTOP-74] 17 p2065 N73-26704
Chemiluminescent emissions from trimethylaluminium, iron pentacarbonyl, and lead tetraethyl upon reaction with oxygen
[AD-762317] 19 p2233 N73-28007
Reaction kinetics and solid solubility of oxygen in molybdenum
22 p2624 N73-31027
OZONE
Aerological data from balloon and rocket flights for Japan and its vicinity, tables for Dec. 1971, and ozone data, tables for Jan. - Dec. 1971
01 p0073 N73-10603
Balloon measurements of aerosol and ozone in Arctic stratosphere
[AD-747256] 02 p0169 N73-11374
Mathematical inversion of light scattering data to obtain atmospheric ozone profile
02 p0196 N73-11586
Inferred ozone profiles from ultraviolet earth radiance data from Nimbus 4
[NASA-TM-X-66108] 03 p0294 N73-12397
Comparison of satellite ozone contours during 1965 geomagnetic storm and L-shell parameters
[WRE-TN-80[WR/D]] 03 p0296 N73-12412
Tabulated data on atmospheric ozone density at UCCLE, Belgium, for 1969
[QR-3] 05 p0539 N73-14386
Ultraviolet flash photolysis of ozone and reaction of O[1 D] with H2O
[DREV-TN-2026/72] 06 p0638 N73-15176
Using simultaneous measurements of ozone profile and solar extinction to obtain absorption coefficient for calculating ozone distribution
[AD-750404] 06 p0668 N73-15429
Ozone tables, ozonagrams, and ascent tables for aerological ozone soundings conducted at Hohenpeissenberg, West Germany
[AD-750166] 06 p0670 N73-15446
Cosmos 121 measurements of total ozone content of earth atmosphere
[JPRS-57976] 07 p0791 N73-16430
Vertical distribution of atmospheric water vapor and ozone over District of Columbia during 1969 and 1970
[AD-751535] 07 p0795 N73-16465
Atmospheric circulation and temperature effects on stratospheric ozone during winter storm period
[AD-751211] 07 p0797 N73-16479
Ozone reaction with mercaptane for elimination of exhaust gas pollution in air
08 p0883 N73-17152
Tabulated data on atmospheric ozone density at Uccle, Belgium for 1969
08 p0918 N73-17522
Approximate values of intensity of natural ultraviolet radiation for different amounts of atmospheric ozone
[AD-752115] 08 p0921 N73-17549
Measurement of total oxidants in atmosphere using potassium iodide absorbing solutions
[LR140[AP]] 08 p0937 N73-17674
Atmospheric ozone as circulation tracer in upper troposphere and lower stratosphere
08 p0972 N73-17940
Photolysis of ozone at 3130 A in presence of excess of nitrogen oxide
[NASA-CR-130794] 09 p1028 N73-18388
Rocket measurements of ozone distribution under varying latitudes and seasonal conditions in stratosphere
[NASA-TM-X-66192] 09 p1028 N73-18391
Analysis of cloud formations, ozone distribution, and meteorological data from Nimbus 4 satellite observations
[NASA-TM-X-66190] 09 p1028 N73-18392
Steady illumination photolysis of ionospheric ozone in near ultraviolet
[NASA-CR-130830] 09 p1029 N73-18399
Ozone and nonreactive gas calibration of mass spectrometer with modified helium-cooled ion sources
[BMBW-FBW-72-32] 09 p1034 N73-18440
Development of technique for inferring atmospheric ozone information from satellite nadir measurements
[NASA-TR-R-399] 10 p1154 N73-19386
Comparison between measured transmission and emission spectra and calculated spectra in upper atmosphere ozone region
[BMFT-FBW-73-01] 11 p1285 N73-20429
Stratospheric photochemical reactions of ozone in relation to climatology and supersonic transport pollution
[NOAA-TM-NESS-47] 12 p1422 N73-21526
CSTR system for measuring ozone reactions in lower atmosphere
13 p1514 N73-22269
Ozone and point discharge measurements under thunderclouds in New Mexico
[AD-758130] 14 p1665 N73-23515
Threat of stratospheric ozone nonequilibrium by SST nitric oxide exhaust gases
[AD-757059] 14 p1719 N73-23949
Nimbus 3 infrared spectrometric data on global ozone distribution in correlation with atmospheric circulation
[COO-1340-30] 15 p1781 N73-24435

Observations of atmospheric ozone at 110.836 GHz
[AD-758819] 15 p1784 N73-24465
Global distribution of total ozone as determined by Nimbus 3 satellite infrared interferometer spectrometer
16 p1895 N73-25326
Mathematical models for studying atmospheric heating by ozone absorption of sunlight
[NASA-CR-132778] 17 p2024 N73-26382
Difficulty and reliability of simultaneous measurement of ozone and nitric oxide
18 p2132 N73-27228
Photochemical mechanisms of ozone and energy budget in atmosphere between 10 and 100 km
18 p2133 N73-27233
Quantum yields of O[D-1] in ozone photolysis near 310 nm
[NASA-CR-122206] 18 p2142 N73-27311
Nitrogen oxides from supersonic transports affecting stratospheric ozone depletion on solar ultraviolet radiation
[AD-761179] 18 p2195 N73-27722
Aerological ozone sounding
[AD-762291] 19 p2297 N73-28469
Photochemical reaction rate constant for hydroxyl radical with ozone in stratosphere
[AD-762195] 20 p2374 N73-29076
Atmospheric ozone transport by atmospheric circulation and vertical air currents
20 p2443 N73-29627
Satellite ozone observations on 17-18 June 1966 between 20 deg south latitude and 60 deg north latitude
20 p2447 N73-29663
Spatial normalized correlation function of total atmospheric ozone content
20 p2448 N73-29669
Nitrogen and ozone kinetics in stratosphere
[AERONOMICA-ACTA-A-118] 21 p2537 N73-30345
Comparison between measured transmission and emission spectra and calculated spectra in 9.6 micron region of ozone
[NASA-TT-F-15110] 22 p2665 N73-31356
Conceptual work on 125 mm ultraviolet spectrometer for measuring ozone
[NASA-CR-132266] 22 p2673 N73-31411
Photochemical ozone theory and microwave spectroscopy using microwave radiometry for remotely verifying mesospheric ozone diurnal variations
[AD-764705] 23 p2789 N73-32314
Seasonal ozone variations in ultraviolet spectra of Mars atmosphere
23 p2841 N73-32704

**OZONOMETRY**
Analysis of statistical characteristics of ozonosphere to provide additional information in satellite ozonometry and interpretation of satellite results
20 p2400 N73-29287

**OZONOSPHERE**
Analysis of statistical characteristics of ozonosphere to provide additional information in satellite ozonometry and interpretation of satellite results
20 p2400 N73-29287

# P

**P WAVES**
Method for whitening spectra of teleseismic P waves for determining event depths
[AD-750781] 06 p0671 N73-15455
**P-I-N DIODES**
U DIODES
U P-I-N JUNCTIONS
**P-I-N JUNCTIONS**
Computerized design and performance of planar germanium P-I-N thermophotovoltaic cells
[AD-748895] 04 p0376 N73-13063
Time discrimination in temporal information sampling at output of planar germanium detector in gamma ray spectrometry
[NAA-SR-MEMO-6728] 07 p0824 N73-16680
Time discrimination in temporal information sampling at output of planar germanium detector in gamma ray spectrometry
[CEA-R-4355] 09 p1069 N73-18719
Conduction processes in field driven semiconductor p-i-n diodes
12 p1437 N73-21643
Low injection reverse recovery switching phenomena in lithium-drifted silicon PIN diodes
13 p1499 N73-22148
**P-N JUNCTIONS**
Electrical properties of p-n junctions formed by ion implantation into GaAs and [Ga,In]As
[NASA-CR-112200] 01 p0087 N73-10717
Experimental characterization of abrupt junctions in avalanche mode
[LAAS-PUBL-939] 04 p0399 N73-13246
Numerical analysis of signal trapping effects in neutron irradiated p-n junctions as function of frequency
[SC-DC-72-1237] 05 p0587 N73-14772
Application of gas transport method for analyzing p-n junction in cadmium selenide monocrystal
[AD-750506] 06 p0711 N73-15800
Computer program for p-n junction diode simulation
08 p0887 N73-17186
Electron- and neutron-induced defects in silicon p-n junctions
[AD-754905] 11 p1332 N73-20812
Comparison of detectivities of p-n junction diode and Schottky internal photoemission diode under background-limited conditions
[AD-757873] 15 p1757 N73-24243
Graded band gap p-n junction gallium arsenide/gallium aluminum arsenide solar cell
[NASA-CASE-LAR-11174-1] 17 p1985 N73-26047
Influence of silicon particle deposition on volt-ampere characteristics of p-n junctions
18 p2186 N73-27652
Resin for protecting p-n semiconductor junction surface
[NASA-CASE-ERC-10339-1] 21 p2561 N73-30532
High field emission and capture of electrons and holes at zinc centers in N-P and P-N junctions
24 p2966 N73-33705
**P-TYPE SEMICONDUCTORS**
Energy distributions of field-emitted electrons from p-type silicon surfaces
[AD-747067] 03 p0346 N73-12825
Spectral and temperature characteristics of natural photoconductivity in p-type GaAs
[AD-750696] 06 p0709 N73-15790
Electromagnetic wave interactions in p type ferromagnetic semiconductors
10 p1198 N73-19751
Current-voltage, load, and spectral characteristics of p- and n-type GaAs
[NASA-TT-F-14859] 11 p1330 N73-20793
Effects of proton bombardment on p- and n-type PbSnTe thin films
[AD-756542] 13 p1567 N73-22696
Charge carrier transport properties in p-type germanium semiconductors
[AD-757232] 14 p1698 N73-23783
**P-84 AIRCRAFT**
U JET PROVOST AIRCRAFT
**P-3 AIRCRAFT**
Analysis of flight crew errors contributing to aircraft accidents on P-3 and F-4 aircraft for improved air safety
[AD-764868] 23 p2746 N73-31979
**P-531 HELICOPTER**
Measurement and effects of triaxial vibration on pilots in P-531 [Scout] helicopter under different flight conditions
[ISVR-TR-58] 07 p0751 N73-16100
**P-1127 AIRCRAFT**
Flight tests to determine longitudinal aerodynamic parameters of P-1127 aircraft with vectored thrust control
[NASA-TN-D-7296] 15 p1734 N73-24066
**PACIFIC ISLANDS**
NT JAPAN
NT NEW GUINEA [ISLAND]
NT PHILIPPINES
Meteorological charts and tables on wind altitude over French Polynesia
[MN-MONO-85] 01 p0073 N73-10602
Simple method for prediction of lowest observed frequency of high frequency propagation paths between Pacific Islands
[AD-757343] 14 p1636 N73-23266
**PACIFIC OCEAN**
Geological charts of Ontong Java Plateau including bathymetric, sedimentary isochron, and structural contour
[AD-743900] 01 p0052 N73-10423
Geologic structure of Ontong Java Plateau determined from continuous reflection profiles taken between 1966 and 1971
[AD-743899] 01 p0052 N73-10425
First-order analyses of wind and current time series from Totem buoy off Oregon coast during 1970
[AD-746832] 02 p0206 N73-11668
Statistical analysis of geography and seasonal variation effects on intensification of tropical cyclones over western North Pacific Ocean
[AD-746130] 02 p0206 N73-11669
Regression analysis of tropical storm and typhoon speed characteristics after recurvature in western North Pacific Ocean
[AD-746880] 02 p0206 N73-11672
Sources and dispersal patterns of suspended sediments in nearshore surface waters of Northeast Pacific Ocean and Hawaiian Islands based on ERTS-1 imagery
[E72-10271] 03 p0291 N73-12370
Hydrographic data from Oregon waters in 1971
[AD-746515] 03 p0297 N73-12421
Hydrographic survey data for Southern Pacific Ocean between Australia and Antarctica
[AD-747792] 04 p0417 N73-13404
Electrical conductivity of ocean basement determined from measurements of geomagnetic time variations on sea floor off Southern California
[AD-749931] 06 p0668 N73-15431
Geothermal data from deep water and bottom sediment measurements in Atlantic and Pacific Oceans
[AD-749983] 06 p0669 N73-15441
Oceanographic equipment and ocean bottom data resulting from Pacific cruise of Iguana
[AD-750679] 06 p0671 N73-15459
Mean monthly hurricane heat potential and sea surface temperature changes associated with storm passage for North Atlantic and North Pacific Oceans
[AD-751590] 07 p0790 N73-16429
Bathymetry, magnetic, and gravity data for North Pacific Ocean areas collected between 1961 and 1970 - Technical Report 50
[NOAA-TR-NOS-50] 07 p0792 N73-16444
Bathymetry, magnetic, and gravity data for North Pacific Ocean areas collected between 1961 and 1970 - Technical Report 49
[NOAA-TR-NOS-49] 07 p0793 N73-16445
Mean monthly winds of upper troposphere for 200, 250, and 300 mb levels over central and eastern Pacific
[AD-751579] 07 p0816 N73-16620
Determination of values for roughness parameters of isotherms in Pacific thermocline using thermistor chain
07 p0858 N73-16954
Dispersal patterns of suspended particles in nearshore surface waters of northeast Pacific Ocean and Hawaiian Islands
[E73-10314] 09 p1023 N73-18346
Bathymetry, magnetic, and gravity data collected between 1961 and 1969 in North Central Pacific
[NOAA-TR-NOS-51] 09 p1029 N73-18401
Bathymetric survey of Pacific Ocean area for oceanographic data to support underwater acoustic experiment
[AD-752840] 09 p1032 N73-18428
Computer procedure for analysis of maritime sea-level pressure and wind fields
[NASA-TM-X-69135] 09 p1058 N73-18630
Characteristics of wind, pressure, cloud, and precipitation fields in intratropical zone of convergence
09 p1059 N73-18633
Revision of tropical cyclone climatology by satellite data for northern Pacific Ocean
[AD-753584] 09 p1061 N73-18658
Global response of atmosphere to persistent anomalous pool of warm sea surface temperatures in extratropical Pacific Ocean
[NASA-CR-130179] 10 p1154 N73-19391
Tidal and lunar data for Point Mugu, San Nicholas Island, and Barking Sands areas for 1973
[AD-752892] 10 p1156 N73-19407
Optical properties of sea water in Atlantic, Pacific, and Caribbean
[AD-753474] 11 p1290 N73-20470
Long term meteorological study of intensity and movement of tropical cyclones and typhoons in western North Pacific
[AD-754349] 11 p1315 N73-20676
Acquisition and analysis of coastal ground truth data in pacific water off California for correlation with ERTS-1 imagery
[E73-10482] 12 p1396 N73-21319
Sources and dispersal patterns of suspended particulates in nearshore surface waters of northeastern Pacific Ocean and Hawaii
[E73-10487] 12 p1396 N73-21323
Computer printouts of oceanographic data collected in North Pacific between 1961 and 1970
[NOAA-TR-NOS-47] 15 p1780 N73-24429
PAPA Ocean Weather Station measurements of wind and wave condition in north Pacific Ocean
[AD-757982] 15 p1806 N73-24638
Sources and dispersal patterns of suspended particles in nearshore surface waters of San Francisco Bay and Gulf of Farallones
[E73-10788] 18 p2137 N73-27264
Atmospheric wind fields and circulation effects on Pacific Ocean hydrologic regime
[TT-70-50129] 18 p2171 N73-27538
Typhoon and tropical storm intensity forecasts in western North Pacific Ocean using statistical regression analysis
[AD-761379] 18 p2174 N73-27561
Analog scheme for analyzing meteorological parameters to determine their predictive value for forecasting intensity changes in western North Pacific tropical cyclones
[AD-761726] 19 p2316 N73-28625
North Pacific tropical vector mean charts
[AD-762044] 19 p2316 N73-28628
Regionalization of lithosphere and asthenosphere of Pacific Ocean from Rayleigh wave phase velocity dispersion curves
20 p2390 N73-29197
Application of infrared data from satellites for use in field of fishery oceanography in Pacific Ocean
[AD-763350] 21 p2542 N73-30380
Oceanographic survey of eastern tropical Pacific Ocean to determine oxygen content, salinity, temperature distribution, and acceleration potential
[NOAA-NMFS-CIRC-330] 22 p2656 N73-31279
Airborne measurements of photochemical pollution in California and adjacent waters of Pacific Ocean
[NASA-TM-X-69504] 22 p2694 N73-31581

Skylab S-193 RADSCAT measurements of Hurricane Ava
[E73-11062] 23 p2781 N73-32238
Multispectral band scanner reconnaissance of Pacific Ocean off Oregon coast
[AD-763428] 23 p2789 N73-32311
Sources and dispersal patterns of suspended particles in nearshore surface waters of northeast Pacific Ocean and seasonal variation in snow cover in Sierra Nevada Mountains
[E73-11099] 24 p2914 N73-33256

**PACKAGES**
NT APOLLO LUNAR SURFACE EXPERIMENTS PACKAGE
NT EREP
NT INSTRUMENT PACKAGES

**PACKAGING**
NT ELECTRONIC PACKAGING
Development of concepts and procedures for preparation of loads for airdrop to reduce time required and increase reliability of operation
[AD-750705] 05 p0612 N73-14976
Feasibility determination for polyethylene packaging of drugs stocked in spacecraft pharmacies
11 p1246 N73-20114
Performance of shipping container for electron tube in shock and vibration tests
[AD-754926] 11 p1301 N73-20558
Electrically conductive wire storage in plastic capsule that allows for unfolding
[NASA-CASE-LAR-10168-1] 13 p1499 N73-22151
Development and characteristics of system for skin packaging articles using thermoplastic film heating and vacuum operated equipment
[NASA-CASE-MFS-20855] 18 p2154 N73-27405

**PACKING DENSITY**
Large scale integrated circuits used for designing 128 words x 72 bits/word memory
[REPT-1404] 03 p0272 N73-12205
Planar Gunn devices in dipole domain mode for high speed logic circuits in PCM equipment, noting thermal resistances and packing density
[FTZ-A-474-TBR-3] 22 p2643 N73-31183

**PACKINGS (SEALS)**
Computer program to determine compressible fluid flow with friction across face seals and through narrow solts
[NASA-TN-D-6787] 07 p0803 N73-16518
Evaluation of polyimide second stage rod seals at high temperatures to determine suitability for application to aircraft systems
[NASA-CR-121124] 08 p0927 N73-17592
Operating characteristics and service life tests of bypass control valve seal and bearing for nuclear engine for rocket vehicles
[NASA-CR-132226] 15 p1792 N73-24526
Design, fabrication, and evaluation of helicopter transmission seals using dual element split ring and circumferential seal configurations
[NASA-CR-120983] 17 p2037 N73-26481
Design and development of gas-film seal using shrouded Rayleigh step lift pads at primary sealing face of gas turbine engine
[NASA-CR-121177] 18 p2155 N73-27415
Irradiation of pyrolytic carbon sealers at high temperatures to determine effects on growth rate and service life
[CONF-730601-5] 21 p2563 N73-30543

**PAINTS**
Application of paints and varnishes as protective coatings for industrial structures and equipment against radiation damage
[AD-745701] 01 p0071 N73-10582
Inorganic binders for utilizing high reflectance of $BaSO_4$ in paints
[NASA-TM-X-66082] 02 p0191 N73-11549
Hydrogen embrittlement of cadmium coated steels due to paint stripping
[AD-747634] 03 p0319 N73-12599
Analysis of temperature sensitive paints to determine validity of coating technique and development of methods for predicting areas of high thermal gradients
[AD-749582] 04 p0409 N73-13331
X ray fluorescence analysis for determining lead content of paint on pencils in Goddard supply system
08 p0876 N73-17097
Comparison of oxygen transport in polymonomethylsiloxane with properties of polydimethylsiloxane to determine degradation mechanisms in pigmented coatings
[AD-753410] 10 p1176 N73-19565
Spectroscopic and chromatographic analysis of outgassing contaminants in potting compound and paint
[NASA-CR-124227] 13 p1488 N73-22061
Electrophoretic flow coating technique for heating oil storage tanks
[NLL-OA-TRANS-833-[6196.3]] 16 p1870 N73-25139
Reduction of photographic heat transfer rate data at wind tunnel test facility
[AD-762928] 20 p2420 N73-29447
Airfield runway marking paint superior to paint presently used
[FAA-RD-73-23] 21 p2520 N73-30213

**PAIR PRODUCTION**
Total cross sections for electron positron annihilation producing hadron pair
[NOTA-INTERNA-420] 18 p2181 N73-27613

**PAKISTAN**
NT WEST PAKISTAN
High altitude meteorological data measured at Sonmiani, Pakistan 1964-1970
[W-119] 18 p2172 N73-27543
Identification of geomorphic features related to known porphyry copper deposit in Pakistan using ERTS-1 imagery
[PAPER-G17] 19 p2265 N73-28248

**PALEOMAGNETISM**
Paleomagnetic study of Mano Lake, California to determine secular variations during past 30,000 years
16 p1895 N73-25325
Vapor condensation of Ni-Fe phases and paleomagnetic records in carbonaceous chondrites
17 p2017 N73-26310

**PALEONTOLOGY**
Tectonic and paleogeologic mapping of Montana using ERTS-1 imagery
[E73-10280] 08 p0914 N73-17488
Tree ring chronology for constructing paleoclimatology of North America and Europe
[AD-757486] 14 p1686 N73-23682
Concentration, composition, and properties of amino acids found in Cenozoic formations of Japan
[NASA-TT-F-15002] 19 p2293 N73-28439

**PALLADIUM**
Corrosion kinetics of Ti-Pd alloy in HCl at room temperature determined by radioactive tracer method
[NLL-TRANS-746-1328-[9022.401]] 05 p0505 N73-14112

**PALLADIUM ALLOYS**
Magnetic properties and phase composition of finely-dispersed nondeformed powders from highly-anisotropic gamma-phase Fe-Pd alloys
[NLL-TRANS-746-1389-[9022.401]] 05 p0560 N73-14553
Analysis of short time elevated temperature properties of platinum, rhodium, and palladium alloys
[NLL-M-22799-[5828.4F]] 11 p1304 N73-20582
Using transition from Ni-61 to obtain Mossbauer absorption spectra with Ni-Pd alloy
[TID-26197] 12 p1414 N73-21461
Ni-61 transition for obtaining Mossbauer absorption spectra with Ni-Pd alloys
18 p2185 N73-27641

**PALLADIUM COMPOUNDS**
Stability constants for chloride complexes of palladium [II]
[AD-758684] 16 p1871 N73-25151

**PALO VERDE VALLEY (CA)**
Utilization of ERTS-1 imagery for mapping and control of pink bollworm in Imperial, Coachella, and Palo Verde Valleys of California
[E73-10858] 19 p2292 N73-28435

**PAM (MODULATION)**
U PULSE AMPLITUDE MODULATION

**PANAMA**
Descriptions of earthquakes and location of epicenters in US, Alaska, Panama Canal Zone, and Virgin Islands during 1970
03 p0294 N73-12393
Annual climatological measurements of evaporation in Panama Canal Zone
[AD-751782] 07 p0817 N73-16621
Analysis of flight hazards caused by bird strikes on aircraft flying in Panama Canal Zone
[AD-763112] 20 p2362 N73-28997
Aerochrome infrared aerial photography over Barro Colorado Island, using multispectral, line scan data for tropical forests
[AD-762583] 20 p2415 N73-29410
Instrumentation available for measuring evaporation in Canal Zone
[AD-763205] 21 p2574 N73-30629

**PANEL FLUTTER**
Interaction characteristics of harmonic forcing excitation and panel flutter
01 p0113 N73-10932
Criteria for predicting, preventing, and evaluating panel flutter
[NASA-SP-8004] 02 p0237 N73-11932
Application of computer techniques for determination of flutter characteristics of aircraft and comparison with model matching data analysis
[AGARD-R-596] 09 p0983 N73-18030
Analysis of effects on in-plane boundary conditions and panel geometry on natural vibration and flutter characteristics of panels exposed to supersonic flow parallel to generators
09 p1094 N73-18933
Experimental method for studying panel flutter
[PUBL-90] 10 p1218 N73-19909
Numerical analysis of panel flutter based on isoperimetric inequality and effect of viscous damping forces
[NASA-CR-131828] 13 p1475 N73-21950
Determination of flutter characteristics for arbitrary yaw angles with two types of corrugation-stiffened panels
[NASA-CR-2265] 14 p1714 N73-23910
Development of methods for approximating aircraft with asymmetric elevator control to calculate flutter characteristics
[ARC-R/M-3256] 15 p1728 N73-24018
Effect of surface pressure fluctuations on response of panels underlying attached and separated turbulent boundary layers and shock waves
20 p2479 N73-29910
Linearized integral theory of three dimensional unsteady compressible flow in shear layer by oscillating wall
[AD-763807] 22 p2654 N73-31264

**PANELS**
NT CURVED PANELS
NT RECTANGULAR PANELS
NT WING PANELS
Shock tube generated blast loads on panels in steel structures
[REPT-1/72] 02 p0237 N73-11926
Fabrication of light weight panel structure using pairs of elongate hollow ribs of semicircular configuration
[NASA-CASE-LAR-11052-1] 04 p0481 N73-13929
Fatigue behavior of hat section stringer stiffened panels compressed in post-buckling range
[AD-748855] 04 p0482 N73-13938
Subsonic numerical panel method for flow calculation applied to delta wing, lifting reentry body, body-wing configurations
[MBB-UFE-889-72-O] 06 p0615 N73-14992
Estimates of LC stress response in aircraft skin panels to random acoustic loads
[ESDU-67028-AMEND-A] 06 p0723 N73-15904
Use of data items on buckling of plates and compression panels manufactured from isotropic materials
[ESDU-72012] 06 p0723 N73-15906
Fabrication of L-1011 aircraft panels to compare costs and service performance characteristics of PRD-49 and fiberglass
[NASA-CR-112250] 11 p1234 N73-20018
Application of vibrational methods for solving problems on theory of elasticity
[AD-754668] 11 p1346 N73-20922
Numerical analysis of panel flutter based on isoperimetric inequality and effect of viscous damping forces
[NASA-CR-131828] 13 p1475 N73-21950
Fabrication of beryllium compression tubes and structural panels for space shuttle application
[NASA-CR-124245] 13 p1533 N73-22420
Effect of transverse shear deformation on large amplitude free vibrations of plates and cylindrical panels
13 p1584 N73-22845
Strains affecting growth rate of edge cracks in acoustically excited panels
[ISVR-TR-59] 13 p1586 N73-22860
Transfer matrix techniques for vibration analysis of curved skin-stringer structures with tuned elastomeric dampers
[AD-758220] 14 p1605 N73-23010
Determination of inplane stress distribution across thickness by two methods for plate loaded in bending
[AD-757207] 14 p1716 N73-23925
Discontinuous functions in problems of strength and stability of elongated cylindrical panels with finite deflections
[AD-758621] 15 p1841 N73-24918
Pressurized panel meteoroid detector
[NASA-CASE-XLA-08916-2] 19 p2299 N73-28487
Life test data for hybrid thermoelectric panel containing lead telluride and silicon germanium thermocouples
[NASA-TM-X-2869] 20 p2364 N73-29010
Analysis of programs for acoustic testing of composite material components and development of theory for predicting natual frequencies, mode shapes, and stresses in composite panels
20 p2480 N73-29918
Test fixture design for boron-aluminum and beryllium test panels
[NASA-CR-124401] 23 p2792 N73-32337
Production engineering for silica reusable surface insulation panels
24 p2938 N73-33462

**PANORAMIC CAMERAS**
Camera installation for multispectral aerial photography using four electrically driven cameras for synchronous photography
[FOA-2-C-2469-52] 06 p0672 N73-15469
Use of Apollo 16 photogrammetry to determine frequency distributions of lunar slopes
12 p1456 N73-21792
Design study of optical system for annular imagery
[AD-758637] 15 p1789 N73-24505
Stereophotography of rain clouds using panoramic rotating-lens cameras
[AD-757882] 15 p1807 N73-24642
Compensation formulas for panoramic aerial photography cameras
[AD-764168] 22 p2676 N73-31431

**PANORAMIC SCANNING**
Pan-frame system model for panoramic camera in aerial triangulation
24 p2925 N73-33363

**PARABOLIC ANTENNAS**
Electrodynamic fundamentals of antenna theory and design
[AD-755689] 13 p1502 N73-22176
Effect of precipitation on parabolic antennas using linear orthogonal polarization at superhigh frequencies
[REPT-53] 16 p1875 N73-25176
Hertz vector analysis of spatial structure of cross polarization radiation in axisymmetric parabolic antennas
20 p2377 N73-29096
Multimode coaxial feeds for parabolic antennas with large aperture reflectors
[FTZ-A-454-TBR-14] 22 p2642 N73-31177
Design and operational technology associated with radio telescope antennas
[JPRS-59985] 23 p2837 N73-32671
Structural methods for increasing effectiveness of fully rotatable parabolic antennas
23 p2837 N73-32673
Method of alignment and technology of fabricating RTI-7.5/250 MVTU radio telescope antennas
23 p2838 N73-32675

**PARABOLIC BODIES**
Transonic flow around slender bodies noting wave drag deceleration and boundary layer transition
[ISL-33/71] 04 p0406 N73-13304
Computerized stability derivative calculations for oscillating parabolic ogives and circular cones in transonic flow field using iterative procedure
[NASA-CR-124033] 07 p0769 N73-16249
Application of exact method for numerical computations of supercavitating hydrofoils of parabolic shape
[AD-763465] 22 p2654 N73-31261

**PARABOLIC DIFFERENTIAL EQUATIONS**
Stability analysis for semilinear parabolic partial differential equations
[NASA-CR-130542] 09 p1056 N73-18608
Variable directions method for solving numerical weather forecasting problems
[AD-752336] 10 p1182 N73-19620
Bifurcation and stability for nonlinear parabolic partial differential equation
[NASA-CR-131896] 14 p1683 N73-23661

**PARABOLIC FLIGHT**
Problems in simulating weightlessness
12 p1367 N73-21090
Blind fish responses to gravitational changes as in parabolic flight
12 p1368 N73-21101

**PARABOLIC REFLECTORS**
NT PARABOLOID MIRRORS
Plural beam antenna with parabolic reflectors
[NASA-CASE-GSC-11013-1] 10 p1133 N73-19234
Acoustic radiation patterns of line source coincident with focal line of parabolic cylinder reflector immersed in water tank
[AD-754063] 11 p1324 N73-20748
Method for measuring mechanical deformations in parabolic dish of metric tracking radar
[AD-758371] 14 p1635 N73-23260
Multimode antenna feed system for microwave and broadband communication
[NASA-CASE-GSC-11046-1] 19 p2234 N73-28013
Performance of 30 cm ion thrusters with dished accelerator grids
[NASA-TM-X-68294] 21 p2589 N73-30744
Multimode coaxial feeds for parabolic antennas with large aperture reflectors
[FTZ-A-454-TBR-14] 22 p2642 N73-31177

**PARABOLOID MIRRORS**
Advanced Figure Sensor for measuring parabolic mirror surfaces
[NASA-CR-130114] 03 p0301 N73-12454
Manufacture and testing silver parabolic mirror cut directly with diamond tool in numerically-controlled lathe
[UCRL-51213] 03 p0335 N73-12734
Large orbiting X ray telescope with high resolution mirror design
[NASA-CR-124001] 10 p1158 N73-19424
Multiple rod pyramid as cyclic suspension for parabolic radiotelescope mirror
[AD-757237] 15 p1789 N73-24503
Off-axis parabolic mirror segments in onboard optical data processing for spacecraft
16 p1923 N73-25557
Optical data processing system using paraboloidal reflecting surfaces
[NASA-CASE-GSC-11296-1] 21 p2579 N73-30666

**PARABOLOIDS**
U PARABOLIC BODIES

**PARACHUTE DESCENT**
Development and operating principles of gas generator for deploying recovery parachutes from space capsules during atmospheric entry
[NASA-CASE-LAR-10549-1] 04 p0477 N73-13898
Development of concepts and procedures for preparation of loads for airdrop to reduce time required and increase reliability of operation
[AD-750705] 05 p0612 N73-14976
Design, stress analysis, and high altitude performance of recovery parachute system
[NASA-CR-130304] 06 p0621 N73-15037
Flight test of 55 foot diameter disk-gap parachute trailing behind bluff body, planetary aeroshell and attached instrument payload
[NASA-TM-X-2671] 06 p0621 N73-15042
Analysis of shock forces generated by opening 35 foot diameter extended-skirt parachute for retardation at 100,000 feet altitude
[AD-749690] 06 p0623 N73-15060
Performance tests of cargo parachutes with pulled down vents for airdrop of supplies from 500 feet altitude
[AD-750585] 06 p0624 N73-15068
Measurement of parachute cord loads using lightweight transmitting load cell
[AD-751913] 08 p0867 N73-17022
Analysis of design features and photographic data to determine cause of Apollo 15 main parachute failure
09 p1088 N73-18879
Postflight analysis of AV-2 balloon launched decelerator flight test to determine parachute system operation in wake of blunt body simulating Viking 75 entry vehicle
[NASA-CR-112177] 11 p1233 N73-20011
Postflight analysis of AV-3 balloon launched decelerator flight test to determine parachute system operation in wake of blunt body simulating Viking 75 entry vehicle
[NASA-CR-112178] 11 p1233 N73-20012
Apollo 16 flight anomaly report to determine cause of burn holes in main parachute canopy
[NASA-TM-X-69127] 11 p1338 N73-20863
Breathing apparatus for parachutists
[AD-756554] 15 p1745 N73-24141
Design criteria and aerodynamic characteristics of decelerator parachutes used for recovery of solid rocket boosters used in space shuttle launching
[NASA-CR-124266] 16 p1861 N73-25072
Evaluation of explosive loaded material during airdrop operations
[AD-759228] 17 p2099 N73-26981
Development of equations of motion for longitudinal suspension line wave motion during parachute deployment process
[NASA-TM-X-69498] 20 p2361 N73-28988
Simulation calculations of parachute deployment dynamics process for Viking 75 entry vehicle
[NASA-TN-D-7415] 21 p2600 N73-30841
Computer program for analyzing characteristics of parachute-payload system during deployment and trajectory
23 p2740 N73-31936
Combined parachute and retrorocket system for low altitude aerial delivery of military cargo
[AD-765422] 24 p2880 N73-32997

**PARACHUTE FABRICS**
Wind tunnel tests to determine effects of aerodynamic configuration, dimensions, and materials on spinning characteristics of cross parachute
[AD-749010] 04 p0374 N73-13045

**PARACHUTES**
NT DRAG CHUTES
NT RECOVERY PARACHUTES
Operational suitability of various airdrop systems
[AD-744811] 01 p0005 N73-10036
System for controlling torque buildup in suspension of gondola connected to balloon by parachute shroud lines
[NASA-CASE-GSC-11077-1] 04 p0370 N73-13008
Wind tunnel tests to determine effects of aerodynamic configuration, dimensions, and materials on spinning characteristics of cross parachute
[AD-749010] 04 p0374 N73-13045
Performance tests of cargo parachutes with pulled down vents for airdrop of supplies from 500 feet altitude
[AD-750585] 06 p0624 N73-15068
Ground and flight test program of Stokes flow parachute
[NASA-CR-112251] 10 p1106 N73-19016
Illuminance measurement of two types of airborne flares
[DREV-R-673/72] 10 p1223 N73-19942
Design and performance of launcher illumination XM-183 flare package for parachutes
[AD-757731] 15 p1844 N73-24940
Wind tunnel tests to determine inflation characteristics of solid, flat, circular model parachutes at subsonic speed and various geometric configurations
[AD-759209] 16 p1863 N73-25087
Analysis of flow field around 18 inch diameter flat circular parachute model using helium bubble technique
[AD-761098] 18 p2106 N73-27034
Wind tunnel tests to determine drag and stability characteristics of solid flat circular and ringslot parachute models
[AD-764364] 22 p2616 N73-30963

**PARACHUTING**
U PARACHUTE DESCENT

**PARAFFINS**
Effects of gravity-induced free convection of melting behavior of paraffin slab for thermal control devices
[NASA-CR-123954] 04 p0385 N73-13130
Role of gravity-induced free convection upon liquefaction dynamics of cylindrical paraffin slab under normal gravity conditions
[NASA-CR-129911] 04 p0385 N73-13131
Optimization of supersonic aircraft C3/C4 polymer fuel by normal paraffins containing 10 to 16 carbon atoms
[DLR-FB-73-32] 22 p2708 N73-31689

**PARAGLIDERS**
NT FLEXIBLE WINGS
NT PARAWINGS

**PARALLEL COMPUTERS**
Design of signal processing computer using arithmetic parallelism
[AD-745950] 02 p0142 N73-11150
Review of macrocellular research for digital computers, noting parallel computers
05 p0517 N73-14205

**PARALLEL DRAINAGE**
U DRAINAGE PATTERNS

**PARALLEL FLOW**
NT GAS FLOW
NT LAMINAR FLOW
NT PIPE FLOW
NT STEADY FLOW
NT THREE DIMENSIONAL FLOW
Parallel heat conducting viscous gas flow in flat channel with sine wave wall perturbation
24 p2906 N73-33189

**PARALLEL PLATES**
Wave propagation in parallel-plate metallic waveguide as eigenvalue problem using complete cold-plasma dielectric tensor
[IPP-4/37] 08 p0948 N73-17764
Parallel plate electrostatic spectrograph as relativistic particle analyzer
15 p1788 N73-24498
Fringing field effect minimization in parallel plate electrostatic spectrograph taking into account condenser plate thickness
15 p1788 N73-24499
Guiding and scattering of acoustic surface waves in solid layer between substrates
15 p1813 N73-24691
Optimization of parallel plate relativistic particle analyzer by reducing z variation of point source image at detector surface
19 p2301 N73-28501
Numerical calculation of electric potential resulting from charged parallel plates of equal width - Part I
[AD-761866] 19 p2321 N73-28676

**PARALLEL PROCESSING (COMPUTERS)**
Optical-to-optical interface device for use in coherent optical parallel processing systems
[NASA-CR-130183] 10 p1188 N73-19671
Modular inverter/converter automatic paralleling and protection system
[NASA-TN-D-7279] 15 p1737 N73-24084
Multiprogramming for scheduling parallel processable tasks for uniprocessor
[AD-760143] 17 p2002 N73-26188
Survey of parallel processing and parallel processor systems
[CIRC-174] 20 p2379 N73-29111

**PARAMAGNETIC AMPLIFIERS**
U MASERS

**PARAMAGNETIC RESONANCE**
NT ELECTRON PARAMAGNETIC RESONANCE
Paramagnetic resonance energy for accelerating charged particles
[NLL-RTS-7598] 05 p0579 N73-14715
Design and development of zero field paramagnetic resonance spectrometer
[AD-759370] 17 p2035 N73-26466

**PARAMAGNETISM**
Magnetism in solids - magnetic moments, properties of diamagnetism and paramagnetism, and coexistence of superconductivity and ferromagnetism
[ITJ-13] 04 p0449 N73-13670
Effect of electron-phonon interaction on temperature dependence of paramagnetic susceptibility in metals
[AD-753984] 11 p1331 N73-20804
Paramagnetic rotation of plane of polarization
[NASA-TT-F-14737] 20 p2454 N73-29724
Uses of cluster materials and related types in antiferromagnetic cooling by adiabatic magnetization and demagnetization of antiferromagnets
[AD-764620] 23 p2826 N73-32592

**PARAMETERIZATION**
Computing equation of state parameters for material which undergoes phase transition
[AD-746611] 03 p0346 N73-12824
Reduction of angle frequency deviation in antenna array by waveguide parameters
[AD-748742] 04 p0389 N73-13164
Applications of least squares method to analysis of parameters and confidence region determination
[LAAS-NT-SIS-72-T-08] 04 p0441 N73-13593
Parameterization and its role in atmospheric modeling
[GARP-PUBL-8] 05 p0573 N73-14654
Parameterization in atmospheric circulation models
05 p0573 N73-14655

Role of radiation in atmospheric models noting equation of transfer for thermal and solar radiation
05 p0573 N73-14656
Parameterization of clouds in numerical circulation model
05 p0573 N73-14657
Two dimensional eddy viscosity coefficients in atmospheric motion noting parameterization of clear air turbulence
05 p0573 N73-14658
Parameterization of gravity waves noting upper boundary conditions
05 p0573 N73-14659
Mesoscale processes in circulation models noting parameterization
05 p0573 N73-14660
Parameterization of turbulent boundary layer in atmospheric circulation model
05 p0573 N73-14661
Parameterization of atmospheric boundary layer
05 p0574 N73-14664
Parameterization of near surface mesoscale circulation
05 p0574 N73-14665
Use of Kelly Repertory Grid Techniques for assessing subjective estimates of important parameters for target acquisition
10 p1227 N73-19973
Sampling procedures for estimation of convex combination of proportions
[AD-754577] 11 p1312 N73-20644
Parametric design analysis to determine characteristics and performance of class of high speed hydrofoil craft
[AD-760355] 17 p2016 N73-26303
Measurement subsystem parameter optimization to enhance estimates
[AD-759175] 17 p2055 N73-26625
Computer algorithm for calculating orbital trajectories by optimization of equation of motion parameters
18 p2211 N73-27846
Application of quadratic programming to optimize parameters of dynamic systems
21 p2515 N73-30172
Parametric study of proposed high Reynolds number transonic wind tunnel
[AD-763725] 21 p2522 N73-30227
Estimation of parameters for nonlinearly observed dynamic systems
21 p2565 N73-30562
Multidimensional linear system parameter estimation computer program using least squares method evaluating mathematical model stability, observability and real time operation
[LAAS-AS-73-1-06] 23 p2813 N73-32491

**PARAMETERS**
U INDEPENDENT VARIABLES

**PARAMETRIC AMPLIFIERS**
Diode passivation techniques and fabrication of semiconductor targets that are stable under electron beam bombardment for use in L band amplifiers
[AD-747868] 03 p0276 N73-12237
Tunable radiation obtained across wide region of electromagnetic spectrum using parametric amplifier
[AD-748849] 04 p0429 N73-13497
Methods for predicting parametric amplifier input noise temperature degradation for pump AM noise levels undergoing signal interference
[AD-751652] 07 p0763 N73-16197
Design and operation of tunable parametric oscillators with range between 1.0 and 5.0 micrometers
[AD-753347] 09 p1044 N73-18517
Micron output increase of Nd YAG laser to pump optical parametric oscillator through visible spectrum
[AD-756809] 14 p1673 N73-23577
Noise properties and circuits to cancel noise in gas parametric amplifiers
15 p1756 N73-24230
Infrared optical parametric fluorescence and parametric oscillation
16 p1944 N73-25729

**PARAMETRIC DIODES**
Frequency multiplier based on snapoff diode and computer program for evaluating performance
08 p0888 N73-17189

**PARAMETRIC FREQUENCY CONVERTERS**
Tunable parametric oscillator using infrared pumping for ultraviolet frequency generation
[AD-756910] 13 p1561 N73-22650
Development of 10.6 micrometer range gated upconversion imaging laser radar receiver with 150 by 150 resolution elements
[AD-759077] 16 p1915 N73-25495
Upconversion method for monochromatic radiation
[NASA-TM-X-2877] 20 p2425 N73-29479
Nonlinear materials including univalent metal iodates for IR image upconversion
[AD-763952] 22 p2701 N73-31630

**PARAMETRIC OSCILLATORS**
U PARAMETRIC AMPLIFIERS

**PARAWINGS**
Application of parafoil equations of motion to predict flight performance of powered parafoil flight vehicle
[AD-754907] 11 p1236 N73-20034

**PARTIAL DIFFERENTIAL EQUATIONS**
NT BURGER EQUATION
NT ELLIPTIC DIFFERENTIAL EQUATIONS
NT FOKKER-PLANCK EQUATION
NT GAUSS EQUATION
NT HELMHOLTZ VORTICITY EQUATION
NT PARABOLIC DIFFERENTIAL EQUATIONS
NT VLASOV EQUATIONS
Two dimensional numerical analysis based on nonlinear partial difference equations of cross sections of long alternators
[AD-744985] 01 p0007 N73-10052
Numerical solution of parabolic partial differential equations with reference to eddy heat conduction in ocean
[AD-746205] 02 p0167 N73-11362
Mathematical model for convective and radiant heat transfer for gas flow and glass tube inner wall noting partial differential equations at boundary conditions
[LAAS-NI-CMOAC-72-I-11] 02 p0243 N73-11976
Solution of partial differential equations by analog networks
[AD-746929] 03 p0272 N73-12206
Gauge invariance, conservation laws, and Korteweg-deVries equation for class of nonlinear partial differential equations
[IPPJ-138] 04 p0440 N73-13589
Lectures on partial differential equations and numerical analysis presented at International Congress on Mathematics
[FOA-2-C-2470-11] 06 p0690 N73-15618
Nonlinear differential equations in partial derivatives for nonsteady motion of liquids and gases in pipelines
[AD-752685] 09 p1017 N73-18296
Inertial gravity wave frequency spectrum in cylindrically confined incompressible two component liquid flow
[AD-752439] 09 p1018 N73-18312
Stability analysis for semilinear parabolic partial differential equations
[NASA-CR-130542] 09 p1056 N73-18608
Variational problems in optimization and control for hyperbolic partial differential equations
09 p1056 N73-18612
Finite difference algorithm for solving quasi-linear gas dynamic systems
[AD-753097] 10 p1143 N73-19309
Variable directions method for solving numerical weather forecasting problems
[AD-752336] 10 p1182 N73-19620
Power series solution to partial differential equation in thermal conductivity analysis on body of variable density
[AD-754256] 10 p1225 N73-19957
Series solutions for reduced wave equation characterizing radiation from point source in two and three dimensions
[AD-754793] 11 p1312 N73-20647
Heat transfer equation with nonlinear boundary condition and final value problem for porous medium equation
[AD-755073] 11 p1350 N73-20951
Partial differential equations for studying laminar boundary layer separations
13 p1508 N73-22221
Invariant-group properties of equations for boundary layer of electrically conductive liquid in magnetic field
[AD-756956] 13 p1513 N73-22257
Bifurcation and stability for nonlinear parabolic partial differential equation
[NASA-CR-131896] 14 p1683 N73-23661
Nonlinear partial differential equations for studying viscous compressible corner flow at subsonic and supersonic Mach numbers
15 p1764 N73-24294
Approximation methods for solving hyperbolic partial differential equations of meteorology and oceanography
[GARP-PUBL-10] 16 p1938 N73-25680
Fourth-order, time dependent, partial differential flow equation solved by coupled pair of finite difference equations
[AD-765323] 23 p2776 N73-32201
Fourth order partial differential equations governing deformation of circular cylindrical shells
[AD-764560] 23 p2854 N73-32809
Integral transformations for compressible laminar partial differential equations of second order boundary layer theory
24 p2907 N73-33198

**PARTIAL PRESSURE**
NT HYPOXEMIA
NT OXYGEN TENSION
Computerized simulation of carbon dioxide partial pressure in spacecraft environment for wide range of operating conditions - Vol. 1
[NASA-CR-128630] 02 p0233 N73-11893
Development of simulation models for computerized simulation of carbon dioxide partial pressure in spacecraft environment - Vol. 2
[NASA-CR-128631] 02 p0233 N73-11894

**PARTICLE ACCELERATION**
Numerical analysis of classical brachistochrone in which particle starts and ends at same elevation with horizontal velocities and does not leave curve of own inertia
[P-4749] 02 p0196 N73-11584
Paramagnetic resonance energy for accelerating charged particles
[NLL-RTS-7598] 05 p0579 N73-14715
Variations of relative abundances of helium, carbon, nitrogen, oxygen, and iron-group nuclei in solar cosmic rays and their relationship to solar particle acceleration
[NASA-TM-X-66228] 12 p1445 N73-21706
Solar flare particle energization by magnetic field reconnection and shock reflection
19 p2336 N73-28799
Acceleration mechanism for heavy nuclei abundance enhancement in solar flares
19 p2337 N73-28801

**PARTICLE ACCELERATOR TARGETS**
Development and characteristics of improved dispensing targets for ion beam particle generators
[NASA-CASE-NPO-13112-1] 20 p2382 N73-29138

**PARTICLE ACCELERATORS**
NT BETATRONS
NT BEVATRON
NT CYCLOTRONS
NT ELECTRON ACCELERATORS
NT ION ACCELERATORS
NT LINEAR ACCELERATORS
NT STORAGE RINGS [PARTICLE ACCELERATORS]
NT SYNCHROCYCLOTRONS
NT SYNCHROPHASOTRONS
NT SYNCHROTRONS
NT VAN DE GRAAFF ACCELERATORS
Vacuum alteration for jet targets from condensed hydrogen, while operating on accelerator internal beam
[JINR-P13-6324] 04 p0402 N73-13275
Design of time of flight chemical accelerator for low center-of-mass energy spreads and measurement of electron affinity of N02
[AD-753133] 09 p1012 N73-18258
Design of particle accelerator using pulsed laser beam
[RLO-2041-71] 10 p1193 N73-19705
Muon proton interactions and elastic scattering for neutron beam generation in accelerator
[BNL-17314] 10 p1193 N73-19710
High intensity proton sources for high energy accelerators
[BNL-17159] 10 p1194 N73-19719
Fast particle injectors for plasma production in thermonuclear installations
[AEC-TR-7389] 11 p1323 N73-20738
Bunch lengthening and power losses due to vacuum chamber walls
[DESY-72/72] 17 p2010 N73-26258
Design of high intensity proton accelerator
[AD-762240] 19 p2250 N73-28140
Collective cyclic accelerator - gyrotron
[AD-762309] 19 p2250 N73-28141
Performance tests of geometrically different sets of dished accelerator grids on ion thruster engines
[NASA-TM-X-71420] 23 p2830 N73-32615

**PARTICLE BEAMS**
NT ATOMIC BEAMS
NT ELECTRON BEAMS
NT ION BEAMS
NT MOLECULAR BEAMS
NT NEUTRON BEAMS
NT PROTON BEAMS
Development of inverse scattering problem and approach to nonrelativistic problem at fixed angular momentum
02 p0199 N73-11608
Application of Schroedinger equation to solve inverse scattering problem at fixed energy in quantum mechanics
02 p0199 N73-11609
Abstracts and bibliographies on research in laser technology, effects of explosions, geosciences, and particle beams
[AD-749488] 04 p0430 N73-13504
USSR research projects involving laser technology, effects of strong explosions, geosciences, and particle beams
[AD-749487] 04 p0489 N73-13998
Toroidal magnetic field spectrometer for experimentation with high energy beams
[LNF-72/59] 11 p1294 N73-20501
Laser technology, strong explosion effects, geosciences, and particle beams bibliographies
[AD-754946] 11 p1353 N73-20982
Laser technology, strong explosion effects, geosciences, and particle beams - bibliographies
[AD-754962] 11 p1353 N73-20988
Wave-wave coupling in cold beam/cold plasma system
12 p1433 N73-21608
Design and performance of high intensity pulsed electron beam system
[FOA-2-C2579-E8] 15 p1788 N73-24493

Computer program for calculating characteristics of charged particles beam transported through focusing and bending magnets
[NASA-TN-D-7352] 18 p2121 N73-27143
Bibliography on lasers, strong explosions, geosciences, particle beams, and material sciences
[AD-759275] 18 p2215 N73-27884
Collective cyclic accelerator - gyrotron
[AD-762309] 19 p2250 N73-28141
Abstracts and bibliographies of Soviet literature on lasers, explosion effects, particle beams, and geosciences
[AD-762376] 19 p2356 N73-28955
Development and characteristics of improved dispensing targets for ion beam particle generators
[NASA-CASE-NPO-13112-1] 20 p2382 N73-29138
Feasibility of using inverse rastering to irridiate large test objects by penetrating radiation beams
22 p2732 N73-31866

**PARTICLE CLOUDS**
U CLOUDS

**PARTICLE COLLISIONS**
Collisional aspects of 45 mtorr Avco experiment with and without applied magnetic field
[AD-745374] 01 p0084 N73-10698
Studying collisions of heavy particles to understand collision of meteoroids with upper atmosphere
01 p0102 N73-10842
Plasma diagnostics by means of collision dominated spherical electrostatic probes including mathematical model
[DLR-FB-71-41] 06 p0705 N73-15756
Proofs for binary collision term in Boltzmann transport equations in kinetic theory of gas and plasma dynamics
[TRITA-EPP-72-25] 07 p0772 N73-16273
Plasma heating by turbulent pulsation of electric field
[NASA-TT-F-14673] 08 p0947 N73-17758
Differential cross section of emitted photon in suprathermal proton bremsstrahlung
08 p0974 N73-17966
Time dependent scattering theory for evaluating transition cross sections in atomic helium collision with charged particle
[NASA-CR-131265] 11 p1326 N73-20761
Influence of collisions on incoherent scattering spectrum of nonequilibrium inhomogeneous absorbing plasma
[CEA-R-4351] 12 p1436 N73-21633
Triple Regge formula for analyzing proton leading effect in proton proton collisions
[LPTHE-73/17] 20 p2456 N73-29740
Debris particle distribution in ionosphere escaping fireball through charge exchange collisions
[AD-764955] 23 p2819 N73-32535
Collision probability method for calculating neutron transport in multidimensional systems
24 p2960 N73-33653

**PARTICLE COUNTERS**
U RADIATION COUNTERS

**PARTICLE DECAY**
U RADIOACTIVE DECAY

**PARTICLE DENSITY (CONCENTRATION)**
NT ELECTRON DENSITY (CONCENTRATION)
NT ELECTRON DENSITY PROFILES
NT ELECTRON DISTRIBUTION
NT ION DENSITY (CONCENTRATION)
NT IONOSPHERIC ELECTRON DENSITY
NT IONOSPHERIC ION DENSITY
NT MAGNETOSPHERIC ELECTRON DENSITY
NT MAGNETOSPHERIC PROTON DENSITY
NT PLASMA DENSITY
NT PROTON DENSITY (CONCENTRATION)
Numerical analysis of ionospheric and plasma sheet particle densities, fluxes, and bulk velocities along auroral magnetic field for ion-exosphere model
[A-N-109-1972] 06 p0664 N73-15400
Rocket and satellite instrument for simulatenous measurements of total mass density and number density of atomic oxygen in lower thermosphere
[AD-751468] 07 p0795 N73-16464
Application of dual-scatter laser velocimeter to measure particle velocity distribution in hypersonic dust erosion facility
[AD-752225] 08 p0930 N73-17618
Models of aerosol dynamics in upper atmosphere
[BNL-17174] 10 p1126 N73-19176
Rheological properties of abrasive powder solutions considering particle dispersion
[AD-756082] 13 p1488 N73-22065
Nuclear interaction models for cosmic ray air showers to determine lateral distribution of particles and fluctuations in particle densities
13 p1574 N73-22752
Conference on cosmic ray and solar particle diffusion and concentration in interstellar space
[NASA-CR-135528] 23 p2834 N73-32646
IMP-7 measurement of very low energy cosmic ray energy spectra and concentration during solar flares
[TR-73-138] 23 p2835 N73-32654

**PARTICLE DETECTORS**
U RADIATION COUNTERS

**PARTICLE DIFFUSION**
NT ELECTRON DIFFUSION
NT IONIC DIFFUSION
Conductivity profiles determined for beryllium diffused silicon for calculating diffusion coefficients
[NASA-CR-129169] 03 p0320 N73-12605
Diffusion coating and residual stress effects on steel product strength
[AD-749089] 05 p0566 N73-14600
Radial diffusion calculations of ionized helium and protons as probe for magnetospheric dynamics
[AD-750861] 06 p0670 N73-15449
Orbit perturbation effects on frequency shift of electrostatic, turbulent, unmagnetized plasma
09 p1071 N73-18738
Microscopic analysis of silver diffusion into gold plate on electrical connector
[AD-755123] 11 p1263 N73-20249
Measurement of phonon scattering by isotopic impurities in helium single crystals
[AD-754475] 11 p1330 N73-20798
X ray analyses of atomic structures in diffusion zones of copper nickel alloys and copper silver alloys
[AD-759195] 16 p1930 N73-25616
One-dimensional time dependent diffusion convection model analysis of cosmic ray modulation during solar maximum
[TR-73-131] 23 p2834 N73-32647
Theory of radial diffusion applied to electron and proton radiation belts of Jupiter
23 p2836 N73-32663

**PARTICLE EMISSION**
NT ELECTRON EMISSION
NT FIELD EMISSION
NT ION EMISSION
NT NEUTRON EMISSION
NT PHOTOELECTRIC EMISSION
NT SECONDARY EMISSION
NT THERMIONIC EMISSION
Supergiant structures in negative polarity magnetic fields of sun and particle emitting flares
01 p0093 N73-10763
Apollo 15 and Apollo 16 spectrometric observation of X rays, gamma rays, and alpha particle emissions on lunar surface
[NASA-TM-X-66068] 01 p0103 N73-10848
Coronal Magnetic field effects on propagation of solar flare energetic particles.
19 p2338 N73-28806

**PARTICLE ENERGY**
NT ELECTRON ENERGY
NT ELECTRON STATES
NT PROTON ENERGY
Development of inverse scattering problem and approach to nonrelativistic problem at fixed angular momentum
02 p0199 N73-11608
Application of Schroedinger equation to solve inverse scattering problem at fixed energy in quantum mechanics
02 p0199 N73-11609
Numerical analysis of quantum mechanical theory of scattering of particle by spherically symmetrical potential
02 p0199 N73-11610
Numerical analysis of inverse scattering problem at fixed angular momentum for nonlocal separable interactions
02 p0199 N73-11611
Intercosmos satellite observation of cosmic rays
15 p1828 N73-24817

**PARTICLE FLUX**
U FLUX (RATE)

**PARTICLE FLUX DENSITY**
NT ELECTRON FLUX DENSITY
NT NEUTRON FLUX DENSITY
NT PROTON FLUX DENSITY
Solar particle composition measurements using nuclear emulsion detectors on sounding rockets
08 p0973 N73-17959
Raw data processing from proton, alpha particle, and electron flux experiments of Azur satellite
[MPI-PAE/EXTRATERR-76] 09 p1081 N73-18818
Numerical analysis of aerosol concentration and deposition flux for several flow configurations with and without electrical force deposition
20 p2386 N73-29172
Balloon flown hodoscopic observations of rapid variations in solar proton flux in 1972
[TR-73-134] 23 p2834 N73-32650
Flux density of low energy solar flare particles measured by IMP-7
[TR-73-137] 23 p2835 N73-32653

**PARTICLE INTENSITY**
Development of inverse scattering problem and approach to nonrelativistic problem at fixed angular momentum
02 p0199 N73-11608

**PARTICLE INTERACTIONS**
NT ELECTRON CAPTURE
NT ELEMENTARY PARTICLE INTERACTIONS
NT ION ATOM INTERACTIONS
NT MOLECULAR COLLISIONS
NT MOLECULAR INTERACTIONS
NT NUCLEAR INTERACTIONS
NT SPIN-ORBIT INTERACTIONS
Triple Regge phenomenology from finite mass sum rules in proton-proton inclusive reactions
[NOTA-INTERNA-379] 01 p0084 N73-10693
Energization of electrons in ionosphere and magnetoplasma by wave particle interaction
[AD-747093] 04 p0415 N73-13391
Analysis of interaction between fluid and discrete particles in turbulent flow field and development of equations of motion
[WTHD-32] 05 p0526 N73-14280
Injection, propagation, and interaction characteristics of solar protons based on HEOS A satellite data
05 p0593 N73-14817
Investigation for attenuation and extinction in interaction between laser beams and flowing particulate clouds
[RM-567] 08 p0929 N73-17605
Turbulent collisions for interpreting excitation processes in plasma
[AEC-TR-7382] 10 p1197 N73-19740
Effects of particle seeding on jet exhaust noise
19 p2251 N73-28150
Bose model for foreign particle interaction with superfluid helium
20 p2455 N73-29732
Picosecond laser beam study of four photon effects and temporal behavior of optical phonons
22 p2680 N73-31465
Statistical analysis on Markovian plasma turbulence using perturbed particle propagator
22 p2702 N73-31644

**PARTICLE MASS**
NT ELECTRON MASS
Computation of neutron star mass based on crystal arrangement of particles
08 p0974 N73-17965
Dynamic particle mass flow model for solar flares
19 p2333 N73-28773

**PARTICLE MOTION**
Numerical analysis of classical brachistochrone in which particle starts and ends at same elevation with horizontal velocities and does not leave curve of own inertia
[P-4749] 02 p0196 N73-11584
Calculation of particle motion in gravitational field using Schwarzschild metric
[ESRO-SR-17-ESOC] 03 p0357 N73-12910
Particle motion in magnetic mirror with high frequency electric field
[COO-2181-7] 06 p0703 N73-15731
Inverse method for exact analytical solutions for particle motion under central Newtonian gravitational force and atmospheric drag force
[AD-751491] 07 p0847 N73-16865
Stochastic derivation of equations of motion for deformable particles immersed in Newtonian fluids
[WTHD-46] 12 p1431 N73-21595
Motion and orbital direction of particle in Kerr gravitational field
[NASA-TR-R-403] 12 p1458 N73-21816
Transport processes of particles in dilute suspensions in turbulent water flow
[PB-213536] 13 p1512 N73-22255
Statistical mechanics of negative temperatures of particles in motion
[NASA-CR-131572] 13 p1562 N73-22664
Particle-fluid interaction corrections for turbulent flow measurements with laser Doppler flowmeter
[NASA-CR-124254] 14 p1649 N73-23379
Instabilities of homogeneous plasmas caused by particle velocity distributions
[AD-755688] 14 p1696 N73-23760
Physical properties of Coulomb collisions
[IPPJ-151] 16 p1949 N73-25773
Anomalous electromagnetic wave propagation in plasma caused by particle resonance motions
[IPPJ-130] 17 p1997 N73-26149
Relativistic particle motion in nonuniform electromagnetic waves
[NASA-CR-133888] 22 p2632 N73-31092
Motion and distribution of particles in steady, tube flows of suspensions of neutrally buoyant, rigid spheres
22 p2649 N73-31223
Dual resonance model with spin for reaction pion nucleon yields omega meson nucleon
[ILL-(TH)-73-12] 22 p2701 N73-31634

**PARTICLE PRODUCTION**
NT PAIR PRODUCTION
Enhanced solar activity effects on fast neutron production at polar latitudes
04 p0465 N73-13791
Dual resonance model for predicting density matrix elements of vector mesons produced in inclusive reactions
[ILL-(TH)-72-11] 05 p0582 N73-14735
Particle production and energy dissipation in stationary fusion plasma
[FOA-4-C-4465-25] 06 p0703 N73-15734
Dual multiperipheral model of hadronic production amplitudes
[NUB-2164] 07 p0823 N73-16672

Fast electron production by absorption of shf wave in collisionless plasma
[AEC-TR-7331] 07 p0827 N73-16700
Streamer chamber for visual observation of proton-proton interactions in accelerator
[BNL-17273] 10 p1138 N73-19271
Laser beam study of proton production cross sections determined for stable and radioactive rare gases
[TID-26183] 12 p1427 N73-21566
Muon production altitude in cosmic ray air showers from lateral and angular muon separation from shower core, and geomagnetic effects on muon charge ratio
13 p1574 N73-22754
Nondiffractive models with n squared approximately 1/s
18 p2182 N73-27616
Heat pipe production of high purity radioiodine for thyroid measurements
[NASA-CASE-LEW-11390-3] 19 p2248 N73-28128
Development and characteristics of improved dispensing targets for ion beam particle generators
[NASA-CASE-NPO-13112-1] 20 p2382 N73-29138
Primary and secondary nuclei production in cosmic rays
22 p2733 N73-31872

**PARTICLE SIZE DISTRIBUTION**
Molecular beam sampling system for measuring size, size distribution, and particle concentration of carbon particles in acetylene-oxygen flame
[AD-744920] 01 p0118 N73-10971
Cascade impactor network for determining gravimetrically particle size distribution of suspended aerosols in urban areas
[AP-108] 03 p0326 N73-12656
Establishment of takeoff and landing environment criteria for V/STOL aircraft with emphasis on airborne particle concentration
[AD-749463] 05 p0495 N73-14034
Flow charts for British standard particle-size distribution for soils
[PB-211721] 06 p0667 N73-15426
Determination of aerodynamic diameter of latex spheres and asbestos fibers using aerosol spiral centrifuge
[BMVG-FBWT-72-10] 07 p0812 N73-16585
Photometric profiles of dust particle size and dust cloud origins during dust storms on Mars as reported by Mars 3 Automatic Interplanetary Station
[NASA-TT-F-14818] 08 p0962 N73-17866
Holographic techniques for particle sizing and velocity distribution
[NASA-TR-R-404] 09 p1035 N73-18448
Wear process and colloidal particle production test on sliding metal surfaces using magnetic measurements
[AD-753251] 09 p1040 N73-18481
Removal and separation of particles by crystallization in carbon-naphthalene system
[AD-753056] 09 p1076 N73-18777
Size distribution of natural aerosol particles, using terrestrial measurements
[AD-756051] 13 p1528 N73-22381
Aerosol particle size determination and distribution with aerodynamically focused impactor, applied to coal mine dust
[BMVG-FBWT-73-1] 14 p1667 N73-23533
Aerodynamic size and mass distribution of aerosol particles determined with spiral centrifuge compared to other precipitators
[BMVG-FBWT-73-3] 14 p1668 N73-23535
Analysis of breakup length and breakup pattern for jets of liquids of different viscosity and surface tension ejected vertically downward into atmosphere
[NLL-RTS-8049] 15 p1764 N73-24291
Working principles of two aerosol particle size spectrometers, based on lateral air jet or asymmetric expansion of aerosol
[BMVG-FBWT-73-6] 15 p1788 N73-24496
Aerosol model of atmosphere based on experimental data regarding aerosol attenuation and particle number concentration and size distribution at various heights
[AD-760393] 17 p2030 N73-26429
Analysis of aluminum oxide to determine material characterization, particle size distribution, and specific surface area
17 p2050 N73-26582
Piezoelectric device for measuring the size and concentration of particles in clouds generated by underground nuclear explosion
[FRNC-TH-298] 17 p2065 N73-26709
Atomized particle dispersion in dryer space
[AD-762221] 19 p2233 N73-28005
Particle size distribution of coagulated aerosols using computer program
[NPL-NAC-35] 22 p2668 N73-31373
Analysis of equal-size droplet injection in fluid flow, noting fuel injection
[DLR-MITT-72-19] 22 p2710 N73-31703
Tear and fatigue crack propogation tests for determining mechanical properties of ultrafine grain alpha titanium
[AD-765329] 23 p2805 N73-32434
Mariner 9 mapping of Mars surface albedo variations
23 p2840 N73-32693
Effect of ocean depth on light scattering and attenuation parameters to include optical properties influenced by concentration, size, and shape of particulate matter
24 p2957 N73-33626

**PARTICLE SPIN**
NT ELECTRON SPIN
Derivation of theorems for spinless particle scattering from Kohn variational principle
[NASA-CR-129259] 03 p0323 N73-12634
Projective invariance of dual resonance models from spin analyticity and Lorentz invariance
[NOTA-INTERNA-388] 03 p0340 N73-12772
Structure of high spin particle propagator
[DPGU-01-73] 20 p2456 N73-29734

**PARTICLE TELESCOPES**
Azur satellite proton and electron telescope measurements in radiation belt, and conclusions regarding magnetospheric processes
[MPI-PAE/EXTRATERR-66] 02 p0226 N73-11821

**PARTICLE THEORY**
Integrable and nonintegrable Lie-algebra representations relative to particle physics
10 p1191 N73-19692

**PARTICLE TRACKS**
U PARTICLE TRAJECTORIES

**PARTICLE TRAJECTORIES**
NT ELECTRON TRAJECTORIES
Numerical simulation of one-dimensional collisionless plasma phenomena - users manual
[AD-745423] 01 p0085 N73-10706
Plastic, nuclear track detectors for recording and measuring multicharged, heavy particles
[NASA-CR-123918] 02 p0213 N73-11725
Calculating trajectories of solid particles entrained by fluid flow in turbine and compressor stators
[AD-749547] 05 p0591 N73-14799
Radial diffusion of charged particles and splitting of drift shells surrounding earth
[AD-750741] 06 p0668 N73-15437
Spreading of charged particles from point source in magnetic dipole field
[AD-750703] 06 p0703 N73-15732
Computer program ELECTRA used to compute paraxial particle trajectories in axially symmetric electrostatic fields
[SGAE-2007] 07 p0824 N73-16678
Ion currents and trajectories for fluid flow diagnostics
[AD-751785] 07 p0824 N73-16681
Constant azimuth cycloids discussing rotating earth trajectory
07 p0859 N73-16970
Relation between photometric track width and velocity of heavy ions in nuclear emulsions
[LUIP-CR-72-13] 08 p0946 N73-17750
Particle entry measurements from IMP 5 of polar or dayside cusp
08 p0972 N73-17949
Three dimensional solid particle trajectories through stationary and rotating turbine cascades
[AD-753364] 09 p1080 N73-18808
Flow patterns of air being aspirated into blunt thickwalled tube, and inertia effects on particle trajectories
[TR-23] 11 p1270 N73-20306
Computerized video display for processing spark and bubble chamber photographs
[JPRS-58713] 12 p1381 N73-21202
Regge pole model for charge exchange processes using isospin amplitudes and daughter trajectories
[TUETP-73-4] 14 p1694 N73-23747
Three dimensional particle trajectories in compressible gas flow in rotating cascade
[AD-757162] 14 p1701 N73-23807
Projected radiation environment profiles of OSO missions from 1974 to 1978
[NASA-TM-X-66264] 16 p1962 N73-25872
Thin plastic flexible gas discharge tubes for automatic particle track chamber
[NOTA-INTERNA-416] 17 p2033 N73-26455
Position sensitive detector with lithium diffused layer as uniform resistive layer
[NASA-CR-133408] 18 p2152 N73-27391
Pitch angle diffusion of relativistic electrons in plasmasphere
[AD-762952] 20 p2414 N73-29405
Particle track research and lunar rock studies
[NASA-CR-134023] 21 p2596 N73-30806
Analysis of etching process in polycarbonate film when aqueous sodium hydroxide is used to develop charged particle tracks
[NASA-CR-124381] 22 p2673 N73-31415
Molecular transition principle for constructing liquid- and solidhydrogen particle track chambers
[JINR-P13-7067] 24 p2960 N73-33658

**PARTICLES**
NT AEROSOLS
NT ALPHA PARTICLES
NT ANTINUCLEONS
NT ANTIPROTONS
NT ARGON PLASMA
NT BARYON RESONANCES
NT BETA PARTICLES
NT BOSONS
NT CESIUM PLASMA
NT CHARGED PARTICLES
NT COLD PLASMAS
NT COLLISIONLESS PLASMAS
NT CONDUCTION ELECTRONS
NT CORPUSCULAR RADIATION
NT COSMIC PLASMA
NT CYCLOTRON RADIATION
NT DEUTERIUM PLASMA
NT DEUTERONS
NT DROPS [LIQUIDS]
NT ELECTRON BEAMS
NT ELECTRON PLASMA
NT ELECTRON PRECIPITATION
NT ELECTRON RADIATION
NT ELECTRONS
NT ELEMENTARY PARTICLES
NT FAST NEUTRONS
NT FERMIONS
NT FOG
NT FREE ELECTRONS
NT HADRONS
NT HELIUM PLASMA
NT HIGH ENERGY ELECTRONS
NT HOT ELECTRONS
NT HYDROGEN PLASMA
NT ION CYCLOTRON RADIATION
NT LEPTONS
NT LIGHT BEAMS
NT MAGNETICALLY TRAPPED PARTICLES
NT MESON RESONANCES
NT MESONS
NT METAL IONS
NT METAL PARTICLES
NT METALLIC PLASMAS
NT MICROPARTICLES
NT NEUTRAL PARTICLES
NT NEUTRINOS
NT NEUTRONS
NT NONEQUILIBRIUM PLASMAS
NT NONUNIFORM PLASMAS
NT NUCLEAR PARTICLES
NT NUCLEONS
NT OUTER RADIATION BELT
NT PARTONS
NT PHOTOELECTRONS
NT PHOTONS
NT PIONS
NT PLASMA CLOUDS
NT PLASMA JETS
NT PLASMA LAYERS
NT PLASMA SHEATHS
NT PLASMA SLABS
NT PLASMAS [PHYSICS]
NT PLATINUM BLACK
NT POLARONS
NT POSITRONS
NT POWDER [PARTICLES]
NT PRIMARY COSMIC RAYS
NT PROTON BELTS
NT PROTONS
NT QUARKS
NT RADIATION BELTS
NT RAINDROPS
NT RAREFIED PLASMAS
NT RECOIL PROTONS
NT RELATIVISTIC PARTICLES
NT RELATIVISTIC PLASMAS
NT ROTATING PLASMAS
NT SOLAR CORPUSCULAR RADIATION
NT SOLAR COSMIC RAYS
NT SOLAR ELECTRONS
NT SOLAR PROTONS
NT SOLAR WIND
NT SOOT
NT THERMAL NEUTRONS
NT THERMAL PLASMAS
NT TOROIDAL PLASMAS
NT TRAPPED PARTICLES
NT TRITONS
Infrared polarimeter for airborne measurement of terrestrial cloud particle sizes and shapes
[NASA-CR-130119] 03 p0301 N73-12458
Kinetic energy of abrasive particles knocked from metal surface during impact
[AD-750500] 06 p0655 N73-15321
Derivation of equations governing modulation of continuous wave whistler-mode transition by resonant particles
[AD-751043] 07 p0797 N73-16482
Measurement of radioisotopes in air and rain water for areas around Helsinki and Ivalo, Finland
[REPT-11] 07 p0815 N73-16604
Energetic particle flux experiments aboard Explorer 34 and 41 satellites
[NASA-CR-130172] 08 p0946 N73-17747
Radial distribution functions and liquid structure factors for fluids of particles interacting through repulsive potentials
[LPTHE-72/45] 10 p1191 N73-19690
Charge form factor of helium and center-of-mass motion
[ISS-72/12] 10 p1191 N73-19693

Coagulation of carbon particles in premixed flames
[AD-755693] 13 p1592 N73-22907
Equation of motion of sand particle under influence of aerodynamic drag developed in inertial coordinate system
[AD-757724] 14 p1653 N73-23405
Low energy particle experiment in earth magnetoplasma
[AD-758101] 15 p1782 N73-24446
Satellite-borne instruments for measurement of heavy particles
[AD-762208] 19 p2302 N73-28510
Analysis of flow pattern of particles in moving bed for application to manufacturing processes
[NLL-RTS-7330] 20 p2386 N73-29167
Sounding rocket measurements of high latitude dayside electric fields and low energy particles
[NASA-TM-X-70450] 20 p2413 N73-29392
Self-contamination of manned orbiting spacecraft from plasma gas or particulate matter
[NASA-CR-133836] 21 p2601 N73-30843
One- and two-dimensional analysis of particle deposition in turbulent slot flow with application to self cleaning air filter design
22 p2649 N73-31225
Multiplier for estimating particle flux from Explorer 8 and 9 satellite data - Part 2
[NASA-CR-132798] 22 p2665 N73-31352
Particle erosion of 2024 aluminum alloys
[AD-764267] 22 p2686 N73-31517

**PARTICULATE FILTERS**
U FLUID FILTERS

**PARTICULATE SAMPLING**
Absorption spectroscopic determination of nickel, chromium, and cobalt in airborne particulates
[NASA-TM-X-2672] 02 p0137 N73-11111
Design and development of device to prevent clogging in hoppers containing particulate materials
[NASA-CASE-LAR-10961-1] 03 p0306 N73-12496
Rotary powder sample divider for preparation of small sub-samples of heterogeneous powders with adverse flow properties
[PB-211838] 05 p0553 N73-14489
Particulate and gaseous pollutant data gathered during 1968 by national, state, and local air surveillance networks
[APTD-0978] 05 p0572 N73-14652
Microbiological assay procedures for spacecraft cabling, antennas, solar panels, and thermal blankets
[NASA-CR-130383] 08 p0877 N73-17109
X ray fluorescence analysis on air pollution particulate sample
[PB-213366] 11 p1254 N73-20173
Development and operation of apparatus for sampling particulates in gases in upper atmosphere
[NASA-CASE-HQN-10037-1] 18 p2150 N73-27376
Nationwide air pollutant trends for hydrocarbons, oxides, and particulates from 1940 to 1970
[AP-115] 18 p2171 N73-27537
Thermal conductivity measurements of particulate materials in vacuum using basalt and soda lime glass beads of various size ranges as samples
[NASA-TM-X-64759] 18 p2205 N73-27801
Performance of commercial multiple crystal spectrometer instruments in analyzing particulate matter
[AD-762061] 19 p2231 N73-27994
Measurement of concentration of volatile and particulate lead compounds in atmosphere at selected road sites
[PB-221663/8] 22 p2695 N73-31592

**PARTITIONS [MATHEMATICS]**
Sequential machine reduction with partition tree
03 p0271 N73-12200

**PARTITIONS [STRUCTURES]**
Dynamic response of light partitions to sonic boom noting theoretical computation and scale model tests
[ISL-23/72] 19 p2220 N73-27910

**PARTONS**
Sum rule for photoproduction amplitudes in isovector Compton scattering and inconsistency of free fermion parton model in deep inelastic limit
[NUB-2169] 07 p0823 N73-16673

**PARTS**
U COMPONENTS

**PASSAGEWAYS**
NT STRAITS
NT TRANSFER TUNNELS

**PASSBANDS**
U BANDPASS FILTERS
U BANDWIDTH

**PASSENGER AIRCRAFT**
NT BO-105 HELICOPTER
NT BOEING 707 AIRCRAFT
NT BOEING 720 AIRCRAFT
NT BOEING 727 AIRCRAFT
NT BOEING 737 AIRCRAFT
NT BOEING 747 AIRCRAFT
NT BREGUET 941 AIRCRAFT
NT CH-3 HELICOPTER
NT CH-47 HELICOPTER
NT COMET 4 AIRCRAFT
NT CONVAIR 880 AIRCRAFT
NT CV-340 AIRCRAFT
NT CV-990 AIRCRAFT
NT DC 8 AIRCRAFT
NT DC 10 AIRCRAFT
NT EUROPEAN AIRBUS
NT F-27 AIRCRAFT
NT F-28 TRANSPORT AIRCRAFT
NT H-53 HELICOPTER
NT HFB-320 AIRCRAFT
NT L-1011 AIRCRAFT
NT TU-144 AIRCRAFT
NT VISCOUNT AIRCRAFT
NT YAK 40 AIRCRAFT
Analysis of current knowledge regarding ride quality factors in passenger transportation and development of criteria based on human factors engineering
01 p0002 N73-10013
Guidelines and criteria for developing ride quality in air transportation based on external and internal environment conditions
01 p0002 N73-10014
Analysis of airline passenger reactions to vibration environments encountered in supersonic transport and commercial jet aircraft
01 p0003 N73-10017
Development of mathematical model to analyze traveler acceptance factors in short haul air carrier operations
01 p0004 N73-10023
Compilation of accident reports involving corporate executive aircraft during 1970
[PB-210247] 01 p0005 N73-10040
Relative economic advantages of 3 STOL aircraft concepts for short haul, high density transportation systems in 1980 time period
[NASA-CR-114466] 01 p0120 N73-10990
Computerized simulation of passenger emergency evacuation efficiency using Boeing 720 aircraft models
[FAA-AM-72-30] 08 p0879 N73-17119
Mission analysis of VTOL passenger transport aircraft to determine optimum engine cycle for minimum direct operating cost
[NASA-TM-X-68186] 10 p1208 N73-19826
Design of perforated tube uniform distribution of fire extinguishing agent into commercial air transport compartments
[FAA-NA-73-3] 11 p1233 N73-20009
Design and development of vertical takeoff aircraft configuration for use with air transportation services between major population centers
13 p1471 N73-21916
Analysis of trans-Atlantic aircraft movements for 1970 - 1971 period to establish base line for passenger forecasts
13 p1474 N73-21935
Aircraft accident involving crash of Turbo Commander aircraft following takeoff and climbout from Greater Pittsburgh Airport, Pennsylvania on 14 Aug. 1972
[NTSB-AAR-73-5] 13 p1474 N73-21936
Analysis of air passenger traffic on North Atlantic air routes to show development of scheduled and chartered operations
13 p1474 N73-21937
Proceedings of conference on short haul air transportation to show development requirements, economic aspects, and urban and environmental impacts
[M73-54] 14 p1600 N73-22974
Fatigue tests on Comet aircraft pressure cabin to determine effects of pressure cycles on structural stability of cabin windows
[ARC-R/M-3248] 15 p1728 N73-24017
Program definition study for improvement of short haul air transportation to show development requirements and operational constraints - Vol. 2
[FAA-QS-73-1-VOL-2] 18 p2213 N73-27869
Design and characteristics of augmentor wing cruise blowing valveless system for STOL passenger aircraft to define requirements for test facilities - Vol. 2
[NASA-CR-114570] 19 p2220 N73-27907
Dynamic tests of seat belt system, seat belt/shoulder harness system, and seat belt airbag system for aircraft
[FAA-NA-73-30] 20 p2371 N73-29052
Analysis of commuter air transportation services to define problems and identify methods for improvements in cost effective operations
23 p2863 N73-32885
Operation of low cost local air service carriers to show methods for improving transportation services
23 p2863 N73-32886
Actions by Civil Aviation Board to regulate and improve commuter air transportation services
23 p2864 N73-32888

**PASSENGERS**
Proceedings of conference on ride qualities of air, surface, and water vehicles with emphasis on human factors engineering for comfort in transportation
[NASA-TM-X-2620] 01 p0002 N73-10012
Survey of passengers flying from Dulles Airport, Virginia during one year period to obtain cross section of typical passengers and destinations
13 p1473 N73-21925
Survey of US tourism potential
13 p1595 N73-22933
Analysis of nonfatal injuries to passengers and flight attendants in airline operations during period 1968 through 1971
[NTSB-AAS-73-1] 14 p1601 N73-22983
Analysis of passenger acceptance of commercial low-density short haul, air transportation
[NASA-CR-132285] 19 p2226 N73-27950
Analytical forecasting methods for air passenger traffic
23 p2861 N73-32864
World air passenger traffic demand
23 p2862 N73-32868

**PASSIVATION**
U PASSIVITY

**PASSIVE L-BAND RADIOMETERS**
Determination of sea surface conditions using Skylab L-band and Radscat passive microwave radiometers
[E73-10847] 19 p2291 N73-28425
Atmospheric effects on radiometric measurements using EREP of Skylab
[E73-10857] 19 p2292 N73-28434
Determination of sea surface conditions using Skylab passive L-band and Radscat microwave radiometers
[E73-10911] 20 p2397 N73-29260

**PASSIVE SATELLITES**
NT ECHO I SATELLITE

**PASSIVITY**
Diode passivation techniques and fabrication of semiconductor targets that are stable under electron beam bombardment for use in L band amplifiers
[AD-747868] 03 p0276 N73-12237
Effects of passivation processes on radiation tolerance of bipolar transistors subjected to neutron or gamma radiation
[SC-DC-72-1232] 05 p0565 N73-14589
Uses and limitations of passive radar
[AD-750855] 06 p0642 N73-15215
Effect of passivation and dissolution phenomena on structural corrosion of Cr-Ni stainless steels
[NLL-RISLEY-TR-2500-[9091.9F]]
11 p1305 N73-20586

**PASTES**
Production of screen-printed inductive components using ferrite pastes
[RAE-LIB-TRANS-1690] 17 p2072 N73-26763

**PASTURES**
U GRASSLANDS

**PATCHING**
U MAINTENANCE

**PATENTS**
Thermal shock resistant hafnia ceramic materials
[NASA-CASE-LAR-10894-1] 05 p0564 N73-14584
Index of bibliographies for patents and patent applications May 1969 through June 1972
[NASA-SP-7039[01]-SECTION-2]
08 p0971 N73-17932
Survey of patents resulting from aeronautical and space research supported by NASA
08 p0976 N73-17984
NASA patent abstracts bibliography
[NASA-SP-7039[2]-SECTION-1]
16 p1976 N73-25976
Indexes to patent abstracts bibliography
[NASA-SP-7039[2]-SECTION-2]
16 p1976 N73-25977

**PATHOLOGICAL EFFECTS**
Metabolic implications in hyperbaric oxygen systems
[AD-749381] 05 p0504 N73-14106
Hyperoxic damage in animal cells, tissues, and organs
10 p1115 N73-19091
Hyperoxic morphological changes in connective rat tissues
10 p1115 N73-19092
Pathophysiological response reactions of rats to acute hypoxia after injection of cysteamine and aminothiol group radioprotector
11 p1239 N73-20059

**PATHOLOGY**
NT HUMAN PATHOLOGY
Physiological and pathological responses of humans exposed to electricity
[NASA-CR-128422] 01 p0008 N73-10065
Pathomorphological changes in internal organs of white rats following 120 MeV proton irradiation and effect of partial shielding on attenuation of damage
11 p1241 N73-20076
Characteristics of pathomorphological changes in rat internal organs subjected to gamma-neutron irradiation with head and stomach shielded
11 p1241 N73-20077
Combined tissue blocks for comparative pathomorphological study of radiation pathology
11 p1243 N73-20090

**PATIENTS**
Salvarsan therapy of luetic patients and behavior of Wassermann reaction
[NASA-TT-F-14618] 02 p0133 N73-11076
NASA contributions to patient monitoring
[NASA-CR-131538] 12 p1373 N73-21138

**PATTERN DISTRIBUTION**
U DISTRIBUTION [PROPERTY]

**PATTERN RECOGNITION**
NT CHARACTER RECOGNITION
Classification and pattern recognition of short lived events using ERTS-1 imagery
[E72-10183] 01 p0045 N73-10362

Electron optics and target study for improved pattern threshold recognition device
[AD-746246] 02 p0147 N73-11192
Demountable electro-optical system tests for improving pattern threshold recognition device
[AD-745915] 02 p0147 N73-11194
Multidimensional Fourier transformation model for human visual pattern recognition in computerized simulation
[AD-745995] 02 p0147 N73-11195
Hardware design and algorithm for image processing on IDECS/PDP system
[AD-743526] 02 p0174 N73-11414
Fourier pattern recognition techniques applied to titanium alloy photomicrographs
[AD-746720] 02 p0188 N73-11528
Optical texture perception and pattern recognition imagery
[AD-746658] 02 p0212 N73-11722
Walsh transformation for two dimensional correlation and convolution in pattern recognition
[AD-746701] 03 p0272 N73-12207
Automatic pattern recognition of urban land use and land use change
[E72-10244] 03 p0289 N73-12344
Automated thematic mapping using multispectral and spatial pattern recognition techniques on ERTS-1 imagery
[E72-10281] 03 p0292 N73-12379
Development of auditory display of two-dimensional patterns to assist blind persons in pattern identification
[NASA-CASE-HQN-10832-1] 03 p0301 N73-12456
Application of pattern recognition to fault diagnosis of internal combustion engines
[AD-747334] 03 p0351 N73-12863
Computer technique for automatic analysis of planar characteristics of chromosome patterns in microscopic observations
[JPRS-57418] 04 p0379 N73-13085
Substantive analyses of optical design, using visual perception
[AD-749372] 05 p0502 N73-14084
Pattern recognition by devices consisting of arrays of cooperating elements
[PB-211238] 05 p0503 N73-14096
Performance of dual wavelength hail detector considering meteorological and radar parameters
[TR-25] 06 p0639 N73-15191
Critical velocity and patterns of stationary motion of filament
[JPRS-57813] 06 p0652 N73-15293
Analysis of earth resources information systems using satellites as sensor platforms to show type of data obtained and data reduction procedures
07 p0782 N73-16360
Application of pattern recognition oriented algorithms for multispectral data analysis software system
[NASA-CR-130757] 08 p0887 N73-17184
Nonparametric method of pattern recognition using computer simulation
[NASA-CR-130824] 09 p1005 N73-18203
Calculation and simulation of effects of complex search situations
10 p1225 N73-19963
Themis Project results on adaptive learning control systems and pattern recognition
[AD-756424] 13 p1550 N73-22562
Word recognition system based on dimensional representation of phoneme-like word segments
14 p1623 N73-23145
Signal processing of speech pattern recognition using PDP 9 Computer
[AD-757109] 14 p1635 N73-23258
Proceedings of conference on pattern information processing
[PB-214617/3] 15 p1743 N73-24129
Interactive digital processing of optical data in investigations of pattern recognition techniques
[AD-758517] 15 p1755 N73-24223
Discriminatory analysis of waveform data for pattern recognition in radar targets
[AD-757564] 16 p1876 N73-25189
Time domain acoustic signal processor for automatic pattern recognition and target discrimination
[AD-757538] 16 p1876 N73-25190
Fourier analysis of boundary curve for identification of three dimensional objects
[AD-758895] 16 p1877 N73-25192
Pattern recognition and detection of short-lived events such as storms, forest fires, volcanoes, and earthquakes using ERTS-1 data
[E73-10678] 16 p1901 N73-25373
Classification of aerial photographic image data sets on basis of computable textural features
[AD-759505] 16 p1915 N73-25498
Holography applied to matched filtering and pattern recognition
16 p1922 N73-25555
Processing and displaying techniques for optical images
[AD-759038] 17 p2001 N73-26183
Computer interpretation of textured visual outdoor scenes
[AD-759712] 17 p2034 N73-26463
Pattern recognition as statistical analysis of confidence level in forensic trace element identification
[IRI-133-72-11] 19 p2240 N73-28056
Computerized acoustic imaging technique with automatic pattern recognition
[AD-761497] 19 p2240 N73-28060
Computerized simulation of optical pattern recognition and image processing system
[AD-761882] 19 p2241 N73-28065
Improved electron optics and target for pattern threshold recognition device
[AD-762164] 19 p2247 N73-28117
Analysis of ERTS-1 multispectral data by automatic pattern recognition procedures for geological mapping of San Juan Basin, Colorado
[PAPER-G25] 19 p2267 N73-28256
Automatic recognition of terrain types from ERTS-1 MSS imagery
[PAPER-I17] 19 p2279 N73-28338
System for displaying low resolution digital grayscale images of ladar target imaging system
[DREV-TN-2075/73] 19 p2307 N73-28552
Computer program for identifying and classifying sensor signals
[AD-762567] 20 p2379 N73-29118
Statistical methods for pattern recognition and classification applications
[NASA-CR-128989] 20 p2436 N73-29566
Digital calculations in classification portion of Hybrid Pattern Recognition System [HYMPS] program
[REPT-2] 20 p2437 N73-29567
Pattern recognition and potential function
[REPT-6] 20 p2437 N73-29571
Concept of fuzzy sets in pattern recognition
[REPT-7] 20 p2437 N73-29572
Pattern recognition and linear discriminant function
[REPT-8] 20 p2437 N73-29573
Linear programming and its application to pattern recognition problems
[REPT-9] 20 p2437 N73-29574
Cluster seeking techniques in pattern recognition
[REPT-10] 20 p2437 N73-29575
Unique approach to feature selection based on Karhunen-Loeve expansion
[TR-29] 20 p2440 N73-29598
Control mechanism in accommodation-vergence eye movement system in human eyes and importance of central and peripheral vision in pattern perception by human beings
21 p2500 N73-30061
Importance of central and peripheral vision in pattern perception
21 p2500 N73-30063
Detection of urban street patterns in ERTS-1 imagery of Lincoln, Nebraska
[E73-10976] 21 p2534 N73-30315
Data analysis, feature extraction, and pattern recognition for automatic target classification
[AD-763493] 21 p2550 N73-30449
Minimum distance classification based on multispectral scanner data using density estimators and Kullback-Leibler numbers as distance measures
[NASA-CR-133796] 21 p2566 N73-30569
Feature extraction process using gray level structure of imagery
22 p2636 N73-31127
Sediment pattern correlation with inflow and tidal action
[E73-10984] 22 p2658 N73-31291
Detection and identification of short-lived events using ERTS-1 imagery
[E73-10990] 22 p2658 N73-31296
Star mapper using solid-state detectors discussing dioptric and mirror objectives, and star recognition algorithms
[ESRO-CR-82] 22 p2698 N73-31610
Identification of radar targets by pattern recognition
[AD-764713] 23 p2759 N73-32080
Recognition algorithm for object localization in pictures
[BMVG-FBWT-73-14] 23 p2760 N73-32091
Threshold selection for interpretation of digital pictures
[AD-764736] 24 p2898 N73-33132
Comparison of preprocessing and classification techniques for pattern recognition applications to MSS data
[E73-11103] 24 p2915 N73-33260

**PATTERN REGISTRATION**
Analysis of sampling mechanism and operation of automatic normalization of character patterns
[REPT-726] 05 p0516 N73-14195
Digital pattern classification for automatic recognition of English language speech
[AD-757492] 14 p1636 N73-23262
Scene analysis and computer perception with breadboard Mars robot operating in laboratory environment containing rocks of various sizes
[NASA-CR-135711] 23 p2770 N73-32156

**PAULI EXCLUSION PRINCIPLE**
Self-consistent Pauli corrections in Brueckner-Hartree-Fock calculations
[NASA-TM-X-68197] 10 p1193 N73-19704

**PAVEMENTS**
Development of fiberglass reinforced polyester for expedient airfield pavement system
[AD-743958] 01 p0114 N73-10941
Deformation and repair of artificial runway surfaces using new structural materials
[AD-746718] 02 p0153 N73-11242
Structural evaluation of cellular plastic as base course material for military expedient pavement to withstand limited number of aircraft coverages
[AD-747048] 02 p0153 N73-11244
Structural design guidance and construction standards for upgrading and extending service life of airport pavements
[FAA-ED-08-2] 10 p1137 N73-19266
FAA research and development in airport paving criteria
13 p1506 N73-22205
Nondestructive replica techniques for studying roadstone surface polishing by electron microscopy
[PB-212720] 13 p1531 N73-22409
Performance of fibrous concrete pavement materials under cargo aircraft and roadway vehicle loads
[AD-741357] 13 p1547 N73-22537
Numerical integration technique used to re-compute influence coefficients used for development of design curves for rigid airfield runway pavements
[AD-755526] 14 p1646 N73-23353
Inspection of pavement grooving at four commercial and one military airfield
[AD-757208] 14 p1647 N73-23355
Inspection of Hunter Army Airfield, Savannah, Georgia to determine condition of runways
[AD-757387] 15 p1763 N73-24285
Development of procedures for repairing damaged runway pavements
[AD-756806] 15 p1763 N73-24286
Strengthening of keyed longitudinal construction joints in rigid pavements
[AD-759570] 18 p2204 N73-27789
All-weather permanent street patching material for flexible and rigid pavements
[NASA-CR-133549] 19 p2312 N73-28595
Evaluation of structural layers in flexible pavement during simulated aircraft traffic
[AD-762131] 20 p2383 N73-29149
Preliminary analysis of possible factors associated with asphaltic concrete airfield pavement defects
[AD-762404] 20 p2383 N73-29150
Finite element model of jointed concrete pavement on nonlinear viscous subgrade dynamic interaction of aircraft-pavement systems
[AD-764243] 22 p2647 N73-31213
Prediction of performance of runway pavements
[AD-763118] 22 p2648 N73-31214
Design methodology for airfield pavements
[AD-763212] 22 p2648 N73-31215
Application of energy concepts for prediction of pavement system performance
23 p2770 N73-32153
Test results and evaluation procedure for nondestructive tests of airfield pavements
[AD-764787] 23 p2798 N73-32382

**PAYLOADS**
Design and launch support for high altitude sounding rocket payloads
[AD-745977] 02 p0235 N73-11914
Development of payload for mission planning for missions to outer planets as function of flight time for various launch years, launch vehicles, and orbit sizes
[NASA-CR-129244] 03 p0354 N73-12887
Payload data bank, space shuttle program risk analysis, reusable launch vehicles, and cost analysis
[NASA-CR-126170] 03 p0355 N73-12897
Identification of mechanical/structural differences resulting from use of tug/payload combination in space space mode as contrasted to ground-based operations
[NASA-CR-125905] 03 p0358 N73-12920
Design and fabrication of balloon to carry 3500 pound payload at 60,000 feet altitude for feasibility test of powering free balloon near minimum wind field
[AD-750542] 05 p0498 N73-14052
Development of facility for determining satellite payloads
05 p0523 N73-14257
Analysis of payloads for space shuttle based on space missions, planetary exploration, and international rendezvous and docking - Vol. 2
[NASA-CR-129844] 05 p0598 N73-14862
Possible reduction of NASA payload costs
[NASA-TM-X-62223] 07 p0844 N73-16835
Design and fabrication of payloads for sounding rockets for use in X ray astronomy
[NASA-CR-130749] 08 p0959 N73-17845
Design and development of large flexible tunnel for use at space shuttle and payload interface
[NASA-CR-124073] 08 p0964 N73-17879
Analysis of space shuttle capability as launch vehicle for delivery of payloads into earth orbit
[NASA-TM-X-68859] 08 p0965 N73-17889
Frangible glass canister capable of deploying payload in space without dynamically disturbing its contents
09 p1088 N73-18875

Fabrication and calibration of Tomahawk sounding rocket payload for magnetic field measurements in ionosphere
[AD-754246] 10 p1157 N73-19413
Analysis of systems for recovering sounding rocket payloads
[ONERA-TP-1153] 10 p1214 N73-19870
Development and characteristics of supporting frame to isolate payloads from multi-gravitational forces
[NASA-CASE-MFS-21680-1] 11 p1297 N73-20525
Program formulation for weight/sizing design synthesis computer program for application to space shuttle development - Vol. 1
[NASA-CR-128867] 11 p1343 N73-20894
Program description of computerized analysis for space shuttle weight analysis to include flow chart and subroutine linkages - Vol. 2
[NASA-CR-128868] 11 p1343 N73-20895
User manual for weight/sizing design synthesis computer program for application to space shuttle payloads - Vol. 3
[NASA-CR-128869] 11 p1343 N73-20896
Economic analysis of space tug operations to include tug definition, spacecraft configurations, payload effects, and costing logic - Vol. 1
[NASA-CR-124142] 11 p1343 N73-20899
Design, fabrication, and evaluation of mechanical devices for supporting external stores on military helicopters
[AD-755532] 13 p1535 N73-22436
Model for estimating impact of manned EVA costs on future payloads - Vol. 3
[NASA-CR-128928] 14 p1614 N73-23083
Development of system concept for shuttle support to orbital operations of low cost unmanned satellites in low earth orbit
[NASA-CR-130239] 15 p1834 N73-24869
T-38 structural flight load data from Williams, Reese, and Moody Air Force Bases, Jun. 1970 to Dec. 1971
[AD-758891] 16 p1861 N73-25076
Rocket-borne chemical release systems for gas, liquid, solid, and explosive payloads
[AD-758766] 16 p1908 N73-25435
Traffic model data for 1973 NASA payload space shuttle
[NASA-TM-X-64751] 17 p2083 N73-26845
Space shuttle traffic and payload data developed from 1971 mission model
[NASA-TM-X-64731] 17 p2086 N73-26878
Spacelab payload analysis, shuttle interface, operational analysis, and design guidelines
[ESS/SS-399-VOL-1] 17 p2089 N73-26902
Zero-gravity cloud physics laboratory for space shuttle payload planning
[NASA-CR-129002] 20 p2449 N73-29674
Design analysis and trade studies to support candidate configurations and payloads for Astronomy Sortie Missions - Vol. 3 Bk. 2
[NASA-CR-124044] 20 p2474 N73-29871
Effects of ascent trajectory mode and tank disposal method on shuttle payload accommodation
[NASA-TM-X-64773] 21 p2599 N73-30831
Payload carrier integrated test for simulated Sortie Lab Missions
[NASA-TM-X-64770] 22 p2647 N73-31207
Safety concerns with shuttle payloads, space stations and space shuttle orbiters
[NASA-CR-134022] 22 p2714 N73-31726
Payloads of ballistic trajectories in Mercury orbit, and interplanetary trajectory characteristics for Venus swingbys to Mercury
[NASA-CR-2298] 23 p2846 N73-32745
Payload definition and integration study to establish planning concepts for life sciences spacecraft laboratories - Vol. 1
[NASA-CR-124411] 23 p2849 N73-32765
Payload and scientific mission of German aeronomy satellite AEROS
[NASA-TT-F-15104] 23 p2850 N73-32779
Statistical decision approach to missile payload discrimination
[AD-764723] 23 p2852 N73-32790
Design, development, and fabrication of prototype storage module with internal restraints for stowage of items launched to support space missions
[NASA-CR-124465] 24 p2983 N73-33832

**PCM [MODULATION]**
U PULSE CODE MODULATION

**PCM TELEMETRY**
Extraction of telemetry data from bit flow of PCM signals
[NASA-TT-F-14657] 07 p0755 N73-16129
Convolutional encoder and decoder for PCM telemetry
[ESRO-CR-165] 22 p2634 N73-31111

**PDM [MODULATION]**
U PULSE DURATION MODULATION

**PDP COMPUTERS**
NT PDP 8 COMPUTER
NT PDP 10 COMPUTER
Hardware design and algorithm for image processing on IDECS/PDP system
[AD-743526] 02 p0174 N73-11414
Assembler language program for Fourier transform spectroscopy with PDP 11 computer
[MSC-1743] 04 p0394 N73-13200
Structure and signal processing capabilities of special speech processor
14 p1631 N73-23222
Signal processing of speech pattern recognition using PDP 9 Computer
[AD-757109] 14 p1635 N73-23258

**PDP 8 COMPUTER**
PDP 8 computer control of linac system used in photonuclear experiments
[CEA-N-1527] 03 p0302 N73-12466
Three-dimensional output from third octave frequency analysis
14 p1631 N73-23221
Development of PDP 8 computer programs for medical biological laboratory in Netherlands
[MBL-1972-4] 14 p1637 N73-23275
PDP 8 computer interfaces for tropospheric radio propagation measurements
[AD-759700] 16 p1879 N73-25214

**PDP 10 COMPUTER**
Simulation of System 10 computer operation for performance evaluation
[ARL/SM-392] 24 p2897 N73-33127

**PEARLITE**
Vulnerability mechanism of pearlitic and austenitic steel alloys during plastic deformation
[NLL-RTS-7426] 02 p0184 N73-11493
Removal of mechanical impurities from AKOR-1 additive by filtration method using perlite
[AD-751947] 10 p1167 N73-19496

**PEDIMENTS**
U PIEDMONTS

**PEDIPLAINS**
U PIEDMONTS

**PEDOLOGY**
U SOIL SCIENCE

**PEENING**
NT SHOT PEENING

**PELLETS**
Low voltage pellet type thermal batteries
[SC-DC-71-4102] 03 p0254 N73-12059
Production of isotopic fuel pellets by vacuum hot pressing
[ORNL-4796] 05 p0579 N73-14711
Design of prototype thermal battery incorporating pelletized alkaline heat source
[SC-RR-69-497-A] 12 p1366 N73-21084
Collisionless plasma with two stream coupling of corona and core in C02 laser-heated pellets
[AD-757790] 15 p1818 N73-24740
Laser beam fusion and plasma generation on pellet
[UCID-16222] 24 p2965 N73-33697

**PELTIER EFFECTS**
Thermoelectricity of solid-liquid phase boundary in ternary semiconductors and alloys
[AD-756899] 13 p1478 N73-21972

**PENDULOUS GYROSCOPES**
U GYROSCOPIC PENDULUMS

**PENDULUMS**
NT GYROSCOPIC PENDULUMS
Numerical analysis of friction forces developed in ball bearing of pendulum support to show dynamic friction torque and arm of rolling friction
[JPRS-57257] 01 p0062 N73-10507
Swinging ball viscosimeter design and calibration for water viscosity measurements
[AD-745252] 04 p0424 N73-13456
Analysis of motion of compound pendulum and two-gimbal gyroscope mounted in artificial satellite with prescribed orbit and constant rate of rotation
07 p0817 N73-16625
Equations for determining pressure profile, forces, and torques on disk pendulum by point source wave theory from acoustics
[NASA-TM-X-69569] 20 p2454 N73-29725
Stability of undisturbed motion of suspension rings of gyropendulum on moving base
23 p2791 N73-32330

**PENETRANTS**
Liquid-penetrant inspection for surface defects
19 p2303 N73-28519
Sensitivity and comparison evaluation of liquid penetrants used in Saturn 5 vehicle hardware to detect surface cracks
[NASA-TM-X-64769] 22 p2688 N73-31529

**PENETRATING PARTICLES**
U CORPUSCULAR RADIATION

**PENETRATION**
Penetration resistance of cohesionless sands with solid obstacles embedded within soil matrix
[NASA-TM-X-58099] 03 p0294 N73-12392
Penetration of truncated cones into ductile targets
[DREV-R-655/72] 09 p1093 N73-18926
Electromagnetic wave penetration into plasma at lower hybrid frequencies
[AEC-TR-7378] 10 p1196 N73-19732
Static penetration resistance of soils
[NASA-CR-133460] 19 p2294 N73-28445
Water penetration properties of multispectral photography
[UCS/72/13] 20 p2412 N73-29387

**PENETRATION BALLISTICS**
U TERMINAL BALLISTICS

**PENETROMETERS**
Portable penetrometer for analyzing soil characteristics
[NASA-CASE-MFS-20774] 10 p1158 N73-19420
Auger-type soil penetrometer for burrowing into soil formations
[NASA-CASE-XNP-05530] 23 p2790 N73-32321

**PENNING DISCHARGE**
Ion energy distribution functions parallel and perpendicular to modified Penning discharge with high kinetic temperatures and Maxwellian velocity distribution of ions
[NASA-TM-X-68150] 01 p0079 N73-10656
Penning ionization gage ion sources for generating heavy ion beams
[LYCEN-7207] 04 p0453 N73-13695
Low frequency oscillations in Penning discharge under conditions of cyclotron ion source
[NASA-TT-F-14649] 06 p0703 N73-15736
Ion energy distribution function measurements parallel and perpendicular to magnetic Penning discharge field
[NASA-TN-D-7167] 07 p0825 N73-16690
Measurement and analysis of fast ions and neutral particles in Penning discharge with ring anode in magnetic field
[TRITA-EPP-72-12] 09 p1071 N73-18739
Penning discharge along magnetic field in collision-free plasma to simulate geomagnetic flux tube conditions
[TRITA-EPP-72-13] 10 p1189 N73-19676
Rotation of ion component of hot cathode Penning discharge plasma
[NASA-TT-F-14931] 16 p1948 N73-25765
Correlation of potential and density fluctuations of plasma resulting from rotational instability of hot cathode Penning discharge
[NASA-TT-F-15026] 20 p2458 N73-29751

**PENNING GAGES**
Penning ionization gage ion sources for generating heavy ion beams
[LYCEN-7207] 04 p0453 N73-13695

**PENNSYLVANIA**
NT DELAWARE RIVER BASIN [US]
NT SUSQUEHANNA RIVER BASIN [MD-NY-PA]
Resource inventory, land use, and pollution within Susquehanna River Basin based on interpretation of ERTS-1 data
[E72-10329] 05 p0531 N73-14317
Development of environmental indices covering land, water, and air quality in Pennsylvania compatible with ERTS-1 imagery
[E73-10505] 13 p1516 N73-22280
Development of environmental indices covering land, water, and air quality compatible with ERTS-1 imagery for two test sites in Pennsylvania
[E73-10709] 16 p1904 N73-25400
EREP imagery for detection of strip mines and reclamation activities in Ohio, West Virginia, and Pennsylvania
[E73-10731] 17 p2020 N73-26337
Combined visual and digital techniques for analyzing ERTS-1 data pertaining to geologic information on selected areas in Pennsylvania
[PAPER-G2] 19 p2263 N73-28234
Digital processing of ERTS-1 data for identification of strip mining areas in west branch area of Susquehanna River and mine drainage in Pennsylvania
[PAPER-E3] 19 p2268 N73-28267
Application of ERTS-1 and U-2 photography to study of urban land use in Pennsylvania
[PAPER-L17] 19 p2275 N73-28312
Mapping of agricultural land use in Lancaster and Lebandon Counties, Pennsylvania from ERTS-1 digital data
[PAPER-L22] 19 p2276 N73-28317
Use of temporal dimension in classifying and mapping central Pennsylvania area from ERTS-1 MSS data
[PAPER-L23] 19 p2276 N73-28318
Identification and mapping of coal refuse banks in Pennsylvania anthracite coal fields from ERTS-1 data
[PAPER-L24] 19 p2276 N73-28319
Comparison of extreme floods statistically predicted for highway bridge design in Pennsylvania to actual floods caused by hurricane Agnes
[PB-220888/2] 21 p2575 N73-30639
Skylab monitoring of surface mining activities and reclamation in Ohio, West Virginia, Pennsylvania, Indiana, Kentucky, and Illinois
[E73-11033] 22 p2663 N73-31337
Comparison of preprocessing and classification techniques for pattern recognition applications to MSS data
[E73-11103] 24 p2915 N73-33260
Operational system for processing both imagery and computer compatible tapes of ERTS-1 and aerial data of Pennsylvania
[E73-11105] 24 p2915 N73-33262
Photointerpretation and digital data mapping of land use in Pennsylvania
[E73-11106] 24 p2915 N73-33263

Mapping of anthracite wastes from mining in Pennsylvania
[E73-11107] 24 p2915 N73-33264
Thematic mapping of land use near Harrisburg, Pennsylvania from ERTS-1 digital data
[E73-11109] 24 p2915 N73-33266
Usefulness of ERTS-1 MSS data for monitoring coal strip mining, detection of acid mine drainage, and determination of effectiveness of reclamation and abatement procedures in Pennsylvania
[E73-11112] 24 p2915 N73-33269
Storage and retrieval of ERTS-1 and underflight imagery of Pennsylvania
[E73-11116] 24 p2916 N73-33273

**PENS**
X ray fluorescence analysis for determining lead content of paint on pencils in Goddard supply system
08 p0876 N73-17097

**PENTAERYTHRITOL TETRANITRATE**
U PETN

**PENTANES**
Measurement of infrared emission spectra of liquid cyclopentane derivatives excited by carbon dioxide laser
[AD-750480] 06 p0681 N73-15544
Concentration fluctuations in critical region of binary liquid mixture 3-methylpentane-nitroethane
[AD-759740] 16 p1872 N73-25158

**PENTANONE**
Toxicity of long term methyl isobutyl ketone exposure in dogs, monkeys, mice, and rats
[NASA-TM-X-69100] 09 p0996 N73-18130

**PENTOBARBITAL SODIUM**
Sodium pentobarbital effects on albino rats in normocapnic and chronically hypercapnic conditions
[AD-751234] 10 p1121 N73-19142

**PENTOSE**
NT RIBOSE

**PENUMBRAS**
Correction of observed penumbral intensities for scattered light
[NP-19732] 24 p2977 N73-33787

**PEPTIDES**
Development of fluorescent reagent and application to automated assay of amino acids and peptides
[PAPER-76A6-747] 21 p2546 N73-30413

**PERCENTAGE**
U RATIOS

**PERCEPTION**
NT AUDITORY PERCEPTION
NT BINAURAL HEARING
NT SENSORY PERCEPTION
NT SOUND LOCALIZATION
NT SPACE PERCEPTION
NT TACTILE DISCRIMINATION
NT VERTICAL PERCEPTION
NT VIBRATION PERCEPTION
NT VISUAL DISCRIMINATION
NT VISUAL PERCEPTION

**PERCHLORATES**
NT ALUMINUM PERCHLORATES
NT AMMONIUM PERCHLORATES
Preparation of tetraperchlorate of methane by displacement of halogen from carbon tetrahalides using halogen perchlorates
[NASA-CR-129168] 02 p0137 N73-11106

**PERFLUORO COMPOUNDS**
Photolysis of perfluorodienes and diacyl fluorides to produce high molecular weight perfluorocarbon polyether gums
[NASA-CR-130552] 08 p0883 N73-17149
Perfluoroalkylene ether polymers for high temperature fuel tank sealants
[NASA-CR-124249] 14 p1680 N73-23635
Process for preparing disilanols with in-chain perfluoroalkyl groups
[NASA-CASE-MFS-20979-2] 23 p2753 N73-32030

**PERFORATED PLATES**
Analog reinforcement for reducing stress concentration around hole in plate
[AD-745116] 01 p0071 N73-10578
Elastoplastic stress concentration and deformations in perforated plates
[ONERA-NT-193] 04 p0482 N73-13936
Applications of transonic wind tunnel with variable geometry perforated walls
[DGT-8652] 13 p1507 N73-22212
Stress and strain distribution along round, circular cavity in infinite space
[AD-764104] 22 p2726 N73-31819
Method for determining stress and displacements infinite plate with hole of various shapes under uniform tension of compression
24 p2988 N73-33882

**PERFORATED SHELLS**
Application of least square point matching for stress analysis of shallow, perforated, cylindrical shell subjected to tension, edge moment, or transverse shear
[AD-750942] 06 p0728 N73-15942
Concentration of stress around holes in thin walled shells
[AD-764169] 22 p2726 N73-31813

**PERFORATING**
Mathematical model for calculating time required for continuous wave CO2 laser to perforate thin metal sheets
[REPT-534] 16 p1923 N73-25562

**PERFORMANCE**
Performance of graphite fiber reinforced polyimide composites as journal bearing materials
[NASA-TN-D-7078] 01 p0062 N73-10505
Effects of intraperitoneally administered hydrazine on electrophysiology, general behavior, and performance of cats
[AD-746014] 02 p0133 N73-11081
Comparison of European and United States of America reproduced broadband microwave components
[FOA-3-A-3750-E6] 02 p0148 N73-11204
Performance evaluation and operating characteristics of different dissolved oxygen analyzers
[RN-1007] 02 p0171 N73-11385
Performance evaluation of iridium/rhodium integrated probe/fluidic temperature sensor up to 3000 F
[AD-745987] 02 p0175 N73-11417
Performance of closed cycle MHD generators
[AD-747661] 03 p0255 N73-12068
Performance characteristics of self lubricating sintered sulfur-iron material used for bushings in naval aircraft
[AD-748175] 03 p0319 N73-12603
Research reports on chemical propulsion systems and performance engineering
03 p0348 N73-12841
Pulse performance data for small monopropellant and hypergolic bipropellant rocket engines
03 p0349 N73-12846
Performance, combustion stability, and combustion efficiency of aerospike rocket engines
03 p0349 N73-12847
Analytical procedure for determining aerospike nozzle performance particularly performance around base area
03 p0349 N73-12848
Rocket nozzle redesign for improving Saturn launch vehicle J-2 engine performance and reliability
03 p0349 N73-12849
Operational and air transport characteristics of civil V/STOL aircraft
[NASA-TT-F-14619] 04 p0371 N73-13012
Performance of wire bound electrical connectors used in integrated and hybrid circuits and low power semiconductor devices
[AD-748788] 04 p0396 N73-13220
Design and performance of breathing metabolic simulator
04 p0472 N73-13850
Development and performance of color television equipment developed for use on Apollo 15 mission
04 p0473 N73-13855
Performance of prototype high pressure space suit glove
[NASA-CR-114532] 06 p0635 N73-15162
Electrical and performance characteristics of Skylab radar altimeter
06 p0663 N73-15386
Operating principles and thermodynamic cycle of ducted fan turbojet engines
[AD-750984] 06 p0715 N73-15833
Measurement of accelerator tube and waveguide system parameters for improving linear accelerator performance
[RISO-M-1518] 07 p0766 N73-16223
Sample classification accuracy of minimum distance and maximum likelihood classifiers and parametric and nonparametric classifiers in remote sensing
[NASA-CR-130030] 07 p0799 N73-16489
Influence of chemical composition and molecular structure of liquid lubricant on its performance
[NASA-TM-X-68183] 07 p0804 N73-16521
Influence of external pressure on foil bearing performance
[AD-751642] 07 p0805 N73-16528
Gain and performance measurement of expanding CO2 laser mixtures at high pressures
[AD-751694] 07 p0807 N73-16547
Performance of translucent beryllium oxide as envelope material for high intensity flash and continuous wave lamps
[AD-751661] 07 p0813 N73-16589
Operating principles and flight test performance of aerosol counter onboard tethered balloon
[AD-751315] 07 p0816 N73-16619
Performance of lunar roving vehicle during Apollo 15 mission
[NASA-TR-R-401] 07 p0841 N73-16817
Performance characteristics of solid state converter system for measuring aircraft noise and sonic boom
[NASA-CR-112260] 09 p0982 N73-18019
Design and preflight analysis of flexible solar array mechanism
09 p1089 N73-18887
Performance capabilities and cycle life of high specific energy batteries for pollution free electric vehicles
[ANL-7953] 10 p1112 N73-19061
Hydrodynamic instability effects on performance of electromagnetic pump under certain operating conditions
[FRNC-CONF-46] 10 p1166 N73-19485
Effects of boundary layer flow patterns on upright cascade blade performance
10 p1205 N73-19803
Mathematical models for measuring inertial qualities of spherical gyroscope rotors with electric suspension
11 p1317 N73-20691
Differential method for evaluating performance of nonlinear accelerometers
11 p1320 N73-20715
Performance of electromagnetic accelerators in high pressure test facilities
[AD-754024] 11 p1328 N73-20779
Survey of USSR missile defense system
[AD-754629] 11 p1353 N73-20983
Influence of various aerodynamic forces on rectangular wing performance with harmonic movement parallel to sieve flow movement
12 p1361 N73-21043
Performance characteristics of erbium doped laser glass material
[AD-755683] 12 p1411 N73-21435
Design and performance of demand regulated liquid breathing systems for mammalian respiration
13 p1478 N73-21976
Design and performance analysis of thermionic diode modules for in-core thermionic power source
[NASA-CR-131602] 13 p1499 N73-22153
Low temperature performance of air electrodes for use in zinc-air and metal-air battery systems
[AD-758171] 14 p1607 N73-23021
Influence of rain on airborne Doppler velocity sensor performance
[AD-757509] 14 p1668 N73-23541
Performance of aircraft gas turbine components in hot corrosion environments
14 p1676 N73-23599
Influence of carrier lifetime in semiconductor material on its performance as radiation detector
[NASA-CR-121187] 14 p1697 N73-23775
Electrical properties and performance of satellite group terminal system
[STC-TM-332] 15 p1749 N73-24178
Performance of combined photoelectric snow depth-robot rain gage system
[NLL-M-22978-[5828.4F]] 16 p1910 N73-25457
Advanced technology for improving performance parameters of ruby laser
16 p1921 N73-25542
Design and performance of stable CO and CO2 lasers
[AD-758774] 16 p1924 N73-25568
Performance of airfield pavement construction joints under heavy aircraft loads
[FAA-RD-72-106] 16 p1969 N73-25926
Performance of hadron laser safety eyeshields in protecting personnel from accidental ocular exposure to common laser radiation
[AD-759921] 17 p1991 N73-26099
Performance and fatigue strength of compressor blades fabricated from carbon fiber composites and boron composite wires
18 p2166 N73-27496
Performance and endurance of compressor disks bound with boron composite wires
18 p2167 N73-27499
Performance and exhaust emission analysis of Williams research Gas Turbine Hornet automobile engine
[PB-218687/2] 18 p2173 N73-27551
Costs, physical characteristics, and performance of urban transportation systems
[PB-219254/0] 18 p2214 N73-27878
Performance characteristics, except direction, of detection receivers in processing known signals
[AD-762048] 19 p2236 N73-28029
Performance of OV-5 and OV-6 alpha and proton particle detector
[AD-760147] 19 p2302 N73-28505
Design, fabrication, and performance evaluation of CO laser
[AD-762334] 19 p2308 N73-28568
Performance of 1972 ford galaxie equipt with rankine cycle power system composed of organic based working fluid and reciprocating expander
[PB-210836] 19 p2329 N73-28739
Dynamic tests of seat belt system, seat belt/shoulder harness system, and seat belt airbag system for aircraft
[FAA-NA-73-30] 20 p2371 N73-29052
Design and performance characteristics of trap loaded cylindrical antennas
21 p2516 N73-30183
High performance annular combustion chambers for use in turboreactors
22 p2709 N73-31696
Design and performance of DSS 14 64 m antenna feed system
22 p2732 N73-31861
Performance analysis of large orbital X ray telescope
[NASA-CR-124429] 23 p2792 N73-32338

Economics and performance characteristics of high speed digital integrated circuits used in nuclear instrumentation
[LBL-1750] 24 p2900 N73-33150
PERFORMANCE CHARACTERISTICS
U PERFORMANCE
PERFORMANCE DECREMENT
U PERFORMANCE
PERFORMANCE PREDICTION
NT PREDICTION ANALYSIS TECHNIQUES
Suboptimal sampling and control behavior of human operator in output prediction task for automatic process
01 p0015 N73-10114
Optimal control model for predicting manual VTOL pilot performance in longitudinal hovering tasks
01 p0017 N73-10134
Phase margin measure for determining human operator control performance in multivariable closed loop system
01 p0018 N73-10135
Evaluating video graphic performance before and after implementation
[P-4830] 01 p0080 N73-10658
Prediction of lateral directional aerodynamic characteristics for twin engine propeller driven airplane
[NASA-TN-D-6946] 02 p0125 N73-11016
Data management system for prediction of Naval student pilot performances
[AD-744984] 02 p0136 N73-11104
Data sheet for prediction of loaded hydrodynamic journal bearing performance
[ESDU-69002-AMEND-A] 02 p0177 N73-11432
Analysis of space base mission and accidents/events involving nuclear hazard to general public - Vol. 3 Pt. 3
[NASA-CR-123846] 02 p0210 N73-11699
Performance prediction for nuclear electric propulsion systems in advanced unmanned missions to outer planets and solar system
[NASA-CR-129134] 02 p0210 N73-11705
Mathematical basis for operational availability, and its relation to performance effectiveness
[NASA-CR-61382] 02 p0245 N73-11987
Reliability probability analysis on ergatic process in spacecraft control during approach and docking with orbital station
03 p0258 N73-12087
Performance characteristics and prediction methods for hypervelocity light gas gun
[NASA-CR-129292] 03 p0300 N73-12450
Development of method for estimating power required to drive ball bearings in turbine engine based on performance of high speed antifriction bearings
[AD-747600] 03 p0308 N73-12514
Development of closed cycle, vortex stabilized nuclear lightbulb engine to show basic design concepts and operating principles
[NASA-CR-129298] 03 p0330 N73-12695
Maximum detection probability of optical image by photoelectric surface with unit quantum efficiency
[NASA-CR-130121] 03 p0334 N73-12725
Computer techniques for prediction and analysis of OTH radar operation
[AD-748588] 04 p0390 N73-13170
Electrical characterization of silicon materials by lifetime, ionized impurity concentration, and noise measurement
05 p0519 N73-14223
Performance of ERTS data collection system in total system context
[E72-10328] 05 p0530 N73-14316
Aerodynamic configurations of swept wings to improve lift performance at stall in higher range of subsonic speeds
06 p0617 N73-15010
Development of mathematical model for optimal takeoff performance of single rotor helicopter in ground effect with various payloads
[AD-750388] 06 p0624 N73-15066
Application of propagation theory to analyze development and effectiveness of loran navigation system in Germany
[AD-750006] 06 p0697 N73-15682
Computerized prediction of noise levels for jet aircraft with or without noise suppression devices
[NASA-CR-114517] 06 p0700 N73-15708
Development and application of procedures for determining service life of gas turbine engines and components
[NASA-TM-X-2664] 06 p0726 N73-15925
Technique for defining aircraft performance model from limited flight test data and predicted aerodynamic and propulsion system characteristics
[NASA-TN-D-7137] 07 p0738 N73-16008
Reliability engineering methods for electronic components
[FTL-A-A16-1] 07 p0803 N73-16517
Predicting flying qualities by wind tunnel tests
08 p0865 N73-17000
Prediction of aeroelastic hinge moment effects on stability and control
08 p0866 N73-17006
Frequency multiplier based on snapoff diode and computer program for evaluating performance
08 p0888 N73-17189
Designs and performance predictions for high performance supersonic ejector systems
[AGARDOGRAPH-163] 08 p0895 N73-17248
Procedure for predicting performance characteristics of second throat diffusers in ejector systems
08 p0895 N73-17250
Ejector flow model for predicting performance characteristics of supersonic ejector systems
08 p0896 N73-17251
Performance prediction for deployable aerodynamic decelerators operating in supersonic wakes using gas dynamics analogy
[AD-751982] 08 p0897 N73-17266
Reliability and its development in time, frequency and probability domain
[TR-72-38] 08 p0927 N73-17595
Monte Carlo simulation of complex reliability systems using logic circuit analysis programs linked to statistics programs
[TR-72-39] 08 p0927 N73-17596
Mathematical model to simulate staging dynamics of proposed space shuttle configuration
[NASA-TM-X-58098] 08 p0965 N73-17886
Optimum service life determination technique for Naval aircraft
[AD-752747] 09 p0987 N73-18057
Computer programs for predicting hydrodynamic forces and vibration characteristics of rocket engine turbopump inducer - Vol. 2 Revised
[NASA-CR-72712-VOL-2-REV]
09 p1078 N73-18797
Approximative prediction for elastic collapse of spherical shell with flat spot region under external pressure
[NASA-CR-130961] 09 p1096 N73-18946
Application of correlation equations to evaluate structural strength and reliability of various materials
[AD-753497] 09 p1097 N73-18956
Predicting loads and stresses on helicopter rotor blades
[NASA-TT-F-14845] 10 p1105 N73-19014
Development of method for analyzing performance of magnetohydrodynamic generator based on thermodynamic properties and flow characteristics
10 p1110 N73-19051
Color vision tests as predictive indicators of flying task performance
10 p1113 N73-19074
Harmonic analysis for predicting long term artificial satellite orbital motion
10 p1178 N73-19579
Application of parafoil equations of motion to predict flight performance of powered parafoil flight vehicle
[AD-754907] 11 p1236 N73-20034
Performance estimates for airborne magnetic drum memories
[AD-754933] 11 p1260 N73-20226
Reliability and failure time prediction for titanium adhesive bonds using multiple regression analysis
[AD-754526] 11 p1301 N73-20560
Mathematical models for measuring operating functions and performance of gyroscope with two degrees of freedom
11 p1318 N73-20696
Methods employed to obtain datum position and velocity information for evaluation of inertial navigation systems and identification of error sources
11 p1320 N73-20716
Nomographs for predicting aerodynamic performance of air launched stores
[AD-754428] 11 p1353 N73-20981
Technique for determining mechanical properties of full-size aircraft tires from tests conducted with small-scale model tires
[NASA-CR-2220] 12 p1357 N73-21006
Analysis of factors inhibiting performance of rotary wing aircraft and mathematical models of rotary wing flow characteristics
12 p1358 N73-21019
Development of method for predictiong performance of heavily loaded propellers and rotors in steady hovering flight
12 p1360 N73-21040
Development of algorithm for calculating inviscid flow about arbitrary planform rotors and application to analyzing various rotary wing configurations
12 p1362 N73-21048
Three different bases for susceptibility prediction to motion sickness
12 p1367 N73-21093
Motion sickness questionnaire and field independence scores as predictors of success in Naval aviation training
12 p1368 N73-21097
Alcohol reference method for predicting drug modifications of central nervous system activity and pilot performance decrease
12 p1369 N73-21112
Effect of steady state circumferential total pressure distortion on loss in compressor stall pressure ratio
[NASA-CR-114577] 12 p1443 N73-21693
Design and evaluation of two airfoils for helicopter rotors for reduction of rotor power requirements
[NASA-CR-112297] 14 p1601 N73-22977
Analysis of liquid metal magnetohydrodynamic energy conversion systems to determine performance limits and identify system parameters
[AD-757065] 14 p1606 N73-23013
Development of self-contained, solid lubricated ball bearings for operation at high speed - Part 2
[AD-756487] 14 p1671 N73-23557
Exponential probability distribution analysis for extrapolating aerospace system performance statistics from test results
14 p1713 N73-23903
Development and application of aircraft performance prediction methods for subsonic and supersonic transport and fighter aircraft
[AGARD-LS-56] 15 p1732 N73-24042
Numerical methods for determining range and radius of action performance of transport and combat aircraft and effects of various parameters on performance
15 p1732 N73-24043
Methods for evaluating and predicting airfield performance of turbojet and turbofan aircraft operating in conventional and short takeoff modes
15 p1732 N73-24044
Development of methods for predicting aircraft flight maneuver and climb performance to show effects of excess power and load factor
15 p1732 N73-24045
Analysis of parameters affecting choice of engines for transport and combat aircraft during design process
15 p1732 N73-24048
Development of computer program for determining minimum time trajectory and comparison with gradient method of computation
15 p1733 N73-24053
Parametric performance characteristics and treatment of temperature coefficients of silicon solar cells for space application
[NASA-CR-132156] 15 p1738 N73-24090
Psychological assessment techniques for determining astronaut attentional flexibility and associate performance
[NASA-CR-128945] 15 p1744 N73-24136
Mean squared error method for predicting fidelity of differential pulse code modulation system
16 p1873 N73-25165
Computerized prediction of radar cross sections for thin wires and comparison with backscatter data
[AD-758757] 16 p1882 N73-25230
Calculated performance map of high pressure ratio turbine designed for turbofan simulator
[NASA-TM-X-2822] 16 p1956 N73-25822
Quantitative evaluations of adaptive physical operator/manipulator control systems
17 p1990 N73-26090
Use of differential phase and gain for predicting performance of ultrahigh frequency telecommunication system
17 p1995 N73-26132
Parametric design analysis to determine characteristics and performance of class of high speed hydrofoil craft
[AD-760355] 17 p2016 N73-26303
Development of techniques for predicting point and path performance of light aircraft
[NASA-CR-2272] 18 p2105 N73-27022
Analysis of dynamics of free-piston expander-compressor machinery
18 p2156 N73-27416
Feasibility analysis and prediction performance of constant temperature heat pipe for space applications
[ESRO-CR[P]-246] 18 p2207 N73-27810
Operation of pulse radar automatic range finders used jointly with search and lock-on system
22 p2628 N73-31061
Prediction of performance of runway pavements
[AD-763118] 22 p2648 N73-31214
Characteristics of axial flow compressors to show compressor parameters during pre-stall conditions and techniques for predicting compressor stall conditions
[AD-763816] 22 p2710 N73-31704
Pilot rating of fighter aircraft in precision heading task using mathematical model for predicting aircraft performance
[AD-764695] 23 p2745 N73-31973
Computer program for predicting pilot rating of pitch stability of T-33 aircraft under vertical turbulence conditions
[AD-764696] 23 p2745 N73-31974
Kalman filter estimation of aircraft pilot performance
[AD-764694] 23 p2752 N73-32026
Application of energy concepts for prediction of pavement system performance
23 p2770 N73-32153
Prediction of overall and blade-element performance for axial flow pumps
[NASA-CR-2301] 23 p2775 N73-32189
Performance of study plan for proposed Skylab experiments concerning metals melting and sphere forming
[NASA-CR-124396] 23 p2796 N73-32368

Development of mechanical equipment reliability prediction techniques
[AD-765367] 23 p2799 N73-32390
Design parameters for optimal cost/cruise performance of subsonic jet transport
23 p2860 N73-32853
International civil aviation organization for air traffic forecasting and airport development
23 p2861 N73-32865
Functional models for airline operations
23 p2862 N73-32870
Performance preduction for tritium powered generators
[LIB/TRANS-437] 24 p2881 N73-33004
Performance characteristics prediction of linearly oscillating electromagnetic pump
24 p2928 N73-33384
Performance calculation of arbitrarily switched gas turbines by simulation with building block system on digital computer
24 p2973 N73-33758

**PERFORMANCE TESTS**

Results of testing and characterization of battery plates for nickel cadmium cells
[NASA-CR-130094] 01 p0006 N73-10050
Experiments and simulations to determine effect of compliance and force feedback on manipulator performance
[NASA-CR-128605] 01 p0019 N73-10151
Performance tests of ball bearings to determine service life during operation without lubrication under various conditions of atmospheres, loads, and speeds
[AD-746034] 01 p0063 N73-10520
Performance of air-to-satellite-to-ground systems for air traffic control
[PB-210378] 01 p0078 N73-10646
Survey of techniques used for turbine engine performance analysis
[AD-744587] 01 p0091 N73-10750
Performance of sealed nickel cadmium storage cells at very low ampere/hour percent recharge for OAO
[NASA-TM-X-66093] 02 p0128 N73-11040
Long-term testing of water electrolysis systems for regenerative life support system in manned space stations
[NASA-CR-128629] 02 p0135 N73-11095
Evaluation of HF/VHF breadboard modeled manpack radio sets
[AD-745918] 02 p0142 N73-11152
Performance tests of scale model of lunar roving vehicle used on Apollo 15 mission to determine vehicle mobility
[NASA-CR-129176] 02 p0152 N73-11234
Mechanical, friction, and gap-effects on semiaxial turbine pump having different blade arrangements
02 p0178 N73-11439
Effects of pavement surface condition on cornering forces developed by automobile tires of different tread design
[NASA-TN-D-6964] 02 p0192 N73-11551
Evaluation of automated air traffic control system and comparison with operator performance using manual system
02 p0207 N73-11683
Design, development, and evaluation of turbine for small, low-cost turbofan engine
[NASA-TM-X-68157] 02 p0223 N73-11803
Performance of prototype monopropellant engines using electrolytic ignition system
[AD-745993] 02 p0224 N73-11808
Performance of solid propellant apogee rocket motor in test firing at simulated altitude
[AD-747018] 02 p0224 N73-11809
Performance of shrouded and unshrouded fans in low noise turbofan engines
03 p0249 N73-12018
Results of testing long life primary cells
[SC-DC-72-1005] 03 p0255 N73-12060
Kapton covered cadmium sulfide solar cell performance tests in aerospace and earth atmosphere environments
[ONERA-DERTS-NT-02-32] 03 p0255 N73-12062
Design, development, and evaluation of pressure transducer using glass fiber bundle to transmit and receive reflected light from pressure diaphragm
[AD-747521] 03 p0304 N73-12480
Performance of high speed overriding clutch assemblies for helicopters
[AD-747807] 03 p0308 N73-12518
Design, development, and performance tests of long pulse liquid laser oscillator and circulatory subsystem
[AD-747964] 03 p0311 N73-12536
Testing hydrophone types for acceleration response
[AD-748038] 03 p0338 N73-12758
Performance, stability, and design of aerospike engines and engine system components
[NASA-TM-X-64690] 03 p0348 N73-12840
Demonstration of duct cooling concept with gaseous hydrogen/oxygen propellant in high pressure thruster - Vol. 2
[NASA-CR-120870] 03 p0350 N73-12859
British Prospero satellite control noting instrumentation, equipment, and experimental performance
[RAE-TR-72088] 03 p0359 N73-12928
Performance tests of Andover C short takeoff transport aircraft on grass, concrete and soil landing sites
[ARC-CP-1220] 04 p0373 N73-13034
Design and performance of rechargeable zinc-air batteries
[AD-748455] 04 p0376 N73-13058
Measurement technique for determining sensitivity and radiated power of oscillator radio receiver
[AD-748826] 04 p0389 N73-13165
Tests of lunar roving vehicle wheels in simulated lunar soil to determine effects of wheel speed, wheel load, presence of fender, travel direction, and soil strength
[NASA-CR-129612] 04 p0401 N73-13263
Performance evaluation of volumetric and mass cryogenic turbine flowmeters
[NBS-TN-624] 04 p0420 N73-13426
Performance tests of ball bearings operating at high dn values
[NAL-TR-284] 04 p0426 N73-13469
Valid tests with temperature gradients and/or rates of discharge as primary variables for accelerated life testing sealed nickel cadmium batteries
[AD-749129] 05 p0499 N73-14061
Comparison of micropower operational amplifiers based on various measurements and performance tests
[GRI/NTP/105] 05 p0520 N73-14225
Performance tests and service life of electroluminescent film display device
[AD-749790] 05 p0521 N73-14235
Experimental data on baffled and unbaffled vibratory cavitation damage tests
[PB-211899] 05 p0525 N73-14270
Performance tests of differential dc voltmeter
[LRBA-PV-9/520/SIE] 05 p0548 N73-14450
Test results of acoustic ranging and bearing measuring system
[AD-749041] 05 p0578 N73-14703
Design, fabrication, and comparison of heat pipes for temperature control in meteorological satellite
[ESRO-CR-59] 05 p0606 N73-14929
Performance tests of crash protective seat belts using energy absorbers to allow system to yield at constant force
[ARL/SM-340] 06 p0619 N73-15023
Physical properties and performance of radioisotope power generator Tristan
[CONF-710444-11] 06 p0627 N73-15083
Design and performance of mechanically rechargeable zinc air battery
[AD-749779] 06 p0627 N73-15086
Development and operation of test facility for high temperature gas turbine experiments
[NAL-TR-282] 06 p0649 N73-15269
Development and test of explosively driven two-stage hypervelocity rocket launcher for use in meteoroid studies
[NASA-CR-2143] 06 p0649 N73-15272
Effect of sea state and atmospheric parameters on satellite altimeter performance
06 p0662 N73-15372
Analysis of gyrocompass performance characteristics to include long term accuracy, statistical attributes, and application as geophysical instrument
[AD-750890] 06 p0697 N73-15685
Development of method for analysis and assessment of turbofan engine performance
[CRANFIELD-SME-2] 06 p0712 N73-15811
Performance comparison of double cornered plug nozzle with conventional convergent-divergent rocket nozzle
[AD-750591] 06 p0714 N73-15830
Nonequilibrium combustion products for calculating rocket engine performance and chemical kinetics of combustion processes
[AD-750169] 06 p0715 N73-15835
Power handling capability and electrical breakdown characteristics of electronic countermeasure antennas
[AD-751309] 07 p0758 N73-16154
Performance of large screen tactical display systems in training devices using cathode ray tubes
[AD-751559] 07 p0767 N73-16228
Design and implementation of fixed-based spin simulator, and spin test results
[AD-751644] 07 p0767 N73-16229
Current voltage characteristics of vapor deposited tungsten niobium planar thermionic converter
[NASA-TM-X-2716] 07 p0819 N73-16639
Fabrication and tests of 2.5-centimeter Kaufman electron bombardment microthruster
[NASA-TM-X-2708] 07 p0836 N73-16774
Performance tests to determine effects of reducing turbine blade thickness on turbine engine performance
[NASA-TN-D-7128] 07 p0836 N73-16776
Tests of grid-translation type beam deflection system on 5-cm diameter mercury ion thruster
[NASA-TM-X-68185] 07 p0836 N73-16777
Performance evaluation of coaxial injectors for use in gaseous hydrogen-liquid oxygen rocket engines
[DLR-FB-71-56] 07 p0836 N73-16779
Tests of Skylab Orbital Workshop ventilation concepts
[NASA-TM-X-64700] 07 p0845 N73-16875
Performance tests to determine effects of increased rotor blade loading on gas turbine operation by reduction of rotor blade inlet diameter
[NASA-TM-X-2730] 08 p0870 N73-17039
Performance and endurance testing of 6 kW organic Rankine cycle power conversion system
[SAN-651-130] 08 p0870 N73-17042
Performance of sensing system having inverse function amplifier
[RD/B/M-2306] 08 p0889 N73-17196
Evaluation of device for rapid detection and location of shallow subsurface tunnels and excavations
[AD-752086] 08 p0919 N73-17531
Compilation of analyses generated during development of electron-proton spectrometer for Skylab program to insure reliability and quality control
[NASA-CR-128705] 08 p0925 N73-17576
Qualification tests of electron-proton spectrometer to determine suitability for use in Skylab program
[NASA-CR-128703] 08 p0925 N73-17580
Test plan for evaluation of redundant sensor strapdown inertial measuring unit to include operating procedures and data and analysis requirements
[NASA-CR-123513] 08 p0941 N73-17711
General test plan for redundant sensor strapdown inertial measuring unit evaluation program
[NASA-CR-130722] 08 p0941 N73-17712
Evaluation of loran antenna modification to determine effect of increased height on radiated power and system performance
[AD-751978] 08 p0942 N73-17714
Cesium oxide/cesium solutions as sources of oxygen and cesium for improved thermionic converter performance
[NASA-CR-121119] 08 p0942 N73-17717
Design, development, and evaluation of solar electric thrust vector control system for ion engine array
[NASA-CR-130622] 08 p0953 N73-17806
Design, fabrication, and testing of thrust vectorable ion optical systems with emphasis on response time and minimal power consumption
[NASA-CR-121142] 08 p0955 N73-17816
Literature review on design and performance of multistage rockets
[AD-752815] 08 p0956 N73-17824
Dynamic testing and structural modeling of aircraft tire properties
[NASA-CR-2219] 09 p0985 N73-18042
Accomplishments during evaluation of automatic inspection, diagnostic, and prognostic maintenance system using UH-1 helicopter as test bed - Vol. 2
[AD-752891] 09 p0987 N73-18059
Performance tests of hydromechanical fuel control system for J-85 engine
[NASA-TN-D-7198] 09 p0990 N73-18082
Design and evaluation of hybrid boost bearings consisting of fluid film bearing coupled with rolling element bearing
[NASA-CR-2226] 09 p1039 N73-18476
Performance of gas lubricated thrust bearing based on minimum surface damage and low value of friction coefficient
[AD-753018] 09 p1041 N73-18493
Terminal ballistic performance of fiber glass epoxy composite material for aerodynamic control surfaces
[AD-752918] 09 p1053 N73-18584
Performance tests on low hub-tip ratio supersonic axial flow compressor
[AD-752585] 09 p1079 N73-18805
Development problems and flight performance evaluation of Apollo lunar module landing gear
09 p1088 N73-18878
Structural configuration and performance tests of 928 sq m solar array
09 p1089 N73-18891
Performance tests of experimental short length annular combustor using one-side-entry dilution airflow technique
[NASA-TN-D-7225] 09 p1099 N73-18967
Tests of combustion chamber with burner device using system of transverse air streams for flame stabilization
[AD-753518] 09 p1100 N73-18977
Determination of aircraft aerodynamic characteristics under captive flight conditions and description of test equipment
10 p1105 N73-19010
Performance of typical V/STOL aircraft and comparison of data obtained with flight simulator against data obtained by actual flight tests
10 p1105 N73-19011
Cold weather tests to determine application of ground effect machines for military logistic purposes in Arctic regions
[AD-753527] 10 p1107 N73-19027
Design and performance tests of prototype self-locking actuator
[NASA-CR-124135] 10 p1163 N73-19459
Performance tests of low-pressure-ratio centrifugal compressor with four different diffuser configurations
[NASA-TN-D-7237] 11 p1231 N73-19997
Performance data analysis for OAO sealed nickel cadmium cells and batteries
[NASA-CR-130233] 11 p1237 N73-20045

Comparison tests of strobe and incandescent beacons to determine suitability as replacement for standard rotating airport beacon
[FAA-NA-73-1] 11 p1255 N73-20182
Performance tests of electron-proton spectrometer for design verification
[NASA-CR-128852] 11 p1292 N73-20486
Evaluation of explosive actuated normally open valve model 1399
[NASA-CR-131401] 11 p1296 N73-20520
Design, development, and evaluation of servoactuator device to include application to optimized system configuration
[NASA-CR-124025] 11 p1297 N73-20524
Operating principles and performance tests results for optical modulator system with mode locked Nd-YAG laser
[NASA-CR-130195] 11 p1302 N73-20569
Design and performance of transverse excited atmospheric carbon dioxide lasers
[AD-754544] 11 p1303 N73-20572
Methods for conducting acceptance tests and reliability tests of gyroscopes as part of inertial platform quality control procedures
11 p1317 N73-20689
Laboratory tests of accelerometers used in inertial guidance systems in French military programs
11 p1320 N73-20714
Performance tests on J-52 turbojet engines to determine acceptable compressor stall margin
[AD-755152] 11 p1334 N73-20832
Evaluation of helicopter handling qualities based on ground-based piloted flight simulator tests
12 p1359 N73-21030
Analysis of effect of grooved runway configurations on aircraft tire braking traction on flooded runway surfaces
[NASA-TN-D-7215] 12 p1363 N73-21057
HF cell performance over different operating conditions after storage
[SC-CR-72-3156] 12 p1366 N73-21085
Life test performance of SNAP 23 prototype mockup system
[WANL-3559-1] 12 p1427 N73-21568
Performance of SNAP 19 RTG for Viking lander system
[IESD-2960-53] 12 p1427 N73-21569
Performance and noise reducing properties of thrust augmentors
[NASA-TM-X-62250] 13 p1472 N73-21921
Performance tests on commercial transport aircraft engines to determine factors contributions to engine malfunctions
[FS-140-72-2] 13 p1473 N73-21933
Evaluation of ground effect machines under various environmental conditions to determine feasibility as rescue vehicles by Coast Guard
[AD-755409] 13 p1475 N73-21947
Solar array development discussing manufacturing, design qualification tests in aerospace environments, and comparison between fold-up and roll-up types
[RAE-TR-72109] 13 p1476 N73-21959
Construction and performance of sealed nickel zinc batteries
[AD-755550] 13 p1477 N73-21967
Development of standard uncertainty methology for analysis of gas turbine engine performance characteristics
[AD-755356] 13 p1571 N73-22733
Performance of Mirage 3 sigma 4 after body
14 p1597 N73-22946
Comparison of aerodynamic lift developed by mechanical high lift systems and lift developed by externally blown flaps on short takeoff aircraft
[NASA-TT-F-14895] 14 p1601 N73-22981
Development of boron composite materials for construction of aircraft landing gear for A-37 aircraft - Vol. 1
[AD-756922] 14 p1603 N73-22996
Design, fabrication, and test of boron composite material landing gear for use as main landing gear on A-37 aircraft - Vol. 2
[AD-756923] 14 p1603 N73-22997
Design, development, and evaluation of organic, Rankine cycle power plant
[AD-757652] 14 p1606 N73-23018
Performance tests of air traffic control system to determine effectiveness in prevention of midair collisions
14 p1690 N73-23713
Space flight tests for determining performance efficiency of ion engine model with surface ionization of cesium on tungsten
14 p1701 N73-23801
Static and cruise tests on series of 13 ft diameter low disc loading rotors with various blade twists
[NASA-CR-114625] 15 p1734 N73-24063
Design and performance of voltage transducers for Mariner spacecraft solar cells
[NASA-CR-132250] 15 p1756 N73-24234
Broadband characteristics of open sleeve dipole antenna mounted in front of metallic reflector
[AD-758755] 15 p1758 N73-24251
Evaluation of image forming ability of infrared line scan system using laboratory and flight test techniques
15 p1786 N73-24476
Cross calibration tests of ultraviolet spectrometer
[NASA-CR-128628] 15 p1789 N73-24506
Effect of blade thickness on shear strength of fasteners
[AD-757997] 15 p1793 N73-24539
Performance test of compressor stage with cantilevered stator and rotating inner shroud under stator at rotor tip speed of 1600 feet per second
[NASA-CR-121141] 15 p1825 N73-24794
Statistical performance test evaluation in aerodynamic development of Dart sailplane
[CRANFIELD-AERO-16] 16 p1859 N73-25059
Performance tests of 2-pound and 3.3-pound disposable zinc air, non-reserve batteries
[AD-759218] 16 p1865 N73-25105
Design and performance of aircraft or spacecraft differential maneuvering simulator
[NASA-TN-D-7304] 16 p1885 N73-25259
Construction and operation of calorimeters for heat of solution and low temperature heat capacitance measurements
[USGS-PP-755] 16 p1912 N73-25470
Design of 10.6 micrometer detector array using 77 K, 1500 MHz photodiodes
[AD-758714] 16 p1915 N73-25496
Performance verification test plan for Apollo ultraviolet spectrometer experiment
[NASA-CR-128573] 16 p1915 N73-25500
Acceptance test plan for bench test equipment of Apollo ultraviolet spectrometer experiment
[NASA-CR-128574] 16 p1916 N73-25508
Aerodynamic design parameters and test performance of two-stage high pressure ratio centrifugal compressor
[AD-759499] 16 p1919 N73-25533
Performance data for single stage axial flow compressor with tandem airfoil blading
[NASA-CR-121145] 16 p1955 N73-25818
Performance tests of nickel cadmium and silver cadmium electric batteries to determine service life and reliability
[NASA-CR-132801] 17 p1985 N73-26046
Analysis of operation of electric alternator feeding into direct current system through rectifying device
[RAE-LIB-TRANS-1679] 17 p1986 N73-26049
Test operation procedure for radar interrogator transmitter
[AD-759227] 17 p1998 N73-26158
Performance of prototype broadband selective ferrite limiters
[AD-759951] 17 p2005 N73-26219
Design and performance tests of solid state A-6 aircraft engine instruments
[AD-760351] 17 p2035 N73-26469
Endurance and performance tests of bore ball bearings lubrication thrust loaded 120-mm to 3 million DN
[NASA-TM-X-68264] 17 p2037 N73-26479
Environmental and performance tests of thermoelectric materials
[MMM-2473-342] 17 p2050 N73-26585
Simulation testing of detector for digitally encoded multifrequency tones
[REPT-6755] 18 p2116 N73-27113
Modifications and testing of portable ultra-sensitive superconducting magnetometer
[AD-759735] 18 p2153 N73-27400
Fabrication and life testing of thermionic converters
[NASA-CR-121180] 18 p2177 N73-27576
Feasibility of small scale, full operating gas core reactor demonstration test
[NASA-CR-121190] 18 p2177 N73-27577
OAO 3 flight test on heat pipe cooling efficiency during weightlessness
18 p2208 N73-27826
Evaluation of air cushion vehicle operations over railroad beds and secondary roads and analysis of dynamic response to geometric obstacles
[AD-762169] 19 p2221 N73-27920
X ray inspection and quality control of AEG cathode life-tests tubes after 44,000/hr life for prediction of communication satellite traveling wave tube durability
[ESRO-TM-148-ESTEC] 19 p2305 N73-28536
Analysis of operation of single stage, high pressure centrifugal compressor during closed loop flow of various gases
[AD-761608] 19 p2331 N73-28750
Performance tests to determine fore and aft elastic response characteristics of aircraft tires with bias ply, bias-belted, and radial-belted design
[NASA-TM-X-69570] 20 p2360 N73-28987
Performance of anti-G valve subjected to varying acceleration forces
[AD-760814] 20 p2372 N73-29062
Evaluation of electrogasdynamic concept for dispersal of warm fog based on injection of charged water droplets into fog
[ASRC-PUBL-207] 20 p2382 N73-29140
Motion simulator for performance testing of satellite attitude control systems
[ESRO-CR-66] 20 p2383 N73-29145
Analysis of flow pattern of particles in moving bed for application to manufacturing processes
[NLL-RTS-7330] 20 p2386 N73-29167
Performance tests of radiation thermoelements to determine stability of detectors and feasibility of daytime measurement of long wave radiation
20 p2403 N73-29309
Fabrication and mechanical testing of high pressure ratio compressor
[NASA-CR-121193] 20 p2423 N73-29463
Flight tests of VHF Omnirange navigation and Tacan systems to determine bearing error curves
[FAA-RD-72-73] 20 p2452 N73-29710
Status of civil airline implementation of all-weather landings in Europe and United Kingdom
[MTR-6211] 20 p2452 N73-29711
Tachistoscopic investigation on electronic and electromechanical cockpit display for performance comparison
[DLR-FB-73-27] 21 p2496 N73-30034
Environmental tests on Symphonie model momentum flywheel
[ESRO-CR-96] 21 p2553 N73-30469
Aero and acoustic design features of single stage fans tested in outdoor acoustic facility
[NASA-TM-X-68289] 21 p2579 N73-30668
Investigation of hollow cathode performance for 30 cm thrusters
[NASA-TM-X-68298] 21 p2588 N73-30739
Performance of 30 cm ion thrusters with dished accelerator grids
[NASA-TM-X-68294] 21 p2589 N73-30744
Altitude test and performance of Aerojet AJ10-179 liquid rocket engine under vacuum conditions
[AD-763727] 21 p2591 N73-30758
Engineering test procedures for heat seeking missiles
[AD-763324] 21 p2602 N73-30853
Supersonic wind tunnel tests of internal performance of rectangular variable geometry air inlets noting effect of incidence
[ARC-CP-1242] 22 p2612 N73-30933
Supersonic wind tunnel tests of internal performance of rectangular variable geometry air inlets at zero incidence
[ARC-CP-1243-PT-1] 22 p2612 N73-30934
Performance tests for Naval global communications system equipment
[AD-764485] 22 p2635 N73-31116
Pyroelectric infrared detector performances investigating strontium and barium niobates, lithium sulfate and TGS materials effects on frequency ranges and sensitivity
[ESRO-CR-67] 22 p2675 N73-31425
Test performance of pump for Pioneer Venus probe mass spectrometer inlet
[NASA-CR-114660] 22 p2678 N73-31448
Hydraulic pump-looped circuit evaluation of candidate silicone base nonflammable hydraulic fluid
[AD-764064] 22 p2679 N73-31456
Design operation and performance of gyro module for SIRU
[NASA-CR-135509] 22 p2698 N73-31608
Performance tests of hydrazine catalytic thruster to determine capability for spacecraft limit-cycle attitude control with short thruster pulse durations
[NASA-CR-135489] 22 p2710 N73-31701
Effects of blade tip clearance and leading edge sweepback of compressor rotor blades on inducer performance and blade pressure loading
[NASA-CR-72712] 23 p2739 N73-31930
Performance tests to determine cornering characteristics of aircraft tire under various runway conditions, ground speeds, and yaw angles with and without braking
[NASA-TN-D-7351] 23 p2742 N73-31948
EMR 549-120 image dissector test and calibration noting geometrical and photometric tube properties
[ELEC-010-72] 23 p2766 N73-32127
Limiting speed and bearing performance of grooved and angular contact ball bearings
[NASA-TT-F-15017] 23 p2796 N73-32364
Performance and environmental tests of National Air Space Enroute Stage air traffic control system
[FAA-NA-73-55] 23 p2817 N73-32518
Performance tests of geometrically different sets of dished accelerator grids on ion thruster engines
[NASA-TM-X-71420] 23 p2830 N73-32615
Performance of Mariner 9 television cameras
23 p2843 N73-32718
Design, fabrication, and performance of multilayer insulation system for modular nuclear vehicle LH2 propellant tank
[NASA-CR-124400] 23 p2856 N73-32824
Simulation of System 10 computer operation for performance evaluation
[ARL/SM-392] 24 p2897 N73-33127
CIT photoheliograph functional verification unit test in Big Bear Solar Observatory vacuum chamber
[NASA-CR-124455] 24 p2925 N73-33364
Acoustic, reentry, and structural load environment tests on mullite insulation for space shuttle
24 p2941 N73-33483
Space environmental testing of silica insulation for space shuttle orbiter
24 p2941 N73-33484

Thermal and structural performance tests on space shuttle orbiter surface insulation materials
24 p2941 N73-33489
Effects of partly filled small gas turbine hydrodynamic converter during starting process of main engines
24 p2973 N73-33759
Relationships between performance, safety, cost, and schedule parameters to generate program models for total space program
[NASA-CR-135903] 24 p2993 N73-33919
Relationships between performance, safety, cost, and schedule parameters to generate program models for total space program
[NASA-CR-135902] 24 p2993 N73-33920

**PERFUSION**
U DIFFUSION

**PERIGEES**
Perigee rotation effects on orbit-integrated proton and electron fluxes for AE-C orbit
[NASA-TM-X-66059] 01 p0103 N73-10855

**PERIHELIONS**
Finite series expansion study on motion of Mercury perihelion
[PB-213059] 11 p1339 N73-20870

**PERIOD EQUATIONS**
U PERIODIC FUNCTIONS

**PERIODIC FUNCTIONS**
NT COSINE SERIES
NT SINE SERIES
NT TANGENTS
NT TRIGONOMETRIC FUNCTIONS
Periodic functional analysis of ultra-short pulse generation and propagation in laser systems
16 p1920 N73-25535
The prediction of instabilities of linear differential equations with periodic coefficients
[ARC-R/M-3713] 24 p2945 N73-33518

**PERIODIC ORBITS**
U ORBITS

**PERIODIC OSCILLATIONS**
U OSCILLATIONS

**PERIODIC PROCESSES**
U CYCLES

**PERIODIC VARIATIONS**
NT ANNUAL VARIATIONS
NT DIURNAL VARIATIONS
Night cloud cover and meteorological parameter variations determined at La Silla, Chile, in 1970
[ESO-BULL-9] 01 p0075 N73-10620
Numerical analysis on electromagnetic wave scattering from periodic surface with arbitrary profile
[AD-747491] 03 p0268 N73-12170
Martinique climate variations noting wind circulation, cyclones and tropical storms recorded from various weather stations and meteorological satellites
[MONO-86] 07 p0815 N73-16610
Tables of Dst hourly variations for July, August, and September 1972
[NASA-TM-X-66156] 07 p0842 N73-16822
Chemical synthesis inhibitor of oceanic species having antibiotic properties
07 p0858 N73-16962
Six-day variation in cosmic ray intensity recorded at different astronomical observatories
07 p0859 N73-16967
Tables and charts of meteorological data gathered at Oarai site for 1970
[JAERI-M-4657] 08 p0939 N73-17685
Intraday time scale variability of infrared, optical, and radio observations from 3C 120, Bl Lac, and OJ 287
[AD-752214] 08 p0962 N73-17871
Analysis of dayside auroral characteristics and hydroxyl airglow variations from 1969 airborne auroral expedition
[NASA-CR-130916] 09 p1025 N73-18367
Hydrometeorological study of periodic precipitation variations over Lesse Basin, Belgium
[PUBL-SER-A-76] 12 p1423 N73-21530
Radar cross section modulation power spectrum in periodic motion of scattering object
[AD-756488] 13 p1494 N73-22109
Prediction of F 2 region critical frequencies from spatial and temporal correlation data
13 p1520 N73-22320
Predicting regular variations in geometric parameters of N[h] profiles and h prime f characteristics of quiet and disturbed ionosphere
13 p1520 N73-22321
Cyclic variations in Es layer with 11 year cycle of solar activity
13 p1521 N73-22329
Photometric measurements on human sensitivity to optical luminosity considering seasonal and monthly fluctuations
14 p1692 N73-23732
Biennial periodicity of blocking systems in atmosphere over Europe-Atlantic region considering cyclonic circulation
[NLL-M-22831-[5828.4F]] 16 p1936 N73-25661
Effect of sunspot cycle on precipitation pattern over U.S. plains states
17 p2056 N73-26629
Prevaling monthly and seasonal surface wind directions for coastal areas around Arctic Ocean
[AD-761074] 18 p2174 N73-27560
Glacio-climatic and geophysical rhythms of earth and space
[NASA-TT-F-14985] 19 p2342 N73-28843
Analysis of long term variations in water surface temperature of North Atlantic Ocean
[NLL-M-23016-[5828.4F]] 20 p2390 N73-29200
Orthogonal functional analysis of unsteadiness in atmospheric circulation
20 p2442 N73-29617
Spectral analysis of variations in meteorological elements for periods ranging from several years to several tens of years
20 p2443 N73-29620
Rocket sounding of two year cyclic variations of zonal wind components in stratosphere and mesosphere up to 100 km
20 p2444 N73-29631
Digital computer techniques for determining changes in brightness periods of variable stars
21 p2595 N73-30792
Structure of global geopotential fields in connection with quasi-biannual cyclicity in equatorial stratosphere
24 p2947 N73-33533

**PERIODICALS**
Military training, combat readiness, and antiaircraft defense
[AD-754834] 11 p1352 N73-20980
Published articles on mining and metallurgy
[TT-70-56005/4] 21 p2561 N73-30527

**PERIODICITY**
U PERIODIC VARIATIONS

**PERIODICITY [BIOLOGY]**
U RHYTHM [BIOLOGY]

**PERIPHERAL CIRCULATION**
Functional state of lymphoid cell in peripheral blood of astronauts and immunoreactivity of individual astronants after space flight
[NASA-TT-F-15089] 22 p2620 N73-30999

**PERIPHERAL JET FLOW**
Analysis of air cushion vehicle landing system operation and computation of air flow requirements
[AD-750936] 06 p0625 N73-15069
Results of aerodynamic jet interference tests for Do-31 aircraft and application to future VSTOL development for lift-loss calculation
[BMVG-FBWT-72-22] 09 p0985 N73-18044

**PERIPHERAL NERVOUS SYSTEM**
Survey of literature and morphological studies of vestibular nerve
[NASA-CR-135746] 24 p2885 N73-33042

**PERIPHERAL VISION**
Control mechanism in accommodation-vergence eye movement system in human eyes and importance of central and peripheral vision in pattern perception by human beings
21 p2500 N73-30061
Importance of central and peripheral vision in pattern perception
21 p2500 N73-30063

**PERIPHERIES**
U BOUNDARIES

**PERISCOPES**
Analysis of high resolution vidicon optics for electronic periscope view simulator
[AD-751023] 07 p0822 N73-16664

**PERMAFROST**
Environmental studies of sedimentation and nearshore marine processes in Cook Inlet, Alaska, and regional study of permafrost regimes in Alaska using ERTS-1 imagery
[E72-10209] 02 p0161 N73-11304
ERTS-1 imagery of permafrost and geologic hazards in Alaska
[E72-10247] 03 p0289 N73-12347
Alaskan arctic and subarctic sediment deposition, permafrost, snow cover, and ice mapping from ERTS-1 imagery
[E73-10279] 08 p0914 N73-17487
ERTS-1 imagery of permafrost and geologic hazards in Alaska
[E73-10320] 09 p1023 N73-18352
Effects of ground effect vehicle tests on ecology of arctic tundra in northern Alaska
[AD-751741] 10 p1107 N73-19026
ERTS-1 imagery of permafrost and geologic hazards in Alaska
[E73-10495] 12 p1397 N73-21331
Mapping of coastal sedimentation and related processes in Cook Inlet, Alaska and distribution and environmental interrelationships of permafrost terrain
[E73-10421] 13 p1515 N73-22275
Mapping permafrost areas of Alaska, correlating snowpack cover of Caribou-Poker Creek with stream runoff, and mapping and inventorying icing on Chena River
[E73-10511] 13 p1516 N73-22286
ERTS-1 imagery of permafrost and geologic hazards in Alaska
[E73-10601] 15 p1772 N73-24362
Analysis and mapping sediment deposition, permafrost areas, snow cover, and icing in Arctic regions of Alaska from ERTS-1 data
[E73-11067] 23 p2781 N73-32243

**PERMALLOYS [TRADEMARK]**
Analysis of effects of heat treatment of magnetic and physical properties of molybdenum permalloy
[NLL-RTS-7641] 04 p0431 N73-13509
Effects of chemical etching on magnetic and storage properties of Permalloy memory films
18 p2178 N73-27589

**PERMEABILITY**
NT DIELECTRIC PERMEABILITY
Permeability of fine-pored carbons as function of mean pressure temperature and gas properties
[AD-749362] 05 p0499 N73-14064
Effects of plasma-neutral gas interactions on equilibrium and stability of permeable Tokamak plasmas noting scaling conditions
[TRITA-EPP-72-26] 07 p0828 N73-16716
Chloride and water permeability parameters for hydraulic brake hose testing
[AD-748083] 13 p1546 N73-22530
Measurement of gas permeability of high porosity nickel powder metallurgy parts
[NLL-LTI-746-1404-[9022.401]]
15 p1797 N73-24564
Probabilistic model of nonisothermal gaseous flow through fine pored homogeneous media
17 p2013 N73-26276

**PERMEATING**
Influence of surface processes on rate of permeation of hydrogen through metals
[NASA-CR-129276] 03 p0312 N73-12548
Time lag method for transient permeation of benzene and acetone vapors through sulfur natural rubber
[NASA-TM-X-64721] 07 p0752 N73-16112
Electrochemical permeation technique and scanning electron microscopy used to determine hydrogen embrittlement in ferrous materials
[AD-752828] 09 p1049 N73-18557
Gas phase hydrogen permeation through alpha iron, 4130 steels, and 304 stainless steels from less than 100 C to near 600 C
[NASA-TN-D-7265] 12 p1412 N73-21442

**PERMITTIVITY**
Methods for determining electric permittivity of inhomogeneous dielectric medium that is uniform in two dimensions and varies according to profile function in other dimension
02 p0201 N73-11622
Static dielectric constant of solid methane at low temperatures and high pressures
15 p1745 N73-24147
Limitations in microelectronic circuits, design of power Schottky diode, and strontium titanate permittivity
16 p1880 N73-25218
Thermal conductivity of complex dielectric crystals at high temperature
16 p1952 N73-25796
Dielectric constant and loss tangent of Eccofoam PT at various packing densities
[NASA-CR-133550] 19 p2312 N73-28594
Dielectric properties of ice, snow, and water at microwave frequencies and thickness measurements of ice and snow layers with radar
[CRC-1242] 21 p2537 N73-30341
Complex permittivity measurements during high temperature recycling of space shuttle antenna window and dielectric heat shield materials
[NASA-CR-2302] 22 p2707 N73-31675
Characteristics of bulk and surface modes in simple metals using modified self-consistent linear response theory
24 p2933 N73-33427

**PERMUTATIONS**
Ordering theories of variables for realization procedures of multithreshold logic circuits
05 p0522 N73-14242
Notes on problem involving permutations as subsequences
[NASA-CR-133103] 17 p2055 N73-26624

**PEROVSKITES**
Lattice potential topography for 180 degree boundary in Perovskite ferroelectrics
[AD-742109] 01 p0088 N73-10724

**PEROXIDES**
NT HYDROGEN PEROXIDE
Microphotometer analysis of absorption spectra, physical and chemical properties of NO2 system in Martian atmosphere
07 p0752 N73-16107
Mechanism of peroxidation of polymers under irradiation conditions
08 p0881 N73-17137

**PERSHING MISSILE**
Advanced guidance techniques for Pershing missile
[AD-745897] 02 p0208 N73-11689

**PERSONALITY**
Psychobiological factors for predicting monotony tolerance and selecting personnel for isolated duty
[AD-747272] 04 p0381 N73-13098

Human performance in schematic concept formation as a function of socio-economic level, personality, intelligence, and race
[AD-744781] 13 p1486 N73-22052

**PERSONALITY TESTS**
Psychological and personality test results and problems in selection of pilots, air traffic controllers, and technicians from Yemen
19 p2226 N73-27956

**PERSONNEL**
NT AIRCRAFT PILOTS
NT ASTRONAUTS
NT COSMONAUTS
NT CREWS
NT ENEMY PERSONNEL
NT FLIGHT CREWS
NT FLYING PERSONNEL
NT GROUND CREWS
NT MEDICAL PERSONNEL
NT NAVIGATORS
NT OPERATORS [PERSONNEL]
NT PHYSICIANS
NT PILOTS [PERSONNEL]
NT POLICE
NT PROGRAMMERS
NT SCIENTISTS
NT SPACECREWS
Results from employment workshop program for unemployed aerospace engineers and scientists
[PB-209366] 01 p0022 N73-10168
Directory of workers in field of fire research and related activities
[NASA-CR-121149] 15 p1845 N73-24954

**PERSONNEL DEVELOPMENT**
Workshop for teaching professional unemployed personnel competitive job searching techniques
[PB-209367] 01 p0020 N73-10159
Effectiveness of underwater acoustic propagation loss models in sonar personnel training devices
[AD-750694] 06 p0701 N73-15719
Cybernetic application of computers in personnel training
[AD-751145] 09 p0998 N73-18143
Development of simulator for training personnel in underwater terrain navigation and reconnaissance
[AD-754091] 11 p1322 N73-20729
Role of man in flight experiment payload missions with application to Spacelab operations - Vol. 1
[NASA-CR-135487] 22 p2623 N73-31020
Role of man in flight experiment payload missions with application to Spacelab operations - Vol. 2
[NASA-CR-135488] 22 p2624 N73-31021

**PERSONNEL MANAGEMENT**
Workshop for teaching professional unemployed personnel competitive job searching techniques
[PB-209367] 01 p0020 N73-10159
Employee communication at NASA Langley Research Center
[NASA-TM-X-68854] 02 p0244 N73-11985
Industrial model for leave and overtime taking behavior of employees exposed to peak work activity periods in relation to health, demography, and job variables
08 p0872 N73-17055
Automated medical history questionnaire for screening industrial personnel and scheduling physical examinations
08 p0872 N73-17060
Computerized multivariate scheduling of physical examinations for NASA personnel in clinical intervention program
08 p0873 N73-17068
Physical exercise effects on health of NASA personnel
08 p0873 N73-17069
Continuous monitoring of hypertension and hypercholesterolemia in NASA employees for prevention of heart disease and disability
08 p0873 N73-17072
Industrial health measures and environmental control to insure worker productivity
08 p0874 N73-17077
Conference on occupational and environmental medical services provided to NASA employees
[NASA-TM-X-69074] 08 p0874 N73-17078
Management of NASA employee health problems by automated medical system
08 p0874 N73-17079
Influence of repeated test and dietary counseling on hypercholesterolemia control in NASA employees
08 p0875 N73-17081
Chronic disease health trends and mortality rates in employee population of NASA Goddard Space Flight Center
08 p0875 N73-17086
Medical services of operating environmental health program for industrial workers
08 p0876 N73-17093
Time-span of discretion as measure of military work and responsibility
[DRAE-M45] 13 p1486 N73-22049
Development of cost effective program for training naval fixed wing pilots in 1974 to 1986 time period - Vol. 1
[AD-756638] 15 p1745 N73-24143
Development of cost effective program for training naval fixed wing pilots in 1974 to 1986 time period - Vol. 2
[AD-756639] 15 p1745 N73-24144
Development of cost effective program for training naval fixed wing pilots in 1974 to 1986 time period - Vol. 3
[AD-756640] 15 p1745 N73-24145
Manpower requirements for aircraft maintenance operations of USAF
[AD-760082] 17 p1991 N73-26097
Military personnel management and human factors engineering
[AD-763168] 21 p2504 N73-30094

**PERSONNEL SELECTION**
NT PILOT SELECTION
Workshop for teaching professional unemployed personnel competitive job searching techniques
[PB-209367] 01 p0020 N73-10159
Comparison of age, education, pre-FAA experience, aptitudes, training course performance, and post-Academy attrition rates of male and female trainees
[FAA-AM-72-22] 02 p0135 N73-11094
Psychobiological factors for predicting monotony tolerance and selecting personnel for isolated duty
[AD-747272] 04 p0381 N73-13098
Tasks analyses to determine technical personnel requirements for maintenance of Navy microelectronic shipboard equipment
[AD-748040] 04 p0384 N73-13123
Optimal linear combination of observable parameters for maximizing correlation between index and criterion variates for sampling classification and personnel selection
[AD-751257] 07 p0813 N73-16596
Multiphase health screening and medical history questionnaire for preventive/occupational physical examinations
08 p0871 N73-17052
Attrition-retention rates of air traffic control trainees recruited during 1960 to 1963 and 1968 to 1970
[FAA-AM-72-33] 11 p1249 N73-20140
Predictability of motion sickness in pilot selection - conferences
[AGARD-CP-109] 12 p1367 N73-21092
Reaction assessment of vestibular disorientation stress for aircrew selection, using visual displays and tasks
12 p1368 N73-21096
Mathematical models for educational planning and personnel selection in Soviet Union
[JPRS-58793] 12 p1419 N73-21497
Motivational patterns underlying devolunteering by submarine graduate school personnel
[AD-749324] 13 p1487 N73-22054
Computation of Coriolis forces in selecting flying personnel for vestibular tolerance
14 p1609 N73-23042
Curriculum development and personnel training for information centers
15 p1753 N73-24205
Psychological and personality test results and problems in selection of pilots, air traffic controllers, and technicians from Yemen
19 p2226 N73-27956

**PERT**
PERT planning run time reduction with special purpose cellular logic computer
03 p0271 N73-12195
Application of program evaluation and review technique for planning and management of air transport operations
[NASA-TT-F-742] 16 p1860 N73-25067

**PERTURBATION**
NT ORBIT PERTURBATION
NT SATELLITE PERTURBATION
Magnetohydrodynamic equilibrium perturbations in toroidal fields with circular cross sections
[CEA-CONF-2014] 06 p0705 N73-15755
Nonlinear and small perturbation linear models for one dimensional heave motion of flexible skirted, air cushion suspension
[PB-212705] 07 p0766 N73-16226
Effect of perturbation on frequency and intensity of thunderstorms in Italy
10 p1181 N73-19608
Investigation of causes of perturbations in Saturns rings
[REPT-14] 10 p1212 N73-19854
Laser Doppler velocimeter for simultaneously measuring orthogonal fluid velocity components without flow field perturbation
[NASA-CASE-ARC-10637-1] 12 p1405 N73-21390
Application of computerized series manipulation system to planetary theory using recursive linearization
12 p1447 N73-21715
Special perturbation methods for improved computational efficiency in numerical integration of artificial satellite orbits
12 p1447 N73-21717
Wave and Einstein equations for studying scaler waves and tensor perturbations in Mixmaster Universe
15 p1829 N73-24823
Multivariable approach to perturbed aerospace vehicle motion, using approximate solutions of nonlinear differential equations
19 p2341 N73-28832
Effect of random perturbations relative to main gyroscope axis on ground gyrocompass readings
20 p2418 N73-29429
Distribution of odd nitrogen in lower stratosphere and perturbations caused by stratospheric air transport
[NASA-CR-2314] 21 p2536 N73-30336
Probabilistic approach to trajectory sensitivity
23 p2835 N73-32657

**PERTURBATION THEORY**
NT VINTI THEORY
Singular perturbation method for predicting pressure distribution on supercavitating hydrofoils with rounded noses
[AD-745791] 01 p0063 N73-10514
Small perturbation theory applied to effects of irregular topography on deflection of wind blowing over industrial area and then residential area and effects on air pollution
[NASA-TM-X-2653] 01 p0074 N73-10610
Development of theories for calculating pressure on perturbed plane wall in presence of viscous boundary layer
[AD-746332] 02 p0158 N73-11278
Lagrangian theory of internal ocean wave interaction
[AD-746149] 02 p0169 N73-11371
Perturbation theory for developing eigenvalues and eigenfunctions in power series expansion for Hill differential equation
02 p0195 N73-11581
Application of reductive perturbation method to electromagnetic waves propagating in cold electron plasma
[IPPJ-136] 02 p0216 N73-11745
Evaluation of edge and membrane effects in moderately thick beams by singular perturbation technique
[AD-746985] 02 p0240 N73-11955
Numerical and perturbation theory solutions for evaluating performance of eddy current flowmeters
[BNWL-SA-4236] 03 p0302 N73-12470
Perturbation theory formulas derived and applied to determine changes in neutron and gamma ray doses due to changes in various radiation shield layers for fixed sources
[NASA-TN-D-7093] 03 p0331 N73-12700
Propagation properties of ion density perturbations and waves in collisionless plasmas with Maxwellian velocity distribution functions
[RISO-257] 03 p0343 N73-12795
Perturbation approach to strains confined to elastic region with small electronic energy changes
[AD-748085] 03 p0347 N73-12829
Development of cosmological models based on Einstein field equations with random perturbations of long wave lengths superimposed on unperturbed models
[AD-747505] 03 p0357 N73-12911
Obtaining first natural frequencies of vibration of noncircular plates by perturbation theory
[AD-748355] 03 p0363 N73-12955
Analysis of heating of electron component of magnetoplasma due to localized time varying magnetic field perturbations
[AD-747094] 04 p0415 N73-13390
Tidal interactions in multiple galaxies
04 p0468 N73-13816
Numerical methods for computing reentry trajectories for space shuttles
[NASA-CR-128652] 04 p0474 N73-13877
Application of perturbation techniques to single blade helicopter rotor dynamics
[NASA-TM-X-62165] 05 p0492 N73-14006
Orbit perturbations due to solar radiation pressure, including disturbing force of satellites with large area to mass ratio
05 p0610 N73-14959
Stability margins for electrical power systems with perturbations in its multiareas
07 p0760 N73-16173
Singular perturbation approach to stability analysis of linear time varying systems
07 p0761 N73-16180
Application of singular perturbation of ordinary differential equations to control system design
07 p0761 N73-16181
Theorems for proving consistency of singular perturbations in physical systems with parasitic elements
07 p0761 N73-16182
Perturbed nonlinear differential equations applied to integral manifolds
[NASA-CR-130277] 07 p0813 N73-16592
Perturbation theoretical and graphical representation of vertical ionization energies and electron affinities of free molecules
08 p0916 N73-17506
Perturbation method for calculating voltage and impedance response of Josephson point contacts to external HF currents
[AD-751911] 08 p0951 N73-17786

Static perturbation method of studying nonlinear equilibrium and stability problems of structural systems and elements
09 p1093 N73-18921
Perturbation analysis of combustion and burning of initially unmixed reactants
[AD-755214] 13 p1592 N73-22906
Transonic perturbation equation for studying steady compressible flow past lifting and nonlifting wings at high subsonic Mach numbers
[NASA-CR-2246] 15 p1766 N73-24312
Perturbation method for separated laminar incompressible flows in divergent channels
16 p1886 N73-25268
Application of perturbation theory and Ritz energy method for analyzing nonlinear flexural gyrations of untwisted, rotating cantilevered blade vibrating in plane of rotation
16 p1968 N73-25923
Perturbation theory of dynamic structure factors in high frequency liquids
[AD-761659] 19 p2230 N73-27987
Analysis of arbitrarily nonuniform, nonadiabatic, two dimensional or axisymmetric basic flows based on inviscid theory of three dimensional perturbations in uniform transonic flow
[AD-761632] 19 p2256 N73-28188
Performance of various types of gyroscopes
[JPRS-59498] 20 p2418 N73-29426
Application of cononical perturbation theory to nonconservative systems
20 p2470 N73-29835
Some regularities in propagation of perturbations of discrete tone in free supersonic jet
[AD-763163] 21 p2581 N73-30681
Development of nonlinear stochastic equations for turbulent field with application to simple electron plasma
[AD-763438] 21 p2584 N73-30710
Matrix perturbation techniques in structural dynamics
[NASA-CR-133795] 21 p2603 N73-30862
Perturbation technique for determining microwave interactions in magnetized waveguide plasma
22 p2702 N73-31643
Calculation of evanescent-wave gain in TE sub Om and TM Om of optical fibers
[CRC-1247] 23 p2769 N73-32147
Perturbation solutions for multicomponent, variable-property forced convection in laminar boundary layers
[AD-764563] 23 p2776 N73-32200
Procedure for determining Rayleigh-Schroe dinger energies and wave functions of degenerate states to high orders
[NASA-CR-135641] 23 p2812 N73-32485
Hydromagnetic gradient waves in ionosphere
24 p2921 N73-33331
Determination of perturbing moments due to solar radiation pressure forces acting on body of revolution
[NASA-TT-F-15072] 24 p2976 N73-33780
Application of perturbation method for computing optimal three dimensional reentry trajectories for shuttle-type spacecraft
24 p2978 N73-33798

**PERU**
Scintillating [VHF] signals fading measurements at Lima, Peru during spring equinox of 1970
[NASA-TM-X-66092] 02 p0166 N73-11347

**PETN**
Optical measurement of RDX and PETN monocrystal detonation velocity along different crystallographic axes
[ISL-28/71-PT-1] 09 p1052 N73-18575

**PETROGRAPHY**
Chemical, petrographic, and textural characteristics of Apollo 16 rock and soil samples
12 p1449 N73-21737
Identification and source of lunar rocks, lunar interior and, lunar magmas
[NASA-CR-133457] 19 p2344 N73-28853

**PETROLEUM**
U CRUDE OIL

**PETROLOGY**
NT PETROGRAPHY
Mineral analysis of lunar samples of crystalline rocks from Apollo 12 flight
[NASA-SP-306] 07 p0844 N73-16837

**PFM [MODULATION]**
U PULSE FREQUENCY MODULATION

**PH**
PH influence on hexachloroiridite and hexachloroiridate ions in aqueous solutions
[IRI-133-73-02-PT-2] 21 p2506 N73-30111

**PH FACTOR**
Oxygen content and hydrogen ion concentration in monkey blood after incapacitating ionizing radiation dosage
[AD-750681] 06 p0632 N73-15134

**PHANTOM AIRCRAFT**
NT F-4 AIRCRAFT

**PHARMACOLOGY**
Pharmacolo~ic investigations of antagonistic effects of pyridines on isolated guinea pig ileum
[BMVG-FBWT-72-14] 07 p0747 N73-16075
Pharmacological measures for prophylactic and restorative treatment of men and animals during space flight
11 p1239 N73-20060
Pharmacological data for aminothiol and indolylalkylamine radioprotectors
11 p1240 N73-20066

**PHASE ANGLE**
U PHASE SHIFT

**PHASE CHANGES**
U PHASE TRANSFORMATIONS

**PHASE COHERENCE**
Design of nonlinear coherence receiver with feedback signal selection for carrier tracking in telecommunications
[NASA-CASE-NPO-11921-1] 14 p1620 N73-23118

**PHASE CONTRAST**
Analysis of single channel phase communication system based on statistical communication theory with application to direction finding
12 p1425 N73-21553

**PHASE CONTROL**
Attenuation and phase constancy propagation criteria of tactical satellite communications using mobile ground terminals
01 p0026 N73-10201
Radiometer quadrature control and measuring system using optical coupling circuitry
[NASA-CASE-MFS-21660-1] 04 p0421 N73-13434
System for generating timing and control signals during repetitive fixed length serial data transmission
[NASA-CASE-NPO-13125-1] 09 p1008 N73-18225
Phase delay control system for stabilizing signals passing through coaxial cables
[NASA-CASE-NPO-13138-1] 11 p1262 N73-20238
Voltage controlled oscillator circuit for two-phase induction motor control
[NASA-CASE-MFS-21465-1] 23 p2768 N73-32145

**PHASE DEMODULATORS**
Digital receiver for detecting moderate data rate phase-shift keyed signals in real time
01 p0025 N73-10196

**PHASE DETECTORS**
Frequency discriminator for on-line measurements of entrainment and synchronization in EEG signals as related to human alertness
[NASA-CR-129173] 02 p0135 N73-11091
Voltage controlled phase shifter with low distortion
[NASA-CASE-MFS-21671-1] 08 p0891 N73-17211
Phase detector with time correlation integrator for frequency multiplexed signals
[NASA-CASE-GSC-11744-1] 14 p1640 N73-23291
Homodyne interferometer for measuring phase variations of laser beam wave front
[AD-756885] 14 p1668 N73-23539
Power equation theory for defining ultrahigh frequency and microwave measurements
[NBS-TN-637] 15 p1750 N73-24182
Small phase difference measuring technique within holographically reconstructed optical fields
16 p1922 N73-25549
Ionosphere D and F region high frequency ray propagation effects and design of high frequency dynamic phase metering instruments
20 p2375 N73-29083

**PHASE DEVIATION**
Détermination of circulation and diameter of vortices from ultrasonic wave phase deviation
[REPT-6/1972] 03 p0285 N73-12308
Phase difference between temperature and density in thermosphere
[NASA-TM-X-66119] 03 p0294 N73-12395
Water evaporation interference in phase measurements by transhorizontal microwave propagation over sea surface
17 p1994 N73-26125
Attenuation and phase dispersion of radio wave in atmosphere due to oxygen microwave spectrum
17 p1994 N73-26126

**PHASE DIAGRAMS**
Ternary phase diagram of magnesium yttrium zinc in magnesium alloy
[AD-746724] 02 p0188 N73-11526
Crystalline structures, physical properties, chemical properties, and phase characteristics of various metal systems and alloys
[AD-746792] 02 p0189 N73-11532
Effects of high-speed heating after cold plastic deformation on phase composition of titanium alloy VT 15
[AD-747516] 03 p0318 N73-12591
Physicochemical and optical properties of glasses of BaO-PbO-Bi2O3-TiO2 system
[AD-747371] 03 p0322 N73-12620
Phase diagram of Ti-Os system
[NLL-TRANS-746-1302-[9022.401]] 05 p0560 N73-14548
Phase equilibrium diagram of intermetallic compound of vanadium and gallium
[AD-752877] 09 p1049 N73-18551
Phase diagram of decorated Ising system in nonzero magnetic field
[NUB-2175] 12 p1428 N73-21576
Concentration fluctuations in critical region of binary liquid mixture 3-methylpentane-nitroethane
[AD-759740] 16 p1872 N73-25158
Development of procedure for estimating solid phase occurrence during oxidation of heavy metal sulfides
[NLL-M-22913-[5828.4F]] 16 p1926 N73-25581
CO2 laser study of ZrO-Y2O3 phase diagram
16 p1931 N73-25629
Thermodynamics of precipitation caused by zinc diffusion into gallium arsenide
18 p2113 N73-27085
Handbook of phase diagrams of silicate and similar systems comprising oxides and fluorides - Vol. I
[TT-71-50040] 21 p2564 N73-30556

**PHASE FADING**
U FADING

**PHASE LOCK DEMODULATORS**
Quasi-optimum digital phase locked loops derived by nonlinear estimation theory
20 p2380 N73-29121

**PHASE LOCKED SYSTEMS**
Digital second order, phase locked loop with counter driven by stable clock pulse source
[NASA-CASE-NPO-11905-1] 03 p0270 N73-12192
Development of frequency modulated diode laser transmitter for point-to-point voice communication system
[AD-747524] 03 p0311 N73-12540
Characteristics of data-aided carrier tracking loop used for tracking carrier in angle modulated communications system
[NASA-CASE-NPO-11282] 07 p0764 N73-16205
Nonlinear programming of multifilter phase-lock loops at low signal-to-noise environments
[NASA-CR-131237] 10 p1127 N73-19184
Numerical integration of Fokker-Planck equation for first order phase locked loop
[AD-754355] 11 p1259 N73-20214
Phase locking of reflex klystron with stable microwave source
[AD-758677] 16 p1882 N73-25235
Design of avionics digital frequency synthesizer with four phase locked loops for aircraft communication and navigational aids
[AD-759699] 16 p1883 N73-25238
Bibliography of literature on phase locked loops
[NASA-CR-133225] 17 p2004 N73-26202
Characteristics of subharmonically injection locked microwave diode oscillators
[AD-759540] 17 p2004 N73-26208
Filter for third order phase locked loops in signal receivers
[NASA-CASE-NPO-11941-1] 18 p2125 N73-27171
Improved phase lock loop for receiver in multichannel telemetry system with suppressed carrier
[NASA-CASE-NPO-11593-1] 19 p2234 N73-28012
Modelling, analysis, and applications of class of all digital phase locked loops
20 p2375 N73-29082
Automatic carrier acquisition system for phase locked loop receiver
[NASA-CASE-NPO-11628-1] 21 p2506 N73-30113
Electronic digital data synchronizing and instrumentation amplification techniques
[AD-763797] 21 p2509 N73-30131
Digital phase-locked loop for accumulator output signal phase-locked to input signal
[NASA-CASE-GSC-11623-1] 22 p2646 N73-31202

**PHASE MODULATION**
NT PHASE SHIFT KEYING
Interchannel interference and Gaussian noise effects on phase modulated digital microwave radio systems
01 p0027 N73-10211
Degradation of spread spectrum modulation performance in airborne multipath communication channels
[AD-747486] 04 p0391 N73-13181
Statistical analyses for detecting frequency shift keyed and phase keyed signals in additive disturbance
[AD-752010] 08 p0886 N73-17173
Power spectrum of satellite radio signal phase modulation caused by F region diffraction
[NASA-CR-131280] 11 p1254 N73-20178
Linear filtration effect on correlation properties of phase manipulated signals
12 p1378 N73-21175
Correlation processing of phase modulated signals
14 p1619 N73-23115
Performance of digital matched filter receiver designed to receive biphase modulated signal in presence of interference
[AD-756841] 14 p1643 N73-23326
Multicarrier communications system for transmitting modulated signals from single transmitter
[NASA-CASE-NPO-11548] 17 p1993 N73-26118
Phase modulation of tone and binary signals on carrier waves in communication systems
[NASA-CASE-GSC-11743-1] 18 p2116 N73-27107

**PHASE SHIFT**
Television picture quality dependence on color tone change from phase shift of color carrier
[NLL-TRANS-2870-[9022.81]] 02 p0139 N73-11125
Radar arrays with no phase shifters for air defense systems
[AD-750328] 06 p0642 N73-15211

Surface wave conversion to longitudinal oscillations in plasma surface layer by perturbation of waveguide
[AEC-TR-7335] 07 p0827 N73-16703
Wave transformation in plasma with nonmonotonic longitudinal distribution under action of superhigh frequency power
[AEC-TR-7338] 07 p0827 N73-16705
Wave transformation region in superhigh frequency argon discharge plasma
[AEC-TR-7339] 07 p0827 N73-16706
Analysis of radio phase differences for determining electron concentration in solar corona
10 p1177 N73-19577
Microwave Doppler shift technique for measuring dynamic bulk modulus of dielectric materials including solid propellants
[NASA-CR-131743] 13 p1546 N73-22532
Phase shift model for induced voltage in current carrying superconducting thin films in superimposed ac and dc magnetic fields including radio and microwave frequency ranges
15 p1820 N73-24748
Production of polycrystalline bismuth-calcium-vanadium garnet phase shifters
[AD-758919] 16 p1881 N73-25224
Ultrahigh frequency coherent radio signal transmission for differential phase shift measurements due to vapor and oxygen absorption lines
17 p1995 N73-26131
Use of differential phase and gain for predicting performance of ultrahigh frequency telecommunication system
17 p1995 N73-26132
Laboratory model of distributed pin diode millimeter wave phase shifter
[AD-762572] 20 p2381 N73-29136
Standard digital data clock-rate generator with programmable digital phase shift for data transmission from communication satellites
[AD-764049] 22 p2635 N73-31117

**PHASE SHIFT CIRCUITS**
NT CIRCULATORS [PHASE SHIFT CIRCUITS]
Development and characteristics of reciprocal latching microwave phase shifters based on ferrimagnetic substrate
[AD-744795] 01 p0033 N73-10255
Design and performance of digital ferrite phase shifter for phased array antenna systems
[AD-748431] 04 p0396 N73-13225
Voltage controlled phase shifter with low distortion
[NASA-CASE-MFS-21671-1] 08 p0891 N73-17211
Transient radiation caused performance degradation in integrated ferrite phase shifter driven circuit
[AD-757618] 14 p1644 N73-23336
Contactless extremum transistorized circuit capable of cutoff, saturation, and generation
16 p1883 N73-25245
Design and fabrication of microwave reciprocal latching ferrite phase shifters
[AD-763216] 21 p2519 N73-30204
Voltage controlled oscillator circuit for two-phase induction motor control
[NASA-CASE-MFS-21465-1] 23 p2768 N73-32145

**PHASE SHIFT KEYING**
Development of communication system for transmitting differential phase shift keyed signals from input data bits without timing or phase reference signals
[NASA-CASE-MSC-14065-1] 01 p0028 N73-10215
Development of differential phase shift keyed signal receiver to resolve differential phase shift in incoming signal
[NASA-CASE-MSC-14066-1] 01 p0034 N73-10269
Computer software to enable any general purpose computer with A/D conversion capability to be used as PSK receiver for low data rate telemetry processing
[NASA-CR-130174] 08 p0887 N73-17185
Multiple phase shift keying communications for improving carrier tracking efficiency and data detection performance
[NASA-CASE-NPO-13103-1] 11 p1255 N73-20180
Phase manipulated signal reception in noise background of unknown statistics
[AD-754603] 11 p1258 N73-20205
TDMA/PSK test equipment noting modulators, demodulators, converters, and transmission system
[ESRO-CR[P]-144] 17 p1998 N73-26157

**PHASE SWITCHING INTERFEROMETERS**
Fixed frequency ionosonde receiver with phase swept interferometer
[KGO-726] 18 p2118 N73-27122

**PHASE TRANSFORMATIONS**
NT ARC MELTING
NT BOILING
NT EVAPORATION
NT FILM BOILING
NT FLASHING [VAPORIZING]
NT FREEZING
NT FUSION [MELTING]
NT LIQUEFACTION
NT MELTING
NT NUCLEATE BOILING
NT PROPELLANT EVAPORATION
NT SUBLIMATION
NT TRANSPIRATION
NT VACUUM MELTING
NT VAPORIZING
NT VIBRATIONAL FREEZING
Experimental and theoretical analysis of martensitic transition of TiNi [Nitinol]
[AD-742767] 02 p0187 N73-11516
Development of general theory for studying large plastic deformation of metals
[AD-746689] 02 p0190 N73-11542
Computing equation of state parameters for material which undergoes phase transition
[AD-746611] 03 p0346 N73-12824
Anomalous capacity for estimating ferroelectric phase transition in Kanzig regions
[AD-747559] 03 p0347 N73-12831
Regularity in phase transitions of magnetic and liquid-gas systems
[COO-1112-63] 03 p0364 N73-12967
Directional martensite transformations in steel and alloy development
[AD-748408] 04 p0436 N73-13553
Structure and phase composition of electrodeposited iron-nickel-chromium alloys analyzed by X ray spectroscopy and electron microscopy
[NLL-TRANS-746-1327-[9022.401]]
05 p0560 N73-14551
Glass transistion characteristics and compatibility of linear poly carborane-siloxane series plastics
[AD-749385] 05 p0566 N73-14597
Fast and accurate technique for iterative solution of saturation adjustment problem
[AD-750083] 05 p0575 N73-14683
Chemical surface reactions, phase transformations, and reaction kinetics in flow systems
[AD-750172] 06 p0712 N73-15808
Critical transport properties in binary liquid phase transition
[AD-752473] 08 p0884 N73-17158
Supercooling analysis for predicting interface stability in plane front solidification of ternary alloys containing one, two, or three phases
[AD-752609] 08 p0933 N73-17639
Transition properties of type I and magnetic properties of type 2 semiconductors with small Ginzburg-Landau parameters
[JUL-854-FF] 10 p1200 N73-19762
Calculation of shock-induced phase transformations in solids
[SC-RR-72-0626] 10 p1201 N73-19770
Deformation of gamma and epsilon phases in intermetallic compounds by extrusion method
[AD-754523] 11 p1307 N73-20605
Volumetric factor of precipitation phase causing X ray diffraction fading in alloys
[JPRS-58761] 12 p1414 N73-21455
Phase structure of crystallizing nickel tin alloy melt during cooling
[JPRS-58681] 12 p1414 N73-21456
Acoustic emission signals by fcc phase transition to fct in In-Ti alloys
[SC-DC-72-1650] 12 p1414 N73-21462
Phase transition and entropy behavior of solid He-3
[COO-1569-96] 12 p1439 N73-21654
Temperatures of various adiabatic and isobaric mixtures of humid atmospheric air with water or ice
[PUBL-SER-B-68] 12 p1465 N73-21866
Development of model for conditions of superplasticity related to maximum interphase surface of fluctuation nuclei of phase transformation
13 p1540 N73-22478
Analysis of alpha to gamma transformation in steel to determine effect of initial state nonequilibrium on starting temperature
13 p1541 N73-22482
Increasing phase change material thermal diffusivity by means of solid fillers
[NASA-CR-124214] 13 p1590 N73-22894
Neutron scattering, computerized simulation, and magnetic resonance techniques for studying phase transitions in magnetic materials
[AD-757223] 14 p1698 N73-23782
Analysis of phase change occurring in molten metals, semiconductors, and alloys when heated to 700 to 900 C above melting point
[NLL-M-21614-[5828.4F]] 15 p1796 N73-24563
Phase transformations in titanium alloy TiAl6V4
[DLR-FB-73-38] 15 p1799 N73-24584
Development of procedure for estimating solid phase occurrence during oxidation of heavy metal sulfides
[NLL-M-22913-[5828.4F]] 16 p1926 N73-25581
Influence of phase composition on mechanical properties of heat resistant vacuum tight cast aluminum alloys
[AD-759645] 16 p1930 N73-25619
Phase characteristics of submonolayer isotopic mixtures of helium adsorbed on Grafoil
18 p2113 N73-27084
Thermodynamics of phase changes occurring in heat treatment of carbon and alloy steels
[AD-762361] 19 p2311 N73-28589
Radiative heat transfer of single crystal surface at phase transition boundary during Czochralski crystal growth
[NLL-RRE-TRANS-386-[8036.625]]
20 p2460 N73-29772
Computer program for application of phase change technique to thin sections with heating on both sides
[NASA-TN-D-7193] 20 p2485 N73-29965
Effect of phase instability during low cycle fatigue on plastic deformation in steels
[AD-763235] 22 p2686 N73-31512
Isothermal and athermal martensitic transformation in beta copper zinc alloys
23 p2803 N73-32417
Characteristics of alpha-beta-transformation of titanium and zirconium alloys based on localization of valency electrons in atoms of elements
23 p2808 N73-32456
Magnetic phase transition in FeCl3
[AD-764982] 23 p2827 N73-32595
Magneto-optic phase change for detecting magnetization reversal in magnetic films
[AD-764549] 24 p2959 N73-33645
Phase transformation and superconductivity in titanium and zirconium alloys
[RLO-2225-T-13-14] 24 p2969 N73-33726

**PHASE VELOCITY**
VLF phase velocity measurements with separated time phase synchronized receivers
[AD-753206] 09 p1003 N73-18188
Regionalization of lithosphere and asthenosphere of Pacific Ocean from Rayleigh wave phase velocity dispersion curves
20 p2390 N73-29197
Velocity and attenuation of wave fronts generated by double diaphragm shock tube
[CEA-R-4365] 22 p2647 N73-31210

**PHASE-SPACE INTEGRAL**
Grid excitation and digitized probe measurements for oscilloscopic display of phase space diagram distribution functions of plasma waves
[IPPJ-147] 09 p1070 N73-18732

**PHASED ARRAYS**
Theoretical analysis of linear semi-infinite array of uniformly spaced elements to determine mutual coupling effects
[AD-745799] 01 p0034 N73-10263
Computerized simulation of planar phased array of circular waveguide elements
[NASA-CR-123820] 02 p0140 N73-11139
Analysis of mutual coupling compensation using microstrip techniques with application to behind-the-array coupling of phased antenna array
[NASA-CR-123819] 02 p0151 N73-11222
Radiation patterns of linear phased array focused in near field
[AD-746997] 03 p0274 N73-12226
Reduction of angle frequency deviation in antenna array by waveguide parameters
[AD-748742] 04 p0389 N73-13164
Adaptive control systems for phased antenna arrays
[AD-748220] 04 p0390 N73-13174
Tracking errors associated with monopulse phased-array radar
[AD-748428] 04 p0391 N73-13175
Design and performance of digital ferrite phase shifter for phased array antenna systems
[AD-748431] 04 p0396 N73-13225
Detailed digital simulation of Army Missile Command experimental array radar system for air defense against low altitude threats
[AD-749501] 05 p0514 N73-14177
Coherent optical processing of phased array radar data, using electron beam addressed, potassium dideuterium phosphate modulator
05 p0610 N73-14957
Electronic scan phased array antenna system and digital clutter mapping system
[AD-751054] 07 p0758 N73-16158
Array techniques for large and sub-arrays for limited scan application
[AD-751274] 07 p0763 N73-16203
Development of phase control coupling for use with phased array antenna
[NASA-CASE-ERC-10285] 07 p0764 N73-16206
Design of airborne electronically steerable phased array system
[NASA-CR-124041] 09 p1007 N73-18219
Experimental array radar ear test bed
[AD-758139] 14 p1636 N73-23261
Solid state, superheterodyne monopulse receiver for experimental array radar
[AD-757610] 14 p1637 N73-23268
Ribbon cabling designs for AEGIS phased arrays
[RE-18-1-14] 14 p1642 N73-23316
Computer manual for experimental array radar ear system simulation program
[AD-758922] 16 p1877 N73-25197
Improving optical compatibility of lidar transmitter-receiver
[NASA-TM-X-64753] 16 p1923 N73-25561
Recursive digital filters in moving target indicator of phased array radars
[AD-759901] 18 p2118 N73-27128
Design of broadband continuous wave amplifier for phased array
[AD-760545] 18 p2124 N73-27167
Interface microprogramming for radar array signal processing computer
[AD-762439] 19 p2238 N73-28041

Development and evaluation of on-line spatial light modulator for application as input transducer for real-time optical data processing system
[NASA-CR-124375] 21 p2508 N73-30121
Development plan for experimental array radar for antimissile defense
[AD-763171] 21 p2509 N73-30132
C band waveguide phased array
[AD-763214] 21 p2517 N73-30193
Broadband space feed system for phased array
[AD-763767] 21 p2518 N73-30195
Target searching procedures with electronically steered phased array radar
[REPT-186] 22 p2632 N73-31094
Evaluation of phased array antennas
[AD-764367] 22 p2634 N73-31113
Digital signal processor for use with experimental MICOM array radar
[AD-764227] 22 p2635 N73-31121
Conception and application of phased arrays
[FTZ-A-454-TBR-15] 22 p2642 N73-31178

**PHENOL FORMALDEHYDE**
Use of phenol formaldehyde plastic foam as thermal insulation for solar water heaters to improve efficiency
[AD-756591] 13 p1548 N73-22543

**PHENOLIC RESINS**
Production of large carbon fibers by impregnation with phenolic resin and carbonizing composite fiber
[NPL-IMS-18] 09 p1052 N73-18580
Research on carbon, graphite, and phenolic resin binders
[NASA-CR-131483] 13 p1547 N73-22539
Stagnation-line analysis of radiative heating of phenolic-nylon ablator
[NASA-CR-112306] 15 p1766 N73-24309
Physical and mechanical properties of high-strength, high-modulus reinforcing fibers and organic resin composite materials
18 p2164 N73-27475

**PHENOLOGY**
Identification of phenological stages and vegetative types for land use classification based on ERTS-1 imagery
[E72-10342] 05 p0532 N73-14330
Identification of phenological events, rangelands, and crops using ERTS-1 imagery
[E72-10351] 05 p0533 N73-14339
ERTS-1 identification of phenological stages and vegetation types in Alaska for land use classification
[E73-10276] 08 p0914 N73-17484
Identification of phenological stages and vegetative types from ERTS-1 imagery for land use classification in Alaska
[E73-10439] 11 p1281 N73-20399
Identifying phenological changes for specific forest and crop types using ERTS-1 imagery
[E73-10498] 12 p1398 N73-21334
Identification of phenological stages and vegetative types in Alaska for land use classification
[E73-10618] 15 p1774 N73-24379
Mapping phenological changes using ERTS-1 imagery
[E73-10660] 16 p1899 N73-25356
Detection of phenological event for specific forest and crop types using ERTS-1 imagery
[PAPER-A19] 19 p2261 N73-28226
ERTS-1 identification of phenological stages and vegetative types for land use classification in Alaska
[E73-10905] 20 p2396 N73-29254
Phenological observations of lilac, honeysuckle, alfalfa, and winter wheat in Rocky Mountain and Columbia Valley Corridors
[E73-10925] 20 p2398 N73-29274
Identification of phenological stages and vegetative types for land use classification in Alaska
[E73-11066] 23 p2781 N73-32242

**PHENOLS**
NT BISPHENOLS
Utilization of lithium p-lithiphenoxide to prepare star polymers
[NASA-CASE-NPO-10998-1] 23 p2753 N73-32029

**PHENOMENOLOGY**
NT PHENOLOGY

**PHENYLS**
NT POLYPHENYLS
Liquid retention in chlorpropamide therapy and water intoxication of patients
[NASA-TT-F-14597] 02 p0133 N73-11077
Antimicrobial phenyl preparations for human urine conservation during space flight
10 p1118 N73-19112

**PHILIPPINES**
Effect of Philippines on intensity, speed and size of typhoons crossing islands
[AD-746131] 02 p0206 N73-11670
Annotated bibliography on nuclear energy research in Philippines
[PAEC[A]-7116-SUPPL-4] 06 p0699 N73-15698
Application of ERTS-1 imagery for determining rice growing areas in Philippines and assessment of crop condition
[PAPER-A5] 19 p2260 N73-28213
Summaries of synoptic meteorological observations for Chinese - Philippine coastal marine areas
[AD-762423] 19 p2318 N73-28645
Identification of rice fields in Philippes from ERTS-1 imagery
[E73-10908] 20 p2397 N73-29257
Solar radio and geophysical studies at Manila Observatory
[AD-760771] 20 p2413 N73-29396
Synoptic meteorological data for Philippine coastal marine surfaces
[AD-762424] 20 p2450 N73-29688
Synoptic meteorological data for Philippine and Vietnam coastal marine surfaces
[AD-762425] 20 p2450 N73-29689

**PHILOSOPHY**
Analysis of development of cosmos, universe, mankind, and space exploration
04 p0470 N73-13833
Philosophical and social psychological study of Apollo moon scientist
[NASA-CR-130832] 09 p0995 N73-18122

**PHOENIX QUADRANGLE [AZ]**
Land use mapping and image enhancement of ERTS-1 imagery of Phoenix Quadrangle
[E73-10090] 08 p0902 N73-17302
Agricultural and urban land use mapping of Phoenix Quadrangle based on ERTS-1 imagery
[E73-10340] 10 p1147 N73-19339
Land use management and mapping for Phoenix Quadrangle from ERTS-1 imagery
[E73-10650] 16 p1897 N73-25346
Land use mapping of Phoenix Quadrangle, Arizona from ERTS-1 Photography
[PAPER-L3] 19 p2273 N73-28299
Land use mapping and modelling for Phoenix Quadrangle using ERTS-1 imagery
[E73-10955] 21 p2531 N73-30297
Land use mapping and modelling for Phoenix Quadrangle
[E73-11098] 24 p2914 N73-33255

**PHONEMES**
Synthesis of letter sounds of alphabet by concatenation of phonemes for digital spelled speech reading machine for blind
14 p1620 N73-23127
Isolated-word phoneme recognition using features derived from wave function parameters
14 p1622 N73-23142
Word recognition system based on dimensional representation of phoneme-like word segments
14 p1623 N73-23145
Phonocode for recognition of natural and artificial speech
14 p1628 N73-23197
Interaction between segmental and nonsegmental factors in speech recognition
14 p1629 N73-23203
Phoneme recognition of continuants in connected English speech by computer
14 p1630 N73-23208
Relation of phonemes to acoustic signals from human vocal tracts as represented by ultrahigh frequency patterns
14 p1631 N73-23218

**PHONEMICS**
Word and phrase stress by rule for reading machine that produces synthetic English speech
14 p1620 N73-23124

**PHONETICS**
Speech messages representing nine emotions for studies on time/frequency distortion effects on prosodic features of speech
[AD-746102] 02 p0141 N73-11146
Phonetic analysis of underwater diver speech and standardization for intelligibility
[AD-751662] 07 p0757 N73-16153
Role of distinctive features in speech production, acoustics, and phonetics
14 p1625 N73-23167
Articulatory occlusion recorder for studying differences in timing in labial stops and rounded vowels
14 p1625 N73-23171
Formants in automatic speech recognition, emphasizing physiological phone in terms of articulatory dynamics
14 p1628 N73-23194
Time domain analysis technique for acoustic phonemic level of speech recognition
14 p1628 N73-23196
Derivation of phonetic representation by combining steady-state and transemic classification in automatic recognition of continuous speech
14 p1629 N73-23200
Using graph search procedure to convert machine-contaminated phonetic descriptions of speaker performance into standard orthography
14 p1629 N73-23201
Spoken word recognition system utilizing word dictionary and phonological rule
14 p1629 N73-23202
Analysis of human performance in synthesis on non-nazalized vowels and input resistance as function of frequency
14 p1630 N73-23213
Three-dimensional output from third octave frequency analysis
14 p1631 N73-23221
Development of procedures and techniques for improved speech analysis based on fast Fourier transform and time compression and analysis
14 p1632 N73-23226
Development of method of speech analysis and synthesis using partial autocorrelation coefficients and optimum quantization technique
14 p1632 N73-23230
Analysis of clipped speed characteristics and zero crossing-related speech phenomena
14 p1632 N73-23233
Development of speech analysis-synthesis system for extracting singing voice signal from background noise on recording device
14 p1632 N73-23234
Automatic recognition algorithm for liquids and glides
[AD-762377] 19 p2237 N73-28032

**PHONONS**
Thermal conductivity measurements of electron and phonon scattering behavior in low temperature solids
[COO-1629-31] 04 p0485 N73-13961
Shell model for phonon dispersion anomalies and lattice instabilities in hard metalcarbides-nitrides and transition metals
08 p0951 N73-17783
Association of surface polaritons with surface magnetoplasmons coupled to surface optical phonons in polar semiconductors
[AD-753484] 09 p1075 N73-18771
Boundary scattering of phonons in germanium and silicon determined from low temperature thermal conductivity measurements
[AD-753494] 09 p1076 N73-18780
Measurement of phonon scattering by isotopic impurities in helium single crystals
[AD-754475] 11 p1330 N73-20798
Phonon dispersions and three particle correlations in liquid helium, and adsorbed helium monolayers
16 p1944 N73-25730
Crystal phonon contribution to free energy of identical atom pairs adsorbed on cubic lattice surface
[AD-759035] 17 p1992 N73-26109
Low temperature measurement of heat pulse and ultrasonic wave interaction with stress-split acceptor states in semiconductors
18 p2186 N73-27647
Picosecond laser beam study of four photon effects and temporal behavior of optical phonons
22 p2680 N73-31465
Theory for thermal boundary, kapitza, resistance to include effects of phonon attenuation near interface
24 p2968 N73-33719

**PHOSPHATES**
NT ADENINES
NT ADENOSINE TRIPHOSPHATE [ATP]
NT NUCLEOTIDES
Determination of quality of zinc phosphate coatings by measurement of electrode potential
[AD-745094] 01 p0070 N73-10571
Refutation of microbial ability to reduce phosphate using thermochemical computations
[NASA-TT-F-14724] 04 p0379 N73-13081
Effect of protective barrier creams on toxic alkyl phosphate penetration of pig skin
[BMVG-FBWT-72-15] 07 p0747 N73-16076
Optimal molecular composition of zirconium phosphate ion exchanger for separation of radioactive actinide series elements
08 p0883 N73-17151
Structural, electrical, and magnetic properties of transition metal oxide phosphate glasses
[AD-758373] 14 p1699 N73-23790
Vibrational spectral study of molecular orientation in vitreous sodium metaphosphate glass fibers
[AD-757751] 15 p1748 N73-24167
Interionic vibrations and glass transitions in ionic oxide metaphosphate glasses
[AD-765344] 23 p2811 N73-32478

**PHOSPHIDES**
NT BORON PHOSPHIDES
NT GALLIUM PHOSPHIDES
NT INDIUM PHOSPHIDES
Development of gallium aluminum phosphide alloys for electroluminescent diodes
[NASA-CR-112182] 03 p0273 N73-12213
Crystal growth and magnetic properties of transition metal chalcogenides
[AD-748864] 04 p0459 N73-13748

**PHOSPHONITRILES**
Synthesis of polyfluoroalkoxy phosphazenes
[AD-747344] 04 p0438 N73-13570
Thermally stable phosphonitrile elastomers for advanced aerospace structures
[NASA-CR-124008] 06 p0687 N73-15593
Synthesis of fire resistant phosphonitrilic plastics and elastomers for marine applications
[AD-755188] 13 p1548 N73-22547

**PHOSPHORESCENCE**
Design of three color plasma panel display device capable of operating at three intensity levels
[AD-752442] 09 p1009 N73-18236

**PHOSPHORIC ACID**
Bacterial reduction of organically bound phosphoric acid in blood
[NASA-TT-F-14723] 04 p0379 N73-13080
Development of phosphoric acid fuel cells operating on hydrogen produced from thermocracking or steam reforming of hydrocarbon
[AD-755206] 13 p1477 N73-21966
Low cost oxygen electrode for phosphoric acid fuel cell
[AD-758179] 15 p1739 N73-24095
**PHOSPHORS**
Photoluminescence, thermoluminescence, photoconductivity, and electrical conductivity measurements in heavily doped ZnS-Cu, In phosphors
17 p2071 N73-26759
**PHOSPHORUS**
Ion concentration profiles of injected boron and phosphorus including substitution of arsenic for phosphorus
05 p0522 N73-14249
Ion implantation of amorphous insulators and switching effects in silicon oxides
[LETI/ME-773] 07 p0832 N73-16744
Effect of acute and chronic hypercapnia on Ca and inorganic P levels in guinea pig blood plasma and erythrocytes
[AD-749323] 13 p1484 N73-22035
**PHOSPHORUS COMPOUNDS**
NT ADENINES
NT ADENOSINE TRIPHOSPHATE [ATP]
NT BORON PHOSPHIDES
NT GALLIUM PHOSPHIDES
NT INDIUM PHOSPHIDES
NT NUCLEOTIDES
NT ORGANIC PHOSPHORUS COMPOUNDS
NT PHOSPHATES
NT PHOSPHIDES
NT PHOSPHONITRILES
NT PHOSPHORIC ACID
**PHOSPHORUS METABOLISM**
Synthesis rate of phospholipids and cytochromes b5 and P 450 in thiamine-deficient rats after treatment with thiamine
[NASA-TT-F-14989] 17 p1987 N73-26064
**PHOSPHORYLATION**
Hydrophobic iminoxyl radicals as uncouplers of photophosphorylation in choloroplasts
[NASA-TT-F-14819] 12 p1376 N73-21160
**PHOTOABSORPTION**
Recoilless resonance photoabsorption by 6.2 keV transition in Ta-181, using W-181 in W and Ta foil sources
[NASA-TT-F-14680] 08 p0946 N73-17745
**PHOTOCATHODES**
Electron energy distribution of semiconductor cold-cathode
[AD-750611] 06 p0646 N73-15247
Research and development of infrared photocathodes
[AD-756239] 13 p1501 N73-22162
Photocathode for high resolution streak camera tube
[UCID-16218] 24 p2898 N73-33137
**PHOTOCELLS**
U PHOTOELECTRIC CELLS
**PHOTOCHEMICAL REACTIONS**
NT PHOTODECOMPOSITION
NT PHOTOLYSIS
NT PHOTOSYNTHESIS
NT RADIOLYSIS
Atmospheric measurement of photochemical smog reactions in San Francisco Bay area
[PB-210422] 01 p0077 N73-10635
Source of C3 in comets
02 p0228 N73-11842
Formation processes for C3 or C2 in comets
02 p0228 N73-11843
Fabricating miniature fluidic elements using photochemical engraving
04 p0426 N73-13472
Analysis of factors affecting environmental chambers used to study photochemical reactions in lower atmosphere
[PB-212715] 06 p0695 N73-15663
Photochemical and transport processes in stratosphere
08 p0972 N73-17941
Numerical and photochemical models for analyzing transport and trace constituents in stratosphere
[COO-2249-1] 10 p1155 N73-19399
CF3I gas laser system for high power operation
[SC-T-72-2560] 12 p1410 N73-21426
Stratospheric photochemical reactions of ozone in relation to climatology and supersonic transport pollution
[NOAA-TM-NESS-47] 12 p1422 N73-21526
Photochemical enhancement of combustion and mixing in supersonic flows
[AD-758802] 15 p1844 N73-24944
Models for radiative heating and cooling and ozone photochemistry in stratosphere
[NASA-CR-132777] 17 p2025 N73-26385
Photochemical mechanisms of ozone and energy budget in atmosphere between 10 and 100 km
18 p2133 N73-27233
NASA supported research in photobiology and photochemistry from 1966 to 1973
[NASA-CR-133459] 19 p2224 N73-27937
Airborne measurements of photochemical pollution in California and adjacent waters of Pacific Ocean
[NASA-TM-X-69504] 22 p2694 N73-31581
Proceedings of conference on mathematical modeling of photochemical smog
[PB-221177/9] 23 p2754 N73-32038
Field program design for verifying photochemical diffusion models
[PB-221300/7] 23 p2814 N73-32502
Gain measurements of excited iodine atom decay rates in photochemical iodine laser
[UCRL-TRANS-10692] 24 p2931 N73-33409
**PHOTOCHEMISTRY**
U PHOTOCHEMICAL REACTIONS
**PHOTOCONDUCTIVE CELLS**
Design of photoelectric sunshine recorder using cadmium sulfide photoconductive cells
[NLL-M-22979-[5828.4F]] 16 p1910 N73-25456
**PHOTOCONDUCTIVITY**
Surface damage to gallium arsenide surfaces from radiation by ruby and neodymium-glass lasers
05 p0555 N73-14507
Photoconductivity of thin dielectric films induced by X ray irradiation
[UCRL-73974] 05 p0586 N73-14770
Spectral and temperature characteristics of natural photoconductivity in p-type GaAs
[AD-750696] 06 p0709 N73-15790
Measurement of picosecond laser pulse width using two-photon conductivity in GaAs and three-photon conductivity in CdS
[AD-750414] 06 p0710 N73-15798
Temperature and intensity dependences of photoconductivity and annealing effects in electro-optical properties of amorphous Ge[.5]Te[.5] films
[AD-752024] 08 p0951 N73-17787
Photoconductivity of cadmium sulfide crystals excited by mode-locked neodymium laser pulses
[AD-753677] 09 p1077 N73-18786
Carrier lifetime measurement by photoconductive decay method
[NBS-TN-736] 13 p1565 N73-22685
Thin film lead and tin selenide photoconductive infrared detectors
[AD-758685] 16 p1915 N73-25499
Photoconductivity of gallium arsenide-, Cadmium sulfide-, and cadmium selenide-semiconductors correlated to laser pulse width
[AD-760560] 18 p2190 N73-27682
Photoconductive effect and absorption of monochromatic sub-mm radiation in n-type germanium
[RR-737] 20 p2462 N73-29782
**PHOTOCONDUCTORS**
Influence of photoconducting layer thickness on sensitivity of vidicons
[NLL-DRIC-TRANS-2965-[3623.66]]
11 p1261 N73-20233
Infrared sensitive photoconductors
[AD-755224] 13 p1560 N73-22647
Feasibility of using RF generated argon plasma for sputter etching Al and SiO2 windows and photoresist
[AD-757878] 15 p1800 N73-24588
Thermoelectric and photothermoelectric effects in semiconductors
15 p1819 N73-24747
Photoconducting semiconductor system for converting stored optical images into video signals
[NASA-CASE-NPO-13131-1] 22 p2680 N73-31467
**PHOTOCURRENTS**
U ELECTRIC CURRENT
U PHOTOELECTRIC EMISSION
**PHOTODECOMPOSITION**
Procedures for improving resistance of Nomex fabric and webbing to actinic degradation
[AD-759217] 17 p2051 N73-26596
**PHOTODIODES**
Design and development of photoparameteric detector-amplifier using indium antimonide photovoltaic reactions
[AD-749034] 04 p0451 N73-13683
Electrical properties of MOS field effect transistors and Schottky barrier photodiode
[AD-748862] 04 p0459 N73-13746
Performance of 10-micron mercury-cadmium-telluride and lead-tin-telluride photodiodes in laser heterodyne communication systems
[NASA-TM-X-66135] 05 p0557 N73-14521
Fabrication of photodiode transistor image sensor array in silicon
[NASA-CR-130036] 07 p0831 N73-16738
Conference on semiconductors, lasers, and photodiodes
[AD-754237] 10 p1202 N73-19782
Comparison of detectivities of p-n junction diode and Schottky internal photoemission diode under background-limited conditions
[AD-757873] 15 p1757 N73-24243
Design of 10.6 micrometer detector array using 77 K, 1500 MHz photodiodes
[AD-758714] 16 p1915 N73-25496
Mercury cadmium telluride 10.6-micron photodiode
[AD-762167] 19 p2248 N73-28122
Development of Hg Cd Te elevated temperature photovoltaic detectors
[AD-762352] 20 p2381 N73-29131
Star mapper breadboard model for satellite attitude control using either photomultipliers or Si photodiodes
[ESRO-CR-162] 22 p2698 N73-31611
Characteristics of direct-coupled photodetector-preamplifier for use in facsimile camera for improved sensitivity and reduced mechanical complexity
[NASA-TN-D-7338] 23 p2769 N73-32148
**PHOTODISSOCIATION**
Photodissociative excitation of carbon dioxide as source of atomic oxygen in Martian atmosphere
[NASA-TM-X-66088] 02 p0229 N73-11856
Solar flux effects on upper atmosphere oxygen photodissociation and heating rates
[AD-747777] 04 p0467 N73-13807
Mass spectroscopy of C state in iodine by crossing of molecular beam with pulsed laser beam and monitoring recoil photofragments
[AD-751611] 07 p0753 N73-16117
Photodissociation and formation of nitric acid in mesosphere and stratosphere
[AERONOMICA-ACTA-A-113] 09 p1027 N73-18382
Measurement of absorption cross section values of nitric acid vapor in stratosphere at different wavelengths
[A-117-1973] 16 p1905 N73-25408
Differential cross sections in photodisintegration of helium-3
16 p1947 N73-25753
**PHOTOELASTIC ANALYSIS**
Application of dynamic photoelasticity to analyze crack branching in homalite sheets
[AD-744661] 01 p0114 N73-10940
Crack propagation and arrest in impacted, edge cracked, tension plates analyzed by dynamic photoelasticity
[AD-745792] 01 p0114 N73-10946
Photoelastic methods of stress analysis applied to fiber reinforced composites
05 p0602 N73-14892
Evaluation of fringe multiplication technique applied to frozen stress approach of three dimensional stress analysis in three dimensions
[AD-751172] 07 p0853 N73-16917
Photoelastic analysis of plane polyester specimens containing fatigue crack to determine effect of plastic yielding on stress distribution near crack
[TAE-155] 09 p1093 N73-18923
Stress analysis of plates with part circular and flat bottomed cracks and various flaw depths using stress intensity factors from photoelastic data
[NASA-CR-132015] 14 p1715 N73-23915
Development of photoelastic stress freezing and slicing method to determine stress intensity around surface flaws
[AD-758140] 14 p1717 N73-23934
Photoelastic stress analysis of NERVA structures
[NASA-CR-132213] 15 p1810 N73-24673
Scattered light photoelastic method for predicting stress distribution in composite epoxy glass structures
[AD-759900] 17 p2052 N73-26601
Analysis of stress-strain state in metal and contact stresses developed during continuous rolling on long mandrel for reducing and drawing metal tubes
[NLL-M-21688-[5828.4F]] 20 p2428 N73-29502
Stress analysis of adhesive lap joint subjected to tension, shear force, and bending moments for various material properties and thickness of adherents
24 p2988 N73-33877
**PHOTOELASTIC MATERIALS**
Photoclastic models of structures containing spherical voids in hexagonal close-packed configuration
[UCRL-73848] 03 p0361 N73-12940
Static and dynamic analyses on fracture mechanics of polyester plastic sheet
[AD-749098] 09 p1097 N73-18954
**PHOTOELASTIC STRESS MEASUREMENT**
U PHOTOELASTIC ANALYSIS
**PHOTOELASTICITY**
Stress freezing and slicing techniques of photoelasticity to analyze local stresses near deep surface flaws under cylindrical bending fields
[AD-746976] 02 p0240 N73-11950
Correlation functions for displacements in semibounded isotropic elastic media
[ITF-72-78-P] 12 p1429 N73-21579
Determination of stress intensity factors from photoelastic data with applications to surface flaw problems
[AD-756872] 13 p1587 N73-22864
Piezobirefringence measurements on amorphous and crystalline semiconductors with zincblende, wurtzite, and rocksalt structures
18 p2184 N73-27637
**PHOTOELECTRIC CELLS**
NT PHOTOCONDUCTIVE CELLS
NT PHOTOVOLTAIC CELLS
Maximum detection probability of optical image by photoelectric surface with unit quantum efficiency
[NASA-CR-130121] 03 p0334 N73-12725
Development of materials and construction processes for improved efficiency of photoelectric converters
04 p0375 N73-13048

Evaluation of dielectric insulation and etched junction contact techniques for fabrication of wraparound contact silicon solar cells
[NASA-CR-121021] 04 p0375 N73-13051
Photoactivated liquid crystal light valve
09 p1065 N73-18692
Analysis of silicon solar cells to show factors controlling blue response and methods for improvement
[NASA-CR-131090] 10 p1111 N73-19059
Effectiveness of solar cells based on CdS-Cu-xS heterojunctions
[AD-756602] 13 p1478 N73-21971
Performance of combined photoelectric snow depth-robot rain gage system
[NLL-M-22978-[5828.4F]] 16 p1910 N73-25457
Methods for measuring photocell linearity and analysis of conditions for accurate assessment of nonlinearity
[PAPER-76A5-731] 21 p2545 N73-30400
**PHOTOELECTRIC EFFECT**
NT PHOTOIONIZATION
Photoelectric tunnel currents in metal-insulator-metal diodes
[AD-751758] 07 p0763 N73-16201
Oscilloscopic measurement of mode locked ultrashort laser pulses produced by linear and nonlinear photoelectric effects
[KFKI-72-41] 07 p0806 N73-16539
Photodielectric recombination and trapping model for low temperature n-type epitaxial gallium arsenide
[NASA-CR-130764] 08 p0950 N73-17779
Photodielectric and conduction properties of amorphous semiconductors
[AD-753053] 09 p1074 N73-18762
Photon detector applications and theoretical considerations of heterojunction photo-effect
[AD-754026] 10 p1202 N73-19784
Characteristics of photomultiplier tubes and application to optics, biophysics, radiometry, and astronomy for detecting weak light flows
[AD-755874] 12 p1384 N73-21226
Characteristics of photoelectric pyrometer for measuring temperature of thin wire during rolling process
[NLL-M-21634-[5828.4F]] 15 p1785 N73-24471
Methods for measuring photocell linearity and analysis of conditions for accurate assessment of nonlinearity
[PAPER-76A5-731] 21 p2545 N73-30400
Photodielectric techniques for analyzing low temperature band structure of gallium arsenide
24 p2891 N73-33080
**PHOTOELECTRIC EMISSION**
Measurements of work function of {110} and {111} faces of crystal from solid solution of osmium in tungsten
[NLL-TRANS-746-1315-[9022.401]]
05 p0585 N73-14760
Angular distribution of photoemitted electrons from activated p-type gallium arsenide surfaces
[AD-750364] 06 p0645 N73-15239
Explorer 31 measurements of photoelectron escape fluxes for equatorial and midlatitude regions
[NASA-TM-X-68921] 07 p0789 N73-16416
Approximative solution for photon emission amplitude in soft photon irradiation by electromagnetic wave field
[NASA-TT-F-14686] 09 p1066 N73-18697
Effects of photoelectron emission on multiple-probe spacecraft near plasmapause
[NASA-TM-X-69313] 12 p1403 N73-21380
Photoelectric emission of gallium arsenide from adsorbed layers of cesium and barium oxide
[NLL-DRIC-TRANS-2293-[3623.66]]
15 p1819 N73-24746
Absolute electron yields and spectral characteristics of X ray induced photoemission from metals
[AD-750875] 16 p1928 N73-25599
Short-range ordering in amorphous Ge thin films studied by photoemission spectrum analysis as function of film preparation at different substrate temperatures
18 p2190 N73-27680
Photoelectric determination of change in center-limb profiles of faint Fraunhofer lines
20 p2472 N73-29854
One-dimensional analysis of electric fields and electric potential near photo emitting plate emmersed in solar wind plasma
23 p2858 N73-32839
**PHOTOELECTRIC GENERATORS**
Design and operation of high voltage photoelectric generator
[AD-745364] 01 p0007 N73-10053
Possibility of using triple semiconductor compounds in thermoelectric and photoelectric converters
[AD-765730] 24 p2970 N73-33734
**PHOTOELECTRIC MATERIALS**
Development of materials and construction processes for improved efficiency of photoelectric converters
04 p0375 N73-13048
Operational characteristics of semiconductor photoconverters as power supply sources for space vehicles
[AD-753063] 09 p1074 N73-18766
Methods for measuring photocell linearity and analysis of conditions for accurate assessment of nonlinearity
[PAPER-76A5-731] 21 p2545 N73-30400
**PHOTOELECTRIC PHOTOMETRY**
U ELECTROPHOTOMETERS
**PHOTOELECTRICITY**
Photoelectric observation of eclipsing variable stars TY Ursae Majoris and AZ Virginis including spectral classification for WY Cancri, AZ Virginis, and TZ Bootis
04 p0468 N73-13818
Analysis of photoelectric properties of gallium arsenide and application to construction of solar cells
[AD-756228] 13 p1477 N73-21962
Electric, photoelectric, and electroluminescence properties of Cu contacts on CdS surface
[AD-756876] 13 p1504 N73-22187
Applications of photoelectronic and thermoelectronic instruments
[JPRS-59951] 22 p2672 N73-31404
Photoelectric sensor for measurement of spectra and concentration of liquid particles in aerosol
[AD-764927] 23 p2794 N73-32353
Optical, photoelectric, and structural properties of amorphous B1-Ge thin films
23 p2824 N73-32572
Photoelectric light curves of eclipsing binary star systems EE Aquarii and AE Phoenicis
23 p2837 N73-32667
Method for comparing photo-electronic and photographic detectors based on product of signal to noise ratio times spatial bandwidth
24 p2958 N73-33634
Techniques for long range vision underwater using range-gating and dual-scan with parallax techniques
24 p2958 N73-33636
**PHOTOELECTROMAGNETIC DETECTORS**
U RADIATION MEASURING INSTRUMENTS
**PHOTOELECTRONICS**
U ELECTRONICS
U PHOTOELECTRICITY
**PHOTOELECTRONS**
Photoelectron effect on second positive system of nitrogen bands in daytime glow of atmosphere from Cosmos 224 data
05 p0536 N73-14360
Valence electron model for calculating ionization energies and excited levels in photoelectron- and absorption-spectra
08 p0945 N73-17741
Energy spectra of ionospheric photoelectrons measured in 30 to 150 eV range from Cosmos 348 satellite in summer 1970
[PR-107] 10 p1155 N73-19400
Photoelectron transport energy for calculating electron and ion temperatures of ionospheric models
[AD-756241] 13 p1525 N73-22362
**PHOTOEMISSION**
U PHOTOELECTRIC EMISSION
**PHOTOEMISSIVITY**
U EMISSIVITY
U PHOTOELECTRIC EMISSION
**PHOTOEMITTERS**
U PHOTOELECTRIC MATERIALS
**PHOTOENGRAVING**
Elastic surface wave encoders and decoders for use in secure, antijam command, control, and communications systems
[AD-758762] 16 p1919 N73-25529
Metal oxide semiconductor photoengraving principles and utilization noting resin properties, procedures, thin film techniques, and metal chemical attack
[LAAS-FI-73-T-11] 24 p2899 N73-33139
**PHOTOGEOLOGY**
Spectral geological mapping of New York using ERTS-1 imagery
[E72-10223] 02 p0163 N73-11317
Role of remote sensing in geologic reconnaissance for tunnel-site selection
[AD-748663] 04 p0416 N73-13399
Compilation of photomaps of Nevada geology from ERTS-1 imagery
[E73-10473] 12 p1395 N73-21310
Relative ages of near side and far side terra plains based on interpretation of Apollo 16 photogeology - Part A
12 p1452 N73-21765
Cayley Formation interpreted as deposited fluidized debris that traveled beyond extent of Imbrium Basin ejecta - Part B
12 p1453 N73-21766
Photogeologic analysis of Apollo 16 metric photography of northern Nectaris Basin - Part F
12 p1453 N73-21770
Structural aspects of distinctive landforms collectively referred to as Imbrium sculpture - Part G
12 p1453 N73-21771
Morphometric analysis of Apollo 16 photography of lunar craters - Part L
12 p1454 N73-21776
Apollo 16 orbital photography of King Crater and surrounding environment - Part M
12 p1454 N73-21777
Effectiveness of snow cover as photogeological enhancement technique for ERTS-1 imagery of western Massachusetts
[E73-10594] 16 p1896 N73-25334
Geological surveys and mapping of New York using ERTS-1 imagery
[E73-10846] 19 p2291 N73-28424
Tectonic and photogeologic mapping of forested and sparsely vegetated terrain of Montana and Idaho
[E73-10900] 20 p2396 N73-29249
Geological surveys of Colorado from Skylab EREP photography
[E73-10919] 20 p2398 N73-29268
Geologic and mineral and water resources of western Colorado from Skylab multispectral photography
[E73-11010] 22 p2660 N73-31315
Reconnaissance geologic mapping in Dry Valleys of Antarctica using ERTS-1 imagery
[E73-11127] 24 p2916 N73-33282
**PHOTOGRAMMETRY**
Computer program for strip triangulation by independent models in aerial photogrammetry
02 p0164 N73-11334
ALGOL computer program for combined photogrammetric-terrestrial cadastral surveying
02 p0165 N73-11338
Computer aided photogrammetric analysis of lunar topography
[AD-744867] 02 p0232 N73-11881
Analysis of image coordinate refinement parameters applied to aerial photography of ground areas for improved aero-triangulation
[AD-747799] 03 p0304 N73-12479
Design of photogrammetric test standards
[AD-749502] 04 p0424 N73-13459
Measurement of lateral erosion rates at proposed river crossing sites of Alaska pipeline by aerial photogrammetry
[AD-748875] 05 p0541 N73-14402
Photogrammetric interpetation of barium cloud developments parallel to geomagnetic field
[EGG-1183-5006] 06 p0666 N73-15418
Least squares method in gravimetric geodesy and photogrammetry
[AD-749873] 06 p0669 N73-15440
Design and performance of two dimensional sensor array system for image area measurements
[AD-750315] 06 p0675 N73-15490
Operational activities of Hungarian National Bureau of Metrology and use of photogrammetry in city planning and modernization
[JPRS-57792] 06 p0731 N73-15965
Use of photogrammetry in city planning and modernization
06 p0732 N73-15967
Improved measurement of photographic images with negative reticles
[AD-753946] 11 p1295 N73-20505
Use of edges of photographic images as specifiers of image quality
[AD-753947] 11 p1295 N73-20512
Influence of displays on image interpreter performance in investigating characteristics of pictorial content of reference material
[AD-754567] 11 p1353 N73-20984
Application of photointerpretation and photogrammetry to analysis of cloud cover type and motion
[NASA-TM-X-64710] 12 p1404 N73-21385
Morphometric analysis of Apollo 16 photography of lunar craters - Part L
12 p1454 N73-21776
Use of laser altimetry in Apollo 16 flight to aid in spacecraft position determination and lunar geological investigation
12 p1455 N73-21790
Photogrammetric techniques from Apollo 15 and 16 flights to provide accurate measurement of lunar topography
12 p1456 N73-21791
Use of Apollo 16 photogrammetry to determine frequency distributions of lunar slopes
12 p1456 N73-21792
Terrain factor analysis and automatic color coded mapping using image processing methods in estimation of construction time relative to prospective military airfields
[AD-755531] 13 p1526 N73-22367
Comparative evaluation of point marking devices and their suitability for photogrammetric problems
13 p1528 N73-22383
Photogrammetric plotting system for graphical and digital plotting of stereopairs
[MBB-UR-150-72-O] 17 p2034 N73-26458
Photogrammetric and densitometric examination of ERTS-1 MSS imagery of Eastern Virginia to determine sources of aerosol pollution
[PAPER-E5] 19 p2269 N73-28269
Research and development in topographic mapping, field surveys, photogrammetry, orthophotomapping, and space technology
[PB-221469] 22 p2669 N73-31384
Ratio scannergrammetry of geology in Wyoming and South Dakota
[E73-11096] 24 p2914 N73-33253

Photogrammetric refraction angles through total refraction A
[NASA-TT-F-15074] 24 p2922 N73-33335

**PHOTOGRAPH INTERPRETATION**
U PHOTOINTERPRETATION

**PHOTOGRAPHIC EMULSIONS**
NT NUCLEAR EMULSIONS

Analysis of characteristic curves of various black and white photographic films and processing methods for typical conditions
[NASA-TT-F-13920] 01 p0058 N73-10473

Evaluation of concept for determining edge sharpness and transfer characteristics of photographic materials
[NASA-TT-F-13922] 05 p0547 N73-14445

Application of Schmidt telescopes to study of galactic clusters and evolution noting new emulsion, infrared surveys, luminosity, and quasars
07 p0845 N73-16849

System for measuring scattered flux from fine grained photographic emulsions
16 p1921 N73-25548

Spectrophotometry accuracy with Kodak IN, IIaO, and II aD photographic emulsions
[RR-3] 19 p2301 N73-28502

**PHOTOGRAPHIC EQUIPMENT**
NT CAMERAS
NT FRAMING CAMERAS
NT HIGH SPEED CAMERAS
NT MULTISPECTRAL BAND CAMERAS
NT PANORAMIC CAMERAS
NT PHOTOGRAPHIC PROCESSING EQUIPMENT
NT SCHMIDT CAMERAS
NT TELEVISION CAMERAS

Method and data reduction tables for determining resolving power of photographic and other optical systems under typical field conditions
[AD-747265] 03 p0303 N73-12475

Design of photogrammetric test standards
[AD-749502] 04 p0424 N73-13459

Characteristics of various types of remote sensors and identification of specific areas of application
07 p0784 N73-16373

Application of aerial photography for remote sensing to include characteristics of cameras, films, and photographic processing
07 p0784 N73-16375

Development of compact, ultrafast streaking camera to include power requirements, electronic circuitry, and performance analysis
[UCRL-73734] 07 p0801 N73-16502

Application of NASA developed techniques, photographic film, and photographic equipment to ecological problems
[NASA-SP-5099] 09 p1034 N73-18437

Analysis of internal precisions and external accuracies of various stereometric systems consisting of single stereometric camera
12 p1404 N73-21384

High speed photographic system for moisture flow visualization in steam turbines
[NASA-TM-X-2763] 12 p1404 N73-21388

Techniques and equipment for field photography of artillery projectiles in flight
[LA-5030] 12 p1405 N73-21396

Color photographic techniques to study vegetation and terrain, improve mapping methods, and to provide photoelectronic color separation using aerial cameras
[AD-756700] 14 p1668 N73-23536

Development of method for determining resolving power of photographic lenses
[NBS-SP-374] 18 p2151 N73-27387

Logistic performance data book for RF-4C photographic reconnaissance system to show reliability, maintainability, logistic support, and operating problems
[AD-762232] 19 p2358 N73-28974

Photographic equipment for recording fracture of zinc single crystals under dynamic stress
20 p2461 N73-29775

**PHOTOGRAPHIC FILM**
NT MICROFILMS

Analysis of characteristic curves of various black and white photographic films and processing methods for typical conditions
[NASA-TT-F-13920] 01 p0058 N73-10473

Use of TV equipment for converting color negative cinefilm into color positive image
[DRIC-TRANS-2835] 02 p0174 N73-11412

Comparison of methods for determining transfer functions of black and white aerial photographic films
[AD-747594] 03 p0304 N73-12483

Photographic film density and density distribution measurements, and mean square deviation of density and energy spectrum
[NASA-TT-F-14614] 04 p0420 N73-13427

Evaluation of concept for determining edge sharpness and transfer characteristics of photographic materials
[NASA-TT-F-13922] 05 p0547 N73-14445

Photographic characteristics of UFSh-4 film used in Orion orbital observatory
[NASA-TT-F-14585] 07 p0799 N73-16492

Comparison of monochrome and color film for air to ground target acquisition
[RAE-TR-72064] 07 p0801 N73-16504

Application of NASA developed techniques, photographic film, and photographic equipment to ecological problems
[NASA-SP-5099] 09 p1034 N73-18437

Graphical techniques for developing photoplastic record card system
[AD-753602] 10 p1162 N73-19453

Reception of positive color television images using negative color motion picture film
[NLL-DRIC-TRANS-2835-[3623.66]] 11 p1291 N73-20480

Bibliography on infrared photography and infrared films
[AD-754600] 11 p1295 N73-20509

Analysis of test films to assess readiness of Apollo 17 radar equipment with emphasis on lunar sounder equipment
[NASA-CR-128883] 11 p1338 N73-20858

High resolution film actinometric measurements of ultraviolet irradiation levels during space flight
15 p1741 N73-24112

Statistical processing of Pioneer front film data - Part I
[NASA-CR-132797] 22 p2665 N73-31351

Automatic shot change detector for pre-programmed corrections of film reproduced by telecine
[BBC-RD-1973/10] 22 p2671 N73-31392

Photographic film for simplified production of equidensities in normal processing operation
[NASA-TT-F-15112] 22 p2673 N73-31410

Mechanical exposure interlock device for preventing film overexposure in oscilloscope camera
[NASA-CASE-LAR-10319-1] 23 p2790 N73-32322

Technical consulting services for earth resources program
[NASA-CR-135793] 24 p2921 N73-33330

**PHOTOGRAPHIC MEASUREMENT**
NT PHOTOGRAMMETRY

Visual and photographic observations of Beta Scorpii occultation by Jupiter
[NASA-CR-129990] 05 p0594 N73-14832

Topler method for studying structure of turbulent diffusion flames
[NASA-TT-F-14842] 10 p1223 N73-19945

Reduction of photographic heat transfer rate data at wind tunnel test facility
[AD-762928] 20 p2420 N73-29447

Spectrometric and photographic analysis of neodymium glass laser produced hydrogen plasma
[AD-764496] 22 p2705 N73-31667

**PHOTOGRAPHIC PLATES**

Schmidt telescopes for astrometry discussing correspondence between flat and curved plates
07 p0845 N73-16845

**PHOTOGRAPHIC PROCESSING**

Analysis of characteristic curves of various black and white photographic films and processing methods for typical conditions
[NASA-TT-F-13920] 01 p0058 N73-10473

Hardware design and algorithm for image processing on IDECS/PDP system
[AD-743526] 02 p0174 N73-11414

Feasibility of multispectral signal encoding on black and white film
[AD-749495] 05 p0548 N73-14455

Photographic water conservation and reclamation processes
[AD-752220] 08 p0926 N73-17585

Processing and enhancement of Earth Resources Program photography
[NASA-CR-131819] 15 p1787 N73-24491

Analysis of ERTS-1 multispectral band scanner imagery to determine cause of anomalous dark patches occurring in photographs of calm ocean surfaces
[E73-10747] 17 p2021 N73-26351

Technical and economic aspects of new industrial radiographic imaging papers
[AD-759907] 17 p2035 N73-26471

Equipment certification and process verification methods for photographic processing control of ERTS images
18 p2211 N73-27854

Contrast enhancement of ERTS-1 imagery by photographic techniques and methods
19 p2286 N73-28381

**PHOTOGRAPHIC PROCESSING EQUIPMENT**

Drying chamber for photographic sheet material
[NASA-CASE-GSC-11074-1] 19 p2300 N73-28489

**PHOTOGRAPHIC RECORDING**

Development of method for measuring temperature of wind tunnel scale model by photographic recording of changes in thin film phase-change temperature indicating material
[NASA-CASE-LAR-11053-1] 02 p0243 N73-11972

Development of method for automatically scanning bubble chamber films based on optical system for detecting information points as vertices
[CEA-R-4329] 03 p0302 N73-12465

Analysis of image coordinate refinement parameters applied to aerial photography of ground areas for improved aero-triangulation
[AD-747799] 03 p0304 N73-12479

Development of map storage and display system using volume holography using iron-doped lithium niobate
[AD-748002] 03 p0311 N73-12541

Analysis of photographic data obtained during manned and unmanned space flight and application to oceanography, hydrology, geography, and geology
04 p0471 N73-13843

Camera installation for multispectral aerial photography using four electrically driven cameras for synchronous photography
[FOA-2-C-2469-52] 06 p0672 N73-15469

Color photographic system using grid projector and telecentric lenses for recording contours of human face for aircrew oxygen mask fitting
[RAE-TR-71184] 07 p0750 N73-16099

Application of airborne and spaceborne photography to determine agricultural and forestry resources
07 p0782 N73-16355

Comparison of imagery obtained with several types of remote sensors over Test Site 701, Mexico
07 p0783 N73-16367

Analysis of oceanography remote sensing using black and white, color, and color infrared photographic recording
07 p0788 N73-16407

Development of compact, ultrafast streaking camera to include power requirements, electronic circuitry, and performance analysis
[UCRL-73734] 07 p0801 N73-16502

Schmidt telescopes for astrometry discussing correspondence between flat and curved plates
07 p0845 N73-16845

Analysis of cloud formations, ozone distribution, and meteorological data from Nimbus 4 satellite observations
[NASA-TM-X-66190] 09 p1028 N73-18392

Graphical techniques for developing photoplastic record card system
[AD-753602] 10 p1162 N73-19453

Analysis of factors affecting quality of electrostatic printing processes and procedures to improve produc:
[AD-755259] 12 p1409 N73-21420

Development of optical and digital techniques for application to synthetic holograms recorded with suboptical sources
[AD-756506] 14 p1674 N73-23583

Reusable photoplastic recording materials in read/write holographic memories
16 p1922 N73-25553

Analysis of time-lapse data processing for dynamic hydrologic conditions based on ERTS-1 imagery and aerial photography
[E73-10729] 17 p2020 N73-26335

Development of technique for producing holograms using propagation of surface waves within layer of photosensitive material
[NASA-CASE-MFS-22040-1] 17 p2039 N73-26500

Characteristics of NOAA 2 meteorological satellite and photographic data of weather conditions over Europe during 1972
[QR-4-PT-4] 17 p2056 N73-26627

Correlation of ERTS-1 data with ground data for determining characteristics of air pollution in Norfolk, Virginia area
[E73-10779] 18 p2135 N73-27255

Evaluation and characterization of possible recording materials for holographic optical elements
[AD-760561] 18 p2159 N73-27441

Image acquisition and enhancement techniques for oceanographic photography using photo-optical and electronic methods
[AD-761663] 19 p2296 N73-28463

Comparison of photographic digital recording systems using laser technology
[AD-761521] 19 p2308 N73-28563

Photographic recording of secondary flows at nozzle exits produced by planar nozzles with rectangular inlets from circular ducts
[AD-762743] 21 p2527 N73-30265

Comparison of film and video as the recording medium in high voltage electron microscopy
[NPL-IMS-20] 21 p2549 N73-30438

Development of photoplastic materials for optical memory storage applications
[AD-764822] 23 p2794 N73-32356

Optical and digital reconstruction techniques applied to synthetic holograms recorded with suboptical sources
23 p2800 N73-32394

Evaluation of holographic-recording photopolymer to determine diffraction efficiencies and development techniques
[CRC-659] 23 p2800 N73-32395

Method for comparing photo-electronic and photographic detectors based on product of signal to noise ratio times spatial bandwidth
24 p2958 N73-33634

**PHOTOGRAPHIC RECORDING INSTRUMENTS**
U OPTICAL MEASURING INSTRUMENTS
U PHOTOGRAPHIC RECORDING

U RECORDING INSTRUMENTS
PHOTOGRAPHIC TRACKING
Soviet camera for tracking satellites and solving geodetic and geophysical problems
[AD-747135] 03 p0303 N73-12476
Photogrammetric interpetation of barium cloud developments parallel to geomagnetic field
[EGG-1183-5006] 06 p0666 N73-15418
Artificial satellite equations of motion approximations for photographic and laser tracking optimization
15 p1832 N73-24848
Wind estimation by photographic tracking of clouds on images from synchronous meteorological satellites
24 p2948 N73-33546

PHOTOGRAPHS
NT CLOUD PHOTOGRAPHS
NT LUNAR PHOTOGRAPHS
NT MOTION PICTURES
NT PHOTOMICROGRAPHS
Mathematical model for geodetic survey of tracking stations using laser range finder and photographs including results of European tracking network
[GRGS-BULL-3] 03 p0294 N73-12398
Mathematical model for geodetic survey of tracking stations using laser range finder and photographs
03 p0294 N73-12399
Digital technique for picture processing
[AD-755701] 13 p1499 N73-22145
Bibliography of developments in field of picture processing by computers during 1972
[AD-755702] 13 p1499 N73-22146
Data tables and photographs of gaas epitaxial layer perfections as influenced by substrate disorientation
18 p2189 N73-27675
Extraction of edges from photographs of quadric bodies
[AD-762589] 20 p2420 N73-29445
Solar-geophysical data for sudden ionospheric disturbance of Dec. 14 to 21 1971
[AD-762483] 20 p2474 N73-29873
Recognition algorithm for object localization in pictures
[BMVG-FBWT-73-14] 23 p2760 N73-32091
Threshold selection for interpretation of digital pictures
[AD-764736] 24 p2898 N73-33132

PHOTOGRAPHY
NT AERIAL PHOTOGRAPHY
NT ALL SKY PHOTOGRAPHY
NT ASTRONOMICAL PHOTOGRAPHY
NT AUTORADIOGRAPHY
NT BLACK AND WHITE PHOTOGRAPHY
NT CHRONOPHOTOGRAPHY
NT CINEMATOGRAPHY
NT CLOUD PHOTOGRAPHY
NT COLOR PHOTOGRAPHY
NT FRACTOGRAPHY
NT FRAME PHOTOGRAPHY
NT HOLOGRAPHY
NT INFRARED IMAGERY
NT INFRARED PHOTOGRAPHY
NT LUNAR PHOTOGRAPHY
NT MULTISPECTRAL PHOTOGRAPHY
NT PHOTOMICROGRAPHY
NT RADAR PHOTOGRAPHY
NT SATELLITE-BORNE PHOTOGRAPHY
NT SCHLIEREN PHOTOGRAPHY
NT SHADOWGRAPH PHOTOGRAPHY
NT SPACEBORNE PHOTOGRAPHY
NT SPECTROPHOTOGRAPHY
NT STEREOPHOTOGRAPHY
NT ULTRAVIOLET PHOTOGRAPHY
NT ULTRAVIOLET PHOTOMETRY
NT UNDERWATER PHOTOGRAPHY
Soviet research in field of photographic metrology
[NASA-TT-F-13921] 01 p0075 N73-10615
Diffraction technique for determining three dimensional frequency spectra of photographic images
[AD-751418] 07 p0822 N73-16663
Stop-motion cinefluorography system for biomedical research
[AD-762412] 19 p2302 N73-28513
User manual for Image Data Processing System, language and control system for processing image data
[NASA-CR-124438] 24 p2897 N73-33122

PHOTOINTERPRETATION
On-line computer technique for evaluating reconnaissance image compression algorithms
01 p0024 N73-10191
Interpretation and mapping large scale structural lineaments in Precambrian shield areas and basins containing younger sediments using ERTS-1 imagery
[E72-10180] 01 p0045 N73-10359
Automatic photointerpretation for land use management in Minnesota
[E72-10227] 02 p0163 N73-11320
Development of computer programs for aerotriangulation with independent models
02 p0164 N73-11333
Application of aerial photography and photointerpretation to analyzing groundwater conditions under various types of landscape and morphological elements
[NASA-TT-F-681] 02 p0174 N73-11409
Hardware design and algorithm for image processing on IDECS/PDP system
[AD-743526] 02 p0174 N73-11414
Computer aided photogrammetric analysis of lunar topography
[AD-744867] 02 p0232 N73-11881
Interpretation of ERTS-1 multispectral data from area in West Pakistan
[E72-10234] 03 p0288 N73-12334
Cultural resources interpretation and map revision from ERTS-1 RBV and MSS imagery of Washington state
[E72-10276] 03 p0291 N73-12374
Automatic photointerpretation for plant species and stress identification using ERTS-1 imagery
[E72-10258] 03 p0300 N73-12448
Automatic plotting of aerial reconnaissance imagery and evaluation of image quality using coherent optical processing techniques
[AD-747803] 03 p0303 N73-12478
Directions of strong Martian winds inferred from Mariner 6 and 7 photographs and relation to dust storms and topographic wind funneling
[NASA-CR-129520] 03 p0354 N73-12885
Theory and practice of aerial photography to include aerial triangulation, stereometric methods of photointerpretation, and production of maps
[AD-748871] 04 p0423 N73-13449
Interpretation of meteorological satellite TV pictures of ice in Baltic Sea
[NLL-M-20841-[5828.4F]] 05 p0529 N73-14306
Influence of atmospheric conditions on remote image transfer and interpretation as determined by laboratory measurements
05 p0537 N73-14370
Computer technique for stereo image processing of Mariner 9 spacecraft color photographs
[NASA-CR-130305] 06 p0644 N73-15226
Photointerpretation and thematic mapping of ERTS-1 imagery of Brownsville, Texas area
[E73-10006] 06 p0658 N73-15342
Photointerpretation of ERTS-1 imagery of Arizona with emphasis on porphyry copper deposits occurring at intersection of major faults and igneous intrusions
[E73-10018] 06 p0659 N73-15354
Analysis of ERTS-1 imagery for identification and discrimination of geological, hydrological, and mineral phenomena in western and central Colorado
[E73-10041] 07 p0776 N73-16304
Crop identification through interpretation of multiband and multidate photography
07 p0785 N73-16385
Test of computerized analysis method for interpreting ERTS 1 photographs of soils and vegetation
[NASA-CR-130021] 07 p0791 N73-16435
Electromagnetic interference identification in infrared line scan imaging patterns
[DREO-TN-72-25] 07 p0821 N73-16652
Development of system for mapping and monitoring natural ecosystems and environmental complexes from ERTS-1 imagery of California, Nevada, Four Corners Area, Louisiana, and Colorado Plateau
[E73-10289] 08 p0915 N73-17495
Interpretation of Mariner 6 and 7 Martian photometry for sediment geomorphology
[NASA-CR-2194] 08 p0962 N73-17869
Soviet space stations for providing earth space photographs used for earth atmosphere and earth surface analysis
[JPRS-58055-1-PT-1] 09 p1026 N73-18372
Analysis of space photographs of earth surface
09 p1026 N73-18374
Reference key for error avoidance in aerial photointerpretation
[AD-752437] 09 p1037 N73-18463
Photointerpretation techniques based on holographic stereogram three dimensional presentations
[AD-753167] 09 p1044 N73-18518
Analysis of design features and photographic data to determine cause of Apollo 15 main parachute failure
09 p1088 N73-18879
Automatic interpretation of ERTS-1 data for forest management in Minnesota
[E73-10365] 10 p1150 N73-19361
Automatic interpretation of forest species and stress identification using ERTS-1 imagery of Minnesota
[E73-10366] 10 p1150 N73-19362
Development of procedure and system for uniform mapping and monitoring of earth resources and environmental complexes using ERTS-1 imagery
[E73-10350] 11 p1275 N73-20344
Location of center pivot sprinkler irrigation systems in Finney County, Kansas, based on ERTS-1 interpretation
[E73-10418] 11 p1279 N73-20380
Physical interpretation of geology, hydrology, and glaciology revealed by ERTS-1 imagery of east central Ohio
[E73-10454] 11 p1283 N73-20413
Coordination and establishment of centralized facilities and services for University of Alaska ERTS-1 survey of Alaskan environment
[E73-10459] 11 p1284 N73-20417
Improved measurement of photographic images with negative reticles
[AD-753946] 11 p1295 N73-20505
Influence of displays on image interpreter performance in investigating characteristics of pictorial content of reference material
[AD-754567] 11 p1353 N73-20984
Computerized video display for processing spark and bubble chamber photographs
[JPRS-58713] 12 p1381 N73-21202
Application of photointerpretation and photogrammetry to analysis of cloud cover type and motion
[NASA-TM-X-64710] 12 p1404 N73-21385
Relative ages of near side and far side terra plains based on interpretation of Apollo 16 photogeology - Part A
12 p1452 N73-21765
Cayley Formation interpreted as deposited fluidized debris that traveled beyond extent of Imbrium Basin ejecta - Part B
12 p1453 N73-21766
Interpretation of Apollo 16 photography of Orientale Basin deposits under earthshine illumination conditions - Part E
12 p1453 N73-21769
Photogeologic analysis of Apollo 16 metric photography of northern Nectaris Basin - Part F
12 p1453 N73-21770
Interpretation of ejecta blanket deposition from King Crater photographs
12 p1454 N73-21778
Land use, urban development, and regional planning for Los Angeles County based on photointerpretation of MSS imagery and multispectral information extraction
[E73-10486] 13 p1515 N73-22277
Development of multistage forest sampling inventory system from interpretation of ERST-1 MSS photography
[E73-10528] 13 p1517 N73-22294
Interpretation of ERTS-1 imagery of man made culture and revision of small-scale maps
[E73-10536] 13 p1518 N73-22300
Investigation of optical properties of natural objects and their aerial photographic imaging characteristics
[AD-756603] 13 p1532 N73-22413
Algorithm for automatic photointerpretation of plant species and stresses in Minnesota imagery
[E73-10639] 15 p1776 N73-24398
Data users note for dissemination of Apollo 16 lunar photographs
[NSSDC-73-01] 15 p1785 N73-24468
Application of sea photo analysis techniques to obtain surface truth descriptors of open ocean from aerial photography
[FAA-RD-72-110] 16 p1905 N73-25412
Survey on remote sensing and photointerpretation
[PB-214864/1] 16 p1914 N73-25490
Photographic determinations of Mars satellites orbital parameters
16 p1961 N73-25860
Photointerpretation of ERTS-1 imagery to map bodies of water in Saline County, Kansas
[E73-10684] 17 p2017 N73-26313
Photointerpretation of ERTS-1 imagery and airborne photography to determine vegetation growth in Iowa
[E73-10715] 17 p2018 N73-26322
Application of ERTS-1 RBV and multispectral scanner imagery for assessment of ocean water color
[E73-10718] 17 p2019 N73-26325
Evaluation of ERTS-1 image sensor spatial resolution in photographic form
[E73-10721] 17 p2019 N73-26328
Application of ERTS-1 imagery for inventory and monitoring of natural vegetation and related resources in arid environment
[E73-10728] 17 p2020 N73-26334
Analysis of ERTS-1 data for interdisciplinary study of estuarine and coastal oceanography of Block Island Sound and adjacent New York coastal waters
[E73-10735] 17 p2020 N73-26341
Analysis of ERTS-1 data for interdisciplinary study of estuarine and coastal oceanography of Block Island Sound and adjacent New York coastal waters
[E73-10736] 17 p2020 N73-26342
In situ spectroradiometric quantification of ERTS-1 data and multispectral photo analysis of Wilcox Playa
[E73-10737] 17 p2020 N73-26343
In situ spectroradiometric quantification of ERTS-1 data based on Arizona test site and Wilcox Playa
[E73-10738] 17 p2021 N73-26344
Possibilities of studying and mapping soil cover on basis of Soyuz, Gemini, Apollo, and Salyut photographs
[NASA-TT-F-14971] 17 p2032 N73-26447
Computer interpretation of textured visual outdoor scenes
[AD-759712] 17 p2034 N73-26463
Correlation of ERTS-1 data with ground data for determining characteristics of air pollution in Norfolk, Virginia area
[E73-10779] 18 p2135 N73-27255

Algorithm for detecting man-made objects from aerial reconnaissance photographs
[AD-760755] 18 p2153 N73-27402
Application of ERTS-1 imagery for vegetation identification in southern Arizona
[PAPER-A7] 19 p2260 N73-28215
Application of ERTS-1 imagery for mapping and identification of vegetation and landforms in Great Basin
[PAPER-A9] 19 p2260 N73-28217
Analysis of ERTS-1 imagery for extrapolating existing soil maps into unmapped areas of Llanos Orientales of Colombia, South America
[PAPER-A13] 19 p2261 N73-28221
Evaluation of ERTS-1 imagery as tool for management of wildlife habitat in Alaska
[PAPER-W11] 19 p2271 N73-28288
Analysis of ERTS-1 imagery by combining human and computer interpretation capabilities
[PAPER-I14] 19 p2279 N73-28335
Interpretation of ERTS-1 MSS imagery of Tennessee Valley
[E73-10854] 19 p2292 N73-28431
Application of multispectral scanning to geology, noting interpretation problems
19 p2295 N73-28453
Interpretation of space photographs of dry piedmont steppe region for hydrologic mapping
[NASA-TT-F-14974] 20 p2411 N73-29382
Use of computer-controlled two-dimensional film densitometer for analysis of photographs of chemical releases at high altitudes
[AD-763082] 20 p2413 N73-29398
Physiographic terrain analysis in Colorado using principles of aerial photointerpretation
20 p2416 N73-29413
General principles of geological interpretation of remote images of earth surface
21 p2534 N73-30319
Selection of standard sections in u.s.s.r. as test sites for geological interpretation of space photography
21 p2534 N73-30321
Tyan-shan section of USSR as test site for geological interpretation of space photography
21 p2534 N73-30322
Caucasian section of USSR as test site for geological interpretation of space photography
21 p2534 N73-30323
Ustyurt section of USSR as test site for geological interpretation of space photography
21 p2535 N73-30324
Interpreting and compiling soil maps from aerial and space survey data
21 p2535 N73-30328
Geological-structural interpretation of photographs of Balkhash region from space and their role in geological survey of Central Kazakhstan
21 p2535 N73-30329
Electrophotometry, photoelectronic images, converters, and television equipment for studying variable stars
[NASA-TT-F-797] 21 p2594 N73-30783
Instrumented methods for finding variable stars on sky photographs
21 p2594 N73-30784
Multi-image photointerpretation system for processing several types of photographs
22 p2636 N73-31125
Photointerpretation of Skylab MSS photography of mineral deposits in Nevada
[E73-10983] 22 p2658 N73-31290
Detection and identification of short-lived events using ERTS-1 imagery
[E73-10990] 22 p2658 N73-31296
Computer interpretation of multispectral data of Chesapeake Bay, Lake Pontchartrain, Louisiana, and lower Mississippi Valley
[E73-11007] 22 p2660 N73-31312
Interpretation techniques for Skylab monitoring of lake eutrophication in New York State
[E73-11011] 22 p2660 N73-31316
Algorithm for assembling continuous boundaries and contours from black and white picture for computer processing and photointerpretation
[NPL-COM-66] 22 p2675 N73-31426
Scale, haze, and image motion effects on human performance in photointerpretation of aerial photography
[AD-763908] 23 p2752 N73-32024
Computerized graphics testbed for photointerpretation
[AD-764353] 23 p2761 N73-32096
Automatic photointerpretation for land use management in Minnesota
[E73-11046] 23 p2779 N73-32222
Automatic photointerpretation of ERTS-1 imagery for land use management in Minnesota
[E73-11058] 23 p2780 N73-32234
Automatic photointerpretation of ERTS-1 imagery for land use management in Minnesota
[E73-11059] 23 p2780 N73-32235
Automatic photointerpretation and mapping for land use management in Minnesota
[E73-11060] 23 p2780 N73-32236
Automatic photointerpretation of ERTS-1 imagery for land use management in Minnesota
[E73-11061] 23 p2780 N73-32237
Automatic photointerpretation for plant species and stress identification in Minnesota
[E73-11063] 23 p2781 N73-32239
Threshold selection for interpretation of digital pictures
[AD-764736] 24 p2898 N73-33132
Operational system for processing both imagery and computer compatible tapes of ERTS-1 and aerial data of Pennsylvania
[E73-11105] 24 p2915 N73-33262
Photointerpretation and digital data mapping of land use in Pennsylvania
[E73-11106] 24 p2915 N73-33263
Snow and fresh water lake ice interpretations from ERTS-1 imagery of Whitefish Bay, Michigan and Green Bay, Wisconsin
[E73-11129] 24 p2917 N73-33284
Interpretation of aerial photographs to generate category maps and textures
[AD-765526] 24 p2928 N73-33382

**PHOTOIONIZATION**
Crossed beam method for measuring photoionization cross section on atomic barium beam
06 p0707 N73-15770
Photoionization of room temperature gas by radiation from hot plasma in electromagnetic T-Tubes
07 p0825 N73-16684
Solution of ionization and thermal equilibrium equations for gas clouds in quasars and Seyfert galaxies ionized by ultraviolet radiation sources
07 p0839 N73-16801
Calculation of photoionization cross sections near autoionizing lines and theoretical cross sections for beryllium and magnesium
[NASA-CR-130884] 09 p1068 N73-18716
Photoionization cross section measurements on excited cesium maser by light beams
[AD-756217] 13 p1564 N73-22677
Solar photoionization rate constants for nitrogen, oxygen, nitrogen oxides and ultraviolet intensities
[AD-756480] 13 p1574 N73-22759
Photoionization cross section of barium and strontium, determined with atomic beam crossed with ultraviolet radiation
[MPI-PAE/EXTRATERR-75] 15 p1781 N73-24440
Ionospheric F-region electron recombination, heating, and electron production
17 p2017 N73-26311
Mathematical model for calculating relative molecular orbital photoionization cross sections in soft X ray region
[UUIP-753] 17 p2066 N73-26714
Multiphoton ionization by laser beam
[AD-760800] 18 p2159 N73-27440

**PHOTOLUMINESCENCE**
NT X RAY FLUORESCENCE
Determining the effects of ion implantation in aluminum oxide including implanted impurities and crystal damage by electrical resistivity and photoluminescence
17 p2071 N73-26755
Photoluminescence, thermoluminescence, photoconductivity, and electrical conductivity measurements in heavily doped ZnS-Cu, In phosphors
17 p2071 N73-26759

**PHOTOLYSIS**
NT RADIOLYSIS
Ultraviolet flash photolysis of ozone and reaction of O[1 D] with H2O
[DREV-TN-2026/72] 06 p0638 N73-15176
Photolysis of ozone at 3130 A in presence of excess of nitrogen oxide
[NASA-CR-130794] 09 p1028 N73-18388
N2O photolyzed at 2139 A producing O[1 D] atoms in H2O and CO
[NASA-CR-130976] 09 p1029 N73-18398
Steady illumination photolysis of ionospheric ozone in near ultraviolet
[NASA-CR-130830] 09 p1029 N73-18399
Photolysis of CH3ONO
[NASA-CR-131355] 11 p1285 N73-20425
Formyl fluoride photochemical laser and energy content of HF photoelimination product
[AD-757743] 15 p1796 N73-24558
Quantum yields of O[D-1] in ozone photolysis near 310 nm
[NASA-CR-122206] 18 p2142 N73-27311
Reaction kinetics of CF3 I flash photolysis iodine laser
[AD-760806] 18 p2158 N73-27436
Kinetics of chemically pumped CO2 and CH2N2-CO2 photolysis laser systems
20 p2424 N73-29469

**PHOTOMAPPING**
Geologic mapping of Basin and Range - Colorado Plateau boundary in Arizona using ERTS-1 imagery
[E72-10157] 01 p0044 N73-10347
Interpretation and mapping large scale structural lineaments in Precambrian shield areas and basins containing younger sediments using ERTS-1 imagery
[E72-10180] 01 p0045 N73-10359
Development of computer programs for aerotriangulation with independent models
02 p0164 N73-11333
Computer program for block analytical aerotriangulation adjustment with independent models
02 p0164 N73-11335
Horizontal accuracy of computerized planimetric block triangulation with independent models
02 p0164 N73-11336
Computerized horizontal block adjustment for aerial mapping using large numbers of points
02 p0165 N73-11337
Photomapping of US using ERTS-1 return beam vidicon imagery
[E72-10274] 03 p0291 N73-12372
Mapping of seismically active faults in Alaska using ERTS-1 imagery
[E72-10352] 05 p0533 N73-14340
Photomapping of US using ERTS-1 MSS and RBV imagery
[E73-10088] 08 p0902 N73-17300
Gradient methods for solving incompatible systems of linear equations of higher order in photomapping problems
10 p1178 N73-19584
European weather maps constructed from ESSA 8 photographs
[QR-2] 10 p1181 N73-19605
Thematic and photomapping of Arizona CARETS, and polar regions from ERTS-1 imagery
[E73-10463] 12 p1394 N73-21302
Photomapping of Phoenix area from ERTS-1 RBV imagery
[E73-10502] 12 p1398 N73-21338
Photomapping of US using ERTS-1 RBV imagery
[E73-10602] 15 p1772 N73-24363
Mapping of seismically active faults in Alaska from ERTS-1 imagery
[E73-10616] 15 p1774 N73-24377
Mapping of major geological structures of African rift system from ERTS-1 imagery
[E73-10622] 15 p1775 N73-24383
Multichannel ocean color data analysis to produce color maps
[TRW-21123-6001-RU-00] 18 p2144 N73-27328
Mapping of strip mine areas in southeastern Ohio from ERTS-1 imagery
19 p2284 N73-28372
Mapping seismically active faults in Alaska using ERTS-1 imagery
[E73-10842] 19 p2291 N73-28420
Mapping rice crops of California and Louisiana and natural vegetation of Colorado Plateau from Skylab photography
[E73-10885] 20 p2394 N73-29236
Tectonic and photogeologic mapping of forested and sparsely vegetated terrain of Montana and Idaho
[E73-10900] 20 p2396 N73-29249
Photomapping of rice crops and natural vegetation in Louisiana and California from Skylab EREP imagery
[E73-10916] 20 p2397 N73-29265
Research and development in topographic mapping, field surveys, photogrammetry, orthophotomapping, and space technology
[PB-221469] 22 p2669 N73-31384
Uniform mapping and monitoring of natural ecosystems and environmental complexes of Colorado Plateau and Sierra-Lahontan areas and estimation of rice crop yields in California and Louisiana
[E73-11070] 23 p2781 N73-32246
Mariner 9 mapping of Mars surface albedo variations
23 p2840 N73-32693
Geomorphology of layered deposits in Mariner 9 observations of Martian polar regions
23 p2840 N73-32697
Mariner 9 television observations of Mars atmosphere variations
23 p2840 N73-32699
Photogrammetric determination of Martian surface coordinates using Mariner 9 photos
23 p2843 N73-32719
Mars surface mapping with Mariner 9 aerographic coordinate system
23 p2843 N73-32720
Photogrammetric evaluation of Mariner 9 Mars surface pictures
23 p2843 N73-32721
Analytical stereophotogrammetric evaluation of Martian topography using Mariner 9 photographs
[CONTRIB-2250] 23 p2843 N73-32722
Cartographic mapping of Martian surface by Mariner 9 digital picture data evaluation
23 p2843 N73-32723
Stereographic albedo map of Mars south polar region using Mariner 9 video data
23 p2844 N73-32724
Methods for primary and secondary triangulation of Martian surface
[NASA-CR-135586] 23 p2845 N73-32732
Mapping lineaments, structures, and lithological formations of African Rift System in Africa and Yemen from ERTS-1 imagery
[E73-11126] 24 p2916 N73-33281

Reconnaissance geologic mapping in Dry Valleys of Antarctica using ERTS-1 imagery
[E73-11127] 24 p2916 N73-33282
Application of ERTS-1 and EREP imagery to geological surveys and mapping of Basin and Range - Colorado Plateau boundary in Arizona
[E73-11131] 24 p2917 N73-33286
**PHOTOMAPS**
Compilation of photomaps of Nevada geology from ERTS-1 imagery
[E73-10473] 12 p1395 N73-21310
Mapping and mosaic applications of ERTS-1 MSS imagery
[E73-10957] 21 p2532 N73-30299
Interpretation of aerial photographs to generate category maps and textures
[AD-765526] 24 p2928 N73-33382
**PHOTOMECHANICS**
U PHOTOGRAPHY
**PHOTOMETERS**
NT ELECTROPHOTOMETERS
NT ULTRAVIOLET SPECTROMETERS
NT ULTRAVIOLET SPECTROPHOTOMETERS
Characteristics of infrared photodetectors manufactured from semiconductor material irradiated by electron beam
[NASA-CASE-LAR-10728-1] 03 p0300 N73-12445
Push button power supply for measuring light output performance of switchboard lamps
[REPT-6688] 04 p0395 N73-13211
Optical feedback technique to extend frequency response of solid state detector systems
[NASA-TM-X-2676] 04 p0421 N73-13430
Erbium laser rangefinder having germanium avalanche photodetector
[AD-748071] 04 p0430 N73-13502
Design and fabrication of annular ring detector consisting of optical fibers terminated with photodetectors
[NASA-CR-124089] 09 p1065 N73-18683
Definition of scientific objectives for outer planet flyby missions
[NASA-CR-130977] 09 p1083 N73-18830
Photometric system, using sodium vapor resonance cell for observing D2 emission line from daytime sky
10 p1146 N73-19328
Digital photometer for recording measurements of ionospheric disturbances
[AD-754436] 10 p1157 N73-19415
Photon detector applications and theoretical considerations of heterojunction photo-effect
[AD-754026] 10 p1202 N73-19784
Characteristics of narrow field of view, sensitive photometers and application to measuring air glow, aurora, sun corona, and barium releases
[LA-DC-72-1422] 12 p1406 N73-21399
MOS photodetector mosaics for application to readout of optical memories with charge storage
13 p1500 N73-22155
Use of remote airborne photopolarimeters to measure soil moisture content in southwestern United States
[NASA-CR-130211] 13 p1522 N73-22332
Analysis of Skylab and EREP coverage of Wyoming and characteristics of field photometer system for measuring object reflectances
[E73-10697] 16 p1903 N73-25389
Analysis of ERTS-1 data to determine aerosol content in atmosphere and comparison with data obtained by sun photometer at Salton Sea, California
[E73-10702] 16 p1903 N73-25394
Polarization photometers in payload of sounding rocket for noctilucent cloud particle sampling
[AD-760149] 17 p2028 N73-26415
Fundamental problems of photoelectric photometry
[PUBL-4] 17 p2031 N73-26439
Stability and temperature characteristics compared for some silicon and selenium photodetectors to determine suitability for photometric or radiometric measurements
[NBS-TN-594-5] 17 p2072 N73-26765
Development of portable transmissometer calibrating unit using laser as projector source
[AD-757282] 18 p2153 N73-27403
Evaluation of Skylab program experiments involving contamination measurement, photometer, and gegenschein zodiacal light
[NASA-CR-61386] 18 p2200 N73-27760
Photometric measurements of airglow and auroral intensity and ionsopheric disturbances by Goose Ionospheric Observatory
[AD-762081] 19 p2297 N73-28471
Design, development, and characteristics of high sensitivity, nonselective pyranometer with black detecting surface and xenon filling
20 p2402 N73-29304
Various infrared detectors, including thermal detectors and photodetectors
[DRIC-TRANS-3179] 21 p2549 N73-30439
Identifying heavy primary cosmic ray particles at energies higher than 1 GeV/nucleon by nuclear emulsion balloonborne photometry
[LUIP-CR-73-02] 21 p2593 N73-30778
Operating principles of various types of photodetectors
21 p2594 N73-30787
**PHOTOMETRY**
NT ASTRONOMICAL PHOTOMETRY
NT ELECTROPHOTOMETRY
NT SPECTROPHOTOMETRY
NT STELLAR SPECTROPHOTOMETRY
NT TELEPHOTOMETRY
NT ULTRAVIOLET PHOTOMETRY
NT VISUAL PHOTOMETRY
Airborne auroral expedition of November and December 1969
[NASA-CR-128392] 01 p0047 N73-10379
Instrumentation for photometry, and amplifier and circuit design
[NBS-TN-594-2] 01 p0056 N73-10459
Lunar Orbiter photographic and photometric data enhancement - framelet joining, digitization, data improvement, and statistical error analysis
[NASA-CR-128581] 01 p0057 N73-10463
Procedures, techniques, and equipment for calibrating luminous intensity, luminous flux, and color temperature of incandescent lamps
[NBS-TN-594-3] 02 p0174 N73-11408
Photometric observations of comets
02 p0228 N73-11840
L alpha photometry of Comet Bennett
02 p0228 N73-11841
Filter photometric data from OAO 2 on blue Ap, band a dwarfs, and giants
[NASA-TM-X-66163] 07 p0843 N73-16826
Relation between photometric track width and velocity of heavy ions in nuclear emulsions
[LUIP-CR-72-13] 08 p0946 N73-17750
Photometric profiles of dust particle size and dust cloud origins during dust storms on Mars as reported by Mars 3 Automatic Interplanetary Station
[NASA-TT-F-14818] 08 p0962 N73-17866
UBV observations of HD 176387
[BULL-174] 10 p1212 N73-19856
UBV photometry of 115 nearby stars
[BULL-176] 10 p1212 N73-19858
Impact of radiometry and photometry on economic, social and environmental problems
[NBS-TN-594-4] 11 p1292 N73-20488
Physical and geological aspects of heiligenschein measurements made from Apollo 16 Flight
12 p1455 N73-21789
Photometric observations of in situ fluorescence and bioluminescence with Biota in New York Bight
[RM-568J] 13 p1479 N73-21978
Radiative light transfer model for aerosol radiance loss in atmospheric photometry
13 p1558 N73-22628
UBV photometry of stars within 25 parsecs of sun, in quasar and galaxy field, in Kapteyn selected areas and of miscellaneous stars including super and red giants
[ROY-OBS-BULL-176] 13 p1578 N73-22789
Star simulator photometric calibration based on Vega spectrum
[RAE-TR-72138] 14 p1646 N73-23346
Photometric and image intensified TV measurements of auroral precipitation patterns and energy input during rocket experiments at Poker Flats, Alaska in Operation Ice Cap
[AD-760042] 17 p2029 N73-26419
Photometric profile of solar limb by optical device for photographic registration of photosphere
[RR-4] 17 p2032 N73-26441
Extraction-Photometric methods for determining impurities in beryllium
[JAERI-1222] 17 p2044 N73-26537
Equations used in analysis of photometric observations of zodiacal light, and zodiacal light models
[NASA-TN-D-7263] 17 p2082 N73-26843
Photometric aspects of interferometry in far ultraviolet
[AD-762151] 19 p2233 N73-28003
Photometric determination of charge spectrum of low energy primary cosmic rays in stack of nuclear photographic emulsions
20 p2468 N73-29823
Narrow-band photometry of Galilean satellites with resolution of approximately 30
[LPL-COMMUN-167] 21 p2591 N73-30763
Spectral albedos of Galilean satellites from broad-band photometry
[LPL-COMMUN-168] 21 p2591 N73-30764
Photometric and polarimetric mapping of water turbidity and water depth
[NASA-CR-134030] 22 p2666 N73-31360
Infrared photometry of variable stars
[AD-764686] 24 p2981 N73-33827
**PHOTOMICROGRAPHS**
Fourier pattern recognition techniques applied to titanium alloy photomicrographs
[AD-746720] 02 p0188 N73-11528
**PHOTOMICROGRAPHY**
Device for displaying and recording angled views of samples to be viewed by microscope
[NASA-CASE-GSC-11690-1] 19 p2301 N73-28499
Combined micrographic and computerized data storage and search system for information processing
[DSIS-TN-13] 23 p2760 N73-32083
Hand-held, lightweight, portable photomicroscope
[NASA-CASE-ARC-10468-1] 24 p2925 N73-33361
**PHOTOMULTIPLIER TUBES**
Quantum efficiencies of photomultiplier range finders for detection of infrared laser light
[AD-749269] 04 p0397 N73-13230
Photomultiplier tubes and laser range finders for infrared detection
[AD-749645] 06 p0646 N73-15245
Characteristics of photomultiplier tubes and application to optics, biophysics, radiometry, and astronomy for detecting weak light flows
[AD-755874] 12 p1384 N73-21226
Control circuit for reducing bias voltage and radiation sensitivity of photomultiplier
[NASA-CASE-ARC-10593-1] 21 p2517 N73-30187
Star mapper breadboard model for satellite attitude control using either photomultipliers or Si photodiodes
[ESRO-CR-162] 22 p2698 N73-31611
Computerized photon counting technique for recording optical images
22 p2700 N73-31622
**PHOTON ABSORPTION**
U ELECTROMAGNETIC ABSORPTION
**PHOTON BEAMS**
NT LIGHT BEAMS
Stark shift measurements and photon resonance perturbations in triplet metastable helium atom near ionization threshold
[KFKI-72-42] 10 p1169 N73-19507
**PHOTON DENSITY**
Electron flux measurements from Cosmos 490 satellite
14 p1660 N73-23477
Detection and estimation of optical images by photon counting techniques
[NASA-CR-135498] 23 p2792 N73-32335
**PHOTON-ELECTRON INTERACTION**
Matrix solution for one dimensional model of radiation field arising from multiple scattered photons in planetary atmosphere
[NASA-CR-130755] 08 p0943 N73-17722
Approximative solution for photon emission amplitude in soft photon irradiation by electromagnetic wave field
[NASA-TT-F-14686] 09 p1066 N73-18697
Photoconductivity of cadmium sulfide crystals excited by mode-locked neodymium laser pulses
[AD-753677] 09 p1077 N73-18786
Light intensity effect on photon resonance in excited atom ionization for determining Stark effect potential
[KFKI-72-68] 10 p1192 N73-19694
Dependence of photon resonance in metastable helium atom ionization on light intensity
[KFKI-72-69] 10 p1192 N73-19695
Modulation of electron beam by laser beam in thin film with production of light
15 p1795 N73-24548
**PHOTONS**
NT LIGHT BEAMS
Evaluation of photon imaging devices and subsystems with emphasis on television camera tubes
[AD-748005] 03 p0275 N73-12234
Photon-echo generation and behavior
[AD-750155] 06 p0681 N73-15540
Supernovae monitoring experiment using ground-based photomultiplier tubes sensitive to secondary fluorescence light
08 p0974 N73-17967
Multiphoton ionization cross section function of atomic polarization
[NASA-TM-X-66179] 09 p1068 N73-18718
Analysis of support properties of scaling function for time-like virtual photons using simple perturbative model
[LPTHE-72/28] 10 p1192 N73-19696
Numerical calculation of ultrahigh energy photon spectrum
[NASA-TM-X-66198] 10 p1193 N73-19703
Measurement of thermal changes encountered during plastic deformation of copper using photon detection system
[AD-756416] 13 p1543 N73-22510
Photon mean free path control of radiative heat transfer in composite materials
[AD-757140] 13 p1548 N73-22544
Generation of laboratory spectra at photon energies from highly ionized atoms
[AD-758606] 16 p1960 N73-25851
Polarization effects in photon echoes and in anisotropic mirror laser cavities
18 p2157 N73-27429
Detection effeciencies of cylindrical detectors for gamma ray photon angular distributions
[NASA-TM-X-70445] 21 p2548 N73-30424
Picosecond laser beam study of four photon effects and temporal behavior of optical phonons
22 p2680 N73-31465
Filtered and unfiltered photon detections obtained during laser ranging operations between McDonald Observatory and Apollo 11, 14, and 15 reflectors
[NASA-CR-133927] 22 p2681 N73-31472
Photon energy and polarization effects on optical absorption spectra of GMO at varying temperatures
23 p2824 N73-32574

**PHOTONUCLEAR REACTIONS**
PDP 8 computer control of linac system used in photonuclear experiments
[CEA-N-1527] 03 p0302 N73-12466
Photonuclear giant resonance data summary
[NBS-SP-380] 12 p1427 N73-21564
Optical high energy scattering models and photoprocesses in nuclei
[CERN-72-20] 15 p1814 N73-24702
Photonuclear activation with Ge L1 detectors
[AD-761992] 19 p2231 N73-27990

**PHOTOPIEZOELECTRICITY**
U PHOTOELECTRICITY
U PIEZOELECTRICITY

**PHOTOPLASTICITY**
Graphical techniques for developing photoplastic record card system
[AD-753602] 10 p1162 N73-19453
Reusable photoplastic recording materials in read/write holographic memories
16 p1922 N73-25553
Analysis of stress-strain state in metal and contact stresses developed during continuous rolling on long mandrel for reducing and drawing metal tubes
[NLL-M-21688-[5828.4F]] 20 p2428 N73-29502
Development of photoplastic materials for optical memory storage applications
[AD-764822] 23 p2794 N73-32356

**PHOTOPRODUCTION**
Sum rule for photoproduction amplitudes in isovector Compton scattering and inconsistency of free fermion parton model in deep inelastic limit
[NUB-2169] 07 p0823 N73-16673
Measurement of positive and negative pion, and double neutral pion photoproduction cross sections for incident gamma ray energies from 600 to 900 MeV
21 p2582 N73-30691

**PHOTORECEPTORS**
Three color receptors of Young-Helmholtz and opponent color types of information processing
10 p1112 N73-19066
Use of photostimulation in electroencephalographic tests of flying personnel and candidates at flight schools
11 p1245 N73-20111
Chromatic induction and spatial intraocular straylight effects in human perception of contrast colors
[IZF-1972-19] 14 p1692 N73-23730

**PHOTORECONNAISSANCE**
Improved multibeam cathode ray tube for real time display of infrared reconnaissance data
[AD-749475] 05 p0520 N73-14228

**PHOTOREDUCTION**
U PHOTOCHEMICAL REACTIONS
U REDUCTION [CHEMISTRY]

**PHOTORESISTIVITY**
U PHOTOCONDUCTIVITY

**PHOTORESISTORS**
U PHOTOCONDUCTORS

**PHOTOSENSITIVITY**
NT LIGHT ADAPTATION
Molten single crystal silver compounds for studying photographic sensitivity
[AD-746294] 02 p0175 N73-11421
Effects of camera lense photosensitivity on signal loss in vidicon tubes
[AD-750530] 05 p0549 N73-14459
Evaluation and characterization of possible recording materials for holographic optical elements
[AD-760561] 18 p2159 N73-27441
Photosensitivity failure analysis on integrated microcircuit caused by surface inversion
[AD-764708] 23 p2766 N73-32132

**PHOTOSENSORS**
U PHOTOELECTRICITY
U RADIATION MEASURING INSTRUMENTS

**PHOTOSPHERE**
Use of telecamera as contrast monitor for photospheric surveys
[RR-1] 17 p2032 N73-26440
Photometric profile of solar limb by optical device for photographic registration of photosphere
[RR-4] 17 p2032 N73-26441
Determination of turbulent velocities in solar photosphere with allowance for influence of instrumental contour
20 p2472 N73-29855

**PHOTOSYNTHESIS**
Photosynthetic energy conversion in membranes, tissues, and reaction centers of bacteria and viruses
[COO-3162-9] 04 p0380 N73-13091
Effect of toxic substances on algae by observing photosynthesis determined by oxygen production of algae
[DRIC-TRANS-2991] 10 p1121 N73-19139
Simazine influence on green algae photosynthetic pigments noting chlorophyll luminescence spectra
[DRIC-TRANS-2992] 13 p1485 N73-22040
Effects of atmospheric oxygen concentration on Chlorella photosynthesis
14 p1608 N73-23032
Comparative studies of photosynthetic activity of pure and mixed crops during vegetative period
20 p2404 N73-29321
Effects of solar radiation on photomorphogenesis of plants based on spectral distribution of solar energy in daytime
20 p2404 N73-29322
Photosynthesis of chlorella
20 p2405 N73-29326
Solar radiation effects on photosynthesis of submerged aquatic plants
20 p2405 N73-29327

**PHOTOTHERMOTROPISM**
U ANISOTROPY
U TEMPERATURE EFFECTS

**PHOTOTRANSISTORS**
Phototransistor imaging system with mosaic of phototransistors on semiconductor substrate
[NASA-CASE-MFS-20809] 04 p0448 N73-13660
Fabrication of photodiode transistor image sensor array in silicon
[NASA-CR-130036] 07 p0831 N73-16738
Electro-optical control for volt-ampere characteristics of avalanche phototransistors
[JPRS-58321] 09 p1008 N73-18226
Phototransistor with base collector junction diode for integration into photo sensor arrays
[NASA-CASE-MFS-20407] 10 p1133 N73-19235

**PHOTOTUBES**
NT PHOTOMULTIPLIER TUBES

**PHOTOVOLTAIC CELLS**
Feasibility of using photovoltaic cells to convert laser energy into electrical energy
[LA-DC-72-468] 03 p0255 N73-12061
Computerized design and performance of planar germanium P-I-N thermophotovoltaic cells
[AD-748895] 04 p0376 N73-13063
Theoretical and experimental investigations of CdS single crystals photovoltaic cells
[NASA-CR-129675] 04 p0457 N73-13730
Optical and electronic properties of single crystal Cu2S-CdS photovoltaic cells
[NASA-CR-121228] 15 p1738 N73-24091
Development of Hg Cd Te elevated temperature photovoltaic detectors
[AD-762352] 20 p2381 N73-29131

**PHOTOVOLTAIC EFFECT**
Empirical equations for calculating photovoltaic characteristics of solar cell array
[NASA-CR-130248] 15 p1737 N73-24085

**PHTHALOCYANIN**
Limiting stabilities and thickening properties of phthalocyanine lubricants in different dispersion media
[AD-752827] 09 p1040 N73-18484

**PHUGOID OSCILLATIONS**
U OSCILLATIONS
U OSCILLATORS
U PITCH [INCLINATION]

**PHYSICAL CHEMISTRY**
Research in solid state physics, materials, and physical chemistry
[AD-746866] 03 p0347 N73-12826
Physicomechanical and antifriction behavior of polycaproamide and Caprolon surfaces
[NLL-RISLEY-TR-2360-[9091.9F]]
05 p0550 N73-14464
Detailed information of physics subfields and interface areas
[NASA-CR-132050] 15 p1813 N73-24693
Solid state physics, physical chemistry, and materials research
[AD-758374] 15 p1821 N73-24764

**PHYSICAL CONSTANTS TESTING REACTOR**
U NUCLEAR RESEARCH AND TEST REACTORS
U WATER COOLED REACTORS

**PHYSICAL ENDURANCE**
U PHYSICAL FITNESS

**PHYSICAL EXAMINATIONS**
Conference on occupational medicine support in NASA programs to prevent health and emotional problems in personnel
[NASA-TM-X-69072] 08 p0871 N73-17048
Medical examinations and protection procedures for NASA employees working in radiologically controlled areas
08 p0871 N73-17050
Physical exercise and physical fitness program for preventing and treating human coronary heart disease
08 p0871 N73-17051
Multiphase health screening and medical history questionnaire for preventive/occupational physical examinations
08 p0871 N73-17052
Automated medical history questionnaire for screening industrial personnel and scheduling physical examinations
08 p0872 N73-17060
Routine proctosigmoidoscopic examinations of asymptotic NASA personnel for cancer prevention
08 p0872 N73-17061
Conference on preventive medical and environmental control measures for NASA and aviation industry personnel management
[NASA-TM-X-69073] 08 p0873 N73-17064
Dynamic electrocardiography in periodic health examinations for detection of cardiac abnormalities
08 p0873 N73-17065
Computerized multivariate scheduling of physical examinations for NASA personnel in clinical intervention program
08 p0873 N73-17068
Continuous monitoring of hypertension and hypercholesterolemia in NASA employees for prevention of heart disease and disability
08 p0873 N73-17072
Periodic health examinations and automatic processing of medical histories for detection and prevention of human diseases
08 p0874 N73-17074
Blood pressure and cholesterol level screening for preventing heart diseases in flight crews of commercial airline
08 p0874 N73-17076
Latent coronary insufficiency detection in flying personnel using barochamber loading
13 p1480 N73-21988
Evaluation of energy expenditures and reactions of cardiovascular and respiratory systems to physical work
[NASA-TT-F-15090] 23 p2749 N73-31997

**PHYSICAL EXERCISE**
Physical exercise and physical fitness program for preventing and treating human coronary heart disease
08 p0871 N73-17051
Long term exercise effects on cardiovascular response in NASA personnel with periodic ergometric evaluation
08 p0873 N73-17067
Physical exercise effects on health of NASA personnel
08 p0873 N73-17069
Feasibility of effective exercise and health evaluation and enhancement program for NASA employees
08 p0875 N73-17091
Influence of NASA stress lab program on physical education in US colleges
08 p0876 N73-17092
Weightlessness simulator for evaluating exercise effects in hypokinetic bed rest test
13 p1482 N73-22018
Exercise and muscle stimulation for preventing metabolism changes during bed rest
13 p1483 N73-22019
Bioelectric monitoring and motion picture surveying for improved physical training of astronauts
14 p1608 N73-23039
Effect of physical and psychological stress on urinary excretions of adrenal harmones in normal man
[NASA-TT-F-15046] 20 p2368 N73-29043
Use of therapeutic exercise for treatment of functional vascular disorders and occlusive lesions of arteries and veins
[NASA-TT-F-15043] 20 p2368 N73-29045
Effects of adverse Northern environment on human physiology and performance under military exercise conditions
[DCIEM-882] 20 p2371 N73-29056

**PHYSICAL FACTORS**
Physical principles of experimental aeromechanics using wind tunnel tests
[AD-751464] 07 p0773 N73-16280
Radiobiological effects of cosmic radiation in animals and standardization of permissible radiation levels for spacecrews
09 p0993 N73-18102
Tables of conversion factors and physical constants in International System of Units
[NASA-SP-7012] 17 p2098 N73-26969
Physical monitoring and aftereffects of two manned space flights
[NASA-TT-F-15076] 22 p2620 N73-30992

**PHYSICAL FITNESS**
Correlation of assessed maximum oxygen intake with predicted performance in running events
[AD-746867] 04 p0380 N73-13093
Physical exercise and physical fitness program for preventing and treating human coronary heart disease
08 p0871 N73-17051
Influence of NASA stress lab program on physical education in US colleges
08 p0876 N73-17092
Human adaptation to hypoxic hypoxia for increased resistance to physical stress
10 p1116 N73-19095
Effects of physical training on human enzyme activity, carbohydrate metabolism, cholesterol level, and adrenal function
[NASA-TT-F-14826] 11 p1243 N73-20093
Sports medicine - parameters necessary for maintaining competitive form
12 p1370 N73-21114
Variations of cell enzymes, glucose, cholesterol, and 17-hydroxycorticosteroid in blood during physical work noting physical training dependence
[DLR-FB-72-48] 21 p2501 N73-30072
Influence of personal characteristics on likelihood of decompression sickness
[NASA-CR-135495] 22 p2621 N73-31002
Physical fitness effects on human thermoregulation during exercise
[NASA-TT-F-15142] 23 p2749 N73-32003

Physiological effects on highly trained subjects when confined to bed, deprived of sleep, or allowed to discontinue training
[NASA-CR-134044] 23 p2750 N73-32008
Performance evaluation of training devices for developing human physical fitness
[NASA-CR-134046] 23 p2752 N73-32023
PHYSICAL PROPERTIES
Physical and functional performance properties of laser safety goggles
[AD-746208] 01 p0022 N73-10170
Method for producing chemiluminescent materials using rhodamine C and material properties
[NASA-TT-F-14423] 01 p0023 N73-10175
Analysis of viscosity of water using distilled water as primary reference standard to show dynamic and kinematic viscosities
[ESDU-65009] 01 p0039 N73-10306
Problems of precise physical measurements of gas density
[EUR-4797-D] 01 p0055 N73-10448
Physical structure of turbulent shear flows in non-reacting gase flow
[AGARD-AR-46] 02 p0156 N73-11262
Physical properties of intermetallic magnesium tin compound
[AD-745942] 02 p0219 N73-11773
Influence of neutron irradiation on physical and chemical properties of vanadium
[IS-2833] 03 p0314 N73-12558
Influence of chemical composition, non-metallic impurities, and production methods on physical properties of molten high alloy steels and special alloys
[AD-747394] 03 p0316 N73-12579
Physical, technological, and wear resistant properties of naturally alloyed metal ceramic material developed from iron powder
[AD-747626] 03 p0322 N73-12626
Thermophysical properties of lunar fines
[NASA-CR-129293] 03 p0354 N73-12888
Chemical and physiochemical properties of wear resistant steels
[AD-749601] 05 p0563 N73-14573
Development and characteristics of Si-As-Te glasses containing Ag and Se as constituent of chalcogenic glasses
[AD-749958] 05 p0567 N73-14603
Numerical calculation of physical and electronic properties of metals
[AD-749546] 05 p0588 N73-14782
Physical properties and performance of radioisotope power generator Tristan
[CONF-710444-11] 06 p0627 N73-15083
Functional dependence of semicircular canal on physical size
06 p0633 N73-15139
Operating principles and physical mechanisms of pulsed gas discharge lasers
[SC-T-72-2524] 06 p0679 N73-15529
Properties of amorphous semiconductors
[AD-750163] 06 p0710 N73-15797
Physical and electrical transport properties of VO2 near its semiconductor-to-metal transition
[AD-751524] 07 p0834 N73-16759
Physical properties and limitations of components used in hybrid microcircuits
[AD-752216] 08 p0891 N73-17216
Plasticization of polyvinyl chloride with various reagents and effect on physicomechanical properties of systems
[AD-751875] 08 p0935 N73-17656
Hardness and physical characteristics of titanium sponge with low residual chloride concentration after vacuum separation
[JPRS-58347] 09 p1048 N73-18544
Influence of heat treatment on physical properties of iron- and chromium-doped rutile
[RR-107] 09 p1073 N73-18760
Physical properties of ply-tear webbing energy absorber
09 p1089 N73-18886
Time dependent two dimensional numerical model for studying structure of squall line thunderstorm
10 p1180 N73-19597
Mechanical and physical properties of discontinuous thermoset carbon fiber reinforced plastic composites
[AD-754034] 11 p1309 N73-20622
Crystal structure and mechanical and physical properties of polymide S-6 - Nylon
[AD-753967] 11 p1309 N73-20624
Physical and chemical nature of N2O flow decay in liquid propellants
[AD-755378] 13 p1489 N73-22070
Application of nuclear gamma resonance for changing structural state of crystal lattice of alloys to improve strength properties
13 p1541 N73-22486
Physical and spectral characteristics of infrared solid state dispersion filters
[NASA-TT-F-14838] 13 p1558 N73-22631
Electrical and physical properties of low temperature grown cubic gallium nitride films
[AD-755237] 13 p1567 N73-22704
Electronic structure and properties of covalent and polar solids
14 p1697 N73-23773
Physical properties of electronic materials, devices, and thin films
[AD-758197] 14 p1700 N73-23793
Physical and chemical processes of solidification of fusion welds and its effects on weldability
[NLL-TI780/GC/72-[9022.305]] 15 p1790 N73-24508
Physical properties, and hydrazine compatibility of rubber compounds
[NASA-CR-131836] 16 p1932 N73-25633
Effect of crystallization kinetics on physical and chemical properties of polymers particularly polyethylene
[AD-750157] 16 p1953 N73-25802
SOM-3 radar design for measuring meteor trail physics and upper atmosphere physical properties
17 p2023 N73-26368
Methods for evaluating physical properties, and causes of failure of materials
[AD-759225] 17 p2047 N73-26563
Structure, composition, and electrophysical properties of autoepitaxial silicon layers from vapor-gas tetrachloride mixture
18 p2186 N73-27653
Procedure for obtaining monocrystalline layers of silicon by rheotaxial methods
18 p2189 N73-27673
Physical properties of aluminum alloys, titanium alloys, and stainless steels for aerospace airframes
[AD-762305] 19 p2311 N73-28587
Production and characteristics of refractory materials for high temperature applications
[NLL-RTS-7942] 20 p2433 N73-29543
Chemical and physical properties of synthetic polyurethane polymer prepared by reacting hydroxy carbonate with organic diisocyanate
[NASA-CASE-MFS-10512] 21 p2505 N73-30099
Multicolor photometric systems for studying physical properties and spectra of variable stars
21 p2594 N73-30790
Degradation, dispersion and movement of oil slicks by wind and ocean as factors influencing applicability of countermeasures
[WMO-359] 23 p2787 N73-32300
Microstructure of molybdenum carbide samples during hot pressing and development of line intensity diagram for various conditions
23 p2808 N73-32449
Structural, compositional, and photometric model of comet Encke
[NASA-CR-135707] 23 p2845 N73-32737
Chemical and physical properties of graphite and carbide-graphite composites developed by powder metallurgy
[LA-5147] 24 p2936 N73-33448
PHYSICAL SCIENCES
Status of National Standard Reference Data System
[NBS-TN-747] 02 p0245 N73-11990
USSR research in meteorology, oceanography, astronautics, astronomy, and geophysics
[JPRS-59278] 18 p2196 N73-27727
Soviet-bloc research in geophysics, astronomy, and space
[JPRS-59490] 18 p2196 N73-27730
PHYSICAL WORK
Work, heat, and oxygen cost of various activities of man
06 p0629 N73-15109
Correlation of physical activity and oxygen consumption between man and mouse
[FOA-1-B-1233-A5] 08 p0877 N73-17108
Adenin-nucleotides NAD[plus] and NADN in skeletal muscles during intensive work and at rest
[NASA-TT-F-14856] 11 p1246 N73-20118
Physiological response to prolonged muscular activity
14 p1724 N73-23990
Quantitative evaluations of adaptive physical operator/manipulator control systems
17 p1990 N73-26090
Variations of cell enzymes, glucose, cholesterol, and 17-hydroxycorticosteroid in blood during physical work noting physical training dependence
[DLR-FB-72-48] 21 p2501 N73-30072
Cooling effects on human tolerance to work induced heat stress and collapse
[NASA-CR-134059] 23 p2750 N73-32005
PHYSICIANS
Analysis of inflow of professional and technical personnel to US from foreign countries
[NSF-72-312] 05 p0611 N73-14969
PHYSICS
Summaries of research in mathematics, physics, chemistry, biophysics-biochemistry, and biology, and related reports - Weizmann Institute of Science
01 p0119 N73-10977
Transformation functions between z basis and jm basis of Lorentz group principal series
[NOTA-INTERNA-386] 03 p0324 N73-12641
Soviet scientific abstracts on physics and mathematics
[JPRS-57242] 03 p0366 N73-12984
Development and application of computer programs as instructional methods for physics laboratory experiments
05 p0516 N73-14198
Core subfields of physics
[NASA-CR-130361] 06 p0700 N73-15706
History of physics with emphasis on nuclear physics and astrophysics
[NASA-TT-F-14670] 07 p0843 N73-16827
High, medium, and low energy physics, mathematics and computers, chemistry, and metallurgy and materials research
[IS-2800] 10 p1189 N73-19678
PHYSIOCHEMISTRY
Rare earth electronic configurations, physiochemical properties, and implications of analytical chemistry
[IS-2966] 10 p1126 N73-19170
PHYSIOGRAPHY
U GEOMORPHOLOGY
PHYSIOLOGICAL DEFENSES
Localized shielding effects on antitissue antibody mobilization in irradiated rats
03 p0258 N73-12086
PHYSIOLOGICAL EFFECTS
NT HEMODYNAMIC RESPONSES
NT PHYSIOLOGICAL RESPONSES
Physiological and pathological responses of humans exposed to electricity
[NASA-CR-128422] 01 p0008 N73-10065
Physiological effects of 12 submarine personnel during prolonged exposure to sonar signals at 85 db [five day exposure]
[AD-744938] 01 p0011 N73-10087
Statistical analysis of occurrence of backache among Royal Air Force flight crews and ground crews to show effects of crew seats on physical comfort
[AD-745177] 01 p0013 N73-10102
Effects of stress upon psychophysiological responses and performance following sleep deprivation
[NASA-CR-128620] 02 p0132 N73-11073
Influence of 45 to 60 day space flight on physiological functions of human body
[NASA-CR-129131] 02 p0132 N73-11074
Construction of sonic boom simulators to determine effects of sonic boom on human heart reactions and analysis of human responses
[UTIAS-TN-180] 02 p0152 N73-11233
Physiological and mental performance effects of underwater work on humans
[AD-747701] 04 p0382 N73-13107
Physiological effects of weightlessness
06 p0628 N73-15099
Tolerance levels, physiological effects, and performance degradation during simultaneous or sequential exposures to environmental stresses
06 p0629 N73-15110
Clinical neurological and neurophysiological aspects of vestibulo-ocular reflex
06 p0633 N73-15145
Diurnal dynamics of psychic performance during 72-hour continuous wakefulness
07 p0744 N73-16056
Physiological effects of high mountain alpinism exercises on human body
07 p0745 N73-16058
Measurements of endocrine metabolic responses to space flight stress on Apollo 14 and Apollo 15 crewmen
09 p0993 N73-18105
Toxic effects of metabolic waste gases on rat organisms
10 p1116 N73-19101
Effect of high intensity laser outputs on behavior and physiology of birds to determine application for reduction of flight hazards
[AD-754269] 11 p1236 N73-20038
Physiological effects on rats of replacement of atmospheric nitrogen by inert gases at high and low temperatures
11 p1244 N73-20095
Diver monitoring system for physiologic studies in all hyperbaric environments
[AD-754399] 11 p1251 N73-20154
Ergometer to measure divers physiological hyperbaric stresses at all explorable depths
[AD-754401] 11 p1295 N73-20513
Self contained automated primate research laboratory to study physiological effects of space environment weightlessness on monkeys
[NASA-CR-131642] 12 p1387 N73-21250
Analysis of atmospheric pollution parameters to show sources, physiological effects, biological effects, and meteorological effects
12 p1421 N73-21519
Physiological effects of long term hypodynamic weightlessness simulation on humans
13 p1482 N73-22010
Physiological adjustments to environmental factors
[AD-753913] 13 p1487 N73-22059
Long term physiological testing of submerged subjects to simulate weightless conditions for space flight
[NASA-TT-F-14884] 13 p1505 N73-22195

Analysis of nonfatal injuries to passengers and flight attendants in airline operations during period 1968 through 1971
[NTSB-AAS-73-1] 14 p1601 N73-22983
Antiradiation drug effects on vestibular analyzer functions
14 p1608 N73-23033
Statistical analysis of effect of simulated sonic booms on sleep patterns of male subjects
[FAA-AM-72-35] 17 p1987 N73-26057
Analysis of physiological and toxicological aspects of smoke produced by combustion of aircraft interior materials - Part 1
[FAA-RD-73-50-PT-1] 18 p2104 N73-27014
Physio-chemical analysis of flammability characteristics and thermal degradation of rigid and flexible urethane foams used in aircraft structures - Part 2
[FAA-RD-73-50-PT-2] 18 p2105 N73-27025
Effects of adverse Northern environment on human physiology and performance under military exercise conditions
[DCIEM-882] 20 p2371 N73-29056
Analysis of physiological effects of diet on personnel of Tenth Soviet Antarctic Expedition
20 p2409 N73-29358
Analysis of sonic boom phenomenon to show generation, propagation, and effects on structures, people, and animals
[ARL/A-NOTE-337] 21 p2493 N73-30007
Design criteria for supersonic overflight to reduce psychophysical effects and decrease glass damage probability
[FAA-RD-73-116] 22 p2724 N73-31800
Physiological effects on highly trained subjects when confined to bed, deprived of sleep, or allowed to discontinue training
[NASA-CR-134044] 23 p2750 N73-32008
Functional disturbances during hypokinesia in man
[NASA-TT-F-15148] 24 p2890 N73-33073

**PHYSIOLOGICAL FACTORS**
NT PHYSICAL FACTORS
Physiological factors in human oculomotor responses to space flight stress
[DR-208-VOL-1] 06 p0632 N73-15136
Physiological factors of human vestibular adaptation to flight and space environments
06 p0633 N73-15146
Prolonged weightlessness effects on physiological functions of dogs
[NASA-TT-F-14672] 08 p0878 N73-17110
Scientific and engineering studies for Physiology of Chimpanzees in Orbit Program
[NASA-CR-131374] 11 p1248 N73-20129
Physiological method for selecting and observing student pilots in Belgian Air Force for motion sickness
12 p1368 N73-21099
Physiological aspects of sleep induction in aircrews after prolonged flight times
12 p1369 N73-21108
Systems analysis of physiological performance related to stresses such as those experienced in high performance aircraft
[AD-754970] 12 p1372 N73-21133
Psychological, physiological, and work hygiene problems in ergonomic technology
[JPRS-58792] 13 p1486 N73-22050
Analysis of aeromedical factors leading to midair collisions and recommended actions to avoid collisions
[AD-758189] 14 p1604 N73-23005
Acoustic and physiological investigation of speaker variabilities relative to speech wave parameters
14 p1623 N73-23150
Contrasting opinions concerning space activity concerning untested physiological effects
[NASA-TT-F-15019] 19 p2342 N73-28842
Preflight and flight stress analysis, its relation to circadian rhythms measured in pilot physiological parameters
[DLR-FB-72-39] 21 p2501 N73-30071
Mathematical models and physiological mechanisms of goal-directed behavior
[JPRS-60091] 24 p2887 N73-33053

**PHYSIOLOGICAL INDEXES**
U PHYSIOLOGICAL TESTS

**PHYSIOLOGICAL RESPONSES**
NT HEMODYNAMIC RESPONSES
Abstracts on microwave radiation effects on human and animal physiological functions and life expectancy
[MBL-1972-6] 01 p0008 N73-10061
Mathematical model for in vivo study of glucose homeostasis in humans
[NASA-CR-129171] 02 p0130 N73-11056
Physiological response of cat semicircular canal dependent units to linear acceleration without angular acceleration
[AMRU-R-70-4] 02 p0131 N73-11061
Effect of space flight on origin, physiological function, and amelioration of coriolis illusion in semicircular canal
[AMRU-R-70-6] 02 p0131 N73-11063
Tests to determine physiological and behavioral response to transitions between rotating and nonrotating environments
[NASA-CR-2130] 02 p0135 N73-11093
Data acquisition and storage system for computerized physiological monitoring system
[AD-746872] 02 p0148 N73-11199
Physiological data acquisition system software
[AD-746874] 02 p0148 N73-11200
Physiological responses to environmental factors related to space flight
[NASA-CR-129518] 03 p0260 N73-12107
Analysis of cosmonaut emotional stress as determined by physiological and behavioral responses
[NASA-TT-F-14654] 03 p0261 N73-12113
Biodynamic response of human head and neck to impact acceleration
[AD-747988] 04 p0382 N73-13106
Influence of time zones on physiological organs and systems and performance of athlete
[NASA-TT-F-14632] 04 p0383 N73-13116
Effects of SO2 decay product toxicity on human physiological functions
05 p0500 N73-14071
Response of pituitary-thyroid axis to microwave radiation
[VR-3490-149] 06 p0630 N73-15122
Functional dependence of semicircular canal on physical size
06 p0633 N73-15139
Anti-compensatory oculomotor responses in human visual tracking and vestibulo-ocular mechanism during rotational head movement in flight
06 p0633 N73-15140
Physiological control system for stabilization of retinal image in humans
06 p0633 N73-15141
Vestibular stimulation effect in human and animal retinal image stabilization
06 p0633 N73-15144
Evolution of neural messages in human adaptation to prolonged zero gravity flight
06 p0634 N73-15154
Physiology of depressed metabolic states and gastrointestinal responses to ionizing radiation
[NASA-CR-130381] 07 p0742 N73-16038
Personality, occupation, and job stress effects on physiological risk factor in human coronary heart disease
08 p0871 N73-17054
Influence of infrasound on human body functions
08 p0875 N73-17085
Influence of 100 percent anhydrous ammonia environment on body functions
08 p0875 N73-17088
Mechanisms for controlling physiological rhythms in Rana pipiens
[NASA-CR-131153] 10 p1112 N73-19064
Effects of space flight noise intensities on human physiological functions
10 p1114 N73-19080
Immersion effects on human physiological motor functions
10 p1114 N73-19081
Hypothermy effects on drug actions in physiological rabbit functions
11 p1240 N73-20064
Dynamics of some characteristics of induced potential of optical region in cerebral cortex in rabbits with increasing hypoxia
11 p1244 N73-20103
Stress reactions of vestibular apparatus to ionizing radiation, coriolis forces, and gravitational stimuli
[AD-753511] 11 p1248 N73-20132
Physiological stress reactions in simulated flight for pilot selection and training
13 p1481 N73-22001
Physiological stress effects of space flight on human body
[JPRS-57139] 13 p1481 N73-22002
Functional reactions of human otorhinolaryngolic organs during hypokinesia
13 p1482 N73-22015
Physiological and hemodynamic adaptations to CO levels and exercise in nonsmoking normal men
[PB-213834/1] 14 p1612 N73-23073
Design of microbial test system for Apollo 16 mission
15 p1740 N73-24103
Physiological responses of parasitic worms and their larvae to solar ultraviolet irradiation and space flight stress
15 p1740 N73-24106
Analytical gas chromatography and mass spectrography for physiological monitoring of astronauts
[NASA-CR-133272] 18 p2110 N73-27059
Human physiological response to heat stress in preflight operation
[AD-759173] 18 p2110 N73-27060
Variations of cell enzymes, glucose, cholesterol, and 17-hydroxycorticosteroid in blood during physical work noting physical training dependence
[DLR-FB-72-48] 21 p2501 N73-30072
Human response to vibration in Great Britain noting test facilities, equipment, experiments and publications
[ISVR-TR-60] 21 p2504 N73-30093
Physical monitoring and aftereffects of two manned space flights
[NASA-TT-F-15076] 22 p2620 N73-30992
Functional state of lymphoid cell in peripheral blood of astronauts and immunoreactivity of individual astronants after space flight
[NASA-TT-F-15089] 22 p2620 N73-30999
Mathematical model and digital computer simulation of cardiovascular control system response to ergometer exercise
24 p2886 N73-33049

**PHYSIOLOGICAL TELEMETRY**
U BIOTELEMETRY

**PHYSIOLOGICAL TESTS**
NT BODY SWAY TEST
NT VESTIBULAR TESTS
Effects of simulated artificial gravity on human performance
[NASA-CR-2129] 03 p0260 N73-12111
Role of social synchronizers in adaptation process of humans to inversion of diurnal sleep and wakefulness regime
11 p1245 N73-20109
Diagnostic physiological tests for selection and training of flying personnel
[NASA-TT-F-687] 13 p1479 N73-21981
Conditioned reflex motion sickness test of statokinetic fitness for flying personnel
13 p1480 N73-21994
Physiological stress reactions in simulated flight for pilot selection and training
13 p1481 N73-22001
Multichannel medical monitoring system to measure physiological parameters from display device at remote control station
[NASA-CASE-MSC-14180-1] 13 p1486 N73-22045
Tracking tasks for clinical evaluation of human movement disorders
[NASA-CR-132275] 18 p2111 N73-27069
Physiological motor function measurements for determining optimal bed rest periods
[NASA-TT-F-15144] 23 p2749 N73-32004

**PHYSIOLOGY**
NT ELECTROPHYSIOLOGY
NT HEMATOPOIETIC SYSTEM
NT NEUROPHYSIOLOGY
NT PSYCHOPHYSIOLOGY
NT RESPIRATORY PHYSIOLOGY
Physiology and dimensional analysis of semicircular canal
[AMRU-R-69-1] 02 p0130 N73-11058
Computer controlled infusion pump for time varying input of calcium into physiological systems
[NASA-CASE-ARC-10447-1] 05 p0503 N73-14092
Physiological research in support of manned space flight
[NASA-CR-128741] 10 p1120 N73-19129
Interface requirements for design and development of Physiology of Chimpanzees in Orbit experiment
[NASA-CR-131397] 11 p1248 N73-20130
Circadian phase relationships of physiological functions of isolated monkeys subjected to varying photoperiod phases
12 p1367 N73-21088
Pathophysiological justifications for using drugs in aerospace medicine
[NASA-TT-F-736] 13 p1484 N73-22033
Influence of monochromatic light on physiological processes of blood
[NASA-TT-F-14941] 16 p1866 N73-25111
Space biology, space medicine, and human physiology
[NASA-TT-F-14964] 16 p1867 N73-25116

**PIASECKI MILITARY AIRCRAFT**
U MILITARY AIRCRAFT

**PICKLING**
U CHEMICAL CLEANING

**PICKOFFS**
U SENSORS

**PICKUPS**
U SENSORS

**PICTURES**
U PHOTOGRAPHS

**PIEDMONT PLAINS**
U PIEDMONTS

**PIEDMONTS**
Interpretation of space photographs of dry piedmont steppe region for hydrologic mapping
[NASA-TT-F-14974] 20 p2411 N73-29382

**PIEZOELECTRIC CRYSTALS**
Transistor circuit with piezoelectric crystal for stable high frequency oscillator
[NASA-CASE-GSC-11513-1] 07 p0761 N73-16185
Development of acoustic surface wave, multiple-tap, delay line structure using sputtered zinc oxide piezoelectric films on metal interdigital arrays on silicon surface
[AD-753674] 09 p1009 N73-18238
Design of microwave signal processing devices for broadband operation
[AD-753168] 09 p1075 N73-18775
Network analysis of transmission line analogs for stacked piezoelectric crystal vibrators
[AD-754545] 11 p1330 N73-20799
Analysis of quartz and piezoelectric ceramic components for application in high frequency bandpass filters
[REPT-4.387] 12 p1383 N73-21219

Properties of piezoelectric lead zirconate titanate ceramic resonator material produced by adding lead niobates to material
[AD-757617] 14 p1681 N73-23644
Acoustic surface wave convolution in piezoelectric crystals with determination of magnitudes of nonlinear coupling constants
[AD-757441] 14 p1682 N73-23648
Elastic and piezoelectric surface waves guided by thin films
[AD-758688] 15 p1823 N73-24776
Analysis of wave propagation in double-layered piezoelectric system using two cadmium selenide and cadmium sulfide crystals
18 p2115 N73-27102
Elastic properties of oxides and application for temperature compensated materials with large piezoelectric moduli
[AD-760766] 18 p2190 N73-27681
Polish research projects on piezoelectronic and acoustoelectronic equipment with specific application to computers and communication systems
21 p2608 N73-30901

**PIEZOELECTRIC GAGES**
Piezoelectric device for measuring the size and concentration of particles in clouds generated by underground nuclear explosion
[FRNC-TH-298] 17 p2065 N73-26709

**PIEZOELECTRIC TRANSDUCERS**
NT PIEZOELECTRIC GAGES
Development of method for producing constant beamwidth over octave frequency bandwidth for underwater signal reception array
[AD-746690] 02 p0143 N73-11160
Nonlinear characteristics of polarized ferroelectric ceramics in operational environment
[AD-748198] 04 p0438 N73-13571
Finite element model for class 4 flextensional underwater transducer shell
[AD-748187] 04 p0482 N73-13940
Performance of piezoelectric transducer for seismic communication in mine environment
[AD-752218] 08 p0885 N73-17169
Turbine inlet gas temperature measurement by ultrasonic impedance
[AD-752602] 08 p0955 N73-17822
Alternate lead and ceramic stave free-flooded cylinder transducers
[AD-752759] 09 p1009 N73-18234
Piezoelectric quartz crystals used as digital transducers in completely digital detection systems for monitoring gas streams
12 p1382 N73-21208
Surface wave device to correlate acoustic velocity and to correct signal phases from pulse bursts
[AD-755198] 13 p1502 N73-22175
Computer program for analyzing piezoelectric transducer acoustic surface wave device
[AD-757485] 14 p1642 N73-23320
Restoration of obliterated stamped serial numbers by ultrasonically induced cavitation in water
[NASA-TM-X-68257] 18 p2213 N73-27866
Electron beam imaging for manufacturing high rfequency surface acoustic wave transducers
[AD-761625] 19 p2245 N73-28101
Piezoelectric pressure transducers for shock tubes, noting electrostatic calibrator
[ARC-CP-1240] 24 p2910 N73-33221

**PIEZOELECTRICITY**
Determining elastic compliance, piezoelectric constant, and dielectric constant by mechanically driving polarized ceramic bar
[AD-748357] 03 p0348 N73-12839
Sonar equipment research project to include determination of temperature and heat dissipation characteristics of ceramics used in high frequency projectors
[AD-749960] 05 p0515 N73-14187
Dynamic theory of crystal lattices and linear theory of elasticity and piezoelectricity
[AD-749111] 05 p0588 N73-14780

**PIEZORESISTIVE TRANSDUCERS**
NT PIEZOELECTRIC GAGES
Pulsed piezoresistive gage bridge operating in NIM configuration
[LA-4939] 03 p0303 N73-12471

**PIGMENTS**
NT CAROTENE
NT CHLOROPHYLLS
NT CYTOCHROMES
NT VISUAL PIGMENTS
Pigments for space-stable thermal control coatings to shield spacecraft from solar radiation
[NASA-CR-124067] 09 p0998 N73-18144
Chemical characteristics of mushroom pigments and mycological classifications
[NASA-TT-F-14865] 11 p1247 N73-20124
Simazine influence on green algae photosynthetic pigments noting chlorophyll luminescence spectra
[DRIC-TRANS-2992] 13 p1485 N73-22040

**PIGS [SWINE]**
U SWINE

**PILE FOUNDATIONS**
Prediction of horizontal wave forces acting on vertical pile structures of floating ocean platforms
[AD-751574] 07 p0794 N73-16460

**PILOT ERROR**
Oculogravic illusion factor in theoretical model of pilot control loss in jet aircraft
06 p0633 N73-15142
Pilot error analysis for airborne navigation procedures
[AD-754214] 11 p1251 N73-20150
Alcohol induced performance degradation in pilot instrument approach landings
12 p1370 N73-21113
Aircraft accident involving L-1011 aircraft crash near Miami, Florida on 29 Dec. 1972 during examination of suspected nose gear malfunction
[NTSB-AAR-73-14] 20 p2360 N73-28984

**PILOT PERFORMANCE**
Human operator model for man machine control behavior in biodynamic flight environment
01 p0014 N73-10105
Control theory model for pilot decision making based on estimated state of linear plant
01 p0014 N73-10107
Design of computerized airborne traffic display device with alphanumerical control for aircraft pilots
01 p0014 N73-10112
Runway separation standards according to reaction time of pilot manual control response to air traffic controller communication
01 p0015 N73-10113
Predictive display with continuous parameter tracking for quasi-linear model of human pilot transfer function in closed loop system
01 p0015 N73-10120
Optimal control model for predicting display requirements in pilot landing performance
01 p0016 N73-10121
Improved pilot performance using simulated pictorial landing display with symbols
01 p0016 N73-10122
Visual display format effects on pilot describing functions in manual tracking performance
01 p0016 N73-10123
Magnetic data tapes containing measurements of pilot scanning behavior, control response and vehicle response during simulated instrument landing approaches
01 p0016 N73-10124
Pilot visual threshold and perception for aircraft movement estimation during unaided visual approach control
01 p0016 N73-10125
Effect of automatic landing system display on pilot information requirements
01 p0016 N73-10126
Optimal control model for predicting manual VTOL pilot performance in longitudinal hovering tasks
01 p0017 N73-10134
Serial segments method for measuring pilot manual control remnant in vicinity of sine waves
01 p0018 N73-10136
Motion cue effects on pilot manual control tracking task
01 p0018 N73-10141
Dynamic model for pilot manual control ability using aural compensatory tracking
01 p0018 N73-10142
Simulator facility used to determine vibration effects on pilot tracking performance using rigid control stick
[AD-745193] 01 p0021 N73-10164
Development of performance criteria to estimate relative proficiency of aircraft pilots during aircraft carrier qualification training with F-4 aircraft
[AD-746095] 02 p0127 N73-11030
Effect on pilot performance and comfort of active vibration isolation system for commercial transport pilot seat
[NASA-CR-2146] 03 p0260 N73-12109
Analysis of instrument system for assisting pilots in making decisions during aircraft takeoff and landing rolls
[FAA-RD-72-112] 03 p0301 N73-12460
Analysis of limitations on helicopter approach and landing during conditions of low visibility
[AD-747732] 03 p0329 N73-12686
Analysis of aircraft pilot experiences during landing approaches in minimum visibility situations
[AD-747654] 03 p0329 N73-12687
Test and evaluation of aural signal device to prompt students to scan for aircraft during flight simulator training
[FAA-RD-72-95] 04 p0373 N73-13030
Analysis of pilot performance in evaluating three types of aircraft altimeters during C-135B simulator flight
[ASD-TR-72-63] 04 p0383 N73-13117
Computerized fast Fourier transform technique for measuring human performance in compensatory tracking task
[AD-748659] 05 p0501 N73-14078
Flight simulator tests to define minimum acceptable levels of static longitudinal stability for aircraft landing approach following failure of stability augmentation systems
[NASA-TM-X-62200] 06 p0620 N73-15034
Human factors engineering to determine maximum control forces capability of female pilots
[FAA-AM-72-27] 06 p0635 N73-15157
Conceptual model for pilot workload
08 p0866 N73-17010
Measurement of pilot performance during aircraft landing simulation to determine significance of vertical acceleration cues during approach and landing maneuver
[NASA-TM-X-62236] 08 p0867 N73-17020
Pilot performance during simulated standard instrument procedure turn with and without predictor display
[NASA-TM-X-62201] 08 p0879 N73-17118
Analysis of fixed base simulator tests to determine effects of two horizontal display panel locations and three map orientations on manual piloting performance
[NASA-TM-X-62198] 08 p0892 N73-17223
Investigation of correlation between pilot disorientation and UH-1 helicopter accidents
[AD-753208] 09 p0986 N73-18049
Measurements of acceleration stress effects on pilot maneuvering ability and flight control performance
[AMRL-TR-72-3] 10 p1123 N73-19134
Ability of aircraft pilot to visually acquire and recognize two and three dimensional targets during diving approach
[AD-754743] 11 p1258 N73-20294
Development of pilot model parameters to provide data base for multiloop, single controller, multi-input analysis of aircraft performance
[AD-755367] 12 p1365 N73-21078
Drug therapy effects on flying effectiveness and psychosomatic fitness of flying personnel
12 p1369 N73-21103
Chemotherapy for air crews in Great Britain
12 p1369 N73-21105
Pilot performance and sleep patterns in long duration flights and control of hypnotic drug and alcohol use
12 p1369 N73-21107
Adaptive tracking task for evaluating drug after-effects on human flight performance
12 p1369 N73-21109
Pilot performance under certain hypnotic, tranquilizer, and barbiturate type drugs
12 p1369 N73-21110
Effects of isoniazid treatment on pilot performance
12 p1369 N73-21111
Alcohol reference method for predicting drug modifications of central nervous system activity and pilot performance decrease
12 p1369 N73-21112
Alcohol induced performance degradation in pilot instrument approach landings
12 p1370 N73-21113
Performance tests to determine capability of aircraft pilots to avoid midair collisions based on visual perception of target and information from pilot warning indicator
12 p1374 N73-21146
Photographic recording of aircraft in near midair collision conditions to determine feasibility of collision avoidance based on visual perception of pilot
[CDC-JL-5] 12 p1374 N73-21147
Analysis of flight tests to determine range of visual detection of aircraft as basis for visual perception to avoid midair collisions
12 p1374 N73-21148
Age limits and flight fitness of civil aviation pilots
13 p1481 N73-21999
Analysis of parameters affecting transition from meteorological visibility range to real visibility range during aircraft landing
[NASA-TT-F-14887] 13 p1536 N73-22607
Psychometric criteria for pilot performance in F-4 aircraft fleet
[AD-755184] 14 p1614 N73-23087
Pilot performance in dual time-sharing tracking task
[AD-755363] 14 p1615 N73-23088
Simulation of pilot decision making process in manual landing operation during fog
14 p1713 N73-23898
Monte Carlo simulation for man machine task sequencing considering pilot performance degradation
14 p1713 N73-23899
Correlation between instructor rating of students and successful completion of military flight training course
[AD-757693] 15 p1745 N73-24146
Changes in diurnal variations of pilot performance in flight simulator compared with performance after transatlantic flights
[DLR-FB-73-25] 16 p1868 N73-25122
Limitations on pilot visual perception of target from low flying aircraft
[AD-759651] 16 p1869 N73-25136
Reports of aircraft accidents occurring in US civil aviation operations during calendar year 1972 - Issue 3
[NTSB-BA-73-4] 17 p1982 N73-26020
Simulator analysis of effect of engine response characteristics on approach and landing operations of powered lift aircraft with externally blown flaps
[NASA-TM-X-62265] 17 p1982 N73-26021

Performance of pilots under simulated conditions to determine response to anti-collision warnings
[FAA-AM-73-6] 18 p2104 N73-27015
Analysis of aircraft structural loads in operational flight to determine effects of pilot performance and aircraft characteristics
[AGARD-R-608] 19 p2218 N73-27895
Diagnosis and prognosis of pilot reaction and tolerance to psychical stress
19 p2227 N73-27962
Tracking performance during whole-body vibration with side-mounted and center mounted control sticks
[AD-761798] 19 p2228 N73-27971
Analysis of pilot performance and short takeoff aircraft characteristics during landing approach
[AD-762566] 20 p2362 N73-29000
Preflight and flight stress analysis, its relation to circadian rhythms measured in pilot physiological parameters
[DLR-FB-72-39] 21 p2501 N73-30071
Medical evaluation of pilots using onboard flight recorders
22 p2619 N73-30986
Performance decrement and response time of current and noncurrent jet Naval pilots
[AD-761463] 22 p2624 N73-31025
Computer program for predicting pilot rating of pitch stability of T-33 aircraft under vertical turbulence conditions
[AD-764696] 23 p2745 N73-31974
Pilot performance under simulated conditions of modified aircraft control dynamics, navigational task complexity, and induced stress
[AD-764760] 23 p2752 N73-32025
Kalman filter estimation of aircraft pilot performance
[AD-764694] 23 p2752 N73-32026
Flight simulation to determine effectiveness of head-up display for improving glide-slope tracking performance during steep visual approach of short takeoff aircraft
24 p2874 N73-32952
Electronic display devices in aircraft control, noting pilot activation and VTOL control
[DLR-MITT-72-04] 24 p2880 N73-32998
Pilot activation in automatic landing by display devices
24 p2880 N73-32999
Utilization of decision and value theory concepts by helicopter pilots to plan attacks
24 p2950 N73-33565

**PILOT PLANTS**
Pilot plant tests of Luch radio distance finder
[AD-763416] 22 p2698 N73-31612
U-25 pilot plant with open cycle MHD generator operating on natural gas
22 p2728 N73-31833

**PILOT SELECTION**
Clinical procedures for selecting pilot personnel based on predisposition to motion sickness
12 p1367 N73-21094
Physiological method for selecting and observing student pilots in Belgian Air Force for motion sickness
12 p1368 N73-21099
Diagnostic physiological tests for selection and training of flying personnel
[NASA-TT-F-687] 13 p1479 N73-21981
Physiological stress reactions in simulated flight for pilot selection and training
13 p1481 N73-22001
Development of cost effective program for training naval fixed wing pilots in 1974 to 1986 time period - Vol. 1
[AD-756638] 15 p1745 N73-24143
Development of cost effective program for training naval fixed wing pilots in 1974 to 1986 time period - Vol. 2
[AD-756639] 15 p1745 N73-24144
Development of cost effective program for training naval fixed wing pilots in 1974 to 1986 time period - Vol. 3
[AD-756640] 15 p1745 N73-24145
Experimental research in underwater medicine, flight stress, and pilot selection
[DLR-FB-73-15] 19 p2226 N73-27951
Pilot selection by means of concentration stress test
19 p2226 N73-27957
Diagnosis and prognosis of pilot reaction and tolerance to psychical stress
19 p2227 N73-27962

**PILOT TRAINING**
Effectiveness of synthetic fixed wing flight training equipment for military purposes
[AD-744447] 01 p0020 N73-10158
Performance evaluation of airborne audio-video recording system as training device in A-7D tactical fighter
[AD-744041] 01 p0021 N73-10161
Development of performance criteria to estimate relative proficiency of aircraft pilots during aircraft carrier qualification training with F-4 aircraft
[AD-746095] 02 p0127 N73-11030
Data management system for prediction of Naval student pilot performances
[AD-744984] 02 p0136 N73-11104
Motion effects in pilot reactions to ground-based flight simulator display evaluation
[AD-749370] 04 p0384 N73-13126
Systems engineering methods for human performance enhancement in signal detection and flight control
[AD-748239] 05 p0503 N73-14098
Validity of ground training for developing flying skill during pilot training
[AD-749621] 06 p0636 N73-15168
Operational effectiveness of jet flight training simulator
[AD-750248] 06 p0636 N73-15170
Analysis of capabilities, characteristics, and effectiveness of flight simulators for developing primary aeronautical skills in single-engine, land aircraft - Vol. I
[FAA-NA-72-102-VOL-1] 08 p0892 N73-17221
Analysis of capabilities, characteristics, and effectiveness of flight simulators for developing primary aeronautical skills in pilots of single-engine, land aircraft Vol. 2
[FAA-NA-72-102-VOL-2-ADD] 08 p0892 N73-17222
Human performance in sequential task training for acquisition of perceptual motor skills under flight stress
10 p1123 N73-19153
Motion sickness questionnaire and field independence scores as predictors of success in Naval aviation training
12 p1368 N73-21097
Development and use of synthetic flight trainers based on degree and fidelity of simulation as key design considerations
[AD-754957] 12 p1388 N73-21260
Visual cue reinforcement for skill retention in pilot simulated space vehicle approach and landing performance
[NASA-CR-128912] 14 p1614 N73-23086
Development of cost effective program for training naval fixed wing pilots in 1974 to 1986 time period - Vol. 1
[AD-756638] 15 p1745 N73-24143
Development of cost effective program for training naval fixed wing pilots in 1974 to 1986 time period - Vol. 2
[AD-756639] 15 p1745 N73-24144
Development of cost effective program for training naval fixed wing pilots in 1974 to 1986 time period - Vol. 3
[AD-756640] 15 p1745 N73-24145
Correlation between instructor rating of students and successful completion of military flight training course
[AD-757693] 15 p1745 N73-24146
Aerial combat acceleration environment testing of human performance capability using human centrifuges
[AD-759174] 16 p1869 N73-25134
Pilot ground training proficiency of flight simulators
[AD-755681] 18 p2112 N73-27081
Relations between sociometric variables and criteria of ability and behavior of student pilots
19 p2226 N73-27954
Guidelines for assessing acceptability of pilot ground trainer devices based on simulated aircraft maneuvers
[FAA-NA-73-15] 20 p2382 N73-29139
Fog chamber low visibility landing simulation film for pilot training
[FAA-RD-73-61] 20 p2452 N73-29707
Combat job performance and training for air cavalry aeroscout pilot and aeroscout observer
[AD-755505] 23 p2753 N73-32027
Optimization of human performance in system design, training, and operation
[AD-764761] 24 p2890 N73-33075

**PILOTED CENTRIFUGES**
U HUMAN CENTRIFUGES

**PILOTLESS AIRCRAFT**
NT DRONE AIRCRAFT

**PILOTS**
Human physiological response to heat stress in preflight operation
[AD-759173] 18 p2110 N73-27060
Inflight heart and respiratory rate recording of pilots, using nose clip transducers
19 p2226 N73-27953

**PILOTS [PERSONNEL]**
NT AIRCRAFT PILOTS
Flight stress effects on cardiovascular reactions of pilots with a therosclerosis
03 p0258 N73-12090
Criterion development in replacement air group, using F-4 aircraft
[AD-748195] 05 p0505 N73-14111
Pilot warning indicators and collision avoidance systems
[PB-212496] 07 p0740 N73-16020
Measurement and effects of triaxial vibration on pilots in P-531 [Scout] helicopter under different flight conditions
[ISVR-TR-58] 07 p0751 N73-16100
Pilot warning indicator system of intruder aircraft
[NASA-CASE-ERC-10226-1] 07 p0798 N73-16483
Color aptitude of dyschromatopsia French navigators and pilots
10 p1113 N73-19068
Influence of long duration flight missions on metabolic and endocrine functions of pilots and navigators
10 p1123 N73-19152
Management of asymptomatic carriers of hepatitis associated antigen in Hellenic Air Force personnel
14 p1611 N73-23060
Application of hologram optical element to pilot head-up display
[AD-758057] 15 p1744 N73-24139

**PINCH EFFECT**
NT PLASMA PINCH
NT THETA PINCH
Gas-embedded z-pinch and numerical simulation of lithium liner for collapsing theta pinch
[AD-745016] 01 p0086 N73-10708
Plasma heating by nonthermal process in linear pinch device
[AD-749688] 06 p0706 N73-15762
Electron gun for pre-ionization of high beta toroidal pinch system
[IPPJ-164] 20 p2458 N73-29757

**PINS**
Elastic stresses in flat plates, strips, and lugs due to interference-fit pins or bushes
[ESDU-71011] 01 p0111 N73-10916
Fatigue tests to determine service life of aluminum alloy lugs with push-fit pins under tensile stress conditions
[ESDU-72020] 06 p0723 N73-15901
Strain fields around tapered interference fit steel pins in aluminum and steel alloy plates
[ARL/SM-NOTE-377] 09 p1093 N73-18919
Frictional processes, electric contact resistance, and wear of pin on disk friction pair
[NASA-TT-F-15049] 24 p2929 N73-33391

**PIONEER F SPACE PROBE**
U PIONEER 10 SPACE PROBE

**PIONEER PROJECT**
Pioneer space probe project to show history, design, development, flight operations, and results accomplished
[NASA-SP-278] 05 p0598 N73-14864
Tracking and data system support of launch, near-earth, and deep space phases of Pioneer 10 space probe flight
[NASA-CR-131373] 11 p1256 N73-20188
Operational aspects of Pioneer program
[NASA-SP-280] 11 p1341 N73-20882
Valve testing for application in inlet system of Pioneer Venus Probe mass spectrometer
[NASA-CR-114627] 16 p1918 N73-25517
Statistical processing of Pioneer front film data - Part 1
[NASA-CR-132797] 22 p2665 N73-31351

**PIONEER SPACE PROBES**
NT PIONEER 6 SPACE PROBE
NT PIONEER 8 SPACE PROBE
NT PIONEER 9 SPACE PROBE
NT PIONEER 10 SPACE PROBE
NT PIONEER 11 SPACE PROBE
Analysis of performance capability improvement for Pioneer F and G spacecraft using electric thrust subsystem
[NASA-CR-114514] 02 p0222 N73-11798
Characteristics of star field attitude sensor for installation in Pioneer Venus spacecraft
[NASA-CR-114516] 03 p0359 N73-12924
Source term calculations for Pioneer radioisotopic thermoelectric generators
[LA-4914] 04 p0448 N73-13658
Pioneer space probe project to show history, design, development, flight operations, and results accomplished
[NASA-SP-278] 05 p0598 N73-14864
Pioneer space probe system design and development, ground support system, tracking and communication, and data processing
[NASA-SP-279-VOL-2] 08 p0964 N73-17882
Tracking and data system support of launch, near-earth, and deep space phases of Pioneer 10 space probe flight
[NASA-CR-131373] 11 p1256 N73-20188
Pioneer F and G missions to Jupiter
[NASA-TM-X-69125] 11 p1338 N73-20859
Operational aspects of Pioneer program
[NASA-SP-280] 11 p1341 N73-20882
Pressure cell sensors for Pioneer 10/G meteoroid detection experiments
[NASA-CR-112273] 12 p1405 N73-21389
Feasibility of mechanical pumps for use with Pioneer-Venus probe mass spectrometer inlet system
[NASA-CR-114581] 14 p1670 N73-23551
Tracking and data system support for Pioneer 6, 7, 8, and 9 missions
[NASA-CR-131818] 15 p1831 N73-24838
Getter pumps applicable to Pioneer Venus Mass Spectrometer Experiment
[NASA-CR-114594] 16 p1918 N73-25518

Design of chemical pumps for Venus Pioneer mass spectrometer used to determine atmospheric composition of Venus
[NASA-CR-114604] 16 p1918 N73-25519
Specifications for Atlas/Centaur 30 Pioneer G Mission
[NASA-TM-X-69267] 16 p1964 N73-25885
Assessment of joint NASA/ESRO Venus orbiter
[SYST/2109/MS/1V] 17 p2089 N73-26906
Design and performance of lightweight cosmic radiation experiment for Pioneer Jupiter mission
18 p2210 N73-27837
Mission planning for Pioneer Saturn/Uranus atmospheric probe missions
[NASA-TM-X-2824] 21 p2595 N73-30800
Thermoelectric generator for Pioneer interplanetary Jupiter flyby mission
[IESD-2873-172] 23 p2818 N73-32529
Modifications to Pioneer meteoroid detection experiment for outer planet mission applications
[NASA-CR-132310] 23 p2845 N73-32739

PIONEER 6 SPACE PROBE
Velocity and outer limits of magnetic bottles ejected by solar proton flares as observed by Pioneer 6
[NASA-TM-X-66243] 15 p1828 N73-24814
Alfven wave refraction by interplanetary inhomogeneities from analysis of Pioneer 6 data
[NASA-TM-X-62270] 16 p1962 N73-25867

PIONEER 8 SPACE PROBE
Particle flux measurements of interplanetary dust and comet orbits by microphone experiments invalidated by micrometeoroid detectors flown on Pioneer 8 and 9
08 p0975 N73-17976
Multiplier for estimating particle flux from Explorer 8 and 9 satellite data - Part 2
[NASA-CR-132798] 22 p2665 N73-31352

PIONEER 9 SPACE PROBE
Simultaneous observations of plasma waves from electric field instruments on Pioneer 9 and OGO 5 to illustrate difference between near-earth and deep space conditions
01 p0096 N73-10795
Particle flux measurements of interplanetary dust and comet orbits by microphone experiments invalidated by micrometeoroid detectors flown on Pioneer 8 and 9
08 p0975 N73-17976
Solar wind plasma and magnetic field measurements from Pioneers 9 and 10 flights
[NASA-TM-X-62291] 18 p2195 N73-27719
Multiplier for estimating particle flux from Explorer 8 and 9 satellite data - Part 2
[NASA-CR-132798] 22 p2665 N73-31352

PIONEER 10 SPACE PROBE
Aerospace engineering including materials, orbits and trajectories, power sources, satellite geodesy, and structural engineering
[NASA-CR-128329] 01 p0119 N73-10981
Summary of Pioneer 10 mission objectives and midcourse maneuver strategies
01 p0120 N73-10987
Pioneer 10 observations of galactic cosmic ray intensity from 1.0 to 2.0 AU heliocentric radial range
[AD-748614] 05 p0593 N73-14823
Solar wind plasma and magnetic field measurements from Pioneers 9 and 10 flights
[NASA-TM-X-62291] 18 p2195 N73-27719
Pioneer-10 measurements of differential and integral cosmic ray gradients between 1 and 3 AU
[NASA-TM-X-66293] 18 p2197 N73-27736

PIONEER 11 SPACE PROBE
Pioneer 11 high field fluxgate magnetometer experiment
[NASA-TM-X-70467] 22 p2672 N73-31405

PIONS
Measurement of missing mass spectrum from pion [minus] plus proton reaction
[NUB-2160] 01 p0083 N73-10686
New tables for forward pion nucleon scattering amplitude analyzing errors and total cross section data
[NOTA-INTERNA-382] 01 p0084 N73-10695
Pion electroproduction cross section measured near threshold by coincidence experiments
[NOTA-INTERNA-383-A] 01 p0084 N73-10696
Experimental and theoretical studies of nuclear structure and pion reaction mechanisms at intermediate energies
[ORO-3948-4] 04 p0453 N73-13697
Production of gamma rays from decay of neutral pions produced by interstellar cosmic ray interactions
[NASA-TM-X-66120] 04 p0467 N73-13803
Preliminary studies of reaction yielding triton pion from proton deuteron interaction
[NASA-TM-X-68187] 07 p0823 N73-16674
Spectra of prompt gamma rays following nuclear pion absorption
[NASA-CR-131398] 11 p1326 N73-20762
Interactions of energetic neon with emulsion nuclei
[AD-754247] 11 p1327 N73-20768
Measurement of positive and negative pion, and double neutral pion photoproduction cross sections for incident gamma ray energies from 600 to 900 MeV
21 p2582 N73-30691
Development of fixed pole solution for pion-pion scattering amplitude and comparison with high energy data
[ILL-[TH]-73-15] 24 p2960 N73-33657

PIPE FLOW
Transients in cooling water systems of thermal power plant discussing mathematical models, computer programs and experiments
[PUBL-101-PT-1] 01 p0041 N73-10326
Design and development of device for moving liquid through pipes without use of mechanical pumps
[NASA-CASE-LAR-10799-1] 03 p0283 N73-12295
Measurement of momentum of two-phase liquid-vapor flow from pipe of circular cross-section
[EUR-4785-I] 03 p0284 N73-12302
Analytical methods for calculating frictional pressure losses in fluid flow through straight pipes
[ESDU-66027] 04 p0403 N73-13282
Numerical solution for magnetohydrodynamic pipe flow with laminar separation at higher Hartmann number
[AD-748766] 04 p0456 N73-13719
Low pressure air-water annular flow in horizontal tube
[AERE-R-6687] 06 p0655 N73-15320
Steady-state one dimensional motion of uniformly dense suspensions
[AD-750924] 06 p0656 N73-15333
Swirling cavity flow breakdown along axis of swirling water flow in circular pipe
[REPT-250] 06 p0724 N73-15913
Laser method for measuring axial solute dispersion in turbulent pipe flow
[AD-753801] 09 p1019 N73-18314
Analysis of oscillating gas flow in open-ended pipe caused by piston operating at or near resonant frequency
[AD-754647] 11 p1272 N73-20321
Laplace transformation and Volterra integral equation for studying heat transfer in laminar flow through pipe with annular space
[NLL-RTS-7525] 11 p1347 N73-20928
Heat transfer and frictional resistance in pipes with cooled walls during turbulent flow of high temperature gases
[NLL-RTS-7640] 11 p1347 N73-20930
Measurement of pipe resistance to instantaneous pulsating nonstationary flow
[NASA-TT-F-14881] 12 p1391 N73-21279
Experimental and theoretical measurement of pulsed flow velocity and pressure in circular pipes
14 p1649 N73-23372
Effect of wall suction on turbulent pipe flow friction coefficient
[AD-757584] 14 p1653 N73-23406
Laser-Doppler anemometer measurements of turbulence in drag reducing flows
[AD-757075] 14 p1669 N73-23545
Characteristics of wall mass transfer coefficient for pulsed laminar flow in pipe of Newtonian fluid containing dissoloved electrolyte
15 p1765 N73-24301
Characteristics of dilute gas-solids suspensions in drag reducing flow
[NASA-CR-2267] 16 p1888 N73-25277
Analysis of heat transfer in laminar flow of gas through constant diameter cylindrical tubes at low wall to bulk temperature ratios
17 p2013 N73-26275
Stability of laminar pipe flow with rigid rotation and small three-dimensional perturbation
[MITT-55] 19 p2256 N73-28184
Measurement of laminar flow in pipes using differential pressure generating devices
[NLL-M-23017-[5828.4F]] 20 p2386 N73-29168
Dynamic response of pipes with fluid flowing in steady and unsteady conditions
[MERL-TN-72-2] 20 p2387 N73-29178
Heat transfer by thermal radiation in forced convective tube flow of radiation gas
20 p2484 N73-29954
Motion and distribution of particles in steady, tube flows of suspensions of neutrally buoyant, rigid spheres
22 p2649 N73-31223
Influence of periodic oscillations of mean flow on mean and turbulent structure of fully developed air flow in smooth circular pipe
24 p2902 N73-33161
Heat transfer from wall to fluid in laminar fluid flow in circular tube
24 p2990 N73-33895

PIPELINES
Measurement of lateral erosion rates at proposed river crossing sites of Alaska pipeline by aerial photogrammetry
[AD-748875] 05 p0541 N73-14402
Computer program for dynamic structural analyses on three dimensional framework and pipework systems
[TRG-1409-REV-1] 06 p0726 N73-15929
Calculation of hydraulic resistances in pipelines
[AD-754322] 10 p1144 N73-19319
Evaluation of nitinol fittings for joining titanium piping for shipboard application
[AD-760322] 17 p2038 N73-26492

PIPES [TUBES]
NT GAS PIPES
NT U BENDS
Friction reducing properties of fibers in turbulent flow of fluids in pipes
[AD-746485] 01 p0043 N73-10337
Mean turbulent flow in entry region of rough pipe
[AD-747278] 02 p0159 N73-11285
Static and fatigue strength of welded tubular joints
[AD-746894] 02 p0179 N73-11453
Analysis of stress formation and changes in physical properties of pipes during rotary swaging using explosion or pulsed magnetic field energy
[AD-747454] 03 p0308 N73-12516
U shaped heated tube for distillation and purification of liquid metals
[NASA-CASE-XNP-08124-2] 04 p0385 N73-13129
Creep rupture tests of Inconel 702 tubes at high temperatures and internal helium pressures to determine service life
[NASA-TM-X-2728] 08 p0932 N73-17628
Creep rupture tests of Hastelloy-X tubes at high temperatures and internal helium pressures to determine service life
[NASA-TM-X-2727] 08 p0932 N73-17629
Influence of liquid oxygen on chromate coated aluminum tubing of breathing apparatus
[AD-752030] 08 p0936 N73-17661
Analysis of oxygen flow in steel pipelines to determine maximum permissible flow and effects of solid particles and restriction on safe flow rate to avoid ignition
[NASA-TT-F-14831] 09 p1016 N73-18290
Nonlinear differential equations in partial derivatives for nonsteady motion of liquids and gases in pipelines
[AD-752685] 09 p1017 N73-18296
Computer program for calculating dynamic FORTRAN response of piping network to sinusoidal excitation
[AD-752743] 09 p1017 N73-18302
Dynamic response of fluidic circuits with blocked and orifice terminated lines
[AD-753384] 09 p1018 N73-18307
Heat transfer and aerodynamic resistance of in-line smooth walled tube arrays in transverse air flow at high Reynolds number
[NLL-RTS-7689] 09 p1098 N73-18959
Controlled nitrogen additions on mechanical properties of tantalum tubing in nuclear reactors
[NASA-TN-D-6999] 11 p1305 N73-20587
Stability of thin elastic tube of infinite length containing rotating inviscid, incompressible fluid flow
13 p1508 N73-22222
Analytical and experimental examination of instability of spatial system of articulated pipes conveying fluid
[NASA-CR-131605] 13 p1510 N73-22236
Fabrication of beryllium compression tubes and structural panels for space shuttle application
[NASA-CR-124245] 13 p1533 N73-22420
Dynamic tear tests for determining fracture safety of Hanford-N reactor coolant piping material
[AD-748590] 13 p1558 N73-22626
Cable guide and restraint device for reefing tubes in uniform manner
[NASA-CASE-LAR-10129-1] 16 p1917 N73-25512
Potential of hot-isostatic pressing, hydrostatic extrusion and deformable die tube tapering processes to production of titanium tubes
[AD-759504] 16 p1919 N73-25532
Differential equations for analyzing nonstationary incompressible viscous fluid flow in elastic cylindrical tube
17 p2014 N73-26290
Effect of wall thickness variations on failure during burst tests of Zircaloy tubing
[WAPD-TM-1104] 17 p2093 N73-26935
Heat exchange between cooled polydisperse granular material and transversely located cylindrical tubes arranged in staggered bundle
[NLL-M-21602-[5828.4F]] 18 p2205 N73-27795
Hot film sensor measurement of turbulent flow of fluids in pipes
[AD-762059] 19 p2258 N73-28199
Design and tests of composite propulsion feedlines for cryogenic space vehicles - Vol. I
[NASA-CR-121137-VOL-1] 19 p2346 N73-28868
Design and tests of composite propulsion feedlines for cryogenic space vehicles - Vol. 2
[NASA-CR-121137-VOL-2] 19 p2346 N73-28869
Design, development, and testing of foldable beryllium copper alloy elastic tubes for hinges on satellite booms
[ESRO-CR-65] 19 p2346 N73-28874
Production of thin walled tubes by drawing and rolling
[NLL-M-21689-[5828.4F]] 20 p2421 N73-29448
Development of method for analyzing stress deformation state of metal during process of lengthwise rolling of tubes
[NLL-M-21655-[5828.4F]] 20 p2428 N73-29501

Analysis of stress-strain state in metal and contact stresses developed during continuous rolling on long mandrel for reducing and drawing metal tubes
[NLL-M-21688-[5828.4F]] 20 p2428 N73-29502
Nonlinear vibrations of pipelines containing pressurized fluids with application to aircraft hydraulic systems
[AD-764154] 22 p2616 N73-30968
Flow characteristics associated with laminar oscillating flow in horizontal tube containing mild axisymmetric constriction
23 p2772 N73-32175
Mechanical processes for developing metal matrix composite Al/B tubes
[NASA-CR-124407] 23 p2797 N73-32370
Differential thermal technique for lining tantalum alloy tubing with tungsten
[NASA-TN-D-7426] 23 p2805 N73-32429
Twisted wire or tube superconductor for filament windings
[NASA-CASE-LEW-11015] 23 p2823 N73-32571
Shock wave propagation at interface between two recilinear ducts noting oblique shock waves and mathematical models
[PUBL-137] 24 p2910 N73-33223
Safety devices and precautions to protect personnel performing radiographic inspections of pipeline welds
24 p2952 N73-33581

**PISTON ENGINES**
NT DIESEL ENGINES
Design principles of gas turbine and piston engines for commercial aircraft
[AD-751510] 07 p0837 N73-16783
Analog simulation of free piston gasifier tests relative to combustion and friction
[ME-240] 14 p1719 N73-23947
Performance of 1972 ford galaxie equipt with rankine cycle power system composed of organic based working fluid and reciprocating expander
[PB-210836] 19 p2329 N73-28739

**PISTON THEORY**
Analysis of dynamics of free-piston expander-compressor machinery
18 p2156 N73-27416
The calculated growth of lift and pitching moment on a swept wing entering a discrete vertical gust at subsonic speeds
[ARC-CP-1241] 22 p2612 N73-30932

**PISTONS**
NT MAGNETIC PISTONS
Piston manometer as absolute standard for vacuum gage calibration in 2 to 500 millitorr range
[NASA-TN-D-7059] 02 p0173 N73-11402
Computation principles and methods of free-piston expander-compressors
05 p0552 N73-14481
Influence of shock-producing piston on structure of electrostatic ion acoustic laminar shocks
[NASA-CR-130994] 09 p1069 N73-18724
Free piston shock tube driver using two stage compression techinque with intermediate diaphragm
[FFA-AU-765] 12 p1376 N73-21161
Analysis of dynamics of free-piston expander-compressor machinery
18 p2156 N73-27416
Methods of reducing damping in pneumatic piston drivers used in cryogenic armatures
22 p2678 N73-31449
Linear and nonlinear theory of elasticity used to determine deformation of cylinder and piston of high strength steel under influence of high pressure
[AD-763971] 22 p2687 N73-31519
Collapsible piston for hypervelocity gun
[NASA-CASE-MSC-13789-1] 23 p2769 N73-32152

**PITCH**
Human perception of musical intervals between simultaneous tones
[IZF-1972-20] 14 p1613 N73-23078
Strapped down gyroscope aligned with sun and star tracker optical axis calibrating roll, yaw and pitch values
[NASA-CASE-ARC-10716-1] 23 p2851 N73-32784

**PITCH [INCLINATION]**
Mathematical model of force coefficient and pitching moment by wing-body configuration
[BMVG-FBWT-72-28] 10 p1103 N73-18997
Pitch angle distribution of 100-300 keV protons measured by ESRO 1B satellite in early morning-late afternoon local magnetic time sector
[NP-19464] 10 p1210 N73-19846
Computerized simulation of roll and pitch effects on shipboard antenna radiation patterns
[AD-754348] 11 p1258 N73-20212
Effects of season altitude and pitch angle on electron precipitation from OGO-D data
[NASA-TM-X-66260] 16 p1962 N73-25868
Analysis of pitch damping moment for hovering helicopter rotary wing and development of formula for calculating pitch damping derivative
[NASA-TT-F-15010] 21 p2495 N73-30027
Effects of alcohol on eye movements and tracking performance during laboratory angular accelerations about yaw and pitch axes
[FAA-AM-72-34] 22 p2619 N73-30989

**PITCH ANGLES**
U PITCH [INCLINATION]

**PITCH ATTITUDE CONTROL**
U LONGITUDINAL CONTROL

**PITCHING MOMENTS**
Analysis of forced-oscillation pitch-damping over small angular amplitude range about nominal angle of attack
[NASA-CR-129522] 03 p0247 N73-12001
Low speed wind tunnel tests on slender variable sweep wing of lift, drag, and pitching moments
[ARC-CP-1227] 05 p0492 N73-14009
Development of automatic system for controlling aircraft under turbulent atmospheric conditions to provide pitch stabilization
[AD-751148] 07 p0741 N73-16028
Inertially coupled equations of motion for analyzing pitching and yawing motions of nonrolling wind tunnel model
[AD-752208] 08 p0926 N73-17586
Wind tunnel tests to determine viscous normal force, pitching moment, side force and yawing moment on bodies of revolution at incidences up to 90 degrees
[WRE-782[WR/D]] 13 p1470 N73-21902
Analysis of aerodynamic loading for symmetrically tapered wings describing simple harmonic pitching oscillations of low frequency in supersonic flow
[ARC-R/M-3298] 15 p1728 N73-24019
Wind tunnel measurements of direct pitching damping and stiffness derivatives for delta wing and swept wing planforms
[ARC-R/M-3419] 16 p1853 N73-25009
Supersonic wind tunnel tests to measure overall normal and side forces, rolling, pitching, and yawing moments on canard aircraft
[ARC-R/M-3226] 16 p1853 N73-25011
Measurement of pitching moment derivatives using free oscillation technique on two dimensional airfoils of double wedge section and single wedge section
[ARC-R/M-3234] 16 p1855 N73-25025
Development and characteristics of test equipment for measurement of direct pitching moment derivatives for two dimensional flow at subsonic and supersonic speeds
[ARC-R/M-3257] 16 p1855 N73-25027
Measurement of drag, lift and pitching momeats on slender winged low aspect ratio gothic planforms at subsonic speed
[ARC-R/M-3720] 21 p2492 N73-30005
Analysis of pitch damping moment for hovering helicopter rotary wing and development of formula for calculating pitch damping derivative
[NASA-TT-F-15010] 21 p2495 N73-30027
The calculated growth of lift and pitching moment on a swept wing entering a discrete vertical gust at subsonic speeds
[ARC-CP-1241] 22 p2612 N73-30932
Wind tunnel apparatus for determining moment cross-derivatives due to pitching and yawing on models at moderate angles of attack and sideslip
[NASA-CR-114663] 22 p2613 N73-30944
Slotted transonic wind tunnel tests on pitching delta wing enable selection of porpous walls for interference free damping derivatives
[ARC-R/M-3715] 24 p2870 N73-32930
Design of pitching axis control system for aircraft with artificial stability
24 p2878 N73-32988

**PITOT STATIC TUBES**
U PITOT TUBES
U SPEED INDICATORS

**PITOT TUBES**
Comparative assessment of three methods of measurement of pressure error corrections for aircraft pitot-static systems
[CRANFIELD-AERO-11] 08 p0924 N73-17570
Analysis of accuracy of Preston tube calibration equations to determine local skin friction in two dimensional supersonic and low hypersonic flow conditions
[NASA-TN-D-7190] 13 p1510 N73-22239
Hot-wire anemometer and pitot static probe measurement of turbulent mixing in axial pressure gradients
[AD-756543] 13 p1511 N73-22244
Numerical analysis of Navier-Stokes equations for steady, viscous, axisymmetric flow with application to flow past pitot tube at low Reynolds numbers
[ARC-R/M-3240] 15 p1725 N73-23998
Development of methods for determining local skin friction of boundary layer and calibration of instruments for analyzing turbulent shear flow
[ARC-R/M-3202] 16 p1854 N73-25016

**PITS**
Topographic depressions in Mars south polar terrain
[CONTRIB-2266] 23 p2840 N73-32696

**PITTING**
Small etching pits in epitaxial layer of gallium arsenide caused by accumulation of impurities
[DRIC-TRANS-2928] 06 p0709 N73-15782
Etch pit study of motion and generation of dislocations in electron irradiated metals and effect of point defects on mechanical properties of metals
[COO-1367-50] 15 p1799 N73-24579

**PITUITARY GLAND**
Response of pituitary-thyroid axis to microwave radiation
[VR-3490-149] 06 p0630 N73-15122

**PIVOTED WING AIRCRAFT**
U TILT WING AIRCRAFT

**PIVOTS**
Detailed design guidance for flexure-pivots with strips crossing midway along lengths and at right angles to each other
[ESDU-67021] 01 p0110 N73-10907

**PL/1**
Use, implementation, and maintenance procedures for data reconfiguration service compiler coded in PL/1
[AD-745751] 01 p0031 N73-10243

**PLAGES [FACULAE]**
U FACULAE

**PLAINS**
NT COASTAL PLAINS
NT FLOOD PLAINS
NT LLANOS ORIENTALES [COLOMBIA]
NT PLAYAS
Identification of playa lakes in Texas High Plains from ERTS-1 imagery
[E72-10257] 03 p0290 N73-12357
Relative ages of near side and far side terra plains based on interpretation of Apollo 16 photogeology - Part A
12 p1452 N73-21765
Dynamics of playa lakes in Texas High Plains analyzed from ERTS-1 imagery
[E73-10598] 15 p1772 N73-24359
Effect of sunspot cycle on precipitation pattern over U.S. plains states
17 p2056 N73-26629
Utilization of Skylab EREP data in making agriculturally oriented decisions in Mississippi Delta alluvial plain region
[E73-11125] 24 p2916 N73-33280

**PLAN POSITION INDICATORS**
Design, development, and evaluation of bistatic radar processor for synchronizing rotation rate of plan position indicator display
[AD-756515] 13 p1495 N73-22121

**PLANAR STRUCTURES**
Group theoretical descriptions of dualities in projective planes
02 p0196 N73-11582
Application of nonlinear finite element analysis to planar and nonplanar plane stress problems
22 p2723 N73-31789

**PLANE WAVES**
Reflection and propagation of plane waves in fiber reinforced materials
[AD-745358] 01 p0070 N73-10576
Approximate solution to covariance of plane wave direction and propagation velocity of signals in array processing scheme
[AD-747591] 03 p0267 N73-12160
Numerical analysis on electromagnetic wave scattering from periodic surface with arbitrary profile
[AD-747491] 03 p0268 N73-12170
Relationship of acoustic surface waves on curved surfaces to corresponding plane surface waves
[AD-748189] 03 p0338 N73-12761
Characteristics of microwave antenna with conical reflectors to generate plane wave front
[NASA-CASE-NPO-11661] 05 p0507 N73-14130
Nonlinear detection of low frequency plane wave by directional circular piston beam
[AD-755167] 12 p1430 N73-21588
Analysis of characteristics of initially plane, strong shock wave propagating into conical convergence using multi-crystal piezoelectric probe
21 p2522 N73-30228
Plane elastic wave propagation through movable wall, calculating flow distribution behind wall
[DLR-FB-72-59] 21 p2525 N73-30246
Transient response of stratified cold plasma to infinite plane impulsive electromagnetic wave incident vertically on ionization
21 p2582 N73-30693

**PLANET EPHEMERIDES**
Chilean astronomical observations of early star spectra, southern star radial velocities, and minor planet positions
05 p0594 N73-14828
Tables of minor planets positions and comparison stars
05 p0594 N73-14831
Utility of Goddard Trajectory Determination System Solar/Lunar/Planetary ephemeris files
[NASA-TM-X-66185] 08 p0976 N73-17983
Planetary ephemerides for Mariner 9 based on radar range data using normal points
23 p2842 N73-32714

**PLANET ORIGINS**
U PLANETARY EVOLUTION

**PLANETARY ATMOSPHERES**
NT JUPITER ATMOSPHERE
NT MARS ATMOSPHERE
NT VENUS ATMOSPHERE

Separation of refractivity gradient components for error elimination and inversion accuracy in occultation measurements on planetary atmospheres
02 p0198 N73-11597
Inversion of radio occultation data for planetary atmospheres by bent ray path technique
02 p0198 N73-11598
Error analysis on Doppler data associated with bent ray path radio occultation of planetary atmospheres
02 p0198 N73-11600
Astrophysical flow problems, planetary atmospheres, and space radiation
04 p0468 N73-13814
Feasibility of atmospheric entry probe missions to Uranus and Neptune
[NASA-CR-129815] 04 p0469 N73-13824
Matrix solution for one dimensional model of radiation field arising from multiple scattered photons in planetary atmosphere
[NASA-CR-130755] 08 p0943 N73-17722
Research in development of detectors for analysis of planetary atmospheres
[NASA-CR-130700] 08 p0959 N73-17841
Spectrometry investigations of planets by USSR astronomical observatories with emphasis on ultraviolet absorption by planetary atmospheres
[NASA-TT-F-747] 09 p1083 N73-18833
Photometric analysis of violet clouds on planet Mars and determination of monochromatic albedo
09 p1083 N73-18834
Spectrophotometric observations of planet Jupiter to determine ultraviolet absorption for different regions of disk
09 p1083 N73-18835
Measurement of ultraviolet absorption by planet Saturn disk at various geographical regions
09 p1083 N73-18836
Derivation of formula for calculating diffuse radiation from limb side of spherical planetary atmosphere
09 p1084 N73-18839
Abiogenic syntheses of aliphatic and aromatic amino acids by ultraviolet radiation
10 p1119 N73-19119
Metabolism and propagation of microbes in outer planets
[NASA-CR-131091] 10 p1120 N73-19127
Probe study to explore atmosphere of Saturn and Uranus
[NASA-CR-131227] 10 p1215 N73-19883
Radiative transfer in dense water vapor atmosphere
[LBL-1324] 12 p1464 N73-21864
Conference on structure and composition of upper atmosphere and planetary atmospheres
[AD-756812] 14 p1662 N73-23489
Analysis of atmospheric entry trajectories for manned and unmanned missions to planet Venus
[NASA-TN-D-7316] 16 p1966 N73-25900
Analysis of data relative to possible Saturn orbiter mission in 1985
[NASA-CR-133033] 16 p1966 N73-25906
Metabolism and propagation of microbial contamination in planetary atmospheres
[NASA-CR-133638] 20 p2369 N73-29049
Synopticostatistical, numerical, and laboratory procedures for studying dynamics of atmospheric circulation in planetary atmospheres including earth
[TT-70-50052] 20 p2442 N73-29615
Atmospheric circulation of planetary atmospheres
20 p2445 N73-29639
Detection techniques for tenuous planetary atmospheres
[NASA-CR-134430] 20 p2473 N73-29869
Infrared laboratory studies of synthetic planetary atmospheres
[NASA-CR-133855] 21 p2597 N73-30810
Solar physics, planetary atmospheres, and space astronomy research programs
[NASA-CR-133773] 21 p2610 N73-30923
Changes in planetary boundary layer wind profiles
[PB-221752/9] 22 p2697 N73-31601
Objectives of experiments on Mariner 9 space probe
[NASA-CR-135726] 24 p2983 N73-33834

**PLANETARY COMPOSITION**
Sensitivity of low weight CPNE for planetary composition analysis
[NASA-CR-132208] 17 p2032 N73-26448
Subsurface characteristics of Mercury and Mars determined by analysis of thermal microwave emission
24 p2979 N73-33801

**PLANETARY ENTRY**
U ATMOSPHERIC ENTRY

**PLANETARY ENVIRONMENTS**
NT JUPITER ATMOSPHERE
NT MARS ATMOSPHERE
NT MARS ENVIRONMENT
NT PLANETARY ATMOSPHERES
NT VENUS ATMOSPHERE
Influence of Uranus, Neptune, and Pluto environments on design of spacecraft used to probe them
[NASA-SP-8103] 02 p0230 N73-11870
Results of Mars 2 and Mars 3 space probes
[NASA-TT-F-14914] 14 p1709 N73-23869
Research in physical phenomena of space and planetary environments, and applications of radio technology
[NASA-CR-133856] 21 p2596 N73-30809

**PLANETARY EVOLUTION**
Possibility of water on planets, and origin and development of worlds
[JPRS-57709] 04 p0475 N73-13882
Pre- and post-Apollo 11 studies on lunar geologic evolution
[NASA-TM-X-65939] 13 p1577 N73-22777
Escape mechanism of Venus atmosphere
[NASA-CR-132025] 14 p1706 N73-23842
Asteroid and comet exploration for studying planetary evolution and solar system history
[NASA-CR-2291] 18 p2196 N73-27726

**PLANETARY EXPLORATION**
U SPACE EXPLORATION

**PLANETARY EXPLORER**
U OUTER PLANETS EXPLORERS

**PLANETARY GRAVITATION**
Numerical integration of artificial satellite orbit perturbation due to planetary gravitational effects, including long period and secular terms
[GRGS-BULL-5] 01 p0105 N73-10868
Zonal and tesseral harmonics of gravitational fields of major planets and constraints placed on models of planet interiors
[NASA-CR-130346] 07 p0841 N73-16810
Satellite and surface gravity data for computing gravimetric geoid
22 p2736 N73-31910

**PLANETARY LANDING**
First-order geometrical optics analysis of quasi-microscope planetary landers
[NASA-TN-D-7129] 07 p0800 N73-16498
Analysis of standards and precedures for planetary quarantine with emphasis on determination of mission specifications
[NASA-CR-130558] 08 p0877 N73-17103

**PLANETARY LONGITUDE**
U PLANET EPHEMERIDES

**PLANETARY MAGNETIC FIELDS**
Plasma and magnetic field measurements in vicinity of Venus from Venera 4 and Mariner 5 flights
[NASA-TT-F-15128] 22 p2716 N73-31743

**PLANETARY MOTION**
U SOLAR ORBITS

**PLANETARY NEBULAE**
UBV and H alpha spectra for detecting interstellar dust and distances to planetary nebulae
12 p1448 N73-21724
Hydrostatic equilibrium models of ionization zone instability causing planetary nebulae
19 p2341 N73-28828
Thermal stability in planetary nebulae
22 p2713 N73-31720
Hydrodynamic model for stellar mass ejection and planetary nebula formation
22 p2734 N73-31885

**PLANETARY ORBITS**
Characteristics and capabilities of solar electric propulsion for orbiter missions of Uranus and Neptune
[NASA-CR-129857] 05 p0594 N73-14827
Application of computerized series manipulation system to planetary theory using recursive linearization
12 p1447 N73-21715
Numerical integration techniques for solution of orbital elements of moon and planets
[AD-755164] 14 p1707 N73-23850
Payloads of ballistic trajectories in Mercury orbit, and interplanetary trajectory characteristics for Venus swingbys to Mercury
[NASA-CR-2298] 23 p2846 N73-32745

**PLANETARY QUAKES**
Characteristics and requirements of instruments for advanced Viking seismic experiments on Mars
[NASA-CR-130358] 06 p0717 N73-15850

**PLANETARY QUARANTINE**
Planetary quarantine procedures for reduction of microbial burden on spacecraft
[NASA-CR-129793] 04 p0379 N73-13086
Soil sampling and microorganism analysis in planetary spacecraft assembly area for prevention of Mars contamination
[NASA-CR-130009] 07 p0745 N73-16059
Analysis of standards and precedures for planetary quarantine with emphasis on determination of mission specifications
[NASA-CR-130558] 08 p0877 N73-17103
Effects of planetary quarantine constraints on advanced planetary mission planning
[NASA-CR-130861] 09 p0995 N73-18123
Metabolism and propagation of microbes in outer planets
[NASA-CR-131091] 10 p1120 N73-19127
Planning and source allocation for planetary quarantine measures for interplanetary automated spacecrafts
[NASA-CR-131291] 11 p1247 N73-20126
Microbial burden estimation for planning planetary quarantine of advanced spacecraft
[NASA-CR-131845] 13 p1485 N73-22039
Microbiological studies of Apollo 17 command module preflight and postflight samples
[NASA-CR-132022] 14 p1610 N73-23056
Probabilistic model of planetary contamination for deciding spacecraft quarantine standards and procedures
[NASA-CR-132001] 14 p1704 N73-23829
Quarantine constraints as applied to satellites
[NASA-CR-132073] 15 p1741 N73-24116
Spacecraft microbial burden reduction for Jupiter due to atmospheric entry heating
[NASA-CR-132072] 15 p1741 N73-24117
Sixth supplement to bibliography on planetary quarantine with indexes
[NASA-CR-131817] 16 p1866 N73-25112
Development of planetary quarantine measures for automated spacecraft
[NASA-CR-133202] 17 p1988 N73-26066
Planetary quarantine requirements for automated spacecraft flights
[NASA-CR-135795] 24 p2885 N73-33040
Satellite quarantine constraints in outer planet mission planning
[NASA-CR-135791] 24 p2885 N73-33041

**PLANETARY RADIATION**
Fourier spectrometer for measuring absolute spectral intensity of emissions from earth and other planets
[NASA-TT-F-14425] 02 p0172 N73-11397
Mathematical model for calculating scanning angle distribution of planetary albedo gamma rays above 100 MeV
[NASA-TM-X-66117] 03 p0353 N73-12874
Satellite observation for acquisition and monitoring of planetary radiation, clouds, particles, and air pollution
[DGLR-PAPER-72-81] 04 p0444 N73-13626
Analysis of quasi-periodic modulation of L-bursts in decametric radiation from planet Jupiter
05 p0594 N73-14833
Derivation of formula for calculating diffuse radiation from limb side of spherical planetary atmosphere
09 p1084 N73-18839

**PLANETARY ROTATION**
Study of 4-day retrograde rotation of external cloud layer of Venus
[NASA-TT-F-14710] 02 p0230 N73-11864
Satellite motion in gravitational field of nonspherical rotating planet
[NASA-TT-F-15073] 24 p2981 N73-33825

**PLANETARY SATELLITES**
U NATURAL SATELLITES

**PLANETARY SPACE FLIGHT**
U INTERPLANETARY FLIGHT

**PLANETARY SPACECRAFT**
U INTERPLANETARY SPACECRAFT

**PLANETARY SURFACES**
NT MARS SURFACE
Photoelectric measurements of brightness distribution and brightness phase dependence of spheres with different colors and roughness to find optical properties of Mars surface
09 p1083 N73-18837
Analysis of high velocity spacecraft crash landing on planetary surfaces for possible encapsulated microorganism release
[NASA-CR-131835] 16 p1966 N73-25904
Measurements of illumination in atmosphere and on surface of planet Venus obtained by automatic interplanetary station Venera-8
[JPRS-59963] 21 p2595 N73-30794
Experimental radio and radar studies on lunar and planetary atmospheres and surfaces, interplanetary medium, and software and hardware conceptions
[NASA-CR-135670] 23 p2845 N73-32734
Subsurface characteristics of Mercury and Mars determined by analysis of thermal microwave emission
24 p2979 N73-33801
Factors affecting temperature of solid or oceanic surface of planet and adjacent layers of atmosphere
[NASA-TT-F-15040] 24 p2979 N73-33806

**PLANETARY TEMPERATURE**
Direct integration transmittance model for 200/2000 cm region of high spectral resolutions and of planetary thermal emissions
[NASA-TM-X-70454] 21 p2548 N73-30429
Factors affecting temperature of solid or oceanic surface of planet and adjacent layers of atmosphere
[NASA-TT-F-15040] 24 p2979 N73-33806

**PLANETOCENTRIC COORDINATES**
Photogrammetric determination of Martian surface coordinates using Mariner 9 photos
23 p2843 N73-32719
Observation equations to utilize lunar laser ranging and very long baseline interferometry measurements for selenodetic control
[NASA-CR-135774] 24 p2931 N73-33404

**PLANETOLOGY**
Conical section method for determining planetary configuration from spaceborne photographic data on triangulation and horizon lines
[JPRS-58304] 09 p1085 N73-18848

**PLANETS**
NT EARTH [PLANET]
NT EXTRASOLAR PLANETS
NT JUPITER [PLANET]

NT MARS [PLANET]
NT MERCURY [PLANET]
NT NEPTUNE [PLANET]
NT SATURN [PLANET]
NT URANUS [PLANET]
NT VENUS [PLANET]
Radar methods of investigating moon and planets
[NASA-TT-F-729] 09 p1084 N73-18847
Problems which could be solved by comparative geological study of planets of solar system
12 p1456 N73-21796
Geophysical data as indicators of planet properties, using geodetic satellite
[NASA-TM-X-66274] 17 p2024 N73-26377
PLANFORMS
NT CARET WINGS
NT DELTA WINGS
NT INFINITE SPAN WINGS
NT RECTANGULAR PANELS
NT RECTANGULAR PLANFORMS
NT RECTANGULAR PLATES
NT RECTANGULAR WINGS
NT SWEPTBACK WINGS
NT VARIABLE SWEEP WINGS
NT WING PLANFORMS
Procedures for calculating velocity potential and pressure distribution of planforms oscillating harmonically in supersonic flow
[FOK-X-440] 11 p1231 N73-19994
Development of algorithm for calculating inviscid flow about arbitrary planform rotors and application to analyzing various rotary wing configurations
12 p1362 N73-21048
PLANIMETRY
U AREA
U DIMENSIONAL MEASUREMENT
PLANKTON
Chlorophyll and plankton population distribution in upwelling waters off northwest coast of Africa and effects of eolian dust particles on surface water chemistry
[E72-10331] 05 p0531 N73-14319
Investigation of phytoplankton populations in waters along eastern coast of US using ERTS-1 imagery and surface measurements
[E73-10097] 08 p0902 N73-17308
Phytoplankton density determination from ocean color measurements
08 p0972 N73-17939
Dynamics of plankton populations in upwelling waters along Arabian Coast, Somali Coast, and Northwest Coast of Africa
[E73-10325] 09 p1024 N73-18357
Relation of chlorophyll and suspended sediment content in lower Chesapeake Bay to ERTS-1 imagery and application of marine station data to study of productivity along eastern shelf waters of US
[E73-10593] 15 p1772 N73-24358
ERTS-1 imagery of plankton populations in upwelling waters off Africa
[E73-10603] 15 p1773 N73-24364
Measurement of chlorophyll and plankton populations of shelf and slope waters off northeastern United States
[E73-10683] 16 p1901 N73-25378
Use of ERTS-1 data to apply marine station data to study of productivity along Eastern Self Expanded Waters of US
[E73-10778] 18 p2135 N73-27254
Investigation of plankton populations in upwelling waters along NW coast of Africa using ERTS-1 imagery
[E73-10795] 18 p2137 N73-27271
Relation of sea truth data from Cape Cod, Massachusetts, and Charleston, South Carolina on plankton composition and chlorophyll values with ERTS-1 data
[E73-10907] 20 p2397 N73-29256
Identification of female specimen of Trichocorixa reticulata in waters of Gulf of California
[E73-10926] 20 p2398 N73-29275
Seasonal plankton collections conducted during Tenth Antarctic Expedition
20 p2409 N73-29363
Collection of phytoplankton and chlorophyll samples from waters of Chesapeake Bay
[E73-11154] 24 p2919 N73-33308
PLANKTON BLOOM
U PLANKTON
PLANNING
NT AIRPORT PLANNING
NT MANAGEMENT PLANNING
NT MISSION PLANNING
NT PRODUCTION PLANNING
NT PROJECT PLANNING
NT REGIONAL PLANNING
NT URBAN PLANNING
Application of mathematics to general job-shop scheduling noting criteria, procedures, and linear programming
[LAAS-OD-73-I-21] 23 p2813 N73-32488
PLANOTRONS
NT CATHODE RAY TUBES
NT CELESCOPES
NT THERMIONIC DIODES
NT THYRATRONS
PLANTS [BOTANY]
NT ALFALFA
NT ALGAE
NT AUTOTROPHS
NT BACILLUS
NT BACTERIA
NT BLUE GREEN ALGAE
NT BRUSH [BOTANY]
NT CHLORELLA
NT CITRUS TREES
NT CONIFERS
NT CORN
NT DECIDUOUS TREES
NT ESCHERICHIA
NT FUNGI
NT GRASSES
NT LEAVES
NT PSEUDOMONAS
NT SPORES
NT STAPHYLOCOCCUS
NT STREPTOCOCCUS
NT TOBACCO
NT TREES [PLANTS]
NT YEAST
Mathematical model for photosynthetic gas exchanges in growing wheat and radish biopaks of life support systems
03 p0257 N73-12081
Distribution and density of phreatophytes and other arid and desert plants
[E72-10243] 03 p0289 N73-12343
Identification of Nevada wildland plants, vegetation, and fire scars from ERTS-1 imagery
[E72-10253] 03 p0289 N73-12353
Monitoring plant development in California rangeland environments using ERTS-1 and supporting aircraft data
[E72-10263] 03 p0290 N73-12362
Automatic photointerpretation for plant species and stress identification using ERTS-1 imagery
[E72-10258] 03 p0300 N73-12448
Remote sensing of native arid plant distribution using ERTS-1
[E72-10314] 04 p0412 N73-13363
Detection of plant diseases and nutrient deficiencies, soil types, and moisture levels in Tennessee using ERTS-1 imagery
[E72-10320] 04 p0413 N73-13368
Effect of above-ground plant mass on spectral curves of brightness coefficients of soil-vegetation system
04 p0443 N73-13613
ERTS-1 imagery of plant growth and annual flooding in Niger River inland delta
[E73-10078] 07 p0780 N73-16339
Distribution and density of phreatophytes and other arid land plants measured from ERTS-1 imagery
[E73-10094] 08 p0902 N73-17306
Detection of plant and forest diseases, nutrient deficiencies, soil types, and soil moisture levels from ERTS-1 imagery of Tennessee
[E73-10311] 09 p1022 N73-18343
Time periods for nutrient solution exchange in optimal biomass yield on porous aggregate
10 p1117 N73-19106
Hydroponic cultivation of plants on clay filters from human mineralized feces
10 p1117 N73-19110
Thermal combustion requirements for burner devices of human vegetative waste products
10 p1118 N73-19111
Gas chromatography-mass spectrometry for analyzing fatty acid and sterol concentrations in plant tissue samples
[NASA-CR-128740] 10 p1120 N73-19131
Identification of native arid plant distribution in Avra Valley, Arizona using ERTS-1 imagery
[E73-10369] 10 p1151 N73-19365
Prediction of ephemeral and perennial range quantity and quality during normal grazing season in Arizona based on ERTS-1 imagery
[E73-10377] 10 p1152 N73-19372
ERTS-1 observations of plant growth and annual flooding in Inland Delta of Niger River in Mali
[E73-10436] 11 p1281 N73-20396
Determination of specific spectral signatures for dominant Arizona desert scrub plant species and soil surface backgrounds
[E73-10466] 11 p1284 N73-20421
Detection of plant diseases and nutrient deficiencies, soil types, and moisture levels from ERTS-1 imagery of Tennessee and Kentucky
[E73-10468] 12 p1395 N73-21305
Identifying phenological changes for specific forest and crop types using ERTS-1 imagery
[E73-10498] 12 p1398 N73-21334
Photometric observations of in situ fluorescence and bioluminescence with Biota in New York Bight
[RM-568] 13 p1479 N73-21978
Mapping distribution and density of phreatophytes and other arid land plant communities in Arizona using ERTS-1 imagery
[E73-10543] 13 p1518 N73-22306
Application of spaceborne photography and aerial photography to ecological resource inventory and analysis of naturally vegetated areas in Arizona
[NASA-CR-131581] 13 p1523 N73-22342
Thermal effects of microwave and radio frequency radiation on biological systems
[MBL-1971-7-PT-1] 14 p1609 N73-23048
Cytological changes in pine tissues treated with lunar materials collected on Apollo 12 quarantine mission
[NASA-CR-128914] 14 p1610 N73-23054
Determination of arid plant distribution in Arizona from ERTS-1 imagery
[E73-10520] 14 p1654 N73-23413
Development of germ-free plants and tissues
[NASA-CR-128947] 15 p1742 N73-24122
Physical and biomedical research by earth orbiting space stations
[AD-756771] 15 p1743 N73-24126
Algorithm for automatic photointerpretation of plant species and stresses in Minnesota imagery
[E73-10639] 15 p1776 N73-24398
Utilization of ERTS-1 imagery to detect plant diseases, nutrient deficiencies, soil types, and moisture levels in Tennessee
[E73-10640] 15 p1776 N73-24399
Determination of native desert plant distributions in Avra Valley, Arizona from ERTS-1 MSS imagery
[E73-10659] 16 p1899 N73-25355
Application of ERTS-1 imagery for inventory and monitoring of natural vegetation and related resources in arid environment
[E73-10728] 17 p2020 N73-26334
Application of ERTS-1 imagery to determine dynamics of distribution and density of phreatophytes and other arid land plant communities
[E73-10790] 18 p2137 N73-27266
Application of ERTS-1 imagery for vegetative and geologic mapping of western Seward Peninsula, Alaska
[PAPER-A8] 19 p2260 N73-28216
ERTS-1 detection of plant diseases and nutrient deficiencies, soil types and moisture levels, forests, and crop identification in Mississippi Delta
[E73-10849] 19 p2292 N73-28427
ERTS-1 multispectral photography of wetlands vegetation and plant species
[E73-10850] 19 p2292 N73-28428
Spectral signatures for dominant desert scrub plant species and soil surface backgrounds in Arizona
[E73-10890] 20 p2394 N73-29239
Phenological observations of lilac, honeysuckle, alfalfa, and winter wheat in Rocky Mountain and Columbia Valley Corridors
[E73-10925] 20 p2398 N73-29274
Radiation regime of vegetation, using spectral composition and three dimensional structure of incident solar radiation and scattered sky light
20 p2404 N73-29316
Effects of solar radiation on photomorphogenesis of plants based on spectral distribution of solar energy in daytime
20 p2404 N73-29322
Effects of radiation and heat balance of active surface on life processes of plants with emphasis on productivity of cotton
20 p2404 N73-29323
Solar radiation effects on photosynthesis of submerged aquatic plants
20 p2405 N73-29327
Spectral energy distribution of Pamir plants at different altitudes above sea level in relation to mountain plant characteristics
20 p2406 N73-29336
Effect of microflora on exogenous dynamics of weathering and crust development
[NASA-TT-F-15032] 20 p2411 N73-29383
Simulation of growth and mineral uptake by plants growing in lunar soil
[NASA-CR-134036] 22 p2619 N73-30988
Inventory and monitoring natural vegetation and plants in arid land of Arizona from satellite-borne photography
[E73-11021] 22 p2661 N73-31325
Automatic photointerpretation for plant species and stress identification in Minnesota
[E73-11063] 23 p2781 N73-32239
Early detection of insect infestations and density/distribution of host citrus trees along Rio Grande River in Texas
[E73-11073] 23 p2782 N73-32248
Skylab detection of insect infestations and density/distribution of host plants in Texas
[E73-11076] 23 p2782 N73-32251
Detection of plant diseases, soil moisture, drainage patterns, forestry types, and sedimentation in Tennessee from ERTS-1 imagery
[E73-11091] 23 p2782 N73-32258
Survey and Mapping of vegetative cover in Susquehanna River Basin to determine accuracy of photographic technology and ERTS-1 imagery
[E73-11111] 24 p2915 N73-33268
PLANTS [INDUSTRIES]
U INDUSTRIAL PLANTS

**PLASMA ACCELERATION**
Acceleration and compression parameters in plasma focus
[LA-TR-72-24] 07 p0826 N73-16694
Research in plasma acceleration, hollow cathode physics, and plasma dynamics
[NASA-CR-131270] 15 p1817 N73-24725
IMP measurements on hydrogen and helium isotope accelerations in solar flares
19 p2336 N73-28797
Chromospheric type 3 radio burst acceleration of solar electrons and coronal streamer
19 p2340 N73-28821

**PLASMA ACCELERATORS**
NT COAXIAL PLASMA ACCELERATORS
Operation of plasma accelerator in quasi-steady mode to determine ratio of energy deposition into kinetic and thermal modes
[NASA-CR-128408] 01 p0035 N73-10275
Impulsive plasma acceleration in inductive device
[AD-746044] 02 p0217 N73-11754
Measurement of plasma ultraviolet radiation for determining collisional momentum transfer cross sections in accelerator
[AD-747339] 03 p0344 N73-12802
Theoretical and numerical analysis of pulsed plasmoid accelerator
[AD-750524] 06 p0707 N73-15764
Exploding wire plasma accelerator simulating hypervelocity micrometeoritic damage at impact
[ISL-26/71] 07 p0821 N73-16657
Principles of magnetohydrodynamic energy generation to include flows in magnetohydrodynamic generator, physical processes, diagnostics, and required equipment - Part 1
[JPRS-57940-1-PT-1] 07 p0825 N73-16687
Principles of magnetohydrodynamic energy generation to include open and closed cycle magnetohydrodynamic generators, liquid-metal plants, and materials for generators - Part 2
[JPRS-57940-2-PT-2] 07 p0825 N73-16688
Energy deposition in parallel plate plasma accelerators operated in quasi-steady mode
10 p1195 N73-19723
Performance of electromagnetic accelerators in high pressure test facilities
[AD-754024] 11 p1328 N73-20779
Impulsive plasma accelerator study of plasma acceleration by magnetic field annihilation
[AD-758880] 16 p1950 N73-25780

**PLASMA ARC SPRAYING**
U ARC SPRAYING
U PLASMA SPRAYING

**PLASMA ARC WELDING**
Plasma arc welding procedure for Hastelloy seams of isotopic strontium titanate fuel capsule
[CONF-720917-1] 10 p1166 N73-19489

**PLASMA ARCS**
U PLASMA JETS

**PLASMA CLOUDS**
Survey of results from barium cloud releases using shaped charge technique in ionosphere and magnetosphere
[MPI-PAE/EXTRATERR-67] 07 p0794 N73-16454
Laboratory simulation of behavior of artificial plasma clouds in ionosphere
[AD-758064] 15 p1782 N73-24442
Solving equations of motion for behavior of plasma clouds in layered model ionosphere
[MPI-PAE/EXTRATERR-73] 22 p2704 N73-31658
Reaction rate characteristics of interstellar matter and cosmic cloud formation
22 p2735 N73-31896

**PLASMA COMPOSITION**
Analysis of solar wind composition obtained by plasma analyzers mounted on various spacecraft
01 p0098 N73-10806
Analysis of instabilities resulting from interaction of electromagnetic waves with active medium or system
[AD-746893] 02 p0143 N73-11159
Spectroscopic measurements on plasma composition in Tokamac-type facility
[JAERI-M-4596] 06 p0705 N73-15752
Charged particle concentrations and plasma temperatures of liquid or film electrode discharges in mercury vapor
[AD-750559] 06 p0706 N73-15759
Computer program for calculating equations of state, thermodynamic functions, and opacities of plasmas
[AD-751607] 07 p0829 N73-16723
Ionic composition of plasmas produced in helium, hydrogen, xenon, and neon gas mixtures
[AD-751327] 07 p0830 N73-16727
Properties of laser generated plasma trapped in stellarator
[NP-19656] 17 p2067 N73-26725
Statistical mechanics for plasma calculations
18 p2182 N73-27619

**PLASMA CONDUCTIVITY**
Fast radial motion of toroidal plasma column in transverse magnetic field resulting in controlled displacement of plasma column
[NP-19401] 06 p0705 N73-15754
High frequency pressure effect on wave propagation along layer of magnetoactive plasma
[AEC-TR-7336] 07 p0826 N73-16698
Models for force-free magnetic fields in plasmas with finite conductivity
[TRITA-EPP-72-24] 07 p0828 N73-16715
Derivation of directional plasma transport equations from Boltzmann equation
[AD-758275] 14 p1697 N73-23768
Direct current conductivity of cesium plasma in magnetic field
22 p2702 N73-31645

**PLASMA CONFINEMENT**
U PLASMA CONTROL

**PLASMA CONTROL**
Dynamic stabilization of plasma confinement and fluid systems
[LRP-53/72] 01 p0085 N73-10701
Influence of axial current on stability of plasma column
[LRP-52/72] 01 p0085 N73-10702
Confinement of electron-free plasmas in quadrupole RF electric trap
[NASA-TM-X-65719] 01 p0085 N73-10703
Anomalous resistivity in turbulent plasma confined in strong magnetic field considering low and high electric field regimes
02 p0216 N73-11748
Influence of Coulomb collisions on plasma ion relaxation in confined circular stabilized magnetic mirror
[EUR-CEA-FC-640] 03 p0341 N73-12783
Laser optics and diagnostic methods for vaporization and heating of confined spherical overdense plasmas
[AD-748260] 04 p0456 N73-13720
Feedback stabilization of theta pinch plasma column by optical signal processor
[LA-DC-72-707] 05 p0584 N73-14750
Behavior of plasma column in high voltage theta pinch with and without magnetic mirrors
[LA-DC-72-703] 05 p0584 N73-14751
Plasma confinement, plasma dynamics, and turbulent heating
[ORO-3458-34] 06 p0704 N73-15738
Research on microinstabilities of finite mirror-confined plasmas
[COO-2168-3] 06 p0704 N73-15747
Microwave measurements of magnetic field local shearing in confined plasma
[EUR-CEA-FC-632] 06 p0705 N73-15749
Observation of nonlinear waves near lower hybrid resonance frequency
[CONF-720804-3] 07 p0756 N73-16137
Nonlinear wave interaction in plasma column
[NASA-CR-130350] 07 p0825 N73-16686
Acceleration and compression parameters in plasma focus
[LA-TR-72-24] 07 p0826 N73-16694
Hot electron plasma control in superconducting toroids
[UCRL-73806] 07 p0826 N73-16699
Scyllac research experiments
[LA-DC-72-896] 07 p0827 N73-16702
Plasma flow effects on axisymmetric equilibria in toroidal geometry
[IPP-6/107] 07 p0828 N73-16708
Research on impermeable plasmas in poloidal magnetic fields for nuclear fusion reactors
[TRITA-EPP-72-21] 07 p0828 N73-16714
Design of feedback geometry for control of rotating plasma confined in magnetic mirror device
[AD-751341] 07 p0830 N73-16728
Circuits for pulse generation in magnetic plasma pinch
[AD-751250] 07 p0830 N73-16732
Containment of deuterium plasma in magnetic mirror well
[UCRL-74087] 08 p0949 N73-17769
Solar wind propagation in low pressure gas and plasma containment in magnetic fields
[AD-753087] 09 p1072 N73-18750
Application of superconducting magnetics for plasma physics experiments and as component for future thermonuclear reactors
10 p1108 N73-19033
Low frequency instabilities in plasma confined by magnetic mirror system
[AD-754004] 10 p1197 N73-19743
Comparison of hot electron distribution between two magnetically confined plasmas
12 p1431 N73-21599
Parallel magnetic multipole confinement of magnetic field-free plasma
12 p1432 N73-21603
Synchrotron radiation from magnetically confined hot electron plasma
12 p1432 N73-21605
Magnetohydrodynamic equations for heavy ion plasma confined in magnetic field and ion source discharges
[LYCEN-7208] 12 p1435 N73-21625
Properties of dense helical microwave plasma source in intense magnetic field
[CEA-EUR-FC-652] 12 p1435 N73-21626
HCN laser study of coherent scattering from waves in plasma confinement and heating experiments
[IPP-4/39] 12 p1435 N73-21631
Passive circuit grids for stabilization of magnetohydrodynamic generator plasma
[TH-72-E-31] 14 p1695 N73-23757
Potential and electron density studies in inertial electrostatic plasma confinement devices
[AD-757228] 14 p1696 N73-23763
Interchange stability of anisotropic guiding-center plasma in axisymmetric magnetic trap
[ORNL-TM-4077] 15 p1817 N73-24728
Vlasov equation for studying anisotropy produced instabilities in confined hot electron plasma
[EUR-CEA-FC-664] 15 p1818 N73-24736
Equilibrium pattern and control of plasma current distribution in diffuse pinch configuration
[IPPJ-158] 16 p1949 N73-25770
Development of self-energized plasma compressor for compressing plasma discharged from coaxial plasma generator
[NASA-CASE-MFS-22145-1] 17 p2067 N73-26721
Polarization of bremsstrahlung from electron-ion collisions by magnetically confined electrons
[ORNL-TM-4103] 17 p2067 N73-26726
Microwave measurements of electron density profiles in mirror contained plasma
[UCRL-51348] 19 p2323 N73-28685
Ion heating and thermonuclear power production characteristics and performance of superconducting bumpy-torus magnetic facility
[NASA-TN-D-7353] 19 p2324 N73-28693
Finite element analysis on cylindrical and toroidal plasma stabilities contained in magnetic field
[JAERI-M-4890] 19 p2324 N73-28700
Superconducting magnetic field trapping device for producing magnetic field in air
[NASA-CASE-XNP-01185] 19 p2326 N73-28710
Maintenance of Tokamak equilibrium by external currents and equilibrium in high pressure Tokamak plasma
[IPPJ-161] 20 p2458 N73-29754
Magnetostatic trap generation for control of cylindrical magnetic domain
20 p2461 N73-29778
Inductive plasma pulverization for protecting mechanical and electronic components
[CEA-CONF-2111] 21 p2583 N73-30701
Optimal control of parabolic systems with boundary conditions involving time delays and with application to plasma confinement
[AD-763738] 21 p2584 N73-30704
Particle insertion and hot plasma containment in stellarator with superconductors
[NASA-TT-F-15111] 22 p2703 N73-31648
Thermonuclear research on Tokamaks, plasma control, and plasma diagnostics
[JAERI-M-5029] 24 p2963 N73-33676
Analysis of spatiotemporal evolution of plasma confined in toroidal magnetic enclosure
[FRNC-TH-371] 24 p2964 N73-33689
Fokker-Planck study of Coulomb collisions in plasma confined by mirror magnetic configurations
[EUR-CEA-FC-687] 24 p2964 N73-33691
Theoretical analysis of laser-created plasmas confined by external magnetic field
[CEA-R-4410] 24 p2965 N73-33695
Plasma transport properties and confinement
[COO-2168-5] 24 p2965 N73-33696
Computerized simulation of electrostatic inertial plasma confinement device
[AD-763826] 24 p2966 N73-33703

**PLASMA CYLINDERS**
Magnetohydrodynamic theory of diurnal oscillations of earth magnetic tail
09 p1029 N73-18395
Spectroscopic methods for temperature measurement in plasmas with self absorption noting methods for plasma column radial temperature distribution
[BMBW-FBK-72-22] 09 p1071 N73-18737
Oscillations of earths magnetic tail studied from model of plasma cylinder with free boundary
14 p1703 N73-23820
Equilibrium characteristics and Kruskal-Shafranov limit of hollow cylindrical plasma pinch in toroidal magnetic field
[LGI/R-72/9/E] 17 p2067 N73-26723
Electromagnetic wave propagation in inhomogeneous plasmas exemplified by cavity resonators and positive column in magnetic field
[IPF-72-8] 17 p2069 N73-26742
Equilibrium of weakly toroidal plasma column surrounded by Tokamak field
[REPT-72-71] 17 p2069 N73-26744
Characteristic oscilations of cylindrical plasma
[IPPJ-133] 19 p2324 N73-28692
Low frequency instabilities and plasma turbulence including steady state and time dependent characteristics of positive column and hollow cathode discharge
[NASA-CR-135669] 23 p2822 N73-32562
Nonlinear diffusion of pulsed magnetic fields in planar and cylindrical plasmas
[LA-5132-MS] 24 p2963 N73-33681

**PLASMA DECAY**

Measurement of effective collision frequency in RF heating through decay instability in Q device plasma
[CONF-720705-2] 07 p0755 N73-16136

Fourier analysis of plasma deformation and feedback in stabilized rectilinear helicoid with pinch mechanism
[LRP-58/72] 10 p1196 N73-19728

OSO-4 solar flare X ray spectrum analysis on plasma cooling mechanisms
19 p2336 N73-28794

Plasma wave decay effects on solar type 3 radio burst profiles at low frequencies
19 p2339 N73-28815

**PLASMA DENSITY**

Electronic and thermodynamic properties of dense plasma interacting with metallic and nonmetallic materials
[CEA-R-4268] 01 p0085 N73-10705

Analysis procedure for radar observations
01 p0102 N73-10835

Laser optics and diagnostic methods for vaporization and heating of confined spherical overdense plasmas
[AD-748260] 04 p0456 N73-13720

Spectroscopic measurements on plasma composition in Tokamac-type facility
[JAERI-M-4596] 06 p0705 N73-15752

Double probe measurements of electromagnetic noise spectra due to thermodynamic plasma density fluctuations for plasma diagnostics
06 p0706 N73-15758

Linear and nonlinear plasma response to impulse electric field
10 p1195 N73-19725

Density fluctuations of stellarator by correlation procedure
[AEC-TR-7376] 11 p1267 N73-20282

Properties of dense helical microwave plasma source in intense magnetic field
[CEA-EUR-FC-652] 12 p1435 N73-21626

Ion-ion hybrid resonance dispersion relation
[IPPJ-157] 16 p1949 N73-25774

Laser interferometry for plasma diagnostic measurements
[INR-1442] 17 p2040 N73-26506

Microwave measurements of electron density profiles in mirror contained plasma
[UCRL-51348] 19 p2323 N73-28685

Correlation of potential and density fluctuations of plasma resulting from rotational instability of hot cathode Penning discharge
[NASA-TT-F-13026] 20 p2458 N73-29751

Dense plasma focus using CO2 laser scattering and infrared bremsstrahlung emission
[COO-2233-2] 22 p2703 N73-31652

Radial collapse of dense plasma spindle focus in z-pinch geometry
[LA-5178-MS] 22 p2704 N73-31656

Tantalum surface bounding of helium discharge plasma considering resonant ion neutralization
[AD-753520] 22 p2706 N73-31670

Doppler study of plasma column changes at solar elongation in Mariner 9 tracking path
23 p2842 N73-32715

Holographic interferometric measurement of plasma density in electron beam diode
[SLA-73-5483] 24 p2927 N73-33376

Time resolved spectroscopic measurements of near infrared and X ray emission from high density plasma in vacuum spark
24 p2961 N73-33661

**PLASMA DIAGNOSTICS**

Analysis of conditions created by intense laser beam focused on plasma with application as plasma diagnostic technique
[DREV-R-676/72] 02 p0181 N73-11463

Plasma parameters in carbon dioxide laser discharge
[DREV-TN-2025/72] 02 p0181 N73-11464

Statistical mechanics of 2 and 3 dimensional plasmas in strong dc magnetic field
[NASA-CR-129177] 02 p0215 N73-11741

Laser selective excitation of doublet transition in atoms of pure potassium plasma
[AD-745964] 02 p0216 N73-11750

Influence of intense laser radiation on plasma generation of large magnetic fields
[AD-746098] 02 p0216 N73-11752

Ionized continuum flows and collisionless plasmas in electric boundary layers on flat plates and cylindrical bodies
[AD-746094] 02 p0217 N73-11753

Multiple-probe reflectometer technique for diagnosing structure of boundary layer plasma formed on reentry vehicles
[AD-747038] 02 p0217 N73-11760

Pulsed ionization chamber for plasma diagnostics, and applications to MHD electrical power generation from gas cooled reactors
[AD-747681] 03 p0343 N73-12800

Measurement of plasma ultraviolet radiation for determining collisional momentum transfer cross sections in accelerator
[AD-747339] 03 p0344 N73-12802

Analysis of linear and nonlinear properties of density gradient driven drift waves instability using single-ended Q-machine
[AD-747852] 03 p0344 N73-12803

Computer codes for determining X ray filter/sound state detector response curves
[AD-748465] 03 p0344 N73-12804

Large amplitude wave study
[COO-3004-3] 04 p0454 N73-13711

Error analysis of line intensity measurements on plasmas with electron temperature fluctuations
[AD-748474] 04 p0456 N73-13722

Microwave probe studies on chemical additives behavior in nitrogen oxygen plasma
[AD-748469] 04 p0456 N73-13724

Operating characteristics of far infrared spectroscopic system for analyzing plasma diagnostics
[AD-748280] 04 p0456 N73-13726

Fluid and plasma dynamics research
[AD-749287] 04 p0457 N73-13729

Electric field amplitude within superhigh frequency wave absorption by plasma using Stark effect analysis
[FTI-413] 06 p0705 N73-15750

Spectroscopic measurements on plasma composition in Tokamac-type facility
[JAERI-M-4596] 06 p0705 N73-15752

Plasma diagnostics by means of collision dominated spherical electrostatic probes including mathematical model
[DLR-FB-71-41] 06 p0705 N73-15756

Computerized simulation of electromagnetic wave coupling modes in plasma diagnostics
[AD-750138] 06 p0706 N73-15763

Electrostatic probes in spacecraft flow field for measuring plasma sheath density during atmospheric reentry
07 p0825 N73-16683

Principles of magnetohydrodynamic energy generation to include flows in magnetohydrodynamic generator, physical processes, diagnostics, and required equipment - Part 1
[JPRS-57940-1-PT-1] 07 p0825 N73-16687

Principles of magnetohydrodynamic energy generation to include open and closed cycle magnetohydrodynamic generators, liquid-metal plants, and materials for generators -Part 2
[JPRS-57940-2-PT-2] 07 p0825 N73-16688

Equilibrium distribution used for analysis of one component, azimuthally symmetric magnetoplasma
[AD-751255] 07 p0830 N73-16730

Microwave scattering from plasma turbulence
[AD-752149] 08 p0886 N73-17175

X ray flash source for laser plasma diagnostics
[AD-752823] 08 p0894 N73-17237

Slowly changing, large magnetic induction in plasma core of rotating magnetic field pinch
[LRP-56/72] 08 p0947 N73-17756

Limitations and applications of electrostatic probes with floating potential for measurements of plasmas with low frequency oscillations
08 p0947 N73-17757

Analysis of wave propagation and amplification properties of molecular electronic plasma to show energy transfer effects
[PSU-IRL-SCI-403] 08 p0948 N73-17759

Investigation of electric pinch, and development of methods for producing cylindrically symmetric plasma
[NASA-CR-130533] 08 p0949 N73-17770

X ray bandpass filters for hot transient plasma diagnostics
[AD-752544] 08 p0950 N73-17775

Diagnostic spectroscopy of plasmas produced in molecular gases
[AD-751938] 08 p0950 N73-17776

Impedance probe and counter-voltage analyzer used on Aeros satellite for plasma diagnostics experiment
[DGLR-PAPER-72-070] 09 p1036 N73-18455

Influence of shock-producing piston on structure of electrostatic ion acoustic laminar shocks
[NASA-CR-130994] 09 p1069 N73-18724

Grid excitation and digitized probe measurements for oscilloscopic display of phase space diagram distribution functions of plasma waves
[IPPJ-147] 09 p1070 N73-18732

Double electrostatic probe for measuring plasma density, temperature, and velocity
[NASA-TN-D-7223] 09 p1070 N73-18733

Mathematical model for dense rotating plasma with centrifugal expansion instability at high beta values
[TRITA-EPP-72-28] 09 p1071 N73-18740

Probe measurements of electron energy in glow discharge of nitrogen plasma and air
[AD-752871] 09 p1071 N73-18744

Papers presented at conference on physics of low temperature plasma
[AD-753061] 09 p1072 N73-18745

Frequency spectrum of laser scattering from dense plasma focus
[AD-753705] 09 p1073 N73-18754

Characteristics of carbon dioxide laser for use as interferometric and light scattering plasma diagnostic radiation source
[LRP-54/72] 10 p1168 N73-19504

Dispersion relations and drift instability in ionized magnetoplasma
[AD-754005] 10 p1198 N73-19744

Plasma interactions with gas flow and magnetic fields
[AD-754018] 10 p1198 N73-19748

HCN laser interferometer for electron density measurements on helium plasma
[NP-19595] 11 p1328 N73-20774

High temperature plasma diagnostics and properties
[AD-754021] 11 p1328 N73-20777

Laser generation of plasma and plasma diagnostics, and laser fusion research
[UCRL-50021-72-1] 12 p1410 N73-21430

Interpretation of signals from cylindrical Langmuir probe for diagnosis of properties of streaming laser-produced plasma
12 p1431 N73-21600

Steady state hot-ion plasma produced by crossed electric and magnetic fields
[NASA-TM-X-2783] 12 p1433 N73-21613

Interaction of plasma streams with stationary, axisymmetric magnetic fields
[AEC-TR-7354] 12 p1434 N73-21620

Experiments on magnetoacoustic oscillations in rotating hydrogen and deuterium plasmas with superimposed high frequency heating
[TRITA-EPP-72-34] 12 p1436 N73-21635

Plasma diagnostic visualization with pulsed carbon dioxide TEA laser and liquid crystal infrared detector, noting spark discharges
[ISL-18/72] 13 p1563 N73-22668

Plasma enhancement and diagnostic possibilities of tunable laser excitation
[AD-755373] 13 p1564 N73-22672

Properties of plasma stream flowing from pulsed magnetoplasmadynamic arc jet
[ISAS-490] 14 p1695 N73-23756

Potential and electron density studies in inertial electrostatic plasma confinement devices
[AD-757228] 14 p1696 N73-23763

Experimental analysis of high Beta, hot, dense plasma
[COO-2233-1] 15 p1817 N73-24732

Plasma diagnostics with infrared schlieren and interferometric techniques using TEA-CO2 laser, exemplified by electric spark transient response
[ISL-19/72] 16 p1950 N73-25779

Impulsive plasma accelerator study of plasma acceleration by magnetic field annihilation
[AD-758880] 16 p1950 N73-25780

User manual for one-dimensional plasma diagnostics computer program
[AD-758809] 16 p1950 N73-25784

Infrared image converter, based on temperature sensitive liquid-solid interface, using GE-AU IR detector
[IPF-72-6] 17 p2033 N73-26457

High power CO2 tea laser for use as plasma diagnostic radiation source
[LRP-54/72] 17 p2040 N73-26505

CO2 laser-plasma heating and diagnostic scattering experiments
[LA-5167-MS] 17 p2040 N73-26509

Atomic and gas dynamical processes in astrophysical plasmas
17 p2066 N73-26719

High quasi-stationary magnetic field production with capacitor-fed magnetic field coil
[IPF-72-7] 17 p2069 N73-26741

Spectral absorption and emission coefficient calculations for argon plasmas
[AD-759571] 17 p2070 N73-26748

Research in plasma physics and laser diagnostics
[NP-19681] 18 p2183 N73-27625

Properties of arc disharges heated by induction and direct current electromagnetic field
[AD-760808] 18 p2183 N73-27629

Microwave probe for observing parametrically excited ion acoustic wave oscillations in argon plasma
[AD-762380] 19 p2325 N73-28705

Collisionless shock waves in argon plasma pinch discharge
[AD-762426] 19 p2325 N73-28707

Development and characteristics of test equipment for determining temperature and electron density of plasma based on derivation of absorption coefficients
[NASA-CASE-ARC-10598-1] 20 p2458 N73-29750

Design and evaluation of ion beam probe plasma diagnostic system
[COO-2229-2] 21 p2583 N73-30700

Development of optical diagnostic techniques to determine plasma refractive index using interferometers to produce space or time resolved density data
[AD-763802] 21 p2584 N73-30706

Carbon dioxide laser scattering by Alfvenic disturbance in helium plasma
23 p2822 N73-32560

Liquid crystal infrared detectors for plasma diagnostics and flow visualization using CO2 laser impulses
[BMVG-FBWT-73-16] 23 p2823 N73-32564

Spectroscopic analysis of plasma diagnostics
[AD-765221] 23 p2823 N73-32567

Thomson scattering diagnosis on pulsed xenon arc plasma flow
[NASA-TM-X-71443] 24 p2962 N73-33669
Thermonuclear research on Tokamaks, plasma control, and plasma diagnostics
[JAERI-M-5029] 24 p2963 N73-33676
Behavior of plasma in Harmonica-Two torus
[EUR-CEA-FC-660] 24 p2964 N73-33692
Feasibility of RF heating for high temperature turbulent plasma production noting diagnostic techniques and CO2 laser scattering
[LRP-64/73] 24 p2966 N73-33702
Digital spectrum analysis for turbulent plasma diagnostics
[AD-765549] 24 p2966 N73-33704

**PLASMA DIFFUSION**
Ion acoustic and ion cyclotron turbulence effects in plasma resistivity, diffusion, and heating
[NASA-CR-130177] 03 p0340 N73-12776
Anomalous radial plasma losses in Q machine with mirror magnetic fields
[UCRL-51207] 03 p0343 N73-12794
Quasi-linear equations for stochastic plasma diffusion processes of trapped particles in magnetosphere using two selected plasma resonances
[TRITA-EPP-73-09] 21 p2593 N73-30777
Laser generation of fusion plasmas
[UCRL-74628] 24 p2964 N73-33685

**PLASMA DIODES**
Transport characteristics for calculating plasma diode design parameters
[TEE-3056-1] 03 p0274 N73-12221

**PLASMA DISCHARGES**
U PLASMA JETS

**PLASMA DISPERSION**
U PLASMA DIFFUSION

**PLASMA DYNAMICS**
Variations of interplanetary scintillation index with wavelength in accordance with smooth, power law spectrum of plasma fluctuations
01 p0097 N73-10802
Development of porous electrode materials for plasma generators and effects of blowing protective gases through plasma
[AD-747369] 03 p0255 N73-12066
Effect of variable magnetic field on emission of helium-neon laser and resulting parameters of discharge plasma
[AD-747443] 03 p0311 N73-12542
Development of test equipment and procedures to simulate thermal environment and fuel region of small models of nuclear lightbulb engine configurations
[NASA-CR-129299] 03 p0330 N73-12692
Development and evaluation of test equipment for high pressure radio frequency plasma experiments and in-reactor tests of nuclear lightbulb engine
[NASA-CR-129501] 03 p0330 N73-12694
Ion acoustic and ion cyclotron turbulence effects in plasma resistivity, diffusion, and heating
[NASA-CR-130177] 03 p0340 N73-12776
Technique for determining influence of axial magnetic field on holdup of argon in coaxially fed argon-helium plasma generated by radio frequency induction
[ORNL-TM-3700] 03 p0341 N73-12779
Dynamics of laser triggered spark discharge channel with nanosecond pulse formation
[AD-747510] 03 p0343 N73-12799
Design of ionospheric plasma simulator for analyzing and modeling high altitude plasma phenomena
[AD-748311] 04 p0417 N73-13401
Analysis of laser light scattered from marginally stable hydrogen plasma
[INR-P-1377] 04 p0429 N73-13491
Resonance effects anomalous electromagnetic wave propagation in plasma
[NASA-CR-129673] 04 p0454 N73-13704
Computerized simulation of electron-electron collisional effects in plasma
[COO-3086-14] 04 p0454 N73-13709
Computerized simulation of nonlinear and turbulent plasma behavior
[AD-750715] 06 p0707 N73-15766
Isotropic models for determining effect of velocity distribution on electron temperature in ionospheric plasma
[NASA-TM-X-66157] 07 p0791 N73-16433
Analysis of plasmas produced by high power laser beam irradiation of beryllium, carbon, and polyethylene targets
[IPPJ-142] 08 p0947 N73-17754
Analysis of electron cyclotron heating characteristics and generation of hot electron plasma in magnetic mirror trap by microwaves
[IPPJ-140] 08 p0947 N73-17755
Analysis of wave propagation and amplification properties of molecular electronic plasma to show energy transfer effects
[PSU-IRL-SCI-403] 08 p0948 N73-17759
Linearized theory for MPD duct flows with exterior magnetic fields and Hall effect
[DLR-FB-72-67] 09 p1069 N73-18726
Computerized simulation of inhomogeneous plasma response to impulse electric field excitation
[AD-753104] 09 p1072 N73-18746
Analysis of performance of pulsed coaxial guns based on snowplow model allowing for variable initial mass-loading distribution
10 p1111 N73-19057
Characteristics of carbon dioxide laser for use as interferometric and light scattering plasma diagnostic radiation source
[LRP-54/72] 10 p1168 N73-19504
Linear and nonlinear plasma response to impulse electric field
10 p1195 N73-19725
Digital computer simulation of one-dimensional plasma behavior in plasma betatron
10 p1195 N73-19726
Return current induced in bounded plasma by electron beam injection
[SC-RR-72-0669] 10 p1196 N73-19729
Literature on thermodynamics of electrostatic waves and ionized plasmas
[AD-754014] 10 p1198 N73-19745
Theoretical research on plasma instabilities
[AD-754019] 10 p1198 N73-19747
Diamagnetic measurements of electrically driven shock tube to determine general conditions of moving plasma in longitudinal magnetic field interactions
[AREAEE-145] 12 p1429 N73-21583
Development of viscous shock layer analysis to determine nonequilibrium flow distributions of plasma layer during reentry conditions
[NASA-CR-2232] 13 p1491 N73-22085
Plasma cell array for capacitor-coupled shift register
[AD-758310] 14 p1639 N73-23285
Instabilities of homogeneous plasmas caused by particle velocity distributions
[AD-755688] 14 p1696 N73-23760
Steady state dynamics of compressible plasma flows across inhomogeneous magnetic fields in ducts with inclined walls
[AD-755944] 14 p1696 N73-23761
Research in plasma acceleration, hollow cathode physics, and plasma dynamics
[NASA-CR-131270] 15 p1817 N73-24725
Feasibility of potassium-cesium mixture for seeding magnetohydrodynamic combustion plasma
[PB-214314/7] 16 p1865 N73-25102
Mathematical model for turbulent flow in electric arc
[AD-759572] 16 p1950 N73-25781
Equations of motion for plasma drift, deformation, and diffusion in magnetic field
[AD-759742] 16 p1950 N73-25782
Development of self-energized plasma compressor for compressing plasma discharged from coaxial plasma generator
[NASA-CASE-MFS-22145-1] 17 p2067 N73-26721
Snowplow calculations of acceleration and compression in coaxial plasma accelerator with focusing equipment
[IFP-72-4] 17 p2069 N73-26740
Research progress in general physics, plasma dynamics, and communication sciences and engineering
[AD-759747] 17 p2099 N73-26983
Numerical analysis of stationary internal structure of plasma in homogeneous carbon dioxide laser discharge
[DREV-TN-2061/73] 18 p2157 N73-27430
Statistical mechanics for plasma calculations
18 p2182 N73-27619
Ionizing wave transport in streamer breakdown of gas
[JPRS-59474] 18 p2183 N73-27622
Plasma kinetic theory and plasma dynamics
[NASA-CR-132785] 18 p2183 N73-27623
Stabilization of ion acoustic waves by electron trapping
[AD-761174] 18 p2183 N73-27628
Literature abstracts for plasma instability research
[UNICP-SR95-PT-2] 19 p2324 N73-28696
Longitudinal electroacoustic wave attenuation in plasma
[AD-762272] 19 p2325 N73-28706
Energy transfer by fluctuations in plasma
20 p2457 N73-29743
Development of nonlinear stochastic equations for turbulent field with application to simple electron plasma
[AD-763438] 21 p2584 N73-30710
Development of test equipment for analyzing characteristics of plasma in gas stream of nitrogen and helium mixture
22 p2703 N73-31649
Snowplow effects and turbulence in expanding plasmas
[COO-3577-3] 22 p2704 N73-31654
Characteristics of radio frequency produced, magnetically confined hot electron plasma
24 p2962 N73-33668

**PLASMA ELECTRODES**
Plasma instability at initial stage of electrode plasma discharge in rarefied plasma
[AD-745458] 01 p0085 N73-10707
Computer analysis of tapered coaxial plasma gun electrodes
[AD-747057] 03 p0343 N73-12797
Design and performance of carbon dioxide laser amplifier with double discharge electrode geometry
[DREV-TN-2022/72] 10 p1134 N73-19240

**PLASMA ENGINES**
Design and tests of advanced colloid thruster system components
[AD-749961] 05 p0591 N73-14801
Procedures for reducing loss mechanism in plasma jet engine
[AD-759272] 16 p1958 N73-25839

**PLASMA FLOW**
U MAGNETOHYDRODYNAMIC FLOW

**PLASMA FLUX MEASUREMENTS**
Microwave signal interaction with plasma medium
[AD-746677] 02 p0144 N73-11164
Development and characteristics of test equipment for determining temperature and electron density of plasma based on derivation of absorption coefficients
[NASA-CASE-ARC-10598-1] 20 p2458 N73-29750
Characteristics of swept frequency impedance probe installed in unmanned satellite to measure impedance of space plasma
[ISAS-495-VOL-38-NO-6] 22 p2672 N73-31403

**PLASMA FREQUENCIES**
Helmholtz equation for solving electromagnetic wave functions of parabolic plasma density profiles
[AD-751669] 07 p0757 N73-16151
Ordinary wave penetration of infinite magnetoplasma slabs
[IPPJ-154] 16 p1949 N73-25772
Linear plasma wave conversion at lower hybrid resonance
[MATT-979] 22 p2704 N73-31657

**PLASMA GENERATION**
U PLASMA GENERATORS

**PLASMA GENERATORS**
NT DUOPLASMATRONS
NT PLASMA GUNS
NT SCYLLA
NT TOKAMAK FUSION REACTORS
Measurement of electron density in carbon plasma created by heating solid target with laser radiation
[AD-746221] 01 p0086 N73-10715
Influence of intense laser radiation on plasma generation of large magnetic fields
[AD-746098] 02 p0216 N73-11752
Development of porous electrode materials for plasma generators and effects of blowing protective gases through plasma
[AD-747369] 03 p0255 N73-12066
Nonequilibrium plasma generation by strong shock waves produced in diaphragm shock tube
[BMBW-FBK-72-5] 04 p0405 N73-13301
Experimental determination of electron density in absorbing layer of laser produced plasmas
[JUL-820-PP] 04 p0454 N73-13706
Plasma production using gas stream kinetic energy in magnetic field
[DLR-FB-71-43] 04 p0455 N73-13714
Laser optics and diagnostic methods for vaporization and heating of confined spherical overdense plasmas
[AD-748260] 04 p0456 N73-13720
Absorption of laser radiation by laser produced plasma
[AD-749043] 04 p0457 N73-13727
Free electron production by Raman scattering in initial phase of laser produced plasma
[IPP-4/40] 05 p0583 N73-14745
Spreading of charged particles from point source in magnetic dipole field
[AD-750703] 06 p0703 N73-15732
Apparatus and program for turbulent torus experiment
[ORO-4087-8] 06 p0704 N73-15737
Plasma generation within magnetic containment field by laser irradiation of solid particle
[COO-3547-2] 06 p0704 N73-15740
Energy variation principle for specific inductance geometry in stable toroidal plasma generation
[NYO-1480-182] 06 p0704 N73-15741
Variational analysis of laser induced gas breakdown employing simplified diffusion models for plasma generation
[AD-750874] 06 p0707 N73-15767
LLL studies of various lasers and analysis of laser produced plasmas
[UCRL-50022-1] 07 p0806 N73-16541
Ion energy distribution function measurements parallel and perpendicular to magnetic Penning discharge field
[NASA-TN-D-7167] 07 p0825 N73-16690
Diagram solutions of circuits forming high frequency electromagnetic fields in plasma devices
[AEC-TR-7326] 07 p0826 N73-16696
Computer modeling of space charge flow in electrogasdynamic generator
[AD-751632] 07 p0829 N73-16720
Gas ionization and plasma generation by explosive shock wave
[AD-751152] 07 p0829 N73-16725
Analysis of plasmas produced by high power laser beam irradiation of beryllium, carbon, and polyethylene targets
[IPPJ-142] 08 p0947 N73-17754

Analysis of electron cyclotron heating characteristics and generation of hot electron plasma in magnetic mirror trap by microwaves
[IPPJ-140] 08 p0947 N73-17755
Laser generation of heavy ion plasma
[CEA-CONF-2022] 08 p0948 N73-17761
Equilibrium plasma produced by theta pinch gun firing into magnetic field
[AD-752498] 08 p0949 N73-17772
Ionization hydrodynamics of laser produced plasma
[AD-751880] 08 p0949 N73-17773
Performance of ion cyclotron plasma generator using radio frequency coil for plasma control
[NASA-TN-D-7187] 09 p1069 N73-18725
Application of superconducting magnetics for plasma physics experiments and as component for future thermonuclear reactors
10 p1108 N73-19033
Fast particle injectors for plasma production in thermonuclear installations
[AEC-TR-7389] 11 p1323 N73-20738
Laser generation of plasma and plasma diagnostics, and laser fusion research
[UCRL-50021-72-1] 12 p1410 N73-21430
Laser production of plasmas and injection of pulsed ion beams
[LYCEN-7253] 12 p1411 N73-21431
Theoretical and experimental studies on microwave transmission through hypersonic air plasma generated about blunt wedge
[SC-CR-72-3164] 12 p1434 N73-21621
Simulation of satellite motion in ionospheric plasma using low energy and high current ion source in vacuum chambers
[ONERA-NT-202] 15 p1762 N73-24280
Performance tests of copper vapor laser and analysis of relaxation of metastable lower levels
15 p1794 N73-24544
Neodymium-glass laser system production of plasmas for research on controlled thermonuclear fusion
15 p1794 N73-24545
Ionizational relaxation in shock-heated mercury vapor
15 p1816 N73-24719
Plasma device for studying ion acoustic solitons
[IPPJ-149] 15 p1816 N73-24723
Production and confinement of hot plasma and electron thermalization in superconducting ring device
[UCRL-74337] 16 p1950 N73-25777
High energy plasma generation by electromagnetic implosion of thin metal foil cylinder
[AD-759826] 16 p1951 N73-25788
Development of self-energized plasma compressor for compressing plasma discharged from coaxial plasma generator
[NASA-CASE-MFS-22145-1] 17 p2067 N73-26721
Properties of laser generated plasma trapped in stellarator
[NP-19656] 17 p2067 N73-26725
Static characteristics of electrohydrodynamic inverted converters
[AD-760966] 18 p2183 N73-27630
Research on lasers and laser produced plasmas
[UCRL-50021-71-REV-1] 19 p2307 N73-28557
Structure of collisionless ion acoustic shocks in plasma device
[NASA-CR-135490] 22 p2703 N73-31651
Characteristics of radio frequency produced, magnetically confined hot electron plasma
24 p2962 N73-33668
Digital simulation of plasma generation in Tokamak device
[EUR-CEA-FC-683] 24 p2963 N73-33677
Analytical solutions to plasma generation near neutral point in magnetic field
[EUR-CEA-FC-685] 24 p2963 N73-33678
Bibliography on plasma generation by lasers
[LS-255] 24 p2964 N73-33688
Laser beam fusion and plasma generation on pellet
[UCID-16222] 24 p2965 N73-33697

**PLASMA GUNS**

Approximation of behavior of matter in plasma focus
[UCRL-73932] 06 p0704 N73-15746
Equilibrium plasma produced by theta pinch gun firing into magnetic field
[AD-752498] 08 p0949 N73-17772
Analysis of performance of pulsed coaxial guns based on snowplow model allowing for variable initial mass-loading distribution
10 p1111 N73-19057
Study of ionizing wave in coaxial plasma guns to explain plasma-neutral gas interaction
[TRITA-EPP-72-31] 16 p1950 N73-25778

**PLASMA HEATING**

Estimation of radio frequency power required to induce direct current in strong magnetic field of thermonuclear fusion device
[IPPJ-135] 02 p0216 N73-11746
Computer simulation of ion heating by pulsed microwaves
[CONF-720705-1] 03 p0336 N73-12739
Ion acoustic and ion cyclotron turbulence effects in plasma resistivity, diffusion, and heating
[NASA-CR-130177] 03 p0340 N73-12776
Theoretical and experimental determination of harmonic ion cyclotron wave propagation in hot, bounded plasma
[ORO-3778-7] 03 p0342 N73-12786
Higher-temperature limit for turbulent heating of plasma by cross-field current
[ORO-4211-4] 03 p0342 N73-12787
Carbon dioxide lasers used for heating of dense arc plasmas to several million degrees
[UCLA-34-P-157-X-3] 03 p0342 N73-12788
Thermal decay of magnetically confined fully ionized arc plasma heated with pulsed CO2 laser energy
[UCLA-34-P-157-X-4] 03 p0342 N73-12789
Nonhomogeneity effects of magnetic field on plasma heating by electron beam in mirror trap of probkotron type
[SFTI-1] 04 p0454 N73-13710
Laser heating of dense plasma through excitation of parametric instabilities
[AD-749970] 05 p0584 N73-14756
Plasma confinement, plasma dynamics, and turbulent heating
[ORO-3458-34] 06 p0704 N73-15738
Theoretical model for laser flux absorption by plasma instability mechanism
[LA-4984] 06 p0704 N73-15739
Requirements for heating large Tokamak device with energetic neutral beams
[CONF-720804-2] 06 p0704 N73-15743
High energy electrons and surface expansion in plasma targets heated by electromagnetic radiation
[LA-4986] 06 p0704 N73-15745
High frequency plasma heating in toroidal traps
[NP-19379] 06 p0705 N73-15753
Plasma heating by nonthermal process in linear pinch device
[AD-749688] 06 p0706 N73-15762
Radio frequency electron drift velocity and parametric instability in plasma heating
[CONF-720705-4] 07 p0756 N73-16138
High frequency and pulsed electron discharge heating of turbulent skin layer in plasma
[AEC-TR-7329] 07 p0826 N73-16695
Relation of gas kinetic particle pressure and discharge field in plasma heating by pulsed longitudinal current
[AEC-TR-7330] 07 p0826 N73-16697
Hot electron plasma control in superconducting toroids
[UCRL-73806] 07 p0826 N73-16699
Shock heating of plasmas based on superposed superconducting circuits and magnetic energy storage
[TRITA-EPP-72-29] 07 p0829 N73-16717
Kinetic energy and X ray conversion in plasma heated by laser
[AD-751048] 07 p0830 N73-16733
High power radio frequency ion heating effects on harmonics of ion cyclotron radiation
[ORO-3871-7] 08 p0889 N73-17197
Plasma heating by turbulent pulsation of electric field
[NASA-TT-F-14673] 08 p0947 N73-17758
Wave propagation in parallel-plate metallic waveguide as eigenvalue problem using complete cold-plasma dielectric tensor
[IPP-4/37] 08 p0948 N73-17764
Dynamic model for calculating radio frequency absorption in perpendicular ion cyclotron resonance heating of hydrogen deuterium plasma
[IPPJ-146] 09 p1070 N73-18730
Computerized simulation of inhomogeneous plasma response to impulse electric field excitation
[AD-753104] 09 p1072 N73-18746
Possible uses of pulsed lasers for controlled fusion, plasma heating, and creation of controlled nuclear microexplosions
[UCRL-73931] 10 p1186 N73-19654
Laser heating of pinched plasma in cavity
[LA-5010] 10 p1196 N73-19730
Mechanism of plasma heating by large amplitude oscillating electric field
[UCB-34-P-128-X-2] 10 p1196 N73-19731
Superhigh frequency plasma heating in toroidal magnetic trap
[AEC-TR-7360] 10 p1197 N73-19741
Steady state hot-ion plasma produced by crossed electric and magnetic fields
[NASA-TM-X-2783] 12 p1433 N73-21613
Lower hybrid frequency damping of longitudinal plasma oscillations and plasma heating
[EUR-CEA-FC-657] 12 p1433 N73-21614
High frequency excitation and instability in plasma heating
[CONF-720705-5] 12 p1434 N73-21617
HCN laser study of coherent scattering from waves in plasma confinement and heating experiments
[IPP-4/39] 12 p1435 N73-21631
Plasma heating by magnetic pulse in theta pinch and nuclear fusion
[AD-757043] 13 p1563 N73-22671
Magnetic field effects in cathode mechanism of electric arc initiation and travel between copper electrodes
[NLL-CE-TRANS-6108-[9022.09]]
15 p1755 N73-24226
Computerized simulation of plasma heating by oscillating electric field
[UCB-34-P-128-X-3] 15 p1817 N73-24731
Experimental determination of ion resonance heating of plasma
[COO-2194-1] 15 p1817 N73-24733
CO2 laser-plasma heating and diagnostic scattering experiments
[LA-5167-MS] 17 p2040 N73-26509
Damping and ion heating mechanisms in hydromagnetic waves around ion cyclotron frequency
[CEA-CONF-2138] 17 p2067 N73-26724
Resistivity and ion energy distribution in turbulent plasma heating
[COO-3165-3] 17 p2067 N73-26727
Radio frequency heating in THM-2 mirror machine
[LPS-95] 17 p2068 N73-26729
Turbulent heating of dense plasma by laser pulses
[JPRS-59027] 18 p2182 N73-27621
Heating and volume recombination effects on gas discharge column equilibrium
[AD-761492] 19 p2325 N73-28704
Electron beam heating of theta pinch plasma
[AD-762418] 19 p2326 N73-28708
Ion-ion hybrid resonance heating of D-T plasmas
[IPPJ-165] 20 p2459 N73-29758
Turbulent heating of plasmas by streaming instabilities
[AD-763777] 21 p2584 N73-30705
Microwave heating of electron plasma
[CONF-720705-8] 24 p2959 N73-33642
Development of plasmas for industrial applications as fusion torches
24 p2961 N73-33663
Laser generation of fusion plasmas
[UCRL-74628] 24 p2964 N73-33685
Heating of plasma confined in Tokamak by injecting fast helium atoms
[EUR-CEA-FC-682] 24 p2964 N73-33690
Plasma heating by electron beam
[COO-3165-4] 24 p2965 N73-33699
Neutral injection heating of plasma
[CONF-730705-3] 24 p2965 N73-33700

**PLASMA INSTABILITY**

U MAGNETOHYDRODYNAMIC STABILITY

**PLASMA INTERACTIONS**

NT PLASMA-ELECTROMAGNETIC INTERACTION

Electronic and thermodynamic properties of dense plasma interacting with metallic and nonmetallic materials
[CEA-R-4268] 01 p0085 N73-10705
Numerical simulation of one-dimensional collisionless plasma phenomena - users manual
[AD-745423] 01 p0085 N73-10706
Analysis of stream-stream interaction between slow solar wind and leading faster solar wind
01 p0097 N73-10800
Solar wind/interstellar gas interactions and Lyman alpha background radiation
[TRITA-EPP-72-03] 01 p0105 N73-10871
Solar wind plasma/interstellar hydrogen gas interactions
01 p0105 N73-10873
Effects of plasma-neutral gas interaction, finite resistivity, and viscosity on gravitational modes in permeable and impermeable plasmas
[TRITA-EPP-72-06] 04 p0455 N73-13713
Simulation of geomagnetic tail by plasma flux interaction with magnetic field of three dimensional dipole
[PR-113] 05 p0584 N73-14753
Effects of plasma-neutral gas interactions on equilibrium and stability of permeable Tokamak plasmas noting scaling conditions
[TRITA-EPP-72-26] 07 p0828 N73-16716
Macroscopic interaction between electromagnetic fields and lossy, anisotropic, compressible plasma
10 p1195 N73-19724
R-Om experimental setup for studying interaction of high frequency magnetic fields with plasma
[AEC-TR-7388] 10 p1197 N73-19737
Plasma interactions with gas flow and magnetic fields
[AD-754018] 10 p1198 N73-19748
Debye parameters of nonideal cesium plasma reached in shock tube
[AD-754015] 10 p1198 N73-19749
Laboratory simulation validity for analysis of spacecraft-plasma interactions
[PB-214611/6] 16 p1908 N73-25438
Study of ionizing wave in coaxial plasma guns to explain plasma-neutral gas interaction
[TRITA-EPP-72-31] 16 p1950 N73-25778
Model of stationary, adiabatic plasma flow in magnetosphere interacting with ionosphere
[TRITA-EPP-72-22-PT-1] 17 p2027 N73-26404
Hypersonic, shock tube generated, plasma flow interaction with strong magnetic fields, studied by inter-

ferometric, pressure, and light emission measurements
[IPF-72-2] 17 p2069 N73-26738
Plasma kinetic theory and plasma dynamics
[NASA-CR-132785] 18 p2183 N73-27623
Computerized simulation of belt pinch experiments including plasma external circuit interactions
[LRP-61/73] 18 p2183 N73-27626
Finite plasma stream adiabatic motion in inhomogeneous, transverse magnetic field
[TRITA-EPP-73-08] 19 p2325 N73-28702
Analysis of linear and nonlinear stage of ion-acoustic instability in low pressure discharge in helium
[AD-763590] 21 p2584 N73-30707
Quasi-linear equations for stochastic plasma diffusion processes of trapped particles in magnetosphere using two selected plasma resonances
[TRITA-EPP-73-09] 21 p2593 N73-30777
Perturbation technique for determining microwave interactions in magnetized waveguide plasma
22 p2702 N73-31643
Development of test equipment for analyzing characteristics of plasma in gas stream of nitrogen and helium mixture
22 p2703 N73-31649
Pressure distribution and stability of a magnetized plasma with neutral gas blanket
[TRITA-EPP-73-12] 22 p2705 N73-31664
Mathematical model for steady state wind-moon interaction
[COO-3577-2] 22 p2711 N73-31712
Electron beam energy loss in plasma
[LA-5269-MS] 24 p2964 N73-33684

**PLASMA JET WIND TUNNELS**

Thermodynamic flow characteristics of arc heater, convergent-divergent nozzle, and underexpanded jet in plasma wind tunnel
[NAL-TR-307] 15 p1766 N73-24308
Altitude test of rocket-borne mass spectrometer cooled by liquid helium in arc heated plasma jet wind tunnel
[DLR-MITT-72-23] 22 p2675 N73-31424

**PLASMA JETS**

Monte Carlo method applied to elementary processes in plasma arc discharge
[LYCEN-7205] 03 p0339 N73-12768
Two dimensional luminous plasma structure in hard core theta pinch at initial preheater breakdown
[AD-748587] 04 p0455 N73-13716
Analysis of nonequilibrium in excited levels of electric ARC heated potassium vapor injected into argon/helium gas flow passing through supersonic nozzle
[AD-750943] 05 p0585 N73-14759
Analysis of sinusoidally varying point induced charge potential in cold, homogeneous, and boundless magnetoplasma
[GRI/TP/109] 06 p0703 N73-15733
Electron and excitation temperature measurements in plasma jets stabilized by air and oxygen
[AD-752694] 09 p1071 N73-18743
Analysis of performance of pulsed coaxial guns based on snowplow model allowing for variable initial mass-loading distribution
10 p1111 N73-19057
Microwave discharge plasma in magnetic fields greater than cyclotron
[AEC-TR-7372] 10 p1196 N73-19735
Metallurgical reports on plasma jets, creep properties of nickel alloys, oxygen and nitrogen interactions with metals, and Mossbauer effect as applied to diffusion mechanisms
[JPRS-58508] 12 p1412 N73-21445
Kinetics and thermodynamics of oxygen conversion from gas to metal phase in tungsten and molybdenum
12 p1412 N73-21446
Nitrogen exchange between furnace atmosphere and argon plasma arc when melting pure iron
12 p1413 N73-21447
Compact sealed beam plasma arc illuminator with integral reflector
[AD-756968] 13 p1564 N73-22678
Properties of plasma stream flowing from pulsed magnetoplasmadynamic arc jet
[ISAS-490] 14 p1695 N73-23756
Numerical prediction of turbulent flow in argon cascade arc
[AD-759183] 16 p1950 N73-25783
Procedures for reducing loss mechanism in plasma jet engine
[AD-759272] 16 p1958 N73-25839
Channeling of supersonic free jet of plasma by axisymmetric magnetic field
20 p2457 N73-29744
Gas dynamic and Langmuir probe analysis of weakly ionized plasma jet
23 p2822 N73-32557

**PLASMA LAYERS**

NT PLASMA SHEATHS

Double layers and two-stream instability in solar flares, noting evacuating mechanism in solar atmosphere
[TRITA-EPP-73-05] 16 p1959 N73-25850
Development of test equipment for analyzing characteristics of plasma in gas stream of nitrogen and helium mixture
22 p2703 N73-31649
Plasma sheet behavior during magnetospheric substorms
[RLO-2229-T-5-3] 24 p2923 N73-33346
Asymptotic solutions for nonlinear equations of oscillating plasma layers
[FEI-359] 24 p2962 N73-33671

**PLASMA LOSS**

Particle loss rate from mirror machines, and radiation coupling in dense plasmas
[COO-2181-9] 06 p0704 N73-15744
Radionuclide measurements on plasma and red cell mass volume losses in Apollo spacecrews
09 p0993 N73-18106
Procedures for reducing loss mechanism in plasma jet engine
[AD-759272] 16 p1958 N73-25839

**PLASMA OSCILLATIONS**

Magnetohydrodynamic instabilities in ELMAX plasma device
[AD-744818] 01 p0086 N73-10711
Electromagnetic wave propagation from oscillating source in suddenly created plasma
[AD-746329] 02 p0142 N73-11151
Characteristic oscillations of plasma in point cusp
[IPPJ-133] 02 p0215 N73-11743
Computerized simulation of instability response of magnetized two ion species plasma to low frequency electric field oscillations
[AD-746109] 02 p0217 N73-11757
Analysis of linear and nonlinear properties of density gradient driven drift waves instability using single-ended Q-machine
[AD-747852] 03 p0344 N73-12803
Low frequency oscillations in Penning discharge under conditions of cyclotron ion source
[NASA-TT-F-14649] 06 p0703 N73-15736
Theoretical model for electromagnetic coupling of Bernstein modes in vacuum boundary of dense plasma
[COO-2181-10] 06 p0704 N73-15742
Model for pulsar radiation mechanism and relativistic plasma
[NP-19402] 07 p0826 N73-16692
Impulse response of low pressure argon magnetoplasma to excitation by electric field
[NASA-TR-R-400] 07 p0826 N73-16693
Surface wave conversion to longitudinal oscillations in plasma surface layer by perturbation of waveguide
[AEC-TR-7335] 07 p0827 N73-16703
Excitation of electromagnetic waves in cold plasma contained in metal wavequide by electron beam
[AEC-TR-7333] 07 p0827 N73-16704
Wave transformation region in superhigh frequency argon discharge plasma
[AEC-TR-7339] 07 p0827 N73-16706
High frequency wave field pressure effect on Langmuir monochromatic plasma oscillations
[AEC-TR-7337] 07 p0827 N73-16707
High frequency force field effect on electromagnetic wave propagation into bounded plasma configuration
[AREAEE-124] 07 p0828 N73-16712
Nonlinear excitation of longitudinal plasma oscillations in inhomogeneous plasma
[AREAEE-125] 07 p0828 N73-16713
Limitations and applications of electrostatic probes with floating potential for measurements of plasmas with low frequency oscillations
08 p0947 N73-17757
Computer simulation of whistler turbulence and velocity space diffusion in magnetospheric type plasma
[AD-753196] 09 p1031 N73-18415
Electron wave amplitude oscillation in plasma due to initial spatial disturbance
[IPPJ-143] 09 p1070 N73-18728
Oscillatory and nonoscillatory solutions to equations on nonlinear saturation of convective heat transfer
[AD-754228] 10 p1179 N73-19594
Dispersion relations and drift instability in ionized magnetoplasma
[AD-754005] 10 p1198 N73-19744
Literature on thermodynamics of electrostatic waves and ionized plasmas
[AD-754014] 10 p1198 N73-19745
Characteristics of low frequency oscillations in excited unmagnetized plasma
[NOAA-TM-ERL-AL-5] 11 p1327 N73-20773
Lower hybrid frequency damping of longitudinal plasma oscillations and plasma heating
[EUR-CEA-FC-657] 12 p1433 N73-21614
Plasma wave transformations into longitudinal oscillations by conducting surface
[AEC-TR-7346] 12 p1434 N73-21615
Experiments on magnetoacoustic oscillations in rotating hydrogen and deuterium plasmas with superimposed high frequency heating
[TRITA-EPP-72-34] 12 p1436 N73-21635
Equations of motion in wave solutions for cold collisional plasma
[AD-755388] 12 p1437 N73-21640
Computer simulation of nonlinear saturation of parametric decay instability in weak turbulence limit
[AD-757265] 14 p1696 N73-23766
Wave-wave coupling equations for plasma oscillations
[AD-758316] 14 p1697 N73-23769
Quasi-hydrodynamic equations for analyzing pressure anisotropy effects on magnetospheric tail oscillations
14 p1703 N73-23821
Rotation of ion component of hot cathode Penning discharge plasma
[NASA-TT-F-14931] 16 p1948 N73-25765
Parametric instabilities generated by electromagnetic pump in quiescent plasma device
[AD-759543] 16 p1951 N73-25786
Literature survey of abstracts on plasma instabilities
[AD-759276] 16 p1951 N73-25787
Spatial growth properties of parametric and backscattering plasma instabilities
[AD-761173] 18 p2184 N73-27631
Ion acoustic wave excitation in ionized plasma by radio frequency heating
[AD-760794] 18 p2184 N73-27633
Characteristic oscilations of cylindrical plasma
[IPPJ-133] 19 p2324 N73-28692
Correlation of potential and density fluctuations of plasma resulting from rotational instability of hot cathode Penning discharge
[NASA-TT-F-15026] 20 p2458 N73-29751
Total energy equation for coherent response of the plasma to linear wave fields
[JUL-895-TP] 20 p2459 N73-29760
Electromagnetic radiation trapped in magnetosphere above plasma frequency
[NASA-CR-133837] 21 p2540 N73-30367
Calculating self-consistent propagation of intense pump beam that excites parametric decay instability for inhomogeneous plasma
[AD-763736] 21 p2584 N73-30708
Asymptotic solutions for nonlinear equations of oscillating plasma layers
[FEI-359] 24 p2962 N73-33671
Plasma oscillations caused by nonlinear wave interactions
[ITF-73-8-E] 24 p2962 N73-33672
Plasma excitation and instabilities
[ORO-3405-37] 24 p2965 N73-33698

**PLASMA PERTURBATION**

U U PLASMA OSCILLATIONS

**PLASMA PHYSICS**

General, nonstationary electron gas equation for noble gas-alkali plasma
[JUL-902-TP] 01 p0085 N73-10704
Intense relativistic electron beam physics
[AD-745369] 01 p0086 N73-10710
Soft X ray emission from plasma produced in theta pinch deuterium discharge seeded with neon
[AD-745736] 01 p0086 N73-10712
Annotated bibliography of atmospheric sounding, geophysics, and plasma physics
[AD-745168] 01 p0121 N73-10997
Cyclotron resonance caused by electromagnetic waves incident on high density gaseous plasma
[IPPJ-134] 02 p0215 N73-11742
Fluid-type equations describing macroscopic behavior of matter-antimatter plasma
[IPPJ-131] 02 p0215 N73-11744
Laser selective excitation of doublet transition in atoms of pure potassium plasma
[AD-745964] 02 p0216 N73-11750
Theory of solar and terrestrial plasma physics
[AD-747034] 03 p0297 N73-12424
Averaged Lagrangian method for obtaining equations which describe nonlinear interactions of wave components in plasma
[NASA-CR-129597] 03 p0340 N73-12777
Abstracts on physics and mathematics, including aerohydrodynamics, magnetohydrodynamics, thermodynamics, and physics of crystals and semiconductors
[JPRS-57312] 03 p0366 N73-12985
Research and development in surface studies, plasma physics, and gas dynamics
[AD-747132] 03 p0368 N73-12996
Resonance excitation by dipole antenna inside hollow cylindrical, cold, uniform, isotropic plasma
[CRC-1230] 04 p0388 N73-13150
Solid state electronics, information systems, plasma and quantum electronics, biomedical electronics, acoustics, and radio sciences
[AD-748281] 04 p0400 N73-13256
Interferometric study of expansion of plasma created by laser
[CEA-R-4299] 04 p0454 N73-13708
Conference on research in nonchemical energy sources in nuclear fusion and plasma physics
[AD-748265] 04 p0456 N73-13725
USSR research projects involving laser technology, effects of strong explosions, geosciences, and particle beams
[AD-749487] 04 p0489 N73-13998
Theoretical and experimental studies on plasma wave propagation and resonance phenomena
[NASA-CR-129915] 05 p0583 N73-14743

Simulation of geomagnetic tail by plasma flux interaction with magnetic field of three dimensional dipole
[FR-113] 05 p0584 N73-14753
Research in electrically driven shock plasmas
[AD-749552] 05 p0584 N73-14755
Research progress in electronic equipment, data processing, plasma physics, and information systems
[AD-750669] 06 p0732 N73-15976
Technique for determining plasma drifts, applied to dynamic processes in topside F region
07 p0774 N73-16288
Statistical mechanics and kinetic theory for two dimensional plasma in uniform magnetic field
07 p0825 N73-16685
Scyllac research experiments
[LA-DC-72-896] 07 p0827 N73-16702
Research projects in plasma physics
[NP-19414] 07 p0828 N73-16710
Research and development in solid state physics, plasma physics, electrical engineering systems and information sciences, and mathematical biosciences and biomedical engineering
[AD-751515] 07 p0834 N73-16757
Laboratory double inverse plasma pinch experiments with argon, hydrogen, and deuterium and relevance to solar flare
07 p0838 N73-16791
Bibliography of Belgian research reports in fluid mechanics and plasma physics from 1957 to 1972
[NT-32-1972] 07 p0860 N73-16975
Research in plasma physics, communication and data processing
[AD-751213] 08 p0944 N73-17729
Laser lines in xenon plasma caused by self-electromagnetic pinching effect
[AD-752085] 08 p0949 N73-17771
Survey of electronic research projects
[AD-753700] 09 p1010 N73-18240
Abstracts of plasma physics publications
[NASA-CR-130983] 09 p1069 N73-18723
On-line programming to measure correlations in plasma using fast buffer memory and digital analysis
[IPPJ-T-12] 09 p1070 N73-18729
Excitation and propagation of free flow electron waves in plasma
[IPPJ-145] 09 p1070 N73-18731
Experiments on rotating plasmas for determining magnetohydrodynamic stability at high beta values
[TRITA-EPP-72-33] 09 p1071 N73-18741
Toroidal vortex annihilation and neutron production in pinched plasma
[AD-753107] 09 p1072 N73-18748
Solar wind propagation in low pressure gas and plasma containment in magnetic fields
[AD-753087] 09 p1072 N73-18750
Research progress in electro-optics, plasma physics, microwaves, wave propagation, telecommunication, data processing
[AD-753710] 09 p1102 N73-18993
Literature on thermodynamics of electrostatic waves and ionized plasmas
[AD-754014] 10 p1198 N73-19745
Theoretical research on plasma instabilities
[AD-754019] 10 p1198 N73-19747
Plasma interactions with gas flow and magnetic fields
[AD-754018] 10 p1198 N73-19748
High pressure plasma research
[AD-754020] 11 p1328 N73-20776
Magnetohydrodynamic equations for heavy ion plasma confined in magnetic field and ion source discharges
[LYCEN-7208] 12 p1435 N73-21625
Application of kinetic gas theory to plasma physics and dynamics of galaxies
[FRNC-TH-247] 12 p1436 N73-21634
Spectrometric analysis of pulsed X ray sources and detectors
[AD-755845] 12 p1436 N73-21639
Magnetospheric radio frequencies attenuations by plasma clouds and energetic particles
[AD-757085] 13 p1493 N73-22106
High altitude plasma physics and experiments simulating release of artificial plasma clouds in ionosphere
[AD-756684] 13 p1525 N73-22364
Technical problems and accomplishments during reporting period
[AD-757637] 14 p1696 N73-23762
Laboratory simulation of behavior of artificial plasma clouds in ionosphere
[AD-758064] 15 p1782 N73-24442
Low energy particle experiment in earth magnetoplasma
[AD-758101] 15 p1782 N73-24446
Research activities in plasma physics at Nagoya University
15 p1816 N73-24724
Summaries of research in plasma sources, hydromagnetic shock waves rotating plasmas, ion cyclotrons, air pollution, and laser diagnostics
[NP-19643] 15 p1817 N73-24727
Computerized simulation of plasmas in controlled thermonuclear fusion devices
[SU-799-X-1] 15 p1817 N73-24730
Feasibility study to develop recombining electron beam-excited plasma into pulsed laser of exceptionally high peak power
[AD-759399] 16 p1925 N73-25579
Abstracts of studies in nuclear physics, solid state physics, and plasma physics
[AD-759252] 16 p1947 N73-25756
Low loss coupling method for RF heating of plasma ions by electrostatic ion cyclotron waves
[IPP-4/30] 16 p1948 N73-25763
Relation of electrostatic oscillations in lossfree plasma to dispersion and energy equation
[IPPJ-152] 16 p1949 N73-25768
Diffused boundary model for magnetohydrodynamic equilibrium in straight and toroidal plasmas
[IPPJ-159] 16 p1949 N73-25769
Physical properties of Coulomb collisions
[IPPJ-151] 16 p1949 N73-25773
Dispersion of electrostatic ion plasma waves near harmonics of ion cyclotron frequency
17 p2066 N73-26716
Low frequency instabilities in plasmas with magnetic shear
17 p2066 N73-26717
Progress in plasma physics, integrated circuits, solid state, and information and digital systems
[AD-759697] 17 p2099 N73-26984
Electric field autocorrelations in guiding center plasma
[NASA-CR-133410] 18 p2183 N73-27624
Research in plasma physics and laser diagnostics
[NP-19681] 18 p2183 N73-27625
Plasma physics theoretical research
[COO-3577-4] 19 p2324 N73-28698
Rate effects on instabilities in slightly ionized plasmas
[NASA-CR-133599] 20 p2458 N73-29753
Theory of dielectric function in magnetized plasma
[AD-762512] 20 p2459 N73-29764
Loss reduction in high voltage LC oscillator circuits by applying cryogenic temperatures
[BMBW-FBK-72-31] 22 p2704 N73-31659
Electric switches for closing high voltage, high Q LC circuits, determining breakdown voltage and open and closed contact resistance
[BMBW-FBK-72-32] 22 p2704 N73-31660
Research on plasma physics, information theory, biophysics, and data processing systems
[AD-765002] 23 p2867 N73-32919
Laser development and applications to plasma physics
[UCRL-50022-4] 24 p2931 N73-33410
Selection of similarity criteria for stream of plasma flying into magnetic dipole by mathematical model
[NASA-TT-F-15057] 24 p2962 N73-33670
Simulation procedures in plasma physics
[JUL-CONF-7] 24 p2963 N73-33680
Instabilities of laser beam interactions with plasmas
[UCID-16272] 24 p2963 N73-33683
Plasma physics and field configurations
[CONF-730705-1] 24 p2964 N73-33687

PLASMA PINCH
NT THETA PINCH
Calculation of neutron energy and flux distributions from D-D reactions in plasma focus and Z pinch discharges
[AD-745955] 02 p0217 N73-11755
Effect of surrounding gas on MHD instabilities in Z pinch
[AD-748985] 04 p0457 N73-13728
Increased plasma stability in shock heated toroidal z-pinch using preionization
[LA-DC-72-726] 05 p0583 N73-14749
Feedback stabilization of theta pinch plasma column by optical signal processor
[LA-DC-72-707] 05 p0584 N73-14750
Screw pinch device with improved torus for stabilization of toroidal plasma
[NP-19381] 06 p0705 N73-15748
Characterization of halo in pinch plasma by image converters and streak camera
[IPP-1/125] 07 p0828 N73-16709
Circuits for pulse generation in magnetic plasma pinch
[AD-751250] 07 p0830 N73-16732
Laboratory double inverse plasma pinch experiments with argon, hydrogen, and deuterium and relevance to solar flare
07 p0838 N73-16791
Slowly changing, large magnetic induction in plasma core of rotating magnetic field pinch
[LRP-56/72] 08 p0947 N73-17756
Investigation of electric pinch, and development of methods for producing cylindrically symmetric plasma
[NASA-CR-130533] 08 p0949 N73-17770
Laser lines in xenon plasma caused by self-electromagnetic pinching effect
[AD-752085] 08 p0949 N73-17771
Toroidal vortex annihilation and neutron production in pinched plasma
[AD-753107] 09 p1072 N73-18748
Bremsstrahlung for enhancing far infrared laser scattering from theta pinch plasma
[AD-753404] 09 p1073 N73-18755
Fourier analysis of plasma deformation and feedback in stabilized rectilinear helicoid with pinch mechanism
[LRP-58/72] 10 p1196 N73-19728
Laser heating of pinched plasma in cavity
[LA-5010] 10 p1196 N73-19730
Parallel wavelength effects on drift waves in collisional potassium Q machine plasmas
12 p1432 N73-21607
Equilibrium pattern and control of plasma current distribution in diffuse pinch configuration
[IPPJ-158] 16 p1949 N73-25770
Comparison of toroidal screw pinch experiments with one-dimensional MHD computer calculations
[REPT-72-72] 17 p2070 N73-26745
X ray emission from dense plasma focus device
[AD-761800] 19 p2325 N73-28703
Radial collapse of dense plasma spindle focus in z-pinch geometry
[LA-5178-MS] 22 p2704 N73-31656
Use of electron beam for preionization in Z-pinch experiment
[AD-765313] 23 p2823 N73-32568

PLASMA POTENTIALS
Analysis of sinusoidally varying point induced charge potential in cold, homogeneous, and boundless magnetoplasma
[GRI/TP/109] 06 p0703 N73-15733
Tabulation of plasma dispersion function with first derivative using postive imaginary part
[AD-753986] 11 p1328 N73-20780
Tabulation of plasma dispersion function and first derivative using saddle point method
[AD-754002] 11 p1328 N73-20781
Collisional effects on ion distribution function and potential in Tonks-Langmuir plasma sheath problem
20 p2457 N73-29745

PLASMA POWER SOURCES
NT PLASMA ENGINES
Principles of magnetohydrodynamic energy generation to include flows in magnetohydrodynamic generator, physical processes, diagnostics, and required equipment - Part 1
[JPRS-57940-1-PT-1] 07 p0825 N73-16687
Principles of magnetohydrodynamic energy generation to include open and closed cycle magnetohydrodynamic generators, liquid-metal plants, and materials for generators -Part 2
[JPRS-57940-2-PT-2] 07 p0825 N73-16688
Characteristics and evaluation of electrodes for use in thermionic converters - Phase 2
[NASA-CR-131838] 16 p1943 N73-25723
Measurement of work functions of oxygen-doped tantalum to determine applicability for use in plasma-mode thermionic converters
[NASA-CR-131837] 16 p1943 N73-25724
Fissioning uranium plasma for use as power source in driver reactor
[NASA-TM-X-68232] 17 p2067 N73-26722

PLASMA PROBES
NT ELECTROSTATIC PROBES
Ion flux probe for low pressure discharge plasma in thin metal plate
[TRITA-EPP-72-20] 02 p0174 N73-11410
Microstrip plasma probe as diagnostic tool in atmospheric entry
[AD-749860] 05 p0585 N73-14757
Multiring ionospheric plasma probe, including plasma parameter and current study
05 p0610 N73-14960
Double probe measurements of electromagnetic noise spectra due to thermodynamic plasma density fluctuations for plasma diagnostics
06 p0706 N73-15758
Distribution of charged particles in magnetic field for determining superhigh frequency wave absorption by palsma
[AEC-TR-7321] 08 p0949 N73-17768
Double electrostatic probe for measuring plasma density, temperature, and velocity
[NASA-TN-D-7223] 09 p1070 N73-18733
Probe measurements of electron energy in glow discharge of nitrogen plasma and air
[AD-752871] 09 p107! N73-18744
Comparison of plasma probe and predicted electrical properties of rocket exhaust plume
17 p2031 N73-26436
Low energy electron measurements by VELA satellite plasma probes and spacecraft potential
[LA-DC-72-1481] 19 p2324 N73-28695
Design and evaluation of ion beam probe plasma diagnostic system
[COO-2229-2] 21 p2583 N73-30700
Characteristics of swept frequency impedance probe installed in unmanned satellite to measure impedance of space plasma
[ISAS-495-VOL-38-NO-6] 22 p2672 N73-31403

PLASMA PROPULSION
Model specifications of pulsed plasma solid propellant microthruster for synchronous meteorological satellite
[NASA-CR-130126] 04 p0463 N73-13778

Fabrication and tests of flight prototype pulsed plasma microthruster propulsion system for Synchronous Meteorological Satellite
[NASA-CR-130133] 05 p0590 N73-14794
Process for fabricating matched pairs of dished screen and accelerator grids for ion thruster accelerator system
[NASA-CASE-LEW-11694-1] 13 p1570 N73-22721
Design parameters of space propulsion ramjet engine using plasma accelerator
[AD-759290] 16 p1958 N73-25840
Comments on plasma propulsion, manned spaceflight, and evolution of solar system
[TRITA-EPP-72-08] 19 p2355 N73-28944

PLASMA RADIATION
Experiment, theory, and simulation of Cerenkov ion acoustic radiation generated by pseudowaves
[ORO-4211-2] 03 p0342 N73-12791
Characterization of halo in pinch plasma by image converters and streak camera
[IPP-1/125] 07 p0828 N73-16709
Plasma ion sources research, including mass spectra, gas discharges, and ion beams
[AD-758040] 15 p1819 N73-24742

PLASMA RESONANCE
Resonance effects anomalous electromagnetic wave propagation in plasma
[NASA-CR-129673] 04 p0454 N73-13704
Theoretical and experimental studies on plasma wave propagation and resonance phenomena
[NASA-CR-129915] 05 p0583 N73-14743
Operating properties of RF resonant plasma with high-intensity electric field
[ITF-72-77-E] 10 p1197 N73-19739
Plasma wave transformations into longitudinal oscillations by conducting surface
[AEC-TR-7346] 12 p1434 N73-21615
Oblique plasma resonance measured from quadrupolar impedance probe noting motion effect of plasma parallel to geomagnetic field
[GRI/NTP/110] 13 p1563 N73-22669
Ion-ion hybrid resonance dispersion relation
[IPPJ-157] 16 p1949 N73-25774
Anomalous electromagnetic wave propagation in plasma caused by particle resonance motions
[IPPJ-130] 17 p1997 N73-26149
Microwave excitation of electroacoustic resonances in afterglow plasmas
[AD-759789] 17 p2070 N73-26746
Accessibility of plane electromagnetic wave to lower hybrid resonance of inhomogeneous, magnetized plasma column
[IPP-IV-51] 20 p2459 N73-29761
Quasi-linear equations for stochastic plasma diffusion processes of trapped particles in magnetosphere using two selected plasma resonances
[TRITA-EPP-73-09] 21 p2593 N73-30777
Mode conversion at lower hybrid plasma resonance
24 p2962 N73-33666

PLASMA RINGS
U TOROIDAL PLASMAS

PLASMA ROCKETS
U PLASMA ENGINES

PLASMA SHEATHS
Near field characteristics of radio antenna when covered by plasma sheath to determine current distribution, input admittance, and radiation pattern
[NASA-CR-130076] 01 p0024 N73-10184
Algorithms and FORTRAN 4 data analysis programs for reflectometer diagnosis of thin boundary layer plasma sheaths - users manual
[AD-747041] 02 p0217 N73-11758
Multiple-probe reflectometer technique for diagnosing structure of boundary layer plasma formed on reentry vehicles
[AD-747038] 02 p0217 N73-11760
Computer analysis of tapered coaxial plasma gun electrodes
[AD-747057] 03 p0343 N73-12797
Multicomponent electron collision frequency model for predicting signal attenuation in plasma sheath surrounding reentry vehicle
[AD-750553] 05 p0585 N73-14758
Electrostatic probes in spacecraft flow field for measuring plasma sheath density during atmospheric reentry
07 p0825 N73-16683
Radio blackout prevention in atmospheric reentry by chemical injection into vehicle plasma sheath
[AD-753077] 09 p1003 N73-18187
Synchronous satellite observations on magnetospheric substorms in relation to plasma sheath structure
[RLO-2229-T-5-2] 10 p1155 N73-19398
Ionospheric noise created by electromagnetic wave propagation through turbulent plasma sheath
[AD-754904] 11 p1328 N73-20782
Electron density distribution in viscous flows as applied to Trailblazer 2 reentry vehicle
[AD-755397] 13 p1564 N73-22674
Analysis of plasma sheath ion current data measured by electric probes on third flight of Trailblazer 2
[AD-758763] 15 p1836 N73-24883
Shielding lengths in magnetospheric and interplanetary plasmas
[AD-760795] 18 p2147 N73-27352
Collisional effects on ion distribution function and potential in Tonks-Langmuir plasma sheath problem
20 p2457 N73-29745
Magnetotail neutral line and associated plasma phenomena in substorms
[ISAS-497-VOL-38-NO-8] 22 p2664 N73-31346
Simultaneous observations of low energy electrons in plasma sheet and in auroral zone
[LMSC-D350709] 22 p2702 N73-31638

PLASMA SLABS
Combined influence of finite Larmor radius corrections and inertia on stability of infinite slab model
[AD-746060] 02 p0168 N73-11365
Reverse deflection and contraction of plasma beam entering a curved magnetic field
[TRITA-EPP-72-32] 17 p2068 N73-26735

PLASMA SOUND WAVES
U MAGNETOHYDRODYNAMIC WAVES
U PLASMA WAVES

PLASMA SPECTRA
Relaxation theory improvements of spectral line broadening in plasmas
24 p2961 N73-33659

PLASMA SPRAYING
Nickel zinc ferrite powders deposited on ceramic substrates by arc plasma spraying
[AD-747771] 03 p0307 N73-12509
Obtaining stable oxygen electrodes by coating with plasma catalyzed polymer film
[AD-748422] 04 p0383 N73-13120
Surface structure of polymer produced by passing ethylene through radio frequency discharge
[AD-758099] 15 p1748 N73-24166
Analysis of thermophysical properties of plasma sprayed materials for use as thermal insulation coating on rocket nozzles
[NASA-CR-121144] 19 p2311 N73-28590

PLASMA STABILITY
U MAGNETOHYDRODYNAMIC STABILITY

PLASMA TEMPERATURE
Relationship between solar wind proton temperature and bulk speed of solar rotation
[NASA-TM-X-66091] 02 p0225 N73-11819
Electron temperature fluctuations of ionized plasma in Q device
[AD-751256] 07 p0830 N73-16731
Ionospheric modification experiments showing enhanced plasma line temperature of approximately 4000 K due to ion-acoustic parametric instability excitation
[AD-752060] 08 p0921 N73-17547
Spectroscopic methods for temperature measurement in plasmas with self absorption noting methods for plasma column radial temperature distribution
[BMBW-FBK-72-22] 09 p1071 N73-18737
Electron density and temperature measurements on negative glow plasma
12 p1433 N73-21609
Argon plasma temperature profile measurement by differential interferometry, based on temperature dependent refractivity
[IPF-71-4] 17 p2069 N73-26737
Development and characteristics of test equipment for determining temperature and electron density of plasma based on derivation of absorption coefficients
[NASA-CASE-ARC-10598-1] 20 p2458 N73-29750
Development of plasmas for industrial applications as fusion torches
24 p2961 N73-33663

PLASMA THEORY
U PLASMA PHYSICS

PLASMA TURBULENCE
Anomalous resistivity in turbulent plasma confined in strong magnetic field considering low and high electric field regimes
02 p0216 N73-11748
Higher-temperature limit for turbulent heating of plasma by cross-field current
[ORO-4211-4] 03 p0342 N73-12787
Numerical analysis of Langmuir wave spectra development in turbulent plasma
[JINR-P9-6432] 04 p0455 N73-13712
Theoretical plasma perturbation model for calculating coupling effects between acoustic gravity waves and electromagnetic waves in ionospheric disturbances
05 p0512 N73-14162
Computerized simulation of nonlinear and turbulent plasma behavior
[AD-750715] 06 p0707 N73-15766
Microwave scattering from plasma turbulence
[AD-752149] 08 p0886 N73-17175
Orbit perturbation effects on frequency shift of electrostatic, turbulent, unmagnetized plasma
09 p1071 N73-18738
Feedback stabilization of magnetohydrodynamic turbulence in plasma column immersed in magnetic field
[AD-753102] 09 p1072 N73-18747
Turbulent collisions for interpreting excitation processes in plasma
[AEC-TR-7382] 10 p1197 N73-19740
Low frequency instabilities in plasma confined by magnetic mirror system
[AD-754004] 10 p1197 N73-19743
Charged particle transport in turbulent astrophysical plasmas
12 p1432 N73-21606
Turbulence spectra of magnetic pulsating nonisothermal plasma
[AEC-TR-7379] 12 p1434 N73-21622
Spectroscopic examination of electric field intensity and ion temperature of turbulent plasma
[AEC-TR-7375] 12 p1434 N73-21623
Analysis of linear and nonlinear stage of ion-acoustic instability in low pressure discharge in helium
[AD-763590] 21 p2584 N73-30707
Generation of MHD plasma turbulence in magnetospheric domains
22 p2657 N73-31282
Statistical analysis on Markovian plasma turbulence using perturbed particle propagator
22 p2702 N73-31644
Snowplow effects and turbulence in expanding plasmas
[COO-3577-3] 22 p2704 N73-31654
Theoretical and numerical approaches to turbulence dominated theta pinches
23 p2822 N73-32558
Carbon dioxide laser scattering by Alfvenic disturbance in helium plasma
23 p2822 N73-32560
Low frequency instabilities and plasma turbulence including steady state and time dependent characteristics of positive column and hollow cathode discharge
[NASA-CR-135669] 23 p2822 N73-32562
Vlasov approximation of plasma turbulence in stochastic external field
[EUR-CEA-FC-690] 24 p2965 N73-33693
Feasibility of RF heating for high temperature turbulent plasma production noting diagnostic techniques and CO2 laser scattering
[LRP-64/73] 24 p2966 N73-33702

PLASMA WAVES
NT ELECTROSTATIC WAVES
Pseudowaves produced by grids in plasma devices and excitation of ion-acoustic pulses
[ORO-4211-6] 03 p0341 N73-12782
Derivation of nonlinear Schroedinger equation for electron plasma waves
[IPPJ-137] 04 p0441 N73-13590
Theoretical and experimental studies on plasma wave propagation and resonance phenomena
[NASA-CR-129915] 05 p0583 N73-14743
Bibliography of publications from OGO E plasma wave investigation
[NASA-CR-130140] 06 p0644 N73-15227
Surface wave conversion to longitudinal oscillations in plasma surface layer by perturbation of waveguide
[AEC-TR-7335] 07 p0827 N73-16703
Wave transformation in plasma with nonmonotonic longitudinal distribution under action of superhigh frequency power
[AEC-TR-7338] 07 p0827 N73-16705
Wave transformation region in superhigh frequency argon discharge plasma
[AEC-TR-7339] 07 p0827 N73-16706
Characterization of electron plasma wave echoes
[EUR-CEA-FC-639] 07 p0828 N73-16711
Plasma instability saturation by resonant mode coupling of shock waves
[AD-751538] 07 p0829 N73-16722
Plasma wave generation in ionosphere by rocket-borne electron beam accelerator
08 p0947 N73-17753
Electron wave amplitude oscillation in plasma due to initial spatial disturbance
[IPPJ-143] 09 p1070 N73-18728
Grid excitation and digitized probe measurements for oscilloscopic display of phase space diagram distribution functions of plasma waves
[IPPJ-147] 09 p1070 N73-18732
Analysis of low density plasma shock waves in expanding discharge
12 p1432 N73-21602
Plasma wave transformations into longitudinal oscillations by conducting surface
[AEC-TR-7346] 12 p1434 N73-21615
Wave interactions between plasma-electron beam system in magnetic fields
[AEC-TR-7355] 12 p1434 N73-21616
Compressional wave spectrum analysis on fissioning vacuum plasma in gas cored nuclear reactor
[NASA-CR-133235] 17 p2061 N73-26673
Explosive instabilities of waves in plasmas relating to dissipation and phase effects
[ITF-72-159-E] 17 p2068 N73-26730
Radiation patterns of electron plasma waves and reception patterns of monopole antennas
[ISAS-491] 18 p2115 N73-27103
Total energy equation for coherent response of the plasma to linear wave fields
[JUL-895-TP] 20 p2459 N73-29760
Research on nonlinear waves and shock-like phenomena in hot plasmas
[NASA-CR-132808] 21 p2582 N73-30695

Computerized simulation of wave field distributions in collisional plasma
22 p2703 N73-31646
Nonlinear interactions of electromagnetic waves in parametric plasmas
[JPRS-59885] 22 p2703 N73-31647
Linear plasma wave conversion at lower hybrid resonance
[MATT-979] 22 p2704 N73-31657
Plasma wave propagation and absorption, and parametric instabilities
[CALT-767-P-2-X-2] 24 p2963 N73-33682
PLASMA-ELECTROMAGNETIC INTERACTION
High frequency plasma heating in toroidal traps
[NP-19379] 06 p0705 N73-15753
Impulse response of low pressure argon magnetoplasma to excitation by electric field
[NASA-TR-R-400] 07 p0826 N73-16693
High frequency and pulsed electron discharge heating of turbulent skin layer in plasma
[AEC-TR-7329] 07 p0826 N73-16695
Excitation of electromagnetic waves in cold plasma contained in metal wavequide by electron beam
[AEC-TR-7333] 07 p0827 N73-16704
Wave transformation in plasma with nonmonotonic longitudinal distribution under action of superhigh frequency power
[AEC-TR-7338] 07 p0827 N73-16705
High frequency force field effect on electromagnetic wave propagation into bounded plasma configuration
[AREAEE-124] 07 p0828 N73-16712
Rotational polarization of electromagnetic waves propagating in magnetized plasma
[JAERI-M-4640] 08 p0948 N73-17766
Electromagnetic wave interactions in stratified and space-time periodic dielectric or plasma streams
[AD-753690] 09 p1004 N73-18196
Ion acoustic wave response to double plasma excitation impulse
[IPPJ-144] 09 p1027 N73-18386
Mechanism of plasma heating by large amplitude oscillating electric field
[UCB-34-P-128-X-2] 10 p1196 N73-19731
Characteristics of low frequency oscillations in excited unmagnetized plasma
[NOAA-TM-ERL-AL-5] 11 p1327 N73-20773
Ionospheric noise created by electromagnetic wave propagation through turbulent plasma sheath
[AD-754904] 11 p1328 N73-20782
High frequency excitation and instability in plasma heating
[CONF-720705-5] 12 p1434 N73-21617
Computer simulation of collisionless plasma with self-electric and magnetic interactions
[COO-2200-1] 12 p1434 N73-21619
Interaction of plasma streams with stationary, axisymmetric magnetic fields
[AEC-TR-7354] 12 p1434 N73-21620
Transient processes due to interaction of shock produced plasma flows with magnetic fields
[IPP-4/41] 12 p1435 N73-21628
Generation of electromagnetic waves and interactions with plasma media
[AD-757901] 15 p1781 N73-24441
Laser interaction with high density lithium plasma
15 p1816 N73-24718
Equations of motion for plasma drift, deformation, and diffusion in magnetic field
[AD-759742] 16 p1950 N73-25782
Anomalous electromagnetic wave propagation in plasma caused by particle resonance motions
[IPPJ-130] 17 p1997 N73-26149
Approximative model for coherent electromagnetic wave scattering from bounded plasma waves
[IPP-4/48] 17 p2067 N73-26728
Electromagnetic wave propagation in inhomogeneous plasmas exemplified by cavity resonators and positive column in magnetic field
[IPF-72-8] 17 p2069 N73-26742
Turbulent heating of dense plasma by laser pulses
[JPRS-59027] 18 p2182 N73-27621
Research in plasma physics and laser diagnostics
[NP-19681] 18 p2183 N73-27625
Ion acoustic wave excitation in ionized plasma by radio frequency heating
[AD-760794] 18 p2184 N73-27633
Interaction to second order of electrostatic and electromagnetic fields with semi-infinite plasma
20 p2457 N73-29747
Parametric instabilities of electromagnetic waves in plasmas
[AD-764610] 23 p2823 N73-32565
Absolute Raman scattering instabilities in inhomogeneous plasma
[AD-764611] 23 p2823 N73-32566
Computerized simulation of inhomogeneous plasma excitation by electric field impulse
24 p2961 N73-33660
Electromagnetic wave interaction and plasma attenuation
[KHFTI-72-24] 24 p2962 N73-33673
Instabilities of laser beam interactions with plasmas
[UCID-16272] 24 p2963 N73-33683
Plasma excitation and instabilities
[ORO-3405-37] 24 p2965 N73-33698
Plasma heating by electron beam
[COO-3165-4] 24 p2965 N73-33699
PLASMA-PARTICLE INTERACTIONS
Computerized simulation of ion acoustic wave and pseudowave generation in plasma including grid effects
[ORO-4211-1] 03 p0342 N73-12792
Experimental determination of energy loss rate of fast ions in dense plasma and comparison of results with predictions of Spitzer formula
[UCRL-51175] 03 p0342 N73-12793
Return current induced in bounded plasma by electron beam injection
[SC-RR-72-0669] 10 p1196 N73-19729
Theoretical analysis of wave particle interactions in magnetosphere and solar wind
[NASA-CR-131573] 13 p1573 N73-22746
Spectroscopic methods used for analysis of beam-plasma instability
[LBL-1531] 17 p2068 N73-26732
Two dimensional analysis of electron-ion streaming instabilities using computerized simulation
[AD-763336] 21 p2583 N73-30703
PLASMAPAUSE
Electric field noise phenomena observed by S3-A spacecraft near plasmapause during magnetic storm
[NASA-CR-129243] 03 p0293 N73-12388
Plasmapause, magnetic recovery, grounded whistler reception, and OGO 4 and 5 data
[NASA-CR-131394] 11 p1284 N73-20422
Effects of photoelectron emission on multiple-probe spacecraft near plasmapause
[NASA-TM-X-69313] 12 p1403 N73-21380
Design and development of radio sounding satellite for measuring composition of plasmapause during entry and exit phases of orbit
[NOAA-TR-ERL-242-AL-8] 18 p2200 N73-27762
ISIS-A electro static probe measurements of electron concentration and temperature of plasmapause at mid-latitudes
[NASA-TM-X-70429] 19 p2293 N73-28442
Indications of dayside midlatitude plasma trough by ISIS-1 electrostatic probe measurements of electron density and temperature in photonosphere
[NASA-TM-X-70436] 21 p2595 N73-30797
PLASMAS [PHYSICS]
NT ARGON PLASMA
NT BETA PARTICLES
NT CESIUM PLASMA
NT COLD PLASMAS
NT COLLISIONAL PLASMAS
NT COLLISIONLESS PLASMAS
NT COSMIC PLASMA
NT DENSE PLASMAS
NT DEUTERIUM PLASMA
NT ELECTRON PLASMA
NT HELIUM PLASMA
NT HIGH TEMPERATURE PLASMAS
NT HYDROGEN PLASMA
NT LASER PLASMAS
NT METALLIC PLASMAS
NT NITROGEN PLASMA
NT NONEQUILIBRIUM PLASMAS
NT NONUNIFORM PLASMAS
NT RAREFIED PLASMAS
NT RELATIVISTIC PLASMAS
NT ROTATING PLASMAS
NT SOLAR WIND
NT THERMAL PLASMAS
NT URANIUM PLASMAS
Prototype multi-wafer plasma anodization process
[AD-746003] 01 p0064 N73-10521
Monte Carlo simulation model for radiation induced plasmas with nonlinear properties
[NASA-CR-128405] 01 p0084 N73-10700
Transient current overshoot to electrostatic probe in slightly ionized plasma
[PB-210383] 01 p0086 N73-10714
Specifications for automatic command and control of real time plasma simulation chamber
[GRI/NTP/102] 02 p0216 N73-11747
Bibliography on controlled fusion and plasma physics
[TID-3557-1971-SUPPL] 03 p0341 N73-12785
Energization of electrons in ionosphere and magnetoplasma by wave particle interaction
[AD-747093] 04 p0415 N73-13391
Experimental data obtained with high frequency radio heating of ionosphere
[AD-748222] 04 p0416 N73-13394
Application of X ray spectrometry to study of multicharged ions in plasmas
[EUR-CEA-FC-629] 04 p0452 N73-13694
Model for U-shaped solar bursts based on one single group of moderately relativistic electrons radiating in cold magnetoplasma
[AD-747033] 04 p0468 N73-13812
Interferometric determination for distribution of electron density of two colliding laser plasmas
[AD-749618] 05 p0584 N73-14754
Alternate methods for soft X ray pulse generation by light flux available with high pulse energy lasers
[AD-750375] 06 p0680 N73-15534
Analysis of sinusoidally varying point induced charge potential in cold, homogeneous, and boundless magnetoplasma
[GRI/TP/109] 06 p0703 N73-15733
Correlation of organic substance oxidation rate parameters in low temperature plasma with high frequency power
[NASA-TT-F-14671] 07 p0753 N73-16113
Linear and nonlinear propagating characteristics of whistlers
[NASA-CR-130349] 07 p0780 N73-16342
Models for force-free magnetic fields in plasmas with finite conductivity
[TRITA-EPP-72-24] 07 p0828 N73-16715
Computer program for calculating equations of state, thermodynamic functions, and opacities of plasmas
[AD-751608] 07 p0829 N73-16724
Equilibrium distribution used for analysis of one component, azimuthally symmetric magnetoplasma
[AD-751255] 07 p0830 N73-16730
Ionospheric irregularities by low-frequency electrostatic gradient-driven instabilities and their nonlinear evolution in equatorial electrojet plasma
08 p0900 N73-17284
Linear variation of magnetic field as inverse Faraday effect in plasma
[FRNC-TH-217] 08 p0948 N73-17762
Laser-produced plasma as radiation source in 1000 to 20 A range, and detection with double-grating spectrometer
[FRNC-TH-216] 08 p0948 N73-17763
Magnetohydrodynamic equilibrium in axisymmetric torus
[IPPJ-141] 09 p1070 N73-18727
Orbit perturbation effects on frequency shift of electrostatic, turbulent, unmagnetized plasma
09 p1071 N73-18738
Generation of magnetic field energy from radiation pressure in laser-produced plasma thermal energy
[AD-748180] 09 p1071 N73-18742
Transport equations for studying radiative transport through dense plasma
[AD-753245] 09 p1072 N73-18753
Electric conductivity of high density xenon plasma
[AD-753489] 09 p1073 N73-18756
Association of surface polaritons with surface magnetoplasmons coupled to surface optical phonons in polar semiconductors
[AD-753484] 09 p1075 N73-18771
Electromagnetic wave penetration into plasma at lower hybrid frequencies
[AEC-TR-7378] 10 p1196 N73-19732
Graphical amplitude characteristics of electromagnetic radiation reflected from anisotropic plasma boundary
[AEC-TR-7368] 10 p1196 N73-19734
Steady-state characteristics of four plasma sources developed for mirror machine
[AD-754233] 10 p1197 N73-19742
Bronze coating of alloys in argon atmosphere
[AD-753985] 11 p1309 N73-20623
Characteristics of low frequency oscillations in excited unmagnetized plasma
[NOAA-TM-ERL-AL-5] 11 p1327 N73-20773
Relativistic electron beam for thermonuclear heating of plasma media
[AD-754621] 11 p1329 N73-20783
Precipitation of auroral and ring current particles in magnetosphere by artificial plasma injection
[AD-755352] 12 p1403 N73-21381
Effect of ionospheric conductivity on barium ion cloud dynamics
[NASA-CR-131533] 12 p1433 N73-21610
Conference on pulsed high-beta plasmas
[IPP-1/127] 12 p1435 N73-21627
Influence of collisions on incoherent scattering spectrum of nonequilibrium inhomogeneous absorbing plasma
[CEA-R-4351] 12 p1436 N73-21633
Recombination electron beam-excited plasma into pulsed laser of high peak power
[AD-756681] 13 p1537 N73-22455
Numerical calculation of current-voltage characteristics for ionized plasma containing negative ions with unequal electron and ion temperatures
[LOG-J7146] 13 p1563 N73-22667
Features of synchrotron radiation which occur when relativistic particles move with small pitch angles in magnetic field
[NASA-CR-131864] 13 p1563 N73-22670
Wave-normal emissivity and ray emissivity formulae for gyro-synchrotron radiation in magnetoactive plasma and in isotropic plasma
[AD-755398] 13 p1564 N73-22676
Status of research on gas discharge, liquid crystal display systems, and ferroelectric ceramics in Europe
[AD-757649] 14 p1668 N73-23538
Development of hollow cathode plasma electron gun for gas lasers
[AD-757086] 14 p1672 N73-23570
Laboratory astrophysics research on defense applications of gas ionization, electron scattering, plasmas, and line broadening
[AD-757721] 14 p1695 N73-23753

Extension of drift instability theory to plasmas of arbitrary beta
[NASA-CR-131880] 14 p1695 N73-23758
Spontaneous generation of magnetic fields associated with laser produced plasmas
[AD-757247] 14 p1695 N73-23759
Kinetic theory of completely ionized plasma
[AD-758612] 15 p1819 N73-24744
Calculation of lower bounds of blackout of plasma-covered antennas
[AD-759790] 16 p1881 N73-25227
Variational and Schelkunoff methods for analyzing microwave propagation in magnetoplasma filled waveguides
16 p1947 N73-25757
Properties of low frequency instability in hollow cathode discharge magnetoplasma
16 p1948 N73-25758
Equations of motion for describing physical picture of anomalous ordinary wave propagation in magnetoplasma
[IPPJ-153] 16 p1949 N73-25767
Alternating direction implicit magnetohydrodynamic code for simulating laser plasmas
[SC-DR-72-0733] 16 p1949 N73-25776
Research on electron beam devices, quantum electronic devices, plasmas, and solid state microwave devices
[AD-760033] 17 p2041 N73-26517
Plasma anodization and oxidation of thin metal film semiconductors
[AD-760171] 17 p2052 N73-26600
Equilibrium characteristics and Kruskal-Shafranov limit of hollow cylindrical plasma pinch in toroidal magnetic field
[LGI/R-72/9/E] 17 p2067 N73-26723
Radiative cascade limit in recombination oxygen plasma
[AD-759010] 17 p2070 N73-26747
Plasma modification associated with electromagnetic waves and parametric instabilities within ionosphere - Parts 1 and 2
[AD-760809] 18 p2147 N73-27351
Gas, chemical, and solid lasers for producing controlled thermonuclear fusion
[LA-UR-73-224] 19 p2307 N73-28558
Electron spin resonance and synchrotron radiation energy in magnetoactive plasma
[AD-762319] 19 p2326 N73-28709
Complex variable theory used in representation of electric field of longitudinal waves in plasma
[AD-762905] 20 p2459 N73-29763
Design of integrated aircraft instrumention display system utilizing plasma display/memory unit
[AD-763599] 21 p2550 N73-30446
Anomalous nonlinear dissipation of high frequency radio waves in plasma
[JPRS-59883] 22 p2631 N73-31083
Propagation of electromagnetic signals through ionized media
[AD-764281] 22 p2635 N73-31114
Data manipulation and sensing in plasma display/storage panel
[AD-763110] 22 p2641 N73-31164
Perturbation technique for determining microwave interactions in magnetized waveguide plasma
22 p2702 N73-31643
Nonlinear interactions of electromagnetic waves in parametric plasmas
[JPRS-59885] 22 p2703 N73-31647
Characteristics of heavy ion plasma produced by laser interaction with matter
[NASA-TT-F-15132] 22 p2703 N73-31650
Linear and nonlinear wave particle cyclotron interaction for whistler mode waves in anisotropic plasma
[AD-763744] 22 p2705 N73-31668
Continuum electrostatic probe theory for collision-dominated plasma
[PB-222088/7] 22 p2706 N73-31669
Sine wave propagation in lossy plasmas
[AD-764721] 23 p2758 N73-32073
Fundamental requirements of fusion feasibility experiment based on flux compression by collapsing liner
[AD-765314] 23 p2819 N73-32534
Electron beam devices, quantum electronic devices, plasmas, and solid state devices
[AD-764808] 24 p2932 N73-33415
Vlasov equations for analyzing plasma equilibrium stability
[IPP-6/117] 24 p2963 N73-33675

**PLASMATRONS**
NT DUOPLASMATRONS

**PLASMOIDS**
U PLASMAS [PHYSICS]

**PLASMONS**
Theoretical analysis of dispersion curves for surface polaritons in semiconductors
[AD-751671] 07 p0833 N73-16750

**PLASTIC ANISOTROPY**
NT ELASTIC ANISOTROPY

**PLASTIC COATINGS**
Obtaining stable oxygen electrodes by coating with plasma catalyzed polymer film
[AD-748422] 04 p0383 N73-13120
Plastic coatings for lining hydrostatic bearings
[AD-750525] 06 p0690 N73-15614
Procedures for cleaning materials and producing corrosion resistant epoxy plastics
[AD-752039] 08 p0936 N73-17664
Fabrication of plastic encapsulated metal containers by rotational molding process
[AD-753344] 10 p1168 N73-19499
Solid film plastic lubricant coatings for rifles
[AD-754568] 11 p1300 N73-20545
Plastic compensating coatings for alignment and assembly of bearing unit
[AD-754591] 11 p1300 N73-20550
Surface structure of polymer produced by passing ethylene through radio frequency discharge
[AD-758099] 15 p1748 N73-24166
Procedures for improving resistance of Nomex fabric and webbing to actinic degradation
[AD-759217] 17 p2051 N73-26596
Development and characteristics of system for skin packaging articles using thermoplastic film heating and vacuum operated equipment
[NASA-CASE-MFS-20855] 18 p2154 N73-27405
Polymer coatings for moisture protection of optical windows in infrared spectroscopy
[NASA-CASE-ARC-10749-1] 23 p2820 N73-32542
Spraying of powdered polymer coatings onto grooves in micromachines
[AD-764933] 24 p2929 N73-33396

**PLASTIC DEFORMATION**
Method for eliminating plastic deformations and residual stresses by high speed impact forming of weld zone
[AD-745457] 01 p0062 N73-10508
Influence of forging deformation degree on mechanical properties of forged parts
[AD-745432] 01 p0062 N73-10510
Vulnerability mechanism of pearlitic and austenitic steel alloys during plastic deformation
[NLL-RTS-7426] 02 p0184 N73-11493
Analysis of structural changes during heating and elongation of two-phase, high chromium content Cr-Ni-Fe alloys over ranges of temperature and concentration
[NLL-TRANS-746-1153-[9022.401]]
02 p0185 N73-11501
Development of general theory for studying large plastic deformation of metals
[AD-746689] 02 p0190 N73-11542
Relationships between continuum metal plastic deformation under multiaxial stress and phenomenological dislocation theory
[AD-746187] 02 p0219 N73-11769
Characteristics of yield surfaces for hardening body as function of preliminary loading path
02 p0238 N73-11937
Validity of generalized theory of small elastico-deformations
[AD-747296] 02 p0241 N73-11957
Correlation of substructure with mechanical properties of 304 and 316 stainless steel plastically deformed at elevated temperatures
03 p0313 N73-12554
Correlation of substructure with mechanical properties of 304 and 316 stainless steel plastically deformed at elevate temperatures
[COO-2107-3] 03 p0315 N73-12568
Recrystallization of hydrostatically extruded molybdenum, and plastic deformation of extruded samples
[AD-747400] 03 p0317 N73-12581
Plastic deformation of oriented single crystals of tungsten
[AD-747569] 03 p0318 N73-12590
Effects of high-speed heating after cold plastic deformation on phase composition of titanium alloy VT 15
[AD-747516] 03 p0318 N73-12591
Ductility theory used as basis for experimental determination of relation between stress and deformation during loading of thin tubular specimens of aluminum alloy AK 6
[AD-747437] 03 p0318 N73-12592
Effects of surface layer on plastic deformation and crack propagation, using Fe-Si alloys
[AD-748098] 03 p0318 N73-12594
Cold plastic deformation process for manufacturing molds and stamps from sintered metal powder ceramic blanks
04 p0432 N73-13519
Critical cold work for grain coarsening of equiaxed alpha Ti-5Al-2.5Sn alloy heated at 1144 K for one hr after plastic tensile deformation
[AD-748352] 04 p0435 N73-13550
Mathematical model of deformed state of metal strips during upsetting
[NLL-M-21511-[5828.4F]] 05 p0561 N73-14560
Analysis of plastification effects in notched, impact-bending specimens of steel
[NLL-RISLEY-TR-2457-[9091.9F]]
05 p0601 N73-14887
High temperature plastic deformation of refractory metals in vacuum during rolling
[AD-750508] 06 p0678 N73-15516
Measurements of positron lifetime distributions used to characterize plastic deformation in crystals
[COO-2128-2] 06 p0708 N73-15779
Space stress and deformation deviators for calculating work done in plastic deformation
[NLL-M-22004-[5828.4F]] 06 p0723 N73-15897
Equation for calculating plastic deformation of metals under tension
[AD-751151] 07 p0810 N73-16571
Analysis of external loads and states of deformation in light elastic structures
[PB-212011] 07 p0852 N73-16911
Theories of plasticity involving plastic deformation and plastic flow
[AD-752139] 08 p0967 N73-17905
Plastic deformation of brittle materials by machining
[AD-753027] 09 p1041 N73-18494
Tin alloying effects on plastic deformation, mechanical, and stress-rupture properties of Ni-Cr alloys
[JPRS-58159] 09 p1048 N73-18546
Numerical analysis of stress and deformation at crack tip for case where finite plastic zone exists along crack line
[NAL-TR-293] 09 p1092 N73-18918
Hydraulic biaxial medium-rate tension-torsion testing machine
[REPT-1047/72] 10 p1161 N73-19449
Fracture mechanics and plastic deformation in high strength steels
[NASA-CR-131102] 10 p1171 N73-19523
Intergranular deformation in creep elongation of platium rhodium alloys
[AD-753508] 10 p1173 N73-19546
Metallurgical investigation of deformation and fatigue using high temperature tests and stress-strain diagrams on heat resistant alloys
[JPRS-58180] 10 p1219 N73-19912
Fatigue tests to determine plastic deformations in composite materials
10 p1219 N73-19913
Cyclic deformation diagrams of heat resistant and austenitic steels
10 p1219 N73-19914
Failure criteria in cyclic elasto-plastic deformation
10 p1219 N73-19915
Role of plastic deformation process in sliding wear of pure Cu and Cu-Al alloy against Type 440 C in cryogenic fuels
[NASA-TN-D-7253] 11 p1305 N73-20591
Process for analysis of strain field of structures subjected to large deformations involving low modulus substrate with thin coating
[NASA-CASE-LAR-10765-1] 11 p1323 N73-20740
Effect of surface layer stress on plastic deformation and crack propagation of steel
[AD-755844] 12 p1415 N73-21467
Flux line lattice effect on critical current in plastically deformed single niobium crystal
[COO-3169-14] 12 p1440 N73-21665
Instrumentation and data handling process of NAE T-33 turbulence research aircraft, stationary gas turbine icing problems, and role of plastic deformation in metal powder compaction
[DME/NAE-1972[4]] 12 p1466 N73-21882
Tooling workpiece interface condition effects on metal flow and product quality in extrusion
[AD-755832] 13 p1535 N73-22439
Measurement of surface strain deformation in materials by holographic interferometry
[NRC-TT-1623] 13 p1536 N73-22447
Measurement of thermal changes encountered during plastic deformation of copper using photon detection system
[AD-756416] 13 p1543 N73-22510
Superplastic flow as common phenomenon during plastic deformation of metals and alloys
[AD-756601] 13 p1544 N73-22512
Influence of plastic deformation on structure and mechanical behavior of glassy amorphous polymers
15 p1801 N73-24595
Thermally activated deformation of crystalline solids
[PB-214537/3] 15 p1823 N73-24774
Numerical analysis of torsion characteristics of bar with constant section in shape of circular ring or circular sector
[NLL-DRIC-TRANS-2995-[3623.66]]
15 p1837 N73-24885
Temperature speed factor, contact friction, and inertial forces on deformation
[AD-758619] 16 p1919 N73-25526
Variational principle for studying elastic-plastic instability of ring stiffened cylindrical shells under external pressure
[AD-757750] 16 p1970 N73-25935
Variational principle of plasticity
[REPT-450] 17 p2044 N73-26535
Internal friction measurements on brass and aluminum alloys during plastic deformation loading
[AD-760145] 17 p2048 N73-26570

Residual stresses and plastic deformations of machined magnesium oxide crystals
[AD-759411] 17 p2073 N73-26776
Constant strain rate deformation of amphibole minerals
[AD-760105] 18 p2149 N73-27372
Constitutive equations for studying finite elastic-plastic deformation of ductile metals
[AD-761635] 19 p2310 N73-28578
Plastic deformation of cold worked metals
[AD-762468] 19 p2310 N73-28583
Plastic deformation of single crystal sapphire filaments
[AD-762302] 19 p2313 N73-28603
Plastic deformation in alpha-brasses
20 p2427 N73-29497
Evaluation and characterization of superplastic properties of aluminum, zinc, and titanium alloys in various microstructural conditions
20 p2429 N73-29509
Stress and strain relations for elastic and plastic deformation in uniaxial strain
[AD-762536] 20 p2464 N73-29797
Stress analysis of large plastic deformations in hollow sphere deformed during impact tests
[NASA-TM-X-68270] 20 p2482 N73-29940
Accomplishments and publications list of two year project on morphology and deformation mechanisms of high polymers
[AD-762780] 21 p2565 N73-30560
Effect of phase instability during low cycle fatigue on plastic deformation in steels
[AD-763235] 22 p2686 N73-31512
Plastic response of metals under dynamic loading
[AD-765522] 24 p2937 N73-33452
Effects of surface layer on plastic deformation and crack propagation
[AD-765519] 24 p2937 N73-33453

**PLASTIC FILMS**
U POLYMERIC FILMS

**PLASTIC FLOW**
Experimental determination of behavior of uncross-linked polymers subjected to constant stretch history for strip biaxial and simple extensional flow
01 p0120 N73-10986
Biaxial testing device for measuring yield point and plastic flow properties of high strength HY-80 steel
[AD-749021] 05 p0548 N73-14454
Change in flow curves of superplastic aluminum-zinc alloy in different states as function of temperature
09 p1046 N73-18531
Construction of continuous rate field in plane steady state plastic flow in bi-cylindrical system of coordinates
[NLL-M-21519-[5828.4F]] 11 p1310 N73-20630
Theoretical analysis of plastic flow and diffusion during sintering of Life, Ag, and Ni systems
20 p2428 N73-29499
Microdynamics of initial plastic flow in tungsten polycrystals
22 p2683 N73-31487
Plastic flow and fracture mechanics of brittle cuperious oxide and gamma 2Cu-Al compounds under high pressure
24 p2967 N73-33709
Theory of elasto-plastic flow applied to work hardening, anisotropy, plastic compressibility and noncontinuous loading in Quasi-linear form
[NASA-CR-2321] 24 p2989 N73-33886

**PLASTIC MATERIALS**
U PLASTICS

**PLASTIC MEMORY**
Constitutive equations for materials with memory
[AD-753460] 10 p1201 N73-19774
Strontium barium niobate for layered optical memory material
[NASA-CR-112261] 11 p1308 N73-20612
Development of nonisothermal theory of viscoelastic fluids with fading memory and application to viscometric flow
[AD-754802] 11 p1349 N73-20948
Nonisothermal constitutive equations and related thermodynamical aspects of simple materials with fading memory
[AD-761634] 19 p2327 N73-28720

**PLASTIC PROPERTIES**
NT ELASTOPLASTICITY
NT PHOTOPLASTICITY
NT THERMOPLASTICITY
NT VISCOPLASTICITY
NT YIELD POINT
Effect of hydrostatic pressure on plasticity of L-62 copper-zinc brass and LS-59-1 brass
[NLL-NEL-TT-2398-[6075.461]]
02 p0185 N73-11497
Bibliographic survey on yield behavior of metal surfaces
[AD-746473] 02 p0188 N73-11524
Deformation of polycrystalline matter to large strains by grain-boundary sliding with diffusional accommodation
[AD-746499] 02 p0218 N73-11767
Conference on mechanics of deformed solids
[AD-748046] 03 p0362 N73-12954
Effects of one dimensional yield strength gradients on plastic zones in notched aluminum specimens
[AD-747783] 04 p0435 N73-13546
Plastic properties and microstructure of alpha-titanium alloys at high temperature
[AD-750964] 05 p0564 N73-14581
Analysis of plastification effects in notched, impact-bending specimens of steel
[NLL-RISLEY-TR-2457-[9091.9F]]
05 p0601 N73-14887
Tensile tests of pressure effects on plastic properties and fracturing of metals
[NLL-NEL-TT-2190-[6075.461]]
06 p0682 N73-15552
Unified theory of thermoviscoplasticity of crystalline solids
[AD-751293] 07 p0833 N73-16756
Theories of plasticity involving plastic deformation and plastic flow
[AD-752139] 08 p0967 N73-17905
Effects of preliminary deformation on superplasticity and other properties of metals and alloys
[JPRS-58997] 09 p1046 N73-18529
Influence of preliminary hot rolling on superplasticity of zinc aluminum eutectoid
09 p1046 N73-18530
Influence of small magnesium additives on effect of superplasticity in aluminum-zinc eutectoid as function of temperature and velocity of deformation
09 p1046 N73-18532
Influence of tensile velocity on plasticity of cold deformed technically pure nickel
09 p1046 N73-18533
Influence of preliminary deformation on superplasticity of alpha brasses and pure copper
09 p1047 N73-18534
Application of theoretical framework of governing equations and extremum principles to classical elasticity and plasticity yield-point problems
[AD-753137] 09 p1096 N73-18948
Elastic-plastic behavior of thick-walled circular cylinders under internal pressure
[AD-753121] 09 p1097 N73-18952
Impurities and plastic fracture in aluminum alloys
[NASA-CR-131100] 10 p1171 N73-19521
Relationship between brittle and plastic fracture of high strength steels owing to void dynamics
[NASA-CR-131101] 10 p1171 N73-19522
Influence of reversible reaction transition superconducting to normal on plastic properties of transition and lead metal and alloy single crystals
[ANL-7903] 10 p1200 N73-19766
Development of method for extending low temperature strain limit of rubber-based solid propellants by induced plasticization
10 p1203 N73-19788
Crack tip plasticity and fracture initiation criteria
[COO-3084-16] 10 p1221 N73-19926
Plastic instability in stainless steels and effects on load bearing capacity of structural components
[COO-2048-8] 12 p1463 N73-21850
Investigation of creep rupture strength and plastic properties of heat resistant alloys
13 p1542 N73-22496
Application of crack opening stretch concept to fracture problems
13 p1585 N73-22846
Plastic properties of alpha-phase Cu-Al single crystals at low and room temperature
17 p2042 N73-26524
Dynamic plastic behavior of metal shell intersection
[AD-760012] 17 p2095 N73-26952
Temperature effects on copper plasticity failure, noting hydrogen role
[DRIC-TRANS-3009] 22 p2685 N73-31508
Finite element method for structural plasticity problems
[AD-764574] 23 p2855 N73-32811
Elastic-plastic theory at finite strain
[AD-764557] 23 p2855 N73-32815
Fused silica coatings for flexible mat insulation of space shuttle surface
24 p2939 N73-33465
Theory of elasto-plastic flow applied to work hardening, anisotropy, plastic compressibility and noncontinuous loading in Quasi-linear form
[NASA-CR-2321] 24 p2989 N73-33886

**PLASTIC TAPES**
Development of flexible thermocouple in form of tape for adaptation to special temperature measuring conditions
[NASA-CASE-LEW-11072-1] 15 p1785 N73-24472

**PLASTIC YIELDING**
U PLASTIC DEFORMATION

**PLASTICITY**
U PLASTIC PROPERTIES

**PLASTICIZERS**
Process for removing plasticizer from hard metal alloy extruded samples during low temperature sintering
23 p2808 N73-32454

**PLASTICS**
NT ACRYLIC RESINS
NT ADDITION RESINS
NT CARBON FIBER REINFORCED PLASTICS
NT EPOXY RESINS
NT NYLON [TRADEMARK]
NT PHENOLIC RESINS
NT POLYAMIDE RESINS
NT POLYBUTADIENE
NT POLYESTER RESINS
NT POLYETHER RESINS
NT POLYETHYLENES
NT POLYISOBUTYLENE
NT POLYMETHYL METHACRYLATE
NT POLYPROPYLENE
NT POLYSTYRENE
NT POLYTETRAFLUOROETHYLENE
NT POLYVINYL CHLORIDE
NT REINFORCED PLASTICS
NT TEFLON [TRADEMARK]
NT THERMOPLASTIC RESINS
NT THERMOSETTING RESINS
NT VINYL COPOLYMERS
Guidance on choice of nonmetallic gear materials, and method of estimating safe load for nonmetallic spur and helical gear
[ESDU-68001] 01 p0060 N73-10488
Optical design and performance evaluation of athermal solid and liquid acoustic lenses
[AD-745734] 01 p0081 N73-10668
Structural evaluation of cellular plastic as base course material for military expedient pavement to withstand limited number of aircraft coverages
[AD-747048] 02 p0153 N73-11244
Plastic, nuclear track detectors for recording and measuring multicharged, heavy particles
[NASA-CR-123918] 02 p0213 N73-11725
Laboratory manual on technology of polycondensation plastics including methods of preparation, analysis, and properties
[AD-747014] 03 p0321 N73-12615
Research data on dielectrics, refractory materials, plastics, ceramics, and glasses
[AD-746686] 03 p0347 N73-12827
Erythrocyte preservation in blood transfusion practice by cryogenic freezing with polyvinylpyrrolidone
[NASA-TT-F-14590] 04 p0378 N73-13076
Polymer optimization with molecular relaxation processes for preparing vibration damping plastic materials
[RAE-LIB-TRANS-1646] 04 p0386 N73-13135
Thermal decomposition of polyhydrazide and polyoxadiazoles
[AD-749853] 05 p0568 N73-14612
Plastic sheaths as lightning conductors for insulating communication cables
[AD-750642] 06 p0647 N73-15252
Optimum temperature rate conditions of VTZ-1 deformation in superplastic state
06 p0683 N73-15563
Plastic compression type seals for long life Ni-Cd batteries
[NASA-CR-130867] 08 p0870 N73-17040
Plasticization of polyvinyl chloride with various reagents and effect on physicomechanical properties of systems
[AD-751875] 08 p0935 N73-17656
Chemical and physical properties and thermal decomposition products of certain natural fibers and synthetic materials
[AD-751899] 08 p0935 N73-17658
Technique for determining bulk modulus and associated loss factor of elastomeric and plastic materials
[AD-752483] 08 p0935 N73-17659
Numerical analysis of incompressible linearly compressible viscoelastic creep and relaxation for plastic materials
[AD-752067] 08 p0967 N73-17903
Formula for evaluating durability of plastic bearings based on fatigue wear theory and including friction, elasticity, strength, and pressure factors
[AD-752820] 09 p1040 N73-18480
Ultrasonic methods for analyzing elastic moduli of materials at high temperatures
[AD-753844] 10 p1176 N73-19567
Feasibility of producing large plastic components for optical systems
[AD-754818] 11 p1299 N73-20543
Simulation of plastic bonded hexanitrostilbene/Teflon explosive for lunar seismology
[NASA-CR-131370] 11 p1349 N73-20949
Synthesis of fire resistant phosphonitrilic plastics and elastomers for marine applications
[AD-755188] 13 p1548 N73-22547
Technical compilation on adhesives and polymeric plastics
[NASA-SP-5961[01]] 14 p1680 N73-23630
Structural stability testing of aerospace components under pyrotechnic loading conditions using subscale plastic models
[NASA-CR-128911] 14 p1715 N73-23914
Plastics fabrication by ultraviolet, infrared, induction, dielectric, and microwave radiation methods
[AD-756214] 15 p1802 N73-24607
Analysis of resistance of reinforced and unreinforced structural plastics to static and fatigue failure
[AD-758626] 15 p1802 N73-24608

Evaluation of GRP rod and rope materials and associated end fittings
[AD-759931] 17 p2053 N73-26607
Different types of lubricants for working of plastics
[NLL-RTS-7852] 20 p2421 N73-29449
Development and characteristics of organic polymers for application to production of heat resistant plastics
[NLL-RISLEY-TR-2615-[9091.9F]] 20 p2434 N73-29546
Compression molding apparatus for thermosetting plastic compositions
[NASA-CASE-LAR-10489-2] 22 p2677 N73-31446
Plastic and powder metal materials for gear production
[NASA-TM-X-71446] 24 p2928 N73-33388
PLASTISOLS
NT SMOKE
PLATE [METAL]
U METAL PLATES
PLATE THEORY
Analysis of vibration characteristics of laminated plates and modifications of plate theory to produce results consistent with continuum theory
[AD-746951] 02 p0240 N73-11949
Modulus theories for determining microstructure elasticity of laminated plates
[AD-754528] 11 p1309 N73-20619
PLATEAUS
NT COLORADO PLATEAU [US]
NT GREAT BASIN [US]
NT PIEDMONTS
ERTS-1 imagery of structural geology and volcanology in Central High Plateau of Bolivian Andes
[E73-10296] 10 p1146 N73-19333
PLATES
Stress distribution in infinite micropolar plate with elliptic hole
[AD-759964] 17 p2095 N73-26949
Distribution of stress across thickness near crack tip in epoxy resin plate subjected to approximate cylindrical bending 20 p2476 N73-29893
Convective heating tests on joints and gaps between surface insulation tiles 24 p2940 N73-33477
PLATES [STRUCTURAL MEMBERS]
NT ANISOTROPIC PLATES
NT CIRCULAR PLATES
NT CORRUGATED PLATES
NT ELASTIC PLATES
NT ORTHOTROPIC PLATES
NT PERFORATED PLATES
NT POROUS PLATES
NT REINFORCED PLATES
Analysis of geometric stress concentrations caused by two equal unreinforced circular holes in infinite flat plates
[ESDU-67023-AMEND-A] 01 p0110 N73-10909
Crack propagation and arrest in impacted, edge cracked, tension plates analyzed by dynamic photoelasticity
[AD-745792] 01 p0114 N73-10946
Numerical analysis of thin skew plates using tensor-matrix techniques for elastic isotropic body
[NLL-RTS-7401] 02 p0236 N73-11916
Obtaining first natural frequencies of vibration of noncircular plates by perturbation theory
[AD-748355] 03 p0363 N73-12955
Pressure loss coefficients for fluid flowing through orifice plates, perforated plates, and cylindrical tubes
[ESDU-72010] 04 p0403 N73-13279
Rayleigh-Ritz analysis of free vibration behavior in plates with discrete elastic supports
[NASA-CR-112220] 04 p0480 N73-13924
Stability of three-layer plates with elastoviscous core subject to time-dependent loads
[AD-749746] 05 p0605 N73-14918
Numerical analysis of stress in face plates of sandwich panel structures subjected to random acoustic loading
[ESDU-72017] 06 p0723 N73-15900
Use of data items on buckling of plates and compression panels manufactured from isotropic materials
[ESDU-72012] 06 p0723 N73-15906
Mechanical properties of elastic rectangular plates with linear variations of thicknesses
[PB-211229] 06 p0727 N73-15932
Research on theory of plates and shells including bending of rectangular cantilever beam and problems in nonsymmetric deformation of mildly sloping shells
[AD-750991] 06 p0729 N73-15946
Analysis of errors recorded by modified Ligtenberg techique while measuring stress, strain, and static and dynamic loading in curved plates
[AD-752127] 08 p0926 N73-17589
Elastoplastic bending of cracked plates including effects of crack closure
[NASA-CR-112268] 09 p1092 N73-18915
Strain fields around tapered interference fit steel pins in aluminum and steel alloy plates
[ARL/SM-NOTE-377] 09 p1093 N73-18919
Distribution and concentration profiles of stress adjacent to orifices in glass fiber-reinforced plastic plates and shells
[AD-753041] 09 p1096 N73-18945
Proposed computer program for dynamic analysis of elasto-plastic, thin, isotropic plates of rectangular planform subjected to blast loads
[AD-752449] 09 p1096 N73-18947
Static, vibration, and thermal stress analyses of laminated plates and shells by hybrid-stress finite element method including transverse shear deformation effects
[AD-753651] 09 p1097 N73-18955
Finite difference technique for determining transient temperature distribution in plane slab with uniform heat sources and radiative boundary conditions 10 p1223 N73-19944
Movement of trench boundary relative to colliding plates in conjunction with down-buckling of descending plate corner
[NASA-TM-X-66212] 11 p1286 N73-20439
Application of finite element method to stress wave in plates
[NASA-CR-112294] 11 p1345 N73-20911
Stress analysis of elastoplastic state of thin circular plate subjected to axisymmetric loading
[AD-753983] 11 p1346 N73-20920
Effect of transverse shear deformation on large amplitude free vibrations of plates and cylindrical panels 13 p1584 N73-22845
Extensional vibrations of simply supported composite plate strips
[AD-756868] 13 p1587 N73-22867
Determination of inplane stress distribution across thickness by two methods for plate loaded in bending
[AD-757207] 14 p1716 N73-23925
Numerical analysis of effects of heating unidimensional plate under nonlinear boundary conditions
[NLL-M-21618-[5828.4F]] 15 p1764 N73-24290
Diffuse shock wave reflection from ridged plates, simulating aerial explosion effects on earth surface
[REPT-7/72] 15 p1766 N73-24305
Application of finite elements of triangular shape for computing plate vibrations 15 p1838 N73-24898
Application of finite element method for analyzing stability of rectangular plates in supersonic air stream 15 p1838 N73-24899
Mathematical methods of calculating strength of thin walled elastic systems
[AD-758028] 15 p1840 N73-24911
Mechanical properties and failure modes of glass fiber reinforced epoxy plates under high tensile loads
[AD-759153] 16 p1933 N73-25640
Nondestructive methods determining composite beam and plate critical loading
[ENSMP-010] 17 p2094 N73-26940
Selected articles concerning theory of plates and shells
[AD-759391] 17 p2095 N73-26945
Theoretical-experimental method of investigating stability of plates and shells
[AD-759242] 17 p2095 N73-26947
Random vibrations of infinite-span plate on rigid supports during cylindrical bending
[AD-761454] 19 p2321 N73-28677
Calculation of dynamic response of ship structural members consisting of beams and rectangular plates
[AD-762008] 19 p2350 N73-28902
Analysis of dynamics of stiffened plates using finite element modelling of flat and curved stiffened panels 20 p2479 N73-29911
Exact solution for free transverse vibrations of annular plate with supported inner and free outer edge-beams 20 p2482 N73-29938
Finite element analysis of behavior of filamentary composite plates with cutouts
[AD-764362] 22 p2689 N73-31538
Linearization method for approximate solution of rectangular plate response to excitation
[AD-763782] 22 p2727 N73-31821
Boundary integral equation method for determining plane elasto-plastic analysis of V-notched plate under bending stress 24 p2987 N73-33869
Development of finite element relations for dynamic structural analysis of linearly elastic beam and plate flexure problems 24 p2987 N73-33873
Analysis of internal buckling of fibers in viscoelastic composite plate based on linear material responses and small deflection theory 24 p2987 N73-33874
Method for determining stress and displacements infinite plate with hole of various shapes under uniform tension of compression 24 p2988 N73-33882
Variational method for numerical analysis of bending and supercritical behavior of heterogeneous slightly curved plates
[AD-765543] 24 p2990 N73-33891
PLATFORMS
Development of timing device for conserving batteries on remote data collection platform by generating synchronous time windows
[NASA-CASE-GSC-11182-1] 23 p2849 N73-32769
Design of floating platforms to capture and use solar radiation 24 p2974 N73-33764
PLATING
NT ELECTROPLATING
NT NICKEL PLATE
Metal plating process employing spraying of metallic powder/peening particle mixture
[NASA-CASE-GSC-11163-1] 23 p2795 N73-32360
PLATINUM
NT PLATINUM BLACK
Quantitative analysis on divacancy to monovacancy concentration ratios in quenched platinum and effects of storage and electropolishing
[COO-3158-5] 04 p0434 N73-13538
Ion microscopic measurements on divacancy and monovacancy concentrations in high purity platinum
[NYO-3504-55] 04 p0434 N73-13541
Analysis of lattice spacings and changes in platinum metals as function of temperature and applied pressure
[NLL-TRANS-746-1316-[9022.401]] 05 p0561 N73-14558
Quantitative analysis and identification of chemical properties of minerals in Japanese placer platinoids
[NASA-TT-F-14625] 09 p1048 N73-18547
Standards and recommendations for calculating platinum resistance thermometer
[NBS-MONOGRAPH-126] 16 p1912 N73-25471
Oxygen exchange between solid electrolyte and platinum electrode in flowing gas 22 p2617 N73-30972
PLATINUM ALLOYS
Platinum-rhodium-tungsten alloys for encapsulating space isotopic heat sources
[ORNL-4813] 08 p0932 N73-17632
Intergranular deformation in creep elongation of platium rhodium alloys
[AD-753508] 10 p1173 N73-19546
Analysis of short time elevated temperature properties of platinum, rhodium, and palladium alloys
[NLL-M-22799-[5828.4F]] 11 p1304 N73-20582
Platinum-rhodium device for stirring viscous fluids
[NBS-TN-771] 13 p1532 N73-22418
Homogeneity regions of superconducting phases in molybdenum - platinum system
[NASA-TT-F-15139] 22 p2706 N73-31674
PLATINUM BLACK
Cathode degradation in platinum black fuel cell
[AD-757714] 14 p1606 N73-23019
PLAYAS
Identification of playa lakes in Texas High Plains from ERTS-1 imagery
[E72-10257] 03 p0290 N73-12357
Utilization of ERTS-1 multispectral photography in evaluating Iranian playas as potential locations for economic and engineering development
[E72-10270] 03 p0291 N73-12369
Dynamics of playa lakes in Texas High Plains
[E73-10042] 07 p0776 N73-16305
Utilization of ERTS-1 imagery for evaluation of Iranian playas as potential locations for economic and engineering development
[E73-10067] 07 p0779 N73-16329
Utilization of ERTS-1 imagery for evaluation of Iranian playas as potential locations for economic and engineering development
[E73-10339] 10 p1147 N73-19338
Spectroradiometric quantification of soil moisture in Willcox Playa, Arizona based on ERTS-1 imagery
[E73-10354] 10 p1149 N73-19350
Regional wet census of playa lakes on Southern High Plains area of Texas and New Mexico from ERTS-1 MSS imagery
[E73-10455] 11 p1283 N73-20414
Utilization of ERTS-1 imagery to evaluate Iranian playas as potential locations for economic or engineering development
[E73-10539] 13 p1518 N73-22303
Spectral reflectance measurements of playas in Great Basin test site
[E73-10561] 14 p1656 N73-23433
Dyaamics of playa lakes in Texas High Plains analyzed from ERTS-1 imagery
[E73-10598] 15 p1772 N73-24359
Dynamics of playa lakes in Texas high plains
[E73-10832] 18 p2141 N73-27302
Application of ERTS-1 imagery for determining location and characteristics of lake basins Texas high plains and semi-arid areas
[PAPER-W13] 19 p2272 N73-28290
Relationship between in situ spectral reflectance measurements and photometric characteristics of ERTS-1 MSS imagery of Willcox Playa, Arizona
[PAPER-I19] 19 p2279 N73-28340
Skylab monitoring of temperatures of lakes and playas and soil moisture in Nevada
[E73-11004] 22 p2660 N73-31309

Evaluation of Iranian playas as potential locations for economic and engineering development
[E73-11026] 22 p2662 N73-31330
Correlation of ERTS-1 imagery signatures with water balance ecosystem and geology of select playa lake basins in West Texas
[E73-11102] 24 p2914 N73-33259
**PLAYBACKS**
Magnetic tape playback and serial time decoder for IFF flight test instrumentation
[AD-750667] 06 p0641 N73-15204
System for maintaining intensity of laser beam constant in thermomagnetic recording and magneto-optic playback system
[NASA-CASE-NPO-11317-2] 22 p2680 N73-31468
**PLENUM CHAMBERS**
Design and performance of exhaust hood with protective air current outside of hood surface
08 p0872 N73-17063
Flow velocity distribution in lower plenum of pressurized water reactor vessel, and design optimization of core catching structure
[BMFT-FBK-73-03] 19 p2255 N73-28182
**PLEXIGLASS [TRADEMARK]**
U POLYMETHYL METHACRYLATE
**PLIES**
U LAYERS
**PLOTTERS**
NT X-Y PLOTTERS
Performance accuracy of precision stereoplotter for aerotriangulation with independent models
02 p0165 N73-11339
Assessment of cartographers role in automatic cartography system
[AD-746019] 02 p0169 N73-11376
Screen touching device for computer graphic display operation
[RHEL/R-248] 03 p0271 N73-12194
Computer subroutine for drawing networks of latitude and longitude lines by plotter
[EDFB-IBP-72-7-PT-2] 06 p0667 N73-15421
Construction of cartographic scanner/plotter for computer aided mapping
[AD-754648] 11 p1288 N73-20452
Semi-automatic device for encoding three dimensional models
21 p2513 N73-30158
Photogrammetric evaluation of Mariner 9 Mars surface pictures
23 p2843 N73-32721
**PLOTTING**
FORTRAN subroutine for plotting computer determined transmission line parameters on Smith chart
[AD-751019] 06 p0645 N73-15243
Geometrical plot of light ray through leaf cross section using Fresnel equations and Snells law
[NASA-CR-132144] 15 p1813 N73-24695
Photogrammetric plotting system for graphical and digital plotting of stereopairs
[MBB-UR-150-72-O] 17 p2034 N73-26458
Satellite data presentation by means of lists, graphs, and three dimensional plots
24 p2985 N73-33859
**PLOTTING INSTRUMENTS**
U PLOTTERS
**PLOWED FIELDS**
U FARMLANDS
**PLSS**
U PORTABLE LIFE SUPPORT SYSTEMS
**PLUG NOZZLES**
Flow field and base pressure of internal-external-expansion truncated plug nozzles for open and closed wake operations
[NASA-CR-123941] 03 p0281 N73-12282
Performance comparison of double cornered plug nozzle with conventional convergent-divergent rocket nozzle
[AD-750591] 06 p0714 N73-15830
Experimental cold flow evaluation of ram air cooled plug nozzle concept for afterburning turbojet engines in static altitude facility
[NASA-TM-X-2811] 16 p1956 N73-25823
Flyover and static tests of noise and thrust performance of two spoke, suppressor plug nozzles and basic plug nozzle
[NASA-TM-X-2856] 19 p2329 N73-28735
Performance tests of twin jet afterbody configurations to determine effect of nozzle spacing, fairing shapes, and angle of attack
[NASA-TM-X-2724] 21 p2491 N73-29994
Plug and spike nozzles applied to rocket propulsion system configurations
24 p2973 N73-33754
**PLUGS**
Termination of flat conductor cable to NASA/MSFC plugs
[NASA-TM-X-64728] 11 p1262 N73-20239
**PLUMBANE**
U LEAD COMPOUNDS
U METAL HYDRIDES
**PLUMES**
NT ROCKET EXHAUST
Space simulation study of plume contamination in reaction control thruster
[NASA-TM-X-68149] 01 p0090 N73-10743
Estuarine coastal water dynamics controlling sediment transport and plume development in Long Island Sound
[E72-10250] 03 p0289 N73-12350
Numerical calculation of supersonic three dimensional jet plum in perfect gas with inviscid and compressible properties
04 p0404 N73-13287
Impulse base flow facility tests of space shuttle stage separation plume impingement loads
[NASA-CR-124000] 06 p0729 N73-15949
ERTS-1 imagery of estuarine and coastal water dynamics controlling sediment transport and plume development in Long Island Sound
[E73-10093] 08 p0902 N73-17305
Effects of rocket motor nozzle geometry on jet plume characteristics and base pressure
[NASA-CR-130967] 09 p1017 N73-18303
ERTS-1 imagery of suspended sediment plumes in Lake Ontario
[E73-10316] 09 p1023 N73-18348
Estuarine and coastal water dynamics controlling sediment transport and plume development in Long Island Sound
[E73-10378] 10 p1152 N73-19373
Dynamics of suspended sediment plumes in Lake Ontario
[E73-10493] 12 p1397 N73-21329
Wind tunnel simulation of high altitude rocket plumes
[AD-755840] 12 p1466 N73-21876
Computerized simulation of plume shapes produced by axially symmetric nozzle geometry
[AD-756380] 13 p1511 N73-22241
ERTS-1 imagery of suspended sediment plumes in Lake Ontario
[E73-10599] 15 p1772 N73-24360
Estuarine and coastal water dynamics controlling sediment transport and plume development in Long Island Sound
[E73-10627] 15 p1775 N73-24387
Monitoring water pollution plume in Lake Champlain using ERTS-1 imagery
[E73-10742] 17 p2021 N73-26347
Hydrocarbon chemistry and chemiluminescence in high altitude plumes
[AD-760793] 18 p2114 N73-27094
ERTS-1 imagery of plume development where Connecticut River flows into Long Island Sound
[PAPER-M5] 19 p2280 N73-28345
Detection of turbidity plumes in Tampa Bay, Florida from ERTS-1 MSS imagery
19 p2287 N73-28388
Development of techniques for simulating infrared emission from turbojet aircraft exhaust plumes
[AD-763123] 20 p2486 N73-29967
ERTS-1 imagery of suspended sediment plumes and turbidity in Lake Ontario
[E73-10956] 21 p2532 N73-30298
Development of fine spectral resolution procedure for determining infrared radiant heat transfer from exhaust plume
[RM-575] 21 p2605 N73-30877
**PLUTONIUM**
NT PLUTONIUM 238
Detection of C, H, and Ni in Pu metal by hot extrusion-combustion method
[FOA-VOL-6-NO-10] 05 p0506 N73-14115
Low temperature properties and specific heat of plutonium and neptunium
[AERE-R-7172] 24 p2934 N73-33432
**PLUTONIUM COMPOUNDS**
NT PLUTONIUM OXIDES
**PLUTONIUM ISOTOPES**
NT PLUTONIUM 238
**PLUTONIUM OXIDES**
Neutron emission rate from plutonium dioxide nuclear fuel
[NASA-CR-129098] 02 p0211 N73-11707
PUO2-Mo cermet spheres for use as isotopic power fuels
[MCM-1887] 03 p0333 N73-12715
Characteristic property data for plutonia molybdenum radioisotopic cermet fuel
[LA-4976] 06 p0698 N73-15694
Development of plutonium dioxide molybdenum cermet nuclear fuels
[MLM-1905] 07 p0820 N73-16643
Performance of pure plutonium oxide fuel under operational conditions
[LA-5160-MS] 21 p2578 N73-30660
Thermodynamic analysis of MHW space electric power generator with plutonium dioxide heat source
[LA-5202-MS] 22 p2699 N73-31616
Compatability of tantalum alloys fuel capsules and [Pu-238]O2 fuels in radioisotopic thermoelectric generators
[LA-UR-73-764] 24 p2955 N73-33610
**PLUTONIUM 238**
Pu-238 grade fuels for supplying power to artificial heart and circulatory assist devices
[LA-DC-72-473] 03 p0261 N73-12115
Properties and processing of plutonium fuel for isotopic power source
[MLM-1983] 17 p2061 N73-26674
**PLUVIOGRAPHS**
U RAIN GAGES
U RECORDING INSTRUMENTS
**PNEUMATIC CONTROL**
Operating force of optimal pulsed electrically controlled pneumatic valve
[FOA-2-C-2481-H5] 02 p0148 N73-11203
Application of pneumatically controlled prosthetic arm to industrial handling problems
[NASA-TT-F-14628] 04 p0383 N73-13115
Optimal performance of infrared pneumatic transducer with capacitive membrane
[ONERA-TP-1150] 09 p1007 N73-18222
Pneumatic foot pedal operated fluidic exercising device
[NASA-CASE-MSC-11561-1] 23 p2751 N73-32014
**PNEUMATIC EQUIPMENT**
NT GAS VALVES
Mathematical models for developing Coanda eductors for pneumatic conveying systems used in underground excavation
[AD-749088] 05 p0552 N73-14485
Experimental analysis of frequency response of pneumatic tee junction
[AD-750369] 06 p0656 N73-15329
Development of pneumatically isolated stabilized platform to provide active control to local gravity vector
[AD-750869] 06 p0697 N73-15686
Design, development, manufacture, and specifications of automatic fuel valves for liquid propellant rocket engines
[AD-750578] 06 p0715 N73-15832
Portable device for detecting pneumatic pressure leaks in hermetically sealed housings
[NASA-CASE-MFS-21761-1] 09 p1035 N73-18444
Development of integrated control system for supersonic aircraft based on pneumatic power generation
10 p1111 N73-19056
Analysis of leakage and pressure drop characteristics across dam of gas film seal under various flow conditions
12 p1389 N73-21267
Development and characteristics of inflatable airbag restraint system for use in general aviation aircraft
[FAA-RD-73-3] 16 p1868 N73-25127
Analysis of shimmy in pneumatic tires due to lateral flexibility for stationary and nonstationary conditions
[WTHD-48] 16 p1917 N73-25515
Inflatable stabilizing system for use on life raft to reduce rocking and preclude capsizing
[NASA-CASE-MSC-12393-1] 17 p1980 N73-26006
Pneumatic analogue decompression computer for real time prediction of safe ascent depth following depth excursion
[DCIEM-884] 22 p2638 N73-31144
Development and characteristics of air cushion landing system for remotely piloted vehicles
[AD-764774] 23 p2747 N73-31985
**PNEUMATIC RESET**
U PNEUMATIC CONTROL
**PNEUMATICS**
Heat generation associated with pneumatic tire operating under various conditions
[NASA-CR-121239] 18 p2205 N73-27799
**PNEUMONIA**
Course of infectious process and functional activity of pulmonary macrophages in mice confined to atmosphere with high oxygen content
24 p2882 N73-33016
**POCKELS EFFECT**
U BIREFRINGENCE
**PODS [EXTERNAL STORES]**
Flight performance evaluation for underwing nacelle installation of auxiliary-inlet ejector nozzle with clamshell flow diverter from Mach 0.6 to 1.3
[NASA-TM-X-2655] 02 p0222 N73-11793
**POGO EFFECTS**
Interaction of space shuttle control system with pogo
[NASA-CR-2154] 04 p0479 N73-13914
Pogo stability model considering time lag, magnitude of feedback, and loss of mass
[NASA-TN-D-7091] 06 p0726 N73-15924
Flow theory calculation of pogo instability in inducer cascades
[NASA-CR-131415] 11 p1271 N73-20313
Analysis of procedures for reducing pogo on space shuttle vehicle based on estimates of pump cavitation compliance
[NASA-CR-2210] 11 p1341 N73-20885
Longitudinal vibration of rockets with liquid fuel engines
[AD-756076] 13 p1572 N73-22736
**POIKILOTHERMIA**
NT FROGS
**POINCARE PROBLEM**
Invariance under Weyl scale transformations and Poincare gauge invariant matter Lagrangian
[RIFP-160] 02 p0195 N73-11578
**POINT DEFECTS**
NT VACANCIES [CRYSTAL DEFECTS]

Analysis of low temperature proton irradiation induced defects in metals
[COO-3431-1] 04 p0434 N73-13542
Dislocation damping in cu single crystals of controlled substructure, and ultrasonic attenuation data
[AD-750712] 06 p0711 N73-15801
Numerical analyses on elastic displacement field and point defect interactions in anisotropic cubic crystals
[JUL-836-FF] 10 p1200 N73-19767
Neutron irradiation effects on pair defect accumulation in thin rectangular isotropic metal plates
14 p1675 N73-23593
Theoretical treatment of neutron irradiation caused crystal lattice defects in ceramic materials
[AECL-4375] 20 p2462 N73-29788
Point, line, and planar defects in metal crystals
[COO-3158-17] 24 p2968 N73-33723
POINT MATCHING METHOD [MATHEMATICS]
U BOUNDARY VALUE PROBLEMS
POINT SOURCES
Analysis of resolvability of point sources of incoherent light by quantum detection, decisions of observers, and error probability
[NASA-CR-130129] 04 p0449 N73-13663
Spreading of charged particles from point source in magnetic dipole field
[AD-750703] 06 p0703 N73-15732
Perturbation theory for determining potential of point source current in cylindrical cell
[AD-756666] 13 p1501 N73-22166
Analyzing behavior of instantaneous point source as it disperses in thick, neutrally stratified, turbulent shear layer by laser light scattering technique
24 p2904 N73-33176
POINTING CONTROL SYSTEMS
Design and performance of optically stabilized telescope pointing system using digital star tracker
[NASA-TN-D-7204] 18 p2125 N73-27173
Design of terminal pointer hand controller for teleoperator applications
[NASA-CR-124307] 18 p2156 N73-27419
Skylark star-pointing attitude control system using strapdown inertial system
[RAE-TR-71241] 18 p2176 N73-27571
Pointing error sensor in star tracker system for OAO 3 attitude control
18 p2208 N73-27822
Adaptive control system for compensatory positioning of optical tracking telescope
18 p2210 N73-27842
Mathematical procedure for determining exact slew reorientation of spacecraft about nonorthogonal axes
18 p2211 N73-27850
Development of infrared earth horizon scanner employing thermistor bolometers providing pitch and roll data of synchronous satellites
[ESRO-CR-161] 19 p2301 N73-28503
Laboratory simulation of scaled single-axis dual-level control system for large space telescope
[NASA-TN-D-7319] 23 p2791 N73-32333
Simulation of experiment pointing system for space shuttle
[NASA-TM-X-64779] 23 p2848 N73-32760
POINTS
Delineation of clustered points in two dimensions by measuring perimeters of convex hulls and applicability in fields of geology and geochemistry
[BM-RI-7565] 05 p0568 N73-14616
POINTS [MATHEMATICS]
NT FIXED POINTS [MATHEMATICS]
NT INFLECTION POINTS
Computerized horizontal block adjustment for aerial mapping using large numbers of points
02 p0165 N73-11337
Generalized Fourier analysis of geophysical data with data points unequally spaced in time
[AD-751908] 08 p0919 N73-17529
Mesh gradient technique for numerical optimization
23 p2812 N73-32481
Planetary ephemerides for Mariner 9 based on radar range data using normal points
23 p2842 N73-32714
POISEUILLE FLOW
U LAMINAR FLOW
POISONING
Epinephrine oxidation and indole production during high pressure oxygen poisoning
[AD-759405] 18 p2110 N73-27061
POISONING [TOXICOLOGY]
U TOXIC DISEASES
POISONS
NT URETHANES
POISSON EQUATION
Numerical solution to Vlasov-Poisson equations and to simplified Fokker-Planck-Poisson equations
[ORO-4211-3] 03 p0324 N73-12639
Comparison of various numerical solutions to nonlinear Vlasov equation with each other and with solutions to Poisson equation
[COO-2059-12] 03 p0324 N73-12640
Development of method for numerical integration of Navier-Stokes equations based on perturbation of Poisson type equation for viscous flow
[NA-7] 05 p0526 N73-14282
Interactive graphics solution, PDQ 3, to Laplace and Poisson equations
[AD-749252] 05 p0569 N73-14621
POISSON PROCESS
U STOCHASTIC PROCESSES
POLAND
Astronomical, mathematical, and neuropathological research projects in Hungary, and scientific development policy in Poland
[JPRS-57271] 02 p0244 N73-11986
Scientific and technical research projects in Poland
[JPRS-57570] 04 p0488 N73-13988
Operational descriptions of some electronics and nuclear laboratories in Poland
[AD-752772] 09 p1011 N73-18257
Polish environmental protection policy and materials for semiconductor radiation detectors
[JPRS-59523] 20 p2487 N73-29976
Improved water and air quality and land use in Poland
20 p2487 N73-29977
POLAR AURORAS
U AURORAS
POLAR CAP ABSORPTION
Geophysical and space data reported from sites throughout the world
[AD-746290] 02 p0226 N73-11822
Auroral substorm model for predicting high frequency radio absorption
[AD-749859] 05 p0542 N73-14408
Forecasting magnitude of solar proton and polar cap absorption events using semi-integrated flux density
[AD-751925] 08 p0957 N73-17835
Literature survey on polar cap ionospheric disturbance characteristics
[AD-754250] 10 p1157 N73-19416
Solar proton penetration into geomagnetic tail and ionospheric polar cap
10 p1210 N73-19843
Effects of polar cap absorption events on performance of Omega navigation system operating in high latitudes
[AD-759009] 16 p1942 N73-25718
Theoretical calculation of heavy particle induced ionization rates during PCA events
[AD-763089] 20 p2415 N73-29407
POLAR CAPS
Influence of interplanetary magnetic field on geomagnetic variations in polar cap
[NASA-CR-129165] 02 p0166 N73-11351
Optical intensity measurements for detecting low energy protons in polar cap
[AD-749857] 05 p0542 N73-14414
Bibliography and abstracts on upper atmospheric phenomena in inner region of polar caps
[AD-751335] 07 p0796 N73-16473
Erosion rate of dayside magnetic flux based on quantitative study of dependence of polar cusp latitude on interplanetary magnetic field
[NASA-TM-X-66256] 15 p1831 N73-24837
Relation between azimuth component of interplanetary magnetic field and geomagnetic field in polar caps
[NASA-CR-133273] 18 p2145 N73-27338
Topographic depressions in Mars south polar terrain
[CONTRIB-2266] 23 p2840 N73-32696
Effects of polar cap absorption events on phase deviations in Omega navigation system
[AD-764521] 24 p2951 N73-33572
Cosmos-378 data on solar cosmic ray penetration into earth polar caps
24 p2976 N73-33782
POLAR COORDINATES
Analysis of orthopolar coordinate system to compensate for ellipsoidal shape of earth and formulas for conversion to geographic system
08 p0923 N73-17561
Mathematical procedure for calculating tectonic plate movement and the secular shift of the mean pole
[NASA-TM-X-66272] 17 p2024 N73-26376
Polar coordinate method applied to program for calculating aerodynamic loads on oscillating wing configurations in subsonic flow
[SAAB-L-0-R64] 21 p2493 N73-30006
POLAR NAVIGATION
Method for transferring spherical quasi-geographic coordinates into geographic coordinates for polar navigation
10 p1185 N73-19640
POLAR ORBITS
Measurement of energy spectra of high energy trapped protons using nuclear emulsions exposed on low altitude polar orbiting satellites
[AD-750474] 06 p0669 N73-15438
Application of TIROS satellite data to mapping of ice fields through development of composite minimum brightness chart
07 p0788 N73-16409
Data processing role of weather stations, polar and synchronous satellites in global experiments
24 p2948 N73-33549
POLAR REGIONS
NT ANTARCTIC REGIONS
NT ARCTIC REGIONS
Very low frequency radio signal transmission during three polar substorms in 1969
[KGO-PREPRINT-72-303] 01 p0050 N73-10404
Polar upper atmosphere data recorded at Kiruna Geophysical Observatory, Sweden, from Jan. - Mar. 1972
02 p0167 N73-11353
Distribution of auroral frequencies in polar regions
[DMI-GEOPHYS-PAPERS-R-28]
02 p0167 N73-11354
Influence of interplanetary magnetic field on geomagnetism in polar regions during sunspot cycles
[DMI-GEOPHYS-PAPERS-R-29]
02 p0167 N73-11355
Analysis of all-sky photographs and ionograms taken during flights and ground magnetic records from auroral zone stations
[AD-746283] 02 p0205 N73-11663
Polar region mapping using ERTS-1 return beam vidicon imagery
[E72-10273] 03 p0291 N73-12371
Magnetospheric convection, currents feeding polar cap ionosphere, and interplanetary magnetic fields
[NASA-CR-130124] 04 p0413 N73-13375
Enhanced solar activity effects on fast neutron production at polar latitudes
04 p0465 N73-13791
Upper atmospheric disturbance near polar cap - bibliographies
[AD-746298] 05 p0539 N73-14390
Auroral effects on HF radiowave propagation traversing polar regions
[AD-749515] 05 p0540 N73-14392
Computerized simulation of optical stellar observations and data reduction to determine diurnal polar motion
[AD-748460] 05 p0541 N73-14401
Polar ionospheric geophysical data recording at Kiruna, Sweden, during Apr.-Jun. 1972
06 p0667 N73-15424
D region ionization during polar cap absorption determined from parachuteborne blunt probe measurements of charged particle conductivity
[AD-750570] 06 p0670 N73-15448
Cartographic applications of ERTS-1 imagery in polar regions
[E73-10051] 07 p0777 N73-16313
Relationship between polar geomagnetic variations and polarity of interplanetary magnetic sectors
[NASA-CR-130270] 07 p0780 N73-16343
Disposition of scattering layers over polar-regions as observed by OGO-6 airglow photometer
[NASA-CR-130271] 07 p0791 N73-16436
High latitude proton precipitation and light ion density profiles during magnetic storm initial phase
[NASA-TM-X-66166] 07 p0792 N73-16438
Electrical and meteorological experimentation in upper atmosphere of polar regions - bibliography
[AD-751336] 07 p0796 N73-16472
OV1-17 satellite, polar cap measurements of solar flare protons with energies down to 12.4 keV
[AD-751467] 07 p0839 N73-16800
Models for warm and cold conditions of winter stratosphere of polar latitudes
09 p1059 N73-18636
Solar proton intensities in magnetosphere over polar regions and comparison to interplanetary intensities
[AD-753679] 09 p1081 N73-18821
Electron, positive ion, and proton flux measurements by small rocket instrumentation over polar cap
[AD-754897] 11 p1289 N73-20457
Anomalous F region ionization patterns during winter in dark ionosphere in polar regions
13 p1520 N73-22318
Kiruna [Sweden] polar geophysic observatory ionospheric data recorded from Jul.-Sep. 1972
13 p1525 N73-22355
Inferring polarity of interplanetary magnetic field from observations of diurnal variation of polar geomagnetic fields
[NASA-CR-131609] 13 p1527 N73-22379
Application of kinetic theory to collisionless regions of polar and solar winds
[AERONOMICA-ACTA-A-N-115-1973]
14 p1702 N73-23812
Analysis of ground and airborne hydroxyl emission observations in northern polar regions
[NASA-CR-130237] 15 p1777 N73-24408
Convection velocity measurements in polar upper ionsphere made by Cosmos 184 Satellite during moderate magnetic disturbance
15 p1780 N73-24430
Lower ionospheric disturbances in polar region
[NDRE-62] 16 p1905 N73-25407
Polar upper atmosphere data recorded at Kiruna Geophysical Observatory, Sweden, from Oct.-Dec. 1972
17 p2028 N73-26410
Photometric and image intensified TV measurements of auroral precipitation patterns and energy input during rocket experiments at Poker Flats, Alaska in Operation Ice Cap
[AD-760042] 17 p2029 N73-26419
Computer code to calculate ionization distribution for polar ionosphere
[AD-760044] 17 p2029 N73-26423
Plasma and neutral atmospheric motion in earths polar ionosphere
18 p2132 N73-27229

High latitude ionospheric patterns during magnetospheric substorms
18 p2133 N73-27232
Efficient separation of two major spectral components in polar motion data for short time windows
18 p2196 N73-27724
Thule riometer observations of polar cap absorption events 1962-1972
[AD-762279] 19 p2296 N73-28467
Low energy electron measurement onboard meteorological rockets in polar region
20 p2411 N73-29375
Cartographic applications of ERTS-1 RBV imagery in polar regions
[E73-10953] 21 p2531 N73-30295
High latitude electric fields and modulations related to interplanetary magnetic field parameters
[NASA-TM-X-70444] 21 p2535 N73-30331
Interpretation of OGO 2, 4, and 6 measurements of near earth magnetic field disturbances in total field at high latitudes
[NASA-TM-X-70443] 21 p2536 N73-30332
OGO 2, 4, and 6 measurements of near earth magnetic field disturbances in total field at high latitudes
[NASA-TM-X-70442] 21 p2536 N73-30333
ESRO rocketborne spectrometric data on neutral particles and temperature of winter lower thermosphere at polar latitudes
[BMBW-FBW-72-29] 22 p2667 N73-31371
Analytical theory for diurnal polar motion as forced response to lunisolar torques
[NASA-TM-X-70470] 23 p2785 N73-32284
Mariner 9 observations of Mars north polar region
[CONTRIB-2249] 23 p2840 N73-32694
Wind erosion effects in Martian polar regions
23 p2840 N73-32695
Geomorphology of layered deposits in Mariner 9 observations of Martian polar regions
23 p2840 N73-32697
Liquid carbon dioxide in Martian polar laminated surface layers
23 p2840 N73-32698
Mariner 9 S band radio occultation measurements of Mars polar and intermediate latitude atmosphere and topography
23 p2843 N73-32716
Stereographic albedo map of Mars south polar region using Mariner 9 video data
23 p2844 N73-32724
Field measurements and earth model of polar motion
[NASA-TT-F-15066] 24 p2922 N73-33334

**POLARIMETERS**
Two beam interferometer-polarimeter
[NASA-CASE-NPO-11239] 03 p0300 N73-12446
Infrared polarimeter for airborne measurement of terrestrial cloud particle sizes and shapes
[NASA-CR-130119] 03 p0301 N73-12458
Definition of scientific objectives for outer planet flyby missions
[NASA-CR-130977] 09 p1083 N73-18830
Characteristics of ellipsometer and techniques for measuring thin films including computer program for determination of optical constants and thickness of film
[NASA-TM-X-64742] 12 p1405 N73-21392
Use of remote airborne photopolarimeters to measure soil moisture content in southwestern United States
[NASA-CR-130211] 13 p1522 N73-22332
Development of X ray polarimeter by detecting secondary fluorescent X rays
[ISAS-489] 14 p1666 N73-23523
Millimeter wave polarimeters and Cotton-Mouton effect in plasmas
[EUR-CEA-FC-675] 24 p2965 N73-33694

**POLARIMETRY**
Photometric and polarimetric measurements of Bruderheim meteorite particles and comparison with astronomical data to determine composition of asteroids
[NASA-CR-131418] 11 p1339 N73-20865
Effects of atmospheric aerosols on image transfer in aerial photography using polarized light
12 p1400 N73-21356
High resolution spectral and polarization behavior of solar Type 3 bursts at 34 MHz
13 p1489 N73-22073
Scintillation and polarimeter measurements of ionospheric column using ATS 1
[AD-759533] 16 p1910 N73-25451
Polarimetric and spectrophotometric observations of late type giant and supergiant stars
17 p2080 N73-26827
Photometric and polarimetric mapping of water turbidity and water depth
[NASA-CR-134030] 22 p2666 N73-31360

**POLARITY**
Behavior of large scale positive polarity magnetic fields and geomagnetic disturbances
01 p0094 N73-10772
Relationship between polar geomagnetic variations and polarity of interplanetary magnetic sectors
[NASA-CR-130270] 07 p0780 N73-16343
Influence of polarity of interplanetary magnetic field on magnetic activity at high latitudes
[GRI/NT/87] 12 p1402 N73-21371
Inferring polarity of interplanetary magnetic field from observations of diurnal variation of polar geomagnetic fields
[NASA-CR-131609] 13 p1527 N73-22379
Electronic structure and properties of covalent and polar solids
14 p1697 N73-23773
Short geomagnetic polarity intervals in marine magnetic profile for anomalies, using Fourier transformations and linear systems
15 p1770 N73-24336

**POLARIZATION**
Stokes parameters for calculating polarization of radio waves reflected from inhomogeneous ionosphere
[NASA-TT-F-14676] 09 p1002 N73-18174
Integration of Ku-band radiator with X-band antenna design for dual band capability
[AD-760816] 18 p2118 N73-27127
Molecular mechanisms of conduction and polarization in water vapor, liquid water, and ice
[AD-762060] 19 p2231 N73-27993

**POLARIZATION [CHARGE SEPARATION]**
NT DIELECTRIC POLARIZATION
Dynamics of polarization in polycrystalline ferroelectric materials
[NLL-RTS-7416] 02 p0218 N73-11762
Photon energy and polarization effects on optical absorption spectra of GMO at varying temperatures
23 p2824 N73-32574

**POLARIZATION [SPIN ALIGNMENT]**
Multiphoton ionization cross section function of atomic polarization
[NASA-TM-X-66179] 09 p1068 N73-18718
Optical excitation of atomic levels for orientation of nuclei, polarized electron production, and magnetic resonance experiments
[NASA-TT-F-14862] 11 p1326 N73-20765
Paramagnetic rotation of plane of polarization
[NASA-TT-F-14737] 20 p2454 N73-29724

**POLARIZATION [WAVES]**
NT CIRCULAR POLARIZATION
NT ELLIPTICAL POLARIZATION
Polarization of wave propagating in ionosphere noting signal fading recorded at Garchy
[GRI/NT/84] 01 p0050 N73-10403
OAO-A2 observations of Be stars, continuous Balmer emission, and interstellar polarization
[NASA-CR-129166] 02 p0226 N73-11828
Rotational polarization of electromagnetic waves propagating in magnetized plasma
[JAERI-M-4640] 08 p0948 N73-17766
Value of gravitational wave observations in relativistic gravity investigations
[NASA-CR-131511] 12 p1398 N73-21340
Polarization measurement of whistler-type radio frequency signals by using auto- and cross-correlation functions of horizontal signal components
[CEPHAG-24/72] 13 p1491 N73-22088
Effect of gravitational field on polarization
15 p1770 N73-24335
Effect of precipitation on parabolic antennas using linear orthogonal polarization at superhigh frequencies
[REPT-53] 16 p1875 N73-25176
Polarization of infrared waves due to propagation through atmosphere
16 p1895 N73-25327
Variations in 8 GHz flux density and linear polarization of extragalactic radio sources monitored by 85 ft reflector with rotating feed horn
16 p1960 N73-25854
Automatic nulling system for interference signal at multichannel receiver by polarization adjustment
[NASA-CASE-NPO-13140-1] 18 p2116 N73-27106
Polarization effects in photon echoes and in ansiotropic mirror laser cavities
18 p2157 N73-27429
Computerized design of polarization interferometer
[AD-760564] 18 p2180 N73-27602
Polarization fluctuation of beam wave propagating in random atmosphere
19 p2234 N73-28014
Digitizer performance under conditions of linear and circular antenna polarization
[FAA-NA-73-49] 20 p2376 N73-29095
Debye polarization theory for determining electromagnetism of sea surface
24 p2957 N73-33620

**POLARIZATION CHARACTERISTICS**
Intensity variation of circularly polarized radio emission during solar flares at 3.15 cm on 10 and 12 July 1968
[AD-747606] 04 p0467 N73-13810
Potentiostatic polarization method for stress corrosion tests on cracking susceptibility of materials
[AD-754205] 10 p1174 N73-19549
Numerical analysis of low frequency radiation and scattering from noncircular cylinders with transverse electric polarization
[NASA-CR-2245] 11 p1255 N73-20187
Absolute polarization and microwave optical photoselection spectroscopy of zerofield transitions of triplet state
[AD-759996] 17 p1993 N73-26115
Polarization measurements of cosmic ray muons arriving at sea level with different energies and from different zenith angles
17 p2079 N73-26815
Polarization fading effect in angle of rotation measurements on ionospheric radio signal scattering
18 p2115 N73-27105
Ultraviolet interstellar polarization measurement
22 p2735 N73-31889
Determination of polarization characteristics of large Pulkovo radio telescope by use of Stokes parameters
23 p2838 N73-32677

**POLARIZATION CHARTS**
U GRAPHS (CHARTS)
U POLARIZATION [WAVES]

**POLARIZED ELECTROMAGNETIC RADIATION**
NT POLARIZED LIGHT
NT SYNCHROTRON RADIATION
Periodic measurements of integrated Stokes parameters from compact radio sources
[AD-749771] 06 p0720 N73-15874
Numerical analysis of low frequency radiation and scattering from noncircular cylinders with transverse electric polarization
[NASA-CR-2245] 11 p1255 N73-20187
Rain depolarization of linearly and circularly polarized microwaves
17 p1995 N73-26127
Application of polarized radar signals for analyzing structure of cumulonimbus clouds
21 p2569 N73-30588
Application of polarized electromagnetic radiation for analyzing parameters of atmospheric formations
21 p2569 N73-30592
Analysis of atmospheric attenuation of circularly polarized electromagnetic radiation from meteorological radar
21 p2570 N73-30595
Characteristics of electromagnetic radiation reflected from invisible objects in troposphere to show effects of electromagnetic radiation polarization
21 p2571 N73-30599
Observations of polarization of radio radiation from local sources on sun and operating principles of polarization receiver equipment
[NRC-TT-1681] 22 p2631 N73-31090

**POLARIZED LIGHT**
Projectile rotation measurement by polarized light modulation
[BMVG-FBWT-72-18] 07 p0766 N73-16225
Use of remote airborne photopolarimeters to measure soil moisture content in southwestern United States
[NASA-CR-130211] 13 p1522 N73-22332
Polarimetric and spectrophotometric observations of late type giant and supergiant stars
17 p2080 N73-26827
Scattering of polarized light by rough and smooth leaf surfaces
20 p2405 N73-29333
Polarization of light reflected from soil and sand with varied surface moisture and texture
[AD-765421] 23 p2788 N73-32309

**POLARIZED RADIATION**
NT POLARIZED ELECTROMAGNETIC RADIATION
NT POLARIZED LIGHT
NT SYNCHROTRON RADIATION
Production and research applications of magnetic bremsstrahlung
[BNL-TR-480] 04 p0452 N73-13689
Earth rotation aperture synthesis technique and polarized interferometry for determining polarized intensity distributions of Cygnus A at 8300 and 9600 MHz
16 p1961 N73-25865
Polarization of bremsstrahlung from electron-ion collisions by magnetically confined electrons
[ORNL-TM-4105] 17 p2067 N73-26726
Glacing incidence telescope for evaluating polarization of light source
18 p2210 N73-27840
Hertz vector analysis of spatial structure of cross polarization radiation in axisymmetric parabolic antennas
20 p2377 N73-29096
Measurement of intensity and wavelength of polarized radiation from variable stars by polarizers
21 p2594 N73-30789

**POLARIZERS**
Waveguide polarizer for horizontal control of antenna radiation patterns
[AD-751449] 07 p0763 N73-16198
Hydrothermal method for growing single crystal zircon polarizers
[AD-752147] 08 p0952 N73-17793
Measurement of intensity and wavelength of polarized radiation from variable stars by polarizers
21 p2594 N73-30789

**POLAROGRAPHS**
U POLAROGRAPHY

**POLAROGRAPHY**
Characterization of non-aqueous electrolytes and solid electrodes
[AD-750079] 06 p0638 N73-15180
**POLARONS**
Dynamic and adiabatic approximation applied to polarons in uniform magnetic field
17 p2071 N73-26753
**POLICE**
Potential application of thermoluminescence in forensic science
10 p1227 N73-19978
Improved visual capability for police helicopters
10 p1228 N73-19984
**POLICIES**
NT PROCUREMENT POLICY
Astronomical, mathematical, and neuropathological research projects in Hungary, and scientific development policy in Poland
[JPRS-57271] 02 p0244 N73-11986
Federal policy for support and use of technology
[NASA-CR-129669] 04 p0488 N73-13987
Conceptual framework for analysis for aiding policy analyst and policy researcher in empirical investigations into policy phenomena
[NASA-CR-130669] 08 p0976 N73-17982
Policy of Justice Department with respect to airline merger within context of Federal Aviation Act
23 p2864 N73-32897
International air transportation policy and application of policy to scheduled and chartered airline services
23 p2865 N73-32903
Congressional hearings on Federal policy, plans, and organization for support and utilization of science and technology
24 p2994 N73-33924
**POLISHED METALS**
U METAL POLISHING
**POLISHING**
NT ELECTROPOLISHING
NT METAL POLISHING
Fine grinding, polishing, and graded etching techniques to eliminate surface yield on optical telescope mirrors
[NASA-CR-112217] 08 p0934 N73-17647
**POLITICS**
Relation between technology and rise of multinational corporations, and impact on nation-state
[NASA-CR-129269] 03 p0367 N73-12988
Political, legal, and international management of space data and space programs
04 p0474 N73-13871
Fiftieth anniversary of formation of USSR with synopsis of accomplishments including rocket flights with animals for space medicine research
07 p0743 N73-16042
Impact on political and organizational policy and decision making of operations research/management science
[NASA-CR-130667] 08 p0976 N73-17981
Analysis of Marxist-Leninist theory based on data in cybernetics, information theory, systems analysis, and semiotics
24 p2993 N73-33918
**POLLUTANTS**
U CONTAMINANTS
**POLLUTION**
NT AIR POLLUTION
NT ENVIRONMENT POLLUTION
NT NOISE POLLUTION
NT THERMAL POLLUTION
NT WATER POLLUTION
Utilization of ERTS-1 imagery for water depth measurement, mapping of Yellowstone Park, atmospheric effects in Colorado, lake ice surveillance, recreational land use, IFYGL Lake Ontario, image enhancement, water quality monitoring, and oil pollution detection
[E72-10201] 02 p0144 N73-11167
Utilization of ERTS-1 imagery for water depth measurement, mapping of Yellowstone Park, atmospheric effects in Colorado, lake ice surveillance, recreational land use, IFYGL Lake Ontario, image enhancement, water quality monitoring, oil pollution detection, and mapping iron compounds
[E72-10198] 02 p0160 N73-11296
Conversion of solar energy to pollution free power
04 p0474 N73-13870
Resource inventory, land use, and pollution within Susquehanna River Basin based on interpretation of ERTS-1 data
[E72-10329] 05 p0531 N73-14317
Utilization of ERT-1 imagery for water depth measurement, Yellowstone Park data, atmospheric effects in Colorado, lake ice surveillance, recreational land use, IFYGL, image enhancement, water quality monitoring, oil pollution detection, and mapping iron compounds
[E73-10086] 08 p0901 N73-17298
Effect of fuel zoning and fuel nozzle design on exhaust pollution emissions at ground idle conditions for double-annular ram-induction combustor for turbofan engines
[NASA-CR-121094] 08 p0968 N73-17916
Modification of world dynamics model to account for pollution abatement
[NASA-TM-X-2832] 23 p2866 N73-32910
Resource inventory, land use, and pollution of Susquehanna River Basin from ERTS-1 data
[E73-11156] 24 p2919 N73-33310
**POLYACRYLATES**
U ACRYLIC RESINS
**POLYAMIDE RESINS**
NT NYLON [TRADEMARK]
Antifriction interaction between metals and steels on polyamide surfaces
[NLL-RTS-7378] 04 p0425 N73-13461
Synthesis of high temperature clothing from hexahydrobenzodipyrrole monomers
[AD-750380] 06 p0689 N73-15609
Radiation induced grafting of fluorinated monomers on polyamide films
[AD-757376] 14 p1617 N73-23100
**POLYATOMIC GASES**
NT DIATOMIC GASES
**POLYATOMIC MOLECULES**
NT DIATOMIC MOLECULES
**POLYBENZIMIDAZOLE**
Thermal stabilization of textiles composed of polybenzimidazole fibers by chemical treatment
[AD-748248] 04 p0440 N73-13584
**POLYBUTADIENE**
Aging of polyurethane elastomers based on hydroxyl terminated polybutadienes
[ERDE-TR-77] 02 p0192 N73-11554
Hydroxyl terminated polybutadiene for solid rocket propellant application
[AD-746338] 02 p0221 N73-11789
HTPB polymer improvement for applications in highly loaded solid propellants
[AD-750551] 05 p0589 N73-14791
Diisocyanate cure rate stabilization with hydroxy-terminated polybutadiene binders
[AD-759960] 17 p2052 N73-26599
Hydroxyl terminated polybutadience polymer for solid propellant binder
[AD-760579] 18 p2168 N73-27507
**POLYCARBONATES**
NT LEXAN [TRADEMARK]
X ray diffraction pattern and electron microscopy of polycarbonate filled with MoS2
[AD-749731] 05 p0567 N73-14604
Mechanical properties of monolithic transparent polycarbonate plastic sheet
[AD-751551] 07 p0813 N73-16590
Rate and time dependent yield behavior of ductile polycarbonates
[AD-753941] 10 p1177 N73-19571
Properties of graphite fiber/polycarbonate and glass fiber/polycarbonate composites as influenced by heat treatment
[AD-757763] 15 p1802 N73-24605
Fracture mechanics of polycarbonates and polyimides under dynamic loads
[AD-759917] 17 p2053 N73-26608
Analysis of etching process in polycarbonate film when aqueous sodium hydroxide is used to develop charged particle tracks
[NASA-CR-124381] 22 p2673 N73-31415
**POLYCRYSTALS**
Dynamics of polarization in polycrystalline ferroelectric materials
[NLL-RTS-7416] 02 p0218 N73-11762
Deformation of polycrystalline matter to large strains by grain-boundary sliding with diffusional accommodation
[AD-746499] 02 p0218 N73-11767
High temperature deformation of polycrystalline halide microstructures by infrared lasers
[AD-751655] 08 p0944 N73-17730
Optical transmission measurements of single crystal and polycrystal CsI
[NASA-TM-X-66178] 08 p0951 N73-17784
Effects of diffusional creep on particle morphology of polycrystalline alloys strengthened by second-phase particles
[NASA-TN-D-7177] 09 p1047 N73-18536
Electrical screening procedure for solid ionic conductors
[NASA-TN-D-7146] 09 p1073 N73-18758
Variations of electrical resistance of hydroextruded polycrystalline beryllium in annealing process
10 p1171 N73-19525
Analysis of fracture of mixed viscous-brittle breakage of polycrystal using raster electron microscope
13 p1540 N73-22479
Mechanical behavior of polycrystalline nickel deformed by tension and simultaneously cathodically charged with hydrogen
[AD-759036] 20 p2432 N73-29535
Absorption and fluorescence of inorganic glasses and polycrystalline discs doped by heavy metal ions
[PAPER-76A6-746] 21 p2546 N73-30412
Microdynamics of initial plastic flow in tungsten polycrystals
22 p2683 N73-31487
Creep tests of fine-grained polycrystalline ice under uniaxial and multiaxial stress conditions to predict time-dependent deformational behavior
22 p2723 N73-31791
**POLYESTER RESINS**
Development of fiberglass reinforced polyester for expedient airfield pavement system
[AD-743958] 01 p0114 N73-10941
Mechanical properties of monolithic transparent polycarbonate plastic sheet
[AD-751551] 07 p0813 N73-16590
**POLYESTERS**
Photoelastic analysis of plane polyester specimens containing fatigue crack to determine effect of plastic yielding on stress distribution near crack
[TAE-155] 09 p1093 N73-18923
Creep properties of composite, plastic reinforced polyester concretes
[AD-752454] 10 p1221 N73-19930
Apparatus for manufacturing polyester drive belts
[NASA-CASE-NPO-13205-1] 22 p2677 N73-31442
**POLYETHER RESINS**
NT POLYMETHYL METHACRYLATE
Photolysis of perfluorodienes and diacyl fluorides to produce high molecular weight perfluorocarbon polyether gums
[NASA-CR-130552] 08 p0883 N73-17149
Preparation of stable polyurethane polymer by reacting polymer with diisocyanate
[NASA-CASE-MFS-10506] 21 p2505 N73-30100
Preparation of fluorohydroxy ethers by reacting fluoroalkylene oxides with alkali salt of polyfluoroalkylene diol
[NASA-CASE-MFS-10507] 21 p2505 N73-30101
Preparation of fluorinated polyethers from 2-hydroperhaloisopropyl alcohols
[NASA-CASE-MFS-11492] 21 p2505 N73-30102
**POLYETHYLENES**
Application of polyethylene materials as screens for actinometric instruments to include analysis of physical, mechanical, and optical properties
[NLL-M-22675-[5828.4F]] 01 p0069 N73-10566
Strength, mechanical properties, and deformation analysis of flexible polyethylene balloons
[AD-746308] 02 p0127 N73-11029
Description of linear polyethylene standard reference material
[NBS-SP-260-42] 02 p0192 N73-11552
Low temperature investigation of polyethylene balloon film mechanical properties and structural factors affecting such properties
[AD-746678] 02 p0194 N73-11572
Antifriction and antiwear properties of medium pressure polyethylene
[AD-748912] 04 p0439 N73-13582
Combustion efficiency of FLOX/polyethylene hybrid propellants
[DGLR-PAPER-72-86] 04 p0462 N73-13766
Optimization of transparent ethylene terpolymer and compilation of engineering data for use as adhesive in polycarbonate composite aircraft transparencies
[AD-750814] 06 p0689 N73-15611
Effects of rebinders on strength of polyethylene and polymethyl methacrylate
[AD-751615] 07 p0812 N73-16587
Rotational injection moulding for designing polythene sheathed closures on large size cables
[REPT-6713] 10 p1164 N73-19474
Stabilization of polyethylene plastics by antioxidants
[AD-753479] 10 p1176 N73-19564
Ultrasonic relaxation measurement of polyethylene and polyethylene oxide from room temperature to melting point
[AD-754391] 11 p1310 N73-20628
Brittleness determination of low density blown polyethylene film balloons to account for high altitude failure
[AD-757885] 15 p1802 N73-24603
Effect of crystallization kinetics on physical and chemical properties of polymers particularly polyethylene
[AD-750157] 16 p1953 N73-25802
Solid amine filter material for humidity control and carbon dioxide removal in space shuttle
[NASA-CR-133963] 18 p2113 N73-27087
Diffusion across modified polyethylene separator in heat sterilizable silver zinc battery
[NASA-CR-133601] 20 p2363 N73-29007
**POLYGONS**
NT HEXAGONS
NT RECTANGLES
NT TRIANGLES
**POLYHEDRONS**
NT CUBES [MATHEMATICS]
**POLYIMIDE RESINS**
Development and application of polyimide films for hybrid and beam lead substrates
[AD-745731] 01 p0033 N73-10260
Thermomechanical behavior of BBB polymer
[AD-749819] 05 p0568 N73-14611
**POLYIMIDES**
NT KAPTON [TRADEMARK]

Performance of graphite fiber reinforced polyimide composites as journal bearing materials
[NASA-TN-D-7078] 01 p0062 N73-10505
Development and fabrication of graphite polyimide wing box beam
[NASA-CR-123959] 04 p0480 N73-13923
Torque measurement of flat polyimide cable crossing hinge or satellite solar array
[ESRO-TN-114-ESTEC] 05 p0603 N73-14904
Chemical analysis, production, and physical properties of polyimide syntactic foam
[SC-DC-72-2297] 07 p0812 N73-16583
Evaluation of polyimide second stage rod seals at high temperatures to determine suitability for application to aircraft systems
[NASA-CR-121124] 08 p0927 N73-17592
Infrared spectroscopic investigation of polyimide films containing silver metal
[TR-62] 09 p1048 N73-18545
Analysis of polymerization mechanism and fabrication of polyimide/graphite fiber composites using A-type polyimide prepolymers as matrix
[NASA-TM-X-2798] 15 p1801 N73-24597
Development and evaluation of polyimide laminates for printed wiring board applications
[NASA-TM-X-64760] 17 p2050 N73-26581
Fracture mechanics of polycarbonates and polyimides under dynamic loads
[AD-759917] 17 p2053 N73-26608
Design, fabrication, and test of boron-polyimide reinforced titanium fan disks to operate at high temperatures
18 p2167 N73-27498
Stable polyimide synthesis from mixtures of monomeric diamines and polycarboxylic acid esters
[NASA-CASE-LEW-11325-1] 19 p2229 N73-27980

**POLYISOBUTYLENE**
Chemical process for production of polyisobutylene compounds and application as solid rocket propellant binder
[NASA-CASE-NPO-10893] 13 p1568 N73-22710

**POLYMER CHEMISTRY**
Review and evaluation of theories on turbulent drag reduction by polymeric additives
[AD-746107] 02 p0158 N73-11277
Laboratory manual on technology of polycondensation plastics including methods of preparation, analysis, and properties
[AD-747014] 03 p0321 N73-12615
Synthesis of polyfluoroalkoxy phosphazenes
[AD-747344] 04 p0438 N73-13570
Chemical processing industries and utilization of NASA technology - conference
[NASA-CR-129827] 05 p0607 N73-14937
Elementary chemical processes involved in degradation of polymers in melts
08 p0881 N73-17133
Pyrolysis mechanisms for three classes of polymers
08 p0881 N73-17134
Patterns and problems in pyrolysis behavior of synthetic addition polymers
08 p0881 N73-17135
Mechanism of peroxidation of polymers under irradiation conditions
08 p0881 N73-17137
Oxidative degradation of polymers and organic compounds via unimolecular decomposition of peroxy radicals
08 p0882 N73-17138
Mechanisms of oxidation of polyolefins below 150 C
08 p0882 N73-17139
Polymer gas reactions in air pollutants such as NO2 and SO2 as function of pressure, UV light, temperature, and morphology
08 p0882 N73-17140
Models for candle-like flames produced by burning of polymers
08 p0883 N73-17146
Surface pyrolysis boundary condition for combustion of polymers
08 p0883 N73-17148
Pyrolysis-molecular weight chromatography of polymers
[AD-758711] 16 p1872 N73-25154
Freezing points of crystalline polymers determined as functions of pressure and temperature
[AD-759007] 17 p2051 N73-26591
Development and characteristics of organic polymers for application to production of heat resistant plastics
[NLL-RISLEY-TR-2615-[9091.9F]]
20 p2434 N73-29546

**POLYMER PHYSICS**
Aerospace engineering including materials, orbits and trajectories, power sources, satellite geodesy, and structural engineering
[NASA-CR-128329] 01 p0119 N73-10981
Experimental determination of behavior of uncrosslinked polymers subjected to constant stretch history for strip biaxial and simple extensional flow
01 p0120 N73-10986
Drag reduction and diffusion accompanying thin slit injections of drag reducing polymer into water turbulent boundary layer of flat plate at high Reynolds number
[AD-747248] 03 p0285 N73-12312
Formation of large polymers in vacuum plumes of large rocket engines following combustion of hydrogen and oxygen under adiabatic conditions
[RM-571] 13 p1590 N73-22893
Thermal quenching of luminescence and conformational transformations in macromolecules of some polymers
[NRC-TT-1631] 15 p1815 N73-24711
Molecular-kinetic theory of nature of polymer friction
[NLL-RISLEY-TR-2577-[9091.9F]]
16 p1931 N73-25628

**POLYMERIC FILMS**
NT KAPTON [TRADEMARK]
NT MYLAR [TRADEMARK]
Low temperature investigation of polyethylene balloon film mechanical properties and structural factors affecting such properties
[AD-746678] 02 p0194 N73-11572
Statistical analysis of adhesive bond strength as function of plasma treatment of polymer films
[AD-749253] 04 p0440 N73-13587
Infrared spectroscopic investigation of polyimide films containing silver metal
[TR-62] 09 p1048 N73-18545
Synthesis of high molecular weight benzobistriazolo phenanthroline polymers for heat resistant plastic films
[AD-753414] 10 p1127 N73-19180
Design of solar energy concentrators with concentric circular seams of plastic films
[AD-755829] 12 p1446 N73-21712
Brittleness determination of low density blown polyethylene film balloons to account for high altitude failure
[AD-757885] 15 p1802 N73-24603
Silicon solar cell with plastic film binding to cover glass
[NASA-CASE-LEW-11065-2] 17 p1985 N73-26048
Conductance of quaternary ammonium salt dispersions in polymeric films
[AD-759073] 17 p2052 N73-26597
Development and characteristics of system for skin packaging articles using thermoplastic film heating and vacuum operated equipment
[NASA-CASE-MFS-20855] 18 p2154 N73-27405
Analysis of etching process in polycarbonate film when aqueous sodium hydroxide is used to develop charged particle tracks
[NASA-CR-124381] 22 p2673 N73-31415

**POLYMERIZATION**
NT VINYL COPOLYMERS
Preparation of thermally and chemically stable fluoropolymers
[AD-747257] 02 p0139 N73-11121
Plasma sprayed catalyst coatings for low pressure polymerization of ethylene
[AD-750718] 05 p0568 N73-14613
Speed of alkaline polymerization of hydrocyanic acid - Part I
[NASA-TT-F-14651] 09 p0998 N73-18145
Chemical composition of polymers formed by alkaline polymerization of hydrocyanic acid - Part 2
[NASA-TT-F-14645] 09 p0998 N73-18146
Radiation induced grafting of fluorinated monomers on polyamide films
[AD-757376] 14 p1617 N73-23100
Surface structure of polymer produced by passing ethylene through radio frequency discharge
[AD-758099] 15 p1748 N73-24166
Analysis of polymerization mechanism and fabrication of polyimide/graphite fiber composites using A-type polyimide prepolymers as matrix
[NASA-TM-X-2798] 15 p1801 N73-24597
Plastics fabrication by ultraviolet, infrared, induction, dielectric, and microwave radiation methods
[AD-756214] 15 p1802 N73-24607
Effects of ionizing radiation and high pressure on polymerization processes of fluoroolefins and fluorocarbon compounds
[AD-750151] 16 p1870 N73-25143
Monomer polymerization by plasma discharge as thin film for water purification membrane
[NASA-CASE-ARC-10643-1] 20 p2374 N73-29074
Statistical elasticity theory for initial stresses in reinforced and filled polymers
20 p2434 N73-29551
Filler effect on tensile strength characteristics of thermosetting polymers
20 p2434 N73-29552
Microtribometric study of self-lubricating composite materials on polymers
20 p2435 N73-29553
Hydrocarbon polymeric binder for advanced solid propellants
[NASA-CR-133615] 20 p2464 N73-29800
Preparation of fluorohydroxy ethers by reacting fluoroalkylene oxides with alkali salt of polyfluoroalkylene diol
[NASA-CASE-MFS-10507] 21 p2505 N73-30101
Preparation of fluorinated polyethers from 2-hydroperhaloisopropyl alcohols
[NASA-CASE-MFS-11492] 21 p2505 N73-30102
Solid rocket propellants with pulsating combustion, based on mixed polymerizates
[ICT-9/72] 23 p2828 N73-32604
Research in dynamics of thin films polymer chemistry mechanical and chemical properties of materials
[NASA-CR-135697] 23 p2865 N73-32906
In situ monomer polarization for polyphenylquinoxaline/graphite
[NASA-TM-X-71454] 24 p2891 N73-33084

**POLYMERS**
Influence of drag, pressure, and turbulent distribution on flow of dilute Polyox WSR-301 solutions in circular cylinders
[AD-745763] 01 p0042 N73-10334
Formation of chaoite and other crystal forms of carbon by CO2 laser irradiation of solid carbons
[AD-747020] 02 p0193 N73-11565
Sorption and desorption of ethylene oxide and methyl bromide gases on polymeric materials during sterilization
03 p0257 N73-12082
Discharge rate and electrical breakdown in polyethylene, polystyrene, polymethyl methacrylate, and polyvinyl chloride
[SC-T-72-2509] 03 p0273 N73-12217
Viscous drag reduction caused by polymer injection in developing turbulent boundary layer
[AD-747274] 03 p0285 N73-12310
Annotated bibliography of research and development of high temperature stable polymeric systems
[NASA-TM-X-2641] 03 p0320 N73-12608
Solid polymer for water electrolysis system to generate oxygen and hydrogen in manned space station
[NASA-CR-112183] 04 p0375 N73-13052
Polymer optimization with molecular relaxation processes for preparing vibration damping plastic materials
[RAE-LIB-TRANS-1646] 04 p0386 N73-13135
Susceptibility of model polymer with diagonal viscosity and weak interaction
[COO-3161-2] 04 p0387 N73-13142
Carbonyl formation data at elevated temperatures for estimating storage life of unstabilized polyolefins
[AD-748827] 04 p0438 N73-13572
Yield strength of rigid polymers, discussing tensile and compression stresses
[D-MAT-180] 05 p0565 N73-14591
Elastic modulus of composite polyblends and polymers having phase inversion
[AD-749973] 05 p0566 N73-14601
Production of carbon fibers from polyacrylonitrile
[AD-750362] 06 p0688 N73-15604
Hydrostatic pressure effects on mechanical behavior and properties of polymers
[AD-750731] 06 p0688 N73-15605
Thermal degradation process and char forming characteristics of polymers and composites
[AD-750396] 06 p0689 N73-15612
Rotating disk measurement of drag reduction and shear properties of various dilute polymers
[AD-751552] 07 p0773 N73-16281
Measurement of microscale turbulence and turbulent flow intensity of dilute polymer solutions about circular cylinders
[AD-751640] 07 p0774 N73-16284
Development of space shuttle semitransparent polyquinoxaline films
[NASA-CR-112213] 07 p0811 N73-16575
Analysis of crosslinked epoxy-urethane polymer filled with aluminum oxide particles to determine mechanical and thermodynamic properties
[SC-DR-70-617] 07 p0812 N73-16584
Solid propellant containing hydrazinium nitroformate oxidizer and polymeric hydrocarbon binder
[NASA-CASE-NPO-12015] 07 p0834 N73-16764
Technique for determining bulk modulus and associated loss factor of elastomeric and plastic materials
[AD-752483] 08 p0935 N73-17659
Linear differential equations for analyzing viscoelastic properties and mechanical behavior of high polymers
08 p0966 N73-17898
Radiation damage of electrically insulating polymeric materials used in electrotechnology
[AD-753367] 09 p1001 N73-18169
Data processing in reducing effort of mechanical testing polymers for flexural deformation and displacement
[ERDE-TR-111] 09 p1052 N73-18578
Changes in oxygen consumption in rats after inoculation with polymer combustion products
10 p1116 N73-19096
Comparison of oxygen transport in polymonomethylsiloxane with properties of polydimethylsiloxane to determine degradation mechanisms in pigmented coatings
[AD-753410] 10 p1176 N73-19565
Absorption of bile acids and cholesterol by polymers
10 p1227 N73-19976

Stability analysis for spinning flow of cylindrical liquid polymer filament with memory function
[AD-755065] 11 p1273 N73-20332
Development of nonisothermal theory of viscoelastic fluids with fading memory and application to viscometric flow
[AD-754802] 11 p1349 N73-20948
Pyrolysis gas chromatography method for rapid identification of organic polymers
[AD-755375] 12 p1377 N73-21168
Calculation of polymer elastic constants using sound speed measurements
[AD-755695] 12 p1429 N73-21586
Effects of drag reducing polymer on turbulent boundary layer of submerged flat plates
[AD-755215] 13 p1513 N73-22260
Research reports on amorphous, laser window, composite, and gradient materials
[AD-755585] 13 p1545 N73-22521
Mechanical properties and behavior of heat resistant alloys semiconductors, polymers and composite materials
[AD-755660] 13 p1549 N73-22552
Chemical process for production of polyisobutylene compounds and application as solid rocket propellant binder
[NASA-CASE-NPO-10893] 13 p1568 N73-22710
Technical compilation on adhesives and polymeric plastics
[NASA-SP-5961[01]] 14 p1680 N73-23630
Perfluoroalkylene ether polymers for high temperature fuel tank sealants
[NASA-CR-124249] 14 p1680 N73-23635
Polybenzimidazole, polyimide, and polyquinoxaline for low wear, lightweight, high strength bearing retainer
[NASA-CR-132217] 15 p1792 N73-24528
Influence of plastic deformation on structure and mechanical behavior of glassy amorphous polymers
15 p1801 N73-24595
Molecular structures and optical properties of polymer chain materials
[AD-758837] 16 p1872 N73-25156
Piezoelectric and pyroelectric properties of polymer electrets
[AD-758730] 16 p1933 N73-25638
Effect of crystallization kinetics on physical and chemical properties of polymers particularly polyethylene
[AD-750157] 16 p1953 N73-25802
Computerized analysis of electro-optical polymer relaxation data
[AD-759421] 17 p1992 N73-26111
Dynamic spring analysis for measuring hardening reaction of polymers
[RAE-LIB-TRANS-1698] 17 p2049 N73-26577
Torsional braid analysis of polymers
[AD-759412] 17 p2051 N73-26593
Procedures for improving resistance of Nomex fabric and webbing to actinic degradation
[AD-759217] 17 p2051 N73-26596
Crack growth in viscoelastic polymers
[AD-759379] 18 p2168 N73-27513
Quadratic programming with regularization for analyzing polymer molecular weight distribution
[AD-761818] 19 p2234 N73-28009
Polymeric monolayer barrier for thin film Josephson junctions
[NASA-CR-121270] 19 p2326 N73-28715
Solid polymer electrolyte regenerative fuel cells for communication satellites
[AD-762923] 20 p2365 N73-29016
High temperature and ultraviolet stability properties of poly[diarylsiloxy]arylazine
[NASA-CASE-ARC-10592-1] 20 p2435 N73-29554
Chemical analysis of structure and strength of polymeric glasses, elastomers, fibers, and solid polymeric systems with high degree of crosslinking
[AD-763398] 21 p2564 N73-30555
Thin layer chromatographic identification and infrared spectrophotometric quantification of antioxidants used in manufacturing polyolefinic polymers
[REPT-6726] 22 p2625 N73-31029
Drag reduction in fluids by addition of polymer additives
[AD-763824] 22 p2654 N73-31263
Temperature effects on structures and mechanical properties of polysulfone and poly[216-dimethyl] phenylene oxide
22 p2688 N73-31528
Properties and structure of polymers crystallized from stirred dilute solutions and sheared polymer melts
22 p2706 N73-31673
Utilization of lithium p-lithiphenoxide to prepare star polymers
[NASA-CASE-NPO-10998-1] 23 p2753 N73-32029
Effects on drag of injecting aqueous solutions of polyethylene oxide into turbulent boundary layer of flat plate
[AD-764896] 23 p2776 N73-32202
Reduction of friction drag in polymers
[AD-757012] 23 p2777 N73-32205
Evaluation of holographic-recording photopolymer to determine diffraction efficiencies and development techniques
[CRC-659] 23 p2800 N73-32395
Impact tests on selected polymers
[AD-764628] 23 p2811 N73-32479
Pyrolysis of heterocyclic polymer compounds
[AD-764720] 24 p2892 N73-33091
Chemical bonding of solid polymers to metal surfaces and formation of organometallics
[NASA-TM-X-71452] 24 p2929 N73-33390
Viscoelastic effects in design of polymeric equipment and structures
[AD-764555] 24 p2989 N73-33890

**POLYMETHYL METHACRYLATE**
Effect of bubble inclusions on mechanical properties of cast polymethyl methacrylate
[AD-746862] 03 p0321 N73-12616
Effects of rebinders on strength of polyethylene and polymethyl methacrylate
[AD-751615] 07 p0812 N73-16587
High resolution laser interferometer investigation of mechanical behavior of polymethyl methacrylate
[SC-DC-72-1174] 08 p0935 N73-17653
Fatigue crack propagation and retardation experiments using polymethyl methacrylate
[AD-756490] 14 p1681 N73-23641
Wear inhibiting effect of automotive oils containing polymethacrylate
[NLL-TRANS-1190-[9022.9]]
15 p1746 N73-24149
Principles of producing glass parts from polymethi methacrylate organic glass and tensile strength tests
[AD-763282] 22 p2690 N73-31542

**POLYMORPHISM**
Mechanical properties and crystal structures of polymorphous metals and alloys
[AD-759753] 17 p2074 N73-26779

**POLYNOMIALS**
NT BINOMIALS
Continuation method for solving eigenvalue problems and finding roots of polynomials
[TAE-152] 09 p1057 N73-18617
One-level polynomial objective analysis of meteorological fields
[NLL-M-22903-[5828.4F]] 18 p2170 N73-27524

**POLYPHENYL ETHER**
Oxygen concentration on boundary lubricating characteristics of unformulated C-ether using ball-on-disk sliding friction apparatus
[NASA-TN-D-7155] 07 p0811 N73-16578

**POLYPHENYLS**
Fabrication and tests of polyphenylene oxide foam panels for application as reusable insulation with LH2 tanks
[NASA-CR-123955] 05 p0565 N73-14586
Characteristics of gelled liquid hydrogen polyphenylene oxide foam open cell insulation
[NASA-CR-124114] 09 p1051 N73-18568
Development of polyphenylquinoxaline graphite fiber reinforced composites for structural materials
[NASA-CR-121109] 11 p1308 N73-20611
In situ monomer polarization for polyphenylquinoxaline/graphite
[NASA-TM-X-71454] 24 p2891 N73-33084

**POLYPROPYLENE**
Comparison of outdoor exposure of elastomers and plastics with exposure in accelerated weathering test chamber using fluorescent source of UV radiation
[ERDE-TR-107] 06 p0688 N73-15600
Flame retardant treatments for cotton fabrics and polypropylene fibers
19 p2230 N73-27982

**POLYQUINOXALINES**
Polyphenylquinoxaline resin systems for high temperature composite materials
[AD-746273] 02 p0193 N73-11559
Development of space shuttle semitransparent polyquinoxaline films
[NASA-CR-112213] 07 p0811 N73-16575
In situ monomer polarization for polyphenylquinoxaline/graphite
[NASA-TM-X-71454] 24 p2891 N73-33084

**POLYSACCHARIDES**
NT CELLULOSE
NT DEXTRANS

**POLYSTYRENE**
Impact damage caused by polystyrene, aluminum, or iron hypervelocity particles on glass
08 p0934 N73-17651
Polystyrene energy transfer studies using nitrostyrene compounds
[TN-257] 09 p0999 N73-18149
Syntheses of polystyrene polymers with skin friction reduction in dilute solutions
[AD-761600] 19 p2233 N73-28008
Combustion characteristics of polystyrene and oxygen-styrene copolymer with ammonium perchlorate composites
22 p2708 N73-31687

**POLYTETRAFLUOROETHYLENE**
Preparation and properties of polytetrafluoroethylene impregnated with rhenium oxides
[NASA-TN-D-7166] 07 p0811 N73-16579
MoS2 and MoS2/PTFE composite layers for dry lubrication of journal bearings in atmosphere or vacuum
[DLR-FB-72-69] 09 p1038 N73-18470
Scanning electron microscope used in friction tests of polytetrafluoroethylene sliding on aluminum single crystals
[NASA-TN-D-7321] 15 p1791 N73-24520
Analysis of compressibility of polytetrafluoroethylene when subjected to single stage and two stage shock loading
[NLL-NEL-TT-2491-[6075.461]]
20 p2386 N73-29170

**POLYURETHANE FOAM**
Shock wave attenuation in foam water mixtures containing Freon and exposed to hydraulic impact
[AD-748350] 04 p0407 N73-13318
Physio-chemical analysis of flammability characteristics and thermal degradation of rigid and flexible urethane foams used in aircraft structures - Part 2
[FAA-RD-73-50-PT-2] 18 p2105 N73-27025
Decomposition products of polyurethane foam related to aircraft cabin flash fires
[AD-763327] 22 p2730 N73-31846

**POLYURETHANE RESINS**
Aging of polyurethane elastomers based on hydroxyl terminated polybutadienes
[ERDE-TR-77] 02 p0192 N73-11554
Sulfur and MOCA cured polyurethane elastomer resistance to water, STF, and STF/water mixture
[ERDE-TR-83-PT-2] 02 p0192 N73-11555
Hydrolytic stability of polyurethane potting compounds in Navy aircraft
[AD-759972] 17 p2053 N73-26604
Thermal expansion instability and effect on creep properties of polyurethane
[AD-762458] 19 p2313 N73-28602
Characteristics of polyurethane film for fabrication of expandable envelopes subjected to solar heating at high altitudes
[AD-762803] 20 p2362 N73-29001
Chemical and physical properties of synthetic polyurethane polymer prepared by reacting hydroxy carbonate with organic diisocyanate
[NASA-CASE-MFS-10512] 21 p2505 N73-30099
Preparation of stable polyurethane polymer by reacting polymer with diisocyanate
[NASA-CASE-MFS-10506] 21 p2505 N73-30100
Preparation of polyurethane polymer by reacting hydroxy polyformal with organic diisocyanate
[NASA-CASE-MFS-10509] 21 p2505 N73-30103
Chemical and elastic properties of fluorinated polyurethanes
[NASA-CASE-NPO-10767-1] 24 p2891 N73-33076

**POLYVINYL CHLORIDE**
Plasticization of polyvinyl chloride with various reagents and effect on physicomechanical properties of systems
[AD-751875] 08 p0935 N73-17656
Experimental verification of theory on fiber formation from polyvinyl chloride and dimethyl formamide solutions in tube filled with water
[AD-753032] 09 p1054 N73-18596

**PONDS**
Inventory of ponds, lakes, and reservoirs in selected areas of State of Massachusetts
[PB-214116/6] 14 p1665 N73-23512
ERTS-1 detection of small ponds in forested areas of Texas
[E73-10673] 16 p1900 N73-25368
Photointerpretation of ERTS-1 imagery to map bodies of water in Saline County, Kansas
[E73-10684] 17 p2017 N73-26313
ERTS-1 and aircraft multispectral scanner data for mapping ponds and lakes near Woodworth, North Dakota to determine changes in continental migratory bird habitat
[E73-10714] 17 p2018 N73-26321
Evaluation of ERTS-1 imagery for determining numbers and distribution of prairie ponds and lakes in North Dakota
[PAPER-W12] 19 p2272 N73-28289

**POPULATION INVERSION**
CO2/N2 laser applied to CO2 excited state population study during supersonic nozzle expansion
[ONERA-NT-204] 10 p1169 N73-19510
Significant population inversion in flow structure behind blast wave
[AD-757881] 15 p1795 N73-24555
Formation mechanism of vibrational level population inversion in gas discharge CO lasers
[AD-759679] 16 p1925 N73-25578
Remote determination profiles of atmospheric structure constants and wind velocity along line-of-sight path by statistical inversion procedure
[AD-760805] 18 p2173 N73-27552
Molecular population inversion by Laval nozzle expansion in N2/He/carbon dioxide laser
[DLR-FB-72-21] 21 p2554 N73-30480
Electron collision excitation of population inversion in ionic argon lasers
23 p2800 N73-32393

**POPULATION THEORY**
Short-period comets and meteor stream genetic origin discussing formation processes
[TRITA-EPP-72-18] 02 p0231 N73-11880

Computational forms for transformed covariance matrix of multivariate normal populations
[REPT-19] 20 p2438 N73-29583

**POPULATIONS**

Census cities experiment in urban land use and change detection using ERRS-1 imagery
[E73-10064] 07 p0778 N73-16326

Urban and regional changes based on city census and remotely sensed imagery
07 p0786 N73-16395

Application of ERTS-1 data for identifying ethnic groups, limits of occupancy, and use of physiographic features in Republic of Mali, West Africa
[E73-10434] 11 p1281 N73-20394

Biostatistics of genetical processes in human populations
[NASA-CR-131508] 12 p1372 N73-21131

Distribution-free confidence intervals and significance tests for population median of random sample
[NASA-CR-131989] 14 p1683 N73-23660

**PORCELAIN**

Elastic modulus and coefficient of linear thermal expansion of perlite-containing porcelain mixes
[AD-747393] 03 p0322 N73-12627

Damping in porcelain enamel coatings at elevated temperatures
[AD-752317] 09 p1055 N73-18598

White porcelain enamal thermal control coating for spacecraft
[NASA-CR-124459] 24 p2938 N73-33459

**PORES**

U POROSITY

**POROSITY**

Changes in porous structure of nickel electrode substrates due to changes in manufacturing processes
[AD-748109] 03 p0255 N73-12067

X ray analysis of B2O3 effects on composition, porosity, and sorption properties of Al2O3
[NLL-M-22796-[5828.4F]] 06 p0682 N73-15553

Production of fibers, plaques, and highly porous sintered nickel materials
[NLL-TRANS-746-1381-[9022.401]]
06 p0687 N73-15592

Infiltrating porous and particulate materials with metallic alloys
[Y-1846] 12 p1414 N73-21458

Porous surface microphones for acoustic measurements in subsonic flow in wind tunnels
[NASA-CR-114593] 14 p1639 N73-23289

**POROUS BOUNDARY LAYER CONTROL**

Upper bound on heat transfer across porous fluid layer heated from below
16 p1973 N73-25956

**POROUS MATERIALS**

Mechanism of heat transfer for exothermic interaction in porous body between oxidizer and reagent
[AD-745460] 01 p0118 N73-10970

Development of porous electrode materials for plasma generators and effects of blowing protective gases through plasma
[AD-747369] 03 p0255 N73-12066

Analysis of friction surfaces of porous materials based on iron after prolonged operation under self lubricating conditions
[AD-748020] 03 p0317 N73-12585

Wind tunnel tests to determine effects of gas stream flow parallel to discharging surface on flow characteristics of wire-form porous material
[NASA-TM-X-2687] 04 p0369 N73-13000

Preparation of porous metal samples for quantitative metallographic analysis and effects of procedure on accuracy of results obtained
[NLL-TRANS-746-1255-[9022.401]]
05 p0561 N73-14555

Physical properties of porous nickel strips used as electrodes in electro-vacuum equipment and methods for controlling expansion during production
[NLL-TRANS-746-1342-[9022.401]]
06 p0682 N73-15551

Analysis of supersonic, three-dimensional flow characteristics to determine effects of material porosity and angle of attack on jet stretcher performance
07 p0765 N73-16215

Development of method and equipment for detecting cracks in materials with porous subsurface matrix covered by impervious coating
[NASA-CASE-MSC-14187-1] 08 p0923 N73-17564

Development of model to describe flow process, energy transfer, and flame front propagation during combustion of porous propellant charges
08 p0968 N73-17910

Design of porous cooled medium surface to maintain specified design temperature while subjected to uniform heating from external source
[NASA-TN-D-7176] 08 p0969 N73-17919

Hardness and physical characteristics of titanium sponge with low residual chloride concentration after vacuum separation
[JPRS-58347] 09 p1048 N73-18544

Analysis of linear elastic wave propagation normal to laminations of periodically laminated porous composite
[AD-753900] 10 p1221 N73-19934

Analysis of porous media of heat pipe wicks to determine effects on permeability and thermal conductivity of materials
10 p1222 N73-19938

Analysis of interaction of rarefied gas with surface of porous moist bodies during heat and mass transfer using visual and photographic methods
[AD-754633] 11 p1272 N73-20325

Development of phosphoric acid fuel cells operating on hydrogen produced from thermocracking or steam reforming of hydrocarbon
[AD-755206] 13 p1477 N73-21966

Porous structure and surface energy of evaporated metal thin films
13 p1565 N73-22683

Development of theory for wind tunnel boundary upwash interference on symmetrical finite wing with arbitrary lift distribution
[AD-757196] 14 p1652 N73-23397

Measurement of gas permeability of high porosity nickel powder metallurgy parts
[NLL-LTI-746-1404-[9022.401]]
15 p1797 N73-24564

Characteristics and production methods of iron nickel-molybdenum carbonyl powders
[NLL-LTI-746-1418-[9022.401]]
16 p1925 N73-25580

Finite element analysis of thermoplasticity and nonlinear mechanics of fluid-saturated porous solids
[AD-758884] 16 p1972 N73-25949

Probabilistic model of nonisothermal gaseous flow through fine pored homogeneous media
17 p2013 N73-26276

Conformal mapping technique for two-dimensional porous media and jet impingement heat transfer
[NASA-TM-X-68276] 20 p2485 N73-29961

Hollow cathode with BaO impregnated, porous tungsten inserts and tips
[NASA-TM-X-71417] 21 p2517 N73-30189

Shock wave effects in porous iron
[AD-763796] 21 p2540 N73-30368

Porous electrode for use in electrochemical cells
[NASA-CASE-GSC-11368-1] 23 p2763 N73-32108

**POROUS PLATES**

Calculation of drag of porous lattice plates in turbulent flow
[IC-AERO-72-20] 03 p0284 N73-12300

Analysis of turbulent boundary layer on porous plate and fluid mechanics of adverse free stream pressure gradients
15 p1765 N73-24303

Stability of horizontal layer of binary gas mixture in porous medium with different upper and lower boundary temperatures
16 p1886 N73-25263

Porosity analysis on silica and mullite composite surface insulation tiles
24 p2939 N73-33472

**POROUS WALLS**

Plane turbulent gradient flow of incompressible fluid along porous surface in presence of blowing or suction
[AD-746933] 02 p0159 N73-11290

Interference theory in slotted wind tunnels extended to subsonic rectangular wind tunnels with ventilated tool, longitudinal slots and perforated screens of arbitrary porosity
[ARC-R/M-3706] 05 p0492 N73-14007

Subsonic diffusers having ribs aligned transverse to flow direction for separation control
13 p1508 N73-22225

Gas injection of turbulent boundary layer through porous wall
[ONERA-NT-201] 13 p1510 N73-22237

Effects of porous wind tunnel wall corrections on transport aircraft models
14 p1648 N73-23366

Kinetic molecular flow distribution at porous wall using one dimensional steady state Boltzmann equation
[VKI-TN-79] 22 p2654 N73-31259

Slotted transonic wind tunnel tests on pitching delta wing enable selection of porpous walls for interference free damping derivatives
[ARC-R/M-3715] 24 p2870 N73-32930

**PORPHYRINS**

NT CHLOROPHYLLS

**PORTABLE EQUIPMENT**

Description, performance specifications, and results of performance tests for Hydrolab 2A portable water quality analyzer
[NOOH-IFS-73006] 01 p0057 N73-10468

Portable radon alpha decay detectors for use in fluorspar mines
[BMBW-FBK-72-14] 03 p0303 N73-12473

Nickel cadmium storage battery for portable power supply of man-pack equipment
[AD-748454] 04 p0376 N73-13055

Design of portable HF/VHF radio set for manpack usage
[AD-749510] 05 p0514 N73-14175

Lightweight, low power combat surveillance Doppler radar
[AD-750370] 06 p0642 N73-15212

Feasibility of mobile nuclear reactor power plants for cargo transportation and development of remote regions on earth
[NASA-TM-X-68164] 06 p0698 N73-15693

Portable instrumentation kit feasibility study
[AD-751188] 07 p0802 N73-16514

Portable device for detecting pneumatic pressure leaks in hermetically sealed housings
[NASA-CASE-MFS-21761-1] 09 p1035 N73-18444

Portable penetrometer for analyzing soil characteristics
[NASA-CASE-MFS-20774] 10 p1158 N73-19420

Portable pulsed laser ranging system for measurements between earth and retroreflecting satellites
[NASA-CR-131513] 12 p1410 N73-21423

Thick film hybrid radio receiver module consisting of intermediate frequency amplifier and discriminator manpack
[AD-756428] 13 p1494 N73-22108

Design and operating characteristics of pulsed ruby laser source used in portable holocamera
16 p1920 N73-25541

Computerized simulation of mobile tracking radar performance
[AD-762338] 19 p2238 N73-28043

Tool exchange capabilities of portable wrench characterized by telescopic sleeve
[NASA-CASE-MFS-22283-1] 21 p2553 N73-30462

Reliability of USAF fire protection systems including portable equipment
[AD-762948] 21 p2610 N73-30925

Hand-held, lightweight, portable photomicroscope
[NASA-CASE-ARC-10468-1] 24 p2925 N73-33361

**PORTABLE LIFE SUPPORT SYSTEMS**

Flight tests of portable diaphragm liquid pump for astronaut cooling
09 p1089 N73-18883

Regenerable CO2 sorbent formulation and fabrication for extravehicular activity
[NASA-CR-114632] 20 p2371 N73-29054

Guidelines for extravehicular and intravehicular activities during space shuttle operation with emphasis on contingency situations - Vol. 2
[NASA-CR-133992] 22 p2622 N73-31007

Pressure suit requirements and characteristics for space shuttle personnel performing EVA and IVA activities - Vol. 3
[NASA-CR-133993] 22 p2622 N73-31008

**PORTS**

Detailed environmental profiles for seven potential Gulf Coast deep water port sites
[AD-758455] 15 p1806 N73-24637

**POSEIDON MISSILES**

Fire control computer program for Poseidon missile failure data processing
[AD-754426] 11 p1260 N73-20230

**POSITION [LOCATION]**

NT SOLAR POSITION

Computerized aerotriangulation with independent models and planimetric point adjustments
02 p0164 N73-11332

Simulation control of European SOREL space probe attitude and position
[S-3-1949-VOL-3] 02 p0235 N73-11907

Fringe rate residuals used for baseline interferometry measurement of radio source positions
[AD-746464] 03 p0266 N73-12155

Electromagnetic compatibility of very high frequency/frequency modulated radio equipment in tactical site selection
[AD-749186] 04 p0391 N73-13179

Geostationary satellite position and attitude determination using picture landmarks
[NOAA-TM-NESS-21] 04 p0474 N73-13875

Device for recording locations of measurements made by hand-held noncontacting probe
[NASA-CASE-LAR-10806-1] 06 p0673 N73-15474

Tracking performance and quality of colocated laser tracking stations
[NASA-TM-X-66158] 07 p0765 N73-16220

Astrometry for determination of absolute positions of stars and their relative motions from Schmidt plates noting accuracy
07 p0845 N73-16843

Astrometric performance of Schmidt plates for stellar positions noting reduction of coordinates
07 p0845 N73-16844

Most probable position in astronomical navigation using celestial body coordinates
07 p0859 N73-16972

Analysis of orthopolar coordinate system to compensate for ellipsoidal shape of earth and formulas for conversion to geographic system
08 p0923 N73-17561

Method for determining relative orientation of coordinate axes of stellar catalogs
[AD-751077] 09 p1085 N73-18855

Characteristics of navigation satellite system and analysis of operation of translocation subsystem
[AD-754173] 10 p1186 N73-19650

PLRACTA interfaced with site acquisition radar at Nike base in Lincoln, Mass.
[AD-754231] 10 p1229 N73-19991

Comparative evaluation of point marking devices and their suitability for photogrammetric problems
13 p1528 N73-22383
Position location in presence of parametric uncertainty
[AD-756251] 14 p1691 N73-23722
Electromagnetic superconducting force producing coil for positioning models in wind tunnel
15 p1762 N73-24276
Location of archeological village sites in Alaska from ERTS-1 imagery
[E73-10638] 15 p1776 N73-24397
Effect of receiving antenna height measurement on three-dimensional position fixing with navy navigation satellite system
[DLR-FB-73-28] 16 p1941.N73-25712
Development of radio locating system for monitoring geographic movement of surface vehicles in metropolitan area using unsynchronized radio broadcasting stations
[NASA-CASE-NPO-13217-1] 17 p1997 N73-26144
Procedures for obtaining position from surface gravity observations and application of geodetic techniques to earth and ocean physics
[NASA-TM-X-66273] 17 p2059 N73-26655
HELOS lunar occultation experiment on X ray galactic and extragalactic source position and angular size determination
17 p2085 N73-26868
Design, development, and test of NASA-GFSC Position Location and Aircraft Communications Equipment [PLACE]
[NASA-TM-X-66287] 18 p2117 N73-27115
Real time measurement of three-dimensional position of light emitting diodes
[AD-762028] 19 p2241 N73-28070
Determination of orientation of instrument trihedrons and applications in inertial navigation
20 p2451 N73-29701
Random distributions and position angle measurements of elliptical and spiral galaxies
20 p2469 N73-29833
Position of earth spin axis with respect to crust computed on basis of Doppler satellite observations
[AD-763362] 21 p2542 N73-30381
Collimator for analyzing spatial location of near and distant sources of radiation
[NASA-CASE-MFS-20546-2] 21 p2543 N73-30389
Angular position of target determined by scanning radar against background of correlated noise
22 p2628 N73-31057
Solution to radio fixes in spherical trigonometry with confidence region and position error analysis
[AD-764465] 22 p2698 N73-31613
Recognition algorithm for object localization in pictures
[BMVG-FBWT-73-14] 23 p2760 N73-32091

**POSITION ERRORS**
Iterative method for localizing position of balloon on earth, using interrogating satellite and correcting for errors due to terrestrial rotation
[NASA-TT-F-14702] 03 p0328 N73-12677
Iterative method for localizing position of balloon on earth, using interrogating satellite and correcting for errors due to terrestrial rotation and Doppler effect
[NASA-TT-F-14703] 03 p0328 N73-12679
Position errors in airspeed calibration methods
[NAL-298] 15 p1786 N73-24477
Formulation of radar glint tracking error reduction using frequency agility and linear amplitude weighting
16 p1874 N73-25171
Solution to radio fixes in spherical trigonometry with confidence region and position error analysis
[AD-764465] 22 p2698 N73-31613

**POSITION INDICATORS**
NT PLAN POSITION INDICATORS
NT RADIO DIRECTION FINDERS
NT SPACECRAFT POSITION INDICATORS
Influence of sea state on short pulse radar satellite altimeter determination of mean surface position
06 p0663 N73-15385
Doppler compensated communication system for locating supersonic transport position
[NASA-CASE-GSC-10087-4] 11 p1254 N73-20174
Iterative directional analysis of ocean waves
[AD-753825] 11 p1289 N73-20460
Determination of ship positions in broad ocean areas using C band radar tracking data
[NASA-CR-62086] 13 p1491 N73-22083
Position reporting and cmmunications systems of aviation and marine rescue operations
[AD-761756] 19 p2228 N73-27967
Aircraft mounted crash location transmitter for emergency signal transmission after crashes
[NASA-CASE-MFS-16609-2] 22 p2631 N73-31084

**POSITIONING**
Tool positioning holder for grinding by ball nose milling cutter
[NASA-CASE-LAR-10450-1] 01 p0061 N73-10504
Rotating generator for angular display of television raster in horizontal and visual simulation systems
[NASA-CASE-FRC-10071-1] 05 p0513 N73-14171
Human horizontal or antiorthostatic position effect in hypodynamic weightlessness test
13 p1482 N73-22011
Screw calculus in kinematic and power analyses on spatial positions of manipulator link mechanisms
17 p1990 N73-26092
Sound beams for position control during manufacturing in space
[NASA-CR-124300] 19 p2321 N73-28671
Satellite based system for L band precision positioning
[NASA-CR-62095] 22 p2697 N73-31604

**POSITIONING DEVICES [MACHINERY]**
NT BOOMS [EQUIPMENT]
NT CAMS
Design and development of test stand system for supporting test items in vacuum chamber
[NASA-CASE-MFS-21362] 11 p1265 N73-20267

**POSITRON ANNIHILATION**
Gravitationally red-shifted positron annihilation radiation produced at surfaces of old neutron stars
[NASA-TM-X-66062] 01 p0100 N73-10818
Electron positron annihilation structure functions calculated with light cone operator product expansions and Callan-Symanzik equation
[ILL-(TH)-72-12] 07 p0823 N73-16670
Investigation of positron annihilation in water and ice by measuring angular correlation
07 p0859 N73-16969
Total cross sections for electron positron annihilation producing hadron pair
[NOTA-INTERNA-420] 18 p2181 N73-27613
Positron annihilation radiation model for neutron star density in galactic disk
22 p2733 N73-31869

**POSITRONS**
Measurements of positron lifetime distributions used to characterize plastic deformation in crystals
[COO-2128-2] 06 p0708 N73-15779
Computerized positron scintillation camera data acquisition and display system for linear accelerator facility
[UCRL-51288] 10 p1161 N73-19447

**POSTFLIGHT ANALYSIS**
Postflight analysis of Atlas/Centaur - 29 and Intelsat 4 launch and orbit establishment
[NASA-TM-X-68649] 01 p0102 N73-10845
Postflight analysis of Apollo 15 LM APS
[NASA-TM-X-68932] 06 p0712 N73-15813
Postflight analysis of Apollo 14 translunar docking anomaly
09 p1089 N73-18884
Postflight analysis of abnormalities in Apollo 17 flight
[NASA-TM-X-69122] 10 p1211 N73-19850
Inoperative conditions of rear steering system of lunar roving vehicle on Apollo 16 flight
[NASA-TM-X-69198] 17 p2010 N73-26256
Results of postflight analysis of APS performance during Apollo 15 mission
[NASA-TM-X-69204] 17 p2077 N73-26801
Results of postflight analysis of APS performance during Apollo 12 Mission
[NASA-TM-X-69529] 17 p2083 N73-26850
Postflight analysis of Apollo 11 glycol temperature control valve failure
[NASA-TM-X-69200] 17 p2088 N73-26896
Inertial subsystem warning and coupling data unit failure indications on Apollo 16 mission
[NASA-TM-X-69199] 17 p2089 N73-26898
Postflight analysis of Apollo 16 scanning telescope system to determine cause of uneven drive rates
[NASA-TM-X-69233] 17 p2089 N73-26899
Radioactivity urinalysis for calculating postflight astronaut cosmic radiation exposure
[NASA-CR-133378] 19 p2224 N73-27939
Steady state performance of LM-10 Descent Propulsion System during descent phase of Apollo 15 Mission
[NASA-TM-X-69506] 22 p2717 N73-31750
Apollo experience report on various phases of postflight testing of command modules to resolve or minimize anomalies discovered during flight
[NASA-TN-D-7435] 22 p2721 N73-31773
Post mission data analysis of Surveyor 5, 6, and 7 chemical data
[NASA-CR-135900] 24 p2979 N73-33802
Postflight analysis of Apollo 15 flight to determine performance of launch vehicle, spacecraft, and lunar roving vehicle and to analyze malfunctions
[NASA-TM-X-69539] 24 p2981 N73-33819
Performance evaluation of SA-206 launch vehicle for Skylab 2 launch to show signficant events and failures and anomalies
[NASA-TM-X-69538] 24 p2981 N73-33820
Performance evaluation of SA-207 launch vehicle for Skylab 3 launch to show significant events and failures and anomalies
[NASA-TM-X-69540] 24 p2981 N73-33821
Evaluation of launch vehicle, spacecraft, and lunar rover performance during Apollo 17 flight to determine malfunctions and recommend corrective actions
[NASA-TM-X-69534] 24 p2981 N73-33822
Postflight analysis of Apollo 16 flight to show spacecraft performance, launch vehicle performance, and malfunctions occuring during flight
[NASA-TM-X-69535] 24 p2981 N73-33823
Postflight analysis of Apollo 14 flight to show spacecraft performance, launch vehicle performance, and malfunctions occurring during flight
[NASA-TM-X-69536] 24 p2981 N73-33824

**POSTURE**
Whole body, plus or minus a[z] vibration on amplitude and frequencies of postural sway in human subjects
[AD-745580] 01 p0013 N73-10098
Dynamic model for nonlinear simulation of human postural control system using sticks
01 p0015 N73-10116
Regulation of vertical posture after Soyuz 6, 7, and 8 flights and after 120-day bed rest experiment
07 p0744 N73-16052
Instrument for measurement of postural equilibrium in human beings
[AD-763096] 20 p2373 N73-29067

**POTABLE LIQUIDS**
NT POTABLE WATER

**POTABLE WATER**
Environmental health measures to prevent cabin atmosphere toxicity and provide drinking water standards in manned space flight applications
08 p0872 N73-17058
Silver-ion bactericidal monitor for Space Shuttle potable water system
[NASA-CR-128884] 11 p1293 N73-20492
Apollo experience report on design and function of Apollo potable water system supplied as byproduct of fuel cells
[NASA-TN-D-7291] 15 p1835 N73-24874
Aerospace distillation water recovery system for reclamation of potable water from domestic wash water
[NASA-TM-X-2896] 22 p2737 N73-31913

**POTASSIUM**
Crossed molecular beam method for measuring elastic differential scattering cross sections of potassium with gaseous media
02 p0213 N73-11729
Laser selective excitation of doublet transition in atoms of pure potassium plasma
[AD-745964] 02 p0216 N73-11750
Splitting aluminosilicates with silicate bacteria for liberation of potassium in soils
[NASA-TT-F-14870] 11 p1286 N73-20437
Plasma enhancement and diagnostic possibilities of tunable laser excitation
[AD-755373] 13 p1564 N73-22672
Feasibility of potassium-cesium mixture for seeding magnetohydrodynamic combustion plasma
[PB-214314/7] 16 p1865 N73-25102
Analysis of nonequilibrium conditions among populations of excited levels of potassium vapor passing through supersonic nozzle
18 p2128 N73-27199
High intensity noise effects on urinary K-Na ratios in rats
20 p2365 N73-29018
Low temperature thermal magnetoresistance of potassium
[COO-3150-12] 22 p2625 N73-31036
Polycrystals and monocrystals of ice grown from KCl solution
[CONTRIB-1247] 22 p2646 N73-31203

**POTASSIUM BROMIDES**
High resolution spectral reflectance of potassium chlorides and bromides at room temperature in far ultraviolet yields new structures
[NOTA-INTERNA-402] 05 p0587 N73-14777
Measurement of volume relaxation and crystal defects associated with interstitial ion in X irradiated KBr during isothermal annealing
07 p0831 N73-16735

**POTASSIUM CHLORIDES**
High resolution spectral reflectance of potassium chlorides and bromides at room temperature in far ultraviolet yields new structures
[NOTA-INTERNA-402] 05 p0587 N73-14777
Dielectric susceptibilities of potassium chloride to lithium and hydroxyl, sodium chloride to hydroxyl, and rubidium chloride to cyanides
[COO-3151-14] 10 p1200 N73-19763
Growth and hardening of potassium chloride single crystals for infrared laser windows
[AD-757893] 15 p1795 N73-24550
Temperature dependence of elastic constants and Debye temperature of NaCl and KCl single crystals
[NASA-TT-F-14932] 16 p1953 N73-25801
High density optical memory and electron spin dependent trapping and tunneling processes in KCl and KCl-NaCl
20 p2460 N73-29768

**POTASSIUM CHROMATES**
Aircraft corrosion prevention by addition of potassium dichromate to rinse water
[AD-753214] 09 p0986 N73-18050

**POTASSIUM COMPOUNDS**
NT POTASSIUM BROMIDES
NT POTASSIUM CHLORIDES
NT POTASSIUM CHROMATES
NT POTASSIUM HYDROXIDES
NT POTASSIUM IODIDES

Potassium ferrioxalate actinometric measurements of solar ultraviolet photobiological energy
15 p1741 N73-24113
Coloring memory crystals by electron bombardment and KCl, Na, Cl for thermoelectric cooling for high density optical memory
[AD-765391] 23 p2762 N73-32105
Growth of potassium tantalate single crystals
[AD-764902] 23 p2828 N73-32603
Infrared absorption spectra of lithium and potassium silicate glasses
[AD-764891] 24 p2893 N73-33092

**POTASSIUM HYDROXIDES**
Leakage of ESRO 4 nickel cadmium batteries noting electrical and pressure measurements and KOH loss
[ESRO-CR[P]-132] 04 p0375 N73-13053
Determination of KOH loss in ESRO 4 nickel cadmium batteries by electrical measurements
[ESRO-CR[P]-132] 04 p0375 N73-13054
Passivating effects of additives on zinc corrosion in potassium hydroxide solutions
[NASA-TT-F-14693] 08 p0884 N73-17155
Diffusion coefficients for zinc electrode in potassium hydroxide solutions
[AD-753096] 09 p0991 N73-18092
Improving resistance of chrysotile asbestos to potassium hydroxide at temperatures above 100 C
[AD-761512] 19 p2223 N73-27931
Fuel cell technology using low temperature potassium hydroxide electrolyte
[NASA-CR-134002] 21 p2499 N73-30056

**POTASSIUM IODIDES**
Spectrophotometric determination of aqueous iodine complexed with potassium iodide showing free iodine optimally determined at isosbestic point for solutions
[NASA-CR-128585] 01 p0022 N73-10172

**POTENTIAL ENERGY**
NT BIOELECTRIC POTENTIAL
NT COULOMB POTENTIAL
NT ELECTRIC POTENTIAL
NT GEOPOTENTIAL HEIGHT
NT IONIZATION POTENTIALS
NT LOW VOLTAGE
NT NUCLEAR POTENTIALS
NT PLASMA POTENTIALS
NT SPIKE POTENTIALS
Mean monthly hurricane heat potential and sea surface temperature changes associated with storm passage for North Atlantic and North Pacific Oceans
[AD-751590] 07 p0790 N73-16429
Conversion of geomagnetic potential into spherical coordinates of optimally offset, inclined dipole using least squares method
[AD-756460] 13 p1526 N73-22366
Stabilities of nitrogen containing heterocyclic radicals, computation of simple potential energy surfaces, and photophysical properties of indolizine
[NASA-CR-133919] 22 p2625 N73-31034

**POTENTIAL FIELDS**
Low energy electron measurements by VELA satellite plasma probes and spacecraft potential
[LA-DC-72-1481] 19 p2324 N73-28695

**POTENTIAL FLOW**
User manual for computer program of potential flow calculation about three-dimensional lifting bodies
[AD-755933] 12 p1393 N73-21292
Computer graphics for solving three dimensional lifting body potential flow nonlinear equations to determine aerodynamic loads
[DGT-7510] 13 p1474 N73-21939
Three dimensional potential flow problems solved by means of inverse formation and finite differences
[AD-760347] 17 p2016 N73-26302
Integral equations for calculating incompressible potential flows around profiles with suction and blowing
[NASA-TT-F-14962] 18 p2130 N73-27209
Calculation of incompressible potential flow of airfoils by conformal mapping potential flow of lifting circles onto airfoils by double transformations
[ARC-R/M-3717] 21 p2492 N73-30002
Computer solutions for potential and viscous flow calculations for engine inlets
[NASA-TM-X-71457] 24 p2905 N73-33184

**POTENTIAL PROBLEMS**
U POTENTIAL THEORY

**POTENTIAL THEORY**
Potential theory for determining electromagnetic field caused by radial electron emission near conducting sphere
[AD-753664] 09 p1068 N73-18714
Method of local potential applied to analysis of turbulent shear flow
[NASA-CR-112322] 16 p1889 N73-25286
Pattern recognition and potential function
[REFT-6] 20 p2437 N73-29571

**POTENTIOMETERS [INSTRUMENTS]**
Model of electrophotometer for recording ratio of two light currents
[AD-750595] 06 p0675 N73-15494
Potentiostatic tests for determining range of crevice corrosion susceptibility in chromium modified cupronickel alloys
[AD-762596] 22 p2687 N73-31524

**POTENTIOMETERS [RESISTORS]**
Characteristics of carbon, cermet, and wire-wound type potentiometers based on service life and environmental tests
[ECR-30] 08 p0924 N73-17569

**POTOMAC RIVER VALLEY [MD-VA-WV]**
Digital analysis of ERTS-1 data to determine sedimentation levels in Potomac and Anacostia Rivers confluence and strip mining in Allegheny County, Maryland
[PAPER-E13] 19 p2270 N73-28277
Development of resources management information system for resources data from Potomac River Basin
[E73-11069] 23 p2781 N73-32245

**POTTING COMPOUNDS**
Nonsporicidal methods for solvent degradation of cured RTV 41 silicon potting compound and chemical curing effects on decontamination properties
[NASA-CR-130720] 08 p0878 N73-17111
Spectroscopic and chromatographic analysis of outgassing contaminants in potting compound and paint
[NASA-CR-124227] 13 p1488 N73-22061
Evaluation of potting compounds by electrical resistivity techniques using continuous current monitoring device
[AD-759005] 16 p1933 N73-25643
Hydrolytic stability of polyurethane potting compounds in Navy aircraft
[AD-759972] 17 p2053 N73-26604
Development of chemical process for determining quantity of contamination buried in potting compounds and removable of spores with amine dissolution and plating techniques
[NASA-CR-133645] 21 p2562 N73-30535
Titanium dioxide doped, silicon rubber, potting compound for satellite-borne channel multipliers noting doping effects, performance tests, and space applications
24 p2927 N73-33378
Titanium dioxide doped silicone rubber potting compound for satellite-borne channel multipliers
24 p2927 N73-33379

**POWDER [PARTICLES]**
NT METAL POWDER
NT PLATINUM BLACK
Rotary powder sample divider for preparation of small sub-samples of heterogeneous powders with adverse flow properties
[PB-211838] 05 p0553 N73-14489
Rheological properties of abrasive powder solutions considering particle dispersion
[AD-756082] 13 p1488 N73-22065
Theoretical analysis of ballistic H powder erosion combustion in acoustic stream
14 p1700 N73-23796
Test equipment and procedure for determining electrical conductivity of stream of hot powdered fuel during combustion process
[JPRS-59752] 20 p2485 N73-29960
Experimental design parameters for Raman spectroscopy of turbid suspensions and powders using ion gas laser light sources and noting S/N improvement
[NOTA-INTERNA-346] 21 p2580 N73-30676
Analysis of properties of powder materials subjected to compressive forces and development of equations of state for determining mechanical properties
[NLL-NEL-RR-2474-[6075.461]]
21 p2603 N73-30858
Spraying of powdered polymer coatings onto grooves in micromachines
[AD-764933] 24 p2929 N73-33396

**POWDER METALLURGY**
Performance of powder metallurgy bronze graphite bearings operating under hydrodynamic conditions at high slipping rates
[AD-747432] 03 p0309 N73-12523
Analysis of friction surfaces of porous materials based on iron after prolonged operation under self lubricating conditions
[AD-748020] 03 p0317 N73-12585
Superalloys from prealloyed powders at high temperatures
[NASA-CASE-LEW-10805-1] 04 p0425 N73-13465
Fabrication and properties of structural materials based on ceramic titanium powders alloyed with molybdenum and aluminum
04 p0432 N73-13520
Antifriction and friction powder metallurgy materials
[AD-749637] 05 p0553 N73-14495
Production of metal powders with emphasis on iron powder
[NLL-TRANS-746-1262-[9022.401]]
05 p0561 N73-14557
Method of thermal desorption used to determine specific surfaces in powder metallurgy
[NLL-TRANS-746-1287-[9022.401]]
06 p0682 N73-15547
Application of powder metallurgical techniques to fabrication of reaction-bonded Si3N4 for use as high temperature engineering ceramic
[AD-750096] 06 p0688 N73-15603
Development of powder metallurgy nickel-base superalloy for application at 1800 to 2000 F
[NASA-CR-121099] 09 p1047 N73-18537
Economic factors affecting titanium powder metallurgy research and development
09 p1047 N73-18539
Powder metallurgy methods to increase cost effectiveness of titanium raw materials processing
[JPRS-58217] 09 p1048 N73-18542
Fabrication and properties of prealloyed steel powders
[AD-753325] 10 p1167 N73-19497
Technical and economic problems and possibilities of developing titanium powder metallurgy
[NLL-LTI-746-1336-[9022.401]]
12 p1411 N73-21438
Determination and identification of gases in powdered carbonyl nickel
[NLL-LTI-746-1353-[9022.401]]
12 p1412 N73-21439
Instrumentation and data handling process of NAE T-33 turbulence research aircraft, stationary gas turbine icing problems, and role of plastic deformation in metal powder compaction
[DME/NAE-1972[4]] 12 p1466 N73-21882
Tooling workpiece interface condition effects on metal flow and product quality in extrusion
[AD-755832] 13 p1535 N73-22439
Development of method for fabricating cermets and analysis of various compositions to show electrical and physical properties
[NASA-CASE-NPO-13120-1] 14 p1679 N73-23629
Measurement of gas permeability of high porosity nickel powder metallurgy parts
[NLL-LTI-746-1404-[9022.401]]
15 p1797 N73-24564
Magnetic properties of highly dispersed iron-cobalt-nickel alloy powders
[NLL-LTI-746-1419-[9022.401]]
15 p1797 N73-24566
Manufacture of military hardware using powder metallurgy
[DREV-TN-2035/72] 15 p1797 N73-24570
Dispersion strengthened nickel-yttria sheet alloy produced from comminuted powders
[NASA-TM-X-68245] 15 p1798 N73-24576
Rotating electrode process for processing 18Ni maraging steel by powder metallurgy
[AD-758439] 15 p1800 N73-24589
Powder neutron diffraction and susceptibility measuring techniques to study magnetic properties of RbMnBr3
[BNL-17519] 15 p1814 N73-24703
Dispersed granulation of metals and titanium alloys
[AD-759625] 17 p2047 N73-26559
Fast freezing for producing aluminum alloys from consolidated powder
[AD-759828] 17 p2048 N73-26569
Effects of metallurgical processes on thermodynamic properties and compatibility of reinforcing fibers for refractory materials
[JPRS-59118] 20 p2430 N73-29518
Production and characteristics of highly dispersed composite powders on copper base containing metal carbides by reducing copper carbonate with hydrogen
23 p2808 N73-32451
Physical and mechanical properties of cermets to include methods for altering characteristics for specific industrial applications
23 p2809 N73-32459
Experimental and theoretical model of deformation and densification of sintered powder metallurgy compacts
24 p2933 N73-33422
Chemical and physical properties of graphite and carbide-graphite composites developed by powder metallurgy
[LA-5147] 24 p2936 N73-33448

**POWDERED METALS**
U METAL POWDER

**POWER AMPLIFIERS**
Comparison of micropower operational amplifiers based on various measurements and performance tests
[GRI/NTP/105] 05 p0520 N73-14225
Surface cooling method for very high frequency power transistor using heat pipe techniques
[AD-752076] 08 p0889 N73-17200
Semiconductor transmitter in S band
[DLR-FB-72-53] 09 p1007 N73-18220
Microwave UHF and SHF semiconductor oscillators and power amplifiers, noting gunn and impatt diode solutions, and integrated circuit development
[DLR-MITT-73-06] 10 p1135 N73-19248
Design equations for electron beam, semiconductor amplifiers with large area diodes to enhance power output
[AD-755806] 12 p1385 N73-21229
Performance tests on transmitter receiver and power amplifier for portable radio manpack
[AD-759953] 17 p2000 N73-26174
Computerized design of power amplifier
[SLA-73-153] 17 p2004 N73-26204
Computerized design of Smith chart and power amplifier
[AD-759701] 17 p2004 N73-26205
Development of linear power transistors and design of broadband UHF amplifiers from these transistors
[AD-757558] 17 p2006 N73-26227

GaAs and InP reflection amplifier noise figure and power gain at extremely high frequencies
[ESRO-CR[P]-262] 19 p2244 N73-28088
Solid state high power UHF broadband amplifier
[AD-762175] 19 p2247 N73-28118
S-band power amplifier using high efficiency silicon avalanche diode
[AD-763104] 20 p2381 N73-29135
Comparative study of TWT and klystron amplifiers for use as power amplifiers in television broadcast satellites
[ESRO-CR[P]-267-VOL-1] 21 p2508 N73-30122
Comparative study of TWT and klystron amplifiers for use as power amplifiers in television broadcast satellites
[ESRO-CR[P]-268] 21 p2508 N73-30123
Comparative study of TWT and klystron amplifiers for use as power amplifiers in television broadcast satellites
[ESRO-CR[P]-269-VOL-3] 21 p2508 N73-30124
Comparative study of TWT and klystron for use as power amplifier in TV broadcast satellites
[ESRO-CR[P]-271] 22 p2634 N73-31109
Comparative study of TWT and klystron for use as power amplifier in TV broadcast satellites
[ESRO-CR[P]-272] 22 p2634 N73-31110
Final design and specifications for solid state, S band, power amplifier
[NASA-CR-124405] 23 p2764 N73-32115

**POWER CONDITIONING**
Silicon-controlled, rectifier series, resonant inverter, power conditioning for electric propulsion from solar array
[NASA-CR-120928] 02 p0223 N73-11804
Power conditioning subsystem for Symphonie satellite with bus voltage regulation
[REPT-72-90] 09 p0991 N73-18085
Electromagnetic interference of power conditioners for solar electric propulsion
[NASA-CR-133229] 17 p2076 N73-26798
Comparative study of TWT and klystron amplifiers for use as power amplifiers in television broadcast satellites
[ESRO-CR[P]-267-VOL-1] 21 p2508 N73-30122
Comparative study of TWT and klystron amplifiers for use as power amplifiers in television broadcast satellites
[ESRO-CR[P]-268] 21 p2508 N73-30123

**POWER CONVERSION**
U ELECTRIC GENERATORS

**POWER DENSITY**
U FLUX DENSITY

**POWER EFFICIENCY**
Optimization of specific power highly efficient radioisotope thermoelectric generator
07 p0819 N73-16636
Dynamic performance criteria for power actuating components of electrohydraulic actuation servosystem
[NASA-TM-X-2736] 09 p0990 N73-18079
Influence of adiabatic oil compression on power of hydraulic motors and pumps
10 p1111 N73-19055
Remote sensing equipment to ensure efficiency in microwave electric power transmission to remote receiving stations
[NASA-CASE-MFS-21470-1] 11 p1264 N73-20257
Analysis of relationship between losses in rotating turbine blade and pitch irregularity after nozzle blade
[NLL-CE-TRANS-6113-[9022.09]]
15 p1824 N73-24782
Hydrofoil design criteria based on model for minimum control power
[AD-759286] 16 p1892 N73-25312
Performance of CO2 laser excited by H-3 [neutron, proton] reaction
16 p1920 N73-25536
Power production and fuel capability of light water cooled cavity test reactor
[NASA-TM-X-2864] 19 p2320 N73-28662
Performance of turboreactor turbines during high pressure stage
22 p2709 N73-31695

**POWER GAIN**
GaAs and InP reflection amplifier noise figure and power gain at extremely high frequencies
[ESRO-CR[P]-262] 19 p2244 N73-28088
Power gain and noise figure of indium phosphide and gallium arsenide microwave reflection amplifiers
19 p2244 N73-28090

**POWER GENERATORS**
U ELECTRIC GENERATORS

**POWER LIMITERS**
Performance of prototype broadband selective ferrite limiters
[AD-759951] 17 p2005 N73-26219

**POWER LINES**
Cable driver and technique for testing shielding effectiveness of exterior connectors for Pershing missile cable shields
[AD-764236] 22 p2645 N73-31196

**POWER PLANTS**
Proceedings of conference to define research requirements for problems involving waste heat transfer from large thermal sources into the environment
02 p0166 N73-11348
Mathematical model for thermodynamic efficiency of combined power plants incorporating magnetohydrodynamic generators
[AD-753031] 09 p0991 N73-18090
Steel construction design parameters for building and operating ZYKLON type wind driven power plants
[NASA-TT-F-14872] 12 p1388 N73-21253
Design and cost estimate of high altitude wind power plant
[NASA-TT-F-14903] 14 p1605 N73-23011
Use of solid rocket engine as power plant for ballistic missiles
15 p1825 N73-24795

**POWER SERIES**
NT TAYLOR SERIES
Power series solution to partial differential equation in thermal conductivity analysis on body of variable density
[AD-754256] 10 p1225 N73-19957

**POWER SPECTRA**
Serial segments method for measuring pilot manual control remnant in vicinity of sine waves
01 p0018 N73-10136
Possible noise sources in power spectra measurement of interplanetary magnetic field
01 p0096 N73-10791
Power spectra of interplanetary magnetic field near earth bow shock
01 p0096 N73-10792
Analysis of refraction of gravity water waves based on group velocity and phase velocity relationships
[AD-747982] 03 p0286 N73-12316
Measurement of energy spectra of high energy trapped protons using nuclear emulsions exposed on low altitude polar orbiting satellites
[AD-750474] 06 p0669 N73-15438
Seismological wave spectra for differentiating between earthquakes and explosions
[AD-749874] 06 p0671 N73-15457
Output and power characteristics of CS2/O2 chemical laser with flow transverse to optical axis
[DREV-R-684/72] 06 p0679 N73-15527
High resolution power spectra of Zurich daily sunspot numbers over 77 years
[NASA-TM-X-64718] 06 p0716 N73-15840
Temporal spectra of fluctuations in atmospherically degraded spherical waves
[AD-751304] 07 p0807 N73-16551
Power spectrum computation for phototube current of laser Doppler velocimeter
[NASA-TM-X-68184] 07 p0824 N73-16675
Computer computation of spectral data for Josephson junction circuit
[NBS-TN-627] 07 p0832 N73-16740
Analysis of turbulent velocity fluctuations in confined jet to determine design parameters for fluid amplifiers
[AD-752041] 08 p0899 N73-17276
Autocorrelation, Chree, and power spectrum analyses of cosmic ray 27-day recurrences
[NP-19466] 08 p0957 N73-17833
Power density spectrum for statistical analysis of radar altimeter return variations due to radar motion
[SC-RR-72-0265] 10 p1129 N73-19197
Average power spectra of zonal and meridional components of velocity for winter and summer
10 p1146 N73-19327
Power spectrum of satellite radio signal phase modulation caused by F region diffraction
[NASA-CR-131280] 11 p1254 N73-20178
Spectral development of wind-generated water waves in laboratory facility
[AD-754113] 11 p1287 N73-20445
Power distribution in fast spectrum thermionic reactor fuel element at core/BeO reflector boundary
[NASA-TM-X-68207] 11 p1323 N73-20735
Designing aircraft for combined effects of vertical, lateral, and longitudinal turbulence by power spectral techniques
[AD-756886] 13 p1475 N73-21951
Radar cross section modulation power spectrum in periodic motion of scattering object
[AD-756488] 13 p1494 N73-22109
Analog charts developed during monitoring and analysis of differential Omega navigation system - Vol. 3
[AD-756026] 13 p1557 N73-22619
Measurement of power spectra of waveforms derived from vibrating blades in axial compressor and application to determine damping factor of blades
[ARC-R/M-3253] 15 p1728 N73-24014
Development of narrow band spectral analyzer for determining power spectra of waveforms derived from vibrating axial compressor blades due to random excitation
[ARC-R/M-3259] 15 p1729 N73-24024
Phase difference temporal spectra measurements of laser beams
[AD-757915] 15 p1795 N73-24553
Root mean square center of gravity accelerations and undercarriage forces for taxiing KC-135 tanker aircraft
[CRANFIELD-AERO-15] 16 p1859 N73-25060
Fourier coefficients and power spectral density calculating device
[IPPJ-T-13] 16 p1949 N73-25766
Spectrum analysis program for computing power spectrum of angle modulated high frequency carrier wave
[NASA-CR-128984] 17 p1997 N73-26145
Geomagnetic latitude distribution of stationary Pc3 micropulsation statistical properties from power spectra cross correlations
17 p2026 N73-26397
Estimating random signal power spectral density by filtering, fluctuating spectrum, and autocorrelation function
17 p2027 N73-26400
Power spectral analysis of solar 2 cm microwave intensity data
[NASA-CR-133228] 17 p2079 N73-26820
Computer program to obtain power spectrum of frequency modulated signal, modulated by voice signal, digital signal, and combinations of both
[FAA-RD-73-56] 18 p2116 N73-27111
Sea spectra and radar scattering
[AD-760693] 18 p2149 N73-27373
Effect of finite source size on power statistics in reverberant room for pure tone excitation
[NASA-CR-132279] 18 p2179 N73-27594
Power spectral analysis of atmospheric circulation types
20 p2445 N73-29640
Basic elements of power spectral analysis
[NASA-CR-133774] 21 p2508 N73-30127
Stress-time relations of automobile rear wheel suspension systems, over various road surface conditions, based on power spectral density
[LBF-TB-102] 21 p2553 N73-30468
Comparison of gust velocities derived from accelerations of Canberra and Vulcan aircraft noting acceleration and wing loading power spectra
[ARC-CP-1244] 22 p2615 N73-30955
Time evolution of finite power density blast waves
[AD-763834] 22 p2656 N73-31278
Power spectral density estimation by spline smoothing ergodic stochastic process
[NASA-CR-133986] 22 p2691 N73-31552
Testing of power spectrum-diffusion coefficient relations of cosmic rays at low energies
22 p2711 N73-31706

**POWER SUPPLIES**
Pu-238 grade fuels for supplying power to artificial heart and circulatory assist devices
[LA-DC-72-473] 03 p0261 N73-12115
Use of Cm-244 as radioisotope power fuel in electric power conversion systems
[CONF-720519-1] 03 p0333 N73-12717
Nickel cadmium storage battery for portable power supply of man-pack equipment
[AD-748454] 04 p0376 N73-13055
Fuel cell applications as power supplies for rail transportation
[AD-747512] 04 p0376 N73-13056
Push button power supply for measuring light output performance of switchboard lamps
[REPT-6688] 04 p0395 N73-13211
Design of power supply voltage monitor for measuring multiple dc voltages simultaneously
[AD-748829] 04 p0424 N73-13453
Conversion of solar energy to pollution free power
04 p0474 N73-13870
Power sources and requirements for human artificial hearts
[COO-2155-4] 05 p0503 N73-14095
Design and safety procedures for operating high voltage capacitor bank
[AD-750535] 09 p1008 N73-18231
Development and characteristics of transducer for use with fluidic generators
[AD-755104] 11 p1273 N73-20334
Design, development, fabrication, and test of coolant circulating pump assemblies for use in Brayton cycle space power system
[NASA-CR-2176] 11 p1297 N73-20529
Design of repetitively pulsed inductive energy storage systems
[AD-755359] 14 p1606 N73-23014
Development of hermetically sealed nickel cadmium battery and associated control logic and charger circuit for aircraft applications
[AD-757535] 14 p1606 N73-23017
Electronics of waveform generator for digital voltage source
[AD-758212] 15 p1758 N73-24247
Weight optimization for energy storage, coil, cryogen, and dewar
[AD-755360] 17 p1986 N73-26054
Design, development, and fabrication of radiator structure for use with thermoelectric space power systems
[NASA-CR-121222] 17 p2088 N73-26892

Development of portable transmissometer calibrating unit using laser as projector source
[AD-757282] 18 p2153 N73-27403
Computer simulation and optimization code for nuclear space power systems for thermoelectric power generation
[NASA-TM-X-2860] 18 p2178 N73-27586
Performance of ac power supply developed for CO2 laser system
[NASA-CASE-GSC-11222-1] 23 p2800 N73-32391

**POWER SUPPLY CIRCUITS**
Operational performance of breadboarded silicon controlled rectifier series inverter circuitry for ion thruster power supply
[NASA-TM-X-2699] 06 p0626 N73-15082
Reliable functioning of avionic power supply equipment through employment of redundant components
[AD-757153] 14 p1602 N73-22988
Integrated circuit power gyrator with Z-matrix design using parallel transistors
[NASA-CASE-MFS-22342-1] 15 p1756 N73-24236
Analysis of operation of electric alternator feeding into direct current system through rectifying device
[RAE-LIB-TRANS-1679] 17 p1986 N73-26049
Power supply electronic tests on single jet disk type cesium thrustor with beam current feedback control
[LAAS-TNPE-73-T-17] 23 p2831 N73-32629

**POWER TRANSMISSION**
Development of design criteria for maximum horsepower to be transmitted using cycloidal cam transmission and application to marine gas turbine engines
[AD-754822] 11 p1301 N73-20554
Nature of power losses in RF superconducting cavities at low and high temperatures
[SLAC-PUB-963] 12 p1383 N73-21213

**PPI [POSITION INDICATORS]**
U PLAN POSITION INDICATORS

**PPM [MODULATION]**
U PULSE POSITION MODULATION

**PRANDTL NUMBER**
Prandtl number values for water and steam, liquid and gaseous heavy water, and sea water
[ESDU-68011] 01 p0038 N73-10301
Numerical analysis of Prandtl mixing path, criteria charcterizing pressure and velocity pulsations in turbulent flow conditions
10 p1141 N73-19294
Rational approach to use of Prandtl mixing length model in free turbulent shear flow calculations
19 p2252 N73-28158

**PRANDTL-MEYER EXPANSION**
NT THERMAL BUCKLING
Machine calculation of unsteady Mach reflections and Prandtl-Meyer supersonic flows
[AD-756195] 13 p1511 N73-22242
Nozzle flow free jet and Prandtl-Meyer expansion rotational relaxation equation used for relaxation time calculation
[REPT-72-5] 14 p1650 N73-23383

**PRASEODYMIUM**
Effects of solvent composition in quenching fluorescence of Pr[3 plus] ions in aprotic solvents
[CRC-TN-657] 21 p2505 N73-30104

**PREAMPLIFIERS**
Microwave preamplifier induction for electron spin resonance spectroscopy
14 p1666 N73-23521
Characteristics of direct-coupled photodetector-preamplifier for use in facsimile camera for improved sensitivity and reduced mechanical complexity
[NASA-TN-D-7338] 23 p2769 N73-32148

**PRECAMBRIAN PERIOD**
Interpretation and mapping large scale structural lineaments in Precambrian shield areas and basins containing younger sediments using ERTS-1 imagery
[E72-10180] 01 p0045 N73-10359
Utilization of ERTS-1 imagery for mapping large scale structural lineamants in Precambrian Shield and basins containing younger sediments and for mineral and petroleum exploration
[E73-10004] 06 p0658 N73-15340
Isotopic composition of carbon in Precambrian graphitoids from various parts of the USSR
[NASA-TT-F-14682] 08 p0918 N73-17520
Distinguishing major lithologic types in rocks of Precambrian age in central Wyoming using multilevel sensing
[E73-10301] 09 p1021 N73-18333
Commercial utility of ERTS-1 imagery in structural reconnaissance of Precambrian Shield for minerals and petroleum
[E73-10523] 14 p1654 N73-23414
ERTS-1 imagery of linear fractures in Precambrian rocks of Laramie Mountains, Wyoming
[E73-10663] 16 p1899 N73-25359
ERTS analysis of geological relationships of Precambrian Greenstone belts and Troctolite series rocks of Minnesota
23 p2784 N73-32271
Hypothesis for enormous accumulation and exclusive occurrence of ferruginous quartzite in Precambrian rock
[NASA-TT-F-15121] 23 p2786 N73-32290

**PRECAUTIONS**
U ACCIDENT PREVENTION

**PRECESSION**
Development of apparatus and technical procedures for measuring system inertia tensor parameters of precession nonrigid systems
05 p0547 N73-14442
Analysis of gyrocompass performance characteristics to include long term accuracy, statistical attributes, and application as geophysical instrument
[AD-750890] 06 p0697 N73-15685
Dependences between braking and precession moments acting on spherical rotor in magnetic suspension
21 p2547 N73-30422

**PRECIOUS METALS**
U NOBLE METALS

**PRECIPITATION**
Meteoroiogical radar observations of clouds and precipitation
[AD-764934] 23 p2815 N73-32510

**PRECIPITATION [CHEMISTRY]**
Gas phase precipitation method for preparing pure zirconium and niobium carbides
[NLL-RTS-7315] 01 p0069 N73-10563
Age hardening and precipation behavior of V-Ti, V-Ti-Si, V-Zr, and V-Hf alloys with reference to interstitial metalloid
[KFK-1680] 15 p1799 N73-24582
Thermodynamics of precipitation caused by zinc diffusion into gallium arsenide
18 p2113 N73-27085
Behavior of hafnium dioxide particles in precipitation-hardened nickel during isothermal annealing
21 p2558 N73-30503

**PRECIPITATION [METEOROLOGY]**
NT DEW
NT HAIL
NT RAIN
NT SNOW
NT SNOW COVER
Hydrometeorologic study of precipitation in Viroin basin, Belgium
[IRMB-PUBL-A-70-2] 01 p0047 N73-10381
Monthly statistics of precipitable water over Australia in atmosphere from 400 mb to surface, determined from daily radiosonde ascents, 1958 through 1969
01 p0074 N73-10609
Global distributions of surface albedo, planetary albedo, and total precipitation - supplementary data for Dec., Jan., and Feb.
[AD-744633] 01 p0076 N73-10628
Design, construction, and calibration of closed circuit wind tunnel for study of aerodynamic behavior of precipitation
[UTIAS-TN-181] 02 p0152 N73-11232
Correlation of total precipitable water in atmosphere with surface absolute humidity for California and Pacific Ocean islands
[AD-745954] 02 p0206 N73-11666
Canadian research on atmospheric precipation in antarctic regions and meteorological radar systems
[AD-746604] 04 p0444 N73-13627
Extremes of precipitation aloft mandatory for design of military equipment capable of operating at altitude anywhere in world
[AD-747482] 04 p0445 N73-13629
Meteorological causes and characteristics of dry spells
[NLL-M-20052-[5828.4F]] 05 p0569 N73-14623
Relation of solar activity to air temperature and precipitation
[NLL-M-20651-[5828.4F]] 05 p0570 N73-14626
Correction of precipitation measurements using parallel gages and shields
[ISBN-87-7478-048-4] 05 p0571 N73-14642
Diurnal variations of precipitation and surface wind for North Carolina
[PB-211614] 05 p0576 N73-14688
Introducing cloud seeding in model for predicting precipitation patterns over synoptic scale
[AD-750730] 05 p0576 N73-14691
Pluviometric and statistical analyses of precipitation and watercourse patterns in Israel
06 p0665 N73-15403
Statistical characteristics of physical structure for various types of precipitation
[NLL-M-20844-[5828.4F]] 06 p0691 N73-15627
Elementary processes of precipitation particle formation
[AD-751501] 07 p0816 N73-16615
Thermal parameters as predictors of precipitation at Ellsworth, S.D.
[AD-753418] 09 p1061 N73-18657
Accuracy and reliability engineering of precipitation measurement by radar
[NLL-M-22841-[5828.4F]] 12 p1420 N73-21505
Hydrometeorological study of periodic precipitation variations over Lesse Basin, Belgium
[PUBL-SER-A-76] 12 p1423 N73-21530
Time dependent two-dimensional atmospheric model used to test hypothesis of increased precipitation downwind from cloud seeding area
[AD-755724] 12 p1425 N73-21551
Variation in maximum intensity of precipitation falling from stratiform and cumulus clouds
13 p1552 N73-22581
Synoptic climatological studies of precipitation in Plateau states from 850, 700, and 500 mb flows during spring
[NOAA-TM-NWS-TDL-48] 13 p1553 N73-22585
Measurement of extreme rainfall intensites and associated liquid water content at altitude in tropical regions
[AD-756832] 13 p1554 N73-22593
Instrumentation to aid radar investigations of cloud and precipitation physics
[AD-755401] 13 p1555 N73-22606
Development of facilities and processing for determining increase in mean seasonal runoff due to cloud seeding in San Juan Mountains, Colorado
16 p1859 N73-25056
Solid aerosol particle capture by water drops at low Reynolds numbers
[AD-759667] 16 p1872 N73-25157
Precipitation scatter experiment to refine coordination procedures in frequency allocations for terrestrial and space services
[NASA-TM-X-66259] 16 p1875 N73-25175
Effect of precipitation on parabolic antennas using linear orthogonal polarization at superhigh frequencies
[REPT-53] 16 p1875 N73-25176
Long-term cyclic fluctuations of atmospheric precipitation in USSR
[NLL-M-22891-[5828.4F]] 16 p1935 N73-25639
Effect of sunspot cycle on precipitation pattern over U.S. plains states
17 p2056 N73-26629
Evaluation of radiometric computations in infrared window and water vapor absorption band regions based on 4-D atmospheric models
[NASA-CR-129007] 18 p2172 N73-27546
Climatology of instantaneous precipitation rates
[AD-760785] 18 p2174 N73-27558
Thermal parameters as predictors of precipitation at Carswell AFB, Texas
[AD-762289] 19 p2318 N73-28644
Estimation of severe attenuation of radio signals due to precipitation at 2 cm on earth satellite paths
20 p2375 N73-29085
Statistical analysis of snowfall in various areas of USSR for application to transportation, agriculture, and urban planning
[TT-70-50181] 20 p2406 N73-29338
Removal of pollutants from atmosphere by precipitation and clouds
[NLL-M-23010-[5828.4F]] 20 p2441 N73-29608
Resevoir vs. tipping bucket rain gages
[NLL-M-23050-[5828.4F]] 20 p2442 N73-29611
Daily and monthly weather charts for Northern Hemisphere and Berlin, Germany for February, 1973
20 p2442 N73-29614
Atmospheric circulation effects on precipitation and temperature regimes of USSR and Northern Hemisphere
20 p2444 N73-29633
Detection of precipitation pattern in west central Kansas from ERTS-1 MSS imagery
[E73-10975] 21 p2533 N73-30314
Evaluation of recording instrument for in-flight determination of size and distribution of hailstones
[NASA-TM-X-2817] 21 p2549 N73-30434
Statistical correlations between maximum intensity of precipitation of different types and mean intensities for given precipitation
[NLL-M-23044-[5828.4F]] 21 p2567 N73-30574
Analysis of radar measurements of precipitation and comparison with ground level observations
21 p2568 N73-30581
Application of radar techniques for measuring precipitation and comparison with measurements obtained from conventional meteorological instruments
21 p2568 N73-30582
Development of radar equation and radar calibration relationships for measuring multiple target reflectivity
21 p2568 N73-30583
Analysis of radar methods for measuring intensity of precipitation and development of mathematical models for radar reflectivity and microwave attenuation
21 p2569 N73-30585
Application of radar signatures for analyzing the turbulent flow structure of earth adjacent layers of subfrontal clouds and precipitation
21 p2570 N73-30597
Analysis of radar data to determine characteristics of precipitation belts resulting from weather modification practices
21 p2571 N73-30603
Method for calculating correlation functions of diurnal precipitation totals and their space time variability over uniform relief
21 p2573 N73-30619
Daily precipitation and snow cover data - 1970
[ISBN-951-697-010-9] 21 p2573 N73-30624
Methods of augmenting precipitation for winter storms of Sierra, Nevada
[PB-220674/6] 21 p2575 N73-30633

Calculation of Mie differential scattering cross section of spherical particles with complex refractivity, for mm wave propagation through precipitation
[FTZ-A-455-TBR-35] 22 p2633 N73-31100
Measurements of Fe, Mn, Fn, Cu, Ni, and Pb in aerosols and precipitation in clean tropospheric air
[NOAA-TR-ERL-248-APCL-24] 22 p2664 N73-31349
Research in development and utilization of atmospheric water resources in Montana
[PB-222004/4] 22 p2695 N73-31591
Propagation path depolarization caused by precipitation
[NASA-CR-132818] 24 p2895 N73-33107

**PRECIPITATION HARDENING**
Effect of titanium additions on aging characteristics of Al-Zn-Mg alloy
[AD-746195] 01 p0068 N73-10561
Neutron irradiation damage in precipitation hardened aluminum alloy component from High Flux Isotope Reactor
[CONF-720604-1] 03 p0313 N73-12555
Short time annealing effect under load on aluminum alloy precipitation hardening process
[DLR-FB-71-111] 03 p0316 N73-12573
Dispersion hardening of complex chromium nickel alloy by zirconium dioxide 04 p0432 N73-13523
Diffusion creep and creep degradation in precipitation hardened TD-NiCr alloy
[NASA-TN-D-7079] 04 p0433 N73-13530
Improved oxidation resistance of dispersion strengthened nickel-chromium alloys and thermomechanical procedure to produce course grain microstructure
[AD-748266] 04 p0436 N73-13556
High temperature dispersion strengthening of Fe-Al alloys by internal oxidation
[BM-RI-7686] 05 p0562 N73-14564
Fabrication and creep strength of precipitation hardened heat resistant alloys
[ITE-MITT-7/1972] 06 p0684 N73-15572
Time dependent edge-notch sensitivity of oxide and gamma dispersion strengthened nickel alloy sheets
[NASA-CR-121123] 06 p0725 N73-15919
Alloying and thermal treatment for improving mechanical properties of ceramics
[AD-753124] 09 p1055 N73-18597
Microstructure and mechanical properties of precipitation hardened-dispersion strengthened aluminum and titanium alloys and refractory materials
[AD-753910] 10 p1174 N73-19550
Phase stabilization and solid solution strengthening in titanium alloys
[AD-754240] 10 p1174 N73-19551
Analysis of strain aging process in high carbon quenched steels caused by plastic deformation of martensite and migration of carbon to crystal defects in microstructure 13 p1541 N73-22484
Dispersion strengthened nickel-yttria sheet alloy produced from comminuted powders
[NASA-TM-X-68245] 15 p1798 N73-24576
Age hardening and precipation behavior of V-Ti, V-Ti-Si, V-Zr, and V-Hf alloys with reference to interstitial metalloid
[KFK-1680] 15 p1799 N73-24582
Tensile properties and creep behavior of tungsten alloys dispersion strengthened by ZrO2 16 p1927 N73-25590
High temperature strength and deformation properties of Ti-Al-Si alloy aged by alpha phase precipitate particles
[NASA-TN-D-7325] 16 p1928 N73-25597
Processing condition effects on microstructures of sheets, wire and bars made from nickel chromium iron alloy 718
[WAPD-TM-1077] 16 p1928 N73-25603
Dispersion strengthened nickel alloys for use as space shuttle thermal protection systems
[NASA-CR-121164] 17 p2043 N73-26526
Dynamics of dislocation pinning by impurity atoms during dynamic strain aging
[AD-760574] 18 p2162 N73-27466
Precipitation hardening of copper alloys and iron
[AD-764150] 22 p2686 N73-31516
Precipitation and age hardening phenomena in vanadium alloys with reference to metalloid additives
[EURFNR-1060] 24 p2935 N73-33439
Prediction of yeld strength on isothermal aging of precipitation-hardening alloy Nimonic PE16
[TRG-REPORT-2267] 24 p2935 N73-33442

**PRECIPITATION PARTICLE MEASUREMENT**
Radar/radiometer system for measuring temporal and spatial precipitation characteristics particularly thunderstorm activity
[NASA-CR-130235] 14 p1667 N73-23532
Multipath rainfall measurements for planning ultrahigh frequency radio link 17 p1996 N73-26137
Ultrahigh frequency precipitation attenuation measurements by ATS 5 weather radar and radiometer 17 p1996 N73-26142

**PREDICTION ANALYSIS TECHNIQUES**
Survey of techniques used for turbine engine performance analysis
[AD-744587] 01 p0091 N73-10750
Nonlinear transformation relating rectangular coordinates to range instrumentation coordinates in guided missile tracking system
[AD-746637] 02 p0144 N73-11163
Comparison of turbulent heating predictions by three different techniques with flight test data of several reentry vehicles
[NASA-CR-130251] 03 p0282 N73-12288
Economic analysis of space shuttle transportation system based on tradeoffs, alternatives, and variations in spacecraft design - Vol. 1
[NASA-CR-129568] 04 p0487 N73-13977
Prediction analysis method to determine influence of geometry parameters on aerodynamic characteristics of body-wing configuration
[DLR-FB-72-63] 06 p0622 N73-15050
Apollo 16 radar echo data for predicting blockiness of lunar surface 12 p1455 N73-21788
Development and application of aircraft performance prediction methods for subsonic and supersonic transport and fighter aircraft
[AGARD-LS-56] 15 p1732 N73-24042
Theoretical prediction of thermal stress waves in metal conductors induced by relativistic electron beam 16 p1926 N73-25587
Multilevel atmospheric prediction model based on primtiive equations of moiton
[DM-8] 16 p1938 N73-25681
Forecasts of aviation activity at selected airports to meet needs of planning personnel for future air traffic control operations 17 p1982 N73-26019
Comparison of plasma probe and predicted electrical properties of rocket exhaust plume 17 p2031 N73-26436
Development of empirical elastohydrodynamic film thickness formula for predicting minimum film thickness occurring in heavily load contacts
[NASA-TM-X-68267] 18 p2155 N73-27411
Meteorological conditions and instruments analysis by Soviet aerometeorological service
[JPRS-59581] 18 p2171 N73-27533
Prediction of acoustic pressure wave oscillations in T burner combustors
[AD-762153] 19 p2328 N73-28728
Development of system for predicting system failure rate and determination of optimal economic replacement interval
[AD-762417] 19 p2357 N73-28966
Development of computer model to simulate air traffic conditions in Los Angeles, California area in 1982
[MTR-6386] 20 p2452 N73-29706
Development of procedures for predicting fatigue life of aircraft structures based on fracture mechanics, crack propagation, and residual static strength anlaysis
[AGARD-LS-62] 20 p2480 N73-29924
Development of fatigue life prediction procedures based on measured stress-time histories and mathematical model for description of random vibrations 20 p2481 N73-29926
Effect of environment and stress-cycling on in-service structural failure of airframes and procedures for predicting safe operational conditions 20 p2481 N73-29929
Application of growth rate data and analytical retardation models for predicting crack growth under variable amplitude loading 20 p2481 N73-29932
Analysis of errors in fatigue life prediction procedures and methods for improving accuracy of prediction analysis techniques 20 p2481 N73-29934
Loss estimation in predicting ionospheric medium frequency sky wave propagation
[BBC-RD-1973/13] 22 p2627 N73-31051
Analytical forecasting methods for air passenger traffic 23 p2861 N73-32864
Analytic methods for evaluating transportation systems with interacting elements 23 p2861 N73-32867
Method for predicting noise generated by deflecting engine exhaust for under-the-wing and over-the-wing versions of externally blown flap configuration
[NASA-TM-X-71449] 24 p2876 N73-32969
Computer program and mathematical model for predicting dynamic response of helicopter in accident involving vertical and lateral impact
[AD-764985] 24 p2879 N73-32996
Technique for predicting thermal conductivity of randomly packed granular materials 24 p2990 N73-33892

**PREDICTIONS**
NT FLOOD PREDICTIONS
NT IMPACT PREDICTION
NT LINEAR PREDICTION
NT PERFORMANCE PREDICTION
Risk scoring system for identifying subjects with high risk to coronary heart disease 08 p0874 N73-17080

**PREDICTORS**
U PREDICTIONS

**PREFLIGHT ANALYSIS**
Design and preflight analysis of flexible solar array mechanism 09 p1089 N73-18887
Preflight and flight stress analysis, its relation to circadian rhythms measured in pilot physiological parameters
[DLR-FB-72-39] 21 p2501 N73-30071

**PREHEATERS**
U HEATING EQUIPMENT

**PREHEATING**
U HEATING

**PRELAUNCH PROBLEMS**
Prelaunch alignment of stable platform to desired orientation
[NASA-CR-128802] 10 p1184 N73-19638
Apollo experience report on development of design loads criteria, methods, and operational procedures for prelaunch, lift-off, and midboost conditions
[NASA-TN-D-7373] 20 p2474 N73-29875

**PRELAUNCH TESTS**
Prelaunch mission operations for space storable propellant module for retro propulsion on unmanned outer planet orbiters
[NASA-CR-129521] 03 p0358 N73-12915

**PRELOADING**
U PRESTRESSING

**PREMIXED FLAMES**
Processes leading to carbon formation in premixed laminar flames of various fuels 08 p0882 N73-17144
Coagulation of carbon particles in premixed flames
[AD-755693] 13 p1592 N73-22907

**PREPARATION**
NT PRESTRESSING

**PREPOLYMERS**
Determination of functionality distribution of prepolymers used for rocket binders
[NASA-CR-129505] 03 p0262 N73-12121

**PRESELECTORS**
U PREAMPLIFIERS

**PRESERVATIVES**
Preservatives for human urine storage and water reclamation in spacecraft cabin 10 p1116 N73-19099

**PRESINTERING**
U SINTERING

**PRESSES**
Isothermal forging of titanium centrifugal compressor impeller
[AD-764266] 22 p2678 N73-31455

**PRESSING [FORMING]**
NT STAMPING
Different types of lubricants for working of plastics
[NLL-RTS-7852] 20 p2421 N73-29449

**PRESSURE**
NT ATMOSPHERIC PRESSURE
NT BASE PRESSURE
NT BLOOD PRESSURE
NT CRITICAL PRESSURE
NT DENSIFICATION
NT DIFFERENTIAL PRESSURE
NT GAS PRESSURE
NT HIGH PRESSURE
NT HIGH VACUUM
NT HYDROSTATIC PRESSURE
NT HYPERTENSION
NT HYPOXEMIA
NT ILLUMINANCE
NT IMPACT LOADS
NT INLET PRESSURE
NT INTERNAL PRESSURE
NT INTRAOCULAR PRESSURE
NT ISOSTATIC PRESSURE
NT LOW PRESSURE
NT LUMINANCE
NT LUMINOUS INTENSITY
NT OVERPRESSURE
NT OXYGEN TENSION
NT PARTIAL PRESSURE
NT RADIATION PRESSURE
NT SOUND PRESSURE
NT STAGNATION PRESSURE
NT STATIC PRESSURE
NT SUPERCRITICAL PRESSURES
NT TRANSIENT PRESSURES
NT ULTRAHIGH VACUUM
NT VACUUM
NT VAPOR PRESSURE
NT WALL PRESSURE
NT WATER PRESSURE
NT WIND PRESSURE
Pressure fluctuations due to interaction of shock wave with turbulent boundary layer
[NASA-CR-123961] 03 p0281 N73-12281
Prediction of fluctuating pressures acting on externally blown flap surfaces
[NASA-CR-112216] 06 p0619 N73-15026

Experimental and theoretical measurement of pulsed flow velocity and pressure in circular pipes
14 p1649 N73-23372
Wind tunnel tests to determine pressure distributions for four percent thick, circular arc, biconvex airfoil at transonic speeds
[ARC-R/M-3180] 16 p1852 N73-25002
Pressure shaping of steels and alloys
[AD-762308] 19 p2306 N73-28549
Measurements of pressure, voltage, and wall heat flux in wall-stabilized arc heater
[NASA-TM-X-69571] 20 p2420 N73-29443
Analysis of acoustic and fluctuating pressure environments for complete flight envelope of space shuttle
[NASA-CR-124347] 20 p2475 N73-29885

PRESSURE BREATHING
Positive pressure breathing for increased human acceleration tolerance
10 p1123 N73-19156

PRESSURE CABINS
U PRESSURIZED CABINS

PRESSURE CHAMBERS
NT HYPERBARIC CHAMBERS
NT VACUUM CHAMBERS
Coding data of 2565 individual human altitude chamber tests
[NASA-CR-114550] 07 p0746 N73-16066
Carbon monoxide content in exhaled air and blood carboxyhemoglobin in subjects confined to insulating protective gear
11 p1245 N73-20106
Pressure chambers for testing effect of oxygen inspiration on fatigue during flight
[JPRS-59041] 14 p1610 N73-23051

PRESSURE COEFFICIENT
U AERODYNAMIC COEFFICIENTS

PRESSURE DISTRIBUTION
Influence of drag, pressure, and turbulent distribution on flow of dilute Polyox WSR-301 solutions in circular cylinders
[AD-745763] 01 p0042 N73-10334
Singular perturbation method for predicting pressure distribution on supercavitating hydrofoils with rounded noses
[AD-745791] 01 p0063 N73-10514
Mathematical models for predicting unsteady aerodynamic effects on axial flow compressor with distorted inflow - Squid project
[AD-746457] 02 p0157 N73-11271
Development of theories for calculating pressure on perturbed plane wall in presence of viscous boundary layer
[AD-746332] 02 p0158 N73-11278
Least squares curve fitting method for smoothing pressure distribution data for various cross sections of circular cylinder
[WRE-TN-688[WR/D]] 02 p0195 N73-11577
FORTRAN computer program for annular airfoil pressure distribution at subsonic speeds
[ARC-CP-1217] 03 p0248 N73-12004
Flow field and base pressure of internal-external-expansion truncated plug nozzles for open and closed wake operations
[NASA-CR-123941] 03 p0281 N73-12282
Wind tunnel simulation of ground effect conditions to determine effect of three dimensional turbulent boundary layer on V/STOL aircraft configurations - Pt. 1
[NASA-CR-114495] 03 p0282 N73-12283
Pressure loads and damping associated with rigid ring baffles in large cylindrical tanks
[NASA-TN-D-6870] 03 p0282 N73-12285
Development of finite difference techniques for computing static pressure distribution downstream of strong shock wave using navier-Stokes equation
[AD-747978] 03 p0286 N73-12318
Calculation of coefficient of resistance of sphere at supersonic velocities and measurement of critical point on free flying bodies
[AD-747513] 03 p0287 N73-12324
Numerical analysis of pressure distribution at parabolic wing tips on circular wing model based on occurrence of logarithmic sets
[AD-748432] 04 p0370 N73-13007
Fluid wave equation for analyzing damage by excited pressure field between two elastic plates
[AD-748340] 04 p0407 N73-13316
Wind tunnel tests to determine pressure distribution on Apollo command module and Saturn launch vehicle at supersonic and hypersonic speeds
[NASA-TM-X-62117] 04 p0477 N73-13904
Integration of unsteady aerodynamic forces and pressure distributions in aeroelastic analysis
[NLR-MP-71013-U] 05 p0492 N73-14011
Wind tunnel measurement of surface pressure distributions on three bodies of revolution at Mach numbers from 0.7 to 2.02
[AD-749934] 05 p0492 N73-14012
Development of iterative procedure for analysis of arbitrary multi-element airfoils in viscous flow
[AD-749484] 05 p0496 N73-14042
Computer program for designing leading edge slats for producing specified pressure distribution on main airfoil
[AD-749485] 05 p0496 N73-14043
Scalar wave scattering on water surface wake generated by moving pressure point
[AD-749113] 05 p0527 N73-14291
Numerical analysis of two dimensional shock wave resulting from mobile wedge moving with supersonic velocity and specific angle of attack into detonation wave
[AD-749650] 05 p0528 N73-14299
Pressure patterns chronology with Bora on Adriatic coast from 1 Jan. 1956 to 31 Dec. 1965
05 p0571 N73-14640
Wind tunnel tests to determine pressure distribution on wing and lower body surface for space shuttle orbiter in launch configuration
[NASA-CR-120075] 05 p0600 N73-14879
Wind tunnel tests to determine heat transfer and pressure distributions of hemisphere cylinders in hypersonic flow environment
[NASA-TN-D-7104] 05 p0605 N73-14925
Pressures and temperatures on the lower surfaces of an externally blown flap system during full-scale ground tests
[NASA-TN-D-7138] 06 p0614 N73-14984
Application of blockage correction factors to wind tunnel test measurements on aircraft models
06 p0617 N73-15006
Analysis of aerodynamic processes occurring in flow past unpowered multi-element airfoils in high lift attitude
06 p0617 N73-15007
Surface pressure distribution on hydrofoil profiles in accelerated cascades, using boundary layer calculations
[REPT-251] 06 p0724 N73-15914
Application of unsteady airfoil theory to determine pressure and lift fluctuations on rotor blades of turbomachinery
07 p0735 N73-15983
Buckling modes of four optimized Mars entry aeroshell configurations at angle of attack loadings based on experimental pressure distributions
[NASA-CR-2087] 07 p0852 N73-16907
Effect of nonuniform upstream flow conditions on shock shape and surface pressure distribution on two dimensional pointed bodies
08 p0895 N73-17244
Technique for predicting shock envelopes and pressure distributions for two dimensional airfoil at angles of attack producing shock detachment and subsonic flow
[NASA-TN-D-7197] 09 p0979 N73-18001
Measurement of unsteady pressures developed on harmonically oscillating wing planform in three dimensional compressible flow
[DLR-FB-72-55] 09 p0980 N73-18007
Force and pressure distribution measurements on wing-body combination with wing of low aspect ratio in compressible flow
[DLR-FB-72-08] 09 p0980 N73-18008
Measurement of surface pressure fluctuations at two locations on XB-70 aircraft at local Mach number range from 0.35 to 2.45
[NASA-TN-D-7226] 09 p0981 N73-18013
Calculation of flow through airfoils in cascade to show pressure distribution under conditions of two dimensional incompressible flow with boundary layer separation at trailing edge
[DLR-FB-72-62] 09 p1014 N73-18276
Experimental investigation of two dimensional cascade flow tests for three cascade configurations - Vol. 4
[NASA-CR-121101] 09 p1015 N73-18282
Numerical analysis of inviscid, fully developed structure of lift-generated vortices behind aircraft wings and extension to arbitrary span-loaded distributions
[NASA-TM-X-62224] 09 p1016 N73-18289
Optimization of working conditions in plasma wind tunnel by pressure distribution control in acceleration section
[DLR-FB-72-70] 09 p1070 N73-18735
ONERA results of work to determine response of solid propellant to pressure and velocity fluctuations
[ONERA-TP-1165] 09 p1098 N73-18963
Numerical analysis of pressure distribution in subsonic wind tunnel resulting from interference of air flow
10 p1140 N73-19287
Turbulent pressure fluctuation measurements for cross section of supersonic diffuser inlet flow model
10 p1140 N73-19288
Wind tunnel measuresments of time-average pressure on external and internal surfaces of large hangar-type building
[NPL-MAR-SCI-10-72] 10 p1140 N73-19292
Flow field, pressure, and heat transfer associated with small fins of half angle cone in supersonic flow
[SCL-RR-72-0339] 10 p1142 N73-19302
Procedures for calculating velocity potential and pressure distribution of planforms oscillating harmonically in supersonic flow
[FOK-X-440] 11 p1231 N73-19994
Method for computing lifting pressure distribution on wing with partial span, swept control surfaces
[NASA-TN-D-7251] 11 p1232 N73-19999
Wind tunnel tests of space shuttle orbiter in various configurations to determine aerodynamic loads and pressure distributions at range of Mach numbers
[NASA-CR-120066] 11 p1342 N73-20890
Design of airfoil sections for low Reynolds numbers based on requirement to achieve transition upstream of major adverse pressure gradient
12 p1355 N73-20995
Analysis of optimum pressure distribution on multi-element airfoils to obtain conditions for maximum lift coefficient
12 p1355 N73-20996
Scale effect on swept wings at subsonic speed on basis of pressure distribution measured in flight and on wind tunnel super VC 10 model
[ARC-R/M-3707] 12 p1355 N73-20999
Development of procedure for calculating ocean currents based on given density field and comparison with current techniques
12 p1421 N73-21516
Numerical forecasts of barometric fields in stratosphere using quasi-geopotential model
13 p1552 N73-22574
Experimental determination of pressure distribution in burning flaws in solid propellant grains
[AD-756912] 13 p1569 N73-22718
Wind tunnel tests to determine pressure distribution of space shuttle launch configuration for various combinations of geometric components and Mach number
[NASA-CR-120058] 14 p1709 N73-23872
Surface pressure tests on Viking lander capsule at Mach 10, including appendages on base cover pressure distribution
[NASA-CR-131983] 14 p1710 N73-23879
Numerical analysis of pressure distribution in incompressible flow on two dimensional airfoils near ground
[ARC-R/M-3238] 15 p1726 N73-24000
Analysis of pressure distribution and surface flow on half models of wings with curved tips and 60 degree sweepback
[ARC-R/M-3244] 15 p1726 N73-24001
Analysis of flow development over plane, half-wing with cropped-delta planform using surface pressure distributions and oil flow patterns with variations in incidence and Mach number
[ARC-R/M-3286] 15 p1727 N73-24008
Analysis of pressure distribution around hemisphere at supersonic speeds with emphasis on differential pressure measurements
[ARC-R/M-3237] 15 p1729 N73-24023
Analysis of decomposition of liquid jet injected normal to supersonic airstream to show generation of high frequency, axially propagating waves
15 p1764 N73-24296
User manual for Streamtube Curvature Analysis program to predict pressure distribution about nacelle at transonic speeds - Vol. 1
[NASA-CR-112239-1] 15 p1767 N73-24313
User manual for Streamtube Curvature Analysis program to predict pressure distribution about nacelle at transonic speeds - Vol. 2
[NASA-CR-112239-2] 15 p1767 N73-24314
User manual for Streamtube Curvature Analysis program to predict pressure distribution about nacelle at transonic speeds - appendix
[NASA-CR-112239-3] 15 p1767 N73-24315
Factors affecting base flow and jet structure behind cylindrical afterbody with central nozzle at mach 2.0 and turbulent boundary layer conditions
[ARC-R/M-3224] 16 p1851 N73-25001
Calculation of spanwise loading on sweptback wings with trailing edge flaps using data obtained from electric tank tests
[ARC-R/M-3487] 16 p1853 N73-25010
Velocity magnitude and direction, static pressure, and skin friction of circular turbulent jet impinging normally on flat surface
[ARC-R/M-3205] 16 p1856 N73-25034
Flow characteristics of axially symmetrical, supersonic, fully-expanded jet to determine relation between static pressure distributions and jet turbulence
[ARC-R/M-3292] 16 p1857 N73-25038
Wind tunnel tests to determine pressure distribution on two dimensional airfoil with pylon mounted stores at subsonic speeds using F-4 aircraft model
[AD-759582] 16 p1859 N73-25053
Analysis of effect of turbulence intensity on aerodynamic characteristics of bodies of various shapes to develop method for measuring initial turbulence
[AD-760264] 17 p2015 N73-26297
Wind tunnel measurements of overall fluctuating pressure levels on seven space shuttle launch configurations at transonic and supersonic speeds
[NASA-TM-X-62280] 17 p2087 N73-26882

Analysis of pressure distribution on plane ground surface under aircraft flying at low altitude with subsonic velocity
[FFA-AU-634-PT-2] 18 p2129 N73-27206
Formulation and development of computer analysis for calculating streamlines and pressure distributions around two-dimensional isolated nacelles at transonic speeds
[NASA-CR-2217] 19 p2217 N73-27890
Development of semi-empirical model for predicting fluctuating pressure distribution resulting from rocket plume- induced separated regions
[NASA-CR-124346] 19 p2352 N73-28922
Solutions for various problems in two dimensional and axisymmetrical steady viscous flow with harmonic pressure field
20 p2387 N73-29175
Interaction between supersonic boundary layer with turbulent flow and inelastic deformable wall to determine stress perturbations and pressure distribution
[TN-86] 20 p2388 N73-29186
Hydrodynamic models for studying pressure and wind fields in low latitudes
20 p2444 N73-29630
Equations for determining pressure profile, forces, and torques on disk pendulum by point source wave theory from acoustics
[NASA-TM-X-69569] 20 p2454 N73-29725
Analysis of surface pressure fluctuations from jet impingement on inclined flat plate with application to design of aircraft with externally blown flaps
20 p2479 N73-29909
Calculation of pressure field induced by free jet exhausted from flat plate into stagnant medium based on solution of Neumann problem in terms of singularity distributions
[NLR-TR-72040-U] 21 p2492 N73-30000
Pressure fields over hypersonic wing-body configuration at moderate incidence
[AD-763762] 21 p2526 N73-30256
System for reducing noise generated by jet impinging on external flap using injection of secondary air from slot near trailing edge of flap
[NASA-CR-132270] 22 p2611 N73-30930
The lift and stalling characteristics of a 35 deg sweptback wing designed to have identical chordwise pressure distributions at all spanwise stations when near maximum lift
[ARC-R/M-3721] 22 p2612 N73-30935
Aerodynamic configurations of series of airfoils used in parametric studies of drag-rise Mach number
[ESDU-71020] 22 p2650 N73-31228
Derivation of charts for predicting drag-rise Mach number for airfoils with specified upper surface pressure distribution
[ESDU-71019] 22 p2650 N73-31229
Effects of rocket plume simulators on pressure distribution of body of revolution at transonic speeds
[NASA-CR-133916] 22 p2651 N73-31238
Local pressure field in turbulent shear flow and its relation to aerodynamic noise generation
[NASA-CR-134493] 22 p2653 N73-31253
Pressure distribution and stability of a magnetized plasma with neutral gas blanket
[TRITA-EPP-73-12] 22 p2705 N73-31664
Effects of blade tip clearance and leading edge sweepback of compressor rotor blades on inducer performance and blade pressure loading
[NASA-CR-72712] 23 p2739 N73-31930
Static pressure and heat transfer rate distributions on conical bodies at hypersonic speeds laminar and turbulent flow conditions
[AD-764983] 23 p2777 N73-32204
Wind tunnel tests to determine aerodynamic loads on flap systems behind engines and vibration modes of flap system
24 p2873 N73-32945
Measurement of fluctuating surface pressures induced on externally blown flaps by jet impingement and relationship to sonic fatigue of airframes
24 p2873 N73-32946
Full-scale ground tests of externally blown flap system on F-111 aircraft wing to determine pressure and temperature distributions on undersurface of wing, vane, and flap
24 p2873 N73-32947
Free jet boundary and distribution of flow within planar jet and pressure distribution at flat panel
[NASA-TT-F-15151] 24 p2905 N73-33180
Relationship between distribution of outflow of acoustic energy over jet boundary and far-field intensity
[NASA-TN-D-7269] 24 p2905 N73-33181

**PRESSURE DRAG**
NT INTERFERENCE DRAG
NT WAVE DRAG

**PRESSURE DROP**
Pressure drop measurements and drag coefficients for grid spacers of hexagonal fuel rod bundles
[NLL-RISLEY-TR-2440-[9091.9F]]
02 p0209 N73-11692
Pressure drop in plate heat exchangers with corrugations
[NLL-RTS-7505] 02 p0241 N73-11960
Pressure loss coefficients for fluid flowing through orifice plates, perforated plates, and cylindrical tubes
[ESDU-72010] 04 p0403 N73-13279
Pressure changes in fluid flow along duct with sudden enlargement of area
[ESDU-72011] 04 p0403 N73-13281
Analytical methods for calculating frictional pressure losses in fluid flow through straight pipes
[ESDU-66027] 04 p0403 N73-13282
Distribution losses in axial compressor over blade cross sections and effects of blade heights
[AD-750931] 06 p0657 N73-15334
Effect of crud deposits on frictional pressure drop in boiling channel
[AEEW-R-767] 07 p0820 N73-16645
Effect of return bends on downstream pressure drop and heat transfer coefficient of condensing refrigerant
[DSR-72591-75] 22 p2652 N73-31246

**PRESSURE EFFECTS**

Behavior of lubricating materials under high temperature and high pressure
[AD-745001] 01 p0062 N73-10509
Influence of shock compression pressure on critical shear in aluminum, copper, and lead
[AD-745365] 01 p0068 N73-10555
Combustion stability with hydrogen-oxygen liquid rocket propellants
03 p0349 N73-12844
Hydrostatic pressure effects on mechanical behavior and properties of polymers
[AD-750731] 06 p0688 N73-15605
Influence of external pressure on foil bearing performance
[AD-751642] 07 p0805 N73-16528
Pressure effects on phonon spectrum, electron-phonon interaction strength, and electron-phonon coupling function in Pb-In superconductors using electron tunneling
07 p0831 N73-16739
Heat transfer to slush hydrogen at 1 atm and at triple-point pressure
08 p0968 N73-17914
Quasi-hydrodynamic equations for analyzing pressure anisotropy effects on magnetospheric tail oscillations
14 p1703 N73-23821
Pressure effects on tangential-injection film cooling in combustor exhaust stream
[NASA-TM-X-2809] 15 p1843 N73-24931
Effects of ionizing radiation and high pressure on polymerization processes of fluoroolefins and fluorocarbon compounds
[AD-750151] 16 p1870 N73-25143
Mechanical properties of amorphous semiconductors at high pressures
[AD-759849] 17 p2075 N73-26784
Stress analysis of pressurized shallow cylindrical shell containing two collinear axial cracks of equal length
[NASA-CR-132271] 17 p2093 N73-26932
Effect of wall thickness variations on failure during burst tests of Zircaloy tubing
[WAPD-TM-1104] 17 p2093 N73-26935
Analysis of transient pressures in externally pressurized cryogenic hydrogen and oxygen tanks to determine effects of design variables on pressure response
[NASA-CR-133962] 18 p2199 N73-27755
Comparison of normal and hydrostatic extruding processes under fluid pressure
[NLL-NEL-TT-2467-[6075.461]]
20 p2422 N73-29453
Analysis of variations in hardness and microstructure of metals subjected to shock wave pressures
[NLL-NEL-TT-2489-[6075.461]]
20 p2429 N73-29514
Development of computer method for solving axisymmetric variational problems of theory of treatment of metals by pressure
[NLL-M-21659-[5828.4F]] 20 p2430 N73-29517
Discrete method for variational problems in treatment of metals by pressure
[NLL-M-21663-[5828.4F]] 21 p2557 N73-30497
Food heating tests in different atmospheres
[NASA-CR-134040] 22 p2622 N73-31012
Vacuum displacement compression molding of tubular bodies from thermosetting plastics
[NASA-CASE-LAR-10782-2] 22 p2677 N73-31444
Equilibrium concentration and catalytic decomposition products of hydrazine at elevated temperatures and pressures
[NASA-CR-135478] 23 p2753 N73-32031
Measurement of fluctuating surface pressures induced on externally blown flaps by jet impingement and relationship to sonic fatigue of airframes
24 p2873 N73-32946
Pressure effects on dynamic viscosity of helium in temperature range 0.4 to 400 K
24 p2908 N73-33208
Pressure dependent absorption of CO2 laser in BCl3 at 10.6 micron
[DREV-TN-2086/73] 24 p2930 N73-33403

**PRESSURE FIELDS**
U PRESSURE DISTRIBUTION

**PRESSURE GAGES**
NT BAROMETERS
NT IONIZATION GAGES
NT MANOMETERS
NT PENNING GAGES
NT PIEZOELECTRIC GAGES
NT VACUUM GAGES
Scale model evaluation of fiber glass wedge and parabolic deflector efficiencies in cylindrical ballistic ranges using pressure transducer measurements
[DREV-TN-2031/72] 06 p0649 N73-15270
Shock tube and wind tunnel calibration tests of large aspect angle total head pressure gage
[AD-755120] 11 p1295 N73-20506
Spacecraft pressure gage reliability studies relative to gas dynamics and metal surface testing
[NASA-CR-112320] 13 p1529 N73-22392
Use of torsional pendulum as high pressure gage and determination of viscosity of helium gas at high pressures
[NASA-TN-D-7241] 14 p1667 N73-23528
Ultrahigh vacuum gauge with two collector electrodes
[NASA-CASE-LAR-02743] 23 p2791 N73-32324

**PRESSURE GAUGES**
U PRESSURE GAGES

**PRESSURE GRADIENTS**

Semiempirical calculations of turbulent boundary layer problems
[AD-745217] 01 p0042 N73-10330
Prediction of pressure gradient on delta wing between uniform and nonuniform supersonic inviscid flow
[ARC-CP-1228] 05 p0492 N73-14010
Mixing length theory used to determine influence of pressure gradients on wall region of turbulent boundary layer
[AD-749371] 05 p0527 N73-14290
Pressure gradient measurements in swine and rats submitted to pressure pulses
[DLR-FB-71-72] 06 p0636 N73-15164
Wind tunnel tests to determine heat transfer of near equilibrium transpired turbulent boundary layer with adverse pressure gradient
[NASA-CR-130291] 06 p0652 N73-15291
Development of momentum integral type method for solving relaxation-diffusion model for turbulent shear stress of incompressible plane turbulent wakes
[REPT-72-FM-5] 06 p0652 N73-15296
Effect of pressure gradients on supersonic turbulent boundary layers and effect of dilation on Reynolds stresses
[IC-AERO-72-21] 07 p0736 N73-15989
Hypersonic axisymmetric turbulent boundary layer compression in adverse pressure gradient along cylindrical axisymmetric body
[NASA-CR-112247] 07 p0770 N73-16253
Normal pressure gradients in hypersonic boundary layers, including systematic derivation of equations of motion and energy equations
07 p0771 N73-16259
Spall calculations in one-dimensional hydrodynamics codes using aluminum and high explosives
[LA-5001] 07 p0855 N73-16935
Calculation of flow through airfoils in cascade to show pressure distribution under conditions of two dimensional incompressible flow with boundary layer separation at trailing edge
[DLR-FB-72-62] 09 p1014 N73-18276
Application of gas dynamics equations to determine magnitude of pressure rise due to sonic boom in stratified atmosphere
[NASA-TN-D-7105] 11 p1233 N73-20010
Analysis of effect on laminar boundary layer resulting from superposed unsteadiness on yawed infinite flat plate in adverse pressure gradient
12 p1389 N73-21265
Analysis of mean and fluctuating flow properties of compressible turbulent boundary layer in shock wave-induced adverse pressure gradient
[NASA-TN-D-7092] 12 p1391 N73-21280
Hot-wire anemometer and pitot static probe measurement of turbulent mixing in axial pressure gradients
[AD-756543] 13 p1511 N73-22244
Compressible turbulent boundary layer in zero-pressure gradient nozzle flow for zero, moderate, and severe heat transfer conditions
[AD-757330] 14 p1651 N73-23391
Effects of wall jets in still air on flat and curved surfaces under external stream in presence and absence of pressure gradient and initial boundary layer
[ARC-R/M-3252] 15 p1729 N73-24025
Numerical analysis of base pressure distribution for supersonic flow over slender wedge or backward facing step
15 p1764 N73-24295
Analysis of turbulent boundary layer on porous plate and fluid mechanics of adverse free stream pressure gradients
15 p1765 N73-24303
Development of mathematical models for turbulent flow and application to prediction of internal flows
[TM/TN/A/18] 15 p1768 N73-24321

Development of formulas for calculating gradients and ordinates of camber surfaces of sweptback wings of arbitrary planform with subsonic leading edges and specified load distribution
[ARC-R/M-3217] 16 p1852 N73-25004
Development of mathematical procedures for determining turbulent boundary layer in arbitrary pressure gradient
[ARC-R/M-3207] 16 p1854 N73-25017
Performance tests of gas turbine engine with highly loaded stages operating at high pressure ratio
[ARC-R/M-3242] 16 p1854 N73-25021
Incompressible free turbulent mixing in adverse and favorable pressure gradients
[AD-758664] 16 p1891 N73-25308
Measurement of effects of sonic booms on light building structures for various building configurations
[RAE-LIB-TRANS-1633] 17 p1981 N73-26011
Analysis of profile characteristics of supersonic turbulent boundary layer in region of moderate adverse pressure gradient
[AD-759915] 17 p2015 N73-26298
Numerical analysis of disturbance pressure due to impinging of plane shock wave of arbitrary strength on moving slender body
19 p2251 N73-28151
Turbulent free shear layers in pressure gradients
19 p2254 N73-28171
Numerical analysis of two dimensional turbulent wakes in constant adverse and favorable pressure gradients
[AD-761389] 19 p2256 N73-28185
Development of semi-empirical model for predicting fluctuating pressure distribution resulting from rocket plume- induced separated regions
[NASA-CR-124346] 19 p2352 N73-28922
Development of computer program for determining airfoil pressure distribution for subcritical attached viscous flow
[NAL-TR-248] 21 p2523 N73-30236
Numerical analysis of parameters of shock waves and dependence on angle of incidence and amplitude of shock wave
[AD-763157] 21 p2526 N73-30253
Calculations of turbulent shear stress distributions for zero pressure gradient and adverse gradient supersonic turbulent boundary layer flow
[AD-763197] 21 p2526 N73-30254
Turbulent mixing layer of different gases in pressure gradient
[AD-763487] 21 p2527 N73-30260
Free stream pressure gradient effects on accuracy of turbulent boundary layer calculations
22 p2648 N73-31219
Parametric linearization for approximating dynamic and thermal boundary layers for nonNewtonian fluids with arbitrary pressure and surface temperature gradients
[AD-764170] 22 p2655 N73-31271
Method of characteristics laser and mixing program for examining chemical laser flows and reactants in axial and lateral pressure gradients
[AD-763906] 22 p2682 N73-31482
Analytical solution for laminar boundary layer with pressure gradient and coolant injection
23 p2771 N73-32165
Incompressible turbulent plane jets exhausting downstream into external flow having favorable longitudinal pressure gradient
[ARC-CP-1236] 24 p2909 N73-33219
Subsonic air flow pressure drop at interface between two rectilinear ducts noting pressure pulses
[PUBL-133] 24 p2910 N73-33222

**PRESSURE MEASUREMENTS**
Measurement of shock and detonation wave pressures by means of shock-induced polarization of Plexiglas disks
[TL-1972-4] 02 p0155 N73-11254
Pressure drop measurements and drag coefficients for grid spacers of hexagonal fuel rod bundles
[NLL-RISLEY-TR-2440-[9091.9F]]
02 p0209 N73-11692
Surface pressure measurements over model delta wing undergoing oscillatory deformation in low speed wind tunnel
[ARC-R/M-3693] 03 p0248 N73-12005
Development of instrument for determining total pressure in calibration chamber and numerical analysis of operating principles
[NASA-TN-D-7058] 03 p0301 N73-12452
Measurement of pressure in Mach reflection of strong shock waves in shock tube
[AD-746613] 03 p0368 N73-12995
Pressure measurements on harmonically oscillating wing-tailplane configurations in incompressible speed range noting wind tunnel tests on aircraft models
[DLR-FB-71-52] 04 p0373 N73-13033
Heat transfer and surface pressure measurements at supersonic speeds on conical delta wings with sharp leading edges
[ARC-CP-1212] 05 p0492 N73-14008
Development of two experimental approaches for analyzing two dimensional flow on high lift devices
06 p0617 N73-15005
Measurement of ray paths and ground overpressures produced by Concorde aircraft during supersonic flight
[R/D-896] 06 p0618 N73-15021
Equations showing relationship between temperature and vapor pressure of liquids emphasizing vapor pressure measurement and Chebyshev polynomials
[NPL-CHEM-19] 06 p0638 N73-15179
Oscillographic pressure measuring system for flow structure in compressor impeller bladings
[NASA-TT-F-14647] 06 p0673 N73-15480
Flow field measurements around ogive-cylinder at angles of attack to 15 degrees and Mach numbers 3.52 and 4.07
[AD-752025] 08 p0898 N73-17268
Measurement of unsteady pressures developed on harmonically oscillating wing planform in three dimensional compressible flow
[DLR-FB-72-55] 09 p0980 N73-18007
Measurement of surface pressure fluctuations at two locations on XB-70 aircraft at local Mach number range from 0.35 to 2.45
[NASA-TN-D-7226] 09 p0981 N73-18013
Techniques and equipment for measuring stationary and nonstationary flow in wind tunnels during pressure and flutter tests
[DLR-MITT-72-25] 10 p1139 N73-19283
Comparison of two total pressure and total temperature measuring instruments for boundary layer investigations at supersonic speeds
10 p1139 N73-19284
Construction, installation, and calibration of wind tunnel models for measuring flutter characteristics of aerodynamic shapes
10 p1140 N73-19286
Turbulent pressure fluctuation measurements for cross section of supersonic diffuser inlet flow model
10 p1140 N73-19288
Error sources in pressure measurements on turbulent supersonic flows by nonstationary microphone
10 p1140 N73-19289
Orifice inclination effect in pressure measurements on hypersonic rarefied flow field of flat plate
10 p1140 N73-19290
Error sources in pressure measurements on turbulent supersonic flows by nonstationary microphone
10 p1184 N73-19629
Wind tunnel tests to determine pressure sensing characteristics of trailing cone device for calibrating aircraft static-pressure systems
[NASA-TN-D-7217] 13 p1470 N73-21906
Intraoral pressure in speech of deaf affecting voice/voiceless distinction
14 p1626 N73-23181
Analysis of atmospheric turbulence characteristics to show discrete gust and spectral presentations and to determine limitations of discrete gust approach
[ARC-R/M-3216] 15 p1729 N73-24026
Atmosphere Explorer satellite absolute pressure measurements of upper atmosphere
[AD-757908] 15 p1782 N73-24447
Measurement of deep ocean hydrostatic pressure fluctuations
[AD-757098] 15 p1783 N73-24458
Base pressure measurements on axially symmetric wind tunnel models in subsonic, transonic and supersonic speeds at high Reynolds numbers
[TAE-134] 16 p1857 N73-25044
Analysis of drag and pressure measurements made in subsonic wind tunnel tests on two annular airfoils noting relation between pressure distribution in compressible flow and at high speed
[ARC-R/M-2718] 21 p2492 N73-30003
Calibration of vacuum gauges for measuring total and partial pressures in ultrahigh vacuum region
[NASA-CASE-XGS-07752] 21 p2544 N73-30390
Absolute pressure measuring device for measuring gas density level in high vacuum range
[NASA-CASE-LAR-10000] 21 p2544 N73-30394
Pilot model expansion tunnel test flow properties obtained from velocity, pressure, and probe measurements
[NASA-TN-D-7310] 24 p2905 N73-33182
Measurements of temperature and pressure behind incident and reflected shocks in shock tube
[ARC-CP-1239] 24 p2909 N73-33220

**PRESSURE MICROPHONES**
U MICROPHONES

**PRESSURE OSCILLATIONS**
Analysis of pressure fluctuations in Nike rocket case and relationship to structural vibrations of rocket case
[NASA-TN-D-6931] 01 p0113 N73-10933
Oscillations and pressure variations in circular jet impacting on wall
[NASA-TT-F-14630] 05 p0527 N73-14284
Turbulent pressure fluctuation measurements for cross section of supersonic diffuser inlet flow model
10 p1140 N73-19288
Analysis of conditions under which coupling occurs between structure of combustion front and periodic oscillations
[NLL-M-22985-[5828.4F]] 15 p1842 N73-24922
Fluctuating pressure characteristics for far field acoustic radiation in mixing region of perturbed and unperturbed round free jet
[AD-759377] 17 p2015 N73-26294
Relation of local pressure fluctuations to large-scale meteorology, and simulation of acoustic-gravity waves in inhomogeneous media
18 p2170 N73-27528

**PRESSURE PROBES**
U PRESSURE SENSORS

**PRESSURE PULSES**
Approximate method for calculating echo signal of finite spherical pulse from elastic cylindrical shell in compressible fluid
16 p1969 N73-25928
Analysis of supersonic jet aircraft noise using fluctuating jet pressures to characterize the sources
[AD-762296] 19 p2222 N73-27923
Subsonic air flow pressure drop at interface between two rectilinear ducts noting pressure pulses
[PUBL-133] 24 p2910 N73-33222

**PRESSURE RECOVERY**
Pressure recovery performance of conical diffusers at high subsonic speeds and range of geometries
[NASA-CR-2299] 22 p2611 N73-30927
Experimental investigation of large scale, two dimensional, mixed compression inlet system
[NASA-TN-D-7445] 23 p2739 N73-31928

**PRESSURE REDUCTION**
Development of method for determining response of fluids under high pressure when released to atmosphere using closed form solution and numerical analysis
03 p0282 N73-12289
Mortality rate of guinea pigs after decompression treatment as function of water balance
[DLR-FB-71-20] 05 p0501 N73-14075
Analysis of pressure loss through single bends of various geometries under conditions of full incompressible flow
[ESDU-67040-AMEND-A] 05 p0525 N73-14272
Analysis of pressure loss conditions created by turbulent flow conditions for wide range of flowmeters
[ESDU-66030-AMEND-A] 05 p0525 N73-14273
Procedure for designing axisymmetric, translating, centerbody inlet bleed system for operation at Mach 3.5
[NASA-CR-2187] 06 p0713 N73-15821
Internal performance of mixed compression axisymmetric inlet model at Mach 0.8 to 2.65
[NASA-TN-D-7320] 16 p1955 N73-25817
Lower body decompression effects on human cardiovascular hemodynamic system
20 p2367 N73-29032
Pneumatic analogue decompression computer for real time prediction of safe ascent depth following depth excursion
[DCIEM-884] 22 p2638 N73-31144
Pressure drop in air flow isothermally across bank of helically wound, L-type fin tubes
[PB-220315/6] 24 p2911 N73-33229

**PRESSURE REGULATORS**
Development of pressure transducer for satellite attitude control feeding signals back to solenoid flow control valve
[RAE-TR-72085] 05 p0548 N73-14453
Analysis of Apollo 16 reaction control system helium pressure regulator filter failure
[NASA-TM-X-69131] 11 p1334 N73-20827
Underwater space suit pressure control regulator
[NASA-CASE-MFS-20332-2] 16 p1868 N73-25125
Development and characteristics of combined pressure regulator and shutoff valve with variable pressure response characteristics
[NASA-CASE-NPO-13201-1] 17 p2036 N73-26474

**PRESSURE RELIEF VALVES**
U RELIEF VALVES

**PRESSURE SENSORS**
Design, development, and evaluation of pressure transducer using glass fiber bundle to transmit and receive reflected light from pressure diaphragm
[AD-747521] 03 p0304 N73-12480
Development of differential pressure control system using motion of mechanical diaphragms to operate electric switch
[NASA-CASE-MFS-14216] 04 p0419 N73-13418
In-flight tests and operational reliability of jet aircraft nullable compressor face rake
[NASA-TN-D-7162] 07 p0769 N73-16247
Durability investigation of strain gage pressure transducers subjected to long term pressure cycling at ambient and elevated temperatures
[NASA-CR-120953] 07 p0800 N73-16497
Performance comparison of three normal-shock position sensors for supersonic mixed compression inlets
[NASA-TM-X-2739] 08 p0955 N73-17817
Initial systole and dicrotic notch detecting circuitry for monitoring arterial pressure pulse
[NASA-CASE-LEW-11581-1] 09 p0997 N73-18139
Portable device for detecting pneumatic pressure leaks in hermetically sealed housings
[NASA-CASE-MFS-21761-1] 09 p1035 N73-18444

Device for measuring stagnation pressure of supersonic gas streams
[NASA-CASE-LAR-11139-1] 11 p1292 N73-20483
Design and performance of strain gage transducer as blood pressure recording device
12 p1374 N73-21144
Pressure cell sensors for Pioneer 10/G meteoroid detection experiments
[NASA-CR-112273] 12 p1405 N73-21389
Modifications in development of high pressure version of vibrating cylinder pressure transducer
[AD-755533] 13 p1502 N73-22173
Development of method for predicting performance of barometric sensing systems used in determining sounding rocket altitude
[NASA-TM-X-65991] 17 p2087 N73-26881
Pressurized panel meteoroid detector
[NASA-CASE-XLA-08916-2] 19 p2299 N73-28487
Design, dynamic response, and operation of electric pressure difference transducer
[NLL-TRANS-2976-[9022.81]]
21 p2543 N73-30387
Piezoelectric pressure transducers for shock tubes, noting electrostatic calibrator
[ARC-CP-1240] 24 p2910 N73-33221

**PRESSURE SUITS**
NT SPACE SUITS
Tactile information presentation using high pressure pulses into anti-G suit
[AD-761796] 19 p2228 N73-27969
Design approaches to application of Boyle's law to emergency suits for fliers
[AD-761797] 19 p2228 N73-27970
Performance of anti-G valve subjected to varying acceleration forces
[AD-760814] 20 p2372 N73-29062
Equipment requirements for space shuttle EVA/IVA pressure suit, life support system, mobility aids, vehicle support provisions, and emergency support
[NASA-CR-133991] 21 p2503 N73-30089
Pressure suit requirements and characteristics for space shuttle personnel performing EVA and IVA activities - Vol. 3
[NASA-CR-133993] 22 p2622 N73-31008

**PRESSURE TRANSDUCERS**
U PRESSURE SENSORS

**PRESSURE VESSEL DESIGN**
Mechanical properties data and fabrication technology for filament wound graphite/epoxy resin pressure vessels
[NASA-CR-120951] 05 p0602 N73-14897
Finite element method computation of 1:5 scale model prestressed concrete high temperature nuclear reactor pressure vessel
[ISD-120] 10 p1221 N73-19927
Investigation of fibers and composites applicable to the design of high pressure vessels for satellites
[MAN-NT-10/72] 13 p1586 N73-22859
Modified high pressure system with small sample vessels for conducting biological reactions
[AD-752978] 16 p1885 N73-25256

**PRESSURE VESSELS**
Changes in brittle-ductile transition temperature of pressure vessel steel following neutron irradiation
[AD-745299] 01 p0067 N73-10552
Development of procedure for determining maximum and minimum stresses produced by uniform pressure on unpierced torispherical closure of cylindrical shell
[ESDU-67017] 01 p0110 N73-10911
Effect of temperature and flange configurations on critical pressure of 90-degree conical acrylic windows for hydrostatic pressure vessels when subjected to short term loading
[AD-748583] 04 p0440 N73-13583
Free-formed, flanged, acrylic shells for service as external pressure hulls with nominal 56-ft depth
[AD-749029] 05 p0603 N73-14908
Development and characteristics of test equipment for investigating thermodynamic properties of gases at high temperatures
[AD-749653] 05 p0607 N73-14936
Subcritical crack propagation in pressure vessel plates due to cyclic loads and stresses
[NASA-CR-120834] 06 p0725 N73-15920
Curves and general equations for design of lightweight glass fiber reinforced metal pressure vessels for space shuttles
[NASA-CR-120917] 09 p1094 N73-18932
Ultrasonic inspection of pressure vessel steel plates
[TR-7209.601-B] 10 p1164 N73-19469
Ultrasonic inspection of pressure vessel steels
[TR-7209.601] 10 p1164 N73-19470
Development of design concepts for metal-lines, glass-fiber composite pressure vessels and comparison with homogeneous metal pressure vessels
[NASA-TM-X-68198] 10 p1220 N73-19922
Technology for applying advanced fibers or resins to high performance high pressure filament-wound pressure vessels
[NASA-TM-X-68196] 10 p1220 N73-19923
Production of glass fiber reinforced plastic pressure tanks and rods
[AD-754679] 11 p1300 N73-20547
Aluminum and tin alloys for stress corrosion cracking and fatigue crack growth studies pertinent to spacecraft and booster pressure vessels
[NASA-CR-120823] 12 p1462 N73-21846
Analysis of fracture and crack growth properties of 304 stainless steel to determine suitability as material for cryogenic fluid storage pressure vessels
[NASA-CR-121025] 12 p1462 N73-21847
Investigation of fibers and composites applicable to design of high pressure gas storage vessels for satellite altitude control
[RRCM/ED/R/10] 13 p1586 N73-22856
Development of guidelines for selection of hardware items for use in manned spacecraft design to obtain five year maintenance-free service life - Vol. 3
[NASA-CR-128907] 14 p1707 N73-23855
Development of formulas for elastic behavior of axisymmetrically loaded cylindrical and spherical pressure vessels under various load conditions
[AD-758496] 14 p1717 N73-23936
Apollo experience report on design and development of cryogenic storage system and related components
[NASA-TN-D-7288] 16 p1964 N73-25889
Effects of irradiation on fracture and strength properties of pressure vessel steel plate and submerged arc weld
[HEDL-SA-387] 17 p2093 N73-26936
Irradiation effects on fracture of heavy section pressure vessel steels
[HEDL-SA-497] 17 p2094 N73-26937
Analysis of transient pressures in externally pressurized cryogenic hydrogen and oxygen tanks to determine effects of design variables on pressure response
[NASA-CR-133962] 18 p2199 N73-27755
Application of stress wave emission method to nondestructive testing of pressure vessels
[ISAS-492] 18 p2203 N73-27781
Flow velocity distribution in lower plenum of pressurized water reactor vessel, and design optimization of core catching structure
[BMFT-FBK-73-03] 19 p2255 N73-28182
Fracture mechanics of cylindrical pressure vessels having weld seam flaws
[AD-761532] 19 p2349 N73-28894
Computer program for estimating peak static pressure from internal explosions in closed vessels
[AD-762402] 19 p2350 N73-28907
Internal pressure vessels with filament of carbon fibers and epoxy resins
[NASA-CR-121138] 22 p2724 N73-31799
Stress analysis of thick wall cylindrical vessels weakened by flaws
[AD-764279] 22 p2726 N73-31811
Steel technology and water reactor pressure vessel safety
[ORNL-4855] 24 p2935 N73-33440
Safety precautions to be followed during radiographic inspection of pressure vessels
24 p2952 N73-33580
Containment design calculations for cylindrical vessel wall response to explosion
[SLA-73-508] 24 p2992 N73-33916

**PRESSURE WAVES**
U ELASTIC WAVES

**PRESSURE WELDING**
NT DIFFUSION WELDING
NT EXPLOSIVE WELDING
NT ULTRASONIC WELDING
Developments in vacuum diffusion welding methods and metallurgical applications of solar energy
[NLL-M-22830-[5828.4F]] 11 p1304 N73-20584
Analysis of friction welding of metal structures with information on friction theory, heat liberation, basic parameters, and recommended regimes
[AD-755753] 13 p1535 N73-22440

**PRESSURIZED CABINS**
Fatigue tests on Comet aircraft pressure cabin to determine effects of pressure cycles on structural stability of cabin windows
[ARC-R/M-3248] 15 p1728 N73-24017

**PRESSURIZED WATER REACTORS**
Flow velocity distribution in lower plenum of pressurized water reactor vessel, and design optimization of core catching structure
[BMFT-FBK-73-03] 19 p2255 N73-28182

**PRESSURIZING**
NT FUEL TANK PRESSURIZATION

**PRESTON TUBES**
U PITOT TUBES
U SPEED INDICATORS

**PRESTRAINING**
U PRESTRESSING

**PRESTRESSING**
Service life of mechanically prestressed glass used in spacecraft windows
09 p1088 N73-18880

**PRETESTS**
U TESTS

**PRETREATMENT**
NT PRESTRESSING

**PRETWISTING**
U PRESTRESSING

**PREVENTION**
NT ACCIDENT PREVENTION
NT CORROSION PREVENTION
NT FIRE PREVENTION
NT ICE PREVENTION

**PRIMARY BATTERIES**
NT ALKALINE BATTERIES
NT MAGNESIUM CELLS
NT METAL AIR BATTERIES
NT NICKEL ZINC BATTERIES
NT THERMAL BATTERIES
NT ZINC-OXYGEN BATTERIES
Results of testing long life primary cells
[SC-DC-72-1005] 03 p0255 N73-12060
Operational characteristics of carbon manganese dioxide electrode for metal air battery
[AD-751693] 09 p0991 N73-18089

**PRIMARY COSMIC RAYS**
NT SOLAR COSMIC RAYS
Evidence for one source mechanism for primary cosmic rays and another mechanism for iron nuclei, based on balloon-borne ionization spectrometer
[NASA-TM-X-66149] 06 p0716 N73-15841
Balloon borne measurement of cosmic ray electron spectrum from 10 to 200 GeV
[NASA-TM-X-66182] 08 p0956 N73-17830
Large cosmic ray air shower, primary energy spectrum, obtained from structure, size, and flux measurements
13 p1573 N73-22750
Arrival directions and anisotropies of large cosmic ray air showers of primary energy larger than 100,000 TeV
13 p1573 N73-22751
Nuclear interaction models for cosmic ray air showers to determine lateral distribution of particles and fluctuations in particle densities
13 p1574 N73-22752
Photometric determination of charge spectrum of low energy primary cosmic rays in stack of nuclear photographic emulsions
20 p2468 N73-29823
Identifying heavy primary cosmic ray particles at energies higher than 1 GeV/nucleon by nuclear emulsion balloonborne photometry
[LUIP-CR-73-02] 21 p2593 N73-30778

**PRIMATES**
NT CHIMPANZEES
NT HUMAN BEINGS
NT MONKEYS
Prolonged weightlessness for 300 plus days and cardiac performance in primates
[NASA-CR-129512] 03 p0256 N73-12075
Self contained automated primate research laboratory to study physiological effects of space environment weightlessness on monkeys
[NASA-CR-131642] 12 p1387 N73-21250
Techniques for determining effects of prolonged weightlessness on cardiovascular system of subhuman primates
[NASA-CR-131890] 13 p1479 N73-21980

**PRINCE WILLIAM SOUND [AK]**
Surface water circulation in Prince William Sound using ERTS-1 imagery
[E73-10291] 08 p0915 N73-17496
ERTS-1 imagery of water circulation in Prince William Sound
[E73-10402] 11 p1277 N73-20364
ERTS-1 imagery of water circulation in Prince William Sound
[E73-10617] 15 p1774 N73-24378
Surface circulation of coastal waters of Prince William Sound Alaska
[E73-10902] 20 p2396 N73-29251
ERTS-1 imagery of water surface circulation of Prince William Sound, Alaska
[E73-11064] 23 p2781 N73-32240

**PRINTED CIRCUITS**
NT LARGE SCALE INTEGRATION
Radio electronics, printed circuitry, miniaturization, microminiaturization, data processing, and radio equipment
[AD-746715] 02 p0151 N73-11224
Algorithms for computerized design of printed circuits with fixed component positions
03 p0278 N73-12255
Development and characteristics of polyimide impregnated laminates with fiberglass cloth backing for application as printed circuit broads
[NASA-CASE-MFS-20408] 03 p0320 N73-12604
Welding leads of integrated circuits to printed circuit boards
[AD-749838] 05 p0523 N73-14254
Printed circuit boards for microminiaturized electronic manufacturing
[AD-750918] 06 p0648 N73-15265
VHF omnidirectional antenna developed as printed current panel from flat plate dipole with low aspect ratio
[TR-72-34] 07 p0756 N73-16142
Processes for developing high quality multilayer printed wiring boards
[BDX-613-382-REV] 07 p0762 N73-16189
Methods for chip mounting and establishing electrical connections in miniaturized printed circuits and thick and thin film hybrid circuits
[ECR-27] 08 p0891 N73-17212

Bibliography on techniques for integrating and packaging printed circuits
[AD-752400] 09 p1010 N73-18241
Device for bending leads projecting from printed circuit boards
[NASA-CASE-MFS-22133-1] 09 p1039 N73-18473
Digitizing system for numerical definition of satellite printed wiring boards
[SC-TM-72-0645] 10 p1134 N73-19243
Printed circuit wiring patterns by efficient automatic procedures
[AD-754451] 11 p1301 N73-20553
Photoresist fabrication of printed circuit boards
[BDX-613-496] 12 p1387 N73-21245
Automatic scanning and display eddy current system for nondestructive testing of printed circuit boards
[ARL/MET-NOTE-84] 15 p1786 N73-24478
Techniques for packaging and mounting printed circuit boards
[NASA-CASE-MFS-21919-1] 16 p1883 N73-25243
Solder joint and printed circuit fatigue measurements by optical cross correlation
16 p1923 N73-25559
Development and evaluation of polyimide laminates for printed wiring board applications
[NASA-TM-X-64760] 17 p2050 N73-26581
Production of screen-printed inductive components using ferrite pastes
[RAE-LIB-TRANS-1690] 17 p2072 N73-26763
Computerized design of printed circuit boards
[AD-762021] 19 p2247 N73-28114
Printed wire routing on multilayer circuit boards
20 p2380 N73-29122
Fast heuristic techniques for placing and wiring printed circuit boards
24 p2898 N73-33134

**PRINTERS**
NT TELEPRINTERS

**PRINTOUTS**
Circuit and plug register diagrams for printout converter
[PHL-1972-4] 02 p0144 N73-11168
Data dump of space shuttle orbiter maneuvering engine performance, weight, envelope, and interface pressure requirements for propellant combinations
[NASA-CR-128675] 04 p0464 N73-13784
Statistical analysis and computer techniques
[NBS-TN-756] 11 p1311 N73-20635
Computer printouts of oceanographic data collected in North Pacific between 1961 and 1970
[NOAA-TR-NOS-47] 15 p1780 N73-24429

**PRIORITIES**
Ice problems in Canada, estimates of economic significance of problems, and order of priorities of research programs and management
[REPT-17] 07 p0788 N73-16412

**PRISMATIC BARS**
Calculation of stress and strain in two fold continuous prismatic bodies with example of calculation for ribbed fuel tube
[KFK-1665] 15 p1839 N73-24906

**PRISMS**
NT PRISMATIC BARS
Analysis of temperature distribution in prism heated by axisymmetrical beam of radiant heat
[NLL-M-21514-[5828.4F]] 05 p0605 N73-14921
Objective prism survey of entire southern sky within 10th to 13th photographic magnitude range by Schmidt telescope equipped with ultraviolet prism
06 p0717 N73-15851
Pros and cons of objective prisms in astronomical spectroscopy noting work in conjunction with Schmidt telescopes and novel techniques
07 p0845 N73-16846
Flint glass objective prism recommended for ESO Schmidt camera due to light transmission properties
07 p0845 N73-16847
Application of Schmidt telescope and objective prism to stellar radial velocity surveys
07 p0845 N73-16848
Interferometer prism and control system for precisely determining direction to remote light source
[NASA-CASE-ARC-10278-1] 16 p1911 N73-25463
Classification of southern carbon stars using objective prism spectra
16 p1960 N73-25857

**PRIVATE AIRCRAFT**
U GENERAL AVIATION AIRCRAFT

**PRIVATE AVIATION**
U CIVIL AVIATION
U GENERAL AVIATION AIRCRAFT

**PROBABILITY**
U PROBABILITY THEORY

**PROBABILITY DENSITY FUNCTIONS**
NT NORMAL DENSITY FUNCTIONS
NT WEIBULL DENSITY FUNCTIONS
Random number generators and use of estimators of probability density functions in data analysis
[NASA-CR-129507] 03 p0269 N73-12178
Time series and probability density function analyses of hypothesis that organized motion exists in air flow above naturally occurring water waves
[AD-749045] 04 p0408 N73-13328
Synoptic cloud cover observations for computing probability of clear lines of sight through atmosphere to ground
[P-4883] 04 p0444 N73-13620
Experimental analysis of probability density function of instantaneous amplitude of speech and effect of filtering and compression
14 p1630 N73-23212
Position location in presence of parametric uncertainty
[AD-756251] 14 p1691 N73-23722
Multivariate analysis on data used in n-station solution tracking technique
[AD-759975] 17 p2000 N73-26172
Theory and application of random Markov processes to analysis of tracking disruption
18 p2169 N73-27520
Analysis of signal and correlated noise for interperiod compensation systems of moving target selection procedures
22 p2629 N73-31069
Probability distribution function of phase difference of sum of signal and noise to determine efficiency of phase interperiod compensation systems
22 p2629 N73-31070

**PROBABILITY DISTRIBUTION FUNCTIONS**
Package enabling simulation of random samples from discrete and continuous distribution
01 p0072 N73-10587
Probability distribution of yield strength for mild steel, and application of numerical techniques to mechanical vibration problems
[NASA-CR-132203] 17 p2043 N73-26527
Collision probability method for calculating neutron transport in multidimensional systems
24 p2960 N73-33653

**PROBABILITY THEORY**
Equations and nomograms depicting probabilities of rare meteorological phenomena
[NLL-M-22672-[5828.4F]] 01 p0073 N73-10598
Ising ferromagnet thermodynamic equilibrium states in low temperature regions
[NOTA-INTERNA-381] 01 p0080 N73-10660
Incomplete state feedback for systems with parameter uncertainty and random disturbances
[NASA-CR-129180] 02 p0150 N73-11219
Chain geometry theorem for Minkowski space
02 p0203 N73-11641
Estimation procedure for fatigue failure probability of some graphites
[AECL-3958] 04 p0438 N73-13567
Probability estimation of survival fatigue failures, using statistics of extremes
[FO-1078] 05 p0568 N73-14615
Data base containing objectively-correlated solar measurements used to obtain parameters for flare prediction
[AD-749869] 06 p0716 N73-15843
Haze-free and cloud-free lines-of-sight through atmosphere
[AD-751264] 07 p0796 N73-16476
Most probable position in astronomical navigation using celestial body coordinates
07 p0859 N73-16972
Probability models of wet and dry days for several stations in Thailand
[THESIS-392] 08 p0938 N73-17684
Estimating confidence intervals of probability of rare events as function of scale of sample
[AD-751953] 08 p0939 N73-17693
Determination of parameters related to interior of Mercury
[NASA-CR-130981] 09 p1082 N73-18823
Probabilistic design model for prediction of heat transfer rate for heat pipes
[AD-752057] 10 p1224 N73-19954
Modelling prediction of probability of acquiring designated target as function of its range as target is approached
10 p1225 N73-19962
Probability of acquiring targets by search aircraft which flies along enemy line of communication
10 p1226 N73-19971
Asymptotic properties of feedback systems containing uncertain parameters and subjected to stochastic perturbations
[NASA-CR-131372] 11 p1264 N73-20260
Biostatistics of genetical processes in human populations
[NASA-CR-131508] 12 p1372 N73-21131
Probabilities models of organizational behavior and human subjective performance
[IZF-1973-3] 14 p1613 N73-23076
Step adaptation algorithms and application of stochastic graphs for analysis of discrete automatic systems
14 p1644 N73-23332
Probabilistic model of planetary contamination for deciding spacecraft quarantine standards and procedures
[NASA-CR-132001] 14 p1704 N73-23829
Numerical analysis of minimum probability of error expression in digital communication system with intersymbol interference
[AD-760057] 17 p1999 N73-26167
Best channel selection in terms of divergence and minimizing probability of misclassification
[REPT-5] 20 p2437 N73-29569
Interclass divergence with fixed number of channels and probability of misclassification
[REPT-5] 20 p2437 N73-29570
Multivariate statistical analysis including divergence, probability of misclassification, information theory, and matrix analysis
[NASA-CR-128990] 20 p2438 N73-29578
Minimal probability of misclassification in feature selection problem of classifying n-dimensional observation vector into one of m-distinct classes
[REPT-26] 20 p2439 N73-29589
Space vehicle design criteria based on interplanetary charged particle environments
[NASA-CR-133600] 20 p2473 N73-29865
Methods for approximating probability of tracking disruptions in automatic control systems
21 p2565 N73-30564
Quantum detection and estimation in optical communication systems
22 p2679 N73-31460
Research on probabilistic information processing
[NASA-CR-133918] 22 p2738 N73-31920
Probabilistic models and statistical inference in reliability life testing, and fatigue failure
[AD-763818] 23 p2798 N73-32380
Minimizing probability of incorrectory classifying spectral observations from multispectral band scanners
[NASA-CR-134058] 23 p2812 N73-32486
Statistical weather forecasting using Gumbel theory noting application to atmospheric temperature long term effects
[MONO-89] 23 p2814 N73-32500
Probabilistic approach to trajectory sensitivity
23 p2835 N73-32657
Stochastic processes and dynamic systems noting Markov and Ito-Markov processes
[LAAS-AS-73-I-09] 24 p2945 N73-33519

**PROBES**
Development of droplet monitoring probe for use in analysis of droplet propagation in mixed-phase fluid stream
[NASA-CASE-NPO-10985] 11 p1291 N73-20478

**PROBLEM SOLVING**
NT ASYMPTOTIC METHODS
NT ITERATIVE SOLUTION
NT THEOREM PROVING
Semiempirical calculations of turbulent boundary layer problems
[AD-745217] 01 p0042 N73-10330
Fricks equation for determining diffusion profiles in two impure semiconductors
[CEA-CONF-1970] 01 p0087 N73-10723
Numerical solution of parabolic partial differential equations with reference to eddy heat conduction in ocean
[AD-746205] 02 p0167 N73-11362
Successive approximations for solving discrete Bolza problem by dynamic programming
[TR-72-43] 02 p0202 N73-11632
Analysis of approximation methods for solving discrete Bolza problem by dynamic programming, and stability and error properties
[USC-113P19-28] 02 p0202 N73-11633
Heuristic algorithm for mixed integer linear programming problems
[NPL-NAC-18] 02 p0202 N73-11637
Simplex method for linear programming problem solving with explanation of terminology
[NPL-NAC-19] 02 p0202 N73-11638
Stochastic solutions of conservative dynamic systems such as particle accelerators and storage rings
[LAAS-PUBL-935] 02 p0203 N73-11640
Procedure for solving nonconservative projectile penetration problems
[AD-746140] 02 p0219 N73-11774
Graphical solution to bending moment of curved strut subjected to end loads
[ESDU-01.01.14] 02 p0236 N73-11919
Influence of end loads and moments on bending moment of straight strut
[ESDU-01.01.15] 02 p0236 N73-11920
Approximate solution to covariance of plane wave direction and propagation velocity of signals in array processing scheme
[AD-747591] 03 p0267 N73-12160
Computerized simulation of artificial robot interaction behavior with complex environment
[NASA-CR-129526] 03 p0269 N73-12179
Solution of partial differential equations by analog networks
[AD-746929] 03 p0272 N73-12206
Graphical method for solving interference problem in asynchronous circuit
[CEA-CONF-1961] 03 p0277 N73-12249
Asymptotic solution of two-dimensional flow of perfect gas past blunt body at given Mach number
[AD-747545] 03 p0287 N73-12327
Solution of boundary value problems by characteristics equations
[NASA-CR-129256] 03 p0324 N73-12637

Conversion and utilization of solar energy to solve energy shortages and pollution problems on earth
04 p0474 N73-13866
Solving problem of noise in single and double injection diodes
[AD-750186] 06 p0645 N73-15240
Numerical solution for cylindrical symmetrical diffusion problem
[FOA-1-C-1409-92] 06 p0653 N73-15306
Finite difference solution to diffusion equation in spherical coordinates
[SCL-DR-72-0017] 06 p0691 N73-15623
Methodology for computer software documentation
[NASA-TM-X-66161] 07 p0759 N73-16162
Mathematical programs for direct problem solving
[NASA-SP-5913[02]] 08 p0887 N73-17180
Development of digital fast-time air traffic control conflict prediction models and application to specific air route traffic control situations
[UTIAS-TN-183] 08 p0941 N73-17708
Development of algorithm for multiple hypothesis testing with application to amplitude comparison monopulse radar system in air traffic control operations
[TN-1973-7] 09 p1002 N73-18173
Problems of radio telemetry systems in manned and unmanned spacecraft
[NASA-TT-F-722] 09 p1002 N73-18175
Techniques for solving for optimum filter for video signal processing
[AD-753132] 09 p1003 N73-18189
Conditions necessary to insure stationarity in solution process for stochastic differential equations
[NASA-CR-130779] 09 p1056 N73-18606
Continuation method for solving eigenvalue problems and finding roots of polynomials
[TAE-152] 09 p1057 N73-18617
ALGOL 60 subroutine for implementation of modified Newton algorithms for problem solving
[NPL-NAC-24] 09 p1057 N73-18622
Algorithms for numerical solution of problems in calculus of variations
[NPL-NAC-28] 09 p1058 N73-18626
Gradient procedures for solving dual optimal control and max-min problems
[AD-753129] 09 p1058 N73-18628
Finite difference algorithm for solving quasi-linear gas dynamic systems
[AD-753097] 10 p1143 N73-19309
Gradient methods for solving incompatible systems of linear equations of higher order in photomapping problems
10 p1178 N73-19584
Liapunov solutions to linear differential equations with periodic coefficients
[NASA-TT-F-14835] 10 p1179 N73-19588
Oscillatory and nonoscillatory solutions to equations on nonlinear saturation of convective heat transfer
[AD-754228] 10 p1179 N73-19594
Graphical computers and computing techniques for real time aid in human problem solving tests
[AD-754282] 11 p1260 N73-20227
Mologenskys solution of geodetic boundary value problems
[AD-754251] 11 p1287 N73-20444
MIMIC programming language for solving Abel integral equations
[AD-754003] 11 p1311 N73-20642
Finite element formulation and thermoelastoviscoplasticity theory for solving problems in nonlinear continuum mechanics
[AD-754952] 11 p1331 N73-20805
Design of FGRAAL type compiler language for solving graph structure algorithm problems
[NASA-CR-131474] 12 p1382 N73-21204
Theorems for oscillatory solutions to differential equations
[NASA-TT-F-14883] 12 p1419 N73-21498
Design and implementation of language for expressing problem solving procedures in artificial intelligence
[NASA-CR-131591] 13 p1497 N73-22130
Existence of periodic solutions for nonautonomous neutral functional differential equations
[NASA-CR-131887] 13 p1550 N73-22556
Intermediate problem technique used to generate difficult eigenvector and boundary value problem solutions
[AD-756672] 13 p1550 N73-22561
Use of remotely sensed data to solve water resource problems of Wolf Creek Watershed, Colorado
[NASA-CR-129001] 14 p1660 N73-23479
Computer program for calculating individual characteristic values and associated solutions of Mathieu equation
[VUB-STR-1] 14 p1683 N73-23655
Search algorithm for component placement problem in computerized design of circuits
[AD-756502] 14 p1684 N73-23663
Use of aerospace technology to solve earth based problems
[NASA-CR-132148] 15 p1846 N73-24961
Application of holographic nondestructive testing to experimental production hardware components and structural problems in aerospace engineering
16 p1921 N73-25546
Event horizon and T-S solutions to Einstein vacuum field equation
[RIFP-177] 16 p1934 N73-25652
Computer solution to Hallens equation on half wavelength elements of planar symmetrical antenna arrays
[AD-761471] 19 p2245 N73-28103
Mathematical technique for optimal control problems with initial conditions
[AD-762253] 19 p2315 N73-28620
Solution to problem of endangered living space
[NRC-TT-1636] 20 p2371 N73-29057
Solutions to quasisteady problems of dynamic weather forecasting
20 p2442 N73-29618
Photometric standards for North Polar Sequence, Kapteyn Areas, and Harvard Standard Areas
21 p2594 N73-30791
Robot computer problem solving system which represents robot exploration vehicle in simulated Mars environment
[NASA-CR-133942] 22 p2638 N73-31146
Methods of solving quasistatic problems in linear theory of thermoviscoelasticity
[AD-763937] 22 p2726 N73-31816
Solution to equation of radiative transfer for homogeneous atmosphere bounded by perfect specular reflector
[AD-764619] 23 p2857 N73-32830
Solution of nonlinear problems of high temperature heat transfer
[AD-765747] 24 p2993 N73-33917

**PROCEDURES**
NT FINITE ELEMENT METHOD
NT OPTICAL CORRECTION PROCEDURE

**PROCEEDINGS**
Research and development of advanced energy sources for United States of America
01 p0120 N73-10988

**PROCESSORS [COMPUTERS]**
U CENTRAL PROCESSING UNITS
U COMPUTERS

**PROCUREMENT**
NT GOVERNMENT PROCUREMENT

**PROCUREMENT MANAGEMENT**
Planning and budgeting in lightweight fighter prototype development for military aviation
13 p1595 N73-22934
Statistical analysis of naval experience in fixed-price incentive contract management for aircraft and missile procurement
[AD-761396] 19 p2355 N73-28946

**PROCUREMENT POLICY**
Incentive schemes as contract management tool noting use in ESRO 4 satellite project
15 p1849 N73-24989

**PRODUCT DESIGN**
U PRODUCT DEVELOPMENT

**PRODUCT DEVELOPMENT**
NT WEAPONS DEVELOPMENT
Technology assessment for thin film development of magneto-optical manganese bismuth memory
04 p0394 N73-13202
Production and properties of special purpose synthetic fibers
[AD-749059] 05 p0567 N73-14607
Theoretical and parametric study of inductive magnetohydrodynamic converters including design of cryogenic experimental 4 kW converter
[DLR-FB-71-74] 06 p0706 N73-15757
Survey of heavy duty composite materials, development, manufacturing, costs, and applications
09 p1052 N73-18577
Errors in design of mechanisms which result in problems during later development stages
09 p1087 N73-18867
Simplified technique and device for producing industrial grade synthetic diamonds
[NASA-CASE-MFS-20698-2] 10 p1163 N73-19457
Development of miniature electronic trimmable thin film resistor chips having precision responses
[BDX-613-728] 12 p1383 N73-21216
Cosmization of Soviet economy
[NASA-TT-F-13958] 14 p1705 N73-23839
Phased development, planning, and management of new industrial products
15 p1848 N73-24980
Degree of innovation and risk in product development contracts
15 p1849 N73-24988
Thermoelectric converter and 5-kwe reactor system integration
[NASA-CR-121230] 16 p1943 N73-25726
Self-healing fuse development
[NASA-CR-121244] 21 p2517 N73-30191
Airfield runway marking paint superior to paint presently used
[FAA-RD-73-23] 21 p2520 N73-30213
High precision quartz astatic gravimeter designated GRK-1
[JPRS-59832] 21 p2548 N73-30426
Research projects to develop and evaluate ceramic materials in areas of refactory structural ceramics and solid electrolyte ceramics
[NASA-CR-133741] 21 p2562 N73-30540
Method for fabricating samarium cobalt permanent magnets
[BM-RI-7784] 21 p2580 N73-30679
Production and characteristics of yttrium subgroup rare earth metal dodecaborides
23 p2808 N73-32452
Process for removing plasticizer from hard metal alloy extruded samples during low temperature sintering
23 p2808 N73-32454
Physical and mechanical properties of cermets to include methods for altering characteristics for specific industrial applications
23 p2809 N73-32459
Applications of mathematics to design and development of electronic equipment, microelectronic devices, and lasers
24 p2900 N73-33147
Laser development and applications to plasma physics
[UCRL-50022-4] 24 p2931 N73-33410
Photographing method for manufacturing multicolor electroluminescent chips
[AD-764943] 24 p2944 N73-33509
Booster rocket engines, mentioning 20T-LOX/LH2, 5T-LOX/kerosene, 13T-LOX/LH2, and 1T-N2O4/UDMH engines
24 p2973 N73-33753
Bibliography of research projects on heat pipe, development, performance, and application - January through March, 1972
[NASA-CR-135956] 24 p2991 N73-33901
Bibliography of heat pipe research and development projects conducted during April through June 1972
[NASA-CR-135955] 24 p2991 N73-33902
Bibliography of heat pipe research and development projects conducted during July through September, 1972
[NASA-CR-135952] 24 p2991 N73-33903
Supplemental report and bibliographies of heat pipe research projects conducted during calendar year 1971
[NASA-CR-135951] 24 p2991 N73-33904

**PRODUCTION ENGINEERING**
NT PRODUCTION PLANNING
Production measures for visible and ultraviolet transmitting reticles for star trackers
[NASA-CASE-GSC-11188-3] 01 p0056 N73-10460
Manufacturing of holmium lithium tetrafluoroytriate laser disk bonded into glass
[AD-747968] 03 p0352 N73-12871
Fabrication of thin film silicon integrated square wave oscillator circuit capacitors
[AD-749266] 04 p0397 N73-13231
Microwire casting development and technology in USSR
[JPRS-57655] 04 p0426 N73-13473
Production engineering methods for metal ceramic structural materials and parts
[JPRS-57487] 04 p0431 N73-13515
Cold plastic deformation process for manufacturing molds and stamps from sintered metal powder ceramic blanks
04 p0432 N73-13519
Construction of electron beam semiconductor pulse amplifier and radio frequency amplifier diode
[AD-748892] 04 p0461 N73-13758
Production of isotopic fuel pellets by vacuum hot pressing
[ORNL-4796] 05 p0579 N73-14711
Development of process for obtaining iron whiskers and description of mechanical and physical properties
[IIS-142-VOL-22-4] 05 p0586 N73-14766
Production processes for fabrication of lithium doped P/N cells
[NASA-CR-130289] 06 p0626 N73-15078
Production yield of electronic materials and associated devices
[AD-749984] 06 p0678 N73-15514
Fabrication and nondestructive tests of beryllium reinforced metal matrix composites
[AD-750764] 06 p0686 N73-15583
Processes for developing high quality multilayer printed wiring boards
[BDX-613-382-REV] 07 p0762 N73-16189
Design, processing, and measurement of precision single sideband crystal units
[AD-751748] 07 p0833 N73-16754
Prototype 12 GHz low noise converter with mounted planar circuit in waveguide
[NASA-TT-F-14656] 09 p1007 N73-18218
Design of automated production facility capable of manufacturing beam-lead CMOS integrated circuits
[NASA-CR-124116] 09 p1038 N73-18465
Digitizing system for numerical definition of satellite printed wiring boards
[SC-TM-72-0645] 10 p1134 N73-19243
Laser forming of sliding friction bearings for instrument construction
[AD-753490] 10 p1169 N73-19511
Production methods, quality control, and metallurgical uses of pure rare earth metals and alloys
[IS-2968] 10 p1172 N73-19538

Design and fabrication of wraparound contact silicon solar cells
[NASA-CR-121003] 11 p1237 N73-20044
Production of glass fiber reinforced plastic pressure tanks and rods
[AD-754679] 11 p1300 N73-20547
Manufacturing of hyperabrupt Si varicaps based on impurity diffusion from double doped substrate
12 p1384 N73-21221
Problems of designing and developing automatic equipment and control systems
[JPRS-58746] 12 p1405 N73-21391
Production methods for preventing deterioration of freeze-dried foods
[NASA-CR-128915] 14 p1614 N73-23085
Material selection for design and manufacture of FCC
14 p1640 N73-23297
Manufacturing and quality control of FCC harnesses with design and installation requirements
14 p1641 N73-23302
Energy pulse bonding method for joining flat cables
14 p1641 N73-23303
Plastics fabrication by ultraviolet, infrared, induction, dielectric, and microwave radiation methods
[AD-756214] 15 p1802 N73-24607
Fabrication method for plutonium-beryllium neutron sources
[BARC-629] 15 p1815 N73-24716
Statistical performance test evaluation in aerodynamic development of Dart sailplane
[CRANFIELD-AERO-16] 16 p1859 N73-25059
Production cost optimization for thermoelectric solar cell
[AD-759812] 16 p1865 N73-25104
Production of polycrystalline bismuth-calcium-vanadium garnet phase shifters
[AD-758919] 16 p1881 N73-25224
Interferometrically controlled ruling machine for manufacturing optical diffraction gratings
[AD-758898] 16 p1946 N73-25745
Manufacturing of metal insulator semiconductor capacitors on single crystal silicon substrates
[AD-760009] 17 p2005 N73-26214
Fabrication and testing of thin walled cylinders made from tungsten lead composite
[LA-511] 17 p2038 N73-26485
Methods for improving heat resistance of alloys
[AD-760273] 17 p2047 N73-26564
Production of screen-printed inductive components using ferrite pastes
[RAE-LIB-TRANS-1690] 17 p2072 N73-26763
Environmental factors influencing Canadian industrial growth
[DRAE-34] 18 p2207 N73-27815
Design of flat conductor cable for interconnecting harness application
[NASA-TM-X-64750] 19 p2243 N73-28085
Development of method for determining cost functions involving aircraft rework and engine repair programs at military installation
[AD-761475] 19 p2249 N73-28135
Sintering theory and practice review enhancing metallurgists and ceramists
[KFK-1713] 19 p2305 N73-28535
Production technology for diffraction gratings as laser beam sampling components
[AD-762306] 19 p2322 N73-28681
Variable measurements in electrolytic production of aluminum
[NLL-TRANS-1059-[9022.04]]
20 p2422 N73-29454
Production of semiconducting films for waveguides and optical device elements
[AD-763101] 20 p2455 N73-29729
Press-brake roll and weld frabrication of prototype large diameter missile cases
[AD-762612] 20 p2466 N73-29815
Technologies for production and utilization of petroleum, natural gas, oil shale and coal
[BM-IC-8612] 21 p2536 N73-30335
Production method of star tracking reticles for transmitting in visible and near ultraviolet regions
[NASA-CASE-GSC-11188-1] 23 p2790 N73-32320
Mechanical processes for developing metal matrix composite Al/B tubes
[NASA-CR-124407] 23 p2797 N73-32370
Bibliography of techniques, procedures, manufacturing methods, time studies, and shop layout in machine shop practice
[AD-765400] 23 p2799 N73-32388
Production of fire protective intumescent coatings to show methods of manufacture and resulting material properties
[NASA-CR-114470] 23 p2810 N73-32468
Manufacturing of high efficiency ultrasonic wave transducer for light modulation using Brillouin effect
[REPT-4.473] 23 p2820 N73-32544
Analysis of alternate space shuttle concepts to examine stage-and-one-half concept for reusable shuttle system and cost of external hydrogen tank development program
[NASA-CR-124421] 23 p2850 N73-32774
Economic factors, financial management, production and marketing for air transport industry
[NASA-CR-135634] 23 p2860 N73-32848
Production forecasting for aircraft manufacturer
23 p2862 N73-32872
Production of silica, mullite, and alumino silicate reusable surface insulation materials for space shuttle orbiters
[NASA-TM-X-2719] 24 p2938 N73-33461
Production engineering for silica reusable surface insulation panels
24 p2938 N73-33462
Production of rigidized mullite composite materials for external insulation of shuttle orbiter
24 p2938 N73-33463

**PRODUCTION MANAGEMENT**
Manual control model structure for industrial management of man machine systems
01 p0015 N73-10115
Control and coordination requirements for fabrication of devices in the thermonuclear research program
[B-159687] 03 p0332 N73-12703
Application of mathematics to general job-shop scheduling noting criteria, procedures, and linear programming
[LAAS-OD-73-1-21] 23 p2813 N73-32488

**PRODUCTION METHODS**
U PRODUCTION ENGINEERING

**PRODUCTION PLANNING**
Production planning with group techniques for welding shops using component and blank classifications
[NLL-M-22594-[5828.4F]] 05 p0550 N73-14467
Interaction between man and electronic computer in operational planning
09 p0997 N73-18138
Economic effectiveness of production planning and automatic control methods in industry
[JPRS-58680] 12 p1467 N73-21884
Phased development, planning, and management of new industrial products
15 p1848 N73-24980
Interface control documenation for design and development of Apollo ultraviolet spectrometer experiment
[NASA-CR-128550] 16 p1917 N73-25511

**PRODUCTS**
Selected bibliography of articles on product liability
[NASA-TM-X-69493] 20 p2488 N73-29985

**PROFICIENCY**
U ABILITIES

**PROFICIENCY MEASUREMENT**
U HUMAN PERFORMANCE
U PERFORMANCE TESTS

**PROFILOMETERS**
Wavelength profilometer based on phase-ranging with VHF - modulated C02 laser
[AD-762453] 20 p2415 N73-29411
Airborne laser profilometer for evaluating surface roughness of landing sites
[AD-763180] 22 p2648 N73-31218

**PROGRAM MANAGEMENT**
U PROJECT MANAGEMENT

**PROGRAMMED INSTRUCTION**
Program instructions for using and running card deck through AIST-O system
[JPRS-57790] 05 p0517 N73-14200
Cybernetic application of computers in personnel training
[AD-751145] 09 p0998 N73-18143
Update of input instructions for operation of FORTRAN computer code TEMOD
[NASA-CR-121225] 19 p2239 N73-28047

**PROGRAMMERS**
Reference material for thermal simulation system for programmers, temperature controls, power regulator, peripheral equipment, and radiant array purchased parts
[NASA-CR-124437] 24 p2901 N73-33155

**PROGRAMMING**
NT QUADRATIC PROGRAMMING

**PROGRAMMING [SCHEDULING]**
NT THRUST PROGRAMMING
User guide for Dynamic Operational Requirements and Cost Analysis Program for space mission planning and project management - Vol. 1
[NASA-CR-123378] 03 p0270 N73-12188
Programmatics of space shuttle supported research facilities for telecommunication and navigation - Vol. 4
[NASA-CR-124139] 10 p1137 N73-19268

**PROGRAMMING LANGUAGES**
NT ALGOL
NT ASSEMBLY LANGUAGE
NT FORTRAN
NT MACHINE ORIENTED LANGUAGES
NT PL/1
Review of commonly used programming languages and their ranges of applicability
[NASA-TT-F-14610] 01 p0030 N73-10237
Internal structure of SQAP natural language parser for question-answer system
[FOA-P-C-8286-11[64]] 02 p0145 N73-11174
HAL programming language for aerospace computer applications
[NASA-CR-129506] 03 p0270 N73-12191
Users manual for interpretive computer program implementation on large computer
[NBS-TN-552] 04 p0393 N73-13193
Modified programming language for X ray diffraction analysis by special purpose computer using internal counting
[AD-748828] 04 p0459 N73-13747
Recognition and parsing algorithms for phrase structure languages
[NLL-SMRE-TRANS-5884-[8313.4]]
06 p0643 N73-15219
Digital simulation language for flight dynamic tests, exemplified by Fiat G-91 and Dornier Do-31 aircraft
[BMVG-FBWT-72-21] 07 p0740 N73-16019
Implementation of FORTRAN extended graph algorithmic language for univac 1108 computer
[NASA-CR-130966] 09 p1006 N73-18212
Automated engineering design for development of problem and user-oriented languages
10 p1131 N73-19221
Representations of language recognition problem for theorem prover in first order logic
[NASA-CR-131402] 11 p1310 N73-20632
MIMIC programming language for solving Abel integral equations
[AD-754003] 11 p1311 N73-20642
Program debugging and monitoring facilities for improving diagnostic capability of compiler
[NBS-TN-763] 12 p1381 N73-21197
Programming language for writing programs conforming to standards of structured programming and modular design
[NASA-CR-131473] 12 p1381 N73-21203
Design of FGRAAL type compiler language for solving graph structure algorithm problems
[NASA-CR-131474] 12 p1382 N73-21204
Design and implementation of language for expressing problem solving procedures in artificial intelligence
[NASA-CR-131591] 13 p1497 N73-22130
Power of programming features in computer languages
[NASA-CR-131895] 14 p1638 N73-23280
Telemetry preprocessing language for telemetry data processing
[NASA-TM-X-66248] 15 p1750 N73-24183
Manual for TMGL self-describing metalanguage with bootstrapping feature
[ESRO-SP-86] 19 p2239 N73-28054
Analysis of languages for design of digital computers
[AD-762381] 19 p2241 N73-28071
Basic programming language for simulation of digital devices
21 p2514 N73-30164
Design of programming language for image processing
22 p2636 N73-31124
Feasibility analysis of GOAL to HAL language translator for use with space shuttle
[NASA-CR-134033] 22 p2638 N73-31141
Space shuttle avionics and GOAL language including impact of error detection and redundancy management
[NASA-CR-134034] 22 p2638 N73-31142
Syntax diagrams handbook for Ground Operations Aerospace Language [GOAL]
[NASA-TM-X-69505] 22 p2639 N73-31148
Concept of comments in programming languages
[NPL-NAC-34] 22 p2639 N73-31154
TENEX computer system, ARPA network, and computer language design for robot development
[NASA-CR-135899] 24 p2897 N73-33124
Description and capabilities of ground Operations Aerospace Language [GOAL]
[NASA-TM-X-69541] 24 p2897 N73-33128
Textbook of Ground Operations Aerospace Language [GOAL]
[NASA-TM-X-69542] 24 p2897 N73-33129

**PROGRAMS**
NT APOLLO PROJECT
NT DEFENSE PROGRAM
NT EARTH RESOURCES PROGRAM
NT EARTH RESOURCES SURVEY PROGRAM
NT ECHO PROJECT
NT EUROPEAN SPACE PROGRAMS
NT GEOGRAPHIC APPLICATIONS PROGRAM
NT MARINER PROGRAM
NT MARS 69 PROJECT
NT MARS 71 PROJECT
NT NASA PROGRAMS
NT NIMBUS PROJECT
NT PIONEER PROJECT
NT PROJECTS
NT QUIET ENGINE PROGRAM
NT ROVER PROJECT
NT SKYLAB PROGRAM
NT SPACE PROGRAMS
NT SQUID PROJECT
NT SURVEYOR PROJECT
NT TEKTITE PROJECT
NT TELSTAR PROJECT
NT U.S.S.R. SPACE PROGRAM
NT UNIVERSITY PROGRAM

**PROJECT MANAGEMENT**
MSFC/Auburn/Alabama 1972 summer faculty fellowship research program report
[NASA-CR-61395] 01 p0120 N73-10992

Planning, control, and management for European space satellite project
[ESRO-SP-70] 01 p0121 N73-10996
Capabilities of Dynamic Operational Requirements and Cost Analysis Program for space mission planning - Vol. 1
[NASA-CR-129263] 03 p0269 N73-12183
Description of functions and capabilities of Dynamic Operational Requirements and Cost Analysis Program - Vol. 4
[NASA-CR-129266] 03 p0270 N73-12186
Programmer manual for Dynamic Operational Requirements and Cost Analysis Program for space mission planning and project management - Vol. 2
[NASA-CR-123379] 03 p0270 N73-12189
Application of Apollo Project managerial practices to solution of problems encountered in modern civilization
04 p0470 N73-13834
Analysis of management procedures applied to Surveyor and Lunar Orbiter projects
[NASA-SP-4901] 04 p0486 N73-13973
Planning process, objectives of program areas, and index of plans for air traffic control system improvements
[AD-750224] 05 p0578 N73-14705
Research and development projects conducted by National Research Council of Canada from July to September 1972
[DME/NAE-1972[3]] 05 p0611 N73-14967
Control over social change through anticipatory project assessment
[NASA-CR-129830] 05 p0611 N73-14968
Project control in ESRO program
05 p0611 N73-14973
Management and use meteorological satellite data to detect severe storms and crop disease
[NASA-CR-130000] 06 p0693 N73-15642
Analysis of weather satellite program management and organization systems
06 p0693 N73-15643
Analysis of technological alternatives involved in development of air traffic control systems - Vol. 2
[PB-212179] 06 p0698 N73-15689
Demand and trade study related to development of air traffic control system based on geographical regions - Vol. 3
[PB-212180] 06 p0698 N73-15690
Analysis of F-15 contract structure and contribution to effective program management
[AD-750849] 06 p0732 N73-15975
Analysis of political, institutional, and economic factors to determine feasibility of conducting earth resources surveys in developing nations
07 p0783 N73-16362
Analysis of remote sensing of earth resources program conducted by Brazil
07 p0783 N73-16364
Accomplishments of United Nations in providing earth resources data to developing nations
07 p0783 N73-16370
Management regulations and systems requirements for Europa 3 launch vehicle
07 p0849 N73-16885
Cryogenic upper stage requirements for Europa 3 launch vehicle analyzing performance, design, structural and test requirements
07 p0850 N73-16886
Project planning and cost estimates for Europa 3 launch vehicle
07 p0850 N73-16889
Selected technical spin-offs from space program
[NASA-TM-X-68943] 08 p0977 N73-17994
Organization and management methods for space programs in Germany
[DGLR-PAPER-72-052] 09 p1101 N73-18990
Management methods for Skylab program to include mission operations support, environmental and thermal design criteria, optical contamination, and materials science
[NASA-TM-X-64725] 11 p1342 N73-20886
Development of computerized training aid for research and development managers based on spacecraft design operations
[NASA-TN-D-7238] 12 p1466 N73-21880
Analysis of NASA programs for 1970 to 1980 period with application to earth orbital experiment program and requirements - Vol. 1
[NASA-CR-112325] 13 p1577 N73-22778
Analysis of space biology projects related to earth orbital experiment program to identify critical issues and methods of conducting experiments - Vol. 3
[NASA-CR-112327] 13 p1577 N73-22780
Guidelines for spacecraft structural design requirements emphasizing project planning and management methods
[ESRO-CR[P]-200] 13 p1586 N73-22857
Guidelines for spacecraft structural design requirements noting management and compilation methods
[HSD-TP-7363] 13 p1586 N73-22858
Process of planning, programming, and evaluating technological projects within federal agencies
[NASA-CR-131846] 13 p1596 N73-22939
Techniques of technology assessment in federal agencies
[NASA-CR-131848] 13 p1596 N73-22940
Mission and responsibilities of federal agencies in technology assessment
[NASA-CR-131847] 13 p1596 N73-22941
Application of NASA type management approach to other fields
[NASA-TM-X-66251] 15 p1846 N73-24956
Conference on project management and project control
[ESRO-SP-90] 15 p1846 N73-24962
Goals, objectives, tasks, and reporting channels of project management organization
15 p1846 N73-24963
Motivation, planning, and management of research and development programs using controlled thermonuclear fusion as examples
15 p1846 N73-24964
Integration of projects and contracts into program of research and development center
15 p1847 N73-24965
Methods, procedures, and means for comprehensive project management system
15 p1847 N73-24966
Project management in aerospace industry
15 p1847 N73-24967
Project management system and application of management method
15 p1847 N73-24968
Organization and management of CERN/ISR project
15 p1847 N73-24969
Organization and management of ESRO 4 satellite project noting planning and contractor relations
15 p1847 N73-24970
Comparison of management, planning and control for Nimrod avionics system and hospital projects
15 p1847 N73-24971
Systems engineering as decision making tool using space system as example
15 p1847 N73-24972
Systems engineering and project management of ESRO I satellite
15 p1847 N73-24973
Managing contract specification system for satellite projects
15 p1847 N73-24974
Phased planning and management
15 p1848 N73-24977
Phase preparation of ground facilities for satellite missions noting procedures used at ESOC
15 p1848 N73-24979
Requirements, functions, and tasks of project control teams within European space program
15 p1848 N73-24982
Data processing in project control illustrated by cost and network analysis and resource allocation modules
15 p1848 N73-24983
Integrated project control for ESRO satellite management
15 p1849 N73-24985
Control of modifications in projects noting contractors and customers viewpoints
15 p1849 N73-24986
Degree of innovation and risk in product development contracts
15 p1849 N73-24988
Project management information requirements in international organization
15 p1849 N73-24990
Management system for functional support demands in multiproject institution
15 p1850 N73-24991
Project system requirements [planning, communication, analysis] and impediments to implementation
15 p1850 N73-24992
Application of ERTS-1 imagery and aerial photography to missions of US Corps of Engineers
19 p2289 N73-28400
Hazard control and safety management role of project manager
[NASA-TM-X-64764] 19 p2354 N73-28937
Program planning, contract administration, manufacturing, and testing of solid propellant rocket engine for space shuttle booster - Vol. 3
[NASA-CR-124238] 20 p2467 N73-29821
Introductory background to planning process, objectives, and indexing for twenty two engineering and development programs with FAA
[FAA-ED-00-A] 21 p2609 N73-30918
Mission project management, and description of Symphonie communication satellite
[DGLR-PAPER-73-043] 24 p2895 N73-33113
**PROJECT PLANNING**
Planning, control, and management for European space satellite project
[ESRO-SP-70] 01 p0121 N73-10996
Project planning and progress for first GARP global experiment, emphasizing satellite subsystem, data management, and oceanographic programs
[GARP-SPEC-REPT-8] 03 p0327 N73-12669
Progress on GARP, GATE, and related subprograms
03 p0327 N73-12670
Scientific and technical research projects in Poland
[JPRS-57570] 04 p0488 N73-13988
Scientific and technical research projects in Czechoslovakia and Hungary
[JPRS-57583] 04 p0488 N73-13989
Project control in ESRO program
05 p0611 N73-14973
Project planning and cost estimates for Europa 3 launch vehicle
07 p0850 N73-16889
Research progress in astronomy, space, radio, engineering, and nuclear physics
[NP-19468] 11 p1352 N73-20979
Program planning for pollution elimination
[AD-754784] 12 p1467 N73-21893
Guidelines for spacecraft structural design requirements emphasizing project planning and management methods
[ESRO-CR[P]-200] 13 p1586 N73-22857
Guidelines for spacecraft structural design requirements noting management and compilation methods
[HSD-TP-7363] 13 p1586 N73-22858
Conference on project management and project control
[ESRO-SP-90] 15 p1846 N73-24962
Goals, objectives, tasks, and reporting channels of project management organization
15 p1846 N73-24963
Project management system and application of management method
15 p1847 N73-24968
Comparison of management, planning and control for Nimrod avionics system and hospital projects
15 p1847 N73-24971
Phased planning and management
15 p1848 N73-24977
Phased project planning and development for operational space missions referring to NASA meteorological and communication satellite programs
15 p1848 N73-24978
Project control at ESTEC, noting network analysis, phased project planning, cost control, and contract management
15 p1848 N73-24981
Contract requirements, negotiation, and management within European space program
15 p1849 N73-24987
Project system requirements [planning, communication, analysis] and impediments to implementation
15 p1850 N73-24992
Program definition study for improvement of short haul air transportation facilities - Vol. 1
[FAA-QS-73-1-VOL-1] 17 p1983 N73-26025
Plans for collection of ground truth data for Skylab-2 mission
[E73-10759] 17 p2022 N73-26359
Site selection, program planning, cost and design studies for support of IMBLMS
[NASA-CR-133961] 17 p2088 N73-26894
History, development, and description of Skylab program
[NASA-EP-107] 24 p2979 N73-33803
**PROJECTED AREAS**
U AREA
U PROJECTIVE GEOMETRY
**PROJECTILE CRATERING**
Firing tests to determine cratering produced by impact of flat ended, high density metal cylinders striking mild steel plate targets
[DREV-TN-2034/72] 06 p0726 N73-15927
Hypervelocity projectile cratering at mirror glass coating impact
[ONERA-NT-01-14-72] 07 p0822 N73-16659
Simulated micrometeoroid impact cratering in lunar materials using electrostatically accelerated microparticles impacting in oligoclase single crystals
[NASA-CR-130356] 07 p0841 N73-16813
Surveyor 3 lunar probe television mirror pit X ray analysis and scanning electron microscopy for micrometeoroid impact study
[ONERA-NT-01-15] 07 p0847 N73-16864
Development of method for predicting crater profiles produced in ductile materials by impact of rigid projectiles at ballistic velocities
[DREV-R-686/73] 18 p2203 N73-27782
**PROJECTILE PENETRATION**
U TERMINAL BALLISTICS
**PROJECTILES**
NT HYPERVELOCITY PROJECTILES
NT SABOT PROJECTILES
Wind tunnel tests and firing tests to determine aerodynamic characteristics and subsonic flight performance of spin stabilized mortar projectile
[AD-746977] 02 p0124 N73-11009
Guidance system for beam-rider projectiles
04 p0447 N73-13647
Application of point position radar data to determine aerodynamic drag of projectile
[AD-750564] 05 p0492 N73-14013
Laser Doppler velocimeter for measuring initial velocity of projectile
[AD-749670] 05 p0559 N73-14539
Methods for determining air resistance to fragmented shrapnel of different shapes
[FOA-2-A-2539-44] 06 p0653 N73-15304

Projectile rotation measurement by polarized light modulation
[BMVG-FBWT-72-18] 07 p0766 N73-16225
Projectile loader for research gas gun
[AD-753008] 09 p1012 N73-18259
In-flight photography of projectiles using film-image synchronized, rotating-slit shuttered drum field camera
[LA-DC-72-909] 10 p1161 N73-19445
Development of thick-walled, Borsic aluminum alloy ring for use as stiffener in 155 millimeter atomic artillery projectile
[SC-DR-72-0706] 10 p1176 N73-19562
Development of base bleed techniques to reduce Magnus moment on long spinning bodies and improved drag characteristics
[AD-754755] 11 p1232 N73-20002
Structural stability of gun launched finned projectile motor case
[AD-754378] 11 p1344 N73-20906
Analysis of phenomenon generated by passage of projectile into water to determine effects of accelerations, aerodynamic configurations, and surface motions
16 p1886 N73-25264
Computer program for shock and blast loading characteristics high explosive projectile detonation in aircraft
[AD-759002] 16 p1975 N73-25972
Analysis of projectile aerodynamic coefficients based on yawsonde and radar imagery data obtained during flight tests
[AD-759482] 17 p1980 N73-26002
Effect of nose shape and tail length on static stability of fin-stabilized projectile at supersonic speeds and various angles of attack
[NASA-TM-X-2831] 19 p2217 N73-27888
Characteristics of vegetation from existing data for predicting munition height of burst in inaccessible areas
[AD-763179] 21 p2607 N73-30891
Manipulation of digital computer source program for terminal ballistics of gun launched guided projectiles
[AD-764225] 22 p2640 N73-31161
Target acquisition model for gun launched guided projectiles
[AD-763909] 22 p2676 N73-31432
Simplified model for heat transfer and subsequent temperature distribution in thin metal target impacted by cylindrical projectile
[AD-763152] 22 p2730 N73-31850

**PROJECTIVE DIFFERENTIAL GEOMETRY**
U PROJECTIVE GEOMETRY

**PROJECTIVE GEOMETRY**
Group theoretical descriptions of dualities in projective planes
02 p0196 N73-11582

**PROJECTS**
NT APOLLO PROJECT
NT APOLLO SOYUZ TEST PROJECT
NT ECHO PROJECT
NT MARS 69 PROJECT
NT MARS 71 PROJECT
NT NIMBUS PROJECT
NT PIONEER PROJECT
NT ROVER PROJECT
NT SQUID PROJECT
NT SURVEYOR PROJECT
NT TELSTAR PROJECT
NT THEMIS PROJECT
Activation analysis applied to industry, agriculture, and geology, including Br determination in vegetables and inactive marking of insects
03 p0262 N73-12126

**PROMINENCES**
NT SOLAR PROMINENCES

**PROPAGATION**
Structure of high spin particle propagator
[DPGU-01-73] 20 p2456 N73-29734

**PROPAGATION (EXTENSION)**
NT CRACK PROPAGATION
NT FLAME PROPAGATION

**PROPAGATION MODES**
Atmospheric effects on laser beam propagation
[AD-746053] 01 p0066 N73-10544
Acoustic gravity wave propagation modes in ionosphere and neutral atmosphere following nuclear explosion
[CONTRIB-1799] 05 p0509 N73-14140
Self wave oscillations in variable depth rotating basins discussing second class modes for three cases
07 p0857 N73-16952
Mode conversion at lower hybrid plasma resonance
24 p2962 N73-33666

**PROPAGATION VELOCITY**
Velocity slowdown calculation for spherical and cubical fragments as function of distance
[TL-1972-16] 14 p1597 N73-22943

**PROPAGATORS**
U PROPAGATION

**PROPANE**
Mathematical model for unsteady one dimensional reaction waves during combustion of gas mixtures including application to air-propane mixture
[DLR-FB-71-66] 06 p0731 N73-15962
Mass spectra of electrochemical propane oxidation
[AD-755254] 12 p1376 N73-21166
Hydrocarbon oxidation by metal catalysts and adsorption layer formation on electrode in propane air fuel cell
[AD-758172] 15 p1748 N73-24168
Propane aerosol dispenser for cold fog dissipation at airfields
[AD-762292] 19 p2317 N73-28635
Propane oxidation using electrochemical mass spectrometry
[AD-762356] 20 p2374 N73-29077
Combustion and expansion of propane-air mixtures near bottom of short cylinder to generate air vortex rings for removing air from cylinder
[AD-764613] 23 p2777 N73-32207

**PROPELLANT ADDITIVES**
NT PROPELLANT BINDERS
NT SOLID ROCKET BINDERS
Detection of Combustion Improver-2 by atomic absorption spectrophotometry in smoke abatement systems
[AD-755723] 13 p1488 N73-22067
Silicone additives for heat flux reduction in hydrazine rocket propellants
[AD-756913] 14 p1700 N73-23798
Binary boron/lithium system as propellant additive of hybrid rocket engines, noting enthalpy and reaction product density
[DLR-MITT-73-08] 17 p2075 N73-26791
Effect of metal admixtures on specific impulse of solid rocket propellants
24 p2970 N73-33736

**PROPELLANT BINDERS**
NT SOLID ROCKET BINDERS
Influence of ammonia perchlorate binder and surface microstructure on combustion velocity development in solid composite propellants
[ONERA-TP-1167] 10 p1222 N73-19941
Chemical process for production of polyisobutylene compounds and application as solid rocket propellant binder
[NASA-CASE-NPO-10893] 13 p1568 N73-22710

**PROPELLANT CHEMISTRY**
Effects of propellant composition variables on acceleration-induced burning rate augmentation of solid propellants
[NASA-TN-D-6923] 01 p0117 N73-10966
Application of ultraviolet absorption, gas-liquid chromatography, and gravimetric analysis to determine diphenylamine and ethyl centralite in solid rocket propellant
[TN-267] 02 p0221 N73-11786

**PROPELLANT COMBUSTION**
NT SOLID PROPELLANT IGNITION
Solid phase reaction and fuel component effects on composite propellant combustion
[NASA-CR-112083] 01 p0089 N73-10738
Theory for combustion of ammonium perchlorate propellant
[NASA-TT-F-14720] 04 p0484 N73-13955
Interaction between acoustic velocities and solid propellant combustion with variations in frequency of oscillation, mean pressure, and propellant formulation
[AD-750142] 06 p0712 N73-15809
Analyses of laminar combustion phenomena in hybrid rockets
08 p0968 N73-17909
Direct mixing and combustion measurements in ducted, particle-laden jets using boron loaded propellant
[AD-754434] 10 p1224 N73-19956
Combustion transients of solid rocket propellants
[AD-757234] 13 p1591 N73-22899
Combustion instability in gas-fired T-burner
[AD-755824] 13 p1591 N73-22903
Theoretical analysis of ballistic H powder erosion combustion in acoustic stream
14 p1700 N73-23796
Analysis of combustion instability in solid propellant rocket engines and characteristics of acoustic waves in T-burner geometry
16 p1973 N73-25958
Matrix isolation technique used to obtain thermodynamic properties of rocket combustion products
[AD-762622] 20 p2486 N73-29966
Effect of metal additives on combustion rate of solid rocket propellants
[AD-764155] 22 p2730 N73-31849
Solid rocket propellants with pulsating combustion, based on mixed polymerizates
[ICT-9/72] 23 p2828 N73-32604

**PROPELLANT DECOMPOSITION**
Catalyst effects on decomposition kinetics of rocket oxidizer ammonium perchlorate
[AD-746728] 02 p0221 N73-11792
Kinetics of liquid hydrazine decomposition on supported rhodium catalyst
[RPE-TR-71/16-PT-4] 10 p1126 N73-19177
Compatibility of Ti and Ni alloys, stainless steels, Al, tungsten carbide, butyl, and Ep rubbers with hydrazine noting decomposition rates and effects of carbonic acid
[ESRO-CR-85-PT-2] 13 p1569 N73-22712

**PROPELLANT EVAPORATION**
Evaporation rates and toxic plume dispersion for defining downwind evacuation areas for populations adjacent to accidental propellent spills on shipping routes
[NASA-TM-X-68188] 07 p0750 N73-16097
Combustion and evaporation of liquid fuels at high pressures
[NASA-CR-121113] 15 p1843 N73-24934

**PROPELLANT GRAINS**
Solid propellant grain design and internal ballistics
[NASA-SP-8076] 06 p0711 N73-15804
Performance of FLOX-70/polyethylene hybrid rocket engine with cartwheel-type propellant grain geometry
[DLR-FB-72-61] 07 p0836 N73-16780
Evaluation of propellant grain configurations for use in hybrid propellant rocket engines - Vol. I
[DLR-FB-72-60-PT-1] 09 p1077 N73-18792
Experimental determination of pressure distribution in burning flaws in solid propellant grains
[AD-756912] 13 p1569 N73-22718
Thermal analysis of thermoviscoelastic behavior of case bonded propellant grains to thermal property variations
[AD-758839] 15 p1824 N73-24780

**PROPELLANT OXIDIZERS**
U ROCKET OXIDIZERS

**PROPELLANT PROPERTIES**
NT PROPELLANT SENSITIVITY
Development of physical model to determine mechanism of condensed phase reaction in combustion of double base rocket propellants
07 p0853 N73-16921
Evaluation of propellant grain configurations for use in hybrid propellant rocket engines - Vol. I
[DLR-FB-72-60-PT-1] 09 p1077 N73-18792
Development of computer program to predict transient and steady state performance and heat transfer characteristics of pulsing gaseous propellant rocket engine
[NASA-CR-128748] 10 p1214 N73-19871
Ballistic design of solid propellant missiles to include analysis of physical properties and determination of reliability
[JPRS-59060] 18 p2200 N73-27759
Combustion characteristics of polystyrene and oxygen-styrene copolymer with ammonium perchlorate composites
22 p2708 N73-31687
Effect of metal admixtures on specific impulse of solid rocket propellants
24 p2970 N73-33736

**PROPELLANT SENSITIVITY**
Thermal analysis of thermoviscoelastic behavior of case bonded propellant grains to thermal property variations
[AD-758839] 15 p1824 N73-24780

**PROPELLANT SPRAYS**
Droplet combustion at high pressures with unsteady effects
[AD-757227] 14 p1720 N73-23957

**PROPELLANT STORAGE**
Orbiting propellant depot safety hazards - management summary
[NASA-CR-123385] 03 p0356 N73-12898
Orbiting propellant depot safety hazards and interactions between depot and space vehicle - technical discussion
[NASA-CR-123384] 03 p0356 N73-12899
Orbital propellant transfer techniques and feasibility of thermal bootstrap propellant transfer concept
[NASA-CR-125909] 03 p0356 N73-12900
Development of analytical and experimental techniques for determining heat transfer characteristics of solid propellant rocket engine storage container system
[AD-758515] 15 p1827 N73-24807
Differential thermal analysis and dilatometry of 4 to 5 years stored ammonium nitrates with amine copper complex additives
[ICT-4/72] 16 p1954 N73-25812
Analysis, design, fabrication, and tests of regeneratively cooled rocket engine for storable propellants
[NASA-CR-133488] 19 p2329 N73-28737

**PROPELLANT TANKS**
Optimization of propellant tank size delivering apogee impulses when positioning synchronous satellites
[ONERA-NT-2/1895-SY] 04 p0479 N73-13915
Fabrication and tests of polyphenylene oxide foam panels for application as reusable insulation with LH2 tanks
[NASA-CR-123955] 05 p0565 N73-14586
Propellant oscillation modes and frequencies for tanks of any shape, fill level, or orientation
[NASA-CR-124277] 16 p1889 N73-25287

Radio frequency resonant cavity mode analysis technique for fluid mass quantity gauging of space shuttle orbiter tankage
[NASA-CR-133393] 18 p2151 N73-27390
Analysis of transient pressures in externally pressurized cryogenic hydrogen and oxygen tanks to determine effects of design variables on pressure response
[NASA-CR-133962] 18 p2199 N73-27755
Effects of ascent trajectory mode and tank disposal method on shuttle payload accommodation
[NASA-TM-X-64773] 21 p2599 N73-30831
Slosh testing of spherical mercury propellant tank with positive expulsion diaphragm
[NASA-CR-133790] 21 p2600 N73-30838
Advanced material composites for use as insulations for space shuttle LH2 tanks
[NASA-CR-124388] 22 p2688 N73-31532
Feasibility of developing toroidal propellant tanks for bipropellant propulsion system
[NASA-CR-114666] 22 p2720 N73-31766
Design, fabrication, and performance of multilayer insulation system for modular nuclear vehicle LH2 propellant tank
[NASA-CR-124400] 23 p2856 N73-32824

**PROPELLANT TRANSFER**
Appendices to support findings of Orbiting Propellant Depot Safety study - Vol. 3
[NASA-CR-123383] 03 p0254 N73-12058
Orbiting propellant depot safety hazards - management summary
[NASA-CR-123385] 03 p0356 N73-12898
Orbiting propellant depot safety hazards and interactions between depot and space vehicle - technical discussion
[NASA-CR-123384] 03 p0356 N73-12899
Orbital propellant transfer techniques and feasibility of thermal bootstrap propellant transfer concept
[NASA-CR-125909] 03 p0356 N73-12900
Liquid propulsion transfer and injection system for Europa 3 in geostationary and interplanetary missions
[URV-47[71]] 11 p1333 N73-20822
Development of computer program for preliminary design of propellant feed system for space shuttle orbiter main engines - Vol. 5A-2
[NASA-CR-133954] 18 p2200 N73-27758
Design and tests of composite propulsion feedlines for cryogenic space vehicles - Vol. 1
[NASA-CR-121137-VOL-1] 19 p2346 N73-28868
Design and tests of composite propulsion feedlines for cryogenic space vehicles - Vol. 2
[NASA-CR-121137-VOL-2] 19 p2346 N73-28869
Analytical model and computer program for studying disturbances of liquid propellants in feedline systems
[NASA-CR-124308] 20 p2388 N73-29188
Feasibility of thermodynamic vent and screen baffle integration for orbital storage and transfer of liquid hydrogen
[NASA-CR-134482] 24 p2970 N73-33737

**PROPELLANTS**
NT AEROZINE
NT COLLOIDAL PROPELLANTS
NT COMPOSITE PROPELLANTS
NT CRYOGENIC ROCKET PROPELLANTS
NT DOUBLE BASE PROPELLANTS
NT DOUBLE BASE ROCKET PROPELLANTS
NT GASEOUS ROCKET PROPELLANTS
NT HIGH ENERGY PROPELLANTS
NT HYBRID PROPELLANTS
NT HYDRAZINE NITROFORM
NT HYPERGOLIC ROCKET PROPELLANTS
NT LIQUID ROCKET PROPELLANTS
NT MONOPROPELLANTS
NT RDX
NT ROCKET PROPELLANTS
NT SLURRY PROPELLANTS
NT SOLID PROPELLANTS
NT SOLID ROCKET PROPELLANTS
NT STORABLE PROPELLANTS
NMR principle for designing propellant mass flow meter
[AD-751507] 07 p0801 N73-16507
Rapid determination of diphenylamine and dinitrotoluene in single base propellants by ultraviolet spectrophotometry analysis
[TM-51] 21 p2587 N73-30730
Military treatment and disposal of high energy materials
[AD-764534] 23 p2858 N73-32835

**PROPELLER BLADES**
Extended natural mode method for calculating flapwise bending, edgewise bending, and torsional vibration modes and frequencies of helicopter rotor blades
[DLR-FB-71-108] 09 p0983 N73-18026
Comparison of thrust and torque forces on ship propeller blades in oblique and axial flow
[DRIC-TRANS-3205] 21 p2525 N73-30249

**PROPELLER DRIVE**
NT HELICOPTER PROPELLER DRIVE

**PROPELLER EFFICIENCY**
Theoretical and experimental analyses of aircraft propeller operating under turbulent ambient conditions
[UTIAS-183] 06 p0621 N73-15039

**PROPELLER FANS**
Model for generation of blade-passage noise caused by interaction of rotor wakes with downstream stator blades in fan stage
[NASA-TM-X-2669] 02 p0222 N73-11797
Effect of various physical and operating parameters on noise produced by low pressure ratio propulsive fans operating at subsonic speeds
[NASA-CR-2188] 09 p0980 N73-18011
Design, characteristics, and performance tests of high-tip-speed, low-loading, transonic fan stage
[NASA-CR-121095] 13 p1570 N73-22727
Analysis of fan noise levels for fan in proximity of side and ground plane to determine effects on harmonic frequencies
[NASA-CR-132306] 21 p2495 N73-30023
Application of variable pitch fan propulsion system for quiet short takeoff aircraft
21 p2496 N73-30030
Evaluation of acoustic radiation from various noise sources in axial fan
[NASA-CR-114576] 22 p2614 N73-30952

**PROPELLER SLIPSTREAMS**
Interference of wing and propeller streams
[AD-745916] 02 p0124 N73-11008
Design, development, fabrication, and test of propulsion system for free balloon using electric motor and 35.4 foot propeller
[AD-760754] 18 p2107 N73-27042

**PROPELLER SYNCHRONIZERS**
U PROPELLERS
U SYNCHRONIZERS

**PROPELLERS**
NT PROPELLER FANS
NT SHROUDED PROPELLERS
NT TILTED PROPELLERS
NT VARIABLE PITCH PROPELLERS
Wing impulse theory applied to determination of propeller slipstream influence on wing aerodynamic characteristics, using airfoil of finite span
[AD-749726] 05 p0498 N73-14051
Theoretical and experimental analyses of aircraft propeller operating under turbulent ambient conditions
[UTIAS-183] 06 p0621 N73-15039
Research projects to determine aerodynamic characteristics of rotary wings and propellers
[AD-750175] 06 p0656 N73-15326
Analysis of whirl stability boundaries and aerodynamic characteristics of tilting rotors
12 p1356 N73-21004
Development of lifting surface theory for statically operating propellers based on vortex-lattice representation
[AD-757264] 14 p1603 N73-22998
Aircraft accident involving crash of Fairchild Hiller FH-227b aircraft near Albany County Airport, New York on 3 March 1972
[NTSB-AAR-73-8] 17 p1982 N73-26018
Design, development, fabrication, and test of propulsion system for free balloon using electric motor and 35.4 foot propeller
[AD-760754] 18 p2107 N73-27042
Comparison of glass fiber reinforced plastic and bronze submarine propellers, based on binding stress analysis and cavitation behavior
[BMVG-FBWT-73-8] 19 p2256 N73-28183
Design, development, and performance tests of wind driven, propeller operated electric generation station
[NASA-TT-F-15037] 20 p2363 N73-29004
Development and construction of wind driven electric power generators for specific European areas
[NASA-TT-F-15050] 20 p2364 N73-29009
Analysis of wakes generated by hovering model propellers and rotors using schlieren photography and hot-wire anemometry
[NASA-CR-2305] 21 p2491 N73-29996
Directional equipment for suppressing noise of Concorde propellers during high speed flight
22 p2613 N73-30942

**PROPORTIONAL CONTROL**
Target maneuvers and sensor noise effects on proportional navigation systems noting Kalman filtering
[AASU-316] 03 p0329 N73-12681
Feedback control techniques for proportional target interception and acceleration
[AD-755795] 13 p1578 N73-22794

**PROPORTIONAL COUNTERS**
Thin film window for gas flow radioisotope proportional counter
[AD-745579] 01 p0058 N73-10477
Coaxial anode scheme for reducing background of X ray astronomy proportional counter
[NASA-CR-130127] 04 p0421 N73-13432
Design of multiwire proportional chamber systems using electromagnetic delay lines for cosmic ray experiments
[RM-5691] 09 p1011 N73-18251
Amplifier design for multiwire proportional chamber signals
[LA-5085] 12 p1383 N73-21215
Design and construction of decoder for processing signals from multiwire proportional chamber
[LA-5073] 12 p1388 N73-21256
Neutron spectral measured proton recoil proportional counters
[KFK-1623] 12 p1431 N73-21598
Development of multiwire proportional chamber for high resolution spatial detector in cosmic ray investigations and analysis of operating parameters
[NASA-CR-128899] 13 p1506 N73-22210
Frequency limited amplifier for proportional counter pulse shape and pulse height control
[NLL-WH-TRANS-343-[9091.9F]] 15 p1755 N73-24227
Engineering specifications for proportional counter hodoscope to be flown on HEAO A mission
[NASA-TN-D-7317] 15 p1828 N73-24816
Proportional chambers with monofilar helical cathodes for high spatial resolution
[LA-5195-MS] 18 p2152 N73-27393
Rocket-borne proportional counter observations of discrete galactic X rays from supernovae
[NASA-TM-X-70463] 22 p2711 N73-31708
Source and diffusion of cosmic rays greater than 4.5 GV in interstellar medium measured by proportional counter-scintillation counter stack
[TR-73-136] 23 p2835 N73-32652
Gas proportional counting of chlorine-36 in iron and iron meteorites
23 p2835 N73-32656

**PROPORTIONAL LIMIT**
Readout electronics and systems for proportional wire chambers
[JINR-P13-6380] 04 p0422 N73-13441

**PROPULSION**
NT ASCENT PROPULSION SYSTEMS
NT AUXILIARY PROPULSION
NT CHEMICAL PROPULSION
NT ELECTRIC PROPULSION
NT ELECTROMAGNETIC PROPULSION
NT ELECTROSTATIC PROPULSION
NT HYBRID PROPULSION
NT ION PROPULSION
NT JET PROPULSION
NT LOW THRUST PROPULSION
NT MARINE PROPULSION
NT NUCLEAR ELECTRIC PROPULSION
NT NUCLEAR PROPULSION
NT PLASMA PROPULSION
NT SOLAR PROPULSION
NT SPACECRAFT PROPULSION
NT UNDERWATER PROPULSION
Determining parameters of rocket capable of 8 km/sec using simplified equations of motion
[REPT-13] 04 p0463 N73-13775
Contamination avoidance devices for poppet-type shutoff valves
[NASA-CR-121125] 09 p1039 N73-18471
Carbon refractory composites for application in rocket motor nozzles, propulsion structures, and planetary atmospheric entry shells
[NASA-CR-131745] 13 p1547 N73-22533

**PROPULSION CALCULATIONS**
U MATHEMATICAL MODELS
U PROPULSION

**PROPULSION SYSTEM CONFIGURATIONS**
NT DESCENT PROPULSION SYSTEMS
Performance of ignition and flame stabilization using gas generator in different ramjet combustion chamber configurations
[DLR-FB-72-47] 01 p0091 N73-10748
Operational procedure for computer program to calculate design point characteristics of gas generator or turbojet lift engine for V/STOL applications
[NASA-TM-X-2656] 02 p0222 N73-11794
Analysis of costs and effectiveness of space missions, aerospace vehicles, and propulsion systems
[NASA-CR-129258] 03 p0358 N73-12917
Reaction engines with shrouded nozzles, reaction engines for boats, and thermodynamics of hot air bubble cooling in liquid
[JPRS-57308] 04 p0404 N73-13292
Design and tests of advanced colloid thruster system components
[AD-749961] 05 p0591 N73-14801
Analysis of propulsion system specifications and components for research VTOL transports
[NASA-TM-X-68168] 06 p0713 N73-15816
Concept of nuclear powered ground effect machine for commercial operations in Arctic regions
[NASA-TM-X-2684] 08 p0977 N73-17991
Design and development of low pressure auxiliary propulsion system for space shuttle orbiter and booster
[NASA-CR-130796] 09 p1078 N73-18796
Design parameters and characteristics of intermittent pulse jet engine for use as auxiliary power source
10 p1110 N73-19047
Propulsion system requirements for aircraft engines installed in high speed commercial transport aircraft - Vol. 3
[NASA-CR-121134] 10 p1207 N73-19822
Analysis of requirements for oxygen-hydrogen auxiliary propulsion system for use with space shuttle vehicle concept - Phase A
[NASA-CR-128820] 10 p1208 N73-19828

Comparison and evaluation of competing concepts of auxiliary propulsion concepts for space shuttle applications - Phase B
[NASA-CR-128823] 10 p1208 N73-19829
Evaluation of concepts for integrating reaction control system and orbit maneuvering system of space shuttle vehicle - Phase C
[NASA-CR-128821] 10 p1209 N73-19830
Evaluation of two alternate oxygen-hydrogen auxiliary propulsion system concepts for space shuttle vehicle - Phase D
[NASA-CR-128822] 10 p1209 N73-19831
Evaluation of monopropellant and bipropellant earth storable reaction control systems for application to space shuttle vehicle - Phase C & E
[NASA-CR-128819] 10 p1209 N73-19832
European space tug auxiliary and main propulsion
[HSD-TP-7264-VOL-3] 10 p1217 N73-19903
Analysis of integrated airframe and engine configuration for hypersonic transport at 70,000 feet altitude and Mach 6.0
[NASA-CR-112300] 11 p1234 N73-20022
Bibliography of supersonic transport aircraft data to include program management, systems engineering, aircraft structures, and operational considerations
[AD-755600] 12 p1365 N73-21076
Design configuration and operating procedures for utilizing thermonuclear propulsion for upper stage of Europa 3 launcher
[NASA-TT-F-14874] 13 p1557 N73-22623
Systems analysis and operations analysis of solid propellant rocket engine configurations for use with space shuttles - Vol. 3
[NASA-CR-123728] 15 p1826 N73-24799
Mass properties and related data for solid propellant rocket engine used with space shuttle vehicle - Vol. 2, Book 4
[NASA-CR-124237] 15 p1826 N73-24800
Safety measures for nuclear space power and propulsion systems
[LA-DC-72-1480] 17 p2061 N73-26676
Development of computer program for space shuttle orbit injection propulsion system to generate parametric feed system pressure histories - Vol. 5 B-4
[NASA-CR-133957] 17 p2087 N73-26885
Characteristics of long range transport aircraft to include reduction of aircraft engine noise and improved engine response during go-around maneuver
[NASA-CR-121243] 18 p2104 N73-27020
Design, development, fabrication, and test of propulsion system for free balloon using electric motor and 35.4 foot propeller
[AD-760754] 18 p2107 N73-27042
Operating principles and application of ion engines for spacecraft propulsion
[JPRS-59061] 18 p2192 N73-27700
Characteristics of propulsion system for subsonic, long-range transport aircraft designed to meet aerodynamic noise level requirements
[NASA-CR-121242] 18 p2193 N73-27704
Analysis of retrorocket exhaust plume of Viking Lander impinging on Martian surface and development of multiple nozzle configurtaion to reduce effects
[NASA-CR-2252] 18 p2197 N73-27737
Development of computer program for preliminary design of propellant feed system for space shuttle orbiter main engines - Vol. 5A-2
[NASA-CR-133954] 18 p2200 N73-27758
Logistic performance data book on propulsion system for KC-135 aircraft to show reliability, maintenance, costs, and problems
[AD-762217] 19 p2357 N73-28962
Computer simulation of aircraft motions and propulsion system dynamics for YF-12 aircraft under supersonic conditions
[NASA-TM-X-62245] 20 p2361 N73-28990
Technical requirements of solid propellant rocket engine for application to space shuttle booster - Vol. 2 Bk. 1
[NASA-CR-123729] 20 p2465 N73-29805
Analysis of earth storable bimodal engine using earth storable propellants and operating in either monopropellant or bipropellant mode
[BELL-8706-933005] 20 p2466 N73-29811
Analysis of solid propellant rocket engine requirements for space shuttle booster application - Vol. 1
[NASA-CR-124236] 20 p2467 N73-29820
Test objectives and mission planning for extended long tank Delta Launch Vehicle
[NASA-CR-133644] 20 p2475 N73-29886
Analysis of various mixed cycle engines and impact of component choices on application of propulsion system
21 p2590 N73-30747
Apollo experience report on service propulsion subsystem development, qualification, and flight performance
[NASA-TN-D-7375] 22 p2719 N73-31763
Feasibility of developing toroidal propellant tanks for bipropellant propulsion system
[NASA-CR-114666] 22 p2720 N73-31766
Computer program for use with thermal-elastic-plastic-creep structural analyzer for structural analysis of spacecraft and propulsion systems - Vol. 2
[NASA-CR-124391] 22 p2725 N73-31806
Design of detonating propellant propulsion system for exploring planets with hot dense atmospheres
22 p2732 N73-31864
Design and development of quiet, clean propuslion systems for short takeoff aircraft with emphasis on engine noise reduction
24 p2875 N73-32961
Selection criteria and characteristics of quiet, clean propulsion systems for use with short takeoff aircraft
24 p2876 N73-32967
Plug and spike nozzles applied to rocket propulsion system configurations
24 p2973 N73-33754
Turbojet and turbine engine performance optimalization by configuration variations, and auxiliary turbine engine converter problem
[DLR-MITT-73-05] 24 p2973 N73-33755
Influence of combustion chamber, compressor, and afterburner configuration on static performance of two-cycle turbojet engines with high bypass ratio
24 p2973 N73-33756

**PROPULSION SYSTEM PERFORMANCE**

Performance of ignition and flame stabilization using gas generator in different ramjet combustion chamber configurations
[DLR-FB-72-47] 01 p0091 N73-10748
Assessment of materials compatibility data for hydrazine monopropellant propulsion systems of space shuttle vehicle in multicycle extended life applications
[NASA-CR-128491] 02 p0221 N73-11788
Design and in-flight performance of Mariner 9 spacecraft propulsion system
[NASA-CR-129097] 02 p0222 N73-11795
Propulsion system characteristics for long range, high subsonic jet commercial transport aircraft
[NASA-CR-121016] 02 p0223 N73-11800
Direct reaction engines for water surface vessels, using admixture of air and outboard water
04 p0404 N73-13295
Evaluation of descent propulsion system for Apollo 12
[NASA-TM-X-68933] 06 p0712 N73-15812
Technique for defining aircraft performance model from limited flight test data and predicted aerodynamic and propulsion system characteristics
[NASA-TN-D-7137] 07 p0738 N73-16008
Performance of FLOX-70/polyethylene hybrid rocket engine with cartwheel-type propellant grain geometry
[DLR-FB-72-61] 07 p0836 N73-16780
Subsonic performance potential of ramjets and ejector ramjets
[AD-751317] 07 p0837 N73-16781
Performance of auxiliary power systems for advanced Army rotary wing aircraft
[AD-751854] 08 p0870 N73-17046
Comparison of chemical [hydrazine and aerozine], electrothermal, electrostatic, and radioisotopic propulsion systems, emphasizing performance and configurations
[ESRO-CR-25-PT-A] 08 p0955 N73-17818
Mathematical model to simulate staging dynamics of proposed space shuttle configuration
[NASA-TM-X-58098] 08 p0965 N73-17886
Techniques for determining dynamic characteristics of hydraulic duct for predicting low frequency vibrations of liquid propellant rocket engines
[ONERA-TP-1160] 09 p1015 N73-18281
Apollo experience report on lunar module ascent propulsion subsystem to identify significant technical problems encountered during all phases of program
[NASA-TN-D-7082] 09 p1090 N73-18900
Analysis of gas turbine engine requirements and performance when main propulsion system furnishes auxiliary power source
10 p1110 N73-19050
Simplified procedures for correlation of experimentally measured and predicted thrust chamber performance
[NASA-CR-131519] 12 p1442 N73-21685
Development of two methods for optimizing design of subsonic, swept wing jet transport aircraft
15 p1733 N73-24054
Theoretic performance of simple lithium compounds in lithergol rocket engines
[DLR-FB-73-23] 15 p1823 N73-24778
Geostationary satellite trajectory optimization by low thrust resistojet propulsion
[AASU-323] 16 p1967 N73-25913
Characteristics of long range transport aircraft to include reduction of aircraft engine noise and improved engine response during go-around maneuver
[NASA-CR-121243] 18 p2104 N73-27020
Four VTOL propulsion concepts compared parametrically for subsonic applications with three types of aircrafts
[NASA-TM-X-68279] 20 p2466 N73-29810
Performance of Apollo 14 lunar module descent propulsion system
[NASA-TM-X-69491] 20 p2466 N73-29813
Application of variable pitch fan propulsion system for quiet short takeoff aircraft
21 p2496 N73-30030
Performance sensitivity analysis of solar electric propulsion thrust subsystem
[NASA-CR-133792] 21 p2590 N73-30748
Research progress in aerodynamics, propulsion, electronics, instrumentation, and mathematical sciences
21 p2609 N73-30917
Current technology in ion and electrothermal propulsion systems and components
[NASA-TM-X-71434] 23 p2830 N73-32618
Technical conditions for airship development, noting weight reduction, propulsion system performance, and maneuverability improvement
24 p2879 N73-32995
High energy rocket engines - propellant physical chemistry, propulsion system performance, hydrogen oxygen engines, boosters, nozzles - conferences
[DLR-MITT-72-09] 24 p2972 N73-33749
Experimental high energy rocket propellant combinations with heterogeneous combustion and FLOX/polyethylene engine performance
24 p2972 N73-33751
Performance tests of hydrogen oxygen rocket engines for various propellant mixing ratios
24 p2973 N73-33752
Turbojet and turbine engine performance optimalization by configuration variations, and auxiliary turbine engine converter problem
[DLR-MITT-73-05] 24 p2973 N73-33755
Performance of two-cycle turbojet engine for multiparameter control under influence of jet vane and fuel throughput variations
24 p2973 N73-33757
Saturn 5 launch vehicle performance during Skylab launch and orbit
[NASA-TM-X-69537] 24 p2984 N73-33848

**PROPULSIVE EFFICIENCY**

NT PROPELLER EFFICIENCY

Direct reaction engines for water surface vessels, using admixture of air and outboard water
04 p0404 N73-13295
Effect of air precooling before compression on propulsive efficiency of liquid hydrogen turbojet engine with afterburning for space shuttle
[DGLR-PAPER-72-60] 04 p0464 N73-13785
Numerical analysis of wake propulsion parameters to show effects of drag, heating, and energy conversion
[RN-64] 08 p0894 N73-17238
Increased propulsive efficiency through improved secondary flow capacity in double flow turbojets
[NASA-TT-F-14904] 14 p1701 N73-23803
Preflight tests on fluorine/ammonia propellants to be used in Europa 2 transfer stage
[BMFT-FBW-73-07] 21 p2587 N73-30731
Method and apparatus for improving operating efficiency and reducing low speed noise for turbine aircraft engines
[NASA-CASE-LAR-11310-1] 22 p2710 N73-31699

**PROPYL COMPOUNDS**

Effectiveness of polymer complex of cysteamine and sulfopropyl ester of dextran as an antiradiation drug on irradiated mice
[DRIC-TRANS-2963] 06 p0631 N73-15125

**PROPYLENE**

Homogeneous cyanoethylation of hydrogen cyanide in presence of alkaline catalysts
[NASA-TT-F-14690] 08 p0884 N73-17154
Analysis of viscosity of saturated hydrocarbons at different temperatures and pressures to show test equipment and procedures
[NLL-NEL-TT-2471-[6075.461]]
20 p2434 N73-29547
High temperature decomposition of propylene in single pulse shock tube to determine products of decomposition and rate of decomposition
[TAE-172] 23 p2754 N73-32036

**PROSPECTING**

U EXPLORATION

**PROSTHETIC DEVICES**

NT ARTIFICIAL EARS

Computerized teleoperator manual control system for remote mechanical hand
01 p0019 N73-10143
Application of pneumatically controlled prosthetic arm to industrial handling problems
[NASA-TT-F-14628] 04 p0383 N73-13115
Power sources and requirements for human artificial hearts
[COO-2155-4] 05 p0503 N73-14095
Design and development of biomedical prosthetic and electronic devices
[NASA-CR-130022] 07 p0750 N73-16093
Bioelectric control system design for reversible slave mechanism manipulator using single muscle input
17 p1990 N73-26088
Prosthetic limb with tactile sensing device
[NASA-CASE-MFS-16570-1] 23 p2751 N73-32013

**PROTECTION**

NT CIRCUIT PROTECTION
NT CORROSION PREVENTION
NT ENVIRONMENT PROTECTION

NT EYE PROTECTION
NT METEOROID PROTECTION
NT RADIATION PROTECTION
NT RADIATION SHIELDING
NT SOLAR RADIATION SHIELDING
NT THERMAL PROTECTION
Bibliography of lighting theory, instrumentation, and protection
[AD-763667] 21 p2540 N73-30366
PROTECTIVE CLOTHING
NT HELMETS
NT PRESSURE SUITS
NT SPACE SUITS
Calculation of thermal resistance of air layers in air permeable clothing for reliable design
[AD-746037] 02 p0136 N73-11099
Tests to evaluate heat loss from Navy diver suits in water of 55, 45, and 35 F
[AD-747276] 02 p0136 N73-11103
Environmental control unit for damage control suit system for use during shipboard operations
[AD-749025] 04 p0384 N73-13125
Performance of battery powered electrically heated suit for reconnaissance divers
[AD-749847] 05 p0504 N73-14101
Synthesis of high temperature clothing from hexahydrobenzodipyrrole monomers
[AD-750380] 06 p0689 N73-15609
Anthropometry for protective equipment evaluation and human impact acceleration experiments
14 p1612 N73-23066
Thermal response of protective fabric/human skin system to JP-4 jet fuel fire
[AD-759525] 17 p1990 N73-26095
Personnel life support clothing for protection against environmental hazards
[AD-762428] 19 p2229 N73-27976
Design, development, and fabrication of liquid cooled space suit using ice pack heat sink - Vol. 1
[NASA-CR-114624-VOL-1] 22 p2622 N73-31006
Operating instructions for functional model icepack heat sink subsystem for cooling system of space suit - Vol. 2
[NASA-CR-114624-VOL-2] 22 p2728 N73-31829
PROTECTIVE COATINGS
NT ANODIC COATINGS
NT CERAMIC COATINGS
B4C-alkali metal carbonates for boronizing steel surfaces
[NLL-RTS-7197] 01 p0069 N73-10562
Application of paints and varnishes as protective coatings for industrial structures and equipment against radiation damage
[AD-745701] 01 p0071 N73-10582
Protective coatings for solar batteries from atmospheric effects
[AD-746325] 02 p0129 N73-11046
Detergent with glyceryl esthers and oil as protective coating to prevent fogging of space suit visor
[NASA-CASE-MSC-13530-2] 02 p0137 N73-11107
Silicone rubber cover for protecting flush-deck nozzles on aircraft carriers
[AD-746841] 02 p0153 N73-11241
High temperature and fatigue tests to determine effects of heat resistant coatings on mechanical and physical properties of nickel-chromium-iron alloys
[NLL-TRANS-746-1236-[9022.401]]
02 p0185 N73-11500
Compatibility of protective coatings for niobium alloy gas turbine blades
[AD-748837] 04 p0439 N73-13575
Proceedings of symposium on laser radiation damage to transparent dielectrics, plasma formation at dielectric surfaces, and damage morphology of thin film coatings
[NBS-SP-372] 05 p0554 N73-14498
Kinetic and structural investigation of ST-4 titanium alloy oxidizability at 700 to 1000 C, unprotected and protected by silicon and molybdenum silicide coatings
[AD-750646] 06 p0686 N73-15585
Fused slurry silicide protective coatings for tantalum heat shielding
[NASA-CR-121022] 06 p0688 N73-15599
Effect of protective barrier creams on toxic alkyl phosphate penetration of pig skin
[BMVG-FBWT-72-15] 07 p0747 N73-16076
Effects of oxidation resistant coatings on thin superalloy sections in high temperature environments
[NASA-CR-121115] 07 p0809 N73-16563
Development of space shuttle semitransparent polyquinoxaline films
[NASA-CR-112213] 07 p0811 N73-16575
Development of method and equipment for detecting cracks in materials with porous subsurface matrix covered by impervious coating
[NASA-CASE-MSC-14187-1] 08 p0923 N73-17564
Influence of liquid oxygen on chromate coated aluminum tubing of breathing apparatus
[AD-752030] 08 p0936 N73-17661
Temperature effects on hydrogen decomposition of wall surface coatings
[NASA-TM-X-2735] 08 p0946 N73-17748
Evaluation of potential coatings for titanium alloy gears to be used in propeller gearbox systems
[AD-753417] 09 p1041 N73-18492
Seven year tropical exposure test to evaluate corrosion resistance effectiveness of finishing systems for aluminum and magnesium
[AD-752907] 09 p1042 N73-18498
Damping in porcelain enamel coatings at elevated temperatures
[AD-752317] 09 p1055 N73-18598
Atom recombination catalytic rates for surface coatings of thermal protection system materials for space shuttles
[NASA-TN-D-7113] 09 p1098 N73-18965
Comparison of oxygen transport in polymonomethylsiloxane with properties of polydimethylsiloxane to determine degradation mechanisms in pigmented coatings
[AD-753410] 10 p1176 N73-19565
Formation and failure of chromium sesquioxide on cobalt-base alloy L-605 during oxidation at high temperatures
[NASA-TN-D-7255] 12 p1414 N73-21454
Refractory metal alloys with protective coatings for use in structural components of turbine engines
14 p1678 N73-23614
Electrophoretic flow coating technique for heating oil storage tanks
[NLL-OA-TRANS-833-[6196.3]]
16 p1870 N73-25139
Corrosion and protective properties of organic complex-forming agents which produce insoluble chelate compounds with various metal surfaces
[DRIC-TRANS-3079] 17 p2046 N73-26551
Suitability determination of redesigned XW18 membrane as expedient surfacing for waterproofing and dustproofing hastily prepared airfields for operations of C-130 aircraft
[AD-761089] 18 p2127 N73-27190
Environmental tests of zinc-rich coatings applied to carbon steels
[NASA-TN-D-7336] 18 p2160 N73-27450
Spectral characteristics of black and white coating on detector surfaces of actinometric instruments
20 p2403 N73-29310
Fused slurry silicide coatings for tantalum reentry heat shielding
[NASA-CR-120877] 20 p2485 N73-29964
Development of organic glass and plastic materials with improved mechanical and physical properties for use with aircraft canopies and protective coatings
[AD-763263] 21 p2497 N73-30039
Enriched aluminide coatings for dispersion strengthened nickel compounds
[NASA-CR-121250] 21 p2558 N73-30506
Resin for protecting p-n semiconductor junction surface
[NASA-CASE-ERC-10339-1] 21 p2561 N73-30532
Inductive plasma pulverization for protecting mechanical and electronic components
[CEA-CONF-2111] 21 p2583 N73-30701
Feasibility of coating glass optical fibers by melting process
[REPT-6803] 22 p2677 N73-31439
Bibliography of reports on sputtering in industrial processes for applying coatings
[AD-763600] 23 p2798 N73-32379
Application of protective layers of refractory oxides and carbide onto high strength fiber substrates
[NASA-CR-134466] 23 p2810 N73-32467
Production of fire protective intumescent coatings to show methods of manufacture and resulting material properties
[NASA-CR-114470] 23 p2810 N73-32468
Experimental and coating processes for fused slurry silicides on niobium alloy heat shields for space shuttles - Vol. 2
[NASA-CR-134483] 23 p2857 N73-32827
PROTECTORS
NT EAR PROTECTORS
Apollo lunar sample return containers for storing and protecting lunar samples
[Y-1867] 21 p2553 N73-30465
Systems for protection of low altitude tethered balloons from effects of atmospheric electricity
[AD-764651] 23 p2746 N73-31978
PROTEIN METABOLISM
Long term hypokinesia effect on protein and nucleic acid content in rat tissue
14 p1607 N73-23027
PROTEINS
NT ADENINES
NT ADENOSINE TRIPHOSPHATE [ATP]
NT CARBOXYHEMOGLOBIN
NT FIBRINOGEN
NT LIPOPROTEINS
NT NUCLEASE
NT NUCLEOTIDES
NT PEPTIDES
Biodegradation of cellulose fibers and reclamation of single cell protein from refuse through fermentation process
[NASA-CR-130300] 06 p0630 N73-15115
Nutrient protein intake of rats and tolerance to acute hypoxia
14 p1608 N73-23035
Protein sterilization of firefly luciferase without denaturation
[NASA-CASE-GSC-10225-1] 18 p2113 N73-27086
Application of fluorescence spectroscopy for analyzing macromolecules of proteins and nucleic acids
[PAPER-76A6-744] 21 p2546 N73-30410
PROTON BEAMS
Nuclear chemistry and geochemistry research projects including isotope separations, meteorite and tektite compositions, and solid gamma spectrometer development
[COO-3236-3] 08 p0884 N73-17156
Scattering of proton beams upon penetration into upper atmosphere
[NASA-TT-F-14802] 15 p1779 N73-24425
PROTON BELTS
Identification of solar neutron events by satellite detection of proton flux increase in outer edge of trapped proton belt
07 p0838 N73-16790
Measurements of differential energy spectra in cosmic ray protons and solar cycle variations of atmospheric secondary protons
[NASA-CR-132056] 15 p1828 N73-24818
Electrostatic wave mechanism in spatial distribution of inner belt protons
16 p1896 N73-25332
PROTON DENSITY [CONCENTRATION]
NT MAGNETOSPHERIC PROTON DENSITY
Analysis of spectra of radial and nonradial velocity components of solar wind, proton density, and proton thermal speed
01 p0097 N73-10803
Azimuthal distribution losses of protons at synchrophasotron ejection determined by scintillation counters
[JINR-P16-6433] 04 p0453 N73-13699
Magnetospheric plasma tail study, using thermal proton density measurements from OGO 4
08 p0972 N73-17948
PROTON ENERGY
Analysis of spectra of radial and nonradial velocity components of solar wind, proton density, and proton thermal speed
01 p0097 N73-10803
Preliminary studies of reaction yielding triton pion from proton deuteron interaction
[NASA-TM-X-68187] 07 p0823 N73-16674
RF stacking in ISABELLE
[BNL-17274] 10 p1193 N73-19709
Axial and planar channeling effects in thin crystals
15 p1820 N73-24750
Proton energy spectra analysis of solar flare for determining altitude limitations on coronal particle storage
19 p2338 N73-28807
PROTON FLUX DENSITY
Analysis of electron and proton fluxes encountered during nominal Tiros-N trajectories
[NASA-TM-X-66107] 03 p0357 N73-12908
Injection, propagation, and interaction characteristics of solar protons based on HEOS A satellite data
05 p0593 N73-14817
Directional measurements of solar protons during low solar activity from HEOS A satellite
05 p0593 N73-14818
Model for energetic solar proton fluxes with applications to earth spacecraft
[NASA-TM-X-70433] 21 p2592 N73-30769
PROTON IMPACT
Fission and spallation by protons, meteorite composition, and radiation detection
[COO-1167-22] 16 p1947 N73-25754
Neutron emission spectra from protons impinging on spacecraft structural materials
[NASA-TN-D-7386] 20 p2468 N73-29825
PROTON IRRADIATION
Analysis of low temperature proton irradiation induced defects in metals
[COO-3431-1] 04 p0434 N73-13542
Effect of proton bombardment on photoelectric characteristics of n-p junctions alloyed with n-type silicon and lithium admixture
[AD-750977] 06 p0709 N73-15783
Various dispositions of silicon solar cells as influenced by temperature gradients and proton irradiation flux
[NASA-TM-X-66169] 07 p0741 N73-16031
Ultraviolet radiation detector in presence of proton radiation using sensor tubes within shielding mechanism
[NASA-CASE-MFS-21577-1] 11 p1237 N73-20042
Reactivity changes of rats to antiradiation drugs with head and stomach shielded during total irradiation
11 p1241 N73-20072
Pathomorphological changes in internal organs of white rats following 120 MeV proton irradiation and effect of partial shielding on attenuation of damage
11 p1241 N73-20076
Effects of proton bombardment on p- and n-type PbSnTe thin films
[AD-756542] 13 p1567 N73-22696

Nuclear properties in neutron interactions with various nuclei in fast breeder reactor
[ANCR-1088] 17 p2062 N73-26677

**PROTON MAGNETIC RESONANCE**
Proton magnetic resonance spectra and calorimetry of interactions between ions, inhibitors, and substrates with two ribonucleases
[BMVG-FBWT-72-7] 07 p0746 N73-16071
Proton magnetic resonance spectra of ribonuclease A inhibitor complexes, noting effect on catalytic activity
[BMVG-FBWT-72-13] 07 p0747 N73-16074

**PROTON PRECIPITATION**
High latitude proton precipitation and light ion density profiles during magnetic storm initial phase
[NASA-TM-X-66166] 07 p0792 N73-16438
Rocket-borne auroral optical measurement of proton and electron precipitation
[SC-RR-72-0543] 07 p0793 N73-16448
Proton 1 rocket charged particle spectrometer for measuring energy spectrum and electron and proton distribution above 20 keV
[NP-19462] 10 p1161 N73-19444
Data from simultaneous satellite measurement of electron and proton precipitation at high latitudes
[NP-19465] 10 p1210 N73-19845
Electron and proton precipitation in different auroral forms from data obtained by TWINS 1 and 2
[NASA-CR-133889] 22 p2667 N73-31367

**PROTON PROTUBERANCES**
Solar flare physics considering proton acceleration mechanism
[AD-755913] 12 p1446 N73-21711
Solar flare associated proton fluxes at increased energies
19 p2337 N73-28802

**PROTON SATELLITES**
NT PROTON 1 SATELLITE

**PROTON SCATTERING**
Muon proton interactions and elastic scattering for neutron beam generation in accelerator
[BNL-17314] 10 p1193 N73-19710
Scattering of proton beams upon penetration into upper atmosphere
[NASA-TT-F-14802] 15 p1779 N73-24425

**PROTON TELESCOPES**
U PARTICLE TELESCOPES

**PROTON 1 SATELLITE**
Proton 1 rocket charged particle spectrometer for measuring energy spectrum and electron and proton distribution above 20 keV
[NP-19462] 10 p1161 N73-19444

**PROTON-PROTON REACTIONS**
Triple Regge phenomenology from finite mass sum rules in proton-proton inclusive reactions
[NOTA-INTERNA-379] 01 p0084 N73-10693
Meson resonance production in missing mass spectra using quark model for negative pion proton yields proton negative x diffraction calculation
[TUEP-72-41] 07 p0823 N73-16667
Streamer chamber for visual observation of proton-proton interactions in accelerator
[BNL-17273] 10 p1138 N73-19271
Diffractive excitation model for evaluation of inelastic part of proton-proton unitarity equation
18 p2182 N73-27614
I.S.R. elastic proton-proton scattering data and Gribovs Reggeon calculus
[LPTHE-73/13] 20 p2456 N73-29737
Triple Regge formula for analyzing proton leading effect in proton proton collisions
[LPTHE-73/17] 20 p2456 N73-29740

**PROTONS**
NT RECOIL PROTONS
NT SOLAR PROTONS
Measurement of missing mass spectrum from pion [minus] plus proton reaction
[NUB-2160] 01 p0083 N73-10686
Perigee rotation effects on orbit-integrated proton and electron fluxes for AE-C orbit
[NASA-TM-X-66059] 01 p0103 N73-10855
Charge exchange cross sections for protons and alkali atoms using classical approximation of Gryzinski
[NASA-CR-129262] 03 p0339 N73-12763
Statistical comparison of regions with and without proton flares
[AD-747426] 04 p0467 N73-13811
Optical intensity measurements for detecting low energy protons in polar cap
[AD-749857] 05 p0542 N73-14414
Enchancement of 0.24-0.96 MeV trapped protons during 25 May 1967 magnetic storm, measured from OV 1-9 polar orbiting satellite
[AD-749866] 05 p0543 N73-14421
Coupling between ionosphere and protonosphere and effects on long term variations of ionospheric electron content
07 p0775 N73-16296
Electron-proton spectrometer for Skylab radiation dose measurements
[NASA-CR-128702] 08 p0925 N73-17575
Thermodynamic and kinetic behavior of protons and deuterons in regular and heavy ice
[NASA-TT-F-14692] 08 p0946 N73-17744
Low energy cosmic ray protons from nuclear interactions of cosmic rays with interstellar medium
[NASA-TM-X-66181] 08 p0956 N73-17829
Differential cross section of emitted photon in suprathermal proton bremsstrahlung
08 p0974 N73-17966
High intensity proton sources for high energy accelerators
[BNL-17159] 10 p1194 N73-19719
Pitch angle distribution of 100-300 keV protons measured by ESRO 1B satellite in early morning-late afternoon local magnetic time sector
[NP-19464] 10 p1210 N73-19846
Variable intensities of geomagnetically trapped protons at low altitudes
[AD-754844] 11 p1288 N73-20448
Quality control procedures for Skylab electron-proton spectrometer equipment and parts
[NASA-CR-128853] 11 p1292 N73-20484
Safety analysis of EPS electron-proton spectrometer
[NASA-CR-128851] 11 p1292 N73-20485
Performance tests of electron-proton spectrometer for design verification
[NASA-CR-128852] 11 p1292 N73-20486
Design of electron-proton spectrometer for mounting externally on Skylab CSM
[NASA-CR-128814] 11 p1293 N73-20490
Electron and proton radiation effects on Cactus accelerometer electric charge
[ONERA-NT-200] 11 p1294 N73-20503
Laser beam study of proton production cross sections determined for stable and radioactive rare gases
[TID-26183] 12 p1427 N73-21566
Laboratory experiments on interaction of fast protons and hydrogen atoms with earth atmosphere
[AD-757505] 14 p1663 N73-23499
NaI[T1] crystal detector for measuring proton induced activity in gamma ray spectrometer
[NASA-TM-X-66241] 15 p1787 N73-24486
Electrostatic wave mechanism in spatial distribution of inner belt protons
16 p1896 N73-25332
Research activities in physics
[COO-535-674] 17 p2010 N73-26259
Black Brant rocket measurements of proton and alpha particle fluxes
[AD-760138] 17 p2028 N73-26417
Uncorrelated jet model in proton-proton and proton-antiproton annihilation integral
18 p2182 N73-27615
Design of high intensity proton accelerator
[AD-762240] 19 p2250 N73-28140
Evening observations of storm-time ring current particle characteristics during beginning of magnetic storms
[NASA-TM-X-70430] 19 p2293 N73-28441
Performance of OV-5 and OV-6 alpha and proton particle detector
[AD-760147] 19 p2302 N73-28505
Interaction of ultrahigh energy cosmic rays protons with relicit radiation in extragalactic space
19 p2332 N73-28766
Discrimination between high energy cosmic ray electrons and interacting protons using cesium iodide
[NASA-TM-X-70446] 20 p2435 N73-29556
Space vehicle design criteria based on interplanetary charged particle environments
[NASA-CR-133600] 20 p2473 N73-29865
User guide to microfilm records of data obtained in energetic particle experiment with OGO-5
[UCRL-51307] 22 p2639 N73-31150
Proton channeling in silver single crystals at 300, 90, and 20 K
23 p2825 N73-32583

**PROTOSTARS**
NT T TAURI STARS

**PROTOTYPES**
Performance of prototype monopropellant engines using electrolytic ignition system
[AD-745993] 02 p0224 N73-11808
Fabrication and tests of flight prototype pulsed plasma microthruster propulsion system for Synchronous Meteorological Satellite
[NASA-CR-130133] 05 p0590 N73-14794
Design and development of prototype moving base gravity gradiometer
[AD-752231] 08 p0926 N73-17587
Fabrication and evaluation of engineering prototype ground signal processing systems for use with satellite television
[NASA-CR-120933] 09 p1002 N73-18178
Design of prototype thermal battery incorporating pelletized alkaline heat source
[SC-RR-69-497-A] 12 p1366 N73-21084
Prototype regional environmental information system based on ERTS-1 imagery of Central Atlantic Regional Ecological Test Site
[E73-10497] 12 p1397 N73-21333
Design, development, fabrication, and testing of laboratory prototype of residual gas analyzer
[NASA-CR-124177] 12 p1404 N73-21386
Design and fabrication of prototype particulate regenerative filter with backflush for spacecraft fluid system
[NASA-CR-115505] 14 p1614 N73-23084
Prototypes of two acoustic delay lines with delays of 0.5 and 7.5 microsec, noting passband enlargement and echo suppression
15 p1757 N73-24239
Performance of prototype broadband selective ferrite limiters
[AD-759951] 17 p2005 N73-26219

**PROTOZOA**
Survival and reproduction of protozoa in simulated Mars environment
10 p1118 N73-19115

**PROTUBERANCES**
NT PROTON PROTUBERANCES
Heat test program for general protuberance shapes on flat plate
[NASA-CR-128400] 01 p0116 N73-10959

**PROUSTITE**
Laser damage in lithium iodate and proustite
[AD-748935] 04 p0451 N73-13682

**PROVING**
NT THEOREM PROVING
Validation and verification of computer simulation models
[P-4891] 12 p1381 N73-21196
Two speaker verification experiments, using single phrase utterances
14 p1627 N73-23189
Listener performance vs. automatic system in speaker verification tasks
14 p1627 N73-23191
Validation tests for ALGOL 60 compiler
[NPL-NAC-33] 22 p2639 N73-31153

**PRUSSIC ACID**
U HYDROCYANIC ACID

**PSEUDOMONAS**
Ammonifying ability of denitrifying bacteria of species pseudomonas fluorescens
[NASA-TT-F-15086] 21 p2501 N73-30068

**PSEUDONOISE**
Pseudonoise test set for communication system performance evaluation based on RMS error testing
[NASA-TM-X-64698] 03 p0265 N73-12146
Linear shift register with feedback logic for generating pseudonoise linear recurring binary sequences
[NASA-CASE-NPO-11406] 03 p0268 N73-12175
Multicarrier communications system for transmitting modulated signals from single transmitter
[NASA-CASE-NPO-11548] 17 p1993 N73-26118
Statistical properties of filtered pseudorandom digital sequences used in multichannel communications system evaluation, coding theory, and modulation format design
[NASA-TM-X-64758] 18 p2169 N73-27516

**PSEUDORANDOM SEQUENCES**
Adaptive Kalman filter approach for identifying submarine trajectory from hydrodynamic parameters
[AD-747315] 02 p0159 N73-11288
Testing machine for sequential systems using pseudorandom sequences and wired models
03 p0271 N73-12196
Extraction of telemetry data from bit flow of PCM signals
[NASA-TT-F-14657] 07 p0755 N73-16129
Quasi-subcycle properties in congruential pseudorandom number generators
[NASA-TM-X-62275] 17 p2054 N73-26618
Statistical properties of filtered pseudorandom digital sequences used in multichannel communications system evaluation, coding theory, and modulation format design
[NASA-TM-X-64758] 18 p2169 N73-27516
Analysis of statistical properties of filtered summed maximum length digital sequences
20 p2436 N73-29564
Synchronization method for pseudorandom binary data sequences in blockwise transmission of nonoverlapping subsequences, based on digital correlation
[FTZ-A-157-TBR-7] 22 p2632 N73-31095
Pseudorandom 160 Mbits/s pulse generation, and digital word synchronization, for 640 Mbit/s PCM waveguide error rate measurements
[FTZ-A-442-TBR-38] 22 p2633 N73-31098

**PSYCHOACOUSTICS**
Mathematical models for deriving loudness function from physical evidence without human judgment
[NASA-TN-D-7297] 15 p1742 N73-24121
Influence of N-type sound wave pressure rise time on guinea pig cochlear and acoustically evoked potentials
[ISL-31/72] 19 p2224 N73-27940

**PSYCHOLOGICAL EFFECTS**
NT OCULOGRAVIC ILLUSIONS
Effect of temporal uncertainty on human energy expenditure during moderate exercise
[AD-743726] 01 p0011 N73-10084
Effects of stress upon psychophysiological responses and performance following sleep deprivation
[NASA-CR-128620] 02 p0132 N73-11073
Effect of mood on testing human performance
04 p0378 N73-13075

Recorded observations of crew member activities during Tektite 2 underwater habitability study
[NASA-CR-130034] 07 p0750 N73-16094

Analysis of air traffic controller responses under stress conditions to show effects of accuracy, quality, and comprehensiveness of available data
14 p1690 N73-23714

Effect of physical and psychological stress on urinary excretions of adrenal harmones in normal man
[NASA-TT-F-15046] 20 p2368 N73-29043

**PSYCHOLOGICAL FACTORS**
Psychological stresses and crew compatibility during interplanetary spacecraft flight
[JPRS-57878] 06 p0629 N73-15113

Psychological, physiological, and work hygiene problems in ergonomic technology
[JPRS-58792] 13 p1486 N73-22050

Presentations on psychological models, cybernetics, methodology, and applications to teaching
[TT-70-57147-3] 21 p2502 N73-30076

Psychological conception of operator participation in ergonomic process
21 p2502 N73-30081

**PSYCHOLOGICAL INDEXES**
U PSYCHOLOGICAL TESTS

**PSYCHOLOGICAL TESTS**
Psychological assessment techniques for determining astronaut attentional flexibility and associate performance
[NASA-CR-128945] 15 p1744 N73-24136

Psychological and personality test results and problems in selection of pilots, air traffic controllers, and technicians from Yemen
19 p2226 N73-27956

Pilot selection by means of concentration stress test
19 p2226 N73-27957

**PSYCHOLOGY**
NT MILITARY PSYCHOLOGY
NT PSYCHOACOUSTICS
NT PSYCHOPHYSICS

Annotated bibliography on reaction times in selected human information processing tasks
[AD-745416] 01 p0012 N73-10095

Sports medicine - parameters necessary for maintaining competitive form
12 p1370 N73-21114

General problems with psychology in scientific and technical creativity
[TT-70-57147-1] 21 p2502 N73-30074

Articles on methodology and historical importance of scientific research in creativity
[TT-70-57147-2] 21 p2502 N73-30075

Problems involved in achieving harmony in life and work of small groups applied to prolonged space flights
24 p2884 N73-33032

**PSYCHOMETRICS**
Relating test anxiety and trait-state anxiety
[AD-746453] 03 p0260 N73-12104

Use of psychometric tests to account for subjective variations in operations performance relative to target acquisition
10 p1227 N73-19974

Automatic processing of French speech
[AD-752811] 13 p1491 N73-22090

Tracking tasks for clinical evaluation of human movement disorders
[NASA-CR-132275] 18 p2111 N73-27069

**PSYCHOMOTOR PERFORMANCE**
NT PSYCHOSOMATICS

Dynamic changes in psychophysiological motor efficiency of cosmonauts in flight
[JPRS-57417] 01 p0019 N73-10144

Standardized performance battery for assessing effects of environmental stressors particularly noise on human performance
[NASA-CR-2149] 08 p0877 N73-17102

Choice reaction tasks for discriminating individual skill potentials in information handling situations
[AD-752073] 08 p0878 N73-17115

Immersion effects on human physiological motor functions
10 p1114 N73-19081

Combined noise and vibration effects on human mental and psychomotor performance
[AMRL-TR-71-115] 10 p1122 N73-19147

Human performance in sequential task training for acquisition of perceptual motor skills under flight stress
10 p1123 N73-19153

Measurements of acceleration stress effects on pilot maneuvering ability and flight control performance
[AMRL-TR-72-3] 10 p1123 N73-19154

Human psychomotor and cognitive performance in humid environment
[AD-756835] 15 p1745 N73-24142

Human psychomotor performance circadian rhythm variations after transmeridian flight noting time shift effect
[DLR-FB-73-52] 22 p2624 N73-31022

Pilot performance under simulated conditions of modified aircraft control dynamics, navigational task complexity, and induced stress
[AD-764760] 23 p2752 N73-32025

**PSYCHOPHYSICS**
NT PSYCHOACOUSTICS

Psychobiological factors for predicting monotony tolerance and selecting personnel for isolated duty
[AD-747272] 04 p0381 N73-13098

Psychophysical analysis of RF sound perception in human subjects
[AD-747684] 05 p0501 N73-14076

Psychophysical method of limits to evaluate experimental variables in sensory areas
[AD-749334] 05 p0502 N73-14083

Accuracy of method of constant stimuli for studying sensory capabilities of man in relation to display systems
[AD-753009] 10 p1121 N73-19141

**PSYCHOPHYSIOLOGY**
Dynamic changes in psychophysiological motor efficiency of cosmonauts in flight
[JPRS-57417] 01 p0019 N73-10144

Psycho-visual problems associated with monocular, bi-ocular, and binocular visual systems
[AD-749450] 05 p0502 N73-14085

Simulated lunar magnetic environment effects on humans, using scotopic critical flicker frequency measurements to indicate psychophysiological stress
[AD-748193] 05 p0502 N73-14088

Research on laser irradiation effects, sensory psychophysiology, and human blood processing for military medicine
[AD-749440] 06 p0631 N73-15130

Choice reaction tasks for discriminating individual skill potentials in information handling situations
[AD-752073] 08 p0878 N73-17115

Human stress expenditures in operational airlift mission flights
10 p1123 N73-19151

Proceedings of symposium on color vision, color perception, visual acuity, and psychophysiology
[AD-754328] 11 p1249 N73-20136

Human psychomotor and cognitive performance in humid environment
[AD-756835] 15 p1745 N73-24142

Psychophysiological aspects in flight personnel visual perception of image indicator
20 p2367 N73-29035

**PSYCHOSOMATICS**
Drug therapy effects on flying effectiveness and psychosomatic fitness of flying personnel
12 p1369 N73-21103

**PSYCHOTHERAPY**
Mental health services for emotional counselling in NASA facilities to insure maximum human performance
08 p0872 N73-17062

**PSYCHROMETERS**
Theory for Assman psychrometer based on exact analysis of diffusion process in laminar boundary layer with thermal gradients
[NLL-M-22691-[5828.4F]] 05 p0570 N73-14627

**PSYCHROPHILES**
Psychrophilic organisms in soil samples of areas for Viking spacecraft assembly
[REPT-2] 17 p1987 N73-26063

**PUBLICATIONS**
U DOCUMENTS

**PUERTO RICO**
Aerial photography used to delineate areas of ocean ground water discharge and detect submarine springs along northwest coast of Puerto Rico
[PB-210754] 01 p0052 N73-10426

Reference file of local factors affecting weather at Ramey AFB, Puerto Rico
[AD-746026] 02 p0205 N73-11661

Discrimination and mapping land use categories in Puerto Rico using various types of multispectral remote sensor imagery
07 p0776 N73-16298

Height error in sea-surface profile over Puerto Rican trench as determined by multi-station tracking aided by GEOS 2 satellite
[NASA-TM-X-69353] 07 p0781 N73-16347

Experimental determination of coupling between normal F region ionosphere and protonosphere using radar backscatter techniques at Arecibo, Puerto Rico
23 p2778 N73-32213

Water depth determination off Puerto Rico from Skylab multispectral imagery
[E73-11141] 24 p2918 N73-33296

**PULLEYS**
State of stress and strain in rectangular belt pulled over cylindrical pulley
[AD-747318] 03 p0307 N73-12507

**PULMONARY CIRCULATION**
Sensory receptors irritation and cardiopulmonary toxicity from fluorocarbon propellants
[AD-751426] 07 p0749 N73-16089

**PULMONARY FUNCTIONS**
Analysis of arterial hypoxemia caused by pulmonary malfunctions and regulation of oxygen during exercise and rest
[AD-746979] 04 p0380 N73-13092

Deep diving pulmonary functions of man using different breathing gas densities
[AD-749028] 05 p0501 N73-14082

Human oxygen metabolism and pulmonary functions during hypodynamic water immersion
10 p1114 N73-19082

Human pulmonary volume decrease during long term bed rest
13 p1482 N73-22016

Centrineurogenic etiology for pulmonary changes of high altitude pulmonary edema
[AD-756940] 15 p1743 N73-24127

**PULSARS**
Matter in neutron stars and relevance to pulsar observation
[NASA-TM-X-66067] 01 p0103 N73-10849

Astronomical techniques for determining physical parameters and energy balance of neutron stars based on pulsar observations
[NASA-TM-X-66066] 01 p0103 N73-10850

Meter wavelength observations of Crab nebula pulsar using very long base-line interferometry techniques
[NASA-TM-X-66071] 01 p0103 N73-10852

Night sky Cerenkov detector for measuring electromagnetic radiation produced by high energy cosmic rays
[AD-746734] 03 p0354 N73-12883

Annotated bibliography on pulsars taken from Nuclear Science Abstracts for 1971
[TID-3320-SUPPL-2] 03 p0357 N73-12909

Short-term temporal studies of X ray emission from Cas A, Tycho and X-1
[NASA-TM-X-66127] 04 p0466 N73-13802

Fluctuations in radio intensity of pulsar emissions
04 p0469 N73-13819

Model for pulsar radiation mechanism and relativistic plasma
[NP-19402] 07 p0826 N73-16692

Optical identification of pulsed X ray source in eclipsing binary system
[NASA-CR-130923] 09 p1082 N73-18824

Balloon observation of pulsed gamma rays above 250 keV from Crab Nebula pulsar NP 0532
12 p1444 N73-21698

Analysis of conditions leading to generation of cosmic rays by acceleration of charged particles caused by electromagnetic field of pulsars
[PPG-144] 12 p1445 N73-21703

Balloon-borne telescopic observations of X ray pulsars in Gum and Crab nebulae
13 p1575 N73-22764

Least squares and cross correlation procedure for determining absolute timing of pulsars
13 p1575 N73-22765

Tensor viral method for modeling and studying pulsars in rapidly rotating magnetosphere
16 p1960 N73-25858

European measurements of diffuse flux and Crab pulsar NP 0532
19 p2331 N73-28758

Time series on optical pulsar candidates
20 p2469 N73-29831

Boundary between open and closed magnetospheres of pulsar atmosphere
[AD-761883] 21 p2598 N73-30822

X ray emission in pulsar model for supernovae remnants
22 p2733 N73-31870

Pulsar magnetospheric model where radiation is produced near surface of neutron star
[NASA-CR-135587] 23 p2844 N73-32731

Rapid flux, relativity, black holes, and pulsar, and quasar models
[NASA-TM-X-62298] 23 p2846 N73-32742

**PULSATING FLOW**
U UNSTEADY FLOW

**PULSE AMPLITUDE**
Construction of electron beam semiconductor pulse amplifier and radio frequency amplifier diode
[AD-748892] 04 p0461 N73-13758

Effect of ocean surface structure on narrow radar pulse shape
06 p0662 N73-15380

Influence of sea state on short pulse radar satellite altimeter determination of mean surface position
06 p0663 N73-15385

Scattering characterization inputs in computerized design of wideband linear amplifiers for pulse operation
[LBL-772] 07 p0762 N73-16188

Analysis of large amplitude elastic wave interaction in bounded medium
16 p1968 N73-25919

Analog to digital converter circuit for pulse height analysis
[NASA-CASE-XNP-00477] 19 p2238 N73-28045

**PULSE AMPLITUDE MODULATION**
Statistical analysis on nonparametric detection of M-ary time varying signals with intersymbol interference and additive noise
[AD-752011] 08 p0886 N73-17174

Adaptive equalization of pulse amplitude modulated signal with noise interference by successive iterative methods
[NASA-TR-R-402] 10 p1128 N73-19190

Frequency limited amplifier for proportional counter pulse shape and pulse height control
[NLL-WH-TRANS-343-[9091.9F]] 15 p1755 N73-24227

**PULSE CODE MODULATION**
NT DELTA MODULATION
Simulation techniques for determining broadcast quality of digital sound signals produced by pulse code modulation transmission system
[BBC-1972/31] 01 p0024 N73-10183
Noise and error effects on differential pulse code modulation transmission of sampled aerial imagery 01 p0024 N73-10190
Systematic convolutional codes for PCM telemetry
[NASA-TM-X-66085] 02 p0140 N73-11138
Bit synchronizer for split phase PCM transmission with two loop systems
[NASA-CASE-MSC-12494-1] 02 p0141 N73-11142
Bit synchronization of PCM communications signal, without separate synchronization channel by digital correlation
[NASA-CASE-NPO-11302-1] 04 p0388 N73-13149
Analysis of digital information coding procedures with application to control of synchronization errors in data transmission on pulse code modulation systems
[NLL-TRANS-2825-[9022.81]] 05 p0507 N73-14127
PCM coding and decoding noting truncated hamming codes and analysis of error rates
[ESRO-TN-112-ESTEC] 05 p0513 N73-14173
Adaptive pulse code modulator for speech signals noting coder and decoder
[SRDE-72001] 05 p0514 N73-14174
Surface and PCM temperature measurement of capacitors during melting and solidification 05 p0608 N73-14945
Extraction of telemetry data from bit flow of PCM signals
[NASA-TT-F-14657] 07 p0755 N73-16129
Digit-error-protection technique for use in multiplex pulse code modulation systems for high quality sound-signal distribution
[BBC-1972/40] 09 p1001 N73-18170
Binary code signals produced by electron beam deflection in magnetic fields 12 p1378 N73-21176
Subjective evaluation of differential pulse code modulation using speech goodness rating scale 14 p1624 N73-23162
Mean squared error method for predicting fidelity of differential pulse code modulation system 16 p1873 N73-25165
Differential pulse code modulation of digital video signals
[BBC-RD-1973/7] 19 p2234 N73-28011
Transmission problems of hybrid PCM system for television signals
[BBC-RD-1973/9] 20 p2376 N73-29088
Development of entropy coded adaptive differential pulse code modulation systems for speech signals
[AD-762606] 20 p2378 N73-29109
Pseudorandom 160 Mbits/s pulse generation, and digital word synchronization, for 640 Mbit/s PCM waveguide error rate measurements
[FTZ-A-442-TBR-38] 22 p2633 N73-31098
Planar Gunn devices in dipole domain mode for high speed logic circuits in PCM equipment, noting thermal resistances and packing density
[FTZ-A-474-TBR-3] 22 p2643 N73-31183
Integrated GaAs digital circuits with Gunn diodes for pulse code modulation
[FTZ-A-62-TBR-3] 22 p2646 N73-31205

**PULSE COMMUNICATION**
Conference on expanded aerospace telecommunication system requirements and digital data transmission methods
[AGARD-CP-103] 01 p0024 N73-10187
Interchannel interference and Gaussian noise effects on phase modulated digital microwave radio systems 01 p0027 N73-10211
Baseband equalization system for correcting response characteristics of high quality coaxial transmission lines
[UCRL-73943] 07 p0756 N73-16141
Digit-error-protection technique for use in multiplex pulse code modulation systems for high quality sound-signal distribution
[BBC-1972/40] 09 p1001 N73-18170
Survey of some oblique sounding systems and selection of system for practical application 10 p1128 N73-19188
Performance of digital voice transmission system with modulator-demodulator network
[AD-754921] 11 p1258 N73-20210
Adaptive maximum likelihood receiver for digital communication channels 16 p1873 N73-25163
Measurement of pulse parameters in wideband receivers including amplitude, frequency, and time of arrival 16 p1873 N73-25166
Numerical analysis of minimum probability of error expression in digital communication system with intersymbol interference
[AD-760057] 17 p1999 N73-26167
Computerized management tools for use in analysis of automatic switching centers and associated tributaries of Autodin communications network
[AD-761479] 19 p2236 N73-28028
Proceedings of conference on spread spectrum techniques and application to digital communications systems
[AGARD-LS-58] 23 p2756 N73-32053
Fundamental concepts of communication theory to include transmission of continuous signals and use of discrete time signals 23 p2756 N73-32054
Characteristics of digital communication systems and processing of bandpass digital signals using spread spectrum techniques for data transmission 23 p2756 N73-32055
Principles and operation of spread spectrum communication system with application to satellite communication systems 23 p2756 N73-32056
Performance of spread spectrum communication systems to include effects of various forms of channel noise and synchronization aspects of system 23 p2756 N73-32057
Applications of spread spectrum communications techniques to avionics systems 23 p2756 N73-32058
Maximum likelihood receiver for pulse communication systems
[AD-764641] 23 p2758 N73-32072

**PULSE COMPRESSION**
Utilization of spiral antenna as pulse compression network
[AD-764354] 22 p2644 N73-31189

**PULSE DOPPLER RADAR**
NT MONOPULSE RADAR
NT PULSE RADAR

**PULSE DURATION**
Turbulent burst and non-turbulent durations in turbulent boundary layer of open channel
[ARL/SM-NOTE-374] 01 p0039 N73-10307
Generator of extended duration high voltage pulses for controlling high-gain light amplifier
[CEA-N-1516] 03 p0280 N73-12272
Temperature controlled piezoelectric crystal oscillator with digital integrated circuitry for timing of pulses
[AECL-4160] 04 p0396 N73-13217
Oscilloscopic measurement of mode locked ultrashort laser pulses produced by linear and nonlinear photoelectric effects
[KFKI-72-41] 07 p0806 N73-16539
DONAR system for digitizing ultrashort sonic wave trains from pulse echo systems
[NASA-CR-130883] 09 p1013 N73-18266
Effect of thruster pulse length on thruster-exhaust damage of S13G white thermal control coatings
[NASA-TM-X-68213] 11 p1348 N73-20940
Electronic pulse generators producing 10 picosec duration pulses with several hundred MHz repetition rates
[DRIC-TRANS-2934] 12 p1379 N73-21185
Methods of generating supernarrow pulses
[NLL-DRIC-TRANS-2934-[3623.66]] 16 p1910 N73-25455
Periodic functional analysis of ultra-short pulse generation and propagation in laser systems 16 p1920 N73-25535
Pulse stretcher for processing narrow pulses between pulse generators and conventional instruments
[NASA-CASE-MSC-14130-1] 17 p2007 N73-26232
Photoconductivity of gallium arsenide-, Cadmium sulfide-, and cadmium selenide-semiconductors correlated to laser pulse width
[AD-760560] 18 p2190 N73-27682
Development and characteristics of sawtooth voltage generator using blocking generator as switch 22 p2630 N73-31081

**PULSE DURATION MODULATION**
Development and characteristics of terminal analog speech synthesizer using pulse width modulation and pulse number modulation techniques 14 p1632 N73-23228
Design and performance of solid state inverter/converter modular system with pulse width modulation
[NASA-TM-X-2795] 15 p1737 N73-24083
Analog and digital computer simulation study of pulse width modulation in feedback control systems 16 p1883 N73-25242
Peak holding circuit for extremely narrow pulses
[NASA-CASE-MSC-14129-1] 17 p2007 N73-26231
Electric modulator circuit for controlling output power of commercial laser
[LA-5166-MS] 17 p2040 N73-26507
Width modulated pulse rebalance electronics loop for strapdown gyroscope
[NASA-CR-124333] 19 p2318 N73-28649

**PULSE FREQUENCY MODULATION**
Development of frequency modulated diode laser transmitter for point-to-point voice communication system
[AD-747524] 03 p0311 N73-12540

**PULSE GENERATORS**
Electron bombarded semiconductor short pulse generator
[AD-748090] 03 p0276 N73-12239
Generator of extended duration high voltage pulses for controlling high-gain light amplifier
[CEA-N-1516] 03 p0280 N73-12272
Experimental design for X ray and electron pulse production
[ISL-10/72] 03 p0303 N73-12472
Alternate methods for soft X ray pulse generation by light flux available with high pulse energy lasers
[AD-750375] 06 p0680 N73-15534
Generation and measurement of ruby laser picosecond pulses
[AD-750789] 06 p0680 N73-15538
Design of pulsed electron beam accelerator with multiple Mylar stripline modules
[AD-751593] 07 p0766 N73-16227
Circuits for pulse generation in magnetic plasma pinch
[AD-751250] 07 p0830 N73-16732
Explosive generator source, switching and matching networks, and bent dipole antenna
[AD-751907] 08 p0894 N73-17234
Generation of narrow high current pulses 10 p1228 N73-19980
Ultrashort pulse generation from mode locked carbon dioxide laser by resonant acoustic loss modulator
[DREV-TN-2024/72] 11 p1302 N73-20566
Electronic pulse generators producing 10 picosec duration pulses with several hundred MHz repetition rates
[DRIC-TRANS-2934] 12 p1379 N73-21185
CF3I gas laser system for high power operation
[SC-T-72-2560] 12 p1410 N73-21426
Delivery of electron beam to X ray target in 50 nanoseconds
[AD-755456] 14 p1646 N73-23347
Methods of generating supernarrow pulses
[NLL-DRIC-TRANS-2934-[3623.66]] 16 p1910 N73-25455
Periodic functional analysis of ultra-short pulse generation and propagation in laser systems 16 p1920 N73-25535
Circuitry for generating random square wave pulses using white noise source
[NASA-CASE-MSC-14131-1] 17 p2003 N73-26199
Computerized design of electron beam semiconductor short pulse generator
[AD-761111] 18 p2191 N73-27693
Variable-length transistorized pulse shaper
[AD-762328] 19 p2246 N73-28112
Development of solid state beacon and radio frequency generator for avionics applications - Vol. I
[AD-761525] 19 p2247 N73-28115
Applications of inverse Fourier transform method of producing high peak power for use with solid state radio beacon - Vol. 2
[AD-761526] 19 p2247 N73-28116
Development and characteristics of sawtooth voltage generator using blocking generator as switch 22 p2630 N73-31081
Pseudorandom 160 Mbits/s pulse generation, and digital word synchronization, for 640 Mbit/s PCM waveguide error rate measurements
[FTZ-A-442-TBR-38] 22 p2633 N73-31098
Minority carrier lifetime and switching time of step recovery diode for pulse generators in microwave equipment
[FTZ-A-651-TBF-3] 22 p2643 N73-31180

**PULSE HEATING**
Relation of gas kinetic particle pressure and discharge field in plasma heating by pulsed longitudinal current
[AEC-TR-7330] 07 p0826 N73-16697
Pulsed electron beam heating for optimal penetration and forming of welds
[AD-754684] 11 p1301 N73-20557
High voltage pulse for igniting electron bombardment mercury ion thruster
[NASA-TM-X-71425] 23 p2765 N73-32119

**PULSE HEIGHT**
U PULSE AMPLITUDE

**PULSE MODULATION**
NT DELTA MODULATION
NT PULSE AMPLITUDE MODULATION
NT PULSE CODE MODULATION
NT PULSE DURATION MODULATION
NT PULSE FREQUENCY MODULATION
NT PULSE POSITION MODULATION
Pulse modulation characteristics of vidicon beam currents
[DRIC-TRANS-2875] 02 p0174 N73-11413
Jamming of surveillance radar station by airborne electronic countermeasures
[FOA-3-C-3645-66] 06 p0639 N73-15187
Recursive plane analysis for phase locking in pulse modulation sampling technique
[AD-756918] 13 p1492 N73-23092

Motor function modeling of human arm by manipulator using myoelectric control pulses
17 p1990 N73-26091

PULSE POSITION MODULATION
Synchronization using pulsed edge tracking in optical PPM communication systems
[NASA-CR-130117] 03 p0265 N73-12143
Pulse position modulation for coding and signal identification by transmitter receiver
[AD-747629] 04 p0391 N73-13180
Pulse position modulation laser communication system for voice transmission
[AD-757258] 14 p1633 N73-23237

PULSE RADAR
NT MONOPULSE RADAR
Phase shift variations of platinotron microwave amplifier oscillator for pulse radar and steerable antennas
[DLR-MITT-73-03] 12 p1379 N73-21187
Pulse radar measurement of mean monthly wind patterns
17 p2023 N73-26367
Suppression of Doppler ambiguities in pulsed random signal radar
20 p2375 N73-29086

PULSE RATE
Electronic pulse generators producing 10 picosec duration pulses with several hundred MHz repetition rates
[DRIC-TRANS-2934] 12 p1379 N73-21185

PULSE RECORDERS
U COUNTERS

PULSE TIME MODULATION
NT PULSE DURATION MODULATION
NT PULSE POSITION MODULATION

PULSE WIDTH
U PULSE DURATION

PULSE WIDTH AMPLITUDE CONVERTERS
Numerical analysis of voltage spectra of electric inverters with pulse width modulation
[NLL-RTS-7639] 11 p1261 N73-20235
Peak holding circuit for extremely narrow pulses
[NASA-CASE-MSC-14129-1] 17 p2007 N73-26231

PULSE WIDTH MODULATION
U PULSE DURATION MODULATION

PULSED LASERS
NT Q SWITCHED LASERS
Computerized simulation of pulsed HF laser pumped by H2 and F2 chain reaction
[AD-745425] 01 p0065 N73-10531
Generation, measurement, and properties of picosecond laser pulses produced by mode locked lasers
[AD-746310] 01 p0066 N73-10543
Organic dye pulsed laser for detecting individual atomic species concentration in upper atmosphere
[AD-747335] 02 p0169 N73-11377
Laser transitions in pulsed neodymium yttrium-aluminum garnet emission
[AD-746218] 02 p0181 N73-11472
Absorption and fluorescence spectra of marine and fresh water algae using pulsed N2/Ne dye laser as excitation source
[NASA-CR-62090] 03 p0310 N73-12527
Operating principles and physical mechanisms of pulsed gas discharge lasers
[SC-T-72-2524] 06 p0679 N73-15529
Safety procedures for using pulsed lasers and making pulsed holograms
[AD-751024] 07 p0808 N73-16555
Transit time measurements between earth and moon by transportable pulsed laser system
[NASA-CR-130986] 09 p1042 N73-18502
Frequency stable Q switched carbon dioxide laser oscillators, free-running and injection locked pulsed lasers, and optical heterodyne measurements of frequency stability
[AD-753605] 09 p1045 N73-18523
Photoconductivity of cadmium sulfide crystals excited by mode-locked neodymium laser pulses
[AD-753677] 09 p1077 N73-18786
Operational requirements and optical components of pulsed holographic interferometry
[LA-5058] 10 p1161 N73-19446
Computerized simulation of parallel plate pulsed transversely excited atmospheric pressure laser
[DREV-TN-2054/72] 10 p1168 N73-19503
Possible uses of pulsed lasers for controlled fusion, plasma heating, and creation of controlled nuclear microexplosions
[UCRL-73931] 10 p1186 N73-19654
Design of particle accelerator using pulsed laser beam
[RLO-2041-71] 10 p1193 N73-19705
Ultrashort pulse generation from mode locked carbon dioxide laser by resonant acoustic loss modulator
[DREV-TN-2024/72] 11 p1302 N73-20566
Portable pulsed laser ranging system for measurements between earth and retroreflecting satellites
[NASA-CR-131513] 12 p1410 N73-21423
Nonlinear pulse interaction in CO2 lasers
[AD-755919] 12 p1411 N73-21436
Remote detection and measurement of clear air turbulence using pulsed laser radar
[NASA-CASE-MFS-21244-1] 12 p1422 N73-21523
Development of satellite geodesy technique for accurate determination of three dimensional coordinates of ground stations
[NASA-CR-132251] 15 p1778 N73-24412
Design and operating characteristics of pulsed ruby laser source used in portable holocamera
16 p1920 N73-25541
Molecular laser model for pulsed carbon monoxide/nitrogen system
[AD-759509] 16 p1924 N73-25571
Development of laser model for analyzing pulsed excitation of molecules in discharge and nonequilibrium discharge of supersonic flow in vacuum
[JPRS-59040] 18 p2158 N73-27432
Turbulent heating of dense plasma by laser pulses
[JPRS-59027] 18 p2182 N73-27621
Holographic investigations using pulsed lasers
[AD-761977] 19 p2308 N73-28565
Optically actuated two position mechanical mover
[NASA-CASE-NPO-13105-1] 20 p2422 N73-29458
Forward scattered light spectrum from pulsed ruby laser in liquid medium
20 p2424 N73-29470
Simulated emission predictions and measurement of H2 pressure effects on pulsed H2-F2 laser outputs
[AD-763716] 21 p2556 N73-30492
Procedure and device for effecting dual mode locking in pulsed Nd-YAG lasers
[NASA-CASE-GSC-11746-1] 23 p2800 N73-32398
Laser beam divergence and measurement of nanosecond laser pulses
[AD-764702] 23 p2802 N73-32407
Laser fusion and parameteric instabilities
[COO-3227-18] 24 p2932 N73-33413
Thomson scattering diagnosis on pulsed xenon arc plasma flow
[NASA-TM-X-71443] 24 p2962 N73-33669

PULSED RADIATION
NT ELECTROMAGNETIC PULSES
Production and current measurement of intense hydrogen-ion beams in pulsed conditions
[NP-19351] 04 p0454 N73-13705
Development and characteristics of cyclically operable, optical shutter for use as focal plane shutter for transmitting single radiation pulses
[NASA-CASE-NPO-10758] 05 p0545 N73-14427
Generation and measurement of ruby laser picosecond pulses
[AD-750789] 06 p0680 N73-15538
Damage thresholds of multilayered dielectric reflecting mirrors subjected to nanosecond laser pulses
[AD-751265] 07 p0808 N73-16553
Displacement of electric arc by magnetron-produced pulsed high frequency heating
[BMVG-FBWT-72-19] 08 p0943 N73-17728
Balloon observation of pulsed gamma rays above 250 keV from Crab Nebula pulsar NP 0532
12 p1444 N73-21698
Frequency modulated [chirped] optical pulses in subpicosecond to microsecond pulse length range
15 p1812 N73-24686
Techniques for producing laser pulses of nanosecond duration
[AD-760752] 18 p2158 N73-27435
Properties of solar coronal pulsations
19 p2339 N73-28817
Mode locking and pulse selection in atmospheric gas lasers
[AD-765350] 23 p2802 N73-32411

PULSEJET ENGINES
Design parameters and characteristics of intermittent pulse jet engine for use as auxiliary power source
10 p1110 N73-19047

PULSES
NT ELECTRIC PULSES
NT ELECTROMAGNETIC PULSES
NT GEOMAGNETIC MICROPULSATIONS
NT GEOMAGNETIC PULSATIONS
NT MICROPULSATIONS
NT PRESSURE PULSES
Comparison of sequential, two-pulse detection scheme with conventional single pulse detection
[PHL-1972-20-EX-19] 02 p0139 N73-11127
Effects of pulse shape on transient response of cylindrical shells and generation of shear waves in cylindrical shells
[NASA-CR-112221] 05 p0602 N73-14891
Computer simulated parallel-formant synthesizer to copy short samples of human speech
14 p1624 N73-23156
High resolution radar transmitting system for transmitting optical pulses to targets
[NASA-CASE-NPO-11426] 17 p1994 N73-26119
Ultrashort optical pulse propagation through resonant media
[AD-762209] 19 p2309 N73-28569
Digital decoder for processing Barker coded pulses in incoherent scatter observations of ionosphere
23 p2778 N73-32212

PULVERIZING
U GRINDING [COMMINUTION]

PUMICE
Investigation for attenuation and extinction in interaction between laser beams and flowing particulate clouds
[RM-567] 08 p0929 N73-17605
Energy budget of pumice desert surface under clear skies during summer
[PB-218791/2] 18 p2146 N73-27347
Energy exchange characteristics of desert, meadow, forest, and marsh sites
[PB-218825/8] 18 p2173 N73-27550

PUMP IMPELLERS
Analysis, design, fabrication, and performance tests to determine effects of impeller blade clearance on efficiency of centrifugal pumps
[NASA-CR-120815] 03 p0305 N73-12493
Rotor design, test apparatus and procedure, and data reduction and evaluation for axial flow pump rotor configurations
[NASA-TN-D-7074] 06 p0613 N73-14982
Iterative method for calculating axial flow resistance in annular slots of impeller pumps
[NLL-NEL-TT-2422-[6075.461]]
11 p1269 N73-20299

PUMP SEALS
High speed bellows shaft seals for rocket engine turbopumps
03 p0348 N73-12842

PUMPS
NT AXIAL FLOW PUMPS
NT CENTRIFUGAL PUMPS
NT CONDENSATION PUMPS
NT DIFFUSION PUMPS
NT ELECTROMAGNETIC PUMPS
NT FUEL PUMPS
NT JET PUMPS
NT TURBINE PUMPS
NT VACUUM PUMPS
Pump for cryogenic liquids using magnetocaloric material
[NASA-CASE-LEW-11672-1] 05 p0551 N73-14479
Flight tests of portable diaphragm liquid pump for astronaut cooling
09 p1089 N73-18883
Gas flow in multilayer insulation systems applied to broadside pumping
[NASA-CR-124130] 10 p1139 N73-19281
Design of hydrostatic shaft guide bearings for sodium pumps
[CEA-CONF-2045] 10 p1166 N73-19486
Design, development, fabrication, and test of coolant circulating pump assemblies for use in Brayton cycle space power system
[NASA-CR-2176] 11 p1297 N73-20529
Design of chemical pumps for Venus Pioneer mass spectrometer used to determine atmospheric composition of Venus
[NASA-CR-114604] 16 p1918 N73-25519
Low noise level fan and pump concept for space shuttle
[NASA-CR-128986] 17 p2037 N73-26477
Operational reliability and economics for instrumentation particularly electric pumps
[AD-762321] 19 p2306 N73-28545
Test performance of pump for Pioneer Venus probe mass spectrometer inlet
[NASA-CR-114660] 22 p2678 N73-31448

PUNCHED CARDS
Program instructions for using and running card deck through AIST-O system
[JPRS-57790] 05 p0517 N73-14200

PUNCHED TAPES
Computer technique for transferring digital television signal to punched tape
[BBC-RD-1973/6] 19 p2238 N73-28044

PUPILLOMETRY
Pupil enlargement in relation to operator stress during adaptive critical tracking task
[AD-749075] 05 p0501 N73-14081
Pupillometry using advanced design oculometer
[AD-752121] 08 p0878 N73-17116

PURGING
Design, development, and evaluation of pressurized purge system for reusable space shuttles and fabrication of multilayer insulation systems
[NASA-CR-123942] 03 p0358 N73-12914
Purge and vent characteristics of GAC-9 insulation system
[NASA-CR-124052] 09 p1050 N73-18565

PURIFICATION
NT AIR PURIFICATION
Development of procedure for removing oxygen from nickel alloys by blowing hydrogen on bath surface and evacuating gases
[NLL-TRANS-746-1347-[9022.401]]
02 p0184 N73-11495
Production, refining, manufacturing, and applications of uranium alloys and compounds
[JPRS-57364] 03 p0313 N73-12552
Development of steel smelting process using inert argon atmosphere for gas saturation and removal of impurities
[JPRS-57542] 03 p0313 N73-12553

Preparation of pure materials, radiation chemistry, and solid state studies
[BARC-599] 05 p0506 N73-14120
Purification of molten lithium fluoride, sodium fluoride, and potassium fluoride salt eutectics for thermal battery electrolyte application
[AD-758001] 15 p1739 N73-24097
Base metal catalysts as platinum substitutes in petroleum refining and automobile emission devices
[NMAB-297] 18 p2113 N73-27088

**PURIFIERS**
U PURIFICATION

**PURINES**
NT ADENINES

**PURITY**
Fricks equation for determining diffusion profiles in two impure semiconductors
[CEA-CONF-1970] 01 p0087 N73-10723
Refracted electron beam temperature as indication of lead sulfide purity
[AD-753556] 09 p1077 N73-18787

**PURSUIT TRACKING**
Input adaptive behavior model of human operator in pursuit tracking task
01 p0014 N73-10108
Sub-optimal control to synthesize feedback controller for two dimensional, nonlinear intercept and pursuit-evasion problems
[AD-746005] 01 p0109 N73-10901

**PWM [MODULATION]**
U PULSE DURATION MODULATION

**PYLONS**
Wind tunnel tests to determine effects of modified engine nacelle on stability and control characteristics of DC-9 aircraft with emphasis on deep stall regime
[NASA-CR-121220] 19 p2219 N73-27904

**PYRANOMETERS**
Development and characteristics of self-contained digital integrator for recording daily solar irradiance
[AD-760318] 17 p2035 N73-26468
Design, development, and characteristics of high sensitivity, nonselective pyranometer with black detecting surface and xenon filling
20 p2402 N73-29304
Development, characteristics, and operation of thermoelectric photopyranometer with hemispherical glass filters
20 p2402 N73-29306
Characteristics of pryanometers and net radiometers, calibrated for short wave radiation
20 p2403 N73-29312
Sensitivity and structural peculiarities of underwater pyranometers
20 p2447 N73-29660

**PYRAZINES**
NT AZINES

**PYRENEES MOUNTAINS [EUROPE]**
Geomorphology, tectonics, and structural relations between Alps and Pyrenees based on ERTS-1 imagery
[E72-10286] 04 p0410 N73-13336

**PYREX [TRADEMARK]**
U BOROSILICATE GLASS

**PYRIDINES**
NT NICOTINIC ACID
Conversion of 2-methyl 5-ethyl pyridine compound into 5-ethyl picoline acid by different methods
[DRIC-TRANS-2951] 06 p0638 N73-15178
Protective effects of pyridinium salts against alkyl phosphate poisoning including influence of chemical and aging
[BMVG-FBWT-72-8] 07 p0746 N73-16072
Pharmacologic investigations of antagonistic effects of pyridines on isolated guinea pig ileum
[BMVG-FBWT-72-14] 07 p0747 N73-16075
Synthesis of high molecular weight benzobistriazolo phenanthroline polymers for heat resistant plastic films
[AD-753414] 10 p1127 N73-19180

**PYRIDOXINE**
Inhibiting and activating effect of mono- and bi-quaternary pyridioxide reactivators on bovine erythrocyte cell membrane
[BMVG-FBWT-72-9] 10 p1121 N73-19138

**PYROELECTRICITY**
Pyroelectric temperature sensors for ignition mechanism of anti-vehicle mines
[LCR-DR-1-71-266/1/R] 12 p1465 N73-21870
Pyroelectric coefficient of lead zirconate titanate
[AD-755520] 13 p1567 N73-22700
Piezoelectric and pyroelectric properties of polymer electrets
[AD-758730] 16 p1933 N73-25638
Pyroelectric infrared detector performances investigating strontium and barium niobates, lithium sulfate and TGS materials effects on frequency ranges and sensitivity
[ESRO-CR-67] 22 p2675 N73-31425

**PYROGRAPHALLOY**
U COMPOSITE MATERIALS
U PYROLYTIC GRAPHITE
U REFRACTORY MATERIALS

**PYROHELIOMETERS**
Comparison of national standards of socialist countries for measuring solar radiation using pyrheliometer test readings
04 p0443 N73-13614

**PYROLYSIS**
Pyrolysis of glassy carbons in inert atmosphere from copolymers of furfuryl alcohol
[AD-746883] 02 p0194 N73-11570
Thermal decomposition of polyhydrazide and polyoxadiazoles
[AD-749853] 05 p0568 N73-14612
Adiabatic compression method for initial stage mechanism study of thermal decomposition of TiCl4
06 p0683 N73-15560
Magnesium thermal reduction method for interaction mechanism of titanium chloride with magnesium
06 p0683 N73-15561
Toxicity of pyrolysis products from chlorotrifluroethylene-ethylene copolymer Halar resin
[AD-751436] 07 p0748 N73-16080
Production of HCN by pyrolysis of hydrocarbons in nitrogen plasma
[NASA-TT-F-14685] 07 p0854 N73-16925
Papers presented at conference on mechanisms of pyrolysis, oxidation, and burning of organic materials
[NBS-SP-357] 08 p0880 N73-17129
Pyrolysis of organic compounds in gas phase
08 p0881 N73-17131
Analysis of pyrolysis mechanisms in hydrocarbons
08 p0881 N73-17132
Pyrolysis mechanisms for three classes of polymers
08 p0881 N73-17134
Patterns and problems in pyrolysis behavior of synthetic addition polymers
08 p0881 N73-17135
Pyrolysis and combustion of cellulosic materials
08 p0883 N73-17147
Surface pyrolysis boundary condition for combustion of polymers
08 p0883 N73-17148
Reaction kinetics of fluoride pyrolysis in liquid rocket propellant
[AD-752564] 08 p0970 N73-17931
Production of large carbon fibers by impregnation with phenolic resin and carbonizing composite fiber
[NPL-IMS-18] 09 p1052 N73-18580
Pyrolysis of rhenium chlorides to yield chemically vapor deposited rhenium thermionic emitters
[NASA-CR-121143] 09 p1073 N73-18759
Pyrolysis gas chromatography method for rapid identification of organic polymers
[AD-755375] 12 p1377 N73-21168
Oxide formations in thermal vacuum decomposition of rare earth oxalates
[BARC-631] 15 p1747 N73-24162
Pyrolysis-molecular weight chromatography of polymers
[AD-758711] 16 p1872 N73-25154
Silicon epitaxial films obtained by thermal decomposition of silane
18 p2188 N73-27666
Effects of crystallization conditions on properties of autoepitaxial and heteroepitaxial layers of silicon obtained by hydride pyrolysis
18 p2188 N73-27667
Pyrolysis products of flame retardant treated cellulose
19 p2351 N73-28913
Decomposition products of polyurethane foam related to aircraft cabin flash fires
[AD-763327] 22 p2730 N73-31846
Pyrolysis of heterocyclic polymer compounds
[AD-764720] 24 p2892 N73-33091

**PYROLYTIC GRAPHITE**
Computation of thermochemical ablation rates of pyrolytic graphite surfaces using FORTRAN 4 computer code - Vol. 1
[AD-745440] 01 p0071 N73-10579
FORTRAN 4 program to compute thermochemical ablation rates of pyrolytic graphite surfaces as function of surface temperature and pressure including flow charts and program listings
[AD-744854] 01 p0117 N73-10969
Pyrolytic carbon deposition in steady state fluidized beds
[AD-748223] 03 p0323 N73-12631
Development of semi-empirical expression for specific surface oxidation rate of soot for application to design of combustion chambers
10 p1223 N73-19943
Preparation and testing of pyrolytic graphite film polymeric matrix laminates
[AD-761124] 18 p2168 N73-27510
Irradiation of pyrolytic carbon sealers at high temperatures to determine effects on growth rate and service life
[CONF-730601-5] 21 p2563 N73-30543

**PYROLYTIC MATERIALS**
NT PYROLYTIC GRAPHITE
Deposition process investigation of steady-state fluid beds to observe carbonization of pyrolytic materials
[AD-757118] 14 p1682 N73-23647

**PYROMETERS**
NT RADIATION PYROMETERS
Measuring flame temperature in exhaust nozzle and combustion chamber by pyrometer
04 p0420 N73-13425
Fabrication and evaluation of cooled-gas pyrometer for application in hypersonic research engine program
[NASA-TM-X-2715] 07 p0800 N73-16496
Characteristics of photoelectric pyrometer for measuring temperature of thin wire during rolling process
[NLL-M-21634-[5828.4F]] 15 p1785 N73-24471
Black body temperature of double pyrgeometer with two net radiometers
20 p2403 N73-29313
Atmospheric attenuation of CO2 laser radiation measured by pyroelectric detection noting fog absorption and optical communication application
[LCR-DR-1-72-67/1/R] 23 p2801 N73-32404

**PYROMETRY**
U TEMPERATURE MEASUREMENT

**PYROTECHNICS**
Bibliography on pyrotechnics
[AD-752700] 09 p1100 N73-18976
Apollo experience report on use of pyrotechnic devices in systems of Apollo spacecraft
[NASA-TN-D-7141] 10 p1215 N73-19878
Generation of narrow high current pulses
10 p1228 N73-19980
Combustion rates for binary pyrotechnic compositions in rarefied air
[AD-756043] 13 p1591 N73-22898
Structural stability testing of aerospace components under pyrotechnic loading conditions using subscale plastic models
[NASA-CR-128911] 14 p1715 N73-23914
Design and performance of launcher illumination XM-183 flare package for parachutes
[AD-757731] 15 p1844 N73-24940
Development and characteristics of squib actuated explosive disconnect for spacecraft release from launch vehicle
[NASA-CASE-NPO-11330] 17 p2096 N73-26958
Bibliography on metallic fuels for pyrotechnic compositions
[AD-759761] 17 p2097 N73-26963
Analysis of chlorate candle generated oxygen
[AD-762276] 19 p2231 N73-27992
Description of pyrotechnic systems principles with application to systems and equipment on space shuttle
[NASA-CR-2292] 21 p2600 N73-30840
Laser ignition of pyrotechnic compositions being considered as drag reducing fumers
[AD-765415] 23 p2858 N73-32834

**PYROXENES**
Chemical analyses of orthopyroxene and clinopyroxene composition of chondrites
[NASA-TM-X-62259] 15 p1830 N73-24835
Terrestrial analogs of placioclase feldspar and pyroxene
[RM-574] 18 p2196 N73-27731
Diopside submicroscopical twinning in lunar and experimentally deformed pyroxenes
[NASA-CR-133271] 20 p2486 N73-29970

**PYROXYLIN**
U CELLULOSE NITRATE

**PYRROLES**
NT INDOLES
Erythrocyte preservation in blood transfusion practice by cryogenic freezing with polyvinylpyrrolidone
[NASA-TT-F-14590] 04 p0378 N73-13076
Synthesis of high temperature clothing from hexahydrobenzodipyrrole monomers
[AD-750380] 06 p0689 N73-15609

**PYRRONES [TRADEMARK]**
Annotated bibliography of research and development of high temperature stable polymeric systems
[NASA-TM-X-2641] 03 p0320 N73-12608
Techniques for preparation of Pyrrone structural foams for use as honeycomb filler
[NASA-CR-2222] 09 p1052 N73-18574

**P3V AIRCRAFT**
U P-3 AIRCRAFT


# Q


**Q DEVICES**
Anomalous radial plasma losses in Q machine with mirror magnetic fields
[UCRL-51207] 03 p0343 N73-12794
Measurement of effective collision frequency in RF heating through decay instability in Q device plasma
[CONF-720705-2] 07 p0755 N73-16136
Electron temperature fluctuations of ionized plasma in Q device
[AD-751256] 07 p0830 N73-16731
Literature on thermodynamics of electrostatic waves and ionized plasmas
[AD-754014] 10 p1198 N73-19745
Parallel wavelength effects on drift waves in collisional potassium Q machine plasmas
12 p1432 N73-21607

Very high stability microwave oscillator with Q superconducting cavity
[AD-763684] 21 p2518 N73-30196
Q FACTORS
Circuit configuration for high Q factor selective amplifier
[REPT-1370] 05 p0522 N73-14245
Configuration of all pass network with negative real poles and Q factor
[PUBL-1367] 05 p0522 N73-14246
Q SWITCHED LASERS
Optical properties of laser resonators with spinning prism Q switch
[WRE-TN-658[AP]] 02 p0180 N73-11461
High speed holography of high speed phase object using Q switched laser outputs
[ISL-10/71] 02 p0181 N73-11471
Design and operation of amplitude stabilized pulsed laser operating at approximately 1.06 microns in fundamental transverse mode
[AD-746512] 02 p0182 N73-11474
Neodymium doped Q-switched laser glass illuminator oscillator
[AD-749511] 04 p0430 N73-13506
Absorption of laser radiation by laser produced plasma
[AD-749043] 04 p0457 N73-13727
Analysis of damage to thin films and substrate surfaces during irradiation by Q switched ruby laser
05 p0556 N73-14512
Analysis of laser damage to thin film coatings caused by radiation from Q switched ruby laser
05 p0556 N73-14514
Focused one joule pulse and Q switched ruby laser for optical production and detection of ultrasonic waves in metals for nondestructive tests
05 p0609 N73-14954
Designing light weight Q switch laser transmitter for rangefinders
[AD-750383] 06 p0680 N73-15536
Laser induced damage in ruby and sapphire crystals at 6943 A
[AD-751928] 08 p0930 N73-17613
Frequency stable Q switched carbon dioxide laser oscillators, free-running and injection locked pulsed lasers, and optical heterodyne measurements of frequency stability
[AD-753605] 09 p1045 N73-18523
Growths of barium and strontium niobate laser materials for electro-optical Q-switching of visible and near infrared radiation
[AD-752445] 09 p1076 N73-18779
Time development of line radiation emitted from plasma produced by Q switched ruby laser onto magnesium target
[AD-755119] 11 p1328 N73-20775
Examination of Q switched ruby laser produced spherical shock waves
13 p1508 N73-22220
Laser interaction with high density lithium plasma
15 p1816 N73-24718
Measurement of resonant second harmonic generation in exciton of copper chloride and zinc oxide using Q-switched ruby laser
20 p2424 N73-29474
Vibration-rotation relaxation using mode locked and Q switch gas lasers
[AD-763292] 21 p2555 N73-30481
Normal mode laser and Q switched laser for vaporization of graphite and carbides
[SLA-73-5233] 22 p2681 N73-31473
QSO [RADIO SOURCES]
U QUASARS
QUADRATIC EQUATIONS
Kalman filter equations for calculating quadratic forms for turn detector
[AD-744582] 01 p0028 N73-10220
QUADRATIC PROGRAMMING
Application of quadratic programming to optimize parameters of dynamic systems
21 p2515 N73-30172
QUADRATURE APPROXIMATION
U QUADRATURES
QUADRATURES
Radiometer quadrature control and measuring system using optical coupling circuitry
[NASA-CASE-MFS-21660-1] 04 p0421 N73-13434
Methods for computing numerical quadrature of integrable function over finite inerval
[NASA-TM-X-66277] 18 p2169 N73-27518
QUADRUPOLE LENSES
U MAGNETIC LENSES
QUADRUPOLES
Confinement of electron-free plasmas in quadrupole RF electric trap
[NASA-TM-X-65719] 01 p0085 N73-10703
Ionospheric transfer impedance of rocket-borne quadrupole probe near lower hybrid resonance
[NRC-TT-1614] 06 p0666 N73-15414
Design and development of mass spectrometer using quadrupole fields to stabilize ions based on mass of ions
06 p0672 N73-15468
Oblique plasma resonance measured from quadrupolar impedance probe noting motion effect of plasma parallel to geomagnetic field
[GRI/NTP/110] 13 p1563 N73-22669
Modified quadrupole mass spectrometer for in situ space simulation thermal vacuum testing of sophisticated payloads
[NASA-TM-X-64775] 21 p2549 N73-30435
QUALITATIVE ANALYSIS
Description of linear polyethylene standard reference material
[NBS-SP-260-42] 02 p0192 N73-11552
Quantitative, qualitative, and cost analyses of ERTS-1 imagery
[REPT-11215-1-F] 09 p1025 N73-18371
Thin layer chromatography for qualitative analyses on steelwork materials
[PB-214232/1] 16 p1871 N73-25148
QUALITY
NT ENVIRONMENTAL QUALITY
QUALITY CONTROL
Regional air pollution study and air quality control
[PB-210017] 01 p0077 N73-10636
ALSEP developments, and environmental and quality control tests
[NASA-CR-128580] 01 p0103 N73-10847
Automatic analog to digital assembly for measuring electronic equipment characteristics
[CEA-CONF-1966] 03 p0302 N73-12468
Photographic film density and density distribution measurements, and mean square deviation of density and energy spectrum
[NASA-TT-F-14614] 04 p0420 N73-13427
History, organization, and functions of the National Bureau of Standards to include description of test equipment used for research projects
[NBS-SP-367] 05 p0524 N73-14259
Evaluation of concept for determining edge sharpness and transfer characteristics of photographic materials
[NASA-TT-F-13922] 05 p0547 N73-14445
Stress wave emission techniques for monitoring weld quality and structural validation
[AD-745822] 05 p0552 N73-14486
Application of ultrasonic nondestructive tests to vehicle tire compliance measurements
[PB-211892] 05 p0553 N73-14491
Bulk characteristics mapping for quality control of semiconductor wafer junctions
[BDX-613-604-REV] 05 p0586 N73-14769
Specification for group delay variation in upper video band of television transmission system based on chrominance pulse tests
[BBC-1972/39] 06 p0638 N73-15181
Assessment of luminous and spectral sensitivity and electro-optical properties of image tubes
[BARC-610] 08 p0888 N73-17194
Computer based automation for performing material handling, assembly, and quality control tasks
[AD-752464] 08 p0928 N73-17601
Production methods, quality control, and metallurgical uses of pure rare earth metals and alloys
[IS-2968] 10 p1172 N73-19538
HCL processing effects on electrical stability and quality of thermally grown SiO2
[AD-754110] 10 p1202 N73-19786
Development of quality monitoring system for water recovery cycle in weightlessness environment
[NASA-CR-112267] 11 p1250 N73-20144
Quality control procedures for Skylab electron-proton spectrometer equipment and parts
[NASA-CR-128853] 11 p1292 N73-20484
Relationship between temperature and surface layer quality of two row roller bearings polished with abrasive cloth
[AD-754678] 11 p1301 N73-20559
Quality control for rawinsonde data dissemination to ships
[NOAA-TM-NWS-NMC-52] 11 p1314 N73-20663
Quality control of welded, brazed, and bonded electrical terminations
[BDX-613-613-REV] 12 p1383 N73-21214
Qualitative reliability indices of semiconductor thermoelectric devices
[AD-756898] 13 p1503 N73-22184
Quality control and composition of grinding wheels discussing microstructure and chemistry
[CRIF-MC-45] 13 p1530 N73-22399
Grinding wheel hardness determined from modulus of elasticity calculation
[CRIF-NT-9] 13 p1530 N73-22401
Application of holographic interferometry for inspection of large aircraft structures during manufacturing and maintenance
[AD-757510] 14 p1604 N73-23000
Reliability and quality control procedures for development of test equipment used on lunar experiment projects - Vol. 3
[NASA-CR-128920] 14 p1705 N73-23837
Development of guidelines for application to production of spacecraft hardware components with long lifetime - Vol. 1
[NASA-CR-128905] 14 p1707 N73-23853
Qualification plan for the Apollo ultraviolet spectrometer experiment, revision
[NASA-CR-128572] 16 p1916 N73-25503
Contamination control program plan for Apollo ultraviolet spectrometer experiment
[NASA-CR-128575] 16 p1916 N73-25506
Quality control requirements for Apollo ultraviolet spectrometer experiment
[NASA-CR-128584] 16 p1916 N73-25510
Interface control documenation for design and development of Apollo ultraviolet spectrometer experiment
[NASA-CR-128550] 16 p1917 N73-25511
Design and testing of high power microwave components for communications satellites
[NASA-CR-120927] 17 p1998 N73-26152
Electronic failure and quality control of microcircuit devices
[AD-759846] 17 p2005 N73-26215
Test methods for evaluating electrical power supply characteristics
[AD-759926] 17 p2005 N73-26218
Nondestructive testing of welded silicon solar cell silver interconnections
[ESS/SS-397] 17 p2038 N73-26487
Design, materials, fabrication, and testing in DART thruster technology development
[LA-5017-MS] 17 p2077 N73-26802
Quality control policies of DOD and application to weapon system acquisition management
[AD-762000] 19 p2305 N73-28540
Fokker F-28 fellowship structure adhesive bonding processes and quality control methods
[FOK-K-67] 21 p2497 N73-30037
Real time holographic interferometry for optical surface testing
[BMFT-FBT-73-01] 22 p2681 N73-31479
Impact of highway transportation control strategies on Los Angeles air pollution and quality
[PB-221301/5] 22 p2696 N73-31597
Transportation control measures to improve air quality standards in Greater Houston area by 1977
[PB-221611/7] 22 p2696 N73-31598
Apollo experience report on reliability of Apollo spacecraft based on application of proven reliability and quality control techniques
[NASA-TN-D-7438] 22 p2720 N73-31769
Michelson interferometry quality control of Schmidt plate replica by [Jouan Quetin] grating copying technique noting Kerber profile
[OPT-001-72] 23 p2794 N73-32351
QUALITY FACTORS
U Q FACTORS
QUANTITATIVE ANALYSIS
Distillation method for quantitative determination of oxygen solubility in sodium
[NLL-RISLEY-TR-2424-[9091.9F]]
02 p0136 N73-11105
Quantitative analysis of HF chemical CW laser including influence of stimulated emission on reacting medium
[AD-746685] 03 p0311 N73-12535
Gas chromatographic method for quantitative analysis on hydrazine and its breakdown products at catalytic activity levels
[NASA-TT-F-14722] 04 p0386 N73-13137
Iodoantimonous acid for quantitative yield estimation of antimony trace concentrations by spectrophotometric method
[AREAEE-126] 04 p0433 N73-13531
Quantitative analysis on divacancy to monovacancy concentration ratios in quenched platinum and effects of storage and electropolishing
[COO-3158-5] 04 p0434 N73-13538
Ion microscopic measurements on divacancy and monovacancy concentrations in high purity platinum
[NYO-3504-55] 04 p0434 N73-13541
Capabilities and limitations for quantitative nondestructive testing of aerospace structures
[NASA-TM-X-64706] 05 p0552 N73-14483
Dual hologram interferometry for calculating density distributions from refraction index changes
[AD-749872] 05 p0559 N73-14538
Preparation of porous metal samples for quantitative metallographic analysis and effects of procedure on accuracy of results obtained
[NLL-TRANS-746-1255-[9022.401]]
05 p0561 N73-14555
Neutron activation analysis applied to determine bismuth content of meteorites and standard rocks
07 p0840 N73-16809
Quantitative, qualitative, and cost analyses of ERTS-1 imagery
[REPT-11215-1-F] 09 p1025 N73-18371
Quantitative analysis of irreversible portion of radiation damage combined with gamma rays and acceleration
11 p1242 N73-20082
Quantitative analysis of radiation measurements from polar and geosynchronous satellites
[NASA-CR-130194] 13 p1551 N73-22568
Accuracy of various tracer methods for measuring body water compartments during bed rest
[NASA-TR-R-406] 15 p1744 N73-24133

Design of counter tube window and X ray fluorescence analyzer for quantitative analysis of Venusian dust and condensates
[NASA-CR-114619] 15 p1786 N73-24484
Quantitative bismuth determination in stainless steels
[PB-214234/7] 16 p1929 N73-25612
Application of phosphorimetry procedures to quantitative chemical analysis of several aqueous solutions
[PAPER-76A6-743] 21 p2546 N73-30409
Data reduction procedure for quantitative electron probe microanalysis
[NBS-TN-769] 21 p2549 N73-30433
Quantitative analysis of stratospehric aerosol characteristics from Skylab data
[E73-11009] 22 p2660 N73-31314
Quantitative determination of Statospheric aerosol composition over western United States
[E73-11138] 24 p2918 N73-33293

**QUANTIZATION**
U MEASUREMENT

**QUANTIZER**
U COUNTERS

**QUANTUM COUNTERS**
Measurement of quantum yields using chemistry, laser technology, photodetector instrumentation, and calorimetry
[PAPER-76A6-742] 21 p2546 N73-30408

**QUANTUM ELECTRODYNAMICS**
Abstracts of papers presented at conference on coherence and quantum optics
[AD-746712] 02 p0183 N73-11487
Diagram solutions of circuits forming high frequency electromagnetic fields in plasma devices
[AEC-TR-7326] 07 p0826 N73-16696
Research and development of lasers and laser-related equipment in the Soviet Union - bibliography
[AD-753098] 09 p1043 N73-18510
Physical equivalence of null plane quantum electrodynamics in null plane gage to conventional electrodynamics in Coulomb gage
09 p1066 N73-18700
Quantum electrodynamics in high magnetic fields
[AD-753042] 09 p1067 N73-18710
Quantization of free spin-two fields on light front
[ILL-(TH)-73-1] 11 p1326 N73-20764
Null plane quantum electrodynamics
15 p1814 N73-24699
Development of classical electron theory
15 p1815 N73-24710
Phonon dispersions and three particle correlations in liquid helium, and adsorbed helium monolayers
16 p1944 N73-25730
Structure of high spin particle propagator
[DPGU-01-73] 20 p2456 N73-29734
Electron beam devices, quantum electronic devices, plasmas, and solid state devices
[AD-764808] 24 p2932 N73-33415

**QUANTUM GENERATORS**
U STIMULATED EMISSION DEVICES

**QUANTUM MECHANICS**
NT PAULI EXCLUSION PRINCIPLE
NT QUANTUM ELECTRODYNAMICS
Charged particle motion in nonhomogeneous field with Coulomb potential
[NOTA-INTERNA-383-B] 01 p0084 N73-10697
Application of Schroedinger equation to solve inverse scattering problem at fixed energy in quantum mechanics
02 p0199 N73-11609
Numerical analysis of quantum mechanical theory of scattering of particle by spherically symmetrical potential
02 p0199 N73-11610
Numerical analysis of inverse scattering problem at fixed angular momentum for nonlocal separable interactions
02 p0199 N73-11611
Analysis of exact and approximate methods for solving inverse scattering problem for transmission lines
02 p0199 N73-11612
Jost-Kohn inversion procedure applied to quantum mechanical problem
02 p0201 N73-11627
Comparative evolution of inverse problems and various mathematical methods used
02 p0201 N73-11629
Chronological development of multidimensional inversion techniques
02 p0202 N73-11630
Generalized Airy functions, using one dimensional, time independent, Schroedinger equation
[NASA-CR-129604] 03 p0324 N73-12638
Gauge invariant atomic orbitals and current conservatism within quantum mechanical formalism
[NASA-CR-129246] 03 p0339 N73-12762
Time evolution of quantum lattice system Hamiltonian discussing automorphism of suitable algebra
[NOTA-INTERNA-393] 03 p0340 N73-12774
Development of cosmological models based on Einstein field equations with random perturbations of long wave lengths superimposed on unperturbed models
[AD-747505] 03 p0357 N73-12911
Analysis of resolvability of point sources of incoherent light by quantum detection, decisions of observers, and error probability
[NASA-CR-130129] 04 p0449 N73-13663
Noncommuting observables in quantum detection and estimation theory, and application to analysis of coherent signal in harmonic oscillator
[NASA-CR-129694] 04 p0449 N73-13664
Research in analytical methods in nonrelativistic field theory and singular perturbation theory in kinetic theory
[AD-750482] 06 p0702 N73-15721
Josephson junctions and superconducting quantum interference devices
[NBS-TN-630] 06 p0707 N73-15772
Quantum mechanics for describing operational properties of gas laser containing saturable absorber in resonator
12 p1409 N73-21421
Quantum mechanical Racah and Stevens operators used in magnetism theory
[RISO-259] 12 p1429 N73-21580
Correlation energy of quantum mechanical electron gas in intense magnetic field
[NUB-2178] 12 p1431 N73-21597
Quantum physics of liquid helium
[MATSCIENCE-73] 15 p1814 N73-24704
Quiton/perception physics of being, time, space, existence, perception, and physical phenomena
[AD-763210] 21 p2580 N73-30680
Quantum detection and estimation in optical communication systems
22 p2679 N73-31460
Density matrix methods developed and applied in investigation of electronic structure of atoms
[AD-763815] 22 p2709 N73-31692

**QUANTUM NUMBERS**
String models for theoretical study of high energy collisions involving large quantum numbers
[LPTHE-73/22] 21 p2581 N73-30688
Mass formula calculations on baryonic resonances using radial excited symmetric quark model
[TR-74-018] 22 p2701 N73-31636

**QUANTUM STATISTICS**
Application of Schroedinger equation to solve inverse scattering problem at fixed energy in quantum mechanics
02 p0199 N73-11609
Off-diagonal long range crystalline order and vortex lattices in Bose system
24 p2967 N73-33708

**QUANTUM THEORY**
Quantum corrections to trajectories of radiating fast electrons in magnetic field
[NASA-TT-F-14495] 01 p0083 N73-10688
Development of inverse scattering problem and approach to nonrelativistic problem at fixed angular momentum
02 p0199 N73-11608
Numerical analysis of inverse scattering problem at fixed angular momentum for nonlocal separable interactions
02 p0199 N73-11611
Analysis of exact and approximate methods for solving inverse scattering problem for transmission lines
02 p0199 N73-11612
C-shaped and symmetric dc and RF, voltage-biased superconducting quantum interference devices
[FOA-2-B-2034-E1] 02 p0218 N73-11763
Model for operating partly resistive superconducting point contact, quantum interference device
[FOA-2-B-2035-E1] 02 p0218 N73-11764
Long-range forces between atoms at large distances, and weak forces arising from neutrino-antineutrino exchange
[TR-73-049] 03 p0339 N73-12764
Bjorken scaling in deep inelastic electron proton scattering and parton models
[NOTA-INTERNA-391] 03 p0340 N73-12773
Development of cosmological models based on Einstein field equations with random perturbations of long wave lengths superimposed on unperturbed models
[AD-747505] 03 p0357 N73-12911
Electron-impurity spin interchange model for analyzing magnetic properties of diluted magnetic alloys at low temperatures
08 p0931 N73-17626
Analysis of support properties of scaling function for time-like virtual photons using simple perturbative model
[LPTHE-72/28] 10 p1192 N73-19696
Necessity of probability conservation law in quantum theories of gravitation
12 p1393 N73-21296
Scalar quantum field theory in closed universe of constant curvature
15 p1813 N73-24690
Nonrenormalizable interactions as low-energy limits of renormalizable ones
15 p1813 N73-24698
Application of Boson method to quantum field theory computations and mixed state of type 2 superconductors
23 p2825 N73-32582

**QUARKS**
Meson resonance production in missing mass spectra using quark model for negative pion proton yields proton negative x diffraction calculation
[TUEP-72-41] 07 p0823 N73-16667
Naive quark pair creation model and centrifugal barrier effect in baryon decays
[LPTHE-73/11] 20 p2456 N73-29736
Harmonic oscillator quark model of hadrons with relativistic internal velocities for quarks
[LPTHE-73/15] 20 p2456 N73-29739
Mass formula calculations on baryonic resonances using radial excited symmetric quark model
[TR-74-018] 22 p2701 N73-31636

**QUARRIES**
U MINES [EXCAVATIONS]

**QUARTZ**
Using quartz oscillators sensitive to temperature variations for frequency stabilized thermostats
[PUBL-1366] 06 p0647 N73-15253
Radiation testing of swept synthetic quartz resonators with high-purity platinum electrodes
[AD-752584] 08 p0891 N73-17209
Quartz tube, tungsten filament lamp bank for characterization of nonmetallic thermal protection materials for high irradiance environment
[AD-752606] 08 p0893 N73-17231
Analysis of quartz and piezoelectric ceramic components for application in high frequency bandpass filters
[REPT-4.387] 12 p1383 N73-21219
Repackaging of broadband quartz torsional accelerometers for borehole use
[AD-755852] 13 p1531 N73-22410
Manufacture of quartz gyroscopes for application to General Relativity Satellite
13 p1593 N73-22920
X ray reflection efficiency of nickel coated quartz optical flats
[NASA-TM-X-64747] 15 p1813 N73-24694

**QUARTZ CRYSTALS**
Use of quartz and corundum monocrystals to verify dilatometric measurements in USSR
[AD-745840] 01 p0059 N73-10480
Development of interaction gradient concept and application to laser radiation damage to quartz crystals, fused quartz, and laser glass samples
05 p0554 N73-14500
Mechanisms for X irradiation induced transient changes in elastic modulus of quartz resonators
[SC-DC-72-1240] 05 p0587 N73-14771
Development of single sideband quartz crystals for use in temperature compensated crystal oscillators
[AD-749642] 06 p0646 N73-15244
Kinetics of quartz crystal growth and radiation effects on quartz resonators
[AD-750467] 06 p0711 N73-15803
Design, processing, and measurement of precision single sideband crystal units
[AD-751748] 07 p0833 N73-16754
Piezoelectric quartz crystals used as digital transducers in completely digital detection systems for monitoring gas streams
12 p1382 N73-21208
Single sideband quartz crystal with long term aging
[AD-761101] 18 p2125 N73-27170
Packaging of precision quartz crystal resonators and effect on aging and thermal hysteresis
[AD-763215] 21 p2519 N73-30202
Contamination tests of Vacuum Chamber A and cryogenic/vacuum study of quartz crystal microbalance
[NASA-TM-X-64776] 21 p2521 N73-30220
Analysis of data from quartz crystal microbalance contamination monitors on Skylab
[NASA-TM-X-64778] 22 p2673 N73-31412

**QUARTZ LAMPS**
Light shield and cooling apparatus for high intensity ultraviolet lamps
[NASA-CASE-LAR-10089-1] 04 p0426 N73-13474

**QUASARS**
Formation of relativistic particles into clouds in quasar and Seifert nuclei, and centimeter, submillimeter, and gamma radiation emissions
[NP-30] 06 p0717 N73-15854
Solution of ionization and thermal equilibrium equations for gas clouds in quasars and Seyfert galaxies ionized by ultraviolet radiation sources
07 p0839 N73-16801
Applications of Schmidt telescopes to study astrometry, photometry, galactic structure, quasars, and stellar spectra
07 p0844 N73-16840
Application of Schmidt telescopes to study of galactic clusters and evolution noting new emulsion, infrared surveys, luminosity, and quasars
07 p0845 N73-16849
Observation of quasars with Schmidt cameras and compilation of light curve for BL Lacertae
07 p0845 N73-16850
Importance of Schmidt telescopes to radio astronomy noting color identification of quasars and Southern Hemisphere sky survey
07 p0845 N73-16851

Luminosity function of quasars based on comparison of data on optically selected quasars and quasars in radio catalog
[NASA-CR-131111] 10 p1213 N73-19864
Results of observing quasar compact components and radio galaxies made with radio interferometer having limited angular resolution
[NASA-TT-F-14902] 14 p1619 N73-23117
Tables on structure of interstellar masers and quasars
14 p1704 N73-23826
Radio interferometer observations of compact components of quasars and radio galaxy cores
[NASA-TT-F-14698] 15 p1831 N73-24839
Properties of optical radiation of variables and quasers
20 p2471 N73-29847
Rapid flux, relativity, black holes, and pulsar, and quasar models
[NASA-TM-X-62298] 23 p2846 N73-32742
QUASI-PARTICLES
U ELEMENTARY EXCITATIONS
QUASI-STELLAR RADIO SOURCES
U QUASARS
QUASILINEARITY
U NONLINEARITY
QUENCHING [COOLING]
Quantitative analysis on divacancy to monovacancy concentration ratios in quenched platinum and effects of storage and electropolishing
[COO-3158-5] 04 p0434 N73-13538
Use of low temperature quenching techniques to retain simple vacancy defects in magnesium
[NLL-CE-TRANS-5944-[9022.09]]
05 p0561 N73-14559
Microstructure and mechanical properties of rapidly quenched liquid and powder metal alloys
[AD-749679] 05 p0564 N73-14578
Measurement of fluorescence yield in self quenched and foreign gas quenched NO2
[NASA-CR-131296] 11 p1285 N73-20426
Billet processing from rapidly quenched liquid metals
[AD-757677] 14 p1678 N73-23621
Thermal quenching of luminescence and conformational transformations in macromolecules of some polymers
[NRC-TT-1631] 15 p1815 N73-24711
Vapor quenching in ultra-high vacuum of amorphous silicon films
[AD-758267] 15 p1821 N73-24765
Induction heating and concomitant quenching for hot winding helical springs
[AD-759906] 17 p2039 N73-26495
QUEUEING THEORY
Variance of Monte Carlo estimates reduced by correlated and antithetic sampling and illustrated by queueing simulation
[NA-70-21] 03 p0324 N73-12643
Combinations of antithetic sampling methods to determine minimum variance linear combination, with queueing simulation example
[NA-72-49] 03 p0325 N73-12646
Combination of several sampling methods to simulate queueing systems
[NA-72-58] 03 p0325 N73-12648
SMAC with two manual methods and one computer program with queueing simulation up to five parallel servers or up to three series servers
05 p0610 N73-14956
Feedback queueing model with interference caused retransmission for space to surface data transmission
[AD-756568] 13 p1492 N73-22093
QUIET ENGINE PROGRAM
Aerodynamic component test results of Fan C, high-bypass-ratio, low-aerodynamic loading, single stage fan
[NASA-CR-120981] 02 p0222 N73-11799
Conference on reduction and suppression of aircraft engine noise
[NASA-SP-311] 03 p0249 N73-12012
Quiet Engine Program technology application to low noise aircraft development
03 p0249 N73-12013
Noise output from quiet engine during simulated takeoff and approach tests
03 p0250 N73-12021

## R

RABBITS
Fever generation in rabbits by intravenous injection of table salt
[NASA-TT-F-14677] 07 p0745 N73-16063
Hypothermy effects on drug actions in physiological rabbit functions
11 p1240 N73-20064
Dynamics of some characteristics of induced potential of optical region in cerebral cortex in rabbits with increasing hypoxia
11 p1244 N73-20103
High altitude acclimatization effects on mice and rabbit tolerances to hypoxia, acceleration, and high temperature
[NASA-TT-F-14861] 11 p1247 N73-20123
Effects of gastrointestinal pressure on rabbit eye nystagmus during barotrauma
13 p1479 N73-21983
Gastrointestinal proprioceptor effects on high altitude rabbit ocular reflexes
13 p1479 N73-21984
Correlation between primary response and late slow oscillation of evoked potential in response to light in awake and anesthetized rabbits
24 p2889 N73-33069
RACAH COEFFICIENT
Quantum mechanical Racah and Stevens operators used in magnetism theory
[RISO-259] 12 p1429 N73-21580
RACKS [FRAMES]
Design and development of test stand system for supporting test items in vacuum chamber
[NASA-CASE-MFS-21362] 11 p1265 N73-20267
RACON BEACONS
U RADAR BEACONS
RADAR
NT COHERENT RADAR
NT CONTINUOUS WAVE RADAR
NT DOPPLER RADAR
NT METEOROLOGICAL RADAR
NT MONOPULSE RADAR
NT MOVING TARGET INDICATORS
NT OPTICAL RADAR
NT PULSE RADAR
NT RADAR MEASUREMENT
NT RANGE AND RANGE RATE TRACKING
NT SATELLITE-BORNE RADAR
NT SEARCH RADAR
NT SIDE-LOOKING RADAR
NT SURVEILLANCE RADAR
NT TRACKING RADAR
Combined radar-radiometer for remote sensing at microwave performance
[NASA-CR-128492] 03 p0265 N73-12145
Design and fabrication of radar attitude sensing system
[NASA-CR-128684] 04 p0388 N73-13157
Computer techniques for prediction and analysis of OTH radar operation
[AD-748588] 04 p0390 N73-13170
Miss distance radar for air defense weapons testing
[AD-750323] 06 p0642 N73-15210
Uses and limitations of passive radar
[AD-750855] 06 p0642 N73-15215
Frequency modulated radar systems for range finding, velocity measurement, and altimeters
16 p1873 N73-25162
Recursive digital filters in moving target indicator of phased array radars
[AD-759901] 18 p2118 N73-27128
Interface microprogramming for radar array signal processing computer
[AD-762439] 19 p2238 N73-28041
Auroral clutter mapping with Homer backscattering radar to study reaction of upper atmosphere to nuclear explosions
[AD-762012] 19 p2297 N73-28474
Dielectric properties of ice, snow, and water at microwave frequencies and thickness measurements of ice and snow layers with radar
[CRC-1242] 21 p2537 N73-30341
Programs for control of SEL 86 radar operating system
[AD-763940] 22 p2635 N73-31119
Experimental radio and radar studies on lunar and planetary atmospheres and surfaces, interplanetary medium, and software and hardware conceptions
[NASA-CR-135670] 23 p2845 N73-32734
RADAR ALTIMETERS
U RADIO ALTIMETERS
RADAR ANTENNAS
Theoretical analysis of linear semi-infinite array of uniformly spaced elements to determine mutual coupling effects
[AD-745799] 01 p0034 N73-10263
Radar arrays with no phase shifters for air defense systems
[AD-750328] 06 p0642 N73-15211
Characteristics of shipboard radar antennas, antenna radiation patterns, and automatic target tracking systems
[AD-750871] 06 p0642 N73-15216
Optical design of radar antenna configurations with desired scattering patterns
[AD-755914] 12 p1380 N73-21193
Method for measuring mechanical deformations in parabolic dish of metric tracking radar
[AD-758371] 14 p1635 N73-23260
Computerized prediction of radar cross sections for thin wires and comparison with backscatter data
[AD-758757] 16 p1882 N73-25230
Properties and applications of radar antennas
[AD-759693] 17 p1998 N73-26159
Sidelobe level increase and gain reduction caused by raindrops on surface of radar antenna radome
[AD-759178] 17 p1998 N73-26160
Integration of Ku-band radiator with X-band antenna design for dual band capability
[AD-760816] 18 p2118 N73-27127
Digitizer performance under conditions of linear and circular antenna polarization
[FAA-NA-73-49] 20 p2376 N73-29095
Computerized simulation of monopulse radar antenna pointing errors due to ground reflection multipath propagation
21 p2507 N73-30114
Radar microwave link antenna pattern measurements
[FAA-RD-73-118] 22 p2631 N73-31087
Evaluation of phased array antennas
[AD-764367] 22 p2634 N73-31113
Low angle tracking and recognition using self focusing radar antenna
[AD-764052] 22 p2635 N73-31118
Dielectric lightweight aircraft radar antenna array
[AD-764685] 23 p2766 N73-32131
RADAR ASTRONOMY
Research in applications of radar and radio techniques to astronomy and space programs
[NASA-CR-129167] 02 p0226 N73-11829
Radio astronomy and radar observation program for Haystack antenna
[NASA-CR-130756] 08 p0959 N73-17842
Research in radio astronomy using Haystack antenna
[NASA-CR-130673] 08 p0960 N73-17852
Research in physical phenomena of space and planetary environments, and applications of radio technology
[NASA-CR-133856] 21 p2596 N73-30809
RADAR ATTENUATION
Doppler radar frequency attenuation in horizontally polarized field over forest
[AD-748104] 04 p0389 N73-13163
Digital computer routines for calculation of radar/radio tropospheric absorption and noise temperature
[AD-753197] 09 p1004 N73-18193
RADAR BACKSCATTER
U BACKSCATTERING
U RADAR SCATTERING
RADAR BEACONS
Simulator test to evaluate use of air traffic control radar beacon code assignment plan to provide interim radar data processing capability
[FAA-RD-72-103] 02 p0207 N73-11681
Discrete address radar beacon system for aircraft tracking and traffic control
[FAA-RD-72-117] 04 p0447 N73-13649
Analysis of methods for obtaining improved accuracy of aircraft position determination in Discrete Address Beacon system of air navigation
[TN-1972-38] 05 p0577 N73-14697
Analysis of excessive interrogation signals from Air Traffic Control Radar Beacon System and effect on operation of Jacksonville, Florida center
[ECAC-PR-72-014] 06 p0696 N73-15675
Analysis of excessive interrogation signals from Air Traffic Control Radar Beacon System and effect on operation of Washington, D.C. center
[ECAC-PR-72-022] 06 p0696 N73-15676
Analysis of excessive interrogation signals from Air Traffic Control Radar Beacon System and effect on operation of Los Angeles, California center
[ECAC-PR-72-044] 06 p0696 N73-15677
Analysis of Air Traffic Control Radar Beacon System performance and effects on several Air Route Traffic Control Centers
[ECAC-PR-72-023] 06 p0696 N73-15678
Survey of Air Traffic Control Beacon System to determine occurrence of excessive interrogation signals within New York air control sector - Final Report
[ECAC-PR-72-031] 07 p0818 N73-16630
Development and evaluation of discrete address beacon system for air traffic control applications
[FAA-RD-73-12] 11 p1255 N73-20184
Analysis of synchronized discrete address beacon system for improved air traffic control capability
[SD-FR-01] 11 p1256 N73-20189
Development and evaluation of aircraft tracking techniques based on radar and beacon target reports from common sensor site
[PX-6392] 12 p1378 N73-21177
Development and evaluation of cross-band radar/beacon system for operation with airport surveillance radar/air traffic control beacon interrogator system
[FAA-RD-73-38] 12 p1379 N73-21182
Portable beacon test site for enroute radar coverage in airport vicinity
[FAA-RD-73-49] 15 p1760 N73-24266
Discretely addressable radar beacon system with airborne transponders and ground-air-ground data link for air traffic control
[FAA-RD-73-48] 16 p1940 N73-25701
Proceedings of conference on operational problems of air traffic control beacon system
[FAA-NA-72-80] 16 p1940 N73-25702

Interface evaluation of digital simulation facility with system support facility for radar beacon target source for air traffic control
[FAA-NA-73-33] 17 p2009 N73-26248
Integration of Ku-band radiator with X-band antenna design for dual band capability
[AD-760816] 18 p2118 N73-27127
Automatic aircraft altitude reporting using air traffic control radar beacon system
[FAA-RD-73-44] 19 p2318 N73-28648
Development of discrete address beacon system for application to air traffic control operations
[FAA-RD-73-101] 21 p2577 N73-30651
Feasibility of ATC radar beacon system based on vehicle surveillance on airport surface in relation to vehicle time of arrival
[AD-763328] 21 p2577 N73-30655
Air traffic control radar beacon system interference in terminal areas
[MTR-6239] 23 p2816 N73-32512
Evaluation of air traffic control beacon alphanumeric system for automatic operation in low density airport towers and terminal facilities
[FAA-NA-73-54] 23 p2816 N73-32516

**RADAR CLUTTER MAPS**
Electronic scan phased array antenna system and digital clutter mapping system
[AD-751054] 07 p0758 N73-16158
Technical evaluation of weather clutter feasibility model to provide air traffic controllers with weather display of air traffic and contour depiction of weather detected by radar
[FAA-NA-73-48] 20 p2376 N73-29094

**RADAR CROSS SECTIONS**
Procedures for measuring radar cross section areas of extremely small objects in superhigh frequency ranges
[AD-749788] 05 p0515 N73-14186
Radio frequency measurement of brightness temperature and radar cross sections for explaining subsurface and atmospheric properties of Venus
07 p0840 N73-16803
Radar cross section measurements of snow and ice
[AD-752900] 09 p1004 N73-18192
Radar echo cross sections from pyramidal shape of reentry vehicle
[AD-753684] 09 p1005 N73-18200
Instrumentation for Nike-Ajax radar to perform real time cross section measurements on airborne targets
[AD-756538] 13 p1493 N73-22103
Radar cross section modulation power spectrum in periodic motion of scattering object
[AD-756488] 13 p1494 N73-22109
Computerized prediction of radar cross sections for thin wires and comparison with backscatter data
[AD-758757] 16 p1882 N73-25230

**RADAR DATA**
High resolution radar scattering data for determining refractive structure in troposphere
02 p0197 N73-11594
Computerized information processing for radar system by subdivisions and multiple decision making processes
04 p0389 N73-13158
Compression of satellite altimeter radar pulses and high resolution sea reflectivity
06 p0663 N73-15389
Processing digital radar data base to create simulated mapping-radar scope images
[AD-755722] 13 p1495 N73-22118
Determination of parameter s for characterizing meteoric distribution from SOM-1 radar data
17 p2023 N73-26371
Algorithm for computerized spectral analysis on linearly swept signals
[AD-760775] 18 p2120 N73-27138
Hybrid autocorrelator for high altitude incoherent scatter observations
20 p2417 N73-29417
Determination of mean time between successive false detections for binary signal detector with variable memory size
22 p2628 N73-31056
Dispersion of angular coordinate estimate during digital processing of radar data based on application of discrete Markov chains
22 p2628 N73-31058
Analysis of ionospheric response to solar eclipse of 7 March 1970 by Thomson scatter radar technique at Millstone Hill Ionospheric Observatory
24 p2912 N73-33239

**RADAR DETECTION**
Detection probability of log-normally distributed signals embedded in log-normally distributed noise as function of signal to noise ratio
[AD-745947] 02 p0143 N73-11157
Reconnaissance and surveillance countermeasures for radio electronic facilities
03 p0266 N73-12152
Radar observations of meteor trains for detecting high altitude gravity waves
05 p0511 N73-14154
Detailed digital simulation of Army Missile Command experimental array radar system for air defense against low altitude threats
[AD-749501] 05 p0514 N73-14177
Performance of dual wavelength hail detector considering meteorological and radar parameters
[TR-25] 06 p0639 N73-15191
Pulse radar sounding of sea ice thickness with video display
[JPRS-57841] 06 p0665 N73-15406
Remote detection and measurement of clear air turbulence using pulsed laser radar
[NASA-CASE-MFS-21244-1] 12 p1422 N73-21523
Design of extended Kalman filter for detection and ranging of ground radar from aircraft
[AD-760764] 18 p2123 N73-27158
Technical evaluation of weather clutter feasibility model to provide air traffic controllers with weather display of air traffic and contour depiction of weather detected by radar
[FAA-NA-73-48] 20 p2376 N73-29094
Application of prior information concerning location of objects in given ranges for calculating radar energy potential
22 p2630 N73-31074
Use of passive radar to determine range to target emitting radio signal
22 p2630 N73-31077
Energy spectrum and autocorrelation function of random processes at output of key detector
22 p2630 N73-31078
Transient effects in pulse radar hydrometeor detection
24 p2956 N73-33616

**RADAR DIRECTION FINDERS**
U RADIO DIRECTION FINDERS

**RADAR ECHOES**
NT CLUTTER
NT LUNAR RADAR ECHOES
NT VENUS RADAR ECHOES
Matrix method for calculating adaptive pre-whitening filter for radar echo signal processing
01 p0025 N73-10197
Radar backscatter produced by chaff cloud as function of position of radar relative to chaff cloud
[AD-744776] 01 p0029 N73-10226
Head echoes of meteoroids
01 p0102 N73-10840
Detection probability of log-normally distributed signals embedded in log-normally distributed noise as function of signal to noise ratio
[AD-745947] 02 p0143 N73-11157
Acoustic radar scattering in lower atmosphere for measuring wind velocity and direction
02 p0197 N73-11592
Numerical analysis of terrain echo spectrum from moving radar altimeter
[SC-DR-72-0261] 04 p0389 N73-13159
Detection of tropospheric turbulence and gravitational waves by radar sounding
05 p0510 N73-14151
RF electric field reflected by finite conducting plane target illuminated by small antenna
[AD-750088] 05 p0514 N73-14183
Aircraft measurements of microscale motions and atmospheric structure associated with thin echo layers in stable stratified zones
[AD-749512] 05 p0540 N73-14393
Matrix method for computing radar scattering cross sections of airplanes
[AD-750486] 06 p0643 N73-15217
Effect of ocean surface structure on narrow radar pulse shape
06 p0662 N73-15380
Sea state effects on altimeter signal scattering and radar wave form estimates
06 p0663 N73-15381
Composite scattering model for explaining rough sea surface scattering cross sections
06 p0663 N73-15383
Influence of sea state on short pulse radar satellite altimeter determination of mean surface position
06 p0663 N73-15385
Target recognition by considering space-time functions in radar echoes
[REPT-1-72] 09 p1003 N73-18184
Radar echo cross sections from pyramidal shape of reentry vehicle
[AD-753684] 09 p1005 N73-18200
Power density spectrum for statistical analysis of radar altimeter return variations due to radar motion
[SC-RR-72-0265] 10 p1129 N73-19197
Microwave frequency reflection characteristics of quasi-tapered anechoic chamber for radar echo tests
[AD-754203] 10 p1138 N73-19275
Load impedance and electromagnetic radar echo scattering
[AD-754899] 11 p1258 N73-20209
Optical design of radar antenna configurations with desired scattering patterns
[AD-755914] 12 p1380 N73-21193
Apollo 16 radar echo data for predicting blockiness of lunar surface
12 p1455 N73-21788
Radar clutter and false alarm probability by high frequency atmospheric noise
[AD-756842] 13 p1493 N73-22104
Auroral ionospheric measurements from incoherent scatter radar facility
[AD-757358] 14 p1664 N73-23504
Mathematical models and computer simulation for predicting spectral parameters of radar echoes from rain clouds
[STC-TM-308] 15 p1750 N73-24180
Feasibility of using computer system for echo detection and identification of moving targets
[AD-758266] 15 p1751 N73-24191
Transfer equation for calculation of doubly scattered lidar returns
17 p2039 N73-26497
Numerical solution for two dimensional electromagnetic scattering
[AD-760773] 18 p2119 N73-27137
Sea spectra and radar scattering
[AD-760693] 18 p2149 N73-27373
Algorithm for discrete transforms for implementing computer programs in radar signal processing
[AD-762437] 19 p2237 N73-28039
Signal modulation and digital processing for real time radar operation
[AD-762438] 19 p2238 N73-28040
Development of theories for radar sea return from wind-roughened waves
[AD-762073] 21 p2539 N73-30362
Application of microwave radar for monitoring tropopause level to determine dynamic instability and turbulence generation in clear atmosphere
[NOAA-TR-ERL-243-WPL-21] 22 p2665 N73-31353

**RADAR EQUIPMENT**
NT PLAN POSITION INDICATORS
NT RADAR ANTENNAS
NT RADAR BEACONS
NT RADAR FILTERS
NT RADAR RECEIVERS
NT RADAR REFLECTORS
NT RADAR TRANSMITTERS
Radar and microwave equipment and materials, and related research and development
[RRE-11] 01 p0023 N73-10181
Design and development of wideband TRAPATT amplifier in microstrip configuration for use in phased-array radar modules in S-band
[AD-747050] 02 p0150 N73-11215
Radar equipment for tracking meteor trails
[AD-745959] 02 p0169 N73-11372
Systems analysis and evaluation of perimeter acquisition radar equipment for use with Safeguard Antiballistic Missile System - Vol. 1B
[AD-748060] 03 p0267 N73-12161
System definition and methodology for selecting perimeter acquisition radar system used with Safeguard Antiballistic Missile System - Vol. 2
[AD-748061] 03 p0267 N73-12162
System definition and criticality analysis of perimeter acquisition radar system used with Safeguard Antiballistic Missile System - Vol. 3 Pt. 1
[AD-748062] 03 p0267 N73-12163
Quality control data and monitoring equipment specifications for hardness testing of antimissile radar defense system
[AD-748063] 03 p0268 N73-12169
Effect of various technical and operational factors on electromagnetic compatibility of radars operating in 2700 to 2900 MHz frequency band
[ECAC-PR-71-033] 04 p0388 N73-13155
Design and development of electronic equipment for antiaircraft defense to include radio equipment, command and control, and electronic countermeasures
[AD-748709] 04 p0400 N73-13254
Determining ion composition using high-potential radar sets with storage elements for detecting non-coherent scattered radio signals
04 p0413 N73-13373
Analysis of problems in mapping Venus surface with radar from orbiting spacecraft
[NASA-CR-129821] 04 p0477 N73-13900
Establishment of radar information transmission network for dissemination of meteorological data
[NLL-M-22692-[5828.4F]] 05 p0507 N73-14128
Target transmission in multistage radar systems
05 p0513 N73-14172
High resolution FM radar at X band for measuring snow and ice thickness
[CRC-TN-646] 06 p0639 N73-15184
Uses and limitations of passive radar
[AD-750855] 06 p0642 N73-15215
Effect of ocean surface structure on narrow radar pulse shape
06 p0662 N73-15380
Electrical and performance characteristics of Skylab radar altimeter
06 p0663 N73-15386
Characteristics and operation of videocoherent system for improved target acquisition and measurement of target velocity
07 p0755 N73-16133

Development and operation of matched incoherent radar systems to improve accuracy in range measurement and increase probability of target detection
07 p0755 N73-16134
Digital optical hybrid correlator for processing pulse Doppler and wideband radar signals
[AD-751695] 07 p0756 N73-16143
Characteristics of various types of remote sensors and identification of specific areas of application
07 p0784 N73-16373
Characteristics of radar equipment and microwave radiometers to show application to earth resources surveys
07 p0784 N73-16377
Operation and characteristics of primary radar system for air traffic control surveillance
[FAA-ED-02-1] 08 p0885 N73-17163
Independent radar systems using information processing, data correlation, and telecommunication
09 p1002 N73-18179
Military technology for marine radar design
[AD-754408] 11 p1259 N73-20215
Analysis of test films to assess readiness of Apollo 17 radar equipment with emphasis on lunar sounder equipment
[NASA-CR-128883] 11 p1338 N73-20858
Application of optimal control theory to design of constant gain filters to minimize weighted average of filtered variances
[AD-755798] 12 p1380 N73-21190
Instrumentation for Nike-Ajax radar to perform real time cross section measurements on airborne targets
[AD-756538] 13 p1493 N73-22103
Design, development, and evaluation of bistatic radar processor for synchronizing rotation rate of plan position indicator display
[AD-756515] 13 p1495 N73-22121
Analysis of radome design techniques and development of specifications for radome construction
[AGARD-AR-53] 14 p1618 N73-23108
Radar system for electromagnetic subsurface profiling
[PB-213892/0] 14 p1665 N73-23514
Design of meterband radar stations
[AD-758253] 15 p1751 N73-24194
Precipitation scatter experiment to refine coordination procedures in frequency allocations for terrestrial and space services
[NASA-TM-X-66259] 16 p1875 N73-25175
Development and characteristics of air traffic control radar and associated signal and display processing equipment
[FAA-RD-73-35] 16 p1875 N73-25178
Improved geodetic phase range only radar
[AD-759756] 16 p1878 N73-25202
VHF radars to probe ion columns left by meteors
[AD-758765] 16 p1908 N73-25434
Analysis of projectile aerodynamic coefficients based on yawsonde and radar imagery data obtained during flight tests
[AD-759482] 17 p1980 N73-26002
Test operation procedure for radar interrogator transmitter
[AD-759227] 17 p1998 N73-26158
Interface evaluation of digital simulation facility with system support facility for radar beacon target source for air traffic control
[FAA-NA-73-33] 17 p2009 N73-26248
Ruby laser radar system for measuring spatial density distribution of atmospheric water vapor
17 p2039 N73-26499
Application of pulsed radars for side scanning from artificial earth satellites and numerical analysis of radar operating parameters
18 p2117 N73-27117
Radar equipment components for fire control vehicle
[AD-761534] 19 p2237 N73-28031
Development and characteristics of radar system for improved air traffic control
[FAA-RD-73-100] 20 p2452 N73-29703
Proceedings of conference on application of radar techniques to meteorological observations and weather forecasting
[TT-70-50120] 21 p2568 N73-30580
Synchronous observations of precipitation microstructure by radar and ground-level instruments to determine accuracy of radar measurements
21 p2568 N73-30584
Characteristics of meteorological radar operating in millimeter wavelength range and methods for improving radar performance
21 p2572 N73-30607
Polish institutes involved in research and development of microwave tubes and recommendations for new research projects
21 p2608 N73-30900
Radar imagery processing techniques to include binary quantized signals, radar meters, interperiod compensation systems, and radar signal detection
[JPRS-56143] 22 p2628 N73-31054
Time-amplitude quantization of pulsed radar signals with numerical analysis of signal to noise relations
22 p2628 N73-31055
Determination of mean time between successive false detections for binary signal detector with variable memory size
22 p2628 N73-31056
Operation of pulse radar automatic range finders used jointly with search and lock-on system
22 p2628 N73-31061
Analysis of radar tracking systems which maintain constant product or quotient of dependent and independent variables
22 p2629 N73-31062
Development of differential equations for analyzing phase radio range finders with mutual automatic scaling frequency control in interrogator and responder
22 p2629 N73-31063
Analysis of signal and correlated noise for interperiod compensation systems of moving target selection procedures
22 p2629 N73-31069
Probability distribution function of phase difference of sum of signal and noise to determine efficiency of phase interperiod compensation systems
22 p2629 N73-31070
Formation of speed characteristics in interperiod compensation systems when using intermittent pulse repetition periods
22 p2630 N73-31072
Design of high frequency radar antenna equipment for radar stations
[AD-764333] 22 p2632 N73-31093
Digital signal processor for use with experimental MICOM array radar
[AD-764227] 22 p2635 N73-31121
Radio frequency interference measurements with common digitizer door opened and closed, and influence of various equipments inside room on interference magnitude and intensity
[FAA-NA-73-41] 23 p2757 N73-32061
Characteristics of three meteorological radar systems to include principles of operation, circuit description, and fuctions of subsystems
[AD-765363] 23 p2759 N73-32076
Operational evaluation of ARTS 2 radar alphanumeric display subsystem
[FAA-NA-73-77] 24 p2951 N73-33569

**RADAR FILTERS**

Optimum resolution filter for radar target enhancement and surface reconstruction
23 p2755 N73-32048

**RADAR IMAGERY**

Radar backscatter produced by chaff cloud as function of position of radar relative to chaff cloud
[AD-744776] 01 p0029 N73-10226
Characteristics and imagery of side-looking radar
03 p0295 N73-12402
Side-looking radar applications to studies of terrain topography and landforms
03 p0295 N73-12405
Optical and digital data processing and handling of SLR imagery
[ESRO-CR[P]-139-VOL-4] 03 p0297 N73-12419
Frequency stability characteristics of single frequency neodymium YAG laser system with coherent ultrashort pulses for high resolution imaging
[AD-747967] 03 p0312 N73-12543
Application of remotely sensed data to determination of resources and conditions in Susquehanna River Basin
04 p0471 N73-13844
Establishment of radar information transmission network for dissemination of meteorological data
[NLL-M-22692-[5828.4F]] 05 p0507 N73-14128
Procedures for measuring radar cross section areas of extremely small objects in superhigh frequency ranges
[AD-749788] 05 p0515 N73-14186
Summary of side-looking radar applications in earth resources noting basic principles of side-looking radar, radar scattering, data handling, and research and development
[ESRO-CR[P]-141] 06 p0641 N73-15200
Development of evaluation method for determining effectiveness of data compression techniques for radar landmass simulation
[AD-750695] 06 p0642 N73-15214
Characteristics of shipboard radar antennas, antenna radiation patterns, and automatic target tracking systems
[AD-750871] 06 p0642 N73-15216
Development and operation of matched incoherent radar systems to improve accuracy in range measurement and increase probability of target detection
07 p0755 N73-16134
Doppler effect continuous wave radar for bird hazard detection and aircraft collision avoidance near airfields
[AD-751985] 08 p0885 N73-17168
Relationship between wave parameters and spatial spectrum of aerial photographs of sea surface and electromagnetic method for measuring conductivity of sea surface
[JPRS-58370] 10 p1153 N73-19381
Derivation of algorithms correlating spectra of ocean wave conditions with two dimensional spectra of aerial photographs and radar imagery
10 p1153 N73-19383
Application of dielectric constant measurements to interpretation of radar imagery of Michigan ground truth for lake ice
[E73-10391] 11 p1276 N73-20353
Application of dielectric constant measurements to interpretation of radar imagery of ground truth
[E73-10429] 11 p1280 N73-20390
Development and evaluation of aircraft tracking techniques based on radar and beacon target reports from common sensor site
[PX-6392] 12 p1378 N73-21177
Design, development, and evaluation of bistatic radar processor for synchronizing rotation rate of plan position indicator display
[AD-756515] 13 p1495 N73-22121
Lake ice surveillance using radar imagery
[E73-10569] 15 p1771 N73-24349
Radar analysis of ice sheets in Antarctic regions conducted during Tenth Soviet Antarctic Expedition
20 p2407 N73-29346
Development and characteristics of radar system for improved air traffic control
[FAA-RD-73-100] 20 p2452 N73-29703
Flight tests of light aircraft to determine detection by terminal radar observer for various conditions of flight
[FAA-NA-73-50] 20 p2452 N73-29705
Proceedings of conference on application of radar techniques to meteorological observations and weather forecasting
[TT-70-50120] 21 p2568 N73-30580
Development of radar equation and radar calibration relationships for measuring multiple target reflectivity
21 p2568 N73-30583
Synchronous observations of precipitation microstructure by radar and ground-level instruments to determine accuracy of radar measurements
21 p2568 N73-30584
Radar imagery processing techniques to include binary quantized signals, radar meters, interperiod compensation systems, and radar signal detection
[JPRS-56143] 22 p2628 N73-31054
Systems for selecting moving targets when using interperiod compensation devices
22 p2629 N73-31067
Numerical analysis of amplitude difference and phase difference for radar signal and correlated noise in interperiod compensation system of moving target indicator
22 p2629 N73-31068
Analysis of signal and correlated noise for interperiod compensation systems of moving target selection procedures
22 p2629 N73-31069
Synthesis and analysis of optimal systems for separation of quasideterminant signals from noise
22 p2630 N73-31073
Application of prior information concerning location of objects in given ranges for calculating radar energy potential
22 p2630 N73-31074
Analysis of radar mapping mission to Venus
[NASA-TM-X-2868] 22 p2714 N73-31728
Image maps of point targets applied to hard limited, synthetic aperture radar application
[AD-763660] 23 p2788 N73-32306

**RADAR MAPS**

NT RADAR IMAGERY

Hydrographic investigations conducted aboard ships of the Tenth Soviet Antarctic Expedition
20 p2407 N73-29344
Analysis of radar mapping mission to Venus
[NASA-TM-X-2868] 22 p2714 N73-31728
Planning for Venus radar mapping orbiter mission and spacecraft to determine technology requirements and cost effectiveness of alternative approaches-Vol. 1
[NASA-CR-114640] 22 p2715 N73-31735
Configuration comparisons and systems evaluation for overall radar mapping mission of planet Venus - Vol. 2
[NASA-CR-114641] 22 p2715 N73-31736
Parametric studies and subsystem comparisons for orbital radar mapping mission to planet Venus - Vol. 3
[NASA-CR-114642] 22 p2715 N73-31737

**RADAR MEASUREMENT**

Radar techniques for measuring turbulent layers in lower stratosphere and rain in troposphere
02 p0197 N73-11593
Development and operation of matched incoherent radar systems to improve accuracy in range measurement and increase probability of target detection
07 p0755 N73-16134
Computerized simulation of instrument limited angular measurement errors in phased array radar
[AD-754922] 11 p1257 N73-20201
High resolution radar system for measuring wind velocity and height of meteor trails
[NASA-CR-131644] 12 p1377 N73-21172

Accuracy and reliability engineering of precipitation measurement by radar
[NLL-M-22841-[5828.4F]] 12 p1420 N73-21505
Effect of Doppler radar pulse volume on atmospheric turbulence measurements
[AD-755440] 12 p1423 N73-21534
Doppler radar measurement of turbulent air associated with stalactite cloud base zone
[AD-755441] 12 p1423 N73-21535
Doppler radar measurement of atmospheric turbulence structure function
[AD-755439] 12 p1423 N73-21536
Bistatic radar investigation of lunar electromagnetic and surface properties from Apollo 16 command and service module
12 p1451 N73-21759
Estimation of random error variance from simultaneous radar measurements
[AD-755402] 13 p1494 N73-22114
Generalized radar equations and Doppler shift in Fresnel region
18 p2115 N73-27097
Radar analysis of ice sheets in Antarctic regions conducted during Tenth Soviet Antarctic Expedition
20 p2407 N73-29346
Analysis of radar measurements of precipitation and comparison with ground level observations
21 p2568 N73-30581
Application of radar techniques for measuring precipitation and comparison with measurements obtained from conventional meteorological instruments
21 p2568 N73-30582
Development of radar equation and radar calibration relationships for measuring multiple target reflectivity
21 p2568 N73-30583
Synchronous observations of precipitation microstructure by radar and ground-level instruments to determine accuracy of radar measurements
21 p2568 N73-30584
Analysis of radar methods for measuring intensity of precipitation and development of mathematical models for radar reflectivity and microwave attenuation
21 p2569 N73-30585
Application of polarized radar signals for analyzing structure of cumulonimbus clouds
21 p2569 N73-30588
Application of radar signatures for analyzing the turbulent flow structure of earth adjacent layers of subfrontal clouds and precipitation
21 p2570 N73-30597
Development of methods for conducting radar measurements of parameters of atmospheric turbulence
21 p2570 N73-30598
Development of backscattering diagrams for sources of reflections from clear sky based on signatures from meteorological radar
21 p2571 N73-30600
Application of pulsed Doppler radar for analyzing motion of sources of reflection from clear skies to show effect of wind
21 p2571 N73-30601
Development and application of meteorological radar for detecting zones of cloudiness, precipitation, and storms for synoptic weather analysis
21 p2571 N73-30604
Equipment and procedures for obtaining meteorological radar information on clouds, cloud systems, and dangerous meteorological formations
21 p2571 N73-30605
Characteristics and development of receiving device for automatic conversion of meteorological radar data
21 p2572 N73-30608
Procedure for determining lower cloud boundaries using dual range meteorological radar operating in vertical sounding mode
21 p2572 N73-30610
Analysis of radar tracking systems which maintain constant product or quotient of dependent and independent variables
22 p2629 N73-31062
Statistical error analysis of amplitude modulated radio altimeters with phase readout
22 p2629 N73-31064
Use of passive radar to determine range to target emitting radio signal
22 p2630 N73-31077

**RADAR NAVIGATION**
Computerized multistage decision process for radar operator aid in collision avoidance trajectory control
14 p1711 N73-23886
Proceedings of conference to develop area navigation system design concept for application to national airspace system for improved air traffic control
17 p2060 N73-26664

**RADAR OBSERVATION**
U RADAR TRACKING

**RADAR PHOTOGRAPHY**
Radar photography of smoke in forest area for predicting bushfire behavior
[DIV-APPL-CHEM-TP-2] 04 p0388 N73-13151
Microwave radar detection and photography of gravitational waves in troposphere
05 p0510 N73-14152
Radar aerial survey and significance in combination with high altitude and space geological research techniques
21 p2535 N73-30325

**RADAR RANGE**
FORTRAN computer program for calculating radar maximum range
[AD-749686] 06 p0642 N73-15208
Operation of pulse radar automatic range finders used jointly with search and lock-on system
22 p2628 N73-31061
Use of passive radar to determine range to target emitting radio signal
22 p2630 N73-31077
Time delay in ranging signal to Mariner 9 orbiter for testing general relativity
23 p2842 N73-32712
Planetary ephemerides for Mariner 9 based on radar range data using normal points
23 p2842 N73-32714

**RADAR RECEIVERS**
Receiver synthesis for air traffic moving target indicator with digital signal processing
[AD-751923] 08 p0885 N73-17170
Solid state, superheterodyne monopulse receiver for experimental array radar
[AD-757610] 14 p1637 N73-23268
Development and characteristics of radar receiver for detecting coherent and incoherent optical signals against background of noise
22 p2630 N73-31075
Analysis of operation of phase autocorrelator with noncoincidence of frequency of received signal and filter tuning frequency
22 p2630 N73-31076

**RADAR RECEPTION**
Mathematical and computer analysis of multiple channel sidelobe canceller
[AD-753571] 09 p1004 N73-18198
Numerical analysis of amplitude difference and phase difference for radar signal and correlated noise in interperiod compensation system of moving target indicator
22 p2629 N73-31068
Analysis of distribution density of process at output of interperiod compensation system
22 p2629 N73-31071
Formation of speed characteristics in interperiod compensation systems when using intermittent pulse repetition periods
22 p2630 N73-31072
Synthesis and analysis of optimal systems for separation of quasideterminant signals from noise
22 p2630 N73-31073
Application of prior information concerning location of objects in given ranges for calculating radar energy potential
22 p2630 N73-31074
Development and characteristics of radar receiver for detecting coherent and incoherent optical signals against background of noise
22 p2630 N73-31075
Analysis of operation of phase autocorrelator with noncoincidence of frequency of received signal and filter tuning frequency
22 p2630 N73-31076

**RADAR REFLECTIONS**
U RADAR ECHOES

**RADAR REFLECTORS**
Application of meteorological radar measurements of atmospheric turbulence using velocities of reflectors located in scattering volume of radar set
21 p2570 N73-30596
Filtered and unfiltered photon detections obtained during laser ranging operations between McDonald Observatory and Apollo 11, 14, and 15 reflectors
[NASA-CR-133927] 22 p2681 N73-31472

**RADAR RESOLUTION**
Development of digital method for smoothing and differentiating output of Doppler radar
01 p0024 N73-10186

**RADAR SCANNING**
Development of evaluation method for determining effectiveness of data compression techniques for radar landmass simulation
[AD-750695] 06 p0642 N73-15214
FM CW radar data of lower atmosphere, including observations on atmospheric turbulence, wave motions, and rain
[AD-752034] 08 p0921 N73-17546
Feasibility of radar system to measure direction of shoreline ocean waves
[AD-755241] 13 p1527 N73-22373
Analysis of data rate requirements for low visibility approach with scanning beam landing guidance system
[AD-758786] 16 p1942 N73-25719

**RADAR SCATTERING**
High resolution radar scattering data for determining refractive structure in troposphere
02 p0197 N73-11594
Optical radar data for probing atmospheric composition and air pollution particulates
02 p0197 N73-11595
Side-looking radar scattering from terrain and ocean surfaces
[ESRO-CR[P]-137] 03 p0266 N73-12153
Measurement of short pulse, X-band radar backscatter from rough water surfaces expressed as cumulative probability distribution functions
[AD-747949] 03 p0267 N73-12159
Airborne and seaborne observations of radar scattering by sea water surfaces
[JPRS-57409] 04 p0388 N73-13156
High frequency radar backscattering technique for determining ionospheric structure and gravity wave disturbances
05 p0511 N73-14155
Lunar surface layer density from radar measurements by satellites and automatic stations
[D-17] 06 p0639 N73-15185
Summary of side-looking radar applications in earth resources noting basic principles of side-looking radar, radar scattering, data handling, and research and development
[ESRO-CR[P]-141] 06 p0641 N73-15200
Matrix method for computing radar scattering cross sections of airplanes
[AD-750486] 06 p0643 N73-15217
Relationship between radar scattering coefficient and ocean wind speed and direction
07 p0774 N73-16289
Analysis of troposcatter data obtained by radar transmitter as signal source to determine index of refraction fluctuations
08 p0900 N73-17285
Load impedance and electromagnetic radar echo scattering
[AD-754899] 11 p1258 N73-20209
Correlation of ocean surface parameters with radar backscatter data
[E73-10530] 13 p1517 N73-22295
Transfer equation for calculation of doubly scattered lidar returns
17 p2039 N73-26497
Sea spectra and radar scattering
[AD-760693] 18 p2149 N73-27373
Radio frequency shadow calculation for airspace obstruction of radar reception considering Fresnel diffraction
[AG-5082-E-1] 20 p2377 N73-29097
Curvature corrected Kirchhoff formulation for radar sea-return from near vertical
22 p2628 N73-31053
Experimental determination of coupling between normal F region ionosphere and protonosphere using radar backscatter techniques at Arecibo, Puerto Rico
23 p2778 N73-32213
Characterization of multipath and Doppler fading in earth scatter communication, navigation, and radar links
24 p2894 N73-33102
Backscattering from two-scale rough surface application to radar sea return
[NASA-CR-2327] 24 p2948 N73-33543
Transient effects in pulse radar hydrometeor detection
24 p2956 N73-33616

**RADAR SIGNATURES**
High frequency radar backscattering technique for determining ionospheric structure and gravity wave disturbances
05 p0511 N73-14155
Radar signal processing methods
[AD-756599] 13 p1492 N73-22095
Asymptotic methods for deriving transient backscattered signatures from artificial satellites
[AD-758245] 15 p1751 N73-24192
Analysis of radar measurements of precipitation and comparison with ground level observations
21 p2568 N73-30581
Analysis of radar signatures for identifying hail-bearing clouds to show effects of geographical conditions and seasons
21 p2569 N73-30586
Analysis of radar data for time variability of cumulonimbus clouds in shower and thunderstorm stages
21 p2569 N73-30587
Application of meteorological radar measurements of atmospheric turbulence using velocities of reflectors located in scattering volume of radar set
21 p2570 N73-30596
Development of methods for conducting radar measurements of parameters of atmospheric turbulence
21 p2570 N73-30598
Characteristics of electromagnetic radiation reflected from invisible objects in troposphere to show effects of electromagnetic radiation polarization
21 p2571 N73-30599
Application of pulsed Doppler radar for analyzing motion of sources of reflection from clear skies to show effect of wind
21 p2571 N73-30601
Analysis of radar data to determine characteristics of precipitation belts resulting from weather modification practices
21 p2571 N73-30603
Development and application of meteorological radar for detecting zones of cloudiness, precipitation, and storms for synoptic weather analysis
21 p2571 N73-30604

Development of equipment and methods for obtaining and processing meteorological radar data
21 p2571 N73-30606
Characteristics and development of receiving device for automatic conversion of meteorological radar data
21 p2572 N73-30608
Procedure for determining lower cloud boundaries using dual range meteorological radar operating in vertical sounding mode
21 p2572 N73-30610
Design and development of meteorological radar for detecting hail-bearing clouds
21 p2572 N73-30611
Radar imagery processing techniques to include binary quantized signals, radar meters, interperiod compensation systems, and radar signal detection
[JPRS-56143] 22 p2628 N73-31054
Time-amplitude quantization of pulsed radar signals with numerical analysis of signal to noise relations
22 p2628 N73-31055
Determination of mean time between successive false detections for binary signal detector with variable memory size
22 p2628 N73-31056
Angular position of target determined by scanning radar against background of correlated noise
22 p2628 N73-31057
Systems for selecting moving targets when using interperiod compensation devices
22 p2629 N73-31067
Probability distribution function of phase difference of sum of signal and noise to determine efficiency of phase interperiod compensation systems
22 p2629 N73-31070
Analysis of distribution density of process at output of interperiod compensation system
22 p2629 N73-31071
Synthesis and analysis of optimal systems for separation of quasideterminant signals from noise
22 p2630 N73-31073
Application of prior information concerning location of objects in given ranges for calculating radar energy potential
22 p2630 N73-31074
Energy spectrum and autocorrelation function of random processes at output of key detector
22 p2630 N73-31078

**RADAR TARGETS**

Signal processing algorithms for estimating from radar data characteristics and trajectory parameters of bodies moving in air
[AD-745421] 01 p0029 N73-10227
Computerized radar target return data processing and identification system
[AD-746323] 02 p0142 N73-11148
Extracting tracks of moving targets from sensor detection
[AD-746513] 02 p0142 N73-11149
Detection probability of log-normally distributed signals embedded in log-normally distributed noise as function of signal to noise ratio
[AD-745947] 02 p0143 N73-11157
Behavior of alpha-beta tracker for maneuvering targets under noise, false target, and fade conditions
[AD-748993] 04 p0391 N73-13182
Target transmission in multistage radar systems
05 p0513 N73-14172
Absorption, reflection, and scattering of electromagnetic waves by plasma media as electronic countermeasures in radar detection
[FOA-3-C-3652-66] 06 p0639 N73-15189
Statistical models of electromagnetic scattering from radar targets
[AD-755936] 11 p1256 N73-20192
Computerized simulation of aircraft as radar target
[AD-755854] 12 p1380 N73-21189
Optimum techniques for detecting and discriminating backscattered electromagnetic radiation associated with impulse radar concept
[AD-757220] 14 p1636 N73-23267
Asymptotic methods for deriving transient backscattered signatures from artificial satellites
[AD-758245] 15 p1751 N73-24192
Discriminatory analysis of waveform data for pattern recognition in radar targets
[AD-757564] 16 p1876 N73-25189
Flight tests of light aircraft to determine detection by terminal radar observer for various conditions of flight
[FAA-NA-73-50] 20 p2452 N73-29705
Development of space-time integral equation for solution of large body problem for smooth convex targets with application to satellite tracking systems
[AD-763794] 21 p2508 N73-30128
Angular position of target determined by scanning radar against background of correlated noise
22 p2628 N73-31057
Systems for selecting moving targets when using interperiod compensation devices
22 p2629 N73-31067
Target searching procedures with electronically steered phased array radar
[REPT-186] 22 p2632 N73-31094
Optimum resolution filter for radar target enhancement and surface reconstruction
23 p2755 N73-32048
Radar detection of underground objects using polarization for target classification
[AD-763155] 23 p2758 N73-32069
Identification of radar targets by pattern recognition
[AD-764713] 23 p2759 N73-32080
Statistical modeling of electromagnetic scattering from radar targets
24 p2893 N73-33099

**RADAR TRACKING**

Measurement of meteor winds based on radar tracking
[AD-745971] 01 p0054 N73-10440
Statistics from synoptic year sample of 20,000 radar meteor observations using eight station radar network
[NASA-CR-2109] 01 p0101 N73-10830
Description of eight-station radar at Havana, Illinois
01 p0101 N73-10832
Equipment for simultaneous radar observations by image-orthicon and optical observations
01 p0101 N73-10833
Antenna pattern calibration for Havana radar systems
01 p0101 N73-10834
Analysis procedure for radar observations
01 p0102 N73-10835
Results from simultaneous radar-television observations
01 p0102 N73-10838
Precise reduction of Super-Schmidt meteors
01 p0102 N73-10841
List of active meteor streams
01 p0102 N73-10844
Nonlinear transformation relating rectangular coordinates to range instrumentation coordinates in guided missile tracking system
[AD-746637] 02 p0144 N73-11163
Radar equipment for tracking meteor trails
[AD-745959] 02 p0169 N73-11372
Frequency sampling of target position and signal processing by linear amplitude weighting to reduce radar glint pointing errors
[AD-747348] 03 p0267 N73-12167
Digital simulation and angle tracking accuracy of tactical radar with multipath propagation
[AD-748384] 03 p0268 N73-12172
Methods for acquiring meteorological parameter data and procedures for analyzing wind data
[AD-747480] 03 p0298 N73-12432
Applying Kalman filtering to radar track-while-scan problem
[AD-747696] 04 p0390 N73-13173
Behavior of alpha-beta tracker for maneuvering targets under noise, false target, and fade conditions
[AD-748993] 04 p0391 N73-13182
Application of point position radar data to determine aerodynamic drag of projectile
[AD-750564] 05 p0492 N73-14013
Fluctuation errors of pulse time tracking systems in radar and radio navigation devices caused by noise signals
[AD-749649] 05 p0578 N73-14704
Characteristics of shipboard radar antennas, antenna radiation patterns, and automatic target tracking systems
[AD-750871] 06 p0642 N73-15216
Problems of radar network scheduling to track satellites
[AD-751290] 07 p0757 N73-16152
Theory of Kalman filtering and applications to real time tracking systems for air traffic control, satellite observation, and aircraft navigation
[AD-751485] 07 p0818 N73-16634
Development of algorithm for multiple hypothesis testing with application to amplitude comparison monopulse radar system in air traffic control operations
[TN-1973-7] 09 p1002 N73-18173
Analysis of aircraft tracking techniques to show sensitivity of tracking performance to data environment
[AD-753114] 09 p1063 N73-18667
Evaluation of associative processor in performance of tracking and conflict detection function in real time ATC terminal environment
[PX-6406-REV-A] 10 p1185 N73-19642
Characteristics of operational airport surveillance radars and methods for improving performance to meet air route surveillance requirements
[ATC-14] 11 p1255 N73-20183
Development and evaluation of aircraft tracking techniques based on radar and beacon target reports from common sensor site
[PX-6392] 12 p1378 N73-21177
Development and evaluation of cross-band radar/beacon system for operation with airport surveillance radar/air traffic control beacon interrogator system
[FAA-RD-73-38] 12 p1379 N73-21182
Application of optimal control theory to design of constant gain filters to minimize weighted average of filtered variances
[AD-755798] 12 p1380 N73-21190
Spectral analysis of data from C band radar tracking GEOS 2 satellite and development of data compaction method
[NASA-CR-62085] 13 p1490 N73-22082
Determination of ship positions in broad ocean areas using C band radar tracking data
[NASA-CR-62086] 13 p1491 N73-22083
Altitude-aided algorithm for determining aircraft position from radar tracking
[AD-756655] 13 p1492 N73-22097
Radar observation of disk-shaped models of proposed nuclear heat source module
[NASA-TM-X-62262] 14 p1601 N73-22978
Jimsphere tracking for determining accuracy of meteorological radars
[AD-757624] 14 p1634 N73-23251
Measure, criteria, and procedure for radar track and search allocation
[AD-757172] 14 p1635 N73-23257
User requirements and instrumentation plans for aircraft tracking and guidance facility at Wallops Station
[NASA-CR-111931-1] 14 p1645 N73-23340
Development of algorithms for calculating modal trajectory estimate, conditional mean state estimate, and weighted least squares trajectory estimate
[AD-757240] 14 p1684 N73-23665
Equipment and mission of Astrophysics Institute in Tadzhikistan relative to radar tracking and wind velocity measurement
[AD-756100] 14 p1706 N73-23848
Formulation of radar glint tracking error reduction using frequency agility and linear amplitude weighting
16 p1874 N73-25171
Optimal algorithms for processing radar data for trajectory estimation
[AD-759947] 17 p2000 N73-26171
Multivariate analysis on data used in n-station solution tracking technique
[AD-759975] 17 p2000 N73-26172
Radar measurement of air mass circulation and meteor trail drift in upper atmosphere during IQSY
[NASA-TT-F-744] 17 p2023 N73-26363
SOM-1 radar measurement of diffusion in meteor zones
17 p2023 N73-26370
Approximation of atmospheric density and winds from radar track of passive inflatable sphere
17 p2057 N73-26633
Mathematical methods for development of improved rocket trajectories from radar tracking data
[AD-762203] 19 p2347 N73-28878
Flight tests of light aircraft to determine detection by terminal radar observer for various conditions of flight
[FAA-NA-73-50] 20 p2452 N73-29705
Development of space-time integral equation for solution of large body problem for smooth convex targets with application to satellite tracking systems
[AD-763794] 21 p2508 N73-30128
Design and development of meteorological radar for detecting hail-bearing clouds
21 p2572 N73-30611
Analysis of radar tracking systems which maintain constant product or quotient of dependent and independent variables
22 p2629 N73-31062
Low angle tracking and recognition using self focusing radar antenna
[AD-764052] 22 p2635 N73-31118
Tracking of reentry vehicles in strong wake echoes using moving target indicators
[AD-763944] 22 p2635 N73-31120
Reduction of midair collision hazard with bats through tracking by radar and use of high intensity lights
[AD-764828] 23 p2746 N73-31982
Angle tracking computer for experimental array radar system
[AD-764224] 23 p2758 N73-32070
Interplanetary distribution of meteors in radar observations
[NASA-CR-2316] 23 p2844 N73-32727

**RADAR TRANSMISSION**

Development of digital method for smoothing and differentiating output of Doppler radar
01 p0024 N73-10186
Analysis of backscatter from radar transmission and effect of field aligned laminae in both E and F layers of ionosphere
[AD-747027] 03 p0297 N73-12426
Target transmission in multistage radar systems
05 p0513 N73-14172
Development of relaxation method and inverse method for solving problems of electromagnetic scattering
[AD-749954] 05 p0515 N73-14184
Doppler frequency of interplanetary radar signal from earth to another planet or to space probe determined according to general relativity
[NASA-CR-130147] 07 p0755 N73-16131
Curves for solving low angle radar transmission problems at microwave frequencies over ocean surface
[TR-72-31] 08 p0885 N73-17165

Analysis of troposcatter data obtained by radar transmitter as signal source to determine index of refraction fluctuations
08 p0900 N73-17285

Radar arithmetic signal processing element with digital filter and Fourier transformation for moving target indication
[AD-754060] 11 p1258 N73-20206

Sector radio measurements of meteor trail drifts by low frequency radar transmissions
17 p2023 N73-26369

Application of discrete transforms in adaptive radar detection systems and effect functional performance
[AD-761219] 18 p2120 N73-27139

Bistatic radar experiments during lunar orbit phases of Apollo 14, 15, and 16
[NASA-CR-134003] 21 p2507 N73-30116

Application of meteorological radar measurements of atmospheric turbulence using velocities of reflectors located in scattering volume of radar set
21 p2570 N73-30596

Characteristics of meteorological radar operating in millimeter wavelength range and methods for improving radar performance
21 p2572 N73-30607

Development of differential equations for analyzing phase radio range finders with mutual automatic scaling frequency control in interrogator and responder
22 p2629 N73-31063

Analysis of distribution density of process at output of interperiod compensation system
22 p2629 N73-31071

Formation of speed characteristics in interperiod compensation systems when using intermittent pulse repetition periods
22 p2630 N73-31072

Modulation of high frequency oscillation period by symmetric and asymmetric signals
22 p2630 N73-31079

**RADAR TRANSMITTERS**

Statistical analysis of ASDE-2 airport radar failures and design modifications
[FAA-RD-72-82] 04 p0388 N73-13154

Effect of various technical and operational factors on electromagnetic compatibility of radars operating in 2700 to 2900 MHz frequency band
[ECAC-PR-71-033] 04 p0388 N73-13155

High resolution radar transmitting system for transmitting optical pulses to targets
[NASA-CASE-NPO-11426] 17 p1994 N73-26119

Low ripple klystron power supply for experimental array radar transmitter
[AD-765515] 24 p2881 N73-33010

**RADARSCOPES**

NT PLAN POSITION INDICATORS

**RADIAL DISTRIBUTION**

Radial distribution functions and liquid structure factors for fluids of particles interacting through repulsive potentials
[LPTHE-72/45] 10 p1191 N73-19690

**RADIAL DRAINAGE PATTERNS**

U DRAINAGE PATTERNS

**RADIAL FLOW**

Radial diffusion calculations of ionized helium and protons as probe for magnetospheric dynamics
[AD-750861] 06 p0670 N73-15449

Performance tests to determine effects of increased rotor blade loading on gas turbine operation by reduction of rotor blade inlet diameter
[NASA-TM-X-2730] 08 p0870 N73-17039

Radial flow balance in turbomachines
[ONERA-NT-209] 15 p1768 N73-24326

Design and operating principles of base plate for regulating performance of radial centrifugal machines
[NLL-NEL-TT-2476-[6075.461]] 20 p2382 N73-29137

**RADIAL VELOCITY**

X-band pulsed-Doppler radar measurement of radial velocity spectra in Arizona light showers
[PB-211388] 05 p0574 N73-14675

Chilean astronomical observations of early star spectra, southern star radial velocities, and minor planet positions
05 p0594 N73-14828

Radial velocity of southern G and K types stars as observed by Cassegrain spectrograph
05 p0594 N73-14830

Application of Schmidt telescope and objective prism to stellar radial velocity surveys
07 p0845 N73-16848

Schmidt telescopes for compilation of stellar spectra and novae maps, galactic structure, and radial velocities
07 p0846 N73-16856

**RADIANCE**

Atmospheric transmittance from sun and sky radiance measurements with Nimbus E infrared temperature profile radiometer prototype used at Mauna Loa Observatory
[NOAA-TR-NESS-61] 01 p0048 N73-10391

Upward and downward radiance calculations for numerous detector locations in atmosphere and ocean
[AD-745282] 01 p0076 N73-10627

Iterative methods and relaxation algorithm for calculating vertical atmospheric structure from noise contaminated infrared spectral measurements
02 p0196 N73-11588

Limb radiance inversion using weighting functions and iterative convergence for nonlinear kernel
02 p0197 N73-11591

Radiant power measuring instrument for measurement of downwelling and reflected radiance within ERTS multispectral scanner bands
[E72-10366] 05 p0535 N73-14354

Night sky spectral radiant sterance at ground level and variation with latitude and nighttime conditions, using Fourier spectroradiometer
[AD-750609] 06 p0669 N73-15442

Measurement of atmospheric aerosol content in Southern California desert areas from ERTS-1 contrast and radiance measurements
[PAPER-12] 19 p2277 N73-28324

Obtaining absolute target reflectances by correcting ERTS-1 radiance measurements for variable target irradiance, atmospheric attenuation, and atmospheric backscatter
[PAPER-13] 19 p2277 N73-28325

**RADIANT ENERGY**

U RADIATION

**RADIANT FLUX DENSITY**

NT ELECTRON FLUX DENSITY
NT ILLUMINANCE
NT IRRADIANCE
NT LUMINANCE
NT LUMINOUS INTENSITY
NT NEUTRON FLUX DENSITY
NT PARTICLE FLUX DENSITY
NT PROTON FLUX DENSITY
NT RADIANCE
NT SOLAR CONSTANT

Aircraft measurement of long wave radiation brightness and angular distribution
[AD-750945] 05 p0544 N73-14424

Six-day variation in cosmic ray intensity recorded at different astronomical observatories
07 p0859 N73-16967

Gas dynamic equation for investigating thermal heating modes during laser radiation flux interaction with material
09 p1043 N73-18509

Computer program for determining radiative flux and flux divergence through nonisothermal gas
[NASA-CR-112307] 15 p1766 N73-24310

Measurement of luminosity distribution of Coma cluster of galaxies and comparison of mass-to-light ratio of cluster with that of individual galaxies
19 p2341 N73-28829

Radiation regime of forest vegetation under plant cover and open areas under various weather conditions
20 p2405 N73-29329

Measurement of ultraviolet radiation flux density emitted by solar simulator using thermopile and spectrometer
[ESRO-TM-149-ESTEC] 21 p2522 N73-30225

Measurement of intensity and wavelength of polarized radiation from variable stars by polarizers
21 p2594 N73-30789

Radiance distribution as function of depth in upper layers of ocean and numerical analysis of inherent and apparent optical properties
24 p2957 N73-33621

**RADIANT HEATING**

Radiative heating rates measured for global atmosphere
[COO-2195-4] 04 p0415 N73-13386

Analysis of temperature distribution in prism heated by axisymmetrical beam of radiant heat
[NLL-M-21514-[5828.4F]] 05 p0605 N73-14921

Technical and economic feasibility of solar powered space heating, air conditioning, and hot water heating systems for residential applications
[NASA-CR-124063] 08 p0968 N73-17911

Thermal effects of microwave and radio frequency radiation on biological systems
[MBL-1971-7-PT-1] 14 p1609 N73-23048

Stagnation-line analysis of radiative heating of phenolic-nylon ablator
[NASA-CR-112306] 15 p1766 N73-24309

Mathematical models for studying atmospheric heating by ozone absorption of sunlight
[NASA-CR-132778] 17 p2024 N73-26382

Radiant array with as many as 144, 13 inches wide, modular radiant heating units mounted in sets of 3 to comprise each adjustable row
[NASA-CR-124435] 24 p2901 N73-33153

**RADIANT INTENSITY**

U RADIANT FLUX DENSITY

**RADIATION**

NT X RAY SOURCES

Numerical analysis of thermal problems in presence of radiation and temperature-dependent thermal conductivities
[EUR-4809-F] 01 p0116 N73-10960

Development of thermopile with sensor surface to receive radiant energy and to provide measurement of energy quantity
[NASA-CASE-NPO-11493] 03 p0300 N73-12447

Development of high temperature high radiation silicon semiconductors
[NASA-CR-124074] 08 p0950 N73-17777

Interactions of radiation with conductive and convective heat transfer in abiation and boundary layer flow determined by normal mode expansion technique
18 p2128 N73-27200

Propagation of multiwavelength laser radiation through atmospheric turbulance
[AD-762516] 20 p2426 N73-29491

Doppler shift arising from radiating body rotation at extreme relativistic speeds
22 p2714 N73-31721

**RADIATION ABSORPTION**

NT ATMOSPHERIC ATTENUATION
NT AURORAL ABSORPTION
NT ELECTROMAGNETIC ABSORPTION
NT MOLECULAR ABSORPTION
NT PHOTOABSORPTION
NT POLAR CAP ABSORPTION
NT SELF ABSORPTION
NT ULTRAVIOLET ABSORPTION
NT X RAY ABSORPTION

Absorption of laser radiation by laser produced plasma
[AD-749043] 04 p0457 N73-13727

Absorption of carbon dioxide laser radiation by gaseous sulfur hexafluorine in air boundary layers
[AD-751016] 06 p0681 N73-15546

Preparation, characterization, and evaluation of materials for infrared windows
[AD-754280] 10 p1169 N73-19512

Effectiveness of combined chemical protectors against mixed gamma-neutron radiation with neutron contributions to absorbed dose
11 p1240 N73-20068

Gamma survey of rocks and soils covered by nonactive radiation absorption layers using aerial reconnaissance and fourier analysis
[AD-755003] 11 p1289 N73-20461

Standards for calorimeter measurement of laser beam absorption by graphite cones
[CEA-CONF-2056] 12 p1411 N73-21432

Absorbed dose rate and equivalent dose rate investigation for galactic cosmic ray protons and alpha particles in manned spacecraft shields
[ORNL-TM-4029] 17 p2089 N73-26901

Ultrasonic absorption in liquid metals and in liquid selenium
18 p2178 N73-27590

Vacuum/tissue interface effect on biological energy absorption from charged particle track
20 p2366 N73-29028

Absorption of direct solar radiation in maize as function of leaf area index and sums altitude
20 p2404 N73-29320

Radiation equilibrium and grayness of clouds
20 p2448 N73-29665

Photoconductive effect and absorption of monochromatic sub-mm radiation in n-type germanium
[RR-737] 20 p2462 N73-29782

Sources, absorption, and detection of cosmic gamma rays
[MPI-PAE/EXTRATERR-83] 24 p2977 N73-33789

**RADIATION BELTS**

NT OUTER RADIATION BELT
NT PROTON BELTS

Vehicle encountered trapped electron and proton fluxes calculated for nominal UK 5 circular equatorial orbits
[NASA-TM-X-66098] 02 p0225 N73-11816

Validity of using only primary protons in Van Allen belt and solar flare proton shielding studies
[ORNL-TM-3785] 03 p0353 N73-12880

Radial diffusion of charged particles and splitting of drift shells surrounding earth
[AD-750741] 06 p0668 N73-15437

Parametric instabilities of VLF waves in radiation belts
[LA-DC-72-746] 07 p0756 N73-16139

Jovian radiation belts investigation, including particle and field studies
08 p0973 N73-17956

Formation of quiet time slot, dividing radiation belt electrons into inner and outer zone
10 p1145 N73-19324

Effect of trapped electron and proton radiation on onboard components and payloads of low thrust orbits through Van Allen belts
[NASA-TM-X-2777] 11 p1335 N73-20840

Model of electrons artificially injected into inner radiation belt by Starfish nuclear explosion
[NASA-TM-X-66211] 11 p1336 N73-20842

Measurements of galactic cosmic ray dose and geomagnetically trapped radiation from OV 1-4 satellite
[AD-756924] 13 p1575 N73-22761

Jovian magnetosphere model with thermal plasma and superimposed radiation belts
[NASA-CR-132960] 16 p1963 N73-25878

Pitch angle diffusion of relativistic electrons in plasmasphere
[AD-762952] 20 p2414 N73-29405

Theories for explaining high energy protons trapped in radiation belts
[AD-763433] 21 p2598 N73-30826
Theory of radial diffusion applied to electron and proton radiation belts of Jupiter
23 p2836 N73-32663

RADIATION CONTROL
U RADIATION PROTECTION

RADIATION COUNTERS
NT CERENKOV COUNTERS
NT ELECTRON COUNTERS
NT GEIGER COUNTERS
NT NEUTRON COUNTERS
NT NEUTRON SPECTROMETERS
NT PARTICLE TELESCOPES
NT PROPORTIONAL COUNTERS
NT QUANTUM COUNTERS
NT SCINTILLATION COUNTERS
NT SPARK CHAMBERS

Portable radon alpha decay detectors for use in fluorspar mines
[BMBW-FBK-72-14] 03 p0303 N73-12473
Measurement of spatial distribution of aerosols and water vapor in earth mixing layer using optical radar, particle counters, and rawinsonde
[NASA-TN-D-7103] 04 p0444 N73-13621
Comparison of simultaneous particle detector and search coil magnetometer measurements of precipitating particles and field aligned currents from OGO-D
[NASA-TM-X-66224] 12 p1401 N73-21367
Apollo 16 particles and fields subsatellite for measuring vector magnetic fields and plasma and energetic particle fluxes
12 p1451 N73-21756
Radiation monitor for cosmic X ray experiment on OSO-1
[NASA-CR-130206] 13 p1573 N73-22747
Design and performance of lightweight cosmic radiation experiment for Pioneer Jupiter mission
18 p2210 N73-27837
Coaxial anode for gas radiation counter for suppressing background ionization interference
[NASA-CASE-GSC-11492-1] 19 p2301 N73-28497
Optimization of parallel plate relativistic particle analyzer by reducing z variation of point source image at detector surface
19 p2301 N73-28501
Position resistive anode wire radiation counters noting counter acting as voltage and current source
[IRI-132-73-02] 19 p2302 N73-28504
Performance of OV-5 and OV-6 alpha and proton particle detector
[AD-760147] 19 p2302 N73-28505
Solid state dectors for indicating energy and point of impact of charged particles
[ISS-72/7] 21 p2548 N73-30431
Radiation or charged particle detector and amplifier
[NASA-CASE-NPO-12128-1] 23 p2790 N73-32317
Explanation of low counting rates for solar neutrinos
[BNL-TR-538] 24 p2977 N73-33786

RADIATION DAMAGE
CO2 laser radiation damage to surface of infrared laser optical material
[DREV-TN-2013/72] 01 p0064 N73-10524
Changes in brittle-ductile transition temperature of pressure vessel steel following neutron irradiation
[AD-745299] 01 p0067 N73-10552
Application of paints and varnishes as protective coatings for industrial structures and equipment against radiation damage
[AD-745701] 01 p0071 N73-10582
Neutron irradiation effects on lithium-doped silicon solar cells in space environment simulation
[AD-745992] 02 p0129 N73-11048
Relationship between damage in materials exposed to high intensity laser radiation and self focusing thresholds
[AD-747290] 02 p0184 N73-11489
Development of computer code for determining survivability of aircraft following exposure to radiation from aerial nuclear explosion
[AD-746015] 02 p0215 N73-11738
Transient radiation effects and damage to semiconductor devices and electronic equipment
[AD-746851] 03 p0279 N73-12260
Neutron irradiation damage in precipitation hardened aluminum alloy component from High Flux Isotope Reactor
[CONF-720604-1] 03 p0313 N73-12555
Influence of fast neutron damage to ceramic insulators on thermionic reactor design
[LA-DC-72-523] 03 p0333 N73-12716
Annealing phase and space charge decay following pulsed irradiation of MOS structures
[AD-748007] 03 p0347 N73-12833
Static magnetic fields inside idealized structures resembling missile cells
[AD-748409] 03 p0360 N73-12932
Argon laser radiation damage to retina of diabetic and nondiabetic patients
[AD-747058] 04 p0381 N73-13099
Design of intense neutron source for studying materials damage in fusion power reactor
[LA-4863] 04 p0402 N73-13272
Laser damage in lithium iodate and proustite
[AD-748935] 04 p0451 N73-13682
Spatial distribution of radiation defects in silicon irradiated by protons, deuterons, and alpha particles
[AD-748734] 04 p0459 N73-13749
Technique for accelerated evaluation of silicon solar cells for use on extended space missions with weapons environment
[AD-749477] 05 p0499 N73-14062
Internally deposited radioisotope effects on cell populations in mammals
[NYO-3970-29] 05 p0500 N73-14074
Effects of gamma and neutron radiation on high frequency characteristics of microwave bipolar transistors
[SC-DC-72-1233] 05 p0519 N73-14220
Vertical profiles of long wave components of total radiation damage in daytime
[AD-749641] 05 p0542 N73-14409
Proceedings of symposium on laser radiation damage to transparent dielectrics, plasma formation at dielectric surfaces, and damage morphology of thin film coatings
[NBS-SP-372] 05 p0554 N73-14498
Characteristics of optical glass materials with specific resistance to effects of laser radiation
05 p0554 N73-14499
Development of interaction gradient concept and application to laser radiation damage to quartz crystals, fused quartz, and laser glass samples
05 p0554 N73-14500
Effects of stoichiometry variation, heat treatment, impurity, and color center content of electrooptic crystals and kinetics of index damage process
05 p0554 N73-14501
Analysis of laser bulk damage in alkali-halides with no self-focusing and measurement of damaging fields considering effects of inclusions on bulk optical strength
05 p0554 N73-14502
Analysis of laser induced surface damage to glass materials at Brewster angle and near normal incidence
05 p0554 N73-14503
Analysis of entrance and exit surface laser induced radiation damage on sapphire crystal samples as function of beam size and divergence at surfaces
05 p0555 N73-14504
Measurements of laser induced surface damage processes at ruby and neodymium YAG laser wavelengths to determine laser damage at different wavelengths to transparent media
05 p0555 N73-14506
Surface damage to gallium arsenide surfaces from radiation by ruby and neodymium-glass lasers
05 p0555 N73-14507
Analysis of self focusing damage in laser rods with subnanosecond pulse
05 p0555 N73-14511
Analysis of damage to thin films and substrate surfaces during irradiation by Q switched ruby laser
05 p0556 N73-14512
Measurement of damage thresholds for multiple layer dielectric mirrors for laser pulses of twenty nanoseconds and twenty picoseconds duration
05 p0556 N73-14513
Analysis of laser damage to thin film coatings caused by radiation from Q switched ruby laser
05 p0556 N73-14514
Analysis of damage threshold and damage mode from laser radiation for multilayer and periodic inhomogeneous film systems
05 p0556 N73-14515
Pressure induced optical distortion in high power, infrared laser system windows and determination of figures of merit based on minimum thickness
05 p0556 N73-14517
Analysis of surface damage mechanisms to mirrors and mirror coatings resulting from irradiation by pulsed carbon dioxide lasers
05 p0556 N73-14519
Diagnostic techniques for characterizing near surface of solids
[UCRL-73925] 05 p0587 N73-14773
Structural effects of various optical coatings on single shot laser induced damage threshold using pulsed neodymium glass laser
[AD-749852] 06 p0680 N73-15531
Physics research on solid state materials - radiation damage, electronic structure, and magnetic, electrical, surface, low temperature, and lattice properties
[ORNL-4779] 06 p0708 N73-15776
Hall coefficient, resistivity, and charge carrier mobility of epitaxial films of n-type and p-type PbS before and after neutron irradiation
[AD-749689] 06 p0710 N73-15791
Kinetics of quartz crystal growth and radiation effects on quartz resonators
[AD-750467] 06 p0711 N73-15803
Electron paramagnetic resonance and formed free radical investigation of ionizing radiation damage by sulfur-containing aliphatic compounds, pyridoxine, and proteins
[BMVG-FBWT-72-6] 07 p0753 N73-16115
Sensitivity of microwave transistor amplifiers to neutron damage in low noise and high power applications
[SC-R-72-2845] 07 p0762 N73-16190
Charge trap structure of pyrolytic alumina layer in metal oxide semiconductor capacitor
[AD-751629] 07 p0762 N73-16195
FORTRAN program for handling radiation effects circuit analysis problems
[AD-751519] 07 p0765 N73-16213
Photographic characteristics of UFSh-4 film used in Orion orbital observatory
[NASA-TT-F-14585] 07 p0799 N73-16492
Damage thresholds of multilayered dielectric reflecting mirrors subjected to nanosecond laser pulses
[AD-751265] 07 p0808 N73-16553
In pile neutron irradiation damage in graphite at high temperature
[CEA-CONF-1894] 07 p0820 N73-16644
Radiation testing of swept synthetic quartz resonators with high-purity platinum electrodes
[AD-752584] 08 p0891 N73-17209
Laser induced damage in ruby and sapphire crystals at 6943 A
[AD-751928] 08 p0930 N73-17613
Radiation damage threshold determination for glass laser materials
[AD-752549] 08 p0931 N73-17622
Effects of ionizing radiation and space flight conditions on microorganisms, plants, animals, enzymes, and immunological preparations
09 p0993 N73-18103
Radiation damage of electrically insulating polymeric materials used in electrotechnology
[AD-753367] 09 p1001 N73-18169
Electron beam irradiation capabilities of facility for materials and structures testing
[AD-752762] 09 p1012 N73-18260
Mathematical model of thermodynamic damage to metals irradiated by laser beams
[DREV-R-672/72] 09 p1043 N73-18503
Phonon emission by laser beams and thermal conductivity of optical crystals
[AD-753698] 09 p1077 N73-18791
Irradiation damage to tungsten rhenium and tungsten rhenium hafnium claddings of unranium nitride fuel pins
[ORNL-TM-3895] 10 p1186 N73-19653
Effects of nuclear radiation on stainless steels
[AD-753457] 10 p1187 N73-19660
LINVILL and IBIS programs for calculating gamma radiation damage to biopolar transistors
[CEA-R-4337] 10 p1194 N73-19718
Radiation effects on current density of superconducting magnets in fusion reactor
[CLM-R-120] 10 p1199 N73-19760
Continuous wave CO2 laser radiation effects on semiconductor materials
[AD-753918] 10 p1202 N73-19785
Quantitative analysis of irreversible portion of radiation damage combined with gamma rays and acceleration
11 p1242 N73-20082
Free amino acid excretion in urine as test for early diagnosis of radiation damage in humans
11 p1243 N73-20092
Infrared beam profile measurements for determining surface damage thresholds of glass laser materials
[AD-755134] 11 p1303 N73-20571
Computer radiation interaction program for calculating material response to X ray and electron beam impact
[AD-755147] 11 p1327 N73-20767
Surface and unambiguous bulk damage to optically transparent materials
[AD-756486] 13 p1559 N73-22638
Device fabrication and radiation effect studies of various semiconductors
[AD-756249] 13 p1566 N73-22689
Analysis of EPR spectra in neutron irradiated silicon for determination of radiation damage in semiconductors
[AD-756907] 13 p1568 N73-22708
Transient radiation caused performance degradation in integrated ferrite phase shifter driven circuit
[AD-757618] 14 p1644 N73-23336
Effect of residual impurity element on sensitivity of low alloy steels to radiation induced embrittlement
[AD-756625] 14 p1679 N73-23622
Radiation damage in semiconductor devices and changes in electrical properties
[AD-755690] 14 p1698 N73-23778
Neutron irradiation damage in indium arsenide semiconductors and effect on electrical crystal properties
[AD-757468] 14 p1699 N73-23792
Effects of polarized radiation on self-focusing thresholds of laser materials
[AD-757789] 15 p1795 N73-24554
Electron irradiation damage as function of accelerating voltage, time, and temperature in stainless steel
[COO-2119-3] 15 p1799 N73-24581

Evaluation of computer program for analyzing radiation effects on complex semiconductor devices and microcircuits
[AD-758883] 16 p1882 N73-25237
Radiation damage in epoxy materials of reduced viscosity
[RHEL/R-249] 16 p1932 N73-25634
Machine assisted human chromosome karyotyping and aberration for radiation damage
[ANL-7960-PT-2] 17 p1988 N73-26068
Surface damage induced in optical materials by laser
[AD-760131] 17 p2042 N73-26519
Formation of cavities in nickel and some austenitic steels irradiated by medium energy heavy ions
[CEA-CONF-2113] 17 p2045 N73-26542
Research in electron and ion collisions and radiation dosimetry
[ORNL-4811] 17 p2064 N73-26700
Near infrared, electron microscopic, ESR, and magnetic susceptibility measurements
[ORO-4049-3] 17 p2065 N73-26705
Influence of prior microstructure on neutron irradiation damage in 316 stainless steel foils
[HEDL-SA-407] 17 p2065 N73-26707
Radiation resistance of thin insulating films deposited with ion beam system
[AD-760118] 17 p2075 N73-26788
Effects of radiation on semiconductor materials and devices
[AD-759946] 17 p2075 N73-26790
Laser induced damage and avalanche breakdown in transparent insulators
[AD-761168] 18 p2158 N73-27439
Ion implantation damage in silicon and semiconductor devices
[AD-761486] 19 p2245 N73-28104
Electrical and optical properties of irradiated mercury cadmium telluride semiconductors
[AD-761488] 19 p2327 N73-28721
Development of lithium-doped silicon solar cells with increased stability, efficiency, and radiation resistance
[AD-762941] 20 p2364 N73-29011
Junction capacitance techniques to characterize radiation damage in silicon
[AD-762482] 20 p2464 N73-29796
Susceptibility of X band point-contact diodes to microwave radiation
[AD-763364] 21 p2518 N73-30197
Second breakdown in diodes and transistors from intense ionizing radiation
[AD-763951] 22 p2644 N73-31192
Boltzmann transport equation for electron bombardment effects in solids
[AD-764637] 23 p2827 N73-32599
Influence of radiation damage on properties of type 2 superconductors
[IPP-4/104] 24 p2969 N73-33724

**RADIATION DETECTORS**
NT DOSIMETERS
NT SILICON RADIATION DETECTORS
NT THRESHOLD DETECTORS [DOSIMETERS]
Far infrared radiation detection with quantum photodetectors, noting application to submillimeter wave communication
[FTZ-A-14-TBR-4] 02 p0141 N73-11144
Whole body counter efficiency calculations using NaI[Tl] detector for measuring point sources
[KFKI-72-30] 03 p0261 N73-12114
Relations between signal shaping noise and timing resolution in nuclear particle detection
[NASA-CR-129613] 04 p0452 N73-13688
Comprehensive listing of ground-based cosmic ray detectors
[AD-749865] 05 p0594 N73-14824
Color film spectroscopy for quantitative optical radiation detection
[EGG-1183-5015] 06 p0674 N73-15483
Efficiencies of germanium semiconductor detectors calculated by Monte Carlo method for 100 keV to 2 MeV gamma rays
[CEA-R-4316] 07 p0832 N73-16745
Calculation of energy deposition distributions for simple geometries
[NASA-TN-D-7195] 08 p0957 N73-17832
System for measuring charge spectra of solar cosmic rays on IMP-6
08 p0973 N73-17960
Semiconductor radiation detectors with lead and mercury compounds
[BMBW-FBK-72-19] 09 p1036 N73-18458
Design and performance of Compton diode radiation detector
[SC-DR-72-0118] 10 p1134 N73-19242
Very low noise amplifiers for semiconductor X ray detectors
[CONF-720559-2] 10 p1200 N73-19769
Ultraviolet radiation detector in presence of proton radiation using sensor tubes within shielding mechanism
[NASA-CASE-MFS-21577-1] 11 p1237 N73-20042
Response of optico-electronic scanning system with antiphase connection of radiation detector elements
12 p1405 N73-21395
Plastic and glass detectors for measuring composition and energy spectra of solar cosmic ray nuclei
12 p1450 N73-21747
Development of multiwire proportional chamber for high resolution spatial detector in cosmic ray investigations and analysis of operating parameters
[NASA-CR-128899] 13 p1506 N73-22210
Cosmic ray air shower investigations with Haverah Park array
[HPNL-8] 13 p1573 N73-22749
Results from Nottingham cosmic ray air shower muon detector
13 p1574 N73-22756
Influence of carrier lifetime in semiconductor material on its performance as radiation detector
[NASA-CR-121187] 14 p1697 N73-23775
NaI[Tl] crystal detector for measuring proton induced activity in gamma ray spectrometer
[NASA-TM-X-66241] 15 p1787 N73-24486
Thin film detector research including detector response to light and heavy ions and accelerated ions
[ORO-2843-22] 15 p1821 N73-24757
Radiation source tracker comprised of sectored matrix of detectors with output voltages corresponding to irradiance levels
[NASA-CASE-NPO-11686] 16 p1911 N73-25462
Fission and spallation by protons, meteorite composition, and radiation detection
[COO-1167-22] 16 p1947 N73-25754
Thick film microelectronic amplifier module for space instruments
[RAE-LIB-TRANS-1643-PT-1]
17 p2007 N73-26233
Position sensitive detector with lithium diffused layer as uniform resistive layer
[NASA-CR-133408] 18 p2152 N73-27391
Position resistive anode wire radiation counters noting counter acting as voltage and current source
[IRI-132-73-02] 19 p2302 N73-28504
Cerenkov light technique for measuring high energy gamma rays in air showers
19 p2332 N73-28760
Detecting antimatter in universe
19 p2333 N73-28771
Spectral characteristics of black and white coating on detector surfaces of actinometric instruments
20 p2403 N73-29310
Bolometric pyrheliometer with balanced resistance bridge and radiation detector having copper wire spiral
20 p2403 N73-29315
Directional low energy gamma ray detector for gamma ray astronomy
[NASA-TM-X-70449] 20 p2419 N73-29442
Characteristics of semiconductor detectors for soft X ray spectrometry
[RT/EL-{72}6] 20 p2462 N73-29787
Polish environmental protection policy and materials for semiconductor radiation detectors
[JPRS-59523] 20 p2487 N73-29976
Materials for semiconductor radiation detectors and infrared techniques
20 p2487 N73-29978
Semiconductor detectors of nuclear radiation
[JPRS-59634] 20 p2487 N73-29979
Detection effeciencies of cylindrical detectors for gamma ray photon angular distributions
[NASA-TM-X-70445] 21 p2548 N73-30424
Mobile test chamber for calibration of fixed incore radiation detectors
[BMBW-FBK-72-26] 22 p2699 N73-31618
X ray and gamma ray semiconductor mercury iodide detectors
[BMFT-FBK-73-09] 22 p2707 N73-31680
Radiation or charged particle detector and amplifier
[NASA-CASE-NPO-12128-1] 23 p2790 N73-32317
Characteristics and application of various radiation safety monitoring devices for application to industrial safety protection
24 p2952 N73-33576
Development, application, and characteristics of radiation measuring devices for protection of personnel performing hazardous industrial work
24 p2952 N73-33577
Sources, absorption, and detection of cosmic gamma rays
[MPI-PAE/EXTRATERR-83] 24 p2977 N73-33789

**RADIATION DISTRIBUTION**
NT ANTENNA RADIATION PATTERNS
NT DIFFRACTION PATTERNS
NT SIDELOBES
Measuring distribution of radiation as function of its angular coordinates by Talbot spectrometer
[AD-749875] 05 p0581 N73-14733
Geographical variations in environmental radiation background measurements over United States of America
[UCRL-73822] 06 p0650 N73-15275
Analysis of intensity distribution of radiation focussed by zone plate optics and computation of radiation flux on sensor area centered about optical axis
[AD-751516] 07 p0822 N73-16661
Surface and volume mechanisms of material evaporation subject to powerful radiation fluxes
09 p0999 N73-18154
Simultaneous investigations of three-dimensional structure of atmospheric radiation fields using equipment installed on airplanes, balloons, satellites, and ground
[AD-750962] 09 p1030 N73-18411
Computation of neutrons and gamma ray distribution for radiation shielding of Europa 3 launch vehicle nuclear upper stage
[TN-3-25] 15 p1811 N73-24680
Radiative processes in intense magnetic fields of white dwarfs and neutron stars
16 p1961 N73-25861
Balloon sounding program to measure all components of atmospheric radiation balance and analysis of atmospheric stratification
20 p2401 N73-29293
Influence of light conditions and understorey tree death on organic matter loss balance in oak underwood
20 p2405 N73-29331
Radiation equilibrium and interaction problems of atmospheric circulation
20 p2443 N73-29623
Matrix equations of radiation diffusion
20 p2472 N73-29857

**RADIATION DOSAGE**
Dosimetric determination of absorbed gamma and neutron radiation on human phantom
[AD-743005] 01 p0010 N73-10077
Method for calculating aircrew radiation dosage near atmospheric nuclear weapon detonation
[AD-745084] 01 p0010 N73-10079
Cosmic radiation dosage measurements on Apollo astronauts by Lexan dosimetry
[AD-745188] 01 p0013 N73-10101
Methods for predicting initial radiation exposure at ground surface resulting from nuclear explosions
[AD-745906] 02 p0133 N73-11084
Total air ionization and tissue dose rate in atmosphere
[HASL-254] 03 p0353 N73-12881
Dosimetric analyses for Biosatellite 2 yeast and artemia radiation exposure experiment
[NASA-CR-127142] 04 p0379 N73-13082
Energy comparisons for lethal doses of gamma radiation and visible light with energy of basal cell metabolism
[AD-746750] 04 p0381 N73-13102
Computer program for calculating constant dose range in air transport of neutron and photon radiation from point source in atmosphere
[LA-DC-13293] 04 p0453 N73-13700
Internally deposited radioisotope effects on cell populations in mammals
[NYO-3970-29] 05 p0500 N73-14074
Occupational hazards and adverse biological effects of ultraviolet radiation
08 p0876 N73-17094
Measurement of radiation exposure of astronauts by radiochemical techniques
[NASA-CR-130538] 08 p0878 N73-17114
Ionization, thermoluminescence, and nuclear photographic emulsion dosimetry for monitoring radiation loads in spacecrews during manned space flight
09 p0992 N73-18100
Cosmic radiation dosage for estimating manned spacecraft shielding requirements
09 p0992 N73-18101
Radiobiological effects of cosmic radiation in animals and standardization of permissible radiation levels for spacecrews
09 p0993 N73-18102
Monte Carlo radiation transport computer codes for calculating dose distributions and cell survival probabilities
[NASA-CR-130965] 09 p0996 N73-18127
Mineral insulated conductors for inorganic magnet coils for withstanding high radiation dosage
[LA-DC-72-1106] 10 p1189 N73-19677
Exposure to gamma rays from Co-60 and transverse loads and effectiveness of cysteamine and AET protection
11 p1242 N73-20086
Microdosimetric pattern of galactic heavy primaries dissipation in tissues during space flight
[NASA-CR-131467] 12 p1372 N73-21132
Neutron activation analysis of cosmic radiation doses in Apollo 14, 15, and 16 astronauts
[NASA-CR-131984] 14 p1612 N73-23070
Ion beam dose and sputtering characteristics of ion implanted semiconductor devices
[NASA-CR-132254] 15 p1820 N73-24754
Research in electron and ion collisions and radiation dosimetry
[ORNL-4811] 17 p2064 N73-26700
Radioactivity urinalysis for calculating postflight astronaut cosmic radiation exposure
[NASA-CR-133378] 19 p2224 N73-27939
Vacuum/tissue interface effect on biological energy absorption from charged particle track
20 p2366 N73-29028
U.S., Soviet, and Polish standards for radiation levels for humans
21 p2608 N73-30905

**RADIATION EFFECTS**
NT RADIATION DAMAGE

NT RADIATION INJURIES
NT RADIOLYSIS
Compilation of data concerning effects of infrared radiation on eye
[NASA-CR-128407] 01 p0008 N73-10064
Neutron and gamma induced transient incapacitation in conditioned Macaca mulatta
[AD-742076] 01 p0010 N73-10080
Human and animal studies on both ionizing and nonionizing radiations
[PB-210613] 01 p0013 N73-10099
Estimate of dose rate, pattern, and distribution of scattered particles and neutrons during irradiation of superconducting synchrotron magnets
[KFK-1468] 01 p0080 N73-10659
Effects of whole body exposure to external radiations, using animal studies applied to man
[CONF-720108-2] 03 p0259 N73-12102
Articles and abstracts of articles concerning radiobiology
[AEC-TR-7306] 03 p0259 N73-12103
Fabricating Ga-As-phosphide mis capacitors using dielectric-growth processes and radiation studies
[AD-747663] 03 p0275 N73-12232
Transient radiation effects and damage to semiconductor devices and electronic equipment
[AD-746851] 03 p0279 N73-12260
Irradiation effects on 17-7 PH stainless steel, 201 carbon steel, and titanium-aluminum-vanadium alloy
[NASA-TM-X-2678] 03 p0313 N73-12550
Effects of irradiation microstructure and creep rupture properties of annealed and cold worked type 316 stainless steel
[CONF-720604-4] 03 p0314 N73-12560
Effect of radiation on semiconductors
[AD-747565] 03 p0347 N73-12832
Detection and measurement of cosmic ray charge spectrum for nuclei heavier than iron with relation to nucleosynthesis and mechanics of supernova
[NASA-TM-X-58102] 03 p0352 N73-12872
Energy comparisons for lethal doses of gamma radiation and visible light with energy of basal cell metabolism
[AD-746750] 04 p0381 N73-13102
Electrical conductivity methods for measuring effects of high energy radiation on dielectric hydrocarbon liquids
[HMI-B-117] 04 p0452 N73-13693
Mechanisms for increases in saturation voltage as result of neutron radiation
[SC-DR-72-0418] 04 p0467 N73-13806
Effect of glass laser radiation on borosilicate crown glass, fused silica, and flint glass with estimates of Kerr effect and electrostriction processes
05 p0555 N73-14510
Effects of irradiation on properties of fluoride tungsten clad uranium carbide-zirconium carbide fueled capsules
[NASA-CR-120995] 05 p0578 N73-14708
Permanent electron beam radiation effects on thin film single junction quantum interferometer devices
[AD-749065] 05 p0582 N73-14740
Numerical analysis of signal trapping effects in neutron irradiated p-n junctions as function of frequency
[SC-DC-72-1237] 05 p0587 N73-14772
Observation of circulating lymphocytoid cell in monkey after exposure to radio waves
[AD-749583] 06 p0631 N73-15128
Research on laser irradiation effects, sensory psychophysiology, and human blood processing for military medicine
[AD-749440] 06 p0631 N73-15130
Bibliography on radio frequency and microwave radiation effects in biological systems
[AD-750271] 06 p0632 N73-15131
Radiation effects on human visual and vestibular analyzer functions
[AD-750499] 06 p0632 N73-15132
Oxygen content and hydrogen ion concentration in monkey blood after incapacitating ionizing radiation dosage
[AD-750681] 06 p0632 N73-15134
Abstracts on radiation and health physics
[BNWL-1651-VOL-2-PT-2] 07 p0746 N73-16069
Deep trap model for predicting capacitance voltage characteristics of irradiated silicon diodes and resistors
08 p0888 N73-17188
Irradiation of three low power microcircuits by Co-60 gamma radiation, low and high energy electrons, and neutrons
[NASA-CR-130750] 08 p0891 N73-17215
Simulation of thermal radiation-airblast interaction effects in conical shock tube
[AD-752023] 08 p0893 N73-17229
Radiation effects research program
[AD-752561] 08 p0951 N73-17791
Effects of high energy radiations in laser materials of calcium tungstates
[AD-753534] 09 p1044 N73-18519
Vestibular analyzer functions in dogs after prolonged ionizing irradiation
10 p1115 N73-19088
Ultraviolet radiation, X rays, freezing, and thawing effects on ribonuclease
10 p1119 N73-19120
On-line laboratory station connected to real time/time-sharing EMR 6130 computer for semiconductor radiation effects studies
[SC-DR-72-0525] 10 p1161 N73-19442
Radiation effects in semiconducting laser materials
[AD-754217] 10 p1170 N73-19516
Irradiation effects on fatigue and creep-fatigue properties of stainless steels
[ANCR-1078] 10 p1173 N73-19539
Physical properties and dimensional changes in graphites caused by high temperature neutron irradiation
[BNWL-1672] 10 p1193 N73-19706
Radioresistance recovery rate with combined exposure to ionizing radiation and dynamic factors [vibration and acceleration]
11 p1242 N73-20080
Effect of cysteamine combined with adrenalin and phenamine on reparative processes following irradiation and overload
11 p1242 N73-20081
Clinical hematological indices for evaluating vibration effect [70 Hz, 0.4 cm amplitude] on radiation reaction in dogs
11 p1242 N73-20084
Morphological changes in liver of dogs subjected to chronic gamma radiation
11 p1244 N73-20101
Proliferative activity of bone marrow in dogs exposed to three-year chronic gamma irradiation
11 p1244 N73-20102
Electron and proton radiation effects on Cactus accelerometer electric charge
[ONERA-NT-200] 11 p1294 N73-20503
Operant behavior of rhesus monkeys in presence of extremely low frequency, low intensity magnetic and electric fields
[AD-754058] 12 p1372 N73-21134
Atmospheric effects on laser propagation and impact on eye safety
[AD-755405] 13 p1485 N73-22044
Application of nuclear gamma resonance for changing structural state of crystal lattice of alloys to improve strength properties
13 p1541 N73-22486
Experimental techniques for achieving high flux, high energy electron irradiation
[AD-749856] 13 p1561 N73-22654
Radiation induced grafting of fluorinated monomers on polyamide films
[AD-757376] 14 p1617 N73-23100
Analysis of effects of high power lasers to include interactions with plasma, metals, dielectrics, semiconductors, and gases
[AD-755820] 14 p1674 N73-23586
Fabrication and analysis of metal insulator semiconductor capacitors for radiation vulnerability studies
16 p1880 N73-25217
Effects of electron and hole trapping on radiation hardness of aluminum oxide MIS devices
[AD-758696] 16 p1882 N73-25229
Effect of fast reactor irradiation on ductility of annealed stainless steels
[HEDL-SA-310] 16 p1929 N73-25606
Neutron irradiation effects on tensile and creep properties of cold worked stainless steel
[HEDL-SA-468] 16 p1929 N73-25607
Projected radiation environment profiles of OSO missions from 1974 to 1978
[NASA-TM-X-66264] 16 p1962 N73-25872
Effects of irradiation on fracture and strength properties of pressure vessel steel plate and submerged arc weld
[HEDL-SA-387] 17 p2093 N73-26936
Irradiation effects on fracture of heavy section pressure vessel steels
[HEDL-SA-497] 17 p2094 N73-26937
Radiation regime of vegetation, using spectral composition and three dimensional structure of incident solar radiation and scattered sky light
20 p2404 N73-29316
Radiation and turbulent heat flux effects on variations of isobaric surface pressure and altitude in Northern Hemisphere
20 p2446 N73-29651
Method for predicting degradation of solar array in space radiation environment
[NASA-CR-133738] 21 p2499 N73-30055
Irradiation of pyrolytic carbon sealers at high temperatures to determine effects on growth rate and service life
[CONF-730601-5] 21 p2563 N73-30543
Radiation effects on reactor structural materials
[AD-763658] 21 p2578 N73-30661
Microwave radiation effects on rats and standards for acceptable radiation dosage of humans
[JPRS-59709] 21 p2608 N73-30903
Microwave radiation effects on rat tissues and length of survival
21 p2608 N73-30904
Atmospheric models for computing radiation effects in ERTS observations
22 p2736 N73-31905
Effects of nuclear radiation on reverse bias electrical characteristics of silicon power diodes
[NASA-TN-D-7423] 23 p2821 N73-32554
Fabrication and radiation effects of high mobility semiconducting films
23 p2824 N73-32576
RADIATION EMISSION
U RADIATION
RADIATION EXPOSURE
U RADIATION DOSAGE
RADIATION FIELDS
U RADIATION DISTRIBUTION
RADIATION HARDENING
Anneal hardening of irradiated molybdenum metals and alloys
[ORO-3612-9] 10 p1173 N73-19545
RADIATION HAZARDS
Theoretical study of biological hazards from exposure to ELF electrical fields and potentials
[AD-743480] 01 p0012 N73-10093
Radiation ecological aspects of environmental pollution and control for human safety
[EUR-4800-2-F-1-E-PT-2] 01 p0082 N73-10680
Radiological safety aspects of manned space missions employing nuclear reactors for electric power and involving extended stay times in low earth orbit - Vol I
[NASA-CR-123842] 02 p0209 N73-11694
Identification of potential and inherent radiological hazards of spacecraft with nuclear reactors for electric power generation and elimination or reduction of hazards - Vol. 2 Pt. 1
[NASA-CR-123838] 02 p0209 N73-11695
Reference design document for power module systems, facilities, launch vehicle, and mission operations of nuclear reactor for space base programs - Vol. 3 pt. 1
[NASA-CR-123844] 02 p0209 N73-11696
Analysis of terrestrial nuclear hazards involving zirconium hydride reactor-Brayton power module for all phases of space base program - Vol. 3 Pt. 2
[NASA-CR-123839] 02 p0209 N73-11697
Analysis of space base mission and accidents/events involving nuclear hazard to general public - Vol. 3 Pt. 3
[NASA-CR-123846] 02 p0210 N73-11699
Analysis of nuclear safety aspects in transport of nuclear payloads to and from earth orbit by space shuttle - Vol. 4 Pt. 1
[NASA-CR-123847] 02 p0210 N73-11700
Guidelines and requirements of space base nuclear system safety applied to nuclear hardware, ground support equipment, and range safety and facilities - Vol. 5 Pt. 1
[NASA-CR-123848] 02 p0210 N73-11701
Guidelines and requirements for space shuttle nuclear system transportation of nuclear payloads, ground support systems, and facilities - Vol. 5 Pt. 2
[NASA-CR-123843] 02 p0210 N73-11702
Qualitative identification of steps required to assure incorporation of radiological system safety principles into all phases of manned space base program - Vol. 6
[DOC-72SD4201-6-VOL-6] 02 p0210 N73-11703
Analysis of technical documents and literature for conducting manned space flight nuclear system safety study - Vol. 7 Pt. 1
[NASA-CR-123850] 02 p0210 N73-11704
Sr, Ba, and Ce fallout from nuclear explosions and weapons tests, monitored in ground-level air, in rain, and in atmosphere
[ORO-2529-30] 03 p0333 N73-12719
Ocular effects of near infrared laser radiation for safety criteria
[AD-746793] 04 p0381 N73-13097
Safety calculations for compaction and coolant voiding by airborne fast reactor
[LA-4977] 06 p0699 N73-15695
Test evaluation of laser protective visors for flight crews
[AD-751470] 07 p0751 N73-16102
Safety procedures for using pulsed lasers and making pulsed holograms
[AD-751024] 07 p0808 N73-16555
Medical examinations and protection procedures for NASA employees working in radiologically controlled areas
08 p0871 N73-17050
Occupational hazards and adverse biological effects of ultraviolet radiation
08 p0876 N73-17094
Bibliography of USAF reports on air, water, noise, and radiation pollution
[AD-751898] 08 p0940 N73-17699
Physical and experimental data obtained by artificial satellites for estimating extraterrestrial radiation hazard in manned space flight
[NASA-TT-F-724] 09 p0992 N73-18098
Radiation hazards and spacecraft shielding requirements for human safety during manned space flight
09 p0992 N73-18099
Effects of ionizing radiation and space flight conditions on microorganisms, plants, animals, enzymes, and immunological preparations
09 p0993 N73-18103
Vacuum pump system for 150 kV neutron generator to reduce tritium hazards
[NASA-TM-X-2650] 09 p1038 N73-18468

Apollo experience report to analyze radiation protection problems on earth and in space
[NASA-TN-D-7080] 09 p1090 N73-18899
Characteristics of electromagnetic radiation with emphasis on radiobiology and procedures to reduce undesirable physiological and environmental effects
[JPRS-58783] 12 p1379 N73-21184
Thermal effects of microwave and radio frequency radiation on biological systems
[MBL-1971-7-PT-1] 14 p1609 N73-23048
Technical notes on electronic products
[PB-213755/2] 16 p1884 N73-25247
Radiation hazards of gallium arsenide diode array lasers
[AD-762277] 19 p2229 N73-27975
Hazardous region surrounding near fields of Navy HF whip antennas
[AD-761979] 19 p2237 N73-28034
Radiation hazards produced by gages used in industrial processes and precautions to avoid exposure of personnel to radiation hazards
24 p2952 N73-33583
Radiation hazards involved in conducting radiographic inspections of tires and protective measures for industrial personnel
24 p2952 N73-33584
Characteristics and performance of radiographic machine for conducting inspections of parcels for contraband using ionizing radiation
24 p2952 N73-33585
Application of X ray fluoroscopy and radiography for determining presence of bombs in suspicious packages and protection measures for personnel
24 p2952 N73-33586
Preparation and enforcement of safety recommendations established by American National Standards Institute
24 p2953 N73-33588
Activities of Food and Drug Administration in enforcing safety measures pertaining to industrial radiation equipment
24 p2953 N73-33590
Function of state governments in enforcing radiation safety and protection regulations for industrial, research, and medical uses of ionizing radiation
24 p2953 N73-33591
Function of National Institute for Occupational Safety and Health in industrial radiation safety
24 p2953 N73-33592
Recommended practices for avoiding exposure of personnel to radiation hazards
24 p2953 N73-33593

**RADIATION HEATING**
U RADIANT HEATING
**RADIATION INDICATORS**
U DOSIMETERS
U INDICATING INSTRUMENTS
**RADIATION INJURIES**
Argon-ion laser used to determine ocular effects of repetitive laser pulses on rhesus monkeys
[AD-746795] 04 p0380 N73-13096
Examination of GaAs laser radiation injuries and thresholds of ocular system during night vision exercises
[AD-750350] 05 p0559 N73-14542
Literature review of experimental studies to assess relationship of exposure to microwaves and subsequent development of cataracts
[UR-3490-103] 06 p0631 N73-15123
Spectral deficits in visual acuity due to laser irradiation
[AD-750394] 06 p0637 N73-15173
Chorioretinal burn hazards of high intensity radiation sources in industry
08 p0873 N73-17071
Retinal damage in monkeys exposed to near infrared gallium arsenide laser pulses
[AD-753419] 11 p1248 N73-20135
Radiation effects on human chromosomal aberrations in peripheral blood lymphocytes
14 p1609 N73-23041
Radiation hazards of gallium arsenide diode array lasers
[AD-762277] 19 p2229 N73-27975
Microscopic morphological changes in dog cardiac muscle after chronic gamma irradiation
20 p2366 N73-29027

**RADIATION INTENSITY**
U RADIANT FLUX DENSITY
**RADIATION LAWS**
NT KIRCHHOFF LAW OF RADIATION
Use of radiation for preparative chemistry in liquid solutions
[NASA-TN-D-7285] 15 p1747 N73-24156
**RADIATION MEASUREMENT**
Exposure distributions for air travelers and radiation workers at 0.54 millirem/year
[AD-743482] 01 p0011 N73-10083
Cosmic radiation dosage measurements on Apollo astronauts by Lexan dosimetry
[AD-745188] 01 p0013 N73-10101
Data acquisition system for spark chamber spectrometer and review of space radiation measurement techniques
[AD-741761] 01 p0059 N73-10482
Radiation diagram measurements on antenna model surface for UHF communication to FPL 35F
[FOA-3-C-3678-61] 02 p0139 N73-11130
Comparison of statistical and iteration methods for obtaining vertical temperature profiles from multispectral radiation measurements
02 p0196 N73-11589
Biophysics topics involving radiation data inversion problems
02 p0201 N73-11624
Development of thermopile with sensor surface to receive radiant energy and to provide measurement of energy quantity
[NASA-CASE-NPO-11493] 03 p0300 N73-12447
Long-wave radiation divergence measurements over water and land compared with calculated divergences from temperature and humidity profiles
[AD-748997] 04 p0418 N73-13410
Comparison of national standards of socialist countries for measuring solar radiation using pyrheliometer test readings
04 p0443 N73-13614
Geographical variations in environmental radiation background measurements over United States of America
[UCRL-73822] 06 p0650 N73-15275
Periodic measurements of integrated Stokes parameters from compact radio sources
[AD-749771] 06 p0720 N73-15874
Energy exchange between earth and space from meteorological satellite measurements of infrared radiant emittance and reflected and scattered solar radiation
[NASA-CR-130152] 07 p0780 N73-16341
Evaluation of aerial survey on terrestrial gamma radiation environment
[EGG-1183-1559] 07 p0793 N73-16447
Instrumentation and measurement data of OGO-F solar cosmic ray experiment
[NASA-CR-130155] 07 p0839 N73-16795
Nomenclature for describing radiation measurements and computations in geophysics
[BMBW-FBW-72-30] 09 p1027 N73-18379
Atmospheric effects on remotely sensed radiation measurements
[NASA-CR-130828] 09 p1028 N73-18389
Measurement of distribution of radioactivity in troposphere and stratosphere to determine aerosol dimensions and variation with time
12 p1421 N73-21513
Annual global average earth-atmospheric system radiation balance determined from Nimbus 3 radiation measurements
[NASA-TN-D-7249] 12 p1445 N73-21702
Quantitative analysis of radiation measurements from polar and geosynchronous satellites
[NASA-CR-130194] 13 p1551 N73-22568
Preparation and processing of nuclear emulsions for radiation measurement systems
[AD-756826] 13 p1562 N73-22657
Evaluation of direct current amplifiers for radiation measurements
[CEA-N-1580] 15 p1757 N73-24237
Aerial natural radiation survey, using Twin Bonanza Beechcraft
[HASL-269] 17 p2027 N73-26403
Ion recombination loss in high intensity radiation dosimetry
[REPT-736] 17 p2064 N73-26698
Characteristics of electron-proton spectrometer to measure geomagnetically trapped radiation in geostationary orbit at 6.6 earth radii in outer radiation belt
[NASA-CR-132786] 18 p2150 N73-27381
Pioneer-10 measurements of differential and integral cosmic ray gradients between 1 and 3 AU
[NASA-TM-X-66293] 18 p2197 N73-27736
Calorimetric measurements on X ray penetration through thin carbon foils
[AD-761826] 19 p2322 N73-28679
Measurement of cosmic gamma ray emission from galactic center, Crab nebula, and diffuse radiation
19 p2331 N73-28757
Measuring ionizing radiation in near-earth space
[NASA-TT-F-754] 19 p2340 N73-28825
Deep space solar activity monitoring platform with video capability, including X ray flux, UV flux, charged particle flux, and radio emission measurements
[AD-761799] 19 p2346 N73-28875
Airborne observations to determine radiation characteristics of underlying surface and clouds over various types of ground conditions
20 p2400 N73-29285
Analysis of sky back radiation intensity measurements for clear and overcast skies conducted at different angles of elevation above the horizon by day and night
20 p2400 N73-29286
Development of numerical procedures for computing true brightness of radiant energy measurements from smoothed brightness
20 p2400 N73-29289
Application of airborne actinometric measurements to determine transmission, absorption, and reflection of solar radiation by clouds
20 p2401 N73-29292
Balloon sounding program to measure all components of atmospheric radiation balance and analysis of atmospheric stratification
20 p2401 N73-29293
Analysis of absorption of solar radiation by atmospheric water vapor to determine effects of various atmospheric parameters
20 p2401 N73-29294
Development of numerical method for determining long wave radiation balance of atmosphere based on effective surface radiation
20 p2401 N73-29295
Development of numerical methods for improving accuracy of calculations of thermal radiation in earth atmosphere
20 p2401 N73-29297
Development of empirical relationship between effective terrestrial radiation, ground temperature, and water vapor pressure in the ground air layer for cloudless skies
20 p2402 N73-29300
Development and characteristics of radiometer for airborne measurement of outgoing long wave radiation from earth surface between 8 and 12 microns
20 p2402 N73-29302
Development, characteristics, and operation of telephotometer for simultaneous measurements of angular and space distribution of absolute solar radiation fluxes
20 p2402 N73-29303
Development, characteristics, and operation of compensated thermoelectric net radiometer to show advantage over standard radiometers
20 p2402 N73-29305
Development, characteristics, and operation of thermoelectric photopyranometer with hemispherical glass filters
20 p2402 N73-29306
Development of actinometric instruments and surface coatings to show performance parameters and construction details
20 p2403 N73-29307
Performance tests of radiation thermoelements for radiation flux measurements of atmospheric radiation
20 p2403 N73-29308
Performance tests of radiation thermoelements to determine stability of detectors and feasibility of daytime measurement of long wave radiation
20 p2403 N73-29309
Measurements of radiation characteristics in multistoreyed overmature oak grove
20 p2405 N73-29332
Automatic pyrometer for measuring true metal temperature with radiation
[JPRS-59661] 20 p2419 N73-29435
Procedures for determining variations of meteorological parameters from satellite radiation measurements
20 p2443 N73-29625
Analysis of methods for measuring quantity of radiation emitted from materials using standard sources and calibrated detectors
[PAPER-76A5-730] 21 p2545 N73-30399
Observations of decametric radiation of Jupiter with very-long-baseline interferometer
23 p2836 N73-32659
Sea/land breeze circulation study, using airborne infrared radiation measurements of surface temperature along upper Texas coast
[REPT-36] 24 p2922 N73-33336
Measurement of atmospheric radiation levels at low altitude in vincinity of Vienna, Austria during 1972
[NP-19751] 24 p2922 N73-33340
Monte Carlo technique for determining transient radiation fields or completely bounded media
24 p2956 N73-33615

**RADIATION MEASURING INSTRUMENTS**
NT ACTINOMETERS
NT BOLOMETERS
NT CERENKOV COUNTERS
NT DOSIMETERS
NT EBERT SPECTROMETERS
NT ELECTRON COUNTERS
NT ELECTROPHOTOMETERS
NT ELECTROSTATIC PROBES
NT GEIGER COUNTERS
NT HODOSCOPES
NT INFRARED DETECTORS
NT INFRARED INSTRUMENTS
NT INFRARED SCANNERS
NT INFRARED SPECTROMETERS
NT INFRARED SPECTROPHOTOMETERS
NT MICROWAVE RADIOMETERS
NT NEUTRON COUNTERS
NT NEUTRON SPECTROMETERS
NT PARTICLE TELESCOPES
NT PASSIVE L-BAND RADIOMETERS
NT PHOTOMETERS
NT PROPORTIONAL COUNTERS
NT PYRANOMETERS
NT QUANTUM COUNTERS

NT RADIATION COUNTERS
NT RADIATION DETECTORS
NT RADIOMETERS
NT RIOMETERS
NT SCINTILLATION COUNTERS
NT SILICON RADIATION DETECTORS
NT SOLAR SPECTROMETERS
NT SPARK CHAMBERS
NT SPECTROHELIOGRAPHS
NT SPECTROPHOTOMETERS
NT SPECTRORADIOMETERS
NT THRESHOLD DETECTORS [DOSIMETERS]
NT ULTRAVIOLET SPECTROMETERS
NT ULTRAVIOLET SPECTROPHOTOMETERS

Computer program for measuring specific radioisotopes contained in human body
[AD-745578] 01 p0010 N73-10078

Principles of radiometric reconnaissance
[FOA-3-C-3675-E1] 02 p0172 N73-11391

Radiac set for surveying areas contaminated with fissionable materials
[AD-747051] 02 p0211 N73-11709

Development of thermopile with sensor surface to receive radiant energy and to provide measurement of energy quantity
[NASA-CASE-NPO-11493] 03 p0300 N73-12447

Characteristics of research instruments used on rockets and satellites for investigating solar ultraviolet radiation
[AD-748276] 04 p0424 N73-13454

Airborne radiological measuring system for use in nuclear safety programs and routine surveillance of areas around nuclear facilities
[EGG-1183-1558] 07 p0800 N73-16501

Instrumentation and measurement data of OGO-F solar cosmic ray experiment
[NASA-CR-130155] 07 p0839 N73-16795

Tables of cosmic ray MT-64 muon monitor measurements from solar rotation 1867 to solar rotation 1879
[AECL-4207] 08 p0957 N73-17834

Phototransistor with base collector junction diode for integration into photo sensor arrays
[NASA-CASE-MFS-20407] 10 p1133 N73-19235

Preflight tests and performance of electronic instrumentation in measuring solar radiation during Aerobee 170 and Black Brant V rockets
[AD-756909] 13 p1532 N73-22412

Technical notes on electronic products
[PB-213755/2] 16 p1884 N73-25247

Development and characteristics of self-contained digital integrator for recording daily solar irradiance
[AD-760318] 17 p2035 N73-26468

Development and characteristics of instrument to measure back reflection of laser radiation
17 p2041 N73-26515

Method and apparatus for measuring electromagnetic radiation
[NASA-CASE-LEW-11159-1] 19 p2299 N73-28488

Satellite-borne instruments for measurement of heavy particles
[AD-762208] 19 p2302 N73-28510

Design of gamma ray spectrometer for measurement of intense radiation using Compton scattering effect
[NASA-CASE-MFS-21441-1] 21 p2544 N73-30392

LUIN, code for calculation of cosmic ray propagation in atmosphere
[HASL-275] 24 p2977 N73-33784

RADIATION MEDICINE
NT RADIOBIOLOGY

RADIATION METERS
U RADIATION MEASURING INSTRUMENTS

RADIATION NOISE
U ELECTROMAGNETIC NOISE

RADIATION PRESSURE
NT ILLUMINANCE
NT LUMINANCE
NT LUMINOUS INTENSITY
NT SOUND PRESSURE

Surface wave conversion to longitudinal oscillations in plasma surface layer by perturbation of waveguide
[AEC-TR-7335] 07 p0827 N73-16703

High frequency force field effect on electromagnetic wave propagation into bounded plasma configuration
[AREAEE-124] 07 p0828 N73-16712

Generation of magnetic field energy from radiation pressure in laser-produced plasma thermal energy
[AD-748180] 09 p1071 N73-18742

RADIATION PROTECTION
NT RADIATION SHIELDING
NT SOLAR RADIATION SHIELDING

Guidelines and requirements of space base nuclear system safety applied to nuclear hardware, ground support equipment, and range safety and facilities - Vol. 5 Pt. 1
[NASA-CR-123848] 02 p0210 N73-11701

Guidelines and requirements for space shuttle nuclear system transportation of nuclear payloads, ground support systems, and facilities - Vol. 5 Pt. 2
[NASA-CR-123843] 02 p0210 N73-11702

Qualitative identification of steps required to assure incorporation of radiological system safety principles into all phases of manned space base program - Vol. 6
[DOC-72SD4201-6-VOL-6] 02 p0210 N73-11703

Protection of humans from radiation injuries by chemical means
[NRC-TT-1609] 06 p0629 N73-15112

Effectiveness of pharmacochemical protective substances on irradiated mice as neutron component increases
[DRIC-TRANS-2961] 06 p0631 N73-15124

Medical examinations and protection procedures for NASA employees working in radiologically controlled areas
08 p0871 N73-17050

IR laser radiation eye protector
[AD-753080] 09 p0998 N73-18142

Hand book on ionizing radiation protection policies at Kennedy Space Center
[NASA-TM-X-69410] 10 p1120 N73-19133

Composition and effects of radioprotectors on acceleration tolerance, hypoxia toxicity, radiation protection, and dynamic space flight stress in animals
[NASA-TT-F-721] 11 p1239 N73-20054

Classification of radioprotectors for radiation sickness prevention effects
11 p1240 N73-20065

Effectiveness of combined chemical protectors against mixed gamma-neutron radiation with neutron contributions to absorbed dose
11 p1240 N73-20068

Elimination of toxic cysteamine in organisms and method for prolonging its radioprotective effect
11 p1240 N73-20069

Contamination radiation safety during space flight, and safety problems at launch
[JPRS-58781] 12 p1374 N73-21149

Degradation and reuse of radiative-thermal protection materials for space shuttle
[NASA-CR-123587] 14 p1709 N73-23866

Proceedings of conference on radiation safety and protection in industrial applications
[DHEW-PUBL-[FDA]73-8012] 24 p2951 N73-33574

Chronology of radiation protection methods instituted in industrial plants to show specific procedures and reasons for enforcing protective measures
24 p2952 N73-33575

Characteristics and application of various radiation safety monitoring devices for application to industrial safety protection
24 p2952 N73-33576

Development, application, and characteristics of radiation measuring devices for protection of personnel performing hazardous industrial work
24 p2952 N73-33577

Safety precautions to be followed during radiographic inspection of pressure vessels
24 p2952 N73-33580

Safety devices and precautions to protect personnel performing radiographic inspections of pipeline welds
24 p2952 N73-33581

Radiation hazards involved in conducting radiographic inspections of tires and protective measures for industrial personnel
24 p2952 N73-33584

Provisions of Occupation Health and Safety Act to show requirements imposed on employers and employees for protection from radiation hazards
24 p2953 N73-33587

Preparation and enforcement of safety recommendations established by American National Standards Institute
24 p2953 N73-33588

Activities of Food and Drug Administration in enforcing safety measures pertaining to industrial radiation equipment
24 p2953 N73-33590

Function of state governments in enforcing radiation safety and protection regulations for industrial, research, and medical uses of ionizing radiation
24 p2953 N73-33591

Function of National Institute for Occupational Safety and Health in industrial radiation safety
24 p2953 N73-33592

Recommended practices for avoiding exposure of personnel to radiation hazards
24 p2953 N73-33593

RADIATION PYROMETERS
Automatic pyrometer for measuring true metal temperature with radiation
[JPRS-59661] 20 p2419 N73-29435

RADIATION RESISTANCE
U RADIATION TOLERANCE

RADIATION SHIELDING
NT SOLAR RADIATION SHIELDING

Development and characteristics of radioisotope safety devices for use with electric propulsion system - Vol. 1
[NASA-CR-114505] 01 p0090 N73-10745

Design, development, and characteristics of radioisotope shielding systems for use with spacecraft electric propulsion system - Vol. 2
[NASA-CR-114506] 01 p0091 N73-10746

Design and analysis of radioisotope shield for thermionic power supply used in spacecraft electric propulsion systems - Vol. 3
[NASA-CR-114507] 01 p0091 N73-10747

Radiological safety aspects of manned space missions employing nuclear reactors for electric power and involving extended stay times in low earth orbit - Vol I
[NASA-CR-123842] 02 p0209 N73-11694

Identification of potential and inherent radiological hazards of spacecraft with nuclear reactors for electric power generation and elimination or reduction of hazards - Vol. 2 Pt. 1
[NASA-CR-123838] 02 p0209 N73-11695

Localized shielding effects on antitissue antibody mobilization in irradiated rats
03 p0258 N73-12086

Perturbation theory formulas derived and applied to determine changes in neutron and gamma ray doses due to changes in various radiation shield layers for fixed sources
[NASA-TN-D-7093] 03 p0331 N73-12700

Validity of using only primary protons in Van Allen belt and solar flare proton shielding studies
[ORNL-TM-3785] 03 p0353 N73-12880

Light shield and cooling apparatus for high intensity ultraviolet lamps
[NASA-CASE-LAR-10089-1] 04 p0426 N73-13474

Performance tests on cryogenic insulation materials for nuclear radiation shielding
[NASA-CR-2162] 05 p0578 N73-14707

Electron transport properties in space environment and spacecraft shielding
[NASA-CR-123998] 06 p0702 N73-15722

Ultraviolet radiation detector in presence of proton radiation using sensor tubes within shielding mechanism
[NASA-CASE-MFS-21577-1] 11 p1237 N73-20042

Influence of head and stomach shielding on radiation sickness and animal survival from gamma-neutron irradiation
11 p1241 N73-20071

Reactivity changes of rats to antiradiation drugs with head and stomach shielded during total irradiation
11 p1241 N73-20072

Influence of shielding head and anterior stomach on course of radiation sickness in dogs subjected to total lethal gamma irradiation
11 p1241 N73-20073

Stomach shielding effects on chromosomal aberration frequency in guinea pig and rat marrow cells after gamma radiation at doses of 50 to 200 r
11 p1241 N73-20074

GAST and GALT aminotransferases activity of dog blood serum following total exposure to gamma rays with stomach or head shielded
11 p1241 N73-20075

Pathomorphological changes in internal organs of white rats following 120 MeV proton irradiation and effect of partial shielding on attenuation of damage
11 p1241 N73-20076

Characteristics of pathomorphological changes in rat internal organs subjected to gamma-neutron irradiation with head and stomach shielded
11 p1241 N73-20077

Characteristics of electromagnetic radiation with emphasis on radiobiology and procedures to reduce undesirable physiological and environmental effects
[JPRS-58783] 12 p1379 N73-21184

Analysis of techniques for shielding manned space vehicles against protons and alpha particles from Van Allen belt, solar flares, and cosmic rays
[NASA-CR-131517] 12 p1461 N73-21841

Seam weld cracking in lithium hydride shielding of SNAP 8 reactor after irradiation
[NASA-CR-121157] 14 p1691 N73-23726

Electron irradiation effect on transmission properties of ceria doped solar cell cover glass
[NASA-TN-D-7245] 15 p1737 N73-24082

Mathematical model for radiation analysis and shielding for 1137400E NERVA engine
[NASA-CR-132228] 15 p1810 N73-24668

Radiation shielding for thermal-nuclear stage of Europa 3 launch vehicle
[TR-TT-4-18/72] 15 p1811 N73-24679

Computation of neutrons and gamma ray distribution for radiation shielding of Europa 3 launch vehicle nuclear upper stage
[TN-3-25] 15 p1811 N73-24680

DOPEX-1D2C steepest descent and one-dimensional two constraint radiation shield optimization code
[NASA-TM-X-2836] 18 p2177 N73-27579

Lithium hydride and depleted uranium shield materials for space power nuclear reactor
[NASA-TM-X-2835] 18 p2177 N73-27580

Computer code for generating gamma ray moments
[AD-761839] 19 p2323 N73-28689

Evaluation of stripe domain light deflector using iron compounds
[AD-762475] 20 p2426 N73-29490

Modular program RSYST for simplifying handling of reactor and shielding problems
[CONF-721018-22] 22 p2699 N73-31615

Geometric codes for calculating space radiation transport in shielding configurations
[NASA-CR-124403] 23 p2821 N73-32551

Measured and calculated fast neutron spectra at surface of lithium hydride and depleted uranium shielded reactors
[NASA-TM-X-2906] 24 p2953 N73-33594
Radiation shielding for zirconium hydride reactor systems
[AI-AEC-13081] 24 p2955 N73-33609

**RADIATION SICKNESS**
Classification of radioprotectors for radiation sickness prevention effects
11 p1240 N73-20065
Influence of head and stomach shielding on radiation sickness and animal survival from gamma-neutron irradiation
11 p1241 N73-20071
Influence of shielding head and anterior stomach on course of radiation sickness in dogs subjected to total lethal gamma irradiation
11 p1241 N73-20073
Influence of cysteamine hydrochlorine and vitamin B and C prophylaxis on radiation sickness in humans
11 p1242 N73-20078
Comparison of peripheral blood of acclimatized and nonacclimatized irradiated rats under prolonged conditions of reduced barometric pressure
11 p1243 N73-20088
Combined tissue blocks for comparative pathomorphological study of radiation pathology
11 p1243 N73-20090

**RADIATION SOURCES**
NT MONOCHROMATORS
NT NEUTRON SOURCES
NT POINT SOURCES
Astronomical techniques for determining physical parameters and energy balance of neutron stars based on pulsar observations
[NASA-TM-X-66066] 01 p0103 N73-10850
Method for obtaining ultraviolet source using Cerenkov radiation
[AD-746174] 02 p0182 N73-11477
Computer program for calculating constant dose range in air transport of neutron and photon radiation from point source in atmosphere
[LA-DC-13293] 04 p0453 N73-13700
Oxidation resistance of capsule materials for cobalt 60 power and heat source
[DP-1300] 05 p0498 N73-14057
Gas scintillation counter for measuring fluorescence of source of radium coated with radon
[PUBL-1410] 06 p0702 N73-15725
Nature of weak high latitude X ray sources
[NASA-TM-X-66168] 07 p0839 N73-16796
Multispectral scanning systems and potential application to earth resources, noting radiation sources, atmospheric effects, and sensor techniques
[ERL/R-243-U] 13 p1531 N73-22403
Dynamic model of solar flare emission sources
13 p1572 N73-22742
Optical heterodyne signal power obtained from finite sized sources of radiation
[AD-756463] 14 p1633 N73-23243
Radiation source tracker comprised of sectored matrix of detectors with output voltages corresponding to irradiance levels
[NASA-CASE-NPO-11686] 16 p1911 N73-25462
Origin of diffuse X ray and gamma ray background
19 p2332 N73-28762
Metagalactic orgin of cosmic rays and gamma ray astronomy
19 p2332 N73-28764
Production of gamma rays from explosive nucleosynthesis and low energy cosmic ray scattering
19 p2332 N73-28765
Synthesis of monopulse angular coordinate meters of harmonic and noiselike radiation
20 p2419 N73-29440
Sources, absorption, and detection of cosmic gamma rays
[MPI-PAE/EXTRATERR-83] 24 p2977 N73-33789

**RADIATION SPECTRA**
NT ABSORPTION SPECTRA
NT BALMER SERIES
NT D LINES
NT ELECTROMAGNETIC SPECTRA
NT ELECTRONIC SPECTRA
NT EMISSION SPECTRA
NT FRAUNHOFER LINES
NT H ALPHA LINE
NT H BETA LINE
NT H GAMMA LINE
NT H LINES
NT INFRARED SPECTRA
NT K LINES
NT LINE SPECTRA
NT MICROWAVE SPECTRA
NT RAMAN SPECTRA
NT SOLAR SPECTRA
NT STELLAR SPECTRA
NT TELLURIC LINES
NT ULTRAVIOLET SPECTRA
NT VIBRATIONAL SPECTRA
Numerical analysis of inverse scattering problem applied to far field relations between incident and scattered radiation in presence of scattering object
02 p0200 N73-11613
RESALE-2 and INHALE computer code modifications for detecting radiative power of C02 in detector
[AD-748293] 04 p0430 N73-13500
Current-voltage, load, and spectral characteristics of p- and n-type GaAs
[NASA-TT-F-14859] 11 p1330 N73-20793
Apollo 15 measurement of cosmic gamma ray spectrum between 0.3 and 27 MeV
19 p2331 N73-28756
OSO-7 observations of gamma ray emission in solar flares
19 p2332 N73-28761
Analysis of sky back radiation intensity measurements for clear and overcast skies conducted at different angles of elevation above the horizon by day and night
20 p2400 N73-29286
Effects of radiation and heat balance of active surface on life processes of plants with emphasis on productivity of cotton
20 p2404 N73-29323
Forward scattered light spectrum from pulsed ruby laser in liquid medium
20 p2424 N73-29470
RALPH - on-line data acquisition and analysis system for processing gamma ray and coincidence data
[NASA-TM-X-69507] 22 p2639 N73-31151
Hodoscope measurements of cosmic ray electron spectra
[TR-73-135] 23 p2834 N73-32651
LUIN, code for calculation of cosmic ray propagation in atmosphere
[HASL-275] 24 p2977 N73-33784

**RADIATION THERAPY**
Safe handling system for iridium isotopes used in radiation therapy
12 p1374 N73-21143
Nuclear research and neutron radiotherapy at Navy laboratory
[PB-221982/2] 22 p2738 N73-31924

**RADIATION TOLERANCE**
Neutron and gamma induced transient incapacitation in conditioned Macaca mulatta
[AD-742076] 01 p0010 N73-10080
Radiation damage recovery characteristics of lithium doped solar silicon cells
[NASA-CR-129183] 02 p0128 N73-11044
Spacecraft environment, radiation, and weightlessness effects on human biological processes in manned space flight
[JPRS-57517] 03 p0256 N73-12076
Examination of GaAs laser radiation injuries and thresholds of ocular system during night vision exercises
[AD-750350] 05 p0559 N73-14542
Effects of passivation processes on radiation tolerance of bipolar transistors subjected to neutron or gamma radiation
[SC-DC-72-1232] 05 p0565 N73-14589
Sensitivity of microwave transistor amplifiers to neutron damage in low noise and high power applications
[SC-R-72-2845] 07 p0762 N73-16190
Development of high temperature high radiation silicon semiconductors
[NASA-CR-124074] 08 p0950 N73-17777
Evolutionary adaptation and resistance of unicellular organisms to solar radiation
10 p1118 N73-19118
Increased toxicity of sympathomimetic amine stimulants on spinal reflexes in irradiated frogs
11 p1240 N73-20063
Mortality rate in antiradiation drug protected mice subjected to gamma radiation overloads
11 p1242 N73-20079
Conference on Apollo 16 experiment for measuring microbial response to space environment
[NASA-TM-X-58103] 15 p1740 N73-24102
Ultraviolet extraterrestrial radiation tolerances of Bacillus subtilis spores and Escherichia coli bacteriophages
15 p1740 N73-24107
Space vacuum and solar ultraviolet irradiation effects on survival of Bacillus subtilis spores
15 p1740 N73-24108
Space flight ultraviolet irradiation effects on Bacillus thuringiensis toxin production capability
15 p1740 N73-24109
Phenotype numbers and survival rates of fungi exposed to space environment during Apollo 16 flight
15 p1740 N73-24110
Control circuit for reducing bias voltage and radiation sensitivity of photomultiplier
[NASA-CASE-ARC-10593-1] 21 p2517 N73-30187
Electrical properties and radiation resistance of capacitor insulation
[ORNL-4842] 21 p2563 N73-30544
Service life and reliability of radiation hardened lithium doped solar cells
23 p2859 N73-32840
Reliability evaluation of radiation hardened dual nand gates
[AD-765173] 24 p2900 N73-33151

**RADIATIVE HEAT TRANSFER**
Implicit finite difference scheme for fully coupled solution of viscous shock layer including effects of radiation and strong blowing
[NASA-TR-R-388] 02 p0156 N73-11266
Thermal resistance of clothing noting radiative body heat transfer, air layers, and clothing thickness
[DRIC-TRANS-2920] 03 p0261 N73-12117
Mapping electron number density distribution in nonequilibrium shock layer with kinetic and radiative processes coupled to gas dynamics
[AD-748833] 04 p0407 N73-13312
Atmospheric effects on thermal radiation from tropospheric nuclear explosion to ground target
[AD-745884] 05 p0539 N73-14389
Analysis of temperature distribution in prism heated by axisymmetrical beam of radiant heat
[NLL-M-21514-[5828.4F]] 05 p0605 N73-14921
Preliminary estimates of thermal radiation heat transfer to aerobraking space tug
05 p0608 N73-14947
Optimal performance of infrared pneumatic transducer with capacitive membrane
[ONERA-TP-1150] 09 p1007 N73-18222
Atmospheric aerosol particles in infrared radiation transfer process
10 p1146 N73-19325
Finite difference technique for determining transient temperature distribution in plane slab with uniform heat sources and radiative boundary conditions
10 p1223 N73-19944
Radiative transfer in dense water vapor atmosphere
[LBL-1324] 12 p1464 N73-21864
Photon mean free path control of radiative heat transfer in composite materials
[AD-757140] 13 p1548 N73-22544
Energy equations to analyze radiative heat transfer from gaseous suspension flow with internal heating
14 p1718 N73-23939
BOMEX array for longwave radiative transfer model of tropical atmosphere
15 p1770 N73-24339
Atmospheric radiation transmission research, including aerosol, sky radiance, and electromagnetic field studies
[AD-758771] 15 p1784 N73-24460
Analysis of relationships governing shielding through radiative heat exchange
[AD-760399] 17 p2097 N73-26967
Net radiation method for analyzing radiation heat transfer in enclosures involving partially transparent walls
[NASA-TN-D-7384] 19 p2351 N73-28915
Iterative technique for solving nonlinear integral equation for radiative transfer
[NASA-TN-D-7292] 19 p2352 N73-28916
Mathematical model of radiation fog from evolution to dispersal
[NLL-M-23054-[5828.4F]] 20 p2441 N73-29610
Radiative heat transfer of single crystal surface at phase transition boundary during Czochralski crystal growth
[NLL-RRE-TRANS-386-[8036.625]] 20 p2460 N73-29772
Evolution and sturcture of HII regions
20 p2470 N73-29837
Radiant heat transfer in surface insulation materials for space shuttle orbiter
24 p2939 N73-33468
Radiative emittance measurements on surface insulation coatings in plasma jet wind tunnel
24 p2943 N73-33501

**RADIATIVE RECOMBINATION**
Radio recombination line emission from galactic H 1 and H 2 regions
16 p1961 N73-25863

**RADIATIVE TRANSFER**
NT RADIATIVE HEAT TRANSFER
Numerical analysis of simplified radiator system to predict steady state system performance and to optimize system parameters for minimum area or minimum mass
[NASA-CR-128596] 01 p0108 N73-10892
Relaxation method for inverse solution to atmospheric parameters appearing as functions in integrand of radiative transfer equation
02 p0197 N73-11590
Gamma, X ray, ultraviolet, and infrared astronomy noting instrumentation and radiative transfer
[ESRO-SP-75] 04 p0476 N73-13889
Role of radiation in atmospheric models noting equation of transfer for thermal and solar radiation
05 p0573 N73-14656
Interaction between radiative transfer and turbulent exchange in lower layers of atmosphere
[NASA-TT-F-14518] 09 p1026 N73-18378
Transport equations for studying radiative transport through dense plasma
[AD-753245] 09 p1072 N73-18753
Radiative light transfer model for aerosol radiance loss in atmospheric photometry
13 p1558 N73-22628

Two flux radiative transfer model for measuring absorption and scattering coefficients for nonhomogeneous minerals
[RE-451J] 13 p1558 N73-22632
Bibliography of research in radiation physics and aerodynamics
[AD-761633] 19 p2356 N73-28952
Biometric and radiant transfer characteristics of forest vegetation
20 p2405 N73-29328
Physical theory of coherent cosmic ray propagation in random magnetic fields
[TR-73-133] 23 p2834 N73-32649
Solution to equation of radiative transfer for homogeneous atmosphere bounded by perfect specular reflector
[AD-764619] 23 p2857 N73-32830
Differential approximation and numerical integration methods for analyzing behavior of wall stabilized electric arcs with radiative transport
[AD-765207] 23 p2857 N73-32831

**RADIATORS**
Development of computer program for simulating performance of space radiator to account for transient and steady state performance
[NASA-CR-128594] 01 p0108 N73-10891
Numerical analysis of simplified radiator system to predict steady state system performance and to optimize system parameters for minimum area or minimum mass
[NASA-CR-128596] 01 p0108 N73-10892

**RADICALS**
Monochromatic isophote determination of particle distribution in bright comet
22 p2735 N73-31898

**RADII**
Influence of cavity radius on energy dissipation rate in liquid filled spherical cavities
01 p0040 N73-10319
Dynamic determination of equatorial radius of earth
[NASA-TM-X-66151] 06 p0666 N73-15411

**RADIO ALTIMETERS**
Phase switching of transmitting signal from radio altimeter to reduce step error in signal processing
[ISAS-484-VOL-37-10] 02 p0172 N73-11389
Numerical analysis of terrain echo spectrum from moving radar altimeter
[SC-DR-72-0261] 04 p0389 N73-13159
Power density spectrum for statistical analysis of radar altimeter return variations due to radar motion
[SC-RR-72-0265] 10 p1129 N73-19197
Mathematical models for processing Skylab S-193 radar altimeter data
[E73-10812] 18 p2139 N73-27287
Statistical error analysis of amplitude modulated radio altimeters with phase readout
22 p2629 N73-31064
Statistical analysis of signals in amplitude modulation radio altimeters with phase read-out
22 p2629 N73-31065
Statistical error analysis of frequency modulated radio altimeter with phase readout
22 p2629 N73-31066
Terrain proximity warning system using downward looking radar for improved flight safety
[FAA-RD-73-134] 22 p2697 N73-31603

**RADIO ANTENNAS**
Near field characteristics of radio antenna when covered by plasma sheath to determine current distribution, input admittance, and radiation pattern
[NASA-CR-130076] 01 p0024 N73-10184
Procedures for producing electric fields in conductive media at extremely low frequencies
[AD-748303] 04 p0391 N73-13177
Evaluation of loran antenna modification to determine effect of increased height on radiated power and system performance
[AD-751978] 08 p0942 N73-17714
Radio astronomy and radar observation program for Haystack antenna
[NASA-CR-130756] 08 p0959 N73-17842
Development of low volume, high power radiating transmitter and antenna array to show radiation pattern, antenna gain, and efficiency
[AD-761793] 19 p2245 N73-28098
Utilization of live trees and inanimate metal structures as efficient HF radio antennas
[AD-763887] 22 p2645 N73-31195

**RADIO ASTRONOMY**
Joint Soviet-US research radio astronomy and plans involving spaceborne telescope
[NLL-M-22684-[5828.4F]] 01 p0100 N73-10823
Astronomical techniques for determining physical parameters and energy balance of neutron stars based on pulsar observations
[NASA-TM-X-66066] 01 p0103 N73-10850
Greenwich time and latitude observations for Oct. to Dec. 1971
01 p0105 N73-10874
Research in applications of radar and radio techniques to astronomy and space programs
[NASA-CR-129167] 02 p0226 N73-11829
Greenwich time and latitude observations - Oct. through Dec. 1971
02 p0244 N73-11983
Fluctuations in radio intensity of pulsar emissions
04 p0469 N73-13819
Relative flux density measurements and spectra of extragalactic radio sources at decimetric wavelengths
07 p0838 N73-16788
Importance of Schmidt telescopes to radio astronomy noting color identification of quasars and Southern Hemisphere sky survey
07 p0845 N73-16851
Multiple element antenna array for receiving Doppler arrival angle spectral measurements in radio astronomy
[AD-751873] 08 p0889 N73-17202
Radio astronomy and radar observation program for Haystack antenna
[NASA-CR-130756] 08 p0959 N73-17842
Research in radio astronomy using Haystack antenna
[NASA-CR-130673] 08 p0960 N73-17852
Development and characteristics of traveling wave maser amplifier for use in radio astronomy and deep space communication experiments
[REPT-107] 09 p1043 N73-18504
Design of traveling wave maser system for use in satellite communication telescopes and radio astronomy
[REPT-109] 09 p1043 N73-18505
Searches for interstellar OH and other molecular emission and recombination lines in radio frequency range
[RR-108] 09 p1084 N73-18845
Greenwich time and latitude observations for Jan. to Mar. 1972
13 p1578 N73-22791
Characteristics of radio astronomy radiometer to include operation, maintenance, data acquisition, and data retrieval
[NASA-CR-131830] 13 p1579 N73-22796
Research in X ray, solar, and radio astronomy
[AD-756459] 15 p1833 N73-24860
Fully steerable, decametric array for radio astronomy near Borrego Springs, California
16 p1960 N73-25853
Emission spectra of interstellar molecules
[NASA-TT-F-14961] 17 p2083 N73-26849
Greenwich time and latitude observations for Apr. to Jun. 1972
18 p2197 N73-27740
Radio astronomy observation of planet Saturn using interferometer at 21.1 centimeters wavelength
[AD-760014] 18 p2198 N73-27746
Solar radio and geophysical studies at Manila Observatory
[AD-760771] 20 p2413 N73-29396
Application of radio astronomical methods for determining attenuation and radio emission of rain from cumulonimbus clouds
21 p2570 N73-30594
Research in physical phenomena of space and planetary environments, and applications of radio technology
[NASA-CR-133856] 21 p2596 N73-30809
Greenwich time and latitude observations, Jul. through Sep. 1972
21 p2598 N73-30820
Experimental radio and radar studies on lunar and planetary atmospheres and surfaces, interplanetary medium, and software and hardware conceptions
[NASA-CR-135670] 23 p2845 N73-32734
Activities of Haystack Observatory, and radio astronomy
[NASA-CR-135773] 24 p2900 N73-33152

**RADIO ASTRONOMY EXPLORER B**
U EXPLORER 49 SATELLITE

**RADIO ASTRONOMY EXPLORER SATELLITE**
Instrument system to acquire attitude determination data for RAE-B spacecraft
[NASA-CR-132782] 18 p2175 N73-27569
Instrument system to acquire attitude determination data for RAE-B spacecraft
[NASA-CR-132783] 18 p2176 N73-27570
Galactic background maps of nonthermal radiation obtained from RAE mapping antenna data
[NASA-TM-X-66280] 18 p2196 N73-27728
Experimental in-orbit verification of mathematical model for RAE spacecraft gravity gradient dynamics
18 p2208 N73-27825
Systems analysis of Radio Astronomy Satellite - B to show mission objective, spacecraft configuration, and launch operations
[NASA-TM-X-69490] 20 p2475 N73-29878
RAE-1 measurements of thunderstorms and ground-based radio noise
[NASA-CR-132810] 23 p2757 N73-32062

**RADIO ATTENUATION**
Thermal and atmospheric noise effects on optimization of underwater low frequency communications
[FOA-3-C-3671-60] 02 p0139 N73-11129
Statistical attenuation analysis on extremely low radio frequency propagation
[AD-747779] 03 p0267 N73-12166
Daytime ionospheric attenuation of very low frequency signal transmission over Greenland ice
[AD-746636] 04 p0389 N73-13161
Radio frequency interference rejection of broadband communication system receiver
[AD-756590] 13 p1492 N73-22096
Magnetospheric radio frequencies attenuations by plasma clouds and energetic particles
[AD-757085] 13 p1493 N73-22106
Influence of jungle environment on transmission of digital signals by transmitting swept frequency and photographically recording received envelope and phase
[AD-755257] 13 p1495 N73-22120
Estimation of severe attenuation of radio signals due to precipitation at 2 cm on earth satellite paths
20 p2375 N73-29085

**RADIO AURORAS**
Radio auroras and nighttime magnetic field disturbances
[AD-750019] 05 p0543 N73-14415

**RADIO BEACONS**
Frequency characteristics optimization in two dimensional antenna pattern synthesis
[AD-747492] 03 p0276 N73-12242
Program listings and output data summaries for differential Omega navigation system monitoring and analysis - Vol. 2
[AD-756025] 13 p1557 N73-22618
Development of solid state beacon and radio frequency generator for avionics applications - Vol. I
[AD-761525] 19 p2247 N73-28115
Applications of inverse Fourier transform method of producing high peak power for use with solid state radio beacon - Vol. 2
[AD-761526] 19 p2247 N73-28116
Ionospheric electron content from satellite beacon measurements
[NASA-CR-133475] 19 p2294 N73-28446

**RADIO BLACKOUT**
U BLACKOUT [PROPAGATION]

**RADIO BROADCASTING**
U BROADCASTING

**RADIO BURSTS**
NT SOLAR RADIO BURSTS
NT TYPE 2 BURSTS
NT TYPE 3 BURSTS
NT TYPE 4 BURSTS
NT TYPE 5 BURSTS
Physical models of radio outbursts in extragalactic radio sources
20 p2375 N73-29087

**RADIO COMMUNICATION**
NT RADIO RELAY SYSTEMS
NT RADIO TELEMETRY
NT TELEPHONY
Interchannel interference and Gaussian noise effects on phase modulated digital microwave radio systems
01 p0027 N73-10211
Systems analyses on external and internal radio frequency communication and tracking assemblies for manned space station
[NASA-CR-128561] 03 p0265 N73-12147
Reconnaissance and surveillance countermeasures for radio electronic facilities
03 p0266 N73-12152
Speech intelligibility in naval aircraft radio communications
[AD-748202] 03 p0268 N73-12173
Fast acquisition methods for TDMA
[AD-748882] 04 p0390 N73-13167
Shipboard antenna height effect on ultrahigh frequency surface of air communication
[AD-748203] 04 p0390 N73-13171
Conference on acoustic gravity wave effects in atmospheric transmission of radio communication signals
[AGARD-CP-115] 05 p0508 N73-14131
Design and testing of non-blocking UHF communication system
[AD-751263] 07 p0758 N73-16156
Survey of air traffic control system to determine areas within system susceptible to radio frequency interference effects
[ECAC-PR-72-008] 07 p0818 N73-16629
Reliability performance analysis of NASA communication system to show major area of interruption and malfunctions of specified circuits
[NASA-TM-X-66220] 11 p1256 N73-20190
Air force radio communication and navigation system development planning
[AD-754930] 11 p1258 N73-20207
Design of experiment to measure communication characteristics of wideband satellite to ground communication links
[NASA-CR-130196] 11 p1294 N73-20497
Application of mathematical procedures for determining correlation properties of radio transmissions and signal processing
12 p1379 N73-21181
Articles on ionospheric disturbances, and techniques for predicting condition of ionosphere for planning radio communication
[NASA-TT-F-746] 13 p1519 N73-22314

Using statistical distribution of F 2 layer critical frequency deviations from sliding median for planning radio communication
13 p1520 N73-22319
Graphical method for calculating field intensity and radio wave absorption by ionosphere along radio communication paths
13 p1521 N73-22326
Influence of F 2 regional disturbances and magnetic activity on short wave radio communications
13 p1521 N73-22327
Automation of technical control centers for operation and maintenance of Armed Forces defense communication system
[AD-757551] 14 p1635 N73-23255
Extremely low frequency radio communication in ocean environment
[PB-213904/6] 14 p1636 N73-23264
Electromagnetic shielding and hardening of radio communication systems against atmospheric nuclear burst effects
[AD-758403] 15 p1751 N73-24196
Feasibility of radio communications at very low frequencies from satellite-borne transmitter to receivers with subsurface antennas
[AD-759258] 16 p1876 N73-25188
Analysis of radio communication links for air traffic control operations to show effects of adjacent channel interference and modulation limitations
[FAA-RD-70-71] 18 p2117 N73-27114
Design, development, and test of NASA-GFSC Position Location and Aircraft Communications Equipment [PLACE]
[NASA-TM-X-66287] 18 p2117 N73-27115
Ionospheric fading effects on microwave space communication links in equatorial zone
18 p2212 N73-27855
Capabilities and limitations of communication satellite data transmission for conducting conferences
[NASA-CR-133591] 20 p2377 N73-29098
Development of analytical capabilities for determining use of satellite communications technology for professional education and medical services
[NASA-CR-133359] 20 p2377 N73-29100
Effects of turbulence in Venus atmosphere on Pioneer Venus radio
[JPL-TM-33-644] 20 p2473 N73-29866
Speech recognition in disturbed ship radio communication systems
[FTZ-416-TBR-5] 22 p2633 N73-31104
Noise tolerant radio telegraphy, using orthogonal carrier modulation
[FTZ-455-TBR-39] 22 p2634 N73-31108
Three level transmission code for digital broadcast signal network
[BBC-RD-1973/21] 24 p2894 N73-33101
Analysis of linear systems to show characteristics and to evaluate distortion on basis of quadratic criteria
24 p2944 N73-33515

**RADIO CONTROL**
Radio controlled robots with computer induced artificial intelligence to act as human substitutes under adverse conditions
[NASA-CR-131593] 13 p1550 N73-22558

**RADIO DIRECTION FINDERS**
Optimal emitter location algorithm using Kalman filtering for computerized airborne direction finding
[AD-745888] 02 p0208 N73-11688
Mathematical model for radio frequency interference time history at ILS localizer radio receivers
[AASU-317] 03 p0329 N73-12682
Development of system for encoding outputs from several omnidirectional antennas and processing into modified signal to provide angle of arrival data for direction finding
[AD-747501] 03 p0329 N73-12684
Analysis of single channel phase communication system based on statistical communication theory with application to direction finding
12 p1425 N73-21553
Direction sensitive radar moving target indication
13 p1489 N73-22072
Geometrical optical analysis for determining point source location of electromagnetic signal reflected from ionosphere
[AD-759488] 16 p1877 N73-25196
Characteristics of airborne radio homing and alerting equipment for use with emergency locator transmitters
[RTCA-SC-124] 17 p2060 N73-26663
Synthesis of monopulse angular coordinate meters of harmonic and noiselike radiation
20 p2419 N73-29440
Application of radar direction finding observations to determine extent and severity of storm centers
21 p2569 N73-30590
Comparative efficiency of monopulse radar direction finding systems
[AD-765545] 24 p2896 N73-33118

**RADIO ECHOES**
Design and implementation of experimental system for receiving and recording partially reflected echoes from D region
[PSU-IRL-SCI-414] 15 p1778 N73-24417
Improvement of system for measuring intensity of radio echoes from meteorological radar
[AD-759759] 16 p1878 N73-25201
Experimental systems for automatic receiving and recording of echoes from D region
[AD-760362] 17 p2030 N73-26428

**RADIO ELECTRONICS**
Reconnaissance and surveillance countermeasures for radio electronic facilities
03 p0266 N73-12152
Correlation methods for radio signal processing in presence of interference noise
09 p1002 N73-18181
Research projects in radio and electronic engineering
[AD-752845] 09 p1008 N73-18228

**RADIO EMISSION**
NT RADIO BURSTS
NT SOLAR RADIO BURSTS
NT SOLAR RADIO EMISSION
NT TYPE 2 BURSTS
NT TYPE 3 BURSTS
NT TYPE 4 BURSTS
NT TYPE 5 BURSTS
Observations and analysis of VLF radio emissions in auroral zone
[AD-748880] 04 p0416 N73-13393
Instrumentation for spectrum analysis of short bursts and pulses of Jovian decametric radio emission recorded on magnetic tape
05 p0547 N73-14440
Model for pulsar radiation mechanism and relativistic plasma
[NP-19402] 07 p0826 N73-16692
Ground antenna total electric field strength of RF emission from cosmic ray air showers at three VHF frequencies
13 p1574 N73-22753
Central radio source and hard X ray emitting region of Scorpius X-1
[NASA-TM-X-66244] 15 p1830 N73-24831
Radio recombination line emission from galactic H 1 and H 2 regions
16 p1961 N73-25863
Cosmos 243 measurements of radioemission properties of land surfaces
[NASA-TT-F-14978] 18 p2143 N73-27320
Computerized simulation of cyclotron resonant electrons interaction with narrow band whistler wave along magnetospheric duct for VLF emission triggering
19 p2340 N73-28827
Short wave radio emission measurements on giant planets during outer planets grand tour
[NASA-CR-133500] 19 p2343 N73-28844

**RADIO ENERGY**
U RADIANT FLUX DENSITY
U RADIO WAVES

**RADIO EQUIPMENT**
NT IONOSONDES
NT RADIO ANTENNAS
NT RADIO BEACONS
NT RADIO FILTERS
NT RADIO RECEIVERS
NT RADIO TELESCOPES
NT RADIO TRANSMITTERS
NT RADIOSONDES
NT RADIOTELEPHONES
NT RAWINSONDES
NT SONOBUOYS
NT SPACECRAFT ANTENNAS
NT SUPERHETERODYNE RECEIVERS
NT TRANSMITTER RECEIVERS
NT TRANSPONDERS
NT VERY HIGH FREQUENCY RADIO EQUIPMENT
Microminiaturization and reliability of electronic radio equipment
[AD-745828] 01 p0034 N73-10265
Evaluation of HF/VHF breadboard modeled manpack radio sets
[AD-745918] 02 p0142 N73-11152
Radio electronics, printed circuitry, miniaturization, microminiaturization, data processing, and radio equipment
[AD-746715] 02 p0151 N73-11224
Development and application of correction information to improve accuracy of differential Omega navigation system
[AD-745878] 02 p0208 N73-11691
Development of electronically tuned automatic antenna matching coupler for radio equipment
[AD-746996] 03 p0274 N73-12227
High power electronically tunable VHF/UHF bandpass filter for radio frequency interference reduction
[AD-748810] 04 p0390 N73-13168
Electromagnetic compatibility of very high frequency/frequency modulated radio equipment in tactical site selection
[AD-749186] 04 p0391 N73-13179
Design and development of electronic equipment for antiaircraft defense to include radio equipment, command and control, and electronic countermeasures
[AD-748709] 04 p0400 N73-13254
Design of portable HF/VHF radio set for manpack usage
[AD-749510] 05 p0514 N73-14175
Performance of radio distance finding net using polygonometric grid
[AD-748866] 06 p0697 N73-15683
Radio navigation system for providing all-weather short baseline navigation capability for Army aeronautical missions
[AD-752466] 08 p0942 N73-17715
Airborne and laboratory tests of square wave very high frequency omnirange navigation system
[FAA-NA-72-60] 09 p1063 N73-18666
Reliability performance analysis of NASA communication system to show major area of interruption and malfunctions of specified circuits
[NASA-TM-X-66220] 11 p1256 N73-20190
Operational principles of ultrasonic devices in radio circuits
[AD-754616] 11 p1263 N73-20248
Research projects to develop all-weather, low level navigation systems based on one way ranging, range-range navigation techniques
[AD-755205] 12 p1426 N73-21556
Development and testing of HF/VHF radio set for manpack usage
[AD-755547] 13 p1494 N73-22113
Logistic performance data book for C-141A aircraft radio navigation system to show reliability, maintainability, logistics support, and operating problems
[AD-762250] 19 p2358 N73-28971
Identification of Polish institutes involved in electron tube development and recommendations for changes in research projects
21 p2608 N73-30899

**RADIO FILTERS**
High Q active filter channel for UHF active filter manifolds
[AD-747012] 02 p0150 N73-11216
Design, development, and evaluation of three channel interference cancellation system for use with ultrahigh frequency communication systems
[AD-747802] 03 p0267 N73-12158
Correlation interferometer for decreasing interference in noisy signal reception
24 p2926 N73-33370

**RADIO FREQUENCIES**
NT C BAND
NT EXTREMELY HIGH FREQUENCIES
NT EXTREMELY LOW RADIO FREQUENCIES
NT HIGH FREQUENCIES
NT LOW FREQUENCIES
NT MICROWAVE FREQUENCIES
NT SUPERHIGH FREQUENCIES
NT ULTRAHIGH FREQUENCIES
NT VERY HIGH FREQUENCIES
NT VERY LOW FREQUENCIES
Characteristic oscillations of plasma in point cusp
[IPPJ-133] 02 p0215 N73-11743
C-shaped and symmetric dc and RF, voltage-biased superconducting quantum interference devices
[FOA-2-B-2034-E1] 02 p0218 N73-11763
Central region of CERN synchrocyclotron, including sequence of acceleration spaces and radio frequency extraction system
[NP-19179] 03 p0280 N73-12273
Development of test equipment and procedures to simulate thermal environment and fuel region of small models of nuclear lightbulb engine configurations
[NASA-CR-129299] 03 p0330 N73-12692
RF electric field in electron ion plasma condenser with and without magnetic field
[EUR-CEA-FC-638] 04 p0454 N73-13707
Psychophysical analysis of RF sound perception in human subjects
[AD-747684] 05 p0501 N73-14076
Operating principles of RF biased SQUID systems
[NBS-TN-629] 06 p0708 N73-15773
Suitibility of Nb surfaces in superconducting RF cavities
[KFK-EXT-3/72-3] 06 p0709 N73-15781
Radio frequency measurement of brightness temperature and radar cross sections for explaining subsurface and atmospheric properties of Venus
07 p0840 N73-16803
Western European research on open adiabatic mirror devices and radio frequency plugging - EURATOM controlled fusion report
[EUR-CEA-FC-628-AG] 08 p0948 N73-17760
Field emission, high intensity electron gun, single RF cavity, and compression system
[IPPJ-T-11] 09 p1011 N73-18249
Operating properties of RF resonant plasma with high-intensity electric field
[ITF-72-77-E] 10 p1197 N73-19739
High frequency excitation and instability in plasma heating
[CONF-720705-5] 12 p1434 N73-21617
Technique and equipment for sputtering using apertured electrode and pulsed substrate bias
[NASA-CASE-LEW-10920-1] 15 p1797 N73-24569
Temporal variations in dawn and dusk 600 km mid-latitude trough position measured by RF capacitive probes on Ariel 3
[NASA-TM-X-66253] 15 p1806 N73-24634

Computer program for selection of radio frequencies used in VOR, ILS, and Tacan/DME air navigation systems
[FAA-NA-73-4] 16 p1940 N73-25700
Optimum design of insulating intersheaths between radio frequency cable braids
[RAE-TR-72151] 17 p1998 N73-26154
Theory for electrical resistivity in wire braid coaxial conduction at low and high radio frequencies
[RAE-TR-72153] 17 p1998 N73-26155
Radio frequency heating in THM-2 mirror machine
[LPS-95] 17 p2068 N73-26729
Radio frequency resonant cavity mode analysis technique for fluid mass quantity gauging of space shuttle orbiter tankage
[NASA-CR-133393] 18 p2151 N73-27390
Systems applications in the 10 to 100 GHz frequency band for optimum utilization of EHF frequencies
[OT/TRER-34] 19 p2235 N73-28019
Geophysical observations made during Tenth Soviet Antarctic Expedition with emphasis on field strength of long and short wave radio transmission
20 p2408 N73-29354
Radio frequency source resistance measuring instruments of varied design
[NASA-CASE-NPO-11291-1] 21 p2543 N73-30388
Magnetic resonance phenomena in domain of radio frequencies
[NASA-TT-F-14733] 22 p2632 N73-31091
Utilization of live trees and inanimate metal structures as efficient HF radio antennas
[AD-763887] 22 p2645 N73-31195
Function of National Institute for Occupational Safety and Health in industrial radiation safety
24 p2953 N73-33592
Characteristics of radio frequency produced, magnetically confined hot electron plasma
24 p2962 N73-33668

**RADIO FREQUENCY DISCHARGE**
Parametric analysis for estimating spectral spreading of radio frequency amplifier output due to nonlinearities
[SC-DR-72-0330] 03 p0274 N73-12222
Influence of absorption magnetic thermal RF breakdown in superconducting cavities
[KFK-EXT-3/72-2] 06 p0708 N73-15780
Performance of ion cyclotron plasma generator using radio frequency coil for plasma control
[NASA-TN-D-7187] 09 p1069 N73-18725

**RADIO FREQUENCY HEATING**
Estimation of radio frequency power required to induce direct current in strong magnetic field of thermonuclear fusion device
[IPPJ-135] 02 p0216 N73-11746
Numerical code for studying double resonance production of ionospheric irregularities
[AD-747495] 03 p0299 N73-12440
Measurement of effective collision frequency in RF heating through decay instability in Q device plasma
[CONF-720705-2] 07 p0755 N73-16136
Radio frequency electron drift velocity and parametric instability in plasma heating
[CONF-720705-4] 07 p0756 N73-16138
Electron heating in F region by high power radio frequency beam detected by intensity changes in atomic oxygen nightglow
07 p0775 N73-16293
High power radio frequency ion heating effects on harmonics of ion cyclotron radiation
[ORO-3871-7] 08 p0889 N73-17197
Displacement of electric arc by magnetron-produced pulsed high frequency heating
[BMVG-FBWT-72-19] 08 p0943 N73-17728
Dynamic model for calculating radio frequency absorption in perpendicular ion cyclotron resonance heating of hydrogen deuterium plasma
[IPPJ-146] 09 p1070 N73-18730
Computerized simulation of plasma heating by oscillating electric field
[UCB-34-P-128-X-3] 15 p1817 N73-24731
Damping and ion heating mechanisms in hydromagnetic waves around ion cyclotron frequency
[CEA-CONF-2138] 17 p2067 N73-26724
Feasibility of RF heating for high temperature turbulent plasma production noting diagnostic techniques and CO2 laser scattering
[LRP-64/73] 24 p2966 N73-33702

**RADIO FREQUENCY IMPEDANCE PROBES**
Radio frequency impedance probe measurement of ionspheric electron density profiles using Veronique rocket for sounding
06 p0667 N73-15423
Oblique plasma resonance measured from quadrupolar impedance probe noting motion effect of plasma parallel to geomagnetic field
[GRI/NTP/110] 13 p1563 N73-22669

**RADIO FREQUENCY INTERFERENCE**
NT ATMOSPHERICS
NT BLACKOUT [PROPAGATION]
NT CHIRP SIGNALS
NT DAWN CHORUS
NT ELECTROMAGNETIC NOISE
NT HISS
NT IONOSPHERICS
NT SHOT NOISE
NT WHISTLERS
Interchannel interference and Gaussian noise effects on phase modulated digital microwave radio systems
01 p0027 N73-10211
Analysis of coupling characteristics and crosswalk between electric cables used in naval environments
[AD-742971] 01 p0032 N73-10253
Noise immunity of optical communication lines with frequency and time multiplexing subcarriers
[JPRS-57178] 02 p0181 N73-11467
Design, development, and evaluation of three channel interference cancellation system for use with ultrahigh frequency communication systems
[AD-747802] 03 p0267 N73-12158
Parametric analysis for estimating spectral spreading of radio frequency amplifier output due to nonlinearities
[SC-DR-72-0330] 03 p0274 N73-12222
Mathematical model for radio frequency interference time history at ILS localizer radio receivers
[AASU-317] 03 p0329 N73-12682
High power electronically tunable VHF/UHF bandpass filter for radio frequency interference reduction
[AD-748810] 04 p0390 N73-13168
Procedures for producing electric fields in conductive media at extremely low frequencies
[AD-748303] 04 p0391 N73-13177
Effects of magnetic and electric coupling parameters on terminal response shielding of braided-shield cables exposed to external electromagnetic fields
[AD-748387] 04 p0396 N73-13221
Conference on acoustic gravity wave effects in atmospheric transmission of radio communication signals
[AGARD-CP-115] 05 p0508 N73-14131
Atmospheric gravity wave effects on ionospheric transequatorial radio wave propagation in presence of traveling ionospheric disturbances
05 p0512 N73-14164
Effects of traveling ionospheric disturbances following nuclear explosion on high frequency band propagation
05 p0513 N73-14167
Fluctuation errors of pulse time tracking systems in radar and radio navigation devices caused by noise signals
[AD-749649] 05 p0578 N73-14704
Airborne survey of very high frequency interference levels over residential areas on American west coast
[SD-72-SA-0100-VOL-1] 06 p0640 N73-15197
Survey of air traffic control system to determine areas within system susceptible to radio frequency interference effects
[ECAC-PR-72-008] 07 p0818 N73-16629
Multimode transponders for tracking and data relay satellites
[NASA-CR-130170] 08 p0888 N73-17191
Tunable filter system for reducing intermodulation noise in radio transmitter
[AD-754938] 11 p1257 N73-20197
Interference rejection by adaptive antenna array in spread spectrum communication system
[AD-754444] 11 p1258 N73-20211
Noise scattered into receiving antenna system by turbulent plasma
[AD-756829] 13 p1492 N73-22094
Radio frequency interference rejection of broadband communication system receiver
[AD-756590] 13 p1492 N73-22096
Radar clutter and false alarm probability by high frequency atmospheric noise
[AD-756842] 13 p1493 N73-22104
Markov model for analyzing tracking disruption in automatic radio operation
14 p1619 N73-23116
Computer program for estimating interference in world extremely low frequency radio transmission
[AD-757080] 14 p1633 N73-23238
Performance of digital matched filter receiver designed to receive biphase modulated signal in presence of interference
[AD-756841] 14 p1643 N73-23326
Interference in digital voice data link between aircraft and ground traffic control
[FAA-RD-73-63] 15 p1750 N73-24185
Antenna capable of receiving weak communication signal in presence of strong interference
[AD-758690] 15 p1758 N73-24250
Detection and measurement of radio frequency interference and methods of logic circuit protection
[NLL-PO-2928-[9022.81]] 15 p1759 N73-24254
Airborne radio frequency measurements using automatic spectrum analyzer
[AD-758772] 16 p1876 N73-25184
Preparation of equipment and procedures for program to perform broadband noise measurements at sea
[AD-759033] 16 p1877 N73-25193
Lower ionospheric disturbances in polar region
[NDRE-62] 16 p1905 N73-25407
Determination of D region electron density distributions from radio propagation data
[AD-759018] 16 p1909 N73-25449
Simulated environment interference tests on adjacent channel signal receivers for frequency assignments of instrument landing systems
[FAA-RD-73-1-VOL-1] 17 p2060 N73-26665
Automatic nulling system for interference signal at multichannel receiver by polarization adjustment
[NASA-CASE-NPO-13140-1] 18 p2116 N73-27106
Analysis of time-sharing voice modulated output of several collocated transmitters and receivers using very high frequencies
[AD-758567] 18 p2120 N73-27140
Radio transmitter and receiver design procedures for elimination of mutual radio frequency interference as function of total link selectivity
[SRDE-72023] 19 p2235 N73-28018
Radio frequency shadow calculation for airspace obstruction of radar reception considering Fresnel diffraction
[AG-3082-E-1] 20 p2377 N73-29097
Computer program to compute MF sky-wave interference
[BBC-RD-1973/8] 20 p2391 N73-29206
Radio frequency interference tests of VHF omnirange, instrument landing systems, and glideslope indicators to determine required geographical separation for ground stations
[REPT-523-0764695-00111M-VOL-2]
20 p2453 N73-29712
Extended automatic avionics interference prediction model
[ECAC-PR-73-002] 22 p2631 N73-31086
Digital error probalities of binary receivers in presence of intersymbol interference in fading channels
23 p2755 N73-32049
Radio frequency interference measurements with common digitizer door opened and closed, and influence of various equipments inside room on interference magnitude and intensity
[FAA-NA-73-41] 23 p2757 N73-32061
Predicting day-to-day variability of mid-latitude ionosphere for application to HF propagation predictions
[AD-764711] 23 p2789 N73-32310
Radio frequency interference tests of VHF omnirange system, localizer, and glideslope receiving equipment to determine geographical separation requirements - Vol. 2 Book 2
[FAA-RD-73-1-VOL-2-BK-2] 23 p2816 N73-32513
Feasibility of using Doppler techniques for determining location of ground based emitters causing RFI with low orbiting satellites
[NASA-TM-X-70483] 24 p2895 N73-33109
Interference control in radio link operation
24 p2895 N73-33110
Correlation interferometer for decreasing interference in noisy signal reception
24 p2926 N73-33370
Effects of polar cap absorption events on phase deviations in Omega navigation system
[AD-764521] 24 p2951 N73-33572

**RADIO FREQUENCY NOISE**
U ELECTROMAGNETIC NOISE

**RADIO FREQUENCY RADIATION**
U RADIO WAVES

**RADIO FREQUENCY SHIELDING**
Detection and measurement of radio frequency interference and methods of logic circuit protection
[NLL-PO-2928-[9022.81]] 15 p1759 N73-24254
Process for making RF shielded cable connector assemblies and resulting structures
[NASA-CASE-GSC-11215-1] 19 p2243 N73-28083

**RADIO GALAXIES**
Observations and characteristics of 1.35-cm emissions of water vapor in galactic sources
07 p0837 N73-16787
Solution of ionization and thermal equilibrium equations for gas clouds in quasars and Seyfert galaxies ionized by ultraviolet radiation sources
07 p0839 N73-16801
Measurements of 8000-MHz flux densities of radio galaxies
08 p0958 N73-17839
Radio continuum survey of elliptical galaxies at 6 cm
[AD-754121] 11 p1339 N73-20872
Radio interferometer observations of compact components of quasars and radio galaxy cores
[NASA-TT-F-14698] 13 p1831 N73-24839

**RADIO INTERFERENCE**
U RADIO FREQUENCY INTERFERENCE

**RADIO INTERFEROMETERS**
Characteristics of directional dipole antenna array for very high frequency radio interferometer
01 p0027 N73-10213
Results of observing quasar compact components and radio galaxies made with radio interferometer having limited angular resolution
[NASA-TT-F-14902] 14 p1619 N73-23117
Radio interferometer observations of compact components of quasars and radio galaxy cores
[NASA-TT-F-14698] 13 p1831 N73-24839
Timing requirements and calibration procedures for very-long-baseline interferometry
[AD-757690] 15 p1833 N73-24857

Remote sensing and RF interferometry for determining sea states
16 p1911 N73-25465

RADIO METEOROLOGY
Application of radio wave propagation and radar signatures for analyzing structure of clouds
21 p2569 N73-30589
Application of radar direction finding observations to determine extent and severity of storm centers
21 p2569 N73-30590
Application of radar techniques for determining microstructure parameters of cumulonimbus clouds
21 p2569 N73-30591
Application of radio astronomy methods for analyzing microwave absorption spectrum and properties of atmospheric cloud formations
21 p2570 N73-30593
Application of radio astronomical methods for determining attenuation and radio emission of rain from cumulonimbus clouds
21 p2570 N73-30594
Analysis of meteorological nature and characteristics of anomalous radio echoes received during vertical sounding of troposphere
21 p2571 N73-30602
Development of system for quantitative evaluation of radio echo intensities received during measurement of atmospheric formations
21 p2572 N73-30609

RADIO METEORS
Statistics from synoptic year sample of 20,000 radar meteor observations using eight station radar network
[NASA-CR-2109] 01 p0101 N73-10830
Head echoes of meteoroids
01 p0102 N73-10840
Precise reduction of Super-Schmidt meteors
01 p0102 N73-10841
Dynamics of meteor streams and new asteroid-meteor and comet-meteor associations
01 p0102 N73-10843

RADIO NAVIGATION
NT HYPERBOLIC NAVIGATION
NT LORAN
NT LORAN C
NT LORAN D
NT TACAN
NT VHF OMNIRANGE NAVIGATION
Design and development of electronic equipment for antiaircraft defense to include radio equipment, command and control, and electronic countermeasures
[AD-748709] 04 p0400 N73-13254
Algorithms for predicting ionospheric effects on pseudo-ranging from synchronous satellite navigation system
[AD-749486] 05 p0539 N73-14391
Fluctuation errors of pulse time tracking systems in radar and radio navigation devices caused by noise signals
[AD-749649] 05 p0578 N73-14704
Radio navigation system for providing all-weather short baseline navigation capability for Army aeronautical missions
[AD-752466] 08 p0942 N73-17715
Performance tests of various Tacan ground station modifications designed to minimize false distance measuring equipment indications
[FAA-NA-72-65] 09 p1062 N73-18664
Airborne and laboratory tests of square wave very high frequency omnirange navigation system
[FAA-NA-72-60] 09 p1063 N73-18666
Angular alignment of inertial reference by non-directional data from radio aids
[NASA-CR-128806] 10 p1185 N73-19639
Design, construction, and demonstration of airborne, low frequency, phase stable receiver for aircraft navigation
[AD-754027] 10 p1186 N73-19651
Analysis of improved signal processing techniques for low frequency, one-way ranging for aircraft radio navigation
[AD-754031] 11 p1322 N73-20727
Research projects to develop all-weather, low level navigation systems based on one way ranging, range-range navigation techniques
[AD-755205] 12 p1426 N73-21556
Atmospheric noise model with application to low frequency radio navigation receivers
[AD-757275] 13 p1493 N73-22101
Evaluation of VORTAC navigation system accuracies required to support present and anticipated operational uses of system
13 p1557 N73-22616
Characteristics of airborne radio homing and alerting equipment for use with emergency locator transmitters
[RTCA-SC-124] 17 p2060 N73-26663
Development of airborne very low frequency navigation system using radio communications stations and comparison with other air navigation systems
17 p2098 N73-26973
Analysis of very low frequency radio signals for aircraft area navigation to show capability for continental flight redundancy and reliability
[AD-761498] 19 p2318 N73-28651
Logistic performance data book for C-141A aircraft radio navigation system to show reliability, maintainability, logistics support, and operating problems
[AD-762250] 19 p2358 N73-28971
Satellite based system for L band precision positioning
[NASA-CR-62095] 22 p2697 N73-31604
Solution to radio fixes in spherical trigonometry with confidence region and position error analysis
[AD-764465] 22 p2698 N73-31613
Radio frequency interference tests of VHF omnirange system, localizer, and glideslope receiving equipment to determine geographical separation requirements - Vol. 2 Book 2
[FAA-RD-73-1-VOL-2-BK-2] 23 p2816 N73-32513

RADIO OBSERVATION
Properties of active and helmet coronal streamers based on radio observations
01 p0093 N73-10769
Observation of interplanetary and solar magnetic field sector structure from 1962 through 1968
01 p0094 N73-10770
Intraday time scale variability of infrared, optical, and radio observations from 3C 120, BI Lac, and OJ 287
[AD-752214] 08 p0962 N73-17871
Sector radio measurements of meteor trail drifts by low frequency radar transmissions
17 p2023 N73-26369

RADIO OCCULTATION
Abel integral transform and ray tracing methods for radio occultation data inversion to obtain refractive index profiles of planetary atmospheres
02 p0197 N73-11596
Separation of refractivity gradient components for error elimination and inversion accuracy in occultation measurements on planetary atmospheres
02 p0198 N73-11597
Inversion of radio occultation data for planetary atmospheres by bent ray path technique
02 p0198 N73-11598
Errors in Doppler residuals of Mariner 6 and 7 Martian atmospheric occultation data
02 p0198 N73-11599
Error analysis on Doppler data associated with bent ray path radio occultation of planetary atmospheres
02 p0198 N73-11600
Mariner 9 S band radio occultation measurements of Mars polar and intermediate latitude atmosphere and topography
23 p2843 N73-32716
Mariner 9 radio occultation approximations of Mars surface and atmosphere
23 p2843 N73-32717

RADIO PHYSICS
Application of radiophysical methods to study of earth atmosphere and earth resources with satellites
[NASA-TT-F-14642] 05 p0538 N73-14381

RADIO PROBING
Observations of solar plasma using interplanetary scintillation techniques and radio scattering methods
01 p0097 N73-10801

RADIO PROPAGATION
U RADIO TRANSMISSION

RADIO RANGES
U RADIO BEACONS

RADIO RECEIVERS
NT SUPERHETERODYNE RECEIVERS
NT TRANSMITTER RECEIVERS
Measurement technique for determining sensitivity and radiated power of oscillator radio receiver
[AD-748826] 04 p0389 N73-13165
Performance of portable Doppler geodetic receiver in satellite tracking system
[AD-751597] 07 p0757 N73-16149
VLF phase velocity measurements with separated time phase synchronized receivers
[AD-753206] 09 p1003 N73-18188
Design and performance of circuit for measuring tuning error of single-sideband receiver
[AD-753612] 09 p1004 N73-18199
Design, construction, and demonstration of airborne, low frequency, phase stable receiver for aircraft navigation
[AD-754027] 10 p1186 N73-19651
Design and development of radio receiver for navigation satellite - Vol. 1
[AD-755149] 11 p1321 N73-20723
Design and development of low cost radio receiver for navigation satellite - Vol. 2
[AD-755150] 11 p1321 N73-20724
Analysis of improved signal processing techniques for low frequency, one-way ranging for aircraft radio navigation
[AD-754031] 11 p1322 N73-20727
Open resonator with volumetric detector for tunable millimeter and submillimeter receiver
[AD-754829] 11 p1323 N73-20739
Radio frequency interference rejection of broadband communication system receiver
[AD-756590] 13 p1492 N73-22096
Atmospheric noise model with application to low frequency radio navigation receivers
[AD-757275] 13 p1493 N73-22101
Thick film hybrid radio receiver module consisting of intermediate frequency amplifier and discriminator manpack
[AD-756428] 13 p1494 N73-22108
Measurement of pulse parameters in wideband receivers including amplitude, frequency, and time of arrival
16 p1873 N73-25166
Satellite telecommunication link in health/education experiment using tuned radio frequency receiver
18 p2213 N73-27864
Radio transmitter and receiver design procedures for elimination of mutual radio frequency interference as function of total link selectivity
[SRDE-72023] 19 p2235 N73-28018
Nonreciprocal YIG filter preselector for radio receiver tuners
[AD-762517] 22 p2645 N73-31198
Communication/electronic receiver performance degradation handbook
[AD-764710] 23 p2759 N73-32079

RADIO REFLECTION
U RADIO ECHOES

RADIO RELAY SYSTEMS
Coherent multiplexing and radio relay array systems for satellite communication with small terminals
[AD-747488] 03 p0268 N73-12171
Computer program for geostationary orbit avoidance by radio relay transmitting antennas
[PB-211500] 05 p0514 N73-14179
Augmentation of signal transmission using microwave radio relay systems
[JPRS-58044] 08 p0885 N73-17162
Development of Tracking and Data Relay Satellite system concept for service of low, medium, and high data rate user spacecraft - Vol. 1
[NASA-CR-130219] 13 p1579 N73-22799
Configuration data and design development for Delta 2914 launched Tracking and Data Relay Satellite system - Vol. 2
[NASA-CR-130220] 13 p1579 N73-22800
Data and design information for Atlas Centaur launched configuration of Tracking and Data Relay Satellite system - Vol. 3
[NASA-CR-130221] 13 p1579 N73-22801
Configuration data and design information for space shuttle launch of Tracking and Data Relay Satellite System - Vol. 4
[NASA-CR-130222] 13 p1580 N73-22802
Automation of technical control centers for operation and maintenance of Armed Forces defense communication system
[AD-757551] 14 p1635 N73-23255
Systems analysis of radio-TV satellite for coverage of West Germany and west European areas with German language
14 p1710 N73-23876
Electrical properties and performance of satellite group terminal system
[STC-TM-332] 15 p1749 N73-24178
Rain attenuation and multipath fading in ultrahigh frequency radio relay systems
17 p1995 N73-26134
Rain attenuation statistics for ultrahigh frequency microwave link using meteorological data
17 p1996 N73-26135
Multipath rainfall measurements for planning ultrahigh frequency radio link
17 p1996 N73-26137
Effects of rain and atmospheric turbulence on ultrahigh frequency space communication radio line
17 p1996 N73-26143
Performance tests on transmitter receiver and power amplifier for portable radio manpack
[AD-759953] 17 p2000 N73-26174
ESRO AEROSAT experiment using stratospheric balloon-borne transponder to relay signals from ground station to aircraft flying over sea
18 p2106 N73-27029
Assessment of communication channels for maritime satellite systems using broad beam and multiple beam antennas for satellite-ship links
18 p2117 N73-27121
Diversity and selection effects for improving microwave relay link performance
[AD-756605] 18 p2120 N73-27141
Global rain rate statistic model for coordination of radio relay and communication satellite service
18 p2212 N73-27857
Spread spectrum modulation technique for use in airborne relay communication link
[AD-761522] 19 p2236 N73-28027
Design, construction, and performance of Gunn local oscillator for radio receiver applications
[SRDE-72028] 20 p2376 N73-29091
Legal considerations of satellite communications system for teleconferencing applications
[NASA-CR-133592] 20 p2377 N73-29099
Development of analytical capabilities for determining use of satellite communications technology for professional education and medical services
[NASA-CR-133359] 20 p2377 N73-29100

SHF transhorizon radio relay system, noting long term effects of tropospheric scatter propagation, layer reflection, and precipitation
[FTZ-A-455-TBR-34] 22 p2633 N73-31099
Time signal transfer by satellite relay systems
[AD-764716] 23 p2759 N73-32078
RADIO SCATTERING
Ray tracing computations of high frequency signal propagation and dispersion in traveling ionospheric disturbances
05 p0512 N73-14165
Multiple scattering and attenuation of radio signals caused by rainfall
17 p1994 N73-26122
Polarization fading effect in angle of rotation measurements on ionospheric radio signal scattering
18 p2115 N73-27105
RADIO SIGNAL ABSORPTION
U ELECTROMAGNETIC ABSORPTION
U RADIO TRANSMISSION
RADIO SIGNAL PROPAGATION
U RADIO TRANSMISSION
RADIO SIGNALS
Development of system for encoding outputs from several omnidirectional antennas and processing into modified signal to provide angle of arrival data for direction finding
[AD-747501] 03 p0329 N73-12684
Power spectrum of satellite radio signal phase modulation caused by F region diffraction
[NASA-CR-131280] 11 p1254 N73-20178
Influence of jungle environment on transmission of digital signals by transmitting swept frequency and photographically recording received envelope and phase
[AD-755257] 13 p1495 N73-22120
Construction method for radio signal correlators using Fourier transformation
13 p1497 N73-22131
Measurement of bandwidth for binary FM and bitenary FM signals
[AD-757139] 14 p1633 N73-23240
Interactions between radio brightness and surface conditions of oceans based on Cosmos 243 data
[NASA-TT-F-14954] 16 p1904 N73-25401
Operating theory and measured results of yttrium-iron garnet frequency selective limiter under varying signal environments
[AD-760817] 18 p2124 N73-27165
Analysis of meteorological nature and characteristics of anomalous radio echoes received during vertical sounding of troposphere
21 p2571 N73-30602
Statistical error analysis of amplitude modulated radio altimeters with phase readout
22 p2629 N73-31064
Statistical analysis of signals in amplitude modulation radio altimeters with phase read-out
22 p2629 N73-31065
Statistical error analysis of frequency modulated radio altimeter with phase readout
22 p2629 N73-31066
RADIO SOURCES [ASTRONOMY]
NT CASSIOPEIA A
NT EXTRAGALACTIC RADIO SOURCES
NT PULSARS
NT QUASARS
NT RADIO GALAXIES
NT RADIO STARS
Fringe rate residuals used for baseline interferometry measurement of radio source positions
[AD-746464] 03 p0266 N73-12155
Extragalactic radio sources
04 p0468 N73-13815
Periodic measurements of integrated Stokes parameters from compact radio sources
[AD-749771] 06 p0720 N73-15874
History of 48-inch Palomar Schmidt telescope noting investigation of galactic red shift and radio sources
07 p0844 N73-16841
Flux density variations of seven strongest variable extragalactic radio sources
08 p0956 N73-17827
Intraday time scale variability of infrared, optical, and radio observations from 3C 120, BI Lac, and OJ 287
[AD-752214] 08 p0962 N73-17871
Analysis of techniques and procedures for determining existence of extraterrestrial intelligent life
[NASA-CR-114445] 09 p1082 N73-18822
Search for Lambda 21 cm absorption in QSS and other sources near to spiral galaxies
[AD-754120] 11 p1339 N73-20871
High frequency observations and theoretical interpretation of recombination line emission in direction of supernova remnant 3
[AD-756085] 15 p1833 N73-24858
Accurate positions of OH emission sources at 1665 and 1667 MHz
[AD-756086] 15 p1833 N73-24859
Radio and optical data on outburst in Cygnus constellation
[AD-756464] 15 p1833 N73-24862
Variations in 8 GHz flux density and linear polarization of extragalactic radio sources monitored by 85 ft reflector with rotating feed horn
16 p1960 N73-25854
High energy particles in cosmic radiation sources
[CONF-710974-6] 17 p2080 N73-26823
Interferometer aperature synthesis in interstellar neutral hydrogen line spectra of radio sources
[AD-760013] 18 p2198 N73-27744
Physical models of radio outbursts in extragalactic radio sources
20 p2375 N73-29087
Monte Carlo analysis of radio source counts from Ohio Survey at 1415 MHz
24 p2978 N73-33794
RADIO SPECTRA
NT MICROWAVE SPECTRA
RADIO SPECTROSCOPY
Spectral characteristics of radio bursts from sun
[AD-745167] 01 p0106 N73-10880
RADIO STARS
NT PULSARS
Results of observing quasar compact components and radio galaxies made with radio interferometer having limited angular resolution
[NASA-TT-F-14902] 14 p1619 N73-23117
RADIO TELEMETRY
Problems of radio telemetry systems in manned and unmanned spacecraft
[NASA-TT-F-722] 09 p1002 N73-18175
Canadian radio telemetry installation in conjuction with seismic array system
12 p1377 N73-21169
RADIO TELESCOPES
Multiple rod pyramid as cyclic suspension for parabolic radiotelescope mirror
[AD-757237] 15 p1789 N73-24503
Radio telescope observation of low velocity interstellar neutral atomic hydrogen in direction of early type stars
19 p2342 N73-28836
Problems in designing large mirror radio telescopes
[JPRS-60153] 23 p2793 N73-32345
Design and operational technology associated with radio telescope antennas
[JPRS-59985] 23 p2837 N73-32671
Synchronous-Tracking drive system for automating observations on RTI-7.50/250 MVTU radio telescope
23 p2837 N73-32672
Method of alignment and technology of fabricating RTI-7.5/250 MVTU radio telescope antennas
23 p2838 N73-32675
Parameters of RT-22 Krao Radio telescope antenna at wavelengths of 3 and 1.35 cm
23 p2838 N73-32676
Determination of polarization characteristics of large Pulkovo radio telescope by use of Stokes parameters
23 p2838 N73-32677
RADIO TRACKING
NT WILDLIFE RADIOLOCATION
Satellite system for tracking of wildlife and birds in natural environment
[NASA-CR-130301] 06 p0627 N73-15090
Markov model for analyzing tracking disruption in automatic radio operation
14 p1619 N73-23116
Elements of block diagrams for automatic radio tracking systems
16 p1875 N73-25179
Doppler difference monochromatic baseline interferometry for tracking lunar roving vehicle
18 p2210 N73-27844
RADIO TRANSMISSION
NT DOUBLE SIDEBAND TRANSMISSION
NT IONOSPHERIC F-SCATTER PROPAGATION
NT IONOSPHERIC PROPAGATION
NT MICROWAVE ATTENUATION
NT MICROWAVE TRANSMISSION
NT MULTIPATH TRANSMISSION
NT SHORT WAVE RADIO TRANSMISSION
NT SINGLE SIDEBAND TRANSMISSION
NT TRANSHORIZON RADIO PROPAGATION
Very low frequency radio signal transmission during three polar substorms in 1969
[KGO-PREPRINT-72-303] 01 p0050 N73-10404
Disturbances determining quality of speech transmitted by radio
[IZF-1972-14] 02 p0139 N73-11128
Statistical attenuation analysis on extremely low radio frequency propagation
[AD-747779] 03 p0267 N73-12166
Coherent multiplexing and radio relay array systems for satellite communication with small terminals
[AD-747488] 03 p0268 N73-12171
Radio telemetry for detecting and tracking sounding rockets
[REPT-11] 04 p0388 N73-13153
Daytime ionospheric attenuation of very low frequency signal transmission over Greenland ice
[AD-746636] 04 p0389 N73-13161
Intensity variation of circularly polarized radio emission during solar flares at 3.15 cm on 10 and 12 July 1968
[AD-747606] 04 p0467 N73-13810
Ray tracing computations of high frequency signal propagation and dispersion in traveling ionospheric disturbances
05 p0512 N73-14165
Application of propagation theory to analyze development and effectiveness of loran navigation system in Germany
[AD-750006] 06 p0697 N73-15682
Solar X-ray spectra for predicting ionospheric radio wave propagation during solar activity
[AD-751575] 07 p0794 N73-16459
Radio blackout prevention in atmospheric reentry by chemical injection into vehicle plasma sheath
[AD-753077] 09 p1003 N73-18187
Polarized ellipticity of VLF signals in radio fields
[AD-753085] 09 p1003 N73-18190
Airborne and laboratory tests of square wave very high frequency omnirange navigation system
[FAA-NA-72-60] 09 p1063 N73-18666
ELF signal propagation statistics in 40 to 70 Hz band at Norway, Saipan, and Greece during May 1972
[AD-753685] 10 p1129 N73-19199
Digital coding and modulation processes in radio transmission
[NLL-PO-2832-[9022.81]] 11 p1254 N73-20177
Calculation of very low frequency radio wave propagation characteristics of earth-ionosphere waveguide
[AD-754033] 11 p1256 N73-20194
Feasibility of underground waveguide for radio signal transmission
[AD-754786] 11 p1257 N73-20198
Very low frequency propagation effect on minimum shift keying communication system signal transmission
[AD-755122] 11 p1258 N73-20213
Application of mathematical procedures for determining correlation properties of radio transmissions and signal processing
12 p1379 N73-21181
Spherical Hankel functions for approximating radio transmission in earth ionosphere
[AD-755391] 12 p1380 N73-21192
Radio propagation loss over ocean surface paths
[AD-755511] 13 p1492 N73-22091
Influence of jungle environment on transmission of digital signals by transmitting swept frequency and photographically recording received envelope and phase
[AD-755257] 13 p1495 N73-22120
Research and development of French programs for FR-1, impedance and electrostatic probes, and very low frequency wave propagation
[GRI/NTP/103] 13 p1595 N73-22936
Operational principles and applications of address code communication systems
14 p1619 N73-23114
Computer program for estimating interference in world extremely low frequency radio transmission
[AD-757080] 14 p1633 N73-23238
Ionospheric radio wave propagation in presence of tropospheric duct
[AD-757198] 14 p1634 N73-23248
Simple method for prediction of lowest observed frequency of high frequency propagation paths between Pacific Islands
[AD-757343] 14 p1636 N73-23266
Azimuthal and diurnal high frequency backscatter and terrestrial radio noise
[AD-758776] 16 p1876 N73-25185
PDP 8 computer interfaces for tropospheric radio propagation measurements
[AD-759700] 16 p1879 N73-25214
Features deduced from radio propagation measurements of electron content in solar wind storms
16 p1959 N73-25843
Nonspherical raindrop depolarization of electromagnetic wave in ultrahigh frequency radio link
17 p1994 N73-26123
Multipath propagation and phase delay of ultrahigh frequency radio wave caused by atmospheric discontinuity
17 p1994 N73-26124
Attenuation and phase dispersion of radio wave in atmosphere due to oxygen microwave spectrum
17 p1994 N73-26126
Ultrahigh frequency coherent radio signal transmission for differential phase shift measurements due to vapor and oxygen absorption lines
17 p1995 N73-26131
Point rainfall rate statistics for predicting ultrahigh frequency radio propagation
17 p1996 N73-26136
Calculation of electromagnetic wave absorption by rain for frequencies close to 30 GHz
17 p1996 N73-26138
Thunderstorm cloud height and fading statistics for ATS 5 ultrahigh frequency signal transmission to earth
17 p1996 N73-26141

TDMA/PSK test equipment noting modulators, demodulators, converters, and transmission system
[ESRO-CR[P]-144] 17 p1998 N73-26157
Doppler shift measurements at 16 GHz over transhorizon path to estimate tropospheric wind velocity
[AD-760119] 17 p1999 N73-26164
Review of research in electromagnetic radiation
[AD-759990] 17 p2008 N73-26235
Development of airborne very low frequency navigation system using radio communications stations and comparison with other air navigation systems
17 p2098 N73-26973
Radiation from apertures in curved panels
[NASA-CR-2263] 18 p2116 N73-27110
Analysis of intermodulation of weak signal with strong signal in ionosphere to determine variations as function of modulation frequency of strong signal
[BBC-RD-1973/5] 19 p2234 N73-28010
Geophysical observations made during Tenth Soviet Antarctic Expedition with emphasis on field strength of long and short wave radio transmission
20 p2408 N73-29354
FORTRAN program for prediction of tropospheric radio transmission loss over irregular terrain
[AD-764476] 22 p2635 N73-31115
Model for prediction of horizontal ray path deviation effects in high frequency ionospheric propagation
24 p2894 N73-33105
Interference control in radio link operation
24 p2895 N73-33110

**RADIO TRANSMITTERS**
NT IONOSONDES
NT RADIO BEACONS
NT RADIOSONDES
NT RADIOTELEPHONES
NT RAWINSONDES
NT SONOBUOYS
NT TRANSMITTER RECEIVERS
Kalman filter theory for estimating sonobuoy reference system in antisubmarine warfare
[AD-753608] 10 p1129 N73-19201
Tunable filter system for reducing intermodulation noise in radio transmitter
[AD-754938] 11 p1257 N73-20197
Frequency and time broadcasts provided by National Bureau of Standards radio stations
[NBS-SP-236] 16 p1873 N73-25164
Development of radio locating system for monitoring geographic movement of surface vehicles in metropolitan area using unsynchronized radio broadcasting stations
[NASA-CASE-NPO-13217-1] 17 p1997 N73-26144
Radiation mechanisms of camouflaged body coupled radio transmitters
[AD-759927] 17 p2000 N73-26173
Radio transmitter and receiver design procedures for elimination of mutual radio frequency interference as function of total link selectivity
[SRDE-72023] 19 p2235 N73-28018
Transmitter network synthesis by calculating coverage parameters of broadcast
[BBC-RD-1973/11] 22 p2626 N73-31044
Aircraft mounted crash location transmitter for emergency signal transmission after crashes
[NASA-CASE-MFS-16609-2] 22 p2631 N73-31084
Bird migration patterns using radio transmitters with application to reduction of aircraft hazards during migration in congested air routes
[AD-764830] 23 p2746 N73-31983

**RADIO WAVE REFRACTION**
Slant path attenuation of ultrahigh frequency signals from sun tracking radiometers
17 p1996 N73-26140

**RADIO WAVES**
NT EXTRATERRESTRIAL RADIO WAVES
NT GALACTIC RADIO WAVES
NT LONG WAVE RADIATION
NT MICROWAVES
NT MILLIMETER WAVES
NT RADIO BURSTS
NT RADIO EMISSION
NT SHORT WAVE RADIATION
NT SKY WAVES
NT SOLAR RADIO BURSTS
NT SOLAR RADIO EMISSION
NT SUBMILLIMETER WAVES
NT TYPE 2 BURSTS
NT TYPE 3 BURSTS
NT TYPE 4 BURSTS
NT TYPE 5 BURSTS
NT WHISTLERS
Radio wave scintillations at equatorial regions
[NASA-TM-X-66074] 01 p0028 N73-10218
Hankel function for calculating radio wave diffraction around earth surface
[AD-742108] 01 p0028 N73-10221
Numerical analysis of effects of lower ionosphere on propagation of radio waves at low frequencies for conditions of quiet day, night, and disturbed night
[FOA-3-C-3673-60] 02 p0140 N73-11131
Derivations of straight line, Abel transform and seismological Herglotz-Wiechert transform for reconstruction of refractivity profiles from radio wave phase data
[NASA-TN-D-7098] 02 p0230 N73-11868
Calculation of unsteady electric field produced by radio waves in lower half space
[AD-747731] 03 p0267 N73-12164
Determining ion composition using high-potential radar sets with storage elements for detecting noncoherent scattered radio signals
04 p0413 N73-13373
Experimental data obtained with high frequency radio heating of ionosphere
[AD-748222] 04 p0416 N73-13394
Atmospheric gravity wave effects on ionospheric transequatorial radio wave propagation in presence of traveling ionospheric disturbances
05 p0512 N73-14164
Observation of circulating lymphocytoid cell in monkey after exposure to radio waves
[AD-749583] 06 p0631 N73-15128
Review of material presented at conference on magnetospheric wave-particle interaction
[AD-751568] 07 p0756 N73-16145
Determination of turbulent structure of atmosphere through analysis of perturbations induced upon radio wave propagation
07 p0775 N73-16292
Solar X-ray spectra for predicting ionospheric radio wave propagation during solar activity
[AD-751575] 07 p0794 N73-16459
Stokes parameters for calculating polarization of radio waves reflected from inhomogeneous ionosphere
[NASA-TT-F-14676] 09 p1002 N73-18174
Digital computer routines for calculation of radar/radio tropospheric absorption and noise temperature
[AD-753197] 09 p1004 N73-18193
Analysis of radio phase differences for determining electron concentration in solar corona
10 p1177 N73-19577
Comparison of charged particle conductivities measured in very low ionosphere with atmospheric parameters and high frequency radio wave absorption measurements
[NASA-CR-131604] 13 p1519 N73-22313
Predicting regular variations in geometric parameters of N[h] profiles and h prime f characteristics of quiet and disturbed ionosphere
13 p1520 N73-22321
Predicting daily variations in geometric parameters of N[h] profiles and h prime f characteristics of quiet and disturbed ionosphere
13 p1520 N73-22322
Predicting geometric parameters of N[h] profiles and h prime f characteristics of F region during disturbances
13 p1520 N73-22323
Predicting arrival angle and skip distance variations of quiet and disturbed ionosphere on basis of N[h] profiles and h prime f characteristics
13 p1520 N73-22324
Graphical method for calculating field intensity and radio wave absorption by ionosphere along radio communication paths
13 p1521 N73-22326
Antenna measurement of millimeter radio signal propagation through rain
[NASA-CR-132074] 15 p1751 N73-24188
Mathematical models for analyzing resonance effects on wave absorption and scattering in meteor trails
17 p2023 N73-26372
Influence of mountain barriers on radio wave propagation by meteors
17 p2023 N73-26373
Graphical determination of meteor radiant point curve
17 p2024 N73-26374
Radio wave propagation prediction using D region model accounting for quiet and disturbed VLF propagation
[AD-760685] 18 p2118 N73-27130
Ionospheric disturbances and fading of radio waves in polar regions
[AD-762282] 19 p2299 N73-28483
VHF - UHF surface wave studies of compliant layers for wedge transducers
[AD-762173] 20 p2378 N73-29106
Total electron content studies of radio waves of ionosphere
[AD-762481] 20 p2414 N73-29403

**RADIOACTIVE AGE DETERMINATION**
Rare gas abundances in Apollo 11 rocks 10017 and 10071, and rock age determinations
07 p0842 N73-16818
Vapor condensation of Ni-Fe phases and paleomagnetic records in carbonaceous chondrites
17 p2017 N73-26310

**RADIOACTIVE CONTAMINANTS**
Aerial surveillance techniques for measuring gaseous environmental pollution from nuclear power plant
[WERLV-1] 03 p0334 N73-12721
Measurement of radioisotopes in air and rain water for areas around Helsinki and Ivalo, Finland
[REPT-11] 07 p0815 N73-16604

**RADIOACTIVE DATING**
U RADIOACTIVE AGE DETERMINATION

**RADIOACTIVE DEBRIS**
Study of relative condenssabilities of radioactive vapors in nuclear debris by use of high-powered lasers
[AD-750263] 05 p0579 N73-14713

**RADIOACTIVE DECAY**
NT ALPHA DECAY
NT NEUTRON EMISSION
Nucleocosmochrometers for short lived Pb-205 s-process nucleosynthesis study
[AD-760535] 18 p2182 N73-27618
Naive quark pair creation model and centrifugal barrier effect in baryon decays
[LPTHE-73/11] 20 p2456 N73-29736

**RADIOACTIVE ELEMENTS**
U RADIOACTIVE ISOTOPES

**RADIOACTIVE FALLOUT PARTICLES**
U FALLOUT
U PARTICLES

**RADIOACTIVE ISOTOPES**
NT CALIFORNIUM ISOTOPES
NT COBALT 60
NT COPPER ISOTOPES
NT CURIUM 244
NT NEPTUNIUM
NT PLUTONIUM
NT PLUTONIUM 238
NT TRANSURANIUM ELEMENTS
NT TRITIUM
NT URANIUM 233
Computer program for measuring specific radioisotopes contained in human body
[AD-745578] 01 p0010 N73-10078
Radioisotope snow cover gage
[NLL-M-22676-[5828.4F]] 01 p0055 N73-10443
Thin film window for gas flow radioisotope proportional counter
[AD-745579] 01 p0058 N73-10477
Activities to develop radioisotope energy conversion systems
[ORNL-TM-3687] 03 p0332 N73-12705
Environmental pollution monitoring for radioactive isotope laboratory
[MLM-1922] 03 p0340 N73-12770
Developing isotopic thermoelectric generators in USSR
[AD-749528] 05 p0499 N73-14065
Internally deposited radioisotope effects on cell populations in mammals
[NYO-3970-29] 05 p0500 N73-14074
Potential of data on radioisotopes in atmosphere for determining climatological parameters
[NLL-M-9221-[5828.4F]] 05 p0529 N73-14305
Documentation and examples of radionuclide X ray fluorescence analysis as instrumental analytic method - Part 3
[NASA-TT-F-14635] 05 p0582 N73-14736
Radionuclide X ray fluorescence radiation excitation and applications in analytical chemistry - Part 2
[NASA-TT-F-14634] 05 p0582 N73-14737
Performance and cost effectiveness of isotope Brayton space power system
[NASA-TM-X-68145] 06 p0626 N73-15081
Characteristic property data for plutonia molybdenum radioisotopic cermet fuel
[LA-4976] 06 p0698 N73-15694
Measurement of radioisotopes in air and rain water for areas around Helsinki and Ivalo, Finland
[REPT-11] 07 p0815 N73-16604
Laser-probe mass spectrometric analysis of solar wind, cosmogenic, and radiogenic gases in Apollo 12, 14, and 15 samples
[NASA-CR-130029] 07 p0841 N73-16811
Monte Carlo calculation of cosmic isotope buildup in iron meteorites
[ORNL-TR-2620] 07 p0846 N73-16861
Platinum-rhodium-tungsten alloys for encapsulating space isotopic heat sources
[ORNL-4813] 08 p0932 N73-17632
Long lived, alpha radioisotopes applied to transfer mechanism of air masses in tropopause
09 p1060 N73-18642
Heat transfer from radioisotope generator, using organic fluids
[CEA-CONF-2042] 10 p1224 N73-19950
Design of split-core heat-pipe radioisotopic reactor for space power applications
[NASA-TM-X-68254] 16 p1943 N73-25722
Properties and processing of plutonium fuel for isotopic power source
[MLM-1983] 17 p2061 N73-26674
Isotopic fuel technologies
[MLM-2014] 17 p2061 N73-26675
Depth profiles of galactic cosmic ray produced radionuclides in lunar samples
17 p2079 N73-26814
Radioactive tracers for studying atmospheric circulation and synoptic conditions
20 p2446 N73-29644

Nondestructive determination of radionuclides in lunar samples using large low-background gamma ray spectrometer and application of least squares fitting
[NASA-TM-X-69581] 22 p2718 N73-31756

**RADIOACTIVE MATERIALS**
Analysis of nuclear safety aspects in transport of nuclear payloads to and from earth orbit by space shuttle - Vol. 4 Pt. 1
[NASA-CR-123847] 02 p0210 N73-11700
Guidelines and requirements for space shuttle nuclear system transportation of nuclear payloads, ground support systems, and facilities - Vol. 5 Pt. 2
[NASA-CR-123843] 02 p0210 N73-11702
Analysis of technical documents and literature for conducting manned space flight nuclear system safety study - Vol. 7 Pt. 1
[NASA-CR-123850] 02 p0210 N73-11704
Artificial radioactivity of cumulus clouds moving horizontally and touching peaks of Mt. Olympus
[AEC-TR-7308] 03 p0296 N73-12413
Analysis of radioactivity in lunar samples returned by Apollo 16 flight and relationship to occurrence of solar flares
[NASA-CR-129291] 03 p0354 N73-12886
Development of solenoid valve failure detection system based on addition of radioactive gas to propellant of cold gas jet attitude control system
[NASA-CR-130931] 10 p1165 N73-19476
Development and characteristics of instrument landing system using radioactive materials along runways for glide slope and alignment information
14 p1689 N73-23707
Design, materials, fabrication, and testing in DART thruster technology development
[LA-5017-MS] 17 p2077 N73-26802
Safety precautions for personnel handling radioactive isotopes to prevent accidental exposure to radiation hazards
24 p2952 N73-33582
Radiation hazards produced by gages used in industrial processes and precautions to avoid exposure of personnel to radiation hazards
24 p2952 N73-33583
Atomic Energy Commission policies and procedures for licensing and regulating industrial uses of radioisotopes
24 p2953 N73-33589

**RADIOACTIVE NUCLIDES**
U RADIOACTIVE ISOTOPES

**RADIOACTIVE WASTES**
Extraterrestrial disposal of radioactive wastes
[NASA-TM-X-68147] 01 p0079 N73-10650
Disposal of liquid and solid radioactive wastes at Trisnia Nuclear Research Center
[NASA-TT-F-14697] 11 p1323 N73-20734
Space disposal of actinide radioactive wastes
[NASA-TM-X-68216] 12 p1426 N73-21562
Possible space destinations and launch vehicles for space disposal of radioactive waste
[NASA-TM-X-68211] 12 p1427 N73-21563
Temperature and internal pressure response of nuclear waste disposal container following impact on earth
[NASA-CR-121186] 16 p1943 N73-25721
Extraterrestrial disposal of radioactive waste from thermoelectric propulsion
[NASA-TM-X-62272] 19 p2225 N73-27943

**RADIOACTIVITY**
Bibliography on environmental monitoring for radioactivity
[ORNL-NSIC-101] 03 p0334 N73-12720
Measurement of distribution of radioactivity in troposphere and stratosphere to determine aerosol dimensions and variation with time
12 p1421 N73-21513
Atmospheric radioactivity measurements for 1972 obtained at Vienna, Austria
[NP-19753] 24 p2922 N73-33339
Industrial applications of radiation technology for conducting nondestructive tests
24 p2952 N73-33578

**RADIOBIOLOGY**
Articles and abstracts of articles concerning radiobiology
[AEC-TR-7306] 03 p0259 N73-12103
Charged particle energy deposition calculations for radiobiological system
[ORO-3798-52] 04 p0380 N73-13090
Internally deposited radioisotope effects on cell populations in mammals
[NYO-3970-29] 05 p0500 N73-14074
Safety procedures for using pulsed lasers and making pulsed holograms
[AD-751024] 07 p0808 N73-16555
Industrial hygiene, radiological health, and spacecraft sanitation studies in NASA Environmental Health Program
08 p0872 N73-17057
Electron-proton spectrometer applied to Skylab program for measurement of electrons and protons resulting from solar flares to determine radiobiological safety factors
[NASA-CR-128704] 08 p0925 N73-17577
Physical and experimental data obtained by artificial satellites for estimating extraterrestrial radiation hazard in manned space flight
[NASA-TT-F-724] 09 p0992 N73-18098
Effects of ionizing radiation and space flight conditions on microorganisms, plants, animals, enzymes, and immunological preparations
09 p0993 N73-18103
Composition and effects of radioprotectors on acceleration tolerance, hypoxia toxicity, radiation protection, and dynamic space flight stress in animals
[NASA-TT-F-721] 11 p1239 N73-20054
Characteristics of electromagnetic radiation with emphasis on radiobiology and procedures to reduce undesirable physiological and environmental effects
[JPRS-58783] 12 p1379 N73-21184
Physical and biomedical research by earth orbiting space stations
[AD-756771] 15 p1743 N73-24126
Proceedings of conference on radiation safety and protection in industrial applications
[DHEW-PUBL-(FDA)73-8012] 24 p2951 N73-33574

**RADIOCHEMICAL SEPARATION**
Application of inorganic exchangers to radiochemical separations on neutron activated high purity materials
[CONF-721069-42] 17 p2050 N73-26584

**RADIOCHEMISTRY**
NT RADIOCHEMICAL SEPARATION
Preparation of pure materials, radiation chemistry, and solid state studies
[BARC-599] 05 p0506 N73-14120
Measurement of radiation exposure of astronauts by radiochemical techniques
[NASA-CR-130538] 08 p0878 N73-17114
Annual report 1971-1972 of Interuniversitair Reactor Institute in Netherlands
10 p1195 N73-19721

**RADIOGRAPHY**
NT AUTORADIOGRAPHY
Radiographic analysis using isodensitometer techniques
[AD-746954] 03 p0303 N73-12477
Bibliography of literature on radiographic techniques for nondestructive tests
[AD-749258] 05 p0533 N73-14488
Nondestructive inspection techniques for examining catapult and arresting gear structures on E-2 aircraft
[AD-752492] 08 p0868 N73-17027
Application of neutron radiography for inspection of fiber glass composite structures
[AD-752457] 08 p0936 N73-17665
Application of electronic image analyzer to dimensional measurements from neutron radiographs of nuclear fuel elements
[NASA-TM-X-68200] 11 p1293 N73-20495
Techniques and software for digital enhancement of radiographs
[NASA-CR-2213] 13 p1497 N73-22135
Technical and economic aspects of new industrial radiographic imaging papers
[AD-759907] 17 p2035 N73-26471
Stop-motion cinefluorography system for biomedical research
[AD-762412] 19 p2302 N73-28513
Radiography for nondestructive evaluation of internal flaws
19 p2303 N73-28521
Computer enhancement of radiographs using digital filtering techniques
[NASA-CR-124393] 22 p2673 N73-31414
Evaluation of radiographic paper system using ultraviolet fluorescent screens including program objectives, technique, and sensitivity data for F-1 screen
[AD-764779] 23 p2794 N73-32355
Application of radiation technology and equipment for nondestructive analysis of commercial aircraft structures during aircraft maintenance periods
24 p2952 N73-33579
Safety precautions to be followed during radiographic inspection of pressure vessels
24 p2952 N73-33580
Safety devices and precautions to protect personnel performing radiographic inspections of pipeline welds
24 p2952 N73-33581
Radiation hazards involved in conducting radiographic inspections of tires and protective measures for industrial personnel
24 p2952 N73-33584
Characteristics and performance of radiographic machine for conducting inspections of parcels for contraband using ionizing radiation
24 p2952 N73-33585

**RADIOISOTOPE BATTERIES**
NT SNAP 19
NT SNAP 23
Optimization of specific power highly efficient radioisotope thermoelectric generator
07 p0819 N73-16636
Performance prediction for tritium powered generators
[LIB/TRANS-437] 24 p2881 N73-33004

**RADIOLOGY**
Emergency radiological and meteorological instrumentation criteria for reactors
[BNWL-1635] 04 p0422 N73-13443
Medical examinations and protection procedures for NASA employees working in radiologically controlled areas
08 p0871 N73-17050

**RADIOLYSIS**
Application of paints and varnishes as protective coatings for industrial structures and equipment against radiation damage
[AD-745701] 01 p0071 N73-10582
Use of radiation for preparative chemistry in liquid solutions
[NASA-TN-D-7285] 15 p1747 N73-24156
Radiolytic preparation of anhydrous tin [2] chloride
[NASA-TM-X-2927] 24 p2891 N73-33082

**RADIOMETERS**
NT INFRARED DETECTORS
NT INFRARED SCANNERS
NT MICROWAVE RADIOMETERS
NT PASSIVE L-BAND RADIOMETERS
NT SPECTRORADIOMETERS
Atmospheric transmittance from sun and sky radiance measurements with Nimbus E infrared temperature profile radiometer prototype used at Mauna Loa Observatory
[NOAA-TR-NESS-61] 01 p0048 N73-10391
Detection of internal ocean waves using three-color infrared radiometer
[AD-745004] 01 p0059 N73-10484
Principles of radiometric reconnaissance
[FOA-3-C-3675-E1] 02 p0172 N73-11391
Combined radar-radiometer for remote sensing at microwave performance
[NASA-CR-128492] 03 p0265 N73-12145
Establishment of radiometric calibration technique to permit absolute reflectance characteristics of ground targets to be determined from ERTS-1 data
[E72-10255] 03 p0290 N73-12355
Design and development of radiometer to observe steady state radiation in vacuum environment
[NASA-CASE-MFS-21108-1] 03 p0301 N73-12455
Design of radiometric emittance measurement system for use at high temperatures
[NASA-CR-123968] 04 p0420 N73-13421
Radiometer quadrature control and measuring system using optical coupling circuitry
[NASA-CASE-MFS-21660-1] 04 p0421 N73-13434
Radiometric calibration technique to permit absolute reflectance characteristics of ground targets to be determined from ERTS-1 data
[E72-10326] 05 p0530 N73-14314
Method for calibrating visible channel of satellite radiometer from orbit by using sunlit area as calibration target
[NOAA-TR-NESS-62] 05 p0547 N73-14441
Smoke plume analysis of steam plant in Huntsville, Alabama, using fan-beam and single-beam radiometers
05 p0608 N73-14942
Characteristics of four types of horn antennas for application as S-band radiometers and modifications to improve beam efficiency
[NASA-CR-2133] 07 p0755 N73-16135
Earth resources laboratory data system for analyzing and processing multispectral, radiometric, photographic, and passive microwave imagery data
[NASA-CR-128693] 07 p0758 N73-16160
Characteristics of radar equipment and microwave radiometers to show application to earth resources surveys
07 p0784 N73-16377
Spectroscopic instrumentation system for zone radiometry
[NASA-CR-124062] 08 p0922 N73-17555
Soil moisture measurements for microwave radiometers onboard Convair 990 aircraft
08 p0971 N73-17935
Arctic ice measurements from airborne microwave radiometers and ground based equipment in Mar. 1971
08 p0971 N73-17937
Multispectral method of determining sea surface temperatures, using Nimbus 2 infrared radiometer
08 p0971 N73-17938
Medium and high resolution radiometer measurements of water vapor absorption regions from Nimbus satellites
08 p0972 N73-17942
ITOS D and Nimbus E radiometer data
08 p0972 N73-17943
Analysis of cloud formations, ozone distribution, and meteorological data from Nimbus 4 satellite observations
[NASA-TM-X-66190] 09 p1028 N73-18392
Design and operation of radiometer deployment subsystem for Nimbus E spacecraft
09 p1088 N73-18877
Precision geometric and radiometric correction of bulk digital ERTS-1 imagery by digital techniques
[E73-10342] 10 p1148 N73-19341

Radiometric calibration technique to permit absolute reflectance characteristics of ground targets to be determined from ERTS-1 imagery
[E73-10349] 11 p1274 N73-20343
Impact of radiometry and photometry on economic, social and environmental problems
[NBS-TN-594-4] 11 p1292 N73-20488
Atmospheric observation techniques using aircraft infrared radiometers as prototypes for spacecraft remote sensing application
[NOAA-TR-NESS-64] 11 p1293 N73-20494
Establishment of radiometric calibration technique to permit absolute reflectance characteristics of ground targets to be determined from ERTS-1 data
[E73-10458] 12 p1394 N73-21300
Utilization of millimeter wave radiation from atmospheric oxygen to provide vertical sensing information to satellite-borne radiometer
[NASA-CR-2229] 13 p1530 N73-22396
Characteristics of radio astronomy radiometer to include operation, maintenance, data acquisition, and data retrieval
[NASA-CR-131830] 13 p1579 N73-22796
Radar/radiometer system for measuring temporal and spatial precipitation characteristics particularly thunderstorm activity
[NASA-CR-130235] 14 p1667 N73-23532
Sea surface temperature measurements from Skylab EREP radiometer data
[E73-10604] 15 p1773 N73-24365
Polyvinylfluoride pyroelectric radiometer
[NASA-TM-X-62271] 16 p1912 N73-25472
Data processing techniques for radiometry
[PB-214184/4] 16 p1939 N73-25689
Four channel radiometer for remote sensing of microwave emission from atmospheric oxygen and water vapor
[AD-759535] 16 p1939 N73-25696
Radiometric measuring system for solar activity and atmospheric attenuation and emission
[NASA-CASE-ERC-10276] 17 p2031 N73-26432
Two channel output, high resolution surface composition mapping radiometer, and thermal channels of MSDS scanner studies onboard Nimbus 5
[NASA-CR-132764] 17 p2031 N73-26437
Determination of variations in spectral signatures for different geological target types and correlation with radiometric measurements from air and ground
[E73-10808] 18 p2139 N73-27283
Determination of variation in spectral signatures for different geological target types using ERTS-1 radiometric data
[E73-10809] 18 p2139 N73-27284
Variations in spectral signatures for different geological types based on ERTS-1 radiometric data
[E73-10810] 18 p2139 N73-27285
Digital system for precision geometric and radiometric correction of ERTS-1 RBV and MSS images
[E73-10827] 18 p2140 N73-27299
Evaluation of radiometric computations in infrared window and water vapor absorption band regions based on 4-D atmospheric models
[NASA-CR-129007] 18 p2172 N73-27546
Visible infrared spin-scan radiometer system for earth and cloud cover photography by synchronous meteorological satellite
18 p2209 N73-27834
Radiometer image data compression system with zero error wideband ground link transmission
18 p2212 N73-27863
Masking of ERTS-1 RBV images to reduce stationary residual inaccuracies in radiometric shading corrections
[PAPER-14] 19 p2277 N73-28326
Machine processing of ERTS-1 radiometric and ground truth data and calibration of radiometers
[E73-10855] 19 p2292 N73-28432
Development of catalogs for backscatter and brightness temperature measurements and atmospheric effects on Skylab S-193 data
[E73-10896] 20 p2395 N73-29245
Development and characteristics of radiometer for airborne measurement of outgoing long wave radiation from earth surface between 8 and 12 microns
20 p2402 N73-29302
Design, development, and characteristics of high sensitivity, nonselective pyranometer with black detecting surface and xenon filling
20 p2402 N73-29304
Development, characteristics, and operation of thermoelectric photopyranometer with hemispherical glass filters
20 p2402 N73-29306
Performance tests of radiation thermoelements for radiation flux measurements of atmospheric radiation
20 p2403 N73-29308
Performance tests of radiation thermoelements to determine stability of detectors and feasibility of daytime measurement of long wave radiation
20 p2403 N73-29309
Characteristics of pryanometers and net radiometers, calibrated for short wave radiation
20 p2403 N73-29312
Black body temperature of double pyrgeometer with two net radiometers
20 p2403 N73-29313
Analysis of temperature and radiation regime above paddie surfaces as obtained by helicopter-borne radiation thermometer
20 p2405 N73-29324
Analysis of methods for measuring quantity of radiation emitted from materials using standard sources and calibrated detectors
[PAPER-76A5-730] 21 p2545 N73-30399
Measurement of density distribution and patterns of stowing mixture in hydraulic installations by radiometric scanning
[ITJ-35] 21 p2549 N73-30436
Precision geometric and radiometric correction of bulk digital ERTS-1 imagery of Baltimore, Maryland by digital method
[E73-11019] 22 p2661 N73-31323
Infrared radiometry and air/sea interaction studies
[AD-763788] 22 p2669 N73-31389
Effect of television camera and radiometer resolution on accuracy of cloud quantity determinations from satellites
22 p2693 N73-31569
Analysis of GARP radiometersonde comparisons
[WMO-358] 23 p2813 N73-32493
Description of intercomparison of radiometersondes
23 p2814 N73-32494
Analysis of radiometersonde comparisons
23 p2814 N73-32495
Analysis of Mariner 9 infrared radiometric Mars surface measurements
23 p2841 N73-32701
Objectives of infrared radiometry experiment
24 p2983 N73-33838

RADIONUCLIDES
U RADIOACTIVE ISOTOPES
RADIOPROTECTIVE AGENTS
U ANTIRADIATION DRUGS
RADIOSENSITIVITY
U RADIATION TOLERANCE
RADIOSONDES
NT IONOSONDES
NT RAWINSONDES
Monthly statistics of precipitable water over Australia in atmosphere from 400 mb to surface, determined from daily radiosonde ascents, 1958 through 1969
01 p0074 N73-10609
Radiosonde height and temperature data for updating asynoptic meteorological measurements
[NOAA-TM-NWS-NMC-51] 01 p0074 N73-10613
Methods for determining atmospheric circulation from satellite pictures
02 p0204 N73-11649
High altitude wind and temperature measurement data from meteorological sounding rockets, and radiosondes for May 1971
02 p0204 N73-11651
High altitude wind and temperature measurement data from meteorological sounding rockets and radiosonde observations - February 1971
02 p0204 N73-11652
Analysis of standard radiosonde system for accurate measurement of meteorological parameters which affect artillery fire
[AD-747759] 03 p0327 N73-12671
Meteorological and climatological radiosonde observations
10 p1180 N73-19601
Design of AMSS prototype rocketsonde and ground antenna
[AD-754895] 11 p1316 N73-20681
Meteorological investigation of stratospheric turbulence using radiosonde data
[NLL-M-22819-[5828.4F]] 12 p1419 N73-21502
Design, construction, and electrical circuits for radiosondes to study warm cloud development
[AD-758073] 14 p1686 N73-23684
Data processing techniques for radiometry
[PB-214184/4] 16 p1939 N73-25689
Investigation of errors introduced into meteorological calculations through use of hypsometric equation
[AD-759489] 16 p1940 N73-25697
Radiosonde measurements of subsidence in free atmosphere over Belgian weather station
[PUBL-SER-B-69] 17 p2057 N73-26637
Aerological ozone sounding
[AD-762291] 19 p2297 N73-28469
Solid state commutator design for radiosonde set AN/AMQ-9
[AD-763085] 20 p2381 N73-29132
International comparisons of sample-type radiosondes from U.S.S.R., Finland, and Japan
20 p2448 N73-29670
Residual temperature-induced humidity errors in radiosondes
[AD-762484] 20 p2450 N73-29694
Analysis of GARP radiometersonde comparisons
[WMO-358] 23 p2813 N73-32493
Description of intercomparison of radiometersondes
23 p2814 N73-32494
Analysis of radiometersonde comparisons
23 p2814 N73-32495

RADIOTELEPHONES
Automatic frequency control circuit for radiotelephone receiver-converter
[AD-758686] 16 p1877 N73-25193
RADIOTHERAPY
U RADIATION THERAPY
RADIUM
NT RADIUM 226
RADIUM ISOTOPES
NT RADIUM 226
RADIUM 226
Gas scintillation counter for measuring fluorescence of source of radium coated with radon
[PUBL-1410] 06 p0702 N73-15725
RADIUS
U RADII
RADOME MATERIALS
Analysis of radome design techniques and development of specifications for radome construction
[AGARD-AR-53] 14 p1618 N73-23108
Water impact damage to radome materials
[AD-759973] 17 p2000 N73-26170
RADOMES
Specifications for fused silica slip-casting radome material
[AD-745332] 01 p0028 N73-10219
Processing specifications for slip-cast fused silica radomes
[AD-745793] 01 p0029 N73-10229
Acceptance criteria specification for slip-cast fused silica radomes
[AD-745743] 01 p0029 N73-10230
Nuclear thermal vulnerability of honey comb sandwich radome panels
[AD-753666] 09 p1056 N73-18605
Analysis of radome design techniques and development of specifications for radome construction
[AGARD-AR-53] 14 p1618 N73-23108
Sidelobe level increase and gain reduction caused by raindrops on surface of radar antenna radome
[AD-759178] 17 p1998 N73-26160
Composite materials, ceramics, textiles, and plastics for radomes - bibliographies
[AD-760960] 18 p2118 N73-27126
Radio frequency interference measurements with common digitizer door opened and closed, and influence of various equipments inside room on interference magnitude and intensity
[FAA-NA-73-41] 23 p2757 N73-32061
RADON
Portable radon alpha decay detectors for use in fluorspar mines
[BMBW-FBK-72-14] 03 p0303 N73-12473
Gas scintillation counter for measuring fluorescence of source of radium coated with radon
[PUBL-1410] 06 p0702 N73-15725
Spark counter for neutron and radon dosimetry discussing use and reproducibility
[BMVG-FBWT-72-33] 10 p1161 N73-19448
Lunar radon emanation measurements, using alpha particle spectrometers on Apollo 16
12 p1451 N73-21754
Influence of wind speed and direction, and temperature on radon gas concentration in atmosphere
17 p2017 N73-26309
RAE-B
U EXPLORER 49 SATELLITE
RAE-1
U EXPLORER 38 SATELLITE
RAFTS
NT LIFE RAFTS
RAIL TRANSPORTATION
Evaluation of effectiveness of indices relating to effect of vehicle vibrations on passenger comfort with application to railroad travel
01 p0003 N73-10018
Fuel cell applications as power supplies for rail transportation
[AD-747512] 04 p0376 N73-13056
National transportation statistics summaries for 1960 to 1970
06 p0732 N73-15969
Design and development of diborane shipping container
[NASA-CR-130808] 09 p1038 N73-18466
Comparison of air pollution from aircraft, automobiles, buses, trucks, railroads, and electric trains in US from 1940-1980
[FAA-EQ-73-2] 12 p1421 N73-21522
Experimental determination of compressive behavior of linear induction motor reaction rail
[NASA-TM-X-69276] 17 p2011 N73-26263
Application of aircraft crash investigation procedures to railroad passenger train derailment
[FAA-AM-73-1] 19 p2218 N73-27896
Evacuation areas for transportation accidents involving propellant tank pressure bursts
[NASA-TM-X-68277] 20 p2488 N73-29987
RAILROADS
U RAIL TRANSPORTATION
RAILS
Snow accumulations on air cushion vehicle track sections
[NRC-12939] 09 p1010 N73-18247

RAIN
Measurement and analysis of depolarization and differential attenuation during propagation of millimeter wave signals through rain
[NASA-CR-130107] 01 p0028 N73-10217
Reducing rainfall-induced blackouts by space diversity for millimeter wave, earth satellite communications systems
[AD-747022] 02 p0143 N73-11162
Radar techniques for measuring turbulent layers in lower stratosphere and rain in troposphere
02 p0197 N73-11593
X-band pulsed-Doppler radar measurement of radial velocity spectra in Arizona light showers
[PB-211388] 05 p0574 N73-14675
Computerized simulation of thunderstorm rainfall characteristics
[PB-211806] 05 p0575 N73-14679
Digital computer program for determining mean rainfall over areas by use of Thiessen method
[PB-211232] 06 p0694 N73-15655
Probability models of wet and dry days for several stations in Thailand
[THESIS-392] 08 p0938 N73-17684
Tropical rainfall patterns and associated mesoscale systems in Southeast Asia and South America
[AD-752467] 08 p0940 N73-17706
Estimation of average daily rainfall from satellite photographs
[NOAA-TM-NESS-44] 09 p1060 N73-18645
Statistical analysis of rainfall frequency in central Valais
[REPT-28] 10 p1181 N73-19609
Annual, monthly, and hourly rainfall for Hilo, Hawaii
[UHMET-72-03] 12 p1422 N73-21527
Reduction of probability of simultaneous rainfall on millimeter wave earth satellite space communication terminals
[AD-757506] 14 p1633 N73-23242
Influence of rain on airborne Doppler velocity sensor performance
[AD-757509] 14 p1668 N73-23541
Antenna measurement of millimeter radio signal propagation through rain
[NASA-CR-132074] 15 p1751 N73-24188
Satellite cloud photography for predicting rainfall in Sudan
[AD-757733] 15 p1783 N73-24452
Methods of forecasting hail, thunderstorms, and amounts of rainfall
[NLL-M-22902-[5828.4F]] 15 p1805 N73-24626
Procedures and facilities in Czechoslovakia for determining pollution of rain water
[NLL-M-22857-[5828.4F]] 15 p1805 N73-24627
Stereophotography of rain clouds using panoramic rotating-lens cameras
[AD-757882] 15 p1807 N73-24642
Digital techniques for reducing variance in reflected rain signals
[METEOROL-STUDY-25] 16 p1875 N73-25181
Point rainfall rate statistics for predicting ultrahigh frequency radio propagation
17 p1996 N73-26136
Effects of rain and atmospheric turbulence on ultrahigh frequency space communication radio line
17 p1996 N73-26143
Global rain rate statistic model for coordination of radio relay and communication satellite service
18 p2212 N73-27857
Simulation of interaction between wind-driven rain and annular air curtain dome and analysis of resulting flow distribution
[UTIAS-TN-182] 20 p2388 N73-29187
Tropical rainfall patterns and associated mesoscale systems for Southeast Asia
[AD-762571] 20 p2450 N73-29693
Application of radio astronomical methods for determining attenuation and radio emission of rain from cumulonimbus clouds
21 p2570 N73-30594
Methods for obtaining vertical motion signs at various atmospheric levels to explain areas of rain and no rain
[NASA-CR-2304] 22 p2694 N73-31577

RAIN EROSION
U WATER EROSION

RAIN GAGES
Correction of precipitation measurements using parallel gages and shields
[ISBN-87-7478-048-4] 05 p0571 N73-14642
Nearly instantaneous precipitation rates measured in several locations of world to determine point frequencies of occurrence
[AD-749878] 05 p0575 N73-14681
Pluviometric and statistical analyses of precipitation and watercourse patterns in Israel
06 p0665 N73-15403
Performance of combined photoelectric snow depth-robot rain gage system
[NLL-M-22978-[5828.4F]] 16 p1910 N73-25457
Reservoir vs. tipping bucket rain gages
[NLL-M-23050-[5828.4F]] 20 p2442 N73-29611

RAIN IMPACT DAMAGE
Water impingement model for raindrop erosion of homogeneous materials
[AD-748790] 04 p0406 N73-13310
Experimental determination of high velocity liquid impact damage for application to rain erosion protection of supersonic aircraft
[AD-753381] 09 p1018 N73-18305
Water impact damage to radome materials
[AD-759973] 17 p2000 N73-26170

RAINDROPS
Real time meteorological radar data for predicting rainfall effects on satellite communication system
[AD-751742] 07 p0757 N73-16147
Precipitation of rain drops from convective clouds over tropical Atlantic Ocean
[NLL-M-22848-[5828.4F]] 16 p1935 N73-25660
Silver iodide particle size effect on water condensation for artificial precipitation
[AD-758857] 17 p1993 N73-26114
Conference on atmospheric attenuation and rainfall effects on ultrahigh frequency telecommunication systems
[AGARD-CP-107] 17 p1994 N73-26121
Multiple scattering and attenuation of radio signals caused by rainfall
17 p1994 N73-26122
Nonspherical raindrop depolarization of electromagnetic wave in ultrahigh frequency radio link
17 p1994 N73-26123
Rain depolarization of linearly and circularly polarized microwaves
17 p1995 N73-26127
Horizontal radio link system for measuring ultrahigh frequency absorption spectrum due to rain
17 p1995 N73-26130
Scattering in transhorizon ultrahigh frequency radio link due to rain
17 p1995 N73-26133
Rain attenuation and multipath fading in ultrahigh frequency radio relay systems
17 p1995 N73-26134
Rain attenuation statistics for ultrahigh frequency microwave link using meteorological data
17 p1996 N73-26135
Calculation of electromagnetic wave absorption by rain for frequencies close to 30 GHz
17 p1996 N73-26138
Sidelobe level increase and gain reduction caused by raindrops on surface of radar antenna radome
[AD-759178] 17 p1998 N73-26160
Attenuation and fading characteristics of ATS 5 15 and 32 GHz millimeter ground-space links
18 p2212 N73-27856
One dimensional elastic collision problem in which two approaching masses are separated by elastic particle
[AD-764514] 22 p2726 N73-31814

RAINSTORMS
NT THUNDERSTORMS
Synoptic-climatological method for long range forecast of heavy rain for European USSR
[NLL-M-22865-[5828.4F]] 11 p1313 N73-20653

RAMAN EFFECT
U RAMAN SPECTRA

RAMAN LASERS
Free electron production by Raman scattering in initial phase of laser produced plasma
[IPP-4/40] 05 p0583 N73-14745
Laser Raman probe for temperature for nitrogen and hydrogen in hydrogen-air flames
[AD-759386] 17 p2034 N73-26465
Spin-flip Raman scattering in cadmium sulfide
[AD-764699] 23 p2827 N73-32598

RAMAN SCATTERING
U RAMAN SPECTRA

RAMAN SPECTRA
Three laser methods of remotely mapping gaseous pollutants of atmosphere
[AD-746280] 02 p0205 N73-11664
Argon laser for spin-flip Raman scattering study in cadmium sulfide at liquid helium temperature
[AD-746219] 02 p0219 N73-11768
Theoretical model of Raman rotational spectrum of gas mixture applied to air mixture of oxygen and nitrogen to determine temperature
[NASA-TN-D-7126] 06 p0679 N73-15525
Absolute intensity, polarization, and relative line intensities of rotational Raman scattering spectra from nitrogen, oxygen, and carbon dioxide
[NASA-CR-121091] 08 p0946 N73-17746
Sea water temperature measurement from Raman spectra
[AD-753481] 11 p1288 N73-20450
Observation of high-order stimulated Raman-antiStokes radiation and its role in initial phase of plasma production by lasers
[IPP-4/40] 12 p1435 N73-21629
Absolute cross sections for rotational Raman scattering derived for nitrogen and oxygen from near UV to infrared
[AD-756808] 13 p1566 N73-22695
Experimental facility for measuring rotational Raman scattering cross sections of nitrogen and oxygen at 10.6 microns
[AD-757111] 14 p1617 N73-23098
Excitation and deexcitation of vibration in gases by nitrogen and oxygen atoms in upper atmosphere
[AD-757050] 14 p1617 N73-23099
Low frequency Raman spectra of ammonium halides measured by double monochromator at high temperature
[NASA-CR-132049] 15 p1747 N73-24160
Raman spectra of Van der Waals complexes in argon, helium, and xenon
[AD-758241] 15 p1748 N73-24171
Raman scattering by polaritons in anisotropic crystals, including noncollinearity of propagation
[AD-757810] 15 p1822 N73-24769
Effects of aluminum oxide on Raman scattering from nitrogen and oxygen
[AD-758913] 15 p1824 N73-24781
Raman scattering techniques in atmospheric temperature measurements
[NASA-TM-X-68250] 16 p1906 N73-25422
Optical activity and Raman scattering in sodium nitrite crystals
16 p1952 N73-25792
Measurement of hydrogen concentration in mass diffusing jets by laser induced Raman scattering
17 p2012 N73-26272
Resonant Raman scattering in wide gap semiconductors
20 p2461 N73-29773
Raman and far infrared spectra of crystalline fluorine obtained in solid phases
[AD-763686] 22 p2626 N73-31039
Absolute Raman scattering instabilities in inhomogeneous plasma
[AD-764611] 23 p2823 N73-32566
Spin-flip Raman scattering in cadmium sulfide
[AD-764699] 23 p2827 N73-32598
Analysis of high frequency vibrational modes in semiconductor materials using Raman scattering techniques
24 p2960 N73-33650

RAMAN SPECTROSCOPY
Diagnostics of flow fields using Raman scattering technique
[AD-757319] 14 p1652 N73-23400
Development and characteristics of nonmetallic electro-optic materials for electronic applications
[AD-758528] 15 p1760 N73-24261
Laser Raman probe for temperature for nitrogen and hydrogen in hydrogen-air flames
[AD-759386] 17 p2034 N73-26465
Laser Raman spectroscopy for calibrating arc heated wind tunnel flow
[AD-761500] 19 p2231 N73-27989
Raman and far infrared spectroscopy for materials characterization
[AD-762303] 19 p2233 N73-28006
Experimental design parameters for Raman spectroscopy of turbid suspensions and powders using ion gas laser light sources and noting S/N improvement
[NOTA-INTERNA-346] 21 p2580 N73-30676
Analysis of high frequeacy vibrational modes in semiconductor materials using Raman scattering techniques
24 p2960 N73-33650

RAMJET ENGINES
NT PULSEJET ENGINES
NT SUPERSONIC COMBUSTION RAMJET ENGINES
Performance of ignition and flame stabilization using gas generator in different ramjet combustion chamber configurations
[DLR-FB-72-47] 01 p0091 N73-10748
Theory and operation of various jet aircraft engines
[AD-747406] 03 p0352 N73-12868
Operational control of ramjet engine with fixed nozzle diffuser geometry
[AD-748708] 04 p0465 N73-13787
Analysis of reaction kinetics, combustion physics, and propellant properties of fuel elements used with rocket and ramjet engines
05 p0590 N73-14793
Subsonic performance potential of ramjets and ejector ramjets
[AD-751317] 07 p0837 N73-16781
Design and characteristics of auxiliary power source to operate electric, hydraulic, and pneumatic subsystems in ramjet powered aerospace vehicles
10 p1110 N73-19048
Analytical models for ignition and complete combustion of aluminized slurry fuels in ramjet engines
[AD-754117] 10 p1203 N73-19792
Analytical determination of mode transition in integral ramjet rocket propulsion system
[AD-753904] 10 p1224 N73-19955
Analysis of integrated airframe and engine configuration for hypersonic transport at 70,000 feet altitude and Mach 6.0
[NASA-CR-112300] 11 p1234 N73-20022

Factors affecting tangential fuel injector design and their effect on efficiency of supersonic combustion processes
[NASA-CR-112302] 11 p1334 N73-20829
Design of fuel injection system for ramjet engines with coaxial inlet
[AD-754852] 11 p1335 N73-20835
Structural design criteria for ramjet combustion chamber
[PB-212691] 11 p1335 N73-20838
Analysis of various mixed cycle engines and impact of component choices on application of propulsion system
21 p2590 N73-30747
Transonic jet engine for ingesting air without compressor
[AD-763173] 21 p2591 N73-30756
Interior ballistic properties of solid fuel ramjet engines to determine regression rate if fuel as function of chamber pressure, inlet air temperature, and air flux rate
[AD-764491] 22 p2709 N73-31691
Development of aft intake system for ramjet powered missile
23 p2851 N73-32785

**RAMJET MISSILES**
Development of aft intake system for ramjet powered missile
23 p2851 N73-32785

**RAMPS [STRUCTURES]**
Flow instabilities of supersonic variable ramp inlets at Mach 2 discussing Concorde aircraft intake
[ARC-R/M-3711] 10 p1104 N73-18999

**RANDOM ACCESS MEMORY**
NT CORE STORAGE
Design and performance of electron beam storage tube for computer random access memory
[AD-753929] 10 p1136 N73-19257
Medium speed mass random access memory module to operate in airborne or tactical field environment with command and control system computer
[AD-755937] 13 p1498 N73-22144

**RANDOM DISTRIBUTIONS**
U STATISTICAL DISTRIBUTIONS

**RANDOM ERRORS**
Estimation of random error variance from simultaneous radar measurements
[AD-755402] 13 p1494 N73-22114
Statistical error model for solar electric propulsion thrust subsystem
[NASA-CR-133232] 17 p2077 N73-26799
Random errors of marine meteorological observations by ships in tropical Atlantic Ocean
20 p2447 N73-29659

**RANDOM LOADS**
NT GUST LOADS
Analysis of response of flexible helicopter rotor blade to random loads with vertical velocity component
[AD-746627] 04 p0374 N73-13038
Estimates of LC stress response in aircraft skin panels to random acoustic loads
[ESDU-67028-AMEND-A] 06 p0723 N73-15904
Forced vibrations of disturbed elastic systems during random loading
[AD-759866] 17 p2095 N73-26950
Hypothesis of spectral addition and application for determination of endurance under random loads
[AD-759869] 17 p2096 N73-26953
Summaries of papers presented to AGARD conference on random load fatigue
[AGARD-AR-54] 19 p2348 N73-28884
Sinusoidal simulation of material fatigue life when subjected to Gaussian narrow band random loading
20 p2477 N73-29896
Fatigue tests with random loads using electrosteel test specimen
[ICAF-DOC-683] 22 p2724 N73-31801
Vibrational energy transfer between connected substructures under random excitation
[NASA-CR-124450] 24 p2988 N73-33878

**RANDOM NOISE**
NT RANDOM SIGNALS
Random Gaussian distribution for input noise approximation in human response tracker modeling
01 p0014 N73-10110
Signal to noise ratios for short term detection of narrowband Gaussian process in Gaussian noise
[AD-751573] 07 p0756 N73-16144
Combination of noise from separate time varying sources
[PB-214250/3] 16 p1945 N73-25738
Formulation of system and sensor configuration control problem for class of linear stochastic systems corrupted by Gaussian noise
22 p2690 N73-31549

**RANDOM NUMBERS**
Random number generators and use of estimators of probability density functions in data analysis
[NASA-CR-129507] 03 p0269 N73-12178
Minimum correlation theory for random numbers with same distribution, applied to negatively correlated random number generation
[NA-71-32] 03 p0324 N73-12644

**RANDOM PROCESSES**
NT RANDOM WALK
Maximum root-mean-square response of square clamped aluminum plate subjected to stationary random excitation
[NASA-CR-129301] 03 p0361 N73-12939
Set of functionals and consistent estimators for spectral analysis of continuous nonstationary random processes
[AD-748341] 04 p0441 N73-13596
Correlation properties of Gaussian random processes under nonlinear transformations
09 p1057 N73-18619
Modelling of random human visual search performance based on physical properties of eye
10 p1225 N73-19961
Method for determining correlation function of normalized random processes
13 p1504 N73-22189
Burst random access channel for satellite computerized data transmission system
[AD-756226] 14 p1635 N73-23252
Random search in problems of optimization, identification, and teaching of automatic systems
14 p1644 N73-23333
Effectiveness of controllers for dynamic systems modeled by ordinary differential equations
[NASA-CR-132054] 15 p1759 N73-24259
Estimates of meteorological autocorrelation and cross-correlation functions
[NLL-M-22887-[5828.4F]] 16 p1934 N73-25646
Circuitry for generating random square wave pulses using white noise source
[NASA-CASE-MSC-14131-1] 17 p2003 N73-26199
Estimation of random process correlation functions, and statistical and sampling errors
17 p2026 N73-26399
Weakly homogeneous binary systems of order two for random search theory
18 p2169 N73-27515
Maximum likelihood estimate of parameters of Gaussian random processes
18 p2170 N73-27522
Effect of random perturbations relative to main gyroscope axis on ground gyrocompass readings
20 p2418 N73-29429
Digital simulation of multicorrelated random processes and its applications
[NASA-CR-62092] 21 p2565 N73-30563

**RANDOM SAMPLING**
Package enabling simulation of random samples from discrete and continuous distribution
01 p0072 N73-10587
Exponential stability of discrete time composite systems with periodic and non-periodic sampling operation
07 p0761 N73-16178
Sampling procedures for estimation of convex combination of proportions
[AD-754577] 11 p1312 N73-20644
Distribution-free confidence intervals and significance tests for population median of random sample
[NASA-CR-131989] 14 p1683 N73-23660

**RANDOM SIGNALS**
Influence of target motion and wave time variation of underwater acoustic signal transmission
[AD-748651] 04 p0450 N73-13678
Loss coefficients and spectral density of random processes in noise filters
09 p1066 N73-18699
Estimating random signal power spectral density by filtering, fluctuating spectrum, and autocorrelation function
17 p2027 N73-26400
Suppression of Doppler ambiguities in pulsed random signal radar
20 p2375 N73-29086

**RANDOM VARIABLES**
Design and analysis of Type 2 correlation-extreme systems composed of control circuits and gages for measuring random functions
14 p1644 N73-23335
Thermal emission from random sea, using Gaussian slope distribution
20 p2391 N73-29207
FORTRAN 4 routine for random number generator continuous random variables
[NASA-CR-133983] 22 p2691 N73-31553
Pseudo-standardized variables and use as elements of shape operators, emphasizing scale and location invariant
[AD-764361] 22 p2692 N73-31561

**RANDOM VIBRATION**
Resonant random vibration test to assess service equipment and sub-assembly mechanical ruggedness
[RARDE-MEMO-18/72] 01 p0113 N73-10937
Dynamic structural response of rectangular panel to subsonic turbulent boundary layer pressure field
[NASA-TN-D-6970] 03 p0360 N73-12934
Computer analysis of random decrement signatures of structures vibrating in random environment
[NASA-CR-2205] 09 p1094 N73-18929

**RANDOM WALK**
Random walk theory for studying electron avalanche formation in helium electric fields
[NASA-TN-D-7224] 12 p1433 N73-21612
Application of Monte Carlo method and Markov random walks to determine molecular diffusion through rarefied gas
[NASA-TN-D-7405] 23 p2776 N73-32197
Application of random walks for search optimization and function space
24 p2944 N73-33514

**RANEY NICKEL**
U CATALYSTS
U NICKEL

**RANGE [EXTREMES]**
NT FREQUENCY RANGES
NT PROPORTIONAL LIMIT
Limiting speed and bearing performance of grooved and angular contact ball bearings
[NASA-TT-F-15017] 23 p2796 N73-32364
Statistical weather forecasting using Gumbel theory noting application to atmospheric temperature long term effects
[MONO-89] 23 p2814 N73-32500

**RANGE AND RANGE RATE TRACKING**
Analysis of range and range rate tracking data from satellite to satellite for geodetic applications
[AD-741683] 01 p0106 N73-10881
Computer programs for aircraft position and stationary satellite orbit determination from radar range and rate measurements
[ESRO-CR-81] 19 p2318 N73-28650

**RANGE CONTROL**
U TRAJECTORY CONTROL

**RANGE ERRORS**
Ionospheric refractivity influence on electromagnetic wave propagation errors discussing electron density profiles
[DLR-MITT-71-31] 03 p0266 N73-12154
Ionospheric range error given by expansion expression in terms of elevation angle and moment of refractivity distribution
[NASA-TM-X-66159] 07 p0790 N73-16426
Instrument for sensing errors in telescope wavefronts using coarse range sensors and fine range sensors
23 p2792 N73-32336
Mariner 9 range and Doppler data analyses for relativistic time delay effects
23 p2842 N73-32711

**RANGE FINDERS**
NT LASER RANGE FINDERS
NT OPTICAL RANGE FINDERS
State space techniques for obtaining mathematical models of flight test vehicles with nonlinear measurement variables in different moving bases
[AD-746657] 02 p0235 N73-11912
Distance measurement using electromagnetic radiation, range finders, and related geodetic research - conference summary
[AD-748067] 04 p0418 N73-13411
Smoothing functions of range and range rate measurements from earth orbiting satellites
[NASA-TM-X-66126] 04 p0475 N73-13881
Performance of radio distance finding net using polygonometric grid
[AD-748866] 06 p0697 N73-15683
Frequency modulated radar systems for range finding, velocity measurement, and altimeters
16 p1873 N73-25162
Improved geodetic phase range only radar
[AD-759756] 16 p1878 N73-25202
Operation of pulse radar automatic range finders used jointly with search and lock-on system
22 p2628 N73-31061
Development of differential equations for analyzing phase radio range finders with mutual automatic scaling frequency control in interrogator and responder
22 p2629 N73-31063
Pilot plant tests of Luch radio distance finder
[AD-763416] 22 p2698 N73-31612

**RANGE INDICATORS**
U INDICATING INSTRUMENTS
U RANGE FINDERS

**RANGE MEASUREMENT**
U RANGEFINDING

**RANGE RESOURCES**
Mapping and managing soil and range resources in Sand Hills Region of Nebraska using ERTS-1 imagery
[E72-10175] 01 p0044 N73-10354
Prediction of ephemeral and perennial range quantity and quality during normal grazing season using ERTS-1 imagery
[E72-10269] 03 p0291 N73-12368
Prediction of range quantity and quality in desert areas of California and Arizona during growing and grazing seasons
[E73-10068] 07 p0779 N73-16330
Forests and range resources inventory and mapping using remote sensors
07 p0785 N73-16388
Mapping and management of soil range resources in Sand Hills Region of Nebraska using ERTS-1 imagery
[E73-10372] 10 p1151 N73-19367

Application of ERTS-1 multisensor data in Great Plains to map ranglands, croplands, and soil formations
[E73-10443] 11 p1282 N73-20403
Utilization of ERTS-1 imagery to predict ephemeral and perennial range quality and quantity during normal grazing season in Arizona and California
[E73-10541] 14 p1654 N73-23418
Mapping and managing soil and range resources in Sand Hills Region of Nebraska using ERTS-1 imagery
[E73-10629] 15 p1775 N73-24389
Mapping and managing soil and range resources in Sand Hills Region of Nebraska using ERTS-1 imagery
[E73-10807] 18 p2139 N73-27282
Results of ERTS-1 investigations of agriculture, forestry, and range resources
19 p2289 N73-28406
Utilization of ERTS-1 imagery in mapping and managing range resources in Sand Hills Region of Nebraska
[E73-11121] 24 p2916 N73-33276

**RANGEFINDING**
NT LUNAR RANGEFINDING
NT SOUND RANGING
Adaptation of lidar to aircraft and missile rangefinding
[NASA-TT-F-14716] 02 p0181 N73-11466
Erbium laser rangefinder having germanium avalanche photodetector
[AD-748071] 04 p0430 N73-13502
One way and two way VHF ranging system performance for tracking and data relay applications
[NASA-TM-X-66134] 05 p0596 N73-14843
Analysis of improved signal processing techniques for low frequency, one-way ranging for aircraft radio navigation
[AD-754031] 11 p1322 N73-20727
Portable pulsed laser ranging system for measurements between earth and retroreflecting satellites
[NASA-CR-131513] 12 p1410 N73-21423
Loop transponder for regenerating code of mu-type ranging system
[NASA-CASE-NPO-11707] 16 p1873 N73-25161
ATS ranging and position fixing experiments
[NASA-CR-132755] 16 p1965 N73-25896
Laser observations of dense natural fog to determine backscatter and slant range visibility for aircraft landing operations
[AD-760128] 17 p2041 N73-26511
Preflight analysis on Skylab very high frequency ranging for rendezvous portion
[NASA-CR-133981] 19 p2235 N73-28020
Determination of bomb range of low drag bombs delivered by fighter aircraft
[AD-762500] 20 p2488 N73-29992
Mathematical model of VHF ranging system to analyze performance of Apollo Soyuz test project
[NASA-CR-134063] 23 p2846 N73-32741
Techniques for long range vision underwater using range-gating and dual-scan with parallax techniques
24 p2958 N73-33636

**RANGELANDS**
Investigation of forest stress in Black Hills, forest inventory at Atlanta test site, and rangeland inventory at Manitou test site using ERTS-1 imagery
[E72-10219] 02 p0162 N73-11313
Monitoring plant development in California rangeland environments using ERTS-1 and supporting aircraft data
[E72-10263] 03 p0290 N73-12362
Identification of phenological events, rangelands, and crops using ERTS-1 imagery
[E72-10351] 05 p0533 N73-14339
Soil mapping, crop identification, and rangeland assessment in Great Plains using ERTS-1 multisensor imagery
[E72-10369] 05 p0536 N73-14357
Prediction of ephemeral and perennial range quality and quantity during normal grazing season based on ERTS-1 imagery
[E73-10061] 07 p0778 N73-16323
ERTS-1 MSS imagery of Great Plains rangeland, croplands, and land systems
[E73-10076] 07 p0780 N73-16338
Forest and rangeland inventory and forest infestation of Atlanta, Manitou, and Black Hills test sites based on ERTS-1 imagery
[E73-10084] 08 p0901 N73-17296
Effectiveness of ERTS-1 imagery in monitoring vegetation conditions of direct concern to range land management and agriculture business decisions in Great Plains Corridor
[E73-10302] 09 p1021 N73-18334
ERTS-1 imagery of vernal advancement and retrogradation of natural rangeland vegetation of Great Plains Corridor
[E73-10303] 09 p1021 N73-18335
Assessment of range fire damage in Sand Hills Region of Nebraska based on ERTS-1 imagery
[E73-10360] 10 p1149 N73-19356
Prediction of ephemeral and perennial range quantity and quality during normal grazing season in Arizona based on ERTS-1 imagery
[E73-10377] 10 p1152 N73-19372
Soil mapping of rangelands in Bennett County, South Dakota using remotely sensed imagery
[NASA-CR-131229] 10 p1155 N73-19395
Inventory of forest and rangeland and detection of insect infestation from ERTS-1 imagery of Black Hills, Atlanta, and Manitou test sites
[E73-10407] 11 p1278 N73-20369
Utilization of ERTS-1 imagery to predict ephemeral and perennial range quality and quantity during normal grazing season in Arizona and California
[E73-10541] 14 p1654 N73-23418
Inventory of forest and rangeland and detection of forest stress at Black Hills, South Dakota, Atlanta, Georgia, and Manitou Forest test sites using ERTS-1 data
[E73-10546] 14 p1655 N73-23421
Broad scale application of ERTS-1 imagery to study and mapping of geological, hydrological, land use, rangelands, and soil cultures in Wyoming
[E73-10554] 14 p1655 N73-23426
Inventory of forests and rangelands, including forest stress, at Black Hills, Atlanta, Georgia, and Manitou, Colorado test sites using Skylab EREP
[E73-10587] 14 p1657 N73-23447
Monitoring vernal advancement and retrogradation of natural rangeland vegetation in Great Plains Corridor
[E73-10643] 16 p1897 N73-25340
Analysis of ERTS-1 data for predicting ephemeral and perennial range quantity and quality during normal grazing season in Arizona and California
[E73-10712] 17 p2018 N73-26319
Inventroy of forest and rangeland resources at Atlanta, Georgia, Black Hills, South Dakota, and Manitou, Colorado test sites using Skylab EREP imagery
[E73-10749] 18 p2133 N73-27237
Detection and inventory of timber and rangelands and forest stresses in Georgia, Colorado, and Black Hills from ERTS-1 imagery
[E73-10805] 18 p2138 N73-27280
Application of ERTS-1 imagery for mapping and managing soil and range resources in Sand Hills region of Nebraska
[PAPER-A10] 19 p2260 N73-28218
Application of ERTS-1 imagery and aerial photography for monitoring forage crop resources in California
[PAPER-A11] 19 p2260 N73-28219
Analysis of ERTS-1 data for application to forest and range mapping in Houston, Texas area
[PAPER-A20] 19 p2262 N73-28227
Inventories of agriculture, forestry, and rangeland resources based on ERTS-1 imagery
19 p2288 N73-28396
Monitoring vegetation conditions of direct concern to rangeland and agriculture management in Great Plains Corridor
[E73-10891] 20 p2394 N73-29240
Skylab inventory of forest and rangeland resources and forest stresses at Atlanta Georgia, Manitou, Colorado, and Black Hills test sites
[E73-10895] 20 p2395 N73-29244
Inventory of forest and rangeland resources and stresses at Atlanta, Georgia, Black Hills, South Dakota, and Manitou, Colorado from Skylab EREP
[E73-11040] 23 p2778 N73-32219
Forest and rangeland inventory and detection of forest stress at Black Hills, South Dakota, Manitou, Colorado, and Atlanta, Georgia test sites
[E73-11052] 23 p2779 N73-32228

**RANGER LUNAR PROBES**
NT RANGER 7 LUNAR PROBE
NT RANGER 9 LUNAR PROBE
Geologic mapping of moon from pictures by Ranger 7, 8, and 9
[NASA-CR-133090] 17 p2082 N73-26839

**RANGER SATELLITES**
U RANGER LUNAR PROBES

**RANGER 7 LUNAR PROBE**
Identification of Ranger 7 and 9 impact craters from Apollo 16 photography - Part J
12 p1454 N73-21774

**RANGER 9 LUNAR PROBE**
Identification of artificial lunar impact craters produced by Ranger 7 and 9 spacecraft and S-4B stage of Apollo 13 and 14 - Part I
12 p1453 N73-21773
Identification of Ranger 7 and 9 impact craters from Apollo 16 photography - Part J
12 p1454 N73-21774

**RANGES [FACILITIES]**
NT BALLISTIC RANGES
NT MISSILE RANGES
NT TEST RANGES

**RANGING**
U RANGEFINDING

**RANKINE CYCLE**
Performance and endurance testing of 6 kW organic Rankine cycle power conversion system
[SAN-651-130] 08 p0870 N73-17042
Design, development, and evaluation of organic, Rankine cycle power plant
[AD-757632] 14 p1606 N73-23018
Performance of 1972 ford galaxie equipt with rankine cycle power system composed of organic based working fluid and reciprocating expander
[PB-210836] 19 p2329 N73-28739
Materials technology programs in support of mercury rankine space power system
[NASA-TN-D-7355] 21 p2558 N73-30508

**RANKINE-HUGONIOT RELATION**
Numerical analysis of discrete traveling waves which propagate with speed determined by Rankine-Hugoniot relations
[COO-3077-20] 08 p0896 N73-17254
Sound wave, Alfven wave and heat flow effects on normal shock waves noting shock wave attenuation, Rankine-Hugoniot relation extension, and application to interplanetary shock waves
24 p2965 N73-33701

**RANKING**
Error formulas and asymptotes for vocabulary size determination for one, two, and three parameter rank distribution
[NASA-CR-132023] 14 p1683 N73-23659

**RAOULT LAW**
Development of differential equation for normal evaporation of nickel-aluminum alloy relating evaporating time to final solute concentration
[NASA-CR-124040] 07 p0808 N73-16558

**RAPID TRANSIT SYSTEMS**
Analysis of criteria for establishing air transportation curricula in community college based on manpower requirements and industrial needs
04 p0486 N73-13969
Design and development of very high speed transportation system to include technological aspects and physical restraints
[P-4874] 04 p0488 N73-13990
Development of high speed ground rapid transit facility using tracked air-cushion vehicles
[PB-211833] 05 p0524 N73-14266
Development and characteristics of tracked air cushion research vehicle for commercial high speed ground transportation
[PB-211216] 05 p0524 N73-14267
Cost effectiveness of high speed ground transportation system using tracked air cushion vehicles for access to Los Angeles airport
[PB-212023] 06 p0651 N73-15290
Economic feasibility analysis on San Francisco rapid transit system extension to serve airport
[PB-212456] 07 p0860 N73-16978
Control technology for air cushion passenger vehicle
11 p1352 N73-20969
Cryogenics applications for development of superconducting levitated system of high speed ground transportation
[NBS-TN-635] 14 p1645 N73-23344
Feasibility of rapid transit service between downtown Washington, D.C. and Dulles Airport in Virginia
[PB-220074/9] 18 p2214 N73-27879

**RARE EARTH ALLOYS**
NT NEODYMIUM ALLOYS
Thermomagnetic analysis of rare earth transition metal alloys as permanent magnet materials
[AD-750746] 06 p0686 N73-15587
Scientific and technological applications of rare earth materials
[IS-2965] 10 p1166 N73-19484
Electromechanical energy conversion devices using both conventional and rare-earth cobalt permanent magnet materials
[AD-756433] 13 p1501 N73-22168
X ray diffraction analysis of Al based rare earth alloys with potential permanent properties
[AD-756245] 14 p1698 N73-23776
Production and characteristics of yttrium subgroup rare earth metal dodecaborides
23 p2808 N73-32452
Effect of rare earth metals on macrostructure, microstructure, strength, and ductility of cast titanium samples
23 p2809 N73-32458

**RARE EARTH COMPOUNDS**
NT CERIUM OXIDES
NT ERBIUM COMPOUNDS
NT EUROPIUM COMPOUNDS
NT NEODYMIUM COMPOUNDS
NT SAMARIUM COMPOUNDS
Preparation and physical properties of rare earth compounds of technological potential
[AD-744980] 01 p0088 N73-10726
Magnetically uniaxial rare earth garnets grown on substrates, using liquid phase epitaxial dipping technique
[AD-745903] 02 p0220 N73-11781
Magnetic properties and crystalline structures of rare earth-cobalt alloys
[AD-748270] 04 p0436 N73-13555
Rare earth-cobalt permanent magnet materials processing
[AD-748264] 04 p0451 N73-13679
Magnetic intermetallic cobalt-rare earth compounds for electromechanical energy converters
[AD-750338] 06 p0645 N73-15242

Micromagnetic interactions of rare earth orthoferrites and Mossbauer spectroscopy
[AD-751995] 08 p0951 N73-17789
Scientific and technological applications of rare earth materials
[IS-2965] 10 p1166 N73-19484
Magnetic and ferroelectric properties of rare earth compounds for signal processing devices
[AD-754775] 11 p1331 N73-20807
Magnetic, optical, and semiconducting properties of rare earth compounds
[AD-755925] 12 p1376 N73-21164
Characterization of thin films produced by epitaxial growth of magnetic rare earth compounds
[AD-755165] 13 p1568 N73-22707
Spectroscopic analysis of energy transfer in rare earth compounds to determine effect of transfer phenomena on lasing efficiency
[AD-757520] 14 p1673 N73-23579
Oxide formations in thermal vacuum decomposition of rare earth oxalates
[BARC-631] 15 p1747 N73-24162
Magnetic properties of cobalt rare earth thin films
16 p1951 N73-25790
Rare earth oxysulfide luminescent films for use in CRT screens
[AD-758760] 16 p1954 N73-25808
Design and development of zero field paramagnetic resonance spectrometer
[AD-759370] 17 p2035 N73-26466
Rare earth orthoferrites and micromagnetic interactions
[AD-764826] 23 p2827 N73-32593
Evaluation of process for burnable poison deposition on zirconium hydride fuel
[AI-AEC-13085] 24 p2955 N73-33606
Rare earth doped gallium phosphide preparation with application to electroluminescence noting physical and chemical properties
24 p2969 N73-33729

**RARE EARTH ELEMENTS**
NT CERIUM
NT DYSPROSIUM
NT ERBIUM
NT GADOLINIUM
NT HOLMIUM
NT LANTHANUM
NT NEODYMIUM
NT PRASEODYMIUM
NT SAMARIUM
NT THULIUM
NT YTTERBIUM

Laser induced infrared quantum counter upconversion experiments utilizing rare earth ions in single crystals
[AD-747415] 03 p0312 N73-12546
Rare earth electronic configurations, physiochemical properties, and implications of analytical chemistry
[IS-2966] 10 p1126 N73-19170
Production methods, quality control, and metallurgical uses of pure rare earth metals and alloys
[IS-2968] 10 p1172 N73-19538
Commercial applications of rare earth elements in ceramics, glasses, and nuclear technology
[IS-2967] 10 p1175 N73-19561
Technology of high performance transition metal, rare earth permanent magnets for critical applications
[AD-754959] 11 p1306 N73-20601
Processing methods for rare earth cobalt compounds as permanent magnets
[AD-754951] 11 p1325 N73-20749
Values for standard heats and Gibbs free energies of formation, entropies, and enthalpies for rare earth elements
[NBS-TN-270-7] 14 p1616 N73-23092
Effects of oxide dispersions and rare earth elements on oxidation of Cr and Al containing alloys
14 p1677 N73-23608
Technological development of high performance transition metal-rare earth magnets for critical applications
[AD-760178] 17 p2048 N73-26566
Materials processing method for optimization of rare earth cobalt compounds as permanent magnets
[AD-760777] 18 p2180 N73-27599
Perturbed angular correlation measurements on attenuations caused by rare earth nuclei implantation into metals
18 p2184 N73-27638
Research and development of rare earth-transition metal alloys as permanent magnet materials
[AD-762304] 20 p2432 N73-29534
Magnetic interactions and spin wave dispersion in rare earth metals
[CONF-730402-10] 20 p2455 N73-29727
Mass spectrometric determination of rare earth concentration in basaltic rocks and luna sample 14305
[FRNC-TH-335] 21 p2597 N73-30813
Mass spectrometric analysis of rare earth elements contained in lunar samples
[CONF-730402-[P1-2]] 24 p2923 N73-33344
Spectrographic study of rare earth crystal absorption spectra in magnetic fields at liquid helium temperature
[NASA-TT-F-14732] 24 p2958 N73-33640

Electron thermal conductivity of thin films of strong coupling superconductors and of superconductors containing rare earth inpurities
24 p2967 N73-33712

**RARE GASES**
NT ARGON
NT ARGON ISOTOPES
NT HELIUM
NT HELIUM ATOMS
NT HELIUM FILM
NT HELIUM ISOTOPES
NT LIQUID HELIUM
NT NEON
NT RADON
NT XENON

General, nonstationary electron gas equation for noble gas-alkali plasma
[JUL-802-TP] 01 p0085 N73-10704
Rare molecular gas beam scattering from single metal crystal surfaces
[AD-748938] 04 p0451 N73-13685
Abundance and isotopic composition of noble gases release from lunar fines
[NASA-CR-130327] 07 p0841 N73-16812
Rare gas abundances in Apollo 11 rocks 10017 and 10071, and rock age determinations
07 p0842 N73-16818
Physiological effects on rats of replacement of atmospheric nitrogen by inert gases at high and low temperatures
11 p1244 N73-20095
Formation of hydrocyanic acid from mixtures of ammonia, metane and noble gas or hydrogen subjected to UHF waves
[NASA-TT-F-14678] 12 p1376 N73-21162
Laser beam study of proton production cross sections determined for stable and radioactive rare gases
[TID-26183] 12 p1427 N73-21566
Computer simulation techniques to determine equilibrium positions and binding energies of inert gas atoms implanted in tungsten crystal
[AD-758501] 15 p1799 N73-24585
Mechanism of inert gas influence on metabolism
[NASA-CR-133214] 16 p1867 N73-25120
Reactive crossed molecular beam studies using free jet sources
18 p2180 N73-27605
Isotope separation in rare gases caused by centrifugal force in plasmas
[TRITA-EPP-72-27] 19 p2325 N73-28701
Dry inert gas glove box for handling of hygroscopic and corrosive materials in spectroscopic and lasers experiments
[CRC-1244] 21 p2548 N73-30430
Stability of nonequilibrium inert gas plasma for use in MHD power generators
22 p2702 N73-31642
Food consumption and morphollogical indices of blood in white mice with replacement of air nitrogen by inert gases in pressurized chamber
24 p2882 N73-33020
Mechanism of inert gas narcosis in human body and mice
[NASA-CR-62096] 24 p2885 N73-33038

**RARIFACTION WAVES**
U ELASTIC WAVES

**RAREFIED GAS DYNAMICS**
Analysis of aerodynamic drag on general convex bodies at zero angle of attack during high speed flow in rarefied air
08 p0895 N73-17242
Numerical analysis of flow of rarefied monatomic gas through two dimensional slot to show characteristics of transition regime
[NASA-CR-124069] 09 p1012 N73-18265
Meksyn asymptotic integration method for studying viscous interaction within hypersonic rarefied gas flow regime
12 p1389 N73-21263
Transport phenomena in rarefied gas flows
[AD-759165] 16 p1891 N73-25300

**RAREFIED GASES**
NT COSMIC GASES
NT INTERSTELLAR GAS

Abstracts of papers presented at conference on rarefied gas dynamics
[AD-745974] 02 p0159 N73-11289
Singular limits of Boltzmann equation solutions for describing qualitative and quantitative properties of rarefied gas
[AD-753691] 10 p1143 N73-19312
Analysis of interaction of rarefied gas with surface of porous moist bodies during heat and mass transfer using visual and photographic methods
[AD-754633] 11 p1272 N73-20325
Analytical models of viscoseal performance with rarefied gas sealant
[NASA-CR-121089] 12 p1408 N73-21409
Numerical methods in theory of rarefied gases with application of Boltzmann equation
[NASA-TT-F-638] 12 p1417 N73-21483
Models for interaction of rarefied gas with solid surface
12 p1418 N73-21491

Electron beam optics for measuring density and temperature of aerodynamic gas flow
[ONERA-PUBL-146] 13 p1559 N73-22635
Combustion rates for binary pyrotechnic compositions in rarefied air
[AD-756043] 13 p1591 N73-22898
Four moment method for studying thermal conductivity in rarefied gas confined in concentric cylinders
16 p1973 N73-25955
Numerical analysis of hypersonic rarefied flow past sharp leading edge of flat plate using finite difference solution of Navier-Stokes equation
19 p2251 N73-28147
Application of Monte Carlo method and Markov random walks to determine molecular diffusion through rarefied gas
[NASA-TN-D-7405] 23 p2776 N73-32197
Analysis of aerodynamic drag on object moving in rarefied gas under nearly free molecular flow conditions
24 p2869 N73-32923
Liquid surface evaporation in rarefied gas atmosphere
[AD-765527] 24 p2893 N73-33095

**RAREFIED PLASMAS**
Analysis of low density plasma shock waves in expanding discharge
12 p1432 N73-21602
Determination of electric potential field and aerodynamic moments for steady rarefied plasma flow past solid sphere
15 p1816 N73-24720
Parametric ion acoustic wave excitation in ionized plasma
23 p2822 N73-32559

**RASERS**
U MASERS

**RATE METERS**
U MEASURING INSTRUMENTS

**RATES [PER TIME]**
NT ACCELERATION [PHYSICS]
NT ACOUSTIC VELOCITY
NT AIRSPEED
NT ANGULAR ACCELERATION
NT ANGULAR VELOCITY
NT ARRHYTHMIA
NT BRADYCARDIA
NT BURNING RATE
NT COLLISION PARAMETERS
NT COLLISION RATES
NT CRITICAL VELOCITY
NT CURRENT DENSITY
NT DECAY RATES
NT DECELERATION
NT DRIFT RATE
NT ELECTRON DECAY RATE
NT ELECTRON FLUX DENSITY
NT EVAPORATION RATE
NT EXHAUST VELOCITY
NT FLOW VELOCITY
NT FLUX [RATE]
NT FLUX DENSITY
NT GROUND SPEED
NT HEART RATE
NT HEAT FLUX
NT HIGH ACCELERATION
NT HIGH GRAVITY ENVIRONMENTS
NT HIGH SPEED
NT HYPERSONIC SPEED
NT ILLUMINANCE
NT IMPACT ACCELERATION
NT ION PRODUCTION RATES
NT IRRADIANCE
NT LIGHT SPEED
NT LOADING RATE
NT LOW SPEED
NT LUMINANCE
NT LUMINOUS INTENSITY
NT MAGNETIC FLUX
NT MASS FLOW RATE
NT NEUTRON FLUX DENSITY
NT PARTICLE ACCELERATION
NT PARTICLE FLUX DENSITY
NT PHASE VELOCITY
NT PHOTON DENSITY
NT PLASMA ACCELERATION
NT PROPAGATION VELOCITY
NT PROTON FLUX DENSITY
NT PULSE RATE
NT RADIAL VELOCITY
NT RADIANCE
NT RADIANT FLUX DENSITY
NT RECOMBINATION COEFFICIENT
NT RELATIVISTIC VELOCITY
NT RESPIRATORY RATE
NT ROTOR SPEED
NT SOLAR CONSTANT
NT SOLAR FLUX
NT SOUND INTENSITY
NT SPIN REDUCTION
NT STRAIN RATE
NT SUBSONIC SPEED
NT SUPERSONIC SPEEDS
NT TERMINAL VELOCITY
NT TIP SPEED

NT TRANSONIC SPEED
NT WIND VELOCITY
Regression analysis of tropical storm and typhoon speed characteristics after recurvature in western North Pacific Ocean
[AD-746880] 02 p0206 N73-11672
Greenwich time report for the Royal Greenwich Observatory Time and Latitude Service during period of January to March 1972
08 p0960 N73-17856
Apparatus and digital technique for coding rate data
[NASA-CASE-LAR-10128-1] 11 p1259 N73-20217
RATINGS
Linear rating scale for selecting tracking task parameters by subjective operator
[AD-752036] 08 p0880 N73-17125
RATIONS
NT SPACE RATIONS
RATIOS
NT ASPECT RATIO
NT FINENESS RATIO
NT FROUDE NUMBER
NT FUEL-AIR RATIO
NT HARTMANN NUMBER
NT HIGH ASPECT RATIO
NT INDEXES [RATIOS]
NT LOW ASPECT RATIO
NT MACH NUMBER
NT MASS RATIOS
NT NUSSELT NUMBER
NT OPTICAL REFLECTION
NT PRANDTL NUMBER
NT REYNOLDS NUMBER
NT SIGNAL TO NOISE RATIOS
NT SIMILARITY NUMBERS
NT STANDING WAVE RATIOS
NT VOID RATIO
Spectral ratio mapping of iron ore deposits in Wind River Range, Wyoming, using ERTS-1 data
[E73-10397] 11 p1276 N73-20359
Ratio mapping iron ore deposits in Atlantic City District, Wyoming
[E73-10575] 15 p1772 N73-24355
RATS
Hyperoxia effects on elimination of carbon monoxide, ammonia, ketones, and aldehydes by rats
03 p0256 N73-12077
Transverse acceleration effects on dioxyribonucleic acid catabolism in rat spleen and liver
03 p0257 N73-12080
Localized shielding effects on antitissue antibody mobilization in irradiated rats
03 p0258 N73-12086
Heat regulation and adaptation of rats exposed to helium oxygen atmosphere
03 p0259 N73-12096
Toxic effects of Freon decomposition products on activity of isoenzymes of lactate dehydrogenase in rat brains
03 p0259 N73-12097
Cellular activation energy effect in rat tolerance to acceleration stress
[AD-749338] 05 p0501 N73-14079
Pressure gradient measurements in swine and rats submitted to pressure pulses
[DLR-FB-71-72] 06 p0636 N73-15164
Morphological changes in juxtaglomerular apparatus in kidneys of rats during multihour exposure to accelerations in different directions
07 p0743 N73-16045
Thermoregulation reactions of rats in hypoxic atmosphere with nitrogen and helium dilution
07 p0743 N73-16046
Effect of prolonged hypodynamia on rat biology
07 p0744 N73-16050
Weightlessness effects on development of vestibular apparatus and ocular nystagmus in rat, using chronic 2g centrifuge
[NASA-CR-114569] 08 p0878 N73-17112
Transverse acceleration effects on rat gastrointestinal response to drugs
10 p1114 N73-19085
Transverse acceleration effects on rat hepatocytic structures
10 p1115 N73-19086
Hyperoxic morphological changes in connective rat tissues
10 p1115 N73-19092
Helium/oxygen breathing effects on rat gas exchange and musculoskeletal heat control
10 p1115 N73-19093
Physiological effects of argon/oxygen breathing on rats noting carbon dioxide level
10 p1116 N73-19094
Changes in oxygen consumption in rats after inoculation with polymer combustion products
10 p1116 N73-19096
Toxicity of gaseous urine and feces emissions on rat organism
10 p1116 N73-19097
Hypoxia adaptation of rats for increased resistance to toxic atmospheric gases
10 p1116 N73-19100
Toxic effects of metabolic waste gases on rat organisms
10 p1116 N73-19101
Calcium metabolism determination in rats by measuring argon isotope in exhaled air after neutron irradiation
[NASA-CR-128816] 10 p1120 N73-19130
Biological and toxicity effects of aluminum and other chemicals in animals
[ORNL-TIP/TIRC-72-76] 10 p1121 N73-19136
Sodium pentobarbital effects on albino rats in normocapnic and chronically hypercapnic conditions
[AD-751234] 10 p1121 N73-19142
Hypoxia and reduced acceleration tolerance of rats after injection of cysteamine radioprotector
11 p1239 N73-20058
Pathophysiological response reactions of rats to acute hypoxia after injection of cysteamine and aminothiol group radioprotector
11 p1239 N73-20059
Effects of radioprotective drugs on motor evacuatory functions in gastrointestinal tracts of healthy and irradiated rats
11 p1239 N73-20062
Reactivity changes of rats to antiradiation drugs with head and stomach shielded during total irradiation
11 p1241 N73-20072
Pathomorphological changes in internal organs of white rats following 120 MeV proton irradiation and effect of partial shielding on attenuation of damage
11 p1241 N73-20076
Comparison of peripheral blood of acclimatized and nonacclimatized irradiated rats under prolonged conditions of reduced barometric pressure
11 p1243 N73-20088
Physiological effects on rats of replacement of atmospheric nitrogen by inert gases at high and low temperatures
11 p1244 N73-20095
In vitro metabolism of antipyrine in rats
[NASA-TT-F-14868] 11 p1246 N73-20116
Effect of some radioprotective preparations on motor and evacuator function of gastrointestinal tract of healthy and irradiated rats
[DRIC-TRANS-2962] 12 p1372 N73-21130
Dystrophic degeneration of suprarenal rat cortex during hypokinesia
13 p1481 N73-22003
Hyperoxic atmosphere effect on rat metabolism and elimination of gaseous wastes
13 p1481 N73-22004
Hemoglobin and erythrocyte increase in rat adaptation to hypoxic hypoxia
13 p1481 N73-22005
Altitude acclimatization period effects on rat resistance to hypoxia
13 p1481 N73-22006
Hypokinetic disturbances of rats after exposure to carbon monoxide
13 p1481 N73-22007
Long term hypokinesia effect on rats hemodynamic system
14 p1607 N73-23026
Long term hypokinesia effect on protein and nucleic acid content in rat tissue
14 p1607 N73-23027
Depressing effect of hypokinesia on rat skeletal muscle functions
14 p1607 N73-23028
Atrophy and metabolic changes in internal organs and skeletal muscles of rats exposed to hypokinesia
14 p1607 N73-23029
Centripetal acceleration for inhibiting cerebellar rat cortex activity
14 p1608 N73-23030
Nutrient protein intake of rats and tolerance to acute hypoxia
14 p1608 N73-23035
Tolerance of hypokinetic rats to carbon monoxide exposure
14 p1609 N73-23043
Synthesis rate of phospholipids and cytochromes b5 and P 450 in thiamine-deficient rats after treatment with thiamine
[NASA-TT-F-14989] 17 p1987 N73-26064
High intensity noise effects on urinary K-Na ratios in rats
20 p2365 N73-29018
Influence of He, N2, and N2O environments on physiological parameters of rats
20 p2365 N73-29019
Microwave radiation effects on rat tissues and length of survival
21 p2608 N73-30904
Circadian rhythms of sleep and cerebral temperature in rats chronically exposed to hot environments
[NASA-TT-F-15082] 22 p2620 N73-30994
RAWINSONDES
Comparison of rawinsonde data with baroclinic cloud motion pictures
[NOAA-TM-NESS-43] 01 p0074 N73-10611
Meteorological data from radiosondes at Berlin
02 p0204 N73-11650
Measurement of spatial distribution of aerosols and water vapor in earth mixing layer using optical radar, particle counters, and rawinsonde
[NASA-TN-D-7103] 04 p0444 N73-13621
Quality control for rawinsonde data dissemination to ships
[NOAA-TM-NWS-NMC-52] 11 p1314 N73-20663
Intergrated error behavior of rawinsonde tracking system
[AD-763890] 22 p2695 N73-31585
RAY TRACING
Ray tracing program for calculating sound intensity from ocean sources
[AD-745313] 01 p0080 N73-10664
Abel integral transform and ray tracing methods for radio occultation data inversion to obtain refractive index profiles of planetary atmospheres
02 p0197 N73-11596
Ray tracing method for calculating paths of acoustic and gravity waves in atmosphere
05 p0508 N73-14133
Computerized simulation of gravity wave perturbed traveling ionospheric disturbances using radio ray paths
05 p0512 N73-14163
Computer program for tracing paths of high frequency electromagnetic rays through two-dimensional models of ionosphere
[AWRE-O-34/72] 06 p0644 N73-15228
Ray tracing of underwater sound in Arctic Ocean
[AD-752056] 08 p0944 N73-17734
Prevention of spurious caustics in ray tracing scheme for sound propagation mapping in sea water
[AD-752080] 08 p0944 N73-17735
Modified ray theory for underwater sound propagation and diffraction
[AD-755460] 12 p1430 N73-21589
Ray tracing method for computerized prediction of underwater sound propagation loss
[AD-755459] 12 p1430 N73-21590
Satellite ionospheric research, including ray tracing program
[AD-757498] 14 p1662 N73-23487
Ray tracing method for calculating underwater acoustic reflection patterns of surface originated signals from objects of arbitrary shape
[AD-757110] 14 p1694 N73-23744
Geometric optical properties of holographic lens systems
[AD-762526] 20 p2426 N73-29486
RAYLEIGH SCATTERING
Operation and data processing system of long period strain seismographs with wave discrimination
[AD-748232] 05 p0549 N73-14460
Concentrated aerosol layer at intermediate levels of pure Rayleigh atmosphere
07 p0775 N73-16295
Rayleigh-Brillouin intensity ratios measured for aqueous electrolytic solutions as function of concentration
[AD-753017] 09 p1001 N73-18166
Stimulated and spontaneous scattering of electromagnetic radiation
[AD-757082] 13 p1559 N73-22639
Radio frequency induced sidebands in Mossbauer and Rayleigh scattering radiation from nickel foils
23 p2755 N73-32050
Measurements of Rayleigh scattering and depolarization ratio for atoms in gaseous state
[NASA-TN-D-7442] 23 p2819 N73-32539
RAYLEIGH WAVES
Semi-infinite homogeneous response to shear and compressional line sources
[UCRL-51233] 06 p0667 N73-15420
Variation of Rayleigh wave reflection coefficient of different interdigital transducer configurations with electric loads
07 p0831 N73-16737
Dispersive delay lines, bandpass filters, and lines with delay above 30 microseconds utilizing Rayleigh surface waves at VHF/UHF frequencies
[REPT-4.427] 12 p1384 N73-21223
Analysis of Rayleigh wave dispersion in continental path and development of filters for vertical high gain seismometer
[AD-761795] 19 p2296 N73-28462
Regionalization of lithosphere and asthenosphere of Pacific Ocean from Rayleigh wave phase velocity dispersion curves
20 p2390 N73-29197
RAYLEIGH-RITZ METHOD
Rayleigh-Ritz solution of wave propagation in thermoviscoelastic rod insulated on lateral surface and driven by sinusoidal stress at one end
[AD-746466] 01 p0115 N73-10952
Evaluation of Rayleigh-Ritz anisotropic plate analysis procedure for determining performance of composite wing for aircraft operating in transonic environment
[AD-745129] 02 p0126 N73-11023
Rayleigh-Ritz analysis of free vibration behavior in plates with discrete elastic supports
[NASA-CR-112220] 04 p0480 N73-13924
Mathematical model for resonant vibration of cylindrical shells using the Rayleigh-Ritz method
[DLR-FB-71-92] 06 p0727 N73-15931

Rayleigh-Ritz modal vibration analysis for ring and/or stringer stiffened noncircular cylindrical shells with arbitrary end conditions
[NASA-CR-2151] 09 p1094 N73-18927

**RB-57 AIRCRAFT**
U B-57 AIRCRAFT

**RBE**
U RELATIVE BIOLOGICAL EFFECTIVENESS [RBE]

**RC CIRCUITS**
RC equivalent network for flueric flip-flop inputs
[AD-752126] 08 p0899 N73-17280
Temperature control system comprised of wheatstone bridge with RC circuit
[NASA-CASE-NPO-11304] 17 p2030 N73-26430

**RDX**
Shock initiation of reaction in RDX/TNT, nitromethane explosives, and double base propellants
[ERDE-TR-103] 05 p0606 N73-14930
Optical measurement of RDX and PETN monocrystal detonation velocity along different crystallographic axes
[ISL-28/71-PT-1] 09 p1052 N73-18575

**REACTION CONTROL**
Shuttle reaction control system cryogenic liquid distribution system
[NASA-TM-X-68913] 07 p0834 N73-16765
Apollo experience report on command and service module reaction control systems
[NASA-TN-D-7151] 16 p1966 N73-25901

**REACTION JET ATTITUDE CONTROL**
U ATTITUDE CONTROL
U JET THRUST

**REACTION JETS**
U JET FLOW
U JET THRUST

**REACTION KINETICS**
Reaction rate field, emphasizing ionization and upper atmosphere processes
[AD-745370] 01 p0051 N73-10414
Reaction rate field data, emphasizing ionization and upper atmosphere processes
[AD-745371] 01 p0051 N73-10415
Differential scanning calorimeter for solid state reaction analysis in pure metals and alloys
[EUR-4802-D] 01 p0055 N73-10449
Modification of uncoupled radiation analysis of diffusion-type chemical laser to determine lasing diatomics of radiatively saturated medium
[AD-745311] 01 p0065 N73-10534
Solid phase reaction and fuel component effects on composite propellant combustion
[NASA-CR-112083] 01 p0089 N73-10738
Rate coefficient data for recombination reaction hydrogen plus oxygen plus argon yields water and argon in mixtures behind incident shock waves
[NASA-TN-D-6990] 01 p0117 N73-10965
Chemorheology of Viton B fluorocarbon elastomer by kinetic analysis of chemical stress relaxation, and infrared and gel permeation chromatography analysis
01 p0119 N73-10985
Drift tube mass spectrometer for measuring reaction rate of uranium atoms and ions with O2 and N2
[AD-746272] 02 p0138 N73-11115
Reaction kinetics of nitroguanidine-nitrogen dioxide mixture
[TDCK-60180] 02 p0221 N73-11787
Analysis of transient and steady-state combustion processes in hybrid rocket system based on gaseous oxidizer flowing within tube of solid fuel
[NASA-CR-112201] 02 p0242 N73-11968
Multistep chemical processes for water decomposition, using nuclear heat for producing hydrogen
[EUR-4776-E] 03 p0263 N73-12132
Abstracts of DNA-sponsored reaction rate research programs for FY 72
[AD-747660] 03 p0299 N73-12441
Evaluation of cooled, flightweight gaseous hydrogen-oxygen reaction control thrusters to determine catalytic igniter operational limits and performance - Vol. 1
[NASA-CR-120869] 03 p0350 N73-12858
Demonstration of duct cooling concept with gaseous hydrogen/oxygen propellant in high pressure thruster - Vol. 2
[NASA-CR-120870] 03 p0350 N73-12859
Ablation of graphite surfaces heated in turbulent flow of air or carbon dioxide and development of method for calculating ablation rate
[AD-747727] 03 p0365 N73-12973
Analysis of motion of chemically active gases to determine heat and mass transfer in turbulent jet system during diffusion combustion
[AD-747571] 03 p0365 N73-12976
Mapping electron number density distribution in nonequilibrium shock layer with kinetic and radiative processes coupled to gas dynamics
[AD-748833] 04 p0407 N73-13312
Development of description for phenomenon of intrinsic unstable combustion in gas rocket
04 p0483 N73-13948
Reaction kinetics when liquid hydrazines adsorbed on supported ruthenium catalyst
[RPE-TR-72/1-PT-5] 05 p0506 N73-14122
Kinetics of Fe and Al atom oxidation reactions at high temperatures
[AD-749380] 05 p0507 N73-14125
Analysis of reaction kinetics, combustion physics, and propellant properties of fuel elements used with rocket and ramjet engines
05 p0590 N73-14793
Laboratory experiments and mathematical models of nitrogen oxide formation in combustion of fossil fuels
[PB-211480] 05 p0606 N73-14932
Computer program for determining influx towards center of spherical metal shell following detonation of spherical, symmetrically placed explosive
[FOA-2-C-2471-25] 06 p0653 N73-15305
Calculation of relaxation kinetics for carbon dioxide-water-nitrogen mixture to determine gas dynamics of escape from slit nozzle
[JPRS-57906] 06 p0654 N73-15310
Aeronomic reaction rate data
[AD-750771] 06 p0668 N73-15436
Characterization of nonequilibrium flow and coupled chemistry associated with rocket exhaust effluent interactions in upper atmosphere
[AD-750878] 06 p0670 N73-15450
Application of quasistatic theory of spectral line broadening to predict values for laser radiation
[AD-750156] 06 p0681 N73-15541
Kinetic and structural investigation of ST-4 titanium alloy oxidizability at 700 to 1000 C, unprotected and protected by silicon and molybdenum silicide coatings
[AD-750646] 06 p0686 N73-15585
High temperature oxidation behavior of Ni3Al with and without yttrium additions and reaction kinetics of Al2O3 layer growth
[AD-750410] 06 p0686 N73-15589
Rutile crystal growth, and hydrogen kinetics, electronic, and optical properties
[AD-748298] 06 p0709 N73-15789
Chemical surface reactions, phase transformations, and reaction kinetics in flow systems
[AD-750172] 06 p0712 N73-15808
High temperature reactions of COF2 with CO and H2 in excess argon behind reflected shock waves
[AD-751270] 07 p0753 N73-16118
Gain and performance measurement of expanding CO2 laser mixtures at high pressures
[AD-751694] 07 p0807 N73-16547
Feasibility of developing stirred chemical reactor laser cavity based on perfectly stirred reactor concept
[AD-751299] 07 p0807 N73-16549
Reaction between molecular hydrogen and molecular oxygen subjected to temperature and pressure pulses in shock tubes
[NASA-TM-X-2707] 07 p0854 N73-16928
Theoretical analysis of reaction kinetics limitations leading to extinction of counterflow diffusion flame
[AD-751053] 07 p0856 N73-16940
Quantitative inconsistencies in low temperature and high temperature oxidation kinetics
08 p0882 N73-17142
Kinetics and mechanisms of gas phase combustion, flames, and flame suppression
08 p0882 N73-17143
Fluorocarbon combustion and theories on fluorine supported combustion kinetics
08 p0883 N73-17145
Ozone reaction with mercaptane for elimination of exhaust gas pollution in air
08 p0883 N73-17152
Homogeneous cyanoethylation of hydrogen cyanide in presence of alkaline catalysts
[NASA-TT-F-14690] 08 p0884 N73-17154
Monte Carlo calculations of reaction rates for collisions of H atoms with vibrationally excited HF
[AD-751910] 08 p0884 N73-17157
Fast computer program for prediction of nonequilibrium rocket plume properties
[AD-751984] 08 p0970 N73-17927
Reaction kinetics of fluoride pyrolysis in liquid rocket propellant
[AD-752564] 08 p0970 N73-17931
Kinetics and rate constant of reaction OH[v equals 0] plus O3 yields HO2 plus O2
[NASA-CR-130858] 09 p0999 N73-18152
Atomic and molecular reaction kinetics in upper atmosphere
[AD-753246] 09 p1000 N73-18158
Reaction rate research, including atom, molecule, and ion interactions and aeronomy
[AD-753016] 09 p1031 N73-18418
Vaporization kinetics and thermodynamics of graphite using high pressure mass spectrometer
[AD-753713] 09 p1055 N73-18601
Abstracts on kinetics and thermodynamics of gases interacting with liquid metals
[JPRS-58282] 09 p1098 N73-18964
Kinetics of liquid hydrazine decomposition on supported rhodium catalyst
[RPE-TR-71/16-PT-4] 10 p1126 N73-19177
Vapor phase chemistry for producing hydrated ions in upper atmosphere
[AD-753940] 10 p1157 N73-19411
Stratospheric chemical reactions and perturbations caused by supersonic aircraft exhaust
[PB-213111] 11 p1290 N73-20464
Survey on aeronomic dynamics of photochemical reactions caused by supersonic aircraft exhaust
[PB-213126] 11 p1290 N73-20466
Solid phase interactions in cobalt-carbide systems
[NLL-LTI-746-1338-[9022.401]]
12 p1415 N73-21468
Reaction rate data for atmospheric chemistry, metal atom oxidation, and nuclear fireball
[AD-756674] 13 p1488 N73-22063
Perturbation analysis of combustion and burning of initially unmixed reactants
[AD-755214] 13 p1592 N73-22906
Bibliography of kinetic data in gas phase reactions of nitrogen, oxygen, and nitrogen oxides
[NBS-SP-371] 14 p1616 N73-23094
Thermodynamics of chemical species relative to aerospace technology including topics in chemical reaction kinetics and heat measurement
[AD-757518] 14 p1617 N73-23097
Analysis of tangential mode, nonlinear wave motion in liquid propellant rocket engine using two phase detonation wave as reaction model
[NASA-CR-121194] 14 p1718 N73-23944
Kinetics of afterburning process following injection of oxidizer into high temperature gas flow
[AD-756098] 14 p1719 N73-23951
Analysis of kinetic and transport factors governing interfacial mass transfer rates in high temperature systems
[AD-758256] 14 p1720 N73-23959
Emission rate constant for infrared chemiluminescent reaction of oxygen with nitric oxide
[NASA-CR-132157] 15 p1747 N73-24158
Monte Carlo calculations on reaction kinetics in hydrogen, deuterium, and fluoride interactions
[AD-758759] 16 p1872 N73-25153
Optical and microwave measurements of reaction kinetics behind shock waves
[AD-757230] 16 p1890 N73-25293
Kinetics of phase layer growth during diffusion coating of nickel with aluminum
[AD-760365] 17 p2054 N73-26611
Coordination chemistry and kinetics of preferential etching on surfaces of TiO2 [rutile]
[AD-759259] 17 p2074 N73-26780
Kinetics of recombination reactions in upper atmosphere
[AD-759847] 18 p2114 N73-27091
Kinetics of far ultraviolet chemiluminescence of exhaust plumes
[AD-760584] 18 p2114 N73-27093
Reaction kinetics of CF3 I flash photolysis iodine laser
[AD-760806] 18 p2158 N73-27436
Kinetics of gas pickling and epitaxial growth of semiconductor materials
18 p2188 N73-27664
Chemical kinetics of nitrogen-hydrogen-fluorine systems for advanced rocket propellant technology
[AD-760770] 18 p2192 N73-27697
Laminar chemically reacting boundary layer at solid fuel/gas interface over vaporizing surface
19 p2230 N73-27981
Sensitivity of coupled reaction rate equations to coefficient uncertainties
[AD-762420] 19 p2232 N73-27995
Fourier analysis on ergodic calculations of reaction kinetic rate coefficients in air dissociation and hydrogen oxygen combustion
[AD-762421] 19 p2232 N73-27996
Energy transfer reactions of electronically excited atomic and diatomic specspecies
[AD-762201] 19 p2298 N73-28481
Kinetic model and computerized simulation of DF-carbon dioxide chemical transfer laser
[AD-762284] 19 p2309 N73-28571
Kinetics of change in electrical resistance of thin films annealed in magnetic field at high temperature
[JPRS-59625] 19 p2309 N73-28575
Analysis of low speed deflagration of initially unmixed reactants under irreversible, two-step chain reaction
[AD-762459] 19 p2353 N73-28930
Photochemical reaction rate constant for hydroxyl radical with ozone in stratosphere
[AD-762195] 20 p2374 N73-29076
Development of invariant models of diffusion and chemical reactions in turbulent flow systems
[NASA-CR-2295] 21 p2505 N73-30106
Molecular population inversion by Laval nozzle expansion in N2/He/carbon dioxide laser
[DLR-FB-72-21] 21 p2554 N73-30480
Reaction kinetics and solid solubility of oxygen in molybdenum
22 p2624 N73-31027
Rate-controlled method of constrained equilibrium applied to chemically reactive open systems
[FML-PUBL-73-6] 22 p2625 N73-31031
Reaction rate characteristics of interstellar matter and cosmic cloud formation
22 p2735 N73-31896

Kinetic deuterium isotope effect in aqueous reaction of methyl radicals with deuterated alpha-alanine and glycine
[NASA-TT-F-15123] 23 p2753 N73-32033
Reports on upper atmosphere reaction rate data
[AD-764647] 23 p2754 N73-32040
Reaction kinetics in upper atmosphere chemistry and nuclear fireball studies
[AD-764892] 23 p2754 N73-32041
Application of laser energy to induce homogeneous exchange reaction of hydrogen and deuterium
24 p2930 N73-33399

**REACTION TIME**
Annotated bibliography on reaction times in selected human information processing tasks
[AD-745416] 01 p0012 N73-10095
Runway separation standards according to reaction time of pilot manual control response to air traffic controller communication
01 p0015 N73-10113
Analysis of reaction time to different visual cuing methods in large displays during secondary task performance
[AD-747688] 03 p0262 N73-12120
Response time of flash blindness recovery in human exposure to constant energy flashes
[AD-747631] 04 p0380 N73-13095
Pilot performance under certain hypnotic, tranquilizer, and barbiturate type drugs
12 p1369 N73-21110
Human continuous reaction time task distribution rates for paced and selfpaced responses to visual stimuli
[IZF-1973-5] 14 p1613 N73-23077
Reaction rate effect on gain and power of CO2-N2 gasdynamic laser in presence of H2 and H2O
[TAE-176] 16 p1920 N73-25539
Reaction time of 27-day density variation in upper atmosphere noting satellite recorded data on drag using regression analysis, cross correlation, and solar spectrum analysis
[BMFT-FBW-73-10] 21 p2538 N73-30352
Performance decrement and response time of current and noncurrent jet Naval pilots
[AD-761463] 22 p2624 N73-31025

**REACTION WHEELS**
Development of spacecraft control system using two speed-baised and speed-modulated reaction wheels with resultant momentum nominally oriented along orbit normal
[AD-745961] 02 p0235 N73-11911
Development and characteristics of rate measuring package for stabilization of Nimbus D satellite
[NASA-CR-130182] 10 p1216 N73-19888
Derivation of equations of motion for small angular displacements from equilibrium position of earth pointing satellite with reaction wheel damping
[ARC-R/M-3276] 16 p1857 N73-25039

**REACTIVITY**
Multidimensional analysis of fast spectrum material replacement measurements for systematic estimation of cross section uncertainties
[NASA-TM-X-2679] 05 p0579 N73-14709
Reactivity changes of rats to antiradiation drugs with head and stomach shielded during total irradiation
11 p1241 N73-20072
Testing association of automotive fuel composition with exhaust reactivity using different engines and gasolines of varied composition
[BM-RI-7756] 18 p2172 N73-27542
Chemical reactivity of hydrogen, nitrogen, and oxygen below 100 K
[NASA-CR-133654] 20 p2456 N73-29742
Reactivity change in fast spectrum space power reactor due to 328 meter/sec impact
[NASA-TM-X-2886] 23 p2818 N73-32532

**REACTOR CHEMISTRY**
U RADIOCHEMISTRY

**REACTOR CORES**
Computerized simulation of stainless steel clad uranium oxide plutonium oxide fuel pin behavior in reactor core
[ORNL-4825] 07 p0819 N73-16640
Post impact behavior of mobile reactor core containment systems
[NASA-TM-X-68176] 07 p0819 N73-16642
Design, construction, and operation of combined principles simulator of gas core nuclear engine
[NASA-CR-2155] 07 p0826 N73-16691
Development of graphite-matrix fuels for booster assemblies in reactor cores
09 p1063 N73-18669
Power distribution in fast spectrum thermionic reactor fuel element at core/BeO reflector boundary
[NASA-TM-X-68207] 11 p1323 N73-20735
Evaluation of uranium nitride for in-core thermionic applications in electrically heated thermal gradient tests and in flat plate thermionic converters
[NASA-CR-131320] 12 p1416 N73-21470
Experimental and analytical determination of one- and two-component flows in spherical chambers for application to open-cycle gaseous-core nuclear rocket
[NASA-CR-2282] 19 p2255 N73-28175
Flow velocity distribution in lower plenum of pressurized water reactor vessel, and design optimization of core catching structure
[BMFT-FBK-73-03] 19 p2255 N73-28182
System of differential equations of hydraulics and heat transfer for porous body, reactor core
[JPRS-59775] 20 p2453 N73-29714
Prototype mechanical drive for boiling water reactor in-core out-core neutron flux detectors
[BMBW-FBK-72-25] 22 p2699 N73-31617
Mobile test chamber for calibration of fixed incore radiation detectors
[BMBW-FBK-72-26] 22 p2699 N73-31618
Heat transfer in fissioning uranium plasma reactor cavity
[NASA-TM-X-2885] 23 p2828 N73-32607
Computer code for thermal/hydraulic stress analysis on liquid metal zirconium hydride reactor core
[AI-AEC-13065] 24 p2954 N73-33596
Zirconium hydride reactor core heat transfer on rod spacers to liquid metal NaK
[AI-AEC-13088] 24 p2955 N73-33607

**REACTOR DESIGN**
Design and performance tests of small transportable nuclear reactors
[AD-745362] 01 p0079 N73-10652
Working on advanced heat source converter design designated as multihundred watt program
[MLM-1896[OP]] 03 p0333 N73-12711
Computer program for high temperature structural design methods for LMFBR components
[ORNL-TM-3845] 03 p0333 N73-12712
Influence of fast neutron damage to ceramic insulators on thermionic reactor design
[LA-DC-72-523] 03 p0333 N73-12716
Cost analysis and design of possible fusion reactor coil systems
[UCRL-73187] 03 p0336 N73-12741
Design and performance analysis of ZrH reactor thermoelectric nuclear power system
[AI-AEC-13039] 12 p1427 N73-21567
Neutronic feasibility of fast spectrum space power reactor design concepts using boron control devices
[NASA-TM-X-2821] 16 p1943 N73-25720
Design of split-core heat-pipe radioisotopic reactor for space power applications
[NASA-TM-X-68254] 16 p1943 N73-25722
Thermoelectric converter and 5-kwe reactor system integration
[NASA-CR-121230] 16 p1943 N73-25726
FORTRAN 4 code for calculating nuclear reactor dimensions and mass from thermal-hydraulic considerations
[NASA-TM-X-68236] 17 p2061 N73-26670
Fissioning uranium plasma for use as power source in driver reactor
[NASA-TM-X-68232] 17 p2067 N73-26722
Design and sizing of gas core nuclear rocket engine system components
[NASA-TM-X-2772] 18 p2176 N73-27575
Evaluation of fuel pin design concepts for fast spectrum lithium cooled compact space power reactor
[NASA-CR-121181] 18 p2178 N73-27584
Nuclear calculations for gas core breeder reactor configurations
19 p2319 N73-28656
Power production and fuel capability of light water cooled cavity test reactor
[NASA-TM-X-2864] 19 p2320 N73-28662
Design of uranium zirconium hydrogen fueled reactor and development of lead tellurium thermoelectric conversion system
[AI-AEC-13046] 19 p2320 N73-28664
Fatigue and creep-fatigue behavior of irradiated austenitic stainless steel used in LMFBR design
[ANCR-1096] 19 p2349 N73-28891
System of differential equations of hydraulics and heat transfer for porous body, reactor core
[JPRS-59775] 20 p2453 N73-29714
Superconducting materials evaluation for magnet in optimal design of Tokamak reactor
[CONF-721111-21] 20 p2462 N73-29784
Computerized simulation models for thermal exhaust reactors
22 p2727 N73-31824

**REACTOR FUELS**
U NUCLEAR FUELS

**REACTOR MATERIALS**
Nuclear and instrumentation research
[AECL-4129] 01 p0079 N73-10651
Influence of neutron irradiation on damage to fuel cladding and reactor structural materials
[HEDL-SA-317] 03 p0332 N73-12709
Design of intense neutron source for studying materials damage in fusion power reactor
[LA-4863] 04 p0402 N73-13272
Properties of solid reactor materials
[REPT-331] 04 p0448 N73-13655
Muhidimensional analysis of fast spectrum material replacement measurements for systematic estimation of cross section uncertainties
[NASA-TM-X-2679] 05 p0579 N73-14709
Fabrication and characteristics of ceramic-metal multilayers for inclusion in experimental breeder reactor
[LA-5021-PR] 07 p0820 N73-16646
Effects of nuclear radiation on stainless steels
[AD-753457] 10 p1187 N73-19660
Dynamic tear tests for determining fracture safety of Hanford-N reactor coolant piping material
[AD-748590] 13 p1558 N73-22626
Chemical compatibility of materials used for lithium cooled space power reactor concept at high temperature
[NASA-TN-D-7259] 15 p1809 N73-24660
Facility for wear testing sodium cooled reactor materials
[KFK-1659] 16 p1944 N73-25727
Neutron capture and total cross sections for isotopes of reactor materials
[COO-3058-27] 17 p2065 N73-26702
Elastic-plastic toughness level of irradiated stainless steels used in fast reactor construction
[AD-761611] 19 p2310 N73-28580
Superconducting materials evaluation for magnet in optimal design of Tokamak reactor
[CONF-721111-21] 20 p2462 N73-29784
Radiation effects on reactor structural materials
[AD-763658] 21 p2578 N73-30661
Effect of FeF2 addition on Hastelloy N compatibility with LiF-BeF2-UF in low temperature convection loop system
[ORNL-TM-4188] 24 p2936 N73-33444

**REACTOR PHYSICS**
NT NUCLEAR FUEL BURNUP
Annual report 1971-1972 of Interuniversitair Reactor Institute in Netherlands
10 p1195 N73-19721

**REACTOR SAFETY**
Ionizing radiation health standards and safety measures around nuclear installations
[EUR-4800-D-F-I-E-PT-1] 01 p0082 N73-10679
Emergency radiological and meteorological instrumentation criteria for reactors
[BNWL-1635] 04 p0422 N73-13443
Safety calculations for compaction and coolant voiding by airborne fast reactor
[LA-4977] 06 p0699 N73-15695
Analysis of temperature-dependent neutron transmission and self-indication measurements on tantalum in unresolved region
[NASA-TN-D-7214] 09 p1064 N73-18678
Safety procedure for testing thermionic reactor in test facility
[NASA-TM-X-68224] 13 p1558 N73-22624
Dynamic tear tests for determining fracture safety of Hanford-N reactor coolant piping material
[AD-748590] 13 p1558 N73-22626
Probability of aircraft crashing into Boardman nuclear power plant
[PB-220715/7] 21 p2578 N73-30662
Steel technology and water reactor pressure vessel safety
[ORNL-4855] 24 p2935 N73-33440

**REACTOR STARTUP TESTS**
Design and performance tests of small transportable nuclear reactors
[AD-745362] 01 p0079 N73-10652
Safety procedure for testing thermionic reactor in test facility
[NASA-TM-X-68224] 13 p1558 N73-22624
Thermal and nucleonic behavior of NERVA reactor during startup transient investigation
[AD-764231] 22 p2699 N73-31620

**REACTOR TECHNOLOGY**
NT NUCLEAR FUEL BURNUP
State of fusion reactor technology at end of 1971
[EUR-4873-E] 01 p0079 N73-10649
Nuclear and instrumentation research
[AECL-4129] 01 p0079 N73-10651
Design and performance tests of small transportable nuclear reactors
[AD-745362] 01 p0079 N73-10652
Nuclear power plants for mobile applications
[NASA-TM-X-68154] 02 p0211 N73-11708
Properties of solid reactor materials
[REPT-331] 04 p0448 N73-13655
Analysis of magnetic device with longitudinal field for experimentation with Adone reactor
[LNF-71/90] 04 p0448 N73-13659
Annual report of German institute for inorganic and nuclear chemistry, 1971
[BMBW-FBK-72-15] 04 p0453 N73-13702
Development of method for determining critical stress intensity for crack propagation and application to reactor components
[RD/B/N-2143] 04 p0481 N73-13934
Fabrication and characteristics of ceramic-metal multilayers for inclusion in experimental breeder reactor
[LA-5021-PR] 07 p0820 N73-16646
Design, construction, and operation of combined principles simulator of gas core nuclear engine
[NASA-CR-2155] 07 p0826 N73-16691
Neutronics analysis of gas core rocket concept using cavity test reactor
[NASA-TM-X-2743] 09 p1063 N73-18676

Commercial applications of rare earth elements in ceramics, glasses, and nuclear technology
[IS-2967] 10 p1175 N73-19561
Method for interpreting Doppler effect measurements and determining their precision
[NASA-TM-X-68199] 11 p1323 N73-20736
Design and performance analysis of ZrH reactor thermoelectric nuclear power system
[AI-AEC-13039] 12 p1427 N73-21567
Engineering problems of controlled thermonuclear reactor power plants
[BNWL-1685] 15 p1811 N73-24682
Isotopic fuel technologies
[MLM-2014] 17 p2061 N73-26675
Flow configurations for maximum nuclear criticality eigenvalue in gas core reactor
[NASA-CR-121191] 18 p2177 N73-27578
Feasibility of bifold nuclear power source using Pu-238 fuel
24 p2951 N73-33573

REACTORS
NT TOKAMAK FUSION REACTORS
Computer program and numerical technique for calculating chemical composition of stirred reactor
[AD-751462] 16 p1974 N73-25967

READERS
Information retrieval system combining magnetic storage and microfilm reader/copier
[CRIF-EL-5] 02 p0147 N73-11188
Technical problems of automatic speech reading machines and methods adopted for their solution
14 p1620 N73-23122
Field evaluation of automated reading system for blind that produces synthetic speech from written text by use of computer and special-purpose devices
14 p1620 N73-23123
Word and phrase stress by rule for reading machine that produces synthetic English speech
14 p1620 N73-23124
Synthesis of letter sounds of alphabet by concatenation of phonemes for digital spelled speech reading machine for blind
14 p1620 N73-23127
Method for quantitative print quality evaluation of large amount of data with determination based on requirements of optical character readers
[REPT-731] 14 p1637 N73-23276

READING
NT LIP READING

READING MACHINES
U READERS

READJUSTMENT
U ADJUSTING

READOUT
Electron recording and readout sensitivity characteristics of amorphous semiconductor thin films
[AD-763253] 21 p2585 N73-30719

REAL GASES
Numerical analysis of real gas effects in supersonic flows over sharp and spherically blunted cones
16 p1887 N73-25274

REAL NUMBERS
NT INTEGERS

REAL TIME OPERATION
Digital receiver for detecting moderate data rate phase-shift keyed signals in real time
01 p0025 N73-10196
Development and design of small real time computers for information systems
[FOA-2-C-2484-E5] 02 p0145 N73-11175
Design of high speed, real time symbiont for analog telemetry processing
[NASA-TM-X-66090] 02 p0146 N73-11183
Specifications for automatic command and control of real time plasma simulation chamber
[GRI/NTP/102] 02 p0216 N73-11747
Iterative method for real time actuator extension transformation analysis on motion simulator
[NASA-TN-D-7067] 03 p0269 N73-12182
Near real time water resources data from Delaware Bay for use in river basin management
[E72-10239] 03 p0288 N73-12339
Multiprogram structure of HRS 101 digital computer and program package for statistical measured data selection and real time presentation
[JPRS-57696] 05 p0516 N73-14192
Program package for statistical measured data selection and visual presentation in real time
05 p0516 N73-14193
Improved multibeam cathode ray tube for real time display of infrared reconnaissance data
[AD-749475] 05 p0520 N73-14228
Real time software for ballistic missile defense data processing system
[AD-750389] 06 p0644 N73-15234
Real time program for alignment of components and subassemblies prior to installation in chamber
[NASA-CR-128712] 07 p0800 N73-16493
Theory of Kalman filtering and applications to real time tracking systems for air traffic control, satellite observation, and aircraft navigation
[AD-751485] 07 p0818 N73-16634
Real time data display and postflight analysis
[NASA-CR-128836] 10 p1132 N73-19229
On-line laboratory station connected to real time/time-sharing EMR 6130 computer for semiconductor radiation effects studies
[SC-DR-72-0525] 10 p1161 N73-19442
Evaluation of associative processor in performance of tracking and conflict detection function in real time ATC terminal environment
[PX-6406-REV-A] 10 p1185 N73-19642
Liquid crystal Fourier plane filter for real time optical image processing
[NASA-CR-130185] 10 p1188 N73-19670
Display device for real time display of computer generated half tone pictures
[AD-753672] 11 p1260 N73-20224
Graphical computers and computing techniques for real time aid in human problem solving tests
[AD-754282] 11 p1260 N73-20227
Real time analysis of multichannel electrophysiological recording, using hybrid computers
14 p1611 N73-23064
Real time software speech synthesis
14 p1624 N73-23160
Computational processing in real time of digitized palatal signals and analog speech waveforms
14 p1626 N73-23172
Three-dimensional output from third octave frequency analysis
14 p1631 N73-23221
Large space bandwidth signal analysis by means of two-dimensional optical processor and synthesis of near real time optical sound-spectrograph
14 p1631 N73-23223
Hard copy of visible speech in real time using electrostatic matrix recorder
14 p1631 N73-23224
Adaptive processing filtering and design of digital signals for real time analysis with algorithm derivation
[AD-757229] 14 p1684 N73-23667
Real time computer technique for mission control and schedule planning
18 p2211 N73-27852
Real time hybrid computer audio synthesis system
[AD-761730] 19 p2228 N73-27968
Signal modulation and digital processing for real time radar operation
[AD-762438] 19 p2238 N73-28040
Real time measurement of three-dimensional position of light emitting diodes
[AD-762028] 19 p2241 N73-28070
Development and evaluation of on-line spatial light modulator for application as input transducer for real-time optical data processing system
[NASA-CR-124375] 21 p2508 N73-30121
Design of real time telemetry processing system for naval aircraft flight tests
[AD-763469] 21 p2509 N73-30130
Real time holographic interferometry for optical surface testing
[BMFT-FBT-73-01] 22 p2681 N73-31479
Transit waveform control program for real time environmental shock tests
22 p2732 N73-31860
Respiratory analysis system to determine gas flow rate and frequency of respiration and expiration cycles in real time
[NASA-CASE-MSC-13436-1] 23 p2751 N73-32015
Multidimensional linear system parameter estimation computer program using least squares method evaluating mathematical model stability, observability and real time operation
[LAAS-AS-73-1-06] 23 p2813 N73-32491
Azur satellite telemetry, noting real time and tape telemetry systems
24 p2985 N73-33853

REAL VARIABLES
NT ABEL FUNCTION
NT ASYMPTOTES
NT BINARY INTEGRATION
NT BURGER EQUATION
NT CALCULUS OF VARIATIONS
NT COSINE SERIES
NT DIFFERENTIAL EQUATIONS
NT EINSTEIN EQUATIONS
NT ELLIPTIC DIFFERENTIAL EQUATIONS
NT EXTREMUM VALUES
NT FOKKER-PLANCK EQUATION
NT FOURIER SERIES
NT FUNCTIONAL INTEGRATION
NT GAUSS EQUATION
NT GREEN FUNCTION
NT HANKEL FUNCTIONS
NT HELMHOLTZ VORTICITY EQUATION
NT HYPERBOLIC FUNCTIONS
NT INTEGRAL CALCULUS
NT LEBESGUE THEOREM
NT LIAPUNOV FUNCTIONS
NT LINEAR EQUATIONS
NT MAXIMA
NT MEASURE AND INTEGRATION
NT NEUMANN PROBLEM
NT NONLINEAR EQUATIONS
NT NUMERICAL INTEGRATION
NT PARABOLIC DIFFERENTIAL EQUATIONS
NT PARTIAL DIFFERENTIAL EQUATIONS
NT PERIODIC FUNCTIONS
NT POISSON EQUATION
NT POWER SERIES
NT QUADRATIC EQUATIONS
NT RUNGE-KUTTA METHOD
NT SERIES [MATHEMATICS]
NT SINE SERIES
NT STURM-LIOUVILLE THEORY
NT TANGENTS
NT TAYLOR SERIES
NT TRIGONOMETRIC FUNCTIONS
NT VECTOR ANALYSIS
NT VLASOV EQUATIONS
NT VORTICITY
NT WEIGHTING FUNCTIONS

REATTACHED FLOW
Calculation of supersonic boundary layer flow separation and reattachment along plane wall with sinusoidal hollow
[REPT-72-4] 14 p1650 N73-23382
Supersonic boundary layer separation and reattachment - finite difference theory solutions
[AD-757062] 14 p1651 N73-23383

REATTACHMENT
U ATTACHMENT

RECEIVERS
NT LOGARITHMIC RECEIVERS
NT RADAR RECEIVERS
NT RADIO RECEIVERS
NT RADIOTELEPHONES
NT SUPERHETERODYNE RECEIVERS
NT TELEVISION RECEIVERS
Design and performance of wideband down-converter for satellite ground terminal
[NASA-CR-128394] 01 p0032 N73-10249
Design study of infrared 10.6 micrometer, quantum noise limited, optical receiver subsystem
[NASA-CR-130091] 01 p0056 N73-10458
Optical design approach for large array of high speed heterodyne receivers for infrared laser radiation
[AD-750402] 06 p0700 N73-15711
Characteristics of noise-resistant receiver for wireless electrical communication circuit for drill speed measurement
[AD-756090] 13 p1495 N73-22122
Design of nonlinear coherence receiver with feedback signal selection for carrier tracking in telecommunications
[NASA-CASE-NPO-11921-1] 14 p1620 N73-23118
Adaptive maximum likelihood receiver for digital communication channels
16 p1873 N73-25163
Experimental systems for automatic receiving and recording of echoes from D region
[AD-760362] 17 p2030 N73-26428
Simulated environment interference tests on adjacent channel signal receivers for frequency assignments of instrument landing systems
[FAA-RD-73-1-VOL-1] 17 p2060 N73-26665
Fixed frequency ionosonde receiver with phase swept interferometer
[KGO-726] 18 p2118 N73-27122
Improved phase lock loop for receiver in multichannel telemetry system with suppressed carrier
[NASA-CASE-NPO-11593-1] 19 p2234 N73-28012
Performance characteristics, except direction, of detection receivers in processing known signals
[AD-762048] 19 p2236 N73-28029
Automatic carrier acquisition system for phase locked loop receiver
[NASA-CASE-NPO-11628-1] 21 p2506 N73-30113
Analysis and simulation of telemetry receivers and bit synchronizers
[NASA-CR-132809] 21 p2507 N73-30120
Digital error probalities of binary receivers in presence of intersymbol interference in fading channels
23 p2755 N73-32049
Adaptive learning receiver for time varying multipath channel transmission
23 p2756 N73-32052
Theory, design, and operation of suppressed carrier data-aided tracking receiver
[NASA-CR-135714] 23 p2757 N73-32065
Maximum likelihood receiver for pulse communication systems
[AD-764641] 23 p2758 N73-32072
Optimum receiver for detection of pulsed angle modulated optical communication system, using maximum posteriori
24 p2931 N73-33406

RECEIVING SYSTEMS
U RECEIVERS

RECEPTACLES [CONTAINERS]
U CONTAINERS

RECEPTORS [PHYSIOLOGY]
Adaptability and receptivity factors affecting motion sickness susceptibility in pilots
12 p1367 N73-21095

RECIPROCATING ENGINES
U PISTON ENGINES

RECIRCULATION
U CIRCULATION

**RECIRCULATIVE FLUID FLOW**
Hot gas recirculation in Do-31 aircraft from scale model to aircraft and trends for future developments of V/STOL aircraft
[BMVG-FBWT-72-29] 10 p1107 N73-19024
**RECLAMATION**
NT MATERIALS RECOVERY
NT WATER RECLAMATION
Application of ERTS-1 imagery to selected Bureau of Reclamation projects
[E72-10238] 03 p0288 N73-12338
Detection and monitoring area strip mining and reclamation in Ohio using ERTS-1 imagery
[E72-10284] 04 p0409 N73-13334
Remote sensing of selected Bureau of Reclamation land projects
[E73-10062] 07 p0778 N73-16324
Application of ERTS-1 remotely sensed imagery to selected reclamation projects
[E73-10066] 07 p0779 N73-16328
Application of ERTS-1 imagery to Bureau of Reclamation studies of geology, agriculture, and urban development
[E73-10336] 10 p1147 N73-19337
Application of ERTS-1 imagery to selected Bureau of Reclamation projects
[E73-10537] 13 p1518 N73-22301
Detection, monitoring, and mapping coal strip mining and reclamation in Ohio from ERTS-1 imagery
[E73-10641] 16 p1896 N73-25338
EREP imagery for detection of strip mines and reclamation activities in Ohio, West Virginia, and Pennsylvania
[E73-10731] 17 p2020 N73-26337
Skylab monitoring of surface mining activities and reclamation in Ohio, West Virginia, Pennsylvania, Indiana, Kentucky, and Illinois
[E73-11033] 22 p2663 N73-31337
Usefulness of ERTS-1 MSS data for monitoring coal strip mining, detection of acid mine drainage, and determination of effectiveness of reclamation and abatement procedures in Pennsylvania
[E73-11112] 24 p2915 N73-33269
**RECOGNITION**
NT CHARACTER RECOGNITION
NT PATTERN RECOGNITION
NT SPEECH RECOGNITION
NT TARGET RECOGNITION
NT TIMBER IDENTIFICATION
**RECOIL PROTONS**
Spectrometer for fast neutrons using proton recoil in stilbene crystal
[BMVG-FBWT-72-4] 09 p1036 N73-18456
**RECOMBINATION COEFFICIENT**
Rate coefficient data for recombination reaction hydrogen plus oxygen plus argon yields water and argon in mixtures behind incident shock waves
[NASA-TN-D-6990] 01 p0117 N73-10965
Three body recombination and dissociation rate coefficients for reversible reactions H2 plus H yields H plus H plus H
[FML-PUBL-72-11] 10 p1126 N73-19169
**RECOMBINATION REACTIONS**
NT ATOMIC RECOMBINATION
NT ELECTRON RECOMBINATION
NT ELECTRON-ION RECOMBINATION
NT HYDROGEN RECOMBINATIONS
NT ION RECOMBINATION
NT OXYGEN RECOMBINATION
NT RADIATIVE RECOMBINATION
Gas phase recombination of hydrogen and deuterium atoms
[NASA-CR-131417] 11 p1252 N73-20162
Atomic oxygen hydrogen reaction with acetylene, and gas discharge shock tube design
13 p1488 N73-22060
Recombination electron beam-excited plasma into pulsed laser of high peak power
[AD-756681] 13 p1537 N73-22455
Recombination coefficients and volume decay coefficient for laser-produced helium plasmas
[CEA-CONF-2102] 15 p1817 N73-24726
Kinetics of recombination reactions in upper atmosphere
[AD-759847] 18 p2114 N73-27091
Heating and volume recombination effects on gas discharge column equilibrium
[AD-761492] 19 p2325 N73-28704
Continuum chromospheric emission and negative results in search for solar recombination lines in frequency range 110-115 GHz
[AD-763719] 22 p2712 N73-31717
**RECOMMENDATIONS**
Theories and definitions of comets and asteroids for proposed recommendations
[NASA-TM-X-71917] 22 p2717 N73-31747
**RECOMPRESSION**
U COMPRESSING
**RECONNAISSANCE**
NT AERIAL RECONNAISSANCE
NT PHOTORECONNAISSANCE
NT SPECTRAL RECONNAISSANCE
Data handling theory, telemetry, and signal frequency determination for signal reconnaissance
[FOA-3-C-3653-66] 02 p0140 N73-11134
Principles of radiometric reconnaissance
[FOA-3-C-3675-E1] 02 p0172 N73-11391
**RECONNAISSANCE AIRCRAFT**
NT BREGUET 1150 AIRCRAFT
NT CL-84 AIRCRAFT
NT EARTH RESOURCES SURVEY AIRCRAFT
NT F-5 AIRCRAFT
NT MIRAGE 3 AIRCRAFT
NT OV-10 AIRCRAFT
NT P-1127 AIRCRAFT
NT U-2 AIRCRAFT
Computer simulation of aircraft motions and propulsion system dynamics for YF-12 aircraft under supersonic conditions
[NASA-TM-X-62245] 20 p2361 N73-28990
Ground vibration tests of YF-12 aircraft to determine frequency response data, measured node lines, and elastic mode shapes for aircraft components
[NASA-TM-X-2880] 20 p2483 N73-29944
**RECONNAISSANCE DRONE AIRCRAFT**
U DRONE AIRCRAFT
U RECONNAISSANCE AIRCRAFT
**RECONNAISSANCE SPACECRAFT**
Application of infrared reconnaissance satellites for detecting missiles and military satellites
[AD-760951] 18 p2152 N73-27395
**RECONSTRUCTION**
NT WAVE FRONT RECONSTRUCTION
**RECORDING**
NT DATA RECORDING
NT DATA SMOOTHING
NT MAGNETIC RECORDING
NT PHOTOGRAPHIC RECORDING
Time base stability and intermachine compatibility in wideband laser recording systems
13 p1536 N73-22444
Hard copy of visible speech in real time using electrostatic matrix recorder
14 p1631 N73-23224
**RECORDING HEADS**
Production of narrow-track video recording head to include characteristics of recording tape and tetrode sputtering equipment
[NHK-LABS-NOTE-154] 07 p0754 N73-16124
Foil bearing model for predicting head to tape separation in magnetic recording system
[NASA-CR-130536] 08 p0885 N73-17167
**RECORDING INSTRUMENTS**
NT LUNAR SEISMOGRAPHS
NT OSCILLOGRAPHS
NT PLOTTERS
NT SEISMOGRAPHS
NT WEATHER DATA RECORDERS
NT X-Y PLOTTERS
Performance evaluation of airborne audio-video recording system as training device in A-7D tactical fighter
[AD-744041] 01 p0021 N73-10161
Variometer recordings at Narssarssuaq Geophysical Observatory 1968 - 1970
02 p0167 N73-11356
Device for recording locations of measurements made by hand-held noncontacting probe
[NASA-CASE-LAR-10806-1] 06 p0673 N73-15474
Magnetic tape transport unit for ERTS recording instruments - Vol. 1
[NASA-CR-130186] 10 p1129 N73-19194
Recording instruments for Earth Resources Technology Satellites - Vol. 2
[NASA-CR-130187] 10 p1129 N73-19195
Analog digitizer for recording non-recurrent signals
[LRP-57/72] 10 p1132 N73-19226
Digital photometer for recording measurements of ionospheric disturbances
[AD-754436] 10 p1157 N73-19415
Graphical techniques for developing photoplastic record card system
[AD-753602] 10 p1162 N73-19453
Characteristics of instrument for measuring and recording water flow and modifications for improved operation
12 p1421 N73-21518
Instruments for recording force deflection from Charpy impact tests on metals
[REPT-527] 13 p1585 N73-22852
Equipment for continuous recording of natural electromagnetic noise of extremely low frequencies
[AD-757482] 14 p1634 N73-23244
Effectiveness of infrared radiometer and digital recording equipment as clear air turbulence warning system
[AD-757501] 14 p1685 N73-23677
Design of photoelectric sunshine recorder using cadmium sulfide photoconductive cells
[NLL-M-22979-[5828.4F]] 16 p1910 N73-25456
Photographic equipment for recording fracture of zinc single crystals under dynamic stress
20 p2461 N73-29775
Evaluation of recording instrument for in-flight determination of size and distribution of hailstones
[NASA-TM-X-2817] 21 p2549 N73-30434
Automatic speech level meter on voice frequency telephone circuit
[REPT-6648] 22 p2672 N73-31402
Magnetograph for recording magnetic fields in solar active region
[AD-762485] 22 p2712 N73-31713
Temperature, shock, vibration, humidity, salt-fog, and electromagnetic tests on automotive disk recorder
24 p2926 N73-33368
**RECORDS**
Design of interactive program to teach accounting techniques
[NASA-CR-129674] 04 p0393 N73-13192
**RECOVERABLE LAUNCH VEHICLES**
Analysis of size, weight, and packaging requirments for aerodynamic decelerator for recovery of expended solid propellant rocket engines used to launch space shuttle vehicles - Vol. 2, Book 5
[NASA-CR-123730] 15 p1826 N73-24801
**RECOVERABLE SATELLITES**
U RECOVERABLE SPACECRAFT
**RECOVERABLE SPACECRAFT**
NT AEROSPACEPLANES
NT APOLLO SPACECRAFT
NT GEMINI SPACECRAFT
NT REUSABLE SPACECRAFT
NT SPACE SHUTTLES
NT VOSTOK SPACECRAFT
Wind tunnel tests to determine stability and control effectiveness of basic configuration of pressure-fed ballistic recoverable booster for space shuttle
[NASA-CR-120073] 02 p0233 N73-11896
Design study of arresting gear system for recovery of space shuttle orbiters
[NASA-TM-X-68881] 04 p0401 N73-13265
Concepts of space shuttle
[NASA-EP-96] 24 p2984 N73-33846
**RECOVERY**
Method for recovery of sunken bodies at depths of between 30 and 50 m
19 p2226 N73-27955
**RECOVERY PARACHUTES**
Wind tunnel tests to determine drag and performance of disk-gap-band parachutes in wake of Viking reentry vehicle scale model from subsonic to supersonic speeds
[AD-746291] 02 p0126 N73-11026
Development and operating principles of gas generator for deploying recovery parachutes from space capsules during atmospheric entry
[NASA-CASE-LAR-10549-1] 04 p0477 N73-13898
Design, stress analysis, and high altitude performance of recovery parachute system
[NASA-CR-130304] 06 p0621 N73-15037
Analysis of shock forces generated by opening 35 foot diameter extended-skirt parachute for retardation at 100,000 feet altitude
[AD-749690] 06 p0623 N73-15060
Apollo 16 flight anomaly report to determine cause of burn holes in main parachute canopy
[NASA-TM-X-69127] 11 p1338 N73-20863
Analysis of size, weight, and packaging requirments for aerodynamic decelerator for recovery of expended solid propellant rocket engines used to launch space shuttle vehicles - Vol. 2, Book 5
[NASA-CR-123730] 15 p1826 N73-24801
Simulation calculations of parachute deployment dynamics process for Viking 75 entry vehicle
[NASA-TN-D-7415] 21 p2600 N73-30841
**RECOVERY TEMPERATURE**
U SKIN TEMPERATURE [NON-BIOLOGICAL]
**RECREATION**
Case studies of meteorological satellite impact on agricultural crops and recreational activities
06 p0693 N73-15641
Computer mapping of Michigan recreational land use using ERTS-1 data
[E73-10392] 11 p1276 N73-20354
Digital recreational land use mapping in Oakland County, Michigan
[E73-10570] 15 p1772 N73-24350
Study of recreational land and open spaces using Skylab multispectral band cameras and scanners
[E73-10724] 17 p2019 N73-26331
Study of recreation land and open space in Oakland County, Michigan using Skylab MSS data
[E73-10915] 20 p2397 N73-29264
Skylab imagery of recreational land and open space in Oakland County, Michigan
[E73-10973] 22 p2657 N73-31285
Multidisciplinary research on water depth measurement, Yellowstone Park, atmospheric effects, lake ice surveillance, recreational land use, IFYGL, image enhancement, water quality, oil pollution detection, and mapping iron compounds from ERTS-1 data
[E73-11119] 23 p2783 N73-32264
Skylab photography of recreational land and urban resources in Oakland County, Michigan
[E73-11150] 24 p2919 N73-33304
**RECRYSTALLIZATION**
Recrystallization of hydrostatically extruded molybdenum, and plastic deformation of extruded samples
[AD-747400] 03 p0317 N73-12581
Recrystallization processes of sheet nichrome containing zirconium dioxide inclusions
[AD-747603] 03 p0318 N73-12589

Structural recrystallization of steels during fast and slow heating to show structural succession caused by different mechanisms of formation of austenite
13 p1541 N73-22481
Microstructure of recrystallized heat resistant steel
[JPRS-58840] 13 p1542 N73-22498
Recrystallization and aging studies of steels
[PB-221302/3] 22 p2687 N73-31526

**RECTANGLES**
Turbulent boundary layers on walls of rectangular water pipe inlets
02 p0155 N73-11259
Noise intensities of rectangular and circular supersonic nozzle geometries
[NASA-CR-130964] 09 p1067 N73-18704
Microwave frequency reflection characteristics of quasi-tapered anechoic chamber for radar echo tests
[AD-754203] 10 p1138 N73-19275
Approximative gain calculations for linear and rectangular arrays using vertically directed noise model
[AD-760690] 18 p2119 N73-27133

**RECTANGULAR BEAMS**
Computer analysis of temperature distributions in circular and rectangular bodies exposed to thermal radiation from nuclear weapon explosions
[AD-745727] 01 p0084 N73-10699
Shock tests on rectangular steel beams, relation of tension-compression properties to moment-curvature equation, and viscoelastic cantilever beam response to shock
[AD-748656] 04 p0482 N73-13941

**RECTANGULAR DRAINAGE**
U DRAINAGE PATTERNS

**RECTANGULAR GUIDES**
Stereo three dimensional gain pattern formation from plane rectangular antenna characteristics
[AD-754782] 11 p1257 N73-20199

**RECTANGULAR PANELS**
Dynamic structural response of rectangular panel to subsonic turbulent boundary layer pressure field
[NASA-TN-D-6970] 03 p0360 N73-12934
Rectangular solar cell stacked panels to generate electrical power aboard spacecraft
[NASA-CASE-NPO-11771] 11 p1237 N73-20040

**RECTANGULAR PLANFORMS**
NT RECTANGULAR PANELS
NT RECTANGULAR PLATES
NT RECTANGULAR WINGS
ALGOL procedures for calculating velocity and pressure distribution on rectangular and triangular planforms oscillating harmonically in supersonic flow - Part 1
[FOK-X-449-PT-1] 13 p1471 N73-21909
ALGOL procedures for calculating velocity and pressure distribution on rectangular and triangular planforms oscillating harmonically in supersonic flow - Part 2
[FOK-X-449-PT-2] 13 p1471 N73-21910
Wake development on models of elliptic, rectangular, swept and delta planforms when plunged in water
[ARC-CP-1238] 24 p2870 N73-32932

**RECTANGULAR PLATES**
Analysis of large deflections of rectangular plates with nonlinear elasticity and hollow shells with hinge-supported edges under external normal pressure uniformly distributed over surface
[AD-756103] 13 p1587 N73-22870
Neutron irradiation effects on pair defect accumulation in thin rectangular isotropic metal plates
14 p1675 N73-23593
Determination of temperature distributions and deformations of rectangular plates with circular elastic inclusions
[AD-756183] 14 p1717 N73-23930
Effect of forced transverse, low frequency vibrations on stability of rectangular plates with brace
14 p1717 N73-23932
Structural stability tests studying buckling of rectangular boron reinforced aluminum plates
[ENSMP-007] 15 p1840 N73-24907
Response of thick rectangular plate of incompressible, isotropic elastic material to tensile forces applied to opposite faces
[AD-761941] 19 p2350 N73-28903

**RECTANGULAR WIND TUNNELS**
Interference theory in slotted wind tunnels extended to subsonic rectangular wind tunnels with ventilated tool, longitudinal slots and perforated screens of arbitrary porosity
[ARC-R/M-3706] 05 p0492 N73-14007

**RECTANGULAR WINGS**
Influence of trailing edge thickness on aerodynamic drag of rectangular wings in transonic and supersonic flow
[DLR-FB-71-85] 06 p0615 N73-14991
Wind tunnel tests to determine effects of ground proximity on lift, drag, and pitching moment of rectangular wing equipped with jet flaps
[NAL-TR-294] 06 p0621 N73-15038
Heat transfer and flow visualization tests of straight wing hypersonic reentry vehicle at angles of attack from 20 to 80 deg
[NASA-TN-D-7108] 09 p0979 N73-18000
Calculation of outer inviscid flow about rectangular wing moving at supersonic speeds
[NASA-CR-130985] 09 p1013 N73-18269
Influence of various aerodynamic forces on rectangular wing performance with harmonic movement parallel to sieve flow movement
12 p1361 N73-21043
Numerical analysis of unsteady supersonic characteristics of space shuttle type vehicles using arbitrary finite element technique
[NASA-CR-112296] 13 p1470 N73-21904
Wind tunnel investigation of three dimensional flow effects on straight wings
14 p1600 N73-22973
Development of continual solution for stress distribution due to thermal stresses near roots of rectangular wings
[ARC-R/M-3236] 15 p1730 N73-24030
Survey of aerodynamic derivative measurements for unswept rectangular wings and delta wings with emphasis on main surface pitching moment derivatives
[ARC-R/M-3232] 16 p1855 N73-25024
Iterative method for calculation of loading on thin rectangular wing
[ARC-R/M-3719] 21 p2492 N73-30004
Analysis of inviscid flow field around rectangular wing of finite thickness in supersonic flow
23 p2771 N73-32166

**RECTIFICATION**
Rectification of ERTS-1 multispectral imagery using digital techniques
[PAPER-16] 19 p2277 N73-28327

**RECTIFIERS**
NT AVALANCHE DIODES
NT CRYSTAL RECTIFIERS
NT GERMANIUM DIODES
NT THYRATRONS
NT THYRISTORS
Analysis of operation of electric alternator feeding into direct current system through rectifying device
[RAE-LIB-TRANS-1679] 17 p1986 N73-26049
Magnetic materials selection for spacecraft transformers used in static inverters, converters, and transformer-rectifier supplies
[NASA-CR-135642] 23 p2764 N73-32118

**RECTUM**
Routine proctosigmoidoscopic examinations of asymptotic NASA personnel for cancer prevention
08 p0872 N73-17061

**RECUPERATORS**
U REGENERATORS

**RECURSION FORMULAS**
U RECURSIVE FUNCTIONS

**RECURSIVE FUNCTIONS**
Bifurcations, for second order recurrence, related to passing through critical case such as real multiplier having modulus equal to one
[LAAS-PUBL-934] 02 p0203 N73-11639
Inclusion problem for monadic recursion schemes
[NASA-CR-131292] 11 p1311 N73-20634
Recursive plane analysis for phase locking in pulse modulation sampling technique
[AD-756918] 13 p1492 N73-22092
Design of mathematical filters with finite precision
16 p1934 N73-25647
Recursive scheme for computing system availability from component elements
[AD-759809] 17 p2055 N73-26623
Geometrical interpretation of 2n-th central difference using simple recursive functions
[NASA-CR-133985] 22 p2691 N73-31554

**RECYCLING**
U CIRCULATION

**RED ARCS**
Vertical distribution of vibrationally excited molecular nitrogen in thermosphere corresponding to stable auroral red arc
[NASA-TM-X-66194] 09 p1028 N73-18390

**RED BLOOD CELLS**
U ERYTHROCYTES

**RED SEA**
Location of wet areas and detection of potential locust breeding sites using ERTS-1 imagery of Red Sea coastal plain of Saudi Arabia
[E73-10462] 12 p1394 N73-21301
Air water interaction in seasonal circulation variations of Red Sea
[PB-214446/7] 16 p1909 N73-25443

**RED SHIFT**
Gravitationally red-shifted positron annihilation radiation produced at surfaces of old neutron stars
[NASA-TM-X-66062] 01 p0100 N73-10818
Derivation of closed formula for relation between luminosity and red shift in expanding Friedman universe
07 p0840 N73-16802
History of 48-inch Palomar Schmidt telescope noting investigation of galactic red shift and radio sources
07 p0844 N73-16841
Determination of wavelength dependence of interstellar reddening law and applicability to all stars
08 p0975 N73-17971
Red shift energy distribution and black body background distortion theories of universal formation
19 p2333 N73-28770

**REDUCED GRAVITY**
Analysis of materials, processing criteria, processing techniques, and apparatus for preparation of composite materials in space
[NASA-CR-124172] 11 p1307 N73-20609
Effects of low Bond number sloshing on thermal stratification of cryogenic liquids
12 p1391 N73-21283
Development and characteristics of neutral buoyancy simulator for duplicating weightless conditions encountered during space missions
13 p1594 N73-22923
Procedures for simulating and studying effects of subgravity on subjects during laboratory experiments and space flight
[NASA-TT-F-14934] 15 p1761 N73-24267
Finite difference solution to thermoacoustic convection of fluids in low gravity environment
[NASA-CR-2269] 17 p2014 N73-26289
Development of restraint system for securing personnel to ergometer while exercising under weightless conditions
[NASA-CASE-MFS-21046-1] 18 p2150 N73-27377
Capabilities of space processes in ground based experiments at low-g periods
[NASA-CR-124385] 22 p2717 N73-31752

**REDUCTION [CHEMISTRY]**
NT DEOXIDIZING
NT HYDROGENATION
Bacterial reduction of organically bound phosphoric acid in blood
[NASA-TT-F-14723] 04 p0379 N73-13080
Refutation of microbial ability to reduce phosphate using thermochemical computations
[NASA-TT-F-14724] 04 p0379 N73-13081
Thermogravimetric analysis of reduction of oxides of nickel and chromium
[NASA-TM-X-2688] 06 p0684 N73-15565
Growth of iron whiskers by hydrogen reduction of iron halide salts
[AD-757588] 14 p1699 N73-23788
Analysis of melt segregation effects on solidification of metals under weightless conditions
[NASA-CR-124358] 21 p2559 N73-30510

**REDUNDANCY**
Algorithm for reducing redundancy during image transmission
01 p0024 N73-10189
Application of active standby redundancy techniques to large electrohydraulic servoactuator
[NASA-CR-124027] 07 p0803 N73-16515
Optimum allocation of redundancy in system of serially connected subsystems
[NASA-TN-D-7164] 09 p1056 N73-18614
Design of prototype quad redundant data terminal and associated multiplexer/demultiplexer units
[NASA-CR-124127] 10 p1130 N73-19203
Enhancement of multispectral aircraft scanner data using scan overlap redundancy
[NASA-CR-131587] 13 p1530 N73-22395
Redundancy elimination in Azur satellite telemetry data
24 p2985 N73-33857

**REDUNDANCY ENCODING**
Arithmetic error correction in redundant residue number systems
05 p0569 N73-14619

**REDUNDANT COMPONENTS**
Procedures for studying reliability characteristics of systems with standbys - Themis project
[AD-745911] 02 p0179 N73-11451
Redundant cells to improve reliability of asynchronous automata
04 p0399 N73-13250
Analysis of controllability and steady-state response of parallel-redundant flight control systems
[NASA-CR-130354] 07 p0737 N73-15998
Reliable functioning of avionic power supply equipment through employment of redundant components
[AD-757152] 14 p1602 N73-22988
Reliability improvement by redundancy in electronic systems
[RAE-TR-72200] 21 p2520 N73-30208

**REDUNDANT STRUCTURES**
U REDUNDANT COMPONENTS

**REENTRY**
NT HYPERBOLIC REENTRY
NT HYPERSONIC REENTRY
NT SPACECRAFT REENTRY
Boundary layer electron concentration profiles for entry of blunt nosed slender body into earth atmosphere
[NASA-TN-D-7332] 18 p2182 N73-27620

**REENTRY ANGLE**
U ANGLES [GEOMETRY]
U REENTRY TRAJECTORIES

**REENTRY BODIES**
U REENTRY VEHICLES

**REENTRY CONDITIONS**
U REENTRY

REENTRY EFFECTS
Analysis of interference heating on surfaces of reentry vehicle configurations and effects of wing sweep, angle of attack, and Reynolds number
[NASA-TN-D-7060] 03 p0364 N73-12964
REENTRY GLIDERS
U LIFTING REENTRY VEHICLES
REENTRY PHYSICS
Development of proton-activated recession sensor based on migration of beryllium isotope in graphite at high temperature and application to nose cone conditions during reentry
[AD-745454] 01 p0109 N73-10899
Guidance method for transition of space shuttle from hypersonic entry to subsonic cruise flight
[NASA-CR-128648] 03 p0357 N73-12905
Solution of viscous shock-layer equations using implicit finite difference scheme for hyperboloid body under conditions simulating atmospheric entry
07 p0768 N73-16238
Numerical analysis of characteristic processes of hyperbolic shock layers generated during atmospheric entry
07 p0768 N73-16242
Development of viscous shock layer analysis to determine nonequilibrium flow distributions of plasma layer during reentry conditions
[NASA-CR-2232] 13 p1491 N73-22085
Research projects on wake turbulence and atmospheric boundary layers, turbulent mixing and shear flows, and high temperature gas dynamics
[AD-755273] 13 p1512 N73-22251
Analysis of aerodynamic characteristics of Gemini spacecraft during reentry and comparison with wind tunnel data
[NASA-TM-X-58100] 13 p1577 N73-22786
Numerical analysis of space shuttle orbiter flight path and performance during approach guidance from space mission - Document 22
[NASA-CR-128962] 16 p1941 N73-25707
Numerical analysis of nonstationary three dimensional motion of reentry vehicles entering atmosphere at hypersonic speeds
16 p1965 N73-25897
Analysis of atmospheric entry trajectories for manned and unmanned missions to planet Venus
[NASA-TN-D-7316] 16 p1966 N73-25900
Wind tunnel tests to determine heat transfer and flow distribution of space shuttle configuration at hypersonic speeds simulating atmospheric entry
[NASA-CR-133405] 18 p2201 N73-27772
Wind tunnel tests to analyze aerothermodynamic control problems of space shuttle attitude control system at hypersonic speed
[NASA-CR-133407] 18 p2201 N73-27773
REENTRY SHIELDING
Simulated rain erosion testing on closed pore insulation for shuttle orbiter
[RM-573] 20 p2434 N73-29548
REENTRY TRAJECTORIES
Newton-Raphson techniques for analyzing reentry trajectories for heat minimization and terminal range maximization
[AD-745998] 01 p0106 N73-10882
Numerical methods for computing reentry trajectories for space shuttles
[NASA-CR-128652] 04 p0474 N73-13877
Spacecraft control over segment of atmospheric reentry trajectory using on-board computers to preclude deflection beyond atmosphere
[AD-750520] 06 p0719 N73-15871
Aerobraking trajectory for return of reusable space tugs
[NASA-CR-124057] 09 p1082 N73-18827
Space shuttle rendezvous, radiation and reentry analysis code
[NASA-TM-X-64768] 21 p2595 N73-30795
Maneuverable reentry body trajectory calculation using optimizing and nonoptimizing programs
[BMBW-FBW-72-15] 21 p2597 N73-30815
REENTRY VEHICLES
NT AEROSPACEPLANES
NT APOLLO SPACECRAFT
NT GEMINI SPACECRAFT
NT LIFTING REENTRY VEHICLES
NT MANEUVERABLE REENTRY BODIES
NT RECOVERABLE SPACECRAFT
NT REUSABLE SPACECRAFT
NT TRAILBLAZER 2 REENTRY VEHICLE
NT VOSTOK SPACECRAFT
NT X-20 AIRCRAFT
Two layer model of compressible turbulent boundary layer flow around reentry vehicle
[AD-743993] 01 p0043 N73-10338
Wind tunnel tests to determine drag and performance of disk-gap-band parachutes in wake of Viking reentry vehicle scale model from subsonic to supersonic speeds
[AD-746291] 02 p0126 N73-11026
Multiple-probe reflectometer technique for diagnosing structure of boundary layer plasma formed on reentry vehicles
[AD-747038] 02 p0217 N73-11760
Postflight evaluation of ballistic vehicle flight test boundary layer transition data
[NASA-CR-129045] 03 p0282 N73-12287
Comparison of turbulent heating predictions by three different techniques with flight test data of several reentry vehicles
[NASA-CR-130251] 03 p0282 N73-12288
Assessing laminar flow on conical vehicles during hyperbolic entry by studying boundary layer transition on ablating cones
[NASA-TM-X-68867] 03 p0283 N73-12293
Analysis of shock interaction and interference heating on military aerospace vehicles at hypersonic speeds
[AD-747765] 03 p0286 N73-12319
Guidance method for transition of space shuttle from hypersonic entry to subsonic cruise flight
[NASA-CR-128648] 03 p0357 N73-12905
Analysis of interference heating on surfaces of reentry vehicle configurations and effects of wing sweep, angle of attack, and Reynolds number
[NASA-TN-D-7060] 03 p0364 N73-12964
Flight tests of disk-gap band parachute behind full-scale simulator of Viking reentry vehicle over maximum range of entry conditions for landing on planet Mars-Vehicle AV-1
[NASA-CR-112176] 04 p0372 N73-13021
Flight tests of disk-gap band parachute behind full-scale simulator of Viking reentry vehicle over maximum range of entry conditions for landing on planet Mars-Vehicle AV-4
[NASA-CR-112179] 04 p0372 N73-13024
Development of auxiliary lifting system to provide ferry capability for entry vehicles
[NASA-CASE-LAR-10574-1] 04 p0400 N73-13257
Development and operating principles of gas generator for deploying recovery parachutes from space capsules during atmospheric entry
[NASA-CASE-LAR-10549-1] 04 p0477 N73-13898
Theoretical analysis of ablation effects on dynamic stability of reentry vehicles
04 p0477 N73-13899
Feasibility study of space rescue, resupply, and reconnaissance with glide-type reentry vehicle
[AD-748346] 04 p0479 N73-13918
Aerodynamic drag coefficients for conical body in near free molecule and transitional flow regimes
[AD-750042] 06 p0615 N73-14994
Flight test of 55 foot diameter disk-gap parachute trailing behind bluff body, planetary aeroshell and attached instrument payload
[NASA-TM-X-2671] 06 p0621 N73-15042
Mass spectrometer for investigating hypersonic air flows in shock tube for application to reentry body problems
[BMVG-FBWT-72-20] 07 p0801 N73-16505
Development of adaptive control system for atmospheric reentry vehicle to meet flying quality requirements
07 p0848 N73-16871
System for eliminating roll rate anomalies occurring during flights of slender ballistic reentry vehicles
[SC-DC-72-2244-A] 07 p0849 N73-16883
Effects of nozzle orientation and configuration on roll control and base pressure of hypersonic reentry vehicle
[SC-DC-72-1187-A] 07 p0849 N73-16884
Buckling modes of four optimized Mars entry aeroshell configurations at angle of attack loadings based on experimental pressure distributions
[NASA-CR-2087] 07 p0852 N73-16907
Heat transfer and flow visualization tests of straight wing hypersonic reentry vehicle at angles of attack from 20 to 80 deg
[NASA-TN-D-7108] 09 p0979 N73-18000
Performance tests of reentry vehicle control with base plane thrusters and fluidic control logic
[SC-DC-72-2244[RD]] 09 p0985 N73-18043
Radar echo cross sections from pyramidal shape of reentry vehicle
[AD-753684] 09 p1005 N73-18200
Impact safety for reentry of Electre nose cones along south coast of France
[ONERA-TP-1152] 09 p1084 N73-18846
Methods for determining inviscid three dimensional flow about smooth shapes at supersonic speeds
[AD-753695] 10 p1143 N73-19311
Computer automated scheme for solving equations of radiating flow over blunt body with or without ablation
[NASA-CR-2235] 11 p1348 N73-20936
Techniques for measuring heat transfer in short duration and rapidly varying flows
[AGARD-AG-165] 11 p1349 N73-20945
Stationary hypersonic overflow of leading point of graphite blunt body by heat conducting stream of air
[AD-755784] 12 p1466 N73-21875
Application of adaptive control algorithms to self adjusting control systems for aeroelastic aircraft, flight vehicle roll, and control during reentry
[AD-756598] 13 p1474 N73-21941
Aerothermodynamic wind tunnel tests of space shuttle configurations performed at Mach number 8 for flow distribution and heat transfer under reentry conditions
[NASA-CR-131486] 13 p1583 N73-22834
Effects of environmental stresses on materials used in constructing glide reentry vehicles
14 p1676 N73-23601
Problems associated with measuring VUV radiation in shock layer around hypersonic reentry vehicles
[AD-757150] 14 p1693 N73-23740
Numerical analysis of nonstationary three dimensional motion of reentry vehicles entering atmosphere at hypersonic speeds
16 p1965 N73-25897
User guide for computer program to analyze compact transpiration cooling system proposed for hypersonic reentry vehicles
[AD-759698] 16 p1975 N73-25974
Wind tunnel tests to determine effect of asymmetric nose bluntness on aerodynamic characteristics of slender cone at Mach 14
[AD-760807] 18 p2102 N73-26998
Fused slurry silicide coatings for tantalum reentry heat shielding
[NASA-CR-120877] 20 p2485 N73-29964
Optimal three dimensional trajectories to maximize landing footprint of lifting reentry vehicle using energy approximations based on flight path
[AD-764132] 22 p2615 N73-30960
Tracking of reentry vehicles in strong wake echoes using moving target indicators
[AD-763944] 22 p2635 N73-31120
Hypersonic, turbulent, cold-wave, skin friction, and heat transfer measurements on axisymmetric sharp cone
[AD-764059] 22 p2655 N73-31269
Flight tests of hydrazine control system performance and its effects on flight behavior of reentry vehicle
[SLA-73-154] 22 p2722 N73-31785
Wind tunnel tests to determine static and dynamic stability coefficients for circular cone with various nose bluntness configurations
[AD-765164] 23 p2740 N73-31934
Application of perturbation method for computing optimal three dimensional reentry trajectories for shuttle-type spacecraft
24 p2978 N73-33798
Entry and impact behavior of isotope heat source for space nuclear power following flight abort to provide safe dispersion
[LA-UR-73-741] 24 p2986 N73-33861
REFERENCE ATMOSPHERES
Reference atmosphere mean temperature and altimetric corrections
07 p0859 N73-16963
REFERENCE STARS
Northern PZT stars observation and astronomical catalogs
01 p0101 N73-10827
Mathematical models for measuring stellar orientation of spacecraft
[JPRS-58389] 09 p1062 N73-18665
REFERENCE SYSTEMS
Computerized file management system for library reference searches
[UCRL-73355-REV-1] 03 p0271 N73-12193
Analysis of orthopolar coordinate system to compensate for ellipsoidal shape of earth and formulas for conversion to geographic system
08 p0923 N73-17561
Parameters of geodetic reference system
[AD-759127] 18 p2147 N73-27355
REFERENCES [STANDARDS]
U STANDARDS
REFINEMENTS
U IMPROVEMENT
U REVISIONS
REFINING
NT ELECTROREFINING
Production, refining, manufacturing, and applications of uranium alloys and compounds
[JPRS-57364] 03 p0313 N73-12552
Refining in-house magnetic forming capability, using 18,000 joule high energy capacitor
[AD-762844] 20 p2424 N73-29468
REFLECTANCE
NT SPECTRAL REFLECTANCE
Reflectivity measurements with 10.6 micrometer infrared radiation from CO2 laser
[AD-746238] 02 p0183 N73-11482
Inorganic binders for utilizing high reflectance of BaSO4 in paints
[NASA-TM-X-66082] 02 p0191 N73-11549
Establishment of radiometric calibration technique to permit absolute reflectance characteristics of ground targets to be determined from ERTS-1 data
[E72-10255] 03 p0290 N73-12355
Vegetation, soil, and water reflectance measurements from ERTS-1 imagery of Hidalgo County, Texas
[E72-10267] 03 p0291 N73-12366
Characteristics of millimeter attenuation and reflection coefficient measurement system and specifications for waveguide standards fabrication
[NBS-TN-619] 03 p0302 N73-12462

Radiometric calibration technique to permit absolute reflectance characteristics of ground targets to be determined from ERTS-1 data
[E72-10326] 05 p0530 N73-14314
ERTS-1 measurement of vegetation, soil, and water reflectance
[E72-10364] 05 p0535 N73-14352
Computer processing for calculating optical constants from reflectance data of InBi
05 p0609 N73-14952
Reflectance, transmittance and absorbance spectra of normal and six types of maize leaves
[NASA-CR-130032] 07 p0745 N73-16065
Variation of Rayleigh wave reflection coefficient of different interdigital transducer configurations with electric loads
07 p0831 N73-16737
Birefringence properties of total reflection of light beam at separation plane
[LPTHE-72/39] 10 p1188 N73-19668
Temperature-modulated reflectivity in fundamental edge region of GaTe
[ISS-72/2] 10 p1199 N73-19755
Radiometric calibration technique to permit absolute reflectance characteristics of ground targets to be determined from ERTS-1 imagery
[E73-10349] 11 p1274 N73-20343
Establishment of radiometric calibration technique to permit absolute reflectance characteristics of ground targets to be determined from ERTS-1 data
[E73-10458] 12 p1394 N73-21300
Accuracy and reliability engineering of precipitation measurement by radar
[NLL-M-22841-[5828.4F]] 12 p1420 N73-21505
Physical and geological aspects of heiligenschein measurements made from Apollo 16 Flight
12 p1455 N73-21789
Development of equations for determining diffuse reflectance and transmittance of inhomogeneous materials for collimated incident radiation at any angle of incidence
[RE-452J] 13 p1559 N73-22633
Far ultraviolet diffuse reflectivity of lunar dust samples
[NASA-CR-128546] 15 p1834 N73-24864
Operation of reflectometer and correct procedure for measuring mirror reflectivity
[AD-760589] 18 p2152 N73-27398
Transmitting and reflecting diffuser
[NASA-CASE-LAR-10385-3] 23 p2819 N73-32538
Surface roughness effects on bidirectional reflectance of metallic surfaces
24 p2955 N73-33611

**REFLECTED RADIATION**
U REFLECTED WAVES

**REFLECTED RAYS**
U REFLECTED WAVES

**REFLECTED WAVES**
Device and method for determining X ray reflection efficiency, scattering properties, and surface finish of optical surfaces
[NASA-CASE-MFS-20243] 04 p0449 N73-13662
Relationship between maize canopy density and reflected energy determined from color and color infrared photographs
[NASA-CR-130370] 07 p0790 N73-16422
Mathematical model for reflection of shock waves
[REPT-9/71] 07 p0794 N73-16453
Reflected energy of vegetative ground cover measured with multispectral band scanners and infrared photographs
[NASA-CR-131575] 13 p1524 N73-22348
Propagation of reflected shock wave after Mach reflection on wedges
[REPT-4/72] 15 p1765 N73-24304
Analysis of electron number density and collision frequency levels behind reflected shock waves and shock wave interactions in argon
16 p1887 N73-25275
Analysis of changes in amplitudes and frequencies of laser oscillations due to effect of weak reflected signal
17 p2041 N73-26516
Spectral density of infrared radiation reflected by earth atmosphere
[AD-763158] 21 p2539 N73-30361
Medium frequency wave ionospheric propagation loss in earth reflected paths
[BBC-RD-1973/17] 22 p2627 N73-31050
Simultaneous satellite observations of infrared and reflected energy measured to infer convective activity of tropical cloud clusters
[NOAA-TM-NESS-50] 23 p2814 N73-32498

**REFLECTING TELESCOPES**
Fine grinding, polishing, and graded etching techniques to eliminate surface yield on optical telescope mirrors
[NASA-CR-112217] 08 p0934 N73-17647

**REFLECTION**
NT RETROREFLECTION
NT SIGNAL REFLECTION
NT SPECULAR REFLECTION
NT ULTRAVIOLET REFLECTION
NT WAVE REFLECTION
Prediction of laser return pulse shape from corner cube retroreflectors on GEOS 1 satellite
[NASA-TM-X-66123] 04 p0428 N73-13490
Optical and back reflection properties of GaAs crystals used as IR window materials
[AD-749083] 04 p0451 N73-13684
Iridescence and selective reflection of cholesteric liquid crystals according to various models
[BMVG-FBWT-72-27] 10 p1190 N73-19684
Analysis of products and techniques for reducing reflections of light from helicopter windshields, rotor blades and rotor hub assembly
[AD-761127] 18 p2107 N73-27037
Polarization of light reflected from soil and sand with varied surface moisture and texture
[AD-765421] 23 p2788 N73-32309

**REFLECTION COEFFICIENT**
U REFLECTANCE

**REFLECTIVITY**
U REFLECTANCE

**REFLECTOMETERS**
NT MICROWAVE REFLECTOMETERS
Computer aided broadband impedance matching technique using comparison reflectometer
[NASA-CR-129567] 04 p0398 N73-13237
Design and operation of bidirectional reflectometer including reflectance data obtained from two samples of stainless steel 304
[AD-750121] 06 p0675 N73-15491
Operation of reflectometer and correct procedure for measuring mirror reflectivity
[AD-760589] 18 p2152 N73-27398
Four-probe reflectometer for X band measurement system
[AD-761821] 19 p2303 N73-28514
Reflectometer for measuring compositional modulation of copper based alloys at room temperature
23 p2803 N73-32418

**REFLECTORS**
NT FRESNEL REFLECTORS
NT PARABOLIC REFLECTORS
NT PARABOLOID MIRRORS
NT RADAR REFLECTORS
Characteristics of microwave antenna with conical reflectors to generate plane wave front
[NASA-CASE-NPO-11661] 05 p0507 N73-14130
Efficiency of laser telemetry tracking for satellites carrying reflectors
05 p0557 N73-14527
Efficiency of laser telemetry tracking for satellite carrying laser reflector sphere
05 p0557 N73-14528
Lunar laser reflector specifications and fabrication, noting test equipment thermal control, and lunar environment simulation
05 p0558 N73-14529
Design of reflector for stabilization and frequency tuning of ruby laser spectrum
[PB-211890] 05 p0558 N73-14537
Analysis of dual reflector antenna system using physical optics and digital computers
[NASA-TM-X-66223] 12 p1379 N73-21183
Compact sealed beam plasma arc illuminator with integral reflector
[AD-756968] 13 p1564 N73-22678

**REFLEXES**
NT RESPIRATORY REFLEXES
Upper eye lid position effects in electro-oculograhic vertical eye movement recordings
06 p0633 N73-15143
Evoked compensatory reflex reactions of rabbit ocular and eyelid muscles during hypoxia
13 p1480 N73-21992
Analysis of electronystagmograms for healthy persons in labyrinthal calorization tests
24 p2883 N73-33024

**REFRACTED RADIATION**
U REFRACTED WAVES

**REFRACTED RAYS**
U REFRACTED WAVES

**REFRACTED WAVES**
Characteristics of deep water waves reaching Port Phillip Heads, Australia to show effects of refraction, shoaling, and friction
13 p1524 N73-22351

**REFRACTION**
NT ATMOSPHERIC REFRACTION
NT BIREFRINGENCE
NT RADIO WAVE REFRACTION
Celestial navigation method using astronomical refraction effects
07 p0859 N73-16971

**REFRACTIVE INDEX**
U REFRACTIVITY

**REFRACTIVITY**
Mathematical analysis of optical refractive index fluctuations due to salinity and temperature microstructure
[AD-746120] 02 p0168 N73-11366
Analysis of dependence of refractive index of gas discharge medium in carbon dioxide laser on amplitude of discharge current
[NLL-DRIC-TRANS-2815-[3623.66]]
02 p0180 N73-11459
Separation of refractivity gradient components for error elimination and inversion accuracy in occultation measurements on planetary atmospheres
02 p0198 N73-11597
Numerical analysis and diagnostics of nonradially stratified media applied to distributions lacking spherical symmetry
02 p0200 N73-11614
Derivations of straight line, Abel transform and seismological Herglotz-Wiechert transform for reconstruction of refractivity profiles from radio wave phase data
[NASA-TN-D-7098] 02 p0230 N73-11868
Dual hologram interferometry for calculating density distributions from refraction index changes
[AD-749872] 05 p0559 N73-14538
Ionospheric range error given by expansion expression in terms of elevation angle and moment of refractivity distribution
[NASA-TM-X-66159] 07 p0790 N73-16426
Absorption coefficient and index of refraction data for Pb[1-x]S n[x] Te thin films
[AD-751650] 07 p0832 N73-16747
Effect of parallactic refraction correction for satellite optical observations in determination of station coordinates
[NASA-TM-X-66208] 10 p1189 N73-19674
Diurnal cycles of atmospheric refractive index structure function coefficient used to describe scintillation and phase fluctuations of electromagnetic radiation propagated in atmosphere
[AD-755808] 12 p1402 N73-21374
Alfven wave refraction by interplanetary inhomogeneities from analysis of Pioneer 6 data
[NASA-TM-X-62270] 16 p1962 N73-25867

**REFRACTORIES**
Deformation processes in forging refractory ceramic oxides
[NASA-CR-131109] 10 p1175 N73-19558
X ray fluorescence analysis of aluminosilicate refractories
[PB-214233/9] 16 p1932 N73-25636

**REFRACTORY MATERIALS**
NT CHROMIUM
NT IRIDIUM
NT MOLYBDENUM
NT MOLYBDENUM ALLOYS
NT NIOBIUM
NT NIOBIUM ALLOYS
NT OSMIUM
NT OSMIUM ALLOYS
NT PORCELAIN
NT REFRACTORIES
NT REFRACTORY METAL ALLOYS
NT REFRACTORY METALS
NT RHENIUM
NT RHENIUM ALLOYS
NT TANTALUM
NT TANTALUM ALLOYS
NT TUNGSTEN
NT TUNGSTEN ALLOYS
Development of chemical model to present properties of carbides for localized and nonlocalized conditions of electrons in crystal structure
[NLL-RTS-7334] 01 p0069 N73-10565
Chemical diffusion coefficient of oxygen in mixed niobates to determine feasibility of modifying oxide defect structures to enhance oxidation protection of elevated temperature materials
[AD-746834] 03 p0316 N73-12574
Development, production, and application of friction cermet and metal plastics materials
[AD-747575] 03 p0323 N73-12630
Research data on dielectrics, refractory materials, plastics, ceramics, and glasses
[AD-746686] 03 p0347 N73-12827
Compilation of reports on transition metal carbides for period 1956 to 1972
[CE-BIB-228] 04 p0437 N73-13560
Production and evaluation of magnetic and electrical materials capable of operating in 800 to 1600 F temperature range for advanced space electric power systems
[NASA-CR-2224] 09 p0990 N73-18084
Microstructure and mechanical properties of precipitation hardened-dispersion strengthened aluminum and titanium alloys and refractory materials
[AD-753910] 10 p1174 N73-19550
Stress-rupture strength testing and principles of creep-rupture in heat resistant alloys
[JPRS-58760] 13 p1542 N73-22494
Carbon refractory composites for application in rocket motor nozzles, propulsion structures, and planetary atmospheric entry shells
[NASA-CR-131745] 13 p1547 N73-22533
Borides, carbides, and nitrides of silicon oxidation resistant refractory compounds for use in gas turbines and reentry vehicles
14 p1678 N73-23616
Microstructure of hot pressed and press forged polycrystalline refractory oxides
[AD-760353] 17 p2053 N73-26606
Stability of refractory compounds in liquid aluminum at high temperatures
[NLL-RTS-7975] 18 p2113 N73-27083

Solar absorber coatings for use with spaceborne Vuilleumier cycle cryogenic refrigerators
[AD-760577] 18 p2167 N73-27505
Effects of metallurgical processes on thermodynamic properties and compatibility of reinforcing fibers for refractory materials
[JPRS-59118] 20 p2430 N73-29518
Production and characteristics of refractory materials for high temperature applications
[NLL-RTS-7942] 20 p2433 N73-29543
Evaluation of high temperature nozzle throat materials for performance in highly oxidizing rocket exhaust environment
[AD-762533] 20 p2467 N73-29816
Refractory chamber meterials for N2O4/amine propellants
[AD-762531] 20 p2467 N73-29818
Research projects to develop and evaluate ceramic materials in areas of refactory structural ceramics and solid electrolyte ceramics
[NASA-CR-133741] 21 p2562 N73-30540
Bibliography on refractory coatings in industrial processes
[AD-763150] 21 p2563 N73-30547
Nonlinear elastic and thermoelastic properties of single crystals of refractory materials
[COO-3418-9] 22 p2689 N73-31535
High melting oxide and carbide materials in electrode walls of magnetohydrodynamic generators
[AD-764969] 24 p2944 N73-33508

**REFRACTORY METAL ALLOYS**
NT MOLYBDENUM ALLOYS
NT NIOBIUM ALLOYS
NT OSMIUM ALLOYS
NT RHENIUM ALLOYS
NT TANTALUM ALLOYS
NT TUNGSTEN ALLOYS
Cladding materials research, including Pt-Rh-W alloy and Ir properties and Ir purification
[ORNL-TM-3865] 04 p0453 N73-13696
Microhardness tests of refractory metal alloys
[AD-750593] 06 p0686 N73-15582
Refractory metal alloys with protective coatings for use in structural components of turbine engines
14 p1678 N73-23614
Oxidation resistant refractory metal alloys for use in high temperature environments
14 p1678 N73-23615
Methods of oxidation and corrosion resistance in refractory metal alloys used in gas turbine engines
14 p1678 N73-23617
Production of high power arc lamp cathodes by casting copper body on thoriated tungsten insert
[NASA-TM-X-2865] 18 p2160 N73-27451
Modification and control of oxide structures on refractory metal alloys and compounds
[AD-761215] 18 p2162 N73-27464
Production and characteristics of highly dispersed composite powders on copper base containing metal carbides by reducing copper carbonate with hydrogen
23 p2808 N73-32451
Solid-phase interaction of refractory metals and refractory compounds at high temperature using electron beam heater
23 p2808 N73-32455

**REFRACTORY METALS**
NT CHROMIUM
NT IRIDIUM
NT MOLYBDENUM
NT NIOBIUM
NT OSMIUM
NT RHENIUM
NT TANTALUM
NT TANTALUM ISOTOPES
NT TUNGSTEN
High temperature reaction of carbon with refractory compounds of groups 4, 5, and 6
[NLL-RTS-7425] 01 p0022 N73-10171
Effect of composition of refractory metal solid solutions on coefficient of thermal expansion
[AD-745847] 01 p0068 N73-10556
Mechanical properties of various metal alloys and operating life of dies during hot deformation of stainless and heat resistant steels and alloys
[AD-745703] 01 p0068 N73-10559
Properties of refractory metals and application to construction of high temperature irradiation facilities
[EUR-4757] 04 p0434 N73-13540
High temperature plastic deformation of refractory metals in vacuum during rolling
[AD-750508] 06 p0678 N73-15516
Shell model for phonon dispersion anomalies and lattice instabilities in hard metalcarbides-nitrides and transition metals
08 p0951 N73-17783
Compilation of eutectics and melting point minima for binary combinations of metals for refractory metal brazing
[NASA-TM-X-68190] 10 p1172 N73-19537
Improved silicide coatings for refractory metals employed in space shuttles and gas turbine engine components
[NASA-CASE-LEW-11179-1] 13 p1540 N73-22474
Thermoelectric converter and 5-kwe reactor system integration
[NASA-CR-121230] 16 p1943 N73-25726
Technique for welding small refractory metal capsules in controlled atmosphere
[AERE-R-2544] 21 p2553 N73-30466
Application of protective layers of refractory oxides and carbide onto high strength fiber substrates
[NASA-CR-134466] 23 p2810 N73-32467
Refractory metal carbide/metal oxide composites for thermal insulation
[LA-5136] 24 p2943 N73-33504

**REFRASIL [TRADEMARK]**
U FIBERS
U SILICON DIOXIDE

**REFRIGERANTS**
Analysis of thermal conductivity of liquid aliphatic hydrocarbons with saturated and unsaturated straight or branch chain carbons
[ESDU-67018] 01 p0116 N73-10955
Analysis of thermal conductivity of liquid halogenated aliphatic hydrocarbons and commercial refrigerants
[ESDU-68024-AMEND-A] 01 p0116 N73-10956
Method to determine surface tension of refrigerants
[NLL-NEL-TT-2480-[6075.461]]
21 p2578 N73-30663
Effect of return bends on downstream pressure drop and heat transfer coefficient of condensing refrigerant
[DSR-72591-75] 22 p2652 N73-31246

**REFRIGERATING**
Thermoelectricity and refrigeration at low temperature
[AD-753405] 10 p1190 N73-19687
Design of Joule-Thomson cascade for refrigeration cooling using liquid helium
[CEA-CONF-2044] 10 p1199 N73-19761

**REFRIGERATING MACHINERY**
NT REFRIGERATORS
Influence of dead volumes on working processes of theoretical gas refrigerator
04 p0484 N73-13954
Absorption cycle refrigeration system for environmental control of space station
[NASA-CR-123970] 05 p0598 N73-14859
Cryogenic cooling methods for spaceborne systems
[AD-755780] 14 p1720 N73-23958
Applications of heat pumps for recovery of unused heat in factories, air conditioned buildings, and refrigeration plants
[NLL-OA-TRANS-1264-[6196.3]]
15 p1842 N73-24921
Calculation of heat removed by gas refrigerators and heat engines
[AD-762261] 19 p2306 N73-28544
Design of standard, special purpose air, and refrigeration screw compressors
[NLL-NEL-TT-2460-[6075.461]]
20 p2422 N73-29452
Low temperature thermoelectric microrefrigerator
[AD-764171] 22 p2708 N73-31686
Cryocooling and electric capacity of refrigerator/electric generator space power unit
[NASA-TM-X-71433] 23 p2748 N73-31992

**REFRIGERATORS**
Solar absorber coatings for use with spaceborne Vuilleumier cycle cryogenic refrigerators
[AD-760577] 18 p2167 N73-27505

**REFUELING**
Development of forward area refueling equipment for servicing military helicopters
[AD-746249] 02 p0154 N73-11245
Orbiting propellant depot safety hazards - management summary
[NASA-CR-123385] 03 p0356 N73-12898
Orbiting propellant depot safety hazards and interactions between depot and space vehicle - technical discussion
[NASA-CR-123384] 03 p0356 N73-12899
Effectiveness of relaxation chamber and static charge reducer in dissipating electrostatic charge during JP-5 refueler loading
[AD-748995] 04 p0462 N73-13772
Automatic controlled pressure system for onshore fueling of navy aircraft
[AD-748211] 04 p0489 N73-13997

**REGENERATION [ENGINEERING]**
Nondestructive tests of welds in regenerative chambers
[NASA-CR-120980-APP] 06 p0677 N73-15509

**REGENERATION [PHYSIOLOGY]**
Physiological regeneration of corneal epithelial mice cells exposed to strong magnetic fields
14 p1608 N73-23034

**REGENERATIVE COOLING**
Thermocouple apparatus for measuring wall temperatures in regeneratively cooled rocket engines having thin walled cooling passages
[NASA-CASE-XLE-05230-2] 04 p0419 N73-13417
Fundemental aspects of regenerative cooled, upper stage rocket plane with external-burning thrust augmentation
[AD-756498] 13 p1583 N73-22832
Analysis of thermal fatigue in nontubular regeneratively cooled combustion chambers and prediction of thermal cycle life capability - Vol. 1
[AD-760582] 18 p2194 N73-27715
Analysis of thermal fatigue in nontubular regeneratively cooled combustion chambers and development of life prediction techniques - Vol. 2
[AD-760583] 18 p2194 N73-27716
Analysis, design, fabrication, and tests of regeneratively cooled rocket engine for storable propellants
[NASA-CR-133488] 19 p2329 N73-28737
Computation of coolant and wall temperatures of regeneratively cooled liquid propellant rocket engines
[DLR-FB-72-29] 21 p2591 N73-30755
Regeneratively cooled rocket engine tests with space storable propellants
[NASA-CR-133915] 22 p2708 N73-31688

**REGENERATIVE CYCLES**
U REGENERATION [ENGINEERING]

**REGENERATIVE FUEL CELLS**
Regenerative fuel cell for space station use
[NASA-CR-128848] 10 p1111 N73-19058

**REGENERATORS**
Loop transponder for regenerating code of mu-type ranging system
[NASA-CASE-NPO-11707] 16 p1873 N73-25161

**REGGE POLES**
Triple Regge phenomenology from finite mass sum rules in proton-proton inclusive reactions
[NOTA-INTERNA-379] 01 p0084 N73-10693
Theoretical model of Regge phenomena in medium x region for kaon proton interactions
[TUEP-72-46] 07 p0823 N73-16668
Dual multiperipheral model of hadronic production amplitudes
[NUB-2164] 07 p0823 N73-16672
Regge pole model for charge exchange processes using isospin amplitudes and daughter trajectories
[TUETP-73-4] 14 p1694 N73-23747
Triple Regge formula for analyzing proton leading effect in proton proton collisions
[LPTHE-73/17] 20 p2456 N73-29740

**REGIONAL PLANNING**
NT URBAN PLANNING
Urban and regional planning in Florida using ERTS-1 imagery
[E72-10254] 03 p0290 N73-12354
Geological evaluation, regional planning, forest management, and water management in North Carolina using ERTS-1 imagery
[E72-10280] 03 p0292 N73-12378
Application of ERTS-1 imagery to regional land use planning in Wisconsin
[E72-10299] 04 p0411 N73-13349
Utilization of ERTS-1 imagery in geological evaluation, regional planning, forest management, and water management in North Carolina
[E72-10317] 04 p0413 N73-13366
Remote sensing techniques for regional planning and managing earth resources, particularly water resources in California
[NASA-CR-129917] 05 p0536 N73-14361
Use of remote sensing data to analyze impact of California State Water Project on regional planning and land use of west side of San Joaquin Valley
05 p0537 N73-14367
Regional airport planning in Germany, noting infrastructural, economic, safety, and noise problems
[DGLR-PAPER-72-033] 06 p0650 N73-15280
Application of aerial and spaceborne photography to urban, regional, and management planning
[NASA-CR-130290] 06 p0673 N73-15473
Regional planning based on ERTS-1 MSS imagery
[E73-10038] 07 p0776 N73-16301
Regional land use mapping and management using remotely sensed imagery
07 p0786 N73-16392
Application of ERTS-1 imagery to regional land use planning in Wisconsin
[E73-10077] 08 p0900 N73-17290
Urban and regional planning in Brevard County, Florida using ERTS-1 imagery
[E73-10083] 08 p0901 N73-17295
Classification of landforms for land use and regional planning using aerial photographic interpretation
[PB-212774] 08 p0918 N73-17525
Utilization of ERTS-1 imagery in geological evaluation, regional planning, forest and water management in North Carolina
[E73-10300] 09 p1021 N73-18332
Application of ERTS-1 imagery to urban and regional planning in Florida
[E73-10423] 11 p1280 N73-20384
Application of ERTS-1 imagery to regional land use planning in Wisconsin
[E73-10448] 11 p1283 N73-20408
Land use, urban development, and regional planning for Los Angeles County based on photointerpretation of MSS imagery and multispectral information extraction
[E73-10486] 13 p1515 N73-22277
Utilization of ERTS-1 imagery in geological evaluation, regional planning, forest and water management in North Carolina
[E73-10688] 16 p1902 N73-25382
State airport system plan for Iowa - Volume 1
[PB-217531/3] 18 p2127 N73-27192
State airport system plan for Iowa - Volume 2
[PB-217532/1] 18 p2128 N73-27193

Utilization of ERTS-1 imagery for monitoring land use change and regional planning in Coachella Valley, California
[PAPER-L5] 19 p2273 N73-28301
Utilization of ERTS-1 data for inventory of critical land resources for regional land use planning in Wisconsin
[PAPER-L16] 19 p2275 N73-28311
Urban development and regional planning for Los Angeles County, California using ERTS-1 imagery
[PAPER-L18] 19 p2275 N73-28313
Utilization of ERTS-1 imagery and data for land use, regional planning, and urban development in Metropolitan Washington area
19 p2285 N73-28377
Utilization of ERTS-1 imagery in resources management on national scale in South Africa
[E73-10931] 20 p2399 N73-29279
Utilization of Skylab EREP imagery for land use and regional planning
[E73-10886] 20 p2417 N73-29418
Application of ecological, geological, and oceanographic ERTS-1 imagery to Delaware coastal resources management and planning
[E73-10934] 21 p2529 N73-30276
Geological evaluation, regional planning, forest management, and water management in North Carolina using ERTS-1 imagery
[E73-10962] 21 p2532 N73-30304
Utilization of Skylab EREP data in geological evaluation, regional planning, forest management, and water management in North Carolina
[E73-10966] 21 p2533 N73-30308
Regional land use planning and management in Tri-State area from ERTS-1 MSS photography
[E73-10986] 22 p2658 N73-31293
Urban development and regional planning in Los Angeles County using ERTS-1 MSS photography
[E73-10989] 22 p2658 N73-31295
Regional airport planning in Germany
[DGLR-PAPER-73-035] 23 p2770 N73-32159
Application of ERTS-1 data and multispectral analysis to regional planning and urban development
[E73-11045] 23 p2779 N73-32221
Regional and local land use planning and mapping of Ohio from Skylab EREP data
[E73-11090] 24 p2914 N73-33252
Utilization of Skylab imagery as information service for investigating land use and natural resources in New York
[E73-11113] 24 p2915 N73-33270

**REGIONS**
NT ANTARCTIC REGIONS
NT ARCTIC REGIONS
NT AURORAL ZONES
NT CENTRAL ATLANTIC REGION [US]
NT D REGION
NT E REGION
NT F REGION
NT FRESNEL REGION
NT HABITATS
NT NEW ENGLAND [US]
NT NULL ZONES
NT POLAR REGIONS
NT REMOTE REGIONS
NT SUBARCTIC REGIONS
NT TEMPERATE REGIONS
NT TROPICAL REGIONS
Application of remote sensing techniques to study of climatology of urban-regional systems
07 p0786 N73-16394
Urban and regional changes based on city census and remotely sensed imagery
07 p0786 N73-16395
ERTS-1 monitoring of grass seed field burning in western Oregon
[E73-10883] 20 p2394 N73-29234

**REGISTERS [COMPUTERS]**
Circuit and plug register diagrams for printout converter
[PHL-1972-4] 02 p0144 N73-11168

**REGRESSION [STATISTICS]**
U REGRESSION ANALYSIS

**REGRESSION ANALYSIS**
Regression relationships between Nimbus 4 SIRS-B clear-column radiances and geopotential heights of 500 mb and 300 mb levels
[AD-743711] 01 p0075 N73-10624
Regression analysis used for numerical-statistical prediction of visibility at sea
[AD-743733] 01 p0076 N73-10625
Regression analysis of tropical storm and typhoon speed characteristics after recurvature in western North Pacific Ocean
[AD-746880] 02 p0206 N73-11672
Computer program to reduce X ray scattering data from cubic alloys by regression analysis
[ORNL-4828] 10 p1194 N73-19716
Application of regression analysis to water quality measurement from remote sensing spectral signature data
[NASA-CR-132997] 16 p1870 N73-25141
Predictive model for failure times of adhesive bonded aluminum under constant stress
[AD-758845] 16 p1919 N73-25528
Typhoon and tropical storm intensity forecasts in western North Pacific Ocean using statistical regression analysis
[AD-761379] 18 p2174 N73-27561
Differential correction schemes in nonlinear regression
[REPT-3] 20 p2437 N73-29568

**REGULATION**
U CONTROL

**REGULATIONS**
Influence of aircraft reliability regulations on STOL takeoff and landing performance
[MBB-UH-13-72-O] 07 p0740 N73-16018
International air transportation policy and application of policy to scheduled and chartered airline services
23 p2865 N73-32903

**REGULATORS**
NT AUTOMATIC FREQUENCY CONTROL
NT CURRENT REGULATORS
NT FLOW REGULATORS
NT FREQUENCY CONTROL
NT OXYGEN REGULATORS
NT PRESSURE REGULATORS
NT RELIEF VALVES
NT SPEED REGULATORS
NT THERMOSTATS
NT VOLTAGE REGULATORS
Development of method for determining optimum setting of regulators on metal working machinery involved in sintering process
[NLL-M-21642-[5828.4F]] 20 p2428 N73-29505

**REHEATING**
U HEATING

**REIGNITION**
U IGNITION

**REINFORCED MATERIALS**
U COMPOSITE MATERIALS

**REINFORCED PLASTICS**
Development of fiberglass reinforced polyester for expedient airfield pavement system
[AD-743958] 01 p0114 N73-10941
Numerical analysis of stress field in semi-infinite elastic-plastic medium under generalized plane deformation
[AD-746046] 01 p0115 N73-10951
Polyphenylquinoxaline resin systems for high temperature composite materials
[AD-746273] 02 p0193 N73-11559
Development of nondestructive test procedures for determining properties of multidirectional fiber reinforced resin matrix composites
[AD-746592] 02 p0193 N73-11562
Charpy toughness of discontinuous fiber reinforced plastics under nonuniform interfacial shear stress
[SC-DR-72-0260] 03 p0320 N73-12611
Resistance to damage from impulsive loading in three dimensionally graphite reinforced phenolic composite materials
[AD-748099] 03 p0323 N73-12628
Production of unidirectional glass reinforced plastics with high mechanical properties
[AD-747549] 03 p0323 N73-12629
Development, production, and application of friction cermet and metal plastics materials
[AD-747575] 03 p0323 N73-12630
Use of unidirectional glass plastics for wound structures of electrical machines and equipment
[AD-748737] 04 p0400 N73-13252
Weakening and fracture of glass reinforced plastics during compression under conditions of one-sided heating
[AD-748526] 04 p0439 N73-13581
Mechanical properties and fracture strengths of glass fiber reinforced plastic composites
[AD-749948] 05 p0567 N73-14608
Evaluation of fiber reinforced films used in high altitude balloons
[AD-749880] 05 p0567 N73-14609
Structural design and load tests on carbon fiber reinforced plastic VC-10 aileron control strut
[ARC-CP-1229] 05 p0603 N73-14903
Production of carbon fibers and reinforced plastics in British installations
[FOA-2-C-2468-91] 06 p0687 N73-15594
Terminal ballistic performance of fiber glass epoxy composite material for aerodynamic control surfaces
[AD-752918] 09 p1053 N73-18584
Optimal design of elastic bodies using fiberglass reinforced plastics or fibers with high modulus of elasticity
[AD-753040] 09 p1054 N73-18589
Distribution and concentration profiles of stress adjacent to orifices in glass fiber-reinforced plastic plates and shells
[AD-753041] 09 p1096 N73-18945
Punch-loading technique effects on mechanical properties of composites reinforced with glass fibers
[REPT-1042/72] 10 p1176 N73-19563
Hysteresis behavior of glass fiber reinforced plastic specimens under compressive cyclic loading
[AD-753823] 10 p1176 N73-19566
Analysis of fundamental behavior of fiber reinforced plastic composite structures to determine
[AD-754249] 10 p1177 N73-19570
Creep properties of composite, plastic reinforced polyester concretes
[AD-752454] 10 p1221 N73-19930
Production of glass fiber reinforced plastic pressure tanks and rods
[AD-754679] 11 p1300 N73-20547
Transverse tension strength and stiffness of unidirectional carbon fiber reinforced plastic
[RAE-TR-72129] 12 p1416 N73-21477
Composite constructions of reinforced plastics with improved rain erosion resistance
[AD-758650] 15 p1803 N73-24610
Combustion phenomena in reinforced plastics ablation under simulated atmospheric reentry using plasma arc jets
[ONERA-NT-195] 15 p1844 N73-24939
Preheating effects of mandrel and glass tape on residual stress magnitude
[AD-759632] 16 p1934 N73-25645
Characteristics of glass fiber reinforced plastics using boron and carbon fibers
[RAE-LIB-TRANS-1687] 17 p2049 N73-26575
Analysis of loss of high temperature strength in composite materials following aging in room temperature environments
[NASA-CR-124290] 17 p2050 N73-26583
Compressive strength and modulus of unidirectional carbon fiber reinforced plastic laminates
[RAE-TR-72096] 17 p2050 N73-26587
Analysis of glass fiber reinforced plastic laminated structures
[MBB-UD-79-72-O] 17 p2094 N73-26942
Physical and mechanical properties of high-strength, high-modulus reinforcing fibers and organic resin composite materials
18 p2164 N73-27475
Analysis of properties of fiber reinforced materials with plastic and metallic matrix composition and application to gas turbine engines
18 p2164 N73-27476
Characteristics of carbon fiber composite materials and application for structures with reduced weight, fatigue reduction, and corrosion resistance
18 p2164 N73-27477
Production of fibrous metal composites by rolling of powder with strong reinforcing wires and application to aerospace vehicle structures
18 p2164 N73-27478
Design of filamentary composite materials for application to construction of airframes and spacecraft structures
18 p2164 N73-27479
Construction of glider aircraft using glass fiber and carbon fiber reinforced plastic composite materials for weight reduction and increased strength
18 p2165 N73-27486
Application of reinforced composite materials for construction of aeronautical gas turbine engines
18 p2165 N73-27490
Development of fiber reinforced composite materials for application to air breathing engines, aeronautical vehicles, and spacecraft components
18 p2166 N73-27491
Preparation and testing of pyrolytic graphite film polymeric matrix laminates
[AD-761124] 18 p2168 N73-27510
Rheological properties of fiber suspensions in reinforced plastics
[AD-762083] 19 p2232 N73-28001
Comparison of glass fiber reinforced plastic and bronze submarine propellers, based on binding stress analysis and cavitation behavior
[BMVG-FBWT-73-8] 19 p2256 N73-28183
Composite materials studies, including compressive strength and reinforced plastics
[JPRS-59610] 20 p2434 N73-29549
Compressive strength and deformation properties of unidirectionally carbon fiber reinforced plastic under uniaxial compression
20 p2434 N73-29550
Application of reinforced fiberglass thermoplastic materials for construction of military aircraft structures
[AD-763470] 21 p2498 N73-30044
Application of fiber glass reinforced plastic materials for ground handling of aviation fuels and hazards of static electricity caused by plastic materials
[AD-764358] 22 p2709 N73-31693
Construction of helicopter airframes and landing gear to show advantages of composite material prototype over metal prototype
[NASA-CR-112333] 23 p2743 N73-31957

**REINFORCED PLATES**
Analysis of fatigue and fail-safe characteristics of composite-reinforced, stiffened metal panels to determine residual strength
[NASA-CR-2136] 07 p0852 N73-16909
Application of principles of fracture mechanics to problem of preventing brittle fracture in sheet structures
[RAE-LIB-TRANS-1648] 17 p2092 N73-26921
Adhesive shear stress distribution in elastic plates reinforced by orthotropic elastic layer
[NASA-CR-132273] 17 p2093 N73-26933

Structural analysis of unsymmetrically laminated anisotropic plates using linear plate theory and strain-displacement relations
24 p2987 N73-33875

**REINFORCED SHELLS**
Iterative solution for free vibrations of ring stiffened toroidal shells
[AD-747024] 04 p0482 N73-13943
User manual and related documentation for six compatible computer programs for structural analysis of ring-stiffened shells of revolution
[NASA-CR-2086] 09 p1094 N73-18930
Effect of eccentricity of reinforcement upon stability of cylindrical shells
[AD-752691] 09 p1096 N73-18943
Optimum structural design of discretely ring-stiffened cylindrical shell
23 p2853 N73-32794

**REINFORCEMENT [PSYCHOLOGY]**
Reinforcement effects on human attention and performance in continuous response to visual stimuli
[AD-747798] 04 p0381 N73-13103
Expedient functioning of automata with normal and disturbed behavior in experiments on reinforcement selection
24 p2887 N73-33057
Relation of conditioned reactions to evaluation of results of forthcoming reinforcement
24 p2889 N73-33065
Behavior of dogs when given choice of various reinforcements
24 p2889 N73-33066
Structure and functions of central mechanisms of reinforcement
24 p2889 N73-33067

**REINFORCEMENT [STRUCTURES]**
Strain rate and temperature dependence of glass fiber reinforced and unreinforced epoxy resins and deformation mechanisms
[REPT-1040/72] 01 p0069 N73-10568
Analog reinforcement for reducing stress concentration around hole in plate
[AD-745116] 01 p0071 N73-10578
Application of integral nonlinear programming and random search techniques for determining minimum weight of reinforcing structures commensurate with strength requirements
01 p0112 N73-10929
Design, fabrication, and flight tests of boron-epoxy reinforced C-130E center wing boxes
[NASA-CR-112126] 04 p0370 N73-13011
Elastic buckling strength of thin walled aluminum alloy tubes fabricated with and without boron/epoxy glass/epoxy composite materials for reinforcement
[NBS-TN-728] 04 p0437 N73-13566
Fabrication of light weight panel structure using pairs of elongate hollow ribs of semicircular configuration
[NASA-CASE-LAR-11052-1] 04 p0481 N73-13929
Analysis of ring and stringer stiffness parameters and proportions for axially compressed stiffened isotropic cylinders with and without internal pressure
[NASA-CR-2165] 04 p0481 N73-13930
Analysis of structural properties produced by selective reinforcement of aluminum compression panels with unidirectional boron epoxy composite materials
[NASA-CR-2145] 08 p0966 N73-17895
Procedures for reducing residual stresses in aircraft metal structures reinforced by filamentary composites
[NASA-CR-112207] 08 p0966 N73-17900
Effects of spatially varying curvature on dynamics of cylindrical panels and stiffened cylindrical shell structures
[AD-752590] 08 p0967 N73-17907
Coated reinforced materials, glass antidiffusion films, and metal binders
[AD-758167] 14 p1682 N73-23649
Numerical analysis of free vibrations of ring stiffened toroidal shells based on linear shell theory
15 p1837 N73-24888
Analysis of general buckling of pressurized stiffened cylinder under axial load
[ARC-R/M-3198] 16 p1857 N73-25040
Evaluation of low cost techniques for forming boron-reinforced aluminum structural shapes from diffusion-bonded flat sheet and plate
[NASA-CR-124279] 16 p1918 N73-25523
Characteristics of carbon fiber composite materials and application for structures with reduced weight, fatigue reduction, and corrosion resistance
18 p2164 N73-27477
Application of composite materials to reinforce metallic structures for low cost improvement in structural stability of airframes
18 p2165 N73-27485
Analysis of dynamics of stiffened plates using finite element modelling of flat and curved stiffened panels
20 p2479 N73-29911
Optimum edge reinforcement around a circular hole in a flat elastic sheet subjected to axial tensile stress
[ARC-R/M-3723] 21 p2604 N73-30869
Structural optimization procedures applied to design of simply supported, corrugated hat stiffened composite panel under uniaxial compression
[NASA-CR-132314] 23 p2853 N73-32798

**REINFORCEMENT RINGS**
Love- and Donnell-type equations for investigating thermal stresses in ring-reinforced oval cylindrical shells subjected to heat inputs
16 p1968 N73-25920
Variational principle for studying elastic-plastic instability of ring stiffened cylindrical shells under external pressure
[AD-757750] 16 p1970 N73-25935

**REINFORCING FIBERS**
NT CARBON FIBERS
Performance of graphite fiber reinforced polyimide composites as journal bearing materials
[NASA-TN-D-7078] 01 p0062 N73-10505
Initial yield surfaces of unidirectional fiber-reinforced composites
[AD-745176] 01 p0070 N73-10572
Titanium alloy composites reinforced with silicon carbide fibers
[AD-745342] 01 p0070 N73-10573
Reflection and propagation of plane waves in fiber reinforced materials
[AD-745358] 01 p0070 N73-10576
High temperature strength and stability of tungsten reinforced copper
[AD-745700] 01 p0071 N73-10581
Bibliography on fiber reinforced plastic composites
[PB-210305] 01 p0071 N73-10585
Effects of molybdenum and tungsten fiber reinforcements on nickel chromium aluminum matrix alloys
[NLL-TRANS-746-1193-[9022.401]]
02 p0191 N73-11546
Glass fiber reinforced composite materials for developing prototype missile fuselages
[AD-746288] 02 p0193 N73-11560
Technology assessment of silicon carbide reinforced composites with aluminum or nickel matrix discussing mechanical resistance at high temperatures
04 p0434 N73-13543
Electrolytic procedure for manufacturing aluminum whisker and pure nickel matrix composites with reinforced fibers
04 p0435 N73-13544
Development, characteristics, and applications of composite materials containing inorganic fiber or metal fiber reinforcement
[NLL-RTS-7657] 04 p0437 N73-13561
Elastic buckling strength of thin walled aluminum alloy tubes fabricated with and without boron/epoxy glass/epoxy composite materials for reinforcement
[NBS-TN-728] 04 p0437 N73-13566
Photoelastic methods of stress analysis applied to fiber reinforced composites
05 p0602 N73-14892
Procedures for reducing residual stresses in aircraft metal structures reinforced by filamentary composites
[NASA-CR-112207] 08 p0966 N73-17900
Time dependent mechanical behavior of boron filament reinforced aluminum composites based on static and dynamic properties
[AD-753706] 09 p1054 N73-18590
Experimental and analytical determination of elastic constants for some fiber reinforced composite materials
[AD-753575] 09 p1055 N73-18602
Development of thick-walled, Borsic aluminum alloy ring for use as stiffener in 155 millimeter atomic artillery projectile
[SC-DR-72-0706] 10 p1176 N73-19562
Mechanical properties of silicon carbide and aluminum oxide sapphire filaments for design of metal matrix composites
[AD-753711] 10 p1176 N73-19568
Analysis of fundamental behavior of fiber reinforced plastic composite structures to determine
[AD-754249] 10 p1177 N73-19570
Development of design concepts for metal-lines, glass-fiber composite pressure vessels and comparison with homogeneous metal pressure vessels
[NASA-TM-X-68198] 10 p1220 N73-19922
Development of polyphenylquinoxaline graphite fiber reinforced composites for structural materials
[NASA-CR-121109] 11 p1308 N73-20611
Modified lamination process for developing boron carbide ribbon reinforced titanium matrix composites
[AD-754478] 11 p1309 N73-20618
Mechanical and physical properties of discontinuous thermoset carbon fiber reinforced plastic composites
[AD-754034] 11 p1309 N73-20622
Role of titanium in fabricating magnesium-graphite fiber composites with improved strength and stiffness
[AD-754570] 11 p1310 N73-20627
Material tests to determine characteristics of fiber reinforced ceramic matrix composites
[AD-757063] 13 p1544 N73-22513
Field problems of concrete containing randomly oriented, uniformly distributed, short fibers
[AD-741358] 13 p1547 N73-22536
Finite element analysis of reinforcement mechanisms in unidirectional metal matrix composites under transverse loads
[AD-756257] 13 p1548 N73-22541
Analysis of melting, mixing, and solidification of metal matrix composite materials in weightless environment
13 p1594 N73-22921
High strength tungsten fiber reinforced oxidation resistant niobium alloy composites for use in gas turbine engines at 2000 F
[AD-757380] 14 p1678 N73-23620
Performance of fibrous reinforced concrete overlay test slabs as runways at Tampa International Airport, Florida
[FAA-RD-72-119] 14 p1680 N73-23634
Computer programs for analysis of shell structures in general and fiber reinforced rocket engine cases
[AD-756465] 14 p1716 N73-23926
Numerical analysis of load absorption of two adjacent filaments in fiber-reinforced material
[AD-759729] 16 p1933 N73-25639
Characteristics of glass fiber reinforced plastics using boron and carbon fibers
[RAE-LIB-TRANS-1687] 17 p2049 N73-26575
Fatigue failure criterion for fiber reinforced laminates under stress
[AD-760146] 17 p2053 N73-26609
Application of glass composites, all carbon composites, and PRD-49 organic fiber material for airframe and spacecraft construction
18 p2164 N73-27482
Rheological properties of fiber suspensions in reinforced plastics
[AD-762083] 19 p2232 N73-28001
Effects of metallurgical processes on thermodynamic properties and compatibility of reinforcing fibers for refractory materials
[JPRS-59118] 20 p2430 N73-29518
Interaction of nickel base ternary matrix system with tungsten reinforcing fibers
20 p2430 N73-29521
Load absorption and interaction of two elastic filaments in fiber reinforced composite material
20 p2433 N73-29542
Optimization method for minimum weight design of structures made from fiber reinforced composites
[AD-763732] 21 p2565 N73-30558
Metal matrix composites with Ni and NiCr20 matrix materials, and Al2O3, SiC, W, and Mo reinforcing fibers
[BMFT-FB-T-73-08] 23 p2810 N73-32471
Analysis of internal buckling of fibers in viscoelastic composite plate based on linear material responses and small deflection theory
24 p2987 N73-33874

**REISSNER THEORY**
Higher order theories and solution techniques for moderately thick shells of revolution using Reissner Theory and Legendre functions
13 p1584 N73-22842

**RELATIVE BIOLOGICAL EFFECTIVENESS [RBE]**
Relative biological effectiveness of fast neutrons with gamma background
11 p1243 N73-20091

**RELATIVISTIC EFFECTS**
Relativistic effects in satellite dynamics and Doppler tracking
[AD-762400] 19 p2344 N73-28859
Time lag test of general relativity and Earth-Mars ephemeris improvement using Mariner 9 tracking data
23 p2842 N73-32713

**RELATIVISTIC PARTICLES**
Formation of relativistic particles into clouds in quasar and Seifert nuclei, and centimeter, submillimeter, and gamma radiation emissions
[NP-30] 06 p0717 N73-15854
Relativistic electron beam for thermonuclear heating of plasma media
[AD-754621] 11 p1329 N73-20783
Relativistic electron beam equilibria in cylindrical plasma geometry
[IPP-6/111] 12 p1435 N73-21630
Parallel plate electrostatic spectrograph as relativistic particle analyzer
15 p1788 N73-24498
Relativistic particle motion in electromagnetic wave traveling in direction of uniform static magnetic field
[NASA-CR-132781] 18 p2181 N73-27610
Optimization of parallel plate relativistic particle analyzer by reducing z variation of point source image at detector surface
19 p2301 N73-28501
Relativistic particle motion in nonuniform electromagnetic waves
[NASA-CR-133888] 22 p2632 N73-31092
Separation of variables in special Hamilton-Jacobi equation and application to dynamical problem of constrained on moving surface
[NASA-TR-R-405] 22 p2691 N73-31557

**RELATIVISTIC PLASMAS**
Intense relativistic electron beam physics
[AD-745369] 01 p0086 N73-10710
Bremsstrahlung theory for relativistic plasma properties
[AEC-TR-7348] 12 p1434 N73-21618
Bulk viscosity in relativistic homogeneous isotropic cosmologies
17 p2081 N73-26829

**RELATIVISTIC THEORY**
Development of relativistic theory of gravity and comparison with post-Newtonian limit
[NASA-CR-129242] 03 p0293 N73-12387
Exterior gravitational field of slowly rotating deformed masses, obtained by generalizing Weyl metrics into rotating Weyl metrics
[RIFP-162] 04 p0449 N73-13667
Euler equations of motion of relativistic, perfect-fluid hydrodynamics, and potential application to stellar stability
07 p0840 N73-16806
Restricted proof that weak equivalence principle implies Einstein equivalence principle
[NASA-CR-131420] 11 p1324 N73-20745
Relativistic principles of magnetohydrodynamics
13 p1562 N73-22661
Quasi-relativistic theory of two finite masses in Euclidean space and Newtonian time
20 p2454 N73-29720
Gravitation and general relativity
[ITF-72-106-P] 21 p2580 N73-30675
Quasirelativistic theory of two-body motion in Euclidean space and Newtonian time
[AD-763431] 21 p2598 N73-30827
Relativistic rigidity of rotating disk
[AD-763330] 21 p2604 N73-30873
Time delay in ranging signal to Mariner 9 orbiter for testing general relativity
23 p2842 N73-32712

**RELATIVISTIC VELOCITY**
Plastic detectors used to confirm acceleration of argon nuclei to relativistic velocities at Princeton Particle Accelerator
[AD-749863] 05 p0549 N73-14458
Relation between photometric track width and velocity of heavy ions in nuclear emulsions
[LUIP-CR-72-13] 08 p0946 N73-17750
Transformation of signal spectrum in communication between spacecrafts moving at relativistic velocities
[AD-758851] 16 p1876 N73-25186
Doppler shift arising from radiating body rotation at extreme relativistic speeds
22 p2714 N73-31721

**RELATIVITY**
Modified scalar Debye potentials for electromagnetic waves in spherical gravity and spherical media
[AD-746047] 01 p0081 N73-10673
Tensor theory applied to special and general relativity, noting gravitational theory
02 p0231 N73-11878
Group theory and general relativity, including Lorentz group
[AD-749516] 04 p0451 N73-13681
Value of gravitational wave observations in relativistic gravity investigations
[NASA-CR-131511] 12 p1398 N73-21340

**RELAXATION [MECHANICS]**
NT SPIN-LATTICE RELAXATION
NT STRESS RELAXATION
Influence of Coulomb collisions on plasma ion relaxation in confined circular stabilized magnetic mirror
[EUR-CEA-FC-640] 03 p0341 N73-12783
Relaxation tests on high temperature bolted metal joints
[NLL-ESB-TRANS-503-[3810.97]]
06 p0683 N73-15555
Ionizational relaxation in shock-heated mercury vapor
15 p1816 N73-24719
Relaxation curves from lateral strain of test pieces
[NLL-CE-TRANS-6101-[9022.09]]
20 p2478 N73-29903

**RELAXATION METHOD [MATHEMATICS]**
Iterative methods and relaxation algorithm for calculating vertical atmospheric structure from noise contaminated infrared spectral measurements
02 p0196 N73-11588
Relaxation method for inverse solution to atmospheric parameters appearing as functions in integrand of radiative transfer equation
02 p0197 N73-11590
Bilocal operator expansion to two jet structure for final states of deep inelastic scattering on hadrons
[ILL-[TH]-73-4] 12 p1430 N73-21592
Relaxation theory improvements of spectral line broadening in plasmas
24 p2961 N73-33659

**RELAXATION TIME**
Laser luminescence and shock heating for hydrogen fluoride vibrational relaxation measurements in shock tube
[AD-745953] 02 p0138 N73-11119
Vibration-translation and vibration-vibration relaxation rates in rapid expansions of N2 and CO2 in argon
[AD-746068] 02 p0216 N73-11751
Fabry-Perot laser interferometer for studying atomic collisional rate and ionization relaxation time in helium shock wave
[AD-749553] 04 p0408 N73-13326
Analyses of vibrational levels by least squares method for determining transition moment probabilities in nitrogen band
[AD-753394] 09 p1075 N73-18774
Ultrasonic relaxation measurement of polyethylene and polyethylene oxide from room temperature to melting point
[AD-754391] 11 p1310 N73-20628
Nozzle flow free jet and Prandtl-Meyer expansion rotational relaxation equation used for relaxation time calculation
[REPT-72-5] 14 p1650 N73-23383
Direct measurement of mesosphere and stratosphere electrical conductivity and relaxation time
15 p1779 N73-24419
Rate constants for vibrational relaxation using Monte Carlo calculations
[AD-758753] 16 p1871 N73-25152
Computerized analysis of electro-optical polymer relaxation data
[AD-759421] 17 p1992 N73-26111
Oscillation relaxation time of CO2 molecular energy levels in temperature intervals 300 to 600 K.
[AD-762436] 19 p2323 N73-28688
Temperature dependence of several vibrational relaxation processes in DF-CO2 mixtures
[AD-762925] 20 p2374 N73-29078
Nuclear spin-lattice relaxation in magnesium metal
24 p2960 N73-33651

**RELAY SATELLITES**
Earthquake prediction and control through satellite relay telemetry of seismic data
07 p0787 N73-16399

**RELEASING**
Delayed simultaneous appendage release mechanism for use on spacecraft equipped with despin mechanisms and releasable components
[NASA-CASE-GSC-10814-1] 11 p1237 N73-20039
Rocket-borne chemical release systems for gas, liquid, solid, and explosive payloads
[AD-758766] 16 p1908 N73-25435
Environmental tests of interocean acoustic release devices and performance of correlation echo sounder processor
[RN-1008] 18 p2151 N73-27385

**RELIABILITY**
NT AIRCRAFT RELIABILITY
NT CIRCUIT RELIABILITY
NT COMPONENT RELIABILITY
NT SPACECRAFT RELIABILITY
NT STRUCTURAL RELIABILITY
Method of determining reliability of computer components and subsystems
[AD-747080] 02 p0148 N73-11198
Performance evaluation and operating characteristics of different dissolved oxygen analyzers
[RN-1007] 02 p0171 N73-11385
Reliability and its development in time, frequency and probability domain
[TR-72-38] 08 p0927 N73-17595
Monte Carlo simulation of complex reliability systems using logic circuit analysis programs linked to statistics programs
[TR-72-39] 08 p0927 N73-17596
Method and device for verifying reliability of fire detectors
[NASA-CASE-GSC-11600-1] 09 p1034 N73-18436
Service life and reliability of radiation hardened lithium doped solar cells
23 p2859 N73-32840

**RELIABILITY ANALYSIS**
Indicators and controls for validating human reliability data
[AD-744551] 01 p0011 N73-10085
Reliability analysis of Abel transformation algorithm applied to mass measurement in hypersonic wakes
[ISL-21/70] 01 p0041 N73-10324
Design, stress analysis, and reliability evaluation of electric rocket engines
[AD-745427] 01 p0091 N73-10751
Implementation of reliability based strength criteria system for determining service life of C-141 aircraft structures - Vol. 2
[AD-742261] 02 p0126 N73-11025
Kapton covered cadmium sulfide solar cell performance tests in aerospace and earth atmosphere environments
[ONERA-DERTS-NT-02-32] 03 p0255 N73-12062
Development of computer program for estimating reliability of self-repair and fault-tolerant systems with respect to selected system and mission parameters
[NASA-CASE-NPO-13086-1] 03 p0305 N73-12495
Statistical analysis of fatigue properties of SAE 4340 steel and description of test equipment used
[NASA-CR-72835] 03 p0313 N73-12551
Fatigue and crack propagation characteristics of aluminum alloy sheet under controlled cycle stress conditions to simulate fuel tank structural failure
[NASA-CR-128600] 03 p0360 N73-12935
Reliability analysis of nickel zinc rechargeable batteries
[AD-748896] 04 p0376 N73-13062
Application of reliability theory to determine risk function, probability of failure, under ultimate load, and wear-out process of aircraft structures
[ARL/SM-REPT-337] 04 p0480 N73-13925
Definition of expendable second stage and space shuttle booster separation system to include modifications required, ground support equipment, and launch operations - Vol. 2 - Bk. 3
[NASA-CR-128673] 05 p0599 N73-14868
Development and application of procedures for determining service life of gas turbine engines and components
[NASA-TM-X-2664] 06 p0726 N73-15925
Reliability of high temperature strain gages while measuring extreme thermal strain
[NAL-TR-287] 07 p0854 N73-16923
Reliability of semiconductor devices as influenced by quality of aluminum wire bonds used in assembly
[NASA-CR-124037] 09 p1038 N73-18469
Preliminary design assessment of turbofan engines for installation on high speed commercial transport aircraft - Vol. 2
[NASA-CR-121133] 10 p1207 N73-19821
Computational formula for reliability analysis on multiple element circuits of silver zinc storage battery
[AD-754725] 11 p1238 N73-20050
Reliability performance analysis of NASA communication system to show major area of interruption and malfunctions of specified circuits
[NASA-TM-X-66220] 11 p1256 N73-20190
Improvements in military helicopter flight test techniques to provide data for safety, maintainability, and reliability
12 p1357 N73-21013
Development of reliability analysis procedure for determining effects of cumulative and maximum operational loads on airplane structures
[AD-757529] 14 p1603 N73-22999
Improvements in intelligibility testing reliability using experienced listeners
14 p1625 N73-23166
Structural and failure rate models for reliability analysis of electrical systems
[AD-758396] 14 p1671 N73-23560
Reliability analysis of unpaced visual inspection tasks
[AD-757608] 14 p1671 N73-23564
Reliability of safety and arming mechanism for NASA/LSPE program
[NASA-CR-131985] 14 p1719 N73-23953
Design, development, and reliability analysis of bearings for turbine pump on nuclear engine for rocket vehicles
[NASA-CR-132227] 15 p1792 N73-24525
Statistical reliability model and analysis of 5-kwe reactor thermoelectric system
[NASA-CR-121205] 15 p1809 N73-24661
Analysis of coolant flow in transpiration-cooled vanes
[NASA-TN-D-7341] 16 p1974 N73-25966
Techniques used for software reliability determination and evaluation
[AD-760144] 17 p2002 N73-26185
Maximum likelihood efficiency estimation procedures for statistical reliability analyses
[AD-760152] 17 p2039 N73-26493
Nuclear electric propulsion reliability analysis
[NASA-CR-133233] 17 p2061 N73-26671
Management concept for reliability assurance from aerospace industry experience applied to shipbuilding
[MBB-UA-60-72-O] 17 p2099 N73-26980
Development of mathematical model for determining replacement criteria for aircraft structural components
[AD-762226] 19 p2222 N73-27921
Logistic performance data book for C-5A aircraft landing gear to show system reliability, maintainability, logistic support cost, and performance data
[AD-762248] 19 p2357 N73-28963
Logistic performance data book for C-130E aircraft propulsion system to show reliability, maintainability, logistic support costs, and operational problems
[AD-762249] 19 p2357 N73-28964
Logistic performance data book for UH-1F helicopter airframe to show reliability, maintainability, logistic costs, and operational problems
[AD-762251] 19 p2357 N73-28965
Logistic performance data book for C-5A airframe to show reliability, maintainability, logistics support, and operating problems
[AD-762233] 19 p2358 N73-28968
Logistic performance data book for F-4D aircraft fire control system to show reliability, maintanability, logistics support, and operating problems
[AD-762229] 19 p2358 N73-28969
Logistics performance data book for RF-4C aircraft landing gear system to show reliability, maintainability, logistics support, and operating problems
[AD-762231] 19 p2358 N73-28970
Logistic performance data book for C-141A aircraft radio navigation system to show reliability, maintainability, logistics support, and operating problems
[AD-762250] 19 p2358 N73-28971
Logistic performance data book for KC-135 aircraft electrical power system to show reliability, maintainability, logistics support, and operating problems
[AD-762225] 19 p2358 N73-28972
Logistic performance data book for F-4E flight control system to show reliability, maintainability, logistic support, and operating problems
[AD-762230] 19 p2358 N73-28973

Logistic performance data book for RF-4C photographic reconnaissance system to show reliability, maintainability, logistic support, and operating problems
[AD-762232] 19 p2358 N73-28974
Procedures for evaluating fatigue quality of aircraft structures based on fatigue life, crack propagation, and residual strength
20 p2480 N73-29925
Application of high strength structural materials for aerospace vehicles and use of fracture control procedures for improved damage tolerance
20 p2481 N73-29928
Reliability analysis and characterization model of adhesive bonds
[AD-763707] 21 p2563 N73-30549
Analytical techniques for determining reliability growth of cyclic equipment
[AD-763341] 22 p2679 N73-31459
Application of reliability analysis to aircraft structures subject to fatigue crack growth and periodic structural inspection
[AD-764775] 23 p2798 N73-32383
Bayesian reliability demonstration for statistical test development
[AD-765172] 24 p2945 N73-33520
Thermal-vacuum tests of flight model spacecraft to determine performance and reliability based on malfunction analysis
[NASA-TN-D-7408] 24 p2984 N73-33851

**RELIABILITY CONTROL**
U QUALITY CONTROL
U RELIABILITY ENGINEERING

**RELIABILITY ENGINEERING**
Reliability analysis of solar generator on ESRO 1 satellite
[NASA-TT-F-14498] 01 p0007 N73-10051
Microminiaturization and reliability of electronic radio equipment
[AD-745828] 01 p0034 N73-10265
Synthesis of delay-free asynchronous sequential switching circuits
[AD-746392] 01 p0035 N73-10273
Application of scatter factors for various Weibull-shaped parameters, fleet sizes, and level of reliability for aircraft structures
[NASA-CR-2100] 01 p0113 N73-10934
Application of reliability based static strength criteria system to analysis of C-141 aircraft - Vol. 1
[AD-742260] 02 p0126 N73-11024
Procedures for studying reliability characteristics of systems with standbys - Themis project
[AD-745911] 02 p0179 N73-11451
Calibration of combined bending-torsion fatigue reliability research machines and reliability data reduction
[NASA-CR-72837] 03 p0306 N73-12497
Analysis of data generated by combined bending-torsion fatigue reliability research machines using probabilistic-graphically and phenomenological techniques
[NASA-CR-72839] 03 p0306 N73-12498
Reliability tests of computer elements used in automatic airport weather stations
[AD-747558] 03 p0328 N73-12673
Development and application of multiple system checkout procedures for use with gimbaled inertial measuring units
[NASA-CR-123953] 03 p0328 N73-12676
Rocket nozzle redesign for improving Saturn launch vehicle J-2 engine performance and reliability
03 p0349 N73-12849
Characteristics of high performance metal castings and procedures for improving reliability
[AD-748462] 04 p0436 N73-13557
Failure tolerant computer design noting component reliability
05 p0517 N73-14206
Production and costs of producing reliable semiconductor integrated circuits
[AD-749834] 05 p0521 N73-14240
Performance data reduction for cadmium spacecraft cells from simulated orbital life tests
[AD-748251] 06 p0627 N73-15088
Characterizing sequences and fault detection in sequential computers
[AD-750266] 06 p0644 N73-15233
Design criteria for highly accurate and reliable GEOS-C satellite altimetry system
06 p0661 N73-15370
Service life and reliability of single transmitter and array modular type satellite altimeter systems
06 p0663 N73-15388
Theorems for proving consistency of singular perturbations in physical systems with parasitic elements
07 p0761 N73-16182
In-flight tests and operational reliability of jet aircraft nullable compressor face rake
[NASA-TN-D-7162] 07 p0769 N73-16247
Reliability engineering methods for electronic components
[FTL-A-A16-1] 07 p0803 N73-16517
Development of highly accurate and reliable telemeter system utilizing integrated circuits
[AD-752481] 08 p0886 N73-17176
Thermal instability and secondary breakdown prediction for low frequency power transistor
[AD-751852] 08 p0890 N73-17203
Long life broadband transistor amplifier chain for very high frequency range
[AD-752444] 09 p1004 N73-18194
Distributional S-N and Goodman diagrams for designing target reliabilities into rotating mechanical components
[NASA-CR-120967] 10 p1164 N73-19465
Reliability aspects of ground support equipment at Kennedy Space Center
[NASA-CR-131362] 11 p1265 N73-20268
Summary of KSC program for investigating reliability of ground support activities
[NASA-CR-131361] 11 p1297 N73-20521
Evaluation of method for combining point estimates of reliability
[AD-754347] 11 p1302 N73-20563
Methods for conducting acceptance tests and reliability tests of gyroscopes as part of inertial platform quality control procedures
11 p1317 N73-20689
Reliability and operational safety of mechanical helicopter transmission boxes
12 p1357 N73-21012
Electrostatic discharge effects in JFET performance and reliability in low humidity environment
[BDX-613-815] 12 p1383 N73-21217
Relationship of relay intermodulation products and constriction resistance with relay life
[AD-755923] 12 p1385 N73-21236
Accuracy and reliability engineering of precipitation measurement by radar
[NLL-M-22841-[5828.4F]] 12 p1420 N73-21505
Research projects in structural reliability engineering for transport vehicles
12 p1466 N73-21878
Method for evaluating physical characteristics of material
[AD-755626] 12 p1467 N73-21892
Reliability tests of reverse biased semiconductor diodes under electron beam bombardment conditions
[AD-755449] 13 p1502 N73-22171
Technical study of tunnel diode and its microwave amplification and oscillation
[AD-756932] 13 p1503 N73-22183
Reliability analysis of thermoelectric module solar energy converter
[AD-757087] 14 p1606 N73-23015
Reliability and quality control procedures for development of test equipment used on lunar experiment projects - Vol. 3
[NASA-CR-128920] 14 p1705 N73-23837
Guidelines for design and development of electrical and electronic components and systems used in spacecraft construction to obtain long service life - Vol. 2
[NASA-CR-128906] 14 p1707 N73-23854
Improved electrostatic accelerator with increased terminal voltage capacity
[UR-NSRL-71] 16 p1885 N73-25255
Quality control requirements for Apollo ultraviolet spectrometer experiment
[NASA-CR-128584] 16 p1916 N73-25510
Design of water activated zinc-air battery
[AD-759932] 17 p1986 N73-26053
Test operation procedure for radar interrogator transmitter
[AD-759227] 17 p1998 N73-26158
Fault detection test methods in combinational digital logic networks
[AD-760543] 18 p2121 N73-27146
Reliability study of multicomponent systems
[AD-760768] 18 p2169 N73-27521
Computer program problems and possible solutions
[AD-762141] 19 p2242 N73-28072
Determination of diagnostic nucleus of digital computer
[AD-762264] 19 p2242 N73-28080
Ferrite logic device for increased reliability of digital electronic systems
[NASA-CR-132265] 19 p2248 N73-28124
Dynamic and rotary machinery, design and reliability
[AD-762440] 19 p2305 N73-28542
Operational reliability and economics for instrumentation particularly electric pumps
[AD-762321] 19 p2306 N73-28545
Development of system for predicting system failure rate and determination of optimal economic replacement interval
[AD-762417] 19 p2357 N73-28966
Development of fatigue life prediction procedures based on measured stress-time histories and mathematical model for description of random vibrations
20 p2481 N73-29926
Analysis of failure modes of blades on CH-47 helicopter rotary wings for improved helicopter reliability and cost reduction
[AD-763187] 21 p2497 N73-30042
Reliability improvement by redundancy in electronic systems
[RAE-TR-72200] 21 p2520 N73-30208
Scanning electron microscope examination of wire bonds from high reliability microelectronic devices
[NBS-TN-785] 21 p2549 N73-30432
Algorithm for optimization of reliability characteristics of redundant digital computer
[AD-763261] 22 p2640 N73-31156
Reliability and failure modes of GaAs Gunn and impatt diodes and Si impatt diodes
[AD-763929] 22 p2644 N73-31193
Parameters and errors of magnetically sensitive elements of ferrosonde gradiometers
22 p2671 N73-31399
Apollo experience report on reliability of Apollo spacecraft based on application of proven reliability and quality control techniques
[NASA-TN-D-7438] 22 p2720 N73-31769
Engineering safety in space programs
[NASA-TT-F-15077] 22 p2721 N73-31777
Construction of reliability cost-model
[NASA-TM-X-64777] 23 p2797 N73-32372
Probabilistic models and statistical inference in reliability life testing, and fatigue failure
[AD-763818] 23 p2798 N73-32380
Development of mechanical equipment reliability prediction techniques
[AD-765367] 23 p2799 N73-32390
Reliability of circular electrical connectors
[AD-765609] 24 p2899 N73-33144

**RELIEF MAPS**
Method to automate and represent relief drawings
[AD-750750] 06 p0670 N73-15453

**RELIEF VALVES**
Redundant hydraulic control system for actuators with three main valve combination
[NASA-CASE-MFS-20944] 04 p0425 N73-13466

**RELIEVING**
NT STRESS RELIEVING

**REMAGNETIZATION**
U MAGNETIZATION

**REMANENCE**
Magnetic hysteresis of lunar surface and permanent remanence in lunar samples
[NASA-TM-X-65941] 10 p1212 N73-19860

**REMELTING**
U MELTING

**REMOTE CONSOLES**
RAF operating procedures for ICL 7020 Remote computer terminal
[RAE-TR-72086] 06 p0644 N73-15231

**REMOTE CONTROL**
NT RADIO CONTROL
Computerized teleoperator manual control system for remote mechanical hand
01 p0019 N73-10143
Remote control manipulator for space maintenance
[DGLR-PAPER-72-098] 06 p0722 N73-15888
Design and development of multichannel laser remote control system using modulated helium-neon laser as transmitter and light collector as receiving antenna
[NASA-CASE-LAR-10311-1] 07 p0806 N73-16536
Concept evaluation and subsystem analyses for design of remote controlled teleoperator visual system
[NASA-CR-124059] 08 p0879 N73-17117
Sophisticated maintenance of orbital space vehicles with application of remotely controlled telemanipulation concept
[NASA-TT-F-14804] 08 p0965 N73-17885
Remotely controlled device for detection of mass changes in selected specimens
[NASA-CASE-MFS-21556-1] 11 p1292 N73-20487
Construction of remote controlled mechanical manipulators using biodynamic principles
[NASA-TT-F-14889] 12 p1374 N73-21152
Long range objectives of design and control study of remote manipulators
[NASA-CR-124191] 13 p1486 N73-22046
Design of automatic controlled remote arm mechanism incorporating feedback information
[NASA-CR-2238] 13 p1487 N73-22055
LORAMS design for remotely collecting weather data
[AD-756682] 13 p1554 N73-22594
Development and evaluation of display and control equipment for remotely piloted vehicles
[AD-757761] 15 p1736 N73-24077
Intelligent telemetry device remotely controlled via communication channels
[AD-758272] 15 p1751 N73-24195
Design of manipulator mechanisms with manual, bioelectric, and automatic control systems
[NASA-TT-F-14336] 17 p1989 N73-26073
Volumetric kinematic analysis on servomechansim of remote handling manipulator
17 p1989 N73-26075
Design requirements for remotely controlled master-slave manipulators
17 p1989 N73-26076
Remote control of underwater manipulator using cables and automatic servomechanics
17 p1989 N73-26078
Structural design of computer controlled manipulator for remote handling
17 p1989 N73-26079

Remotely controlled manipulators with independent follow-up and force reproduction mechanisms
17 p1989 N73-26082
Miniature, remote controlled land and water vehicles and components
[AD-761665] 19 p2356 N73-28953
Energy transfer control and compressor bleed concepts of remote lift fan control
[NASA-TM-X-2863] 21 p2590 N73-30749
REMOTE HANDLING
Prototype elbow joint for remote control of heavy duty cargo boom
[AD-749520] 05 p0553 N73-14487
Experiments in video camera positioning with regard to remote manipulators
[NASA-CR-124190] 11 p1249 N73-20139
Dry inert gas glove box for handling of hygroscopic and corrosive materials in spectroscopic and lasers experiments
[CRC-1244] 21 p2548 N73-30430
REMOTE REGIONS
NT ANTARCTIC REGIONS
NT ARCTIC REGIONS
ERTS-1 retransmission of water level data collected at remote locations in Canada
[E73-10469] 12 p1395 N73-21306
Development of techniques for evaluation of ERTS-1 imagery of natural resources in remote and unexplored areas of Venezuela
[E73-10481] 12 p1396 N73-21318
ERTS-1 retransmission of water resources data collected from remote regions of Canada
[E73-10504] 13 p1515 N73-22279
LORAMS design for remotely collecting weather data
[AD-756682] 13 p1554 N73-22594
REMOTE SENSORS
ERTS-1 remote sensing of chlorophyll measurements in upwelling areas of oceans
[E72-10196] 01 p0047 N73-10375
Visible fluorescence of earth surface materials and potential applications in remote sensing
[PB-210621] 01 p0053 N73-10434
Remotely operated boundary layer probe for use in three dimensional measurements
[AD-745215] 01 p0059 N73-10481
Thermal sounding experiment by Meteor satellite
[NASA-TT-F-14493] 01 p0104 N73-10861
Detection and mapping snow cover from ERTS-1 remotely sensed imagery of western US and Arctic
[E72-10202] 02 p0160 N73-11299
Definition of characteristics and boundaries of vegetation-soil types in Southern Idaho from ERTS-1 remotely sensed imagery
[E72-10203] 02 p0161 N73-11300
Determination of in-flight optical transfer functions of orbital earth resources multispectral sensors
[E72-10212] 02 p0162 N73-11307
Forest resources evaluation, planning, protection, and management using remotely sensed imagery
[E72-10220] 02 p0162 N73-11314
Remote sensing in forestry using aerial and satellite-borne photography and imaging techniques
[E72-10221] 02 p0162 N73-11315
Location of water current boundaries in Gulf of Mexico by sensing color change associated with cyclonic edge of zone of maximum horizontal velocity shear
[E72-10233] 02 p0163 N73-11326
Feasibility of obtaining estimate of waterfowl production using remote sensing technology
[USGS-IR-215] 02 p0165 N73-11343
Use of remote sensing data from spacecraft and aircraft to assist technology in tropical tuna and Alaska salmon fisheries
[AD-745774] 02 p0169 N73-11370
Airborne and satellite-borne, microwave radiometer, remote sensing systems
[CRC-1231] 02 p0172 N73-11387
Design of precision sensors for optical tracking systems
[AD-746742] 02 p0176 N73-11424
One-dimensional and multi-dimensional inversion techniques for processing remote atmospheric and ionospheric sounding data
[NASA-TM-X-62150] 02 p0196 N73-11585
Combined radar-radiometer for remote sensing at microwave performance
[NASA-CR-128492] 03 p0265 N73-12145
Monitoring and surveillance of state of eutrophication of inland lakes in California and Nevada
[E72-10207] 03 p0288 N73-12330
Land use planning on Mississippi Gulf Coast utilizing ERTS-1 remotely sensed data
[E72-10262] 03 p0290 N73-12361
Stratigraphy, structure, and geologic history of Sangre de Cristo Mountains of Colorado based on aerial remote sensing
[NASA-CR-129519] 03 p0293 N73-12385
Analyzing and processing remotely sensed earth resources data
[NASA-CR-61399] 03 p0293 N73-12390
Potential application of SLR to remote sensing of earth resources
[ESRO-CR[P]-138] 03 p0295 N73-12401
Characteristics and imagery of side-looking radar
03 p0295 N73-12402
Side-looking radar for agricultural applications, noting crop identification and growth
03 p0295 N73-12403
Geological applications of side-looking radar, noting mineral exploration, engineering geology, and soil science
03 p0295 N73-12406
Side-looking radar applications to transportation noting route planning, shipping lanes, and traffic
03 p0295 N73-12409
Design and development of radiometer to observe steady state radiation in vacuum environment
[NASA-CASE-MFS-21108-1] 03 p0301 N73-12455
Absorption and fluorescence spectra of marine and fresh water algae using pulsed N2/Ne dye laser as excitation source
[NASA-CR-62090] 03 p0310 N73-12527
Infrared spectral emittance data, and infrared spectrometry studies
[NASA-CR-128646] 03 p0335 N73-12730
Remote detection of water content and spectral properties of leaves in different soybean crop species
04 p0378 N73-13070
Thermal remote sensing of infrared radiant temperatures in alpine/periglacial environments
04 p0409 N73-13332
Control of pink bollworm infestation in southern California cotton fields using ERTS-1 remotely sensed imagery
[E72-10285] 04 p0409 N73-13335
Remote sensing of Thailand earth resources using ERTS-1 imagery
[E72-10298] 04 p0411 N73-13348
Investigation of natural resources in remote and unexplored areas of Venezuela using ERTS-1 remotely sensed imagery
[E72-10311] 04 p0412 N73-13360
Remote sensing of native arid plant distribution using ERTS-1
[E72-10314] 04 p0412 N73-13363
Development of operational remote sensing water quality monitoring system
[NASA-CR-129797] 04 p0414 N73-13378
Role of remote sensing in geologic reconnaissance for tunnel-site selection
[AD-748663] 04 p0416 N73-13399
Remote recording of speed with laser Doppler anemometry
[RISO-M-1489] 04 p0422 N73-13442
Survey of methods for sounding atmospheric temperature profile by remote measurement
[NASA-CR-130110] 04 p0442 N73-13601
Application of remote sensing techniques for solution of ecological management problems
04 p0471 N73-13838
Development of airborne instrumentation and application of remote earth observations for determining stream discharge prediction for water management program
04 p0471 N73-13839
Feasibility of monitoring global air pollution using optical sensors installed in orbiting satellites
04 p0471 N73-13840
Application of remotely sensed, multispectral observations for assessment of earth resources and environmental quality in Alabama
04 p0471 N73-13841
Application of remotely sensed data to determination of resources and conditions in Susquehanna River Basin
04 p0471 N73-13844
Development of remote sensing devices to measure jet exhaust fluctuating density gradients, mean and turbulent velocity, and mean temperature Vol. 6
[AD-749143] 05 p0496 N73-14041
Application of remote sensing techniques to public health
[NASA-CR-129822] 05 p0500 N73-14069
ERTS-1 remotely sensed imagery to support study of Lake Ontario basin as part of International Field Year for the Great Lakes
[E72-10354] 05 p0534 N73-14342
Remote sensing techniques for regional planning and managing earth resources, particularly water resources in California
[NASA-CR-129917] 05 p0536 N73-14361
Remote sensing of California water systems
05 p0536 N73-14362
Use of resource indicators and remote sensing to plan and manage hydrologic and water resource systems
05 p0536 N73-14364
Remote sensing data for determining land use potential of northern California coastal zone
05 p0536 N73-14365
Use of remote sensing data to analyze impact of California State Water Project on regional planning and land use of west side of San Joaquin Valley
05 p0537 N73-14367
Impact of California Water Project on environmental quality and resources in southern California
05 p0537 N73-14368
Digital facility for handling and processing remotely sensed earth resources data
05 p0537 N73-14369
Influence of atmospheric conditions on remote image transfer and interpretation as determined by laboratory measurements
05 p0537 N73-14370
Geology photography infrared imagery, and remote sensing evaluation of Klondike Mining District, Nevada
[NASA-CR-129934] 05 p0537 N73-14371
Evaluation of image dissector sensor for Earth Resources program
[NASA-CR-130131] 05 p0547 N73-14443
Development of proton-activated sensors to measure graphite nosetip recession due to ablation during nose cone reentry
[AD-748289] 05 p0548 N73-14456
Dual gas correlation spectrometer measurements of sulfur dioxide and nitrogen dioxide in industrial area of southern California
[PB-210717] 05 p0575 N73-14676
Research on chemical reactions, remote sensors, pollution, and transportation
[NASA-CR-61396] 05 p0607 N73-14938
Remote sensors for data acquisition on soils, water conditions, microclimatic conditions, flora, and land use
05 p0609 N73-14948
Conference on dynamic wave effects on satellite-borne sea surface measurements
[NASA-CR-129993] 06 p0664 N73-15392
Effect of wind wave energy balance on remote microwave sensing of sea surface
06 p0664 N73-15395
Calibration and temperature control system for airborne interferometer
[AD-749876] 06 p0667 N73-15427
Evaluation of utility of available remote sensor returns in analysis of slope failure phenomena
[AD-750735] 06 p0671 N73-15462
Mapping of distribution of slope failure forms as depicted by remote sensor returns
[AD-750733] 06 p0672 N73-15463
Annotated bibliography of technical characteristics of remote sensors and technological experiments developed under NASA programs for earth observation
[NASA-TM-X-66144] 06 p0674 N73-15482
Remote sensing techniques for detection and prevention of Rocky Mountain spotted fever, Encephalitis, Malaria, and Red Tide environmental health problems
[NASA-CR-128727] 07 p0745 N73-16060
Multispectral remote sensing techniques for identification of corn blight disease
[NASA-TM-X-69055] 07 p0745 N73-16064
Remote chemical detectors for vehicle identification by exhaust gases
[AD-751740] 07 p0753 N73-16116
Remote automatic multipurpose station for collecting oceanographic and meteorological data in Arctic regions
[AD-751039] 07 p0758 N73-16139
Transform coding and block quantization for remote aircraft scanner data and digitized satellite imagery compression
[NASA-CR-130365] 07 p0759 N73-16161
Handling and analysis of remote sensing data on 1971 corn blight
[NASA-CR-130368] 07 p0759 N73-16164
Discrimination and mapping land use categories in Puerto Rico using various types of multispectral remote sensor imagery
07 p0776 N73-16298
Remote sensing of selected Bureau of Reclamation land projects
[E73-10062] 07 p0778 N73-16324
Application of ERTS-1 remotely sensed imagery to selected reclamation projects
[E73-10066] 07 p0779 N73-16328
Proceedings of conference on earth resources survey systems to show applications of remote sensing to agriculture, forestry, oceanography, and urban development - Vol. I
[NASA-SP-283-VOL-1] 07 p0781 N73-16348
Analysis of earth resources based on mapping, human needs, minerals, water, and food and contributions made by remote sensing satellites
07 p0781 N73-16350
Objectives of NASA Earth Resources Survey Program to include types of sensors used and data acquired by aircraft, spacecraft, and ground observations
07 p0782 N73-16351
International aspects of Earth Resources Survey Program to include proposals for data availability and assistance to be provided by various nations
07 p0782 N73-16352
Employment of Earth Resources Technology Satellite capabilities for determining distribution of earth resources
07 p0782 N73-16353

Application of remote sensing from aircraft and spacecraft to geology, hydrology, and geographical data acquisition
07 p0782 N73-16354
Application of airborne and spaceborne photography to determine agricultural and forestry resources
07 p0782 N73-16355
Application of electromagnetic sensors for remote sensing of oceanographic processes to determine available resources
07 p0782 N73-16356
Application of remote sensors for determining meteorological and environmental parameters with emphasis on data obtained by satellite infrared sensors
07 p0782 N73-16357
Development of steps and procedures for determining and evaluating environmental quality through use of remote sensors
07 p0782 N73-16358
Analysis of NASA Earth Resources Program to include ERTS satellites, Skylab program, and earth resources survey aircraft
07 p0782 N73-16359
Analysis of earth resources information systems using satellites as sensor platforms to show type of data obtained and data reduction procedures
07 p0782 N73-16360
Characteristics and capabilities of remote sensor systems to collect and analyze earth resource data
07 p0783 N73-16361
Comparison of imagery obtained with several types of remote sensors over Test Site 701, Mexico
07 p0783 N73-16367
Organization, planning, and development of remote sensor programs for Canada
07 p0784 N73-16371
Identification of organizations and activities concerning French programs in aerial photography and earth resources technology
07 p0784 N73-16372
Characteristics of various types of remote sensors and identification of specific areas of application
07 p0784 N73-16373
Design and characteristics of television cameras used for remote sensing and comparison with imagery of photographic film cameras
07 p0784 N73-16374
Application of aerial photography for remote sensing to include characteristics of cameras, films, and photographic processing
07 p0784 N73-16375
Analysis of factors affecting design and application of remote sensors for earth observation
07 p0784 N73-16376
Characteristics of multispectral sensors and methods for interpreting multispectral data obtained during earth resources surveys
07 p0784 N73-16378
Application of remote sensing techniques for detecting environmental changes at and near earth surface
07 p0784 N73-16379
Analysis of effects of various parameters inherent in remote sensors to show distortions and errors produced in remotely sensed data
07 p0784 N73-16380
Organization and functions of interdisciplinary teams for analyzing and interpreting remotely sensed data on earth resources
07 p0784 N73-16381
Proceedings of conference on earth resources survey systems - Vol. 2
[NASA-TM-X-68912] 07 p0785 N73-16382
Detection of citrus tree anomalies by remote sensing with infrared color aerial photography
07 p0785 N73-16384
Development and application of field data collection techniques for remote sensing applications
07 p0785 N73-16386
Forests and range resources inventory and mapping using remote sensors
07 p0785 N73-16388
Remote detection of insect damage and stress symptoms in forests of Black Hills
07 p0785 N73-16389
Planimetric, topographic, and thematic mapping using remotely sensed imagery
07 p0786 N73-16391
Acquisition of data concerning urban housing quality using remotely sensed imagery
07 p0786 N73-16393
Application of remote sensing techniques to study of climatology of urban-regional systems
07 p0786 N73-16394
Urban and regional changes based on city census and remotely sensed imagery
07 p0786 N73-16395
Multispectral remote sensing techniques applied to study changes in wildlife habitats
07 p0786 N73-16396
Detection, identification, measurement, and monitoring environmental pollution by remote sensing devices and techniques
07 p0786 N73-16397
Control and mapping of water pollution using remote sensors
07 p0787 N73-16398
Application of remote sensing techniques and models to geophysics
07 p0787 N73-16401
Snow line delineation using satellite remotely sensed data
07 p0787 N73-16402
Application of TIROS satellite data to mapping of ice fields through development of composite minimum brightness chart
07 p0788 N73-16409
Development of method for determining sea surface temperature using remote sensors in earth orbiting satellites
07 p0788 N73-16410
Airborne multispectral scanning of maize canopy to determine temporal characteristics, and relation of leaf area index to spectral response curves
[NASA-CR-130369] 07 p0789 N73-16421
Relationship between maize canopy density and reflected energy determined from color and color infrared photographs
[NASA-CR-130370] 07 p0790 N73-16422
Automatic processing of remote sensed data to aid in land use mapping and agricultural conservation
[NASA-CR-130372] 07 p0790 N73-16423
Application of multispectral remote sensing to soil survey research in Indiana
[NASA-CR-130033] 07 p0790 N73-16424
Airborne multispectral scanning of maize canopy to determine density, and comparision to leaf area index
[NASA-CR-130363] 07 p0790 N73-16425
Anomalous scattering effects of haze layer in remote sensing data on corn blight distribution
[NASA-CR-130028] 07 p0790 N73-16428
Remote sensing of rapid mass wastage, mudflow, and debris slide
[NASA-CR-130379] 07 p0792 N73-16443
Sample classification accuracy of minimum distance and maximum likelihood classifiers and parametric and nonparametric classifiers in remote sensing
[NASA-CR-130030] 07 p0799 N73-16489
Statistical three-stage sampling model for estimating resources from remote sensor applications
[NASA-CR-130026] 07 p0800 N73-16494
Importance of ground truth data in remote sensing
[NASA-CR-130020] 07 p0800 N73-16495
Abstracts on remote sensing of turbulence and waves in planetary boundary layer
[AD-751110] 07 p0816 N73-16618
Curriculum of training course on basics and state-of-the-art of remote sensing and developments in parameter optimization
[NASA-CR-128713] 07 p0848 N73-16876
Secondary subsystems of ITOS 1
[NASA-CR-130164] 07 p0849 N73-16881
Theoretical procedure for estimating social benefits of remote sensing
[NASA-CR-130027] 07 p0857 N73-16947
Remote sensing of areas in Italy using infrared scanners for thermal radiation map
07 p0859 N73-16968
Application of pattern recognition oriented algorithms for multispectral data analysis software system
[NASA-CR-130757] 08 p0887 N73-17184
Importance of ground truth data by remote sensing
[REPT-120371] 08 p0916 N73-17508
Earth resource survey using remote sensing techniques to improve land use and management in Michigan
[NASA-CR-130758] 08 p0917 N73-17514
Use of remote sensing for assessing impact of highway construction on land use management in Michigan
[NASA-CR-130761] 08 p0917 N73-17515
Application of remote sensors carried in aircraft and satellites to survey extent of usage of recreational facilities
[NASA-CR-130752] 08 p0917 N73-17517
Remote gas filter correlation instrument for monitoring air pollution by satellites
[NASA-CR-112137] 08 p0938 N73-17682
Digital data processing system for infrared video scan
[AD-752069] 08 p0944 N73-17731
Research on remote sensing applications and satellite observation data - conferences
[NASA-SP-312] 08 p0971 N73-17934
Remote sensing with meteorological radar equipment
[AD-753813] 09 p1004 N73-18197
Data processing for synthetic aperture radar used as satellite-borne earth resources remote sensor
[NASA-CR-2193] 09 p1005 N73-18202
Survey and mapping Colorado geology using airborne remote sensors
[NASA-CR-130822] 09 p1025 N73-18370
Spaceborne remote sensing for agricultural and forest resource surveys
[NASA-CR-130798] 09 p1036 N73-18376
Atmospheric effects on remotely sensed radiation measurements
[NASA-CR-130828] 09 p1028 N73-18389
Ross Barnett Reservoir remote sensing project to determine water sediment, investigate erosion, and improve land use
[NASA-CR-130960] 09 p1029 N73-18396
Operational system for employment of remote sensing and automated information in urban land management
[NASA-CR-130969] 09 p1030 N73-18410
Multiband airborne remote sensor devices for collecting data on reflective and emissive terrain properties
[AD-752420] 09 p1033 N73-18430
Basic mechanism underlying generation of Moire patterns in line scanner data acquisition
[NASA-CR-130829] 09 p1035 N73-18442
Design and development of two long wavelength, focal plane, and cooler assemblies for use in multispectral scanner installed in earth observations aircraft
[NASA-CR-128743] 10 p1137 N73-19262
Optimized method of remote haze detection using ERTS-1 imagery
[E73-10344] 10 p1148 N73-19343
Application of remote sensing techniques and laboratory analyses for determining water pollution caused by carbonaceous materials
[NASA-CR-128824] 10 p1154 N73-19387
Correlation and regression analysis of aerial photography and soil samples to determine principal soil limitations
[NASA-CR-131110] 10 p1154 N73-19392
Soil mapping of rangelands in Bennett County, South Dakota using remotely sensed imagery
[NASA-CR-131229] 10 p1155 N73-19395
Angular distribution of outgoing shortwave radiation intensity in atmosphere with continuous cloud cover
[AD-753975] 10 p1157 N73-19417
Application of remote sensing and aerial photography to Houston metropolitan area
[NASA-CR-128746] 10 p1159 N73-19431
Design, development, and configuration of astronomical observatory for space shuttle to show telescope capabilities and characteristics of various remote sensors
[NASA-CR-128841] 10 p1215 N73-19879
Development of attitude control system jitter specification for Tiros-N satellite three axis orientation capability
[NASA-TM-X-66201] 10 p1216 N73-19886
Remote sensing equipment to ensure efficiency in microwave electric power transmission to remote receiving stations
[NASA-CASE-MFS-21470-1] 11 p1264 N73-20257
Catalogue of selected remote sensing data for New Jersey environment protection and management
[E73-10383] 11 p1275 N73-20347
Application of remote sensing to Pantano Wash for balance between environment and urban growth for Tucson
[NASA-CR-131279] 11 p1286 N73-20436
Mineral prospecting in tropical areas by application of geochemical, botanical, geophysical, and remote sensing techniques
[PB-213230] 11 p1289 N73-20456
Atmospheric observation techniques using aircraft infrared radiometers as prototypes for spacecraft remote sensing application
[NOAA-TR-NESS-64] 11 p1293 N73-20494
Research in aircraft noise and sonic booms reduction, remote sensing of water pollution, and earth surface changes
[DLR-MITT-72-15] 12 p1375 N73-21153
Remote sensing techniques for managing California earth resources
[NASA-CR-131392] 12 p1399 N73-21347
Remote sensing and automatic data processing techniques for earth resources survey in California
12 p1399 N73-21348
Management planning for California water resource information gathering system
12 p1399 N73-21349
Remote sensing techniques for acquiring hydrological resource information to be used in California water management
12 p1399 N73-21350
Feasibility of remote sensing techniques for hydrology and watershed management in California
12 p1399 N73-21351
Satellite television photography of geomorphological indices for developing stream meander pattern
12 p1400 N73-21352
Digital systems for automatic processing of remote earth resources sensing data
12 p1400 N73-21355
Remote sensing techniques for water management and land use classification in California coastal zone considering river deltas
12 p1400 N73-21357
Research and applications of remote sensing to local and state governments
[NASA-CR-131643] 12 p1400 N73-21360

Analysis of earth based remote sensing data and infrared observations to determine nature of Apollo 16 landing site
12 p1455 N73-21787
Long range objectives of design and control study of remote manipulators
[NASA-CR-124191] 13 p1486 N73-22046
Remote sensing of fallow soil moisture, using visible and infrared scanners
13 p1514 N73-22267
Application of Earth Resources Experiment Package data to development of commercial mining activities
[MCR-73-62] 13 p1518 N73-22308
Use of remote airborne photopolarimeters to measure soil moisture content in southwestern United States
[NASA-CR-130211] 13 p1522 N73-22332
Use of remote sensor techniques for wildlands vegetation management
[NASA-CR-131580] 13 p1522 N73-22336
Space and supporting aircraft photography for interpretation and analysis of non-forest vegetation
[NASA-CR-131585] 13 p1522 N73-22338
Application of remote sensing techniques in forestry and range disciplines for timber inventory, weather forecasting, land classification, and snowfield monitoring
[NASA-CR-131583] 13 p1523 N73-22340
Remote sensing techniques for evaluating vigor loss in black spruce due to eastern dwarf mistletoe
[NASA-CR-131582] 13 p1523 N73-22341
Use of digitized remote sensor data and automatic data processing techniques in preparation of forest cover mapping to aid in forest resources management
[NASA-CR-131578] 13 p1523 N73-22344
Feasibility of detecting subsurface coal fires in Wyoming and Montana from ground observation, aerial photography, and satellite imagery
13 p1528 N73-22384
Earth resources remote sensing project using multispectral band scanners to detect and measure thermal radiation from ground vegetation
[NASA-CR-124219] 13 p1529 N73-22393
Passive microwave radiometry and its application to earth resources surveys
[ESRO-CR-116] 13 p1530 N73-22402
Multispectral scanning systems and potential application to earth resources, noting radiation sources, atmospheric effects, and sensor techniques
[ERL/R-243-U] 13 p1531 N73-22403
Appraisal of meteorological satellite data as aid in weather modification programs
[NASA-CR-131876] 13 p1553 N73-22583
Weather forecasting and atmospheric activity detection using meteorological radar and remote sensing equipment
[AD-755438] 13 p1554 N73-22597
Preparation for multidisciplinary study of Wyoming test sites using EREP remotely sensed data from Skylab
[E73-10552] 14 p1655 N73-23425
Use of remotely sensed data to solve water resource problems of Wolf Creek Watershed, Colorado
[NASA-CR-129001] 14 p1660 N73-23479
Mission planning for European earth resources survey aircraft
[ESRO-CR[P]-117] 14 p1661 N73-23484
Mesoscale variation of outgoing spectral radiation near 15 microns
[AD-757622] 14 p1663 N73-23500
Remote sensor system aboard Skylab in support of EREP oceanographic program
[AD-755715] 14 p1663 N73-23501
Computer program for extracting features from remotely sensed data presented in digital image form
[NASA-TN-D-7312] 15 p1778 N73-24410
Critical evaluation of existing optical remote sensors for HCl vapor detection in solid rocket propellant plumes
[NASA-CR-112274] 15 p1780 N73-24431
Geologic mapping of Bonanza Test Site Colorado using remotely sensed data
[NASA-CR-132231] 15 p1780 N73-24433
Application of regression analysis to water quality measurement from remote sensing spectral signature data
[NASA-CR-132997] 16 p1870 N73-25141
Development of electronic detection system for remotely determining number and movement of enemy personnel
[NASA-CASE-ARC-10097-2] 16 p1873 N73-25160
Atmospheric effects on remote sensing of nonuniform temperature sources applied to Skylab and ERTS missions
[NASA-CR-129004] 16 p1905 N73-25413
Application of remote sensing techniques of ERTS and other sources for solution of environmental problems in Oregon
[NASA-CR-133034] 16 p1906 N73-25420
Remote sensing of thermal and industrial discharges along shoreline of Lake Michigan
[PB-214503/5] 16 p1908 N73-25436
Aerial reconnaissance of thermal discharges along shoreline of Lake Michigan
[PB-214407/9] 16 p1908 N73-25437
Development of remote sensing activities in countries with limited resources
[PB-214861/7] 16 p1909 N73-25446
Airborne laser remote sensing of coastal waters
[AD-759781] 16 p1910 N73-25454
Remote sensing and RF interferometry for determining sea states
16 p1911 N73-25465
Survey on remote sensing and photointerpretation
[PB-214864/1] 16 p1914 N73-25490
Multispectral remote sensing techniques for measuring light absorption, scattering, and particle concentrations in water
[AD-759668] 16 p1914 N73-25491
Four channel radiometer for remote sensing of microwave emission from atmospheric oxygen and water vapor
[AD-759535] 16 p1939 N73-25696
Remote low power mineralogical analysis of lunar, planetary, or asteroid soils, using X ray diffraction
[NASA-CR-124271] 16 p1963 N73-25879
Image processing techniques and applications to Earth Resources Technology Satellite program
[NASA-CR-124285] 16 p1967 N73-25910
Fokker F-27 as European earth resources survey aircraft noting design, remote sensors, and program
[ESRO-CR[P]-128] 17 p1984 N73-26035
Application of ERTS-1 remotely sensed data and ground truth information to predict and manage water quantity and quality in river basins
[E73-10689] 17 p2018 N73-26314
Application of airborne microwave radiometers for remote monitoring of soil moisture in selected areas of Texas and Oklahoma
[NASA-CR-133102] 17 p2031 N73-26438
Application of airborne microwave radiometry for remote sensing of soil moisture in southwest US
[NASA-TM-X-66265] 17 p2032 N73-26444
Statistical classification of earth resources in remote sensing data
[NASA-CR-128988] 17 p2054 N73-26615
Remote barometric altimetry and estimation of meteorological field variables
[AD-759910] 17 p2058 N73-26650
Side-looking radar for aerial imagery of earth surface
[JPRS-59391] 18 p2116 N73-27108
Remote sensing of thermal emission from sea surface and atmosphere
[NASA-TT-F-14972] 18 p2142 N73-27317
Remote sensing methods and equipment
[NASA-TT-F-14973] 18 p2142 N73-27318
Remote sensing techniques for earth resources, water pollution, and vegetation growth
[PUBL-21] 18 p2143 N73-27321
Water balance, micrometeorology, thermal structure, and heat content of Great Lakes as determined by remote sensors during International Field Year
[IFYGL-BULL-4] 18 p2143 N73-27322
Aerosol physical properties from horizon inversion by satellite
[NASA-CR-112311] 18 p2144 N73-27330
Bibliography of remote sensing applications to agriculture, civil engineering, and geology
[PB-219104/7] 18 p2147 N73-27356
Bibliography on remote sensing for agriculture and geological surveys
[PB-219103/9] 18 p2147 N73-27357
Remote color aerial photography for soil mapping and highway engineering applications
[PB-220317/6] 18 p2148 N73-27363
Multispectral band scanner for Earth Resources Technology Satellite A imagery
18 p2209 N73-27831
Performance of return beam vidicon multispectral camera system for remote ERTS imagery
18 p2209 N73-27832
Visible infrared spin-scan radiometer system for earth and cloud cover photography by synchronous meteorological satellite
18 p2209 N73-27834
High resolution radiometer for visible and infrared imagery onboard meteorological satellite
18 p2209 N73-27836
Proceedings of conference on significant results obtained from ERTS-1 - Vol. 1, Parts A and B
[E73-10824] 19 p2259 N73-28207
Digital analysis of ERTS-1 imagery for southeastern South Dakota to determine cultivated areas and to identify crops
[PAPER-A3] 19 p2259 N73-28211
Analysis of ERTS-1 to include specifications of sensors, data acquisition, orbital mechanics, and data processing
19 p2287 N73-28391
Application of remote sensing techniques to geology of Bonanza volcanic center
[NASA-CR-133499] 19 p2294 N73-28448
Multispectral scanning systems applied to agriculture and forestry
19 p2295 N73-28452
Passive microwave radiometry for remote sensing of earth resources and environmental monitoring programs
[ESRO-CR-75] 19 p2295 N73-28458
Application of satellite-borne remote sensors to survey of earth resources and environment
[NASA-TM-X-68266] 20 p2412 N73-29384
Analysis of Milwaukee county, Wisconsin land use by machine processing of ERTS-1 remotely sensed data
[NASA-CR-133643] 20 p2412 N73-29385
Requirements of earth resources aircraft facility for remote sensing of European terrain
[ESRO-CR-97] 20 p2413 N73-29394
Sequential photography for coastal oceanography
[AD-760713] 20 p2413 N73-29399
Wavelength profilometer based on phase-ranging with VHF - modulated C02 laser
[AD-762453] 20 p2415 N73-29411
Aircraft gamma surveys of moisture content in soil detention layer
20 p2448 N73-29667
Survey of remote sensing applications for transportation and traffic engineering studies
[NASA-CR-129011] 20 p2488 N73-29989
Geometric aspects in digital analysis of multispectral scanner data
[NASA-CR-133641] 21 p2511 N73-30137
Papers presented at meeting of Soviet-American working group on remote sensing of natural environment from space
[JPRS-59739] 21 p2534 N73-30317
General principles of geological interpretation of remote images of earth surface
21 p2534 N73-30319
Determination of optimal spectral intervals for remote sensing of earth surface from space
21 p2535 N73-30327
Requirements for international laws of remote sensing
[NASA-TT-F-15055] 21 p2535 N73-30330
Proceedings of international conference on remote sensing of environment
[NASA-CR-133784] 21 p2540 N73-30370
Feasibility of using satellite-borne instruments to detect atmospheric pollution
[PB-220394/1] 21 p2541 N73-30372
Glossary of aerial photography and remote sensing in geology and earth science
[PB-220154/9] 21 p2541 N73-30373
Identification of conjugate, or corresponding points in multitemporal imagery for obtaining coefficients of misregistration
[NASA-CR-133640] 21 p2566 N73-30565
Direct determination of electromagnetic reflection properties of smooth brackish water by remote measurement technique
[PB-221372/6TR-48] 22 p2635 N73-31122
Use of spatial information for improving classification accuracy of remotely sensed data
[NASA-CR-133988] 22 p2637 N73-31130
Detection and monitoring of oil pollution from Skylab EREP sensors
[E73-11016] 22 p2661 N73-31320
Research needs in ocean color data analysis
[NASA-TM-X-70466] 22 p2665 N73-31355
Estimating crop acreage from space-simulated multispectral scanner data
[NASA-CR-134029] 22 p2666 N73-31359
Performances and limitations of geological remote sensing from earth resources survey aircraft and satellites
[BMBW-FBW-72-28] 22 p2667 N73-31370
Directory of European activities in remote sensing of earth resources
[ESRO/JPPC-73-20-ADD-1] 22 p2667 N73-31372
Equations for determining ground resolution on surface of earth observed by satellite-borne sensor
[AD-764246] 22 p2668 N73-31375
Thermal infrared imagery of North American Arctic for different seasons
[AD-764239] 22 p2668 N73-31376
Theory and application of active and passive remote sensors in air pollution engineering
22 p2671 N73-31395
Use of Cholesky decomposition technique in feature selection and classification algorithms
[NASA-CR-133990] 22 p2690 N73-31550
Design and performance of remote sensing system for optical sensing of emissions
[PB-221073/0] 22 p2696 N73-31599
Remote sensing methods for earth observation missions by aircraft and satellites
22 p2736 N73-31900
Multispectral ERTS imagery for polar ice mapping
22 p2736 N73-31901
Remote sensing of Arctic Sea ice motion by ERTS instrumentation
22 p2736 N73-31902
Satellite applications for earth and ocean dynamic studies
22 p2736 N73-31909
Geophysical survey of Nevada from Skylab remote sensors
[E73-10998] 23 p2778 N73-32215
Remote sensing geophysics and geology from Skylab EREP
[E73-11072] 23 p2781 N73-32247

Surface water transport in western Lake Superior
23 p2783 N73-32267
Application of remote sensing data to analysis of spring snowmelt floods in Minnesota and surrounding areas
23 p2784 N73-32270
ERTS analysis of geological relationships of Precambrian Greenstone belts and Troctolite series rocks of Minnesota
23 p2784 N73-32271
Models for sensitivity of apparent temperature and backscattering coefficient to variations of soil moisture as function of vegetation
[NASA-CR-135593] 23 p2784 N73-32275
Remote sensor data, particularly photography, applied to geological mapping of Rio Grande rift zone
[NASA-CR-135636] 23 p2785 N73-32279
Remote sensing techniques in Michigan for resource management and environmental protection in both public and private interests
[NASA-CR-135639] 23 p2785 N73-32282
Multispectral scanning systems and potential application to earth resources surveys - bibliography
[ERL/R-249-U] 23 p2787 N73-32299
European program in multispectral scanning systems and application to earth resources surveys
[ERL/R-247-U] 23 p2787 N73-32301
Photochemical ozone theory and microwave spectroscopy using microwave radiometry for remotely verifying mesospheric ozone diurnal variations
[AD-764705] 23 p2789 N73-32314
Accurate and reliable prototype earth horizon sensor head employing logic locator concept
[NASA-CR-132267] 23 p2792 N73-32334
Photoelectric sensor for measurement of spectra and concentration of liquid particles in aerosol
[AD-764927] 23 p2794 N73-32353
Study of terrestrial resources by satellites, and international law
[NASA-TT-F-15094] 23 p2846 N73-32740
Urban transportation planning using satellite-borne remote sensors
[NASA-CR-124433] 23 p2859 N73-32846
Contamination of sensors installed in spacecraft and recommendations for eliminating or correcting
[NASA-TM-X-70487] 24 p2926 N73-33367
Solar radiation effects on upper earth atmosphere
[AD-764599] 24 p2977 N73-33790

**REMOTELY PILOTED VEHICLES**
Design, development, and production of low cost remotely piloted vehicles based on innovative approach for aircraft engineering procedures
[P-4902] 12 p1363 N73-21060
Development and evaluation of display and control equipment for remotely piloted vehicles
[AD-757761] 15 p1736 N73-24077
Application of ground effect machine landing systems for recovery of remotely piloted vehicles
[AD-758789] 15 p1736 N73-24079
Criteria for acceptance of early design information with application to design studies and cost estimates for liquid hydrogen fueled aircraft and remotely piloted vehicles
[NASA-TM-X-62303] 22 p2613 N73-30943
Development and characteristics of air cushion landing system for remotely piloted vehicles
[AD-764774] 23 p2747 N73-31985

**RENAL FUNCTION**
Renal component of antigravitational function in body
07 p0743 N73-16043
Renin-angiotension system in simulated hypervolemia induced by immersion
[NASA-TT-F-14885] 13 p1484 N73-22036

**RENDEZVOUS**
NT LUNAR ORBITAL RENDEZVOUS
NT ORBITAL RENDEZVOUS
NT SPACE RENDEZVOUS
Feasibility of flyby or rendezvous cometary mission
02 p0229 N73-11852
Details and problems of docking technology, mutual aid and rescue for disasters, search and rendezvous means, and cabin atmospheric parameters for Soviet-American flight
[NASA-TT-F-15096] 23 p2844 N73-32726

**RENDEZVOUS GUIDANCE**
Guidance and rendezvous sub-systems of European space tug
[HSD-TP-7227-APP-4] 10 p1217 N73-19896
Preflight analysis on Skylab very high frequency ranging for rendezvous portion
[NASA-CR-133981] 19 p2235 N73-28020

**RENDEZVOUS SPACECRAFT**
Space shuttle rendezvous, radiation and reentry analysis code
[NASA-TM-X-64768] 21 p2595 N73-30795

**RENDEZVOUS TRAJECTORIES**
Optimum rendezvous maneuver of space vehicles on elliptical trajectories for minimum fuel consumption
[NASA-TT-F-14644] 07 p0843 N73-16828
Rendezvous targeting program for space shuttle missions
[NASA-CR-128963] 16 p1965 N73-25898
Apollo experience report on evolution of rendezvous maneuver plan for lunar landing missions
[NASA-TN-D-7388] 20 p2475 N73-29882
Preflight assessment of Skylab VHF ranging coverage for rendezvous portion of SL-1/SL-3 mission
[NASA-CR-133996] 22 p2631 N73-31085

**REPAIRING**
U MAINTENANCE

**REPETITION**
High energy capacitors of six designs for moderate repetition rate
[AD-746991] 02 p0150 N73-11214

**REPLICAS**
Nondestructive replica techniques for studying roadstone surface polishing by electron microscopy
[PB-212720] 13 p1531 N73-22409
Michelson interferometry quality control of Schmidt plate replica by [Jouan Quetin] grating copying technique noting Kerber profile
[OPT-001-72] 23 p2794 N73-32351

**REPORTS**
Evaluation of current US Air Force aircraft engine status reporting system
[AD-750910] 06 p0624 N73-15067
Annotated bibliography of reports, articles, and documents introduced into NASA scientific and technical information system in 1972
[NASA-SP-7500(07)] 15 p1845 N73-24946

**REPRODUCTION**
Effects of real or simulated sonic booms of six pounds per square foot over-pressure on reproduction in farm-raised mink
[FAA-EQ-72-2] 03 p0251 N73-12028

**REPRODUCTION [COPYING]**
Information retrieval system combining magnetic storage and microfilm reader/copier
[CRIF-EL-5] 02 p0147 N73-11188
Prototype of high resolution duplicator for large scale integration circuit masks
[REPT-3424] 16 p1914 N73-25488

**REPRODUCTIVE SYSTEMS**
NT TESTES
Advantages of breeding Rhesus monkeys in compounds for biomedical research
14 p1611 N73-23063

**REPUBLIC AIRCRAFT**
NT F-105 AIRCRAFT

**REPUBLIC MILITARY AIRCRAFT**
U MILITARY AIRCRAFT

**REPUBLIC OF CHINA**
U CHINA

**REPUBLIC OF VIETNAM**
U VIETNAM

**REPULSION**
U FORCE

**REQUIREMENTS**
Contract end item specifications for defining hardware end items required by expendable second stage of space shuttle booster system - Vol. 8 Pt. 1
[NASA-CR-128663] 05 p0599 N73-14874
Preliminary system specification for design, operation, and performance of expendable second stage for reusable space shuttle booster - Vol. 9
[NASA-CR-128664] 05 p0599 N73-14875
Financial requirements of air transportation industry
23 p2861 N73-32861

**RESCUE OPERATIONS**
Executive summary of advanced missions safety study involving space shuttle rescue capability, experiment safety, and emergency crew transfer - Vol. 1
[NASA-CR-129099] 02 p0231 N73-11871
Analysis of space rescue mission capability of Earth Orbit Shuttle and concepts for increasing capability - Vol. 2 Pt. 1
[NASA-CR-129104] 02 p0231 N73-11872
Analysis of emergency crew transfer operations using Earth Orbit Shuttle to determine mission effectiveness and cost requirements - Vol. 2 Pt. 3
[NASA-CR-129102] 02 p0231 N73-11874
Analysis of space shuttle rescue capability based on mission, shuttle configuration and performance, and ground launched ascent and rendezvous time - Vol. 3 Pt. 1
[NASA-CR-129101] 02 p0231 N73-11875
Feasibility study of space rescue, resupply, and reconnaissance with glide-type reentry vehicle
[AD-748346] 04 p0479 N73-13918
Measurements of launch g forces and line tensions in aerial recovery of dummies for long-line loiter personnel retrieval system
[AD-749518] 05 p0497 N73-14045
Helicopter performance in civilian air rescue operations
[AD-748695] 05 p0502 N73-14087
Design development, and evaluation of hoist for H-3 helicopter rescue system
[AD-750289] 06 p0623 N73-15054
Avionics requirements for multimission, fixed wing, twin engine aircraft designed for search and rescue operations
[AD-750463] 06 p0624 N73-15064
Design, development, and evaluation of flywheel powered hoist for personnel rescue missions conducted by helicopters
[AD-751217] 07 p0741 N73-16029
Avionics requirements for HH-53C helicopter engaged in search and rescue operations
[AD-752625] 09 p0986 N73-18047
Evaluation of ground effect machines under various environmental conditions to determine feasibility as rescue vehicles by Coast Guard
[AD-755409] 13 p1475 N73-21947
Module for automatic dock and detumble device for orbital rescue operations
[NASA-CR-131592] 13 p1581 N73-22816
Position reporting and communications systems of aviation and marine rescue operations
[AD-761756] 19 p2228 N73-27967
Analysis of US Navy aviation combat casualty experiences in Southeast Asia to determine effectiveness of rescue and recovery operations under combat conditions
[AD-761636] 19 p2228 N73-27972
Operational investigation of combined all weather capabilities of Coast Guard motor lifeboat and 70 knot surface effect rescue vehicle
[AD-761460] 19 p2229 N73-27974
Global system for search and rescue
[NASA-TM-X-70437] 21 p2537 N73-30339
Details and problems of docking technology, mutual aid and rescue for disasters, search and rendezvous means, and cabin atmospheric parameters for Soviet-American flight
[NASA-TT-F-15096] 23 p2844 N73-32726
Systems analysis of avionics and aircraft equipment for search and rescue helicopters to determine cost effective improvements - Vol. 7
[AD-764914] 24 p2927 N73-33381
Dynamics and control of detumbling disabled spacecraft during rescue operations
[NASA-CR-135788] 24 p2983 N73-33831

**RESEARCH**
NT CRITICAL PATH METHOD
NT DYNAMIC PROGRAMMING
NT GAME THEORY
NT HIGH TEMPERATURE RESEARCH
NT LINEAR PROGRAMMING
NT MARKET RESEARCH
NT NONLINEAR PROGRAMMING
NT NUCLEAR RESEARCH
NT OPERATIONS RESEARCH
NT SADDLE POINTS [GAME THEORY]
Research in solid state physics, materials, and physical chemistry
[AD-746866] 03 p0347 N73-12826
Soviet research in meteorology, geophysics, space, and astronomy
[JPRS-57989] 07 p0843 N73-16829
Solid state physics, materials, and semiconductor research
[AD-752063] 09 p1053 N73-18581
Naval research in aerodynamics, ballistics, mathematics, and physics
[AD-754397] 11 p1268 N73-20292
Chemical and molecular laser research
[AD-754792] 11 p1303 N73-20575
Long term frequency stability, service life, and reproducibility of NASA hydrogen maser in relation to world standards
[NASA-TM-X-66229] 12 p1410 N73-21425
Behavioral and social science advancement in USSR after 50 years
[JPRS-58686] 12 p1467 N73-21883
Solid state physics, physical chemistry, and materials research
[AD-758374] 15 p1821 N73-24764
Research in X ray, solar, and radio astronomy
[AD-756459] 15 p1833 N73-24860
Directory of workers in field of fire research and related activities
[NASA-CR-121149] 15 p1845 N73-24954
Navy research reports on electronics, optical physics, and information systems
[PB-215342/7] 16 p1977 N73-25992
International cooperation in noctilucent cloud research
[NASA-TT-F-14950] 17 p2026 N73-26390
Research on fluid codes and heat transfer in shock tubes
[COO-3086-17] 17 p2068 N73-26733
Astronomical research and instrument development by Professor M. G. Pereira de Barros
17 p2081 N73-26837
Documentation of electrohydrodynamics research
[NASA-CR-133456] 19 p2255 N73-28180
Research on lasers and laser produced plasmas
[UCRL-50021-71-REV-1] 19 p2307 N73-28557
Methods and procedures for ergonomic research
21 p2503 N73-30086
Research on plasma physics, information theory, biophysics, and data processing systems
[AD-765002] 23 p2867 N73-32919

**RESEARCH AIRCRAFT**
NT B-70 AIRCRAFT
NT FD 2 AIRCRAFT
NT H-126 AIRCRAFT

NT U-2 AIRCRAFT
NT X-14 AIRCRAFT
NT X-15 AIRCRAFT
NT X-20 AIRCRAFT
NT X-22 AIRCRAFT
NT X-24 AIRCRAFT
NT XH-51 HELICOPTER
NT XV-5 AIRCRAFT
Analysis and application of load alleviation and mode suppression system for YF-12A aircraft to determine extent of design risks
[NASA-CR-2158] 06 p0620 N73-15033
Feasibility of modifying supersonic drone configuration into remotely controlled research vehicle
[NASA-CR-112323] 15 p1733 N73-24057
**RESEARCH AND DEVELOPMENT**
Radar and microwave equipment and materials, and related research and development
[RRE-11] 01 p0023 N73-10181
Progress in ALSEP program
[NASA-CR-128597] 01 p0057 N73-10464
Research and development of ceramic systems for use as structural components in hypersonic missile applications
[AD-745744] 01 p0071 N73-10580
Soviet research in field of photographic metrology
[NASA-TT-F-13921] 01 p0075 N73-10615
Hearings concerning research and development requirements for future energy needs
01 p0119 N73-10980
Articles concerning European scientific research
[AD-742336] 02 p0245 N73-11993
European scientific research
[AD-743929] 02 p0245 N73-11994
Points of contact for scientific and technical information
[AD-746615] 02 p0246 N73-11997
Effects of gravitational and inertial forces on cardiovascular and respiratory dynamics
[NASA-CR-129603] 03 p0256 N73-12074
Prolonged weightlessness for 300 plus days and cardiac performance in primates
[NASA-CR-129512] 03 p0256 N73-12075
Research in field of time measurements
[CEA-CONF-1980] 03 p0302 N73-12467
Annotated bibliography of research and development of high temperature stable polymeric systems
[NASA-TM-X-2641] 03 p0320 N73-12608
Research in nuclear physics
[AEC-TR-7223/5-6] 03 p0332 N73-12704
Working on advanced heat source converter design designated as multihundred watt program
[MLM-1896(OP)] 03 p0333 N73-12711
Abstracts of Research and Technology Operating Plans used for management review and control of research for NASA programs
[NASA-TM-X-68856] 03 p0366 N73-12978
Measurement of research and development and technological progress impact on national economic growth - Part 1
[NASA-CR-129502] 03 p0366 N73-12980
Abstracts on aeronautical, marine, mechanical, automotive, civil, and industrial engineering
[JPRS-57311] 03 p0366 N73-12986
Research on various theoretical and applied scientific disciplines and technical fields in east Europe
[JPRS-57372] 03 p0367 N73-12989
Papers on research conducted at Riso in nuclear physics
[RISO-256] 03 p0367 N73-12993
Research and development in surface studies, plasma physics, and gas dynamics
[AD-747132] 03 p0368 N73-12996
Research in plasma dynamics, communication and general physics
[AD-747350] 03 p0368 N73-12998
Engineering psychology for developing practical designs of man machine systems
[AD-748237] 04 p0384 N73-13121
Scripps Institute research on oceanographic instruments, stabilized floating platforms, ocean bottom accelerometers, and surface waves
[AD-748024] 04 p0417 N73-13407
Review of Soviet publication on development of hydrology in USSR
04 p0443 N73-13616
Research in physics
[LUNP-7201] 04 p0452 N73-13690
Research in control of infectious diseases weather forecasting, and epidemic of Q fever without pneumonia
[JPRS-57663] 04 p0475 N73-13886
Contributions of military technology, research, and development to civil aviation programs - Vol. 1
[NASA-CR-129572] 04 p0487 N73-13982
Military technology, research, and development contributions to civil aviation programs - Vol. 2
[NASA-CR-129573] 04 p0487 N73-13983
Military technology, research, and development contributions to US aviation advances since 1925 - Exec. Summary
[NASA-CR-129574] 04 p0487 N73-13984
Progress in development of Deep Space Network
[NASA-CR-129831] 05 p0523 N73-14258
Expanded research program in materials sciences
[AD-749068] 05 p0588 N73-14785
Congressional hearings on earthbound potential utilization of solar energy
05 p0592 N73-14812
Research in space physics at University of Iowa
[NASA-CR-129878] 05 p0594 N73-14825
Research and development projects conducted to improve weapon systems and to conduct ionospheric and upper atmosphere experiments in Australia
05 p0611 N73-14965
Research projects conducted by French research facility during 1971 with application to aerospace industry
05 p0611 N73-14966
Research and development projects conducted by National Research Council of Canada from July to September 1972
[DME/NAE-1972[3]] 05 p0611 N73-14967
Research and development in Army aviation medical science and problems
[AD-749456] 06 p0631 N73-15129
Photon-echo generation and behavior
[AD-750155] 06 p0681 N73-15540
Study of optical masers
[AD-750711] 06 p0681 N73-15543
Research and development involved in design and implementation of air traffic control system - Vol. 5
[PB-212182] 06 p0698 N73-15692
Research in analytical methods in nonrelativistic field theory and singular perturbation theory in kinetic theory
[AD-750482] 06 p0702 N73-15721
Research on microinstabilities of finite mirror-confined plasmas
[COO-2168-3] 06 p0704 N73-15747
Cryogenic research and development on slush hydrogen heat transfer and hydrocarbon suspension
[NASA-CR-130362] 06 p0729 N73-15950
Research in inorganic materials
[LBL-425] 06 p0732 N73-15970
European research and development programs
[AD-750267] 06 p0732 N73-15972
Research activities of Battelle Institute
07 p0856 N73-16942
Aeronautical research for 1971-1972
07 p0856 N73-16943
Atomic energy and space research in India for 1971 and 1972
[NP-19407] 07 p0860 N73-16974
Brief articles concerning recent developments in European Scientific Research
[AD-751630] 07 p0860 N73-16980
Role of free-flight models in aircraft research and development
08 p0865 N73-17002
Research progress in functional network theory and microcircuit systems
[AD-752243] 08 p0891 N73-17217
Research and development in topographic mapping
[NASA-CR-130540] 08 p0918 N73-17527
CMB-13 research on carbon and graphite
[NASA-CR-130539] 08 p0935 N73-17652
Research in plasma physics, communication and data processing
[AD-751213] 08 p0944 N73-17729
Research in superconductors
[AD-751855] 08 p0952 N73-17796
Solid state research at Lincoln Laboratory
[AD-752556] 08 p0952 N73-17798
Research in radio astronomy using Haystack antenna
[NASA-CR-130673] 08 p0960 N73-17852
Abstracts and bibliographic lists on major research projects completed in September, 1972
[AD-751956] 08 p0977 N73-17996
Bibliography of armed forces research and development bibliographies - Vol. 1
[AD-752150] 08 p0978 N73-17997
Annotated bibliography of military research and development bibliographies - Vol. 2
[AD-752160] 08 p0978 N73-17998
Economic factors affecting titanium powder metallurgy research and development
09 p1047 N73-18539
Developments in air pollution research program
09 p1060 N73-18650
Annual report for 1971 of university institute in field of nuclear, elementary particle, and solid state physics
[BMBW-FBK-72-21] 09 p1069 N73-18720
University program accomplishments in materials science and engineering research
[AD-753845] 09 p1077 N73-18789
General trends in guided missile development since World War 2
[AD-753510] 09 p1092 N73-18912
Distribution of federal funds for research and development
[NSF-72-317-VOL-21] 09 p1100 N73-18980
Research and development in theoretical and applied sciences in Eastern Europe
[JPRS-58121] 09 p1101 N73-18982
Graphs, tables, and analysis of Federal R and D funding by budget function and by primary purpose
[NSF-72-313] 09 p1101 N73-18987
Research activities supported by National Science Foundation
[NSF-73-1] 09 p1101 N73-18988
Urgent problems connected with contemporary scientific and technological revolution
[AD-751509] 09 p1102 N73-18992
Physiological research in support of manned space flight
[NASA-CR-128741] 10 p1120 N73-19129
Research and development in Fast Reactor Program
[EURFNR-1034] 10 p1187 N73-19656
Research in theoretical physics
[PUBL-100] 10 p1187 N73-19662
Study program for Geodetic Satellite applications
[NASA-CR-130180] 10 p1214 N73-19868
Quarterly report of JPL research and development
[NASA-CR-131152] 10 p1227 N73-19975
Research in protecting equipment from tropical environment and seas
10 p1228 N73-19986
Present international status of research and development of electrochemistry and fuel cells
[AD-755106] 11 p1238 N73-20048
Air force radio communication and navigation system development planning
[AD-754930] 11 p1258 N73-20207
Research and development of transpiration cooled inflatable nozzle extension
[NASA-CR-124165] 11 p1269 N73-20300
Congressional assessment of governmental role in industrial and social aspects of aerospace and related technology
11 p1292 N73-20482
Research in high energy laser technology
[AD-754410] 11 p1303 N73-20573
Research and development with glassy carbon
[AD-755146] 11 p1310 N73-20629
Atomic science and engineering developments in USSR
[AD-754040] 11 p1327 N73-20766
High pressure plasma research
[AD-754020] 11 p1328 N73-20776
Energy requirements of Department of Defense and identification of research and development activities
[AD-754824] 11 p1333 N73-20819
Statistical analysis on expense increase funding for technological systems
11 p1351 N73-20963
Management of development and research costs for advancement of technology in aerospace systems
11 p1351 N73-20964
Congressional hearings on research and development of environmentally safe electric power production
11 p1352 N73-20976
Articles concerning research and development in scientific disciplines and technological fields, and research management
[JPRS-58615] 11 p1352 N73-20978
Articles on European scientific research
[AD-754406] 11 p1353 N73-20985
Guide to literature of engineering, mathematics and physical science
[AD-754382] 11 p1353 N73-20989
Cybernetic integration of experiments into CVT system
[NASA-CR-124150] 12 p1373 N73-21136
Annual report of German aerospace research institute, 1972
12 p1388 N73-21259
Thermoelectric outer planets spacecraft advanced systems technology project
[NASA-CR-131451] 12 p1426 N73-21561
Infrared spectrometer for use with ground based telescope
[NASA-CR-131512] 12 p1448 N73-21726
Annual AGARD meeting in Brussels, Belgium
12 p1466 N73-21881
Scientific conferences held in east Europe
[JPRS-58769] 12 p1467 N73-21886
Proceedings of conference on research and development projects conducted by US Air Force Research and Development Command
[AD-753071] 12 p1467 N73-21890
Soviet research and development of solar batteries and power cells for spacecraft
[AD-756039] 13 p1478 N73-21973
Progress in deep space network - Jan. and Feb. 1973
[NASA-CR-131493] 13 p1490 N73-22081
Research and development of infrared photocathodes
[AD-756239] 13 p1501 N73-22162
FAA research and development in airport paving criteria
13 p1506 N73-22205
Research on carbon, graphite, and phenolic resin binders
[NASA-CR-131483] 13 p1547 N73-22539
Numerical weather prediction activities of NMC
13 p1553 N73-22582
Research activities of ESO
13 p1576 N73-22773
Research and developments in technology utilization program
[NASA-CR-131568] 13 p1593 N73-22914
Congressional study of future governmental role in scientific and technological research and development
13 p1594 N73-22927

Congressional study on historical background of energy research and development
13 p1594 N73-22928
Research and development progress in telecommunications and electronics engineering
[REPT-73-00567] 14 p1619 N73-23111
Research and development with gas lasers
[AD-758405] 14 p1674 N73-23587
Technical problems and accomplishments during reporting period
[AD-757637] 14 p1696 N73-23762
Research and development conducted at Spanish universities on solid state and low temperature physics
[AD-757991] 14 p1700 N73-23795
Astronomical studies at Hale Observatories
14 p1704 N73-23828
Factors for determining army requirements for research
14 p1723 N73-23982
Development technology for communication systems
[JPRS-59221] 15 p1750 N73-24184
Research and development progress on solid state microwave oscillator and amplifier
[AD-758244] 15 p1757 N73-24241
Bibliography of Soviet research and development of lasers
[AD-758259] 15 p1795 N73-24552
Effect of scientific and technical progress on economic control parameters in USSR
[JPRS-58976] 15 p1845 N73-24952
Scope of Federal funding for scientific research and development
[NSF-72-317] 15 p1846 N73-24958
Price trends affecting research and development at academic institutions
[NSF-72-310] 15 p1846 N73-24959
Summary of national patterns of R and D funding and manpower allocations
[NSF-73-303] 15 p1846 N73-24960
Industrial policy of ESRO noting distribution of contracts, relations with industry, multinational consortiums, and technological research
15 p1848 N73-24975
Research and development in analytical chemistry
[AD-758805] 16 p1871 N73-25150
Bibliography of JPL reports for 1972
[NASA-CR-132994] 16 p1976 N73-25983
Abstracts and bibliographic lists of Soviet technical literature on research and development
[AD-758784] 16 p1977 N73-25995
Research and development on microwave oscillators, diode structures, and ion implantation and diffusion
[AD-759542] 17 p1998 N73-26161
Research activities in physics
[COO-535-674] 17 p2010 N73-26259
Research and development in coastal engineering
[AD-759283] 17 p2028 N73-26413
Theoretical and experimental investigations of superconductivity, and amorphous semiconductors, superconductivity and magnetism
[NASA-CR-133234] 17 p2072 N73-26767
Research and development in Project SQUID
[AD-759977] 17 p2078 N73-26809
Research and development at Belgium nuclear center
[BLG-467] 17 p2099 N73-26979
Research and development on chemical and molecular lasers
[AD-760701] 18 p2158 N73-27438
Potential applications of high pressure technology
[AD-760714] 18 p2191 N73-27686
Soviet-bloc research in geophysics, astronomy, and space research
[JPRS-59390] 18 p2196 N73-27733
Research conducted in School of Electrical Engineering at Purdue University during 1972
18 p2213 N73-27871
Research and development of thin cathode ray display tubes
[AD-762115] 19 p2246 N73-28108
Research and development of electronic equipment for night combat surveillance
[AD-762351] 19 p2302 N73-28507
Research activities for DREV during 1972
[DREV-692/73] 19 p2307 N73-28553
Research and development program plan for air traffic control technology involving data display and data entry
[FAA-ED-16-1] 19 p2318 N73-28647
Cooling histories of lunar rocks
[NASA-CR-133333] 19 p2343 N73-28851
Air Force research and technology accomplishments during calendar year 1971
[AD-762269] 19 p2357 N73-28967
Development and progress in theoretical and scientific disciplines
[JPRS-59769] 20 p2487 N73-29981
Articles concerning development and progress in theoretical and applied sciences of leading East European scientific organizations
[JPRS-59756] 20 p2488 N73-29982
Theoretical and developmental work on high efficiency avalanche diode sources and amplifiers
[FAA-RD-73-93] 21 p2517 N73-30186
Research and development of electronic equipment and techniques
[AD-763729] 21 p2520 N73-30210
Reserach and development in metallurgical thermodynamics
[TT-71-56066] 21 p2561 N73-30528
Abstracts on research projects inclusive of flight dynamics to heating of swimming pools using solar collector
[ISBN-0-85494-200-9] 21 p2609 N73-30910
Planned 1973 AGARD meetings, and list of 1972 AGARD publications
[AGARD-BUL-73-1] 21 p2610 N73-30919
Research and development progress in solid state physics, chemistry, electronics, and materials science
[AD-763501] 21 p2610 N73-30924
Abstracts of research projects on adaptive telemetry systems
[NASA-CR-130228] 22 p2631 N73-31088
Research and development in topographic mapping, field surveys, photogrammetry, orthophotomapping, and space technology
[PB-221469] 22 p2669 N73-31384
Summaries of materials research projects
[AD-764819] 23 p2828 N73-32601
Development of US commercial air transport industry
23 p2860 N73-32849
Articles concerning development of scientific disciplines and technical fields in Eastern Europe
[JPRS-60063] 23 p2865 N73-32904
Advances in technology and armament in USSR
[AD-763323] 23 p2866 N73-32917
Research and development in solid state lasers, gas lasers, component development, diognostics, design analysis, advanced concepts, laser plasmas and laser fusion
[UCRL-50021-72-2] 24 p2931 N73-33408

**RESEARCH FACILITIES**

Research facilities, and educational and research programs of Institute of Industrial Science, University of Tokyo
01 p0035 N73-10277
Laboratory facility for regional air pollution study at St. Louis, Missouri
[PB-210019] 01 p0077 N73-10638
Descriptions of Federal Government environmental research and development facilities
[PB-209751] 02 p0153 N73-11239
Inventory listing of Federal Government environmental research facilities
[PB-209752] 02 p0153 N73-11240
Employee communication at NASA Langley Research Center
[NASA-TM-X-68854] 02 p0244 N73-11985
Experimental facilities for nuclear particle physics research at proton energy level of 300 GeV
[CERN-1050] 04 p0402 N73-13274
Compilation of technical reports prepared by Aerospace Laboratories of US Air Force for calendar year 1971
[AD-746707] 04 p0487 N73-13974
Organization and functions of research facility for conducting projects involving low temperature effects
04 p0487 N73-13976
Development of facility for determining satellite payloads
05 p0523 N73-14257
History, organization, and functions of the National Bureau of Standards to include description of test equipment used for research projects
[NBS-SP-367] 05 p0524 N73-14259
Design and operation of 5 MeV Van de Graaff ion accelerator at Central Research Institute for Physics in Budapest, Hungary
[KFKI-71-47] 05 p0524 N73-14260
Origins and history of Los Alamos meson physics facility
[LA-5000] 05 p0524 N73-14261
Research and development projects conducted to improve weapon systems and to conduct ionospheric and upper atmosphere experiments in Australia
05 p0611 N73-14965
Research projects conducted by French research facility during 1971 with application to aerospace industry
05 p0611 N73-14966
Research and development projects conducted by National Research Council of Canada from July to September 1972
[DME/NAE-1972[3]] 05 p0611 N73-14967
Simulator research at Netherlands National Aerospace Laboratory
[AD-750589] 06 p0650 N73-15283
Analysis of political, institutional, and economic factors to determine feasibility of conducting earth resources surveys in developing nations
07 p0783 N73-16362
Administration, structure, personnel, and research plans of East European scientific organizations and institutions
[JPRS-57952] 07 p0857 N73-16946
Feasibility of effective exercise and health evaluation and enhancement program for NASA employees
08 p0875 N73-17091
Operating principles of force measuring and generating equipment in NBS research facilities
[NBS-SP-370] 09 p1010 N73-18243
Programmatics of space shuttle supported research facilities for telecommunication and navigation - Vol. 4
[NASA-CR-124139] 10 p1137 N73-19268
Microbiological inspections of NASA food handling facilities
[NASA-TM-X-64734] 11 p1247 N73-20127
Description of turbopropulsion laboratory in aeronautics department at Naval Postgraduate School
[AD-754380] 11 p1268 N73-20287
Research activities of electronic laboratory in development of inertial navigation systems to include applications for space missions and commercial aviation
11 p1316 N73-20686
Disposal of liquid and solid radioactive wastes at Trisaia Nuclear Research Center
[NASA-TT-F-14697] 11 p1323 N73-20734
History and organization of German Society for Aerospace Research
11 p1351 N73-20961
Organization and management of aerospace research institute
11 p1351 N73-20962
Management models for large research institute considering aerospace sciences
11 p1351 N73-20968
Annual report of German aerospace research institute, 1972
12 p1388 N73-21259
Role of USSR scientific centers in economic development
[JPRS-58683] 12 p1467 N73-21887
Problems of library and information services to large research center
15 p1753 N73-24204
Description and operating experience of experimental MHD facility
[JUL-883-TP-VOL-10] 17 p2068 N73-26734
Ion heating and thermonuclear power production characteristics and performance of superconducting bumpy-torus magnetic facility
[NASA-TN-D-7353] 19 p2324 N73-28693
Mission definition and analysis for manned earth observatory based on projected technology for 1980 time period - Vol. 2
[NASA-CR-124340] 19 p2343 N73-28847
Conceptual design of earth observation facility to include sensor payload, crew functions and accomodations, and common core equipment - Vol. 3
[NASA-CR-124338] 19 p2343 N73-28848
Schedules, costs, requirements, and equipment for manned earth observatory missions - Vol 4
[NASA-CR-124339] 19 p2343 N73-28849
Technology planning objectives and supporting technical goals for Air Force Flight Dynamics Laboratory during Fiscal Year 1974
[AD-762300] 19 p2356 N73-28950
Cost analysis of large research institutes in Germany
[DLR-FB-73-64] 24 p2995 N73-33931

**RESEARCH MANAGEMENT**

Research plan for regional air pollution study
[PB-210018] 01 p0077 N73-10637
Abstracts of Research and Technology Operating Plans used for management review and control of research for NASA programs
[NASA-TM-X-68856] 03 p0366 N73-12978
Scientific and technical research projects in Poland
[JPRS-57570] 04 p0488 N73-13988
Scientific and technical research projects in Czechoslovakia and Hungary
[JPRS-57583] 04 p0488 N73-13989
Research management of eastern Europe scientific affairs
[JPRS-57765] 05 p0595 N73-14838
Core subfields of physics
[NASA-CR-130361] 06 p0700 N73-15706
Ice problems in Canada, estimates of economic significance of problems, and order of priorities of research programs and management
[REPT-17] 07 p0788 N73-16412
Overview of scientific and technological research in Yugoslavia on NBS grants, 1971 - 1972
[NBS-TN-753] 08 p0976 N73-17979
Research activities supported by National Science Foundation
[NSF-73-1] 09 p1101 N73-18988
Management and organization in aerospace science and technology research
11 p1350 N73-20955
History and organization of German Society for Aerospace Research
11 p1351 N73-20961
Organization and management of aerospace research institute
11 p1351 N73-20962
Management of development and research costs for advancement of technology in aerospace systems
11 p1351 N73-20964

Research management for technical applications
11 p1351 N73-20967
Articles concerning research and development in scientific disciplines and technological fields, and research management
[JPRS-58615] 11 p1352 N73-20978
Analysis of NASA programs during post-Apollo period to show organization of field centers, planning activities, operational activities, and resources utilization
[NASA-CR-131931] 12 p1466 N73-21879
Techniques of technology assessment in federal agencies
[NASA-CR-131848] 13 p1596 N73-22940
Mission and responsibilities of federal agencies in technology assessment
[NASA-CR-131847] 13 p1596 N73-22941
Observations of various organizations and individuals on certain aspects of federal support of problem oriented research
[B-133183] 14 p1721 N73-23964
Conference on human performance under sustained work, and interdisciplinary research
[AD-744782] 14 p1723 N73-23981
Aspects of interdisciplinary research in graduate programs
14 p1723 N73-23984
Research strategy and precise definition of continuous operations
14 p1724 N73-23991
Motivation, planning, and management of research and development programs using controlled thermonuclear fusion as examples
15 p1846 N73-24964
Research management of East European scientific affairs
[JPRS-59273] 18 p2213 N73-27865
Survey of characteristics and attitudes of immigrant scientists and engineers in US
19 p2354 N73-28938
Articles on methodology and historical importance of scientific research in creativity
[TT-70-57147-2] 21 p2502 N73-30075
Research in development and utilization of atmospheric water resources in Montana
[PB-222004/4] 22 p2695 N73-31591
Airborne research management and shuttle sortie planning
[NASA-TM-X-62287] 22 p2715 N73-31729
Methodology of planning experiments under nonuniform conditions
24 p2944 N73-33513
Deficiencies in development of hydrometeorological science
24 p2947 N73-33536
Automation of processes of gathering and primary processing of scientific information on expeditions of Arctic and Antarctic Scientific Research Institute
24 p2947 N73-33537
Congressional hearings on Federal policy, plans, and organization for support and utilization of science and technology
24 p2994 N73-33924

**RESEARCH PROJECTS**

Research report on tidal hydraulics
[AD-744784] 01 p0051 N73-10412
Analysis of laser applications in medicine, biology, research, chemical processing, initiation of thermonuclear reactions, and weapon systems
[AD-743098] 01 p0066 N73-10541
MSFC/Auburn/Alabama 1972 summer faculty fellowship research program report
[NASA-CR-61395] 01 p0120 N73-10992
History of Radcliffe Observatory and its scientific research activities and personnel
02 p0152 N73-11231
Descriptions of Federal Government environmental research and development facilities
[PB-209751] 02 p0153 N73-11239
Research and development of fluidics systems and applications to industrial processes
[NASA-SP-5112] 02 p0155 N73-11260
Research activities in nuclear physics, solid state detectors and theoretical physics
[AECL-4257] 02 p0213 N73-11726
Astronomical, mathematical, and neuropathological research projects in Hungary, and scientific development policy in Poland
[JPRS-57271] 02 p0244 N73-11986
Scientific research projects in Europe relative to aerospace technology, biology, computer development, physical sciences, and microwaves
[AD-746879] 02 p0246 N73-11996
Abstracts of DNA-sponsored reaction rate research programs for FY 72
[AD-747660] 03 p0299 N73-12441
USSR research projects in geosphysics, astronomy, and space - No. 288
[JPRS-57505] 03 p0357 N73-12906
Developments in laser technology to include chemical lasers, electric discharge lasers, high power glass lasers, and laser techniques
[AD-748178] 04 p0429 N73-13498
Abstracts and bibliographies on research in laser technology, effects of explosions, geosciences, and particle beams
[AD-749488] 04 p0430 N73-13504
Nuclear research projects with fast electron accelerator and theoretical physics of neutron decay reactions
04 p0452 N73-13687
Compilation of technical reports prepared by Aerospace Laboratories of US Air Force for calendar year 1971
[AD-746707] 04 p0487 N73-13974
Aerospace sciences and flight mechanics research projects
04 p0487 N73-13975
Congressional hearings to establish government supported projects for fire research and safety
04 p0487 N73-13981
Scientific and technical research projects in Poland
[JPRS-57570] 04 p0488 N73-13988
Scientific and technical research projects in Czechoslovakia and Hungary
[JPRS-57583] 04 p0488 N73-13989
Analysis of factors involved in transfer of technology from Department of Defense developments to solution of problems in civilian community
[B-175132] 04 p0488 N73-13994
Collection of European scientific research reports
[AD-747959] 04 p0488 N73-13996
Identification of human factors research projects in support of civil aviation for accomplishment by NASA research centers
05 p0493 N73-14015
Chemistry research program for Air Force
[AD-749544] 05 p0507 N73-14124
Proceedings of conference on automation of scientific research through use of computers
[JPRS-57826] 05 p0516 N73-14199
History, organization, and functions of the National Bureau of Standards to include description of test equipment used for research projects
[NBS-SP-367] 05 p0524 N73-14259
Development and characteristics of tracked air cushion research vehicle for commercial high speed ground transportation
[PB-211216] 05 p0524 N73-14267
Research projects in flow mechanics and gas dynamics
05 p0526 N73-14278
Publications of carbon and graphite research results
[NYO-1710-106] 05 p0565 N73-14590
Interdisciplinary research on materials science
[AD-749383] 05 p0612 N73-14974
Research on laser irradiation effects, sensory psychophysiology, and human blood processing for military medicine
[AD-749440] 06 p0631 N73-15130
Research projects to determine aerodynamic characteristics of rotary wings and propellers
[AD-750175] 06 p0656 N73-15326
International research on aerospace instrumentation systems
[AD-750653] 06 p0675 N73-15493
Research and development involved in design and implementation of air traffic control system - Vol. 5
[PB-212182] 06 p0698 N73-15692
Annotated bibliography on nuclear energy research in Philippines
[PAEC[A]-7116-SUPPL-4] 06 p0699 N73-15698
Research and development projects compiled at Army science conference
[AD-750300] 06 p0732 N73-15973
Operational problems and scientific research activities at cyclotron
[AD-751539] 07 p0767 N73-16230
Organization, planning, and development of remote sensor programs for Canada
07 p0784 N73-16371
Identification of organizations and activities concerning French programs in aerial photography and earth resources technology
07 p0784 N73-16372
Research projects in plasma physics
[NP-19414] 07 p0828 N73-16710
Guide to National Science Foundation programs and grants - information for proposals
[NSF-72-23] 07 p0857 N73-16945
Administration, structure, personnel, and research plans of East European scientific organizations and institutions
[JPRS-57952] 07 p0857 N73-16946
Nuclear chemistry and geochemistry research projects including isotope separations, meteorite and tektite compositions, and solid gamma spectrometer development
[COO-3236-3] 08 p0884 N73-17156
Scientific reports on adaptive control system theory for aerospace engineering
[AD-751941] 08 p0887 N73-17187
Radio astronomy and radar observation program for Haystack antenna
[NASA-CR-130756] 08 p0959 N73-17842
Stellar, planetary, and comet observations at astronomical observatory during 1973
08 p0960 N73-17850
Armed Forces science conference report with list of principle authors
[AD-750326] 08 p0977 N73-17992
Armed Forces science conference report with list of principle authors
[AD-750360] 08 p0977 N73-17993
Physical and chemical energy sources for earth, sea, and space
[AD-753828] 09 p0992 N73-18093
Review of papers presented at Conference on Space Biology and Aerospace Medicine
[JPRS-58345] 09 p0995 N73-18125
Research projects in radio and electronic engineering
[AD-752845] 09 p1008 N73-18228
Survey of electronic research projects
[AD-753700] 09 p1010 N73-18240
Guide to research in air pollution for 1972
[AP-47] 09 p1060 N73-18649
Research on amorphous semiconductor materials
[AD-752798] 09 p1074 N73-18761
Research activities in solid state physics
[AD-753255] 09 p1075 N73-18770
Conference on Air Force science and engineering research
[AD-753072] 09 p1101 N73-18991
Air Force research and development programs in aircraft electrical power systems to show planning process for developing specific classes of technology
10 p1111 N73-19052
Theoretical research on plasma instabilities
[AD-754019] 10 p1198 N73-19747
Plasma interactions with gas flow and magnetic fields
[AD-754018] 10 p1198 N73-19748
Grants and awards for scientific research
[NSF-73-2] 10 p1229 N73-19987
Organization and research projects for 1971
10 p1229 N73-19988
Research and development projects of Federal Aviation Administration to provide improved weather data acquisition and distribution
[FAA-ED-15-1] 11 p1314 N73-20662
Research activities of electronic laboratory in development of inertial navigation systems to include applications for space missions and commercial aviation
11 p1316 N73-20686
Research and development projects conducted by Federal Aviation Administration to improve air traffic control and flight safety
[FAA-EM-73-2] 11 p1321 N73-20720
Research projects in metals and ceramics
[ORNL-4820] 11 p1330 N73-20796
German cooperation with AGARD research in aerospace sciences
11 p1350 N73-20958
German cooperation in international aeronautical research
11 p1351 N73-20959
Organization, management, and research activities at National Institute for Aerospace Research of the Netherlands
11 p1351 N73-20960
Tabulation of research reports published in German technical document series during calendar year 1972
[DLR-MITT-73-01] 11 p1352 N73-20971
Review of Naval research activities
[PB-212475] 11 p1354 N73-20993
Environmental quality program, environmental forecasting program, and seabed assessment program for international decade of ocean exploration
12 p1400 N73-21359
Analysis of transition region of subsonic turbulent jets to determine noise producing potential based on far field acoustic density
[NASA-TN-D-7242] 12 p1428 N73-21573
Research projects in atomic and molecular spectroscopy
[NASA-CR-131829] 13 p1495 N73-22119
Research projects in geophysics, astronomy, and satellite applications
[JPRS-58885] 13 p1577 N73-22776
Analysis of NASA programs for 1970 to 1980 period with application to earth orbital experiment program and requirements - Vol. 1
[NASA-CR-112325] 13 p1577 N73-22778
Analysis of space biology projects related to earth orbital experiment program to identify critical issues and methods of conducting experiments - Vol. 3
[NASA-CR-112327] 13 p1577 N73-22780
Development of space astronomy projects identified during orbital experiment program and requirements study - Vol. 4
[NASA-CR-112328] 13 p1577 N73-22781
Development of space communications and navigation projects involved in earth orbital experimest program and requirements study - Vol. 5
[NASA-CR-112329] 13 p1577 N73-22782
Definition of supporting technology development requirements for earth orbital experiment program and requirements study - Vol. 7
[NASA-CR-112331] 13 p1577 N73-22784

Data management systems, instrumentation concepts, and biotechnology laboratory for earth orbital experiment program and requirements study - Vol. 8
[NASA-CR-112332] 13 p1577 N73-22785
Proceedings of conference on materials and structures to include materials research, fracture control, and aerospace vehicle dynamics and control
[NASA-TM-X-69227] 13 p1585 N73-22850
Research projects conducted as part of NASA programs during period May 1970 through May 1972
[NASA-TM-X-64723] 13 p1593 N73-22915
Process of planning, programming, and evaluating technological projects within federal agencies
[NASA-CR-131846] 13 p1596 N73-22939
Preliminary design of V/STOL tilting rotor aircraft for performance of research flights - Vol. 2
[NASA-CR-114438] 14 p1599 N73-22965
Research activities in exobiology and aerospace medicine
[JPRS-59015] 14 p1607 N73-23024
Research on semiconductor and solid state physics
[AD-757521] 14 p1697 N73-23771
Research projects involving aerodynamics, aerodynamic heating, aerodynamic forces, airframes, structural analysis, and fluid mechanics - Vol. 1
15 p1725 N73-23995
Research projects involving boundary layer flow, heat transfer during aerodynamic heating, atmospheric turbulence effects, and airframe structural analysis - Vol. 2
15 p1727 N73-24011
Cryobiological and space biological studies
[JPRS-59129] 15 p1742 N73-24120
Conference on materials research
[AD-758571] 15 p1802 N73-24609
Research activities in plasma physics at Nagoya University
15 p1816 N73-24724
List of NASA inventions available for licensing in foreign countries
[NASA-SP-7038[01]] 15 p1845 N73-24947
Research activities at University of Toronto for 1972
15 p1845 N73-24949
Integration of projects and contracts into program of research and development center
15 p1847 N73-24965
Research projects in theoretical and practical aerodynamics - Vol. 1
16 p1851 N73-24999
Research projects in solid state chemistry and materials science
[AECL-4351] 16 p1871 N73-25145
Supporting research plan for Apollo 17 ultraviolet spectrometer experiment
[NASA-CR-128547] 16 p1916 N73-25507
Aerospace research projects
16 p1976 N73-25980
French-Soviet cooperation in space research
[AD-759106] 16 p1978 N73-25996
Progress report, abstracts, and principle results of research project to develop computer software
[NASA-CR-130209] 17 p2001 N73-26180
Review of research in electromagnetic radiation
[AD-759990] 17 p2008 N73-26235
USSR research projects in geophysics, astronomy, and aerospace subjects - May 1973
[JPRS-59136] 17 p2024 N73-26379
Research projects conducted by organizations of National Research Council of Canada on structural analysis, jet fuels, air pollution, and very low frequency navigation
[DME/NAE-1973[1]] 17 p2098 N73-26970
Proceedings of conference on military applications of V/STOL aircraft to include current and proposed research projects to meet military requirements
[AGARD-CP-126-VOL-1] 18 p2102 N73-27000
Lists on research activities in medium energy nuclear physics
[NASA-CR-132280] 18 p2181 N73-27612
Research on solid state devices and microelectronics
[AD-760815] 18 p2190 N73-27683
USSR research in meteorology, oceanography, astronautics, astronomy, and geophysics
[JPRS-59278] 18 p2196 N73-27727
Soviet-bloc research in geophysics, astronomy, and space
[JPRS-59490] 18 p2196 N73-27730
Astronomical and astrophysical research reports
[PB-219589/9] 18 p2198 N73-27747
Plasma physics theoretical research
[COO-3577-4] 19 p2324 N73-28698
Research on solar high energy physics - conference summary
19 p2340 N73-28822
ONERA activities for 1972
19 p2354 N73-28933
Analysis of Tenth Soviet Antarctic Expedition to show preparations, logistic support, and operational accomplishments
20 p2406 N73-29340
Objectives, scope of work, and funding requirements of research project for improvement of aircraft safety
[FAA-ED-18-1] 21 p2493 N73-30008
National Environmental Research Center research projects for FY 73 on air pollution and control equipment
[PB-220259/6] 21 p2574 N73-30630
Eastern Europe research projects involving hydrometeorology, semiconductor materials, microelectronics, and piezoelectronics
[JPRS-59617] 21 p2607 N73-30893
Research projects involving development and application of semiconductor materials and process for measuring properties of semiconductors at high pressures
21 p2607 N73-30894
Identification of Polish institutes involved in electron tube development and recommendations for changes in research projects
21 p2608 N73-30899
Polish research projects involving development and application of magnetically soft ferrite materials
21 p2608 N73-30902
Congressional hearings to review NASA program accomplishments and to predict advantages to accrue from space programs
21 p2609 N73-30916
Studies in hypoxia and phylogenetics by USSR aerospace medical scientist
[NASA-TT-F-15101] 22 p2619 N73-30991
Summary of research projects in Earth Resources Data Analysis Program
[NASA-CR-133982] 22 p2664 N73-31348
Summary of biochemistry and biology research projects
[NASA-CR-135650] 22 p2667 N73-31366
Research in heavy ion scattering reactions
[CONF-720669] 22 p2702 N73-31641
Scientific research in geophysics, astronomy, meteorology, oceanography, astronautics from soviet-block
[JPRS-59935] 22 p2716 N73-31738
Research in solid state semiconductor physics
[PB-220703/3] 22 p2738 N73-31923
Computer science and technology research programs
[AD-764659] 23 p2762 N73-32101
Scientific research projects in engineering, chemistry, and social sciences
23 p2859 N73-32844
Research project to determine factors involved in expansion of air freight traffic and prospects for future expansion
23 p2863 N73-32884
USSR research in solid state physics, laser technology, geosciences, and materials
[AD-763742] 23 p2866 N73-32916
USSR research in solid state physics, plasma physics, atmospheric physics, and seismology
[AD-763743] 23 p2866 N73-32918
Characteristics and performance of piloted simulator for application as research tool in design and development of experimental aircraft
24 p2874 N73-32955
Application of skill requirement method for determining skills required of on-orbit crew personnel performing earth-orbital research
[NASA-CR-124452] 24 p2982 N73-33830
Cumulative bibliography of research and development projects conducted on heat pipe technology and applications
[NASA-CR-135953] 24 p2991 N73-33900
Bibliography of research projects on heat pipe, development, performance, and application - January through March, 1972
[NASA-CR-135956] 24 p2991 N73-33901
Bibliography of heat pipe research and development projects conducted during April through June 1972
[NASA-CR-135955] 24 p2991 N73-33902
Bibliography of heat pipe research and development projects conducted during July through September, 1972
[NASA-CR-135952] 24 p2991 N73-33903
Supplemental report and bibliographies of heat pipe research projects conducted during calendar year 1971
[NASA-CR-135951] 24 p2991 N73-33904
**RESEARCH TORPEDO CONFIGURATIONS**
U TORPEDOES
**RESEARCH VEHICLES**
Development of simulator for training personnel in underwater terrain navigation and reconnaissance
[AD-754091] 11 p1322 N73-20729
**RESERVOIRS**
Environmental and ecological impact of construction and operation of dam and impoundment on Sangamon River in Illinois
[E72-10216] 02 p0162 N73-11310
Effect of dam construction and staged filling of reservoirs in Illinois on environment and ecology
[E72-10217] 02 p0162 N73-11311
Environmental and ecological impact of construction and staged filling of reservoirs in Illinois
[E72-10309] 04 p0412 N73-13358
Reservoir and watershed management utilizing ERTS-1 imagery
[E73-10055] 07 p0778 N73-16317
Environmental and ecological impact of construction and filling of reservoir on Sangamon River in Illinois
[E73-10082] 08 p0901 N73-17294
Reservoir management and operation using ERTS-1 imagery
[E73-10308] 09 p1022 N73-18340
Ross Barnett Reservoir remote sensing project to determine water sediment, investigate erosion, and improve land use
[NASA-CR-130960] 09 p1029 N73-18396
Environmental and ecological impact of construction and operation of Oakley Dam and Friends Creek impoundment located on Sangamon River in East Central Illinois
[E73-10484] 12 p1396 N73-21321
Rapid vaporization of liquid hydrogen in noninsulated reservoir placed in water
[CEA-CONF-2082] 12 p1429 N73-21582
Reservoir and water management in Maine using ERTS-1 data collection platforms and imagery
[E73-10585] 14 p1657 N73-23445
Inventory of ponds, lakes, and reservoirs in selected areas of State of Massachusetts
[PB-214116/6] 14 p1665 N73-23512
Environmental and ecological impact of construction and operation of Oakley Dam and Friends Creek impoundment located on Sangamon River in East Central Illinois
[E73-10655] 16 p1898 N73-25351
Analysis of water turbidity in two federal reservoirs in Kansas using ERTS-1 multispectral band scanners
[PAPER-E12] 19 p2270 N73-28276
Environmental and ecological impact of construction and operation of Oakley Dam and Friends Creek Impoundment located on Sangamon River in East central Illinois
[E73-10882] 20 p2394 N73-29233
Environmental and ecological impact of major construction of reservoirs in Illinois
[E73-10892] 20 p2395 N73-29241
Analysis of albedo of reservoirs from observations of total and reflected radiation measured near floating island stations
20 p2402 N73-29301
Detection and monitoring of water quality parameters in reservoirs and lakes in Kansas from Skylab imagery
[E73-10938] 21 p2529 N73-30280
Detection and monitoring water quality in Kansas reservoirs from Skylab data
[E73-10939] 21 p2529 N73-30281
Investigation of New England reservoirs, land use, streams, flooding, and vegetation from Skylab imagery
[E73-10993] 22 p2659 N73-31299
General geology and potential geologic problems of proposed Deer Creek Reservoir in Converse County, Wyoming
22 p2666 N73-31358
Effect of construction and staged filling of Oakley Dam and Friends Creek impoundment in Illinois on environment and ecology
[E73-11124] 24 p2916 N73-33279
**RESIDENTIAL AREAS**
Evaporation rates and toxic plume dispersion for defining downwind evacuation areas for populations adjacent to accidental propellent spills on shipping routes
[NASA-TM-X-68188] 07 p0750 N73-16097
Acoustic measurement methods for evaluating aircraft noise pollution in urban areas
[PB-212875] 11 p1326 N73-20757
**RESIDUAL GAS**
Design, development, fabrication, and testing of laboratory prototype of residual gas analyzer
[NASA-CR-124177] 12 p1404 N73-21386
**RESIDUAL STRESS**
Residual stresses and mechanical properties in circumferentially wrapped composite cylinders
[SC-DC-72-1291] 03 p0361 N73-12942
Determination of temperature and residual stresses and deformations caused by welding process
[AD-749529] 04 p0428 N73-13487
Development of technique for measuring residual stresses in thin coatings based on analysis of stress induced deflections of substrate
[NASA-CR-130813] 09 p1051 N73-18566
Improvements in welding techniques to increase productivity and quality of performance of bonded joints
[JPRS-58291] 10 p1163 N73-19460
Hydrocompression treatment to lower residual stresses in weld joints of forge-welded carbon steel vessels
10 p1163 N73-19461
Continuous measurement of residual stress in thin cylindrical pieces using deflection-etching techniques
[CRIF-MC-47] 12 p1409 N73-21418

Experimental method of measuring direction and residual stress in steel using surface displacements around indentations
[AD-756869] 13 p1546 N73-22526
Preheating effects of mandrel and glass tape on residual stress magnitude
[AD-759632] 16 p1934 N73-25645
Analysis of residual stresses in pressure displacement converter diaphragm occurring during manufacturing
16 p1968 N73-25921
Residual stresses and plastic deformations of machined magnesium oxide crystals
[AD-759411] 17 p2073 N73-26776

**RESIDUES**
Serial segments method for measuring pilot manual control remnant in vicinity of sine waves
01 p0018 N73-10136

**RESIN BONDING**
Mechanical and thermal properties and oxidation resistance of seal ring carbon graphite materials with resin impregnants
[NASA-CR-120955] 10 p1165 N73-19480
Improved carbon graphite materials for high temperature self-acting seals
[NASA-CR-121092] 10 p1165 N73-19481
Improved resin adhesion by depositing silicon carbide whiskers on carbon fibers
[AD-757659] 14 p1681 N73-23642
Silicon solar cell with plastic film binding to cover glass
[NASA-CASE-LEW-11065-2] 17 p1985 N73-26048
Aging tests of light alloys bonded with various adhesives and development of new aging test criteria
[RAE-LIB-TRANS-1662] 17 p2043 N73-26528

**RESINS**
NT ACRYLIC RESINS
NT ADDITION RESINS
NT EPOXY RESINS
NT ION EXCHANGE RESINS
NT NYLON [TRADEMARK]
NT PHENOLIC RESINS
NT POLYAMIDE RESINS
NT POLYESTER RESINS
NT POLYETHER RESINS
NT POLYIMIDE RESINS
NT POLYMETHYL METHACRYLATE
NT POLYURETHANE RESINS
NT SILICONE RESINS
NT THERMOPLASTIC RESINS
NT THERMOSETTING RESINS
NT VINYL COPOLYMERS
Development of process for bonding resinous body in cavities of honeycomb structures
[NASA-CASE-MSC-12357] 03 p0305 N73-12489
Selection of resin matrices for composites with improved unidirectional strength
[NASA-TM-X-68166] 06 p0687 N73-15597
Numerical analysis of incompressible linearly compressible viscoelastic creep and relaxation for plastic materials
[AD-752067] 08 p0967 N73-17903
Brittleness determination of low density blown polyethylene film balloons to account for high altitude failure
[AD-757885] 15 p1802 N73-24603
Computerized prediction and actual carbon dioxide adsorption performance of solid amine resin
[NASA-CR-112324] 16 p1870 N73-25140
Resin for protecting p-n semiconductor junction surface
[NASA-CASE-ERC-10339-1] 21 p2561 N73-30532
Shear, flexural, and tensile strength performance of carbon fiber composites made from epoxy, phenolic, polyester, and polyimide resins
[AQD/NM-000198] 22 p2689 N73-31536
Properties of dielectric layers of negative electrosensitive resin noting masking capability and application to MOS circuit manufacturing
[REPT-5.497] 23 p2765 N73-32124
Metal oxide semiconductor photoengraving principles and utilization noting resin properties, procedures, thin film techniques, and metal chemical attack
[LAAS-FI-73-T-11] 24 p2899 N73-33139

**RESISTANCE**
Sulfur and MOCA cured polyurethane elastomer resistance to water, STF, and STF/water mixture
[ERDE-TR-83-PT-2] 02 p0192 N73-11555
Variable resistance tension and lubrication device, using oil-saturated leather wiper
[NASA-CASE-KSC-10723-1] 14 p1670 N73-23553
Microhardness and corrosion resistance of Zr-Nb alloy prepared by reaction of ZrC with Nb2O5
[BARC-612] 15 p1799 N73-24583

**RESISTANCE COEFFICIENTS**
U COEFFICIENTS
U RESISTANCE

**RESISTANCE HEATING**
MHD equations for calculating joule heating and winds from geomagnetic storms in thermosphere
[NASA-CR-124071] 08 p0915 N73-17498
Joule heating model for cathode surface structure effect on metal evaporation in vacuum discharge
[TH-73-E-33] 14 p1643 N73-23329
Thermospheric heating due to EUV absorption and Joule dissipation
[AD-758758] 15 p1784 N73-24464
Properties of arc disharges heated by induction and direct current electromagnetic field
[AD-760808] 18 p2183 N73-27629
Circulation in high latitude thermosphere due to electric fields and joule heating
20 p2391 N73-29203

**RESISTANCE THERMOMETERS**
Determining time constant of resistance thermometer by double heating
[NASA-TT-F-14494] 02 p0173 N73-11398
Thermal stability of high temperature tungsten and platinum resistance thermometers
[NBS-TN-764] 13 p1529 N73-22391

**RESISTIVITY**
U ELECTRICAL RESISTIVITY

**RESISTOJET ENGINES**
Engineering model of 20 millipound thrust monopropellant hydrazine resistojet program
[NASA-CR-130762] 16 p1956 N73-25828
Feasibility demonstration of biowaste propellant resistojet engines for space station attitude control system
[NASA-CR-132269] 18 p2193 N73-27706

**RESISTOJETS**
U RESISTOJET ENGINES

**RESISTORS**
NT POTENTIOMETERS [RESISTORS]
NT THERMISTORS
Microstructure of thick film resistors
[AD-747980] 03 p0276 N73-12238
Development of allpass, highpass, bandpass, and stopband electric filter circuits using only resistors as passive components
[REPT-1404] 05 p0522 N73-14244
Development of miniature electronic trimmable thin film resistor chips having precision responses
[BDX-613-728] 12 p1383 N73-21216
High isolation RF signal selection switches
[NASA-CASE-NPO-13081-1] 14 p1618 N73-23106
Nondestructive tests and failure analysis of Vamistor resistors
[NASA-TM-X-64754] 18 p2122 N73-27154

**RESOLUTION**
NT ANGULAR RESOLUTION
NT HIGH RESOLUTION
NT RADAR RESOLUTION
NT SPECTRAL RESOLUTION
Method and data reduction tables for determining resolving power of photographic and other optical systems under typical field conditions
[AD-747265] 03 p0303 N73-12475
Evaluation of concept for determining edge sharpness and transfer characteristics of photographic materials
[NASA-TT-F-13922] 05 p0547 N73-14445
Determination of meteorological information of ERTS-1 MSS bulk data at 0.6 - 0.7 microns as function of resolution
[E73-10085] 08 p0901 N73-17297
Atmospheric effects on ERTS-1 imagery and spatial resolution of MSS data
[E73-10394] 11 p1276 N73-20356
Coherent optical system for display of spatial resolution of ERTS-1 MSS photography
[E73-10449] 11 p1283 N73-20409
Increase in resolving power of camera tubes by changing form and size of electron gun aperture noting electron beam density distribution
[DRIC-TRANS-3025] 13 p1500 N73-22160
Development of method for determining resolving power of photographic lenses
[NBS-SP-374] 18 p2151 N73-27387
Microwave holography describing lateral and axial resolution, computerized wave front reconstruction, and application to moving objects
[REPT-6-72] 20 p2425 N73-29484

**RESOLVENTS**
U PROBLEM SOLVING

**RESOLVING POWER**
U RESOLUTION

**RESONANCE**
NT BARYON RESONANCES
NT CYCLOTRON RESONANCE
NT ELECTRON PARAMAGNETIC RESONANCE
NT FERROMAGNETIC RESONANCE
NT MAGNETIC RESONANCE
NT MESON RESONANCES
NT MICROWAVE RESONANCE
NT NUCLEAR MAGNETIC RESONANCE
NT OPTICAL RESONANCE
NT PARAMAGNETIC RESONANCE
NT PLASMA RESONANCE
NT PROTON MAGNETIC RESONANCE
NT RESONANT VIBRATION
NT SPIN RESONANCE
Interrelation of divergence, flutter and autoparametric resonance in cantilever beams
[AD-746695] 03 p0285 N73-12311
Numerical code for studying double resonance production of ionospheric irregularities
[AD-747495] 03 p0299 N73-12440
Resonance capture of Toro asteroid perturbed orbit by earth
[TRITA-EPP-72-19] 07 p0846 N73-16863
Recoilless resonance photoabsorption by 6.2 keV transition in Ta-181, using W-181 in W and Ta foil sources
[NASA-TT-F-14680] 08 p0946 N73-17745
Light intensity effect on photon resonance in excited atom ionization for determining Stark effect potential
[KFKI-72-68] 10 p1192 N73-19694
Dependence of photon resonance in metastable helium atom ionization on light intensity
[KFKI-72-69] 10 p1192 N73-19695
Numerical analysis of resonance interactions in dynamic stability of elastic shells under compression
[AD-756237] 14 p1715 N73-23918
Mathematical models for analyzing resonance effects on wave absorption and scattering in meteor trails
17 p2023 N73-26372
Ultrashort optical pulse propagation through resonant media
[AD-762209] 19 p2309 N73-28569
Ion-ion hybrid resonance heating of D-T plasmas
[IPPJ-165] 20 p2459 N73-29758
Fifteenth order resonance on decaying orbit of TETR-3
[NASA-TM-X-70484] 24 p2979 N73-33805

**RESONANCE PROBES**
Infrasonic resonant tube determination of wind and temperature variabilities in lower troposphere
[AD-745912] 02 p0206 N73-11667

**RESONANCE SCATTERING**
Predissociation by rotation and curve crossing in diatomic molecules
[NASA-CR-131262] 15 p1747 N73-24159

**RESONANCE TESTING**
Ionospheric transfer impedance of rocket-borne quadrupole probe near lower hybrid resonance
[NRC-TT-1614] 06 p0666 N73-15414

**RESONANT CAVITIES**
U CAVITY RESONATORS

**RESONANT FREQUENCIES**
Procedures for computing upper and lower bounds to bending frequencies and estimates of mode shapes of beams with constant stiffness and mass - Part 1
[AD-747241] 02 p0239 N73-11946
Computer program user guide for determining limits to bending frequencies and mode shape estimates for free nonuniform beams with attached masses - Part 2
[AD-747242] 02 p0239 N73-11947
Analysis of vibration characteristics of laminated plates and modifications of plate theory to produce results consistent with continuum theory
[AD-746951] 02 p0240 N73-11949
Rotor frequency response to shaft pitching and rolling oscillations, and steady response and frequency response data at high advance ratios for hingeless rotors
[NASA-CR-114519] 03 p0251 N73-12032
Application of small rate theory to resonant acoustic oscillations with damping
[AD-746981] 03 p0337 N73-12745
Analysis of finite amplitude standing waves in air at ambient temperature contained in rigid walled rectangular cavity
[AD-747522] 03 p0337 N73-12749
Obtaining first natural frequencies of vibration of noncircular plates by perturbation theory
[AD-748355] 03 p0363 N73-12955
Design of reflector for stabilization and frequency tuning of ruby laser spectrum
[PB-211890] 05 p0558 N73-14537
Influence of inhomogeneity of magnetic field on oscillations of plasma layer of magnetosphere tail
06 p0665 N73-15407
Mathematical model for resonant vibration of cylindrical shells using the Rayleigh-Ritz method
[DLR-FB-71-92] 06 p0727 N73-15931
Observation of nonlinear waves near lower hybrid resonance frequency
[CONF-720804-3] 07 p0756 N73-16137
Existence of natural radio noise between electron plasma frequency and upper hybrid resonance frequency as detected by long electric antennas of IMP-6 satellite
[NASA-CR-130273] 07 p0843 N73-16832
Technique for determining bulk modulus and associated loss factor of elastomeric and plastic materials
[AD-752483] 08 p0935 N73-17639
Application of statistical methods for determination of dynamic system parameters influence on spectrum of natural frequencies
[AD-752695] 09 p1067 N73-18707
Natural vibrations of gyroscope with flexible rotor shaft and elastic axial cardan suspension
10 p1184 N73-19633
Analysis of oscillating gas flow in open-ended pipe caused by piston operating at or near resonant frequency
[AD-754647] 11 p1272 N73-20321

Calculating resonance frequency of cylindrical cavity frequency meter
[REPT-6659] 14 p1666 N73-23522
Natural frequencies and dynamic response of NERVA engine thrust train
[NASA-CR-132224] 15 p1809 N73-24664
Resonance tests of delta wing aircraft model to determine effect of stiffness changes of wing spars on frequencies and modes of vibration
[ARC-R/M-3268] 16 p1856 N73-25031
Propellant oscillation modes and frequencies for tanks of any shape, fill level, or orientation
[NASA-CR-124277] 16 p1889 N73-25287
Development of electrical circuit for suppressing oscillations across inductor operating in resonant mode
[NASA-CASE-ERC-10403-1] 17 p2007 N73-26228
Numerical analysis of nonlinear resonance phenomena in systems of solids having rotating and vibrating parts
17 p2092 N73-26928
Computer program incorporating capability to perform free vibration analysis for natural frequencies
[AD-761370] 18 p2204 N73-27792
Results of Resonant Infrasonic Gauging System development
[NASA-CR-124314] 19 p2301 N73-28500
Effect of friction in compont on frequency of natural vibrations
[AD-761558] 19 p2306 N73-28550
Measurement of resonant second harmonic generation in exciton of copper chloride and zinc oxide using Q-switched ruby laser
20 p2424 N73-29474
Nonlinear vibrations of pipelines containing pressurized fluids with application to aircraft hydraulic systems
[AD-764154] 22 p2616 N73-30968
Effect of homogeneous dielectric sphere on electromagnetic radiation from simple source
22 p2646 N73-31201
Development of program for obtaining resonant frequencies, modal amplitudes, and damping of structure from sinusoidal force-controlled vibration test
[NASA-TM-X-2789] 22 p2724 N73-31802

**RESONANT VIBRATION**
Resonant random vibration test to assess service equipment and sub-assembly mechanical ruggedness
[RARDE-MEMO-18/72] 01 p0113 N73-10937
Instrumentation and techniques for measuring viscosity of liquids by vibration method
[AD-759389] 17 p2034 N73-26464
Ghost-free dual resonance models
[LPTHE-73/16] 20 p2456 N73-29738
Resonant vibration structural analysis of cylindrical sandwich shells
[TUB-IR-1972/2] 22 p2725 N73-31808
Vibrational cross section resonances of excited state in nitrogen and carbon monoxide
[AD-764596] 23 p2754 N73-32042
Investigation of evolution of orbit-orbit resonances
[NASA-CR-135674] 23 p2844 N73-32728
Resonance stabilization of air cushion between liquid and oscillation source
[IPP-2/209] 24 p2963 N73-33674

**RESONATORS**
NT CAVITY RESONATORS
NT MULTIMODE RESONATORS
GaAs wafer development, diode construction, and resonator design
[AD-746655] 02 p0150 N73-11213
Optical properties of laser resonators with spinning prism Q switch
[WRE-TN-658[AP]] 02 p0180 N73-11461
Mechanisms for X irradiation induced transient changes in elastic modulus of quartz resonators
[SC-DC-72-1240] 05 p0587 N73-14771
Kinetics of quartz crystal growth and radiation effects on quartz resonators
[AD-750467] 06 p0711 N73-15803
Radiation testing of swept synthetic quartz resonators with high-purity platinum electrodes
[AD-752584] 08 p0891 N73-17209
Theory of finite aperture waveguide gas laser resonators representing external reflectors by matrices
[NASA-TM-X-66186] 08 p0929 N73-17608
Properties of piezoelectric lead zirconate titanate ceramic resonator material produced by adding lead niobates to material
[AD-757617] 14 p1681 N73-23644
Selective bandpass resonators using bandstop resonator pairs for microwave frequency operation
[NASA-CASE-GSC-10990-1] 17 p2003 N73-26195
Analysis of power loss for coupled transmission and reaction resonator circuits
[AD-762252] 19 p2248 N73-28126
Resonator design for low cost microwave bandpass filter
[NHK-LABS-NOTE-162] 20 p2381 N73-29128
Packaging of precision quartz crystal resonators and effect on aging and thermal hysteresis
[AD-763215] 21 p2519 N73-30202
Effect of connecting aperture in resonator mirror on radiation power of CO2 laser
[AD-763254] 21 p2555 N73-30484
Analyses of sonic resonators and transducers
24 p2925 N73-33362

**RESOURCE ALLOCATION**
Critique of methods for allocation of resources for defense projects
[AD-753817] 11 p1354 N73-20994
Analysis of NASA programs during post-Apollo period to show organization of field centers, planning activities, operational activities, and resources utilization
[NASA-CR-131931] 12 p1466 N73-21879
Simultaneous equation production functions for decisions pertaining to sea-based tactical air resources
17 p2054 N73-26612
Indicators for describing state of science in US for setting priorities in allocating resources
[NSB73-1] 19 p2354 N73-28939
Judge ranking projects for resource allocations
[AD-761392] 19 p2355 N73-28945
Multi-criteria resource allocation decision aid
23 p2812 N73-32480
Congressional hearings on causes and implications of impending shortages of gasoline, heating oil, diesel fuel, jet fuel, and electricity
24 p2994 N73-33928

**RESOURCES**
NT EARTH RESOURCES
NT GEOTHERMAL RESOURCES
NT RANGE RESOURCES
Proceedings of Congressional committee on use of recycled materials in NASA programs and requirement for recycling legislation for environmental and economy improvement
11 p1308 N73-20614

**RESOURCES MANAGEMENT**
NT FOREST MANAGEMENT
NT LAND MANAGEMENT
Mapping and managing soil and range resources in Sand Hills Region of Nebraska using ERTS-1 imagery
[E72-10175] 01 p0044 N73-10354
Application of ERTS-1 imagery data to protection and management of New Jersey coastal environment
[E72-10178] 01 p0045 N73-10357
Monitoring by ERTS-1 imagery for resource inventory, planning, land use zoning, and resource development in Oregon
[E72-10182] 01 p0045 N73-10361
Forest resources evaluation, planning, protection, and management using remotely sensed imagery
[E72-10220] 02 p0162 N73-11314
Inventory and management of geological, botanical, and agricultural resources in Wyoming using satellite and airborne imagery and ground control data
[E72-10229] 02 p0163 N73-11322
Near real time water resources data from Delaware Bay for use in river basin management
[E72-10239] 03 p0288 N73-12339
Timber resource management and information system
[E72-10245] 03 p0289 N73-12345
Natural resource inventory in Arizona using ERTS-1 imagery
[E72-10287] 04 p0410 N73-13337
Management of wildlife habitat in Alaska using ERTS-1 imagery
[E72-10293] 04 p0410 N73-13343
Management of earth resources in France and Spain through automatic mapping inventory
[E72-10303] 04 p0411 N73-13352
Earth resource surveys for management and development of resources in Ohio
04 p0472 N73-13845
Resource inventory, land use, and pollution within Susquehanna River Basin based on interpretation of ERTS-1 data
[E72-10329] 05 p0531 N73-14317
Remote sensing techniques for regional planning and managing earth resources, particularly water resources in California
[NASA-CR-129917] 05 p0536 N73-14361
Remote sensing data for determining land use potential of northern California coastal zone
05 p0536 N73-14365
Use of remote sensing data to analyze impact of California State Water Project on regional planning and land use of west side of San Joaquin Valley
05 p0537 N73-14367
Resources inventory and land use management in Oregon using ERTS-1 imagery
[E73-10008] 06 p0658 N73-15344
Mapping and inventories of land use and natural resources in New York based on ERTS-1 imagery
[E73-10024] 06 p0660 N73-15358
Resources management in Ohio utilizing ERTS-1 imagery
[E73-10032] 06 p0661 N73-15365
Microanalytic analysis of satellite meteorology on resource utilization, commerce, and agriculture
06 p0692 N73-15637
Development and application of field data collection techniques for remote sensing applications
07 p0785 N73-16386
Utilization of ERTS-1 imagery for water resources management in Delaware River Basin
07 p0787 N73-16404
Earth resources surveys and management in California using ERTS-1 and supporting aircraft data
[E73-10027] 08 p0900 N73-17287
Use of remote sensing for assessing impact of highway construction on land use management in Michigan
[NASA-CR-130761] 08 p0917 N73-17515
Effectiveness of ERTS-1 imagery in monitoring vegetation conditions of direct concern to range land management and agriculture business decisions in Great Plains Corridor
[E73-10302] 09 p1021 N73-18334
Reservoir management and operation using ERTS-1 imagery
[E73-10308] 09 p1022 N73-18340
Management of wildlife habitats in Alaska using ERTS-1 imagery
[E73-10335] 10 p1147 N73-19336
Mapping and management of soil range resources in Sand Hills Region of Nebraska using ERTS-1 imagery
[E73-10372] 10 p1151 N73-19367
Land use, water quality, and air quality indices useful to environmental resources managers and data processing equipment and techniques for production of indices
[E73-10376] 10 p1151 N73-19371
Conservational and rational use of natural resources and wildlife to preserve biosphere environment
[JPRS-58429] 11 p1250 N73-20145
Timber inventory and management in Washington using ERTS-1 imagery
[E73-10411] 11 p1278 N73-20373
Application of ecological, geological, and oceanographic ERTS-1 imagery to coastal resources management and planning in Delaware
[E73-10426] 11 p1280 N73-20387
Resources management in Ohio using ERTS-1 imagery
[E73-10437] 11 p1281 N73-20397
Natural resources management and inventory of Arizona using ERTS-1 imagery
[E73-10442] 11 p1282 N73-20402
Wildland resource evaluation in Nevada using ERTS-1 imagery
[E73-10450] 11 p1283 N73-20410
Environmental engineering for conservation of ocean resources
[PB-212634] 11 p1290 N73-20467
Utilization of ERTS-1 imagery to evaluate Iranian playas as potential locations for economic or engineering development
[E73-10539] 13 p1518 N73-22303
Use of remote sensor techniques for wildlands vegetation management
[NASA-CR-131580] 13 p1522 N73-22336
Resources inventory, planning, land use zoning, and resources development in Oregon using ERTS-1 imagery
[E73-10579] 14 p1656 N73-23440
Wildland resource and vegetation monitoring in Nevada and Great Basin using ERTS-1 imagery
[E73-10606] 15 p1773 N73-24367
Updating land use and resources data in Guatemala based on ERTS-1 imagery
[E73-10609] 15 p1773 N73-24370
Relevance of ERTS-1 imagery to land use, resources, and environment management in Ohio
[E73-10621] 15 p1775 N73-24382
Mapping and managing soil and range resources in Sand Hills Region of Nebraska using ERTS-1 imagery
[E73-10629] 15 p1775 N73-24389
Application of ecological, geological, and oceanographic ERTS-1 imagery to Delaware coastal resources management and planning
[E73-10631] 15 p1776 N73-24391
Use of ERTS multispectral data to solve development and management problems of agricultural resources in Lynn County, Texas
[NASA-CR-132956] 15 p1778 N73-24411
Taxonomic identification and natural resource inventory using ERTS-1 data
[E73-10666] 16 p1899 N73-25361
Application of ERTS-1 data to develop and implement utilization of living marine resources in Mississippi Sound
[E73-10707] 16 p1904 N73-25398
Land use management and planning in Maryland based on ERTS-1 data
[E73-10732] 17 p2020 N73-26338
Management of natural resources in France and Spain by automatic cartographic inventories from ERTS-1 data
[E73-10725] 18 p2133 N73-27234
Resources management, land use mapping, and water quality management in Ohio based on ERTS-1 imagery
[E73-10775] 18 p2135 N73-27251
Wildlife management in Alaska using ERTS-1 data
[E73-10791] 18 p2137 N73-27267
Mapping and managing soil and range resources in Sand Hills Region of Nebraska using ERTS-1 imagery
[E73-10807] 18 p2139 N73-27282

Analysis of ERTS-1 imagery of New Jersey coastal resources to assist in resource management and allocation of funds for environmental control
[PAPER-E9] 19 p2269 N73-28273
Application of ERTS-1 multispectral imagery to water resources development in lower Mekong River basin in southeast Asia
[PAPER-W3] 19 p2271 N73-28283
Evaluation of stream flow data for Verde River watershed in central Arizona provided by ERTS-1 imagery
[PAPER-W8] 19 p2271 N73-28286
Evaluation of ERTS-1 imagery as tool for management of wildlife habitat in Alaska
[PAPER-W11] 19 p2271 N73-28288
Utilization of ERTS-1 data for land use and resources survey in Michigan
[PAPER-L26] 19 p2276 N73-28321
Resources and land use management and planning in Oregon using ERTS-1 data
[PAPER-R2] 19 p2282 N73-28360
Application of ERTS-1 imagery to resource management in Ohio
[PAPER-R3] 19 p2283 N73-28361
ERTS-1 imagery of desertification, hydrology, vegetation, forage, and water resources in Republic of Mali
[PAPER-R5] 19 p2283 N73-28363
Application of ERTS-1 for mapping California, identifying natural resources, and developing programs for environmental improvement
19 p2287 N73-28390
Application of ERTS-1 imagery for geologic development of natural resources in Alaska
19 p2287 N73-28393
Application of ERTS-1 imagery for multidisciplinary survey to aid in management of Alaskan resources
19 p2288 N73-28394
Inventories of agriculture, forestry, and rangeland resources based on ERTS-1 imagery
19 p2288 N73-28396
Development of land management programs based on ERTS-1 imagery and computer compatible tapes for machine processing of data
19 p2288 N73-28397
Application of ERTS-1 imagery for controlling quantity and quality of ground water resources
19 p2288 N73-28399
Application of ERTS-1 imagery and aerial photography to missions of US Corps of Engineers
19 p2289 N73-28400
Application of ERTS-1 imagery to programs conducted by Department of Interior
19 p2289 N73-28401
Assessment of ERTS-1 imagery for identification of marine resources to include sources of pollution, beach erosion, and navigation in ice-filled waterways
19 p2289 N73-28402
Application of ERTS-1 data to water resources management in State of California
19 p2289 N73-28403
Application of ERTS-1 imagery to land use and resource management in State of Mississippi
19 p2289 N73-28404
Utilization of Skylab imagery as information service for investigating land use and natural resources in New York State
[E73-10829] 19 p2290 N73-28414
Utilization of ERTS-1 data for regulation, protection, and management of New Jersey coastal environment
[E73-10845] 19 p2291 N73-28423
Application of ERTS-1 imagery to land use inventory, land capability evaluation, and land use suitability in Maryland
[E73-10873] 20 p2393 N73-29224
Resources management in France through automatic cartographic inventory
[E73-10894] 20 p2395 N73-29243
Utilization of ERTS-1 imagery in resources management on national scale in South Africa
[E73-10931] 20 p2399 N73-29279
Application of ecological, geological, and oceanographic ERTS-1 imagery to Delaware coastal resources management and planning
[E73-10934] 21 p2529 N73-30276
Water, agriculture, and soil resources management and planning in California using ERTS-1 imagery
[E73-10935] 21 p2529 N73-30277
Application of ERTS-1 imagery to resources management and planning in Ohio
[E73-10987] 22 p2658 N73-31294
Remote sensing methods for earth observation missions by aircraft and satellites
22 p2736 N73-31900
Development of resources management information system for resources data from Potomac River Basin
[E73-11069] 23 p2781 N73-32245
Remote sensing techniques in Michigan for resource management and environmental protection in both public and private interests
[NASA-CR-135639] 23 p2785 N73-32282
Utilization of ERTS-1 imagery in mapping and managing range resources in Sand Hills Region of Nebraska
[E73-11121] 24 p2916 N73-33276
Development of land use, water quality, and air quality indices from ERTS-1 imagery for environmental resources management in Susquehanna River Basin and Quantico, Virginia test areas
[E73-11143] 24 p2918 N73-33298
Resource inventory, land use, and pollution of Susquehanna River Basin from ERTS-1 data
[E73-11156] 24 p2919 N73-33310
Utilization of ERTS-1 imagery of topography and drainage patterns for resources inventory and management in Arizona
[E73-11159] 24 p2919 N73-33312

**RESPIRATION**
NT HIGH ALTITUDE BREATHING
NT LIQUID BREATHING
NT PRESSURE BREATHING
Changes in lung capacity, air passage resistance, and dynamic compliance of humans during water immersion to simulate weightlessness
07 p0744 N73-16053
Gas chromatographic and mass spectrometric determinations of trace elements in human breath samples
[AD-750141] 09 p1000 N73-18159
Human ability to note changes in composition of inhaled air
10 p1115 N73-19090
Carbon monoxide content in exhaled air and blood carboxyhemoglobin in subjects confined to insulating protective gear
11 p1245 N73-20106

**RESPIRATORY DISEASES**
NT INFLUENZA
NT PNEUMONIA

**RESPIRATORY IMPEDANCE**
Respiratory impedance effects on electrical activities of bulbar respiratory neurons, respiratory muscles, and pulmonary ventilation in anesthesized cats
03 p0257 N73-12084

**RESPIRATORY PHYSIOLOGY**
Acute and subacute inhalation toxicity experiments with organic solvents, rocket propellants, and various hydrocarbons in confined environments
[NASA-CR-131675] 13 p1485 N73-22043
Role of respiratory enzymes on human adaptation to hypoxia
[NASA-TT-F-15058] 21 p2500 N73-30060

**RESPIRATORY RATE**
Correlation of respiratory distress and ultrasonic transmission with severe decompression sickness in hampsters
[AD-743475] 01 p0012 N73-10091
Automatic device for measuring human metabolic oxygen rate and breathing dynamics
[NASA-CASE-MFS-21415-1] 06 p0635 N73-15156
Pathogenesis of some respiratory and circulatory reactions accompanying drop in barometric pressure
07 p0743 N73-16047
Transverse acceleration effects on human respiratory rate and oxygen metabolism
10 p1114 N73-19084
Influence of isolated heating of spinal column on respiratory rate and panting in dogs
[NASA-TT-F-14998] 18 p2109 N73-27054
Inflight heart and respiratory rate recording of pilots, using nose clip transducers
19 p2226 N73-27953
Influence of He, N2, and N2O environments on physiological parameters of rats
20 p2365 N73-29019
Human circadian rhythms of blood circulation, respiration and catabolism under flight simulation stress
[DLR-FB-72-49] 21 p2501 N73-30073
Respiratory analysis system to determine gas flow rate and frequency of respiration and expiration cycles in real time
[NASA-CASE-MSC-13436-1] 23 p2751 N73-32015

**RESPIRATORY REFLEXES**
Barotrauma mechanoreceptor reflex effects on animal respiratory and circulatory system
13 p1479 N73-21982

**RESPIRATORY SYSTEM**
NT LUNGS
Effects of gravitational and inertial forces on cardiovascular and respiratory dynamics
[NASA-CR-129603] 03 p0256 N73-12074
Factors relevant to respiratory support and equipment design
06 p0628 N73-15102
Respiratory models for studying hazards of air pollution
[UR-3490-169] 06 p0630 N73-15121
Cardiovascular and respiratory systems reactions in cosmonauts during space flight
10 p1114 N73-19079
Investigation of vocal cord regulatory mechanism of register, pitch, and intensity of voice during singing
14 p1632 N73-23225
Instrumentation and techniques for determining effects of gravitational and inertial forces on cardiovascular and respiratory dynamics
[NASA-CR-133212] 16 p1867 N73-25119
Evaluation of energy expenditures and reactions of cardiovascular and respiratory systems to physical work
[NASA-TT-F-15090] 23 p2749 N73-31997
Change in impulse activity of neurons in respiratory center during electric stimulation of vestibular nerve and dorsal roots in spinal cord
24 p2882 N73-33017

**RESPIROMETERS**
Automatic device for measuring human metabolic oxygen rate and breathing dynamics
[NASA-CASE-MFS-21415-1] 06 p0635 N73-15156

**RESPONDERS**
U TRANSPONDERS

**RESPONSE BIAS**
Dynamic response of vestibular nuclei neurons of decerebrated cats subjected to sinusoidal rotation
[AMRU-R-70-2] 02 p0130 N73-11059
Asymmetric response of cat semicircular canal neurons to symmetric sinusoidal rotation
[AMRU-R-69-2] 02 p0130 N73-11060
Response characteristics of vestibulo-ocular reflex arc
[AMRU-R-71-2] 02 p0132 N73-11067
Mechanical response of otolith-dependent units of cats to sinusoidal linear rotation
[AMRU-R-69-3] 02 p0132 N73-11068

**RESPONSES**
NT DYNAMIC RESPONSE
NT FREQUENCY RESPONSE
NT GALVANIC SKIN RESPONSE
NT HEMODYNAMIC RESPONSES
NT MODAL RESPONSE
NT PHYSIOLOGICAL RESPONSES
NT TIME RESPONSE
NT TRANSIENT RESPONSE
System for monitoring condition responsive devices by using frequency division multiplex technique
[NASA-CASE-KSC-10521] 11 p1254 N73-20176
Response variations of microphone worn on human body
[BM-RI-7810] 20 p2371 N73-29058

**REST**
NT BED REST
Adenin-nucleotides NAD[plus] and NADN in skeletal muscles during intensive work and at rest
[NASA-TT-F-14856] 11 p1246 N73-20118

**RESTARTABLE ROCKET ENGINES**
Launch program cost comparisons of restartable high energy upper stage rocket engine
[NASA-CR-130275] 07 p0835 N73-16768
SERT 2 hollow cathode multiple restarts in space
[NASA-TM-X-68292] 21 p2589 N73-30742

**RESTRAINTS**
U CONSTRAINTS

**RESTRICTIONS**
U CONSTRICTIONS

**RETARDANTS**
Application of space program fire retardant technology to housing
[NASA-TN-D-7370] 19 p2312 N73-28592

**RETENTION [PSYCHOLOGY]**
Overview of literature concerning retention of learned skills with emphasis on space flight skill retention
[NASA-CR-128611] 01 p0020 N73-10152
Short-term memory results from connected speech experiments using adult listeners
14 p1625 N73-23169

**RETICLES**
Production measures for visible and ultraviolet transmitting reticles for star trackers
[NASA-CASE-GSC-11188-3] 01 p0056 N73-10460
Method for producing reticles for use in outer space
[NASA-CASE-GSC-11188-2] 10 p1184 N73-19630
Improved measurement of photographic images with negative reticles
[AD-753946] 11 p1295 N73-20505
Reconstructing information of reticulated spectroscopy
[RR-2] 16 p1913 N73-25480
Production method of star tracking reticles for transmitting in visible and near ultraviolet regions
[NASA-CASE-GSC-11188-1] 23 p2790 N73-32320

**RETINA**
NT FOVEA
NT VISUAL PIGMENTS
Argon-ion laser used to determine ocular effects of repetitive laser pulses on rhesus monkeys
[AD-746795] 04 p0380 N73-13096
Ocular effects of near infrared laser radiation for safety criteria
[AD-746793] 04 p0381 N73-13097
Argon laser radiation damage to retina of diabetic and nondiabetic patients
[AD-747058] 04 p0381 N73-13099
Chorioretinal burn hazards of high intensity radiation sources in industry
08 p0873 N73-17071

Modelling of random human visual search performance based on physical properties of eye
10 p1225 N73-19961
Retinal damage in monkeys exposed to near infrared gallium arsenide laser pulses
[AD-753419] 11 p1248 N73-20135
Influence of excitation surface with liminary brightness on different regions of the retina
[NASA-TT-F-15124] 23 p2751 N73-32017
RETINAL ADAPTATION
NT DARK ADAPTATION
NT LIGHT ADAPTATION
Literature concerning retinal adaptation to varying light intensities
[NASA-TT-F-15036] 24 p2890 N73-33074
RETINAL IMAGES
Visual image generation as textured flight information resembling retinal images for airborne flight simulation
01 p0017 N73-10128
Physiological control system for stabilization of retinal image in humans
06 p0633 N73-15141
Vestibular stimulation effect in human and animal retinal image stabilization
06 p0633 N73-15144
Optical modulation transfer functions of human eye for white light
[IZF-1973-2] 14 p1609 N73-23047
RETIREMENT
Motivational patterns underlying devoluntteering by submarine graduate school personnel
[AD-749324] 13 p1487 N73-22054
RETORC [TORPEDOES]
U TORPEDOES
RETRACTABLE LANDING GEAR
U LANDING GEAR
RETRIEVAL
NT DATA RETRIEVAL
NT INFORMATION RETRIEVAL
Optimum inclination of inclination non-sensitive satellites for shuttle retrieval
[NASA-TM-X-64780] 22 p2715 N73-31730
RETROACTION
U RETROTHRUST
RETROGRESSIVE SHORELINES
U BEACHES
RETROREFLECTION
Computer programs for calculating transfer functions of retroreflector laser arrays carried by orbiting satellites
[NASA-CR-130696] 08 p0888 N73-17190
Portable pulsed laser ranging system for measurements between earth and retroreflecting satellites
[NASA-CR-131513] 12 p1410 N73-21423
RETROROCKET ENGINES
Combined parachute and retrorocket system for low altitude aerial delivery of military cargo
[AD-765422] 24 p2880 N73-32997
RETROSEQUENCING
U SEQUENTIAL CONTROL
RETROTHRUST
Combined parachute and retrorocket system for low altitude aerial delivery of military cargo
[AD-765422] 24 p2880 N73-32997
RETURN BEAM VIDICONS
Ocean water color assessment of Monterey Bay, California, from ERTS-1 RBV and MSS imagery
[E72-10190] 01 p0046 N73-10369
ERTS-1 return beam vidicon imagery of Lake Champlain region and Vermont
[E72-10252] 03 p0289 N73-12352
Polar region mapping using ERTS-1 return beam vidicon imagery
[E72-10273] 03 p0291 N73-12371
Photomapping of US using ERTS-1 return beam vidicon imagery
[E72-10274] 03 p0291 N73-12372
Thematic mapping using ERTS-1 return beam vidicon imagery
[E72-10275] 03 p0291 N73-12373
Cultural resources interpretation and map revision from ERTS-1 RBV and MSS imagery of Washington state
[E72-10276] 03 p0291 N73-12374
Overall evaluation of ERTS-1 RBV and MSS imagery for cartographic applications
[E72-10278] 03 p0292 N73-12376
Ocean water color assessment from ERTS-1 RBV and MSS imagery
[E73-10002] 06 p0658 N73-15338
Photomapping of US using ERTS-1 MSS and RBV imagery
[E73-10088] 08 p0902 N73-17300
Photomapping of Phoenix area from ERTS-1 RBV imagery
[E73-10502] 12 p1398 N73-21338
Detection and mapping of sea ice in Arctic regions using ERTS-1 RBV and MSS data
[E73-10595] 14 p1658 N73-23452
Photomapping of US using ERTS-1 RBV imagery
[E73-10602] 15 p1772 N73-24363
Application of ERTS-1 return beam vidicon and multispectral scanner imagery for ocean water color assessment in Caribbean Sea
[E73-10726] 17 p2019 N73-26332
Digital system for precision geometric and radiometric correction of ERTS-1 RBV and MSS images
[E73-10827] 18 p2140 N73-27299
Masking of ERTS-1 RBV images to reduce stationary residual inaccuracies in radiometric shading corrections
[PAPER-I4] 19 p2277 N73-28326
Application of digital techniques to processing of ERTS-1 MSS and RBV image data
[PAPER-I7] 19 p2278 N73-28328
Conference on significant results obtained from ERTS-1 MSS and RBV data - Vol. 3
[E73-10826] 19 p2289 N73-28405
Cartographic applications of ERTS-1 RBV imagery in polar regions
[E73-10953] 21 p2531 N73-30295
Assessment of water color in Caribbean from ERTS-1 RBV and MSS imagery.
[E73-11006] 22 p2660 N73-31311
REUSABLE LAUNCH VEHICLES
Analysis of space program costs and launch vehicle traffic based on either expendable, partially reusable, or fully reusable launch vehicle fleet
[NASA-CR-125847] 03 p0355 N73-12896
Payload data bank, space shuttle program risk analysis, reusable launch vehicles, and cost analysis
[NASA-CR-126170] 03 p0355 N73-12897
REUSABLE ROCKET ENGINES
Composite materials for use as internal LH2 tank insulation for reusable boosters
[NASA-CR-124222] 13 p1546 N73-22528
REUSABLE SPACECRAFT
NT AEROSPACEPLANES
NT SPACE SHUTTLES
Atmospheric turbulence response of reusable space shuttle configuration during ascent flight
[NASA-CR-123952] 03 p0357 N73-12913
Spacecraft configurations and aerodynamic characteristics of space shuttle systems with two reusable stages
[NASA-CASE-MSC-12433] 05 p0597 N73-14854
Design, development, and characteristics of expendable second stage for use with reusable space shuttle booster - Vol. 1
[NASA-CR-128671] 05 p0598 N73-14865
Definition of system for expendable second stage and reusable space shuttle booster system - Vol. 2 - Bk. 1
[NASA-CR-128670] 05 p0598 N73-14866
Definition of expendable second stage for use with reusable space shuttle booster to include structural, propulsion, and avionics systems design - Vol. 2 - Bk. 2
[NASA-CR-128672] 05 p0599 N73-14867
Definition of expendable second stage and space shuttle booster separation system to include modifications required, ground support equipment, and launch operations - Vol. 2 - Bk. 3
[NASA-CR-128673] 05 p0599 N73-14868
Wind tunnel tests to determine aerodynamic characteristics of expendable second stage and payload configurations for reusable space shuttle booster - Vol. 3
[NASA-CR-128674] 05 p0599 N73-14869
Analysis of mass properties of reusable space shuttle booster and expendable second stage for three specified payloads - Vol. 4
[NASA-CR-128659] 05 p0599 N73-14870
Analysis of operations and resources required to support expendable second stage reusable space shuttle booster - Vol. 5
[NASA-CR-128660] 05 p0599 N73-14871
Definition of major expendable second stage interfaces with specified space shuttle booster components including interface control drawings - Vol. 6
[NASA-CR-128661] 05 p0599 N73-14872
Preliminary design drawings of expendable second stage reusable space shuttle booster to define specific payloads and configurations - Vol. 7
[NASA-CR-128662] 05 p0599 N73-14873
Contract end item specifications for defining hardware end items required by expendable second stage of space shuttle booster system - Vol. 8 Pt. 1
[NASA-CR-128663] 05 p0599 N73-14874
Preliminary system specification for design, operation, and performance of expendable second stage for reusable space shuttle booster - Vol. 9
[NASA-CR-128664] 05 p0599 N73-14875
Analysis of technology requirements for expendable second stage of space shuttle booster system - Vol. 10
[NASA-CR-128665] 05 p0600 N73-14876
Design requirements and data for expendable second stage of reusable space shuttle booster - Vol. 12
[NASA-CR-128667] 05 p0600 N73-14877
Costs of space tug refurbishment
[NASA-CR-130366] 07 p0841 N73-16815
Liquid hydrogen booster propellant tank internal insulation system for use in reusable spacecraft
[NASA-CR-121102] 15 p1842 N73-24925
Design and development of pressurization system for reusable space shuttle multilayer insulation systems
[NASA-CR-124380] 22 p2722 N73-31782
Design, development, and configuration of reusable lunar shuttlecraft
[NASA-CR-135794] 24 p2984 N73-33849
REVERBERATION
Acoustic noise, transmission loss, and reverberation measurements in West Greenland Sea
[AD-746839] 02 p0169 N73-11373
Effect of reverberation and interfering noise on speech intelligibility as determined from physical description of running speech
14 p1631 N73-23219
REVERSE TIME
U REACTION TIME
REVERSED FLOW
Evaluation of concept of reverse flow engine for APS engine
[NASA-CR-120881] 04 p0464 N73-13783
REVERSING
Systems engineering for design of two dimensional automatic manipulator control system using reversible follow-up
17 p1989 N73-26081
REVIEWING
Principles of classical mechanics and quantum mechanics in theoretical physics
[ITF-71-104-P] 04 p0414 N73-13383
Review of papers presented at Conference on Space Biology and Aerospace Medicine
[JPRS-58345] 09 p0995 N73-18125
Review of high density computer storage devices for recorded data
[AD-753626] 09 p1007 N73-18217
Review of Naval research activities
[PB-212475] 11 p1354 N73-20993
REVISIONS
Interpretation of ERTS-1 imagery of man made culture and revision of small-scale maps
[E73-10536] 13 p1518 N73-22300
Proposed 50 to 100 km revision to US Standard Atmosphere, 1962
[AD-753394] 13 p1526 N73-22371
Control of modifications in projects noting contractors and customers viewpoints
15 p1849 N73-24986
REYNOLDS EQUATION
Analytical solution of Reynolds equation and application to hydrodynamic lubrication to show characteristics of lubrication film
[TAE-153] 09 p1057 N73-18618
REYNOLDS LAW
U REYNOLDS EQUATION
REYNOLDS NUMBER
Estimating local or average turbulent skin friction on flat plates from Reynolds numbers
[NASA-TN-D-6945] 01 p0040 N73-10315
Drag measurement in wake of oscillating cylinder at low Reynolds number using hot-wire technique
[DLR-FB-71-42] 09 p0981 N73-18015
Dependence of turbulent line vortices decay on Reynolds number
[AD-753131] 09 p1017 N73-18297
Heat transfer and aerodynamic resistance of in-line smooth walled tube arrays in transverse air flow at high Reynolds number
[NLL-RTS-7689] 09 p1098 N73-18959
Determining open-loop response of Reynolds number depeadent process as analog of drop-vaporization burning-rate process
[NASA-CR-121167] 11 p1269 N73-20301
Analysis of Reynolds stress in turbulent boundary layer on smooth wall with zero pressure gradient
[AD-754758] 11 p1272 N73-20319
Design of airfoil sections for low Reynolds numbers based on requirement to achieve transition upstream of major adverse pressure gradient
12 p1355 N73-20995
Analysis of effects of Reynolds number on aerodynamic stalling of rotary wings and relationship of Reynolds number to aerodynamic coefficients of blade elements
14 p1598 N73-22957
Mach number effect on motion of sphere in compressible low Reynolds number flow
15 p1765 N73-24298
Influence of free stream Reynolds number on transition in boundary layer on infinite swept wing
17 p2013 N73-26280
Present and future need for high Reynolds number transonic wind tunnels including analysis of design selection and requirements
17 p2013 N73-26282
Reynolds stress in turbulent boundary layer on smooth wall
22 p2650 N73-31233
Measurement of wall shearing stress and velocity and temperature profiles of turbulent boundary layer to derive Reynolds number
[ARC-R/M-3712] 24 p2870 N73-32928
Vortex pairing in turbulent shear layer at moderate Reynolds numbers
24 p2903 N73-33169

**RF-4 AIRCRAFT**
U F-4 AIRCRAFT
**RF-8 AIRCRAFT**
U F-8 AIRCRAFT
**RH-2 HELICOPTER**
U UH-1 HELICOPTER
**RHENIUM**
Pyrolysis of rhenium chlorides to yield chemically vapor deposited rhenium thermionic emitters
[NASA-CR-121143] 09 p1073 N73-18759
**RHENIUM ALLOYS**
Performance of rhenium alloy electron tube cathodes
[AD-755828] 12 p1385 N73-21232
**RHENIUM COMPOUNDS**
Preparation and properties of polytetrafluoroethylene impregnated with rhenium oxides
[NASA-TN-D-7166] 07 p0811 N73-16579
Growth of single crystals of rhenium and iridium dioxides
[NASA-CR-133213] 17 p2072 N73-26768
**RHEOGRAPHY**
U RECORDING INSTRUMENTS
**RHEOLOGY**
Feasibility of multichannel rheography for studying cardiovascular system on centrifuge
03 p0259 N73-12094
Rheological investigation of lubricating media using displacement equations for three special cases
[FOA-1-C-1408-92] 06 p0672 N73-15470
Rheological model - for behavior of nonNewtonian fluid
[WTHD-42] 06 p0699 N73-15701
Rheological behavior of lubricant in rolling and sliding elastohydrodynamic lubricated contact
[NASA-CR-2206] 12 p1408 N73-21413
Rheological properties of abrasive powder solutions considering particle dispersion
[AD-756082] 13 p1488 N73-22065
Elastohydrodynamic theory for predicting spin friction of ball in nonconforming groove, using rheological model
[NASA-TN-D-7280] 15 p1790 N73-24514
Anomalous rheological characteristics of high-internal-phase-ratio emulsions containing 97 to 98 percent liquid fuel as dispersed phase
[AD-758908] 15 p1823 N73-24779
Rheological properties of fiber suspensions in reinforced plastics
[AD-762083] 19 p2232 N73-28001
Methods of solving quasistatic problems in linear theory of thermoviscoelasticity
[AD-763937] 22 p2726 N73-31816
Effect of fibrinogen concentration on viscosity of human blood
[DLR-FB-73-54] 24 p2886 N73-33046
Comparison of rheological equations of state and constrained shear recovery results for two polyisobutylene melts
[RR-203] 24 p2891 N73-33078
**RHODE ISLAND**
NT BLOCK ISLAND SOUND [RI]
Land use in northern megalopolis of Massachusetts, Connecticut, and Rhode Island
[E73-10506] 13 p1516 N73-22281
Land use of northern megalopolis of Massachusetts, Connecticut, and Rhode Island from ERTS-1 imagery
[E73-10630] 15 p1776 N73-24390
Application of ERTS-1 imagery to determine land use in Massachusetts, Connecticut, and Rhode Island
[E73-10723] 17 p2019 N73-26330
Mapping and digitization of land use in northern megalopolis of Masssachusetts, Connecticut, and Rhode Island using ERTS-1 data
[PAPER-L12] 19 p2274 N73-28308
**RHODIUM**
Kinetics of liquid hydrazine decomposition on supported rhodium catalyst
[RPE-TR-71/16-PT-4] 10 p1126 N73-19177
**RHODIUM ALLOYS**
Platinum-rhodium-tungsten alloys for encapsulating space isotopic heat sources
[ORNL-4813] 08 p0932 N73-17632
Intergranular deformation in creep elongation of platium rhodium alloys
[AD-753508] 10 p1173 N73-19546
Analysis of short time elevated temperature properties of platinum, rhodium, and palladium alloys
[NLL-M-22799-[5828.4F]] 11 p1304 N73-20582
Platinum-rhodium device for stirring viscous fluids
[NBS-TN-771] 13 p1532 N73-22418
**RHYTHM [BIOLOGY]**
NT CIRCADIAN RHYTHMS
Effects of prolonged bed rest on body temperature and heart rate periodicity in man
09 p0994 N73-18113
Prolonged bed rest effects on human blood hormone level periodicities
09 p0994 N73-18114
Mechanisms for controlling physiological rhythms in Rana pipiens
[NASA-CR-131153] 10 p1112 N73-19064
Spectral analysis on human biorhythmic performance to evaluate tranquilizer effects
12 p1370 N73-21116
Effects of human biorhythms on chemotherapy and drug evaluation
12 p1370 N73-21119
**RIBBONS**
Controlled diffusion reaction process for masking substrate of twisted multifilament superconductive ribbon
[NASA-CASE-LEW-11726-1] 17 p2070 N73-26752
**RIBONUCLEIC ACIDS**
Proton magnetic resonance spectra of ribonuclease A inhibitor complexes, noting effect on catalytic activity
[BMVG-FBWT-72-13] 07 p0747 N73-16074
Ultraviolet radiation, X rays, freezing, and thawing effects on ribonuclease
10 p1119 N73-19120
Synthesis rate of phospholipids and cytochromes b5 and P 450 in thiamine-deficient rats after treatment with thiamine
[NASA-TT-F-14989] 17 p1987 N73-26064
**RIBOSE**
Ultracentrifugation of biological materials
[NASA-CR-114673] 23 p2750 N73-32009
**RIBS [SUPPORTS]**
Fabrication of light weight panel structure using pairs of elongate hollow ribs of semicircular configuration
[NASA-CASE-LAR-11052-1] 04 p0481 N73-13929
Calculation of harmonic vibrations of elastic rectangular plates supported at two edges and reinforced vertically with eccentric ribs
[AD-748906] 04 p0483 N73-13944
Effect of arrangement of stiffening ribs for cylindrical shell on critical load value
[AD-758029] 15 p1840 N73-24912
**RICCATI EQUATION**
FORTRAN program for numerical solution of steady state matrix Riccati equation of quadratic cost optimal control problem
[AD-745862] 01 p0072 N73-10589
Theorems for optimization of Riccati equation in singular discrete time filtering and control problems
[NASA-CR-130360] 06 p0690 N73-15621
Riccati controlled feedback for guiding spacecraft during unpowered terminal phase of flight
23 p2847 N73-32751
**RICE**
Atmospheric effects on recognition of rice and corn in ERTS-1 imagery of Sacramento Valley
[E73-10390] 11 p1276 N73-20352
Mapping and monitoring natural ecosystems and environmental complexes and estimation of rice crop yield in California and Louisiana from ERTS-1 imagery
[E73-10669] 16 p1899 N73-25364
Application of ERTS-1 imagery for identifying citrus groves and rice fields in Valencia region of Eastern Spain
[PAPER-A4] 19 p2260 N73-28212
Application of ERTS-1 imagery for determining rice growing areas in Philippines and assessment of crop condition
[PAPER-A5] 19 p2260 N73-28213
Mapping rice crops of California and Louisiana and natural vegetation of Colorado Plateau from Skylab photography
[E73-10885] 20 p2394 N73-29236
Identification of rice fields in Philippes from ERTS-1 imagery
[E73-10908] 20 p2397 N73-29257
Photomapping of rice crops and natural vegetation in Louisiana and California from Skylab EREP imagery
[E73-10916] 20 p2397 N73-29265
Uniform mapping of rice crops in Louisiana and California and desert vegetation in southwestern Colorado from Skylab imagery
[E73-10979] 22 p2657 N73-31286
Uniform mapping and monitoring of natural ecosystems and environmental complexes of Colorado Plateau and Sierra-Lahontan areas and estimation of rice crop yields in California and Louisiana
[E73-11070] 23 p2781 N73-32246
Uniform mapping of vegetation and rice in Colorado Plateau, Sierra-Lahontan, California, and Louisiana coastal plain from Skylab multispectral photography
[E73-11149] 24 p2919 N73-33303
**RICHARDSON-DUSHMAN EQUATION**
U TEMPERATURE EFFECTS
U THERMIONIC EMISSION
**RIDGES**
Apollo 16 photography of V-shaped ridges associated with secondary craters - Part K
12 p1454 N73-21775
Volcanic origin of mare ridges and sinuous rilles on lunar surface
12 p1454 N73-21780
**RIEMANN INTEGRAL**
U MEASURE AND INTEGRATION
**RIEMANN PROBLEM**
U CAUCHY PROBLEM
**RIFLES**
Solid film plastic lubricant coatings for rifles
[AD-754568] 11 p1300 N73-20545
**RIFT VALLEYS**
U VALLEYS
**RIFTS**
U GEOLOGICAL FAULTS
**RIGID BODIES**
U RIGID STRUCTURES
**RIGID ROTOR HELICOPTERS**
NT CH-3 HELICOPTER
NT XH-51 HELICOPTER
**RIGID ROTORS**
Rotor frequency response to shaft pitching and rolling oscillations, and steady response and frequency response data at high advance ratios for hingeless rotors
[NASA-CR-114519] 03 p0251 N73-12032
Application of equations of motion to investigate effects of mode shape and coning angle on stability boundaries of hingeless helicopter rotor blades
[NASA-CR-114525] 07 p0739 N73-16015
Analytic methods for calculating blade loads and shaft-transmitted vibratory forces in stiff bladed hingeless rotors operating at various advance ratios - Vol. I
[NASA-CR-114562] 09 p0984 N73-18034
Descriptions, geometry, and technical data for three rotary wing systems used in determining vibration and loads in hingeless rotary wings - Vol. 2
[NASA-CR-114568] 09 p0984 N73-18035
Effect of elastic flapping of rotor blades on stability and control of helicopter equipped with hingeless rotor system
12 p1358 N73-21016
Flight tests of Westland Scout helicopter fitted with reduced scale version of rigid rotor to determine airworthiness and handling characteristics
12 p1358 N73-21017
Analysis of helicopter blade flutter for both hinged and hingeless rotor blades
[AGARD-R-607] 13 p1472 N73-21920
Design, development, and testing of inflexible blade, hingeless rotor system with hydraulic rotor control system
[AD-758514] 15 p1736 N73-24081
Numerical analysis of bending of rotating beams with application to linear flap-lag stability of hingeless rotary wings using nonlinear equations
[NASA-TM-X-2770] 15 p1838 N73-24897
Rundown time and rotor imbalance of electrostatic gyroscope with spherical rigid rotor
20 p2419 N73-29434
**RIGID STRUCTURES**
NT RIGID ROTORS
NT RIGID WINGS
Derivation of minimum dimension sets of discrete coordinate and hybrid coordinate equations of motion for hinge connected rigid bodies assembled in tree topology
[NASA-CR-129950] 05 p0602 N73-14900
Mathematical model for development of first-order secular solutions to rotational motions of triaxial rigid body - Part 2
[NASA-CR-131878] 13 p1549 N73-22555
Relativistic rigidity of rotating disk
[AD-763330] 21 p2604 N73-30873
**RIGID WINGS**
Calculation of induced load effects on controllability of rigid and flexible aircraft
08 p0865 N73-17004
**RILLS**
U VALLEYS
**RING CURRENTS**
OGO 3 and 5 observations of inner magnetosphere and ring currents
08 p0972 N73-17947
Variable intensities of geomagnetically trapped protons at low altitudes
[AD-754844] 11 p1288 N73-20448
Precipitation of auroral and ring current particles in magnetosphere by artificial plasma injection
[AD-755352] 12 p1403 N73-21381
Evening observations of storm-time ring current particle characteristics during beginning of magnetic storms
[NASA-TM-X-70430] 19 p2293 N73-28441
**RING LASERS**
Analysis of fluctuations in difference frequency in ring lasers operating in single mode
17 p2040 N73-26501
**RING STRUCTURES**
NT REINFORCEMENT RINGS
NT RING WINGS
Analysis of ring and stringer stiffness parameters and proportions for axially compressed stiffened isotropic cylinders with and without internal pressure
[NASA-CR-2165] 04 p0481 N73-13930
Mathematical solution to compressive bulk formation for calibrating ring test specimens using constant interface friction factor
[AD-750885] 06 p0675 N73-15492
Butt welding of titanium alloy rings and flanges to improve mechanical properties
10 p1163 N73-19463
Damping of liquid oscillations using flexible ring baffles
[NASA-TM-X-64730] 12 p1390 N73-21273
Fabrication of full-size structural rings from composite materials
[NASA-CR-124253] 15 p1793 N73-24532

Numerical analysis of free vibrations of ring stiffened toroidal shells based on linear shell theory
15 p1837 N73-24888
Nuclear magnetic resonance spectrum analysis for rings inversion rate in benzodiazepine derivatives
[RAE-LIB-TRANS-1628] 17 p1991 N73-26103
Ultrasonic inspection and examination of large size cast steel ring prior to machining
[TR-7212.624] 20 p2422 N73-29456
Optimum structural design of discretely ring-stiffened cylindrical shell
23 p2853 N73-32794
RING WINGS
Subsonic wind tunnel tests of ring-wing canard configurations for air to surface antitank missiles
[AD-763899] 22 p2723 N73-31788
RINGS [MATHEMATICS]
Operator theory of n-th order modular forms
[NASA-TT-F-15006] 19 p2313 N73-28605
RIOMETERS
Thule riometer observations of polar cap absorption events 1962-1972
[AD-762279] 19 p2296 N73-28467
RIOMETRY
U MEASUREMENT
U RIOMETERS
RISK
Risk scoring system for identifying subjects with high risk to coronary heart disease
08 p0874 N73-17080
RITZ AVERAGING METHOD
Application of perturbation theory and Ritz energy method for analyzing nonlinear flexural gyrations of untwisted, rotating cantilevered blade vibrating in plane of rotation
16 p1968 N73-25923
RIVER BASINS
NT CHENA RIVER BASIN [AK]
NT DELAWARE RIVER BASIN [US]
NT SUSQUEHANNA RIVER BASIN [MD-NY-PA]
NT WABASH RIVER BASIN [IL-IN-OH]
Near real time water resources data from Delaware Bay for use in river basin management
[E72-10239] 03 p0288 N73-12339
Aircraft and spacecraft observation of riverbed formation and flow patterns
04 p0472 N73-13846
ERTS-1 sensing of fall snow melting in Chena River Basin, Alaska
[E72-10345] 05 p0533 N73-14333
Fluvial environment of Arctic coastal plain in Northern Alaska
[AD-749150] 05 p0542 N73-14412
Fluvial environmental charts for Arctic coastal plain in Northern Alaska
[AD-749151] 05 p0542 N73-14413
Utilization of ERTS-1 imagery for water resources management in Delaware River Basin
07 p0787 N73-16404
ERTS-1 relayed water resources data collected from Delaware River Basin
[E73-10451] 12 p1394 N73-21299
Satellite television photography of geomorphological indices for developing stream meander pattern
12 p1400 N73-21352
Hydrometeorological study of periodic precipitation variations over Lesse Basin, Belgium
[PUBL-SER-A-76] 12 p1423 N73-21530
Statistical tests for determining Colorado River Basin response to natural or induced changes
[PB-214114/1] 14 p1665 N73-23513
Hydrological investigation of drainage basin characteristics from ERTS-1 imagery for improved regression estimates of water flow
[E73-10652] 16 p1898 N73-25348
Application of ERTS-1 remotely sensed data and ground truth information to predict and manage water quantity and quality in river basins
[E73-10689] 17 p2018 N73-26314
RIVERS
One and two dimensional models of tidal propagation in St. Lawrence River
[NRC-12764] 01 p0048 N73-10382
Water resources survey and river monitoring in Canada using ERTS-1 imagery
[E72-10230] 02 p0163 N73-11323
Land use mapping, limnology, wetlands, geomorphic and landform surveys, and river monitoring of Lake Champlain Basin and Vermont using ERTS-1 imagery
[E72-10282] 03 p0292 N73-12380
ERTS-1 imagery of California nearshore processes including estuarine flushing, currents, season river discharges, and sediment dispersion
[E72-10363] 05 p0535 N73-14351
Meander patterns of Feather and Colorado Rivers
05 p0537 N73-14366
Measurement of lateral erosion rates at proposed river crossing sites of Alaska pipeline by aerial photogrammetry
[AD-748875] 05 p0541 N73-14402
Fluvial environment of Arctic coastal plain in Northern Alaska
[AD-749150] 05 p0542 N73-14412
Fluvial environmental charts for Arctic coastal plain in Northern Alaska
[AD-749151] 05 p0542 N73-14413
Marine weather program for providing weather and river advisories to public sector
06 p0663 N73-15382
Sedimentation levels in rivers and shoal estuarine waters based on ERTS-1 imagery
[E73-10048] 07 p0777 N73-16310
Geographical, physicomathematical, and hydrological engineering treatment of river runoff in USSR
[TT-70-50058] 07 p0781 N73-16346
Repetitive ERTS-1 imagery of surface water variability and flooding along rivers and low-lying areas in Virginia, Iowa, and California
[E73-10046] 08 p0900 N73-17289
ERTS-1 observations of plant growth and annual flooding in Inland Delta of Niger River in Mali
[E73-10436] 11 p1281 N73-20396
Analysis of interactions between marine water and freshwater at river mouth for understanding dissemination of sediment
[AD-755158] 14 p1664 N73-23507
Thematic mapping of Mississippi River from ERTS-1 imagery
[E73-10628] 15 p1775 N73-24388
Mineral concentration in ground and river waters of Porkhov determined from their specific electroconductivity
[NASA-TT-F-14991] 17 p1992 N73-26105
Application of ERTS-1 imagery for hydrometric and hydrographic surveys of Canada
[E73-10777] 18 p2135 N73-27253
Stream and river drainage network analysis from Skylab imagery
[E73-10818] 18 p2140 N73-27293
Application of ERTS-1 imagery for determining course of Ebro River in northeast Spain
[PAPER-W2] 19 p2271 N73-28282
Application of ERTS-1 multispectral imagery to water resources development in lower Mekong River basin in southeast Asia
[PAPER-W3] 19 p2271 N73-28283
Assessment of flood damage in Arizona using ERTS-1 MSS imagery to show extent of inundation and sediment deposition
[PAPER-W6] 19 p2271 N73-28284
Evaluation of stream flow data for Verde River watershed in central Arizona provided by ERTS-1 imagery
[PAPER-W8] 19 p2271 N73-28286
Application of ERTS-1 data to North Carolina forest and water resources management
[PAPER-R1] 19 p2282 N73-28359
Analysis of thermal radiation brightness of river strip as basis for determining actual temperature from data provided by satellite
20 p2400 N73-29288
RIVETED JOINTS
Secondary bending effect on aluminum alloy riveted joint fatigue strength determined by comparetive program fatigue tests
[NLR-TR-72007-U] 13 p1586 N73-22862
Effect of friction forces on fatigue breakdown of bolted and riveted joints in airframes
[AD-761446] 19 p2305 N73-28539
RIVETING
Methods for designing and developing aircraft structural components by riveting, welding, and gluing aluminum alloys parts
[AD-753513] 09 p1041 N73-18491
RNA
U RIBONUCLEIC ACIDS
ROADS
NT HIGHWAYS
Soil stabilization during road and airport construction
[AD-748153] 03 p0299 N73-12442
ROBOTS
Design, development, and characteristics of industrial robot machinery to show load capacity, positioning accuracy, power actuators, and method of controls
01 p0060 N73-10486
Computerized simulation of artificial robot interaction behavior with complex environment
[NASA-CR-129526] 03 p0269 N73-12179
Telecommunication jamming of robot aircraft control system by pulse amplitude modulation or pulse time modulation
[FOA-3-C-3649-66] 06 p0639 N73-15188
Computerized simulation of three dimensional robots using generalized cylinder descriptions
[AD-755139] 11 p1251 N73-20152
Radio controlled robots with computer induced artificial intelligence to act as human substitutes under adverse conditions
[NASA-CR-131593] 13 p1550 N73-22558
Artificial intelligence research projects with emphasis on design, implementation, and integration of system for control of robot
[NASA-CR-131991] 14 p1638 N73-23279
Application of artificial intelligence to control of mobile automatons
[NASA-CR-132996] 16 p1874 N73-25173
Performance of combined photoelectric snow depth-robot rain gage system
[NLL-M-22978-[5828.4F]] 16 p1910 N73-25457
Vision model for robot object recognition system
[NASA-CR-133458] 19 p2224 N73-27936
Computer programming for hierarchial robot intelligence system
[AD-761641] 19 p2240 N73-28061
Automation of computer controlled robot manipulators
[JPRS-59717] 20 p2371 N73-29051
Robot buoy for study of relation between marine environment and weather in Sea of Japan
[NLL-M-23049-[5828.4F]] 21 p2567 N73-30573
Robot computer problem solving system which represents robot exploration vehicle in simulated Mars environment
[NASA-CR-133942] 22 p2638 N73-31146
Scene analysis and computer perception with breadboard Mars robot operating in laboratory environment containing rocks of various sizes
[NASA-CR-135711] 23 p2770 N73-32156
TENEX computer system, ARPA network, and computer language design for robot development
[NASA-CR-135899] 24 p2897 N73-33124
ROCKET BOOSTERS
U BOOSTER ROCKET ENGINES
ROCKET CHAMBERS
U COMBUSTION CHAMBERS
U THRUST CHAMBERS
ROCKET COMBUSTORS
U COMBUSTION CHAMBERS
U THRUST CHAMBERS
ROCKET ENGINE CASES
Analysis of pressure fluctuations in Nike rocket case and relationship to structural vibrations of rocket case
[NASA-TN-D-6931] 01 p0113 N73-10933
Performance of prototype monopropellant engines using electrolytic ignition system
[AD-745993] 02 p0224 N73-11808
Development of flow visualization and flow measurement techniques and application to flow problems of turbines, aircraft engines, and missile propulsion
[AD-747613] 03 p0287 N73-12328
Components and performance of solid propellant rocket engines
[AD-752865] 08 p0956 N73-17823
Design and fabrication of fiberglass, graphite, and maraging steel composite motor cases
[AD-753959] 10 p1176 N73-19569
Computer programs for analysis of shell structures in general and fiber reinforced rocket engine cases
[AD-756465] 14 p1716 N73-23926
Thermal conductivity of rocket motor walls with variable heat exchange coefficients
[AD-759815] 16 p1958 N73-25836
Failure analysis of fiber reinforced composite rocket engine case using distortional energy and maximum strain theories of failure
18 p2167 N73-27500
Application of ultrasonic inspection techniques for detecting separation of solid propellant rocket case-liner and liner-propellant interfaces
[NAL-TR-308] 18 p2193 N73-27703
Analysis of cost data for fabrication of large solid rocket engine cases based on process complexity factor
[NASA-CR-133412] 18 p2200 N73-27764
Fabrication and hydrotests of shear spun rocket engine cases
[AD-761129] 18 p2201 N73-27770
Design, fabrication, manufacture, and verification of composite material rocket engine cases for antitank missiles - Vol. 1
[AD-760566] 18 p2202 N73-27774
Design calculations, tooling sketches, manufacturing and inspection records of composite material rocket engine cases for antitank missiles - Vol. 2
[AD-760569] 18 p2202 N73-27775
Press-brake roll and weld frabrication of prototype large diameter missile cases
[AD-762612] 20 p2466 N73-29815
ROCKET ENGINE DESIGN
Analysis of heat balance characteristics of nuclear lightbulb engine to determine effects on engine performance, space radiator requirements, and cooling sequence
[NASA-CR-129295] 03 p0331 N73-12696
Colloidal thrustor propellant performance discussing thrustor design and propellant choice
[ESRO-CR-53] 03 p0349 N73-12851
Development and application of systematic procedures for estimating life cycle costs of solid rocket motor booster configurations
[NASA-CR-129255] 03 p0350 N73-12857
Demonstration of duct cooling concept with gaseous hydrogen/oxygen propellant in high pressure thruster - Vol. 2
[NASA-CR-120870] 03 p0350 N73-12859
Development of description for phenomenon of intrinsic unstable combustion in gas rocket
04 p0483 N73-13948

Components and performance of solid propellant rocket engines
[AD-752865] 08 p0956 N73-17823
Literature review on design and performance of multistage rockets
[AD-752815] 08 p0956 N73-17824
Development and characteristics of molecular beam mass spectrometer system for sampling rocket engine combustion chambers
[NASA-CR-130933] 10 p1137 N73-19267
Evaluation of scale model of low pressure rocket engine used for secondary injection studies and modifications required for full scale simulation
[NASA-CR-124176] 12 p1443 N73-21690
Dynamic compatibility of liquid and gaseous fluorine and chlorine pentafluoride propellants with designated metals for rocket engine design criteria
[AD-756916] 13 p1569 N73-22719
Design, development, and operation of water electrolysis system to provide gaseous hydrogen and oxygen for satellite propulsion system
[AD-755384] 13 p1571 N73-22735
Characteristics of ion rocket engine with combination keeper electrode and electron baffle
[NASA-CASE-NPO-11880] 15 p1824 N73-24783
Technical analysis of solid propellant rocket engines for use with space shuttle vehicle - Vol. 2, Book 2
[NASA-CR-123926] 15 p1826 N73-24798
Analysis of cost data for fabrication of large solid rocket engine cases based on process complexity factor
[NASA-CR-133412] 18 p2200 N73-27764
Technical requirements of solid propellant rocket engine for application to space shuttle booster - Vol. 2 Bk. 1
[NASA-CR-123729] 20 p2465 N73-29805
Analysis of earth storable bimodal engine using earth storable propellants and operating in either monopropellant or bipropellant mode
[BELL-8706-933005] 20 p2466 N73-29811
Analysis of solid propellant rocket engine requirements for space shuttle booster application - Vol. 1
[NASA-CR-124236] 20 p2467 N73-29820
Program planning, contract administration, manufacturing, and testing of solid propellant rocket engine for space shuttle booster - Vol. 3
[NASA-CR-124238] 20 p2467 N73-29821
Regeneratively cooled rocket engine tests with space storable propellants
[NASA-CR-133915] 22 p2708 N73-31688
Monograph for design and development of combustion chambers for liquid propellant rocket engines
[NASA-SP-8087] 22 p2709 N73-31697
Performance tests of hydrazine catalytic thruster to determine capability for spacecraft limit-cycle attitude control with short thruster pulse durations
[NASA-CR-135489] 22 p2710 N73-31701
Determination of vapor pressure, viscosity, and thermal conductivity of several liquid rocket propellants
24 p2972 N73-33750

**ROCKET ENGINES**

NT AJ-10 ENGINE
NT BOOSTER ROCKET ENGINES
NT ELECTRIC ROCKET ENGINES
NT ELECTROSTATIC ENGINES
NT HYBRID PROPELLANT ROCKET ENGINES
NT HYDRAZINE ENGINES
NT HYDROGEN OXYGEN ENGINES
NT J-2 ENGINE
NT LIQUID PROPELLANT ROCKET ENGINES
NT LITHERGOL ROCKET ENGINES
NT NUCLEAR ENGINE FOR ROCKET VEHICLES
NT NUCLEAR LIGHTBULB ENGINES
NT NUCLEAR ROCKET ENGINES
NT RESTARTABLE ROCKET ENGINES
NT RETROROCKET ENGINES
NT REUSABLE ROCKET ENGINES
NT SOLID PROPELLANT ROCKET ENGINES
NT UPPER STAGE ROCKET ENGINES
Small rocket wire deployment for simulating electrical properties of large rocket engine to study lightning triggering or diversion
[AD-746309] 01 p0078 N73-10644
Space simulation study of plume contamination in reaction control thruster
[NASA-TM-X-68149] 01 p0090 N73-10743
Stability of small amplitude oscillations in combustion chambers for one and three dimensional problems
[AD-746132] 02 p0224 N73-11807
Performance, stability, and design of aerospike engines and engine system components
[NASA-TM-X-64690] 03 p0348 N73-12840
High speed bellows shaft seals for rocket engine turbopumps
03 p0348 N73-12842
NPSH technique for two phase pumping of cryogenic propellants in turbopumps and rocket engines
03 p0348 N73-12843
Performance, combustion stability, and combustion efficiency of aerospike rocket engines
03 p0349 N73-12847
Analytical procedure for determining aerospike nozzle performance particularly performance around base area
03 p0349 N73-12848
Flow equations for water/steam reaction engine with shrouded nozzles
04 p0404 N73-13293
Thermocouple apparatus for measuring wall temperatures in regeneratively cooled rocket engines having thin walled cooling passages
[NASA-CASE-XLE-05230-2] 04 p0419 N73-13417
Numerical method for determining mass flow rates in two phase gas-solid rocket nozzle flow
[AD-750038] 05 p0591 N73-14804
Nonequilibrium combustion products for calculating rocket engine performance and chemical kinetics of combustion processes
[AD-750169] 06 p0715 N73-15835
Fabrication and evaluation of cooled-gas pyrometer for application in hypersonic research engine program
[NASA-TM-X-2715] 07 p0800 N73-16496
Tests of grid-translation type beam deflection system on 5-cm diameter mercury ion thruster
[NASA-TM-X-68185] 07 p0836 N73-16777
Analysis of turbulent diffusion in rocket combustion chamber to determine Lagrangian correlation coefficient and intensity of turbulence in chamber
08 p0967 N73-17908
Electrothermal acoustics model for predicting and suppressing combustion instability in rocket motors
[AD-753111] 09 p1079 N73-18807
Rocket engines and components
[AD-754320] 10 p1210 N73-19839
Evaluation of scale model of low pressure rocket engine used for secondary injection studies and modifications required for full scale simulation
[NASA-CR-124176] 12 p1443 N73-21690
Wind tunnel simulation of high altitude rocket plumes
[AD-755840] 12 p1466 N73-21876
Research progress on radio wave propagation, electronic warfare, rocket engines, and weapon systems
[PB-213217] 12 p1467 N73-21891
Feasibility of laser induced ablation thruster for space propulsion system
[NASA-CR-131744] 13 p1537 N73-22449
Thiokol TE-M-521-5 solid propellant apogee kick rocket motor tests at 46 rpm spin at simulated altitude conditions
[NASA-CR-131987] 14 p1702 N73-23810
Improved version of modified machine gun for use as combustion stability rating device with various rocket combustors
[NASA-TM-X-2792] 15 p1842 N73-24928
Improving preformance of magnetoplasmadynamic arc rocket engine
[NASA-CASE-LEW-11180-1] 16 p1948 N73-25760
Rocket nozzle coolant channel thermal analysis program
[NASA-CR-132185] 16 p1957 N73-25832
Condensation in rocket exhaust plumes
[AD-760039] 17 p2097 N73-26966
Active-standby servoactuator for failure detection of space shuttle main engine hydraulic actuation system
[NASA-CR-124299] 18 p2156 N73-27418
Design and fabrication of monopropellant hydrazine thruster
[NASA-CR-132784] 18 p2193 N73-27702
Handbook on radiant emission and absorption of combustion gases for application to design of rocket combustion chambers and exhausts, turbojet engines, and industrial furnaces
[NASA-SP-3080] 18 p2206 N73-27807
Analysis, design, fabrication, and tests of regeneratively cooled rocket engine for storable propellants
[NASA-CR-133488] 19 p2329 N73-28737
Air Force Rocket Propulsion Laboratory computer programs
[AD-763094] 20 p2467 N73-29817
Performance analysis and high frequency combustion stability of high pressure rocket motor
20 p2484 N73-29956
Investigation of hollow cathode performance for 30 cm thrusters
[NASA-TM-X-68298] 21 p2588 N73-30739
Exhaust pressure and density of pulsed thrustor systems
[NASA-TM-X-68299] 21 p2589 N73-30740
Durability test of five cm diameter ion thruster for 9700 hours
[NASA-TM-X-68284] 21 p2589 N73-30741
Hollow cathode neutralizer for 30-cm diameter bombardment thruster
[NASA-TM-X-68291] 21 p2589 N73-30743
Performance of 30 cm ion thrusters with dished accelerator grids
[NASA-TM-X-68294] 21 p2589 N73-30744
Application of gas analysis techniques to determine combustion efficiency in turbine engines and rocket engine combustion chambers
[AGARD-AG-168] 22 p2728 N73-31830
Effects of high pressure hydrogen environments on mechanical properties of alloys considered as candidate materials for high performance rocket engine construction
[NASA-CR-124410] 23 p2804 N73-32428
Radiative behavior of rocket exhaust plumes at high altitude
[AD-764908] 23 p2857 N73-32832

**ROCKET EXHAUST**

Chemical spray scrubber for cleaning toxic products from rocket exhaust gases
[AD-747023] 02 p0224 N73-11810
Wind tunnel tests to determine space shuttle ascent configuration plumes with pressure-fed and solid rocket motor boosters - Vol. 4
[NASA-CR-120086] 02 p0234 N73-11904
Analysis of propellant gases emitted by attitude control system to determine interference with experiments due to flow fields and plume density
[NASA-CR-114508] 03 p0363 N73-12958
Wind tunnel study of basic nature of plume induced flow separation
[NASA-CR-112218] 04 p0404 N73-13288
Development of vortex fluid amplifier for throttling rocket exhaust
[NASA-CASE-LEW-10374-1] 04 p0463 N73-13773
Characterization of nonequilibrium flow and coupled chemistry associated with rocket exhaust effluent interactions in upper atmosphere
[AD-750878] 06 p0670 N73-15450
Deleterious effects of electrostatic rocket exhaust [cesium, mercury] and materials of rocket construction on spacecraft surfaces
[NASA-CR-131092] 10 p1208 N73-19823
Spectroscopic measurements of flame composition an temperature of composite solid propellants during unstable combustion
10 p1222 N73-19939
High altitude plume impingement of Titan 3
[NASA-CR-124093] 10 p1222 N73-19940
Toxicological properties of rocket exhaust products and blood analysis for beryllium oxide content
[AD-754936] 11 p1248 N73-20131
Effect of thruster pulse length on thruster-exhaust damage of S13G white thermal control coatings
[NASA-TM-X-68213] 11 p1348 N73-20940
Exhaust plume and contamination characteristics of bipropellant [MMH/N2O4] RCS thruster in liquid helium cooled, environmental facility
[NASA-TM-X-68212] 11 p1348 N73-20941
Changes in optical properties of various materials due to exposure to exhaust plume of bipropellant rocket
[NASA-TM-X-68204] 11 p1349 N73-20942
Dual channel infrared spectroradiometric analyses of rocket engine exhaust spectra
[NASA-CR-124207] 12 p1404 N73-21387
Computerized simulation of plume shapes produced by axially symmetric nozzle geometry
[AD-756380] 13 p1511 N73-22241
Formation of large polymers in vacuum plumes of large rocket engines following combustion of hydrogen and oxygen under adiabatic conditions
[RM-571] 13 p1590 N73-22893
Critical evaluation of existing optical remote sensors for HCl vapor detection in solid rocket propellant plumes
[NASA-CR-112274] 15 p1780 N73-24431
Effects of aluminum oxide on Raman scattering from nitrogen and oxygen
[AD-758913] 15 p1824 N73-24781
Barometric gravity tube discharger for liquid cooling of rocket exhaust gas and analysis of improvement with air vent
[DLR-MITT-73-10] 17 p2011 N73-26262
Comparison of plasma probe and predicted electrical properties of rocket exhaust plume
17 p2031 N73-26436
Possible condensation in rocket exhaust plumes, using frozen gas mixture
[AD-760040] 17 p2097 N73-26965
Comparison of wind tunnel measurements of impact pressure and species number density of simulated high altitude rocket exhaust plume with computer calculated values
[AD-759838] 17 p2097 N73-26968
Analysis of retrorocket exhaust plume of Viking Lander impinging on Martian surface and development of multiple nozzle configurtaion to reduce effects
[NASA-CR-2252] 18 p2197 N73-27737
Development of semi-empirical model for predicting fluctuating pressure distribution resulting from rocket plume- induced separated regions
[NASA-CR-124346] 19 p2352 N73-28922
Molecular flux measurement in back flow region of nozzle plume in high vacuum
[NASA-CR-133602] 20 p2388 N73-29184
Base region thermal environment test of scale model of Saturn S-2 stage - Vol. 1
[NASA-CR-129009] 20 p2475 N73-29883
Development of fine spectral resolution procedure for determining infrared radiant heat transfer from exhaust plume
[RM-575] 21 p2605 N73-30877

Effects of rocket plume simulators on pressure distribution of body of revolution at transonic speeds
[NASA-CR-133916] 22 p2651 N73-31238
Dispersion predictions for effluents from exhaust gases from Saturn 5 and Scout-Algol 3 launch vehicles
[NASA-TM-X-2935] 24 p2921 N73-33327
ROCKET FIRING
Algorithm for targeting finite burn maneuvers
[NASA-TM-X-66180] 08 p0961 N73-17859
ROCKET FLIGHT
Bubble formation analysis in plain and fiber reinforced metals melted and solidified under weightless conditions, using Aerobee and Black Brant rocket vehicles
[NASA-TM-X-64665] 16 p1964 N73-25886
Altitude test of rocket-borne mass spectrometer cooled by liquid helium in arc heated plasma jet wind tunnel
[DLR-MITT-72-23] 22 p2675 N73-31424
ROCKET FUEL TANKS
U PROPELLANT TANKS
ROCKET LAUNCHING
Meteorological and ballistics data for launching of Athena rocket flight 134, vehicle H-004J
[AD-749436] 04 p0445 N73-13633
Meteorological and ballistics data for launching 13901 Little John, missile number 2172, round number 684 AM
[AD-749435] 04 p0445 N73-13634
Meteorological and ballistics data for launching 13401 Honest John, missile number 2632, round number 626 ROL
[AD-749434] 04 p0445 N73-13635
Meteorological and ballistics data for launching of Lance Missile 2143, vehicle 159
[AD-749429] 04 p0445 N73-13636
Meteorological and ballistics data for launching of Honest John Laser, missile flight 205, vehicle 624
[AD-749430] 04 p0446 N73-13637
Meteorological and ballistics data for launching of Honest John Missile flight 1755, vehicle 625
[AD-749431] 04 p0446 N73-13638
Meteorological and ballistics data for launching of Lance Missile 2168, vehicle 160
[AD-749432] 04 p0446 N73-13639
Meteorological and ballistics data for launching of Lance Missile 2159, vehicle 161
[AD-749433] 04 p0446 N73-13640
Meteorological and ballistics data for launching of Little John, missile number 3175, round 687 RO
[AD-749439] 05 p0574 N73-14669
Meteorological and ballistics data for launching of Little John, missile number 2253, round 683 RO
[AD-749437] 05 p0574 N73-14670
Meteorological and ballistics data for launching of Honest John, missile number 3116, round 686
[AD-749438] 05 p0574 N73-14671
Index of reports prepared by data center concerning rocket and satellite launches and satellite sightings
05 p0611 N73-14964
Meteorological and ballistics data for launching of 11601 Lance Missile number 2154, round number 163 RBL
[AD-752088] 08 p0939 N73-17690
Meteorological and ballistics data for launching of 11602 Lance Missile number 5175, round number 164 ESL
[AD-752090] 08 p0940 N73-17695
Meteorological and ballistics data for launching of 13901 Little John Missile number 1463, round number 692 RG
[AD-752091] 08 p0940 N73-17696
Meteorological and ballistics data for launching of 14101 Little John RIP missile number 12751
[AD-752092] 08 p0940 N73-17697
Meteorological and ballistics data for launching of 13801 Little John ARM-P Ripple, missile numbers 3102, 3142 and 3257, round numbers 693, 694 and 695 RO
[AD-752095] 08 p0940 N73-17698
Meteorological and ballistics data for launching of Lance missile, number 2183, round no. 167 APT
[AD-752098] 08 p0940 N73-17700
Meteorological and ballistics data for launching of 15001 Little John missile no. 1508, round no. 697 RG
[AD-754558] 11 p1314 N73-20665
Meteorological and ballistics data for launching of 14801 Lance missile no. 2184, round no. 168 APT 9
[AD-754556] 11 p1315 N73-20669
Meteorological data for launch of Little John probe of upper atmosphere
[AD-754561] 11 p1315 N73-20671
Meteorological and ballistics data for launching of 12802 Lance missile no. 2150, round no. 174 ESL
[AD-754563] 11 p1316 N73-20678
Meteorological and ballistics data for launching of 11602 Lance missile, number 2174, round 181
[AD-755773] 12 p1424 N73-21539
Meteorological and ballistics data for launching of 12893 Lance missile, number 2354, round 182
[AD-755774] 12 p1424 N73-21540
Meteorological and ballistics data for launching of 14101 RIP missile, numbers 12723/12720, rounds 3/4
[AD-755775] 12 p1424 N73-21541
Meteorological and ballistics data for launching of Athena rocket vehicle, flight 137, vehicle H-005
[AD-755776] 12 p1424 N73-21542
Meteorological and ballistics data for launching of Athena rocket vehicle, flight 136, vehicle H-009
[AD-755779] 12 p1424 N73-21547
Analysis of military helicopter control and stability characteristics to determine suitability as rocket launching platform
[AD-756436] 13 p1474 N73-21944
Meteorological and ballistics data for launching of Lance missile, number 2149, round 180
[AD-755772] 13 p1555 N73-22599
Meteorological and ballistics data for launching of Athena rocket flight 138, vehicle H-008
[AD-758866] 15 p1807 N73-24645
Meteorological and ballistics data for launching Athena rocket flight 139, vehicle H-006
[AD-758867] 15 p1807 N73-24646
Meteorological and ballistics data for launching of 14101 RIP missile nos. 9623/9034, round nos. 5/6
[AD-758861] 15 p1807 N73-24647
Meteorological and ballistics data for launching of 03702 Honest John missile number 1003, round number 631 AML
[AD-758869] 15 p1807 N73-24650
Meteorological data for launching of RIP 14101, missile numbers 12712 and 12716
[AD-758863] 15 p1808 N73-24651
Meteorological and ballistics data for launching of Honest John missile number 359, round 629,
[AD-758862] 16 p1938 N73-25684
Meteorological and ballistics data for launching of Honest John missile number 627, round 632
[AD-758868] 16 p1938 N73-25685
Meteorological and ballistics data for launching of Honest John, missile number 1002, round 630
[AD-758865] 16 p1938 N73-25686
Meteorological and ballistics data for launching of Lance missile, number 2237, round 185
[AD-758864] 16 p1939 N73-25687
Index of international scientific rocketlaunches
[NASA-TM-X-69350] 18 p2196 N73-27732
Catalog of international rocket and satellite launching data
18 p2199 N73-27750
NASA/MSFC multilayer diffusion models and computer program for operational prediction of toxic fuel hazards
[NASA-CR-129006] 19 p2239 N73-28050
Meteorological data for launching of Honest John, missile number 1763, round 685
[AD-762158] 19 p2317 N73-28632
Meteorological and ballistics data for launching of 13401 Honest John missile no. 2542, round no. 634 RMI
[AD-762157] 19 p2317 N73-28633
Meteorological data for launching of Honest John, missile number 305, round 633
[AD-762155] 19 p2317 N73-28636
Meteorological data for launching of Lance missile, number 2238, round 187
[AD-762162] 19 p2317 N73-28638
Meteorological and ballistic data gathered for launching Athena flight 140
[AD-762160] 19 p2317 N73-28639
Solar monitoring information for SPARCS-equipped rocket launches
[NASA-CR-114635] 22 p2711 N73-31707
Logistics support for launches of sounding rockets
[AD-765231] 23 p2852 N73-32789
ROCKET LININGS
Dimpled array liners used as augmentor acoustic devices for controlling low frequency combustion instabilities
[AD-750902] 06 p0731 N73-15963
ROCKET MOTOR CASES
U ROCKET ENGINE CASES
ROCKET NOSE CONES
Aerodynamic heating analysis on sounding rocket tangent ogive nose wall
[NASA-TM-X-69896] 17 p1979 N73-26001
ROCKET NOZZLES
Effective thermal conductivities of four metal-ceramic composite coatings in hydrogen-oxygen rocket firings
[NASA-TN-D-7055] 01 p0116 N73-10961
Analytical procedure for determining aerospike nozzle performance particularly performance around base area
03 p0349 N73-12848
Variational problem for computation of maximum thrust nozzles
[AD-746618] 03 p0351 N73-12864
Prediction of shock shapes and wall shock traces encountered in secondary injection into conical rocket nozzle
[AD-750081] 05 p0528 N73-14295
Measurement of surface recession of ablative materials in rocket nozzles by spectroscopic analysis
[AD-749968] 06 p0714 N73-15829
Effects of rocket motor nozzle geometry on jet plume characteristics and base pressure
[NASA-CR-130967] 09 p1017 N73-18303
Research and development of transpiration cooled inflatable nozzle extension
[NASA-CR-124165] 11 p1269 N73-20300
Carbon refractory composites for application in rocket motor nozzles, propulsion structures, and planetary atmospheric entry shells
[NASA-CR-131745] 13 p1547 N73-22533
Design analysis of NERVA nozzle including structural elements of nozzle jacket and various aspects of coolant passages
[NASA-CR-132223] 15 p1810 N73-24669
Design fabrication, and nondestructive testing of six experimental cylinder assemblies of selected composite graphites for NERVA nozzle extension
[NASA-CR-132233] 15 p1810 N73-24674
Tests and evaluation of seal for movable rocket nozzle systems
[AD-762944] 20 p2423 N73-29467
Plug and spike nozzles applied to rocket propulsion system configurations
24 p2973 N73-33754
ROCKET OXIDIZERS
NT FLOX
Catalyst effects on decomposition kinetics of rocket oxidizer ammonium perchlorate
[AD-746728] 02 p0221 N73-11792
Utilization of inorganic metal-oxidizer materials in solid rocket propellants resulting in increased combustion efficiency
[NASA-CASE-NPO-11975-1] 08 p0953 N73-17802
Evaluation of methods for detection of fluorine-containing missile oxidizers
[AD-756525] 13 p1569 N73-22713
Prevention of N2O4 flow decay by means of contaminant removal through distillation and filtration
[AD-755380] 13 p1569 N73-22717
ROCKET PLANES
NT X-15 AIRCRAFT
ROCKET PROPELLANT TANKS
U PROPELLANT TANKS
ROCKET PROPELLANTS
NT AEROZINE
NT CRYOGENIC ROCKET PROPELLANTS
NT DOUBLE BASE ROCKET PROPELLANTS
NT GASEOUS ROCKET PROPELLANTS
NT HYPERGOLIC ROCKET PROPELLANTS
NT LIQUID ROCKET PROPELLANTS
NT MONOPROPELLANTS
NT SLURRY PROPELLANTS
NT SOLID ROCKET PROPELLANTS
Acute and subacute inhalation toxicity experiments with organic solvents, rocket propellants, and various hydrocarbons in confined environments
[NASA-CR-131675] 13 p1485 N73-22043
Evaluation of active and passive rupture disk designs for performance at cryogenic temperatures
[NASA-CR-121118] 14 p1670 N73-23554
Analysis of kinetic and transport factors governing interfacial mass transfer rates in high temperature systems
[AD-758256] 14 p1720 N73-23959
Matrix isolation technique used to obtain thermodynamic properties of rocket combustion products
[AD-762622] 20 p2486 N73-29966
ROCKET PROPELLED SLEDS
Avian hazards to Air Force rocket sled test tract at Holloman AFB, New Mexico
[AD-755833] 12 p1389 N73-21261
ROCKET SONDES
U SOUNDING ROCKETS
ROCKET SOUNDING
Meteorological parameters of stratosphere from rocket sounding data
[NLL-M-22213-[5828.4F]] 01 p0073 N73-10594
Automatic meteorological stations, and rocket investigations of atmosphere
[AD-746738] 02 p0206 N73-11671
Solar flare forecasts and comparisons with rocket-borne observations for flare class greater than or equal to 2F
[NASA-CR-114511] 02 p0225 N73-11814
Radio frequency impedance probe measurement of ionspheric electron density profiles using Veronique rocket for sounding
06 p0667 N73-15423
Aerobee mass spectrometer data on neutral gas composition of Arctic thermosphere
08 p0899 N73-17282
Rocket measurements of ozone distribution under varying latitudes and seasonal conditions in stratosphere
[NASA-TM-X-66192] 09 p1028 N73-18391
Meteorological data gathered for Little John launching 14101
[AD-754560] 11 p1316 N73-20679
Rocket-borne chemical release systems for gas, liquid, solid, and explosive payloads
[AD-758766] 16 p1908 N73-25435
ESRO sounding rocket experiment R-175 in presence of noctilucent clouds on polar summer upper atmosphere structure, composition, and ionization
[AP-7] 17 p2027 N73-26406
Photometric and image intensified TV measurements of auroral precipitation patterns and energy

input during rocket experiments at Poker Flats, Alaska in Operation Ice Cap
[AD-760042] 17 p2029 N73-26419
Woomera atmospheric parameters measured during falling sphere ejection from rocket soundings between Feb. and Jun. 1972 noting comparison with atmospheric models
[WRE-TN-787] 18 p2146 N73-27341
High altitude meteorological data measured at Sonmiani, Pakistan 1964-1970
[W-119] 18 p2172 N73-27543
Circulation structure of stratosphere and troposphere over Southern Hemisphere as determined by rocket soundings
20 p2444 N73-29629
Rocket sounding of two year cyclic variations of zonal wind components in stratosphere and mesosphere up to 100 km
20 p2444 N73-29631
Instrumentation for atmospheric rocket sounding by occultation including infrared interferometer, Fabry-Perot interference filter, and vacuum spectrometer
[BMBW-FBW-72-14-PT-1] 22 p2667 N73-31368
Experimental and theoretical IR spectra of atmospheric hydrocarbon gases CO, CO2, and NH4 for occultation sounding
[BMBW-FBW-72-14-PT-2] 22 p2667 N73-31369
ESRO rocketborne spectrometric data on neutral particles and temperature of winter lower thermosphere at polar latitudes
[BMBW-FBW-72-29] 22 p2667 N73-31371
Parachute-borne blunt probe measurement of mesospheric ionization
[NASA-CR-135637] 23 p2784 N73-32277

**ROCKET THRUST**
NT RETROTHRUST
Characteristics of solid propellant rocket engine with controlled rate of thrust buildup operating in vacuum environment
[NASA-CASE-NPO-11559] 15 p1824 N73-24784

**ROCKET VEHICLES**
NT AEROBEE ROCKET VEHICLE
NT ARCAS ROCKET VEHICLES
NT ASTROBEE ROCKET VEHICLES
NT ATHENA ROCKET VEHICLE
NT ATLAS CENTAUR LAUNCH VEHICLE
NT ATLAS LAUNCH VEHICLES
NT BLACK BRANT SOUNDING ROCKETS
NT CENTAUR LAUNCH VEHICLE
NT HONEST JOHN ROCKET VEHICLE
NT LITTLE JOHN ROCKET VEHICLE
NT LOKI ROCKET VEHICLE
NT MULTISTAGE ROCKET VEHICLES
NT NIKE ROCKET VEHICLES
NT NIKE-TOMAHAWK ROCKET VEHICLE
NT SATURN LAUNCH VEHICLES
NT SATURN S-2 STAGE
NT SATURN S-4B STAGE
NT SATURN 1B LAUNCH VEHICLES
NT SATURN 5 LAUNCH VEHICLES
NT SCOUT LAUNCH VEHICLE
NT SKYLARK ROCKET VEHICLE
NT SOUNDING ROCKETS
NT TITAN LAUNCH VEHICLES
NT TITAN 3 LAUNCH VEHICLES
NT VERONIQUE ROCKET VEHICLES
Air density at 200 km heights analyzed from Cosmos 286 rocket orbit decay, emphasizing annual variations and geomagnetic disturbances
[RAE-TR-72071] 03 p0296 N73-12417
Design and performance of vibratory output gyro using asymmetrical rotor for rocket inertial attitude control
[NAL-TR-290] 04 p0447 N73-13645
Procedures for calculating attitude of rocket from gyroscopic roll, pitch and yaw
[AD-758764] 15 p1809 N73-24659
Summary of COSPAR meetings and reports on news from national and international organizations about rockets and propelled vehicles
24 p2994 N73-33922

**ROCKET-BORNE INSTRUMENTS**
Rocket-borne auroral optical measurement of proton and electron precipitation
[SC-RR-72-0543] 07 p0793 N73-16448
Galactic and background radiation measurements by rocket-borne submillimeter detectors
07 p0840 N73-16808
Solar observation and research using rocket-borne instruments, in German programs
[BMBW-FBW-72-27] 07 p0846 N73-16862
Plasma wave generation in ionosphere by rocket-borne electron beam accelerator
08 p0947 N73-17753
Atmospheric sounding and ionospheric disturbance measurements by rocket-borne instruments
[AD-754244] 10 p1157 N73-19412
Rocket measurement of solar fluxes at 1216 A, 1450 A and 1710 A
[AERONOMICA-ACTA-A-111] 10 p1210 N73-19842
Rocket-borne mass spectrometer experiment with cryo-cooled ion source to determine neutral atmosphere composition between 85 and 125 km altitude
[BMFT-FBW-73-03] 11 p1285 N73-20431
Rocket-borne mass spectrometric measurements of atmospheric ion composition
15 p1779 N73-24421
ESRO sounding rocket experiment R-175 in presence of noctilucent clouds on polar summer upper atmosphere structure, composition, and ionization
[AP-7] 17 p2027 N73-26406
Altitude test of rocket-borne mass spectrometer cooled by liquid helium in arc heated plasma jet wind tunnel
[DLR-MITT-72-23] 22 p2675 N73-31424

**ROCKETRY**
U ROCKETS

**ROCKETS**
Soviet Cosmos satellite and rocket programs
[NASA-TT-F-14641] 04 p0478 N73-13913

**ROCKS**
NT ANORTHOSITE
NT BASALT
NT COAL
NT IGNEOUS ROCKS
NT LUNAR ROCKS
NT PUMICE
NT SEDIMENTARY ROCKS
NT SHALES
Feasibility assessment of rapid excavation of hard rock by means of continuous fluid jets with pressures of 20,000 to 80,000 psi
[AD-744014] 01 p0051 N73-10416
Geological applications of side-looking radar, noting mineral exploration, engineering geology, and soil science
03 p0295 N73-12406
ERTS-1 imagery of Quaternary landforms and materials in Midwest and Great Plains
[E72-10272] 04 p0409 N73-13333
FORTRAN 4 computer program for one-dimensional stress wave analysis of linear viscoelastic rock
[BM-IC-8563] 05 p0516 N73-14197
Determination of paleotectonic principal stress orientation and spacings of joints in outcrops, and development of optical diffraction analysis method
[BM-RI-7706] 06 p0665 N73-15409
Distinguishing major lithologic types in rocks of Precambrian age in central Wyoming using multilevel sensing
[E73-10301] 09 p1021 N73-18333
Gamma survey of rocks and soils covered by nonactive radiation absorption layers using aerial reconnaissance and fourier analysis
[AD-755003] 11 p1289 N73-20461
Aeromagnetic survey of Amchitka Island, Alaska and adjacent insular shelf for studying tertiary volcanic rocks
[USGS-PP-707] 14 p1661 N73-23481
Rock densities within gravitational anomalies of Ukrainian shield
[AD-757540] 15 p1783 N73-24455
Differentiation of serpentinitic from nonserpentinitic ultramafic rocks in Maryland Piedmont using ERTS-1 MSS imagery
[E73-10632] 16 p1896 N73-25337
Effectiveness of crushed and graded stone aggregate in preventing or retarding rate of flame propagation from fixed ignition source for aircraft fuels
[FAA-NA-73-13] 17 p2097 N73-26962
Significance of biological factors in weathering of rocks and minerals
[NASA-TT-F-14892] 18 p2142 N73-27316
Velocities of elastic waves during deformation and failure of rocks under compression
[AD-759993] 18 p2149 N73-27374
Influence of blue green algae on crystalline calcium carbonate formation on river rocks
[NASA-TT-F-15028] 20 p2368 N73-29046
Mapping exposed silicate rock types and exposed ferric and ferrous compounds from Skylab
[E73-10877] 20 p2393 N73-29228
Effects of microflora on rock weathering and edaphic factor
[NASA-TT-F-15033] 20 p2411 N73-29380
Magnetic variation station for recording geomagnetic variations on ocean bottom
21 p2547 N73-30419
Electrical properties of dry rocks
[NASA-CR-133886] 22 p2666 N73-31364
ERTS analysis of geological relationships of Precambrian Greenstone belts and Troctolite series rocks of Minnesota
23 p2784 N73-32271
Hypothesis for enormous accumulation and exclusive occurrence of ferruginous quartzite in Precambrian rock
[NASA-TT-F-15121] 23 p2786 N73-32290

**ROCKY MOUNTAINS (NORTH AMERICA)**
Detection of phenological event for specific forest and crop types using ERTS-1 imagery
[PAPER-A19] 19 p2261 N73-28226
Mapping of snow cover in western areas of US based on ERTS-1 data
[PAPER-W18] 19 p2272 N73-28295
Phenological observations of lilac, honeysuckle, alfalfa, and winter wheat in Rocky Mountain and Columbia Valley Corridors
[E73-10925] 20 p2398 N73-29274
Interdisciplinary analysis of Colorado Rocky Mountain environments using ADP techniques
[E73-11039] 23 p2778 N73-32218

**RODENTS**
NT GUINEA PIGS
NT HAMSTERS
NT MICE
NT RABBITS
NT RATS

**RODS**
NT CONTROL RODS
Rayleigh-Ritz solution of wave propagation in thermoviscoelastic rod insulated on lateral surface and driven by sinusoidal stress at one end
[AD-746466] 01 p0115 N73-10952
Measurement of axial velocity profiles and resulting acoustical fields of rod under continuous-wave excitation
[AD-747209] 02 p0239 N73-11945
Propagation of axisymmetric harmonic waves across interface of two semi-infinite rods composed of different isotropic materials
[AD-746721] 02 p0239 N73-11948
Iterative algorithm for determining thermal instabilities in viscoelastic rod under cyclic loads
[AD-746470] 02 p0240 N73-11953
Analytical model for parallel flow-induced vibrations experimentally checked on single rod test facility in water loop
[EUR-4771] 03 p0284 N73-12301
Lateral inertia effects on elastic-plastic wave propagation in slender rods
[AD-750102] 06 p0728 N73-15938
Series expansion method for calculating longitudinal load impact on rod of rate-dependent material
[AD-751979] 08 p0967 N73-17904
Thermal simulation of oxide fuel rod by heated rods of different geometry
[EURFNR-1026] 10 p1187 N73-19655
Elastoplastic deformation of slender rod subjected to impact loads
[AD-754241] 10 p1221 N73-19935
Production of glass fiber reinforced plastic pressure tanks and rods
[AD-754679] 11 p1300 N73-20547
Arc welding of joints and hard surfaces using longitudinally notched ceramic rods
[AD-756944] 13 p1535 N73-22435
Theoretical and experimental analysis of flow induced by harmonic oscillation of rods with arbitrary cross sections containing incompressible, viscous, Newtonian fluid
23 p2774 N73-32183
Synthesis of polycrystalline oxide ceramic laser rods
[AD-765345] 23 p2802 N73-32413

**ROGALLO WINGS**
U FLEXIBLE WINGS
U FOLDING STRUCTURES

**ROLL**
Visual and vestibular effects in human oculomotor response during head rotation in yaw and roll
06 p0633 N73-15147
Forced oscillation test equipment for measuring dynamic stability of roll velocity on lifting bodies
[AD-762258] 19 p2250 N73-28139

**ROLL CONTROL**
U LATERAL CONTROL

**ROLL FORMING**
Determination of friction and lead during rolling by electrical contact procedure and by method of core impressions
[AD-747670] 03 p0308 N73-12517
Influence of preliminary hot rolling on superplasticity of zinc aluminum eutectoid
09 p1046 N73-18530

**ROLLER BEARINGS**
Design and evaluation of hybrid boost bearings consisting of fluid film bearing coupled with rolling element bearing
[NASA-CR-2226] 09 p1039 N73-18476
Defect effect in geometric shape of antifriction bearings on balancing precision of rigid rotors
[AD-754610] 11 p1300 N73-20551
Relationship between temperature and surface layer quality of two row roller bearings polished with abrasive cloth
[AD-754678] 11 p1301 N73-20559
Optimum roller bearing design for use in heavy lift helicopter rotor transmission second stage planetary system
[AD-755535] 15 p1794 N73-24540
Computer programs for analyses of free or forced undamped vibrations of rolling contact supported rotors
[NASA-CR-132220] 15 p1810 N73-24672
Thermodynamic analysis of high speed tapered roller bearings operating with fluid lubrication under combined loads
[NASA-CR-121207] 17 p2037 N73-26482

Performance tests of gas turbine engine mainshaft roller bearings to determine stress and lubrication parameters
[AD-760563] 18 p2157 N73-27426
Wear tests of ceramic materials for rolling contact bearings
[AD-761200] 18 p2168 N73-27506
Low mass rolling element bearing assembly
[NASA-CASE-LEW-11087-1] 21 p2552 N73-30458
Development of high temperature rolling bearings for operation in liquid sodium
[NYO-4117-9] 22 p2678 N73-31452
Roller bearings technology - material, design, and lubricants
[NASA-TM-X-71441] 24 p2929 N73-33389

ROLLING
Metal temperature effect on friction factor in cold rolling within 20 to 250 C
[AD-746935] 02 p0180 N73-11455
Hot pressing and hot rolling procedures for producing aluminum reinforced with high strength steel strips
[NLL-TRANS-746-1355-[9022.401]] 05 p0561 N73-14554
Pack rolling effects on bond strength between Nb and Cu
[AD-750511] 06 p0678 N73-15517
Characteristics of photoelectric pyrometer for measuring temperature of thin wire during rolling process
[NLL-M-21634-[5828.4F]] 15 p1785 N73-24471
Strip rolling mill for high speed rolling of iron and titanium powders
[AD-759241] 17 p2047 N73-26556
Production of fibrous metal composites by rolling of powder with strong reinforcing wires and application to aerospace vehicle structures 18 p2164 N73-27478
Production of thin walled tubes by drawing and rolling
[NLL-M-21689-[5828.4F]] 20 p2421 N73-29448
Different types of lubricants for working of plastics
[NLL-RTS-7852] 20 p2421 N73-29449
Proceedings of conference on rolling mills for production of work hardened, heat treated metal products
[NLL-M-21649-[5828.4F]] 20 p2421 N73-29450

ROLLING CONTACT BEARINGS
U ANTIFRICTION BEARINGS

ROLLING CONTACT LOADS
Analysis of electrical contact occurrences between rolling surfaces with application to elastohydrodynamic lubrication
[NASA-TN-D-7134] 06 p0690 N73-15620

ROLLING MOMENTS
Procedure for determining rolling moment derivatives of aircraft due to rolling, yawing, and sideslip
[ESDU-AIRCRAFT-06.01.00] 07 p0735 N73-15978
System for eliminating roll rate anomalies occurring during flights of slender ballistic reentry vehicles
[SC-DC-72-2244-A] 07 p0849 N73-16883
Effects of nozzle orientation and configuration on roll control and base pressure of hypersonic reentry vehicle
[SC-DC-72-1187-A] 07 p0849 N73-16884
Development of procedure for determining characteristics of aircraft roll coupling moment caused by flow induced by deflected wings and cross flow
[ISAS-488-VOL-37-NO-14] 14 p1597 N73-22945
Measurements of roll damping derivative of three wing planforms using free light roll balance technique for Mach numbers from 0.7 to 1.4
[ARC-R/M-3274] 15 p1726 N73-24005
Numerical analysis of aircraft rolling performance and effect of cross-coupling of lateral and longitudinal motions
[ARC-R/M-3349] 15 p1727 N73-24010
Supersonic wind tunnel tests to measure overall normal and side forces, rolling, pitching, and yawing moments on canard aircraft
[ARC-R/M-3226] 16 p1853 N73-25011
Numerical analysis of lift and roll stability of ram air cushion vehicle to determine equations for rolling moment coefficient
[PB-219820/8] 18 p2106 N73-27032
Development of rolling maneuver fatigue load data for F-5 and F-105 aircraft based on statistical flight loads data
[AD-761491] 19 p2221 N73-27915

ROLLUP SOLAR ARRAYS
U SOLAR ARRAYS

ROOFS
Sheba triangular thin shell element application to calculation of coding towers, toruses, and roofs
[ISD-127] 09 p1095 N73-18936

ROOM TEMPERATURE
Room temperature electrical properties of SiGe thermoelectric alloys
[SC-DC-72-1020] 07 p0812 N73-16581
Design allowables for room temperature vulcanizing silicone rubber based adhesives for attaching reusable surface insulation to space shuttle structures
[NASA-CR-128887] 11 p1308 N73-20615
Effect of load variables on fatigue crack growth at room temperture in Ti-6Al-4V alloy
[NASA-CR-2239] 11 p1345 N73-20913
Electrical conductivity of ThO2 at room and high temperatures and in high intensity gamma radiation fields
[BNWL-1671] 12 p1416 N73-21475
Thermal and electrical conductivity of Nd-Y alloy system at room temperature
[AD-756595] 13 p1566 N73-22693
Volumetric expansion of silver alloy at room temperature
[TID-26251] 16 p1928 N73-25602
Crack arresting in single edge notch A533 B steel at room temperature
[HSSTP-TR-27] 19 p2349 N73-28892
Lithium anode cells operating at room temperature using electrolytic solutions in inorganic solutions
[AD-763478] 23 p2754 N73-32039
Reflectometer for measuring compositional modulation of copper based alloys at room temperature 23 p2803 N73-32418

ROOMS
NT CLEAN ROOMS

ROOT-MEAN-SQUARE ERRORS
Pseudonoise test set for communication system performance evaluation based on RMS error testing
[NASA-TM-X-64698] 03 p0265 N73-12146
Maximum root-mean-square response of square clamped aluminum plate subjected to stationary random excitation
[NASA-CR-129301] 03 p0361 N73-12939
Root mean square center of gravity accelerations and undercarriage forces for taxiing KC-135 tanker aircraft
[CRANFIELD-AERO-15] 16 p1859 N73-25060
Mean squared error method for predicting fidelity of differential pulse code modulation system 16 p1873 N73-25165

ROOTS OF EQUATIONS
Continuation method for solving eigenvalue problems and finding roots of polynomials
[TAE-152] 09 p1057 N73-18617
Algorithms for developing equations yielding root locus diagram
[TT-7303] 14 p1683 N73-23653

ROSETTE SHAPES
Development of curves for determining magnitude and direction of principal stresses and strains in plane stress field from strain gage readings
[ESDU-72014] 05 p0601 N73-14890

ROSSBY REGIMES
Numerical analysis of stability and convergence conditions based on mathematical model of Arctic Ocean
[AD-745182] 01 p0053 N73-10429

ROTARY DRIVES
U MECHANICAL DRIVES

ROTARY GYROSCOPES
Design and performance of vibratory output gyro using asymmetrical rotor for rocket inertial attitude control
[NAL-TR-290] 04 p0447 N73-13645
Determination of gimbal errors of astatic gyroscope with allowance for drift 05 p0546 N73-14435
Synchronizing control of drag-cup gyro motor using dynamic gas bearing
[NAL-TR-304] 15 p1756 N73-24232

ROTARY STABILITY
NT GYROSCOPIC STABILITY
Analysis of whirl stability boundaries and aerodynamic characteristics of tilting rotors 12 p1356 N73-21004

ROTARY WING AIRCRAFT
NT BO-105 HELICOPTER
NT CH-3 HELICOPTER
NT CH-47 HELICOPTER
NT H-53 HELICOPTER
NT HELICOPTERS
NT MILITARY HELICOPTERS
NT OH-6 HELICOPTER
NT OH-13 HELICOPTER
NT P-531 HELICOPTER
NT SH-3 HELICOPTER
NT TANDEM ROTOR HELICOPTERS
NT UH-1 HELICOPTER
NT UH-2 HELICOPTER
NT XH-51 HELICOPTER
Flight mechanics of rotary wing aircraft
[DLR-MITT-71-15] 05 p0493 N73-14021
Performance of auxiliary power systems for advanced Army rotary wing aircraft
[AD-751854] 08 p0870 N73-17046
Aircraft control system for rotary wing aircraft
[NASA-CASE-ERC-10439] 10 p1104 N73-19004
Synthesis of hover autopilots for rotary wing VTOL aircraft
[NASA-CR-132053] 15 p1735 N73-24071
Feedback control for rotary wing aircraft steep approach profiles
[MBB-UFE-1021-O] 23 p2744 N73-31967
Rotary wing aircraft steep instrument approach limits
[MBB-UD-101-73-O] 23 p2745 N73-31969

ROTARY WINGS
NT LIFTING ROTORS
NT RIGID ROTORS
NT TILTING ROTORS
NT TIP DRIVEN ROTORS
Computer program listings for analysis of main rotor free wake geometry effects on blade air loads and response for helicopters in steady maneuvers - Vol. 2
[NASA-CR-2111] 02 p0124 N73-11006
Fabrication of helicopter rotary wings from composite materials of stainless steel liner overwrapped with fiberglass
[NASA-CR-112191] 03 p0251 N73-12031
Development and characteristics of test facility for measuring three dimensional boundary layers on helicopter rotor blade under various conditions
[NASA-CR-112194] 03 p0252 N73-12042
Development of equations for large amplitude coupled flap-lag motion of hingeless elastic helicopter blades
[NASA-CR-114485] 03 p0252 N73-12043
Evaluation of helicopter rotary wing configuration consisting of conventional pitch horn linkages inboard and aerodynamic control flap outboard for controllable twist
[AD-747808] 03 p0254 N73-12054
Application of metal-polyfluoroethylene bearings in helicopter rotor hinges for operation with and without lubrication
[AD-747428] 03 p0308 N73-12512
Foreign process for developing spiral bevel gear for CH-47 helicopter
[AD-747857] 03 p0309 N73-12522
Vortex model for calculating blade circulation flow of helicopter rotor
[NASA-TT-F-14637] 04 p0371 N73-13014
Effects of aerodynamic stall on helicopter rotor blade element in three dimensional rotating environment
[NASA-CR-114489] 04 p0372 N73-13028
Helicopter design data to include kinematic and power diagrams of basic components of helicopter structures
[AD-748751] 04 p0373 N73-13035
Analysis of response of flexible helicopter rotor blade to random loads with vertical velocity component
[AD-746627] 04 p0374 N73-13038
Analysis of model helicopter rotor blade response to random excitation during simulated forward flight using electromechanical apparatus
[AD-748457] 04 p0374 N73-13040
Proceedings of conference to analyze static and dynamic loads exerted on helicopter rotary wings and application to improved helicopter design
[AGARD-R-595] 05 p0491 N73-14000
Developments in unsteady aerodynamics of helicopter rotary wings to analyze stall flutter, transient effects of interactions, and wake induced instabilities 05 p0491 N73-14001
Application of model helicopter rotor experiments to determining dynamic stall of rotary wings and predicting aerodynamic loads developed 05 p0491 N73-14002
Numerical analysis of unsteady aerodynamic forces on helicopter rotor blades to determine lift distribution as function of velocity component normal to blades 05 p0491 N73-14003
Application of perturbation techniques to single blade helicopter rotor dynamics
[NASA-TM-X-62165] 05 p0492 N73-14006
Exact theory for helicopter rotor wake calculation 05 p0494 N73-14025
Design analysis of repairable main rotor blades applicable to UH-1H helicopter
[AD-749283] 05 p0494 N73-14028
Calculation method for effect of compressible three dimensional relief on torque required for helicopter rotor
[AD-750179] 05 p0498 N73-14053
Analysis of stability characteristics of hingeless rotary wing on flap and lead-lag degrees of freedom of single blade
[AD-750359] 06 p0623 N73-15053
Modification of UH-1 helicopter rotor to determine effects of injecting tip vortex of rotor blade with mass of linearly directed air
[AD-750634] 06 p0625 N73-15074
Design and development of sectionalized main rotor blade for UH-1 helicopter
[AD-750633] 06 p0625 N73-15075
Research projects to determine aerodynamic characteristics of rotary wings and propellers
[AD-750175] 06 p0656 N73-15326
Numerical analysis of characteristics of rotary wing aircraft when considered as two coupled rigid bodies representing rotor and fuselage 07 p0737 N73-15994
Application of equations of motion to investigate effects of mode shape and coning angle on stability boundaries of hingeless helicopter rotor blades
[NASA-CR-114525] 07 p0739 N73-16015
Development of dynamic helicopter performance and control model based on force and rotor aerodynamic equations
[AD-751460] 07 p0740 N73-16022

Effect of dynamic absorbers and damping on noise generated by CH-47 helicopter rotor transmission
[AD-752579] 08 p0868 N73-17031

Development of computer programs to calculate helicopter rotor tip vortex geometry in hover and forward flight to include calculation of rotor harmonic air loads
[AD-752628] 08 p0869 N73-17032

Modifications to helicopter active transmission isolation system to provide method for measuring forces on rotary wing of CH-53 helicopter
[NASA-CR-112245] 09 p0982 N73-18024

Dynamic and aeroelastic problems of stop-rotors of V/STOL aircraft occurring during retracting and stowing of rotary wings
[DLR-FB-72-65-PT-1] 09 p0983 N73-18027

Analytic methods for calculating blade loads and shaft-transmitted vibratory forces in stiff bladed hingeless rotors operating at various advance ratios - Vol. 1
[NASA-CR-114562] 09 p0984 N73-18034

Descriptions, geometry, and technical data for three rotary wing systems used in determining vibration and loads in hingeless rotary wings - Vol. 2
[NASA-CR-114568] 09 p0984 N73-18035

Analysis of aerodynamic stall characteristics of airfoils at various angles of attack with application to control forces of H-53 helicopter
[AD-752917] 09 p0986 N73-18053

Analysis of effects of rotary wing configuration on aerodynamic noise generation during hovering flight
[AD-753397] 09 p0989 N73-18070

Analysis of aerodynamic noise generated by tips of helicopter rotary wings during acceleration to near sonic speed
[AD-752301] 09 p0989 N73-18072

Analysis of airload and blade response of rotary wings to determine sources of rotor vibratory loads in level and maneuvering flight of NH-3A and CH-53A helicopters
[NASA-CR-2225] 10 p1103 N73-18996

Predicting loads and stresses on helicopter rotor blades
[NASA-TT-F-14845] 10 p1105 N73-19014

Application of equations of motion to develop analog computer simulation of helicopter rotor system
[AD-754547] 11 p1235 N73-20024

Application of momentum theory to determine performance limits of propellers, and lifting rotors with axes parallel to undisturbed flow
[AD-754072] 11 p1235 N73-20025

Numerical analysis of ideal and real gas equations for application to lift generated by helicopter rotors
[AD-754420] 11 p1235 N73-20026

Fatigue damage of helicopter rotary wing structures - bibliographies
[AD-754062] 11 p1235 N73-20027

Three component wake velocity measurements of full scale OH-13 helicopter rotary wing during hovering flight
[AD-754644] 11 p1235 N73-20030

Proceedings of conference on rotary wing aircraft developments to include operational experience, flight tests, and evaluation of structural concepts
[AGARD-CP-121] 12 p1357 N73-21008

Effect of elastic flapping of rotor blades on stability and control of helicopter equipped with hingeless rotor system
12 p1358 N73-21016

Flight tests of Westland Scout helicopter fitted with reduced scale version of rigid rotor to determine airworthiness and handling characteristics
12 p1358 N73-21017

Analysis of factors inhibiting performance of rotary wing aircraft and mathematical models of rotary wing flow characteristics
12 p1358 N73-21019

Survey of problems encountered in prediction of structural design loads and aeroelastic stability margins during development of rotary wing aircraft
12 p1358 N73-21020

Structural concepts of rotary wing system capabilities to show changes in design of specific vertical takeoff aircraft components
12 p1358 N73-21021

Aerodynamic characteristics of circulation controlled rotor and fundamental problems of stopped rotor aircraft
12 p1359 N73-21024

Development of jet-flap rotor and application to heavy helicopter and stoppable rotor designs
12 p1359 N73-21025

Development of rotary wings with cold, hot, and mixed cycle tip jet propulsion systems and application for torque-free rotor drive system
12 p1359 N73-21026

Review of tilting rotor technology and comparison of tilting rotor performance with standard rotary wings
12 p1359 N73-21027

Development of advancing blade concept rotary wing and wind tunnel tests of full scale model
12 p1359 N73-21029

Proceedings of conference on fluid dynamics of rotary wings and aerodynamic characteristics of rotary wing systems
[AGARD-CP-111] 12 p1359 N73-21031

Analytical and experimental techniques to define geometry of vortex field of hovering rotary wing and effect on rotor performance
12 p1359 N73-21032

Development of actuator disc theory for predicting time-averaged downwash distribution and response characteristics of helicopter rotors in forward flight
12 p1360 N73-21033

Procedures for measuring velocity distribution through helicopter rotor blade tip vortex using single full scale rotor blade
12 p1360 N73-21034

Development of procedure for determining geometry and strength distribution of vortex wake generated by single-bladed hovering helicopter rotor
12 p1360 N73-21035

Parameters for enhancing performance of helicopter rotors during stationary flight
12 p1360 N73-21036

Wind tunnel tests of rotary wing to determine retreating blade stall at several preset parameters and effect of reverse flow area
12 p1360 N73-21037

Improvements in basic rotary wing design and tests to determine effects on helicopter performance
12 p1360 N73-21038

Aerodynamic characteristics of rotary wings under axial flow conditions and development of numerical analysis techniques
12 p1360 N73-21039

Development of method for predictiong performance of heavily loaded propellers and rotors in steady hovering flight
12 p1360 N73-21040

Analysis of unsteady aerodynamic environment of rotary wings and research projects to improve understanding of rotor unsteady airfoils
12 p1361 N73-21041

Analysis of unsteady aerodynamic loading on reference section of helicopter rotor blade in axial or hovering flight under compressible flow conditions
12 p1361 N73-21044

Effect of rotary wing airfoil modifications on performance, stability, and control of helicopters
12 p1361 N73-21045

Developments in techniques for analyzing boundary layer characteristics of rotary wings based on unsteady viscous-inviscid interaction
12 p1361 N73-21046

Development of technique for rotor blade design and measurement of pressure distributions along the blade chord and across blade wake near rotor tip in flight
12 p1361 N73-21047

Development of algorithm for calculating inviscid flow about arbitrary planform rotors and application to analyzing various rotary wing configurations
12 p1362 N73-21048

Wind tunnel tests to determine effects of blade twist and aeroelasticity on tilt rotor performance from hover to mach number 0.7
12 p1362 N73-21049

Development of concept of circulation control applied to rotary wings to show effects on hover, transition, and high speed cruise performance
12 p1362 N73-21050

Aerodynamic, dynamic, and aeroelastic problems in rotary wing design for helicopters and V/STOL aircraft with application to hingeless rotor systems
12 p1362 N73-21051

Analysis of aerodynamic noise produced by rotary wings and methods for noise reduction based on shed vortex wakes and blade tip modification
12 p1362 N73-21053

Generation of aerodynamic noise by turbulent wake behind rotary wing airfoil and relationship to drag and lift coefficients
12 p1362 N73-21054

Noise spectrum characteristics and directivity patterns for rotary wings as function of blade tip speed, total rotor thrust, and angle of rotor disc plane
12 p1362 N73-21056

Analysis of electrical charge generated by helicopter rotor operating near particulate matter with seeded vortex
[AD-755282] 12 p1366 N73-21080

Analysis of helicopter blade flutter for both hinged and hingeless rotor blades
[AGARD-R-607] 13 p1472 N73-21920

Proceedings of conference on rotary wings to investigate rotor wakes, aerodynamic characteristics at hover and high advance ratio, and aerodynamic noise properties
13 p1473 N73-21931

Analysis of helicopter performance with functioning engines, disengaged transmission, and steady autorotation of coaxial rotary wings
[AD-756592] 13 p1474 N73-21942

Analysis of aerodynamic and dynamic properties of rotary wing aircraft for application to design, development, and evaluation of helicopters
[AGARD-LS-63] 14 p1597 N73-22948

Aerodynamic characteristics of helicopters with emphasis on airloads, aeroelasticity, and mechanical instabilities
14 p1597 N73-22949

Fundamentals of rotary wing aerodynamics and application to performance considerations of helicopters
14 p1598 N73-22950

Basic dynamics of rotary wings, mechanics of helicopter flight, and aerodynamic characteristics of advanced rotary wing concepts and configurations
14 p1598 N73-22951

Effects of aeroelasticity on performance of rotary wings and procedures for predicting aerodynamic forces on rotary wing blades
14 p1598 N73-22952

Effects of aerodynamic drag on rotary wing performance and methods for reducing influence of stall and compressibility parameters
14 p1598 N73-22954

Procedures for testing rotary wing aircraft models in wind tunnels to include design of test facilities, cost of models and facilities, and methods for obtaining data
14 p1598 N73-22955

Analysis of effects of Reynolds number on aerodynamic stalling of rotary wings and relationship of Reynolds number to aerodynamic coefficients of blade elements
14 p1598 N73-22957

Analysis of effects of aerodynamic and dynamic parameters on design synthesis of rotary wings and application of optimization techniques
14 p1598 N73-22958

Flight test procedures for rotary wing aircraft with emphasis on performance and flying qualities
14 p1598 N73-22959

Analysis of aerodynamic noise produced by rotor operating at supersonic speed
[TT-7213] 14 p1599 N73-22967

Design and evaluation of two airfoils for helicopter rotors for reduction of rotor power requirements
[NASA-CR-112297] 14 p1601 N73-22977

Analysis of vortex shedding from airfoils with application to vortex noise generated by helicopter rotary wings
[AD-757167] 14 p1602 N73-22989

Environmental endurance testing of elastomeric pitch change bearing for use on H-1 Aircraft
[AD-758463] 14 p1671 N73-23561

Feasibility and cost effectiveness of expendable main rotor blades on UH-1 helicopter
[AD-758464] 15 p1736 N73-24078

Design, development, and testing of inflexible blade, hingeless rotor system with hydraulic rotor control system
[AD-758514] 15 p1736 N73-24081

Optimum roller bearing design for use in heavy lift helicopter rotor transmission second stage planetary system
[AD-755535] 15 p1794 N73-24540

Numerical analysis of bending of rotating beams with application to linear flap-lag stability of hingeless rotary wings using nonlinear equations
[NASA-TM-X-2770] 15 p1838 N73-24897

Research projects in theoretical and practical aerodynamics - Vol. 2
16 p1854 N73-25020

Development of method for calculating spanwise loading on helicopter rotor blades in forward flight at various azimuth angles
[ARC-R/M-3318] 16 p1856 N73-25032

Design studies and model test results of folding-proprotor aircraft concept
[AD-759534] 16 p1862 N73-25086

Aerodynamic characteristics and noise attenuation effects of leading edge serrations on rotary wings
[AD-759028] 16 p1863 N73-25088

Development of procedures for determining service life of helicopter airframes and rotor blades
[RAE-LIB-TRANS-1520] 17 p1981 N73-26013

Technique for realistic prediction and electronic synthesis of helicopter rotor noise
[AD-759955] 17 p1984 N73-26037

Design and feasibility analysis of field-replaceable rotor blade pocket
[AD-759956] 17 p1984 N73-26038

Wind tunnel tests to determine acoustic properties of helicopter rotor and wind tunnel calibration techniques
[RAE-LIB-TRANS-1683] 17 p2009 N73-26249

Analysis of products and techniques for reducing reflections of light from helicopter windshields, rotor blades and rotor hub assembly
[AD-761127] 18 p2107 N73-27037

Effect of engine vibration, shaft whirling, and dynamic instabilities on helicopter performance and standardization of vibration limit specifications
[AD-761100] 18 p2107 N73-27039

Application of glass reinforced and carbon reinforced composite materials for helicopter structures and rotary wings
18 p2165 N73-27483

Design, reliability analysis, maintainability, and cost effectiveness of expendable rotor blades for UH-1 helicopter rotary wing
[AD-762198] 19 p2222 N73-27926
Numerical methods for determining unsteady aerodynamic forces on helicopter rotor blades to show lift distribution as function of velocity component normal to blades
[NASA-TT-F-15039] 20 p2360 N73-28981
Analysis of wakes generated by hovering model propellers and rotors using schlieren photography and hot-wire anemometry
[NASA-CR-2305] 21 p2491 N73-29996
Design, development, and flight test of stowed folding tilt rotor aircraft and comparison with nonfolding tilt rotor aircraft - Vol. 5
[NASA-CR-114598] 21 p2493 N73-30009
Application of composite materials in development of tilting rotor for vertical takeoff aircraft - Vol. 6
[NASA-CR-114599] 21 p2493 N73-30010
Development of feedback control in tilt rotor aircraft using swashplate cyclic and collective controls in addition to direct lift control - Vol. 7
[NASA-CR-114600] 21 p2493 N73-30011
Real time piloted simulation to investigate handling qualities and performance of tilting rotor aircraft - Vol. 9
[NASA-CR-114602] 21 p2493 N73-30012
Analysis of discrete frequency and broad band noise generation by subsonic rotary wings for vertical takeoff aircraft
[NASA-CR-2077] 21 p2494 N73-30014
Analysis of pitch damping moment for hovering helicopter rotary wing and development of formula for calculating pitch damping derivative
[NASA-TT-F-15010] 21 p2495 N73-30027
Analysis of failure modes of blades on CH-47 helicopter rotary wings for improved helicopter reliability and cost reduction
[AD-763187] 21 p2497 N73-30042
Wind tunnel and rotor whirl cage tests to determine stability and control parameters of scale model of tilting rotor aircraft model - Vol. 6
[NASA-CR-114615] 22 p2614 N73-30950
Dynamic structural analysis of fully articulated rotor blade on helicopter rotary wing for three degrees of freedom
[AD-763934] 22 p2615 N73-30957
Helicopter gust response to include unsteady aerodynamic stall effects under short-term, control-fixed conditions
[AD-763957] 22 p2615 N73-30958
Aerodynamic characteristics of low speed flight using heavily loaded ducted fans, single bladed hovering rotor, and tensioned sheets with cutouts
[AD-764264] 22 p2616 N73-30964
Bibliography of technical reports of helicopter engines and rotary wings
[AD-764900] 23 p2746 N73-31981
Wind tunnel tests of high harmonic circulation control rotary wing model to show instruments required and data acquisition procedures
[AD-765320] 23 p2747 N73-31984

**ROTATING**
U ROTATION

**ROTATING BODIES**
NT COMPRESSOR ROTORS
NT FLYWHEELS
NT IMPELLERS
NT LIFTING ROTORS
NT LUNAR ROTATION
NT PUMP IMPELLERS
NT RIGID ROTORS
NT ROTARY WINGS
NT ROTATING CYLINDERS
NT ROTATING DISKS
NT ROTATING SPHERES
NT ROTORS
NT TILTING ROTORS
NT TIP DRIVEN ROTORS
NT TURBINE WHEELS
Large-diameter rotary vacuum chamber with servo controlled angular positioning and readout
[LBL-769] 03 p0281 N73-12275
Exact solution of gravitational field of rotating mass
[RIFP-161] 04 p0449 N73-13666
Exterior gravitational field of slowly rotating deformed masses, obtained by generalizing Weyl metrics into rotating Weyl metrics
[RIFP-162] 04 p0449 N73-13667
Rotating target providing high yield neutrons by He-4 reaction for cancer therapy
[NASA-TM-X-68179] 07 p0746 N73-16067
Numerical analysis of viscous, compressible, and heat conducting fluid flow patterns in rotating nozzles
07 p0768 N73-16241
Magnus effect in supersonic laminar boundary layer on spinning body of revolution
[SC-DC-72-1173] 07 p0772 N73-16269
Variational equations for studying rotational motion of orbiting rigid body about its center of mass under conservative and nonconservative torques
07 p0817 N73-16624
Relationship between laminar film condensation on inside of rotating non-capillary heat pipe and pipe heat transfer capabilities
[NASA-CR-130373] 07 p0854 N73-16926
Mathematical model and analysis of attitude stability and control of spinning flexible satellite in force-free environment
08 p0964 N73-17876
Formulation of mathematical model for predicting dynamic behavior of rotating flexible space station configurations - Vol. 1
[NASA-CR-112243] 10 p1189 N73-19672
User's manual for computer program to predict dynamic behavior of rotating flexible space station configurations - Vol. 2
[NASA-CR-112244] 10 p1189 N73-19673
Optical rotating intensity modulator for measuring positions and magnitudes of stars
10 p1211 N73-19848
High speed water jets from vertically accelerated cones partially filled with water
[MT-64] 11 p1270 N73-20302
Cartesian and curvilinear coordinates for studying axial symmetrical deformation of rotatory bodies
[NLL-M-22827-[5828.4F]] 11 p1344 N73-20907
Orbital retrieval technology associated with spinning uncooperative satellites
[NASA-CR-131510] 12 p1459 N73-21826
Solution of axisymmetric finite deformation equations for arbitrary shallow orthotropic shell of revolution subjected to uniform pressure and edge loading
13 p1584 N73-22844
Modal analysis for Liapunov stability of rotating elastic bodies
[NASA-CR-124258] 15 p1839 N73-24904
Computer program for dynamic analysis of shells of revolution
[NASA-CR-132752] 17 p2001 N73-26177
Numerical analysis of nonlinear resonance phenomena in systems of solids having rotating and vibrating parts
17 p2092 N73-26928
Design of dynamic and rotary machines - Vol. 2
[AD-762441] 19 p2306 N73-28543
Development and characteristics of annular momentum control device for two axis stabilization of spacecraft
[NASA-CASE-LAR-11051-1] 19 p2318 N73-28646
Turbulent flow of gas-solid suspensions about ellipsoid of revolution
20 p2385 N73-29163
Steady, supersonic, three dimensional flow in rotating and stationary annular cascades treated by method of characteristics in three independent variables
[DLR-FB-73-12] 21 p2525 N73-30247
Second order thermal boundary layer theory for steady, laminar, compressible flow over cambered two dimensional or rotational bodies
[DLR-FB-73-31] 22 p2653 N73-31256
Calculation of heat exchange between rotating body and moving fluid
[AD-763941] 22 p2656 N73-31275
Inviscid, isentropic, three-dimensional flow theory for rotating thin blade row in cylindrical duct
23 p2775 N73-32193
Structural methods for increasing effectiveness of fully rotatable parabolic antennas
23 p2837 N73-32673
Attitude stability of spinning elastic bodies based on modal analysis and criteria for idealized spinning flexible spacecraft
24 p2950 N73-33564
Approximate solution for free vibrations of rotating uniform cantilever beams
[NASA-TM-X-62299] 24 p2989 N73-33885

**ROTATING CONES**
U CONICAL BODIES
U ROTATING BODIES

**ROTATING CYLINDERS**
Free surface secondary flow of Newtonian liquid between rotating concentric cylinders
24 p2906 N73-33188

**ROTATING DISKS**
Analysis of laminar fluid flow between two rotating coaxial disks
[ISAS-485-VOL-37-11] 02 p0155 N73-11257
Rotating disk measurement of drag reduction and shear properties of various dilute polymers
[AD-751552] 07 p0773 N73-16281
Design of elastically geared circular disk wave drive motor and telemanipulator
[NASA-TT-F-14803] 10 p1165 N73-19482
Absorbing power with enclosed partially submerged rotating disk in turbulent viscous shearing of water
[NASA-TN-D-7234] 15 p1767 N73-24316
Design, fabrication, and test of boron-polyimide reinforced titanium fan disks to operate at high temperatures
18 p2167 N73-27498
Performance and endurance of compressor disks bound with boron composite wires
18 p2167 N73-27499
Stability characteristics of stratified and unstratified air flow between two horizontal, infinite disks rotating at slightly different rotation rates
20 p2384 N73-29154
Turbulent fluid friction of rotating disks in incompressible flow calculations
20 p2384 N73-29155
Transition from laminar to turbulent flow for radially inward throughflow of incompressible Newtonian fluid between closely spaced parallel corotating disks
20 p2385 N73-29159
Relativistic rigidity of rotating disk
[AD-763330] 21 p2604 N73-30873

**ROTATING ELECTRICAL MACHINES**
Numerical analysis of electrical field of capacitance generator to determine potential at points in gas gap
[AD-747570] 03 p0256 N73-12069
Determination of dynamic zone sparkless commutation for linear and sinusoidal load current changes in dc machines
[NLL-RTS-7771] 18 p2122 N73-27149

**ROTATING ENVIRONMENTS**
Direction-specific adaptation effects acquired by humans in slowly rotating room
[NASA-CR-129063] 01 p0008 N73-10062
Dynamic model of rotating spacecraft force effects on human vestibular system
01 p0015 N73-10119
Tests to determine physiological and behavioral response to transitions between rotating and nonrotating environments
[NASA-CR-2130] 02 p0135 N73-11093
Effects of simulated artificial gravity on human performance
[NASA-CR-2129] 03 p0260 N73-12111
Analysis of axially symmetric motions of viscous neutral stratified gas in spherical layer resulting from rotation of inner sphere
[NASA-TT-F-14661] 08 p0897 N73-17260
Application of perturbation theory and Ritz energy method for analyzing nonlinear flexural gyrations of untwisted, rotating cantilevered blade vibrating in plane of rotation
16 p1968 N73-25923

**ROTATING FLUIDS**
NT ROTATING LIQUIDS
Sphere free motion in rotating fluid noting Taylor instability existence
[DLR-FB-71-32] 03 p0285 N73-12309
Structure and behavior of confined jet flow in rotating fluid
06 p0653 N73-15301
Molecular diffusion in mixing binary flow and separation of uranium isotopes by fixed wall centrifugation
06 p0653 N73-15302
Lectures on properties and characteristics of rotating and stratified fluids
[AD-754066] 11 p1272 N73-20320
Near axial zone of flow reversal of rotating supersonic unexpanded jet and helical gas flow
[AD-754617] 11 p1272 N73-20327
Computations of turbulent mixing and combustion of swirling jets in coaxial stream
[NASA-CR-2231] 11 p1348 N73-20935
Stability of thin elastic tube of infinite length containing rotating inviscid, incompressible fluid flow
13 p1508 N73-22222
Measurement of fluid velocity and surface deformation during fluid discharge from rotating cylindrical tank
13 p1509 N73-22232
Numerical analysis of steady state laminar motion of viscous, incompressible, and binary fluids for rotating flow in cylindrical geometry
18 p2129 N73-27204
Stability of laminar pipe flow with rigid rotation and small three-dimensional perturbation
[MITT-55] 19 p2256 N73-28184
Numerical analysis of solitary wave propagation in incompressible rotating fluids
20 p2385 N73-29160
Hydrodynamic stability of circular magnetic fields and revolving fluids
22 p2650 N73-31234
Boundary and shear layers in rotating and stratified fluids
22 p2651 N73-31235

**ROTATING GENERATORS**
NT AC GENERATORS
NT DYNAMOMETERS
NT TURBOGENERATORS
Rotating generator for angular display of television raster in horizontal and visual simulation systems
[NASA-CASE-FRC-10071-1] 05 p0513 N73-14171
Development of superconducting homopolar machines with multiple discs and superconducting field winding using liquid metals for armature sliding contacts
10 p1109 N73-19037

**ROTATING LIQUIDS**
Self wave oscillations in variable depth rotating basins discussing second class modes for three cases
07 p0857 N73-16952

Existence of undamped Kelvin waves in semiinfinite rotating basin with step change in depth
22 p2653 N73-31250

**ROTATING PLASMAS**
Design of feedback geometry for control of rotating plasma confined in magnetic mirror device
[AD-751341] 07 p0830 N73-16728
Mathematical model for dense rotating plasma with centrifugal expansion instability at high beta values
[TRITA-EPP-72-28] 09 p1071 N73-18740
Experiments on rotating plasmas for determining magnetohydrodynamic stability at high beta values
[TRITA-EPP-72-33] 09 p1071 N73-18741
Experiments on magnetoacoustic oscillations in rotating hydrogen and deuterium plasmas with superimposed high frequency heating
[TRITA-EPP-72-34] 12 p1436 N73-21635
Instability of rotating plasmas at beta value before reaching critical velocity
[TRITA-EPP-73-01] 12 p1436 N73-21636
Tensor viral method for modeling and studying pulsars in rapidly rotating magnetosphere
16 p1960 N73-25858
Experiments on velocity distribution and critical velocity of rotating hydrogen plasma
[TRITA-EPP-73-06] 17 p2068 N73-26736
Isotope separation in rare gases caused by centrifugal force in plasmas
[TRITA-EPP-72-27] 19 p2325 N73-28701
Correlation of potential and density fluctuations of plasma resulting from rotational instability of hot cathode Penning discharge
[NASA-TT-F-13026] 20 p2458 N73-29751
Stablity of plasma rotating in crossed electrical and magnetic fields
[NASA-TT-F-15021] 20 p2458 N73-29752
Stability of indicating gyrostabilizer in viscous suspension of forced rotation of three stage gyroscopes
23 p2791 N73-32331

**ROTATING SHAFTS**
NT SHAFTS [MACHINE ELEMENTS]
NT TURBOSHAFTS
Torsional bending and longitudinal vibrations of rotating shafts and application to free vibrations of individual rotor blades, blade cascades, and shrouded blades
[NASA-TT-F-14627] 04 p0372 N73-13029
Evaluation of exact point speed and least squares procedures for determining balance of flexible rotating machinery
[NASA-CR-121035] 05 p0551 N73-14477
Procedure for balancing high speed, light weight rotary machinery resting on gas lubricated bearings
[AD-750951] 06 p0623 N73-15055
Bearing sectors for controlling self excited instability of journal bearing shafts rotating at high speeds in low viscosity lubricants
[NASA-CASE-LEW-11076-2] 11 p1298 N73-20533
Dynamic behavior of eccentric rotating shaft subject to linearly varying or constant tension
13 p1532 N73-22414
Vibration effects on self-acting and hydrodynamic shaft seals in gas turbine engines
[NASA-TM-X-68214] 13 p1534 N73-22430
Methods of testing rotating components of turbomachines compared with tests on complete turbomachines
[AGARD-AG-167] 17 p2077 N73-26800
Digital servocontroller for rotating antenna shaft
[NASA-CASE-KSC-10769-1] 18 p2122 N73-27153
Development of optical system for detecting defective components in rotating machinery with emphasis on bearing assemblies
[NASA-CASE-KSC-10752-1] 18 p2154 N73-27407
FORTRAN 4 computer program for calculating critical speeds of rotating shafts
[NASA-TN-D-7385] 19 p2347 N73-28881
High speed, self-acting shaft seal
[NASA-CASE-LEW-11274-1] 20 p2422 N73-29457

**ROTATING SPHERES**
Analysis of axially symmetric motions of viscous neutral stratified gas in spherical layer resulting from rotation of inner sphere
[NASA-TT-F-14661] 08 p0897 N73-17260
Dependences between braking and precession moments acting on spherical rotor in magnetic suspension
21 p2547 N73-30422
Doppler shift arising from radiating body rotation at extreme relativistic speeds
22 p2714 N73-31721
Exact solution to nonlinear Euler equations pertaining to problem of thermally stratified compressible fluid motion on rotating sphere with gravitation
[AD-764684] 23 p2788 N73-32308

**ROTATING VEHICLES**
U ROTATING BODIES
U VEHICLES

**ROTATION**
NT AUTOROTATION
NT EARTH ROTATION
NT MOLECULAR ROTATION
NT PLANETARY ROTATION
NT SATELLITE ROTATION
NT SOLAR ROTATION
NT STELLAR ROTATION
Vestibulo-ocular response of man to oscillatory rotation during sleep
[AMRU-R-70-3] 02 p0131 N73-11066
Shape and rotation rate of asteroid bodies
02 p0228 N73-11850
Human semicircular canal response to rotational stimuli in yaw, pitch, and roll planes of the head
06 p0632 N73-15137
Anti-compensatory oculomotor response of pilot to rotational head stimuli
06 p0632 N73-15138
Electronic circuits for synchronous rotation of rotors suspended in magnetic field
[SRARI-P-120] 06 p0647 N73-15257
Projectile rotation measurement by polarized light modulation
[BMVG-FBWT-72-18] 07 p0766 N73-16225
Rotational polarization of electromagnetic waves propagating in magnetized plasma
[JAERI-M-4640] 08 p0948 N73-17766
Observation of eastward diurnal driving forces in thermospheric superrotation phenomenon
[NASA-TM-X-66222] 11 p1286 N73-20438
Mathematical model for development of first-order secular solutions to rotational motions of triaxial rigid body - Part 2
[NASA-CR-131878] 13 p1549 N73-22555
Kinematics of orientation in rotating coordinate system and determination of orientation of instrument trihedrons
[JPRS-59162] 20 p2451 N73-29700
Kinematics of stability of orientation in rotating coordinate system signal processing
20 p2451 N73-29702

**ROTATIONAL FLOW**
U FLUID FLOW
U VORTICES

**ROTONS**
Damping of accelerated isothermal superfluid helium flow by roton polarization
[NOTA-INTERNA-395] 03 p0336 N73-12743
Elementary excitation spectrum of superfluid helium
10 p1198 N73-19750
Low temperature energy spectrum near roton minimum region in superfluid helium
17 p2064 N73-26696

**ROTOR AERODYNAMICS**
Analysis of response of flexible helicopter rotor blade to random loads with vertical velocity component
[AD-746627] 04 p0374 N73-13038
Application of perturbation techniques to single blade helicopter rotor dynamics
[NASA-TM-X-62165] 05 p0492 N73-14006
Nonlinear instability in flap-lag of rotor blades in forward flight
[NASA-CR-114524] 08 p0867 N73-17017
Proceedings of conference on rotary wings to investigate rotor wakes, aerodynamic characteristics at hover and high advance ratio, and aerodynamic noise properties
13 p1473 N73-21931
Performance of seismic angular vibration transducer using gas rotor
[RAE-TM-IR-128] 13 p1530 N73-22400
Design, characteristics, and performance tests of high-tip-speed, low-loading, transonic fan stage
[NASA-CR-121095] 13 p1570 N73-22727
Static and cruise tests on series of 13 ft diameter low disc loading rotors with various blade twists
[NASA-CR-114625] 15 p1734 N73-24063

**ROTOR BLADES**
Development of equations for large amplitude coupled flap-lag motion of hingeless elastic helicopter blades
[NASA-CR-114485] 03 p0252 N73-12043
Vortex model for calculating blade circulation flow of helicopter rotor
[NASA-TT-F-14637] 04 p0371 N73-13014
Effects of aerodynamic stall on helicopter rotor blade element in three dimensional rotating environment
[NASA-CR-114489] 04 p0372 N73-13028
Design and development of sectionalized main rotor blade for UH-1 helicopter
[AD-750633] 06 p0625 N73-15075
Nonlinear instability in flap-lag of rotor blades in forward flight
[NASA-CR-114524] 08 p0867 N73-17017
Extended natural mode method for calculating flapwise bending, edgewise bending, and torsional vibration modes and frequencies of helicopter rotor blades
[DLR-FB-71-108] 09 p0983 N73-18026
Development of advancing blade concept rotary wing and wind tunnel tests of full scale model
12 p1359 N73-21029
Procedures for measuring velocity distribution through helicopter rotor blade tip vortex using single full scale rotor blade
12 p1360 N73-21034
Wind tunnel tests of rotary wing to determine retreating blade stall at several preset parameters and effect of reverse flow area
12 p1360 N73-21037
Development of technique for rotor blade design and measurement of pressure distributions along the blade chord and across blade wake near rotor tip in flight
12 p1361 N73-21047
Analysis of helicopter blade flutter for both hinged and hingeless rotor blades
[AGARD-R-607] 13 p1472 N73-21920
Analysis of reverberant-field noise produced by three lift fan models operating at various rotor tip speeds
[NASA-TM-X-68243] 17 p1981 N73-26014
Wind tunnel tests to determine acoustic properties of helicopter rotor and wind tunnel calibration techniques
[RAE-LIB-TRANS-1683] 17 p2009 N73-26249
Application of boron/aluminum composite material for construction of turbine blades with low notch sensitivity in high cycle fatigue
18 p2166 N73-27497
Far field sound propagation calculation for ducted fan rotor-stator interaction
[NRC-13260] 18 p2179 N73-27592
Rotor noise reduction by serrated brass strip attachment to blade leading edges
[NASA-TN-D-7371] 19 p2219 N73-27898
Design, reliability analysis, maintainability, and cost effectiveness of expendable rotor blades for UH-1 helicopter rotary wing
[AD-762198] 19 p2222 N73-27926
Flight tests of CH-47 helicopter to determine structural performance of boron-reinforced epoxy aft rotor blades
[AD-762199] 19 p2222 N73-27927
Numerical analysis of variable pitch compressor rotor blades for reduction of rotor vibrations
[AD-762228] 19 p2330 N73-28746
Dynamic and aeroelastic problems of V/STOL aircraft stop-rotors occurring during retracting and stowing of rotor blades
[DLR-FB-73-19] 21 p2496 N73-30035
Analysis of failure modes of blades on CH-47 helicopter rotary wings for improved helicopter reliability and cost reduction
[AD-763187] 21 p2497 N73-30042
Analysis of failure modes of tail rotor on OH-58 helicopter for improved reliability and cost reduction
[AD-763188] 21 p2497 N73-30043
Dynamic structural analysis of fully articulated rotor blade on helicopter rotary wing for three degrees of freedom
[AD-763934] 22 p2615 N73-30957
Pulsed laser holographic interferometry of shock waves within transonic fan rotors
[NASA-TM-X-71430] 23 p2801 N73-32402

**ROTOR BLADES [TURBOMACHINERY]**
Rotor design, test apparatus and procedure, and data reduction and evaluation for axial flow pump rotor configurations
[NASA-TN-D-7074] 06 p0613 N73-14982
Analysis of radial distributions of flow conditions at inlet and outlet of high speed rotors to determine effects of blade part-span dampers on rotor performance
[NASA-TM-X-2696] 06 p0614 N73-14985
Procedure for balancing high speed, light weight rotary machinery resting on gas lubricated bearings
[AD-750951] 06 p0623 N73-15055
Application of unsteady airfoil theory to determine pressure and lift fluctuations on rotor blades of turbomachinery
07 p0735 N73-15983
Two dimensional cascade test of highly loaded, low solidity, tandem airfoil turbine rotor blade
[NASA-TM-X-2729] 08 p0954 N73-17814
Performance test of compressor stage with cantilevered stator and rotating inner shroud under stator at rotor tip speed of 1600 feet per second
[NASA-CR-121141] 15 p1825 N73-24794
Axial flow turbomachine response to upstream disturbances
[AD-759029] 16 p1866 N73-25107
Design and feasibility analysis of field-replaceable rotor blade pocket
[AD-759956] 17 p1984 N73-26038
Design, development, and evaluation of centrifugal compressor with six to one pressure ratio and two pounds per second air flow
[NASA-CR-120941] 17 p2037 N73-26483
One dimensional stationary analysis of air cooled, ducted gas turbines nozzle vanes
[AD-761451] 19 p2330 N73-28744
Analysis of operation of single stage, high pressure centrifugal compressor during closed loop flow of various gases
[AD-761608] 19 p2331 N73-28750
Boundary layer theory for flow and heat transfer problems in turbomachine blades
21 p2590 N73-30751
Computer program for analyzing general nonaxisymmetric and nonsynchronous transient and steady-state performance of flexible rotor bearing system
[NASA-CR-121276] 22 p2677 N73-31440
Method for determining time to failure of blades on aircraft gas turbine engines at steady mode and transient mode of operation
[NASA-TT-F-15113] 22 p2710 N73-31700

Effects of blade tip clearance and leading edge sweepback of compressor rotor blades on inducer performance and blade pressure loading
[NASA-CR-72712] 23 p2739 N73-31930
Noise comparison of two STOL pressure ratio fans with 15 and 42 rotor blades
[NASA-TM-X-2891] 23 p2829 N73-32609
Capacitive method for measuring blade tip clearance in running turbocompressors
[DLR-FB-72-40] 23 p2831 N73-32628

**ROTOR DISKS**
U TURBINE WHEELS

**ROTOR HUBS**
U HUBS
U ROTORS

**ROTOR SPEED**
Computer program for analyzing general nonaxisymmetric and nonsynchronous transient and steady-state performance of flexible rotor bearing system
[NASA-CR-121276] 22 p2677 N73-31440

**ROTORCRAFT**
U ROTARY WING AIRCRAFT

**ROTORS**
NT COMPRESSOR ROTORS
NT FLYWHEELS
NT IMPELLERS
NT LIFTING ROTORS
NT PUMP IMPELLERS
NT RIGID ROTORS
NT ROTARY WINGS
NT TILTING ROTORS
NT TIP DRIVEN ROTORS
NT TURBINE WHEELS
Rotary vane attenuator with two stators and intermediary rotor, using resistive and orthogonally disposed cards
[NASA-CASE-NPO-11418-1] 04 p0420 N73-13420
Electronic circuits for synchronous rotation of rotors suspended in magnetic field
[SRARI-P-120] 06 p0647 N73-15257
Elastic gyro rotor with stable orientation of readout axis by point mass system
07 p0817 N73-16623
Equations of motion for calculating flexible rotor influence on two gimbaled gyroscope motion
08 p0922 N73-17554
Flight characteristics and performance of Fenestron type helicopter tail rotor
12 p1359 N73-21028
Computing rotor potential of electrostatic gyroscope
13 p1556 N73-22610
Algorithm for computing unrelieved electromagnetic forces of attraction of rotors in EDG electric motors
17 p2059 N73-26657
Analysis of products and techniques for reducing reflections of light from helicopter windshields, rotor blades and rotor hub assembly
[AD-761127] 18 p2107 N73-27037
Process for welding compressor and turbine blades to rotors and discs of jet engines
[NASA-CASE-LEW-10533-1] 19 p2303 N73-28515
Development of improved cooling system for low-flow gas turbine rotor
[AD-761452] 19 p2330 N73-28743
Elastic deformation of gimbal suspension on gyroscope nutation, moments acting on spherical rotor in magnetic suspension, and differentiating linear accelerometer
[JPRS-59740] 21 p2547 N73-30420
Dependences between braking and precession moments acting on spherical rotor in magnetic suspension
21 p2547 N73-30422
Equations of motion formulated to compute transient response of multi-mass flexible rotors
[NASA-CR-2300] 23 p2797 N73-32374

**ROUGHNESS**
NT SEA ROUGHNESS
NT SURFACE ROUGHNESS

**ROUND TRIP TRAJECTORIES**
Interplanetary trajectory characteristics of Saturn swingby mission to Uranus
[NASA-TM-X-2914] 22 p2714 N73-31727

**ROUNDED LEADING EDGES**
U LEADING EDGES

**ROUTES**
Side-looking radar applications to transportation noting route planning, shipping lanes, and traffic
03 p0295 N73-12409
Compilation of Instrument Flight Rules Off-Airway Non-95 Routes for US and Alaska, November 1972
05 p0577 N73-14696
Computerized optimal ship routing considering ocean meteorological charts
[AD-761620] 19 p2319 N73-28652

**ROUTINES**
Text, syntax, and description of PL 516 assembler noting ALGOL, one track, one pass syntax, and design philosophy
[NPL-COM-SCI-65] 23 p2761 N73-32093

**ROVER PROJECT**
Monte Carlo use in Rover nuclear rocket engine development program
[LA-DC-72-1078] 08 p0937 N73-17673

**ROVING VEHICLES**
NT LUNAR ROVING VEHICLES
Application of laser rangefinder on autonomous Martian roving vehicle for navigation and mid-range path selection
[NASA-CR-128398] 01 p0064 N73-10523
Experimental design and scientific exploration of Mars surface by MARV
[NASA-TM-X-64719] 07 p0765 N73-16219
Unmanned roving vehicle design for surface exploration of Mars
16 p1884 N73-25252
Autonomous Martian roving vehicle determination of terrain gradients from laser measurements
[NASA-CR-133498] 19 p2307 N73-28556

**RPV**
U REMOTELY PILOTED VEHICLES

**RUBBER**
NT CHLOROPRENE RESINS
NT ELASTOMERS
NT LATEX
NT SILICONE RUBBER
NT SYNTHETIC RUBBERS
NT VITON RUBBER [TRADEMARK]
Three different equations of state used for computing stress-strain curves of rubber in tension
[AD-747664] 03 p0322 N73-12621
Frictional properties of rubbers in presence of greases and graphite lubricants
[AD-747447] 03 p0322 N73-12622
Compatibility with explosives and propellants of natural, butyl and chloroprene rubbers containing Octamine or Flectol H as antioxidants
[ERDE-TN-55] 05 p0565 N73-14592
Time lag method for transient permeation of benzene and acetone vapors through sulfur natural rubber
[NASA-TM-X-64721] 07 p0752 N73-16112
Application of data processing to flexural and tensile tests on rubber
[ERDE-TR-114] 09 p1052 N73-18579
Application of tension stress relaxation measurements to determine physical and mechanical properties of rubber networks during chemical reactions
[RR-204] 24 p2987 N73-33868

**RUBBER COATINGS**
Intumescent paint containing nitrile rubber for fire protection
[NASA-CASE-ARC-10196-1] 04 p0437 N73-13562

**RUBIDIUM**
NT RUBIDIUM ISOTOPES
Acoustic measurements and sound velocity calculations for molten rubidium at high pressures
[AD-746838] 02 p0138 N73-11120
Operational frequency stability of rubidium and cesium frequency standards
[NASA-TN-D-7063] 08 p0943 N73-17724

**RUBIDIUM COMPOUNDS**
Dielectric susceptibilities of potassium chloride to lithium and hydroxyl, sodium chloride to hydroxyl, and rubidium chloride to cyanides
[COO-3151-14] 10 p1200 N73-19763
Powder neutron diffraction and susceptibility measuring techniques to study magnetic properties of $RbMnBr_3$
[BNL-17519] 15 p1814 N73-24703

**RUBIDIUM ISOTOPES**
Measurement errors and working signal structure of rubidium vapor M sub Z magnetometers and design of observatory vector magnetometer
[JPRS-58950] 15 p1786 N73-24480
Measurement errors of rubidium vapor M sub Z magnetometer
15 p1786 N73-24481
Structure of working signal of rubidium vapor M sub Z magnetometer
15 p1786 N73-24482
Electronic design of rubidium-87 maser
[NASA-CR-132770] 17 p2040 N73-26502

**RUBY**
Sliding friction experiments in air with polycrystalline copper and ruby riders
[NASA-TN-D-7232] 11 p1298 N73-20530
Chromium concentration effect on duration and width of luminescent lines in ruby spectrum
[AD-761374] 18 p2191 N73-27692

**RUBY LASERS**
Improving divergence in ruby laser radiation by holographic transformation of light field coherence
[AD-746646] 02 p0183 N73-11486
Application of continuous wave gas laser and pulsed ruby laser to analyze laminar and turbulent films of air at porous wall with carbon dioxide and helium injected into air stream
[AD-747511] 03 p0287 N73-12323
Experimental determination of electron density in absorbing layer of laser produced plasmas
[JUL-820-PP] 04 p0454 N73-13706
Surface damage to gallium arsenide surfaces from radiation by ruby and neodymium-glass lasers
05 p0555 N73-14507
French Pic du Midi ruby laser telemetry station, noting positioning devices and optical data processing
05 p0557 N73-14525
Design of reflector for stabilization and frequeacy tuning of ruby laser spectrum
[PB-211890] 05 p0558 N73-14537
Measurement of vertical distribution of atmospheric water vapor by ruby laser rod
[PB-211891] 05 p0575 N73-14680
Generation and measurement of ruby laser picosecond pulses
[AD-750789] 06 p0680 N73-15538
Examination of Q switched ruby laser produced spherical shock waves
13 p1508 N73-22220
Plasma enhancement and diagnostic possibilities of tunable laser excitation
[AD-755373] 13 p1564 N73-22672
Design and operating characteristics of pulsed ruby laser source used in portable holocamera
16 p1920 N73-25541
Advanced technology for improving performance parameters of ruby laser
16 p1921 N73-25542
Holographic technique to record front surface detail from high velocity target
16 p1921 N73-25547
Ruby laser radar system for measuring spatial density distribution of atmospheric water vapor
17 p2039 N73-26499
Holographic interferometry using pulsed ruby lasers to measure electron density in toroidal plasmas
[REPT-72-70] 17 p2069 N73-26743
Forward scattered light spectrum from pulsed ruby laser in liquid medium
20 p2424 N73-29470
Variations in beam characteristics of ruby laser used in lidar system
[SLA-73-347] 24 p2931 N73-33407
Scattering of ruby laser beam by plasma focus of coaxial gun
[CEA-R-4430] 24 p2931 N73-33411

**RULES**
NT INSTRUMENT FLIGHT RULES
NT SUM RULES

**RUMBLE INSTABILITY**
U ACOUSTIC INSTABILITY

**RUN TIME [COMPUTERS]**
PERT planning run time reduction with special purpose cellular logic computer
03 p0271 N73-12195

**RUNGE-KUTTA METHOD**
Application of Runge-Kutta process to circular geostationary orbit equations of motion
[RAE-TR-72118] 13 p1578 N73-22790
Development of equations of condition necessary for determining coefficients for Runge-Kutta methods used to solve ordinary differential equations
[NASA-CR-130902] 15 p1803 N73-24613
Runge-Kutta-Nystrom formulas of eighth and lower order derived for special second order differential equations
[NASA-TR-R-410] 15 p1803 N73-24614

**RUNNING**
Correlation of assessed maximum oxygen intake with predicted performance in running events
[AD-746867] 04 p0380 N73-13093

**RUNOFFS**
U DRAINAGE

**RUNUP**
U ENGINE TESTS

**RUNWAY ALIGNMENT**
Runway separation standards according to reaction time of pilot manual control response to air traffic controller communication
01 p0015 N73-10113

**RUNWAY CONDITIONS**
Mu-meter and diagonal braked vehicle measurements of runway friction at ten airports
[PSC-107] 01 p0036 N73-10281
Visual inspection of runway conditions at Fort Polk Army Airfield, Louisiana
[AD-743858] 01 p0037 N73-10292
Visual inspection of runway conditions at Butts Army Airfield, Fort Carson, Colorado
[AD-743859] 01 p0037 N73-10293
Visual inspection of runway pavement conditions at Forney Army Airfield, Fort Leonard Wood, Missouri
[AD-743856] 01 p0037 N73-10294
Visual inspection of runway conditions at Redstone Army Airfield, Huntsville, Ala.
[AD-743857] 01 p0037 N73-10295
Braking effects on aircraft tire tread wear and runway surface characteristics
[NASA-TN-D-6963] 02 p0125 N73-11021
Performance tests of Andover C short takeoff transport aircraft on grass, concrete and soil landing sites
[ARC-CP-1220] 04 p0373 N73-13034
Analysis of effect of grooved runway configurations on aircraft tire braking traction on flooded runway surfaces
[NASA-TN-D-7215] 12 p1363 N73-21057
Development of procedures for repairing damaged runway pavements
[AD-756806] 15 p1763 N73-24286

**RUNWAY LIGHTS**
Development, characteristics, and operation of test facility for determining effectiveness of runway lighting systems under various atmospheric conditions
[FAA-RD-71-94] 20 p2382 N73-29141

**RUNWAYS**
Mu-meter and diagonal braked vehicle measurements of runway friction at ten airports
[PSC-107] 01 p0036 N73-10281
Visual investigation of runway and taxiway pavements at Campbell Army Airfield, Fort Campbell, Kentucky
[AD-743462] 01 p0037 N73-10291
Visual survey of runway and taxiway conditions at Davison Army Airfield, Fort Belvoir, Virginia
[AD-743463] 01 p0038 N73-10296
Determining optimal runway orientation for minimizing frequency of crosswinds and headwind reversals at Cape Kennedy
[NASA-CR-128995] 01 p0075 N73-10617
Deformation and repair of artificial runway surfaces using new structural materials
[AD-746718] 02 p0153 N73-11242
Structural evaluation of cellular plastic as base course material for military expedient pavement to withstand limited number of aircraft coverages
[AD-747048] 02 p0153 N73-11244
Cost effectiveness analysis of propane operated fog dispersal system and evaluation of runway visual range improvement
[FAA-RD-72-123] 06 p0649 N73-15267
Observation, measurement, and automatic calculation of runway visibilities
[NLL-M-20785-[5828.4F]] 07 p0814 N73-16597
Evaluation of aluminum 1 by 12 ft extruded light-duty landing mat with symmetrical butt-type end connectors
[AD-752079] 08 p0893 N73-17233
Evaluation of aluminum runway surface concepts as possible aid to aircraft braking
[NASA-TN-D-7186] 09 p0985 N73-18040
Design, construction, and maintenance of landing fields and runways
[AD-751400] 09 p1012 N73-18263
Analysis of effect of grooved runway configurations on aircraft tire braking traction on flooded runway surfaces
[NASA-TN-D-7215] 12 p1363 N73-21057
Development of mathematical and simulation models to calculate capacity of single runway under instrument flight rules conditions
[MTR-4102-REV-2] 14 p1645 N73-23345
Numerical integration technique used to re-compute influence coefficients used for development of design curves for rigid airfield runway pavements
[AD-755526] 14 p1646 N73-23353
Inspection of pavement grooving at four commercial and one military airfield
[AD-757208] 14 p1647 N73-23355
Performance of fibrous reinforced concrete overlay test slabs as runways at Tampa International Airport, Florida
[FAA-RD-72-119] 14 p1680 N73-23634
Inspection of Hunter Army Airfield, Savannah, Georgia to determine condition of runways
[AD-757387] 15 p1763 N73-24285
Analysis of dual lane runway operations at high density airport terminals using computerized simulation techniques
[ATC-17] 16 p1885 N73-25254
Performance of airfield pavement construction joints under heavy aircraft loads
[FAA-RD-72-106] 16 p1969 N73-25926
Airport planning studies, and procedures for determining airfield capacity, operations, and delays
[FAA-RD-73-11-VOL-2] 17 p2010 N73-26255
Worldwide airfield climatic data for Eastern Europe and USSR - Part 1
[AD-759794] 17 p2057 N73-26640
Worldwide airfield climatic data for Eastern Europe, and USSR - Part 2
[AD-759795] 17 p2057 N73-26641
Evaluation of aluminum honeycomb core landing mat with modified hinges
[AD-758840] 18 p2127 N73-27186
Suitability determination of redesigned XW18 membrane as expedient surfacing for waterproofing and dustproofing hastily prepared airfields for operations of C-130 aircraft
[AD-761089] 18 p2127 N73-27190
Strengthening of keyed longitudinal construction joints in rigid pavements
[AD-759570] 18 p2204 N73-27789
Analysis and recommendations concerning relaxation of spacing requirements for independent IFR parallel approaches into closely spaced runways
[MTR-6282] 19 p2249 N73-28129
Guidelines for evaluation and maintenance of expedient-surfaced airfield facilities
[AD-762126] 19 p2249 N73-28137
Installation of XM19 airfield landing mat and ancillary items
[AD-762137] 20 p2383 N73-29148
Evaluation of structural layers in flexible pavement during simulated aircraft traffic
[AD-762131] 20 p2383 N73-29149
Preliminary analysis of possible factors associated with asphaltic concrete airfield pavement defects
[AD-762404] 20 p2383 N73-29150
Analysis of factors affecting feasibility of minimizing runway spacings for increased air terminal operational capacity - Vol. 2
[FAA-RD-72-58-VOL-2] 20 p2452 N73-29709
Airfield runway marking paint superior to paint presently used
[FAA-RD-73-23] 21 p2520 N73-30213
Analysis of glide path parameters, approach control system precision, and separation standards for extension of runway capacity under instrument flight rule conditions
[AD-763142] 21 p2578 N73-30657
Finite element model of jointed concrete pavement on nonlinear viscous subgrade dynamic interaction of aircraft-pavement systems
[AD-764243] 22 p2647 N73-31213
Prediction of performance of runway pavements
[AD-763118] 22 p2648 N73-31214
Design methodology for airfield pavements
[AD-763212] 22 p2648 N73-31215
Test results and evaluation procedure for non-destructive tests of airfield pavements
[AD-764787] 23 p2798 N73-32382

**RUPTURING**
Influence of transverse force on impeller bearing rupture of centrifugal pumps
02 p0179 N73-11446
Relationship between structure and high temperature creep and creep rupture of metals
[SU-326-P-17-X-3] 03 p0315 N73-12566
Diaphragm rupture effects on expanding flow in evacuated tube
[AD-752605] 08 p0899 N73-17277
Extrapolating stress-rupture test results of heat resistant alloys
13 p1542 N73-22495
Durability of metal films to rupture as thickness of film increases
[AD-756616] 14 p1679 N73-23623

**RURAL AREAS**
Monitoring rural landscape changes in eastern Tennessee through interpretation of ERTS-1 imagery
[E72-10177] 01 p0045 N73-10356
Geographic applications of ERTS-1 imagery to rural landscape change in Tennessee
[E72-10355] 05 p0534 N73-14343
Aerial photointerpretation of impact of highway construction on rural area in Thailand
20 p2417 N73-29414

**RUTHENIUM**
NT RUTHENIUM COMPOUNDS
Reaction kinetics when liquid hydrazines adsorbed on supported ruthenium catalyst
[RPE-TR-72/1-PT-5] 05 p0506 N73-14122

**RUTHENIUM ALLOYS**
Effect of ruthenium on passivating capacity and corrosion resistance of titanium
[NLL-TRANS-746-1375-[9022.401]] 05 p0560 N73-14550

**RUTHENIUM COMPOUNDS**
Electrical resistance of thick film ruthenium dioxide resistor circuits
[AD-756254] 14 p1644 N73-23337

**RUTILE**
Rutile crystal growth, and hydrogen kinetics, electronic, and optical properties
[AD-748298] 06 p0709 N73-15789
Influence of heat treatment on physical properties of iron- and chromium-doped rutile
[RR-107] 09 p1073 N73-18760
Coordination chemistry and kinetics of preferential etching on surfaces of TiO2 [rutile]
[AD-759259] 17 p2074 N73-26780
Experimental analysis of rutile properties including crystal growth, hydrogen diffusion, and magnetic resonance determination of defects
[AD-760667] 18 p2190 N73-27684
Growth of rutile single crystals by chemical vapor transport
[AD-760733] 18 p2191 N73-27687
Heat treated chromium doped rutile for L-band traveling wave masers
[RR-111] 24 p2930 N73-33402
Temperature dependence of spin-Hamiltonian parameters for chromium doped rutile
[RR-110] 24 p2968 N73-33721

**RYAN MILITARY AIRCRAFT**
U MILITARY AIRCRAFT

**RYAN AIRCRAFT**
NT XC-142 AIRCRAFT
NT XV-5 AIRCRAFT


## S


**S BAND**
U SUPERHIGH FREQUENCIES
U ULTRAHIGH FREQUENCIES

**S MATRIX THEORY**
Jost-Kohn inversion procedure applied to quantum mechanical problem
02 p0201 N73-11627
Location of poles of scattering matrix
02 p0201 N73-11628
Derivation of doubling equations for scattering and transmission functions for a homogeneous isotropically scattering atmosphere using scattering matrix
[USC-113P19-32] 02 p0202 N73-11631
Derivation of theorems for spinless particle scattering from Kohn variational principle
[NASA-CR-129259] 03 p0323 N73-12634
Long-range forces between atoms at large distances, and weak forces arising from neutrino-antineutrino exchange
[TR-73-049] 03 p0339 N73-12764
Composite scattering model for explaining rough sea surface scattering cross sections
06 p0663 N73-15383
Physical equivalence of null plane quantum electrodynamics in null plane gage to conventional electrodynamics in Coulomb gage
09 p1066 N73-18700

**S WAVES**
Effects of pulse shape on transient response of cylindrical shells and generation of shear waves in cylindrical shells
[NASA-CR-112221] 05 p0602 N73-14891
Numerical solution to problem of gravitational-shear waves in flow with arbitrary temperature stratification
24 p2947 N73-33532

**S-N DIAGRAMS**
Fatigue tests of notched and unnotched Ti6Al4V bars compared to other Ti-alloys
[LBF-TM-62/71] 06 p0685 N73-15574
Fatigue strength of notched titanium aluminum vanadium alloy between 1 million and 10 million stress cycles
[LBF-TM-63/71] 06 p0685 N73-15575
Distributional S-N and Goodman diagrams for designing target reliabilities into rotating mechanical components
[NASA-CR-120967] 10 p1164 N73-19465

**S-3 SATELLITE**
U EXPLORER 12 SATELLITE

**S-16 SATELLITE**
U OSO-1

**S-18 SATELLITE**
U OAO

**S-27 SATELLITE**
U ALOUETTE 1 SATELLITE

**S-49 SATELLITE**
U OGO-A

**S-74 SATELLITE**
U EXPLORER 18 SATELLITE

**S-2 AIRCRAFT**
Performance tests of aircraft arresting gear to determine allowable operating restraints on angular displacement and off-center engagements
[NATF-R125] 06 p0649 N73-15268

**S-3 AIRCRAFT**
Role of flight simulation in development of S-3 and F-14 aircraft
08 p0865 N73-17001

**S-67 HELICOPTER**
Addition of feel augmentation system to improve flight control of S-67 helicopter
[AD-749284] 05 p0494 N73-14029

**SABOT PROJECTILES**
Strain wave propagation in metal cones with compressive pulse applied at base and application to design of gun launchers
[AD-762504] 22 p2727 N73-31822

**SABRE AIRCRAFT**
U F-86 AIRCRAFT

**SACRAMENTO VALLEY [CA]**
ERTS-1 imagery of structures and lithology of Northern California Coast Ranges and Sacramento Valley, California
[E72-10214] 03 p0288 N73-12332
ERTS-1 imagery of structure and lithology of Northern California Coast Ranges and Sacramento Valley
[E72-10333] 05 p0531 N73-14321
Atmospheric effects on recognition of rice and corn in ERTS-1 imagery of Sacramento Valley
[E73-10390] 11 p1276 N73-20352
ERTS-1 imagery of structural and lithological properties of Northern Coast Ranges and Sacramento Valley, California
[E73-10478] 12 p1396 N73-21315
Structural and lithological investigation of Northern Coast Ranges and Sacramento Valley, California
[E73-10577] 14 p1656 N73-23438
Preparation of recognition map to determine crop species and mensuration accuracy in Sacramento Valley, California
[PAPER-A22] 19 p2262 N73-28229
Analysis of ERTS-1 imagery of Northern Coast Ranges and Sacramento Valley, California for locating mercury deposits and oil and gas fields
[PAPER-G18] 19 p2265 N73-28249

Structural and lightological systems of Sierra Nevada Mountains and Sacramento Valley of California from ERTS-1 imagery
[E73-10942] 21 p2530 N73-30284
SADDLE POINTS
NT SADDLE POINTS [GAME THEORY]
SADDLE POINTS [GAME THEORY]
Saddle point method for exact wave plane solution of Burger equation in shock zone
[AD-758409] 15 p1814 N73-24706
SAFEGUARD SYSTEM
Systems analysis and evaluation of perimeter acquisition radar equipment for use with Safeguard Antiballistic Missile System - Vol. 1B
[AD-748060] 03 p0267 N73-12161
System definition and methodology for selecting perimeter acquisition radar system used with Safeguard Antiballistic Missile System - Vol. 2
[AD-748061] 03 p0267 N73-12162
System definition and criticality analysis of perimeter acquisition radar system used with Safeguard Antiballistic Missile System - Vol. 3 Pt. 1
[AD-748062] 03 p0267 N73-12163
SAFETY
NT AIRCRAFT SAFETY
NT FLIGHT SAFETY
NT INDUSTRIAL SAFETY
NT REACTOR SAFETY
Safety procedures for using pulsed lasers and making pulsed holograms
[AD-751024] 07 p0808 N73-16555
Application of ERTS-1 imagery to fracture related mine safety hazards in coal mining industry in Indiana and Illinois
[E73-10096] 09 p1020 N73-18321
Application of ERTS-1 imagery to fracture related mine safety hazards in coal mining industry in Indiana and Illinois
[E73-10371] 10 p1151 N73-19366
Safety analysis of EPS electron-proton spectrometer
[NASA-CR-128851] 11 p1292 N73-20485
Contamination radiation safety during space flight, and safety problems at launch
[JPRS-58781] 12 p1374 N73-21149
Guide for preparation of contractor safety plans at Cape Kennedy Space Center
[NASA-TM-X-69492] 20 p2488 N73-29986
Investigation of backfires and explosions occuring in vacuum pumps of oxygen test stands
[AD-763370] 21 p2554 N73-30474
Application of ERTS-1 imagery to fracture-related mine safety hazards in Ohio coal mining industry
[E73-11034] 22 p2663 N73-31338
Abstracts of NASA-ASRDI publications on aerospace safety research
[NASA-TM-X-71428] 23 p2866 N73-32911
Application of ERTS-1 imagery to fracture related coal mine safety hazards and environmental problems in mining in Indiana
[E73-11148] 24 p2918 N73-33302
SAFETY DEVICES
NT ABORT APPARATUS
NT ARRESTING GEAR
NT EJECTION SEATS
NT ESCAPE CAPSULES
NT ESCAPE ROCKETS
NT HELMETS
NT SEAT BELTS
NT SPACE SUITS
Design, development, and evaluation of aircrew restraint system for forward-facing, nonejection seat for military aircraft
[AD-746631] 02 p0128 N73-11038
Safety devices for preventing surge tank explosions in liquid nitrogen system of hypersonic wind tunnels
[SC-DC-72-1260] 03 p0280 N73-12274
Development, design, fabrication, and testing of a self-generating overheat detection system for USAF aircraft
[AD-749474] 05 p0495 N73-14031
Ionization, thermoluminescence, and nuclear photographic emulsion dosimetry for monitoring radiation loads in spacecrews during manned space flight
09 p0992 N73-18100
Cosmic radiation dosage for estimating manned spacecraft shielding requirements
09 p0992 N73-18101
Design of perforated tube uniform distribution of fire extinguishing agent into commercial air transport compartments
[FAA-NA-73-3] 11 p1233 N73-20009
Decelerator sled simulation for testing air bag restraint system effects in passenger motor vehicle crash
[PB-212706] 11 p1251 N73-20155
Development of collision protection equipment for ground effect machines operating in arctic regions
[AD-758359] 14 p1604 N73-23004
System failure and safety features of superconducting magnetic suspension systems
15 p1762 N73-24277
Comparison of effectiveness of yielding and elastic restraint systems for crash protection to show effects of slack and yield at constant load
[ARL/SM-382] 15 p1837 N73-24890
Development of fibrous flame arrestor materials to provide explosion and fire protection for aircraft fuel tanks
[AD-759193] 16 p1863 N73-25090
Development and characteristics of inflatable airbag restraint system for use in general aviation aircraft
[FAA-RD-73-3] 16 p1868 N73-25127
Performance of hadron laser safety eyeshields in protecting personnel from accidental ocular exposure to common laser radiation
[AD-759921] 17 p1991 N73-26099
Safety measures for nuclear space power and propulsion systems
[LA-DC-72-1480] 17 p2061 N73-26676
Acoustic measurement and recording system for noise generated by air bag automobile safety device
[AD-761836] 19 p2229 N73-27977
Hazard control and safety management role of project manager
[NASA-TM-X-64764] 19 p2354 N73-28937
Dynamic tests of seat belt system, seat belt/shoulder harness system, and seat belt airbag system for aircraft
[FAA-NA-73-30] 20 p2371 N73-29052
Reliability of USAF fire protection systems including portable equipment
[AD-762948] 21 p2610 N73-30925
Impact resistance of crash helmets for agricultural aviation pilots
[ARL/SM-NOTE-390] 22 p2623 N73-31014
SAFETY FACTORS
Analysis of current knowledge regarding ride quality factors in passenger transportation and development of criteria based on human factors engineering
01 p0002 N73-10013
Reference design document for power module systems, facilities, launch vehicle, and mission operations of nuclear reactor for space base programs - Vol. 3 pt. 1
[NASA-CR-123844] 02 p0209 N73-11696
Guidelines and requirements of space base nuclear system safety applied to nuclear hardware, ground support equipment, and range safety and facilities - Vol. 5 Pt. 1
[NASA-CR-123848] 02 p0210 N73-11701
Guidelines and requirements for space shuttle nuclear system transportation of nuclear payloads, ground support systems, and facilities - Vol. 5 Pt. 2
[NASA-CR-123843] 02 p0210 N73-11702
Qualitative identification of steps required to assure incorporation of radiological system safety principles into all phases of manned space base program - Vol. 6
[DOC-72SD4201-6-VOL-6] 02 p0210 N73-11703
Analysis of instrument system for assisting pilots in making decisions during aircraft takeoff and landing rolls
[FAA-RD-72-112] 03 p0301 N73-12460
Development and characteristics of terminal area simulation for analysis of air traffic control requirements and improvement in flight safety conditions
[NASA-CR-112195] 05 p0577 N73-14699
Electrostatic charging and discharging of helicopters in flight and personnel safety
[AD-750617] 06 p0701 N73-15718
Design and safety procedures for operating high voltage capacitor bank
[AD-750535] 09 p1008 N73-18231
Compilation of mishaps in manned space flight program for 1970 to 1971
[NASA-CR-120999] 09 p1090 N73-18897
Health hazards in using electron beams for welding beryllium alloys
10 p1172 N73-19531
Apollo 17 Calibration Facility safety plan covering ultraviolet spectrometer components
[NASA-CR-128833] 10 p1229 N73-19990
Microbiological investigation of neutral buoyancy simulator for weightless space environment testing
[NASA-TM-X-64736] 12 p1371 N73-21127
Development of procedure for designing elevated temperature structures to achieve safety factors and structural integrity of room temperature conditions
[NASA-CR-124232] 13 p1585 N73-22851
National Transportation Safety Board studies in aircraft and surface transportation safety
21 p2609 N73-30909
Engineering safety in space programs
[NASA-TT-F-15077] 22 p2721 N73-31777
SAFETY HAZARDS
U HAZARDS
SAFETY MANAGEMENT
Radiological safety aspects of manned space missions employing nuclear reactors for electric power and involving extended stay times in low earth orbit - Vol 1
[NASA-CR-123842] 02 p0209 N73-11694
Identification of potential and inherent radiological hazards of spacecraft with nuclear reactors for electric power generation and elimination or reduction of hazards - Vol. 2 Pt. 1
[NASA-CR-123838] 02 p0209 N73-11695
Reference design document for power module systems, facilities, launch vehicle, and mission operations of nuclear reactor for space base programs - Vol. 3 pt. 1
[NASA-CR-123844] 02 p0209 N73-11696
Analysis of terrestrial nuclear hazards involving zirconium hydride reactor-Brayton power module for all phases of space base program - Vol. 3 Pt. 2
[NASA-CR-123839] 02 p0209 N73-11697
Development of abort sequence trees for reference zirconium hydride reactor power module for each phase of space base program mission - Vol. 3 Pt. 2A
[NASA-CR-123845] 02 p0209 N73-11698
Analysis of space base mission and accidents/events involving nuclear hazard to general public - Vol. 3 Pt. 3
[NASA-CR-123846] 02 p0210 N73-11699
Analysis of nuclear safety aspects in transport of nuclear payloads to and from earth orbit by space shuttle - Vol. 4 Pt. 1
[NASA-CR-123847] 02 p0210 N73-11700
Guidelines and requirements of space base nuclear system safety applied to nuclear hardware, ground support equipment, and range safety and facilities - Vol. 5 Pt. 1
[NASA-CR-123848] 02 p0210 N73-11701
Guidelines and requirements for space shuttle nuclear system transportation of nuclear payloads, ground support systems, and facilities - Vol. 5 Pt. 2
[NASA-CR-123843] 02 p0210 N73-11702
Analysis of technical documents and literature for conducting manned space flight nuclear system safety study - Vol. 7 Pt. 1
[NASA-CR-123850] 02 p0210 N73-11704
Operational hazards and safety regulations for liquid and gaseous oxygen system handling
[NASA-CR-120922-VOL-2] 05 p0580 N73-14717
Personnel protection and emergencies handling for oxygen systems
[NASA-CR-120922-VOL-4] 05 p0580 N73-14718
Airborne radiological measuring system for use in nuclear safety programs and routine surveillance of areas around nuclear facilities
[EGG-1183-1558] 07 p0800 N73-16501
Characteristics of electromagnetic radiation with emphasis on radiobiology and procedures to reduce undesirable physiological and environmental effects
[JPRS-58783] 12 p1379 N73-21184
Instructions for implementing safety program for KSC
[NASA-TM-X-69219] 12 p1467 N73-21885
Handbook of basic requirements and guidelines for preparing system safety engineering analysis
[NASA-CR-131886] 13 p1593 N73-22913
Grounding, bonding, and shielding practices for operational reliability enhancement in air traffic control electronic facilities
[FAA-RD-73-51] 14 p1645 N73-23341
System safety plan for Apollo ultraviolet spectrometer experiment
[NASA-CR-128570] 16 p1916 N73-25505
Safety standards for Air Force nuclear weapons systems
[AD-759574] 17 p2062 N73-26681
Hazard control and safety management role of project manager
[NASA-TM-X-64764] 19 p2354 N73-28937
Installation standards for NASA Aerospace Safety Information System [NASIS] data base management system - Vol. 1
[NASA-CR-134455] 21 p2511 N73-30139
Overviews of NASA Aerospace Safety Information [NASIS] to introduce system features and component capabilities - Vol. 2
[NASA-CR-134456] 21 p2511 N73-30140
Data set specifications for NASA Aerospace Safety Information System [NASIS] to show standard format for every data set required by system - Vol. 3
[NASA-CR-134457] 21 p2511 N73-30141
Design specifications for programs and modules within NASA Aerospace Safety Information System [NASIS] - Vol. 4
[NASA-CR-134458] 21 p2511 N73-30142
Characteristics and operation of retrieval command subsystem for NASA Aerospace Safety Information System [NASIS] - Vol. 5
[NASA-CR-134459] 21 p2511 N73-30143
Definition and functions of message terms used in NASA Aerospace Safety Information System [NASIS] - Vol. 6
[NASA-CR-134460] 21 p2511 N73-30144
Operation specifications, Installation, and Modifications of NASA Aerospace Safety Information System [NASIS] - Vol. 7
[NASA-CR-134461] 21 p2511 N73-30145
Development of data base administrator user guide for use with NASA Aerospace Safety Information System [NASIS] - Vol. 8
[NASA-CR-134462] 21 p2512 N73-30146
Installation standards for NASA Aerospace Safety Information System [NASIS] data base management system using IBM 360-1370 OS MVT computer - Vol. 1
[NASA-CR-134470] 22 p2637 N73-31132

Overviews of NASA Aerospace Safety Information System [NASIS] to introduce system features and capability of IBM 360/370 OS MVT computer - Vol. 2
[NASA-CR-134471] 22 p2637 N73-31133
Data set specifications for NASA Aerospace Safety Information System [NASIS] to show formats used with IBM 360/370 OS MVT computer - Vol. 3
[NASA-CR-134472] 22 p2637 N73-31134
Design specifications for programs and modules within NASA Aerospace Safety Information System [NASIS] using IBM 360/370 OS MV computer - Vol. 4
[NASA-CR-134473] 22 p2637 N73-31135
Characteristics and operation of retrieval command subsystem for NASA Aerospace Safety Information System [NASIS] using IBM 360/370 OS MVT computer - Vol. 5
[NASA-CR-134474] 22 p2637 N73-31136
Definition and functions of message terms used in NASA Aerospace Safety Information System [NASIS] using IBM 360/370 OS MVT computer - Vol. 6
[NASA-CR-134475] 22 p2637 N73-31137
Development of data base administrator user guide for use with NASA Aerospace Safety Information System [NASIS] using IBM 360/370 OS MVT computer - Vol. 7
[NASA-CR-134476] 22 p2637 N73-31138
Proceedings of conference on radiation safety and protection in industrial applications
[DHEW-PUBL-[FDA]73-8012] 24 p2951 N73-33574
Chronology of radiation protection methods instituted in industrial plants to show specific procedures and reasons for enforcing protective measures
24 p2952 N73-33575
Characteristics and application of various radiation safety monitoring devices for application to industrial safety protection
24 p2952 N73-33576
Development, application, and characteristics of radiation measuring devices for protection of personnel performing hazardous industrial work
24 p2952 N73-33577
Safety precautions for personnel handling radioactive isotopes to prevent accidental exposure to radiation hazards
24 p2952 N73-33582
Provisions of Occupation Health and Safety Act to show requirements imposed on employers and employees for protection from radiation hazards
24 p2953 N73-33587
Preparation and enforcement of safety recommendations established by American National Standards Institute
24 p2953 N73-33588
Atomic Energy Commission policies and procedures for licensing and regulating industrial uses of radioisotopes
24 p2953 N73-33589
Activities of Food and Drug Administration in enforcing safety measures pertaining to industrial radiation equipment
24 p2953 N73-33590

**SAINT VENANT FLEXURE PROBLEM**
U SAINT VENANT PRINCIPLE

**SAINT VENANT PRINCIPLE**
Torsion of an orthotropic, inhomogeneous bar with cylindrical anisotropy including solution by Saint Venant principle
[DRIC-TRANS-2995] 12 p1463 N73-21856

**SALINE SOILS**
U SOILS

**SALINITY**
Mathematical analysis of optical refractive index fluctuations due to salinity and temperature microstructure
[AD-746120] 02 p0168 N73-11366
Mapping, evaluation, and monitoring of coastal and saline wetlands ecology and shallow water environments using ERTS-1 imagery
[E72-10290] 04 p0410 N73-13340
Temperature-salinity profiles of Tyrrhenian Sea
[CONTRIB-2725] 07 p0858 N73-16957
Measurements of oceanographic temperature distribution and salinity in northern Baffin Bay during midsummer 1970
[CG-373-54] 11 p1286 N73-20434
Problems of sea chemistry
[TT-70-57237] 16 p1907 N73-25427
Oceanographic survey of eastern tropical Pacific Ocean to determine oxygen content, salinity, temperature distribution, and acceleration potential
[NOAA-NMFS-CIRC-330] 22 p2656 N73-31279
Indepth comparative analysis of multispectral remote sensing techniques applied to salinity and drainage problems in Columbia Basin, Washington
22 p2656 N73-31280
Land use, forest density, soil mapping, erosion, drainage, and salinity limitations in Greece from ERTS-1 data
[E73-10969] 22 p2657 N73-31283
Salinity effects on extinction coefficient of sea ice
[AD-763882] 24 p2924 N73-33355

**SALIVA**
Statistical analysis of steroid levels in parotid secretions of humans under prolonged mental stress
[AD-747682] 04 p0381 N73-13104
Feasibility of saliva analysis for measuring mental stress in man
[AD-747671] 04 p0382 N73-13111

**SALT BATHS**
Effect of constant applied stress in crack initiation of aluminum and titanium alloys exposed to salt solution and organic fluids
[NASA-CR-124110] 09 p1045 N73-18525

**SALT MARSHES**
U MARSHLANDS

**SALT SPRAY TESTS**
Stress corrosion cracking in saline water of TA6V and TU2 titanium alloys
[ONERA-P-145] 04 p0435 N73-13545
Environmental salt spray tests of closed pore insulation for space shuttle orbiter thermal protection system
[RM-570] 09 p1051 N73-18572
Sea salt and radiant heat effects on crystalline properties of mullite/silica composite thermal insulation for space shuttle
24 p2941 N73-33486

**SALTS**
Coefficients of electrical conductivity for determining concentration of water soluble salts in soils
[NASA-TT-F-15045] 20 p2411 N73-29379

**SALYUT SPACE STATION**
Stellar spectrograms from Salyut space station of alpha Lyrae and beta Centauri
[NASA-TT-F-14582] 07 p0843 N73-16831
Morphological composition of peripheral blood of crew members of Soyuz-9 and Salyut-1
11 p1245 N73-20104

**SAMARITAN AIRCRAFT**
U C-131 AIRCRAFT

**SAMARIUM**
Analysis of cobalt alloys containing samarium additives to determine effects on saturation magnetization, residual magnetization, and coercive forces
[NLL-M-21478-[5828.4F]] 02 p0185 N73-11499
Design of ironless armature torque motor using samarium cobalt permanent magnets
[NASA-CR-130224] 13 p1532 N73-22416
Method for fabricating samarium cobalt permanent magnets
[BM-RI-7784] 21 p2580 N73-30679

**SAMARIUM COMPOUNDS**
Mass spectra of doublets in samarium and gadolinium chlorides
24 p2959 N73-33648

**SAMPLED DATA**
U DATA SAMPLING

**SAMPLED DATA SYSTEMS**
U DATA SAMPLING

**SAMPLERS**
Polarization photometers in payload of sounding rocket for noctilucent cloud particle sampling
[AD-760149] 17 p2028 N73-26415
Portable vacuum probe surface sampler for sampling large surface areas with relatively light loading densities of microorganisms
[NASA-CASE-LAR-10623-1] 21 p2544 N73-30395
Sample-and-hold circuit for monitoring system calibration
[AD-764242] 22 p2676 N73-31434

**SAMPLES**
Quality control of welded joints
[AD-761587] 19 p2306 N73-28548

**SAMPLING**
NT AIR SAMPLING
NT CORE SAMPLING
NT DATA SAMPLING
NT PARTICULATE SAMPLING
NT RANDOM SAMPLING
Suboptimal sampling and control behavior of human operator in output prediction task for automatic process
01 p0015 N73-10114
Variance of Monte Carlo estimates reduced by correlated and antithetic sampling and illustrated by queueing simulation
[NA-70-21] 03 p0324 N73-12643
Antithetic and control variate sampling methods for probability estimation in simulation, with telephony traffic example
[NA-71-41] 03 p0324 N73-12645
Combinations of antithetic sampling methods to determine minimum variance linear combination, with queueing simulation example
[NA-72-49] 03 p0325 N73-12646
Antithetic sampling for variance reduction in stochastic system simulation
[NA-72-57] 03 p0325 N73-12647
Combination of several sampling methods to simulate queueing systems
[NA-72-58] 03 p0325 N73-12648
Automatic swabbing apparatus for sampling of microbiological surfaces
[NASA-CASE-LAR-11069-1] 07 p0745 N73-16061
Statistical three-stage sampling model for estimating resources from remote sensor applications
[NASA-CR-130026] 07 p0800 N73-16494
Optimal linear combination of observable parameters for maximizing correlation between index and criterion variates for sampling classification and personnel selection
[AD-751257] 07 p0813 N73-16596
Spherical sampling functions related to spherical-harmonic functions applied to geophysics
[NASA-CR-130745] 08 p0918 N73-17519
Recursive plane analysis for phase locking in pulse modulation sampling technique
[AD-756918] 13 p1492 N73-22092
Estimation of random process correlation functions, and statistical and sampling errors
17 p2026 N73-26399
Pattern recognition as statistical analysis of confidence level in forensic trace element identification
[IRI-133-72-11] 19 p2240 N73-28056
Sampling strategies for automatic thematic land use mapping of Washington D.C., Maryland counties, and Alice Springs, Australia using Skylab multispectral photography
[E73-11018] 22 p2661 N73-31322
Digital to analog converter for sampled signal reconstruction
[NASA-CASE-MSC-12458-1] 23 p2759 N73-32081
Sampling strategies in land use mapping using Skylab EREP multispectral photography
[E73-11139] 24 p2918 N73-33294

**SAMPLING DEVICES**
U SAMPLERS

**SAN FRANCISCO BAY [CA]**
Airport planning recommendations and procedures for San Francisco Bay Area
[REPT-73-00316] 13 p1506 N73-22208
Sources and dispersal patterns of suspended particles in nearshore surface waters of San Francisco Bay and Gulf of Farallones
[E73-10788] 18 p2137 N73-27264
Pseudocolor transformation of ERTS-1 imagery of Monterey Bay-San Francisco, California area
[PAPER-I12] 19 p2278 N73-28333

**SAN MARCO SATELLITE**
NT SAN MARCO 3 SATELLITE

**SAN MARCO 3 SATELLITE**
Instrumentation of San Marco 3 satellite for neutral atmosphere composition experiments
[NASA-TM-X-66269] 17 p2024 N73-26380

**SAND HILLS REGION [NE]**
Mapping and managing soil and range resources in Sand Hills Region of Nebraska using ERTS-1 imagery
[E72-10175] 01 p0044 N73-10354
Assessment of range fire damage in Sand Hills Region of Nebraska based on ERTS-1 imagery
[E73-10360] 10 p1149 N73-19356
Mapping and management of soil range resources in Sand Hills Region of Nebraska using ERTS-1 imagery
[E73-10372] 10 p1151 N73-19367
Mapping and managing soil and range resources in Sand Hills Region of Nebraska using ERTS-1 imagery
[E73-10629] 15 p1775 N73-24389
Mapping and managing soil and range resources in Sand Hills Region of Nebraska using ERTS-1 imagery
[E73-10807] 17 p2139 N73-27282
Application of ERTS-1 imagery for mapping and managing soil and range resources in Sand Hills region of Nebraska
[PAPER-A10] 19 p2260 N73-28218
Utilization of ERTS-1 imagery in mapping and managing range resources in Sand Hills Region of Nebraska
[E73-11121] 24 p2916 N73-33276

**SANDS**
Calibration of rotating sand erosion test apparatus simulating turbocompressor wear
[AD-743309] 01 p0059 N73-10483
Morphology, provenance, and movement of desert sand seas in Africa, Asia, and Australia
[E72-10249] 03 p0289 N73-12349
Penetration resistance of cohesionless sands with solid obstacles embedded within soil matrix
[NASA-TM-X-58099] 03 p0294 N73-12392
Morphology, provenance, and movement of desert sand seas in Africa, Asia, and Australia
[E73-10058] 07 p0778 N73-16320
Morphology, provenance, and desert sand sea movements in Asia, Australia, and Africa
[E73-10060] 07 p0778 N73-16322
ERTS-1 imagery of morphology, provenance, and movement of desert sand seas in Africa, Asia, and Australia
[E73-10409] 11 p1278 N73-20371
Equation of motion of sand particle under influence of aerodynamic drag developed in inertial coordinate system
[AD-757724] 14 p1653 N73-23405
ERTS-1 imagery of morphology, provenance, and movement of desert sand areas in Africa, Asia, and Australia
[E73-10710] 17 p2018 N73-26317

ERTS-1 imagery of morphology, provenance, and movement of desert sand seas in Africa, Asia, and Australia
[E73-10786] 18 p2136 N73-27262
Wind erosion and sandstorm effects on Mars surface topography
23 p2839 N73-32692

SANDWICH CONSTRUCTION
U SANDWICH STRUCTURES

SANDWICH PLATES
U PLATES [STRUCTURAL MEMBERS]
U SANDWICH STRUCTURES

SANDWICH STRUCTURES
Design and fabrication of honeycomb resin-composite sandwich panels for shuttle orbiter thermal shielding
[NASA-CR-128610] 01 p0061 N73-10503
Equipment for tensile, shear, bending, and hydrostatic pressure tests of sandwich elements
[FOA-4-C-4472-E6] 02 p0172 N73-11390
Structural analysis of sandwich panels with close-packed conical shells and honeycombs as fillers
[AD-747403] 03 p0362 N73-12953
Development of aerodynamic structural design data to reduce effects of acoustic fatigue on flat and singly-curved sandwich panels - Part 2
[AGARD-AG-162-PT-2] 05 p0602 N73-14898
Axisymmetric bending of round sandwich plate with rigid isotropic layers
[AD-749767] 05 p0604 N73-14915
University course on dimensioning, construction, and manufacturing of nonmetallic structural sandwich elements
[FOA-4-C-4467-61] 06 p0677 N73-15506
Dynamic frequency response of curved or flat honeycomb sandwich panels having cores of negligible flexural stiffness
[ESDU-72016] 06 p0723 N73-15898
Numerical analysis of stress in face plates of sandwich panel structures subjected to random acoustic loading
[ESDU-72017] 06 p0723 N73-15900
Transverse shear stiffnesses of sandwich panels with corrugated core and equal face plates
[ESDU-07.03.01] 06 p0723 N73-15903
Design parameters for torsion of airframe sandwich strips having trapezoidal, rectangular, and triangular cross sections
[AD-752619] 08 p0868 N73-17029
Nuclear thermal vulnerability of honey comb sandwich radome panels
[AD-753666] 09 p1056 N73-18605
Vibration analysis of shallow spherical sandwich shells based on effects of thickness-shear deformation and rotary inertia
12 p1462 N73-21843
Fatigue behavior of composite-reinforced, integrally stiffened metal panels
[NASA-CR-112148] 13 p1585 N73-22853
Development of stability matrices of displacement type for multilayer sandwich beam, rectangular, and triangular plate elements
14 p1714 N73-23908
Combustion tests of ammonium perchlorate-binder sandwich structures
[AD-757347] 14 p1719 N73-23952
Development and testing of beryllium honeycomb sandwich composite panels
[NASA-CR-130648] 15 p1838 N73-24896
Evaluation of aluminum honeycomb core landing mat with modified hinges
[AD-758840] 18 p2127 N73-27186
Application of composite materials and sandwich structures to reduce vulnerability of aircraft structures to projectile impact
18 p2165 N73-27487
Application of constrained optimal design approaches for minimum mass designs of damped, linear, continuous sandwich beam
[AD-761881] 19 p2349 N73-28896
Sonic fatigue characteristics of titanium sandwich structures and numerical analysis of natural frequencies and static stress values
20 p2480 N73-29919
Resonant vibration structural analysis of cylindrical sandwich shells
[TUB-IR-1972/2] 22 p2725 N73-31808
Creep induced buckling of infinitely long sandwich panel under uniform pressure and uniform temperature
[AD-764311] 22 p2725 N73-31810

SANITATION
Sanitizing agents for cleansing and decontaminating spacecraft environment
[NASA-CR-128591] 01 p0019 N73-10149
Industrial hygiene, radiological health, and spacecraft sanitation studies in NASA Environmental Health Program
08 p0872 N73-17057
Analysis of factors involved in selection of suitable sites for sanitary land fills with emphasis on economic and social problems
[NASA-CR-128745] 10 p1229 N73-19989
Analysis of microclimate of living and service quarters during Tenth Soviet Antarctic Expedition
20 p2409 N73-29359
Environmental sanitation handbook for occupational medicine and health procedures at Kennedy Space Center
[NASA-TM-X-69522] 23 p2752 N73-32020

SAPPHIRE
Analysis of entrance and exit surface laser induced radiation damage on sapphire crystal samples as function of beam size and divergence at surfaces
05 p0555 N73-14504
Increase in laser damage threshold of sapphire surfaces by polishing with energetic argon ion beams
05 p0555 N73-14505
Laser induced damage in ruby and sapphire crystals at 6943 A
[AD-751928] 08 p0930 N73-17613
High temperature bonding of sapphire to sapphire by eutectic Al2O3 and ZrO2 mixture to form sapphire rubidium maser cell
[NASA-CASE-GSC-11577-1] 10 p1164 N73-19467
Mechanical properties of silicon carbide and aluminum oxide sapphire filaments for design of metal matrix composites
[AD-753711] 10 p1176 N73-19568
Variations in electrical properties of silicon films on sapphire using MOS Hall technique
13 p1564 N73-22679
Formation of current filaments in thin film silicon-on-sapphire diodes
16 p1952 N73-25795
Plastic deformation of single crystal sapphire filaments
[AD-762302] 19 p2313 N73-28603

SARCOMA
U CANCER

SAS
U SMALL ASTRONOMY SATELLITES

SAS-B
Star sensor/mapper with two data channels with memory for SAS-B
[NASA-CR-129192] 02 p0173 N73-11403
SAS-2 observation of high energy gamma radiation
19 p2331 N73-28759

SAS-C
Small Astronomy Satellite-C equipment for X ray source location and flow energy spectral analysis
17 p2084 N73-26859

SATAN [SENSOR]
U TERRAIN ANALYSIS

SATELLITE ANTENNAS
Computer program for mapping satellite-borne narrow beam antenna footprints on earth
[NASA-CR-129283] 03 p0265 N73-12149
Test range for Symphonie satellite antennas and onboard communication equipment
[DGLR-PAPER-72-89] 06 p0640 N73-15199
Source and form of altitude errors obtained from antenna/satellite attitude errors
06 p0664 N73-15390
Analysis of parameters affecting design of synthetic aperture radar antennas for satellites
[NASA-TM-X-66162] 07 p0755 N73-16130
Effect of receiving antenna height measurement on three-dimensional position fixing with navy navigation satellite system
[DLR-FB-73-28] 16 p1941 N73-25712
Mechanical drives for communication satellite antennas and solar arrays
[DGLR-PAPER-73-050] 24 p2986 N73-33864

SATELLITE ATTITUDE CONTROL
Attitude stability criteria and nutation decay times of dual-spin satellite with large flexible solar array
[AD-743258] 01 p0109 N73-10897
High resolution attitude sensor for sensing spacecraft attitude relative to light source
[NASA-CASE-LAR-10586-1] 02 p0174 N73-11406
Magnetic attitude control of ESRO 4 satellite noting magnetorquer and maneuver simulation
[ESRO-TN-108-ESTEC] 02 p0235 N73-11909
Development of spacecraft control system using two speed-baised and speed-modulated reaction wheels with resultant momentum nominally oriented along orbit normal
[AD-745961] 02 p0235 N73-11911
Cartographic evaluation of ERTS-1 orbit and attitude data
[E72-10277] 03 p0292 N73-12375
Application of active control for stability augmentation of passive gradient satellites based on impulses from control jet engines
[NASA-CR-130112] 03 p0356 N73-12904
Momentum wheel design for spacecraft attitude control and magnetic drum and head system for data storage
[NASA-CASE-NPO-11481] 04 p0446 N73-13644
Development of pressure transducer for satellite attitude control feeding signals back to solenoid flow control valve
[RAE-TR-72085] 05 p0548 N73-14453
Source and form of altitude errors obtained from antenna/satellite attitude errors
06 p0664 N73-15390
Magnetic attitude acquisition and control system for automatic despinning of satellite
[NASA-CR-130145] 06 p0673 N73-15477
Fabrication and tests of magnetic control assembly designed as add-on unit for components of Nimbus and ERTS attitude control system
[NASA-CR-130142] 06 p0673 N73-15479
Design and qualification of hydrazine attitude control engines for Aeros satellite
[DGLR-PAPER-72-79] 06 p0714 N73-15824
Pressurized gas and electrothermal hydrazine engine for European satellite attitude control
[DGLR-PAPER-72-78] 06 p0714 N73-15825
Design and operation of Aeros satellite attitude control system during acquisition phase
[DGLR-PAPER-72-62] 06 p0721 N73-15885
Standardization of satellite control systems by using onboard computers, exemplified by proposal for Aeros satellite
[DGLR-PAPER-72-064] 06 p0721 N73-15886
Dynamics of satellite gravitational stabilization systems with gyrodamping
[AD-750555] 06 p0722 N73-15892
Attitude dynamics of nearly spherical dual spin satellite with asymmetrical bodies, orbital results for OSO 7, and critical mass properties
07 p0848 N73-16877
Comparison of chemical [hydrazine and aerozine], electrothermal, electrostatic, and radioisotopic propulsion systems, emphasizing performance and configurations
[ESRO-CR-25-PT-A] 08 p0955 N73-17818
Mathematical model and analysis of attitude stability and control of spinning flexible satellite in force-free environment
08 p0964 N73-17876
Design of solar ephemeris synthesizer for LES-8/9 stationkeeping system
[AD-752250] 08 p0965 N73-17891
Aluminum rods for gas cooling requirements of satellite attitude and orbit control using hydrazine as low thrust propellant
[RAE-TR-72161] 09 p0991 N73-18086
Development of attitude control system jitter specification for Tiros-N satellite three axis orientation capability
[NASA-TM-X-66201] 10 p1216 N73-19886
Development and characteristics of rate measuring package for stabilization of Nimbus D satellite
[NASA-CR-130182] 10 p1216 N73-19888
Effects of solar pressure and gravity gradient on attitude motions of artificial satellite near far moon side libration point
12 p1447 N73-21722
Manufacture of quartz gyroscopes for application to General Relativity Satellite
13 p1593 N73-22920
Computerized simulation of multiloop attitude control system for satellite with flexible booms
14 p1712 N73-23890
Derivation of equations of motion for small angular displacements from equilibrium position of earth pointing satellite with reaction wheel damping
[ARC-R/M-3276] 16 p1857 N73-25039
Development of autonomous stationkeeping system for controlling longitude of synchronous satellite by onboard navigation aids
[AD-759806] 16 p1942 N73-25716
Brushless dc torque motor in-orbit performance of ITOS with improved attitude controls and earth splitting technique
[NASA-TM-X-66267] 17 p2060 N73-26662
HELOS spacecraft subsystems for attitude control, tracking, telecommand, and X ray source detection
17 p2085 N73-26869
Soundings and imagings from geostationary satellites and numerical analysis of satellite stability parameters
[NASA-CR-132799] 18 p2200 N73-27761
ESRO 1A [Aurorae] satellite dynamic model derived from attitude sensor data using smoothing factor in spline function subroutine
[RA-SAT-3.4-C-006] 18 p2201 N73-27767
Attitude computer facility for unmanned satellite control from ground base
18 p2211 N73-27848
Computerized ground-air-ground information system for error estimation and alignment of spacecraft attitude sensors
18 p2211 N73-27849
Mathematical procedure for determining exact slew reorientation of spacecraft about nonorthogonal axes
18 p2211 N73-27850
Three axes motion simulator for satellite attitude control systems
[ESRO-CR-61] 19 p2349 N73-28132
Development, characteristics, and performance of ion thruster engine for attitude control and station-keeping of synchronous satellite
[NASA-CR-121183] 19 p2329 N73-28736
Motion simulator for performance testing of satellite attitude control systems
[ESRO-CR-66] 20 p2383 N73-29145

Star mapper using solid-state detectors discussing dioptric and mirror objectives, and star recognition algorithms
[ESRO-CR-82] 22 p2698 N73-31610
Star mapper breadboard model for satellite attitude control using either photomultipliers or Si photodiodes
[ESRO-CR-162] 22 p2696 N73-31611
Development of test equipment, propellants, and control equipment for interplanetary spacecraft
[NASA-CR-133863] 22 p2731 N73-31858
Hybrid programmable attitude control electronic analog digital system for preflight and in-flight changes in planetary missions
22 p2731 N73-31859
Gimballed attitude gyros for Symphonie satellite stabilization
[DGLR-PAPER-73-058] 24 p2927 N73-33377
Azur satellite attitude determination, based on coordinate transformation matrix and angle measurement
24 p2985 N73-33858
Dynamic flight simulation of Symphonie satellite attitude control system
[DGLR-PAPER-73-045] 24 p2986 N73-33862
Use of mercury ion engines for attitude control of communication satellites
[DGLR-PAPER-73-048] 24 p2986 N73-33863
Equations of motion for Lincoln Experimental Satellites with gimbaled momentum wheel and gyroscope to analyze attitude control dynamics
[AD-765548] 24 p2986 N73-33867

**SATELLITE ATTITUDE DISTURBANCE**
U ATTITUDE STABILITY
U SPACECRAFT STABILITY

**SATELLITE COMMUNICATIONS**
U SPACECRAFT COMMUNICATION

**SATELLITE COMMUNICATIONS SHIPS**
Feasibility of radio communications at very low frequencies from satellite-borne transmitter to receivers with subsurface antennas
[AD-759258] 16 p1876 N73-25188
Assessment of communication channels for maritime satellite systems using broad beam and multiple beam antennas for satellite-ship links
18 p2117 N73-27121

**SATELLITE CONFIGURATIONS**
Design of satellite and satellite components for Atmospheric Explorer missions to include electrical, mechanical, and environmental interfaces
[NASA-CR-130085] 01 p0049 N73-10395
Magnetic tests of UK 4 spacecraft to determine magnetic characteristics and to provide desirable magnetic conditions
[NASA-TM-X-66125] 04 p0478 N73-13912
Configuration and functions of ITOS D and E system of meteorological satellites to expand basic capability of TIROS M/ITOS system
[NASA-CR-130160] 09 p1086 N73-18863
Design and development of interplanetary Helios satellite
[DGLR-PAPER-72-104] 09 p1091 N73-18905
Design, development, and characteristics of Tracking and Data Relay Satellite System - Vol. 1
[NASA-CR-130216] 13 p1582 N73-22820
Linear stability analyses for four satellite configurations using passive elements for attitude control
16 p1964 N73-25883
German astronomical satellite configuration and subsystems for launching Scout D vehicle
[BMBW-FB-W-72-26] 23 p2852 N73-32787

**SATELLITE CONTROL**
NT SATELLITE ATTITUDE CONTROL
Optimum design of format synchronizer for ESRO control center
[ESRO-CR[P]-127] 02 p0141 N73-11143
British Prospero satellite control noting instrumentation, equipment, and experimental performance
[RAE-TR-72088] 03 p0359 N73-12928
Orbit determination for self-contained stationkeeping systems, equations of satellite motion, orbit control, gravitational effects, and synchronous satellite drift
[NAL-TR-295] 04 p0469 N73-13826
Investigation of fibers and composites applicable to design of high pressure gas storage vessels for satellite altitude control
[RRCM/ED/R/10] 13 p1586 N73-22856
Automatic flight control system AOOSY for satellite control, tested with Azur satellite
[MBB-UA-56-72-O] 18 p2126 N73-27183
Design and analysis of Viking Orbiter 1975 guidance and control system
[NASA-CR-135649] 21 p2600 N73-30836
Application of Runge-Kutta, multi-step, and extrapolation methods for numerical integration of equations of motion on controlled satellite
[NASA-CR-124416] 23 p2848 N73-32762

**SATELLITE DESIGN**
Design of satellite and satellite components for Atmospheric Explorer missions to include electrical, mechanical, and environmental interfaces
[NASA-CR-130085] 01 p0049 N73-10395
Development and characteristics of four spacecraft configurations for communications satellite applications - Vol. 1
[NASA-CR-120873-VOL-1] 02 p0234 N73-11899
Structural design, subsystem analysis and mechanical integration of synchronous meteorological satellite - Vol. 3
[NASA-TM-X-68839] 02 p0234 N73-11900
Development and characteristics of four spacecraft configurations for communications satellite applications - Vol. 2
[NASA-CR-120873-VOL-2] 02 p0236 N73-11915
Program requirements, operational support, and systems analysis for IMP satellite to identify responsibilities of launching organizations
[NASA-CR-129258] 03 p0358 N73-12916
Fundamentals for designing thermal control of satellites
04 p0447 N73-13646
Analysis of parametric resonance in rotating crossed-dipole satellites and method for determining regions of instability
07 p0847 N73-16868
Design criteria for SOREL drag-free space probe discussing attitude control and orbital position estimation
[S-3-1949-VOL-1/2] 09 p1091 N73-18904
Design and development of interplanetary Helios satellite
[DGLR-PAPER-72-104] 09 p1091 N73-18905
Design, development, and characteristics of spacecraft systems and equipment used with Tracking and Data Relay Satellite System - Vol. 3
[NASA-CR-130218] 13 p1582 N73-22822
Design and development of radio sounding satellite for measuring composition of plasmapause during entry and exit phases of orbit
[NOAA-TR-ERL-242-AL-8] 18 p2200 N73-27762
Parameters affecting design of AEROSAT navigation satellite for aircraft communication and air traffic control
18 p2201 N73-27768
Systems analysis of Radio Astronomy Satellite - B to show mission objective, spacecraft configuration, and launch operations
[NASA-TM-X-69490] 20 p2475 N73-29878

**SATELLITE DRAG**
Accuracy of harmonics of diurnal density variations in thermosphere determined from satellite drag data and Jacchia empirical atmospheric model
[NASA-TM-X-66160] 07 p0790 N73-16427
Supplemental catalog of atmospheric densities from satellite drag analysis
[NASA-CR-131646] 12 p1398 N73-21341
Effect of spurious forces on electrostatic suspension of ultrasensitive accelerometers
[ONERA-NT-197] 13 p1530 N73-22397

**SATELLITE GROUND SUPPORT**
Design and performance of wideband down-converter for satellite ground terminal
[NASA-CR-128394] 01 p0032 N73-10249
Program requirements, operational support, and systems analysis for IMP satellite to identify responsibilities of launching organizations
[NASA-CR-129268] 03 p0358 N73-12916
TD-1A satellite ground checkout stations noting spacecraft communication and data transmission
[ESRO-TM-140-ESTEC] 04 p0402 N73-13277
Systems analysis of Radio Astronomy Satellite - B to show mission objective, spacecraft configuration, and launch operations
[NASA-TM-X-69490] 20 p2475 N73-29878

**SATELLITE GUIDANCE**
Design, development, and operation of water electrolysis system to provide gaseous hydrogen and oxygen for satellite propulsion system
[AD-755384] 13 p1571 N73-22735
Design and analysis of Viking Orbiter 1975 guidance and control system
[NASA-CR-135649] 21 p2600 N73-30836

**SATELLITE INSTRUMENTS**
NT LASER ALTIMETERS
British Prospero satellite control noting instrumentation, equipment, and experimental performance
[RAE-TR-72088] 03 p0359 N73-12928
Effect of sea state and atmospheric parameters on satellite altimeter performance
06 p0662 N73-15372
Equipment, data processing, and results of Intercosmos observations of cosmic rays
[JPRS-57913] 06 p0716 N73-15839
Remote gas filter correlation instrument for monitoring air pollution by satellites
[NASA-CR-112137] 08 p0938 N73-17682
Effect of cloud conditions on satellite infrared spectrometer temperature retrievals
[NOAA-TR-NESS-63] 09 p1034 N73-18435
Electron and proton radiation effects on Cactus accelerometer electric charge
[ONERA-NT-200] 11 p1294 N73-20503
Wide field reflective optical scanning system for use in satellite based earth surveillance activities
[NASA-CASE-MSC-14096-1] 13 p1529 N73-22388
Nimbus 4 satellite users guide detailing instrumentation, configuration, and experimentation
[NASA-TM-X-69887] 13 p1580 N73-22803
Instrumentation of San Marco 3 satellite for neutral atmosphere composition experiments
[NASA-TM-X-66269] 17 p2024 N73-26380
Development of satellite equipment for solving inverse problems of meteorological satellites
20 p2447 N73-29661
Assessment of US and USSR technology and instrumentation for obtaining, transmitting, and processing earth images from space
21 p2534 N73-30318

**SATELLITE LAUNCHING**
U SPACECRAFT LAUNCHING

**SATELLITE LIFETIME**
List of artificial satellites launched between 1 Jan. 1969 and 31 Dec. 1971 giving details of lifetime, orbit, mass, and size
[RAE-TR-72127] 03 p0359 N73-12929
Orbits, size, mass of space vehicles launched between 31 Dec. 1971 and 30 Jun. 1972
[RAE-TM-SPACE-182-SUPPL] 03 p0360 N73-12930

**SATELLITE MANEUVERS**
U SPACECRAFT MANEUVERS

**SATELLITE NAVIGATION SYSTEMS**
Evaluation of worldwide empirical ionospheric model to assist in design of satellite navigational system - Vol. 1
[AD-753081] 09 p1031 N73-18419
Evaluation of worldwide empirical ionospheric model to assist in design of satellite navigational system - Vol. 2
[AD-753082] 09 p1031 N73-18420
Evaluation of worldwide empirical ionospheric model to assist in design of satellite navigational system - Vol. 3
[AD-753083] 09 p1032 N73-18421
Effect of receiving antenna height measurement on three-dimensional position fixing with navy navigation satellite system
[DLR-FB-73-28] 16 p1941 N73-25712

**SATELLITE NETWORKS**
Orbit sharing and deployment problems of high power satellite communication systems
01 p0026 N73-10205
Characteristics and operation of educational satellite networks
[NASA-CR-129257] 03 p0265 N73-12148
Calculation of ephemeris for Navy navigation satellites
[AD-753807] 09 p1092 N73-18914
Least squares adjustment of geometrical global satellite network data
[NASA-CR-131535] 12 p1459 N73-21823
Burst random access channel for satellite computerized data transmission system
[AD-756226] 14 p1635 N73-23252
Global rain rate statistic model for coordination of radio relay and communication satellite service
18 p2212 N73-27857
Onboard processing for data collection satellite systems
[NASA-CR-132792] 19 p2239 N73-28049

**SATELLITE OBSERVATION**
ATS 5 and Intelsat 1 observations of L band and VHF signals during ionospheric scintillation
[NASA-TM-X-66060] 01 p0028 N73-10216
Low energy electron precipitation observed as function of substorm phase by polar satellites
[NASA-TM-X-66063] 01 p0049 N73-10393
Contributions of Smithsonian Astrophysical Observatory to International Satellite Geodesy program
[NASA-CR-128396] 01 p0100 N73-10825
Apollo 15 and Apollo 16 spectrometric observation of X rays, gamma rays, and alpha particle emissions on lunar surface
[NASA-TM-X-66068] 01 p0103 N73-10848
Iterative method for localizing position of balloon on earth, using interrogating satellite and correcting for errors due to terrestrial rotation
[NASA-TT-F-14702] 03 p0328 N73-12677
Method for localizing position of balloon on earth, using interrogating satellite and correcting for electronic errors in distance measurement
[NASA-TT-F-14707] 03 p0328 N73-12678
Iterative method for localizing position of balloon on earth, using interrogating satellite and correcting for errors due to terrestrial rotation and Doppler effect
[NASA-TT-F-14703] 03 p0328 N73-12679
Analysis of computer programs for plotting geographical and political features of world based on observations from artificial satellites
[NASA-CR-129282] 03 p0356 N73-12903
Physical-statistical inference model using satellite infrared data for estimating cloud distribution from empirical histographs of equivalent black body temperatures
04 p0441 N73-13597
Satellite observation for acquisition and monitoring of planetary radiation, clouds, particles, and air pollution
[DGLR-PAPER-72-81] 04 p0444 N73-13626
Cinetheodolite observations of Explorer 24 satellite between Nov. 1965 and Mar. 1966, using azimuth and elevation values
[ROE-STS-131] 04 p0479 N73-13916
Determination of location and time of solar flare observed from HEOS A and ESRO 2 satellites
05 p0592 N73-14814

HEOS 1 satellite recorded data on solar proton event in 1970
05 p0593 N73-14815

Index of reports prepared by data center concerning rocket and satellite launches and satellite sightings
05 p0611 N73-14964

Combined marine astrogravimetry and marine geodetic acoustic techniques for accurate determination of global marine geoid
06 p0662 N73-15374

Ocean circulation effects on orbiting satellite gravimetry
06 p0664 N73-15394

Numerical analysis on hypothetical satellite altimeter detection of tides and tsunamis
06 p0664 N73-15396

European climatological maps constructed from ESSA 8 satellite photographic observations during first quarter of 1972
06 p0691 N73-15630

Legal liability of US Government in handling meteorological data obtained by satellites
06 p0692 N73-15638

Meteorological satellites for detecting and aiding southern corn leaf blight disease
06 p0693 N73-15645

Error analyses of satellite orbital parameters based on simulations of observational variances, observation equations, and normal equations
[NASA-CR-130357] 06 p0720 N73-15878

Cinetheodolite observation of 1963-30 D [Dash 2] satellite between Nov. 1965 and Mar. 1966
[ROE-STS-132] 06 p0722 N73-15890

Analysis of earth resources information systems using satellites as sensor platforms to show type of data obtained and data reduction procedures
07 p0782 N73-16360

Application of TIROS satellite data to mapping of ice fields through development of composite minimum brightness chart
07 p0788 N73-16409

Diurnal electron content tables obtained at Hawaii during 1971
07 p0789 N73-16419

Geostationary satellite observation of convective tropical cloud trajectories and velocity
07 p0814 N73-16602

Application of remote sensors carried in aircraft and satellites to survey extent of usage of recreational facilities
[NASA-CR-130752] 08 p0917 N73-17517

Research on remote sensing applications and satellite observation data - conferences
[NASA-SP-312] 08 p0971 N73-17934

Satellite vs aircraft imagery of Saudi Arabia for mineral exploration
08 p0971 N73-17936

Evaluation of type 3 solar radio burst theories using low frequency satellite observations
08 p0974 N73-17961

Configuration and functions of ITOS D and E system of meteorological satellites to expand basic capability of TIROS M/ITOS system
[NASA-CR-130160] 09 p1086 N73-18863

Cinetheodolite observations of satellites between 3 and 26 Nov. 1965
[ROE-STS-134] 09 p1091 N73-18907

Synchronous satellite observations on magnetospheric substorms in relation to plasma sheath structure
[RLO-2229-T-5-2] 10 p1155 N73-19398

Effect of parallactic refraction correction for satellite optical observations in determination of station coordinates
[NASA-TM-X-66208] 10 p1189 N73-19674

Analysis of soundings and imaging measurements obtained from geostationary satellites during 1 Nov. 1972 to 31 Jan. 1973
[NASA-CR-130175] 10 p1215 N73-19884

Performance of OSO-7 spacecraft during twelve months after launch and description of satellite components and subsystems
[NASA-CR-130184] 10 p1215 N73-19885

Neutral atmospheric models compatible with satellite orbital decay and incoherent scatter measurements
[NASA-CR-131294] 11 p1285 N73-20427

Geodetic quality determination of Soviet satellite data, using camera sites at Riga, Uzhgorod, and Helsinki
[AD-754070] 11 p1287 N73-20446

Satellite observations of soft X ray height distribution and directionality in solar flares
[AD-754772] 11 p1336 N73-20845

Satellite solar occultation absorption measurements of pollutant concentrations and spectral properties of molecules in infrared region
[REPT-011023-1-T] 12 p1444 N73-21700

OSUGOP computer program for adjusting geometrical or optical satellite observations
[NASA-CR-131532] 12 p1448 N73-21728

Effects of solar activity and geocoronal emissions on atmospheric boundary layer as observed by Prognoz satellite
12 p1461 N73-21840

Government contracts and grants relative to documents on environmental satellites
[NOAA-TM-NESS-46] 13 p1524 N73-22349

Solar gamma ray and neutron observations from OSO-7 during 2B and 3B flares
[NASA-CR-131866] 13 p1574 N73-22758

Data catalog of Nimbus 4 satellite performance capacity, experimentation, and instrumentation - Vol. 2
[NASA-TM-X-69889] 13 p1580 N73-22805

Nimbus 4 satellite catalog of observations for period 1 July through 31 August, 1970 - Vol. 3
[NASA-TM-X-69890] 13 p1580 N73-22806

Catalog of Nimbus 4 satellite observations for 1 November through 31 December, 1970 - Vol. 5
[NASA-TM-X-69892] 13 p1580 N73-22808

Data catalog of Nimbus 4 satellite performance capacity, experimentation, and instrumentation - Vol. 6
[NASA-TM-X-69893] 13 p1580 N73-22809

Nimbus 4 data catalog for 1 May 1971 to 30 Apr. 1972, including IDCS, THIR, IRIS, AND SIRS
[NASA-TM-X-69895] 13 p1580 N73-22811

Partial derivative analysis using equations of motion for recovering gravity anomalies from satellite observations
[NASA-CR-130240] 14 p1661 N73-23483

Solar X ray flux distribution from 0.1 to 8.0A using fluxes measured from Solrad 9 satellite
[CRC-1241] 14 p1702 N73-23813

Statistical comparison of simultaneous satellite solar wind observations
[AD-758194] 14 p1703 N73-23816

Development of accurate geoidal map based on gravimetric and satellite data for determining precise location of tracking stations
[NASA-CR-131869] 14 p1710 N73-23874

Development of satellite geodesy technique for accurate determination of three dimensional coordinates of ground stations
[NASA-CR-132251] 15 p1778 N73-24412

Satellite monitoring of open pit mining operations
[BM-IC-8530] 15 p1780 N73-24432

Use of spaceborne microwave radiation measurements to detect fires, subsurface water, and surface temperature
[NASA-TT-F-14975] 17 p1998 N73-26153

Magnetospheric proton density from satellite and ground observation of type Pc3 geomagnetic micropulsations
17 p2026 N73-26396

Conference on X ray experiments onboard different astronomical observatories for galactic and extragalactic X ray source position and size determination
[ESRO-SP-87] 17 p2084 N73-26855

Comparison of HELOS mission with other X ray astronomy missions
17 p2085 N73-26874

Dynamics and morphology of Beaufort Sea ice determined from satellites, aircraft, and drifting stations
[NASA-TM-X-66291] 18 p2144 N73-27333

Polar motion and earth tides applicable to satellite studies of earth elasticity
[NASA-CR-133414] 18 p2145 N73-27339

Soundings and imagings from geostationary satellites and numerical analysis of satellite stability parameters
[NASA-CR-132799] 18 p2200 N73-27761

HEOS A 2 experimental design for solar wind and magnetospheric low frequency wave measurement
[DSRI-73-01] 19 p2295 N73-28457

SAS-2 observation of high energy gamma radiation
19 p2331 N73-28759

Explorer 38 observations of solar type 3 radio bursts
19 p2339 N73-28813

Zonal, hemispherical, and global averages for satellite measurements of albedo and outgoing long wave radiation
[NOAA-TM-NESS-48] 19 p2340 N73-28823

Application of satellite observation data for determining statistical relationship between cloud field and outgoing short wave radiation in earth atmosphere
20 p2399 N73-29283

Analysis of statistical characteristics of ozonosphere to provide additional information in satellite ozonometry and interpretation of satellite results
20 p2400 N73-29287

Analysis of thermal radiation brightness of river strip as basis for determining actual temperature from data provided by satellite
20 p2400 N73-29288

Satellite ozone observations on 17-18 June 1966 between 20 deg south latitude and 60 deg north latitude
20 p2447 N73-29663

Reaction time of 27-day density variation in upper atmosphere noting satellite recorded data on drag using regression analysis, cross correlation, and solar spectrum analysis
[BMFT-FBW-73-10] 21 p2538 N73-30352

Position of earth spin axis with respect to crust computed on basis of Doppler satellite observations
[AD-763362] 21 p2542 N73-30381

Priority basis for satellite applications to communications, navigation, and surveillance for aircraft over contiguous US
[NASA-CR-132794] 22 p2722 N73-31784

Injun 5 satellite extended mission analysis discussing experiments, data processing telemetry, and geophysical data
[BMBW-FBW-72-24] 22 p2722 N73-31786

Satellite measurements on lunar and planetary environments in solar system
22 p2735 N73-31891

Atmospheric models for computing radiation effects in ERTS observations
22 p2736 N73-31905

Satellite applications for earth and ocean dynamic studies
22 p2736 N73-31909

Satellite and surface gravity data for computing gravimetric geoid
22 p2736 N73-31910

Simultaneous satellite observations of infrared and reflected energy measured to infer convective activity of tropical cloud clusters
[NOAA-TM-NESS-50] 23 p2814 N73-32498

Flux density of low energy solar flare particles measured by IMP-7
[TR-73-137] 23 p2835 N73-32653

Optimum use of infrared data as obtained from satellites for meteorological and oceanographic applications
24 p2911 N73-33233

Balloon and GEOS satellite observations of auroral X rays from Scandinavia to Greenland
[NP-19738] 24 p2923 N73-33343

Satellite measurement of cosmic ray abundances and spectra in charge range 2 equal to or less than 7 equal to or less than 10
[NASA-CR-135786] 24 p2976 N73-33777

Satellite data presentation by means of lists, graphs, and three dimensional plots
24 p2985 N73-33859

**SATELLITE ORBIT CALCULATION**
U ORBIT CALCULATION

**SATELLITE ORBITS**
NT POLAR ORBITS
NT STATIONARY ORBITS
NT TWENTY-FOUR HOUR ORBITS

Orbit sharing and deployment problems of high power satellite communication systems
01 p0026 N73-10205

Postflight analysis of Atlas/Centaur - 29 and Intelsat 4 launch and orbit establishment
[NASA-TM-X-68649] 01 p0102 N73-10845

Disturbing functions of artificial satellite orbit perturbation by solar and lunar gravitational effects
01 p0105 N73-10869

Tables of data on artificial satellites launched during period 1957 to 1971 to include chronology of manned space flight and emission frequencies of various satellites
[F-22] 01 p0107 N73-10885

Vehicle encountered trapped electron and proton fluxes calculated for nominal UK 5 circular equatorial orbits
[NASA-TM-X-66098] 02 p0225 N73-11816

Development and characteristics of four spacecraft configurations for communications satellite applications - Vol. 1
[NASA-CR-120873-VOL-1] 02 p0234 N73-11899

Development and characteristics of four spacecraft configurations for communications satellite applications - Vol. 2
[NASA-CR-120873-VOL-2] 02 p0236 N73-11915

Modification to Dynamic Operational Requirements and Cost Analysis Program to perform traffic analyses of automated satellite program - Vol. 5
[NASA-CR-129267] 03 p0270 N73-12187

Cartographic evaluation of ERTS-1 orbit and attitude data
[E72-10277] 03 p0292 N73-12375

Analysis of electron and proton fluxes encountered during nominal Tiros-N trajectories
[NASA-TM-X-66107] 03 p0357 N73-12908

List of artificial satellites launched between 1 Jan. 1969 and 31 Dec. 1971 giving details of lifetime, orbit, mass, and size
[RAE-TR-72127] 03 p0359 N73-12929

Mathematical model for short period terms in satellite orbits including comparison between analytical theory and numerical integration
[GRGS-BULL-2] 05 p0596 N73-14845

Mathematical model for short period terms in satellite orbits, including comparison between analytical theory and numerical integration
05 p0596 N73-14846

Comparison of satellite orbit elements, using analytic theory and numerical integration
05 p0596 N73-14847

Use of aerodynamic drag for transfer from hyperbolic trajectories to satellite orbits noting spacecraft guidance
[D-149] 05 p0596 N73-14849

Accuracy of atmospheric density predictions for satellite orbit determination
[D-151] 05 p0596 N73-14850

Evaluation of 15th order harmonics by analysis of orbit decay of Ariel 3, Transit 1b, Cosmos 373 and Cosmos 387 satellites
[RAE-TR-72115] 05 p0597 N73-14851
Tables of data on artificial satellites launched during period 1957 to 1971 to include chronology of manned space flight and emission frequencies of various satellites
[F-23] 05 p0598 N73-14861
Use of GEOS-C satellite height for determining earth gravitational field and physical ocean surface variations
06 p0662 N73-15375
Short arc tracking procedure for determining GEOS-C satellite altitude
06 p0662 N73-15376
Description of computer program, main subroutines, input, output, and program requirements of Goddard Brouwer Orbit Bulletin
[NASA-TM-X-66141] 06 p0719 N73-15869
Error analyses of satellite orbital parameters based on simulations of observational variances, observation equations, and normal equations
[NASA-CR-130357] 06 p0720 N73-15878
Computer program for orbit comparison plots - users manual
[NASA-TM-X-66164] 07 p0759 N73-16165
Evaluation of Halo and Hummingbird satellites for lunar libration point satellite to provide tracking and communications link with far side of moon
[NASA-CR-130135] 07 p0844 N73-16836
Development of technique for inferring atmospheric ozone information from satellite nadir measurements
[NASA-TR-R-399] 10 p1154 N73-19386
Harmonic analysis for predicting long term artificial satellite orbital motion
10 p1178 N73-19579
Parametric design of aerodynamic control system for compensating artificial satellite orbit perturbations
10 p1178 N73-19580
Numerical method for determining optimal satellite control system with discontinuous links
10 p1178 N73-19581
OGO-5 fluxgate magnetometer for measuring magnetic field over range of OGO-5 orbit
[NASA-CR-130205] 11 p1294 N73-20498
Special perturbation methods for improved computational efficiency in numerical integration of artificial satellite orbits
12 p1447 N73-21717
Tables of cataloged data collected by Nimbus 4 satellite
[NASA-TM-X-69894] 13 p1580 N73-22810
Cartographic evaluation of ERTS-1 orbit and attitude data
[E73-10544] 14 p1654 N73-23419
Eleventh order resonant terms in geopotential from orbit of Vanguard 3
[NASA-TM-X-66246] 15 p1778 N73-24415
Photographic determinations of Mars satellites orbital parameters
16 p1961 N73-25860
Design and development of radio sounding satellite for measuring composition of plasmapause during entry and exit phases of orbit
[NOAA-TR-ERL-242-AL-8] 18 p2200 N73-27762
Vinti equations of motion solved for position and velocity of orbiting satellite
[NASA-TM-X-70418] 19 p2343 N73-28846
Optimum inclination of inclination non-sensitive satellites for shuttle retrieval
[NASA-TM-X-64780] 22 p2715 N73-31730
Techniques for analysis of geodynamic effects using laser data in estimating satellite orbits
[NASA-TM-X-70459] 22 p2716 N73-31739
Telescopic detection and ranging system for satellite orbital trajectory determination
[AD-764727] 23 p2820 N73-32546
Fifteenth order resonance on decaying orbit of TETR-3
[NASA-TM-X-70484] 24 p2979 N73-33805
Selection of Azur satellite additional information for telemetry data processing
24 p2985 N73-33856

**SATELLITE ORIENTATION**
Geostationary satellite position and attitude determination using picture landmarks
[NOAA-TM-NESS-21] 04 p0474 N73-13875
Astronomical techniques for spacecraft orientation and aircraft instrument errors
[JPRS-57704] 05 p0577 N73-14693
Astronomical techniques for spacecraft orientation
05 p0577 N73-14694
Stability of dual-spin satellite system during momentum wheel spin-up maneuver
[NASA-CR-130130] 05 p0597 N73-14858
Analysis of parametric resonance in rotating crossed-dipole satellites and method for determining regions of instability
07 p0847 N73-16868
Mathematical models for measuring stellar orientation of spacecraft
[JPRS-58389] 09 p1062 N73-18665
Development of attitude control system jitter specification for Tiros-N satellite three axis orientation capability
[NASA-TM-X-66201] 10 p1216 N73-19886
Numerical analysis of satellite stability parameters with application to stability of Skylab satellite
[NASA-CR-124223] 13 p1581 N73-22815
Algorithm for computing satellite orientation and tables of gravitational constants used for computations
[NASA-TT-F-14699] 15 p1831 N73-24840
Onboard control systems for spacecraft
[JPRS-60179] 23 p2847 N73-32755
Orientation system for Molniya-1 communications satellite
23 p2848 N73-32756

**SATELLITE PERTURBATION**
Numerical integration of artificial satellite orbit perturbation due to planetary gravitational effects, including long period and secular terms
[GRGS-BULL-5] 01 p0105 N73-10868
Disturbing functions of artificial satellite orbit perturbation by solar and lunar gravitational effects
01 p0105 N73-10869
Secular and long period terms of artificial satellite perturbed equation of motion noting planetary gravitational effects
01 p0105 N73-10870
Error analyses of satellite orbital parameters based on simulations of observational variances, observation equations, and normal equations
[NASA-CR-130357] 06 p0720 N73-15878
Analysis of parametric resonance in rotating crossed-dipole satellites and method for determining regions of instability
07 p0847 N73-16868
Analysis of satellite stability of motion using Liapunov system as applied to flexible bodies
07 p0848 N73-16869
Formulation of disturbing function for computing lunisolar perturbations in satellite motion
[NASA-CR-130743] 08 p0941 N73-17709
Second degree Love number values from analysis of lunar-solar tidal perturbations of GEOS 1 and 2 inclinations
[NASA-TM-X-66176] 08 p0960 N73-17857
Gravitational field models for solution of satellite geopotential using optical data processing
[NASA-TM-X-66207] 11 p1341 N73-20883
Effects of solar, lunar, and earth gravity perturbations on synchronous satellite
13 p1576 N73-22767
Application of variational equations for analysis of rapidly spinning triaxial body moving in elliptical orbit
[NASA-CR-131871] 13 p1581 N73-22813
Earth satellite orbit perturbation due to fluid tidal effects and temporal geopotential variations
[GRGS-BULL-7] 14 p1706 N73-23847
Determination of electric potential field and aerodynamic moments for steady rarefied plasma flow past solid sphere
15 p1816 N73-24720
Soundings and imagings from geostationary satellites and numerical analysis of satellite stability parameters
[NASA-CR-132799] 18 p2200 N73-27761
Satellite motion in gravitational field of nonspherical rotating planet
[NASA-TT-F-15073] 24 p2981 N73-33825

**SATELLITE RENDEZVOUS**
U ORBITAL RENDEZVOUS

**SATELLITE ROTATION**
Attitude stability criteria and nutation decay times of dual-spin satellite with large flexible solar array
[AD-743258] 01 p0109 N73-10897
Application of variational equations for analysis of rapidly spinning triaxial body moving in elliptical orbit
[NASA-CR-131871] 13 p1581 N73-22813
Numerical analysis of satellite stability parameters with application to stability of Skylab satellite
[NASA-CR-124223] 13 p1581 N73-22815
Spin scan camera photography of Jupiter from rotating outer planet orbiters
[NASA-TM-X-62260] 15 p1830 N73-24836
Translational-rotational magnetized satellite equations of motion in geomagnetic field
15 p1832 N73-24847

**SATELLITE TELEVISION**
Combination satellite television system with local cable system for Federal Post Office
[NASA-TT-F-14660] 06 p0640 N73-15195
Technical and economical factors of satellite television reception
[NASA-TT-F-14659] 06 p0640 N73-15196
Development of Hurricane Inez, 1966 as shown by Nimbus 2 radiometer data and ESSA-1 and 3 television photographs
[NASA-TM-X-65943] 10 p1182 N73-19616
Technological and economical factors of satellite television network in India
[PB-213226] 11 p1258 N73-20208
Collection of data relating to Mariner 9 TV pictures
[NASA-CR-131416] 11 p1337 N73-20850
Satellite television photography of geomorphological indices for developing stream meander pattern
12 p1400 N73-21352
Development of processing satellite data to show quantity of data and time required for various techniques
[BMFT-FBW-73-04] 14 p1638 N73-23277
Ground terminal optimization and cost effectiveness of satellite television broadcasting
18 p2115 N73-27100
Statistical weather analysis for optimum picture quality design of satellite television broadcasting system
18 p2115 N73-27101
Comparative study of TWT and klystron amplifiers for use as power amplifiers in television broadcast satellites
[ESRO-CR[P]-267-VOL-1] 21 p2508 N73-30122
Comparative study of TWT and klystron for use as power amplifier in TV broadcast satellites
[ESRO-CR[P]-271] 22 p2634 N73-31109
Comparative study of TWT and klystron for use as power amplifier in TV broadcast satellites
[ESRO-CR[P]-272] 22 p2634 N73-31110
Radio frequency bandwidth for satellite frequency modulated television broadcasting
[BBC-RD-1973/19] 24 p2893 N73-33097

**SATELLITE TEMPERATURE**
Research and development of high performance satellite thermal control louver array actuator including single blade and multiple blade actuation system
[ESRO-CR[P]-247] 18 p2201 N73-27766

**SATELLITE TRACKING**
Application of satellite tracking and precision traversing data to improve accuracy of geodetic triangulation
[NASA-CR-128402] 01 p0047 N73-10377
Analysis of range and range rate tracking data from satellite to satellite for geodetic applications
[AD-741683] 01 p0106 N73-10881
Errors in localization in measurement of distance to balloon-satellites
[NASA-TT-F-14701] 02 p0207 N73-11678
Tracking and orbit calculation of Cosmos 316 to determine upper atmospheric wind
[RAE-TR-72062] 02 p0235 N73-11910
Modification to Dynamic Operational Requirements and Cost Analysis Program to perform traffic analyses of automated satellite program - Vol. 5
[NASA-CR-129267] 03 p0270 N73-12187
Effects of tracking system errors of satellite orbit when single station provides satellite tracking in immediate area of altimeter evaluation
[NASA-TM-X-69352] 03 p0301 N73-12457
Soviet camera for tracking satellites and solving geodetic and geophysical problems
[AD-747135] 03 p0303 N73-12476
VLBI time delay, satellite tracking technique for synchronous satellites
[NASA-TM-X-66122] 04 p0475 N73-13887
Laser tracking techniques used for geodetic applications in space
[GRGS-BULL-1] 05 p0557 N73-14522
Laser range finding for satellite angular coordinate determination using echo recorded by Schmidt telescope
05 p0557 N73-14523
Effects of spacecraft stabilization on laser tracking efficiency
05 p0558 N73-14531
Laser ranging techniques applied to ground base line measurements between French South Coast and Corsica
05 p0558 N73-14532
Optical satellite tracking of Cosmos and other artificial satellites, Edinburgh, Aug. 1972
[ROE-STS-129] 05 p0601 N73-14883
Optical satellite tracking of Cosmos and other artificial satellites, Edinburgh, Sep. 1972
[ROE-STS-130] 05 p0601 N73-14884
Satellite system for tracking of wildlife and birds in natural environment
[NASA-CR-130301] 06 p0627 N73-15090
Short arc tracking procedure for determining GEOS-C satellite altitude
06 p0662 N73-15376
Capabilities and projected accuracy of various satellite tracking systems
06 p0662 N73-15379
Probability of further developments of satellite geodesy
[AD-750749] 06 p0672 N73-15466
Optical satellite tracking of Cosmos and other artificial satellites, Edinburgh, Oct. 1972
[ROE-STS-133] 06 p0722 N73-15891
Application of digital techniques for control of large antennas used for satellite tracking
[NASA-TM-X-66154] 07 p0754 N73-16127
Performance of portable Doppler geodetic receiver in satellite tracking system
[AD-751597] 07 p0757 N73-16149
Problems of radar network scheduling to track satellites
[AD-751290] 07 p0757 N73-16152
Optical satellite tracking of Cosmos and other artificial satellites, Edinburgh, Nov. 1972
[ROE-STS-135] 09 p1091 N73-18908

Cinetheodolite observations of satellites between 30 Nov. 1965 and 17 Jan. 1966
[ROE-STS-136] 09 p1091 N73-18909
Cinetheodolite observations of satellites between 18 and 31 Jan. 1966
[ROE-STS-137] 09 p1091 N73-18910
Synchronous satellite tracking by planetary radar system
[AD-754937] 11 p1257 N73-20196
Problems in estimation theory with applications to orbit determinations
[AD-755802] 12 p1458 N73-21820
Determining preliminary orbital elements of earth satellite from angle-only observations
[AD-755399] 13 p1578 N73-22793
Optical satellite tracking of Cosmos and other artificial satellites, Edinburgh, Dec. 1972
[ROE-STS-138] 13 p1582 N73-22824
Optical tracking of artificial satellites between Oct. and Dec. 1972
[ROE-STS-139] 13 p1582 N73-22825
Cinetheodolite satellite tracking at Earlyburn between 15 and 18 Feb. 1966
[ROE-STS-142] 13 p1582 N73-22829
Cinetheodolite satellite tracking at Earlyburn between 19 Feb. and 1 Mar. 1966
[ROE-STS-143] 13 p1583 N73-22830
Vaisala method of stellar triangulation
[AD-757542] 15 p1783 N73-24456
Improved earth gravitational model from combination of satellite tracking and surface mean free-air gravity anomaly data
[AD-756177] 15 p1783 N73-24459
Artificial satellite motion and tracking
[GRGS-BULL-6] 15 p1832 N73-24846
Artificial satellite equations of motion approximations for photographic and laser tracking optimization
15 p1832 N73-24848
Optical satellite tracking of Cosmos and other artificial satellites, Edinburgh, Feb. 1973
[ROE-STS-147] 15 p1836 N73-24881
Cinetheodolite satellite tracking at Earlyburn between 2 and 10 Mar. 1966
[ROE-STS-148] 15 p1836 N73-24882
Laser ranging technique to determine distance from satellites to ground
[NASA-CR-2264] 16 p1906 N73-25419
Satellite tracking camera for geometric geodesy
[PUBL-27] 16 p1913 N73-25479
ATS ranging and position fixing experiments
[NASA-CR-132755] 16 p1965 N73-25896
Optical satellite tracking of Cosmos and other artificial satellites, Edinburgh, Jan. 1973
[ROE-STS-141] 16 p1967 N73-25912
HELOS spacecraft subsystems for attitude control, tracking, telecommand, and X ray source detection
17 p2085 N73-26869
Cinetheodolite satellite tracking at Earlyburn between 11 and 29 Mar. 1966
[ROE-STS-149] 17 p2089 N73-26905
Simultaneous satellite photographic and Doppler observations for determining space triangulation chord direction
[AD-759096] 18 p2127 N73-27188
Simultaneous observation solutions for NASA-MOTS and SPEOPT station positions on North American Datum
[NASA-TM-X-66297] 18 p2145 N73-27336
Input usage guide for mission planning program
[AD-760796] 18 p2201 N73-27769
Error drift projection for ERTS orbit maintenance calculation using ground tracking data
18 p2211 N73-27847
Optical satellite tracking of Cosmos and other artificial satellites, Edinburgh, Jan. 1973
[ROE-STS-151] 19 p2346 N73-28872
Optical satellite tracking of Cosmos and other artificial satellites, Edinburgh, Apr. 1973
[ROE-STS-152] 19 p2346 N73-28873
Extensions to short arc geodetic adjustment for reduction of Doppler operations in satellite geodesy
[AD-760791] 20 p2414 N73-29401
Development of space-time integral equation for solution of large body problem for smooth convex targets with application to satellite tracking systems
[AD-763794] 21 p2508 N73-30128
Azur satellite orbit perturbation recorded from Weilheim-Lichtenau ground station
[BMBW-FBW-72-18] 21 p2597 N73-30816
Hewitt camera satellite tracking at Earlyburn, England, between 1 Jan. and 31 May 1973
[ROE-STS-153] 21 p2602 N73-30850
Optical satellite tracking of Cosmos and other artificial satellites, Edinburgh, May 1973
[ROE-STS-154] 21 p2602 N73-30851
Laser tracking of satellite for measuring polar motion and solid earth tide
22 p2737 N73-31911
Telescopic detection and ranging system for satellite orbital trajectory determination
[AD-764727] 23 p2820 N73-32546
Celestial mechanics analysis on Mariner 9 Doppler tracking data for determining Mars gravitational field
23 p2841 N73-32706
Mariner 9 Doppler tracking short data arcs for determining Mars gravitational field
23 p2841 N73-32707
Mariner 9 Doppler tracking data filtering method for determining Mars gravity
23 p2841 N73-32708
Doppler data range change measurements for Mariner 9 celestial mechanics experiment
23 p2842 N73-32709
Range points in relativistic test of celestial mechanics in Mariner 9 Doppler tracking data analysis for Mars gravity
23 p2842 N73-32710
Time delay in ranging signal to Mariner 9 orbiter for testing general relativity
23 p2842 N73-32712
Time lag test of general relativity and Earth-Mars ephemeris improvement using Mariner 9 tracking data
23 p2842 N73-32713
Doppler study of plasma column changes at solar elongation in Mariner 9 tracking path
23 p2842 N73-32715
Characteristics of minitrack tracking function to show minitrack hardware, system calibration, and quadratic listing - Vol. 2
[NASA-TM-X-70482] 24 p2901 N73-33156

**SATELLITE TRANSMISSION**

Tables of data on artificial satellites launched during period 1957 to 1971 to include chronology of manned space flight and emission frequencies of various satellites
[F-22] 01 p0107 N73-10885
Tables of data on artificial satellites launched during period 1957 to 1971 to include chronology of manned space flight and emission frequencies of various satellites
[F-23] 05 p0598 N73-14861
Mariner 9 space probe microfiche library
[NASA-CR-130925] 10 p1128 N73-19193
Performance of OSO-7 spacecraft during twelve months after launch and description of satellite components and subsystems
[NASA-CR-130184] 10 p1215 N73-19885
Development of Tracking and Data Relay Satellite system concept for service of low, medium, and high data rate user spacecraft - Vol. 1
[NASA-CR-130219] 13 p1579 N73-22799
Configuration data and design development for Delta 2914 launched Tracking and Data Relay Satellite system - Vol. 2
[NASA-CR-130220] 13 p1579 N73-22800
Data and design information for Atlas Centaur launched configuration of Tracking and Data Relay Satellite system - Vol. 3
[NASA-CR-130221] 13 p1579 N73-22801
Configuration data and design information for space shuttle launch of Tracking and Data Relay Satellite System - Vol. 4
[NASA-CR-130222] 13 p1580 N73-22802
Design, development, and characteristics of Tracking and Data Relay Satellite System - Vol. 1
[NASA-CR-130216] 13 p1582 N73-22820
Design and development of telecommunications equipment for use with Tracking and Data Relay Satellite System - Vol. 2
[NASA-CR-130217] 13 p1582 N73-22821
Comparison of voice coding technique for satellite-based air traffic control system
14 p1630 N73-23209
Amplitude fading of superhigh frequency geostationary communications satellite signals considering atmospheric refraction
17 p1996 N73-26139
USSR automatic stations on mars and venus, lunar continental region samples, and 24 hour satellite earth watching
[NASA-TT-F-14929] 19 p2342 N73-28841
Stability of multistation satellite communications system
[JPRS-59753] 20 p2376 N73-29092
Requirements for international laws of remote sensing
[NASA-TT-F-15055] 21 p2535 N73-30330

**SATELLITE-BORNE INSTRUMENTS**

Determination of in-flight optical transfer functions of orbital earth resources multispectral sensors
[E72-10212] 02 p0162 N73-11307
Efficiency of laser telemetry tracking for satellites carrying reflectors
05 p0557 N73-14527
Failure analysis of tape recorders for spacecraft applications
[NASA-SP-307] 06 p0643 N73-15225
Spaceborne laser ranging system for accurately mapping ocean surface
06 p0662 N73-15377
Conference on dynamic wave effects on satellite-borne sea surface measurements
[NASA-CR-129993] 06 p0664 N73-15392
Telemetry data processing systems for experiments flown on Injun 5 satellite, OV-3 satellite, OV-4 satellite, OV-5 satellite, OV-6 satellite, and OV-15 satellite
[AD-751508] 07 p0759 N73-16166



Two satellite microwave occultation system for determining pressure levels in atmosphere using infrared sensors
07 p0775 N73-16294
Computer programs for calculating transfer functions of retroreflector laser arrays carried by orbiting satellites
[NASA-CR-130696] 08 p0888 N73-17190
Design of traveling wave maser system for use in satellite communication telescopes and radio astronomy
[REPT-109] 09 p1043 N73-18505
Scientific space mission of small spin stabilized astronomical satellite with X ray and IR experiments
09 p1081 N73-18817
Simulation of logical functions for construction of computerized control system for onboard spacecraft instrumentation
10 p1177 N73-19573
Simulation of program sequencing functions in design of computerized digital control system for onboard spacecraft instrumentation
10 p1177 N73-19574
Design and development of brushless, direct drive solar array reorientation control system for satellites
[NASA-CR-130153] 11 p1261 N73-20236
Satellite-borne electric field measurement in magnetosphere
[NASA-CR-131419] 11 p1287 N73-20442
Design, construction, and evaluation of 12.2 GHz, 4.0 kW-CW coupled-cavity traveling wave tube for satellite-borne television broadcast transmitters
[NASA-CR-120920] 12 p1382 N73-21209
Utilization of millimeter wave radiation from atmospheric oxygen to provide vertical sensing information to satellite-borne radiometer
[NASA-CR-2229] 13 p1530 N73-22396
Satellite measurements of sea surface temperatures
[NASA-TM-X-66235] 14 p1659 N73-23467
Conference on X ray experiments onboard different astronomical observatories for galactic and extragalactic X ray source position and size determination
[ESRO-SP-87] 17 p2084 N73-26855
OAO-C X ray experimental design
17 p2084 N73-26857
Small Astronomy Satellite-C equipment for X ray source location and flow energy spectral analysis
17 p2084 N73-26859
X ray Astronomical Netherlands Satellite experimental design for soft and hard source identification and spectral analysis
17 p2084 N73-26860
Corsa 1 and 2 instruments, experimental design, and data systems for X ray astronomy
17 p2084 N73-26864
OSO-J experimental design, and equipment for soft X ray sources and diffuse components in 0.01 to 2.0 keV range
17 p2085 N73-26865
HEAO-A experimental design and equipment for mapping celestial X ray sources and spectral analysis over 0.2 to 150 keV
17 p2085 N73-26866
HELOS lunar occultation experiment on X ray galactic and extragalactic source position and angular size determination
17 p2085 N73-26868
HELOS spacecraft subsystems for attitude control, tracking, telecommand, and X ray source detection
17 p2085 N73-26869
HEAO-B Bragg crystal spectrometer for stellar X ray spectral analysis
17 p2085 N73-26870
HEAO-B cosmic ray experiment for diffuse sky brightness determination
17 p2085 N73-26871
HEAO-C X ray focusing telescopes for spectrometric and polarization studies
17 p2085 N73-26872
HEAO-C soft X ray telescope
17 p2085 N73-26873
Observability of high altitude aerosol and atmospheric scattering layers by satellite-borne optical detector
[NASA-CR-112309] 18 p2144 N73-27329
Scanning radiometer imagery of Northern Hemisphere cloud cover obtained during May, 1973 by enivoramental satellite
18 p2171 N73-27535
Cloud data for November and December 1972, obtained by environmental satellite imagery
18 p2171 N73-27536
Ionospheric electron content from satellite beacon measurements
[NASA-CR-133475] 19 p2294 N73-28446
Performance of OV-5 and OV-6 alpha and proton particle detector
[AD-760147] 19 p2302 N73-28505
Satellite-borne instruments for measurement of heavy particles
[AD-762208] 19 p2302 N73-28510
Feasibility of using satellite-borne instruments to detect atmospheric pollution
[PB-220394/1] 21 p2541 N73-30372

Analysis of interferometric characteristics of stellar figure sensor for orbiting astronomical telescope
[NASA-CR-132795] 22 p2673 N73-31408
ERTS-1 sensor analysis of air pollution and air pollution related injuries to plant vegetation in metropolitan Minnesota
23 p2784 N73-32269
Vertical temperature profile data obtained by satellite radiometer sounding
[NOAA-TR-NESS-65] 23 p2786 N73-32291
Accurate and reliable prototype earth horizon sensor head employing logic locator concept
[NASA-CR-132267] 23 p2792 N73-32334
OGO-6 measurements of solar neutrons
23 p2833 N73-32639
Urban transportation planning using satellite-borne remote sensors
[NASA-CR-124433] 23 p2859 N73-32846
Metric cartographic potential of geostationary/geosynchronous satellite camera
24 p2912 N73-33238
Titanium dioxide doped, silicon rubber, potting compound for satellite-borne channel multipliers noting doping effects, performance tests, and space applications
24 p2927 N73-33378
Titanium dioxide doped silicone rubber potting compound for satellite-borne channel multipliers
24 p2927 N73-33379

**SATELLITE-BORNE PHOTOGRAPHY**
Evaluation of simultaneous ERTS-1 and aerial photography of Arizona
[E72-10213] 02 p0162 N73-11308
Remote sensing in forestry using aerial and satellite-borne photography and imaging techniques
[E72-10221] 02 p0162 N73-11315
Methods for determining atmospheric circulation from satellite pictures
02 p0204 N73-11649
Geostationary satellite position and attitude determination using picture landmarks
[NOAA-TM-NESS-21] 04 p0474 N73-13875
Atlas of reconstructed lunar photographs taken by Lunar Orbiters during 1966 and 1967
[NASA-SP-206] 04 p0475 N73-13879
Interpretation of meteorological satellite TV pictures of ice in Baltic Sea
[NLL-M-20841-[5828.4F]] 05 p0529 N73-14306
Application of aerial and spaceborne photography to urban, regional, and management planning
[NASA-CR-130290] 06 p0673 N73-15473
European climatological maps constructed from ESSA 8 satellite photographic observations during first quarter of 1972
06 p0691 N73-15630
History of Nimbus satellite project and selected photography
[NASA-CR-130144] 06 p0720 N73-15877
Snow line delineation using satellite remotely sensed data
07 p0787 N73-16402
UV imagery of earth and moon at varied wavelengths
12 p1451 N73-21751
Space and supporting aircraft photography for interpretation and analysis of non-forest vegetation
[NASA-CR-131585] 13 p1522 N73-22338
Classification of forest land use and detection of forest disturbances using space and high altitude aerial photography
[NASA-CR-131584] 13 p1523 N73-22339
Data catalog tables and pictorial montages from Nimbus 4 satellite observation
[NASA-TM-X-69891] 13 p1580 N73-22807
Weather forecasts using satellite information
[NLL-M-22897-[5828.4F]] 15 p1804 N73-24625
Application of ERTS-1 imagery to cartography, geomorphology, agronomy, and hydrology of Bolivia
[E73-10695] 16 p1902 N73-25387
Application of Skylab and EREP imagery for uniform mapping of earth resources and environmental complexes
[E73-10706] 16 p1904 N73-25397
Application of remote sensing techniques of ERTS and other sources for solution of environmental problems in Oregon
[NASA-CR-133034] 16 p1906 N73-25420
Development of rotary solenoid shutter drive assembly and inertia damper for use with cameras mounted in satellites
[NASA-CASE-GSC-11560-1] 17 p2003 N73-26198
Application of ERTS-1 remotely sensed data and ground truth information to predict and manage water quantity and quality in river basins
[E73-10689] 17 p2018 N73-26314
Photointerpretation of ERTS-1 imagery and airborne photography to determine vegetation growth in Iowa
[E73-10715] 17 p2018 N73-26322
Evaluation of utility of ERTS-1 satellite and aircraft remotely sensed data to integrated processes of state planning and land use in Maryland
[E73-10716] 17 p2019 N73-26323
Evaluation of ERTS-1 image data compression technique
[E73-10717] 17 p2019 N73-26324
Application of ERTS-1 RBV and multispectral scanner imagery for assessment of ocean water color
[E73-10718] 17 p2019 N73-26325
Establishment of data management system for ERTS-1 data by National Marine Fisheries Service Engineering Laboratory
[E73-10720] 17 p2019 N73-26327
Evaluation of ERTS-1 image sensor spatial resolution in photographic form
[E73-10721] 17 p2019 N73-26328
Application of ERTS-1 imagery for tectonic analysis of Bighorn Mountains region and effect of snow cover and low sun angle on identifying topographical features
[E73-10722] 17 p2019 N73-26329
Application of ERTS-1 imagery to determine land use in Massachusetts, Connecticut, and Rhode Island
[E73-10723] 17 p2019 N73-26330
Application of ERTS-1 return beam vidicon and multispectral scanner imagery for ocean water color assessment in Caribbean Sea
[E73-10726] 17 p2019 N73-26332
Evaluation of ERTS-1 image data compression techniques to show four ERTS MSS tapes recorded on single compressed tape
[E73-10730] 17 p2020 N73-26336
In situ spectroradiometric quantification of ERTS-1 data and multispectral photo analysis of Willcox Playa
[E73-10737] 17 p2020 N73-26343
In situ spectroradiometric quantification of ERTS-1 data based on Arizona test site and Willcox Playa
[E73-10738] 17 p2021 N73-26344
Detection and analysis of fracture systems using ERTS-1 imagery of snow cover conditions as enhancement tool
[E73-10741] 17 p2021 N73-26346
Analysis of ERTS-1 multispectral band scanner imagery to determine cause of anomalous dark patches occurring in photographs of calm ocean surfaces
[E73-10747] 17 p2021 N73-26351
Application of ERTS-1 imagery for determining availability and distribution of menhaden within Mississippi Sound adjacent waters
[E73-10751] 17 p2022 N73-26354
Characteristics of NOAA 2 meteorological satellite and photographic data of weather conditions over Europe during 1972
[QR-4-PT-4] 17 p2056 N73-26627
Evaluation of satellite remote sensing and automatic data techniques for analysis of wetlands and marshlands using ERTS-1 imagery
[E73-10740] 18 p2133 N73-27235
Analysis of ERTS-1 imagery for area measurement of land use categories in Finney County, Kansas
[E73-10764] 18 p2134 N73-27241
Survey of lake flooding in Lake Champlain basin using ERTS-1 imagery
[E73-10771] 18 p2134 N73-27247
Use of ERTS-1 data to apply marine station data to study of productivity along Eastern Self Expanded Waters of US
[E73-10778] 18 p2135 N73-27254
Application of ERTS-1 imagery for defining ice formations, ocean currents, beach erosion, and estuarine circulation
[E73-10780] 18 p2136 N73-27256
Application of ERTS-1 imagery to determine dynamics of distribution and density of phreatophytes and other arid land plant communities
[E73-10790] 18 p2137 N73-27266
Application of ERTS-1 imagery for vegetation identification in southern Arizona
[PAPER-A7] 19 p2260 N73-28215
Application of ERTS-1 imagery for mapping and identification of vegetation and landforms in Great Basin
[PAPER-A9] 19 p2260 N73-28217
Analysis of ERTS-1 imagery for extrapolating existing soil maps into unmapped areas of Llanos Orientales of Colombia, South America
[PAPER-A13] 19 p2261 N73-28221
Application of ERTS-1 imagery for delineation of major soil association in loess region of Obion County, Tennessee
[PAPER-A14] 19 p2261 N73-28222
Mapping of cotton fields in Southern California using ERTS-1 data for control of pink bollworm growth
[PAPER-A15] 19 p2261 N73-28223
Analysis of ERTS-1 data for studies of hydrogeology, geomorphology, and paleoclimatology in Bolivia, Argentina, Chile, and Peru
[PAPER-W1] 19 p2270 N73-28281
Cartographic quality of ERTS-1 RBV and MSS imagery
[PAPER-L1] 19 p2273 N73-28297
Application of ERTS-1 TV imagery to map-making
19 p2283 N73-28366
Mapping of strip mine areas in southeastern Ohio from ERTS-1 imagery
19 p2284 N73-28372
ERTS-1 imagery of algal blooms in Lake Erie and Utah Lake, Ohio
19 p2285 N73-28376
Contrast enhancement of ERTS-1 imagery by photographic techniques and methods
19 p2286 N73-28381
Application of ERTS-1 imagery to study of coastal areas and processes
19 p2286 N73-28386
Proceedings of conference on significant results obtained by ERTS-1 - Vol. 2
[E73-10825] 19 p2287 N73-28389
Analysis of ERTS-1 to include specifications of sensors, data acquisition, orbital mechanics, and data processing
19 p2287 N73-28391
Analysis of ERTS data on ice formation in Bering Sea and correlation with ice observations by aerial reconnaissance
[E73-10865] 20 p2392 N73-29216
Application of ERTS data for mapping snow cover in Arizona and California and correlation with aerial photography
[E73-10866] 20 p2392 N73-29217
Application of ERTS data for mapping distribution of glacioluvial deposits and associated glacial landforms
[E73-10867] 20 p2392 N73-29218
Photographic recordings and meteorological data obtained by Environmental Research Satellite during January 1973
20 p2475 N73-29879
Photographic recordings and meteorological data obtained by Environmental Research Satellite During June 1973
20 p2475 N73-29880
Detection and identification of short-lived events using ERTS-1 imagery
[E73-10990] 22 p2658 N73-31296
Aerotriangulation with very small scale Skylab photography
[E73-10995] 22 p2659 N73-31301
Inventory and monitoring natural vegetation and plants in arid land of Arizona from satellite-borne photography
[E73-11021] 22 p2661 N73-31325
Equations for determining ground resolution on surface of earth observed by satellite-borne sensor
[AD-764246] 22 p2668 N73-31375
Aerotriangulation with very small scale photography from Skylab
[E73-11117] 24 p2916 N73-33274
Remote sensing of oceanic gamefish from ERTS-1 imagery
[E73-11135] 24 p2917 N73-33290
Analysis of grizzly bear habitats from ERTS-1 photography
[NASA-CR-135776] 24 p2920 N73-33319

**SATELLITE-BORNE RADAR**
Principles, installation, and operation of side-looking radar in aircraft and satellites for earth resources sensing
[ESRO-CR[P]-136-VOL-1] 03 p0296 N73-12418
Analysis of problems in mapping Venus surface with radar from orbiting spacecraft
[NASA-CR-129821] 04 p0477 N73-13900
Data processing for synthetic aperture radar used as satellite-borne earth resources remote sensor
[NASA-CR-2193] 09 p1005 N73-18202
Layout of scientific experiments in Aeros satellite, including description and function of satellite-borne instruments
[DGLR-PAPER-72-069] 09 p1091 N73-18906

**SATELLITES**
NT AEROS SATELLITE
NT ALOUETTE SATELLITES
NT ALOUETTE 1 SATELLITE
NT ALOUETTE 2 SATELLITE
NT APPLICATIONS TECHNOLOGY SATELLITES
NT ARIEL 3 SATELLITE
NT ARTIFICIAL SATELLITES
NT ASTRONOMICAL NETHERLANDS SATELLITE
NT ATS 1
NT ATS 3
NT ATS 5
NT ATS-6
NT AZUR SATELLITE
NT BIOSATELLITE 2
NT COMMUNICATION SATELLITES
NT COSMOS SATELLITES
NT COSMOS 213 SATELLITE
NT COSMOS 224 SATELLITE
NT COSMOS 381 SATELLITE
NT DIADEME SATELLITES
NT DIAL SATELLITE
NT EARTH RESOURCES TECHNOLOGY SATELLITE 1
NT EARTH RESOURCES TECHNOLOGY SATELLITES
NT EARTH SATELLITES
NT ECHO 1 SATELLITE
NT ENVIRONMENTAL RESEARCH SATELLITES
NT EOLE SATELLITES
NT EROS [SATELLITES]
NT ESRO 1 SATELLITE

NT ESRO 2 SATELLITE
NT ESSA 8 SATELLITE
NT EXPLORER SATELLITES
NT EXPLORER 12 SATELLITE
NT EXPLORER 18 SATELLITE
NT EXPLORER 21 SATELLITE
NT EXPLORER 24 SATELLITE
NT EXPLORER 27 SATELLITE
NT EXPLORER 31 SATELLITE
NT EXPLORER 32 SATELLITE
NT EXPLORER 33 SATELLITE
NT EXPLORER 34 SATELLITE
NT EXPLORER 35 SATELLITE
NT EXPLORER 38 SATELLITE
NT EXPLORER 40 SATELLITE
NT EXPLORER 41 SATELLITE
NT EXPLORER 49 SATELLITE
NT FR-1 SATELLITE
NT GEODETIC SATELLITES
NT GEOS 1 SATELLITE
NT GEOS 2 SATELLITE
NT GEOS-C SATELLITE
NT GOE SATELLITES
NT GRAVITY GRADIENT SATELLITES
NT HELIOS SATELLITES
NT HEOS A SATELLITE
NT HEOS B SATELLITE
NT HEOS SATELLITES
NT IMP
NT IMPROVED TIROS OPERATIONAL SATELLITES
NT INJUN 3 SATELLITE
NT INTELSAT SATELLITES
NT INTERCOSMOS SATELLITES
NT ISIS SATELLITES
NT ISIS-A
NT ITOS 1
NT ITOS 2
NT ITOS 3
NT ITOS 4
NT LINCOLN EXPERIMENTAL SATELLITES
NT LUNAR ORBITER
NT LUNAR SATELLITES
NT METEOROLOGICAL SATELLITES
NT METEOSAT SATELLITE
NT MOLNIYA SATELLITES
NT MOON
NT NATURAL SATELLITES
NT NAVIGATION SATELLITES
NT NIMBUS SATELLITES
NT NIMBUS 2 SATELLITE
NT NIMBUS 3 SATELLITE
NT NIMBUS 4 SATELLITE
NT NIMBUS 5 SATELLITE
NT OAO
NT OGO
NT OGO-A
NT ORBITAL SPACE STATIONS
NT ORBITAL WORKSHOPS
NT OSO
NT OSO-J
NT OSO-I
NT OSO-5
NT OSO-6
NT OSO-7
NT OV-1 SATELLITES
NT PROTON 1 SATELLITE
NT RADIO ASTRONOMY EXPLORER SATELLITE
NT RELAY SATELLITES
NT SAN MARCO 3 SATELLITE
NT SAS-B
NT SAS-C
NT SCIENTIFIC SATELLITES
NT SMALL ASTRONOMY SATELLITES
NT SPUTNIK SATELLITES
NT SYMPHONIE SATELLITES
NT SYNCHRONOUS METEOROLOGICAL SATELLITE
NT SYNCHRONOUS SATELLITES
NT TD-1 SATELLITE
NT TDR SATELLITES
NT TIROS M
NT TIROS SATELLITES
NT TRANSIT SATELLITES
NT UHURU SATELLITE
NT UK SATELLITES
NT UK 4 SATELLITE
NT VANGUARD 3 SATELLITE
NT VELA SATELLITES
NT VENERA SATELLITES
NT VENERA 8 SATELLITE

Systems and studies for direct TV reception from satellite in Germany
[DGLR-PAPER-72-50] 04 p0389 N73-13160

Digitizing system for numerical definition of satellite printed wiring boards
[SC-TM-72-0645] 10 p1134 N73-19243

**SATURATION**

IR laser study of absorption and saturation properties of molecular gases
[NASA-CR-132769] 19 p2307 N73-28554

**SATURN**

Investigation of causes of perturbations in Saturns rings
[REPT-14] 10 p1212 N73-19854

**SATURN [PLANET]**

NT SATURN RINGS

Composition, temperature, and optical properties of Jupiter and Saturn atmospheres
[NLL-M-20702-[5828.4F]] 06 p0716 N73-15845

Measurement of ultraviolet absorption by planet Saturn disk at various geographical regions
09 p1083 N73-18836

Probe study to explore atmosphere of Saturn and Uranus
[NASA-CR-131227] 10 p1215 N73-19883

Spectrophotometric analyses of Jovian and Saturnian limb darkenings
[NASA-CR-131891] 13 p1576 N73-22772

Characteristics of ring system around planet Saturn and sequence of space missions to acquire data on ring system composition
[NASA-CR-132952] 15 p1831 N73-24841

Analysis of data relative to possible Saturn orbiter mission in 1985
[NASA-CR-133033] 16 p1966 N73-25906

Radio astronomy observation of planet Saturn using interferometer at 21.1 centimeters wavelength
[AD-760014] 18 p2198 N73-27746

Mission planning for Pioneer Saturn/Uranus atmospheric probe missions
[NASA-TM-X-2824] 21 p2595 N73-30800

Observations of atmospheric limb darkening in visual continuium and multiple scattering analysis of jupiter and saturns atmospheres
22 p2713 N73-31719

Interplanetary trajectory characteristics of Saturn swingby mission to Uranus
[NASA-TM-X-2914] 22 p2714 N73-31727

Saturn satellite encounter opportunities for Mariner Jupiter-Saturn 1977 project
23 p2858 N73-32838

**SATURN LAUNCH VEHICLES**

NT SATURN 1B LAUNCH VEHICLES
NT SATURN 5 LAUNCH VEHICLES

Rocket nozzle redesign for improving Saturn launch vehicle J-2 engine performance and reliability
03 p0349 N73-12849

Wind tunnel tests to determine pressure distribution on Apollo command module and Saturn launch vehicle at supersonic and hypersonic speeds
[NASA-TM-X-62117] 04 p0477 N73-13904

**SATURN RINGS**

Rings of Saturn, their composition, and their thickness
[NASA-TT-F-14617] 02 p0230 N73-11867

Dark side illumination of Saturns ring by scattering
[REPT-13] 10 p1212 N73-19855

Characteristics of ring system around planet Saturn and sequence of space missions to acquire data on ring system composition
[NASA-CR-132952] 15 p1831 N73-24841

**SATURN S-2 STAGE**

Test data tabulation, statistical analysis, and heating rate contours for base region thermal environment of Saturn S-2 stage scale model - Vol. 2
[NASA-CR-129010] 20 p2382 N73-29144

Base region thermal environment test of scale model of Saturn S-2 stage - Vol. 1
[NASA-CR-129009] 20 p2475 N73-29883

**SATURN S-4B STAGE**

Identification of artificial lunar impact craters produced by Ranger 7 and 9 spacecraft and S-4B stage of Apollo 13 and 14 - Part I
12 p1453 N73-21773

**SATURN STAGES**

NT SATURN S-2 STAGE
NT SATURN S-4B STAGE

**SATURN WORKSHOPS**

Preflight assessment of Skylab VHF ranging coverage for rendezvous portion of SL-1/SL-3 mission
[NASA-CR-133996] 22 p2631 N73-31085

**SATURN 1B LAUNCH VEHICLES**

Performance evaluation of SA-206 launch vehicle for Skylab 2 launch to show signficant events and failures and anomalies
[NASA-TM-X-69538] 24 p2981 N73-33820

Performance evaluation of SA-207 launch vehicle for Skylab 3 launch to show significant events and failures and anomalies
[NASA-TM-X-69540] 24 p2981 N73-33821

Pseudo-Nyquist analysis technique for hybrid sampled-data control systems
[NASA-CR-2345] 24 p2984 N73-33847

**SATURN 5 LAUNCH VEHICLES**

Design of cryogenic flow control components for Saturn 5 S-1C launch vehicle
03 p0349 N73-12850

Postflight trajectory for Apollo/Saturn V AS-511 spent S-4B/IU stage from CSM separation to lunar impact
[NASA-CR-123975] 05 p0594 N73-14826

Ground-based measurements of electrical length of vehicle and plume and of atmospheric electricity during Apollo 13 and 14 launches
[NASA-CR-130535] 08 p0916 N73-17503

Wind tunnel pressure signatures for scale model of Saturn 5-Apollo launch vehicle with simulated exhaust plumes
[NASA-TM-X-62129] 21 p2599 N73-30830

Sensitivity and comparison evaluation of liquid penetrants used in Saturn 5 vehicle hardware to detect surface cracks
[NASA-TM-X-64769] 22 p2688 N73-31529

Dispersion predictions for effluents from exhaust gases from Saturn 5 and Scout-Algol 3 launch vehicles
[NASA-TM-X-2935] 24 p2921 N73-33327

Postflight analysis of Apollo 15 flight to determine performance of launch vehicle, spacecraft, and lunar roving vehicle and to analyze malfunctions
[NASA-TM-X-69539] 24 p2981 N73-33819

Evaluation of launch vehicle, spacecraft, and lunar rover performance during Apollo 17 flight to determine malfunctions and recommend corrective actions
[NASA-TM-X-69534] 24 p2981 N73-33822

Postflight analysis of Apollo 16 flight to show spacecraft performance, launch vehicle performance, and malfunctions occuring during flight
[NASA-TM-X-69535] 24 p2981 N73-33823

Postflight analysis of Apollo 14 flight to show spacecraft performance, launch vehicle performance, and malfunctions occurring during flight
[NASA-TM-X-69536] 24 p2981 N73-33824

Saturn 5 launch vehicle performance during Skylab launch and orbit
[NASA-TM-X-69537] 24 p2984 N73-33848

**SAUDI ARABIA**

ERTS-1 multispectral data of northwest Saudi Arabia
[E72-10295] 04 p0410 N73-13345

ERTS-1 detection of potential locust breeding sites in Saudi Arabian desert
[E73-10098] 08 p0902 N73-17309

Satellite vs aircraft imagery of Saudi Arabia for mineral exploration
08 p0971 N73-17936

Dynamics of plankton populations in upwelling waters along Arabian Coast, Somali Coast, and Northwest Coast of Africa
[E73-10325] 09 p1024 N73-18357

Analysis of ERTS-1 multispectral imagery of Northwest Saudi Arabia
[E73-10380] 10 p1152 N73-19375

Location of wet areas and detection of potential locust breeding sites using ERTS-1 imagery of Red Sea coastal plain of Saudi Arabia
[E73-10462] 12 p1394 N73-21301

ERTS-1 imagery of morphology, provenance, and movement of desert sand areas in Africa, Asia, and Australia
[E73-10710] 17 p2018 N73-26317

**SAVANNAHS**

U GRASSLANDS

**SAWS**

Flexural strength of aluminum oxide substrates separated by lasers and diamond sawing
[SC-DC-71-4496] 03 p0321 N73-12613

**SAWTOOTH WAVEFORMS**

Development and characteristics of sawtooth voltage generator using blocking generator as switch
22 p2630 N73-31081

**SCALARS**

Scalar quantum field theory in closed universe of constant curvature
15 p1813 N73-24690

**SCALE [CORROSION]**

Transport properties of oxide scales formed on oxidation resistant alloys
14 p1676 N73-23604

Vaporization thermodynamics of Cr2O3 protective scales under transonic flow conditions
14 p1677 N73-23607

Oxidation resistant refractory metal alloys for use in high temperature environments
14 p1678 N73-23615

**SCALE EFFECT**

Parameterization and its role in atmospheric modeling
[GARP-PUBL-8] 05 p0573 N73-14654

**SCALE MODELS**

Scale model for design of large modular subsonic wind tunnel
[DLR-MITT-72-21] 01 p0037 N73-10288

Wind tunnel static stability and control data for delta wing booster of scale model of space shuttle
[NASA-CR-119994-VOL-3] 01 p0107 N73-10886

Performance tests of scale model of lunar roving vehicle used on Apollo 15 mission to determine vehicle mobility
[NASA-CR-129176] 02 p0152 N73-11234

Instrumentation and methods used with acoustic studio scale model
[BBC-1972/34] 04 p0419 N73-13413

Design and development of scale model of parallel burn space shuttle to represent low frequency structural dynamic characteristics
[NASA-CR-112205] 04 p0478 N73-13909

Wind tunnel tests of space shuttle model to determine performance, stability, and control characteristics of launch configuration
[NASA-CR-120088] 04 p0478 N73-13910

Development of structural dynamics model of space shuttle and evaluation of structural and hydroelastic analysis methods
[NASA-CR-112196] 04 p0478 N73-13911

Development of space shuttle scale model for thermodynamic analysis of internal and external heat flow fields
[NASA-CR-128849] 10 p1215 N73-19882
Technique for determining mechanical properties of full-size aircraft tires from tests conducted with small-scale model tires
[NASA-CR-2220] 12 p1357 N73-21006
Evaluation of scale model of low pressure rocket engine used for secondary injection studies and modifications required for full scale simulation
[NASA-CR-124176] 12 p1443 N73-21690
Wind tunnel tests of space shuttle orbiter scale model to determine low speed aerodynamic characteristics of spacecraft components
[NASA-CR-120092] 12 p1460 N73-21832
Aerodynamic coefficients for calculating transport aircraft performance using wind tunnel and scale models
15 p1732 N73-24046
Feasibility of small scale, full operating gas core reactor demonstration test
[NASA-CR-121190] 18 p2177 N73-27577
Supersonic wind tunnel tests on scale model space shuttle orbiter configuration
[NASA-TM-X-2804] 19 p2248 N73-28123
Test data tabulation, statistical analysis, and heating rate contours for base region thermal environment of Saturn S-2 stage scale model - Vol. 2
[NASA-CR-129010] 20 p2382 N73-29144
Base region thermal environment test of scale model of Saturn S-2 stage - Vol. 1
[NASA-CR-129009] 20 p2475 N73-29883
Semi-automatic device for encoding three dimensional models
21 p2513 N73-30158
Wind tunnel pressure signatures for scale model of Saturn 5-Apollo launch vehicle with simulated exhaust plumes
[NASA-TM-X-62129] 21 p2599 N73-30830
Thermal-vacuum tests of flight model spacecraft to determine performance and reliability based on malfunction analysis
[NASA-TN-D-7408] 24 p2984 N73-33851

**SCALERS**
Design of logic counters and scalers based on continued quotients for digital function generators
03 p0278 N73-12253
Wave and Einstein equations for studying scaler waves and tensor perturbations in Mixmaster Universe
15 p1829 N73-24823

**SCALING LAWS**
Similarity analysis of transient temperature and thermal stress for deriving scaling relations for modeling thermal shock
[SC-RR-71-0657] 04 p0485 N73-13962
Effects of plasma-neutral gas interactions on equilibrium and stability of permeable Tokamak plasmas noting scaling conditions
[TRITA-EPP-72-26] 07 p0828 N73-16716
Hot gas recirculation in Do-31 aircraft from scale model to aircraft and trends for future developments of V/STOL aircraft
[BMVG-FBWT-72-29] 10 p1107 N73-19024
Analysis of support properties of scaling function for time-like virtual photons using simple perturbative model
[LPTHE-72/28] 10 p1192 N73-19696
Bilocal operator expansion to two jet structure for final states of deep inelastic scattering on hadrons
[ILL-(TH)-73-4] 12 p1430 N73-21592
Scaling relations for critical exponents of modified F model
[NUB-2172] 12 p1438 N73-21653
Scaling laws, constructional problems, and optimum model size associated with wind tunnel tests of helicopters and rotary wing aircraft
17 p2009 N73-26246
Analysis of transonic scaling effect on quasi, two-dimensional airfoil model of C-141 aircraft
[AD-762285] 19 p2222 N73-27924
Scaling phenomena of collapse of wake of self-propelled body in stratified fluid
[AD-762454] 19 p2258 N73-28201
Vortex age as scaling parameter in wake turbulence development and dissipation
[NASA-CR-132312] 22 p2652 N73-31245
Scaling laws to predict supersonic jet noise generated by rectangular and axisymmetric nozzles
[PB-221855/0] 22 p2700 N73-31629

**SCANNERS**
NT FLYING SPOT SCANNERS
NT HORIZON SCANNERS
NT INFRARED SCANNERS
NT OPTICAL SCANNERS
Ultrasonic scanner for inspection and evaluation of in-place brazed tube joints
[NASA-TM-X-64702] 02 p0178 N73-11445
Performance of scanning acoustical imaging telescope at microwave frequencies
07 p0820 N73-16648
Scan processor and symbol scanner for program documentation
10 p1132 N73-19224
Very bright field ionization and evaporation ion sources for use in ion probes of scanning instruments
[IPP-9/6] 10 p1194 N73-19717
Construction of cartographic scanner/plotter for computer aided mapping
[AD-754648] 11 p1288 N73-20452
Response of optico-electronic scanning system with antiphase connection of radiation detector elements
12 p1405 N73-21395
Time base stability and intermachine compatibility in wideband laser recording systems
13 p1536 N73-22444

**SCANNING**
NT FREQUENCY SCANNING
NT PANORAMIC SCANNING
NT RADAR SCANNING
Scanning electron microscopy applied to surface fracture mechanics study, composite materials, and powder metallurgy
[DLR-MITT-71-32] 03 p0315 N73-12571
Array techniques for large and sub-arrays for limited scan application
[AD-751274] 07 p0763 N73-16203
Electronic optical transfer function analyzer using scanning image dissection system to produce representative output signal
[NASA-CASE-MFS-21672-1] 13 p1558 N73-22630
Automatic scanning and display eddy current system for nondestructive testing of printed circuit boards
[ARL/MET-NOTE-84] 15 p1786 N73-24478
Use of argon-ion laser transverse mode locking to produce high resolution scanning beam
15 p1794 N73-24546
Scanning auger spectroscopy for surface analysis of solid state devices
[AD-760550] 18 p2153 N73-27399

**SCANNING DEVICES**
U SCANNERS

**SCARS (GEOLOGY)**
U EROSION

**SCAT**
U SUPERSONIC COMMERCIAL AIR TRANSPORT

**SCATTER PROPAGATION**
NT IONOSPHERIC F-SCATTER PROPAGATION
Numerical analysis and diagnostics of nonradially stratified media applied to distributions lacking spherical symmetry
02 p0200 N73-11614
Characterization of multipath and Doppler fading in earth scatter communication, navigation, and radar links
24 p2894 N73-33102

**SCATTERED CLOUDS**
U CLOUDS (METEOROLOGY)

**SCATTERERS**
U SCATTERING

**SCATTERING**
NT ACOUSTIC SCATTERING
NT ATMOSPHERIC SCATTERING
NT BACKSCATTERING
NT COHERENT SCATTERING
NT COMPTON EFFECT
NT ELASTIC SCATTERING
NT ELECTROMAGNETIC SCATTERING
NT ELECTRON SCATTERING
NT FORWARD SCATTERING
NT INCOHERENT SCATTERING
NT INELASTIC SCATTERING
NT IONOSPHERIC F-SCATTER PROPAGATION
NT LIGHT SCATTERING
NT MICROWAVE SCATTERING
NT MIE SCATTERING
NT NEUTRON SCATTERING
NT NUCLEAR SCATTERING
NT PROTON SCATTERING
NT RADAR SCATTERING
NT RAMAN SPECTRA
NT RAYLEIGH SCATTERING
NT RESONANCE SCATTERING
NT REVERBERATION
NT THOMSON SCATTERING
NT TROPOSPHERIC SCATTERING
NT WAVE SCATTERING
NT X RAY SCATTERING
Spontaneous and stimulating scattering and molecular spectra
[AD-746497] 02 p0212 N73-11718
Rare molecular gas beam scattering from single metal crystal surfaces
[AD-748938] 04 p0451 N73-13685
Dark side illumination of Saturns ring by scattering
[REPT-13] 10 p1212 N73-19855
Sound speed modulation by bubbles in upper ocean
[AD-754372] 11 p1325 N73-20754
Scattering kernel analysis on monatomic gas interaction with solid surface
[AD-755838] 13 p1489 N73-22069
Optical high energy scattering models and photoprocesses in nuclei
[CERN-72-20] 15 p1814 N73-24702
Scattering by charged particle density fluctuations of plasma for zero magnetic field
[NASA-CR-133808] 21 p2582 N73-30694
Observations of atmospheric limb darkening in visual continuum and multiple scattering analysis of jupiter and saturns atmospheres
22 p2713 N73-31719

**SCATTERING AMPLITUDE**
New tables for forward pion nucleon scattering amplitude analyzing errors and total cross section data
[NOTA-INTERNA-382] 01 p0084 N73-10695
Scattered acoustic wave amplitudes of plane wave incident on perforated screen with periodic array of circular or elliptic apertures
[AD-747648] 03 p0338 N73-12755
Scattering characterization inputs in computerized design of wideband linear amplifiers for pulse operation
[LBL-772] 07 p0762 N73-16188
Sum rule for photoproduction amplitudes in isovector Compton scattering and inconsistency of free fermion parton model in deep inelastic limit
[NUB-2169] 07 p0823 N73-16673
Development of equations for determining diffuse reflectance and transmittance of inhomogeneous materials for collimated incident radiation at any angle of incidence
[RE-452J] 13 p1559 N73-22633
Development of fixed pole solution for pion-pion scattering amplitude and comparison with high energy data
[ILL-(TH)-73-15] 24 p2960 N73-33657

**SCATTERING COEFFICIENTS**
Two flux radiative transfer model for measuring absorption and scattering coefficients for nonhomogeneous minerals
[RE-451J] 13 p1558 N73-22632
Development of equations for determining diffuse reflectance and transmittance of inhomogeneous materials for collimated incident radiation at any angle of incidence
[RE-452J] 13 p1559 N73-22633
Rayleigh equations for determining axial sound wave scattering coefficients by torus
[REPT-208.138/1] 14 p1692 N73-23731
Comparison of absorption and scattering coefficients for air
[LA-UR-73-708] 24 p2923 N73-33348

**SCATTERING CROSS SECTIONS**
Relation between momentum transfer and capture, and total scattering cross sections for ion-dipole collisions
[NASA-TM-X-68151] 01 p0083 N73-10685
Determination of longitudinal cross section in inelastic electron proton scattering in Delta(1236) resonance region
02 p0213 N73-11728
Crossed molecular beam method for measuring elastic differential scattering cross sections of potassium with gaseous media
02 p0213 N73-11729
FORTRAN 4 programs and subroutines for generating potential parameters from energy dependence of elastic scattering cross sections
[NASA-CR-129179] 03 p0269 N73-12180
Composite scattering model for explaining rough sea surface scattering cross sections
06 p0663 N73-15383
Differential cross section of emitted photon in suprathermal proton bremsstrahlung
08 p0974 N73-17966
Charge transfer cross sections of alkali metals
[AD-752909] 09 p1000 N73-18161
Time dependent scattering theory for evaluating transition cross sections in atomic helium collision with charged particle
[NASA-CR-131265] 11 p1326 N73-20761
Laser beam study of proton production cross sections determined for stable and radioactive rare gases
[TID-26183] 12 p1427 N73-21566
Equations of motion for calculating collision dynamics of diatomic molecules
[NASA-CR-131527] 12 p1431 N73-21594
Differential and integral scattering cross sections for H and He atoms in hydrogen
[NASA-TT-F-14900] 13 p1561 N73-22655
Absolute cross sections for rotational Raman scattering derived for nitrogen and oxygen from near UV to infrared
[AD-756808] 13 p1566 N73-22695
Experimental facility for measuring rotational Raman scattering cross sections of nitrogen and oxygen at 10.6 microns
[AD-757111] 14 p1617 N73-23098
Differential scattering of hydrogen and oxygen atoms in methane molecules
[NASA-TT-F-14898] 14 p1694 N73-23751
Collision cross section of D line radiated into sodium atoms for one 3 P2 state
[NASA-TT-F-14853] 14 p1695 N73-23752
Electron energy loss spectra and scattering cross sections
[NASA-CR-132174] 15 p1749 N73-24172

Differential scattering from collision of metastable atoms of He[2 3S] with molecules of N2 and O2
[NASA-TT-F-14801] 15 p1815 N73-24712
Axial and planar channeling effects in thin crystals
15 p1820 N73-24750
Reactive crossed molecular beam studies using free jet sources
18 p2180 N73-27605
Optical models for electron scattering from atoms and molecules
18 p2181 N73-27608
Optical potential approach to electron-atom impact ionization threshold problem
[NASA-TM-X-66282] 18 p2181 N73-27609
Total cross sections for electron positron annihilation producing hadron pair
[NOTA-INTERNA-420] 18 p2181 N73-27613
Regularity in dip positions of elastic differential cross sections
[LPTPE-73/18] 20 p2456 N73-29741
Measurement of positive and negative pion, and double neutral pion photoproduction cross sections for incident gamma ray energies from 600 to 900 MeV
21 p2582 N73-30691
Calculation of Mie differential scattering cross section of spherical particles with complex refractivity, for mm wave propagation through precipitation
[FTZ-A-455-TBR-35] 22 p2633 N73-31100
Cross section for collision processes between molecular oxygen and electron with collision energy below 100 eV
[NASA-TT-F-15048] 23 p2821 N73-32550

**SCATTERING FUNCTIONS**
Application of scatter factors for various Weibull-shaped parameters, fleet sizes, and level of reliability for aircraft structures
[NASA-CR-2100] 01 p0113 N73-10934
Light scattering by particles in sea water based on volume scattering function and point spread function
24 p2957 N73-33628

**SCATTERING MATRIX**
U S MATRIX THEORY

**SCATTEROMETERS**
Characteristics of radar equipment and microwave radiometers to show application to earth resources surveys
07 p0784 N73-16377
Characteristics of microwave radiometer scatterometer system for Skylab program
22 p2671 N73-31394
Skylab S-193 RADSCAT measurements of Hurricane Ava
[E73-11062] 23 p2781 N73-32238

**SCF**
U SELF CONSISTENT FIELDS

**SCHEDULING**
NT PREDICTION ANALYSIS TECHNIQUES
Scheduling management, and costs of St. Louis air pollution facility
[PB-210020] 01 p0077 N73-10639
Generation of random experiment schedules for space station using Monte Carlo technique
[NASA-TM-X-64557] 03 p0355 N73-12894
Production of software in NASA within predictable schedule and budget constraints and reasonable tolerances - App. C
[NASA-CR-129818] 05 p0516 N73-14191
Environmental factors affecting OAO and related computer programs for data processing and scheduling observations
[NASA-TM-X-66145] 06 p0721 N73-15882
Problems of radar network scheduling to track satellites
[AD-751290] 07 p0757 N73-16152
Automated medical history questionnaire for screening industrial personnel and scheduling physical examinations
08 p0872 N73-17060
Computerized multivariate scheduling of physical examinations for NASA personnel in clinical intervention program
08 p0873 N73-17068
Human continuous reaction time task distribution rates for paced and selfpaced responses to visual stimuli
[IZF-1973-5] 14 p1613 N73-23077
Work-rest schedule for optimum performance of monitoring tasks
14 p1723 N73-23987
Model for updating aerospace research and development as function of perturbations in program time
[NASA-TM-X-64748] 15 p1845 N73-24948
Computerized support system for complex spacecraft mission scheduling
18 p2211 N73-27851
Forward algorithm for scheduling process monitor in time sharing computer sample data control
[AD-761668] 19 p2240 N73-28058
Heuristic method for scheduling aircraft maintenance
[AD-761494] 19 p2355 N73-28947
Application of mathematics to general job-shop scheduling noting criteria, procedures, and linear programming
[LAAS-OD-73-I-21] 23 p2813 N73-32488

**SCHEELITE**
Gamma spectroscopic activation analysis of scheelite deposits
03 p0262 N73-12124

**SCHELKUNOFF PRINCIPLE**
Variational and Schelkunoff methods for analyzing microwave propagation in magnetoplasma filled waveguides
16 p1947 N73-25757

**SCHEMATICS**
U CIRCUIT DIAGRAMS

**SCHLIEREN PHOTOGRAPHY**
Wake transition of blunt cones in hypersonic flight using schlieren photography and opto-electronic laser system
[ISL-12/72] 03 p0310 N73-12531
Quantitative schlieren photography with semishadow of edge in photograph allowing calibration
[WB-2/72] 09 p1037 N73-18459
High speed schlieren film of pulsating flow in transonic turbine cascade
10 p1207 N73-19818
Topler schlieren photographic study of diffusion flame structure
[NASA-TT-F-14843] 10 p1223 N73-19946
Schlieren method adapted as flow visualization technique to study cavitation development on axisymmetric bodies in water tunnel
[AD-757078] 14 p1652 N73-23402
Electromechanical focal plane shutters for spectrographic and color schlieren camera systems
[DREV-TN-1997/72] 15 p1785 N73-24475
Plasma diagnostics with infrared schlieren and interferometric techniques using TEA-CO2 laser, exemplified by electric spark transient response
[ISL-19/72] 16 p1950 N73-25779
Analysis of wakes generated by hovering model propellers and rotors using schlieren photography and hot-wire anemometry
[NASA-CR-2305] 21 p2491 N73-29996
Device for observing diaphragm surface vibration angular displacement based on two dimensional schlieren techniques
[REPT-10/1972] 22 p2674 N73-31420
Color schlieren photography of ammonium perchlorate binder sandwich combustion
[AD-764489] 23 p2857 N73-32829

**SCHMIDT CAMERAS**
Objective prism survey of entire southern sky within 10th to 13th photographic magnitude range by Schmidt telescope equipped with ultraviolet prism
06 p0717 N73-15851
Applications of Schmidt telescopes to study astrometry, photometry, galactic structure, quasars, and stellar spectra
07 p0844 N73-16840
History of 48-inch Palomar Schmidt telescope noting investigation of galactic red shift and radio sources
07 p0844 N73-16841
Application of Schmidt telescopes and three color photometry to galactic clusters, star distribution in galactic disk and halo and galactic white stars.
07 p0845 N73-16842
Astrometry for determination of absolute positions of stars and their relative motions from Schmidt plates noting accuracy
07 p0845 N73-16843
Astrometric performance of Schmidt plates for stellar positions noting reduction of coordinates
07 p0845 N73-16844
Schmidt telescopes for astrometry discussing correspondence between flat and curved plates
07 p0845 N73-16845
Pros and cons of objective prisms in astronomical spectroscopy noting work in conjunction with Schmidt telescopes and novel techniques
07 p0845 N73-16846
Flint glass objective prism recommended for ESO Schmidt camera due to light transmission properties
07 p0845 N73-16847
Application of Schmidt telescope and objective prism to stellar radial velocity surveys
07 p0845 N73-16848
Application of Schmidt telescopes to study of galactic clusters and evolution noting new emulsion, infrared surveys, luminosity, and quasars
07 p0845 N73-16849
Observation of quasars with Schmidt cameras and compilation of light curve for BL Lacertae
07 p0845 N73-16850
Importance of Schmidt telescopes to radio astronomy noting color identification of quasars and Southern Hemisphere sky survey
07 p0845 N73-16851
Galactic brightness distribution obtained by imaging galaxies on Schmidt plates, selecting one as photometric standard and applying microdensitometric scans
07 p0845 N73-16852
Schmidt telescopes in Southern Hemisphere survey noting possible sites and study of Magellanic clouds
07 p0846 N73-16853
Infrared sky survey in Southern Hemisphere for finding late M stars
07 p0846 N73-16854
Identification of infrared stars using Schmidt telescopes, infrared photometry, and slit spectra
07 p0846 N73-16855
Schmidt telescopes for compilation of stellar spectra and novae maps, galactic structure, and radial velocities
07 p0846 N73-16856
Investigation of stellar density distribution and luminosity function in high galactic altitudes using Schmidt telescopes
07 p0846 N73-16857
Design of Schmidt telescope with possibility of converting to Cassegrain configuration and noting achromatic corrector and angular resolution
07 p0846 N73-16858
Parameters and components of ESO Schmidt telescope
07 p0846 N73-16859
Applications of Tautenburg 134-cm Schmidt telescope noting instrument efficiency and astrophysical statistics
07 p0846 N73-16860
Michelson interferometry quality control of Schmidt plate replica by [Jouan Quetin] grating copying technique noting Kerber profile
[OPT-001-72] 23 p2794 N73-32351
Kerber profile Schmidt plates uses in optical combinations with applications to cameras
[OPT-01-72] 23 p2794 N73-32352

**SCHOOLS**
Silent alarm system for mutiple room facility or school
[NASA-CASE-NPO-11307-1] 21 p2519 N73-30205

**SCHOTTKY BARRIER DIODES**
U SCHOTTKY DIODES

**SCHOTTKY DIODES**
Design and performance of traveling wave gallium arsenide amplifier with Schottky barrier
[AD-757219] 14 p1642 N73-23321
Schottky barrier diodes for electron beam semiconductor applications
[AD-757749] 15 p1757 N73-24240
Comparison of detectivities of p-n junction diode and Schottky internal photoemission diode under background-limited conditions
[AD-757873] 15 p1757 N73-24243
Limitations in microelectronic circuits, design of power Schottky diode, and strontium titanate permittivity
16 p1880 N73-25218

**SCHOTTKY EFFECT**
U WORK FUNCTIONS

**SCHROEDINGER EQUATION**
Application of Schroedinger equation to solve inverse scattering problem at fixed energy in quantum mechanics
02 p0199 N73-11609
Generalized Airy functions, using one dimensional, time independent, Schroedinger equation
[NASA-CR-129604] 03 p0324 N73-12638
Derivation of nonlinear Schroedinger equation for electron plasma waves
[IPPJ-137] 04 p0441 N73-13590
Plasma device for studying ion acoustic solitons
[IPPJ-149] 15 p1816 N73-24723
Nonlinear Schrodinger equation for studying nonlinear wave modulation in magnetized collisionless plasma
[IPPJ-162] 20 p2458 N73-29755
Procedure for determining Rayleigh-Schroe dinger energies and wave functions of degenerate states to high orders
[NASA-CR-135641] 23 p2812 N73-32485

**SCHUMANN-RUNGE BANDS**
Absorption cross sections of Schumann-Runge bands of molecular oxygen
[A-107-1972] 04 p0385 N73-13127
Tables on molecular oxygen absorption in schumann-runge band
[AERONOMICA-ACTA-A-107-PT-2] 05 p0506 N73-14114
Tables of O2 absorption cross sections in Schumann-Runge band
[A-N-107-1972] 07 p0752 N73-16108
Tables of absorption cross sections of molecular oxygen in Schumann-Runge bands
[AERONOMICA-ACTA-A-107-1972-V-1] 12 p1375 N73-21157
Tables of absorption cross sections of molecular oxygen in Schumann-Runge bands
[AERONOMICA-ACTA-A-107-1972-V-2] 12 p1375 N73-21158

**SCHWARZSCHILD METRIC**
Calculation of particle motion in gravitational field using Schwarzschild metric
[ESRO-SR-17-ESOC] 03 p0357 N73-12910
Boundary conditions and singularities in gravitational collapse and gravitational radiation
[MATSCIENCE-72] 15 p1781 N73-24437
Spherical and nonspherical gravitational collapse and Schwarzschild black holes
15 p1829 N73-24822

SCIENCE
Joint meetings in Sweden on business economics, industrial economics, and scientific theory
[FOA-P-C-8280-10] 02 p0244 N73-11984
Astronomical, mathematical, and neuropathological research projects in Hungary, and scientific development policy in Poland
[JPRS-57271] 02 p0244 N73-11986
Relationship between law and scientific and technical progress in socialist systems
[JPRS-57318] 03 p0367 N73-12992
Scientific and technical research projects in Poland
[JPRS-57570] 04 p0488 N73-13988
Scientific and technical research projects in Czechoslovakia and Hungary
[JPRS-57583] 04 p0488 N73-13989
Collection of European scientific research reports
[AD-747959] 04 p0488 N73-13996
Research management of eastern Europe scientific affairs
[JPRS-57765] 05 p0595 N73-14838
Research and development projects compiled at Army science conference
[AD-750300] 06 p0732 N73-15973
Guide to National Science Foundation programs and grants - information for proposals
[NSF-72-23] 07 p0857 N73-16945
Bibliography of Nuclear Science Abstracts from 1964 to 1970
[AED-C-21-10] 08 p0942 N73-17720
Overview of scientific and technological research in Yugoslavia on NBS grants, 1971 - 1972
[NBS-TN-753] 08 p0976 N73-17979
Conference on Air Force science and engineering research
[AD-753072] 09 p1101 N73-18991
Development of scientific centers in USSR during past 50 years and considerations for future development
[JPRS-58596] 11 p1267 N73-20281
Index of international scientific rocketlaunches
[NASA-TM-X-69350] 18 p2196 N73-27732
Research management of East European scientific affairs
[JPRS-59273] 18 p2213 N73-27865
Scientific research in geophysics, astronomy, meteorology, oceanography, astronautics from soviet-block
[JPRS-59935] 22 p2716 N73-31738

SCIENTIFIC SATELLITES
NT APPLICATIONS TECHNOLOGY SATELLITES
NT ATS 1
NT ATS 3
NT ATS 5
NT ATS 6
NT AZUR SATELLITE
NT DIAL SATELLITE
NT ENVIRONMENTAL RESEARCH SATELLITES
NT OV-1 SATELLITES
NT UK SATELLITES
NT UK 4 SATELLITE
Vehicle encountered trapped electron and proton fluxes calculated for nominal UK 5 circular equatorial orbits
[NASA-TM-X-66098] 02 p0225 N73-11816
Ionospheric electron content and satellite signal scintillation
[AD-747507] 03 p0298 N73-12430
Design and employment of Soviet satellite of Cosmos series
[AD-749725] 05 p0601 N73-14886
Measurement of energy spectra of high energy trapped protons using nuclear emulsions exposed on low altitude polar orbiting satellites
[AD-750474] 06 p0669 N73-15438
Development of Large Space Telescope for conducting astronomical observations from unmanned satellites and analysis of constraints and tradeoffs during design phase - Vol. I
[NASA-TM-X-64726-VOL-1] 09 p1035 N73-18449
Ionospheric sounding by scientific satellites
[AD-756483] 14 p1662 N73-23490
Launching Radio Exploration Satellite using Mu-4S-4 rocket for studying ionosphere and magnetosphere
17 p2088 N73-26888
Lightweight reprogrammable data system for small scientific satellite
18 p2208 N73-27823
Techniques for assessment and control of contamination in scientific satellites
[NASA-TN-D-7433] 23 p2845 N73-32738
German astronomical satellite configuration and subsystems for launching Scout D vehicle
[BMBW-FB-W-72-26] 23 p2852 N73-32787

SCIENTISTS
History of Radcliffe Observatory and its scientific research activities and personnel
02 p0152 N73-11231
Analysis of inflow of professional and technical personnel to US from foreign countries
[NSF-72-312] 05 p0611 N73-14969
Utilization of scientific and technical personnel by urban governments
[PB-212762] 07 p0860 N73-16979
Philosophical and social psychological study of Apollo moon scientist
[NASA-CR-130832] 09 p0995 N73-18122
Research and development in theoretical and applied sciences in Eastern Europe
[JPRS-58121] 09 p1101 N73-18982
Training of scientists and engineers for German Department of the Defense
11 p1351 N73-20965
Leading scientists of USSR space programs
[NASA-TT-F-14882] 13 p1595 N73-22935
Survey of characteristics and attitudes of immigrant scientists and engineers in US
19 p2354 N73-28938
Graduate science students and manpower resources
[NSF-73-304] 21 p2609 N73-30908

SCINTILLATION
Variations of interplanetary scintillation index with wavelength in accordance with smooth, power law spectrum of plasma fluctuations
01 p0097 N73-10802
Spectral form of irregularities in electron density causing interplanetary scintillation of small angular diameter radio sources
01 p0098 N73-10804
Ionospheric electron content and satellite signal scintillation
[AD-747507] 03 p0298 N73-12430
Scintillation reductions in multiwavelength laser propagation by near field transmitter apertures
[AD-747640] 03 p0337 N73-12751
Analysis of laser beam scintillation due to atmospheric turbulence
[AD-752565] 08 p0930 N73-17620
Laser beam scintillation caused by atmospheric turbulence
[AD-757562] 14 p1674 N73-23580
Cerium and silver containing silicate and borate systems for developing high density scintillation glass for nuclear cascade detectors
[NASA-CR-133960] 17 p2049 N73-26580
HF and VHF oblique backscatter and scintillation study at Plum Island
[AD-760783] 18 p2146 N73-27349
Observations of amplitude scintillations produced in F region in equatorial areas based on Applications Technology Satellite transmissions
[NASA-TM-X-70478] 24 p2921 N73-33326

SCINTILLATION COUNTERS
Comparison of neutron spectra measured with three sizes of organic liquid scintillators using differentiation analysis
[NASA-TM-X-2646] 03 p0331 N73-12699
Gas scintillation counter for measuring fluorescence of source of radium coated with radon
[PUBL-1410] 06 p0702 N73-15725
Computerized positron scintillation camera data acquisition and display system for linear accelerator facility
[UCRL-51288] 10 p1161 N73-19447
Handbook on scintillation counters with emphasis on cesium iodide scintillators for HEAO experiments
[NASA-TM-X-64741] 13 p1530 N73-22398
Scintillation and polarimeter measurements of ionospheric column using ATS 1
[AD-759533] 16 p1910 N73-25451
Experimental system for conducting ionospheric scintillation measurements using ATS geostationary satellites at 136 and 1550 MHz
[PB-220564/9] 21 p2509 N73-30133
Portable nuclear radiation spectrometer for field measurement of mixed isotopic contaminants
[LA-5203-MS] 22 p2674 N73-31418
Gamma ray telescope using double Compton process and measuring extraterrestrial gamma ray fluxes in energy range 1-10 MeV
[MPI-PAE/EXTRATERR-74] 22 p2674 N73-31421
Balloon observations of solar neutrons by scintillation counter
[NASA-CR-135496] 22 p2712 N73-31714
Source and diffusion of cosmic rays greater than 4.5 GV in interstellar medium measured by proportional counter-scintillation counter stack
[TR-73-136] 23 p2835 N73-32652

SCINTILLATION SPECTROMETERS
U SCINTILLATION COUNTERS
U SPECTROMETERS

SCINTILLATORS
U SCINTILLATION COUNTERS

SCINTILLOMETERS
U SCINTILLATION COUNTERS

SCORPIO CONSTELLATION
U SCORPIUS CONSTELLATION

SCORPIUS CONSTELLATION
Lyman and Werner molecular hydrogen bands in ultraviolet intersteller spectrum of delta Scorpii
[NASA-TM-X-66102] 02 p0230 N73-11865
Visual and photographic observations of Beta Scorpii occultation by Jupiter
[NASA-CR-129990] 05 p0594 N73-14832
Aerobee rocket observation of ultraviolet line spectra of Delta Scorpii and Zeta Ophiuchi
08 p0958 N73-17838
Stellar X ray temporal variations from observations of Sco X-1 and Cyg X-1
08 p0974 N73-17969
Central radio source and hard X ray emitting region of Scorpius X-1
[NASA-TM-X-66244] 15 p1830 N73-24831

SCOTLAND
Small scale mapping of England and Scotland from ERTS-1 imagery
[E73-10817] 18 p2140 N73-27292
Report of the Astronomer Royal for Scotland for the year ending 31 March 1973
22 p2718 N73-31760

SCOUT HELICOPTER
U P-531 HELICOPTER

SCOUT LAUNCH VEHICLE
Aerodynamic characteristics of Scout vehicle during launch through high velocity horizontal winds
[NASA-CR-112175] 01 p0108 N73-10888
German astronomical satellite configuration and subsystems for launching Scout D vehicle
[BMBW-FB-W-72-26] 23 p2852 N73-32787
Dispersion predictions for effluents from exhaust gases from Saturn 5 and Scout-Algol 3 launch vehicles
[NASA-TM-X-2935] 24 p2921 N73-33327

SCR [RECTIFIERS]
U SILICON CONTROLLED RECTIFIERS

SCRAMBLING [COMMUNICATION]
Rate distortion theory for providing privacy transformations in data banks
[P-4952] 14 p1619 N73-23113

SCRAMJET ENGINES
U SUPERSONIC COMBUSTION RAMJET ENGINES

SCRAMJETS
U SUPERSONIC COMBUSTION RAMJET ENGINES

SCREEN EFFECT
Screening factor which reduces densities at which carbon ignition can occur in helium, exhausted carbon, and oxygen stellar core models
[UCRL-74669-REV-1] 24 p2992 N73-33913

SCREENS
Development of mosaic image conversion panels sensitive to ultraviolet, X ray, near infrared, and visible light
[AD-745757] 01 p0033 N73-10262
Application of polyethylene materials as screens for actinometric instruments to include analysis of physical, mechanical, and optical properties
[NLL-M-22675-[5828.4F]] 01 p0069 N73-10566
Millimeter wave image conversion panel using p-i-n diode structures for carrier injection and bulk conductivity modulation
[AD-747409] 03 p0276 N73-12241
Accelerated electron ring focusing by image forces in conducting cylindrical screen
[JINR-P9-6421] 05 p0580 N73-14724
Performance of large screen tactical display systems in training devices using cathode ray tubes
[AD-751559] 07 p0767 N73-16228

SCREWS
Estimating effect of inclined nut seating on fatigue strength of steel screw thread
[ESDU-67034] 01 p0060 N73-10487
Fatigue tests of steel screw threads with large root radii under axial loading to determine fatigue strength and point of failure
[ESDU-67020-AMEND-A] 01 p0110 N73-10906
Tensile and stripping strength data in terms of failure probability for bolts, nuts, screws, and threaded rods
[ESDU-67019] 01 p0110 N73-10908

SCRUBS [BOTANY]
U BRUSH [BOTANY]

SCYLLA
Plasma experiments on helical equilibria in Scyllac theta pinch sector
[LA-DC-72-706] 05 p0584 N73-14752
Scyllac research experiments
[LA-DC-72-896] 07 p0827 N73-16702

SEA ICE
NT ICE FLOES
NT ICEBERGS
Surveillance and mapping of sea ice in Arctic regions based on ERTS-1 imagery
[E72-10199] 02 p0160 N73-11297
Winter wind and ocean conditions in Labrador fishing waters, and effects on pack ice drifting and icing hazards
[NLL-M-22670-[5828.4F]] 05 p0570 N73-14630
Energy balance equations for parameterization of hydrological processes effecting atmospheric circulation
05 p0573 N73-14663
Pulse radar sounding of sea ice thickness with video display
[JPRS-57841] 06 p0665 N73-15406
Mapping Arctic sea ice from ERTS-1 MSS imagery
[E73-10278] 08 p0914 N73-17486

Arctic ice measurements from airborne microwave radiometers and ground based equipment in Mar. 1971
08 p0971 N73-17937
Detection and mapping Arctic sea ice using ERTS-1 imagery
[E73-10374] 10 p1151 N73-19369
Sea ice and surface water circulation in Cook Inlet, Alaska, and along continental shelves
[E73-10370] 11 p1275 N73-20346
ERTS-1 imagery of sea ice and surface water circulation along Alaskan contiental shelf
[E73-10416] 11 p1279 N73-20378
Mapping Arctic sea ice from ERTS-1 imagery of Hudson Bay, M'Clure Strait, Beaufort Sea, and Greenland Sea
[E73-10447] 11 p1282 N73-20407
Sea ice dynamics, heat and mass budget of Arctic sea ice, desalinization, thermal and mechanical stresses, bearing capacity of floating ice, and interaction of oil and ice
[AD-754118] 11 p1290 N73-20463
Sonar mapping of underside of sea ice
[AD-755243] 13 p1527 N73-22374
Continuous observations of structural changes in deforming polycrystalline ice
[AD-755336] 13 p1527 N73-22375
Detection and mapping of sea ice in Arctic regions using ERTS-1 RBV and MSS data
[E73-10595] 14 p1658 N73-23452
ERTS-1 imagery of sea ice and surface water circulation along Alaskan Continental Shelf
[E73-10620] 15 p1775 N73-24381
Solar and terrestrial radiation fluxes over Arctic pack ice
[AD-758060] 15 p1828 N73-24820
ERTS-1 imagery of icebergs and sea ice in Antarctic region
[E73-10686] 16 p1902 N73-25380
Survey of Antarctic icebergs using ERTS-1 imagery
[E73-10692] 16 p1902 N73-25385
Application of ERTS-1 imagery for defining ice formations, ocean currents, beach erosion, and estuarine circulation
[E73-10780] 18 p2136 N73-27256
Skylab 4 microwave radiometry of lake and sea ice in Gulf of St. Lawrence and Lake Ontario
[E73-10820] 18 p2140 N73-27295
Dynamics and morphology of Beaufort Sea ice determined from satellites, aircraft, and drifting stations
[NASA-TM-X-66291] 18 p2144 N73-27333
Influence of sea ice on coastal marine environment of Beaufort Sea, Alaska
[PAPER-M7] 19 p2280 N73-28346
Detection and mapping Arctic sea ice from ERTS-1 imagery
[PAPER-M14] 19 p2281 N73-28353
Sea ice and surface water circulation along Alaskan continental shelf
[E73-10901] 20 p2396 N73-29250
Analysis of ice conditions existing in Antarctic waters during Tenth Soviet Antarctic Expedition
20 p2407 N73-29342
Marine ice observations during Tenth Soviet Antarctic Expedition to measure formation, growth, disintegration, and physicomechanical properties
20 p2408 N73-29351
Analysis of physicomechanical properties of ice conducted during Tenth Soviet Antarctic Expedition with emphasis on ice cover temperature effects
20 p2408 N73-29352
Analysis of ice conditions existing in Alasheyev Bight during Tenth Soviet Antarctic Expedition
20 p2409 N73-29362
Spectral analysis of wind-wave spectrum at ice edge in Arctic Basin
21 p2573 N73-30621
Application of ERTS-1 data to detection and mapping of sea ice in Beaufort Sea and Bering Sea areas
[E73-11037] 22 p2663 N73-31341
Ice motion and interior flow field
[PB-221714/9] 22 p2669 N73-31387
Air stress predictions for synoptic scale ice dynamics model
[PB-222057/2] 22 p2669 N73-31388
Remote sensing of Arctic Sea ice motion by ERTS instrumentation
22 p2736 N73-31902
Mesoscale movement and deformation of sea ice in Beaufort Sea
[E73-11153] 24 p2919 N73-33307
Salinity effects on extinction coefficient of sea ice
[AD-763882] 24 p2924 N73-33355

**SEA KING HELICOPTER**
U SH-3 HELICOPTER

**SEA OF JAPAN**
Robot buoy for study of relation between marine environment and weather in Sea of Japan
[NLL-M-23049-[5828.4F]] 21 p2567 N73-30573

**SEA ROUGHNESS**
Analysis of factors affecting ride quality of water vehicles and human reactions to motion caused by rough water
01 p0003 N73-10022
Analysis of long-period wave phenomenon for means of forecasting and control in seaport operations
04 p0443 N73-13612
Composite scattering model for explaining rough sea surface scattering cross sections
06 p0663 N73-15383
Doppler return spectra from rough ocean surface
19 p2320 N73-28667
Curvature corrected Kirchhoff formulation for radar sea-return from near vertical
22 p2628 N73-31053

**SEA STATES**
Side-looking radar applied to oceanography noting sensing of sea states, pollution, and waves
03 p0295 N73-12408
Statistical eigenfunctions used for analysis and prediction of sea level surges
04 p0443 N73-13611
Effects of vertical jet breakwaters on wind generated deep water waves
[AD-748190] 05 p0528 N73-14293
Effect of sea state and atmospheric parameters on satellite altimeter performance
06 p0662 N73-15372
Sea state effects on altimeter signal scattering and radar wave form estimates
06 p0663 N73-15381
Influence of sea state on short pulse radar satellite altimeter determination of mean surface position
06 p0663 N73-15385
Ocean circulation effects on orbiting satellite gravimetry
06 p0664 N73-15394
Empirical data on probable sea state conditions to be encountered by space shuttle booster recovery forces
[NASA-TM-X-68631] 07 p0792 N73-16440
Remote sensing and RF interferometry for determining sea states
16 p1911 N73-25465
Two-reservoir exchange model for Baltic Sea material balance
[GH-4] 17 p2027 N73-26407
Laboratory investigations of whitecaps, spray and capillary waves
[AD-759407] 18 p2149 N73-27369
Sea spectra and radar scattering
[AD-760693] 18 p2149 N73-27373
Influence of atmospheric cyclones on circulation and mixing of sea water in motionless uniformly rotating baroclinic ocean
19 p2258 N73-28202
ERTS-1 detection of oceanic eddies in Lesser Antilles
[E73-10922] 20 p2398 N73-29271
Development of theories for radar sea return from wind-roughened waves
[AD-762073] 21 p2539 N73-30362

**SEA WALLS**
U BREAKWATERS

**SEA WATER**
Analysis of density of water in forms of ice, water and steam, liquid and gaseous heavy water, and sea water
[ESDU-68010-AMEND-A] 01 p0038 N73-10302
Solution of Navier-Stokes equation for sea water pressure determination
[NOTA-INTERNA-377] 01 p0042 N73-10328
Ocean water color assessment of Monterey Bay, California, from ERTS-1 RBV and MSS imagery
[E72-10190] 01 p0046 N73-10369
Analysis of thermal fluctuations in San Diego Bay, California and factors which affect thermodynamic properties
[AD-744921] 01 p0052 N73-10420
MINOS DOM oxygen monitor for measuring dissolved oxygen in sea water to depths of 3000 meters
[NOAA-IFS-73004] 01 p0057 N73-10466
Vertical and horizontal turbulent mixing coefficients of sea water determined from attenuation coefficient
[NLL-RTS-7536] 02 p0160 N73-11294
Mathematical analysis of optical refractive index fluctuations due to salinity and temperature microstructure
[AD-746120] 02 p0168 N73-11366
Mean irradiance distribution of finite cross section laser beam propagating in sea water
[AD-745956] 02 p0183 N73-11483
Deterioration in sea water of materials and underwater system components
[AD-747245] 02 p0194 N73-11567
Optical parameter effects of sea water and spatial-temporal structure of light impulses
[JPRS-57332] 03 p0335 N73-12733
Airborne and seaborne observations of radar scattering by sea water surfaces
[JPRS-57409] 04 p0388 N73-13156
Bubble distributions in quiescent ocean calculated from bubble transport equation
[AD-749046] 04 p0408 N73-13329
Sea, ice, and surface water circulation in Alaskan Continental Shelf
[E72-10347] 05 p0533 N73-14335
Natural convection in liquid layers of differing density
[AD-750762] 06 p0656 N73-15330
Ocean water color assessment from ERTS-1 RBV and MSS imagery
[E73-10002] 06 p0658 N73-15338
Geothermal data from deep water and bottom sediment measurements in Atlantic and Pacific Oceans
[AD-749983] 06 p0669 N73-15441
Depth effect on underwater ambient noise intensity in Caribbean Sea
[AD-750693] 06 p0670 N73-15447
Chemical synthesis inhibitor of oceanic species having antibiotic properties
07 p0858 N73-16962
Gain and impedance measurements on ultrahigh frequency antennas near surface of simulated sea water
[AD-751922] 08 p0890 N73-17205
Prevention of spurious caustics in ray tracing scheme for sound propagation mapping in sea water
[AD-752080] 08 p0944 N73-17735
Development of method for determining conductivity of surface layer of sea by recording field of remote transmitters operating in superlong wavelength range
10 p1153 N73-19382
Penetration and transmission of light in sea water
[AD-753029] 10 p1156 N73-19409
Sea water temperature measurement from Raman spectra
[AD-753481] 11 p1288 N73-20450
Optical properties of sea water in Atlantic, Pacific, and Caribbean
[AD-753474] 11 p1290 N73-20470
Transmission of light through randomly scattering medium
[AD-754074] 11 p1325 N73-20752
Environmental quality program, environmental forecasting program, and seabed assessment program for international decade of ocean exploration
12 p1400 N73-21359
Stress corrosion cracking tests of aluminum alloys in synthetic sea water
[NASA-TM-X-64733] 13 p1488 N73-22062
Radio propagation loss over ocean surface paths
[AD-755511] 13 p1492 N73-22091
Statistical analysis of underwater sound speed fluctuation in upper ocean region
[AD-756570] 13 p1560 N73-22641
Marine luminescence data for monitoring algal and pollutant concentrations
[NASA-CR-114578] 16 p1867 N73-25114
Collection of marine fluorescence data from Atlantic, Gulf, and Pacific sites
[NASA-CR-114579] 16 p1867 N73-25115
Problems of sea chemistry
[TT-70-57237] 16 p1907 N73-25427
Airborne laser remote sensing of coastal waters
[AD-759781] 16 p1910 N73-25454
Application of ERTS-1 RBV and multispectral scanner imagery for assessment of ocean water color
[E73-10718] 17 p2019 N73-26325
Numerical analysis of horizontal diffusion in ocean water to determine lifetime and spatial extent of submarine wakes in various turbulent media
[AD-762046] 19 p2256 N73-28186
Analysis of wake collapse in sea water and stratified fluids with emphasis on final stages of decay
[AD-761622] 19 p2257 N73-28189
ERTS-1 imagery of sea surface circulation and sediment transport in Cook Inlet, Alaska
[PAPER-M8] 19 p2280 N73-28347
Hydrological investigations conducted during Tenth Soviet Antarctic Expedition to determine temperature and salinity of ocean
20 p2407 N73-29343
Hydrological investigations of Davis Sea conducted during Tenth Soviet Antarctic Expedition
20 p2408 N73-29353
Physical oceanography problems
[AD-760704] 20 p2413 N73-29395
Airborne radiometer for continuously measuring sea water temperature
[NASA-TT-F-15070] 20 p2419 N73-29441
Direct determination of electromagnetic reflection properties of smooth brackish water by remote measurement technique
[PB-221372/6TR-48] 22 p2635 N73-31122
Dipole receiver characteristics in presence of sea water
[AD-763722] 22 p2644 N73-31187
Assessment of water color in Caribbean from ERTS-1 RBV and MSS imagery.
[E73-11006] 22 p2660 N73-31311
Circulation and mixing of sea water due to stationary and transitory axisymmetric atmospheric cyclones
[AD-763930] 22 p2669 N73-31383
ERTS-1 imagery of sea, ice, and surface water circulation along Alaskan continental shelf
[E73-11050] 23 p2779 N73-32226
Proceedings of conference on electromagnetic and optical properties of sea water for application to surveillance, mapping, communications, and visibility
[AGARD-LS-61] 24 p2956 N73-33619

Debye polarization theory for determining electromagnetism of sea surface
24 p2957 N73-33620
Radiance distribution as function of depth in upper layers of ocean and numerical analysis of inherent and apparent optical properties
24 p2957 N73-33621
Debye polarization theory for determining electromagnetic wave propagation in sea
24 p2957 N73-33622
Optical properties of pure and turbulent sea water
24 p2957 N73-33624
Techniques for predicting effects of thermal and saline inhomogeneities on optical imaging systems with application to optical properties of sea water
24 p2957 N73-33625
Effect of ocean depth on light scattering and attenuation parameters to include optical properties influenced by concentration, size, and shape of particulate matter
24 p2957 N73-33626
Mathematical theories for determining light propagation by sea water
24 p2957 N73-33627
Light scattering by particles in sea water based on volume scattering function and point spread function
24 p2957 N73-33628
Effect of various parameters on long range underwater vision for narrow and broad beam illumination
24 p2958 N73-33630
Effects of resolution, signal to noise ratio, and contrast on underwater imaging systems performance
24 p2958 N73-33631
Computer programs for analyzing optical properties of sea water
24 p2958 N73-33638

**SEALANTS**
U SEALERS
**SEALERS**
Application of continued fractions to rational scale counter design
05 p0517 N73-14208
Improved carbon graphite materials for high temperature self-acting seals
[NASA-CR-121092] 10 p1165 N73-19481
Analytical models of viscoseal performance with rarefied gas sealant
[NASA-CR-121089] 12 p1408 N73-21409
Perfluoroalkylene ether polymers for high temperature fuel tank sealants
[NASA-CR-124249] 14 p1680 N73-23635
**SEALING**
NT SELF SEALING
**SEALS [ANIMALS]**
Receiver operating characteristics for underwater signal detection performance of sea lions
[AD-746520] 04 p0382 N73-13113
**SEALS [STOPPERS]**
NT GASKETS
NT GLANDS [SEALS]
NT HERMETIC SEALS
NT O RING SEALS
NT PACKINGS [SEALS]
NT PLUGS
NT PUMP SEALS
Complex variable method of planar elastic stress for lubricated rectangular seal
02 p0178 N73-11444
High temperature ceramic to metal seal capable of operation at 1200 C for 3 to 5 years
[NASA-CR-120831] 05 p0552 N73-14484
Abradable buffered labyrinth seal for control of gas path leakage in tip-turbine driven lift fan
[NASA-CR-121131] 07 p0804 N73-16524
Plastic compression type seals for long life Ni-Cd batteries
[NASA-CR-130867] 08 p0870 N73-17040
LOX-cooled bearing and seal start cycling performance
[MBB-UR-84-71] 10 p1167 N73-19493
Tests on bearings and seals undergoing repeated starts of turbine pumps
[SEP-NT-3058/71-M] 10 p1167 N73-19494
Load factors for pressure balancing of gas film seals under various flow conditions
[NASA-TM-X-68227] 12 p1408 N73-21412
Vibration effects on self-acting and hydrodynamic shaft seals in gas turbine engines
[NASA-TM-X-68214] 13 p1534 N73-22430
Designs of high temperature seals for gaps between structure and aerodynamic control surfaces of space shuttle orbiter
[NASA-CR-128951] 16 p1965 N73-25891
Interfacial wear reactions in nickel and molybdenum alloy mechanical face seals
[AD-762076] 19 p2306 N73-28546
High speed, self-acting shaft seal
[NASA-CASE-LEW-11274-1] 20 p2422 N73-29457
Tests and evaluation of seal for movable rocket nozzle systems
[AD-762944] 20 p2423 N73-29467
Leak detector with high vacuum seals
[NASA-CASE-LAR-11237-1] 23 p2793 N73-32344
Development of high temperature resistant elastomeric sealant
[AD-764589] 23 p2811 N73-32473
**SEAMS [JOINTS]**
Design of solar energy concentrators with concentric circular seams of plastic films
[AD-755829] 12 p1446 N73-21712
**SEARCH PROFILES**
Characterization of interaction between detection and visibility processes with application to search policies
15 p1743 N73-24130
Technology transfer and information dissemination services provided by Technology Use Studies Center
[NASA-CR-132963] 16 p1977 N73-25991
Development of report search code for computer generated bibliographic data in machine readable form
[DSIS-TN-11] 24 p2897 N73-33125
**SEARCH RADAR**
Range-gated moving target indicator for use with search radar
[AD-757259] 14 p1636 N73-23265
Development and characteristics of air traffic control radar and associated signal and display processing equipment
[FAA-RD-73-35] 16 p1875 N73-25178
Computer manual for experimental array radar ear system simulation program
[AD-758922] 16 p1877 N73-25197
Determining mean and covariance errors in alpha-beta filter operating in Cartesian coordinates
[AD-759011] 16 p1935 N73-25656
Angular resolution and target discrimination in pulsed search radar
[AD-759350] 17 p1999 N73-26162
Error reduction in two-gimbal, airborne search radar system
[AD-760551] 18 p2119 N73-27131
Target searching procedures with electronically steered phased array radar
[REPT-186] 22 p2632 N73-31094
**SEARCHING**
NT SEARCH PROFILES
Reliability of search strategies for information retrieval by aerospace personnel
[AD-751977] 08 p0977 N73-17995
Conference on human visual search and perception
[AD-754327] 11 p1248 N73-20133
Weakly homogeneous binary systems of order two for random search theory
18 p2169 N73-27515

**SEAS**
NT BALTIC SEA
NT BARENTS SEA
NT BEAUFORT SEA [NORTH AMERICA]
NT BERING SEA
NT BLACK SEA
NT CARIBBEAN SEA
NT MEDITERRANEAN SEA
NT RED SEA
NT SEA OF JAPAN
Thermal emission from random sea, using Gaussian slope distribution
20 p2391 N73-29207
**SEASONAL VARIATIONS**
U ANNUAL VARIATIONS
**SEASONS**
NT SUMMER
NT WINTER
Survey of seasonal snow cover of Alaska from ERTS-1 imagery
[E72-10344] 05 p0532 N73-14332
Monitoring vernal advancement and retrogradation of natural rangeland vegetation in Great Plains Corridor
[E73-10643] 16 p1897 N73-25340
Time of formation of elementary circulation mechanisms related to annual fluctuation in solar activity
[NLL-M-23014-[5828.4F]] 20 p2390 N73-29199
Survey of seasonal snow cover of North Slope and Alaska Range from ERTS-1 data
[E73-11086] 24 p2913 N73-33249
**SEASPRITE HELICOPTER**
U UH-2 HELICOPTER
**SEAT BELTS**
Performance tests of crash protective seat belts using energy absorbers to allow system to yield at constant force
[ARL/SM-340] 06 p0619 N73-15023
Comparison of effectiveness of yielding and elastic restraint systems for crash protection to show effects of slack and yield at constant load
[ARL/SM-382] 15 p1837 N73-24890
**SEATS**
NT BARANY CHAIR
NT EJECTION SEATS
Statistical analysis of impact injuries to seated human responding to square wave energy absorption of vertical deceleration pulse representing helicopter crash
[AD-745919] 02 p0136 N73-11102
Development of aircraft seat for high acceleration tolerance of flight crew personnel by elevating pelvis and legs forward
[AD-756630] 14 p1605 N73-23009
**SECANTS**
U TRIGONOMETRIC FUNCTIONS
**SECONDARY AIR**
U AIR
**SECONDARY COSMIC RAYS**
Atmospheric model for secondary gamma ray production
22 p2733 N73-31871
**SECONDARY EMISSION**
Development of X ray polarimeter by detecting secondary fluorescent X rays
[ISAS-489] 14 p1666 N73-23523
Secondary electron densities in two-electrode interspace in ac current present during multipactor discharge
[REPT-73-74] 19 p2244 N73-28091
Electron scattering and secondary emission from tungsten crystal surface
[AD-761876] 19 p2328 N73-28726
Finiteness of radiative corrections to semileptonic decays in unified gauge theories
[TR-74-021] 22 p2701 N73-31637
**SECONDARY FLOW**
Secondary flow phenomena and associated losses in high-deflection turbine rotor cascade
[AD-750183] 05 p0528 N73-14300
Experiments with cascade secondary flows
10 p1206 N73-19811
Characteristics of secondary flows around and downstream of protuberances in laminar boundary layers and conditions for development of turbulence
22 p2649 N73-31222
Secondary flow in curved channel of square cross section
[AD-764502] 22 p2655 N73-31267
Jet noise emission and reduction by secondary cold annular flow for SST and military aircraft
23 p2820 N73-32543
Free surface secondary flow of Newtonian liquid between rotating concentric cylinders
24 p2906 N73-33188
**SECONDARY FRONTS**
U FRONTS [METEOROLOGY]
**SECONDARY HARMONIC GENERATION**
U HARMONIC GENERATIONS
**SECONDARY INJECTION**
Gas or liquid injection for secondary injection thrust control
[NAL-TR-286T] 04 p0463 N73-13774
Prediction of shock shapes and wall shock traces encountered in secondary injection into conical rocket nozzle
[AD-750081] 05 p0528 N73-14295
**SECONDARY WAVES**
U S WAVES
**SECRETIONS**
NT ENDOCRINE SECRETIONS
NT HORMONES
NT INSULIN
NT SWEAT
**SECTORS**
Bearing sectors for controlling self excited instability of journal bearing shafts rotating at high speeds in low viscosity lubricants
[NASA-CASE-LEW-11076-2] 11 p1298 N73-20533
**SECULAR PERTURBATION**
U LONG TERM EFFECTS
**SECURITY**
Cost effective data security safeguards in personal information databanks
[P-4871] 02 p0145 N73-11178
Liapunov type methods for checking dynamic security in power system stability theory
07 p0760 N73-16174
Rate distortion theory for providing privacy transformations in data banks
[P-4952] 14 p1619 N73-23113
**SEDATIVES**
Neuronal changes in cortical motor region cells during pharmacological induced sleep
13 p1483 N73-22028
**SEDIMENT TRANSPORT**
Estuarine coastal water dynamics controlling sediment transport and plume development in Long Island Sound
[E72-10250] 03 p0289 N73-12350
Sediment pattern correlation with tidal and inflow action in Chesapeake Bay using ERTS-1 data
[E72-10334] 05 p0531 N73-14322
ERTS-1 imagery of California nearshore processes including estuarine flushing, currents, season river discharges, and sediment dispersion
[E72-10363] 05 p0535 N73-14351
ERTS-1 imagery of estuarine and coastal water dynamics controlling sediment transport and plume development in Long Island Sound
[E73-10093] 08 p0902 N73-17305
Measurement of coastal currents and processes and seaward extent of suspended sediment transport in waters of California
[E73-10375] 10 p1151 N73-19370

Estuarine and coastal water dynamics controlling sediment transport and plume development in Long Island Sound
[E73-10378] 10 p1152 N73-19373
Sources and dispersal patterns of suspended particulates in nearshore surface waters of northeastern Pacific Ocean and Hawaii
[E73-10487] 12 p1396 N73-21323
ERTS-1 imagery of California nearshore sediment transport, coastal processes, and tidal currents
[E73-10525] 13 p1517 N73-22292
Estuarine and coastal water dynamics controlling sediment transport and plume development in Long Island Sound
[E73-10627] 15 p1775 N73-24387
Sediment pattern correlation with inflow and tidal action in Chesapeake Bay
[E73-10623] 16 p1896 N73-25336
ERTS-1 imagery of inner shelf and coastal sediment transport in Beaufort Sea
[E73-10649] 16 p1897 N73-25345
Problems of sea chemistry
[TT-70-57237] 16 p1907 N73-25427
Sources and dispersal patterns of suspended particles in nearshore surface waters of San Francisco Bay and Gulf of Farallones
[E73-10788] 18 p2137 N73-27264
Correlation of sediment patterns with inflow and tidal action using MSS and I2S imagery
[E73-10794] 18 p2137 N73-27270
Littoral transport of sedimention coastal region of France
[E73-10822] 18 p2140 N73-27297
ERTS-1 imagery of littoral drift and sedimentation patterns of beach and nearshore areas of Maryland section of Chesapeake Bay
[PAPER-M2] 19 p2280 N73-28342
ERTS-1 imagery of sea surface circulation and sediment transport in Cook Inlet, Alaska
[PAPER-M8] 19 p2280 N73-28347
Sediment distribution, water currents, and water circulation in Cook Inlet, Alaska
[PAPER-M9] 19 p2281 N73-28348
Distribution and movement of suspended sediment in Gulf of Mexico off Texas coast
[PAPER-M10] 19 p2281 N73-28349
Application of ERTS-1 data to North Carolina forest and water resources management
[PAPER-R1] 19 p2282 N73-28359
ERTS-1 imagery of suspended sediment plumes and turbidity in Lake Ontario
[E73-10956] 21 p2532 N73-30298
Sediment pattern correlation with inflow and tidal action
[E73-10984] 22 p2658 N73-31291
Sources and dispersal patterns of suspended particles in nearshore surface waters of northeast Pacific Ocean and seasonal variation in snow cover in Sierra Nevada Mountains
[E73-11099] 24 p2914 N73-33256

**SEDIMENTARY ROCKS**
NT COAL
NT SHALES
Chemical analysis of krypton and xenon isotopes in three meteorites and for melt extractions on samples of five terrestrial sedimentary rocks
08 p0958 N73-17836
Oil exploration in large intercratonic sedimentary basins in Oklahoma using ERTS-1 imagery
[E73-10646] 16 p1897 N73-25342
Evaluation of ERTS-1 imagery for geological surveys and topographical analysis of various terrains in New York State
[PAPER-G1] 19 p2263 N73-28233
Combined visual and digital techniques for analyzing ERTS-1 data pertaining to geologic information on selected areas in Pennsylvania
[PAPER-G2] 19 p2263 N73-28234
Analysis of ERTS-1 MSS imagery to determine geological and structural features in sedimentary basin in France
[PAPER-G6] 19 p2263 N73-28237
Organic geochemistry of amino acids in sedimentary rocks
[NASA-TT-F-14986] 23 p2787 N73-32295

**SEDIMENTS**
Sediment pattern correlations with inflow and tidal action in Chesapeake Bay based on ERTS-1 imagery
[E72-10169] 01 p0044 N73-10350
Environmental studies of sedimentation and nearshore marine processes in Cook Inlet, Alaska, and regional study of permafrost regimes in Alaska using ERTS-1 imagery
[E72-10209] 02 p0161 N73-11304
ERTS-1 imagery of inner shelf and coastal sedimentation environment of Beaufort Sea
[E72-10248] 03 p0289 N73-12348
Strip mine identification, land use assessment, smoke plume detection, and sedimentation patterns in Sandusky Bay from ERTS-1 imagery of Ohio
[E72-10259] 03 p0290 N73-12358
Sources and dispersal patterns of suspended sediments in nearshore surface waters of Northeast Pacific Ocean and Hawaiian Islands based on ERTS-1 imagery
[E72-10271] 03 p0291 N73-12370
Dynamic behavior of coastal sedimentation in Lions Gulf
[E72-10289] 04 p0410 N73-13339
Development and evaluation of equipment for monitoring long term sea floor foundation settlement and tilting
[AD-750258] 06 p0669 N73-15444
Sedimentation levels in rivers and shoal estuarine waters based on ERTS-1 imagery
[E73-10048] 07 p0777 N73-16310
ERTS-1 imagery of suspended sediment plumes in Lake Ontario
[E73-10057] 07 p0778 N73-16319
Seismic reflection and refraction surveys of thickness of coastal plain sediments in Virginia
[PB-212604] 07 p0794 N73-16455
Alaskan arctic and subarctic sediment deposition, permafrost, snow cover, and ice mapping from ERTS-1 imagery
[E73-10279] 08 p0914 N73-17487
Interpretation of Mariner 6 and 7 Martian photometry for sediment geomorphology
[NASA-CR-2194] 08 p0962 N73-17869
Dispersal patterns of suspended particles in nearshore surface waters of northeast Pacific Ocean and Hawaiian Islands
[E73-10314] 09 p1023 N73-18346
ERTS-1 imagery of suspended sediment plumes in Lake Ontario
[E73-10316] 09 p1023 N73-18348
Ross Barnett Reservoir remote sensing project to determine water sediment, investigate erosion, and improve land use
[NASA-CR-130960] 09 p1029 N73-18396
Study of suspended sediment and aquatic fronts in Delaware Bay using ERTS-1 imagery
[E73-10368] 10 p1150 N73-19364
ERTS-1 imagery of inner shelf and coastal sedimentation environment of Beaufort Sea, Alaska
[E73-10412] 11 p1278 N73-20374
Correlation of chlorophyll and suspended sediments in Chesapeake Bay to ERTS-1 imagery
[E73-10424] 11 p1280 N73-20385
ERTS-1 imagery of inner shelf and coastal sedimentation environment of Beaufort Sea
[E73-10492] 12 p1397 N73-21328
Dynamics of suspended sediment plumes in Lake Ontario
[E73-10493] 12 p1397 N73-21329
Mapping of coastal sedimentation and related processes in Cook Inlet, Alaska and distribution and environmental interrelationships of permafrost terrain
[E73-10421] 13 p1515 N73-22275
ERTS-1 imagery of suspended matter and hydrologic interfaces in Delaware Bay
[E73-10515] 14 p1653 N73-23409
Relation of chlorophyll and suspended sediment content in lower Chesapeake Bay to ERTS-1 imagery and application of marine station data to study of productivity along eastern shelf waters of US
[E73-10593] 15 p1772 N73-24358
ERTS-1 imagery of suspended sediment plumes in Lake Ontario
[E73-10599] 15 p1772 N73-24360
Physical properties and suspended matter of surface waters in southeastern Atlantic Ocean
[PB-214813/8] 15 p1784 N73-24467
Paleomagnetic study of Mano Lake, California to determine secular variations during past 30,000 years
16 p1895 N73-25325
Movement of suspended particle and solute concentrations with inflow and tidal action in Chesapeake Bay
[E73-10662] 16 p1899 N73-25358
Digital analysis of ERTS-1 data to determine sedimentation levels in Potomac and Anacostia Rivers confluence and strip mining in Allegheny County, Maryland
[PAPER-E13] 19 p2270 N73-28277
Assessment of flood damage in Arizona using ERTS-1 MSS imagery to show extent of inundation and sediment deposition
[PAPER-W6] 19 p2271 N73-28284
Application of ERTS-1 imagery to analysis of suspended sediments and aquatic fronts in Delaware Bay
[PAPER-M3] 19 p2280 N73-28343
Correlation of ERTS-1 multispectral imagery with suspended matter and chlorophyll in lower Chesapeake Bay
[PAPER-M4] 19 p2280 N73-28344
ERTS-1 imagery of water pollution, sedimentation, and geology of southeastern France and western Alps
[PAPER-R6] 19 p2283 N73-28364
Relation of chlorophyll and suspended sediments in waters of lower Chesapeake Bay to ERTS-1 imagery
[E73-10851] 19 p2292 N73-28429
Marine geological research of submarine relief and ocean bottom sediments conducted during Tenth Soviet Antarctic Expedition
20 p2407 N73-29345
Microbiology of sediments and its geological aspects
[NASA-TT-F-15022] 20 p2411 N73-29381
Wave flume and oscillating water tunnel for bed forms generated by wave action
22 p2731 N73-31856
Analysis and mapping sediment deposition, permafrost areas, snow cover, and icing in Arctic regions of Alaska from ERTS-1 data
[E73-11067] 23 p2781 N73-32243
Detection of plant diseases, soil moisture, drainage patterns, forestry types, and sedimentation in Tennessee from ERTS-1 imagery
[E73-11091] 23 p2782 N73-32258

**SEEBECK COEFFICIENT**
U SEEBECK EFFECT

**SEEBECK EFFECT**
Galvanomagnetic and thermoelectric properties of monocrystalline alloys of bismuth and antimony at liquid nitrogen temperature
[AD-745865] 01 p0089 N73-10734

**SEEDING [INOCULATION]**
U INOCULATION

**SEEKERS**
U HOMING DEVICES

**SEGMENTS**
Automatic speech recognition program to provide segmentation, acoustical parameters, and phonetic feature classifications in speech
14 p1623 N73-23146

**SEISMIC WAVES**
NT LOVE WAVES
NT RAYLEIGH WAVES
Systematic regional stress variations in fault zones in competent rocks
[AD-743837] 01 p0052 N73-10422
Large aperture seismic array, seismometer and amplifier performance, and seismograph calibration
[AD-745753] 01 p0053 N73-10433
Uncorrected accelerometer data resulting from San Fernando, California earthquake of Feb. 1971
[PB-208529] 01 p0054 N73-10439
Detection and classification of earthquakes and nuclear explosions by Swedish observatory
[FOA-4-A-4503-TR78] 01 p0101 N73-10828
Application of Monte Carlo inversion to seismic data
02 p0200 N73-11617
Application of Backus-Gilbert theory for geophysical inverse problems to seismic body wave travel-time problem
02 p0200 N73-11618
Evaluation of methods for analyzing short-period seismic records to detect multiple events
[AD-747764] 03 p0298 N73-12434
Application of ray-tracing to seismic event location near island arc structures
[AD-747762] 03 p0298 N73-12435
Computing theoretical amplitude ratio of shear waves to compressional waves using double-couple representations of earthquakes
[AD-747763] 03 p0299 N73-12436
Tsai method for seismic discrimination, using parameterized reduced displacement potential function
[AD-749894] 05 p0542 N73-14407
Method for whitening spectra of teleseismic P waves for determining event depths
[AD-750781] 06 p0671 N73-15455
Seismological wave spectra for differentiating between earthquakes and explosions
[AD-749874] 06 p0671 N73-15457
Regional seismic reflection survey of Strait of Sicily, using multichannel digital techniques
[SACLANTCEN-CONF-PROC-7] 07 p0789 N73-16418
Response spectra of earthquake motion accelerograms
[PB-212602] 07 p0794 N73-16457
Fourier amplitude spectra for earthquake ground motions and structural response accelerations
[PB-212603] 07 p0794 N73-16458
Research in network evaluation
[AD-751523] 07 p0795 N73-16467
Formation of seismic waves in surface soils during underground explosions
[AD-751070] 07 p0797 N73-16481
Performance of piezoelectric transducer for seismic communication in mine environment
[AD-752218] 08 p0885 N73-17169
Geological structure effect on seismic wave propagation in earth and upper mantle
[AD-753110] 10 p1156 N73-19408
Crustal structure from high resolution seismic refraction profile across transition zone from Basin and Range provinces into Middle Rocky Mountains
[AD-753850] 11 p1289 N73-20462
Fatigue damage due to seismic loads of materials with different yield strength and various ductility
[NASA-CR-133099] 17 p2091 N73-26916
Bibliography of literature concerning electromagnetic and seismic noise and propagation
[PB-217500/8] 18 p2118 N73-27125
Analysis of Rayleigh wave dispersion in continental path and development of filters for vertical high gain seismometer
[AD-761795] 19 p2296 N73-28462

**SEISMOGRAMS**
Evaluation of data processing systems for Alaskan and Norwegian seismic arrays
[AD-756905] 13 p1525 N73-22360
Algorithm for adaptive convergence rate on weak noise components in seismic signal processing
[AD-756904] 13 p1525 N73-22361

**SEISMOGRAPHS**
NT LUNAR SEISMOGRAPHS
Large aperture seismic array, seismometer and amplifier performance, and seismograph calibration
[AD-745753] 01 p0053 N73-10433
Optimized antenna design for medium artillery delivered seismic detection system sensor
[AD-748825] 04 p0396 N73-13219
Compensating and matching short period seismometers for laboratory inertial guidance and control
[AD-748245] 04 p0424 N73-13455
Operation and data processing system of long period strain seismographs with wave discrimination
[AD-748232] 05 p0549 N73-14460
Development of pneumatically isolated stabilized platform to provide active control to local gravity vector
[AD-750869] 06 p0697 N73-15686
Characteristics and requirements of instruments for advanced Viking seismic experiments on Mars
[NASA-CR-130358] 06 p0717 N73-15850
Repackaging of broadband quartz torsional accelerometers for borehole use
[AD-755852] 13 p1531 N73-22410

**SEISMOLOGY**
Description of magnetic and seismic facility at Great Whale River, Canada and analysis of data acquired during calendar year 1969 - Vol. 43, No. 3
[M70-43/3] 01 p0043 N73-10343
Description of equipment installed in magnetic and seismic observatory at Mould Bay, Canada and analysis of data acquired during 1969 - Vol 43. No. 4
[M70-43/4] 01 p0043 N73-10344
Description of magnetic and seismic facility at Baker Lake, Canada and analysis of data acquired during calendar year 1969 - Vol. 43, No. 2
[M70-43/2] 01 p0044 N73-10345
Dourbes [Belgium] Geophysical Observatory data on geomagnetism, ionospheric propagation, seismology, cosmic rays, and atmospheric electricity, Nov. 1971
01 p0050 N73-10401
Dourbes [Belgium] Geophysical Observatory data on geomagnetism, ionospheric propagation, seismology, cosmic rays, and atmospheric electricity, Dec. 1971
01 p0050 N73-10405
Analysis of subbottom acoustic reflection profiles along track line from Monrovia, Liberia to Lesser Antilles
[PB-209872] 01 p0053 N73-10427
Seismological effects of explosions and earthquakes and structural dynamics of earth crust and upper mantle
[AD-746031] 01 p0054 N73-10435
Preliminary evaluation of Norwegian long period seismic array
[AD-746009] 02 p0167 N73-11361
Seismological experiments and evaluation of instrumentation in program of long range seismic measurements
[AD-746666] 02 p0170 N73-11382
Derivations of straight line, Abel transform and seismological Herglotz-Wiechert transform for reconstruction of refractivity profiles from radio wave phase data
[NASA-TN-D-7098] 02 p0230 N73-11868
Descriptions of earthquakes and location of epicenters in US, Alaska, Panama Canal Zone, and Virgin Islands during 1970
03 p0294 N73-12393
Maximum likelihood fit of straight line to pairs of seismological magnitudes having variations and measurement errors
[FOA-4-C-4474-A1] 04 p0440 N73-13588
Mapping of seismically active faults in Alaska using ERTS-1 imagery
[E72-10352] 05 p0533 N73-14340
Evaluation of research projects involving seismic arrays, long period arrays, seismometers, and seismic signal processing
[AD-750759] 06 p0669 N73-15439
Earthquake prediction and control through satellite relay telemetry of seismic data
07 p0787 N73-16399
Seismic reflection and refraction surveys of thickness of coastal plain sediments in Virginia
[PB-212604] 07 p0794 N73-16455
Digital signal processing applied to ocean bottom seismic reflection data
[PB-212155] 07 p0794 N73-16456
Development of phase contrast enhancement techniques for seismic holography without use of spatial filters
[BM-RI-7721] 07 p0806 N73-16537
Seismic detection of nuclear explosions and earthquakes
[AD-751243] 08 p0918 N73-17526
Mapping seismically active faults in Alaska from ERTS-1 imagery
[E73-10283] 09 p1020 N73-18326
Dourbes, Belgium, geophysical observatory data on geomagnetism, ionospheric propagation, seismology, cosmic rays, and atmospheric electricity, Feb. 1972
09 p1030 N73-18403
Dourbes, Belgium, geophysical observatory data on geomagnetism, ionospheric propagation, seismology, cosmic rays, and atmospheric electricity, Mar. 1972
09 p1030 N73-18404
Dourbes, Belgium, geophysical observatory data on geomagnetism, ionospheric propagation, seismology, cosmic rays, and atmospheric electricity, Apr. 1972
09 p1030 N73-18405
Dourbes, Belgium, geophysical observatory data on geomagnetism, ionospheric propagation, seismology, cosmic rays, and atmospheric electricity, May 1972
09 p1030 N73-18406
Dourbes, Belgium, geophysical observatory data on geomagnetism, ionospheric propagation, seismology, cosmic rays, and atmospheric electricity, Jun. 1972
09 p1030 N73-18407
Dourbes, Belgium, geophysical observatory data on geomagnetism, ionospheric propagation, seismology, cosmic rays, and atmospheric electricity, Jul. 1972
09 p1030 N73-18408
Mapping of seismically active faults in Alaska using ERTS-1 imagery to determine areas of earthquake occurrence
[E73-10405] 11 p1277 N73-20367
Explosives for lunar seismic studies
[NASA-CR-128876] 11 p1348 N73-20939
Canadian radio telemetry installation in conjuction with seismic array system
12 p1377 N73-21169
Mapping of seismically active faults in Alaska from ERTS-1 imagery
[E73-10616] 15 p1774 N73-24377
Application of ERTS-1 data for development and operation of volcano surveillance network
[E73-10711] 17 p2018 N73-26318
Dourbes [Belgium] geophysical observatory data on geomagnetism, ionospheric propagation, seismology, cosmic rays, and atmospheric electricity, Aug. 1972
17 p2028 N73-26411
Dourbes [Belgium] geophysical observatory data on geomagnetism, ionospheric propagation, seismology, cosmic rays, and atmospheric electricity, Sep. 1972
17 p2028 N73-26412
Application of ERTS-1 imagery for seismic conditions and recent fault formations in eastern California and western and central Nevada
[E73-10769] 18 p2134 N73-27245
Mapping seismically active faults in Alaska using ERTS-1 imagery
[E73-10842] 19 p2291 N73-28420
Long term broad band vertical earth noise structure at very long period experiment sites
[AD-761812] 19 p2297 N73-28473
Peculiarities of common deep point composite tapes
[JPRS-59754] 20 p2439 N73-29591
Dourbes [Belgium] geophysical observatory data on geomagnetism, ionospheric propagation, seismology, cosmic rays, and atmospheric electricity. Nov. 1972
24 p2924 N73-33353
Geophysical observatory data obtained at Dourbes, Belgium in Dec. 1972 on geomagnetism, ionospheric propagation, seismology, cosmic rays, and atmospheric electricity
24 p2924 N73-33354

**SEISMOMETERS**
U SEISMOGRAPHS

**SEL COMPUTERS**
Programs for control of SEL 86 radar operating system
[AD-763940] 22 p2635 N73-31119

**SELECTION**
NT PERSONNEL SELECTION
NT PILOT SELECTION

**SELECTIVE DISSEMINATION OF INFORMATION**
Design and operational services of small data centers to technical users
[AGARD-CP-117] 15 p1752 N73-24201
Information dissemination services to industry
15 p1753 N73-24210
Information dissemination services of technical information service of National Research Council of Canada
15 p1753 N73-24211

**SELECTORS**
Nonreciprocal YIG filter preselector for radio receiver tuners
[AD-762517] 22 p2645 N73-31198

**SELENIDES**
NT CADMIUM SELENIDES
NT GALLIUM SELENIDES
NT LEAD SELENIDES
NT ZINC SELENIDES
Hall resistivity and electromagnetic properties of bismuth selenide crystals for cryogenic magnetometers
[NASA-TN-D-7057] 03 p0344 N73-12809
Crystal growth and magnetic properties of transition metal chalcogenides
[AD-748864] 04 p0459 N73-13748
Thermal stability of amorphous arsenic compound glasses and electron diffraction analyses on semiconducting arsenic selenide films
[AD-752993] 09 p1076 N73-18778
X ray and electron diffraction spectra of amorphous arsenic sellenide semiconductors
[AD-762367] 20 p2463 N73-29792
Analysis of electrical switching phenomena in amorphous arsenic telluride-arsenic selenide system
24 p2966 N73-33707

**SELENIUM**
Development and characteristics of Si-As-Te glasses containing Ag and Se as constituent of chalcogenic glasses
[AD-749958] 05 p0567 N73-14603
Electrical and photoelectrical properties of trigonal selenium single crystals, including Hall mobility
[PUBL-170] 06 p0707 N73-15771
Ultrasonic absorption in liquid metals and in liquid selenium
18 p2178 N73-27590

**SELENIUM ALLOYS**
Crystal structures, electrical properties, and electronic applications of metal selenides
[JPRS-58293] 10 p1198 N73-19752

**SELENIUM COMPOUNDS**
NT CADMIUM SELENIDES
NT GALLIUM SELENIDES
NT LEAD SELENIDES
NT SELENIDES
NT ZINC SELENIDES

**SELENOGRAPHY**
Determining optimal selenodetic control network on moon
04 p0469 N73-13822
Proceedings of colloquium on lunar dynamics and observational coordinate systems
[NASA-CR-131263] 11 p1337 N73-20849
Estimates of moon geometry using lunar orbiter imagery and Apollo laser altimeter data
[NASA-TR-R-407] 23 p2846 N73-32743

**SELENOLOGY**
NT LUNAR CORE
Research in intepretation of lunar data developed during Apollo Program
[NASA-CR-133302] 18 p2190 N73-27679

**SELF ABSORPTION**
Spectroscopic methods for temperature measurement in plasmas with self absorption noting methods for plasma column radial temperature distribution
[BMBW-FBK-72-22] 09 p1071 N73-18737

**SELF ADAPTIVE CONTROL SYSTEMS**
Optimization of stochastic systems including introduction to self adaptive systems
05 p0569 N73-14618
Design analysis for reversible, self adaptive manipulator control system
17 p1989 N73-26083
Error analysis on manipulator activation system using reversible self adaptive control mechanism
17 p1989 N73-26084
Adaptive control system for compensatory positioning of optical tracking telescope
18 p2210 N73-27842
One class of adaptive systems and results of computer modeling of their self instruction
24 p2887 N73-33056

**SELF ALIGNMENT**
Advanced procedures for self alignment and calibration of inertial platforms
11 p1319 N73-20706

**SELF CONSISTENT FIELDS**
Vlasov approximation of plasma turbulence in stochastic external field
[EUR-CEA-FC-690] 24 p2965 N73-33693

**SELF DEPLOYING SPACE STATIONS**
U SELF ERECTING DEVICES
U SPACE STATIONS

**SELF DIFFUSION**
U DIFFUSION

**SELF ERECTING ANTENNAS**
U ANTENNAS
U SELF ERECTING DEVICES

**SELF ERECTING DEVICES**
Design, development, and testing of foldable beryllium copper alloy elastic tubes for hinges on satellite booms
[ESRO-CR-65] 19 p2346 N73-28874

**SELF EXCITATION**
Analysis of wind induced vibration in vertical cantilever beam and square sagging suspended cable
[AD-750550] 05 p0604 N73-14913
Ion acoustic wave response to double plasma excitation impulse
[IPPJ-144] 09 p1027 N73-18386

**SELF FOCUSING**
Relationship between damage in materials exposed to high intensity laser radiation and self focusing thresholds
[AD-747290] 02 p0184 N73-11489
Analysis of laser bulk damage in alkali-halides with no self-focusing and measurement of damaging fields considering effects of inclusions on bulk optical strength
05 p0554 N73-14502

Analysis of time dependent, self focusing optical beams with elliptical constant intensity contours
05 p0555 N73-14509
Analysis of self focusing damage in laser rods with subnanosecond pulse
05 p0555 N73-14511
Effects of polarized radiation on self-focusing thresholds of laser materials
[AD-757789] 15 p1795 N73-24554
Low angle tracking and recognition using self focusing radar antenna
[AD-764052] 22 p2635 N73-31118
Stability theory of laser beam self focusing
[LA-UR-73-671] 24 p2932 N73-33414
Self focusing of laser beams
[AD-765541] 24 p2932 N73-33416
SELF INDUCED VIBRATION
NT PANEL FLUTTER
NT SUBSONIC FLUTTER
NT SUPERSONIC FLUTTER
NT TRANSONIC FLUTTER
SELF LUBRICATING MATERIALS
Performance characteristics of self lubricating sintered sulfur-iron material used for bushings in naval aircraft
[AD-748175] 03 p0319 N73-12603
Plasma-sprayed metal-glass and metal-glass fluoride coatings for lubrication
[NASA-TM-X-71432] 24 p2929 N73-33392
SELF REGULATING
U AUTOMATIC CONTROL
SELF SEALING
Improved carbon graphite materials for high temperature self-acting seals
[NASA-CR-121092] 10 p1165 N73-19481
SELF STIMULATION
Theoretical analysis of motivation stimulation
24 p2888 N73-33062
SELSYNS [TRADEMARK]
U SERVOMOTORS
SEMICIRCULAR CANALS
Physiology and dimensional analysis of semicircular canal
[AMRU-R-69-1] 02 p0130 N73-11058
Asymmetric response of cat semicircular canal neurons to symmetric sinusoidal rotation
[AMRU-R-69-2] 02 p0130 N73-11060
Physiological response of cat semicircular canal dependent units to linear acceleration without angular acceleration
[AMRU-R-70-4] 02 p0131 N73-11061
Effect of space flight on origin, physiological function, and amelioration of coriolis illusion in semicircular canal
[AMRU-R-70-6] 02 p0131 N73-11063
Response characteristics of vestibulo-ocular reflex arc
[AMRU-R-71-2] 02 p0132 N73-11067
Physiological factors in human oculomotor responses to space flight stress
[DR-208-VOL-1] 06 p0632 N73-15136
Human semicircular canal response to rotational stimuli in yaw, pitch, and roll planes of the head
06 p0632 N73-15137
Functional dependence of semicircular canal on physical size
06 p0633 N73-15139
Physiological control system for stabilization of retinal image in humans
06 p0633 N73-15141
Vestibular stimulation effect in human and animal retinal image stabilization
06 p0633 N73-15144
Clinical neurological and neurophysiological aspects of vestibulo-ocular reflex
06 p0633 N73-15145
Semicircular canal plugging response in cats to rotary stimulation
06 p0634 N73-15151
Semicircular canal model with flow visualization chamber for dynamic recording of canal fluid response to angular velocity effects
06 p0634 N73-15153
Determination of angular acceleration equivalent to effect of coriolis acceleration on receptors of semicircular canals
11 p1246 N73-20112
SEMICONDUCTING FILMS
Identification by country and research facility of thin film studies
[AD-746719] 02 p0220 N73-11779
Growths and applications of compound semiconductor materials and devices
[AD-746882] 02 p0220 N73-11783
Nucleation and film growth mechanisms in heteroepitaxial semiconductor
[AD-748424] 04 p0460 N73-13753
Electrical conductivity of thin films during nucleation and film growth
[AD-748269] 04 p0460 N73-13756
Hall coefficient, resistivity, and charge carrier mobility of epitaxial films of n-type and p-type PbS before and after neutron irradiation
[AD-749689] 06 p0710 N73-15791
Laplace transform amplitude function generator utilizing thin film semiconductor
[AD-750590] 06 p0710 N73-15792
Reaction diffusion method used for growing semiconductive two-layer structures of zinc telluride on zinc selenide
[AD-751476] 07 p0833 N73-16752
Methods for chip mounting and establishing electrical connections in miniaturized printed circuits and thick and thin film hybrid circuits
[ECR-27] 08 p0891 N73-17212
Sputtering deposition of semiconductor film devices
[AD-752081] 08 p0928 N73-17599
Temperature and intensity dependences of photoconductivity and annealing effects in electro-optical properties of amorphous Ge[.5]Te[.5] films
[AD-752024] 08 p0951 N73-17787
Mossbauer spectroscopic analysis of order-disorder transitions in vacuum deposited Te films
[AD-753272] 09 p1074 N73-18769
Temperature and thickness effects on electrical conductivity of amorphous germanium semiconducting films
[AD-753827] 09 p1076 N73-18782
Effect of flaws on chemical, electrical, mechanical, and masking properties of Si3N4 films
[NLL-DRIC-TRANS-2902-[3623.66]]
11 p1329 N73-20789
Homoepitaxial films of GaAs deposited from vapor phase
[AD-754821] 11 p1331 N73-20800
Electronic switching phenomena in organic thin films
[AD-755267] 12 p1442 N73-21682
Material properties of thin single crystal silicon films on insulator/polycrystalline silicon substrates
[AD-756646] 13 p1503 N73-22179
Nucleation and film growth mechanisms in heteroepitaxial semiconductor thin films
[AD-755529] 13 p1568 N73-22706
Structures and optical absorption spectra of mercury telluride/cadmium telluride thin films
[AD-756093] 13 p1568 N73-22709
Gallium arsenide epitaxial thin films as active elements for electrooptic modulation of carbon dioxide laser radiation
[AD-757792] 15 p1796 N73-24559
Thin film lead and tin selenide photoconductive infrared detectors
[AD-758685] 16 p1915 N73-25499
Metallurgical and electrical properties of thin film Pb[0.9]Sn[0.1]Se photoconductive infrared detectors
[AD-758519] 17 p2064 N73-26693
Electrical properties of semiconducting film configurations with contacts to chalcogenide glasses
[AD-760335] 17 p2074 N73-26781
Growth and crystal structure of Si, Ge, and GaAs thin films
[JPRS-59279-PT-2] 18 p2186 N73-27650
Experimental analysis of disappearance phenomena of packing defects in silicon epitaxial films during thermal oxidation in wet oxygen
18 p2187 N73-27662
Kinetics of gas pickling and epitaxial growth of semiconductor materials
18 p2188 N73-27664
Variation of electrophysical parameters of epitaxial films of germanium as result of gas etching
18 p2188 N73-27665
Silicon epitaxial films obtained by thermal decomposition of silane
18 p2188 N73-27666
Effects of crystallization conditions on properties of autoepitaxial and heteroepitaxial layers of silicon obtained by hydride pyrolysis
18 p2188 N73-27667
Flow velocity, GeCl4 concentration, and temperature effects on growth and morphology of autoepitaxial Ge films
18 p2189 N73-27674
Data tables and photographs of gaas epitaxial layer perfections as influenced by substrate disorientation
18 p2189 N73-27675
Production of semiconducting films for waveguides and optical device elements
[AD-763101] 20 p2455 N73-29729
Thin film optical waveguides in III-V semiconductors
[AD-763120] 20 p2455 N73-29730
Waveguide and luminescent properties of thin film Pb-salt injection lasers
[AD-763757] 21 p2556 N73-30488
Electrical conduction in nondegenerate, nonsymmetrical, epitaxial semiconducting films
21 p2585 N73-30713
Electron recording and readout sensitivity characteristics of amorphous semiconductor thin films
[AD-763253] 21 p2585 N73-30719
Observation of amorphous to crystalline transition in vacuum deposited tellurium films using Mossbauer spectroscopy
[AD-763408] 21 p2586 N73-30724
Fabrication and radiation effects of high mobility semiconducting films
23 p2824 N73-32576
Electrical properties and switching behavior of amorphous semiconductor films
[AD-765346] 24 p2970 N73-33732
SEMICONDUCTOR DEVICES
NT AVALANCHE DIODES
NT FIELD EFFECT TRANSISTORS
NT GALLIUM ARSENIDE LASERS
NT GERMANIUM DIODES
NT JUNCTION DIODES
NT JUNCTION TRANSISTORS
NT LIGHT EMITTING DIODES
NT METAL OXIDE SEMICONDUCTORS
NT MIS [SEMICONDUCTORS]
NT NEURISTORS
NT PARAMETRIC DIODES
NT PHOTODIODES
NT PHOTOTRANSISTORS
NT PHOTOVOLTAIC CELLS
NT SCHOTTKY DIODES
NT SEMICONDUCTOR LASERS
NT SILICON TRANSISTORS
NT THERMISTORS
NT THYRISTORS
NT TRANSISTOR AMPLIFIERS
NT TRANSISTORS
NT VARACTOR DIODES
Development, characteristics, and application of solar electric power generators used in USSR spacecraft - Part 1
[AD-741524] 01 p0007 N73-10056
Capacity of geometric codes and increased effectiveness of semiconductor storage units using number block structures
[JPRS-57251] 02 p0145 N73-11177
Numerical analysis of semiconductor saturable absorber and extablishment of criteria for operation of laser saturable resonator in bistable regime
[AD-746736] 02 p0183 N73-11488
Techniques for generation and processing microwave signals using elastic, electromagnetic and carrier space charge waves in solid media
[AD-747047] 02 p0220 N73-11782
Design, development, and evaluation of three channel interference cancellation system for use with ultrahigh frequency communication systems
[AD-747802] 03 p0267 N73-12158
Electrical overstress failures in silicon semiconductor devices
[AD-747795] 03 p0275 N73-12230
Diode passivation techniques and fabrication of semiconductor targets that are stable under electron beam bombardment for use in L band amplifiers
[AD-747868] 03 p0276 N73-12237
Transient radiation effects and damage to semiconductor devices and electronic equipment
[AD-746851] 03 p0279 N73-12260
Nuclear spectrometry with semiconductor detectors
[CEA-CONF-1964] 03 p0345 N73-12812
Evaluation of dielectric insulation and etched junction contact techniques for fabrication of wraparound contact silicon solar cells
[NASA-CR-121021] 04 p0375 N73-13051
Performance of wire bound electrical connectors used in integrated and hybrid circuits and low power semiconductor devices
[AD-748788] 04 p0396 N73-13220
Solid states physics and manufacturing methods for microwave generation, amplification, and control devices
[AD-749500] 04 p0397 N73-13234
High amplitude gamma current pulse degradation of semiconductor devices
[SC-RR-72-0515] 04 p0399 N73-13245
Magnetic, optical, and transport properties of semiconductors
[AD-747692] 04 p0460 N73-13752
Trends in microwave solid state power generation
[AD-749503] 05 p0499 N73-14063
Effects of low frequency background noise on electrical properties of semiconductor materials and components
05 p0519 N73-14222
Production and costs of producing reliable semiconductor integrated circuits
[AD-749834] 05 p0521 N73-14240
Development and characteristics of hermetically sealed coaxial package for containing microwave semiconductor components
[NASA-CASE-GSC-10791-1] 05 p0550 N73-14469
Permanent electron beam radiation effects on thin film single junction quantum interferometer devices
[AD-749065] 05 p0582 N73-14740
Bulk characteristics mapping for quality control of semiconductor wafer junctions
[BDX-613-604-REV] 05 p0586 N73-14769
Angular distribution of photoemitted electrons from activated p-type gallium arsenide surfaces
[AD-750364] 06 p0645 N73-15239
High resistivity semiconductor waveguides for device and circuit functions
[AD-750317] 06 p0645 N73-15241
Electron energy distribution of semiconductor cold-cathode
[AD-750611] 06 p0646 N73-15247

Pulse voltage distribution over series connected silicon rectifiers
[AD-750969] 06 p0648 N73-15260
Production yield of electronic materials and associated devices
[AD-749984] 06 p0678 N73-15514
Charge trap structure of pyrolytic alumina layer in metal oxide semiconductor capacitor
[AD-751629] 07 p0762 N73-16195
Method for selecting silicon planar semiconductor devices for long life
[NASA-CR-124036] 07 p0803 N73-16516
Design, fabrication, and performance evaluation of Faraday effect far infrared isolators
[AD-751319] 07 p0808 N73-16552
Threshold commutation in amorphous semiconductors
[CEA-CONF-1972] 07 p0832 N73-16741
Efficiencies of germanium semiconductor detectors calculated by Monte Carlo method for 100 keV to 2 MeV gamma rays
[CEA-R-4316] 07 p0832 N73-16745
Sputtering deposition of semiconductor film devices
[AD-752081] 08 p0928 N73-17599
Semiconductor transmitter in S band
[DLR-FB-72-53] 09 p1007 N73-18220
Development of acoustic surface wave, multiple-tap, delay line structure using sputtered zinc oxide piezoelectric films on metal interdigital arrays on silicon surface
[AD-753674] 09 p1009 N73-18238
Reliability of semiconductor devices as influenced by quality of aluminum wire bonds used in assembly
[NASA-CR-124037] 09 p1038 N73-18469
Extension of frequency spectrum and improvement of semiconductor devices and techniques in microwave spectrum
[AD-753266] 09 p1044 N73-18514
Solid state physics, materials, and semiconductor research
[AD-752063] 09 p1053 N73-18581
Electromagnetic radiation screening of semiconductor devices for long life applications
[NASA-CR-124119] 09 p1073 N73-18757
Operational characteristics of semiconductor photoconverters as power supply sources for space vehicles
[AD-753063] 09 p1074 N73-18766
Measurement methods for semiconductor materials, process control, and devices
[AD-753642] 09 p1076 N73-18785
Microwave UHF and SHF semiconductor oscillators and power amplifiers, noting gunn and impatt diode solutions, and integrated circuit development
[DLR-MITT-73-06] 10 p1135 N73-19248
Process for automatically contacting, testing, and handling beam lead semiconductor devices
[BDX-613-779] 10 p1166 N73-19487
Very low noise amplifiers for semiconductor X ray detectors
[CONF-720559-2] 10 p1200 N73-19769
HCL processing effects on electrical stability and quality of thermally grown SiO2
[AD-754110] 10 p1202 N73-19786
Electromagnetic waves propagation and impedance analysis of double stream interaction in semiconductors
[NASA-CR-131293] 11 p1329 N73-20791
Electron- and neutron-induced defects in silicon p-n junctions
[AD-754905] 11 p1332 N73-20812
Characteristics of photomultiplier tubes and application to optics, biophysics, radiometry, and astronomy for detecting weak light flows
[AD-755874] 12 p1384 N73-21226
Design equations for electron beam, semiconductor amplifiers with large area diodes to enhance power output
[AD-755806] 12 p1385 N73-21229
Reliability tests of reverse biased semiconductor diodes under electron beam bombardment conditions
[AD-755449] 13 p1502 N73-22171
Fabrication of monolithic light emitting diode display system on single wafers of gallium phosphide
[AD-755204] 13 p1502 N73-22172
High power transcalent silicon semiconductor thyristor device including metallization techniques and heat pipe construction
[AD-755553] 13 p1502 N73-22174
Qualitative reliability indices of semiconductor thermoelectric devices
[AD-756898] 13 p1503 N73-22184
Hot electron effects in SCL diodes and MOSFETS
13 p1565 N73-22680
Device fabrication and radiation effect studies of various semiconductors
[AD-756249] 13 p1566 N73-22689
Research on semiconductor and solid state physics
[AD-757521] 14 p1697 N73-23771
Radiation damage in semiconductor devices and changes in electrical properties
[AD-755690] 14 p1698 N73-23778
Generation and processing of microwave signals using elastic, electro-magnetic, and carrier space charge waves in solid media
[AD-757555] 14 p1699 N73-23784
Development of guidelines for selection of manned spacecraft equipment and recommendations for performance and quality control tests
[NASA-CR-128909] 14 p1708 N73-23857
Schottky barrier diodes for electron beam semiconductor applications
[AD-757749] 15 p1757 N73-24240
Utilization of semiconductor in systematic analysis of Al after subjected to neutron irradiation
[FRNC-CONF-75] 15 p1788 N73-24495
Ion beam dose and sputtering characteristics of ion implanted semiconductor devices
[NASA-CR-132254] 15 p1820 N73-24754
Abstracts on properties of semiconductors and semiconductor devices
[AD-758053] 15 p1822 N73-24767
Evaluation of computer program for analyzing radiation effects on complex semiconductor devices and microcircuits
[AD-758883] 16 p1882 N73-25237
Multistable semiconductor devices and integrated circuits
16 p1951 N73-25791
Formation of current filaments in thin film silicon-on-sapphire diodes
16 p1952 N73-25795
Current carrier mobility near charged semiconductor surface
[AD-758973] 16 p1953 N73-25804
Electrical properties of silicon semiconductor under shock loads
[AD-759003] 16 p1971 N73-25945
Electron beam semiconductor S-band amplifier
[AD-759948] 17 p2005 N73-26212
Research on electron beam devices, quantum electronic devices, plasmas, and solid state microwave devices
[AD-760033] 17 p2041 N73-26517
Feasibility determination of using ultrahigh fluences of implanted oxygen ions to create usable oxide layer on silicon for semiconductor device applications
[AD-760350] 17 p2075 N73-26785
Microwave solid state devices and circuits
[AD-759833] 17 p2075 N73-26787
Electrical conductivity and carrier lifetimes in gold doped silicon wafer
[AD-760150] 17 p2075 N73-26789
Effects of radiation on semiconductor materials and devices
[AD-759946] 17 p2075 N73-26790
Apollo 16 flight anomaly report on malfunction of water/glycol temperature control circuit
[NASA-TM-X-69234] 17 p2089 N73-26900
Fabrication of cold cathode optoelectronic electron emitter with emission properties suitable for practical applications
[AD-760601] 18 p2123 N73-27162
Noise in metal nitride oxide semiconductor devices
[AD-760544] 18 p2124 N73-27163
Fabrication of array of silicon diodes for application in electron beam semiconductor device
[AD-760602] 18 p2124 N73-27164
Computerized design of electron beam semiconductor short pulse generator
[AD-761111] 18 p2191 N73-27693
Ion implantation damage in silicon and semiconductor devices
[AD-761486] 19 p2245 N73-28104
Semiconductor microcircuits for recording of optical radiation, mechanical stresses, and magnetic fields
[AD-762312] 19 p2247 N73-28119
Image converter based on multilayer semiconductor dielectric structures
[JPRS-59636] 19 p2326 N73-28714
Characteristics of semiconductor detectors for soft X ray spectrometry
[RT/EL-[72]6] 20 p2462 N73-29787
Design and performance of semiconductor limiters for microwave isolation
[AD-762168] 20 p2463 N73-29794
Polish environmental protection policy and materials for semiconductor radiation detectors
[JPRS-59523] 20 p2487 N73-29976
Materials for semiconductor radiation detectors and infrared techniques
20 p2487 N73-29978
Semiconductor detectors of nuclear radiation
[JPRS-59634] 20 p2487 N73-29979
Development and progress in theoretical and scientific disciplines
[JPRS-59769] 20 p2487 N73-29981
Dynamic electric field profiles in electron beam semiconductor devices
[AD-763296] 21 p2517 N73-30192
Electron beam semiconductor S-band amplifier
[AD-763223] 21 p2518 N73-30200
NBS methods for measuring properties of semiconductor materials, process control, and devices
[NBS-TN-788] 21 p2585 N73-30717
Development of semiconductor electro-optical devices in Poland with emphasis on management planning and research projects to establish capability
21 p2608 N73-30898
Failure analysis of semiconductor devices by metallography
[DLR-MITT-72-20] 22 p2643 N73-31184
Photoconducting semiconductor system for converting stored optical images into video signals
[NASA-CASE-NPO-13131-1] 22 p2680 N73-31467
X ray and gamma ray semiconductor mercury iodide detectors
[BMFT-FBK-73-09] 22 p2707 N73-31680
Bulk semiconductor dielectric waveguide functional circuits
[AD-763888] 22 p2707 N73-31681
Manufacturing high resolution active and passive semiconductor devices noting field effect transistors and transistor logic
[REPT-3.462] 23 p2766 N73-32126
Photosensitivity failure analysis on integrated microcircuit caused by surface inversion
[AD-764708] 23 p2766 N73-32132
Semiconductor panel modulation for millimeter image conversion
[AD-765418] 23 p2767 N73-32133
Traveling wave amplification in Ge and InSb semiconductors
23 p2824 N73-32573
Two dimensional elastic-plastic hydrodynamics code for calculating dynamic response of semiconductor configuration to electron loading
[AD-763943] 23 p2826 N73-32590

**SEMICONDUCTOR JUNCTIONS**
NT JOSEPHSON JUNCTIONS
NT N-P-N JUNCTIONS
NT P-I-N JUNCTIONS
NT P-N JUNCTIONS
NT SILICON JUNCTIONS
Bulk characteristics mapping for quality control of semiconductor wafer junctions
[BDX-613-604-REV] 05 p0586 N73-14769
Luminescence of ZnSe and ZnS crystals compared to electroluminescence of MS and MIS structures, preparation of heterojunction structures, and solution growth of wafers
[AD-749135] 05 p0588 N73-14784
Light generated current output of vertical multijunction solar cell
[AD-754901] 11 p1238 N73-20047
Tunneling biases into interfaces of semiconductor junctions
[AD-755656] 12 p1441 N73-21676
Inversion layer silicon solar cells with induced junctions
[NASA-CR-131840] 16 p1865 N73-25100
Fabrication of niobium thin film superconductive tunnel junctions using semiconductor barrier
17 p2072 N73-26761
Analysis of tunneling in metal semiconductor junctions
18 p2185 N73-27640
Sensitivity and optoelectronic properties of semiconductor heterojunctions
20 p2460 N73-29770
Resin for protecting p-n semiconductor junction surface
[NASA-CASE-ERC-10339-1] 21 p2561 N73-30532

**SEMICONDUCTOR LASERS**
NT GALLIUM ARSENIDE LASERS
Tunable diode laser for air pollution gas analysis
[PB-214240/5] 16 p1871 N73-25149

**SEMICONDUCTORS [MATERIALS]**
NT ACCEPTOR MATERIALS
NT AMORPHOUS SEMICONDUCTORS
NT DONOR MATERIALS
NT METAL OXIDE SEMICONDUCTORS
NT MIS [SEMICONDUCTORS]
NT N-TYPE SEMICONDUCTORS
NT ORGANIC SEMICONDUCTORS
NT P-TYPE SEMICONDUCTORS
NT PHOTOCONDUCTORS
Survey on materials and manufacturing processes for solid state electronic devices
[AD-745745] 01 p0034 N73-10266
Fricks equation for determining diffusion profiles in two impure semiconductors
[CEA-CONF-1970] 01 p0087 N73-10723
Preparation and physical properties of rare earth compounds of technological potential
[AD-744980] 01 p0088 N73-10726
Optical properties and band structure of solids studied with electroreflectance and other optical modulation
[AD-746271] 01 p0089 N73-10736
Compensating impurities in semiconductors which give majority charge carriers
[NLL-RTS-7358] 02 p0218 N73-11761
Semiconductor theory of barrier layer and point-contact rectifiers
[NASA-TT-F-14708] 02 p0218 N73-11766
Electrical and transport properties in polycyclic semiconductor compounds
[AD-745988] 02 p0219 N73-11771

Physical properties of intermetallic magnesium tin compound
[AD-745942] 02 p0219 N73-11773
Growths and applications of compound semiconductor materials and devices
[AD-746882] 02 p0220 N73-11783
Electron bombarded semiconductor short pulse generator
[AD-748090] 03 p0276 N73-12239
Characteristics of infrared photodetectors manufactured from semiconductor material irradiated by electron beam
[NASA-CASE-LAR-10728-1] 03 p0300 N73-12445
Single crystal growth of ceramic oxides and compound semiconductors in space
[NASA-CR-123951] 03 p0344 N73-12806
Optical and magnetic properties of actinide and rare earth ions in insulators and semiconductors
[RLO-2221-T-6-14] 03 p0345 N73-12815
Effect of radiation on semiconductors
[AD-747565] 03 p0347 N73-12832
Synthesis of rare earth compounds and determination of their magnetic, optical, and semiconducting properties
[AD-747839] 03 p0348 N73-12835
Solid state research from 1 Feb. through 30 Apr. 1972
[AD-748836] 03 p0348 N73-12837
Design and development of photoparameteric detector-amplifier using indium antimonide photovoltaic reactions
[AD-749034] 04 p0451 N73-13683
Secondary ionic emission procedure for studying semiconductor properties
[CEA-CONF-1969] 04 p0459 N73-13745
Crystal growing of iron monosulfide, crystallographic studies on titanium oxide semiconductor, emission of zinc selenide diode, and electroreflectance of gallium arsenide
[AD-748336] 04 p0459 N73-13750
Czochralski technique for growing GaAs and III and V semiconductor crystals
[AD-748344] 04 p0461 N73-13759
Technique for accelerated evaluation of silicon solar cells for use on extended space missions with weapons environment
[AD-749477] 05 p0499 N73-14062
Electrical characterization of silicon materials by lifetime, ionized impurity concentration, and noise measurement
05 p0519 N73-14223
Waveguiding in thin silver strip vacuum deposited on bismuth germanium oxide
[AD-750612] 06 p0648 N73-15262
Application of light emitting diodes to pumping of solid-state laser rods
[AD-750576] 06 p0681 N73-15545
Effect of proton bombardment on photoelectric characteristics of n-p junctions alloyed with n-type silicon and lithium admixture
[AD-750977] 06 p0709 N73-15783
X ray and electron diffraction analysis of A[3]B[5] semiconductor crystal structure
[AD-750966] 06 p0709 N73-15787
Optical and electrical properties of amorphous germanium and silicon semiconductors
[AD-748856] 06 p0709 N73-15788
Electrical properties of insulating and semiconducting CdF2 with trivalent Ce and Gd codopants
[AD-750937] 06 p0711 N73-15799
Application of gas transport method for analyzing p-n junction in cadmium selenide monocrystal
[AD-750506] 06 p0711 N73-15800
Optical materials and design of optical equipment
[AD-751496] 07 p0822 N73-16660
Theoretical analysis of dispersion curves for surface polaritons in semiconductors
[AD-751671] 07 p0833 N73-16750
Physical and electrical transport properties of VO2 near its semiconductor-to-metal transition
[AD-751524] 07 p0834 N73-16759
Defect structure of semiconducting III-V compounds and determination of vibrational properties of imperfect systems
[AD-751052] 07 p0834 N73-16762
Development of high temperature high radiation silicon semiconductors
[NASA-CR-124074] 08 p0950 N73-17777
Nuclear magnetic resonance technique to obtain calibrations of charged defects in semiconducting compounds
[NASA-CR-112224] 08 p0950 N73-17781
Electronic transport properties in band properties
[AD-752100] 08 p0951 N73-17790
Radiation effects research program
[AD-752561] 08 p0951 N73-17791
Contacts between chalcogenide glasses, metals and semiconductors
[AD-752560] 08 p0952 N73-17797
Research on amorphous semiconductor materials
[AD-752798] 09 p1074 N73-18761
Research activities in solid state physics
[AD-753255] 09 p1075 N73-18770
Association of surface polaritons with surface magnetoplasmons coupled to surface optical phonons in polar semiconductors
[AD-753484] 09 p1075 N73-18771
Required doping levels for germanium and silicon infrared windows at microwave energies
[AD-753466] 09 p1075 N73-18772
Thermal stability of amorphous arsenic compound glasses and electron diffraction analyses on semiconducting arsenic selenide films
[AD-752993] 09 p1076 N73-18778
Measurement methods for semiconductor materials, process control, and devices
[AD-753642] 09 p1076 N73-18785
On-line laboratory station connected to real time/time-sharing EMR 6130 computer for semiconductor radiation effects studies
[SC-DR-72-0525] 10 p1161 N73-19442
Radiation effects in semiconducting laser materials
[AD-754217] 10 p1170 N73-19516
Conference on semiconductors, lasers, and photodiodes
[AD-754237] 10 p1202 N73-19782
Continuous wave CO2 laser radiation effects on semiconductor materials
[AD-753918] 10 p1202 N73-19785
Synthesis of stoichiometric crystals of InP doped with impurities for obtaining semiconductor with desired resistance
[NLL-RRE-TRANS-381-[8036.625]]
11 p1329 N73-20790
NBS activities in developing measuring methods for semiconductors
[NASA-CR-131275] 11 p1330 N73-20792
Magnetic, optical, and semiconducting properties of rare earth compounds
[AD-755925] 12 p1376 N73-21164
Conduction processes in field driven semiconductor p-i-n diodes
12 p1437 N73-21643
Dynamic interface effects on electromagnetic response of magnetic semiconductors
[AD-755861] 12 p1442 N73-21681
Synthesis of compound semiconducting materials and application to planar microwave acoustic equipment using gallium arsenide thin films as active layer
[AD-755947] 12 p1442 N73-21684
Analysis of photoelectric properties of gallium arsenide and application to construction of solar cells
[AD-756228] 13 p1477 N73-21962
Thermoelectricity of solid-liquid phase boundary in ternary semiconductors and alloys
[AD-756899] 13 p1478 N73-21972
Mechanical properties and behavior of heat resistant alloys semiconductors, polymers and composite materials
[AD-755660] 13 p1549 N73-22552
Analysis of EPR spectra in neutron irradiated silicon for determination of radiation damage in semiconductors
[AD-756907] 13 p1568 N73-22708
Effects of various gases on conductivity of four organic semiconductors at very low pressures
[REPT-1972-19] 14 p1697 N73-23772
Influence of carrier lifetime in semiconductor material on its performance as radiation detector
[NASA-CR-121187] 14 p1697 N73-23775
New methods for growth and characterization of GaAs and mixed semiconductor crystals
[AD-756259] 14 p1698 N73-23777
Research in solid state physics including semiconductor lasers and laser spectroscopy
[AD-757559] 14 p1698 N73-23779
Study of electrical properties of amorphous semiconductors using Green's function
[AD-757432] 14 p1699 N73-23786
Magnetic bubble material and magnetic properties of Mott transition
[AD-757435] 14 p1699 N73-23787
Neutron irradiation damage in indium arsenide semiconductors and effect on electrical crystal properties
[AD-757468] 14 p1699 N73-23792
Physical properties of electronic materials, devices, and thin films
[AD-758197] 14 p1700 N73-23793
Evaluation of semiconductive metal halides as cathode material for high energy-density batteries
[AD-757883] 15 p1739 N73-24094
Fabrication and characterization of monolithic acoustic surface wave amplifiers
15 p1755 N73-24229
Industrial application of ion implantation for doped semiconducting structures
[NLL-TRANS-861-[5022.64]]
15 p1759 N73-24257
Thermoelectric and photothermoelectric effects in semiconductors
15 p1819 N73-24747
Composite conductors of 19-Nb3Sn filaments in normal metal matrix, using heat treatment
[BNL-17425] 15 p1821 N73-24756
Electronic state density of semiconductor compounds A[3] B[5], using law of dispersion
[AD-758168] 15 p1822 N73-24766
Abstracts on properties of semiconductors and semiconductor devices
[AD-758053] 15 p1822 N73-24767
Aluminum ribbon wire for ultrasonic bonding of semiconductor microelectronic interconnections
[AD-758981] 16 p1881 N73-25223
Research and development progress on electronic equipment, integrated circuits, semiconductors, and digital computers
[AD-759180] 16 p1884 N73-25251
Density and light radiation measurements of molten metals, semiconductors, and alloys
[NLL-M-21580-[5828.4F]] 16 p1951 N73-25789
Improvement in methods of measurement for semiconductor materials, process control, and devices
[NASA-CR-133030] 16 p1953 N73-25800
Lattice dynamical calculation for soft mode semiconductor surface reconstruction
[AD-758723] 16 p1953 N73-25806
Nonlinear optical susceptibilities for electromagnetic wave coupling of semiconductors
17 p2071 N73-26758
Conference on growth and synthesis of semiconductor crystals and films
[JPRS-59208] 17 p2072 N73-26762
Pseudo-binary crystal model for electron mobility variation with composition of gallium indium arsenide semiconducting alloys
18 p2181 N73-27607
Piezobirefringence measurements on amorphous and crystalline semiconductors with zincblende, wurtzite, and rocksalt structures
18 p2184 N73-27637
Low temperature measurement of heat pulse and ultrasonic wave interaction with stress-split acceptor states in semiconductors
18 p2186 N73-27647
Synthesis and characterization of semiconducting diamond and boron phosphide crystals
18 p2186 N73-27648
Utilization of sandwich method to obtain epitaxial layers of Si, GaAs, and heteroepitaxial GaAs-Ge
18 p2186 N73-27654
Effect of various growth and doping parameters on GaN for LED applications
[NASA-CR-132263] 18 p2189 N73-27676
Photoconductivity of gallium arsenide-, Cadmium sulfide-, and cadmium selenide-semiconductors correlated to laser pulse width
[AD-760560] 18 p2190 N73-27682
Electron spin resonance studies in single crystals of CaS and CdS
[AD-760803] 18 p2191 N73-27691
Electrical and optical properties of irradiated mercury cadmium telluride semiconductors
[AD-761488] 19 p2327 N73-28721
Magnetic and electrical properties of ferromagnetic semiconductors
[AD-762103] 19 p2327 N73-28725
Resonant Raman scattering in wide gap semiconductors
20 p2461 N73-29773
Neutron activation analyses of trace elements in germanium, silicon, and selenium semiconductors
[CONF-721069-29] 20 p2462 N73-29786
Infrared optical reflectivity analysis for determining free carrier parameters of irradiated gallium arsenide
[AD-762273] 20 p2463 N73-29791
Research and development of laser materials, semiconductor materials, and magnetic materials
[AD-763709] 21 p2555 N73-30486
Analysis of structural-eutectic transformations in liquid phase of metal-metal and metal-semiconductor systems
[NLL-M-21665-[5828.4F]] 21 p2557 N73-30496
NBS methods for measuring properties of semiconductor materials, process control, and devices
[NBS-TN-788] 21 p2585 N73-30717
Characterization and growth of GaAs crystals by gradient freeze and traveling heater methods
[AD-763761] 21 p2586 N73-30722
Epitaxic sublimation methods for studying pseudo-binary semiconductor alloys
[AD-763488] 21 p2586 N73-30723
Research on ternary diamond-like semiconductors as long wavelength infrared detectors
[AD-763466] 21 p2586 N73-30725
Evaluation of Gallium nitride for active microwave devices
[AD-763413] 21 p2586 N73-30726
Eastern Europe research projects involving hydrometeorology, semiconductor materials, microelectronics, and piezoelectronics
[JPRS-59617] 21 p2607 N73-30893
Research projects involving development and application of semiconductor materials and process for measuring properties of semiconductors at high pressures
21 p2607 N73-30894
Research projects involving design and technology of semiconductor devices, metal oxide semiconductor field transistors, and electron storage for memory purposes
21 p2607 N73-30895

Polish research projects on piezoelectronic and acoustoelectronic equipment with specific application to computers and communication systems
21 p2608 N73-30901
Influence of electronic states, electronic transport, and radiative transitions on luminescent defects in pure and doped single crystal compound semiconductors
[AD-764278] 22 p2708 N73-31683
Luminescence modulation and negative resistance modulation of semiconductors and high temperature semiconductors
[AD-763840] 22 p2708 N73-31685
Metal oxide semiconductor photoengraving principles and utilization noting resin properties, procedures, thin film techniques, and metal chemical attack
[LAAS-FI-73-T-11] 24 p2899 N73-33139
Analysis of high frequency vibrational modes in semiconductor materials using Raman scattering techniques
24 p2960 N73-33650
Diagnostic technique for determining excess free carrier lifetime and ambipolar diffusion coefficient in localized regions within semiconductors
24 p2966 N73-33706
Cyclotron resonance linewidth in semiconductors
24 p2968 N73-33716
Rare earth doped gallium phosphide preparation with application to electroluminescence noting physical and chemical properties
24 p2969 N73-33729
Possibility of using triple semiconductor compounds in thermoelectric and photoelectric converters
[AD-765730] 24 p2970 N73-33734

**SEMIEMPIRICAL EQUATIONS**
Semiempirical calculations of turbulent boundary layer problems
[AD-745217] 01 p0042 N73-10330
Semiempiricial methods for designing ejectors for various applications
08 p0896 N73-17252
Semiempirical model for development of round turbulent jet in cross flow using asymptotic solution for jet excess velocity
[NLR-TR-71107-U] 10 p1142 N73-19307
Semiempirical calculations of gf values, LS transition arrays, and spin-orbit matrices
[SAO-SPECIAL-REPT-351] 16 p1904 N73-25405

**SEMIMETALS**
U METALLOIDS

**SEMISPAN MODELS**
Wind tunnel tests to determine acoustic properties of semispan wing with externally blown jet flap to include effects of flap size, vertical location and forward speed
[NASA-TM-X-2749] 09 p0985 N73-18041

**SENDERS**
U TRANSMITTERS

**SENEGAL**
Evaluation of hydrology and vegetation in Sahelian zone of Mali, Mauritania, and Senegal during dry season/drought period based on ERTS-1 imagery
[E73-10488] 12 p1396 N73-21324

**SENSE ORGANS**
NT BARORECEPTORS
NT COCHLEA
NT EAR
NT EYE [ANATOMY]
NT FOVEA
NT GRAVIRECEPTORS
NT LABYRINTH
NT MIDDLE EAR
NT OCULOMOTOR NERVES
NT OTOLITH ORGANS
NT PHOTORECEPTORS
NT RETINA
NT SEMICIRCULAR CANALS
NT VESTIBULES

**SENSES**
U SENSORY PERCEPTION

**SENSIBILITY**
U SENSITIVITY

**SENSING**
U DETECTION

**SENSITIVITY**
NT IMPACT RESISTANCE
NT LIGHT ADAPTATION
NT NOTCH SENSITIVITY
NT PHOTOSENSITIVITY
NT PROPELLANT SENSITIVITY
NT RADIATION TOLERANCE
Transient and steady state response characteristics of sandwich-type wavelength selective bolometer
[AD-750264] 06 p0675 N73-15496
Evaluation of sex difference in thermal sensitivity in men and women
[NASA-CR-114564] 08 p0878 N73-17113
Influence of photoconducting layer thickness on sensitivity of vidicons
[NLL-DRIC-TRANS-2965-[3623.66]] 11 p1261 N73-20233
Sensitivity testing of hydrophones using Univac 1108 computer
[AD-754099] 11 p1262 N73-20244
Trajectory sensitivity during perturbations in dynamic systems
[AD-754919] 11 p1312 N73-20643
Low cost highly sensitive 12 GHz low noise converter for communication between broadcast satellites and ground stations
[NHK-LABS-NOTE-161] 20 p2380 N73-29127
Design of low cost highly sensitive SHF microwave components
[NHK-LABS-NOTE-163] 20 p2381 N73-29129
Increased sensitivity of laser gyroscopes
[AD-763284] 21 p2550 N73-30443
Threshold of sensitivity of laser gyroscope lowered by use of Zeeman effect
[AD-763160] 21 p2550 N73-30444
Electron recording and readout sensitivity characteristics of amorphous semiconductor thin films
[AD-763253] 21 p2585 N73-30719
Optimized sensitivity of computer controlled microwave spectrometer for trace element detection
[BMVG-FBWT-73-18] 23 p2754 N73-32037
Sensitivity of gravitational detector with positive electromechanical transducers
[ITF-72-90-E] 24 p2926 N73-33374

**SENSOR-AIRBORNE TERRAIN ANALYSIS**
U SENSORS
U TERRAIN ANALYSIS

**SENSORIMOTOR PERFORMANCE**
NT PSYCHOMOTOR PERFORMANCE
NT PSYCHOSOMATICS
Motor reaction model for hand motion in decision making manual task
[AD-761518] 19 p2229 N73-27973

**SENSORS**
Nucleonic sensor for detecting metal in recirculating lubricating oil systems
[AD-752580] 08 p0926 N73-17588
Wind tunnel calibration and requirements for in-flight use of fixed hemispherical head of angle of attack and angle of sideslip sensors
[NASA-TN-D-6986] 09 p0981 N73-18014
Techniques for casting large area polysulfone film capacitors onto thick aluminum substrates for application as meteoroid impact sensors
[NASA-CR-128862] 10 p1160 N73-19441
Effects of sensor deadband and actuator breakout torque control system nonlinearities on performance of Apollo telescope mount pointing capability
[NASA-TN-D-7247] 15 p1834 N73-24868
Conference on technology utilization in spacecraft guidance, ground operations, communications and navigation systems, and sensor development
[NASA-SP-326] 18 p2207 N73-27816

**SENSORY DISCRIMINATION**
NT BRIGHTNESS DISCRIMINATION
NT TACTILE DISCRIMINATION
NT VISUAL DISCRIMINATION
Attention sharing effects on human operator performing simultaneously dynamic compensatory tracking control tasks
01 p0018 N73-10140

**SENSORY PERCEPTION**
NT AUDITORY PERCEPTION
NT SPACE PERCEPTION
NT TACTILE DISCRIMINATION
NT TOUCH
NT VERTICAL PERCEPTION
NT VIBRATION PERCEPTION
NT VISUAL DISCRIMINATION
NT VISUAL PERCEPTION
Psychophysical method of limits to evaluate experimental variables in sensory areas
[AD-749334] 05 p0502 N73-14083
Bioastronautics research, including stress effects, sensory perception, and human performance
[NASA-SP-3006] 06 p0627 N73-15091
Sensory receptors irritation and cardiopulmonary toxicity from fluorocarbon propellants
[AD-751426] 07 p0749 N73-16089
Effect of cigarette smoking on sensory perception and performance parameters of flight crews
[AD-754421] 14 p1612 N73-23071
Model of speech processing with perceptual asymmetry
14 p1626 N73-23173
Importance of central and peripheral vision in pattern perception
21 p2500 N73-30063
Prosthetic limb with tactile sensing device
[NASA-CASE-MFS-16570-1] 23 p2751 N73-32013

**SENSORY STIMULATION**
Vestibular analyzer functions in dogs after prolonged ionizing irradiation
10 p1115 N73-19088
Use of motivational relations to find acceptor of action with conditioned stimuli
24 p2888 N73-33064
Various types of corticopetal influences from deep-seated emotiogenic formations of brain
24 p2889 N73-33068

**SENTENCES**
NT SYLLABLES
NT WORDS [LANGUAGE]
Computer program for machine recognition of distinctive features in words and sentences
14 p1623 N73-23147
Recognition of spoken sentences by visual examination of spectrograms
14 p1628 N73-23199

**SEPARATED FLOW**
NT BOUNDARY LAYER SEPARATION
Computation of steady conical flow past a yawed slender delta wing with leading edge separation using vortex sheet model and Newton-Raphson iteration
[IC-AERO-72-17] 01 p0001 N73-10005
Procedure for calculating sectional lift coefficient as function of angle of attack and free stream Reynolds number at angles of attack beyond maximum coefficient of lift
[AD-746505] 01 p0002 N73-10008
Heat transfer rate measurements in separated flow region behind series of eight axisymmetric backward facing step models
[AD-735745] 01 p0037 N73-10289
Characteristics of turbulent separated flows, and calculations of momentum and heat transfer in them
[EF/TN/A/49] 01 p0039 N73-10308
Incompressible boundary layer flow separation over moving boundaries
[AD-746869] 02 p0159 N73-11292
Wind tunnel study of basic nature of plume induced flow separation
[NASA-CR-112218] 04 p0404 N73-13288
Analysis of laminar part of separation bubbles in two dimensional incompressible flow for various shaped objects
06 p0616 N73-15000
Development of method for calculating small separation zones near leading edge of airfoil at incidence
06 p0616 N73-15002
Dissipative losses in separation nozzle flow determined for uranium isotope separation conditions from Pitot tube measurements
[KFK-1562] 07 p0772 N73-16271
Couette flows used to determine effect of injection and curvature of walls on flow separation
[AD-753501] 09 p1019 N73-18317
Magnetohydrodynamic wall flow with laminar separation
[AD-753149] 09 p1072 N73-18751
Analysis of fluid flow over two dimensional flat plate wedge configuration for application to deep submersible vehicles
[NASA-CR-131888] 13 p1510 N73-22233
Visualization and integral methods for studying three-dimensional supersonic flow separation on delta wing
14 p1600 N73-22970
Three-dimensional representation of hypersustentation during separated flow
[REF-8467] 14 p1648 N73-23371
Wind tunnel tests to determine effect of approaching boundary layer on separated flow behind downstream facing step
[NLR-TR-70033-U] 15 p1768 N73-24322
Finite difference calculations of laminar flow past blunt-nosed cone with spherical after body injecting mass into air
[AD-758009] 15 p1844 N73-24943
Perturbation method for separated laminar incompressible flows in divergent channels
16 p1886 N73-25268
Structural and gas dynamic parameters at flow separation boundary in compressor cascades
[AD-762238] 19 p2257 N73-28197
Integral solution to internal separated flow problems in nozzles and orifices
23 p2772 N73-32174
Rocket motor chamber pressure and orifice effects in hydraulic flip
[AD-764730] 23 p2832 N73-32630

**SEPARATORS**
NT AIR FILTERS
NT CLASSIFIERS
NT DIVIDERS
NT DRYING APPARATUS
NT EVAPORATORS
NT FLUID FILTERS
NT SIEVES
NT STILLS
Fluid mechanics and dynamic energy separation in steady flow, nonsteady flow, and cryptosteady flow
[AD-747316] 03 p0286 N73-12314
Device for removing air from water for use in life support systems in manned space flight
[NASA-CASE-XLA-8914] 03 p0305 N73-12492
Design and evaluation of electrochemical nitrogen-hydrogen separator for use in spacecraft nitrogen generator
[NASA-CR-114580] 13 p1534 N73-22431
Diffusion across modified polyethylene separator in heat sterilizable silver zinc battery
[NASA-CR-133601] 20 p2363 N73-29007
Separation of fine metallic powders using air in combination with fluidized bed
23 p2809 N73-32462

**SEQUENCING**
Linear shift register with feedback logic for generating pseudonoise linear recurring binary sequences
[NASA-CASE-NPO-11406] 03 p0268 N73-12175

Approximative parameters and probabilistic sequential subsets for modeling linear and renewal sources in communication theory
06 p0639 N73-15186
Abstract algebraic techniques to determine synchronization properties of binary, linear, and maximal length sequences
[AD-744101] 13 p1550 N73-22560
Computer code which reorganizes old FORTRAN programs so that statement numbers are added sequentially and extraneous statements are deleted
[NASA-TM-X-62286] 22 p2636 N73-31128
Sequential communication systems with information feedback
24 p2893 N73-33098

**SEQUENTIAL ANALYSIS**
Automatic sequential processing, technique for unsupervised classification, or clustering, of multispectral remote sensing data, using digital computer program
[NASA-CR-128999] 03 p0323 N73-12633
Analysis of statistical properties of filtered summed maximum length digital sequences
20 p2436 N73-29564
Event sequence detector with several input and shift register responsive to clock pulses
[NASA-CASE-NPO-11703-1] 23 p2768 N73-32144

**SEQUENTIAL COMPUTERS**
Testing machine for sequential systems using pseudorandom sequences and wired models
03 p0271 N73-12196
On-line failure testing of synchronous sequential computers
03 p0271 N73-12197
Sequential machine reduction with partition tree
03 p0271 N73-12200
Total machine language conception for sequential automaton from modular evolution
04 p0394 N73-13201
Asynchronous sequential circuit model with input delays and feedback
04 p0400 N73-13251
Statistical and deterministic tests for failure analysis of sequential computer storage devices
05 p0517 N73-14203
Serial digital data bus for integrated avionics system interface
14 p1713 N73-23902
Computer aided procedure for complete design of sequential machines
[AD-759959] 17 p2002 N73-26191
Computer programming for sequential machine design
[AD-762163] 19 p2241 N73-28069

**SEQUENTIAL CONTROL**
Shift register with feedback for generating pseudorandom binary sequences
[REPT-6707] 08 p0887 N73-17183
Differential games, nonlinear sequential machines, hyperbolic partial differential equations, and iterative solutions
[JPRS-58069] 09 p1056 N73-18609
Multidimensional Laplace-Galois transform for nonlinear sequential machines
09 p1056 N73-18611
Monte Carlo simulation for man machine task sequencing considering pilot performance degradation
14 p1713 N73-23899
Design of sequential circuits using edge and level sensitive flip-flops
24 p2900 N73-33146

**SEQUENTIAL DETECTION**
U SEQUENTIAL ANALYSIS

**SERIES [MATHEMATICS]**
NT COSINE SERIES
NT FOURIER SERIES
NT POWER SERIES
NT SINE SERIES
NT TAYLOR SERIES
Figure series for digital data presentation
[IZF-1972-11] 02 p0145 N73-11170
Transformation functions between z basis and jm basis of Lorentz group principal series
[NOTA-INTERNA-386] 03 p0324 N73-12641
Series expansion of functions using eigenfunctions and applications to initial and boundary value problems of orbital mechanics
[BMBW-FBW-72-33] 09 p1084 N73-18844

**SERIES EXPANSION**
U SERIES [MATHEMATICS]

**SEROTONIN**
Diurnal changes in human histamine and serotonin metabolism and effects of work-sleep cycle
03 p0258 N73-12089

**SERT 2 SPACECRAFT**
Dished high perveance grids on throttlable 15 cm hollow cathode ion thruster
[NASA-CR-121038] 04 p0464 N73-13782
Tests of mercury-fed hollow cathode in bell jar at SERT 2 neutralizer conditions
[NASA-TM-X-2785] 15 p1825 N73-24793
SERT 2 hollow cathode multiple restarts in space
[NASA-TM-X-68292] 21 p2589 N73-30742

**SERUMS**
Stabilization methods in collecting and shipping of human sera for chemical analyses
08 p0871 N73-17053

**SERVICE LIFE**
Failure analysis of Geiger counters used in nucleonic oil gauging system of USAF aircraft
[AD-746267] 01 p0059 N73-10485
Performance tests of ball bearings to determine service life during operation without lubrication under various conditions of atmospheres, loads, and speeds
[AD-746034] 01 p0063 N73-10520
Implementation of reliability based strength criteria system for determining service life of C-141 aircraft structures - Vol. 2
[AD-742261] 02 p0126 N73-11025
Aircraft tire dynamometer tests to determine effects of tire deflection on rolling resistance and tire life
[AD-746304] 02 p0127 N73-11031
Diffusion metallizing and service life of gas turbine engine blades
[NASA-TT-F-13914] 02 p0223 N73-11801
Rate of discharge of accelerated life tests of nickel cadmium cells
[AD-748253] 04 p0377 N73-13065
Temperature and temperature gradients for accelerated life tests of nickel cadmium cells
[AD-748252] 04 p0377 N73-13066
Valid tests with temperature gradients and/or rates of discharge as primary variables for accelerated life testing sealed nickel cadmium batteries
[AD-749129] 05 p0499 N73-14061
Performance tests and service life of electroluminescent film display device
[AD-749790] 05 p0521 N73-14235
Influence of humidity on thermal life determination of electrical insulation
[AD-749926] 05 p0521 N73-14238
Lubricant supply for mechanical antenna bearings
[NLL-RISLEY-TR-2308-[9091.9F]]
05 p0550 N73-14463
Performance data reduction for cadmium spacecraft cells from simulated orbital life tests
[AD-748251] 06 p0627 N73-15088
Service life and reliability of single transmitter and array modular type satellite altimeter systems
06 p0663 N73-15388
Fatigue tests to determine service life of aluminum alloy lugs with push-fit pins under tensile stress conditions
[ESDU-72020] 06 p0723 N73-15901
Development and application of procedures for determining service life of gas turbine engines and components
[NASA-TM-X-2664] 06 p0726 N73-15925
Durability investigation of strain gage pressure transducers subjected to long term pressure cycling at ambient and elevated temperatures
[NASA-CR-120953] 07 p0800 N73-16497
Method for selecting silicon planar semiconductor devices for long life
[NASA-CR-124036] 07 p0803 N73-16516
Accelerated life tests and reliability predictions for ageing components
[AD-751616] 07 p0805 N73-16529
Design parameters that contribute to cycle life of sealed, heat-sterilized silver oxide-zinc cells
[NASA-CR-130723] 08 p0869 N73-17038
Elastic-plastic solution for calculating influence of energy dissipation on drawn wire fatigue
[AD-752017] 08 p0928 N73-17600
Optimum service life determination technique for Naval aircraft
[AD-752747] 09 p0987 N73-18057
Formula for evaluating durability of plastic bearings based on fatigue wear theory and including friction, elasticity, strength, and pressure factors
[AD-752820] 09 p1040 N73-18480
Electromagnetic radiation screening of semiconductor devices for long life applications
[NASA-CR-124119] 09 p1073 N73-18757
Fuel expulsion efficiency and service life of Arde metallic diaphragm used in Atmospheric Explorer propulsion subsystem
[NASA-TM-X-66191] 09 p1078 N73-18794
Service life of mechanically prestressed glass used in spacecraft windows
09 p1088 N73-18880
Performance capabilities and cycle life of high specific energy batteries for pollution free electric vehicles
[ANL-7953] 10 p1112 N73-19061
Structural design guidance and construction standards for upgrading and extending service life of airport pavements
[FAA-ED-08-2] 10 p1137 N73-19266
Test plan for extending service life of E-2A arresting gear
[AD-754752] 11 p1267 N73-20284
Test plan for extending life of C-2A arresting hook A-frame to 3000 arrested landings
[AD-754076] 11 p1268 N73-20289
Development of methods for determining service life of rolling bearings based on fatigue of bearing materials
[NLL-RISLEY-TR-2524-[9091.9F]]
12 p1407 N73-21406
Long term frequency stability, service life, and reproducibility of NASA hydrogen maser in relation to world standards
[NASA-TM-X-66229] 12 p1410 N73-21425
Life test performance of SNAP 23 prototype mockup system
[WANL-3559-1] 12 p1427 N73-21568
Service life and operation of military equipment in subzero Siberian environments
[AD-756478] 13 p1554 N73-22595
Carrier lifetime measurement by photoconductive decay method
[NBS-TN-736] 13 p1565 N73-22685
Cost effectiveness analysis of helicopter transmission components to determine effect of extended overhaul life up to 6,000 hours
[AD-758465] 14 p1604 N73-23007
Guidelines for design and development of electrical and electronic components and systems used in spacecraft construction to obtain long service life - Vol. 2
[NASA-CR-128906] 14 p1707 N73-23854
Performance tests to determine stress-life exponent for vacuum-processed steel ball bearing operating at 500 F
[NASA-TM-X-68240] 15 p1791 N73-24521
Increased service life of rolling element radial bearings in nuclear engine for rocket vehicles by liquid hydrogen cooling and bearing modifications
[NASA-CR-132229] 15 p1792 N73-24531
Service life extension of cyclically loaded copper specimens by application of electroplated layers of nickel
16 p1927 N73-25595
Development of procedures for determining service life of helicopter airframes and rotor blades
[RAE-LIB-TRANS-1520] 17 p1981 N73-26013
Statistical analysis of counting accelerometer data obtained on Navy and Marine fleet aircraft from 1 Jan. 1962 to 1 Jan. 1972
[AD-760321] 17 p1985 N73-26041
Endurance and performance tests of bore ball bearings lubrication thrust loaded 120-mm to 3 million DN
[NASA-TM-X-68264] 17 p2037 N73-26479
Flight evaluation of composite for use in aircraft structures
[NASA-TM-X-2761] 17 p2049 N73-26579
Service life of turbine blades operating under stochastic conditions
[AD-759874] 17 p2078 N73-26812
Performance tests and failure analyses on silver zinc cells with inorganic separator materials
[NASA-CR-121215] 18 p2108 N73-27049
Performance tests of spur gears with and without tip relief to determine service life of M-50 and Super Nitralloy metals
[NASA-TM-X-68269] 18 p2155 N73-27413
Effect of lubricant active additives on rolling-element fatigue life using five-ball fatigue tester
[NASA-TN-D-7383] 18 p2156 N73-27417
Performance tests of gas turbine engine mainshaft roller bearings to determine stress and lubrication parameters
[AD-760563] 18 p2157 N73-27426
Life tests of niobium coatings used on alkali metal arc lamps
[AD-761204] 18 p2168 N73-27508
Fabrication and life testing of thermionic converters
[NASA-CR-121180] 18 p2177 N73-27576
Analysis of thermal fatigue in nontubular regeneratively cooled combustion chambers and prediction of thermal cycle life capability - Vol. 1
[AD-760582] 18 p2194 N73-27715
Analysis of thermal fatigue in nontubular regeneratively cooled combustion chambers and development of life prediction techniques - Vol. 2
[AD-760583] 18 p2194 N73-27716
Analysis of effects of flying time on service life of wing fastening knee plates on transport aircraft
[AD-761468] 19 p2221 N73-27919
Development of mathematical model for determining replacement criteria for aircraft structural components
[AD-762226] 19 p2222 N73-27921
Cost history of F-111 aircraft airframe system to show logistics organization, support costs, reliability and maintainability, and development problems
[AD-762213] 19 p2356 N73-28958
Logistics performance data book on bombing and navigation system for A-7D aircraft to show reliability, maintainability, cost, and problems
[AD-762215] 19 p2357 N73-28960
Logistic performance data book on propulsion system for KC-135 aircraft to show reliability, maintenance, costs, and problems
[AD-762217] 19 p2357 N73-28962

Logistic performance data book for C-5A airframe to show reliability, maintainability, logistics support, and operating problems
[AD-762233] 19 p2358 N73-28968
Life test data for hybrid thermoelectric panel containing lead telluride and silicon germanium thermocouples
[NASA-TM-X-2869] 20 p2364 N73-29010
Development of lithium-doped silicon solar cells with increased stability, efficiency, and radiation resistance
[AD-762941] 20 p2364 N73-29011
Development of procedures for predicting fatigue life of aircraft structures based on fracture mechanics, crack propagation, and residual static strength anlaysis
[AGARD-LS-62] 20 p2480 N73-29924
Development of fatigue life prediction procedures based on measured stress-time histories and mathematical model for description of random vibrations
20 p2481 N73-29926
Procedures for predicting fatigue life of aircraft flying under various load conditions using data obtained by counting accelerometer
20 p2481 N73-29927
Effect of environment and stress-cycling on in-service structural failure of airframes and procedures for predicting safe operational conditions
20 p2481 N73-29929
Durability test of five cm diameter ion thruster for 9700 hours
[NASA-TM-X-68284] 21 p2589 N73-30741
Method for determining time to failure of blades on aircraft gas turbine engines at steady mode and transient mode of operation
[NASA-TT-F-15113] 22 p2710 N73-31700
Service life and reliability of radiation hardened lithium doped solar cells
23 p2859 N73-32840
Vibration tests of flight control moment gyros and bearing life test fixtures
[NASA-CR-124449] 24 p2926 N73-33365

**SERVICE MODULES**
Apollo experience report on command and service module reaction control systems
[NASA-TN-D-7151] 16 p1966 N73-25901
Apollo experience report on command and service module instrumentation subsystem to show requirements determination and conceptual design
[NASA-TN-D-7374] 22 p2719 N73-31761
Apollo experience report on service propulsion subsystem development, qualification, and flight performance
[NASA-TN-D-7375] 22 p2719 N73-31763

**SERVICES**
NT MEDICAL SERVICES
NT METEOROLOGICAL SERVICES

**SERVO LOOPS**
U FEEDBACK CONTROL
U SERVOCONTROL

**SERVOACTUATORS**
U ACTUATORS
U SERVOMOTORS

**SERVOCONTROL**
Large-diameter rotary vacuum chamber with servo controlled angular positioning and readout
[LBL-769] 03 p0281 N73-12275
Design, development, and evaluation of servoactuator device to include application to optimized system configuration
[NASA-CR-124025] 11 p1297 N73-20524
Design of IDFF servovalve applicable for controlling hydraulic systems
[NAL-TR-303] 15 p1824 N73-24787
Improved design of high-response slotted plate overboard bypass valve for supersonic inlets
[NASA-TM-X-2812] 16 p1864 N73-25097
Construction of reversible self synchronous control system for manipulator
17 p1989 N73-26080
Systems engineering for design of two dimensional automatic manipulator control system using reversible follow-up
17 p1989 N73-26081
Remotely controlled manipulators with independent follow-up and force reproduction mechanisms
17 p1989 N73-26082
Digital servocontroller for rotating antenna shaft
[NASA-CASE-KSC-10769-1] 18 p2122 N73-27153

**SERVOMECHANISMS**
NT SERVOMOTORS
Design, development, and characteristics of industrial robot machinery to show load capacity, positioning accuracy, power actuators, and method of controls
01 p0060 N73-10486
Development and characteristics of rotary actuator for use on spacecraft to deploy and support pivotal structures such as solar panels
[NASA-CASE-NPO-10680] 05 p0597 N73-14855
Dynamic performance criteria for power actuating components of electrohydraulic actuation servosystem
[NASA-TM-X-2736] 09 p0990 N73-18079
Design and performance tests of prototype self-locking actuator
[NASA-CR-124135] 10 p1163 N73-19459
Comparison of computed torque method and conventional position servo computer controlled manipulator
[NASA-CR-131521] 12 p1381 N73-21198
Transistorized feedback servomechanism design for cryogenic oxygen flow control
[NASA-TM-X-68234] 15 p1759 N73-24258
Design of manipulator mechanisms with manual, bioelectric, and automatic control systems
[NASA-TT-F-14336] 17 p1989 N73-26073
Volumetric kinematic analysis on servomechansim of remote handling manipulator
17 p1989 N73-26075
Remote control of underwater manipulator using cables and automatic servomechanics
17 p1989 N73-26078
Systems engineering for design of two dimensional automatic manipulator control system using reversible follow-up
17 p1989 N73-26081
Synchronization kinetics in control of movement links in human extremities
17 p1990 N73-26089
Automatic control systems with variable coupling between functional elements
24 p2900 N73-33149

**SERVOMOTORS**
Development and characteristics of cyclically operable, optical shutter for use as focal plane shutter for transmitting single radiation pulses
[NASA-CASE-NPO-10758] 05 p0545 N73-14427
Development and characteristics of rotary actuator for use on spacecraft to deploy and support pivotal structures such as solar panels
[NASA-CASE-NPO-10680] 05 p0597 N73-14855
Application of active standby redundancy techniques to large electrohydraulic servoactuator
[NASA-CR-124027] 07 p0803 N73-16515
Design of automatic controlled remote arm mechanism incorporating feedback information
[NASA-CR-2238] 13 p1487 N73-22055
Construction of reversible self synchronous control system for manipulator
17 p1989 N73-26080
Single channel wheel system with electrohydraulic servoactuators for flight control feel system
22 p2731 N73-31855

**SERVOSTABILITY CONTROL**
U SERVOCONTROL

**SET THEORY**
NT EQUIVALENCE
NT THRESHOLD LOGIC
Algorithm for determining optimal partition of points into mutually exclusive and exhaustive subsets or clusters according to objective function defined on set of all partitions
[P-4878] 01 p0072 N73-10586
Statistics of parallel dimers on mxn lattice
[NUB-2166] 07 p0813 N73-16594
Theorems regarding oscillation and nonoscillation conditions for canonic linear sets of differential equations
[NASA-TT-F-14816] 09 p1057 N73-18615
Linear vector space theory used to develop general representation of random vectors and data sets
[NASA-TR-R-398] 09 p1057 N73-18620
Numerical analysis of projected gradient method and operator formed from any linearly independent subset of gradients
[DLR-FB-73-26] 11 p1311 N73-20636
Markovian decision processes with limited state observability and unobservable costs
[P-4925] 12 p1419 N73-21496
Topologies on directed graphs
[NASA-CR-133342] 18 p2169 N73-27517
Concept of fuzzy sets in pattern recognition
[REPT-7] 20 p2437 N73-29572

**SEWAGE**
Raw water sewage treatment
[NASA-CASE-NPO-13224-1] 22 p2622 N73-31011

**SEX GLANDS**
NT TESTES

**SH-3 HELICOPTER**
Development of equipment for securing external stores SH-3G helicopter and analysis of failure modes
[AD-757001] 13 p1474 N73-21943

**SHADOWGRAPH PHOTOGRAPHY**
NT SCHLIEREN PHOTOGRAPHY
Monopulse laser emission study of moving objects during shadow photography
[AD-747607] 03 p0311 N73-12539
Sequential spark method for measuring cone wake velocity profiles
[AD-759159] 16 p1893 N73-25317
Shadowgraph photography of boundary layer transition of spinning cones
[AD-762564] 22 p2656 N73-31276

**SHADOWGRAPHS**
U SHADOWGRAPH PHOTOGRAPHY

**SHADOWS**
Quantitative schlieren photography with semishadow of edge in photograph allowing calibration
[WB-2/72] 09 p1037 N73-18459
Atmospheric model for acoustic pressure produced in shadow zone by wind and temperature gradients
[AD-754634] 11 p1324 N73-20747
Shadowing mounds on ruled gratings for X ray and far ultraviolet spectra
[AD-757894] 15 p1814 N73-24705

**SHAFTS (MACHINE ELEMENTS)**
NT TURBOSHAFTS
Analysis of factors affecting design of interference-fit collars on rotating shafts
[ESDU-68002] 01 p0061 N73-10496
Numerical analysis of nominal interface pressures and stresses for shafts with interference fit collars
[ESDU-68003-AMEND-A] 01 p0061 N73-10497
Methods for increasing stability of rotors with gas bearings
[AD-745858] 01 p0063 N73-10517
Static, ballistic, and impact behavior of glass/graphite drive shaft sections to determine suitability for heavy lift helicopters
[AD-743938] 01 p0091 N73-10752
Guide for using data on effects of buckling and deflections in beams, struts, and shafts
[ESDU-SS3] 01 p0112 N73-10922
Elastic interface pressure and stress calculations on assemblies of shafts with interference-fit collars
[ESDU-68004-PT-3] 02 p0177 N73-11433
Fatigue tests on solid shafts with interference-fit collars
[ESDU-68005-PT-4] 02 p0177 N73-11434
Effect of galvanic and thermodiffusive coatings on wear resistance of shafts and hinged joints
[AD-750533] 05 p0553 N73-14494
Actuator shaft sealing techniques for long term interplanetary spacecraft missions
[NASA-CR-130927] 10 p1165 N73-19479
Time integration of transient equations in shaft dynamics analysis
[AD-754341] 10 p1168 N73-19500
Development of beryllium-copper bearings for use with stainless steel shafts under high bearing stress levels imposed by airframes
[AD-754759] 11 p1299 N73-20540
Design and development of gas-film seal using shrouded Rayleigh step lift pads at primary sealing face of gas turbine engine
[NASA-CR-121177] 18 p2155 N73-27415
Fatigue life of hybrid antifriction bearings at ultrahigh speeds
[NASA-CASE-LEW-11152-1] 23 p2795 N73-32359

**SHAKING**
NT DITHERS

**SHALES**
Regional environmental impact from oil shale development on private and public lands in Wyoming, Colorado, and Utah - Vol. 1
[EIS-AA-72-5242-D-1-VOL-1]
20 p2410 N73-29367
Energy alternatives to prototype oil shale leasing program for Wyoming, Colorado, and Utah - Vol. 2
[EIS-AA-72-5242-D-2-VOL-2]
20 p2410 N73-29368
Description of proposed leases for oil-shale program in Wyoming, Utah, and Colorado, and potential environmental impacts - Vol. 3
[EIS-AA-72-5242-D-3-VOL-3]
20 p2410 N73-29369

**SHALLOW WATER**
Shallow flowing water channel for hydraulic analogy of gas flow in transonic to hypersonic range
[ICT-4/71] 01 p0036 N73-10286
Model 735 dissolved oxygen analyzer for continuous measurement of dissolved oxygen concentration in shallow fresh water
[NOAA-IFS-73003] 01 p0057 N73-10465
Hydrophone measurement of acoustic propagation and CW signals from underwater explosions in shallow Bering Sea
[AD-745735] 01 p0081 N73-10667
Shallow flowing water channel for hydraulic analogy of gas flow in transonic to hypersonic range
[GRI/NTP/100] 02 p0146 N73-11186
Wind-driven currents and surges with bottom slipping in shallow water
09 p1059 N73-18639
Calculation of water depth off Little Bahama Bank from ERTS-1 data for use in upgrading and mapping world navigation charts of shallow waters
[PAPER-M20] 19 p2282 N73-28358

**SHANKS**
U JOINTS (JUNCTIONS)

**SHANNON INFORMATION THEORY**
U INFORMATION THEORY

**SHAPED CHARGES**
Development and operation of facility for investigating effect of spin on aerodynamic characteristics of shaped charges
[DREV-TN-2037/72] 06 p0649 N73-15271

Survey of results from barium cloud releases using shaped charge technique in ionosphere and magnetosphere
[MPI-PAE/EXTRATERR-67] 07 p0794 N73-16454
Apollo experience report on use of pyrotechnic devices in systems of Apollo spacecraft
[NASA-TN-D-7141] 10 p1215 N73-19878

**SHAPES**
NT CONVEXITY
NT ELLIPTICITY
NT ROSETTE SHAPES
NT T SHAPE
Stress concentration effects due to shape discontinuity, inclusions, or local load distributions
[ESDU-65004-AMEND-A-B-C] 01 p0112 N73-10925
Shape and rotation rate of asteroid bodies
02 p0228 N73-11850
Automatic land use classification based on optical density and shapes from ERTS-1 imagery
[E73-10816] 18 p2140 N73-27291
Elastic and shape memory properties of beta-brass alloys at various temperatures
[AD-764472] 22 p2686 N73-31515

**SHARP LEADING EDGES**
Flow characteristics around semi-infinite plate with sharp leading edge inserted in hypersonic uniform air stream
[NAL-TR-289T] 06 p0613 N73-14979

**SHATTERING**
U FRAGMENTATION

**SHEAR**
Development of mathematical relationships to define the behavior of multilayer, thin shell structures under various conditions of shear and bending
02 p0238 N73-11936

**SHEAR DISTURBANCES**
U S WAVES

**SHEAR FATIGUE**
U SHEAR STRESS

**SHEAR FLOW**
Physical structure of turbulent shear flows in nonreacting gase flow
[AGARD-AR-46] 02 p0156 N73-11262
Development of mathematical models to analyze stability characteristics of thermally stratified shear flow in atmosphere
[ORO-4199-1] 03 p0296 N73-12414
Review of linear viscous stability theory for stably stratified parallel shear flow
[CONF-720632-1] 07 p0772 N73-16270
Nonlinear analysis of gravity wave moving over horizontal bed into vertical shear flow
[AD-754646] 11 p1272 N73-20322
Calculation of nonlinear evolution of disturbance in unbounded viscous fluid with uniform shear using Navier-Stokes equations
[NASA-TN-D-7284] 14 p1648 N73-23363
Absorbing power with enclosed partially submerged rotating disk in turbulent viscous shearing of water
[NASA-TN-D-7234] 15 p1767 N73-24316
Shear stabilization of drift instability in hydrogen plasma
[EUR-CEA-FC-646] 15 p1818 N73-24734
Method of local potential applied to analysis of turbulent shear flow
[NASA-CR-112322] 16 p1889 N73-25286
Low frequency instabilities in plasmas with magnetic shear
17 p2066 N73-26717
Proceedings of conference to develop data on free turbulent shear flows to include two dimensional shear layers and axisymmetric jets
[NASA-SP-321-VOL-2] 18 p2130 N73-27213
Phenomenological approach to turbulent shear flows
[AD-760765] 18 p2132 N73-27223
Proceedings of conference on free turbulent shear flows - Vol. I
[NASA-SP-321-VOL-1] 19 p2252 N73-28154
Rational approach to use of Prandtl mixing length model in free turbulent shear flow calculations
19 p2252 N73-28158
Analysis of free turbulent shear flows by numerical methods
19 p2252 N73-28160
Predictions of axisymmetric free turbulent shear flows using generalized eddy viscosity approach
19 p2253 N73-28163
Comparison of six different turbulence models for prediction of free shear flows
19 p2253 N73-28165
Local eddy viscosity model for turbulent shear flow
19 p2254 N73-28168
Integral turbulent kinetic energy analysis of free shear flows
19 p2254 N73-28170
General classification of approaches used for prediction of turbulent shear flows
19 p2254 N73-28173
Numerical analysis of two dimensional turbulent wakes in constant adverse and favorable pressure gradients
[AD-761389] 19 p2256 N73-28185
Local pressure field in turbulent shear flow and its relation to aerodynamic noise generation
[NASA-CR-134493] 22 p2653 N73-31253
Sharp interface in unbounded turbulent shear flows determined by linear array of hot-wire probes
23 p2773 N73-32178
Stochastic modeling of turbulent heat and mass transport in anisotropic shear flow
23 p2773 N73-32181
Comparison of rheological equations of state and constrained shear recovery results for two polyisobutylene melts
[RR-203] 24 p2891 N73-33078
Computation of kinetic fluctuation energy of turbulent shear flow from mean velocity distribution
24 p2908 N73-33211
Rheological and optical properties of deformable particles in laminar shear flows
24 p2959 N73-33647

**SHEAR LAYERS**
Proceedings of conference to develop data on free turbulent shear flows to include two dimensional shear layers and axisymmetric jets
[NASA-SP-321-VOL-2] 18 p2130 N73-27213
Critical review of experimental data for developed free turbulent shear layers
19 p2252 N73-28156
Turbulent free shear layers in pressure gradients
19 p2254 N73-28171
VHF - UHF surface wave studies of compliant layers for wedge transducers
[AD-762173] 20 p2378 N73-29106
Analytical and experimental study of spatially growing disturbances in shear layers between parallel streams
22 p2650 N73-31231
Boundary and shear layers in rotating and stratified fluids
22 p2651 N73-31235
Linearized integral theory of three dimensional unsteady compressible flow in shear layer by oscillating wall
[AD-763807] 22 p2654 N73-31264
Hydrodynamic stability of axisymmetric free shear layers
24 p2902 N73-33165
Vortex pairing in turbulent shear layer at moderate Reynolds numbers
24 p2903 N73-33169
Analyzing behavior of instantaneous point source as it disperses in thick, neutrally stratified, turbulent shear layer by laser light scattering technique
24 p2904 N73-33176

**SHEAR PROPERTIES**
NT SHEAR STRENGTH
Microwave measurements of magnetic field local shearing in confined plasma
[EUR-CEA-FC-632] 06 p0705 N73-15749
Rotating disk measurement of drag reduction and shear properties of various dilute polymers
[AD-751552] 07 p0773 N73-16281
Analysis of dynamic stability of elastic orthotropic cylindrical shell to determine shell parameters, shear moduli, and buckling mode
17 p2093 N73-26930

**SHEAR STRENGTH**
Torsion, bending, and shear in concrete beams reinforced with stirrups
[D-10-72] 02 p0238 N73-11938
Transverse shear stiffnesses of sandwich panels with corrugated core and equal face plates
[ESDU-07.03.01] 06 p0723 N73-15903
Improvement in interlaminar shear strength of organic matrix composites using plasma deposited coupling agents
[AD-753857] 09 p1055 N73-18599
Effect of blade thickness on shear strength of fasteners
[AD-757997] 15 p1793 N73-24539
Shear, flexural, and tensile strength performance of carbon fiber composites made from epoxy, phenolic, polyester, and polyimide resins
[AQD/NM-000198] 22 p2689 N73-31536

**SHEAR STRESS**
NT TORSIONAL STRESS
Reduction of peak shear stress in bonded joint
[NASA-CASE-LAR-10900-1] 01 p0061 N73-10499
Influence of shock compression pressure on critical shear in aluminum, copper, and lead
[AD-745365] 01 p0068 N73-10555
Determining maximum shear stress at hole boundary in axially loaded bar
[ESDU-66011-AMEND-A] 01 p0111 N73-10913
Elastic stresses in flat plates, strips, and lugs due to interference-fit pins or bushes
[ESDU-71011] 01 p0111 N73-10916
Mean velocity, turbulence intensity, and turbulent shear stress in turbulent boundary layer
[WTHD-41] 02 p0155 N73-11255
Subsequent yield curves for axial stressed-shear stressed surfaces of annealed SAE 1017 steel
[AD-746474] 02 p0188 N73-11523
Charpy toughness of discontinuous fiber reinforced plastics under nonuniform interfacial shear stress
[SC-DR-72-0260] 03 p0320 N73-12611
Effects of free edge shear stresses on failure of fiber-reinforced angle ply laminates
[AD-747343] 03 p0322 N73-12625
Structural analysis of sandwich panels with close-packed conical shells and honeycombs as fillers
[AD-747403] 03 p0362 N73-12953
Development of curves for determining magnitudes and directions of principal stress in plane using components of direct and shear stress
[ESDU-72013] 05 p0601 N73-14889
Development of curves for determining magnitude and direction of principal stresses and strains in plane stress field from strain gage readings
[ESDU-72014] 05 p0601 N73-14890
Development of momentum integral type method for solving relaxation-diffusion model for turbulent shear stress of incompressible plane turbulent wakes
[REPT-72-FM-5] 06 p0652 N73-15296
Shearing mode stress intensity for finite length crack in bimaterial composite
[AD-750498] 06 p0727 N73-15937
Viscous wall flow in turbulent boundary layer including shear stress
07 p0771 N73-16266
Effect of degree of saturation on susceptibility to onset of plastic instability in pure shear for solid solution of copper-zinc system
[COO-2048-6-PT-2] 08 p0967 N73-17901
Closed form solution using four harmonic functions for elastic solid with plane crack subjected to concentrated shears parallel to edge of crack
[NASA-CR-112317] 13 p1585 N73-22848
Chemistry and physics of thin liquid films in contact with solid substrates and application to boundary lubrication of propulsion systems
[AD-757061] 14 p1670 N73-23556
Numerical analysis of torsion characteristics of bar with constant section in shape of circular ring or circular sector
[NLL-DRIC-TRANS-2995-[3623.66]]
15 p1837 N73-24885
Development of electrical circuitry for analysis of stress deformation state of delta wing model based on discrete design diagram
[AD-760948] 18 p2108 N73-27044
Effects of shear, rotatory inertia and inplane forces on transverse vibration of thin plates, and effect of shear on buckling
19 p2347 N73-28879
Interaction between supersonic boundary layer with turbulent flow and inelastic deformable wall to determine stress perturbations and pressure distribution
[TN-86] 20 p2388 N73-29186
Calculations of turbulent shear stress distributions for zero pressure gradient and adverse gradient supersonic turbulent boundary layer flow
[AD-763197] 21 p2526 N73-30254
Numerical procedure for determining relationship between shear stress and turbulent kinetic energy in two dimensional flow
22 p2649 N73-31221
Effects on drag of injecting aqueous solutions of polyethylene oxide into turbulent boundary layer of flat plate
[AD-764896] 23 p2776 N73-32202
Measurement of wall shearing stress and velocity and temperature profiles of turbulent boundary layer to derive Reynolds number
[ARC-R/M-3712] 24 p2870 N73-32928
Turbulent shear stress profiles in boundary layer flow at sine wave pressure perturbations
24 p2906 N73-33194

**SHEAR WAVES**
U S WAVES

**SHEARING STRESS**
U SHEAR STRESS

**SHEATHS**
NT PLASMA SHEATHS
Rotational injection moulding for designing polythene sheathed closures on large size cables
[REPT-6713] 10 p1164 N73-19474

**SHEET METAL**
U METAL SHEETS

**SHEETS**
Fluid model for analyzing nonlinear magnetosonic wave propagation in magnetic neutral sheet
[IPPJ-139] 04 p0388 N73-13152

**SHELL STABILITY**
Nondestructive evaluation of stability of shells and development of mechanical device for crash simulator
04 p0480 N73-13922
Procedures for determining shell stability under various types of dynamic loads
07 p0852 N73-16906
Development of mixed finite-difference scheme for free vibration analysis of simply supported closed noncircular cylindrical shells
[NASA-TN-D-7107] 07 p0852 N73-16908
Effect of eccentricity of reinforcement upon stability of cylindrical shells
[AD-752691] 09 p1096 N73-18943
Field method for linear static analysis on open branch shells of revolution under asymmetric loads
[NASA-CR-112270] 11 p1311 N73-20638

Effect of stress state nonhomogeneity and initial imperfections on stability of cylindrical shells
[AD-758027] 15 p1840 N73-24910
Statistical method used to examine stability of cylindrical shell under influence of axial forces
[AD-759394] 16 p1970 N73-25938
Vibration stability contact and interfacial crack propagation for partially delaminated layered circular cylindrical shells
20 p2476 N73-29891

**SHELL THEORY**
Analysis of shell theory parameters to determine relationship between stress and displacement fields predicted by shell theory and corresponding actual fields
[WTHD-40] 05 p0602 N73-14895
Recent results in general theory of elastic shells
[AD-749091] 05 p0603 N73-14907
Application of three dimensional theory of elasticity to dynamic response of freely supported circular cylindrical shell
06 p0725 N73-15921
Development of mixed finite-difference scheme for free vibration analysis of simply supported closed noncircular cylindrical shells
[NASA-TN-D-7107] 07 p0852 N73-16908
Shell model for phonon dispersion anomalies and lattice instabilities in hard metalcarbides-nitrides and transition metals
08 p0951 N73-17783
Shell theories by direct approach based on Cosserat surface theory
[AD-754803] 11 p1346 N73-20924
Shell theory and three dimensional analysis of cylindrical shells subjected to axisymmetric tangential surface loads
13 p1584 N73-22838
Higher-order shell equations for vibrations of thick orthotropic circular cylindrical shells
[AD-756649] 13 p1589 N73-22884
Higher-order shell theory for thick circular cylinders under arbitrary load and boundary conditions
[AD-756648] 13 p1589 N73-22885
Numerical analysis of free vibrations of ring stiffened toroidal shells based on linear shell theory
15 p1837 N73-24888
Dual finite element and shell theory analyses of linear and nonlinear structures
[AD-758790] 16 p1970 N73-25933
Derivation of equations for multilayer anisotropic shells with lateral shift considered
[AD-762224] 19 p2351 N73-28908
Structure of high spin particle propagator
[DPGU-01-73] 20 p2456 N73-29734
Matrix displacement analysis of shells using curved SHEBA elements to approximate surface geometry
[ISD-134] 20 p2483 N73-29947

**SHELLS (STRUCTURAL FORMS)**
NT ANISOTROPIC SHELLS
NT CIRCULAR SHELLS
NT CONICAL SHELLS
NT CYLINDRICAL SHELLS
NT DOMES [STRUCTURAL FORMS]
NT ELASTIC SHELLS
NT HEMISPHERICAL SHELLS
NT LIQUID FILLED SHELLS
NT METAL SHELLS
NT ORTHOTROPIC SHELLS
NT PERFORATED SHELLS
NT RADOMES
NT REINFORCED SHELLS
NT SPHERICAL CAPS
NT SPHERICAL SHELLS
NT THIN WALLED SHELLS
NT TOROIDAL SHELLS
Computer program for stress, stability, and vibration analyses of segmented, ring-stiffened, branched shells of rotation
[NASA-CR-2116] 02 p0237 N73-11931
Development of mathematical relationships to define the behavior of multilayer, thin shell structures under various conditions of shear and bending
02 p0238 N73-11936
Linear and nonlinear analysis of static equilibrium stability, and vibrations of shell of revolution subjected to unsymmetric loadings
[AD-745967] 02 p0238 N73-11939
Nondestructive evaluation of stability of shells and development of mechanical device for crash simulator
04 p0480 N73-13922
Application of finite element method to determine deformation of elastic plates, shells, and membranes
[AD-749565] 04 p0483 N73-13946
Analysis of shell theory parameters to determine relationship between stress and displacement fields predicted by shell theory and corresponding actual fields
[WTHD-40] 05 p0602 N73-14895
Limit equilibrium of axially symmetrical shells made from multilayered structurally-orthotropic and uniform material
[AD-747715] 05 p0603 N73-14905
Finite element method with continuity of slope for stress analysis on arbitrary shell
[PB-211759] 05 p0604 N73-14909
Research on theory of plates and shells including bending of rectangular cantilever beam and problems in nonsymmetric deformation of mildly sloping shells
[AD-750991] 06 p0729 N73-15946
Development of mixed finite-difference scheme for free vibration analysis of simply supported closed noncircular cylindrical shells
[NASA-TN-D-7107] 07 p0852 N73-16908
Theory for nonlinear collapse analysis of shells with general shape
[AD-751702] 07 p0853 N73-16916
Development of series of computer programs for structural analysis of axisymmetric shell structures to analyze different modes of structural response
[NASA-CR-2085] 08 p0966 N73-17897
Stress and displacement of structures consisting of alternatingly elastic and hyperbolic paraboloidal shells with rectangular planform
[PB-212649] 08 p0967 N73-17902
Effects of spatially varying curvature on dynamics of cylindrical panels and stiffened cylindrical shell structures
[AD-752590] 08 p0967 N73-17907
Procedures for calculating sonic fields radiated and diffracted by elastic bodies and passage of sound through elastic plates and shells - Vol. 2
[JPRS-58146-2-PT-2] 09 p1015 N73-18284
Univac 1108 computer for three dimensional stress analysis of complex structures
[AD-753211] 09 p1096 N73-18944
Distribution and concentration profiles of stress adjacent to orifices in glass fiber-reinforced plastic plates and shells
[AD-753041] 09 p1096 N73-18945
Static, vibration, and thermal stress analyses of laminated plates and shells by hybrid-stress finite element method including transverse shear deformation effects
[AD-753651] 09 p1097 N73-18955
Analysis of structural response of light aircraft to crash loadings based on dynamic buckling of discretely stiffened shells
10 p1219 N73-19910
Vibration analysis of shallow spherical sandwich shells based on effects of thickness-shear deformation and rotary inertia
12 p1462 N73-21843
Limit equilibrium of axially symmetrical shells made from multilayered structurally-orthotropic and uniform materials
[NLL-DRIC-TRANS-2854-[3623.66]]
12 p1462 N73-21844
Analysis of large deflections of rectangular plates with nonlinear elasticity and hollow shells with hinge-supported edges under external normal pressure uniformly distributed over surface
[AD-756103] 13 p1587 N73-22870
Equations of motion for shell developed in general orthogonal coordinates using Hamilton principle
[AD-755239] 13 p1588 N73-22878
Variational principle for finite deformations of quasi-shallow shells
[AD-756187] 13 p1589 N73-22886
Numerical analysis of thermoelastic state of shells subjected to thermal impact on the surface of the shell
14 p1715 N73-23912
Computer programs for analysis of shell structures in general and fiber reinforced rocket engine cases
[AD-756465] 14 p1716 N73-23926
Analysis of free transverse oscillations of closed prismatic shell of flexible rectangular panels and filled with compressible inviscid liquid
[AD-755416] 14 p1716 N73-23927
Development of finite difference method for calculating boundary value problem for nonsymmetrical deformation of random shells of revolution
[NLL-DRIC-TRANS-2996-[3623.66]]
15 p1836 N73-24884
Numerical analysis of free vibrations of ring stiffened toroidal shells based on linear shell theory
15 p1837 N73-24888
Formulation and checkout problems for computer code for analyzing large deflection elastic-plastic dynamic response of stiffened shells of revolution
[NASA-CR-132044] 15 p1839 N73-24902
Mathematical methods of calculating strength of thin walled elastic systems
[AD-758028] 15 p1840 N73-24911
Viscoplastic characteristics of structural shells
[AD-758074] 15 p1841 N73-24915
Analysis of residual stresses in pressure displacement converter diaphragm occurring during manufacturing
16 p1968 N73-25921
Computer program for dynamic analysis of shells of revolution
[NASA-CR-132752] 17 p2001 N73-26177
Analysis of structural stability of shells weakened by holes to develop numerical analysis of stress concentration
17 p2093 N73-26929
Numerical technique for determining thermo-elastic deformations in segment of hollow cylinder subjected to varying forces
[AECL-4308] 17 p2094 N73-26939
Selected articles concerning theory of plates and shells
[AD-759391] 17 p2095 N73-26945
Theoretical-experimental method of investigating stability of plates and shells
[AD-759242] 17 p2095 N73-26947
Dynamic plastic behavior of metal shell intersection
[AD-760012] 17 p2095 N73-26952
Computer program incorporating capability to perform free vibration analysis for natural frequencies
[AD-761370] 18 p2204 N73-27792
Nonlinear vibrations and failure of shallow shells of random shape under stress of white noise
[AD-761449] 19 p2349 N73-28898
Modification of input/output procedures to computer code for structural analysis of general shells
[AD-761806] 19 p2350 N73-28905
Development of numerical procedures for buckling analysis of truncated conical shells with rigid edge constraint using load displacement criterion
20 p2477 N73-29894
Nonlinear parametric vibrations of closed cylindrical shells
20 p2482 N73-29939
Computer analysis to three structural shell problems, including linear stress, free vibration, bifurcation buckling, elastic and inelastic collapse, and transient response
[AD-762946] 20 p2483 N73-29949
Comprehensive computer code for collapse of general shape shells
[AD-762543] 20 p2484 N73-29951
Computer program for elastic-plastic dynamic analysis of shells of revolution by finite element method
[AD-764244] 22 p2726 N73-31812
Theoretical analysis background for shell theory automated for rotational structures [STARS-2] program - Vol. 1
[NASA-CR-2273-VOL-1] 23 p2854 N73-32801
Procedure for structural analysis of stiffened shells of revolution to describe computer program and types of shapes and cross sections of specimens - Vol. 2
[NASA-CR-2273-VOL-2] 23 p2854 N73-32802
User manual for shell theory automated for rotational structures [STAR 2B, 2V] - Vol. 3
[NASA-CR-2273-VOL-3] 23 p2854 N73-32803
Engineering programming information for digital computer program developed for structural analysis of shells - Vol. 4
[NASA-CR-2273-VOL-4] 23 p2854 N73-32804
Engineering programming information for digital computer program developed to analyze buckling characteristics of shell structures - Vol. 5
[NASA-CR-2273-VOL-5] 23 p2854 N73-32805
Engineering programming information for digital computer program developed to analyze vibration effects on shell structures - Vol. 6
[NASA-CR-2273-VOL-6] 23 p2854 N73-32806
Satellite programs for computer program applied to structural analysis of shells to include user and programming information - Vol. 7
[NASA-CR-2273-VOL-7] 23 p2854 N73-32807
Development of set of equations for analysis of thick shell structures to include effects of geometric thickness and transverse strain
24 p2987 N73-33870
Variational method for numerical analysis of bending and supercritical behavior of heterogeneous slightly curved plates
[AD-765543] 24 p2990 N73-33891

**SHELTERS**
Design of ground electronic equipment shelters in mobile systems for military ground support application
[AD-748808] 04 p0400 N73-13253
Analysis of temperature conditions in hermetically sealed room to determine human tolerances under various climatic conditions
[FOA-1-A-1527-76] 07 p0854 N73-16924

**SHIELDING**
NT ELECTROMAGNETIC SHIELDING
NT HEAT SHIELDING
NT MAGNETIC SHIELDING
NT RADIATION SHIELDING
NT RADIO FREQUENCY SHIELDING
NT REENTRY SHIELDING
NT SOLAR RADIATION SHIELDING
NT SPACECRAFT SHIELDING
Plastic sheaths as lightning conductors for insulating communication cables
[AD-750642] 06 p0647 N73-15252
Shielding lengths in magnetospheric and interplanetary plasmas
[AD-760795] 18 p2147 N73-27352
Cable driver and technique for testing shielding effectiveness of exterior connectors for Pershing missile cable shields
[AD-764236] 22 p2645 N73-31196
Assessment of jets as acoustic shields by comparison of single and multitube suppressor nozzle data
[NASA-TM-X-71450] 24 p2904 N73-33179

**SHIFT REGISTERS**
Linear shift register with feedback logic for generating pseudonoise linear recurring binary sequences
[NASA-CASE-NPO-11406] 03 p0268 N73-12175

Two-phase charge-coupled shift registers
[NASA-CR-2148] 07 p0761 N73-16187
Shift register with feedback for generating pseudorandom binary sequences
[REPT-6707] 08 p0887 N73-17183
Design and performance of metal oxide semiconductor analog shift register as image sensor and reading aid for blind persons
[AD-753259] 09 p1075 N73-18776
Family of m-ary linear feedback shift register with binary logic
[NASA-CASE-NPO-11868] 11 p1264 N73-20254
Plasma cell array for capacitor-coupled shift register
[AD-758310] 14 p1639 N73-23285
Nonrecursive counting digital filter containing shift register
[NASA-CASE-NPO-11821-1] 17 p2000 N73-26175
DOT blocking shift register and tip blocking for ferromagnetic research
[AD-763086] 20 p2365 N73-29017
Design and construction of thin magnetic film shift register
[NHK-LABS-NOTE-164] 20 p2379 N73-29112
Propagation schemes and domain distribution in magnetic shift registers for domain memory devices
20 p2461 N73-29779
Hybrid computer multiplication-division modular unit for ASMODEE minicomputer noting three state gate circuits, integrated circuits, and algorithms
[LAAS-TNPE-73-I-07] 23 p2761 N73-32094
Event sequence detector with several input and shift register responsive to clock pulses
[NASA-CASE-NPO-11703-1] 23 p2768 N73-32144
Two phase, charge coupled shift registers using polysilicon gates overlapped by aluminum gates
[NASA-CR-132304] 24 p2968 N73-33722

**SHIMS**
U COMPENSATORS

**SHIP HULLS**
Numerical analysis of radiation damping of thin finite rectangular plates immersed in heavy and light fluid media
[AD-746460] 01 p0115 N73-10950
Calculated relationships of potential distribution over ship hulls for electrochemical protection from seawater corrosion
[DRIC-TRANS-2877] 02 p0149 N73-11208
Structural behavior of glass hulls under external hydrostatic and cyclic pressure
[AD-746878] 03 p0362 N73-12947
Orthogonal coordinate systems for three dimensional boundary layer calculations on ship hull geometry
[AD-749774] 05 p0529 N73-14301
Analytical methods for evaluating high performance ship design concepts particularly hydrofoil concepts
[AD-759376] 17 p2009 N73-26251
Boundary layer calculation and wind tunnel model test of ships
24 p2909 N73-33214

**SHIP PROPULSION**
U MARINE PROPULSION

**SHIPS**
NT AIRCRAFT CARRIERS
NT SATELLITE COMMUNICATIONS SHIPS
NT SUBMARINES
NT TANKER SHIPS
Satellite communication terminal for ships
01 p0026 N73-10204
Design and evaluation of inertial microphone headset system
[AD-745088] 01 p0032 N73-10254
Application of time frequency techniques to improve navigation of ships and reduce risk of collision
[NASA-TT-F-14718] 02 p0207 N73-11679
Tasks analyses to determine technical personnel requirements for maintenance of Navy microelectronic shipboard equipment
[AD-748040] 04 p0384 N73-13123
Environmental control unit for damage control suit system for use during shipboard operations
[AD-749025] 04 p0384 N73-13125
Shipboard antenna height effect on ultrahigh frequency surface of air communication
[AD-748203] 04 p0390 N73-13171
Analysis of geometrical, analytical, and semi-analytical inertial navigation systems for application to shipbuilding industry
[JPRS-57694] 04 p0447 N73-13650
Satellites for mobile aircraft and ship communications
04 p0472 N73-13852
Four-component wind coefficients for nine different ship models
[A-3] 05 p0523 N73-14256
Performance tests with halogenated hydrocarbon-foam generating fire extinguishing system for ships
[AD-749022] 05 p0612 N73-14975
Reliability analysis of digital computer used in system for ship navigation
[AD-750990] 06 p0697 N73-15687
National transportation statistics summaries for 1960 to 1970
06 p0732 N73-15969
Operation and maintenance of shipboard meteorological systems
[AD-751691] 07 p0816 N73-16617
Computerized simulation of roll and pitch effects on shipboard antenna radiation patterns
[AD-754348] 11 p1258 N73-20212
Effectiveness and cost of high performance watercraft for selected missions of US Coast Guard
[AD-754917] 11 p1268 N73-20295
Digital simulation method to study wind tunnel model ship configurations
[AD-755005] 11 p1273 N73-20333
Determination of ships orientation from accelerometer signals
11 p1319 N73-20703
Analysis of procedures and problems involved in operating helicopters from decks of ships
12 p1357 N73-21010
Determination of ship positions in broad ocean areas using C band radar tracking data
[NASA-CR-62086] 13 p1491 N73-22083
Design specifications for shipborne real time environmental data processing system
[AD-757458] 14 p1638 N73-23283
Analysis of meteorological parameters and climatological effects leading to heavy icing of ships
[NLL-M-22981-[5828.4F]] 16 p1935 N73-25657
Management concept for reliability assurance from aerospace industry experience applied to shipbuilding
[MBB-UA-60-72-O] 17 p2099 N73-26980
Computerized optimal ship routing considering ocean meteorological charts
[AD-761620] 19 p2319 N73-28652
Calculation of dynamic response of ship structural members consisting of beams and rectangular plates
[AD-762008] 19 p2350 N73-28902
Random errors of marine meteorological observations by ships in tropical Atlantic Ocean
20 p2447 N73-29659
Formation and prevention of ice on ships
[NLL-M-23007-[5828.4F]] 21 p2528 N73-30270
Speech recognition in disturbed ship radio communication systems
[FTZ-416-TBR-5] 22 p2633 N73-31104
Use of differential magnetometers with mobile carriers for earth magnetic field measurements
22 p2671 N73-31398
Compensation of static fields for ferrosonde magnetometer mounted on mobile carrier
22 p2672 N73-31400
Computerized simulation of interactions of VTOL aircraft taking off from or landing on deck of ship moving in irregular or random seaway
[AD-764865] 23 p2746 N73-31980

**SHIVERING**
NT DITHERS

**SHOCK ABSORBERS**
Statistical analysis of impact injuries to seated human responding to square wave energy absorption of vertical deceleration pulse representing helicopter crash
[AD-745919] 02 p0136 N73-11102
Development of statistical technique for determining injury reduction capability of energy absorber equipment
[AD-749333] 05 p0497 N73-14044
Use of cyclic struts as energy absorbers for Apollo couch
09 p1088 N73-18881
Physical properties of ply-tear webbing energy absorber
09 p1089 N73-18886
Effects of trapped air on operation of aircraft hydraulic systems and methods for removing air contamination
[NLL-NEL-TT-2420-[6075.461]]
11 p1232 N73-20005
Numerical analysis of aircraft shock absorber operation to show initial charging, motion, and force parameters during static and dynamic compression of landing gear
[AD-754609] 11 p1236 N73-20031
Development and characteristics of supporting frame to isolate payloads from multi-gravitational forces
[NASA-CASE-MFS-21680-1] 11 p1297 N73-20525
Shock absorbing systems used by US guided missile silos
[AD-761577] 19 p2356 N73-28954
Viscoelastic shock absorbing mount for electrical circuit board
[NASA-CASE-NPO-13253-1] 22 p2677 N73-31445

**SHOCK DIFFUSERS**
U DIFFUSERS
U SHOCK WAVE ATTENUATION

**SHOCK DISCONTINUITY**
Microwave reflection from electron density ramps produced behind shock waves in nitrogen oxygen mixtures
07 p0824 N73-16682
Nonlinear interaction of fast magnetogasdynamic shock with tangential discontinuity
[NASA-TM-X-69178] 14 p1695 N73-23754
Numerical integration techniques for shock discontinuity in one dimensional unsteady channel flow
[PUBL-138] 22 p2654 N73-31258

**SHOCK FRONTS**
Calculation of shock normals using least squares technique on combined magnetic field and plasma data from single spacecraft
01 p0097 N73-10798
Calculating shock front for terminal flow of solar wind
17 p2079 N73-26816

**SHOCK HEATING**
Solar atmospheric heating model for mechanical heating in stellar chromospheres
04 p0466 N73-13797
Increased plasma stability in shock heated toroidal z-pinch using preionization
[LA-DC-72-726] 05 p0583 N73-14749
Shock heating of plasmas based on superposed superconducting circuits and magnetic energy storage
[TRITA-EPP-72-29] 07 p0829 N73-16717
Effects of heating within oblique shock wave on its aerothermodynamic and geometric properties
[DLR-FB-73-21] 16 p1858 N73-25050
Semiempirical solution of six types of shock interference heating in hypersonic flows
[NASA-TN-D-7139] 16 p1888 N73-25283
Computer programs for predicting supersonic and hypersonic interference flow fields and heating
[NASA-TM-X-2725] 16 p1889 N73-25285

**SHOCK LAYERS**
Inverse method for calculating hypersonic flow shock layer around axisymmetrical two-dimensional blunt bodies
[ISL-42/71] 01 p0041 N73-10325
Implicit finite difference scheme for fully coupled solution of viscous shock layer including effects of radiation and strong blowing
[NASA-TR-R-388] 02 p0156 N73-11266
Shock wave structure in gas consisting of ideally elastic, rigid spherical molecules
12 p1418 N73-21488
Problems associated with measuring VUV radiation in shock layer around hypersonic reentry vehicles
[AD-757150] 14 p1693 N73-23740
Viscous shock layer in hypersonic flow of perfect gas past axisymmetric blunt nosed body
15 p1764 N73-24297

**SHOCK LOADS**
NT BLAST LOADS
Electrical properties of silicon semiconductor under shock loads
[AD-759003] 16 p1971 N73-25945
X ray diffraction analysis of single crystals of high purity copper subjected to shock loading
[AD-762146] 19 p2311 N73-28586

**SHOCK MEASURING INSTRUMENTS**
Development of pulsed power strain gage system for use in presence of high amplitude electrical noise
[SC-DC-72-1413] 07 p0801 N73-16503

**SHOCK RESISTANCE**
NT IMPACT RESISTANCE
Thermal shock resistant hafnia ceramic materials
[NASA-CASE-LAR-10894-1] 05 p0564 N73-14584
Sonic boom nitroglycerin resistance noting shock simulation and sonic boom effect on detonation
[ISL-14/72] 07 p0822 N73-16658
Dynamic and static response to blast loads of thin circular plates free or embedded using Timoshenko model and finite difference theory
[ISL-4/72] 09 p1094 N73-18934
Performance of shipping container for electron tube in shock and vibration tests
[AD-754926] 11 p1301 N73-20558
Detonation sensitivity and shock resistance of explosives at impact
[ISL-2/73] 19 p2353 N73-28923

**SHOCK SENSITIVITY**
U SHOCK RESISTANCE

**SHOCK SIMULATORS**
Light gas gun generating high intensity shock waves
[ISL-6/72] 05 p0527 N73-14288

**SHOCK SPECTRA**
Shock test of electron-proton spectrometer structural test unit to verify structural integrity of spectrometer design and to analyze shock response of electronic housing
[NASA-CR-128698] 08 p0924 N73-17574

**SHOCK TESTS**
Shock tests on rectangular steel beams, relation of tension-compression properties to moment-curvature equation, and viscoelastic cantilever beam response to shock
[AD-748656] 04 p0482 N73-13941
Shock test of electron-proton spectrometer structural test unit to verify structural integrity of spectrometer design and to analyze shock response of electronic housing
[NASA-CR-128698] 08 p0924 N73-17574
Model of jet aircraft shock cell noise generation and reduction
[NRC-12923] 10 p1188 N73-19666

Maximum and minimum possible values of dynamic load factors for damped and undamped simple oscillators
[AD-755168] 13 p1588 N73-22875

SHOCK TUBES
NT SHOCK TUNNELS
Shock tube measurements of surface oxidation rates of soot formed during combustion of hydrocarbon fuels
[FML-PUBL-72-8] 01 p0023 N73-10176
Shock deactivation cross sections of metastable barium and thallium atoms in shock tube
[MPI-PAE/EXTRATERR-65] 02 p0214 N73-11734
Shock tube generated blast loads on panels in steel structures
[REPT-1/72] 02 p0237 N73-11926
Heating characteristics of internal resistance
[NASA-TN-D-7070] 03 p0280 N73-12268
Application of small rate theory to resonant acoustic oscillations with damping
[AD-746981] 03 p0337 N73-12745
Nonequilibrium plasma generation by strong shock waves produced in diaphragm shock tube
[BMBW-FBK-72-5] 04 p0405 N73-13301
Numerical simulation and study of collisional plasmas and shock tube phenomena
[COO-3086-15] 05 p0583 N73-14748
Mass spectrometer for investigating hypersonic air flows in shock tube for application to reentry body problems
[BMVG-FBWT-72-20] 07 p0801 N73-16505
Photoionization of room temperature gas by radiation from hot plasma in electromagnetic T-Tubes
07 p0825 N73-16684
Reaction between molecular hydrogen and molecular oxygen subjected to temperature and pressure pulses in shock tubes
[NASA-TM-X-2707] 07 p0854 N73-16928
Simulation of thermal radiation-airblast interaction effects in conical shock tube
[AD-752023] 08 p0893 N73-17229
Fundamental problem of complete expansion into evacuated tube
[AD-751983] 08 p0897 N73-17265
Interaction of two equally strong shock waves reflecting from plane wall in double shock tube
[BMVG-FBWT-72-35] 09 p1011 N73-18254
Cryogenic shock tubes for studying shock wave interactions and generating large Mach number flows
[AD-753134] 09 p1012 N73-18261
Compression of helium to high pressures and temperatures using ballistic piston apparatus with shock tube
[NASA-CR-131230] 10 p1141 N73-19298
Debye parameters of nonideal cesium plasma reached in shock tube
[AD-754015] 10 p1198 N73-19749
Shock tube and wind tunnel calibration tests of large aspect angle total head pressure gage
[AD-755120] 11 p1295 N73-20506
Free piston shock tube driver using two stage compression techinque with intermediate diaphragm
[FFA-AU-765] 12 p1376 N73-21161
Development of electrically driven shock tube for generation of high velocity shock waves and analysis of physical properties of shock waves
[AREAEE-149] 12 p1388 N73-21258
Diamagnetic measurements of electrically driven shock tube to determine general conditions of moving plasma in longitudinal magnetic field interactions
[AREAEE-145] 12 p1429 N73-21583
Effects of nozzle geometry and diaphragm location on starting process in Ludwieg tubes
[AD-755357] 13 p1511 N73-22248
Use of finite difference theory to calculate nonsteady flow in linear magnetohydrodynamic generators
[AD-755203] 13 p1564 N73-22673
Design and development of shock tube facility for eliminating effect of plane walls on plane shock waves
[BMVG-FBWT-72-35] 15 p1766 N73-24307
Ionizational relaxation in shock-heated mercury vapor
15 p1816 N73-24719
Research on fluid codes and heat transfer in shock tubes
[COO-3086-17] 17 p2068 N73-26733
Hypersonic, shock tube generated, plasma flow interaction with strong magnetic fields, studied by interferometric, pressure, and light emission measurements
[IPF-72-2] 17 p2069 N73-26738
TOPAL computer program for investigating metal-liquid thermal interactions under shock tube conditions
[GRO/44/91/26-PT-1] 18 p2125 N73-27174
Analysis of shock wave strenghtening by positive density gradient in cryogenic shock tube
20 p2386 N73-29173
Velocity and attenuation of wave fronts generated by double diaphragm shock tube
[CEA-R-4365] 22 p2647 N73-31210
High temperature decomposition of propylene in single pulse shock tube to determine products of decomposition and rate of decomposition
[TAE-172] 23 p2754 N73-32036
Dynamic testing of fabrics and Mylar in shock tubes
[NASA-CR-132284] 23 p2770 N73-32157
Measurements of temperature and pressure behind incident and reflected shocks in shock tube
[ARC-CP-1239] 24 p2909 N73-33220
Piezoelectric pressure transducers for shock tubes, noting electrostatic calibrator
[ARC-CP-1240] 24 p2910 N73-33221

SHOCK TUNNELS
Shock wave generation with rechargeable compressed air bottles for large diameter shock tunnel
[REPT-2/72] 02 p0151 N73-11228
Analysis of hydrogen mixing and combustion in hypersonic air stream to show hydrogen concentration and pressure distribution
[AD-746341] 02 p0243 N73-11978
Numerical analysis of shock tunnel performance operated by reflected shock technique to determine effects of disturbance to flow at nozzle entry caused by reflected waves
[ARC-R/M-3265] 15 p1725 N73-23999
High enthalpy arc-heated helium shock tunnel for gas dynamic research
[NASA-TM-X-2814] 16 p1885 N73-25258
Pilot model expansion tunnel test flow properties obtained from velocity, pressure, and probe measurements
[NASA-TN-D-7310] 24 p2905 N73-33182

SHOCK WAVE ATTENUATION
Shock wave generation and attenuation in tunnel noting computer programming based on characteristics method
[ISL-36/71] 04 p0406 N73-13305
Shock wave propagation and attenuation in tunnels noting computer programming based on method of characteristics
[ISL-11/72] 04 p0406 N73-13307
Shock wave attenuation in foam water mixtures containing Freon and exposed to hydraulic impact
[AD-748350] 04 p0407 N73-13318
Scale model evaluation of fiber glass wedge and parabolic deflector efficiencies in cylindrical ballistic ranges using pressure transducer measurements
[DREV-TN-2031/72] 06 p0649 N73-15270
Solar flare particle energization by magnetic field reconnection and shock reflection
19 p2336 N73-28799
Sound wave, Alfven wave and heat flow effects on normal shock waves noting shock wave attenuation, Rankine-Hugoniot relation extension, and application to interplanetary shock waves
24 p2965 N73-33701

SHOCK WAVE CONTROL
Numerical analysis of parameters of shock waves and dependence on angle of incidence and amplitude of shock wave
[AD-763157] 21 p2526 N73-30253

SHOCK WAVE GENERATORS
NT SHOCK TUBES
NT SHOCK TUNNELS
Shock wave generation and attenuation in tunnel noting computer programming based on characteristics method
[ISL-36/71] 04 p0406 N73-13305
Auroral infrasonic shock wave generation by supersonic electrojet arcs
05 p0508 N73-14137
Acoustic gravity wave generation by transient sources in isothermal atmosphere
05 p0508 N73-14139
Light gas gun generating high intensity shock waves
[ISL-6/72] 05 p0527 N73-14288
Theta pinch generation of ionizing shock waves in argon plasma
[AD-751659] 07 p0829 N73-16721
Cryogenic shock tubes for studying shock wave interactions and generating large Mach number flows
[AD-753134] 09 p1012 N73-18261
Analysis of structure of collisionless shock waves using oblique shock apparatus and calculation of effects of various dissipative mechanisms
12 p1390 N73-21268
Examination of Q switched ruby laser produced spherical shock waves
13 p1508 N73-22220

SHOCK WAVE INTERACTION
Analysis of hydrogen mixing and combustion in hypersonic air stream to show hydrogen concentration and pressure distribution
[AD-746341] 02 p0243 N73-11978
Finite difference method for calculating interaction between spherical shock waves from underwater explosion and ocean surface
[AD-749818] 06 p0656 N73-15325
Laboratory simulation of solar wind interaction with geomagnetic field, and measurements of magnetosphere at shock wave front and of field configuration on noctunal side
[D-15] 06 p0716 N73-15838
Numerical solution of shock wave interaction with supersonic blunt body flow exemplified by circular cylinder and parabolic body
[DLR-FB-72-68] 07 p0736 N73-15990
Numerical analysis of discrete traveling waves which propagate with speed determined by Rankine-Hugoniot relations
[COO-3077-20] 08 p0896 N73-17254
Interaction of two equally strong shock waves reflecting from plane wall in double shock tube
[BMVG-FBWT-72-35] 09 p1011 N73-18254
Interaction of shock wave with turbulent boundary layer at moderate supersonic Mach numbers
10 p1206 N73-19815
Shock wave boundary layer interaction in compressor cascades
10 p1207 N73-19816
Design and development of shock tube facility for eliminating effect of plane walls on plane shock waves
[BMVG-FBWT-72-35] 15 p1766 N73-24307
Sound wave, Alfven wave and heat flow effects on normal shock waves noting shock wave attenuation, Rankine-Hugoniot relation extension, and application to interplanetary shock waves
24 p2965 N73-33701

SHOCK WAVE PROFILES
Shock structure characterization of normal ionizing shock waves in argon
[AD-751594] 07 p0829 N73-16719
Development of electrically driven shock tube for generation of high velocity shock waves and analysis of physical properties of shock waves
[AREAEE-149] 12 p1388 N73-21258
Analysis of shock wave propagation in direction of decreasing air density following aerial explosion
[AD-755173] 12 p1465 N73-21873

SHOCK WAVE PROPAGATION
Turbulent and laminar boundary layer behind blast waves generated in shock tubes
[ISL-5/72] 04 p0406 N73-13306
Shock wave propagation and attenuation in tunnels noting computer programming based on method of characteristics
[ISL-11/72] 04 p0406 N73-13307
Acoustic gravity wave propagation modes in ionosphere and neutral atmosphere following nuclear explosion
[CONTRIB-1799] 05 p0509 N73-14140
Infrasonic wave generation and atmospheric propagation of gravity acoustic waves
05 p0509 N73-14142
Excitation of Lamb atmospheric edge mode by tail of large atmospheric explosion
05 p0509 N73-14143
Hydrodynamic calculations and experimental observations of ionospheric shock front propagation following nuclear explosion
05 p0510 N73-14150
Continuous wave Doppler radar observations of ionospheric disturbances generated by Saturn-Apollo launchings
05 p0511 N73-14157
Infrasonic detection of propagating atmospheric shock waves caused by supersonic aircraft
05 p0512 N73-14161
Shock tube simulation of propagation of shock waves over and beyond walls, including slope effect
[REPT-10/71] 05 p0527 N73-14286
Shock wave reflection from water surface
07 p0769 N73-16250
Numerical analysis of discrete traveling waves which propagate with speed determined by Rankine-Hugoniot relations
[COO-3077-20] 08 p0896 N73-17254
Collisionless ion acoustic shocks with high Mach number in plasma
[IPPJ-119] 08 p0948 N73-17765
Model of shock wave propagation parallel to external magnetic field in hot collisionless plasma with turbulent dissipation based on garden hose instability
[MPI-PAE/EXTRATERR-69] 09 p1071 N73-18736
Development of precursor waves in helium and analysis of wave speed, electron temperatures, and densities using nuclear data handling techniques
12 p1387 N73-21249
Analysis of structure of collisionless shock waves using oblique shock apparatus and calculation of effects of various dissipative mechanisms
12 p1390 N73-21268
Shock wave propagation and attenuation in tunnels noting computer programming based on method of characteristics and wall skin friction
[ISL-17/72-PT-4] 12 p1392 N73-21287
Analysis of shock wave propagation in direction of decreasing air density following aerial explosion
[AD-755173] 12 p1465 N73-21873
Shock heated argon expansion through nozzle and spherical shock wave front
[AD-756455] 13 p1511 N73-22245
Propagation of reflected shock wave after Mach reflection on wedges
[REPT-4/72] 15 p1765 N73-24304
Diffuse shock wave reflection from ridged plates, simulating aerial explosion effects on earth surface
[REPT-7/72] 15 p1766 N73-24305

Design and development of shock tube facility for eliminating effect of plane walls on plane shock waves
[BMVG-FBWT-72-35] 15 p1766 N73-24307
Flare induced magnetohydrodynamic disturbance propagation in solar corona considering Moreton surface waves and type 2 shocks
19 p2339 N73-28816
Plane elastic wave propagation through movable wall, calculating flow distribution behind wall
[DLR-FB-72-59] 21 p2525 N73-30246
Structure of collisionless ion acoustic shocks in plasma device
[NASA-CR-135490] 22 p2783 N73-31651
Shock wave propagation at interface between two rectilinear ducts noting oblique shock waves and mathematical models
[PUBL-137] 24 p2910 N73-33223

SHOCK WAVES
NT DETONATION WAVES
NT NORMAL SHOCK WAVES
NT OBLIQUE SHOCK WAVES
NT SONIC BOOMS

Shock properties for steady, irrotational, transonic flow
[NASA-TN-D-6997] 01 p0040 N73-10314
Numerical analysis of finite-strength, isentropic pressure waves transverse to axis of circular cylinder
[NASA-CR-2138] 01 p0041 N73-10321
Propagation of weak shock wave through slightly inhomogeneous turbulent medium
[AD-745728] 01 p0081 N73-10670
Nonlinear theory using fourth order Hugoniot curves for compression shocks in cubic crystals
01 p0087 N73-10720
Approximate analytic theory of acoustic shock propagation in nonuniform media for motion determination of flare generated, shock wave in corona
01 p0095 N73-10783
Theoretical models of interplanetary shock waves and solar wind disturbances with large scale characteristics
01 p0096 N73-10794
Corotating forward shock at 1 AU
01 p0097 N73-10796
Shock pair observation from HEOS 1
01 p0097 N73-10797
Analysis of solar flare energetics based on shock velocity, ambient solar wind velocity and density, and ambient azimuthal Mach number
01 p0097 N73-10799
Principles of nuclear reactions and different types of nuclear explosions
[AD-745857] 01 p0121 N73-10998
Measurement of shock and detonation wave pressures by means of shock-induced polarization of Plexiglas disks
[TL-1972-4] 02 p0155 N73-11254
Analysis of diffusive separation in front of blunt body in low density binary mixture of supersonic flows using electron beam densitometer
[AD-745960] 02 p0157 N73-11274
Microwave attenuation and neutral gas density profile measurements behind shock waves in air
[AD-745969] 02 p0158 N73-11282
Possible shock effect associated with seaquakes
[NASA-TM-X-66096] 02 p0166 N73-11344
Influence of inhomogeneity on structure of collisionless turbulent shock wave in high beta infinite plasma
[AD-746467] 02 p0217 N73-11756
Greenstadt binary index criterion for distinguishing between laminar and pulsating bow shock crossings expressed as critical angle between shock normal and magnetic field
[NASA-TM-X-66105] 02 p0225 N73-11817
Analysis of short time response of cylindrical, elastic segment to shock wave engulfment based on focusing effects due to curved geometry
[AD-745962] 02 p0238 N73-11940
Procedure for predicting structural and acoustic response of full scale structures to sonic booms using scale models and laboratory techniques
[FAA-RD-72-116] 03 p0251 N73-12029
Analysis of sonic boom data recorded on strain gages mounted on windows to record overpressures and relation to window size
[FAA-RD-72-114] 03 p0251 N73-12030
Pressure fluctuations due to interaction of shock wave with turbulent boundary layer
[NASA-CR-123961] 03 p0281 N73-12281
Development of finite difference techniques for computing static pressure distribution downstream of strong shock wave using navier-Stokes equation
[AD-747978] 03 p0286 N73-12318
Analysis of shock interaction and interference heating on military aerospace vehicles at hypersonic speeds
[AD-747765] 03 p0286 N73-12319
Measurement of heat transfer in gas flow behind shock wave
[AD-747604] 03 p0286 N73-12320
Characteristics of flow around bluff body at supersonic speed with emphasis on leading shock wave formation and changes in withdrawal value for argon and nitrogen
[AD-747407] 03 p0287 N73-12325
Analysis of laser induced two dimensional wave motions in hydrogen plasma
[AD-746681] 03 p0343 N73-12798
Corrections for sidewall waveguide slots to microwave transmission data for shock-ionized air
[AD-748075] 03 p0343 N73-12801
Flare-associated interplanetary shock data of 15-16 Feb. 1967 analyzed for estimation of ecliptic plane geometry of shock surface near 1 AU
[NASA-TM-X-66115] 03 p0353 N73-12875
Analysis of magnetogasdynamic shock fronts caused by solar winds and development of theoretical concepts and models for phenomenon
[NASA-TM-X-66106] 03 p0353 N73-12876
Measurement of pressure in Mach reflection of strong shock waves in shock tube
[AD-746613] 03 p0368 N73-12995
Development of mathematical model for viscous inviscid interaction analysis and solution of boundary layer equations by finite difference scheme
[AD-748342] 04 p0408 N73-13322
Fabry-Perot laser interferometer for studying atomic collisional rate and ionization relaxation time in helium shock wave
[AD-749553] 04 p0408 N73-13326
Stress behavior of lithium fluoride crystals exposed to shock wave impact
[AD-748267] 04 p0460 N73-13757
Analysis of acoustic properties of shock associated noise in narrow band spectrum produced by jet flows - Vol. 5 App. 2
[AD-749142] 05 p0496 N73-14040
Characteristics of mixing shock in mixing tube of water jet-gas pump to determine pressure distribution
[WTHD-31] 05 p0526 N73-14281
Prediction of shock shapes and wall shock traces encountered in secondary injection into conical rocket nozzle
[AD-750081] 05 p0528 N73-14295
Shock wave instability in one dimensional and two dimensional problems
[AD-750009] 05 p0528 N73-14298
Numerical analysis of two dimensional shock wave resulting from mobile wedge moving with supersonic velocity and specific angle of attack into detonation wave
[AD-749650] 05 p0528 N73-14299
Multiple tone acoustic radiations phenomenon in transonic fans
[ARC-CP-1226] 05 p0580 N73-14726
Aerodynamic heating of supersonic models due to shock wave impingement
[AD-749946] 06 p0655 N73-15324
Effect of high pressure shock waves on mechanical properties of bimetals produced by different cladding techniques
[AD-750958] 06 p0677 N73-15513
Aerodynamic configurations and characteristics of airfoils designed to reduce formation of shock waves during supersonic flight
[NASA-TT-F-749] 07 p0736 N73-15987
High temperature reactions of COF2 with CO and H2 in excess argon behind reflected shock waves
[AD-751270] 07 p0753 N73-16118
Numerical analysis of oscillating wedge in supersonic perfect gas flow to evaluate trends for wedge and to analyze unsteady flows
07 p0767 N73-16235
Solution of viscous shock-layer equations using implicit finite difference scheme for hyperboloid body under conditions simulating atmospheric entry
07 p0768 N73-16238
Mathematical model for reflection of shock waves
[REPT-9/71] 07 p0794 N73-16453
Plasma instability saturation by resonant mode coupling of shock waves
[AD-751538] 07 p0829 N73-16722
Gas ionization and plasma generation by explosive shock wave
[AD-751152] 07 p0829 N73-16725
Analysis of uniform jet flow around airfoil with separated shock wave at low supersonic velocities of incident flow
[NASA-TT-F-14813] 08 p0896 N73-17259
Angles of attack for shock wave detachment from sharp leading edge of five delta wing models with flat compression surfaces
[AD-752206] 08 p0898 N73-17271
Focusing effects of distortion of near sonic shocks by weakly turbulent layers with random temperature and pressure variations
[AD-752472] 08 p0899 N73-17279
Technique for predicting shock envelopes and pressure distributions for two dimensional airfoil at angles of attack producing shock detachment and subsonic flow
[NASA-TN-D-7197] 09 p0979 N73-18001
Flight test measurements and analysis of sonic booms to determine caustics produced by variations in flight speed and to develop method for predicting shock wave-ground intersections
[NASA-CR-2167] 09 p0982 N73-18022
Development of model for analyzing propagation of weak normal shock wave through turbulent atmosphere and application to sonic boom characteristics
[NRC-12981] 09 p0983 N73-18028
Mach reflection in solids, liquids, and explosives using annular shock wave generated by explosion of cylinder coatings
[BMVG-FBWT-72-3] 09 p1016 N73-18292
Solution of Chaplygin equation by straight line method to describe gas flow around profile at high subsonic speed with local supersonic curved shock wave
[AD-753557] 09 p1019 N73-18318
Nonstationary shock models and wear processes
[AD-753117] 09 p1042 N73-18497
Influence of shock-producing piston on structure of electrostatic ion acoustic laminar shocks
[NASA-CR-130994] 09 p1069 N73-18724
Dissociation of HBr behind shock waves and at temperatures from 1450 to 2300 K in pure HBr
[AD-753395] 10 p1143 N73-19310
Dynamic functions of air blast parameters in detonation of spherical trinitrotoluene charge
[AD-753805] 10 p1187 N73-19659
Computer program for calculating structure and supersonic combustion flow with chemical reactions and shock waves
[NASA-CR-112303] 11 p1271 N73-20311
Geometrical shock wave transmission model used to determine water surface peak spall velocities above single charge cratering detonations in medium overlain with water
[AD-755099] 11 p1273 N73-20329
Variable energy blast wave theory applied to two phase detonation and liquid monopropellant ignition by shock wave
[AD-754525] 11 p1333 N73-20818
Construction of discrete models of nonlinear wave phenomena in elastic rods based on finite element analysis of shock waves in hyperelastic solids
[AD-754953] 11 p1346 N73-20921
Development of precursor waves in helium and analysis of wave speed, electron temperatures, and densities using nuclear data handling techniques
12 p1387 N73-21249
Development of electrically driven shock tube for generation of high velocity shock waves and analysis of physical properties of shock waves
[AREAEE-149] 12 p1388 N73-21258
Analysis of mean and fluctuating flow properties of compressible turbulent boundary layer in shock wave-induced adverse pressure gradient
[NASA-TN-D-7092] 12 p1391 N73-21280
Integration of nonlinear differential equations describing one-dimensional steady flow across normal shock wave, considering transport, degree of freedom relaxation, and chemical reactions
[DLR-FB-72-54] 12 p1392 N73-21288
Diamagnetic measurements of electrically driven shock tube to determine general conditions of moving plasma in longitudinal magnetic field interactions
[AREAEE-145] 12 p1429 N73-21583
Analysis of low density plasma shock waves in expanding discharge
12 p1432 N73-21602
Transient processes due to interaction of shock produced plasma flows with magnetic fields
[IPP-4/41] 12 p1435 N73-21628
Bibliography on shock waves in solids
[AD-755429] 12 p1441 N73-21679
Influence of small periodic oscillations on viscous shock waves structure and sonic boom rise time caused by supersonic transport vibrations
13 p1507 N73-22217
Research projects on wake turbulence and atmospheric boundary layers, turbulent mixing and shear flows, and high temperature gas dynamics
[AD-755273] 13 p1512 N73-22251
Vibrational relaxation of DF behind incident shock waves
[AD-756462] 13 p1562 N73-22658
Propagation of shock and continuous waves in solid plastic media, and wave interaction with elements of structures
[AD-742421] 13 p1586 N73-22854
Analysis of supersaturation conditions in Mach 7.5 wind tunnel in expansion region of nozzle and technique for visualization of shock waves and shear layers
[ARL/A-139] 14 p1648 N73-23367
Normal shock wave conditions in elements of axial supersonic compressor
[AD-756102] 14 p1650 N73-23384
Application of integral relations to analyzing inviscid supercritical flow about lifting airfoils with embedded shock wave
[AD-755762] 14 p1651 N73-23390
Nonlinear interaction of fast magnetogasdynamic shock with tangential discontinuity
[NASA-TM-X-69178] 14 p1695 N73-23754
Construction of transfer functions in problems of weak shock interactions with cylindrical and spherical surfaces
14 p1715 N73-23913

Numerical analysis of shock tunnel performance operated by reflected shock technique to determine effects of disturbance to flow at nozzle entry caused by reflected waves
[ARC-R/M-3265] 15 p1725 N73-23999
Wind tunnel tests to determine effects of leading edge modifications on flow and forces on untapered wing with 50 degree leading edge sweep and Mach numbers from 0.60 to 1.20
[ARC-R/M-3270] 15 p1726 N73-24003
Analysis of flow pattern on tapered, sweptback wing at Mach numbers between 0.6 and 1.6 and 12 degree angle of incidence
[ARC-R/M-3271] 15 p1726 N73-24004
Analysis of flow development over plane, half-wing with cropped-delta planform using surface pressure distributions and oil flow patterns with variations in incidence and Mach number
[ARC-R/M-3286] 15 p1727 N73-24008
Design and development of shock tube facility for eliminating effect of plane walls on plane shock waves
[BMVG-FBWT-72-35] 15 p1766 N73-24307
Creation shape and flow of tridimensional spark by focused radiation
[NASA-CR-2230] 15 p1766 N73-24311
Development of test facility for determining interaction of sonic boom with surface of body of water
[NASA-TT-F-14917] 15 p1767 N73-24318
Numerical method of characteristics for unsteady propagation processes considering dissipative terms in equations for supersonic mixing processes
[NASA-TT-F-14825] 15 p1767 N73-24320
Electromagnetic dispersion relation for two counterstreaming ion beams flowing parallel to direct current magnetic field
[NASA-CR-132953] 15 p1814 N73-24701
Saddle point method for exact wave plane solution of Burger equation in shock zone
[AD-758409] 15 p1814 N73-24706
Electrical response of capacitor triggered by shock wave effect on Fermi energy level
[AD-759059] 16 p1883 N73-25239
Analysis of electron number density and collision frequency levels behind reflected shock waves and shock wave interactions in argon
16 p1887 N73-25275
Optical and microwave measurements of reaction kinetics behind shock waves
[AD-757230] 16 p1890 N73-25293
Wave compression and expansion effects on laminar gas boundary flow
[AD-759768] 16 p1893 N73-25320
Observation of laminar electrostatic shock waves in collisionless plasma generated by ion beam
[IPPJ-156] 16 p1949 N73-25771
Reflected wave detonation of gaseous mixture in shock tube for simulating hydrogen/oxygen rocket plume
16 p1974 N73-25963
Measurement of effects of sonic booms on light building structures for various building configurations
[RAE-LIB-TRANS-1633] 17 p1981 N73-26011
Structure of weak shock wave in vibrationally relaxing gas undergoing wall reflection
17 p2013 N73-26277
Application of holographic interferometry techniques for determining asymmetric flow distribution encountered near wing-fuselage junction at transonic speed
[AD-759967] 17 p2015 N73-26296
CONSHOC computer program for locating shock waves and contours of flow variables in finite difference flow fields
[AD-759898] 17 p2016 N73-26301
Methods for computing shock flows including one dimensional unsteady flow
[AD-760015] 18 p2131 N73-27219
Possibility of similarity solution to describe flow field at juncture of sonic line and shock in flows with high subsonic Mach numbers
[AD-760801] 18 p2132 N73-27224
Thermomechanical processing of nickel-base superalloys by explosive shock wave deformation
[AD-761218] 18 p2162 N73-27462
Defined shock wave effects on miniature swine, describing organ injuries
19 p2227 N73-27965
Numerical analysis of disturbance pressure due to impinging of plane shock wave of arbitrary strength on moving slender body
19 p2251 N73-28151
Detonation sensitivity and shock resistance of explosives at impact
[ISL-2/73] 19 p2353 N73-28923
Analysis of interaction of detonation wave with boundary gas based on formation of low velocity detonation wave
20 p2384 N73-29153
Effect of shock wave interaction in parallel, two-dimensional, stratified flow of heavy and light gases
20 p2384 N73-29157
Analysis of compressibility of polytetrafluoroethylene when subjected to single stage and two stage shock loading
[NLL-NEL-TT-2491-(6075.461)] 20 p2386 N73-29170
Analysis of shock wave strenghtening by positive density gradient in cryogenic shock tube
20 p2386 N73-29173
Effect of wall cooling on shock wave laminar boundary layer interactions in hypersonic two dimensional flow
[AD-762937] 20 p2389 N73-29192
Analysis of properties of copper, titanium, and nickel specimens following hardening by shock waves at pressures up to 1,200 kilobars
[NLL-RTS-8047] 20 p2428 N73-29500
Analysis of variations in hardness and microstructure of metals subjected to shock wave pressures
[NLL-NEL-TT-2489-(6075.461)] 20 p2429 N73-29514
Laboratory analysis of high Beta collision-free plasma shock waves
20 p2457 N73-29749
Large amplitude electron plasma wave with trailing wave train in collisionless plasma
[IPPJ-163] 20 p2458 N73-29756
Gas dynamics of plane shock wave propagation in steady state moving medium
20 p2472 N73-29860
Effect of surface pressure fluctuations on response of panels underlying attached and separated turbulent boundary layers and shock waves
20 p2479 N73-29910
Development of technique and apparatus for optically detonating insensitive high explosives
[NASA-CASE-NPO-11743-1] 20 p2485 N73-29959
Analysis of sonic boom phenomenon to show generation, propagation, and effects on structures, people, and animals
[ARL/A-NOTE-337] 21 p2493 N73-30007
Motion of sources for type 2 and type 4 radio bursts and flare-associated interplanetary disturbances
[NASA-TM-X-70452] 21 p2507 N73-30117
Analysis of characteristics of initially plane, strong shock wave propagating into conical convergence using multi-crystal piezoelectric probe
21 p2522 N73-30228
Perpendicular fast reverse shock wave found in interplanetary plasma and magnetic field data from Explorers 33 and 35
[NASA-TM-X-70451] 21 p2523 N73-30235
Numerical analysis of parameters of shock waves and dependence on angle of incidence and amplitude of shock wave
[AD-763157] 21 p2526 N73-30253
Numerical analysis of flow characteristics on upper surface of wedge moving at supersonic speed when plane shock wave is incident on wedge
[AD-763283] 21 p2527 N73-30267
Shock wave effects in porous iron
[AD-763796] 21 p2540 N73-30368
Research on nonlinear waves and shock-like phenomena in hot plasmas
[NASA-CR-132808] 21 p2582 N73-30695
Method for estimating drag-rise mach number of smooth, nonducted, axisymmetric bodies at zero incidence without discontinuities in surface slope
[ESDU-71008] 22 p2650 N73-31230
Prediction and measurement of heat transfer rates for shock-induced unsteady laminar boundary layer on flat plate
[NASA-CR-114582] 22 p2651 N73-31241
Time evolution of finite power density blast waves
[AD-763834] 22 p2656 N73-31278
Transit waveform control program for real time environmental shock tests
22 p2732 N73-31860
Analysis of sonic boom characteristics based on second order solutions for flow distribution around slender bodies in supersonic flow - Part 1
[NASA-CR-2339] 23 p2739 N73-31927
Development of wind tunnel with self correcting apparatus based on sensors to determine flow conditions on tunnel surfaces and method for varying wall geometry
[AD-764957] 23 p2771 N73-32161
Shock wave pattern and stability in axial flow supersonic compressor using simulated rotating cascade test facility
23 p2775 N73-32196
Pulsed laser holographic interferometry of shock waves within transonic fan rotors
[NASA-TM-X-71430] 23 p2801 N73-32402
Production of intermetallic compounds by effect of shock waves from explosions and compaction of powder
[NASA-CASE-MFS-20861-1] 23 p2806 N73-32437
Photographic recording of dynamic behavior of flames in explosive gases caused by ignition of equimolar acetylene-oxygen mixture
[NASA-CR-135672] 23 p2856 N73-32825
Flow characteristics of merged layer regime in hypersonic, low density flow past semi-infinite sharp cone
24 p2903 N73-33168
Asymptotic expansion analysis of shock supported arrhenius reactions and ignition delay
24 p2903 N73-33172
Laminar boundary layers at continuously moving wall and behind shock wave, noting fuel combustion problem
24 p2906 N73-33192
Measurements of temperature and pressure behind incident and reflected shocks in shock tube
[ARC-CP-1239] 24 p2909 N73-33220
Propagation of shock waves following explosion of finite cylindrical charge based on finite difference numerical analysis
24 p2991 N73-33907

**SHOOTING STAR AIRCRAFT**
See U T-33 AIRCRAFT

**SHOPS**
Production planning with group techniques for welding shops using component and blank classifications
[NLL-M-22594-(5828.4F)] 05 p0550 N73-14467

**SHORT CIRCUITS**
Failure detector for dc to ac inverter circuit
[NASA-CASE-NPO-13160-1] 14 p1667 N73-23525

**SHORT HAUL AIRCRAFT**
See NT MERCURE AIRCRAFT

Development of mathematical model to analyze traveler acceptance factors in short haul air carrier operations
01 p0004 N73-10023
Flight test program to determine effects of low frequency vibration on passenger comfort in short haul aircraft
01 p0004 N73-10025
Development and characteristics of civilian V/STOL aircraft with application to short haul commercial air traffic
[NASA-TT-F-14629] 01 p0005 N73-10034
Relative economic advantages of 3 STOL aircraft concepts for short haul, high density transportation systems in 1980 time period
[NASA-CR-114466] 01 p0120 N73-10990
Airport planning, economics, computer program, and arena characteristics for short haul, high density transportation systems in 1980 time period
[NASA-CR-114467] 01 p0120 N73-10991
Aircraft accident prevention analysis of air taxi/commuter operations to identify safety factors and enhance safety of operations
[NTSB-AAS-72-9] 05 p0493 N73-14016
Technical and economic feasibility of V/STOL lift-fan commercial aircraft for short haul transport applications
[NASA-CR-2184] 06 p0621 N73-15041
Technical documentation to support V/STOL aircraft implementation and utilization based on short haul air transportation requirements - Vol. 2
[NASA-CR-114518] 07 p0739 N73-16009
Analysis of factors affecting development and operation of satellite airport system as method for relieving congestion at metropolitan airports
07 p0765 N73-16216
Analysis of performance potential of buoyant systems and flexible structures for use with short haul passenger transport aircraft
[NASA-TM-X-62168] 08 p0866 N73-17014
Aerodynamic configuration and predicted performance of short takeoff aircraft for short haul passenger transportation
[CRANFIELD-AERO-12-PT-1] 08 p0867 N73-17019
Conceptual designs of V/STOL lift fan commercial short haul transport aircraft to determine technical and economic feasibility
[NASA-CR-2183] 09 p0984 N73-18038
Analysis of system concepts, design criteria, operating procedures, and terminal facilities for short haul transportation aircraft and supporting systems
[NASA-TM-X-62235] 10 p1105 N73-19013
Economic analysis of high density short haul air market to show aircraft requirements, engine development, and funding sources
[NASA-CR-2227] 10 p1106 N73-19017
Analysis of factors involving commercial application of short takeoff aircraft for short haul airline operations
[NASA-TM-X-62239] 11 p1234 N73-20016
Proceedings of conference on short haul air transportation to show development requirements, economic aspects, and urban and environmental impacts
[M73-54] 14 p1600 N73-22974
Characteristics of Yak 40 aircraft and application for short haul service to isolated areas of USSR
[NASA-TT-F-14943] 16 p1859 N73-25057
Effect of gust loads on wing and T-tail airworthiness requirements for short haul aircraft
[FOK-K-66] 16 p1859 N73-25058
Characteristics of quiet turbofan short takeoff aircraft for short haul air transportation and analysis of economic and sociological factors affecting operation Vol. 1
[NASA-CR-114612] 16 p1860 N73-25065
Analysis of quiet turbofan short takeoff aircraft for short haul air transportation to show research and development requirements and advanced technology benefits - Vol. 2
[NASA-CR-114613] 16 p1860 N73-25066

Program definition study for improvement of short haul air transportation facilities - Vol. 1
[FAA-QS-73-1-VOL-1] 17 p1983 N73-26025
Program definition study for improvement of short haul air transportation to show development requirements and operational constraints - Vol. 2
[FAA-QS-73-1-VOL-2] 18 p2213 N73-27869
Design, development, and characteristics of quiet turbofan short takeoff aircraft for short haul air transportation - Vol. 2
[NASA-CR-114607] 19 p2219 N73-27899
Airport siting, design, cost, operation, and implementation for STOL aircraft short-haul air transportation system - Vol. 3
[NASA-CR-114608] 19 p2219 N73-27900
Marketing survey to determine acceptance and utilization of STOL aircraft for short-haul air transportation system - Vol. 4
[NASA-CR-114609] 19 p2219 N73-27901
Analysis of economic factors affecting operation of STOL aircraft for short-haul air transportation system - Vol. 5
[NASA-CR-114610] 19 p2219 N73-27902
Future of short haul air transport in Western Europe - V/STOL Working Group
[SP-73-001] 22 p2737 N73-31915
Application of short takeoff aircraft for short haul air transportation with identification of critical technology, economics, and social viability
[NASA-CR-135481] 23 p2741 N73-31941
Dynamic response of short haul aircraft to gust loads
[FOK-K66] 23 p2744 N73-31960
Economics, traffic demand, and community acceptance of short haul air transportation system in California Corridor - Vol. 1
[NASA-CR-114634] 23 p2859 N73-32842
Forecast model for predicting economic factors involved in short haul air transportation in California Corridor - Vol. 2
[NASA-CR-114634[1]] 23 p2859 N73-32843
Analysis of commuter air transportation services to define problems and identify methods for improvements in cost effective operations
23 p2863 N73-32885
Operation of low cost local air service carriers to show methods for improving transportation services
23 p2863 N73-32886
Evaluation of new forms of air transport service for improving short haul air travel market
23 p2863 N73-32887
Actions by Civil Aviation Board to regulate and improve commuter air transportation services
23 p2864 N73-32888
Proceedings of conference on short takeoff and landing aircraft to determine aerodynamic characteristics and short haul transportation applications
[NASA-SP-320] 24 p2871 N73-32934
Analysis of short-haul air transportation requirements to include aircraft development programs, economic factors, and environmental considerations
24 p2871 N73-32935
Objectives and findings of study to determine applicability of short takeoff aircraft for short-haul air transportation systems
24 p2872 N73-32936
Economic and environmental aspects of short takeoff aircraft used for short-haul air transportation systems
24 p2872 N73-32937
Short takeoff aircraft technology development related to requirements for expanded and improved short-haul air transportation system capabilities
24 p2872 N73-32938
Short haul aircraft operations in terminal area with concurrent conventional aircraft operations to show methods for improved utilization of facilities
24 p2874 N73-32953
Systems analysis of problems created in terminal area by application of short takeoff aircraft for providing high speed, short haul air transportation service
24 p2874 N73-32958
Specification of thrust control system for Airbus A 300 B, tested in Boeing 707
24 p2877 N73-32981

**SHORT RANGE BALLISTIC MISSILES**

Design optimization of SRAM inertial navigation and guidance
11 p1319 N73-20705

**SHORT TAKEOFF AIRCRAFT**

NT BREGUET 941 AIRCRAFT

Simulated STOL aircraft flight to determine effects of cruise and terminal area maneuvers on ride quality and passenger comfort
01 p0003 N73-10016
Relative economic advantages of 3 STOL aircraft concepts for short haul, high density transportation systems in 1980 time period
[NASA-CR-114466] 01 p0120 N73-10990
Airport planning, economics, computer program, and arena characteristics for short haul, high density transportation systems in 1980 time period
[NASA-CR-114467] 01 p0120 N73-10991
Noise caused by jet exhaust and wing for STOL engine-over-wing configuration
[NASA-TM-X-68159] 02 p0125 N73-11018
Influence of split ground belt on aerodynamic characteristics of high lift STOL aircraft with blown flap
[UTIAS-TN-173] 02 p0152 N73-11230
Suppression of fan noise and effects on short takeoff aircraft systems design
03 p0250 N73-12023
Noise sources and noise scaling laws of externally blown STOL flaps
03 p0250 N73-12024
Design of augmentor wing jet flap configuration with minimum noise generation for jet STOL transport aircraft
03 p0250 N73-12025
Traffic environment and operational procedures for intercity STOL transportation system
[NASA-CR-114523] 03 p0367 N73-12990
Flight tests of rotating cylinder flap on YOV-10 aircraft modified to STOL configuration
[NASA-CR-2135] 04 p0371 N73-13020
Performance tests of Andover C short takeoff transport aircraft on grass, concrete and soil landing sites
[ARC-CP-1220] 04 p0373 N73-13034
Location of soil types with potential for generating atmospheric sand and dust with application to analysis of V/STOL operational environment
[AD-749462] 05 p0495 N73-14033
Establishment of takeoff and landing environment criteria for V/STOL aircraft with emphasis on airborne particle concentration
[AD-749463] 05 p0495 N73-14034
Research on air transport with VTOL and STOL aircraft
[PUBL-1352] 06 p0613 N73-14977
Evaluation of subjective annoyance caused by noise generated by turbofan short takeoff aircraft and comparison with noise of conventional takeoff aircraft
[NASA-TN-D-7102] 06 p0621 N73-15040
Market research, economic analysis, and technology of conventional STOL aircraft in Europe
[DGLR-PAPER-72-54] 06 p0622 N73-15046
Integration of STOL aircraft instruments and approach control for new approach profiles
[DGLR-PAPER-72-096] 06 p0622 N73-15047
Short takeoff aircraft lift augmentation and prevention of airflow separation on cambered elliptical airfoil section using circulation control
[AD-751045] 07 p0736 N73-15992
Development and application of computer programs for evaluating performance of powered-lift STOL aircraft to include static, takeoff, and landing performance
[NASA-TM-X-62217] 07 p0738 N73-16007
Flight simulator evaluations of flight control, flight path, and airspeed for approach and landing of powered lift jet short takeoff aircraft
[NASA-TM-X-62203] 07 p0739 N73-16014
Comparison of mechanical high lift flaps with externally blown flaps for STOL aircraft
[MBB-UH-12-72-O] 07 p0739 N73-16017
Influence of aircraft reliability regulations on STOL takeoff and landing performance
[MBB-UH-13-72-O] 07 p0740 N73-16018
Aerodynamic configuration and predicted performance of short takeoff aircraft for short haul passenger transportation
[CRANFIELD-AERO-12-PT-1] 08 p0867 N73-17019
Design and development of stability augmentation system to eliminate coupling effects during landing of short takeoff aircraft
[NASA-CR-130543] 08 p0867 N73-17021
Analysis of internal flow conditions of inlet with centerbody retracted for short takeoff and landing aircraft takeoff and approach operations
[NASA-TN-D-7185] 09 p0980 N73-18010
Detail design features of short takeoff and landing commercial aircraft and impact on design caused by STOL requirement - Part 2
[AERO-13-PT-2] 09 p0984 N73-18033
Proceedings of conference on flight test technology to analyze results of flight test and comparison with data obtained using flight simulators for short takeoff aircraft
[DLR-MITT-72-18] 10 p1104 N73-19005
Comparison of simulation and flight test results for automatic short takeoff aircraft landing system
10 p1105 N73-19006
Comparison of validity of results obtained by flight simulation with results obtained from actual flight test of short takeoff aircraft
10 p1105 N73-19007
Analysis of system concepts, design criteria, operating procedures, and terminal facilities for short haul transportation aircraft and supporting systems
[NASA-TM-X-62235] 10 p1105 N73-19013
Development of techniques for reduction of aircraft noise generated by short takeoff aircraft
[NASA-TM-X-68195] 10 p1106 N73-19021
Analysis of gust alleviation system for short takeoff aircraft for improved performance under random turbulence conditions
[NASA-TN-D-7201] 11 p1233 N73-20013
Analysis of factors involving commercial application of short takeoff aircraft for short haul airline operations
[NASA-TM-X-62239] 11 p1234 N73-20016
Annotated bibliography of aerodynamic configurations and characteristics of short takeoff aircraft
[AD-754500] 11 p1236 N73-20037
Development of jet-flap rotor and application to heavy helicopter and stoppable rotor designs
12 p1359 N73-21025
Development of pilot model parameters to provide data base for multiloop, single controller, multi-input analysis of aircraft performance
[AD-755367] 12 p1365 N73-21078
Wind tunnel tests to determine static longitudinal aerodynamic characteristics of jet transport wing-body with upper surface blown jet flap for lift augmentation
[NASA-TN-D-7183] 13 p1470 N73-21907
Dynamic simulation used to analyze various aspects of STOL aircraft operations within air traffic control system
[FAA-NA-72-95] 13 p1472 N73-21919
Wind tunnel tests to determine acoustic properties of externally blown jet flap and augmentor wing short takeoff aircraft concepts
[NASA-TM-X-62251] 13 p1472 N73-21924
Design and aerodynamic characteristics of tilt propeller aircraft for short takeoff and landing operations - Vol. 1
[NASA-CR-114441] 13 p1473 N73-21926
Development of high performance, low volume thrust augmentation using combined Coanda inlet and jet flap diffusion techniques
[AD-756895] 13 p1476 N73-21954
Dynamic stability information for space shuttles, high performance military aircraft, and short takeoff aircraft at high angles of attack
[NASA-CR-114583] 13 p1505 N73-22201
Forecasting demand potential for STOL transportation
[NASA-CR-114572] 13 p1595 N73-22932
Wind gust effects on STOL type aircraft
14 p1600 N73-22971
Comparison of aerodynamic lift developed by mechanical high lift systems and lift developed by externally blown flaps on short takeoff aircraft
[NASA-TT-F-14895] 14 p1601 N73-22981
Development of computer programs to predict performance of thrust reversal and thrust vector control systems on short takeoff transport aircraft - Vol. 1
[AD-756860] 14 p1603 N73-22993
Design and development of thrust reverser and thrust vectoring systems for application to short takeoff transport aircraft - Vol. 2
[AD-756861] 14 p1603 N73-22994
Development of air navigation system to provide four dimensional guidance for short takeoff aircraft operating in terminal area
[NASA-TM-X-62234] 14 p1687 N73-23686
Analysis of short takeoff and landing aircraft landing guidance systems and application of air traffic control procedures for improved sequencing
14 p1688 N73-23703
Development of stability augmentation systems for decoupling response of short takeoff and landing aircraft in longitudinal and lateral-directional flight modes
15 p1732 N73-24041
Methods for evaluating and predicting airfield performance of turbojet and turbofan aircraft operating in conventional and short takeoff modes
15 p1732 N73-24044
Analysis of manual control theory of vertical situation displays for short takeoff aircraft
[NASA-CR-114620] 15 p1734 N73-24061
Characteristics of flight control system for approach flight path control of augmentor wing on powered-lift short takeoff aircraft configuration
[NASA-CR-114574] 15 p1734 N73-24062
Application of cold thrust augmentation techniques for improved performance of short takeoff aircraft performance
[AD-758202] 15 p1735 N73-24073
Two dimensional unsteady separation and stall phenomena over airfoils oscillating in pitch with application to short takeoff aircraft
[AD-758899] 15 p1736 N73-24080
Development of air traffic control procedure to permit short takeoff aircraft landing along curved approach trajectory and analysis of data transmission requirements
16 p1859 N73-25055
Characteristics of Yak 40 aircraft and application for short haul service to isolated areas of USSR
[NASA-TT-F-14943] 16 p1859 N73-25057
Development of simulation model and computer code for evaluation of operation of short takeoff aircraft for commercial airline operations
[NASA-CR-114631] 16 p1860 N73-25062
Characteristics of quiet turbofan short takeoff aircraft for short haul air transportation and analysis of economic and sociological factors affecting operation Vol. 1
[NASA-CR-114612] 16 p1860 N73-25065

Analysis of quiet turbofan short takeoff aircraft for short haul air transportation to show research and development requirements and advanced technology benefits - Vol. 2
[NASA-CR-114613] 16 p1860 N73-25066
Design and development of STOL and V/STOL aircraft to show design requirements, performance characteristics, and air traffic control problems
[PB-217102] 16 p1862 N73-25085
Direct side force control for STOL crosswind landings with analysis of manual and automatic control modes
[AD-759555] 16 p1863 N73-25091
Cockpit and control display design criteria for tactical STOL and V/STOL aircraft
[AD-758787] 16 p1914 N73-25489
Operational procedures and modes of experimental guidance system for short takeoff aircraft to provide arrival time control and automatic tracking
[NASA-TM-X-62233] 16 p1941 N73-25710
Mechanical cross coupling of STOL transport aircraft engines
[CRANFIELD-AERO-14] 16 p1955 N73-25819
Wind tunnel tests to determine acoustic properties of jet augmented lifting flap configuration
[NASA-TT-F-14951] 17 p1983 N73-26030
Flight tests for determining handling qualities and operational characteristics of Breguet 941 STOL aircraft
18 p2103 N73-27008
Propulsive-lift technology program for development of short takeoff aircraft propulsion systems and lift augmentation devices
18 p2103 N73-27009
Design, development, and evaluation of Buffalo/Spey Augmentor-Wing research aircraft using internally blown flap for lift augmentation
18 p2103 N73-27010
Design, development, and requirements for short takeoff transport aircraft for military applications using civil aircraft production procedures
18 p2103 N73-27011
Analysis of aerodynamic characteristics affecting selection of short takeoff transport aircraft
18 p2103 N73-27012
Analysis of research and development programs involving construction of short takeoff transport aircraft in Germany
18 p2103 N73-27013
Development and characteristics of control system for short takeoff transport aircraft for ride-smoothing effect
[NASA-CR-2276] 18 p2105 N73-27026
Comparison of automatic short takeoff aircraft landings based on simulation and flight test results
[NASA-TT-F-14995] 18 p2105 N73-27028
Conceptual development and cost analysis of elevated short takeoff and landing facility for test purposes
[FAA-RD-73-15] 18 p2126 N73-27179
Wind tunnel tests of short takeoff and landing fan stage model to determine airflow conditions around rotor and stator and stage pressure ratio
[NASA-TM-X-2837] 18 p2192 N73-27701
Two dimensional flow, low speed wind tunnel tests of trapped vortex-high lift airfoil to reduce blowing requirements for lift augmentation
[AD-762077] 19 p2218 N73-27893
Aerodynamic noise of STOL engine-over-wing configuration using nozzle deflector
[NASA-TM-X-2871] 19 p2219 N73-27897
Design, development, and characteristics of quiet turbofan short takeoff aircraft for short haul air transportation - Vol. 2
[NASA-CR-114607] 19 p2219 N73-27899
Airport siting, design, cost, operation, and implementation for STOL aircraft short-haul air transportation system - Vol. 3
[NASA-CR-114608] 19 p2219 N73-27900
Marketing survey to determine acceptance and utilization of STOL aircraft for short-haul air transportation system - Vol. 4
[NASA-CR-114609] 19 p2219 N73-27901
Analysis of economic factors affecting operation of STOL aircraft for short-haul air transportation system - Vol. 5
[NASA-CR-114610] 19 p2219 N73-27902
Systems analysis of quiet turbofan STOL aircraft for short-haul air transportation operations - Vol. 6
[NASA-CR-114611] 19 p2219 N73-27903
Design and characteristics of augmentor wing cruise blowing valveless system for STOL passenger aircraft to define requirements for test facilities - Vol. 2
[NASA-CR-114570] 19 p2220 N73-27907
Analysis of passenger acceptance of commercial low-density short haul, air transportation
[NASA-CR-132285] 19 p2226 N73-27950
Social and technological impact of STOL aircraft potential
[NASA-CR-133356] 19 p2355 N73-28942
Simulator tests to determine short takeoff transport aircraft terminal area characteristics and longitudinal handling qualities
[MDC-J5575L] 20 p2360 N73-28983
Analysis of pilot performance and short takeoff aircraft characteristics during landing approach
[AD-762566] 20 p2362 N73-29000
Computer simulated loading of Army Brigade and equipment into several medium short takeoff transport aircraft configurations
[AD-762916] 20 p2362 N73-29002
Development of computer programs for designing engine inlets for VTOL and STOL aircraft based on axisymmetric potential flow parameter
[NASA-TM-X-68278] 20 p2388 N73-29182
Influence of noise requirements on STOL propulsion systems design
[NASA-TM-X-68280] 20 p2465 N73-29807
Aerodynamic characteristics of high lift wing concepts for application to commercial short takeoff transport aircraft
20 p2479 N73-29908
Development and characteristics of experimental aircraft for demonstrating augmentor wing jet short takeoff concept using modified C-8A aircraft - Vol. 1
[NASA-CR-114503] 21 p2494 N73-30016
Flight tests of modified C-8A aircraft to demonstrate augmentor wing, short takeoff concept - Vol. 2
[NASA-CR-114504] 21 p2494 N73-30017
Effect of wing aspect ratio and flap span on aerodynamic characteristics of short takeoff model with externally blown jet flap
[NASA-TN-D-7205] 21 p2494 N73-30020
Wind tunnel tests to determine effects of variations in Reynolds number and leading edge configurations on aerodynamic characteristics of STOL transport with externally blown flaps
[NASA-TN-D-7194] 21 p2494 N73-30021
Flight tests of various steep gradient approaches to ground level short takeoff and landing runway to determine aircraft performance and navigation aids required
[FAA-NA-72-77] 21 p2495 N73-30025
Simulation tests of short takeoff transport aircraft to determine airport and air space requirements under normal operating conditions
[NASA-TN-D-7300] 21 p2495 N73-30026
Application of variable pitch fan propulsion system for quiet short takeoff aircraft
21 p2496 N73-30030
Aerodynamic wind tunnel performance of high bypass pressure ratio fan engine for STOL aircraft
[NASA-TM-X-71445] 23 p2740 N73-31931
Takeoff and landing performance characteristics and field length requirements for jet short takeoff transport aircraft with full span, externally blown flaps
[NASA-TN-D-7441] 23 p2741 N73-31939
Application of short takeoff aircraft for short haul air transportation with identification of critical technology, economics, and social viability
[NASA-CR-135481] 23 p2741 N73-31941
Flight paths for short takeoff aircraft landing approach consistent with pilot preference passenger comfort, and microwave landing system limitations
[NASA-TN-D-7298] 23 p2742 N73-31949
Evaluation of low speed flying qualities of short takeoff aircraft with externally blown flap wing or augmentor wing using flight simulator
[NASA-TN-D-7454] 23 p2742 N73-31951
Display devices for short takeoff aircraft landing
[DGLR-PAPER-73-038] 23 p2744 N73-31961
Noise reducing approach and takeoff profiles for short takeoff aircraft
[MBB-UH-06-73-O] 23 p2744 N73-31968
Noise comparison of two STOL pressure ratio fans with 15 and 42 rotor blades
[NASA-TM-X-2891] 23 p2829 N73-32609
Economic risk analysis for propeller STOL transport market
23 p2861 N73-32866
Proceedings of conference on short takeoff and landing aircraft to determine aerodynamic characteristics and short haul transportation applications
[NASA-SP-320] 24 p2871 N73-32934
Objectives and findings of study to determine applicability of short takeoff aircraft for short-haul air transportation systems
24 p2872 N73-32936
Economic and environmental aspects of short takeoff aircraft used for short-haul air transportation systems
24 p2872 N73-32937
Short takeoff aircraft technology development related to requirements for expanded and improved short-haul air transportation system capabilities
24 p2872 N73-32938
Aerodynamic and performance characteristics of short takeoff aircraft equipped with externally blown flaps
24 p2872 N73-32939
Wind tunnel tests to determine aerodynamic characteristics of five configurations of short takeoff aircraft wind tunnel models
24 p2872 N73-32944
Simulations of powered-lift STOL transport aircraft with either externally blown flap configuration or augmentor wing configuration
24 p2873 N73-32948
Flight simulation to determine manual control of flight path and airspeed for approach and landing of powered lift jet short takeoff aircraft
24 p2873 N73-32949
Wind tunnel tests to determine magnitude of adverse ground effects on longitudinal aerodynamic coefficients of powered-lift short takeoff aircraft
24 p2873 N73-32950
Development and evaluation of active control system to provide ride smoothing on short takeoff aircraft
24 p2873 N73-32951
Flight simulation to determine effectiveness of head-up display for improving glide-slope tracking performance during steep visual approach of short takeoff aircraft
24 p2874 N73-32952
Flight tests of augmentor-wing jet STOL research aircraft to compare wind tunnel data with flight data for dynamic characteristics and limitations
24 p2874 N73-32954
Air traffic control problems created by introduction of large numbers of STOL aircraft into high density terminal area
24 p2874 N73-32956
Development and characteristics of 4-D guidance system for traffic control of STOL aircraft operating in congested areas
24 p2874 N73-32957
Systems analysis of problems created in terminal area by application of short takeoff aircraft for providing high speed, short haul air transportation service
24 p2874 N73-32958
Program plan to develop criteria for airworthiness standards applied to short takeoff aircraft used as transport service
24 p2875 N73-32959
Analysis of human reactions to short takeoff aircraft aerodynamic noise for predicting community acceptance of short haul air service operations
24 p2875 N73-32960
Design and development of quiet, clean propulsion systems for short takeoff aircraft with emphasis on engine noise reduction
24 p2875 N73-32961
Characteristics of aerodynamic noise generated by interaction of airstream with flap surface to show location and control of noise sources
24 p2875 N73-32963
Wind tunnel tests to determine acoustic properties of externally blown flap and augmentor wing for short takeoff aircraft configurations
24 p2875 N73-32965
Aerodynamic noise characteristics of short takeoff aircraft with externally blown flaps and engines mounted over and under wing
24 p2876 N73-32966
Selection criteria and characteristics of quiet, clean propulsion systems for use with short takeoff aircraft
24 p2876 N73-32967
Fan and core engine noise suppression for STOL aircraft
[NASA-TM-X-71448] 24 p2971 N73-33741

**SHORT WAVE RADIATION**
NT MICROWAVES
NT MILLIMETER WAVES
NT SUBMILLIMETER WAVES
Short wave radio emission measurements on giant planets during outer planets grand tour
[NASA-CR-133500] 19 p2343 N73-28844
Development of mathematical relationships to determine short-wave thermal radiation under cloudy and cloudless conditions
20 p2401 N73-29291
Characteristics of pryanometers and net radiometers, calibrated for short wave radiation
20 p2403 N73-29312
Short wave radiation regime compared to atmospheric radiation regime for vegetation
20 p2404 N73-29318

**SHORT WAVE RADIO TRANSMISSION**
Monitoring Northern Hemisphere transmissions in Antarctica and some oblique sounding systems
[JPRS-58205] 10 p1128 N73-19186
Peculiarities of short wave propagation over long distance radio links connecting Antarctia with Northern Hemisphere
10 p1128 N73-19187
Influence of F 2 regional disturbances and magnetic activity on short wave radio communications
13 p1521 N73-22327

**SHOT NOISE**
Noise measurements on n-junction gold silicon and aluminum silicon diodes at avalanche potential considering leakage current
[FRNC-CONF-29] 05 p0519 N73-14221

**SHOT PEENING**
Statistical test of difference in fatigue life results is conventional and shot peening in aluminum-titanium alloy
[AD-758624] 15 p1794 N73-24542

**SHRAPNEL**
Methods for determining air resistance to fragmented shrapnel of different shapes
[FOA-2-A-2539-44] 06 p0653 N73-15304

SHRINKAGE
Sintering temperature and tungsten content effects on volumetric shrinkage of ferrotungsten alloy briquets
04 p0432 N73-13518
Compactibility, shrinkage, and microhardness of electrolytic titanium powders obtained at low temperatures from melts
04 p0432 N73-13521
SHROUDED BODIES
U SHROUDS
SHROUDED NOZZLES
Flow equations for water/steam reaction engine with shrouded nozzles
04 p0404 N73-13293
SHROUDED PROPELLERS
Design, development, and evaluation of helicopter control system using fan in fin configuration for antitorque and directional control
[AD-747806] 03 p0254 N73-12055
Computerized simulation of shrouded propeller low field in cross flow using vortex lattice models
[AD-751463] 07 p0773 N73-16274
Vortice diatribution field for calculating inlet flow of ducted propeller
[AD-754114] 10 p1144 N73-19318
SHROUDS
Performance of shrouded and unshrouded fans in low noise turbofan engines
03 p0249 N73-12018
SHUNTS
U BYPASSES
U CIRCUITS
SHUTTLE BOOSTERS
U SPACE SHUTTLE BOOSTERS
SHUTTLE ORBITERS
U SPACE SHUTTLE ORBITERS
SI
U INTERNATIONAL SYSTEM OF UNITS
SIBERIA
Blocking anticyclones over Siberia during winter, and meteorological conditions for forecasting their occurrence
13 p1552 N73-22577
Service life and operation of military equipment in subzero Siberian environments
[AD-756478] 13 p1554 N73-22595
SICKNESSES
NT ALTITUDE SICKNESS
NT DECOMPRESSION SICKNESS
SID [IONOSPHERIC DISTURBANCES]
U SUDDEN IONOSPHERIC DISTURBANCES
SIDE INLETS
Three dimensional boundary layer separation and shock wave generation in flow field of supersonic conical intake mounted on fuselage side
[ARL/ME-137] 08 p0863 N73-16981
SIDE-LOOKING RADAR
NT RADAR IMAGERY
Side-looking radar scattering from terrain and ocean surfaces
[ESRO-CR[P]-137] 03 p0266 N73-12153
Potential application of SLR to remote sensing of earth resources
[ESRO-CR[P]-138] 03 p0295 N73-12401
Characteristics and imagery of side-looking radar
03 p0295 N73-12402
Side-looking radar for agricultural applications, noting crop identification and growth
03 p0295 N73-12403
Side-looking radar applications to forestry management, and timber inventory and identification
03 p0295 N73-12404
Side-looking radar applications to studies of terrain topography and landforms
03 p0295 N73-12405
Geological applications of side-looking radar, noting mineral exploration, engineering geology, and soil science
03 p0295 N73-12406
Hydrological applications of side-looking radar, noting soil moisture, ground water, and water loss
03 p0295 N73-12407
Side-looking radar applied to oceanography noting sensing of sea states, pollution, and waves
03 p0295 N73-12408
Side-looking radar applications to transportation noting route planning, shipping lanes, and traffic
03 p0295 N73-12409
Principles, installation, and operation of side-looking radar in aircraft and satellites for earth resources sensing
[ESRO-CR[P]-136-VOL-1] 03 p0296 N73-12418
Optical and digital data processing and handling of SLR imagery
[ESRO-CR[P]-139-VOL-4] 03 p0297 N73-12419
Bibliography on side-looking radar for remote sensing of earth resources, agriculture, oceanography, geology, hydrology, geography - noting data processing and photointerpretation
[ESRO-CR[P]-142-VOL-7] 06 p0640 N73-15198
First-order statistics of terrain clutter
[AD-750668] 06 p0641 N73-15205
Side-looking sonar system with coherent electrical processing
[AD-757253] 14 p1669 N73-23549
Operator performance in interpreting side-looking airborne radar real-time imagery
[AD-759495] 16 p1878 N73-25204
Side-looking radar for aerial imagery of earth surface
[JPRS-59391] 18 p2116 N73-27108
Application of pulsed radars for side scanning from artificial earth satellites and numerical analysis of radar operating parameters
18 p2117 N73-27117
Training program for improving performance of operators in locating targets in side-looking airborne radar
[AD-762342] 19 p2229 N73-27979
Description of Breguet 1150 to be used as European earth resources survey aircraft noting sensor payload
21 p2538 N73-30353
SIDEBANDS
Radio frequency induced sidebands in Mossbauer and Rayleigh scattering radiation from nickel foils
23 p2755 N73-32050
SIDELOBES
Mathematical and computer analysis of multiple channel sidelobe canceller
[AD-753571] 09 p1004 N73-18198
Sidelobe level increase and gain reduction caused by raindrops on surface of radar antenna radome
[AD-759178] 17 p1998 N73-26160
SIDERITE METEORITES
U IRON METEORITES
SIDESLIP
Wind tunnel calibration and requirements for in-flight use of fixed hemispherical head of angle of attack and angle of sideslip sensors
[NASA-TN-D-6986] 09 p0981 N73-18014
SIERRA NEVADA MOUNTAINS (CA)
Evaluation of ERTS-1 imagery for hydrologic information in Sierra Nevada Mountains and Lake Ontario
[E72-10170] 01 p0044 N73-10351
Study of crustal structure from eastern Sierra Nevada to Colorado Plateau using ERTS-1 imagery
[E72-10192] 01 p0046 N73-10371
Detection and monitoring forest insect infestation in Sierra Nevada Mountains of California using ERTS-1 imagery
[E72-10301] 04 p0411 N73-13351
ERTS-1 imagery of structure and lithology of Northern California Coast Ranges and Sacramento Valley
[E72-10333] 05 p0531 N73-14321
Evaluation of ERTS-1 imagery for hydrological information in Sierra Nevada Mountains and Lake Ontario areas
[E73-10016] 06 p0659 N73-15352
ERTS-1 imagery of crustal structure of area from eastern Sierra Nevada to Colorado Plateau
[E73-10028] 06 p0660 N73-15361
Detection and monitoring forest insect infestations in Sierra Nevada Mountains of California using ERTS-1 imagery
[E73-10312] 09 p1022 N73-18344
ERTS-1 imagery of crustal structure of strip from eastern Sierra Nevada to Colorado Plateau
[E73-10355] 10 p1149 N73-19351
Analysis of ERTS-1 data to detect and map areas of tree mortality due to insect outbreaks using color infrared positive transparencies
[E73-10351] 11 p1275 N73-20345
ERTS-1 imagery of forest insect infestation in Sierra Nevada Mountains of California
[E73-10440] 11 p1282 N73-20400
Evaluation of ERTS-1 data for hydrologic information in Sierra Nevada and Lake Ontario
[E73-10485] 12 p1396 N73-21322
ERTS-1 imagery of crustal structure of strip from eastern Sierra Nevada to Colorado Plateau
[E73-10529] 14 p1654 N73-23416
Detection and monitoring of forest insect infestation in Sierra Nevada Mountains of California
[E73-10668] 16 p1899 N73-25363
Comparison of Skylab/EREP imagery with television and radiometric measurements from other satellites for snow cover survey in Sierra Nevada Mountains and Great Plains
[E73-10755] 17 p2022 N73-26358
Application of ERTS-1 MSS imagery to study of tectonics and crustal structure of area from eastern Sierra Nevada to Colorado Plateau
[E73-10774] 18 p2135 N73-27250
Mapping snow cover in central Arizona mountains and southern Sierra Nevada of California from ERTS-1 imagery
[E73-10833] 18 p2141 N73-27303
Analysis of ERTS-1 data and underflight photography for detection of insect infestation and timber resources in Sierra Nevada Mountains of California
[PAPER-A16] 19 p2261 N73-28224
Analysis of ERTS data for detection and monitoring of forest insect infestations in Sierra Nevada Mountains of California
[E73-10868] 20 p2392 N73-29219
ERTS-1 imagery of snow cover, ice conditions, and soil moisture in Sierra Nevada Mountains and Lake Ontario Basin
[E73-10869] 20 p2393 N73-29220
Structural and lightological systems of Sierra Nevada Mountains and Sacramento Valley of California from ERTS-1 imagery
[E73-10942] 21 p2530 N73-30284
ERTS-1 reconnaissance of crustal structure of strip from eastern Sierra Nevada to Colorado Plateau
[E73-10985] 22 p2658 N73-31292
Sources and dispersal patterns of suspended particles in nearshore surface waters of northeast Pacific Ocean and seasonal variation in snow cover in Sierra Nevada Mountains
[E73-11099] 24 p2914 N73-33256
Detection and monitoring forest insect infestation in Sierra Nevada Mountains of California from ERTS-1 data
[E73-11133] 24 p2917 N73-33288
SIEVES
Adsorption properties of synthetic zeolites
[AD-754324] 11 p1253 N73-20170
Influence of various aerodynamic forces on rectangular wing performance with harmonic movement parallel to sieve flow movement
12 p1361 N73-21043
SIGHT
U VISUAL PERCEPTION
SIGNAL ANALYSIS
Pulse position modulation for coding and signal identification by transmitter receiver
[AD-747629] 04 p0391 N73-13180
Input signal dynamics for analyzing gain stability and linearity of electronic circuit working with large signals
[INR-1371] 04 p0398 N73-13240
Noncommuting observables in quantum detection and estimation theory, and application to analysis of coherent signal in harmonic oscillator
[NASA-CR-129694] 04 p0449 N73-13664
Digit-error-protection technique for use in multiplex pulse code modulation systems for high quality sound-signal distribution
[BBC-1972/40] 09 p1001 N73-18170
FORTRAN programs for statistical analysis of signal and linear and nonlinear systems
[ANTHRO-MITT-3/72] 09 p1006 N73-18208
Analysis of single channel phase communication system based on statistical communication theory with application to direction finding
12 p1425 N73-21553
Influence of jungle environment on transmission of digital signals by transmitting swept frequency and photographically recording received envelope and phase
[AD-755257] 13 p1495 N73-22120
Correlation processing of phase modulated signals
14 p1619 N73-23115
Pitch-synchronous, nonharmonic analysis of speech signals by application of FFT to single pitch periods
14 p1621 N73-23135
Three stage algorithm for representing human speech by time ordered sets of Hanning cosine modulated wavefunctions
14 p1630 N73-23214
Large space bandwidth signal analysis by means of two-dimensional optical processor and synthesis of near real time optical sound-spectrograph
14 p1631 N73-23223
Phase detector with time correlation integrator for frequency multiplexed signals
[NASA-CASE-GSC-11744-1] 14 p1640 N73-23291
SIGNAL ANALYZERS
Beat frequency detector algorithm for multichannel signal analysis
[AD-746682] 03 p0266 N73-12157
Sea bottom classifier device designed for use with towed underwater vehicle
[AD-748611] 04 p0415 N73-13392
Design and operation of coherent analyzer
[NASA-TT-F-14595] 06 p0673 N73-15476
Correlation methods for radio signal processing in presence of interference noise
09 p1002 N73-18181
Device for performing statistical time-series analysis of complex electrical signal waveforms
[NASA-CASE-MSC-12428-1] 16 p1883 N73-25240
Pulse stretcher for processing narrow pulses between pulse generators and conventional instruments
[NASA-CASE-MSC-14130-1] 17 p2007 N73-26232
SIGNAL DETECTION
NT CORRELATION DETECTION
Kalman filtering algorithm for detecting continuous wave interference signals in digital telecommunications
01 p0027 N73-10210
Comparison of sequential, two-pulse detection scheme with conventional single pulse detection
[PHL-1972-20-EX-19] 02 p0139 N73-11127
Modulation and detection of signals on optical carriers
[NASA-CR-129181] 02 p0180 N73-11460

Receiver operating characteristics for underwater signal detection performance of sea lions
[AD-746520] 04 p0382 N73-13113
Signal to noise ratios for short term detection of narrowband Gaussian process in Gaussian noise
[AD-751573] 07 p0756 N73-16144
Detection scheme with threshold learning for amplitude shift keyed signals
[AD-752009] 08 p0886 N73-17171
Detection of time varying signals in amplitude shift keyed signals with additive disturbance
[AD-752008] 08 p0890 N73-17208
Detecting point radiator in presence of nongaussian interference
[AD-752712] 09 p1004 N73-18191
Loss coefficients and spectral density of random processes in noise filters
09 p1066 N73-18699
Review of 10.6 micrometer detection techniques
[DREV-TN-2052/73] 11 p1302 N73-20567
Application of matched filtering techniques for detection of mode locked laser signals
17 p2039 N73-26496
Correlation receivers for detecting binary array signals with directional interference
22 p2627 N73-31047
Quantum detection and estimation in optical communication systems
22 p2679 N73-31460
Robust detection schemes for time varying signals in additive noise
23 p2756 N73-32051
Communication/electronic receiver performance degradation handbook
[AD-764710] 23 p2759 N73-32079

**SIGNAL DETECTORS**
Digital receiver for detecting moderate data rate phase-shift keyed signals in real time
01 p0025 N73-10196
Maximum detection probability of optical image by photoelectric surface with unit quantum efficiency
[NASA-CR-130121] 03 p0334 N73-12725
Expressions for generalized signal to noise ratio at output of optimal detector of optical signal
12 p1378 N73-21179
Failure detector for dc to ac inverter circuit
[NASA-CASE-NPO-13160-1] 14 p1667 N73-23525
Evaluation of Pc1 geomagnetic micropulsations with automatic signal detectors, noting dispersion
17 p2027 N73-26401
Frascati gravitational wave detector signal to noise ratio optimization
18 p2145 N73-27340
Noise model for optimal signal to noise ratio in sonar detector design
19 p2235 N73-28015
Detectors for signals in non-Guassian additive noise
19 p2235 N73-28016
Performance characteristics, except direction, of detection receivers in processing known signals
[AD-762048] 19 p2236 N73-28029
Visibility and optimum light characteristics of marks for sighting devices
20 p2368 N73-29039

**SIGNAL DISCRIMINATORS**
U SIGNAL DETECTORS

**SIGNAL DISTORTION**
Specification for group delay variation in upper video band of television transmission system based on chrominance pulse tests
[BBC-1972/39] 06 p0638 N73-15181
Distortion of sonar signals transmitted through random and inhomogeneous media
[AD-750755] 06 p0641 N73-15202
Sea state effects on altimeter signal scattering and radar wave form estimates
06 p0663 N73-15381
Methods for predicting parametric amplifier input noise temperature degradation for pump AM noise levels undergoing signal interference
[AD-751652] 07 p0763 N73-16197
Analysis of major sources of distortion in AM baseband telemetry systems and techniques for optimum baseband design
16 p1874 N73-25169

**SIGNAL ENCODING**
Pulse position modulation for coding and signal identification by transmitter receiver
[AD-747629] 04 p0391 N73-13180
PCM coding and decoding noting truncated hamming codes and analysis of error rates
[ESRO-TN-112-ESTEC] 05 p0513 N73-14173
Adaptive pulse code modulator for speech signals noting coder and decoder
[SRDE-72001] 05 p0514 N73-14174
Feasibility of multispectral signal encoding on black and white film
[AD-749495] 05 p0548 N73-14455
Digital coding and modulation processes in radio transmission
[NLL-PO-2832-[9022.81]] 11 p1254 N73-20177
Operational principles and applications of address code communication systems
14 p1619 N73-23114
Formant extraction technique using adaptive predictive coding
14 p1622 N73-23137
Comparison of voice coding technique for satellite-based air traffic control system
14 p1630 N73-23209
Thermomagnetic recording of analog signals on CrO2 magnetic tape
[NHK-LABS-NOTE-157] 18 p2116 N73-27112
Data error protection in disturbed binary channels by linear systematic codes, applied to 50 Kbaud telephone channel transmission
[FTZ-A-441-TBR-1] 22 p2632 N73-31097
High density bipolar encoder and decoder for code transparent digital channels
[FTZ-44-TBR-35] 22 p2633 N73-31103
Convolutional encoder and decoder for PCM telemetry
[ESRO-CR-165] 22 p2634 N73-31111
Evaluation of computer storage requirements for TV camera tubes with signal encoding test program
[ELEC-011-72] 23 p2794 N73-32350

**SIGNAL FADEOUT**
U SIGNAL FADING

**SIGNAL FADING**
Signal dropout detection and counting tester for magnetic tape measurements
[NBS-TN-739] 01 p0030 N73-10236
Polarization of wave propagating in ionosphere noting signal fading recorded at Garchy
[GRI/NT/84] 01 p0050 N73-10403
Scintillating [VHF] signals fading measurements at Lima, Peru during spring equinox of 1970
[NASA-TM-X-66092] 02 p0166 N73-11347
Simultaneous ultrahigh and very high frequency ionospheric effects from ATS 5 at the magnetic equator
[NASA-TM-X-65948] 12 p1378 N73-21173
Fading frequency characteristics of Es layer
13 p1521 N73-22330
Nonspherical raindrop depolarization of electromagnetic wave in ultrahigh frequency radio link
17 p1994 N73-26123
Multipath propagation and phase delay of ultrahigh frequency radio wave caused by atmospheric discontinuity
17 p1994 N73-26124
Rain attenuation and multipath fading in ultrahigh frequency radio relay systems
17 p1995 N73-26134
Point rainfall rate statistics for predicting ultrahigh frequency radio propagation
17 p1996 N73-26136
Calculation of electromagnetic wave absorption by rain for frequencies close to 30 GHz
17 p1996 N73-26138
Amplitude fading of superhigh frequency geostationary communications satellite signals considering atmospheric refraction
17 p1996 N73-26139
Slant path attenuation of ultrahigh frequency signals from sun tracking radiometers
17 p1996 N73-26140
Thunderstorm cloud height and fading statistics for ATS 5 ultrahigh frequency signal transmission to earth
17 p1996 N73-26141
Effects of rain and atmospheric turbulence on ultrahigh frequency space communication radio line
17 p1996 N73-26143
Polarization fading effect in angle of rotation measurements on ionospheric radio signal scattering
18 p2115 N73-27105
Ionospheric fading effects on microwave space communication links in equatorial zone
18 p2212 N73-27855
Attenuation and fading characteristics of ATS 5 15 and 32 GHz millimeter ground-space links
18 p2212 N73-27856
Balloon measurements of stellar scintillation for predicting fading on space to ground laser propagation path
18 p2212 N73-27858
Performance of neodymium-yag optical data transmission system and development of channel simulator
18 p2212 N73-27859
Ionospheric disturbances and fading of radio waves in polar regions
[AD-762282] 19 p2299 N73-28483
Doppler and surface effects in backscattered signal fading
22 p2627 N73-31052
Digital error probalities of binary receivers in presence of intersymbol interference in fading channels
23 p2755 N73-32049

**SIGNAL GENERATORS**
NT FREQUENCY SYNTHESIZERS
NT FUNCTION GENERATORS
Minimum correlation theory for random numbers with same distribution, applied to negatively correlated random number generation
[NA-71-32] 03 p0324 N73-12644
System for generating timing and control signals during repetitive fixed length serial data transmission
[NASA-CASE-NPO-13125-1] 09 p1008 N73-18225
Design of light modulator for generation of periodic visual stimuli
[AD-754562] 11 p1250 N73-20149
Test set for signal conditioner modules
[NASA-CASE-KSC-10750-1] 14 p1667 N73-23527
Development and characteristics of sawtooth voltage generator using blocking generator as switch
22 p2630 N73-31081
Optimal accumulation time in superlong-baseline interferometer and frequency stability of sinusoidal signal generators used as heterodynes at receiving points
23 p2838 N73-32678
COLFTAR real time electro-optical system for generating optical Fourier transforms of two-dimensional video signals
24 p2956 N73-33613

**SIGNAL MEASUREMENT**
Signal dropout detection and counting tester for magnetic tape measurements
[NBS-TN-739] 01 p0030 N73-10236
Measurement of signal strength variations in beam currents of vidicon targets
[DRIC-TRANS-2965] 06 p0645 N73-15238
Polarization measurement of whistler-type radio frequency signals by using auto- and cross-correlation functions of horizontal signal components
[CEPHAG-24/72] 13 p1491 N73-22088
Analytical method for determination of large signal characteristics of impatt amplifiers
18 p2122 N73-27151

**SIGNAL NOISE**
U SIGNAL TO NOISE RATIOS

**SIGNAL PROCESSING**
Development of system for eliminating constant luminance failure in color television systems by modifying coding process
[BBC-1972/29] 01 p0023 N73-10180
Fast Fourier transform digital processor as spectrum analyzer and adaptive filter
01 p0025 N73-10198
Estimation of magnitude-squared coherence function spectrum
[AD-743945] 01 p0029 N73-10227
Signal processing algorithms for estimating from radar data characteristics and trajectory parameters of bodies moving in air
[AD-745421] 01 p0029 N73-10227
Development of differential phase shift keyed signal receiver to resolve differential phase shift in incoming signal
[NASA-CASE-MSC-14066-1] 01 p0034 N73-10269
Functional analysis and logical construction systematics for signal processing equipment design
02 p0140 N73-11136
Design of signal processing computer using arithmetic parallelism
[AD-745950] 02 p0142 N73-11150
Phase switching of transmitting signal from radio altimeter to reduce step error in signal processing
[ISAS-484-VOL-37-10] 02 p0172 N73-11389
Intensity modulation of electrical signals recorded on film using two oscilloscopes
[FOA-3-C-3677-62] 02 p0172 N73-11392
Modulation and detection of signals on optical carriers
[NASA-CR-129181] 02 p0180 N73-11460
Composite signals for lane identification in Omega
[AD-746503] 02 p0208 N73-11686
Techniques for generation and processing microwave signals using elastic, electromagnetic and carrier space charge waves in solid media
[AD-747047] 02 p0220 N73-11782
Approximate solution to covariance of plane wave direction and propagation velocity of signals in array processing scheme
[AD-747591] 03 p0267 N73-12160
Application of pattern recognition to fault diagnosis of internal combustion engines
[AD-747334] 03 p0351 N73-12865
Characteristics of digital data processor using pulse from clock source to derive binary singles to show state of various indicators in processor
[NASA-CASE-GSC-10975-1] 04 p0392 N73-13187
Signal processing element users reference manual for radar, sonar, and communication systems
[AD-748592] 04 p0394 N73-13205
Development of delay cable to display simultaneous signals in nanosecond region in single trace oscilloscope
[IPPJ-T-9] 04 p0395 N73-13212
Research on speech recognition, spectrum analyzers and design of digital filters
[AD-748212] 04 p0396 N73-13223
Binaural processing of speech intelligibility in light aircraft
[FAA-AM-72-31] 05 p0503 N73-14094
Minicomputer application in processing underwater sound signals
[AD-749095] 05 p0514 N73-14176
Microprogrammed control, buffer store, and storage control units for all applications digital computer for signal processing in radar, sonar, and communication systems
[AD-748996] 05 p0520 N73-14227

Error performances of several digital signaling methods as function of specified signal to noise ratio
05 p0609 N73-14953
Digital phase measuring device for mutual phase position of two signals, emphasizing LF and VLF waves
[AD-750472] 06 p0675 N73-15497
European study of optical and signal processing problems in laser anemometry
[ET/TN/A/20] 06 p0679 N73-15526
Characteristics of two channel telemetry system with two data rate channels for high and low data rate communication
[NASA-CASE-NPO-11572] 07 p0754 N73-16121
Digital optical hybrid correlator for processing pulse Doppler and wideband radar signals
[AD-751695] 07 p0756 N73-16143
Estimation of time delays generated by random field propagating across array of noise sensors in optimal processing of multiple sensor data
[AD-751555] 07 p0756 N73-16146
Digital signal processing applied to ocean bottom seismic reflection data
[PB-212155] 07 p0794 N73-16456
Microwave acoustic signal processing with time-variant distributed networks using surface amplifiers
07 p0820 N73-16649
Design and development of universal voice processor system
[NASA-CR-128739] 08 p0885 N73-17161
Fabrication and evaluation of engineering prototype ground signal processing systems for use with satellite television
[NASA-CR-120933] 09 p1002 N73-18178
Influence of autocorrelation and its parameters on phase manipulated signal passed through n stage resonance filter
09 p1002 N73-18180
Techniques for solving for optimum filter for video signal processing
[AD-753132] 09 p1003 N73-18189
DONAR system for digitizing ultrashort sonic wave trains from pulse echo systems
[NASA-CR-130883] 09 p1013 N73-18266
Basic mechanism underlying generation of Moire patterns in line scanner data acquisition
[NASA-CR-130829] 09 p1035 N73-18442
Design of microwave signal processing devices for broadband operation
[AD-753168] 09 p1075 N73-18775
Nonlinear programming of multifilter phase-lock loops at low signal-to-noise environments
[NASA-CR-131237] 10 p1127 N73-19184
Analysis of effects of nonlinear electronic devices on bandpass signals consisting of modulated sine waves
[CRC-1234] 10 p1128 N73-19189
Fast electronics technology in signal processing
[CEA-CONF-1897] 10 p1129 N73-19196
Phase manipulated signal reception in noise background of unknown statistics
[AD-754603] 11 p1258 N73-20205
Linear filtration effect on correlation properties of phase manipulated signals
12 p1378 N73-21175
Integral equation for calculating influence of linear channels on correlation processing of noise signals
12 p1378 N73-21180
Application of mathematical procedures for determining correlation properties of radio transmissions and signal processing
12 p1379 N73-21181
Surface acoustic waves used with devices for parametric signal processing and long delay lines
[AD-755943] 12 p1385 N73-21235
Design and construction of decoder for processing signals from multiwire proportional chamber
[LA-5073] 12 p1388 N73-21256
Compensation of vidicon signal dark component
[DRIC-TRANS-2967] 13 p1491 N73-22089
Radar signal processing methods
[AD-756599] 13 p1492 N73-22095
Maximum likelihood testing algorithm for estimating monopulse radar signal amplitude in air traffic control
[AD-756844] 13 p1493 N73-22105
Digital quadrature methods for processing bandpass signals
[AD-755473] 13 p1494 N73-22110
Surface wave device to correlate acoustic velocity and to correct signal phases from pulse bursts
[AD-755198] 13 p1502 N73-22175
Characteristics of signal conditioning electronics for vector velocity laser velocimeter
[NASA-CR-131475] 13 p1538 N73-22459
Facilities for handling light signals from long range spacecraft
14 p1618 N73-23107
Application of digital signal processing to design of phase vocoder analyzer
14 p1621 N73-23131
Design and implementation of adaptive delta modulator with integrated circuit hardware for encoding of speech signals
14 p1621 N73-23132
Properties of spectra derived by linear prediction in spectral analysis of speech
14 p1622 N73-23138
Decoding of information in acoustic waveform of human speech using signal processing techniques
14 p1623 N73-23148
Acoustic theory of speech production for definition of terminal analog speech synthesizer configuration using digital signal processing techniques
14 p1623 N73-23152
Speech synthesis using Hadamard-Walsh transform
14 p1624 N73-23158
Structure and signal processing capabilities of special speech processor
14 p1631 N73-23222
Signal processing of speech pattern recognition using PDP 9 Computer
[AD-757109] 14 p1635 N73-23258
Estimation method for correlation between two stationary random signals in noise
[AD-757459] 14 p1636 N73-23263
Optimum techniques for detecting and discriminating backscattered electromagnetic radiation associated with impulse radar concept
[AD-757220] 14 p1636 N73-23267
Synthesis and analysis of systems combining extreme principle of control with correlation processing of signals entering from object being controlled
14 p1644 N73-23334
Adaptive processing filtering and design of digital signals for real time analysis with algorithm derivation
[AD-757229] 14 p1684 N73-23667
Analysis of Loran C signal processing techniques using hybrid simulation procedure
[AD-757586] 14 p1691 N73-23725
Generation and processing of microwave signals using elastic, electro-magnetic, and carrier space charge waves in solid media
[AD-757555] 14 p1699 N73-23784
Feasibility of using computer system for echo detection and identification of moving targets
[AD-758266] 15 p1751 N73-24191
Acousto-optic interactions in guided wave structure for optical modulation, deflection and signal processing
[AD-758719] 15 p1752 N73-24198
Digital techniques for reducing variance in reflected rain signals
[METEOROL-STUDY-25] 16 p1875 N73-25181
Transformation of signal spectrum in communication between spacecrafts moving at relativistic velocities
[AD-758851] 16 p1876 N73-25186
Automatic frequency control circuit for radiotelemetype receiver-converter
[AD-758686] 16 p1877 N73-25193
Development of 10.6 micrometer range gated upconversion imaging laser radar receiver with 150 by 150 resolution elements
[AD-759077] 16 p1915 N73-25495
Techniques and circuitry for designing adaptive high Q notch filter
[AD-759031] 17 p2004 N73-26210
Bulk elastic wave signals and design of acoustic filter
[AD-760020] 17 p2006 N73-26223
Correlation loss of Gaussian signal passed through odd quantizer
[AD-760310] 17 p2006 N73-26225
Pulse stretcher for processing narrow pulses between pulse generators and conventional instruments
[NASA-CASE-MSC-14130-1] 17 p2007 N73-26232
Three estimation techniques for bearing of arrival of transient signals
[AD-760691] 18 p2119 N73-27134
Application of discrete transforms in adaptive radar detection systems and effect functional performance
[AD-761219] 18 p2120 N73-27139
Switched antennas and digital signal processing of high performance, low cost, surveillance radar
[AD-759179] 18 p2120 N73-27142
Performance characteristics, except direction, of detection receivers in processing known signals
[AD-762048] 19 p2236 N73-28029
Algorithm for discrete transforms for implementing computer programs in radar signal processing
[AD-762437] 19 p2237 N73-28039
Signal modulation and digital processing for real time radar operation
[AD-762438] 19 p2238 N73-28040
Signal processing facility for underwater acoustics consisting of digital computer and Fourier analyzer
[REPT-5-72] 19 p2239 N73-28055
Signal processing digital computer for microprogramming all applications computer
[AD-761610] 19 p2242 N73-28081
Analysis of Rayleigh wave dispersion in continental path and development of filters for vertical high gain seismometer
[AD-761795] 19 p2296 N73-28462
Development of electro-hydrofluidic transducer for control of turbine engines
[AD-762298] 19 p2330 N73-28745
Development of entropy coded adaptive differential pulse code modulation systems for speech signals
[AD-762606] 20 p2378 N73-29109
Analysis of quantized signal dependent control of continuous process by computerized simulation
20 p2378 N73-29110
Computer program for identifying and classifying sensor signals
[AD-762567] 20 p2379 N73-29118
Development of space-time integral equation for solution of large body problem for smooth convex targets with application to satellite tracking systems
[AD-763794] 21 p2508 N73-30128
Measurement system for physical quantity represented by or converted to variable frequency signal
[NASA-CASE-MFS-20658-1] 21 p2543 N73-30386
Time-amplitude quantization of pulsed radar signals with numerical analysis of signal to noise relations
22 p2628 N73-31055
Determination of mean time between successive false detections for binary signal detector with variable memory size
22 p2628 N73-31056
Spectral correlation characteristics of pair of orthogonal binary random signals
22 p2628 N73-31060
Statistical analysis of signals in amplitude modulation radio altimeters with phase read-out
22 p2629 N73-31065
Statistical error analysis of frequency modulated radio altimeter with phase readout
22 p2629 N73-31066
Analysis of distribution density of process at output of interperiod compensation system
22 p2629 N73-31071
Formation of speed characteristics in interperiod compensation systems when using intermittent pulse repetition periods
22 p2630 N73-31072
Analysis of operation of phase autocorrelator with noncoincidence of frequency of received signal and filter tuning frequency
22 p2630 N73-31076
Modulation of high frequency oscillation period by symmetric and asymmetric signals
22 p2630 N73-31079
Digital signal processor for use with experimental MICOM array radar
[AD-764227] 22 p2635 N73-31121
Algorithm for calculating correcting signals in flight control systems with high speed digital computer
[AD-764310] 22 p2640 N73-31157
Capabilities of surface wave devices as signal processors for spread spectrum communications systems
[AD-763881] 22 p2645 N73-31197
Design and performance of stacked crystal filters for frequency control and signal processing
[AD-765416] 23 p2758 N73-32074
Digital to analog converter for sampled signal reconstruction
[NASA-CASE-MSC-12458-1] 23 p2759 N73-32081
Digital decoder for processing Barker coded pulses in incoherent scatter observations of ionosphere
23 p2778 N73-32212
DO-31 aircraft integrated flight control system for vertical velocity regulation in gliding, noting signal processing requirements
24 p2878 N73-32983
Symphonie satellite transponder parameters, noting intelligible crosstalk
[DGLR-PAPER-73-056] 24 p2896 N73-33115
Statistical design of nonrecursive digital filters for signal processing
[AD-764595] 24 p2899 N73-33142

**SIGNAL RECEPTION**
NT SYLLABLES
NT SYMBOLS
NT TELEVISION RECEPTION
Development of system for eliminating constant luminance failure in color television systems by modifying coding process
[BBC-1972/29] 01 p0023 N73-10180
Simulation techniques for determining broadcast quality of digital sound signals produced by pulse code modulation transmission system
[BBC-1972/31] 01 p0024 N73-10183
Development of differential phase shift keyed signal receiver to resolve differential phase shift in incoming signal
[NASA-CASE-MSC-14066-1] 01 p0034 N73-10269
Development of method for producing constant beamwidth over octave frequency bandwidth for underwater signal reception array
[AD-746690] 02 p0143 N73-11160
Analysis of Microwave Landing System performance to determine signal formats and to reduce effects of multipath transmission
[AG-5011-B-1] 07 p0818 N73-16628
Multiple element antenna array for receiving Doppler arrival angle spectral measurements in radio astronomy
[AD-751873] 08 p0889 N73-17202

Analysis of single channel phase communication system based on statistical communication theory with application to direction finding
12 p1425 N73-21553
Filter for third order phase locked loops in signal receivers
[NASA-CASE-NPO-11941-1] 18 p2125 N73-27171
Multi-impedance loading of linear antennas to improve transmitting and receiving characteristics
21 p2516 N73-30184
Electromechanical actuator for producing mechanical force and/or motion in response to electrical signals
[NASA-CASE-NPO-11738-1] 21 p2516 N73-30185
Analysis of operation of phase autocorrelator with noncoincidence of frequency of received signal and filter tuning frequency
22 p2630 N73-31076
Energy spectrum and autocorrelation function of random processes at output of key detector
22 p2630 N73-31078
Modulation of high frequency oscillation period by symmetric and asymmetric signals
22 p2630 N73-31079
SHF transhorizon radio relay system, noting long term effects of tropospheric scatter propagation, layer reflection, and precipitation
[FTZ-A-455-TBR-34] 22 p2633 N73-31099
Requirements for design, fabrication, performance, and testing of optical heterodyne receiver subsystem for use in laser communication system - Vol. 1 Pt. 3
[NASA-CR-132805] 22 p2681 N73-31471
Fundamental concepts of communication theory to include transmission of continuous signals and use of discrete time signals
23 p2756 N73-32054

**SIGNAL REFLECTION**
Algorithm for underwater echo signals from elastic spherical shell subjected to incident pulse
[AD-746220] 01 p0082 N73-10676
Data analysis on reflected oblique soundings of ionosphere using short pulses
[AD-749766] 05 p0543 N73-14417
Tables on ionospheric data measured by vertical echo sounding
[REPT-316-F] 08 p0916 N73-17507
Depths of reflection zone characteristics for classifying ultrasonic echoes in weld testing
[NLL-CE-TRANS-5993-[9022.09]]
11 p1324 N73-20742
Digital techniques for reducing variance in reflected rain signals
[METEOROL-STUDY-25] 16 p1875 N73-25181
Doppler return spectra from rough ocean surface
19 p2320 N73-28667
Influence of solar, sky, and ground radiation on signal reflection under cloudless daytime sky
[AD-763893] 22 p2712 N73-31716
Improvement of instrument landing systems with respect to multipath propagation effects and surface reflections
[DGLR-PAPER-73-017] 23 p2817 N73-32521

**SIGNAL STABILIZATION**
Adaptive equalization of pulse amplitude modulated signal with noise interference by successive iterative methods
[NASA-TR-R-402] 10 p1128 N73-19190
Phase delay control system for stabilizing signals passing through coaxial cables
[NASA-CASE-NPO-13138-1] 11 p1262 N73-20238
Automatic nulling system for interference signal at multichannel receiver by polarization adjustment
[NASA-CASE-NPO-13140-1] 18 p2116 N73-27106
Stability of multistation satellite communications system
[JPRS-59753] 20 p2376 N73-29092

**SIGNAL TO NOISE RATIOS**
Signal to noise ratio performance of optimum digitalized FM demodulator
01 p0025 N73-10195
Attenuation and phase constancy propagation criteria of tactical satellite communications using mobile ground terminals
01 p0026 N73-10201
Human recognition of contrasting target in noisy environment with diversion of attention
[FOA-2-C-2482-H5] 02 p0135 N73-11092
Detection probability of log-normally distributed signals embedded in log-normally distributed noise as function of signal to noise ratio
[AD-745947] 02 p0143 N73-11157
Feasibility of mounting geophone arrays on pack ice to provide passive sonar system with improved signal to noise ratios over hydrophone arrays
[AD-747327] 02 p0143 N73-11161
Fast digital noise filter capable of locating spectral peaks and shoulders by using techniques of convoluting integers
[NASA-TM-X-64707] 03 p0273 N73-12212
Degradation of spread spectrum modulation performance in airborne multipath communication channels
[AD-747486] 04 p0391 N73-13181
Modification principle for synchronous amplifier to improve sensitivity
[NASA-TT-F-14719] 04 p0395 N73-13213
Signal ratio measurements for determining terminal invariant parameters in microwave system calibration
[SC-DR-72-0315] 04 p0395 N73-13216
Noise measurements on n-junction gold silicon and aluminum silicon diodes at avalanche potential considering leakage current
[FRNC-CONF-29] 05 p0519 N73-14221
Signal filtration in amplitude spectrometry system
[JINR-P13-6428] 05 p0548 N73-14448
Fluctuation errors of pulse time tracking systems in radar and radio navigation devices caused by noise signals
[AD-749649] 05 p0578 N73-14704
Airborne survey of very high frequency interference levels over residential areas on American west coast
[SD-72-SA-0100-VOL-1] 06 p0640 N73-15197
Signal to noise ratios for short term detection of narrowband Gaussian process in Gaussian noise
[AD-751573] 07 p0756 N73-16144
Estimation of time delays generated by random field propagating across array of noise sensors in optimal processing of multiple sensor data
[AD-751555] 07 p0756 N73-16146
Time discrimination in temporal information sampling at output of planar germanium detector in gamma ray spectrometry
[NAA-SR-MEMO-6728] 07 p0824 N73-16680
Statistical analyses for detecting frequency shift keyed and phase keyed signals in additive disturbance
[AD-752010] 08 p0886 N73-17173
Statistical analysis on nonparametric detection of M-ary time varying signals with intersymbol interference and additive noise
[AD-752011] 08 p0886 N73-17174
Detection of time varying signals in amplitude shift keyed signals with additive disturbance
[AD-752008] 08 p0890 N73-17208
Correlation methods for radio signal processing in presence of interference noise
09 p1002 N73-18181
Loss coefficients and spectral density of random processes in noise filters
09 p1066 N73-18699
Time discrimination in temporal information sampling at output of planar germanium detector in gamma ray spectrometry
[CEA-R-4355] 09 p1069 N73-18719
Nonlinear programming of multifilter phase-lock loops at low signal-to-noise environments
[NASA-CR-131237] 10 p1127 N73-19184
Phase manipulated signal reception in noise background of unknown statistics
[AD-754603] 11 p1258 N73-20205
Experimental verification of output signal to noise ratio and time of arrival estimate of tapped delay line matched filter using surface elastic waves
12 p1377 N73-21171
Expressions for generalized signal to noise ratio at output of optimal detector of optical signal
12 p1378 N73-21179
Interpolative estimation for error reduction during video signal demodulation in noise environment
[NASA-CR-131873] 13 p1490 N73-22080
Algorithm for adaptive convergence rate on weak noise components in seismic signal processing
[AD-756904] 13 p1525 N73-22361
Stimulus time interval and response mode methods using signal to noise ratios to test speech intelligibility
14 p1625 N73-23164
Enhancement of speech intelligibility through appropriate spectral weighting and effect of passing through optimum filter on signal to noise ratios
14 p1630 N73-23211
Development of speech analysis-synthesis system for extracting singing voice signal from background noise on recording device
14 p1632 N73-23234
Electroacoustic effects of speech communication circuits on speech intelligibility
[AD-757326] 14 p1633 N73-23236
Estimation method for correlation between two stationary random signals in noise
[AD-757459] 14 p1636 N73-23263
Digital filter with dither for correlation detection of weak signal in jamming environment
[AD-757013] 14 p1643 N73-23325
Signal to noise ratio of frequency locked loop FM demodulator
16 p1874 N73-25168
Estimation of signal-to-noise ratio in spacecraft data channel
16 p1879 N73-25207
Signal to noise ratio determination circuit using bandpass limiter
[NASA-CASE-GSC-11239-1] 16 p1883 N73-25241
Application of discrete transforms in adaptive radar detection systems and effect functional performance
[AD-761219] 18 p2120 N73-27139
Noise in metal nitride oxide semiconductor devices
[AD-760544] 18 p2124 N73-27163
Frascati gravitational wave detector signal to noise ratio optimization
18 p2145 N73-27340
Adaptive phased antenna array simulation for optimal design of tracking data relay satellite very high frequency beam
18 p2210 N73-27841
Noise model for optimal signal to noise ratio in sonar detector design
19 p2235 N73-28015
Detectors for signals in non-Gaussian additive noise
19 p2235 N73-28016
Analysis of digital communication systems disturbed by non-Gaussian noise
19 p2235 N73-28017
Channel length effect on field effect transistor noise in hot electron regime
19 p2326 N73-28713
Experimental design parameters for Raman spectroscopy of turbid suspensions and powders using ion gas laser light sources and noting S/N improvement
[NOTA-INTERNA-346] 21 p2580 N73-30676
Correlation receivers for detecting binary array signals with directional interference
22 p2627 N73-31047
Time-amplitude quantization of pulsed radar signals with numerical analysis of signal to noise relations
22 p2628 N73-31053
Numerical analysis of amplitude difference and phase difference for radar signal and correlated noise in interperiod compensation system of moving target indicator
22 p2629 N73-31068
Synthesis and analysis of optimal systems for separation of quasideterminant signals from noise
22 p2630 N73-31073
Frequency domain analysis on noise in avalanche diode microwave oscillator
22 p2641 N73-31166
Robust detection schemes for time varying signals in additive noise
23 p2756 N73-32051
Signal to noise ratios in coherent bandpass limiters
[NASA-CR-135781] 23 p2765 N73-32122
Amplification of low light level optical signals by preferential integration in imaging tubes
[AD-763724] 23 p2766 N73-32129
Correlation interferometer for decreasing interference in noisy signal reception
24 p2926 N73-33370
Effects of resolution, signal to noise ratio, and contrast on underwater imaging systems performance
24 p2958 N73-33631
Method for comparing photo-electronic and photographic detectors based on product of signal to noise ratio times spatial bandwidth
24 p2958 N73-33634

**SIGNAL TRANSMISSION**
NT AUTOMATIC PICTURE TRANSMISSION
NT BIOTELEMETRY
NT DATA TRANSMISSION
NT DOUBLE SIDEBAND TRANSMISSION
NT IONOSPHERIC F-SCATTER PROPAGATION
NT IONOSPHERIC PROPAGATION
NT MESSAGES
NT MICROWAVE ATTENUATION
NT MICROWAVE TRANSMISSION
NT MULTIPATH TRANSMISSION
NT PCM TELEMETRY
NT RADAR TRANSMISSION
NT RADIO TELEMETRY
NT RADIO TRANSMISSION
NT SATELLITE TRANSMISSION
NT SHORT WAVE RADIO TRANSMISSION
NT SINGLE SIDEBAND TRANSMISSION
NT TELEMETRY
NT TELEVISION TRANSMISSION
Simulation techniques for determining broadcast quality of digital sound signals produced by pulse code modulation transmission system
[BBC-1972/31] 01 p0024 N73-10183
Propagation characteristics of satellite-borne television transmitter and ground receiver for communication satellite system
[NASA-CR-123909] 01 p0028 N73-10214
Influence of temperature on cable parameter variations in wideband transmission system
[REPT-6670] 01 p0034 N73-10268
Spurious signals introduced into system from external cabling in electromagnetic pulse environment
[AWRE-O-47/71] 01 p0034 N73-10270
Difference frequency modulation technique for signal transmission
[NLL-TRANS-2835-[9022.81]]
02 p0139 N73-11124
Correlation of signals with various frequency spacing for tropospheric propagation
[FOA-3-A-3748-60[63]] 02 p0140 N73-11132
Bit synchronizer for split phase PCM transmission with two loop systems
[NASA-CASE-MSC-12494-1] 02 p0141 N73-11142
Ionospheric electron content and satellite signal scintillation
[AD-747507] 03 p0298 N73-12430

Input signal dynamics for analyzing gain stability and linearity of electronic circuit working with large signals
[INR-1371] 04 p0398 N73-13240
Influence of target motion and wave time variation of underwater acoustic signal transmission
[AD-748651] 04 p0450 N73-13678
Bubble frequencies of air gun sources for at-sea experiments
[AD-748586] 04 p0451 N73-13680
Distortion of sonar signals transmitted through random and inhomogeneous media
[AD-750755] 06 p0641 N73-15202
Spatial grid method for solving hyperbolic equations for signal propagation on three wire transmission line
[UCRL-73796] 07 p0764 N73-16209
Analysis of Microwave Landing System performance to determine signal formats and to reduce effects of multipath transmission
[AG-5011-B-1] 07 p0818 N73-16628
Augmentation of signal transmission using microwave radio relay systems
[JPRS-58044] 08 p0885 N73-17162
Optimization of noise immunity of analog signal transmission channels by preemphasis, exemplified for AM or FM channel
[DLR-FB-73-09] 12 p1379 N73-21188
Graphical method for calculating field intensity and radio wave absorption by ionosphere along radio communication paths
13 p1521 N73-22326
Automatic frequency control circuit for radioteletype receiver-converter
[AD-758686] 16 p1877 N73-25193
Device for locating electrically nonlinear objects and determining distance to object by FM signal transmission
[NASA-CASE-KSC-10108] 16 p1911 N73-25461
Discrete unitary transforms with fast algorithm for encoding images for transmission
[NASA-CR-132771] 17 p2055 N73-26622
Coherent and incoherent components of sound scattered at time dependent rough surface with application to wind-blown water waves
[AD-760306] 17 p2064 N73-26695
Phase modulation of tone and binary signals on carrier waves in communication systems
[NASA-CASE-GSC-11743-1] 18 p2116 N73-27107
Computer program to obtain power spectrum of frequency modulated signal, modulated by voice signal, digital signal, and combinations of both
[FAA-RD-73-56] 18 p2116 N73-27111
Analysis of intermodulation of weak signal with strong signal in ionosphere to determine variations as function of modulation frequency of strong signal
[BBC-RD-1973/5] 19 p2234 N73-28010
Differential pulse code modulation of digital video signals
[BBC-RD-1973/7] 19 p2234 N73-28011
Signal transmission in visible and infrared portions of electromagnetic spectrum of cloud free, lines of sight through atmosphere at Grand Forks, Fargo, and Minot, North Dakota
[AD-763083] 20 p2415 N73-29408
Television multiplexing system, using single crystal controlled clock for signal synchronization
[NASA-CASE-KSC-10654-1] 21 p2507 N73-30115
Aircraft mounted crash location transmitter for emergency signal transmission after crashes
[NASA-CASE-MFS-16609-2] 22 p2631 N73-31084
Special purpose slide rule to compute free space propagation delay between synchronous satellite and points on earth surface
[NBS-TN-638] 22 p2638 N73-31139
Adaptive learning receiver for time varying multipath channel transmission
23 p2756 N73-32052

**SIGNALS**
Conversion of electrical signals into hydraulic signals using electrostatic hydraulic converter with no moving parts
[AD-751246] 07 p0759 N73-16168
Analog digitizer for recording non-recurrent signals
[LRP-57/72] 10 p1132 N73-19226
Photoconducting semiconductor system for converting stored optical images into video signals
[NASA-CASE-NPO-13131-1] 22 p2680 N73-31467

**SIGNATURES**
NT MAGNETIC SIGNATURES
NT RADAR SIGNATURES
NT SPECTRAL SIGNATURES

**SIGNS [SYMBOLS]**
U SYMBOLS

**SIGNS AND SYMPTOMS**
NT BRADYCARDIA
NT LEUKOPENIA
Influence of infrasound on human body functions
08 p0875 N73-17085

**SIKORSKY AIRCRAFT**
NT CH-3 HELICOPTER
NT H-53 HELICOPTER
NT S-67 HELICOPTER
NT SH-3 HELICOPTER

**SIKORSKY HSS-2 HELICOPTER**
U SH-3 HELICOPTER

**SIKORSKY S-65 HELICOPTER**
U H-53 HELICOPTER

**SIKORSKY S-67 HELICOPTER**
U S-67 HELICOPTER

**SILANES**
Silicon epitaxial films obtained by thermal decomposition of silane
18 p2188 N73-27666

**SILICA**
U SILICON DIOXIDE

**SILICA GLASS**
Feasibility of using terbium-silicate glass as Faraday rotator-isolator in high power laser
[AD-749919] 05 p0559 N73-14543
Fused silica coatings for flexible mat insulation of space shuttle surface
24 p2939 N73-33465
Silica fiber materials for surface insulation of space shuttle orbiters
24 p2939 N73-33467

**SILICATES**
NT ALUMINUM SILICATES
NT AMPHIBOLES
NT FELDSPARS
NT GARNETS
NT PYROXENES
NT YTTRIUM-ALUMINUM GARNET
NT YTTRIUM-IRON GARNET
NT ZEOLITES
Superconductivity of multifilamentary wires consisting of vanadium silicates
[BNL-16891] 03 p0346 N73-12818
Crystal chemistry of anhydrous and hydrous layer silicates
[NRC-TT-1479] 04 p0458 N73-13734
Spectral analysis of nonconducting siliceous materials by luminescent discharge
[CEA-CONF-2060] 12 p1405 N73-21397
Thermodynamic properties of solid and molten silicate systems
[NPL-CHEM-21] 15 p1844 N73-24938
Mapping exposed silicate rock types and exposed ferric and ferrous compounds from Skylab
[E73-10877] 20 p2393 N73-29228
Ceramic to metal bonding, noting improvement of Mo-Mn silicate method, and use of interfacially active metals
[BMFT-FB-T-73/07] 23 p2798 N73-32377
Infrared absorption spectra of lithium and potassium silicate glasses
[AD-764891] 24 p2893 N73-33092
Production of silica, mullite, and alumino silicate reusable surface insulation materials for space shuttle orbiters
[NASA-TM-X-2719] 24 p2938 N73-33461
Production engineering for silica reusable surface insulation panels
24 p2938 N73-33462
Amorphous silica material characterizations for thermal reusable insulation of space shuttle orbiter
24 p2939 N73-33470
Porosity analysis on silica and mullite composite surface insulation tiles
24 p2939 N73-33472
Simulated reentry heating tests on silica surface insulation material for space shuttle
24 p2940 N73-33482
Space environmental testing of silica insulation for space shuttle orbiter
24 p2941 N73-33484
Thermal cycling effects on properties of silica, mullite, and alumino-silicate insulation coatings
24 p2941 N73-33487
Cost effectiveness of silica insulation in space shuttle thermal protection system design
24 p2942 N73-33496
Thermostructural evaluation of mullite and silica composite materials for space shuttle surface insulation system design
24 p2942 N73-33498
Cristobalite transformation effects on tensile strength of silica surface insulation materials
24 p2943 N73-33500

**SILICIDES**
Improved silicide coatings for refractory metals employed in space shuttles and gas turbine engine components
[NASA-CASE-LEW-11179-1] 13 p1540 N73-22474
Kinetic of interstital contamination and defect growth in fused slurry silicide coated columbium alloys
[NASA-TN-D-7324] 18 p2160 N73-27448
Fused slurry silicide coatings for tantalum reentry heat shielding
[NASA-CR-120877] 20 p2485 N73-29964
Fused slurry silicide protective coatings for niobium alloy reentry heat shields for space shuttles - Vol. 1
[NASA-CR-121216] 23 p2857 N73-32826
Experimental and coating processes for fused slurry silicides on niobium alloy heat shields for space shuttles - Vol. 2
[NASA-CR-134483] 23 p2857 N73-32827

**SILICON**
Effects of electron-hole scattering on mobility to carriers in silicon at high injected carrier densities
01 p0087 N73-10718
Substitutional element diffusion coefficients in silicon
[AD-745945] 01 p0089 N73-10735
Radiation damage recovery characteristics of lithium doped solar silicon cells
[NASA-CR-129183] 02 p0128 N73-11044
Hydrolytically grown aluminum oxide films on silicon
[AD-747019] 02 p0193 N73-11564
Fabrication processes for silicon Schottky barrier diodes
[FRNC-TH-179] 03 p0274 N73-12218
Electrical overstress failures in silicon semiconductor devices
[AD-747795] 03 p0275 N73-12230
Conductivity profiles determined for beryllium diffused silicon for calculating diffusion coefficients
[NASA-CR-129169] 03 p0320 N73-12605
Spectral absorption coefficients of argon and silicon and spectral reflectivity of aluminum as function of pressure, temperature, and wave number
[NASA-CR-129300] 03 p0335 N73-12727
X ray diffraction analysis of crack propagation in deformed, notched, wedge shaped silicon crystal
[AD-746275] 03 p0346 N73-12820
Energy distributions of field-emitted electrons from p-type silicon surfaces
[AD-747067] 03 p0346 N73-12825
Chemical reaction of Si, SiC, and Si-SiC mixtures in CO and N at high temperature
[AD-747718] 04 p0438 N73-13569
Spatial distribution of radiation defects in silicon irradiated by protons, deuterons, and alpha particles
[AD-748734] 04 p0459 N73-13749
Design and performance of cylindrical silicon germanium thermoelectric generators
06 p0626 N73-15080
Operational performance of breadboarded silicon controlled rectifier series inverter circuitry for ion thruster power supply
[NASA-TM-X-2699] 06 p0626 N73-15082
Pulse voltage distribution over series connected silicon rectifiers
[AD-750969] 06 p0648 N73-15260
Optical and electrical properties of amorphous germanium and silicon semiconductors
[AD-748856] 06 p0709 N73-15788
Method for selecting silicon planar semiconductor devices for long life
[NASA-CR-124036] 07 p0803 N73-16516
Reduction of oxidation attack of nickel-base superalloy B-1900 by addition of one percent silicon
[NASA-TM-X-68191] 07 p0809 N73-16564
Fabrication of photodiode transistor image sensor array in silicon
[NASA-CR-130036] 07 p0831 N73-16738
Deep trap model for predicting capacitance voltage characteristics of irradiated silicon diodes and resistors
08 p0888 N73-17188
Thin film broadband absorber for use in underwater acoustics using silicon oils
[BMVG-FBWT-72-2] 09 p1067 N73-18703
Charge composition of cosmic rays for elements silicon to nickel
[LUIP-CR-72-16] 09 p1069 N73-18721
Autoradiograms of deformed silicon and germanium single crystal surfaces
[AD-753039] 09 p1074 N73-18765
Required doping levels for germanium and silicon infrared windows at microwave energies
[AD-753466] 09 p1075 N73-18772
Boundary scattering of phonons in germanium and silicon determined from low temperature thermal conductivity measurements
[AD-753494] 09 p1076 N73-18780
Growth of large-area silicon ribbons for application to large area solar cells and arrays
10 p1228 N73-19981
Electron- and neutron-induced defects in silicon p-n junctions
[AD-754905] 11 p1332 N73-20812
High power transcalent silicon semiconductor thyristor device including metallization techniques and heat pipe construction
[AD-755553] 13 p1502 N73-22174
Material properties of thin single crystal silicon films on insulator/polycrystalline silicon substrates
[AD-756646] 13 p1503 N73-22179
Microwave amplifier circuit for testing avalanche diode
[AD-756520] 13 p1503 N73-22180
Hall mobility measurements on single crystal silicon ribbons grown from graphite dies
[NASA-CR-131601] 13 p1565 N73-22686
Storage time loss in metal oxide capacitors caused by surface damage in silicon wafer
[AD-756250] 13 p1566 N73-22690

Analysis of EPR spectra in neutron irradiated silicon for determination of radiation damage in semiconductors
[AD-756907] 13 p1568 N73-22708
Borides, carbides, and nitrides of silicon oxidation resistant refractory compounds for use in gas turbines and reentry vehicles
14 p1678 N73-23616
Desilification in alumina and cement production by sintering disintegration method
[NLL-LIB-TRANS-1725-[5205.9]]
15 p1746 N73-24150
Electrical properties of silicon semiconductor under shock loads
[AD-759003] 16 p1971 N73-25945
Annealing properties and electron emission of amorphous and crystalline silicon
17 p2072 N73-26760
Feasibility determination of using ultrahigh fluences of implanted oxygen ions to create usable oxide layer on silicon for semiconductor device applications
[AD-760350] 17 p2075 N73-26785
Electrical conductivity and carrier lifetimes in gold doped silicon wafer
[AD-760150] 17 p2075 N73-26789
Electrical properties of silicon under dynamic loading
18 p2185 N73-27639
Influence of silicon particle deposition on volt-ampere characteristics of p-n junctions
18 p2186 N73-27652
Mechanism of silicon autoepitaxy during transport in sandwich process
18 p2187 N73-27655
Growth and properties of epitaxial silicon films treated with hydrogen of high purity
18 p2187 N73-27657
Effect of growth conditions and properties of silicon films deposited by chloride method
18 p2187 N73-27658
Transport coefficients of donor and acceptor mixtures for epitaxial growth of silicon by sandwich method
18 p2187 N73-27659
Alloying epitaxial layers of silicon with boron and arsenic using gas discharge
18 p2187 N73-27660
Distribution profiles of admixtures in epitaxial silicon layers prepared with hydrogen of high purity
18 p2187 N73-27661
Silicon epitaxial films obtained by thermal decomposition of silane
18 p2188 N73-27666
Effects of crystallization conditions on properties of autoepitaxial and heteroepitaxial layers of silicon obtained by hydride pyrolysis
18 p2188 N73-27667
Analysis of optimal conditions of selective growth of epitaxial layers of germanium and silicon
18 p2188 N73-27669
Procedure for obtaining monocrystalline layers of silicon by rheotaxial methods
18 p2189 N73-27673
Ion implantation damage in silicon and semiconductor devices
[AD-761486] 19 p2245 N73-28104
Quantitative deposition by standard techniques of adsorbates containing C and Si
[NASA-CR-124309] 19 p2343 N73-28850
Development of lithium-doped silicon solar cells with increased stability, efficiency, and radiation resistance
[AD-762941] 20 p2364 N73-29011
Shape of crystal interface and impurity striations in single crystals of silicon grown by Czochralski method
[NLL-RRE-TRANS-387-[8036.625]]
20 p2460 N73-29771
Junction capacitance techniques to characterize radiation damage in silicon
[AD-762482] 20 p2464 N73-29796
Effect of copper and silicon on selected mechanical properties of hot rolled medium carbon steels
[BM-RI-7777] 21 p2558 N73-30504
Performance calculation for Schottky field effect transistor on resistive substrate
22 p2641 N73-31167
Optical and electrical properties of amorphous Si and their dependence on thermal history
23 p2807 N73-32440
Interaction of powders of carbides of zirconium, niobium, and molybdenum with silicon using X ray and chemical analysis to determine reaction products
23 p2809 N73-32461
Effects of nuclear radiation on reverse bias electrical characteristics of silicon power diodes
[NASA-TN-D-7423] 23 p2821 N73-32554

**SILICON ALLOYS**
Thermodynamic properties of transition metal/silicon binary alloys
[NPL-CHEM-18] 03 p0365 N73-12970
Silicon additions and borax-glass coatings used to reduce surface hot shortness of copper-bearing steels
[PB-212660] 11 p1307 N73-20607
Effects of carbon and copper on magnetic properties of iron and iron-silicon alloys
[NASA-TT-F-14857] 12 p1428 N73-21574
Short range order effect on interatomic reaction and heat of displacement in molten nickel and silicon alloys
[NLL-M-21597-[5828.4F]] 15 p1797 N73-24568
Cause and prevention of smoky spots occurring on surface of silicon alloyed with boron after chemical polishing
18 p2188 N73-27663
Vapor phase heteroepitaxial growth of silicon germanium alloys by hydrogen reduction of tetrachlorides
20 p2460 N73-29767
Application of divergent beam X ray microdiffraction technique for measuring residual and impressed stresses and strains in iron-silicon alloy transformer sheet
[NBS-MONOGRAPH-130] 22 p2672 N73-31407

**SILICON CARBIDES**
Titanium alloy composites reinforced with silicon carbide fibers
[AD-745342] 01 p0070 N73-10573
Mechanical properties of heat resistant silicon carbide-graphite composite
[AD-745434] 01 p0070 N73-10577
Compressive surface layer formation on hot pressed silicon carbide and nitride to improve impact resistance
[NASA-CR-121002] 02 p0222 N73-11796
Single crystal alpha SiC for GEISHA device with electron carrier velocity up to 8,200,000 cm/sec on 10 to 17th power/cu cm uncompensated n-type crystals
[AD-747270] 03 p0275 N73-12228
Silicon graphite and heat resistant titanium alloys
[JPRS-57679] 04 p0433 N73-13526
Properties and uses of silicon graphite
04 p0433 N73-13527
Technology assessment of silicon carbide reinforced composites with aluminum or nickel matrix discussing mechanical resistance at high temperatures
04 p0434 N73-13543
Chemical reaction of Si, SiC, and Si-SiC mixtures in CO and N at high temperature
[AD-747718] 04 p0438 N73-13569
Thermogravimetric measurements for oxidation of hot pressed silicon carbide
[AD-748351] 04 p0439 N73-13578
Fracture behavior of silicon nitride and silicon carbide ceramics
[NASA-CR-129671] 05 p0564 N73-14585
Liquid hot pressing of silicon carbide whiskers for reinforcing aluminum alloy composites
[AD-752589] 08 p0936 N73-17666
Synthesis of SiC single crystals free from carbon particle inclusions
[AD-752227] 08 p0952 N73-17792
Mechanical properties of silicon carbide and aluminum oxide sapphire filaments for design of metal matrix composites
[AD-753711] 10 p1176 N73-19568
Influence of annealing on thin films of beta SiC
[AD-755792] 12 p1442 N73-21683
Development of high strength composite tungsten alloy and silicon carbide filaments for high temperature applications
[AD-756867] 13 p1549 N73-22551
Improved resin adhesion by depositing silicon carbide whiskers on carbon fibers
[AD-757659] 14 p1681 N73-23642
High temperature testing of silicon carbide ceramics for use in gas turbine vanes
[AD-757796] 15 p1802 N73-24602
Compatibility of silicon carbide fibers with tungsten substrate and titanium matrix
20 p2430 N73-29520
Temperature relationship of work function of silicon carbide for application to direct conversion of thermal energy to electrical energy
23 p2807 N73-32443
Characteristics of silicon carbide samples produced by hot casting under pressure
23 p2808 N73-32450
Hot pressing behavior of SiC with Al2O3
[AD-764639] 23 p2811 N73-32475

**SILICON COMPOUNDS**
NT ALUMINUM SILICATES
NT FELDSPARS
NT FLINT
NT GARNETS
NT NEPHELITE
NT PYROXENES
NT QUARTZ
NT SILANES
NT SILICATES
NT SILICIDES
NT SILICON CARBIDES
NT SILICON DIOXIDE
NT SILICON NITRIDES
NT SILICON OXIDES
NT YTTRIUM-ALUMINUM GARNET
NT YTTRIUM-IRON GARNET
Analysis of thermal expansion coefficients and elastic moduli of solid solutions of silicon in given solutions
[AD-745825] 01 p0068 N73-10557
Development and characteristics of Si-As-Te glasses containing Ag and Se as constituent of chalcogenic glasses
[AD-749958] 05 p0567 N73-14603
Effect of proton bombardment on photoelectric characteristics of n-p junctions alloyed with n-type silicon and lithium admixture
[AD-750977] 06 p0709 N73-15783
Room temperature electrical properties of SiGe thermoelectric alloys
[SC-DC-72-1020] 07 p0812 N73-16581
Evaluation of ceramic materials for application as high temperature gas bearing material
[AD-753858] 09 p1042 N73-18499
Friction, wear, and thermal stability of some organotin and organosilicon compounds
[NASA-TN-D-7175] 09 p1051 N73-18569
Bulk, surface, and superficial analysis of semiconductor grade silicon and gallium arsenide
[CONF-721069-36] 17 p2073 N73-26770
Capability of portable SF6 chromatograph to detect and determine behavior of plume out to 100 km
[BNL-17478] 22 p2674 N73-31417
Process for preparing disilanols with in-chain perfluoroalkyl groups
[NASA-CASE-MFS-20979-2] 23 p2753 N73-32030

**SILICON CONTROLLED RECTIFIERS**
Minority carrier lifetime optimization for gallium silicon diffusion thyristor
11 p1330 N73-20795

**SILICON DIOXIDE**
NT QUARTZ
Specifications for fused silica slip-casting radome material
[AD-745332] 01 p0028 N73-10219
Processing specifications for slip-cast fused silica radomes
[AD-745793] 01 p0029 N73-10229
Effect of heat treatment on adsorption properties of titano-silica gel and interactions of adsorbed molecules with silanol groups
[NLL-RTS-7360] 01 p0069 N73-10564
Characteristics of ion transport in silicon dioxide, interface phenomena, and photoelectric method of storing charge in floating gate MOS memory
[AD-746999] 03 p0346 N73-12823
Ion migration in SiO2 layer of integrated circuit oxides
[AD-747435] 03 p0348 N73-12836
Effect of glass laser radiation on borosilicate crown glass, fused silica, and flint glass with estimates of Kerr effect and electrostriction processes
05 p0555 N73-14510
Optical surface correction method for laser reflectors based on vacuum silica vapor differential deposition
05 p0558 N73-14530
Analysis of particle erosion of solid surfaces using model of erosion pit nucleation and growth for solid spherical particles impacting on plane surface of elastic half space
[AD-752221] 08 p0935 N73-17657
HCL processing effects on electrical stability and quality of thermally grown SiO2
[AD-754110] 10 p1202 N73-19786
Feasibility of using RF generated argon plasma for sputter etching Al and SiO2 windows and photoresist
[AD-757878] 15 p1800 N73-24588
Mathematical models for surface ablation of silica-reinforced composites
15 p1801 N73-24596
Effects of ion implantation displacement damage in silicon diodide insulator of MIS capacitor
[AD-758695] 16 p1881 N73-25228
Properties of silicon-silicon dioxide interface properties in thin oxide metal oxide semiconductor structures
24 p2968 N73-33718

**SILICON FILMS**
Carrier mobility in epitaxial silicon film deposited on spinel crystal surface
[NLL-TRANS-2768-[9022.81]]
05 p0585 N73-14781
Variations in electrical properties of silicon films on sapphire using MOS Hall technique
13 p1564 N73-22679
Formation of current filaments in thin film silicon-on-sapphire diodes
16 p1952 N73-25795
Thermodynamic analysis of Si film growth rate in vertical reactor
18 p2186 N73-27651
Structure, composition, and electrophysical properties of autoepitaxial silicon layers from vapor-gas tetrachloride mixture
18 p2186 N73-27653
Low temperature epitaxial development of Ge and Si layers by chloride method
18 p2187 N73-27656

Selective growth of epitaxial silicon layers in chloride process
18 p2188 N73-27668
Growth of monocrystalline films of silicon base
18 p2189 N73-27672

**SILICON JUNCTIONS**
Manufacturing of hyperabrupt Si varicaps based on impurity diffusion from double doped substrate
12 p1384 N73-21221
Design of vertical multijunction silicon solar cells with prolonged lifetimes
[AD-760172] 17 p1986 N73-26052
High bias tunneling of silicon and aluminum semiconductor junctions
19 p2326 N73-28712
Design and performance of silicon Schottky barrier avalanche diodes
23 p2764 N73-32113
Minority carrier lifetime control in n-type base regions of gallium diffused silicon power thyristors and diodes
[BMFT-FB-T-73-05] 23 p2765 N73-32123
Fluxon coupling force measurements on superconducting dc transformers noting film thickness and silicon monoxide layer
24 p2898 N73-33135

**SILICON NITRIDES**
Annealing effect on amorphous silicon nitride protective film defects
[DRIC-TRANS-2902] 02 p0192 N73-11557
Compressive surface layer formation on hot pressed silicon carbide and nitride to improve impact resistance
[NASA-CR-121002] 02 p0222 N73-11796
Annotated bibliography of sintered and hot pressed silicon nitride
[AD-747785] 03 p0322 N73-12624
Fracture behavior of silicon nitride and silicon carbide ceramics
[NASA-CR-129671] 05 p0564 N73-14585
Application of powder metallurgical techniques to fabrication of reaction-bonded Si3N4 for use as high temperature engineering ceramic
[AD-750096] 06 p0688 N73-15603
Fatigue tests of hot pressed silicon nitride ball bearings
[NASA-TM-X-68174] 06 p0725 N73-15922
Reactive hot pressing for producing silicon nitrides
[AD-757748] 15 p1802 N73-24604
Characteristics and production of silicon nitride-alumina sintered materials
[NLL-RTS-7988] 16 p1931 N73-25627
Microstructure of hot pressed and press forged polycrystalline refractory oxides
[AD-760353] 17 p2053 N73-26606
Survey of Soviet literature on use of silicon nitride for gas turbine applications
[AD-760329] 17 p2078 N73-26810
Production of silicon nitride layers on silicon by growth from gas phase and properties of resulting layers
18 p2189 N73-27670
Force and wear analysis in ceramic processing for alumina and silicon nitride
[AD-762522] 20 p2436 N73-29561

**SILICON OXIDES**
NT NEPHELITE
NT QUARTZ
NT SILICON DIOXIDE
Mechanical properties of thin films of Ni-SiO
[NLL-TRANS-746-1329-[9022.401]]
05 p0564 N73-14582
Ion implantation of amorphous insulators and switching effects in silicon oxides
[LETI/ME-773] 07 p0832 N73-16744

**SILICON POLYMERS**
NT SILICONE RESINS
NT SILICONES
NT SILOXANES

**SILICON RADIATION DETECTORS**
X ray spectrometer using cooled Si[Li] detectors
[CEA-CONF-1963] 03 p0336 N73-12736
Application of multichannel analyzer with lithium drifted silicon detector to determine spectral distribution of low energy X ray devices
[BDX-613-704] 04 p0450 N73-13672
Scanning spectrometer for fluorescence measurements, and silicon detector for alpha counting
[BARC-628] 19 p2230 N73-27984

**SILICON RECTIFIERS**
U CRYSTAL RECTIFIERS

**SILICON SOLAR CELLS**
U SOLAR CELLS

**SILICON TRANSISTORS**
Numerical analysis to obtain error estimate for thermal resistance measurements on uncoated silicon microwave transistors as result of temperature gradients
[AD-748073] 03 p0276 N73-12235
Design and performance of transistorized broadband logarithmic amplifier using hybrid thick film technology
[ECR-32] 12 p1382 N73-21210

**SILICONE RESINS**
Comparison of oxygen transport in polymonomethylsiloxane with properties of polydimethylsiloxane to determine degradation mechanisms in pigmented coatings
[AD-753410] 10 p1176 N73-19565
High temperature silicone adhesive formulations for thermal protection systems used with space shuttle mission
[NASA-CR-124389] 22 p2688 N73-31533

**SILICONE RUBBER**
Silicone rubber cover for protecting flush-deck nozzles on aircraft carriers
[AD-746841] 02 p0153 N73-11241
Carbon black additives used to improve heat-aging resistance in silicone rubber vulcanizates
[AD-747769] 03 p0321 N73-12619
Design allowables for room temperature vulcanizing silicone rubber based adhesives for attaching reusable surface insulation to space shuttle structures
[NASA-CR-128887] 11 p1308 N73-20615
Polycondensation syntheses of heat resistant siloxane polymers with fluoro aromatic groups at silicon atoms
[RAE-LIB-TRANS-1669] 17 p1991 N73-26104
High performance vulcanized elastomers produced by nitrile and silicone rubber covulcanization
[RAE-TR-72184] 17 p2050 N73-26588
Titanium dioxide doped silicone rubber potting compound for satellite-borne channel multipliers
24 p2927 N73-33379

**SILICONES**
Low temperature bonding of solar panel materials
[AD-746684] 05 p0553 N73-14493
Silicone base nonflammable hydraulic fluid to aid wear resistance in military aircraft
[AD-758361] 14 p1671 N73-23562
Silicone additives for heat flux reduction in hydrazine rocket propellants
[AD-756913] 14 p1700 N73-23798
Hydraulic pump-looped circuit evaluation of candidate silicone base nonflammable hydraulic fluid
[AD-764064] 22 p2679 N73-31456
Elastomeric silicone adhesive systems for surface insulation attachment to space shuttle
24 p2942 N73-33491

**SILOS [MISSILE STORAGE]**
U MISSILE SILOS

**SILOXANES**
Wide Temperature range, nonpolymeric, large molecular weight lubricants based on combination of siloxane and aromatic groups, for equipment near spacecraft nuclear reactors
[NASA-CR-123966] 04 p0447 N73-13654
Glass transition characteristics and compatibility of linear poly carborane-siloxane series plastics
[AD-749385] 05 p0566 N73-14597
Thermomechanical behavior and structure of poly[carborane-siloxane]s containing icosahedral cages in nitrogen environment
[AD-749364] 05 p0566 N73-14598
Infrared and NMB spectra of poly[carborane-siloxane] s containing icosahedral cages in nitrogen environment
[AD-749386] 05 p0566 N73-14599
Relationship of molecular structure to thermo-oxidative stability of carborane-siloxane polymers with icosohedral CB10H10C cages
[AD-749820] 05 p0567 N73-14610
Fluid polydimethylsiloxane resin with low outgassing properties in cured state
[NASA-CASE-GSC-11358-1] 17 p1991 N73-26100
Utilization of thiophenyl ether disiloxane and trisiloxane as lubricant fluids in severe environment including space
[NASA-CASE-MFS-22411-1] 19 p2304 N73-28532

**SILTS**
U SEDIMENTS

**SILVER**
Manufacture and testing silver parabolic mirror cut directly with diamond tool in numerically-controlled lathe
[UCRL-51213] 03 p0335 N73-12734
Development and characteristics of Si-As-Te glasses containing Ag and Se as constituent of chalcogenic glasses
[AD-749958] 05 p0567 N73-14603
Waveguiding in thin silver strip vacuum deposited on bismuth germanium oxide
[AD-750612] 06 p0648 N73-15262
Influence of surface finishing on adherence of radio frequency sputtered molybdenum disulfide on silver, gold, copper, and bronze
[NASA-TN-D-7169] 07 p0804 N73-16523
Infrared spectroscopic investigation of polyimide films containing silver metal
[TR-62] 09 p1048 N73-18545
Microscopic analysis of silver diffusion into gold plate on electrical connector
[AD-755123] 11 p1263 N73-20249
Silver-ion bactericidal monitor for Space Shuttle potable water system
[NASA-CR-128884] 11 p1293 N73-20492
Creep processes in vacuum sintered copper and silver
12 p1407 N73-21407
Theoretical analysis of plastic flow and diffusion during sintering of Li6, Ag, and Ni systems
20 p2428 N73-29499
Lateral diffusion in thin [film] couples of gold and silver
23 p2825 N73-32579
Proton channeling in silver single crystals at 300, 90, and 20 K
23 p2825 N73-32583
Wavelength modulation spectra of copper, gold, silver, gallium phosphide, and indium phosphide
[LBL-1125] 24 p2927 N73-33375

**SILVER ALLOYS**
Effects of growth speed and heat treatment on deformation of aligned Ag3 Mg-AgMg and Al-Ag2 Al eutectics at minus 196 to 300 C
[AD-747310] 02 p0190 N73-11541
Effects of interatomic forces on diffusion mechanisms in silver cadmium alloys, silver indium alloys and silver lead alloys
[CEA-R-4292] 03 p0333 N73-12714
Materials for ball bearings for space applications using chromium steel and silver-indium alloy
[REPT-781-4.4] 10 p1166 N73-19490
Volumetric expansion of silver alloy at room temperature
[TID-26251] 16 p1928 N73-25602
Creep properties of aligned silver-magnesium eutectic alloy
[AD-763375] 21 p2561 N73-30531
Transverse magneto-resistance and Hall resistivity in pure cadmium and in dilute crystal alloys of Cd-Ag and Cd-In
23 p2825 N73-32585

**SILVER CADMIUM BATTERIES**
Performance tests of nickel cadmium and silver cadmium electric batteries to determine service life and reliability
[NASA-CR-132801] 17 p1985 N73-26046

**SILVER CHLORIDES**
Luminescence of normal and deformed single crystals of AgCl of different thickness measured at minus 180 C
[AD-755430] 12 p1441 N73-21677

**SILVER COMPOUNDS**
NT SILVER CHLORIDES
NT SILVER HALIDES
NT SILVER IODIDES
Molten single crystal silver compounds for studying photographic sensitivity
[AD-746294] 02 p0175 N73-11421
Preparation of thin film metal fluoride electrodes from elemental constituents to obtain high purity and variations in size and shape
[NASA-TM-X-2690] 04 p0386 N73-13140

**SILVER HALIDES**
NT SILVER CHLORIDES
NT SILVER IODIDES
Large silver halide single crystals as charged particle track detectors in regions of damaged lattice
05 p0609 N73-14951

**SILVER IODIDES**
Silver iodide particle size effect on water condensation for artificial precipitation
[AD-758857] 17 p1993 N73-26114
Theoretical determination of heterogeneous nucleation rate of supercooled water droplets from thermally generated AgI particles
[AD-758858] 18 p2114 N73-27095
Feasibility of electrochemical silver/silver iodide/iodine battery
[SC-RR-72-0386] 24 p2881 N73-33006

**SILVER OXIDE ZINC BATTERIES**
U SILVER ZINC BATTERIES

**SILVER ZINC BATTERIES**
High energy density storage system with encapsulated silver zinc cells for deep ocean applications
[AD-750719] 06 p0627 N73-15085
Chemical stability, electrochemical properties and wetting characteristics of polyvinyl and polyethylene membrane separators for alkaline silver zinc batteries
[NASA-CR-130154] 07 p0741 N73-16030
Design parameters that contribute to cycle life of sealed, heat-sterilized silver oxide-zinc cells
[NASA-CR-130723] 08 p0869 N73-17038
Computational formula for reliability analysis on multiple element circuits of silver zinc storage battery
[AD-754725] 11 p1238 N73-20050
Effect of active, inductive and capacitive resistance of elements of asymmetric alternating current battery charger on discharged characteristics of silver zinc batteries
[AD-756955] 13 p1478 N73-21970
Oxygen gas production during stand and discharge in silver zinc batteries
[NASA-CR-128933] 15 p1738 N73-24087
Current distribution in flooded, porous electrodes
[NASA-CR-131839] 16 p1864 N73-25098
Performance tests and failure analyses on silver zinc cells with inorganic separator materials
[NASA-CR-121215] 18 p2108 N73-27049

Diffusion across modified polyethylene separator in heat sterilizable silver zinc battery
[NASA-CR-133601] 20 p2363 N73-29007
Activation and cycling of silver zinc batteries
[AD-761186] 20 p2364 N73-29013

**SIMICOR [IMAGE CORRELATOR]**
U IMAGE CORRELATORS

**SIMILARITY NUMBERS**
Similarity analysis of transient temperature and thermal stress for deriving scaling relations for modeling thermal shock
[SC-RR-71-0657] 04 p0485 N73-13962

**SIMILITUDE LAW**
Similitude theory for design optimization of automatic control systems for aircraft gas turbine engines
[AD-764683] 23 p2832 N73-32631
Aerothermodynamic study of air cushion vehicles buffeting noting dynamical stability, nonlinear behavior, and similitude law
[NT-33-1973] 24 p2870 N73-32933

**SIMPLIFICATION**
Simplification of Boolean functions adapted to incompletely specified functions
03 p0325 N73-12649

**SIMULATION**
NT ALTITUDE SIMULATION
NT ANALOG SIMULATION
NT ATMOSPHERIC ENTRY SIMULATION
NT COMPUTERIZED SIMULATION
NT CONTROL SIMULATION
NT DIGITAL SIMULATION
NT ENVIRONMENT SIMULATION
NT EXHAUST FLOW SIMULATION
NT FLIGHT SIMULATION
NT LANDING SIMULATION
NT SPACE ENVIRONMENT SIMULATION
NT THERMAL SIMULATION
NT WEIGHTLESSNESS SIMULATION
Global distributions of mean January surface wind stress, diabatic heating rate, and rate of moisture addition as simulated in 30-day integration with atmospheric general circulation model
[AD-745752] 01 p0077 N73-10640
Gas-embedded z-pinch and numerical simulation of lithium liner for collapsing theta pinch
[AD-745016] 01 p0086 N73-10708
Space simulation study of plume contamination in reaction control thruster
[NASA-TM-X-68149] 01 p0090 N73-10743
Simulating radiant heating of propellant stream of nuclear light bulb engine
[NASA-CR-129499] 03 p0330 N73-12693
Fast flux neutron source for cyclotron simulation of reactor core
[AERE-R-6626] 04 p0402 N73-13269
Simulation of flow of compressible gas through water channel of varying cross section
[AD-749134] 04 p0408 N73-13327
Magnetization experiments to simulate cusp coil tests
[ORNL-TM-3887] 04 p0459 N73-13744
Numerical simulation and study of collisional plasmas and shock tube phenomena
[COO-3086-15] 05 p0583 N73-14748
Response of cylindrical shells to traveling load simulation of x ray blow-off impulse
[AD-750336] 06 p0727 N73-15933
Performance test of aluminum alloy landing mats under heavy duty loads
[AD-753935] 10 p1138 N73-19276
Dynamic functions of air blast parameters in detonation of spherical trinitrotoluene charge
[AD-753805] 10 p1187 N73-19659
Simulation of plastic bonded hexanitrostilbene/Teflon explosive for lunar seismology
[NASA-CR-131370] 11 p1349 N73-20949
Laboratory simulation of meteors and meteoroid impact
[NASA-CR-131468] 12 p1448 N73-21725
Processing digital radar data base to create simulated mapping-radar scope images
[AD-755722] 13 p1495 N73-22118
Sinusoidal simulation of material fatigue life when subjected to Gaussian narrow band random loading
20 p2477 N73-29896
Simulated tank fragmentation test
[NASA-TM-X-68282] 20 p2482 N73-29942
Simulation of growth and mineral uptake by plants growing in lunar soil
[NASA-CR-134036] 22 p2619 N73-30988
Effects of rocket plume simulators on pressure distribution of body of revolution at transonic speeds
[NASA-CR-133916] 22 p2651 N73-31238

**SIMULATOR TRAINING**
U TRAINING SIMULATORS

**SIMULATORS**
NT COCKPIT SIMULATORS
NT CONTROL SIMULATION
NT ENVIRONMENT SIMULATORS
NT FLIGHT SIMULATORS
NT SHOCK SIMULATORS
NT SOLAR SIMULATORS
NT SPACE SIMULATORS
NT SPACECRAFT CABIN SIMULATORS
NT TARGET SIMULATORS
NT TRAINING SIMULATORS
NT VIBRATION SIMULATORS
Construction of sonic boom simulators to determine effects of sonic boom on human heart reactions and analysis of human responses
[UTIAS-TN-180] 02 p0152 N73-11233
Iterative method for real time actuator extension transformation analysis on motion simulator
[NASA-TN-D-7067] 03 p0269 N73-12182
Procedures for analyzing very thick walled cylindrical shells used in constructing hydrospace simulators
[AD-747963] 03 p0362 N73-12952
Spacecraft simulation techniques applicable to flight simulator motion systems
[NASA-CR-128653] 04 p0401 N73-13266
Design of ionospheric plasma simulator for analyzing and modeling high altitude plasma phenomena
[AD-748311] 04 p0417 N73-13401
Design and performance of breathing metabolic simulator
04 p0472 N73-13850
Simulator research at Netherlands National Aerospace Laboratory
[AD-750589] 06 p0650 N73-15283
Fabrication and performance of real-time jet engine simulator for development of jet engine components and control systems
[NAL-TR-283] 06 p0713 N73-15820
Design, construction, and operation of combined principles simulator of gas core nuclear engine
[NASA-CR-2155] 07 p0826 N73-16691
Simulation of thermal radiation-airblast interaction effects in conical shock tube
[AD-752023] 08 p0893 N73-17229
Development of digital fast-time air traffic control conflict prediction models and application to specific air route traffic control situations
[UTIAS-TN-183] 08 p0941 N73-17708
Development of simulator for training personnel in underwater terrain navigation and reconnaissance
[AD-754091] 11 p1322 N73-20729
Cylindrical chamber for simulating electrical impedance of whip antenna
[AD-757141] 13 p1501 N73-22167
Star simulator photometric calibration based on Vega spectrum
[RAE-TR-72138] 14 p1646 N73-23346
Initiator ignition effect in laboratory glass and polythene vessel studying dummy hand injuries during simulated accidents
[ERDE-TRANS-1] 15 p1744 N73-24137
Digital radar landmass simulation for determining optimum specification of digital radar training devices
[AD-758363] 15 p1763 N73-24284
Attached manipulator system for simulating and demonstrating shuttle manipulator cargo handling operations under weightless conditions
[NASA-CR-133964] 18 p2126 N73-27176
Feedback control loop stability analysis for dynamic solar array simulator, based on frequency response and using digital computer
[ESRO-CR(P)-261] 19 p2223 N73-27929
Deep sea simulator facilities in USA in 1972
[AD-761899] 19 p2249 N73-28136
Comparative evaluation of conventional and solid state simulators for A-7 aircraft electrical system
[AD-762295] 19 p2250 N73-28142
Daytime fog simulator system modifications
[FAA-RD-73-130] 22 p2647 N73-31208
Effects of rocket plume simulators on pressure distribution of body of revolution at transonic speeds
[NASA-CR-133916] 22 p2651 N73-31238

**SIMULTANEOUS EQUATIONS**
Asymptotic properties of full information estimators in dynamic autoregressive simultaneous equations
[P-4924] 12 p1418 N73-21494

**SIMULTANEOUS IMAGE CORRELATOR**
U IMAGE CORRELATORS

**SINE**
U TRIGONOMETRIC FUNCTIONS

**SINE SERIES**
Function generators for producing complex vibration mode patterns used to identify vibration mode data
[NASA-CASE-LAR-10310-1] 11 p1263 N73-20253

**SINE WAVES**
Development of procedure for measuring sinusoidal vibration displacement amplitude using laser homodyne system
[RM-5601] 03 p0310 N73-12526
Measurement of sinusoidal waves in flumes with transducers using non-contacting capacitive sensing
[NRC-MI-836] 05 p0522 N73-14243
Solution of Laplace equation in space bounded by flat and sinusoidal surface for determination of precision of noncontacting capacitive wave transducers
[AD-752021] 09 p1008 N73-18229
Stiffness of flat strips in compression under sinusiodally distributed bending couples at their edges
[ESDU-05.01.30-AMEND-A] 14 p1714 N73-23906
Characteristics of turbulent flow over wavy surface using sinusoidal waves of three sizes to determine variations of flow with wave size
16 p1887 N73-25273
Development of program for obtaining resonant frequencies, modal amplitudes, and damping of structure from sinusoidal force-controlled vibration test
[NASA-TM-X-2789] 22 p2724 N73-31802
Sine wave propagation in lossy plasmas
[AD-764721] 23 p2758 N73-32073
Brushless electromechanical generator for sine and cosine functions
[NASA-CASE-LAR-11389-1] 23 p2765 N73-32121
Characteristics of flow about spherical body undergoing rectilinear, sinusoidal oscillations in viscous, incompressible fluid
23 p2773 N73-32180
Turbulent shear stress profiles in boundary layer flow at sine wave pressure perturbations
24 p2906 N73-33194

**SINGLE CRYSTALS**
NT WHISKERS [SINGLE CRYSTALS]
Analysis of oxidation of high purity tantalum single crystals and large-grained tantalum sheets
[AD-745341] 01 p0068 N73-10554
Molten single crystal silver compounds for studying photographic sensitivity
[AD-746294] 02 p0175 N73-11421
Single crystal alpha SiC for GEISHA device with electron carrier velocity up to 8,200,000 cm/sec on 10 to 17th power/cu cm uncompensated n-type crystals
[AD-747270] 03 p0275 N73-12228
Plastic deformation of oriented single crystals of tungsten
[AD-747569] 03 p0318 N73-12590
Single crystal growth of ceramic oxides and compound semiconductors in space
[NASA-CR-123951] 03 p0344 N73-12806
Technology for determining mechanical properties of single crystal and polycrystals at low temperature
[AD-748744] 03 p0348 N73-12838
Theoretical and experimental investigations of CdS single crystals photovoltaic cells
[NASA-CR-129675] 04 p0457 N73-13730
Beryllium and beryllium-lithium complexes in single crystal silicon with acceptor levels 191 and 145 MeV
[NASA-TR-R-395] 04 p0458 N73-13736
Determination of activation parameters and microcreep in niobium single crystals at low temperature
[COO-1198-909] 04 p0458 N73-13742
Single crystal shaped as turbine blade, both hollow and solid
[AD-748519] 04 p0465 N73-13786
Magnetic properties of single crystal nickel powers
[NLL-TRANS-746-1390-[9022.401]]
05 p0585 N73-14762
Single crystal growth of indium antimonide
05 p0608 N73-14940
Electrical and photoelectrical properties of trigonal selenium single crystals, including Hall mobility
[PUBL-170] 06 p0707 N73-15771
Dislocation damping in cu single crystals of controlled substructure, and ultrasonic attenuation data
[AD-750712] 06 p0711 N73-15801
Crystallographic fatigue crack growth in aluminum single crystals
[AD-751603] 07 p0810 N73-16567
Optical transmission measurements of single crystal and polycrystal CsI
[NASA-TM-X-66178] 08 p0951 N73-17784
Synthesis of SiC single crystals free from carbon particle inclusions
[AD-752227] 08 p0952 N73-17792
Hydrothermal method for growing single crystal zircon polarizers
[AD-752147] 08 p0952 N73-17793
Mechanical properties of unidirectionally solidified, in-situ grown composites
[ONERA-TP-1147] 09 p1051 N73-18570
Growth of FeS[x] and NbO2 single crystals
[AD-753270] 09 p1074 N73-18768
Elucidation of satellite lines of manganese-doped zinc selenide single crystals in electron paramagnetic resonance spectrum
[AD-753507] 09 p1077 N73-18788
Thermal dilatation coefficients of explosive monocrystals determined by extensometry
[ISL-24/71] 09 p1099 N73-18969
Measurement of phonon scattering by isotopic impurities in helium single crystals
[AD-754475] 11 p1330 N73-20798
Luminescence of normal and deformed single crystals of AgCl of different thickness measured at minus 180 C
[AD-755430] 12 p1441 N73-21677
Single crystals of high melting point metals in solid solution
[NASA-CR-124212] 13 p1540 N73-22476
Hall mobility measurements on single crystal silicon ribbons grown from graphite dies
[NASA-CR-131601] 13 p1565 N73-22686
Static longitudinal and transverse susceptibilities calculated for iron fluoride as function of temperature
[AD-757009] 14 p1698 N73-23781
Preflight, inflight, and post flight operations evaluation analyses for Skylab gallium arsenide single crystal growth facility - Appendix J
[NASA-CR-61386-APP-J] 14 p1708 N73-23863

Optical and electronic properties of single crystal Cu2S-CdS photovoltaic cells
[NASA-CR-121228] 15 p1738 N73-24091
Growth and hardening of potassium chloride single crystals for infrared laser windows
[AD-757893] 15 p1795 N73-24550
Axial and planar channeling effects in thin crystals 15 p1820 N73-24750
Anomalous X ray transmission through single germanium crystals 16 p1952 N73-25793
Temperature dependence of elastic constants and Debye temperature of NaCl and KCl single crystals
[NASA-TT-F-14932] 16 p1953 N73-25801
Plastic properties of alpha-phase Cu-Al single crystals at low and room temperature 17 p2042 N73-26524
Piezo- and thermo-optical properties of bismuth germanium oxide single crystals 17 p2071 N73-26754
Optical spectra and crystal field parameters of neodymium in lanthanum aluminate 17 p2071 N73-26757
Growth of single crystals of rhenium and iridium dioxides
[NASA-CR-133213] 17 p2072 N73-26768
Preparation of single crystal films by reactive sputtering process
[AD-760715] 18 p2123 N73-27160
High temperature effects on dislocation mobility of LiF single crystals 18 p2185 N73-27642
Theoretical treatment of Schwarz-Hora effect in which electron beam passing through crystal is modulated by laser light and reproduces it on striking nonluminescent target 18 p2185 N73-27643
Electronic properties of beryllium single crystals with emphasis on microwave surface impedance 18 p2185 N73-27646
Growth of monocrystalline films of silicon base 18 p2189 N73-27672
Procedure for obtaining monocrystalline layers of silicon by rheotaxial methods 18 p2189 N73-27673
X ray diffraction analysis of single crystals of high purity copper subjected to shock loading
[AD-762146] 19 p2311 N73-28586
Plastic deformation of single crystal sapphire filaments
[AD-762302] 19 p2313 N73-28603
Development of low energy diffraction system for observing surface structure of low-index single crystal metal surfaces with and without absorbates 20 p2429 N73-29510
Characteristics of single crystals of metals with melting points and effects of crystal growth under zero-gravity conditions
[NASA-CR-124354] 20 p2432 N73-29532
Shape of crystal interface and impurity striations in single crystals of silicon grown by Czochralski method
[NLL-RRE-TRANS-387-[8036.625]] 20 p2460 N73-29771
Photographic equipment for recording fracture of zinc single crystals under dynamic stress 20 p2461 N73-29775
Growth of high quality, single crystalline, Pb Sn Te by vapor-phase epitaxy for infrared detectors
[AD-762344] 20 p2463 N73-29795
Using single crystals to determine ionization energies of organic semiconductors
[NASA-CR-133827] 21 p2517 N73-30188
Adsorption kinetics of CO on [100] face of molybdenum single crystal
[CEA-CONF-2194] 22 p2684 N73-31499
Nonlinear elastic and thermoelastic properties of single crystals of refractory materials
[COO-3418-9] 22 p2689 N73-31535
Proton channeling in silver single crystals at 300, 90, and 20 K 23 p2825 N73-32583
Crack propagation velocities in NaCl crystals 23 p2826 N73-32586
Pulling single crystal silicon in space environment
[NASA-CR-124439] 23 p2826 N73-32588
Absence of S band energy gap in single crystal niobium
[AD-764906] 23 p2827 N73-32594
Interaction of supersaturated vacancies and vacancy clusters with dislocations in copper single crystals 24 p2967 N73-33715

**SINGLE SIDEBAND DEMODULATION**
U SINGLE SIDEBAND TRANSMISSION

**SINGLE SIDEBAND MODULATION**
U SINGLE SIDEBAND TRANSMISSION

**SINGLE SIDEBAND RECEIVERS**
U SINGLE SIDEBAND TRANSMISSION

**SINGLE SIDEBAND TRANSMISSION**
Design and fabrication of high stability, temperature compensated, crystal oscillator for advanced SSB communication equipment
[AD-745914] 02 p0149 N73-11212
Development of single sideband quartz crystals for use in temperature compensated crystal oscillators
[AD-749642] 06 p0646 N73-15244
System performance with single and double sideband doppler low level receiver maintenance simulation
[FAA-RD-72-67] 07 p0818 N73-16627
Design, processing, and measurement of precision single sideband crystal units
[AD-751748] 07 p0833 N73-16754
Design and performance of circuit for measuring tuning error of single-sideband receiver
[AD-753612] 09 p1004 N73-18199
Speech modulated, single sideband, suppressed carrier systems for speech reception 14 p1630 N73-23215
Frequency division multiplexer for operation in double or single sideband channel
[NASA-CR-124250] 14 p1640 N73-23293
Single sideband quartz crystal with long term aging
[AD-761101] 18 p2125 N73-27170

**SINGLE STAGE ROCKET VEHICLES**
NT ARCAS ROCKET VEHICLES
NT BLACK BRANT SOUNDING ROCKETS
NT HONEST JOHN ROCKET VEHICLE
NT LITTLE JOHN ROCKET VEHICLE
NT LOKI ROCKET VEHICLE
NT VERONIQUE ROCKET VEHICLES

**SINGULARITY [MATHEMATICS]**
Light cone and hyperbaloid contributions to structure functions in Bjorken limit
[TR-73-076] 06 p0702 N73-15726
Singularity method for calculating incompressible flow through cascades with separation 10 p1205 N73-19802
Calculation of pressure field induced by free jet exhausted from flat plate into stagnant medium based on solution of Neumann problem in terms of singularity distributions
[NLR-TR-72040-U] 21 p2492 N73-30000
Treatment of singularities in solution of Laplace equation by integral equation method based on Green function, applied to flow distribution and transmission lines
[NPL-NAC-31] 23 p2813 N73-32490

**SINKS**
NT HEAT SINKS
U STRUCTURAL BASINS

**SINKS [GEOLOGY]**
U STRUCTURAL BASINS

**SINTERING**
Annotated bibliography of sintered and hot pressed silicon nitride
[AD-747785] 03 p0322 N73-12624
Sintering behavior of UO2 powder compacts under hydrogen atmosphere
[CEA-R-4285] 04 p0427 N73-13477
Pressure sintering of beryllium oxide powder blended with aluminum oxide powder
[AD-748389] 04 p0439 N73-13576
Fatigue properties of sintered test bars for bending and axial loads
[LBF-TM-58/71] 05 p0563 N73-14570
Production of fibers, plaques, and highly porous sintered nickel materials
[NLL-TRANS-746-1381-[9022.401]] 06 p0687 N73-15592
Sintered Cd-Ni electrodes for alkaline batteries
[AD-754257] 10 p1112 N73-19063
Creep processes in vacuum sintered copper and silver 12 p1407 N73-21407
Electrical and ionic conductivity of calcium oxide-doped nonstoichiometric cerium dioxide at various temperature ranges
[COO-1441-16] 12 p1416 N73-21473
Sintering heat resistant nickel alloys 13 p1543 N73-22501
Development of method for fabricating cermets and analysis of various compositions to show electrical and physical properties
[NASA-CASE-NPO-13120-1] 14 p1679 N73-23629
Desilification in alumina and cement production by sintering disintegration method
[NLL-LIB-TRANS-1725-[5205.9]] 15 p1746 N73-24150
Measurement of gas permeability of high porosity nickel powder metallurgy parts
[NLL-LTI-746-1404-[9022.401]] 15 p1797 N73-24564
Characteristics and production methods of iron nickel-molybdenum carbonyl powders
[NLL-LTI-746-1418-[9022.401]] 16 p1925 N73-25580
Characteristics and production of silicon nitride-alumina sintered materials
[NLL-RTS-7988] 16 p1931 N73-25627
Sintering theory and practice review enhancing metallurgists and ceramists
[KFK-1713] 19 p2305 N73-28535
Theoretical analysis of plastic flow and diffusion during sintering of Life, Ag, and Ni systems 20 p2428 N73-29499
Development of method for determining optimum setting of regulators on metal working machinery involved in sintering process
[NLL-M-21642-[5828.4F]] 20 p2428 N73-29505
Development of procedures for stabilizing snow to permit helicopter landings
[AD-763231] 21 p2497 N73-30040
Analysis of properties of powder materials subjected to compressive forces and development of equations of state for determining mechanical properties
[NLL-NEL-RR-2474-[6075.461]] 21 p2603 N73-30858
Sintering kinetics and mechanical properties of high purity mullite 22 p2688 N73-31527
Application of hot pressing, hot extruding, and sintering processes for production of composite materials
[JPRS-59873] 23 p2807 N73-32441
Sintering kinetics of zirconium and titanium carbides by hot extrusion in regions of homogeneity 23 p2808 N73-32448
Production and characteristics of sintered titanium diboride-molybdenum compacts 23 p2808 N73-32453
Process for removing plasticizer from hard metal alloy extruded samples during low temperature sintering 23 p2808 N73-32454
Experimental and theoretical model of deformation and densification of sintered powder metallurgy compacts 24 p2933 N73-33422

**SINUSOIDS**
U SINE WAVES

**SIOUX HELICOPTER**
U OH-13 HELICOPTER

**SIRENS**
Application of siren as test technique for determining response and life of aircraft structures subject to engine noise field excitation 20 p2480 N73-29922

**SITES**
NT LANDING SITES
NT LAUNCHING SITES
NT LUNAR LANDING SITES
Atmospheric models for evaluating nuclear facility sites
[BNWL-1651-VOL-2-PT-1] 24 p2885 N73-33044

**SIZE DETERMINATION**
NT PRECIPITATION PARTICLE MEASUREMENT
HELOS lunar occultation experiment on X ray galactic and extragalactic source position and angular size determination 17 p2085 N73-26868

**SIZE PERCEPTION**
U SPACE PERCEPTION

**SIZE SEPARATION**
Jet impactor for size separation of aerosol particles
[BMVG-FBWT-72-11] 07 p0805 N73-16526

**SIZING [SEPARATION]**
U SIZE SEPARATION

**SKELETON**
U MUSCULOSKELETAL SYSTEM

**SKEWNESS**
Numerical analysis of thin skew plates using tensor-matrix techniques for elastic isotropic body
[NLL-RTS-7401] 02 p0236 N73-11916

**SKIDDING**
Performance tests to determine cornering characteristics of cantilever aircraft tire on dry, damp, and flooded runway surfaces over range of yaw angles
[NASA-TN-D-7203] 12 p1363 N73-21058

**SKILLS**
U ABILITIES

**SKIN [ANATOMY]**
Effect of mood on human performance, possibility of using skin analyzer for communication, and effect of prolonged exposure to depths of 160 m on mental functioning
[JPRS-57541] 04 p037E N73-13072
Use of skin analyzer as communication channel in controlling activity 04 p0378 N73-13074
Effect of protective barrier creams on toxic alkyl phosphate penetration of pig skin
[BMVG-FBWT-72-15] 07 p0747 N73-16076
Evaluation of sex difference in thermal sensitivity in men and women
[NASA-CR-114564] 08 p0878 N73-17113
Bactericidal activity of human skin at different times of day 11 p1245 N73-20110
Immunological effectiveness of X ray irradiation on histocompatibility of mice skin transplants 13 p1481 N73-22008
Thermal response of protective fabric/human skin system to JP-4 jet fuel fire
[AD-759525] 17 p1990 N73-26095
Human skin reactions to lotions and distilled water during hypokinesia 24 p2884 N73-33034

**SKIN [STRUCTURAL MEMBER]**
Acoustic fatigue tests of aluminum alloy structural elements under narrow-band, random loading with zero mean stress in skin 20 p2480 N73-29921

**SKIN FRICTION**
NT AERODYNAMIC DRAG
NT FRICTION DRAG
Tests of fabric friction on human skin for aircrew tropical clothing comfort
[RAE-TR-72037] 01 p0020 N73-10157
Estimating local or average turbulent skin friction on flat plates from Reynolds numbers
[NASA-TN-D-6945] 01 p0040 N73-10315
Wind tunnel tests to determine effects of hypersonic flow interaction on thrustor nozzle configurations and procedures to prevent excess heating
[NASA-CR-129914] 05 p0597 N73-14857
Methods for determining air resistance to fragmented shrapnel of different shapes
[FOA-2-A-2539-44] 06 p0653 N73-15304
Analysis of unsteady flow over moving boundaries to determine characteristics of boundary layer separation
[AD-750398] 06 p0655 N73-15322
Analysis of skin friction measurement techniques for incompressible flow to show instruments required and areas of difference
[FFA-AU-726] 08 p0895 N73-17246
Shock wave propagation and attenuation in tunnels noting computer programming based on method of characteristics and wall skin friction
[ISL-17/72-PT-4] 12 p1392 N73-21287
Analysis of accuracy of Preston tube calibration equations to determine local skin friction in two dimensional supersonic and low hypersonic flow conditions
[NASA-TN-D-7190] 13 p1510 N73-22239
Calculation of coupled skin friction and heat transfer in two and three dimensional turbulent boundary layers
[AD-757871] 15 p1768 N73-24327
Calculation of two-dimensional turbulent skin friction under arbitrary compressible flow conditions
[AD-757872] 15 p1769 N73-24329
Development of methods for determining local skin friction of boundary layer and calibration of instruments for analyzing turbulent shear flow
[ARC-R/M-3202] 16 p1854 N73-25016
Flight tests of XB-70 aircraft to determine skin friction coefficients and boundary layer profiles at Mach numbers up to 2.5
[NASA-TN-D-7220] 16 p1887 N73-25276
Syntheses of polystyrene polymers with skin friction reduction in dilute solutions
[AD-761600] 19 p2233 N73-28008
Computation of skin friction and heat transfer on sharp cone in axisymmetric turbulent hypersonic flow
[AD-761602] 19 p2353 N73-28929
Hypersonic, turbulent, cold-wave, skin friction, and heat transfer measurements on axisymmetric sharp cone
[AD-764059] 22 p2655 N73-31269
Measurement of wall shearing stress and velocity and temperature profiles of turbulent boundary layer to derive Reynolds number
[ARC-R/M-3712] 24 p2870 N73-32928
Effect of heat transfer on velocity distribution and skin friction in turbulent wall boundary layers
24 p2906 N73-33195
Comparison of theories for skin friction coefficient in turbulent compressible boundary layers
24 p2907 N73-33203

**SKIN FRICTION DRAG**
U FRICTION DRAG

**SKIN TEMPERATURE [NON-BIOLOGICAL]**
Analysis of thermal failures in combustion chambers of J-57 jet engine and system for detecting burn-through prior to engine case rupture
[FAA-NA-72-92] 07 p0835 N73-16772

**SKULL**
NT CRANIUM

**SKY**
NT NIGHT SKY
Digital computer model to predict spectral irradiance on ground target from sun and sky
[AD-758877] 16 p1945 N73-25739

**SKY BRIGHTNESS**
Results of computations pertaining to brilliance of atmospheric haze and daytime sky
[NASA-TT-F-14421] 01 p0049 N73-10397
Measurements of isotropy of cosmic background radiation at 6 cm determined from apparent sky brightness temperature differences
07 p0838 N73-16789
HEAO-B cosmic ray experiment for diffuse sky brightness determination
17 p2085 N73-26871
Development of numerical procedures for computing true brightness of radiant energy measurements from smoothed brightness
20 p2400 N73-29289
Influence of solar, sky, and ground radiation on signal reflection under cloudless daytime sky
[AD-763893] 22 p2712 N73-31716
Measurement of night-sky brightness in visible and ultraviolet spectral regions using photometers on Cosmos-51 and Cosmos-213 satellites
[NASA-TT-F-15154] 24 p2980 N73-33814
Measurement of night-sky brightness in visible and ultraviolet spectral regions using photometers on Cosmos-51 satellite
[NASA-TT-F-15153] 24 p2980 N73-33815

**SKY RADIATION**
NT AIRGLOW
NT DAYGLOW
NT GEOCORONAL EMISSIONS
NT NIGHTGLOW
NT TWILIGHT GLOW
Atmospheric radiative transfer model for predicting solar and daytime sky irradiance of ground target
[AD-757149] 14 p1693 N73-23739
Mesospheric diffuse skylight measurement onboard Centaure sounding rockets launched from Kiruna during August 1969
[ISL-16/72-PT-1] 15 p1781 N73-24439
Analysis of sky back radiation intensity measurements for clear and overcast skies conducted at different angles of elevation above the horizon by day and night
20 p2400 N73-29286
Development of numerical procedures for computing true brightness of radiant energy measurements from smoothed brightness
20 p2400 N73-29289
Measurement of night-sky brightness in visible and ultraviolet spectral regions using photometers on Cosmos-51 and Cosmos-213 satellites
[NASA-TT-F-15154] 24 p2980 N73-33814
Measurement of night-sky brightness in visible and ultraviolet spectral regions using photometers on Cosmos-51 satellite
[NASA-TT-F-15153] 24 p2980 N73-33815

**SKY WAVES**
NT WHISTLERS
Ionospheric disturbance effects on sky wave bearing measurement
05 p0511 N73-14159
Computer program to compute MF sky-wave interference
[BBC-RD-1973/8] 20 p2391 N73-29206
Loss estimation in predicting ionospheric medium frequency sky wave propagation
[BBC-RD-1973/13] 22 p2627 N73-31051

**SKYHAWK AIRCRAFT**
U A-4 AIRCRAFT

**SKYHOOK BALLOONS**
Skyhook balloon flight operations
[AD-761657] 19 p2221 N73-27913

**SKYLAB PROGRAM**
Astronaut manual performance limits in intravehicular Skylab environment
[NASA-CR-128590] 01 p0019 N73-10150
Manual space navigation research projects conducted by US Air Force in support of Skylab project
[AD-747479] 03 p0329 N73-12683
Analysis of Skylab program to show construction of spacecraft, test facilities, personnel accomodations, and research projects
04 p0470 N73-13831
Analyses of Experiment S183, Ultraviolet Panorama [MSFC] for evaluating Skylab performance
[NASA-CR-61386-APP-N] 04 p0475 N73-13885
Transient thermodynamic simulation of Apollo fuel cell/radiator system for proposed Skylab mission
[NASA-CR-129824] 05 p0598 N73-14860
Microwave measurements and Skylab S193 analysis of wind field over ocean
[CONTRIB-118] 06 p0663 N73-15384
Electrical and performance characteristics of Skylab radar altimeter
06 p0663 N73-15386
Analyses of Skylab crew quarters and habitability - App. D
[NASA-CR-61386-APP-D] 06 p0721 N73-15880
Human factors characteristics and geometry of expandable structures for use as airlocks, escape capsules, and crew transfer tunnels on Skylab program
[AD-749131] 06 p0722 N73-15896
Hypervelocity impact tests of Skylab electrical cables for simulation of micrometeoroid environment
[NASA-TN-D-7178] 07 p0761 N73-16186
Analysis of NASA Earth Resources Program to include ERTS satellites, Skylab program, and earth resources survey aircraft
07 p0782 N73-16359
Tests of Skylab Orbital Workshop ventilation concepts
[NASA-TM-X-64700] 07 p0848 N73-16875
List of facilities and environmental measurements to be monitored in support of Skylab 2 at Launch Complex 39
[NASA-TM-X-68916] 07 p0849 N73-16879
Electron-proton spectrometer for Skylab radiation dose measurements
[NASA-CR-128702] 08 p0925 N73-17575
Electron-proton spectrometer applied to Skylab program for measurement of electrons and protons resulting from solar flares to determine radiobiological safety factors
[NASA-CR-128704] 08 p0925 N73-17577
Qualification tests of electron-proton spectrometer to determine suitability for use in Skylab program
[NASA-CR-128703] 08 p0925 N73-17580
Earth resources requirements for Skylab missions - Appendix B
[NASA-TM-X-69137] 09 p1029 N73-18402
Aluminum-copper eutectic solidification experiment to be run in M518 multipurpose electric furnace during Skylab mission
[NASA-CR-124103] 09 p1045 N73-18526
Tissue culture laboratory for first manned Skylab mission for performing experiments to detect effects of zero gravity on living human cells
09 p1088 N73-18874
Status of space shuttle and Skylab programs and shuttle facilities
10 p1215 N73-19880
Vehicle telemetry measurements for Skylab 2 spacecraft and identification of data sources
[NASA-TM-X-69142] 10 p1216 N73-19887
Dermatological testing of personal hygiene cleansing agents and laundry detergents for possible use in Skylab Program
[NASA-CR-128880] 11 p1250 N73-20143
Design of electron-proton spectrometer for mounting externally on Skylab CSM
[NASA-CR-128814] 11 p1293 N73-20490
Developing facility on Skylab mission for electromagnetic suspension of small molten spheres in space
[NASA-CR-124134] 11 p1297 N73-20522
Analysis of KC-135 flight samples of Star-J Satellite solidified in near-zero gravity
[NASA-CR-124179] 11 p1308 N73-20610
Management methods for Skylab program to include mission operations support, environmental and thermal design criteria, optical contamination, and materials science
[NASA-TM-X-64725] 11 p1342 N73-20886
Numerical analysis of satellite stability parameters with application to stability of Skylab satellite
[NASA-CR-124223] 13 p1581 N73-22815
Collection and measurement of atmospheric contaminants during Skylab AM/MDA unmanned altitude chamber test
[NASA-CR-128903] 13 p1582 N73-22823
Development of manufacturing in space processes for Skylab program to include operating sequence description and results obtained
13 p1594 N73-22922
Space rations and menus developed for Skylab missions
[NASA-CR-128910] 14 p1614 N73-23080
Remote sensor system aboard Skylab in support of EREP oceanographic program
[AD-755715] 14 p1663 N73-23501
Double-gimbaled control moment gyro system for maintaining Skylab attitude control without excessive fuel consumption after failure of main gyro system
[NASA-TM-X-64746] 14 p1707 N73-23851
Preflight, inflight, and post flight operations evaluation analyses for Skylab materials processing facility - Appendix E
[NASA-CR-61386-APP-E] 14 p1708 N73-23859
Preflight, inflight, and post flight operations evaluation analyses for Skylab metals melting experiment facility - Appendix F
[NASA-CR-61386-APP-F] 14 p1708 N73-23860
Preflight, inflight, and post flight operations evaluation analyses for Skylab exothermic brazing experiment facility - Appendix G
[NASA-CR-61386-APP-G] 14 p1708 N73-23861
Preflight, inflight, and post flight operations evaluation analyses for Skylab sphere forming experiment facility - Appendix H
[NASA-CR-61386-APP-H] 14 p1708 N73-23862
Preflight, inflight, and post flight operations evaluation analyses for Skylab gallium arsenide single crystal growth facility - Appendix J
[NASA-CR-61386-APP-J] 14 p1708 N73-23863
Preflight, inflight, and post flight operations evaluation analyses for Skylab contamination measurement sample array - Appendix S
[NASA-CR-61386-APP-S] 14 p1708 N73-23864
Congressional hearings on Skylab program, Apollo/Soyuz test project; and other planned space missions
14 p1721 N73-23965
Data analysis for predicting human personal hygienic needs during long term space flight
[NASA-CR-128929] 15 p1743 N73-24132
Performance tests of L-band truss cable meteoroid shielding on Skylab space station at minus 180 degrees Fahrenheit
[NASA-TM-X-64743] 15 p1834 N73-24867
Skylab television camera system to record launch and tests
[NASA-TM-X-69526] 16 p1875 N73-25174
Atmospheric effects on remote sensing of nonuniform temperature sources applied to Skylab and ERTS missions
[NASA-CR-129004] 16 p1905 N73-25413
Manual for 70mm hand held photography from Skylab
[NASA-TM-X-66262] 16 p1912 N73-25475
Materials fatigue test machine for use aboard Skylab or space shuttles
[NASA-CR-132260] 16 p1913 N73-25476

Congressional hearing to determine malfunction on Skylab 1 workshop and proposed methods for correcting malfunction
16 p1964 N73-25884
Atlas S183 experiment for ultraviolet stellar spectrophotometry onboard Skylab manned space station
17 p2033 N73-26454
Mission events for Skylab 2 flight
[NASA-TM-X-69197] 17 p2088 N73-26893
Evaluation of Skylab program experiments involving contamination measurement, photometer, and gegenschein zodiacal light
[NASA-CR-61386] 18 p2200 N73-27760
Preflight analysis on Skylab very high frequency ranging for rendezvous portion
[NASA-CR-133981] 19 p2235 N73-28020
Skylab experiments on convection and molten metal flow and solidification under reduced gravity
[NASA-CR-124329] 19 p2343 N73-28852
Guidance and navigation error analysis for Skylab 3
[NASA-CR-133997] 21 p2576 N73-30642
Preflight assessment of Skylab VHF ranging coverage for rendezvous portion of SL-1/SL-3 mission
[NASA-CR-133996] 22 p2631 N73-31085
Characteristics of microwave radiometer scatterometer system for Skylab program
22 p2671 N73-31394
Analysis of data from quartz crystal microbalance contamination monitors on Skylab
[NASA-TM-X-64778] 22 p2673 N73-31412
Congressional hearing to determine causes of malfunctions of Skylab space vehicle
22 p2737 N73-31914
Skylab, solar studies, and usefulness of Apollo telescope mount
[NASA-EP-119] 23 p2834 N73-32645
Payload definition and integration study to establish planning concepts for life sciences spacecraft laboratories - Vol. 1
[NASA-CR-124411] 23 p2849 N73-32765
Simulated launch countdown, liftoff, and flight test to demonstrate compatibility of Skylab rescue space vehicle systems, ground support, and off-site support facilities
[NASA-TM-X-69520] 23 p2850 N73-32776
Skylab rescue space vehicle flight readiness test
[NASA-TM-X-69519] 23 p2850 N73-32777
Flammability of engineering materials in gaseous oxygen environments and applicability to Skylab program
[NASA-TM-X-64783] 24 p2891 N73-33081
Information management for Skylab earth resources experiments in oceanography and marine science
[NOAA-TM-NESS-51] 24 p2921 N73-33328
History, development, and description of Skylab program
[NASA-EP-107] 24 p2979 N73-33803
Skylab education program for high school students - Vol. 1
[NASA-EP-110] 24 p2980 N73-33811
Skylab education program for high school students - Vol. 2
[NASA-EP-111] 24 p2980 N73-33812
Performance evaluation of SA-206 launch vehicle for Skylab 2 launch to show signficant events and failures and anomalies
[NASA-TM-X-69538] 24 p2981 N73-33820
Performance evaluation of SA-207 launch vehicle for Skylab 3 launch to show significant events and failures and anomalies
[NASA-TM-X-69540] 24 p2981 N73-33821
Saturn 5 launch vehicle performance during Skylab launch and orbit
[NASA-TM-X-69537] 24 p2984 N73-33848

**SKYLAB SPACE STATION [UNMANNED]**
U SKYLAB 1

**SKYLAB 1**
Congressional hearing on Skylab 1 solar array system failure
23 p2866 N73-32912

**SKYLARK**
U SKYLARK ROCKET VEHICLE

**SKYLARK ROCKET VEHICLE**
Performance of attitude sensors determined from Skylark 586 payload flight test
[RAE-TR-72066] 03 p0359 N73-12927
Electron temperature and density profiles obtained with Skylark rocket-borne double electrostatic probes
[TRITA-EPP-72-14-REV] 12 p1402 N73-21370
Skylark star-pointing attitude control system using strapdown inertial system
[RAE-TR-71241] 18 p2176 N73-27571

**SL 1**
U SKYLAB 1

**SLABS**
FORTRAN program for solving transport problem for neutrons in multilayer slab system
[EUR-4839-E] 01 p0082 N73-10681
Lateral gas expansion behind explosive detonating slab
[ISL-19/71] 09 p1016 N73-18291
Finite difference technique for determining transient temperature distribution in plane slab with uniform heat sources and radiative boundary conditions
10 p1223 N73-19944
Electromagnetic properties of plane slab of finite thickness immersed in uniform magnetic field
[VTH-169] 13 p1559 N73-22637
Nondestructive measurement of dielectric properties of slab-type materials
[AD-762359] 19 p2312 N73-28599

**SLAGS**
Identification and mapping of coal refuse banks in Pennsylvania anthracite coal fields from ERTS-1 data
[PAPER-L24] 19 p2276 N73-28319

**SLANT PERCEPTION**
U SPACE PERCEPTION

**SLATS**
U LEADING EDGE SLATS

**SLEDS**
NT ROCKET PROPELLED SLEDS

**SLEEP**
Sleep stage classification analysis on heart rate data recordings
[AD-740946] 01 p0021 N73-10167
Vestibulo-ocular response of man to oscillatory rotation during sleep
[AMRU-R-70-3] 02 p0131 N73-11066
Diurnal changes in human histamine and serotonin metabolism and effects of work-sleep cycle
03 p0258 N73-12089
Activity cycle data for spacecrews of Soyuz 3 to 9 spacecrafts before, during and after space flights
[JPRS-58173] 07 p0746 N73-16068
Electrophysiological sleep patterns of human and animal brains
[NASA-TT-F-740] 13 p1483 N73-22023
Electropolygraphic analyses of sleep patterns in humans with neurological disorders
13 p1483 N73-22024
Neurophysiology of sleep and wakefulness in fish, amphibians, birds, and reptiles
13 p1483 N73-22025
Bioelectrical activity differentiations in cat cortex during sleep inhibition
13 p1483 N73-22026
Interdependence of slow and rapid brain waves during sleep
13 p1483 N73-22027
Neuronal changes in cortical motor region cells during pharmacological induced sleep
13 p1483 N73-22028
Somnofunctional mapping of deep brain waves in neurological patients
13 p1484 N73-22029
Thalamic cat cell activities during sleep and wakefulness phases
13 p1484 N73-22030
Bioelectric activity and excitability of cat brain structures during sleep phases
13 p1484 N73-22031
Bioelectric activity changes in brains of sleeping children caused by aging factor
13 p1484 N73-22032
Statistical analysis of effect of simulated sonic booms on sleep patterns of male subjects
[FAA-AM-72-35] 17 p1987 N73-26057
Electroencephalographic and behavioral responses of humans to aircraft noise during sleep
[NASA-CR-2279] 18 p2109 N73-27058
Human body temperature dynamics in adaptation to changed work-sleep cycles
20 p2367 N73-29036
Rhythm disturbances in sleep and wakefulness cycles of Soyuz 3 and 9 crews before, during, and after space flight
[NASA-TT-F-15103] 20 p2369 N73-29048
Effect of simulated sonic booms and overpressure on EEG waveform patterns and disturbance judgments
[FAA-RD-73-115] 21 p2500 N73-30066
Circadian rhythms of sleep and cerebral temperature in rats chronically exposed to hot environments
[NASA-TT-F-15082] 22 p2620 N73-30994
Prototype automatic sleep analyzer for clinical applications
[NASA-CR-134049] 23 p2793 N73-32346

**SLEEP DEPRIVATION**
Effects of stress upon psychophysiological responses and performance following sleep deprivation
[NASA-CR-128620] 02 p0132 N73-11073
Diurnal dynamics of psychic performance during 72-hour continuous wakefulness
07 p0744 N73-16056
Pilot performance and sleep patterns in long duration flights and control of hypnotic drug and alcohol use
12 p1369 N73-21107
Physiological aspects of sleep induction in aircrews after prolonged flight times
12 p1369 N73-21108
Effects of work-rest schedules, circadian rhythms, continuous work, and sleep loss on sustained performance
14 p1723 N73-23988
Biological effects of sleep deprivation, and effects of prolonged work on performance under combat conditions
14 p1723 N73-23989
Effect of sleep deprivation and heat stress on human performance in visual and auditory tasks
[OES-8/72] 22 p2624 N73-31024
Sleep deprivation effects, airborne simulator feel system, bed forms, and V/STOL engine model tests
[DME/NAE-1973(2)] 22 p2731 N73-31853
Sleep deprivation effects on accuracy and speed of response selection and execution
22 p2731 N73-31854
Physiological effects on highly trained subjects when confined to bed, deprived of sleep, or allowed to discontinue training
[NASA-CR-134044] 23 p2750 N73-32008

**SLEEVES**
Rotational injection moulding for designing polythene sheathed closures on large size cables
[REPT-6713] 10 p1164 N73-19474
Tool exchange capabilities of portable wrench characterized by telescopic sleeve
[NASA-CASE-MFS-22283-1] 21 p2553 N73-30462

**SLENDER BODIES**
NT SLENDER CONES
Computation of steady conical flow past a yawed slender delta wing with leading edge separation using vortex sheet model and Newton-Raphson iteration
[IC-AERO-72-17] 01 p0001 N73-10005
Linear and nonlinear parts of slender body of revolution aerodynamic coefficients in supersonic flow, noting influence of incidence on pressure distribution
[DLR-FB-72-42] 01 p0001 N73-10006
Cross flexure sting designed for measuring dynamic stability of slender bodies of revolution with delta wings in supersonic wind tunnel tests
[FFA-AU-637] 01 p0035 N73-10278
Transonic flow around slender bodies noting wave drag deceleration and boundary layer transition
[ISL-33/71] 04 p0406 N73-13304
Perturbation approximation method for determining velocity potential and aerodynamic forces of slender body of elliptical cross section in airstream
[AD-748353] 04 p0407 N73-13317
Coning motion, autorotation and vortex system of slender missiles
[BMVG-FBWT-72-31] 10 p1103 N73-18998
Development of method for estimating normal force, axial force, and pitching moment coefficients for slender bodies of varying cross section equipped with lifting surfaces
[NASA-TN-D-7228] 12 p1355 N73-20998
Analysis of viscous hypersonic flow around slender sharp wedges and unyawed cones
[AD-757037] 14 p1650 N73-23386
Development of slender body theory for analyzing flow past thin, conically cambered, delta wing with exact boundary conditions
[ARC-R/M-3249] 15 p1726 N73-24002
Wind tunnel tests to determine effect of asymmetric nose bluntness on aerodynamic characteristics of slender cone at Mach 14
[AD-760807] 18 p2102 N73-26998
Numerical analysis of disturbance pressure due to impinging of plane shock wave of arbitrary strength on moving slender body
19 p2251 N73-28151
Numerical procedure for calculating viscous shock-layer flow near sharp leading edge of two dimensional and axisymmetric slender bodies
[AD-762505] 20 p2389 N73-29190
Aerodynamic drag on slender bodies in transonic flow
[AD-763437] 21 p2527 N73-30264
Analysis of sonic boom characteristics based on second order solutions for flow distribution around slender bodies in supersonic flow - Part 1
[NASA-CR-2339] 23 p2739 N73-31927

**SLENDER CONES**
Effect of ablation on aerodynamic characteristics of blunted slender cone during free flight ablating conditions
[NASA-TN-D-7196] 09 p0979 N73-18002

**SLENDER WINGS**
NT INFINITE SPAN WINGS
Low speed pull-up maneuvers for slender wing transport aircraft with stability and control augmentation
[ARC-CP-1231] 04 p0369 N73-13004
Vortex sheet and increased lift caused by blowing from leading edges of slender delta wing
[ARC-R/M-3692] 09 p0981 N73-18016
Application of modified slender wing theory to analyze aerodynamic characteristics of slender, lifting, wings with curved leading edges at supersonic speeds
[ARC-R/M-3278] 15 p1727 N73-24006
Effect of jet stream blowing downwards from lower surface of slender delta wing to obtain lift augmentation for takeoff and landing
[ARC-R/M-3288] 15 p1727 N73-24009

Evaluation of double integral equation for calculation of wave drag due to volume and aerodynamic lift of slender wings
[ARC-R/M-3221] 16 p1852 N73-25006
Application of slender body theory for calculating minimum values of zero lift wave drag of slender wings with unswept trailing edge
[ARC-R/M-3222] 16 p1852 N73-25007
Design criteria for slender warped wings with unswept trailing edge with zero load along leading edge and near planar vortex sheet at trailing edge for design lift coefficient
[ARC-R/M-3406] 16 p1852 N73-25008
Comparison of linearized theories to determine aerodynamic characteristics of slender wings in supersonic flow
[RAE-LIB-TRANS-1677] 17 p1981 N73-26010
Aerodynamic characteristics of slender delta wings to show performance under various conditions of airspeed, angle of attack, and ground effect
[NASA-TT-F-14949] 17 p1983 N73-26031
Measurement of drag, lift and pitching moments on slender winged low aspect ratio gothic planforms at subsonic speed
[ARC-R/M-3720] 21 p2492 N73-30005
Wind tunnel tests to determine flow characteristics around sharp-edged slender delta wing at large angles of attack
[NASA-TT-F-15107] 22 p2611 N73-30928

**SLEWING**
Mathematical procedure for determining exact slew reorientation of spacecraft about nonorthogonal axes
18 p2211 N73-27850

**SLICKS**
U OIL SLICKS

**SLIDING FRICTION**
Estimation of rising interface temperature in sliding friction of two surfaces
[AD-746830] 02 p0180 N73-11456
Sliding friction and wear of Fe, Co, Cu, Ag, Mg, and Al in oxygen-nitrogen mixture of pressures between 760 torr and 0.2 microtorr
[BAM-BR-13] 03 p0306 N73-12503
Sliding friction and natural vibration of solid with rigid connection moving over dry surface
[AD-749521] 04 p0428 N73-13488
Dry sliding friction characteristics of iron ceramic materials using solid lubricants
04 p0432 N73-13517
X ray analysis to determine occurrence of metal surface texturing as result of sliding friction
[NASA-TN-D-7136] 06 p0677 N73-15508
Friction, wear, and transfer of carbon and graphite to copper, chromium, and aluminum metal surfaces in vacuum
[NASA-TN-D-7206] 09 p1039 N73-18475
Wear process and colloidal particle production test on sliding metal surfaces using magnetic measurements
[AD-753251] 09 p1040 N73-18481
Reversible sliding and lubrication effects in internal stress friction on thin plate
[AD-751723] 09 p1097 N73-18957
Friction induced surface activity of some hydrocarbons with clean and oxide-covered iron
[NASA-TN-D-7233] 11 p1297 N73-20527
Sliding friction experiments in air with polycrystalline copper and ruby riders
[NASA-TN-D-7232] 11 p1298 N73-20530
Role of plastic deformation process in sliding wear of pure Cu and Cu-Al alloy against Type 440 C in cryogenic fuels
[NASA-TN-D-7253] 11 p1305 N73-20591
Scanning electron microscope used in friction tests of polytetrafluoroethylene sliding on aluminum single crystals
[NASA-TN-D-7321] 15 p1791 N73-24520
Effect of contact-surface-active vapors on wear behavior of soft steel during sliding friction
[NASA-TT-F-14935] 15 p1791 N73-24523
Auger analysis of chemisorption of various gases to metal surfaces and sliding friction effects on interaction
[NASA-TN-D-7340] 16 p1918 N73-25520
Effects of boundary surface active vapors on behavior of steel during sliding friction
[NASA-TT-F-14993] 19 p2304 N73-28531
Deformation of dry steel surfaces during high velocity sliding contact
20 p2427 N73-29496
Boundary layer friction data under ion pumped vacuum
[NASA-CR-135480] 23 p2796 N73-32366
Fatigue life tests of ball motion and sliding friction in arched outer race ball bearing under thrust load
[NASA-TM-X-71442] 23 p2797 N73-32375

**SLIP BANDS**
U EDGE DISLOCATIONS

**SLIP CASTING**
Specifications for fused silica slip-casting radome material
[AD-745332] 01 p0028 N73-10219
Processing specifications for slip-cast fused silica radomes
[AD-745793] 01 p0029 N73-10229
Acceptance criteria specification for slip-cast fused silica radomes
[AD-745743] 01 p0029 N73-10230

**SLIP FLOW**
Vortex generation and propagation under perfect slip flow conditions, for thin elliptical cylinder
24 p2908 N73-33206

**SLIPSTREAMS**
NT PROPELLER SLIPSTREAMS
Numerical determination of augmented lift due to wing-slipstream interaction for application to V/STOL aircraft
[AD-743257] 01 p0005 N73-10035
Analysis of aerodynamic characteristics of free, semibounded slipstream of straight-jet laminar gas flames
[NASA-TT-F-14688] 07 p0855 N73-16934
Iterative method for analyzing feathering characteristics in airfoil whirlwinds
[DEP/PRA/NT/88/72] 14 p1600 N73-22968

**SLITS**
Procedure for fabricating element with cavity closed by thin wall with precisely shaped slit
[NASA-CASE-LAR-10409-1] 11 p1297 N73-20526
Exit slit mirrors for Ebert ultraviolet spectrometer Apollo experiment
[NASA-CR-128549] 16 p1916 N73-25504
Heat transfer in slit-like channels
[AD-762793] 22 p2730 N73-31851

**SLOPES**
NT GLIDE PATHS
Autonomous Martian roving vehicle determination of terrain gradients from laser measurements
[NASA-CR-133498] 19 p2307 N73-28556
Tensile and fatigue data for irradiated and unirradiated AISI 310 stainless steel and titanium-5 percent aluminum-2.5 percent tin applied to universal slopes
[NASA-TM-X-2883] 22 p2683 N73-31494

**SLOSHING**
U LIQUID SLOSHING

**SLOT ANTENNAS**
Turnstile slot antenna system for spacecraft or missile telemetry and command control
[NASA-CASE-GSC-11428-1] 02 p0149 N73-11206
Power handling capability and electrical breakdown characteristics of electronic countermeasure antennas
[AD-751309] 07 p0758 N73-16154
Mathematical models for predicting microwave breakdown in fringing field of rectangular slot antenna
[AD-751320] 07 p0763 N73-16202
Gain and impedance measurements on ultrahigh frequency antennas near surface of simulated sea water
[AD-751922] 08 p0890 N73-17205
Electrical characteristics of flush-mounted multimode slot antenna with scan capability
[AD-757907] 15 p1757 N73-24244
Radiation characteristics of grounded slotted dielectric slab
[AD-760129] 17 p1999 N73-26165
Radiation from apertures in curved panels
[NASA-CR-2263] 18 p2116 N73-27110
Slot antenna mounted symmetrically on square plate with symmetrical antenna pattern
[AD-762056] 19 p2237 N73-28038
Intergral equations for incident electromagnetic wave scattering by slotted spherical antenna
[AD-764880] 23 p2758 N73-32075

**SLOTS**
NT WING SLOTS
Effect of longitudinal slot in circular waveguide
[PB-208160] 01 p0034 N73-10267
Iterative method for calculating axial flow resistance in annular slots of impeller pumps
[NLL-NEL-TT-2422-[6075.461]]
11 p1269 N73-20299
Short curved wall, axisymmetric subsonic diffusers, using slot suction to prevent flow separation
[NASA-CR-2209] 11 p1270 N73-20305
Design and aerodynamic performance of low speed fan stage for low noise turboengine
[NASA-CR-121148] 12 p1364 N73-21070
Admittance of axial slot backed by cylindrical cavity inside infinite cylinder
[AD-759568] 16 p1946 N73-25748
Slot line transitions to coaxial line and to microstrip
[AD-761765] 19 p2244 N73-28095
Three dimensional effects on slot cooling in hypersonic flight
[AD-762624] 20 p2388 N73-29189

**SLOTTED ANTENNAS**
U SLOT ANTENNAS

**SLOTTED WIND TUNNELS**
Finite difference solutions for oscillatory lift interference in slotted wind tunnel compressible and incompressible flow
[ARC-R/M-3700-PT-1-FT-2] 03 p0284 N73-12297
Finite difference solutions for oscillatory lift interference parameters for slotted wind tunnel incompressible flow
03 p0284 N73-12298
Finite difference solutions for oscillatory lift interference parameters for slotted wind tunnel compressible flow
03 p0284 N73-12299
Interference theory in slotted wind tunnels extended to subsonic rectangular wind tunnels with ventilated tool, longitudinal slots and perforated screens of arbitrary porosity
[ARC-R/M-3706] 05 p0492 N73-14007
Transonic flow studies in slotted wind tunnels
[AD-753911] 10 p1144 N73-19320
Performance tests of working section of variable pressure, supersonic wind tunnel to show effects of inclination of slotted walls on Mach number accuracy
[ARC-R/M-3228] 15 p1730 N73-24032
Design of ventilated walls for transonic wind tunnels with analysis of parameters affecting noise generation
17 p2014 N73-26285
Slotted transonic wind tunnel tests on pitching delta wing enable selection of porpous walls for interference free damping derivatives
[ARC-R/M-3715] 24 p2870 N73-32930

**SLOW NEUTRONS**
U THERMAL NEUTRONS

**SLURRY PROPELLANTS**
Analytical models for ignition and complete combustion of aluminized slurry fuels in ramjet engines
[AD-754117] 10 p1203 N73-19792
Effects of additives on high speed ignition and combustion characteristics of slurry fuels using magnesium and lithium fluoride
[AD-762615] 20 p2465 N73-29802

**SLUSH**
Hydrocarbon suspensions in slush hydrogen and heat transfer to slush hydrogen
[NASA-CR-130550] 08 p0968 N73-17912
Preparation of hydrocarbon suspensions in slush hydrogen for nuclear fuel element corrosion inhibition in rocket engines
08 p0968 N73-17913
Heat transfer to slush hydrogen at 1 atm and at triple-point pressure
08 p0968 N73-17914

**SM-65 MISSILE**
U ATLAS LAUNCH VEHICLES

**SMALL ASTRONOMY SATELLITES**
SAS-2 measurements of gamma rays from galactic plane
[NASA-TM-X-70486] 24 p2976 N73-33778
Celestial diffuse gamma radiation above 30 MeV observed by SAS-2
[NASA-TM-X-70485] 24 p2976 N73-33779

**SMALL PERTURBATION FLOW**
Stability of laminar pipe flow with rigid rotation and small three-dimensional perturbation
[MITT-55] 19 p2256 N73-28184
Turbulent shear stress profiles in boundary layer flow at sine wave pressure perturbations
24 p2906 N73-33194
Theory for small perturbation laminar boundary layer stability at longitudinally curved walls
24 p2909 N73-33212

**SMELTING**
Development of steel smelting process using inert argon atmosphere for gas saturation and removal of impurities
[JPRS-57542] 03 p0313 N73-12553
Analysis of melt segregation effects on solidification of metals under weightless conditions
[NASA-CR-124358] 21 p2559 N73-30510

**SMITH CHART**
FORTRAN subroutine for plotting computer determined transmission line parameters on Smith chart
[AD-751019] 06 p0645 N73-15243
Computerized design of Smith chart and power amplifier
[AD-759701] 17 p2004 N73-26205

**SMOG**
Atmospheric measurement of photochemical smog reactions in San Francisco Bay area
[PB-210422] 01 p0077 N73-10635
Users manual for photochemical smog simulation diffusion/kinetics code
[PB-220243/0] 22 p2697 N73-31600
Proceedings of conference on mathematical modeling of photochemical smog
[PB-221177/9] 23 p2754 N73-32038

**SMOKE**
Sulfur oxides, smoke, and air pollution tables from Belgian weather stations, Oct. 1971
01 p0075 N73-10619
Sulfur oxides, smoke, and air pollution tables from Belgian weather stations, Dec. 1971
02 p0205 N73-11659
Strip mine identification, land use assessment, smoke plume detection, and sedimentation patterns in Sandusky Bay from ERTS-1 imagery of Ohio
[E72-10259] 03 p0290 N73-12358
Sulfur oxides, smoke, and air pollution tables from Belgian weather stations, Nov. 1971
03 p0327 N73-12663
Sulfur oxides, smoke, and air pollution tables from Belgian weather stations, Jan. 1972
05 p0574 N73-14668
Smoke plume analysis of steam plant in Huntsville, Alabama, using fan-beam and single-beam radiometers
05 p0608 N73-14942

Sulfur oxides, smoke, and air pollution tables from Belgian weather stations, Feb. 1972
08 p0939 N73-17686
Atmospheric pollution in Belgium from 1 Apr. 1969 to 31 Mar. 1970
[PUBL-SER-A-78] 10 p1182 N73-19618
Detection of smoke pollution in Virginia by photogrammetric and densitometric analysis of ERTS-1 imagery
[E73-10419] 11 p1279 N73-20381
Influence of altitude and drugs on cerebral circulation in smokers and non-smokers
12 p1371 N73-21125
Detection of Combustion Improver-2 by atomic absorption spectrophotometry in smoke abatement systems
[AD-755723] 13 p1488 N73-22067
Sulfur oxides, smoke, and air pollution tables from Belgian weather stations, Mar. 1972
13 p1553 N73-22587
Sulfur oxides, smoke, and air pollution tables from Belgian weather stations, Apr. 1972
13 p1553 N73-22590
Sulfur oxides, smoke, and air pollution tables from Belgian weather stations, Jul. 1972
20 p2449 N73-29686
Smoke generation data on organic polymeric materials
[DSL-REPT-560] 22 p2729 N73-31837
Sulfur oxides, smoke, and air pollution tables from Belgian weather stations, Aug. 1972
24 p2949 N73-33559
Sulfur oxides, smoke, and air pollution tables from Belgian weather stations, Sep. 1972
24 p2949 N73-33560

**SMOKE TRAILS**
Radar photography of smoke in forest area for predicting bushfire behavior
[DIV-APPL-CHEM-TP-2] 04 p0388 N73-13151

**SMOOTHING**
NT DATA SMOOTHING

**SMS**
U SYNCHRONOUS METEOROLOGICAL SATELLITE

**SNAKING**
U LATERAL OSCILLATION

**SNAP**
NT SNAP 8
NT SNAP 10A
NT SNAP 19
NT SNAP 23
Physics measurements for SPF Zirconium Hydride Reactor
[AI-AEC-13023] 03 p0332 N73-12706
NaK loop testing of thermoelectric converter modules for SNAP program
[NASA-CR-121192] 14 p1691 N73-23727
Statistical reliability model and analysis of 5-kwe reactor thermoelectric system
[NASA-CR-121205] 15 p1809 N73-24661
Design of expansion joint unit for coolant piping loop of reactor thermoelectric system - SNAP program
[NASA-CR-121209] 15 p1809 N73-24663
Computer codes for designing volume accumulator units
[NASA-CR-121246] 18 p2178 N73-27583
FORTRAN program, ZIP, for time sharing in SNAP reactor parametric studies
[AI-AEC-13076-VOL-1] 24 p2954 N73-33603
Heat transfer-lifetime code for SNAP reactor analysis
[AI-AEC-13076-VOL-5] 24 p2955 N73-33604
Library of 28-group neutron cross sections designed for SNAP reactor analysis
[AI-AEC-13076-VOL-4] 24 p2955 N73-33605

**SNAP 8**
Seam weld cracking in lithium hydride shielding of SNAP 8 reactor after irradiation
[NASA-CR-121157] 14 p1691 N73-23726
Materials technology programs in support of mercury rankine space power system
[NASA-TN-D-7355] 21 p2558 N73-30508

**SNAP 10A**
Dual throat thermoelectric NaK development pump for use on reactor thermoelectric system
[NASA-CR-121231] 16 p1918 N73-25521

**SNAP 19**
Performance of SNAP 19 RTG for Viking lander system
[ESD-2960-53] 12 p1427 N73-21569

**SNAP 23**
Life test performance of SNAP 23 prototype mockup system
[WANL-3559-1] 12 p1427 N73-21568

**SNELLS LAW**
Geometrical plot of light ray through leaf cross section using Fresnel equations and Snells law
[NASA-CR-132144] 15 p1813 N73-24695

**SNOW**
Light and ultraviolet albedo of grass and snow including effect of sun altitude, cloud cover, and state of underlying surface on magnitude of albedo
04 p0442 N73-13609
ERTS-1 sensing of fall snow melting in Chena River Basin, Alaska
[E72-10345] 05 p0533 N73-14333
High resolution FM radar at X band for measuring snow and ice thickness
[CRC-TN-646] 06 p0639 N73-15184
Performance of mathematical snowmelt models and statistical analysis of avalanche forecasts
06 p0665 N73-15402
Water equivalent of snow determined from aerial detection of natural terrestrial radiation
[EGG-1183-1533] 06 p0667 N73-15419
Aerial snow gaging, using transmitted terrain gamma radiation
[EGG-1183-1557] 07 p0800 N73-16500
Radar cross section measurements of snow and ice
[AD-752900] 09 p1004 N73-18192
Snow accumulations on air cushion vehicle track sections
[NRC-12939] 09 p1010 N73-18247
Survey and mapping of snow and ground water levels in Norway using ERTS-1 imagery
[E73-10324] 09 p1024 N73-18356
Tabular and graphical data for moderate and heavy snow for Loring AFB, Maine
[AD-756881] 13 p1555 N73-22605
Electromagnetic wave scattering from snow, ice, and sea ice
[AD-758071] 15 p1783 N73-24454
Performance of combined photoelectric snow depth-robot rain gage system
[NLL-M-22978-[5828.4F]] 16 p1910 N73-25457
Characteristics and operational problems of overflow snow gage
[NLL-M-22982-[5828.4F]] 18 p2150 N73-27375
Ground based silver iodide cloud seeding for modifying snowfall in northern Rockies near Montana
[PB-2180512] 18 p2173 N73-27548
Analysis of ice conditions existing in Antarctic waters during Tenth Soviet Antarctic Expedition
20 p2407 N73-29342
Development of procedures for stabilizing snow to permit helicopter landings
[AD-763231] 21 p2497 N73-30040
Dielectric properties of ice, snow, and water at microwave frequencies and thickness measurements of ice and snow layers with radar
[CRC-1242] 21 p2537 N73-30341
Cup-type snow gage, using kerosene to prevent evaporation
[NLL-M-23051-[5828.4F]] 21 p2567 N73-30572
Daily precipitation and snow cover data - 1970
[ISBN-951-697-010-9] 21 p2573 N73-30624
Effects of snow cover and snow surface conditions on image glide path systems for aircraft approach control
[FAA-RD-72-85] 22 p2697 N73-31602
Application of remote sensing data to analysis of spring snowmelt floods in Minnesota and surrounding areas
23 p2784 N73-32270
Snow and fresh water lake ice interpretations from ERTS-1 imagery of Whitefish Bay, Michigan and Green Bay, Wisconsin
[E73-11129] 24 p2917 N73-33284
Forecasting of spring flow runoff and snow data collection network design
24 p2922 N73-33338

**SNOW AERIAL APPLICATOR AIRCRAFT S-2B**
U S-2 AIRCRAFT

**SNOW AIRCRAFT**
NT S-2 AIRCRAFT

**SNOW COVER**
Radioisotope snow cover gage
[NLL-M-22676-[5828.4F]] 01 p0055 N73-10443
Detection and mapping snow cover from ERTS-1 remotely sensed imagery of western US and Arctic
[E72-10202] 02 p0160 N73-11299
Geological fracture mapping based on enhancement of ERTS-1 snow cover imagery of Massachusetts, Connecticut, and Feather River/Lake Tahoe area
[E72-10205] 02 p0161 N73-11302
Mapping and detection of snow cover changes on land and on glaciers in Alaska, British Columbia, and Washington using ERTS-1 imagery
[E72-10237] 03 p0288 N73-12337
Survey of seasonal snow cover of Alaska from ERTS-1 imagery
[E72-10344] 05 p0532 N73-14332
Application of ERTS-1 imagery to study of caribou movements and winter dispersal in relation to prevailing snow cover
[E72-10346] 05 p0533 N73-14334
Energy balance equations for parameterization of hydrological processes effecting atmospheric circulation
05 p0573 N73-14663
Snow enhancement in New England test areas based on ERTS-1 imagery
[E73-10001] 06 p0657 N73-15337
Mapping and detection of changes of snow cover on land and glaciers
[E73-10063] 07 p0778 N73-16325
Snow line delineation using satellite remotely sensed data
07 p0787 N73-16402
Nimbus 3 and 4 observations of snow cover and hydrological features in Western Himalayas
07 p0787 N73-16403
Mapping snow cover in western US using ERTS-1 MSS imagery
[E73-10087] 08 p0901 N73-17299
Application of ERTS-1 imagery to thematic mapping of open water, ice and snow cover, vegetation, and works of man
[E73-10089] 08 p0902 N73-17301
Alaskan arctic and subarctic sediment deposition, permafrost, snow cover, and ice mapping from ERTS-1 imagery
[E73-10279] 08 p0914 N73-17487
Survey and mapping of freeze-up and break-up patterns of seasonal snow and ice covers in Alaska
[E73-10282] 08 p0914 N73-17489
Application of ERTS-1 imagery to study of caribou movements and winter dispersal in relation to snow cover
[E73-10285] 08 p0914 N73-17491
ERTS-1 imagery of snow cover and break-up characteristics in Chena River Basin, Alaska
[E73-10292] 08 p0915 N73-17497
Simulation of monthly variation of local surface energy budget and sub-surface temperature regime in Antarctica
10 p1146 N73-19326
Geologic and land use exploitation of ERTS-1 imagery of New England using snow enhancement techniques
[E73-10345] 10 p1148 N73-19344
Detection and mapping snow cover in Salt-Verde Watershed of Arizona using ERTS-1 imagery
[E73-10361] 10 p1149 N73-19357
Mapping and detection of snow cover on land and glaciers in Cascade Range using ERTS-1 imagery
[E73-10379] 10 p1152 N73-19374
Utilization of ERTS-1 imagery for study of caribou movements and winter dispersal in relation to prevailing Alaskan snow cover
[E73-10401] 11 p1277 N73-20363
Analysis of ERTS-1 imagery using electronic satellite image analysis console to display and measure snowfield extent, glacier development, and hydrologic features
[E73-10415] 11 p1279 N73-20377
Survey of seasonal snow and ice covers in Alaska using ERTS-1 imagery
[E73-10438] 11 p1281 N73-20398
Mapping permafrost areas of Alaska, correlating snowpack cover of Caribou-Poker Creek with stream runoff, and mapping and inventorying icing on Chena River
[E73-10511] 13 p1516 N73-22286
Detection and mapping changes of snow cover on land and glaciers from ERTS-1 imagery
[E73-10559] 14 p1655 N73-23431
Snow cover survey and vegetation growth in Swiss Alps using ERTS-1 imagery
[E73-10586] 14 p1657 N73-23446
Application of ERTS-1 imagery to study of caribou movements and winter dispersal in relation to prevailing snow cover in Alaska
[E73-10615] 15 p1774 N73-24376
ERTS-1 imagery of snow cover break-up in Chena River Basin, Alaska
[E73-10619] 15 p1774 N73-24380
Survey of seasonal snow cover in Alaska using ERTS-1 imagery
[E73-10637] 15 p1776 N73-24396
Effectiveness of snow cover as photogeological enhancement technique for ERTS-1 imagery of western Massachusetts
[E73-10594] 16 p1896 N73-25334
Application of ERTS-1 imagery for tectonic analysis of Bighorn Mountains region and effect of snow cover and low sun angle on identifying topographical features
[E73-10722] 17 p2019 N73-26329
Analysis of time-lapse data processing for dynamic hydrologic conditions based on ERTS-1 imagery and aerial photography
[E73-10729] 17 p2020 N73-26335
Survey of snow cover and vegetation growth in high mountains of Swiss Alps based on ERTS-1 imagery
[E73-10733] 17 p2020 N73-26339
Detection and analysis of fracture systems using ERTS-1 imagery of snow cover conditions as enhancement tool
[E73-10741] 17 p2021 N73-26346
Application of ERTS-1 data for identification of ice formations in Lake Erie and snow mapping in American River basin
[E73-10750] 17 p2022 N73-26353
Comparison of Skylab/EREP imagery with television and radiometric measurements from other satellites for snow cover survey in Sierra Nevada Mountains and Great Plains
[E73-10755] 17 p2022 N73-26358

Spaceborne imagery of snow cover and glaciers in mountainous regions
[NASA-TT-F-14969] 17 p2025 N73-26387
Mapping snow cover in central Arizona mountains and southern Sierra Nevada of California from ERTS-1 imagery
[E73-10833] 18 p2141 N73-27303
Analysis of ERTS-1 imagery to determine enhancement of ground fracture detail produced by snow cover
[PAPER-G12] 19 p2264 N73-28243
Mapping of snow cover in western areas of US based on ERTS-1 data
[PAPER-W18] 19 p2272 N73-28295
Measurement of percentage of snow cover area on specific drainage basins in Cascade Mountains in Washington state using ERTS-1 imagery
[PAPER-W19] 19 p2273 N73-28296
ERTS-1 imagery of snow cover on northern foothills of Brooks Range and Wrangell Mountains, Alaska
19 p2285 N73-28374
ERTS-1 imagery of caribou movements and winter habitats in Alaska in relation to prevailing snow cover
[E73-10840] 19 p2290 N73-28418
Application of ERTS data for mapping snow cover in Arizona and California and correlation with aerial photography
[E73-10866] 20 p2392 N73-29217
ERTS-1 imagery of snow cover, ice conditions, and soil moisture in Sierra Nevada Mountains and Lake Ontario Basin
[E73-10869] 20 p2393 N73-29220
ERTS-1 imagery of snow melt in Chena River Basin of Alaska
[E73-10903] 20 p2396 N73-29252
Survey of freeze-up and breakup patterns of seasonal snow and ice covers in Alaska
[E73-10920] 20 p2398 N73-29269
Statistical analysis of snowfall in various areas of USSR for application to transportation, agriculture, and urban planning
[TT-70-50181] 20 p2406 N73-29338
Daily and monthly weather charts for Northern Hemisphere and Berlin, Germany for February, 1973
20 p2442 N73-29614
Mapping of fracture-lineaments in New England using snow enhancement techniques
[E73-10930] 21 p2528 N73-30273
Snow cover surveys of Sierra Nevada, Cascades, and Wasatch mountains using Skylab EREP data
[E73-11036] 22 p2663 N73-31340
Detection and mapping snow cover in Arizona and California from ERTS-1 imagery
[E73-11038] 23 p2778 N73-32217
Analysis and mapping sediment deposition, permafrost areas, snow cover, and icing in Arctic regions of Alaska from ERTS-1 data
[E73-11067] 23 p2781 N73-32243
Snowmelt model for Chena River Basin
[E73-11085] 24 p2913 N73-33248
Survey of seasonal snow cover of North Slope and Alaska Range from ERTS-1 data
[E73-11086] 24 p2913 N73-33249
Sources and dispersal patterns of suspended particles in nearshore surface waters of northeast Pacific Ocean and seasonal variation in snow cover in Sierra Nevada Mountains
[E73-11099] 24 p2914 N73-33256
Survey of snow cover to predict risk of spring flood and snow storage in areas of hydroelectric power stations in Norway
[E73-11160] 24 p2919 N73-33313

**SNOW PACKS**
U SNOW

**SNOW S-2 AIRCRAFT**
U S-2 AIRCRAFT

**SNOWPLOW EFFECT**
U PLASMA DYNAMICS

**SOAPS**
Dermatological testing of personal hygiene cleansing agents and laundry detergents for possible use in Skylab Program
[NASA-CR-128880] 11 p1250 N73-20143
Oil base effect on lubricating performance of lithium greases and soaps containing hydrocarbons
[AD-754593] 11 p1300 N73-20549

**SOARING**
Numerical analysis of minimum flight time for sail plane performance while performing cross country flight
[ME-68] 15 p1733 N73-24055
Analysis of three dimensional weakly controlled soaring procedures for increased sailplane performance
19 p2218 N73-27894

**SOCIAL FACTORS**
Evolution of man-machine-hybrid integration in evolving social structure
[AMRU-R-68-3] 02 p0132 N73-11069
Relationship between law and scientific and technical progress in socialist systems
[JPRS-57318] 03 p0367 N73-12992
Theory of preference and theory of optimization treated from order and topology vantage point, and application to social analysis
[NASA-CR-129593] 04 p0441 N73-13592
Influence of space technology and exploration on earthbound human problems
04 p0473 N73-13859
Use of ERTS data to manage and solve social problems associated with earth resources in California
05 p0536 N73-14363
Catalog of economic, social, and educational institutions in Houston Area Test Site
[NASA-CR-128719] 07 p0856 N73-16944
Theoretical procedure for estimating social benefits of remote sensing
[NASA-CR-130027] 07 p0857 N73-16947
Conceptual framework for analysis for aiding policy analyst and policy researcher in empirical investigations into policy phenomena
[NASA-CR-130669] 08 p0976 N73-17982
Impact of radiometry and photometry on economic, social and environmental problems
[NBS-TN-594-4] 11 p1292 N73-20488
Management of technological progress and effects on society
11 p1351 N73-20966
Human performance in schematic concept formation as a function of socio-economic level, personality, intelligence, and race
[AD-744781] 13 p1486 N73-22052
Relations between sociometric variables and criteria of ability and behavior of student pilots
19 p2226 N73-27954
Social and technological impact of STOL aircraft potential
[NASA-CR-133356] 19 p2355 N73-28942
Social, philosophical, and humanistic impacts of possible existence of extraterrestrial life
[NASA-SP-328] 21 p2596 N73-30807

**SOCIAL ISOLATION**
Composition of human gastrointestinal microflora during prolonged isolation
20 p2367 N73-29037

**SOCIOLOGY**
NT SOCIAL FACTORS
Control over social change through anticipatory project assessment
[NASA-CR-129830] 05 p0611 N73-14968
Philosophical and social psychological study of Apollo moon scientist
[NASA-CR-130832] 09 p0995 N73-18122
Behavioral and social science advancement in USSR after 50 years
[JPRS-58686] 12 p1467 N73-21883
Analysis of complex social systems relative to information, communication, and behavior
[P-4951] 14 p1721 N73-23963
Scientific research projects in engineering, chemistry, and social sciences
23 p2859 N73-32844
Airport establishment and operation with emphasis on regional planning, social factors, and economic forces
23 p2863 N73-32877

**SODIUM**
NT LIQUID SODIUM
NT SODIUM VAPOR
Distillation method for quantitative determination of oxygen solubility in sodium
[NLL-RISLEY-TR-2424-[9091.9F]]
02 p0136 N73-11105
Research on fuel cycle technology, sodium technology, fast reactor materials properties, liquid metal and molten salt chemistry, and reactor safety
[ANL-7850] 03 p0263 N73-12136
Reaction of Fe-Ni-Cr alloys with oxygen-containing sodium
[IS-T-508] 04 p0433 N73-13534
Spectral line thickness and temperature distribution in inhomogeneous sodium plasma confined between parallel mirrors
[INR-1388] 06 p0705 N73-15751
Sulfur, sodium, and chloride contaminants in gas turbines
14 p1677 N73-23610
Collision cross section of D line radiated into sodium atoms for one 3 P2 state
[NASA-TT-F-14853] 14 p1695 N73-23752
High intensity noise effects on urinary K-Na ratios in rats
20 p2365 N73-29018
Wedging corrosion and mass transport in sodium/zirconium/stainless steel system at high temperature - Part 1
[RD/B/N-2521-PT-1] 21 p2559 N73-30517

**SODIUM CARBONATES**
Effectiveness of sodium hydrocarbonate as means for treating and preventing motion sickness
07 p0745 N73-16057

**SODIUM CHLORIDES**
Effect of sodium chloride on mechanical properties of superalloys at elevated temperature
[NASA-TM-X-64701] 02 p0186 N73-11510
Composition of diffuse reflective coating containing sodium chloride in combination with diol solvent and organic wetting and drying agents
[NASA-CASE-GSC-11214-1] 04 p0385 N73-13128
Fever generation in rabbits by intravenous injection of table salt
[NASA-TT-F-14677] 07 p0745 N73-16063
Positron annihilation center decrease through migrating anion vacancies in thermal annealing of radiation damaged sodium chloride crystals
[CONF-720530-6] 10 p1194 N73-19715
Dielectric susceptibilities of potassium chloride to lithium and hydroxyl, sodium chloride to hydroxyl, and rubidium chloride to cyanides
[COO-3151-14] 10 p1200 N73-19763
Temperature dependence of elastic constants and Debye temperature of NaCl and KCl single crystals
[NASA-TT-F-14932] 16 p1953 N73-25801
Apparatus for measuring thermal conductivities to 2 degrees K used for measurements in single crystal halides as function of dislocation density
[AD-759552] 17 p2034 N73-26462
High deasity optical memory and electron spin dependent trapping and tunneling processes in KCl and KCl-NaCl
20 p2460 N73-29768
Crack propagation velocities in NaCl crystals
23 p2826 N73-32586

**SODIUM COMPOUNDS**
NT CRYOLITE
NT SODIUM CARBONATES
NT SODIUM CHLORIDES
NT SODIUM FLUORIDES
NT SODIUM HYDROXIDES
NT SODIUM NITRATES
Effects of sodium salts on hot corrosion mechanism in Ni-8Cr-6Al
[AD-748349] 04 p0435 N73-13551
Half wave voltage for optimum orientation for barium sodium niobate transverse light modulator
[CRC-1229] 04 p0457 N73-13733
Calorimetric analysis of low temperature heat capacities and high temperature enthalpies for sodium chromate
[BM-RI-7691] 05 p0605 N73-14924
Influence of Na2SO4 oxidation of Ni-20Cr-2ThO2 gas turbine corrosion
[AD-751259] 07 p0810 N73-16573
Single crystals of hematitic Fe2O3 grown from Na2B4O7 and occuring as plates, rods, hoppers, and equidimensional solid crystals
[AD-755349] 13 p1567 N73-22697
Barium sodium niobate as nonlinear optical material
[AD-758221] 14 p1682 N73-23650
Standard enthalpies of formation for all undisputed compound members in Na-Ti-O system
[BM-RI-7778] 21 p2562 N73-30534

**SODIUM COOLING**
Corrosion behavior of interstitial alloying elements in canning steels for sodium cooled fast breeder reactor
[NLL-RISLEY-TR-2444-[9091.9F]]
02 p0209 N73-11693
Thermohydraulic test facility for design of fuel elements for water and sodium cooled reactors
[NT-31-1972] 05 p0579 N73-14712

**SODIUM D-LINE**
U D LINES

**SODIUM FLUORIDES**
Application of alkali halides for holographic recording and recovery at room temperatures for high density data storage systems
[AD-748027] 03 p0311 N73-12537

**SODIUM HYDROXIDES**
Thermodynamic stability diagrams for iron, nickel, and chromium in fused sodium hydroxide
22 p2625 N73-31028
Analysis of etching process in polycarbonate film when aqueous sodium hydroxide is used to develop charged particle tracks
[NASA-CR-124381] 22 p2673 N73-31415

**SODIUM NITRATES**
Optical activity and Raman scattering in sodium nitrite crystals
16 p1952 N73-25792

**SODIUM VAPOR**
Photometric system, using sodium vapor resonance cell for observing D2 emission line from daytime sky
10 p1146 N73-19328

**SOFT LANDING**
Results of Mars 2 and Mars 3 space probes
[NASA-TT-F-14914] 14 p1709 N73-23869

**SOFT LANDING SPACECRAFT**
NT AEROSPACEPLANES
NT APOLLO SPACECRAFT
NT GEMINI SPACECRAFT
NT LUNAR LANDING MODULES
NT LUNAR MODULE
NT SURVEYOR LUNAR PROBES
NT SURVEYOR 3 LUNAR PROBE
NT VOSTOK SPACECRAFT

**SOFT RECOVERY**
U SOFT LANDING

**SOFTWARE [COMPUTERS]**
U COMPUTER PROGRAMS

U COMPUTER SYSTEMS PROGRAMS
SOIL EROSION
Inventory and mapping extent and spread of wind erosion of soils in west Texas
[E73-10834] 18 p2141 N73-27304
Application of ERTS-1 imagery for monitoring accelerated soil erosion in southern Arizona
[PAPER-G7] 19 p2264 N73-28238
Detection and mapping of soil erosion and flooding in southern Arizona
[E73-10950] 21 p2531 N73-30292
Erosional latitudinal debris distribution on Mars surface
23 p2839 N73-32689
Wind erosion and sandstorm effects on Mars surface topography
23 p2839 N73-32692
SOIL MAPPING
Mapping and managing soil and range resources in Sand Hills Region of Nebraska using ERTS-1 imagery
[E72-10175] 01 p0044 N73-10354
Identification and mapping geologic, soil, agriculture, geographic, and land use features using ERTS-1 imagery of Central US
[E72-10232] 02 p0163 N73-11325
Crop identification, acreage estimation, urban land use, soil mapping, and earth resources identification in Wabash River Basin using ERTS-1 imagery
[E72-10208] 03 p0288 N73-12331
Spectral analysis of soil boundaries in Collin County, Texas
[E72-10260] 03 p0290 N73-12359
Location of soil types with potential for generating atmospheric sand and dust with application to analysis of V/STOL operational environment
[AD-749462] 05 p0495 N73-14033
Soil mapping, crop identification, and rangeland assessment in Great Plains using ERTS-1 multisensor imagery
[E72-10369] 05 p0536 N73-14357
Delineation of flood plain hazard zones by means of detailed soil surveys and by means of aerial photointerpretation
[PB-211325] 05 p0541 N73-14398
Multispectral data and computer processing technique for mapping soil patterns and multispectral radiation changes from corn crop canopy
[NASA-CR-130035] 07 p0789 N73-16420
Application of multispectral remote sensing to soil survey research in Indiana
[NASA-CR-130033] 07 p0790 N73-16424
Procedure for defining spectrally separable classes for soil survey research
[NASA-CR-130031] 07 p0791 N73-16434
Mapping of soil-vegetation groupings in Arizona using ERTS-1 imagery
[E73-10290] 09 p1020 N73-18327
Detection of plant and forest diseases, nutrient deficiencies, soil types, and soil moisture levels from ERTS-1 imagery of Tennessee
[E73-10311] 09 p1022 N73-18343
Evaluation of ERTS-1 imagery of major crops and soil associations for selected sites in central United States
[E73-10323] 09 p1024 N73-18355
Crop identification, soil mapping, water resources, and urban land use analysis in Wabash River Basin based on ERTS-1 imagery
[E73-10364] 10 p1150 N73-19360
Mapping and management of soil range resources in Sand Hills Region of Nebraska using ERTS-1 imagery
[E73-10372] 10 p1151 N73-19367
Correlation and regression analysis of aerial photography and soil samples to determine principal soil limitations
[NASA-CR-131110] 10 p1154 N73-19392
Soil mapping of rangelands in Bennett County, South Dakota using remotely sensed imagery
[NASA-CR-131229] 10 p1155 N73-19395
Evaluation and comparison of ERTS-1 measurements of major crops and soil conditions for selected areas in Central United States
[E73-10384] 11 p1275 N73-20348
Detection of plant diseases and nutrient deficiencies, soil types, and moisture levels from ERTS-1 imagery of Tennessee and Kentucky
[E73-10468] 12 p1395 N73-21305
Identification and mapping soil in Tennessee Valley from ERTS-1 imagery
[E73-10477] 12 p1395 N73-21314
Utilization of ERTS-1 data for crop identification and acreage estimation, soil mapping, urban land use, water resources, atmospheric modeling, and earth surface feature identification in Wabash River Basin
[E73-10549] 14 p1655 N73-23422
Mapping and managing soil and range resources in Sand Hills Region of Nebraska using ERTS-1 imagery
[E73-10629] 15 p1775 N73-24389
Identification and mapping of soils, vegetation, and water resources in Texas from ERTS-1 MSS digital data
[E73-10670] 16 p1899 N73-25365
Identification of soil associations in Great Plains from ERTS-1 imagery
[E73-10679] 16 p1901 N73-25374
Possibilities of studying and mapping soil cover on basis of Soyuz, Gemini, Apollo, and Salyut photographs
[NASA-TT-F-14971] 17 p2032 N73-26447
Soil analysis and mapping from Skylab EREP imagery
[E73-10756] 18 p2133 N73-27238
Mapping and managing soil and range resources in Sand Hills Region of Nebraska using ERTS-1 imagery
[E73-10807] 18 p2139 N73-27282
Remote color aerial photography for soil mapping and highway engineering applications
[PB-220376] 18 p2148 N73-27363
Application of ERTS-1 imagery for delineation of major soil association in loess region of Obion County, Tennessee
[PAPER-A14] 19 p2261 N73-28222
Computer analysis of ERTS-1 MSS data for identification and mapping of soils, vegetation, and water resources in Lynn County, Texas
19 p2287 N73-28392
Utilization of ERTS-1 imagery for soil mapping, land use, and urban mapping in Wabash River Basin
[E73-10862] 20 p2392 N73-29213
Application of space photography for small-scale mapping and analysis of farm lands
21 p2535 N73-30326
Interpreting and compiling soil maps from aerial and space survey data
21 p2535 N73-30328
Land use, forest density, soil mapping, erosion, drainage, and salinity limitations in Greece from ERTS-1 data
[E73-10969] 22 p2657 N73-31283
Crop identification, soil mapping, and atmospheric modeling in Wabash River Basin using ERTS-1 data
[E73-11082] 23 p2782 N73-32257
Utilization of ERTS-1 imagery in mapping and managing range resources in Sand Hills Region of Nebraska
[E73-11121] 24 p2916 N73-33276
ERTS-1 measurements of major crops and soil associations in Indiana, North Dakota, Iowa, Nebraska, Kansas, and Texas
[E73-11155] 24 p2919 N73-33309
SOIL MECHANICS
Penetration resistance of cohesionless sands with solid obstacles embedded within soil matrix
[NASA-TM-X-58099] 03 p0294 N73-12392
Location of soil types with potential for generating atmospheric sand and dust with application to analysis of V/STOL operational environment
[AD-749462] 05 p0495 N73-14033
Establishment of takeoff and landing environment criteria for V/STOL aircraft with emphasis on airborne particle concentration
[AD-749463] 05 p0495 N73-14034
Development and evaluation of equipment for monitoring long term sea floor foundation settlement and tilting
[AD-750258] 06 p0669 N73-15444
Development of model to describe characteristics of one dimensional lunar ash flow with and without heat transfer effects
[NASA-CR-130697] 08 p0895 N73-17245
Soil mechanics for lunar soils near landing site for Apollo 16 mission
12 p1449 N73-21740
Performance of aircraft taxiing on dirt surfaces
[AD-756588] 16 p1861 N73-25077
Energy budget of pumice desert surface under clear skies during summer
[PB-218791/2] 18 p2146 N73-27347
Static penetration resistance of soils
[NASA-CR-133460] 19 p2294 N73-28445
Effects of microflora on rock weathering and edaphic factor
[NASA-TT-F-15033] 20 p2411 N73-29380
SOIL MOISTURE
Identification of agricultural crops and soil moisture stress in Iowa using ERTS-1 imagery
[E72-10335] 05 p0531 N73-14323
Detection of plant and forest diseases, nutrient deficiencies, soil types, and soil moisture levels from ERTS-1 imagery of Tennessee
[E73-10311] 09 p1022 N73-18343
Spectroradiometric quantification of soil moisture in Willcox Playa, Arizona based on ERTS-1 imagery
[E73-10354] 10 p1149 N73-19350
Airborne electrical scanning microwave radiometric measurements of soil moisture in Texas, California, and Arizona
[NASA-CR-130204] 11 p1284 N73-20423
Detection of plant diseases and nutrient deficiencies, soil types, and moisture levels from ERTS-1 imagery of Tennessee and Kentucky
[E73-10468] 12 p1395 N73-21305
Analysis of soil moisture distribution in test sites for Skylab 3
[E73-10815] 18 p2140 N73-27290
ERTS-1 detection of plant diseases and nutrient deficiencies, soil types and moisture levels, forests, and crop identification in Mississippi Delta
[E73-10849] 19 p2292 N73-28427
Application of multispectral scanning to hydrology and water resources, noting measurement of soil moisture, water depth, and water quality
19 p2295 N73-28454
ERTS-1 imagery of snow cover, ice conditions, and soil moisture in Sierra Nevada Mountains and Lake Ontario Basin
[E73-10869] 20 p2393 N73-29220
Collection of ground truth data in Great Basin for support of aerial and Skylab overflights
[E73-10884] 20 p2394 N73-29235
Acquisition of land use, soil moisture, and hydrological data of Ontario, Canada and Syracuse, New York for Skylab-3
[E73-10888] 20 p2394 N73-29237
Soil moisture and vegetation surveys of Kansas and Texas for Skylab investigations
[E73-10944] 21 p2530 N73-30286
Skylab monitoring of temperatures of lakes and playas and soil moisture in Nevada
[E73-11004] 22 p2660 N73-31309
Humic soil acid effects in silicate mineral weathering with aluminum migration
[NASA-TT-F-15134] 23 p2754 N73-32034
Detection of plant diseases, soil moisture, drainage patterns, forestry types, and sedimentation in Tennessee from ERTS-1 imagery
[E73-11091] 23 p2782 N73-32258
Skylab detection of soil moisture in Texas
[E73-11101] 24 p2914 N73-33258
SOIL SCIENCE
Flow charts for British standard particle-size distribution for soils
[PB-211721] 06 p0667 N73-15426
Analysis of imagery obtained from infrared color and color photography used for highway and railroad engineering applications
07 p0783 N73-16368
Graphical method for determining soil temperature from air temperature and humidity measurements
[NLL-M-22802-[5828.4F]] 11 p1274 N73-20339
Application of ERTS-1 multisensor data in Great Plains to map ranglands, croplands, and soil formations
[E73-10443] 11 p1282 N73-20403
Splitting aluminosilicates with silicate bacteria for liberation of potassium in soils
[NASA-TT-F-14870] 11 p1286 N73-20437
Use of remote airborne photopolarimeters to measure soil moisture content in southwestern United States
[NASA-CR-130211] 13 p1522 N73-22332
Identification of soil associations in Great Plains from ERTS-1 imagery
[E73-10679] 16 p1901 N73-25374
Application of ERTS-1 data to locate wind erosion sites in West Texas and to determine extent and spread of wind erosion
[E73-10719] 17 p2019 N73-26326
Soil analysis and mapping from Skylab EREP imagery
[E73-10756] 18 p2133 N73-27238
Analysis of ERTS-1 imagery for multi-disciplinary resource inventory of soils, vegetation, and geology in Big Summit Prairie area of oregon
[E73-10770] 18 p2134 N73-27246
Analysis of soil moisture distribution in test sites for Skylab 3
[E73-10815] 18 p2140 N73-27290
Application of ERTS-1 imagery for delineation of major soil association in loess region of Obion County, Tennessee
[PAPER-A14] 19 p2261 N73-28222
Identification of soil associations in western South Dakota using ERTS-1 imagery
[PAPER-L11] 19 p2274 N73-28307
Electric conductivity of water extracts from soil as measure of ionic strength
[NASA-TT-F-15044] 20 p2411 N73-29377
Coefficients of electrical conductivity for determining concentration of water soluble salts in soils
[NASA-TT-F-15045] 20 p2411 N73-29379
Water, agriculture, and soil resources management and planning in California using ERTS-1 imagery
[E73-10935] 21 p2529 N73-30277
Interpretation of seasonal changes in vegetation and soils in Idaho from ERTS-1 imagery
[E73-10936] 21 p2529 N73-30278
Comparison of ERTS-1 spectral reflectance measurements of major crops and soil associations for selected sites in Iowa, Kansas, North Dakota, and Texas
[E73-10981] 22 p2657 N73-31288
Auger-type soil penetrometer for burrowing into soil formations
[NASA-CASE-XNP-05530] 23 p2790 N73-32321
Application of ERTS-1 imagery to land use, forest density, and soil investigations in Greece
[E73-10988] 24 p2913 N73-33244
SOILS
NT ALLUVIUM
NT LUNAR DUST
NT LUNAR SOIL
NT PERMAFROST
NT SANDS

Procedure for assaying enzyme activity in soils and application to presumptive life tests in Martian soil
[NASA-CR-128399] 01 p0008 N73-10059
Definition of characteristics and boundaries of vegetation-soil types in Southern Idaho from ERTS-1 remotely sensed imagery
[E72-10203] 02 p0161 N73-11300
Vegetation, soil, and water reflectance measurements from ERTS-1 imagery of Hidalgo County, Texas
[E72-10267] 03 p0291 N73-12366
Measuring electromagnetic parameters of soil samples in VHF/UHF range to determine properties that limit target detection
[AD-747346] 03 p0299 N73-12439
Soil stabilization during road and airport construction
[AD-748153] 03 p0299 N73-12442
Gas chromatographic-mass spectrometric analysis of volatile organic metabolic products in terrestrial soils
[NASA-CR-129602] 04 p0386 N73-13134
ERTS-1 imagery of Quaternary landforms and materials in Midwest and Great Plains
[E72-10272] 04 p0409 N73-13333
Spectral signatures for dominant desert scrub plant species of Arizona and soil surface backgrounds
[E72-10318] 04 p0413 N73-13367
Detection of plant diseases and nutrient deficiencies, soil types, and moisture levels in Tennessee using ERTS-1 imagery
[E72-10320] 04 p0413 N73-13368
Utilization of ERTS-1 imagery to map soils and vegetation in Idaho
[E72-10356] 05 p0534 N73-14344
ERTS-1 measurement of vegetation, soil, and water reflectance
[E72-10364] 05 p0535 N73-14352
Mathematical characterization of mechanical behavior of porous frictional granular media
[NASA-CR-124006] 06 p0661 N73-15368
Soil sampling and microorganism analysis in planetary spacecraft assembly area for prevention of Mars contamination
[NASA-CR-130009] 07 p0745 N73-16059
Soil moisture measurements for microwave radiometers onboard Convair 990 aircraft
08 p0971 N73-17935
Freezing effects on structure of soils and biological tissues
[CNRS/LA-PUBL-440] 09 p0999 N73-18150
Multidisciplinary analysis of forestry, agriculture, soils, and landforms in Michigan using ERTS-1 imagery
[E73-10310] 09 p1022 N73-18342
Utilization of ERTS-1 imagery for mapping Quaternary deposits and landforms in Great Plains and Midwest
[E73-10381] 10 p1152 N73-19376
ERTS-1 spectral reflectance measurements of vegetation, soil, and water in Rio Grande Valley, New Mexico
[E73-10408] 11 p1278 N73-20370
Determination of specific spectral signatures for dominant Arizona desert scrub plant species and soil surface backgrounds
[E73-10466] 11 p1284 N73-20421
Gamma survey of rocks and soils covered by nonactive radiation absorption layers using aerial reconnaissance and fourier analysis
[AD-755003] 11 p1289 N73-20461
Mass fragmentography-computer for identification and quantitation of amino acids in soil
[NASA-CR-131507] 12 p1376 N73-21159
Application of ERTS-1 data to analysis of agricultural crops, forests, soils, landforms, and acreage estimates in Michigan
[E73-10483] 12 p1396 N73-21320
Remote sensing of fallow soil moisture, using visible and infrared scanners
13 p1514 N73-22267
Identification of vegetation and soils in Idaho using ERTS-1 remotely sensed imagery
[E73-10512] 13 p1516 N73-22287
Broad scale application of ERTS-1 imagery to study and mapping of geological, hydrological, land use, rangelands, and soil cultures in Wyoming
[E73-10554] 14 p1655 N73-23426
Utilization of ERTS-1 imagery to detect plant diseases, nutrient deficiencies, soil types, and moisture levels in Tennessee
[E73-10640] 15 p1776 N73-24399
Thermoradiation sterilization of naturally occurring microorganisms in soil from Kennedy Space Center
[NASA-CR-132197] 16 p1904 N73-25404
Remote low power mineralogical analysis of lunar, planetary, or asteroid soils, using X ray diffraction
[NASA-CR-124271] 16 p1963 N73-25879
Psychrophilic organisms in soil samples of areas for Viking spacecraft assembly
[REPT-2] 17 p1987 N73-26063
Spaceborne photography of vegetation, soils, and agricultural land use
[NASA-TT-F-14967] 17 p2025 N73-26393
Application of airborne microwave radiometers for remote monitoring of soil moisture in selected areas of Texas and Oklahoma
[NASA-CR-133102] 17 p2031 N73-26438
Application of airborne microwave radiometry for remote sensing of soil moisture in southwest US
[NASA-TM-X-66265] 17 p2032 N73-26444
Ionic migration and weathering in frozen Antarctic soils
[NASA-CR-2283] 18 p2143 N73-27326
Field sampling taxonomic units within geomorphic-soil-vegetation mapping units in Arizona
[E73-10889] 20 p2394 N73-29238
Spectral signatures for dominant desert scrub plant species and soil surface backgrounds in Arizona
[E73-10890] 20 p2394 N73-29239
Use of soil-vegetation system brightness coefficients to measure vegetation quantity and crop yield
20 p2406 N73-29334
Aircraft gamma surveys of moisture content in soil detention layer
20 p2448 N73-29667
SL-2 MSS photography of soils, water, and vegetation in Texas
[E73-10943] 21 p2530 N73-30285
ERTS-1 measurements of seasonal changes in reflectance of soils, vegetation, and water in Hidalgo County, Texas
[E73-10946] 21 p2530 N73-30288
Approximate theory for wheel-soil interaction
[NASA-CR-133860] 21 p2580 N73-30673
Lime-cement combination for soil stabilization in road and airfield construction
[AD-762552] 22 p2690 N73-31545
Polarization of light reflected from soil and sand with varied surface moisture and texture
[AD-765421] 23 p2788 N73-32309
Soil burrowing mole apparatus
[NASA-CASE-XNP-07169] 23 p2796 N73-32362

**SOLAR ACTIVITY**
NT FACULAE
NT SOLAR FLARES
NT SOLAR PROMINENCES
NT SOLAR STORMS
NT SUNSPOTS
Solar flares, magnetic storms, ionospheric disturbances, and geophysical observations recorded by weather stations in India during Feb. 1972
[RRC-A-201-PT-2] 01 p0048 N73-10386
Synoptic charts and catalogs of solar activity centers and chromospheric filaments
01 p0099 N73-10817
Cosmos 224 observations of N2 ions during medium solar activity
03 p0293 N73-12389
Enhanced solar activity effects on fast neutron production at polar latitudes
04 p0465 N73-13791
Prediting mean annual runoff from solar activity
[NLL-M-20715-[5828.4F]] 05 p0529 N73-14303
Relation of solar activity to air temperature and precipitation
[NLL-M-20651-[5828.4F]] 05 p0570 N73-14626
Solar phenomenon, based on dynamo model
[PUBL-5] 05 p0592 N73-14809
Preliminary results from HEOS A satellite in electron and proton events, solar wind and interplanetary magnetic field measurement, and propagation of charged particles
[ESRO-SP-74] 05 p0592 N73-14813
Directional measurements of solar protons during low solar activity from HEOS A satellite
05 p0593 N73-14818
High resolution power spectra of Zurich daily sunspot numbers over 77 years
[NASA-TM-X-64718] 06 p0716 N73-15840
Research projects to determine nature of Sun as ultraviolet variable star and description of MUSE experiment
[NASA-TM-X-66142] 06 p0719 N73-15868
Latitude-time variations of ionospheric electron densities at high latitudes during periods of solar activity
07 p0791 N73-16431
Solar particle composition measurements using nuclear emulsion detectors on sounding rockets
08 p0973 N73-17959
Radio telescope and satellite studies of atmosphere, ionosphere, and magnetosphere under disturbed conditions produced by enhanced solar activity
[AD-754252] 10 p1157 N73-19410
Relationship between solar activity and atmospheric pressure of Northern Hemisphere
[NLL-M-22858-[5828.4F]] 11 p1313 N73-20651
Prediction of solar activity and geophysical effects, including X ray burst data
[AD-755920] 12 p1403 N73-21379
Effects of solar activity and geocoronal emissions on atmospheric boundary layer as observed by Proghoz satellite
12 p1461 N73-21840
Cyclic variations in Es layer with 11 year cycle of solar activity
13 p1521 N73-22329
Solar-geophysical activity associated with major ground level cosmic ray event of 24 January 1971
[UAG-24-PT-1] 13 p1572 N73-22737
Solar-geophysical activity associated with major ground level solar cosmic ray event of 1 September 1971
[UAG-24-PT-2] 13 p1572 N73-22738
Oscillation and supergranulation motions in solar atmosphere
[NASA-CR-131606] 13 p1579 N73-22797
Tabular ionospheric data acquired by vertical incidence sounding techniques
[RRC-A207-PT-2] 16 p1905 N73-25409
Tables on solar and magnetic activity
[RRC-A210-PT-2] 16 p1907 N73-25424
Tables on solar and magnetic activity
[RRC-A203-PT-2] 16 p1907 N73-25425
Radiometric measuring system for solar activity and atmospheric attenuation and emission
[NASA-CASE-ERC-10276] 17 p2031 N73-26432
Power spectral analysis of solar 2 cm microwave intensity data
[NASA-CR-133228] 17 p2079 N73-26820
Proving solar activity effect on biosphere by correlation between activity indices with biological indices
[NASA-TT-F-14984] 17 p2079 N73-26821
Analysis of velocity signals of solar active regions
[AD-760124] 18 p2195 N73-27723
Deep space solar activity monitoring platform with video capability, including X ray flux, UV flux, charged particle flux, and radio emission measurements
[AD-761799] 19 p2346 N73-28875
Time of formation of elementary circulation mechanisms related to annual fluctuation in solar activity
[NLL-M-23014-[5828.4F]] 20 p2390 N73-29199
Analysis of cause of nonlinear relationship between solar constant and solar activity to show possible climatic consequences
[NLL-M-23053-[5828.4F]] 20 p2390 N73-29201
Pyrheliometers errors with various aperture angles associated with solar aurora effects
20 p2403 N73-29311
Effects of solar activity on present day changes of climate
[NLL-M-23005-[5828.4F]] 20 p2442 N73-29612
Solar-geophysical data for sudden ionospheric disturbance of Dec. 14 to 21 1971
[AD-762483] 20 p2474 N73-29873
Complex system of tidal forces on sun, created by all planets of solar system
[NLL-M-23039-[5828.4F]] 21 p2591 N73-30760
Influence of solar activity on biological indices and disease of living organisms in biosphere
[NRC-TT-1679] 21 p2592 N73-30771
Solar magnetic sector structure effects on tropospheric and lower stratospheric vorticity
[NASA-CR-133842] 21 p2592 N73-30773
Solar magnetic sector structure related to earth atmospheric circulation during winter
[NASA-CR-133850] 21 p2593 N73-30774
Magnetograph for recording magnetic fields in solar active region
[AD-762485] 22 p2712 N73-31713
Skylab, solar studies, and usefulness of Apollo telescope mount
[NASA-EP-119] 23 p2834 N73-32645
One-dimensional time dependent diffusion convection model analysis of cosmic ray modulation during solar maximum
[TR-73-131] 23 p2834 N73-32647

**SOLAR ACTIVITY EFFECTS**
Relationship between atmospheric gravity waves and spread F conditions caused by solar activity
05 p0509 N73-14146
Electron flux density recorded onboard HEOS 1 in 1969 and 1970, discussing solar activity effects and comparing proton flux density
05 p0593 N73-14816
Solar X-ray spectra for predicting ionospheric radio wave propagation during solar activity
[AD-751575] 07 p0794 N73-16459
Formulation of disturbing function for computing lunisolar perturbations in satellite motion
[NASA-CR-130743] 08 p0941 N73-17709
Analysis of semiannual density variation in thermosphere during period of increasing solar activity
[SMFT-FBW-73-02] 11 p1285 N73-20430
Night sky luminescence in upper atmosphere during IQSY
[NASA-TT-F-14927] 14 p1660 N73-23478
ERTS/Nimbus satellite observations of electron flux levels as function of solar cycle
[NASA-TM-X-66236] 14 p1703 N73-23814
Dichotomy in geomagnetic disturbance and its solar origin
[AD-759791] 16 p1909 N73-25447
Large scale structure of solar wind including proton results, solar cycles, interplanetary medium, and high heliographic latitude activities
[NASA-TM-X-69342] 19 p2340 N73-28826

Analysis of cause of nonlinear relationship between solar constant and solar activity to show possible climatic consequences
[NLL-M-23053-[5828.4F]] 20 p2390 N73-29201
Solar activity effects on terrestrial climate
[AD-762227] 20 p2468 N73-29827
Doppler study of plasma column changes at solar elongation in Mariner 9 tracking path
23 p2842 N73-32715

**SOLAR ARRAYS**
Attitude stability criteria and nutation decay times of dual-spin satellite with large flexible solar array
[AD-743258] 01 p0109 N73-10897
Computer program for determining solar array output characteristics while accounting for effects of temperature,incidence angle on solar arrays
[NASA-CR-130109] 02 p0129 N73-11045
Silicon-controlled, rectifier series, resonant inverter, power conditioning for electric propulsion from solar array
[NASA-CR-120928] 02 p0223 N73-11804
Single axis orientation mechanism for solar arrays on high power synchronous satellites with 116 liquid metal slip rings
[NASA-CR-120954] 04 p0395 N73-13215
Torque measurement of flat polyimide cable crossing hinge or satellite solar array
[ESRO-TN-114-ESTEC] 05 p0603 N73-14904
Optimal design of baseline configuration for solar array panel with deployable beam
[NASA-CR-130287] 06 p0626 N73-15079
Design and performance of solar array for Helios solar probe
[DGLR-PAPER-72-091] 06 p0627 N73-15084
Design and preflight analysis of flexible solar array mechanism
09 p1089 N73-18887
Structural configuration and performance tests of 928 sq m solar array
09 p1089 N73-18891
Growth of large-area silicon ribbons for application to large area solar cells and arrays
10 p1228 N73-19981
Design and development of brushless, direct drive solar array reorientation control system for satellites
[NASA-CR-130153] 11 p1261 N73-20236
Solar array development discussing manufacturing, design qualification tests in aerospace environments, and comparison between fold-up and roll-up types
[RAE-TR-72109] 13 p1476 N73-21959
Design and tests of liquid metal slip ring/solar orientation mechanism
[NASA-CR-120885] 14 p1640 N73-23292
Empirical equations for calculating photovoltaic characteristics of solar cell array
[NASA-CR-130248] 15 p1737 N73-24085
Dynamic characteristics of large flexible solar arrays and interaction between spacecraft attitude dynamics and elastic degrees of freedom
[UTIAS-179] 15 p1835 N73-24878
Mariner 9 solar array design, manufacture, and performance
[NASA-CR-132991] 16 p1912 N73-25469
Feedback control loop stability analysis for dynamic solar array simulator, based on frequency response and using digital computer
[ESRO-CR[P]-261] 19 p2223 N73-27929
Method for predicting degradation of solar array in space radiation environment
[NASA-CR-133738] 21 p2499 N73-30055
Space station solar array technology evaluation program
[MSC-07163] 21 p2499 N73-30057
Optimized electric welding technique for silicon solar cell arrays
[LCR-DR-1-72-52/1/R] 21 p2553 N73-30470
Analysis and Mechanical design of solar array stowage and deployment arrangements for use in Small Applications Technology Satellite spacecraft
[NASA-CR-132800] 22 p2720 N73-31767
Congressional hearing on Skylab 1 solar array system failure
23 p2866 N73-32912
High voltage solar array for ion thruster electric propulsion system
[NASA-TM-X-71462] 24 p2880 N73-33002
Computer program for calculating roll-up solar array performance characteristics
[NASA-CR-135898] 24 p2880 N73-33003
Mechanical drives for communication satellite antennas and solar arrays
[DGLR-PAPER-73-050] 24 p2986 N73-33864
Direct broadcasting TV satellite solar arrays, and heat budget subsystems
[DGLR-PAPER-73-051] 24 p2986 N73-33865

**SOLAR ATMOSPHERE**
Theoretical study of sunspots and electrical and thermal conductivities of solar magnetoplasma
[AD-752230] 08 p0962 N73-17872
Short-duration solar microwave bursts and associated soft X ray emission
[NASA-CR-130859] 09 p1081 N73-18816
Solar meridional circulation and latitudinal sunspot drift analysis
[AD-751268] 09 p1081 N73-18820
Correlation of solar magnetograms with interplanetary magnetic field
[NASA-CR-131607] 13 p1577 N73-22775
Oscillation and supergranulation motions in solar atmosphere
[NASA-CR-131606] 13 p1579 N73-22797
Research in X ray, solar, and radio astronomy
[AD-756459] 15 p1833 N73-24860
Isotopic composition of chemical elements in solar atmosphere
[AD-758769] 18 p2198 N73-27748
Structure and physics of solar and stellar atmosphere including physical processes in nonstationary stars
[NASA-TT-F-760] 20 p2470 N73-29840
Determination of turbulent velocities in solar photosphere with allowance for influence of instrumental contour
20 p2472 N73-29855

**SOLAR AZIMUTH**
U AZIMUTH
U SOLAR POSITION

**SOLAR CELLS**
Design and operation of high voltage photoelectric generator
[AD-745364] 01 p0007 N73-10053
Development, characteristics, and application of solar electric power generators used in USSR spacecraft - Part I
[AD-741524] 01 p0007 N73-10056
Potential plume contamination effects from two 300 lb bipropellant engines in satellite environment and electrical power loss study
[AD-746306] 01 p0007 N73-10057
Design optimization for gallium arsenide solar cell parameters
[NASA-CR-129214] 02 p0128 N73-11041
Performance characteristics of gallium arsenide solar cells with zinc or beryllium ion implantations
[NASA-CR-129199] 02 p0128 N73-11042
Radiation damage recovery characteristics of lithium doped solar silicon cells
[NASA-CR-129183] 02 p0128 N73-11044
Protective coatings for solar batteries from atmospheric effects
[AD-746325] 02 p0129 N73-11046
Neutron irradiation effects on lithium-doped silicon solar cells in space environment simulation
[AD-745992] 02 p0129 N73-11048
Feasibility of using photovoltaic cells to convert laser energy into electrical energy
[LA-DC-72-468] 03 p0255 N73-12061
Kapton covered cadmium sulfide solar cell performance tests in aerospace and earth atmosphere environments
[ONERA-DERTS-NT-02-32] 03 p0255 N73-12062
High altitude balloon flights for solar cell calibration
[NASA-CR-129794] 04 p0375 N73-13050
Evaluation of dielectric insulation and etched junction contact techniques for fabrication of wraparound contact silicon solar cells
[NASA-CR-121021] 04 p0375 N73-13051
Technique for accelerated evaluation of silicon solar cells for use on extended space missions with weapons environment
[AD-749477] 05 p0499 N73-14062
Production processes for fabrication of lithium doped P/N cells
[NASA-CR-130289] 06 p0626 N73-15078
Design and performance of solar array for Helios solar probe
[DGLR-PAPER-72-091] 06 p0627 N73-15084
Various dispositions of silicon solar cells as influenced by temperature gradients and proton irradiation flux
[NASA-TM-X-66169] 07 p0741 N73-16031
Coatings of borosilicate glasses deposited on silicon solar cells by radio frequency sputtering for enhanced protection
[ESRO-CR-68] 09 p0991 N73-18087
Development of processing techniques for fabrication of lithium doped solar cells noting behavior during electron irradiation and annealing
[ESRO-CR-94] 09 p0991 N73-18088
Ultraviolet and charged particle irradiation of solar cell coverslide materials and conductive coatings for Helios satellites
[NASA-TM-X-65945] 09 p1051 N73-18571
Analysis of silicon solar cells to show factors controlling blue response and methods for improvement
[NASA-CR-131090] 10 p1111 N73-19059
Cellular arrays as iterative logical and memory structures
[NASA-CR-130936] 10 p1132 N73-19227
Apollo experience report on design philosophy and experience of Apollo spacecraft electrical power generation system
[NASA-TN-D-7142] 10 p1214 N73-19873
Growth of large-area silicon ribbons for application to large area solar cells and arrays
10 p1228 N73-19981
Rectangular solar cell stacked panels to generate electrical power aboard spacecraft
[NASA-CASE-NPO-11771] 11 p1237 N73-20040
Design and fabrication of wraparound contact silicon solar cells
[NASA-CR-121003] 11 p1237 N73-20044
Light generated current output of vertical multijunction solar cell
[AD-754901] 11 p1238 N73-20047
Effects of electron irradiation and temperature on 1 ohm-cm and 10 ohm-cm solar cells
[NASA-TM-X-66231] 12 p1366 N73-21083
Analysis of photoelectric properties of gallium arsenide and application to construction of solar cells
[AD-756228] 13 p1477 N73-21962
Effectiveness of solar cells based on CdS-Cu-xS heterojunctions
[AD-756602] 13 p1478 N73-21971
Electron irradiation effect on transmission properties of ceria doped solar cell cover glass
[NASA-TN-D-7245] 15 p1737 N73-24082
Parametric performance characteristics and treatment of temperature coefficients of silicon solar cells for space application
[NASA-CR-132156] 15 p1738 N73-24090
Design and performance of voltage transducers for Mariner spacecraft solar cells
[NASA-CR-132250] 15 p1756 N73-24234
Development of high efficiency gallium arsenide solar cells using ion implantation techniques
[NASA-CR-131842] 16 p1865 N73-25099
Inversion layer silicon solar cells with induced junctions
[NASA-CR-131840] 16 p1865 N73-25100
Production cost optimization for thermoelectric solar cell
[AD-759812] 16 p1865 N73-25104
Graded band gap p-n junction gallium arsenide/gallium aluminum arsenide solar cell
[NASA-CASE-LAR-11174-1] 17 p1985 N73-26047
Silicon solar cell with plastic film binding to cover glass
[NASA-CASE-LEW-11065-2] 17 p1985 N73-26048
Design of vertical multijunction silicon solar cells with prolonged lifetimes
[AD-760172] 17 p1986 N73-26052
Nondestructive testing of welded silicon solar cell silver interconnections
[ESS/SS-397] 17 p2038 N73-26487
Design, development, and application of 10,000 watt solar array panel for application to three possible space missions and review of solar cell technology
[NASA-CR-133616] 20 p2363 N73-29006
Development of lithium-doped silicon solar cells with increased stability, efficiency, and radiation resistance
[AD-762941] 20 p2364 N73-29011
Optimized electric welding technique for silicon solar cell arrays
[LCR-DR-1-72-52/1/R] 21 p2553 N73-30470
Techniques for improving performance of gallium arsenide solar cells by ion implantation
[NASA-CR-135510] 22 p2618 N73-30977
Fabrication techniques for lithium-doped silicon solar cells
[AD-764357] 22 p2618 N73-30982
Thermoelastic analysis for predicting thermal stress failure in silicon solar cell array
[NASA-CR-135713] 23 p2748 N73-31993
Electroforming of aluminum solar cell contacts
[AD-764816] 23 p2748 N73-31995
Service life and reliability of radiation hardened lithium doped solar cells
23 p2859 N73-32840

**SOLAR CHROMOSPHERE**
U CHROMOSPHERE
U SOLAR ATMOSPHERE

**SOLAR COLLECTORS**
Low temperature bonding of solar panel materials
[AD-746684] 05 p0553 N73-14493
Optimal design of baseline configuration for solar array panel with deployable beam
[NASA-CR-130287] 06 p0626 N73-15079
Analysis of silicon solar cells to show factors controlling blue response and methods for improvement
[NASA-CR-131090] 10 p1111 N73-19059
Design of solar energy concentrators with concentric circular seams of plastic films
[AD-755829] 12 p1446 N73-21712
Analysis of methods for meeting national energy requirements with emphasis on technology for using solar energy
[NASA-TM-X-68230] 13 p1573 N73-22748
Net radiation method for analyzing radiation heat transfer in enclosures involving partially transparent walls
[NASA-TN-D-7384] 19 p2351 N73-28915
Abstracts on research projects inclusive of flight dynamics to heating of swimming pools using solar collector
[ISBN-0-85494-200-9] 21 p2609 N73-30910
Flat plate collector performance evaluation using simulated sun
[NASA-TM-X-71427] 23 p2835 N73-32655
Analysis of linear focused collectors for solar power
[SLA-73-5319] 24 p2881 N73-33007

**SOLAR CONSTANT**
Ultraviolet solar irradiance in selected wavelength bands
[NASA-TM-X-66143] 07 p0838 N73-16794
Analysis of cause of nonlinear relationship between solar constant and solar activity to show possible climatic consequences
[NLL-M-23053-[5828.4F]] 20 p2390 N73-29201
**SOLAR CONVERTERS**
U SOLAR GENERATORS
**SOLAR CORONA**
Mathematical models for studying coronal magnetic fields and solar wind
01 p0092 N73-10762
Current sheet magnetic field model for computing three dimensional currents flowing in solar corona
01 p0093 N73-10764
Physical model for determining structure of neutral sheets in solar corona
01 p0093 N73-10765
Properties of active and helmet coronal streamers based on radio observations
01 p0093 N73-10769
Inference of coronal and interplanetary magnetic fields and H-alpha patterns from high resolution photography
01 p0094 N73-10771
Theoretical analysis of energy supply to quiet solar wind
01 p0094 N73-10773
Approximate analytic theory of acoustic shock propagation in nonuniform media for motion determination of flare generated, shock wave in corona
01 p0095 N73-10783
Coronal Alfven waves in solar wind at 1 AU
01 p0096 N73-10793
Numerical computations for quiescent solar prominence formation by condensation from solar corona
04 p0465 N73-13790
Possibility of current sheets serving as pathways for transport of cosmic rays in solar corona
08 p0973 N73-17958
Analysis of radio phase differences for determining electron concentration in solar corona
10 p1177 N73-19577
Photographic observations of solar corona by Apollo 16 command module from lunar orbit
12 p1456 N73-21794
Development of dynamic model of solar corona based on equations for ideal, inviscid, fully ionized hydrogen gas in gravitational field
13 p1572 N73-22740
High resolution solar X ray astronomy from Aerobee rockets
[NASA-CR-132984] 16 p1959 N73-25849
Coronal Magnetic field effects on propagation of solar flare energetic particles.
19 p2338 N73-28806
Proton energy spectra analysis of solar flare for determining altitude limitations on coronal particle storage
19 p2338 N73-28807
Energetic particle storage in solar corona
19 p2338 N73-28809
Solar type 3 radio burst position measurements for coronal density determination
19 p2338 N73-28812
Properties of solar coronal pulsations
19 p2339 N73-28817
**SOLAR CORPUSCULAR RADIATION**
NT SOLAR ELECTRONS
NT SOLAR PROTONS
Electron flux density recorded onboard HEOS 1 in 1969 and 1970, discussing solar activity effects and comparing proton flux density
05 p0593 N73-14816
Identification of solar neutron events by satellite detection of proton flux increase in outer edge of trapped proton belt
07 p0838 N73-16790
**SOLAR COSMIC RAYS**
Ion sensitive emulsion detection system for use in cycloidal focusing mass spectrometer for measuring atomic species of solar plasma
[NASA-CR-130134] 05 p0592 N73-14810
Theoretical response of neutron monitor to anisotropic flux of solar cosmic rays
[AD-751275] 07 p0802 N73-16511
Instrumentation and measurement data of OGO-F solar cosmic ray experiment
[NASA-CR-130155] 07 p0839 N73-16795
Solar particle composition measurements using nuclear emulsion detectors on sounding rockets
08 p0973 N73-17959
System for measuring charge spectra of solar cosmic rays on IMP-6
08 p0973 N73-17960
IMP 6 measurements of light element composition of solar cosmic rays during flares of Apr. and Sept. 1971
[NASA-TM-X-65947] 09 p1080 N73-18814
Variations of relative abundances of helium, carbon, nitrogen, oxygen, and iron-group nuclei in solar cosmic rays and their relationship to solar particle acceleration
[NASA-TM-X-66228] 12 p1445 N73-21706
Plastic and glass detectors for measuring composition and energy spectra of solar cosmic ray nuclei
12 p1450 N73-21747
Solar cosmic ray, solar wind, solar flare, and neutron albedo measurements, using mineral detectors onboard Apollo 16
12 p1450 N73-21749
Solar diurnal and semidiurnal variations in cosmic ray neutron monitor data
[NP-19650] 15 p1828 N73-24819
Isotopic composition of hydrogen and helium in solar cosmic ray measurements by OGO F
19 p2336 N73-28798
Cosmic ray modulation in solar envelope
19 p2337 N73-28803
Energy spectra of solar cosmic rays
22 p2733 N73-31876
Cosmos-378 data on solar cosmic ray penetration into earth polar caps
24 p2976 N73-33782
**SOLAR CYCLES**
NT SUNSPOT CYCLE
Supergiant structures in negative polarity magnetic fields of sun and particle emitting flares
01 p0093 N73-10763
Archimedes spiral and solar wind induced structures in interplanetary magnetic field
01 p0093 N73-10766
Large scale structure of solar wind during fading and maximum portions of two different cycles
01 p0094 N73-10774
Development of method for distinguishing between phenomena related to solar wind and those related to solar extreme ultraviolet emission
01 p0099 N73-10816
References to measurements of cosmic ray intensity in and above atmosphere during solar cycles and high energy cosmic ray interactions at sea level
[AD-745331] 01 p0100 N73-10821
Application of Avco data analysis and prediction techniques to derivation of algorithms for predicting future sunspot activity
[NASA-CR-123925] 02 p0224 N73-11811
Ultraviolet solar irradiance in selected wavelength bands
[NASA-TM-X-66143] 07 p0838 N73-16794
Autocorrelation, Chree, and power spectrum analyses of cosmic ray 27-day recurrences
[NP-19466] 08 p0957 N73-17833
Solar meridional circulation and latitudinal sunspot drift analysis
[AD-751268] 09 p1081 N73-18820
Relating glaciation cycles to cosmic rhythms
[NASA-TT-F-14827] 14 p1659 N73-23469
Measurements of differential energy spectra in cosmic ray protons and solar cycle variations of atmospheric secondary protons
[NASA-CR-132056] 15 p1828 N73-24818
Changes in cosmic ray intensity over last solar modulation cycle
[AD-760789] 20 p2468 N73-29828
**SOLAR DISK**
U SUN
**SOLAR ECLIPSES**
Solar eclipse of 4 January 1973, visible in Argentina
06 p0717 N73-15853
Ionograms and cosmic radio noise absorption studies of anomalous behavior of F region during solar eclipse of 22 Sept. 1968
[RSD-73] 07 p0789 N73-16414
Studies of solar X ray fluxes during total eclipse of 7 March 1970
[NASA-CR-130698] 08 p0959 N73-17843
Solar eclipse effects on atmosphere, measured by three pitot probe rocket soundings
08 p0972 N73-17944
Electron density, electron and ion temperature, and ion composition values obtained during eclipse on 7 Mar. 1970
[UILU-ENG-73-2501] 10 p1154 N73-19390
ATS-3 satellite measurement of ionospheric effects during partial solar eclipses of July 10, 1972
[AD-758855] 15 p1784 N73-24461
Partial annular eclipse of 4 January 1973 in Argentina
[NP-19597] 21 p2597 N73-30811
Observations of polarization of radio radiation from local sources on sun and operating principles of polarization receiver equipment
[NRC-TT-1681] 22 p2631 N73-31090
Feasibility study for use of YF-12 aircraft as scientific instrument platform for observing 1970 solar eclipse
[NASA-CR-135482] 23 p2845 N73-32735
Analysis of ionospheric response to solar eclipse of 7 March 1970 by Thomson scatter radar technique at Millstone Hill Ionospheric Observatory
24 p2912 N73-33239
Temperature and ion composition measurements of F 1 region during solar eclipse on 7 March 1970
24 p2921 N73-33329
**SOLAR ELECTRIC PROPULSION**
Characteristics and capabilities of solar electric propulsion for orbiter missions of Uranus and Neptune
[NASA-CR-129857] 05 p0594 N73-14827
Effects and prevention of possible mercury pollution from failure of solar electric propulsion spacecraft using mercury propellant
[NASA-CR-130286] 06 p0717 N73-15855
Investigation of solar electric propulsion as method for exploring space beyond reach of ballistic missions - Vol. 1
[NASA-CR-130701] 08 p0954 N73-17811
Solar electric propulsion system integration technology study to show spacecraft and mission applications - Vol. 2
[NASA-CR-130702] 08 p0954 N73-17812
Solar electric propulsion system integration technology study to show spacecraft and mission applications - Vol. 3
[NASA-CR-130703] 08 p0954 N73-17813
Solar electric propulsion for unmanned exploration of solar system
[NASA-CR-130245] 15 p1826 N73-24803
Earth-based orbit determination for SEP spacecraft in multistation tracking
[NASA-CR-132154] 15 p1830 N73-24832
Selected solar electric propulsion and ballistic missions
[NASA-CR-132753] 16 p1956 N73-25826
Optimum trajectory and spacecraft data for unmanned interplanetary missions from 1975 to 1990 using solar electric propulsion
[NASA-CR-132765] 16 p1966 N73-25907
Electromagnetic interference of power conditioners for solar electric propulsion
[NASA-CR-133229] 17 p2076 N73-26798
Statistical error model for solar electric propulsion thrust subsystem
[NASA-CR-133232] 17 p2077 N73-26799
Natural environment design requirement for solar electric power stage based on radiation atmospheric conditions at orbital altitudes
[NASA-TM-X-64761] 18 p2193 N73-27708
Performance sensitivity analysis of solar electric propulsion thrust subsystem
[NASA-CR-133792] 21 p2590 N73-30748
**SOLAR ELECTRONS**
Low energy solar X ray burst data detected by OGO E proportional counter
19 p2334 N73-28782
Gyrosynchrotron and magnetoactive absorption processes in solar microwave emission
19 p2335 N73-28787
Gyrosynchrotron radiation of relativistic electrons in solar magnetoactive plasma
19 p2335 N73-28788
Hard X radiation from solar flares caused by bremsstrahlung of nonthermal electron streams
19 p2335 N73-28789
Solar flares and relativistic electron events in interplanetary space
[NASA-CR-135491] 22 p2712 N73-31715
Hodoscope measurements of cosmic ray electron spectra
[TR-73-135] 23 p2834 N73-32651
**SOLAR ENERGY**
Photoelectric, thermoelectric, and thermoemission methods of converting solar to electrical energy
[AD-747293] 02 p0129 N73-11050
Conversion and utilization of solar energy to solve energy shortages and pollution problems on earth
04 p0474 N73-13866
Conversion of solar energy to pollution free power
04 p0474 N73-13870
Congressional hearings on earthbound potential utilization of solar energy
05 p0592 N73-14812
Development of surfaces and coatings for solar energy conversion systems
[NASA-TT-F-14650] 06 p0688 N73-15598
Onboard spacecraft propulsion using nuclear fuels and solar energy - pt. 1
[JPRS-58612-1-PT-1] 10 p1209 N73-19833
Rectangular solar cell stacked panels to generate electrical power aboard spacecraft
[NASA-CASE-NPO-11771] 11 p1237 N73-20040
Analysis of methods for meeting national energy requirements with emphasis on technology for using solar energy
[NASA-TM-X-68230] 13 p1573 N73-22748
Reliability analysis of thermoelectric module solar energy converter
[AD-757087] 14 p1606 N73-23015
Textbook of solar physics
[NASA-SP-303] 16 p1959 N73-25846
Applications of solar energy to heat and power requirements
[NASA-CR-133101] 17 p2079 N73-26818
High energy astrophysics and solar astronomy
22 p2732 N73-31868
Solar energy effect in galactic cosmic ray modulation
22 p2733 N73-31875

Solar energy, thermonuclear energy, and fossile fuel energy sources
[UCRL-74697] 24 p2881 N73-33005
Analysis of linear focused collectors for solar power
[SLA-73-5319] 24 p2881 N73-33007
Influence of solar energy absorption and air water interactions on seasonal thermocline of sea
24 p2957 N73-33623
Conference on use of solar energy in Mediterranean
[BULL-22] 24 p2974 N73-33762
Heliotechnique for utilizing solar energy on earth
24 p2974 N73-33763
Measurement of air-sea temperature in relation to incident solar energy
24 p2975 N73-33773

SOLAR FACULAE
U FACULAE

SOLAR FLARES
Sunspot, solar flare, magnetic storm, and SID data, Delhi - Dec. 1971
[RRC-A-199-PT-2] 01 p0048 N73-10385
Sunspot, solar flare, magnetic storm, and SID data, Delhi Jan. 1972
[RRC-A-200-PT-2] 01 p0048 N73-10387
Supergiant structures in negative polarity magnetic fields of sun and particle emitting flares
01 p0093 N73-10763
Analysis of solar flare energetics based on shock velocity, ambient solar wind velocity and density, and ambient azimuthal Mach number
01 p0097 N73-10799
Observations of solar wind helium enhancements following major solar flares and relation to flare piston plasma
01 p0098 N73-10808
Analysis of chromospheric patterns produced by changes in interplanetary and geomagnetic fields
[AD-745100] 01 p0106 N73-10877
Solar flare forecasts and comparisons with rocket-borne observations for flare class greater than or equal to 2F
[NASA-CR-114511] 02 p0225 N73-11814
Forecasting solar flares of classes 1N and 1B based on solar radio temperature contour maps at 3 mm wavelength
[NASA-CR-114510] 02 p0225 N73-11815
Flare-associated interplanetary shock data of 15-16 Feb. 1967 analyzed for estimation of ecliptic plane geometry of shock surface near 1 AU
[NASA-TM-X-66115] 03 p0353 N73-12875
Analysis of magnetogasdynamic shock fronts caused by solar winds and development of theoretical concepts and models for phenomenon
[NASA-TM-X-66106] 03 p0353 N73-12876
Analysis of radioactivity in lunar samples returned by Apollo 16 flight and relationship to occurrence of solar flares
[NASA-CR-129291] 03 p0354 N73-12886
Intensity variation of circularly polarized radio emission during solar flares at 3.15 cm on 10 and 12 July 1968
[AD-747606] 04 p0467 N73-13810
Statistical comparison of regions with and without proton flares
[AD-747426] 04 p0467 N73-13811
Model for U-shaped solar bursts based on one single group of moderately relativistic electrons radiating in cold magnetoplasma
[AD-747033] 04 p0468 N73-13812
Optical intensity measurements for detecting low energy protons in polar cap
[AD-749857] 05 p0542 N73-14414
Determination of location and time of solar flare observed from HEOS A and ESRO 2 satellites
05 p0592 N73-14814
Data base containing objectively-correlated solar measurements used to obtain parameters for flare prediction
[AD-749869] 06 p0716 N73-15843
Laboratory double inverse plasma pinch experiments with argon, hydrogen, and deuterium and relevance to solar flare
07 p0838 N73-16791
Ultraviolet solar irradiance in selected wavelength bands
[NASA-TM-X-66143] 07 p0838 N73-16794
Theory of gamma ray line emission from solar flares
[NASA-TM-X-66165] 07 p0839 N73-16797
Influence of solar flares on thunderstorms and meteorological phenomena over Mediterranean Sea
07 p0859 N73-16965
Evolution of solar active region and solar flare from observations of OSO-7 spectroheliograph
08 p0973 N73-17957
IMP 6 measurements of light element composition of solar cosmic rays during flares of Apr. and Sept. 1971
[NASA-TM-X-65947] 09 p1080 N73-18814
Apollo experience report to analyze radiation protection problems on earth and in space
[NASA-TN-D-7080] 09 p1090 N73-18899
Satellite observations of soft X ray height distribution and directionality in solar flares
[AD-754772] 11 p1336 N73-20845
Analysis of two dimensional pattern of interplanetary shock waves based on solar longitude dependence of time intervals between geomagnetic storms and solar flares
[NASA-TM-X-66226] 12 p1445 N73-21704
Propagation pattern of shock waves emitted by solar flares occurring in active region of McMath No. 9740 from 23 Oct. - 4 Nov. 1968
[NASA-TM-X-66227] 12 p1445 N73-21705
Cosmic ray disturbances following solar flare occurrences in August 1972 recorded by neutron monitoring
12 p1446 N73-21709
Solar flare physics considering proton acceleration mechanism
[AD-755913] 12 p1446 N73-21711
Solar flare producing large amounts of low energy nuclei measured by Apollo 16
12 p1450 N73-21748
Ionospheric disturbance and geophysical effects caused by proton burst on X/28/1963 at 0135 UT
13 p1519 N73-22317
Dynamic model of solar flare emission sources
13 p1572 N73-22742
Solar gamma ray and neutron observations from OSO-7 during 2B and 3B flares
[NASA-CR-131866] 13 p1574 N73-22758
Velocity and outer limits of magnetic bottles ejected by solar proton flares as observed by Pioneer 6
[NASA-TM-X-66243] 15 p1828 N73-24814
Solar flare activity in Mc Math region 10789 during disk passage of 12 to 15 June 1970
[AD-756827] 15 p1833 N73-24855
Double layers and two-stream instability in solar flares, noting evacuating mechanism in solar atmosphere
[TRITA-EPP-73-05] 16 p1959 N73-25850
Generation of laboratory spectra at photon energies from highly ionized atoms
[AD-758606] 16 p1960 N73-25851
Observation analysis of August 1972 solar flares using spectrophotographic techniques
[NASA-CR-132195] 16 p1963 N73-25881
Analysis of X ray data obtained during solar flares
[NASA-CR-133341] 18 p2195 N73-27721
OSO-7 observations of gamma ray emission in solar flares
19 p2332 N73-28761
Conference on solar high energy interactions
[NASA-TM-X-66290] 19 p2333 N73-28772
Dynamic particle mass flow model for solar flares
19 p2333 N73-28773
Fast electron production by protons trapped in sunspot magnetic field as energy source for solar flares
19 p2333 N73-28774
Magnetic field rearrangement model for solar infall-impact flares
19 p2333 N73-28775
Optical properties of solar flare spectra
19 p2333 N73-28776
Properties of energetic electrons accelerated during solar flare flashes
19 p2333 N73-28777
Microwave features of proton bursts during solar flares
19 p2334 N73-28778
Millimeter polarization spectra of solar activities for estimating chromospheric magnetic fields
19 p2334 N73-28780
ERS 18 measurements of gamma ray fluxes during solar flare
19 p2334 N73-28784
Polarimetric measurements of high energy solar X ray emission processes
19 p2335 N73-28785
Theory of microwave and X ray emission mechanisms in solar flares considering nosthermal electrons
19 p2335 N73-28786
Hard X radiation from solar flares caused by bremsstrahlung of nonthermal electron streams
19 p2335 N73-28789
Optical X ray, H alpha, and microwave emissions during solar flares
19 p2335 N73-28790
Relative variations in extreme ultraviolet solar flare spectrum
19 p2335 N73-28791
Ground based ionospheric observations of extreme ultraviolet fluxes during solar flares
19 p2335 N73-28792
Analyses of soft X ray spectra obtained during solar flares by OSO satellites
19 p2336 N73-28793
OSO-4 solar flare X ray spectrum analysis on plasma cooling mechanisms
19 p2336 N73-28794
Gamma ray and neutron emissions during solar flares
19 p2336 N73-28795
Properties of nuclear gamma ray line emissions during solar flares
19 p2336 N73-28796
IMP measurements on hydrogen and helium isotope accelerations in solar flares
19 p2336 N73-28797
Isotopic composition of hydrogen and helium in solar cosmic ray measurements by OGO F
19 p2336 N73-28798
Solar flare particle energization by magnetic field reconnection and shock reflection
19 p2336 N73-28799
Composition and energy spectra of energetic particles emitted during solar flares
19 p2337 N73-28800
Acceleration mechanism for heavy nuclei abundance enhancement in solar flares
19 p2337 N73-28801
Solar flare associated proton fluxes at increased energies
19 p2337 N73-28802
Low energy solar flare alpha to proton flux ratios
19 p2337 N73-28804
Evidence of electron acceleration and type 3 radio bursts during solar flares
19 p2337 N73-28805
Coronal Magnetic field effects on propagation of solar flare energetic particles.
19 p2338 N73-28806
Magnetic field structure effects on coronal propagation of solar charged particle event
19 p2338 N73-28808
Flare induced magnetohydrodynamic disturbance propagation in solar corona considering Moreton surface waves and type 2 shocks
19 p2339 N73-28816
Improved performance of visual perception of solar patrol observers monitoring sun activity
[AD-760802] 20 p2372 N73-29063
Analysis of cause of nonlinear relationship between solar constant and solar activity to show possible climatic consequences
[NLL-M-23053-[5828.4F]] 20 p2390 N73-29201
Construction and testing of matched pair solar telescopes
[AD-762274] 20 p2420 N73-29444
Motion of sources for type 2 and type 4 radio bursts and flare-associated interplanetary disturbances
[NASA-TM-X-70452] 21 p2507 N73-30117
Sunspot motion and flaring in M482
[NASA-CR-133848] 21 p2593 N73-30775
Solar monitoring information for SPARCS-equipped rocket launches
[NASA-CR-114635] 22 p2711 N73-31707
Bremsstrahlung radiation from beam of electrons in solar chromosphere, and total energy of solar flares
[NASA-CR-133943] 22 p2711 N73-31710
Solar flares and relativistic electron events in interplanetary space
[NASA-CR-135491] 22 p2712 N73-31715
Synchrotron and X ray modulations produced by solar flare effects
22 p2733 N73-31878
Soft X ray and hydrogen alpha structure of solar flare
22 p2734 N73-31879
Structure of isolated solar flare point
22 p2734 N73-31880
Satellite instrumentation for determining origin and energetics of solar flares
22 p2734 N73-31881
Flux density of low energy solar flare particles measured by IMP-7
[TR-73-137] 23 p2835 N73-32653
IMP-7 measurement of very low energy cosmic ray energy spectra and concentration during solar flares
[TR-73-138] 23 p2835 N73-32654
Nature of solar flare emissions and geophysical disturbances
[NASA-TM-X-70479] 24 p2976 N73-33781

SOLAR FLUX
Solar flux effects on upper atmosphere oxygen photodissociation and heating rates
[AD-747777] 04 p0467 N73-13807
Rocket measurement of solar fluxes at 1216 A, 1450 A and 1710 A
[AERONOMICA-ACTA-A-111] 10 p1210 N73-19842
Solar X ray flux distribution from 0.1 to 8.0A using fluxes measured from Solrad 9 satellite
[CRC-1241] 14 p1702 N73-23813
Ionospheric F-region electron recombination, heating, and electron production
17 p2017 N73-26311
ERS 18 measurements of gamma ray fluxes during solar flare
19 p2334 N73-28784
Ground based ionospheric observations of extreme ultraviolet fluxes during solar flares
19 p2335 N73-28792
Solar flare associated proton fluxes at increased energies
19 p2337 N73-28802
Cosmic ray modulation in solar envelope
19 p2337 N73-28803
Low energy solar flare alpha to proton flux ratios
19 p2337 N73-28804
Modification of JPL space simulator for simulating solar intensities at Mercury
[NASA-CR-133791] 21 p2521 N73-30217
Model for energetic solar proton fluxes with applications to earth spacecraft
[NASA-TM-X-70433] 21 p2592 N73-30769

**SOLAR FLUX DENSITY**
NT SOLAR CONSTANT
**SOLAR FURNACES**
Developments in vacuum diffusion welding methods and metallurgical applications of solar energy
[NLL-M-22830-[5828.4F]] 11 p1304 N73-20584
**SOLAR GENERATORS**
NT SOLAR CELLS
Reliability analysis of solar generator on ESRO 1 satellite
[NASA-TT-F-14498] 01 p0007 N73-10051
Operational characteristics of semiconductor photoconverters as power supply sources for space vehicles
[AD-753063] 09 p1074 N73-18766
Photoelectric solar converter using cadmium sulfide and cadmium selenide tablets or thin films
[AD-756594] 13 p1476 N73-21960
Soviet research and development of solar batteries and power cells for spacecraft
[AD-756039] 13 p1478 N73-21973
Analysis of methods for meeting national energy requirements with emphasis on technology for using solar energy
[NASA-TM-X-68230] 13 p1573 N73-22748
State-of-the-art techniques for harnessing solar and wind power
[AD-765783] 24 p2881 N73-33011
**SOLAR GRAVITATION**
Mathematical modeling of solar gravitational fields
[ITF-71-130-P] 07 p0793 N73-16452
**SOLAR HEAT FLOW**
U HEAT FLUX
U SOLAR FLUX
**SOLAR HEATING**
Feasibility of thermal energy storage and solar heating as means of conservation and more efficient utilization of electric power
[PB-210359] 01 p0118 N73-10976
Technical and economic feasibility of solar powered space heating, air conditioning, and hot water heating systems for residential applications
[NASA-CR-124063] 08 p0968 N73-17911
Boiler surface coating effects on water heated by solar energy
[NASA-TT-F-14850] 11 p1237 N73-20043
Use of phenol formaldehyde plastic foam as thermal insulation for solar water heaters to improve efficiency
[AD-756591] 13 p1548 N73-22543
Solar heating and air conditioning as energy conservation alternatives to nuclear power
[NASA-TM-X-70468] 23 p2748 N73-31990
**SOLAR INSTRUMENTS**
NT SPECTROHELIOGRAPHS
**SOLAR LIMB**
Photometric profile of solar limb by optical device for photographic registration of photosphere
[RR-4] 17 p2032 N73-26441
Photoelectric determination of change in center-limb profiles of faint Fraunhofer lines
20 p2472 N73-29854
Asymmetry of selected Fraunhofer lines at center of solar disk and near limb
20 p2472 N73-29856
**SOLAR MAGNETIC FIELD**
Diurnal variations of sunspot classification, areas, and magnetic fields for June and July 1972
[BULL-171] 01 p0092 N73-10759
Conference on magnetic structure of interplanetary and solar magnetic fields and solar wind
[NASA-SP-308] 01 p0092 N73-10760
Review of solar rotation and solar magnetic fields
01 p0092 N73-10761
Mathematical models for studying coronal magnetic fields and solar wind
01 p0092 N73-10762
Supergiant structures in negative polarity magnetic fields of sun and particle emitting flares
01 p0093 N73-10763
Current sheet magnetic field model for computing three dimensional currents flowing in solar corona
01 p0093 N73-10764
Observation of interplanetary and solar magnetic field sector structure from 1962 through 1968
01 p0094 N73-10770
Behavior of large scale positive polarity magnetic fields and geomagnetic disturbances
01 p0094 N73-10772
Statistical analysis of magnetic assymetry and variations of general solar magnetic field
[AD-746717] 04 p0476 N73-13892
Effect of solar magnetic sector structure on stratospheric circulation
[NASA-CR-130551] 08 p0916 N73-17505
Interplanetary sector structure and heliomagnetic equator
[AD-751909] 08 p0963 N73-17874
Analysis of boundaries between solar magnetic sectors and comparison with observations of stellar magnetism
[NASA-CR-131832] 13 p1579 N73-22795
Magnetic field rearrangement model for solar infall-impact flares
19 p2333 N73-28775
Millimeter polarization spectra of solar activities for estimating chromospheric magnetic fields
19 p2334 N73-28780
Solar flare particle energization by magnetic field reconnection and shock reflection
19 p2336 N73-28799
Coronal Magnetic field effects on propagation of solar flare energetic particles.
19 p2338 N73-28806
Magnetic field structure effects on coronal propagation of solar charged particle event
19 p2338 N73-28808
Solar magnetic sector structure effects on tropospheric and lower stratospheric vorticity
[NASA-CR-133842] 21 p2592 N73-30773
Magnetograph for recording magnetic fields in solar active region
[AD-762485] 22 p2712 N73-31713
Solar magnetic field effects on galactic cosmic ray spectrum
22 p2733 N73-31877
**SOLAR NEBULA**
U SOLAR CORONA
**SOLAR NOISE**
U SOLAR RADIO EMISSION
**SOLAR OBSERVATORIES**
NT OSO
NT OSO-J
NT OSO-1
NT OSO-7
Design details of photoheliograph thermal concepts
[NASA-CR-124255] 15 p1787 N73-24492
**SOLAR ORBITS**
NT PERIHELIONS
Solar sonde in earth-sun orbit with 0.26 AU perihelion
[NASA-TT-F-14700] 01 p0104 N73-10860
**SOLAR PHYSICS**
Comet probe for analyzing properties of solar wind and direction of type 1 comet tails
02 p0228 N73-11845
Theory of solar and terrestrial plasma physics
[AD-747034] 03 p0297 N73-12424
Solar observation and research using rocket-borne instruments, in German programs
[BMBW-FBW-72-27] 07 p0846 N73-16862
Solar flare physics considering proton acceleration mechanism
[AD-755913] 12 p1446 N73-21711
Research projects for ground-based and space-based astronomy to show present capabilities and future potential
[PB-212965] 12 p1458 N73-21819
Study of effects of solar activity on geophysical phenomena using numerical techniques
13 p1514 N73-22264
Upper atmosphere, magnetosphere, and solar physics and solar-terrestrial interactions
[AD-757874] 15 p1782 N73-24444
Textbook of solar physics
[NASA-SP-303] 16 p1959 N73-25846
Conference on solar high energy interactions
[NASA-TM-X-66290] 19 p2333 N73-28772
Theory of microwave and X ray emission mechanisms in solar flares considering nonthermal electrons
19 p2335 N73-28786
Gyrosynchrotron and magnetoactive absorption processes in solar microwave emission
19 p2335 N73-28787
Research on solar high energy physics - conference summary
19 p2340 N73-28822
Solar physics, planetary atmospheres, and space astronomy research programs
[NASA-CR-133773] 21 p2610 N73-30923
**SOLAR PLASMA [RADIATION]**
U SOLAR WIND
**SOLAR POSITION**
Multislot shadow transducer for maintaining solar orientation
20 p2419 N73-29439
**SOLAR POWER GENERATION**
U SOLAR GENERATORS
**SOLAR POWER SOURCES**
U SOLAR GENERATORS
**SOLAR PROBES**
Solar sonde in earth-sun orbit with 0.26 AU perihelion
[NASA-TT-F-14700] 01 p0104 N73-10860
Tensor analysis application to relativity theory and measurements of solar gravitational fields using European geodetic solar probes
[ESRO-SN-118-ESTEC] 02 p0231 N73-11877
Precision measurements of solar gravitational fields by European drag-free and twin geodetic space probes
02 p0231 N73-11879
Design and performance of solar array for Helios solar probe
[DGLR-PAPER-72-091] 06 p0627 N73-15084
Onboard data processing system for Helios solar probe
[DGLR-PAPER-72-092] 06 p0644 N73-15229
Solar probe orbit perturbation calculation assuming circular gravitating asteroid ring with center at sun
[ESRO-SR-19] 19 p2344 N73-28856
**SOLAR PROMINENCES**
Synoptic charts and catalogs of solar activity centers and chromospheric filaments
01 p0099 N73-10817
Numerical computations for quiescent solar prominence formation by condensation from solar corona
04 p0465 N73-13790
Equivalent widths and line intensities for prominences observed during 1964 to 1965
20 p2472 N73-29852
Helium excitation and structure of quiescent solar prominences
20 p2472 N73-29859
**SOLAR PROPULSION**
NT SOLAR ELECTRIC PROPULSION
Design, development, and evaluation of solar electric thrust vector control system for ion engine array
[NASA-CR-130622] 08 p0953 N73-17806
Solar electric power plants in unmanned spacecraft
[NASA-CR-131360] 11 p1333 N73-20824
Combined chemical solar electric transfer stage for inserting Europa 3 satellites into twenty-four hour orbits
[MBB-UR-V-49-71] 15 p1832 N73-24851
**SOLAR PROTONS**
Relationship between solar wind proton temperature and bulk speed of solar rotation
[NASA-TM-X-66091] 02 p0225 N73-11819
Validity of using only primary protons in Van Allen belt and solar flare proton shielding studies
[ORNL-TM-3785] 03 p0353 N73-12880
Preliminary results from HEOS A satellite in electron and proton events, solar wind and interplanetary magnetic field measurement, and propagation of charged particles
[ESRO-SP-74] 05 p0592 N73-14813
HEOS 1 satellite recorded data on solar proton event in 1970
05 p0593 N73-14815
Injection, propagation, and interaction characteristics of solar protons based on HEOS A satellite data
05 p0593 N73-14817
Directional measurements of solar protons during low solar activity from HEOS A satellite
05 p0593 N73-14818
OV1-17 satellite, polar cap measurements of solar flare protons with energies down to 12.4 keV
[AD-751467] 07 p0839 N73-16800
Forecasting magnitude of solar proton and polar cap absorption events using semi-integrated flux density
[AD-751925] 08 p0957 N73-17835
Solar proton intensities in magnetosphere over polar regions and comparison to interplanetary intensities
[AD-753679] 09 p1081 N73-18821
Solar proton penetration into geomagnetic tail and ionospheric polar cap
10 p1210 N73-19843
Ionospheric disturbance and geophysical effects caused by proton burst on X/28/1963 at 0135 UT
13 p1519 N73-22317
Solar proton anisotropies in interplanetary space as measured by Explorer 35 solid state detectors
13 p1573 N73-22744
Velocity and outer limits of magnetic bottles ejected by solar proton flares as observed by Pioneer 6
[NASA-TM-X-66243] 15 p1828 N73-24814
Microwave features of proton bursts during solar flares
19 p2334 N73-28778
Low energy solar flare alpha to proton flux ratios
19 p2337 N73-28804
Proton energy spectra analysis of solar flare for determining altitude limitations on coronal particle storage
19 p2338 N73-28807
Proceedings of conference on solar proton event of Nov. 1969
[AD-763081] 20 p2468 N73-29830
Model for energetic solar proton fluxes with applications to earth spacecraft
[NASA-TM-X-70433] 21 p2592 N73-30769
Operational processing of solar proton monitor data from ITOS
[NOAA-TM-NESS-49] 21 p2592 N73-30772
Theories for explaining high energy protons trapped in radiation belts
[AD-763433] 21 p2598 N73-30826
Cost effective measures for preventing solar proton interference with interplanetary spacecraft operation
22 p2732 N73-31863
Conference on cosmic ray and solar particle diffusion and concentration in interstellar space
[NASA-CR-135528] 23 p2834 N73-32646
Direct charge state measurements of low energy solar carbon and oxygen in interplanetary space
[TR-73-132] 23 p2834 N73-32648
Balloon flown hodoscopic observations of rapid variations in solar proton flux in 1972
[TR-73-134] 23 p2834 N73-32650

SOLAR RADIATION
NT SOLAR CORPUSCULAR RADIATION
NT SOLAR COSMIC RAYS
NT SOLAR ELECTRONS
NT SOLAR PROTONS
NT SOLAR RADIO BURSTS
NT SOLAR RADIO EMISSION
NT SOLAR WIND
NT SOLAR X-RAYS
NT SUNLIGHT
NT TYPE 2 BURSTS
NT TYPE 3 BURSTS
NT TYPE 4 BURSTS
NT TYPE 5 BURSTS
Soil and plant identification in tropical environment by incident and reflected solar radiation
[AD-743931] 01 p0051 N73-10417
Observations of solar wind helium enhancements following major solar flares and relation to flare piston plasma
01 p0098 N73-10808
Development of method for distinguishing between phenomena related to solar wind and those related to solar extreme ultraviolet emission
01 p0099 N73-10816
Geophysical and space data reported from sites throughout the world
[AD-746290] 02 p0226 N73-11822
Correlation between solar radiation and monthly and seasonal variations for calculating atmospheric turbidity in Belgium
[PUBL-SER-A-75] 03 p0354 N73-12882
Ultraviolet photometry experiment for Atmosphere Explorer C, D, and E missions to record solar irradiance
[NASA-TM-X-66130] 04 p0422 N73-13437
Characteristics of research instruments used on rockets and satellites for investigating solar ultraviolet radiation
[AD-748276] 04 p0424 N73-13454
Method for calibrating visible channel of satellite radiometer from orbit by using sunlit area as calibration target
[NOAA-TR-NESS-62] 05 p0547 N73-14441
Geophysics and space data bulletin
[AD-749815] 05 p0597 N73-14852
Orbit perturbations due to solar radiation pressure, including disturbing force of satellites with large area to mass ratio
05 p0610 N73-14959
Mesoscale interaction models for effects of orography on momentum and energy transfer in atmosphere and interaction of solar radiation with earth atmosphere
[AD-750727] 06 p0694 N73-15657
Research projects to determine nature of Sun as ultraviolet variable star and description of MUSE experiment
[NASA-TM-X-66142] 06 p0719 N73-15868
Ultraviolet solar irradiance in selected wavelength bands
[NASA-TM-X-66143] 07 p0838 N73-16794
Solar radiation pressure on Mariner 9 Mars Orbiter
[NASA-CR-130724] 08 p0957 N73-17831
Solar neutrinos and influences of opacity, thermal instability, additional sources, and central black hole on solar models
[NASA-TM-X-68847] 08 p0959 N73-17844
Scattered solar radiation distribution in cloud absence by sky zones in entire spectrum, including visible and ultraviolet sections
09 p1059 N73-18637
Short-duration solar microwave bursts and associated soft X ray emission
[NASA-CR-130859] 09 p1081 N73-18816
Analysis of silicon solar cells to show factors controlling blue response and methods for improvement
[NASA-CR-131090] 10 p1111 N73-19039
Evolutionary adaptation and resistance of unicellular organisms to solar radiation
10 p1118 N73-19118
Physics of high energy particles, cosmic showers, modulation of cosmic rays, high atmospheric meteorology, and application of solar radiation to other areas
[NP-19366] 10 p1211 N73-19847
Investigation of causes of perturbations in Saturns rings
[REPT-14] 10 p1212 N73-19854
Effects of solar pressure and gravity gradient on attitude motions of artificial satellite near far moon side libration point
12 p1447 N73-21722
Preflight tests and performance of electronic instrumentation in measuring solar radiation during Aerobee 170 and Black Brant V rockets
[AD-756909] 13 p1532 N73-22412
Development of dynamic model of solar corons based on equations for ideal, inviscid, fully ionized hydrogen gas in gravitational field
13 p1572 N73-22740
Solar gamma ray and neutron observations from OSO-7 during 2B and 3B flares
[NASA-CR-131866] 13 p1574 N73-22758
Solar photoionization rate constants for nitrogen, oxygen, nitrogen oxides and ultraviolet intensities
[AD-756480] 13 p1574 N73-22759
Characteristics of radio astronomy radiometer to include operation, maintenance, data acquisition, and data retrieval
[NASA-CR-131830] 13 p1579 N73-22796
Reliability analysis of thermoelectric module solar energy converter
[AD-757087] 14 p1606 N73-23015
Atmospheric radiative transfer model for predicting solar and daytime sky irradiance of ground target
[AD-757149] 14 p1693 N73-23739
Geophysical and space data bulletin
[AD-755839] 14 p1706 N73-23849
Physiological responses of parasitic worms and their larvae to solar ultraviolet irradiation and space flight stress
15 p1740 N73-24106
Solar and terrestrial radiation fluxes over Arctic pack ice
[AD-758060] 15 p1828 N73-24820
Environmental impact of increased intensities of solar ultraviolet radiation resulting from operation of supersonic transport aircraft
[PB-215324/0] 16 p1862 N73-25079
Two rocket measurements of atmospheric oxygen concentration during twilight
16 p1895 N73-25331
Vertical incidence sounding techniques to determine ionospheric effects of solar activity
[RRC-A208-PT-2] 16 p1905 N73-25410
Solar and geophysical data obtained by ionospheric sounding over India for April, 1972
[RRC-A202-PT-2] 16 p1907 N73-25423
Design, fabrication, and tests of experimental flight packages capable of measuring long term solar degradation of thermal control coatings
[AD-759083] 16 p1968 N73-25916
Development and characteristics of self-contained digital integrator for recording daily solar irradiance
[AD-760318] 17 p2035 N73-26468
Solar particle contributions to diurnal variations of neutron intensity in upper atmosphere
[AD-760950] 18 p2146 N73-27350
Analysis of ionospheric response to fluctuations of solar radiation based on sensitivity and delay of electron content
[NASA-CR-133474] 19 p2294 N73-28447
OSO-H observations of solar thermal and nonthermal X ray bursts
19 p2334 N73-28783
Characteristics of polyurethane film for fabrication of expandable envelopes subjected to solar heating at high altitudes
[AD-762803] 20 p2362 N73-29001
Application of airborne actinometric measurements to determine transmission, absorption, and reflection of solar radiation by clouds
20 p2401 N73-29292
Analysis of absorption of solar radiation by atmospheric water vapor to determine effects of various atmospheric parameters
20 p2401 N73-29294
Development, characteristics, and operation of telephotometer for simultaneous measurements of angular and space distribution of absolute solar radiation fluxes
20 p2402 N73-29303
Radiation regime of vegetation, using spectral composition and three dimensional structure of incident solar radiation and scattered sky light
20 p2404 N73-29316
Optimal use of solar energy for high capacity crop growth
20 p2404 N73-29317
Pyranometer measurements of direct and total solar radiation in crops and semiempirical relations
20 p2404 N73-29319
Absorption of direct solar radiation in maize as function of leaf area index and sums altitude
20 p2404 N73-29320
Effects of solar radiation on photomorphogenesis of plants based on spectral distribution of solar energy in daytime
20 p2404 N73-29322
Effects of radiation and heat balance of active surface on life processes of plants with emphasis on productivity of cotton
20 p2404 N73-29323
Solar radiation effects on photosynthesis of submerged aquatic plants
20 p2405 N73-29327
Influence of solar radiation in mountainous areas on crop capacity and grain yield of spring wheat
20 p2406 N73-29335
Arizona-NASA atlas of infrared solar spectrum in 13350 - 34100 A wavelength
[LPL-COMMUN-166] 21 p2591 N73-30762
Geophysics and space data, including magnetometer, cosmic ray, and ELF noise data - 1973
[AD-763507] 21 p2593 N73-30779
Balloon observations of solar neutrons by scintillation counter
[NASA-CR-135496] 22 p2712 N73-31714
Solar flares and relativistic electron events in interplanetary space
[NASA-CR-135491] 22 p2712 N73-31715
Influence of solar, sky, and ground radiation on signal reflection under cloudless daytime sky
[AD-763893] 22 p2712 N73-31716
Continuum chromospheric emission and negative results in search for solar recombination lines in frequency range 110-115 GHz
[AD-763719] 22 p2712 N73-31717
Application of radiant solar energy for welding and soldering materials
[AD-764938] 23 p2799 N73-32386
State-of-the-art techniques for harnessing solar and wind power
[AD-765783] 24 p2881 N73-33011
Design of floating platforms to capture and use solar radiation
24 p2974 N73-33764
Analog measurement of useful energy stored in thermocollector several years
24 p2974 N73-33766
Heliothermic conversion of solar radiation for industrial use
24 p2975 N73-33767
Production of vegetables in arid zones using controlled solar greenhouses
24 p2975 N73-33768
Solar still greenhouse for using desalinated water to produce vegetables in arid regions
24 p2975 N73-33769
Influence of solar radiation on thermodynamic balance and biological processes of earth
24 p2975 N73-33770
Utilization of solar rays as internal light sources in architectural designs
24 p2975 N73-33771
Filter for determining long wave solar spectral reflection by plane surfaces
24 p2975 N73-33772
Determination of perturbing moments due to solar radiation pressure forces acting on body of revolution
[NASA-TT-F-15072] 24 p2976 N73-33780
Computer program for correcting solar intensity measurements in elliptical sunspots for stray light
[NP-135] 24 p2977 N73-33785
Explanation of low counting rates for solar neutrinos
[BNL-TR-538] 24 p2977 N73-33786
Solar radiation effects on upper earth atmosphere
[AD-764599] 24 p2977 N73-33790
SOLAR RADIATION OBSERVATION
U SOLAR RADIATION
SOLAR RADIATION SHIELDING
Pigments for space-stable thermal control coatings to shield spacecraft from solar radiation
[NASA-CR-124067] 09 p0998 N73-18144
Apollo experience report to analyze radiation protection problems on earth and in space
[NASA-TN-D-7080] 09 p1090 N73-18899
Analysis of techniques for shielding manned space vehicles against protons and alpha particles from Van Allen belt, solar flares, and cosmic rays
[NASA-CR-131517] 12 p1461 N73-21841
SOLAR RADIO BURSTS
NT TYPE 2 BURSTS
NT TYPE 3 BURSTS
NT TYPE 4 BURSTS
NT TYPE 5 BURSTS
Spectral characteristics of radio bursts from sun
[AD-745167] 01 p0106 N73-10820
Type 4 solar radio bursts and their relation to expanding magnetic bottles
[NASA-TM-X-66217] 11 p1336 N73-20844
Conference on solar high energy interactions
[NASA-TM-X-66290] 19 p2333 N73-28772
Microwave features of proton bursts during solar flares
19 p2334 N73-28778
Statistical analysis on flux density spectra of solar microwave bursts
19 p2334 N73-28779
Millimeter polarization spectra of solar activities for estimating chromospheric magnetic fields
19 p2334 N73-28780
Solar burst observations at millimeter wavelengths
19 p2334 N73-28781
Low energy solar X ray burst data detected by OGO E proportional counter
19 p2334 N73-28782
Optical X ray, H alpha, and microwave emissions during solar flares
19 p2335 N73-28790
Dynamic spectra of solar type 3 radio bursts at kilometer wavelengths
19 p2338 N73-28810
Decay times of type 3 solar radio bursts
19 p2338 N73-28811
Review of solar type 2 and type 3 radio burst theory
19 p2339 N73-28814
Positions and sizes of solar type 3 radio bursts associated with electron propagation in interplanetary space
19 p2339 N73-28818

Decametric dynamic spectra of solar type 3 radio bursts
19 p2339 N73-28819
High resolution spectra and position measurements on solar radio bursts
19 p2339 N73-28820
Chromospheric type 3 radio burst acceleration of solar electrons and coronal streamer
19 p2340 N73-28821
Stabilization of electron streams in Type 3 solar radio bursts
[NASA-CR-133844] 21 p2593 N73-30776

**SOLAR RADIO EMISSION**
NT SOLAR RADIO BURSTS
NT TYPE 2 BURSTS
NT TYPE 3 BURSTS
NT TYPE 4 BURSTS
NT TYPE 5 BURSTS
Forecasting solar flares of classes 1N and 1B based on solar radio temperature contour maps at 3 mm wavelength
[NASA-CR-114510] 02 p0225 N73-11815
Radio observations of distribution of chromospheric brightness temperature
[AD-747021] 04 p0467 N73-13809
Solar radio interferometry for traveling ionospheric disturbance detection
05 p0511 N73-14158
High resolution spectral and polarization behavior of solar Type 3 bursts at 34 MHz
13 p1489 N73-22073
Solar flare activity in Mc Math region 10789 during disk passage of 12 to 15 June 1970
[AD-756827] 15 p1833 N73-24855
Solar radio and geophysical studies at Manila Observatory
[AD-760771] 20 p2413 N73-29396
Observations of polarization of radio radiation from local sources on sun and operating principles of polarization receiver equipment
[NRC-TT-1681] 22 p2631 N73-31090
Solar monitoring information for SPARCS-equipped rocket launches
[NASA-CR-114635] 22 p2711 N73-31707

**SOLAR RADIO WAVES**
U SOLAR RADIO EMISSION

**SOLAR ROTATION**
Review of solar rotation and solar magnetic fields
01 p0092 N73-10761
Relationship between solar wind proton temperature and bulk speed of solar rotation
[NASA-TM-X-66091] 02 p0225 N73-11819
Tables of cosmic ray MT-64 muon monitor measurements from solar rotation 1867 to solar rotation 1879
[AECL-4207] 08 p0957 N73-17834
Analysis of boundaries between solar magnetic sectors and comparison with observations of stellar magnetism
[NASA-CR-131832] 13 p1579 N73-22795

**SOLAR SENSORS**
Mariner Mars 1971 sun sensor model development and simulation
[NASA-CR-132990] 16 p1912 N73-25468
Multislot shadow transducer for maintaining solar orientation
20 p2419 N73-29439

**SOLAR SIMULATORS**
FORTRAN computer program for solar simulator optimization
[DLR-FB-71-34] 03 p0281 N73-12277
Measurement of ultraviolet radiation flux density emitted by solar simulator using thermopile and spectrometer
[ESRO-TM-149-ESTEC] 21 p2522 N73-30225

**SOLAR SPECTRA**
Methane mixing ratios in stratosphere deduced from balloon-observed solar infrared spectra
[AERONOMICA-ACTA-A-105] 01 p0092 N73-10757
Analysis on OSO-H observations of solar X ray burst spectra
[NASA-CR-131245] 11 p1336 N73-20841
Computer program to analyze solar observational data
[AD-755921] 14 p1703 N73-23815
OSO-1 Bragg crystal spectrometer for solar and stellar X ray source analysis
17 p2084 N73-26863
Analysis of velocity signals of solar active regions
[AD-760124] 18 p2195 N73-27723
Approximate determination of optical depth in different parts of Fraunhofer line contour
20 p2472 N73-29853
Telluric lines in solar spectrum region lambda lambda 6327.5 to 6330.0 AA
20 p2472 N73-29858
Attenuation of solar spectral intensity by pollution in boundary layer of New Haven, Connecticut atmosphere
23 p2833 N73-32641

**SOLAR SPECTROMETERS**
Aerobee-borne spectrometer/monochromator for advanced studies of solar X-ray line emissions and preliminary results
[NASA-CR-130359] 07 p0838 N73-16793

**SOLAR STORMS**
Observations of solar wind helium enhancements following major solar flares and relation to flare piston plasma
01 p0098 N73-10808
Analysis of two dimensional pattern of interplanetary shock waves based on solar longitude dependence of time intervals between geomagnetic storms and solar flares
[NASA-TM-X-66226] 12 p1445 N73-21704
Propagation pattern of shock waves emitted by solar flares occurring in active region of McMath No. 9740 from 23 Oct. - 4 Nov. 1968
[NASA-TM-X-66227] 12 p1445 N73-21705
Features deduced from radio propagation measurements of electron content in solar wind storms
16 p1959 N73-25843

**SOLAR STREAMS**
U SOLAR CORPUSCULAR RADIATION

**SOLAR SYSTEM**
Performance prediction for nuclear electric propulsion systems in advanced unmanned missions to outer planets and solar system
[NASA-CR-129134] 02 p0210 N73-11705
Computing free fall trajectories from one point to another specified point in solar system based on numerical optimization
[NASA-CR-128644] 03 p0356 N73-12901
Gravity-assisted exploration of outer planets of solar system in 1980s
[AERO-72/3] 04 p0470 N73-13827
Contributions of astronomy to understanding solar system and initiating manned space flight and exploration
04 p0471 N73-13837
Space technology for ground based economic support and investigating solar system origins
04 p0473 N73-13857
Comparison of accuracy of patched-conic and linearization methods for predicting trajectories in sun-planet system
[AD-748345] 04 p0476 N73-13891
History and future of solar system observation, exploration and exploitation
[NASA-TT-F-767] 07 p0844 N73-16839
Research in support of definition phase of Outer Planets Mission
[NASA-CR-130917] 09 p1082 N73-18826
Summary of advanced mission planning for solar system exploration
[NASA-CR-131395] 11 p1350 N73-20954
Problems which could be solved by comparative geological study of planets of solar system
12 p1456 N73-21796
Composition and physical characteristics of meteorites and meteoritic craters
[SAO-909-42] 14 p1704 N73-23827
Solar electric propulsion for unmanned exploration of solar system
[NASA-CR-130245] 15 p1826 N73-24803
Asteroid and comet exploration for studying planetary evolution and solar system history
[NASA-CR-2291] 18 p2196 N73-27726
Isotope separation in rare gases caused by centrifugal force in plasmas
[TRITA-EPP-72-27] 19 p2325 N73-28701
Comments on plasma propulsion, manned spaceflight, and evolution of solar system
[TRITA-EPP-72-08] 19 p2355 N73-28944
Satellite measurements on lunar and planetary environments in solar system
22 p2735 N73-31891
Explosive carbon burning effects of observed nuclei in solar system and constraints on supernova explosions
[LA-UR-73-489] 24 p2992 N73-33911

**SOLAR TEMPERATURE**
Solar neutrinos and influences of opacity, thermal instability, additional sources, and central black hole on solar models
[NASA-TM-X-68847] 08 p0959 N73-17844

**SOLAR WIND**
Conference on magnetic structure of interplanetary and solar magnetic fields and solar wind
[NASA-SP-308] 01 p0092 N73-10760
Mathematical models for studying coronal magnetic fields and solar wind
01 p0092 N73-10762
Archimedes spiral and solar wind induced structures in interplanetary magnetic field
01 p0093 N73-10766
Effect of solar wind velocity on interplanetary magnetic field properties
01 p0093 N73-10767
Theoretical analysis of energy supply to quiet solar wind
01 p0094 N73-10773
Large scale structure of solar wind during fading and maximum portions of two different cycles
01 p0094 N73-10774
Autocorrelation analysis of velocity structure temporal evolution in solar wind
01 p0094 N73-10775
Vela 4 observation of solar wind electron average thermal characteristics
01 p0094 N73-10776
Calculation of hydromagnetic wave induced energy transfer in solar wind
01 p0094 N73-10777
Generalized magnetic Weber-Davis model for calculating magnetic latitude effects in solar wind
01 p0094 N73-10778
Transition from supersonic to subsonic solar wind by increased density at corona base
01 p0095 N73-10779
Conversion of magnetic field energy into kinetic energy in solar wind as function of heliocentric distance
01 p0095 N73-10780
Physical implications of solar wind measurements at 1 AU within framework of two fluid solar wind model equations
01 p0095 N73-10781
Two fluid, solar wind model of energy transfer
01 p0095 N73-10782
Problems of solar and stellar spindown and theory, emphasizing angular momentum flux of solar wind
01 p0095 N73-10784
Problems of solar and stellar spindown and theory, emphasizing changes in angular velocity of surface regions of sun and stars
01 p0095 N73-10785
Theoretical constraints on microscale fluctuations in solar wind, emphasizing hydromagnetic waves
01 p0096 N73-10788
Electric field oscillations in upstream solar wind, using OGO-5 observations
01 p0096 N73-10789
Magnetic field merging in solar wind in terms of steady state merging
01 p0096 N73-10790
Theoretical models of interplanetary shock waves and solar wind disturbances with large scale characteristics
01 p0096 N73-10794
Corotating forward shock at 1 AU
01 p0097 N73-10796
Shock pair observation from HEOS 1
01 p0097 N73-10797
Analysis of solar flare energetics based on shock velocity, ambient solar wind velocity and density, and ambient azimuthal Mach number
01 p0097 N73-10799
Analysis of stream-stream interaction between slow solar wind and leading faster solar wind
01 p0097 N73-10800
Observations of solar plasma using interplanetary scintillation techniques and radio scattering methods
01 p0097 N73-10801
Analysis of spectra of radial and nonradial velocity components of solar wind, proton density, and proton thermal speed
01 p0097 N73-10803
Effect of sputtering corotating source of thin solar plasma streams on electron content of solar wind
01 p0098 N73-10805
Analysis of solar wind composition obtained by plasma analyzers mounted on various spacecraft
01 p0098 N73-10806
Analysis of isotopic composition of solar wind based on collecting foils and lunar material
01 p0098 N73-10807
Correlation between geomagnetic field increases or storm commencements with variations in electron content of solar wind
01 p0098 N73-10810
Characteristics of solar wind and interaction with interstellar plasma and magnetic field
01 p0099 N73-10811
Development of model of scattering of solar Lyman alpha from spatial distribution of neutral hydrogen in interplanetary space
01 p0099 N73-10813
Calculation of velocity distribution of helium ion in solar wind at one astronomical unit
01 p0099 N73-10814
Effect of flow of interstellar neutral particles on loss of field angular momentum by solar wind
01 p0099 N73-10815
Development of method for distinguishing between phenomena related to solar wind and those related to solar extreme ultraviolet emission
01 p0099 N73-10816
Solar wind/interstellar gas interactions and Lyman alpha background radiation
[TRITA-EPP-72-03] 01 p0105 N73-10871
Background Lyman alpha radiation and interstellar hydrogen gas taking into account radiative heat transfer
01 p0105 N73-10872
Solar wind plasma/interstellar hydrogen gas interactions
01 p0105 N73-10873
Solar wind interaction with Comet Bennett during period 23 March to 5 April 1970
[NASA-TM-X-66087] 02 p0224 N73-11813

Relationship between solar wind proton temperature and bulk speed of solar rotation
[NASA-TM-X-66091] 02 p0225 N73-11819
On variational relationships between solar wind parameters, magnetospheric magnetic activity, and magnetospheric storm electrons
02 p0225 N73-11820
Ionization of gas emitted by comets
02 p0228 N73-11844
Comet probe for analyzing properties of solar wind and direction of type I comet tails
02 p0228 N73-11845
Analysis of magnetogasdynamic shock fronts caused by solar winds and development of theoretical concepts and models for phenomenon
[NASA-TM-X-66106] 03 p0353 N73-12876
Evaluation of solar wind data obtained from Pioneer 6, Mariner 5, and Explorer 35 for velocity variations, magnetopause motion, and geomagnetic disturbances
[NASA-CR-129880] 05 p0591 N73-14806
Analyses of solar wind plasma data obtained by Explorer 33 and Explorer 35
[NASA-CR-129923] 05 p0592 N73-14807
Correlative studies of effects of solar wind and interplanetary magnetic field on bow shock and geomagnetic cavity
[NASA-CR-129924] 05 p0592 N73-14808
Ion sensitive emulsion detection system for use in cycloidal focusing mass spectrometer for measuring atomic species of solar plasma
[NASA-CR-130134] 05 p0592 N73-14810
HEOS A satellite measurement of solar wind parameters
05 p0593 N73-14820
Solar wind angular measurements and correlation with solar activity, magnetic storms, plasma flow, in magnetosheath
05 p0593 N73-14821
Amplitudes of natural oscillations of geomagnetic tail excited by solar wind
06 p0665 N73-15404
Differential energy spectra of cosmic ray protons and helium nuclei dominated by solar modulation of local interstellar spectra, and numerical solutions to transport equation
[NASA-CR-130298] 06 p0715 N73-15837
Laboratory simulation of solar wind interaction with geomagnetic field, and measurements of magnetosphere at shock wave front and of field configuration on noctunal side
[D-15] 06 p0716 N73-15838
Ionizing flow in solar wind passage through cometary coma
[TRITA-EPP-71-33] 06 p0716 N73-15842
Calculation of interplanetary magnetic field induced asymmetries in forward stagnation region of solar-wind magnetospheric interaction
07 p0838 N73-16792
Effects of Alfven waves in solar wind on angular momentum, wave pressure, and Poynting flux
[MPI-PAE/EXTRATERR-70] 07 p0839 N73-16799
Laser-probe mass spectrometric analysis of solar wind, cosmogenic, and radiogenic gases in Apollo 12, 14, and 15 samples
[NASA-CR-130029] 07 p0841 N73-16811
Magnetic field around spherical moon and downstream cylindrical cavity formed by solar wind, derived for parallel and perpendicular interplanetary magnetic fields
[NASA-TM-X-62227] 08 p0960 N73-17851
Electron density profiles from Mariner 5 and solar wind maintenance of nighttime Venus ionosphere
08 p0973 N73-17951
Solar wind propagation in low pressure gas and plasma containment in magnetic fields
[AD-753087] 09 p1072 N73-18750
Asymptotic behavior of kinetic solar wind model
[AERONOMICA-ACTA-A-108] 09 p1080 N73-18812
Solar wind composition experiment onboard Apollo 16
12 p1450 N73-21746
Solar cosmic ray, solar wind, solar flare, and neutron albedo measurements, using mineral detectors onboard Apollo 16
12 p1450 N73-21749
Principles governing ionospheric disturbances
13 p1519 N73-22315
Correlation between ionospheric disturbance and solar wind velocity, density, and positive ion flux of interplanetary medium
13 p1519 N73-22316
Low frequency transverse waves in two-fluid solar wind having radial magnetic field and streaming velocity
[NASA-CR-131570] 13 p1573 N73-22745
Theoretical analysis of wave particle interactions in magnetosphere and solar wind
[NASA-CR-131573] 13 p1573 N73-22746
Validity of CGL equations in solar wind problems of exosphere
[AD-756501] 13 p1575 N73-22760
Application of kinetic theory to collisionless regions of polar and solar winds
[AERONOMICA-ACTA-A-N-115-1973]
14 p1702 N73-23812
Statistical comparison of simultaneous satellite solar wind observations
[AD-758194] 14 p1703 N73-23816
Calculation of shape of earth magnetopause for various orientations of solar wind stream with respect to earth dipole axis
16 p1895 N73-25328
Ion optical design with applications to solar wind mass spectrometer
[NASA-CR-133053] 16 p1913 N73-25481
Cyclotron damping by suprathermal fluxes of protons and electrons in interplanetary medium
[NASA-TM-X-66254] 16 p1959 N73-25847
Calculating shock front for terminal flow of solar wind
17 p2079 N73-26816
Continuum methods for studying solar wind interaction with interstellar neutral particles
18 p2194 N73-27717
Solar wind plasma and magnetic field measurements from Pioneers 9 and 10 flights
[NASA-TM-X-62291] 18 p2195 N73-27719
HEOS A 2 experimental design for solar wind and magnetospheric low frequency wave measurement
[DSRI-73-01] 19 p2295 N73-28457
Gyrosynchrotron radiation of relativistic electrons in solar magnetoactive plasma
19 p2335 N73-28788
Large scale structure of solar wind including proton results, solar cycles, interplanetary medium, and high heliographic latitude activities
[NASA-TM-X-69342] 19 p2340 N73-28826
Space vehicle design criteria based on interplanetary charged particle environments
[NASA-CR-133600] 20 p2473 N73-29865
Analysis of steady state flow of solar wind and effect on magnetic field of dipole
[NASA-TT-F-15071] 22 p2711 N73-31709
Mathematical model for steady state wind-moon interaction
[COO-3577-2] 22 p2711 N73-31712
Variations in solar wind He-4 ion abundance occurring primarily in lower corona
23 p2834 N73-32643
One-dimensional analysis of electric fields and electric potential near photo emitting plate emmersed in solar wind plasma
23 p2858 N73-32839

**SOLAR X-RAYS**
Computer program for rapid reduction of Vela satellite data on solar X rays
[AD-743921] 01 p0100 N73-10822
Explorer 44 measurement of solar X rays and ultraviolet radiation
[AD-748992] 04 p0479 N73-13919
Solar X-ray spectra for predicting ionospheric radio wave propagation during solar activity
[AD-751575] 07 p0794 N73-16459
Aerobee-borne spectrometer/monochromator for advanced studies of solar X-ray line emissions and preliminary results
[NASA-CR-130359] 07 p0838 N73-16793
Solar X ray based calculations of K alpha line emission from sulfur, argon, calcium, and iron
[NASA-TM-X-66210] 11 p1335 N73-20839
Analysis on OSO-H observations of solar X ray burst spectra
[NASA-CR-131245] 11 p1336 N73-20841
Satellite observations of soft X ray height distribution and directionality in solar flares
[AD-754772] 11 p1336 N73-20845
Prediction of solar activity and geophysical effects, including X ray burst data
[AD-755920] 12 p1403 N73-21379
Solar X ray flux distribution from 0.1 to 8.0A using fluxes measured from Solrad 9 satellite
[CRC-1241] 14 p1702 N73-23813
Generation of laboratory spectra at photon energies from highly ionized atoms
[AD-758606] 16 p1960 N73-25851
Analysis of X ray data obtained during solar flares
[NASA-CR-133341] 18 p2195 N73-27721
Low energy solar X ray burst data detected by OGO E proportional counter
19 p2334 N73-28782
OSO-H observations of solar thermal and nonthermal X ray bursts
19 p2334 N73-28783
Polarimetric measurements of high energy solar X ray emission processes
19 p2335 N73-28785
Theory of microwave and X ray emission mechanisms in solar flares considering nonthermal electrons
19 p2335 N73-28786
Hard X radiation from solar flares caused by bremsstrahlung of nonthermal electron streams
19 p2335 N73-28789
Optical X ray, H alpha, and microwave emissions during solar flares
19 p2335 N73-28790
OSO-4 solar flare X ray spectrum analysis on plasma cooling mechanisms
19 p2336 N73-28794
Synchrotron and X ray modulations produced by solar flare effects
22 p2733 N73-31878

**SOLDERED JOINTS**
Solder joint and printed circuit fatigue measurements by optical cross correlation
16 p1923 N73-25559
Strength of printed circuit joints for reliability, based on electrical resistivity
[DLR-FB-73-33] 24 p2899 N73-33140

**SOLDERING**
Soldering process of graphite materials such as zirconium carbide with composition like stoichiometric
[AD-754050] 11 p1300 N73-20552
Cable fabrication and encapsulation inclusive of, string-pulling machine and solder sleeve processing
[BDX-613-775] 21 p2553 N73-30467
Application of radiant solar energy for welding and soldering materials
[AD-764938] 23 p2799 N73-32386

**SOLENOID VALVES**
Development of pressure transducer for satellite attitude control feeding signals back to solenoid flow control valve
[RAE-TR-72085] 05 p0548 N73-14453
Electrohydraulic directional valves with fluidic ball elements
[DLR-FB-73-35] 15 p1793 N73-24535
Automatically operable self-leveling load table with plurality of solenoid valves
[NASA-CASE-MFS-22639-1] 21 p2548 N73-30428

**SOLENOIDS**
Development of solenoid valve failure detection system based on addition of radioactive gas to propellant of cold gas jet attitude control system
[NASA-CR-130931] 10 p1165 N73-19476
Superconductors in marine technology, including coils, solenoids, and magnetic systems
[AD-755711] 13 p1567 N73-22702
Development of rotary solenoid shutter drive assembly and inertia damper for use with cameras mounted in satellites
[NASA-CASE-GSC-11560-1] 17 p2003 N73-26198

**SOLID ARGON**
U SOLIDIFIED GASES

**SOLID LUBRICANTS**
Behavior of lubricating materials under high temperature and high pressure
[AD-745001] 01 p0062 N73-10509
High temperature friction and wear properties of PbO for solid lubricant applications including tests in room air, controlled atmospheres, and vacuum
[NAL-TR-285] 04 p0426 N73-13470
Dry sliding friction characteristics of iron ceramic materials using solid lubricants
04 p0432 N73-13517
Properties and applications of solid lubricant coatings using molybdenum disulfide base
[AD-750998] 06 p0678 N73-15518
Fatigue behavior of thin solid films induced by moving surface load
[AD-753411] 09 p1041 N73-18490
Solid lubricants for moderate to extremely high temperature applications
[NASA-TM-X-68201] 11 p1298 N73-20537
Solid film plastic lubricant coatings for rifles
[AD-754568] 11 p1300 N73-20545
Development of self-contained, solid lubricated ball bearings for operation at high speed - Part 2
[AD-756487] 14 p1671 N73-23557
Wear processes and compressive stress of graphite fluoride lubricated machine surfaces
[AD-759560] 17 p2038 N73-26489
Handbook for liquid and solid lubricants in aerospace industry
[NASA-CR-130490] 23 p2796 N73-32365

**SOLID PHASES**
Solid phase reaction and fuel component effects on composite propellant combustion
[NASA-CR-112083] 01 p0039 N73-10738
Mechanical properties as function of temperature for unidirectionally solidified eutectic composites
[NASA-CR-124094] 09 p1046 N73-18527
Solid phase interactions in cobalt-carbide systems
[NLL-LTI-746-1338-[9022.401]]
12 p1415 N73-21468
Diffision in niobium of beryllium and aluminum from solid phase at 900 to 1300 deg
[NLL-CE-TRANS-5121-[9022.09]]
20 p2429 N73-29513
Effect of thermal cycling of structure and properties of directionally solidified eutectic composite
[NASA-CR-121249] 21 p2562 N73-30537
Solid-phase interaction of refractory metals and refractory compounds at high temperature using electron beam heater
23 p2808 N73-32455
Role of solid phase heterogeneity on low pressure L-star instability of nonmetallized rocket propellants
[NASA-CR-135766] 24 p2970 N73-33735

**SOLID PROPELLANT IGNITION**
Asymptotic analysis of radiant and hypergolic ignition of solid propellant undergoing exothermic

heterogeneous Arrphenius reaction with gaseous oxidizer
[AD-751303] 07 p0856 N73-16939
SOLID PROPELLANT ROCKET ENGINES
Suppression devices for controlling acoustic combustion instability in solid propellant engines
[AD-743701] 01 p0090 N73-10740
Performance of solid propellant apogee rocket motor in test firing at simulated altitude
[AD-747018] 02 p0224 N73-11809
Colloidal thrustor propellant performance discussing thrustor design and propellant choice
[ESRO-CR-53] 03 p0349 N73-12851
Application of secondary injection to obtain controllable roll moment solid rocket propelled launch vehicles
03 p0350 N73-12856
Development and application of systematic procedures for estimating life cycle costs of solid rocket motor booster configurations
[NASA-CR-129255] 03 p0350 N73-12857
Numerical analysis of nonlinear longitudinal combustion instability in metallized solid propellant rocket engines - Vol. 1
[AD-748415] 04 p0462 N73-13767
Numerical analysis of nonlinear longitudinal combustion instability in metallized solid propellant rocket engines - Vol. 2
[AD-748417] 04 p0462 N73-13768
Cool-down problem of solid propellant rocket engine incorporating dewetting
[AD-749036] 04 p0462 N73-13770
Lightweight insulation for long duration low pressure planetary orbiter-type rocket engine applications
[NASA-CR-114513] 04 p0485 N73-13959
Analysis of reaction kinetics, combustion physics, and propellant properties of fuel elements used with rocket and ramjet engines
05 p0590 N73-14793
Analysis and design study of solid rocket motor for space shuttle booster
[NASA-CR-124002] 07 p0835 N73-16769
Application of holography for nondestructive tests of solid propellant rocket engine to detect unbonding between liner and propellant
[NASA-CR-112225] 08 p0929 N73-17606
Components and performance of solid propellant rocket engines
[AD-752865] 08 p0956 N73-17823
Ascent control studies of 049 and ATP parallel burn solid rocket motor shuttle
[NASA-TM-X-64720] 08 p0960 N73-17854
Analytical determination of mode transition in integral ramjet rocket propulsion system
[AD-753904] 10 p1224 N73-19955
Interdependence of combustion processes and physico-mechanical behavior of solid fuels
[AD-754827] 11 p1333 N73-20817
Static-aerodynamic forces and moments of 162-inch diameter solid rocket booster with and without strakes
[NASA-CR-120090] 11 p1342 N73-20888
Elements, units and characteristics of solid rocket engines
[AD-755411] 12 p1444 N73-21697
Three-dimensional finite element studies
[AD-755539] 13 p1571 N73-22734
Excitation of low frequency instability during powder combustion of rocket engine
14 p1718 N73-23942
Characteristics of solid propellant rocket engine with controlled rate of thrust buildup operating in vacuum environment
[NASA-CASE-NPO-11559] 15 p1824 N73-24784
Use of solid rocket engine as power plant for ballistic missiles
15 p1825 N73-24795
Technical analysis of solid propellant rocket engines for use with space shuttle vehicle - Vol. 2, Book 2
[NASA-CR-123926] 15 p1826 N73-24798
Systems analysis and operations analysis of solid propellant rocket engine configurations for use with space shuttles - Vol. 3
[NASA-CR-123728] 15 p1826 N73-24799
Mass properties and related data for solid propellant rocket engine used with space shuttle vehicle - Vol. 2, Book 4
[NASA-CR-124237] 15 p1826 N73-24800
Analysis of size, weight, and packaging requirments for aerodynamic decelerator for recovery of expended solid propellant rocket engines used to launch space shuttle vehicles - Vol. 2, Book 5
[NASA-CR-123730] 15 p1826 N73-24801
Cost analysis of various solid propellant rocket engines for use with space shuttle - Vol. 4
[NASA-CR-124239] 15 p1826 N73-24802
Development of analytical and experimental techniques for determining heat transfer characteristics of solid propellant rocket engine storage container system
[AD-758515] 15 p1827 N73-24807
Manual of CDC 6400 computer program for predicting nozzleless rocket motor internal ballistics
[AD-759559] 16 p1958 N73-25838
Analysis of combustion instability in solid propellant rocket engines and characteristics of acoustic waves in T-burner geometry
16 p1973 N73-25958
Application of ultrasonic inspection techniques for detecting separation of solid propellant rocket case-liner and liner-propellant interfaces
[NAL-TR-308] 18 p2193 N73-27703
Ballistic design of solid propellant missiles to include analysis of physical properties and determination of reliability
[JPRS-59060] 18 p2200 N73-27759
Analysis of cost data for fabrication of large solid rocket engine cases based on process complexity factor
[NASA-CR-133412] 18 p2200 N73-27764
Fabrication and hydrotests of shear spun rocket engine cases
[AD-761129] 18 p2201 N73-27770
Technical requirements of solid propellant rocket engine for application to space shuttle booster - Vol. 2 Bk. 1
[NASA-CR-123729] 20 p2465 N73-29805
Analysis of solid propellant rocket engine requirements for space shuttle booster application - Vol. 1
[NASA-CR-124236] 20 p2467 N73-29820
Program planning, contract administration, manufacturing, and testing of solid propellant rocket engine for space shuttle booster - Vol. 3
[NASA-CR-124238] 20 p2467 N73-29821
Simulated altitude firing test on solid propellant rocket motor
[NASA-CR-135485] 22 p2710 N73-31705
Design characteristics of solid propellant rocket engines
24 p2972 N73-33746
Heat transfer characteristics of container stored rocket motor
[AD-764536] 24 p2974 N73-33760
SOLID PROPELLANTS
NT COMPOSITE PROPELLANTS
NT DOUBLE BASE ROCKET PROPELLANTS
NT SOLID ROCKET PROPELLANTS
Effects of propellant composition variables on acceleration-induced burning rate augmentation of solid propellants
[NASA-TN-D-6923] 01 p0117 N73-10966
Fluid dynamic and chemical processes occurring in solid propellant gas generator
[AD-749144] 05 p0589 N73-14790
ONERA results of work to determine response of solid propellant to pressure and velocity fluctuations
[ONERA-TP-1165] 09 p1098 N73-18963
Influence of ammonia perchlorate binder and surface microstructure on combustion velocity development in solid composite propellants
[ONERA-TP-1167] 10 p1222 N73-19941
Carborane burning catalysts for solid propellants
[AD-755379] 13 p1489 N73-22068
Chemical process for production of polyisobutylene compounds and application as solid rocket propellant binder
[NASA-CASE-NPO-10893] 13 p1568 N73-22710
Nonacoustic combustion instability of composite solid propellants
[AD-755825] 13 p1569 N73-22715
Ignition and deflagration of in nitrocellulose based solid propellants
[AD-756880] 13 p1570 N73-22720
Vacuum effects on mechanical properties of composite heat ablator and solid problem material
15 p1801 N73-24594
Combustion stability theory for solid propellant treated as elastic body
[AD-759819] 16 p1975 N73-25973
Laminar chemically reacting boundary layer at solid fuel/gas interface over vaporizing surface
19 p2230 N73-27981
Design of high temperature combustor for use as solid fuel MHD generator and thermodynamic analysis of combustion conditions
[AD-764153] 22 p2730 N73-31848
SOLID ROCKET BINDERS
Determination of functionality distribution of prepolymers used for rocket binders
[NASA-CR-129505] 03 p0262 N73-12121
Diisocyanate cure rate stabilization with hydroxy-terminated polybutadiene binders
[AD-759960] 17 p2052 N73-26599
Hydroxyl terminated polybutadience polymer for solid propellant binder
[AD-760579] 18 p2168 N73-27507
Hydrocarbon polymeric binder for advanced solid propellants
[NASA-CR-133615] 20 p2464 N73-29800
SOLID ROCKET PROPELLANTS
NT DOUBLE BASE ROCKET PROPELLANTS
Application of ultraviolet absorption, gas-liquid chromatography, and gravimetric analysis to determine diphenylamine and ethyl centralite in solid rocket propellant
[TN-267] 02 p0221 N73-11786
Hydroxyl terminated polybutadiene for solid rocket propellant application
[AD-746338] 02 p0221 N73-11789
Analysis of crack propagation properties of solid rocket propellants based on relation between crack tip stress intensity factor and crack velocity
[AD-747531] 03 p0350 N73-12853
Solid propellant flame as source of amplification for acoustic pressure waves
[AD-746616] 03 p0365 N73-12971
Strain measurement of viscoelastic solid propellant materials with birefringent coating
[NAL-TR-261] 04 p0461 N73-13765
Microwave continuous measuring technique for solid propellant burning rates rapid depressurization, emphasizing carboxyl terminated polybutadiene and ammoaium perchlorate composite
[AD-748256] 04 p0462 N73-13769
Steklov-Lebesgue norm used in stress analysis of solid rocket propellants to determine viscoelastic response with aging
[AD-748943] 04 p0462 N73-13771
Model specifications of pulsed plasma solid propellant microthruster for synchronous meteorological satellite
[NASA-CR-130126] 04 p0463 N73-13778
HTPB polymer improvement for applications in highly loaded solid propellants
[AD-750551] 05 p0589 N73-14791
Solid propellant grain design and internal ballistics
[NASA-SP-8076] 06 p0711 N73-15804
Interaction between acoustic velocities and solid propellant combustion with variations in frequency of oscillation, mean pressure, and propellant formulation
[AD-750142] 06 p0712 N73-15809
Solid propellant containing hydrazinium nitroformate oxidizer and polymeric hydrocarbon binder
[NASA-CASE-NPO-12015] 07 p0834 N73-16764
Evaluation of magnesium-aluminum eutectic to improve combustion efficiency in low burning rate propellants
[NASA-TN-D-7133] 07 p0836 N73-16775
Utilization of inorganic metal-oxidizer materials in solid rocket propellants resulting in increased combustion efficiency
[NASA-CASE-NPO-11975-1] 08 p0953 N73-17802
Correlation of mechanical properties for stored and carton sampled solid rocket propellants
[AD-752612] 08 p0953 N73-17804
Development of model to describe flow process, energy transfer, and flame front propagation during combustion of porous propellant charges
08 p0968 N73-17910
Acoustic combustion instability in solid propellant rockets
[AD-752205] 08 p0970 N73-17926
Mechanisms of detonation initiation in solid rocket propellants by low amplitude stimuli
[AD-752242] 08 p0970 N73-17928
Evaluation of propellant grain configurations for use in hybrid propellant rocket engines - Vol. 1
[DLR-FB-72-60-PT-1] 09 p1077 N73-18792
Combustion instability of solid rocket propellants
[AD-753835] 09 p1078 N73-18795
Fabrication and testing of 22 sounding rockets using solid propellants
[AD-753089] 09 p1092 N73-18911
Thermochemical combustion effects of fuel-rich boron compound as solid rocket propellant
[AD-753105] 09 p1099 N73-18971
Telemetric monitor for in-situ transmission of solid propellant mechanical property data
[AD-754253] 10 p1162 N73-19454
Development of method for extending low temperature strain limit of rubber-based solid propellants by induced plasticization
10 p1203 N73-19788
Spectroscopic measurements of flame composition an temperature of composite solid propellants during unstable combustion
10 p1222 N73-19939
Direct mixing and combustion measurements in ducted, particle-laden jets using boron loaded propellant
[AD-754434] 10 p1224 N73-19956
Interdependence of combustion processes and physico-mechanical behavior of solid fuels
[AD-754827] 11 p1333 N73-20817
Motion picture study to provide combustion mechanism observations of ammonium perchlorate composite propellants
12 p1463 N73-21857
Microwave Doppler shift technique for measuring dynamic bulk modulus of dielectric materials including solid propellants
[NASA-CR-131743] 13 p1546 N73-22532
Automated processing system for mechanical property test data of composite solid propellants and binders
[AD-755515] 13 p1569 N73-22714
Experimental determination of pressure distribution in burning flaws in solid propellant grains
[AD-756912] 13 p1569 N73-22718
Combustion transients of solid rocket propellants
[AD-757234] 13 p1591 N73-22899
Acoustic combustion instability of solid propellants in radial burner
[AD-755826] 13 p1592 N73-22904

Microfilm system and update for acquisition, storage, and retrieval of solid propellant mechanical behavior data
[AD-757245] 14 p1700 N73-23799
Experimental determination of composite solid propellant deflagration and component processes
[AD-757066] 14 p1701 N73-23800
Thiokol TE-M-521-5 solid propellant apogee kick rocket motor tests at 46 rpm spin at simulated altitude conditions
[NASA-CR-131987] 14 p1702 N73-23810
Theoretic performance of simple lithium compounds in lithergol rocket engines
[DLR-FB-73-23] 15 p1823 N73-24778
Aging effects on chemical structure of solid rocket propellant
[AD-759564] 16 p1955 N73-25815
Diisocyanate cure rate stabilization with hydroxy-terminated polybutadiene binders
[AD-759960] 17 p2052 N73-26599
Viscoelastic fracture characterization of cracking rocket motor
[AD-759968] 17 p2076 N73-26792
Preparation and structure of complex metal hydrides for high energy solid rocket propellants
[AD-760346] 17 p2076 N73-26794
Nonsteady combustion and extinguishment tests to determine acoustic instabilities of solid rocket propellants during combustion
[AD-760788] 18 p2207 N73-27813
Prediction of acoustic pressure wave oscillations in T burner combustors
[AD-762153] 19 p2328 N73-28728
Sensitivity of solid rocket propellant stress to linear thermal expansion
[AD-761815] 19 p2328 N73-28729
Analysis of flame front propagation in porous propellant charges to show wave propagation speed and mass fraction of propellant burned during flame propagation
[AD-762063] 19 p2353 N73-28928
Combustion instability analysis of solid propellants
[AD-762841] 20 p2464 N73-29801
Mathematical structure and stress constitutive problem of materials with permanent memory particularly filled propellants
[AD-763753] 21 p2587 N73-30732
Application of holographic interferometry for detecting dewetted zones in solid rocket propellants
[AD-764470] 22 p2708 N73-31690
Magnetic field effects on burning rate of solid rocket propellants
[AD-763894] 22 p2730 N73-31847
Effect of metal additives on combustion rate of solid rocket propellants
[AD-764155] 22 p2730 N73-31849
Development of test equipment, propellants, and control equipment for interplanetary spacecraft
[NASA-CR-133863] 22 p2731 N73-31858
Solid rocket propellants with pulsating combustion, based on mixed polymerizates
[ICT-9/72] 23 p2828 N73-32604
Strain history effects in solid rocket propellant deformation
[AD-764666] 23 p2832 N73-32635
Role of solid phase heterogeneity on low pressure L-star instability of nonmetallized rocket propellants
[NASA-CR-135766] 24 p2970 N73-33735
Effect of metal admixtures on specific impulse of solid rocket propellants
24 p2970 N73-33736

**SOLID ROTATION**
U ROTATING BODIES

**SOLID SOLUTIONS**
Effect of composition of refractory metal solid solutions on coefficient of thermal expansion
[AD-745847] 01 p0068 N73-10556
Analysis of thermal expansion coefficients and elastic moduli of solid solutions of silicon in given solutions
[AD-745825] 01 p0068 N73-10557
Concentration of solute atoms, interaction range between solute atoms and distortion, and interaction strength of solid solution hardening
[NASA-TT-F-14711] 02 p0137 N73-11112
Roentgenographic measurement of coefficient of thermal expansion for chromium and solid chromium based solutions
[AD-747399] 03 p0317 N73-12580
Effects of atomic ordering in ternary solid solutions containing alloys of nickel and iron and relation of Youngs modulus with temperature
[NLL-RTS-7654] 04 p0431 N73-13511
Equation for normal freezing for ideal ternary liquid solutions solidified into ideal solid solutions of pseudobinary type
[NASA-CR-129935] 05 p0562 N73-14563
Solid solution hardening in alloys of niobium-hafnium, niobium-tungsten, and niobium-tantalum
[COO-916-25] 05 p0587 N73-14774
Phase stabilization and solid solution strengthening in titanium alloys
[AD-754240] 10 p1174 N73-19551
Single crystals of high melting point metals in solid solution
[NASA-CR-124212] 13 p1540 N73-22476
Dynamic compression and release of simple homogeneous mechanical mixtures of solids in phase change
[AD-759150] 16 p1933 N73-25644
Formation of solid solutions and fluidity of alloys based on aluminum and titanium
[AD-763491] 21 p2560 N73-30522
Strain rate sensitivity and yield stress of Fe-Mo, Fe-Ti, and Fe-Re solid solutions
21 p2602 N73-30855

**SOLID STATE**
Solid state and fusion resistance spot welding of TD-NiCr sheet
[NASA-TN-D-7256] 12 p1412 N73-21443
Determination of limiting solubility of carbon in cobalt in solid state
[NLL-M-21664-[5828.4F]] 21 p2504 N73-30096
Solid state dectors for indicating energy and point of impact of charged particles
[ISS-72/7] 21 p2548 N73-30431

**SOLID STATE DEVICES**
NT AVALANCHE DIODES
NT CRYOTRONS
NT CRYSTAL RECTIFIERS
NT FIELD EFFECT TRANSISTORS
NT GALLIUM ARSENIDE LASERS
NT GERMANIUM DIODES
NT JUNCTION DIODES
NT JUNCTION TRANSISTORS
NT METAL OXIDE SEMICONDUCTORS
NT MIS [SEMICONDUCTORS]
NT NEURISTORS
NT PARAMETRIC DIODES
NT PHOTODIODES
NT PHOTOTRANSISTORS
NT PHOTOVOLTAIC CELLS
NT RUBY LASERS
NT SEMICONDUCTOR DEVICES
NT SEMICONDUCTOR LASERS
NT SILICON TRANSISTORS
NT SOLID STATE LASERS
NT THERMISTORS
NT THYRISTORS
NT TRANSISTOR AMPLIFIERS
NT TRANSISTORS
NT VARACTOR DIODES
NT YAG LASERS
Survey on materials and manufacturing processes for solid state electronic devices
[AD-745745] 01 p0034 N73-10266
Ionosonde using solid state analog components and digital arrays for continuously monitoring ionosphere
[AD-745965] 02 p0167 N73-11359
Analysis of conditions required to produce superconductivity in materials under high pressure
[NLL-NEL-TT-2402-[6075.461]]
02 p0186 N73-11505
Research activities in nuclear physics, solid state detectors and theoretical physics
[AECL-4257] 02 p0213 N73-11726
Bibliography of solid state electronics
[AD-748739] 03 p0279 N73-12262
Transferred electron and avalanche diodes and solid state materials, for solid state microwave oscillators and amplifiers
[AD-748241] 04 p0460 N73-13755
Feasibility of solid state electric switch gear for aircraft and spacecraft
[NASA-CR-121140] 09 p1007 N73-18223
Application of solid state switching, multiplexing, and electrically programmable logic to aircraft electrical systems
10 p1111 N73-19053
Development of electrical generation and distribution systems for supersonic aircraft using solid state switching and remote control of protective devices
10 p1111 N73-19054
Quantum electronics, solid state devices, and solid microelectronics
[AD-754945] 11 p1331 N73-20806
Thin film physics, cohesive and dielectric properties, and solid state theory
[COO-623-190] 12 p1439 N73-21658
Solar proton anisotropies in interplanetary space as measured by Explorer 35 solid state detectors
13 p1573 N73-22744
Design and performance of solid state inverter/converter modular system with pulse width modulation
[NASA-TM-X-2795] 15 p1737 N73-24083
Design and tests of hybrid microelectronics solid state relay for 2500 volts isolation and minus 120 C to 80 C thermal cycling range
[NASA-TM-X-68248] 15 p1756 N73-24235
Research and development progress on solid state microwave oscillator and amplifier
[AD-758244] 15 p1757 N73-24241
Development and characteristics of solid state cosmic ray telescope for use on IMP F and G missions
[NASA-CR-132767] 16 p1912 N73-25473
Influence of supersaturation on nucleation behavior in continuous agitated cooling crystallizers
[WTHD-44] 16 p1953 N73-25799
Design and performance tests of solid state A-6 aircraft engine instruments
[AD-760351] 17 p2035 N73-26469
Scanning auger spectroscopy for surface analysis of solid state devices
[AD-760550] 18 p2153 N73-27399
Research on solid state devices and microelectronics
[AD-760815] 18 p2190 N73-27683
Determination of susceptibility limits and desensitization of solid state electronic equipment to power line transients
[AD-762403] 19 p2246 N73-28110
Development of solid state beacon and radio frequency generator for avionics applications - Vol. 1
[AD-761525] 19 p2247 N73-28115
Solid state high power UHF broadband amplifier
[AD-762175] 19 p2247 N73-28118
Comparative evaluation of conventional and solid state simulators for A-7 aircraft electrical system
[AD-762295] 19 p2250 N73-28142
Solid state switch for variable circuit switching
[NASA-CASE-NPO-10817-1] 21 p2510 N73-30135
Polish research projects on piezoelectronic and acoustoelectronic equipment with specific application to computers and communication systems
21 p2608 N73-30901
Solid state avalanche diodes for use as microwave amplifiers and oscillators
[NASA-CR-132300] 22 p2642 N73-31172
Star mapper using solid-state detectors discussing dioptric and mirror objectives, and star recognition algorithms
[ESRO-CR-82] 22 p2698 N73-31610
Final design and specifications for solid state, S band, power amplifier
[NASA-CR-124405] 23 p2764 N73-32115
Economics and performance characteristics of high speed digital integrated circuits used in nuclear instrumentation
[LBL-1750] 24 p2900 N73-33150
Electron beam devices, quantum electronic devices, plasmas, and solid state devices
[AD-764808] 24 p2932 N73-33415

**SOLID STATE LASERS**
NT GALLIUM ARSENIDE LASERS
NT RUBY LASERS
High-efficiency, self-contained, small neodymium laser for pyrotechnic ignition
10 p1228 N73-19979
Solid state laser multiwavelength identification and display system for detection and spectrum analysis of air pollutants
[AD-755161] 13 p1554 N73-22598
Performance capabilities of erbium lasers and tabulation of laser materials to show chemical composition, mode of operation, frequency and output characteristics
[PHL-1973-12] 14 p1672 N73-23565
Solid state laser induced excitation of HF second vibration rotation energy levels
15 p1794 N73-24547
Research and development in solid state lasers, gas lasers, component development, diognostics, design analysis, advanced concepts, laser plasmas and laser fusion
[UCRL-50021-72-2] 24 p2931 N73-33408

**SOLID STATE PHYSICS**
Research in solid state physics, materials, and physical chemistry
[AD-746866] 03 p0347 N73-12826
Solid state research from 1 Feb. through 30 Apr. 1972
[AD-748836] 03 p0348 N73-12837
Solid states physics and manufacturing methods for microwave generation, amplification, and control devices
[AD-749500] 04 p0397 N73-13234
Preparation of pure materials, radiation chemistry, and solid state studies
[BARC-599] 05 p0506 N73-14120
Numerical calculation of physical and electronic properties of metals
[AD-749546] 05 p0588 N73-14782
Physics research on solid state materials - radiation damage, electronic structure, and magnetic, electrical, surface, low temperature, and lattice properties
[ORNL-4779] 06 p0708 N73-15776
Theoretical studies of solid surfaces, electron diffraction experiments, and electronic charge distribution
[AD-750481] 06 p0711 N73-15802
Research and development in solid state physics, plasma physics, electrical engineering systems and information sciences, and mathematical biosciences and biomedical engineering
[AD-751515] 07 p0834 N73-16757
Research and development in advance electronics including applications to digital computers, air traffic control, and solid state physics
[AD-751308] 07 p0834 N73-16758
Solid state research at Lincoln Laboratory
[AD-752556] 08 p0952 N73-17798
Survey of electronic research projects
[AD-753700] 09 p1010 N73-18240

Solid state physics, materials, and semiconductor research
[AD-752063] 09 p1053 N73-18581
Research activities in solid state physics
[AD-753255] 09 p1075 N73-18770
Proceedings of conference on application of superconductivity techniques to auxiliary power systems for aircraft and missiles
[AGARD-CP-104] 10 p1108 N73-19030
Naval research in aerodynamics, ballistics, mathematics, and physics
[AD-754397] 11 p1268 N73-20292
Quantum electronics, solid state devices, and solid microelectronics
[AD-754945] 11 p1331 N73-20806
Surface chemistry and physics of inorganic solids
[AD-754453] 11 p1332 N73-20814
Research on semiconductor and solid state physics
[AD-757521] 14 p1697 N73-23771
Papers on crystallography and liquid and solid structures
[NASA-CR-132048] 15 p1820 N73-24752
Solid state physics, physical chemistry, and materials research
[AD-758374] 15 p1821 N73-24764
Abstracts of studies in nuclear physics, solid state physics, and plasma physics
[AD-759252] 16 p1947 N73-25756
Magnetic phenomena in solid state physics
[COO-3150-10] 16 p1953 N73-25803
Research and development in solid state physics, antenna arrays, and control theory
[AD-760008] 17 p2074 N73-26783
Developments in data systems air traffic control, and solid state physics
[AD-763731] 21 p2587 N73-30727
Research and development progress in solid state physics, chemistry, electronics, and materials science
[AD-763501] 21 p2610 N73-30924
Research in solid state semiconductor physics
[PB-220703/3] 22 p2738 N73-31923
Electron network model of solid interfaces, surface defects, planar defects, and thin films
23 p2825 N73-32584
USSR research in solid state physics, plasma physics, atmospheric physics, and seismology
[AD-763743] 23 p2866 N73-32918

**SOLID SURFACES**
NT CRYSTAL SURFACES
Mathematical models for determining impact of supersonic gas jet on solid surfaces
[NLL-RTS-7551] 02 p0154 N73-11248
Estimation of impact pressures of drops against solid surface
[AD-748731] 03 p0363 N73-12956
Phonon emission by laser beams and thermal conductivity of optical crystals
[AD-753698] 09 p1077 N73-18791
Low energy electron diffraction and Auger electron spectroscopy used for determination of structure of adsorbed gases on solid surfaces
[LBL-878] 10 p1193 N73-19708
Scattering kernel analysis on monatomic gas interaction with solid surface
[AD-755838] 13 p1489 N73-22069
Contact interaction and friction and wear of solid bodies
[AD-755710] 13 p1535 N73-22438

**SOLID SUSPENSIONS**
Influence of solid suspended particles on turbulent flow properties
06 p0652 N73-15300

**SOLID-SOLID INTERFACES**
Moving point force on solid-solid interface
[AD-750252] 05 p0604 N73-14916
Tunneling biases into interfaces of semiconductor junctions
[AD-755656] 12 p1441 N73-21676
Electrical properties of solid-solid interfaces for charge transfer phenomena used in image transducer and metal-semiconductor devices
18 p2123 N73-27156
Ceramic to metal bonding, noting improvement of Mo-Mn silicate method, and use of interfacially active metals
[BMFT-FB-T-73/07] 23 p2798 N73-32377

**SOLIDIFICATION**
Electrotransport effect on solidification of some Sn-Bi and Sn-Pb alloys
[IS-T-532] 03 p0315 N73-12567
Mathematical model for phase change solidification in thermal control devices, including natural convection effects and transient, two dimensional, finite difference solution
[NASA-CR-129910] 04 p0385 N73-13132
Aluminum-copper eutectic solidification experiment to be run in M518 multipurpose electric furnace during Skylab mission
[NASA-CR-124103] 09 p1045 N73-18526
Effect of solidification under high isostatic pressure on high strength steels
[AD-753958] 11 p1306 N73-20596
Analysis of KC-135 flight samples of Star-J Satellite solidified in near-zero gravity
[NASA-CR-124179] 11 p1308 N73-20610
Physical and chemical processes of solidification of fusion welds and its effects on weldability
[NLL-T1780/GC/72-[9022.305]]
15 p1790 N73-24508
Skylab experiments on convection and molten metal flow and solidification under reduced gravity
[NASA-CR-124329] 19 p2343 N73-28852
Carbon fiber/cobalt/chromium system tensile and high temperature strength noting different solidification modes
[DLR-FB-73-37] 21 p2560 N73-30519

**SOLIDIFIED GASES**
Melting characteristics and thermophysical properties of solid hydrogen
[AD-748847] 04 p0387 N73-13144
Electron microscopic analysis of epitaxial growth and nucleation in condensed gas crystals
[AD-753108] 10 p1201 N73-19773
Helium crystal growth in preferred orientations
[AD-754442] 11 p1330 N73-20797
Phase transition and entropy behavior of solid He-3
[COO-1569-96] 12 p1439 N73-21654
Three body exchange effects on Neel temperature of solid He-3
[COO-1569-97] 12 p1439 N73-21655
Molecular transition principle for constructing liquid- and solidhydrogen particle track chambers
[JINR-P13-7067] 24 p2960 N73-33658
Ion motions in liquid and solid helium
[COO-2027-6] 24 p2969 N73-33728

**SOLIDS**
NT SOLIDIFIED GASES
Mechanical wave front propagation in fluid mixtures and isotropic solids
[AD-746617] 02 p0158 N73-11281
Wetting of alumina, magnesia, zirconia, and carbides and borides of vanadium, titanium, and zirconium by palladium melts
[NLL-RTS-7321] 02 p0190 N73-11544
Laser interferometer instrumentation techniques for study of plane stress wave propagation in solids
[SC-DC-70-5465] 03 p0310 N73-12529
Computing equation of state parameters for material which undergoes phase transition
[AD-746611] 03 p0346 N73-12824
Solid polymer for water electrolysis system to generate oxygen and hydrogen in manned space station
[NASA-CR-112183] 04 p0375 N73-13052
Properties of solid reactor materials
[REPT-331] 04 p0448 N73-13655
Magnetism in solids - magnetic moments, propertism of diamagnetism and paramagnetism, and coexistence of superconductivity and ferromagnetism
[ITJ-13] 04 p0449 N73-13670
Preparation of solid homogeneous materials in space
04 p0473 N73-13861
Plasma generation within magnetic containment field by laser irradiation of solid particle
[COO-3547-2] 06 p0704 N73-15740
Darcy-Weisback equation for investigating solid-liquid flow in noncircular pipes
[BM-RI-7725] 09 p1013 N73-18271
Calculation of shock-induced phase transformations in solids
[SC-RR-72-0626] 10 p1201 N73-19770
Riemann-Hilbert solution to steady state crack propagation in orthotropic solid
[AD-754529] 11 p1332 N73-20810
Heat transfer solutions for solids with moving boundaries and for viscous liquid flow
[AD-754639] 11 p1349 N73-20950
Bibliography on shock waves in solids
[AD-755429] 12 p1441 N73-21679
Physical and spectral characteristics of infrared solid state dispersion filters
[NASA-TT-F-14838] 13 p1558 N73-22631
Increasing phase change material thermal diffusivity by means of solid fillers
[NASA-CR-124214] 13 p1590 N73-22894
Open circuit voltage measurements on solid beta alumina electrolytic cells
[NASA-TN-D-7322] 15 p1738 N73-24089
High optical resolution derivative spectrometer for measuring optical properties of solids in vacuum UV and far IR range
15 p1785 N73-24474
Characteristics of dilute gas-solids suspensions in drag reducing flow
[NASA-CR-2267] 16 p1888 N73-25277
Adhesion, friction, and wear behavior of glasses and ionic solids
[NASA-TM-X-68255] 16 p1932 N73-25632
Structural properties and stability of solid materials and structures with different geometric configurations
[AD-759558] 16 p1971 N73-25942
Periodic excitation of finite three dimensional standard, linear viscoelastic solid
[AD-759485] 16 p1972 N73-25951
Crack initiation and fatigue fracture in overload mechanism of solid structures
[AD-760007] 17 p2048 N73-26568
Low energy X ray absorption and electron ionization cross section measurements on solids
[CONF-720404-VOL-2] 19 p2322 N73-28683
Optical wavelength - modulation spectroscopy of solids
[LBL-1402] 21 p2549 N73-30437
Mechanical effects resulting from interactions of laser beams with gases, liquids, and solids
[AD-763258] 21 p2555 N73-30482
Boltzmann transport equation for electron bombardment effects in solids
[AD-764637] 23 p2827 N73-32599

**SOLIDS FLOW**
Laser-Doppler velocity measurement of large particles in two-phase gas-solid nozzle flow
[VKI-TN-81] 10 p1142 N73-19305
Dynamic characteristics of solid particles in particulate flow through turbine and compressor cascades
17 p2013 N73-26278
Analysis of flow pattern of particles in moving bed for application to manufacturing processes
[NLL-RTS-7330] 20 p2386 N73-29167

**SOLUBILITY**
Distillation method for quantitative determination of oxygen solubility in sodium
[NLL-RISLEY-TR-2424-[9091.9F]]
02 p0136 N73-11105
Thermodynamics of oxygen solubility in lanthanum uranium oxide measured on solid state electrolytic cell
[KFK-1649] 12 p1376 N73-21163
Two-phase flow of two immiscible fluids considered for motion in diverging channel
[AD-756341] 13 p1513 N73-22259
Temperature dependence of sparingly soluble electrolytes and nonelectrolytes
[AD-757504] 14 p1617 N73-23102
Influence of zirconium additions on diffusivity and solubility of hydrogen and deuterium in niobium alloys at high temperature
[BNWL-SA-4473] 17 p2065 N73-26706
Coefficients of electrical conductivity for determining concentration of water soluble salts in soils
[NASA-TT-F-15045] 20 p2411 N73-29379
Determination of limiting solubility of carbon in cobalt in solid state
[NLL-M-21664-[5828.4F]] 21 p2504 N73-30096
Solubility curves from 25 to 70 C for K2HfF-K2ZrF6-HF system
[BM-RI-7785] 21 p2558 N73-30505
Observation of oxide particles below apparent oxygen solubility limit in tantalum
[NASA-TM-X-2889] 21 p2558 N73-30509

**SOLUTES**
Laser method for measuring axial solute dispersion in turbulent pipe flow
[AD-753801] 09 p1019 N73-18314
Specific wavelength colorimeter for measuring given solute concentration in test sample
[NASA-CASE-MSC-14081-1] 09 p1035 N73-18443
Gas model of solute diffusion in liquid metals
[NASA-TR-R-417] 23 p2753 N73-32032

**SOLUTIONS**
NT AQUEOUS SOLUTIONS
NT DETONABLE GAS MIXTURES
NT GAS MIXTURES
NT NUCLEAR EMULSIONS
NT PHOTOGRAPHIC EMULSIONS
NT SOLID SOLUTIONS
Electrons in metal ammonia solutions - abstracts of conference papers
[AD-752915] 10 p1127 N73-19179

**SOLVENTS**
Chemical synthesis of formaldehyde based disinfectants without penetrating odor and eye and ear irritation properties
[NASA-CASE-NPO-12115-1] 08 p0884 N73-17153
High energy batteries based on aprotic organic electrolytes
[AD-763140] 21 p2506 N73-30112

**SOMALIA**
Dynamics of plankton populations in upwelling waters along Arabian Coast, Somali Coast, and Northwest Coast of Africa
[E73-10325] 09 p1024 N73-18357
Somali current and southwest monsoon arising from ocean atmosphere instability associated with Coriolis force
[NASA-TM-X-70471] 23 p2786 N73-32285

**SOMMERFELD APPROXIMATION**
Orr-Sommerfeld equation for studying laminar boundary layer stability on elastic surface
[NASA-TT-F-14855] 11 p1270 N73-20307

**SONAR**
NT SONOBUOYS
Physiological effects of 12 submarine personnel during prolonged exposure to sonar signals at 85 db [five day exposure]
[AD-744938] 01 p0011 N73-10087
Development and characteristics of digital beamformer for narrowband sonar systems
[AD-745302] 01 p0029 N73-10224
Digital data coding instructions for underwater acoustics and environmental data bank
[AD-746507] 01 p0082 N73-10675
Human tolerance and adaptation in long term exposure to sonar signals at elevated intensities
[AD-746103] 02 p0134 N73-11089

Feasibility of infrared laser/sonar beam communication system between submarine and aircraft and effects of air water interaction
[AD-746106] 02 p0143 N73-11156
Development of method for producing constant beamwidth over octave frequency bandwidth for underwater signal reception array
[AD-746690] 02 p0143 N73-11160
Feasibility of mounting geophone arrays on pack ice to provide passive sonar system with improved signal to noise ratios over hydrophone arrays
[AD-747327] 02 p0143 N73-11161
Computer aided analysis on radiative characteristics of sonar transducer with spaced sensor element array
[AD-747281] 03 p0266 N73-12156
Sonar equipment research project to include determination of temperature and heat dissipation characteristics of ceramics used in high frequency projectors
[AD-749960] 05 p0515 N73-14187
Test results of acoustic ranging and bearing measuring system
[AD-749041] 05 p0578 N73-14703
Decision making behavior of sonar operator in target detection and reporting
[AD-750761] 06 p0637 N73-15174
Distortion of sonar signals transmitted through random and inhomogeneous media
[AD-750755] 06 p0641 N73-15202
Effectiveness of underwater acoustic propagation loss models in sonar personnel training devices
[AD-750694] 06 p0701 N73-15719
Effects of quantized luminance levels and display contrast on sonar target recognition
[AD-751711] 07 p0757 N73-16148
Acoustic properties of ocean bottom and relevance to sonar performance
[AD-753265] 09 p1032 N73-18429
Computer program for estimating position and shape of surface shadow zone in sonar operations
[AD-753443] 10 p1129 N73-19200
Design of towed sonar transducer array for bathymetric mapping of ocean bottom topography
[AD-755113] 11 p1259 N73-20216
Digital quadrature methods for processing bandpass signals
[AD-755473] 13 p1494 N73-22110
Analysis of vibratory characteristics of sonar transducer element using finite element three dimensional mathematical model
[AD-755177] 13 p1495 N73-22117
Passive electrical dummy load for simulating transducers in large sonar arrays
[AD-755174] 13 p1495 N73-22123
Sonar mapping of underside of sea ice
[AD-755243] 13 p1527 N73-22374
Design of sonar array using standard amplitude shading technique
[AD-755481] 14 p1633 N73-23241
Adaptation of Acoustic Research Tank Facility for parametric sonar experiments
[AD-756176] 14 p1634 N73-23249
Side-looking sonar system with coherent electrical processing
[AD-757253] 14 p1669 N73-23549
Approximative gain calculations for linear and rectangular arrays using vertically directed noise model
[AD-760690] 18 p2119 N73-27133
Three estimation techniques for bearing of arrival of transient signals
[AD-760691] 18 p2119 N73-27134
Noise model for optimal signal to noise ratio in sonar detector design
19 p2235 N73-28015
Analysis of acoustic volume scattering in Bermuda Ocean to show daily variability and diurnal variations
[AD-761976] 19 p2296 N73-28465
Thermal properties of ceramics for design of sonar arrays
[AD-764572] 23 p2758 N73-32071

**SONDES**
NT DROPSONDES
NT IONOSONDES
NT RADIOSONDES
NT RAWINSONDES

**SONIC BOOMS**
Aircraft maneuvers for reducing sonic boom intensity during horizontal turns
[AD-744859] 02 p0126 N73-11022
Sonic boom effects on individuals compensatory tracking performance for unstable system
[UTIAS-TN-179] 02 p0135 N73-11098
Construction of sonic boom simulators to determine effects of sonic boom on human heart reactions and analysis of human responses
[UTIAS-TN-180] 02 p0152 N73-11233
Effects of real or simulated sonic booms of six pounds per square foot over-pressure on reproduction in farm-raised mink
[FAA-EQ-72-2] 03 p0251 N73-12028
Procedure for predicting structural and acoustic response of full scale structures to sonic booms using scale models and laboratory techniques
[FAA-RD-72-116] 03 p0251 N73-12029
Analysis of sonic boom data recorded on strain gages mounted on windows to record overpressures and relation to window size
[FAA-RD-72-114] 03 p0251 N73-12030
Analysis of sonic boom pressure signatures recorded during reentry of Apollo 15 command module and correlation with wind tunnel signatures
[NASA-TM-X-62111] 04 p0371 N73-13016
Measurement of ray paths and ground overpressures produced by Concorde aircraft during supersonic flight
[R/D-896] 06 p0618 N73-15021
Wind tunnel tests to determine effect of wing planform on generation of sonic boom at various Mach numbers
[NASA-TN-D-7160] 06 p0700 N73-15709
Development of computer program for calculating flow field resulting from sonic boom focusing
[NASA-CR-2127] 07 p0739 N73-16013
Sonic boom nitroglycerin resistance noting shock simulation and sonic boom effect on detonation
[ISL-14/72] 07 p0822 N73-16658
Focusing effects of distortion of near sonic shocks by weakly turbulent layers with random temperature and pressure variations
[AD-752472] 08 p0899 N73-17279
Performance characteristics of solid state converter system for measuring aircraft noise and sonic boom
[NASA-CR-112260] 09 p0982 N73-18019
Flight test measurements and analysis of sonic booms to determine caustics produced by variations in flight speed and to develop method for predicting shock wave-ground intersections
[NASA-CR-2167] 09 p0982 N73-18022
Development of model for analyzing propagation of weak normal shock wave through turbulent atmosphere and application to sonic boom characteristics
[NRC-12981] 09 p0983 N73-18028
Low sonic boom overpressure profiles for supersonic transport aircraft configurations
[NASA-TM-X-2746] 09 p0984 N73-18039
Application of gas dynamics equations to determine magnitude of pressure rise due to sonic boom in stratified atmosphere
[NASA-TN-D-7105] 11 p1233 N73-20010
Effect of sonic boom on fish and fish eggs during developmental stage
[FAA-RD-73-29] 11 p1247 N73-20121
Correlation of sonic boom pressure signatures recorded during reentry of Apollo 16 command module with wind tunnel signatures
[NASA-TM-X-62073] 12 p1365 N73-21073
Research in aircraft noise and sonic booms reduction, remote sensing of water pollution, and earth surface changes
[DLR-MITT-72-15] 12 p1375 N73-21153
Flight tests to determine magnitude of groundtrack overpressure generated by oblique wing transport aircraft at Mach 1.4 and 45,000 feet
[NASA-TM-X-62247] 13 p1472 N73-21922
Prediction of sonic boom effect on avalanches to prepare mirage 3 flight over Lavey Valley
[ISL-13/72] 13 p1474 N73-21940
Influence of small periodic oscillations on viscous shock waves structure and sonic boom rise time caused by supersonic transport vibrations
13 p1507 N73-22217
Various atmospheric disturbances including turbulence, sonic boom, and shock wave propagation
13 p1514 N73-22271
Jet aircraft noise and sonic boom measuring device which converts sound pressure into electric current
[NASA-CASE-LAR-11173-1] 13 p1529 N73-22387
Sonic boom minimization design for supersonic transport aircraft
[NASA-TN-D-7218] 15 p1734 N73-24065
Development of test facility for determining interaction of sonic boom with surface of body of water
[NASA-TT-F-14917] 15 p1767 N73-24318
Measurement of effects of sonic booms on light building structures for various building configurations
[RAE-LIB-TRANS-1633] 17 p1981 N73-26011
Statistical analysis of effect of simulated sonic booms on sleep patterns of male subjects
[FAA-AM-72-35] 17 p1987 N73-26057
Development of statistical prediction model for determining probability of glass breakage caused by sonic boom overpressures
[FAA-RD-73-79] 18 p2104 N73-27018
Dynamic response of light partitions to sonic boom noting theoretical computation and scale model tests
[ISL-23/72] 19 p2220 N73-27910
Lesion threshold in guinea pig auditory sensation areas due to sonic booms
[ISL-33/72] 19 p2228 N73-27966
Analysis of sonic boom phenomenon to show generation, propagation, and effects on structures, people, and animals
[AEL/A-NOTE-337] 21 p2493 N73-30007
Data base for abatement and control of aircraft noise and sonic boom for rule making criteria
[FAA-ED-20-2] 21 p2495 N73-30022
Effect of simulated sonic booms and overpressure on EEG waveform patterns and disturbance judgments
[FAA-RD-73-115] 21 p2500 N73-30066
Design criteria for supersonic overflight to reduce psychophysical effects and decrease glass damage probability
[FAA-RD-73-116] 22 p2724 N73-31800
Analysis of sonic boom characteristics based on second order solutions for flow distribution around slender bodies in supersonic flow - Part I
[NASA-CR-2339] 23 p2739 N73-31927
Theory for predicting sonic boom intensity and techniques for sonic boom suppression
[FAA-RD-73-4] 23 p2741 N73-31944

**SONIC FLOW**
U TRANSONIC FLOW

**SONIC NOZZLES**
Suppression of turbofan engine sonic inlet noise in STOL propulsion by use of acoustic nozzle insert
03 p0250 N73-12026

**SONIC SPEED**
U ACOUSTIC VELOCITY

**SONIC WAVEGUIDES**
U ACOUSTIC DELAY LINES

**SONOBUOYS**
Kalman filter theory for estimating sonobuoy reference system in antisubmarine warfare
[AD-753608] 10 p1129 N73-19201

**SOOT**
Shock tube measurements of surface oxidation rates of soot formed during combustion of hydrocarbon fuels
[FML-PUBL-72-8] 01 p0023 N73-10176
Development of semi-empirical expression for specific surface oxidation rate of soot for application to design of combustion chambers
10 p1223 N73-19943

**SORBENTS**
NT ABSORBENTS
Computer prediction of performance of sorbent beds for CO2 or water removal
[NASA-CR-112098] 01 p0022 N73-10173
Bactericidal properties of sorbents in spacecraft water regeneration system
20 p2367 N73-29038
Regenerable CO2 sorbent formulation and fabrication for extravehicular activity
[NASA-CR-114632] 20 p2371 N73-29054

**SORPTION**
NT ADSORPTION
NT CHEMISORPTION
Sorption and desorption of ethylene oxide and methyl bromide gases on polymeric materials during sterilization
03 p0257 N73-12082
X ray analysis of B2O3 effects on composition, porosity, and sorption properties of Al2O3
[NLL-M-22796-[5828.4F]] 06 p0682 N73-15553
Systems design for amine carbon dioxide sorber bed to be used in manned spacecraft
[NASA-CR-111849] 22 p2623 N73-31018

**SORTIE CAN**
U SPACELAB

**SORTIE LAB**
U SPACELAB

**SORTING**
U CLASSIFYING

**SOUND**
U ACOUSTICS

**SOUND ABSORPTION**
U SOUND TRANSMISSION

**SOUND BARRIER**
U ACOUSTIC VELOCITY

**SOUND DETECTORS**
U SOUND TRANSDUCERS

**SOUND FIELDS**
Dependence of timbre on location in diffuse sound fields
[IZF-1972-15] 02 p0211 N73-11711
Far and near sound fields of Do-31 aircraft, and noise reduction for future VSTOL aircraft
[BMVG-FBWT-72-23] 09 p0985 N73-18045
Affect of sound and vibration on convective heat transfer and flow distribution on boundary layers of cylindrical bodies
[AD-754006] 10 p1143 N73-19316
Acoustic radiation patterns of line source coincident with focal line of parabolic cylinder reflector immersed in water tank
[AD-754063] 11 p1324 N73-20748

**SOUND GENERATORS**
Analysis of aerodynamic noise generated by tips of helicopter rotary wings during acceleration to near sonic speed
[AD-752301] 09 p0989 N73-18072
Excitation and sound generating effects on laminar flames, and stabilizing and noise reducing effect of sound on turbulent flames
[REPT-8/1972] 09 p1099 N73-18970
Calculation of unsteady, subsonic flow through infinite, two-dimensional flat plate blade
[ARC-R/M-3709] 13 p1510 N73-22240

Development and characteristics of terminal analog speech synthesizer using pulse width modulation and pulse number modulation techniques
14 p1632 N73-23228
Computer simulation to demonstrate feasibility of delta modulation as method for encoding control signals of voiced speech synthesizer
14 p1632 N73-23231
Development of equipment and system for real-time analysis of speech transients
14 p1632 N73-23232
Quantitative data on propagation and directivity of parametric array in air
[AD-757034] 14 p1693 N73-23737
Application of siren as test technique for determining response and life of aircraft structures subject to engine noise field excitation
20 p2480 N73-29922
Fluid mechanics of hole tone whistle designed as efficient producer of discrete frequency sound
24 p2903 N73-33170

**SOUND INTENSITY**
Ray tracing program for calculating sound intensity from ocean sources
[AD-745313] 01 p0080 N73-10664
Aural analysis of sound into bands of frequencies
[NASA-TT-F-13912] 02 p0212 N73-11715
Loudness level perception of human ear and reference level for telephone engineering
[NLL-PO-2831-(9022.81)] 15 p1812 N73-24684
Analysis of relative intensity profiles of density fluctuations based on acoustic properties of subsonic and supersonic unheated jet flow
[NASA-CR-124563] 16 p1861 N73-25073
Analysis of noise problems created by supersonic transport aircraft, conventional aircraft, and short takeoff aircraft to show methods for jet exhaust noise reduction
21 p2495 N73-30024

**SOUND LOCALIZATION**
Acoustic properties of sound emitted from arbitrary point in parallel or nearly parallel turbulent shear flow confined to region near solid boundaries
[NASA-TN-D-7118] 07 p0821 N73-16653
Filtering and vertical sensor position effects on human speech detection in jungle evnironment
[AD-753650] 10 p1190 N73-19686
Acoustic shielding baffle for determining jet noise source location
[NASA-TN-D-7229] 16 p1944 N73-25734

**SOUND MEASUREMENT**
U ACOUSTIC MEASUREMENTS

**SOUND PERCEPTION**
U AUDITORY PERCEPTION

**SOUND PRESSURE**
Measurement of indoor and outdoor sound pressure levels at airport control towers during aircraft takeoff and landing
[AD-752535] 09 p1012 N73-18262
Acoustic properties and sound pressure of jet flow
[AD-754422] 10 p1144 N73-19321
Jet aircraft noise and sonic boom measuring device which converts sound pressure into electric current
[NASA-CASE-LAR-11173-1] 13 p1529 N73-22387
Effect of finite source size on power statistics in reverberant room for pure tone excitation
[NASA-CR-132279] 18 p2179 N73-27594

**SOUND PROPAGATION**
NT VOICE
Analysis of effects of rotary wing configuration on aerodynamic noise generation during hovering flight
[AD-753397] 09 p0989 N73-18070
Model of jet aircraft shock cell noise generation and reduction
[NRC-12923] 10 p1188 N73-19666
Modified ray theory for underwater sound propagation and diffraction
[AD-755460] 12 p1430 N73-21589
Ray tracing method for computerized prediction of underwater sound propagation loss
[AD-755459] 12 p1430 N73-21590
Calculating acoustic source distributions in turbulent flows when average velocity distribution is known
[NASA-TT-F-14946] 17 p2063 N73-26689
Coherent and incoherent components of sound scattered at time dependent rough surface with application to wind-blown water waves
[AD-760306] 17 p2064 N73-26695
Far field sound propagation calculation for ducted fan rotor-stator interaction
[NRC-13260] 18 p2179 N73-27592
Analysis of fluctuating density with high temperature subsonic jet and characteristics of noise radiated to surroundings
[NASA-CR-133789] 21 p2524 N73-30241
Analysis of sound propagation in elliptic ducts to determine acoustic effects produced by variations from symmetry in circular ducts
[NASA-CR-132307] 21 p2579 N73-30672
Ultrasonic wave propagation in He-Ar and He-Xe mixtures
24 p2956 N73-33614

**SOUND RANGING**
Artillery sound ranging computer simulations
[AD-745887] 02 p0212 N73-11719
Sea bottom classifier device designed for use with towed underwater vehicle
[AD-748611] 04 p0415 N73-13392
Underwater equipment for locating and recovery of objects from ocean bottom by whales
[AD-747612] 04 p0417 N73-13403
Underwater devices for target detection on sea bottom
[JPRS-58916] 14 p1667 N73-23529
Pulse-echo technique for measuring ultrasonic attenuation in Bi12GeO20 single crystals at low temperature
16 p1952 N73-25798

**SOUND TRANSDUCERS**
NT ELECTROACOUSTIC TRANSDUCERS
NT HYDROPHONES
NT MICROPHONES
Underwater sound transducer calibration system for 0.3 to 2000 Hz frequency range at hydrostatic pressure to 6.89 MPa
[AD-751536] 07 p0822 N73-16662
Design and performance of strain gage transducer as blood pressure recording device
12 p1374 N73-21144
Nonlinear detection of low frequency plane wave by directional circular piston beam
[AD-755167] 12 p1430 N73-21588
Synthesis of microwave network having surface acoustic wave transducer
[AD-759934] 17 p2008 N73-26236
Subsonic intrinsic noise reduction of sound pressure transducers in air flow
[RAE-LIB-TRANS-1660] 17 p2063 N73-26687
Analyses of sonic resonators and transducers
24 p2925 N73-33362

**SOUND TRANSMISSION**
Acoustic measurements and sound velocity calculations for molten rubidium at high pressures
[AD-746838] 02 p0138 N73-11120
Acoustic noise, transmission loss, and reverberation measurements in West Greenland Sea
[AD-746839] 02 p0169 N73-11373
Sound transmission at extremely low frequency in far field radiation from turbulent wake
[AD-747238] 02 p0212 N73-11721
Analysis of finite amplitude standing waves in air at ambient temperature contained in rigid walled rectangular cavity
[AD-747522] 03 p0337 N73-12749
Scattered acoustic wave amplitudes of plane wave incident on perforated screen with periodic array of circular or elliptic apertures
[AD-747648] 03 p0338 N73-12755
Development of unified theory of jet engine noise based on fluctuating motions in fluids - Vol. 3
[AD-749138] 05 p0496 N73-14037
Development of theory for jet noise generated by turbulence, noise radiation from upstream sources, and combustion noise - Vol. 4
[AD-749139] 05 p0496 N73-14038
Analysis of acoustic properties of shock associated noise in narrow band spectrum produced by jet flows - Vol. 5 App. 2
[AD-749142] 05 p0496 N73-14040
Acoustic properties of air and sound absorption anomalies due to molecular relaxation
[AD-750220] 05 p0581 N73-14732
Effect of sound absorbing exhaust duct on rear quadrant noise of J-65 engine and contributions of internal and jet components
[NASA-TM-X-2718] 07 p0739 N73-16011
Acoustic properties of sound emitted from arbitrary point in parallel or nearly parallel turbulent shear flow confined to region near solid boundaries
[NASA-TN-D-7118] 07 p0821 N73-16653
Measurement of sound transmission and attenuation in Tyrrhenian Sea discussing experimental design and results
07 p0858 N73-16959
Ray tracing of underwater sound in Arctic Ocean
[AD-752056] 08 p0944 N73-17734
Prevention of spurious caustics in ray tracing scheme for sound propagation mapping in sea water
[AD-752080] 08 p0944 N73-17735
Procedures for calculating sonic fields radiated and diffracted by elastic bodies and passage of sound through elastic plates and shells - Vol. 1
[JPRS-58146-1-PT-1] 09 p1015 N73-18283
Procedures for calculating sonic fields radiated and diffracted by elastic bodies and passage of sound through elastic plates and shells - Vol. 2
[JPRS-58146-2-PT-2] 09 p1015 N73-18284
Analysis of hydrodynamics of helium isotopes to determine entrainment of sound in moving fluid
10 p1159 N73-19278
Development of electromagnetic pulse sounding probe for detection and delineation of geological anomalies in hard rock medium
[AD-754847] 11 p1288 N73-20454
Fundamentals of helicopter noise generation and propagation to include noise control procedures and cost effectiveness of noise reduction
14 p1598 N73-22953
Development and characteristics of terminal analog speech synthesizer using pulse width modulation and pulse number modulation techniques
14 p1632 N73-23228
Saddle point method for exact wave plane solution of Burger equation in shock zone
[AD-758409] 15 p1814 N73-24706
Parametric difference frequency generation of sound in air through interaction of two intense high frequency sound waves
[AD-758682] 16 p1946 N73-25747
Analysis of acoustic volume scattering in Bermuda Ocean to show daily variability and diurnal variations
[AD-761976] 19 p2296 N73-28465
Development of model for analyzing pressure excitation spectrum and acoustic impedance of sound absorbers in presence of grazing flow
[NASA-TM-X-71418] 21 p2523 N73-30231
Analysis of fluctuating density with high temperature subsonic jet and characteristics of noise radiated to surroundings
[NASA-CR-133789] 21 p2524 N73-30241
Some regularities in propagation of perturbations of discrete tone in free supersonic jet
[AD-763163] 21 p2581 N73-30681
Atmospheric attenuation of sound transmissions in air
[AD-764286] 22 p2675 N73-31428

**SOUND VELOCITY**
U ACOUSTIC VELOCITY

**SOUND WAVES**
NT AERODYNAMIC NOISE
NT AIRCRAFT NOISE
NT ELECTROACOUSTIC WAVES
NT ENGINE NOISE
NT ION ACOUSTIC WAVES
NT JET AIRCRAFT NOISE
NT LAMB WAVES
NT NOISE [SOUND]
NT SONIC BOOMS
Diffraction of acoustic and electromagnetic waves on wavy surfaces
[AD-748037] 03 p0268 N73-12168
Acoustic emission testing to broaden nondestructive testing capability
[LA-4724] 03 p0302 N73-12464
Acoustic field of infinite circular cylindrical transducer partially covered by layer of sound-soft material
[JPRS-57367] 03 p0335 N73-12732
Relationship of acoustic surface waves on curved surfaces to corresponding plane surface waves
[AD-748189] 03 p0338 N73-12761
Psychophysical analysis of RF sound perception in human subjects
[AD-747684] 05 p0501 N73-14076
Conference on acoustic gravity wave effects in atmospheric transmission of radio communication signals
[AGARD-CP-115] 05 p0508 N73-14131
Comparison of ionospheric radio wave propagation and acoustic gravity wave propagation
05 p0508 N73-14132
Auroral infrasonic sound wave generation and downward propagation into lower atmosphere
05 p0508 N73-14134
Effects of acoustic gravity wave diffusion on atmospheric boundaries
05 p0508 N73-14136
Acoustic gravity wave generation by transient sources in isothermal atmosphere
05 p0508 N73-14139
Nuclear source model for generating ionospheric disturbances through acoustic gravity waves
05 p0509 N73-14141
Excitation of Lamb atmospheric edge mode by tail of large atmospheric explosion
05 p0509 N73-14143
Ionospheric oscillations caused by infrasonic waves propagating from thunderstorms
05 p0510 N73-14148
Electromagnetic cross modulation and very low frequency propagation techniques for measuring acoustic gravity waves in ionospheric D region
05 p0511 N73-14153
Nonlinear propagation and ionospheric coupling of atmospheric waves following nuclear explosion
05 p0513 N73-14168
Multiple tone acoustic radiations phenomenon in transonic fans
[ARC-CP-1226] 05 p0580 N73-14726
Bessel function analysis on acoustic wave propagation in curved ducts
[NASA-TM-X-2698] 06 p0700 N73-15705
Wave scattering by lenses and microsound elastic waveguides
[AD-750766] 06 p0701 N73-15717
Ultrasonic nondestructive tests of sound waves emitted from stress corrosion cracking - Part 2
[AD-751529] 07 p0810 N73-16570
Nonlinear interaction and modulation in parametric acoustic array for spherical wave field
07 p0821 N73-16650
Application of acoustic emission analysis to nondestructive testing on crack formation
[RFP-TRANS-101] 07 p0821 N73-16656

Flight test measurements and analysis of sonic booms to determine caustics produced by variations in flight speed and to develop method for predicting shock wave-ground intersections
[NASA-CR-2167] 09 p0982 N73-18022
DONAR system for digitizing ultrashort sonic wave trains from pulse echo systems
[NASA-CR-130883] 09 p1013 N73-18266
Procedures for calculating sonic fields radiated and diffracted by elastic bodies and passage of sound through elastic plates and shells - Vol. 1
[JPRS-58146-1-PT-1] 09 p1015 N73-18283
Procedures for calculating sonic fields radiated and diffracted by elastic bodies and passage of sound through elastic plates and shells - Vol. 2
[JPRS-58146-2-PT-2] 09 p1015 N73-18284
Dimensions and mechanical properties of elastic spherical shells measured by sound echo signals
10 p1188 N73-19667
Series solutions for reduced wave equation characterizing radiation from point source in two and three dimensions
[AD-754793] 11 p1312 N73-20647
Atmospheric model for acoustic pressure produced in shadow zone by wind and temperature gradients
[AD-754634] 11 p1324 N73-20747
Design of noise source for simulating supersonic spinning modes in duct acoustics
[NASA-CR-2260] 12 p1364 N73-21067
Detection of acoustic emission signals from fatigue cracks during cyclic bend tests
[NASA-TM-X-68228] 12 p1462 N73-21848
Interferometric measurement of hypersonic sound wave attenuation in liquid helium transition region
13 p1558 N73-22629
Decoding of information in acoustic waveform of human speech using signal processing techniques
14 p1623 N73-23148
Computer simulated parallel-formant synthesizer to copy short samples of human speech
14 p1624 N73-23156
Nonlinear acoustic and gravity waves in earth atmosphere
[TR-48] 14 p1659 N73-23466
Rayleigh equations for determining axial sound wave scattering coefficients by torus
[REPT-208.138/1] 14 p1692 N73-23731
Measured and calculated transmission losses of sound waves through helium layer
[NASA-TN-D-7230] 14 p1692 N73-23735
Holographic interferograms of supersonic jet aircraft acoustic field
[PB-214112/5] 14 p1693 N73-23743
Development of long acoustic damping device for various chamber flow conditions based on nonlinearity of orifice flow upon passage of high intensity wave
15 p1765 N73-24299
Fluctuating pressure characteristics for far field acoustic radiation in mixing region of perturbed and unperturbed round free jet
[AD-759377] 17 p2015 N73-26294
Measurement of electromagnetically excited acoustic standing-wave resonance
18 p2159 N73-27444
Acoustic pressure radiation from infinite elastic plate excited by point source
19 p2320 N73-28666
Convolution of surface acoustic waves on barium titanate crystal
[AD-761880] 19 p2327 N73-28724
Prediction of acoustic pressure wave oscillations in T burner combustors
[AD-762153] 19 p2328 N73-28728
Transmission of wave energy in curved ducts
[NASA-TM-X-68287] 20 p2377 N73-29101
Analysis of sonic boom phenomenon to show generation, propagation, and effects on structures, people, and animals
[ARL/A-NOTE-337] 21 p2493 N73-30007
Application of acoustic transducers for suspending object at center of chamber under near weightless conditions
[NASA-CASE-NPO-13263-1] 22 p2677 N73-31443
Ultrasonic attenuation of longitudial sound waves in superconducting molybdenum single crystals
23 p2825 N73-32581
Analyses of sonic resonators and transducers
24 p2925 N73-33362

**SOUND-SOUND INTERACTIONS**
Excitation and sound generating effects on laminar flames, and stabilizing and noise reducing effect of sound on turbulent flames
[REPT-8/1972] 09 p1099 N73-18970

**SOUNDERS**
U SOUNDING

**SOUNDING**
NT BALLOON SOUNDING
NT IONOSPHERIC SOUNDING
NT ROCKET SOUNDING
Survey of methods for sounding atmospheric temperature profile by remote measurement
[NASA-CR-130110] 04 p0442 N73-13601
Triaxial accelerometer for determining upper air density, temperature, and pressure
[AD-749881] 05 p0543 N73-14422
Monitoring Northern Hemisphere transmissions in Antarctica and some oblique sounding systems
[JPRS-58205] 10 p1128 N73-19186
Survey of some oblique sounding systems and selection of system for practical application
10 p1128 N73-19188
Design of upper atmosphere chemical release package
[AD-760141] 17 p2028 N73-26416
Environmental tests of interocean acoustic release devices and performance of correlation echo sounder processor
[RN-1008] 18 p2151 N73-27385

**SOUNDING ROCKETS**
NT AEROBEE ROCKET VEHICLE
NT ARCAS ROCKET VEHICLES
NT ASTROBEE ROCKET VEHICLES
NT BLACK BRANT SOUNDING ROCKETS
NT LOKI ROCKET VEHICLE
NT SKYLARK ROCKET VEHICLE
NT VERONIQUE ROCKET VEHICLES
Hole area for evacuating and degassing of far ultraviolet sounding rocket photometer
[MPI-PAE/EXTRATERR-68] 02 p0174 N73-11411
High altitude wind and temperature measurement data from meteorological sounding rockets, and radiosondes for May 1971
02 p0204 N73-11651
High altitude wind and temperature measurement data from meteorological sounding rockets and radiosonde observations - February 1971
02 p0204 N73-11652
Meteorological rocket sounding data on stratospheric and mesospheric structures and circulations
[NASA-TR-R-391] 02 p0205 N73-11657
Design and launch support for high altitude sounding rocket payloads
[AD-745977] 02 p0235 N73-11914
High resolution X ray astronomy using rocketborne telescopes
[NASA-CR-130166] 03 p0357 N73-12912
Radio telemetry for detecting and tracking sounding rockets
[REPT-11] 04 p0388 N73-13153
Performance of temperature compensated rocketborne MOSFET electrometer amplifier for measurement of electron and ion densities in lower ionosphere
[FOA-3-C-3640-E1] 04 p0420 N73-13424
Characteristics of research instruments used on rockets and satellites for investigating solar ultraviolet radiation
[AD-748276] 04 p0424 N73-13454
Technical engineering services in support of Nike-Tomahawk sounding rocket vehicles
[NASA-CR-130123] 04 p0478 N73-13906
Sounding rocket launches and air and ground support equipment
[AD-750544] 05 p0515 N73-14185
System for deploying and ejecting releasable clamshell fairing sections from spinning sounding rockets
[NASA-CASE-GSC-10590-1] 05 p0597 N73-14853
Design, development and flight tests of Super Loki Dart Meteorological Rocket Systems
[AD-750796] 06 p0722 N73-15895
Meteorological data for launching 11601 Lance, missile 2138, round number 165
[AD-752093] 08 p0939 N73-17689
Techniques for determining attitude of rocket axis for vehicle AH 7.886
[AD-751937] 08 p0965 N73-17890
Determination of atmospheric density numbers by sounding rocket carrying mass spectrometer with cryo ion source
[BMBW-FBW-72-34] 09 p1027 N73-18381
Lidar anemometry for quick determination of aerological data above launching site prior to rocket firing
[ONERA-TP-1151] 09 p1027 N73-18385
Fabrication and testing of 22 sounding rockets using solid propellants
[AD-753089] 09 p1092 N73-18911
Fabrication and calibration of Tomahawk sounding rocket payload for magnetic field measurements in ionosphere
[AD-754246] 10 p1157 N73-19413
Analysis of systems for recovering sounding rocket payloads
[ONERA-TP-1153] 10 p1214 N73-19870
Meteorological data of upper atmosphere from sounding rockets for Lance missile launch
[AD-754554] 11 p1314 N73-20666
Design of AMSS prototype rocketsonde and ground antenna
[AD-754895] 11 p1316 N73-20681
Modification of double-deck EUV spectrophotometer recovered from previous rocket flight
[AD-756917] 13 p1528 N73-22380
Observation of venus far ultraviolet spectrum by sounding rockets
13 p1572 N73-22741
Eridan rocket probe performance in experimental vehicles
14 p1718 N73-23940
Meteorological and ballistics data for launching of 14101 RIP missile nos. 9623/9034, round nos. 5/6
[AD-758861] 15 p1807 N73-24647
High time resolution measurements of energetic electrons in auroral breakup using sounding rockets
16 p1895 N73-25324
Sounding rocket injection of controlled beam of energetic electrons into trapping region of magnetosphere
16 p1895 N73-25329
Dynamics of sounding rockets at burnout
[SC-DC-72-1613] 16 p1967 N73-25911
Polarization photometers in payload of sounding rocket for noctilucent cloud particle sampling
[AD-760149] 17 p2028 N73-26415
Development of method for predicting performance of barometric sensing systems used in determining sounding rocket altitude
[NASA-TM-X-65991] 17 p2087 N73-26881
Measurement of positive ion composition in midlatitude sporadic E layer using rocket-borne ion mass spectrometer
[NASA-TM-X-66276] 18 p2142 N73-27313
Sounding rocket instrument for measuring polar electrojet position and current parameters
[AD-760767] 18 p2152 N73-27396
Rate integrated gyro attitude control system for sounding rockets
18 p2208 N73-27820
Charge neutralization and echo analysis using electron gun in magnetosphere onboard sounding rocket during Electron Echo I experiment
19 p2258 N73-28204
Rocket produced infrared emissions for analyzing auroral atmospheric mechanisms
[AD-762206] 19 p2298 N73-28478
Low energy electron measurement onboard meteorological rockets in polar region
20 p2411 N73-29375
Sounding rocket measurements of high latitude dayside electric fields and low energy particles
[NASA-TM-X-70450] 20 p2413 N73-29392
Development and characteristics of servoed roll gimbal to isolate gyroscopes of stabilized platform from effects of vehicle spin
[AD-764903] 23 p2818 N73-32527
Feasibility of actively guiding sounding rockets to reduce impact dispersion at White Sands Missile Range
[NASA-TM-X-70474] 23 p2851 N73-32780
Logistics support for launches of sounding rockets
[AD-765231] 23 p2852 N73-32789

**SOUNDS [TOPOGRAPHIC FEATURES]**
NT BLOCK ISLAND SOUND [RI]
NT PRINCE WILLIAM SOUND [AK]

**SOUTH AFRICA**
Value of ERTS-1 imagery in resource evaluation on national scale in South Africa
[E73-10071] 07 p0779 N73-16333
Differentiation between mine dumps in South Africa having varying degrees of vegetative cover based on ERTS-1 imagery
[E73-10326] 10 p1147 N73-19334
Identification of mine dumps in South Africa by growth and decline of vegetation
[E73-10642] 16 p1896 N73-25339
ERTS-1 imagery applied to definition of geotectonic domains of southern African crystalline shield
[PAPER-G26] 19 p2267 N73-28257
ERTS-1 imagery analysis to determine varying degrees of vegetation on mine dumps in South Africa
[PAPER-4E] 19 p2268 N73-28268
Application of ERTS-1 band six imagery to determine rate of spread of grass fires in Zambesi Basin of South Africa
[PAPER-E6] 19 p2269 N73-28270
Utilization of ERTS-1 imagery in resources management on national scale in South Africa
[E73-10931] 20 p2399 N73-29279

**SOUTH AMERICA**
Tropical rainfall patterns and associated mesoscale systems in Southeast Asia and South America
[AD-752467] 08 p0940 N73-17706
Geologic mapping and mineral resource inventory in South America from ERTS-1 imagery
[E73-10648] 16 p1897 N73-25344
Analysis of ERTS-1 imagery for extrapolating existing soil maps into unmapped areas of Llanos Orientales of Colombia, South America
[PAPER-A13] 19 p2261 N73-28221
Classification of coastal environments along Americas and Africa
[AD-761193] 20 p2415 N73-29412

**SOUTH CAROLINA**
Mapping southeastern coastal marshlands and wetlands of South Carolina and Georgia using ERTS-1 imagery
[E73-10362] 10 p1150 N73-19358
Mapping wetlands ecology of Chesapeake Bay, South Carolina, and Georgia from ERTS-1 imagery
[E73-10507] 13 p1516 N73-22282
Application of Skylab multispectral photography to mineral and land resources of South Carolina
[E73-10831] 18 p2141 N73-27301

Relation of sea truth data from Cape Cod, Massachusetts, and Charleston, South Carolina on plankton composition and chlorophyll values with ERTS-1 data
[E73-10907] 20 p2397 N73-29256
Application of Skylab multispectral photography to mineral and land resources of South Carolina and Georgia
[E73-11140] 24 p2918 N73-33295
SOUTH DAKOTA
NT BLACK HILLS (SD-WY)
Crop identification and acreage measurement in Idaho, Missouri, Kansas, and South Dakota using ERTS-1 imagery
[E72-10179] 01 p0045 N73-10358
Crop identification and acreage measurement in Missouri, Kansas, South Dakota, and Idaho using ERTS-1 imagery
[E72-10336] 05 p0531 N73-14324
Crop identification and acreage measurement in Missouri, Kansas, South Dakata, and Idaho based on ERTS-1 imagery and aerial photography
[E73-10328] 09 p1024 N73-18359
Thermal parameters as predictors of precipitation at Ellsworth, S.D.
[AD-753418] 09 p1061 N73-18657
Soil mapping of rangelands in Bennett County, South Dakota using remotely sensed imagery
[NASA-CR-131229] 10 p1155 N73-19395
ERTS-1 imagery of flood damage to farmlands in South Dakota
[NASA-CR-131641] 12 p1401 N73-21361
Utilization of ERTS-1 imagery for crop identification and acreage measurement in South Dakota, Kansas, Missouri, and Idaho
[E73-10734] 17 p2020 N73-26340
Digital analysis of ERTS-1 imagery for southeastern South Dakota to determine cultivated areas and to identify crops
[PAPER-A3] 19 p2259 N73-28211
Application of ERTS-1 imagery for differentiating quaternary surface deposits and landforms in Illinois, Iowa, Missouri, Kansas, Nebraska, and South Dakota
[PAPER-G13] 19 p2264 N73-28244
Identification of soil associations in western South Dakota using ERTS-1 imagery
[PAPER-L11] 19 p2274 N73-28307
Acquisition of ground truth data and site selection for SL-3 EREP experiments in South Dakota
[E73-10945] 21 p2530 N73-30287
Ratio scannergrammetry of geology in Wyoming and South Dakota
[E73-11096] 24 p2914 N73-33253
SOUTH KOREA
U KOREA
SOUTH VIETNAM
U VIETNAM
SOUTHEAST ASIA
Data from marine surface observations in Southeast Asian coastal marine areas
[AD-749936] 05 p0576 N73-14686
Summary of synoptic meteorological observations in Southeast Asian coastal marine areas
[AD-749937] 05 p0576 N73-14687
Tropical rainfall patterns and associated mesoscale systems in Southeast Asia and South America
[AD-752467] 08 p0940 N73-17706
Time series analysis of summer monsoon data from Southeast Asia for 1967 and 1968
[AD-759788] 16 p1939 N73-25691
Structural framework of Sunda Shelf and vicinity
[PB-218671/6] 18 p2146 N73-27346
Application of ERTS-1 imagery for determining rice growing areas in Philippines and assessment of crop condition
[PAPER-A5] 19 p2260 N73-28213
Application of ERTS-1 multispectral imagery to water resources development in lower Mekong River basin in southeast Asia
[PAPER-W3] 19 p2271 N73-28283
Tropical rainfall patterns and associated mesoscale systems for Southeast Asia
[AD-762571] 20 p2450 N73-29693
Comparison of surface cloud cover observations and cloud cover estimates determined by satellite measurements for Southeast Asia
[AD-763098] 20 p2451 N73-29695
SOUTHERN CALIFORNIA
Computer program for analysis of ERTS-1 MSS imagery of haze in Southern California test area
[E73-10346] 10 p1148 N73-19345
Mapping of cotton fields in Southern California using ERTS-1 data for control of pink bollworm growth
[PAPER-A15] 19 p2261 N73-28223
Application of ERTS-1 imagery to identify, locate, and map faults showing geomorphic evidence of geologically recent breakage in Southern California
[PAPER-G22] 19 p2266 N73-28253
Identification of fifty mile wide tectonic zone across Southern California using ERTS-1 imagery
[PAPER-G33] 19 p2268 N73-28264
Measurement of atmospheric aerosol content in Southern California desert areas from ERTS-1 contrast and radiance measurements
[PAPER-I2] 19 p2277 N73-28324
Enhancement of ERTS-1 images by density slicing and application to mapping of Yucca trees in Mojave Desert of Southern California and Nevada
[PAPER-I11] 19 p2278 N73-28332
ERTS-1 detection and monitoring of tectonic and vegetational patterns, urban development, and agricultural processes in Southern California
[PAPER-R4] 19 p2283 N73-28362
Application of Skylab imagery to analysis of fault tectonics and earthquake hazards in Peninsular Ranges of Southern California
[E73-10863] 20 p2392 N73-29214
Correlation of coastal ground truth data from Southern California waters with ERTS imagery
[E73-10864] 20 p2392 N73-29215
Urban development and regional planning in Los Angeles County using ERTS-1 MSS photography
[E73-10989] 22 p2658 N73-31295
Application of Skylab imagery to analysis of fault tectonics and earthquake hazards in Peninsular Ranges of Southern California
[E73-10999] 22 p2659 N73-31304
Impact of highway transportation control strategies on Los Angeles air pollution and quality
[PB-221301/5] 22 p2696 N73-31597
Identification and interpretation of tectonic features from ERTS-1 imagery of Southern California and Baja California
[E73-11084] 24 p2913 N73-33247
Application of Skylab imagery to analysis of fault tectonics and earthquake hazards in Peninsular Ranges, Southern California
[E73-11134] 24 p2917 N73-33289
SOUTHERN HEMISPHERE
NT ANTARCTIC REGIONS
EOLE satellite tracking of meteorological balloons released in Southern Hemisphere to trace horizontal motion of air masses
[NASA-TM-X-66152] 06 p0694 N73-15651
Importance of Schmidt telescopes to radio astronomy noting color identification of quasars and Southern Hemisphere sky survey
07 p0845 N73-16851
Schmidt telescopes in Southern Hemisphere survey noting possible sites and study of Magellanic clouds
07 p0846 N73-16853
Infrared sky survey in Southern Hemisphere for finding late M stars
07 p0846 N73-16854
Divergence at 200 mb level in Southern Hemisphere atmospheric circulation inferred from EOLE data
08 p0918 N73-17523
Magnitude and UBV colors for 900 stars brighter than magnitude 5.0 and south of plus 10 deg declination
[ANNALS-7] 08 p0960 N73-17849
Analysis of energy conservation constraints on circulation of Southern Hemisphere atmosphere and oceans based on radiant, latent, and sensible heat energy transfers
[METEOROL-STUDY-26] 09 p1027 N73-18387
Profiles of neutral atmospheric density at high and middle latitudes in Southern Hemisphere from OV1-15
[AD-755396] 13 p1526 N73-22370
Distribution of tropospheric infrared radiative fluxes and associated heating and cooling rates in Southern hemisphere
15 p1771 N73-24340
Cloud cover mosaics developed from environmental satellite imagery for April, 1973
18 p2171 N73-27534
Circulation structure of stratosphere and troposphere over Southern Hemisphere as determined by rocket soundings
20 p2444 N73-29629
SOVIET UNION
U U.S.S.R.
SOYBEANS
Remote detection of water content and spectral properties of leaves in different soybean crop species
04 p0378 N73-13070
SOYUZ SPACECRAFT
Welding experiments during flight of Soyuz 6
[AD-749745] 05 p0553 N73-14496
Activity cycle data for spacecrews of Soyuz 3 to 9 spacecrafts before, during and after space flights
[JPRS-58173] 07 p0746 N73-16068
Morphological composition of peripheral blood of crew members of Soyuz-9 and Salyut-1
11 p1245 N73-20104
Orbital mechanics involved in rendezvous between space shuttle and Soyuz spacecraft
[NASA-TT-F-13955] 14 p1705 N73-23838
Rhythm disturbances in sleep and wakefulness cycles of Soyuz 3 and 9 crews before, during, and after space flight
[NASA-TT-F-15103] 20 p2369 N73-29048
SPACE
Time dependent correlation functions between magnetohydrodynamics and space transport coefficients
13 p1562 N73-22660
SPACE BASES
Optimization of propulsion stage selection for space-based transportation
[AD-744979] 01 p0109 N73-10900
Orbital propellant transfer techniques and feasibility of thermal bootstrap propellant transfer concept
[NASA-CR-125909] 03 p0356 N73-12900
Identification of mechanical/structural differences resulting from use of tug/payload combination in space space mode as contrasted to ground-based operations
[NASA-CR-125905] 03 p0358 N73-12920
Cost estimates for base basing, space shuttles, and systems analysis
[NASA-CR-125985] 03 p0359 N73-12921
SPACE BIOLOGY
U EXOBIOLOGY
SPACE CAPSULES
NT ESCAPE CAPSULES
Electrochemical process for recovery of oxygen from atmospheres of manned space capsules
[NASA-CR-114573] 16 p1869 N73-25130
SPACE CHARGE
Annealing phase and space charge decay following pulsed irradiation of MOS structures
[AD-748007] 03 p0347 N73-12833
Computer modeling of space charge flow in electrogasdynamic generator
[AD-751632] 07 p0829 N73-16720
Effects of acceleration or retardation on electric strength of gas
[AD-755848] 12 p1429 N73-21584
Electric charge, momentum, and mass of elliptic universe
[AD-756902] 13 p1561 N73-22649
Generation and processing of microwave signals using elastic, electro-magnetic, and carrier space charge waves in solid media
[AD-757555] 14 p1699 N73-23784
SPACE COMMUNICATION
NT SPACECRAFT COMMUNICATION
Conference on expanded aerospace telecommunication system requirements and digital data transmission methods
[AGARD-CP-103] 01 p0024 N73-10187
Digital telecommunication techniques and network planning for aerospace systems
01 p0024 N73-10188
Noise and error effects on differential pulse code modulation transmission of sampled aerial imagery
01 p0024 N73-10190
Design and performance of C band traveling wave tube amplifier for space communication application
[NASA-CR-112125] 01 p0032 N73-10250
Design and development of closed-loop, digital data communication system using optimum number of interconnecting wires
[NASA-CASE-MSC-13912-1] 03 p0266 N73-12151
Evaluation of Halo and Hummingbird satellites for lunar libration point satellite to provide tracking and communications link with far side of moon
[NASA-CR-130135] 07 p0844 N73-16836
Problems of radio telemetry systems in manned and unmanned spacecraft
[NASA-TT-F-722] 09 p1002 N73-18175
Antenna design and transionospheric propagation relative to space communication - conference
[AD-754061] 11 p1256 N73-20193
Conceptual designs for manned, space shuttle sortie mission laboratory for communications and navigation experiments - Vol. 1 - Exec. Summary
[NASA-CR-124136] 11 p1266 N73-20273
Selection and definition of candidate experiments and associated instrumentation requirements for space shuttle communication/navigation experiments laboratory - Vol. 2
[NASA-CR-124137] 11 p1266 N73-20274
Design of experiment to measure communication characteristics of wideband satellite to ground communication links
[NASA-CR-130196] 11 p1294 N73-20497
Development of space communications and navigation projects involved in earth orbital experiment program and requirements study - Vol. 5
[NASA-CR-112329] 13 p1577 N73-22782
Reduction of probability of simultaneous rainfall on millimeter wave earth satellite space communication terminals
[AD-757506] 14 p1633 N73-23242
Design, development, and evaluation of optical detectors used in high speed digital laser communication links
[NASA-CR-132772] 17 p2032 N73-26446
Earth surface scattering model for multiphase prediction of radiowave communication between earth satellites
[NASA-CR-132791] 18 p2116 N73-27109
Design of tunable waveguide carbon dioxide laser for optical heterodyne communication system between satellites
18 p2212 N73-27860
Proceedings of international telecommunication organization on peaceful uses of outer space with emphasis frequency assignments for space communication
[REPT-12] 21 p2507 N73-30118

Application of laser systems to space communication using carbon dioxide laser for two way communication with ATS-F satellite - Vol. 1 Pt. 1
[NASA-CR-132803] 22 p2680 N73-31469
Application of carbon dioxide laser for space communication to include ground equipment, data acquisition, and data processing - Vol. 1 Pt. 2
[NASA-CR-132804] 22 p2681 N73-31470
Requirements for design, fabrication, performance, and testing of optical heterodyne receiver subsystem for use in laser communication system - Vol. 1 Pt. 3
[NASA-CR-132805] 22 p2681 N73-31471
Theory, design, and operation of suppressed carrier data-aided tracking receiver
[NASA-CR-135714] 23 p2757 N73-32065

**SPACE ENVIRONMENT**
U AEROSPACE ENVIRONMENTS

**SPACE ENVIRONMENT SIMULATION**
NT WEIGHTLESSNESS SIMULATION
Human physiological and psychological responses in long time exposure to simulated space station atmosphere as observed by critical tracking task
01 p0017 N73-10133
Experiments and simulations to determine effect of compliance and force feedback on manipulator performance
[NASA-CR-128605] 01 p0019 N73-10151
Neutron irradiation effects on lithium-doped silicon solar cells in space environment simulation
[AD-745992] 02 p0129 N73-11048
Pumping system of space environment simulation vacuum chamber noting vacuum and diffusion pumps, valves, cryogenic section, and automatic control system
[ESDO-TN-113-ESTEC] 05 p0524 N73-14262
Performance data reduction for cadmium spacecraft cells from simulated orbital life tests
[AD-748251] 06 p0627 N73-15088
Comparison of three different space environment simulators
[DLR-FB-71-44] 06 p0650 N73-15277
Hypervelocity impact tests of Skylab electrical cables for simulation of micrometeoroid environment
[NASA-TN-D-7178] 07 p0761 N73-16186
Hypodynamia effect on human transverse acceleration tolerance
10 p1114 N73-19083
Microorganism survival in simulated Mars environment
10 p1118 N73-19116
Design and performance of photostat for simulating Mars environment
10 p1118 N73-19117
Microbiological investigation of neutral buoyancy simulator for weightless space environment testing
[NASA-TM-X-64736] 12 p1371 N73-21127
Self contained automated primate research laboratory to study physiological effects of space environment weightlessness on monkeys
[NASA-CR-131642] 12 p1387 N73-21250
Human visual/motor response to tracking task during long term confinement in simulated space station
[NASA-CR-2240] 15 p1744 N73-24134
Simulation of satellite motion in ionospheric plasma using low energy and high current ion source in vacuum chambers
[ONERA-NT-202] 15 p1762 N73-24280
Laboratory simulation validity for analysis of spacecraft-plasma interactions
[PB-214611/6] 16 p1908 N73-25438
Tests of potential thermal degradation of ATS-F radiant cooler form contaminants generated by hydrazine thruster in simulated space
[NASA-CR-132988] 16 p1974 N73-25965
Screw calculus in kinematic and power analyses on spatial positions of manipulator link mechanisms
17 p1990 N73-26092
German test facilities for environment simulation
19 p2249 N73-28133
Motion simulator for performance testing of satellite attitude control systems
[ESRO-CR-66] 20 p2383 N73-29145
Laboratory simulation of scaled single-axis dual-level control system for large space telescope
[NASA-TN-D-7319] 23 p2791 N73-32333
Space environment simulation tests on space shuttle reusable surface insulation materials
[NASA-TM-X-2720] 24 p2940 N73-33475
Acoustic, reentry, and structural load environment tests on mullite insulation for space shuttle
24 p2941 N73-33483
Space environmental testing of silica insulation for space shuttle orbiter
24 p2941 N73-33484
Meteoroid impact simulation tests on bonded fiber/aluminum skin panels for space shuttle insulation
24 p2941 N73-33485
Space environment effects on space shuttle thermal protection system design
[NASA-TM-X-2721] 24 p2941 N73-33490

**SPACE ERECTABLE STRUCTURES**
Expandable space frames with high expansion to collapse ratio
[NASA-CASE-ERC-10365-1] 23 p2847 N73-32749

**SPACE EXPLORATION**
NT VIKING MARS PROGRAM
Influence of Uranus, Neptune, and Pluto environments on design of spacecraft used to probe them
[NASA-SP-8103] 02 p0230 N73-11870
Development of payload for mission planning for missions to outer planets as function of flight time for various launch years, launch vehicles, and orbit sizes
[NASA-CR-129244] 03 p0354 N73-12887
Proceedings of conference on benefits of space exploration conducted at Huntsville, Alabama Nov. 1971
[NASA-SP-313] 04 p0470 N73-13829
Analysis of development of cosmos, universe, mankind, and space exploration
04 p0470 N73-13833
Influence of space technology on man and his environment
04 p0472 N73-13847
Flyby missions to outer planets
04 p0473 N73-13858
Influence of space technology and exploration on earthbound human problems
04 p0473 N73-13859
Extraterrestrial space for supplying earth with vanishing minerals, materials, and needed electric power
04 p0473 N73-13863
Use of space exploration and benefits to procure world peace
04 p0474 N73-13872
Experimental design and scientific exploration of Mars surface by MARV
[NASA-TM-X-64719] 07 p0765 N73-16219
History and future of solar system observation, exploration and exploitation
[NASA-TT-F-767] 07 p0844 N73-16839
Research in support of definition phase of Outer Planets Mission
[NASA-CR-130917] 09 p1082 N73-18826
Summary of advanced mission planning for solar system exploration
[NASA-CR-131395] 11 p1350 N73-20954
Presidential report on progress and activities of various aerospace programs in 1972 and comments on future mission planning
11 p1352 N73-20975
Research projects in geophysics, astronomy, and satellite applications
[JPRS-58885] 13 p1577 N73-22776
Research projects for space exploration by out-of-ecliptic spacecraft
[NASA-CR-131865] 13 p1578 N73-22792
Model for estimating cost of unmanned lunar and planetary exploration programs
[NASA-CR-131897] 14 p1705 N73-23840
Manned orbital space station for geophysical and astronomical research
[NASA-TT-F-13957] 14 p1709 N73-23868
Some effects of space research on society
[NASA-TM-X-66233] 14 p1721 N73-23968
Solar electric propulsion for unmanned exploration of solar system
[NASA-CR-130245] 15 p1826 N73-24803
Achievements in space exploration to include spacecraft design, planetary composition, lunar missions, and predicted space accomplishments
[NASA-TT-F-737] 15 p1830 N73-24829
Artificial intelligence for identifying practical applications to unmanned spacecraft to explore solar system in 1980 time period - Vol. 1
[NASA-CR-132256] 16 p1962 N73-25873
Analysis of requirements for unmanned spacecraft mission to planet Mars and characteristics of lander vehicles for planetary exploration - Vol. 3
[NASA-CR-132258] 16 p1962 N73-25875
Analysis of data relative to possible Saturn orbiter mission in 1985
[NASA-CR-133033] 16 p1966 N73-25906
Synopsis of past, present, and future progress in aerospace engineering and manned space exploration
[UTIAS-REV-37] 16 p1976 N73-25979
Self-propelled vehicle with wheel, track laying, and walking capability for exploratory expolaration
[NASA-CASE-NPO-11366] 17 p2008 N73-26238
Asteroid and comet exploration for studying planetary evolution and solar system history
[NASA-CR-2291] 18 p2196 N73-27726
DSN progress in planetary flight support
[NASA-CR-133651] 20 p2473 N73-29867
Soviet space exploration and research during 1972
[JPRS-59778] 20 p2488 N73-29983
Design of detonating propellant propulsion system for exploring planets with hot dense atmospheres
22 p2732 N73-31864
Cosmonaut activities onboard orbiting space stations
[NASA-TT-F-15152] 23 p2850 N73-32778
Application of aerospace engineering to planetary exploration and spacecraft shielding problems
[NASA-CR-135529] 23 p2858 N73-32836
Saturn satellite encounter opportunities for Mariner Jupiter-Saturn 1977 project
23 p2858 N73-32838

**SPACE FLIGHT**
NT APOLLO FLIGHTS
NT APOLLO 9 FLIGHT
NT APOLLO 11 FLIGHT
NT APOLLO 12 FLIGHT
NT APOLLO 13 FLIGHT
NT APOLLO 14 FLIGHT
NT APOLLO 15 FLIGHT
NT APOLLO 16 FLIGHT
NT APOLLO 17 FLIGHT
NT GEMINI FLIGHTS
NT HYPERBOLIC REENTRY
NT HYPERSONIC REENTRY
NT INTERPLANETARY FLIGHT
NT MANNED SPACE FLIGHT
NT MERCURY FLIGHTS
NT SPACECRAFT REENTRY
NT VIKING MARS PROGRAM
Soviet bloc research in astronomy, meteorology, oceanography, geology, and space science - 3 Oct. 1972
[JPRS-57162] 01 p0104 N73-10856
Soviet Bloc research in astronomy, meteorology, oceanography, geology, and space science - 1 Nov. 1972
[JPRS-57392] 03 p0355 N73-12895
Visual perception during space flight
06 p0629 N73-15104
Vestibular neuron response to rotational stimuli in space flight environment
06 p0634 N73-15150
Soviet research on astronomy, meteorology, oceanography, and space science - 27 Dec. 1972
[JPRS-57858] 06 p0717 N73-15856
Soviet bloc research in astromony, meteorology, oceanography, geology, and space science - 31 Jan. 1973
[JPRS-58112] 08 p0961 N73-17860
Effects of ionizing radiation and space flight conditions on microorganisms, plants, animals, enzymes, and immunological preparations
09 p0993 N73-18103
Soviet Bloc research in astronomy, meteorology, oceanography, geology, and space science - Feb. 1973
[JPRS-58218] 09 p1085 N73-18851
Functional morphology of various organs and tissues subjected to space flight
[NASA-TT-F-738] 10 p1119 N73-19126
System for analysis and classification of voice communications associated with space missions or simulations
[NASA-CR-128837] 10 p1128 N73-19191
Medical biological and other problems of space flight
[JPRS-58678] 12 p1367 N73-21089
Review of bibliography on medical and biological research during space flights
12 p1367 N73-21091
Contamination radiation safety during space flight, and safety problems at launch
[JPRS-58781] 12 p1374 N73-21149
BIOSTACK experiment on Apollo 16 for studying combined action of heavy high energy loss nuclei and space flight factors on resting biological systems
14 p1611 N73-23062
Analysis of major problems in early stages of manned spaceflight, Vostok and Mercury flights, and Mars exploration
[NASA-TT-F-14916] 14 p1709 N73-23867
Procedures for simulating and studying effects of subgravity on subjects during laboratory experiments and space flight
[NASA-TT-F-14934] 15 p1761 N73-24267
Soviet bloc research in astronomy, meteorology, oceanography and space science Aug. 1973
[JPRS-59673] 20 p2473 N73-29861
Soviet block research in astronomy meteorology, geology, and space science Aug. 1973
[JPRS-59789] 20 p2473 N73-29863
Schedule of NASA space missions through 1991
[NASA-TM-X-64739] 20 p2488 N73-29984
Scheduling of work-rest cycle for cosmonauts during space flights
22 p2618 N73-30984
Soviet bloc research in astronomy, meteorology, oceanography, geology, and space science - September 1973
[JPRS-60035] 22 p2716 N73-31740

**SPACE FLIGHT FEEDING**
Analysis of nutrient intake and absorption during Apollo 16 flight
[NASA-TM-X-58096] 03 p0260 N73-12110
Space rations and menus developed for Skylab missions
[NASA-CR-128910] 14 p1614 N73-23080

**SPACE FLIGHT STRESS**
Dynamic changes in psychophysiological motor efficiency of cosmonauts in flight
[JPRS-57417] 01 p0019 N73-10144
Effect of space flight on origin, physiological function, and amelioration of coriolis illusion in semicircular canal
[AMRU-R-70-6] 02 p0131 N73-11063
Analysis of cosmonaut emotional stress as determined by physiological and behavioral responses
[NASA-TT-F-14654] 03 p0261 N73-12113
Regulation of vertical posture after Soyuz 6, 7, and 8 flights and after 120-day bed rest experiment
07 p0744 N73-16052

Conference on human endocrine secretions and hormone metabolisms during space flight stress
[NASA-TM-X-58093] 09 p0993 N73-18104
Measurements of endocrine metabolic responses to space flight stress on Apollo 14 and Apollo 15 crewmen
09 p0993 N73-18105
Measurement of antidiuretic hormone excretions in human urine as indication of neurosecretory stress response during space flight
09 p0993 N73-18108
Human adrenocorticotropin level measurements as indication of adaptation to space flight stress
09 p0993 N73-18109
Pharmacological measures for prophylactic and restorative treatment of men and animals during space flight
11 p1239 N73-20060
Scientific and engineering studies for Physiology of Chimpanzees in Orbit Program
[NASA-CR-131374] 11 p1248 N73-20129
Physiological stress effects of space flight on human body
[JPRS-57139] 13 p1481 N73-22002
Long term physiological testing of submerged subjects to simulate weightless conditions for space flight
[NASA-TT-F-14884] 13 p1505 N73-22195
Research activities in exobiology and aerospace medicine
[JPRS-59015] 14 p1607 N73-23024
Conference on Apollo 16 experiment for measuring microbial response to space environment
[NASA-TM-X-58103] 15 p1740 N73-24102
Physiological responses of parasitic worms and their larvae to solar ultraviolet irradiation and space flight stress
15 p1740 N73-24106
Space vacuum and solar ultraviolet irradiation effects on survival of Bacillus subtilis spores
15 p1740 N73-24108
Phytological and physiological problems caused by rest-work cycles of cosmonauts during space flight
[NASA-TT-F-14990] 17 p1990 N73-26093
Human hydroxycorticosteroid and aldosterone excretions during hypodynamic space flight conditions
20 p2367 N73-29031
Rhythm disturbances in sleep and wakefulness cycles of Soyuz 3 and 9 crews before, during, and after space flight
[NASA-TT-F-15103] 20 p2369 N73-29048

**SPACE GLIDERS**
U LIFTING REENTRY VEHICLES

**SPACE LABORATORIES**
NT MANNED ORBITAL LABORATORIES
NT MANNED ORBITAL RESEARCH LABORATORIES
Congressional hearing to establish national science policy and priorities act of 1972
03 p0367 N73-12991
Payload definition and integration study to establish planning concepts for life sciences spacecraft laboratories - Vol. 1
[NASA-CR-124411] 23 p2849 N73-32765
Life sciences payload definition and integration study to show design of space laboratory for space shuttle and cost analysis of project - Vol. 2
[NASA-CR-124412] 23 p2849 N73-32766
Research equipment requirements for space laboratory concepts involved in conducting life sciences experiments in space - Vol. 3
[NASA-CR-124414] 23 p2849 N73-32767
Specification catalog to identify test equipment for use in conducting life sciences experiments aboard space laboratory - Vol. 4
[NASA-CR-124413] 23 p2849 N73-32768
Development and characteristics of advanced technology laboratory for use with space shuttle concept
[NASA-TM-X-2813] 23 p2851 N73-32781

**SPACE LAW**
Political, legal, and international management of space data and space programs
04 p0474 N73-13871
Information system for space law
[NASA-CR-130746] 08 p0976 N73-17986
Television broadcasting and communication systems using communication satellites, noting space law and regional coverage
23 p2757 N73-32068
Utilization of extra-atmospheric space
[NASA-TT-F-15118] 24 p2980 N73-33818

**SPACE LOGISTICS**
Analysis of space tug operating techniques and requirements to include engineering support, off-site facility requirements, and checkout procedures
[NASA-CR-129163] 02 p0232 N73-11887
Appendices to support findings of Orbiting Propellant Depot Safety study - Vol. 3
[NASA-CR-123383] 03 p0254 N73-12058

**SPACE MAINTENANCE**
Analysis of space tug operating techniques and requirements to include engineering support, off-site facility requirements, and checkout procedures
[NASA-CR-129163] 02 p0232 N73-11887
Remote control manipulator for space maintenance
[DGLR-PAPER-72-098] 06 p0722 N73-15888
Findings and data products developed during crew interface specification study for inflight maintenance and stowage functions in future manned space flights
[NASA-CR-128685] 07 p0849 N73-16878
Sophisticated maintenance of orbital space vehicles with application of remotely controlled telemanipulation concept
[NASA-TT-F-14804] 08 p0965 N73-17885

**SPACE MANUFACTURING**
NASA MS/MS program for manufacturing materials during space shuttle missions
04 p0473 N73-13860
Preparation of solid homogeneous materials in space
04 p0473 N73-13861
Space manufacturing of biological and electronic materials
04 p0473 N73-13862
Extraterrestrial space for supplying earth with vanishing minerals, materials, and needed electric power
04 p0473 N73-13863
Analysis of materials, processing criteria, processing techniques, and apparatus for preparation of composite materials in space
[NASA-CR-124172] 11 p1307 N73-20609
Preflight, inflight, and post flight operations evaluation analyses for Skylab metals melting experiment facility - Appendix F
[NASA-CR-61386-APP-F] 14 p1708 N73-23860
Preflight, inflight, and post flight operations evaluation analyses for Skylab exothermic brazing experiment facility - Appendix G
[NASA-CR-61386-APP-G] 14 p1708 N73-23861
Preflight, inflight, and post flight operations evaluation analyses for Skylab sphere forming experiment facility - Appendix H
[NASA-CR-61386-APP-H] 14 p1708 N73-23862
Liquid-solid transition for materials processing in space
[NASA-CR-124294] 18 p2179 N73-27596
Physical phenomena related to crystal growth in space environment
[NASA-CR-2281] 18 p2189 N73-27677
Development and employment of orbital space stations to conduct earth resources surveys and provide space manufacturing facilities
[JPRS-59650] 18 p2199 N73-27754
Sound beams for position control during manufacturing in space
[NASA-CR-124300] 19 p2321 N73-28671
Characteristics of single crystals of metals with melting points and effects of crystal growth under zero-gravity conditions
[NASA-CR-124354] 20 p2432 N73-29532
Performed investigations and results on composite materials in space
[NASA-CR-124365] 21 p2562 N73-30542
Application of acoustic transducers for suspending object at center of chamber under near weightless conditions
[NASA-CASE-NPO-13263-1] 22 p2677 N73-31443

**SPACE MECHANICS**
NT CELESTIAL MECHANICS
NT MINIMUM VARIANCE ORBIT DETERMINATION
NT ORBITAL MECHANICS

**SPACE MISSIONS**
Control and display sequences for four space shuttle orbiter mission phases - Vol. 4
[NASA-CR-128579] 01 p0019 N73-10148
Tables of data on artificial satellites launched during period 1957 to 1971 to include chronology of manned space flight and emission frequencies of various satellites
[F-22] 01 p0107 N73-10885
Development of abort sequence trees for reference zirconium hydride reactor power module for each phase of space base program mission - Vol. 3 Pt. 2A
[NASA-CR-123845] 02 p0209 N73-11698
Development of long range plan for solar system exploration to define space missions, equipment, and trajectories for interplanetary flight
[NASA-CR-129132] 02 p0226 N73-11823
Definition of requirements for flight simulator to provide space shuttle systems and space mission analysis and performance - Vol. 1
[NASA-CR-128621] 02 p0229 N73-11860
Development of requirements for space shuttle vehicle and mission simulation - Vol. 2
[NASA-CR-128622] 02 p0230 N73-11861
Analysis of space shuttle systems and space shuttle mission requirements for development of mission simulator - Vol. 3
[NASA-CR-128623] 02 p0230 N73-11862
Analysis of external interfaces, crew procedures, visual cues, and aural cues for space shuttle vehicle and mission simulation - Vol. 4
[NASA-CR-128624] 02 p0230 N73-11863
Executive summary of advanced missions safety study involving space shuttle rescue capability, experiment safety, and emergency crew transfer - Vol. 1
[NASA-CR-129099] 02 p0231 N73-11871
Analysis of space rescue mission capability of Earth Orbit Shuttle and concepts for increasing capability - Vol. 2 Pt. 1
[NASA-CR-129104] 02 p0231 N73-11872
Analysis of emergency crew transfer operations using Earth Orbit Shuttle to determine mission effectiveness and cost requirements - Vol. 2 Pt. 3
[NASA-CR-129102] 02 p0231 N73-11874
Analysis of space shuttle rescue capability based on mission, shuttle configuration and performance, and ground launched ascent and rendezvous time - Vol. 3 Pt. 1
[NASA-CR-129101] 02 p0231 N73-11875
Analysis of hazards involved in transporting experimental equipment on space shuttle and recommended precautionary measures - Vol. 3 Pt. 2
[NASA-CR-129100] 02 p0231 N73-11876
Capabilities of Dynamic Operational Requirements and Cost Analysis Program for space mission planning - Vol. 1
[NASA-CR-129263] 03 p0269 N73-12183
Guide for coding Dynamic Operational Requirements and Cost Analysis Program to show subroutines and flow charts - Vol. 2
[NASA-CR-129264] 03 p0270 N73-12184
Program listing for Dynamic Operational Requirements and Cost Analysis Program to provide space mission planning and project management capability - Vol. 3
[NASA-CR-129265] 03 p0270 N73-12185
Description of functions and capabilities of Dynamic Operational Requirements and Cost Analysis Program - Vol. 4
[NASA-CR-129266] 03 p0270 N73-12186
User guide for Dynamic Operational Requirements and Cost Analysis Program for space mission planning and project management - Vol. 1
[NASA-CR-123378] 03 p0270 N73-12188
Programmer manual for Dynamic Operational Requirements and Cost Analysis Program for space mission planning and project management - Vol. 2
[NASA-CR-123379] 03 p0270 N73-12189
Program listing for Dynamic Operational Requirements and Cost Analysis Program to provide space mission planning and project management capability - Vol. 3
[NASA-CR-123380] 03 p0270 N73-12190
Design and development of zero-gravity atmospheric cloud physics experiment laboratory for installation in orbiting spacecraft
[NASA-CR-128998] 03 p0280 N73-12270
Design and development of space shuttle system for delivering payload to earth orbit or celestial orbit
[NASA-CASE-MSC-12391] 03 p0354 N73-12884
Development of payload for mission planning for missions to outer planets as function of flight time for various launch years, launch vehicles, and orbit sizes
[NASA-CR-129244] 03 p0354 N73-12887
Analysis of asteroids selected for space mission objectives to show significant parameters
[NASA-CR-129248] 03 p0355 N73-12890
Analysis of pointing and stability problems of space shuttle sortie mission and application to earth observation and astronomy experiments
[NASA-TM-X-64692] 03 p0355 N73-12892
Analysis of space program costs and launch vehicle traffic based on either expendable, partially reusable, or fully reusable launch vehicle fleet
[NASA-CR-125847] 03 p0355 N73-12896
Analysis of magnetic field near planet Mars from data obtained by Mars 2 and Mars 3 spacecraft
[NASA-TM-X-66116] 03 p0357 N73-12907
Design requirements for space tug systems and cost analysis of maintenance and operation during space missions
[NASA-CR-129253] 03 p0358 N73-12918
Analysis of Skylab program to show construction of spacecraft, test facilities, personnel accomodations, and research projects
04 p0470 N73-13831
Impact of space shuttle operations on national economy, technological superiority, and development of future space activities
04 p0470 N73-13832
Operations summary and mission planning for IMP-H spacecraft
[NASA-TM-X-68880] 04 p0478 N73-13907
Analysis of economic merits of three alternative space transportation systems for use during 1980 time period - Vol. 3
[NASA-CR-129569] 04 p0487 N73-13979
Tables of data on artificial satellites launched during period 1957 to 1971 to include chronology of manned space flight and emission frequencies of various satellites
[F-23] 05 p0598 N73-14861
Analysis of payloads for space shuttle based on space missions, planetary exploration, and international rendezvous and docking - Vol. 2
[NASA-CR-129844] 05 p0598 N73-14862
Pioneer space probe project to show history, design, development, flight operations, and results accomplished
[NASA-SP-278] 05 p0598 N73-14864

Analysis of operations and resources required to support expendable second stage reusable space shuttle booster - Vol. 5
[NASA-CR-128660] 05 p0599 N73-14871
Development of concept of space shuttle orbiter/tug orbital insertion and application to specific space missions
[NASA-TM-X-64715] 06 p0718 N73-15862
Effect of Apollo project accomplishments on earth resources surveys and conduct of earth resources investigations in future space missions
07 p0781 N73-16349
Analysis of earth resources based on mapping, human needs, minerals, water, and food and contributions made by remote sensing satellites
07 p0781 N73-16350
Objectives of NASA Earth Resources Survey Program to include types of sensors used and data acquired by aircraft, spacecraft, and ground observations
07 p0782 N73-16351
Analysis of NASA Earth Resources Program to include ERTS satellites, Skylab program, and earth resources survey aircraft
07 p0782 N73-16359
Launch vehicle estimating factors for planning advanced solar system and earth orbital missions
[NHB-7100.5B] 07 p0847 N73-16866
Investigation of solar electric propulsion as method for exploring space beyond reach of ballistic missions - Vol. 1
[NASA-CR-130701] 08 p0954 N73-17811
Analysis of space shuttle capability as launch vehicle for delivery of payloads into earth orbit
[NASA-TM-X-68859] 08 p0965 N73-17889
Mission description and system design for Large Space Telescope used on unmanned satellites - Vol. 2
[NASA-TM-X-64726-VOL-2] 09 p1036 N73-18450
Scientific space mission of small spin stabilized astronomical satellite with X ray and IR experiments
09 p1081 N73-18817
Payload deployment aspects of control system optimization of spacecraft maneuvers involved in stationkeeping and docking - Vol. 1
[NASA-CR-124050] 09 p1086 N73-18860
Tracking and data system support of launch, near-earth, and deep space phases of Pioneer 10 space probe flight
[NASA-CR-131373] 11 p1256 N73-20188
Proceedings of conference on economic aspects of space shuttle system to show basis for cost effectiveness determinations and system selection
[NASA-CR-131421] 11 p1337 N73-20848
Design, functional operation, and recommended expansion and enhancements for Space Ultrareliable Modular Computer interpretive simulator
[NASA-CR-124202] 12 p1380 N73-21194
Hardware manual for Space Ultrareliable Modular Computer-Demonstration Vehicle including assembly, physical and basic electrical tests
[NASA-CR-124205] 12 p1380 N73-21195
Description of Apollo 16 flight
12 p1448 N73-21731
Development of computerized multistage failure process simulation to evaluate risk in solar electric space mission
[NASA-CR-131518] 12 p1457 N73-21813
Analysis of NASA programs for 1970 to 1980 period with application to earth orbital experiment program and requirements - Vol. 1
[NASA-CR-112325] 13 p1577 N73-22778
Analysis of manned space flight capability development for support of earth orbital experiment program and requirements - Vol. 2
[NASA-CR-112326] 13 p1577 N73-22779
Analysis of space biology projects related to earth orbital experiment program to identify critical issues and methods of conducting experiments - Vol. 3
[NASA-CR-112327] 13 p1577 N73-22780
Development of space astronomy projects identified during orbital experiment program and requirements study - Vol. 4
[NASA-CR-112328] 13 p1577 N73-22781
Earth observation experiments identified during earth orbital experiment program and requirements study - Vol. 6
[NASA-CR-112330] 13 p1577 N73-22783
Definition of supporting technology development requirements for earth orbital experiment program and requirements study - Vol. 7
[NASA-CR-112331] 13 p1577 N73-22784
Data management systems, instrumentation concepts, and biotechnology laboratory for earth orbital experiment program and requirements study - Vol. 8
[NASA-CR-112332] 13 p1577 N73-22785
Operational and engineering aspects of Apollo 17 lunar landing mission
[NASA-TM-X-69292] 14 p1706 N73-23844
Analysis of major problems in early stages of manned spaceflight, Vostok and Mercury flights, and Mars exploration
[NASA-TT-F-14916] 14 p1709 N73-23867
Performance of solar electric propulsion modules for out of ecliptic and cometary missions of Europa 3
15 p1826 N73-24804
Achievements in space exploration to include spacecraft design, planetary composition, lunar missions, and predicted space accomplishments
[NASA-TT-F-737] 15 p1830 N73-24829
Characteristics of ring system around planet Saturn and sequence of space missions to acquire data on ring system composition
[NASA-CR-132952] 15 p1831 N73-24841
Numerical analysis of space navigation parameters for interplanetary Mars spacecraft based on equations of motion of spacecraft
[NASA-TT-F-14897] 16 p1940 N73-25704
Consolidation of navigation and guidance for space shuttle vehicles for all phases of space mission - Document 21
[NASA-CR-128961] 16 p1941 N73-25708
Analysis of requirements for unmanned spacecraft mission to planet Mars and characteristics of lander vehicles for planetary exploration - Vol. 3
[NASA-CR-132258] 16 p1962 N73-25875
Apollo 17 flight plan for prelaunch checkout support and continuous support to be provided during mission - Revision A
[NASA-TM-X-69530] 17 p2083 N73-26853
Development and employment of orbital space stations to conduct earth resources surveys and provide space manufacturing facilities
[JPRS-59650] 18 p2199 N73-27754
Evaluation of Skylab program experiments involving contamination measurement, photometer, and gegenschein zodiacal light
[NASA-CR-61386] 18 p2200 N73-27760
Mission definition and analysis for manned earth observatory based on projected technology for 1980 time period - Vol. 2
[NASA-CR-124340] 19 p2343 N73-28847
Conceptual design of earth observation facility to include sensor payload, crew functions and accomodations, and common core equipment - Vol. 3
[NASA-CR-124338] 19 p2343 N73-28848
Schedules, costs, requirements, and equipment for manned earth observatory missions - Vol 4
[NASA-CR-124339] 19 p2343 N73-28849
Design, development, and application of 10,000 watt solar array panel for application to three possible space missions and review of solar cell technology
[NASA-CR-133616] 20 p2363 N73-29006
Design analysis and tradeoff studies for defining Astronomy Sortie Mission based on mission requirements and payload limitations - Vol. 3 Bk. 1
[NASA-CR-124047] 20 p2473 N73-29870
Design analysis and trade studies to support candidate configurations and payloads for Astronomy Sortie Missions - Vol. 3 Bk. 2
[NASA-CR-124044] 20 p2474 N73-29871
Program development requirements for selected Astronomy Sortie Missions concept to show rationale and explanations of guidelines and assumptions - Vol. 4
[NASA-CR-124046] 20 p2474 N73-29872
Soviet space exploration and research during 1972
[JPRS-59778] 20 p2488 N73-29983
Congressional hearings to review NASA program accomplishments and to predict advantages to accrue from space programs
21 p2609 N73-30916
Payload carrier integrated test for simulated Sortie Lab Missions
[NASA-TM-X-64770] 22 p2647 N73-31207
Apollo experience report on process of crew procedures development for systems procedures and flight procedures
[NASA-TN-D-7436] 22 p2721 N73-31772
Apollo experience report on various phases of post-flight testing of command modules to resolve or minimize anomalies discovered during flight
[NASA-TN-D-7435] 22 p2721 N73-31773
Projected space missions to comets and scientific goals
22 p2735 N73-31899
Mariner 9 missions operations summary
23 p2844 N73-32725
Life sciences payload definition and integration study to show design of space laboratory for space shuttle and cost analysis of project - Vol. 2
[NASA-CR-124412] 23 p2849 N73-32766
Research equipment requirements for space laboratory concepts involved in conducting life sciences experiments in space - Vol. 3
[NASA-CR-124414] 23 p2849 N73-32767
Payload and scientific mission of German aeronomy satellite AEROS
[NASA-TT-F-15104] 23 p2850 N73-32779
Development and characteristics of advanced technology laboratory for use with space shuttle concept
[NASA-TM-X-2813] 23 p2851 N73-32781
Technique for determining fuel optimal, impulsive, fixed time trajectories based on comparison of two neighboring trajectories with application to ascent rendezvous
24 p2978 N73-33799
Performance evaluation of SA-206 launch vehicle for Skylab 2 launch to show significant events and failures and anomalies
[NASA-TM-X-69538] 24 p2981 N73-33820
Performance evaluation of SA-207 launch vehicle for Skylab 3 launch to show significant events and failures and anomalies
[NASA-TM-X-69540] 24 p2981 N73-33821
Evaluation of launch vehicle, spacecraft, and lunar rover performance during Apollo 17 flight to determine malfunctions and recommend corrective actions
[NASA-TM-X-69534] 24 p2981 N73-33822
Postflight analysis of Apollo 16 flight to show spacecraft performance, launch vehicle performance, and malfunctions occuring during flight
[NASA-TM-X-69535] 24 p2981 N73-33823
Postflight analysis of Apollo 14 flight to show spacecraft performance, launch vehicle performance, and malfunctions occurring during flight
[NASA-TM-X-69536] 24 p2981 N73-33824
Application of skill requirement method for determining skills required of on-orbit crew personnel performing earth-orbital research
[NASA-CR-124452] 24 p2982 N73-33830
Design, development, and fabrication of prototype storage module with internal restraints for stowage of items launched to support space missions
[NASA-CR-124465] 24 p2983 N73-33832

**SPACE NAVIGATION**

Evaluation of five candidate navigation systems for earth orbit missions
[NASA-CR-128582] 01 p0102 N73-10846
Comparison of open and closed loop applications of second order guidance algorithm using minimum distance strategy for Earth-Mars transfer
[NASA-CR-129170] 02 p0227 N73-11830
Manual space navigation research projects conducted by US Air Force in support of Skylab project
[AD-747479] 03 p0329 N73-12683
Momentum wheel design for spacecraft attitude control and magnetic drum and head system for data storage
[NASA-CASE-NPO-11481] 04 p0446 N73-13644
Astronomical techniques for spacecraft orientation
05 p0577 N73-14694
Characteristics of inertial guidance systems to include minimizing of errors, forces on electrostatic gyroscope, and parameters of electromagnetic load cell
[JPRS-57746] 06 p0695 N73-15664
Analysis of lateral velocity measurement errors of inertial guidance system and development of system to compensate for errors
06 p0695 N73-15665
Guidance, navigation and control system analysis report for Apollo 15
[NASA-TM-X-68934] 06 p0696 N73-15673
Guidance, navigation, and control system performance analysis report for Apollo 16 mission
[NASA-TM-X-68931] 06 p0696 N73-15674
Spacecraft control over segment of atmospheric reentry trajectory using on-board computers to preclude deflection beyond atmosphere
[AD-750520] 06 p0719 N73-15871
Computerized simulation of approach navigation accuracy and guidance requirements for 1977 Grand Tour mission to outer planets
08 p0941 N73-17707
Method for producing reticles for use in outer space
[NASA-CASE-GSC-11188-2] 10 p1184 N73-19630
Evaluation of ultraviolet flux from stars used as inertial-hold pointing directions during Apollo 17 flight
[NASA-CR-128834] 10 p1213 N73-19866
Conceptual designs for manned, space shuttle sortie mission laboratory for communications and navigation experiments - Vol. 1 - Exec. Summary
[NASA-CR-124136] 11 p1266 N73-20273
Selection and definition of candidate experiments and associated instrumentation requirements for space shuttle communication/navigation experiments laboratory - Vol. 2
[NASA-CR-124137] 11 p1266 N73-20274
Proceedings of conference on inertial navigation components and systems with emphasis on concepts and techniques involving cost and performance tradeoffs
[AGARD-CP-116] 11 p1316 N73-20684
Development of space communications and navigation projects involved in earth orbital experiment program and requirements study - Vol. 5
[NASA-CR-112329] 13 p1577 N73-22782
Apollo experience report on engineering simulation in support of Apollo guidance and control system
[NASA-TN-D-7287] 15 p1835 N73-24873
Numerical analysis of space navigation parameters for interplanetary Mars spacecraft based on equations of motion of spacecraft
[NASA-TT-F-14897] 16 p1940 N73-25704
Procedure for aligning inertial reference unit of space shuttle by celestial references - Document 20
[NASA-CR-128964] 16 p1941 N73-25706
Analysis of inflight performance of Apollo 13 spacecraft guidance, navigation, and control equipment
[NASA-TM-X-69528] 17 p2060 N73-26666
Guidance and navigation error analysis for Skylab 3
[NASA-CR-133997] 21 p2576 N73-30642

Stellar-inertial measurement system trade study on spacecraft orbital ephemeris and attitude errors for landmark location
[NASA-CR-134042] 24 p2984 N73-33845
SPACE PERCEPTION
Bayesian model for stimuli processing in visual space perception
01 p0016 N73-10127
Operator visual perception mapping during parameter adjustment in dynamic control system
01 p0017 N73-10129
Measurements of automobile driver response functions in simulated steering control task with visual field display
01 p0017 N73-10130
Motion cue effects on pilot manual control tracking task
01 p0018 N73-10141
Training procedure for improving divers distance estimation ability in clear and turbid water
[AD-752976] 10 p1121 N73-19140
Improving distance under water and long-term effectiveness of training
[AD-752979] 16 p1869 N73-25128
Differences in speed of mentally processing displays containing information about right and left
[AD-759723] 17 p1988 N73-26070
Factors affecting stereoscopic vision and depth perception in human beings
[AD-759261] 20 p2369 N73-29050
Infrared sensitive television camera for horizon and depth perception in whiteout
[DREO-TN-73-11] 23 p2791 N73-32332
SPACE PHOTOGRAPHY
U SPACEBORNE PHOTOGRAPHY
SPACE POWER REACTORS
NT SNAP 8
NT SNAP 10A
NT SPACE POWER UNIT REACTORS
Performance and cost effectiveness of isotope Brayton space power system
[NASA-TM-X-68145] 06 p0626 N73-15081
Research and development program with space electric power systems
[LA-4690] 11 p1238 N73-20046
Design of split-core heat-pipe radioisotopic reactor for space power applications
[NASA-TM-X-68254] 16 p1943 N73-25722
Evaluation of fuel pin design concepts for fast spectrum lithium cooled compact space power reactor
[NASA-CR-121181] 18 p2178 N73-27584
Design and performance modeling of liquid metal reactor thermoelectric space power system
[NASA-CR-121241] 19 p2320 N73-28661
Cryocooling and electric capacity of refrigerator/electric generator space power unit
[NASA-TM-X-71433] 23 p2748 N73-31992
Reactivity change in fast spectrum space power reactor due to 328 meter/sec impact
[NASA-TM-X-2886] 23 p2818 N73-32532
Molybdenum reflector reactivity and space power reactor control
[NASA-TM-X-2922] 23 p2819 N73-32533
SPACE POWER UNIT REACTORS
Effects of backlash and dead band on temperature control of primary loop of conceptual nuclear Brayton space powerplant
[NASA-TM-X-2754] 09 p1064 N73-18679
UC-ZrC fuel elements for space power reactor system
[GULF-GA-A-11073] 12 p1428 N73-21571
Chemical compatibility of materials used for lithium cooled space power reactor concept at high temperature
[NASA-TN-D-7259] 15 p1809 N73-24660
Neutronic feasibility of fast spectrum space power reactor design concepts using boron control devices
[NASA-TM-X-2821] 16 p1943 N73-25720
Lithium hydride and depleted uranium shield materials for space power nuclear reactor
[NASA-TM-X-2835] 18 p2177 N73-27580
SPACE PROBES
NT EXPLORER 18 SATELLITE
NT JUPITER PROBES
NT LUNAR PROBES
NT LUNIK 16 LUNAR PROBE
NT LUNIK 20 LUNAR PROBE
NT MARINER SPACE PROBES
NT MARINER SPACECRAFT
NT MARINER VENUS-MERCURY 1973
NT MARINER 3 SPACE PROBE
NT MARINER 7 SPACE PROBE
NT MARINER 9 SPACE PROBE
NT MARS PROBES
NT MARS 2 SPACECRAFT
NT PIONEER SPACE PROBES
NT PIONEER 6 SPACE PROBE
NT PIONEER 8 SPACE PROBE
NT PIONEER 9 SPACE PROBE
NT PIONEER 10 SPACE PROBE
NT PIONEER 11 SPACE PROBE
NT RANGER LUNAR PROBES
NT RANGER 7 LUNAR PROBE
NT RANGER 9 LUNAR PROBE
NT SOLAR PROBES
NT SURVEYOR LUNAR PROBES
NT SURVEYOR 3 LUNAR PROBE
NT VENERA SATELLITES
NT VENERA 8 SATELLITE
NT VENUS PROBES
NT VIKING MARS PROGRAM
Feasibility study for laser transponder onboard SOREL space probe
[ESRO-CR[P]-123] 02 p0149 N73-11207
Development of long range plan for solar system exploration to define space missions, equipment, and trajectories for interplanetary flight
[NASA-CR-129132] 02 p0226 N73-11823
Simulation control of European SOREL space probe attitude and position
[S-3-1949-VOL-3] 02 p0235 N73-11907
Threshold of accelerometer and drag free probe detector
[ONERA-NT-199] 04 p0423 N73-13448
Evaluation of solar wind data obtained from Pioneer 6, Mariner 5, and Explorer 35 for velocity variations, magnetopause motion, and geomagnetic disturbances
[NASA-CR-129880] 05 p0591 N73-14806
Cost effectiveness and mission value comparisons of three propulsion systems for delivery of advanced probe spacecraft
[NASA-TM-X-2751] 09 p1079 N73-18802
Scientific aspect of interplanetary investigation by Helios satellite
[DGLR-PAPER-72-068] 09 p1085 N73-18853
Design criteria for SOREL drag-free space probe discussing attitude control and orbital position estimation
[S-3-1949-VOL-1/2] 09 p1091 N73-18904
Spacecraft pressure gage reliability studies relative to gas dynamics and metal surface testing
[NASA-CR-112320] 13 p1529 N73-22392
Sensitivity of low weight CPNE for planetary composition analysis
[NASA-CR-132208] 17 p2032 N73-26448
SPACE PROGRAMS
NT APOLLO PROJECT
NT EUROPEAN SPACE PROGRAMS
NT FRENCH SPACE PROGRAMS
NT GEOGRAPHIC APPLICATIONS PROGRAM
NT SURVEYOR PROJECT
NT TEKTITE PROJECT
NT U.S.S.R. SPACE PROGRAM
Contributions of science and technology to success of US as world leader
04 p0470 N73-13835
Impact of space program on efforts to improve standards of living and to reduce harmful pollution of environment
04 p0471 N73-13836
Contributions of astronomy to understanding solar system and initiating manned space flight and exploration
04 p0471 N73-13837
Political, legal, and international management of space data and space programs
04 p0474 N73-13871
Development of facility for determining satellite payloads
05 p0523 N73-14257
Analysis of earth resources based on mapping, human needs, minerals, water, and food and contributions made by remote sensing satellites
07 p0781 N73-16350
Possible reduction of NASA payload costs
[NASA-TM-X-62223] 07 p0844 N73-16835
Solar observation and research using rocket-borne instruments, in German programs
[BMBW-FBW-72-27] 07 p0846 N73-16862
Organization and management methods for space programs in Germany
[DGLR-PAPER-72-052] 09 p1101 N73-18990
Presidential report on progress and activities of various aerospace programs in 1972 and comments on future mission planning
11 p1352 N73-20975
Reference to aerospace-related events for 1970
[NASA-SP-4015] 14 p1705 N73-23833
NASA participation in international space programs
[NASA-TM-X-69259] 15 p1846 N73-24957
History of NASA
[NASA-NEWS-RELEASE-73-134]
18 p2213 N73-27868
Objectives and accomplishments of geosynchronous platform definition study
[NASA-CR-133968] 19 p2345 N73-28860
Program results and supporting data obtained in geosynchronous platform definition study
[NASA-CR-133969] 19 p2345 N73-28861
Mission characteristics data compiled in geosynchronous platform definition study
[NASA-CR-133970] 19 p2345 N73-28862
Baseline traffic model resulting from traffic analysis and system requirements data generated in geosynchronous platform definition study
[NASA-CR-133971] 19 p2345 N73-28863
Traffic analysis and system requirements for new traffic model developed in geosynchronous platform definition study
[NASA-CR-133972] 19 p2345 N73-28864
Platform configurations, support subsystems, mission equipment, and servicing concepts generated in geosynchronous platform definition study
[NASA-CR-133973] 19 p2345 N73-28865
Program evaluation and recommendations of geosynchronous platform definition study
[NASA-CR-133974] 19 p2345 N73-28866
Interfaces between space platforms and space transportation system established in geosynchronous platform definition study
[NASA-CR-133975] 19 p2345 N73-28867
Engineering safety in space programs
[NASA-TT-F-15077] 22 p2721 N73-31777
Space applications research in astronomy and earth physics
[NASA-SP-331] 22 p2732 N73-31867
Utilization of extra-atmospheric space
[NASA-TT-F-15118] 24 p2980 N73-33818
Relationships between performance, safety, cost, and schedule parameters to generate program models for total space program
[NASA-CR-135903] 24 p2993 N73-33919
Relationships between performance, safety, cost, and schedule parameters to generate program models for total space program
[NASA-CR-135902] 24 p2993 N73-33920
SPACE RADIATION
U EXTRATERRESTRIAL RADIATION
SPACE RADIATORS
U SPACECRAFT RADIATORS
SPACE RATIONS
Space rations and menus developed for Skylab missions
[NASA-CR-128910] 14 p1614 N73-23080
SPACE RENDEZVOUS
NT LUNAR ORBITAL RENDEZVOUS
NT ORBITAL RENDEZVOUS
HILTOP - variational calculus program for generating electric propulsion data on rendezvous missions to comet Encke
[NASA-CR-114491] 01 p0104 N73-10857
Analysis of asteroids selected for space mission objectives to show significant parameters
[NASA-CR-129248] 03 p0355 N73-12890
Dynamic testing for determining flight readiness of Apollo docking system hardware
09 p1089 N73-18885
Development of computerized multistage failure process simulation to evaluate risk in solar electric space mission
[NASA-CR-131518] 12 p1457 N73-21813
Apollo experience report on evolution of rendezvous maneuver plan for lunar landing missions
[NASA-TN-D-7388] 20 p2475 N73-29882
Technique for determining fuel optimal, impulsive, fixed time trajectories based on comparison of two neighboring trajectories with application to ascent rendezvous
24 p2978 N73-33799
SPACE RENDEZVOUS MANEUVERS
U SPACE RENDEZVOUS
U SPACECRAFT MANEUVERS
SPACE SCIENCES
U AEROSPACE SCIENCES
SPACE SHUTTLE BOOSTERS
Effect of air precooling before compression on propulsive efficiency of liquid hydrogen turbojet engine with afterburning for space shuttle
[DGLR-PAPER-72-60] 04 p0464 N73-13785
Design, development, and characteristics of expendable second stage for use with reusable space shuttle booster - Vol. 1
[NASA-CR-128671] 05 p0598 N73-14865
Definition of system for expendable second stage and reusable space shuttle booster system - Vol. 2 - Bk. 1
[NASA-CR-128670] 05 p0598 N73-14866
Definition of expendable second stage for use with reusable space shuttle booster to include structural, propulsion, and avionics systems design - Vol. 2 - Bk. 2
[NASA-CR-128672] 05 p0599 N73-14867
Definition of expendable second stage and space shuttle booster separation system to include modifications required, ground support equipment, and launch operations - Vol. 2 - Bk. 3
[NASA-CR-128673] 05 p0599 N73-14868
Wind tunnel tests to determine aerodynamic characteristics of expendable second stage and payload configurations for reusable space shuttle booster - Vol. 3
[NASA-CR-128674] 05 p0599 N73-14869
Analysis of mass properties of reusable space shuttle booster and expendable second stage for three specified payloads - Vol. 4
[NASA-CR-128659] 05 p0599 N73-14870
Analysis of operations and resources required to support expendable second stage reusable space shuttle booster - Vol. 5
[NASA-CR-128660] 05 p0599 N73-14871
Definition of major expendable second stage interfaces with specified space shuttle booster components including interface control drawings - Vol. 6
[NASA-CR-128661] 05 p0599 N73-14872

Preliminary design drawings of expendable second stage reusable space shuttle booster to define specific payloads and configurations - Vol. 7
[NASA-CR-128662] 05 p0599 N73-14873
Contract end item specifications for defining hardware end items required by expendable second stage of space shuttle booster system - Vol. 8 Pt. 1
[NASA-CR-128663] 05 p0599 N73-14874
Preliminary system specification for design, operation, and performance of expendable second stage for reusable space shuttle booster - Vol. 9
[NASA-CR-128664] 05 p0599 N73-14875
Analysis of technology requirements for expendable second stage of space shuttle booster system - Vol. 10
[NASA-CR-128665] 05 p0600 N73-14876
Design requirements and data for expendable second stage of reusable space shuttle booster - Vol. 12
[NASA-CR-128667] 05 p0600 N73-14877
Development of procedure for computing normal force, axial force, and pitching moment coefficients with application to space shuttle booster characteristics
[NASA-TN-D-6996] 06 p0614 N73-14988
Application of autopilot techniques to control and stabilize vibration modes of two space shuttle configurations at liftoff flight condition
[NASA-CR-112202] 06 p0721 N73-15884
Empirical data on probable sea state conditions to be encountered by space shuttle booster recovery forces
[NASA-TM-X-68631] 07 p0792 N73-16440
Analysis and design study of solid rocket motor for space shuttle booster
[NASA-CR-124002] 07 p0835 N73-16769
Design and development of low pressure auxiliary propulsion system for space shuttle orbiter and booster
[NASA-CR-130796] 09 p1078 N73-18796
Parametric studies of space shuttle booster, orbiter and launch vehicle concepts
[NASA-CR-124090] 09 p1086 N73-18862
Wind tunnel tests to determine pressure distribution on space shuttle launch configuration consisting of delta wing orbiter and swept wing booster - Vol. 1 Pt. A
[NASA-CR-120034-VOL-1-PT-A] 11 p1342 N73-20891
Wind tunnel tests to determine pressure distribution on space shuttle launch configurations consisting of delta wing orbiter and swept wing booster - Vol. 1 Pt. B
[NASA-CR-120034-VOL-1-PT-B] 11 p1342 N73-20892
Wind tunnel tests to determine pressure distribution on space shuttle launch configuration consisting of space shuttle orbiter in presence of booster - Vol. 2
[NASA-CR-120034-VOL-2] 11 p1342 N73-20893
Wind tunnel tests to determine heat transfer properties of space shuttle orbiter, booster, and launch configurations for various angles of attack and yaw
[NASA-CR-128891] 12 p1460 N73-21830
Gas dynamic simulation of plumes from orbiter propulsion system for determining power-on aerodynamic flight characteristics of orbiter
[NASA-CR-124217] 13 p1581 N73-22814
Quantitative tests of space shuttle booster recovery in open seas
[NASA-TM-X-69273] 16 p1965 N73-25892
Analysis and design of closed loop control for slowly time-varying linear systems for space shuttle booster
[NASA-CR-128972] 16 p1966 N73-25905
Technical requirements of solid propellant rocket engine for application to space shuttle booster - Vol. 2 Bk. 1
[NASA-CR-123729] 20 p2465 N73-29805
Analysis of solid propellant rocket engine requirements for space shuttle booster application - Vol. 1
[NASA-CR-124236] 20 p2467 N73-29820

**SPACE SHUTTLE ORBITERS**

Utilization of simplified man machine interface concept to manage and control complex space system involving multiple redundant computers that control multiple redundant systems - Vol. 1
[NASA-CR-128576] 01 p0019 N73-10145
Space shuttle orbiter subsystems and control and display data required for crew operations - Vol. 2
[NASA-CR-128577] 01 p0019 N73-10146
Space shuttle orbiter subsystems, formats and format trees, and coding of sample format - Vol. 3
[NASA-CR-128578] 01 p0019 N73-10147
Control and display sequences for four space shuttle orbiter mission phases - Vol. 4
[NASA-CR-128579] 01 p0019 N73-10148
Design and fabrication of honeycomb resin-composite sandwich panels for shuttle orbiter thermal shielding
[NASA-CR-128610] 01 p0061 N73-10503
Comparison of longitudinal and lateral stability and control characteristics of Phase B Grumman H-33 space shuttle orbiter
[NASA-CR-120080] 01 p0108 N73-10889
Comparison of longitudinal and lateral stability and control characteristics of baseline 040A space shuttle orbiter
[NASA-CR-120081] 01 p0109 N73-10894
Space shuttle orbiter guidance and control software functions for horizontal flight operations
[NASA-TM-X-68857] 02 p0207 N73-11682
Wind tunnel tests to determine lee surface flow characteristics and aerodynamic heating of space shuttle orbiters at supersonic speed with large angles of attack
[NASA-TN-D-7088] 02 p0233 N73-11890
Wind tunnel tests of scale model of orbiter 040A configuration in ground effect
[NASA-CR-120082] 02 p0233 N73-11895
Methodology for combining thermal structural loads as design criteria for thermal protection system of space shuttle orbiter
[NASA-CR-2102] 02 p0234 N73-11898
Calculation of optimal gliding flight paths associated with space shuttle orbiter transition from entry to cruising flight
[NASA-CR-128647] 03 p0359 N73-12922
Wind tunnel results of static stability and control effectiveness of shuttle orbiter
[NASA-CR-120070] 03 p0359 N73-12923
High temperature insulation materials for reradiative thermal protection system of shuttle orbiter vehicle
[NASA-CR-123945] 03 p0363 N73-12957
Design study of arresting gear system for recovery of space shuttle orbiters
[NASA-TM-X-68881] 04 p0401 N73-13265
Data dump of space shuttle orbiter maneuvering engine performance, weight, envelope, and interface pressure requirements for propellant combinations
[NASA-CR-128675] 04 p0464 N73-13784
Organizational and decision processes for determining essential scheduled maintenance requirements for space shuttle orbiter
[NASA-TM-X-69004] 04 p0478 N73-13908
Calculation of heat transfer on shuttle type configurations including effects of variable entropy at boundary layer edge
[NASA-CR-112180] 04 p0484 N73-13958
Wind tunnel tests to determine subsonic aerodynamic characteristics of model of space shuttle orbiter configuration with swept trapezoidal wing and swept fixed glove
[NASA-TM-X-2701] 05 p0491 N73-14005
Wind tunnel tests to determine pressure distribution on wing and lower body surface for space shuttle orbiter in launch configuration
[NASA-CR-120075] 05 p0600 N73-14879
Procurement specification for space shuttle orbiter windshield pane and factors influencing development
[NASA-CR-112209] 05 p0600 N73-14882
Development of concept of space shuttle orbiter/tug orbital insertion and application to specific space missions
[NASA-TM-X-64715] 06 p0718 N73-15862
Development and testing of primary structural elements of windshield system for space shuttle orbiter
[NASA-CR-112234] 06 p0720 N73-15879
Application of autopilot techniques to control and stabilize vibration modes of two space shuttle configurations at liftoff flight condition
[NASA-CR-112202] 06 p0721 N73-15884
Configuration and requirements for general purpose optical research facility to investigate earth atmosphere from space shuttle orbiter vehicle
[NASA-CR-128732] 08 p0893 N73-17226
Program and technical alternatives to design of space shuttle orbiter to include aerodynamic configurations and predicted performance
[NASA-CR-130747] 08 p0964 N73-17877
Parametric weight analysis of heat rejection systems for environmental control/life support system space shuttle orbiter
[NASA-CR-128735] 08 p0965 N73-17884
Effects of chemical nonequilibrium of inviscid flow in windward plane of symmetry for space shuttle orbiter configurations
[NASA-TN-D-7189] 09 p1015 N73-18287
Techniques and instrumentation for nondestructive testing of high performance multilayer thermal insulation for space shuttle orbiters
[NASA-CR-124106] 09 p1051 N73-18567
Design and development of low pressure auxiliary propulsion system for space shuttle orbiter and booster
[NASA-CR-130796] 09 p1078 N73-18796
Parametric studies of space shuttle booster, orbiter and launch vehicle concepts
[NASA-CR-124090] 09 p1086 N73-18862
Habitability study of shuttle orbiter
[NASA-CR-128863] 10 p1124 N73-19162
Habitability study of shuttle orbiter
[NASA-CR-128864] 10 p1124 N73-19163
Data distribution subsystem for space shuttle orbiters
[NT-SES/11/71/030] 10 p1133 N73-19233
Fatigue test facility for space shuttle orbiters
10 p1138 N73-19273
Cavity resonators for measuring cryogenic propellant content in space shuttle orbiter tanks under weightlessness
10 p1162 N73-19452
Boron-aluminum radiators for space shuttle orbiters
[NASA-CR-128805] 10 p1164 N73-19468
Carbon fiber reinforced metal structures for space shuttles
[SOR-W-13] 10 p1167 N73-19495
Auxiliary propulsion for space shuttle orbiters
[SEP-NT-3054/71-M] 10 p1209 N73-19835
Combined orbital maneuvering and attitude control propulsion system for space shuttles
[MBB-UR-82-71] 10 p1209 N73-19836
Auxiliary propulsion system for space shuttle orbiter
[REPT-D-9/71-MK/DH] 10 p1209 N73-19837
Formulation, evaluation, and demonstration of various procedures for analytically coupling two or more substructures to obtain modal data for assembly
[NASA-CR-112252] 10 p1215 N73-19881
Composite material for cargo door of space shuttle
[R-1525] 10 p1221 N73-19928
Wind tunnel tests of scale model of space shuttle orbiter to determine low subsonic aerodynamic characteristics
[NASA-TM-X-2712] 11 p1232 N73-20000
Problem formulation and numerical procedures for solving flow equations for flow distribution of viscous shock layer on nose of shuttle orbiter during reentry - Vol. 1
[NASA-CR-128871] 11 p1271 N73-20309
Development of computer programs for analyzing flow distribution in nose region of blunt body at arbitrary speed and altitude - Vol. 2
[NASA-CR-128872] 11 p1271 N73-20310
Wind tunnel tests of space shuttle orbiter in various configurations to determine aerodynamic loads and pressure distributions at range of Mach numbers
[NASA-CR-120066] 11 p1342 N73-20890
Wind tunnel tests to determine pressure distribution on space shuttle launch configuration consisting of delta wing orbiter and swept wing booster - Vol. 1 Pt. A
[NASA-CR-120034-VOL-1-PT-A] 11 p1342 N73-20891
Wind tunnel tests to determine pressure distribution on space shuttle launch configurations consisting of delta wing orbiter and swept wing booster - Vol. 1 Pt. B
[NASA-CR-120034-VOL-1-PT-B] 11 p1342 N73-20892
Wind tunnel tests to determine pressure distribution on space shuttle launch configuration consisting of space shuttle orbiter in presence of booster - Vol. 2
[NASA-CR-120034-VOL-2] 11 p1342 N73-20893
Orbital retrieval technology associated with spinning uncooperative satellites
[NASA-CR-131510] 12 p1459 N73-21826
Low speed wind tunnel tests of scale model of space shuttle orbiter to determine longitudinal and lateral-directional aerodynamic characteristics
[NASA-CR-123851] 12 p1460 N73-21829
Wind tunnel tests to determine heat transfer properties of space shuttle orbiter, booster, and launch configurations for various angles of attack and yaw
[NASA-CR-128891] 12 p1460 N73-21830
Trisonic wind tunnel tests to determine force and moment characteristics of space shuttle orbiter and modified external tank and solid rocket booster
[NASA-CR-120089] 12 p1460 N73-21831
Wind tunnel tests of space shuttle orbiter scale model to determine low speed aerodynamic characteristics of spacecraft components
[NASA-CR-120092] 12 p1460 N73-21832
Wind tunnel tests of space shuttle orbiter scale model to determine aerodynamic characteristics at hypersonic speed in various configurations
[NASA-CR-128754] 12 p1461 N73-21838
Optimization of basic ceramic insulation for space shuttle orbiters - Part 2
[NASA-CR-112257] 13 p1546 N73-22531
Wind tunnel tests to determine aerodynamic characteristics of delta wing space shuttle orbiter model at various angles of attack and sideslip
[NASA-TM-X-2748] 15 p1733 N73-24058
Integrated digital flight control system for space shuttle orbiter
[NASA-CR-128936] 15 p1834 N73-24871
Numerical analysis of space shuttle orbiter flight path and performance during approach guidance from space mission - Document 22
[NASA-CR-128962] 16 p1941 N73-25707
Designs of high temperature seals for gaps between structure and aerodynamic control surfaces of space shuttle orbiter
[NASA-CR-128951] 16 p1965 N73-25891
Design parameters and systems analysis of crew compartment for space shuttle orbiter - Summary Report
[NASA-CR-128949] 16 p1965 N73-25893
Design parameters and systems analysis of crew compartment for space shuttle orbiter - Final Report
[NASA-CR-128950] 16 p1965 N73-25894

Aerodynamic characteristics of space shuttle orbiter model in wind tunnel test
[NASA-TM-X-2786] 17 p1979 N73-25998
Low subsonic aerodynamic characteristics of 60 deg swept delta wing space shuttle orbiter
[NASA-TM-X-2762] 17 p2087 N73-26880
Development of computer program for preliminary design of propellant feed system for space shuttle orbiter main engines - Vol. 5A-2
[NASA-CR-133954] 18 p2200 N73-27758
Supersonic wind tunnel tests on scale model space shuttle orbiter configuration
[NASA-TM-X-2804] 19 p2248 N73-28123
Wind tunnel tests to determine effects of control surface modifications on stability and control of space shuttle orbiter
[NASA-CR-133979] 19 p2346 N73-28870
Development and characteristics of hydrogen-oxygen power unit for application to onboard systems of space shuttle orbiter vehicle
[NASA-TM-X-68262] 20 p2363 N73-29005
Shuttle sortie simulation using lear jet aircraft
[NASA-TM-X-62283] 20 p2473 N73-29868
Integrated digital flight control system for rotational and translational control of space shuttle orbiters
[NASA-CR-134001] 21 p2600 N73-30835
Reusable ablative heat shielding for space shuttle orbiters
[NASA-CR-132282] 21 p2605 N73-30880
Development and application of self evacuating multilayer insulation system for application to space shuttle orbiter liquid hydrogen tanks
[NASA-CR-121166] 21 p2606 N73-30883
Safety concerns with shuttle payloads, space stations and space shuttle orbiters
[NASA-CR-134022] 22 p2714 N73-31726
Design of metal shear web selectively reinforced with filamentary composites for space shuttle application
[NASA-CR-132320] 22 p2721 N73-31774
Component fabrication of metal shear web selectively reinforced with filamentary composites for space shuttle application
[NASA-CR-132321] 22 p2721 N73-31775
Component testing and analysis in program to evaluate metal shear web selectively reinforced with filamentary composites for space shuttle application
[NASA-CR-132322] 22 p2721 N73-31776

**SPACE SHUTTLES**

Wind tunnel tests of space shuttle models to determine effects of body and wing geometry on hypersonic shock structure and on surface impingement of interior flow field shock waves
[NASA-CR-128587] 01 p0040 N73-10317
Wind tunnel tests to determine convective heat distribution for space shuttle configurations based on viscous/inviscid interactions of three dimensional flow fields
[NASA-CR-128586] 01 p0040 N73-10318
Laboratory prototype flash evaporator design, fabrication, and testing for space shuttle environmental control expendable heat sink
[NASA-CR-128608] 01 p0057 N73-10470
Technology for developing hydrogen-oxygen thruster for space shuttle ACPS
[NASA-TM-X-68146] 01 p0090 N73-10744
Heat sink and cooling system concepts for space shuttle baseline thermal protection systems
[NASA-CR-123912] 01 p0107 N73-10884
Wind tunnel static stability and control data for delta wing booster of scale model of space shuttle
[NASA-CR-119994-VOL-3] 01 p0107 N73-10886
Test results of booster and orbiter configurations
[NASA-CR-119994-VOL-4] 01 p0108 N73-10887
Simulation for use in dynamics and control analysis during boost from liftoff to orbit insertion
[NASA-CR-128592] 01 p0108 N73-10890
Nondestructive analysis techniques for detection of defects in rigidized surface insulation for space shuttle thermal protection
[NASA-CR-128607] 01 p0108 N73-10893
Hypervelocity wind tunnel tests of aerothermal characteristics of ...nged space shuttle booster model
[NASA-TM-X-2642] 01 p0109 N73-10895
TD nickel chromium, dispersion-strengthened alloy for thermal protection system of space shuttle
[NASA-CR-120796] 02 p0187 N73-11512
Development and evaluation of internal insulation materials for use with liquid hydrogen tanks on space shuttle
[NASA-CR-123928] 02 p0191 N73-11547
Analysis of nuclear safety aspects in transport of nuclear payloads to and from earth orbit by space shuttle - Vol. 4 Pt. 1
[NASA-CR-123847] 02 p0210 N73-11700
Guidelines and requirements for space shuttle nuclear system transportation of nuclear payloads, ground support systems, and facilities - Vol. 5 Pt. 2
[NASA-CR-123843] 02 p0210 N73-11702
Assessment of materials compatibility data for hydrazine monopropellant propulsion systems of space shuttle vehicle in multicycle extended life applications
[NASA-CR-128491] 02 p0221 N73-11788
Definition of requirements for flight simulator to provide space shuttle systems and space mission analysis and performance - Vol. 1
[NASA-CR-128621] 02 p0229 N73-11860
Development of requirements for space shuttle vehicle and mission simulation - Vol. 2
[NASA-CR-128622] 02 p0230 N73-11861
Analysis of space shuttle systems and space shuttle mission requirements for development of mission simulator - Vol. 3
[NASA-CR-128623] 02 p0230 N73-11862
Analysis of external interfaces, crew procedures, visual cues, and aural cues for space shuttle vehicle and mission simulation - Vol. 4
[NASA-CR-128624] 02 p0230 N73-11863
Executive summary of advanced missions safety study involving space shuttle rescue capability, experiment safety, and emergency crew transfer - Vol. 1
[NASA-CR-129099] 02 p0231 N73-11871
Analysis of space rescue mission capability of Earth Orbit Shuttle and concepts for increasing capability- Vol. 2 Pt. 1
[NASA-CR-129104] 02 p0231 N73-11872
Analysis of potential hazards caused by carrying experimental equipment on Earth Orbit Shuttle and recommendations for eliminating or reducing hazards- Vol.2 Pt.2
[NASA-CR-129103] 02 p0231 N73-11873
Analysis of emergency crew transfer operations using Earth Orbit Shuttle to determine mission effectiveness and cost requirements - Vol. 2 Pt. 3
[NASA-CR-129102] 02 p0231 N73-11874
Analysis of space shuttle rescue capability based on mission, shuttle configuration and performance, and ground launched ascent and rendezvous time -Vol. 3 Pt. 1
[NASA-CR-129101] 02 p0231 N73-11875
Analysis of hazards involved in transporting experimental equipment on space shuttle and recommended precautionary measures - Vol. 3 Pt. 2
[NASA-CR-129100] 02 p0231 N73-11876
Aerospace Vehicle Synthesis Program for simulating space shuttles
[NASA-CR-129135] 02 p0232 N73-11886
Development and evaluation of space shuttle main landing gear door constructed of boron/epoxy composite material ribs on titanium panel
[NASA-CR-112172] 02 p0233 N73-11889
Wind tunnel tests to determine static aerodynamic characteristics of single-stage-to-orbit space shuttle at Mach numbers of 2.60, 3.85 and 4.64
[NASA-TM-X-2667] 02 p0233 N73-11891
Wind tunnel tests to determine stability and control effectiveness of basic configuration of pressure-fed ballistic recoverable booster for space shuttle
[NASA-CR-120073] 02 p0233 N73-11896
Wind tunnel tests to determine aerodynamic characteristics and aerodynamic interference of various configurations of space shuttle ascent vehicle-Vol. 1
[NASA-CR-120083] 02 p0234 N73-11901
Wind tunnel tests to determine aerodynamic characteristics of space shuttle ascent configurations with parallel burn pressure-fed and SRM boosters and tank T3 installation - Vol. 2
[NASA-CR-120084] 02 p0234 N73-11902
Wind tunnel tests to determine aerodynamic characteristics of space shuttle ascent configurations with parallel burn pressure-fed and SRM boosters and tank T4 installation - Vol. 3
[NASA-CR-120085] 02 p0234 N73-11903
Wind tunnel tests to determine space shuttle ascent configuration plumes with pressure-fed and solid rocket motor boosters - Vol. 4
[NASA-CR-120086] 02 p0234 N73-11904
Wind tunnel tests to determine aerodynamic characteristics of space shuttle ascent configurations with orbiter, tanks, and booster alone installations - Vol. 5
[NASA-CR-120087] 02 p0234 N73-11905
Analysis of shock interaction and interference heating on military aerospace vehicles at hypersonic speeds
[AD-747765] 03 p0286 N73-12319
Space shuttle avionics design and cost analysis
[NASA-CR-123962] 03 p0300 N73-12449
Design and development of space shuttle system for delivering payload to earth orbit or celestial orbit
[NASA-CASE-MSC-12391] 03 p0354 N73-12884
Analysis of pointing and stability problems of space shuttle sortie mission and application to earth observation and astronomy experiments
[NASA-TM-X-64692] 03 p0355 N73-12892
Analysis of space program costs and launch vehicle traffic based on either expendable, partially reusable, or fully reusable launch vehicle fleet
[NASA-CR-125847] 03 p0355 N73-12896
Payload data bank, space shuttle program risk analysis, reusable launch vehicles, and cost analysis
[NASA-CR-126170] 03 p0355 N73-12897
Guidance method for transition of space shuttle from hypersonic entry to subsonic cruise flight
[NASA-CR-128648] 03 p0357 N73-12905
Atmospheric turbulence response of reusable space shuttle configuration during ascent flight
[NASA-CR-123952] 03 p0357 N73-12913
Design, development, and evaluation of pressurized purge system for reusable space shuttles and fabrication of multilayer insulation systems
[NASA-CR-123942] 03 p0358 N73-12914
Analysis of costs and effectiveness of space missions, aerospace vehicles, and propulsion systems
[NASA-CR-129258] 03 p0358 N73-12917
Cost estimates for base basing, space shuttles, and systems analysis
[NASA-CR-125985] 03 p0359 N73-12921
Evaluation of concept of reverse flow engine for APS engine
[NASA-CR-120881] 04 p0464 N73-13783
Impact of space shuttle operations on national economy, technological superiority, and development of future space activities
04 p0470 N73-13832
NASA MS/MS program for manufacturing materials during space shuttle missions
04 p0473 N73-13860
Numerical methods for computing reentry trajectories for space shuttles
[NASA-CR-128652] 04 p0474 N73-13877
Design and development of scale model of parallel burn space shuttle to represent low frequency structural dynamic characteristics
[NASA-CR-112205] 04 p0478 N73-13909
Wind tunnel tests of space shuttle model to determine performance, stability, and control characteristics of launch configuration
[NASA-CR-120088] 04 p0478 N73-13910
Development of structural dynamics model of space shuttle and evaluation of structural and hydroelastic analysis methods
[NASA-CR-112196] 04 p0478 N73-13911
Interaction of space shuttle control system with pogo
[NASA-CR-2154] 04 p0479 N73-13914
Development of computational techniques for design optimization of thermal protection systems for space shuttle vehicle
[NASA-CR-128618] 04 p0484 N73-13951
Economic analysis of space shuttle transportation system based on tradeoffs, alternatives, and variations in spacecraft design - Vol. 1
[NASA-CR-129568] 04 p0487 N73-13977
Projected space missions and space transportation system with payload and cost analysis for space shuttle system - Vol. 2
[NASA-CR-129571] 04 p0487 N73-13978
Economic analysis of space transportation system for use during 1980 time period based on various configurations of space shuttle and space tug - Executive Summary
[NASA-CR-129570] 04 p0487 N73-13980
Charts for selecting suitable earth orbits for solar observations from space shuttles
[NASA-TM-X-64709] 05 p0595 N73-14840
Spacecraft configurations and aerodynamic characteristics of space shuttle systems with two reusable stages
[NASA-CASE-MSC-12433] 05 p0597 N73-14854
Preliminary design of selected Research and Applications Module [RAM] concepts, operations, and missions
[NASA-CR-129828] 05 p0597 N73-14856
Analysis of payloads for space shuttle based on space missions, planetary exploration, and international rendezvous and docking - Vol. 2
[NASA-CR-129844] 05 p0598 N73-14862
Computational techniques for design optimization of thermal protection for space shuttle
[NASA-CR-128658] 05 p0598 N73-14863
Analysis of natural environment design requirements for space tug to show orbital environmental impacts and short-period atmospheric density variation effects
[NASA-TM-X-64713] 05 p0600 N73-14881
Hydrogen oxygen engine for space shuttle attitude control and stationary or pulsed operation
[MBB-UR-158-72-O] 06 p0714 N73-15823
Proceedings of Space Shuttle Sortie Workshop
[NASA-TM-X-68841] 06 p0719 N73-15866
Advanced technology, experimental and instrument design, and mission planning for space shuttle sortie workshop - conference working group reports
[NASA-TM-X-68842] 06 p0719 N73-15867
Application of autopilot techniques to control and stabilize vibration modes of two space shuttle configurations at liftoff flight condition
[NASA-CR-112202] 06 p0721 N73-15884
Impulse base flow facility tests of space shuttle stage separation plume impingement loads
[NASA-CR-124000] 06 p0729 N73-15949
Shuttle reaction control system cryogenic liquid distribution system
[NASA-TM-X-68913] 07 p0834 N73-16765
Launch vehicle estimating factors for planning advanced solar system and earth orbital missions
[NHB-7100.5B] 07 p0847 N73-16866
Payload guidelines for space shuttle/tug
[NASA-CR-130025] 07 p0848 N73-16872
Technology base for multiplexed data bus subsystem design for space shuttles
[NASA-CR-124030] 07 p0848 N73-16874

Improvement and evaluation of mullite reusable surface insulation material for thermal protection system of space shuttle
[NASA-CR-124053] 08 p0934 N73-17646
Ascent control studies of 049 and ATP parallel burn solid rocket motor shuttle
[NASA-TM-X-64720] 08 p0960 N73-17854
Design and development of large flexible tunnel for use at space shuttle and payload interface
[NASA-CR-124073] 08 p0964 N73-17879
Updated structural design criteria for manned space shuttle missions
[NASA-SP-8057-REV] 08 p0964 N73-17881
Development of computer program to optimize space shuttle environmental and thermal control life support system
[NASA-CR-128736] 08 p0964 N73-17883
Mathematical model to simulate staging dynamics of proposed space shuttle configuration
[NASA-TM-X-58098] 08 p0965 N73-17886
Space shuttle design recommendations based on aircraft maintenance experience
[NASA-TM-X-68646] 08 p0965 N73-17888
Analysis of space shuttle capability as launch vehicle for delivery of payloads into earth orbit
[NASA-TM-X-68859] 08 p0965 N73-17889
Relative rain erosion resistance of low-density-thermal protection materials for space shuttles at subsonic velocities
[NASA-CR-130541] 08 p0969 N73-17924
Environmental salt spray tests of closed pore insulation for space shuttle orbiter thermal protection system
[RM-570] 09 p1051 N73-18572
Analytical and experimental evaluation of high pressure thrust chamber concepts for hydrogen oxygen auxiliary propulsion for space shuttle vehicle
[NASA-CR-120895] 09 p1079 N73-18800
Design and tests of low pressure thrust chamber concepts for hydrogen oxygen auxiliary propulsion for space shuttle vehicle
[NASA-CR-120896] 09 p1079 N73-18801
Baseline astronomy sortie mission concept for space shuttle
[NASA-CR-124043] 09 p1084 N73-18842
Baseline experiment definition documents for candidate astronomy sortie mission telescopes and arrays to be used on space shuttle
[NASA-CR-124045] 09 p1084 N73-18843
Resource requirements for single-stage earth-orbital vehicle
[NASA-CR-124091] 09 p1086 N73-18858
Analysis of control and simulation methods for space shuttle manipulator
09 p1089 N73-18889
Analysis of relationships between changes in space shuttle weights and costs with changes in weight of structural subsystems
[NASA-CR-2164] 09 p1090 N73-18894
Curves and general equations for design of lightweight glass fiber reinforced metal pressure vessels for space shuttles
[NASA-CR-120917] 09 p1094 N73-18932
Atom recombination catalytic rates for surface coatings of thermal protection system materials for space shuttles
[NASA-TN-D-7113] 09 p1098 N73-18965
Application of finite element method to calculation of supersonic flutter of thermal protection panel for space shuttles
[VF-12] 10 p1104 N73-19001
Computation of supersonic flutter for thermal protection panel of space shuttles
[VF-16] 10 p1104 N73-19002
Rendezvous and docking radar for space shuttle
10 p1129 N73-19198
Programmatics of space shuttle supported research facilities for telecommunication and navigation - Vol. 4
[NASA-CR-124139] 10 p1137 N73-19268
Precision State and Filter Weighting Matrix Extrapolation routine for space shuttle guidance navigation
[NASA-CR-128803] 10 p1184 N73-19631
Development and characteristics of auxiliary propulsion system for space shuttle applications - Summary
[NASA-CR-128818] 10 p1208 N73-19827
Analysis of requirements for oxygen-hydrogen auxiliary propulsion system for use with space shuttle vehicle concept - Phase A
[NASA-CR-128820] 10 p1208 N73-19828
Comparison and evaluation of competing concepts of auxiliary propulsion concepts for space shuttle applications - Phase B
[NASA-CR-128823] 10 p1208 N73-19829
Evaluation of concepts for integrating reaction control system and orbit maneuvering system of space shuttle vehicle - Phase C
[NASA-CR-128821] 10 p1209 N73-19830
Evaluation of two alternate oxygen-hydrogen auxiliary propulsion system concepts for space shuttle vehicle - Phase D
[NASA-CR-128822] 10 p1209 N73-19831
Evaluation of monopropellant and bipropellant earth storable reaction control systems for application to space shuttle vehicle - Phase C & E
[NASA-CR-128819] 10 p1209 N73-19832
Design, development, and configuration of astronomical observatory for space shuttle to show telescope capabilities and characteristics of various remote sensors
[NASA-CR-128841] 10 p1215 N73-19879
Status of space shuttle and Skylab programs and shuttle facilities
10 p1215 N73-19880
Development of space shuttle scale model for thermodynamic analysis of internal and external heat flow fields
[NASA-CR-128849] 10 p1215 N73-19882
Non-metallic thermal protection panels for space shuttles
[TASS-72-Z-1095] 10 p1224 N73-19953
Software conceptual designs for space shuttle simulator requirements
[NASA-CR-128882] 11 p1266 N73-20270
Conceptual designs for manned, space shuttle sortie mission laboratory for communications and navigation experiments - Vol. 1 - Exec. Summary
[NASA-CR-124136] 11 p1266 N73-20273
Selection and definition of candidate experiments and associated instrumentation requirements for space shuttle communication/navigation experiments laboratory - Vol. 2
[NASA-CR-124137] 11 p1266 N73-20274
Conceptual design of space shuttle comm/nav research laboratory and identification of major laboratory equipment - Vol. 3
[NASA-CR-124138] 11 p1266 N73-20275
Development of numerical model of eddy diffusive transport of emitted gases from space shuttle wake to show chemical reactions between emitted gases and ambient atmosphere
[NASA-TM-X-66215] 11 p1287 N73-20440
Silver-ion bactericidal monitor for Space Shuttle potable water system
[NASA-CR-128884] 11 p1293 N73-20492
Design allowables for room temperature vulcanizing silicone rubber based adhesives for attaching reusable surface insulation to space shuttle structures
[NASA-CR-128887] 11 p1308 N73-20615
Development of design data for adhesives for attaching reusable surface insulation on space shuttle
[NASA-CR-128888] 11 p1308 N73-20616
Proceedings of conference on inertial navigation components and systems with emphasis on concepts and techniques involving cost and performance tradeoffs
[AGARD-CP-116] 11 p1316 N73-20684
Proceedings of conference on economic aspects of space shuttle system to show basis for cost effectiveness determinations and system selection
[NASA-CR-131421] 11 p1337 N73-20848
Influence of combined loading criteria on space shuttle structural performance
[NASA-CR-124113] 11 p1340 N73-20874
Development of mathematical model of lateral motion of flexible space shuttle vehicle during ascent
[NASA-CR-124159] 11 p1340 N73-20876
Analysis of procedures for reducing pogo on space shuttle vehicle based on estimates of pump cavitation compliance
[NASA-CR-2210] 11 p1341 N73-20885
Program formulation for weight/sizing design synthesis computer program for application to space shuttle development - Vol. 1
[NASA-CR-128867] 11 p1343 N73-20894
Program description of computerized analysis for space shuttle weight analysis to include flow chart and subroutine linkages - Vol. 2
[NASA-CR-128868] 11 p1343 N73-20895
User manual for weight/sizing design synthesis computer program for application to space shuttle payloads - Vol. 3
[NASA-CR-128869] 11 p1343 N73-20896
MASS computer models for analyzing space shuttles and space shuttle payload operations
[NASA-CR-112286] 11 p1343 N73-20897
Experimental design for space shuttle sortie mission payloads
[NASA-CR-112287] 11 p1343 N73-20898
Effect of nose geometry on aerothermodynamic environment of shuttle entry configurations
[NASA-CR-128873] 11 p1348 N73-20937
Design, development, and capabilities of space shuttle mission simulator to show types of training available and cost effectiveness of facility
[NASA-CR-128885] 12 p1387 N73-21251
Thermal design of filamentary composite materials for primary structures on space shuttles
[NASA-CR-124206] 12 p1415 N73-21469
Structural load reduction of space shuttle booster/orbiter configuration using load relief guidance technique
[NASA-TM-X-64738] 12 p1457 N73-21812
Development of computer program for parametric ascent trajectory optimization for application to space shuttle vehicle operation
[NASA-CR-129000] 12 p1458 N73-21815
Application of optimal control technology to design of controller for space shuttle descent
[NASA-CR-124183] 12 p1459 N73-21824
Development of dissipative energy approach for predicting damping of four component space shuttle model using modal parameters for individual components
12 p1459 N73-21827
Development of empirical structural damping law for space shuttle by dynamic analysis of vibration test data
[NASA-CR-124203] 12 p1460 N73-21828
Dynamic stability information for space shuttles, high performance military aircraft, and short takeoff aircraft at high angles of attack
[NASA-CR-114583] 13 p1505 N73-22201
Space shuttle mission simulator requirements
[NASA-CR-128890] 13 p1506 N73-22203
Training requirements of mission phase for crews and ground support personnel
[NASA-CR-128886] 13 p1506 N73-22204
Fabrication of beryllium compression tubes and structural panels for space shuttle application
[NASA-CR-124245] 13 p1533 N73-22420
Improved silicide coatings for refractory metals employed in space shuttles and gas turbine engine components
[NASA-CASE-LEW-11179-1] 13 p1540 N73-22474
Configuration data and design information for space shuttle launch of Tracking and Data Relay Satellite System - Vol. 4
[NASA-CR-130222] 13 p1580 N73-22802
Aerothermodynamic wind tunnel tests of space shuttle configurations performed at Mach number 8 for flow distribution and heat transfer under reentry conditions
[NASA-CR-131486] 13 p1583 N73-22834
Effect of biaxial loading on flaw growth rate of aluminum alloys used in space shuttle cryogenic tankage
[NASA-CR-128904] 13 p1586 N73-22855
Development and application of composite materials for weight reduction of space shuttle structural hardware
13 p1593 N73-22917
Conceptual designs of versatile EVA work-stations - Vol. 2
[NASA-CR-128927] 14 p1614 N73-23082
Orbital mechanics involved in rendezvous between space shuttle and Soyuz spacecraft
[NASA-TT-F-13955] 14 p1705 N73-23838
Degradation and reuse of radiative-thermal protection materials for space shuttle
[NASA-CR-123587] 14 p1709 N73-23866
Wind tunnel tests to determine aerodynamic interference between space shuttle orbiter, external tank, and solid rocket booster in ascent configuration
[NASA-CR-120060] 14 p1709 N73-23871
Wind tunnel tests to determine pressure distribution of space shuttle launch configuration for various combinations of geometric components and Mach number
[NASA-CR-120058] 14 p1709 N73-23872
Design, development, and manufacture of boron-aluminum alloy for use as space shuttle structural components
[NASA-CR-124242] 14 p1709 N73-23873
Operational cost and technological development aspects in design of space shuttle avionic systems
14 p1711 N73-23884
Simulation model for optimum spaceborne computer system design controlling shuttle booster subsystems
14 p1712 N73-23891
Onboard computer system for in-flight monitoring of space shuttle in support of flight crew
14 p1712 N73-23893
Hardware phase of digital capacitance measuring system
[REPT-2873-2143-116] 15 p1754 N73-24218
Space shuttle visual simulation system design study
[NASA-CR-128940] 15 p1760 N73-24265
Potential valve closures for space shuttle auxiliary propulsion system
[NASA-CR-120976] 15 p1791 N73-24516
Technical analysis of solid propellant rocket engines for use with space shuttle vehicle - Vol. 2, Book 2
[NASA-CR-123926] 15 p1826 N73-24798
Systems analysis and operations analysis of solid propellant rocket engine configurations for use with space shuttles - Vol. 3
[NASA-CR-123728] 15 p1826 N73-24799
Mass properties and related data for solid propellant rocket engine used with space shuttle vehicle - Vol. 2, Book 4
[NASA-CR-124237] 15 p1826 N73-24800
Analysis of size, weight, and packaging requirments for aerodynamic decelerator for recovery of expended solid propellant rocket engines used to launch space shuttle vehicles - Vol. 2, Book 5
[NASA-CR-123730] 15 p1826 N73-24801
Cost analysis of various solid propellant rocket engines for use with space shuttle - Vol. 4
[NASA-CR-124239] 15 p1826 N73-24802
Space shuttle energy management, approach, and landing analysis
[NASA-CR-128937] 15 p1830 N73-24830

Nuclear waste disposal into space, using space shuttle and nonexpendable and expendable orbital stages
[NASA-TM-X-68235] 15 p1830 N73-24834
Development of system concept for shuttle support to orbital operations of low cost unmanned satellites in low earth orbit
[NASA-CR-130239] 15 p1834 N73-24869
Identification of requirements and systems for intravehicular activity and extravehicular activity during space shuttle missions - Vol. 1
[NASA-CR-128941] 15 p1835 N73-24875
Identification of requirements and systems for intravehicular activity during space shuttle missions - Vol. 2
[NASA-CR-128942] 15 p1835 N73-24876
Design criteria and aerodynamic characteristics of decelerator parachutes used for recovery of solid rocket boosters used in space shuttle launching
[NASA-CR-124266] 16 p1861 N73-25072
HCl acid aerosol production by space shuttle exhaust products and atmosphere
[NASA-CR-132993] 16 p1870 N73-25142
Design and programming techniques for space shuttle software
[NASA-CR-128971] 16 p1879 N73-25211
Materials fatigue test machine for use aboard Skylab or space shuttles
[NASA-CR-132260] 16 p1913 N73-25476
Procedure for aligning inertial reference unit of space shuttle by celestial references - Document 20
[NASA-CR-128964] 16 p1941 N73-25706
Consolidation of navigation and guidance for space shuttle vehicles for all phases of space mission - Document 21
[NASA-CR-128961] 16 p1941 N73-25708
Development of equations of motion for energy dissipation phase of shuttle reentry and landing approach - Document 23
[NASA-CR-128960] 16 p1941 N73-25709
Rendezvous targeting program for space shuttle missions
[NASA-CR-128963] 16 p1965 N73-25898
Bibliography of technical documents pertinent to development of system for recovering space shuttle solid rocket booster motors from ocean
[LPC-DOC-SRM-143] 16 p1965 N73-25899
Lightweight evacuated multilayer insulation systems for space shuttle vehicle
[NASA-CR-121105] 16 p1966 N73-25902
Space shuttle related technology development and utilization
[NASA-CR-124260] 16 p1977 N73-25988
Earth resources survey applications of space shuttle sortie mode
[NASA-CR-132207] 17 p2026 N73-26394
Low noise level fan and pump concept for space shuttle
[NASA-CR-128986] 17 p2037 N73-26477
Dispersion strengthened nickel alloys for use as space shuttle thermal protection systems
[NASA-CR-121164] 17 p2043 N73-26526
Traffic model data for 1973 NASA payload space shuttle
[NASA-TM-X-64751] 17 p2083 N73-26845
Development of engineering analysis and computer code for predicting space shuttle orbiter longitudinal aerodynamic characteristics during abort separation
[NASA-CR-128974] 17 p2086 N73-26877
Space shuttle traffic and payload data developed from 1971 mission model
[NASA-TM-X-64731] 17 p2086 N73-26878
Wind tunnel measurements of overall fluctuating pressure levels on seven space shuttle launch configurations at transonic and supersonic speeds
[NASA-TM-X-62280] 17 p2087 N73-26882
Development of computer program and data base for design of cryogenic systems used in space shuttles and spacecraft - Vol. 5 B-1
[NASA-CR-133955] 17 p2087 N73-26883
Computer programmers manual for mathematical model used in design of cryogenic supply systems for space shuttles and spacecraft - Vol. 5 B-2 Part 1
[NASA-CR-133956] 17 p2087 N73-26884
Development of computer program for space shuttle orbit injection propulsion system to generate parametric feed system pressure histories - Vol. 5 B-4
[NASA-CR-133957] 17 p2087 N73-26885
Computer programmers manual for parametric analysis of attitude control propulsion system using converted liquid cryogenics reaction system - Vol. 5 B-3 Part 2
[NASA-CR-133958] 17 p2087 N73-26886
Analysis of parameters for optimization of cryogenic supply system for space shuttles - Vol. 6
[NASA-CR-133959] 17 p2087 N73-26887
Analysis of space shuttle cryogenic fluid storage system to determine heat absorption capability and design of radiators for additional cooling capability - Vol. 4
[NASA-CR-133952] 17 p2088 N73-26895
Design and tests of breadboard cryogenic hydrogen and Freon heat exchanger for space shuttle missions
[NASA-CR-128987] 17 p2096 N73-26959
Aerodynamic characteristics of two space shuttle concepts with delta wing configurations at hypersonic speed using helium flow visualization technique
[NASA-TN-D-7282] 18 p2102 N73-26997
Attached manipulator system for simulating and demonstrating shuttle manipulator cargo handling operations under weightless conditions
[NASA-CR-133964] 18 p2126 N73-27176
Development of hardware and software specifications for procurement of space shuttle mission training simulator for crew training
[NASA-CR-133965] 18 p2126 N73-27177
Calculation of three-dimensional boundary layer flows on aircraft and space shuttle configurations
[NASA-CR-2285] 18 p2130 N73-27214
Active-standby servoactuator for failure detection of space shuttle main engine hydraulic actuation system
[NASA-CR-124299] 18 p2156 N73-27418
Natural environment design requirement for solar electric power stage based on radiation atmospheric conditions at orbital altitudes
[NASA-TM-X-64761] 18 p2193 N73-27708
Design and development of optimized cryogenic fuel supply systems for space shuttle vehicles - Vol. 2
[NASA-CR-128993] 18 p2199 N73-27751
Evaluation of candidate systems for cryogenic fuel supply system used on space shuttle vehicle - Vol. 3
[NASA-CR-128994] 18 p2199 N73-27752
Flight simulation to determine navigation, guidance, and control problems involving terminal area approach and landing of space shuttle using CV-990 aircraft
[NASA-TM-X-62285] 18 p2199 N73-27753
Analysis of cryogenic supply system for space shuttle vehicles and evaluation of candidate systems - Vol. 1
[NASA-CR-128992] 18 p2199 N73-27756
Development of integrated mathematical model for optimization of cryogenic fluid storage and supply systems for spacecraft - Vol. 5A-1
[NASA-CR-133953] 18 p2199 N73-27757
Wind tunnel tests to determine heat transfer and flow distribution of space shuttle configuration at hypersonic speeds simulating atmospheric entry
[NASA-CR-133405] 18 p2201 N73-27772
Wind tunnel tests to analyze aerothermodynamic control problems of space shuttle attitude control system at hypersonic speed
[NASA-CR-133407] 18 p2201 N73-27773
Storage stability of intermediate moisture foods for space shuttle
[NASA-CR-133978] 19 p2225 N73-27944
Analysis of various aircraft antiskid braking systems to determine appropriate antiskid braking system for space shuttle vehicle
[NASA-CR-124349] 19 p2294 N73-28449
Development and characteristics of closed pore ceramic foam insulation material for use as heat shield on space shuttle vehicle
[NASA-CR-2254] 19 p2312 N73-28591
Congressional hearing concerning GAO cost analysis of NASA estimates for space shuttle 19 p2354 N73-28936
Zero-gravity cloud physics laboratory for space shuttle payload planning
[NASA-CR-129002] 20 p2449 N73-29674
Program planning, contract administration, manufacturing, and testing of solid propellant rocket engine for space shuttle booster - Vol. 3
[NASA-CR-124238] 20 p2467 N73-29821
Design analysis and tradeoff studies for defining Astronomy Sortie Mission based on mission requirements and payload limitations - Vol. 3 Bk. 1
[NASA-CR-124047] 20 p2473 N73-29870
Design analysis and trade studies to support candidate configurations and payloads for Astronomy Sortie Missions - Vol. 3 Bk. 2
[NASA-CR-124044] 20 p2474 N73-29871
Space vehicle design criteria based on interplanetary charged particle environments
[NASA-CR-124341] 20 p2474 N73-29876
Analysis of acoustic and fluctuating pressure environments for complete flight envelope of space shuttle
[NASA-CR-124347] 20 p2475 N73-29885
Equipment requirements for space shuttle EVA/IVA pressure suit, life support system, mobility aids, vehicle support provisions, and emergency support
[NASA-CR-133991] 21 p2503 N73-30089
Space shuttle environmental and thermal control/life support system
[NASA-CR-134009] 21 p2504 N73-30091
Development of visual simulation system design for space shuttle mission simulator to include cost analysis and alternate concepts
[NASA-CR-134020] 21 p2522 N73-30221
Stochastic model of atmosphere between 30 and 90 km was developed for use in Monte Carlo space shuttle entry studies
[NASA-TM-X-69567] 21 p2536 N73-30337
Space shuttle rendezvous, radiation and reentry analysis code
[NASA-TM-X-64768] 21 p2595 N73-30795
Effects of ascent trajectory mode and tank disposal method on shuttle payload accommodation
[NASA-TM-X-64773] 21 p2599 N73-30831
Development and characteristics of variable ratio, mixed-mode, bilateral master-slave control system for space shuttle remote manipulator system
[NASA-CASE-MSC-14245-1] 21 p2599 N73-30832
Description of pyrotechnic systems principles with application to systems and equipment on space shuttle
[NASA-CR-2292] 21 p2600 N73-30840
Self-contamination of manned orbiting spacecraft from plasma gas or particulate matter
[NASA-CR-133836] 21 p2601 N73-30843
Development of alternate space shuttle concepts to show modified avionics, vehicle subsystems, and thermal protection system
[NASA-CR-124345] 21 p2601 N73-30844
Development of damping system to compensate for wind loads on space shuttle vehicle during launch operations
[NASA-CR-124367] 21 p2601 N73-30845
Analytical solution of nonlinear aeroelastic galloping instability, with reference to space shuttle ground wind response, and application to U beams
[DLR-FB-73-18] 21 p2601 N73-30848
Guidelines for extravehicular and intravehicular activities during space shuttle operation with emphasis on contingency situations - Vol. 2
[NASA-CR-133992] 22 p2622 N73-31007
Pressure suit requirements and characteristics for space shuttle personnel performing EVA and IVA activities - Vol. 3
[NASA-CR-133993] 22 p2622 N73-31008
Requirements for mobility aids and restraint devices for use by personnel of space shuttle - Vol. 4
[NASA-CR-133994] 22 p2622 N73-31009
Requirements and equipment for space shuttle emergency intravehicular activity and effectiveness of emergency procedures - Vol. 5
[NASA-CR-133995] 22 p2622 N73-31010
Feasibility analysis of GOAL to HAL language translator for use with space shuttle
[NASA-CR-134033] 22 p2638 N73-31141
Space shuttle avionics and GOAL language including impact of error detection and redundancy management
[NASA-CR-134034] 22 p2638 N73-31142
Advanced material composites for use as insulations for space shuttle LH2 tanks
[NASA-CR-124388] 22 p2688 N73-31532
High temperature silicone adhesive formulations for thermal protection systems used with space shuttle mission
[NASA-CR-124389] 22 p2688 N73-31533
Complex permittivity measurements during high temperature recycling of space shuttle antenna window and dielectric heat shield materials
[NASA-CR-2302] 22 p2707 N73-31675
Identification, selection, and description of earth observation experiments for shuttle sortie missions in 1980's
[NASA-CR-124368] 22 p2717 N73-31751
Ultrasonic technique for assessing structural integrity of primary surface of space shuttle vehicles
[NASA-CR-133859] 22 p2721 N73-31778
Ultrasonic technique for assessing structural integrity of primary surface of space shuttle vehicles
[NASA-CR-133815] 22 p2721 N73-31779
Zero leakage separable and semipermanent ducting joints for space flight vehicles
[NASA-CR-124386] 22 p2722 N73-31780
Simplified analysis procedure for determining static and dynamic aeroelastic loads for space shuttle dynamics
[NASA-CR-124370] 22 p2722 N73-31781
Design and development of pressurization system for reusable space shuttle multilayer insulation systems
[NASA-CR-124380] 22 p2722 N73-31782
Congressional hearings on cost of space shuttle program to show differences between Government Accounting Office and NASA projections 22 p2737 N73-31916
Senate hearings concerning GAO analysis of space shuttle cost estimates 22 p2738 N73-31919
Payload carrier simlation data for design of manned space shuttle missions
[NASA-CR-124430] 23 p2751 N73-32018
Design, development and operation of laser communication system developed for potential space shuttle application
[NASA-CR-124440] 23 p2801 N73-32400
Evaluating reusable surface insulation for space shuttle over range of heat transfer rate and surface temperature
[NASA-TM-X-2823] 23 p2809 N73-32465
Space shuttle guidance, navigation, and control design equations
[NASA-TM-X-69524] 23 p2816 N73-32514
Logistics of orbital vehicle servicing computer specification to improve utilization of space shuttle and tug
[NASA-CR-135709] 23 p2845 N73-32736

Numerical solutions to optimal three glide/thrust atmosphere skip maneuver
[NASA-TN-D-7211] 23 p2848 N73-32759
Simulation of experiment pointing system for space shuttle
[NASA-TM-X-64779] 23 p2848 N73-32760
Design and development of logic scheme for control of Omni-Axis Secondary Thrust Vector Control system for use on space shuttle pressure fed engine
[NASA-CR-124428] 23 p2848 N73-32761
Analysis of unsteady aerodynamics of space shuttle vehicles
[NASA-CR-124424] 23 p2848 N73-32763
Life sciences payload definition and integration study to show design of space laboratory for space shuttle and cost analysis of project - Vol. 2
[NASA-CR-124412] 23 p2849 N73-32766
Research equipment requirements for space laboratory concepts involved in conducting life sciences experiments in space - Vol. 3
[NASA-CR-124414] 23 p2849 N73-32767
Specification catalog to identify test equipment for use in conducting life sciences experiments aboard space laboratory - Vol. 4
[NASA-CR-124413] 23 p2849 N73-32768
Representative shuttle mission applications
[NASA-CR-124431] 23 p2850 N73-32771
Design and cost analysis of space shuttle systems - Vol. 2, Part 1
[NASA-CR-124417] 23 p2850 N73-32772
Design and cost analysis of space shuttle systems - Vol. 2, Part 2
[NASA-CR-124422] 23 p2850 N73-32773
Analysis of alternate space shuttle concepts to examine stage-and-one-half concept for reusable shuttle system and cost of external hydrogen tank development program
[NASA-CR-124421] 23 p2850 N73-32774
Aerodynamic characteristics of alternate space shuttle configurations and trajectory analysis with external drop tanks installed
[NASA-CR-124418] 23 p2850 N73-32775
Development and characteristics of advanced technology laboratory for use with space shuttle concept
[NASA-TM-X-2813] 23 p2851 N73-32781
Convective heat transfer determination for nose region of space shuttle entry configurations, using three dimensional flow field study
[NASA-CR-134057] 23 p2851 N73-32782
Trisonic wind tunnel tests of baseline launch configuration space shuttle model to determine effects of model parametric variations on static stability characteristics
[NASA-CR-128778] 23 p2851 N73-32783
Fused slurry silicide protective coatings for niobium alloy reentry heat shields for space shuttles - Vol. 1
[NASA-CR-121216] 23 p2857 N73-32826
Experimental and coating processes for fused slurry silicides on niobium alloy heat shields for space shuttles - Vol. 2
[NASA-CR-134483] 23 p2857 N73-32827
Space environment effects on space shuttle thermal protection system design
[NASA-TM-X-2721] 24 p2941 N73-33490
Concepts of space shuttle
[NASA-EP-96] 24 p2984 N73-33846
Design, development, and configuration of reusable lunar shuttlecraft
[NASA-CR-135794] 24 p2984 N73-33849

**SPACE SIMULATORS**

Reflectance spectra of contaminants in space simulation chamber
[NASA-CR-128716] 07 p0799 N73-16486
Development and characteristics of neutral buoyancy simulator for duplicating weightless conditions encountered during space missions
13 p1594 N73-22923
Radioactive isotope measurements and neutron activation analyses for identifying contaminants in space environment simulator
[NASA-CR-128931] 15 p1815 N73-24709
Marshall system for aerospace system simulation
[NASA-CR-124288] 17 p2010 N73-26252
Large space simulation chambers realizing true ultimate vacuum
[NASA-TM-X-68272] 20 p2382 N73-29142
Modification of JPL space simulator for simulating solar intensities at Mercury
[NASA-CR-133791] 21 p2521 N73-30217
Development of visual simulation system design for space shuttle mission simulator to include cost analysis and alternate concepts
[NASA-CR-134020] 21 p2522 N73-30221
Modified quadrupole mass spectrometer for in situ space simulation thermal vacuum testing of sophisticated payloads
[NASA-TM-X-64775] 21 p2549 N73-30435

**SPACE STATIONS**

NT ORBITAL SPACE STATIONS
NT ORBITAL WORKSHOPS
NT SALYUT SPACE STATION
NT SKYLAB 1

Functional design criteria for multiprocessor computer system to provide computational capability for space station
[NASA-CR-128601] 01 p0030 N73-10235
Mass properties for Modular Space Station Program, Phase B Definition
[NASA-CR-128409] 01 p0107 N73-10883
Long-term testing of water electrolysis systems for regenerative life support system in manned space stations
[NASA-CR-128629] 02 p0135 N73-11095
Radiological safety aspects of manned space missions employing nuclear reactors for electric power and involving extended stay times in low earth orbit - Vol 1
[NASA-CR-123842] 02 p0209 N73-11694
Identification of potential and inherent radiological hazards of spacecraft with nuclear reactors for electric power generation and elimination or reduction of hazards - Vol. 2 Pt. 1
[NASA-CR-123838] 02 p0209 N73-11695
Reference design document for power module systems, facilities, launch vehicle, and mission operations of nuclear reactor for space base programs - Vol. 3 pt. 1
[NASA-CR-123844] 02 p0209 N73-11696
Analysis of terrestrial nuclear hazards involving zirconium hydride reactor-Brayton power module for all phases of space base program - Vol. 3 Pt. 2
[NASA-CR-123839] 02 p0209 N73-11697
Development of abort sequence trees for reference zirconium hydride reactor power module for each phase of space base program mission - Vol. 3 Pt. 2A
[NASA-CR-123845] 02 p0209 N73-11698
Analysis of space base mission and accidents/events involving nuclear hazard to general public - Vol. 3 Pt. 3
[NASA-CR-123846] 02 p0210 N73-11699
Guidelines and requirements of space base nuclear system safety applied to nuclear hardware, ground support equipment, and range safety and facilities - Vol. 5 Pt. 1
[NASA-CR-123848] 02 p0210 N73-11701
Qualitative identification of steps required to assure incorporation of radiological system safety principles into all phases of manned space base program - Vol. 6
[DOC-72SD4201-6-VOL-6] 02 p0210 N73-11703
Analysis of technical documents and literature for conducting manned space flight nuclear system safety study - Vol. 7 Pt. 1
[NASA-CR-123850] 02 p0210 N73-11704
Systems analyses on external and internal radio frequency communication and tracking assemblies for manned space station
[NASA-CR-128561] 03 p0265 N73-12147
REPRI program using Monte Carlo techniques for support compatibility studies for space station
[NASA-CR-123948] 03 p0268 N73-12174
Generation of random experiment schedules for space station using Monte Carlo technique
[NASA-TM-X-64557] 03 p0355 N73-12894
Analytical assessment of potential methods for replenishing auxiliary propulsion onboard orbiting space stations
[NASA-CR-123947] 04 p0461 N73-13764
Conceptual design of thermal control system for space stations
[NASA-CR-123956] 04 p0484 N73-13950
Absorption cycle refrigeration system for environmental control of space station
[NASA-CR-123970] 05 p0598 N73-14859
Results of multiprocessor systems design review
[NASA-CR-124026] 07 p0848 N73-16873
Analysis of visual observation data gathered by Soviet manned spacecraft
[JPRS-58055-2-PT-2] 08 p0960 N73-17853
Visual observations of atmospheric structure and land and water surfaces by cosmonauts from manned orbiting space stations
09 p1026 N73-18373
Structural configuration and performance tests of 928 sq m solar array
09 p1089 N73-18891
Regenerative fuel cell for space station use
[NASA-CR-128848] 10 p1111 N73-19058
Computer simulation of space station computer-steered high gain antenna
[NASA-CR-128749] 10 p1134 N73-19239
Formulation of mathematical model for predicting dynamic behavior of rotating flexible space station configurations - Vol. 1
[NASA-CR-112243] 10 p1189 N73-19672
User's manual for computer program to predict dynamic behavior of rotating flexible space station configurations - Vol. 2
[NASA-CR-112244] 10 p1189 N73-19673
Baseline design of central multiprocessor for manned space station application
[NASA-CR-124151] 11 p1259 N73-20219
Conceptual designs of versatile EVA work-stations - Vol. 2
[NASA-CR-128927] 14 p1614 N73-23082
Evolutionary, gradual, and step-wise spacecraft systems technology development of interim space station program
[NASA-TM-X-69243] 14 p1706 N73-23845

Physical and biomedical research by earth orbiting space stations
[AD-756771] 15 p1743 N73-24126
Water content of Mars atmospheres as measured by Mars 3 automatic space station
[JPRS-59231] 15 p1830 N73-24833
Performance tests of L-band truss cable meteoroid shielding on Skylab space station at minus 180 degrees Fahrenheit
[NASA-TM-X-64743] 15 p1834 N73-24867
Habitability study of earth orbital space stations
[NASA-CR-124276] 16 p1869 N73-25132
Feasibility demoastration of biowaste propellant resistojet engines for space station attitude control system
[NASA-CR-132269] 18 p2193 N73-27706
Satellite nuclear power station, transmitting power safely to ground by microwave beam
[NASA-CR-121254] 19 p2319 N73-28653
Cost and applications for satellite nuclear power station
19 p2319 N73-28658
USSR automatic stations on mars and venus, lunar continental region samples, and 24 hour satellite earth watching
[NASA-TT-F-14929] 19 p2342 N73-28841
Space station solar array technology evaluation program
[MSC-07163] 21 p2499 N73-30057
Design, fabrication and acceptance testing of zero gravity whole body shower
[NASA-CR-134066] 22 p2623 N73-31019
Safety concerns with shuttle payloads, space stations and space shuttle orbiters
[NASA-CR-134022] 22 p2714 N73-31726

**SPACE STORAGE**

Prelaunch mission operations for space storable propellant module for retro propulsion on unmanned outer planet orbiters
[NASA-CR-129521] 03 p0358 N73-12915
Findings and data products developed during crew interface specification study for inflight maintenance and stowage functions in future manned space flights
[NASA-CR-128685] 07 p0849 N73-16878
Analysis and Mechanical design of solar array stowage and deployment arrangements for use in Small Applications Technology Satellite spacecraft
[NASA-CR-132800] 22 p2720 N73-31767
Apollo experience report on equipment storage and stowage arrangement in spacecraft for maximum operational performance
[NASA-TN-D-7434] 22 p2720 N73-31771
Feasibility of thermodynamic vent and screen baffle integration for orbital storage and transfer of liquid hydrogen
[NASA-CR-134482] 24 p2970 N73-33737
Design, development, and fabrication of prototype storage module with internal restraints for stowage of items launched to support space missions
[NASA-CR-124465] 24 p2983 N73-33832

**SPACE SUITS**

Performance of prototype high pressure space suit glove
[NASA-CR-114532] 06 p0635 N73-15162
Development of prototype high pressure space suit glove assembly
[NASA-CR-114535] 08 p0879 N73-17120
Underwater space suit pressure control regulator
[NASA-CASE-MFS-20332-2] 16 p1868 N73-25125
Automatic temperature controller for liquid cooled garment based on total evaporative water loss during exercise
[NASA-TN-D-7311] 16 p1868 N73-25126
Automatic temperature control for liquid cooled space suit
[NASA-CASE-ARC-10599-1] 17 p1988 N73-26071
Process for developing flame retardant elastomeric composition textiles for use in space suits
[NASA-CASE-MSC-14331-1] 18 p2167 N73-27501
Design, development, and fabrication of liquid cooled space suit using ice pack heat sink - Vol. 1
[NASA-CR-114624-VOL-1] 22 p2622 N73-31006
Operating instructions for functional model icepack heat sink subsystem for cooling system of space suit - Vol. 2
[NASA-CR-114624-VOL-2] 22 p2728 N73-31829
Cooling effects on human tolerance to work induced heat stress and collapse
[NASA-CR-134059] 23 p2750 N73-32005
Intra- and extravehicular life support space suite for Apollo astronauts
[NASA-CASE-MSC-12609-1] 23 p2751 N73-32012

**SPACE SYSTEMS ENGINEERING**

U AEROSPACE ENGINEERING

**SPACE TRANSPORTATION**

Optimization of propulsion stage selection for space-based transportation
[AD-744979] 01 p0109 N73-10900
Analysis of nuclear safety aspects in transport of nuclear payloads to and from earth orbit by space shuttle - Vol. 4 Pt. 1
[NASA-CR-123847] 02 p0210 N73-11700
Guidelines and requirements for space shuttle nuclear system transportation of nuclear payloads, ground support systems, and facilities - Vol. 5 Pt. 2
[NASA-CR-123843] 02 p0210 N73-11702

Economic analysis of space shuttle transportation system based on tradeoffs, alternatives, and variations in spacecraft design - Vol. 1
[NASA-CR-129568] 04 p0487 N73-13977
Projected space missions and space transportation system with payload and cost analysis for space shuttle system - Vol. 2
[NASA-CR-129571] 04 p0487 N73-13978
Analysis of economic merits of three alternative space transportation systems for use during 1980 time period - Vol. 3
[NASA-CR-129569] 04 p0487 N73-13979
Economic analysis of space transportation system for use during 1980 time period based on various configurations of space shuttle and space tug - Executive Summary
[NASA-CR-129570] 04 p0487 N73-13980
Space disposal of actinide radioactive wastes
[NASA-TM-X-68216] 12 p1426 N73-21562
Results of tug turnaround cost study and space transportation system abort modes and effects study
[NASA-CR-135765] 24 p2983 N73-33833

**SPACE TUGS**
Analysis of space tug operating techniques and requirements to include engineering support, off-site facility requirements, and checkout procedures
[NASA-CR-129163] 02 p0232 N73-11887
Design requirements for space tug systems and cost analysis of maintenance and operation during space missions
[NASA-CR-129253] 03 p0358 N73-12918
Identification of mechanical/structural differences resulting from use of tug/payload combination in space space mode as contrasted to ground-based operations
[NASA-CR-125905] 03 p0358 N73-12920
Analysis of economic merits of three alternative space transportation systems for use during 1980 time period - Vol. 3
[NASA-CR-129569] 04 p0487 N73-13979
Economic analysis of space transportation system for use during 1980 time period based on various configurations of space shuttle and space tug - Executive Summary
[NASA-CR-129570] 04 p0487 N73-13980
Analysis of natural environment design requirements for space tug to show orbital environmental impacts and short-period atmospheric density variation effects
[NASA-TM-X-64713] 05 p0600 N73-14881
Preliminary estimates of thermal radiation heat transfer to aerobraking space tug
05 p0608 N73-14947
Development of concept of space shuttle orbiter/tug orbital insertion and application to specific space missions
[NASA-TM-X-64715] 06 p0718 N73-15862
Costs of space tug refurbishment
[NASA-CR-130366] 07 p0841 N73-16815
Payload guidelines for space shuttle/tug
[NASA-CR-130025] 07 p0848 N73-16872
Aerobraking trajectory for return of reusable space tugs
[NASA-CR-124057] 09 p1082 N73-18827
Preliminary analysis of proposed European space tug
[MBB-URV-38-71-SUMMARY] 10 p1216 N73-19889
European space tug - prephase A extension
[MBB-URV-44-71] 10 p1216 N73-19890
Preliminary defination of European space tug
[HSD-TP-7227] 10 p1216 N73-19891
Study digest for European space tug
[HSD-TP-7264A] 10 p1216 N73-19892
Study logic and activities scheduling for European space tug
[HSD-TP-7227-APP-1] 10 p1216 N73-19893
Vehicle selection and economic analysis for European space tug
[HSD-TP-7227-APP-2] 10 p1216 N73-19894
Propellant control and propulsion study for European space tug
[HSD-TP-7227-APP-3] 10 p1217 N73-19895
Guidance and rendezvous sub-systems of European space tug
[HSD-TP-7227-APP-4] 10 p1217 N73-19896
Integrated electronics for European space tug
[HSD-TP-7227-APP-5] 10 p1217 N73-19897
Structure and configuration of European space tug
[HSD-TP-7227-APP-6] 10 p1217 N73-19898
Mass summary, test facilities, costs and PERT for European space tug
[HSD-TP-7227-APP-7] 10 p1217 N73-19899
European space tug study summary
[HSD-TP-7264] 10 p1217 N73-19900
European space tug alternative concepts and objectives
[HSD-TP-7264-VOL-1] 10 p1217 N73-19901
Concept definition of European space tug
[HSD-TP-7264-VOL-2] 10 p1217 N73-19902
European space tug auxiliary and main propulsion
[HSD-TP-7264-VOL-3] 10 p1217 N73-19903
European space tug guidance control rendezvous and integrated electronics
[HSD-TP-7264-VOL-4] 10 p1218 N73-19904
Structure and configuration of European space tug
[HSD-TP-7264-VOL-5] 10 p1218 N73-19905
European space tug development including analyses of performance, economics, weights, reliability, and costs
[HSD-TP-7264-VOL-6] 10 p1218 N73-19906
European space tug concepts and feasibility analyses
[HSD-TP-7316] 10 p1218 N73-19907
European space tug - Prephase A study
[MBB-URV-38-71] 10 p1218 N73-19908
Economic analysis of space tug operations to include tug definition, spacecraft configurations, payload effects, and costing logic - Vol. 1
[NASA-CR-124142] 11 p1343 N73-20899
Comparative analysis of space tug concepts to show overall approach and data generation - Vol. 2, Pt. 1
[NASA-CR-124143] 11 p1343 N73-20900
Economic principles for cost effectiveness and cost benefit analysis of space tug operations - Vol. 2, Pt. 2
[NASA-CR-124144] 11 p1343 N73-20901
Development of data base to show space tug characteristics, costs, and performance for comparison of concepts - Vol. 2 Appendix
[NASA-CR-124146] 11 p1344 N73-20902
Cost analysis of single stage space tug operations with several types of liquid propellant rocket engine propulsion systems - Vol. 3
[NASA-CR-124147] 11 p1344 N73-20903
Design and analysis of low speed hydrogen and oxygen inducers applicable to space tugs
[NASA-CR-124233] 13 p1570 N73-22722
Strategies for European geosynchronous space tug mission
[VTH-171] 13 p1583 N73-22831
European space tug phase A study
[MBB-URV-53-72-VOL-2-PT-1] 18 p2200 N73-27765
Space tug geosynchronous mission simulation
[NASA-CR-135706] 23 p2844 N73-32730
Logistics of orbital vehicle servicing computer specification to improve utilization of space shuttle and tug
[NASA-CR-135709] 23 p2845 N73-32736
Results of tug turnaround cost study and space transportation system abort modes and effects study
[NASA-CR-135765] 24 p2983 N73-33833

**SPACE VEHICLE CONTROL**
U SPACECRAFT CONTROL

**SPACE VEHICLES**
U SPACECRAFT

**SPACE-TIME CONTINUUM**
U RELATIVITY

**SPACE-TIME FUNCTIONS**
Target recognition by considering space-time functions in radar echoes
[REPT-1-72] 09 p1003 N73-18184
Space time laws governing F-scattering at various latitudes
13 p1521 N73-22328
Space-variant image motion degradation and restoration in linear incoherent optical systems
15 p1812 N73-24687
Method for calculating correlation functions of diurnal precipitation totals and their space time variability over uniform relief
21 p2573 N73-30619

**SPACE-TIME METRIC**
U SPACE-TIME FUNCTIONS

**SPACEBORNE ASTRONOMY**
Development of Large Space Telescope for conducting astronomical observations from unmanned satellites and analysis of constraints and tradeoffs during design phase - Vol. 1
[NASA-TM-X-64726-VOL-1] 09 p1035 N73-18449
Mission description and system design for Large Space Telescope used on unmanned satellites - Vol. 2
[NASA-TM-X-64726-VOL-2] 09 p1036 N73-18450
Development and characteristics of optical telescope assembly system for Large Space Telescope based on mission-related and optical parameters - Vol. 3
[NASA-TM-X-64726-VOL-3] 09 p1036 N73-18451
Development and characteristics of scientific instrument package for use with Large Space Telescope - Vol. 4
[NASA-TM-X-64726-VOL-4] 09 p1036 N73-18452
Development and characteristics of support systems module for use with Large Space Telescope - Vol. 5
[NASA-TM-X-64726-VOL-5] 09 p1036 N73-18453
Baseline astronomy sortie mission concept for space shuttle
[NASA-CR-124043] 09 p1084 N73-18842
Baseline experiment definition documents for candidate astronomy sortie mission telescopes and arrays to be used on space shuttle
[NASA-CR-124045] 09 p1084 N73-18843
Feasibility determination of astronomy sortie missions concept including definitions of support hardware, mission profiles, and interfaces with space shuttle and sortie lab
[NASA-CR-124042] 10 p1211 N73-19851
Design, development, and configuration of astronomical observatory for space shuttle to show telescope capabilities and characteristics of various remote sensors
[NASA-CR-128841] 10 p1215 N73-19879
Research projects for ground-based and space-based astronomy to show present capabilities and future potential
[PB-212965] 12 p1458 N73-21819
Development of space astronomy projects identified during orbital experiment program and requirements study - Vol. 4
[NASA-CR-112328] 13 p1577 N73-22781
Experimental design, research programs, and equipment design activities of Astronomical Space Laboratory for 1971 to 1972
[RAP-01-72] 17 p2011 N73-26261
Design of optical instrument package for large space telescope
18 p2210 N73-27839
Glacing incidence telescope for evaluating polarization of light source
18 p2210 N73-27840
Design analysis and tradeoff studies for defining Astronomy Sortie Mission based on mission requirements and payload limitations - Vol. 3 Bk. 1
[NASA-CR-124047] 20 p2473 N73-29870
Design analysis and trade studies to support candidate configurations and payloads for Astronomy Sortie Missions - Vol. 3 Bk. 2
[NASA-CR-124044] 20 p2474 N73-29871
Program development requirements for selected Astronomy Sortie Missions concept to show rationale and explanations of guidelines and assumptions - Vol. 4
[NASA-CR-124046] 20 p2474 N73-29872
Solar physics, planetary atmospheres, and space astronomy research programs
[NASA-CR-133773] 21 p2610 N73-30923

**SPACEBORNE PHOTOGRAPHY**
NT SATELLITE-BORNE PHOTOGRAPHY
Satellite cloud photographs of BOMEX area
04 p0442 N73-13600
Analysis of photographic data obtained during manned and unmanned space flight and application to oceanography, hydrology, geography, and geology
04 p0471 N73-13843
Mariner 6 and 7 television photographs of Mars
[NASA-SP-263] 04 p0475 N73-13878
Analysis of cloud console devices used in displaying meteorological satellite imagery
[AD-750085] 05 p0575 N73-14684
Computer technique for stereo image processing of Mariner 9 spacecraft color photographs
[NASA-CR-130305] 06 p0644 N73-15226
Application of remote sensing from aircraft and spacecraft to geology, hydrology, and geographical data acquisition
07 p0782 N73-16354
Application of airborne and spaceborne photography to determine agricultural and forestry resources
07 p0782 N73-16355
Regional agricultural survey using small scale aerial and space photography
07 p0785 N73-16383
Analysis of oceanography remote sensing using black and white, color, and color infrared photographic recording
07 p0788 N73-16407
Analysis of photography from Apollo 9 flight to determine origin, movement, and dissipation of masses of discolored water near shores of North and South Carolina
07 p0788 N73-16408
Application of remote sensors carried in aircraft and satellites to survey extent of usage of recreational facilities
[NASA-CR-130752] 08 p0917 N73-17517
Development of mathematical methods for calibrating lunar orbiter photography
[NASA-CR-128279] 08 p0924 N73-17572
Interpretation of Mariner 6 and 7 Martian photometry for sediment geomorphology
[NASA-CR-2194] 08 p0962 N73-17869
Soviet space stations for providing earth space photographs used for earth atmosphere and earth surface analysis
[JPRS-58055-1-PT-1] 09 p1026 N73-18372
Analysis of space photographs of earth surface
09 p1026 N73-18374
Spaceborne remote sensing for agricultural and forest resource surveys
[NASA-CR-130798] 09 p1026 N73-18376
Conference on parallel image processing for earth observation systems
[NASA-TM-X-66175] 09 p1065 N73-18684
Digital image processing for processing pictures from space vehicles
09 p1065 N73-18687
Conical section method for determining planetary configuration from spaceborne photographic data on triangulation and horizon lines
[JPRS-58304] 09 p1085 N73-18848
Tests and equipment for measuring performance characteristics of camera systems for space applications
[NASA-CR-128825] 10 p1160 N73-19438
Technique for using satellite pictures to analyze and forecast tropical cyclone intensities
[NOAA-TM-NESS-45] 10 p1182 N73-19611

Photographic summary for Apollo 16 flight
12 p1449 N73-21734
Photogrammetric techniques from Apollo 15 and 16 flights to provide accurate measurement of lunar topography
12 p1456 N73-21791
Photographic observations of solar corona by Apollo 16 command module from lunar orbit
12 p1456 N73-21794
Features of lunar furrows and ridges from telescopic and satellite photographs
12 p1457 N73-21808
Application of spaceborne photography and aerial photography to ecological resource inventory and analysis of naturally vegetated areas in Arizona
[NASA-CR-131581] 13 p1523 N73-22342
Earth observation experiments identified during earth orbital experiment program and requirements study - Vol. 6
[NASA-CR-112330] 13 p1577 N73-22783
Availability of Mariner 9 TV picture data
[NASA-TM-X-69216] 14 p1704 N73-23822
Satellite monitoring of open pit mining operations
[BM-IC-8530] 15 p1780 N73-24432
Manual for 70mm hand held photography from Skylab
[NASA-TM-X-66262] 16 p1912 N73-25475
Method for evaluating image errors of mapping camera locked to stellar cameras
[AD-759491] 16 p1915 N73-25497
Erratic operation of mapping camera extension mechanism on Apollo spacecraft
[NASA-TM-X-69269] 16 p1967 N73-25909
Analysis of ERTS-1 imagery to interpret three seasonal nearshore processes along California coast
[E73-10727] 17 p2020 N73-26333
Cartographic evaluation of ERTS-1 imagery for area of Bristol, England to show natural and man-made features
[E73-10739] 17 p2021 N73-26345
Application of EREP data in geological evaluation, regional planning, forest management, and water management in North Carolina
[E73-10754] 17 p2022 N73-26357
Comparison of Skylab/EREP imagery with television and radiometric measurements from other satellites for snow cover survey in Sierra Nevada Mountains and Great Plains
[E73-10755] 17 p2022 N73-26358
Spaceborne imagery of snow cover and glaciers in mountainous regions
[NASA-TT-F-14969] 17 p2025 N73-26387
Geomorphological structure of earth surface from spaceborne photography
[NASA-TT-F-14968] 17 p2025 N73-26388
Geobotanical mapping based on spaceborne photography
[NASA-TT-F-14976] 17 p2026 N73-26392
Spaceborne photography of vegetation, soils, and agricultural land use
[NASA-TT-F-14967] 17 p2026 N73-26393
Possibilities of studying and mapping soil cover on basis of Soyuz, Gemini, Apollo, and Salyut photographs
[NASA-TT-F-14971] 17 p2032 N73-26447
Development of techniques for processing Skylab multispectral scanner data and comparison with ERTS-1 and aircraft scanner data processed by same technique
[E73-10758] 17 p2036 N73-26473
EREP 463 imagery of fault tectonics and earthquake hazards in peninsular ranges of southern California
[E73-10781] 18 p2136 N73-27257
Study of recreational land and open space with Skylab imagery EREP 443
[E73-10783] 18 p2136 N73-27259
Skylab and EREP remote sensing data for tectonic analysis of Bighorn Mountains of Wyoming and Montana
[E73-10784] 18 p2136 N73-27260
Aerial and space photographic methods for geographic research
[NASA-TT-F-14966] 19 p2293 N73-28440
Interpretation of space photographs of dry piedmont steppe region for hydrologic mapping
[NASA-TT-F-14974] 20 p2411 N73-29382
Sequence design and picture coverage catalog for Mariner Mars 1971 television pictures
[NASA-CR-133614] 20 p2473 N73-29864
Papers presented at meeting of Soviet-American working group on remote sensing of natural environment from space
[JPRS-59739] 21 p2534 N73-30317
Assessment of US and USSR technology and instrumentation for obtaining, transmitting, and processing earth images from space
21 p2534 N73-30318
General principles of geological interpretation of remote images of earth surface
21 p2534 N73-30319
Solution of certain regional geological problems using space photography
21 p2534 N73-30320
Selection of standard sections in u.s.s.r. as test sites for geological interpretation of space photography
21 p2534 N73-30321
Tyan-shan section of USSR as test site for geological interpretation of space photography
21 p2534 N73-30322
Caucasian section of USSR as test site for geological interpretation of space photography
21 p2534 N73-30323
Ustyurt section of USSR as test site for geological interpretation of space photography
21 p2535 N73-30324
Application of space photography for small-scale mapping and analysis of farm lands
21 p2535 N73-30326
Determination of optimal spectral intervals for remote sensing of earth surface from space
21 p2535 N73-30327
Interpreting and compiling soil maps from aerial and space survey data
21 p2535 N73-30328
Geological-structural interpretation of photographs of Balkhash region from space and their role in geological survey of Central Kazakhstan
21 p2535 N73-30329
Aerotriangulation with very small scale photography from Skylab
[E73-10994] 22 p2659 N73-31300
Mariner 9 television observations of Martian planets Phobos and Deimos
23 p2841 N73-32705
Photogrammetric evaluation of Mariner 9 Mars surface pictures
23 p2843 N73-32721
Analytical stereophotogrammetric evaluation of Martian topography using Mariner 9 photographs
[CONTRIB-2250] 23 p2843 N73-32722

**SPACEBORNE TELESCOPES**
NT LARGE SPACE TELESCOPE
Joint Soviet-US research radio astronomy and plans involving spaceborne telescope
[NLL-M-22684-[5828.4F]] 01 p0100 N73-10823
High resolution X ray astronomy using rocketborne telescopes
[NASA-CR-130166] 03 p0357 N73-12912
Determination of optical/mechanical properties of low expansion glass ceramic material for use as lightweight substrate for primary mirror on large spaceborne telescope
[NASA-CR-130141] 06 p0674 N73-15481
Stellar spectrograms from Salyut space station of alpha Lyrae and beta Centauri
[NASA-TT-F-14582] 07 p0843 N73-16831
Development of Large Space Telescope for conducting astronomical observations from unmanned satellites and analysis of constraints and tradeoffs during design phase - Vol. 1
[NASA-TM-X-64726-VOL-1] 09 p1035 N73-18449
Development and characteristics of optical telescope assembly system for Large Space Telescope based on mission-related and optical parameters - Vol. 3
[NASA-TM-X-64726-VOL-3] 09 p1036 N73-18451
Development and characteristics of scientific instrument package for use with Large Space Telescope - Vol. 4
[NASA-TM-X-64726-VOL-4] 09 p1036 N73-18452
Development and characteristics of support systems module for use with Large Space Telescope - Vol. 5
[NASA-TM-X-64726-VOL-5] 09 p1036 N73-18453
Baseline experiment definition documents for candidate astronomy sortie mission telescopes and arrays to be used on space shuttle
[NASA-CR-124045] 09 p1084 N73-18843
Design, development, and configuration of astronomical observatory for space shuttle to show telescope capabilities and characteristics of various remote sensors
[NASA-CR-128841] 10 p1215 N73-19879
Balloon-borne telescopic observations of X ray pulsars in Gum and Crab nebulae
13 p1575 N73-22764
Postflight analysis of Apollo 16 scanning telescope system to determine cause of uneven drive rates
[NASA-TM-X-69233] 17 p2089 N73-26899
Design of ultraviolet Explorer satellite for spaceborne astronomy
18 p2210 N73-27838
LST phase A design update study
[NASA-TM-X-64763] 19 p2300 N73-28494
TD-1A telescope optical surface chemical contamination investigation of thermal vacuum tests and volatile condensable material screening
[ESRO-TN-86-ESTEC] 21 p2601 N73-30847
Requirements of telescopes for extra-atmospheric astronomical observations
[NASA-TT-F-15119] 22 p2715 N73-31732
Laboratory simulation of scaled single-axis dual-level control system for large space telescope
[NASA-TN-D-7319] 23 p2791 N73-32333

**SPACECRAFT**
Research in aerospace, biological, and solar sciences
[AD-746143] 02 p0133 N73-11080
Space vehicle descent into Mars, Jupiter, and Venus atmospheres
[NASA-TT-F-768] 07 p0844 N73-16838
Facilities for handling light signals from long range spacecraft
14 p1618 N73-23107
Advanced wiring system for aircraft and space vehicle application
14 p1642 N73-23311
Optimal control, guidance, and trajectory for low thrust acceleration spacecraft
15 p1829 N73-24827
Integrated thermal protection and structural meteoroid protection system in space vehicles - Vol. 1
[NASA-CR-121103] 15 p1834 N73-24865
Space vehicle integrated thermal protection/structural meteoroid protection system - Vol. 2
[NASA-CR-121104] 15 p1834 N73-24866
Design and performance of aircraft or spacecraft differential maneuvering simulator
[NASA-TN-D-7304] 16 p1885 N73-25259
Development, fabrication, and evaluation of heat pipe thermal conditioning panels for temperature control of spacecraft electronic equipment - Technical Report
[NASA-CR-124451] 24 p2991 N73-33898

**SPACECRAFT ANTENNAS**
Orientation of Symphonie satellite antennas with accuracy effect
[DGLR-PAPER-72-063] 09 p1003 N73-18182
Design, fabrication, and testing of lightweight, foldable 4.27 meter spacecraft antenna
09 p1087 N73-18870
Collapsible support for antenna reflector applied to installation of spacecraft antennas
[NASA-CASE-NPO-11751] 15 p1749 N73-24176
Development of large furlable spacecraft antennas using conical main reflectors
[NASA-CR-132989] 16 p1880 N73-25219
Complex permittivity measurements during high temperature recycling of space shuttle antenna window and dielectric heat shield materials
[NASA-CR-2302] 22 p2707 N73-31675

**SPACECRAFT CABIN ATMOSPHERES**
Spacecraft environment, radiation, and weightlessness effects on human biological processes in manned space flight
[JPRS-57517] 03 p0256 N73-12076
Aerogenic microbial contamination of manned pressurized cabin atmosphere at reduced temperature and high humidity
03 p0259 N73-12098
Design and performance of prototype nitrogen/oxygen supply unit using water/hydrazine electrolysis to provide cabin leakage makeup in manned spacecraft
[NASA-CR-128688] 06 p0635 N73-15159
Environmental health measures to prevent cabin atmosphere toxicity and provide drinking water standards in manned space flight applications
08 p0872 N73-17058
Toxicity of atmospheric dichloromethane levels in simulated space cabin atmosphere on dogs, rats, mice, and monkeys
[NASA-TM-X-69099] 09 p0996 N73-18129
Nitrogen oxide and ammonia removal from spacecabin atmosphere by catalytic oxidation with ruthenium and adsorption on silica gel
[NASA-CR-2132] 09 p0999 N73-18151
Medical and biological problems of manned space flight
[NASA-TT-F-719] 10 p1114 N73-19077
Oxidation of atmospheric impurities in space cabin and purity of reciamated water
10 p1117 N73-19104
Temperature and humidity control in air quality modeling for optimal life support system of spacecraft cabin
15 p1743 N73-24131
Electrochemical process for recovery of oxygen from atmospheres of manned space capsules
[NASA-CR-114573] 16 p1869 N73-25130

**SPACECRAFT CABIN SIMULATORS**
Analysis of external interfaces, crew procedures, visual cues, and aural cues for space shuttle vehicle and mission simulation - Vol. 4
[NASA-CR-128624] 02 p0230 N73-11863
Design, development, and capabilities of space shuttle mission simulator to show types of training available and cost effectiveness of facility
[NASA-CR-128885] 12 p1387 N73-21251
Space shuttle mission simulator requirements
[NASA-CR-128890] 13 p1506 N73-22203
Training requirements of mission phase for crews and ground support personnel
[NASA-CR-128886] 13 p1506 N73-22204
Development of hardware and software specifications for procurement of space shuttle mission training simulator for crew training
[NASA-CR-133965] 18 p2126 N73-27177
Payload carrier integrated test for simulated Sortie Lab Missions
[NASA-TM-X-64770] 22 p2647 N73-31207

**SPACECRAFT CABINS**
Analyses of Skylab crew quarters and habitability - App. D
[NASA-CR-61386-APP-D] 06 p0721 N73-15880

Design parameters and systems analysis of crew compartment for space shuttle orbiter - Summary Report
[NASA-CR-128949] 16 p1965 N73-25893
Design parameters and systems analysis of crew compartment for space shuttle orbiter - Final Report
[NASA-CR-128950] 16 p1965 N73-25894
Interrelationship and reaction of human subjects to spacecraft cabin environment
[NASA-TT-F-15020] 20 p2368 N73-29041

SPACECRAFT COMMUNICATION
Attenuation and phase constancy propagation criteria of tactical satellite communications using mobile ground terminals
01 p0026 N73-10201
Wideband tactical satellite communications systems using onboard processing
01 p0026 N73-10202
Measurement methods and error analyses by ground terminals for optimizing satellite communications link
01 p0026 N73-10203
Satellite communication terminal for ships
01 p0026 N73-10204
Orbit sharing and deployment problems of high power satellite communication systems
01 p0026 N73-10205
Satellite communications and defense
[AD-746165] 02 p0142 N73-11147
Turnstile slot antenna system for spacecraft or missile telemetry and command control
[NASA-CASE-GSC-11428-1] 02 p0149 N73-11206
Characteristics of diversity satellite-to-ground communication link measured using ATS 5 15.3 GHz downlink
[NASA-CR-130118] 03 p0265 N73-12144
TD-1A satellite ground checkout stations noting spacecraft communication and data transmission
[ESRO-TM-140-ESTEC] 04 p0402 N73-13277
Analysis of electromagnetic interference between satellite frequency modulated television signal and television signal for commercial broadcasting
[NHK-LABS-NOTE-153] 07 p0754 N73-16123
Real time meteorological radar data for predicting rainfall effects on satellite communication system
[AD-751742] 07 p0757 N73-16147
Feasibility of efficient multiamplitude communication in earth satellite systems
10 p1228 N73-19983
Spacecraft communications terminal breadboard components
[NASA-CR-128859] 11 p1255 N73-20181
Design of experiment to measure communication characteristics of wideband satellite to ground communication links
[NASA-CR-130196] 11 p1294 N73-20497
Design of communication repeater subsystems for advanced multifunctional communications satellites
[NASA-CR-132296] 13 p1581 N73-22819
Design, development, and characteristics of spacecraft systems and equipment used with Tracking and Data Relay Satellite System - Vol. 3
[NASA-CR-130218] 13 p1582 N73-22822
Estimation of signal-to-noise ratio in spacecraft data channel
16 p1879 N73-25207
Design technology of aeronautical satellite communication system for air traffic control over Atlantic Ocean
[FAA-ED-17-1] 18 p2115 N73-27104
Characteristics of low cost mass producible earth terminal antenna system for broadcast satellite
18 p2122 N73-27152
Conference on technology utilization in spacecraft guidance, ground operations, communications and navigation systems, and sensor development
[NASA-SP-326] 18 p2207 N73-27816
Ionospheric fading effects on microwave space communication links in equatorial zone
18 p2212 N73-27855
Attenuation and fading characteristics of ATS 5 15 and 32 GHz millimeter ground-space links
18 p2212 N73-27856
Amplitude control method for equalizing low level phonemes in satellite voice communication system
18 p2212 N73-27862
Radiometer image data compression system with zero error wideband ground link transmission
18 p2212 N73-27863
Modelling, experimentation, and estimation for multipath signals between ground terminal and aerospace vehicle
20 p2376 N73-29089
Low cost highly sensitive 12 GHz low noise converter for communication between broadcast satellites and ground stations
[NHK-LABS-NOTE-161] 20 p2380 N73-29127
Compendium of worldwide satellite communications programs to Aug. 1971
[NASA-TM-X-70435] 21 p2599 N73-30834
Computer programs for analyzing satellite communication links
[REPT-6806] 24 p2895 N73-33108

SPACECRAFT COMPONENTS
NT COMMAND MODULES
NT SERVICE MODULES
NT SPACECRAFT CABINS
NT SPACECRAFT MODULES
Analysis of potential hazards caused by carrying experimental equipment on Earth Orbit Shuttle and recommendations for eliminating or reducing hazards-Vol.2 Pt.2
[NASA-CR-129103] 02 p0231 N73-11873
Development and evaluation of space shuttle main landing gear door constructed of boron/epoxy composite material ribs on titanium panel
[NASA-CR-112172] 02 p0233 N73-11889
Wind tunnel tests to determine aerodynamic characteristics and aerodynamic interference of various configurations of space shuttle ascent vehicle-Vol. 1
[NASA-CR-120083] 02 p0234 N73-11901
Wind tunnel tests to determine aerodynamic characteristics of space shuttle ascent configurations with parallel burn pressure-fed and SRM boosters and tank T3 installation - Vol. 2
[NASA-CR-120084] 02 p0234 N73-11902
Wind tunnel tests to determine aerodynamic characteristics of space shuttle ascent configurations with parallel burn pressure-fed and SRM boosters and tank T4 installation - Vol. 3
[NASA-CR-120085] 02 p0234 N73-11903
Wind tunnel tests to determine aerodynamic characteristics of space shuttle ascent configurations with orbiter, tanks, and booster alone installations - Vol. 5
[NASA-CR-120087] 02 p0234 N73-11905
Magnetic bearings for spacecraft applications
[NASA-TM-X-66111] 03 p0306 N73-12499
Design requirements for space tug systems and cost analysis of maintenance and operation during space missions
[NASA-CR-129253] 03 p0358 N73-12918
Rate of discharge of accelerated life tests of nickel cadmium cells
[AD-748253] 04 p0377 N73-13065
Manual of chemical processes related to spacecraft development technology
[NASA-TM-X-2635] 05 p0506 N73-14117
Design, development, and characteristics of expendable second stage for use with reusable space shuttle booster - Vol. 1
[NASA-CR-128671] 05 p0598 N73-14865
Definition of system for expendable second stage and reusable space shuttle booster system - Vol. 2 - Bk. 1
[NASA-CR-128670] 05 p0598 N73-14866
Definition of expendable second stage for use with reusable space shuttle booster to include structural, propulsion, and avionics systems design - Vol. 2 - Bk. 2
[NASA-CR-128672] 05 p0599 N73-14867
Definition of expendable second stage and space shuttle booster separation system to include modifications required, ground support equipment, and launch operations - Vol. 2 - Bk. 3
[NASA-CR-128673] 05 p0599 N73-14868
Wind tunnel tests to determine aerodynamic characteristics of expendable second stage and payload configurations for reusable space shuttle booster - Vol. 3
[NASA-CR-128674] 05 p0599 N73-14869
Wind tunnel tests to determine pressure distribution on wing and lower body surface for space shuttle orbiter in launch configuration
[NASA-CR-120075] 05 p0600 N73-14879
Development of space stable thermal control coatings for application to spacecraft surfaces
[NASA-CR-124003] 07 p0854 N73-16922
Microbiological assay procedures for spacecraft cabling, antennas, solar panels, and thermal blankets
[NASA-CR-130383] 08 p0877 N73-17109
Program and technical alternatives to design of space shuttle orbiter to include aerodynamic configurations and predicted performance
[NASA-CR-130747] 08 p0964 N73-17877
Design and development of large flexible tunnel for use at space shuttle and payload interface
[NASA-CR-124073] 08 p0964 N73-17879
Squib actuated disconnect for spacecraft coupling to launch vehicle
[NASA-CASE-NPO-13172-1] 08 p0969 N73-17917
Control equipment for sterilization facility used to thermally inactivate microbes on interplanetary space vehicle components
[NASA-CR-131103] 10 p1119 N73-19122
Fabrication and evaluation of wire harnesses from small gage wire round conductor cables - Vol. 2
[NASA-CR-128846] 11 p1262 N73-20242
Cost comparison of flat versus round conductor cable based on spacecraft electric wiring system specifications - Vol. 3
[NASA-CR-128847] 11 p1262 N73-20243
Development and characteristics of supporting frame to isolate payloads from multi-gravitational forces
[NASA-CASE-MFS-21680-1] 11 p1297 N73-20525
Development of dissipative energy approach for predicting damping of four component space shuttle model using modal parameters for individual components
12 p1459 N73-21827
Soviet research and development of solar batteries and power cells for spacecraft
[AD-756039] 13 p1478 N73-21973
Degradation of cold optical systems on orbiting spacecraft by cryodeposition
[AD-756772] 13 p1560 N73-22644
Analysis of telemetry data from prelaunch, launch, and flight activation phases of ERTS-1 spacecraft
[NASA-CR-130150] 13 p1581 N73-22817
Flight performance analysis of ERTS-1 spacecraft components during orbits 1300 to 2600
[NASA-CR-130207] 13 p1581 N73-22818
Development of guidelines for application to production of spacecraft hardware components with long lifetime - Vol. 1
[NASA-CR-128905] 14 p1707 N73-23853
Guidelines for design and development of electrical and electronic components and systems used in spacecraft construction to obtain long service life - Vol. 2
[NASA-CR-128906] 14 p1707 N73-23854
Development of guidelines for selection of hardware items for use in manned spacecraft design to obtain five year maintenance-free service life - Vol. 3
[NASA-CR-128907] 14 p1707 N73-23855
Development of guidelines for spacecraft equipment selection based on quality control and test procedures during manufacturing - Vol. 4
[NASA-CR-128908] 14 p1707 N73-23856
Development of guidelines for selection of manned spacecraft equipment and recommendations for performance and quality control tests
[NASA-CR-128909] 14 p1708 N73-23857
Development and characteristics of movable mass control system to convert tumbling motions of disabled spacecraft into simple spin movements
[NASA-CR-131867] 14 p1710 N73-23875
Cryogenic cooling methods for spaceborne systems
[AD-755780] 14 p1720 N73-23958
Performance tests of L-band truss cable meteoroid shielding on Skylab space station at minus 180 degrees Fahrenheit
[NASA-TM-X-64743] 15 p1834 N73-24867
Serpentine teleoperator device for simulating intravehicular and extravehicular activities in space
[NASA-TR-R-414] 16 p1879 N73-25210
Congressional hearing to determine malfunction on Skylab 1 workshop and proposed methods for correcting malfunction
16 p1964 N73-25884
Dry heat inactivation of atypical Bacillus subtilis var. niger spores in and on interplanetary space vehicle components
[NASA-CR-133224] 17 p1987 N73-26059
Development of computer program and data base for design of cryogenic systems used in space shuttles and spacecraft - Vol. 5 B-1
[NASA-CR-133955] 17 p2087 N73-26883
Computer programmers manual for mathematical model used in design of cryogenic supply systems for space shuttles and spacecraft - Vol. 5 B-2 Part 1
[NASA-CR-133956] 17 p2087 N73-26884
Computer programmers manual for parametric analysis of attitude control propulsion system using converted liquid cryogenics reaction system - Vol. 5 B-3 Part 2
[NASA-CR-133958] 17 p2087 N73-26886
NASA space vehicle design criteria on accelerometer applications
[NASA-SP-8102] 17 p2088 N73-26891
Apollo 16 flight anomaly report on malfunction of water/glycol temperature control circuit
[NASA-TM-X-69234] 17 p2089 N73-26900
Solar absorber coatings for use with spaceborne Vuilleumier cycle cryogenic refrigerators
[AD-760577] 18 p2167 N73-27505
Design and development of optimized cryogenic fuel supply systems for space shuttle vehicles - Vol. 2
[NASA-CR-128993] 18 p2199 N73-27751
Evaluation of candidate systems for cryogenic fuel supply system used on space shuttle vehicle - Vol. 3
[NASA-CR-128994] 18 p2199 N73-27752
Analysis of cryogenic supply system for space shuttle vehicles and evaluation of candidate systems - Vol. 1
[NASA-CR-128992] 18 p2199 N73-27756
Development of integrated mathematical model for optimization of cryogenic fluid storage and supply systems for spacecraft - Vol. 5A-1
[NASA-CR-133953] 18 p2199 N73-27757
Biodetection grinder for sampling aerospace materials for microorganisms
[NASA-TM-X-64765] 20 p2372 N73-29059
Development and characteristics of variable ratio, mixed-mode, bilateral master-slave control system for space shuttle remote manipulator system
[NASA-CASE-MSC-14245-1] 21 p2599 N73-30832
Description of pyrotechnic systems principles with application to systems and equipment on space shuttle
[NASA-CR-2292] 21 p2600 N73-30840
Computer program for use with thermal-elastic-plastic-creep structural analyzer for structural analysis of spacecraft and propulsion systems - Vol. 2
[NASA-CR-124391] 22 p2725 N73-31806
White porcelain enamal thermal control coating for spacecraft
[NASA-CR-124459] 24 p2938 N73-33459

Design, development, and fabrication of prototype storage module with internal restraints for stowage of items launched to support space missions
[NASA-CR-124465] 24 p2983 N73-33832

SPACECRAFT CONFIGURATIONS
NT APOLLO TELESCOPE MOUNT
NT SATELLITE CONFIGURATIONS
Wind tunnel tests of space shuttle models to determine effects of body and wing geometry on hypersonic shock structure and on surface impingement of interior flow field shock waves
[NASA-CR-128587] 01 p0040 N73-10317
Wind tunnel tests to determine convective heat distribution for space shuttle configurations based on viscous/inviscid interactions of three dimensional flow fields
[NASA-CR-128586] 01 p0040 N73-10318
Wind tunnel tests to determine aerodynamic characteristics and aerodynamic interference of various configurations of space shuttle ascent vehicle-Vol. 1
[NASA-CR-120083] 02 p0234 N73-11901
Wind tunnel tests to determine aerodynamic characteristics of space shuttle ascent configurations with parallel burn pressure-fed and SRM boosters and tank T4 installation - Vol. 3
[NASA-CR-120085] 02 p0234 N73-11903
Wind tunnel tests to determine space shuttle ascent configuration plumes with pressure-fed and solid rocket motor boosters - Vol. 4
[NASA-CR-120086] 02 p0234 N73-11904
Wind tunnel tests to determine aerodynamic characteristics of space shuttle ascent configurations with orbiter, tanks, and booster alone installations - Vol. 5
[NASA-CR-120087] 02 p0234 N73-11905
Development of payload for mission planning for missions to outer planets as function of flight time for various launch years, launch vehicles, and orbit sizes
[NASA-CR-129244] 03 p0354 N73-12887
Design and development of scale model of parallel burn space shuttle to represent low frequency structural dynamic characteristics
[NASA-CR-112205] 04 p0478 N73-13909
Wind tunnel tests of space shuttle model to determine performance, stability, and control characteristics of launch configuration
[NASA-CR-120088] 04 p0478 N73-13910
Wind tunnel tests to determine subsonic aerodynamic characteristics of model of space shuttle orbiter configuration with swept trapezoidal wing and swept fixed glove
[NASA-TM-X-2701] 05 p0491 N73-14005
Spacecraft configurations and aerodynamic characteristics of space shuttle systems with two reusable stages
[NASA-CASE-MSC-12433] 05 p0597 N73-14854
Analysis of payloads for space shuttle based on space missions, planetary exploration, and international rendezvous and docking - Vol. 2
[NASA-CR-129844] 05 p0598 N73-14862
Definition of system for expendable second stage and reusable space shuttle booster system - Vol. 2 - Bk. 1
[NASA-CR-128670] 05 p0598 N73-14866
Definition of expendable second stage for use with reusable space shuttle booster to include structural, propulsion, and avionics systems design - Vol. 2 - Bk. 2
[NASA-CR-128672] 05 p0599 N73-14867
Definition of expendable second stage and space shuttle booster separation system to include modifications required, ground support equipment, and launch operations - Vol. 2 - Bk. 3
[NASA-CR-128673] 05 p0599 N73-14868
Analysis of mass properties of reusable space shuttle booster and expendable second stage for three specified payloads - Vol. 4
[NASA-CR-128659] 05 p0599 N73-14870
Definition of major expendable second stage interfaces with specified space shuttle booster components including interface control drawings - Vol. 6
[NASA-CR-128661] 05 p0599 N73-14872
Preliminary design drawings of expendable second stage reusable space shuttle booster to define specific payloads and configurations - Vol. 7
[NASA-CR-128662] 05 p0599 N73-14873
Contract end item specifications for defining hardware end items required by expendable second stage of space shuttle booster system - Vol. 8 Pt. 1
[NASA-CR-128663] 05 p0599 N73-14874
Preliminary system specification for design, operation, and performance of expendable second stage for reusable space shuttle booster - Vol. 9
[NASA-CR-128664] 05 p0599 N73-14875
Design requirements and data for expendable second stage of reusable space shuttle booster - Vol. 12
[NASA-CR-128667] 05 p0600 N73-14877
Application of multivariate control theory to design of hierarchial attitude control system for CARD space vehicle
[NASA-CR-124087] 09 p1086 N73-18859
Apollo experience report of structural subsystem, structural configuration, and design verification of lunar module spacecraft
[NASA-TN-D-7084] 09 p1091 N73-18901
Evaluation of monopropellant and bipropellant earth storable reaction control systems for application to space shuttle vehicle - Phase C & E
[NASA-CR-128819] 10 p1209 N73-19832
Development of computer program to size launch vehicles for optimal trajectories and application for general purpose branched trajectory optimization
[NASA-CR-128725] 10 p1214 N73-19869
Formulation, evaluation, and demonstration of various procedures for analytically coupling two or more substructures to obtain modal data for assembly
[NASA-CR-112252] 10 p1215 N73-19881
Proceedings of conference on economic aspects of space shuttle system to show basis for cost effectiveness determinations and system selection
[NASA-CR-131421] 11 p1337 N73-20848
Development of mathematical model of lateral motion of flexible space shuttle vehicle during ascent
[NASA-CR-124159] 11 p1340 N73-20876
Development of dynamic loads computation capability for application to unified flexible spacecraft simulation program
[NASA-CR-124168] 11 p1340 N73-20878
Wind tunnel tests to determine pressure distribution on space shuttle launch configuration consisting of delta wing orbiter and swept wing booster - Vol. 1 Pt. A
[NASA-CR-120034-VOL-1-PT-A] 11 p1342 N73-20891
Wind tunnel tests to determine pressure distribution on space shuttle launch configurations consisting of delta wing orbiter and swept wing booster - Vol. 1 Pt. B
[NASA-CR-120034-VOL-1-PT-B] 11 p1342 N73-20892
Wind tunnel tests to determine pressure distribution on space shuttle launch configuration consisting of space shuttle orbiter in presence of booster - Vol. 2
[NASA-CR-120034-VOL-2] 11 p1342 N73-20893
Economic analysis of space tug operations to include tug definition, spacecraft configurations, payload effects, and costing logic - Vol. 1
[NASA-CR-124142] 11 p1343 N73-20899
Comparative analysis of space tug concepts to show overall approach and data generation - Vol. 2, Pt. 1
[NASA-CR-124143] 11 p1343 N73-20900
Economic principles for cost effectiveness and cost benefit analysis of space tug operations - Vol. 2, Pt. 2
[NASA-CR-124144] 11 p1343 N73-20901
Development of data base to show space tug characteristics, costs, and performance for comparison of concepts - Vol. 2 Appendix
[NASA-CR-124146] 11 p1344 N73-20902
Cost analysis of single stage space tug operations with several types of liquid propellant rocket engine propulsion systems - Vol. 3
[NASA-CR-124147] 11 p1344 N73-20903
Effect of nose geometry on aerothermodynamic environment of shuttle entry configurations
[NASA-CR-128873] 11 p1348 N73-20937
Wind tunnel tests of space shuttle orbiter scale model to determine low speed aerodynamic characteristics of spacecraft components
[NASA-CR-120092] 12 p1460 N73-21832
Description of canonical set of equations which governs behavior of n-body spacecraft connected by dissipative elastic joints
[NASA-CR-132155] 15 p1835 N73-24872
Dynamic characteristics of large flexible solar arrays and interaction between spacecraft attitude dynamics and elastic degrees of freedom
[UTIAS-179] 15 p1835 N73-24878
Artificial intelligence for identifying practical applications to unmanned spacecraft to explore solar system in 1980 time period - Vol. 1
[NASA-CR-132256] 16 p1962 N73-25873
Handbook of data on passive thermal control coatings and surfaces for heat transfer and temperature regulation of spacecraft
[NASA-CR-124287] 16 p1975 N73-25969
Wind tunnel measurements of overall fluctuating pressure levels on seven space shuttle launch configurations at transonic and supersonic speeds
[NASA-TM-X-62280] 17 p2087 N73-26882
Spacelab configurations noting thermal control, life support, electrical power, communication, and altitude control subsystems
[ESS/SS-399-VOL-2] 17 p2089 N73-26903
Development of alternate space shuttle concepts to show modified avionics, vehicle subsystems, and thermal protection system
[NASA-CR-124345] 21 p2601 N73-30844
Apollo experience report on equipment storage and stowage arrangement in spacecraft for maximum operational performance
[NASA-TN-D-7434] 22 p2720 N73-31771
Simplified analysis procedure for determining static and dynamic aeroelastic loads for space shuttle dynamics
[NASA-CR-124370] 22 p2722 N73-31781
Congressional hearing to determine causes of malfunctions of Skylab space vehicle
22 p2737 N73-31914
Analysis of alternate space shuttle concepts to examine stage-and-one-half concept for reusable shuttle system and cost of external hydrogen tank development program
[NASA-CR-124421] 23 p2850 N73-32774
Development and characteristics of advanced technology laboratory for use with space shuttle concept
[NASA-TM-X-2813] 23 p2851 N73-32781
Spacecraft mass properties data for use in mission planning for Apollo/Soyuz Test Project
[NASA-TM-X-69502] 24 p2980 N73-33813
Thermal-vacuum tests of flight model spacecraft to determine performance and reliability based on malfunction analysis
[NASA-TN-D-7408] 24 p2984 N73-33851

SPACECRAFT CONSTRUCTION MATERIALS
Effects of high temperature cycling on structural properties of boron reinforced aluminum alloys used in spacecraft structures
[NASA-CR-124369] 21 p2562 N73-30541

SPACECRAFT CONTAMINATION
Aerogenic microbial contamination of manned pressurized cabin atmosphere at reduced temperature and high humidity
03 p0259 N73-12098
Infrared absorption spectra analysis of contaminant materials and binary mixtures to determine contamination of spacecraft by material outgassing
[NASA-CR-124072] 08 p0934 N73-17645
Development of procedures of identification of microorganisms on orbiting spacecraft
[NASA-CR-128747] 10 p1120 N73-19132
Theoretical analysis of effects of outgassing and waste dumping on contamination of orbiting spacecraft
[NASA-CR-124131] 11 p1340 N73-20875
Preflight, inflight, and post flight operations evaluation analyses for Skylab contamination measurement sample array - Appendix S
[NASA-CR-61386-APP-S] 14 p1708 N73-23864
Molecular contamination performance determination for space chamber tests, including molecular flow conditions and parameters
[NASA-TN-D-7250] 15 p1760 N73-24264
Psychrophilic organisms in soil samples of areas for Viking spacecraft assembly
[REPT-2] 17 p1987 N73-26063
Self-contamination of manned orbiting spacecraft from plasma gas or particulate matter
[NASA-CR-133836] 21 p2601 N73-30843
TD-1A telescope optical surface chemical contamination investigation of thermal vacuum tests and volatile condensable material screening
[ESRO-TN-86-ESTEC] 21 p2601 N73-30847
Thermal stress and mechanical shock effects on release of bacterial spores from stainless steel surfaces with application to Mars landing
[NASA-CR-133868] 22 p2619 N73-30987
Techniques for assessment and control of contamination in scientific satellites
[NASA-TN-D-7433] 23 p2845 N73-32738

SPACECRAFT CONTROL
NT SATELLITE ATTITUDE CONTROL
NT SATELLITE CONTROL
Utilization of simplified man machine interface concept to manage and control complex space system involving multiple redundant computers that control multiple redundant systems - Vol. 1
[NASA-CR-128576] 01 p0019 N73-10145
Space shuttle orbiter subsystems and control and display data required for crew operations - Vol. 2
[NASA-CR-128577] 01 p0019 N73-10146
Control and display sequences for four space shuttle orbiter mission phases - Vol. 4
[NASA-CR-128579] 01 p0019 N73-10148
Corrector module and spacecraft dynamics program
[NASA-CR-130108] 01 p0031 N73-10238
Reliability probability analysis on ergatic process in spacecraft control during approach and docking with orbital station
03 p0258 N73-12087
Analysis of pointing and stability problems of space shuttle sortie mission and application to earth observation and astronomy experiments
[NASA-TM-X-64692] 03 p0355 N73-12892
Characteristics of star field attitude sensor for installation in Pioneer Venus spacecraft
[NASA-CR-114516] 03 p0359 N73-12924
Interaction of space shuttle control system with pogo
[NASA-CR-2154] 04 p0479 N73-13914
Guidance, navigation and control system analysis report for Apollo 15
[NASA-TM-X-68934] 06 p0696 N73-15673
Guidance, navigation, and control system performance analysis report for Apollo 16 mission
[NASA-TM-X-68931] 06 p0696 N73-15674
Application of on-board digital computers for stabilization of missile and rocket control systems
[JPRS-57893] 06 p0721 N73-15881
Development of computer model to simulate pulse mode performance operation of liquid bipropellant attitude control engines
[AD-752610] 08 p0955 N73-17819

Attitude control of space vehicles using single movable mass to generate control torques with application to cable-connected, artificial gravity configuration
[NASA-CR-124081] 08 p0964 N73-17880
Role of cosmonaut in spacecraft control
09 p0997 N73-18137
Application of multivariate control theory to design of hierarchial attitude control system for CARD space vehicle
[NASA-CR-124087] 09 p1086 N73-18859
Payload deployment aspects of control system optimization of spacecraft maneuvers involved in stationkeeping and docking - Vol. 1
[NASA-CR-124050] 09 p1086 N73-18860
Digital implementation of high frequency cutoff filter for spacecraft control system optimization based on word length, sampling rate, accuracy, and computing time requirements - Vol. 2
[NASA-CR-124051] 09 p1086 N73-18861
Analysis of control and simulation methods for space shuttle manipulator
09 p1089 N73-18889
Mathematical and numerical methods for solving spacecraft control problems and mapping of celestial bodies
[NASA-TT-F-731] 10 p1177 N73-19572
Computer control of Atmosphere Explorer spacecraft
[NASA-TM-X-66209] 11 p1341 N73-20884
Wind tunnel tests of space shuttle orbiter scale model to determine low speed aerodynamic characteristics of spacecraft components
[NASA-CR-120092] 12 p1460 N73-21832
Proceedings of conference on materials and structures to include materials research, fracture control, and aerospace vehicle dynamics and control
[NASA-TM-X-69227] 13 p1585 N73-22850
Development and characteristics of movable mass control system to convert tumbling motions of disabled spacecraft into simple spin movements
[NASA-CR-131867] 14 p1710 N73-23875
Feasibility of automated spacecraft monitoring using real time computer telemetry
14 p1711 N73-23888
Mathematical models for human performance in manned spacecraft control
14 p1712 N73-23897
Development of electrostatically focused image dissector tube for use in spacecraft attitude control star trackers
[NASA-CR-132153] 15 p1787 N73-24487
Algorithm for computer simulation of Eulerian angles for spacecraft attitude
[NAL-TR-305] 15 p1803 N73-24612
Space shuttle energy management, approach, and landing analysis
[NASA-CR-128937] 15 p1830 N73-24830
Integrated digital flight control system for space shuttle orbiter
[NASA-CR-128936] 15 p1834 N73-24871
Steady-state attitude control propulsion system simulation program
[NASA-CR-128916] 16 p1955 N73-25820
Elastic structural models for dynamics and control of advanced space vehicles
[NASA-CR-124272] 16 p1967 N73-25908
Flight simulation to determine navigation, guidance, and control problems involving terminal area approach and landing of space shuttle using CV-990 aircraft
[NASA-TM-X-62285] 18 p2199 N73-27753
Wind tunnel tests to analyze aerothermodynamic control problems of space shuttle attitude control system at hypersonic speed
[NASA-CR-133407] 18 p2201 N73-27773
Technological modification to OSO-G launch vehicle for improved guidance and control
18 p2208 N73-27817
Real time computer technique for mission control and schedule planning
18 p2211 N73-27852
Flight tests of hydrazine control system performance and its effects on flight behavior of reentry vehicle
[SLA-73-154] 22 p2722 N73-31785
Dynamics and control of detumbling disabled spacecraft during rescue operations
[NASA-CR-135788] 24 p2983 N73-33831
Pseudo-Nyquist analysis technique for hybrid sampled-data control systems
[NASA-CR-2345] 24 p2984 N73-33847

**SPACECRAFT DESIGN**
NT SATELLITE DESIGN
Reference design document for power module systems, facilities, launch vehicle, and mission operations of nuclear reactor for space base programs - Vol. 3 pt. 1
[NASA-CR-123844] 02 p0209 N73-11696
Influence of Uranus, Neptune, and Pluto environments on design of spacecraft used to probe them
[NASA-SP-8103] 02 p0230 N73-11870
Criteria and guidelines for combining loads during ascent phase of space flight
[NASA-SP-8099] 02 p0234 N73-11897
Criteria for predicting, preventing, and evaluating panel flutter
[NASA-SP-8004] 02 p0237 N73-11932
Analysis of costs and effectiveness of space missions, aerospace vehicles, and propulsion systems
[NASA-CR-129258] 03 p0358 N73-12917
Design requirements for space tug systems and cost analysis of maintenance and operation during space missions
[NASA-CR-129253] 03 p0358 N73-12918
Analysis of Skylab program to show construction of spacecraft, test facilities, personnel accomodations, and research projects
04 p0470 N73-13831
Design and development of scale model of parallel burn space shuttle to represent low frequency structural dynamic characteristics
[NASA-CR-112205] 04 p0478 N73-13909
Development of design data for metallic materials, fasteners, joints, and structural elements used in aerospace vehicle design
[AD-748268] 04 p0479 N73-13917
Pioneer space probe project to show history, design, development, flight operations, and results accomplished
[NASA-SP-278] 05 p0598 N73-14864
Design, development, and characteristics of expendable second stage for use with reusable space shuttle booster - Vol. 1
[NASA-CR-128671] 05 p0598 N73-14865
Analysis of technology requirements for expendable second stage of space shuttle booster system - Vol. 10
[NASA-CR-128665] 05 p0600 N73-14876
Design requirements and data for expendable second stage of reusable space shuttle booster - Vol. 12
[NASA-CR-128667] 05 p0600 N73-14877
Design and employment of Soviet satellite of Cosmos series
[AD-749725] 05 p0601 N73-14886
History of USSR space program to include design of manned spacecraft, solution of space flight problems, and chronology of manned USSR space flights
[NLL-M-22222-[5828.4F]] 06 p0720 N73-15876
Design of orthotropic cylindrical shell as structural adapter for Helios solar probe
[DGLR-PAPER-72-101] 06 p0722 N73-15889
Wind tunnel determination of supersonic aerodynamic characteristics of variable geometry spacecraft designed for high hypersonic performance
[NASA-TM-X-2703] 07 p0735 N73-15985
ITOS system and design of TIROS M spacecraft
[NASA-CR-130163] 07 p0849 N73-16880
Program and technical alternatives to design of space shuttle orbiter to include aerodynamic configurations and predicted performance
[NASA-CR-130747] 08 p0964 N73-17877
Pioneer space probe system design and development, ground support system, tracking and communication, and data processing
[NASA-SP-279-VOL-2] 08 p0964 N73-17882
Characteristics of Performance Analysis and Design Synthesis computer program for determining size of launch vehicles for optimal trajectories - Vol. 2, Pt. 1
[NASA-CR-128678] 09 p1083 N73-18831
Description of QL module Performance Analysis and Design Synthesis computer program for determining optimal trajectory of launch vehicles - Vol. 2, Pt. 2
[NASA-CR-128657] 09 p1083 N73-18832
Analysis of relationships between changes in space shuttle weights and costs with changes in weight of structural subsystems
[NASA-CR-2164] 09 p1090 N73-18894
Apollo experience report of structural subsystem, structural configuration, and design verification of lunar module spacecraft
[NASA-TN-D-7084] 09 p1091 N73-18901
Management methods for Skylab program to include mission operations support, environmental and thermal design criteria, optical contamination, and materials science
[NASA-TM-X-64725] 11 p1342 N73-20886
Space vehicle design to withstand adverse conditions involved in handling and transportation from factory to launch site
[NASA-SP-8104] 12 p1461 N73-21839
Development of computerized training aid for research and development managers based on spacecraft design operations
[NASA-TN-D-7238] 12 p1466 N73-21880
Development of method for determining optimal lunar landing gear design parameter values for front-foot touchdown mode
13 p1579 N73-22798
Guidelines for spacecraft structural design requirements emphasizing project planning and management methods
[ESRO-CR[P]-200] 13 p1586 N73-22857
Guidelines for spacecraft structural design requirements noting management and compilation methods
[HSD-TP-7363] 13 p1586 N73-22858
Development of guidelines for application to production of spacecraft hardware components with long lifetime - Vol. I
[NASA-CR-128905] 14 p1707 N73-23853
Guidelines for design and development of electrical and electronic components and systems used in spacecraft construction to obtain long service life - Vol. 2
[NASA-CR-128906] 14 p1707 N73-23854
Development of guidelines for selection of hardware items for use in manned spacecraft design to obtain five year maintenance-free service life - Vol. 3
[NASA-CR-128907] 14 p1707 N73-23855
Development of guidelines for spacecraft equipment selection based on quality control and test procedures during manufacturing - Vol. 4
[NASA-CR-128908] 14 p1707 N73-23856
Development of guidelines for selection of manned spacecraft equipment and recommendations for performance and quality control tests
[NASA-CR-128909] 14 p1708 N73-23857
Achievements in space exploration to include spacecraft design, planetary composition, lunar missions, and predicted space accomplishments
[NASA-TT-F-737] 15 p1830 N73-24829
Unmanned roving vehicle design for surface exploration of Mars
16 p1884 N73-25252
Design parameters and systems analysis of crew compartment for space shuttle orbiter - Summary Report
[NASA-CR-128949] 16 p1965 N73-25893
Design parameters and systems analysis of crew compartment for space shuttle orbiter - Final Report
[NASA-CR-128950] 16 p1965 N73-25894
Development of computer program and data base for design of cryogenic systems used in space shuttles and spacecraft - Vol. 5 B-1
[NASA-CR-133955] 17 p2087 N73-26883
Computer programmers manual for mathematical model used in design of cryogenic supply systems for space shuttles and spacecraft - Vol. 5 B-2 Part 1
[NASA-CR-133956] 17 p2087 N73-26884
Computer programmers manual for parametric analysis of attitude control propulsion system using converted liquid cryogenics reaction system - Vol. 5 B-3 Part 2
[NASA-CR-133958] 17 p2087 N73-26886
Analysis of parameters for optimization of cryogenic supply system for space shuttles - Vol. 6
[NASA-CR-133959] 17 p2087 N73-26887
Guidance for assessment and control of spacecraft temperatures
[NASA-SP-8105] 17 p2088 N73-26890
Design of double gimballed flywheel for spacecraft stability
[ESRO-CR[P]-135] 17 p2090 N73-26907
Apollo experience report on development of design loads criteria, methods, and operational procedures for prelaunch, lift-off, and midboost conditions
[NASA-TN-D-7373] 20 p2474 N73-29875
Development of alternate space shuttle concepts to show modified avionics, vehicle subsystems, and thermal protection system
[NASA-CR-124345] 21 p2601 N73-30844
Feasibility and cost benefits of nuclear-powered standardized spacecraft
[NASA-CR-133743] 21 p2601 N73-30846
Summary of attitude dynamic analysis for IMP-J S/C wire antenna spacecraft
[NASA-TM-X-70465] 22 p2720 N73-31764
Design and cost analysis of space shuttle systems - Vol. 2, Part 1
[NASA-CR-124417] 23 p2850 N73-32772
Design and cost analysis of space shuttle systems - Vol. 2, Part 2
[NASA-CR-124422] 23 p2850 N73-32773
Design, development, and configuration of reusable lunar shuttlecraft
[NASA-CR-135794] 24 p2984 N73-33849

**SPACECRAFT DOCKING**
Fail safe latching mechanism for spacecraft docking
[NASA-CASE-MSC-12549-1] 02 p0178 N73-11443
Executive summary of advanced missions safety study involving space shuttle rescue capability, experiment safety, and emergency crew transfer - Vol. I
[NASA-CR-129099] 02 p0231 N73-11871
Reliability probability analysis on ergatic process in spacecraft control during approach and docking with orbital station
03 p0258 N73-12087
Simulating liquid propellant motion in partially filled containers during docking maneuver in orbit
[NASA-CR-124055] 09 p1013 N73-18268
Design of docking system of androgynous and peripheral type for creation of compatible system for US and Soviet spacecraft
09 p1087 N73-18869
Computer program used for dynamic analysis of Apollo-Salyut/Soyuz docking
09 p1087 N73-18871
Postflight analysis of Apollo 14 translunar docking anomaly
09 p1089 N73-18884
Dynamic testing for determining flight readiness of Apollo docking system hardware
09 p1089 N73-18885
Rendezvous and docking radar for space shuttle
10 p1129 N73-19198

High energy absorption docking system design for docking large spacecraft
[NASA-CASE-MFS-20863] 17 p2086 N73-26876
Development of spacecraft docking system for optical alignment of spacecraft using television camera system
[NASA-CASE-MSC-12559-1] 17 p2086 N73-26879
Orbital docking technology for spacecraft
[NASA-TT-F-15105] 22 p2716 N73-31741
Details and problems of docking technology, mutual aid and rescue for disasters, search and rendezvous means, and cabin atmospheric parameters for Soviet-American flight
[NASA-TT-F-15096] 23 p2844 N73-32726

**SPACECRAFT ELECTRONIC EQUIPMENT**
NT AIRBORNE/SPACEBORNE COMPUTERS
Development of rationale and requirements for conducting accelerated life tests on spacecraft electronic systems
[NASA-CR-129096] 02 p0233 N73-11892
Recording instruments for Earth Resources Technology Satellites - Vol. 2
[NASA-CR-130187] 10 p1129 N73-19195
Vibration and acoustic tests for spacecraft electronic equipment design
[NASA-TN-D-7159] 11 p1345 N73-20914
Guidelines for design and development of electrical and electronic components and systems used in spacecraft construction to obtain long service life - Vol. 2
[NASA-CR-128906] 14 p1707 N73-23854
Development of guidelines for spacecraft equipment selection based on quality control and test procedures during manufacturing - Vol. 4
[NASA-CR-128908] 14 p1707 N73-23856
Development of guidelines for selection of manned spacecraft equipment and recommendations for performance and quality control tests
[NASA-CR-128909] 14 p1708 N73-23857
Parametric performance characteristics and treatment of temperature coefficients of silicon solar cells for space application
[NASA-CR-132156] 15 p1738 N73-24090
Development, manufacture, and testing of optical beam steerer for use in spaceborne optical radar systems
[NASA-CR-124283] 16 p1884 N73-25246
Guidelines for selection and application of three types of tantalum electrolytic capacitors for design of circuits in spacecraft components
[NASA-TM-X-64755] 17 p2003 N73-26200
Development of test equipment, propellants, and control equipment for interplanetary spacecraft
[NASA-CR-133863] 22 p2731 N73-31858
Magnetic materials selection for spacecraft transformers used in static inverters, converters, and transformer-rectifier supplies
[NASA-CR-135642] 23 p2764 N73-32118
Development, fabrication, and evaluation of heat pipe thermal conditioning panels for temperature control of spacecraft electronic equipment - Executive Summary
[NASA-CR-124453] 24 p2991 N73-33899

**SPACECRAFT ENVIRONMENTS**
Computerized simulation of carbon dioxide partial pressure in spacecraft environment for wide range of operating conditions - Vol. 1
[NASA-CR-128630] 02 p0233 N73-11893
Development of simulation models for computerized simulation of carbon dioxide partial pressure in spacecraft environment - Vol. 2
[NASA-CR-128631] 02 p0233 N73-11894
Spacecraft environment, radiation, and weightlessness effects on human biological processes in manned space flight
[JPRS-57517] 03 p0256 N73-12076
Development of technology for design and application of self controlled, variable conductance heat pipes for spacecraft thermal control
[NASA-CR-114530] 06 p0730 N73-15957
Industrial hygiene, radiological health, and spacecraft sanitation studies in NASA Environmental Health Program
08 p0872 N73-17057
Development of computer program to optimize space shuttle environmental and thermal control life support system
[NASA-CR-128736] 08 p0964 N73-17883
Use of cyclic struts as energy absorbers for Apollo couch
09 p1088 N73-18881
Cryogenic heat exchanger for removal of waste heat from spacecraft environmental control life support system
[NASA-CR-124301] 18 p2111 N73-27071
Dual stage check valve for cryogenic supply systems used in space flight environmental control system
[NASA-CASE-MSC-13587-1] 21 p2552 N73-30459
Guidelines for extravehicular and intravehicular activities during space shuttle operation with emphasis on contingency situations - Vol. 2
[NASA-CR-133992] 22 p2622 N73-31007
Computer program for calculation of steady, state and/or transient thermal environments for space system during lunar surface, deep space, or thermal vacuum
[NASA-CR-134031] 22 p2729 N73-31842

**SPACECRAFT GUIDANCE**
NT SATELLITE GUIDANCE
Closed-form solutions for motion of rocket-powered vehicle during atmospheric ascent and unpowered atmospheric reentry
[NASA-TM-X-64694] 02 p0207 N73-11677
Space shuttle orbiter guidance and control software functions for horizontal flight operations
[NASA-TM-X-68857] 02 p0207 N73-11682
Comparison of open and closed loop applications of second order guidance algorithm using minimum distance strategy for Earth-Mars transfer
[NASA-CR-129170] 02 p0227 N73-11830
Analysis of factors involved in specification, design, and evaluation of gyroscopes for spaceborne sensor applications
[NASA-SP-8096] 03 p0328 N73-12680
Characteristics of blowdown-pressurized hydrazine propulsion system for trajectory correction of spacecraft during outer planet flyby missions
[NASA-CR-129796] 04 p0464 N73-13780
Characteristics of thermoelectric outer planet spacecraft attitude propulsion subsystem
[NASA-CR-129795] 04 p0464 N73-13781
Use of aerodynamic drag for transfer from hyperbolic trajectories to satellite orbits noting spacecraft guidance
[D-149] 05 p0596 N73-14849
Guidance, navigation and control system analysis report for Apollo 15
[NASA-TM-X-68934] 06 p0696 N73-15673
Guidance, navigation, and control system performance analysis report for Apollo 16 mission
[NASA-TM-X-68931] 06 p0696 N73-15674
Erasable-memory programs for guidance computers in command and lunar modules
[NASA-CR-128689] 07 p0817 N73-16626
Computerized simulation of approach navigation accuracy and guidance requirements for 1977 Grand Tour mission to outer planets
08 p0941 N73-17707
Comparison of several first and second order deterministic low-thrust guidance methods
08 p0963 N73-17875
Guidance strategies and analysis for low thrust navigation
[NASA-CR-130862] 09 p1062 N73-18663
Precision State and Filter Weighting Matrix Extrapolation routine for space shuttle guidance navigation
[NASA-CR-128803] 10 p1184 N73-19631
Apollo experience report on evolution of attitude time line
[NASA-TN-D-7086] 10 p1214 N73-19872
Algorithm for space vehicle re-orientation through angular velocity control by jet momentum
12 p1425 N73-21555
Guidance and control concepts for structural control interactions and dynamic loads
[NASA-TM-X-64732] 12 p1461 N73-21834
Development of electrostatically focused image dissector tube for use in spacecraft attitude control star trackers
[NASA-CR-132153] 15 p1787 N73-24487
Apollo experience report on engineering simulation in support of Apollo guidance and control system
[NASA-TN-D-7287] 15 p1835 N73-24873
Numerical analysis of space shuttle orbiter flight path and performance during approach guidance from space mission - Document 22
[NASA-CR-128962] 16 p1941 N73-25707
Apollo experience report on development of Apollo digital autopilots for primary attitude control during all phases of lunar landing mission
[NASA-TN-D-7289] 16 p1964 N73-25888
Analysis of inflight performance of Apollo 13 spacecraft guidance, navigation, and control equipment
[NASA-TM-X-69528] 17 p2060 N73-26666
Conference on technology utilization in spacecraft guidance, ground operations, communications and navigation systems, and sensor development
[NASA-SP-326] 18 p2207 N73-27816
Guidance and navigation error analysis for Skylab 3
[NASA-CR-133997] 21 p2576 N73-30642
Space shuttle guidance, navigation, and control design equations
[NASA-TM-X-69524] 23 p2816 N73-32514
Riccati controlled feedback for guiding spacecraft during unpowered terminal phase of flight
23 p2847 N73-32751

**SPACECRAFT INSTRUMENTS**
NT LASER ALTIMETERS
NT SATELLITE INSTRUMENTS
NT SPACECRAFT POSITION INDICATORS
Star scanner for spin-stabilized spacecraft
[NASA-CASE-GSC-11569-1] 02 p0173 N73-11404
Fourier analysis for characterizing force field of superconducting suspension for spacecraft elements
03 p0335 N73-12731
Improved electrochemical storage batteries for spacecraft
[NASA-TM-X-66129] 04 p0375 N73-13049
Problems of radio telemetry systems in manned and unmanned spacecraft
[NASA-TT-F-722] 09 p1002 N73-18175
Environmental and flight readiness tests of scanning mirror for infrared sensors
09 p1089 N73-18888
Atmospheric observation techniques using aircraft infrared radiometers as prototypes for spacecraft remote sensing application
[NOAA-TR-NESS-64] 11 p1293 N73-20494
Apollo experience report on instrument calibration data to provide correct engineering data for tests and mission support
[NASA-TN-D-7144] 11 p1341 N73-20881
Scientific instrument package for large space telescope
[NASA-CR-130214] 13 p1529 N73-22394
In-depth analysis of UV instruments, nondeployed solar payload, and on-orbit access
[NASA-CR-131892] 13 p1576 N73-22770
Design of counter tube window and X ray fluorescence analyzer for quantitative analysis of Venusian dust and condensates
[NASA-CR-114619] 15 p1786 N73-24484
Design and development of thermomechanical pump for transmitting warming fluid through fluid circuit to control temperature of spacecraft instrumentation
[NASA-CASE-NPO-11417] 15 p1790 N73-24513
Thick film microelectronic amplifier module for space instruments
[RAE-LIB-TRANS-1643-PT-1]
17 p2007 N73-26233
UK-5 X ray experimental design performance
17 p2084 N73-26858
Characteristics of microwave radiometer scatterometer system for Skylab program
22 p2671 N73-31394
Contamination of sensors installed in spacecraft and recommendations for eliminating or correcting
[NASA-TM-X-70487] 24 p2926 N73-33367
Opto-electronic instruments for spacecraft
[JPRS-60199-1-PT-1] 24 p2926 N73-33372
Opto-electronic instruments for spacecraft
[JPRS-60199-2-PT-2] 24 p2926 N73-33373

**SPACECRAFT LANDING**
NT LUNAR LANDING
NT MARS LANDING
NT PLANETARY LANDING
Visual cue reinforcement for skill retention in pilot simulated space vehicle approach and landing performance
[NASA-CR-128912] 14 p1614 N73-23086
Space shuttle energy management, approach, and landing analysis
[NASA-CR-128937] 15 p1830 N73-24830
Consolidation of navigation and guidance for space shuttle vehicles for all phases of space mission - Document 21
[NASA-CR-128961] 16 p1941 N73-25708
Development of equations of motion for energy dissipation phase of shuttle reentry and landing approach - Document 23
[NASA-CR-128960] 16 p1941 N73-25709
Analysis of high velocity spacecraft crash landing on planetary surfaces for possible encapsulated microorganism release
[NASA-CR-131835] 16 p1966 N73-25904
Flight simulation to determine navigation, guidance, and control problems involving terminal area approach and landing of space shuttle using CV-990 aircraft
[NASA-TM-X-62285] 18 p2199 N73-27753
Optimal three dimensional trajectories to maximize landing footprint of lifting reentry vehicle using energy approximations based on flight path
[AD-764132] 22 p2615 N73-30960

**SPACECRAFT LAUNCHING**
Extraterrestrial disposal of radioactive wastes
[NASA-TM-X-68147] 01 p0079 N73-10650
Postflight analysis of Atlas/Centaur - 29 and Intelsat 4 launch and orbit establishment
[NASA-TM-X-68649] 01 p0102 N73-10845
Program requirements, operational support, and systems analysis for IMP satellite to identify responsibilities of launching organizations
[NASA-CR-129268] 03 p0358 N73-12916
Orbits, size, mass of space vehicles launched between 31 Dec. 1971 and 30 Jun. 1972
[RAE-TM-SPACE-182-SUPPL] 03 p0360 N73-12930
Application of Apollo Project managerial practices to solution of problems encountered in modern civilization
04 p0470 N73-13834
Continuous wave Doppler radar observations of ionospheric disturbances generated by Saturn-Apollo launchings
05 p0511 N73-14157
Index of reports prepared by data center concerning rocket and satellite launches and satellite sightings
05 p0611 N73-14964

List of facilities and environmental measurements to be monitored in support of Skylab 2 at Launch Complex 39
[NASA-TM-X-68916] 07 p0849 N73-16879
Ground-based measurements of electrical length of vehicle and plume and of atmospheric electricity during Apollo 13 and 14 launches
[NASA-CR-130535] 08 p0916 N73-17503
European satellites to be launched between 1980 and 1990
[NASA-TT-F-14695] 08 p0965 N73-17887
Mariner Mars 1971 development through launch and trajectory correction maneuver
[NASA-CR-131268] 11 p1338 N73-20855
Analysis of size, weight, and packaging requirments for aerodynamic decelerator for recovery of expended solid propellant rocket engines used to launch space shuttle vehicles - Vol. 2, Book 5
[NASA-CR-123730] 15 p1826 N73-24801
Apollo 17 flight plan for prelaunch checkout support and continuous support to be provided during mission - Revision A
[NASA-TM-X-69530] 17 p2083 N73-26853
Wind tunnel measurements of overall fluctuating pressure levels on seven space shuttle launch configurations at transonic and supersonic speeds
[NASA-TM-X-62280] 17 p2087 N73-26882
Development and characteristics of squib actuated explosive disconnect for spacecraft release from launch vehicle
[NASA-CASE-NPO-11330] 17 p2096 N73-26958
Apollo experience report on development of design loads criteria, methods, and operational procedures for prelaunch, lift-off, and midboost conditions
[NASA-TN-D-7373] 20 p2474 N73-29875
Table of space vehicles launched during 1958 - 1972 detailing mass, size, shape, orbit, and launch date.
[RAE-TR-73006] 22 p2722 N73-31787
Space vehicles launched between January and August 1973
[TECH-MEMO-SPACE-199] 23 p2847 N73-32753
Performance evaluation of SA-206 launch vehicle for Skylab 2 launch to show signficant events and failures and anomalies
[NASA-TM-X-69538] 24 p2981 N73-33820
Performance evaluation of SA-207 launch vehicle for Skylab 3 launch to show significant events and failures and anomalies
[NASA-TM-X-69540] 24 p2981 N73-33821
Evaluation of launch vehicle, spacecraft, and lunar rover performance during Apollo 17 flight to determine malfunctions and recommend corrective actions
[NASA-TM-X-69534] 24 p2981 N73-33822
Postflight analysis of Apollo 16 flight to show spacecraft performance, launch vehicle performance, and malfunctions occuring during flight
[NASA-TM-X-69535] 24 p2981 N73-33823
Postflight analysis of Apollo 14 flight to show spacecraft performance, launch vehicle performance, and malfunctions occurring during flight
[NASA-TM-X-69536] 24 p2981 N73-33824

**SPACECRAFT MANEUVERS**
NT MANEUVERABLE REENTRY BODIES
Summary of Pioneer 10 mission objectives and midcourse maneuver strategies
01 p0120 N73-10987
Payload deployment aspects of control system optimization of spacecraft maneuvers involved in stationkeeping and docking - Vol. 1
[NASA-CR-124050] 09 p1086 N73-18860
Digital implementation of high frequency cutoff filter for spacecraft control system optimization based on word length, sampling rate, accuracy, and computing time requirements - Vol. 2
[NASA-CR-124051] 09 p1086 N73-18861
Mariner Mars 1971 development through launch and trajectory correction maneuver
[NASA-CR-131268] 11 p1338 N73-20855

**SPACECRAFT MODELS**
Extended theory of imperfect modeling with error approximation for application to thermal modeling of spacecrafts
04 p0483 N73-13949
Thermal vacuum testing of spacecraft performance using flight models to determine malfunctions
[NASA-TM-X-66188] 09 p1090 N73-18895
Elastic structural models for dynamics and control of advanced space vehicles
[NASA-CR-124272] 16 p1967 N73-25908
Traffic model data for 1973 NASA payload space shuttle
[NASA-TM-X-64751] 17 p2083 N73-26845
Traffic model data for 1973 expendable launch vehicle
[NASA-TM-X-64752] 17 p2083 N73-26846
Stochastic optimal controller for n-body spacecraft
[NASA-CR-133788] 21 p2600 N73-30839

**SPACECRAFT MODULES**
NT LUNAR LANDING MODULES
NT LUNAR MODULE
Mass properties for Modular Space Station Program, Phase B Definition
[NASA-CR-128409] 01 p0107 N73-10883
Development and characteristics of thermal control system for maintaining constant temperature within spacecraft module with wide variations of component heat transfer
[NASA-CASE-GSC-11018-1] 21 p2599 N73-30829

**SPACECRAFT MOTION**
Data transmission and processing system for balanced air bearing stabilized platform for satellite motion simulator
[ESRO-CR-54] 01 p0037 N73-10287
Spacecraft simulation techniques applicable to flight simulator motion systems
[NASA-CR-128653] 04 p0401 N73-13266
Aberration due to high velocity satellites for laser telemetry
05 p0557 N73-14526
Development of mathematical model to represent small motions relative to inertial reference coordinate system of spacecraft in low, circular earth orbit
07 p0847 N73-16867
Algorithm for targeting finite burn maneuvers
[NASA-TM-X-66180] 08 p0961 N73-17859
Dynamics and control of escape and rescue from tumbling spacecraft
[NASA-CR-130549] 08 p0964 N73-17878
Attitude control of space vehicles using single movable mass to generate control torques with application to cable-connected, artificial gravity configuration
[NASA-CR-124081] 08 p0964 N73-17880
Mathematical model for optimal control of spacecraft flight considering error and perturbation factors
10 p1178 N73-19583
Simulation of satellite motion in ionospheric plasma using low energy and high current ion source in vacuum chambers
[ONERA-NT-202] 15 p1762 N73-24280
Laboratory simulation validity for analysis of spacecraft-plasma interactions
[PB-214611/6] 16 p1908 N73-25438
Semi-analytical solution of oceanic tidal perturbations in motion of artificial satellites
[NASA-TM-X-66298] 18 p2200 N73-27763
Multivariable approach to perturbed aerospace vehicle motion, using approximate solutions of nonlinear differential equations
19 p2341 N73-28832
Motion simulator for performance testing of satellite attitude control systems
[ESRO-CR-66] 20 p2383 N73-29145
Analysis of tethered body problems and determination of relative molton orbit - Parts 1 and 2
[NASA-CR-132780] 22 p2714 N73-31723

**SPACECRAFT ORBITS**
NT POLAR ORBITS
NT SATELLITE ORBITS
NT STATIONARY ORBITS
NT TRANSFER ORBITS
NT TWENTY-FOUR HOUR ORBITS
Orbits, size, mass of space vehicles launched between 31 Dec. 1971 and 30 Jun. 1972
[RAE-TM-SPACE-182-SUPPL] 03 p0360 N73-12930
Nonlinear filter estimation of interplanetary spacecraft orbits during simulated Jupiter flyby and Jupiter orbiter missions
17 p2081 N73-26834
Table of space vehicles launched during 1958 - 1972 detailing mass, size, shape, orbit, and launch date.
[RAE-TR-73006] 22 p2722 N73-31787
Stellar-inertial measurement system trade study on spacecraft orbital ephemeris and attitude errors for landmark location
[NASA-CR-134042] 24 p2984 N73-33845

**SPACECRAFT PERFORMANCE**
Capabilities of Dynamic Operational Requirements and Cost Analysis Program for space mission planning - Vol. 1
[NASA-CR-129263] 03 p0269 N73-12183
Guide for coding Dynamic Operational Requirements and Cost Analysis Program to show subroutines and flow charts - Vol. 2
[NASA-CR-129264] 03 p0270 N73-12184
Program listing for Dynamic Operational Requirements and Cost Analysis Program to provide space mission planning and project management capability - Vol. 3
[NASA-CR-129265] 03 p0270 N73-12185
Program listing for Dynamic Operational Requirements and Cost Analysis Program to provide space mission planning and project management capability - Vol. 3
[NASA-CR-123380] 03 p0270 N73-12190
Operations summary and mission planning for IMP-H spacecraft
[NASA-TM-X-68880] 04 p0478 N73-13907
Development of procedure for computing normal force, axial force, and pitching moment coefficients with application to space shuttle booster characteristics
[NASA-TN-D-6996] 06 p0614 N73-14988
Mathematical model to simulate staging dynamics of proposed space shuttle configuration
[NASA-TM-X-58098] 08 p0965 N73-17886
Analysis of space shuttle capability as launch vehicle for delivery of payloads into earth orbit
[NASA-TM-X-68859] 08 p0965 N73-17889
Thermal vacuum testing of spacecraft performance using flight models to determine malfunctions
[NASA-TM-X-66188] 09 p1090 N73-18895
Formulation of mathematical model for predicting dynamic behavior of rotating flexible space station configurations - Vol. 1
[NASA-CR-112243] 10 p1189 N73-19672
User's manual for computer program to predict dynamic behavior of rotating flexible space station configurations - Vol. 2
[NASA-CR-112244] 10 p1189 N73-19673
Apollo experience report on propulsion system for descent stage of lunar module with emphasis on throttling capability and cryogenic helium pressurization system
[NASA-TN-D-7143] 10 p1215 N73-19877
ERTS-1 performance during orbits 0 to 1300
[NASA-CR-130178] 11 p1286 N73-20435
Development of mathematical model of lateral motion of flexible space shuttle vehicle during ascent
[NASA-CR-124159] 11 p1340 N73-20876
Comparative analysis of space tug concepts to show overall approach and data generation - Vol. 2, Pt. 1
[NASA-CR-124143] 11 p1343 N73-20900
Economic principles for cost effectiveness and cost benefit analysis of space tug operations - Vol. 2, Pt. 2
[NASA-CR-124144] 11 p1343 N73-20901
Development of data base to show space tug characteristics, costs, and performance for comparison of concepts - Vol. 2 Appendix
[NASA-CR-124146] 11 p1344 N73-20902
Time variations of instantaneous orbital parameters and topocentric range and range rate of spacecraft moving in gravitational field of oblate large body
[JPL-TM-33-594] 12 p1458 N73-21814
Wind tunnel tests of space shuttle orbiter scale model to determine aerodynamic characteristics at hypersonic speed in various configurations
[NASA-CR-128754] 12 p1461 N73-21838
Analysis of telemetry data from prelaunch, launch, and flight activation phases of ERTS-1 spacecraft
[NASA-CR-130150] 13 p1581 N73-22817
Flight performance analysis of ERTS-1 spacecraft components during orbits 1300 to 2600
[NASA-CR-130207] 13 p1581 N73-22818
Achievements in space exploration to include spacecraft design, planetary composition, lunar missions, and predicted space accomplishments
[NASA-TT-F-737] 15 p1830 N73-24829
Numerical analysis of space shuttle orbiter flight path and performance during approach guidance from space mission - Document 22
[NASA-CR-128962] 16 p1941 N73-25707
Consolidation of navigation and guidance for space shuttle vehicles for all phases of space mission - Document 21
[NASA-CR-128961] 16 p1941 N73-25708
Characteristics of spacecraft control systems to provide examples of attitude control and stabilization for manual and automatic operation
[NASA-TT-F-774] 16 p1966 N73-25903
Analysis of inflight performance of Apollo 13 spacecraft guidance, navigation, and control equipment
[NASA-TM-X-69528] 17 p2060 N73-26666
Flight simulation to determine navigation, guidance, and control problems involving terminal area approach and landing of space shuttle using CV-990 aircraft
[NASA-TM-X-62285] 18 p2199 N73-27753
Performance and growth capability of orbital test satellite for European communication satellite program
[DGLR-PAPER-73-044] 21 p2602 N73-30849
Apollo experience report on process of crew procedures development for systems procedures and flight procedures
[NASA-TN-D-7436] 22 p2721 N73-31772
Postflight analysis of Apollo 15 flight to determine performance of launch vehicle, spacecraft, and lunar roving vehicle and to analyze malfunctions
[NASA-TM-X-69539] 24 p2981 N73-33819

**SPACECRAFT POSITION INDICATORS**
Device for determining relative angular position of spacecraft and radiating celestial body
[NASA-CASE-GSC-11444-1] 19 p2300 N73-28490
Spacecraft attitude sensing system design with narrow field of view sensor rotating about spacecraft x-y axis
[NASA-CASE-GSC-10890-1] 21 p2575 N73-30640

**SPACECRAFT POWER SUPPLIES**
Development, characteristics, and application of solar electric power generators used in USSR spacecraft - Part 1
[AD-741524] 01 p0007 N73-10056
Control circuit for nuclear thermionic converter power source for spacecraft
[NASA-CASE-NPO-13114-1] 04 p0448 N73-13656
Measurement of magnetic field emission of spacecraft power system units at low frequencies
[ESRO-CR-57] 05 p0548 N73-14452

Modifications and test performance of 2 to 15 kilowatt Brayton cycle electrical subsystem
[NASA-TM-X-2757] 09 p0990 N73-18083
Production and evaluation of magnetic and electrical materials capable of operating in 800 to 1600 F temperature range for advanced space electric power systems
[NASA-CR-2224] 09 p0990 N73-18084
Apollo experience report on design philosophy and experience of Apollo spacecraft electrical power generation system
[NASA-TN-D-7142] 10 p1214 N73-19873
Apollo experience report on procedures and techniques for predicting consumables usage for Apollo missions
[NASA-TN-D-7140] 10 p1214 N73-19874
Rectangular solar cell stacked panels to generate electrical power aboard spacecraft
[NASA-CASE-NPO-11771] 11 p1237 N73-20040
Accelerated life test program for space batteries
[NASA-SP-323] 13 p1476 N73-21958
Method and device for providing banded transformer cores for use in spacecraft power systems
[NASA-CASE-NPO-11966] 13 p1499 N73-22150
Optimization of oxygen hydrogen fuel cell power system for advanced spacecraft
[NASA-CR-121136] 17 p1986 N73-26050
Spacelab configurations noting thermal control, life support, electrical power, communication, and altitude control subsystems
[ESS/SS-399-VOL-2] 17 p2089 N73-26903
Magnetic field interference of transformers for dc/dc converters for spacecraft power supplies
[ESRO-CR-84] 19 p2223 N73-27930
Design and evaluation of mini-Brayton compressor-alternator-turbine system for spacecraft power supplies
[NASA-CR-133810] 21 p2553 N73-30463
Onboard control systems for spacecraft
[JPRS-60179] 23 p2847 N73-32755
Synthesis of optimal control system for nuclear power plant and power supplies onboard spacecraft
23 p2848 N73-32758

**SPACECRAFT PROPULSION**
NT ELECTROMAGNETIC PROPULSION
NT ELECTROSTATIC PROPULSION
NT ION PROPULSION
NT PLASMA PROPULSION
NT SOLAR PROPULSION
Advanced nuclear rocket propulsion system based on chain of exploding thermonuclear micro-bombs ignited before concave magnetic reflector
[AD-746027] 01 p0079 N73-10653
Development and characteristics of radioisotope safety devices for use with electric propulsion system - Vol. 1
[NASA-CR-114505] 01 p0090 N73-10745
Design, development, and characteristics of radioisotope shielding systems for use with spacecraft electric propulsion system - Vol. 2
[NASA-CR-114506] 01 p0091 N73-10746
Design and analysis of radioisotope shield for thermionic power supply used in spacecraft electric propulsion systems - Vol. 3
[NASA-CR-114507] 01 p0091 N73-10747
Wind tunnel tests to determine space shuttle ascent configuration plumes with pressure-fed and solid rocket motor boosters - Vol. 4
[NASA-CR-120086] 02 p0234 N73-11904
Advanced concepts in conventional chemical rocketry
[AD-750554] 06 p0714 N73-15827
Investigation of solar electric propulsion as method for exploring space beyond reach of ballistic missions - Vol. 1
[NASA-CR-130701] 08 p0954 N73-17811
Solar electric propulsion system integration technology study to show spacecraft and mission applications - Vol. 2
[NASA-CR-130702] 08 p0954 N73-17812
Solar electric propulsion system integration technology study to show spacecraft and mission applications - Vol. 3
[NASA-CR-130703] 08 p0954 N73-17813
Onboard spacecraft propulsion using nuclear fuels and solar energy - pt. 1
[JPRS-58612-1-PT-1] 10 p1209 N73-19833
Onboard spacecraft thermoelectric and chemical propulsion systems - Pt. 2
[JPRS-58612-2-PT-2] 10 p1209 N73-19834
Apollo experience report on procedures and techniques for predicting consumables usage for Apollo missions
[NASA-TN-D-7140] 10 p1214 N73-19874
Feasibility of using nuclear propulsion systems in spacecraft
[JPRS-58457] 11 p1323 N73-20737
Kaufman thruster development of 5 cm and 30 cm sizes
[NASA-TM-X-68202] 11 p1334 N73-20828
Development of computerized multistage failure process simulation to evaluate risk in solar electric space mission
[NASA-CR-131518] 12 p1457 N73-21813
Feasibility of laser induced ablation thruster for space propulsion system
[NASA-CR-131744] 13 p1537 N73-22449
Mission engineering analysis of nuclear-thermionic electric propulsion spacecraft for unmanned interplanetary and geocentric mission
[NASA-CR-131599] 13 p1570 N73-22724
Mission engineering analysis of nuclear-thermionic electric propulsion spacecraft for unmanned interplanetary and geocentric missions
[NASA-CR-131600] 13 p1570 N73-22725
Description of research and air breathing engine test facility at University of Stuttgart
[AD-758150] 15 p1827 N73-24806
Development of computer program for space shuttle orbit injection propulsion system to generate parametric feed system pressure histories - Vol. 5 B-4
[NASA-CR-133957] 17 p2087 N73-26885
Operating principles and application of ion engines for spacecraft propulsion
[JPRS-59061] 18 p2192 N73-27700
Apollo experience report on service propulsion subsystem development, qualification, and flight performance
[NASA-TN-D-7375] 22 p2719 N73-31763

**SPACECRAFT RADIATORS**
Design and tests of passive radiative cooler for spacecraft
09 p1088 N73-18873
Spacecraft advanced radiator design system program for environmental control in long duration space flights
[NASA-CR-128913] 14 p1719 N73-23946

**SPACECRAFT RECOVERY**
Analysis of systems for recovering sounding rocket payloads
[ONERA-TP-1153] 10 p1214 N73-19870
Module for automatic dock and detumble device for orbital rescue operations
[NASA-CR-131592] 13 p1581 N73-22816

**SPACECRAFT REENTRY**
Finite difference solution of film cooling as alternate thermal protection system for spacecraft during reentry
[NASA-CR-112192] 01 p0116 N73-10958
Electrostatic probes in spacecraft flow field for measuring plasma sheath density during atmospheric reentry
07 p0825 N73-16683
Stochastic model of atmosphere between 30 and 90 km was developed for use in Monte Carlo space shuttle entry studies
[NASA-TM-X-69567] 21 p2536 N73-30337

**SPACECRAFT RELIABILITY**
Organizational and decision processes for determining essential scheduled maintenance requirements for space shuttle orbiter
[NASA-TM-X-69004] 04 p0478 N73-13908

**SPACECRAFT RENDEZVOUS**
U SPACE RENDEZVOUS

**SPACECRAFT SENSORS**
U SPACECRAFT INSTRUMENTS

**SPACECRAFT SHIELDING**
Electron transport properties in space environment and spacecraft shielding
[NASA-CR-123998] 06 p0702 N73-15722
Radiation hazards and spacecraft shielding requirements for human safety during manned space flight
09 p0992 N73-18099
Cosmic radiation dosage for estimating manned spacecraft shielding requirements
09 p0992 N73-18101
Pigments for space-stable thermal control coatings to shield spacecraft from solar radiation
[NASA-CR-124067] 09 p0998 N73-18144
Analysis of techniques for shielding manned space vehicles against protons and alpha particles from Van Allen belt, solar flares, and cosmic rays
[NASA-CR-131517] 12 p1461 N73-21841
Performance tests of L-band truss cable meteoroid shielding on Skylab space station at minus 180 degrees Fahrenheit
[NASA-TM-X-64743] 15 p1834 N73-24867
Absorbed dose rate and equivalent dose rate investigation for galactic cosmic ray protons and alpha particles in manned spacecraft shields
[ORNL-TM-4029] 17 p2089 N73-26901
Cost effective measures for preventing solar proton interference with interplanetary spacecraft operation
22 p2732 N73-31863
Application of aerospace engineering to planetary exploration and spacecraft shielding problems
[NASA-CR-135529] 23 p2858 N73-32836

**SPACECRAFT STABILITY**
Analysis of performance capability improvement for Pioneer F and G spacecraft using electric thrust subsystem
[NASA-CR-114514] 02 p0222 N73-11798
Bearing flexibility effect on triple-spin satellite attitude stability
[ESRO-SN-121] 03 p0359 N73-12926
Effects of spacecraft stabilization on laser tracking efficiency
05 p0558 N73-14531
Application of autopilot techniques to control and stabilize vibration modes of two space shuttle configurations at liftoff flight condition
[NASA-CR-112202] 06 p0721 N73-15884
Dynamics of satellite gravitational stabilization systems with gyrodamping
[AD-750555] 06 p0722 N73-15892
Pogo stability model considering time lag, magnitude of feedback, and loss of mass
[NASA-TN-D-7091] 06 p0726 N73-15924
Development of mathematical model to represent small motions relative to inertial reference coordinate system of spacecraft in low, circular earth orbit
07 p0847 N73-16867
Attitude control of space vehicles using single movable mass to generate control torques with application to cable-connected, artificial gravity configuration
[NASA-CR-124081] 08 p0964 N73-17880
Formulation of mathematical model for predicting dynamic behavior of rotating flexible space station configurations - Vol. 1
[NASA-CR-112243] 10 p1189 N73-19672
User's manual for computer program to predict dynamic behavior of rotating flexible space station configurations - Vol. 2
[NASA-CR-112244] 10 p1189 N73-19673
Development of mathematical model of lateral motion of flexible space shuttle vehicle during ascent
[NASA-CR-124159] 11 p1340 N73-20876
Analysis of procedures for reducing pogo on space shuttle vehicle based on estimates of pump cavitation compliance
[NASA-CR-2210] 11 p1341 N73-20885
Numerical analysis of satellite stability parameters with application to stability of Skylab satellite
[NASA-CR-124223] 13 p1581 N73-22815
Development and characteristics of movable mass control system to convert tumbling motions of disabled spacecraft into simple spin movements
[NASA-CR-131867] 14 p1710 N73-23875
Description of canonical set of equations which governs behavior of n-body spacecraft connected by dissipative elastic joints
[NASA-CR-132155] 15 p1835 N73-24872
Dynamic characteristics of large flexible solar arrays and interaction between spacecraft attitude dynamics and elastic degrees of freedom
[UTIAS-179] 15 p1835 N73-24878
Characteristics of spacecraft control systems to provide examples of attitude control and stabilization for manual and automatic operation
[NASA-TT-F-774] 16 p1966 N73-25903
Device for automatically balancing spinning spacecraft
17 p2059 N73-26654
Development of engineering analysis and computer code for predicting space shuttle orbiter longitudinal aerodynamic characteristics during abort separation
[NASA-CR-128974] 17 p2086 N73-26877
Development and characteristics of annular momentum control device for two axis stabilization of spacecraft
[NASA-CASE-LAR-11051-1] 19 p2318 N73-28646
Optimal detumbling of large manned spacecraft using internal moving mass
[NASA-CR-135515] 22 p2722 N73-31783
Dynamics and control of detumbling disabled spacecraft during rescue operations
[NASA-CR-135788] 24 p2983 N73-33831

**SPACECRAFT STERILIZATION**
Sanitizing agents for cleansing and decontaminating spacecraft environment
[NASA-CR-128591] 01 p0019 N73-10149
Terminal sterilization process for unmanned lander spacecraft
[NASA-CR-129513] 03 p0259 N73-12100
Sterilization parameters for spacecraft
[NASA-CR-129272] 03 p0259 N73-12101
Planetary quarantine procedures for reduction of microbial burden on spacecraft
[NASA-CR-129793] 04 p0379 N73-13086
Analysis of standards and precedures for planetary quarantine with emphasis on determination of mission specifications
[NASA-CR-130558] 08 p0877 N73-17103
Nonsporicidal methods for solvent degradation of cured RTV 41 silicon potting compound and chemical curing effects on decontamination properties
[NASA-CR-130720] 08 p0878 N73-17111
Evaluation of sterile access technique for repair and adjustment of sterile spacecraft
[NASA-TN-D-7147] 08 p0879 N73-17122
Control equipment for sterilization facility used to thermally inactivate microbes on interplanetary space vehicle components
[NASA-CR-131103] 10 p1119 N73-19122
Bibliography of citations relating to planetary quarantine from 1966 to 1971
[NASA-CR-131889] 13 p1485 N73-22038
Microbial burden estimation for planning planetary quarantine of advanced spacecraft
[NASA-CR-131845] 13 p1485 N73-22039

Probabilistic model of planetary contamination for deciding spacecraft quarantine standards and procedures
[NASA-CR-132001] 14 p1704 N73-23829
Thermal inactivation of Bacillus subtilis var. niger spores on Viking lander
[NASA-CR-133223] 17 p1987 N73-26058
Dry heat inactivation of atypical Bacillus subtilis var. niger spores in and on interplanetary space vehicle components
[NASA-CR-133224] 17 p1987 N73-26059
Development of planetary quarantine measures for automated spacecraft
[NASA-CR-133202] 17 p1988 N73-26066
Sterilization for unmanned landers
[NASA-CR-133742] 21 p2500 N73-30064
Planetary quarantine requirements for automated spacecraft flights
[NASA-CR-135795] 24 p2885 N73-33040

**SPACECRAFT STRUCTURES**
Development and characteristics of four spacecraft configurations for communications satellite applications - Vol. 1
[NASA-CR-120873-VOL-1] 02 p0234 N73-11899
Structural design, subsystem analysis and mechanical integration of synchronous meteorological satellite - Vol. 3
[NASA-TM-X-68839] 02 p0234 N73-11900
Development and characteristics of four spacecraft configurations for communications satellite applications - Vol. 2
[NASA-CR-120873-VOL-2] 02 p0236 N73-11915
Development of procedures for determining contamination characteristics of materials which become volatile in space environment
[NASA-CR-130132] 05 p0600 N73-14878
Design of orthotropic cylindrical shell as structural adapter for Helios solar probe
[DGLR-PAPER-72-101] 06 p0722 N73-15889
Updated structural design criteria for manned space shuttle missions
[NASA-SP-8057-REV] 08 p0964 N73-17881
Computer programmer manual for NASA structural analysis program
[NASA-SP-223[01]] 08 p0966 N73-17892
Contamination avoidance devices for poppet-type shutoff valves
[NASA-CR-121125] 09 p1039 N73-18471
Apollo 15 deployable boom anomaly and subsequent design changes
09 p1087 N73-18868
Service life of mechanically prestressed glass used in spacecraft windows
09 p1088 N73-18880
Analysis of relationships between changes in space shuttle weights and costs with changes in weight of structural subsystems
[NASA-CR-2164] 09 p1090 N73-18894
Deleterious effects of electrostatic rocket exhaust [cesium, mercury] and materials of rocket construction on spacecraft surfaces
[NASA-CR-131092] 10 p1208 N73-19823
Handbook for design of isogrid, triangular integrated stiffened structures for spacecraft structures and components
[NASA-CR-124075] 10 p1219 N73-19911
Delayed simultaneous appendage release mechanism for use on spacecraft equipped with despin mechanisms and releasable components
[NASA-CASE-GSC-10814-1] 11 p1237 N73-20039
X ray detection of incomplete weldment and surface oxidation in welded aluminum spacecraft structures
[NASA-CR-124167] 11 p1298 N73-20536
Influence of combined loading criteria on space shuttle structural performance
[NASA-CR-124113] 11 p1340 N73-20874
Development of composite structures for spacecraft to serve as anti-meteoroid device
[NASA-CASE-LAR-10788-1] 11 p1341 N73-20880
Technical development and future use of materials in aerospace systems
[AD-755371] 12 p1415 N73-21466
Design, development, and characteristics of spacecraft systems and equipment used with Tracking and Data Relay Satellite System - Vol. 3
[NASA-CR-130218] 13 p1582 N73-22822
Guidelines for spacecraft structural design requirements emphasizing project planning and management methods
[ESRO-CR[P]-200] 13 p1586 N73-22857
Guidelines for spacecraft structural design requirements noting management and compilation methods
[HSD-TP-7363] 13 p1586 N73-22858
Development and application of composite materials for weight reduction of space shuttle structural hardware
13 p1593 N73-22917
Meteoroid impact resistance of bumper protected laminated spacecraft mainwalls
[NASA-CR-2262] 14 p1714 N73-23909
Copper coating of welded aluminum spacecraft structures to resist oxidation and aid detection of incomplete penetration
[NASA-CR-124251] 15 p1791 N73-24515
Thesaurus of terms for information on mechanics of structural failure modes and mechanisms for aerospace structures
[NASA-CR-121199] 17 p2091 N73-26917
Register of experts for information on mechanics of structural failure to support safety and technology aspects of aerospace industry
[NASA-CR-121200] 17 p2091 N73-26918
Identification of sources for specialized information on failure modes and mechanisms of aerospace structures
[NASA-CR-121201] 17 p2091 N73-26919
Bibliography of citations related to problem areas in mechanics of failure in aerospace structures
[NASA-CR-121202] 17 p2091 N73-26920
Development of nondestructive inspection procedures for determining quality of welded joints in aluminum spacecraft structures
[NASA-CR-124332] 18 p2156 N73-27420
Proceedings of conference on application of composite materials in construction of aerospace vehicles and propulsion systems
[AGARD-CP-112] 18 p2163 N73-27474
Design and manufacturing of composite materials with organic matrices for use in aerospace vehicle structures subjected to high temperatures
18 p2165 N73-27489
Development of fiber reinforced composite materials for application to air breathing engines, aeronautical vehicles, and spacecraft components
18 p2166 N73-27491
Pressurized panel meteoroid detector
[NASA-CASE-XLA-08916-2] 19 p2299 N73-28487
Neutron emission spectra from protons impinging on spacecraft structural materials
[NASA-TN-D-7386] 20 p2468 N73-29825
Analysis and simulation of Mariner Mars 1971 scan platform, and spacecraft dynamic interaction
[NASA-CR-133793] 21 p2600 N73-30837
Extended torsional tests of interlocked bi-stem satellite boom
[NASA-TN-D-7365] 22 p2724 N73-31798
Compilation of outgassing data for spacecraft materials
[NASA-TN-D-7362] 23 p2810 N73-32469
Structural heat pipe for spacecraft wall thermal insulation system
[NASA-CASE-GSC-11619-1] 23 p2857 N73-32828

**SPACECRAFT TELEVISION**
NT SATELLITE TELEVISION
Television experiment on Mariner 9
24 p2983 N73-33841

**SPACECRAFT TRACKING**
NT SATELLITE TRACKING
Directory of principal tracking facilities used by NASA to include Deep Space Network and several radio telescopes - Vol. 1
[NASA-CR-130071] 01 p0036 N73-10279
Pioneer space probe system design and development, ground support system, tracking and communication, and data processing
[NASA-SP-279-VOL-2] 08 p0964 N73-17882
Tracking and data system report for Mariner Mars 1971 mission
[NASA-CR-132955] 15 p1761 N73-24270
Apollo 17 flight plan for prelaunch checkout support and continuous support to be provided during mission - Revision A
[NASA-TM-X-69530] 17 p2083 N73-26853
Ground station S band tracking in Doppler mode for calibrating Mariner 9 in deep space
18 p2210 N73-27845
Deep Space Network tracking support of planetary and interplanetary flight projects - Vol. 17
[NASA-CR-135708] 23 p2757 N73-32064
Theory, design, and operation of suppressed carrier data-aided tracking receiver
[NASA-CR-135714] 23 p2757 N73-32065

**SPACECRAFT TRAJECTORIES**
NT EARTH-MARS TRAJECTORIES
NT INTERPLANETARY TRAJECTORIES
NT LUNAR TRAJECTORIES
Position of satellite with respect to earth magnetosphere
[AD-746469] 02 p0232 N73-11883
Obtaining rocket trajectories by anological-hybrid computation
04 p0470 N73-13828
Optimum trajectory and spacecraft data for unmanned interplanetary missions from 1975 to 1990 using solar electric propulsion
[NASA-CR-132765] 16 p1966 N73-25907

**SPACECREWS**
Space shuttle orbiter subsystems and control and display data required for crew operations - Vol. 2
[NASA-CR-128577] 01 p0019 N73-10146
Psychological stresses and crew compatibility during interplanetary spacecraft flight
[JPRS-57878] 06 p0629 N73-15113
Activity cycle data for spacecrews of Soyuz 3 to 9 spacecrafts before, during and after space flights
[JPRS-58173] 07 p0746 N73-16068
Occupational medicine procedures for personnel in lunar receiving laboratory for Apollo 11 crew members
08 p0871 N73-17049
Ionization, thermoluminescence, and nuclear photographic emulsion dosimetry for monitoring radiation loads in spacecrews during manned space flight
09 p0992 N73-18100
Cosmic radiation dosage for estimating manned spacecraft shielding requirements
09 p0992 N73-18101
Radiobiological effects of cosmic radiation in animals and standardization of permissible radiation levels for spacecrews
09 p0993 N73-18102
Radionuclide measurements on plasma and red cell mass volume losses in Apollo spacecrews
09 p0993 N73-18106
Apollo experience report on development of flight simulators for spacecrew training to show functional uses, characteristics, and problems
[NASA-TN-D-7112] 10 p1214 N73-19876
Development and characteristics of neutral buoyancy simulator for duplicating weightless conditions encountered during space missions
13 p1594 N73-22923
Development of hardware and software specifications for procurement of space shuttle mission training simulator for crew training
[NASA-CR-133965] 18 p2126 N73-27177
Design and test performance of space crew waste collection system
[NASA-CR-133977] 19 p2225 N73-27945
Role of man in flight experiment payload missions with application to Spacelab operations - Vol. 1
[NASA-CR-135487] 22 p2623 N73-31020
Role of man in flight experiment payload missions with application to Spacelab operations - Vol. 2
[NASA-CR-135488] 22 p2624 N73-31021
Application of skill requirement method for determining skills required of on-orbit crew personnel performing earth-orbital research
[NASA-CR-124452] 24 p2982 N73-33830

**SPACELAB**
Advanced technology, experimental and instrument design, and mission planning for space shuttle sortie workshop - conference working group reports
[NASA-TM-X-68842] 06 p0719 N73-15867
Feasibility determination of astronomy sortie missions concept including definitions of support hardware, mission profiles, and interfaces with space shuttle and sortie lab
[NASA-CR-124042] 10 p1211 N73-19851
Experimental design for space shuttle sortie mission payloads
[NASA-CR-112287] 11 p1343 N73-20898
Preliminary definition study of sortie laboratory noting structural design, subsystems and shuttle interface
[MBB-SL-72-04] 13 p1582 N73-22826
Preliminary definition study of sortie module/pallet system noting configurations, thermal control, attitude control, power and communications subsystems
[ESRO-CR[P]-239] 13 p1582 N73-22827
Preliminary definition study of a sortie module/pallet system noting configurations, thermal control, attitude control, power and communications subsystems
[ESRO-CR[P]-240] 13 p1582 N73-22828
Spacelab payload analysis, shuttle interface, operational analysis, and design guidelines
[ESS/SS-399-VOL-1] 17 p2089 N73-26902
Spacelab configurations noting thermal control, life support, electrical power, communication, and altitude control subsystems
[ESS/SS-399-VOL-2] 17 p2089 N73-26903
Sortie Lab system evaluation, future growth, and IR astronomy experiment accommdation
[ESS/SS-399-VOL-3] 17 p2089 N73-26904
Shuttle sortie simulation using lear jet aircraft
[NASA-TM-X-62283] 20 p2473 N73-29868
Role of man in flight experiment payload missions with application to Spacelab operations - Vol. 1
[NASA-CR-135487] 22 p2623 N73-31020
Role of man in flight experiment payload missions with application to Spacelab operations - Vol. 2
[NASA-CR-135488] 22 p2624 N73-31021
Payload carrier integrated test for simulated Sortie Lab Missions
[NASA-TM-X-64770] 22 p2647 N73-31207
Development of flight experiment work performance and workstation interface requirements for Sortie Lab
[NASA-CR-124409] 23 p2845 N73-32733

**SPACERS**
Pressure drop measurements and drag coefficients for grid spacers of hexagonal fuel rod bundles
[NLL-RISLEY-TR-2440-[9091.9F]]
02 p0209 N73-11692

**SPACING**
NT AIRCRAFT APPROACH SPACING

**SPAIN**
Management of earth resources in France and Spain through automatic mapping inventory
[E72-10303] 04 p0411 N73-13352

English, French, and Spanish vocabulary of aircraft aeronautical terminology
[DOC-8800-VOL-1] 06 p0616 N73-14996
Geomagnetic annuals for Spanish observatories
15 p1777 N73-24400
Geomagnetic measurements for 1970 at Toledo
15 p1777 N73-24401
Geomagnetic data for 1970 at Almeria
15 p1777 N73-24402
Geomagnetic data for 1970 at Logrono
15 p1777 N73-24403
Geomagnetic data for 1970 at Santa Cruz, Tenerife
15 p1777 N73-24404
Management of natural resources in France and Spain by automatic cartographic inventories from ERTS-1 data
[E73-10725] 18 p2133 N73-27234
Application of ERTS-1 imagery for identifying citrus groves and rice fields in Valencia region of Eastern Spain
[PAPER-A4] 19 p2260 N73-28212
Application or ERTS-1 imagery for determining course of Ebro River in northeast Spain
[PAPER-W2] 19 p2271 N73-28282
Timber inventory and land use in Province of Huelva-Spain based on ERTS-1 imagery
[PAPER-L9] 19 p2274 N73-28305

**SPALLATION**
Effect of aging time on spallation of 2024-T6 aluminum subjected to impulsive loading
[AD-746955] 05 p0564 N73-14579
Production of iodine isotope by high energy bombardment of cesium heat pipe causing spallation reaction
[NASA-CASE-LEW-11390-2] 11 p1326 N73-20763
Hypervelocity meteoritic impact resulting in structural damage of orbital space stations
[NASA-CR-124241] 14 p1705 N73-23841
Spallation reactions of light nuclei during galactic cosmic radiation interaction with interstellar gas
[FRNC-TH-333] 21 p2597 N73-30812
Proton spallation of neon and lithium production in stellar flares
22 p2701 N73-31631

**SPALLING**
Spall calculations in one-dimensional hydrodynamics codes using aluminum and high explosives
[LA-5001] 07 p0855 N73-16935
Application of finite element method to stress wave in plates
[NASA-CR-112294] 11 p1345 N73-20911
Alpha particle beam spalling production of aluminum, oxygen, carbon, and beryllium isotopes, and cosmic ray transport theory
13 p1561 N73-22651
Cyclic furnace tests of nickel-, cobalt-, and iron-base alloys oxidation resistance considering scale spalling
[NASA-TM-X-68252] 16 p1870 N73-25144

**SPARE PARTS**
Effectiveness of DOD guidelines in determining time of aircraft engine replacements
[AD-745396] 01 p0091 N73-10749
Quality control procedures for Skylab electron-proton spectrometer equipment and parts
[NASA-CR-128853] 11 p1292 N73-20484
Spares and repair parts support plan for ultraviolet spectrometer Apollo experiment
[NASA-CR-128571] 16 p1885 N73-25260
Thermionic cathode development for Apollo telescope mount camera tube Spares Program
[NASA-CR-124342] 19 p2243 N73-28087

**SPARK CHAMBERS**
Data acquisition system for spark chamber spectrometer and review of space radiation measurement techniques
[AD-741761] 01 p0059 N73-10482
Spark counter for neutron and radon dosimetry discussing use and reproducibility
[BMVG-FBWT-72-33] 10 p1161 N73-19448
Wide gap spark chamber system for NAL experiment 2-B
[ORO-2504-202] 21 p2522 N73-30223
Time resolved spectroscopic measurements of near infrared and X ray emission from high density plasma in vacuum spark
24 p2961 N73-33661

**SPARK DISCHARGES**
U ELECTRIC SPARKS

**SPARK GAPS**
Voltage characteristics of electrical discharges over long air gaps
[AD-746853] 02 p0213 N73-11723
Analysis of electronic circuit and performance of spark gap assembly
[CERN-72-6] 04 p0399 N73-13244
Optical laser triggering of high voltage spark gap
[IPP-4/102] 17 p2040 N73-26504
Application of laser radiation to control operation of spark gaps to show breakdown synchronization and time characteristics
[JPRS-59677] 20 p2425 N73-29476

**SPARK IGNITION**
Application of laser radiation to control operation of spark gaps to show breakdown synchronization and time characteristics
[JPRS-59677] 20 p2425 N73-29476

**SPARK MACHINING**
Experimental and theoretical study of electro-erosion of metals
24 p2933 N73-33423

**SPARK SHADOWGRAPH PHOTOGRAPHY**
U SHADOWGRAPH PHOTOGRAPHY

**SPARKS**
NT ELECTRIC SPARKS
Electrostatic repulsion criteria for dc high voltage spark breakdown of gas
[ORO-4211-5] 03 p0336 N73-12742

**SPATIAL DEPENDENCIES**
Use of spatial information for improving classification accuracy of remotely sensed data
[NASA-CR-133988] 22 p2637 N73-31130

**SPATIAL DISTRIBUTION**
NT STAR DISTRIBUTION
Spatial distribution model of reflectivity in storm cells for digital radar data
[NASA-TM-X-66118] 03 p0327 N73-12661
Spatial distribution of radiation defects in silicon irradiated by protons, deuterons, and alpha particles
[AD-748734] 04 p0459 N73-13749
Metixenum and Meclocin under double blind comparison test conditions against motion sickness
12 p1368 N73-21100
Development of multiwire proportional chamber for high resolution spatial detector in cosmic ray investigations and analysis of operating parameters
[NASA-CR-128899] 13 p1506 N73-22210
Electrostatic wave mechanism in spatial distribution of inner belt protons
16 p1896 N73-25332
Ruby laser radar system for measuring spatial density distribution of atmospheric water vapor
17 p2039 N73-26499
Proportional chambers with monofilar helical cathodes for high spatial resolution
[LA-5195-MS] 18 p2152 N73-27393
Spatial distribution of soft X ray and EUV emission associated with chromospheric flare of importance 1B August 2, 1972
[NASA-TM-X-66299] 18 p2195 N73-27720
Spatial normalized correlation function of total atmospheric ozone content
20 p2448 N73-29669
Spatial distribution of stars in area surrounding cluster NGC 6913
20 p2471 N73-29843
Analytical and experimental study of spatially growing disturbances in shear layers between parallel streams
22 p2650 N73-31231
Growth characteristics of hypersonic turbulent wakes with spatially resolved measurements
[DREV-R-687/73] 24 p2869 N73-32925
Method for comparing photo-electronic and photographic detectors based on product of signal to noise ratio times spatial bandwidth
24 p2958 N73-33634
Interpretation of data on crater distribution on surface of moon
[NASA-TT-F-15122] 24 p2979 N73-33808

**SPATIAL FILTERING**
Synthesis of complex spatial filters for coherent optical data processing
09 p1065 N73-18693
Chromatic induction and spatial intraocular straylight effects in human perception of contrast colors
[IZF-1972-19] 14 p1692 N73-23730
Spatial filtering techniques in connection with coherent light optical data processing
[LCR-DR-1-71-253/1/R] 15 p1754 N73-24220
Hybrid optical processing system
16 p1922 N73-25552

**SPATIAL ISOTROPY**
U ISOTROPY
U SPATIAL DISTRIBUTION

**SPATIAL ORIENTATION**
U ATTITUDE [INCLINATION]

**SPECIFIC HEAT**
NT HEAT OF DISSOCIATION
Using specific heat method to study vacancies
[AD-743695] 01 p0088 N73-10725
Specific heat capacity at constant temperature and pressure of water substances
[ESDU-68008] 01 p0116 N73-10957
Thermal expansion, specific heat, and thermal conductivity of carbon reentry materials to 3000 C
[SC-CR-72-3139] 03 p0320 N73-12610
Anomalous capacity for estimating ferroelectric phase transition in Kanzig regions
[AD-747559] 03 p0347 N73-12831
Calorimetric analysis of low temperature heat capacities and high temperature enthalpies for sodium chromate
[BM-RI-7691] 05 p0605 N73-14924
Model for studying excessive specific heat that glasses exhibit at low temperatures
[AD-752471] 08 p0970 N73-17930
Two dimensional unsteady transonic flow of perfect gas with specific heat
[AD-753221] 09 p1018 N73-18310
Calorimeter for measuring high temperature specific heat of Ti and Ti based alloys during intermetallic phase
[AD-754954] 11 p1306 N73-20599
Research projects in solid state physics, low temperature physics, superconducting films, and quantum liquids and crystals
[COO-1569-93] 12 p1439 N73-21657
Specific heat and thermodynamic properties of heat accumulating materials
14 p1718 N73-23941
Specific heat measurements of He-4 monolayers on sintered and gas monolayer coated copper
16 p1973 N73-25957
Computation of bulk moduli of synthetic hydrocarbon hydraulic fluid
[AD-760776] 18 p2163 N73-27471
Specific heat measurements on rubidium tungsten bronze and aluminum film superconductors
18 p2184 N73-27636
Electrical, magnetic, and thermal properties of dilute and concentrated magnetic alloys
[AD-763820] 22 p2707 N73-31682
Method for determining heat capacity of ceramic materials by measuring heat transfer during condensation process
23 p2807 N73-32445
Thermophysical properties of synthetic resin-base materials with fillers to show errors in development of mathematical relationships
23 p2807 N73-32446
Coefficient of thermal conductivity for composite materials by using axial thermal flow method
23 p2807 N73-32447
Low temperature properties and specific heat of plutonium and neptunium
[AERE-R-7172] 24 p2934 N73-33432
Magnetic and specific heat measurements of carbides, nitrides, and uranium and thorium sulfides
[CEA-R-4453] 24 p2943 N73-33506
Thermodynamic properties of electron gas in magnetic fields of varying strengths to include magnetic susceptibility, internal energy, and specific heat
24 p2990 N73-33896
Heat capacity of liquid metals and stainless steels
[ORO-3291-17] 24 p2992 N73-33914

**SPECIFIC IMPULSE**
Development of fluidic control system for stabilizing aircraft ejection seat in pitch plane during rocket motor burn portion of ejection sequence
[AD-747630] 03 p0254 N73-12056
Specific impulse of auxiliary rocket thrusters using liquefied gases
[NASA-TT-F-14878] 12 p1444 N73-21694
Effect of metal admixtures on specific impulse of solid rocket propellants
24 p2970 N73-33736

**SPECIFICATIONS**
NT AIRCRAFT SPECIFICATIONS
NT EQUIPMENT SPECIFICATIONS
Processing specifications for slip-cast fused silica radomes
[AD-745793] 01 p0029 N73-10229
Acceptance criteria specification for slip-cast fused silica radomes
[AD-745743] 01 p0029 N73-10230
Cleaning processes and postcleaning inspection procedures for meeting oxygen system cleaning requirements
[NASA-SP-3072] 06 p0634 N73-15155
Findings and data products developed during crew interface specification study for inflight maintenance and stowage functions in future manned space flights
[NASA-CR-128685] 07 p0849 N73-16878
Military specifications for flat connectors and cables
14 p1641 N73-23306
Managing contract specification system for satellite projects
15 p1847 N73-24974
Specifications for threaded fasteners
[NASA-CR-124415] 23 p2849 N73-32764

**SPECTRA**
NT ABSORPTION SPECTRA
NT ATOMIC SPECTRA
NT BALMER SERIES
NT D LINES
NT ELECTROMAGNETIC SPECTRA
NT ELECTRONIC SPECTRA
NT EMISSION SPECTRA
NT ENERGY SPECTRA
NT FRAUNHOFER LINES
NT H ALPHA LINE
NT H BETA LINE
NT H GAMMA LINE
NT H LINES
NT INFRARED SPECTRA
NT K LINES
NT LINE SPECTRA

NT MASS SPECTRA
NT MICROWAVE SPECTRA
NT MOLECULAR SPECTRA
NT NEUTRON SPECTRA
NT NOISE SPECTRA
NT OXYGEN SPECTRA
NT PLASMA SPECTRA
NT POWER SPECTRA
NT RADIATION SPECTRA
NT RAMAN SPECTRA
NT SCHUMANN-RUNGE BANDS
NT SHOCK SPECTRA
NT SOLAR SPECTRA
NT SPECTRAL BANDS
NT STELLAR SPECTRA
NT TELLURIC LINES
NT UBV SPECTRA
NT ULTRAVIOLET SPECTRA
NT VIBRATIONAL SPECTRA

Numerical calculation of ultrahigh energy photon spectrum
[NASA-TM-X-66198] 10 p1193 N73-19703

Spectral and statistical characteristics of surface wave velocity fields
20 p2446 N73-29654

**SPECTRAL ABSORPTION**
U ABSORPTION SPECTRA

**SPECTRAL ANALYSIS**
U SPECTRUM ANALYSIS

**SPECTRAL BANDS**
NT ABSORPTION SPECTRA
NT FRAUNHOFER LINES
NT SCHUMANN-RUNGE BANDS
NT TELLURIC LINES

Development of narrow band spectral analyzer for determining power spectra of waveforms derived from vibrating axial compressor blades due to random excitation
[ARC-R/M-3259] 15 p1729 N73-24024

Appropriate line profiles for radiation modeling in detection of atmospheric pollutants
[NASA-CR-132303] 20 p2448 N73-29672

Determination of optimal spectral intervals for remote sensing of earth surface from space
21 p2535 N73-30327

**SPECTRAL EMISSION**

Influence of wind stress and bottom friction on spectral response of two layer beta plane ocean currents
[AD-746506] 02 p0168 N73-11367

Shape and rotation rate of asteroid bodies
02 p0228 N73-11850

Remote detection of water content and spectral properties of leaves in different soybean crop species
04 p0378 N73-13070

Characteristics of cryogenic interferometric spectrometer and application to measuring low level emittance or absorption in optical elements
05 p0556 N73-14518

Spectral characteristics of normal and nutrient-deficient maize leaves
[NASA-CR-132145] 15 p1742 N73-24119

Mathematical models and computer simulation for predicting spectral parameters of radar echoes from rain clouds
[STC-TM-308] 15 p1750 N73-24180

Spectral emissions of liquid titanium, vanadium, zirconium, molybdenum, and platinum at fusion temperatures
[BM-RI-7743] 15 p1798 N73-24575

Measurement of spectral flux density of universal diffuse X ray background between 2 and 200 KeV
19 p2331 N73-28755

Equivalent widths and line intensities for prominences observed during 1964 to 1965
20 p2472 N73-29852

**SPECTRAL ENERGY DISTRIBUTION**

Determination of comet chemical nature from comet spectral energy
02 p0228 N73-11847

Parametric analysis for estimating spectral spreading of radio frequency amplifier output due to nonlinearities
[SC-DR-72-0330] 03 p0274 N73-12222

Line spectra and spectral energy distribution of early type stars
05 p0594 N73-14829

Vertical radiation heat flux profiles and spectral distribution
09 p1059 N73-18632

Fourier coefficients and power spectral density calculating device
[IPPJ-T-13] 16 p1949 N73-25766

Spectral energy distribution of Pamir plants at different altitudes above sea level in relation to mountain plant characteristics
20 p2406 N73-29336

Spectrophotometric measurements of spectral composition of conifer and decidous forests
20 p2406 N73-29337

Numerical analysis of one form of distribution of spectral energy density of thermal radiation
[JPRS-59660] 20 p2485 N73-29958

**SPECTRAL LINE WIDTH**

Equivalent widths and line intensities for prominences observed during 1964 to 1965
20 p2472 N73-29852

Line strengths in spectra of seven double-lined Am binary stars
[ROY-OBS-BULL-177] 21 p2598 N73-30819

Nitric oxide spectral line width for stratospheric aeronomical analysis
[A-114-1973] 23 p2819 N73-32536

Collision frequency and velocity effects on ion cyclotron resonance line shape
[NASA-CR-135724] 23 p2821 N73-32552

Relaxation theory improvements of spectral line broadening in plasmas
24 p2961 N73-33659

**SPECTRAL LINES**
U LINE SPECTRA

**SPECTRAL NOISE**
U WHITE NOISE

**SPECTRAL RECONNAISSANCE**

Soil and plant identification in tropical environment by incident and reflected solar radiation
[AD-743931] 01 p0051 N73-10417

Microwave radiometer technique for detecting and identifying man-made objects and discriminating them from natural objects
[DREO-R-661] 04 p0449 N73-13669

Employment of Earth Resources Technology Satellite capabilities for determining distribution of earth resources
07 p0782 N73-16353

Application of electromagnetic sensors for remote sensing of oceanographic processes to determine available resources
07 p0782 N73-16356

Characteristics and capabilities of remote sensor systems to collect and analyze earth resource data
07 p0783 N73-16361

Analysis of factors affecting design and application of remote sensors for earth observation
07 p0784 N73-16376

Procedure for defining spectrally separable classes for soil survey research
[NASA-CR-130031] 07 p0791 N73-16434

Multichannel ocean color data analysis to produce color maps
[TRW-21123-6001-RU-00] 18 p2144 N73-27328

**SPECTRAL REFLECTANCE**

Spectral absorption coefficients of argon and silicon and spectral reflectivity of aluminum as function of pressure, temperature, and wave number
[NASA-CR-129300] 03 p0335 N73-12727

Bidirectional reflectance of metallic surfaces as function of wavelength and surface roughness
[UILU-ENG-72-4001] 03 p0335 N73-12728

Theory of spectral reflectance or emittance of particulate minerals
[NASA-CR-128638] 03 p0335 N73-12729

Effect of above-ground plant mass on spectral curves of brightness coefficients of soil-vegetation system
04 p0443 N73-13613

High resolution spectral reflectance of potassium chlorides and bromides at room temperature in far ultraviolet yields new structures
[NOTA-INTERNA-402] 05 p0587 N73-14777

Reflectance spectra of contaminants in space simulation chamber
[NASA-CR-128716] 07 p0799 N73-16486

ERTS-1 spectral reflectance measurements of vegetation, soil, and water in Rio Grande Valley, New Mexico
[E73-10408] 11 p1278 N73-20370

Spectral reflectance measurements of playas in Great Basin test site
[E73-10561] 14 p1656 N73-23433

Relationship between in situ spectral reflectance measurements and photometric characteristics of ERTS-1 MSS imagery of Willcox Playa, Arizona
[PAPER-119] 19 p2279 N73-28340

DCP-collected absolute target reflectance measurements to assist interpretation of ERTS-1 imagery of forest stresses in Black Hills, South Dakota
19 p2283 N73-28365

Design, development, and characteristics of high sensitivity, nonselective pyranometer with black detecting surface and xenon filling
20 p2402 N73-29304

Development and characteristics of single reflector interference spectrometer and associated drive system
[NASA-CASE-NPO-11932-1] 20 p2419 N73-29438

ERTS-1 measurements of seasonal changes in reflectance of soils, vegetation, and water in Hidalgo County, Texas
[E73-10946] 21 p2530 N73-30288

Comparison of ERTS-1 spectral reflectance measurements of major crops and soil associations for selected sites in Iowa, Kansas, North Dakota, and Texas
[E73-10981] 22 p2657 N73-31288

Bidirectional reflectance of zinc oxide in ultraviolet and infrared spectral bands
[NASA-CR-135494] 22 p2678 N73-31450

Mathematical model for identification of crops from directional reflectance
[NASA-CR-133989] 22 p2691 N73-31555

Filter for determining long wave solar spectral reflection by plane surfaces
24 p2975 N73-33772

**SPECTRAL RESOLUTION**

Gray scale reproduction capability for characterizing aerial television reconnaissance system
[AD-747632] 03 p0267 N73-12165

Auxiliary corrective windings for increased resolution and decreased distortions in cathode ray tubes
[AD-751879] 08 p0889 N73-17201

Derivation of algorithms correlating spectra of ocean wave conditions with two dimensional spectra of aerial photographs and radar imagery
10 p1153 N73-19383

Nimbus 4 IRIS spectra in 750-1250/cm atmospheric window region
[NASA-TM-X-66281] 18 p2142 N73-27315

Direct integration transmittance model for 200/2000 cm region of high spectral resolutions and of planetary thermal emissions
[NASA-TM-X-70454] 21 p2548 N73-30429

Development of fine spectral resolution procedure for determining infrared radiant heat transfer from exhaust plume
[RM-575] 21 p2605 N73-30877

**SPECTRAL SIGNATURES**

Spectral signatures for dominant desert scrub plant species of Arizona and soil surface backgrounds
[E72-10318] 04 p0413 N73-13367

Loss coefficients and spectral density of random processes in noise filters
09 p1066 N73-18699

Determination of specific spectral signatures for dominant Arizona desert scrub plant species and soil surface backgrounds
[E73-10466] 11 p1284 N73-20421

Multispectral scanning systems and potential application to earth resources noting spectral properties of common earth materials
[ERL/R-244-U] 13 p1531 N73-22404

Application of regression analysis to water quality measurement from remote sensing spectral signature data
[NASA-CR-132997] 16 p1870 N73-25141

Determination of variations in spectral signatures for different geological target types and correlation with radiometric measurements from air and ground
[E73-10808] 18 p2139 N73-27283

Determination of variation in spectral signatures for different geological target types using ERTS-1 radiometric data
[E73-10809] 18 p2139 N73-27284

Variations in spectral signatures for different geological types based on ERTS-1 radiometric data
[E73-10810] 18 p2139 N73-27285

Multispectral scanning systems applied to agriculture and forestry
19 p2295 N73-28452

Spectral signatures for dominant desert scrub plant species and soil surface backgrounds in Arizona
[E73-10890] 20 p2394 N73-29239

Determination of seasonal, meteorological, and statistical variations in spectral signatures for geological target types from ERTS-1 data
[E73-10933] 21 p2529 N73-30275

Correlation of ERTS-1 imagery signatures with water balance ecosystem and geology of select playa lake basins in West Texas
[E73-11102] 24 p2914 N73-33259

Infrared signatures of high performance jet aircraft and evaluation of air to air missile effectiveness
[SLA-73-5271] 24 p2994 N73-33929

**SPECTROGRAMS**

Discrimination of liquids and glides in automatic speech recognition system using syntactic recognition algorithms in analysis of digital spectrograms
14 p1623 N73-23149

Recognition of spoken sentences by visual examination of spectrograms
14 p1628 N73-23199

Hierarchial models of words and sentence recognition
14 p1629 N73-23205

Extraction of formant information from discrete spectrograms in speech recognition processes
14 p1630 N73-23216

Analysis and classification of spectrograms of some southern red variables
19 p2341 N73-28834

**SPECTROGRAPHS**

Energy calibration of Orion spectrograph for operation in wavelength range from 2000 to 3800
[NASA-TT-F-14584] 07 p0799 N73-16491

Large space bandwidth signal analysis by means of two-dimensional optical processor and synthesis of near real time optical sound-spectrograph
14 p1631 N73-23223

Electromechanical focal plane shutters for spectrographic and color schlieren camera systems
[DREV-TN-1997/72] 15 p1785 N73-24475

Spectrographic study of rare earth crystal absorption spectra in magnetic fields at liquid helium temperature
[NASA-TT-F-14732] 24 p2958 N73-33640
**SPECTROHELIOGRAPHS**
Photoheliographic data on sunspots for 1962, 1963, and 1964 - tables
01 p0101 N73-10829
Evolution of solar active region and solar flare from observations of OSO-7 spectroheliograph
08 p0973 N73-17957
Design feasibility of thermal subsystem concepts for photoheliographs
[NASA-CR-124268] 16 p1913 N73-25483
**SPECTROHELIOSCOPES**
U SPECTROHELIOGRAPHS
**SPECTROMETERS**
NT EBERT SPECTROMETERS
NT FILTER WHEEL INFRARED SPECTROMETERS
NT INFRARED SPECTROMETERS
NT MASS SPECTROMETERS
NT NEUTRON SPECTROMETERS
NT SOLAR SPECTROMETERS
NT SPECTROHELIOGRAPHS
NT TIME OF FLIGHT SPECTROMETERS
NT ULTRAVIOLET SPECTROMETERS
Transmission characteristics of commercially available, laser eye protectors with Cary 14 spectrophotometer
[AD-746293] 02 p0136 N73-11100
Empirical corrections for quantitative multi-element analyses using combined wavelenth- and energy-dispersive systems
[NASA-TM-X-66103] 02 p0137 N73-11113
Stabilization of base line at output of amplifiers for gamma spectrometry chain
[CEA-N-1514] 03 p0277 N73-12248
Development of alpha and X ray spectrometers for use on Apollo 15 and 16 flights
[NASA-CR-128649] 03 p0301 N73-12461
Nuclear spectrometry with semiconductor detectors
[CEA-CONF-1964] 03 p0345 N73-12812
Mossbauer spectrometer with high efficiencies in both transmission and backscattering techniques
[NASA-CASE-LAR-11155-1] 04 p0421 N73-13433
Signal filtration in amplitude spectrometry system
[JINR-P13-6428] 05 p0548 N73-14448
Throughput, multiplex systems, and free spectral range in spectrometers
[AD-749858] 05 p0553 N73-14492
Dual gas correlation spectrometer measurements of sulfur dioxide and nitrogen dioxide in industrial area of southern California
[PB-210717] 05 p0575 N73-14676
Nondestructive neutron activation and spectrum analysis using gamma ray spectrometer coupled to PDP 9 computer
[IRI-133-71-03] 05 p0582 N73-14739
Radial velocity of southern G and K types stars as observed by Cassegrain spectrograph
05 p0594 N73-14830
Airborne spectrometer measurements of cloud droplet size
[NASA-CR-130138] 06 p0693 N73-15650
Nuclear chemistry and geochemistry research projects including isotope separations, meteorite and tektite compositions, and solid gamma spectrometer development
[COO-3236-3] 08 p0884 N73-17156
Characteristics and vibrational test of structural test unit for electron-proton spectrometer under simulated flight conditions
[NASA-CR-128699] 08 p0924 N73-17573
Shock test of electron-proton spectrometer structural test unit to verify structural integrity of spectrometer design and to analyze shock response of electronic housing
[NASA-CR-128698] 08 p0924 N73-17574
Electron-proton spectrometer for Skylab radiation dose measurements
[NASA-CR-128702] 08 p0925 N73-17575
Compilation of analyses generated during development of electron-proton spectrometer for Skylab program to insure reliability and quality control
[NASA-CR-128705] 08 p0925 N73-17576
Electron-proton spectrometer applied to Skylab program for measurement of electrons and protons resulting from solar flares to determine radiobiological safety factors
[NASA-CR-128704] 08 p0925 N73-17577
Qualification tests of electron-proton spectrometer to determine suitability for use in Skylab program
[NASA-CR-128703] 08 p0925 N73-17580
Multichannel digital spectrometer for measuring ion temperature of Circe 25-kW device
[EUR-CEA-FC-641] 08 p0925 N73-17582
Survival of heavy nuclei in cosmic ray source environments from Goddard balloon spectrometer experiment
08 p0974 N73-17964
Spectrometer for fast neutrons using proton recoil in stilbene crystal
[BMVG-FBWT-72-4] 09 p1036 N73-18456
Laser operation in vacuum and active scattering particle spectrometers
[NASA-CR-124111] 10 p1159 N73-19425
Proton 1 rocket charged particle spectrometer for measuring energy spectrum and electron and proton distribution above 20 keV
[NP-19462] 10 p1161 N73-19444
Rocket measurement of solar fluxes at 1216 A, 1450 A and 1710 A
[AERONOMICA-ACTA-A-111] 10 p1210 N73-19842
Quality control procedures for Skylab electron-proton spectrometer equipment and parts
[NASA-CR-128853] 11 p1292 N73-20484
Safety analysis of EPS electron-proton spectrometer
[NASA-CR-128851] 11 p1292 N73-20485
Performance tests of electron-proton spectrometer for design verification
[NASA-CR-128852] 11 p1292 N73-20486
Design of electron-proton spectrometer for mounting externally on Skylab CSM
[NASA-CR-128814] 11 p1293 N73-20490
Electron-proton spectrometer providing signals for determining energy
[NASA-CR-128850] 11 p1293 N73-20493
Toroidal magnetic field spectrometer for experimentation with high energy beams
[LNF-72/59] 11 p1294 N73-20501
Computerized control and recording system for magnetic spectrometer
[FRNC-TH-268] 11 p1294 N73-20502
Low energy particles on front detector in coincidence in electron spectrometer on OV1-13 satellite
[AD-755789] 12 p1406 N73-21401
Two cavity spectrometer for studying microwave transmission through gallium single crystals
12 p1438 N73-21647
Far UV camera/spectrograph deployed on lunar surface in Apollo 16 mission
12 p1450 N73-21745
Gamma ray spectrometer experiment during transearth coast period of Apollo 16 flight
12 p1451 N73-21752
X ray fluorescence spectrometer for orbital mapping of lunar composition and X ray galactic observations
12 p1451 N73-21753
Lunar radon emanation measurements, using alpha particle spectrometers on Apollo 16
12 p1451 N73-21754
Effects of successive concave optical gratings in spectrograph on X ray diffraction patterns
[AD-757014] 13 p1560 N73-22640
Design of tunable electron paramagnetic resonance spectrometer with quartz stabilization
13 p1565 N73-22684
Development of narrow band spectral analyzer for determining power spectra of waveforms derived from vibrating axial compressor blades due to random excitation
[ARC-R/M-3259] 15 p1729 N73-24024
High optical resolution derivative spectrometer for measuring optical properties of solids in vacuum UV and far IR range
15 p1785 N73-24474
NaI[T1] crystal detector for measuring proton induced activity in gamma ray spectrometer
[NASA-TM-X-66241] 15 p1787 N73-24486
Working principles of two aerosol particle size spectrometers, based on lateral air jet or asymmetric expansion of aerosol
[BMVG-FBWT-73-6] 15 p1788 N73-24496
Parallel plate electrostatic spectrograph as relativistic particle analyzer
15 p1788 N73-24498
Fringing field effect minimization in parallel plate electrostatic spectrograph taking into account condenser plate thickness
15 p1788 N73-24499
Neutron inelastic scattering spectroscopy for studying problems in materials science
[COO-3352-4] 15 p1815 N73-24713
Preventive maintenance of internal combustion engines and transmissions using spectrochemical oil analysis techniques
[PB-216168/5] 16 p1919 N73-25525
Electron-proton spectrometer component derating
[NASA-CR-128706] 17 p2033 N73-26450
Thermal/vacuum tests of engineering test unit of electron-proton spectrometer
[NASA-CR-128701] 17 p2033 N73-26451
Data base of electron and proton spectrometer, Orbiting Geophysical Observatory, and fluxgate magnetometer experiments
[UCRL-51314] 17 p2033 N73-26453
Design and development of zero field paramagnetic resonance spectrometer
[AD-759370] 17 p2035 N73-26466
Characteristics of electron-proton spectrometer to measure geomagnetically trapped radiation in geostationary orbit at 6.6 earth radii in outer radiation belt
[NASA-CR-132786] 18 p2150 N73-27381
Scanning spectrometer for fluorescence measurements, and silicon detector for alpha counting
[BARC-628] 19 p2230 N73-27984
High resolution interferometer spectrometer measurements of auroral infrared emissions to simulate high altitude nuclear explosions
[AD-762013] 19 p2297 N73-28475
Dual purpose optical instrument capable of simultaneously acting as spectrometer and diffractometer
[NASA-CASE-XNP-05231] 19 p2300 N73-28491
Development, construction, and operation of polarization fourier spectrometer for conducting astronomical observations
19 p2300 N73-28492
Integration of spectrometer capability with imagery function of facsimile cameras for use on planetary landers
[NASA-CASE-LAR-11207-1] 19 p2300 N73-28496
Correlation between Ge crystal and spectrometer properties of Ge[L1] detector made from Ge crystal
[AECL-4369] 19 p2327 N73-28718
Development of actinometric instruments and surface coatings to show performance parameters and construction details
20 p2403 N73-29307
Development and characteristics of single reflector interference spectrometer and associated drive system
[NASA-CASE-NPO-11932-1] 20 p2419 N73-29438
Development of nitrogen-laser-pumped tunable-dye laser for application as spectroscopic light source
20 p2424 N73-29473
Design of gamma ray spectrometer for measurement of intense radiation using Compton scattering effect
[NASA-CASE-MFS-21441-1] 21 p2544 N73-30392
Conceptual work on 125 mm ultraviolet spectrometer for measuring ozone
[NASA-CR-132266] 22 p2673 N73-31411
Portable nuclear radiation spectrometer for field measurement of mixed isotopic contaminants
[LA-5203-MS] 22 p2674 N73-31418
CO2 laser and spectrophone for CO2 and water vapor absorption measurements
22 p2679 N73-31462
Spectrometric and photographic analysis of neodymium glass laser produced hydrogen plasma
[AD-764496] 22 p2705 N73-31667
Study of galactic nuclei using image tube spectrographic techniques
22 p2713 N73-31718
Spectrometric measurement of D/H ratio in Jupiter atmosphere
24 p2978 N73-33797
**SPECTROMETRY**
U SPECTROMETERS
**SPECTROPHOTOGRAPHY**
Observation analysis of August 1972 solar flares using spectrophotographic techniques
[NASA-CR-132195] 16 p1963 N73-25881
**SPECTROPHOTOMETERS**
NT INFRARED SPECTROPHOTOMETERS
NT ULTRAVIOLET SPECTROPHOTOMETERS
Biological oceanography by airborne spectrophotometer
[NASA-CR-133325] 18 p2147 N73-27353
Measurements of upward radiation flux from ground and atmosphere using airborne spectrophotometer
20 p2400 N73-29284
Spectrophotometric measurements of spectral composition of conifer and decidous forests
20 p2406 N73-29337
Development and characteristics of spectrophotometer for measuring transmittance of solid and liquid materials
[PAPER-76A5-729] 21 p2545 N73-30398
Analysis of methods for measuring quantity of radiation emitted from materials using standard sources and calibrated detectors
[PAPER-76A5-730] 21 p2545 N73-30399
**SPECTROPHOTOMETRY**
NT STELLAR SPECTROPHOTOMETRY
Spectrophotometric determination of aqueous iodine complexed with potassium iodide showing free iodine optimally determined at isosbestic point for solutions
[NASA-CR-128585] 01 p0022 N73-10172
Application of high pass broadband filters to absorption spectrophotometry
[IRI-133-72-08] 03 p0274 N73-12223
Iodoantimonous acid for quantitative yield estimation of antimony trace concentrations by spectrophotometric method
[AREAEE-126] 04 p0433 N73-13531
Spectrophotometric observation of earth atmosphere and underlying surfaces near twilight horizon from manned spacecraft
09 p1026 N73-18375
Spectrophotometric observations of planet Jupiter to determine ultraviolet absorption for different regions of disk
09 p1083 N73-18835
Photoelectric measurements of solar phase brightness relationship of planet Jupiter Galilean satellites to show porous nature of surface layers of satellites
09 p1083 N73-18838

Ionospheric investigation of auroral activity using rocket-borne spectrophotometric techniques
[NASA-CR-131484] 13 p1519 N73-22311

Atomic absorption spectrophotometric analysis of chromium in stainless steels
[AD-755809] 13 p1545 N73-22522

Spectrophotometric analyses of Jovian and Saturnian limb darkenings
[NASA-CR-131891] 13 p1576 N73-22772

Chemical composition and structure of metal surface corrosion protective chelate coatings
[DRIC-TRANS-3020] 14 p1616 N73-23095

Spectrophotometric analysis of terminal epoxy and olefinic compounds
[TN-287] 15 p1746 N73-24155

Polarimetric and spectrophotometric observations of late type giant and supergiant stars
17 p2080 N73-26827

Spectrophotometry accuracy with Kodak IN, IIaO, and II aD photographic emulsions
[RR-3] 19 p2301 N73-28502

Analysis of tungsten in tungsten steel by precipitation with cinchonine and spectrophotometric measurement of hydroquinone color
[AD-762122] 19 p2310 N73-28579

Simultaneous electrophotometric and spectral observations of N Del in 1967
20 p2471 N73-29848

Spectrum of class M supergiants in region lambda lambda 7000 to 6000 A
20 p2471 N73-29851

Proceedings of conference on accuracy in spectrophotometry and luminescence measurements
[NBS-SP-378] 21 p2544 N73-30396

Techniques and equipment for achieving high accuracy spectrophotometric measurements
[PAPER-76A5-728] 21 p2544 N73-30397

Analysis of physical parameters involved in spectrophotometry with high accuracy to show effects of stray light and interference
[PAPER-76A5-732] 21 p2545 N73-30401

Procedures for standardization in clinical spectrophotometric and fluorometric measurements
[PAPER-76A5-735] 21 p2545 N73-30404

Spectrophotometric procedures applied to medical services in clinical chemistry laboratories and analysis of sources of error in diagnoses
[PAPER-76A5-736] 21 p2545 N73-30405

Analysis of parameters involved in establishing spectrophotometric standards
[PAPER-76A5-737] 21 p2546 N73-30406

Photometric standards for North Polar Sequence, Kapteyn Areas, and Harvard Standard Areas
21 p2594 N73-30791

Spectrophotometric analysis of electrochemical reactions on transparent mercury/platinum electrode
[AD-763265] 22 p2626 N73-31043

Compilation, reduction, and correlation of spectrophotometric data obtained during NASA airborne auroral expedition
[NASA-CR-135497] 23 p2785 N73-32278

Spectrophotometric determination of B, Cu, and Ta in Ni base alloys
[JAERI-M-5094] 24 p2934 N73-33431

**SPECTRORADIOMETERS**

In situ spectroradiometric quantification of ERTS-1 imagery of Arizona and Texas
[E72-10173] 01 p0055 N73-10444

In situ spectroradiometric quantification of ERTS-1 MSS and RBV imagery
[E72-10174] 01 p0055 N73-10445

Night sky spectral radiant sterance at ground level and variation with latitude and nighttime conditions, using Fourier spectroradiometer
[AD-750609] 06 p0669 N73-15442

Spectroradiometric quantification of soil moisture in Willcox Playa, Arizona based on ERTS-1 imagery
[E73-10354] 10 p1149 N73-19350

Dual channel infrared spectroradiometric analyses of rocket engine exhaust spectra
[NASA-CR-124207] 12 p1404 N73-21387

Preparation of field spectroradiometer equipment and tapes for Skylab S-191 experiment
[E73-10760] 17 p2022 N73-26360

High resolution radiometer for visible and infrared imagery onboard meteorological satellite
18 p2209 N73-27836

Relationship between in situ spectral reflectance measurements and photometric characteristics of ERTS-1 MSS imagery of Willcox Playa, Arizona
[PAPER-I19] 19 p2279 N73-28340

Development, characteristics, and operation of compensated thermoelectric net radiometer to show advantage over standard radiometers
20 p2402 N73-29305

In situ spectroradiometric quantification of ERTS-1 imagery of Arizona agriculture
[E73-10967] 21 p2533 N73-30309

Analysis of absolute spectrofluorometry procedures and establishment of standards for calibrating spectrofluorometers
[PAPER-76A6-741] 21 p2546 N73-30407

Spectroradiometric calibration of EREP imagery and oceanography of Block Island Sound
[E73-11015] 22 p2660 N73-31319

**SPECTROSCOPES**

U SPECTROMETERS

**SPECTROSCOPIC ANALYSIS**

Absorption spectroscopic determination of nickel, chromium, and cobalt in airborne particulates
[NASA-TM-X-2672] 02 p0137 N73-11111

Empirical corrections for quantitative multi-element analyses using combined wavelenth- and energy-dispersive systems
[NASA-TM-X-66103] 02 p0137 N73-11113

Neutron activation analysis using gamma ray spectroscopy for determination of trace elements and short-lived nuclides
[BMBW-FBK-72-13] 03 p0262 N73-12122

Spectroscopic measurements on plasma composition in Tokamac-type facility
[JAERI-M-4596] 06 p0705 N73-15752

Measurement of surface recession of ablative materials in rocket nozzles by spectroscopic analysis
[AD-749968] 06 p0714 N73-15829

Infrared absorption spectra analysis of contaminant materials and binary mixtures to determine contamination of spacecraft by material outgassing
[NASA-CR-124072] 08 p0934 N73-17645

Spectroscopic studies of electrical and optical properties of amorphous semiconductors
[AD-753903] 10 p1202 N73-19779

Spectroscopic, photometric, and electron microscope analyses of metal wear particles in JT3D turbojet engine oil
[DLR-FB-73-06] 12 p1409 N73-21417

Spectroscopic examination of electric field intensity and ion temperature of turbulent plasma
[AEC-TR-7375] 12 p1434 N73-21623

Spectrometric determination of copper, iron, cobalt, nickel, and manganese complexes in biological samples
13 p1483 N73-22022

Spectroscopic analysis of atmospheric water vapor at 6943.8 Angstrom line in telluric spectrum
19 p2258 N73-28203

Proceedings of conference on mass spectrometry of metal containing compounds
20 p2431 N73-29527

Spectrochemical analysis of nonconducting materials using cathodes from sample in Grim glow discharge tube
[NASA-TT-F-15031] 20 p2454 N73-29723

Techniques and equipment for achieving high accuracy spectrophotometric measurements
[PAPER-76A5-728] 21 p2544 N73-30397

Analysis of methods for measuring quantity of radiation emitted from materials using standard sources and calibrated detectors
[PAPER-76A5-730] 21 p2545 N73-30399

Analysis of physical parameters involved in spectrophotometry with high accuracy to show effects of stray light and interference
[PAPER-76A5-732] 21 p2545 N73-30401

Procedures for standardization in clinical spectrophotometric and fluorometric measurements
[PAPER-76A5-735] 21 p2545 N73-30404

Spectrophotometric procedures applied to medical services in clinical chemistry laboratories and analysis of sources of error in diagnoses
[PAPER-76A5-736] 21 p2545 N73-30405

Analysis of parameters involved in establishing spectrophotometric standards
[PAPER-76A5-737] 21 p2546 N73-30406

Application of phosphorimetry procedures to quantitative chemical analysis of several aqueous solutions
[PAPER-76A6-743] 21 p2546 N73-30409

Application of fluorescence spectroscopy for analyzing macromolecules of proteins and nucleic acids
[PAPER-76A6-744] 21 p2546 N73-30410

Development of fluorometric methods for analysis of biological compounds based on production of fluorescence by enzymic reaction
[PAPER-76A6-745] 21 p2546 N73-30411

Dry inert gas glove box for handling of hygroscopic and corrosive materials in spectroscopic and lasers experiments
[CRC-1244] 21 p2548 N73-30430

Spectroscopic analysis of plasma diagnostics
[AD-765221] 23 p2823 N73-32567

Development of high resolving power interferometer for line shape measurement applications
[AD-764719] 24 p2927 N73-33380

**SPECTROSCOPIC TELESCOPES**

NT STRATOSCOPE TELESCOPES

Spectroscopic observation of Comets Tago-Sato-Kosaka and Bennett
02 p0228 N73-11848

**SPECTROSCOPY**

NT ABSORPTION SPECTROSCOPY
NT ASTRONOMICAL SPECTROSCOPY
NT AURORAL SPECTROSCOPY
NT GAS SPECTROSCOPY
NT INFRARED SPECTROSCOPY
NT MAGNETIC SPECTROSCOPY
NT MASS SPECTROSCOPY
NT MOLECULAR SPECTROSCOPY
NT OPTICAL EMISSION SPECTROSCOPY
NT RADIO SPECTROSCOPY
NT RAMAN SPECTROSCOPY
NT SPECTROPHOTOGRAPHY
NT SPECTROPHOTOMETRY
NT SPECTROSCOPIC ANALYSIS
NT STELLAR SPECTROPHOTOMETRY
NT ULTRAVIOLET SPECTROSCOPY
NT VACUUM SPECTROSCOPY
NT X RAY SPECTROSCOPY

Microstructural studies of adhesion, wear, friction, and lubrication using LEED, Auger emission spectroscopy analysis, and field ion microscopy
[NASA-TM-X-68152] 01 p0058 N73-10471

Spectroscopic studies of luminescence emitted by dyes irradiated by lasers
[AD-750377] 06 p0680 N73-15335

Auger electron spectroscopy of surface segregation in binary alloys
[NASA-TN-D-6982] 06 p0683 N73-15564

Spectroscopic instrumentation system for zone radiometry
[NASA-CR-124062] 08 p0922 N73-17555

Laser-produced plasma as radiation source in 1000 to 20 A range, and detection with double-grating spectrometer
[FRNC-TH-216] 08 p0948 N73-17763

Spectroscopic methods for temperature measurement in plasmas with self absorption noting methods for plasma column radial temperature distribution
[BMBW-FBK-72-22] 09 p1071 N73-18737

High power tunable organic dye laser excitation of atomic fluorescence spectroscopy
12 p1409 N73-21422

Microwave preamplifier induction for electron spin resonance spectroscopy
14 p1666 N73-23521

Research in solid state physics including semiconductor lasers and laser spectroscopy
[AD-757559] 14 p1698 N73-23779

Reconstructing information of reticulated spectroscopy
[RR-2] 16 p1913 N73-25480

Auger analysis of chemisorption of various gases to metal surfaces and sliding friction effects on interaction
[NASA-TN-D-7340] 16 p1918 N73-25520

Chemical analysis of iron, steel, and nonmetallic materials
[PB-214230/5] 16 p1929 N73-25609

High resolution Brillouin spectroscopic study of hypersonic sound velocity and attenuation as function of temperature in acrylic monomers
16 p1944 N73-25731

Spectral line features of neon beam-foil spectroscopy
16 p1947 N73-25752

Spectroscopic methods used for analysis of beam-plasma instability
[LBL-1531] 17 p2068 N73-26732

Low energy electron diffraction and auger spectroscopy of [100] surfaces of aluminum and aluminum-copper alloys
18 p2159 N73-27445

Determination of rotational temperatures in flow gas discharges containing nitrogen using sidelight spectroscopy techniques
[AD-762290] 19 p2233 N73-28002

Mossbauer spectra of ferrite catalysts used in oxidative dehydrogenation
[NASA-CR-133740] 21 p2506 N73-30108

Spectroscopic determination of induced emission cross section of 3 P 0 yields 3 F 2 and P 0 yields 3 H 6 transitions of Pr[3 plus] ion in SeCl2 and SnClr
[CRC-1243] 21 p2579 N73-30671

Baryon spectroscopy and regularities between SU[6] and SU[3] mass breaking parameters
[LPTHE-73/21] 21 p2581 N73-30687

**SPECTRUM ANALYSIS**

Windowing or tapering of surface wave time series and spectrum analysis
[AD-742845] 01 p0050 N73-10407

Generation spectrum of excited DF molecules obtained during chemical reactions in D2/F2/N2/O2 laser system
[NLL-DRIC-TRANS-2816-[3623.66]]
02 p0180 N73-11458

Spectral line profiles of helium triplet diffuse series and quasi-static approximation for ions and electrons
[NASA-TN-D-6954] 02 p0214 N73-11731

Spectrum of total diffuse and discrete cosmic gamma ray background over 0.3 to 27 MeV range
[NASA-TM-X-66104] 02 p0225 N73-11818

Determination of comet chemical nature from comet spectral energy
02 p0228 N73-11847

Fast digital noise filter capable of locating spectral peaks and shoulders by using techniques of convoluting integers
[NASA-TM-X-64707] 03 p0273 N73-12212

Spectral analysis of soil boundaries in Collin County, Texas
[E72-10260] 03 p0290 N73-12359

Evaluation of methods for analyzing short-period seismic records to detect multiple events
[AD-747764] 03 p0298 N73-12434

Numerical analysis of terrain echo spectrum from moving radar altimeter
[SC-DR-72-0261] 04 p0389 N73-13159

Research on speech recognition, spectrum analyzers and design of digital filters
[AD-748212] 04 p0396 N73-13223
Iron absorption band analysis for discrimination of iron-rich zones in California and Nevada
[E72-10294] 04 p0410 N73-13344
Onboard digital correlator for spacecraft VLF radio wave studies
04 p0423 N73-13446
Set of functionals and consistent estimators for spectral analysis of continuous nonstationary random processes
[AD-748341] 04 p0441 N73-13596
Line spectra analysis for temperature distribution in stellar atmosphere
04 p0466 N73-13793
Ground based line spectra analyses for determining stellar chromospheres
04 p0466 N73-13795
Photoelectric observation of eclipsing variable stars TY Ursae Majoris and AZ Virginis including spectral classification for WY Cancri, AZ Virginis, and TZ Bootis
04 p0468 N73-13818
Instrumentation for spectrum analysis of short bursts and pulses of Jovian decametric radio emission recorded on magnetic tape
05 p0547 N73-14440
Discharge compositions of gas laser emissions from mercury and copper halides
[AD-749938] 05 p0559 N73-14541
Nondestructive neutron activation and spectrum analysis using gamma ray spectrometer coupled to PDP 9 computer
[IRI-133-71-03] 05 p0582 N73-14739
Computer programs for curve-of-growth analysis using dimensions of stellar lines as input
[ROY-OBS-BULL-171] 06 p0644 N73-15230
Response spectra of earthquake motion accelerograms
[PB-212602] 07 p0794 N73-16457
Fourier amplitude spectra for earthquake ground motions and structural response accelerations
[PB-212603] 07 p0794 N73-16458
Relative flux density measurements and spectra of extragalactic radio sources at decimetric wavelengths
07 p0838 N73-16788
Balloon-borne X ray telescope survey of Cygnus region on 10 June and 17 July 1969 in 20 to 300 keV energy range
07 p0840 N73-16804
Fourier series and fourier integral formulations for improving spectrum analysis and display computer program
[AD-752113] 08 p0886 N73-17177
Electron spin overlap model for quantitative analyses on magnetic spectra of coordination compounds with unpaired electrons
08 p0945 N73-17740
Valence electron model for calculating ionization energies and excited levels in photoelectron- and absorption-spectra
08 p0945 N73-17741
Absolute intensity, polarization, and relative line intensities of rotational Raman scattering spectra from nitrogen, oxygen, and carbon dioxide
[NASA-CR-121091] 08 p0946 N73-17746
Balloon borne measurement of cosmic ray electron spectrum from 10 to 200 GeV
[NASA-TM-X-66182] 08 p0956 N73-17830
Digital on-line spectrum analysis using cross correlation and fast Fourier transformation techniques
[ARC-CP-1225] 09 p1006 N73-18209
Electronic desk calculator for automatic X ray spectrometry data processing
[Y-1854] 10 p1132 N73-19231
Spectral analysis of turbulent fluctuations over ocean waves
[AD-753624] 10 p1156 N73-19406
Measurement of line spectra produced by high resolution mass spectrometer and application to identifying organic compounds in samples from Apollo 11 and 12 flights
[NASA-CR-128840] 10 p1160 N73-19436
X ray attenuation coefficients in absorption spectra of titanium, iron, cobalt, nickel, copper, and zinc
[UCRL-73923] 10 p1189 N73-19675
Antiproton and antinucleon energy spectrum analysis
[LPTHE-73/1] 10 p1191 N73-19691
Computer programming for gamma ray spectra analysis applicable to neutron activation analysis
[IRI-133-72-09] 10 p1194 N73-19720
Computer program for analysis of mass spectra of GaTe and GaSe
[ISS-72/11] 10 p1199 N73-19754
Comparison between measured transmission and emission spectra and calculated spectra in upper atmosphere ozone region
[BMFT-FBW-73-01] 11 p1285 N73-20429
Spectra of prompt gamma rays following nuclear pion absorption
[NASA-CR-131398] 11 p1326 N73-20762
Analysis on OSO-H observations of solar X ray burst spectra
[NASA-CR-131245] 11 p1336 N73-20841
Jovian emission spectrum analysis for temperature and ammonia profiles, and Martian infrared limb profile analysis for atmospheric temperature and water vapor
[NASA-CR-131266] 11 p1337 N73-20847
Spectral analysis of nonconducting siliceous materials by luminescent discharge
[CEA-CONF-2060] 12 p1405 N73-21397
Satellite solar occultation absorption measurements of pollutant concentrations and spectral properties of molecules in infrared region
[REPT-011023-1-T] 12 p1444 N73-21700
Spectral analysis of data from C band radar tracking GEOS 2 satellite and development of data compaction method
[NASA-CR-62085] 13 p1490 N73-22082
Molecular orbital energies in spectra of tervalent titanium chlorocomplexes
13 p1542 N73-22493
Solid state laser multiwavelength identification and display system for detection and spectrum analysis of air pollutants
[AD-755161] 13 p1554 N73-22598
Vibronic interaction in electron paramagnetic resonance spectra of yttrium and scandium doped single strontium chloride crystals
[NASA-CR-131295] 13 p1561 N73-22653
Observation of venus far ultraviolet spectrum by sounding rockets
13 p1572 N73-22741
Properties of spectra derived by linear prediction in spectral analysis of speech
14 p1622 N73-23138
Development of procedures and techniques for improved speech analysis based on fast Fourier transform and time compression and analysis
14 p1632 N73-23226
Development of equipment and system for real-time analysis of speech transients
14 p1632 N73-23232
Development of speech analysis-synthesis system for extracting singing voice signal from background noise on recording device
14 p1632 N73-23234
Interfacing and programming of minicomputer for Doppler spectrum analysis
[NOAA-TR-ERL-241-AL-7] 14 p1692 N73-23733
Airborne radio frequency measurements using automatic spectrum analyzer
[AD-758772] 16 p1876 N73-25184
High frequency plasma line fluctuation for ionospheric heating analysis
[AD-758779] 16 p1907 N73-25433
Reconstructing information of reticulated spectroscopy
[RR-2] 16 p1913 N73-25480
Spectrum analysis program for computing power spectrum of angle modulated high frequency carrier wave
[NASA-CR-128984] 17 p1997 N73-26145
Mathematical model for calculating relative molecular orbital photoionization cross sections in soft X ray region
[UUIP-753] 17 p2066 N73-26714
Energy spectra analysis for heavy nuclei charge compositions in galactic cosmic rays
[NASA-TM-X-66136] 17 p2079 N73-26817
Power spectral analysis of solar 2 cm microwave intensity data
[NASA-CR-133228] 17 p2079 N73-26820
HEAO-A experimental design and equipment for mapping celestial X ray sources and spectral analysis over 0.2 to 150 keV
17 p2085 N73-26866
HEAO-B Bragg crystal spectrometer for stellar X ray spectral analysis
17 p2085 N73-26870
Frequency response of structural systems excited by transient and random loads using cross correlation and spectral analysis techniques
[ISVR-TR-57] 18 p2180 N73-27598
Application of infrared detectors for location and identification of asteroids during sky survey activities
[AD-760107] 18 p2198 N73-27745
Spectral and cospectral analyses of turbulence data obtained over natural ocean waves
[AD-761504] 19 p2316 N73-28624
Relative variations in extreme ultraviolet solar flare spectrum
19 p2335 N73-28791
Analyses of soft X ray spectra obtained during solar flares by OSO satellites
19 p2336 N73-28793
OSO-4 solar flare X ray spectrum analysis on plasma cooling mechanisms
19 p2336 N73-28794
Decametric dynamic spectra of solar type 3 radio bursts
19 p2339 N73-28819
High resolution spectra and position measurements on solar radio bursts
19 p2339 N73-28820
Analysis of gamma ray pulse-height spectra from lunar surface
[NASA-TM-X-70421] 19 p2340 N73-28824
Analysis and classification of spectrograms of some southern red variables
19 p2341 N73-28834
Effects of solar radiation on photomorphogenesis of plants based on spectral distribution of solar energy in daytime
20 p2404 N73-29322
Spectral analysis of variations in meteorological elements for periods ranging from several years to several tens of years
20 p2443 N73-29620
Physical processes associated with infrared millimeter component of spectra from nuclei of Seyfert galaxies
20 p2469 N73-29834
Basic elements of power spectral analysis
[NASA-CR-133774] 21 p2508 N73-30127
Spectral analysis of wind-wave spectrum at ice edge in Arctic Basin
21 p2573 N73-30621
Statistical analysis of NASA multivariate spectrum analysis program performance after modifications
[NASA-CR-134011] 22 p2620 N73-30995
Structural and spectral analysis of lineaments and circular features for discrimination of iron-rich zones in Nevada
[E73-11020] 22 p2661 N73-31324
Geochemical analyses on lunar gamma ray spectra obtained during Apollo orbits
22 p2735 N73-31895
Application of ERTS-1 data and multispectral analysis to regional planning and urban development
[E73-11045] 23 p2779 N73-32221
Atmospheric infrared transmission spectral analysis discussing computed and measured data, and absorption due to atmospheric components
[BMVG-FBWT-73-11] 23 p2787 N73-32297
Analysis of Mariner 9 infrared radiometric Mars surface measurements
23 p2841 N73-32701
Digital spectrum analysis for turbulent plasma diagnostics
[AD-765549] 24 p2966 N73-33704
Structural and spectral studies of sunspots
[NASA-CR-135787] 24 p2975 N73-33776

**SPECULAR REFLECTION**

Solution to equation of radiative transfer for homogeneous atmosphere bounded by perfect specular reflector
[AD-764619] 23 p2857 N73-32830

**SPEECH**

NT ARTICULATION
NT PHONEMES
NT PHONETICS
NT SYLLABLES
NT WORDS [LANGUAGE]

Binaural improvement in normal and defective ears in background of other voices
[AD-746101] 01 p0013 N73-10103
Disturbances determining quality of speech transmitted by radio
[IZF-1972-14] 02 p0139 N73-11128
Speech messages representing nine emotions for studies on time/frequency distortion effects on prosodic features of speech
[AD-746102] 02 p0141 N73-11146
Voice variability for assessing performance of communication system
[AD-746104] 02 p0143 N73-11155
Transmission line inversion problem applied to speech communication process
02 p0201 N73-11625
Speech intelligibility in naval aircraft radio communications
[AD-748202] 03 p0268 N73-12173
Adaptive pulse code modulator for speech signals noting coder and decoder
[SRDE-72001] 05 p0514 N73-14174
On-line and off-line evaluation of HeO2 unscramblers speech intelligibility
[AD-751034] 07 p0758 N73-16157
Speech tests and typical naval noise spectra for use in evaluating voice communication equipment
[AD-753207] 09 p1003 N73-18185
Principles for regulation of timing in speech
14 p1624 N73-23155
Computer simulated parallel-formant synthesizer to copy short samples of human speech
14 p1624 N73-23156
Speech synthesis aided by recursive filter approximating transfer function of nasalized vocal tract
14 p1624 N73-23157
Speech synthesis using Hadamard-Walsh transform
14 p1624 N73-23158
Use of orthogonal Walsh and Hadamard transforms to reduce bit rate for speech communication
14 p1624 N73-23159
Real time software speech synthesis
14 p1624 N73-23160
Diagnostic evaluation of intelligibility in digital vocoders
14 p1624 N73-23161
Subjective evaluation of differential pulse code modulation using speech goodness rating scale
14 p1624 N73-23162

Definition of equivalent peak level in objective speech level measurement
14 p1625 N73-23163
Stimulus time interval and response mode methods using signal to noise ratios to test speech intelligibility
14 p1625 N73-23164
Role of distinctive features in speech production, acoustics, and phonetics
14 p1625 N73-23167
Perceptive evaluation of acoustic signal parts displaying rapid changes and short durations
14 p1625 N73-23170
Model of speech processing with perceptual asymmetry
14 p1626 N73-23173
Experimental computer-based system of speech training aids for deaf
14 p1626 N73-23178
Intraoral pressure in speech of deaf affecting voice/voiceless distinction
14 p1626 N73-23181
Visual vocoder for aiding in speech teaching to deaf
14 p1627 N73-23184
Low order terms of cepstrum for compact digital form of continuous speech
14 p1628 N73-23195
Analysis of human performance in synthesis on non-nazalized vowels and input resistance as function of frequency
14 p1630 N73-23213
Three stage algorithm for representing human speech by time ordered sets of Hanning cosine modulated wavefunctions
14 p1630 N73-23214
Speech modulated, single sideband, suppressed carrier systems for speech reception
14 p1630 N73-23215
Structure and signal processing capabilities of special speech processor
14 p1631 N73-23222
Hard copy of visible speech in real time using electrostatic matrix recorder
14 p1631 N73-23224
Nature, investigative instrumentation, and practical application of speech and linguistics
[AD-762373] 19 p2237 N73-28036
Analysis and perception of nonspeech marine sounds
[OES-6/72] 22 p2624 N73-31023
Mathematics of linear predictive filtering and application to speech analysis and synthesis
[AD-765176] 24 p2896 N73-33117

**SPEECH DISCRIMINATION**
U SPEECH RECOGNITION

**SPEECH RECOGNITION**
Modulation transfer function in room acoustics as predictor of speech intelligibility
[IZF-1972-13] 02 p0211 N73-11710
Effect of breathing hydrogen at depths greater than 1000 feet on speech intelligibility
[AD-749320] 04 p0392 N73-13184
Effect of breathing hydrogen at 200 feet below sea level on speech intelligibility
[AD-749322] 04 p0392 N73-13186
Research on speech recognition, spectrum analyzers and design of digital filters
[AD-748212] 04 p0396 N73-13223
Binaural processing of speech intelligibility in light aircraft
[FAA-AM-72-31] 05 p0503 N73-14094
Depth effect on microphone sensitivity in underwater speech communication
[AD-750650] 06 p0642 N73-15213
Digitized grammar for signal analysis and speech recognition accuracy in command and control system
[AD-746333] 06 p0643 N73-15218
Underwater divers and speech communication problems
[AD-751665] 07 p0757 N73-16150
Phonetic analysis of underwater diver speech and standardization for intelligibility
[AD-751662] 07 p0757 N73-16153
Structural vibration and noise effects on man in aerospace operations
[AGARDOGRAPH-151] 08 p0876 N73-17098
Noise effects on hearing conservation in aircrew and ground support personnel of aerospace operations
08 p0876 N73-17101
Development of computerized speech recognition and voice communication system
[AD-752244] 08 p0886 N73-17172
Real time, small vocabulary, connected-word speech recognition system
[AD-753176] 09 p1006 N73-18211
Reference manual for SAID [speech analog input to digitizer] hardware system which performs preliminary preprocessing of speech signal before entering into computer
[AD-753012] 09 p1006 N73-18215
Filtering and vertical sensor position effects on human speech detection in jungle evnironment
[AD-753650] 10 p1190 N73-19686
Synthetic speech generation and recognition under hybrid computer control, using one set of linguistic rules
13 p1496 N73-22127
Papers presented at conference on speech communication and processing
[AD-742236] 14 p1620 N73-23119
Survey of digital speech processing activity in US and abroad
14 p1620 N73-23120
Need and feasibility of automatic speech reading machines for blind people
14 p1620 N73-23121
Technical problems of automatic speech reading machines and methods adopted for their solution
14 p1620 N73-23122
Field evaluation of automated reading system for blind that produces synthetic speech from written text by use of computer and special-purpose devices
14 p1620 N73-23123
Word and phrase stress by rule for reading machine that produces synthetic English speech
14 p1620 N73-23124
System for automated speech synthesis from ordinary English text
14 p1620 N73-23125
System for generating speech from English text punched on paper tape using small digital computer and parametric speech synthesizer
14 p1620 N73-23126
Synthesis of letter sounds of alphabet by concatenation of phonemes for digital spelled speech reading machine for blind
14 p1620 N73-23127
Electronic time compressor/expander for audio using digital technology
14 p1621 N73-23129
Time induced orthogonality for simplified voice control of speech recognition machines
14 p1621 N73-23130
Design and implementation of adaptive delta modulator with integrated circuit hardware for encoding of speech signals
14 p1621 N73-23132
Voicing adaptive speech digitization technique with delta modulation for effective operation at 9600 bits/second
14 p1621 N73-23133
Pitch-synchronous time-compression speech sampling method for greater intelligibility
14 p1621 N73-23134
Pitch-synchronous, nonharmonic analysis of speech signals by application of FFT to single pitch periods
14 p1621 N73-23135
Real time pitch period extraction by adaptive prediction of speech waveform
14 p1622 N73-23136
Formant extraction technique using adaptive predictive coding
14 p1622 N73-23137
Properties of spectra derived by linear prediction in spectral analysis of speech
14 p1622 N73-23138
Automatic formant and fundamental frequency extraction from digital inverse filter formulation
14 p1622 N73-23139
Accuracy of formant parameter estimation based on method of Prony
14 p1622 N73-23140
Real time, adaptive isolated-word speech recognition system using minicomputer to time normalize word duration
14 p1622 N73-23141
Isolated-word phoneme recognition using features derived from wave function parameters
14 p1622 N73-23142
Word recognition by Walsh transform computer program
14 p1622 N73-23143
Evaluation of various parameters in spoken digits recognition
14 p1622 N73-23144
Automatic speech recognition program to provide segmentation, acoustical parameters, and phonetic feature classifications in speech
14 p1623 N73-23146
Computer program for machine recognition of distinctive features in words and sentences
14 p1623 N73-23147
Decoding of information in acoustic waveform of human speech using signal processing techniques
14 p1623 N73-23148
Discrimination of liquids and glides in automatic speech recognition system using syntactic recognition algorithms in analysis of digital spectrograms
14 p1623 N73-23149
Acoustic and physiological investigation of speaker variabilities relative to speech wave parameters
14 p1623 N73-23150
Fundamental acoustic models for synthesis of speech operating on articulatory parameters
14 p1623 N73-23151
Acoustic theory of speech production for definition of terminal analog speech synthesizer configuration using digital signal processing techniques
14 p1623 N73-23152
Model of speech production mechanism based on anatomical structures and physiological natures of articulatory organs
14 p1624 N73-23153
Generative model for prosody of connected speech in Japanese
14 p1624 N73-23154
Measurement of monosyllabic speech communication using adaptive methodology
14 p1625 N73-23165
Improvements in intelligibility testing reliability using experienced listeners
14 p1625 N73-23166
Linguistic and perceptual role of syntactic hypotheses in speech recognition systems
14 p1625 N73-23168
Short-term memory results from connected speech experiments using adult listeners
14 p1625 N73-23169
Articulatory occlusion recorder for studying differences in timing in labial stops and rounded vowels
14 p1625 N73-23171
Computational processing in real time of digitized palatal signals and analog speech waveforms
14 p1626 N73-23172
Dichotic signs of recognition of speech elements in normals, temporal lobectomies, and hemispherectomies
14 p1626 N73-23174
Aids for speech perception and speech training
14 p1626 N73-23176
Three parameter speech display, including phonemes, pitch, and loudness
14 p1627 N73-23182
Speech display simulation system, using CDC 1604 computer
14 p1627 N73-23183
Visual vocoder evaluation in speech therapy, foreign language pronunciation, and music interpretation
14 p1627 N73-23185
Two speaker verification experiments, using single phrase utterances
14 p1627 N73-23189
Construction of combined identification system of individual voices under natural speech conditions
14 p1627 N73-23190
Listener performance vs. automatic system in speaker verification tasks
14 p1627 N73-23191
Speaker adaptation to automatic speech recognition system, extracting acoustic and phonetic features from continuous speech
14 p1628 N73-23192
Automatic segmentation of repeated utterances of isolated words
14 p1628 N73-23193
Formants in automatic speech recognition, emphasizing physiological phone in terms of articulatory dynamics
14 p1628 N73-23194
Time domain analysis technique for acoustic phonemic level of speech recognition
14 p1628 N73-23196
Phonocode for recognition of natural and artificial speech
14 p1628 N73-23197
Mechanical recognition of spoken words by incomplete learning samples
14 p1628 N73-23198
Recognition of spoken sentences by visual examination of spectrograms
14 p1628 N73-23199
Derivation of phonetic representation by combining steady-state and transemic classification in automatic recognition of continuous speech
14 p1629 N73-23200
Using graph search procedure to convert machine-contaminated phonetic descriptions of speaker performance into standard orthography
14 p1629 N73-23201
Spoken word recognition system utilizing word dictionary and phonological rule
14 p1629 N73-23202
Interaction between segmental and nonsegmental factors in speech recognition
14 p1629 N73-23203
Analysis-by-synthesis models of speech perception with emphasis on efficient machine realization of model
14 p1629 N73-23204
Hierarchial models of words and sentence recognition
14 p1629 N73-23205
Implementation strategy for vocal data management system
14 p1629 N73-23206
Prosodic signals for parenthesis in algebraic expressions
14 p1629 N73-23207
Phoneme recognition of continuants in connected English speech by computer
14 p1630 N73-23208
Proceedings of international workshop on helium speech processing
14 p1630 N73-23210
Enhancement of speech intelligibility through appropriate spectral weighting and effect of passing through optimum filter on signal to noise ratios
14 p1630 N73-23211

Experimental analysis of probability density function of instantaneous amplitude of speech and effect of filtering and compression
14 p1630 N73-23212
Extraction of formant information from discrete spectrograms in speech recognition processes
14 p1630 N73-23216
Relation of phonemes to acoustic signals from human vocal tracts as represented by ultrahigh frequency patterns
14 p1631 N73-23218
Effect of reverberation and interfering noise on speech intelligibility as determined from physical description of running speech
14 p1631 N73-23219
Segmentation and classification of speech using low Q single-tuned filters
14 p1631 N73-23220
Development of procedures and techniques for improved speech analysis based on fast Fourier transform and time compression and analysis
14 p1632 N73-23226
Development and characteristics of computer controlled voice response system
14 p1632 N73-23227
Development of method of speech analysis and synthesis using partial autocorrelation coefficients and optimum quantization technique
14 p1632 N73-23230
Computer simulation to demonstrate feasibility of delta modulation as method for encoding control signals of voiced speech synthesizer
14 p1632 N73-23231
Development of equipment and system for real-time analysis of speech transients
14 p1632 N73-23232
Analysis of clipped speed characteristics and zero crossing-related speech phenomena
14 p1632 N73-23233
Electroacoustic effects of speech communication circuits on speech intelligibility
[AD-757326] 14 p1633 N73-23236
Signal processing of speech pattern recognition using PDP 9 Computer
[AD-757109] 14 p1635 N73-23258
Proceedings of workshop on processing helium speech
[AD-757329] 14 p1635 N73-23259
Digital pattern classification for automatic recognition of English language speech
[AD-757492] 14 p1636 N73-23262
Design of speech-understanding computer system
[AD-757049] 14 p1637 N73-23270
Feasibility of hybrid voice coding system for speech transmission
[AD-756519] 14 p1637 N73-23272
Speech discrimination by personnel with hearing loss at 3 kHz in noise
[AD-752974] 16 p1867 N73-25118
Effects of underwater breathing of helium oxygen mixture on speech recognition
[AD-759413] 16 p1878 N73-25205
Machine perception of speech and vision
[AD-760153] 17 p2002 N73-26187
Broad based computer science research and development, including speech understanding systems and techniques for I/O capability extension
[AD-760024] 17 p2002 N73-26189
Amplitude control method for equalizing low level phonemes in satellite voice communication system
18 p2212 N73-27862
Automatic recognition algorithm for liquids and glides
[AD-762377] 19 p2237 N73-28032
A priori digital speech analysis
[AD-762029] 19 p2237 N73-28037
Development of entropy coded adaptive differential pulse code modulation systems for speech signals
[AD-762606] 20 p2378 N73-29109
Analysis and perception of nonspeech marine sounds
[OES-6/72] 22 p2624 N73-31023
Speech recognition in disturbed ship radio communication systems
[FTZ-416-TBR-5] 22 p2633 N73-31104
Automatic speech level meter on voice frequency telephone circuit
[REPT-6648] 22 p2672 N73-31402
Mathematical voice model for a priori digital speech analysis
24 p2894 N73-33104
Adaptive speech synthesizer operation and associated software
24 p2894 N73-33106
Speech and picture processing
[AD-764968] 24 p2898 N73-33131

**SPEED**
U VELOCITY

**SPEED BRAKES**
U BRAKES [FOR ARRESTING MOTION]

**SPEED CONTROL**
Optimization of radar acquisition of moving targets by blind speed zone eliminations
[AD-753963] 11 p1256 N73-20195
Feasibility of producing constant speed drive with aid of gyroscope
[AD-763256] 21 p2550 N73-30445

**SPEED INDICATORS**
NT ANEMOMETERS
NT HOT-FILM ANEMOMETERS
NT HOT-WIRE ANEMOMETERS
NT TACHOMETERS
Development and evaluation of three axis fluidic airspeed sensor system for use with standard aircraft power supplies
[NASA-CR-112167] 01 p0058 N73-10472
Bibliography on laser Doppler velocimeter theory and usage
[AD-746634] 02 p0176 N73-11427
Laser Doppler velocimeter for measuring initial velocity of projectile
[AD-749670] 05 p0559 N73-14539
Aircraft instrument errors
05 p0577 N73-14695
Comparative assessment of three methods of measurement of pressure error corrections for aircraft pitot-static systems
[CRANFIELD-AERO-11] 08 p0924 N73-17570
Flight test of instrument for determining low airspeeds to evaluate suitability for helicopter airspeed indicator
[AD-753343] 09 p0989 N73-18071
Analysis of accuracy of Preston tube calibration equations to determine local skin friction in two dimensional supersonic and low hypersonic flow conditions
[NASA-TN-D-7190] 13 p1510 N73-22239
Influence of rain on airborne Doppler velocity sensor performance
[AD-757509] 14 p1668 N73-23541
Performance tests of hemispherical flow-direction sensor mounted on F-104 aircraft to develop Mach number position error calibration curve
[NASA-TN-D-7461] 23 p2743 N73-31956

**SPEED REGULATION**
U SPEED CONTROL

**SPEED REGULATORS**
Synchronizing control of drag-cup gyro motor using dynamic gas bearing
[NAL-TR-304] 15 p1756 N73-24232
Design and operating principles of base plate for regulating performance of radial centrifugal machines
[NLL-NEL-TT-2476-[6075.461]] 20 p2382 N73-29137

**SPEEDOMETERS**
U SPEED INDICATORS

**SPERMATOGENESIS**
Morphological changes in testes and spermatogenesis process of dogs subjected to chronic and combined gamma irradiation
07 p0743 N73-16048

**SPHERES**
NT FALLING SPHERES
NT ROTATING SPHERES
Analytical method to compute squeeze film thickness, pressure, and load relations between rigid ball and rigid groove when lubricated by fluid with exponential pressure-viscosity relationship
[NASA-CR-2139] 01 p0062 N73-10506
Sphere free motion in rotating fluid noting Taylor instability existence
[DLR-FB-71-32] 03 p0285 N73-12309
Measurement of hypersonic free molecular sphere drag at varying wall temperature ratios
[AD-748618] 04 p0407 N73-13320
Efficiency of laser telemetry tracking for satellite carrying laser reflector sphere
05 p0557 N73-14528
Potential theory for determining electromagnetic field caused by radial electron emission near conducting sphere
[AD-753664] 09 p1068 N73-18714
Laminar heat transfer problem on spheres and cylinders solved by laminar boundary layer theory
[VKI-TN-84] 10 p1142 N73-19306
Streaming flow of viscous fluid past sphere in uniform magnetic field at low Hartmann numbers
[AD-755060] 11 p1329 N73-20784
Velocity slowdown calculation for spherical and cubical fragments as function of distance
[TL-1972-16] 14 p1597 N73-22943
Pulsed electron motion equations for surface current analysis on conducting sphere
[AD-757190] 14 p1694 N73-23745
Preflight, inflight, and post flight operations evaluation analyses for Skylab sphere forming experiment facility - Appendix H
[NASA-CR-61386-APP-H] 14 p1708 N73-23862
Development of formulas for elastic behavior of axisymmetrically loaded cylindrical and spherical pressure vessels under various load conditions
[AD-758496] 14 p1717 N73-23936
Electrostatic suspension of conducting sphere in electric field between electrodes
[JPRS-59675] 20 p2380 N73-29123
Stress analysis of large plastic deformations in hollow sphere deformed during impact tests
[NASA-TM-X-68270] 20 p2482 N73-29940
Effect of homogeneous dielectric sphere on electromagnetic radiation from simple source
22 p2646 N73-31201
Motion and distribution of particles in steady, tube flows of suspensions of neutrally buoyant, rigid spheres
22 p2649 N73-31223
Characteristics of flow about spherical body undergoing rectilinear, sinusoidal oscillations in viscous, incompressible fluid
23 p2773 N73-32180
Performance of study plan for proposed Skylab experiments concerning metals melting and sphere forming
[NASA-CR-124396] 23 p2796 N73-32368
Analysis of aerodynamic drag on object moving in rarefied gas under nearly free molecular flow conditions
24 p2869 N73-32923
Characteristics of laminar and turbulent wakes of spherical bodies at hypersonic speed in nitrogen atmosphere
[DREV-R-683/72] 24 p2904 N73-33178
Supersonic stationary flow around atmosphere retained by gravitational force of spherical body
24 p2905 N73-33183

**SPHERICAL ANTENNAS**
Effect of homogeneous dielectric sphere on electromagnetic radiation from simple sources treated as boundary value problem and solution obtained by technique of dyadic Green functions
[NASA-CR-2211] 12 p1378 N73-21178

**SPHERICAL CAPS**
Development of procedure for determining maximum and minimum stresses produced by uniform pressure on unpierced torispherical closure of cylindrical shell
[ESDU-67017] 01 p0110 N73-10911
Measured maximal laminar heat transfer on cone with spherical nose in hot hypersonic flow
07 p0771 N73-16263

**SPHERICAL HARMONICS**
Spherical sampling functions related to spherical-harmonic functions applied to geophysics
[NASA-CR-130745] 08 p0918 N73-17519
Use of vector spherical harmonics for numerical weather forecasting
[AD-752569] 08 p0921 N73-17548
Empirical method for determining spherical harmonic coefficients of lunar gravity field
12 p1447 N73-21718
Transformation matrices between spherical harmonics and spherical sampling functions
[AD-755486] 14 p1664 N73-23509
Methods for improving 1967 geodetic reference system
[AD-755418] 14 p1665 N73-23510
Representation of Jacchia thermospheric models in spherical harmonics
[NASA-TM-X-66247] 15 p1778 N73-24416
Spherical harmonics presentation of anomalous gravity potential from satellite and terrestrial data at 9km aove sea level
[AD-759909] 18 p2147 N73-27358
Energetics of transient zonal and planetary scale waves in wintertime lower stratosphere investigated using surface spherical harmonics
20 p2389 N73-29193
Features of earth gravity anomalies in form expansion in spherical functions
[AD-761942] 21 p2542 N73-30384

**SPHERICAL SHELLS**
NT SPHERICAL CAPS
Influence of cavity radius on energy dissipation rate in liquid filled spherical cavities
01 p0040 N73-10319
Free vibrations of complex system of ring with added mass, connected to thin spherical or cylindrical shell
01 p0112 N73-10930
Calculation of coefficient of resistance of sphere at supersonic velocities and measurement of critical point on free flying bodies
[AD-747513] 03 p0287 N73-12324
Computer program for determining influx towards center of spherical metal shell following detonation of spherical, symmetrically placed explosive
[FOA-2-C-2471-25] 06 p0653 N73-15305
Theory of shallow spherical shells including effect of transverse shear deformation
[AD-749966] 06 p0727 N73-15935
Theory of plates and shields to include response of structurally loaded shells of cylindrical and spherical configurations
[AD-751502] 07 p0852 N73-16913
Approximative prediction for elastic collapse of spherical shell with flat spot region under external pressure
[NASA-CR-130961] 09 p1096 N73-18946
Dimensions and mechanical properties of elastic spherical shells measured by sound echo signals
10 p1188 N73-19667
Slow toroidal oscillations of thin spherical shell of conducting fluid in magnetic field
[AD-755059] 11 p1273 N73-20331

Vibrational characteristics, mechanical properties, and stress analysis of thin shell structures of various cross sections
[NASA-SP-288] 17 p2092 N73-26924
Elastic deformation of gimbal suspension on gyroscope nutation, moments acting on spherical rotor in magnetic suspension, and differentiating linear accelerometer
[JPRS-59740] 21 p2547 N73-30420
Discovery of small hollow spherules of glass containing various gases in peat bogs where Tungus meteorite fell
[NASA-TT-F-15125] 22 p2716 N73-31742
Dynamic stability of harmonically varying forced vibrations of thin spherical shell submerged in acoustic medium medium
22 p2723 N73-31792
Inelastic buckling of deep spherical shell subject to uniformly distributed external pressure
[AD-764085] 22 p2726 N73-31815

**SPHERICAL TANKS**
Slosh testing of spherical mercury propellant tank with positive expulsion diaphragm
[NASA-CR-133790] 21 p2600 N73-30838

**SPHERICAL WAVES**
Temporal spectra of fluctuations in atmospherically degraded spherical waves
[AD-751304] 07 p0807 N73-16551
Examination of Q switched ruby laser produced spherical shock waves
13 p1508 N73-22220
Shock heated argon expansion through nozzle and spherical shock wave front
[AD-756455] 13 p1511 N73-22245
Fluctuations of spherical wave through turbulent layer over receiving aperture
[AD-756928] 13 p1561 N73-22648
Creation shape and flow of tridimensional spark by focused radiation
[NASA-CR-2230] 15 p1766 N73-24311

**SPHEROIDS**
NT OBLATE SPHEROIDS

**SPIKE ANTENNAS**
U MONOPOLE ANTENNAS

**SPIKE NOZZLES**
Plug and spike nozzles applied to rocket propulsion system configurations
24 p2973 N73-33754

**SPIKE POTENTIALS**
Bioelectrical activity differentiations in cat cortex during sleep inhibition
13 p1483 N73-22026

**SPILLING**
Evaporation rates and toxic plume dispersion for defining downwind evacuation areas for populations adjacent to accidental propellent spills on shipping routes
[NASA-TM-X-68188] 07 p0750 N73-16097

**SPIN**
NT ELECTRON CAPTURE
NT ELECTRON SPIN
NT METAL SPINNING
NT PARTICLE SPIN
NT SPIN-ORBIT INTERACTIONS
Fuel tanks, spinup techniques, and thruster-CG misalignment problems for synchronous orbiting satellites
[AD-746845] 03 p0360 N73-12931
Improved Venus spin vector and probe position estimates
08 p0973 N73-17953
Correlation between lateral-directional static stability characteristics and spin susceptibility
[AD-753905] 10 p1107 N73-19029
Spin reorientation of nonsymmetric body with energy dissipation, using ATS5
[NASA-CR-131320] 11 p1316 N73-20683
Spin energy transfer processes at low temperatures
[AD-762618] 20 p2455 N73-29731

**SPIN DYNAMICS**
Deployable flexible ventral fins providing triangular planform of flexible material for spin recovery of aircraft
[NASA-CASE-LAR-10753-1] 01 p0004 N73-10031
Isocyanide spin label for studying conformational transitions in cytochrome c, emphasizing heme group
[NASA-TT-F-14623] 03 p0259 N73-12099
Cable connected spinning spacecraft, canonical and Lagrange equations, and urban mass transportation
05 p0610 N73-14961
Development of base bleed techniques to reduce Magnus moment on long spinning bodies and improved drag characteristics
[AD-754755] 11 p1232 N73-20002
Quantization of free spin-two fields on light front
[ILL-[TH]-73-1] 11 p1326 N73-20764
Nutation damper for use on spinning body
[NASA-CASE-GSC-11205-1] 16 p1917 N73-25513

**SPIN EXCHANGE**
Regge pole model for charge exchange processes using isospin amplitudes and daughter trajectories
[TUETP-73-4] 14 p1694 N73-23747

**SPIN FORGING**
U METAL SPINNING

**SPIN REDUCTION**
Magnetic attitude acquisition and control system for automatic despinning of satellite
[NASA-CR-130145] 06 p0673 N73-15477
Design of despin mechanism noting thermal and stress analysis of beryllium and aluminum as structural materials
[ESRO-CR[P]-226] 13 p1534 N73-22432
Design study of despin mechanism noting alignment accuracy, lubrication system, load carrying capacity and bearings
[ESRO-CR[P]-227-APP] 13 p1535 N73-22433
Design of despin mechanism noting angular stiffness, stress analysis, signal transmission, power transmission, instrumentation and ground support equipment
[ESRO-CR[P]-228] 13 p1535 N73-22434

**SPIN RESONANCE**
Projective invariance of dual resonance models from spin analyticity and Lorentz invariance
[NOTA-INTERNA-388] 03 p0340 N73-12772
Electron spin overlap model for quantitative analyses on magnetic spectra of coordination compounds with unpaired electrons
08 p0945 N73-17740
Dual resonance model with spin for reaction pion nucleon yields omega meson nucleon
[ILL-[TH]-73-12] 22 p2701 N73-31634

**SPIN STABILIZATION**
Attitude stability criteria and nutation decay times of dual-spin satellite with large flexible solar array
[AD-743258] 01 p0109 N73-10897
Wind tunnel tests and firing tests to determine aerodynamic characteristics and subsonic flight performance of spin stabilized mortar projectile
[AD-746977] 02 p0124 N73-11009
Spin stabilized gyroscope having spining rotor and stationary platform
[NASA-CASE-GSC-11479-1] 02 p0207 N73-11680
Stability of dual-spin satellite system during momentum wheel spin-up maneuver
[NASA-CR-130130] 05 p0597 N73-14858
Development and operation of facility for investigating effect of spin on aerodynamic characteristics of shaped charges
[DREV-TN-2037/72] 06 p0649 N73-15271
Pitot pressure survey of laminar boundary layer on supersonic spinning ogive cylinder
[AD-755694] 12 p1393 N73-21294
Results of wind tunnel measurements of normal force, pitching moment, and Magnus force and moment on M823 research store with fixed and freely spinning stabilizers
[AD-757658] 13 p1471 N73-21912
Analysis of Magnus forces on high fineness ratio body of revolution with ogive forebody at varying angles of attack
[AD-759987] 17 p1980 N73-26003

**SPIN-LATTICE RELAXATION**
Nuclear spin-lattice relaxation in magnesium metal
24 p2960 N73-33651

**SPIN-ORBIT INTERACTIONS**
NT ELECTRON CAPTURE
Dual resonance model with spin for reaction pion nucleon yields omega meson nucleon
[ILL-[TH]-73-12] 22 p2701 N73-31634

**SPINAL CORD**
Influence of isolated heating of spinal column on respiratory rate and panting in dogs
[NASA-TT-F-14998] 18 p2109 N73-27054
Change in impulse activity of neurons in respiratory center during electric stimulation of vestibular nerve and dorsal roots in spinal cord
24 p2882 N73-33017

**SPINEL**
Carrier mobility in epitaxial silicon film deposited on spinel crystal surface
[NLL-TRANS-2768-[9022.81]]
05 p0585 N73-14761
Hot pressed polycristalline garnets and ferrites of spinel type to be used at UHF
19 p2236 N73-28026

**SPINNING [METALLURGY]**
U METAL SPINNING

**SPIRAL ANTENNAS**
Numerical analysis of parameters affecting design and characteristics of spiral top loaded antennas
10 p1134 N73-19238
Impedance measurement for two planar, equiangular, printed circuit, two arm, spiral antennas
[AD-756706] 14 p1643 N73-23322
Analysis of some slow-wave conical log-spiral and helical antennas
[AD-757913] 15 p1757 N73-24242
Utilization of spiral antenna as pulse compression network
[AD-764354] 22 p2644 N73-31189

**SPIRAL GALAXIES**
NT MILKY WAY GALAXY
Archimedes spiral and solar wind induced structures in interplanetary magnetic field
01 p0095 N73-10766
Synthesis observations of neutral hydrogen emission in two spiral galaxies NGC 6946 and IC 342
[AD-744679] 01 p0106 N73-10876
Astronomical mapping of rotating spiral Maffei qalaxy
[AD-752042] 08 p0962 N73-17873
Bar shaped density wave theory of barred spiral galaxies
19 p2341 N73-28835
Random distributions and position angle measurements of elliptical and spiral galaxies
20 p2469 N73-29833

**SPIRALS**
Three basic forms of cyclonic cloud vortices to trace spirals
[AD-763170] 21 p2540 N73-30363

**SPLASH POINTS**
U WATER LANDING

**SPLASHING**
Analysis of phenomenon generated by passage of projectile into water to determine effects of accelerations, aerodynamic configurations, and surface motions
16 p1886 N73-25264

**SPLEEN**
Transverse acceleration effects on dioxyribonucleic acid catabolism in rat spleen and liver
03 p0257 N73-12080

**SPLICING**
FCC transition splices and cost comparison of FCC vs. RCC
14 p1641 N73-23304

**SPLINE FUNCTIONS**
Bicubic spline approximations over two dimensional region derived with dynamic programming
[USC-113P19-33] 02 p0202 N73-11635
Spline approximation of initial value problem and successive application of finite difference and spline interpolation operators for heat equation
[AD-748774] 04 p0441 N73-13594
FORTRAN routines for interpolation and integration of approximation with cubic splines
[FOA-2-C-2476-11] 06 p0643 N73-15223
Closed form, Romberg, and Gaussian procedures for calculating transonic wave drag integral using cubic splines
[NAL-TN-35] 06 p0652 N73-15299
Algorithms for variable order filters from extensions of spline function concepts
[AD-751124] 07 p0813 N73-16595
Numerical smoothing and interpolation methods noting spline function method
[ONERA-NT-205] 15 p1804 N73-24619
Interpolation of functions of one variable by cubic spline functions
21 p2512 N73-30152
Theory of spline interpolation extended to case of two independent variables
21 p2512 N73-30153
Spline smoothing of histograms by linear programming
[NASA-CR-133987] 22 p2691 N73-31551
Power spectral density estimation by spline smoothing ergodic stochastic process
[NASA-CR-133986] 22 p2691 N73-31552
Least squares fitting of bicubic spline surfaces to general data at arbitrary points noting householder orthogonal transformation, solution stability, and ranking
[NPL-NAC-22] 23 p2813 N73-32489
Estimation and approximation of integrand in J for spline function study
[NASA-CR-124454] 24 p2945 N73-33516

**SPLITS [GEOLOGY]**
U GEOLOGICAL FAULTS

**SPOILERS**
Fixed base flight simulator evaluation of wing spoilers for longitudinal flight path control of Cessna aircraft during instrument landing system approach
[NASA-CR-2121] 02 p0125 N73-11015
Wind tunnel tests to determine effects of slot spoilers on longitudinal and lateral aerodynamic characteristics of twin engine light aircraft
[NASA-TN-D-7315] 21 p2496 N73-30033

**SPONTANEOUS IGNITION TEMPERATURE**
U IGNITION TEMPERATURE

**SPORADIC E LAYER**
Formation theory of sporadic E by tidal wind systems
17 p2017 N73-26306

**SPORES**
Nonsporicidal methods for solvent degradation of cured RTV 41 silicon potting compound and chemical curing effects on decontamination properties
[NASA-CR-130720] 08 p0878 N73-17111
Space vacuum and solar ultraviolet irradiation effects on survival of Bacillus subtilis spores
15 p1740 N73-24108
Development of chemical process for determining quantity of contamination buried in potting compounds and removable of spores with amine dissolution and plating techniques
[NASA-CR-133645] 21 p2562 N73-30535
Thermal stress and mechanical shock effects on release of bacterial spores from stainless steel surfaces with application to Mars landing
[NASA-CR-133868] 22 p2619 N73-30987

**SPOT WELDS**
Electric resistance spot welding and brazing for producing metal bonds with superior mechanical and structural characteristics
[NASA-CASE-LAR-11072-1] 11 p1298 N73-20535
Solid state and fusion resistance spot welding of TD-NiCr sheet
[NASA-TN-D-7256] 12 p1412 N73-21443
**SPRAY CHARACTERISTICS**
Analysis of drop trajectories transition of boundary layer structure and flow regime for binary spray flow over upstream surface of isothermal cylinder
20 p2386 N73-29171
Effects of accelerating gas flow on atomization characteristics of liquid sprays produced by impinging two liquid jets - Part 1
[NASA-CR-134478] 22 p2652 N73-31247
Secondary atomization produced by accelerating gas flow to show effects on liquid sprays produced by impinging two liquid jets - Part 2
[NASA-CR-134479] 22 p2652 N73-31248
**SPRAYED COATINGS**
Process for spraying metal coatings on aluminum alloys and resulting antifriction properties
[NLL-TRANS-746-1290-[9022.401]]
05 p0550 N73-14465
Superconducting properties of sprayed thin films
[JINR-P8-6863] 19 p2327 N73-28717
Metal plating process employing spraying of metallic power/peening particle mixture
[NASA-CASE-GSC-11163-1] 23 p2795 N73-32360
Spraying of powdered polymer coatings onto grooves in micromachines
[AD-764933] 24 p2929 N73-33396
**SPRAYED PROTECTIVE COATINGS**
U PROTECTIVE COATINGS
U SPRAYED COATINGS
**SPRAYING**
NT ARC SPRAYING
NT PLASMA SPRAYING
**SPREAD F**
Relationship between atmospheric gravity waves and spread F conditions caused by solar activity
05 p0509 N73-14146
**SPREAD REFLECTION**
U DIFFUSE RADIATION
U REFLECTION
**SPRINGS (ELASTIC)**
Numerical analysis of elastic stresses and deflections of helical compression springs made of round wire
[ESDU-65005] 01 p0112 N73-10926
Analysis of factors affecting choice of material and manufacturing methods for production of helical compression springs
[ESDU-65006] 01 p0112 N73-10927
Characteristics of symmetrical springs for elastic field between rotor and housing of gyroscopic instruments and numerical analysis of radial stiffness
06 p0696 N73-15669
Brake clearance controlling mechanism with split bush screwed into body and with components as springing elements
[AD-742704] 13 p1533 N73-22424
Induction heating and concomitant quenching for hot winding helical springs
[AD-759906] 17 p2039 N73-26495
Solutions to problems involving helical springs under load
[AD-762776] 21 p2604 N73-30871
Finite difference method and equations of motion for studying nonlinear vibrations of one and two degree of freedom spring mass systems
22 p2724 N73-31796
**SPRINKLING**
Location of center pivot sprinkler irrigation systems in Finney County, Kansas, based on ERTS-1 interpretation
[E73-10418] 11 p1279 N73-20380
**SPUR (REACTORS)**
U SPACE POWER UNIT REACTORS
**SPUTNIK SATELLITES**
Analyzing component measurements of geomagnetic field by Sputniks for solving geophysical problems
[NASA-TT-F-14446] 01 p0105 N73-10865
**SPUTTERING**
Development of procedure for producing thin transparent films of zinc oxide on transparent refractory substrate
[NASA-CASE-FRC-10019] 03 p0304 N73-12487
Analysis of microstructure of radio frequency-sputtered, thin lead-dielectric cermet films using transmission electron microscopy
[NASA-TR-R-393] 03 p0345 N73-12811
Numerically controlled ion beam sputtering process for manufacturing solid optical surfaces
[AD-750347] 05 p0581 N73-14730
Influence of surface finishing on adherence of radio frequency sputtered molybdenum disulfide on silver, gold, copper, and bronze
[NASA-TN-D-7169] 07 p0804 N73-16523
Characteristics of molybdenum disulfide films radio frequency sputtered on aluminum and nickel surfaces at elevated, ambient, and liquid nitrogen temperatures
[NASA-TN-D-7170] 08 p0927 N73-17593
Sputtering deposition of semiconductor film devices
[AD-752081] 08 p0928 N73-17599
Coatings of borosilicate glasses deposited on silicon solar cells by radio frequency sputtering for enhanced protection
[ESRO-CR-68] 09 p0991 N73-18087
Technique and equipment for sputtering using apertured electrode and pulsed substrate bias
[NASA-CASE-LEW-10920-1] 15 p1797 N73-24569
Ion beam dose and sputtering characteristics of ion implanted semiconductor devices
[NASA-CR-132254] 15 p1820 N73-24754
Experimental conditions for depositing crystalline and amorphous VO2 thin films by RF and dc sputtering
[CEA-CONF-2133] 17 p2073 N73-26774
Preparation of single crystal films by reactive sputtering process
[AD-760715] 18 p2123 N73-27160
Sputtering of multicomponent materials by ion bombardment
[AD-762813] 20 p2423 N73-29466
Bibliography of reports on sputtering in industrial processes for applying coatings
[AD-763600] 23 p2798 N73-32379
Sputter erosion and deposition in discharge chamber of small mercury ion thruster
[NASA-TM-X-71424] 23 p2829 N73-32611
**SQUALL LINES**
U SQUALLS
**SQUALLS**
Time dependent two dimensional numerical model for studying structure of squall line thunderstorm
10 p1180 N73-19597
Gravity current model applied to analysis of squall-line gust front
12 p1419 N73-21504
Study of severe local storm of 22 Apr. 71, near Norman, Oklahoma
[AD-756571] 13 p1554 N73-22592
**SQUARE WAVES**
Circuitry for generating random square wave pulses using white noise source
[NASA-CASE-MSC-14131-1] 17 p2003 N73-26199
**SQUID PROJECT**
Research reports on SQUID programs related to fluid mechanics, and atomic and molecular collisions
[AD-752037] 08 p0955 N73-17820
Research and development in Project SQUID
[AD-759977] 17 p2078 N73-26809
**SR-N2 GROUND EFFECT MACHINE**
U WESTLAND GROUND EFFECT MACHINES
**SR-N3 GROUND EFFECT MACHINE**
U WESTLAND GROUND EFFECT MACHINES
**SR-N5 GROUND EFFECT MACHINE**
U WESTLAND GROUND EFFECT MACHINES
**ST VENANT FLEXURE PROBLEM**
U SAINT VENANT PRINCIPLE
**STABILITY**
NT ACOUSTIC INSTABILITY
NT AERODYNAMIC STABILITY
NT AIRCRAFT STABILITY
NT ATTITUDE STABILITY
NT BOUNDARY LAYER STABILITY
NT COMBUSTION STABILITY
NT CONTROL STABILITY
NT DIRECTIONAL STABILITY
NT DYNAMIC STABILITY
NT FLAME STABILITY
NT FLOW STABILITY
NT FREQUENCY STABILITY
NT GYROSCOPIC STABILITY
NT HOVERING STABILITY
NT LATERAL STABILITY
NT LONGITUDINAL STABILITY
NT LOW SPEED STABILITY
NT MAGNETOHYDRODYNAMIC STABILITY
NT MAGNETOSPHERIC INSTABILITY
NT ROTARY STABILITY
NT SHELL STABILITY
NT SPACECRAFT STABILITY
NT STATIC STABILITY
NT STORAGE STABILITY
NT STRUCTURAL STABILITY
NT SURFACE STABILITY
NT SYSTEMS STABILITY
NT THERMAL STABILITY
L2 stability in low and high frequency distributed feedback systems
[NASA-CR-129599] 03 p0277 N73-12245
Equilibrium stability of orthotropic cylindrical shell
[AD-747724] 03 p0362 N73-12948
Metallic surface effects on radiative stability and focusing effects of electron ring
[JINR-P9-6318] 04 p0452 N73-13692
Computerized simulation of inductor performance constraints
[AD-749685] 06 p0646 N73-15249
Parametric instabilities of VLF waves in radiation belts
[LA-DC-72-746] 07 p0756 N73-16139
Pigments for space-stable thermal control coatings to shield spacecraft from solar radiation
[NASA-CR-124067] 09 p0998 N73-18144
Stability analysis for semilinear parabolic partial differential equations
[NASA-CR-130542] 09 p1056 N73-18608
Stability criteria for incompressible elastic materials
[AD-753459] 10 p1221 N73-19931
Bearing sectors for controlling self excited instability of journal bearing shafts rotating at high speeds in low viscosity lubricants
[NASA-CASE-LEW-11076-2] 11 p1298 N73-20533
Stability of thin elastic tube of infinite length containing rotating inviscid, incompressible fluid flow
13 p1508 N73-22222
Stability of molecular gas discharges typical of those used in high power lasers
[AD-757083] 13 p1537 N73-22456
Bifurcation and stability for nonlinear parabolic partial differential equation
[NASA-CR-131896] 14 p1683 N73-23661
Properties of low frequency instability in hollow cathode discharge magnetoplasma
16 p1948 N73-25758
Stability and temperature characteristics compared for some silicon and selenium photodetectors to determine suitability for photometric or radiometric measurements
[NBS-TN-594-5] 17 p2072 N73-26765
Stability of refractory compounds in liquid aluminum at high temperatures
[NLL-RTS-7975] 18 p2113 N73-27083
Stability of deep beam subjected to concentrated, transverse follower force applied at center of beam
[AD-762124] 19 p2350 N73-28900
Kinematics of stability of orientation in rotating coordinate system signal processing
20 p2451 N73-29702
Multidimensional linear system parameter estimation computer program using least squares method evaluating mathematical model stability, observability and real time operation
[LAAS-AS-73-I-06] 23 p2813 N73-32491
Dynamic behavior and stability classification of one-dimensional wave propagation systems
24 p2893 N73-33096
Potentiometric stability data analyses for nickel, lead, and zinc organic acetate complexes
[JINR-E12-6776] 24 p2935 N73-33436
Functional stability calculations for organometallic complexes of copper and cadmium
[JINR-E12-6775] 24 p2935 N73-33437
Stability constants correlation for metal-inorganic ligands in organometallic cadmium, rhodium, and lead compounds
[JINR-E12-6773] 24 p2935 N73-33438
**STABILITY AUGMENTATION**
U FEEDBACK CONTROL
U STABILIZATION
**STABILITY DERIVATIVES**
NT PITCHING MOMENTS
NT ROLLING MOMENTS
NT YAWING MOMENTS
High angle of attack characteristics of high performance aircraft and correlation with dynamic directional-stability parameter
[NASA-TN-D-6993] 01 p0005 N73-10033
Definitions of aircraft longitudinal stability to account for effects of aircraft structure distortion and compressibility effects
[ESDU-00.00.03] 02 p0124 N73-11010
Digital analysis of dynamic response data, aerodynamic forces and stability derivatives, of free flight models
[ARC-R/M-3699] 03 p0248 N73-12006
Analysis of stall and post-stall characteristics of F-111 aircraft and development of regression techniques to obtain aerodynamic derivatives
06 p0617 N73-15013
Time vector technique for determining stability and control derivatives by simultaneous analysis of two maneuvers which differ by dependent control input
[NASA-TM-X-2722] 07 p0739 N73-16010
Application of equations of motion to investigate effects of mode shape and coning angle on stability boundaries of hingeless helicopter rotor blades
[NASA-CR-114525] 07 p0739 N73-16015
Computerized stability derivative calculations for oscillating parabolic ogives and circular cones in transonic flow field using iterative procedure
[NASA-CR-124033] 07 p0769 N73-16249
Analysis of parametric resonance in rotating crossed-dipole satellites and method for determining regions of instability
07 p0847 N73-16868
Analysis of satellite stability of motion using Liapunov system as applied to flexible bodies
07 p0848 N73-16869
Aerodynamic characteristics of two-stage, flexible, variable-mass missile with internal flow, discrete masses, and aerodynamic forces in powered flight
07 p0848 N73-16870
Evaluation of stability derivatives obtained from dynamic tests of model in cold magnetic balance wind tunnel facility
[NASA-CR-112305] 11 p1267 N73-20279

Application of maximum likelihood criterion and optimal input design for analyzing flight test data to obtain aircraft stability and control derivatives
[NASA-CR-2200] 12 p1364 N73-21071
Wind tunnel tests to determine oscillatory longitudinal derivatives of thin delta wing with 0.8 aspect ratio over range of incidences
[ATN-7105] 13 p1470 N73-21903
Applying sequential estimation technique of system identification to determination of unknown coefficients in vertical plane equation of motion of hydrofoil
[AD-755738] 13 p1512 N73-22253
Analysis of aircraft rolling moment derivatives caused by rolling, yawing, and sideslip
[ESDU-06.01.00-AMEND-A-C] 14 p1599 N73-22963
Analysis of aerodynamic loading for symmetrically tapered wings describing simple harmonic pitching oscillations of low frequency in supersonic flow
[ARC-R/M-3298] 15 p1728 N73-24019
Determination of electric potential field and aerodynamic moments for steady rarefied plasma flow past solid sphere 15 p1816 N73-24720
Wind tunnel tests to determine subsonic derivatives for oscillating M-wing planform
[ARC-R/M-3214] 16 p1854 N73-25022
Survey of aerodynamic derivative measurements for unswept rectangular wings and delta wings with emphasis on main surface pitching moment derivatives
[ARC-R/M-3232] 16 p1855 N73-25024
Measurement of pitching moment derivatives using free oscillation technique on two dimensional airfoils of double wedge section and single wedge section
[ARC-R/M-3234] 16 p1855 N73-25025
Development and characteristics of test equipment for measurement of direct pitching moment derivatives for two dimensional flow at subsonic and supersonic speeds
[ARC-R/M-3257] 16 p1855 N73-25027
Design and characteristics of test equipment for measuring longitudinal oscillatory aerodynamic derivatives in high speed wind tunnel
[ARC-R/M-3260] 16 p1855 N73-25029
Aircraft configuration for reducing effects of nose-down pitching moments due to high lift forces, loss of trim lift, and engine-out yawing moments
[NASA-CASE-LAR-11252-1] 17 p1980 N73-26007
Longitudinal stability derivatives from flight data by model with automatic parameter adjustment
[DLR-FB-73-13] 17 p1984 N73-26033
Analysis of descent trajectories to determine static and dynamic stability of free-fall stores with freely spinning stabilizer devices
[AD-760677] 18 p2102 N73-26999
Development and characteristics of pitch/yaw dynamic stability, forced-oscillation test mechanism for measuring stability derivatives of lifting reentry vehicles
[AD-762286] 19 p2250 N73-28143
Development of procedures for determining stability parameters of balloons tethered under steady wind conditions
[NASA-TN-D-7222] 21 p2493 N73-30013
Analysis of pitch damping moment for hovering helicopter rotary wing and development of formula for calculating pitch damping derivative
[NASA-TT-F-15010] 21 p2495 N73-30027
Stability derivative analysis of tethered balloon in steady wind conditions to determine balloon aerodynamics buoyancy, mass, and static forces resulting from tether cable
[NASA-TN-D-7272] 23 p2743 N73-31955
Jet aircraft flight tests for stability derivative determination comparing various measuring techniques
[BMVG-FBWT-73-12] 23 p2745 N73-31971
Trisonic wind tunnel tests of baseline launch configuration space shuttle model to determine effects of model parametric variations on static stability characteristics
[NASA-CR-128778] 23 p2851 N73-32783

**STABILITY TESTS**
NT FLIGHT STABILITY TESTS
NT WIND TUNNEL STABILITY TESTS
Structural stability tests studying buckling of rectangular boron reinforced aluminum plates
[ENSMP-007] 15 p1840 N73-24907
Capabilities of space processes in ground based experiments at low-g periods
[NASA-CR-124385] 22 p2717 N73-31752

**STABILIZATION**
NT SIGNAL STABILIZATION
NT SPIN STABILIZATION
Development of fluidic control system for stabilizing aircraft ejection seat in pitch plane during rocket motor burn portion of ejection sequence
[AD-747630] 03 p0254 N73-12056
System for controlling torque buildup in suspension of gondola connected to balloon by parachute shroud lines
[NASA-CASE-GSC-11077-1] 04 p0370 N73-13008
Effect of internal spinning fly wheel on air launched missile stability and resulting launch disturbance
[AD-749027] 04 p0375 N73-13047
Aerodynamic characteristics of two-stage, flexible, variable-mass missile with internal flow, discrete masses, and aerodynamic forces in powered flight 07 p0848 N73-16870
Stabilization methods in collecting and shipping of human sera for chemical analyses 08 p0871 N73-17053
Intensity stabilization and development of tunable ultranarrowband dye laser
[AD-754112] 10 p1170 N73-19517
Automatic motion stabilization system controlling foil lift of hydrofoil
[AD-758286] 15 p1769 N73-24332
Development of aerodynamic control system to control flutter over large range of oscillatory frequencies using stability augmentation techniques
[NASA-CASE-LAR-10682-1] 17 p1980 N73-26004
Kinematics of gyroscopes and gimbals and effects on missile stability
[AD-763147] 21 p2549 N73-30440
Boron radiation hardening for stabilizing gate threshold potential of MOS devices
[NASA-CASE-GSC-11425-2] 23 p2764 N73-32114

**STABILIZED PLATFORMS**
Data transmission and processing system for balanced air bearing stabilized platform for satellite motion simulator
[ESRO-CR-54] 01 p0037 N73-10287
Analysis of factors involved in specification, design, and evaluation of gyroscopes for spaceborne sensor applications
[NASA-SP-8096] 03 p0328 N73-12680
Scripps Institute research on oceanographic instruments, stabilized floating platforms, ocean bottom accelerometers, and surface waves
[AD-748024] 04 p0417 N73-13407
Characteristics of inertial guidance systems to include minimizing of errors, forces on electrostatic gyroscope, and parameters of electromagnetic load cell
[JPRS-57746] 06 p0695 N73-15664
Analysis of lateral velocity measurement errors of inertial guidance system and development of system to compensate for errors 06 p0695 N73-15665
Development of pneumatically isolated stabilized platform to provide active control to local gravity vector
[AD-750869] 06 p0697 N73-15686
Prediction of horizontal wave forces acting on vertical pile structures of floating ocean platforms
[AD-751574] 07 p0794 N73-16460
Vibration of foundation block test-pad imbedded in or resting on elastic substratum
[AD-751332] 07 p0853 N73-16915
Analysis of gyroscopic instrument performance during acceleration and method for determining position of vehicle in geopolar regions
[JPRS-57990] 08 p0923 N73-17557
Development of matrix method for determining gimbal errors of three-axis gyrostabilized platform with constant drift rate 08 p0923 N73-17558
Prelaunch alignment of stable platform to desired orientation
[NASA-CR-128802] 10 p1184 N73-19638
Numerical analysis of effects of various parameters affecting accuracy and stability of strapdown inertial navigation systems 11 p1316 N73-20685
Research activities of electronic laboratory in development of inertial navigation systems to include applications for space missions and commercial aviation 11 p1316 N73-20686
Development and evaluation of failure detection and isolation technique for use with four gimbaled inertial measuring units 11 p1317 N73-20687
Development of single-degree-of-freedom gyroscope for application to strapdown inertial guidance system 11 p1317 N73-20688
Methods for conducting acceptance tests and reliability tests of gyroscopes as part of inertial platform quality control procedures 11 p1317 N73-20689
Development of low cost inertial measurement unit with navigational accuracy performance based on optimum size design of inertial instruments and platform 11 p1317 N73-20690
Optimization of integrated navigation systems combining several independent navigation sensors to provide self-contained aircraft navigation capability 11 p1317 N73-20694
Three axis gyro stabilized torpedo platform 11 p1318 N73-20702
Application of cluster rotation to improvement of existing platforms in strike aircraft 11 p1319 N73-20704
Floating stable platforms for combat and civilian use
[AD-754783] 11 p1353 N73-20986
Stability of steady state motions of gyroscope with spring limiters on rotating platform in Newtonian central field of forces 13 p1556 N73-22611
Preliminary definition study of sortie laboratory noting structural design, subsystems and shuttle interface
[MBB-SL-72-04] 13 p1582 N73-22826
Preliminary definition study of sortie module/pallet system noting configurations, thermal control, attitude control, power and communications subsystems
[ESRO-CR[P]-239] 13 p1582 N73-22827
Preliminary definition study of a sortie module/pallet system noting configurations, thermal control, attitude control, power and communications subsystems
[ESRO-CR[P]-240] 13 p1582 N73-22828
Objectives and accomplishments of geosynchronous platform definition study
[NASA-CR-133968] 19 p2345 N73-28860
Program results and supporting data obtained in geosynchronous platform definition study
[NASA-CR-133969] 19 p2345 N73-28861
Mission characteristics data compiled in geosynchronous platform definition study
[NASA-CR-133970] 19 p2345 N73-28862
Baseline traffic model resulting from traffic analysis and system requirements data generated in geosynchronous platform definition study
[NASA-CR-133971] 19 p2345 N73-28863
Traffic analysis and system requirements for new traffic model developed in geosynchronous platform definition study
[NASA-CR-133972] 19 p2345 N73-28864
Platform configurations, support subsystems, mission equipment, and servicing concepts generated in geosynchronous platform definition study
[NASA-CR-133973] 19 p2345 N73-28865
Program evaluation and recommendations of geosynchronous platform definition study
[NASA-CR-133974] 19 p2345 N73-28866
Interfaces between space platforms and space transportation system established in geosynchronous platform definition study
[NASA-CR-133975] 19 p2345 N73-28867
Deep space solar activity monitoring platform with video capability, including X ray flux, UV flux, charged particle flux, and radio emission measurements
[AD-761799] 19 p2346 N73-28875
Development of kinematic equations for analyzing performance of gimballess inertial navigation system
[JPRS-59688] 20 p2452 N73-29704
Development and characteristics of servoed roll gimbal to isolate gyroscopes of stabilized platform from effects of vehicle spin
[AD-764903] 23 p2818 N73-32527
Dynamic calibration of inertial navigation system using extended Kalman filtering and command torquing of platform gyros 24 p2950 N73-33566

**STABILIZERS [AGENTS]**
Stabilization of aqueous prussic acid during synthesis from ammonia by carbon dioxide
[NASA-TT-F-14691] 07 p0752 N73-16110
Storage instability of hydrocyanic acid mixed with stabilizing agents - Part 3
[NASA-TT-F-14652] 09 p0998 N73-18147
Stabilization of polyethylene plastics by antioxidants
[AD-753479] 10 p1176 N73-19564
Influence of carbon stabilizing elements and temperature on cold worked austenitic stainless steel corrosion
[CEA-CONF-2119] 21 p2560 N73-30518

**STABILIZERS [FLUID DYNAMICS]**
NT HORIZONTAL TAIL SURFACES
Static and vibration tests of graphite-epoxy stabilizer system for A-4 Skyhawk aircraft
[AD-750778] 06 p0689 N73-15610
CDC 6600 computer analysis of numerical stabilizer effects on computing time for second order accurate schemes
[AD-753165] 09 p1018 N73-18308
Static tests of redesigned graphite horizontal stabilizers
[AD-758718] 15 p1803 N73-24611
Inflatable stabilizing system for use on life raft to reduce rocking and preclude capsizing
[NASA-CASE-MSC-12393-1] 17 p1980 N73-26006

**STACKING FAULT ENERGY**
Deformation and different orientation effects on lattice defect energies in copper crystals
[JUL-855-FF] 10 p1194 N73-19713

**STACKING FAULTS**
U CRYSTAL DEFECTS

**STACKS**
Remote fire stack igniter on vent stack with flame cage near top
[NASA-CASE-MFS-21675-1] 22 p2727 N73-31826
Design and performance of stacked crystal filters for frequency control and signal processing
[AD-765416] 23 p2758 N73-32074

STAGE SEPARATION
Impulse base flow facility tests of space shuttle stage separation plume impingement loads
[NASA-CR-124000] 06 p0729 N73-15949
Nutation and damping theory of Dial satellite after last stage separation
[DLR-FB-72-74] 12 p1461 N73-21842
Gas dynamic simulation of plumes from orbiter propulsion system for determining power-on aerodynamic flight characteristics of orbiter
[NASA-CR-124217] 13 p1581 N73-22814
Alternate concepts study on two and one half stage, stage and one half, and SRM interim booster systems for establishing performance, costs, and schedules
[NASA-CR-124344] 24 p2982 N73-33829
STAGING [ROCKETS]
U STAGE SEPARATION
STAGNATION
U STAGNATION POINT
STAGNATION FLOW
Numerical analysis of fluid containment near stagnation point and within self-confined stagnation region for bi-component mixture
[NASA-CR-2172] 03 p0283 N73-12292
Techniques and equipment for measuring stationary and nonstationary flow in wind tunnels during pressure and flutter tests
[DLR-MITT-72-25] 10 p1139 N73-19283
STAGNATION POINT
Numerical analysis of fluid containment near stagnation point and within self-confined stagnation region for bi-component mixture
[NASA-CR-2172] 03 p0283 N73-12292
Wind tunnel tests to determine effects of hypersonic flow interaction on thrustor nozzle configurations and procedures to prevent excess heating
[NASA-CR-129914] 05 p0597 N73-14857
Laminar and turbulent boundary layers, including hypersonic flow, wall flow and stagnation area
[DLR-MITT-71-13] 07 p0770 N73-16256
Visualization of longitudinal vortices in stagnation area of circular cylinder in turbulent flow with splitting plate
07 p0771 N73-16264
Calculation of interplanetary magnetic field induced asymmetries in forward stagnation region of solar-wind magnetospheric interaction
07 p0838 N73-16792
Laminar heat transfer problem on spheres and cylinders solved by laminar boundary layer theory
[VKI-TN-84] 10 p1142 N73-19306
User manual for computer program to solve equations of fully coupled viscous, radiating flow at stagnation point of blunt body which may be ablating or non-ablating
[NASA-CR-2237] 11 p1347 N73-20933
Nonstationary heat and mass transfer developed by transverse flow around cylindrical body to determine conditions at stagnation point
[AD-760396] 17 p2016 N73-26299
Analysis of stagnation point on blunt body in massive ablation condition to show effects of absorption coefficient enhancement on mass loss rate
19 p2351 N73-28912
Static pressure and heat transfer rate distributions on conical bodies at hypersonic speeds laminar and turbulent flow conditions
[AD-764983] 23 p2777 N73-32204
STAGNATION PRESSURE
Techniques and equipment for measuring stationary and nonstationary flow in wind tunnels during pressure and flutter tests
[DLR-MITT-72-25] 10 p1139 N73-19283
Device for measuring stagnation pressure of supersonic gas streams
[NASA-CASE-LAR-11139-1] 11 p1292 N73-20483
STAGNATION REGION
U STAGNATION POINT
STAINLESS STEELS
NT AUSTENITIC STAINLESS STEELS
NT FERRITIC STAINLESS STEELS
NT MARTENSITIC STAINLESS STEELS
Mechanical property and stress corrosion evaluation of Custom 455 stainless steel alloy at cryogenic temperatures
[NASA-TM-X-64682] 02 p0186 N73-11509
Strain hardened properties of 304L stainless steel surfaces under combined tension and torsion
[AD-746472] 02 p0188 N73-11525
Measurement of surface, grain boundary, and coherent twin boundary free energies in 304 stainless steel at elevated temperatures using method of zero creep coupled with electron microscopy
[AD-747267] 02 p0189 N73-11535
Fabrication of helicopter rotary wings from composite materials of stainless steel liner overwrapped with fiberglass
[NASA-CR-112191] 03 p0251 N73-12031
Statistical analysis of fatigue properties of SAE 4340 steel and description of test equipment used
[NASA-CR-72835] 03 p0313 N73-12551
Fast reactor irradiation effects on creep behavior of annealed type 316 stainless steels
[HEDL-SA-300] 03 p0314 N73-12559
Effects of irradiation microstructure and creep rupture properties of annealed and cold worked type 316 stainless steel
[CONF-720604-4] 03 p0314 N73-12560
Time controlled creep-fatigue interaction for type 403 stainless steels at high temperature
[ORNL-4757] 03 p0315 N73-12565
Computer calculations of growth rates of voids in stainless steel during neutron irradiation
[HEDL-TME-72-35] 03 p0316 N73-12576
Effect of neutron irradiation on fatigue crack propagation in stainless steel samples at high temperatures using fracture mechanics approach
[AD-747950] 03 p0316 N73-12578
Effect of foil thickness on mechanical behavior of stainless steel in tension
[AD-747698] 03 p0318 N73-12596
Installation of stainless steel lining to stop water leakage from 2MV HOR swimming pool reactors
[IRI-131-72-01] 03 p0334 N73-12723
Mechanical properties of types 304 and 304 plus 0.15 percent Ti stainless steel after irradiation at temperatures in range of 400 to 820 C
[ORNL-TM-3733] 05 p0562 N73-14569
Design and operation of bidirectional reflectometer including reflectance data obtained from two samples of stainless steel 304
[AD-750121] 06 p0675 N73-15491
Propagation of fatigue cracks in gas-tungsten-arc welded 304 stainless steels
[HEDL-SA-329] 06 p0677 N73-15510
Evaluation of tantalum/316 stainless steel transition joints
[NASA-CR-121111] 07 p0804 N73-16519
Mechanical properties of welded joints in stainless and low-alloy steels at temperatures of 900 to 1300 F
[ORNL-4781] 07 p0804 N73-16525
Irradiation effects on fatigue and creep-fatigue properties of stainless steels
[ANCR-1078] 10 p1173 N73-19539
Effects of nuclear radiation on stainless steels
[AD-753457] 10 p1187 N73-19660
Creep tests and transmission electron microscopic observation of grain boundary structure in stainless steel bicrystals
[CEA-R-4317] 10 p1200 N73-19768
Mechanical properties and stress corrosion cracking of 431 stainless steel alloy at low temperatures
[NASA-TM-X-64729] 12 p1412 N73-21441
Effects of hydrogen environment embrittlement of steels and alloys
[NASA-CR-2163] 12 p1412 N73-21444
Analysis of fracture and crack growth properties of 304 stainless steel to determine suitability as material for cryogenic fluid storage pressure vessels
[NASA-CR-121025] 12 p1462 N73-21847
Plastic instability in stainless steels and effects on load bearing capacity of structural components
[COO-2048-8] 12 p1463 N73-21850
Stress corrosion cracking in 410 stainless steel due to hydrogen embrittlement
13 p1539 N73-22471
Vibration damping ability of steel compressor blades subjected to different heat treatments
[AD-743119] 13 p1543 N73-22502
Atomic absorption spectrophotometric analysis of chromium in stainless steels
[AD-755809] 13 p1545 N73-22522
Mechanical properties of aluminum stainless steel composites and associated interface microstructures
[AD-756673] 13 p1548 N73-22542
Feasibility and cost effectiveness of expendable main rotor blades on UH-1 helicopter
[AD-758464] 15 p1736 N73-24078
Electron irradiation damage as function of accelerating voltage, time, and temperature in stainless steel
[COO-2119-3] 15 p1799 N73-24581
Effect of heat treatment on structure and properties of stainless steels
[NLL-M-21566-[5828.4F]] 16 p1926 N73-25585
Effect of fast reactor irradiation on ductility of annealed stainless steels
[HEDL-SA-310] 16 p1929 N73-25606
Neutron irradiation effects on tensile and creep properties of cold worked stainless steel
[HEDL-SA-468] 16 p1929 N73-25607
Correction factor technique for X ray fluorescent analysis on stainless steel
[PB-214231/3] 16 p1929 N73-25611
Quantitative bismuth determination in stainless steels
[PB-214234/7] 16 p1929 N73-25612
Influence of prior microstructure on neutron irradiation damage in 316 stainless steel foils
[HEDL-SA-407] 17 p2065 N73-26707
Temperature effects on hot extrusion of stainless steels
[AD-761538] 19 p2306 N73-28551
Elastic-plastic toughness level of irradiated stainless steels used in fast reactor construction
[AD-761611] 19 p2310 N73-28580
Physical properties of aluminum alloys, titanium alloys, and stainless steels for aerospace airframes
[AD-762305] 19 p2311 N73-28587
Analysis of effects of plastic deformation on internal structure of austenitic steels as shown by anomalies in tensile stress-strain curves
[NLL-M-23029-[5828.4F]] 20 p2428 N73-29504
Effect of high hydrostatic pressure on flow stress of 18-8 stainless steel
[NLL-NEL-TT-2458-[6075.461]]
20 p2430 N73-29516
Wedging corrosion and mass transport in sodium/zirconium/stainless steel system at high temperature - Part I
[RD/B/N-2521-PT-1] 21 p2559 N73-30517
Tensile and fatigue data for irradiated and unirradiated AISI 310 stainless steel and titanium-5 percent aluminum-2.5 percent tin applied to universal slopes
[NASA-TM-X-2883] 22 p2683 N73-31494
Mossbauer effect study of high temperature oxidation and breakaway in 302 stainless steel
22 p2706 N73-31671
Stainless steel and Hastelloy corrosion by boron trifluoride, air, and argon mixtures
[ORNL-TM-4172] 24 p2892 N73-33087
Acetone decomposition by stainless steel and other metal compounds
[AERE-R-7407] 24 p2892 N73-33088
Heat to heat variation in fatigue and creep-fatigue behavior of AISI Type 304 stainless steel, and fatigue behavior of type 308 stainless steel weld material
[ANCR-1097] 24 p2936 N73-33450
Creep characterization tests on stainless steels
[ORNL-TM-4105] 24 p2954 N73-33597
Heat capacity of liquid metals and stainless steels
[ORO-3291-17] 24 p2992 N73-33914
STALL
U BOUNDARY LAYER SEPARATION
STALLING
Time variant distortion in supersonic inlet related to stall in compressor
[NASA-TM-X-68189] 10 p1208 N73-19825
Analysis of steady-state and dynamic pressure conditions in F-111 aircraft engine to determine causes of engine compressor stalls
[NASA-TN-D-7328] 20 p2465 N73-29806
STAMPING
Frictionless plane contact between elastic layer on elastic half space with compression loads by frictionless rigid stamp
[WB-1/72] 09 p1040 N73-18478
STANDARD ATMOSPHERES
U REFERENCE ATMOSPHERES
STANDARDIZATION
Status of National Standard Reference Data System
[NBS-TN-747] 02 p0245 N73-11990
Standardization criteria for nominal sizes and test conditions of extension strain gages with bound metallic measuring grids
[NLL-NEL-TT-2414-[6075.461]]
05 p0545 N73-14426
Determination of flat notched fatigue test specimens form numbers by stress optical method and finite element method, noting standardization
[LBF-TM-61/71] 06 p0685 N73-15573
Standardization of satellite control systems by using onboard computers, exemplified by proposal for Aeros satellite
[DGLR-PAPER-72-064] 06 p0721 N73-15886
Standardization of tests and classification of color perception abnormalities in military personnel
10 p1113 N73-19071
Standardization values for grinding forces and surface roughness in cylindrical grinding, noting steels
[CRIF-MC-46] 10 p1167 N73-19491
NBS activities in developing measuring methods for semiconductors
[NASA-CR-131275] 11 p1330 N73-20792
Standards for calorimeter measurement of laser beam absorption by graphite cones
[CEA-CONF-2056] 12 p1411 N73-21432
Application of ANSI Y14.5 rules to designing connectors for interchangeability
14 p1641 N73-23309
Standardization of geodetic instruments in U.S.S.R. research facility
[AD-759687] 16 p1914 N73-25492
Systems theory in analysis and system of analytical quantity ranges
[NASA-TT-F-15029] 20 p2423 N73-29460
STANDARDS
NT FREQUENCY STANDARDS
NT REFERENCE ATMOSPHERES
Evaluation of ice-water mixture thermocouple reference chamber discussing best operating parameter combination for high accuracy
[RAE-TR-72035] 01 p0058 N73-10475
Description of linear polyethylene standard reference material
[NBS-SP-260-42] 02 p0192 N73-11552
Design of photogrammetric test standards
[AD-749502] 04 p0424 N73-13459
Comparison of national standards of socialist countries for measuring solar radiation using pyrheliometer test readings
04 p0443 N73-13614

History, organization, and functions of the National Bureau of Standards to include description of test equipment used for research projects
[NBS-SP-367] 05 p0524 N73-14259
Research and development related to maintaining national standards of measurement of physical quantities in Australia
[NP-19392] 06 p0650 N73-15276
Data compiled in international comparative creep rupture program using two types of steel as test materials
[PB-211174] 06 p0685 N73-15578
Preparation, testing, and use of superconductive fixed point devices incorporating lead, indium, aluminum, zinc, or cadmium as standard reference materials
[NBS-SP-260-44] 06 p0707 N73-15768
Public health exposure limits to nitrogen oxide, hydrogen chloride, and hydrogen fluoride air pollutants
[AD-751438] 07 p0748 N73-16084
Public health exposure limits for air pollutants
[AD-751437] 07 p0749 N73-16088
Organometallic and physical property standards for diluent oil calibration
[NBS-TN-751] 08 p0883 N73-17150
Industrial conversion to metrication standards
[NASA-CR-130534] 08 p0925 N73-17584
Overview of scientific and technological research in Yugoslavia on NBS grants, 1971 - 1972
[NBS-TN-753] 08 p0976 N73-17979
Radiobiological effects of cosmic radiation in animals and standardization of permissible radiation levels for spacecrews
09 p0993 N73-18102
Electrochemical methods for determining acidity standard, atomic weight, stoichiometric composition, and trace contaminants
[NBS-TN-583] 09 p0999 N73-18153
Improvement to primary standard of measurement associated with International System of Units
[NPL-QU-AR-71] 10 p1161 N73-19450
Improvement in methods of measurement for semiconductor materials, process control, and devices
[NASA-CR-133030] 16 p1953 N73-25800
Catalog on standard reference materials, their properties, compositions, and characterizations
[NBS-SP-260] 17 p2049 N73-26573
Termination resistance as standard for calibrating low noise temperature in electronic equipment
[NASA-TT-F-15016] 19 p2243 N73-28086
Noise standards for habitable houses, rest homes, hospitals, camps, public facilities, and streets in residential areas
[NASA-TT-F-15065] 21 p2503 N73-30088
Photometric standards for North Polar Sequence, Kapteyn Areas, and Harvard Standard Areas
21 p2594 N73-30791
Microwave radiation effects on rats and standards for acceptable radiation dosage of humans
[JPRS-59709] 21 p2608 N73-30903
U.S., Soviet, and Polish standards for radiation levels for humans
21 p2608 N73-30905

**STANDING WAVE RATIOS**
Voltage standing wave ratio measurement and evaluation of aircraft antenna systems
[AD-761031] 18 p2123 N73-27161

**STANDING WAVES**
Conditions of coherence in diffraction spectra produced in liquids on ultrasonic standing waves
[NASA-TT-F-13925] 02 p0211 N73-11713
Analysis of finite amplitude standing waves in air at ambient temperature contained in rigid walled rectangular cavity
[AD-747522] 03 p0337 N73-12749

**STANDS**
U SUPPORTS

**STANNIDES**
NT NIOBIUM STANNIDES

**STAPHYLOCOCCUS**
Methods for improving bacterial transport media
[NASA-CR-128958] 16 p1866 N73-25113

**STAR CLUSTERS**
NT VIRGO STAR CLUSTER
Extended two color photometry of faint stars by telescope with objective grating
[BULL-172] 07 p0842 N73-16819
Mass-luminosity relationship of binary stars in Hyades cluster
[ROY-OBS-BULL-175] 13 p1578 N73-22788
Asymptotic branch evolution of globular cluster star of low mass
16 p1960 N73-25856
Measurement of luminosity distribution of Coma cluster of galaxies and comparison of mass-to-light ratio of cluster with that of individual galaxies
19 p2341 N73-28829
Star cluster data used to obtain absorption values for different galactic longitudes in northern part of Milky Way
20 p2471 N73-29842
Spatial distribution of stars in area surrounding cluster NGC 6913
20 p2471 N73-29843
Comparison of color index and formation conditions of cluster and field galaxies
[NLL-RTS-8000] 21 p2593 N73-30780

**STAR DISTRIBUTION**
Characteristics of star field attitude sensor for installation in Pioneer Venus spacecraft
[NASA-CR-114516] 03 p0359 N73-12924
Origin and evolution of stars, stellar matter, and galaxies
[AD-749734] 06 p0720 N73-15875
Application of Schmidt telescopes and three color photometry to galactic clusters, star distribution in galactic disk and halo and galactic white stars.
07 p0845 N73-16842
Investigation of stellar density distribution and luminosity function in high galactic altitudes using Schmidt telescopes
07 p0846 N73-16857
Holographic starfield and landmark tracker with two reference beam, coherent optical matched filter technique
[NASA-CR-112143] 10 p1168 N73-19505

**STAR FIELDS**
U STAR DISTRIBUTION

**STAR TRACKERS**
Production measures for visible and ultraviolet transmitting reticles for star trackers
[NASA-CASE-GSC-11188-3] 01 p0056 N73-10460
Star sensor/mapper with two data channels with memory for SAS-B
[NASA-CR-129192] 02 p0173 N73-11403
Star scanner for spin-stabilized spacecraft
[NASA-CASE-GSC-11569-1] 02 p0173 N73-11404
Characteristics of star field attitude sensor for installation in Pioneer Venus spacecraft
[NASA-CR-114516] 03 p0359 N73-12924
Evaluation of electro-optic direction sensor
[NASA-CR-130928] 10 p1160 N73-19437
Method for producing reticles for use in outer space
[NASA-CASE-GSC-11188-2] 10 p1184 N73-19630
Optimization of optical filtering for tracking faint stars
[NASA-CR-130199] 11 p1293 N73-20496
Development of electrostatically focused image dissector tube for use in spacecraft attitude control star trackers
[NASA-CR-132153] 15 p1787 N73-24487
Development of automated astronomic positioning system using vertically oriented telescope to produce accurate astronomic latitude and longitude
[AD-760108] 17 p2060 N73-26668
Design and performance of optically stabilized telescope pointing system using digital star tracker
[NASA-TN-D-7204] 18 p2125 N73-27173
Skylark star-pointing attitude control system using strapdown inertial system
[RAE-TR-71241] 18 p2176 N73-27571
Technological modification to OSO-G launch vehicle for improved guidance and control
18 p2208 N73-27817
Rate integrated gyro attitude control system for sounding rockets
18 p2208 N73-27820
Pointing error sensor in star tracker system for OAO 3 attitude control
18 p2208 N73-27822
Star mapper using solid-state detectors discussing dioptric and mirror objectives, and star recognition algorithms
[ESRO-CR-82] 22 p2698 N73-31610
Star mapper breadboard model for satellite attitude control using either photomultipliers or Si photodiodes
[ESRO-CR-162] 22 p2698 N73-31611
Production method of star tracking reticles for transmitting in visible and near ultraviolet regions
[NASA-CASE-GSC-11188-1] 23 p2790 N73-32320
Strapped down gyroscope aligned with sun and star tracker optical axis calibrating roll, yaw and pitch values
[NASA-CASE-ARC-10716-1] 23 p2851 N73-32784

**STAR TRACKING**
U STAR TRACKERS

**STARFIGHTER AIRCRAFT**
U F-104 AIRCRAFT

**STARK EFFECT**
Electric field amplitude within superhigh frequency wave absorption by plasma using Stark effect analysis
[FTI-413] 06 p0705 N73-15750
Stark shift measurements and photon resonance perturbations in triplet metastable helium atom near ionization threshold
[KFKI-72-42] 10 p1169 N73-19507
Light intensity effect on photon resonance in excited atom ionization for determining Stark effect potential
[KFKI-72-68] 10 p1192 N73-19694
Spectroscopic analyses of molecular energy levels in crystals
[AD-753382] 10 p1201 N73-19776
Analysis of dynamic Stark effect in laser-atom interactions to show distortion of atomic structure in high intensity laser fields
[CEA-CONF-2135] 20 p2425 N73-29481

**STARLIFTER AIRCRAFT**
U C-141 AIRCRAFT

**STARS**
NT A STARS
NT B STARS
NT BINARY STARS
NT BLACK HOLES [ASTRONOMY]
NT CEPHEID VARIABLES
NT EARLY STARS
NT ECLIPSING BINARY STARS
NT GIANT STARS
NT HOT STARS
NT INFRARED STARS
NT LATE STARS
NT MAIN SEQUENCE STARS
NT NEUTRON STARS
NT NOVAE
NT O STARS
NT PULSARS
NT RADIO STARS
NT REFERENCE STARS
NT STELLAR GRAVITATION
NT SUN
NT SUPERGIANT STARS
NT SUPERNOVAE
NT T TAURI STARS
NT VARIABLE STARS
NT WHITE DWARF STARS
Problems of solar and stellar spindown and theory, emphasizing angular velocity inside sun and stars
01 p0095 N73-10786
Tidal interactions in multiple galaxies
04 p0468 N73-13816
Atomic and molecular spectra of SC stars
04 p0469 N73-13821
Radial velocity of southern G and K types stars as observed by Cassegrain spectrograph
05 p0594 N73-14830
Tables of minor planets positions and comparison stars
05 p0594 N73-14831
Filter photometric data from OAO 2 on blue Ap, band a dwarfs, and giants
[NASA-TM-X-66163] 07 p0843 N73-16826
Application of Schmidt telescope and objective prism to stellar radial velocity surveys
07 p0845 N73-16848
Proper motions for 3478 faint stars
[NASA-CR-130693] 09 p1085 N73-18850
Method for determining relative orientation of coordinate axes of stellar catalogs
[AD-751077] 09 p1085 N73-18855
Mass-luminosity relationship of Hyades and other stars
[BULL-175] 10 p1212 N73-19857
UBV photometry of 115 nearby stars
[BULL-176] 10 p1212 N73-19858
Computation of optical sensor output relative to known star magnitudes for attitude control of spacecraft
[NASA-CR-130926] 10 p1212 N73-19859
UBV photometry of stars within 25 parsecs of sun, in quasar and galaxy field, in Kapteyn selected areas and of miscellaneous stars including super and red giants
[ROY-OBS-BULL-176] 13 p1578 N73-22789
Definitions of stellar terms
14 p1705 N73-23834
Classification of southern carbon stars using objective prism spectra
16 p1960 N73-25857
Numerical approach to study of convective and semi-convective stability
20 p2470 N73-29836
Computational method for obtaining models for fast and differentially rotating upper main sequence stars in radiative equilibrium
20 p2470 N73-29838
Galilean satellites, Venus clouds, and astronomical observatories
[NASA-CR-133826] 21 p2591 N73-30761
Narrow-band photometry of Galilean satellites with resolution of approximately 30
[LPL-COMMUN-167] 21 p2591 N73-30763
Spectral albedos of Galilean satellites from broad-band photometry
[LPL-COMMUN-168] 21 p2591 N73-30764
Line strengths in spectra of seven double-lined Am binary stars
[ROY-OBS-BULL-177] 21 p2598 N73-30819
Listing of double star observations for 1900 and 1960
22 p2717 N73-31748
Ultraviolet interstellar polarization measurement
22 p2735 N73-31889
Using UBUH gamma photometry and spectral classifications for 48 stars in monoceros region to study dispersed part of 1 Mon association
23 p2836 N73-32658
Kinematic properties of carbon stars
24 p2977 N73-33791

**STARTERS**
NT ENGINE STARTERS

**STARTING**
Tests on bearings and seals undergoing repeated starts of turbine pumps
[SEP-NT-3058/71-M] 10 p1167 N73-19494

Liquid hydrogen turbopump rapid start program with cooled and uncooled system tests
[NASA-CR-124262] 16 p1918 N73-25522
STATE EQUATIONS
U EQUATIONS OF STATE
STATE ESTIMATION
U ORBITAL POSITION ESTIMATION
STATIC AERODYNAMIC CHARACTERISTICS
Wind tunnel tests to determine static aerodynamic characteristics of single-stage-to-orbit space shuttle at Mach numbers of 2.60, 3.85 and 4.64
[NASA-TM-X-2667] 02 p0233 N73-11891
Effect of wing aspect ratio and flap span on aerodynamic characteristics of short takeoff model with externally blown jet flap
[NASA-TN-D-7205] 21 p2494 N73-30020
STATIC DEFORMATION
Surface pressure measurements over model delta wing undergoing oscillatory deformation in low speed wind tunnel
[ARC-R/M-3693] 03 p0248 N73-12005
Temperature effects on measurement accuracy of static deformation of semiconductor resistance strain gages
[NASA-TT-F-14616] 04 p0481 N73-13928
STATIC ELECTRICITY
Electrostatic charging and discharging of helicopters in flight and personnel safety
[AD-750617] 06 p0701 N73-15718
Papers presented at conference on lightning and static electricity
[AD-752551] 08 p0922 N73-17552
Static charge generation in hydrocarbon fuels during flow through pipes
[AD-753386] 09 p1067 N73-18706
Analysis of electrical charge generated by helicopter rotor operating near particulate matter with seeded vortex
[AD-755282] 12 p1366 N73-21080
Application of fiber glass reinforced plastic materials for ground handling of aviation fuels and hazards of static electricity caused by plastic materials
[AD-764358] 22 p2709 N73-31693
STATIC INVERTERS
Motor starting characteristics of Brayton electric engine using static inverter
[NASA-TM-X-2738] 09 p0990 N73-18080
Modular inverter/converter automatic paralleling and protection system
[NASA-TN-D-7279] 15 p1737 N73-24084
Magnetic materials selection for spacecraft transformers used in static inverters, converters, and transformer-rectifier supplies
[NASA-CR-135642] 23 p2764 N73-32118
STATIC LOADS
Holographic interferometry for measuring surface deflections of statically loaded turbine blades
16 p1921 N73-25543
Simplified analysis procedure for determining static and dynamic aeroelastic loads for space shuttle dynamics
[NASA-CR-124370] 22 p2722 N73-31781
STATIC PRESSURE
NT HYDROSTATIC PRESSURE
Wind tunnel tests to determine pressure sensing characteristics of trailing cone device for calibrating aircraft static-pressure systems
[NASA-TN-D-7217] 13 p1470 N73-21906
Flow characteristics of axially symmetrical, supersonic, fully-expanded jet to determine relation between static pressure distributions and jet turbulence
[ARC-R/M-3292] 16 p1857 N73-25038
Computer program for estimating peak static pressure from internal explosions in closed vessels
[AD-762402] 19 p2350 N73-28907
STATIC STABILITY
NT SHELL STABILITY
NT STRUCTURAL STABILITY
Definitions of aircraft longitudinal stability to account for effects of aircraft structure distortion and compressibility effects
[ESDU-00.00.03] 02 p0124 N73-11010
Effects of various external stores characteristics, spanwise positions, and Mach number on static longitudinal stability of several military aircraft
[AD-750120] 06 p0624 N73-15063
Analysis of external loads and states of deformation in light elastic structures
[PB-212011] 07 p0852 N73-16911
Effect of ablation on aerodynamic characteristics of blunted slender cone during free flight ablating conditions
[NASA-TN-D-7196] 09 p0979 N73-18002
Correlation between lateral-directional static stability characteristics and spin susceptibility
[AD-753905] 10 p1107 N73-19029
Tables and graphs on static stability and axial force characteristics of flat faced right circular cylinders at subsonic and supersonic speed
[AD-754920] 11 p1273 N73-20330
Effect of nose shape and tail length on static stability of fin-stabilized projectile at supersonic speeds and various angles of attack
[NASA-TM-X-2831] 19 p2217 N73-27888
Effect of inflated air cushion landing gear on subsonic static stability of high performance aircraft operating out of ground effect
[AD-763365] 21 p2498 N73-30048
Effects of artificial aircraft stability control on damping, and static stability recovery by controllers
24 p2878 N73-32987
STATIC TESTS
Static and vibration tests of graphite-epoxy stabilizer system for A-4 Skyhawk aircraft
[AD-750778] 06 p0689 N73-15610
Static and wind tunnel tests to determine performance of four cowl cascade thrust reverser configurations at forward velocity
[NASA-TM-X-2665] 07 p0835 N73-16773
Static tests of redesigned graphite horizontal stabilizers
[AD-758718] 15 p1803 N73-24611
Flyover and static tests for determining effects of flight velocity on F-106B exhaust nozzle noise
[NASA-TM-X-2854] 19 p2329 N73-28734
Flyover and static tests of noise and thrust performance of two spoke, suppressor plug nozzles and basic plug nozzle
[NASA-TM-X-2856] 19 p2329 N73-28735
Decision methodology on static tests of large aircraft vehicles
[NASA-CR-124366] 21 p2604 N73-30866
Definition of criteria and techniques of design, analysis, and test for using single major structural test article for performing dynamic, fatigue, and static testing
[NASA-CR-124404] 23 p2853 N73-32799
STATICS
NT ELECTROSTATICS
NT HYDROSTATICS
STATIONARY FRONTS
U FRONTS [METEOROLOGY]
STATIONARY ORBITS
Application of Runge-Kutta process to circular geostationary orbit equations of motion
[RAE-TR-72118] 13 p1578 N73-22790
Geostationary satellite trajectory optimization by low thrust resistojet propulsion
[AASU-323] 16 p1967 N73-25913
Juridical problems in use of stationary orbits for artificial earth satellites
[JPRS-59819] 20 p2473 N73-29862
STATIONKEEPING
Design of high frequency mercury ion engine for application to communication satellite stationkeeping
[DGLR-PAPER-72-88] 03 p0351 N73-12861
Orbit determination for self-contained stationkeeping systems, equations of satellite motion, orbit control, gravitational effects, and synchronous satellite drift
[NAL-TR-295] 04 p0469 N73-13826
Analysis of military helicopter formation flight techniques with emphasis on station keeping based on nominal point coordinate system
[AD-751459] 07 p0740 N73-16021
Design of solar ephemeris synthesizer for LES-8/9 stationkeeping system
[AD-752250] 08 p0965 N73-17891
Development of autonomous stationkeeping system for controlling longitude of synchronous satellite by onboard navigation aids
[AD-759806] 16 p1942 N73-25716
Development, characteristics, and performance of ion thruster engine for attitude control and stationkeeping of synchronous satellite
[NASA-CR-121183] 19 p2329 N73-28736
Flight tests of modified F-100 aircraft to determine effectiveness of fast-acting flaps as direct-lift-control devices to improve station keeping
[NASA-TM-X-2936] 24 p2876 N73-32970
STATIONS
NT DEEP SPACE INSTRUMENTATION FACILITY
NT GLOBAL TRACKING NETWORK
NT GROUND STATIONS
NT HYDROELECTRIC POWER STATIONS
NT INTEGRATED MISSION CONTROL CENTER
NT ORBITAL SPACE STATIONS
NT ORBITAL WORKSHOPS
NT SALYUT SPACE STATION
NT SPACE STATIONS
NT TRACKING STATIONS
NT WEATHER STATIONS
STATISTICAL ANALYSIS
NT AMPLITUDE DISTRIBUTION ANALYSIS
NT CORRELATION COEFFICIENTS
NT MAXWELL-BOLTZMANN DENSITY FUNCTION
NT MULTIVARIATE STATISTICAL ANALYSIS
NT NONPARAMETRIC STATISTICS
NT NORMAL DENSITY FUNCTIONS
NT PROBABILITY DENSITY FUNCTIONS
NT PROBABILITY DISTRIBUTION FUNCTIONS
NT REGRESSION ANALYSIS
NT SEQUENTIAL ANALYSIS
NT STATISTICAL CORRELATION
NT STATISTICAL DECISION THEORY
NT STATISTICAL TESTS
NT VARIANCE [STATISTICS]
NT WEIBULL DENSITY FUNCTIONS
Statistical analysis of turbulent motion using Navier-Stokes equations - Part I
[NASA-TT-F-14560] 01 p0039 N73-10310
Evaluation of bucket and intake system for measuring sea surface temperature and statistical analysis of data obtained from international ship observations
[WMO-336] 01 p0050 N73-10406
Statistical analysis of normal acceleration, airspeed, altitude, and flight loads on military aircraft
[AD-747285] 02 p0127 N73-11035
Statistical analysis of impact injuries to seated human responding to square wave energy absorption of vertical deceleration pulse representing helicopter crash
[AD-745919] 02 p0136 N73-11102
Programs and techniques for statistical analysis and reduction of ionospheric physics data
[AD-745966] 02 p0167 N73-11360
Maximum probability and minimum variance methods for interpreting remote soundings on meteorological structure of atmosphere
02 p0196 N73-11587
Comparison of statistical and iteration methods for obtaining vertical temperature profiles from multispectral radiation measurements
02 p0196 N73-11589
Statistical analysis of geography and seasonal variation effects on intensification of tropical cyclones over western North Pacific Ocean
[AD-746130] 02 p0206 N73-11669
Statistical analysis of stream meteor composition
02 p0229 N73-11851
Estimation of censoring, truncation, transformation, and partial data vectors for predicting and measuring assembly performance in biological and physical situations
[NASA-CR-129503] 03 p0323 N73-12632
Fields, statistics and non-Abelian gauge groups
[NOTA-INTERNA-387] 03 p0340 N73-12771
Statistical analysis of ASDE-2 airport radar failures and design modifications
[FAA-RD-72-82] 04 p0388 N73-13154
Statistical analysis of adhesive bond strength as function of plasma treatment of polymer films
[AD-749253] 04 p0440 N73-13587
Analysis of mean distribution maps for altitude and temperature of tropopause over Northern Hemisphere in Jan. and July between 1957 and 1965
04 p0442 N73-13607
Statistical analysis of magnetic assymetry and variations of general solar magnetic field
[AD-746717] 04 p0476 N73-13892
Statistical analysis of thermal stability and service life of electrical insulation
[AD-749925] 05 p0521 N73-14239
Probability estimation of survival fatigue failures, using statistics of extremes
[FO-1078] 05 p0568 N73-14615
Statistical estimation and decision techniques applied to time series and multivariate analyses for communication, tracking, and physiological monitoring
[AD-749542] 05 p0569 N73-14620
Inherent statistical properties of bubble field in two phase flow determined by correlation functions
[EUR-4840] 06 p0655 N73-15319
Pluviometric and statistical analyses of precipitation and watercourse patterns in Israel
06 p0665 N73-15403
Coefficients for estimated values of location and scale parameters from ordered statistical samples, applied to Gumbel and Weibull distributions
[FOA-P-B-8010-11] 06 p0690 N73-15619
Statistical supplement for capital investment in transportation modes
[PB-212308] 07 p0860 N73-16977
Statistical analyses for detecting frequency shift keyed and phase keyed signals in additive disturbance
[AD-752010] 08 p0886 N73-17173
Statistical analysis on nonparametric detection of M-ary time varying signals with intersymbol interference and additive noise
[AD-752011] 08 p0886 N73-17174
Monte Carlo simulation of complex reliability systems using logic circuit analysis programs linked to statistics programs
[TR-72-39] 08 p0927 N73-17596
Statistical analysis of strength and fracture characteristics of materials with application to fiber composites using Weibull density functions
[JPL-TM-33-580] 08 p0934 N73-17650
FORTRAN programs for statistical analysis of signal and linear and nonlinear systems
[ANTHRO-MITT-3/72] 09 p1006 N73-18208
Distribution function inequalities in order statistics
[NASA-CR-130962] 09 p1058 N73-18627
Calculating error in temporal statistical structure of zonal and meridional velocity components of ground wind
09 p1060 N73-18641
Diffusion random model for statistical analysis of light propagation in turbulent medium
09 p1066 N73-18698

Methods for obtaining statistical morphological characteristics of lunar surface using photographic imagery
09 p1084 N73-18840
Statistical analysis of engine failure/malfunction accidents for US fixedwing aircraft of general aviation category during 1965 to 1969
[NTSB-AAS-72-10] 10 p1106 N73-19015
Power density spectrum for statistical analysis of radar altimeter return variations due to radar motion
[SC-RR-72-0265] 10 p1129 N73-19197
ELF signal propagation statistics in 40 to 70 Hz band at Norway, Saipan, and Greece during May 1972
[AD-753685] 10 p1129 N73-19199
Statistical analysis of rainfall frequency in central Valais
[REPT-28] 10 p1181 N73-19609
Statistical anlaysis of aircraft accidents occurring in US civil aviation during calendar year 1971
[NTSB-BA-73-1] 11 p1234 N73-20015
Statistical models of electromagnetic scattering from radar targets
[AD-753936] 11 p1256 N73-20192
Phase manipulated signal reception in noise background of unknown statistics
[AD-754603] 11 p1258 N73-20205
Development of statistical methods for estimating annual operations at non-tower airports and establishment of standardized estimation procedure
[SCI-2040] 11 p1267 N73-20278
Statistical properties measurements of atmospheric turbulence at altitudes below 1000 ft over hilly and flat terrain
[LR-567] 11 p1285 N73-20428
Evaluation of method for combining point estimates of reliability
[AD-754347] 11 p1302 N73-20563
Development of procedures for accurately estimating annual air traffic levels at airports without tower control
[SCI-2-2040] 11 p1321 N73-20722
Statistical analysis on expense increase funding for technological systems
11 p1351 N73-20963
Failure modes and mechanisms for integrated circuits with stressed pin pair combinations
[AD-755807] 12 p1387 N73-21247
Calculation of expected anomaly criteria for some meteorological fields using statistical analysis methods
[NLL-M-22804-[5828.4F]] 12 p1420 N73-21507
Analysis of air passenger traffic on North Atlantic air routes to show development of scheduled and chartered operations
13 p1474 N73-21937
Application of adaptive control algorithms to self adjusting control systems for aeroelastic aircraft, flight vehicle roll, and control during reentry
[AD-756598] 13 p1474 N73-21941
Characteristics of deep water waves reaching Port Phillip Heads, Australia to show effects of refraction, shoaling, and friction
13 p1524 N73-22351
Statistical description of wind field in upper troposphere and lower stratosphere for time scales from 6 to 72 hours
13 p1552 N73-22572
Statistical analysis of phase data on three Omega navigation stations to determine positioning accuracies - Vol. 1
[AD-756024] 13 p1557 N73-22617
Program listings and output data summaries for differential Omega navigation system monitoring and analysis - Vol. 2
[AD-756025] 13 p1557 N73-22618
Analog charts developed during monitoring and analysis of differential Omega navigation system - Vol. 3
[AD-756026] 13 p1557 N73-22619
Psychophysical and statistical experiments on auditory speech perception
14 p1626 N73-23175
Analysis and modeling of ionospheric data collected worldwide
[AD-757480] 14 p1662 N73-23491
Investigation of ultraviolet interstellar extinction
[NASA-CR-131990] 14 p1706 N73-23843
Exponential probability distribution analysis for extrapolating aerospace system performance statistics from test results
14 p1713 N73-23903
Application of statistical analysis techniques in telecommunication, tracking, and control
[AD-758260] 15 p1751 N73-24193
Structural stability of thin imperfect cylindrical shells as determined by statistical analysis
[AD-758030] 15 p1840 N73-24913
Statistical analysis of effect of simulated sonic booms on sleep patterns of male subjects
[FAA-AM-72-35] 17 p1987 N73-26057
Maximum likelihood efficiency estimation procedures for statistical reliability analyses
[AD-760152] 17 p2039 N73-26493
Statistical classification of earth resources in remote sensing data
[NASA-CR-128988] 17 p2054 N73-26615
Statistical analysis of aircraft accidents occurring in US civil aviation operations during calendar year 1972 - Issue 4
[NTSB-BA-73-6] 18 p2105 N73-27024
Reliability study of multicomponent systems
[AD-760768] 18 p2169 N73-27521
Research in intepretation of lunar data developed during Apollo Program
[NASA-CR-133302] 18 p2190 N73-27679
Statistical analysis of load-carrying capacity of smooth cylindrical shells
[AD-760946] 18 p2204 N73-27787
Pattern recognition as statistical analysis of confidence level in forensic trace element identification
[IRI-133-72-11] 19 p2240 N73-28056
Specialized digital computer for correlation analysis
[AD-761586] 19 p2241 N73-28066
Statistical prediction of malfunction in digital computer
[AD-762263] 19 p2242 N73-28079
Statistical analysis of surface and upper air rawinsonde for White Sands Missile Range, New Mexico
[AD-762159] 19 p2297 N73-28472
Data compression preserving statistical independence
[NASA-TM-X-70419] 19 p2313 N73-28606
Statistical analysis of upper confidence levels for system failure rates
[AD-761758] 19 p2314 N73-28612
Statistical analysis on flux density spectra of solar microwave bursts
19 p2334 N73-28779
Evaluation of statistical energy analysis methods for vibrating structures
[NASA-CR-124322] 19 p2349 N73-28890
Statistical analysis of naval experience in fixed-price incentive contract management for aircraft and missile procurement
[AD-761396] 19 p2355 N73-28946
Analysis of long term variations in water surface temperature of North Atlantic Ocean
[NLL-M-23016-[5828.4F]] 20 p2390 N73-29200
Analysis of thermal radiation brightness of river strip as basis for determining actual temperature from data provided by satellite
20 p2400 N73-29288
Statistical analysis of snowfall in various areas of USSR for application to transportation, agriculture, and urban planning
[TT-70-50181] 20 p2406 N73-29338
Statistical methods for pattern recognition and classification applications
[NASA-CR-128989] 20 p2436 N73-29566
Sufficient statistics for divergence and brattacharyya distance
[REPT-13] 20 p2438 N73-29579
Sufficient statistics for divergence and probability of misclassification
[REPT-14] 20 p2438 N73-29580
Subroutines SYMAT and COVAR for use as test procedures in matrix calculations
[REPT-17] 20 p2438 N73-29581
Nearest neighbor algorithms for pattern classification
[REPT-18] 20 p2438 N73-29582
Optimal methods for processing observations
20 p2439 N73-29593
Methods for determining most probable value of recurring errors
20 p2439 N73-29594
Statistical properties of atmospheric circulation particularly geopotential fields on global basis
20 p2442 N73-29619
Comparative analysis of upper troposphere maximum wind strength maps and ground surface synoptic maps
20 p2445 N73-29642
Four dimensional processing of a synchronously arriving meteorological data based on dynamic statistical approach
20 p2447 N73-29664
Statistical analysis of meteorological parameters during fog at US airports
[FAA-RD-72-39] 20 p2448 N73-29673
Statistics of extreme values of meteorological parameters
[MONO-89] 21 p2566 N73-30568
Statistical procedures for hydrometeorological and weather forecasting and climate control
[JPRS-59580] 21 p2572 N73-30612
Statistical analysis of large scale fluctuations in water surface temperature of North Atlantic Ocean
21 p2572 N73-30614
Statistical structure and automated monitoring of meteorological and hydrometeorological fields
21 p2573 N73-30623
Statistical analysis of Civil Aviation midair collisions occurring during period January 1964 to December 1971
[MTR-6334] 22 p2614 N73-30946
Operational parameters for UH-1H helicopters during combat flights in Southeast Asia to determine helicopter performance and reliability
[AD-764260] 22 p2616 N73-30965
Performance decrement and response time of current and noncurrent jet Naval pilots
[AD-761463] 22 p2624 N73-31025
Statistical analysis of signals in amplitude modulation radio altimeters with phase read-out
22 p2629 N73-31065
Statistical error analysis of frequency modulated radio altimeter with phase readout
22 p2629 N73-31066
Statistical study of nonlinear energy transfer interactions in turbulence models
22 p2649 N73-31224
Statistical processing of Pioneer front film data - Part I
[NASA-CR-132797] 22 p2665 N73-31351
Statistical analysis of annual maximum temperatures of Paris
[MN-MONO-90] 22 p2694 N73-31580
Statistical analysis of aircraft accidents occurring in US Civil Aviation during calenadar year 1972 - Issue 5
[NTSB-BA-73-7] 23 p2741 N73-31942
Probabilistic models and statistical inference in reliability life testing, and fatigue failure
[AD-763818] 23 p2798 N73-32380
Atmospheric field decomposition by systems of orthogonal functions
[AD-764942] 23 p2815 N73-32509
Statistical analysis of computational round-off errors associated with cutting plane solution ot linear integer programming problems
[NASA-TN-D-7457] 24 p2945 N73-33517

**STATISTICAL COMMUNICATION THEORY**
U COMMUNICATION THEORY

**STATISTICAL CORRELATION**

Correlation techniques and measurements of surface wave height statistics
[NASA-CR-2153] 04 p0405 N73-13298
Second order coherence function discriminating between thermal and laser radiation
[ONERA-NT-196] 04 p0450 N73-13675
Selection of statistically significant relationships for predictors in long range weather forecasting
[NLL-M-22803-[5828.4F]] 11 p1313 N73-20657
Statistical comparison of simultaneous satellite solar wind observations
[AD-758194] 14 p1703 N73-23816
Statistical correlation of gulls and USAF aircraft hazards
[AD-759824] 16 p1863 N73-25092
Retrevial of dispersive and convective transport phenomena in fluids using time domain analysis
[NASA-TN-D-7240] 19 p2255 N73-28178
Statistical correlations between maximum intensity of precipitation of different types and mean intensities for given precipitation
[NLL-M-23044-[5828.4F]] 21 p2567 N73-30574

**STATISTICAL DECISION THEORY**

Contradictions and inconsistencies in use of Bayesian approach for production of sampling theory point estimators
[AD-747325] 03 p0325 N73-12650
Statistical decision approach to missile payload discrimination
[AD-764723] 23 p2852 N73-32790

**STATISTICAL DISTRIBUTIONS**
NT PROBABILITY DISTRIBUTION FUNCTIONS

Analysis of deterministic and random flight data
01 p0056 N73-10455
Measurement of short pulse, X-band radar backscatter from rough water surfaces expressed as cumulative probability distribution functions
[AD-747949] 03 p0267 N73-12159
Minimum correlation theory for random numbers with same distribution, applied to negatively correlated random number generation
[NA-71-32] 03 p0324 N73-12644
Applicability of various laws of statistics of extremal values for approximating empirical distributions of maximum wind velocities
04 p0442 N73-13608
Algorithm for calculating distribution functions of meteorological parameters by computer technique
[AD-749588] 04 p0446 N73-13642
Theoretical statistical distribution model representing worldwide cloud cover
[NASA-TM-X-64714] 05 p0573 N73-14653
Analysis of stresses in compressor blades with emphasis on conditions in dove tail joints at base of blades
[AD-750497] 06 p0727 N73-15936
Virial theorem for analyzing structure of clusters in galaxies
08 p0959 N73-17840
Using statistical distribution of F 2 layer critical frequency deviations from sliding median for planning radio communication
13 p1520 N73-22319
Definition of equivalent peak level in objective speech level measurement
14 p1625 N73-23163
Analysis of Loran C signal processing techniques using hybrid simulation procedure
[AD-757586] 14 p1691 N73-23725

Analysis of statistical properties of filtered summed maximum length digital sequences
20 p2436 N73-29564
Spectral and statistical characteristics of surface wave velocity fields
20 p2446 N73-29654
Random distributions and position angle measurements of elliptical and spiral galaxies
20 p2469 N73-29833
Fiber distribution and orientation of aerodynamically spun nonwoven fabrics
24 p2907 N73-33196

**STATISTICAL MECHANICS**
Statistical mechanics of 2 and 3 dimensional plasmas in strong dc magnetic field
[NASA-CR-129177] 02 p0215 N73-11741
Statistical mechanics of negative temperatures of particles in motion
[NASA-CR-131572] 13 p1562 N73-22664
Statistical mechanics for relating material properties to their atomic and molecular structures
[AD-758257] 15 p1814 N73-24708
Statistical mechanics for plasma calculations
18 p2182 N73-27619
Application of statistical turbulence theory for validity determination of turbulence phenomenology
19 p2252 N73-28157

**STATISTICAL MOMENTS**
U DISTRIBUTION MOMENTS

**STATISTICAL PROBABILITY**
U PROBABILITY THEORY

**STATISTICAL TESTS**
Statistical and deterministic tests for failure analysis of sequential computer storage devices
05 p0517 N73-14203
Application of statistical methods for determination of dynamic system parameters influence on spectrum of natural frequencies
[AD-752695] 09 p1067 N73-18707
Sampling procedures for estimation of convex combination of proportions
[AD-754577] 11 p1312 N73-20644
Statistical tests for determining Colorado River Basin response to natural or induced changes
[PB-214114/1] 14 p1665 N73-23513
Analytical techniques for determining reliability growth of cyclic equipment
[AD-763341] 22 p2679 N73-31459
Bayesian reliability demonstration for statistical test development
[AD-765172] 24 p2945 N73-33520

**STATISTICAL WEATHER FORECASTING**
Statistical eigenfunctions used for analysis and prediction of sea level surges
04 p0443 N73-13611
Statistical characteristics of physical structure for various types of precipitation
[NLL-M-20844-[5828.4F]] 06 p0691 N73-15627
Variational optimization technique used as analysis scheme for application to high energy portion of hurricane
15 p1805 N73-24632
Global rain rate statistic model for coordination of radio relay and communication satellite service
18 p2212 N73-27857
Application of model output statistics to predict ceiling and visibility
[FAA-RD-73-14] 19 p2315 N73-28621
Statistical determination of temperature at mandatory pressure levels in Arctic region
[AD-761474] 19 p2316 N73-28627
Synopticostatistical, numerical, and laboratory procedures for studying dynamics of atmospheric circulation in planetary atmospheres including earth
[TT-70-50052] 20 p2442 N73-29615
Multiparameter method for forecasting monthly mean air temperature anomalies in U.S.S.R.
[NLL-M-23038-[5828.4F]] 21 p2567 N73-30577
Evaluation of procedure for three to ten day synoptic-hydrodynamic-statistical weather forecasting
22 p2692 N73-31567
Forecasting mean monthly air temperature anomalies for Oct. in northern part of European territory of USSR
22 p2693 N73-31575
Statistical weather forecasting using Gumbel theory noting application to atmospheric temperature long term effects
[MONO-89] 23 p2814 N73-32500

**STATOR BLADES**
Flow conditions around exit and downstream of stator blades with varying trailing-edge geometries and thicknesses
[NASA-TM-X-2659] 01 p0001 N73-10003
Cold air experiment in two-dimensional cascade to determine aerodynamic performance of turbine stator blade with suction-surface cooling
[NASA-TM-X-2685] 06 p0713 N73-15818
Flow characteristics of tandem bladed compressor stators at various inlet incidence angles
[NASA-TM-X-2734] 08 p0863 N73-16986
Experimental determination of effect of angle of rotation of stator blades on operation of small size turbine stage
[AD-754683] 11 p1335 N73-20834
Heat transfer between gas and turbine casing in intervane channels of stators and guide vanes
[NASA-TT-F-15051] 21 p2588 N73-30737
Measurement of flow parameters in midspan double-circular-arc section of stator in subsonic flow and comparison with computed performance
[NASA-TN-D-7425] 23 p2740 N73-31932

**STAYS**
U GUY WIRES

**STEADY FLOW**
NT COUETTE FLOW
Shock properties for steady, irrotational, transonic flow
[NASA-TN-D-6997] 01 p0040 N73-10314
Explicit difference method for steady two dimensional or axisymmetric hypersonic flow
[DGLR-PAPER-72-66] 04 p0405 N73-13303
Numerical analysis of nonlinear elliptic-hyperbolic mixing about wing profiles at Mach 1
14 p1597 N73-22944
Analysis of spoiler plate characteristics to eliminate effects of installation disturbance when conducting flow rate measurements
[NLL-NEL-TT-2439-[6075.461]]
15 p1763 N73-24288
Dynamic response of pipes with fluid flowing in steady and unsteady conditions
[MERL-TN-72-2] 20 p2387 N73-29178
Asymptotic expansion analysis of shock supported arrhenius reactions and ignition delay
24 p2903 N73-33172

**STEADY STATE**
Fast periodic steady state analysis of nonlinear large signal electronic circuits
[AD-745639] 01 p0034 N73-10271
Steady state response of semi-infinite solid with overlying semi-infinite fluid subjected to moving point load at supersonic speed
[AD-747252] 03 p0286 N73-12313
Transient and steady state response characteristics of sandwich-type wavelength selective bolometer
[AD-750264] 06 p0675 N73-15496
Solution for steady state motion of atmosphere about rotating earth
[AD-754248] 10 p1157 N73-19414
Derivation of phonetic representation by combining steady-state and transemic classification in automatic recognition of continuous speech
14 p1629 N73-23200
Steady-state response of interface to disturbance moving with constant velocity
16 p1886 N73-25267
Feasibility analysis and prediction performance of constant temperature heat pipe for space applications
[ESRO-CR[P]-246] 18 p2207 N73-27810

**STEADY STATE FLOW**
U EQUILIBRIUM FLOW

**STEAM**
Prandtl number values for water and steam, liquid and gaseous heavy water, and sea water
[ESDU-68011] 01 p0038 N73-10301
Dynamic viscosity data for water and steam, liquid and gaseous heavy water, and sea water
[ESDU-68009] 01 p0038 N73-10303
Influence of steam on fusion in electron beam welding
[DRIC-TRANS-2927] 03 p0307 N73-12505
Theoretical investigation of rocket steam generator with emphasis on trajectories and spectrum of injected drops and their vaporization for Europa 1 launch vehicle
[DLR-FB-71-36] 09 p1011 N73-18253
Triple wall tube exchanger/steam generator for sodium cooled fast breeder reactor
[BMBW-FBK-72-28] 22 p2699 N73-31619
Steam reactor system for manned spacecraft waste processing
[NASA-CR-134048] 23 p2752 N73-32021

**STEAM FLOW**
Computer calculations of two-phase flow transients in once-through steam generators
[CEA-CONF-2009] 06 p0655 N73-15318

**STEAM GENERATORS**
U BOILERS

**STEAM TURBINES**
Wet-steam tunnel facility design and program for future use
[PB-210654] 01 p0038 N73-10298
Computerized analysis of droplet size effect on erosion rate in wet steam turbine stage
[PB-211901] 05 p0527 N73-14292
High speed photographic system for moisture flow visualization in steam turbines
[NASA-TM-X-2763] 12 p1404 N73-21388

**STEEL STRUCTURES**
Shock tube generated blast loads on panels in steel structures
[REPT-1/72] 02 p0237 N73-11926
Firing tests to determine cratering produced by impact of flat ended, high density metal cylinders striking mild steel plate targets
[DREV-TN-2034/72] 06 p0726 N73-15927
Stress corrosion cracking of steel double cantilever beam specimens produced by loading sequence in aqueous environment
[AD-752215] 08 p0933 N73-17637
Fatigue tests with random loads using electrosteel test specimen
[ICAF-DOC-683] 22 p2724 N73-31801
Steel technology and water reactor pressure vessel safety
[ORNL-4855] 24 p2935 N73-33440

**STEELS**
NT AUSTENITIC STAINLESS STEELS
NT CARBON STEELS
NT CHROMIUM STEELS
NT FERRITIC STAINLESS STEELS
NT HIGH STRENGTH STEELS
NT MARAGING STEELS
NT MARTENSITIC STAINLESS STEELS
NT NICKEL STEELS
NT STAINLESS STEELS
Changes in brittle-ductile transition temperature of pressure vessel steel following neutron irradiation
[AD-745299] 01 p0067 N73-10552
Stress history effect on incubation time for stress corrosion crack growth in E-4340 HR steel
[AD-745308] 01 p0068 N73-10553
Fatigue tests of steel screw threads with large root radii under axial loading to determine fatigue strength and point of failure
[ESDU-67020-AMEND-A] 01 p0110 N73-10906
Hard alloy shaping tools for extruding steels and nonferrous materials
[NLL-NEL-TT-2400-[6075.461]]
02 p0177 N73-11435
Fatigue strength of tensile strained 45 and 40Kh steel
[NLL-SMRE-TRANS-5862-[8313.4]]
02 p0184 N73-11494
Subsequent yield curves for axial stressed-shear stressed surfaces of annealed SAE 1017 steel
[AD-746474] 02 p0188 N73-11523
Nonmetallic inclusion effects on crack growth rate in two alloy steels
[AD-746950] 02 p0189 N73-11530
Formation mechanism and strength of adhesive bond between polyvinyl acetate and steel
[NLL-RTS-7520] 02 p0190 N73-11543
Corrosion behavior of interstitial alloying elements in canning steels for sodium cooled fast breeder reactor
[NLL-RISLEY-TR-2444-[9091.9F]]
02 p0209 N73-11693
Fatigue tests on unnotched steel specimens during bending and axial loading
[ESDU-FAT-E.07.04] 02 p0236 N73-11924
X ray fluorescence analysis of manganese and trace elements in mild steels
[NPL-CHEM-16-PT-1] 03 p0264 N73-12140
Electric arc bonding of aluminum bronze onto clean steel surface
[AD-747768] 03 p0307 N73-12510
Irradiation effects on 17-7 PH stainless steel, 201 carbon steel, and titanium-aluminum-vanadium alloy
[NASA-TM-X-2678] 03 p0313 N73-12550
Development of steel smelting process using inert argon atmosphere for gas saturation and removal of impurities
[JPRS-57542] 03 p0313 N73-12553
Determination of oxygen, silicon, phosphorus, and copper in iron and steel by 14-MeV neutron activation analysis
[EURISOTOP-57] 03 p0313 N73-12556
Effect of mechanical-thermal pretreatments on time-to-rupture and creep strength of nickel-chromium steels
[KFK-1535] 03 p0313 N73-12557
Influence of chemical composition, non-metallic impurities, and production methods on physical properties of molten high alloy steels and special alloys
[AD-747394] 03 p0316 N73-12579
Corrosion fatigue behavior of 4340 steel above K sub Iscc in distilled water
[AD-747700] 03 p0317 N73-12584
Hydrogen embrittlement of cadmium coated steels due to paint stripping
[AD-747634] 03 p0319 N73-12599
Analysis of crack tip deformation in boron-aluminum sheet and laminar steel sheet resulting from crack propagation
[AD-747760] 03 p0322 N73-12623
Plastic-strain controlled failure criteria and design parameters
[COO-2048-4] 03 p0361 N73-12941
Antifriction interaction between metals and steels on polyamide surfaces
[NLL-RTS-7378] 04 p0425 N73-13461
Hot pressing of chromium carbide alloy matrice tools for cold drawing of pipes
04 p0432 N73-13522
Lowered ductility and crack initiation in neutron irradiated steels after tensile testing
[STU-70-419/U-350-A] 04 p0433 N73-13533
Physical and chemical properties of steel surfaces exposed to deoxidation products
[AD-747828] 04 p0435 N73-13547
Electrochemical analysis of cathodic hydrogen absorption by iron and steel
[BARC-585] 05 p0506 N73-14116

Results of ultrasonic inspection of cast steel cylinders
[TR-7208.594] 05 p0551 N73-14471

Effect of heat input and post-weld heat treatment on mild and low alloy steel submerged arc weld deposits
[CRANFIELD-MAT-8] 05 p0551 N73-14475

Research trends in steels with reduced nickel content for cryogenic applications
[NLL-TRANS-746-1266-[9022.401]] 05 p0561 N73-14556

Chemical and physiochemical properties of wear resistant steels
[AD-749601] 05 p0563 N73-14573

Effect of friction and external environment on fatigue strength of medium C steels
[AD-749749] 05 p0564 N73-14580

Diffusion coating and residual stress effects on steel product strength
[AD-749089] 05 p0566 N73-14600

Analysis of plastification effects in notched, impact-bending specimens of steel
[NLL-RISLEY-TR-2457-[9091.9F]] 05 p0601 N73-14887

Elastoplastic deformation of steel samples under cyclic loads during torsion tests
[AD-749768] 05 p0604 N73-14914

Crack formation during stress-relief annealing in heat-affected zones of weld seams in low-alloy steels
[NLL-RISLEY-TR-2507-[9091.9F]] 06 p0676 N73-15499

Copper brass bimetal cladding layers on steel strips for manufacturing elastic current conducting springs
[NLL-M-21498-[5828.4F]] 06 p0682 N73-15554

Data compiled in international comparative creep rupture program using two types of steel as test materials
[PB-211174] 06 p0685 N73-15578

Analysis of mild and low alloy steels by multichannel ARL 72000 X ray spectrometer
[PB-211170] 06 p0685 N73-15579

Microstructural analysis of 1010 modified steel and titanium alloy grains
[AD-748101] 06 p0686 N73-15584

Corrosion behavior of structural materials during condensation of alkylphenol with formalin and ammonia
[AD-751249] 07 p0753 N73-16119

Production of ball bearing steel ingots with emphasis on effects of temperature, surface defects, and casting methods
[AD-751252] 07 p0805 N73-16533

Solutions to problem of wear processes experienced by steel industry
[PB-211173] 07 p0809 N73-16565

Ductility as criterion of performance of quenched and tempered steel
[AD-751534] 07 p0810 N73-16568

Stress corrosion cracking of titanium alloys and steels - Part I
[AD-751544] 07 p0810 N73-16569

Determination of heat transfer and flow friction characteristics of fibrous metals for application to heat exchanger design
[AD-751633] 07 p0856 N73-16937

Crack growth characteristics of steel and structural failure of F-111 aircraft frame
[AD-752223] 08 p0868 N73-17024

Microwave gauge for measuring thickness of hot steel product during production
[PB-212210] 08 p0925 N73-17583

Measurement of fatigue crack propagation rates in heat treated steels
[PB-212208] 08 p0932 N73-17635

Direct current electrical resistance crack monitoring technique for detection of crack propagation in steels
[PB-212206] 08 p0933 N73-17636

Phenomenological criterion for uniaxial yield of ductile materials
[AD-752573] 08 p0952 N73-17795

Low cost arc welding technique for thick sections of HY-150 steels
[NASA-CR-120994] 09 p1039 N73-18472

Influence of microdoping with cerium on quality of fractures in structural steels
09 p1047 N73-18535

Comparison of fatigue strength of steel joints produced by friction welding and by electrocontact welding with fusion method
[AD-753488] 09 p1049 N73-18553

Compilation of fracture mechanics data on high strength aluminum alloys, alloy steels, stainless steels, and titanium alloys
[AD-753774] 09 p1049 N73-18554

Macroscopic and microscopic fracture criteria for steels
[AD-752446] 09 p1049 N73-18559

Simulation of ratcheting behavior of loaded structural components subjected to nonuniform thermal cycling
[AD-753686] 09 p1050 N73-18563

Temperature measurement of heavy nonferrous metals and alloys, steels, titanium, and other metals in plastic zone
[NLL-RTS-6867] 10 p1163 N73-19456

Ultrasonic inspection of steel gear parts
[REPT-7210.614] 10 p1164 N73-19466

Ultrasonic inspection of pressure vessel steel plates
[TR-7209.601-B] 10 p1164 N73-19469

Ultrasonic inspection of pressure vessel steels
[TR-7209.601] 10 p1164 N73-19470

Ultrasonic inspection and control of cast steel parts for use as machine gears
[TR-7210.617] 10 p1164 N73-19471

Ultrasonic inspection of cast steel blocks, steel plates, and welded seams
[TR-7210.607] 10 p1164 N73-19472

Standardization values for grinding forces and surface roughness in cylindrical grinding, noting steels
[CRIF-MC-46] 10 p1167 N73-19491

Fabrication and properties of prealloyed steel powders
[AD-753325] 10 p1167 N73-19497

Reports on electrical and mechanical properties of beryllium, chromium-manganese austenitic steels, and martensitic conversion during deformation
[JPRS-58357] 10 p1171 N73-19524

Effect of warm rolling on mechanical properties of unstable chromium-manganese austenitic steels
10 p1171 N73-19526

Interrelation of martensitic conversion during deformation and structural properties of trip steel
10 p1171 N73-19527

Effect of order of welding and heat treatment operations on mechanical properties of weld joints of N18K9M5T
10 p1171 N73-19529

Cyclic deformation diagrams of heat resistant and austenitic steels
10 p1219 N73-19914

Friction and wear measurements of CVM M-50 steel lubricated with three C-ether formulations
[NASA-TN-D-7254] 11 p1298 N73-20532

Quantitative analysis of hydrogen-induced slow crack growth in low alloy steel in gaseous hydrogen and distilled water environments
[NASA-TM-X-62253] 11 p1305 N73-20589

Reaction of nickel oxide with steel in argon and vacuum atmospheres
[AD-754776] 11 p1306 N73-20600

Effect of reverse abrasive friction exoelectron emission and steel corrosion
[AD-754666] 11 p1307 N73-20603

Shear instabilities and tensile fracture characteristics of cold worked 1080 pearlitic steel
[AD-755102] 11 p1307 N73-20604

Silicon additions and borax-glass coatings used to reduce surface hot shortness of copper-bearing steels
[PB-212660] 11 p1307 N73-20607

Gas phase hydrogen permeation through alpha iron, 4130 steels, and 304 stainless steels from less than 100 C to near 600 C
[NASA-TN-D-7265] 12 p1412 N73-21442

Effect of surface layer stress on plastic deformation and crack propagation of steel
[AD-755844] 12 p1415 N73-21467

Strength mechanism of stress wave emission in steel and aluminum alloys during tensile testing
[RFP-TRANS-104] 12 p1463 N73-21854

Determination of corrosion resistance of coatings on low alloy steel and susceptibility to exfoliation of 7178 aluminum alloy using Lawrence corrosion detection gauge
[AD-755163] 13 p1531 N73-22405

Aluminum alloy sheet bonding with steel sheets to form high strength composites
[TN-279] 13 p1533 N73-22421

Creation of discontinuities in high strength steels to evaluate effects on mechanical properties of welds
[AD-755524] 13 p1535 N73-22437

Structural recrystallization of steels during fast and slow heating to show structural succession caused by different mechanisms of formation of austenite
13 p1541 N73-22481

Analysis of alpha to gamma transformation in steel to determine effect of initial state nonequilibrium on starting temperature
13 p1541 N73-22482

Analysis of strain aging process in high carbon quenched steels caused by plastic deformation of martensite and migration of carbon to crystal defects in microstructure
13 p1541 N73-22484

Effect of deformation performed during heat treatment on structure and mechanical properties of E1437B alloy
13 p1541 N73-22485

Microstructure of recrystallized heat resistant steel
[JPRS-58840] 13 p1542 N73-22498

Thermal processing procedures for strain hardening TRIP steels
[AD-756953] 13 p1543 N73-22505

Cyclic transformation treatments on structural and mechanical properties of austenitic steels
[AD-756240] 13 p1543 N73-22506

Evaluating fatigue strength of steel with nonstationary loading
[AD-756945] 13 p1545 N73-22523

Notch sensitivity and static strength of laminated steels
[AD-756556] 13 p1545 N73-22524

Experimental method of measuring direction and residual stress in steel using surface displacements around indentations
[AD-756869] 13 p1546 N73-22526

Analysis of fatigue performance of titanium alloys and steels to identify variations based on shape parameter for reliability engineering of airframes
[AD-758219] 14 p1605 N73-23008

Ultrasonic inspection and control of laminated steel blocks prior to machining
[TR-7212.620] 14 p1670 N73-23550

Effect of residual impurity element on sensitivity of low alloy steels to radiation induced embrittlement
[AD-756625] 14 p1679 N73-23622

Effect of contact-surface-active vapors on wear behavior of soft steel during sliding friction
[NASA-TT-F-14935] 15 p1791 N73-24523

Analysis of effect of rigidity of stressed state in corrosion cracking under biaxial stress conditions for steel and titanium alloys
[NLL-LTI-746-1413-[9022.401]] 15 p1837 N73-24886

Chemical analysis of iron, steel, and nonmetallic materials
[PB-214230/5] 16 p1929 N73-25609

Irradiation strengthening and fracture embrittlement of A533-B steel and arc weldment metal
[HEDL-SA-323] 16 p1969 N73-25931

Probability distribution of yield strength for mild steel, and application of numerical techniques to mechanical vibration problems
[NASA-CR-132203] 17 p2043 N73-26527

Irradiation effects on fracture of heavy section pressure vessel steels
[HEDL-SA-497] 17 p2094 N73-26937

Fatigue life of reactor pressure vessel steels in high temperature aqueous environment
[CONF-721104-6] 17 p2094 N73-26938

Separation of short half life O-15 and N-13 isotopes from alkali metals, steels, copper, and indium by gamma activation analysis
[CONF-721069-24] 18 p2160 N73-27453

Chemical machining of steels, iron, nickel, cobalt, copper, and light alloys
18 p2161 N73-27454

Effects of mechanical and metallurgical factors on crack propagation and ductile fracturing resistance of steels
[PB-218919] 18 p2161 N73-27458

Bibliography of test equipment and procedures for determining physical and mechanical properties of iron and steel products
[PB-219047] 18 p2161 N73-27459

Accelerated test technique for determination of K ISCC in steels
[PB-217215/3] 18 p2161 N73-27460

Instability model for stress corrosion and fatigue crack propagation in 4340 steel
[AD-761148] 18 p2162 N73-27461

Effects of boundary surface active vapors on behavior of steel during sliding friction
[NASA-TT-F-14993] 19 p2304 N73-28531

Dynamic and rotary machinery, design and reliability
[AD-762440] 19 p2305 N73-28542

Design of dynamic and rotary machines - Vol. 2
[AD-762441] 19 p2306 N73-28543

Pressure shaping of steels and alloys
[AD-762308] 19 p2306 N73-28549

Numerical analysis of fatigue strength of steel specimens under symmetric loading cycles
[AD-761469] 19 p2310 N73-28581

Thermodynamics of phase changes occurring in heat treatment of carbon and alloy steels
[AD-762361] 19 p2311 N73-28589

Crack arresting in single edge notch A533 B steel at room temperature
[HSSTP-TR-27] 19 p2349 N73-28892

Analysis of physical and mechanical properties of nonmagnetic steels and suitability for producing tubes and forgings
[NLL-M-21647-[5828.4F]] 20 p2422 N73-29451

Ultrasonic inspection and examination of large size cast steel ring prior to machining
[TR-7212.624] 20 p2422 N73-29456

Ultrasonic inspection and control for laminated steel disc
[TR-73-2-640] 20 p2423 N73-29461

Deformation of dry steel surfaces during high velocity sliding contact
20 p2427 N73-29496

Development of procedures for determining molybdenum in iron and steel with emphasis on factors affecting stability and temperature dependence
[TN-303] 20 p2431 N73-29529

Flourescent X ray spectrography of low alloy steel specimens to determine presence of eight elements
[BM-RI-7773] 20 p2433 N73-29539

Temperature characterization of below K sub Iscc corrosion fatigue behavior of HY-130 steel
20 p2477 N73-29899

Fatigue life and inelastic strain response under complex histories for alloy steel
20 p2478 N73-29900
Friction and lubrication in steel wire drawing
[NLL-RTS-7851] 21 p2552 N73-30454
Effect of internal weld defects on fatigue behavior in mild structural steel butt welded connections
[PB-220896/5] 21 p2554 N73-30475
Microstructural determination of bonding strength of steel bimetal produced by pressure working
[NLL-M-21699-[5828.4F]] 21 p2557 N73-30499
Effect of O2-H2 atmosphere, H2, Ar, and room air on fatigue crack propagation in 4340 steel
[COO-3166-4] 21 p2559 N73-30513
Fusion welding of aluminum to steels
[AD-764322] 22 p2678 N73-31454
Use of nickel steels for cryogenic tanks
[AD-763947] 22 p2679 N73-31457
Argon-arc welding of aluminum and aluminum alloys to steels
[AD-763948] 22 p2679 N73-31458
Embrittlement and cracking of steels
[CEA-BIB-204] 22 p2685 N73-31506
Linear and nonlinear theory of elasticity used to determine deformation of cylinder and piston of high strength steel under influence of high pressure
[AD-763971] 22 p2687 N73-31519
Thermal embrittlement of 4340 steels at high temperatures
[AD-763900] 22 p2687 N73-31521
Acoustic emission from aqueous stress corrosion cracking in various tempers of steel
[AD-764048] 22 p2687 N73-31522
Recrystallization and aging studies of steels
[PB-221302/3] 22 p2687 N73-31526
Method of testing materials based on teflon and Kel-F for friction at low temperatures by using X18H9T steel in helium medium for different slip rates and loads
22 p2688 N73-31531
Stress corrosion cracking of steels in liquid ammonia environments
24 p2932 N73-33420
Wear testing of Zircaloy 2 on Zircaloy 2 and of Zircaloy 2 on steel considering debris generation
[DUN-8075] 24 p2935 N73-33441

**STEEP GRADIENT AIRCRAFT**
U V/STOL AIRCRAFT

**STEEPEST ASCENT METHOD**
U STEEPEST DESCENT METHOD

**STEEPEST DESCENT METHOD**
DOPEX-1D2C steepest descent and one-dimensional two constraint radiation shield optimization code
[NASA-TM-X-2836] 18 p2177 N73-27579
Method of steepest descents used in analysis of traveling wave instabilities
[AD-763091] 20 p2378 N73-29108

**STEERABLE ANTENNAS**
Systems analysis for determining cause of steerable antenna oscillations during Apollo 14 and 15 missions
[NASA-TM-X-68901] 05 p0519 N73-14218
Application of digital techniques for control of large antennas used for satellite tracking
[NASA-TM-X-66154] 07 p0754 N73-16127
Design of airborne electronically steerable phased array system
[NASA-CR-124041] 09 p1007 N73-18219
Phase shift variations of platinotron microwave amplifier oscillator for pulse radar and steerable antennas
[DLR-MITT-73-03] 12 p1379 N73-21187
Amplitude steered antenna array approximating performance of electronically steered phased array
[NASA-CASE-GSC-11446-1] 23 p2764 N73-32117

**STELLAR ATMOSPHERES**
NT CHROMOSPHERE
NT SOLAR ATMOSPHERE
Phase variation and hydrostatic atmospheric models for eta Aquilae
[NASA-TT-F-14717] 02 p0229 N73-11857
Conference on stellar chromospheres and their compositions
[NASA-SP-317] 04 p0465 N73-13792
Line spectra analysis for temperature distribution in stellar atmosphere
04 p0466 N73-13793
Radiative equilibrium and empirical models for stellar chromospheres
04 p0466 N73-13794
Ground based line spectra analyses for determining stellar chromospheres
04 p0466 N73-13795
Spaceborne ultraviolet emission lines in stellar sources as chromospheric indicators
04 p0466 N73-13796
Solar atmospheric heating model for mechanical heating in stellar chromospheres
04 p0466 N73-13797
Summary of physical and theoretical work on stellar chromospheres
04 p0466 N73-13800
Deviations in local thermodynamic equilibrium in stellar atmospheres
[NASA-CR-130792] 09 p1082 N73-18829
Rotating atmospheric model for Altair
17 p2081 N73-26833
Application of line-blanketed model stellar atmospheres to Sirius
19 p2342 N73-28837
Structure and physics of solar and stellar atmosphere including physical processes in nonstationary stars
[NASA-TT-F-760] 20 p2470 N73-29840
Boundary between open and closed magnetospheres of pulsar atmosphere
[AD-761883] 21 p2598 N73-30822
Far ultraviolet photometry of peculiar B and A stars by OAO 2
22 p2734 N73-31883

**STELLAR DOPPLER SHIFT**
U DOPPLER EFFECT
U EXTRATERRESTRIAL RADIATION

**STELLAR EVOLUTION**
Stellar evolution and atmospheric turbulence dynamics for chromospheric activity model
04 p0466 N73-13799
Origin and evolution of stars, stellar matter, and galaxies
[AD-749734] 06 p0720 N73-15875
Evolutionary sequences for high-mass stars from zero-age main sequence to end of core helium burning, computed with Ledoux criterion for convective instability
[NASA-TM-X-68914] 07 p0841 N73-16814
Evolution of stars with suppressed core convection
[NASA-TM-X-68944] 08 p0959 N73-17846
Computer programs for differential curve of growth analysis of solar type stars
[BULL-171] 08 p0960 N73-17848
Research projects for ground-based and space-based astronomy to show present capabilities and future potential
[PB-212965] 12 p1458 N73-21819
Asymptotic branch evolution of globular cluster star of low mass
16 p1960 N73-25856
Evolution and sturcture of HII regions
20 p2470 N73-29837
Theoretical evolution of extremely metal poor stars
20 p2470 N73-29839
Theory of toroidal stages in stellar evolution
20 p2470 N73-29841

**STELLAR FIELDS**
U STAR DISTRIBUTION

**STELLAR GRAVITATION**
Analysis of post-Newtonian effects on instability of white dwarf stars, neutron stars, and supermassive stars
[NASA-CR-129241] 03 p0355 N73-12893
Approximate analytic and numerical methods for describing encounter of star with sun-comet system and resulting gravitational perturbations of cometary orbits
07 p0840 N73-16805
Preferred frame effects on stellar stability
[NASA-CR-135517] 22 p2717 N73-31754

**STELLAR INERTIAL NAVIGATION**
U CELESTIAL NAVIGATION
U INERTIAL NAVIGATION

**STELLAR LUMINOSITY**
Development of photoelectric and photographic standards for Magellanic clouds and analysis of differences in stellar population of regions
02 p0227 N73-11832
Luminosity, mass, and elemental abundances of line-blanketed model stellar atmospheres
[NASA-CR-129670] 04 p0469 N73-13825
Investigation of stellar density distribution and luminosity function in high galactic altitudes using Schmidt telescopes
07 p0846 N73-16857
Mass-luminosity relationship of binary stars in Hyades cluster
[ROY-OBS-BULL-175] 13 p1578 N73-22788
Brightness changes in WZ Cas in photographic and visible light
20 p2471 N73-29844
Brightness changes of MZ Cas and TZ Cas in B- and V-light
20 p2471 N73-29845
Electrophotometry, photoelectronic images, converters, and television equipment for studying variable stars
[NASA-TT-F-797] 21 p2594 N73-30783
Argelander, Pickering, and Neyland-Blazhko methods for visually estimating variable star brightness
21 p2594 N73-30785
Determination of magnitude and brightness of variable stars by photographic photometry
21 p2594 N73-30786
Photoelectronic devices for amplifying brightness image of variable stars
21 p2594 N73-30788
Digital computer techniques for determining changes in brightness periods of variable stars
21 p2595 N73-30792
Surface brightness of reflection nebulae
24 p2978 N73-33796

**STELLAR MAGNETIC FIELDS**
NT SOLAR MAGNETIC FIELD
Radiative processes in intense magnetic fields of white dwarfs and neutron stars
16 p1961 N73-25861

**STELLAR MASS**
NT STELLAR GRAVITATION
Analysis of post-Newtonian effects on instability of white dwarf stars, neutron stars, and supermassive stars
[NASA-CR-129241] 03 p0355 N73-12893
Mass-luminosity relationship of binary stars in Hyades cluster
[ROY-OBS-BULL-175] 13 p1578 N73-22788

**STELLAR MASS EJECTION**
Nuclear reactions in hydrogen exhausted zone of star during supernova explosion and nuclei syntheses through nitrogen conversion
13 p1575 N73-22762
Mechanisms by which stars radiate excess infrared energy, and correlation between rapid mass loss and infrared excesses in stars
13 p1575 N73-22766
Asymptotic branch evolution of globular cluster star of low mass
16 p1960 N73-25856
Proton spallation of neon and lithium production in stellar flares
22 p2701 N73-31631
Hydrodynamic model for stellar mass ejection and planetary nebula formation
22 p2734 N73-31885

**STELLAR MOTIONS**
NT STELLAR ROTATION
Astrometry for determination of absolute positions of stars and their relative motions from Schmidt plates noting accuracy
07 p0845 N73-16843
Catalog of proper motion for 691 stars of Southern Hemisphere
11 p1338 N73-20861
Dynamics of axisymmetric stellar systems applied to collapse and violent relaxation of rotating stellar systems
24 p2977 N73-33792

**STELLAR OCCULTATION**
Calculation of all occultations by planet Jupiter of stars brighter than magnitude 6.55 for period 1951 to 2000
[NASA-TT-F-14626] 01 p0104 N73-10862
Visual and photographic observations of Beta Scorpii occultation by Jupiter
[NASA-CR-129990] 05 p0594 N73-14832
Tables on occulation of stars by moon
[PUBL-28] 17 p2081 N73-26835
Observations of lunar behavior in stellar occulation
[PUBL-25] 17 p2081 N73-26836

**STELLAR RADIATION**
Gravitationally red-shifted positron annihilation radiation produced at surfaces of old neutron stars
[NASA-TM-X-66062] 01 p0100 N73-10818
Evaluation of ultraviolet flux from stars used as inertial-hold pointing directions during Apollo 17 flight
[NASA-CR-128834] 10 p1213 N73-19866
OSO-I graphite crystal polarimeter for stellar X ray astronomy
17 p2084 N73-26862
Catalog of ultraviolet stellar observations using celescope on OAO 2
[NASA-CR-133259] 17 p2088 N73-26889
Possible origin of soft gamma ray bursts from stellar superflares
[NASA-TM-X-66294] 18 p2197 N73-27735
Computational method for obtaining models for fast and differentially rotating upper main sequence stars in radiative equilibrium
20 p2470 N73-29838
Properties of optical radiation of variables and quasers
20 p2471 N73-29847
Star electrophotometer for operation in photon-counting regime
20 p2471 N73-29849

**STELLAR REFRACTION**
U ATMOSPHERIC REFRACTION
U STELLAR RADIATION

**STELLAR ROTATION**
NT SOLAR ROTATION
Rotating atmospheric model for Altair
17 p2081 N73-26833
Analysis of rotational velocities in close visual binary stars
19 p2341 N73-28833
Computational method for obtaining models for fast and differentially rotating upper main sequence stars in radiative equilibrium
20 p2470 N73-29838
Dynamics of axisymmetric stellar systems applied to collapse and violent relaxation of rotating stellar systems
24 p2977 N73-33792

**STELLAR SPECTRA**
NT SOLAR SPECTRA

High dispersion Coude spectrograms of zeta Oph and Per, and molecular absorption in interstellar medium
[NASA-TM-X-66073] 02 p0224 N73-11812
OAO-A2 observations of Be stars, continuous Balmer emission, and interstellar polarization
[NASA-CR-129166] 02 p0226 N73-11828
Chilean astronomical observations of early star spectra, southern star radial velocities, and minor planet positions
05 p0594 N73-14828
Computer programs for curve-of-growth analysis using dimensions of stellar lines as input
[ROY-OBS-BULL-171] 06 p0644 N73-15230
Extended two color photometry of faint stars by telescope with objective grating
[BULL-172] 07 p0842 N73-16819
Pros and cons of objective prisms in astronomical spectroscopy noting work in conjunction with Schmidt telescopes and novel techniques
07 p0845 N73-16846
Identification of infrared stars using Schmidt telescopes, infrared photometry, and slit spectra
07 p0846 N73-16855
Schmidt telescopes for compilation of stellar spectra and novae maps, galactic structure, and radial velocities
07 p0846 N73-16856
Star simulator photometric calibration based on Vega spectrum
[RAE-TR-72138] 14 p1646 N73-23346
High frequency observations and theoretical interpretation of recombination line emission in direction of supernova remnant 3
[AD-756085] 15 p1833 N73-24858
OSO-1 Bragg crystal spectrometer for solar and stellar X ray source analysis
17 p2084 N73-26863
Multicolor photometric systems for studying physical properties and spectra of variable stars
21 p2594 N73-30790
Line strengths in spectra of seven double-lined Am binary stars
[ROY-OBS-BULL-177] 21 p2598 N73-30819
Blue to violet intensity distributions in S, C-S, and C stars
23 p2837 N73-32666

**STELLAR SPECTROPHOTOMETRY**
Transformations for converting b-y color excesses for Cepheids into B-V excesses
[NASA-TM-X-66061] 01 p0103 N73-10854
Use of objective grating for extension of magnitudes and colors beyond those available photoelectrically
[ROY-OBS-BULL-172] 06 p0674 N73-15486
Photographic magnetudes of T Tauri and normal stars in Orion I
06 p0716 N73-15846
Photographic V and R magnitudes of 130 T Tauri and H alpha emission stars in Orion I
06 p0716 N73-15847
Objective prism survey of entire southern sky within 10th to 13th photographic magnitude range by Schmidt telescope equipped with ultraviolet prism
06 p0717 N73-15851
Stellar spectrograms from Salyut space station of alpha Lyrae and beta Centauri
[NASA-TT-F-14582] 07 p0843 N73-16831
Laser illumination for stellar interferometry
[AD-752902] 09 p1068 N73-18712
Near infrared spectrophotometry of cool stars in galactic anticenter
16 p1960 N73-25852
Atlas S183 experiment for ultraviolet stellar spectrophotometry onboard Skylab manned space station
17 p2033 N73-26454
Report of the Astronomer Royal for Scotland for the year ending 31 March 1973
22 p2718 N73-31760

**STELLAR STRUCTURE**
Evolution of stars with suppressed core convection
[NASA-TM-X-68944] 08 p0959 N73-17846
Optical rotating intensity modulator for measuring positions and magnitudes of stars
10 p1211 N73-19848
Tables on structure of interstellar masers and quasars
14 p1704 N73-23826
Interstellar molecular hydrogen lines in ultraviolet spectrum of delta Scorpii
22 p2734 N73-31886

**STELLARATORS**
Density fluctuations of stellarator by correlation procedure
[AEC-TR-7376] 11 p1267 N73-20282
Transient behavior of currents and forces in coil system of stellarator during operational disturbances
[NASA-TT-F-15014] 18 p2126 N73-27182
Numerical analysis of transient currents and forces in toroidal coils for stellarators and effects of sudden disturbance of normal operation
[NASA-TT-F-15013] 18 p2179 N73-27595
Particle insertion and hot plasma containment in stellarator with superconductors
[NASA-TT-F-15111] 22 p2703 N73-31648

**STEP FAULTS**
U GEOLOGICAL FAULTS

**STEPPES**
Interpretation of space photographs of dry piedmont steppe region for hydrologic mapping
[NASA-TT-F-14974] 20 p2411 N73-29382

**STEPS**
Supersonic laminar flow reattachment and redevelopment behind two-dimensional rearward facing step
[AD-753358] 09 p1018 N73-18306
Theoretical analysis of flow recompression, reattachment, and redevelopment associated with supersonic laminar flow past rearward facing step
20 p2385 N73-29162

**STEREOGRAPHY**
U STEREOPHOTOGRAPHY

**STEREOPHOTOGRAPHY**
Performance accuracy of precision stereoplotter for aerotriangulation with independent models
02 p0165 N73-11339
Stereoradiography study of depth and geometrical dimensions of internal flaws in weldments
[AD-749459] 04 p0428 N73-13486
Spurious image and color rendition problems in producing multicolor holograms
[AD-751560] 07 p0801 N73-16508
Optical reconstruction applied to holograms recorded at microwave, acoustic, or other suboptical frequencies producing longitudinally distorted image
[AD-751408] 07 p0801 N73-16509
Safety procedures for using pulsed lasers and making pulsed holograms
[AD-751024] 07 p0808 N73-16555
Analysis of internal precisions and external accuracies of various stereometric systems consisting of single stereometric camera
12 p1404 N73-21384
Photogrammetric plotting system for graphical and digital plotting of stereopairs
[MBB-UR-150-72-O] 17 p2034 N73-26458
Coherent laser light measurement of ceramic material surface roughness
[AD-761198] 18 p2168 N73-27512
Cartographic mapping of Martian surface by Mariner 9 digital picture data evaluation
23 p2843 N73-32723

**STEREOSCOPIC PHOTOGRAPHY**
U STEREOPHOTOGRAPHY

**STEREOSCOPIC VISION**
Vision model for robot object recognition system
[NASA-CR-133458] 19 p2224 N73-27936
Factors affecting stereoscopic vision and depth perception in human beings
[AD-759261] 20 p2369 N73-29050

**STEREOSCOPY**
NT STEREOPHOTOGRAPHY
Acoustic holographic signals for designing underground geological viewing system
[AD-746498] 02 p0184 N73-11490
Development of map storage and display system using volume holography using iron-doped lithium niobate
[AD-748002] 03 p0311 N73-12541

**STERILIZATION**
NT SPACECRAFT STERILIZATION
Analysis of resistance of cultured and natural microbes in ethylene oxide sterilization method
[NASA-TT-F-14612] 04 p0379 N73-13078
Radiation sterilization with Van de Graaff accelerators
[NASA-TT-F-14821] 11 p1247 N73-20120
Environmentally controlled suit for working in sterile chamber
[NASA-CASE-LAR-10076-1] 11 p1249 N73-20137
Development of germ-free plants and tissues
[NASA-CR-128947] 15 p1742 N73-24122
Thermoradiation sterilization of naturally occurring microorganisms in soil from Kennedy Space Center
[NASA-CR-132197] 16 p1904 N73-25404
Protein sterilization of firefly luciferase without denaturation
[NASA-CASE-GSC-10225-1] 18 p2113 N73-27086

**STERILIZATION EFFECTS**
NT CHEMICAL EFFECTS
NT CORROSION
NT DECONTAMINATION
NT DEGRADATION
NT THERMAL DEGRADATION
Sorption and desorption of ethylene oxide and methyl bromide gases on polymeric materials during sterilization
03 p0257 N73-12082

**STERNS**
U AFTERBODIES

**STEROIDS**
NT ALDOSTERONE
NT CHOLESTEROL
NT CORTICOSTEROIDS
Statistical analysis of steroid levels in parotid secretions of humans under prolonged mental stress
[AD-747682] 04 p0381 N73-13104
Gas chromatography-mass spectrometry for analyzing fatty acid and sterol concentrations in plant tissue samples
[NASA-CR-128740] 10 p1120 N73-19131

**STIFF STRUCTURES**
U RIGID STRUCTURES

**STIFFENING**
Effect of arrangement of stiffening ribs for cylindrical shell on critical load value
[AD-758029] 15 p1840 N73-24912
Analysis of dynamics of stiffened plates using finite element modelling of flat and curved stiffened panels
20 p2479 N73-29911

**STIFFNESS**
Cataloging elastomer stiffness and damping properties in terms of viscoelastic model constants
[NASA-CR-120965] 01 p0113 N73-10931
Transverse shear stiffnesses of sandwich panels with corrugated core and equal face plates
[ESDU-07.03.01] 06 p0723 N73-15903
Stiffness of flat strips in compression under sinusoidally distributed bending couples at their edges
[ESDU-02.01.30-AMEND-A] 06 p0723 N73-15905
Elastic properties of thin walled U beam lateral stiffness under flexing torsional stresses
[ISD-130] 09 p1095 N73-18939
Transverse tension strength and stiffness of unidirectional carbon fiber reinforced plastic
[RAE-TR-72129] 12 p1416 N73-21477
Design of despin mechanism noting angular stiffness, stress analysis, signal transmission, power transmission, instrumentation and ground support equipment
[ESRO-CR[P]-228] 13 p1535 N73-22434
Stiffness of flat strips in compression under sinusiodally distributed bending couples at their edges
[ESDU-05.01.30-AMEND-A] 14 p1714 N73-23906
Wind tunnel measurements of direct pitching damping and stiffness derivatives for delta wing and swept wing planforms
[ARC-R/M-3419] 16 p1853 N73-25009
Conjugate basis functions and consistent stresses for finite element stiffness method
[AD-758675] 16 p1972 N73-25948

**STILBENE**
Spectrometer for fast neutrons using proton recoil in stilbene crystal
[BMVG-FBWT-72-4] 09 p1036 N73-18456

**STILLS**
Solar still greenhouse for using desalinated water to produce vegetables in arid regions
24 p2975 N73-33769

**STIMULANT**
NT ATROPINE
NT CENTRAL NERVOUS SYSTEM STIMULANTS
Stimulating and tranquilizing drug effects on human performance indices
13 p1483 N73-22021

**STIMULATED EMISSION DEVICES**
NT ARGON LASERS
NT CARBON DIOXIDE LASERS
NT CARBON MONOXIDE LASERS
NT CHEMICAL LASERS
NT GALLIUM ARSENIDE LASERS
NT GAS LASERS
NT GAS MASERS
NT HCN LASERS
NT HELIUM-NEON LASERS
NT INFRARED LASERS
NT INJECTION LASERS
NT LASERS
NT LIQUID LASERS
NT MASERS
NT ORGANIC LASERS
NT PULSED LASERS
NT Q SWITCHED LASERS
NT RAMAN LASERS
NT RING LASERS
NT RUBY LASERS
NT SEMICONDUCTOR LASERS
NT SOLID STATE LASERS
NT TRAVELING WAVE MASERS
Laser technology and utilization
[NASA-TT-F-14871] 11 p1302 N73-20568

**STIMULATION**
NT AUDITORY STIMULI
NT SENSORY STIMULATION

**STIMULI**
Mathematical models for studying vestibuli adaptation to stimuli in humans
[AMRU-R-70-1] 02 p0131 N73-11062
Human attention and reaction performance as function of type and latency in response to signal stimulus
[AD-747801] 04 p0382 N73-13110
Sound, light, and proprioceptive stimuli for inhibiting vestibular illusion in man
10 p1115 N73-19087
Accuracy of method of constant stimuli for studying sensory capabilities of man in relation to display systems
[AD-753009] 10 p1121 N73-19141

**STIRLING CYCLE**
Structural analysis of mechanical rhombic drives for machines operating on Stirling cycle
[AD-761594] 19 p2330 N73-28749

**STIRRING**
Platinum-rhodium device for stirring viscous fluids
[NBS-TN-771] 13 p1532 N73-22418

**STOCHASTIC PROCESSES**
NT MARKOV CHAINS
NT MARKOV PROCESSES
NT RANDOM PROCESSES
NT RANDOM WALK
Markov chain model for classifying stochastic automation
02 p0195 N73-11579
Application of stochastic inverse theory for solutions to linear system of integral equations representing reduced gross earth data
02 p0201 N73-11621
Stochastic solutions of conservative dynamic systems such as particle accelerators and storage rings [LAAS-PUBL-935] 02 p0203 N73-11640
Antithetic sampling for variance reduction in stochastic system simulation [NA-72-57] 03 p0325 N73-12647
Maximum likelihood fit of straight line to pairs of seismological magnitudes having variations and measurement errors [FOA-4-C-4474-A1] 04 p0440 N73-13588
Extreme values of irregularity factor of bandpass filters for realizing steady Gauss processes with one-peak power density spectrum [LBF-TM-64/72] 05 p0523 N73-14250
Optimization of stochastic systems including introduction to self adaptive systems
05 p0569 N73-14618
Existing stochastic models of galactic magnetic field [NASA-CR-130158] 08 p0959 N73-17847
Conditions necessary to insure stationarity in solution process for stochastic differential equations [NASA-CR-130779] 09 p1056 N73-18606
One dimensional search directions from sequential Monte Carlo optimization of unconstrained stochastic systems [AD-754413] 11 p1312 N73-20649
Averaging time and maxima for dependent observations [AD-754788] 11 p1315 N73-20674
Optimal control and measurement techniques of decentralization for stochastic linear dynamic systems [AD-754984] 12 p1419 N73-21501
Statistical models for smoothing environmental economics and communications data
13 p1549 N73-22554
Step adaptation algorithms and application of stochastic graphs for analysis of discrete automatic systems
14 p1644 N73-23332
Effectiveness of controllers for dynamic systems modeled by ordinary differential equations [NASA-CR-132054] 15 p1759 N73-24259
Analysis of improved numerical solutions to stochastic collection equation for cloud droplets
15 p1805 N73-24629
Mathematical models for stochastic feedback processes in optimal adaptive control systems [AD-757900] 16 p1935 N73-25655
Structure identification of multivariable stochastic systems [TR-31] 17 p2054 N73-26614
Survey of articles dealing with stochastic approximation [AD-761766] 19 p2314 N73-28613
Stochastic control theory for homing guidance laws for tactical missiles [AD-761626] 19 p2347 N73-28876
Time optimal control in stochastic dynamic systems
20 p2436 N73-29565
Aerospace applications of stochastic continuous-time nonlinear programming [AD-763805] 21 p2515 N73-30178
Decentralized control of stochastic large scale systems [NASA-CR-133857] 21 p2519 N73-30207
Development of nonlinear stochastic equations for turbulent field with application to simple electron plasma [AD-763438] 21 p2584 N73-30710
Stochastic optimal controller for n-body spacecraft [NASA-CR-133788] 21 p2600 N73-30839
Stochastic and deterministic approaches to vegetation canopy reflectance models [AD-763222] 22 p2668 N73-31381
Power spectral density estimation by spline smoothing ergodic stochastic process [NASA-CR-133986] 22 p2691 N73-31552
**STOICHIOMETRY**
Intrinsic and extrinsic nonstoichiometry in lead zirconate titanate system [LBL-880] 10 p1126 N73-19172
Thermodynamic analysis of nonstoichiometric cerium dioxide in temperature range from 700 to 1500 C and reduced atmospheric pressure conditions [COO-1441-18] 10 p1175 N73-19560
Synthesis of stoichiometric crystals of InP doped with impurities for obtaining semiconductor with desired resistance [NLL-RRE-TRANS-381-[8036.625]]
11 p1329 N73-20790
Electrical conductivity of sintered nonstoichiometric CeO[2-x] as function of temperature [COO-1441-17] 12 p1416 N73-21474
High temperature tests to determine thermodynamic properties of nonstoichiometric vanadium nitrides [NLL-M-21551-[5828.4F]] 12 p1464 N73-21858
Stoichiometric gas turbines using hot cascades, aerodynamic cascades, and combustor rigs [EDR-7460] 21 p2589 N73-30746
**STOKES FLOW**
Ground and flight test program of Stokes flow parachute [NASA-CR-112251] 10 p1106 N73-19016
Two-phase flow of two immiscible fluids considered for motion in diverging channel [AD-756341] 13 p1513 N73-22259
**STOKES THEOREM [VECTOR CALCULUS]**
Stokes parameters for calculating polarization of radio waves reflected from inhomogeneous ionosphere [NASA-TT-F-14676] 09 p1002 N73-18174
Determination of polarization characteristics of large Pulkovo radio telescope by use of Stokes parameters
23 p2838 N73-32677
Monte Carlo technique using Stokes vectors of Lyman alpha radiation
24 p2975 N73-33774
**STOL AIRCRAFT**
U SHORT TAKEOFF AIRCRAFT
**STOMACH**
Hypoxia effects on human gastric motor functions in pressure chamber experiments using electrogastrography
03 p0257 N73-12085
Stomach shielding effects on chromosomal aberration frequency in guinea pig and rat marrow cells after gamma radiation at doses of 50 to 200 r
11 p1241 N73-20074
**STONES [ROCKS]**
U ROCKS
**STONY METEORITES**
NT BRUDERHEIM METEORITE
NT CARBONACEOUS METEORITES
NT CHONDRITES
NT TEKTITES
NT TUNGUSK METEORITE
**STOPPING**
Improved indication of stops, using transposer as lip reading aid
14 p1626 N73-23180
**STOPPING POWER**
Geometric codes for calculating space radiation transport in shielding configurations [NASA-CR-124403] 23 p2821 N73-32551
**STORABLE PROPELLANTS**
NT AIRCRAFT FUELS
Prelaunch mission operations for space storable propellant module for retro propulsion on unmanned outer planet orbiters [NASA-CR-129521] 03 p0358 N73-12915
Analysis of earth storable bimodal engine using earth storable propellants and operating in either monopropellant or bipropellant mode [BELL-8706-933005] 20 p2466 N73-29811
Regeneratively cooled rocket engine tests with space storable propellants [NASA-CR-133915] 22 p2708 N73-31688
**STORAGE BATTERIES**
NT NICKEL CADMIUM BATTERIES
NT NICKEL ZINC BATTERIES
NT SILVER CADMIUM BATTERIES
NT SILVER ZINC BATTERIES
Performance of lithium battery with inorganic electrolyte [AD-746633] 02 p0129 N73-11052
Improved electrochemical storage batteries for spacecraft [NASA-TM-X-66129] 04 p0375 N73-13049
Nickel cadmium storage battery for portable power supply of man-pack equipment [AD-748454] 04 p0376 N73-13055
Design and performance of rechargeable zinc-air batteries [AD-748455] 04 p0376 N73-13058
Design and performance of mechanically rechargeable zinc air battery [AD-749779] 06 p0627 N73-15086
Formulation of stress strain model for storage batteries [AD-752257] 08 p0870 N73-17045
Design and tests of mechanically rechargable zinc air batteries [AD-753361] 09 p0991 N73-18091
High charge and discharge rate lead/acid battery for hybrid heat-engine/electric vehicle [PB-213257] 13 p1477 N73-21969
Evaluation of semiconductive metal halides as cathode material for high energy-density batteries [AD-757883] 15 p1739 N73-24094
Design, development, and evaluation of zinc-oxygen battery with mechanically rechargeable feature [AD-762573] 20 p2364 N73-29012
**STORAGE RINGS [PARTICLE ACCELERATORS]**
Stochastic solutions of conservative dynamic systems such as particle accelerators and storage rings [LAAS-PUBL-935] 02 p0203 N73-11640
Cost estimates and design of electron synchrotron injector for high energy rings [DNPL/R-13] 04 p0401 N73-13268
Metallic surface effects on radiative stability and focusing effects of electron ring [JINR-P9-6318] 04 p0452 N73-13692
Accelerated electron ring focusing by image forces in conducting cylindrical screen [JINR-P9-6421] 05 p0580 N73-14724
Analysis of single electron bunch transfer tolerance for intersecting storage accelerators [BNL-17275] 10 p1194 N73-19711
Alignment and field distribution of coil currents in storage accelerators using superconducting magnets [BNL-17272] 10 p1194 N73-19712
Collective method for developing charged ion accelerator [AD-754624] 11 p1268 N73-20293
Design of warm vacuum system for superconducting storage rings [BNL-17239] 12 p1440 N73-21670
Organization and management of CERN/ISR project
15 p1847 N73-24969
Production and confinement of hot plasma and electron thermalization in superconducting ring device [UCRL-74337] 16 p1950 N73-25777
**STORAGE STABILITY**
Carbonyl formation data at elevated temperatures for estimating storage life of unstabilized polyolefins [AD-748827] 04 p0438 N73-13572
Long-term storability and decomposition kinetics of monopropellant formulations containing hydrazine, hydrazine azide, and ammonia [AD-750900] 06 p0711 N73-15806
Storage instability of hydrocyanic acid mixed with stabilizing agents - Part 3 [NASA-TT-F-14652] 09 p0998 N73-18147
HF cell performance over different operating conditions after storage [SC-CR-72-3156] 12 p1366 N73-21085
Storage stability of intermediate moisture foods for space shuttle [NASA-CR-133978] 19 p2225 N73-27944
**STORAGE TANKS**
Tank heater for lowering viscosity of highly viscous liquids in storage tanks [NASA-CASE-WLP-10040-1] 04 p0426 N73-13475
Development of digital computer program for evaluating vibrational characteristics of large liquid-filled rigid wall tanks of general shape [NASA-CR-124070] 08 p0953 N73-17801
Performance of storable liquid system components and tankage under severe conditions of humidity and temperature [AD-755383] 13 p1569 N73-22716
Incendiary vulnerability of dry bays adjacent to jet fuel tanks under gunfire [AD-764732] 23 p2867 N73-32920
Cryogenic tanking and partial jettison tests of Centaur launch vehicle and Centaur standard shroud to develop insulation, purge, and vent systems [NASA-TM-X-71455] 24 p2984 N73-33850
**STORMS**
NT CYCLONES
NT HURRICANES
NT IONOSPHERIC STORMS
NT MAGNETIC STORMS
NT RAINSTORMS
NT SOLAR STORMS
NT STORMS [METEOROLOGY]
NT SUDDEN IONOSPHERIC DISTURBANCES
NT THUNDERSTORMS
NT TORNADOES
NT TROPICAL STORMS
NT TYPHOONS
Two-dimensional curve fitting technique for analyzing data acquired by Doppler radar and application to study of convective storms [AD-755946] 12 p1424 N73-21537
Structure of dust storms determined from ITOS-1 television pictures [NLL-M-23033-[5828.4F]] 21 p2528 N73-30272
**STORMS [METEOROLOGY]**
NT HURRICANES
NT RAINSTORMS
NT THUNDERSTORMS
NT TORNADOES
NT TROPICAL STORMS
NT TYPHOONS
Spatial distribution model of reflectivity in storm cells for digital radar data [NASA-TM-X-66118] 03 p0327 N73-12661
Utilization of ERTS-1 imagery to study short-lived events such as fires, volcanism, storms, and earthquakes [E73-10025] 06 p0660 N73-15359
Long term meteorological study of intensity and movement of tropical cyclones and typhoons in western North Pacific [AD-754349] 11 p1315 N73-20676
Gravity current model applied to analysis of squall-line gust front
12 p1419 N73-21504

Study of severe local storm of 22 Apr. 71, near Norman, Oklahoma
[AD-756571] 13 p1554 N73-22592
Pattern recognition and detection of short-lived events such as storms, forest fires, volcanoes, and earthquakes using ERTS-1 data
[E73-10678] 16 p1901 N73-25373
Analysis of radar signatures for identifying hail-bearing clouds to show effects of geographical conditions and seasons
21 p2569 N73-30586
Equipment and procedures for obtaining meteorological radar information on clouds, cloud systems, and dangerous meteorological formations
21 p2571 N73-30605
Study of low level boundary layer jet streams for predicting dangerous atmospheric conditions
21 p2573 N73-30622
ERTS-1 imagery of short-lived events such as forest fires, oil spills, volcanic activity, floods, and storms
[E73-11048] 23 p2779 N73-32224

**STOSS-AND-LEE TOPOGRAPHY**
U GLACIAL DRIFT

**STRAIGHT WINGS**
U RECTANGULAR WINGS

**STRAIN AGING**
U PRECIPITATION HARDENING

**STRAIN DISTRIBUTION**
U STRESS CONCENTRATION

**STRAIN ENERGY METHODS**
Application of strainrange partitioning method to high temperature fatigue
[NASA-TM-X-68171] 06 p0725 N73-15923
Inequalities satisfied by strain energy functions for isotopic elastic material
[AD-761624] 19 p2315 N73-28616
Strain energy density and surface layer energy for crack-like ellipse
[NASA-CR-132338] 24 p2988 N73-33879

**STRAIN FATIGUE**
U FATIGUE [MATERIALS]

**STRAIN GAGE BALANCES**
One-component strain gage for measuring axial forces on low density wind tunnel models
[DLR-MITT-71-30] 04 p0423 N73-13447

**STRAIN GAGES**
Superconducting magnetometer as strain transducer in liquid helium cooled gravitational wave antenna
[NOTA-INTERNA-373] 01 p0058 N73-10476
Temperature effects on measurement accuracy of static deformation of semiconductor resistance strain gages
[NASA-TT-F-14616] 04 p0481 N73-13928
Standardization criteria for nominal sizes and test conditions of extension strain gages with bound metallic measuring grids
[NLL-NEL-TT-2414-[6075.461]]
05 p0543 N73-14426
Development of curves for determining magnitude and direction of principal stresses and strains in plane stress field from strain gage readings
[ESDU-72014] 05 p0601 N73-14890
Design and tests of counting strain gages for high-g naval aircraft
[AD-750692] 06 p0676 N73-15498
Durability investigation of strain gage pressure transducers subjected to long term pressure cycling at ambient and elevated temperatures
[NASA-CR-120953] 07 p0800 N73-16497
Development of pulsed power strain gage system for use in presence of high amplitude electrical noise
[SC-DC-72-1413] 07 p0801 N73-16503
Reliability of high temperature strain gages while measuring extreme thermal strain
[NAL-TR-287] 07 p0854 N73-16923
Measurement of parachute cord loads using lightweight transmitting load cell
[AD-751913] 08 p0867 N73-17022
Development of strain gage ambiguity sensor for measuring alignment of optical mirror segments
[NASA-CASE-MFS-20506-1] 08 p0923 N73-17563
Strain gage, smoke flow photograph, and hot-wire anemometer studies for determining magnus characteristics
09 p1015 N73-18286
High temperature electric resistance wire strain gages
[NASA-CR-112241] 09 p1035 N73-18446
Evaluation of airframe fatigue life gage under constant and variable amplitude loading
[AD-753800] 09 p1037 N73-18464
Design and performance of strain gage transducer as blood pressure recording device
12 p1374 N73-21144
Turnbuckle device for tensile stress load measurements
[NASA-CASE-MFS-21488-1] 14 p1667 N73-23526
Data analysis from A-37 aircraft flights to evaluate electronic strain-level counter as fatigue damage monitor
[AD-757210] 14 p1668 N73-23540
Design of torsional gage with step response for strain-rate measurements
[AD-757527] 14 p1668 N73-23542
Production and performance of strain gage embedded in boron/epoxy materials
[AD-759548] 16 p1915 N73-25493
Development of strain gage mounting assembly for amplifying measurable deformation applied to strain gage
[NASA-CASE-NPO-13170-1] 19 p2300 N73-28495
Strength, creep, and transmission coefficient of adhesives for attaching strain gages
[AD-761470] 19 p2302 N73-28506
Strain gage bridge calibrations on wing structure at elevated temperatures to establish thermal and mechanical loads due to aerodynamic heating
[NASA-TN-D-7390] 19 p2348 N73-28883
Acquisition of stress data and aerodynamic loads on F-5 aircraft using mechanical strain gages and oscillograph recorders for service life determination
[AD-760567] 20 p2361 N73-28991
Analysis of state of mechanically heterogeneous material during deformation using optically sensitive coatings
[NLL-M-21653-[5828.4F]] 21 p2602 N73-30856

**STRAIN HARDENING**
Fatigue strength of tensile strained 45 and 40Kh steel
[NLL-SMRE-TRANS-5862-[8313.4]]
02 p0184 N73-11494
Strain hardened properties of 304L stainless steel surfaces under combined tension and torsion
[AD-746472] 02 p0188 N73-11525
Effect of strain hardening on fatigue crack resistance after single cycle peak overload in Ti-6Al-4V Ti alloy
[AD-753899] 10 p1174 N73-19553
Thermal processing procedures for strain hardening TRIP steels
[AD-756953] 13 p1543 N73-22505
Temperature dependence of strain hardening in metals
[RAE-LIB-TRANS-1672] 17 p2043 N73-26531
Exponential equation for power law strain hardening behavior during tensile tests of structural alloys
[RAE-LIB-TRANS-1689] 17 p2092 N73-26922
Measurments of monotonic and cyclic strain hardening parameters by five alloys
[AD-762610] 20 p2433 N73-29540
Thermoplastic strengthening of martensite steels and titanium alloys
[AD-760953] 21 p2560 N73-30520

**STRAIN RATE**
Strain rate and temperature dependence of glass fiber reinforced and unreinforced epoxy resins and deformation mechanisms
[REPT-1040/72] 01 p0069 N73-10568
Plastic-strain controlled failure criteria and design parameters
[COO-2048-4] 03 p0361 N73-12941
Yield strength of rigid polymers, discussing tensile and compression stresses
[D-MAT-180] 05 p0565 N73-14591
Strain fields around tapered interference fit steel pins in aluminum and steel alloy plates
[ARL/SM-NOTE-377] 09 p1093 N73-18919
Literature review of strain rate effects on mechanical properties of metals at high temperatures
[AD-754243] 10 p1174 N73-19548
Influence of strain rate on inelastic properties of Udimet alloys at elevated temperatures and presentation in form of hodograph
10 p1219 N73-19917
Process for analysis of strain field of structures subjected to large deformations involving low modulus substrate with thin coating
[NASA-CASE-LAR-10765-1] 11 p1323 N73-20740
Influence of axial impact loads on dynamic properties and strain wave speeds in polycarbonate Lexan
[AD-755457] 12 p1417 N73-21482
Design of torsional gage with step response for strain-rate measurements
[AD-757527] 14 p1668 N73-23542
Viscoplastic characteristics of structural shells
[AD-758074] 15 p1841 N73-24915
Constant strain rate deformation of amphibole minerals
[AD-760105] 18 p2149 N73-27372
Effect of temperature and strain rate on tensile properties of aluminum-boron, epoxy-boron, and epoxy-graphite composites
[AD-763656] 21 p2564 N73-30551
Strain rate sensitivity and yield stress of Fe-Mo, Fe-Ti, and Fe-Re solid solutions
21 p2602 N73-30855

**STRAIN SOFTENING**
U PLASTIC DEFORMATION

**STRAITS**
Mimi field test of July 1970 for underwater acoustic study in Straits of Florida
[AD-744982] 01 p0080 N73-10662
Bathymetry, free air gravity anomaly, and magnetic field intensity data on Strait of Sicily, gathered from 1965 to 1971
[SACLANTCEN-CONF-PROC-7]8 p0915 N73-17501

**STRAPDOWN INERTIAL GUIDANCE**
Performance tests of strapdown air to air tracking system for short range weapons control system
[AD-751654] 07 p0818 N73-16633
Test plan for evaluation of redundant sensor strapdown inertial measuring unit to include operating procedures and data and analysis requirements
[NASA-CR-123513] 08 p0941 N73-17711
General test plan for redundant sensor strapdown inertial measuring unit evaluation program
[NASA-CR-130722] 08 p0941 N73-17712
Dynamic testing procedures for strapdown sensors with motion induced error torques
[NASA-CR-124126] 10 p1185 N73-19641
Motion induced error in tuned, flexure-mounted strapdown gyro
[NASA-CR-124161] 11 p1316 N73-20682
Proceedings of conference on inertial navigation components and systems with emphasis on concepts and techniques involving cost and performance tradeoffs
[AGARD-CP-116] 11 p1316 N73-20684
Numerical analysis of effects of various parameters affecting accuracy and stability of strapdown inertial navigation systems
11 p1316 N73-20685
Development of single-degree-of-freedom gyroscope for application to strapdown inertial guidance system
11 p1317 N73-20688
Dynamically tuned gyros in strapdown systems
11 p1318 N73-20697
Development of electrostatic gyro systems
11 p1318 N73-20698
Inertial grade instrumentation for precision strapdown reference system
11 p1318 N73-20699
Development of strapdown electrically suspended gyroscope components for increased readout accuracy
[NASA-CR-112206] 11 p1321 N73-20721
Analysis of algorithms for failure detection, isolation, and correction of redundant inertial instruments in strapdown dodecahedron configuration
[NASA-CR-124234] 13 p1556 N73-22608
Application of Kalman-Bucy filter theory to post-flight guidance error analysis
[NAL-TR-302] 15 p1808 N73-24652
Software description and program documentation for strapdown inertial reference unit system
[NASA-CR-128965] 18 p2175 N73-27567
Skylark star-pointing attitude control system using strapdown inertial system
[RAE-TR-71241] 18 p2176 N73-27571
Test performance of computerized strapdown inertial attitude reference system
[NASA-TM-X-2848] 20 p2453 N73-29713
Design operation and performance of gyro module for SIRU
[NASA-CR-135509] 22 p2698 N73-31608
Three axis inertial system in Apollo gimbal for fine grain evaluation of strapdown system performance in dynamic environments
[NASA-CR-135484] 22 p2698 N73-31609
Strapped down gyroscope aligned with sun and star tracker optical axis calibrating roll, yaw and pitch values
[NASA-CASE-ARC-10716-1] 23 p2851 N73-32784

**STRATA**
NT SUBSTRATES

**STRATEGY**
Strategies for European geosynchronous space tug mission
[VTH-171] 13 p1583 N73-22831
Differential game theory applied to military operations, such as antimissile missile problem and air warfare
[BMVG-FBWT-73-9] 19 p2314 N73-28609

**STRATHS**
U VALLEYS

**STRATIFICATION**
NT ATMOSPHERIC STRATIFICATION
Analysis of natural vibrations on stratified fluid in rectangular vessel and computer program for solving continuous density distribution
12 p1390 N73-21275
Effects of low Bond number sloshing on thermal stratification of cryogenic liquids
12 p1391 N73-21283
Numerical analysis of turbulent diffusion in stratified fluid to show variations in diffusion coefficient with changes in ocean water depth
[AD-761653] 19 p2257 N73-28190

**STRATIFIED FLOW**
Convection and mixing of stratified fluids in rotating tank
[NASA-TR-R-392] 01 p0039 N73-10312
Review of linear viscous stability theory for stably stratified parallel shear flow
[CONF-720632-1] 07 p0772 N73-16270
Lectures on properties and characteristics of rotating and stratified fluids
[AD-754066] 11 p1272 N73-20320

Approximate solution of two-dimensional problem of non-steady state stratal flow with movable gas-liquid interface
[AD-754828] 11 p1273 N73-20328
Collapse of homogeneous fluid mass immersed in vertically stratified fluid
[AD-757995] 15 p1769 N73-24330
Relationship between eddy-transport and second-order closure models for stratified media and for vortices
19 p2253 N73-28161
Analysis of wake collapse in sea water and stratified fluids with emphasis on final stages of decay
[AD-761622] 19 p2257 N73-28189
Scaling phenomena of collapse of wake of self-propelled body in stratified fluid
[AD-762454] 19 p2258 N73-28201
Stability characteristics of stratified and unstratified air flow between two horizontal, infinite disks rotating at slightly different rotation rates
20 p2384 N73-29154
Effect of shock wave interaction in parallel, two-dimensional, stratified flow of heavy and light gases
20 p2384 N73-29157
Numerical analysis of collapse of homogeneous fluid mass in stratified fluid
[AD-763657] 21 p2526 N73-30257
Mathematical model formulated for mean disturbance created in linear stratified fluid by growth and collapse of localized region of turbulent mixed fluid
[AD-764050] 24 p2910 N73-33224

**STRATIGRAPHY**
Stratigraphy, structure, and geologic history of Sangre de Cristo Mountains of Colorado based on aerial remote sensing
[NASA-CR-129519] 03 p0293 N73-12385
Radar system for electromagnetic subsurface profiling
[PB-213892/0] 14 p1665 N73-23514
Differentiation of serpentinitic from nonserpentinitic ultramafic rocks in Maryland Piedmont using ERTS-1 MSS imagery
[E73-10632] 16 p1896 N73-25337

**STRATOCUMULUS CLOUDS**
Analysis of aircraft measurements of long-wave radiation fluxes, water content, and temperature in presence of stratified and stratocumulus clouds
22 p2693 N73-31574

**STRATOFORTRESS AIRCRAFT**
U B-52 AIRCRAFT

**STRATOSCOPE TELESCOPES**
High resolution imagery of Uranus obtained by Stratoscope 2
[NASA-CR-132024] 14 p1706 N73-23846

**STRATOSCOPE 1 TELESCOPE**
U STRATOSCOPE TELESCOPES

**STRATOSCOPE 2 TELESCOPE**
U STRATOSCOPE TELESCOPES

**STRATOSPHERE**
Aperiodic processes and formation of seasonal temperature and wind fields in stratosphere in Northern Hemisphere, and tropospheric influences
[NLL-M-20086-[5828.4F]] 01 p0043 N73-10342
Meteorological parameters of stratosphere from rocket sounding data
[NLL-M-22213-[5828.4F]] 01 p0073 N73-10594
Methane mixing ratios in stratosphere deduced from balloon-observed solar infrared spectra
[AERONOMICA-ACTA-A-105] 01 p0092 N73-10757
Vertical distribution and dissociation of methane in stratosphere and CO production
[A-N-103-1972] 02 p0164 N73-11329
Infrared absorption spectra of stratospheric nitrogen dioxide
02 p0164 N73-11330
Balloon measurements of aerosol and ozone in Arctic stratosphere
[AD-747256] 02 p0169 N73-11374
Meteorological rocket sounding data on stratospheric and mesospheric structures and circulations
[NASA-TR-R-391] 02 p0205 N73-11657
Stratospheric water vapor mixing ratio altitude profile from spectral observations of downward emission from vapor lines
[AD-747031] 03 p0297 N73-12423
Momentum, energy, and mass budgets of stratosphere
[COO-2195-2] 04 p0415 N73-13385
Increase of water vapor in stratosphere due to fleet of SSTs
[AD-748797] 04 p0416 N73-13397
Stratospheric weather maps for Northern Hemisphere based on rawinsonde and rocketsonde observations - Vol. 124, No. 3
05 p0570 N73-14632
Stratospheric daily altitude maps and monthly mean maps of Northern Hemisphere
05 p0570 N73-14633
Stratospheric daily altitude maps and monthly mean maps of Northern Hemisphere
05 p0571 N73-14634
Vertical distribution of atmospheric water vapor and ozone over District of Columbia during 1969 and 1970
[AD-751535] 07 p0795 N73-16465
Stratospheric nitric oxide production from past nuclear explosions and its relevance to projected SST pollution
[AD-751295] 07 p0795 N73-16466
Atmospheric circulation and temperature effects on stratospheric ozone during winter storm period
[AD-751211] 07 p0797 N73-16479
Effect of solar magnetic sector structure on stratospheric circulation
[NASA-CR-130551] 08 p0916 N73-17505
Attenuation of nitric oxide dissociation in mesosphere and stratosphere
[PSU-IRL-SCI-407] 08 p0917 N73-17518
Atmospheric ozone as circulation tracer in upper troposphere and lower stratosphere
08 p0972 N73-17940
Photochemical and transport processes in stratosphere
08 p0972 N73-17941
Photodissociation and formation of nitric acid in mesosphere and stratosphere
[AERONOMICA-ACTA-A-113] 09 p1027 N73-18382
Relative importance of processes determining vertical distribution of nitrogen oxides in stratosphere
[AERONOMICA-ACTA-A-110] 09 p1027 N73-18383
Dissociation of nitric oxide in mesosphere and stratosphere by attenuation
[AERONOMICA-ACTA-A-112] 09 p1027 N73-18384
Rocket measurements of ozone distribution under varying latitudes and seasonal conditions in stratosphere
[NASA-TM-X-66192] 09 p1028 N73-18391
Temperature and wind conditions in stratosphere and troposphere of equatorial latitudes in Indian Ocean
09 p1059 N73-18634
Models for warm and cold conditions of winter stratosphere of polar latitudes
09 p1059 N73-18636
Numerical and photochemical models for analyzing transport and trace constituents in stratosphere
[COO-2249-1] 10 p1155 N73-19399
Meteorological charts of upper atmosphere of Northern Hemisphere
[QR-4-PT-4] 10 p1181 N73-19604
Relationship between surface temperature anomalies in European USSR and seasonal variations of stratospheric circulation
[NLL-M-22851-[5828.4F]] 11 p1274 N73-20336
Aerosynoptic wind and temperature conditions contributing to atmospheric turbulence at altitude of 18 km over European USSR
[NLL-M-22822-[5828.4F]] 11 p1274 N73-20342
Hydrodynamic and chemical properties of stratospheric aircraft wake
[PB-213114] 11 p1290 N73-20465
Meteorological investigation of stratospheric turbulence using radiosonde data
[NLL-M-22819-[5828.4F]] 12 p1419 N73-21502
Stratospheric photochemical reactions of ozone in relation to climatology and supersonic transport pollution
[NOAA-TM-NESS-47] 12 p1422 N73-21526
Long term climatological study of meteorological parameters for Northern Hemisphere
13 p1551 N73-22565
Stratospheric weather maps for Northern Hemisphere
[QTSE-1] 13 p1551 N73-22570
Numerical forecasts of barometric fields in stratosphere using quasi-geopotential model
13 p1552 N73-22574
Direct measurement of mesosphere and stratosphere electrical conductivity and relaxation time
15 p1779 N73-24419
Measurement of atmospheric transport properties in stratosphere
[AD-757927] 15 p1782 N73-24445
Wind calculations of stratosphere in Northern Hemisphere at 100, 50, 30 and 10 mb
15 p1804 N73-24622
Phenomenological concepts of earth electrical structure controlled by neutral atmosphere dynamics of stratospheric tides
16 p1895 N73-25330
Measurement of absorption cross section values of nitric acid vapor in stratosphere at different wavelengths
[A-117-1973] 16 p1905 N73-25408
Models for radiative heating and cooling and ozone photochemistry in stratosphere
[NASA-CR-132777] 17 p2025 N73-26385
Seasonal variations in tropospheric and stratospheric carbon dioxide concentration determined from commercial aircraft sampling within Northern Hemisphere
[AC-24-PT-3] 17 p2028 N73-26409
Stratospheric backscattering measurements using airborne lidar system onboard Convair 990 aircraft
18 p2132 N73-27227
Nitrogen oxides from supersonic transports affecting stratospheric ozone depletion on solar ultraviolet radiation
[AD-761179] 18 p2195 N73-27722
Energetics of transient zonal and planetary scale waves in wintertime lower stratosphere investigated using surface spherical harmonics
20 p2389 N73-29193
Distribution of odd nitrogen in lower stratosphere and perturbations caused by stratospheric air transport
[NASA-CR-2314] 21 p2536 N73-30336
Nitrogen and ozone kinetics in stratosphere
[AERONOMICA-ACTA-A-118] 21 p2537 N73-30345
Stratospheric and tropospheric composition and chemical reactions
[AP-12] 21 p2539 N73-30357
Quantitative analysis of stratospehric aerosol characteristics from Skylab data
[E73-11009] 22 p2660 N73-31314
Quantitative determination of Statospheric aerosol composition over western United States
[E73-11138] 24 p2918 N73-33293
Computer codes for calculating trace contaminant effects on stratospheric transport processes
[COO-2249-2] 24 p2923 N73-33345
Effect of spatial variability of wind in stratosphere on flight of supersonic transports
24 p2946 N73-33529
Structure of global geopotential fields in connection with quasi-biannual cyclicity in equatorial stratosphere
24 p2947 N73-33533

**STRATOSPHERE RADIATION**
Measurement of distribution of radioactivity in troposphere and stratosphere to determine aerosol dimensions and variation with time
12 p1421 N73-21513

**STRATOTANKER AIRCRAFT**
U C-135 AIRCRAFT

**STRATUS CLOUDS**
Variation in maximum intensity of precipitation falling from stratiform and cumulus clouds
13 p1552 N73-22581
Analysis of aircraft measurements of long-wave radiation fluxes, water content, and temperature in presence of stratified and stratocumulus clouds
22 p2693 N73-31574

**STREAM FUNCTIONS [FLUIDS]**
Numerical analysis of effect of streamwise coordinate of basic flow on stability characteristics of boundary layer flow
17 p2012 N73-26270
Analytical and experimental study of spatially growing disturbances in shear layers between parallel streams
22 p2650 N73-31231
Formation and structure of vortex rings formed by stream deceleration
22 p2653 N73-31251

**STREAMLINE FLOW**
U LAMINAR FLOW

**STREAMLINED BODIES**
NT FAIRINGS
Aerodynamic drag for streamline bodies at small angles of incidence
[ESDU-BODIES-02.04.00] 07 p0735 N73-15979
Numerical analysis of drag of streamlined bodies of revolution for various length to diameter ratios
[ESDU-BODIES-02.04.02] 14 p1647 N73-23362

**STREAMS**
NT GAS STREAMS
Meteoroid stream search among photographic meteors
[CONTRIB-15] 11 p1337 N73-20853
Stream and river drainage network analysis from Skylab imagery
[E73-10818] 18 p2140 N73-27293
Heat transfer across interface between high speed steam jet and external coaxial cocurrent water flow
[AD-763696] 21 p2527 N73-30262
Investigation of New England reservoirs, land use, streams, flooding, and vegetation from Skylab imagery
[E73-10993] 22 p2659 N73-31299
Interpretation of land use and stream drainage in Pawnee River Basin, Kansas
[E73-11005] 22 p2660 N73-31310
Streaming in liquid metals due to thermal surface tension gradient
[TRITA-EPP-73-10] 22 p2700 N73-31626

**STREETS**
All-weather permanent street patching material for flexible and rigid pavements
[NASA-CR-133549] 19 p2312 N73-28595
Detection of urban street patterns in ERTS-1 imagery of Lincoln, Nebraska
[E73-10976] 21 p2534 N73-30315

**STRENGTH OF MATERIALS**
U MECHANICAL PROPERTIES

**STREPTOCOCCUS**
Methods for improving bacterial transport media
[NASA-CR-128958] 16 p1866 N73-25113

**STRESS [BIOLOGY]**
Detection of vegetation stress and damage associated with highways and highway facilities in Maine
[E73-10611] 15 p1773 N73-24372
Algorithm for automatic photointerpretation of plant species and stresses in Minnesota imagery
[E73-10639] 15 p1776 N73-24398
Masking phenomenon for measuring state of fatigue and stress of nervous system
[AD-752975] 16 p1869 N73-25129

**STRESS [PHYSIOLOGY]**
NT ACCELERATION STRESSES [PHYSIOLOGY]
NT CENTRIFUGING STRESS
Underwater submersion and prolonged underwater submersion effects on diver tactile sensitivity
[AD-743709] 01 p0010 N73-10082
Visual evoked cortical response as measure of stress in naval environment, using rapid flash rates
[AD-744934] 01 p0011 N73-10088
Concepts for reduction of fatigue in sustained tactical operations
[AD-746643] 02 p0134 N73-11090
Noise and response complexity effects on human attention and performance in visual perception task
[AD-747797] 04 p0381 N73-13105
Pupil enlargement in relation to operator stress during adaptive critical tracking task
[AD-749075] 05 p0501 N73-14081
Bioastronautics research, including stress effects, sensory perception, and human performance
[NASA-SP-3006] 06 p0627 N73-15091
Heat and cold stress effects in humans
06 p0628 N73-15094
Tolerance levels, physiological effects, and performance degradation during simultaneous or sequential exposures to environmental stresses
06 p0629 N73-15110
Analysis of temperature conditions in hermetically sealed room to determine human tolerances under various climatic conditions
[FOA-1-A-1527-76] 07 p0854 N73-16924
Dynamic electrocardiography in periodic health examinations for detection of cardiac abnormalities
08 p0873 N73-17065
Electrocardiographic stress testing for determining influence of occupational and other stresses on ischemic heart disease
08 p0875 N73-17082
Combined stress effects in human communication and motion sickness biodynamics
10 p1122 N73-19144
Temperature and noise irradiation effects on human energetic metabolism during vigilance task
10 p1123 N73-19155
Automatic interpretation of forest species and stress identification using ERTS-1 imagery of Minnesota
[E73-10366] 10 p1150 N73-19362
Stress reactions of vestibular apparatus to ionizing radiation, coriolis forces, and gravitational stimuli
[AD-753511] 11 p1248 N73-20132
Reaction assessment of vestibular disorientation stress for aircrew selection, using visual displays and tasks
12 p1368 N73-21096
Hashish smoking effects on human oxygen consumption during physical stress and safe driving ability
12 p1370 N73-21115
Analysis of self-destructive tendencies created by psychological stress and relationship to aircraft accidents
[FAA-AM-73-5] 18 p2104 N73-27016
Physiological responses of flying personnel to multiple stresses
[AD-759565] 18 p2113 N73-27082
Hypoxia effects on release of gaseous wastes from rat vital functions
20 p2366 N73-29025
Aerospace Medical Research Laboratory handbook to medical monitoring and treatment of environmental stresses
[AD-760813] 20 p2372 N73-29061
Subjective and physiological indicators of fatigue and performance during vigilance task
[AD-761503] 21 p2502 N73-30077
Effect of sleep deprivation and heat stress on human performance in visual and auditory tasks
[OES-8/72] 22 p2624 N73-31024
Physiological stress effects of aerospace environment on human body and animals
[NASA-TT-F-15081] 23 p2749 N73-32001
Aerospace psychology and physiology
[JPRS-60248] 24 p2882 N73-33014
Cross correlation analysis of stress rhythm during stimuli of varying biological significance
24 p2890 N73-33071

**STRESS [PSYCHOLOGY]**
Statistical analysis of steroid levels in parotid secretions of humans under prolonged mental stress
[AD-747682] 04 p0381 N73-13104
Noise and response complexity effects on human attention and performance in visual perception task
[AD-747797] 04 p0381 N73-13105
Cognitive functioning test to measure human performance in underwater diving stress
[AD-748036] 04 p0382 N73-13108
Feasibility of saliva analysis for measuring mental stress in man
[AD-747671] 04 p0382 N73-13111
Personality, occupation, and job stress effects on physiological risk factor in human coronary heart disease
08 p0871 N73-17054
Standardized performance battery for assessing effects of environmental stressors particularly noise on human performance
[NASA-CR-2149] 08 p0877 N73-17102
Indices of emotional stress in cosmonauts during Voskhod 2 and Soyuz flights
[JPRS-58039] 08 p0877 N73-17104
Combined stress effects in human communication and motion sickness biodynamics
10 p1122 N73-19144
Pilot selection by means of concentration stress test
19 p2226 N73-27957
Aerospace psychology and physiology
[JPRS-60248] 24 p2882 N73-33014

**STRESS ANALYSIS**
NT PHOTOGRAPHIC MEASUREMENT
Numerical procedures for designing cams with radial followers for conditions of straight line travel and flat faced followers with faces normal to direction of motion
[ESDU-66009] 01 p0060 N73-10490
Numerical analysis of contact stresses between cam and follower mechanisms for combinations of materials, surface finish, and lubrication conditions
[ESDU-66002] 01 p0060 N73-10492
Numerical analysis of performance of sinusoidal acceleration cams using radial followers and no opening or closing ramps
[ESDU-66026-AMEND-A] 01 p0060 N73-10494
Analysis of factors affecting design of interference-fit collars on rotating shafts
[ESDU-68002] 01 p0061 N73-10496
Numerical analysis of nominal interface pressures and stresses for shafts with interference fit collars
[ESDU-68003-AMEND-A] 01 p0061 N73-10497
Design, stress analysis, and reliability evaluation of electric rocket engines
[AD-745427] 01 p0091 N73-10751
Analysis of geometric stress concentrations caused by two equal unreinforced circular holes in infinite flat plates
[ESDU-67023-AMEND-A] 01 p0110 N73-10909
Development of procedure for determining maximum and minimum stresses produced by uniform pressure on unpierced torispherical closure of cylindrical shell
[ESDU-67017] 01 p0110 N73-10911
Stress and strength guide for engineering design
[ESDU-SS1] 01 p0111 N73-10917
Calculation of geometric stress concentration factors in two adjacent, unreinforced circular holes in infinite flat plates
[ESDU-66035] 01 p0111 N73-10919
Application of periodic Dirichlet problems to analysis of planar theory of elasticity
[AD-741924] 01 p0115 N73-10948
Numerical analysis of stress field in semi-infinite elastic-plastic medium under generalized plane deformation
[AD-746046] 01 p0115 N73-10951
Elastic interface pressure and stress calculations on assemblies of shafts with interference-fit collars
[ESDU-68004-PT-3] 02 p0177 N73-11433
Complex variable method of planar elastic stress for lubricated rectangular seal
02 p0178 N73-11444
Effects of pavement surface condition on cornering forces developed by automobile tires of different tread design
[NASA-TN-D-6964] 02 p0192 N73-11551
Numerical analysis of thin skew plates using tensor-matrix techniques for elastic isotropic body
[NLL-RTS-7401] 02 p0236 N73-11916
Development of method for classifying stresses in isotropic work hardening media using polarized light
[NLL-M-21475-[5828.4F]] 02 p0236 N73-11918
Definition of basic terms, notation, and forms of presentation for fatigue data
[ESDU-70016] 02 p0237 N73-11925
Computer program for stress, stability, and vibration analyses of segmented, ring-stiffened, branched shells of rotation
[NASA-CR-2116] 02 p0237 N73-11931
Development of mathematical relationships to define the behavior of multilayer, thin shell structures under various conditions of shear and bending
02 p0238 N73-11936
Stress freezing and slicing techniques of photoelasticity to analyze local stresses near deep surface flaws under cylindrical bending fields
[AD-746976] 02 p0240 N73-11950
Approximate method for computing consistent conjugate stresses in elastic finite elements
[AD-746024] 02 p0240 N73-11954
Analysis of data generated by combined bending-torsion fatigue reliability research machines using probabilistic-graphically and phenomenological techniques
[NASA-CR-72839] 03 p0306 N73-12498
Analysis of stress formation and changes in physical properties of pipes during rotary swaging using explosion or pulsed magnetic field energy
[AD-747454] 03 p0308 N73-12516
Mapping-collocation method for elastostatic stress analysis of orthotropic rectangular plates with centrally located traction-free cracks
[NASA-TN-D-7119] 03 p0360 N73-12933
Numerical analysis of dynamic buckling modes of elastic systems under intensive loading in finite time segment
03 p0360 N73-12937
Torsional bending and longitudinal vibrations of rotating shafts and application to free vibrations of individual rotor blades, blade cascades, and shrouded blades
[NASA-TT-F-14627] 04 p0372 N73-13029
Elastic stress analysis of bi-material plate with crack normal to interfaces, using finite element method
[AD-748299] 04 p0439 N73-13579
Steklov-Lebeague norm used in stress analysis of solid rocket propellants to determine viscoelastic response with aging
[AD-748943] 04 p0462 N73-13771
Development of method for determining critical stress intensity for crack propagation and application to reactor components
[RD/B/N-2143] 04 p0481 N73-13934
Development of curves for determining magnitudes and directions of principal stress in plane using components of direct and shear stress
[ESDU-72013] 05 p0601 N73-14889
Development of curves for determining magnitude and direction of principal stresses and strains in plane stress field from strain gage readings
[ESDU-72014] 05 p0601 N73-14890
Analysis of shell theory parameters to determine relationship between stress and displacement fields predicted by shell theory and corresponding actual fields
[WTHD-40] 05 p0602 N73-14895
Application of optimality criteria to automation of structural design with emphasis on aerospace applications
[NASA-TN-D-7115] 05 p0603 N73-14901
Finite element method with continuity of slope for stress analysis on arbitrary shell
[PB-211759] 05 p0604 N73-14909
Stress deformation in anisotropic elastic thin walled shells
[AD-749955] 05 p0604 N73-14911
Design and fabrication of X ray diffractometer and application to determination of residual stresses in polycrystalline samples
[NAL-TN-34] 06 p0672 N73-15467
Effect of residual compressive stresses on fatigue strength and service life of aluminum alloy 7079 specimens
[NLR-TR-71105-U] 06 p0684 N73-15567
Fatigue tests of aluminum alloy specimens used for aircraft structures under simulated acoustic loading conditions
[ESDU-72015] 06 p0723 N73-15899
Numerical analysis of stress in face plates of sandwich panel structures subjected to random acoustic loading
[ESDU-72017] 06 p0723 N73-15900
Application of cumulative damage theory to internal stress caused by cyclic loading in notched bars
[LBF-FB-100/72] 06 p0726 N73-15930
Analysis of stresses in compressor blades with emphasis on conditions in dove tail joints at base of blades
[AD-750497] 06 p0727 N73-15936
Application of least square point matching for stress analysis of shallow, perforated, cylindrical shell subjected to tension, edge moment, or transverse shear
[AD-750942] 06 p0728 N73-15942
Relations between fuel swelling and clad strain for cylindrical uranium dioxide pins with niobium zirconium cladding
[NASA-TM-X-2717] 07 p0819 N73-16638
Procedures for estimating stresses in titanium and high strength steel panels and comparison of estimated and measured stresses
[ESDU-72005-AMEND-A] 07 p0850 N73-16894
Analysis of response of structure to acoustic excitation to include vibration of structure, natural frequencies and damping, and noise field characteristics
[ESDU-72001-AMEND-A] 07 p0850 N73-16895
Procedures for determining shell stability under various types of dynamic loads
07 p0852 N73-16906
Evaluation of fringe multiplication technique applied to frozen stress approach of three dimensional stress analysis in three dimensions
[AD-751172] 07 p0853 N73-16917
Measurement of parachute cord loads using lightweight transmitting load cell
[AD-751913] 08 p0867 N73-17022

Development of technique for measuring residual stresses in thin coatings based on analysis of stress induced deflections of substrate
[NASA-CR-130813] 09 p1051 N73-18566
Computer programs for predicting hydrodyaamic forces and vibration characteristics of rocket engine turbopump inducer - Vol. 2 Revised
[NASA-CR-72712-VOL-2-REV] 09 p1078 N73-18797
Stress analysis of ITOS D and E structural members - Vol. 3
[NASA-CR-130162] 09 p1087 N73-18865
Numerical analysis of stress and deformation at crack tip for case where finite plastic zone exists along crack line
[NAL-TR-293] 09 p1092 N73-18918
Photoelastic analysis of plane polyester specimens containing fatigue crack to determine effect of plastic yielding on stress distribution near crack
[TAE-155] 09 p1093 N73-18923
Development of three stage model for fatigue failure of structure with several critical regions for initial failure
[ARL/SM-NOTE-338] 09 p1093 N73-18924
Stress analysis of uniaxial steel wire-plastic composite material, using finite element method
[ISD-131] 09 p1095 N73-18940
Static, vibration, and thermal stress analyses of laminated plates and shells by hybrid-stress finite element method including transverse shear deformation effects
[AD-753651] 09 p1097 N73-18955
Reversible sliding and lubrication effects in internal stress friction on thin plate
[AD-751723] 09 p1097 N73-18957
Effect of discontinuous changes in strain rate on relationship between strain rate, strain and stress in Udimet 700 alloy at elevated temperatures
10 p1219 N73-19916
Influence of strain rate on inelastic properties of Udimet alloys at elevated temperatures and presentation in form of hodograph
10 p1219 N73-19917
Numerical analysis of displacement of cylindrical shell subjected to cylindrical wave in acoustic medium
10 p1219 N73-19918
Stress analysis on lap joint subjected to loads
[AD-753469] 10 p1221 N73-19929
IBM 360 FORTRAN computer program for three dimensional stress analysis of structural parts
[AD-753617] 10 p1221 N73-19932
Analysis of Reynolds stress in turbulent boundary layer on smooth wall with zero pressure gradient
[AD-754758] 11 p1272 N73-20319
Characteristics of metal drawing processes based on hypotheses of plane cross sections and deformation zone equilibrium conditions
[NLL-M-21553-[5828.4F]] 11 p1296 N73-20518
Process for analysis of strain field of structures subjected to large deformations involving low modulus substrate with thin coating
[NASA-CASE-LAR-10765-1] 11 p1323 N73-20740
Analysis of thermal static bending forces on deployable interlocked booms and comparison with thermal bending of seamless tubes
[NASA-TN-D-7243] 11 p1345 N73-20915
Seminumerical analysis of three dimensional elastic properties of finite geometry solids with traction-free cracks
[NASA-TN-D-7213] 11 p1345 N73-20917
Stress analysis of elastoplastic state of thin circular plate subjected to axisymmetric loading
[AD-753983] 11 p1346 N73-20920
Design of despin mechanism noting thermal and stress analysis of beryllium and aluminum as structural materials
[ESRO-CR[P]-226] 13 p1534 N73-22432
Design of despin mechanism noting angular stiffness, stress analysis, signal transmission, power transmission, instrumentation and ground support equipment
[ESRO-CR[P]-228] 13 p1535 N73-22434
Higher order theories and solution techniques for moderately thick shells of revolution using Reissner Theory and Legendre functions
13 p1584 N73-22842
Survey of optimal structural design techniques to include method of fully stressed design and linear programming problems
[REPT-10432] 14 p1714 N73-23911
Numerical analysis of thermoelastic state of shells subjected to thermal impact on the surface of the shell
14 p1715 N73-23912
Stress analysis of plates with part circular and flat bottomed cracks and various flaw depths using stress intensity factors from photoelastic data
[NASA-CR-132015] 14 p1715 N73-23915
Development of photoelastic stress freezing and slicing method to determine stress intensity around surface flaws
[AD-758140] 14 p1717 N73-23934
Development of formulas for elastic behavior of axisymmetrically loaded cylindrical and spherical pressure vessels under various load conditions
[AD-758496] 14 p1717 N73-23936
Numerical analysis of effects of heating unidimensional plate under nonlinear boundary conditions
[NLL-M-21618-[5828.4F]] 15 p1764 N73-24290
Thermal and stress analyses of interfaces for nozzles and nozzle extensions
[NASA-CR-132211] 15 p1768 N73-24324
Photoelastic stress analysis of NERVA structures
[NASA-CR-132213] 15 p1810 N73-24673
Development of finite difference method for calculating boundary value problem for nonsymmetrical deformation of random shells of revolution
[NLL-DRIC-TRANS-2996-[3623.66]] 15 p1836 N73-24884
Numerical analysis of torsion characteristics of bar with constant section in shape of circular ring or circular sector
[NLL-DRIC-TRANS-2995-[3623.66]] 15 p1837 N73-24885
Analysis of effect of rigidity of stressed state in corrosion cracking under biaxial stress conditions for steel and titanium alloys
[NLL-LTI-746-1413-[9022.401]] 15 p1837 N73-24886
Analysis for stresses and buckling of heated composite stiffened structures
[NASA-CR-112227] 15 p1838 N73-24894
Computer program for thermal stress and instability analyses of structures
[NASA-CR-112228] 15 p1838 N73-24895
Application of finite element method for analyzing stability of rectangular plates in supersonic air stream
15 p1838 N73-24899
Numerical analysis of elasto-plastic bending of plates with V-notch on one edge and subjected to pure bending
[NASA-CR-132225] 15 p1839 N73-24900
Research projects in theoretical and practical aerodynamics - Vol. 1
16 p1851 N73-24999
Stress analysis verification of structural integrity of Apollo ultraviolet spectrometer experiment
[NASA-CR-128551] 16 p1916 N73-25501
Aerospace application of holography through nondestructive testing and flow visualization
16 p1922 N73-25550
Analysis of residual stresses in pressure displacement converter diaphragm occurring during manufacturing
16 p1968 N73-25921
Measurement of effects of sonic booms on light building structures for various building configurations
[RAE-LIB-TRANS-1633] 17 p1981 N73-26011
Analysis of fatigue behavior of airframe components and development of methods for predicting service life of aircraft structures
[RAE-LIB-TRANS-1678] 17 p1981 N73-26012
Development of procedures for determining service life of helicopter airframes and rotor blades
[RAE-LIB-TRANS-1520] 17 p1981 N73-26013
Vibrational characteristics, mechanical properties, and stress analysis of thin shell structures of various cross sections
[NASA-SP-288] 17 p2092 N73-26924
Analysis of structural stability of shells weakened by holes to develop numerical analysis of stress concentration
17 p2093 N73-26929
Stress analysis of pressurized shallow cylindrical shell containing two collinear axial cracks of equal length
[NASA-CR-132271] 17 p2093 N73-26932
Stress analysis of elastic plane containing elastic inclusion using singular integral equations
[NASA-CR-132272] 17 p2093 N73-26934
Stress analysis of impact in composite plates
[NASA-CR-121110] 18 p2203 N73-27786
Automation of input/output routines for use with computerized data processing of finite element structural analyses
[AD-761154] 18 p2204 N73-27793
Analysis of aircraft structural loads in operational flight to determine effects of pilot performance and aircraft characteristics
[AGARD-R-608] 19 p2218 N73-27895
Generally used practical methods of strain sensing
19 p2304 N73-28527
Development of method for analyzing stress deformation state of metal during process of lengthwise rolling of tubes
[NLL-M-21655-[5828.4F]] 20 p2428 N73-29501
Analysis of stress-strain state in metal and contact stresses developed during continuous rolling on long mandrel for reducing and drawing metal tubes
[NLL-M-21688-[5828.4F]] 20 p2428 N73-29502
Analysis of fracture and creep properties of metals after extension under conditions of hydrostatic pressure as function of time
[NLL-NEL-TT-2475-[6075.461]] 20 p2429 N73-29515
Statistical elasticity theory for initial stresses in reinforced and filled polymers
20 p2434 N73-29551
Fatigue strength criteria for stressed materials
[AD-761447] 20 p2463 N73-29790
Elastic stress analysis of aluminum-epoxy plate with crack normal to interfaces
20 p2478 N73-29901
Bending stresses produced by internal pressure in thin walled hollow cylinders with out-of-round cross section
[NLL-CE-TRANS-6040-[9022.09]] 20 p2478 N73-29902
Analysis of effect of damping on response of structure to acoustic excitation and experimental method for determining damping coefficients
20 p2479 N73-29917
Analysis of programs for acoustic testing of composite material components and development of theory for predicting natual frequencies, mode shapes, and stresses in composite panels
20 p2480 N73-29918
Development of rational analytic theory for analyzing fatigue of airframes based on maximum stress-field parameter and maximum load excursion ratio
20 p2481 N73-29931
Development of procedure for estimating fatigue life of airframes to eliminate errors caused by neglecting effect of stress redistribution after localized yielding
20 p2481 N73-29933
Analysis of errors in fatigue life prediction procedures and methods for improving accuracy of prediction analysis techniques
20 p2481 N73-29934
Stress analysis of large plastic deformations in hollow sphere deformed during impact tests
[NASA-TM-X-68270] 20 p2482 N73-29940
Development of electronic computer process for analyzing contact stress oscillograms
[NLL-M-21662-[5828.4F]] 21 p2511 N73-30136
Analysis of state of mechanically heterogeneous material during deformation using optically sensitive coatings
[NLL-M-21653-[5828.4F]] 21 p2602 N73-30856
Computer program for analysis of nonlinear deformation and fatigue response of components subjected to complex load histories
[AD-763780] 21 p2604 N73-30870
Application of divergent beam X ray microdiffraction technique for measuring residual and impressed stresses and strains in iron-silicon alloy transformer sheet
[NBS-MONOGRAPH-130] 22 p2672 N73-31407
Simplified analysis procedure for determining static and dynamic aeroelastic loads for space shuttle dynamics
[NASA-CR-124370] 22 p2722 N73-31781
Application of nonlinear finite element analysis to planar and nonplanar plane stress problems
22 p2723 N73-31789
Creep tests of fine-grained polycrystalline ice under uniaxial and multiaxial stress conditions to predict time-dependent deformational behavior
22 p2723 N73-31791
Semidirect boundary integral method to obtain numerical solution for elastic stress and strain fields in V-notched beams in pure bending
[NASA-TN-D-7424] 22 p2725 N73-31803
BOPACE program for advanced thermal-elastic-plastic-creep structural analysis
[NASA-CR-124390] 22 p2725 N73-31805
Stress analysis of thick wall cylindrical vessels weakened by flaws
[AD-764279] 22 p2726 N73-31811
Concentration of stress around holes in thin walled shells
[AD-764169] 22 p2726 N73-31813
Stress and strain distribution along round, circular cavity in infinite space
[AD-764104] 22 p2726 N73-31819
Stress analysis of vacuum deposited nickel films to determine correlation between microstructure and measured stress
23 p2804 N73-32424
Theoretical analysis background for shell theory automated for rotational structures [STARS-2] program - Vol. 1
[NASA-CR-2273-VOL-1] 23 p2854 N73-32801
Engineering programming information for digital computer program developed for structural analysis of shells - Vol. 4
[NASA-CR-2273-VOL-4] 23 p2854 N73-32804
Elastic-plastic theory at finite strain
[AD-764557] 23 p2855 N73-32815
Analysis of equations of finite elasticity to show nonapplicability of rest state constraint associated with strain energy function
[AD 764667] 23 p2855 N73-32817
Linear elastic fracture mechanics applied to graphite under multiaxial stress conditions
[CONF-730707-2] 24 p2943 N73-33507
Computer code for thermal/hydraulic stress analysis on liquid metal zirconium hydride reactor core
[AI-AEC-13065] 24 p2954 N73-33596
Development of set of equations for analysis of thick shell structures to include effects of geometric thickness and transverse strain
24 p2987 N73-33870

Dynamic buckling of thin, elastic beam subjected to constant, compressive axial displacement
24 p2987 N73-33871
Application of finite element analysis techniques to determine characteristics of curved elements in thin, elastic shells
24 p2987 N73-33872
Analysis of internal buckling of fibers in viscoelastic composite plate based on linear material responses and small deflection theory
24 p2987 N73-33874
Analysis of size effects related to fatigue strength of metals under conditions of geometrical stress concentrations producing stress and strain gradients
24 p2988 N73-33876
Stress analysis of adhesive lap joint subjected to tension, shear force, and bending moments for various material properties and thickness of adherents
24 p2988 N73-33877
Method for determining stress and displacements infinite plate with hole of various shapes under uniform tension of compression
24 p2988 N73-33882
Variational method for numerical analysis of bending and supercritical behavior of heterogeneous slightly curved plates
[AD-765543] 24 p2990 N73-33891

**STRESS CALCULATIONS**
U STRESS ANALYSIS

**STRESS CONCENTRATION**
Analog reinforcement for reducing stress concentration around hole in plate
[AD-745116] 01 p0071 N73-10578
Stress field intensity in opening interface crack in composite materials
[AD-746033] 01 p0071 N73-10583
Stress effects around holes in flat plates under various combinations of loads
[ESDU-70005] 01 p0110 N73-10902
Analysis of geometric stress concentrations caused by two equal unreinforced circular holes in infinite flat plates
[ESDU-67023-AMEND-A] 01 p0110 N73-10909
Calculation of geometric stress concentration factors in two adjacent, unreinforced circular holes in infinite flat plates
[ESDU-66035] 01 p0111 N73-10919
Stress concentration effects due to shape discontinuity, inclusions, or local load distributions
[ESDU-65004-AMEND-A-B-C] 01 p0112 N73-10925
Finite analysis of effects of varying radii of circumferential fillets in transition of cylindrical shells
[ORNL-TM-3766] 03 p0361 N73-12943
Stress-rupture strength of turbine blade root joints at elevated temperature and prolonged stress loads
[AD-749589] 04 p0465 N73-13788
Elastoplastic stress concentration and deformations in perforated plates
[ONERA-NT-193] 04 p0482 N73-13936
Influence of thermal stresses and loads on endurance properties of heat resistant alloys used to manufacture turbine blades
[AD-749752] 05 p0591 N73-14805
Automatic systems for analyzing fatigue crack propagation and for conducting constant stress intensity factor fatigue tests with servo-hydraulic machine
[RD/B/N-2013] 06 p0726 N73-15928
Numerical solution for stress concentration factors in isotropic and layered composites with parallel and collinear cracks
[WB-5/72] 09 p1052 N73-18576
Distribution and concentration profiles of stress adjacent to orifices in glass fiber-reinforced plastic plates and shells
[AD-753041] 09 p1096 N73-18945
Mechanical and microstructural behavior of Al-Zn alloy in superplastic region at high temperature
10 p1170 N73-19518
NASTRAN computer program for determining stress concentration at holes in isotropic finite strips
[AD-753574] 10 p1221 N73-19933
Solution of Hertz contact problem for case involving indentation of elastic half space by rigid axisymmetric punch under monotonically applied normal force with assumed Coulomb friction
[AD-755071] 11 p1299 N73-20544
Application of Schwarz-Neumann alternating method to stress intensity solutions of edge and surface crack problems
[NASA-CR-112299] 11 p1345 N73-20912
Three-dimensional finite element analysis of stress concentration near holes in laminated composites
[AD-756454] 13 p1548 N73-22545
Stress distribution in lap joints under cleavage and tension-shear loading conditions
13 p1584 N73-22843
Determination of stress intensity factors from photoelastic data with applications to surface flaw problems
[AD-756872] 13 p1587 N73-22864
Determination of inplane stress distribution across thickness by two methods for plate loaded in bending
[AD-757207] 14 p1716 N73-23925
Circular geometry and mixed boundary value problems in three dimensional elasticity
[NASA-TN-D-7266] 15 p1837 N73-24891
Stresses and displacements of elastic-plastic trusses
[AD-758726] 15 p1841 N73-24920
Effects of stress concentration ahead of running crack in sheets with centrally located hole
[AD-759734] 16 p1972 N73-25950
Constant-stress irradiation creep capsules for application of load to several graphite samples by single pneumatic bellows
[BNWL-SA-4199] 17 p2050 N73-26586
Scattered light photoelastic method for predicting stress distribution in composite epoxy glass structures
[AD-759900] 17 p2052 N73-26601
Stress distribution in infinite micropolar plate with elliptic hole
[AD-759964] 17 p2095 N73-26949
Distribution of stress across thickness near crack tip in epoxy resin plate subjected to approximate cylindrical bending
20 p2476 N73-29893
Relaxation curves from lateral strain of test pieces
[NLL-CE-TRANS-6101-[9022.09]]
20 p2478 N73-29903
Effects of experimental error on stress intensity fractors from fracture testing
[NASA-TM-X-68285] 20 p2482 N73-29941
Concentration of stress around holes in thin walled shells
[AD-764169] 22 p2726 N73-31813
Low energy blow technique to determine dimensional changes and development of cracking in Charpy V-notch impact test
[CRANFIELD-MAT-10] 24 p2988 N73-33880

**STRESS CORROSION**
NT STRESS CORROSION CRACKING
Stress history effect on incubation time for stress corrosion crack growth in E-4340 HR steel
[AD-745308] 01 p0068 N73-10553
Stress corrosion cracking test for armor alloys with self-loading
[AD-746251] 01 p0068 N73-10560
Mechanical property and stress corrosion evaluation of Custom 455 stainless steel alloy at cryogenic temperatures
[NASA-TM-X-64682] 02 p0186 N73-11509
Interactions between residual elements, inclusion, toughness, and stress corrosion resistance in high strength steel
[PB-209655] 02 p0187 N73-11515
Development of airframe integrity investigation procedures to determine structural deficiencies and modifications required to airframes for increased service life
[AD-746881] 03 p0253 N73-12049
Bibliographic survey on stress corrosion cracking of high strength aluminum alloys, including oxide effects
[DLR-FB-71-105] 03 p0316 N73-12572
Wedge procedure for determining stress corrosion cracking susceptibility of 5000 series aluminum alloy sheets
[AD-747944] 03 p0316 N73-12577
Corrosion fatigue behavior of 4340 steel above K sub Iscc in distilled water
[AD-747700] 03 p0317 N73-12584
Mechanisms of corrosion fatigue crack propagation in Al-Zn-Mg including effect of cyclic stress waveform
[AD-747709] 03 p0319 N73-12597
Effect of thermomechanical treatment on stress corrosion cracking susceptibility of Beta 3 titanium
[AD-748359] 03 p0319 N73-12602
Electron fractography of stress corrosion fracture surfaces of aircraft materials as high strength steels, Al-Zn-Mg, Al-Cu and Ti alloys
[NLR-TR-71038-U] 03 p0361 N73-12945
Stress corrosion cracking in saline water of TA6V and TU2 titanium alloys
[ONERA-P-145] 04 p0435 N73-13545
Effect of thickness on sustained load crack propagation in Ti-6Al-4V alloy tested in 3-1/2 percent NaCl solution
[AD-748591] 04 p0435 N73-13548
Stress corrosion cracking of sensitized austenitic stainless steels in oxygenated high temperature water
[BMI-1927] 05 p0562 N73-14565
Effect of sodium chloride solution and distilled water on stress corrosion crack propagation in aluminum alloy 7075
[NLR-TR-71090-U-PT-1] 06 p0685 N73-15577
Stress corrosion cracking of titanium and titanium alloys in organic liquids and vapors
[AD-751528] 07 p0810 N73-16572
Significance of grain boundary microstructure and pH in chloride ion solution as stress corrosives in 7075 aluminum alloys
[RM-564] 08 p0931 N73-17624
Stress corrosion cracking of steel double cantilever beam specimens produced by loading sequence in aqueous environment
[AD-752215] 08 p0933 N73-17637
Effect of constant applied stress in crack initiation of aluminum and titanium alloys exposed to salt solution and organic fluids
[NASA-CR-124110] 09 p1045 N73-18525
Corrosion behavior of grain boundary constituents in Al-Zn-Mg alloys
[AD-753273] 09 p1049 N73-18556
Environmental tests of crystallographic and stress corrosive properties of reactor related metal alloys
[AECL-4353] 09 p1063 N73-18668
Stress-corrosion cracking of zirconium alloys in nuclear reactor environment
09 p1063 N73-18670
Stress-corrosion cracking of zirconium alloy fuel element sheaths subjected to tension stress in iodine vapor environment
09 p1063 N73-18671
Summary of conference on stress corrosion testing methods
[AGARD-AR-52] 09 p1094 N73-18931
Apollo experience report on causes of stress-corrosion cracking of structural materials and corrective actions
[NASA-TN-D-7111] 10 p1214 N73-19875
Mechanical properties and stress corrosion cracking of 431 stainless steel alloy at low temperatures
[NASA-TM-X-64729] 12 p1412 N73-21441
Aluminum and tin alloys for stress corrosion cracking and fatigue crack growth studies pertinent to spacecraft and booster pressure vessels
[NASA-CR-120823] 12 p1462 N73-21846
Various applications of explosive welding
[AD-758844] 16 p1919 N73-25530
Instability model for stress corrosion and fatigue crack propagation in 4340 steel
[AD-761148] 18 p2162 N73-27461
Influence of heat treatment on stress corrosion susceptibility of ternary Al-Zn-Mg alloy
[AD-761207] 18 p2162 N73-27467
Stress corrosion behavior of titanium and aluminum alloys with and without surface layer
[AD-760529] 18 p2163 N73-27469
Electron microscopic study of stress corrosion cracking behavior of austenitic stainless steel having increased nitrogen content in boiling MgC42
20 p2427 N73-29495
Metallurgical and environmental factors influencing stress corrosion cracking
[AD-762541] 20 p2431 N73-29528
Compact, portable nondestructive test instrument for susceptability determination to stress corrosion cracking
[AD-762777] 20 p2433 N73-29538
Temperature characterization of below K sub Iscc corrosion fatigue behavior of HY-130 steel
20 p2477 N73-29899
Adjustable deflection, multispecimen, bent beam test fixture for conditioning sheet specimens used in hot salt stress corrosion tests of titanium alloys
[AD-763704] 21 p2561 N73-30529
Theoretical and experimental approach to stress corrosion cracking in metal alloys
21 p2603 N73-30859
Acoustic emission from aqueous stress corrosion cracking in various tempers of steel
[AD-764048] 22 p2687 N73-31522
Stress corrosion cracking of steels in liquid ammonia environments
24 p2932 N73-33420
Stress corrosion cracking in gaseous and aqueous environments
24 p2933 N73-33426

**STRESS CORROSION CRACKING**
Stress corrosion cracking of titanium alloys and steels - Part I
[AD-751544] 07 p0810 N73-16569
Ultrasonic nondestructive tests of sound waves emitted from stress corrosion cracking - Part 2
[AD-751529] 07 p0810 N73-16570
Potentiostatic polarization method for stress corrosion tests on cracking susceptibility of materials
[AD-754205] 10 p1174 N73-19549
Stress corrosion cracking tests of aluminum alloys in synthetic sea water
[NASA-TM-X-64733] 13 p1488 N73-22062
Stress corrosion cracking in 410 stainless steel due to hydrogen embrittlement
13 p1539 N73-22471
Stress corrosion cracking in high strength aluminum alloys due to hydrogen embrittlement
13 p1539 N73-22472
Composition effects on stress corrosion cracking of titanium alloys in aqueous environments
[NASA-CR-131872] 13 p1540 N73-22475
Fracture toughness and aqueous stress corrosion resistance of high strength commercial Ti alloy
[NLR-TR-72107-U] 13 p1542 N73-22492
Effect of stress corrosion cracking and hydrogen embrittlement on failure of high strength spacecraft fasteners
[AD-758754] 15 p1800 N73-24591
Analysis of effect of rigidity of stressed state in corrosion cracking under biaxial stress conditions for steel and titanium alloys
[NLL-LTI-746-1413-[9022.401]]

15 p1837 N73-24886
Oxidation and stress corrosion cracking of high strength steel in gaseous environment
[AD-758848] 16 p1929 N73-25608
Effect of thermomechanical treatment on stress corrosion cracking susceptibility of Beta 3 titanium alloy
[AD-759166] 16 p1930 N73-25618
Stress corrosion cracking of titanium alloys by hydrofluoric acid released during Viton B thermal degradation
[D-MAT-191] 18 p2161 N73-27455
Stress corrosion cracking in aluminum and titanium alloys
[NASA-CR-124352] 20 p2431 N73-29531

**STRESS CYCLES**
Development of test equipment for random and constant amplitude loading on resonant and electrohydraulic fatigue machines
[RAE-TR-72226] 17 p2009 N73-26250
Numerical analysis of fatigue strength of steel specimens under symmetric loading cycles
[AD-761469] 19 p2310 N73-28581
Analysis of factors affecting variability in fatigue life of materials to show effects of material type, load applications, and test conditions on scatter of data
[ARL/SM-REPT-342] 23 p2853 N73-32796
Cyclic mechanical and fatigue properties of ferroanelastic beta prime gold-cadmium
24 p2933 N73-33421
High temperature low cycle effects on directly stressed, notched fatigue specimens
[RD/B/N-1996] 24 p2989 N73-33888

**STRESS DISTRIBUTION**
U STRESS CONCENTRATION

**STRESS FUNCTIONS**
Space stress and deformation deviators for calculating work done in plastic deformation
[NLL-M-22004-[5828.4F]] 06 p0723 N73-15897

**STRESS MEASUREMENT**
Determination of paleotectonic principal stress orientation and spacings of joints in outcrops, and development of optical diffraction analysis method
[BM-RI-7706] 06 p0665 N73-15409
Development of pulsed power strain gage system for use in presence of high amplitude electrical noise
[SC-DC-72-1413] 07 p0801 N73-16503
Development of technique for measuring residual stresses in thin coatings based on analysis of stress induced deflections of substrate
[NASA-CR-130813] 09 p1051 N73-18566
Measures to determine psychophysiological reactions of military flight crews to flying stress
10 p1122 N73-19148
Continuous measurement of residual stress in thin cylindrical pieces using deflection-etching techniques
[CRIF-MC-47] 12 p1409 N73-21418
Correlation between microstructure and measured stress of vacuum deposited nickel films
[COO-623-183] 12 p1439 N73-21659
Mathematical and mechanical consideration of finite strip compressed between two rough rigid stamps
[NASA-CR-112318] 13 p1585 N73-22849
Turnbuckle device for tensile stress load measurements
[NASA-CASE-MFS-21488-1] 14 p1667 N73-23526
Development of strain gage mounting assembly for amplifying measurable deformation applied to strain gage
[NASA-CASE-NPO-13170-1] 19 p2300 N73-28495

**STRESS RELAXATION**
Chemorheology of Viton B fluorocarbon elastomer by kinetic analysis of chemical stress relaxation, and infrared and gel permeation chromatography analysis
01 p0119 N73-10985
Creep measurements on metals for calculating stress-strain-time relaxation curves
02 p0186 N73-11507
Stress state and deformation characteristics of hardening carbon steel with decreasing temperatures
[AD-746723] 02 p0188 N73-11527
Creep and stress relaxation tests on Cr-Ni austenitic steel at 700 C
[STU-70-419/U-350-B] 04 p0481 N73-13932
Role of isothermal stresses generated during oxidation and modes of stress relaxation
14 p1676 N73-23605
Wave front stress relaxation in suddenly loaded semi-infinite rod of nonlinear viscoelastic materials with random temperature distributions
[AD-760324] 17 p2096 N73-26956
Equations for creep and stress relaxation in nickel-based alloy bolted joints subjected to vibration
[AD-761455] 19 p2349 N73-28897

**STRESS RELIEVING**
Method for eliminating plastic deformations and residual stresses by high speed impact forming of weld zone
[AD-745457] 01 p0062 N73-10508
Crack formation during stress-relief annealing in heat-affected zones of weld seams in low-alloy steels
[NLL-RISLEY-TR-2507-[9091.9F]]
06 p0676 N73-15499
Procedures for reducing residual stresses in aircraft metal structures reinforced by filamentary composites
[NASA-CR-112207] 08 p0966 N73-17900
Analysis of stresses in magnet windings due to thermal contraction and temperature gradient stresses and impregnation with epoxy resins to reduce effects
[RHEL/R-264-PT-1] 20 p2435 N73-29558

**STRESS RUPTURE STRENGTH**
U CREEP RUPTURE STRENGTH

**STRESS WAVES**
Facility monitoring of stress wave emission as nondestructive testing method
[AD-745729] 01 p0114 N73-10945
Wave propagation in half space due to interior point load parallel to surface
[AD-747306] 02 p0170 N73-11381
Stress wave emission nondestructive inspection technique for detecting flaw criticality in structural parts
[AD-747225] 02 p0176 N73-11426
Laser interferometer instrumentation techniques for study of plane stress wave propagation in solids
[SC-DC-70-5465] 03 p0310 N73-12529
FORTRAN 4 computer program for one-dimensional stress wave analysis of linear viscoelastic rock
[BM-IC-8563] 05 p0516 N73-14197
Stress wave emission techniques for monitoring weld quality and structural validation
[AD-745822] 05 p0552 N73-14486
Application of finite element method to stress wave in plates
[NASA-CR-112294] 11 p1345 N73-20911
Numerical analysis of dynamic problem of axisymmetrically impacting finite-length rods
[AD-754119] 11 p1346 N73-20923
Detection and application of stress waves to nondestructive testing
[RFP-TRANS-114] 12 p1463 N73-21853
Strength mechanism of stress wave emission in steel and aluminum alloys during tensile testing
[RFP-TRANS-104] 12 p1463 N73-21854
Stress wave diffraction models for crack propagation induced by dynamic loads
13 p1584 N73-22839
Computer program for finite element stress wave analysis
[AD-755393] 13 p1587 N73-22871
Theoretical prediction of thermal stress waves in metal conductors induced by relativistic electron beam
16 p1926 N73-25587
Application of stress wave emission method to nondestructive testing of pressure vessels
[ISAS-492] 18 p2203 N73-27781
Nondestructive evaluation methods recently introduced
19 p2304 N73-28528
Strain waves propagating in linear viscoelastic plates of various thicknesses
20 p2477 N73-29897
Wave propagation and impact in composite materials
[NASA-CR-121226] 20 p2482 N73-29935
Bibliography on stress wave emission, 1950-1972
[ARL/MET-BIBL-1] 21 p2557 N73-30500
Strain wave propagation in metal cones with compressive pulse applied at base and application to design of gun launchers
[AD-762504] 22 p2727 N73-31822
Behavior of impact-generated elastic stress waves propagating in rods of unidirectional composite material
23 p2852 N73-32792

**STRESS-STRAIN DIAGRAMS**
State of stress and strain in rectangular belt pulled over cylindrical pulley
[AD-747318] 03 p0307 N73-12507
Three different equations of state used for computing stress-strain curves of rubber in tension
[AD-747664] 03 p0322 N73-12621
Relationship of stress-strain rates and loading histories on material hardening
03 p0360 N73-12936
Compressive stress-strain properties of aircraft materials
[ESDU-00.01.01-AMEND-A] 06 p0723 N73-15902
Formulation of stress strain model for storage batteries
[AD-752257] 08 p0870 N73-17045
Analysis of errors recorded by modified Ligtenberg techique while measuring stress, strain, and static and dynamic loading in curved plates
[AD-752127] 08 p0926 N73-17589
Series expansion method for calculating longitudinal load impact on rod of rate-dependent material
[AD-751979] 08 p0967 N73-17904
Irradiation effects on fatigue and creep-fatigue properties of stainless steels
[ANCR-1078] 10 p1173 N73-19539
Kinetic theory of stress-strain relations and temperature induced dislocation in crystal lattices
[AD-753576] 10 p1201 N73-19777
Metallurgical investigation of deformation and fatigue using high temperature tests and stress-strain diagrams on heat resistant alloys
[JPRS-58180] 10 p1219 N73-19912
Cyclic deformation diagrams of heat resistant and austenitic steels
10 p1219 N73-19914
Extrapolating stress-rupture test results of heat resistant alloys
13 p1542 N73-22495
Standardized stress strain curves
[ESDU-00.01.00] 14 p1675 N73-23588
Sensitivity of solid rocket propellant stress to linear thermal expansion
[AD-761815] 19 p2328 N73-28729
Development of method for analyzing stress deformation state of metal during process of lengthwise rolling of tubes
[NLL-M-21655-[5828.4F]] 20 p2428 N73-29501
Analysis of stress-strain state in metal and contact stresses developed during continuous rolling on long mandrel for reducing and drawing metal tubes
[NLL-M-21688-[5828.4F]] 20 p2428 N73-29502
Stress and strain relations for elastic and plastic deformation in uniaxial strain
[AD-762536] 20 p2464 N73-29797
Fatigue life and inelastic strain response under complex histories for alloy steel
20 p2478 N73-29900
Stress-strain diagrams and mechanical properties of metal wires as determined by tranverse impact method
[AD-764105] 22 p2687 N73-31523

**STRESS-STRAIN DISTRIBUTION**
U STRESS CONCENTRATION

**STRESS-STRAIN RELATIONSHIPS**
U STRESS-STRAIN DIAGRAMS

**STRESS-STRAIN-TIME RELATIONS**
Creep measurements on metals for calculating stress-strain-time relaxation curves
02 p0186 N73-11507
Time dependent inelastic behavior of metals and metal structures
[AD-746340] 02 p0240 N73-11951
Stress-time relations of automobile rear wheel suspension systems, over various road surface conditions, based on power spectral density
[LBF-TB-102] 21 p2553 N73-30468
Methods of solving quasistatic problems in linear theory of thermoviscoelasticity
[AD-763937] 22 p2726 N73-31816
Strain history effects in solid rocket propellant deformation
[AD-764666] 23 p2832 N73-32635

**STRESSED-SKIN STRUCTURES**
Space stress and deformation deviators for calculating work done in plastic deformation
[NLL-M-22004-[5828.4F]] 06 p0723 N73-15897

**STRESSES**
NT AXIAL STRESS
NT COMBINED STRESS
NT CRITICAL LOADING
NT RESIDUAL STRESS
NT SHEAR STRESS
NT TENSILE STRESS
NT THERMAL STRESSES
NT TORSIONAL STRESS
NT TRIAXIAL STRESSES
NT VIBRATIONAL STRESS
Systematic regional stress variations in fault zones in competent rocks
[AD-743837] 01 p0052 N73-10422
Curves for determining maximum elastic stresses and deflections for initially flat circular plates of uniform thickness under uniform pressure with various edge conditions
[ESDU-65002] 01 p0112 N73-10923
Maximum deflection and stresses for initially flat circular plates under uniform pressure
[ESDU-65003] 01 p0112 N73-10924
Method of potential applied to three-dimensional elastic and thermoelastic stress problems and fracture mechanics
[SCL-DR-71-0026] 01 p0113 N73-10935
Automatic photointerpretation for plant species and stress identification using ERTS-1 imagery
[E72-10258] 03 p0300 N73-12448
Effect of circular inclusion on stresses around two collinear finite line cracks in plate under tension
[AD-749901] 05 p0604 N73-14910
Stress singularities associated with crack inclined to bimaterial interface
[AD-750367] 06 p0689 N73-15607
Subcritical crack propagation in pressure vessel plates due to cyclic loads and stresses
[NASA-CR-120834] 06 p0725 N73-15920
Procedure for measuring flow stresses of metals during closed die forging
[AD-752588] 08 p0928 N73-17602
Stress and displacement of structures consisting of alternatingly elastic and hyperbolic paraboloidal shells with rectangular planform
[PB-212649] 08 p0967 N73-17902
Internal stress field and elastic moduli of fibrous compositions
[AD-752866] 09 p1053 N73-18587
Fatigue tests of 7075-T6 aluminum alloy under synchronous pulsating triaxial stresses
[AD-754414] 10 p1174 N73-19552
Optical system for measuring passive stress conditions in xenon flash lamps for use in high power lasers
[UCRL-50022-3] 12 p1410 N73-21427

Effect of surface layer stress on plastic deformation and crack propagation of steel
[AD-755844] 12 p1415 N73-21467
Inventory of forest and rangeland and detection of forest stress at Black Hills, South Dakota, Atlanta, Georgia, and Manitou Forest test sites using ERTS-1 data
[E73-10546] 14 p1655 N73-23421
Inventory of forests and rangelands, including forest stress, at Black Hills, Atlanta, Georgia, and Manitou, Colorado test sites using Skylab EREP
[E73-10587] 14 p1657 N73-23447
Development of approximate equation for determining stress intensities for quarter circular cracks emanating from circular hole in sheet material
[AD-757550] 14 p1716 N73-23928
Calculation of stress and strain in two fold continuous prismatic bodies with example of calculation for ribbed fuel tube
[KFK-1665] 15 p1839 N73-24906
Effect of stress state nonhomogeneity and initial imperfections on stability of cylindrical shells
[AD-758027] 15 p1840 N73-24910
Elastic stresses due to axial loads on nozzle intersecting cylindrical shell
[AD-758075] 15 p1841 N73-24916
Simple thickness modes for couple stress theory for laminated media
[AD-759133] 16 p1933 N73-25642
Conjugate basis functions and consistent stresses for finite element stiffness method
[AD-758675] 16 p1972 N73-25948
Effect of stress intensity on fatigue crack growth in 5456-H117 aluminum alloys
[AD-760668] 18 p2162 N73-27465
Quality control of welded joints
[AD-761587] 19 p2306 N73-28548
Interaction between circular inclusion and arbitrarily oriented crack
[NASA-CR-132291] 19 p2348 N73-28886
Stability of freely supported circular cylindrical shell subjected to random stresses
[AD-761541] 19 p2350 N73-28901
Computer program for modeling UO2 cladding strain resulting from irradiation
[NASA-TM-X-68281] 20 p2453 N73-29715
Influence of applied stress, magnetic and electric fields, and impurity concentration on electrical conductance of n-type germanium at very low temperatures
[RR-738] 20 p2462 N73-29783
Technique for dealing with problem of elastic domain containing arbitrarily oriented internal crack
[NASA-CR-132289] 20 p2482 N73-29937
Effect of stress on fatigue crack propagation in metals
[AD-763776] 21 p2560 N73-30523
Stress and corrosion effects on fatigue behavior 7075-T6 aluminum alloy
[AD-763455] 21 p2560 N73-30525

**STRETCH FORMING**
Characteristics of metal drawing processes based on hypotheses of plane cross sections and deformation zone equilibrium conditions
[NLL-M-21553-[5828.4F]] 11 p1296 N73-20518

**STRETCHING**
Experimental determination of behavior of uncrosslinked polymers subjected to constant stretch history for strip biaxial and simple extensional flow
01 p0120 N73-10986
Device for securing together structural members with axially stretched bolt and nut
[NASA-CASE-GSC-11149-1] 21 p2552 N73-30457

**STRIATION**
Striations in large barium ion clouds in two stage process
[AD-757916] 15 p1807 N73-24643
Influence of gaseous atmospheres on aluminum alloy, titanium, and refractory alloy fatigue striations
[ONERA-NT-192] 17 p2045 N73-26548
Striation of ion cloud in Oosik barium release experiment
[LA-UR-73-677] 24 p2923 N73-33349

**STRINGERS**
Analysis of ring and stringer stiffness parameters and proportions for axially compressed stiffened isotropic cylinders with and without internal pressure
[NASA-CR-2165] 04 p0481 N73-13930

**STRIP MINING**
Mapping ecological effects of coal strip mining in Ohio
[E72-10256] 03 p0290 N73-12356
Strip mine identification, land use assessment, smoke plume detection, and sedimentation patterns in Sandusky Bay from ERTS-1 imagery of Ohio
[E72-10259] 03 p0290 N73-12358
ERTS-1 imagery of landscape changes in Tennessee and Kentucky due to strip mining
[E72-10265] 03 p0291 N73-12364
Detection and monitoring area strip mining and reclamation in Ohio using ERTS-1 imagery
[E72-10284] 04 p0409 N73-13334
Environmental and ecological effects of coal strip mining in Ohio
[E73-10003] 06 p0658 N73-15339
Application of ERTS-1 imagery for locating coal refuse deposits, analysis of geologic formations and mapping of agricultural areas in Pennsylvania
[E73-10327] 09 p1024 N73-18358
Ecological effects of coal strip mining in Ohio
[E73-10430] 11 p1281 N73-20391
Satellite monitoring of open pit mining operations
[BM-IC-8530] 15 p1780 N73-24432
Detection, monitoring, and mapping coal strip mining and reclamation in Ohio from ERTS-1 imagery
[E73-10641] 16 p1896 N73-25338
ERTS-1 imagery of strip mining activity in Cumberland Plateau, Tennessee Test Site and agricultural areas in Alabama, Georgia, and Tennessee
[E73-10694] 16 p1902 N73-25386
EREP imagery for detection of strip mines and reclamation activities in Ohio, West Virginia, and Pennsylvania
[E73-10731] 17 p2020 N73-26337
Application of ERTS-1 imagery to determine ecological effects of strip mining in eastern Ohio
[PAPER-E2] 19 p2268 N73-28266
Digital processing of ERTS-1 data for identification of strip mining areas in west branch area of Susquehanna River and mine drainage in Pennsylvania
[PAPER-E3] 19 p2268 N73-28267
Digital analysis of ERTS-1 data to determine sedimentation levels in Potomac and Anacostia Rivers confluence and strip mining in Allegheny County, Maryland
[PAPER-E13] 19 p2270 N73-28277
Mapping of strip mine areas in southeastern Ohio from ERTS-1 imagery
19 p2284 N73-28372
ERTS-1 imagery of landscape changes, strip mines, timber, agriculture, and water resources in eastern Tennessee
[E73-10843] 19 p2291 N73-28421
Skylab monitoring of surface mining activities and reclamation in Ohio, West Virginia, Pennsylvania, Indiana, Kentucky, and Illinois
[E73-11033] 22 p2663 N73-31337
Usefulness of ERTS-1 MSS data for monitoring coal strip mining, detection of acid mine drainage, and determination of effectiveness of reclamation and abatement procedures in Pennsylvania
[E73-11112] 24 p2915 N73-33269

**STRIP TRANSMISSION LINES**
Analysis of mutual coupling compensation using microstrip techniques with application to behind-the-array coupling of phased antenna array
[NASA-CR-123819] 02 p0151 N73-11222
Numerical techniques for analysis of microstrip transmission line configurations
[AD-746059] 02 p0151 N73-11223
Stripline n-input, n-output cascade network analysis
03 p0278 N73-12254
Feasibility determination for use of p-i-n diodes as switching elements to control impulse signals in strip transmission line
[AD-749125] 05 p0520 N73-14229
Microstrip plasma probe as diagnostic tool in atmospheric entry
[AD-749860] 05 p0585 N73-14757
Fourier and Galerkin techniques for analyzing discontinuities and coupling phenomena in microstrip lines
[AD-750737] 06 p0648 N73-15264
Development of method for calculating characteristics of coupled microstrip lines and directional couplers
[REPT-6731] 10 p1136 N73-19261
Strip transmission line circulators using ferrites, noting new densification method for polycrystalline ferrimagnetic materials
[REPT-8.422] 12 p1384 N73-21222

**STRIPPING**
Hydrogen embrittlement of cadmium coated steels due to paint stripping
[AD-747634] 03 p0319 N73-12599

**STRONTIUM**
Photoionization cross section of barium and strontium, determined with atomic beam crossed with ultraviolet radiation
[MPI-PAE/EXTRATERR-75] 15 p1781 N73-24440

**STRONTIUM COMPOUNDS**
NT STRONTIUM TITANATES
Vibronic interaction in electron paramagnetic resonance spectra of yttrium and scandium doped single strontium chloride crystals
[NASA-CR-131295] 13 p1561 N73-22653
Potential use of strontium barium metaniobate crystals for electro-optics
[AD-762740] 22 p2687 N73-31520

**STRONTIUM TITANATES**
Limitations in microelectronic circuits, design of power Schottky diode, and strontium titanate permittivity
16 p1880 N73-25218
Dielectric, ferroelectric barium strontium titanate for electronic tuning
[AD-765417] 23 p2769 N73-32150

**STRUCTURAL ANALYSIS**
NT BERNSTEIN ENERGY PRINCIPLE
NT DYNAMIC STRUCTURAL ANALYSIS
NT ENERGY METHODS
NT EQUILIBRIUM METHODS
NT FLUTTER ANALYSIS
NT MATRIX METHODS
NT STRAIN ENERGY METHODS
Classification system for indexing and retrieving documents on structural analysis
[ESDU-00.00.01] 01 p0112 N73-10928
Application of integral nonlinear programming and random search techniques for determining minimum weight of reinforcing structures commensurate with strength requirements
01 p0112 N73-10929
Application of reliability based static strength criteria system to analysis of C-141 aircraft - Vol. 1
[AD-742260] 02 p0126 N73-11024
Implementation of reliability based strength criteria system for determining service life of C-141 aircraft structures - Vol. 2
[AD-742261] 02 p0126 N73-11025
Low temperature investigation of polyethylene balloon film mechanical properties and structural factors affecting such properties
[AD-746678] 02 p0194 N73-11572
Development of computer programs to provide finite element method solutions to problems involving elastic and inelastic structures
[AD-746175] 02 p0239 N73-11942
Procedures for computing upper and lower bounds to bending frequencies and estimates of mode shapes of beams with constant stiffness and mass - Part I
[AD-747241] 02 p0239 N73-11946
Flight loads data recording system for F-102 aircraft maneuver load analysis for data acquisition and application to development of structural design criteria
[AD-747016] 03 p0253 N73-12047
Development of airframe integrity investigation procedures to determine structural deficiencies and modifications required to airframes for increased service life
[AD-746881] 03 p0253 N73-12049
Analysis of forces imposed on aircraft wing from landing gear impact in relation to weight of wing, damping, and frequency of periodic load
[AD-747381] 03 p0254 N73-12052
References on fatigue and fracture of aircraft structures and materials to include instruments, sonic fatigue, and mechanical fasteners
[AD-748100] 03 p0254 N73-12053
Procedures for using liquid crystal tape for thermographic testing of bonded structures for aircraft
[NASA-CR-123932] 03 p0300 N73-12451
Numerical analysis of dynamic buckling modes of elastic systems under intensive loading in finite time segment
03 p0360 N73-12937
Photoelastic models of structures containing spherical voids in hexagonal close-packed configuration
[UCRL-73848] 03 p0361 N73-12940
Structural analysis of sandwich panels with close-packed conical shells and honeycombs as fillers
[AD-747403] 03 p0362 N73-12953
Evaluation of structure safety against brittle fracture based on transition temperature, fracture toughness, and crack opening displacement
[ZJE-118] 04 p0481 N73-13933
Elasto-viscoplastic behavior of structures subjected to complex loads and thermal gradients
[ONERA-NT-194] 04 p0482 N73-13937
Stress wave emission techniques for monitoring weld quality and structural validation
[AD-745822] 05 p0552 N73-14486
Development of curves for determining magnitudes and directions of principal stress in plane using components of direct and shear stress
[ESDU-72013] 05 p0601 N73-14889
Analysis of shell theory parameters to determine relationship between stress and displacement fields predicted by shell theory and corresponding actual fields
[WTHD-40] 05 p0602 N73-14895
Derivation of minimum dimension sets of discrete coordinate and hybrid coordinate equations of motion for hinge connected rigid bodies assembled in tree topology
[NASA-CR-129950] 05 p0602 N73-14900
Application of optimality criteria to automation of structural design with emphasis on aerospace applications
[NASA-TN-D-7115] 05 p0603 N73-14901
Analysis of natural vibration characteristics of plate-beam combination structures during supersonic flight
[NAL-TR-291] 06 p0725 N73-15917
Computer program for dynamic structural analyses on three dimensional framework and pipework systems
[TRG-1409-REV-1] 06 p0726 N73-15929
Analysis of response of structure to acoustic excitation to include vibration of structure, natural frequencies and damping, and noise field characteristics
[ESDU-72001-AMEND-A] 07 p0850 N73-16895
Structural analysis of two bonded half planes with finite crack perpendicular to and passing through interface
[NASA-CR-2181] 07 p0852 N73-16910

Analysis of external loads and states of deformation in light elastic structures
[PB-212011] 07 p0852 N73-16911
Theory for nonlinear collapse analysis of shells with general shape
[AD-751702] 07 p0853 N73-16916
Fatigue tests to determine aervice life of catapult structure on C-2 aircraft
[AD-752493] 08 p0868 N73-17028
Development and application of design synthesis methodology for composite structures
[AD-752158] 08 p0936 N73-17667
Computer programmer manual for NASA structural analysis program
[NASA-SP-223[01]] 08 p0966 N73-17892
Development of series of computer programs for structural analysis of axisymmetric shell structures to analyze different modes of structural response
[NASA-CR-2085] 08 p0966 N73-17897
Mechanical properties of unidirectionally solidified, in-situ grown composites
[ONERA-TP-1147] 09 p1051 N73-18570
Computer analysis of random decrement signatures of structures vibrating in random environment
[NASA-CR-2205] 09 p1094 N73-18929
User manual and related documentation for six compatible computer programs for structural analysis of ring-stiffened shells of revolution
[NASA-CR-2086] 09 p1094 N73-18930
FORTRAN subroutines for matrix operations encountered in finite element analysis of structures, noting application to flat plates
[ARC-CP-1223] 09 p1095 N73-18941
Univac 1108 computer for three dimensional stress analysis of complex structures
[AD-753211] 09 p1096 N73-18944
Finite element method of continuum and structural analysis using computer programs - users manual
[AD-753120] 09 p1097 N73-18951
Analysis of fundamental behavior of fiber reinforced plastic composite structures to determine
[AD-754249] 10 p1177 N73-19570
Structure and configuration of European space tug
[HSD-TP-7227-APP-6] 10 p1217 N73-19898
Structural analysis of laminated aluminum alloy sheets to determine flaw growth behavior in roll diffusion bonded and adhesive bonded structures
[NASA-CR-128844] 10 p1220 N73-19921
Influence of combined loading criteria on space shuttle structural performance
[NASA-CR-124113] 11 p1340 N73-20874
Optimization of aircraft structures by finite element modeling and automated structural optimization computer program
[AD-754915] 11 p1344 N73-20905
Addition of three-dimensional isoparametric elements to NASTRAN structural analysis program
[NASA-CR-112269] 11 p1345 N73-20916
Development of structural optimization algorithm used with large finite element program based on displacement method of structural analysis
12 p1356 N73-21005
Three-dimensional finite element studies
[AD-755539] 13 p1571 N73-22734
Development of procedure for designing elevated temperature structures to achieve safety factors and structural integrity of room temperature conditions
[NASA-CR-124232] 13 p1585 N73-22851
Analysis of Michell framework for uniform load between fixed supports
[REPT-1054/73] 13 p1586 N73-22861
Engineer manual for use of MAGIC 3 automated general purpose program for structural analysis
[AD-755368] 13 p1588 N73-22879
User manual for MAGIC 3 automated general purpose program for structural analysis
[AD-755369] 13 p1589 N73-22880
Programmer manual for use with MAGIC 3 automated general purpose program for structural analysis
[AD-755370] 13 p1589 N73-22881
Development of reliability analysis procedure for determining effects of cumulative and maximum operational loads on airplane structures
[AD-757529] 14 p1603 N73-22999
Development of stability matrices of displacement type for multilayer sandwich beam, rectangular, and triangular plate elements
14 p1714 N73-23908
Structural design criteria to develop structures with minimum weight and safe equilibration of externally applied loads
[ARC-R/M-3303] 15 p1730 N73-24029
Numerical analysis of bending of rotating beams with application to linear flap-lag stability of hingeless rotary wings using nonlinear equations
[NASA-TM-X-2770] 15 p1838 N73-24897
Holography and optical filtering techniques for structural analysis, material tests, and astronomical observation - conference
[NASA-SP-299] 16 p1920 N73-25540
Analysis of optimal configurations for thin walled, axisymmetric, laminated shells based on shell configuration, loading, fiber alignment, and material properties of composite structure
16 p1969 N73-25924
Dual finite element and shell theory analyses of linear and nonlinear structures
[AD-758790] 16 p1970 N73-25933
Register of experts for information on mechanics of structural failure to support safety and technology aspects of aerospace industry
[NASA-CR-121200] 17 p2091 N73-26918
Structural inspection for maintaining airworthiness of older aircraft
[NASA-TM-X-2845] 17 p2092 N73-26925
Analysis of glass fiber reinforced plastic laminated structures
[MBB-UD-79-72-O] 17 p2094 N73-26942
Research projects conducted by organizations of National Research Council of Canada on structural analysis, jet fuels, air pollution, and very low frequency navigation
[DME/NAE-1973[1]] 17 p2098 N73-26970
Analysis of fatigue fracture under combined stress conditions for specimens of various cross sections
[NLL-RTS-7770] 18 p2202 N73-27776
Devleopment of computer program for determining ultimate optimum behavior of dynamically loaded structural-mechanical system
[NASA-CR-2268] 18 p2203 N73-27783
Automation of input/output routines for use with computerized data processing of finite element structural analyses
[AD-761154] 18 p2204 N73-27793
Application of oscillation theory and mathematical statistics to problems of aircraft structures and aerodynamic loads on aircraft and missiles
[NASA-TT-F-753] 19 p2220 N73-27908
Development of mathematical model for determining replacement criteria for aircraft structural components
[AD-762226] 19 p2222 N73-27921
Development of doubly curved triangular finite element for use in small deformation analysis of thin shells containing cutouts and irregular boundaries
[RE-453] 19 p2347 N73-28882
Modification of input/output procedures to computer code for structural analysis of general shells
[AD-761806] 19 p2350 N73-28905
Natural mode vibration analysis of aircraft structural systems by direct and component mode synthesis techniques applied to tilt rotor VTOL aircraft aeroelasticity - Vol. 2
[NASA-TM-X-69496] 20 p2359 N73-28977
Research projects involving aeroelastic stability and response, stability of thin shell structures, and suspension system concept for control of vehicle responses
[AD-762568] 20 p2359 N73-28979
Evaluation of structural layers in flexible pavement during simulated aircraft traffic
[AD-762131] 20 p2383 N73-29149
Proceedings of conference on acoustic fatigue to show effects of aerodynamic loads, response of structures, structural design, and fatigue test methods
[AGARD-CP-113] 20 p2478 N73-29905
Analysis of dynamics of stiffened plates using finite element modelling of flat and curved stiffened panels
20 p2479 N73-29911
Analysis of response and fatigue characteristics of light alloy integrally machined planks with emphasis on acoustic fatigue properties
20 p2479 N73-29912
Analysis of structural response to acoustic loading and preparation of data sheets for various conditions of acoustic loads
20 p2479 N73-29914
Structural response and endurance tests of aircraft structural components to determine effect of critical environment on acoustic fatigue
20 p2480 N73-29920
Acoustic fatigue tests of aluminum alloy structural elements under narrow-band, random loading with zero mean stress in skin
20 p2480 N73-29921
Development of fatigue life prediction procedures based on measured stress-time histories and mathematical model for description of random vibrations
20 p2481 N73-29926
Application of high strength structural materials for aerospace vehicles and use of fracture control procedures for improved damage tolerance
20 p2481 N73-29928
Application of growth rate data and analytical retardation models for predicting crack growth under variable amplitude loading
20 p2481 N73-29932
Development of procedure for estimating fatigue life of airframes to eliminate errors caused by neglecting effect of stress redistribution after localized yielding
20 p2481 N73-29933
Exact solution for free transverse vibrations of annular plate with supported inner and free outer edge-beams
20 p2482 N73-29938
Ground vibration tests of YF-12 aircraft to determine frequency response data, measured node lines, and elastic mode shapes for aircraft components
[NASA-TM-X-2880] 20 p2483 N73-29944
Development of methods for analyzing thermal stress, heat conduction, structural theory, and thermoelastic wave propagation
[AD-762479] 20 p2484 N73-29952
Derivation of finite element properties in terms of stress functions for structural and nonstructural applications
[AD-762947] 20 p2484 N73-29953
Analysis of flight test procedures for evaluating strength of airframes for aircraft and helicopters
[NASA-TT-F-769] 21 p2494 N73-30019
Development of digital computer program for generating individual component or entire aircraft mass and aerodynamic models for vehicle inelastic bending response analysis
[AD-763701] 21 p2498 N73-30045
Analysis of equipment and procedures for conducting sonic fatigue tests of airframes at elevated temperatures
[AD-763798] 21 p2498 N73-30052
Effects of wind loads on structures and structural design criteria based on wind speed, structural shape, and aerodynamic coefficients
[NLL-LIB-TRANS-1705-[5205.9]]
21 p2602 N73-30857
Application of Galerkin method in nonconservative stability problems relating to thin elastic plates and slender elastic rods
[NRC-TT-1673] 21 p2603 N73-30860
Matrix perturbation techniques in structural dynamics
[NASA-CR-133795] 21 p2603 N73-30862
Development of linear analysis method for predicting buckling of composite structures with arbitrary uniform cross section
[NASA-CR-2216] 21 p2603 N73-30863
Computer program for analysis of nonlinear deformation and fatigue response of components subjected to complex load histories
[AD-763780] 21 p2604 N73-30870
Finite element method to determine post-buckling strength of B-1 aircraft aft intermediate fuselage following combined torque and axial loading
[AD-763813] 22 p2615 N73-30956
FORTRAN matrix abstraction program for structural analysis of aerospace structures, Vol. 2 - Digital computer program description
[AD-764360] 22 p2640 N73-31158
FORTRAN matrix abstraction program for structural analysis of aerospace structures, Vol. 5 - Engineering user and technical report
[AD-763812] 22 p2640 N73-31159
FORTRAN matrix abstraction program for structural analysis of aerospace structures, Vol. 6 - Digital computer program Phase 1 description
[AD-764366] 22 p2640 N73-31160
BOPACE program for advanced thermal-elastic-plastic-creep structural analysis
[NASA-CR-124390] 22 p2725 N73-31805
Computer program for use with thermal-elastic-plastic-creep structural analyzer for structural analysis of spacecraft and propulsion systems - Vol. 2
[NASA-CR-124391] 22 p2725 N73-31806
Resonant vibration structural analysis of cylindrical sandwich shells
[TUB-IR-1972/2] 22 p2725 N73-31808
Proceedings of conference on structural analysis with application to ships, guns, hydrofoils, marine propellers, and radar antennas
[AD-764508] 22 p2726 N73-31818
General purpose computer program for inelastic dynamic response of plane structure
[PB-221260/3] 22 p2727 N73-31823
Condensation method and computer program for reducing truncation errors for vibration analysis of complex structures
[NASA-CR-124446] 23 p2812 N73-32484
Nonlinear analysis for thin elastic shells using modal expansion method of linear vibration analysis extended to nonlinear analog
23 p2852 N73-32793
Optimum structural design of discretely ring-stiffened cylindrical shell
23 p2853 N73-32794
Structural optimization procedures applied to design of simply supported, corrugated hat stiffened composite panel under uniaxial compression
[NASA-CR-132314] 23 p2853 N73-32798
Theoretical analysis background for shell theory automated for rotational structures [STARS-2] program - Vol. 1
[NASA-CR-2273-VOL-1] 23 p2854 N73-32801
Procedure for structural analysis of stiffened shells of revolution to describe computer program and types of shapes and cross sections of specimens - Vol. 2
[NASA-CR-2273-VOL-2] 23 p2854 N73-32802
User manual for shell theory automated for rotational structures [STAR 2B, 2V] - Vol. 3
[NASA-CR-2273-VOL-3] 23 p2854 N73-32803
Engineering programming information for digital computer program developed for structural analysis of shells - Vol. 4
[NASA-CR-2273-VOL-4] 23 p2854 N73-32804

Engineering programming information for digital computer program developed to analyze buckling characteristics of shell structures - Vol. 5
[NASA-CR-2273-VOL-5] 23 p2854 N73-32805
Engineering programming information for digital computer program developed to analyze vibration effects on shell structures - Vol. 6
[NASA-CR-2273-VOL-6] 23 p2854 N73-32806
Satellite programs for computer program applied to structural analysis of shells to include user and programming information - Vol. 7
[NASA-CR-2273-VOL-7] 23 p2854 N73-32807
Development of procedures for simultaneous structure and parameter identification of linear dynamical systems
[TAE-173] 23 p2854 N73-32808
Elastic-plastic analysis of wheel rolling on rigid track
[AD-764575] 23 p2855 N73-32812
Post yield behavior of beam with partial end fixity
[AD-764576] 23 p2855 N73-32813
Structural analysis of unsymmetrically laminated anisotropic plates using linear plate theory and strain-displacement relations
24 p2987 N73-33875
Nonlinear analysis of structures by finite element method as supplement to linear analysis
[WTHD-51] 24 p2988 N73-33881

**STRUCTURAL BASINS**
NT GREAT BASIN [US]
NT LAKE CHAMPLAIN BASIN [NY-VT]
NT RIVER BASINS
NT WABASH RIVER BASIN [IL-IN-OH]
NT WATERSHEDS
Interpretation and mapping large scale structural lineaments in Precambrian shield areas and basins containing younger sediments using ERTS-1 imagery
[E72-10180] 01 p0045 N73-10359
Processing of IFYGL data for Lake Ontario and its drainage basin
[E73-10393] 11 p1276 N73-20355
Interpretation of Apollo 16 photography of Orientale Basin deposits under earthshine illumination conditions - Part E
12 p1453 N73-21769
Discovery of previously unknown structural basin and crater on Apollo 16 photography of far side highlands near eastern limb of moon - Part H
12 p1453 N73-21772
Automatic processing of ERTS-1 data for physiography and geologic mapping of San Juan Basin, Colorado
[NASA-CR-131577] 13 p1524 N73-22346
Oil exploration in large intercratonic sedimentary basins in Oklahoma using ERTS-1 imagery
[E73-10646] 16 p1897 N73-25342
Lithological and structural surveys of sedimentary basin in France from ERTS-1 MSS imagery
[E73-10656] 16 p1898 N73-25352
Structural geology of Massif Central and Parisian Basins, France from ERTS-1 imagery
[E73-10657] 16 p1898 N73-25353
Analysis of ERTS-1 MSS imagery to determine geological and structural features in sedimentary basin in France
[PAPER-G6] 19 p2263 N73-28237
Geomorphology of Martian and lunar large multi-ringed circular basins
23 p2839 N73-32687

**STRUCTURAL BEAMS**
U BEAMS [SUPPORTS]

**STRUCTURAL DESIGN**
NT PRESSURE VESSEL DESIGN
Design of satellite and satellite components for Atmospheric Explorer missions to include electrical, mechanical, and environmental interfaces
[NASA-CR-130085] 01 p0049 N73-10395
Guide to early stage design choice of thrust bearing
[ESDU-67033] 01 p0060 N73-10489
Early stage design and choice of journal bearings
[ESDU-65007] 01 p0061 N73-10495
Design and fabrication of honeycomb resin-composite sandwich panels for shuttle orbiter thermal shielding
[NASA-CR-128610] 01 p0061 N73-10503
Detailed design guidance for flexure-pivots with strips crossing midway along lengths and at right angles to each other
[ESDU-67021] 01 p0110 N73-10907
General design principles for minimizing fatigue failure in structures and components
[ESDU-71009] 01 p0111 N73-10914
Stress and strength guide for engineering design
[ESDU-SS1] 01 p0111 N73-10917
Design optimization for gallium arsenide solar cell parameters
[NASA-CR-129214] 02 p0128 N73-11041
Functional analysis and logical construction systematics for signal processing equipment design
02 p0140 N73-11136
Data for major dimension determination for straight spur and helical gears
[ESDU-68040-AMEND-A] 02 p0176 N73-11428
Design of steadily loaded, pressure fed, 360 degree, hydrodynamic journal bearings
[ESDU-66023] 02 p0177 N73-11431
Structural changes in high bypass ratio engines for fan noise reduction to jet noise level
03 p0249 N73-12017
Suppression of fan noise and effects on short takeoff aircraft systems design
03 p0250 N73-12023
Transport characteristics for calculating plasma diode design parameters
[TEE-3056-1] 03 p0274 N73-12221
Structural design of implosion-driven hypervelocity launchers
[AD-742993] 03 p0281 N73-12280
Design and performance of rechargeable zinc-air batteries
[AD-748455] 04 p0376 N73-13058
Cost estimates and design of electron synchrotron injector for high energy rings
[DNPL/R-13] 04 p0401 N73-13268
Design of quadrupolar focusing lenses for drift tubes of heavy ion accelerator
[LYCEN-7179] 04 p0402 N73-13270
Swinging ball viscosimeter design and calibration for water viscosity measurements
[AD-745252] 04 p0424 N73-13456
Design and development of very high speed transportation system to include technological aspects and physical restraints
[P-4874] 04 p0488 N73-13990
Structural design and load tests on carbon fiber reinforced plastic VC-10 aileron control strut
[ARC-CP-1229] 05 p0603 N73-14903
Design, fabrication, and comparison of heat pipes for temperature control in meteorological satellite
[ESRO-CR-59] 05 p0606 N73-14929
Airfoil with cambered trailing edge section for supersonic flight
[NASA-CASE-LAR-10585-1] 06 p0613 N73-14981
Optimal design of baseline configuration for solar array panel with deployable beam
[NASA-CR-130287] 06 p0626 N73-15079
Design and performance of mechanically rechargeable zinc air battery
[AD-749779] 06 p0627 N73-15086
Electrical and structural criteria for design optimization of integrated circuits
[AD-750947] 06 p0648 N73-15261
Design and performance of optical altimeter with shaft angle recording
[AD-749964] 06 p0675 N73-15488
Design and performance of flash lamps with nanosecond light pulses
[AD-750788] 06 p0701 N73-15720
Design of high power air cooled microwave S band junction circulator using YIG rod and boron nitride transformers
[AD-751743] 07 p0762 N73-16194
Design of hopping transporter for lunar exploration
[NASA-CR-130010] 07 p0765 N73-16217
Design of pulsed electron beam accelerator with multiple Mylar stripline modules
[AD-751593] 07 p0766 N73-16227
Design and performance of exhaust hood with protective air current outside of hood surface
08 p0872 N73-17063
Concept evaluation and subsystem analyses for design of remote controlled teleoperator visual system
[NASA-CR-124059] 08 p0879 N73-17117
Multivariate limits for describing cockpit related anthropometric features of aviation personnel
[AD-752032] 08 p0880 N73-17124
Parametric design optimization for multiple element short backfire antenna array
[AD-751918] 08 p0889 N73-17199
Design modules for optical equipment
[AD-751964] 08 p0944 N73-17732
Updated structural design criteria for manned space shuttle missions
[NASA-SP-8057-REV] 08 p0964 N73-17881
Structural configuration and performance tests of 928 sq m solar array
09 p1089 N73-18891
Design and performance of metabolic gas analyzer using mass spectrometer and digital data printout
[NASA-CR-128842] 10 p1124 N73-19160
Design and performance of carbon dioxide laser amplifier with double discharge electrode geometry
[DREV-TN-2022/72] 10 p1134 N73-19240
Design and performance of Compton diode radiation detector
[SC-DR-72-0118] 10 p1134 N73-19242
Structural design guidance and construction standards for upgrading and extending service life of airport pavements
[FAA-ED-08-2] 10 p1137 N73-19266
Design and performance tests of prototype self-locking actuator
[NASA-CR-124135] 10 p1163 N73-19459
Design of elastically geared circular disk wave drive motor and telemanipulator
[NASA-TT-F-14803] 10 p1165 N73-19482
Design of hydrostatic shaft guide bearings for sodium pumps
[CEA-CONF-2045] 10 p1166 N73-19486
Handbook for design of isogrid, triangular integrated stiffened structures for spacecraft structures and components
[NASA-CR-124075] 10 p1219 N73-19911
Design of pyrotechnical gas generator for gate valve control
[AD-754963] 11 p1301 N73-20556
Design of noise source for simulating supersonic spinning modes in duct acoustics
[NASA-CR-2260] 12 p1364 N73-21067
Development and design of satellite cable boom
[HSD-TP-7356] 12 p1366 N73-21086
Design of hemoglobin tester, flow ventilation systems, blood viscometer, isotope handling equipment, and blood pressure measuring device
[NASA-TM-X-66214] 12 p1373 N73-21139
Design of electrophoretic mass screening tester for sickle cell anemia
12 p1373 N73-21140
Design of anesthetic flow valve canister system for exhaust gas absorption and laminar ventilation system for operating rooms
12 p1373 N73-21141
Design of relative velocity blood viscometer
12 p1373 N73-21142
Design of solar energy concentrators with concentric circular seams of plastic films
[AD-755829] 12 p1446 N73-21712
Guidance and control concepts for structural control interactions and dynamic loads
[NASA-TM-X-64732] 12 p1461 N73-21834
Design of despin mechanism noting thermal and stress analysis of beryllium and aluminum as structural materials
[ESRO-CR[P]-226] 13 p1534 N73-22432
Design study of despin mechanism noting alignment accuracy, lubrication system, load carrying capacity and bearings
[ESRO-CR[P]-227-APP] 13 p1535 N73-22433
Design of despin mechanism noting angular stiffness, stress analysis, signal transmission, power transmission, instrumentation and ground support equipment
[ESRO-CR[P]-228] 13 p1535 N73-22434
Design of tunable electron paramagnetic resonance spectrometer with quartz stabilization
13 p1565 N73-22684
Preliminary definition study of a sortie module/pallet system noting configurations, thermal control, attitude control, power and communications subsystems
[ESRO-CR[P]-240] 13 p1582 N73-22828
Guidelines for spacecraft structural design requirements emphasizing project planning and management methods
[ESRO-CR[P]-200] 13 p1586 N73-22857
Guidelines for spacecraft structural design requirements noting management and compilation methods
[HSD-TP-7363] 13 p1586 N73-22858
Design, fabrication, and evaluation of boron-epoxy reinforced C-130 center wing boxes
[NASA-CR-112272] 14 p1601 N73-22979
Design and cost estimate of high altitude wind power plant
[NASA-TT-F-14903] 14 p1605 N73-23011
Design and fabrication of prototype particulate regenerative filter with backflush for spacecraft fluid system
[NASA-CR-115505] 14 p1614 N73-23084
Design of test facility for turbofan engines at subsonic operation
[AD-757197] 14 p1646 N73-23352
Feasibility of modifying supersonic drone configuration into remotely controlled research vehicle
[NASA-CR-112323] 15 p1733 N73-24057
Design and operation of superconducting quantum point contact interference device
[PB-214758/5] 15 p1823 N73-24775
Interface control documenation for design and development of Apollo ultraviolet spectrometer experiment
[NASA-CR-128550] 16 p1917 N73-25511
Design of high temperature and high pressure furnace for crystal growth
[AD-759786] 16 p1954 N73-25811
Design of vertical multijunction silicon solar cells with prolonged lifetimes
[AD-760172] 17 p1986 N73-26052
Design of water activated zinc-air battery
[AD-759932] 17 p1986 N73-26053
Conference on manipulator design considering basic elements
17 p1989 N73-26074
Design requirements for remotely controlled master-slave manipulators
17 p1989 N73-26076
Manipulator kinematics in selecting geometrical shapes of containers and chambers
17 p1990 N73-26087
Analytical methods for evaluating high performance ship design concepts particularly hydrofoil concepts
[AD-759376] 17 p2009 N73-26251

Design procedure for hydrostatic ring thrust bearings
[NRC-13180PT-3] 17 p2037 N73-26478
Design and performance of momentum wheel suspended by magnetic bearings for rotor operation in space environment
18 p2209 N73-27829
Design of torque motor with armature windings cast in epoxy cylinder and conductors cast integrally with aluminum mounting ring
18 p2209 N73-27830
Nonlinear programming algorithms for variable design of structural cylindrical shell
[AD-761645] 19 p2240 N73-28062
Design of MOS floating gate transistor amplifier
[AD-761660] 19 p2244 N73-28092
Design and performance modeling of liquid metal reactor thermoelectric space power system
[NASA-CR-121241] 19 p2320 N73-28661
Optimization method for minimum weight design of structures made from fiber reinforced composites
[AD-763732] 21 p2565 N73-30558
Design methodology for airfield pavements
[AD-763212] 22 p2648 N73-31215
Design and performance of silicon Schottky barrier avalanche diodes
23 p2764 N73-32113
Design and operational technology associated with radio telescope antennas
[JPRS-59985] 23 p2837 N73-32671
Structural methods for increasing effectiveness of fully rotatable parabolic antennas
23 p2837 N73-32673
Method for iterative reanalysis in automated structural designs using direct stiffness approach
[NASA-TN-D-7357] 23 p2853 N73-32797
Space environment effects on space shuttle thermal protection system design
[NASA-TM-X-2721] 24 p2941 N73-33490
Optical property effect in thermal design for insulation coating attachments
24 p2942 N73-33492
Design of rigid ceramic foam insulation for space shuttle surface thermal protection
24 p2942 N73-33493
Flexible ceramic mat surface insulation for space shuttle thermal protection system design
24 p2942 N73-33497
Thermostructural evaluation of mullite and silica composite materials for space shuttle surface insulation system design
24 p2942 N73-33498
Interference heating in gaps between surface insulation tiles for space shuttle thermal protection system design
24 p2942 N73-33499
Computer programs for three dimensional civil engineering lattice structures noting matrix methods, computerized design, and repetitive lattices
[CRIF-MT-82] 24 p2989 N73-33889
Viscoelastic effects in design of polymeric equipment and structures
[AD-764555] 24 p2989 N73-33890

**STRUCTURAL DESIGN CRITERIA**

Methodology for combining thermal structural loads as design criteria for thermal protection system of space shuttle orbiter
[NASA-CR-2102] 02 p0234 N73-11898
Criteria for predicting, preventing, and evaluating panel flutter
[NASA-SP-8004] 02 p0237 N73-11932
Development of aerodynamic structural design data to reduce effects of acoustic fatigue on flat and singly-curved sandwich panels - Part 2
[AGARD-AG-162-PT-2] 05 p0602 N73-14898
Application of optimality criteria to automation of structural design with emphasis on aerospace applications
[NASA-TN-D-7115] 05 p0603 N73-14901
Criteria for designing launch vehicle structural reliability
[NT-D3-71.040] 07 p0850 N73-16890
Development and application of design synthesis methodology for composite structures
[AD-752158] 08 p0936 N73-17667
Structural design criteria for ramjet combustion chamber
[PB-212691] 11 p1335 N73-20838
Optimization of aircraft structures by finite element modeling and automated structural optimization computer program
[AD-754915] 11 p1344 N73-20905
FAA research and development in airport paving criteria
13 p1506 N73-22205
Preliminary definition study of sortie laboratory noting structural design, subsystems and shuttle interface
[MBB-SL-72-04] 13 p1582 N73-22826
Survey of optimal structural design techniques to include method of fully stressed design and linear programming problems
[REPT-10432] 14 p1714 N73-23911
Structural design criteria to develop structures with minimum weight and safe equilibration of externally applied loads
[ARC-R/M-3303] 15 p1730 N73-24029
Design criteria and analysis procedures to minimize occurrence of major structural failures in airframes due to undetected damage
[AD-757870] 15 p1735 N73-24074
Optimization of mass distribution of solid beams and panels for structural design of airframes and panels
[AD-759169] 16 p1859 N73-25054
Hydrofoil design criteria based on model for minimum control power
[AD-759286] 16 p1892 N73-25312
Stress analysis verification of structural integrity of Apollo ultraviolet spectrometer experiment
[NASA-CR-128551] 16 p1916 N73-25501
Analysis of optimal configurations for thin walled, axisymmetric, laminated shells based on shell configuration, loading, fiber alignment, and material properties of composite structure
16 p1969 N73-25924
Development of formula for determining ideal weight of shell-type aircraft fuselages with body of revolution cross section
[RAE-LIB-TRANS-1688] 17 p1981 N73-26009
Analysis of fatigue behavior of airframe components and development of methods for predicting service life of aircraft structures
[RAE-LIB-TRANS-1678] 17 p1981 N73-26012
Register of experts for information on mechanics of structural failure to support safety and technology aspects of aerospace industry
[NASA-CR-121200] 17 p2091 N73-26918
Bibliography of citations related to problem areas in mechanics of failure in aerospace structures
[NASA-CR-121202] 17 p2091 N73-26920
Laminated composite cylindrical shell buckling strength criteria
[AD-759537] 17 p2095 N73-26944
Airport construction procedures to include general requirements, construction materials, and operational maintenance
[AD-759243] 18 p2127 N73-27191
Design criteria and materials for reducing structural weight of hydrofoil boats
[AD-761123] 18 p2132 N73-27222
Development of computer program for optimum design of submarine hulls with frame stiffened cylindrical structures
[AD-761643] 19 p2349 N73-28893
Application of constrained optimal design approaches for minimum mass designs of damped, linear, continuous sandwich beam
[AD-761881] 19 p2349 N73-28896
Analysis of structural response to acoustic loading and preparation of data sheets for various conditions of acoustic loads
20 p2479 N73-29914
Effects of wind loads on structures and structural design criteria based on wind speed, structural shape, and aerodynamic coefficients
[NLL-LIB-TRANS-1705-[5205.9]]
21 p2602 N73-30857
Criteria for acceptance of early design information with application to design studies and cost estimates for liquid hydrogen fueled aircraft and remotely piloted vehicles
[NASA-TM-X-62303] 22 p2613 N73-30943
Optimum structural design of discretely ring-stiffened cylindrical shell
23 p2853 N73-32794
Thermal and structural performance tests on space shuttle orbiter surface insulation materials
24 p2941 N73-33489
Containment design calculations for cylindrical vessel wall response to explosion
[SLA-73-508] 24 p2992 N73-33916

**STRUCTURAL DYNAMICS**
U DYNAMIC STRUCTURAL ANALYSIS

**STRUCTURAL ENGINEERING**

Aerospace engineering including materials, orbits and trajectories, power sources, satellite geodesy, and structural engineering
[NASA-CR-128329] 01 p0119 N73-10981
Use of data items on buckling of plates and compression panels manufactured from isotropic materials
[ESDU-72012] 06 p0723 N73-15906
Development of optimized aircraft structures based on vibratory strain energy distribution using damped forced response
[AD-751809] 07 p0741 N73-16027
Literature review on design and performance of multistage rockets
[AD-752815] 08 p0956 N73-17824
Development of series of computer programs for structural analysis of axisymmetric shell structures to analyze different modes of structural response
[NASA-CR-2085] 08 p0966 N73-17897
Computer techniques and test facilities for structural engineering at German university institute
[ISD-119] 09 p1095 N73-18935
Structural design criteria to develop structures with minimum weight and safe equilibration of externally applied loads
[ARC-R/M-3303] 15 p1730 N73-24029

**STRUCTURAL FAILURE**

General design principles for minimizing fatigue failure in structures and components
[ESDU-71009] 01 p0111 N73-10914
Buckling characteristics of perfect and imperfect circular cylindrical shells subjected to dynamic axial loading
[NASA-CR-129086] 02 p0237 N73-11927
Aircraft accident involving Beechcraft 18 aircraft on air taxi flight from Cleveland, Ohio airport on 22 June, 1972
[NTSB-AAR-72-33] 07 p0738 N73-16006
Development of three stage model for fatigue failure of structure with several critical regions for initial failure
[ARL/SM-NOTE-338] 09 p1093 N73-18924
Fracture mechanics and structural fatigue of nickel alloys, aluminum alloys, and molybdenum alloys at elevated temperatures
[AD-753687] 09 p1097 N73-18958
Space vehicle design to withstand adverse conditions involved in handling and transportation from factory to launch site
[NASA-SP-8104] 12 p1461 N73-21839
Analysis of resistance of reinforced and unreinforced structural plastics to static and fatigue failure
[AD-758626] 15 p1802 N73-24608
High temperature strength and deformation properties of Ti-Al-Si alloy aged by alpha phase precipitate particles
[NASA-TN-D-7325] 16 p1928 N73-25597
Fatigue failure criterion for fiber reinforced laminates under stress
[AD-760146] 17 p2053 N73-26609
Bibliography of citations related to problem areas in mechanics of failure in aerospace structures
[NASA-CR-121202] 17 p2091 N73-26920
Nonlinear vibrations and failure of shallow shells of random shape under stress of white noise
[AD-761449] 19 p2349 N73-28898
Fatigue failure of notched samples of titanium alloy
[AD-761588] 19 p2350 N73-28904
Aircraft accident involving crash of TU-144 aircraft at Paris Air Show in 1973
[NASA-TT-F-15062] 20 p2360 N73-28982
Preliminary analysis of possible factors associated with asphaltic concrete airfield pavement defects
[AD-762404] 20 p2383 N73-29150
Address on problems of acoustic fatigue
20 p2478 N73-29906
Techniques for controlling time to fatigue crack initiation in design of aircraft structures and application of residual stress analyses
20 p2481 N73-29930
Development of rational analytic theory for analyzing fatigue of airframes based on maximum stress-field parameter and maximum load excursion ratio
20 p2481 N73-29931
Application of growth rate data and analytical retardation models for predicting crack growth under variable amplitude loading
20 p2481 N73-29932
Analysis of errors in fatigue life prediction procedures and methods for improving accuracy of prediction analysis techniques
20 p2481 N73-29934
Mathematical models for determining dynamic response of strain sensitive materials and structure to dynamic loads
22 p2724 N73-31797
Design criteria for supersonic overflight to reduce psychophysical effects and decrease glass damage probability
[FAA-RD-73-116] 22 p2724 N73-31800
Cristobalite transformation effects on tensile strength of silica surface insulation materials
24 p2943 N73-33500

**STRUCTURAL FATIGUE**
U FATIGUE [MATERIALS]

**STRUCTURAL FOUNDATIONS**
U FOUNDATIONS

**STRUCTURAL MATERIALS**
U CONSTRUCTION MATERIALS

**STRUCTURAL MEMBERS**
NT ANISOTROPIC PLATES
NT BEAMS [SUPPORTS]
NT BOX BEAMS
NT CANTILEVER BEAMS
NT CIRCULAR PLATES
NT COLUMNS [SUPPORTS]
NT CORRUGATED PLATES
NT ELASTIC PLATES
NT FLAT PLATES
NT I BEAMS
NT MEMBRANE STRUCTURES
NT ORTHOTROPIC PLATES
NT PERFORATED PLATES
NT PLATES [STRUCTURAL MEMBERS]
NT POROUS PLATES
NT RECTANGULAR BEAMS
NT REINFORCED PLATES

NT SKIN [STRUCTURAL MEMBER]
NT STRINGERS
NT STRUTS
NT TRUSSES
NT WING PANELS
Stress wave emission nondestructive inspection technique for detecting flaw criticality in structural parts
[AD-747225] 02 p0176 N73-11426
Production engineering methods for metal ceramic structural materials and parts
[JPRS-57487] 04 p0431 N73-13515
Design and technical characteristics of rotary automatic devices for pressing and gauging of metal ceramic structural parts
04 p0432 N73-13524
Fabrication of light weight panel structure using pairs of elongate hollow ribs of semicircular configuration
[NASA-CASE-LAR-11052-1] 04 p0481 N73-13929
Simulation of ratcheting behavior of loaded structural components subjected to nonuniform thermal cycling
[AD-753686] 09 p1050 N73-18563
Stress analysis of ITOS D and E structural members - Vol. 3
[NASA-CR-130162] 09 p1087 N73-18865
Application of correlation equations to evaluate structural strength and reliability of various materials
[AD-753497] 09 p1097 N73-18956
Apollo experience report on causes of stress-corrosion cracking of structural materials and corrective actions
[NASA-TN-D-7111] 10 p1214 N73-19875
Methods for bounding life of structures subjected to constant loads and temperature within creep range
[RD/B/N-2257] 10 p1220 N73-19925
IBM 360 FORTRAN computer program for three dimensional stress analysis of structural parts
[AD-753617] 10 p1221 N73-19932
NASTRAN computer program for determining stress cencentration at holes in isotropic finite strips
[AD-753574] 10 p1221 N73-19933
Plastic instability in stainless steels and effects on load bearing capacity of structural components
[COO-2048-8] 12 p1463 N73-21850
Acoustic fatigue characteristics of flat multi-layered structural panel
[NASA-CR-124079] 13 p1546 N73-22529
Calculation of effect of short-term impulse loads on structures with finite and infinite numbers of degrees of freedom
[AD-756959] 13 p1587 N73-22868
Pulsed holographic measurement of wave propagation in thin walled shells and vibration modes in steel rectangular plates at high temperature
16 p1921 N73-25544
Structural properties and stability of solid materials and structures with different geometric configurations
[AD-759558] 16 p1971 N73-25942
Statistical energy and deterministic analyses on dynamic response of coupled rods to longitudinal acoustic excitation
[AD-760276] 17 p2095 N73-26951
Analysis of programs for acoustic testing of composite material components and development of theory for predicting natual frequencies, mode shapes, and stresses in composite panels
20 p2480 N73-29918
Device for securing together structural members with axially stretched bolt and nut
[NASA-CASE-GSC-11149-1] 21 p2552 N73-30457
Analysis of buckling behavior of viscoelastic structural member
[PB-221835/2] 22 p2726 N73-31817
Hot forging of aluminum alloy structural parts
[AD-764618] 23 p2798 N73-32384
Laws governing stress-rupture strength for structural materials under conditions of cyclic loading
[AD-764665] 23 p2854 N73-32810

**STRUCTURAL PROPERTIES [GEOLOGY]**
Interpretation and mapping large scale structural lineaments in Precambrian shield areas and basins containing younger sediments using ERTS-1 imagery
[E72-10180] 01 p0045 N73-10359
Study of crustal structure from eastern Sierra Nevada to Colorado Plateau using ERTS-1 imagery
[E72-10192] 01 p0046 N73-10371
Lithological and structural surveys of African rift system using ERTS-1 imagery
[E72-10194] 01 p0046 N73-10373
Geological fracture mapping based on enhancement of ERTS-1 snow cover imagery of Massachusetts, Connecticut, and Feather River/Lake Tahoe area
[E72-10205] 02 p0161 N73-11302
Recognition of geologic framework for copper porphyry-type deposits on ERTS-1 imagery
[E72-10210] 02 p0161 N73-11305
ERTS-1 imagery of structures and lithology of Northern California Coast Ranges and Sacramento Valley, California
[E72-10214] 03 p0288 N73-12332
Stratigraphy, structure, and geologic history of Sangre de Cristo Mountains of Colorado based on aerial remote sensing
[NASA-CR-129519] 03 p0293 N73-12385
Geomorphology, tectonics, and structural relations between Alps and Pyrenees based on ERTS-1 imagery
[E72-10286] 04 p0410 N73-13336
Identification of continental crust geostructures and their relation to mineral resources based on ERTS-1 imagery
[E72-10296] 04 p0410 N73-13346
Spectral geological mapping in diverse terranes of New York using ERTS-1 imagery
[E72-10302] 05 p0530 N73-14309
Geological structural surveys of North Carolina based on ERTS-1 imagery
[E72-10325] 05 p0530 N73-14313
Utility of ERTS-1 imagery in study of geological structures and exploration for economic mineral deposits in Utah and Nevada
[E72-10332] 05 p0531 N73-14320
ERTS-1 imagery of structure and lithology of Northern California Coast Ranges and Sacramento Valley
[E72-10333] 05 p0531 N73-14321
Mapping of regional fracture patterns and related structural features of Wind River Mountains using ERTS-1 imagery
[E72-10349] 05 p0533 N73-14337
Utilization of ERTS-1 imagery for mapping large scale structural lineamants in Precambrian Shield and basins containing younger sediments and for mineral and petroleum exploration
[E73-10004] 06 p0658 N73-15340
Geological structure of selected areas of East Africa based on ERTS-1 imagery
[E73-10005] 06 p0658 N73-15341
Recognition of geologic framework of copper and molybdenum porphyry deposits on ERTS-1 imagery of Navada and Utah
[E73-10020] 06 p0659 N73-15356
Mapping of major geological structures of African Rift System using ERTS-1 imagery
[E73-10026] 06 p0660 N73-15360
ERTS-1 imagery of crustal structure of area from eastern Sierra Nevada to Colorado Plateau
[E73-10028] 06 p0660 N73-15361
Geological mapping of New York State using ERTS-1 imagery
[E73-10031] 06 p0660 N73-15364
Regional geologic, tectonic, and volcanic surveys of Bolivia using ERTS-1 imagery
[E73-10286] 08 p0914 N73-17492
Identification and interpretation of tectonic features of Colorado, California, and Sonora, Mexico
[E73-10275] 09 p1020 N73-18324
Evaluation of ERTS-1 imagery for mapping geological structures in New York
[E73-10298] 09 p1021 N73-18330
Evaluation of ERTS-1 imagery for study of geological structures and features and exploration of mineral deposits in Utah and Nevada
[E73-10313] 09 p1022 N73-18345
ERTS-1 imagery of geostructures of Alaskan continental crust and relation to mineral resources
[E73-10321] 09 p1024 N73-18353
ERTS-1 imagery of structural geology and volcanology in Central High Plateau of Bolivian Andes
[E73-10296] 10 p1146 N73-19333
Geologic and land use exploitation of ERTS-1 imagery of New England using snow enhancement techniques
[E73-10345] 10 p1148 N73-19344
ERTS-1 imagery of crustal structure of strip from eastern Sierra Nevada to Colorado Plateau
[E73-10355] 10 p1149 N73-19351
Evaluation of geologic applications of ERTS-1 imagery for New Mexico
[E73-10358] 10 p1149 N73-19354
Utilization of ERTS-1 imagery in structural reconnaissance for minerals and oil in Alaska, Canada, Montana, Colorado, New Mexico, and Texas
[E73-10414] 11 p1279 N73-20376
Mapping of major structural lineaments of Ethiopian rift using ERTS-1 imagery
[E73-10431] 11 p1281 N73-20392
ERTS-1 imagery applied to geological and water resources investigations of Basin and Range - Colorado Plateau boundary in northwestern and north central Arizona
[E73-10441] 11 p1282 N73-20401
ERTS-1 imagery of geological structures and terrains of New York
[E73-10457] 11 p1284 N73-20416
ERTS-1 imagery of structural and lithological properties of Northern Coast Ranges and Sacramento Valley, california
[E73-10478] 12 p1396 N73-21315
ERTS-1 imagery of permafrost and geologic hazards in Alaska
[E73-10495] 12 p1397 N73-21331
Identification of geostructures of continental crust and relation to mineral resources
[E73-10496] 12 p1397 N73-21332
Cayley Formation interpreted as deposited fluidized debris that traveled beyond extent of Imbrium Basin ejecta - Part B
12 p1453 N73-21766
Structural aspects of distinctive landforms collectively referred to as Imbrium sculpture - Part G
12 p1453 N73-21771
Mineral exploration in Utah and Nevada based on ERTS-1 imagery of structural fracture and fault trends
[E73-10510] 13 p1516 N73-22285
Recognition of characteristic geological structures associated with mineral deposits of copper molybdenum porphyry type
[E73-10526] 13 p1517 N73-22293
ERTS-1 imagery of structural features in Colorado Plateau margin near Flagstaff, Arizona
[E73-10517] 14 p1654 N73-23411
Commercial utility of ERTS-1 imagery in structural reconnaissance of Precambrian Shield for minerals and petroleum
[E73-10523] 14 p1654 N73-23414
ERTS-1 imagery of crustal structure of strip from eastern Sierra Nevada to Colorado Plateau
[E73-10529] 14 p1654 N73-23416
Relationship of geological structures to iron-rich zones in Nevada based on ERTS-1 imagery
[E73-10555] 14 p1655 N73-23427
Structural and lithological investigation of Northern Coast Ranges and Sacramento Valley, California
[E73-10577] 14 p1656 N73-23438
Geological surveys and mapping of Netherlands based on ERTS-1 imagery
[E73-10584] 14 p1657 N73-23444
Mapping of major geological structures of African rift system from ERTS-1 imagery
[E73-10622] 15 p1775 N73-24383
Lithological and structural surveys of sedimentary basin in France from ERTS-1 MSS imagery
[E73-10656] 16 p1898 N73-25352
Structural geology of Massif Central and Parisian Basins, France from ERTS-1 imagery
[E73-10657] 16 p1898 N73-25353
Major fracture and fault zones of Baltic Shield in Finland and relationships to mineral deposits
[E73-10682] 16 p1901 N73-25377
Tectonic and structural mapping in Alaska using ERTS-1 imagery
[E73-10685] 16 p1901 N73-25379
Identification of copper/molybdenum porphyry mineral deposits in characteristic geologic setting in Nevada, Arizona, Colorado, Australia, Alaska, and New Guinea
[E73-10762] 17 p2023 N73-26362
Application of ERTS-1 MSS imagery to study of tectonics and crustal structure of area from eastern Sierra Nevada to Colorado Plateau
[E73-10774] 18 p2135 N73-27250
Identification of geostructures of continental crust and relation to mineral resources
[E73-10787] 18 p2136 N73-27263
Application of ERTS-1 and EREP imagery to geologically investigations of Basin and Range-Colorado Plateau boundary in Arizona
[E73-10799] 18 p2138 N73-27275
Application of Skylab EREP imagery to fracture-related mine safety hazards and environmental problems in mining
[E73-10802] 18 p2138 N73-27277
Mineral resources, geological structures, and landform surveys from ERTS-1 imagery
19 p2289 N73-28408
Geological surveys and mapping of New York using ERTS-1 imagery
[E73-10846] 19 p2291 N73-28424
Mapping of fracture-lineaments in New England using snow enhancement techniques
[E73-10930] 21 p2528 N73-30273
Structural and lightological systems of Sierra Nevada Mountains and Sacramento Valley of California from ERTS-1 imagery
[E73-10942] 21 p2530 N73-30284
Synoptic identification and mapping of Quaternary geologic and geomorphic units in Midwest-Great Plains area
[E73-10951] 21 p2531 N73-30293
Geology of photo linear elements, Great Divide, Wyoming
[E73-10958] 21 p2532 N73-30300
Recognition of geologic framework for ERTS-1 identification of mineral deposits of copper/molybdenum prophyry type in Colorado, Nevada, Arizona, and Australia
[E73-10960] 21 p2532 N73-30302
ERTS-1 reconnaissance of crustal structure of strip from eastern Sierra Nevada to Colorado Plateau
[E73-10985] 22 p2658 N73-31292
Structural and spectral analysis of lineaments and circular features for discrimination of iron-rich zones in Nevada
[E73-11020] 22 p2661 N73-31324
Identification of geostructures of continental crust from ERTS-1 imagery and relationship to mineral resources in Alaska
[E73-11023] 22 p2662 N73-31327
Mineral exploration and fracture trends in Utah and Nevada from ERTS-1 imagery
[E73-11032] 22 p2663 N73-31336

Identification of geostructures of continental crust in Alaska and relation to mineral resources and exploration
[E73-11035] 22 p2663 N73-31339
.Oil exploration using ERTS-1 imagery of lithology and geological structures
[E73-11053] 23 p2780 N73-32229
Inventories of mineral deposits and geologic structures in Susquehanna River Basin from Skylab EREP data
[E73-11056] 23 p2780 N73-32232
Mapping lineaments, structures, and lithological formations of African Rift System in Africa and Yemen from ERTS-1 imagery
[E73-11126] 24 p2916 N73-33281

**STRUCTURAL RELIABILITY**
Criteria for designing launch vehicle structural reliability
[NT-D3-71.040] 07 p0850 N73-16890
Time dependent mechanical behavior of boron filament reinforced aluminum composites based on static and dynamic properties
[AD-753706] 09 p1054 N73-18590
Application of correlation equations to evaluate structural strength and reliability of various materials
[AD-753497] 09 p1097 N73-18956
Cyclic transformation treatments on structural and mechanical properties of austenitic steels
[AD-756240] 13 p1543 N73-22506
Statistical analysis on vibration intensity and structural reliability of turbomachine blades
[AD-760279] 17 p2078 N73-26811

**STRUCTURAL RIGIDITY**
U STRUCTURAL STABILITY

**STRUCTURAL STABILITY**
NT SHELL STABILITY
Engineering data for aeronautical structures under loads
[ESDU-SS2] 01 p0111 N73-10918
Procedure for predicting structural and acoustic response of full scale structures to sonic booms using scale models and laboratory techniques
[FAA-RD-72-116] 03 p0251 N73-12029
Structural behavior of glass hulls under external hydrostatic and cyclic pressure
[AD-746878] 03 p0362 N73-12947
Design, fabrication, and flight tests of boron-epoxy reinforced C-130E center wing boxes
[NASA-CR-112126] 04 p0370 N73-13011
Analysis of stability of cylindrical shells with filler under axial compression and development of linearized equations of stability
[AD-750953] 05 p0605 N73-14919
Fatigue tests to determine service life of catapult structure on C-2 aircraft
[AD-752493] 08 p0868 N73-17028
Analysis of structural properties produced by selective reinforcement of aluminum compression panels with unidirectional boron epoxy composite materials
[NASA-CR-2145] 08 p0966 N73-17895
Effects of spatially varying curvature on dynamics of cylindrical panels and stiffened cylindrical shell structures
[AD-752590] 08 p0967 N73-17907
Static perturbation method of studying nonlinear equilibrium and stability problems of structural systems and elements
09 p1093 N73-18921
Handbook for design of isogrid, triangular integrated stiffened structures for spacecraft structures and components
[NASA-CR-124075] 10 p1219 N73-19911
Structural stability of gun launched finned projectile motor case
[AD-754378] 11 p1344 N73-20906
Development of structural optimization algorithm used with large finite element program based on displacement method of structural analysis
12 p1356 N73-21005
Research projects in structural reliability engineering for transport vehicles
12 p1466 N73-21878
Analysis of aircraft construction methods to compare riveting, welded joints, and bonded joints for structural stability
[AD-755754] 13 p1475 N73-21948
Improved latching device for joining structural components in motionless relationship
[NASA-CASE-MFS-21606-1] 13 p1532 N73-22417
Development of procedure for designing elevated temperature structures to achieve safety factors and structural integrity of room temperature conditions
[NASA-CR-124232] 13 p1585 N73-22851
Analysis of structural reliability of large scale bonded joints for advanced composite wing to determine service life of boron epoxy to titanium scarf joint
[AD-756893] 14 p1603 N73-22995
Development of stability matrices of displacement type for multilayer sandwich beam, rectangular, and triangular plate elements
14 p1714 N73-23908
Structural stability testing of aerospace components under pyrotechnic loading conditions using subscale plastic models
[NASA-CR-128911] 14 p1715 N73-23914
Dynamic structural analysis of helicopter structures using single point excitation techniques - Vol. 2
[AD-756390] 14 p1716 N73-23922
Dynamic structural analysis of helicopter structures using free-body response techniques - Vol. 3
[AD-756391] 14 p1716 N73-23923
Dynamic structural analysis of helicopter subsystems based on equations for combination of mobility matrices - Vol. 4
[AD-756392] 14 p1716 N73-23924
Stability of cylindrical shell stiffened by frames and loaded with external pressure
[AD-757726] 14 p1717 N73-23929
Effect of forced transverse, low frequency vibrations on stability of rectangular plates with brace
14 p1717 N73-23932
Fatigue tests on Comet aircraft pressure cabin to determine effects of pressure cycles on structural stability of cabin windows
[ARC-R/M-3248] 15 p1728 N73-24017
Development of equations of motion for vibration frequencies of cantilever and elastically supported-free thin circular cylindrical shell
15 p1837 N73-24887
Low frequency structural response and damping characteristics of XB-70 aircraft during subsonic and supersonic flight
[NASA-TN-D-7227] 15 p1837 N73-24892
Computer program for linear instability analyses of biaxially loaded composite structures
[NASA-CR-112226] 15 p1838 N73-24893
Computer program for thermal stress and instability analyses of structures
[NASA-CR-112228] 15 p1838 N73-24895
Application of finite element method for analyzing stability of rectangular plates in supersonic air stream
Structural stability tests studying buckling of rectangular boron reinforced aluminum plates
[ENSMP-007] 15 p1840 N73-24907
Stability of cylindrical shells with consideration of initial imperfections
[AD-757728] 15 p1840 N73-24909
Structural stability of thin imperfect cylindrical shells as determined by statistical analysis
[AD-758030] 15 p1840 N73-24913
Equations for structural stability of orthotropic plates and cylindrical shells
[AD-758327] 15 p1840 N73-24914
Discontinuous functions in problems of strength and stability of elongated cylindrical panels with finite deflections
[AD-758621] 15 p1841 N73-24918
Wind tunnel measurements of direct pitching damping and stiffness derivatives for delta wing and swept wing planforms
[ARC-R/M-3419] 16 p1853 N73-25009
Structural properties and stability of solid materials and structures with different geometric configurations
[AD-759558] 16 p1971 N73-25942
Carrying capacity of cylindrical shells under dynamic loads
[AD-759103] 16 p1971 N73-25944
Feasibility of using Galkerin method to control cantilevered beam subjected to nonconservative force
17 p2091 N73-26913
Buckling and structural response of two magnesium ring stiffened conical shells subjected to uniform external pressure
[NASA-TN-D-7303] 17 p2092 N73-26926
Analysis of structural stability of shells weakened by holes to develop numerical analysis of stress concentration
17 p2093 N73-26929
Analysis of dynamic stability of elastic orthotropic cylindrical shell to determine shell parameters, shear moduli, and buckling mode
17 p2093 N73-26930
Hypothesis of spectral addition and application for determination of endurance under random loads
[AD-759869] 17 p2096 N73-26953
Application of composite materials for structural purposes to show limitations and failure characteristics
18 p2164 N73-27481
Application of oscillation theory and mathematical statistics to problems of aircraft structures and aerodynamic loads on aircraft and missiles
[NASA-TT-F-753] 19 p2220 N73-27908
Loading force diagrams and structural properties of landing gear
[AD-761644] 19 p2221 N73-27918
Stability of freely supported circular cylindrical shell subjected to random stresses
[AD-761541] 19 p2350 N73-28901
Stability of cylindrical shell under nonuniform radial loads
[AD-762242] 19 p2351 N73-28909
Wind tunnel tests to determine aeroelastic stability of thin isotropic circular cylindrical shells at subsonic and supersonic air speeds
20 p2359 N73-28975
Research projects involving aeroelastic stability and response, stability of thin shell structures, and suspension system concept for control of vehicle responses
[AD-762568] 20 p2359 N73-28979
Development of numerical procedures for buckling analysis of truncated conical shells with rigid edge constraint using load displacement criterion
20 p2477 N73-29894
Application of high strength structural materials for aerospace vehicles and use of fracture control procedures for improved damage tolerance
20 p2481 N73-29928
Development of rational analytic theory for analyzing fatigue of airframes based on maximum stress-field parameter and maximum load excursion ratio
20 p2481 N73-29931
Development of procedure for estimating fatigue life of airframes to eliminate errors caused by neglecting effect of stress redistribution after localized yielding
20 p2481 N73-29933
Analysis of sonic boom phenomenon to show generation, propagation, and effects on structures, people, and animals
[ARL/A-NOTE-337] 21 p2493 N73-30007
Analysis of flight test procedures for evaluating strength of airframes for aircraft and helicopters
[NASA-TT-F-769] 21 p2494 N73-30019
Development of digital computer program for generating individual component or entire aircraft mass and aerodynamic models for vehicle inelastic bending response analysis
[AD-763701] 21 p2498 N73-30045
Ultrasonic technique for assessing structural integrity of primary surface of space shuttle vehicles
[NASA-CR-133859] 22 p2721 N73-31778
Ultrasonic technique for assessing structural integrity of primary surface of space shuttle vehicles
[NASA-CR-133815] 22 p2721 N73-31779
Nonlinear analysis for thin elastic shells using modal expansion method of linear vibration analysis extended to nonlinear analog
23 p2852 N73-32793
Theoretical analysis background for shell theory automated for rotational structures [STARS-2] program - Vol. 1
[NASA-CR-2273-VOL-1] 23 p2854 N73-32801
User manual for shell theory automated for rotational structures [STAR 2B, 2V] - Vol. 3
[NASA-CR-2273-VOL-3] 23 p2854 N73-32803
Development of set of equations for analysis of thick shell structures to include effects of geometric thickness and transverse strain
24 p2987 N73-33870
Nonlinear analysis of structures by finite element method as supplement to linear analysis
[WTHD-51] 24 p2988 N73-33881

**STRUCTURAL STRAIN**
Analysis of sonic boom data recorded on strain gages mounted on windows to record overpressures and relation to window size
[FAA-RD-72-114] 03 p0251 N73-12030
Development of curves for determining magnitudes and directions of principal stress in plane using components of direct and shear stress
[ESDU-72013] 05 p0601 N73-14889
Structural analysis of two bonded half planes with finite crack perpendicular to and passing through interface
[NASA-CR-2181] 07 p0852 N73-16910
Determination of inplane stress distribution across thickness by two methods for plate loaded in bending
[AD-757207] 14 p1716 N73-23925
Effect of arrangement of stiffening ribs for cylindrical shell on critical load value
[AD-758029] 15 p1840 N73-24912
Effect of environment and stress-cycling on in-service structural failure of airframes and procedures for predicting safe operational conditions
20 p2481 N73-29929
Finite element method for structural plasticity problems
[AD-764574] 23 p2855 N73-32811
Elastic-plastic theory at finite strain
[AD-764557] 23 p2855 N73-32815

**STRUCTURAL VIBRATION**
NT BENDING VIBRATION
NT FLUTTER
NT PANEL FLUTTER
NT SUBSONIC FLUTTER
NT SUPERSONIC FLUTTER
NT TORSIONAL VIBRATION
NT TRANSONIC FLUTTER
Iterative solution for free vibrations of ring stiffened toroidal shells
[AD-747024] 04 p0482 N73-13943
Algebraic criteria for connective stability of large scale dynamic systems subjected to structural perturbations
07 p0760 N73-16177
Development of mixed finite-difference scheme for free vibration analysis of simply supported closed noncircular cylindrical shells
[NASA-TN-D-7107] 07 p0852 N73-16908
Vibration of foundation block test-pad imbedded in or resting on elastic substratum
[AD-751332] 07 p0853 N73-16915
Structural vibrations in aerospace operations and effects on man
08 p0876 N73-17099

Thermal stress vibrations in prebuckled region of orthotropic trapezoidal plates with two parallel opposite sides and various boundary conditions
[NASA-CR-2174] 09 p1094 N73-18928

Computer analysis of random decrement signatures of structures vibrating in random environment
[NASA-CR-2205] 09 p1094 N73-18929

Effect of ovality of radial thrust bearing balls on axial vibration of rapidly rotating rotor of engine
[AD-754615] 11 p1300 N73-20546

Acoustic amplification in fluid circuit and reactor heat exchanger vibration
[NLL-CE-TRANS-5913-(9022.09)] 12 p1390 N73-21271

Higher-order shell equations for vibrations of thick orthotropic circular cylindrical shells
[AD-756649] 13 p1589 N73-22884

Transfer matrix techniques for vibration analysis of curved skin-stringer structures with tuned elastomeric dampers
[AD-758220] 14 p1605 N73-23010

Effect of forced transverse, low frequency vibrations on stability of rectangular plates with brace 14 p1717 N73-23932

Statistical analysis on vibration intensity and structural reliability of turbomachine blades
[AD-760279] 17 p2078 N73-26811

Equations of motion for high frequency vibrations of thin crystal plates
[AD-760323] 17 p2095 N73-26948

Random vibrations of infinite-span plate on rigid supports during cylindrical bending
[AD-761454] 19 p2321 N73-28677

Evaluation of statistical energy analysis methods for vibrating structures
[NASA-CR-124322] 19 p2349 N73-28890

Natural mode vibration analysis of aircraft structural systems by direct and component mode synthesis techniques applied to tilt rotor VTOL aircraft aeroelasticity - Vol. 2
[NASA-TM-X-69496] 20 p2359 N73-28977

Vibrational energy transfer between connected substructures under random excitation
[NASA-CR-124450] 24 p2988 N73-33878

**STRUCTURAL WEIGHT**

Analysis of relationships between changes in space shuttle weights and costs with changes in weight of structural subsystems
[NASA-CR-2164] 09 p1090 N73-18894

Structure and configuration of European space tug
[HSD-TP-7264-VOL-5] 10 p1218 N73-19905

Analysis of optimal configurations for thin walled, axisymmetric, laminated shells based on shell configuration, loading, fiber alignment, and material properties of composite structure 16 p1969 N73-25924

Design criteria and materials for reducing structural weight of hydrofoil boats
[AD-761123] 18 p2132 N73-27222

Proceedings of conference on structural analysis with application to ships, guns, hydrofoils, marine propellers, and radar antennas
[AD-764508] 22 p2726 N73-31818

Structural optimization procedures applied to design of simply supported, corrugated hat stiffened composite panel under uniaxial compression
[NASA-CR-132314] 23 p2853 N73-32798

**STRUTS**

Bending moment at center of strut due to initial curvature under combined action of end loads and equal restraining moments
[ESDU-01.01.12] 01 p0110 N73-10904

Guide for using data on effects of buckling and deflections in beams, struts, and shafts
[ESDU-SS3] 01 p0112 N73-10922

Graphical solution to bending moment of curved strut subjected to end loads
[ESDU-01.01.14] 02 p0236 N73-11919

Influence of end loads and moments on bending moment of straight strut
[ESDU-01.01.15] 02 p0236 N73-11920

Buckling of constant flexural rigid composite struts
[ESDU-01.01.23] 02 p0236 N73-11921

Bending moments at ends of strut due to end load and triangularly distributed side load
[ESDU-01.01.25] 02 p0236 N73-11923

Structural design and load tests on carbon fiber reinforced plastic VC-10 aileron control strut
[ARC-CP-1229] 05 p0603 N73-14903

Use of cyclic struts as energy absorbers for Apollo couch 09 p1088 N73-18881

Numerical analysis of bending flutter and torsional flutter in flexible hydrofoil struts
[AD-757645] 14 p1717 N73-23935

Collapsible support for antenna reflector applied to installation of spacecraft antennas
[NASA-CASE-NPO-11751] 15 p1749 N73-24176

Determination of ventilation characteristics of blunt-based surface piercing struts in calm water and in waves
[AD-759046] 16 p1892 N73-25314

**STUDENTS**

Computer-based pupil/tracking monitoring system for Mesa Public Schools, Mesa Arizona 10 p1228 N73-19985

Electronic procedures for selecting and teaching students at Moscow Institute of Electronic Engineering
[JPRS-58550] 12 p1386 N73-21242

Relations between sociometric variables and criteria of ability and behavior of student pilots 19 p2226 N73-27954

**STUDS [STRUCTURAL MEMBERS]**

Fatigue tests to determine service life of aluminum alloy lugs with push-fit pins under tensile stress conditions
[ESDU-72020] 06 p0723 N73-15901

**STURM-LIOUVILLE OPERATOR**

U STURM-LIOUVILLE THEORY

**STURM-LIOUVILLE THEORY**

Discussion of Sturm-Liouville theory and canonical system of arbitrary number of differential equations
[NASA-TT-F-14696] 08 p0937 N73-17671

**STYLUSES**

U PENS

**STYRENES**

NT POLYSTYRENE

Time temperature superposition in heterophase block copolymers, using viscoelastic behavior of styrene-butadiene-styrene block
[AD-748213] 04 p0438 N73-13574

Viscoelastic properties of styrene butadiene plastic homopolymers and styrene-butadiene-styrene block copolymers
[AD-752622] 08 p0936 N73-17660

Radiation induced grafting of fluorinated monomers on polyamide films
[AD-757376] 14 p1617 N73-23100

Systems design for amine carbon dioxide sorber bed to be used in manned spacecraft
[NASA-CR-111849] 22 p2623 N73-31018

**SUBARCTIC REGIONS**

Effects of adverse Northern environment on human physiology and performance under military exercise conditions
[DCIEM-882] 20 p2371 N73-29056

**SUBASSEMBLIES**

Real time program for alignment of components and subassemblies prior to installation in chamber
[NASA-CR-128712] 07 p0800 N73-16493

Design and sizing of gas core nuclear rocket engine system components
[NASA-TM-X-2772] 18 p2176 N73-27575

**SUBCARRIER WAVES**

U CARRIER WAVES

**SUBCIRCUITS**

U CIRCUITS

U SUBASSEMBLIES

**SUBCOOLING**

U SUPERCOOLING

**SUBCRITICAL FLOW**

Mathematical models for calculating subcritical and supercritical compressible flow about blade cascades 14 p1649 N73-23378

**SUBGRAVITY**

U REDUCED GRAVITY

**SUBLATTICES**

U LATTICES [MATHEMATICS]

**SUBLAYERS**

U SUBSTRATES

**SUBLETHAL DOSAGE**

Effects of antiradiation drug dosage on mice and rat tolerance to transverse acceleration overloads 11 p1239 N73-20055

**SUBLIMATION**

Theory of dynamic viscous pressure interaction applied to surface ablation by sublimation
[AD-759186] 16 p1967 N73-25915

**SUBMARINES**

Physiological effects of 12 submarine personnel during prolonged exposure to sonar signals at 85 db [five day exposure]
[AD-744938] 01 p0011 N73-10087

Adaptive Kalman filter approach for identifying submarine trajectory from hydrodynamic parameters
[AD-747315] 02 p0159 N73-11288

Noise sources in towed ELF H-field antenna
[AD-754949] 11 p1263 N73-20250

Motivational patterns underlying devolunteering by submarine graduate school personnel
[AD-749324] 13 p1487 N73-22054

Comparison of glass fiber reinforced plastic and bronze submarine propellers, based on binding stress analysis and cavitation behavior
[BMVG-FBWT-73-8] 19 p2256 N73-28183

Numerical analysis of horizontal diffusion in ocean water to determine lifetime and spatial extent of submarine wakes in various turbulent media
[AD-762046] 19 p2256 N73-28186

Development of computer program for optimum design of submarine hulls with frame stiffened cylindrical structures
[AD-761643] 19 p2349 N73-28893

Advanced marine technology, including submerged navigation, transfer at sea, and bottom reconnaissance
[AD-763372] 23 p2788 N73-32305

**SUBMERGED BODIES**

NT DIVING [UNDERWATER]

Method for recovery of sunken bodies at depths of between 30 and 50 m 19 p2226 N73-27955

Computer program for calculating acoustic impedance of submerged vibrating structure
[AD-762007] 19 p2322 N73-28680

Influence of blue green algae on crystalline calcium carbonate formation on river rocks
[NASA-TT-F-15028] 20 p2368 N73-29046

**SUBMERGING**

Changes in lung capacity, air passage resistance, and dynamic compliance of humans during water immersion to simulate weightlessness 07 p0744 N73-16053

Water immersion model for simulating renin, aldosterone, and natriuresis effects of prolonged weightlessness on man 09 p0993 N73-18110

Immersion effects on human physiological motor functions 10 p1114 N73-19081

Long term physiological testing of submerged subjects to simulate weightless conditions for space flight
[NASA-TT-F-14884] 13 p1505 N73-22195

**SUBMILLIMETER WAVES**

Far infrared radiation detection with quantum photodetectors, noting application to submillimeter wave communication
[FTZ-A-14-TBR-4] 02 p0141 N73-11144

Formation of relativistic particles into clouds in quasar and Seifert nuclei, and centimeter, submillimeter, and gamma radiation emissions
[NP-30] 06 p0717 N73-15854

Millimeter and submillimeter wave detection and mixing with superconducting weak links
[AD-754083] 10 p1202 N73-19783

Analysis of electron number density and collision frequency levels behind reflected shock waves and shock wave interactions in argon 16 p1887 N73-25275

**SUBREFLECTORS**

Dish antenna having switching beamwidth with truncated concave ellipsoid subreflector
[NASA-CASE-GSC-11760-1] 23 p2764 N73-32116

**SUBROUTINE LIBRARIES [COMPUTERS]**

Library of numerical linear algebra programs
[AD-745430] 01 p0072 N73-10588

**SUBROUTINES**

Policy iteration subroutine package for IBM 360 computer
[FOA-P-C-8287-X9] 02 p0145 N73-11173

Subroutines for use of IBM 1627 x-y plotter associated with IBM 1130 computer
[LAAS-NT-SIS-72-T-09] 02 p0147 N73-11190

Subroutines for optimization of criteria under constraints using gradient projection method and HEATHER computer program
[LAAS-NI-CH-72-03] 02 p0147 N73-11191

Computer subroutines for propagating experimental numerical errors, rounding off numbers, checking validity of assumptions, and finding weak links in experiments 03 p0323 N73-12636

Subroutines for estimating linear system parameters by matrix methods
[LAAS-AS-72-I-14] 04 p0394 N73-13204

FORTRAN 4 subroutines for time series analysis
[FOA-3-C-3672-64[11]] 06 p0643 N73-15221

Computer subroutine for drawing networks of latitude and longitude lines by plotter
[EDFB-IBP-72-7-PT-2] 06 p0667 N73-15421

On-line dialog and testing program for control of real time FORTRAN program 08 p0887 N73-17182

ALGOL 60 subroutine for implementation of modified Newton algorithms for problem solving
[NPL-NAC-24] 09 p1057 N73-18622

FORTRAN subroutines for matrix operations encountered in finite element analysis of structures, noting application to flat plates
[ARC-CP-1223] 09 p1095 N73-18941

Subroutines SYMAT and COVAR for use as test procedures in matrix calculations
[REPT-17] 20 p2438 N73-29581

Numerical integration subroutines built into NASA-JSC computer
[NASA-CR-134021] 22 p2714 N73-31725

Satellite programs for computer program applied to structural analysis of shells to include user and programming information - Vol. 7
[NASA-CR-2273-VOL-7] 23 p2854 N73-32807

**SUBSETS [MATHEMATICS]**

U SET THEORY

**SUBSIDENCE**

Application of ERTS-1 imagery to fracture related mine safety hazards in coal mining industry and identification of mine subsidence areas in Indiana
[E73-10681] 16 p1901 N73-25376

Radiosonde measurements of subsidence in free atmosphere over Belgian weather station
[PUBL-SER-B-69] 17 p2057 N73-26637

**SUBSONIC AIRCRAFT**

Method for computing effects of meteorological conditions on sound in vicinity of subsonic aircraft
[SC-DC-72-1007] 03 p0253 N73-12044

FORTRAN program for calculating aerodynamic coefficients of subsonic aircraft at high speeds 04 p0370 N73-13010

Numerical analysis of minimum flight time for sail plane performance while performing cross country flight
[ME-68] 15 p1733 N73-24055

Analysis of three dimensional weakly controlled soaring procedures for increased sailplane performance
19 p2218 N73-27894

**SUBSONIC FLOW**

Steady state response of semi-infinite fluid-solid interface subjected to subsonic and intersonic load velocities
[AD-747253] 02 p0159 N73-11287

ALGOL program for lift distribution determination on thin wing in subsonic flow
[NLR-TR-70088-U] 03 p0274 N73-12224

Method of electroprofiling utilizing natural electromagnetic fields in subsonic frequency range
[AD-747557] 03 p0298 N73-12431

Analysis procedure for three dimensional, subsonic, duct flow
[AD-748649] 04 p0407 N73-13313

Navier-Stokes equations governing flow of subsonic or supersonic jets mixing with surrounding atmosphere
[AD-750185] 05 p0528 N73-14296

Subsonic numerical panel method for flow calculation applied to delta wing, lifting reentry body, bodywing configurations
[MBB-UFE-889-72-O] 06 p0615 N73-14992

Predicting base pressure in subsonic two dimensional steady base flow
[DLR-FB-72-57] 09 p1014 N73-18274

Solution of Chaplygin equation by straight line method to describe gas flow around profile at high subsonic speed with local supersonic curved shock wave
[AD-753557] 09 p1019 N73-18318

Numerical analysis of pressure distribution in subsonic wind tunnel resulting from interference of air flow
10 p1140 N73-19287

Magnus forces on center of gravity and rotational startup response of self-spinning rotor in subsonic air stream
[AD-755108] 11 p1232 N73-20001

Flow and acoustic characteristics determined for subsonic and supersonic jets and supersonic suppressors
[NASA-CR-131297] 11 p1233 N73-20006

Calculation of flows in subsonic and transonic portions of circular nozzles
[NASA-TT-F-14847] 11 p1270 N73-20308

Theoretical calculation of generalized forces and load distribution on wings oscillating at general frequency in subsonic stream
[ARC-R/M-3710] 13 p1470 N73-21908

Calculation of unsteady, subsonic flow through infinite, two-dimensional flat plate blade
[ARC-R/M-3709] 13 p1510 N73-22240

Derivation of equations governing temporal and spatial variation for amplitudes and phase of capillary and gravity waves in case of second harmonic resonance
[AD-756218] 13 p1513 N73-22262

Feasibility of using iron magnetic support to extend cold magnetic balance wind tunnel system to subsonic flow regimes and continuous spinning aircraft configurations
15 p1762 N73-24275

Time dependent flow field model for subsonic diffuser section of supersonic inlet
[AD-758803] 16 p1957 N73-25835

Analysis of jet penetration and mixing of multiple cold air jets into ducted subsonic heated mainstream flow
[NASA-CR-121217] 17 p2014 N73-26286

Subsonic intrinsic noise reduction of sound pressure transducers in air flow
[RAE-LIB-TRANS-1660] 17 p2063 N73-26687

Development of computer program for subsonic and shock-free transonic flow solution on hub-shroud midchannel flow surface of turbomachine - Vol. I
[NASA-TN-D-7343] 18 p2102 N73-26996

Four VTOL propulsion concepts compared parametrically for subsonic applications with three types of aircrafts
[NASA-TM-X-68279] 20 p2466 N73-29810

Load near apex of lifting swept wing in linearized subsonic flow
[ARC-R/M-3716] 21 p2492 N73-30001

Pressure recovery performance of conical diffusers at high subsonic speeds and range of geometries
[NASA-CR-2299] 22 p2611 N73-30927

Subsonic air flow pressure drop at interface between two rectilinear ducts noting pressure pulses
[PUBL-133] 24 p2910 N73-33222

**SUBSONIC FLUTTER**

Dynamic structural response of rectangular panel to subsonic turbulent boundary layer pressure field
[NASA-TN-D-6970] 03 p0360 N73-12934

Developments in unsteady aerodynamics of helicopter rotary wings to analyze stall flutter, transient effects of interactions, and wake induced instabilities
05 p0491 N73-14001

Flutter characteristics of thin cantilever wings at transonic and supersonic speeds
[NAL-TR-288] 06 p0618 N73-15022

**SUBSONIC SPEED**

Development of computer program for analyzing mono-element and multi-element airfoils at subsonic speed with attached air flow - Vol. 2
[AD-740124] 01 p0031 N73-10242

Guidance method for transition of space shuttle from hypersonic entry to subsonic cruise flight
[NASA-CR-128648] 03 p0357 N73-12905

Aerodynamic configurations of swept wings to improve lift performance at stall in higher range of subsonic speeds
06 p0617 N73-15010

Wind tunnel tests to determine structural integrity of birds under conditions simulating ingestion of birds into inlets of high speed aircraft
[NASA-TM-X-68163] 06 p0629 N73-15114

Subsonic performance potential of ramjets and ejector ramjets
[AD-751317] 07 p0837 N73-16781

Development of two dimensional theory for unsteady flow disturbances caused by aeroelastic deformation of thick wing at high subsonic speeds
[NASA-CR-112114] 08 p0896 N73-17258

Effect of various physical and operating parameters on noise produced by low pressure ratio propulsive fans operating at subsonic speeds
[NASA-CR-2188] 09 p0980 N73-18011

Wind tunnel tests of scale model of space shuttle orbiter to determine low subsonic aerodynamic characteristics
[NASA-TM-X-2712] 11 p1232 N73-20000

Numerical analysis of minimum time climbing procedure and minimum fuel climbing procedure for typical subsonic aircraft
15 p1733 N73-24052

Low subsonic aerodynamic characteristics of 60 deg swept delta wing space shuttle orbiter
[NASA-TM-X-2762] 17 p2087 N73-26880

Analysis of pressure distribution on plane ground surface under aircraft flying at low altitude with subsonic velocity
[FFA-AU-634-PT-2] 18 p2129 N73-27206

Characteristics of propulsion system for subsonic, long-range transport aircraft designed to meet aerodynamic noise level requirements
[NASA-CR-121242] 18 p2193 N73-27704

Numerical analysis of supercritical flow about C-141 aircraft wing using finite difference, relaxation algorithm
[NASA-TN-D-6933] 19 p2217 N73-27889

Wind tunnel tests to determine aeroelastic stability of thin isotropic circular cylindrical shells at subsonic and supersonic air speeds
20 p2359 N73-28975

Wind tunnel tests to determine performance of lobed-display mixer nozzle with convergent nozzle at subsonic speeds
[NASA-TM-X-2806] 21 p2491 N73-29995

Effect of inflated air cushion landing gear on subsonic static stability of high performance aircraft operating out of ground effect
[AD-763365] 21 p2498 N73-30048

Wind tunnel tests to determine two dimensional characteristics of airfoil optimized for maximum lift coefficient at various angles of attack
[NASA-TN-D-7071] 22 p2611 N73-30929

Subsonic jet noise measurements by means of directional microphone system
24 p2956 N73-33612

**SUBSONIC WIND TUNNELS**

Scale model for design of large modular subsonic wind tunnel
[DLR-MITT-72-21] 01 p0037 N73-10288

Interference theory in slotted wind tunnels extended to subsonic rectangular wind tunnels with ventilated tool, longitudinal slots and perforated screens of arbitrary porosity
[ARC-R/M-3706] 05 p0492 N73-14007

Numerical analysis of pressure distribution in subsonic wind tunnel resulting from interference of air flow
10 p1140 N73-19287

Large subsonic wind tunnel design for German industry
[REPT-EA-317-A] 13 p1507 N73-22213

Analysis of problems involved in operation of large wind tunnels at subsonic and supersonic speeds
[AGARD-R-601] 17 p2008 N73-26239

Influence of free stream turbulence on turbulent boundary layer in relation to wind tunnel testing at subsonic speeds
17 p2014 N73-26283

**SUBSTANCES**
U MATERIALS

**SUBSTITUTES**

Nuclear magnetic resonance spectrum analysis for rings inversion rate in benzodiazepine derivatives
[RAE-LIB-TRANS-1628] 17 p1991 N73-26103

**SUBSTITUTION**
U SUBSTITUTES

**SUBSTRATES**

Flexural strength of aluminum oxide substrates separated by lasers and diamond sawing
[SC-DC-71-4496] 03 p0321 N73-12613

Influence of substrate temperature on properties of epitaxial layers of GaAs during growth
[NLL-RRE-TRANS-370-[8036.625]] 05 p0585 N73-14763

Effects of substrates on stability of superconductor and electrical properties of superconductors for various conditions
10 p1108 N73-19031

Interpretation of ERTS-1 geologic data for Nevada and evaluation of materials used in compiling photomaps
[E73-10398] 11 p1277 N73-20360

Preparation techniques and quality control of GaAs substrates for use in epitaxy
13 p1566 N73-22688

Procedure for obtaining monocrystalline layers of silicon by rheotaxial methods
18 p2189 N73-27673

Performance calculation for Schottky field effect transistor on resistive substrate
22 p2641 N73-31167

Geomorphology of layered deposits in Mariner 9 observations of Martian polar regions
23 p2840 N73-32697

**SUBSTRUCTURES**

Development and evaluation of equipment for monitoring long term sea floor foundation settlement and tilting
[AD-750258] 06 p0669 N73-15444

**SUBTRACTORS**
U ADDING CIRCUITS

**SUBTROPICAL REGIONS**
U TEMPERATE REGIONS
U TROPICAL REGIONS

**SUBZERO TEMPERATURE**

Service life and operation of military equipment in subzero Siberian environments
[AD-756478] 13 p1554 N73-22595

**SUCTION**

Steady state heat and mass transfer in suction boiling
15 p1842 N73-24923

Integral equations for calculating incompressible potential flows around profiles with suction and blowing
[NASA-TT-F-14962] 18 p2130 N73-27209

**SUD AVIATION AIRCRAFT**
NT CONCORDE AIRCRAFT

**SUDDEN IONOSPHERIC DISTURBANCES**

Sunspot, solar flare, magnetic storm, and SID data, Delhi - Dec. 1971
[RRC-A-199-PT-2] 01 p0048 N73-10385

Sunspot, solar flare, magnetic storm, and SID data, Delhi Jan. 1972
[RRC-A-200-PT-2] 01 p0048 N73-10387

Solar-geophysical data for sudden ionospheric disturbance of Dec. 14 to 21 1971
[AD-762483] 20 p2474 N73-29873

Nature of solar flare emissions and geophysical disturbances
[NASA-TM-X-70479] 24 p2976 N73-33781

**SUGARS**
NT DEXTRANS
NT GLUCOSE
NT MONOSACCHARIDES
NT RIBOSE

**SUITS**
NT PRESSURE SUITS
NT SPACE SUITS

**SULFATES**

Inorganic binders for utilizing high reflectance of $BaSO_4$ in paints
[NASA-TM-X-66082] 02 p0191 N73-11549

Pyroelectric infrared detector performances investigating strontium and barium niobates, lithium sulfate and TGS materials effects on frequency ranges and sensitivity
[ESRO-CR-67] 22 p2675 N73-31425

**SULFATION**

Potassium exchange on sulfocation resins containing divinylbenzene for drinking water regeneration
03 p0257 N73-12078

**SULFIDES**
NT CADMIUM SULFIDES
NT COPPER SULFIDES
NT HYDROGEN SULFIDE
NT LEAD SULFIDES
NT MOLYBDENUM DISULFIDES
NT MOLYBDENUM SULFIDES
NT ZINC SULFIDES

Ozone reaction with mercaptane for elimination of exhaust gas pollution in air
08 p0883 N73-17152

Thermodynamic properties of iridium sulfides at equilibrium pressures
[AD-753897] 11 p1253 N73-20168

Multicomponent diffusion theory as applied to oxidation, corrosion, and sulfation of complex heat resistant alloys
14 p1677 N73-23609
Development of procedure for estimating solid phase occurrence during oxidation of heavy metal sulfides
[NLL-M-22913-[5828.4F]] 16 p1926 N73-25581

SULFONES
Liquid retention in chlorpropamide therapy and water intoxication of patients
[NASA-TT-F-14597] 02 p0133 N73-11077

SULFUR
Influence of atmospheric sulfur budget on biosphere
[BNL-16906] 04 p0415 N73-13387
Auger spectroscopy of oxygen and sulfur interactions with clean iron surface and rubbing contact effect on interactions
[NASA-TN-D-7283] 14 p1670 N73-23555
Sulfur, sodium, and chloride contaminants in gas turbines
14 p1677 N73-23610
Atmospheric sulfur budget for northern Europe with model for deposition variations with distance from source
[AC-17] 17 p2027 N73-26408
Use of lithium/sulfur batteries as load-leveling devices in electrical utility networks
[ANL-7958] 21 p2499 N73-30058
Decomposition of hydrogen sulfide, in electrical discharge, to elemental sulfur
[BM-RI-7780] 21 p2505 N73-30105
Sulfur line density in spectrographic scan of Orion nebula
22 p2734 N73-31888

SULFUR COMPOUNDS
NT CADMIUM SULFIDES
NT COPPER SULFIDES
NT HYDROGEN SULFIDE
NT LEAD SULFIDES
NT MOLYBDENUM DISULFIDES
NT MOLYBDENUM SULFIDES
NT SULFATES
NT SULFIDES
NT SULFONES
NT SULFUR FLUORIDES
NT SULFUR OXIDES
NT SULFURIC ACID
NT THIOLS
NT ZINC SULFIDES
Mass spectrometric analysis of aromatic hydrocarbons and sulfur compounds
[NLL-TRANS-1193-[9022.9]]
15 p1746 N73-24151

SULFUR FLUORIDES
Absorption of carbon dioxide laser radiation by gaseous sulfur hexafluorine in air boundary layers
[AD-751016] 06 p0681 N73-15546

SULFUR OXIDES
Sulfur oxides, smoke, and air pollution tables from Belgian weather stations, Oct. 1971
01 p0075 N73-10619
Sulfur oxides, smoke, and air pollution tables from Belgian weather stations, Dec. 1971
02 p0205 N73-11659
Sulfur oxides, smoke, and air pollution tables from Belgian weather stations, Nov. 1971
03 p0327 N73-12663
Effects of SO2 decay product toxicity on human physiological functions
05 p0500 N73-14071
Sulfur oxides, smoke, and air pollution tables from Belgian weather stations, Jan. 1972
05 p0574 N73-14668
Dual gas correlation spectrometer measurements of sulfur dioxide and nitrogen dioxide in industrial area of southern California
[PB-210717] 05 p0575 N73-14676
High concentration sulfur dioxide pollution over Osaka, Japan during summer
[NLL-M-20713-[5828.4F]] 06 p0692 N73-15634
Polymer gas reactions in air pollutants such as NO2 and SO2 as function of pressure, UV light, temperature, and morphology
08 p0882 N73-17140
Sulfur oxides, smoke, and air pollution tables from Belgian weather stations, Feb. 1972
08 p0939 N73-17686
Atmospheric pollution in Belgium from 1 Apr. 1969 to 31 Mar. 1970
[PUBL-SER-A-78] 10 p1182 N73-19618
Sulfur oxides, smoke, and air pollution tables from Belgian weather stations, Mar. 1972
13 p1553 N73-22587
Sulfur oxides, smoke, and air pollution tables from Belgian weather stations, Apr. 1972
13 p1553 N73-22590
Mass spectrographic determination of ions and neutral reactions in glow discharge of helium-sulfur dioxide-carbon monoxide
[BM-RI-7747] 15 p1747 N73-24157
Sulfur oxides, smoke, and air pollution tables from Belgian weather stations, Jul. 1972
20 p2449 N73-29686
Increased optical efficiency of flame photometric detector for detection of SO2 in air
[PB-220480/8] 21 p2551 N73-30453
Sulfur oxides, smoke, and air pollution tables from Belgian weather stations, Aug. 1972
24 p2949 N73-33559
Sulfur oxides, smoke, and air pollution tables from Belgian weather stations, Sep. 1972
24 p2949 N73-33560

SULFURIC ACID
Sulfuric acid in Venus clouds by photolytic decomposition of hydrogen bromide
[LPL-COMMUN-171] 21 p2592 N73-30767

SUM RULES
Triple Regge phenomenology from finite mass sum rules in proton-proton inclusive reactions
[NOTA-INTERNA-379] 01 p0084 N73-10693
Sum rule for photoproduction amplitudes in isovector Compton scattering and inconsistency of free fermion parton model in deep inelastic limit
[NUB-2169] 07 p0823 N73-16673

SUMMARIES
NT ABSTRACTS
Mariner 9 missions operations summary
23 p2844 N73-32725

SUMMER
High concentration sulfur dioxide pollution over Osaka, Japan during summer
[NLL-M-20713-[5828.4F]] 06 p0692 N73-15634
Average power spectra of zonal and meridional components of velocity for winter and summer
10 p1146 N73-19327

SUMS
Sum of two scattering matrices connected together by two hybrid circuits
[NLL-M-22701-[5828.4F]] 05 p0568 N73-14614

SUN
Problems of solar and stellar spindown and theory, emphasizing angular velocity inside sun and stars
01 p0095 N73-10786
Research in aerospace, biological, and solar sciences
[AD-746143] 02 p0133 N73-11080
Research projects to determine nature of Sun as ultraviolet variable star and description of MUSE experiment
[NASA-TM-X-66142] 06 p0719 N73-15868
Utility of Goddard Trajectory Determination System Solar/Lunar/Planetary ephemeris files
[NASA-TM-X-66185] 08 p0976 N73-17983
Solar flare activity in Mc Math region 10789 during disk passage of 12 to 15 June 1970
[AD-756827] 15 p1833 N73-24855
Digital computer model to predict spectral irradiance on ground target from sun and sky
[AD-758877] 16 p1945 N73-25739
Skylab, solar studies, and usefulness of Apollo telescope mount
[NASA-EP-119] 23 p2834 N73-32645
Analysis of isotopic composition of chemical elements in solar structure using photospheric and sunspot spectra
[NP-19727] 24 p2981 N73-33826

SUN SENSORS
U SOLAR SENSORS

SUNLIGHT
Design of photoelectric sunshine recorder using cadmium sulfide photoconductive cells
[NLL-M-22979-[5828.4F]] 16 p1910 N73-25456

SUNRISE
Structure and variation of topside ionosphere at mid-latitudes during sunrise period based on Alouette 1 electron density measurements
[AD-748430] 03 p0299 N73-12443

SUNSPOT CYCLE
Influence of interplanetary magnetic field on geomagnetism in polar regions during sunspot cycles
[DMI-GEOPHYS-PAPERS-R-29]
02 p0167 N73-11355
Night sky luminescence in upper atmosphere during IQSY
[NASA-TT-F-14927] 14 p1660 N73-23478

SUNSPOTS
Sunspot, solar flare, magnetic storm, and SID data, Delhi - Dec. 1971
[RRC-A-199-PT-2] 01 p0048 N73-10385
Sunspot, solar flare, magnetic storm, and SID data, Delhi Jan. 1972
[RRC-A-200-PT-2] 01 p0048 N73-10387
Diurnal variations of sunspot classification, areas, and magnetic fields for June and July 1972
[BULL-171] 01 p0092 N73-10759
Photoheliographic data on sunspots for 1962, 1963, and 1964 - tables
01 p0101 N73-10829
Application of Avco data analysis and prediction techniques to derivation of algorithms for predicting future sunspot activity
[NASA-CR-123925] 02 p0224 N73-11811
High resolution power spectra of Zurich daily sunspot numbers over 77 years
[NASA-TM-X-64718] 06 p0716 N73-15840
Theoretical study of sunspots and electrical and thermal conductivities of solar magnetoplasma
[AD-752230] 08 p0962 N73-17872
Solar meridional circulation and latitudinal sunspot drift analysis
[AD-751268] 09 p1081 N73-18820
Effect of sunspot cycle on precipitation pattern over U.S. plains states
17 p2056 N73-26629
Analysis of cause of nonlinear relationship between solar constant and solar activity to show possible climatic consequences
[NLL-M-23053-[5828.4F]] 20 p2390 N73-29201
Sunspot motion and flaring in M482
[NASA-CR-133848] 21 p2593 N73-30775
Solar data on daily total areas of sunspot groups, for Oct. 1972 by Rome, Italy Astronomical Observatory
[BULL-174] 21 p2597 N73-30817
Solar data on daily total areas of sunspot groups, for Nov. 1972 by Rome, Italy Astronomical Observatory
[BULL-175] 21 p2598 N73-30818
Structural and spectral studies of sunspots
[NASA-CR-135787] 24 p2975 N73-33776
Computer program for correcting solar intensity measurements in elliptical sunspots for stray light
[NP-19735] 24 p2977 N73-33785
Solar data on daily total areas of sunspot groups for Apr. 1973 by Rome Astronomical Observatory
[PUBL-180] 24 p2977 N73-33788
Analysis of isotopic composition of chemical elements in solar structure using photospheric and sunspot spectra
[NP-19727] 24 p2981 N73-33826

SUPER SABRE AIRCRAFT
U F-100 AIRCRAFT

SUPERALLOYS
U HEAT RESISTANT ALLOYS

SUPERCAVITATING FLOW
Singular perturbation method for predicting pressure distribution on supercavitating hydrofoils with rounded noses
[AD-745791] 01 p0063 N73-10514
Application of exact method for numerical computations of supercavitating hydrofoils of parabolic shape
[AD-763465] 22 p2654 N73-31261

SUPERCAVITATION
U SUPERCAVITATING FLOW

SUPERCONDUCTING MAGNETS
Acquisition and reduction of data acquired from superconducting magnetic suspension and balance facility
[NASA-CR-112186] 01 p0035 N73-10276
Estimate of dose rate, pattern, and distribution of scattered particles and neutrons during irradiation of superconducting synchrotron magnets
[KFK-1468] 01 p0080 N73-10659
MHD parameter optimization procedure for determining optimum coil geometry for 10 MW level superconducting magnet system
[AD-745322] 02 p0212 N73-11717
Projections for superconductor costs for dc fusion magnets
[BNL-16748] 03 p0335 N73-12735
Influence of position and dimension on field errors of synchrotron bending magnet with winding cross section
[NP-19323] 03 p0345 N73-12813
Design of coils and switches for superconducting magnetic energy storage and transfer
[LA-DC-72-470] 03 p0345 N73-12816
Superconducting magnet systems, high-power turbogenerators with superconducting field windings, and synchronous generators with superconducting inductors
[JPRS-57638] 04 p0458 N73-13735
Dipole configuration of pulsed superconducting synchrotron magnet
[KFK-1354] 04 p0458 N73-13739
Optimization and cost factors for cryogenic and superconducting magnets in plasma physics
[IPP-4/96] 04 p0458 N73-13740
Fabrication of Nb-Ti and Al composite for use in superconducting rod
[COO-3311-1] 05 p0587 N73-14775
Application of superconducting magnetics for plasma physics experiments and as component for future thermonuclear reactors
10 p1108 N73-19033
Analysis of effect of mass on operation of airborne superconductor magnetic system with aluminum stabilized conductor
10 p1108 N73-19034
Characteristics of large, lightweight, saddle-coil, superconducting dipole magnet for airborne magnetohydrodynamic generators
10 p1109 N73-19038
Characteristics of superconducting electric generators to show effect of electromechanical, electromagnetic, and cryogenic parameters on design
10 p1109 N73-19039
Features and characteristics of superconducting electrical machines and design of synchronous electric generator for airborne use
10 p1109 N73-19040
Radiation effects on current density of superconducting magnets in fusion reactor
[CLM-R-120] 10 p1199 N73-19760

Direct current superconducting beam splitting magnet system
[BNL-17221] 10 p1200 N73-19765
Coil configuration influence on current distribution of superconducting dipoles and quadrupoles
[BNL-17168] 10 p1201 N73-19771
Modified GRACY magnet program for computing magnetization effects in superconducting magnets
[BNL-17219] 10 p1201 N73-19772
Superconducting properties of niobium titanium multifilamentary magnet material
[BNL-17193] 12 p1388 N73-21255
Epoxy resins for use in superconducting magnets at liquid helium temperatures
[RHEL/R-251] 12 p1416 N73-21476
Current lead optimization for minimizing heat loss of superconducting magnet
[BNL-17233] 12 p1439 N73-21661
Design of warm vacuum system for superconducting storage rings
[BNL-17239] 12 p1440 N73-21670
Redesign of Argas 2 facility for using superconducting magnet
[NASA-TT-F-14876] 13 p1562 N73-22662
Cryogenics applications for development of superconducting levitated system of high speed ground transportation
[NBS-TN-635] 14 p1645 N73-23344
Superconducting electromagnetic suspension and balance and supersonic wind tunnel facility for dynamic stability studies
[NASA-CR-132255] 15 p1761 N73-24271
System failure and safety features of superconducting magnetic suspension systems
15 p1762 N73-24277
Helium cooled current leads in refrigerated superconductive magnet system
[DESY-72/65] 17 p2073 N73-26769
Pulsed superconducting magnet systems for high energy synchrotrons
[CONF-720565-2] 19 p2249 N73-28131
Ion heating and thermonuclear power production characteristics and performance of superconducting bumpy-torus magnetic facility
[NASA-TN-D-7353] 19 p2324 N73-28693
Superconducting materials evaluation for magnet in optimal design of Tokamak reactor
[CONF-721111-21] 20 p2462 N73-29784
Multipole production in superconducting dipole and quadrupole synchrotron magnets
[NP-19692] 20 p2462 N73-29785
Conference on flux pumps and ac superconducting components
[CONF-720908] 21 p2580 N73-30674
Superconducting materials for high field ac magnets with one second field risetime
[BMFT-FBT-73-03] 22 p2685 N73-31509
Superconducting magnets for use in high field synchrotrons
[LBL-1703] 22 p2707 N73-31677
Supercritical helium cooling of superconducting magnet for use in dc beam line elements
[RHEL/R-258] 24 p2969 N73-33725

**SUPERCONDUCTIVITY**

Superconducting magnetometer as strain transducer in liquid helium cooled gravitational wave antenna
[NOTA-INTERNA-373] 01 p0058 N73-10476
Analysis of conditions required to produce superconductivity in materials under high pressure
[NLL-NEL-TT-2402-[6075.461]]
02 p0186 N73-11505
Fourier analysis for characterizing force field of superconducting suspension for spacecraft elements
03 p0335 N73-12731
Superconductivity of multifilamentary wires consisting of vanadium silicates
[BNL-16891] 03 p0346 N73-12818
Superconductive tunable filter having broad tuning range with inductance and capacitance varied simultaneously
[AD-749237] 04 p0397 N73-13226
Weak-link apparatus for superconducting instrumentation
[LNF-72/4] 04 p0422 N73-13439
Magnetism in solids - magnetic moments, propertism of diamagnetism and paramagnetism, and coexistence of superconductivity and ferromagnetism
[ITJ-13] 04 p0449 N73-13670
Two sector, superconducting dipole in direct current
[LNF-72/6] 04 p0458 N73-13738
Inductive reactances of superconducting synchronous machine
[AD-749326] 05 p0499 N73-14066
Bumpy torus magnet facility with 12 superconducting coils, each 19 cm and capable of 3.0 tesla on their axes
[NASA-TM-X-68165] 06 p0648 N73-15266
Influence of absorption magnetic thermal RF breakdown in superconducting cavities
[KFK-EXT-3/72-2] 06 p0708 N73-15780
Fluctuation-induced diamagnetism in bulk Al and Al alloys above superconducting transition temperature
[AD-750275] 06 p0710 N73-15794
Abstracts of experimental studies on superconductivity
[AD-751869] 08 p0952 N73-17794
Superconducting energy gap structure and physical properties of dysprosium-dysprosium oxide-lead tunnel junctions
[AD-753847] 09 p1077 N73-18790
Proceedings of conference on application of superconductivity techniques to auxiliary power systems for aircraft and missiles
[AGARD-CP-104] 10 p1108 N73-19030
Large helium systems for superconducting power applications and high energy physics
[BNL-17228] 10 p1200 N73-19764
Influence of reversible reaction transition superconducting to normal on plastic properties of transition and lead metal and alloy single crystals
[ANL-7903] 10 p1200 N73-19766
High field superconductivity in alkali metal [Na, K, Rb, and Cs] intercalates of MoS2
[NASA-TM-X-68206] 11 p1330 N73-20794
Shunted junction model applied to point contact Josephson junctions, using dc characteristics as function of temperature, contact pressure, and RF power
[AD-754082] 11 p1331 N73-20801
Application of many body theory to superconductivity and superfluidity
[AD-754961] 11 p1331 N73-20808
Research projects in solid state physics, low temperature physics, superconducting films, and quantum liquids and crystals
[COO-1569-93] 12 p1439 N73-21657
Superconducting properties and damage susceptibility of composite wire conductors
[BNL-17222] 12 p1439 N73-21660
Superconducting properties of crystalline films of aluminum on silicon, considering fluctuating critical temperatures
[BNL-17240] 12 p1441 N73-21672
Effect of dissolved hydrogen on mechanical and superconducting properties of molybdenum
13 p1565 N73-22681
Application of cryogenic and superconductive systems for propulsion of ships
[AD-758431] 14 p1694 N73-23746
Research and development conducted at Spanish universities on solid state and low temperature physics
[AD-757991] 14 p1700 N73-23795
Magnetic coil design and physical phenomena responsible for ac losses in superconductivity
15 p1761 N73-24273
Hartree approximation of extra conductivity in quasi-superconducting thin films considering nonlinear external field effect
[LNF-72/76] 15 p1821 N73-24758
Apparatus for measuring magnetization curve of superconducting coil
[EUR-CEA-FC-661] 15 p1821 N73-24760
Inductance of cryogenic synchronous equipment with damping system
[AD-759235] 16 p1884 N73-25250
Studies of electron mirror microscopy and its application to superconductivity and magnetism
16 p1952 N73-25797
Fabrication of niobium thin film superconductive tunnel junctions using semiconductor barrier
17 p2072 N73-26761
Theoretical and experimental investigations of superconductivity, and amorphous semiconductors, superconductivity and magnetism
[NASA-CR-133234] 17 p2072 N73-26767
Alloying effect on superconducting temperature La3In
[IS-M-2] 17 p2073 N73-26771
Superconducting lead film thickness effect on magnetic properties
[ISS-72/6-PT-2] 17 p2073 N73-26773
Superconductive materials for military rotating electrical machinery
[AD-760330] 17 p2074 N73-26782
Low temperature superconductivity research at Danish universities
[AD-760317] 17 p2075 N73-26786
Superconducting magnetic field trapping device for producing magnetic field in air
[NASA-CASE-XNP-01185] 19 p2326 N73-28710
Superconducting properties of sprayed thin films
[JINR-P8-6863] 19 p2327 N73-28717
Apparatus for deposition of superconducting thin films on large surfaces of complex configuration
[JINR-P8-6855] 20 p2463 N73-29789
Homogeneity regions of superconducting phases in molybdenum - platinum system
[NASA-TT-F-15139] 22 p2706 N73-31674
Problems and applications of superconductive energy storage
[NASA-TT-F-15109] 22 p2707 N73-31676
Casting and heat treatments for fabricating ductile superconducting copper base alloys
[CALT-822-51] 22 p2707 N73-31678
Superconductivity of copper containing small amounts of niobium
[CALT-822-50] 22 p2707 N73-31679
Fluctuation diamagnetism of aluminum and aluminum alloys above superconducting transition temperature
23 p2804 N73-32422
Behavior of macroscopic quantum interferometer composed of superconducting tin rings containing two Josephson junctions
24 p2967 N73-33710
Phase transformation and superconductivity in titanium and zirconium alloys
[RLO-2225-T-13-14] 24 p2969 N73-33726

**SUPERCONDUCTORS**

Development of superconducting magnet system for magnetohydrodynamic power generation
[AD-745321] 01 p0032 N73-10247
Model for operating partly resistive superconducting point contact, quantum interference device
[FOA-2-B-2035-E1] 02 p0218 N73-11764
Multifilamentary niobium-titanium superconductors for winding pulsed magnets
[BNL-16764] 03 p0345 N73-12817
Ac measurements of cold worked superconducting niobium-titanium alloy
[CONF-720513-4] 03 p0346 N73-12819
Experimental and theoretical determination of intrinsic fluctuations in superconducting flux detector ring closed by Josephson junction
[AD-749101] 04 p0424 N73-13458
Superconductor interactions and properties, and amorphous semiconducting and magnetic materials
[NASA-CR-129524] 04 p0457 N73-13731
Heat transfer in superconducting matrix as magnet coils
[BNL-16615] 04 p0459 N73-13743
Electric parameter of rectangular superconductors immersed in cavities of electric motors
[REPT-123] 05 p0586 N73-14764
Josephson junctions and superconducting quantum interference devices
[NBS-TN-630] 06 p0707 N73-15772
Operating, principles of RF biased SQUID systems
[NBS-TN-629] 06 p0708 N73-15773
Pulsed magnetic field apparatus, and microstructure influence on critical current density of superconducting Nb3Sn strips in pulsed fields
[LBL-448] 06 p0708 N73-15778
Local oscillator and mixer forming Josephson frequency conversion in superconducting point contact junctions
[AD-750775] 06 p0709 N73-15784
Use of very high Q superconducting microwave cavities to obtain strong coupling between electromagnetic field and Josephson junction
[AD-749986] 06 p0710 N73-15795
Properties of evaporated Josephson junctions coupled to high q superconducting microwave cavities
[AD-749981] 06 p0710 N73-15796
Littles theory of high temperature superconductors
[AD-751038] 07 p0753 N73-16120
Shock heating of plasmas based on superposed superconducting circuits and magnetic energy storage
[TRITA-EPP-72-29] 07 p0829 N73-16717
Pressure effects on phonon spectrum, electron-phonon interaction strength, and electron-phonon coupling function in Pb-In superconductors using electron tunneling
07 p0831 N73-16739
Vibration simulation of space probe model, superconducting energy storage coil
[LA-DC-72-724] 07 p0832 N73-16742
Chemical process for producing continuous fine superconducting filaments
[AD-751545] 07 p0832 N73-16746
Synthesis of superconducting intercalated and intermetallic compounds
[AD-751497] 07 p0833 N73-16751
Magnetic measurements of superconducting iron-shielded dipoles
[BNL-17190] 08 p0893 N73-17227
Response of self-driven, weakly connected superconducting ring incorporating small voltage-biased Josephson junction
[AD-752213] 08 p0951 N73-17788
Research in superconductors
[AD-751855] 08 p0952 N73-17796
Manufacturing of superconducting cylindrical films of niobium and niobium nitride by sputter etch techniques
[AD-752593] 08 p0952 N73-17799
Cryogenics, superconductors, and electromagnets - conference
[AD-753456] 09 p1067 N73-18705
Magnetic impurities and boundary effects in metals and superfluids
[AD-753100] 09 p1074 N73-18763
Research activities in solid state physics
[AD-753255] 09 p1075 N73-18770
Effects of substrates on stability of superconductor and electrical properties of superconductors for various conditions
10 p1108 N73-19031
Analysis of alternating current loss mechanisms in superconductors with comparison of performance in coil and cable configurations
10 p1108 N73-19032

Development of high magnetic fields using superconductors with high current densities and application to power conversion and energy storage
10 p1108 N73-19035

Characteristics of conventional alternators and aircraft electrical power systems and comparison with electric systems using superconductors
10 p1109 N73-19036

Development of superconducting homopolar machines with multiple discs and superconducting field winding using liquid metals for armature sliding contacts
10 p1109 N73-19037

Utilization of superconductors to store and discharge electric energy
10 p1109 N73-19041

Application of superconducting coils for energy storage and determination of optimizing parameters for inductive energy storage
10 p1109 N73-19042

Effects of electromagnetic forces, energy radiation, and discharge losses on design of superconducting coils for energy storage elements
10 p1109 N73-19043

Analysis of biaxial gyrostabilizer system and synthesis of spherical superconducting suspensions with maximum lift
[JPRS-58356] 10 p1159 N73-19428

Synthesis of superconducting magnetic field suspensions with maximum lift using Fourier coefficients
10 p1159 N73-19430

Electromagnetic response of Pb superconducting film as function of magnetic field in microwave range
[ISS-72/5] 10 p1199 N73-19756

Magnetic properties of superconducting films
[ISS-72/6] 10 p1199 N73-19758

Transition properties of type 1 and magnetic properties of type 2 semiconductors with small Ginzburg-Landau parameters
[JUL-854-FF] 10 p1200 N73-19762

State of superconducting science in Switzerland
[AD-754235] 10 p1202 N73-19781

Millimeter and submillimeter wave detection and mixing with superconducting weak links
[AD-754083] 10 p1202 N73-19783

Nature of power losses in RF superconducting cavities at low and high temperatures
[SLAC-PUB-963] 12 p1383 N73-21213

Theoretical and experimental investigation of flux-flow noise in type 2 superconductors
12 p1437 N73-21642

Modification of resistive transition in superconductors by thermodynamic fluctuations
12 p1438 N73-21648

Performance prediction model and scaling laws for flux pinning in superconducting niobium zirconium and niobium titanium alloys
[COO-3169-13] 12 p1440 N73-21664

Magnetic instabilities in Type-2 superconductors
[CEA-N-1552] 12 p1440 N73-21667

Application of electron tunneling process to superconductor technology
[AD-756081] 13 p1566 N73-22692

Evaluation of cryogenic devices for application in surveillance, radiation detection, and communications
[AD-756175] 14 p1668 N73-23537

Cryogenic superconducting magnetic suspension and balance facility designs
15 p1761 N73-24272

Phase shift model for induced voltage in current carrying superconducting thin films in superimposed ac and dc magnetic fields including radio and microwave frequency ranges
15 p1820 N73-24748

Electric field and current in thin aluminum film superconductor near critical temperature
[LNF-72/77] 15 p1821 N73-24759

Microwave surface resistance of niobium tantalum - and lead indium-superconducting alloys considering thermodynamic vortices
[AD-757875] 15 p1822 N73-24770

Design and operation of superconducting quantum point contact interference device
[PB-214758/5] 15 p1823 N73-24775

Design and performance of superconducting quantum interference devices
[PB-214757/7] 16 p1954 N73-25810

Superconducting cavity stabilized oscillator of high stability
[AD-760339] 17 p2006 N73-26221

Meissner effects and magnetization curves for superconductors - conference
[LA-5115] 17 p2010 N73-26257

Controlled diffusion reaction process for masking substrate of twisted multifilament superconductive ribbon
[NASA-CASE-LEW-11726-1] 17 p2070 N73-26752

Metal cryostat for studying superconductors in liquid helium
[IPP-4/95] 17 p2072 N73-26766

Metallic chain compounds and organometallic complexes for high temperature superconductor materials
[AD-759767] 17 p2074 N73-26778

Specific heat measurements on rubidium tungsten bronze and aluminum film superconductors
18 p2184 N73-27636

High frequency transport coefficients of clean type 2 superconductor near upper critical field
18 p2185 N73-27644

Metastable states of superconductors in presence of magnetic fields
18 p2185 N73-27645

Chemical vapor deposition of stoichiometric niobium gallium superconducting film
[NASA-CR-2308] 20 p2455 N73-29726

Influence of epoxy resins on mechanical properties of superconducting windings
[RHEL/R-265-PT-2] 22 p2689 N73-31534

Design, construction, and performance of large superconducting magnetic shield
[NASA-CR-135486] 22 p2700 N73-31627

Twisted wire or tube superconductor for filament windings
[NASA-CASE-LEW-11015] 23 p2823 N73-32571

Hypersound attenuation in superconducting aluminum and cadmium
23 p2825 N73-32580

Application of Boson method to quantum field theory computations and mixed state of type 2 superconductors
23 p2825 N73-32582

Quasiparticle tunneling into superconducting transition metals
[AD-764905] 23 p2826 N73-32591

Fluxon coupling force measurements on superconducting dc transformers noting film thickness and silicon monoxide layer
24 p2898 N73-33135

Electron thermal conductivity of thin films of strong coupling superconductors and of superconductors containing rare earth inpurities
24 p2967 N73-33712

Influence of radiation damage on properties of type 2 superconductors
[IPP-4/104] 24 p2969 N73-33724

Electromagnetic characteristics of single crystal niobium, niobium alloy, and molybdenum alloy superconductors
[AD-765368] 24 p2970 N73-33731

Enhanced electron field emission in resonant niobium superconducting cavity
[AD-765336] 24 p2970 N73-33733

Bench and thermal-vacuum testing of superconductors and heat pipe systems to determine failure characteristics
[NASA-TN-D-7395] 24 p2992 N73-33909

**SUPERCOOLING**

High temperature contact nucleation of supercooled water by organic chemicals for fog and cloud seeding
[AD-753465] 10 p1127 N73-19181

Void fraction in subcooled trichlorotrifluoroethane boiling at high pressures
[NASA-CR-2241] 14 p1718 N73-23938

Organic compounds for nucleating supercooled water
[AD-758002] 15 p1748 N73-24169

Volt-ampere characteristics of heated electric wire during cryogenic cooling in liquid helium
[AD-759958] 17 p2005 N73-26211

Theoretical determination of heterogeneous nucleation rate of supercooled water droplets from thermally generated AgI particles
[AD-758858] 18 p2114 N73-27095

Subcooled forced convection film boiling in vertical annulus
23 p2856 N73-32819

Cooling of 60 to 400 cm length circular tubes with superfluid helium
[KFK-1786] 24 p2992 N73-33910

**SUPERCRITICAL FLOW**

Mathematical models for calculating subcritical and supercritical compressible flow about blade cascades
14 p1649 N73-23378

Application of integral relations to analyzing inviscid supercritical flow about lifting airfoils with embedded shock wave
[AD-755762] 14 p1651 N73-23390

Numerical analysis of supercritical flow about C-141 aircraft wing using finite difference, relaxation algorithm
[NASA-TN-D-6933] 19 p2217 N73-27889

**SUPERCRITICAL PRESSURES**

Thermophysical properties of helium-4 under various conditions of temperature and pressure
[NASA-CR-128445] 02 p0242 N73-11966

**SUPERFLUID FLOW**

U SUPERFLUIDITY

**SUPERFLUIDITY**

Application of Doppler-shifted fourth sound techniques for analyzing current states in rotating superfluid helium contained in superleak
[AD-745316] 01 p0118 N73-10974

Cooling rates of neutron stars with maximum and zero superfluidity
[NASA-TM-X-66101] 02 p0230 N73-11866

Damping of accelerated isothermal superfluid helium flow by roton polarization
[NOTA-INTERNA-395] 03 p0336 N73-12743

Elementary excitation spectrum of superfluid helium
10 p1198 N73-19750

Application of many body theory to superconductivity and superfluidity
[AD-754961] 11 p1331 N73-20808

Investigation of He-3 impurities in He-4 for development of microscopic theory of He-3 quasiparticles
12 p1375 N73-21153

Liquid helium experiments on ac Josephson effect in superfluid helium and superfluid critical velocities
16 p1944 N73-25728

Theory of mobility of ions in superfluid helium
22 p2701 N73-31632

Measurement of viscosity of solution of He 3 in He 4 at superflow temperatures
[JINR-P8-7009] 24 p2892 N73-33086

Cooling of 60 to 400 cm length circular tubes with superfluid helium
[KFK-1786] 24 p2992 N73-33910

**SUPERGIANT STARS**

Analysis of post-Newtonian effects on instability of white dwarf stars, neutron stars, and supermassive stars
[NASA-CR-129241] 03 p0355 N73-12893

Polarimetric and spectrophotometric observations of late type giant and supergiant stars
17 p2080 N73-26827

Spectrum of class M supergiants in region lambda lambda 7000 to 6000 A
20 p2471 N73-29851

**SUPERHEATING**

Influence of grain size and cold working on static corrosion of Incoloy 800 alloy in superheated steam
[EURFNR-965] 03 p0315 N73-12570

**SUPERHETERODYNE RECEIVERS**

Design of infrared detector array using multielement heterodyne technology
[AD-754443] 11 p1325 N73-20751

Design of miniaturized 37 GHz low noise receiver
[AD-763402] 21 p2509 N73-30129

**SUPERHIGH FREQUENCIES**

Measurement of short pulse, X-band radar backscatter from rough water surfaces expressed as cumulative probability distribution functions
[AD-747949] 03 p0267 N73-12159

Investigation of nonlinearities in X band IMPATT reflection amplifiers
[AD-747796] 03 p0275 N73-12231

One watt pulsed solid state source for X-band navigational beacons
[TR-70-3] 05 p0518 N73-14213

Characteristics of four types of horn antennas for application as S-band radiometers and modifications to improve beam efficiency
[NASA-CR-2133] 07 p0755 N73-16135

Design of high power air cooled microwave S band junction circulator using YIG rod and boron nitride transformers
[AD-751743] 07 p0762 N73-16194

Development of broadband S band hybrid traveling wave tube
[AD-751262] 07 p0763 N73-16200

Fast electron production by absorption of shf wave in collisionless plasma
[AEC-TR-7331] 07 p0827 N73-16700

Wave transformation region in superhigh frequency argon discharge plasma
[AEC-TR-7339] 07 p0827 N73-16706

Striction and thermal mechanisms of superhigh frequency, self stress in collisionless plasma
[AEC-TR-7374] 10 p1196 N73-19733

Superhigh frequency emission of collisionless magnetized plasma on its interaction with pumping wave in microwave range
[AEC-TR-7373] 10 p1197 N73-19736

Superhigh frequency plasma heating in toroidal magnetic trap
[AEC-TR-7360] 10 p1197 N73-19741

Strip transmission line circulators using ferrites, noting new densification method for polycrystalline ferrimagnetic materials
[REPT-8.422] 12 p1384 N73-21222

Magnetic properties and superhigh frequency behavior of yttrium-aluminum and -iron garnets with substitutions of Gd, Al, Sn, and In
12 p1384 N73-21225

Use of superhigh frequency transponder on Apollo 16 subsatellite to measure lunar gravitational field as preliminary investigation of lunar mass
12 p1451 N73-21758

Ku-band microminiature modulators for converting 10 mW signal at 400 MHz to 10 mW signal at 15 GHz
[NASA-CR-130230] 13 p1490 N73-22078

Magnetoelastic transmission delay lines for S band noting insertion loss reduction
[REPT-8.425] 13 p1491 N73-22087

Influence of flare shapes on element factors and gain as function of scan angle of 40 element linear array at superhigh frequencies
[PHL-1973-10] 14 p1639 N73-23288

Effect of precipitation on parabolic antennas using linear orthogonal polarization at superhigh frequencies
[REPT-53] 16 p1875 N73-25176

Amplitude fading of superhigh frequency geostationary communications satellite signals considering atmospheric refraction
17 p1996 N73-26139
Wideband SHF ferrite microelectronics
19 p2236 N73-28025
Four-probe reflectometer for X band measurement system
[AD-761821] 19 p2303 N73-28514
Design of low cost highly sensitive SHF microwave components
[NHK-LABS-NOTE-163] 20 p2381 N73-29129
S-band power amplifier using high efficiency silicon avalanche diode
[AD-763104] 20 p2381 N73-29135
Susceptibility of X band point-contact diodes to microwave radiation
[AD-763364] 21 p2518 N73-30197
Electron beam semiconductor S-band amplifier
[AD-763223] 21 p2518 N73-30200
Dynamic characteristics of microwave synchronized oscillators
22 p2643 N73-31185
Final design and specifications for solid state, S band, power amplifier
[NASA-CR-124405] 23 p2764 N73-32115
Summary of S band occultation experiment
24 p2983 N73-33837

**SUPERMAGNETS**
U HIGH FIELD MAGNETS

**SUPERNOVAE**
Spectroscopy and photography of novae and supernovae
[AD-743955] 01 p0106 N73-10875
Supernovae monitoring experiment using ground-based photomultiplier tubes sensitive to secondary fluorescence light
08 p0974 N73-17967
Attenuation of X rays emitted by supernovae remnants and Crab Nebula
[NASA-TM-X-64722] 12 p1445 N73-21701
Five possible supernova remnants mapped by aperture synthesis interferometry
12 p1447 N73-21721
Nuclear reactions in hydrogen exhausted zone of star during supernova explosion and nuclei syntheses through nitrogen conversion
13 p1575 N73-22762
High frequency observations and theoretical interpretation of recombination line emission in direction of supernova remnant 3
[AD-756085] 15 p1833 N73-24858
Concept of nuclear fusion chain reactions for supernovae and controlled fusion reactors
[SM-170/49] 17 p2062 N73-26678
Observations of recombination line emission in direction of supernova remnants
[AD-762002] 21 p2598 N73-30825
Rocket-borne proportional counter observations of discrete galactic X rays from supernovae
[NASA-TM-X-70463] 22 p2711 N73-31708
X ray emission in pulsar model for supernovae remnants
22 p2733 N73-31870
Survey of properties of supernova remnants
24 p2978 N73-33793
Explosive carbon burning effects of observed nuclei in solar system and constraints on supernova explosions
[LA-UR-73-489] 24 p2992 N73-33911

**SUPERSATURATION**
Supersaturation and condensation in cloud chamber expansion
[AD-745348] 01 p0058 N73-10478
Growth rate of liquid droplets formed in supersaturated vapors
[AD-753074] 09 p1017 N73-18301
Temperature effects on supersaturation in thermal diffusion chamber
[AD-758137] 14 p1646 N73-23354
Analysis of supersaturation conditions in Mach 7.5 wind tunnel in expansion region of nozzle and technique for visualization of shock waves and shear layers
[ARL/A-139] 14 p1648 N73-23367
Condensible vapor supersonic nozzle flows at supersaturation collapse near condensation point
[AD-756471] 14 p1651 N73-23393
Influence of supersaturation on nucleation behavior in continuous agitated cooling crystallizers
[WTHD-44] 16 p1953 N73-25799

**SUPERSONIC AIRCRAFT**
NT B-70 AIRCRAFT
NT CONCORDE AIRCRAFT
NT F-4 AIRCRAFT
NT F-5 AIRCRAFT
NT F-8 AIRCRAFT
NT F-14 AIRCRAFT
NT F-15 AIRCRAFT
NT F-100 AIRCRAFT
NT F-102 AIRCRAFT
NT F-104 AIRCRAFT
NT F-106 AIRCRAFT
NT F-111 AIRCRAFT
NT MIRAGE 3 AIRCRAFT
NT SUPERSONIC COMMERCIAL AIR TRANSPORT
NT SUPERSONIC TRANSPORTS
NT T-38 AIRCRAFT
NT TU-144 AIRCRAFT
NT X-15 AIRCRAFT
Optical control theory and energy-state approximation to determine parameters for minimum time flight path of supersonic aircraft
[AD-748219] 03 p0329 N73-12689
Aerodynamic analytical model for reducing supersonic jet exhaust noise
[AD-747774] 03 p0337 N73-12752
Development of numerical method for designing minimum drag supersonic wing camber surfaces of arbitrary planform for given lift characteristics
[NASA-TN-D-7097] 04 p0369 N73-13001
Increase of water vapor in stratosphere due to fleet of SST's
[AD-748797] 04 p0416 N73-13397
Research project to analyze and evaluate supersonic jet noise generation and radiation - Vol. 1
[AD-749428] 05 p0495 N73-14035
Analysis of noise sources associated with supersonic jet noise and establishment of effects of refraction on radiated field of sources - Vol. 5 App. 1
[AD-749141] 05 p0496 N73-14039
Analysis of acoustic properties of shock associated noise in narrow band spectrum produced by jet flows - Vol. 5 App. 2
[AD-749142] 05 p0496 N73-14040
Development of remote sensing devices to measure jet exhaust fluctuating density gradients, mean and turbulent velocity, and mean temperature Vol. 6
[AD-749143] 05 p0496 N73-14041
Infrasonic detection of propagating atmospheric shock waves caused by supersonic aircraft
05 p0512 N73-14161
Acoustic properties of supersonic jet noise and refraction effects on noise field
[AD-749140] 05 p0581 N73-14728
Application of power method for reducing base drag of long range supersonic aircraft at supersonic speeds
[AD-750950] 06 p0623 N73-15056
Reduction of transonic drag for high performance aircraft by injecting air in rear of aircraft to alter transonic flow distribution on aft section
[AD-751269] 07 p0736 N73-15991
Optimized design of supersonic aircraft wing based on linear combination of weight of wing and aerodynamic drag minimization
07 p0737 N73-15997
Climatic changes resulting from upper atmosphere perturbation by supersonic aircraft exhausts
[PB-212427] 07 p0816 N73-16612
Effect of engine failure on aerodynamic characteristics of supersonic aircraft
08 p0865 N73-17003
Application of active controls to suppression of flutter for supersonic aircraft
08 p0865 N73-17005
Artificial stabilization to correct control deficiencies for high performance aircraft
08 p0866 N73-17009
Low sonic boom overpressure profiles for supersonic transport aircraft configurations
[NASA-TM-X-2746] 09 p0984 N73-18039
Experimental determination of high velocity liquid impact damage for application to rain erosion protection of supersonic aircraft
[AD-753381] 09 p1018 N73-18305
Development of electrical generation and distribution systems for supersonic aircraft using solid state switching and remote control of protective devices
10 p1111 N73-19054
Stratospheric chemical reactions and perturbations caused by supersonic aircraft exhaust
[PB-213111] 11 p1290 N73-20464
Survey on aeronomic dynamics of photochemical reactions caused by supersonic aircraft exhaust
[PB-213126] 11 p1290 N73-20466
Atmospheric models for fluid dynamic and chemical impacts of supersonic aircraft on climatology
[PB-212819] 11 p1291 N73-20473
Preliminary appraisal of hydrogen and methane fuel and fuel tank configuration in Mach 2.7 supersonic transport
[NASA-TM-X-68222] 13 p1568 N73-22711
Holographic interferograms of supersonic jet aircraft acoustic field
[PB-214112/5] 14 p1693 N73-23743
Local flow measurements at inlet spike tip of Mach 3 supersonic cruise aircraft
[NASA-TN-D-6987] 15 p1731 N73-24037
Automated design optimization of supersonic airplane wing structures under dynamic constraints
[NASA-CR-112319] 16 p1860 N73-25063
Development of techniques for real time, on-line, optimum flight path conditions and minimum time maneuvers for supersonic aircraft
[AD-758799] 16 p1862 N73-25083
Wake model program for computing wake height and width
[PB-218820/9] 18 p2106 N73-27030
Development of digital computing system for synthesis and optimization of military flight vehicle preliminary designs
[AD-760568] 18 p2108 N73-27045
Design and development of cryptosteady energy separator for use with turbojet engines on supersonic aircraft
[AD-762032] 19 p2331 N73-28752
Design of aircraft with rotatable wing for producing high speed aerodynamic configuration
[NASA-CASE-ARC-10470-2] 21 p2494 N73-30018
Optical holographic measurement of jet noise in supersonic air/nitrogen and helium jets at Mach numbers from 1.5 to 3.4
[PB-220641/5] 21 p2581 N73-30686
Optimization of supersonic aircraft C3/C4 polymer fuel by normal paraffins containing 10 to 16 carbon atoms
[DLR-FB-73-32] 22 p2708 N73-31689

**SUPERSONIC AIRFOILS**
Airfoil with cambered trailing edge section for supersonic flight
[NASA-CASE-LAR-10585-1] 06 p0613 N73-14981
Minimum weight design of supersonic aircraft wing with finite element modeling to meet strength, stability, frequency, and flutter requirements
12 p1356 N73-21003

**SUPERSONIC BOUNDARY LAYERS**
Effect of pressure gradients on supersonic turbulent boundary layers and effect of dilation on Reynolds stresses
[IC-AERO-72-21] 07 p0736 N73-15989

**SUPERSONIC COMBUSTION**
Analysis of hydrogen mixing and combustion in hypersonic air stream to show hydrogen concentration and pressure distribution
[AD-746341] 02 p0243 N73-11978
Ignition and combustion characteristics of high density storable fuels injected into supersonic and subsonic air streams
[AD-746063] 02 p0244 N73-11980
Analysis of subsonic and supersonic burning in ramjet combustors to determine effects of nozzle configurations
[AD-747030] 03 p0351 N73-12862
Analytical determination of mode transition in integral ramjet rocket propulsion system
[AD-753904] 10 p1224 N73-19955
Factors affecting tangential fuel injector design and their effect on efficiency of supersonic combustion processes
[NASA-CR-112302] 11 p1334 N73-20829
Exponential laws for temperature, velocity, and CO-concentration profiles in nitrogen hot gas jet or nitrogen-propane flame in free atmosphere, in application to supersonic combustion
[DLR-FB-73-05] 12 p1465 N73-21867
Photochemical enhancement of combustion and mixing in supersonic flows
[AD-758802] 15 p1844 N73-24944
Mixing and ignition of enclosed supersonic diffusion flames
[AD-760804] 18 p2207 N73-27811
Supersonic combustion and turbulent mixing processes required for advanced weapon systems
[AD-762599] 20 p2486 N73-29969
Optimization of supersonic aircraft C3/C4 polymer fuel by normal paraffins containing 10 to 16 carbon atoms
[DLR-FB-73-32] 22 p2708 N73-31689
Experimental data analysis for sonic injection of hydrogen from backward facing step in parallel direction to main supersonic stream
[NASA-TM-X-2828] 22 p2728 N73-31828

**SUPERSONIC COMBUSTION RAMJET ENGINES**
Effect of nonequilibrium conditions on performance of combustors employing supersonic flows
[NASA-CR-120932] 02 p0242 N73-11969
Analysis of subsonic and supersonic burning in ramjet combustors to determine effects of nozzle configurations
[AD-747030] 03 p0351 N73-12862
Mixing and ignition of hydrogen jets injected normally into supersonic two dimensional flow and effect on combustion performance of hyersonic ramjet engine
[ONERA-TP-973] 09 p1098 N73-18962

**SUPERSONIC COMBUSTION RAMJET MISSILE**
U RAMJET MISSILES
U SUPERSONIC COMBUSTION RAMJET ENGINES

**SUPERSONIC COMMERCIAL AIR TRANSPORT**
NT TU-144 AIRCRAFT
Analysis of airline passenger reactions to vibration environments encountered in supersonic transport and commercial jet aircraft
01 p0003 N73-10017
Threat of stratospheric ozone nonequilibrium by SST nitric oxide exhaust gases
[AD-757059] 14 p1719 N73-23949
Environmental impact of increased intensities of solar ultraviolet radiation resulting from operation of supersonic transport aircraft
[PB-215524/0] 16 p1862 N73-25079

**SUPERSONIC COMPRESSORS**
Performance tests on low hub-tip ratio supersonic axial flow compressor
[AD-752585] 09 p1079 N73-18805
Blockage ring used for inlet stall problem with supersonic axial flow compressor stage having tip Mach number of 2.0
[AD-757217] 14 p1702 N73-23809

**SUPERSONIC DIFFUSERS**
Turbulent pressure fluctuation measurements for cross section of supersonic diffuser inlet flow model
10 p1140 N73-19288

**SUPERSONIC FLIGHT**
Aircraft maneuvers for reducing sonic boom intensity during horizontal turns
[AD-744859] 02 p0126 N73-11022
Numerical prediction of exhaust products released to stratosphere during supersonic flight along definite air routes
[NASA-TT-F-14622] 04 p0371 N73-13013
Measurement of ray paths and ground overpressures produced by Concorde aircraft during supersonic flight
[R/D-896] 06 p0618 N73-15021
Analysis of natural vibration characteristics of plate-beam combination structures during supersonic flight
[NAL-TR-291] 06 p0725 N73-15917
Effects of thrust characteristics on longitudinal stability in supersonic flight
08 p0865 N73-16997
Numerical analysis of unsteady supersonic characteristics of space shuttle type vehicles using arbitrary finite element technique
[NASA-CR-112296] 13 p1470 N73-21904
Flight tests to determine magnitude of groundtrack overpressure generated by oblique wing transport aircraft at Mach 1.4 and 45,000 feet
[NASA-TM-X-62247] 13 p1472 N73-21922
Supersonic wind tunnel tests on scale model space shuttle orbiter configuration
[NASA-TM-X-2804] 19 p2248 N73-28123
Design criteria for supersonic overflight to reduce psychophysical effects and decrease glass damage probability
[FAA-RD-73-116] 22 p2724 N73-31800
Exhaust emission measurements on turbojet engine plume at simulated supersonic flight
[AD-764717] 23 p2832 N73-32632

**SUPERSONIC FLOW**
Linear and nonlinear parts of slender body of revolution aerodynamic coefficients in supersonic flow, noting influence of incidence on pressure distribution
[DLR-FB-72-42] 01 p0001 N73-10006
Method of characteristics for analyzing supersonic flow past oscillating flat plate cascades with leading edge locus
[AD-745838] 01 p0042 N73-10332
Numerical analysis of supersonic, inviscid, steady flow past blunt-nosed cone at yaw
[AD-745782] 01 p0042 N73-10333
Application of flow field models, combustion, mixing, and nonequilibrium chemistry data to development of chemical lasers
[AD-745419] 01 p0066 N73-10536
Analysis of diffusive separation in front of blunt body in low density binary mixture of supersonic flows using electron beam densitometer
[AD-745960] 02 p0157 N73-11274
Numerical analysis of viscous-inviscid interaction in supersonic flow around blunt body
[AD-746891] 02 p0160 N73-11293
Effect of nonequilibrium conditions on performance of combustors employing supersonic flows
[NASA-CR-120932] 02 p0242 N73-11969
Steady state response of semi-infinite solid with overlying semi-infinite fluid subjected to moving point load at supersonic speed
[AD-747252] 03 p0286 N73-12313
Calculation of coefficient of resistance of sphere at supersonic velocities and measurement of critical point on free flying bodies
[AD-747513] 03 p0287 N73-12324
Characteristics of flow around bluff body at supersonic speed with emphasis on leading shock wave formation and changes in withdrawal value for argon and nitrogen
[AD-747407] 03 p0287 N73-12325
Analysis of flow around conical body at small angles of attack in uniform supersonic flow of ideal gas
[AD-747408] 03 p0287 N73-12326
Base pressure effect of external shocks or expansions intersecting wake of two dimensional blunt body in supersonic flow
04 p0403 N73-13285
Breakup of liquid jet injected normal to supersonic airstream
[AD-747494] 04 p0406 N73-13309
Prediction of pressure gradient on delta wing between uniform and nonuniform supersonic inviscid flow
[ARC-CP-1228] 05 p0492 N73-14010
Ballistic tube for drag measurement on firing models into oncoming supersonic flow
[AD-749839] 05 p0525 N73-14271
Supersonic characteristics of sonic nozzle gas flow expansion
[AD-749764] 05 p0528 N73-14297
Application of holography to jet breakup in supersonic flow fields and analytical method for reducing holographic droplet data
[AD-749854] 05 p0529 N73-14302
Dynamic response of fluid-solid interface to supersonic disturbance
[AD-750253] 05 p0604 N73-14917
Acoustic properties of supersonic fan
[NASA-TN-D-7096] 06 p0619 N73-15025
Supersonic flow past solid cylindrical and circular jet barriers on flat plates
[AD-750522] 06 p0656 N73-15327
Numerical solution of shock wave interaction with supersonic blunt body flow exemplified by circular cylinder and parabolic body
[DLR-FB-72-68] 07 p0736 N73-15990
Numerical analysis of oscillating wedge in supersonic perfect gas flow to evaluate trends for wedge and to analyze unsteady flows
07 p0767 N73-16235
Stability of liquid films interacting with high pressure supersonic airstream
[SC-DC-72-1225] 07 p0772 N73-16268
Boltzmann equations for kinetic modeling of supersonically flowing electrically excited laser system
[NASA-TM-X-62196] 07 p0806 N73-16538
Finite difference solution for supersonic laminar flow over two dimensional compression corner
08 p0894 N73-17241
Designs and performance predictions for high performance supersonic ejector systems
[AGARDOGRAPH-163] 08 p0895 N73-17248
Conservation equations for analyzing supersonic and mixing flow regimes of supersonic ejectors
08 p0895 N73-17249
Ejector flow model for predicting performance characteristics of supersonic ejector systems
08 p0896 N73-17251
Analysis of uniform jet flow around airfoil with separated shock wave at low supersonic velocities of incident flow
[NASA-TT-F-14813] 08 p0896 N73-17259
Supersonic aerodynamic influence coefficients for isolated and parallel interfering coplanar and noncoplanar wings
[NASA-CR-2168] 09 p0979 N73-18003
Analysis of downstream mixing of transverse hydrogen injection from single and multiple orifices in Mach 4 boundary layer over flat plate
[NASA-CR-112254] 09 p1015 N73-18285
Supersonic laminar flow reattachment and redevelopment behind two-dimensional rearward facing step
[AD-753358] 09 p1018 N73-18306
Model for liquid fuel sprayed into supersonic gaseous stream and two phase flow of dispersed liquid
[AD-753515] 09 p1019 N73-18316
Mathematical model for predicting erosion rate of graphite surface exposed to hot supersonic stream of hydrogen gas
[NASA-CR-130812] 09 p1050 N73-18564
Application of optimal control theory to design of control system for supersonic inlet of turbojet engine
[NASA-TN-D-7188] 09 p1079 N73-18803
Analysis of effects on in-plane boundary conditions and panel geometry on natural vibration and flutter characteristics of panels exposed to supersonic flow parallel to generators
09 p1094 N73-18933
Development of steel wedge probe for measurement of three dimensional wake flow in subsonic and transonic flow fields
10 p1140 N73-19285
Error sources in pressure measurements on turbulent supersonic flows by nonstationary microphone
10 p1140 N73-19289
Initial temperature effects on diffusion burning of hydrogen flame in closed channel with supersonic flow
[NASA-TT-F-14844] 10 p1141 N73-19295
Error sources in pressure measurements on turbulent supersonic flows by nonstationary microphone
10 p1184 N73-19629
Interaction of shock wave with turbulent boundary layer at moderate supersonic Mach numbers
10 p1206 N73-19815
Boundary layer behavior in supersonic straight and annular blade cascades of fixed and mobile types
10 p1207 N73-19817
Flow and acoustic characteristics determined for subsonic and supersonic jets and supersonic suppressors
[NASA-CR-131297] 11 p1233 N73-20006
Computer program for calculating structure and supersonic combustion flow with chemical reactions and shock waves
[NASA-CR-112303] 11 p1271 N73-20311
Navier-Stokes equations for generating and maintaining straight oblique shock wave in steady supersonic flow and computing inviscid flow field downstream of shock wave
[AD-754095] 11 p1271 N73-20317
Development and characteristics of supersonic nozzles with perforated edges for wind tunnel applications
[AD-754601] 11 p1272 N73-20323
Device for measuring stagnation pressure of supersonic gas streams
[NASA-CASE-LAR-11139-1] 11 p1292 N73-20483
Development of computer program and algorithm for determining interference between lifting surface elements at various Mach numbers
[NASA-CR-112264] 12 p1390 N73-21272
Finite difference method for evaluating supersonic flow over sharp cone
[AD-755862] 12 p1392 N73-21290
Pitot pressure survey of laminar boundary layer on supersonic spinning ogive cylinder
[AD-755694] 12 p1393 N73-21294
Effects of nose bluntness on natural and induced boundary layer transition on axisymmetric bodies in supersonic flow
[AD-755843] 12 p1393 N73-21295
Finite difference solution to right angle circular cone streamline swallowing phenomenon during supersonic and hypersonic flow
13 p1508 N73-22218
Compressible laminar boundary layer on cone near plane of symmetry and stagnation point boundary layer with hydrogen injection
13 p1509 N73-22228
Analysis of accuracy of Preston tube calibration equations to determine local skin friction in two dimensional supersonic and low hypersonic flow conditions
[NASA-TN-D-7190] 13 p1510 N73-22239
Machine calculation of unsteady Mach reflections and Prandtl-Meyer supersonic flows
[AD-756195] 13 p1511 N73-22242
Visualization and integral methods for studying three-dimensional supersonic flow separation on delta wing
14 p1600 N73-22970
Finite difference method for blunt body supersonic flow computation
[DLR-FB-73-10] 14 p1650 N73-23381
Normal shock wave conditions in elements of axial supersonic compressor
[AD-756102] 14 p1650 N73-23384
Numerical analysis of gas flow ahead of supersonic cascade
[AD-756079] 14 p1650 N73-23385
Oscillating bodies [cone, wedge, and flat plate] in supersonic flow
[AD-757254] 14 p1650 N73-23387
Supersonic boundary layer separation and reattachment - finite difference theory solutions
[AD-757062] 14 p1651 N73-23388
Analysis of aerodynamic loading for symmetrically tapered wings describing simple harmonic pitching oscillations of low frequency in supersonic flow
[ARC-R/M-3298] 15 p1728 N73-24019
Analysis of pressure distribution around hemisphere at supersonic speeds with emphasis on differential pressure measurements
[ARC-R/M-3237] 15 p1729 N73-24023
Numerical analysis of base pressure distribution for supersonic flow over slender wedge or backward facing step
15 p1764 N73-24295
Analysis of decomposition of liquid jet injected normal to supersonic airstream to show generation of high frequency, axially propagating waves
15 p1764 N73-24296
Development of model to predict formation and detection of molecular cluster size distribution for various materials in supersonic free jet
15 p1765 N73-24300
Numerical method of characteristics for unsteady propagation processes considering dissipative terms in equations for supersonic mixing processes
[NASA-TT-F-14825] 15 p1767 N73-24320
Nonlinear stability of liquid adjacent to supersonic stream
[AD-758103] 15 p1769 N73-24328
Application of finite element method for analyzing stability of rectangular plates in supersonic air stream
15 p1838 N73-24899
Performance tests of gas turbines with high pressure ratios per stage to determine flow characteristics of supersonic nozzles for turbines
[ARC-R/M-3273] 16 p1856 N73-25037
Effect of humidity on laminar recovery temperature measurements during supersonic air flow in wind tunnels
[ARC-R/M-3215] 16 p1857 N73-25042
Numerical analysis of real gas effects in supersonic flows over sharp and spherically blunted cones
16 p1887 N73-25274
Effect of adjacent jets on turbulent mixing rate of coaxial helium jet in Mach 4 air stream
[NASA-CR-112292] 16 p1888 N73-25281

Performance tests of terminal shock and restart control system of two dimensional twin-duct compression inlet
[NASA-TM-X-2818] 16 p1956 N73-25824
Comparison of linearized theories to determine aerodynamic characteristics of slender wings in supersonic flow
[RAE-LIB-TRANS-1677] 17 p1981 N73-26010
Analysis of profile characteristics of supersonic turbulent boundary layer in region of moderate adverse pressure gradient
[AD-759915] 17 p2015 N73-26298
Analysis of condensation effects in supersonic nozzle flows for homogeneous and heterogeneous nucleation conditions
18 p2128 N73-27195
Analysis of nonequilibrium conditions among populations of excited levels of potassium vapor passing through supersonic nozzle
18 p2128 N73-27199
Analysis of characteristics of supersonic flow of helium around right circular cones at zero angle of attack and Mach numbers from 1.5 to 30.0
[NASA-SP-3078] 18 p2130 N73-27208
Characteristics method for calculating supersonic flow fields
[NASA-CR-132274] 18 p2130 N73-27210
Analysis of supersonic flow involving viscous and inviscid flow using unified solution technique
19 p2251 N73-28148
Development of theoretical model for supersonic turbulent near wakes of planar and axisymmetric configuration in supersonic flow
20 p2384 N73-29151
Theoretical analysis of flow recompression, reattachment, and redevelopment associated with supersonic laminar flow past rearward facing step
20 p2385 N73-29162
Interaction between supersonic boundary layer with turbulent flow and inelastic deformable wall to determine stress perturbations and pressure distribution
[TN-86] 20 p2388 N73-29186
Channeling of supersonic free jet of plasma by axisymmetric magnetic field
20 p2457 N73-29744
Irrotational planar supersonic cascade ideal gas flow computation using method of characteristics
[DLR-FB-73-34] 21 p2491 N73-29998
Development of numerical code to calculate two dimensional flow field when supersonic flow encounters double wedge configuration
[NASA-CR-134010] 21 p2524 N73-30242
Study of supersonic flow in inlets using holographic interfereometry
[AD-763335] 21 p2525 N73-30250
Calculations of turbulent shear stress distributions for zero pressure gradient and adverse gradient supersonic turbulent boundary layer flow
[AD-763197] 21 p2526 N73-30254
Numerical analysis of flow characteristics on upper surface of wedge moving at supersonic speed when plane shock wave is incident on wedge
[AD-763283] 21 p2527 N73-30267
Some regularities in propagation of perturbations of discrete tone in free supersonic jet
[AD-763163] 21 p2581 N73-30681
Study of supersonic conical flow by solving exact conical flow equations
[ISAD-4980-VOL-38-NO-9] 22 p2651 N73-31236
Supersonic flow configurations at inlet and exit of infinite two dimensional straight cascade of flat plates
22 p2652 N73-31244
Effects of flow turning, flow acceleration, and supersonic flow on hydrogen film cooling
[NASA-CR-121235] 22 p2729 N73-31841
Wind tunnel tests to determine boundary layer flow characteristics in supersonic axisymmetric inlet
[NASA-TM-X-2902] 23 p2739 N73-31926
Analysis of sonic boom characteristics based on second order solutions for flow distribution around slender bodies in supersonic flow - Part I
[NASA-CR-2339] 23 p2739 N73-31927
Flow interference between supersonic intake and airframe to show three dimensional separation of boundary layer
23 p2775 N73-32194
Shock wave pattern and stability in axial flow supersonic compressor using simulated rotating cascade test facility
23 p2775 N73-32196
Supersonic stationary flow around atmosphere retained by gravitational force of spherical body
24 p2905 N73-33183
Flow through supersonic Laval nozzle with several contractions
24 p2909 N73-33216

**SUPERSONIC FLOW INLETS**
U SUPERSONIC INLETS

**SUPERSONIC FLUTTER**
Flutter characteristics of thin cantilever wings at transonic and supersonic speeds
[NAL-TR-288] 06 p0618 N73-15022
Application of finite element method to calculation of supersonic flutter of thermal protection panel for space shuttles
[VF-12] 10 p1104 N73-19001
Computation of supersonic flutter for thermal protection panel of space shuttles
[VF-16] 10 p1104 N73-19002

**SUPERSONIC INLETS**
Wind tunnel tests of mixed compression axisymmetric inlet with large transonic mass flow at Mach numbers 0.6 to 2.65
[NASA-TN-D-6971] 04 p0463 N73-13777
Three dimensional boundary layer separation and shock wave generation in flow field of supersonic conical intake mounted on fuselage side
[ARL/ME-137] 08 p0863 N73-16981
Performance comparison of three normal-shock position sensors for supersonic mixed compression inlets
[NASA-TM-X-2739] 08 p0955 N73-17817
Application of optimal control theory to design of control system for supersonic inlet of turbojet engine
[NASA-TN-D-7188] 09 p1079 N73-18803
Flow instabilities of supersonic variable ramp inlets at Mach 2 discussing Concorde aircraft intake
[ARC-R/M-3711] 10 p1104 N73-18999
Time variant distortion in supersonic inlet related to stall in compressor
[NASA-TM-X-68189] 10 p1208 N73-19825
Improved design of high-response slotted plate overboard bypass valve for supersonic inlets
[NASA-TM-X-2812] 16 p1864 N73-25097
Dynamic response of Mach 2.5 supersonic mixed compression axisymmetric inlet operating with turbofan engine
[NASA-TM-X-2833] 18 p2193 N73-27709
Supersonic wind tunnel tests of internal performance of rectangular variable geometry air inlets noting effect of incidence
[ARC-CP-1242] 22 p2612 N73-30933
Supersonic wind tunnel tests of internal performance of rectangular variable geometry air inlets at zero incidence
[ARC-CP-1243-PT-1] 22 p2612 N73-30934

**SUPERSONIC JET FLOW**
Mathematical models for determining impact of supersonic gas jet on solid surfaces
[NLL-RTS-7551] 02 p0154 N73-11248
Numerical calculation of supersonic three dimensional jet plum in perfect gas with inviscid and compressible properties
04 p0404 N73-13287
Navier-Stokes equations governing flow of subsonic or supersonic jets mixing with surrounding atmosphere
[AD-750185] 05 p0528 N73-14296
Properties of axisymmetric supersonic free jet including relation between jet structure and discrete noise frequencies
[ISL-29/72] 12 p1365 N73-21075
Computer programs for predicting supersonic and hypersonic interference flow fields and heating
[NASA-TM-X-2725] 16 p1889 N73-25285
Density profiles of supersonic jet target of hydrogen-deuterium in vacuum
[LA-UR-73-231] 17 p2010 N73-26260

**SUPERSONIC NOZZLES**
Calibration of aerodynamic wind tunnel with supersonic nozzle flow
[AD-749513] 05 p0524 N73-14264
Performance tests of wedge nozzle with cold primary and secondary flows for supersonic cruise and takeoff configurations to analyze noise suppression effects
[NASA-TM-X-2689] 06 p0714 N73-15822
Noise intensities of rectangular and circular supersonic nozzle geometries
[NASA-CR-130964] 09 p1067 N73-18704
CO2/N2 laser applied to CO2 excited state population study during supersonic nozzle expansion
[ONERA-NT-204] 10 p1169 N73-19510
Analysis of deflection forces and deflection angles generated by thrust vector control nozzle at various Mach numbers and exit pressures
[AD-758521] 15 p1827 N73-24808
Performance tests of gas turbines with high pressure ratios per stage to determine flow characteristics of supersonic nozzles for turbines
[ARC-R/M-3273] 16 p1856 N73-25037
Vapor condensation by homogeneous nucleation in supersonic nozzle flows
17 p1991 N73-26101
Scaling laws to predict supersonic jet noise generated by rectangular and axisymmetric nozzles
[PB-221855/0] 22 p2700 N73-31629
Friction forces on pneumatically drawn fibers with supersonic nozzle
24 p2906 N73-33193

**SUPERSONIC PRESSURE DISTRIBUTION**
U PRESSURE DISTRIBUTION
U SUPERSONIC FLOW

**SUPERSONIC SPEEDS**
Effects of location of wing pivot and geometry of wing on static longitudinal aerodynamic characteristics of variable-sweep supersonic fighter aircraft model
[NASA-TM-X-2674] 03 p0247 N73-12000
Vaporization rates of liquid injected into high temperature, supersonic gas flow using aviation gasoline injected by Laval nozzle into air stream
[AD-747456] 03 p0286 N73-12317
Ultrasonic velocity measurements for determining adiabatic compressibilities of ionic solutions and molten salts
[AD-749353] 04 p0451 N73-13686
Wind tunnel tests to determine pressure distribution on Apollo command module and Saturn launch vehicle at supersonic and hypersonic speeds
[NASA-TM-X-62117] 04 p0477 N73-13904
Analysis of nonequilibrium in excited levels of electric ARC heated potassium vapor injected into argon/helium gas flow passing through supersonic nozzle
[AD-750943] 05 p0585 N73-14759
Flow characteristics of two-dimensional, tangential-slot injection into turbulent boundary layer at Mach 2.4 freestream velocity
[NASA-CR-2128] 06 p0654 N73-15313
Aerodynamic configurations and characteristics of airfoils designed to reduce formation of shock waves during supersonic flight
[NASA-TT-F-749] 07 p0736 N73-15987
Development of computer program for calculating flow field resulting from sonic boom focusing
[NASA-CR-2127] 07 p0739 N73-16013
Aeroelastic divergence of transport aircraft flying at supersonic speeds and design techniques to eliminate adverse effects
[NASA-CR-112262] 09 p0984 N73-18036
Performance tests of reentry vehicle control with base plane thrusters and fluidic control logic
[SC-DC-72-2244[RD]] 09 p0985 N73-18043
Calculation of outer inviscid flow about rectangular wing moving at supersonic speeds
[NASA-CR-130985] 09 p1013 N73-18269
Comparison of two total pressure and total temperature measuring instruments for boundary layer investigations at supersonic speeds
10 p1139 N73-19284
Effect of plume-induced boundary layer separation on afterbody during powered supersonic flight
[AD-754640] 11 p1272 N73-20326
Analysis of requirements, instruments, and procedures for measurement of aircraft temperatures up to Mach 2.3 and altitudes up to 80,000 feet
[AGARD-AG-160-VOL-2] 11 p1294 N73-20499
Theories, numerical methods, and computer programs for determining inviscid three dimensional flow around spherically-capped smooth bodies and wings at supersonic speeds
[AD-753696] 12 p1356 N73-21002
Measurement of aerodynamic heating on nose of Fairey Delta aircraft at 40,000 feet and Mach numbers to 1.65 during climb and level flight
[ARC-R/M-3280] 15 p1725 N73-23996
Application of modified slender wing theory to analyze aerodynamic characteristics of slender, lifting, wings with curved leading edges at supersonic speeds
[ARC-R/M-3278] 15 p1727 N73-24006
Wind tunnel tests to determine characteristics of turbine rotor blades with inter-blade passages operating at supersonic speed
[ARC-R/M-3275] 15 p1728 N73-24016
Numerical methods for determining effect of aerodynamic lag on bending response of aircraft wings at supersonic speeds
[NAL-TN-36] 15 p1733 N73-24056
Wind tunnel tests to determine aerodynamic characteristics of two missile configurations with common body at transonic and supersonic speeds
[NASA-TM-X-2780] 19 p2218 N73-27891
Analysis of supersonic jet aircraft noise using fluctuating jet pressures to characterize the sources
[AD-762296] 19 p2222 N73-27923
Numerical analysis of disturbance pressure due to impinging of plane shock wave of arbitrary strength on moving slender body
19 p2251 N73-28151
Wind tunnel tests to determine aeroelastic stability of thin isotropic circular cylindrical shells at subsonic and supersonic air speeds
20 p2359 N73-28975
Computer simulation of aircraft motions and propulsion system dynamics for YF-12 aircraft under supersonic conditions
[NASA-TM-X-62245] 20 p2361 N73-28990
Effect of ablation modes and flow field distribution on cross hatching phenomenon at supersonic speeds
[TN-85] 20 p2485 N73-29963

**SUPERSONIC STRIKE AIRCRAFT**
U ATTACK AIRCRAFT
U SUPERSONIC AIRCRAFT

**SUPERSONIC TRANSPORTS**
NT CONCORDE AIRCRAFT
NT SUPERSONIC COMMERCIAL AIR TRANSPORT

Effect of external air flowing across exhaust nozzles on jet noise produced by supersonic transport aircraft at high takeoff speeds
[NASA-TM-X-68161] 03 p0250 N73-12027
Analysis of jet noise produced by supersonic transport aircraft with augmentor wing and four duct burning turbofan engines
[NASA-TM-X-68177] 06 p0619 N73-15028
Mission performance analysis of three supersonic transport configurations and effects of limitations on allowable engine noise
[NASA-TM-X-68178] 06 p0620 N73-15032
Doppler compensated communication system for locating supersonic transport position
[NASA-CASE-GSC-10087-4] 11 p1254 N73-20174
Bibliography of supersonic transport aircraft data to include program management, systems engineering, aircraft structures, and operational considerations
[AD-755600] 12 p1365 N73-21076
Stratospheric photochemical reactions of ozone in relation to climatology and supersonic transport pollution
[NOAA-TM-NESS-47] 12 p1422 N73-21526
Flight tests to determine magnitude of groundtrack overpressure generated by oblique wing transport aircraft at Mach 1.4 and 45,000 feet
[NASA-TM-X-62247] 13 p1472 N73-21922
Influence of small periodic oscillations on viscous shock waves structure and sonic boom rise time caused by supersonic transport vibrations
13 p1507 N73-22217
Sonic boom minimization design for supersonic transport aircraft
[NASA-TN-D-7218] 15 p1734 N73-24065
Chemical kinetics and atmospheric dynamics data base for digital modeling of climatological aircraft exhaust effects
[PB-214100/0] 16 p1908 N73-25441
Influence of combined rotary flow inductors and dry turbojets on side line noise levels of supersonic transports
[NASA-TM-X-68233] 20 p2466 N73-29809
Stratospheric electricity due to operating supersonic transport fleets
[AD-763471] 21 p2540 N73-30365
Modification of Olympus turbojet engine to meet supersonic civil transport requirements
21 p2590 N73-30752
Effect of spatial variability of wind in stratosphere on flight of supersonic transports
24 p2946 N73-33529

**SUPERSONIC WAKES**
Performance prediction for deployable aerodynamic decelerators operating in supersonic wakes using gas dynamics analogy
[AD-751982] 08 p0897 N73-17266
Hydrodynamic and chemical properties of stratospheric aircraft wake
[PB-213114] 11 p1290 N73-20465

**SUPERSONIC WIND TUNNELS**
Calibration of aerodynamic wind tunnel with supersonic nozzle flow
[AD-749513] 05 p0524 N73-14264
Feasibility of porous jet stretcher nozzle for angle of attack testing of missiles in supersonic wind tunnel
[AD-750867] 06 p0651 N73-15288
Wind tunnel determination of supersonic aerodynamic characteristics of variable geometry spacecraft designed for high hypersonic performance
[NASA-TM-X-2703] 07 p0735 N73-15985
Analysis of design flow in open jet wind tunnel and examination of processes for starting supersonic wind tunnels
[ARL/ME-138] 10 p1137 N73-19264
Performance tests of working section of variable pressure, supersonic wind tunnel to show effects of inclination of slotted walls on Mach number accuracy
[ARC-R/M-3228] 15 p1730 N73-24032
Superconducting electromagnetic suspension and balance and supersonic wind tunnel facility for dynamic stability studies
[NASA-CR-132255] 15 p1761 N73-24271
Cryogenic superconducting magnetic suspension and balance facility designs
15 p1761 N73-24272
Electric discharges in supersonic high pressure gas flow to improve carbon dioxide laser power
[ISL-20/72] 19 p2307 N73-28560

**SUPINE POSITION**
Acceleration effects on mechanical impedance of human body in supine position
19 p2227 N73-27963

**SUPPLEMENTS**
Supplement to bibliography on Aerospace Medicine and Biology, October 1972
[NASA-SP-7011[107]] 04 p0377 N73-13069

**SUPPORT INTERFERENCE**
Systems analysis for determining cause of steerable antenna oscillations during Apollo 14 and 15 missions
[NASA-TM-X-68901] 05 p0519 N73-14218
Analysis of interference occurring in subsonic and transonic wind tunnels caused by model support system
17 p2009 N73-26242

**SUPPORT SYSTEMS**
NT GROUND OPERATIONAL SUPPORT SYSTEM
NT GROUND SUPPORT SYSTEMS
NT PORTABLE LIFE SUPPORT SYSTEMS
Eole and support operations planning
[NASA-TT-F-14709] 03 p0249 N73-12011
Development and characteristics of support systems module for use with Large Space Telescope - Vol. 5
[NASA-TM-X-64726-VOL-5] 09 p1036 N73-18453
Development of system concept for shuttle support to orbital operations of low cost unmanned satellites in low earth orbit
[NASA-CR-130239] 15 p1834 N73-24869
Management system for functional support demands in multiproject institution
15 p1850 N73-24991
Manufacturing of large structural mirror supports for space telescopes using titanium alloys
18 p2209 N73-27828
Textbook of Ground Operations Aerospace Language [GOAL]
[NASA-TM-X-69542] 24 p2897 N73-33129

**SUPPORTS**
NT PYLONS
Rayleigh-Ritz analysis of free vibration behavior in plates with discrete elastic supports
[NASA-CR-112220] 04 p0480 N73-13924
Design and development of test stand system for supporting test items in vacuum chamber
[NASA-CASE-MFS-21362] 11 p1265 N73-20267
Development and characteristics of supporting frame to isolate payloads from multi-gravitational forces
[NASA-CASE-MFS-21680-1] 11 p1297 N73-20525
Analysis of Michell framework for uniform load between fixed supports
[REPT-1054/73] 13 p1586 N73-22861
Collapsible support for antenna reflector applied to installation of spacecraft antennas
[NASA-CASE-NPO-11751] 15 p1749 N73-24176
Viscoelastic shock absorbing mount for electrical circuit board
[NASA-CASE-NPO-13253-1] 22 p2677 N73-31445
Optical radar angle tracking mount
[AD-765213] 23 p2759 N73-32077

**SUPPRESSORS**
Suppression devices for controlling acoustic combustion instability in solid propellant engines
[AD-743701] 01 p0090 N73-10740
Conference on reduction and suppression of aircraft engine noise
[NASA-SP-311] 03 p0249 N73-12012
Design and performance of suppressors for acoustic noise reduction in turbofan engines
03 p0249 N73-12015
Estimates of reduced noise levels for turbofan engines with sound suppressors
03 p0250 N73-12022
Suppression of fan noise and effects on short takeoff aircraft systems design
03 p0250 N73-12023
Surge divertor breakdown voltage characteristics
[AD-747622] 03 p0276 N73-12236
Performance of lightning and surge suppressors for digital transmission equipment
[AD-752448] 09 p1004 N73-18195
Flow and acoustic characteristics determined for subsonic and supersonic jets and supersonic suppressors
[NASA-CR-131297] 11 p1233 N73-20006
Performance of baffles as energy dissipation suppressors in liquid filled precessing cavities
16 p1888 N73-25280
Characterization of electromagnetic pulse shunt protective devices
[AD-763886] 22 p2644 N73-31191

**SURFACE CHEMISTRY**
U SURFACE REACTIONS

**SURFACE COATINGS**
U COATING

**SURFACE COOLING**
Analysis of factors affecting cooling of liners in gas turbine combustion chambers
[NAL-TR-196] 06 p0713 N73-15819
Surface cooling method for very high frequency power transistor using heat pipe techniques
[AD-752076] 08 p0889 N73-17200
Determination of optimum conditions for lubrication and cooling during grinding by abrasive discs of synthetic superhard materials
[AD-754665] 11 p1302 N73-20562
Analysis of heat exchange between liquid and bodies on which liquid flows during catalytic chemical reactions on surface of bodies
[AD-761607] 19 p2353 N73-28927

**SURFACE CRACKS**
Scanning electron microscopy applied to surface fracture mechanics study, composite materials, and powder metallurgy
[DLR-MITT-71-32] 03 p0315 N73-12571
Electron fractography of stress corrosion fracture surfaces of aircraft materials as high strength steels, Al-Zn-Mg, Al-Cu and Ti alloys
[NLR-TR-71038-U] 03 p0361 N73-12945
Storage time loss in metal oxide capacitors caused by surface damage in silicon wafer
[AD-756250] 13 p1566 N73-22690
Evaluation of nondestructive testing methods for fatigue crack detection
[NASA-CR-128946] 15 p1839 N73-24901
Sensitivity and comparison evaluation of liquid penetrants used in Saturn 5 vehicle hardware to detect surface cracks
[NASA-TM-X-64769] 22 p2688 N73-31529
Oxidative stress cracking in nylon fibers immersed in alkaline aqueous medium saturated with molecular oxygen at elevated temperature
24 p2937 N73-33455

**SURFACE DEFECTS**
Fracture strength of aluminum alloys 7075-T6 and 2024-T3 with surface flaws and corner cracks at holes
[NLR-TR-71033-U] 06 p0685 N73-15576
Determination of stress intensity factors from photoelastic data with applications to surface flaw problems
[AD-756872] 13 p1587 N73-22864
Stress analysis of thick wall cylindrical vessels weakened by flaws
[AD-764279] 22 p2726 N73-31811
Electron network model of solid interfaces, surface defects, planar defects, and thin films
23 p2825 N73-32584
Point, line, and planar defects in metal crystals
[COO-3158-17] 24 p2968 N73-33723

**SURFACE DIFFUSION**
Lateral diffusion in thin [film] couples of gold and silver
23 p2825 N73-32579

**SURFACE DISTORTION**
Measurement of fluid velocity and surface deformation during fluid discharge from rotating cylindrical tank
13 p1509 N73-22232
Measurement of surface strain deformation in materials by holographic interferometry
[NRC-TT-1623] 13 p1536 N73-22447
Holographic interferometry for measuring surface deflections of statically loaded turbine blades
16 p1921 N73-25543

**SURFACE ENERGY**
Measurement of surface, grain boundary, and coherent twin boundary free energies in 304 stainless steel at elevated temperatures using method of zero creep coupled with electron microscopy
[AD-747267] 02 p0189 N73-11535
Surface and volume mechanisms of material evaporation subject to powerful radiation fluxes
09 p0999 N73-18154
Porous structure and surface energy of evaporated metal thin films
13 p1565 N73-22683
Strain energy density and surface layer energy for crack-like ellipse
[NASA-CR-132338] 24 p2988 N73-33879

**SURFACE EROSION**
U EROSION

**SURFACE FINISHING**
B4C-alkali metal carbonates for boronizing steel surfaces
[NLL-RTS-7197] 01 p0069 N73-10562
Development of procedure for producing thin transparent films of zinc oxide on transparent refractory substrate
[NASA-CASE-FRC-10019] 03 p0304 N73-12487
Device and method for determining X ray reflection efficiency, scattering properties, and surface finish of optical surfaces
[NASA-CASE-MFS-20243] 04 p0449 N73-13662
Optical surface correction method for laser reflectors based on vacuum silica vapor differential deposition
05 p0558 N73-14530
Influence of surface finishing on adherence of radio frequency sputtered molybdenum disulfide on silver, gold, copper, and bronze
[NASA-TN-D-7169] 07 p0804 N73-16523
Argon ion gun for cleaning surfaces and specimens for use in electron spectrometer
[ECRC/N486] 10 p1125 N73-19165
Nondestructive replica techniques for studying roadstone surface polishing by electron microscopy
[PB-212720] 13 p1531 N73-22409
Tooling workpiece interface condition effects on metal flow and product quality in extrusion
[AD-755832] 13 p1535 N73-22439
Influence of surface preparation, surface texture, and initial oxidation on metal surface crystallization
14 p1676 N73-23603
Digital system for programmed control of maching process for turbine blade foil
[AD-759682] 17 p2077 N73-26804
Location of adhesive bond failure on Al surface during coupon surface treatment by radioactive tracing
[AD-761073] 18 p2168 N73-27509

**SURFACE GEOMETRY**
Matrix displacement analysis of shells using curved SHEBA elements to approximate surface geometry
[ISD-134] 20 p2483 N73-29947

Least squares fitting of bicubic spline surfaces to general data at arbitrary points noting householder orthogonal transformation, solution stability, and ranking
[NPL-NAC-22] 23 p2813 N73-32489
SURFACE INTERACTIONS
U SURFACE REACTIONS
SURFACE IONIZATION
Space flight tests for determining performance efficiency of ion engine model with surface ionization of cesium on tungsten
14 p1701 N73-23801
SURFACE LAYERS
NT MONOMOLECULAR FILMS
Compressive surface layer formation on hot pressed silicon carbide and nitride to improve impact resistance
[NASA-CR-121002] 02 p0222 N73-11796
Measurement of diurnal heat budget in tropical Atlantic surface layers
07 p0857 N73-16953
Surface instability of liquid layer subjected to perpendicular motion
[NASA-TT-F-14880] 12 p1390 N73-21274
Sources and dispersal patterns of suspended particulates in nearshore surface waters of northeastern Pacific Ocean and Hawaii
[E73-10487] 12 p1396 N73-21323
Effect of surface layer stress on plastic deformation and crack propagation of steel
[AD-755844] 12 p1415 N73-21467
Position sensitive detector with lithium diffused layer as uniform resistive layer
[NASA-CR-133408] 18 p2152 N73-27391
Stress corrosion behavior of titanium and aluminum alloys with and without surface layer
[AD-760529] 18 p2163 N73-27469
Utilization of sandwich method to obtain epitaxial layers of Si, GaAs, and heteroepitaxial GaAs-Ge
18 p2186 N73-27654
Mechanism of silicon autoepitaxy during transport in sandwich process
18 p2187 N73-27655
Low temperature epitaxial development of Ge and Si layers by chloride method
18 p2187 N73-27656
Film growth transient measurements for stress corrosion cracking susceptibility analyses on metals
23 p2804 N73-32421
Theoretical calculation of surface mobility in MOS surface inversion layers at room temperature
23 p2825 N73-32578
Mechanical attachment of surface insulation tiles to space shuttle structure
24 p2942 N73-33494
Flexible ceramic mat surface insulation for space shuttle thermal protection system design
24 p2942 N73-33497
SURFACE NAVIGATION
Application of time frequency techniques to improve navigation of ships and reduce risk of collision
[NASA-TT-F-14718] 02 p0207 N73-11679
Review of Soviet publication on navigational hydrometeorology
04 p0443 N73-13617
Analysis of geometrical, analytical, and semi-analytical inertial navigation systems for application to shipbuilding industry
[JPRS-57694] 04 p0447 N73-13650
Reliability analysis of digital computer used in system for ship navigation
[AD-750990] 06 p0697 N73-15687
Kalman filtering applied to surface and air navigation using celestial body coordinates
07 p0860 N73-16973
Development and evaluation of Geographic Position Locator for accurate, long-term, land based inertial navigation
[UCRL-51130-VOL-1] 08 p0941 N73-17713
Characteristics of navigation satellite system and analysis of operation of translocation subsystem
[AD-754173] 10 p1186 N73-19650
Proceedings of conference on inertial navigation components and systems with emphasis on concepts and techniques involving cost and performance tradeoffs
[AGARD-CP-116] 11 p1316 N73-20684
Design, development, and test of NASA-GFSC Position Location and Aircraft Communications Equipment [PLACE]
[NASA-TM-X-66287] 18 p2117 N73-27115
Observational errors and algorithms in determining position of ships
[JPRS-59638] 20 p2439 N73-29592
Optimal methods for processing observations
20 p2439 N73-29593
Methods for determining most probable value of recurring errors
20 p2439 N73-29594
Algorithms for solving differential-range bearing in rectangular geocentric system of coordinates
20 p2439 N73-29595
Velocity integration in navigational digital computers
20 p2440 N73-29596
SURFACE PRESSURE
U PRESSURE
SURFACE PROPERTIES
NT ADHESION
NT COEFFICIENT OF FRICTION
NT INTERFACIAL TENSION
NT SKIN TEMPERATURE [NON-BIOLOGICAL]
NT SPECTRAL REFLECTANCE
NT SURFACE CRACKS
NT SURFACE DEFECTS
NT SURFACE ENERGY
NT SURFACE ROUGHNESS
NT SURFACE STABILITY
NT SURFACE TEMPERATURE
NT WALL TEMPERATURE
Mu-meter and diagonal braked vehicle measurements of runway friction at ten airports
[PSC-107] 01 p0036 N73-10281
Subsequent yield curves for axial stressed-shear stressed surfaces of annealed SAE 1017 steel
[AD-746474] 02 p0188 N73-11523
Wetting of alumina, magnesia, zirconia, and carbides and borides of vanadium, titanium, and zirconium by palladium melts
[NLL-RTS-7321] 02 p0190 N73-11544
Progress in multidisciplinary research leading to utilization of extraterrestrial resources
[NASA-CR-129109] 02 p0226 N73-11827
Characteristics of yield surfaces for hardening body as function of preliminary loading path
02 p0238 N73-11937
Surface properties study of thermionic electrodes, using quasi-equilibrium model for oxygen reactions with refractory metals
[NASA-CR-129598] 03 p0254 N73-12057
Measurement of short pulse, X-band radar backscatter from rough water surfaces expressed as cumulative probability distribution functions
[AD-747949] 03 p0267 N73-12159
Influence of surface processes on rate of permeation of hydrogen through metals
[NASA-CR-129276] 03 p0312 N73-12548
Bibliographic survey on stress corrosion cracking of high strength aluminum alloys, including oxide effects
[DLR-FB-71-105] 03 p0316 N73-12572
Analysis of friction surfaces of porous materials based on iron after prolonged operation under self lubricating conditions
[AD-748020] 03 p0317 N73-12585
Research and development in surface studies, plasma physics, and gas dynamics
[AD-747132] 03 p0368 N73-12996
Physical and chemical properties of steel surfaces exposed to deoxidation products
[AD-747828] 04 p0435 N73-13547
Measurement of physical and chemical properties of well characterized surfaces for application to optical elements in high power laser development
05 p0555 N73-14508
Optical surface correction method for laser reflectors based on vacuum silica vapor differential deposition
05 p0558 N73-14530
Diagnostic techniques for characterizing near surface of solids
[UCRL-73925] 05 p0587 N73-14773
Method of thermal desorption used to determine specific surfaces in powder metallurgy
[NLL-TRANS-746-1287-[9022.401]]
06 p0682 N73-15547
Auger electron spectroscopy of surface segregation in binary alloys
[NASA-TN-D-6982] 06 p0683 N73-15564
Development of surfaces and coatings for solar energy conversion systems
[NASA-TT-F-14650] 06 p0688 N73-15598
Automatic swabbing apparatus for sampling of microbiological surfaces
[NASA-CASE-LAR-11069-1] 07 p0745 N73-16061
Production of ball bearing steel ingots with emphasis on effects of temperature, surface defects, and casting methods
[AD-751252] 07 p0805 N73-16533
Theoretical analysis of dispersion curves for surface polaritons in semiconductors
[AD-751671] 07 p0833 N73-16750
Surface properties and gas-solid interface phenomena in engineering materials
[AD-753099] 09 p1000 N73-18165
Autoradiograms of deformed silicon and germanium single crystal surfaces
[AD-753039] 09 p1074 N73-18765
Association of surface polaritons with surface magnetoplasmons coupled to surface optical phonons in polar semiconductors
[AD-753484] 09 p1075 N73-18771
Refracted electron beam temperature as indication of lead sulfide purity
[AD-753556] 09 p1077 N73-18787
Photoelectric measurements of solar phase brightness relationship of planet Jupiter Galilean satellites to show porous nature of surface layers of satellites
09 p1083 N73-18838
Performance test of aluminum alloy landing mats under heavy duty loads
[AD-753935] 10 p1138 N73-19276
Development of technique for production of beryllium foil with high surface finish
[RFP-1842] 10 p1166 N73-19483
Classification of land use in California using textural information in ERTS-1 MSS imagery
[E73-10461] 11 p1284 N73-20419
Determination of specific spectral signatures for dominant Arizona desert scrub plant species and soil surface backgrounds
[E73-10466] 11 p1284 N73-20421
Surface chemistry and physics of inorganic solids
[AD-754453] 11 p1332 N73-20814
Establishment of radiometric calibration technique to permit absolute reflectance characteristics of ground targets to be determined from ERTS-1 data
[E73-10458] 12 p1394 N73-21300
Interaction of nonsaturated surface gravity ocean waves with nondispersive internal waves
[AD-754281] 12 p1403 N73-21377
Correlation of ocean surface parameters with radar backscatter data
[E73-10530] 13 p1517 N73-22295
Exoelectronic emission and relationship with various surface properties of metals and alloys
[AD-756943] 13 p1543 N73-22509
Influence of surface conditions on Ti-6Al-4V alloy fatigue life
[AD-755385] 13 p1544 N73-22516
Experimental method of measuring direction and residual stress in steel using surface displacements around indentations
[AD-756869] 13 p1546 N73-22526
Detection of changes in water quality and surface area in Tahoka Lake, Texas using ERTS-1 imagery
[E73-10518] 14 p1654 N73-23412
Chemistry and physics of thin liquid films in contact with solid substrates and application to boundary lubrication of propulsion systems
[AD-757061] 14 p1670 N73-23556
Influence of surface preparation, surface texture, and initial oxidation on metal surface crystallization
14 p1676 N73-23603
Atmospheric radiative transfer model for predicting solar and daytime sky irradiance of ground target
[AD-757149] 14 p1693 N73-23739
Results of Venera 8 unmanned spacecraft probe
[NASA-TT-F-14915] 14 p1709 N73-23870
Analysis of kinetic and transport factors governing interfacial mass transfer rates in high temperature systems
[AD-758256] 14 p1720 N73-23959
Surface structure of polymer produced by passing ethylene through radio frequency discharge
[AD-758099] 15 p1748 N73-24166
Inspection of Hunter Army Airfield, Savannah, Georgia to determine condition of runways
[AD-757387] 15 p1763 N73-24285
Development of procedures for repairing damaged runway pavements
[AD-756806] 15 p1763 N73-24286
Development of test facility for determining interaction of sonic boom with surface of body of water
[NASA-TT-F-14917] 15 p1767 N73-24318
Measurement of gas permeability of high porosity nickel powder metallurgy parts
[NLL-LTI-746-1404-[9022.401]]
15 p1797 N73-24564
Microwave surface resistance of niobium tantalum - and lead indium-superconducting alloys considering thermodynamic vortices
[AD-757875] 15 p1822 N73-24770
Lattice dynamical calculation for soft mode semiconductor surface reconstruction
[AD-758723] 16 p1953 N73-25806
Cavitation data on surface irregularities applied to design problems
[AD-759030] 17 p2015 N73-26295
Surface damage induced in optical materials by laser
[AD-760131] 17 p2042 N73-26519
Surface potential and wear measurements on carbamate, amine, and phosphorothioate lubricant additives
[AD-759126] 17 p2051 N73-26595
Cosmos 243 measurements of radioemission properties of land surfaces
[NASA-TT-F-14978] 18 p2143 N73-27320
Electronic properties of beryllium single crystals with emphasis on microwave surface impedance
18 p2185 N73-27646
Formation of longitudinal edge waviness and center camber on sheets as measure of sheet flatness
[NLL-M-21611-[5828.4F]] 18 p2202 N73-27777
Ablation article and surface for analyzing flow transition on ablative surface
[NASA-CASE-LAR-10439-1] 18 p2205 N73-27796
Determination of sea surface conditions using Skylab L-band and Radscat passive microwave radiometers
[E73-10847] 19 p2291 N73-28425
Determination of sea surface conditions using Skylab passive L-band and Radscat microwave radiometers
[E73-10911] 20 p2397 N73-29260

Development of low energy diffraction system for observing surface structure of low-index single crystal metal surfaces with and without absorbates
20 p2429 N73-29510
Conference on contact surface requirements for electric contacts and connectors
[AD-763213] 21 p2519 N73-30203
Outdoor weathering influence on polyester and epoxy glasscloth reinforced laminate flexural strength and surface appearance
[FOK-R-1627] 21 p2563 N73-30546
Structure and composition of anodic coatings formed on magnesium dry cell
[AD-764253] 22 p2618 N73-30980
Effect of surface properties on tensile properties of beryllium under hydrostatic pressure
[NEL-537] 22 p2684 N73-31502
Performance tests to determine cornering characteristics of aircraft tire under various runway conditions, ground speeds, and yaw angles with and without braking
[NASA-TN-D-7351] 23 p2742 N73-31948
Characteristics of bulk and surface modes in simple metals using modified self-consistent linear response theory
24 p2933 N73-33427
Debye polarization theory for determining electromagnetism of sea surface
24 p2957 N73-33620
Properties of silicon-silicon dioxide interface properties in thin oxide metal oxide semiconductor structures
24 p2968 N73-33718
Mars surface properties working group
24 p2984 N73-33842

**SURFACE REACTIONS**
Antifriction interaction between metals and steels on polyamide surfaces
[NLL-RTS-7378] 04 p0425 N73-13461
Analysis of laser induced surface damage to glass materials at Brewster angle and near normal incidence
05 p0554 N73-14503
Analysis of entrance and exit surface laser induced radiation damage on sapphire crystal samples as function of beam size and divergence at surfaces
05 p0555 N73-14504
Increase in laser damage threshold of sapphire surfaces by polishing with energetic argon ion beams
05 p0555 N73-14505
Measurements of laser induced surface damage processes at ruby and neodymium YAG laser wavelengths to determine laser damage at different wavelengths to transparent media
05 p0555 N73-14506
Measurement of physical and chemical properties of well characterized surfaces for application to optical elements in high power laser development
05 p0555 N73-14508
Measurement of surface recession of ablative materials in rocket nozzles by spectroscopic analysis
[AD-749968] 06 p0714 N73-15829
Mathematical models for gas surface interactions and calculating aerodynamic coefficients for simple geometric shapes and high Mach number flow past thin airfoils
[AD-752245] 08 p0899 N73-17278
Influence of liquid oxygen on chromate coated aluminum tubing of breathing apparatus
[AD-752030] 08 p0936 N73-17661
Technique for obtaining Auger spectra of electron desorbable surface species on time independent basis
[NASA-TN-D-7257] 11 p1252 N73-20161
Orr-Sommerfeld equation for studying laminar boundary layer stability on elastic surface
[NASA-TT-F-14855] 11 p1270 N73-20307
Role of gas-surface interactions in reduction of OGO 6 neutral-particle mass spectrometer data
[NASA-TN-D-7239] 11 p1286 N73-20432
X ray detection of incomplete weldment and surface oxidation in welded aluminum spacecraft structures
[NASA-CR-124167] 11 p1298 N73-20536
Effect of contact-surface-active vapors on wear behavior of soft steel during sliding friction
[NASA-TT-F-14935] 15 p1791 N73-24523
Current carrier mobility near charged semiconductor surface
[AD-758973] 16 p1953 N73-25804
Chemical spot test for identifying magnesium or magnesium alloys used in aerospace applications
[NASA-CASE-LAR-10953-1] 18 p2160 N73-27446
Effects of boundary surface active vapors on behavior of steel during sliding friction
[NASA-TT-F-14993] 19 p2304 N73-28531
Electronic structure of solid surfaces
[AD-762372] 19 p2328 N73-28727
Approximate theory for wheel-soil interaction
[NASA-CR-133860] 21 p2580 N73-30673
Spectrophotometric analysis of electrochemical reactions on transparent mercury/platinum electrode
[AD-763265] 22 p2626 N73-31043

**SURFACE ROUGHNESS**
Effects of striated roughness and grooving on load carrying capacity of lubricating films
[AD-747307] 02 p0180 N73-11457
Performance tests of Andover C short takeoff transport aircraft on grass, concrete and soil landing sites
[ARC-CP-1220] 04 p0373 N73-13034
Boundary layer approach to analysis of atmospheric motion over surface obstruction
[NASA-CR-2182] 07 p0769 N73-16244
Fine grinding, polishing, and graded etching techniques to eliminate surface yield on optical telescope mirrors
[NASA-CR-112217] 08 p0934 N73-17647
Standardization values for grinding forces and surface roughness in cylindrical grinding, noting steels
[CRIF-MC-46] 10 p1167 N73-19491
Apollo 16 radar echo data for predicting blockiness of lunar surface
12 p1455 N73-21788
Nondestructive replica techniques for studying roadstone surface polishing by electron microscopy
[PB-212720] 13 p1531 N73-22409
Inspection of pavement grooving at four commercial and one military airfield
[AD-757208] 14 p1647 N73-23355
Kirchhoff approximation correction for application to electromagnetic wave scattering by rough surfaces
[NASA-CR-112263] 16 p1875 N73-25180
Wind tunnel investigation of turbulent boundary layer response to lateral surface roughness discontinuities
18 p2129 N73-27202
Coherent laser light measurement of ceramic material surface roughness
[AD-761198] 18 p2168 N73-27512
Doppler return spectra from rough ocean surface
19 p2320 N73-28667
Scattering of polarized light by rough and smooth leaf surfaces
20 p2405 N73-29333
Airborne laser profilometer for evaluating surface roughness of landing sites
[AD-763180] 22 p2648 N73-31218
Surface roughness effects on bidirectional reflectance of metallic surfaces
24 p2955 N73-33611

**SURFACE ROUGHNESS EFFECTS**
Diffraction of acoustic and electromagnetic waves on wavy surfaces
[AD-748037] 03 p0268 N73-12168
Bidirectional reflectance of metallic surfaces as function of wavelength and surface roughness
[UILU-ENG-72-4001] 03 p0335 N73-12728
Literature survey on wave scattering from rough surfaces
[FOA-2-C-2486-E1] 04 p0449 N73-13668
Compression of satellite altimeter radar pulses and high resolution sea reflectivity
06 p0663 N73-15389
Conference on dynamic wave effects on satellite-borne sea surface measurements
[NASA-CR-129993] 06 p0664 N73-15392
Configuration and structure of turbulent boundary layer flow over lateral uneven surface roughness
[AD-749944] 06 p0694 N73-15656
Effect of electromagnetic scattering from ocean surface on spherical waves of dipole antenna
07 p0761 N73-16184
Numerical simulation of air flow in atmospheric layer over inhomogeneous surface considering wind, temperature, shear stress, and turbulent energy
[AD-751589] 07 p0795 N73-16462
Surface roughness effects on elastohydrodynamic lubrication
[NASA-CR-2195] 07 p0804 N73-16522
Laser scattering from curved aluminum and titanium aircraft surfaces in clear atmosphere
08 p0884 N73-17159
Joule heating model for cathode surface structure effect on metal evaporation in vacuum discharge
[TH-73-E-33] 14 p1643 N73-23329
Numerical analysis of effects on bearing load carrying capacity of opposing surfaces with striated roughness on both surfaces
[AD-761169] 18 p2156 N73-27423
Stress-time relations of automobile rear wheel suspension systems, over various road surface conditions, based on power spectral density
[LBF-TB-102] 21 p2553 N73-30468

**SURFACE STABILITY**
Surface instability of liquid layer subjected to perpendicular motion
[NASA-TT-F-14880] 12 p1390 N73-21274

**SURFACE TEMPERATURE**
NT SKIN TEMPERATURE [NON-BIOLOGICAL]
NT WALL TEMPERATURE
Estimation of rising interface temperature in sliding friction of two surfaces
[AD-746830] 02 p0180 N73-11456
Corrections for airborne sea surface temperature measurements by infrared techniques
[AD-747011] 03 p0297 N73-12425
Long-wave radiation divergence measurements over water and land compared with calculated divergences from temperature and humidity profiles
[AD-748997] 04 p0418 N73-13410
Time development of anode surface temperatures for vacuum arc discharges of microsecond duration
[SC-DC-72-2267] 05 p0580 N73-14723
Analytical prediction of transient surface heat flux and temperature on cooled turbine blade due to gas stream inlet temperature change
[NASA-TN-D-7101] 06 p0730 N73-15955
Mean monthly hurricane heat potential and sea surface temperature changes associated with storm passage for North Atlantic and North Pacific Oceans
[AD-751590] 07 p0790 N73-16429
Multispectral method of determining sea surface temperatures, using Nimbus 2 infrared radiometer
08 p0971 N73-17938
Analysis of correlation between Martian surface temperature deviations and theory of nitrogen oxides on Mars
10 p1211 N73-19849
Near-surface air and sea-surface temperatures for hurricanes in Gulf of Mexico
[AD-754353] 11 p1315 N73-20677
Analysis of interrelation of ocean and atmosphere based on temperature of surface layer of water in Atlantic and Pacific Oceans
12 p1421 N73-21514
Satellite measurements of sea surface temperatures
[NASA-TM-X-66235] 14 p1659 N73-23467
Sea surface temperature measurements from Skylab EREP radiometer data
[E73-10604] 15 p1773 N73-24365
Temperature rise at heat transfer surfaces caused by magnetite, humus, calcium, and copper deposits
[AE-459] 15 p1844 N73-24937
Sea surface temperature anomalies and model generated meteorological histories
[NASA-CR-132756] 16 p1938 N73-25679
Use of spaceborne microwave radiation measurements to detect fires, subsurface water, and surface temperature
[NASA-TT-F-14975] 17 p1998 N73-26133
Frequency and duration of extreme surface temperatures and effects on missile systems development in hot-dry climates
[AD-759899] 17 p2059 N73-26652
Application of multispectral scanning to sea surface temperature, coastal topography and water sediment load, marine biology, sea ice, and oil slicks
19 p2295 N73-28455
Oceanographical observations from Danish light vessels and coastal stations - 1972
[ISBN-87-7478-080-6] 20 p2412 N73-29386
Annual variations of Garda Lake surface temperature using airborne bolometric equipment and earth based infrared video equipment
[IFA-STR-23] 23 p2787 N73-32298
Evaluating reusable surface insulation for space shuttle over range of heat transfer rate and surface temperature
[NASA-TM-X-2823] 23 p2809 N73-32465

**SURFACE TENSION**
U INTERFACIAL TENSION

**SURFACE TO AIR MISSILES**
NT NIKE MISSILES
NT NIKE-AJAX MISSILE
NT NIKE-HERCULES MISSILE
NT TERRIER MISSILE
Point defense missile simulation program
[AD-759969] 17 p2099 N73-26985

**SURFACE TO SURFACE MISSILES**
NT ANTITANK MISSILES
NT CRUISE MISSILES
NT LANCE MISSILE
NT MINUTEMAN ICBM
NT PERSHING MISSILE
NT POSEIDON MISSILES
NT SHORT RANGE BALLISTIC MISSILES
Design of Penguin missile inertial navigation system for midcourse guidance
11 p1320 N73-20711
Shock absorbing systems used by US guided missile silos
[AD-761577] 19 p2356 N73-28954

**SURFACE TO SURFACE ROCKETS**
NT HONEST JOHN ROCKET VEHICLE
NT LITTLE JOHN ROCKET VEHICLE

**SURFACE TREATMENT**
U SURFACE FINISHING

**SURFACE VEHICLES**
NT AIRCRAFT CARRIERS
NT AUTOMOBILES
NT LIFEBOATS
NT LUNAR ROVING VEHICLES
NT LUNAR SURFACE VEHICLES
NT MANNED LUNAR SURFACE VEHICLES
NT ROCKET PROPELLED SLEDS
NT ROVING VEHICLES
NT SATELLITE COMMUNICATIONS SHIPS
NT TANKER SHIPS
NT TRACTORS
NT TRUCKS
Proceedings of conference on ride qualities of air, surface, and water vehicles with emphasis on human factors engineering for comfort in transportation
[NASA-TM-X-2620] 01 p0002 N73-10012

Evaluation of effectiveness of indices relating to effect of vehicle vibrations on passenger comfort with application to railroad travel
01 p0003 N73-10018
Analysis of vibration environment in aerospace and surface vehicles with definitions of effect on human comfort and performance
01 p0003 N73-10021
Analysis of research activities conducted to determine criteria for passenger comfort in various methods of transportation
01 p0004 N73-10024
Application of laser rangefinder on autonomous Martian roving vehicle for navigation and mid-range path selection
[NASA-CR-128398] 01 p0064 N73-10523
Development of high speed ground rapid transit facility using tracked air-cushion vehicles
[PB-211833] 05 p0524 N73-14266
Numerical analysis of vertical and lateral motion of road vehicle trains with arbitrary number of components
[TT-7211] 08 p0892 N73-17220
Simulation and evaluation of proposed path selection systems for autonomous Martian Roving vehicle
[NASA-CR-130978] 09 p1010 N73-18242
Comparison of air pollution from aircraft, automobiles, buses, trucks, railroads, and electric trains in US from 1940-1980
[FAA-EQ-73-2] 12 p1421 N73-21522
Analysis and design of capsule landing system and surface vehicle control system for Mars exploration
[NASA-CR-131515] 12 p1459 N73-21825
Characteristics of nickel-zinc electric battery and application to propulsion of hybrid electric surface vehicles
[AD-756431] 13 p1477 N73-21963
Development of radio locating system for monitoring geographic movement of surface vehicles in metropolitan area using unsynchronized radio broadcasting stations
[NASA-CASE-NPO-13217-1] 17 p1997 N73-26144
Self-propelled vehicle with wheel, track laying, and walking capability for exploratory expolaration
[NASA-CASE-NPO-11366] 17 p2008 N73-26238
Radar equipment components for fire control vehicle
[AD-761534] 19 p2237 N73-28031
Miniature, remote controlled land and water vehicles and components
[AD-761665] 19 p2356 N73-28953
National Transportation Safety Board studies in aircraft and surface transportation safety
21 p2609 N73-30909

**SURFACE WATER**
ERTS-1 imagery of sea ice and surface water circulation along Alaskan Continental Shelf
[E73-10620] 15 p1775 N73-24381
ERTS-1 measurement of surface area of water bodies in Houston and Galveston, Texas area
[E73-10675] 16 p1900 N73-25370
Sources and dispersal patterns of suspended particles in nearshore surface waters of San Francisco Bay and Gulf of Farallones
[E73-10788] 18 p2137 N73-27264
Sea ice and surface water circulation along Alaskan continental shelf
[E73-10901] 20 p2396 N73-29250
Acquisition of Skylab data and determination of surface water areas from digital data
[E73-10912] 20 p2397 N73-29261
ERTS-1 imagery of surface water aera in Quivera National Wildlife Refuge, Kansas
[E73-10974] 21 p2533 N73-30313
Mapping dynamic hydrologic conditions of surface water changes in south Florida
[E73-11028] 22 p2662 N73-31332
ERTS-1 imagery of sea, ice, and surface water circulation along Alaskan continental shelf
[E73-11050] 23 p2779 N73-32226
Sources and dispersal patterns of suspended particles in nearshore surface waters of northeast Pacific Ocean and seasonal variation in snow cover in Sierra Nevada Mountains
[E73-11099] 24 p2914 N73-33256

**SURFACE WAVES**
NT BAROCLINIC WAVES
NT GRAVITY WAVES
Growth of mechanically generated surface water waves when subjected to turbulent channel air flow
[AD-746493] 01 p0042 N73-10336
Windowing or tapering of surface wave time series and spectrum analysis
[AD-742845] 01 p0050 N73-10407
Interaction of internal and surface waves in water
[AD-747332] 02 p0159 N73-11291
Nonlinear interactions among standing surface and internal gravity waves
[AD-746138] 02 p0168 N73-11368
Relationship of acoustic surface waves on curved surfaces to corresponding plane surface waves
[AD-748189] 03 p0338 N73-12761
Approximation technique applied to elastic surface waveguides utilizing curved thin films
[AD-748646] 04 p0390 N73-13169
Analysis of long-period wave phenomenon for means of forecasting and control in seaport operations
04 p0443 N73-13612
Attenuation of surface elastic waves as related to mass defects and applied to lunar geology
08 p0958 N73-17837
Line source beneath free surface of semi-infinite fluid
[AD-753140] 09 p1018 N73-18311
Acoustic surface wave matched filters
[AD-754283] 11 p1262 N73-20245
Design and fabrication of microwave acoustic surface wave delay lines
[AD-754896] 11 p1263 N73-20252
Magnetostatic and magnetoelastic surface wave interactions in magnetized yttrium-iron garnet film
[AD-754106] 11 p1331 N73-20802
Experimental verification of output signal to noise ratio and time of arrival estimate of tapped delay line matched filter using surface elastic waves
12 p1377 N73-21171
Surface acoustic waves used with devices for parametric signal processing and long delay lines
[AD-755943] 12 p1385 N73-21235
Correlation functions for displacements in semiboundless isotropic elastic media
[ITF-72-78-P] 12 p1429 N73-21579
Surface wave device to correlate acoustic velocity and to correct signal phases from pulse bursts
[AD-755198] 13 p1502 N73-22175
Subsonic diffusers having ribs aligned transverse to flow direction for separation control
13 p1508 N73-22225
Characteristics of deep water waves reaching Port Phillip Heads, Australia to show effects of refraction, shoaling, and friction
13 p1524 N73-22351
Feasibility of radar system to measure direction of shoreline ocean waves
[AD-755241] 13 p1527 N73-22373
Surface wave interaction and thermal microstructure of sea water
[AD-757425] 14 p1664 N73-23502
Construction of transfer functions in problems of weak shock interactions with cylindrical and spherical surfaces
14 p1715 N73-23913
Fabrication and characterization of monolithic acoustic surface wave amplifiers
15 p1755 N73-24229
Guiding and scattering of acoustic surface waves in solid layer between substrates
15 p1813 N73-24691
Elastic and piezoelectric surface waves guided by thin films
[AD-758688] 15 p1823 N73-24776
Characteristics of turbulent flow over wavy surface using sinusoidal waves of three sizes to determine variations of flow with wave size
16 p1887 N73-25273
Elastic surface wave encoders and decoders for use in secure, antijam command, control, and communications systems
[AD-758762] 16 p1919 N73-25529
Ray tracing method for kinematic analysis of mechanical waves in nonlinear elastic materials
[AD-760438] 17 p2096 N73-26955
Mathematical models for studying energy spectra and nonlinear surface waves of ocean
[AD-759541] 18 p2149 N73-27371
Electromechanical coupling coefficient of interdigital surface wave transducer on piezoelectric ceramic
[AD-761879] 19 p2246 N73-28105
Convolution of surface acoustic waves on barium titanate crystal
[AD-761880] 19 p2327 N73-28724
Spectral and statistical characteristics of surface wave velocity fields
20 p2446 N73-29654
Capabilities of surface wave devices as signal processors for spread spectrum communications systems
[AD-763881] 22 p2645 N73-31197
Turbulent, surface, and internal motions of ocean
[AD-763804] 22 p2670 N73-31390
Test facility for generating and analyzing internal waves
[AD-763444] 22 p2670 N73-31391
Surface water transport in western Lake Superior
23 p2783 N73-32267
Influence of wind drift and capillarity on blockage of short surface waves
[AD-764559] 24 p2924 N73-33358

**SURFACES**
Estimation of rising interface temperature in sliding friction of two surfaces
[AD-746830] 02 p0180 N73-11456
Doppler and surface effects in backscattered signal fading
22 p2627 N73-31052

**SURGERY**
NT LABYRINTHECTOMY
Surgical liquification pump for removing macerated tissue from eye
[NASA-CASE-LEW-12051-1] 23 p2749 N73-32000

**SURGES**
Transients in cooling water systems of thermal power plant discussing mathematical models, computer programs and experiments
[PUBL-101-PT-1] 01 p0041 N73-10326
Hydraulic transients in cooling water system of thermal power plants, figures and computer programs
[PUBL-101-PT-2] 01 p0041 N73-10327
Surge divertor breakdown voltage characteristics
[AD-747622] 03 p0276 N73-12236
Number of surge series of turbulent velocity pulsations with Gaussian distribution
09 p1059 N73-18635
Wind-driven currents and surges with bottom slipping in shallow water
09 p1059 N73-18639

**SURGICAL INSTRUMENTS**
Ultrasonic device for ophthalmic eye surgery with safe removal of macerated material
[NASA-CASE-LEW-11669-1] 18 p2110 N73-27062
Surgical liquification pump for removing macerated tissue from eye
[NASA-CASE-LEW-12051-1] 23 p2749 N73-32000

**SURINAM**
Geophysical survey off Surinam coast including seismics, magnetics, and gravity
[SP-6] 14 p1660 N73-23476

**SURVEILLANCE**
Performance of air-to-satellite-to-ground systems for air traffic control
[PB-210378] 01 p0078 N73-10646
Surveillance and mapping of sea ice in Arctic regions based on ERTS-1 imagery
[E72-10199] 02 p0160 N73-11297
Monitoring and surveillance of state of eutrophication of inland lakes in California and Nevada
[E72-10207] 03 p0288 N73-12330
Prototype volcano surveillance network in Alaska and Cascade Mountains
[E72-10242] 03 p0289 N73-12342
Aerial surveillance techniques for measuring gaseous environmental pollution from nuclear power plant
[WERLV-1] 03 p0334 N73-12721
Volcano and earthquake surveillance network in Alaska, California, Washington, Hawaii, El Salvador, Nicaragua, Iceland, and Guatemala
[E73-10337] 09 p1025 N73-18365
Establishment of prototype volcano surveillance network using ERTS data collection platforms
[E73-10545] 14 p1654 N73-23420
Prototype surveillance network of volcanoes in Western Hemisphere using data from ERTS data collection platforms
[E73-10558] 14 p1655 N73-23430
Application of ERTS-1 data for development and operation of volcano surveillance network
[E73-10711] 17 p2018 N73-26318
Computerized simulation of tactical ground surveillance system
[AD-761805] 19 p2240 N73-28059
Research and development of electronic equipment for night combat surveillance
[AD-762351] 19 p2302 N73-28507

**SURVEILLANCE RADAR**
ATC surveillance/communication analysis and planning activities from 1 June to 31 Aug. 1972
[FAA-RD-72-107] 01 p0078 N73-10645
Jamming of surveillance radar station by airborne electronic countermeasures
[FOA-3-C-3645-66] 06 p0639 N73-15187
Optimal moving target indicator for long range air traffic control surveillance radars
[AD-750747] 06 p0642 N73-15209
Lightweight, low power combat surveillance Doppler radar
[AD-750370] 06 p0642 N73-15212
Operation and characteristics of primary radar system for air traffic control surveillance
[FAA-ED-02-1] 08 p0885 N73-17163
Systems planning for improved airport surveillance radar equipment using dual airborne antenna switching for air traffic control
[FAA-RD-72-136] 09 p1002 N73-18176
Characteristics of operational airport surveillance radars and methods for improving performance to meet air route surveillance requirements
[ATC-14] 11 p1255 N73-20183
Switched antennas and digital signal processing of high performance, low cost, surveillance radar
[AD-759179] 18 p2120 N73-27142
Positional accuracy of aircraft radar targets as displayed in air traffic control airport surveillance radar system
[FAA-NA-72-87-PT-2] 21 p2577 N73-30650

**SURVEYOR LUNAR PROBES**
NT SURVEYOR 3 LUNAR PROBE
Post mission data analysis of Surveyor 5, 6, and 7 chemical data
[NASA-CR-135900] 24 p2979 N73-33802

**SURVEYOR PROJECT**
Analysis of management procedures applied to Surveyor and Lunar Orbiter projects
[NASA-SP-4901] 04 p0486 N73-13973

**SURVEYOR 3 LUNAR PROBE**
Surveyor 3 lunar probe television mirror pit X ray analysis and scanning electron microscopy for micrometeoroid impact study
[ONERA-NT-01-15] 07 p0847 N73-16864

**SURVEYS**
NT GEODETIC SURVEYS
NT GEOLOGICAL SURVEYS
Multispectral band survey and mapping of earth in 18 days
[E73-10044] 07 p0777 N73-16307
Surveying and mapping earth resources over large areas utilizing ERTS-1 imagery
[E73-10049] 07 p0777 N73-16311
Analysis of political, institutional, and economic factors to determine feasibility of conducting earth resources surveys in developing nations
07 p0783 N73-16362
Survey and mapping of snow and ground water levels in Norway using ERTS-1 imagery
[E73-10324] 09 p1024 N73-18356
Utilization of artificial satellites and spacecraft for surveying and mapping earth resources
[NASA-TT-F-739] 09 p1026 N73-18377
Surveys of electroplating methods and techniques generated from NASA programs
[NASA-SP-5114] 13 p1533 N73-22426
Survey of digital speech processing activity in US and abroad
14 p1620 N73-23120
Urban mapping activities assisted by aerial photography and ground surveying in connection with urban planning and community development
[PB-214305/5] 16 p1915 N73-25494
Literature survey on jet propagation and interference in lifting surface aerodynamics
[NASA-TT-F-14957] 19 p2217 N73-27886
Survey of articles dealing with stochastic approximation
[AD-761766] 19 p2314 N73-28613

**SURVIVAL**
Microorganism survival in simulated Mars environment
10 p1118 N73-19116
Influence of head and stomach shielding on radiation sickness and animal survival from gamma-neutron irradiation
11 p1241 N73-20071
Space vacuum and solar ultraviolet irradiation effects on survival of Bacillus subtilis spores
15 p1740 N73-24108
Thermal inactivation of Bacillus subtilis var. niger spores on Viking lander
[NASA-CR-133223] 17 p1987 N73-26058
Crew survival after emergency landing or ditching in unpopulated areas
[NASA-TT-F-15047] 20 p2371 N73-29053

**SURVIVAL EQUIPMENT**
Analysis of US Navy aviation combat casualty experiences in Southeast Asia to determine effectiveness of rescue and recovery operations under combat conditions
[AD-761636] 19 p2228 N73-27972

**SUSCEPTIBILITY (MAGNETISM)**
U MAGNETIC PERMEABILITY

**SUSPENDING (HANGING)**
NT MAGNETIC SUSPENSION
Procedure for predicting aeroelastic behavior of Huber suspension bridge
[NPL-R102] 06 p0726 N73-15926
Dynamically tuned gyros in strapdown systems
11 p1318 N73-20697
Effect of spurious forces on electrostatic suspension of ultrasensitive accelerometers
[ONERA-NT-197] 13 p1530 N73-22397
Multiple rod pyramid as cyclic suspension for parabolic radiotelescope mirror
[AD-757237] 15 p1789 N73-24503
Stability of undisturbed motion of suspension rings of gyropendulum on moving base
23 p2791 N73-32330

**SUSPENDING (MIXING)**
Light beam attenuation in suspensions of algae
20 p2405 N73-29325
Two phase detonation in fuel sprays suspended in gaseous oxidizing atmospheres
20 p2484 N73-29957
Turbulent boundary layer flow of gas-solid suspension
24 p2906 N73-33190

**SUSPENSION SYSTEMS (VEHICLES)**
Stress-time relations of automobile rear wheel suspension systems, over various road surface conditions, based on power spectral density
[LBF-TB-102] 21 p2553 N73-30468
Optimized design for vehicle suspension systems
[PB-220553/2] 22 p2648 N73-31216

**SUSPENSIONS**
Steady-state one dimensional motion of uniformly dense suspensions
[AD-750924] 06 p0636 N73-15333
Preparation of hydrocarbon suspensions in slush hydrogen for nuclear fuel element corrosion inhibition in rocket engines
08 p0968 N73-17913
Electrostatic suspension of conducting sphere in electric field between electrodes
[JPRS-59675] 20 p2380 N73-29123
Turbulent flow of gas-solid suspensions about ellipsoid of revolution
20 p2385 N73-29163

**SUSQUEHANNA RIVER BASIN (MD-NY-PA)**
Application of ERTS-1 imagery for locating coal refuse deposits, analysis of geologic formations and mapping of agricultural areas in Pennsylvania
[E73-10327] 09 p1024 N73-18358
Digital processing of ERTS-1 data for identification of strip mining areas in west branch area of Susquehanna River and mine drainage in Pennsylvania
[PAPER-E3] 19 p2268 N73-28267
Inventories of mineral deposits and geologic structures in Susquehanna River Basin from Skylab EREP data
[E73-11056] 23 p2780 N73-32232
Survey and inventory of forest resources in Susquehanna River Basin to determine accuracy achieved in mapping vegetation classes using ERTS-1 imagery
[E73-11110] 24 p2915 N73-33267
Survey and Mapping of vegetative cover in Susquehanna River Basin to determine accuracy of photographic technology and ERTS-1 imagery
[E73-11111] 24 p2915 N73-33268
Computer programs for processing multispectral scanner data of Susquehanna River Basin
[E73-11114] 24 p2915 N73-33271
Development of land use, water quality, and air quality indices from ERTS-1 imagery for environmental resources management in Susquehanna River Basin and Quantico, Virginia test areas
[E73-11143] 24 p2918 N73-33298
Resource inventory, land use, and pollution of Susquehanna River Basin from ERTS-1 data
[E73-11136] 24 p2919 N73-33310
Processing ERTS-1 MSS digital data of Susquehanna River Basin
[E73-11165] 24 p2920 N73-33318

**SWAGING**
Analysis of stress formation and changes in physical properties of pipes during rotary swaging using explosion or pulsed magnetic field energy
[AD-747454] 03 p0308 N73-12516

**SWAMPS**
U MARSHLANDS

**SWASH**
U SPLASHING

**SWEAT**
Sweat rate and heat conductance in thermoregulatory system during rest and exercise
[NASA-TT-F-14562] 01 p0009 N73-10074

**SWEAT COOLING**
Computer program for compact transpiration cooling with free jet tests and theory comparison
[AD-753109] 09 p1017 N73-18299
Research and development of transpiration cooled inflatable nozzle extension
[NASA-CR-124165] 11 p1269 N73-20300
User guide for computer program to analyze compact transpiration cooling system proposed for hypersonic reentry vehicles
[AD-759698] 16 p1975 N73-25974
Analytical model for transpiration cooling of gas turbine blades
[AD-759190] 17 p2077 N73-26805
Wake effects in transpiration cooling of gas turbine blades
[AD-759191] 17 p2078 N73-26806
Computer manual for transpiration cooling analysis on gas turbine blades
[AD-759192] 17 p2078 N73-26807
Analysis of water table simulation of transpirationally cooled nozzle, and formulation of two flow models of water table boundary layer
[NASA-TM-X-2884] 22 p2710 N73-31702

**SWEDEN**
Polar upper atmosphere data recorded at Kiruna Geophysical Observatory, Sweden, from Jan. - Mar. 1972
02 p0167 N73-11353
Joint meetings in Sweden on business economics, industrial economics, and scientific theory
[FOA-P-C-8280-10] 02 p0244 N73-11984
Polar ionospheric geophysical data recording at Kiruna, Sweden, during Apr.-Jun. 1972
06 p0667 N73-15424
Kiruna [Sweden] polar geophysic observatory ionospheric data recorded from Jul.-Sep. 1972
13 p1525 N73-22355
Polar upper atmosphere data recorded at Kiruna Geophysical Observatory, Sweden, from Oct.-Dec. 1972
17 p2028 N73-26410
Polar ionospheric geophysical data recording in Sweden, Jan-Mar. 1973
19 p2295 N73-28459
Survey of terminal moraines in western Sweden and southeastern Norway from ERTS-1 imagery
[E73-11122] 24 p2916 N73-33277

**SWEEP ANGLE**
Application of methods for prediction of boundary layer transition on sheared wings
17 p2013 N73-26281

**SWEEP FREQUENCY**
Hybrid computer program for processing several channels of sweep frequency data simultaneously
[NASA-TM-X-2753] 09 p1005 N73-18206
Algorithm for computerized spectral analysis on linearly swept signals
[AD-760775] 18 p2120 N73-27138

**SWELLING**
Relations between fuel swelling and clad strain for cylindrical uranium dioxide pins with niobium zirconium cladding
[NASA-TM-X-2717] 07 p0819 N73-16638
Temperature effects on swelling of nickel irradiated by medium energy heavy ions
[CEA-CONF-2052] 17 p2044 N73-26540
Swelling study of metals irradiated by small angle scattering of X rays applied to Al irradiated by fast neutrons
[CEA-CONF-2115] 17 p2045 N73-26543
Para-benzoquinone dioxime and concentrated mineral acid processed to yield intumescent or fire resistant, heat insulating materials
[NASA-CASE-ARC-10304-1] 17 p2048 N73-26572
Unrestrained swelling of uranium nitride fuel irradiated at temperatures ranging from 1100 to 1400 K
[NASA-TM-X-2907] 21 p2578 N73-30659

**SWEPT WINGS**
NT DELTA WINGS
NT SWEPTBACK WINGS
Longitudinal and lateral aerodynamic characteristics of cruise missile with swept wing and conventional aft tails at various Mach numbers
[NASA-TN-D-7069] 01 p0001 N73-10002
Evaluation of Rayleigh-Ritz anisotropic plate analysis procedure for determining performance of composite wing for aircraft operating in transonic environment
[AD-745129] 02 p0126 N73-11023
Effects of location of wing pivot and geometry of wing on static longitudinal aerodynamic characteristics of variable-sweep supersonic fighter aircraft model
[NASA-TM-X-2674] 03 p0247 N73-12000
Contribution of straight-tapered swept wing to rolling moment derivative due to yawing under conditions where flow remains fully attached to surface
[ESDU-72021] 07 p0735 N73-15980
Effects of various leading edge slat devices on static aerodynamic characteristics of twin-jet, swept wing fighter model
[NASA-TN-D-6921] 07 p0736 N73-15988
Turbulent heat transfer and pressure on leading edge of fin, swept wing, or antenna
[SCL-RR-72-0308] 12 p1464 N73-21863
Theoretical calculation of generalized forces and load distribution on wings oscillating at general frequency in subsonic stream
[ARC-R/M-3710] 13 p1470 N73-21908
Wind tunnel tests of swept augmentor wing aerodynamic characteristics
[NASA-TM-X-62252] 13 p1472 N73-21923
Analysis of aerodynamic loading for symmetrically tapered wings describing simple harmonic pitching oscillations of low frequency in supersonic flow
[ARC-R/M-3298] 15 p1728 N73-24019
Development of two methods for optimizing design of subsonic, swept wing jet transport aircraft
15 p1733 N73-24054
Wind tunnel measurements of direct pitching damping and stiffness derivatives for delta wing and swept wing planforms
[ARC-R/M-3419] 16 p1853 N73-25009
Numerical analysis of incompressible laminar boundary layer on infinite swept wing with arbitrary velocity and suction distribution
[ARC-R/M-3241] 16 p1854 N73-25018
Survey of aerodynamic derivative measurements for unswept rectangular wings and delta wings with emphasis on main surface pitching moment derivatives
[ARC-R/M-3232] 16 p1855 N73-25024
Influence of free stream Reynolds number on transition in boundary layer on infinite swept wing
17 p2013 N73-26280
Load near apex of lifting swept wing in linearized subsonic flow
[ARC-R/M-3716] 21 p2492 N73-30001
The calculated growth of lift and pitching moment on a swept wing entering a discrete vertical gust at subsonic speeds
[ARC-CP-1241] 22 p2612 N73-30932
Wake development on models of elliptic, rectangular, swept and delta planforms when plunged in water
[ARC-CP-1238] 24 p2870 N73-32932
Wind tunnel tests to determine basic performance of swept augmentor wing configuration and effect on longitudinal characteristics of aircraft
24 p2872 N73-32941

**SWEPTBACK WINGS**
NT DELTA WINGS

Three dimensional transonic flows past lifting configurations having finite leading edge swept angles
[AD-747266] 02 p0159 N73-11284
Development of computer programs for analyzing and predicting properties of transonic flows around certain types of wing-body combinations
[NASA-CR-2157] 03 p0247 N73-11999
Computation of loading on sweptback wings noting extra collocation points
[ARC-CP-1213] 03 p0247 N73-12002
Analysis of aerodynamic stall characteristics of wing sections with high lift devices in two dimensional flow
06 p0617 N73-15008
Aerodynamic configurations of swept wings to improve lift performance at stall in higher range of subsonic speeds
06 p0617 N73-15010
Numerical analysis of aerodynamic load distribution on swept back wing mounted on infinite circular cylinder fuselage at zero angle of attack
[AD-756075] 13 p1475 N73-21952
Development of theory for wind tunnel boundary upwash interference on symmetrical finite wing with arbitrary lift distribution
[AD-757196] 14 p1652 N73-23397
Analysis of pressure distribution and surface flow on half models of wings with curved tips and 60 degree sweepback
[ARC-R/M-3244] 15 p1726 N73-24001
Analysis of flow pattern on tapered, sweptback wing at Mach numbers between 0.6 and 1.6 and 12 degree angle of incidence
[ARC-R/M-3271] 15 p1726 N73-24004
Wind tunnel tests to determine aerodynamic characteristics of model of sweptback wing with warp distribution to produce constant spanwise coefficient of lift
[ARC-R/M-3385] 15 p1727 N73-24007
Calculation of spanwise loading on sweptback wings with trailing edge flaps using data obtained from electric tank tests
[ARC-R/M-3487] 16 p1853 N73-25010
Equivalence rule and transonic flows involving lift around thin smooth configuration with swept leading edge
[AD-760349] 17 p1985 N73-26042
The lift and stalling characteristics of a 35 deg sweptback wing designed to have identical chordwise pressure distributions at all spanwise stations when near maximum lift
[ARC-R/M-3721] 22 p2612 N73-30935

**SWIMMING POOL REACTORS**
Installation of stainless steel lining to stop water leakage from 2MV HOR swimming pool reactors
[IRI-131-72-01] 03 p0334 N73-12723

**SWINE**
Effect of calcium-deficient diet on bone structure of pigs and dogs
[NASA-TT-F-13917] 01 p0008 N73-10067
Pressure gradient measurements in swine and rats submitted to pressure pulses
[DLR-FB-71-72] 06 p0636 N73-15164
Defined shock wave effects on miniature swine, describing organ injuries
19 p2227 N73-27965
Hematology of miniature pigs after rapid decompression
[DLR-FB-73-63] 24 p2886 N73-33047

**SWINGBY TECHNIQUE**
Interplanetary trajectory characteristics of Saturn swingby mission to Uranus
[NASA-TM-X-2914] 22 p2714 N73-31727

**SWIRLING**
Aerodynamics structure of swirling flow in short cylindrical combustion chamber
[AD-747455] 03 p0365 N73-12975
Analysis of swirling jet of gas injected into vacuum and effect of centrifugal force on separation of constituents
[ISAS-487-VOL-37-NO-13] 05 p0526 N73-14283
Fuel injectors with high frequency swirl generators
[AD-751079] 09 p1080 N73-18810
Development and mixing of coaxial fluid jet with axisymmetric swirling vortex flow in cylindrical chamber
[AD-754613] 11 p1272 N73-20324
Visualization of swirling flow in rotating tube and measurement of velocity distribution by laser-Doppler anemometry
[NASA-CR-2284] 18 p2131 N73-27216
Swirl can, full-annulus combustion chambers for high performance gas turbine engines
[NASA-CASE-LEW-11326-1] 21 p2579 N73-30665

**SWIRLING WAKES**
U TURBULENT WAKES

**SWITCHES**
NT CAPACITANCE SWITCHES
NT CRYOTRONS
NT ELECTRIC RELAYS
NT ELECTRIC SWITCHES
NT FLUID SWITCHING ELEMENTS
NT SWITCHING CIRCUITS
NT THERMOSTATS
Logic and design procedures for multifunction mode switching controls in jet aircraft cockpits
[AD-764617] 23 p2767 N73-32141

**SWITCHING**
NT BEAM SWITCHING
NT MAGNETIC SWITCHING
NT MICROWAVE SWITCHING
Universal cellular network for combinational switching functions with simple failure testing
03 p0278 N73-12252
Ion implantation of amorphous insulators and switching effects in silicon oxides
[LETI/ME-773] 07 p0832 N73-16744
Mass and momentum of control signals in switching mechanism of fluid bistable amplifiers
[AD-756583] 13 p1511 N73-22243
Switching processes in selected amorphous compounds
[AD-758133] 14 p1699 N73-23791
Minority carrier lifetime and switching time of step recovery diode for pulse generators in microwave equipment
[FTZ-A-651-TBF-3] 22 p2643 N73-31180

**SWITCHING CIRCUITS**
NT FLUID SWITCHING ELEMENTS
Synthesis of delay-free asynchronous sequential switching circuits
[AD-746392] 01 p0035 N73-10273
Optimum switching of large number of low voltage power generating elements with nonlinear volt-ampere characteristics
[AD-747560] 03 p0275 N73-12233
Electronic video editor for switching video input signals to common output channel
[NASA-CASE-KSC-10003] 04 p0398 N73-13235
Construction of electron beam semiconductor pulse amplifier and radio frequency amplifier diode
[AD-748892] 04 p0461 N73-13758
Feasibility determination for use of p-i-n diodes as switching elements to control impulse signals in strip transmission line
[AD-749125] 05 p0520 N73-14229
Analysis of intermodulation and cross modulation distortions in broadband balanced bridge switching state MOSFET mixer
[AD-749064] 05 p0521 N73-14234
High isolation RF signal selection switches
[NASA-CASE-NPO-13081-1] 14 p1618 N73-23106
Plated thin magnetic film wire element for high speed main memories
[REPT-732] 14 p1619 N73-23112
Computer aided procedure for complete design of sequential machines
[AD-759959] 17 p2002 N73-26191
Switched antennas and digital signal processing of high performance, low cost, surveillance radar
[AD-759179] 18 p2120 N73-27142
Packet switching, bilateral broadcasting, and burst random access capabilities
[AD-761544] 19 p2237 N73-28035
Diagnostics of malfunctions in logic circuits and switching circuits
[AD-762234] 20 p2379 N73-29116
Solid state switch for variable circuit switching
[NASA-CASE-NPO-10817-1] 21 p2510 N73-30135
Operation of switching electronic power regulator for Skylab/Apollo telescope mount
[NASA-CR-124445] 23 p2748 N73-31989
Manually and automatically operable video switching system
[NASA-CASE-KSC-10782-1] 23 p2757 N73-32063
Transparent switchboard which permits optical display devices to be adapted for use in man machine communications
[NASA-CASE-MSC-13746-1] 23 p2768 N73-32143

**SWITCHING ELEMENTS**
U SWITCHING CIRCUITS

**SWITCHING FUNCTIONS**
U BOOLEAN FUNCTIONS
U SWITCHING

**SWITCHING THEORY**
Bang-bang controller operating in chatter mode for disturbance regulation in linear system
[AD-745896] 02 p0203 N73-11643
Syntheses of logical circuits by composing common inputs and common variables
[AD-748165] 03 p0279 N73-12263
Computerized management tools for use in analysis of automatic switching centers and associated tributaries of Autodin communications network
[AD-761479] 19 p2236 N73-28028

**SWITZERLAND**
NT ALPS MOUNTAINS [EUROPE]
Bibliography on meteorological phenomena in Switzerland
[REPT-71-II] 05 p0571 N73-14643
Bibliography on meteorological phenomena in Switzerland
[REPT-72-I] 05 p0571 N73-14644
Tabulation of relative humidity data obtained from network of weather stations in Switzerland
05 p0572 N73-14645
Annual report of meteorological observations conducted by weather stations in Switzerland during calendar year 1970
05 p0572 N73-14646
Statistical analysis of rainfall frequency in central Valais
[REPT-28] 10 p1181 N73-19609
Foehn wind of canton Valais
10 p1181 N73-19610
State of superconducting science in Switzerland
[AD-754235] 10 p1202 N73-19781
Snow cover survey and vegetation growth in Swiss Alps using ERTS-1 imagery
[E73-10586] 14 p1657 N73-23446
Survey of snow cover and vegetation growth in high mountains of Swiss Alps based on ERTS-1 imagery
[E73-10733] 17 p2020 N73-26339

**SYLLABLES**
NT MESSAGES
Word recognition system based on dimensional representation of phoneme-like word segments
14 p1623 N73-23145
Discrimination of liquids and glides in automatic speech recognition system using syntactic recognition algorithms in analysis of digital spectrograms
14 p1623 N73-23149

**SYMBOLIC PROGRAMMING**
NT COMPUTER PROGRAMMING

**SYMBOLS**
NT MESSAGES
Design of circular symbol and video inset generator for television display devices
[AD-757621] 14 p1634 N73-23246
Symbol designs for graphic symbol subset of ASCII in warning and control systems
[AD-759807] 17 p2004 N73-26206

**SYMMETRICAL BODIES**
NT AXISYMMETRIC BODIES
NT BODIES OF REVOLUTION
NT CONICAL BODIES
NT CYLINDRICAL BODIES
NT ELLIPSOIDS
NT FAIRINGS
NT PARABOLIC BODIES
NT ROTATING CYLINDERS
NT ROTATING SPHERES
NT SLENDER CONES
NT SPHERES
NT STREAMLINED BODIES
NT TORUSES

**SYMMETRY**
Numerical solution for cylindrical symmetrical diffusion problem
[FOA-1-C-1409-92] 06 p0653 N73-15306
Deviation from rotational symmetry of electric arcs in transverse magnetic fields
[AD-754022] 11 p1328 N73-20778

**SYMPATHOMIMETICS**
U ADRENERGICS

**SYMPHONIE SATELLITES**
Test range for Symphonie satellite antennas and onboard communication equipment
[DGLR-PAPER-72-89] 06 p0640 N73-15199
Power conditioning subsystem for Symphonie satellite with bus voltage regulation
[REPT-72-90] 09 p0991 N73-18085
Orientation of Symphonie satellite antennas with accuracy effect
[DGLR-PAPER-72-063] 09 p1003 N73-18182
Specifications and capabilities of Franco-German telecommunications satellite - Symphonie
[NASA-TT-F-14875] 12 p1461 N73-21836
Mission project management, and description of Symphonie communication satellite
[DGLR-PAPER-73-043] 24 p2895 N73-33113
Symphonie satellite transponder parameters, noting intelligible crosstalk
[DGLR-PAPER-73-056] 24 p2896 N73-33115
Gimballed attitude gyros for Symphonie satellite stabilization
[DGLR-PAPER-73-058] 24 p2927 N73-33377
Dynamic flight simulation of Symphonie satellite attitude control system
[DGLR-PAPER-73-045] 24 p2986 N73-33862

**SYMPTOMS**
U SIGNS AND SYMPTOMS

**SYNCHROCYCLOTRONS**
Central region of CERN synchrocyclotron, including sequence of acceleration spaces and radio frequency extraction system
[NP-19179] 03 p0280 N73-12273

**SYNCHRONISM**
NT BIT SYNCHRONIZATION
NT FREQUENCY SYNCHRONIZATION
Synchronization using pulsed edge tracking in optical PPM communication systems
[NASA-CR-130117] 03 p0265 N73-12143
Electronic circuits for synchronous rotation of rotors suspended in magnetic field
[SRARI-P-120] 06 p0647 N73-15257
Mathematical models for analyzing synchronous functions of multimachine electrical power systems
07 p0760 N73-16175

Abstract algebraic techniques to determine synchronization properties of binary, linear, and maximal length sequences
[AD-744101] 13 p1550 N73-22560
Nonlinear and parametric effects on synchronization and mixing of electron transfer microwave oscillators
18 p2123 N73-27155
Resynchronization of circadian rhythms following transmeridian flight observed in two group of students
19 p2227 N73-27958
Time shift effects on human 17-hydroxy corticosteroid diurnal excretion noting transmeridian flights
[DLR-FB-73-58] 21 p2501 N73-30070
Technology for evaluating ground station sites based on effectiveness in disseminating time synchronization
[FAA-RD-73-102] 23 p2770 N73-32155
Time synchronization in optical communication as problem of estimating arrival time of known transmitted field
[NASA-CR-132813] 23 p2801 N73-32401

**SYNCHRONIZATION**
U SYNCHRONISM

**SYNCHRONIZED OSCILLATORS**
Dynamic characteristics of microwave synchronized oscillators
22 p2643 N73-31185

**SYNCHRONIZERS**
Bit synchronizer for split phase PCM transmission with two loop systems
[NASA-CASE-MSC-12494-1] 02 p0141 N73-11142
System for generating timing and control signals during repetitive fixed length serial data transmission
[NASA-CASE-NPO-13125-1] 09 p1008 N73-18225
Analysis and simulation of telemetry receivers and bit synchronizers
[NASA-CR-132809] 21 p2507 N73-30120
Monte Carlo simulation of self bit synchronizer for binary overlapping signals
23 p2755 N73-32046

**SYNCHRONOUS DETECTORS**
U CORRELATORS

**SYNCHRONOUS METEOROLOGICAL SATELLITE**
Fabrication and tests of flight prototype pulsed plasma microthruster propulsion system for Synchronous Meteorological Satellite
[NASA-CR-130133] 05 p0590 N73-14794
Geoisochronous satellites for obtaining and transmitting meteorological data
20 p2447 N73-29658
Wind estimation by photographic tracking of clouds on images from synchronous meteorological satellites
24 p2948 N73-33546

**SYNCHRONOUS MOTORS**
Inductive reactances of superconducting synchronous machine
[AD-749526] 05 p0499 N73-14066
Hysteretic synchronous motor equivalent circuits
[LRBA-E-603-NT-1/SIE] 15 p1738 N73-24093
Synchronizing control of drag-cup gyro motor using dynamic gas bearing
[NAL-TR-304] 15 p1756 N73-24232
Inductive reactances of direct sequence of synchronous machine with ferromagnetic screen
[AD-759879] 17 p2039 N73-26494

**SYNCHRONOUS SATELLITES**
NT AEROS SATELLITE
NT GOE SATELLITES
NT SYNCHRONOUS METEOROLOGICAL SATELLITE
Multipath propagation between aeronautical relay satellite in synchronous earth orbit and aircraft flying over ocean
[NASA-TM-X-66094] 02 p0141 N73-11140
Fuel tanks, spinup techniques, and thruster-CG misalignment problems for synchronous orbiting satellites
[AD-746845] 03 p0360 N73-12931
Single axis orientation mechanism for solar arrays on high power synchronous satellites with 116 liquid metal slip rings
[NASA-CR-120954] 04 p0395 N73-13215
Orbit determination for self-contained stationkeeping systems, equations of satellite motion, orbit control, gravitational effects, and synchronous satellite drift
[NAL-TR-295] 04 p0469 N73-13826
VLBI time delay, satellite tracking technique for synchronous satellites
[NASA-TM-X-66122] 04 p0475 N73-13887
Optimization of propellant tank size delivering apogee impulses when positioning synchronous satellites
[ONERA-NT-2/1895-SY] 04 p0479 N73-13915
Algorithms for predicting ionospheric effects on pseudo-ranging from synchronous satellite navigation system
[AD-749486] 05 p0539 N73-14391
Antenna systems for Ku band synchronous orbit communication satellite
05 p0608 N73-14941
Comparison of chemical [hydrazine and aerozine], electrothermal, electrostatic, and radioisotopic propulsion systems, emphasizing performance and configurations
[ESRO-CR-25-PT-A] 08 p0955 N73-17818
Analysis of soundings and imaging measurements obtained from geostationary satellites during 1 Nov. 1972 to 31 Jan. 1973
[NASA-CR-130175] 10 p1215 N73-19884
Synchronous satellite tracking by planetary radar system
[AD-754937] 11 p1257 N73-20196
Meteorological measurements from geosynchronous satellites
[NASA-CR-130246] 15 p1834 N73-24870
Development of autonomous stationkeeping system for controlling longitude of synchronous satellite by onboard navigation aids
[AD-759806] 16 p1942 N73-25716
Development of infrared earth horizon scanner employing thermistor bolometers providing pitch and roll data of synchronous satellites
[ESRO-CR-161] 19 p2301 N73-28503
Objectives and accomplishments of geosynchronous platform definition study
[NASA-CR-133968] 19 p2345 N73-28860
Program results and supporting data obtained in geosynchronous platform definition study
[NASA-CR-133969] 19 p2345 N73-28861
Mission characteristics data compiled in geosynchronous platform definition study
[NASA-CR-133970] 19 p2345 N73-28862
Baseline traffic model resulting from traffic analysis and system requirements data generated in geosynchronous platform definition study
[NASA-CR-133971] 19 p2345 N73-28863
Traffic analysis and system requirements for new traffic model developed in geosynchronous platform definition study
[NASA-CR-133972] 19 p2345 N73-28864
Platform configurations, support subsystems, mission equipment, and servicing concepts generated in geosynchronous platform definition study
[NASA-CR-133973] 19 p2345 N73-28865
Program evaluation and recommendations of geosynchronous platform definition study
[NASA-CR-133974] 19 p2345 N73-28866
Interfaces between space platforms and space transportation system established in geosynchronous platform definition study
[NASA-CR-133975] 19 p2345 N73-28867
Special purpose slide rule to compute free space propagation delay between synchronous satellite and points on earth surface
[NBS-TN-638] 22 p2638 N73-31139
Time signal transfer by satellite relay systems
[AD-764716] 23 p2759 N73-32078
Space tug geosynchronous mission simulation
[NASA-CR-135706] 23 p2844 N73-32730
Data processing role of weather stations, polar and synchronous satellites in global experiments
24 p2948 N73-33549

**SYNCHROPHASOTRONS**
Azimuthal distribution losses of protons at synchrophasotron ejection determined by scintillation counters
[JINR-P16-6433] 04 p0453 N73-13699

**SYNCHROTRON NOISE**
U ELECTROMAGNETIC NOISE
U SYNCHROTRON RADIATION

**SYNCHROTRON RADIATION**
Production and research applications of magnetic bremsstrahlung
[BNL-TR-480] 04 p0452 N73-13689
Computerized control of synchrotron beam lines and power supply system
[DNPL/R-22] 12 p1388 N73-21254
Synchrotron radiation from magnetically confined hot electron plasma
12 p1432 N73-21605
Investigation of emissivity and circular polarization of synchrotron radiation
[NASA-CR-131526] 12 p1457 N73-21811
Features of synchrotron radiation which occur when relativistic particles move with small pitch angles in magnetic field
[NASA-CR-131864] 13 p1563 N73-22670
Energy loss method for calculating synchrotron-Cerenkov radiation of relativistic electrons in cold magnetoplasma
[AD-755387] 13 p1564 N73-22675
Wave-normal emissivity and ray emissivity formulae for gyro-synchrotron radiation in magnetoactive plasma and in isotropic plasma
[AD-755398] 13 p1564 N73-22676
Electron spin resonance and synchrotron radiation energy in magnetoactive plasma
[AD-762319] 19 p2326 N73-28709
Gyrosynchrotron and magnetoactive absorption processes in solar microwave emission
19 p2335 N73-28787
Gyrosynchrotron radiation of relativistic electrons in solar magnetoactive plasma
19 p2335 N73-28788
Synchrotron and X ray modulations produced by solar flare effects
22 p2733 N73-31878

**SYNCHROTRONS**
NT BEVATRON
NT STORAGE RINGS [PARTICLE ACCELERATORS]
Estimate of dose rate, pattern, and distribution of scattered particles and neutrons during irradiation of superconducting synchrotron magnets
[KFK-1468] 01 p0080 N73-10659
Development and characteristics of synchrotrons with steady-state field in energy range of 35 to 300 giga electron volts
[JPRS-57489] 03 p0280 N73-12271
Proceedings of Zero Gradient Synchrotron Workshops
[ANL/HEP-7208-VOL-1] 03 p0281 N73-12276
Detailed design study for synchrotron booster magnets and associated power supplies and orbit calculations
[DNPL/R-13[VOL-2]] 06 p0649 N73-15274
Pulsed superconducting magnet systems for high energy synchrotrons
[CONF-720565-2] 19 p2249 N73-28131
Multipole production in superconducting dipole and quadrupole synchrotron magnets
[NP-19692] 20 p2462 N73-29785
Superconducting magnets for use in high field synchrotrons
[LBL-1703] 22 p2707 N73-31677

**SYNCLINAL VALLEYS**
U VALLEYS

**SYNCODERS**
Neural model as pulse interval processor
[AD-746007] 01 p0022 N73-10169

**SYNCOPE**
NT BLACKOUT PREVENTION

**SYNDROMES**
U SIGNS AND SYMPTOMS

**SYNOPTIC MEASUREMENT**
Synoptic analysis of ocean surface currents in Northern Hemisphere
07 p0858 N73-16955
Aerosynoptic wind and temperature conditions contributing to atmospheric turbulence at altitude of 18 km over European USSR
[NLL-M-22822-[5828.4F]] 11 p1274 N73-20342
Synoptic weather maps of Northern Hemisphere for October 1972 obtained in Berlin
13 p1551 N73-22564

**SYNOPTIC METEOROLOGY**
Radiosonde height and temperature data for updating asynoptic meteorological measurements
[NOAA-TM-NWS-NMC-51] 01 p0074 N73-10613
Synoptic weather charts of daily and monthly heights and temperature for Northern Hemisphere from Jan. to Dec. 1968
[AD-746659] 02 p0206 N73-11673
Synoptic meteorological data for weather stations, Belgium, Oct. 1971
03 p0327 N73-12665
Synoptic meteorological data for weather stations, Belgium, Nov. 1971
03 p0327 N73-12666
Summary of synoptic meteorological observations for Southeast Asian Coastal Marine Areas
[AD-747638] 03 p0328 N73-12674
Analysis of natural synoptic seasons prior to winter to determine forecasting indications of extremely warm periods
04 p0442 N73-13605
Synoptic cloud cover observations for computing probability of clear lines of sight through atmosphere to ground
[P-4883] 04 p0444 N73-13620
Two methods of analyzing persistence of weather map types, using January MSL pressure data for Colorado map typing window
[AD-749130] 04 p0446 N73-13641
Synoptic meteorological data for weather stations, Belgium, Dec. 1971
05 p0574 N73-14666
Numerical analysis through proportional differences for analyzing meteorological satellite data and predicting synoptic weather patterns
[AD-749072] 05 p0574 N73-14672
Summary of synoptic meteorological observations in Southeast Asian coastal marine areas
[AD-749937] 05 p0576 N73-14687
Daily and monthly meteorological charts for Europe obtained during June, 1972 at Berlin
06 p0691 N73-15629
Daily and monthly meteorological charts for Europe obtained during May, 1972 at Berlin
06 p0692 N73-15631
Synoptic meteorological weather charts for Northern Hemisphere obtained at ground level, 500 mb, and 850 mb during July, 1972, at Berlin
06 p0692 N73-15635
Tables of synoptic meteorological observations for Southeast Asian coastal marine areas
[AD-750159] 06 p0694 N73-15658
Atmospheric energetics as related to cyclogenesis over eastern United States
[NASA-CR-2189] 07 p0815 N73-16607
Practical statistical prediction techniques applied to time series analysis and statistical meteorology
[AD-753714] 09 p1058 N73-18629

Computer procedure for analysis of maritime sea-level pressure and wind fields
[NASA-TM-X-69135] 09 p1058 N73-18630
Tables of synoptic meteorological observations for Okinawa, Sakishima Islands, and southern East China Sea
[AD-753216] 09 p1061 N73-18656
Development of Hurricane Inez, 1966 as shown by Nimbus 2 radiometer data and ESSA-1 and 3 television photographs
[NASA-TM-X-65943] 10 p1182 N73-19616
Tables of synoptic meteorological observations for Japanese and Korean coastal marine areas.
[AD-753468] 10 p1182 N73-19619
Synoptic-climatological method for long range forecast of heavy rain for European USSR
[NLL-M-22865-[5828.4F]] 11 p1313 N73-20653
Tables of synoptic meteorological observations of Japan coastal marine areas
[AD-754773] 11 p1314 N73-20668
Development of agrometeorological forecasts with emphasis on optimal decisions on taking preventive measures for frost control
12 p1421 N73-21517
Analysis of synoptic wind scale spectra over Caribbean and tropical Atlantic region
[COO-2153-1] 12 p1422 N73-21528
Computer-derived synoptic weather forecast maps
[AD-755898] 12 p1423 N73-21532
Long term climatological study of meteorological parameters for Northern Hemisphere
13 p1551 N73-22565
Synoptic climatological studies of precipitation in Plateau states from 850, 700, and 500 mb lows during spring
[NOAA-TM-NWS-TDL-48] 13 p1553 N73-22585
Synoptic meteorological data for weather stations, Belgium, Jan. 1972
13 p1553 N73-22588
Synoptic meteorological data for weather stations, Belgium, Feb. 1972
13 p1553 N73-22589
Tables of synoptic meteorological observations for Japanese and Korean coastal marine areas
[AD-757107] 14 p1685 N73-23674
Macrosynoptic tropopause formula for long range weather forecasts in Budapest
[NLL-M-22839-[5828.4F]] 16 p1894 N73-25322
Synoptic meteorology of large dust cloud over west coast of Africa
[NLL-M-22850-[5828.4F]] 16 p1936 N73-25662
Synoptic weather maps and data tables on daily and monthly Northern Hemisphere stratospheric height and temperature
[QTSR-3] 17 p2056 N73-26626
Daily and monthly synoptic weather maps for Northern Hemisphere and Berlin vicinity, December 1972
17 p2056 N73-26628
Annual report of WMO noting World Weather Watch, global atmospheric research program, education, technical cooperation, environmental and oceanographic aspects
[WMO-348] 17 p2057 N73-26639
Synoptic marine meteorological observations of Chinese and Taiwan coastal areas - Vol. 2
[AD-760333] 17 p2058 N73-26647
Statistical processing of Nimbus infrared data for synoptic atmospheric climatology
18 p2170 N73-27523
Application of meteorological satellite data in analysis and forecasting
[ESSA-TR-NESC-51-SUPPL-2] 18 p2171 N73-27532
Summaries of synoptic meteorological observations for Chinese - Philippine coastal marine areas
[AD-762423] 19 p2318 N73-28645
Synoptic charts for 50mb in Northern Hemisphere from January to June, 1972
[QR-1/2-PT-1/2] 20 p2442 N73-29613
Effect of orography on climatic wind distribution and geopotential fields
20 p2444 N73-29632
Influence of circulation poles and anticyclones on synopticoclimatology
20 p2445 N73-29643
Radioactive tracers for studying atmospheric circulation and synoptic conditions
20 p2446 N73-29644
Development and application of meteorological radar for detecting zones of cloudiness, precipitation, and storms for synoptic weather analysis
21 p2571 N73-30604
Sorting analogs to composite-kinematic maps of natural synoptic periods
21 p2573 N73-30618
Evaluation of procedure for three to ten day synoptic-hydrodynamic-statistical weather forecasting
22 p2692 N73-31567
Forecasting mean monthly air temperature anomalies for Oct. in northern part of European territory of USSR
22 p2693 N73-31575
Dependence of clear air turbulence on evolution of baric field and effect on synoptic forecasting
24 p2946 N73-33526

**SYNTAX**
NT SENTENCES
NT SYLLABLES
NT WORDS [LANGUAGE]
Discrimination of liquids and glides in automatic speech recognition system using syntactic recognition algorithms in analysis of digital spectrograms
14 p1623 N73-23149
Linguistic and perceptual role of syntactic hypotheses in speech recognition systems
14 p1625 N73-23168
Syntax diagrams handbook for Ground Operations Aerospace Language [GOAL]
[NASA-TM-X-69505] 22 p2639 N73-31148

**SYNTHESIS**
Chemical and physical properties of three petroleum resistant elastomers suitable for use under low temperature conditions
[AD-745900] 02 p0194 N73-11569
Frequency characteristics optimization in two dimensional antenna pattern synthesis
[AD-747492] 03 p0276 N73-12242
Syntheses of logical circuits by composing common inputs and common variables
[AD-748165] 03 p0279 N73-12263
Stabilization of aqueous prussic acid during synthesis from ammonia by carbon dioxide
[NASA-TT-F-14691] 07 p0752 N73-16110
Chemical synthesis of formaldehyde based disinfectants without penetrating odor and eye and ear irritation properties
[NASA-CASE-NPO-12115-1] 08 p0884 N73-17153
Synthesis of high molecular weight benzobistriazolo phenanthroline polymers for heat resistant plastic films
[AD-753414] 10 p1127 N73-19180
Synthesis and characterization of tetrahydroborates of lanthanum, neodymium, and erbium
[AD-759372] 17 p1992 N73-26110
Preparation and structure of complex metal hydrides for high energy solid rocket propellants
[AD-760346] 17 p2076 N73-26794
Stable polyimide synthesis from mixtures of monomeric diamines and polycarboxylic acid esters
[NASA-CASE-LEW-11325-1] 19 p2229 N73-27980

**SYNTHESIZERS**
Computer simulation to demonstrate feasibility of delta modulation as method for encoding control signals of voiced speech synthesizer
14 p1632 N73-23231
Adaptive speech synthesizer operation and associated software
24 p2894 N73-33106

**SYNTHETIC ARRAYS**
Analysis of parameters affecting design of synthetic aperture radar antennas for satellites
[NASA-TM-X-66162] 07 p0755 N73-16130
Interferometer aperature synthesis in interstellar neutral hydrogen line spectra of radio sources
[AD-760013] 18 p2198 N73-27744
Radiant array with as many as 144, 13 inches wide, modular radiant heating units mounted in sets of 3 to comprise each adjustable row
[NASA-CR-124435] 24 p2901 N73-33153

**SYNTHETIC FIBERS**
NT DACRON [TRADEMARK]
NT GLASS FIBERS
NT NYLON [TRADEMARK]
Development, characteristics, and applications of composite materials containing inorganic fiber or metal fiber reinforcement
[NLL-RTS-7657] 04 p0437 N73-13561
Production and properties of special purpose synthetic fibers
[AD-749059] 05 p0567 N73-14607
Experimental verification of theory on fiber formation from polyvinyl chloride and dimethyl formamide solutions in tube filled with water
[AD-753032] 09 p1054 N73-18596
Torsional device for testing small diameter single synthetic fibers
[AD-755932] 14 p1680 N73-23638
Physical and mechanical properties of high-strength, high-modulus reinforcing fibers and organic resin composite materials
18 p2164 N73-27475
Design of filamentary composite materials for application to construction of airframes and spacecraft structures
18 p2164 N73-27479
Failure analysis of fiber reinforced composite rocket engine case using distortional energy and maximum strain theories of failure
18 p2167 N73-27500
Development of unidirectional fiber composite materials with emphasis on improving compressive strength
[NASA-CR-112334] 18 p2203 N73-27784
Friction forces on pneumatically drawn fibers with supersonic nozzle
24 p2906 N73-33193
Meteoroid impact simulation tests on bonded fiber/aluminum skin panels for space shuttle insulation
24 p2941 N73-33485

**SYNTHETIC RESINS**
NT ACRYLIC RESINS
NT ADDITION RESINS
NT EPOXY RESINS
NT NYLON [TRADEMARK]
NT PHENOLIC RESINS
NT POLYAMIDE RESINS
NT POLYESTER RESINS
NT POLYETHER RESINS
NT POLYMETHYL METHACRYLATE
NT THERMOPLASTIC RESINS
NT THERMOSETTING RESINS
NT VINYL COPOLYMERS

**SYNTHETIC RUBBERS**
NT CHLOROPRENE RESINS
NT ELASTOMERS
NT VITON RUBBER [TRADEMARK]
Heat treatment and aging behavior of rubbers
[AD-755827] 13 p1548 N73-22548
Physical properties, and hydrazine compatibility of rubber compounds
[NASA-CR-131836] 16 p1932 N73-25633
Polycondensation syntheses of heat resistant siloxane polymers with fluoro aromatic groups at silicon atoms
[RAE-LIB-TRANS-1669] 17 p1991 N73-26104
High performance vulcanized elastomers produced by nitrile and silicone rubber covulcanization
[RAE-TR-72184] 17 p2050 N73-26588
Effect of high temperature and oil immersion on rubbers
[AD-760066] 18 p2167 N73-27503

**SYPHILIS**
Salvarsan therapy of luetic patients and behavior of Wassermann reaction
[NASA-TT-F-14618] 02 p0133 N73-11076

**SYSTEM EFFECTIVENESS**
Effectiveness of synthetic fixed wing flight training equipment for military purposes
[AD-744447] 01 p0020 N73-10158
Mathematical basis for operational availability, and its relation to performance effectiveness
[NASA-CR-61382] 02 p0245 N73-11987
Data 620 minicomputer system performance in acquiring and processing data
[AD-751636] 07 p0759 N73-16167
Dynamic testing for determining flight readiness of Apollo docking system hardware
09 p1089 N73-18885
Program debugging and monitoring facilities for improving diagnostic capability of compiler
[NBS-TN-763] 12 p1381 N73-21197
Reliability and performance of landbased and shipboard Air Force instrumentation systems
[AD-755916] 12 p1389 N73-21262
Effectiveness of infrared radiometer and digital recording equipment as clear air turbulence warning system
[AD-757501] 14 p1685 N73-23677

**SYSTEM FAILURES**
Statistical analysis of ASDE-2 airport radar failures and design modifications
[FAA-RD-72-82] 04 p0388 N73-13154
Errors in design of mechanisms which result in problems during later development stages
09 p1087 N73-18867
Analysis of design features and photographic data to determine cause of Apollo 15 main parachute failure
09 p1088 N73-18879
Fault detection possibilities in integrated navigation system employing Kalman filtering
11 p1320 N73-20712
Fault isolation and maintenance concepts of advanced inertial navigation system
11 p1320 N73-20713
Fault-tolerant clock apparatus for use in digital logic systems which maintains output pulses during component failure
[NASA-CASE-MSC-12531-1] 13 p1528 N73-22386
Double-gimbaled control moment gyro system for maintaining Skylab attitude control without excessive fuel consumption after failure of main gyro system
[NASA-TM-X-64746] 14 p1707 N73-23851
System failure and safety features of superconducting magnetic suspension systems
15 p1762 N73-24277
Precision and reliability characteristics of combined gyroscopic and correction channel
17 p2059 N73-26659
Computer program problems and possible solutions
[AD-762141] 19 p2242 N73-28072
Statistical analysis of upper confidence levels for system failure rates
[AD-761758] 19 p2314 N73-28612
Congressional hearing on Skylab 1 solar array system failure
23 p2866 N73-32912

**SYSTEM LIFE**
U RELIABILITY

**SYSTEMIZATION**
U SYSTEMS ENGINEERING

**SYSTEMS**
Design factors resulting from hydrodynamic loads induced on large underwater structures by impulsive motion
[AD-753603] 09 p1019 N73-18315

SYSTEMS ANALYSIS

Thermodynamic equilibria and carbon deposition in carbon-hydrogenaoxygen system of high temperature fuel cells
[ARL/ME-NOTE-333] 01 p0006 N73-10048

Numerical analysis of simplified radiator system to predict steady state system performance and to optimize system parameters for minimum area or minimum mass
[NASA-CR-128596] 01 p0108 N73-10892

Survey of aerospace industry to determine various techniques used in considering interactions of handling qualities, stability, control, and load alleviation devices on structural loads
[AGARD-R-593] 02 p0125 N73-11020

Development and application of computer program for simulation of continuous systems expressed as ordinary differential and logical equations
[EUR-4836-E] 02 p0144 N73-11169

Performance of equipment and software of SAAC [LASA] system
[AD-745874] 02 p0169 N73-11375

Procedures for studying reliability characteristics of systems with standbys - Themis project
[AD-745911] 02 p0179 N73-11451

Development and application of correction information to improve accuracy of differential Omega navigation system
[AD-745878] 02 p0208 N73-11691

Design and in-flight performance of Mariner 9 spacecraft propulsion system
[NASA-CR-129097] 02 p0222 N73-11795

Analysis of space shuttle systems and space shuttle mission requirements for development of mission simulator - Vol. 3
[NASA-CR-128623] 02 p0230 N73-11862

Development of rationale and requirements for conducting accelerated life tests on spacecraft electronic systems
[NASA-CR-129096] 02 p0233 N73-11892

Systems analyses on external and internal radio frequency communication and tracking assemblies for manned space station
[NASA-CR-128561] 03 p0265 N73-12147

System definition and methodology for selecting perimeter acquisition radar system used with Safeguard Antiballistic Missile System - Vol. 2
[AD-748061] 03 p0267 N73-12162

System definition and criticality analysis of perimeter acquisition radar system used with Safeguard Antiballistic Missile System - Vol. 3 Pt. 1
[AD-748062] 03 p0267 N73-12163

Design features and capabilities of quasi analog and hybrid computers
[AD-747579] 03 p0273 N73-12210

Operating characteristics of small pulsed HF chemical lasers
[AD-747210] 03 p0310 N73-12533

Basic principles of holography and applications
[AD-747380] 03 p0311 N73-12538

Comparison of various numerical solutions to nonlinear Vlasov equation with each other and with solutions to Poisson equation
[COO-2059-12] 03 p0324 N73-12640

Program requirements, operational support, and systems analysis for IMP satellite to identify responsibilities of launching organizations
[NASA-CR-129268] 03 p0358 N73-12916

Cost estimates for base basing, space shuttles, and systems analysis
[NASA-CR-125985] 03 p0359 N73-12921

Systems analysis for determining cause of steerable antenna oscillations during Apollo 14 and 15 missions
[NASA-TM-X-68901] 05 p0519 N73-14218

Problems involved with construction of Silund high current induction linear accelerator of nanosecond range
[AD-749613] 05 p0524 N73-14265

Development, characteristics, and applications of Loran C navigation system for air navigation and microsecond clock synchronization
[NBS-MONO-129] 05 p0577 N73-14700

Definition of expendable second stage for use with reusable space shuttle booster to include structural, propulsion, and avionics systems design - Vol. 2 - Bk. 2
[NASA-CR-128672] 05 p0599 N73-14867

Comparison of three different space environment simulators
[DLR-FB-71-44] 06 p0650 N73-15277

Analysis of weather satellite program management and organization systems
06 p0693 N73-15643

Guidance, navigation and control system analysis report for Apollo 15
[NASA-TM-X-68934] 06 p0696 N73-15673

Guidance, navigation, and control system performance analysis report for Apollo 16 mission
[NASA-TM-X-68931] 06 p0696 N73-15674

Development and characteristics of air traffic control system to show system performance tradeoffs and technonogical alternatives - Vol. 1
[PB-212178] 06 p0698 N73-15688

Air traffic control system development to show factors involved in system selection - Vol. 4
[PB-212181] 06 p0698 N73-15691

FM distortion and FASP computer program for design and analysis of linear dynamic systems
[NASA-CR-130272] 07 p0754 N73-16125

Liapunov functions for analyzing stability properties of various large scale electrical power systems - conferences
07 p0760 N73-16169

Stability analysis of electric power systems
07 p0760 N73-16170

Stability margins for electrical power systems with perturbations in its multiareas
07 p0760 N73-16173

Analysis of factors affecting design and application of remote sensors for earth observation
07 p0784 N73-16376

Underwater sound transducer calibration system for 0.3 to 2000 Hz frequency range at hydrostatic pressure to 6.89 MPa
[AD-751536] 07 p0822 N73-16662

Analysis and design study of solid rocket motor for space shuttle booster
[NASA-CR-124002] 07 p0835 N73-16769

Analysis of guidance systems used with guided missiles
[AD-751089] 07 p0850 N73-16892

Concept evaluation and subsystem analyses for design of remote controlled teleoperator visual system
[NASA-CR-124059] 08 p0879 N73-17117

Evaluation of sterile access technique for repair and adjustment of sterile spacecraft
[NASA-TN-D-7147] 08 p0879 N73-17122

Theoretical relationships among displacement, velocity, acceleration, and cue duration for single degree of freedom flight simulator system during sharp onset acceleration profile
[AD-752222] 08 p0893 N73-17230

Development of computer program to optimize space shuttle environmental and thermal control life support system
[NASA-CR-128736] 08 p0964 N73-17883

UH-1 helicopter test bed program for evaluation of automatic inspection, diagnosis, and prognostic maintenance functions on selected subsystems - Vol. 1
[AD-752890] 09 p0987 N73-18058

FORTRAN programs for statistical analysis of signal and linear and nonlinear systems
[ANTHRO-MITT-3/72] 09 p1006 N73-18208

Design and evalution of lunar roving vehicle deployment mechanism
09 p1088 N73-18876

Theoretical and experimental analysis of digital processing in various communication systems
10 p1127 N73-19183

Analysis of biaxial gyrostabilizer system and synthesis of spherical superconducting suspensions with maximum lift
[JPRS-58356] 10 p1159 N73-19428

Application of averaging method to biaxial gyrostabilizer analysis
10 p1159 N73-19429

Parametric design of aerodynamic control system for compensating artificial satellite orbit perturbations
10 p1178 N73-19580

Numerical method for determining optimal satellite control system with discontinuous links
10 p1178 N73-19581

Performance of OSO-7 spacecraft during twelve months after launch and description of satellite components and subsystems
[NASA-CR-130184] 10 p1215 N73-19885

Proposal for hierarchical description of software systems
[NASA-TN-D-7200] 12 p1381 N73-21200

Performance of ERTS data collection system in total system context
[E73-10494] 12 p1397 N73-21330

Dynamic simulation used to analyze various aspects of STOL aircraft operations within air traffic control system
[FAA-NA-72-95] 13 p1472 N73-21919

Application of systems analysis techniques to improve management controls within biomedical research programs
[NBS-TN-761] 13 p1478 N73-21977

Statistical analysis of phase data on three Omega navigation stations to determine positioning accuracies - Vol. 1
[AD-756024] 13 p1557 N73-22617

Preliminary definition study of sortie laboratory noting structural design, subsystems and shuttle interface
[MBB-SL-72-04] 13 p1582 N73-22826

Preliminary definition study of sortie module/pallet system noting configurations, thermal control, attitude control, power and communications subsystems
[ESRO-CR[P]-239] 13 p1582 N73-22827

Preliminary definition study of a sortie module/pallet system noting configurations, thermal control, attitude control, power and communications subsystems
[ESRO-CR[P]-240] 13 p1582 N73-22828

Evaluation of multifiltration water reclamation subsystem to reclaim domestic clothes wash water
[NASA-TM-X-2781] 13 p1595 N73-22931

Design characteristics and advantage of FCC use
14 p1640 N73-23295

Application of graph theory to Air Force systems design and analysis
[AD-757235] 14 p1684 N73-23666

Systems analysis of radio-TV satellite for coverage of West Germany and west European areas with German language
14 p1710 N73-23876

Analysis of complex social systems relative to information, communication, and behavior
[P-4951] 14 p1721 N73-23963

FAA communications system description for 1973
[FAA-RD-73-36] 15 p1750 N73-24186

Design analysis and integration of MOS threshold logic gates
[AD-758021] 15 p1759 N73-24260

Minitrack tracking function description - Vol. 1
[NASA-TM-X-66213] 15 p1762 N73-24279

Characteristics of emitting-receiving ultrasonic probe including beam configuration and determination of electric equivalent circuit of transducer
[EUR-4774] 15 p1788 N73-24494

Systems analysis of civil airport surface traffic control
[FAA-ED-08-1] 15 p1808 N73-24655

Timing requirements and calibration procedures for very-long-baseline interferometry
[AD-757690] 15 p1833 N73-24857

Systems analysis of active thermal control using thermoelectric devices
[NASA-CR-124256] 15 p1843 N73-24935

Application of cybernetics and systems analysis techniques to economic problems in USSR
[JPRS-58935] 15 p1845 N73-24951

Construction and tests of MHD generator channel and electrical power converter
[AD-758783] 16 p1866 N73-25106

Computerized design of aircraft control optimization stabilization systems
[NASA-CR-133002] 16 p1935 N73-25653

System modeling and performance optimization for analyzing parameters and disturbances for dynamic precision weapon delivery - Vol. 1
[AD-751505] 16 p1976 N73-25985

Analytical methods for evaluating high performance ship design concepts particularly hydrofoil concepts
[AD-759376] 17 p2009 N73-26251

Present and future need for high Reynolds number transonic wind tunnels including analysis of design selection and requirements
17 p2013 N73-26282

Sortie Lab system evaluation, future growth, and IR astronomy experiment accommdation
[ESS/SS-399-VOL-3] 17 p2089 N73-26904

Voltage standing wave ratio measurement and evaluation of aircraft antenna systems
[AD-761031] 18 p2123 N73-27161

Statistical properties of filtered pseudorandom digital sequences used in multichannel communications system evaluation, coding theory, and modulation format design
[NASA-TM-X-64758] 18 p2169 N73-27516

Software description and program documentation for strapdown inertial reference unit system
[NASA-CR-128965] 18 p2175 N73-27567

Systems analysis of quiet turbofan STOL aircraft for short-haul air transportation operations - Vol. 6
[NASA-CR-114611] 19 p2219 N73-27903

Analysis of electronic digital computer inaccuracies
[AD-762235] 19 p2241 N73-28068

Comparative evaluation of conventional and solid state simulators for A-7 aircraft electrical system
[AD-762295] 19 p2250 N73-28142

Analysis of various aircraft antiskid braking systems to determine appropriate antiskid braking system for space shuttle vehicle
[NASA-CR-124349] 19 p2294 N73-28449

Logistic performance data book for electronic countermeasures system of B-52G aircraft to show reliability, maintenance, costs, and problems
[AD-762216] 19 p2357 N73-28961

Logistic performance data book for UH-1F helicopter airframe to show reliability, maintainability, logistic costs, and operational problems
[AD-762251] 19 p2357 N73-28965

Development of system for predicting system failure rate and determination of optimal economic replacement interval
[AD-762417] 19 p2357 N73-28966

Logistic performance data book for F-4D aircraft fire control system to show reliability, maintanability, logistics support, and operating problems
[AD-762229] 19 p2358 N73-28969

Logistic performance data book for F-4E flight control system to show reliability, maintainability, logistic support, and operating problems
[AD-762230] 19 p2358 N73-28973

Analysis of quantized signal dependent control of continuous process by computerized simulation
20 p2378 N73-29110

Survey of parallel processing and parallel processor systems
[CIRC-174] 20 p2379 N73-29111
Airport surface traffic control requirements analysis
[AD-762442] 20 p2383 N73-29147
Development of kinematic equations for analyzing performance of gimballess inertial navigation system
[JPRS-59688] 20 p2452 N73-29704
Examination of man machine systems efficiency in relation to cost criteria
21 p2503 N73-30087
Spaceborne TR 16 digital computer systems analysis
[BMBW-FBW-72-22] 22 p2639 N73-31152
Theoretical and experimental analysis of transferred electron amplifiers
22 p2641 N73-31169
Payload carrier simlation data for design of manned space shuttle missions
[NASA-CR-124430] 23 p2751 N73-32018
Performance analysis of large orbital X ray telescope
[NASA-CR-124429] 23 p2792 N73-32338
Techniques for assessment and control of contamination in scientific satellites
[NASA-TN-D-7433] 23 p2845 N73-32738
Development and evaluation of active control system to provide ride smoothing on short takeoff aircraft
24 p2873 N73-32951
Theory of systems for effective behavior predictions
24 p2887 N73-33054
Analysis of linear systems to show characteristics and to evaluate distortion on basis of quadratic criteria
24 p2944 N73-33515

**SYSTEMS COMPATIBILITY**
System characteristics of amorphous semiconductor thin film and electron beam storage devices
[AD-749282] 05 p0587 N73-14778
Construction materials and electrolytes for electrochemical fuel cells
[AD-750152] 06 p0627 N73-15089
Fuel-oxide can compatability and reaction during fabrication of fuel elements for fast reactors
[NLL-CE-TRANS-6049-[9022.09]]
11 p1322 N73-20732

**SYSTEMS DESIGN**
U SYSTEMS ENGINEERING

**SYSTEMS ENGINEERING**
NT COMPUTER SYSTEMS DESIGN
Operational suitability of various airdrop systems
[AD-744811] 01 p0005 N73-10036
Minimum quadratic cost optimal control technology for design of F-4C aircraft manual control system
01 p0018 N73-10137
Functional design criteria for multiprocessor computer system to provide computational capability for space station
[NASA-CR-128601] 01 p0030 N73-10235
Design and evaluation of inertial microphone headset system
[AD-745088] 01 p0032 N73-10254
Design of satellite and satellite components for Atmospheric Explorer missions to include electrical, mechanical, and environmental interfaces
[NASA-CR-130085] 01 p0049 N73-10395
Development of airborne flight data acquisition and data processing systems
[AGARD-LS-50] 01 p0055 N73-10450
Design of aircraft flight test instrumentation systems
01 p0055 N73-10451
Increased load capacities of self-generating gas bearings with circular supply
[AD-745827] 01 p0063 N73-10518
Development of hydrocarbon fuels and fuel systems for advanced air breathing engines
[AD-746334] 01 p0090 N73-10741
Design, development, and characteristics of radioisotope shielding systems for use with spacecraft electric propulsion system - Vol. 2
[NASA-CR-114506] 01 p0091 N73-10746
Mass properties for Modular Space Station Program, Phase B Definition
[NASA-CR-128409] 01 p0107 N73-10883
Telecommunications systems design techniques for deep space network application
[NASA-CR-129108] 02 p0140 N73-11137
Design of high speed, real time symbiont for analog telemetry processing
[NASA-TM-X-66090] 02 p0146 N73-11183
Design and fabrication of high stability, temperature compensated, crystal oscillator for advanced SSB communication equipment
[AD-745914] 02 p0149 N73-11212
Synthesis of adaptive control tracking systems using Liapunov second method
[NASA-CR-129175] 02 p0150 N73-11220
Systems engineering study for proposed lunar colony
[NASA-CR-129164] 02 p0152 N73-11236
Laboratory restraint chair for squirrel monkeys
[AD-746661] 02 p0154 N73-11246
Design operation, testing, and calibration of Mariner Mars 1971 ultra violet spectrometer
[NASA-CR-128493] 02 p0172 N73-11396
Functional design of electrostatic camera system for application on outer planets explorers
[NASA-CR-129093] 02 p0173 N73-11399
Design and operation of amplitude stabilized pulsed laser operating at approximately 1.06 microns in fundamental transverse mode
[AD-746512] 02 p0182 N73-11474
Acoustic holographic signals for designing underground geological viewing system
[AD-746498] 02 p0184 N73-11490
Evaluation of automated air traffic control system and comparison with operator performance using manual system
02 p0207 N73-11683
Functions of automated system for processing flight data and surveillance functions with development plan for improved capability
[FAA-ED-12-2] 02 p0208 N73-11684
Analysis of space tug operating techniques and requirements to include engineering support, off-site facility requirements, and checkout procedures
[NASA-CR-129163] 02 p0232 N73-11887
Structural design, subsystem analysis and mechanical integration of synchronous meteorological satellite - Vol. 3
[NASA-TM-X-68839] 02 p0234 N73-11900
Mathematical basis for operational availability, and its relation to performance effectiveness
[NASA-CR-61382] 02 p0245 N73-11987
Systems engineering for incorporating human factors in design of transportation
[NASA-CR-129092] 02 p0245 N73-11989
Appendices to support findings of Orbiting Propellant Depot Safety study - Vol. 3
[NASA-CR-123383] 03 p0254 N73-12058
Design features and capabilities of quasi analog and hybrid computers
[AD-747579] 03 p0273 N73-12210
Space shuttle avionics design and cost analysis
[NASA-CR-123962] 03 p0300 N73-12449
Development of computer program for estimating reliability of self-repair and fault-tolerant systems with respect to selected system and mission parameters
[NASA-CASE-NPO-13086-1] 03 p0305 N73-12495
Progressive technological processes and equipment for hot shaping
[AD-747402] 03 p0309 N73-12519
Manual space navigation research projects conducted by US Air Force in support of Skylab project
[AD-747479] 03 p0329 N73-12683
Design, development, and evaluation of pressurized purge system for reusable space shuttles and fabrication of multilayer insulation systems
[NASA-CR-123942] 03 p0358 N73-12914
Design and development of active control system for air cushion vehicle to reduce or eliminate effects of excessive vertical vibratory acceleration
[NASA-CASE-LAR-10531-1] 04 p0372 N73-13023
Improvement in V/STOL aircraft performance with yaw control augmentation to reduce cross coupling effects
[AD-749489] 04 p0375 N73-13046
Design and fabrication of radar attitude sensing system
[NASA-CR-128684] 04 p0388 N73-13157
Design of ionospheric plasma simulator for analyzing and modeling high altitude plasma phenomena
[AD-748311] 04 p0417 N73-13401
Design of power supply voltage monitor for measuring multiple dc voltages simultaneously
[AD-748829] 04 p0424 N73-13453
Design of low power high performance MOS random access memory unit
[NASA-CR-123943] 04 p0457 N73-13732
Dipole configuration of pulsed superconducting synchrotron magnet
[KFK-1354] 04 p0458 N73-13739
Design and performance of breathing metabolic simulator
04 p0472 N73-13850
Design of systems for utilizing communication satellite data in education
04 p0474 N73-13873
Conceptual design of thermal control system for space stations
[NASA-CR-123956] 04 p0484 N73-13950
Addition of feel augmentation system to improve flight control of S-67 helicopter
[AD-749284] 05 p0494 N73-14029
Systems engineering methods for human performance enhancement in signal detection and flight control
[AD-748239] 05 p0503 N73-14098
Fabrication and tests of L band, RF pulse amplifier
[AD-749791] 05 p0514 N73-14182
Design technique for control systems of large space telescope mirrors
[NASA-TN-D-7090] 05 p0522 N73-14247
Pioneer space probe project to show history, design, development, flight operations, and results accomplished
[NASA-SP-278] 05 p0598 N73-14864
Definition of major expendable second stage interfaces with specified space shuttle booster components including interface control drawings - Vol. 6
[NASA-CR-128661] 05 p0599 N73-14872
Research and development projects conducted by National Research Council of Canada from July to September 1972
[DME/NAE-1972[3]] 05 p0611 N73-14967
Analysis of parameters affecting dynamic compatibility in helicopter propulsion systems
[AD-750387] 06 p0624 N73-15065
Improved universal time system implemented on 1 Jan. 1972 eliminating changing-frequency offset and increasing size of step-time adjustments
[NASA-TN-D-7065] 06 p0639 N73-15192
Design and functional description of digital computer system
[FOA-3-C-3657-63] 06 p0643 N73-15220
Design criteria for highly accurate and reliable GEOS-C satellite altimetry system
06 p0661 N73-15370
Design and operation of coherent analyzer
[NASA-TT-F-14595] 06 p0673 N73-15476
Fabrication and tests of magnetic control assembly designed as add-on unit for components of Nimbus and ERTS attitude control system
[NASA-CR-130142] 06 p0673 N73-15479
Investigation of high performance variable speed 10 hp machine tool spindle drive system
[E/C-3] 06 p0677 N73-15505
Design and operation of picosecond neodymium glass laser in terawatt range
[UCRL-TRANS-10633] 06 p0679 N73-15528
Technique for extending viewing angle of hologram to three hundred and sixty degrees
[AD-750250] 06 p0681 N73-15539
Design of linear feedback control system in Hilbert space
[AD-750784] 06 p0691 N73-15624
Application of control theory to design of actual systems
[AD-750490] 06 p0691 N73-15626
Development and characteristics of air traffic control system to show system performance tradeoffs and technonogical alternatives - Vol. 1
[PB-212178] 06 p0698 N73-15688
Analysis of technological alternatives involved in development of air traffic control systems - Vol. 2
[PB-212179] 06 p0698 N73-15689
Air traffic control system development to show factors involved in system selection - Vol. 4
[PB-212181] 06 p0698 N73-15691
Procedure for predicting aeroelastic behavior of Huber suspension bridge
[NPL-R102] 06 p0726 N73-15926
DESIGN OF HEAT EXCHANGERS FOR FLUID VAPORIZATION
[CEA-CONF-2010] 06 p0731 N73-15960
FM distortion and FASP computer program for design and analysis of linear dynamic systems
[NASA-CR-130272] 07 p0754 N73-16125
Baseband equalization system for correcting response characteristics of high quality coaxial transmission lines
[UCRL-73943] 07 p0756 N73-16141
Design and tests of one kilowatt L band solid state power amplifier
[AD-751279] 07 p0758 N73-16155
Design and testing of non-blocking UHF communication system
[AD-751263] 07 p0758 N73-16156
Application of singular perturbation of ordinary differential equations to control system design
07 p0761 N73-16181
Two-phase charge-coupled shift registers
[NASA-CR-2148] 07 p0761 N73-16187
Design and operation of Orion orbital astrophysical observatory
[NASA-TT-F-14581] 07 p0766 N73-16221
Proceedings of conference on earth resources survey systems to show applications of remote sensing to agriculture, forestry, oceanography, and urban development - Vol. 1
[NASA-SP-283-VOL-1] 07 p0781 N73-16348
Design of Brewster angle acousto-optic modulator for high power mode locked C02 laser
[AD-751680] 07 p0807 N73-16544
Description of Geographical Position Locator system with emphasis on means for automatically reducing position errors
[UCRL-74039] 07 p0818 N73-16631
Test programs for TIROS M
[NASA-CR-130165] 07 p0849 N73-16882
Operation and characteristics of primary radar system for air traffic control surveillance
[FAA-ED-02-1] 08 p0885 N73-17163
Techniques for reduction of damage to models caused by launching accelerations in hypervelocity launcher
[AD-752554] 08 p0893 N73-17232
Designs and performance predictions for high performance supersonic ejector systems
[AGARDOGRAPH-163] 08 p0895 N73-17248
Semiempiricial methods for designing ejectors for various applications
08 p0896 N73-17252

Design of electron gun and laser cavity for carbon monoxide lasers
[AD-752818] 08 p0931 N73-17623
Space shuttle design recommendations based on aircraft maintenance experience
[NASA-TM-X-68646] 08 p0965 N73-17888
Design and safety procedures for operating high voltage capacitor bank
[AD-750535] 09 p1008 N73-18231
Design of three color plasma panel display device capable of operating at three intensity levels
[AD-752442] 09 p1009 N73-18236
Development and characteristics of support systems module for use with Large Space Telescope - Vol. 5
[NASA-TM-X-64726-VOL-5] 09 p1036 N73-18453
Design of traveling wave maser system for use in satellite communication telescopes and radio astronomy
[REPT-109] 09 p1043 N73-18505
Image intensifier system for daytime missile tracking telescopes
[AD-753342] 09 p1068 N73-18715
Digital implementation of high frequency cutoff filter for spacecraft control system optimization based on word length, sampling rate, accuracy, and computing time requirements - Vol. 2
[NASA-CR-124051] 09 p1086 N73-18861
Design characteristics of data handling equipment for ITOS D and E meteorological satellites - Vol. 2
[NASA-CR-130161] 09 p1087 N73-18864
Design of docking system of androgynous and peripheral type for creation of compatible system for US and Soviet spacecraft
09 p1087 N73-18869
Design and tests of passive radiative cooler for spacecraft
09 p1088 N73-18873
Design and preflight analysis of flexible solar array mechanism
09 p1089 N73-18887
Characteristics of power generating systems and application in missiles for production of hydraulic and electric energy
10 p1110 N73-19044
Design principles of auxiliary power units of secondary power system for operation of aircraft equipment
10 p1110 N73-19046
Design and characteristics of auxiliary power source to operate electric, hydraulic, and pneumatic subsystems in ramjet powered aerospace vehicles
10 p1110 N73-19048
Rendezvous and docking radar for space shuttle
10 p1129 N73-19198
Design of prototype quad redundant data terminal and associated multiplexer/demultiplexer units
[NASA-CR-124127] 10 p1130 N73-19203
Automated computer program documentation as feature of total system design
10 p1131 N73-19212
Design of nonlinear feedback system with significant plant ignorance for prescribed time domain tolerances
[NASA-CR-127489] 10 p1136 N73-19260
Active optics simulation system for designing mirror control system for large space telescope
[NASA-CR-112259] 10 p1159 N73-19433
Hydrodynamic design of thrust slide bearings
[AD-753965] 10 p1168 N73-19501
Design of Joule-Thomson cascade for refrigeration cooling using liquid helium
[CEA-CONF-2044] 10 p1199 N73-19761
Reliability performance analysis of NASA communication system to show major area of interruption and malfunctions of specified circuits
[NASA-TM-X-66220] 11 p1256 N73-20190
System designs for automating GC/MS analyzing system
[NLL-RTS-7572] 11 p1259 N73-20218
Design and fabrication of microwave acoustic surface wave delay lines
[AD-754896] 11 p1263 N73-20252
Conceptual design of space shuttle comm/nav research laboratory and identification of major laboratory equipment - Vol. 3
[NASA-CR-124138] 11 p1266 N73-20275
Design and construction of 200 kV ion accelerator
[AD-754274] 11 p1268 N73-20290
Research and development projects conducted by Federal Aviation Administration to improve air traffic control and flight safety
[FAA-EM-73-2] 11 p1321 N73-20720
Design of fuel injection system for ramjet engines with coaxial inlet
[AD-754852] 11 p1335 N73-20835
Management methods for Skylab program to include mission operations support, environmental and thermal design criteria, optical contamination, and materials science
[NASA-TM-X-64725] 11 p1342 N73-20886
Validation and verification of computer simulation models
[P-4891] 12 p1381 N73-21196
Steel construction design parameters for building and operating ZYKLON type wind driven power plants
[NASA-TT-F-14872] 12 p1388 N73-21253
Design, assembly, and operation of gaseous hydrogen system with solutions to specific problems
[SC-DR-72-0593] 12 p1388 N73-21257
CF3I gas laser system for high power operation
[SC-T-72-2560] 12 p1410 N73-21426
Design and performance of demand regulated liquid breathing systems for mammalian respiration
13 p1478 N73-21976
Design and performance analysis of thermionic diode modules for in-core thermionic power source
[NASA-CR-131602] 13 p1499 N73-22153
Design of ironless armature torque motor using samarium cobalt permanent magnets
[NASA-CR-130224] 13 p1532 N73-22416
Design of welded bellows for cryogenic turbomachinery face seal applications
[NASA-CR-121117] 13 p1533 N73-22423
LORAMS design for remotely collecting weather data
[AD-756682] 13 p1554 N73-22594
Infrared sensitive photoconductors
[AD-755224] 13 p1560 N73-22647
Design of communication repeater subsystems for advanced multifunctional communications satellites
[NASA-CR-132296] 13 p1581 N73-22819
Handbook of basic requirements and guidelines for preparing system safety engineering analysis
[NASA-CR-131886] 13 p1593 N73-22913
Design of repetitively pulsed inductive energy storage systems
[AD-755359] 14 p1606 N73-23014
Parameters requiring consideration by planners and designers when planning EVA functions for astronauts - Vol. 1
[NASA-CR-128926] 14 p1614 N73-23081
Conceptual designs of versatile EVA work-stations - Vol. 2
[NASA-CR-128927] 14 p1614 N73-23082
Implementation strategy for vocal data management system
14 p1629 N73-23206
Design of circular symbol and video inset generator for television display devices
[AD-757621] 14 p1634 N73-23246
Measure, criteria, and procedure for radar track and search allocation
[AD-757172] 14 p1635 N73-23257
Flat conductor cabling system for electrical/electronic interwiring
14 p1641 N73-23305
Synthesis and analysis of systems combining extreme principle of control with correlation processing of signals entering from object being controlled
14 p1644 N73-23334
Design of tunable carbon dioxide laser using integrated optics technique
[AD-757068] 14 p1672 N73-23569
Feasibility analysis and design of bleachable absorber laser amplifier and detector
[AD-757361] 14 p1672 N73-23571
Application of graph theory to Air Force systems design and analysis
[AD-757235] 14 p1684 N73-23666
Design, construction, and electrical circuits for radiosondes to study warm cloud development
[AD-758073] 14 p1686 N73-23684
Development of method for estimating power output of helicopter gas turbine engines operating at full power
[AD-758461] 14 p1702 N73-23811
Development of guidelines for application to production of spacecraft hardware components with long lifetime - Vol. 1
[NASA-CR-128905] 14 p1707 N73-23853
Revised edition of human engineering guide to equipment design
[AD-758339] 15 p1744 N73-24140
Design and operational services of small data centers to technical users
[AGARD-CP-117] 15 p1752 N73-24201
Design and operation of Turkish information systems
15 p1752 N73-24202
Management methods for developing information systems
15 p1753 N73-24209
Systems design of facilities for studying flight problems of VTOL aircraft
[NAL-TR-306] 15 p1760 N73-24263
Functional characteristics and operating data of experimental, aerodynamic three-phase electric power plant constructed in Crimea
[NASA-TT-F-14933] 15 p1761 N73-24268
Cryogenic superconducting magnetic suspension and balance facility designs
15 p1761 N73-24272
Design and implementation of experimental system for receiving and recording partially reflected echoes from D region
[PSU-IRL-SCI-414] 15 p1778 N73-24417
Measurement errors and working signal structure of rubidium vapor M sub Z magnetometers and design of observatory vector magnetometer
[JPRS-58950] 15 p1786 N73-24480
Design and operation of observatory vector magnetometer
15 p1786 N73-24483
Design and applications of air bearings
[Y-DA-4834] 15 p1793 N73-24534
Optimum roller bearing design for use in heavy lift helicopter rotor transmission second stage planetary system
[AD-755535] 15 p1794 N73-24540
Design of expansion joint unit for coolant piping loop of reactor thermoelectric system - SNAP program
[NASA-CR-121209] 15 p1809 N73-24663
Development of system concept for shuttle support to orbital operations of low cost unmanned satellites in low earth orbit
[NASA-CR-130239] 15 p1834 N73-24869
Design and performance of launcher illumination XM-183 flare package for parachutes
[AD-757731] 15 p1844 N73-24940
Conference on project management and project control
[ESRO-SP-90] 15 p1846 N73-24962
Systems engineering as decision making tool using space system as example
15 p1847 N73-24972
Systems engineering and project management of ESRO 1 satellite
15 p1847 N73-24973
Research projects in theoretical and practical aerodynamics - Vol. 1
16 p1851 N73-24999
Progress in DSN flight project support, research and technology, and network engineering
[NASA-CR-133032] 16 p1874 N73-25172
Factors affecting design of charge-coupled image sensors
[AD-758741] 16 p1882 N73-25234
Design and performance of aircraft or spacecraft differential maneuvering simulator
[NASA-TN-D-7304] 16 p1885 N73-25259
Design feasibility of thermal subsystem concepts for photoheliographs
[NASA-CR-124268] 16 p1913 N73-25483
Design of 10.6 micrometer detector array using 77 K, 1500 MHz photodiodes
[AD-758714] 16 p1915 N73-25496
Improvement in methods of measurement for semiconductor materials, process control, and devices
[NASA-CR-133030] 16 p1953 N73-25800
Design engineering for radio communication systems considering troposphere transmission characteristics
17 p1995 N73-26128
Criteria for planning ultrahigh frequency telecommunication system considering radioelectrical and meteorological measurements
17 p1995 N73-26129
Astronomical research and instrument development by Professor M. G. Pereira de Barros
17 p2081 N73-26837
NASA space vehicle design criteria on accelerometer applications
[NASA-SP-8102] 17 p2088 N73-26891
Statistical weather analysis for optimum picture quality design of satellite television broadcasting system
18 p2115 N73-27101
Design technology of aeronautical satellite communication system for air traffic control over Atlantic Ocean
[FAA-ED-17-1] 18 p2115 N73-27104
Modifications and testing of portable ultra-sensitive superconducting magnetometer
[AD-759735] 18 p2153 N73-27400
Design of gas turbines for furnishing hot gases for turbine drives and analysis of limitations imposed by thermal stresses
[NASA-SP-8081] 18 p2193 N73-27705
Parameters affecting design of AEROSAT navigation satellite for aircraft communication and air traffic control
18 p2201 N73-27768
Design, construction, and performance of crossed beams tandem mass spectrometer for study of low energy ionic collisions
[AD-762450] 19 p2231 N73-27991
Design of high intensity proton accelerator
[AD-762240] 19 p2250 N73-28140
Design of automatic throttle control for Navy carrier based A-7 E aircraft
[AD-761764] 19 p2329 N73-28740
Objectives and accomplishments of geosynchronous platform definition study
[NASA-CR-133968] 19 p2345 N73-28860
Program results and supporting data obtained in geosynchronous platform definition study
[NASA-CR-133969] 19 p2345 N73-28861
Mission characteristics data compiled in geosynchronous platform definition study
[NASA-CR-133970] 19 p2345 N73-28862
Baseline traffic model resulting from traffic analysis and system requirements data generated in geosynchronous platform definition study
[NASA-CR-133971] 19 p2345 N73-28863

Traffic analysis and system requirements for new traffic model developed in geosynchronous platform definition study
[NASA-CR-133972] 19 p2345 N73-28864
Platform configurations, support subsystems, mission equipment, and servicing concepts generated in geosynchronous platform definition study
[NASA-CR-133973] 19 p2345 N73-28865
Program evaluation and recommendations of geosynchronous platform definition study
[NASA-CR-133974] 19 p2345 N73-28866
Interfaces between space platforms and space transportation system established in geosynchronous platform definition study
[NASA-CR-133975] 19 p2345 N73-28867
Collection generation, and analysis of MIL-HDBK-5 allowable design data for aerospacecraft
[AD-761817] 19 p2347 N73-28877
Logistics performance data book for RF-4C aircraft landing gear system to show reliability, maintainability, logistics support, and operating problems
[AD-762231] 19 p2358 N73-28970
Design and development of prototype moving base gravity gradiometers
[AD-760799] 20 p2414 N73-29400
Design of standard, special purpose air, and refrigeration screw compressors
[NLL-NEL-TT-2460-[6075.461]] 20 p2422 N73-29452
Development of satellite equipment for solving inverse problems of meteorological satellites 20 p2447 N73-29661
Ergonomic research and design principles for automatic control and man machine systems
[NASA-TT-F-716] 21 p2502 N73-30079
Military personnel management and human factors engineering
[AD-763168] 21 p2504 N73-30094
FAA engineering and development program for terminal air traffic control
[FAA-ED-14-2] 21 p2521 N73-30215
Wide gap spark chamber system for NAL experiment 2-B
[ORO-2504-202] 21 p2522 N73-30223
Global system for search and rescue
[NASA-TM-X-70437] 21 p2537 N73-30339
Measurement system for physical quantity represented by or converted to variable frequency signal
[NASA-CASE-MFS-20658-1] 21 p2543 N73-30386
Design and construction of vacuum system and safety interlocks for photoionization mass spectrometer
[AD-763685] 21 p2550 N73-30447
Holographic system for nondestructive testing
[NASA-CASE-MFS-21704-1] 21 p2554 N73-30478
System design and test plan for NASA position location and aircraft communications equipment at C band using USNS Vanguard and ATS 3 and ATS 5 satellites
[NASA-TM-X-70447] 21 p2576 N73-30646
Engineering design handbook on infrared systems for military applications
[AD-763495] 21 p2581 N73-30684
Design of MHD generators with fuel gas and air turbine
[JUL-892-TP-VOL-11] 21 p2583 N73-30699
Introductory background to planning process, objectives, and indexing for twenty two engineering and development programs with FAA
[FAA-ED-00-A] 21 p2609 N73-30918
Portable open cycle fuel cell power plant capable of operation on military fuels
[AD-764285] 22 p2618 N73-30979
Systems design for advanced water recovery and waste processing in aerospace and domestic applications
[NASA-CR-134028] 22 p2623 N73-31017
Multi-image photointerpretation system for processing several types of photographs 22 p2636 N73-31125
Optimized design for vehicle suspension systems
[PB-220553/2] 22 p2648 N73-31216
Design, fabrication, production and testing of data collection platforms and platform field test sets for Earth Resources Program
[E73-11008] 22 p2660 N73-31313
Technology related to design and operation of magnetometers
[JPRS-59674] 22 p2671 N73-31396
Design and flight tests of helicopter airspeed indicator
[AD-764240] 22 p2675 N73-31430
Design and performance of remote sensing system for optical sensing of emissions
[PB-221073/0] 22 p2696 N73-31599
Development of test equipment, propellants, and control equipment for interplanetary spacecraft
[NASA-CR-133863] 22 p2731 N73-31858
Design of detonating propellant propulsion system for exploring planets with hot dense atmospheres 22 p2732 N73-31864
Psychological concept for developing cybernetic control devices
[JPRS-60103] 23 p2752 N73-32019
Evaluation of radiographic paper system using ultraviolet fluorescent screens including program objectives, technique, and sensitivity data for F-1 screen
[AD-764779] 23 p2794 N73-32355
Combined parachute and retrorocket system for low altitude aerial delivery of military cargo
[AD-765422] 24 p2880 N73-32997
Optimization of human performance in system design, training, and operation
[AD-764761] 24 p2890 N73-33075
Computer aided design of optimal control systems 24 p2896 N73-33119
Statistical design of nonrecursive digital filters for signal processing
[AD-764595] 24 p2899 N73-33142
Design of precision vertical alignment system using laser with gravitationally sensitive cavity
[NASA-CASE-ARC-10444-1] 24 p2930 N73-33397
Design and development of thermionic reactor power system for future interplanetary exploration - Vol. 4
[GULF-GA-C-12308-VOL-4] 24 p2954 N73-33602
Design of floating platforms to capture and use solar radiation 24 p2974 N73-33764
Computer programs for three dimensional civil engineering lattice structures noting matrix methods, computerized design, and repetitive lattices
[CRIF-MT-82] 24 p2989 N73-33889
Bimodal system of improving urban transportation
[NASA-TT-F-15056] 24 p2994 N73-33925

**SYSTEMS FOR NUCLEAR AUXILIARY POWER**
U SNAP

**SYSTEMS MANAGEMENT**
Cost effective data security safeguards in personal information databanks
[P-4871] 02 p0145 N73-11178
Project control in ESRO program 05 p0611 N73-14973
Management regulations and systems requirements for Europa 3 launch vehicle 07 p0849 N73-16885
Phased development, planning, and management of new industrial products 15 p1848 N73-24980
Design and programming techniques for space shuttle software
[NASA-CR-128971] 16 p1879 N73-25211

**SYSTEMS STABILITY**
Iterative solution for characteristic exponents of linear differential equations with periodic coefficients
[ARC-CP-1218] 03 p0324 N73-12642
Liapunov functions for analyzing stability properties of various large scale electrical power systems - conferences 07 p0760 N73-16169
Stability analysis of electric power systems 07 p0760 N73-16170
Liapunov direct method for studying transient stability of multimachine power system 07 p0760 N73-16171
Output stability analysis on nonlinear feedback and transient power systems 07 p0760 N73-16172
Stability margins for electrical power systems with perturbations in its multiareas 07 p0760 N73-16173
Liapunov type methods for checking dynamic security in power system stability theory 07 p0760 N73-16174
Mathematical models for analyzing synchronous functions of multimachine electrical power systems 07 p0760 N73-16175
Principle and vector Liapunov functions for studying stability in large scale dynamic systems 07 p0760 N73-16176
Algebraic criteria for connective stability of large scale dynamic systems subjected to structural perturbations 07 p0760 N73-16177
Exponential stability of discrete time composite systems with periodic and non-periodic sampling operation 07 p0761 N73-16178
Estimates of differential functions for proving system stability 07 p0761 N73-16179
Singular perturbation approach to stability analysis of linear time varying systems 07 p0761 N73-16180
Theorems for proving consistency of singular perturbations in physical systems with parasitic elements 07 p0761 N73-16182
Stability of two coordinate angle tracking optical automatic tracking systems
[AD-762106] 19 p2250 N73-28138
Development and characteristics of annular momentum control device for two axis stabilization of spacecraft
[NASA-CASE-LAR-11051-1] 19 p2318 N73-28646
The prediction of instabilities of linear differential equations with periodic coefficients
[ARC-R/M-3713] 24 p2945 N73-33518

## T

**T SHAPE**
Buckling tests on double T shaped Protenax steel beams
[CRIF-MT-78] 04 p0481 N73-13935

**T TAIL SURFACES**
Effect of gust loads on wing and T-tail airworthiness requirements for short haul aircraft
[FOK-K-66] 16 p1859 N73-25058

**T TAURI STARS**
Photographic magnetudes of T Tauri and normal stars in Orion I 06 p0716 N73-15846
Photographic V and R magnitudes of 130 T Tauri and H alpha emission stars in Orion I 06 p0716 N73-15847

**T-33 AIRCRAFT**
Flight tests to determine lateral-directional performance and roll-sideslip coupling of T-33 aircraft at subsonic speed - Vol. 2
[AD-748436] 06 p0622 N73-15051
Computerized simulation of aircraft as radar target
[AD-755854] 12 p1380 N73-21189
Instrumentation and data handling process of NAE T-33 turbulence research aircraft, stationary gas turbine icing problems, and role of plastic deformation in metal powder compaction
[DME/NAE-1972[4]] 12 p1466 N73-21882
Computer program for predicting pilot rating of pitch stability of T-33 aircraft under vertical turbulence conditions
[AD-764696] 23 p2745 N73-31974

**T-38 AIRCRAFT**
T-38 structural flight load data from Williams, Reese, and Moody Air Force Bases, Jun. 1970 to Dec. 1971
[AD-758891] 16 p1861 N73-25076
Ground-based devices for spatial orientation training in T-38 aircraft
[AD-764740] 24 p2901 N73-33157

**TABLES [DATA]**
NT CONVERSION TABLES
Prandtl number values for water and steam, liquid and gaseous heavy water, and sea water
[ESDU-68011] 01 p0038 N73-10301
Dynamic viscosity data for water and steam, liquid and gaseous heavy water, and sea water
[ESDU-68009] 01 p0038 N73-10303
Translation of titles, subtitles, and table of contents for Soviet publication on Problems of Physics of Atmosphere
[NASA-TT-F-14424] 01 p0049 N73-10396
Ionospheric sounding and cosmic ray neutron flux density tables, Dourbes, Belgium, Feb. 1972 01 p0050 N73-10402
Meteorological charts and tables on wind altitude over French Polynesia
[MN-MONO-85] 01 p0073 N73-10602
Meteorological parameter table for Belgian weather stations, June 1972 01 p0075 N73-10618
Sulfur oxides, smoke, and air pollution tables from Belgian weather stations, Oct. 1971 01 p0075 N73-10619
Tables on Atlantic tropical cyclone strike probabilities - 24 hour movement
[AD-744916] 01 p0076 N73-10630
Tables on Atlantic tropical cyclone strike probabilities - 48 hour movement
[AD-744917] 01 p0076 N73-10631
Data tables of atomic spectra derived from optical analyses
[NSRDS-NBS-3-SECT-6] 01 p0082 N73-10677
New tables for forward pion nucleon scattering amplitude analyzing errors and total cross section data
[NOTA-INTERNA-382] 01 p0084 N73-10695
Uncorrected and barometer-corrected hourly rate data on cosmic ray neutrons at Deep River, Ontario - 1960
[AECL-4209] 01 p0092 N73-10758
Photoheliographic data on sunspots for 1962, 1963, and 1964 - tables 01 p0101 N73-10829
Thermal conductivities of liquid alcohols at their saturation pressures
[ESDU-67030] 01 p0115 N73-10953
Ionospheric sounding and cosmic ray neutron flux density tables, Dourbes, Belgium, Mar. 1972 02 p0166 N73-11352
Tables on geodetic satellite gravity observations 09.0 deg E to 37.9 deg W along equator
[AD-746465] 02 p0170 N73-11379
Sulfur oxides, smoke, and air pollution tables from Belgian weather stations, Dec. 1971 02 p0205 N73-11659
Simulation of alternate expressions for meteorological phenomena of atmospheric boundary layer - tables
[AD-746247] 02 p0205 N73-11665
Magnetospheric and upper atmospheric physics data obtained during 1971
[AD-746326] 02 p0232 N73-11882
Ionospheric sounding and cosmic ray neutron flux density tables, Dourbes, Belgium, Apr. 1972 03 p0297 N73-12420

Hydrographic data from Oregon waters in 1971
[AD-746515] 03 p0297 N73-12421
Sulfur oxides, smoke, and air pollution tables from Belgian weather stations, Nov. 1971
03 p0327 N73-12663
Meteorological parameter tables for Belgian weather stations, Aug. 1972
03 p0327 N73-12664
Synoptic meteorological data for weather stations, Belgium, Oct. 1971
03 p0327 N73-12665
Synoptic meteorological data for weather stations, Belgium, Nov. 1971
03 p0327 N73-12666
Meteorological parameter tables for Belgian weather stations, Sep. 1972
03 p0327 N73-12668
Tables of earth magnetic field intensity measurements at Sao Jose dos Campos, Brazil
[AD-747060] 04 p0415 N73-13389
Lake, river, and land-fast sea ice thickness in North American Arctic and subarctic regions during 1968-1969 and 1969-1970
[AD-746256] 04 p0416 N73-13400
Hydrographic survey data for Southern Pacific Ocean between Australia and Antarctica
[AD-747792] 04 p0417 N73-13404
Temperature, pressure, and related climatological data for Australia - tables for [May, 1972]
04 p0441 N73-13598
Temperature, pressure, and related climatological data for Australia - tables for [April 1972]
04 p0442 N73-13599
Meteorological and ballistics data for launching of Athena rocket flight 134, vehicle H-004J
[AD-749436] 04 p0445 N73-13633
Meteorological and ballistics data for launching 13901 Little John, missile number 2172, round number 684 AM
[AD-749435] 04 p0445 N73-13634
Meteorological and ballistics data for launching 13401 Honest John, missile number 2632, round number 626 ROL
[AD-749434] 04 p0445 N73-13635
Meteorological and ballistics data for launching of Lance Missile 2143, vehicle 159
[AD-749429] 04 p0445 N73-13636
Meteorological and ballistics data for launching of Honest John Laser, missile flight 205, vehicle 624
[AD-749430] 04 p0446 N73-13637
Meteorological and ballistics data for launching of Honest John Missile flight 1755, vehicle 625
[AD-749431] 04 p0446 N73-13638
Meteorological and ballistics data for launching of Lance Missile 2168, vehicle 160
[AD-749432] 04 p0446 N73-13639
Meteorological and ballistics data for launching of Lance Missile 2159, vehicle 161
[AD-749433] 04 p0446 N73-13640
Tables on molecular oxygen absorption in schumann-runge band
[AERONOMICA-ACTA-A-107-PT-2]
05 p0506 N73-14114
Data tables and computer generated profile plots obtained in evaluation tests of circumferential airflow uniformity entering combustors from two advanced engine compressors
[NASA-CR-121010] 05 p0526 N73-14277
Synoptic meteorological data for weather stations, Belgium, Dec. 1971
05 p0574 N73-14666
Various Belgian climates associated to different air mass origins
[MISC-SER-A-2] 05 p0574 N73-14667
Microphysical and meteorological data on fog cycle in California valley
[AD-750086] 05 p0576 N73-14685
Computer index on bibliographical references to microscopic neutron data
05 p0582 N73-14734
Analyses of solar wind plasma data obtained by Explorer 33 and Explorer 35
[NASA-CR-129923] 05 p0592 N73-14807
Line spectra and spectral energy distribution of early type stars
05 p0594 N73-14829
Tables of minor planets positions and comparison stars
05 p0594 N73-14831
Aeronomic reaction rate data
[AD-750771] 06 p0668 N73-15436
Meteorological parameter tables for Belgian weather stations, Oct. 1972
06 p0694 N73-15654
Tables of synoptic meteorological observations for Southeast Asian coastal marine areas
[AD-750159] 06 p0694 N73-15658
Tables of thermophysical properties of helium 4
[NBS-TN-631] 06 p0730 N73-15953
Tables of O2 absorption cross sections in Schumann-Runge band
[A-N-107-1972] 07 p0752 N73-16108
Tables of geomagnetic and geoelectric magnetograms and tellurigrams measured at Kakioka Magnetic Observatory, Japan
[REPT-12] 07 p0788 N73-16411
Tables of Dst hourly variations for July, August, and September 1972
[NASA-TM-X-66156] 07 p0842 N73-16822
Tables on ionospheric data measured by vertical echo sounding
[REPT-316-F] 08 p0916 N73-17507
Tabulated data on atmospheric ozone density at Uccle, Belgium for 1969
08 p0918 N73-17522
Ionospheric sounding and cosmic ray neutron flux density tables, Dourbes, Belgium, Jun. 1972
08 p0918 N73-17524
Tables on airborne and ground based measurements of optical atmospheric properties in central New Mexico
[AD-751936] 08 p0919 N73-17534
Tables and charts of meteorological data gathered at Oarai site for 1970
[JAERI-M-4657] 08 p0939 N73-17685
Sulfur oxides, smoke, and air pollution tables from Belgian weather stations, Feb. 1972
08 p0939 N73-17686
Meteorological parameter tables for Belgian weather stations, Nov. 1972
08 p0939 N73-17687
Meteorological and ballistics data for launching of 11601 Lance Missile number 2154, round number 163 RBL
[AD-752088] 08 p0939 N73-17690
Meteorological and ballistics data for launching of 11602 Lance Missile number 5175, round number 164 ESL
[AD-752090] 08 p0940 N73-17695
Meteorological and ballistics data for launching of 13901 Little John Missile number 1463, round number 692 RG
[AD-752091] 08 p0940 N73-17696
Meteorological and ballistics data for launching of 14101 Little John RIP missile number 12751
[AD-752092] 08 p0940 N73-17697
Meteorological and ballistics data for launching of 13801 Little John ARM-P Ripple, missile numbers 3102, 3142 and 3257, round numbers 693, 694 and 695 RO
[AD-752095] 08 p0940 N73-17698
Tables of cosmic ray MT-64 muon monitor measurements from solar rotation 1867 to solar rotation 1879
[AECL-4207] 08 p0957 N73-17834
Test data on liquid dielectric breakdown mechanisms
[AD-752819] 09 p1053 N73-18585
Survey of climatological conditions in Martinique
[MN-MONO-86] 09 p1060 N73-18644
Meteorological parameter tables for Belgian weather stations, Dec. 1972
09 p1061 N73-18651
Tables of synoptic meteorological observations for Okinawa, Sakishima Islands, and southern East China Sea
[AD-753216] 09 p1061 N73-18656
Oceanographic data collection on Caribbean Sea and Gulf of Mexico environments
[AD-752494] 10 p1156 N73-19404
Tables of synoptic meteorological observations for Japanese and Korean coastal marine areas
[AD-753468] 10 p1182 N73-19619
Equatorial Dst tables for Nov. and Dec. 1972
[NASA-TM-X-66197] 10 p1212 N73-19861
Development of tables of gasdynamic functions in three dimensional, axisymmetric, and plane gas flows past blunt bodies of revolution
[NASA-TT-F-715] 11 p1231 N73-19996
Tables and graphs on static stability and axial force characteristics of flat faced right circular cylinders at subsonic and supersonic speed
[AD-754920] 11 p1273 N73-20330
Meteorological and ballistics data for launching of 15001 Little John missile no. 1508, round no. 697 RG
[AD-754558] 11 p1314 N73-20665
Tables of synoptic meteorological observations of Japan coastal marine areas
[AD-754773] 11 p1314 N73-20668
Meteorological and ballistics data for launching of 14801 Lance missile no. 2184, round no. 168 APT 9
[AD-754556] 11 p1315 N73-20669
Meteorological and ballistics data for launching of 12802 Lance missile no. 2150, round no. 174 ESL
[AD-754563] 11 p1316 N73-20678
Approximate thermochemical tables for some C-H and C-H-O species
[NASA-CR-2178] 11 p1347 N73-20932
Tables of absorption cross sections of molecular oxygen in Schumann-Runge bands
[AERONOMICA-ACTA-A-107-1972-V-1]
12 p1375 N73-21157
Tables of absorption cross sections of molecular oxygen in Schumann-Runge bands
[AERONOMICA-ACTA-A-107-1972-V-2]
12 p1375 N73-21158
Tables on geomagnetic observations made by Kakioka Magnetic Observatory
[REPT-86] 12 p1399 N73-21345
Tables on geomagnetic observations made by Kanoya Magnetic Observatory
[REPT-88] 12 p1399 N73-21346
Tables on geomagnetic observations made by Memambetsu Magnetic Observatory
[REPT-87] 12 p1400 N73-21358
Photonuclear giant resonance data summary
[NBS-SP-380] 12 p1427 N73-21564
Ionospheric sounding and cosmic ray neutron flux density tables, Dourbes, Belgium, Aug. 1972
13 p1524 N73-22354
Sulfur oxides, smoke, and air pollution tables from Belgian weather stations, Mar. 1972
13 p1553 N73-22587
Synoptic meteorological data for weather stations, Belgium, Jan. 1972
13 p1553 N73-22588
Synoptic meteorological data for weather stations, Belgium, Feb. 1972
13 p1553 N73-22589
Sulfur oxides, smoke, and air pollution tables from Belgian weather stations, Apr. 1972
13 p1553 N73-22590
Meteorological parameter tables for Belgian weather stations, Jan. 1973
13 p1553 N73-22591
Tabular and graphical data for moderate and heavy snow for Loring AFB, Maine
[AD-756881] 13 p1555 N73-22605
Catalog of data acquired from Nimbus 4 meteorological satellite from 18 Apr. through 22 May 1970
[NASA-TM-X-69888] 13 p1580 N73-22804
Data catalog tables and pictorial montages from Nimbus 4 satellite observation
[NASA-TM-X-69891] 13 p1580 N73-22807
Tables of cataloged data collected by Nimbus 4 satellite
[NASA-TM-X-69894] 13 p1580 N73-22810
Catalog of data in World Data Center C2 for Geomagnetism
14 p1658 N73-23456
Data tables on nonmetallic materials for offgassing CO and hydrocarbons in 5 psia O2
[NASA-TM-X-64745] 14 p1680 N73-23631
Daily and monthly meteorological charts for Northern Hemisphere obtained during November, 1972 at Berlin
14 p1684 N73-23668
Tables of synoptic meteorological observations for Japanese and Korean coastal marine areas
[AD-757107] 14 p1685 N73-23674
Tabular listing of minimum and maximum temperatures for use in specifying fuel and lubricant properties needed in different geographical areas
[AD-756420] 14 p1685 N73-23675
Tables of climatological conditions for selected areas of Virginia
[PB-213881/3] 14 p1686 N73-23681
Tables on structure of interstellar masers and quasars
14 p1704 N73-23826
Tables of thermophysical properties of materials
[AD-758175] 15 p1747 N73-24164
Ionospheric sounding and cosmic ray neutron flux density tables from Dourbes, Belgium for Oct. 1972
15 p1781 N73-24438
Meteorological parameter tables for Belgian weather stations, Feb. 1973
15 p1806 N73-24636
Meteorological and ballistics data for launching of Athena rocket flight 138, vehicle H-008
[AD-758866] 15 p1807 N73-24645
Meteorological and ballistics data for launching Athena rocket flight 139, vehicle H-006
[AD-758867] 15 p1807 N73-24646
Meteorological and ballistics data for launching of 14101 RIP missile nos. 9623/9034, round nos. 5/6
[AD-758861] 15 p1807 N73-24647
Meteorological and ballistics data for launching of 03702 Honest John missile number 1003, round number 631 AM1.
[AD-758869] 15 p1807 N73-24650
Collection of marine fluorescence data from Atlantic, Gulf, and Pacific sites
[NASA-CR-114579] 16 p1867 N73-25115
Daily tidal current tables for stations along Atlantic coast of North America - 1973
16 p1904 N73-25403
Mineral yearbook containing domestic industry data
[PB-214329/5] 16 p1905 N73-25411
Solar and geophysical data obtained by ionospheric sounding over India for April, 1972
[RRC-A202-PT-2] 16 p1907 N73-25423
Tables on solar and magnetic activity
[RRC-A210-PT-2] 16 p1907 N73-25424
Tables on solar and magnetic activity
[RRC-A203-PT-2] 16 p1907 N73-25425
Ionospheric sounding and cosmic ray neutron flux density tables, Dourbes, Belgium, Sep. 1972
16 p1907 N73-25428
Ionospheric sounding data from Monte Capellino Observatory, Italy, 1972
16 p1907 N73-25430
Geomagnetic field direction intensity hourly variations recorded at Roburent Observatory, Italy, for 1972
16 p1907 N73-25431

Synoptic weather maps and data tables on daily and monthly Northern Hemisphere stratospheric height and temperature
[QTSR-3] 17 p2056 N73-26626
Meteorological tables and charts on Berlin temperature
17 p2057 N73-26635
Meteorological parameter tables for Belgian weather stations, Mar. 1973
17 p2057 N73-26638
Tables on Antarctic cosmic ray measurements obtained during 1969
[NP-19680] 17 p2080 N73-26824
Tables on occulation of stars by moon
[PUBL-28] 17 p2081 N73-26835
Tables on harmonic coefficients of isostatic reduction potential U
[NASA-TM-X-66292] 18 p2145 N73-27334
Ionospheric sounding and cosmic ray neutron flux density tables, Dourbes, Belgium, Dec. 1972
18 p2146 N73-27342
Ionospheric sounding and cosmic ray neutron flux density tables, Dourbes, Belgium, Nov. 1972
18 p2146 N73-27343
Data tables and photographs of gaas epitaxial layer perfections as influenced by substrate disorientation
18 p2189 N73-27675
Galactic background maps of nonthermal radiation obtained from RAE mapping antenna data
[NASA-TM-X-66280] 18 p2196 N73-27728
Compilation of card-gap and projectile impact sensitivity data for wide variety of explosive compositions
[BM-IC-8605] 18 p2206 N73-27802
Tabulation of environmental tests on microelectronic devices
[AD-761951] 19 p2247 N73-28113
Tables of Greenwich time and latitude observations
19 p2293 N73-28437
Meteorological and ballistics data for launching of 13401 Honest John missile no. 2542, round no. 634 RMI
[AD-762157] 19 p2317 N73-28633
Tabular data from helicopter downdraft fog dispersal experiments
[AD-762189] 19 p2318 N73-28643
Yearbook of meteorological parameters measured for Denmark and Faroe Islands - 1968
20 p2449 N73-29683
Sulfur oxides, smoke, and air pollution tables from Belgian weather stations, Jul. 1972
20 p2449 N73-29686
Ionospheric sounding and cosmic ray neutron flux density tables, Dourbes, Belgium, Mar. 1973
21 p2539 N73-30354
Ionospheric sounding and cosmic ray neutron flux density tables, Dourbes, Belgium, Apr. 1973
21 p2539 N73-30355
Meteorological parameter tables for Belgian weather stations, May 1973
21 p2574 N73-30628
Automobile exhaust emission surveillance of light-duty vehicles
[PB-220755/3] 21 p2575 N73-30638
Tables on time and latitude observations made by Greenwich Time and Latitude service
22 p2664 N73-31345
Atmospheric radioactivity measurements for 1972 obtained at Vienna, Austria
[NP-19753] 24 p2922 N73-33339
Ionospheric sounding and cosmic ray neutron flux density tables, Dourbes, Belgium Jan. 1973
24 p2923 N73-33350
Ionospheric sounding and cosmic ray neutron flux density tables, Dourbes, Belgium, Feb. 1973
24 p2923 N73-33351
Geophysical data tables and graphs for Dourbes, Belgium
24 p2924 N73-33352
Sulfur oxides, smoke, and air pollution tables from Belgian weather stations, Aug. 1972
24 p2949 N73-33559
Falling sphere measurement data on atmospheric parameters
[WRE-TN-799[WR/D]] 24 p2958 N73-33639

**TACAN**
Performance tests of various Tacan ground station modifications designed to minimize false distance measuring equipment indications
[FAA-NA-72-65] 09 p1062 N73-18664
Feasibility of modifying Tacan/DME system to broadcast digital data for area navigation
[FAA-RD-73-2] 15 p1808 N73-24656
Computer program for selection of radio frequencies used in VOR, ILS, and Tacan/DME air navigation systems
[FAA-NA-73-4] 16 p1940 N73-25700
Flight tests of VHF Omnirange navigation and Tacan systems to determine bearing error curves
[FAA-RD-72-73] 20 p2452 N73-29710
Description of sector-Tacan and DME-supported instrument landing systems
[DGLR-73-019] 23 p2817 N73-32523

**TACHISTOSCOPES**
Tachistoscopic investigation on electronic and electromechanical cockpit display for performance comparison
[DLR-FB-73-27] 21 p2496 N73-30034

**TACHOMETERS**
Development of instantaneous reading tachometer for measuring electrocardiogram signal rate
[NASA-CASE-MFS-20418] 15 p1785 N73-24473

**TACTICAL AIR NAVIGATION**
U TACAN

**TACTICS**
Survivability and confidence assessment of military weapon systems with reference to tactics, threat, and environment
[AD-746061] 02 p0235 N73-11913
Helicopter flight performance in tactical environment
12 p1357 N73-21009
Operational performance of helicopters in French Army
12 p1357 N73-21011
Utilization of decision and value theory concepts by helicopter pilots to plan attacks
24 p2950 N73-33565

**TACTILE DISCRIMINATION**
Feasibility determination of cutaneous communication system for working divers
[AD-750268] 06 p0636 N73-15169
Electrocutaneous parameters for designing dynamic tactual communication system
12 p1373 N73-21135
Lipreading aid indicating voice/voiceless feature, using visual or tactile sense
14 p1626 N73-23179
Flight control system using tactile displays under instrument flying conditions
[AD-757344] 14 p1669 N73-23543
Angular resolution and target discrimination in pulsed search radar
[AD-759350] 17 p1999 N73-26162

**TACTILE SENSATION**
U TOUCH

**TAGGING**
U MARKING

**TAIL ASSEMBLIES**
Performance tests of twin jet afterbody configurations to determine effect of nozzle spacing, fairing shapes, and angle of attack
[NASA-TM-X-2724] 21 p2491 N73-29994

**TAIL MOUNTINGS**
U TAIL ASSEMBLIES

**TAIL PLANES**
U HORIZONTAL TAIL SURFACES

**TAIL SURFACES**
NT HORIZONTAL TAIL SURFACES
NT T TAIL SURFACES

**TAILLESS AIRCRAFT**
NT F-102 AIRCRAFT
NT F-106 AIRCRAFT
NT FD 2 AIRCRAFT
NT MIRAGE 3 AIRCRAFT
NT VULCAN AIRCRAFT

**TAILORING.**
U DESIGN

**TAILS [ASSEMBLIES]**
U TAIL ASSEMBLIES

**TAKEOFF**
NT VERTICAL TAKEOFF
Analysis of instrument system for assisting pilots in making decisions during aircraft takeoff and landing rolls
[FAA-RD-72-112] 03 p0301 N73-12460
Analysis of loading conditions imposed on commercial aircraft during turning maneuvers on ground
[NASA-TN-D-7132] 04 p0372 N73-13027
Measurement of critical atmospheric turbulence for aircraft takeoff and landing
[AD-750131] 06 p0694 N73-15660
Crash of DC-8 aircraft during takeoff from Anchorage International Airport, Alaska on 27 Nov. 1970
[NTSB-AAR-72-12] 07 p0737 N73-15999
Aircraft accident involving Beechcraft Queen Air aircraft on takeoff from Albuquerque, New Mexico airport on 19 May, 1972
[NTSB-AAR-72-32] 07 p0738 N73-16003
Analysis of internal flow conditions of inlet with centerbody retracted for short takeoff and landing aircraft takeoff and approach operations
[NASA-TN-D-7185] 09 p0980 N73-18010
Analysis of procedures and problems involved in operating helicopters from decks of ships
12 p1357 N73-21010
Aircraft accident involving attempted takeoff of Sabre Mark 5 aircraft at Sacramento, California airport on 24 Sept. 1972
[NTSB-AAR-73-6] 14 p1602 N73-22985
Methods for evaluating and predicting airfield performance of turbojet and turbofan aircraft operating in conventional and short takeoff modes
15 p1732 N73-24044
Development of methods for presenting aircraft performance data and comparison of specific methods to show sources of discrepancies
15 p1733 N73-24050
Numerical analysis of aircraft takeoff performance based on phases of takeoff and forces exerted on aircraft as basis for aircraft design
15 p1733 N73-24051
Development of perturbation guidance system for maintaining tilting rotor vertical takeoff aircraft on predetermined flight path during takeoff and landing
[NASA-CR-132043] 15 p1735 N73-24072
Aircraft accident involving Lear jet aircraft following takeoff from Atlanta, Georgia Airport on 26 Feb. 1973
[NTSB-AAR-73-12] 17 p1984 N73-26036
Ground based visual aid to alleviate spatial disorientation during takeoff and landing
[FAA-RD-73-26] 21 p2521 N73-30216
Noise reducing approach and takeoff profiles for short takeoff aircraft
[MBB-UH-06-73-O] 23 p2744 N73-31968

**TAKEOFF RUNS**
Development of computer program for complete simulation of factors involved in aircraft takeoff and landing
[AD-741942] 01 p0006 N73-10042
Effect of external air flowing across exhaust nozzles on jet noise produced by supersonic transport aircraft at high takeoff speeds
[NASA-TM-X-68161] 03 p0250 N73-12027
Analysis of velocity profiles in boundary layer produced by incompressible flow during takeoff
06 p0616 N73-15001
Aircraft accident involving Boeing 707 aircraft at San Francisco, California airport following rejected takeoff on 13 Sept. 1972
[NTSB-AAR-73-4] 12 p1363 N73-21062
Aerodynamic characteristics and aircraft performance of jet aircraft during takeoff run
[AD-764314] 22 p2615 N73-30959
Aircraft accident involving Boeing 707 aircraft following aborted takeoff at Kennedy International Airport, New York, on 13 August, 1972
[NTSB-AAR-73-7] 23 p2741 N73-31943

**TAKEOFF SYSTEMS**
U AIRCRAFT LAUNCHING DEVICES

**TALKING**
NT SYLLABLES
NT WORDS [LANGUAGE]

**TALON AIRCRAFT**
U T-38 AIRCRAFT

**TANDEM ROTOR HELICOPTERS**
NT CH-47 HELICOPTER
Single stage experimental evaluation of D and E stage design of tandem airfoil rotor and stator blading for compressors
[NASA-CR-121008] 04 p0463 N73-13779
Development of method for calculating downwash interference and longitudinal stability of tandem rotor helicopter
[ARC-R/M-3223] 15 p1729 N73-24022

**TANGENTS**
Integrated circuit tangnet function generator
[NASA-CASE-MSC-13907-1] 17 p2007 N73-26230

**TANKER SHIPS**
Problems and prospects for marine transportation of oil
[NASA-CR-133854] 21 p2553 N73-30464

**TANKS [CONTAINERS]**
NT CYLINDRICAL TANKS
NT FUEL TANKS
NT PROPELLANT TANKS
NT SPHERICAL TANKS
NT STORAGE TANKS
Convection and mixing of stratified fluids in rotating tank
[NASA-TR-R-392] 01 p0039 N73-10312
Tank design for forced circulation oil lubricating systems
[ESDU-68039] 02 p0177 N73-11429
Pressure loads and damping associated with rigid ring baffles in large cylindrical tanks
[NASA-TN-D-6870] 03 p0282 N73-12285
Design and development of device to prevent clogging in hoppers containing particulate materials
[NASA-CASE-LAR-10961-1] 03 p0306 N73-12496
Design, development, and tests of liquid diborane
[NASA-CR-130303] 06 p0676 N73-15502
Instruction manual for safe and efficient use of 200-pound diborane shipping container
[NASA-CR-131290] 11 p1296 N73-20519
Ship model basin for simulating aircraft vortex wake
[AD-758893] 16 p1890 N73-25291
Floating baffle for tank drain
[NASA-CASE-KSC-10639] 17 p2036 N73-26472
Simulated tank fragmentation test
[NASA-TM-X-68282] 20 p2482 N73-29942

**TANTALUM**
NT TANTALUM ISOTOPES
Analysis of oxidation of high purity tantalum single crystals and large-grained tantalum sheets
[AD-745341] 01 p0068 N73-10554

Evaluation of tantalum/316 stainless steel transition joints
[NASA-CR-121111] 07 p0804 N73-16519
Analysis of temperature-dependent neutron transmission and self-indication measurements on tantalum in unresolved region
[NASA-TN-D-7214] 09 p1066 N73-18678
Controlled nitrogen additions on mechanical properties of tantalum tubing in nuclear reactors
[NASA-TN-D-6999] 11 p1305 N73-20587
Measurement of work functions of oxygen-doped tantalum to determine applicability for use in plasma-mode thermionic converters
[NASA-CR-131837] 16 p1943 N73-25724
Guidelines for selection and application of three types of tantalum electrolytic capacitors for design of circuits in spacecraft components
[NASA-TM-X-64755] 17 p2003 N73-26200
Effect of oxygen on corrosion of niobium and tantalum by liquid lithium at 600 C
[ORNL-TM-4069] 17 p2045 N73-26547
Observation of oxide particles below apparent oxygen solubility limit in tantalum
[NASA-TM-X-2889] 21 p2558 N73-30509
Using average transmission and self-indication ratio measurements to investigate temperature dependence of resonance self-shielding effect in depleted uranium and tantalum
[NASA-TM-X-69565] 21 p2585 N73-30715
Tantalum surface bounding of helium discharge plasma considering resonant ion neutralization
[AD-753520] 22 p2706 N73-31670
Growth of potassium tantalate single crystals
[AD-764902] 23 p2828 N73-32603

**TANTALUM ALLOYS**
Influence of creep damage on low cycle thermal-mechanical fatigue behavior of two tantalum base alloys
[NASA-CR-121001] 04 p0431 N73-13514
Fused slurry silicide protective coatings for tantalum heat shielding
[NASA-CR-121022] 06 p0688 N73-15599
Development of advanced high strength tantalum alloys
[NASA-CR-120818] 07 p0809 N73-16562
Effect of metallurgical conditions on mechanical properties of ASTAR-811C sheet
[NASA-CR-121096] 08 p0931 N73-17625
Metallurgical evaluations of factors influencing ductility of aged T-111
[NASA-CR-120865] 09 p1047 N73-18540
Hydrogen embrittlement of tantalum alloy cladding for uranium mononitride nuclear fuel pins at high temperatures
[NASA-TM-X-2732] 09 p1063 N73-18675
Removal of lithium from 1040 C aged tantalum alloy by liquid ammonia and vacuum distillation techniques
[NASA-TM-X-2775] 11 p1305 N73-20590
Oxygen diffusion in gettered tantalum alloy heat pipes at startup
[NASA-TM-X-2793] 14 p1675 N73-23589
Modified filler metal composite for reducing or eliminating underbread cracking in multipass gas tungsten arc plate welds of T-111
[NASA-CR-121198] 19 p2304 N73-28530
Hydrogen embrittlement of aged tantalum and niobium alloys
[NASA-TM-X-68293] 20 p2431 N73-29525
Fused slurry silicide coatings for tantalum reentry heat shielding
[NASA-CR-120877] 20 p2485 N73-29964
Vacuum creep behavior of tantalum alloys and tungsten
[NASA-CR-134481] 22 p2684 N73-31496
Design and operation of tantalum alloy clad uranium mononitride irradiated fuel pins
[NASA-TM-X-2878] 22 p2698 N73-31614
Differential thermal technique for lining tantalum alloy tubing with tungsten
[NASA-TN-D-7426] 23 p2805 N73-32429
Compatability of tantalum alloys fuel capsules and [Pu-238]O2 fuels in radioisotopic thermoelectric generators
[LA-UR-73-764] 24 p2955 N73-33610

**TANTALUM COMPOUNDS**
NT TANTALUM OXIDES

**TANTALUM ISOTOPES**
Recoilless resonance photoabsorption by 6.2 keV transition in Ta-181, using W-181 in W and Ta foil sources
[NASA-TT-F-14680] 08 p0946 N73-17745

**TANTALUM OXIDES**
Electrical and thermal breakdown properties of tantalum oxide and hafnium oxides capacitors
22 p2641 N73-31168

**TAPE MERGING**
U DATA PROCESSING
U MAGNETIC TAPES

**TAPE RECORDERS**
Failure analysis of tape recorders for spacecraft applications
[NASA-SP-307] 06 p0643 N73-15225
Production of narrow-track video recording head to include characteristics of recording tape and tetrode sputtering equipment
[NHK-LABS-NOTE-154] 07 p0754 N73-16124
Video tape recorder with scan conversion playback for color television signals
[NASA-CASE-NPO-10166-1] 13 p1490 N73-22076
Video bandwith tape recorder for ERTS A imagery
18 p2209 N73-27833
Specifications of portable magnetic video tape recorder for television signal reproduction
[JPRS-59611] 19 p2235 N73-28021

**TAPERED WINGS**
U SWEPT WINGS

**TAPES**
Diffusion bonding of plasma sprayed boron reinforced magnesium monolayer tapes by hot pressing
[SC-DR-72-0677] 10 p1166 N73-19488
Evaluation of Puller tapes applied to military use
[AD-754925] 11 p1353 N73-20987

**TARE (DATA REDUCTION)**
U DATA REDUCTION

**TARGET ACQUISITION**
Measuring electromagnetic parameters of soil samples in VHF/UHF range to determine properties that limit target detection
[AD-747346] 03 p0299 N73-12439
Subjective tests of target acquisition time using television with image enhancement possibilities
[MBB-UFE-892-72-O] 06 p0636 N73-15165
Characteristics and operation of videocoherent system for improved target acquisition and measurement of target velocity
07 p0755 N73-16133
Comparison of monochrome and color film for air to ground target acquisition
[RAE-TR-72064] 07 p0801 N73-16504
AGARD conference on air-to-ground target acquisition
[AGARD-CP-100] 10 p1225 N73-19959
Application of extra-foveal vision to predicting target acquisition in air-to-ground search
10 p1225 N73-19960
Modelling prediction of probability of acquiring designated target as function of its range as target is approached
10 p1225 N73-19962
Calculation and simulation of effects of complex search situations
10 p1225 N73-19963
Relationship between subjective effect of structured target backgrounds on acquisition performance
10 p1226 N73-19964
Peripheral acuity with complex stimuli at two viewing distances
10 p1226 N73-19965
Model for inherent contrast conditions in full-form objects
10 p1226 N73-19966
Air-to-ground visibility of lights at low background levels
10 p1226 N73-19967
Air-to-ground target acquisition with flare illumination
10 p1226 N73-19968
Biomedical problems with helmet mounted sight and visual target acquisition system
10 p1226 N73-19969
Application of night vision technology helicopter night scouts
10 p1226 N73-19970
Probability of acquiring targets by search aircraft which flies along enemy line of communication
10 p1226 N73-19971
Effect of briefing information on target acquisition performance of observer
10 p1227 N73-19972
Use of Kelly Repertory Grid Techniques for assessing subjective estimates of important parameters for target acquisition
10 p1227 N73-19973
Use of psychometric tests to account for subjective variations in operations performance relative to target acquisition
10 p1227 N73-19974
Ability of aircraft pilot to visually acquire and recognize two and three dimensional targets during diving approach
[AD-754743] 11 p1268 N73-20294
Calibration of missile infrared track and acquisition system
[AD-754944] 11 p1295 N73-20507
Instrumentation for Nike-Ajax radar to perform real time cross section measurements on airborne targets
[AD-756538] 13 p1493 N73-22103
Calibration of target acquisition system using infrared tracking
[AD-756845] 13 p1595 N73-22937
Development of electronic detection system for remotely determining number and movement of enemy personnel
[NASA-CASE-ARC-10097-2] 16 p1873 N73-25160
Discriminatory analysis of waveform data for pattern recognition in radar targets
[AD-757564] 16 p1876 N73-25189
Time domain acoustic signal processor for automatic pattern recognition and target discrimination
[AD-757538] 16 p1876 N73-25190
Angular resolution and target discrimination in pulsed search radar
[AD-759350] 17 p1999 N73-26162
Angular position of target determined by scanning radar against background of correlated noise
22 p2628 N73-31057
Target acquisition model for gun launched guided projectiles
[AD-763909] 22 p2676 N73-31432
Feasibility of using gravity measuring techniques as unattended sensors for detection and classification of military targets
[AD-763889] 22 p2738 N73-31922

**TARGET PENETRATION**
U TERMINAL BALLISTICS

**TARGET RECOGNITION**
Literature review on psychophysiological factors affecting visual perception of colored signal light
[AD-746297] 02 p0133 N73-11083
Human recognition of contrasting target in noisy environment with diversion of attention
[FOA-2-C-2482-H5] 02 p0135 N73-11092
Computerized radar target return data processing and identification system
[AD-746323] 02 p0142 N73-11148
Microwave radiometer technique for detecting and identifying man-made objects and discriminating them from natural objects
[DREO-R-661] 04 p0449 N73-13669
Influence of target motion and wave time variation of underwater acoustic signal transmission
[AD-748651] 04 p0450 N73-13678
Decision making behavior of sonar operator in target detection and reporting
[AD-750761] 06 p0637 N73-15174
Development of evaluation method for determining effectiveness of data compression techniques for radar landmass simulation
[AD-750695] 06 p0642 N73-15214
Partial wave analysis solutions for acoustic scattering patterns and target recognition in antisubmarine warfare
[AD-750754] 06 p0700 N73-15710
Evaluation of device to train forward air controllers to communicate target locations
[AD-751292] 07 p0751 N73-16103
Effects of quantized luminance levels and display contrast on sonar target recognition
[AD-751711] 07 p0757 N73-16148
Target recognition by considering space-time functions in radar echoes
[REPT-1-72] 09 p1003 N73-18184
Relationship between subjective effect of structured target backgrounds on acquisition performance
10 p1226 N73-19964
Strip photography used in simulation study of very low altitude detection of small stationary targets at very slow speeds
[AD-754928] 11 p1250 N73-20146
Optimization of radar acquisition of moving targets by blind speed zone eliminations
[AD-753963] 11 p1256 N73-20195
Ability of aircraft pilot to visually acquire and recognize two and three dimensional targets during diving approach
[AD-754743] 11 p1268 N73-20294
Underwater devices for target detection on sea bottom
[JPRS-58916] 14 p1667 N73-23529
Characterization of interaction between detection and visibility processes with application to search policies
15 p1743 N73-24130
Limitations on pilot visual perception of target from low flying aircraft
[AD-759651] 16 p1869 N73-25136
Operator performance in interpreting side-looking airborne radar real-time imagery
[AD-759495] 16 p1878 N73-25204
Vision model for robot object recognition system
[NASA-CR-133458] 19 p2224 N73-27936
Training program for improving performance of operators in locating targets in side-looking airborne radar
[AD-762342] 19 p2229 N73-27979
Data analysis, feature extraction, and pattern recognition for automatic target classification
[AD-763493] 21 p2550 N73-30469
Low angle tracking and recognition using self focusing radar antenna
[AD-764052] 22 p2635 N73-31118
Identification of radar targets by pattern recognition
[AD-764713] 23 p2759 N73-32088
Optimization of human performance in system design, training, and operation
[AD-764761] 24 p2890 N73-33075

**TARGET SIMULATORS**
Interface evaluation of digital simulation facility with system support facility for radar beacon target source for air traffic control
[FAA-NA-73-33] 17 p2009 N73-26240

**TARGETS**
NT PARTICLE ACCELERATOR TARGETS

NT RADAR TARGETS
Bistatic target areas of three simple targets for seven bistatic angles
[FOA-3-C-3676-E1] 02 p0172 N73-11393
SAL storage for AN/UPA-59/60 IFF (identification friend or foe) decoders for displaying aircraft targets
[AD-746445] 02 p0208 N73-11685
Target design for cyclotron irradiation using iodine nucleus
[NASA-TM-X-68156] 02 p0214 N73-11733
Establishment of radiometric calibration technique to permit absolute reflectance characteristics of ground targets to be determined from ERTS-1 data
[E72-10255] 03 p0290 N73-12355
Psychophysical functions of range and time estimates by ground and aerial observers
[AD-747271] 04 p0380 N73-13094
Vacuum alteration for jet targets from condensed hydrogen, while operating on accelerator internal beam
[JINR-P13-6324] 04 p0402 N73-13275
Radiometric calibration technique to permit absolute reflectance characteristics of ground targets to be determined from ERTS-1 data
[E72-10326] 05 p0530 N73-14314
Measurement of signal strength variations in beam currents of vidicon targets
[DRIC-TRANS-2965] 06 p0645 N73-15238
Rotating target providing high yield neutrons by He-4 reaction for cancer therapy
[NASA-TM-X-68179] 07 p0746 N73-16067
Radiometric calibration technique to permit absolute reflectance characteristics of ground targets to be determined from ERTS-1 imagery
[E73-10349] 11 p1274 N73-20343
Digital computer model to predict spectral irradiance on ground target from sun and sky
[AD-758877] 16 p1945 N73-25739
Improved electron optics and target for pattern threshold recognition device
[AD-762164] 19 p2247 N73-28117
Image maps of point targets applied to hard limited, synthetic aperture radar application
[AD-763660] 23 p2788 N73-32306
TASK COMPLEXITY
Human performance in sequential task training for acquisition of perceptual motor skills under flight stress
10 p1123 N73-19153
Pilot performance under certain hypnotic, tranquilizer, and barbiturate type drugs
12 p1369 N73-21110
Effects of fatigue, age, and degree of difficulty on eye-hand coordination performance
24 p2887 N73-33051
TASK SEQUENCERS
U CONTROL EQUIPMENT
U SEQUENTIAL CONTROL
TASKS
NT AUDITORY TASKS
NT VISUAL TASKS
Model for awarding hazardous pay to employees
08 p0876 N73-17095
Combat job performance and training for air cavalry aeroscout pilot and aeroscout observer
[AD-755505] 23 p2753 N73-32027
TAURID METEOROIDS
Mass spectrometer identification of positive metal ions in Comet Encke beta Taurids meteor shower
[NASA-TM-X-66084] 02 p0229 N73-11855
TAXIING
Analysis of loading conditions imposed on commercial aircraft during turning maneuvers on ground
[NASA-TN-D-7132] 04 p0372 N73-13027
Active control in landing gear of aircraft for reducing fatigue damage from ground induced vibration during taxiing
[AD-750137] 06 p0678 N73-15515
Application of power spectral density method to analyze vibrations induced in aircraft during taxiing
[AD-757283] 14 p1602 N73-22991
Root mean square center of gravity accelerations and undercarriage forces for taxiing KC-135 tanker aircraft
[CRANFIELD-AERO-15] 16 p1859 N73-25060
Performance of aircraft taxiing on dirt surfaces
[AD-756588] 16 p1861 N73-25077
TAXONOMY
Chemiotaxionomic survey of carotenoid pigments in several species and groups of Basidiomycetes
[NASA-TT-F-14858] 11 p1246 N73-20117
Taxonomic identification and natural resource inventory using ERTS-1 data
[E73-10666] 16 p1899 N73-25361
Field sampling taxonomic units within geomorphic-soil-vegetation mapping units in Arizona
[E73-10889] 20 p2394 N73-29238
TAYLOR INSTABILITY
Sphere free motion in rotating fluid noting Taylor instability existence
[DLR-FB-71-32] 03 p0285 N73-12309
Nonoscillatory characteristics of Taylor vortices occurring in Couette flows based on evolution of eigenvalues and analytic continuation - Part 3
[AD-754480] 12 p1392 N73-21289
TAYLOR SERIES
Programming implementation of Taylor series method for numerical solution of ordinary differential equations
[NASA-TM-X-70438] 21 p2566 N73-30567
TAYLOR THEOREM
U TAYLOR SERIES
TD SATELLITES
NT TD-1 SATELLITE
TD-1 SATELLITE
TD-1A satellite ground checkout stations noting spacecraft communication and data transmission
[ESRO-TM-140-ESTEC] 04 p0402 N73-13277
TD-1A telescope optical surface chemical contamination investigation of thermal vacuum tests and volatile condensable material screening
[ESRO-TN-86-ESTEC] 21 p2601 N73-30847
TDR SATELLITES
One way and two way VHF ranging system performance for tracking and data relay applications
[NASA-TM-X-66134] 05 p0596 N73-14843
Multimode transponders for tracking and data relay satellites
[NASA-CR-130170] 08 p0888 N73-17191
Propagation path simulator for channel between Tracking and Data Relay Satellite and user spacecraft
[NASA-CR-130173] 11 p1255 N73-20185
Development of Tracking and Data Relay Satellite system concept for service of low, medium, and high data rate user spacecraft - Vol. 1
[NASA-CR-130219] 13 p1579 N73-22799
Configuration data and design development for Delta 2914 launched Tracking and Data Relay Satellite system - Vol. 2
[NASA-CR-130220] 13 p1579 N73-22800
Data and design information for Atlas Centaur launched configuration of Tracking and Data Relay Satellite system - Vol. 3
[NASA-CR-130221] 13 p1579 N73-22801
Configuration data and design information for space shuttle launch of Tracking and Data Relay Satellite System - Vol. 4
[NASA-CR-130222] 13 p1580 N73-22802
Design, development, and characteristics of Tracking and Data Relay Satellite System - Vol. 1
[NASA-CR-130216] 13 p1582 N73-22820
Design and development of telecommunications equipment for use with Tracking and Data Relay Satellite System - Vol. 2
[NASA-CR-130217] 13 p1582 N73-22821
Design, development, and characteristics of spacecraft systems and equipment used with Tracking and Data Relay Satellite System - Vol. 3
[NASA-CR-130218] 13 p1582 N73-22822
Adaptive phased antenna array simulation for optimal design of tracking data relay satellite very high frequency beam
18 p2210 N73-27841
TEA LASERS
U CARBON DIOXIDE LASERS
Construction of carbon dioxide transversely excited atmospheric laser and application to absorption studies of laser induced plasmas
[AD-745842] 01 p0066 N73-10542
Plasma parameters in carbon dioxide laser discharge
[DREV-TN-2025/72] 02 p0181 N73-11464
Design and performance of carbon dioxide laser amplifier with double discharge electrode geometry
[DREV-TN-2022/72] 10 p1134 N73-19240
Computerized simulation of parallel plate pulsed transversely excited atmospheric pressure laser
[DREV-TN-2054/72] 10 p1168 N73-19503
Characteristics of carbon dioxide laser for use as interferometric and light scattering plasma diagnostic radiation source
[LRP-54/72] 10 p1168 N73-19504
Ultrashort pulse generation from mode locked carbon dioxide laser by resonant acoustic loss modulator
[DREV-TN-2024/72] 11 p1302 N73-20566
Dynamic processes for laser emission in pulsed pumping of transversely excited atmospheric carbon dioxide laser
[DREV-TN-2036/73] 23 p2800 N73-32396
TEACHING
U EDUCATION
TEACHING MACHINES
Design of interactive program to teach accounting techniques
[NASA-CR-129674] 04 p0393 N73-13192
Aids for speech perception and speech training
14 p1626 N73-23176
TEARING
Energy-absorbing efficiency of ply-tear webbings and discussion of warp and weft count and binder property effects
[RAE-TR-72051] 01 p0113 N73-10936
Dynamic tear tests for determining fracture resistance properties of aluminum alloys
[AD-755436] 12 p1415 N73-21465
TECHNICAL WRITING
Analysis of technical documents and literature for conducting manned space flight nuclear system safety study - Vol. 7 Pt. 1
[NASA-CR-123850] 02 p0210 N73-11704
Compilation of technical reports prepared by Aerospace Laboratories of US Air Force for calendar year 1971
[AD-746707] 04 p0487 N73-13974
Tabulation of research reports published in German technical document series during calendar year 1972
[DLR-MITT-73-01] 11 p1352 N73-20971
Cumulative bibliography of research and development projects conducted on heat pipe technology and applications
[NASA-CR-135953] 24 p2991 N73-33900
TECHNIQUES
U METHODOLOGY
TECHNOLOGICAL FORECASTING
Urgent problems connected with contemporary scientific and technological revolution
[AD-751509] 09 p1102 N73-18992
Review and analysis of air carrier/reliever airport grant allocations and technological forecast of airport demands
[FAA-AV-72-4] 17 p2010 N73-26253
Technology planning objectives and supporting technical goals for Air Force Flight Dynamics Laboratory during Fiscal Year 1974
[AD-762300] 19 p2356 N73-28950
TECHNOLOGIES
NT BIOTECHNOLOGY
NT MARINE TECHNOLOGY
NT MILITARY TECHNOLOGY
NT REACTOR TECHNOLOGY
Abstracts of Research and Technology Operating Plans used for management review and control of research for NASA programs
[NASA-TM-X-68856] 03 p0366 N73-12978
Bibliography of economic impact of stimulated aerospace technology activity
[NASA-CR-129515] 03 p0366 N73-12981
Relationship between law and scientific and technical progress in socialist systems
[JPRS-57318] 03 p0367 N73-12992
Abstracts on theory, design, and applications of analog and digital computers and digital control systems
[JPRS-57529] 04 p0392 N73-13189
Soviet interest in West German technological advances in welding techniques
[AD-747834] 04 p0427 N73-13480
Manual of chemical processes related to spacecraft development technology
[NASA-TM-X-2635] 05 p0506 N73-14117
Overview of scientific and technological research in Yugoslavia on NBS grants, 1971 - 1972
[NBS-TN-753] 08 p0976 N73-17979
Accounts of scientific and technological cooperation in Eastern Europe
[JPRS-58053] 08 p0977 N73-17990
Management and organization in aerospace science and technology research
11 p1350 N73-20955
History of German aeronautical development during the first half of the century
11 p1350 N73-20956
Electromagnetic technology for radar, air traffic control, and communication systems
[AD-756482] 13 p1493 N73-22107
Bibliography on welding by electron beam, ultrasonic radiation, laser beam, and friction
[ORNL-TM-4133] 17 p2038 N73-26486
General problems with psychology in scientific and technical creativity
[TT-70-57147-1] 21 p2502 N73-30074
Orbital docking technology for spacecraft
[NASA-TT-F-15105] 22 p2716 N73-31741
TECHNOLOGY ASSESSMENT
Survey of nondestructive technology
[NASA-CR-129245] 03 p0305 N73-12491
Role of law in technology assessment
[NASA-CR-129270] 03 p0367 N73-12987
Technology of aircraft construction
[AD-748712] 04 p0374 N73-13043
Influence of space technology on man and his environment
04 p0472 N73-13847
French space programs and benefits to mankind
04 p0474 N73-13874
Advanced technology relative to chemical upper stages
[NASA-CR-129587] 04 p0477 N73-13903
Alternatives in complement and structure of NASA teleprocessing resources for years 1975 through 1985 including options of minicomputers, mass storage devices, and software development
[NASA-CR-129825] 05 p0515 N73-14188
Evaluation of scientific and technical experiments for space missions
05 p0610 N73-14963
Theoretical procedure for estimating social benefits of remote sensing
[NASA-CR-130027] 07 p0857 N73-16947
Congressional assessment of governmental role in industrial and social aspects of aerospace and related technology
11 p1292 N73-20482

Solar array development discussing manufacturing, design qualification tests in aerospace environments, and comparison between fold-up and roll-up types
[RAE-TR-72109] 13 p1476 N73-21959
Assessment of technology for environmental impact studies
[AD-754458] 13 p1527 N73-22376
Process of planning, programming, and evaluating technological projects within federal agencies
[NASA-CR-131846] 13 p1596 N73-22939
Techniques of technology assessment in federal agencies
[NASA-CR-131848] 13 p1596 N73-22940
Mission and responsibilities of federal agencies in technology assessment
[NASA-CR-131847] 13 p159[illegible] N73-22941
Present technology and prospects for creation of national communications television broadcast network in USSR during 1971 - 1975
[JPRS-58928] 14 p1637 N73-23273
Congressional hearings on aeronautics and space technology
14 p1721 N73-23967
Sortie Lab system evaluation, future growth, and IR astronomy experiment accommdation
[ESS/SS-399-VOL-3] 17 p2089 N73-26904
Potential applications of high pressure technology
[AD-760714] 18 p2191 N73-27686
Technology assessment of fog modification
[AD-762207] 19 p2316 N73-28631
Indicators for describing state of science-in US for setting priorities in allocating resources
[NSB73-1] 19 p2354 N73-28939
Social and technological impact of STOL aircraft potential
[NASA-CR-133356] 19 p2355 N73-28942
Assessment of technological readiness for coated columbium thermal projection systems
[NASA-TM-X-2858] 20 p2431 N73-29530
Space station solar array technology evaluation program
[MSC-07163] 21 p2499 N73-30057
Assessment of US and USSR technology and instrumentation for obtaining, transmitting, and processing earth images from space
21 p2534 N73-30318
Fabrication techniques for lithium-doped silicon solar cells
[AD-764357] 22 p2618 N73-30982
Articles concerning development of scientific disciplines and technical fields in Eastern Europe
[JPRS-60063] 23 p2865 N73-32904
Delphi forecasts of utilization and social impacts of large-scale educational telecommunications technology
[NASA-CR-135477] 23 p2866 N73-32909
Scope of technology assessment
[NASA-CR-135783] 23 p2866 N73-32913
Implications of technology assessment function for effective public decision making process
[NASA-CR-135782] 23 p2866 N73-32914
Meteorological satellite technology and operation
[PUBL-SER-B-70] 24 p2949 N73-33558

**TECHNOLOGY TRANSFER**

Proceedings of conference on benefits of space exploration conducted at Huntsville, Alabama Nov. 1971
[NASA-SP-313] 04 p0470 N73-13829
Impact of space shuttle operations on national economy, technological superiority, and development of future space activities
04 p0470 N73-13832
Use of space technology to solve medical problems and improve medical equipment
04 p0472 N73-13848
Aerospace technology for solving domestic solid waste disposal, water purification, and water recovery problems
04 p0472 N73-13849
Space technology for developing ground based integrated medical laboratory
04 p0472 N73-13851
Revolutionization of communications by satellite systems
04 p0472 N73-13854
Influence of space technology and exploration on earthbound human problems
04 p0473 N73-13859
Analysis of factors involved in transfer of technology from Department of Defense developments to solution of problems in civilian community
[B-175132] 04 p0488 N73-13994
Advanced NASA and DOD technology management techniques, and application to NATO programs for defense and civil needs
06 p0732 N73-15968
Technology transfer in nondestructive testing and visual displays
[NASA-CR-130302] 07 p0856 N73-16941
Technology transfer of biomedical data for use in research of cardiovascular diseases
[NASA-CR-131246] 11 p1238 N73-20053
NASA contributions to patient monitoring
[NASA-CR-131538] 12 p1373 N73-21138
Technical development and future use of materials in aerospace systems
[AD-755371] 12 p1415 N73-21466
Technical compilation on adhesives and polymeric plastics
[NASA-SP-5961[01]] 14 p1680 N73-23630
Congressional hearings on NASA technology applications program budget
14 p1721 N73-23966
Pilot program for transfer of aerospace technology to city management
[NASA-CR-131918] 14 p1724 N73-23992
Use of aerospace technology to solve earth based problems
[NASA-CR-132148] 15 p1846 N73-24961
Role of NASA programs and technologies in developing better communication links among people
[NASA-CR-133052] 16 p1876 N73-25183
Development of remote sensing activities in countries with limited resources
[PB-214861/7] 16 p1909 N73-25446
Technology transfer and information dissemination services provided by Technology Use Studies Center
[NASA-CR-132963] 16 p1977 N73-25991
Application of high power electron tube technology to cylindrical electron gun design
[AD-760047] 17 p2006 N73-26226
Technology transfer activities of NC/STRC
[NASA-CR-133301] 18 p2214 N73-27874
Transfer of technology developed for aerospace program to specific industrial problems of developing nation [Korea]
[NASA-CR-133358] 19 p2355 N73-28943
Medically related NASA technology applications and transfer activities
[NASA-CR-135527] 22 p2621 N73-31001
Research activities for technology transfer and impact studies
[NASA-CR-135720] 23 p2859 N73-32847
Technical consulting services for earth resources program
[NASA-CR-135793] 24 p2921 N73-33330

**TECHNOLOGY UTILIZATION**

Impact of technological development on airborne data acquisition system and ground data processing station
01 p0056 N73-10457
Research in applications of radar and radio techniques to astronomy and space programs
[NASA-CR-129167] 02 p0226 N73-11829
Transfer of unemployed aerospace professionals to small businesses
[NASA-CR-129504] 03 p0366 N73-12979
Measurement of research and development and technological progress impact on national economic growth - Part 1
[NASA-CR-129502] 03 p0366 N73-12980
Congressional hearing to establish national science policy and priorities act of 1972
03 p0367 N73-12991
Applications of aerospace technology to biomedical research
[NASA-CR-129588] 04 p0378 N73-13071
Proceedings of conference on benefits of space exploration conducted at Huntsville, Alabama Nov. 1971
[NASA-SP-313] 04 p0470 N73-13829
Application of unmanned spacecraft for research purposes to show benefits from Communication and Navigation satellites and Earth Observation satellites
04 p0470 N73-13830
Impact of space program on efforts to improve standards of living and to reduce harmful pollution of environment
04 p0471 N73-13836
Influence of space technology on man and his environment
04 p0472 N73-13847
Utilization of space technology to supply earth demands for thermal and electric energy
04 p0473 N73-13864
Workshop for educating public to space benefits in education
04 p0474 N73-13867
Advances in educational communication and meteorology as derived from satellite technology
04 p0474 N73-13869
Use of space exploration and benefits to procure world peace
04 p0474 N73-13872
New knowledge gain from crew life support aspect of manned space program and applicability to earth-based problems
[NASA-CR-129514] 04 p0486 N73-13970
Federal policy for support and use of technology
[NASA-CR-129669] 04 p0488 N73-13987
Analysis of technology requirements for expendable second stage of space shuttle booster system - Vol. 10
[NASA-CR-128665] 05 p0600 N73-14876
Chemical processing industries and utilization of NASA technology - conference
[NASA-CR-129827] 05 p0607 N73-14937
Technology utilization in biomedical areas for November 1972
[NASA-CR-129998] 06 p0632 N73-15135
Technical and economical factors of satellite television reception
[NASA-TT-F-14659] 06 p0640 N73-15196
Legal liabilities and impact of satellite meteorology on agricultural crops and economics
[NASA-CR-129994] 06 p0692 N73-15636
Comprehension and use of weather forecasts by Wisconsin agricultural groups
06 p0692 N73-15639
Applications of aerospace technology in biology and medicine
[NASA-CR-130544] 08 p0871 N73-17047
Applications of visual display systems developed by aerospace technology
[NASA-CR-130634] 08 p0924 N73-17566
Growth and characterization of crystals and metallic whiskers in zero gravity environment during Skylab and Apollo flights
[NASA-CR-124065] 08 p0950 N73-17778
Survey of patents resulting from aeronautical and space research supported by NASA
08 p0976 N73-17984
Armed Forces science conference report with list of principle authors
[AD-750326] 08 p0977 N73-17992
Armed Forces science conference report with list of principle authors
[AD-750360] 08 p0977 N73-17993
Selected technical spin-offs from space program
[NASA-TM-X-68943] 08 p0977 N73-17994
Utilization of aerospace technology in biomedical field - Southwest Research Institute report for Jan. 1973
[NASA-CR-130984] 09 p0992 N73-18097
Studies of biomedical applications of NASA technology
[NASA-CR-130809] 09 p0997 N73-18135
Technology application team program
[NASA-CR-130990] 09 p1100 N73-18979
Scientific and technological applications of rare earth materials
[IS-2965] 10 p1166 N73-19484
Management of technological progress and effects on society
11 p1351 N73-20966
Research management for technical applications
11 p1351 N73-20967
Impact of technological progress on economic development
[NASA-CR-131289] 11 p1352 N73-20977
Technical utilization of advanced equipment for oceanological exploitation by US
[JPRS-58696] 12 p1401 N73-21363
Technical development and future use of materials in aerospace systems
[AD-755371] 12 p1415 N73-21466
Analysis of NASA programs for 1970 to 1980 period with application to earth orbital experiment program and requirements - Vol. 1
[NASA-CR-112325] 13 p1577 N73-22778
Definition of supporting technology development requirements for earth orbital experiment program and requirements study - Vol. 7
[NASA-CR-112331] 13 p1577 N73-22784
Research and developments in technology utilization program
[NASA-CR-131568] 13 p1593 N73-22914
Congressional study of future governmental role in scientific and technological research and development
13 p1594 N73-22927
Application of flat conductor technology to surface mounted housewiring
14 p1642 N73-23314
Technical compilation on adhesives and polymeric plastics
[NASA-SP-5961[01]] 14 p1680 N73-23630
Cosmization of Soviet economy
[NASA-TT-F-13958] 14 p1705 N73-23839
Evolutionary, gradual, and step-wise spacecraft systems technology development of interim space station program
[NASA-TM-X-69243] 14 p1706 N73-23845
Use of aerospace technology to solve earth based problems
[NASA-CR-132148] 15 p1846 N73-24961
Development of remote sensing activities in countries with limited resources
[PB-214861/7] 16 p1909 N73-25446
Advanced technology for improving performance parameters of ruby laser
16 p1921 N73-25542
Technology utilization program relating to hydrogen effects on metal alloys and mechanical properties of recently developed alloys
[NASA-SP-5940[03]] 16 p1928 N73-25598
Effects of techno-economic and organizational factors on adoption of NASA innovations by commercial firms in US
16 p1975 N73-25975
Government-owned patent survey for technology utilization in commercial enterprises
16 p1976 N73-25981
Space shuttle related technology development and utilization
[NASA-CR-124260] 16 p1977 N73-25988

Role of NASA in accident prevention
[NASA-CR-133051] 16 p1977 N73-25989
Applications of aerospace technology in biology and medicine
[NASA-CR-133226] 17 p1988 N73-26067
Chemical machining of steels, iron, nickel, cobalt, copper, and light alloys
18 p2161 N73-27454
Conference on technology utilization in spacecraft guidance, ground operations, communications and navigation systems, and sensor development
[NASA-SP-326] 18 p2207 N73-27816
Technology transfer activities of NC/STRC
[NASA-CR-133301] 18 p2214 N73-27874
Identification of feasible and practical applications of space teleoperator technology for problems of handicapped
[NASA-CR-133357] 19 p2225 N73-27949
Principles and applications of nondestructive tests
[NASA-SP-5113] 19 p2303 N73-28517
Application of space program fire retardant technology to housing
[NASA-TN-D-7370] 19 p2312 N73-28592
Abstracts of 1972 NASA Tech Briefs
[NASA-SP-5021[13]] 19 p2355 N73-28941
Air Force research and technology accomplishments during calendar year 1971
[AD-762269] 19 p2357 N73-28967
Application of aerospace medicine research in science and technology
[JPRS-59803] 20 p2368 N73-29040
Industrial applications of cryogenic technology
[AD-762315] 20 p2455 N73-29728
Technologies for production and utilization of petroleum, natural gas, oil shale and coal
[BM-IC-8612] 21 p2536 N73-30335
Application of NASA management techniques to problems of community violence
[NASA-CR-133830] 21 p2609 N73-30915
United States cooperation with the USSR and Japan in science and technology
22 p2737 N73-31917
NASA bioinstrumentation list for public utilization
[NASA-SP-5958[01]] 23 p2750 N73-32007
Improving air transportation to low density population regions
[NASA-CR-114484] 23 p2865 N73-32905
Utilization of extra-atmospheric space
[NASA-TT-F-15118] 24 p2980 N73-33818
Industrial utilization of NASA generated aerospace technology
[NASA-TM-X-71435] 24 p2994 N73-33923
Congressional hearings on Federal policy, plans, and organization for support and utilization of science and technology
24 p2994 N73-33924

**TECTONIC MOVEMENT**
U TECTONICS

**TECTONICS**
Geologic structure of Ontong Java Plateau determined from continuous reflection profiles taken between 1966 and 1971
[AD-743899] 01 p0052 N73-10425
Detection of regional tectonic structures and mineral exploration in Arizona using ERTS-1 imagery
[E72-10218] 02 p0162 N73-11312
Geomorphology, tectonics, and structural relations between Alps and Pyrenees based on ERTS-1 imagery
[E72-10286] 04 p0410 N73-13336
Tectonic analysis of Bighorn Mountains using ERTS-1 imagery
[E72-10310] 04 p0412 N73-13359
Tectonic analysis of Southwestern Wyoming from ERTS-1 imagery
[E72-10337] 05 p0532 N73-14325
Determination of paleotectonic principal stress orientation and spacings of joints in outcrops, and development of optical diffraction analysis method
[BM-RI-7706] 06 p0665 N73-15409
Tectonic analysis of Bighorn Mountains using ERTS-1 imagery
[E73-10036] 08 p0900 N73-17288
Tectonic and paleogeologic mapping of Montana using ERTS-1 imagery
[E73-10280] 08 p0914 N73-17488
Regional geologic, tectonic, and volcanic surveys of Bolivia using ERTS-1 imagery
[E73-10286] 08 p0914 N73-17492
Identification and interpretation of tectonic features of Colorado, California, and Sonora, Mexico
[E73-10275] 09 p1020 N73-18324
Vegetation analysis and preparation of tectonic map overlay of Bighorn Mountains region based on ERTS-1 data
[E73-10420] 11 p1279 N73-20382
Identification and interpretation of tectonic features and mercury deposited in California coast ranges and western transverse ranges
[E73-10446] 11 p1282 N73-20406
Utilization of ERTS-1 imagery for tectonic analysis and geological mapping of Bighorn Mountains
[E73-10583] 14 p1657 N73-23443
Detection of regional tectonic structures related to mineralization in Arizona
[E73-10591] 14 p1657 N73-23450
Tectonic and structural mapping in Alaska using ERTS-1 imagery
[E73-10685] 16 p1901 N73-25379
ERTS-1 imagery of Bighorn-Pryor mountains of Wyoming and Montana applied to analysis of regional tectonic relationships
[E73-10704] 16 p1903 N73-25395
Application of ERTS-1 imagery for tectonic analysis of Bighorn Mountains region and effect of snow cover and low sun angle on identifying topographical features
[E73-10722] 17 p2019 N73-26329
Mathematical procedure for calculating tectonic plate movement and the secular shift of the mean pole
[NASA-TM-X-66272] 17 p2024 N73-26376
Evolution of earth and moon tectonic elements
[NASA-TT-F-14947] 17 p2083 N73-26848
Application of ERTS-1 MSS imagery to study of tectonics and crustal structure of area from eastern Sierra Nevada to Colorado Plateau
[E73-10774] 18 p2135 N73-27250
EREP 463 imagery of fault tectonics and earthquake hazards in peninsular ranges of southern California
[E73-10781] 18 p2136 N73-27257
Skylab and EREP remote sensing data for tectonic analysis of Bighorn Mountains of Wyoming and Montana
[E73-10784] 18 p2136 N73-27260
Structural framework of Sunda Shelf and vicinity
[PB-218671/6] 18 p2146 N73-27346
Application of ERTS-1 imagery to identify, locate, and map faults showing geomorphic evidence of geologically recent breakage in Southern California
[PAPER-G22] 19 p2266 N73-28253
ERTS-1 imagery of western portion of Nicaragua following December 1972 earthquake to determine lineaments of fault systems related to earthquake
[PAPER-G24] 19 p2266 N73-28255
ERTS-1 imagery applied to definition of geotectonic domains of southern African crystalline shield
[PAPER-G26] 19 p2267 N73-28257
Analysis of tectonic situation in Alps and Apennine mountains using ERTS-1 imagery of previously inaccessible areas
[PAPER-G27] 19 p2267 N73-28258
Assessment of ERTS-1 imagery for mapping geologic features of Gaspe Peninsula, Quebec and determination of lithologic lineaments
[PAPER-G28] 19 p2267 N73-28259
Identification of fifty mile wide tectonic zone across Southern California using ERTS-1 imagery
[PAPER-G33] 19 p2268 N73-28264
ERTS-1 detection and monitoring of tectonic and vegetational patterns, urban development, and agricultural processes in Southern California
[PAPER-R4] 19 p2283 N73-28362
Application of ERTS-1 data to geomorphotectonics, earthquake studies, and mineral exploration at Los Angeles, California, and New Jersey coastal plain
19 p2284 N73-28367
Application of Skylab imagery to analysis of fault tectonics and earthquake hazards in Peninsular Ranges of Southern California
[E73-10863] 20 p2392 N73-29214
Identification and interpretation of tectonics from ERTS-1 imagery of California, Mexico, and Baja California
[E73-10875] 20 p2393 N73-29226
Tectonic and photogeologic mapping of forested and sparsely vegetated terrain of Montana and Idaho
[E73-10900] 20 p2396 N73-29249
Geology of photo linear elements, Great Divide, Wyoming
[E73-10958] 21 p2532 N73-30300
Simulation of San Andreas fault for determining relative motion of plates
[NASA-TM-X-70439] 21 p2537 N73-30338
Application of Skylab imagery to analysis of fault tectonics and earthquake hazards in Peninsular Ranges of Southern California
[E73-10999] 22 p2659 N73-31304
Tectonic analysis and mapping of Bighorn Mountains from ERTS-1 imagery
[E73-11049] 23 p2779 N73-32225
Identification and interpretation of tectonic features from ERTS-1 imagery of Southern California and Baja California
[E73-11084] 24 p2913 N73-33247
Application of Skylab imagery to analysis of fault tectonics and earthquake hazards in Peninsular Ranges, Southern California
[E73-11134] 24 p2917 N73-33289
Tectonic analysis of Bighorn Mountains of Montana and Wyoming and Black Hills of South Dakota and Wyoming from Skylab imagery
[E73-11151] 24 p2919 N73-33305

**TEE**
U T SHAPE

**TEETH**
Unified approach to biomechanics of dental implantology
10 p1227 N73-19977

**TEFLON [TRADEMARK]**
Applying dislocation scattering of phonons to measurement of thermal conductivity of Teflon
[AD-746516] 02 p0220 N73-11777
Ultrasonic testing of Teflon and composite materials considering phase velocity
[AD-756385] 13 p1560 N73-22642
Physical and detonation properties of dry blended hexanitrostilbene/Teflon explosive charges used on Apollo 17 seismic experiment
[NASA-CR-133838] 21 p2606 N73-30886
Method of testing materials based on teflon and Kel-F for friction at low temperatures by using X18H9T steel in helium medium for different slip rates and loads
22 p2688 N73-31531

**TEKTITE PROJECT**
Recorded observations of crew member activities during Tektite 2 underwater habitability study
[NASA-CR-130034] 07 p0750 N73-16094

**TEKTITES**
Nuclear chemistry and geochemistry research projects including isotope separations, meteorite and tektite compositions, and solid gamma spectrometer development
[COO-3236-3] 08 p0884 N73-17156
Discovery and geographical distribution of tektites
[NASA-TT-F-15052] 20 p2411 N73-29378

**TELECHIRICS**
U REMOTE HANDLING

**TELECOMMUNICATION**
NT AIRCRAFT COMMUNICATION
NT AUTOMATIC PICTURE TRANSMISSION
NT BIOTELEMETRY
NT BROADCASTING
NT CLOSED CIRCUIT TELEVISION
NT COLOR TELEVISION
NT COMMUNICATION
NT DATA LINKS
NT DEFENSE COMMUNICATIONS SATELLITE SYSTEM
NT EDUCATIONAL TELEVISION
NT FACSIMILE COMMUNICATION
NT GROUND-AIR-GROUND COMMUNICATIONS
NT MULTICHANNEL COMMUNICATION
NT OPTICAL COMMUNICATION
NT PULSE COMMUNICATION
NT RADIO COMMUNICATION
NT RADIO RELAY SYSTEMS
NT RADIO TELEMETRY
NT RADIOTELEPHONES
NT SATELLITE TELEVISION
NT SPACE COMMUNICATION
NT SPACECRAFT ANTENNAS
NT SPACECRAFT COMMUNICATION
NT SPACECRAFT TELEVISION
NT TELEMETRY
NT TELEPHONY
NT TRANSOCEANIC COMMUNICATION
NT VIDEO COMMUNICATION
NT VOICE COMMUNICATION
NT VOICE DATA PROCESSING
NT WIDEBAND COMMUNICATION
NT WIRELESS COMMUNICATIONS
Conference on expanded aerospace telecommunication system requirements and digital data transmission methods
[AGARD-CP-103] 01 p0024 N73-10187
Digital telecommunication techniques and network planning for aerospace systems
01 p0024 N73-10188
Digital computer techniques for filtering and transmission of telecommunication data
01 p0025 N73-10192
Numerical control of delta modulated vocal signals in air navigation telecommunication system
01 p0025 N73-10194
Attenuation and phase constancy propagation criteria of tactical satellite communications using mobile ground terminals
01 p0026 N73-10201
Wideband tactical satellite communications systems using onboard processing
01 p0026 N73-10202
Measurement methods and error analyses by ground terminals for optimizing satellite communications link
01 p0026 N73-10203
Satellite communication terminal for ships
01 p0026 N73-10204
Orbit sharing and deployment problems of high power satellite communication systems
01 p0026 N73-10205
Real time computerized message switching and data transmission systems for military communications network
01 p0026 N73-10206
Automated technical control system for military communications facility
01 p0027 N73-10207
Operational performance and transmission measurements on worldwide Defense Communications System network
01 p0027 N73-10208

Feasibility of all-digital implementation of worldwide analog communications systems
01 p0027 N73-10209
Kalman filtering algorithm for detecting continuous wave interference signals in digital telecommunications
01 p0027 N73-10210
Intermodulation interference effects of metal surface transmitters and receivers in near field locations of transmission system
01 p0027 N73-10212
Telecommunications by satellite, and operation of Intelsat network
[NLL-TRANS-2860-[9022.81]]
02 p0139 N73-11126
Telecommunications systems design techniques for deep space network application
[NASA-CR-129108] 02 p0140 N73-11137
Pseudonoise test set for communication system performance evaluation based on RMS error testing
[NASA-TM-X-64698] 03 p0265 N73-12146
Legal restraints on dissemination of instructional materials by educational communications systems
[NASA-CR-129271] 03 p0366 N73-12983
Application of graph theory to network analysis and coding problems in communication systems
[AD-748290] 04 p0391 N73-13178
Phase coherent frequency synthesizer for improving digital voice and data transmission in communication systems
04 p0472 N73-13853
Revolutionization of communications by satellite systems
04 p0472 N73-13854
Algorithms for construction of minimum cost communication networks
[PB-211233] 05 p0514 N73-14178
Resource sharing computer communication networks and some aspects of distributed computation
[AD-749378] 05 p0518 N73-14210
Feasibility determination of cutaneous communication system for working divers
[AD-750268] 06 p0636 N73-15169
Telecommunication jamming of robot aircraft control system by pulse amplitude modulation or pulse time modulation
[FOA-3-C-3649-66] 06 p0639 N73-15188
Adaptive routing techniques for message switching computer-communication networks
[AD-749678] 06 p0646 N73-15246
Mathematical modeling of communication systems transponders and receivers at circuit detail and block levels
[NASA-CR-124097] 09 p1001 N73-18172
Independent radar systems using information processing, data correlation, and telecommunication
09 p1002 N73-18179
Computerized simulation of global communication system
[AD-753115] 09 p1003 N73-18186
Computer network with random access storage for teletype data transmission system
[NASA-CR-130500] 09 p1006 N73-18214
Research progress in electro-optics, plasma physics, microwaves, wave propagation, telecommunication, data processing
[AD-753710] 09 p1102 N73-18993
Theoretical and experimental analysis of digital processing in various communication systems
10 p1127 N73-19183
Programmatics of space shuttle supported research facilities for telecommunication and navigation - Vol. 4
[NASA-CR-124139] 10 p1137 N73-19268
Portable telephone system for transmission of electroencephalographical data diagnostic center
[NASA-CR-128877] 11 p1255 N73-20186
Light communication systems using fiber optics
[AD-754566] 11 p1257 N73-20200
Technological and economical factors of satellite television network in India
[PB-213226] 11 p1258 N73-20208
Computer communications systems
[AD-754461] 11 p1260 N73-20225
Interface data processing system for telecommunication computer network
[AD-754441] 11 p1260 N73-20228
Source coding, modulation/channel coding, and systems techniques for application to teleconferencing over high data rate digital communication satellite links
[NASA-CR-114561] 11 p1342 N73-20889
German telecommunication research and development
12 p1379 N73-21186
Handbook on defense and commercial communication systems
[AD-755917] 12 p1380 N73-21191
Specifications and capabilities of Franco-German telecommunications satellite - Symphonie
[NASA-TT-F-14875] 12 p1461 N73-21836
Design of all digital low data rate communication system with potential cost reduction
[NASA-CR-130234] 13 p1490 N73-22077
Survivability analysis of command and control communication systems
[AD-755846] 13 p1495 N73-22116
Design and development of telecommunications equipment for use with Tracking and Data Relay Satellite System - Vol. 2
[NASA-CR-130217] 13 p1582 N73-22821
Research and development progress in telecommunications and electronics engineering
[REPT-73-00567] 14 p1619 N73-23111
Design of nonlinear coherence receiver with feedback signal selection for carrier tracking in telecommunications
[NASA-CASE-NPO-11921-1] 14 p1620 N73-23118
Automation of technical control centers for operation and maintenance of Armed Forces defense communication system
[AD-757551] 14 p1635 N73-23255
Evaluation of cryogenic devices for application in surveillance, radiation detection, and communications
[AD-756175] 14 p1668 N73-23537
FAA communications system description for 1973
[FAA-RD-73-36] 15 p1750 N73-24186
Application of statistical analysis techniques in telecommunication, tracking, and control
[AD-758260] 15 p1751 N73-24193
Satellite telecommunications systems for childhood education
[NASA-CR-133028] 16 p1869 N73-25131
Skylab television camera system to record launch and tests
[NASA-TM-X-69526] 16 p1875 N73-25174
Physical properties of electro-optical switching devices for telecommunication
[REPT-61] 16 p1875 N73-25177
Role of NASA programs and technologies in developing better communication links among people
[NASA-CR-133052] 16 p1876 N73-25183
Relationships between United States of America and Latin American telecommunication institutions
[PB-214619/9] 16 p1876 N73-25187
Artificial ultralow frequency generation in ionosphere and magnetosphere for global communication system
[AD-759012] 16 p1878 N73-25199
Multicarrier communications system for transmitting modulated signals from single transmitter
[NASA-CASE-NPO-11548] 17 p1993 N73-26118
Conference on atmospheric attenuation and rainfall effects on ultrahigh frequency telecommunication systems
[AGARD-CP-107] 17 p1994 N73-26121
Design engineering for radio communication systems considering troposphere transmission characteristics
17 p1995 N73-26128
Criteria for planning ultrahigh frequency telecommunication system considering radioelectrical and meteorological measurements
17 p1995 N73-26129
Horizontal radio link system for measuring ultrahigh frequency absorption spectrum due to rain
17 p1995 N73-26130
Use of differential phase and gain for predicting performance of ultrahigh frequency telecommunication system
17 p1995 N73-26132
Effects of rain and atmospheric turbulence on ultrahigh frequency space communication radio line
17 p1996 N73-26143
Phase modulation of tone and binary signals on carrier waves in communication systems
[NASA-CASE-GSC-11743-1] 18 p2116 N73-27107
Conference on communications policy research from 17 to 18 November 1972, Washington, D.C.
[PB-218981/9] 18 p2118 N73-27124
Satellite telecommunication link in health/education experiment using tuned radio frequency receiver
18 p2213 N73-27864
Analysis of digital communication systems disturbed by non-Gaussian noise
19 p2235 N73-28017
Systems applications in the 10 to 100 GHz frequency band for optimum utilization of EHF frequencies
[OT/TRER-34] 19 p2235 N73-28019
Technique for hybrid addition of both digital and analog data in troposcatter communication system
[AD-761523] 19 p2236 N73-28030
Design of communications processor for access control to computer system
[AD-761804] 19 p2241 N73-28064
Synchronized digital communication system
[NASA-CASE-XNP-03623] 19 p2243 N73-28084
Capabilities and limitations of communication satellite data transmission for conducting conferences
[NASA-CR-133591] 20 p2377 N73-29098
Legal considerations of satellite communications system for teleconferencing applications
[NASA-CR-133592] 20 p2377 N73-29099
Development of analytical capabilities for determining use of satellite communications technology for professional education and medical services
[NASA-CR-133359] 20 p2377 N73-29100
Design, development, and control of large scale educational telecommunication system using satellites
[NASA-CR-133646] 20 p2377 N73-29104
Research progress in coding, synchronization, data processing, and communication systems
[AD-762542] 20 p2379 N73-29117
Proceedings of international telecommunication organization on peaceful uses of outer space with emphasis frequency assignments for space communication
[REPT-12] 21 p2507 N73-30118
Performance tests for Naval global communications system equipment
[AD-764485] 22 p2635 N73-31116
Assembly language programs required to interface ALOHA system to IBM telecommunication time sharing operation
[NASA-CR-133853] 22 p2639 N73-31155
Delphi forecasts of utilization and social impacts of large-scale educational telecommunications technology
[NASA-CR-135477] 23 p2866 N73-32909
Sequential communication systems with information feedback
24 p2893 N73-33098

**TELEGRAPH SYSTEMS**
Noise tolerant radio telegraphy, using orthogonal carrier modulation
[FTZ-455-TBR-39] 22 p2634 N73-31108

**TELEGRAPHY**
U TELEGRAPH SYSTEMS

**TELEMETERS**
U TELEMETRY

**TELEMETRY**
NT BIOTELEMETRY
NT PCM TELEMETRY
NT RADIO TELEMETRY
Remote automatic multipurpose station for collecting oceanographic and meteorological data in Arctic regions
[AD-746496] 01 p0038 N73-10300
Data handling theory, telemetry, and signal frequency determination for signal reconnaissance
[FOA-3-C-3653-66] 02 p0140 N73-11134
Systematic convolutional codes for PCM telemetry
[NASA-TM-X-66085] 02 p0140 N73-11138
Design of high speed, real time symbiont for analog telemetry processing
[NASA-TM-X-66090] 02 p0146 N73-11183
Performance tests of scale model of lunar roving vehicle used on Apollo 15 mission to determine vehicle mobility
[NASA-CR-129176] 02 p0152 N73-11234
Radio telemetry for detecting and tracking sounding rockets
[REPT-11] 04 p0388 N73-13153
Laser telemetry discussing equipment specifications, errors, and noise reduction
05 p0557 N73-14524
Aberration due to high velocity satellites for laser telemetry
05 p0557 N73-14526
Efficiency of laser telemetry tracking for satellites carrying reflectors
05 p0557 N73-14527
Efficiency of laser telemetry tracking for satellite carrying laser reflector sphere
05 p0557 N73-14528
Characteristics of two channel telemetry system with two data rate channels for high and low data rate communication
[NASA-CASE-NPO-11572] 07 p0754 N73-16121
Telemetry data processing systems for experiments flown on Injun 5 satellite, OV-3 satellite, OV-4 satellite, OV-5 satellite, OV-6 satellite, and OV-15 satellite
[AD-751508] 07 p0759 N73-16166
Earthquake prediction and control through satellite relay telemetry of seismic data
07 p0787 N73-16399
Principles of spacecraft telemetry data management
[ESRO-TN-121-ESOC] 08 p0885 N73-17166
Development of highly accurate and reliable telemeter system utilizing integrated circuits
[AD-752481] 08 p0886 N73-17176
Computer software to enable any general purpose computer with A/D conversion capability to be used as PSK receiver for low data rate telemetry processing
[NASA-CR-130174] 08 p0887 N73-17185
Modification of Auburn University Model S-2 FM television transmitter through use of integrated circuits and conversion to receive telemetry signals
[NASA-CR-124082] 09 p1001 N73-18171
Monitoring Northern Hemisphere transmissions in Antarctica and some oblique sounding systems
[JPRS-58205] 10 p1128 N73-19186
Survey of some oblique sounding systems and selection of system for practical application
10 p1128 N73-19188
Telemetric monitor for in-situ transmission of solid propellant mechanical property data
[AD-754253] 10 p1162 N73-19454
Vehicle telemetry measurements for Skylab 2 spacecraft and identification of data sources
[NASA-TM-X-69142] 10 p1216 N73-19887

Feasibility of efficient multiamplitude communication in earth satellite systems
10 p1228 N73-19983
Instrumented dolphins for surveying oceanographic parameters and relaying information to tracking aircraft
[AD-754761] 11 p1256 N73-20191
Analysis of telemetry data from prelaunch, launch, and flight activation phases of ERTS-1 spacecraft
[NASA-CR-130150] 13 p1581 N73-22817
Development of processing satellite data to show quantity of data and time required for various techniques
[BMFT-FBW-73-04] 14 p1638 N73-23277
Development of system for collection and processing of telemetered magnetometer data received from artificial satellite
[GAMMA-17-167S] 14 p1658 N73-23457
Telemetry preprocessing language for telemetry data processing
[NASA-TM-X-66248] 15 p1750 N73-24183
Telemetry and transmission system with programmed sampling and multiplexing
[NASA-CASE-GSC-11388-1] 15 p1750 N73-24187
Intelligent telemetry device remotely controlled via communication channels
[AD-758272] 15 p1751 N73-24195
Analysis of major sources of distortion in AM baseband telemetry systems and techniques for optimum baseband design
16 p1874 N73-25169
Telemetry data from data processing system for spherical electrostatic analyzer experiment onboard ISIS-A satellite
[AD-760148] 17 p2001 N73-26179
Telemetry and investigative methods in space biology
[NASA-TT-F-14996] 18 p2109 N73-27057
Failure analysis of telemetry anomalies during Apollo 17 flight
[NASA-TM-X-69367] 18 p2117 N73-27118
Improved phase lock loop for receiver in multichannel telemetry system with suppressed carrier
[NASA-CASE-NPO-11593-1] 19 p2234 N73-28012
Technical facilities for data links in teleautomatic queueing system
[JPRS-59662] 19 p2235 N73-28022
Analysis and simulation of telemetry receivers and bit synchronizers
[NASA-CR-132809] 21 p2507 N73-30120
Design of real time telemetry processing system for naval aircraft flight tests
[AD-763469] 21 p2509 N73-30130
Abstracts of research projects on adaptive telemetry systems
[NASA-CR-130228] 22 p2631 N73-31088
Characteristics of swept frequency impedance probe installed in unmanned satellite to measure impedance of space plasma
[ISAS-495-VOL-38-NO-6] 22 p2672 N73-31403
Azur satellite telemetry data processing - conferences
[BMFT-FB-W-73-04] 24 p2985 N73-33852
Azur satellite telemetry, noting real time and tape telemetry systems
24 p2985 N73-33853
Preprocessing of Azur satellite telemetry data to provide several output tape formats
24 p2985 N73-33854
Time allocation in Azur satellite telemetry data, noting onboard clock and world time deviations on tapes
24 p2985 N73-33855
Selection of Azur satellite additional information for telemetry data processing
24 p2985 N73-33856
Redundancy elimination in Azur satellite telemetry data
24 p2985 N73-33857

**TELEMETRY AUTO REDUCTION SYSTEM**
U DATA REDUCTION
U TELEMETRY

**TELEOPERATORS**
Computerized teleoperator manual control system for remote mechanical hand
01 p0019 N73-10143
Concept evaluation and subsystem analyses for design of remote controlled teleoperator visual system
[NASA-CR-124059] 08 p0879 N73-17117
Sophisticated maintenance of orbital space vehicles with application of remotely controlled telemanipulation concept
[NASA-TT-F-14804] 08 p0965 N73-17885
Research projects conducted as part of NASA programs during period May 1970 through May 1972
[NASA-TM-X-64723] 13 p1593 N73-22915
Development and evaluation of free flying teleoperators to include semiexoskeletal master control unit, joystick-analog unit, and three dimensional television system
13 p1594 N73-22925
Computerized teleoperator applications in manned aerospace systems
14 p1713 N73-23904
Conceptual design study for teleoperator visual system
[NASA-CR-124273] 16 p1869 N73-25133
Serpentine teleoperator device for simulating intravehicular and extravehicular activities in space
[NASA-TR-R-414] 16 p1879 N73-25210
Design of terminal pointer hand controller for teleoperator applications
[NASA-CR-124307] 18 p2156 N73-27419
Identification of feasible and practical applications of space teleoperator technology for problems of handicapped
[NASA-CR-133357] 19 p2225 N73-27949

**TELEPHONES**
NT RADIOTELEPHONES
Portable telephone system for transmission of electroencephalographical data diagnostic center
[NASA-CR-128877] 11 p1255 N73-20186
Development and characteristics of audio response unit for use with telephone exchange to answer tax inquiries from subscribers
14 p1632 N73-23229

**TELEPHONY**
Automatic equalizers of telephone channels for fast transmission of digital data
01 p0025 N73-10199
Antithetic and control variate sampling methods for probability estimation in simulation, with telephony traffic example
[NA-71-41] 03 p0324 N73-12645
System parameters for satellite communications system to provide remote area telephone and television service
[REPT-6741] 14 p1619 N73-23109
Operation of electronic telephone exchange in France
[NLL-PO-2957-[9022.81]] 15 p1749 N73-24175
Data error protection in disturbed binary channels by linear systematic codes, applied to 50 Kbaud telephone channel transmission
[FTZ-A-441-TBR-1] 22 p2632 N73-31097
Luminescent diode and liquid crystal display devices for telephony, using COS/MOS and TTL logic
[FTZ-421-TBR-4] 22 p2633 N73-31105

**TELEPHOTOMETERS**
U TELEPHOTOMETRY

**TELEPHOTOMETRY**
Development, characteristics, and operation of telephotometer for simultaneous measurements of angular and space distribution of absolute solar radiation fluxes
20 p2402 N73-29303

**TELEPRINTERS**
Analog to digital converter with teleprinter for multiple printout of projectile ballistic measurements
[PHL-1972-4] 01 p0032 N73-10245

**TELESCOPES**
NT APOLLO TELESCOPE MOUNT
NT ASTRONOMICAL TELESCOPES
NT CELESCOPES
NT HELIOMETERS
NT LARGE SPACE TELESCOPE
NT PARTICLE TELESCOPES
NT PYROHELIOMETERS
NT RADIO TELESCOPES
NT REFLECTING TELESCOPES
NT SCHMIDT CAMERAS
NT SPACEBORNE TELESCOPES
NT SPECTROSCOPIC TELESCOPES
NT STRATOSCOPE TELESCOPES
NT X RAY TELESCOPES
Correction of axisymmetric deformations in space telescope mirrors by thermally induced elastic strains
[NASA-TM-X-2673] 06 p0672 N73-15472
Performance of scanning acoustical imaging telescope at microwave frequencies
07 p0820 N73-16648
Image intensifier system for daytime missile tracking telescopes
[AD-753342] 09 p1068 N73-18715
Design and construction of 3.5 m telescope in Italy
16 p1911 N73-25466
Development and characteristics of solid state cosmic ray telescope for use on IMP F and G missions
[NASA-CR-132767] 16 p1912 N73-25473
Thermoelastic response model for actively controlling primary mirror surface error of orbiting telescope
[NASA-CR-124286] 17 p2033 N73-26449
Glacing incidence telescope for evaluating polarization of light source
18 p2210 N73-27840
Adaptive control system for compensatory positioning of optical tracking telescope
18 p2210 N73-27842
Ritchey-Chretien telescope responsive to images located off telescope optical axis
[NASA-CASE-GSC-11487-1] 21 p2544 N73-30393
Instrument for sensing errors in telescope wavefronts using coarse range sensors and fine range sensors
23 p2792 N73-32336
Telescopic detection and ranging system for satellite orbital trajectory determination
[AD-764727] 23 p2820 N73-32546

**TELETYPEWRITER SYSTEMS**
Analytic model for teletype communication networks, using queueing theory
[AD-744467] 01 p0028 N73-10222
Software module for teletypes connected to HP ALOHA SYSTEM multiplexer
[NASA-CR-130492] 09 p1006 N73-18213

**TELETYPEWRITERS**
NT TELEPRINTERS

**TELEVISION CAMERAS**
Evaluation of photon imaging devices and subsystems with emphasis on television camera tubes
[AD-748005] 03 p0275 N73-12234
Encoding action of pair of dichroic gratings suitable for single tube color television camera
[BBC-1972/32] 04 p0419 N73-13414
Failure analysis of malfunction of Apollo 16 television camera monitor on command module
[NASA-TM-X-68930] 06 p0639 N73-15190
Design and characteristics of television cameras used for remote sensing and comparison with imagery of photographic film cameras
07 p0784 N73-16374
Specifications and characteristics of ground-commanded color television assembly used on Apollo 15 flight
[NASA-CR-128829] 10 p1128 N73-19192
Design modifications to WX-5419B SEC camera tube
[NASA-CR-130934] 10 p1160 N73-19434
Electronic equipment for infrared television camera used in terrain analysis
[LCR-DR-1-71-210/1/R] 13 p1500 N73-22157
Various imaging systems and techniques for possible use aboard Grand Tour Spacecraft
[NASA-CR-132014] 14 p1704 N73-23824
Skylab television camera system to record launch and tests
[NASA-TM-X-69526] 16 p1875 N73-25174
Method and equipment for testing lag response in television camera tubes
[AD-763339] 22 p2644 N73-31186
Effect of television camera and radiometer resolution on accuracy of cloud quantity determinations from satellites
22 p2693 N73-31569
Infrared sensitive television camera for horizon and depth perception in whiteout
[DREO-TN-73-11] 23 p2791 N73-32332
Evaluation of computer storage requirements for TV camera tubes with signal encoding test program
[ELEC-011-72] 23 p2794 N73-32350
Performance of Mariner 9 television cameras
23 p2843 N73-32718

**TELEVISION EQUIPMENT**
NT IMAGE DISSECTOR TUBES
NT TELEVISION CAMERAS
NT TELEVISION RECEIVERS
Development of graphical method for determining chromaticity and relative luminance of test color reproduced by color television display
[BBC-1972/30] 01 p0023 N73-10182
Use of TV equipment for converting color negative cinefilm into color positive image
[DRIC-TRANS-2835] 02 p0174 N73-11412
Development of auditory display of two-dimensional patterns to assist blind persons in pattern identification
[NASA-CASE-HQN-10832-1] 03 p0301 N73-12456
Rotating generator for angular display of television raster in horizontal and visual simulation systems
[NASA-CASE-FRC-10071-1] 05 p0513 N73-14171
Characteristics of video tape recording film and procedures for controlling magnetic properties during production
[NHK-LABS-NOTE-155] 07 p0754 N73-16122
Design and characteristics of television cameras used for remote sensing and comparison with imagery of photographic film cameras
07 p0784 N73-16374
Design, construction, and evaluation of 12.2 GHz, 4.0 kW-CW coupled-cavity traveling wave tube for satellite-borne television broadcast transmitters
[NASA-CR-120920] 12 p1382 N73-21209
Correction of scanning beam velocity nonuniformity in vidicons by deflection of current pulse
[DRIC-TRANS-2758] 12 p1384 N73-21224
Development of spacecraft docking system for optical alignment of spacecraft using television camera system
[NASA-CASE-MSC-12559-1] 17 p2086 N73-26879
Television multiplexing system, using single crystal controlled clock for signal synchronization
[NASA-CASE-KSC-10654-1] 21 p2507 N73-30115

**TELEVISION RECEIVERS**
Central ground station and local receivers for direct TV broadcasting satellite system
[DGLR-PAPER-73-055] 24 p2895 N73-33114

**TELEVISION RECEPTION**
Development of graphical method for determining chromaticity and relative luminance of test color reproduced by color television display
[BBC-1972/30] 01 p0023 N73-10182
Systems and studies for direct TV reception from satellite in Germany
[DGLR-PAPER-72-50] 04 p0389 N73-13160

Television reviewing conditions, including contrast handling requirements of color TV display
[BBC-1972/37] 06 p0638 N73-15182
Fabrication and evaluation of engineering prototype ground signal processing systems for use with satellite television
[NASA-CR-120933] 09 p1002 N73-18178
Temporary loss of Apollo 14 command module color television picture by ground station converter
[NASA-TM-X-69296] 15 p1751 N73-24189
Direct satellite FM-TV broadcasting experiment, with receiver operating near threshold and with 24 and 32 MHz IF band widths
[ESRO-CR[P]-251] 18 p2117 N73-27119
Direct satellite FM-TV broadcasting experiment, with receiver operating near threshold and with 20 MHz IF bandwidth
[ESRO-CR[P]-252] 18 p2117 N73-27120

**TELEVISION SYSTEMS**
NT CLOSED CIRCUIT TELEVISION
NT COLOR TELEVISION
NT EDUCATIONAL TELEVISION
NT SATELLITE TELEVISION
NT SPACECRAFT TELEVISION

Propagation characteristics of satellite-borne television transmitter and ground receiver for communication satellite system
[NASA-CR-123909] 01 p0028 N73-10214
Analysis procedure for television observations and simultaneous observations
01 p0102 N73-10836
Results from simultaneous radar-television observations
01 p0102 N73-10838
Gray scale reproduction capability for characterizing aerial television reconnaissance system
[AD-747632] 03 p0267 N73-12165
Analysis of problems and effects in reducing sampling frequency in 625 line television digital codes to improve transmission
[REPT-1972/36] 05 p0507 N73-14129
Subjective tests of target acquisition time using television with image enhancement possibilities
[MBB-UFE-892-72-O] 06 p0636 N73-15165
Design and characteristics of television cameras used for remote sensing and comparison with imagery of photographic film cameras
07 p0784 N73-16374
Modification of Auburn University Model S-2 FM television transmitter through use of integrated circuits and conversion to receive telemetry signals
[NASA-CR-124082] 09 p1001 N73-18171
German needs for television transmission via satellite
[DGLR-PAPER-72-051] 09 p1003 N73-18183
Technological and economical factors of satellite television network in India
[PB-213226] 11 p1258 N73-20208
Cross and square command symbol and video inset generator to display flight command data on aircraft television screen
[AD-755160] 13 p1494 N73-22111
Feasibility analysis and planning for two aircraft television transmission over Federal Republic of Germany
[DLR-MITT-73-09] 14 p1633 N73-23235
Design of circular symbol and video inset generator for television display devices
[AD-757621] 14 p1634 N73-23246
Design of attitude line generator for use with aircraft-type television displays
[AD-757620] 14 p1634 N73-23247
Present technology and prospects for creation of national communications television broadcast network in USSR during 1971 - 1975
[JPRS-58928] 14 p1637 N73-23273
Availability of Mariner 9 TV picture data
[NASA-TM-X-69216] 14 p1704 N73-23822
MJS imaging and baseline TV system
[NASA-CR-132012] 14 p1704 N73-23825
Systems analysis of radio-TV satellite for coverage of West Germany and west European areas with German language
14 p1710 N73-23876
Television readout devices for color display of data and picture blending
[NLL-PO-2958-[9022.81]] 15 p1755 N73-24225
Communication satellite systems for educational television vision
[NASA-TT-F-775] 15 p1845 N73-24953
Low light level television system for coherent optical matched filtering for meteor trail detection
16 p1922 N73-25554
Infrared television system used for HF laser flow visualization with selected nozzle configurations
[AD-759803] 16 p1925 N73-25577
Exploration of natural landscape using TV pictures from meteorological satellites
[NASA-TT-F-14965] 17 p2025 N73-26389
On-line binary scan converter for converting pictorial from computer output to raster form suitable for TV display
19 p2238 N73-28046
Application of ERTS-1 TV imagery to map-making
19 p2283 N73-28366
Facsimile data transmitted simultaneously with television
[NHK-LABS-NOTE-160] 20 p2377 N73-29103
Geodetic control net of Mars based on Mariner 9 television pictures
[NASA-CR-133845] 21 p2596 N73-30808
Data transmission interference after television field synchronizing signal
[BBC-RD-1973/12] 22 p2627 N73-31049

**TELEVISION TRANSMISSION**
Development and performance of color television equipment developed for use on Apollo 15 mission
04 p0473 N73-13855
Analysis of problems and effects in reducing sampling frequency in 625 line television digital codes to improve transmission
[REPT-1972/36] 05 p0507 N73-14129
Combination satellite television system with local cable system for Federal Post Office
[NASA-TT-F-14660] 06 p0640 N73-15195
Technical and economical factors of satellite television reception
[NASA-TT-F-14659] 06 p0640 N73-15196
Analysis of electromagnetic interference between satellite frequency modulated television signal and television signal for commercial broadcasting
[NHK-LABS-NOTE-153] 07 p0754 N73-16123
Automatic frequency control circuit for FM television transmitter
[NASA-CASE-MFS-21540-1] 09 p1002 N73-18177
Specifications and characteristics of ground-commanded color television assembly used on Apollo 15 flight
[NASA-CR-128829] 10 p1128 N73-19192
System parameters for satellite communications system to provide remote area telephone and television service
[REPT-6741] 14 p1619 N73-23109
Feasibility analysis and planning for two aircraft television transmission over Federal Republic of Germany
[DLR-MITT-73-09] 14 p1633 N73-23235
Multiplexing still picture broadcasting by cable system
[NHK-LABS-NOTE-158] 18 p2115 N73-27099
Direct satellite FM-TV broadcasting experiment, with receiver operating near threshold and with 24 and 32 MHz IF band widths
[ESRO-CR[P]-251] 18 p2117 N73-27119
Direct satellite FM-TV broadcasting experiment, with receiver operating near threshold and with 20 MHz IF bandwidth
[ESRO-CR[P]-252] 18 p2117 N73-27120
Transmission problems of hybrid PCM system for television signals
[BBC-RD-1973/9] 20 p2376 N73-29088
Characteristics of Orbita-2 satellite communications system
[JPRS-59751] 20 p2376 N73-29093
Comparative study of TWT and klystron amplifiers for use as power amplifiers in television broadcast satellites
[ESRO-CR[P]-268] 21 p2508 N73-30123
Structure of dust storms determined from ITOS-1 television pictures
[NLL-M-23033-[5828.4F]] 21 p2528 N73-30272
Digital methods of television signal timing corrections
[BBC-RD-1973/15] 22 p2627 N73-31048
Television broadcasting wave depolarization measurement for multiple utilization of assigned frequencies
[FTZ-A-455-TBR-36] 22 p2633 N73-31101
Experimental television transmission system with vestigeal sideband amplitude/frequency modulation
[FTZ-44-TBR-33] 22 p2633 N73-31102
Usability of 42 and 85 GHz mm waves for terrestrial television broadcasting
[FTZ-455-TBR-37] 22 p2634 N73-31107
Omnidirectional polygon reflector antenna with cosecant radiation pattern for TV transmission in SHF range
[FTZ-A-454-TBR-16] 22 p2643 N73-31179
User guide to Mariner 9 television reduced data record
[NASA-CR-135712] 23 p2793 N73-32347
Mariner 9 television observations of Martian planets Phobos and Deimos
23 p2841 N73-32705
Simplification of television synchronization signal by reducing duration
[BBC-RD-1973/20] 24 p2894 N73-33100
Direct TV broadcasting communication satellites
[DGLR-PAPER-73-040] 24 p2895 N73-33112
Central ground station and local receivers for direct TV broadcasting satellite system
[DGLR-PAPER-73-055] 24 p2895 N73-33114
Direct broadcasting TV satellite solar arrays, and heat budget subsystems
[DGLR-PAPER-73-051] 24 p2986 N73-33865
Direct broadcasting TV communication satellite temperature control by louvers, heat pipes, radiators, heat storage, and coatings
[DGLR-PAPER-73-052] 24 p2986 N73-33866

**TELLEGEN THEORY**
U GYRATORS
U NETWORK ANALYSIS
U NETWORK SYNTHESIS

**TELLURIC CURRENT MICROPULSATIONS**
U MICROPULSATIONS
U TELLURIC CURRENTS

**TELLURIC CURRENTS**
Magnetotelluric analysis of geological structure of various locations in Rhine River Valley, Germany
[GAMMA-20] 01 p0048 N73-10388
Geophysical observations of horizontal and vertical components of earth magnetic field at Feurstenfeldbruck, Germany for 1972
14 p1660 N73-23473
Phenomenological concepts of earth electrical structure controlled by neutral atmosphere dynamics of stratospheric tides
16 p1895 N73-25330
Effect of magnetic induction anomaly on magnetotelluric fields in Oahu, Hawaii
[PB-214444/2] 16 p1908 N73-25440

**TELLURIC FIELDS**
U ELECTRIC FIELDS
U TELLURIC CURRENTS

**TELLURIC LINES**
Development and improvement of magnetovariation station for conducting magnetotelluric soundings
[JPRS-57678] 04 p0401 N73-13262
Telluric lines in solar spectrum region lambda lambda 6327.5 to 6330.0 AA
20 p2472 N73-29858

**TELLURIDES**
NT CADMIUM TELLURIDES
NT LEAD TELLURIDES
NT MERCURY TELLURIDES
NT TIN TELLURIDES

Silver addition in Si-As-Te glasses to permit introduction of substantial amounts of selenium and to produce infrared transmitting glasses with increased softening ranges
[AD-747333] 02 p0193 N73-11563
Effect of external electric field on optical absorption of GaSe and GaTe single crystals and solid solutions
[AD-749750] 05 p0589 N73-14789
Temperature-modulated reflectivity in fundamental edge region of GaTe
[ISS-72/2] 10 p1199 N73-19755
Analysis of electrical switching phenomena in amorphous arsenic telluride-arsenic selenide system
24 p2966 N73-33707

**TELLURIUM**
Mossbauer spectroscopic analysis of order-disorder transitions in vacuum deposited Te films
[AD-753272] 09 p1074 N73-18769
Observation of amorphous to crystalline transition in vacuum deposited tellurium films using Mossbauer spectroscopy
[AD-763408] 21 p2586 N73-30724

**TELLURIUM COMPOUNDS**
NT CADMIUM TELLURIDES
NT LEAD TELLURIDES
NT MERCURY TELLURIDES
NT TELLURIDES
NT TIN TELLURIDES

**TELSTAR PROJECT**
Compendium of worldwide satellite communications programs to Aug. 1971
[NASA-TM-X-70435] 21 p2599 N73-30834

**TEMPERATE REGIONS**
Analytical expressions for geographic distribution of midday ionization of F 2 layer in temperate latitudes
13 p1521 N73-22331

**TEMPERATURE**
NT AMBIENT TEMPERATURE
NT ATMOSPHERIC TEMPERATURE
NT BODY TEMPERATURE
NT BRIGHTNESS TEMPERATURE
NT COMBUSTION TEMPERATURE
NT CRITICAL TEMPERATURE
NT FLAME TEMPERATURE
NT FLASH POINT
NT GAS TEMPERATURE
NT HIGH TEMPERATURE
NT IGNITION TEMPERATURE
NT ION TEMPERATURE
NT LOW TEMPERATURE
NT NEEL TEMPERATURE
NT NOISE TEMPERATURE
NT PLANETARY TEMPERATURE
NT PLASMA TEMPERATURE
NT ROOM TEMPERATURE
NT SATELLITE TEMPERATURE
NT SKIN TEMPERATURE [NON-BIOLOGICAL]
NT SOLAR TEMPERATURE
NT SUBZERO TEMPERATURE
NT SURFACE TEMPERATURE
NT TRANSITION TEMPERATURE
NT WALL TEMPERATURE
NT WATER TEMPERATURE

Theoretical model of Raman rotational spectrum of gas mixture applied to air mixture of oxygen and nitrogen to determine temperature
[NASA-TN-D-7126] 06 p0679 N73-15525
Temperatures of various adiabatic and isobaric mixtures of humid atmospheric air with water or ice
[PUBL-SER-B-68] 12 p1465 N73-21866
Statistical mechanics of negative temperatures of particles in motion
[NASA-CR-131572] 13 p1562 N73-22664
Static longitudinal and transverse susceptibilities calculated for iron fluoride as function of temperature
[AD-757009] 14 p1698 N73-23781
Determination of vibrational temperature of molecular nitrogen in high atmosphere by chemical release of hydrogen iodide from sounding rocket
[AD-757909] 15 p1782 N73-24448
Cavity temperature and flow characteristics in gas-core reactor for testing fissioning uranium plasmas
[NASA-TM-X-2797] 15 p1809 N73-24662
Analysis of wing leading edge buckling due to aerodynamic heating to show effect of shear modulus of material and geometry of leading edge on buckling onset
[ARC-R/M-3197] 16 p1851 N73-25000
Fluorinated esters of polycarboxylic acid and lubricating compositions for use at extreme temperature
[NASA-CASE-MFS-21040-1] 21 p2505 N73-30098
Statistical analysis of annual maximum temperatures of Paris
[MN-MONO-90] 22 p2694 N73-31580

**TEMPERATURE COMPENSATION**

Development of temperature compensated light source with components and circuitry for maintaining luminous intensity independent of temperature variations
[NASA-CASE-ARC-10467-1] 05 p0518 N73-14214

**TEMPERATURE CONTROL**

Laboratory prototype flash evaporator design, fabrication, and testing for space shuttle environmental control expendable heat sink
[NASA-CR-128608] 01 p0057 N73-10470
Effects of gravity-induced free convection of melting behavior of paraffin slab for thermal control devices
[NASA-CR-123954] 04 p0385 N73-13130
Mathematical model for phase change solidification in thermal control devices, including natural convection effects and transient, two dimensional, finite difference solution
[NASA-CR-129910] 04 p0385 N73-13132
Mathematical model and experimental evaluation of performance of phase change thermal control devices containing high thermal conductivity metal matrices
[NASA-CR-129909] 04 p0385 N73-13133
Atomic hydrogen maser with bulb temperature control by output frequency difference signal for wall shift elimination
[NASA-CASE-HQN-10654-1] 04 p0428 N73-13489
Fundamentals for designing thermal control of satellites
04 p0447 N73-13646
Conceptual design of thermal control system for space stations
[NASA-CR-123956] 04 p0484 N73-13950
Design, fabrication, and comparison of heat pipes for temperature control in meteorological satellite
[ESRO-CR-59] 05 p0606 N73-14929
Thermal control of scientific instrument package in large scale telescope
05 p0608 N73-14946
Development of technology for design and application of self controlled, variable conductance heat pipes for spacecraft thermal control
[NASA-CR-114530] 06 p0730 N73-15957
Development of space stable thermal control coatings for application to spacecraft surfaces
[NASA-CR-124003] 07 p0854 N73-16922
Analytical methods for estimating circumferential and longitudinal temperature distributions in large space telescope
[NASA-TN-D-7174] 07 p0855 N73-16931
Analysis of heat supply requirements and heating availability in geographical areas of USSR
[JPRS-58114] 08 p0917 N73-17513
Analysis of effect of chord size and cooling methods on cooling requirements for air cooled turbine blades - Vol. 1
[NASA-CR-120882-BK-1] 08 p0954 N73-17809
Analysis of effect of chord size and cooling methods on cooling requirements for air cooled turbine blades - Vol. 2
[NASA-CR-120882] 08 p0954 N73-17810
Parametric weight analysis of heat rejection systems for environmental control/life support system space shuttle orbiter
[NASA-CR-128735] 08 p0965 N73-17884
Design of porous cooled medium surface to maintain specified design temperature while subjected to uniform heating from external source
[NASA-TN-D-7176] 08 p0969 N73-17919
Effects of backlash and dead band on temperature control of primary loop of conceptual nuclear Brayton space powerplant
[NASA-TM-X-2754] 09 p1064 N73-18679
Influence of immersion in temperature controlled bath on circulation and water balance in human body
[NASA-TT-F-14834] 10 p1119 N73-19124
Design and development of thermomechanical pump for transmitting warming fluid through fluid circuit to control temperature of spacecraft instrumentation
[NASA-CASE-NPO-11417] 15 p1790 N73-24513
Automatic temperature controller for liquid cooled garment based on total evaporative water loss during exercise
[NASA-TN-D-7311] 16 p1868 N73-25126
Automatic temperature control for liquid cooled space suit
[NASA-CASE-ARC-10599-1] 17 p1988 N73-26071
Temperature control system comprised of wheatstone bridge with RC circuit
[NASA-CASE-NPO-11304] 17 p2030 N73-26430
Thermal/vacuum tests of engineering test unit of electron-proton spectrometer
[NASA-CR-128701] 17 p2033 N73-26451
Guidance for assessment and control of spacecraft temperatures
[NASA-SP-8105] 17 p2088 N73-26890
Postflight analysis of Apollo 11 glycol temperature control valve failure
[NASA-TM-X-69200] 17 p2088 N73-26896
Research and development of high performance satellite thermal control louver array actuator including single blade and multiple blade actuation system
[ESRO-CR[P]-247] 18 p2201 N73-27766
Feasibility analysis and prediction performance of constant temperature heat pipe for space applications
[ESRO-CR[P]-246] 18 p2207 N73-27810
Space shuttle environmental and thermal control/life support system
[NASA-CR-134009] 21 p2504 N73-30091
Development and characteristics of thermal control system for maintaining constant temperature within spacecraft module with wide variations of component heat transfer
[NASA-CASE-GSC-11018-1] 21 p2599 N73-30829
Methanol heat pipe using nitrogen gas for temperature control
[NASA-CR-114597] 21 p2606 N73-30884
Temperature control of welding equipment by detection of discrete bands of infrared radiation from objects being heated
[NASA-CASE-MFS-20781-2] 22 p2672 N73-31401
System controls description for 36 zone thermal simulation system for operation and maintenance
[NASA-CR-124436] 24 p2901 N73-33154
Reference material for thermal simulation system for programmers, temperature controls, power regulator, peripheral equipment, and radiant array purchased parts
[NASA-CR-124437] 24 p2901 N73-33155
Direct broadcasting TV communication satellite temperature control by louvers, heat pipes, radiators, heat storage, and coatings
[DGLR-PAPER-73-052] 24 p2986 N73-33866
Development, fabrication, and evaluation of heat pipe thermal conditioning panels for temperature control of spacecraft electronic equipment - Technical Report
[NASA-CR-124451] 24 p2991 N73-33898
Development, fabrication, and evaluation of heat pipe thermal conditioning panels for temperature control of spacecraft electronic equipment - Executive Summary
[NASA-CR-124453] 24 p2991 N73-33899

**TEMPERATURE DIFFERENCES**

U TEMPERATURE GRADIENTS

**TEMPERATURE DISTRIBUTION**

Computer analysis of temperature distributions in circular and rectangular bodies exposed to thermal radiation from nuclear weapon explosions
[AD-745727] 01 p0084 N73-10699
Transient heat transfer analysis of space radiator heat rejection system under conditions of aerodynamic heating, solar, albedo, and planetary radiation
[NASA-CR-128595] 01 p0117 N73-10964
Development of equations and computer program for determining temperature distribution in walls of three eccentric annuli
[AD-747697] 03 p0287 N73-12322
Analysis of temperature sensitive paints to determine validity of coating technique and development of methods for predicting areas of high thermal gradients
[AD-749582] 04 p0409 N73-13331
Transient, two dimensional temperature field of laser pulse in solid
[SC-DR-72-0393] 04 p0429 N73-13495
Variability of temperature field of troposphere, stratosphere, and mesosphere in winter
04 p0442 N73-13606
Line spectra analysis for temperature distribution in stellar atmosphere
04 p0466 N73-13793
Analytic solution for temperature distribution in thermally insulated cylinder bar to determine time-variable thermal stresses
[DGLR-PAPER-72-112] 04 p0485 N73-13963
Approximation method for calculation of temperature distribution in microcircuit
[AD-749762] 05 p0523 N73-14255
Analysis of temperature distribution in prism heated by axisymmetrical beam of radiant heat
[NLL-M-21514-[5828.4F]] 05 p0605 N73-14921
Pressures and temperatures on the lower surfaces of an externally blown flap system during full-scale ground tests
[NASA-TN-D-7138] 06 p0614 N73-14984
Diurnal and annual variations in intensity of urban heat island in Austin, Texas
[REPT-34] 08 p0938 N73-17679
Stratospheric turbulence as an effect of jet streams, vorticity, temperature gradients, and temperature distribution
[NLL-M-22823-[5828.4F]] 11 p1274 N73-20338
Measurements of oceanographic temperature distribution and salinity in northern Baffin Bay during midsummer 1970
[CG-373-54] 11 p1286 N73-20434
Meaning coefficients for heat flows and temperature fields of simple shaped bodies with III order boundary conditions
[NLL-M-21522-[5828.4F]] 11 p1347 N73-20929
Analysis of two-dimensional liquid metal slot jet impinging normally against uniformly heated flat plate
[NASA-TN-D-7260] 11 p1348 N73-20938
Numerical analysis of temperature distribution of complex two-dimensional body with various boundary conditions including radiation effects
[N8110R:72-040] 12 p1464 N73-21860
Effect of heat transfer on flow and temperature fields in separation nozzle measured with free molecular pressure and temperature probes
[KFK-1634] 12 p1464 N73-21865
Analysis of linear oscillating temperature distribution to determine thermal diffusivity coefficient of gases
[BER-1/73] 13 p1590 N73-22895
Temperature field calculations on cylinder solidification in axial and radial axial heat transfer
[AD-755871] 13 p1591 N73-22901
Propagation of waves in elastic-viscoplastic media in temperature field
[AD-755274] 13 p1592 N73-22905
Cooled film anemometry applied to determination of temperature and velocity distributions in wake of projectiles travelling at hypersonic speeds in free flight range
[DREV-R-648/72] 14 p1648 N73-23365
Determination of temperature distributions and deformations of rectangular plates with circular elastic inclusions
[AD-756183] 14 p1717 N73-23930
Calculating temperature distribution by applying Green function to two dimensional Laplace equation
[NAL-TR-297] 15 p1842 N73-24924
Volumetric temperature fields of internally cooled rotating blade
[AD-759246] 16 p1958 N73-25841
Calculation of temperature fields of solids under conditions of natural heat exchange with atmosphere
[AD-762494] 20 p2486 N73-29968
Efficient technique for determining apparent temperature distributions from antenna temperature measurements
[NASA-CR-2310] 21 p2538 N73-30350
Measurement of temperatures of airfoil immersed in stream of combustion gases to determine effectiveness of two phase cooling system
[ARL/ME-338] 21 p2605 N73-30876
Oceanographic survey of eastern tropical Pacific Ocean to determine oxygen content, salinity, temperature distribution, and acceleration potential
[NOAA-NMFS-CIRC-330] 22 p2656 N73-31279
Holographic interferometric measurements of three dimensional temperature fields
22 p2680 N73-31463
Simplified model for heat transfer and subsequent temperature distribution in thin metal target impacted by cylindrical projectile
[AD-763152] 22 p2730 N73-31850
Vertical temperature profile data obtained by satellite radiometer sounding
[NOAA-TR-NESS-65] 23 p2786 N73-32291
Full-scale ground tests of externally blown flap system on F-111 aircraft wing to determine pressure and temperature distributions on undersurface of wing, vane, and flap
24 p2873 N73-32947

**TEMPERATURE EFFECTS**

Development of computer model to analyze effects of temperature variations on six basic electronic components
[AD-745189] 01 p0033 N73-10256
Influence of temperature on cable parameter variations in wideband transmission system
[REPT-6670] 01 p0034 N73-10268

Analysis of sensitivity of elevated temperature deformation of nickel alloy to grain size and shape under tension and creep conditions
[NASA-CR-128403] 01 p0067 N73-10549
Nuclear magnetic resonance spectroscopy to measure order parameter in diatomic molecule rotational ordering transitions
[NOTA-INTERNA-376] 01 p0083 N73-10691
Computer program for determining solar array output characteristics while accounting for effects of temperature,incidence angle on solar arrays
[NASA-CR-130109] 02 p0129 N73-11045
Aluminizing of titanium and aluminum alloys in powder form with use of electric heating methods
[NLL-M-21479-[5828.4F]] 02 p0185 N73-11503
Chromium superalloy damage and temperature effects
[NASA-TN-D-7073] 03 p0312 N73-12549
Temperature and concentration dependence of Debye-Waller factor for superconducting Nb-Zr alloy system
[BNL-TR-483] 03 p0315 N73-12569
Influence of temperature on creep and strength characteristics of organic PRD49 fiber/epoxy composites
[NASA-TN-D-7120] 03 p0320 N73-12607
Sintering temperature and tungsten content effects on volumetric shrinkage of ferrotungsten alloy briquets
04 p0432 N73-13518
Effects of high temperature brazing and thermal cycling on mechanical properties of Hastelloy X
[NASA-TM-X-2704] 04 p0433 N73-13529
Temperature effects on tensile-, fracture toughness-, and crack growth-properties of aluminum alloy forgings
[AD-748257] 04 p0436 N73-13554
Temperature effects on measurement accuracy of static deformation of semiconductor resistance strain gages
[NASA-TT-F-14616] 04 p0481 N73-13928
Permeability of fine-pored carbons as function of mean pressure temperature and gas properties
[AD-749362] 05 p0499 N73-14064
Numerical analysis of thermal resistance of air layers in air permeable clothing
[NLL-DRIC-TRANS-2717-(3623.66)]
05 p0502 N73-14089
Cyclically changing temperature effects on monitoring behavior and physiological responses of man
[AD-748451] 05 p0505 N73-14110
Mechanical properties of uranium alloys containing additions of aluminum, iron, molybdenum, silicon, and chromium over temperature range from 20 to 640 C
[UJV-2802-M] 05 p0562 N73-14567
Yield strength of rigid polymers, discussing tensile and compression stresses
[D-MAT-180] 05 p0565 N73-14591
Influence of substrate temperature on properties of epitaxial layers of GaAs during growth
[NLL-RRE-TRANS-370-[8036.625]]
05 p0585 N73-14763
Influence of absorption magnetic thermal RF breakdown in superconducting cavities
[KFK-EXT-3/72-2] 06 p0708 N73-15780
Various dispositions of silicon solar cells as influenced by temperature gradients and proton irradiation flux
[NASA-TM-X-66169] 07 p0741 N73-16031
Procedure for repairing and recovering voice data from heat damaged magnetic tapes
[NASA-CASE-MSC-14219-1] 07 p0755 N73-16132
Atmospheric circulation and temperature effects on stratospheric ozone during winter storm period
[AD-751211] 07 p0797 N73-16479
Analysis of temperature conditions in hermetically sealed room to determine human tolerances under various climatic conditions
[FOA-1-A-1527-76] 07 p0854 N73-16924
Temperature effects on hydrogen decomposition of wall surface coatings
[NASA-TM-X-2735] 08 p0946 N73-17748
Temperature influence on atmospheric diffusion and turbulence near ground level
[AD-753350] 09 p1033 N73-18434
Interaction of velocity and temperature fields in lubricating layer of thrust slide bearings and analysis of viscosity variation along length and thickness of lubricating layer
[AD-753044] 09 p1041 N73-18487
Mechanical properties as function of temperature for unidirectionally solidified eutectic composites
[NASA-CR-124094] 09 p1046 N73-18527
Change in flow curves of superplastic aluminum-zinc alloy in different states as function of temperature
09 p1046 N73-18531
Fracture mechanics and structural fatigue of nickel alloys, aluminum alloys, and molybdenum alloys at elevated temperatures
[AD-753687] 09 p1097 N73-18958
Ultraviolet radiation, X rays, freezing, and thawing effects on ribonuclease
10 p1119 N73-19120
Initial temperature effects on diffusion burning of hydrogen flame in closed channel with supersonic flow
[NASA-TT-F-14844] 10 p1141 N73-19295
Kinetic theory of stress-strain relations and temperature induced dislocation in crystal lattices
[AD-753576] 10 p1201 N73-19777
Effect of cooling air discharged into air-gas flow of turbine engine to improve effeciency of gas turbine engine operation
[AD-753969] 10 p1210 N73-19840
Methods for bounding life of structures subjected to constant loads and temperature within creep range
[RD/B/N-2257] 10 p1220 N73-19925
Thermodynamic properties of high altitude balloons to show effects of ascent, sunrise, surface coating, and thermal insulation
[TAMRF-921-7305] 11 p1234 N73-20021
Relationship between temperature and surface layer quality of two row roller bearings polished with abrasive cloth
[AD-754678] 11 p1301 N73-20559
Ultrasonic relaxation measurement of polyethylene and polyethylene oxide from room temperature to melting point
[AD-754391] 11 p1310 N73-20628
Effects of electron irradiation and temperature on 1 ohm-cm and 10 ohm-cm solar cells
[NASA-TM-X-66231] 12 p1366 N73-21083
Electrical conductivity of sintered nonstoichiometric CeO[2-x] as function of temperature
[COO-1441-17] 12 p1416 N73-21474
Analysis of interrelation of ocean and atmosphere based on temperature of surface layer of water in Atlantic and Pacific Oceans
12 p1421 N73-21514
Structural recrystallization of steels during fast and slow heating to show structural succession caused by different mechanisms of formation of austenite
13 p1541 N73-22481
Analysis of alpha to gamma transformation in steel to determine effect of initial state nonequilibrium on starting temperature
13 p1541 N73-22482
Temperature dependence of sparingly soluble electrolytes and nonelectrolytes
[AD-757504] 14 p1617 N73-23102
Temperature effects on supersaturation in thermal diffusion chamber
[AD-758137] 14 p1646 N73-23354
Numerical analysis of thermoelastic state of shells subjected to thermal impact on the surface of the shell
14 p1715 N73-23912
Analysis of heat transfer properties of air, helium, and carbon dioxide and effects of variations of fluid properties with temperature
[ARC-R/M-3246] 15 p1729 N73-24021
Development of continual solution for stress distribution due to thermal stresses near roots of rectangular wings
[ARC-R/M-3236] 15 p1730 N73-24030
Post buckling behavior of circular plate following heating at center and heating at edge and effects of restraints on final configuration
[ARC-R/M-3245] 15 p1730 N73-24031
Temperature dependence of mercury telluride band gap
15 p1820 N73-24749
Temperature dependence of elastic constants and Debye temperature of NaCl and KCl single crystals
[NASA-TT-F-14932] 16 p1953 N73-25801
Influence of wind speed and direction, and temperature on radon gas concentration in atmosphere
17 p2017 N73-26309
Temperature dependence of strain hardening in metals
[RAE-LIB-TRANS-1672] 17 p2043 N73-26531
Temperature effects on swelling of nickel irradiated by medium energy heavy ions
[CEA-CONF-2052] 17 p2044 N73-26540
Stability and temperature characteristics compared for some silicon and selenium photodetectors to determine suitability for photometric or radiometric measurements
[NBS-TN-594-5] 17 p2072 N73-26765
Effect of high temperature and oil immersion on rubbers
[AD-760066] 18 p2167 N73-27503
Flow velocity, GeCl4 concentration, and temperature effects on growth and morphology of autoepitaxial Ge films
18 p2189 N73-27674
Numerical analysis of temperature and stresses in cylindrical body heated with constant heat flow
[NLL-M-21601-[5828.4F]] 18 p2205 N73-27794
Heat exchange between cooled polydisperse granular material and transversely located cylindrical tubes arranged in staggered bundle
[NLL-M-21602-[5828.4F]] 18 p2205 N73-27795
Influence of atmospheric pressure and temperature on viscosity and density of mineral oil and siloxane liquids
[AD-761590] 19 p2232 N73-27999
Temperature effects on hot extrusion of stainless steels
[AD-761538] 19 p2306 N73-28551
Temperature interrelationships between rat brain tissues and cerebral blood supply
20 p2366 N73-29026
Temperature dependence of several vibrational relaxation processes in DF-CO2 mixtures
[AD-762925] 20 p2374 N73-29078
Analysis of relationships of dissociation elasticity of vanadium mononitride to composition and temperature based on thermodynamic theory of non-stoichiometric compounds
[NLL-M-21638-[5828.4F]] 20 p2428 N73-29506
Ultrasonic absorption and dielectric loss as function of temperature in heterophase block copolymers
[AD-762452] 20 p2435 N73-29559
Analysis of maximum fuel pin temperature during nominal operation of advanced power reactor to show possible variations in maximum temperature
[NASA-TM-X-68217] 20 p2453 N73-29716
Analysis of structure dependent and temperature dependent variables affecting flow curves of metals
[BLL-RAE-LIB-TRANS-1675] 21 p2556 N73-30494
Solubility curves from 25 to 70 C for K2HfF-K2ZrF6-HF system
[BM-RI-7785] 21 p2558 N73-30505
Influence of carbon stabilizing elements and temperature on cold worked austenitic stainless steel corrosion
[CEA-CONF-2119] 21 p2560 N73-30518
Effect of temperature and strain rate on tensile properties of aluminum-boron, epoxy-boron, and epoxy-graphite composites
[AD-763656] 21 p2564 N73-30551
Temperature effects and effect of addition of lithium fluoride on conductivity of magnesium oxide
[NLL-M-23040-[5828.4F]] 21 p2585 N73-30711
Using average transmission and self-indication ratio measurements to investigate temperature dependence of resonance self-shielding effect in depleted uranium and tantalum
[NASA-TM-X-69565] 21 p2585 N73-30715
Thermal effects on planar epitaxial silicon power transistors
[AD-763903] 22 p2645 N73-31194
Universal diagram representing changes in viscosity of liquid metals as function of temperature
[FRNC-CONF-45] 22 p2684 N73-31501
Effect of temperature and extension rate on tensile properties of SAP
[AREAEE-159] 22 p2685 N73-31507
Temperature effects on copper plasticity failure, noting hydrogen role
[DRIC-TRANS-3009] 22 p2685 N73-31508
Temperature effects on structures and mechanical properties of polysulfone and poly[216-dimethyl] phenylene oxide
22 p2688 N73-31528
Properties and structure of polymers crystallized from stirred dilute solutions and sheared polymer melts
22 p2706 N73-31673
Properties of materials in high pressure hydrogen at cryogenic, room, and elevated temperatures
[NASA-CR-124394] 22 p2725 N73-31804
Equilibrium concentration and catalytic decomposition products of hydrazine at elevated temperatures and pressures
[NASA-CR-135478] 23 p2753 N73-32031
Optical and electrical properties of amorphous Si and their dependence on thermal history
23 p2807 N73-32440
Role of water temperature in bradycardia during facial immersion
[NASA-TT-F-15025] 24 p2890 N73-33072
Characteristics of natural convection induced in cylindrical layer of fluid by uniform heating from below
24 p2902 N73-33163
Self diffusion in liquid metals conducted over wide temperature intervals
[COO-841-30] 24 p2934 N73-33434
Effect of aging temperature and time on impact and tensile properties of L-605 cobalt alloy
[ORNL-TM-3734] 24 p2934 N73-33435
Influence of alloy additives on strength of nickel base alloys at temperatures from 25 to 650 C
[ORNL-TM-4173] 24 p2936 N73-33446
Susceptibility of Zircaloy 4 and niobium base alloy to hydrogen embrittlement at elevated temperature
[LA-5169] 24 p2936 N73-33447
Temperature dependence of second-order elastic constants of cubic crystalline materials derived on basis of quasiharmonic anisotropic continuum model
24 p2968 N73-33717
Temperature dependence of spin-Hamiltonian parameters for chromium doped rutile
[RR-110] 24 p2968 N73-33721
Measurement of heat conductivity of He 3 and He 4 at superflow temperature
[JINR-P8-7008] 24 p2992 N73-33912

**TEMPERATURE FIELDS**
U TEMPERATURE DISTRIBUTION
**TEMPERATURE GRADIENTS**
NT THERMOCLINES

Experimental procedure for estimating rate of thermal flow and heat transfer from longitudinally swept surfaces using unstable thermal regime method
[AD-746011] 02 p0243 N73-11977
Sterilization parameters for spacecraft
[NASA-CR-129272] 03 p0259 N73-12101
Analysis of temperature sensitive paints to determine validity of coating technique and development of methods for predicting areas of high thermal gradients
[AD-749582] 04 p0409 N73-13331
Temperature corrected circuit for gyroscope or accelerometer of digital rebalance type
[NASA-CASE-NPO-13044-1] 04 p0421 N73-13436
Development of temperature compensated light source with components and circuitry for maintaining luminous intensity independent of temperature variations
[NASA-CASE-ARC-10467-1] 05 p0518 N73-14214
Theory for Assman psychrometer based on exact analysis of diffusion process in laminar boundary layer with thermal gradients
[NLL-M-22691-[5828.4F]] 05 p0570 N73-14627
Analysis of heat transfer characteristics of hot wire normal to incompressible air flow and influence of frequency on sensitivity and temperature distribution along wire
[WTHD-33] 05 p0605 N73-14922
Investigation of urban heat island phenomena in Austin, Texas, using two-dimensional, time-dependent, earth atmosphere mathematical model
[REPT-32] 08 p0938 N73-17681
Method and device for verifying reliability of fire detectors
[NASA-CASE-GSC-11600-1] 09 p1034 N73-18436
Computational procedure for determining heat resistance of different graphites in broad temperature range
10 p1175 N73-19557
Physiological effects on rats of replacement of atmospheric nitrogen by inert gases at high and low temperatures
11 p1244 N73-20095
Stratospheric turbulence as an effect of jet streams, vorticity, temperature gradients, and temperature distribution
[NLL-M-22823-[5828.4F]] 11 p1274 N73-20338
Aerosynoptic wind and temperature conditions contributing to atmospheric turbulence at altitude of 18 km over European USSR
[NLL-M-22822-[5828.4F]] 11 p1274 N73-20342
Modification of resistive transition in superconductors by thermodynamic fluctuations
12 p1438 N73-21648
Temperature anomaly studies along 30 deg W meridian of Atlantic Ocean
[NLL-M-22849-[5828.4F]] 16 p1894 N73-25323
Helium migration in aluminum matrices under temperature gradients
16 p1926 N73-25586
Beam position monitor which operates by detection of temperature differences
[AERE-M-2372] 17 p2033 N73-26452
Numerical analysis of turbulent diffusion in stratified fluid to show variations in diffusion coefficient with changes in ocean water depth
[AD-761653] 19 p2257 N73-28190
Thermal and infrared testing for nondestructive evaluation of flaws
19 p2304 N73-28523
Atmospheric circulation effects on precipitation and temperature regimes of USSR and Northern Hemisphere
20 p2444 N73-29633
Statistical analysis of large scale fluctuations in water surface temperature of North Atlantic Ocean
21 p2572 N73-30614
Thermal analysis of carbon migration in carbide and oxycarbide systems
[AERE-R-6897] 21 p2606 N73-30885
Parametric linearization for approximating dynamic and thermal boundary layers for nonNewtonian fluids with arbitrary pressure and surface temperature gradients
[AD-764170] 22 p2655 N73-31271
Streaming in liquid metals due to thermal surface tension gradient
[TRITA-EPP-73-10] 22 p2700 N73-31626
Diurnal temperature variations and upper atmospheric tides
22 p2736 N73-31908
Spatial structure of temperature fluctuations in seas
24 p2947 N73-33535

**TEMPERATURE INDICATORS**
U INDICATING INSTRUMENTS
U TEMPERATURE MEASURING INSTRUMENTS

**TEMPERATURE INSTRUMENTS**
U TEMPERATURE MEASURING INSTRUMENTS

**TEMPERATURE INVERSIONS**
NT CENTRIFUGING STRESS
NT INTERFACIAL TENSION
NT STRUCTURAL STRAIN

Energetic role of trade wind inversion in tropical subalpine ecosystem
15 p1806 N73-24633
Aerosol physical properties from horizon inversion by satellite
[NASA-CR-112311] 18 p2144 N73-27330
Analysis of atmospheric temperature inversion conditions and requirements for thermal convection for removal of temperature inversion effects
[NLL-M-23034-[5828.4F]] 20 p2391 N73-29204

**TEMPERATURE MEASUREMENT**
Evaluation of bucket and intake system for measuring sea surface temperature and statistical analysis of data obtained from international ship observations
[WMO-336] 01 p0050 N73-10406
Design, development, and specifications of thermohygrometer for measuring fluctuations in temperature due to clouds and precipitation
[NLL-M-20703-[5828.4F]] 01 p0055 N73-10442
Temperature measurements on vibrational excited microwave discharged nitrogen
[AD-746327] 02 p0138 N73-11118
Metal temperature effect on friction factor in cold rolling within 20 to 250 C
[AD-746935] 02 p0180 N73-11455
High altitude wind and temperature measurement data from meteorological sounding rockets and radiosonde observations - February 1971
02 p0204 N73-11652
Recirculation flow velocities and temperatures of VTOL lift engines
[DLR-FB-72-50] 02 p0223 N73-11806
Development of method for measuring temperature of wind tunnel scale model by photographic recording of changes in thin film phase-change temperature indicating material
[NASA-CASE-LAR-11053-1] 02 p0243 N73-11972
Procedure for determining temperature distribution along linear dimension of stator of electrostatic generator
[AD-747425] 03 p0256 N73-12070
Phase difference between temperature and density in thermosphere
[NASA-TM-X-66119] 03 p0294 N73-12395
Development of system to correct upper atmosphere temperature readings to ambient air temperature
[AD-747973] 03 p0298 N73-12433
Bibliography on theory, calibration, pyrometric devices, and temperature measurements
[NBS-SP-373] 03 p0364 N73-12962
Thermocouple apparatus for measuring wall temperatures in regeneratively cooled rocket engines having thin walled cooling passages
[NASA-CASE-XLE-05230-2] 04 p0419 N73-13417
Temperature measurement of air layer directly over ocean surface
[NLL-M-20745-[5828.4F]] 05 p0529 N73-14308
Thermochromic compositions for detecting heat levels in electronic circuits and devices
[NASA-CASE-NPO-10764-1] 05 p0545 N73-14428
Surface and PCM temperature measurement of capacitors during melting and solidification
05 p0608 N73-14945
Geothermal data from deep water and bottom sediment measurements in Atlantic and Pacific Oceans
[AD-749983] 06 p0669 N73-15441
Comparative inter-laboratory creep rupture tests on temperature measurement and control
[PB-211172] 06 p0674 N73-15487
Preparation, testing, and use of superconductive fixed point devices incorporating lead, indium, aluminum, zinc, or cadmium as standard reference materials
[NBS-SP-260-44] 06 p0707 N73-15768
Analysis of combustion liner wall temperatures under steady-state and convective heat balance conditions and comparison with experimental values
[NASA-TM-X-2711] 06 p0730 N73-15959
Development of method for determining sea surface temperature using remote sensors in earth orbiting satellites
07 p0788 N73-16410
Measurement of cloud base temperature with infrared detector and comparison with lidar and radiosonde results
[BMVG-FBWT-72-17] 07 p0815 N73-16611
Development of solid state magnetic digital temperature transducer - Vol. I
[NASA-CR-133832] 08 p0923 N73-17556
Characteristics of noble metal thermocouples under prescribed temperature ranges and environmental conditions to determine effects on accuracy and stability of temperature measurements
[NASA-CR-120990] 08 p0925 N73-17578
Multichannel digital spectrometer for measuring ion temperature of Circe 25-kW device
[EUR-CEA-FC-641] 08 p0925 N73-17582
Influence of urban and suburban area on wind and temperature profiles at Austin, Texas
[REPT-33] 08 p0938 N73-17680
System for measuring turbine blade temperature
[NASA-CR-124056] 08 p0953 N73-17805
Rotational temperature measurement in nitrogen using unresolved rotational spectra
[DLR-FB-72-15] 09 p0998 N73-18148
Methods for measuring temperature in wind tunnels with electric contact thermometers
[DLR-MITT-72-27] 09 p1010 N73-18246
Effect of cloud conditions on satellite infrared spectrometer temperature retrievals
[NOAA-TR-NESS-63] 09 p1034 N73-18435
Spectroscopic methods for temperature measurement in plasmas with self absorption noting methods for plasma column radial temperature distribution
[BMBW-FBK-72-22] 09 p1071 N73-18737
Comparison of two total pressure and total temperature measuring instruments for boundary layer investigations at supersonic speeds
10 p1139 N73-19284
Local measurements and their statistical interpretation for high velocity two phase flow with high void fraction
[CEA-CONF-2043] 10 p1141 N73-19300
Temperature measurement of heavy nonferrous metals and alloys, steels, titanium, and other metals in plastic zone
[NLL-RTS-6867] 10 p1163 N73-19456
Thermocouple measurement of gas velocity and temperature near liquid rocket injector face
[NASA-CR-121100] 11 p1270 N73-20304
Relationship between surface temperature anomalies in European USSR and seasonal variations of stratospheric circulation
[NLL-M-22851-[5828.4F]] 11 p1274 N73-20336
Sea water temperature measurement from Raman spectra
[AD-753481] 11 p1288 N73-20450
Analysis of requirements, instruments, and procedures for measurement of aircraft temperatures up to Mach 2.3 and altitudes up to 80,000 feet
[AGARD-AG-160-VOL-2] 11 p1294 N73-20499
Techniques for measuring heat transfer in short duration and rapidly varying flows
[AGARD-AG-165] 11 p1349 N73-20945
Measurement of Mediterranean Sea temperature profiles using free drifting, self-recording drogues equipped with thermistor chains
[AD-753442] 12 p1402 N73-21372
Diagnostics of flow fields using Raman scattering technique
[AD-757319] 14 p1652 N73-23400
Upper atmospheric wind velocity and temperature measurements
[NASA-TT-F-14921] 14 p1659 N73-23470
Measurements and techniques of low temperature acoustic thermometry
[NBS-TN-765] 14 p1666 N73-23518
Measurement of aerodynamic heating on nose of Fairey Delta aircraft at 40,000 feet and Mach numbers to 1.65 during climb and level flight
[ARC-R/M-3280] 15 p1725 N73-23996
Characteristics of photoelectric pyrometer for measuring temperature of thin wire during rolling process
[NLL-M-21634-[5828.4F]] 15 p1785 N73-24471
Characteristics of system for obtaining continuous profiles of ocean conductivity, temperature, and sound velocity as functions of depth
[NOAA-IFS-73009] 15 p1787 N73-24489
Electron beam probing technique for measuring hypersonic rarefied gas density, vibration, and rotational temperature
[ONERA-P-146] 15 p1788 N73-24497
Effect of humidity on laminar recovery temperature measurements during supersonic air flow in wind tunnels
[ARC-R/M-3215] 16 p1857 N73-25042
Raman scattering techniques in atmospheric temperature measurements
[NASA-TM-X-68250] 16 p1906 N73-25422
Transient temperature measurement errors in intrinsic thermocouples caused by heat transfer
[SC-RR-72-0719] 16 p1975 N73-25970
Upper atmosphere wind and temperature measurements from Sonmiani, Pakistan, using rocket grenades - 1965 - 1967
[NASA-CR-133401] 18 p2144 N73-27331
Thermal conductivity measurements of particulate materials in vacuum using basalt and soda lime glass beads of various size ranges as samples
[NASA-TM-X-64759] 18 p2205 N73-27801
Determination of rotational temperatures in flow gas discharges containing nitrogen using sidelight spectroscopy techniques
[AD-762290] 19 p2233 N73-28002
ISIS-A electro static probe measurements of electron concentration and temperature of plasmapause at mid-latitudes
[NASA-TM-X-70429] 19 p2293 N73-28442
Measurement of ionic conductivity and temperature in Apollo 15 plume
[AD-761484] 19 p2353 N73-28924
Collection of ground truth data in Great Basin for support of aerial and Skylab overflights
[E73-10884] 20 p2394 N73-29235

Development of catalogs for backscatter and brightness temperature measurements and atmospheric effects on Skylab S-193 data
[E73-10896] 20 p2395 N73-29245
Preparation of backscatter and brightness temperature measurement catalogs and atmospheric effects on Skylab S-193 data
[E73-10897] 20 p2395 N73-29246
Analysis of thermal radiation brightness of river strip as basis for determining actual temperature from data provided by satellite
20 p2400 N73-29288
Analytic function of electron temperature measurements in ionosphere by high frequency probe method
20 p2410 N73-29372
Electron concentration and temperature measurements, using cylindrical Langmuir probes
20 p2410 N73-29374
Airborne radiometer for continuously measuring sea water temperature
[NASA-TT-F-15070] 20 p2419 N73-29441
Analysis of maximum fuel pin temperature during nominal operation of advanced power reactor to show possible variations in maximum temperature
[NASA-TM-X-68217] 20 p2453 N73-29716
Ground-based radiation thermometry mapping of volcanology in Central America
[E73-10937] 21 p2529 N73-30279
Measurement of temperatures of airfoil immersed in stream of combustion gases to determine effectiveness of two phase cooling system
[ARL/ME-338] 21 p2605 N73-30876
Exhaust blast velocities and temperatures at ground level for various aircraft and wing tip vortex velocity for C-5 aircraft
[AD-764228] 22 p2616 N73-30961
Measurements of temperature and pressure behind incident and reflected shocks in shock tube
[ARC-CP-1239] 24 p2909 N73-33220
Effect of friction term on equations of motion of liquid helium and measurement of temperature along axis of channel carrying supercritical heat current
24 p2990 N73-33894

**TEMPERATURE MEASURING INSTRUMENTS**
NT PYROMETERS
NT RADIATION PYROMETERS
NT RESISTANCE THERMOMETERS
NT TEMPERATURE PROBES
NT THERMOMETERS
Bibliography on theory, calibration, pyrometric devices, and temperature measurements
[NBS-SP-373] 03 p0364 N73-12962
Ingestible miniaturized telemetry device for deep body temperature measurements on humans and animals
[NASA-CASE-ARC-10583-1] 05 p0503 N73-14093
Fabrication and evaluation of cooled-gas pyrometer for application in hypersonic research engine program
[NASA-TM-X-2715] 07 p0800 N73-16496
Design and performance of wire grid temperature probes for flowing media
11 p1294 N73-20500
Design of katathermometer for measuring environmental cooling effects in simulated space flight
14 p1608 N73-23036
Calibration of liquid helium-cooled germanium bolometers to determine responsitivity at different chopper frequencies and cryostat temperatures
[BMFT-FBW-73-05] 14 p1666 N73-23524
Development of flexible thermocouple in form of tape for adaptation to special temperature measuring conditions
[NASA-CASE-LEW-11072-1] 15 p1785 N73-24472
Various infrared detectors, including thermal detectors and photodetectors
[DRIC-TRANS-3179] 21 p2549 N73-30439
Trivane measured fluctuations of wind and temperature over an inland lake
22 p2694 N73-31578

**TEMPERATURE PHOTOMETERS**
U PHOTOMETERS
U TEMPERATURE MEASURING INSTRUMENTS

**TEMPERATURE PROBES**
Organic amine and nitroaromatic mixed compound for heat change detection in microelectronic components
[NASA-CASE-NPO-10764-2] 11 p1264 N73-20259

**TEMPERATURE PROFILES**
Thermal sounding experiment by Meteor satellite
[NASA-TT-F-14493] 01 p0104 N73-10861
Possibilities of obtaining temperature profiles for Mars atmosphere by thermal sounding
[NASA-TT-F-14715] 02 p0229 N73-11859
Survey of methods for sounding atmospheric temperature profile by remote measurement
[NASA-CR-130110] 04 p0442 N73-13601
Temperature-salinity profiles of Tyrrhenian Sea
[CONTRIB-2725] 07 p0858 N73-16957
Density and temperature profiles of HI lines in interstellar dust clouds
12 p1448 N73-21723
Exponential laws for temperature, velocity, and CO-concentration profiles in nitrogen hot gas jet or nitrogen-propane flame in free atmosphere, in application to supersonic combustion
[DLR-FB-73-05] 12 p1465 N73-21867
Systems analysis of active thermal control using thermoelectric devices
[NASA-CR-124256] 15 p1843 N73-24935
Temperature characteristics of film cooled and non-film cooled vanes incorporating impingement cooling
[NASA-TM-X-2819] 18 p2205 N73-27798
Development of numerical methods for computation of vertical divergence of thermal radiation
20 p2400 N73-29290
Surface boundary layer temperature profiles and turbulent heat flux during onshore flow
[REPT-38] 21 p2524 N73-30239
Variability of eigenvectors and eigenvalues using autocorrelation matrices of vertical temperature profiles on regional latitudes
[AD-763145] 21 p2539 N73-30360
Influence of temperature and wind profiles on water upwelling
24 p2974 N73-33765

**TEMPERATURE SENSORS**
NT THERMISTORS
Performance evaluation of iridium/rhodium integrated probe/fluidic temperature sensor up to 3000 F
[AD-745987] 02 p0175 N73-11417
Analysis of temperature sensitive paints to determine validity of coating technique and development of methods for predicting areas of high thermal gradients
[AD-749582] 04 p0409 N73-13331
Pyroelectric temperature sensors for ignition mechanism of anti-vehicle mines
[LCR-DR-1-71-266/1/R] 12 p1465 N73-21870
C-130 aircraft flights to obtain simulated operation of Skylab multispectral scanner, thermal scanner, and cameras
[E73-10761] 17 p2023 N73-26361

**TEMPERATURE TRANSDUCERS**
U TEMPERATURE MEASURING INSTRUMENTS
U TEMPERATURE SENSORS

**TENNESSEE**
NT TENNESSEE VALLEY [AL-KY-TN]
Monitoring rural landscape changes in eastern Tennessee through interpretation of ERTS-1 imagery
[E72-10177] 01 p0045 N73-10356
Analysis and interpretation of ERTS-1 ecologic, geographic, and agricultural data for Tennessee Valley
[E72-10231] 02 p0163 N73-11324
ERTS-1 imagery of landscape changes in Tennessee and Kentucky due to strip mining
[E72-10265] 03 p0291 N73-12364
Geographic applications of ERTS-1 imagery to land use and landscape changes in Tennessee
[E72-10315] 04 p0412 N73-13364
Detection of plant diseases and nutrient deficiencies, soil types, and moisture levels in Tennessee using ERTS-1 imagery
[E72-10320] 04 p0413 N73-13368
Geographic applications of ERTS-1 imagery to rural landscape change in Tennessee
[E72-10355] 05 p0534 N73-14343
Geographic applications of ERTS-1 imagery to rural landscape changes in eastern Tennessee
[E73-10040] 07 p0776 N73-16303
Detection of plant and forest diseases, nutrient deficiencies, soil types, and soil moisture levels from ERTS-1 imagery of Tennessee
[E73-10311] 09 p1022 N73-18343
Determination of ecosystem-vegetation boundaries from ERTS-1 imagery of Tennessee
[E73-10417] 11 p1279 N73-20379
Detection of plant diseases and nutrient deficiencies, soil types, and moisture levels from ERTS-1 imagery of Tennessee and Kentucky
[E73-10468] 12 p1395 N73-21305
Utilization of ERTS-1 imagery to detect plant diseases, nutrient deficiencies, soil types, and moisture levels in Tennessee
[E73-10640] 15 p1776 N73-24399
Geographic analysis and mapping of landscape changes in Tennessee from ERTS-1 imagery
[E73-10661] 16 p1899 N73-25357
ERTS-1 imagery of strip mining activity in Cumberland Plateau, Tennessee Test Site and agricultural areas in Alabama, Georgia, and Tennessee
[E73-10694] 16 p1902 N73-25386
Application of ERTS-1 imagery for delineation of major soil association in loess region of Obion County, Tennessee
[PAPER-A14] 19 p2261 N73-28222
Geographic applications of ERTS-1 data to landscape changes in eastern Tennessee
[PAPER-L10] 19 p2274 N73-28306
ERTS-1 imagery of landscape changes, strip mines, timber, agriculture, and water resources in eastern Tennessee
[E73-10843] 19 p2291 N73-28421
Airport environment compatibility plan for Jackson, Tennessee
[PB-221129] 22 p2648 N73-31217
Detection of plant diseases, soil moisture, drainage patterns, forestry types, and sedimentation in Tennessee from ERTS-1 imagery
[E73-11091] 23 p2782 N73-32258

**TENNESSEE VALLEY [AL-KY-TN]**
Digital processing of ERTS-1 imagery of Tennessee Valley
[E73-10054] 07 p0778 N73-16316
Computer processing, enhancement, and recognition of ERTS imagery of Tennessee Valley
[E73-10056] 07 p0778 N73-16318
Identification and mapping soil in Tennessee Valley from ERTS-1 imagery
[E73-10477] 12 p1395 N73-21314
Processing techniques for ERTS-1 imagery of Tennessee Valley
[E73-10633] 15 p1776 N73-24392
Interpretation of ERTS-1 MSS imagery of Tennessee Valley
[E73-10854] 19 p2292 N73-28431
Delineation of major terrain features, land uses, and crop species in Tennessee Valley through computerized analysis
[E73-11089] 24 p2913 N73-33251

**TENSILE CREEP**
Neutron irradiation effects on tensile and creep properties of cold worked stainless steel
[HEDL-SA-468] 16 p1929 N73-25607

**TENSILE DEFORMATION**
Influence of tensile velocity on plasticity of cold deformed technically pure nickel
09 p1046 N73-18533
Role of microstructure on acoustic emission in deformation of Al-CuAl2 composites
[AD-758378] 14 p1679 N73-23628
Influence of microstructure on tensile deformation and fracture in high strength Al-Zn-Mg alloys
[ARL/MET-NOTE-86] 18 p2160 N73-27447

**TENSILE PROPERTIES**
Relationship of tensile properties and fracture toughness levels to microstructure of Ti6Al2Sn4Zr6Mo
[AD-751530] 07 p0810 N73-16566
Analysis of relation between fracture toughness and yield strength in high strength titanium alloys
[AD-752575] 08 p0933 N73-17643
Effect of discontinuous changes in strain rate on relationship between strain rate, strain and stress in Udimet 700 alloy at elevated temperatures
10 p1219 N73-19916
Controlled nitrogen additions on mechanical properties of tantalum tubing in nuclear reactors
[NASA-TN-D-6999] 11 p1305 N73-20587
Superplastic flow as common phenomenon during plastic deformation of metals and alloys
[AD-756601] 13 p1544 N73-22512
Analysis of relationship between texture development and normal anisotropy in cold-rolled, low carbon steel
[NLL-M-21627-[5828.4F]] 15 p1797 N73-24567
Effects of O2 on mechanical properties, elastic limit, and tension resistance of nonferrous metals
[EURISOTOP-59] 15 p1798 N73-24577
Tensile properties and creep behavior of tungsten alloys dispersion strengthened by ZrO2
16 p1927 N73-25590
High temperature strength and deformation properties of Ti-Al-Si alloy aged by alpha phase precipitate particles
[NASA-TN-D-7325] 16 p1928 N73-25597
Effect of Al-Zn-Mg-Cu alloy composition variations on fracture strength and tensile properties
[RAE-TR-72173] 17 p2046 N73-26549
Effect of temperature and strain rate on tensile properties of aluminum-boron, epoxy-boron, and epoxy-graphite composites
[AD-763656] 21 p2564 N73-30551
Effect of surface properties on tensile properties of beryllium under hydrostatic pressure
[NEL-537] 22 p2684 N73-31502
Effect of temperature and extension rate on tensile properties of SAP
[AREAEE-159] 22 p2685 N73-31507
Short-term tensile and low-cycle fatigue behavior of zirconium-copper at 482C to 593C
[NASA-CR-121260] 24 p2934 N73-33430
Effect of aging temperature and time on impact and tensile properties of L-605 cobalt alloy
[ORNL-TM-3734] 24 p2934 N73-33435

**TENSILE STRENGTH**
Tensile and stripping strength data in terms of failure probability for bolts, nuts, screws, and threaded rods
[ESDU-67019] 01 p0110 N73-10908
Influence of interlamellar spacing on strength of Ni3Al-Ni3Cb eutectic
[AD-748658] 03 p0319 N73-12601
Tensile strength determined for two commercial boron filaments
[AD-752505] 08 p0936 N73-17663
Large diameter, carbon-carbon composite, monofilaments from pyrolysis of organic precursor resins
[NASA-CR-120973] 12 p1408 N73-21414

Transverse tension strength and stiffness of unidirectional carbon fiber reinforced plastic
[RAE-TR-72129] 12 p1416 N73-21477
Strength mechanism of stress wave emission in steel and aluminum alloys during tensile testing
[RFP-TRANS-104] 12 p1463 N73-21854
Application of nuclear gamma resonance for changing structural state of crystal lattice of alloys to improve strength properties
13 p1541 N73-22486
Analysis of production and characteristics of ultrahigh strength steels based on survey of literature
[ARL/SM-NOTE-378] 14 p1675 N73-23591
Tensile strength testing of multilayer thin metal film structures
[AD-757723] 14 p1681 N73-23645
Development of high temperature titanium alloys with improved tensile strength
[AD-759215] 16 p1930 N73-25614
Micromechanical failure criteria for tensile and shear strengths of composites
[AD-761221] 18 p2167 N73-27504
Filler effect on tensile strength characteristics of thermosetting polymers
20 p2434 N73-29552
Effects of microstructure differences on tensile strength of graphite fibers
[AD-763687] 21 p2564 N73-30557
Shear, flexural, and tensile strength performance of carbon fiber composites made from epoxy, phenolic, polyester, and polyimide resins
[AQD/NM-000198] 22 p2689 N73-31536

**TENSILE STRESS**
Elastic stresses in flat plates, strips, and lugs due to interference-fit pins or bushes
[ESDU-71011] 01 p0111 N73-10916
Elastic stresses in single lap joints under compression or tension
[ESDU-67008] 01 p0111 N73-10920
Computation of tensile stress in shackles assuming elastic deformation
[NPL-NAC-17] 02 p0179 N73-11447
Fatigue strength of tensile strained 45 and 40Kh steel
[NLL-SMRE-TRANS-5862-[8313.4]]
02 p0184 N73-11494
Strain hardened properties of 304L stainless steel surfaces under combined tension and torsion
[AD-746472] 02 p0188 N73-11525
Numerical analysis of stresses produced in bolt or similar threaded object from application of known tightening torque to bolt head or engaged nut
[ESDU-72022] 05 p0601 N73-14888
Fatigue tests to determine service life of aluminum alloy lugs with push-fit pins under tensile stress conditions
[ESDU-72020] 06 p0723 N73-15901
Application of least square point matching for stress analysis of shallow, perforated, cylindrical shell subjected to tension, edge moment, or transverse shear
[AD-750942] 06 p0728 N73-15942
Equation for calculating plastic deformation of metals under tension
[AD-751151] 07 p0810 N73-16571
Hydraulic biaxial medium-rate tension-torsion testing machine
[REPT-1047/72] 10 p1161 N73-19449
Buckling and vibration behavior of tensioned sheets with elliptical openings
13 p1584 N73-22840
Device for measuring tensile forces applied to tension members
[NASA-CASE-MFS-21728-1] 16 p1912 N73-25467
Fatigue mechanics of boron-aluminum composites under oscillating tensile loads
[AD-757213] 16 p1932 N73-25635
Mechanical properties and failure modes of glass fiber reinforced epoxy plates under high tensile loads
[AD-759153] 16 p1933 N73-25640
Analysis of fracture and creep properties of metals after extension under conditions of hydrostatic pressure as function of time
[NLL-NEL-TT-2475-[6075.461]]
20 p2429 N73-29515
Optimum edge reinforcement around a circular hole in a flat elastic sheet subjected to axial tensile stress
[ARC-R/M-3723] 21 p2604 N73-30869
Application of tension stress relaxation measurements to determine physical and mechanical properties of rubber networks during chemical reactions
[RR-204] 24 p2987 N73-33868

**TENSILE TESTERS**
U TENSILE TESTS

**TENSILE TESTS**
Effect of foil thickness on mechanical behavior of stainless steel in tension
[AD-747698] 03 p0318 N73-12596
Data processing and recording applications in tensile testing of thermoplastics
[ERDE-TR-99] 05 p0565 N73-14593
Application of data processing to flexural and tensile tests on rubber
[ERDE-TR-114] 09 p1052 N73-18579
Dynamic tear tests for determining fracture resistance properties of aluminum alloys
[AD-755436] 12 p1415 N73-21465
Comprehensive and tensile load tests on three-inch cubes of concrete
[AD-756926] 14 p1715 N73-23919
Standards for metallic specimens to include methods of mechanical and technological testing
[JPRS-59280] 17 p2044 N73-26538
Exponential equation for power law strain hardening behavior during tensile tests of structural alloys
[RAE-LIB-TRANS-1689] 17 p2092 N73-26922
Constant strain rate tensile tests to determine long-time dynamic compatibility of elastomeric materials with hydrazine
[NASA-CR-133794] 21 p2562 N73-30538
Short-term tensile and low-cycle fatigue behavior of zirconium-copper at 482C to 593C
[NASA-CR-121260] 24 p2934 N73-33430
Method for determining stress and displacements infinite plate with hole of various shapes under uniform tension of compression
24 p2988 N73-33882

**TENSION**
Supersonic wind tunnel tests on three dimensional turbulent boundary layer growth on wires leading to calculation of tension and skin friction on aircraft towlines
[ARC-CP-1235] 23 p2740 N73-31933

**TENSION TESTERS**
U TENSILE TESTS

**TENSOMETERS**
Development of curves for determining magnitude and direction of principal stresses and strains in plane stress field from strain gage readings
[ESDU-72014] 05 p0601 N73-14890

**TENSOR ANALYSIS**
Tensor analysis application to relativity theory and measurements of solar gravitational fields using European geodetic solar probes
[ESRO-SN-118-ESTEC] 02 p0231 N73-11877
Tensor theory applied to special and general relativity, noting gravitational theory
02 p0231 N73-11878
Development of apparatus and technical procedures for measuring system inertia tensor parameters of precession nonrigid systems
05 p0547 N73-14442
Tensor analysis of strength and failure of composite materials
[AD-761994] 19 p2313 N73-28600
Analysis of equations of finite elasticity to show nonapplicability of rest state constraint associated with strain energy function
[AD-764667] 23 p2855 N73-32817

**TERMINAL BALLISTICS**
Procedure for solving nonconservative projectile penetration problems
[AD-746140] 02 p0219 N73-11774
Shock wave attenuation in foam water mixtures containing Freon and exposed to hydraulic impact
[AD-748350] 04 p0407 N73-13318
Terminal ballistic performance of fiber glass epoxy composite material for aerodynamic control surfaces
[AD-752918] 09 p1053 N73-18584
Computerized simulation of terminal homing missile trajectory
[AD-754543] 11 p1344 N73-20904
Velocity slowdown calculation for spherical and cubical fragments as function of distance
[TL-1972-16] 14 p1597 N73-22943
Analysis of threshold penetration of spherical projectiles impacting aluminum single wall targets at hypervelocity speeds
[NASA-TN-D-7308] 21 p2603 N73-30865
Computerized simulation of weapon system terminal ballistics and impact effectiveness
[AD-764884] 23 p2867 N73-32921

**TERMINAL FACILITIES**
Satellite communication terminal for ships
01 p0026 N73-10204
Design, development, and evaluation of mockup of control tower for airport traffic control functions
[FAA-NA-72-63] 02 p0152 N73-11235
Simulator test to evaluate use of air traffic control radar beacon code assignment plan to provide interim radar data processing capability
[FAA-RD-72-103] 02 p0207 N73-11681
Evaluation of automated air traffic control system and comparison with operator performance using manual system
02 p0207 N73-11683
Characteristics of air traffic control system to include components of system and application of automation to obtain system safety
[MTR-6152-REV-1] 05 p0577 N73-14698
Development and characteristics of terminal area simulation for analysis of air traffic control requirements and improvement in flight safety conditions
[NASA-CR-112195] 05 p0577 N73-14699
Design and development of microwave landing system for operation of civil and military aircraft in conventional and V/STOL configurations
[AD-749505] 05 p0578 N73-14702
Analysis of Canadian air traffic control system to include human factors aspects, automation, and environmental engineering
[DCIEM-825] 06 p0696 N73-15670
Analysis of factors affecting development and operation of satellite airport system as method for relieving congestion at metropolitan airports
07 p0765 N73-16216
Analysis of airport operations to show importance to community, effect on environment, and application of new technologies for airport development
10 p1183 N73-19625
Comparison tests of strobe and incandescent beacons to determine suitability as replacement for standard rotating airport beacon
[FAA-NA-73-1] 11 p1255 N73-20182
Characteristics of operational airport surveillance radars and methods for improving performance to meet air route surveillance requirements
[ATC-14] 11 p1255 N73-20183
Analysis of technical and economic feasibility of constructing offshore airport in New York Metropolitan area
[FAA-RD-73-45] 11 p1267 N73-20280
Research and development projects conducted by Federal Aviation Administration to improve air traffic control and flight safety
[FAA-EM-73-2] 11 p1321 N73-20720
Analysis of impact of major airport operations on economy, ecology, and urban development
13 p1505 N73-22199
Proceedings of conference on short haul air transportation to show development requirements, economic aspects, and urban and environmental impacts
[M73-54] 14 p1600 N73-22974
Development of wake vortex avoidance system for airports to reduce hazards caused by aircraft wakes and permit increased utilization of terminal facilities
[FAA-ED-21-1] 14 p1645 N73-23342
Stochastic network to model materials handling operations at air cargo terminals
[AD-757629] 14 p1647 N73-23356
Activity network to model cargo flow through air cargo terminal
[AD-757628] 14 p1647 N73-23357
Development of air navigation system to provide four dimensional guidance for short takeoff aircraft operating in terminal area
[NASA-TM-X-62234] 14 p1687 N73-23686
Analysis of terminal air traffic control procedures to determine impact of automation on air traffic controller personnel
14 p1688 N73-23700
Numerical anlaysis of optimal control and sequencing of air traffic control operations in near terminal area
14 p1688 N73-23701
Analysis of development program for improving US air traffic control procedures for 1980 time period
14 p1690 N73-23718
Development of air traffic control procedure to permit short takeoff aircraft landing along curved approach trajectory and analysis of data transmission requirements
16 p1859 N73-25055
Analysis of economics and finances of airport operations to determine procedures for improved management and operation
[REPT-73-01210] 16 p1884 N73-25253
Analysis of dual lane runway operations at high density airport terminals using computerized simulation techniques
[ATC-17] 16 p1885 N73-25254
GERTS 3Q simulation model and data base for air cargo terminal
[AD-753925] 16 p1885 N73-25257
Objectives, goals, and program structure of project to improve performance of air traffic and control and navigation facilities within National Airspace System
[FAA-ED-21-2] 16 p1940 N73-25703
Analysis of control and display device testing for microwave landing system - Vol. I
[AD-758791] 16 p1942 N73-25713
Analysis of data rate requirements for low visibility approach with scanning beam landing guidance system
[AD-758786] 16 p1942 N73-25719
Forecasts of aviation activity at selected airports to meet needs of planning personnel for future air traffic control operations
17 p1982 N73-26019
Review and analysis of air carrier/reliever airport grant allocations and technological forecast of airport demands
[FAA-AV-72-4] 17 p2010 N73-26253
Conceptual development and cost analysis of elevated short takeoff and landing facility for test purposes
[FAA-RD-73-15] 18 p2126 N73-27179
Development of procedures for determining capacity of airports and causes of airport delays - Vol. I
[FAA-RD-73-11-VOL-1] 18 p2126 N73-27180

Airport siting, design, cost, operation, and implementation for STOL aircraft short-haul air transportation system - Vol. 3
[NASA-CR-114608] 19 p2219 N73-27900
Development of noise standard for permissible noise levels in air traffic control and navigational facilities
[FAA-RD-72-47] 20 p2452 N73-29708
Analysis of factors affecting feasibility of minimizing runway spacings for increased air terminal operational capacity - Vol. 2
[FAA-RD-72-58-VOL-2] 20 p2452 N73-29709
Flight tests of various steep gradient approaches to ground level short takeoff and landing runway to determine aircraft performance and navigation aids required
[FAA-NA-72-77] 21 p2495 N73-30025
Simulation tests of short takeoff transport aircraft to determine airport and air space requirements under normal operating conditions
[NASA-TN-D-7300] 21 p2495 N73-30026
Statistical analysis of air traffic conditions predicted for Los Angeles, California area in 1982 - Vol. 1
[MTR-6387-VOL-1] 21 p2577 N73-30653
Statistical analysis of air traffic conditions predicted for Los Angeles, California area in 1982 - Vol. 2
[MTR-6387-VOL-2] 21 p2577 N73-30654
Analysis of glide path parameters, approach control system precision, and separation standards for extension of runway capacity under instrument flight rule conditions
[AD-763142] 21 p2578 N73-30657
Numerical analysis of curved approach paths and landing sequence for multiple aircraft using same terminal facilities to provide maximum system performance
23 p2740 N73-31935
Analysis and simulation of intermittent positive control of air traffic by fully automated ground facility
23 p2816 N73-32511
Air traffic control radar beacon system interference in terminal areas
[MTR-6239] 23 p2816 N73-32512
Evaluation of air traffic control beacon alphanumeric system for automatic operation in low density airport towers and terminal facilities
[FAA-NA-73-54] 23 p2816 N73-32516
Air traffic control evaluation to determine feasibility of combining smaller aircraft into gaps on flow of normal traffic to increase effectiveness of terminal facilites
[FAA-AFS-500-1] 23 p2816 N73-32517
Patterns of behavior of airlines and air travellers in air transportation network and effects on use of satellite airports
23 p2862 N73-32876
Short haul aircraft operations in terminal area with concurrent conventional aircraft operations to show methods for improved utilization of facilities
24 p2874 N73-32953
Air traffic control problems created by introduction of large numbers of STOL aircraft into high density terminal area
24 p2874 N73-32956
Development and characteristics of 4-D guidance system for traffic control of STOL aircraft operating in congested areas
24 p2874 N73-32957
Systems analysis of problems created in terminal area by application of short takeoff aircraft for providing high speed, short haul air transportation service
24 p2874 N73-32958

**TERMINAL GUIDANCE**
Newton-Raphson techniques for analyzing reentry trajectories for heat minimization and terminal range maximization
[AD-745998] 01 p0106 N73-10882
Analysis of propagating and non-propagating motions produced by earth tides and earth rates and effects on inertial instrument performance
[AD-748274] 03 p0330 N73-12691
Analysis of guidance systems used with guided missiles
[AD-751089] 07 p0850 N73-16892
Riccati controlled feedback for guiding spacecraft during unpowered terminal phase of flight
23 p2847 N73-32751

**TERMINAL VELOCITY**
Radar observation of disk-shaped models of proposed nuclear heat source module
[NASA-TM-X-62262] 14 p1601 N73-22978

**TERMINALS**
Reduction of probability of simultaneous rainfall on millimeter wave earth satellite space communication terminals
[AD-757506] 14 p1633 N73-23242

**TERMINOLOGY**
English, French, and Spanish vocabulary of aircraft aeronautical terminology
[DOC-8800-VOL-1] 06 p0616 N73-14996
English, Spanish, and French definitions for international civil aviation terminology
[DOC-8800-VOL-2] 06 p0616 N73-14997
Definitions of stellar terms
14 p1705 N73-23834
Glossary of acronyms, abbreviations, initials, code words and phrases used at John F. Kennedy Space Center
[NASA-TM-X-69523] 23 p2866 N73-32908

**TERMS**
Definition of basic terms, notation, and forms of presentation for fatigue data
[ESDU-70016] 02 p0237 N73-11925

**TERNARY ALLOYS**
Supercooling analysis for predicting interface stability in plane front solidification of ternary alloys containing one, two, or three phases
[AD-752609] 08 p0933 N73-17639
Thermoelectricity of solid-liquid phase boundary in ternary semiconductors and alloys
[AD-756899] 13 p1478 N73-21972
Interaction of nickel base ternary matrix system with tungsten reinforcing fibers
20 p2430 N73-29521

**TERNARY SYSTEMS**
Thermodynamic properties of solid and molten silicate systems
[NPL-CHEM-21] 15 p1844 N73-24938
Research on ternary diamond-like semiconductors as long wavelength infrared detectors
[AD-763466] 21 p2586 N73-30725

**TERNARY SYSTEMS (DIGITAL)**
U DIGITAL SYSTEMS

**TERRACES (LANDFORMS)**
NT PLATEAUS

**TERRAIN**
Monitoring rural landscape changes in eastern Tennessee through interpretation of ERTS-1 imagery
[E72-10177] 01 p0045 N73-10356
Side-looking radar scattering from terrain and ocean surfaces
[ESRO-CR[P]-137] 03 p0266 N73-12153
First-order statistics of terrain clutter
[AD-750668] 06 p0641 N73-15205
Automatic computer mapping of infrared scanner data of terrain classes in Yellowstone National Park
07 p0787 N73-16400
Comparative evaluation of ERTS-1 imagery for inventorying and monitoring vegetation-terrain relationships in arid environments of Arizona
[E73-10413] 11 p1279 N73-20375
ERTS-1 imagery of geological structures and terrains of New York
[E73-10457] 11 p1284 N73-20416
Detection of surface specific points by local parallel processing of discrete terrain elevation data
[AD-753701] 11 p1289 N73-20459
Simulation of digital radar landmass simulator
[AD-756219] 14 p1634 N73-23250
ERTS-1 applications in water depth calculation, terrain classification, land use mapping, water pollution, and mineral exploration
[E73-10565] 15 p1771 N73-24345
Terrain classification mapping of Yellowstone Park from ERTS-1 imagery
[E73-10567] 15 p1771 N73-24347
Identification, definition, and mapping of terrestrial ecosystems in interior Alaska from ERTS-1 imagery
[E73-10634] 15 p1776 N73-24393
Terrain classification maps of Yellowstone Park from ERTS-1 imagery
[PAPER-L27] 19 p2277 N73-28322
Autonomous Martian roving vehicle determination of terrain gradients from laser measurements
[NASA-CR-133498] 19 p2307 N73-28556
Influence of ground concentration, hilly terrain, and wind velocity on distribution of pollutants considering initial elevation
20 p2446 N73-29648
Influence of solar, sky, and ground radiation on signal reflection under cloudless daytime sky
[AD-763893] 22 p2712 N73-31716

**TERRAIN ANALYSIS**
Side-looking radar applications to studies of terrain topography and landforms
03 p0295 N73-12405
Infrared spectral emittance data, and infrared spectrometry studies
[NASA-CR-128646] 03 p0335 N73-12730
Development of evaluation method for determining effectiveness of data compression techniques for radar landmass simulation
[AD-750695] 06 p0642 N73-15214
Evaluation of utility of available remote sensor returns in analysis of slope failure phenomena
[AD-750735] 06 p0671 N73-15462
Mapping of distribution of slope failure forms as depicted by remote sensor returns
[AD-750733] 06 p0672 N73-15463
Criteria development for recognizing and identifying slope failure forms, based on pattern, color contrast, and geometric form
[AD-750732] 06 p0672 N73-15464
Thematic mapping and terrain analysis using diffraction patterns of ERTS-1 imagery
[E73-10385] 10 p1153 N73-19378
Automated thematic mapping and analysis of terrain in Arizona, Texas, Washington, Utah, Louisiana, and California using ERTS-1 imagery
[E73-10386] 10 p1153 N73-19379
Terrain classification mapping of Yellowstone National Park
[E73-10389] 11 p1276 N73-20351
Electronic equipment for infrared television camera used in terrain analysis
[LCR-DR-1-71-210/1/R] 13 p1500 N73-22157
Methods for meeting terrain intelligence needs of airmobile division in tactical situation
[AD-756191] 13 p1531 N73-22411
Ecology, hydrology, geomorphology, and terrain modeling of Colorado mountain environments from ERTS-2 data
[E73-10551] 14 p1655 N73-23424
Color photographic techniques to study vegetation and terrain, improve mapping methods, and to provide photoelectronic color separation using aerial cameras
[AD-756700] 14 p1668 N73-23536
Application of ERTS-1 data for multidisciplinary analysis of Michigan resources and development of computerized procedure for map coordinates correlation
[E73-10703] 17 p2018 N73-26316
Automatic recognition of terrain types from ERTS-1 MSS imagery
[PAPER-I17] 19 p2279 N73-28338
Physiographic terrain analysis in Colorado using principles of aerial photointerpretation
20 p2416 N73-29413
Satellite applications for earth and ocean dynamic studies
22 p2736 N73-31909
Analysis of terrain properties and topography from Skylab altimetry
[E73-11081] 23 p2782 N73-32256
Geomorphology of fretted and chaotic terrains on Mars surface
[CONTRIB-2264] 23 p2839 N73-32686
Martian surface cratering analysis using Mariner 9 observations
23 p2839 N73-32688
Erosional latitudinal debris distribution on Mars surface
23 p2839 N73-32689
Liquid carbon dioxide in Martian polar laminated surface layers
23 p2840 N73-32698
Delineation of major terrain features, land uses, and crop species in Tennessee Valley through computerized analysis
[E73-11089] 24 p2913 N73-33251

**TERRESTRIAL MAGNETISM**
U GEOMAGNETISM

**TERRESTRIAL RADIATION**
Inferred ozone profiles from ultraviolet earth radiance data from Nimbus 4
[NASA-TM-X-66108] 03 p0294 N73-12397
Water equivalent of snow determined from aerial detection of natural terrestrial radiation
[EGG-1183-1533] 06 p0667 N73-15419
Evaluation of aerial survey on terrestrial gamma radiation environment
[EGG-1183-1559] 07 p0793 N73-16447
Analysis of methods for interpreting satellite radiation measurements to determine physical parameters of atmosphere which affect earth radiation field
20 p2399 N73-29281
Application of satellite observation data for determining statistical relationship between cloud field and outgoing short wave radiation in earth atmosphere
20 p2399 N73-29283
Measurements of upward radiation flux from ground and atmosphere using airborne spectrophotometer
20 p2400 N73-29284
Airborne observations to determine radiation characteristics of underlying surface and clouds over various types of ground conditions
20 p2400 N73-29285
Development of numerical method for determining long wave radiation balance of atmosphere based on effective surface radiation
20 p2401 N73-29295
Development of numerical methods for improving accurracy of calculations of thermal radiation in earth atmosphere
20 p2401 N73-29297
Development of empirical relationship between effective terrestrial radiation, ground temperature, and water vapor pressure in the ground air layer for cloudless skies
20 p2402 N73-29300
Development, characteristics, and operation of thermoelectric photopyranometer with hemispherical glass filters
20 p2402 N73-29306

**TERRIER MISSILE**
Analysis of computing methods for Terrier fire control system
[AD-758499] 14 p1724 N73-23993

**TESSERAL HARMONICS**
Zonal and tesseral harmonics of gravitational fields of major planets and constraints placed on models of planet interiors
[NASA-CR-130346] 07 p0841 N73-16810

**TEST BEDS**
U TEST EQUIPMENT
**TEST CHAMBERS**
NT ANECHOIC CHAMBERS
NT HYPERBARIC CHAMBERS
NT PRESSURE CHAMBERS
NT VACUUM CHAMBERS
Analysis of factors affecting environmental chambers used to study photochemical reactions in lower atmosphere
[PB-212715] 06 p0695 N73-15663
Thin plastic flexible gas discharge tubes for automatic particle track chamber
[NOTA-INTERNA-416] 17 p2033 N73-26455
Mobile test chamber for calibration of fixed incore radiation detectors
[BMBW-FBK-72-26] 22 p2699 N73-31618
**TEST EQUIPMENT**
Signal dropout detection and counting tester for magnetic tape measurements
[NBS-TN-739] 01 p0030 N73-10236
Calibration of rotating sand erosion test apparatus simulating turbocompressor wear
[AD-743309] 01 p0059 N73-10483
Equipment and procedures for measuring flow of liquids and gases to identify application of specific types of equipment
[NLL-TRANS-45-[3958.4]] 02 p0154 N73-11249
Equipment for tensile, shear, bending, and hydrostatic pressure tests of sandwich elements
[FOA-4-C-4472-E6] 02 p0172 N73-11390
Load cell for combined axial load and torque with good sensitivity reliability and low cross talk
[AD-746671] 02 p0175 N73-11420
On-line data acquisition and instrumentation improvements for transonic turbine test rig
[AD-746727] 02 p0175 N73-11422
Analysis of potential hazards caused by carrying experimental equipment on Earth Orbit Shuttle and recommendations for eliminating or reducing hazards-Vol.2 Pt.2
[NASA-CR-129103] 02 p0231 N73-11873
Analysis of hazards involved in transporting experimental equipment on space shuttle and recommended precautionary measures - Vol. 3 Pt. 2
[NASA-CR-129100] 02 p0231 N73-11876
Quality control data and monitoring equipment specifications for hardness testing of antimissile radar defense system
[AD-748063] 03 p0268 N73-12169
Testing machine for sequential systems using pseudorandom sequences and wired models
03 p0271 N73-12196
Instruction manual for Model 600F Data Transmission Test Set
[NASA-TM-X-68833] 03 p0301 N73-12453
Test equipment and procedures for determining foaming and aeration characteristics of aircraft engine lubricants
[AD-747804] 03 p0321 N73-12618
Development and evaluation of test equipment for high pressure radio frequency plasma experiments and in-reactor tests of nuclear lightbulb engine
[NASA-CR-129501] 03 p0330 N73-12694
Development of troubleshooting skills to isolate causes of malfunctions in complex electronic assemblies
[BDX-613-337-REV] 04 p0398 N73-13241
Equipment for vibration testing of assemblies, components, and other articles
[NASA-CASE-GSC-11302-1] 04 p0419 N73-13416
History, organization, and functions of the National Bureau of Standards to include description of test equipment used for research projects
[NBS-SP-367] 05 p0524 N73-14259
Experimental data on baffled and unbaffled vibratory cavitation damage tests
[PB-211899] 05 p0525 N73-14270
Development and characteristics of coulometric detector for conducting chromatographic analyses
[NLL-TRANS-857-[9022.64]]
05 p0545 N73-14425
Biaxial testing device for measuring yield point and plastic flow properties of high strength HY-80 steel
[AD-749021] 05 p0548 N73-14454
Application and advantages of ultrasonic inspection for thick walled components
[NLL-RISLEY-TR-2209-[9091.9F]]
05 p0550 N73-14466
Lunar laser reflector specifications and fabrication, noting test equipment thermal control, and lunar environment simulation
05 p0558 N73-14529
Development and characteristics of test equipment for investigating thermodynamic properties of gases at high temperatures
[AD-749653] 05 p0607 N73-14936
Application of small digital computer to improve operation of electronic maintenance system
[Y-1837] 06 p0647 N73-15258
Tester controlled by fluidic logic system for testing safety functions of missile safe and arm devices
[AD-751127] 07 p0802 N73-16512
Development of test probe device for simultaneous determination of condition of cells in multi-cell storage battery
[NASA-CASE-MFS-20761-1] 08 p0869 N73-17037
Design and development of ultrasonic instrumentation to facilitate quantitative nondestructive evaluation of defects in materials
[NASA-CR-124021] 08 p0923 N73-17562
Characteristics and vibrational test of structural test unit for electron-proton spectrometer under simulated flight conditions
[NASA-CR-128699] 08 p0924 N73-17573
Compilation of analyses generated during development of electron-proton spectrometer for Skylab program to insure reliability and quality control
[NASA-CR-128705] 08 p0925 N73-17576
Qualification tests of electron-proton spectrometer to determine suitability for use in Skylab program
[NASA-CR-128703] 08 p0925 N73-17580
Evaluation of infrared laser beams using thin membrane type displays of cholestric liquid crystals
[AD-752201] 08 p0930 N73-17616
Design, fabrication, and test of flight qualified heat pipe diode for Advanced Thermal Control Flight Experiment
[NASA-CR-114526] 08 p0968 N73-17915
Developments in aerodynamic test facilities to show past experience, present status, free flight techniques, and future plans
[AGARD-R-603] 09 p1011 N73-18250
Comparison of two total pressure and total temperature measuring instruments for boundary layer investigations at supersonic speeds
10 p1139 N73-19284
Hydraulic biaxial medium-rate tension-torsion testing machine
[REPT-1047/72] 10 p1161 N73-19449
Design and development of test stand system for supporting test items in vacuum chamber
[NASA-CASE-MFS-21362] 11 p1265 N73-20267
Development and characteristics of transducer for use with fluidic generators
[AD-755104] 11 p1273 N73-20334
Apollo experience report on instrument calibration data to provide correct engineering data for tests and mission support
[NASA-TN-D-7144] 11 p1341 N73-20881
Design of electrophoretic mass screening tester for sickle cell anemia
12 p1373 N73-21140
Low cost magnetic tape recording system for test instrumentation use
[AD-757011] 13 p1493 N73-22102
Acoustic combustion instability of solid propellants in radial burner
[AD-755826] 13 p1592 N73-22904
Development and characteristics of analog wake drag evaluation system for use in test section of low speed wind tunnel
[FFA-AU-860] 14 p1648 N73-23368
Development and characteristics of voltmeter and electronic suppression circuit for high accuracy readings
[REPT-6734] 14 p1666 N73-23519
Test set for signal conditioner modules
[NASA-CASE-KSC-10750-1] 14 p1667 N73-23527
Torsional device for testing small diameter single synthetic fibers
[AD-755932] 14 p1680 N73-23638
Reliability and quality control procedures for development of test equipment used on lunar experiment projects - Vol. 3
[NASA-CR-128920] 14 p1705 N73-23837
Device for extravehicular microbe exposures to space environment during Apollo 16 flight
15 p1740 N73-24104
Operational handling of test equipment for microorganism exposure to space environment
15 p1740 N73-24105
Characteristics of system for obtaining continuous profiles of ocean conductivity, temperature, and sound velocity as functions of depth
[NOAA-IFS-73009] 15 p1787 N73-24489
Development and characteristics of test equipment for measurement of direct pitching moment derivatives for two dimensional flow at subsonic and supersonic speeds
[ARC-R/M-3257] 16 p1855 N73-25027
Design and characteristics of test equipment for measuring longitudinal oscillatory aerodynamic derivatives in high speed wind tunnel
[ARC-R/M-3260] 16 p1855 N73-25029
Acceptance test plan for bench test equipment of Apollo ultraviolet spectrometer experiment
[NASA-CR-128574] 16 p1916 N73-25508
Design, fabrication, and tests of experimental flight packages capable of measuring long term solar degradation of thermal control coatings
[AD-759083] 16 p1968 N73-25916
TDMA/PSK test equipment noting modulators, demodulators, converters, and transmission system
[ESRO-CR[P]-144] 17 p1998 N73-26157
Development of test equipment for random and constant amplitude loading on resonant and electrohydraulic fatigue machines
[RAE-TR-72226] 17 p2009 N73-26250
Thermal/vacuum tests of engineering test unit of electron-proton spectrometer
[NASA-CR-128701] 17 p2033 N73-26451
Nondestructive test equipment using acousto-optical imaging techniques
[AD-760554] 18 p2152 N73-27397
Construction and operation of bend tester at temperature ranges from minus 197 to 650 C
[NASA-TM-X-2853] 18 p2160 N73-27452
Bibliography of test equipment and procedures for determining physical and mechanical properties of iron and steel products
[PB-219047] 18 p2161 N73-27459
Forced oscillation test equipment for measuring dynamic stability of roll velocity on lifting bodies
[AD-762258] 19 p2250 N73-28139
Development, characteristics, and operation of telephotometer for simultaneous measurements of angular and space distribution of absolute solar radiation fluxes
20 p2402 N73-29303
Analysis of operations at ground station during Tenth Soviet Antarctic Expedition to show equipment requirements and mission accomplishments
20 p2408 N73-29356
Development and characteristics of device for head space analysis used with dual column gas chromatographs
[NLL-M-23025-[5828.4F]] 20 p2417 N73-29415
Design, operation, and maintence of digital recording CW system for Minuteman 2 missiles
[AD-763115] 20 p2488 N73-29991
Development and characteristics of spectrophotometer for measuring transmittance of solid and liquid materials
[PAPER-76A5-729] 21 p2545 N73-30398
Methods for measuring photocell linearity and analysis of conditions for accurate assessment of nonlinearity
[PAPER-76A5-731] 21 p2545 N73-30400
Analysis of physical parameters involved in spectrophotometry with high accuracy to show effects of stray light and interference
[PAPER-76A5-732] 21 p2545 N73-30401
Analysis of parameters involved in establishing spectrophotometric standards
[PAPER-76A5-737] 21 p2546 N73-30406
Analysis of absolute spectrofluorometry procedures and establishment of standards for calibrating spectrofluorometers
[PAPER-76A6-741] 21 p2546 N73-30407
Measurement of quantum yields using chemistry, laser technology, photodetector instrumentation, and calorimetry
[PAPER-76A6-742] 21 p2546 N73-30408
Application of phosphorimetry procedures to quantitative chemical analysis of several aqueous solutions
[PAPER-76A6-743] 21 p2546 N73-30409
Adjustable deflection, multispecimen, bent beam test fixture for conditioning sheet specimens used in hot salt stress corrosion tests of titanium alloys
[AD-763704] 21 p2561 N73-30529
Design and characteristics of capsule assembly to evaluate tungsten emitter and carbide fuel combinations for thermionic fuel elements
[NASA-TM-X-2887] 21 p2578 N73-30658
Design, fabrication, production and testing of data collection platforms and platform field test sets for Earth Resources Program
[E73-11008] 22 p2660 N73-31313
Development and characteristics of apparatus for measuring intensity of electric field in atmosphere
[NASA-CASE-KSC-10730-1] 23 p2790 N73-32318
Test equipment to prevent buckling of small diameter specimens during compression tests
[NASA-CASE-LAR-10440-1] 23 p2790 N73-32323
Test fixture design for boron-aluminum and beryllium test panels
[NASA-CR-124401] 23 p2792 N73-32337
Specification catalog to identify test equipment for use in conducting life sciences experiments aboard space laboratory - Vol. 4
[NASA-CR-124413] 23 p2849 N73-32768
Development of instrument to measure steady and oscillatory aerodynamic forces on stiag-mounted model using forced oscillation technique
[ATN-7101] 24 p2926 N73-33366
**TEST FACILITIES**
NT ANECHOIC CHAMBERS
NT BALLISTIC RANGES
NT BLOWDOWN WIND TUNNELS
NT CASCADE WIND TUNNELS
NT ENGINE TESTING LABORATORIES
NT ENVIRONMENTAL LABORATORIES
NT HYPERSONIC WIND TUNNELS
NT HYPERVELOCITY WIND TUNNELS
NT LOW DENSITY WIND TUNNELS
NT LOW SPEED WIND TUNNELS
NT MISSILE RANGES
NT PLASMA JET WIND TUNNELS
NT RECTANGULAR WIND TUNNELS

NT SHOCK TUNNELS
NT SLOTTED WIND TUNNELS
NT SUBSONIC WIND TUNNELS
NT SUPERSONIC WIND TUNNELS
NT TEST RANGES
NT TEST STANDS
NT TRANSONIC WIND TUNNELS
NT WIND TUNNELS
Acquisition and reduction of data acquired from superconducting magnetic suspension and balance facility
[NASA-CR-112186] 01 p0035 N73-10276
Description of equipment installed in magnetic and seismic observatory at Mould Bay, Canada and analysis of data acquired during 1969 - Vol 43. No. 4
[M70-43/4] 01 p0043 N73-10344
Magnetic test facilities at ESTEC, Netherlands, noting coils and magnetometers
[ESRO-TM-152-ESTEC] 02 p0153 N73-11238
Preliminary evaluation of Norwegian long period seismic array
[AD-746009] 02 p0167 N73-11361
Seismological experiments and evaluation of instrumentation in program of long range seismic measurements
[AD-746666] 02 p0170 N73-11382
Development and characteristics of test facility for measuring three dimensional boundary layers on helicopter rotor blade under various conditions
[NASA-CR-112194] 03 p0252 N73-12042
Laboratory tests to determine corrosion failure mechanisms in electronic equipment exposed to humid tropical environments
[AD-747757] 03 p0279 N73-12261
Heating characteristics of internal resistance
[NASA-TN-D-7070] 03 p0280 N73-12268
Design and development of zero-gravity atmospheric cloud physics experiment laboratory for installation in orbiting spacecraft
[NASA-CR-128998] 03 p0280 N73-12270
Analysis of isothermal liquid inflow patterns in spherical container during weightless conditions
[NASA-TM-X-2670] 03 p0283 N73-12291
Apparatus for low temperature cavitation testing of materials at increased static pressure
[AD-748108] 03 p0304 N73-12482
Major problems associated with use and usefulness of aeronautical test facilities
04 p0400 N73-13258
Properties of refractory metals and application to construction of high temperature irradiation facilities
[EUR-4757] 04 p0434 N73-13540
Gravity observations near San Juan Moutains in Colorado
[PB-211430] 05 p0540 N73-14395
Thermohydraulic test facility for design of fuel elements for water and sodium cooled reactors
[NT-31-1972] 05 p0579 N73-14712
Bumpy torus magnet facility with 12 superconducting coils, each 19 cm and capable of 3.0 tesla on their axes
[NASA-TM-X-68165] 06 p0648 N73-15266
Development and operation of test facility for high temperature gas turbine experiments
[NAL-TR-282] 06 p0649 N73-15269
Development and operation of facility for investigating effect of spin on aerodynamic characteristics of shaped charges
[DREV-TN-2037/72] 06 p0649 N73-15271
Instrumentation handbook for operational support systems of Space and Missile Test Centers in California, Hawaii, and Pacific Ocean area
[AD-750944] 06 p0651 N73-15285
Evaluation of research projects involving seismic arrays, long period arrays, seismometers, and seismic signal processing
[AD-750759] 06 p0669 N73-15439
Development of method for analysis and assessment of turbofan engine performance
[CRANFIELD-SME-2] 06 p0712 N73-15811
Impulse base flow facility tests of space shuttle stage separation plume impingement loads
[NASA-CR-124000] 06 p0729 N73-15949
Operational activities of Hungarian National Bureau of Metrology and use of photogrammetry in city planning and modernization
[JPRS-57792] 06 p0731 N73-15965
Role and activities of Hungarian National Bureau of Metrology
06 p0731 N73-15966
Test facility for combustion flow in open cycle magnetohydrodynamic generator
[AD-751251] 07 p0742 N73-16036
Configuration and requirements for general purpose optical research facility to investigate earth atmosphere from space shuttle orbiter vehicle
[NASA-CR-128732] 08 p0893 N73-17226
Unique field-laboratory methodology for assessing human response to noise
[NASA-CR-2221] 09 p0995 N73-18124
Developments in aerodynamic test facilities to show past experience, present status, free flight techniques, and future plans
[AGARD-R-603] 09 p1011 N73-18250
Electron beam irradiation capabilities of facility for materials and structures testing
[AD-752762] 09 p1012 N73-18260
Application of ERTS-1 data collection platform system in Arizona ecological test site
[E73-10332] 09 p1024 N73-18362
Application of ERTS-1 data collection system platforms in Arizona ecological test site
[E73-10333] 09 p1025 N73-18363
Low cycle fatigue testing at high temperatures
[AGARD-R-604] 09 p1092 N73-18916
Computer techniques and test facilities for structural engineering at German university institute
[ISD-119] 09 p1095 N73-18935
Analysis of selected problems in formation of simulation models of V/STOL aircraft
10 p1105 N73-19009
Fatigue test facility for space shuttle orbiters
10 p1138 N73-19273
Tests and equipment for measuring performance characteristics of camera systems for space applications
[NASA-CR-128825] 10 p1160 N73-19438
Research facility for studying noise generated by bluff body flow interaction inside ducted fuel combustion system
[AD-754094] 11 p1268 N73-20286
Description of turbopropulsion laboratory in aeronautics department at Naval Postgraduate School
[AD-754380] 11 p1268 N73-20287
Performance of electromagnetic accelerators in high pressure test facilities
[AD-754024] 11 p1328 N73-20779
Avian hazards to Air Force rocket sled test tract at Holloman AFB, New Mexico
[AD-755833] 12 p1389 N73-21261
Postoperational examination of externally configured test thermionic converter
[NASA-CR-131523] 12 p1426 N73-21560
Development of jet noise test facility for flow and acoustic measurements of mean and turbulent velocities in jet flow
[RE-450] 13 p1505 N73-22196
Development of multiwire proportional chamber for high resolution spatial detector in cosmic ray investigations and analysis of operating parameters
[NASA-CR-128899] 13 p1506 N73-22210
Compressor face distortion dependence on test cell inlet design configurations
[AD-756540] 13 p1507 N73-22215
Safety procedure for testing thermionic reactor in test facility
[NASA-TM-X-68224] 13 p1558 N73-22624
Analysis of factors involved in design of wind tunnel for testing V/STOL aircraft models
14 p1598 N73-22956
Facilities for handling light signals from long range spacecraft
14 p1618 N73-23107
Adaptation of Acoustic Research Tank Facility for parametric sonar experiments
[AD-756176] 14 p1634 N73-23249
Calibration and electromagnetic field mapping for continuous wave test facility
[AD-757638] 14 p1647 N73-23358
Preflight, inflight, and post flight operations evaluation analyses for Skylab materials processing facility - Appendix E
[NASA-CR-61386-APP-E] 14 p1708 N73-23859
Preflight, inflight, and post flight operations evaluation analyses for Skylab contamination measurement sample array - Appendix S
[NASA-CR-61386-APP-S] 14 p1708 N73-23864
Antenna pattern and steering measurements of Wisconsin Test Facility transmissions
[AD-758648] 15 p1752 N73-24200
Systems design of facilities for studying flight problems of VTOL aircraft
[NAL-TR-306] 15 p1760 N73-24263
Portable beacon test site for enroute radar coverage in airport vicinity
[FAA-RD-73-49] 15 p1760 N73-24266
Procedures for simulating and studying effects of subgravity on subjects during laboratory experiments and space flight
[NASA-TT-F-14934] 15 p1761 N73-24267
Cryogenic superconducting magnetic suspension and balance facility designs
15 p1761 N73-24272
Superconducting magnetic suspension and balance facility data acquisition and data reduction errors
15 p1762 N73-24274
Feasibility of using iron magnetic support to extend cold magnetic balance wind tunnel system to subsonic flow regimes and continuous spinning aircraft configurations
15 p1762 N73-24275
Description of research and air breathing engine test facility at University of Stuttgart
[AD-758150] 15 p1827 N73-24806
High enthalpy arc-heated helium shock tunnel for gas dynamic research
[NASA-TM-X-2814] 16 p1885 N73-25258
Facility for wear testing sodium cooled reactor materials
[KFK-1659] 16 p1944 N73-25727
Analysis of problems involved in operation of large wind tunnels at subsonic and supersonic speeds
[AGARD-R-601] 17 p2008 N73-26239
Analysis of minimum run times required for instationary measurements at transonic speeds during wind tunnel tests
17 p2009 N73-26243
Conceptual development and cost analysis of elevated short takeoff and landing facility for test purposes
[FAA-RD-73-15] 18 p2126 N73-27179
Principles of nondestructive testing and organization of Soviet metallography laboratories at industries
[JPRS-59424] 18 p2160 N73-27449
Evaluation of Skylab program experiments involving contamination measurement, photometer, and gegenschein zodiacal light
[NASA-CR-61386] 18 p2200 N73-27760
German test facilities for environment simulation
19 p2249 N73-28133
Development and characteristics of pitch/yaw dynamic stability, forced-oscillation test mechanism for measuring stability derivatives of lifting reentry vehicles
[AD-762286] 19 p2250 N73-28143
Evaluation of electrogasdynamic concept for dispersal of warm fog based on injection of charged water droplets into fog
[ASRC-PUBL-207] 20 p2382 N73-29140
Development, characteristics, and operation of test facility for determining effectiveness of runway lighting systems under various atmospheric conditions
[FAA-RD-71-94] 20 p2382 N73-29141
Design characteristics, and operation of ion thruster test facility
[RAE-TR-73061] 20 p2382 N73-29143
Analysis of operations at ground station during Tenth Soviet Antarctic Expedition to show equipment requirements and mission accomplishments
20 p2408 N73-29356
Functions and operations of ground station during Tenth Soviet Antarctic Expedition including construction procedures and equipment installation
20 p2409 N73-29361
Development of method for determining response of box type structures subjected to high intensity acoustic loading
20 p2479 N73-29915
Vibrational temperature and density of molecular oxygen component in expansion tube
[NASA-TN-D-7273] 22 p2653 N73-31249
Test facility for generating and analyzing internal waves
[AD-763444] 22 p2670 N73-31391
Transit waveform control program for real time environmental shock tests
22 p2732 N73-31860
Specification catalog to identify test equipment for use in conducting life sciences experiments aboard space laboratory - Vol. 4
[NASA-CR-124413] 23 p2849 N73-32768
Hydrazine engine tests and small bipropellant engine calibration in Molsink facility
23 p2858 N73-32837

TEST FIRING
Miss distance radar for air defense weapons testing
[AD-750323] 06 p0642 N73-15210
Simulated altitude firing test on solid propellant rocket motor
[NASA-CR-135485] 22 p2710 N73-31705
TEST METHODS
U TESTS
TEST PROGRAMS
U TESTS
TEST RANGES
NT BALLISTIC RANGES
NT MISSILE RANGES
Test range for Symphonie satellite antennas and onboard communication equipment
[DGLR-PAPER-72-89] 06 p0640 N73-15199
Experimental array radar ear test bed
[AD-758139] 14 p1636 N73-23261
TEST STANDS
Equipment for tensile, shear, bending, and hydrostatic pressure tests of sandwich elements
[FOA-4-C-4472-E6] 02 p0172 N73-11390
Test stand for precise measurement of impulse bit and thrust vector of reaction jet thrusters in attitude control system
[NASA-TN-D-7402] 22 p2719 N73-31762
TEST VEHICLES
NT FLIGHT TEST VEHICLES
Eridan rocket probe performance in experimental vehicles
14 p1718 N73-23940
TESTERS
U TEST EQUIPMENT
TESTES
Morphological changes in testes and spermatogenesis process of dogs subjected to chronic and combined gamma irradiation
07 p0743 N73-16048

TESTING MACHINES
U TEST EQUIPMENT
TESTS
NT SALT SPRAY TESTS
New and revised test methods for cathode ray electron storage tubes
[AD-754139] 11 p1263 N73-20251
Test methods for evaluating electrical power supply characteristics
[AD-759926] 17 p2005 N73-26218
Payload carrier integrated test for simulated Sortie Lab Missions
[NASA-TM-X-64770] 22 p2647 N73-31207
TETHERED BALLOONS
Operating principles and flight test performance of aerosol counter onboard tethered balloon
[AD-751315] 07 p0816 N73-16619
Analytical and experimental dynamic behavior of tethered balloons
[AD-762210] 19 p2222 N73-27925
Computer programs for computing stability characteristics of tethered balloon under steady wind conditions
[NASA-TM-X-2740] 23 p2742 N73-31952
Stability derivative analysis of tethered balloon in steady wind conditions to determine balloon aerodynamics buoyancy, mass, and static forces resulting from tether cable
[NASA-TN-D-7272] 23 p2743 N73-31955
Ship to shore transportation of military cargo using tethered balloons
[AD-765352] 23 p2747 N73-31987
TETHERLINES
Measurements of launch g forces and line tensions in aerial recovery of dummies for long-line loiter personnel retrieval system
[AD-749518] 05 p0497 N73-14045
Analysis of tethered body problems and determination of relative molton orbit - Parts 1 and 2
[NASA-CR-132780] 22 p2714 N73-31723
TETRACHLORIDES
Flow velocity, GeCl4 concentration, and temperature effects on growth and morphology of autoepitaxial Ge films
18 p2189 N73-27674
Vapor phase heteroepitaxial growth of silicon germanium alloys by hydrogen reduction of tetrachlorides
20 p2460 N73-29767
TETRACHLOROMETHANE
U CARBON TETRACHLORIDE
TETRAGONS
NT RECTANGLES
TETRAZOLES
Reaction of azotetrazole anion and nitric, sulfuric and hydrochloric acid noting giving of 5-hydrazinotetrazole and 5-azidotetrazole
[ERDE-TN-44] 05 p0507 N73-14123
TEXAS
In situ spectroradiometric quantification of ERTS-1 imagery of Arizona and Texas
[E72-10173] 01 p0055 N73-10444
Reference file of factors affecting weather at Kelly AFB, Texas
[AD-746028] 02 p0205 N73-11662
Identification of playa lakes in Texas High Plains from ERTS-1 imagery
[E72-10257] 03 p0290 N73-12357
Spectral analysis of soil boundaries in Collin County, Texas
[E72-10260] 03 p0290 N73-12359
Vegetation, soil, and water reflectance measurements from ERTS-1 imagery of Hidalgo County, Texas
[E72-10267] 03 p0291 N73-12366
Automatic mapping of geologic features of Fannin County, Texas using MSS imagery from ERTS-1
[E72-10306] 04 p0412 N73-13355
Monitoring changing geologic features along Texas Gulf Coast using ERTS-1 imagery
[E72-10323] 05 p0530 N73-14311
Photointerpretation and thematic mapping of ERTS-1 imagery of Brownsville, Texas area
[E73-10006] 06 p0658 N73-15342
Dynamics of playa lakes in Texas High Plains
[E73-10042] 07 p0776 N73-16305
Catalog of economic, social, and educational institutions in Houston Area Test Site
[NASA-CR-128719] 07 p0856 N73-16944
Automated thematic mapping and analysis of terrain in Arizona, Texas, Washington, Utah, Louisiana, and California using ERTS-1 imagery
[E73-10386] 10 p1153 N73-19379
Evaluation and comparison of ERTS-1 measurements of major crops and soil conditions for selected areas in Central United States
[E73-10384] 11 p1275 N73-20348
Utilization of ERTS-1 imagery in structural reconnaissance for minerals and oil in Alaska, Canada, Montana, Colorado, New Mexico, and Texas
[E73-10414] 11 p1279 N73-20376
Regional wet census of playa lakes on Southern High Plains area of Texas and New Mexico from ERTS-1 MSS imagery
[E73-10455] 11 p1283 N73-20414
Airborne electrical scanning microwave radiometric measurements of soil moisture in Texas, California, and Arizona
[NASA-CR-130204] 11 p1284 N73-20423
Interpretation of geologic map of Fannin County, Texas, prepared by ADP techniques from ERTS MSS data
[NASA-CR-131574] 13 p1522 N73-22333
Effectiveness of ERTS-1 MSS photography in characterizing watershed runoff in Texas
[E73-10513] 14 p1653 N73-23408
Detection of changes in water quality and surface area in Tahoka Lake, Texas using ERTS-1 imagery
[E73-10518] 14 p1654 N73-23412
Dynamics of playa lakes in Texas High Plains analyzed from ERTS-1 imagery
[E73-10598] 15 p1772 N73-24359
Use of ERTS multispectral data to solve development and management problems of agricultural resources in Lynn County, Texas
[NASA-CR-132956] 15 p1778 N73-24411
Identification and mapping of soils, vegetation, and water resources in Texas from ERTS-1 MSS digital data
[E73-10670] 16 p1899 N73-25365
Delineation of lakes and water turbidity identification in ERTS-1 imagery of Houston, Texas area
[E73-10672] 16 p1900 N73-25367
ERTS-1 detection of small ponds in forested areas of Texas
[E73-10673] 16 p1900 N73-25368
ERTS-1 detection of prescribed burn in Sam Houston National Forest and subsequent effects on vegetation
[E73-10674] 16 p1900 N73-25369
ERTS-1 measurement of surface area of water bodies in Houston and Galveston, Texas area
[E73-10675] 16 p1900 N73-25370
ERTS-1 detection and measurement of coastal marshes in Houston area test site
[E73-10676] 16 p1900 N73-25371
Commercial application of ERTS-1 imagery in structural reconnaissance for minerals and petroleum
[E73-10700] 16 p1903 N73-25392
Application of ERTS-1 data to locate wind erosion sites in West Texas and to determine extent and spread of wind erosion
[E73-10719] 17 p2019 N73-26326
Collection of ground truth and meteorological data for Skylab test sites in Texas and Kansas
[E73-10752] 17 p2022 N73-26355
Land use models for Houston area
[NASA-CR-128991] 17 p2096 N73-26975
Dynamics of playa lakes in Texas high plains
[E73-10832] 18 p2141 N73-27302
Inventory and mapping extent and spread of wind erosion of soils in west Texas
[E73-10834] 18 p2141 N73-27304
Analysis of ERTS-1 data for application to forest and range mapping in Houston, Texas area
[PAPER-A20] 19 p2262 N73-28227
Application of ERTS-1 imagery to determine geological evidence of mineral and hydrocarbon accumulations in Alaska, Canada, Montana, Colorado, New Mexico, and Texas
[PAPER-G30] 19 p2267 N73-28261
Application of ERTS-1 imagery for determining location and characteristics of lake basins Texas high plains and semi-arid areas
[PAPER-W13] 19 p2272 N73-28290
Land use mapping and inventory of Houston, Texas using ERTS-1 and high altitude photography
[PAPER-L20] 19 p2276 N73-28315
Processing and interpretation of ERTS-1 MSS data for Lake Livingston, Texas
[PAPER-I8] 19 p2278 N73-28329
Distribution and movement of suspended sediment in Gulf of Mexico off Texas coast
[PAPER-M10] 19 p2281 N73-28349
Application of classification algorithms to ERTS-1 MSS imagery of Texas land and water coastal features
19 p2286 N73-28383
Computer analysis of ERTS-1 MSS data for identification and mapping of soils, vegetation, and water resources in Lynn County, Texas
19 p2287 N73-28392
Thermal parameters as predictors of precipitation at Carswell AFB, Texas
[AD-762289] 19 p2318 N73-28644
SL-2 MSS photography of soils, water, and vegetation in Texas
[E73-10943] 21 p2530 N73-30285
Soil moisture and vegetation surveys of Kansas and Texas for Skylab investigations
[E73-10944] 21 p2530 N73-30286
ERTS-1 measurements of seasonal changes in reflectance of soils, vegetation, and water in Hidalgo County, Texas
[E73-10946] 21 p2530 N73-30288
Comparison of ERTS-1 spectral reflectance measurements of major crops and soil associations for selected sites in Iowa, Kansas, North Dakota, and Texas
[E73-10981] 22 p2657 N73-31288
Transportation control measures to improve air quality standards in Greater Houston area by 1977
[PB-221611/7] 22 p2696 N73-31598
Early detection of insect infestations and density/distribution of host citrus trees along Rio Grande River in Texas
[E73-11073] 23 p2782 N73-32248
Early detection of insect infestations and density/distribution of host citrus trees in Texas
[E73-11074] 23 p2782 N73-32249
Detection of insect infestations and density/distribution of host citrus trees in Texas
[E73-11075] 23 p2782 N73-32250
Skylab detection of insect infestations and density/distribution of host plants in Texas
[E73-11076] 23 p2782 N73-32251
Detection of insect infestations and density/distribution of host citrus trees in Texas
[E73-11077] 23 p2782 N73-32252
Skylab detection of soil moisture in Texas
[E73-11101] 24 p2914 N73-33258
Correlation of ERTS-1 imagery signatures with water balance ecosystem and geology of select playa lake basins in West Texas
[E73-11102] 24 p2914 N73-33259
ERTS-1 measurements of major crops and soil associations in Indiana, North Dakota, Iowa, Nebraska, Kansas, and Texas
[E73-11155] 24 p2919 N73-33309
Sea/land breeze circulation study, using airborne infrared radiation measurements of surface temperature along upper Texas coast
[REPT-36] 24 p2922 N73-33336
Pilot balloon observations of lower tropospheric winds along upper Texas coast
[REPT-35] 24 p2948 N73-33544
TEXTBOOKS
Textbook on hydraulic systems
[AD-746713] 02 p0158 N73-11280
TEXTILES
NT COTTON FIBERS
Thermal stabilization of textiles composed of polybenzimidazole fibers by chemical treatment
[AD-748248] 04 p0440 N73-13584
Chemical and physical properties and thermal decomposition products of certain natural fibers and synthetic materials
[AD-751899] 08 p0935 N73-17658
Process for developing flame retardant elastomeric composition textiles for use in space suits
[NASA-CASE-MSC-14331-1] 18 p2167 N73-27501
TEXTS
Field evaluation of automated reading system for blind that produces synthetic speech from written text by use of computer and special-purpose devices
14 p1620 N73-23123
System for automated speech synthesis from ordinary English text
14 p1620 N73-23125
System for generating speech from English text punched on paper tape using small digital computer and parametric speech synthesizer
14 p1620 N73-23126
TEXTURES
Optical texture perception and pattern recognition imagery
[AD-746658] 02 p0212 N73-11722
Autocorrelation evaluation for texture indicator for lunar ground photos
05 p0609 N73-14955
Classification of land use in California using textural information in ERTS-1 MSS imagery
[E73-10461] 11 p1284 N73-20419
Algorithm for classifying land use categories of ERTS-1 data by textural features
[PAPER-I16] 19 p2279 N73-28337
TF-34 ENGINE
Fan and core engine noise suppression for STOL aircraft
[NASA-TM-X-71448] 24 p2971 N73-33741
TFX AIRCRAFT
U F-111 AIRCRAFT
THAILAND
Remote sensing of Thailand earth resources using ERTS-1 imagery
[E72-10298] 04 p0411 N73-13348
Probability models of wet and dry days for several stations in Thailand
[THESIS-392] 08 p0938 N73-17684
Application of ERTS-1 imagery for identifying and mapping rivers, agricultural areas, forest, mineral resources, and water conditions in Thailand
[E73-10746] 17 p2021 N73-26350
Aerial photointerpretation of impact of highway construction on rural area in Thailand
20 p2417 N73-29414
Utilization of ERTS-1 imagery for studies of agriculture, forestry, cartography, geography, hydrology, meteorology, geology, and oceanography in Thailand
[E73-10996] 22 p2659 N73-31302
Application of ERTS-1 imagery to agriculture, forestry, meteorology, and hydrology in Thailand
[E73-11145] 24 p2918 N73-33299

THALAMUS
Thalamic cat cell activities during sleep and wakefulness phases
13 p1484 N73-22030

THALLIUM
NT THALLIUM COMPOUNDS
Phase diagram of Ti-Os system
[NLL-TRANS-746-1302-[9022.401]]
05 p0560 N73-14548
Acoustic emission signals by fcc phase transition to fct in In-Ti alloys
[SC-DC-72-1650] 12 p1414 N73-21462

THALLIUM ALLOYS
Phase diagram of Ti-Os system
[NLL-TRANS-746-1302-[9022.401]]
05 p0560 N73-14548

THALLIUM COMPOUNDS
Magnetic properties of powdered samples of Dy2Ti2O7
[NASA-TM-X-68219] 12 p1428 N73-21575
Elastic constants and electrical transition in Ti2O3 and V doped Ti2O3
23 p2824 N73-32577

THAWING
U MELTING

THEMATIC MAPPING
Thematic mapping using ERTS-1 return beam vidicon imagery
[E72-10275] 03 p0291 N73-12373
Automated thematic mapping using multispectral and spatial pattern recognition techniques on ERTS-1 imagery
[E72-10281] 03 p0292 N73-12379
Land use mapping of northern megalopolis using ERTS-1 imagery
[E72-10368] 05 p0535 N73-14356
Photointerpretation and thematic mapping of ERTS-1 imagery of Brownsville, Texas area
[E73-10006] 06 p0658 N73-15342
Automated thematic mapping and interpretation of hydrologic and agricultural resources using ERTS-1 imagery
[E73-10023] 06 p0660 N73-15357
Planimetric, topographic, and thematic mapping using remotely sensed imagery
07 p0786 N73-16391
Application of ERTS-1 imagery to thematic mapping of open water, ice and snow cover, vegetation, and works of man
[E73-10089] 08 p0902 N73-17301
Thematic mapping and terrain analysis using diffraction patterns of ERTS-1 imagery
[E73-10385] 10 p1153 N73-19378
Automated thematic mapping and analysis of terrain in Arizona, Texas, Washington, Utah, Louisiana, and California using ERTS-1 imagery
[E73-10386] 10 p1153 N73-19379
Thematic and photomapping of Arizona CARETS, and polar regions from ERTS-1 imagery
[E73-10463] 12 p1394 N73-21302
Application of ERTS-1 imagery to thematic mapping of Washington-Baltimore corridors
[E73-10500] 12 p1398 N73-21336
Thematic mapping of Mississippi River from ERTS-1 imagery
[E73-10628] 15 p1775 N73-24388
Automated thematic mapping and change detection of hydrological and agricultural resources from ERTS-1 imagery
[E73-10644] 16 p1897 N73-25341
Thematic mapping of wetlands, forests, open water, and Mississippi River flooding from ERTS-1 imagery
[E73-10952] 21 p2531 N73-30294
Sampling strategies for automatic thematic land use mapping of Washington D.C., Maryland counties, and Alice Springs, Australia using Skylab multispectral photography
[E73-11018] 22 p2661 N73-31322
Thematic mapping of land use near Harrisburg, Pennsylvania from ERTS-1 digital data
[E73-11109] 24 p2915 N73-33266
Utilization of Skylab imagery for thematic mapping
[E73-11162] 24 p2920 N73-33315

THEMIS PROJECT
Procedures for studying reliability characteristics of systems with standbys - Themis project
[AD-745911] 02 p0179 N73-11451
Themis Project results on adaptive learning control systems and pattern recognition
[AD-756424] 13 p1350 N73-22562
Processes of metal working in Themis project
[AD-763122] 20 p2423 N73-29464

THEODOLITES
NT CINETHEODOLITES
Use of gyrotheodolites for azimuth determinations on orienting points
[AD-744684] 01 p0052 N73-10419
Theodolitic errors in processing time dependent geodetic data
[AD-760109] 17 p2029 N73-26421

THEOREM PROVING
Multi-terminal network flow realizability, analysis, and synthesis
[AD-748773] 04 p0441 N73-13595
Estimates of differential functions for proving system stability
07 p0761 N73-16179
Theorems for proving consistency of singular perturbations in physical systems with parasitic elements
07 p0761 N73-16182
Stability analysis for semilinear parabolic partial differential equations
[NASA-CR-130542] 09 p1056 N73-18608
Representations of language recognition problem for theorem prover in first order logic
[NASA-CR-131402] 11 p1310 N73-20632
Israel-Carter conjecture of black hole physics and baryon number
15 p1829 N73-24825

THEOREMS
NT BAYES THEOREM
NT LEBESGUE THEOREM
NT MICHELL THEOREM
NT STOKES THEOREM [VECTOR CALCULUS]
NT UNIQUENESS THEOREM
Derivation of theorems for spinless particle scattering from Kohn variational principle
[NASA-CR-129259] 03 p0323 N73-12634
Theorems for optimization of Riccati equation in singular discrete time filtering and control problems
[NASA-CR-130360] 06 p0690 N73-15621
Theorems regarding oscillation and nonoscillation conditions for canonic linear sets of differential equations
[NASA-TT-F-14816] 09 p1057 N73-18615
Theorems for oscillatory solutions to differential equations
[NASA-TT-F-14883] 12 p1419 N73-21498
Extension of theorems concerning spectrum of one-dimensional and multidimensional differential operators on vector functions
[NASA-TT-F-14960] 17 p2055 N73-26620
Theorem for specifying sufficient number of input frequencies for identification through Liapunov methods
[NASA-CR-135668] 23 p2812 N73-32482

THEORETICAL PHYSICS
NT QUANTUM THEORY
Asymptotic behavior of elastic form factors and light cone expansion for matrix elements
[TR-73-039] 01 p0083 N73-10683
Theoretical constraints on microscale fluctuations in solar wind, emphasizing hydromagnetic waves
01 p0096 N73-10788
Invariance under Weyl scale transformations and Poincare gauge invariant matter Lagrangian
[RIFP-160] 02 p0195 N73-11578
Numerical analysis of classical brachistochrone in which particle starts and ends at same elevation with horizontal velocities and does not leave curve of own inertia
[P-4749] 02 p0196 N73-11584
Research activities in nuclear physics, solid state detectors and theoretical physics
[AECL-4257] 02 p0213 N73-11726
Statistical mechanics of 2 and 3 dimensional plasmas in strong dc magnetic field
[NASA-CR-129177] 02 p0215 N73-11741
Development of relativistic theory of gravity and comparison with post-Newtonian limit
[NASA-CR-129242] 03 p0293 N73-12387
Light cone singularities, DGS representations, and asymptotic behavior of forward scattering amplitudes
[TR-73-059] 03 p0339 N73-12765
Light cone analysis of large momentum transfer limit of electroproduction structure function at constant missing mass and of its connection with Bjorken limit
[TR-73-066] 03 p0339 N73-12766
Fields, statistics and non-Abelian gauge groups
[NOTA-INTERNA-387] 03 p0340 N73-12771
Principles of classical mechanics and quantum mechanics in theoretical physics
[ITP-71-104-P] 04 p0414 N73-13383
Exact solution of gravitational field of rotating mass
[RIFP-161] 04 p0449 N73-13666
Exterior gravitational field of slowly rotating deformed masses, obtained by generalizing Weyl metrics into rotating Weyl metrics
[RIFP-162] 04 p0449 N73-13667
Nuclear research projects with fast electron accelerator and theoretical physics of neutron decay reactions
04 p0452 N73-13687
Light cone and hyperbaloid contributions to structure functions in Bjorken limit
[TR-73-076] 06 p0702 N73-15726
Noncanonically renormalized phi to 4th power theory in 4-epsilon dimensions and systematic use of Callan-Symanzik equations
[TR-73-020] 06 p0702 N73-15727
Theoretical model of Regge phenomena in medium x region for kaon proton interactions
[TUEP-72-46] 07 p0823 N73-16668
Dual multiperipheral model of hadronic production amplitudes
[NUB-2164] 07 p0823 N73-16672
Calculation of photoionization cross sections near autoionizing lines and theoretical cross sections for beryllium and magnesium
[NASA-CR-130884] 09 p1068 N73-18716
Research in theoretical physics
[PUBL-100] 10 p1187 N73-19662
Theoretical analysis of ion cyclotron wave dynamics in cold plasma
[IPPJ-150] 15 p1816 N73-24722
Global properties of collapsing matter [black holes]
[JINR-E2-6831] 15 p1832 N73-24850
Brief summaries of 13th International Congress of Theoretical and Applied Mechanics
[NASA-CR-132236] 15 p1846 N73-24955
Plasma physics theoretical research
[COO-3577-4] 19 p2324 N73-28698
Quiton/perception physics of being, time, space, existence, perception, and physical phenomena
[AD-763210] 21 p2580 N73-30680
Baryon spectroscopy and regularities between SU[6] and SU[3] mass breaking parameters
[LPTHE-73/21] 21 p2581 N73-30687
String models for theoretical study of high energy collisions involving large quantum numbers
[LPTHE-73/22] 21 p2581 N73-30688
Development of symmetric stress-energy-momentum pseudo-tensor for gravitational fields of Brans-Dicke theory and application to formation of black holes
24 p2978 N73-33800

THEORIES
Development of general theory for studying large plastic deformation of metals
[AD-746689] 02 p0190 N73-11542

THERAPY
NT CHEMOTHERAPY
NT PSYCHOTHERAPY
NT RADIATION THERAPY
Absorption of fructose in saline mixture used for enteritis therapy of children
[NASA-TT-F-14596] 02 p0133 N73-11078
Therapeutic value of mineral water diets especially Karlsbad Muhlbrunn water
[NASA-TT-F-14620] 04 p0379 N73-13079
Oxygen breathing in decompression sickness and remedial recompression of human beings
[DRIC-TRANS-3095] 17 p1988 N73-26069
Extreme aeroembolism case and successful therapy in hyperbaric chamber
19 p2227 N73-27959
Use of therapeutic exercise for treatment of functional vascular disorders and occlusive lesions of arteries and veins
[NASA-TT-F-15043] 20 p2368 N73-29045

THERMAL ABSORPTION
NT POLAR CAP ABSORPTION
Theoretical model for laser flux absorption by plasma instability mechanism
[LA-4984] 06 p0704 N73-15739
Direct thermal energy conversion using thermal absorption principle
[NASA-CASE-ARC-10461-1] 11 p1347 N73-20931
Effect of thruster pulse length on thruster-exhaust damage of S13G white thermal control coatings
[NASA-TM-X-68213] 11 p1348 N73-20940

THERMAL AGITATION
U THERMAL ENERGY

THERMAL BATTERIES
Low voltage pellet type thermal batteries
[SC-DC-71-4102] 03 p0254 N73-12059
Preliminary evaluation of lithium aluminum electrode for thermal batteries
[AD-757007] 13 p1477 N73-21964
Purification of molten lithium fluoride, sodium fluoride, and potassium fluoride salt eutectics for thermal battery electrolyte application
[AD-758001] 15 p1739 N73-24097
Materials for immobilization of electrolyte in pellet-type thermal batteries
[SC-RR-66-202-A] 22 p2618 N73-30978

THERMAL BLOOMING
Theoretical description of thermal blooming of pulsed, focused laser beams in gases
[AD-745739] 01 p0066 N73-10539
Computer program for propagation and thermal blooming of pulsed, focused laser beams
[AD-748991] 04 p0430 N73-13503
Thermal blooming of laser beams in viscous and thermally conductive fluids
[AD-748994] 04 p0431 N73-13508
Thermal blooming of carbon dioxide laser during atmospheric propagation
[AD-765520] 24 p2932 N73-33418

THERMAL BOUNDARY LAYER
Approximative heat transfer in thermal boundary laer on gas turbine blade
[AD-752676] 08 p0956 N73-17825
Surface boundary layer temperature profiles and turbulent heat flux during onshore flow
[REPT-38] 21 p2524 N73-30239
Second order thermal boundary layer theory for steady, laminar, compressible flow over cambered two dimensional or rotational bodies
[DLR-FB-73-31] 22 p2653 N73-31256

Parametric linearization for approximating dynamic and thermal boundary layers for nonNewtonian fluids with arbitrary pressure and surface temperature gradients
[AD-764170] 22 p2655 N73-31271
Integral relations of velocity and thermal boundary layer for approximation purposes
24 p2909 N73-33213
Theory for thermal boundary, kapitza, resistance to include effects of phonon attenuation near interface
24 p2968 N73-33719

THERMAL BUCKLING
Post buckling behavior of circular plate following heating at center and heating at edge and effects of restraints on final configuration
[ARC-R/M-3245] 15 p1730 N73-24031

THERMAL CONDUCTIVITY
Calculation of hydromagnetic wave induced energy transfer in solar wind
01 p0094 N73-10777
Development of proton-activated recession sensor based on migration of beryllium isotope in graphite at high temperature and application to nose cone conditions during reentry
[AD-745454] 01 p0109 N73-10899
Thermal conductivities of liquid alcohols at their saturation pressures
[ESDU-67030] 01 p0115 N73-10953
Thermal conductivity of H20 and D2O
[ESDU-67031-AMEND-A] 01 p0115 N73-10954
Analysis of thermal conductivity of liquid aliphatic hydrocarbons with saturated and unsaturated straight or branch chain carbons
[ESDU-67018] 01 p0116 N73-10955
Analysis of thermal conductivity of liquid halogenated aliphatic hydrocarbons and commercial refrigerants
[ESDU-68024-AMEND-A] 01 p0116 N73-10956
Numerical analysis of thermal problems in presence of radiation and temperature-dependent thermal conductivities
[EUR-4809-F] 01 p0116 N73-10960
Effective thermal conductivities of four metal-ceramic composite coatings in hydrogen-oxygen rocket firings
[NASA-TN-D-7055] 01 p0116 N73-10961
Transient heat transfer analysis of space radiator heat rejection system under conditions of aerodynamic heating, solar, albedo, and planetary radiation
[NASA-CR-128595] 01 p0117 N73-10964
Applying dislocation scattering of phonons to measurement of thermal conductivity of Teflon
[AD-746516] 02 p0220 N73-11777
Thermal conductivity of liquid glycols, glycerols and their aqueous solutions
[ESDU-70004] 02 p0241 N73-11961
Procedure for determining temperature distribution along linear dimension of stator of electrostatic generator
[AD-747425] 03 p0256 N73-12070
Phase method for measuring thermal conductivity of gases at high temperature
[AD-747620] 03 p0264 N73-12142
Thermal expansion, specific heat, and thermal conductivity of carbon reentry materials to 3000 C
[SC-CR-72-3139] 03 p0320 N73-12610
Thermal conductivity, thermal properties, and thermal diffusivity of uranium-fissium alloy
[ANL-7889] 03 p0332 N73-12710
Electron temperatures and thermal conduction in high energy theta pinches
[LA-4930] 03 p0341 N73-12780
Mathematical model and experimental evaluation of performance of phase change thermal control devices containing high thermal conductivity metal matrices
[NASA-CR-129909] 04 p0385 N73-13133
Effect of nature, structure, temperature, volume weight, and moisture content on coefficient of heat transfer for heat insulation materials
[AD-748748] 04 p0438 N73-13573
Equations based on theory of elastic moduli of composite materials used to calculate electrical and thermal conductivities of two phase systems
[AD-748304] 04 p0439 N73-13580
Thermal conductivity measurements of electron and phonon scattering behavior in low temperature solids
[COO-1629-31] 04 p0485 N73-13961
Development of proton-activated sensors to measure graphite nosetip recession due to ablation during nose cone reentry
[AD-748289] 05 p0548 N73-14456
Thermal conductivity of air and nitrogen at high temperatures
[AD-749842] 05 p0607 N73-14934
Measurements of thermal conductivity in boulder clay and effects of soil moisture conductivity
[NASA-TT-F-14664] 07 p0793 N73-16446
Theoretical study of sunspots and electrical and thermal conductivities of solar magnetoplasma
[AD-752230] 08 p0962 N73-17872
Boundary scattering of phonons in germanium and silicon determined from low temperature thermal conductivity measurements
[AD-753494] 09 p1076 N73-18780
Phonon emission by laser beams and thermal conductivity of optical crystals
[AD-753698] 09 p1077 N73-18791
Transient hot-wire measurement of thermal conductivity of electrolytic solutions
[RISO-264] 10 p1126 N73-19173
Transient hot-wire determination of thermal conductivity of pure, dielectric liquids
[RISO-263] 10 p1126 N73-19174
Analysis of porous media of heat pipe wicks to determine effects on permeability and thermal conductivity of materials
10 p1222 N73-19938
Power series solution to partial differential equation in thermal conductivity analysis on body of variable density
[AD-754256] 10 p1225 N73-19957
Approximative solution for first boundary value problem of thermal conductivity
[AD-754255] 11 p1349 N73-20947
Mathematical theory of viscous incompressible flow and solutions to Navier-Stokes equations
[AD-754995] 11 p1350 N73-20953
Review and compilation of technical data on Lorenz ratio of metals and alloys to include electrical resistivity and thermal conductivity
[NBS-TN-634] 12 p1413 N73-21451
Solution of temperature distribution in hollow cylinder for asymptotic regime and variable heat conductivity coefficient
[AD-755251] 12 p1465 N73-21872
Thermal conductivity of Kondo superconductor Zn-Mn
13 p1565 N73-22682
Thermal and electrical conductivity of Nd-Y alloy system at room temperature
[AD-756595] 13 p1566 N73-22693
Analysis of magnon contribution to total heat current and magneto-elastic coupling in antiferromagnetic materials
16 p1932 N73-25630
Phonon scattering by conduction electrons in transition metal carbides
[COO-1198-937] 16 p1947 N73-25755
Thermal conductivity of complex dielectric crystals at high temperature
16 p1952 N73-25796
Thermal conductivity of rocket motor walls with variable heat exchange coefficients
[AD-759815] 16 p1958 N73-25836
Four moment method for studying thermal conductivity in rarefied gas confined in concentric cylinders
16 p1973 N73-25955
Analysis of thermodynamic conditions for rapid start up of high temperature, gas loaded heat pipe
[NASA-TM-X-2840] 18 p2205 N73-27800
Thermal conductivity measurements of particulate materials in vacuum using basalt and soda lime glass beads of various size ranges as samples
[NASA-TM-X-64759] 18 p2205 N73-27801
Analysis of thermophysical properties of plasma sprayed materials for use as thermal insulation coating on rocket nozzles
[NASA-CR-121144] 19 p2311 N73-28590
Thermal conductivity and electrical resistivity ATJS graphite
[AD-762301] 19 p2313 N73-28601
Development of methods for analyzing thermal stress, heat conduction, structural theory, and thermoelastic wave propagation
[AD-762479] 20 p2484 N73-29952
Numerical solution of multidimensional linear thermal conductivity problems with complex boundary conditions which occur with heating of metals
[NLL-M-21666-[5828.4F]] 21 p2557 N73-30495
Thermal and electrical properties of titanium alloyed with vanadium and high temperature creep of metal with fcc lattice
[JPRS-59623] 22 p2683 N73-31490
Thermal conductivity and electrical properties of titanium alloyed with vanadium at 100 to 350 K
22 p2683 N73-31491
Thermal conductivity of germanium in boundary scattering regime
[AD-764122] 23 p2826 N73-32589
Electrostatically controlled heat transfer system for conducting thermal energy
[NASA-CASE-NPO-11942-1] 23 p2855 N73-32818
Electron thermal conductivity of thin films of strong coupling superconductors and of superconductors containing rare earth inpurities
24 p2967 N73-33712
Determination of vapor pressure, viscosity, and thermal conductivity of several liquid rocket propellants
24 p2972 N73-33750
Technique for predicting thermal conductivity of randomly packed granular materials
24 p2990 N73-33892

THERMAL CONDUCTIVITY GAGES
Apparatus for measuring thermal conductivities to 2 degrees K used for measurements in single crystal halides as function of dislocation density
[AD-759552] 17 p2034 N73-26462

THERMAL CONDUCTORS
Determining mechanical properties of high conductivity metals and alloys
[NASA-CR-133890] 22 p2684 N73-31498

THERMAL CONTROL COATINGS
Incremental theory and numerical procedure for analyzing three dimensional thermoplastic structure used in nonmetallic thermal protection system
[NASA-CR-124005] 06 p0729 N73-15948
Development of space stable thermal control coatings for application to spacecraft surfaces
[NASA-CR-124003] 07 p0854 N73-16922
Pigments for space-stable thermal control coatings to shield spacecraft from solar radiation
[NASA-CR-124067] 09 p0998 N73-18144
Degradation rate of thermal control coatings exposed to solar ultraviolet irradiation
[NASA-CR-124149] 11 p1307 N73-20608
Effect of thruster pulse length on thruster-exhaust damage of S13G white thermal control coatings
[NASA-TM-X-68213] 11 p1348 N73-20940
Refractory porcelain enamel passive thermal control coating for high temperature alloys
[NASA-CASE-MFS-22324-1] 12 p1416 N73-21471
Systems analysis of active thermal control using thermoelectric devices
[NASA-CR-124256] 15 p1843 N73-24935
Thermal ultraviolet spectrometer model vacuum test performance
[NASA-CR-128562] 16 p1916 N73-25509
Design, fabrication, and tests of experimental flight packages capable of measuring long term solar degradation of thermal control coatings
[AD-759083] 16 p1968 N73-25916
Handbook of data on passive thermal control coatings and surfaces for heat transfer and temperature regulation of spacecraft
[NASA-CR-124287] 16 p1975 N73-25969
Passivation of pigment particles for thermal coatings
[NASA-CR-124448] 24 p2937 N73-33457
White porcelain enamal thermal control coating for spacecraft
[NASA-CR-124459] 24 p2938 N73-33459
Thermal cycling effects on properties of silica, mullite, and alumino-silicate insulation coatings
24 p2941 N73-33487

THERMAL CONVECTION
U FREE CONVECTION

THERMAL CURRENTS
U CONVECTIVE FLOW

THERMAL CYCLING TESTS
Influence of thermal cycles on weld properties of all weld metal heat affected zone and base metal
[AD-746886] 02 p0179 N73-11452
Temperature and temperature gradients for accelerated life tests of nickel cadmium cells
[AD-748252] 04 p0377 N73-13066
Influence of creep damage on low cycle thermal-mechanical fatigue behavior of two tantalum base alloys
[NASA-CR-121001] 04 p0431 N73-13514
Simulation of ratcheting behavior of loaded structural components subjected to nonuniform thermal cycling
[AD-753686] 09 p1050 N73-18563
Thermal cycling tests of molybdenum foil-zirconium cloth insulation system
[ALO-2832-45] 10 p1224 N73-19951
NaK loop testing of thermoelectric converter modules for SNAP program
[NASA-CR-121192] 14 p1691 N73-23727
Accelerated life tests of copper/acetone heat pipe for meteorological satellite temperature control, including thermal cycling tests
14 p1719 N73-23948
Parametric performance characteristics and treatment of temperature coefficients of silicon solar cells for space application
[NASA-CR-132156] 15 p1738 N73-24090
Effects of thermal cycling at high temperature on rates of distortion of UO2/clad fuel elements
[NASA-CR-133236] 17 p2061 N73-26672
Correlation of creep rate with microstructural changes during high temperature creep
[NASA-CR-135698] 23 p2804 N73-32426
Thermal cycling tests of gas turbine components
[AD-764930] 23 p2833 N73-32637
Plasma arc thermal cycling tests on surface insulation materials for space shuttle
24 p2940 N73-33480
Cyclic convective heating evaluation of surface insulation materials for space shuttles
24 p2940 N73-33481
Sea salt and radiant heat effects on crystalline properties of mullite/silica composite thermal insulation for space shuttle
24 p2941 N73-33486
Thermal cycling effects on properties of silica, mullite, and alumino-silicate insulation coatings
24 p2941 N73-33487

THERMAL DECOMPOSITION
U PYROLYSIS

THERMAL DEFOCUSING
U THERMAL BLOOMING

**THERMAL DEGRADATION**
Carbonyl formation data at elevated temperatures for estimating storage life of unstabilized polyolefins
[AD-748827] 04 p0438 N73-13572
Thermal degradation process and char forming characteristics of polymers and composites
[AD-750396] 06 p0689 N73-15612
Elementary chemical processes involved in degradation of polymers in melts
08 p0881 N73-17133
Tests of potential thermal degradation of ATS-F radiant cooler form contaminants generated by hydrazine thruster in simulated space
[NASA-CR-132988] 16 p1974 N73-25965
Stress corrosion cracking of titanium alloys by hydrofluoric acid released during Viton B thermal degradation
[D-MAT-191] 18 p2161 N73-27455
Electrical and thermal breakdown properties of tantalum oxide and hafnium oxides capacitors
22 p2641 N73-31168
Thermal aging of plastic insulated silver-plated copper aircraft electrical wire
[AD-764731] 23 p2767 N73-32135

**THERMAL DIFFUSION**
Diffusion interaction of components during calorization of niobium alloys with 5 to 50 wt. percent titanium
[AD-747429] 03 p0318 N73-12588
Thermal conductivity, thermal properties, and thermal diffusivity of uranium-fissium alloy
[ANL-7889] 03 p0332 N73-12710
Thermal decay of magnetically confined fully ionized arc plasma heated with pulsed CO2 laser energy
[UCLA-34-P-157-X-4] 03 p0342 N73-12789
Temperature effects on supersaturation in thermal diffusion chamber
[AD-758137] 14 p1646 N73-23354
Two-dimensional submerged slot jets to diffuse thermally buoyant water jets into moving water stream
[PB-213461/7] 14 p1651 N73-23395
Thermal analysis of carbon migration in carbide and oxycarbide systems
[AERE-R-6897] 21 p2606 N73-30885

**THERMAL DIFFUSIVITY**
Increasing phase change material thermal diffusivity by means of solid fillers
[NASA-CR-124214] 13 p1590 N73-22894
Analysis of linear oscillating temperature distribution to determine thermal diffusivity coefficient of gases
[BER-1/73] 13 p1590 N73-22895

**THERMAL DISSOCIATION**
Mass spectra and dissociation energies of high temperature gaseous molecules containing aluminum
[NASA-TN-D-7123] 04 p0386 N73-13138
Analysis of approximate transport properties of high temperature air in dissociation equilibrium
[ESDU-00.01.07-AMEND-A] 07 p0853 N73-16919
Gas jets, seeding, and thermal excitation for producing neutral molecular beams
[DLR-FB-72-52] 09 p1068 N73-18717
Three body recombination and dissociation rate coefficients for reversible reactions H2 plus H yields H plus H plus H
[FML-PUBL-72-11] 10 p1126 N73-19169

**THERMAL EFFECTS**
U TEMPERATURE EFFECTS

**THERMAL EFFICIENCY**
U THERMODYNAMIC EFFICIENCY

**THERMAL EMISSION**
NT THERMIONIC EMISSION
Properties of active and helmet coronal streamers based on radio observations
01 p0093 N73-10769
Comparison of Nimbus interferometer spectrometer observations and theoretical radiances between 425 to 1450/cm
[NASA-TM-X-66275] 18 p2142 N73-27314
Direct integration transmittance model for 200/2000 cm region of high spectral resolutions and of planetary thermal emissions
[NASA-TM-X-70454] 21 p2548 N73-30429
Radiometric emittance measurements on reusable external insulation materials
24 p2939 N73-33473

**THERMAL ENERGY**
Dissipation of kinetic and thermal energy in mixed surface layer of ocean from measurements made in Barbados oceanographic and meteorological experiment
[AD-745343] 01 p0053 N73-10431
Utilization of space technology to supply earth demands for thermal and electric energy
04 p0473 N73-13864
Design, fabrication, and test of flight qualified heat pipe diode for Advanced Thermal Control Flight Experiment
[NASA-CR-114526] 08 p0968 N73-17915
Direct thermal energy conversion using thermal absorption principle
[NASA-CASE-ARC-10461-1] 11 p1347 N73-20931
Experimental and theoretical investigation of trajectory and growth of thermal effluents with variable discharge velocities and temperatures
[NASA-TM-X-69221] 12 p1392 N73-21284
Deep-seated thermal processes, social-economic heat utilization, and geothermal observation improvement
[JPRS-59496] 18 p2143 N73-27324
Analysis of thermodynamic conditions for rapid start up of high temperature, gas loaded heat pipe
[NASA-TM-X-2840] 18 p2205 N73-27800
Analysis of atmospheric temperature inversion conditions and requirements for thermal convection for removal of temperature inversion effects
[NLL-M-23034-[5828.4F]] 20 p2391 N73-29204
Electrostatically controlled heat transfer system for conducting thermal energy
[NASA-CASE-NPO-11942-1] 23 p2855 N73-32818

**THERMAL ENERGY STORAGE**
U HEAT STORAGE

**THERMAL ENVIRONMENTS**
Apollo experience report on techniques to define aerothermodynamic environment of Apollo spacecraft during post boost phase and to predict structural temperatures
[NASA-TN-D-7085] 09 p1091 N73-18903
Computer program for calculation of steady, state and/or transient thermal environments for space system during lunar surface, deep space, or thermal vacuum
[NASA-CR-134031] 22 p2729 N73-31842

**THERMAL EXPANSION**
NT THERMAL BUCKLING
Supersaturation and condensation in cloud chamber expansion
[AD-745348] 01 p0058 N73-10478
Effect of composition of refractory metal solid solutions on coefficient of thermal expansion
[AD-745847] 01 p0068 N73-10556
Analysis of thermal expansion coefficients and elastic moduli of solid solutions of silicon in given solutions
[AD-745825] 01 p0068 N73-10557
Roentgenographic measurement of coefficient of thermal expansion for chromium and solid chromium based solutions
[AD-747399] 03 p0317 N73-12580
Thermal expansion, specific heat, and thermal conductivity of carbon reentry materials to 3000 C
[SC-CR-72-3139] 03 p0320 N73-12610
Analysis of lattice spacings and changes in platinum metals as function of temperature and applied pressure
[NLL-TRANS-746-1316-[9022.401]]
05 p0561 N73-14558
Determination of coefficients of linear expansion for turbine parts as result of heating by Chevenard dilatometer
[AD-749735] 05 p0607 N73-14935
Thermal dilatation coefficients of explosive monocrystals determined by extensometry
[ISL-24/71] 09 p1099 N73-18969
Volumetric expansion of silver alloy at room temperature
[TID-26251] 16 p1928 N73-25602
Ordinary wave penetration of infinite magnetoplasma slabs
[IPPJ-154] 16 p1949 N73-25772
Thermal expansion instability and effect on creep properties of polyurethane
[AD-762458] 19 p2313 N73-28602
Sensitivity of solid rocket propellant stress to linear thermal expansion
[AD-761815] 19 p2328 N73-28729
Differential thermal technique for lining tantalum alloy tubing with tungsten
[NASA-TN-D-7426] 23 p2805 N73-32429

**THERMAL FATIGUE**
Fatigue test facility for space shuttle orbiters
10 p1138 N73-19273

**THERMAL INSTABILITY**
Iterative algorithm for determining thermal instabilities in viscoelastic rod under cyclic loads
[AD-746470] 02 p0240 N73-11953
Numerical analysis of relation between thermal fluctuations in nonequilibrium systems and nonlinear properties of systems
03 p0364 N73-12963
Flow characteristics in earth liquid core
[NRC-TT-1635] 16 p1904 N73-25402

**THERMAL INSULATION**
Calculation of thermal resistance of air layers in air permeable clothing for reliable design
[AD-746037] 02 p0136 N73-11099
Construction and properties of guarded hot plate apparatus for thermal insulation study
[PB-210118] 02 p0175 N73-11415
Development and evaluation of internal insulation materials for use with liquid hydrogen tanks on space shuttle
[NASA-CR-123928] 02 p0191 N73-11547
Heat transfer mechanisms in fibrous insulation materials
[PB-210117] 02 p0192 N73-11558
Development and characteristics of multilayer insulations for long term cryogenic storage
[NASA-CR-123938] 03 p0320 N73-12606
Design, development, and evaluation of pressurized purge system for reusable space shuttles and fabrication of multilayer insulation systems
[NASA-CR-123942] 03 p0358 N73-12914
High temperature insulation materials for reradiative thermal protection system of shuttle orbiter vehicle
[NASA-CR-123945] 03 p0363 N73-12957
Effect of nature, structure, temperature, volume weight, and moisture content on coefficient of heat transfer for heat insulation materials
[AD-748748] 04 p0438 N73-13573
Lightweight insulation for long duration low pressure planetary orbiter-type rocket engine applications
[NASA-CR-114513] 04 p0485 N73-13959
Evaluation of high temperature, space vacuum performance of electrical materials, capacitors, and compression sealed pyrolytic boron nitride slot insulation
[NASA-CR-120785] 05 p0518 N73-14216
Fabrication and tests of polyphenylene oxide foam panels for application as reusable insulation with LH2 tanks
[NASA-CR-123955] 05 p0565 N73-14586
Examination of physical processes governing heat transfer through air-penetrable clothing in wind
[DRIC-TRANS-2921] 06 p0636 N73-15166
Development of space stable thermal control coatings for application to spacecraft surfaces
[NASA-CR-124003] 07 p0854 N73-16922
Improvement and evaluation of mullite reusable surface insulation material for thermal protection system of space shuttle
[NASA-CR-124053] 08 p0934 N73-17646
Techniques and instrumentation for nondestructive testing of high performance multilayer thermal insulation for space shuttle orbiters
[NASA-CR-124106] 09 p1051 N73-18567
Environmental salt spray tests of closed pore insulation for space shuttle orbiter thermal protection system
[RM-570] 09 p1051 N73-18572
Atom recombination catalytic rates for surface coatings of thermal protection system materials for space shuttles
[NASA-TN-D-7113] 09 p1098 N73-18965
Development of methods for protecting aircraft compartments from aerodynamic heating effects
[AD-754606] 11 p1236 N73-20036
Development of design data for adhesives for attaching reusable surface insulation on space shuttle
[NASA-CR-128888] 11 p1308 N73-20616
Optimization of basic ceramic insulation for space shuttle orbiters - Part 2
[NASA-CR-112257] 13 p1546 N73-22531
Use of phenol formaldehyde plastic foam as thermal insulation for solar water heaters to improve efficiency
[AD-756591] 13 p1548 N73-22543
Thermophysical and mechanical properties of closed pore insulation
[NASA-CR-112295] 15 p1843 N73-24930
Apollo experience report on design and development of cryogenic storage system and related components
[NASA-TN-D-7288] 16 p1964 N73-25889
Handbook of data on passive thermal control coatings and surfaces for heat transfer and temperature regulation of spacecraft
[NASA-CR-124287] 16 p1975 N73-25969
Para-benzoquinone dioxime and concentrated mineral acid processed to yield intumescent or fire resistant, heat insulating materials
[NASA-CASE-ARC-10304-1] 17 p2048 N73-26572
Simulated rain erosion testing on closed pore insulation for shuttle orbiter
[RM-573] 20 p2434 N73-29548
Development and characteristics of thermal control system for maintaining constant temperature within spacecraft module with wide variations of component heat transfer
[NASA-CASE-GSC-11018-1] 21 p2599 N73-30829
Cryogenic insulation of liquid oxygen dewars for aircraft pilot breathing masks
[AD-763325] 22 p2624 N73-31026
Advanced material composites for use as insulations for space shuttle LH2 tanks
[NASA-CR-124388] 22 p2688 N73-31532
Thermal aging of plastic insulated silver-plated copper aircraft electrical wire
[AD-764731] 23 p2767 N73-32135
Evaluating reusable surface insulation for space shuttle over range of heat transfer rate and surface temperature
[NASA-TM-X-2823] 23 p2809 N73-32465
Structural heat pipe for spacecraft wall thermal insulation system
[NASA-CASE-GSC-11619-1] 23 p2857 N73-32828
Fabrication and evaluation of composite thermal engine insulation
[NASA-CR-124457] 24 p2938 N73-33458

Production of rigidized mullite composite materials for external insulation of shuttle orbiter
24 p2938 N73-33463
Glass ceramic foam materials for space shuttle heat shielding system
24 p2938 N73-33464
Fused silica coatings for flexible mat insulation of space shuttle surface
24 p2939 N73-33465
Alumina silicate based composite materials for space shuttle heat shielding system
24 p2939 N73-33466
Silica fiber materials for surface insulation of space shuttle orbiters
24 p2939 N73-33467
Radiant heat transfer in surface insulation materials for space shuttle orbiter
24 p2939 N73-33468
Hafnium pigmentation for mullite composite thermophysical optimization
24 p2939 N73-33469
Amorphous silica material characterizations for thermal reusable insulation of space shuttle orbiter
24 p2939 N73-33470
Porosity analysis on silica and mullite composite surface insulation tiles
24 p2939 N73-33472
Space environment simulation tests on space shuttle reusable surface insulation materials
[NASA-TM-X-2720] 24 p2940 N73-33475
Space environment aerodynamic heating tests on mullite and silica fiber surface insulation panels
24 p2940 N73-33476
Convective heating tests on joints and gaps between surface insulation tiles
24 p2940 N73-33477
Plasma jet wind tunnel tests on space shuttle surface insulation materials
24 p2940 N73-33479
Plasma arc thermal cycling tests on surface insulation materials for space shuttle
24 p2940 N73-33480
Cyclic convective heating evaluation of surface insulation materials for space shuttles
24 p2940 N73-33481
Thermal and structural performance tests on space shuttle orbiter surface insulation materials
24 p2941 N73-33489
Optical property effect in thermal design for insulation coating attachments
24 p2942 N73-33492
Design of rigid ceramic foam insulation for space shuttle surface thermal protection
24 p2942 N73-33493
Mechanical attachment of surface insulation tiles to space shuttle structure
24 p2942 N73-33494
Ceramic reinforced mullite thermal protection system design for space shuttle surface
24 p2942 N73-33495
Cost effectiveness of silica insulation in space shuttle thermal protection system design
24 p2942 N73-33496
Thermostructural evaluation of mullite and silica composite materials for space shuttle surface insulation system design
24 p2942 N73-33498
Interference heating in gaps between surface insulation tiles for space shuttle thermal protection system design
24 p2942 N73-33499
Cristobalite transformation effects on tensile strength of silica surface insulation materials
24 p2943 N73-33500
Radiative emittance measurements on surface insulation coatings in plasma jet wind tunnel
24 p2943 N73-33501
Refractory metal carbide/metal oxide composites for thermal insulation
[LA-5136] 24 p2943 N73-33504

**THERMAL NEUTRONS**

Effects of heavy particle external ionization source on carbon dioxide laser efficiency
[COO-2007-24] 10 p1169 N73-19509
Thermal neutron scattering theory for fluid state of matter
[SGAE-2054] 15 p1815 N73-24715

**THERMAL PLASMAS**

Particle production and energy dissipation in stationary fusion plasma
[FOA-4-C-4465-25] 06 p0703 N73-15734
Theory and applications of induction arc
[AD-750742] 06 p0706 N73-15761
Statistical mechanics and kinetic theory for two dimensional plasma in uniform magnetic field
07 p0825 N73-16685
Electron temperature fluctuations of ionized plasma in Q device
[AD-751256] 07 p0830 N73-16731
Lowering of ionization potentials of hydrogen and carbon atoms immersed in high temperature and high density thermal plasma
[AD-733247] 09 p1072 N73-18752
Computing electrical conductivity of thermal plasma taking nonelastic collisions into account
[AD-753972] 10 p1198 N73-19746
Production and confinement of hot plasma and electron thermalization in superconducting ring device
[UCRL-74337] 16 p1950 N73-25777
Damping and saturation of second order electron plasma wave echo
24 p2961 N73-33662

**THERMAL POLLUTION**

Proceedings of conference to define research requirements for problems involving waste heat transfer from large thermal sources into the environment
02 p0166 N73-11348
Development of steps and procedures for determining and evaluating environmental quality through use of remote sensors
07 p0782 N73-16358
Analysis of tidal currents, turbulent diffusion, and local shears in currents found in Trinity Bay, Texas
[NASA-CR-128734] 08 p0916 N73-17510
Man induced changes in earth climate by environment pollution and heat production
[PB-213676/2] 14 p1613 N73-23074
Remote sensing of thermal and industrial discharges along shoreline of Lake Michigan
[PB-214503/5] 16 p1908 N73-25436
Aerial reconnaissance of thermal discharges along shoreline of Lake Michigan
[PB-214407/9] 16 p1908 N73-25437
Thermal and water quality parameters of Tennessee River
[NASA-CR-133089] 17 p2024 N73-26378

**THERMAL POWER**

U TURBOGENERATORS

**THERMAL PROPERTIES**

U THERMODYNAMIC PROPERTIES

**THERMAL PROTECTION**

Heat sink and cooling system concepts for space shuttle baseline thermal protection systems
[NASA-CR-123912] 01 p0107 N73-10884
Nondestructive analysis techniques for detection of defects in rigidized surface insulation for space shuttle thermal protection
[NASA-CR-128607] 01 p0108 N73-10893
Finite difference solution of film cooling as alternate thermal protection system for spacecraft during reentry
[NASA-CR-112192] 01 p0116 N73-10958
TD nickel chromium, dispersion-strengthened alloy for thermal protection system of space shuttle
[NASA-CR-120796] 02 p0187 N73-11512
Methodology for combining thermal structural loads as design criteria for thermal protection system of space shuttle orbiter
[NASA-CR-2102] 02 p0234 N73-11898
High temperature insulation materials for reradiative thermal protection system of shuttle orbiter vehicle
[NASA-CR-123945] 03 p0363 N73-12957
Computational techniques for design optimization of thermal protection for space shuttle
[NASA-CR-128658] 05 p0598 N73-14863
Incremental theory and numerical procedure for analyzing three dimensional thermoplastic structure used in nonmetallic thermal protection system
[NASA-CR-124005] 06 p0729 N73-15948
Relative rain erosion resistance of low-density-thermal protection materials for space shuttles at subsonic velocities
[NASA-CR-130541] 08 p0969 N73-17924
Environmental salt spray tests of closed pore insulation for space shuttle orbiter thermal protection system
[RM-570] 09 p1051 N73-18572
Apollo experience report on techniques to define aerothermodynamic environment of Apollo spacecraft during post boost phase and to predict structural temperatures
[NASA-TN-D-7085] 09 p1091 N73-18903
Application of finite element method to calculation of supersonic flutter of thermal protection panel for space shuttles
[VF-12] 10 p1104 N73-19001
Computation of supersonic flutter for thermal protection panel of space shuttles
[VF-16] 10 p1104 N73-19002
Non-metallic thermal protection panels for space shuttles
[TASS-72-Z-1095] 10 p1224 N73-19953
Thermal design of filamentary composite materials for primary structures on space shuttles
[NASA-CR-124206] 12 p1415 N73-21469
Degradation and reuse of radiative-thermal protection materials for space shuttle
[NASA-CR-123587] 14 p1709 N73-23866
Design of thermal protection system for 8-foot HTST combustor
[NASA-CR-112310] 15 p1760 N73-24262
Integrated thermal protection and structural meteoroid protection system in space vehicles - Vol. 1
[NASA-CR-121103] 15 p1834 N73-24865
Space vehicle integrated thermal protection/structural meteoroid protection system - Vol. 2
[NASA-CR-121104] 15 p1834 N73-24866
Handbook of data on passive thermal control coatings and surfaces for heat transfer and temperature regulation of spacecraft
[NASA-CR-124287] 16 p1975 N73-25969
Dispersion strengthened nickel alloys for use as space shuttle thermal protection systems
[NASA-CR-121164] 17 p2043 N73-26526
Methods for repairing coated columbian thermal protection system
[NASA-CR-124295] 18 p2206 N73-27809
Assessment of technological readiness for coated columbium thermal projection systems
[NASA-TM-X-2858] 20 p2431 N73-29530
Development of alternate space shuttle concepts to show modified avionics, vehicle subsystems, and thermal protection system
[NASA-CR-124345] 21 p2601 N73-30844
High temperature silicone adhesive formulations for thermal protection systems used with space shuttle mission
[NASA-CR-124389] 22 p2688 N73-31533
Flexible ceramic mat surface insulation for space shuttle thermal protection system design
24 p2942 N73-33497

**THERMAL RADIATION**

Computer analysis of temperature distributions in circular and rectangular bodies exposed to thermal radiation from nuclear weapon explosions
[AD-745727] 01 p0084 N73-10699
Thermal surveillance of volcanoes of Cascade Range and Iceland using ERTS-1 imagery and data collection platforms
[E72-10246] 03 p0289 N73-12346
Simulating radiant heating of propellant stream of nuclear light bulb engine
[NASA-CR-129499] 03 p0330 N73-12693
Thermal remote sensing of infrared radiant temperatures in alpine/periglacial environments
04 p0409 N73-13332
Long-wave radiation divergence measurements over water and land compared with calculated divergences from temperature and humidity profiles
[AD-748997] 04 p0418 N73-13410
Second order coherence function discriminating between thermal and laser radiation
[ONERA-NT-196] 04 p0450 N73-13675
Solar and terrestrial radiation regimes over arctic ice packs
[AD-748214] 04 p0467 N73-13808
Actinometric equipment on Soviet meteorological satellites for thermal radiation measurements of earth atmosphere
[AD-749622] 04 p0479 N73-13920
Atmospheric effects on thermal radiation from tropospheric nuclear explosion to ground target
[AD-745884] 05 p0539 N73-14389
Preliminary estimates of thermal radiation heat transfer to aerobraking space tug
05 p0608 N73-14947
Application of thermal infrared scanner data to agriculture
07 p0785 N73-16387
Remote sensing of areas in Italy using infrared scanners for thermal radiation map
07 p0859 N73-16968
Simulation of thermal radiation-airblast interaction effects in conical shock tube
[AD-752023] 08 p0893 N73-17229
Quartz tube, tungsten filament lamp bank for characterization of nonmetallic thermal protection materials for high irradiance environment
[AD-752606] 08 p0893 N73-17231
Computer program for solving radiation-hydrodynamic problems in complex geometries
[AD-752066] 08 p0970 N73-17929
Thermal surveillance of volcanoes of Cascade Range and Iceland using ERTS-1 DCP systems and imagery
[E73-10317] 09 p1023 N73-18349
Simultaneous investigations of three-dimensional structure of atmospheric radiation fields using equipment installed on airplanes, balloons, satellites, and ground
[AD-750962] 09 p1030 N73-18411
Nuclear thermal vulnerability of honey comb sandwich radome panels
[AD-753666] 09 p1056 N73-18605
Angular distribution of outgoing shortwave radiation intensity in atmosphere with continuous cloud cover
[AD-753975] 10 p1157 N73-19417
Nonsteady combustion and extinguishment effects, including external thermal radiation effects, steady flame temperature, and L-stability limit
[AD-755860] 12 p1442 N73-21686
Earth resources remote sensing project using multispectral band scanners to detect and measure thermal radiation from ground vegetation
[NASA-CR-124219] 13 p1529 N73-22393
Thermal surveillance of active volcanoes in Washington, California, and Iceland
[E73-10556] 14 p1655 N73-23428

Characteristics of thermal radiation of Greenland ice measurements by Cosmos-243
[NASA-TT-F-14953] 15 p1780 N73-24427
Attenuation of thermal radiation by transpiration of absorbing gas using porous Porolloy plate
15 p1812 N73-24685
Solar and terrestrial radiation fluxes over Arctic pack ice
[AD-758060] 15 p1828 N73-24820
Interactions between radio brightness and surface conditions of oceans based on Cosmos 243 data
[NASA-TT-F-14954] 16 p1904 N73-25401
Galilean satellite thermal radiation measurements
16 p1961 N73-25866
Remote sensing of thermal emission from sea surface and atmosphere
[NASA-TT-F-14972] 18 p2142 N73-27317
Thermal emission from random sea, using Gaussian slope distribution
20 p2391 N73-29207
Development of numerical methods for computation of vertical divergence of thermal radiation
20 p2400 N73-29290
Development of mathematical relationships to determine short-wave thermal radiation under cloudy and cloudless conditions
20 p2401 N73-29291
Development of numerical methods for improving accurracy of calculations of thermal radiation in earth atmosphere
20 p2401 N73-29297
Development of method for determining atmospheric transmission function with allowance for divergence of thermal radiation
20 p2401 N73-29298
Heat transfer by thermal radiation in forced convective tube flow of radiation gas
20 p2484 N73-29954
Numerical analysis of one form of distribution of spectral energy density of thermal radiation
[JPRS-59660] 20 p2485 N73-29958
External heat transfer problems under space conditions
[NASA-TT-F-783] 21 p2605 N73-30879
Temperature relationship of monochromatic coefficients of radiation of titanium, niobium, and zirconium monocarbides in regions of homogeneity
23 p2807 N73-32442
Aerial thermal infrared surveillance of active volcanoes in northern Cascade Range
[E73-11100] 24 p2914 N73-33257

**THERMAL RADIO EMISSION**
U RADIO EMISSION
U THERMAL EMISSION

**THERMAL REACTORS**
Design and evaluation of automobile thermal reactors with ceramic material construction
[NASA-TM-X-68148] 01 p0069 N73-10567
Testing reactor-equipped vehicle for assessment of emissions control
[PB-218639/3] 18 p2173 N73-27554
Fuel system for thermal nuclear reactor which uses inorganic ion exchanger
[NASA-CASE-LEW-11645-2] 19 p2319 N73-28660
Computerized simulation models for thermal exhaust reactors
22 p2727 N73-31824

**THERMAL RESISTANCE**
Mechanical properties of heat resistant silicon carbide-graphite composite
[AD-745434] 01 p0070 N73-10577
Polyphenylquinoxaline resin systems for high temperature composite materials
[AD-746273] 02 p0193 N73-11559
Thermal resistance of clothing noting radiative body heat transfer, air layers, and clothing thickness
[DRIC-TRANS-2920] 03 p0261 N73-12117
Numerical analysis to obtain error estimate for thermal resistance measurements on uncoated silicon microwave transistors as result of temperature gradients
[AD-748073] 03 p0276 N73-12235
Carbon black additives used to improve heat-aging resistance in silicone rubber vulcanizates
[AD-747769] 03 p0321 N73-12619
Derivation of formulas for calculating interfacial thermal resistance and condensation coefficient during condensation of metal vapors
[AD-748048] 03 p0365 N73-12972
Increased heat and impact resistance of ceramics made of zirconium dioxide reinforced with mullite whiskers
[JPRS-57770] 05 p0565 N73-14588
Synthesis of high molecular weight benzobistriazolo phenanthroline polymers for heat resistant plastic films
[AD-753414] 10 p1127 N73-19180
Properties of thermal resistant electrical insulating papers based on inorganic fibers
[NLL-RTS-7740] 10 p1175 N73-19554
Computational procedure for determining heat resistance of different graphites in broad temperature range
10 p1175 N73-19557
High-speed oscillating and thermal resistance tests of 25 self-lubricating composites
[AD-755112] 11 p1299 N73-20539
Ni/ZrO2 composite material for designing high strength thermal switches
[HIT-527] 12 p1383 N73-21212
Microstructure of recrystallized heat resistant steel
[JPRS-58840] 13 p1542 N73-22498
Synthesis of fire resistant phosphonitrilic plastics and elastomers for marine applications
[AD-755188] 13 p1548 N73-22547
High temperature carbon polymeric composite materials
[AD-759963] 17 p2052 N73-26598
Numerical technique for calculating thermal spreading resistance
[NASA-CR-12412] 19 p2352 N73-28921
Planar Gunn devices in dipole domain mode for high speed logic circuits in PCM equipment, noting thermal resistances and packing density
[FTZ-A-474-TBR-3] 22 p2643 N73-31183
Development of high temperature resistant elastomeric sealant
[AD-764589] 23 p2811 N73-32473

**THERMAL SHIELDING**
U HEAT SHIELDING

**THERMAL SHOCK**
Similarity analysis of transient temperature and thermal stress for deriving scaling relations for modeling thermal shock
[SC-RR-71-0657] 04 p0485 N73-13962
Thermal shock resistant hafnia ceramic materials
[NASA-CASE-LAR-10894-1] 05 p0564 N73-14584

**THERMAL SIMULATION**
Thermal simulation of oxide fuel rod by heated rods of different geometry
[EURFNR-1026] 10 p1187 N73-19655
German test facilities for environment simulation
19 p2249 N73-28133
Development of techniques for simulating infrared emission from turbojet aircraft exhaust plumes
[AD-763123] 20 p2486 N73-29967
Radiant array with as many as 144, 13 inches wide, modular radiant heating units mounted in sets of 3 to comprise each adjustable row
[NASA-CR-124435] 24 p2901 N73-33153
System controls description for 36 zone thermal simulation system for operation and maintenance
[NASA-CR-124436] 24 p2901 N73-33154
Reference material for thermal simulation system for programmers, temperature controls, power regulator, peripheral equipment, and radiant array purchased parts
[NASA-CR-124437] 24 p2901 N73-33155

**THERMAL STABILITY**
Equipment and procedures for measuring variation of strength of sheet specimens of glass under conditions of tension, compression, and shear
[AD-743694] 01 p0067 N73-10551
Mechanical properties of various metal alloys and operating life of dies during hot deformation of stainless and heat resistant steels and alloys
[AD-745703] 01 p0068 N73-10559
High temperature strength and stability of tungsten reinforced copper
[AD-745700] 01 p0071 N73-10581
Experimental procedure for estimating rate of thermal flow and heat transfer from longitudinally swept surfaces using unstable thermal regime method
[AD-746011] 02 p0243 N73-11977
Design, development, and performance tests of long pulse liquid laser oscillator and circulatory subsystem
[AD-747964] 03 p0311 N73-12536
Thermal stabilization of textiles composed of polybenzimidazole fibers by chemical treatment
[AD-748248] 04 p0440 N73-13584
Influence of humidity on thermal life determination of electrical insulation
[AD-749926] 05 p0521 N73-14238
Statistical analysis of thermal stability and service life of electrical insulation
[AD-749925] 05 p0521 N73-14239
Thermomechanical analysis of physical transitions and stability of poly[norbornadiene] in nitrogen
[AD-749374] 05 p0566 N73-14596
Relationship of molecular structure to thermo-oxidative stability of carborane-siloxane polymers with icosohedral CB10H10C cages
[AD-749820] 05 p0567 N73-14610
Thermally stable phosphonitrile elastomers for advanced aerospace structures
[NASA-CR-124008] 06 p0687 N73-15593
Thermal instability and secondary breakdown prediction for low frequency power transistor
[AD-751852] 08 p0890 N73-17203
Evaluation of ceramic materials for application as high temperature gas bearing material
[AD-753858] 09 p1042 N73-18499
Friction, wear, and thermal stability of some organotin and organosilicon compounds
[NASA-TN-D-7175] 09 p1051 N73-18569
Thermal stability of amorphous arsenic compound glasses and electron diffraction analyses on semiconducting arsenic selenide films
[AD-752993] 09 p1076 N73-18778
Thermal stability of high temperature tungsten and platinum resistance thermometers
[NBS-TN-764] 13 p1529 N73-22391
Thermodynamic stability diagrams of high temperature O2 corrosion reactions
14 p1676 N73-23602
Design feasibility of thermal subsystem concepts for photoheliographs
[NASA-CR-124268] 16 p1913 N73-25483
Hydrolytic stability of polyurethane potting compounds in Navy aircraft
[AD-759972] 17 p2053 N73-26604
Thermostability of titanium hydridonitrides
20 p2430 N73-29522
High temperature and ultraviolet stability properties of poly[diarylsiloxy]arylazine
[NASA-CASE-ARC-10592-1] 20 p2435 N73-29554
Thermal stabilization of component dimensions for gyro devices
[AD-763148] 21 p2549 N73-30441
Thermal stability in planetary nebulae
22 p2713 N73-31720
Thermal response of glassy fibrous mullite insulation to entry environment simulation
24 p2940 N73-33478
Plasma jet wind tunnel tests on space shuttle surface insulation materials
24 p2940 N73-33479
Simulated reentry heating tests on silica surface insulation material for space shuttle
24 p2940 N73-33482

**THERMAL STRESSES**
Transient heat transfer analysis of space radiator heat rejection system under conditions of aerodynamic heating, solar, albedo, and planetary radiation
[NASA-CR-128595] 01 p0117 N73-10964
Application of strain compatibility equations to evaluate thermal stresses in unidirectional graphite composites bonded to aluminum structures
[NASA-CR-112162] 02 p0125 N73-11014
Procedures for using liquid crystal tape for thermographic testing of bonded structures for aircraft
[NASA-CR-123932] 03 p0300 N73-12451
Finite element solution for axisymmetric transient heat conduction and thermal stress problems
[AD-747523] 03 p0362 N73-12950
Determination of temperature and residual stresses and deformations caused by welding process
[AD-749529] 04 p0428 N73-13487
Cool-down problem of solid propellant rocket engine incorporating dewetting
[AD-749036] 04 p0462 N73-13770
Elasto-viscoplastic behavior of structures subjected to complex loads and thermal gradients
[ONERA-NT-194] 04 p0482 N73-13937
Similarity analysis of transient temperature and thermal stress for deriving scaling relations for modeling thermal shock
[SC-RR-71-0657] 04 p0485 N73-13962
Analytic solution for temperature distribution in thermally insulated cylinder bar to determine time-variable thermal stresses
[DGLR-PAPER-72-112] 04 p0485 N73-13963
Solid solution hardening in alloys of niobium-hafnium, niobium-tungsten, and niobium-tantalum
[COO-916-25] 05 p0587 N73-14774
Influence of thermal stresses and loads on endurance properties of heat resistant alloys used to manufacture turbine blades
[AD-749752] 05 p0591 N73-14805
Correction of axisymmetric deformations in space telescope mirrors by thermally induced elastic strains
[NASA-TM-X-2673] 06 p0672 N73-15472
Analysis of thermal lensing in high power laser window materials
[AD-751266] 07 p0808 N73-16554
Analysis of thermal failures in combustion chambers of J-57 jet engine and system for detecting burnthrough prior to engine case rupture
[FAA-NA-72-92] 07 p0835 N73-16772
Simulation of ratcheting behavior of loaded structural components subjected to nonuniform thermal cycling
[AD-753686] 09 p1050 N73-18563
Laboratory method for thermal fracture of graphite
[AD-753392] 09 p1054 N73-18592
Thermal stress vibrations in prebuckled region of orthotropic trapezoidal plates with two parallel opposite sides and various boundary conditions
[NASA-CR-2174] 09 p1094 N73-18928
Effect of discontinuous changes in strain rate on relationship between strain rate, strain and stress in Udimet 700 alloy at elevated temperatures
10 p1219 N73-19916
Influence of strain rate on inelastic properties of Udimet alloys at elevated temperatures and presentation in form of hodograph
10 p1219 N73-19917
Sea ice dynamics, heat and mass budget of Arctic sea ice, desalinization, thermal and mechanical stresses, bearing capacity of floating ice, and interaction of oil and ice
[AD-754118] 11 p1290 N73-20463

Analysis of thermal static bending forces on deployable interlocked booms and comparison with thermal bending of seamless tubes
[NASA-TN-D-7243] 11 p1345 N73-20915
Role of isothermal stresses generated during oxidation and modes of stress relaxation
14 p1676 N73-23605
Development of continual solution for stress distribution due to thermal stresses near roots of rectangular wings
[ARC-R/M-3236] 15 p1730 N73-24030
Post buckling behavior of circular plate following heating at center and heating at edge and effects of restraints on final configuration
[ARC-R/M-3245] 15 p1730 N73-24031
Thermal and stress analyses of interfaces for nozzles and nozzle extensions
[NASA-CR-132211] 15 p1768 N73-24324
Computer program for thermal stress and instability analyses of structures
[NASA-CR-112228] 15 p1838 N73-24895
Analysis of wing leading edge buckling due to aerodynamic heating to show effect of shear modulus of material and geometry of leading edge on buckling onset
[ARC-R/M-3197] 16 p1851 N73-25000
Creep test measurement of stresses generated during high temperature oxidation of copper and nickel
16 p1926 N73-25588
Temperature and internal pressure response of nuclear waste disposal container following impact on earth
[NASA-CR-121186] 16 p1943 N73-25721
Love- and Donnell-type equations for investigating thermal stresses in ring-reinforced oval cylindrical shells subjected to heat inputs
16 p1968 N73-25920
Analysis of thermal fatigue in nontubular regeneratively cooled combustion chambers and prediction of thermal cycle life capability - Vol. 1
[AD-760582] 18 p2194 N73-27715
Analysis of thermal fatigue in nontubular regeneratively cooled combustion chambers and development of life prediction techniques - Vol. 2
[AD-760583] 18 p2194 N73-27716
Numerical analysis of temperature and stresses in cylindrical body heated with constant heat flow
[NLL-M-21601-[5828.4F]] 18 p2205 N73-27794
Analysis of stresses in magnet windings due to thermal contraction and temperature gradient stresses and impregnation with epoxy resins to reduce effects
[RHEL/R-264-PT-1] 20 p2435 N73-29558
Development of methods for analyzing thermal stress, heat conduction, structural theory, and thermoelastic wave propagation
[AD-762479] 20 p2484 N73-29952
Effects of high temperature cycling on structural properties of boron reinforced aluminum alloys used in spacecraft structures
[NASA-CR-124369] 21 p2562 N73-30541
Thermal stress and mechanical shock effects on release of bacterial spores from stainless steel surfaces with application to Mars landing
[NASA-CR-133868] 22 p2619 N73-30987
Thermal stress ratcheting of structures subjected to mechanical and cyclic thermal stresses
22 p2723 N73-31790
Thermoelastic analysis for predicting thermal stress failure in silicon solar cell array
[NASA-CR-135713] 23 p2748 N73-31993
Effect of high ambient temperature on calcium content of human bone tissue
24 p2884 N73-33033

**THERMAL VACUUM TESTS**
Performance tests of OAO-C spacecraft heat pipes under thermal-vacuum conditions
[NASA-TM-X-66072] 02 p0242 N73-11967
Thermal vacuum testing of spacecraft performance using flight models to determine malfunctions
[NASA-TM-X-66188] 09 p1090 N73-18895
Thermal and ultraviolet vacuum tests on adhesives, thermoplastic, and thermosetting resins for space environment simulation
[RV-106] 19 p2312 N73-28596
Modified quadrupole mass spectrometer for in situ space simulation thermal vacuum testing of sophisticated payloads
[NASA-TM-X-64775] 21 p2549 N73-30435
TD-1A telescope optical surface chemical contamination investigation of thermal vacuum tests and volatile condensable material screening
[ESRO-TN-86-ESTEC] 21 p2601 N73-30847
Performance evaluation of heat transfer testing of heat pipes with thermal-vacuum and beach testing
[NASA-TN-D-7219] 22 p2728 N73-31827

**THERMALIZATION [ENERGY ABSORPTION]**
High time resolution measurements of energetic electrons in auroral breakup using sounding rockets
16 p1895 N73-25324

**THERMIONIC CATHODES**
Steady-state characteristics of four plasma sources developed for mirror machine
[AD-754233] 10 p1197 N73-19742
Autocathode as gas discharge ion source for ion engines, noting field emission mechanism
[DLR-FB-72-73] 12 p1444 N73-21696
Thermionic cathode development for Apollo telescope mount camera tube Spares Program
[NASA-CR-124342] 19 p2243 N73-28087
Technical and economical effiency of thermionic cathode
[AD-761535] 19 p2248 N73-28121
Hollow cathode with BaO impregnated, porous tungsten inserts and tips
[NASA-TM-X-71417] 21 p2517 N73-30189

**THERMIONIC CONVERSION SYSTEMS**
U THERMIONIC POWER GENERATION

**THERMIONIC CONVERTERS**
Design and manufacturing of gasoline fueled, flame-heated thermionic diode
[AD-746255] 02 p0129 N73-11047
Low cost efficient thermionic converter for use in nuclear reactors
[NASA-CASE-NPO-13121-1] 03 p0332 N73-12702
Basic physical processes in thermionic and magnetohydrodynamic converters of thermal energy into electrical energy
[AD-748707] 04 p0376 N73-13061
Computerized design and performance of planar germanium P-I-N thermophotovoltaic cells
[AD-748895] 04 p0376 N73-13063
Control circuit for nuclear thermionic converter power source for spacecraft
[NASA-CASE-NPO-13114-1] 04 p0448 N73-13656
Current voltage characteristics of vapor deposited tungsten niobium planar thermionic converter
[NASA-TM-X-2716] 07 p0819 N73-16639
Cesium oxide/cesium solutions as sources of oxygen and cesium for improved thermionic converter performance
[NASA-CR-121119] 08 p0942 N73-17717
Useful life of high temperature thermocouples for in-core and out-of-core thermionic applications in vacuum
[NASA-CR-120898] 09 p1035 N73-18447
Evaluation of uranium nitride for in-core thermionic applications in electrically heated thermal gradient tests and in flat plate thermionic converters
[NASA-CR-131520] 12 p1416 N73-21470
Postoperational examination of externally configured test thermionic converter
[NASA-CR-131523] 12 p1426 N73-21560
Conference papers on thermionic power generation
[AD-758620] 15 p1739 N73-24098
Characteristics and evaluation of electrodes for use in thermionic converters - Phase 2
[NASA-CR-131838] 16 p1943 N73-25723
Measurement of work functions of oxygen-doped tantalum to determine applicability for use in plasma-mode thermionic converters
[NASA-CR-131837] 16 p1943 N73-25724
Thermoelectric converter and 5-kwe reactor system integration
[NASA-CR-121230] 16 p1943 N73-25726
Experimental determination of width of near anode region in knudsen mode of thermionic converter having variable interelectrode gap filled by Ba plus Cs mixture
[AD-760394] 17 p2062 N73-26682
Fabrication and life testing of thermionic converters
[NASA-CR-121180] 18 p2177 N73-27576
Design of tubular thermoelectric module for astronuclear power conversion system
[NASA-CR-121210] 19 p2319 N73-28659

**THERMIONIC DIODES**
Design and manufacturing of gasoline fueled, flame-heated thermionic diode
[AD-746255] 02 p0129 N73-11047
Design and performance analysis of thermionic diode modules for in-core thermionic power source
[NASA-CR-131602] 13 p1499 N73-22153
Basic processes in thermionic diodes and application to achievement of practical thermionic energy conversion
[AD-755955] 14 p1606 N73-23020
Collector/heat pipe cooled, externally configured thermionic diode for use in thermionic electric power source
[NASA-CR-135785] 24 p2954 N73-33600

**THERMIONIC EMISSION**
Thermionic emission from oxide-coated cathodes at low temperatures
[AD-747319] 02 p0150 N73-11218
Measurement of work functions of copper and copper-nickel single crystals at low pressures and determination of thermionic emission constant
16 p1927 N73-25593
Characteristics and evaluation of electrodes for use in thermionic converters - Phase 2
[NASA-CR-131838] 16 p1943 N73-25723
Measurement of work functions of oxygen-doped tantalum to determine applicability for use in plasma-mode thermionic converters
[NASA-CR-131837] 16 p1943 N73-25724

**THERMIONIC EMITTERS**
Pyrolysis of rhenium chlorides to yield chemically vapor deposited rhenium thermionic emitters
[NASA-CR-121143] 09 p1073 N73-18759

**THERMIONIC POWER GENERATION**
Power distribution in fast spectrum thermionic reactor fuel element at core/BeO reflector boundary
[NASA-TM-X-68207] 11 p1323 N73-20735
Evaluation of uranium nitride for in-core thermionic applications in electrically heated thermal gradient tests and in flat plate thermionic converters
[NASA-CR-131520] 12 p1416 N73-21470
Design and performance analysis of thermionic diode modules for in-core thermionic power source
[NASA-CR-131602] 13 p1499 N73-22153
Mission engineering analysis of nuclear-thermionic electric propulsion spacecraft for unmanned interplanetary and geocentric mission
[NASA-CR-131599] 13 p1570 N73-22724
Mission engineering analysis of nuclear-thermionic electric propulsion spacecraft for unmanned interplanetary and geocentric missions
[NASA-CR-131600] 13 p1570 N73-22725
Basic processes in thermionic diodes and application to achievement of practical thermionic energy conversion
[AD-755955] 14 p1606 N73-23020
Thermionic reactor development program
[LA-5113] 15 p1738 N73-24092
Conference papers on thermionic power generation
[AD-758620] 15 p1739 N73-24098
Irradiation tests on tungsten clad uranium carbide/zirconium carbide thermionic emitter fuel configurations
[NASA-TM-X-2834] 18 p2178 N73-27587
Design and characteristics of capsule assembly to evaluate tungsten emitter and carbide fuel combinations for thermionic fuel elements
[NASA-TM-X-2887] 21 p2578 N73-30658
Collector/heat pipe cooled, externally configured thermionic diode for use in thermionic electric power source
[NASA-CR-135785] 24 p2954 N73-33600
Design and development of thermionic reactor power system for future interplanetary exploration - Vol. 4
[GULF-GA-C-12308-VOL-4] 24 p2954 N73-33602

**THERMIONIC REACTORS**
U ION ENGINES
U NUCLEAR ROCKET ENGINES

**THERMISTORS**
Method and application of linearizing characteristics of thermistor element
[NLL-M-22863-[5828.4F]] 11 p1291 N73-20479
Measurement of Mediterranean Sea temperature profiles using free drifting, self-recording drogues equipped with thermistor chains
[AD-753442] 12 p1402 N73-21372
Upper atmospheric wind velocity and temperature measurements
[NASA-TT-F-14921] 14 p1659 N73-23470
Development of infrared earth horizon scanner employing thermistor bolometers providing pitch and roll data of synchronous satellites
[ESRO-CR-161] 19 p2301 N73-28503

**THERMO-PHOTOVOLTAIC GENERATORS**
U PHOTOELECTRIC GENERATORS
U THERMOELECTRIC GENERATORS

**THERMOAEROELASTICITY**
U AEROELASTICITY
U THERMOELASTICITY

**THERMOCHEMICAL PROPERTIES**
NT HEAT OF COMBUSTION
NT HEAT OF DISSOCIATION
NT HEAT OF VAPORIZATION
Approximate thermochemical tables for some C-H and C-H-O species
[NASA-CR-2178] 11 p1347 N73-20932
Synthesis, thermodynamics, and electrochemical properties of graphite fluorides
[AD-755934] 12 p1377 N73-21167
Mass spectrometric measurements of high temperature gaseous tungsten fluoride compounds
[AD-757231] 14 p1617 N73-23103
FORTRAN program for calculating thermodynamic properties of complex gas molecules
[AD-762614] 22 p2626 N73-31042

**THERMOCHEMISTRY**
Chemical reactions involved with molybdenum, tungsten, vanadium, and chromium additives in hydrogen-oxygen flames seeded with potassium
[AD-743514] 01 p0023 N73-10179
Analysis of entropy rate admissibility criterion for solutions of hyperbolic conservation laws
[NASA-CR-129594] 04 p0484 N73-13956
Design and operation of galvanic cells involving solid electrolytes to determine accuracy in thermochemical measurements
[LBL-839] 07 p0742 N73-16034
Thermochemical combustion effects of fuel-rich boron compound as solid rocket propellant
[AD-753105] 09 p1099 N73-18971
Thermal combustion requirements for burner devices of human vegetative waste products
10 p1118 N73-19111
Thermodyaamics of chemical species relative to aerospace technology including topics in chemical reaction kinetics and heat measurement
[AD-757518] 14 p1617 N73-23097

**THERMOCHROMATIC MATERIALS**
Thermochromic compositions for detecting heat levels in electronic circuits and devices
[NASA-CASE-NPO-10764-1] 05 p0545 N73-14428

**THERMOCLINES**
Analysis of thermal fluctuations in San Diego Bay, California and factors which affect thermodynamic properties
[AD-744921] 01 p0052 N73-10420
Natural convection in liquid layers of differing density
[AD-750762] 06 p0656 N73-15330
Determination of values for roughness parameters of isotherms in Pacific thermocline using thermistor chain
07 p0858 N73-16954
Review of underwater acoustical measurements revealing layered regions at various ocean depths
[AD-753445] 10 p1156 N73-19405
Characteristics of system for obtaining continuous profiles of ocean conductivity, temperature, and sound velocity as functions of depth
[NOAA-IFS-73009] 15 p1787 N73-24489
Analysis of wake collapse in sea water and stratified fluids with emphasis on final stages of decay
[AD-761622] 19 p2257 N73-28189
Model for calculating thickness of quasiuniform layer of ocean
22 p2693 N73-31572
Influence of solar energy absorption and air water interactions on seasonal thermocline of sea
24 p2957 N73-33623

**THERMOCOMPRESSION**
U COMPRESSING
U HEATING

**THERMOCOUPLES**
NT THERMOPILES
Evaluation of ice-water mixture thermocouple reference chamber discussing best operating parameter combination for high accuracy
[RAE-TR-72035] 01 p0058 N73-10475
Thermocouple apparatus for measuring wall temperatures in regeneratively cooled rocket engines having thin walled cooling passages
[NASA-CASE-XLE-05230-2] 04 p0419 N73-13417
Electrical resistance butt welder for welding fine gauge tungsten/rhenium thermocouple wire
[NASA-CASE-LAR-10103-1] 05 p0550 N73-14468
W/Re thermocouples and high temperature irradiation program
[KFK-1556] 06 p0649 N73-15273
Local quantities in two phase flow measured with anemometer, electrical probe, microthermocouple, and optical sensor techniques
[CEA-CONF-2033] 08 p0897 N73-17263
Characteristics of noble metal thermocouples under prescribed temperature ranges and environmental conditions to determine effects on accuracy and stability of temperature measurements
[NASA-CR-120990] 08 p0925 N73-17578
Useful life of high temperature thermocouples for in-core and out-of-core thermionic applications in vacuum
[NASA-CR-120898] 09 p1035 N73-18447
Thermocouple measurement of gas velocity and temperature near liquid rocket injector face
[NASA-CR-121100] 11 p1270 N73-20304
Development of flexible thermocouple in form of tape for adaptation to special temperature measuring conditions
[NASA-CASE-LEW-11072-1] 15 p1785 N73-24472
Transient temperature measurement errors in intrinsic thermocouples caused by heat transfer
[SC-RR-72-0719] 16 p1975 N73-25970
Transient thermocouple measurement of gas flow direction velocity, and temperature near injector of liquid propellant rocket
18 p2129 N73-27201
Heat transfer in permeable thermocouple
[AD-761556] 19 p2302 N73-28511
Life test data for hybrid thermoelectric panel containing lead telluride and silicon germanium thermocouples
[NASA-TM-X-2869] 20 p2364 N73-29010

**THERMODYNAMIC CYCLES**
NT BRAYTON CYCLE
NT RANKINE CYCLE
NT STIRLING CYCLE
Operating principles and thermodynamic cycle of ducted fan turbojet engines
[AD-750984] 06 p0715 N73-15833
Reduction in heat exchanger size with use of gas mixtures in closed gas turbine installations
[AD-750905] 06 p0715 N73-15836
Fluid flow analysis in mold heating and cooling control loop
[BDX-613-742] 10 p1142 N73-19303
Cryogenic cooling methods for spaceborne systems
[AD-755780] 14 p1720 N73-23958
Three thermodynamic cycles of advanced nuclear MHD power plant systems
19 p2319 N73-28657

**THERMODYNAMIC EFFICIENCY**
Analysis of thermomechanical compressor to include principles of operation and specific applications
05 p0552 N73-14482
Mathematical model for thermodynamic efficiency of combined power plants incorporating magnetohydrodynamic generators
[AD-753031] 09 p0991 N73-18090

**THERMODYNAMIC EQUILIBRIUM**
Ising ferromagnet thermodynamic equilibrium states in low temperature regions
[NOTA-INTERNA-381] 01 p0080 N73-10660
Thermodynamic equilibrium model for simulating pressure transient propagation in two phase water flow with mass transfer
08 p0896 N73-17255
Deviations in local thermodynamic equilibrium in stellar atmospheres
[NASA-CR-130792] 09 p1082 N73-18829
Thermodynamic equilibrium calculations for uranium hexafluoride decomposition at high temperatures
10 p1126 N73-19168
Thermohydrodynamic stability in channel flow heat and mass transfer considering variable cross section area
[AD-758748] 16 p1889 N73-25289
Computer program for thermodynamic equilibrium calculations
[PB-214372/5] 16 p1975 N73-25971
Composition calculation of nitrogen plasma in local thermodynamic equilibrium for determining electrical conductivity and continuum radiation
[DLR-FB-73-51] 23 p2822 N73-32563
Mass flow rate of laminar dissociated equilibrium boundary layer
24 p2907 N73-33200

**THERMODYNAMIC PROPERTIES**
NT CRITICAL POINT
NT CRITICAL PRESSURE
NT CRITICAL TEMPERATURE
NT EMISSIVITY
NT ENTHALPY
NT ENTROPY
NT FREE ENERGY
NT GIBBS FREE ENERGY
NT HEAT OF COMBUSTION
NT HEAT OF VAPORIZATION
NT MELTING POINTS
NT PYROELECTRICITY
NT SPECIFIC HEAT
NT SUPERCRITICAL PRESSURES
NT SURFACE ENERGY
NT THERMAL BUCKLING
NT THERMAL CONDUCTIVITY
NT THERMAL DIFFUSION
NT THERMAL DIFFUSIVITY
NT THERMAL EXPANSION
NT THERMAL INSTABILITY
NT THERMAL STABILITY
NT THERMOCHEMICAL PROPERTIES
NT THERMOPHYSICAL PROPERTIES
NT VAPOR PRESSURE
NT VOLATILITY
Electronic and thermodynamic properties of dense plasma interacting with metallic and nonmetallic materials
[CEA-R-4268] 01 p0085 N73-10705
Vela 4 observation of solar wind electron average thermal characteristics
01 p0094 N73-10776
Development of computer program for simulating performance of space radiator to account for transient and steady state performance
[NASA-CR-128594] 01 p0108 N73-10891
Transient heat transfer analysis of space radiator heat rejection system under conditions of aerodynamic heating, solar, albedo, and planetary radiation
[NASA-CR-128595] 01 p0117 N73-10964
Analysis of velocity and temperature distribution in unsteady thermal boundary layer by approximate integral method
[NASA-TN-D-7054] 01 p0117 N73-10967
Thermodynamic properties and heat transfer characteristics of forced-convection boiling of Freon-113 in vertical annular test section
[NASA-CR-2137] 01 p0117 N73-10968
Analysis of laminar film condensation on inside of truncated, rotating cone and noncapillary, rotating heat pipe with distilled water as working fluid
[AD-743730] 01 p0118 N73-10973
Molecular-kinetic theory for determining temperature dependence of simple liquid viscosity
[AD-747089] 02 p0159 N73-11286
Electrical-, thermal-, and magnetic-properties of zirconium and niobium carbide solid solutions
[AD-746217] 02 p0219 N73-11772
Performance tests of OAO-C spacecraft heat pipes under thermal-vacuum conditions
[NASA-TM-X-66072] 02 p0242 N73-11967
Oscillatory combustion and fuel vaporization tests to determine thermodynamic properties of droplets under various conditions
[NASA-CR-120974] 02 p0242 N73-11971
Analysis of production method for manufacturing ablative heat shield panels using press filling and curing of ablation material
[NASA-CR-112124] 02 p0243 N73-11975
Experimental procedure for estimating rate of thermal flow and heat transfer from longitudinally swept surfaces using unstable thermal regime method
[AD-746011] 02 p0243 N73-11977
Design and development of device for moving liquid through pipes without use of mechanical pumps
[NASA-CASE-LAR-10799-1] 03 p0283 N73-12295
Analysis of heat balance characteristics of nuclear lightbulb engine to determine effects on engine performance, space radiator requirements, and cooling sequence
[NASA-CR-129295] 03 p0331 N73-12696
Thermal conductivity, thermal properties, and thermal diffusivity of uranium-fissium alloy
[ANL-7889] 03 p0332 N73-12710
Thermophysical properties of lunar fines
[NASA-CR-129293] 03 p0354 N73-12888
Development of computer program for determining thermodynamic and transport properties of para and equilibrium hydrogen
[NASA-CR-129261] 03 p0363 N73-12959
Thermodynamic properties of transition metal/silicon binary alloys
[NPL-CHEM-18] 03 p0365 N73-12970
Thermodynamic system cycle for direct transformation of thermal energy into electrical, considering simultaneous temperature changes
[AD-747618] 04 p0376 N73-13060
Tables of pressure, volume, density, and temperature for liquid states of oxygen, nitrogen, argon, and parahydrogen
[NBS-TN-361-REV] 04 p0386 N73-13139
Differential-difference equation describing thermodynamic interactions of hot air bubbling cooling in surrounding liquid
04 p0404 N73-13294
Handbook of thermophysical properties of liquid and gaseous oxygen
[NASA-SP-3071] 04 p0484 N73-13952
Sonar equipment research project to include determination of temperature and heat dissipation characteristics of ceramics used in high frequency projectors
[AD-749960] 05 p0515 N73-14187
Analysis of thermomechanical compressor to include principles of operation and specific applications
05 p0552 N73-14482
Thermomechanical analysis of physical transitions and stability of poly[norbornadiene] in nitrogen
[AD-749374] 05 p0566 N73-14596
Thermomechanical behavior and structure of poly[carborane-siloxane]s containing icosahedral cages in nitrogen environment
[AD-749364] 05 p0566 N73-14598
Thermomechanical behavior of BBB polymer
[AD-749819] 05 p0568 N73-14611
Calorimetric analysis of low temperature heat capacities and high temperature enthalpies for sodium chromate
[BM-RI-7691] 05 p0605 N73-14924
Effect of space-time integral of thermodynamic pressure on thermodynamic potential for compressible, adiabatic flow
[NASA-TM-X-66139] 05 p0606 N73-14926
Development and characteristics of test equipment for investigating thermodynamic properties of gases at high temperatures
[AD-749653] 05 p0607 N73-14936
Calculation of relaxation kinetics for carbon dioxide-water-nitrogen mixture to determine gas dynamics of escape from slit nozzle
[JPRS-57906] 06 p0654 N73-15310
Electrical, mechanical, and thermal properties of transparent optical adhesives
[AD-750571] 06 p0688 N73-15602
Thermodynamic efficiencies of accelerators for liquid metal magnetohydrodynamic converter considering vapor liquefying effect on flow characteristics
[JPRS-57915] 06 p0703 N73-15735
Spectral and temperature characteristics of natural photoconductivity in p-type GaAs
[AD-750696] 06 p0709 N73-15790
Individual and combined effects on heat transfer properties of air jets impinging on concave side of right circular semicylinder
[NASA-TN-D-7127] 06 p0730 N73-15952
Computer program for determining thermodynamic and transport properties of complex mixtures to include rocket performance, shock properties, and detonation properties
[NASA-TN-D-7056] 06 p0730 N73-15954
Development of technology for design and application of self controlled, variable conductance heat pipes for spacecraft thermal control
[NASA-CR-114530] 06 p0730 N73-15957
Analysis of approximate transport properties of high temperature air in dissociation equilibrium
[ESDU-00.01.07-AMEND-A] 07 p0853 N73-16919
Analysis of pressure drop, heat transfer, and flow characteristics for forced convection boiling in helical coils
[AEEW-R-757] 07 p0855 N73-16936

Thermodynamic and kinetic behavior of protons and deuterons in regular and heavy ice
[NASA-TT-F-14692] 08 p0946 N73-17744
Damping in porcelain enamel coatings at elevated temperatures
[AD-752317] 09 p1055 N73-18598
Development of method for analyzing performance of magnetohydrodynamic generator based on thermodynamic properties and flow characteristics
10 p1110 N73-19051
Langmuir measurements of thermodynamic lead vapor properties
[IS-2871] 10 p1173 N73-19542
Thermodynamic analysis of nonstoichiometric cerium dioxide in temperature range from 700 to 1500 C and reduced atmospheric pressure conditions
[COO-1441-18] 10 p1175 N73-19560
Observations of kinematic and thermodynamic fields over Barbados
10 p1180 N73-19596
Thermodynamic properties of high altitude balloons to show effects of ascent, sunrise, surface coating, and thermal insulation
[TAMRF-921-7305] 11 p1234 N73-20021
Handbook on thermodynamic and thermophysical properties of high propellant combustion products
[AD-754329] 11 p1253 N73-20165
Thermodynamic properties of iridium sulfides at equilibrium pressures
[AD-753897] 11 p1253 N73-20168
Design and performance of wire grid temperature probes for flowing media
11 p1294 N73-20500
Effects of excessive HfC on mechanical properties of W-Re-Hf-C alloys
[NASA-TN-D-7210] 11 p1305 N73-20588
Thermodynamic properties of open cycle gaseous core nuclear rocket engine
[NASA-TM-X-2784] 11 p1323 N73-20733
Effect of electron-phonon interaction on temperature dependence of paramagnetic susceptibility in metals
[AD-753984] 11 p1331 N73-20804
Development of nonisothermal theory of viscoelastic fluids with fading memory and application to viscometric flow
[AD-754802] 11 p1349 N73-20948
Numerical analysis of hydrodynamic properties of liquid helium based on quantum statistical mechanics
12 p1396 N73-21270
High temperature tests to determine thermodynamic properties of nonstoichiometric vanadium nitrides
[NLL-M-21551-[5828.4F]] 12 p1464 N73-21858
Numerical analysis of temperature distribution of complex two-dimensional body with various boundary conditions including radiation effects
[N8110R:72-040] 12 p1464 N73-21860
Calculation of heat of evaporation of liquid chlorine into calorimeter for rocket propulsion
[AD-755894] 12 p1466 N73-21874
Calculation of thermodynamic and transport properties for chemically reacting gases
[AD-756597] 13 p1488 N73-22064
Measurement of thermal changes encountered during plastic deformation of copper using photon detection system
[AD-756416] 13 p1543 N73-22510
Numerical analysis of nonequilibrium nozzle expansions from reservoir at high specific enthalpy
[LOG-J7197] 14 p1649 N73-23375
Effects of environmental variables on physical, thermal, and mechanical properties of resin matrix and metal matrix composite materials
[AD-757524] 14 p1681 N73-23640
Specific heat and thermodynamic properties of heat accumulating materials
14 p1718 N73-23941
Analysis of heat transfer properties of air, helium, and carbon dioxide and effects of variations of fluid properties with temperature
[ARC-R/M-3246] 15 p1729 N73-24021
Thermal analysis of thermoviscoelastic behavior of case bonded propellant grains to thermal property variations
[AD-758839] 15 p1824 N73-24780
Thermophysical and mechanical properties of closed pore insulation
[NASA-CR-112295] 15 p1843 N73-24930
Thermodynamic properties of UF6 measured with ballistic piston compressor
[NASA-CR-132051] 15 p1843 N73-24936
Equilibrium compositions and thermodynamic properties of mixed plasmas, including argon-hydrogen plasmas at .01 to 100 atmospheres between 2,000 K and 35,000 K
16 p1948 N73-25764
Analysis of uniform heat energy generation and conduction heat transfer for semi-infinite thin plate with air blowing over one surface and insulated on other
16 p1973 N73-25959
Analysis of heat transfer properties and thermophysical properties of materials used for aircraft and spacecraft construction
[AGARD-R-606] 16 p1975 N73-25968
Thermal response of protective fabric/human skin system to JP-4 jet fuel fire
[AD-759525] 17 p1990 N73-26095
Thermodynamic properties of cycloalkane and cyclobutane epoxy compounds for synthetic high energy fuels
[AD-760156] 17 p1993 N73-26116
Analysis of space shuttle cryogenic fluid storage system to determine heat absorption capability and design of radiators for additional cooling capability - Vol. 4
[NASA-CR-133952] 17 p2088 N73-26895
Development of linear system of equations for computing errors of volume fractions or partial pressures at calculated equilibrium compositions
[NRC-TT-1665] 17 p2096 N73-26960
TOPAL computer program for investigating metal-liquid thermal interactions under shock tube conditions
[GRO/44/91/26-PT-1] 18 p2125 N73-27174
Development of method for identifying nonlinear material behavior using finite element techniques
[PB-219090/8] 18 p2204 N73-27788
Tables and graphs of thermodynamic and transport properties of gaseous CF4 in chemical equilibrium
[NASA-TN-D-7181] 18 p2206 N73-27805
Utilization of thiophenyl ether disiloxane and trisiloxane as lubricant fluids in severe environment including space
[NASA-CASE-MFS-22411-1] 19 p2304 N73-28532
Thermodynamic properties of solid Ni-Ga alloys at temperatures between 837 and 1100 K
[AD-762337] 19 p2311 N73-28588
Nonisothermal constitutive equations and related thermodynamical aspects of simple materials with fading memory
[AD-761634] 19 p2327 N73-28720
Development of performance equations for cryptosteady-flow energy separator over widest range of operating conditions for turbojet engines
[AD-762030] 19 p2330 N73-28747
Analysis of methods for determining thermoelectric cooling and heating devices using pure resistance principle
[AD-762324] 19 p2353 N73-28926
Load-carrying and thermal characteristics of flat conductor cable
[NASA-TM-X-64767] 20 p2380 N73-29125
Test data tabulation, statistical analysis, and heating rate contours for base region thermal environment of Saturn S-2 stage scale model - Vol. 2
[NASA-CR-129010] 20 p2382 N73-29144
Development of method for determining atmospheric transmission function with allowance for divergence of thermal radiation
20 p2401 N73-29298
Numerical analysis of dependence of transmission function of atmosphere on temperature of radiation source
20 p2402 N73-29299
Analysis of relationships of dissociation elasticity of vanadium mononitride to composition and temperature based on thermodynamic theory of non-stoichiometric compounds
[NLL-M-21638-[5828.4F]] 20 p2428 N73-29506
Effects of metallurgical processes on thermodynamic properties and compatibility of reinforcing fibers for refractory materials
[JPRS-59118] 20 p2430 N73-29518
Thermodynamic properties of zirconium carbide in 0 to 3000 K temperature range
20 p2430 N73-29519
Matrix isolation technique used to obtain thermodynamic properties of rocket combustion products
[AD-762622] 20 p2486 N73-29966
Determination of thermal characteristics of electroluminescent diode
[NASA-TM-X-70440] 21 p2517 N73-30190
Analytical methods, thermal model, and user manual for extravehicular mobility unit routines
[NASA-CR-134005] 21 p2521 N73-30218
Analytical methods, thermal model, and user manual for extravehicular mobility unit routines
[NASA-CR-134006] 21 p2521 N73-30219
Thermodynamic properties of solid alloys of chromium with nickel and iron
[COO-1791-4] 21 p2559 N73-30516
Standard enthalpies of formation for all undisputed compound members in Na-Ti-O system
[BM-RI-7778] 21 p2562 N73-30534
Analysis of ignition properties of hypergolic fluids under low pressure conditions to determine relations of time, temperature, and thermodynamic properties
21 p2605 N73-30878
Thermodynamic stability diagrams for iron, nickel, and chromium in fused sodium hydroxide
22 p2625 N73-31028
Determining thermodynamic properties of liquid copper-magnesium alloys by magnesium vapor pressure
[BARC-613] 22 p2685 N73-31504
High temperature research of thermophysical and electrophysical properties of matter and pilot plant with magnetohydrodynamic power generator
[JPRS-59983] 22 p2728 N73-31831
Thermodynamic and transport properties of saturated liquid sodium
[RD/B/M-2479] 22 p2730 N73-31844
Thermal properties of ceramics for design of sonar arrays
[AD-764572] 23 p2758 N73-32071
Cobalt-tungsten alloys with superior strength at elevated temperatures
[NASA-CASE-LEW-10436-1] 23 p2803 N73-32415
Method for determining heat capacity of ceramic materials by measuring heat transfer during condensation process
23 p2807 N73-32445
Thermophysical properties of synthetic resin-base materials with fillers to show errors in development of mathematical relationships
23 p2807 N73-32446
Coefficient of thermal conductivity for composite materials by using axial thermal flow method
23 p2807 N73-32447
Thermal and mechanical properties of low density elastomeric ablation material
[NASA-CR-132281] 23 p2809 N73-32463
Holographic interferometric analysis of thermal response in ferroelectric crystal to laser radiation
[AD-764703] 23 p2820 N73-32547
Temperature dependence and measurement of crystalline electric fields at ytterbium impurities in thulium metal
[AD-764633] 23 p2827 N73-32596
Thermodynamics of low and high molecular weight liquids
23 p2859 N73-32841
Thermodynamic property measurements of solid chromium sesquioxide and chromium in solid alloys with iron and nickel
[TID-26322] 24 p2934 N73-33433
Thermodynamic properties of uranium-based Mo, Nb, Zr, and Ti alloys from 77 to 1500 K
[ORNL-TM-4253] 24 p2936 N73-33445
Thermal and magnetic properties of magnetic crystals
[COO-3574-95] 24 p2969 N73-33727
Thermodynamic state in cascade argon arc after initiation of step increase in electrode voltage from initial steady-state D.C. level
24 p2990 N73-33893
Thermodynamic properties of electron gas in magnetic fields of varying strengths to include magnetic susceptibility, internal energy, and specific heat
24 p2990 N73-33896
Stability of vapor film formed on horizontal cylinders during stable film boiling using variational approach
24 p2991 N73-33906

**THERMODYNAMICS**
NT AEROTHERMODYNAMICS
NT COMBUSTION PHYSICS

Calculation of transition processes in thermoelectric devices
[AD-744683] 01 p0007 N73-10054
Evaluation of several thermographic infrared techniques and their applicability to detection of unbonded areas in babbitted bearings
[AD-745730] 01 p0063 N73-10516
Thermal analysis routine with capability for performing thermal analysis of systems containing flowing fluids
[NASA-CR-128593] 01 p0117 N73-10963
Effects of thermomechanical treatment on mechanical, microstructural, and stress corrosion resistance properties of Al alloys
[AD-748361] 04 p0427 N73-13483
Extended theory of imperfect modeling with error approximation for application to thermal modeling of spacecrafts
04 p0483 N73-13949
Conservation laws and entropy production inequality applied to continuum thermodynamics
[AD-748654] 04 p0485 N73-13965
Computer program for solution of transient thermal problems in electrical power systems using concept of temperature calculations by analogy
[PB-211904] 05 p0607 N73-14933
Effects of prior deformation and transformations on microstructure of iron nickel alloy
[AD-750716] 06 p0687 N73-15591
Cavitation in liquid cryogens with determination of flow and thermodynamic conditions of cavitating hydrofoil
[NASA-CR-2156] 07 p0770 N73-16255
METROC computer program for producing wind and thermodynamic data from raw upper atmospheric data
[AD-751780] 07 p0816 N73-16616
Computer program for calculating equations of state, thermodynamic functions, and opacities of plasmas
[AD-751608] 07 p0829 N73-16724
Mathematical model of thermodynamic damage to metals irradiated by laser beams
[DREV-R-672/72] 09 p1043 N73-18503
Vaporization kinetics and thermodynamics of graphite using high pressure mass spectrometer
[AD-753713] 09 p1055 N73-18601

Abstracts on kinetics and thermodynamics of gases interacting with liquid metals
[JPRS-58282] 09 p1098 N73-18964
Dynamic behavior of flames in explosive acetylene oxygen mixture
[NASA-CR-130963] 09 p1099 N73-18973
Magnetic tape version of substance-property index and bibliographies
[NBS-TN-760] 11 p1260 N73-20223
Heat transfer equation with nonlinear boundary condition and final value problem for porous medium equation
[AD-755073] 11 p1350 N73-20951
Thermodynamics of oxygen solubility in lanthanum uranium oxide measured on solid state electrolytic cell
[KFK-1649] 12 p1376 N73-21163
Vaporization kinetics and thermodynamics of graphite using high pressure mass spectrometers
[AD-755853] 12 p1376 N73-21165
Thermodynamic analysis of combined machine installation operating on Brighton cycle and thermoelectric generator as low temperature superstructure
[AD-756805] 13 p1476 N73-21961
Solution of thermodynamic forces and flows in magnetic field using Gibbs equation
[AD-756901] 13 p1592 N73-22909
Mathematical model for thermal behavior of flat conductor cable under load
14 p1640 N73-23299
Increased propulsive efficiency through improved secondary flow capacity in double flow turbojets
[NASA-TT-F-14904] 14 p1701 N73-23803
Thermodynamic flow characteristics of arc heater, convergent-divergent nozzle, and underexpanded jet in plasma wind tunnel
[NAL-TR-307] 15 p1766 N73-24308
Thermally activated deformation of crystalline solids
[PB-214537/3] 15 p1823 N73-24774
Effect of thermomechanical treatment on stress corrosion cracking susceptibility of Beta 3 titanium alloy
[AD-759166] 16 p1930 N73-25618
Thermodynamic analysis of high speed tapered roller bearings operating with fluid lubrication under combined loads
[NASA-CR-121207] 17 p2037 N73-26482
Formulation of second law of thermodynamics for system in thermal nonequilibrium by assumption of relationship between entropy and temperature
[AD-759970] 17 p2097 N73-26964
Acoustic emission from ferrous martensites as function of thermomechanical history
[AD-761220] 18 p2163 N73-27472
Thermodynamic analysis of Si film growth rate in vertical reactor
18 p2186 N73-27651
Heat transfer and temperature oscillations in chemical vapor transport crystal growth
[AD-760732] 18 p2191 N73-27688
Thermodynamics of phase changes occurring in heat treatment of carbon and alloy steels
[AD-762361] 19 p2311 N73-28589
Automatic pyrometer for measuring true metal temperature with radiation
[JPRS-59661] 20 p2419 N73-29435
Thermodynamic effects on liquid metal magnetohydrodynamic converter flow
[AD-761548] 20 p2459 N73-29762
Reserach and development in metallurgical thermodynamics
[TT-71-56066] 21 p2561 N73-30528
Thermodynamic, structural, and magnetization phenomena during hydrogen reaction with RCo5 type systems
22 p2625 N73-31033
Design of high temperature combustor for use as solid fuel MHD generator and thermodynamic analysis of combustion conditions
[AD-764153] 22 p2730 N73-31848
Thermodynamics of lambda transition in liquid helium and phase transformations
23 p2856 N73-32820
Thermodynamic state of thin helium films for precise measurements of third sound velocity and attenuation
24 p2968 N73-33720
Feasibility of thermodynamic vent and screen baffle integration for orbital storage and transfer of liquid hydrogen
[NASA-CR-134482] 24 p2970 N73-33737

**THERMOELASTICITY**

Method of potential applied to three-dimensional elastic and thermoelastic stress problems and fracture mechanics
[SCL-DR-71-0026] 01 p0113 N73-10935
Development of general mixed finite element models of nonlinear thermomechanical response of dissipative media
[AD-745994] 02 p0239 N73-11944
Derivation of perturbed equations of motion and heat conduction for thermoelastic solid using finite element method
[AD-754542] 11 p1346 N73-20919
Numerical analysis of thermoelastic state of shells subjected to thermal impact on the surface of the shell
14 p1715 N73-23912
Finite element analysis of thermoplasticity and nonlinear mechanics of fluid-saturated porous solids
[AD-758884] 16 p1972 N73-25949
Thermoelastic response model for actively controlling primary mirror surface error of orbiting telescope
[NASA-CR-124286] 17 p2033 N73-26449
Nonlinear elastic and thermoelastic properties of single crystals of refractory materials
[COO-3418-9] 22 p2689 N73-31535
Stress and strain distribution along round, circular cavity in infinite space
[AD-764104] 22 p2726 N73-31819
Thermoelastic analysis for predicting thermal stress failure in silicon solar cell array
[NASA-CR-135713] 23 p2748 N73-31993

**THERMOELECTRIC CONVERSION SYSTEMS**

U THERMOELECTRIC POWER GENERATION

**THERMOELECTRIC COOLING**

Optimized construction of thermoelectric cooling batteries
[AD-757467] 14 p1606 N73-23016
Design and development of volume accumulator units for thermoelectric reactor coolant loops
[NASA-CR-121245] 18 p2177 N73-27582
Analysis of methods for determining thermoelectric cooling and heating devices using pure resistance principle
[AD-762324] 19 p2353 N73-28926
Low temperature thermoelectric microrefrigerator
[AD-764171] 22 p2708 N73-31685
Coloring memory crystals by electron bombardment and KCl, Na, Cl for thermoelectric cooling for high density optical memory
[AD-765391] 23 p2762 N73-32105

**THERMOELECTRIC GENERATORS**

NT SNAP 10A
NT SNAP 19
NT SNAP 23
Calculation of transition processes in thermoelectric devices
[AD-744683] 01 p0007 N73-10054
Aerospace engineering including materials, orbits and trajectories, power sources, satellite geodesy, and structural engineering
[NASA-CR-128329] 01 p0119 N73-10981
Feasibility analysis for use of xenon-filled silicon germanium thermoelectric generators in outer planetary exploration
01 p0119 N73-10984
Network synthesis and analysis of thermoelectric generators to show relation between physical properties and elements of internal structure
[AD-747617] 03 p0256 N73-12071
Thermodynamic system cycle for direct transformation of thermal energy into electrical, considering simultaneous temperature changes
[AD-747618] 04 p0376 N73-13060
Organic fluid capsule test and thermoelectric module test in isotope kilowatt program
[ORNL-TM-3805] 04 p0448 N73-13657
Source term calculations for Pioneer radioisotopic thermoelectric generators
[LA-4914] 04 p0448 N73-13658
Developing isotopic thermoelectric generators in USSR
[AD-749528] 05 p0499 N73-14065
Design and performance of cylindrical silicon germanium thermoelectric generators
06 p0626 N73-15080
Physical properties and performance of radioisotope power generator Tristan
[CONF-710444-11] 06 p0627 N73-15083
Optimization of specific power highly efficient radioisotope thermoelectric generator
07 p0819 N73-16636
Principles of magnetohydrodynamic energy generation to include flows in magnetohydrodynamic generator, physical processes, diagnostics, and required equipment - Part 1
[JPRS-57940-1-PT-1] 07 p0825 N73-16687
Principles of magnetohydrodynamic energy generation to include open and closed cycle magnetohydrodynamic generators, liquid-metal plants, and materials for generators -Part 2
[JPRS-57940-2-PT-2] 07 p0825 N73-16688
Thermodynamic analysis of combined machine installation operating on Brighton cycle and thermoelectric generator as low temperature superstructure
[AD-756805] 13 p1476 N73-21961
Reliability analysis of thermoelectric module solar energy converter
[AD-757087] 14 p1606 N73-23015
Optimal operational temperature for thermoelectric generator using organic fuel heat
[AD-762266] 19 p2223 N73-27932
Heat transfer in permeable thermocouple
[AD-761556] 19 p2302 N73-28511
Design and performance modeling of liquid metal reactor thermoelectric space power system
[NASA-CR-121241] 19 p2320 N73-28661
Thermoelectric generator for Pioneer interplanetary Jupiter flyby mission
[IESD-2873-172] 23 p2818 N73-32529
Compatability of tantalum alloys fuel capsules and [Pu-238]O2 fuels in radioisotopic thermoelectric generators
[LA-UR-73-764] 24 p2955 N73-33610
Possibility of using triple semiconductor compounds in thermoelectric and photoelectric converters
[AD-765730] 24 p2970 N73-33734

**THERMOELECTRIC MATERIALS**

Room temperature electrical properties of SiGe thermoelectric alloys
[SC-DC-72-1020] 07 p0812 N73-16581
Environmental and performance tests of thermoelectric materials
[MMM-2473-342] 17 p2050 N73-26585

**THERMOELECTRIC OUTER PLANET SPACECRAFT**

U TOPS [SPACECRAFT]

**THERMOELECTRIC POWER GENERATION**

Onboard spacecraft thermoelectric and chemical propulsion systems - Pt. 2
[JPRS-58612-2-PT-2] 10 p1209 N73-19834
Design and performance analysis of ZrH reactor thermoelectric nuclear power system
[AI-AEC-13039] 12 p1427 N73-21567
Thermodynamic analysis of combined machine installation operating on Brighton cycle and thermoelectric generator as low temperature superstructure
[AD-756805] 13 p1476 N73-21961
NaK loop testing of thermoelectric converter modules for SNAP program
[NASA-CR-121192] 14 p1691 N73-23727
Statistical reliability model and analysis of 5-kwe reactor thermoelectric system
[NASA-CR-121205] 15 p1809 N73-24661
Design of expansion joint unit for coolant piping loop of reactor thermoelectric system - SNAP program
[NASA-CR-121209] 15 p1809 N73-24663
Dual throat thermoelectric NaK development pump for use on reactor thermoelectric system
[NASA-CR-121231] 16 p1918 N73-25521
Computer codes for designing volume accumulator units
[NASA-CR-121246] 18 p2178 N73-27583
Computer simulation and optimization code for nuclear space power systems for thermoelectric power generation
[NASA-TM-X-2860] 18 p2178 N73-27586
Extraterrestrial disposal of radioactive waste from thermoelectric propulsion
[NASA-TM-X-62272] 19 p2225 N73-27943
Design of tubular thermoelectric module for astronuclear power conversion system
[NASA-CR-121210] 19 p2319 N73-28659
Design of uranium zirconium hydrogen fueled reactor and development of lead tellurium thermoelectric conversion system
[AI-AEC-13046] 19 p2320 N73-28664
Life test data for hybrid thermoelectric panel containing lead telluride and silicon germanium thermocouples
[NASA-TM-X-2869] 20 p2364 N73-29010

**THERMOELECTRIC SPACECRAFT**

U TOPS [SPACECRAFT]

**THERMOELECTRICITY**

Thermoelectric processes in electronic devices and possibilities for use in small-size, very low frequency devices
[AD-749611] 05 p0520 N73-14231
Characteristics of noble metal thermocouples under prescribed temperature ranges and environmental conditions to determine effects on accuracy and stability of temperature measurements
[NASA-CR-120990] 08 p0925 N73-17578
Thermoelectricity and refrigeration at low temperature
[AD-753405] 10 p1190 N73-19687
Thermoelectricity of solid-liquid phase boundary in ternary semiconductors and alloys
[AD-756899] 13 p1478 N73-21972
Qualitative reliability indices of semiconductor thermoelectric devices
[AD-756898] 13 p1503 N73-22184
Effect of charge carrier heating on volt-ampere characteristics of thermoelectric indicators of microwave emissions
[AD-756561] 13 p1531 N73-22407
Development of flexible thermocouple in form of tape for adaptation to special temperature measuring conditions
[NASA-CASE-LEW-11072-1] 15 p1785 N73-24472
Thermoelectric and photothermoelectric effects in semiconductors
15 p1819 N73-24747
Systems analysis of active thermal control using thermoelectric devices
[NASA-CR-124256] 15 p1843 N73-24935
Design and development of electric batteries for use with thermoelectric air conditioning systems
[AD-759239] 17 p1986 N73-26051

Design, development, and fabrication of radiator structure for use with thermoelectric space power systems
[NASA-CR-121222] 17 p2088 N73-26892
Device for measuring thermoelectric properties of materials under high pressure
[NASA-CASE-NPO-11749] 19 p2299 N73-28486
Effect of irradiation on absolute thermal EMF of alloys, metals, and thermocouple materials
[NASA-TT-F-15015] 19 p2309 N73-28574
Development, characteristics, and operation of compensated thermoelectric net radiometer to show advantage over standard radiometers
20 p2402 N73-29305
Applications of photoelectronic and thermoelectronic instruments
[JPRS-59951] 22 p2672 N73-31404
Electrical, magnetic, and thermal properties of dilute and concentrated magnetic alloys
[AD-763820] 22 p2707 N73-31682
Contact resistance of thermoelectric semiconductors by increasing switching layers
[AD-765769] 24 p2959 N73-33646

THERMOGRAMS
U RECORDING INSTRUMENTS
U TEMPERATURE MEASURING INSTRUMENTS

THERMOGRAPHS
U RECORDING INSTRUMENTS
U TEMPERATURE MEASURING INSTRUMENTS

THERMOGRAVIMETRY
Thermogravimetric analysis of reduction of oxides of nickel and chromium
[NASA-TM-X-2688] 06 p0684 N73-15565

THERMOLUMINESCENCE
Effects of atmospheric pressure on thermoluminescence of crystalline powder
[AD-746442] 02 p0219 N73-11770
Method for detecting oxygen in gas by thermoluminescence
[NASA-CASE-LAR-10668-1] 07 p0752 N73-16106
Potential application of thermoluminescence in forensic science
10 p1227 N73-19978
Visible fluorescence and thermoluminescence of YAlO3 crystals containing Er, Eu, Nd, Tb or Yb and other optically active centers
[AD-759161] 17 p1992 N73-26112
Photoluminescence, thermoluminescence, photoconductivity, and electrical conductivity measurements in heavily doped ZnS-Cu, In phosphors
17 p2071 N73-26759
Study of trivalent Y3Al5O12 ionic crystals by radiation stimulated thermoluminescence
20 p2461 N73-29781

THERMOMECHANICS
U THERMODYNAMICS

THERMOMETERS
NT RESISTANCE THERMOMETERS
Design, development, and specifications of thermohygrometer for measuring fluctuations in temperature due to clouds and precipitation
[NLL-M-20703-[5828.4F]] 01 p0055 N73-10442
Methods for measuring temperature in wind tunnels with electric contact thermometers
[DLR-MITT-72-27] 09 p1010 N73-18246
Measurements and techniques of low temperature acoustic thermometry
[NBS-TN-765] 14 p1666 N73-23518
Standards and recommendations for calculating platinum resistance thermometer
[NBS-MONOGRAPH-126] 16 p1912 N73-25471
Increase in heat exchange rate between thermometric sensing element and cryogenic fluid
[NASA-TM-X-68251] 16 p1913 N73-25477
Transient thermal response of globe thermometers in relation to heat transfer parameters
[DCIEM-859] 20 p2418 N73-29431

THERMOMETRY
U TEMPERATURE MEASUREMENT

THERMONUCLEAR ENERGY
U THERMONUCLEAR POWER GENERATION

THERMONUCLEAR POWER GENERATION
Control and coordination requirements for fabrication of devices in the thermonuclear research program
[B-159687] 03 p0332 N73-12703
Application of superconducting magnetics for plasma physics experiments and as component for future thermonuclear reactors
10 p1108 N73-19033
Fast particle injectors for plasma production in thermonuclear installations
[AEC-TR-7389] 11 p1323 N73-20738
Ion heating and thermonuclear power production characteristics and performance of superconducting bumpy-torus magnetic facility
[NASA-TN-D-7353] 19 p2324 N73-28693
Solar energy, thermonuclear energy, and fossile fuel energy sources
[UCRL-74697] 24 p2881 N73-33005
Ignition of mini-atomic bomb to produce thermonuclear power with capacitor produced electron beams
24 p2907 N73-33199

THERMONUCLEAR PROPULSION
U NUCLEAR PROPULSION

THERMONUCLEAR REACTIONS
NT CONTROLLED FUSION
NT NUCLEAR FUSION
High speed ballistic injection of solid spherical pellet of deuterium into thermonuclear reactor plasma to analyze dynamics of pellet evaporation
[AD-751294] 07 p0830 N73-16726
Relativistic electron beam for thermonuclear heating of plasma media
[AD-754621] 11 p1329 N73-20783
Neodymium-glass laser system production of plasmas for research on controlled thermonuclear fusion
15 p1794 N73-24545
Engineering problems of controlled thermonuclear reactor power plants
[BNWL-1685] 15 p1811 N73-24682
Concept of nuclear fusion chain reactions for supernovae and controlled fusion reactors
[SM-170/49] 17 p2062 N73-26678
Thermonuclear research on Tokamaks, plasma control, and plasma diagnostics
[JAERI-M-5029] 24 p2963 N73-33676

THERMOPHILIC PLANTS
NT BLUE GREEN ALGAE

THERMOPHYSICAL PROPERTIES
NT CRITICAL POINT
NT CRITICAL PRESSURE
NT CRITICAL TEMPERATURE
NT EMISSIVITY
NT MELTING POINTS
NT PYROELECTRICITY
NT SPECIFIC HEAT
NT SUPERCRITICAL PRESSURES
NT THERMAL CONDUCTIVITY
NT THERMAL DIFFUSION
NT THERMAL DIFFUSIVITY
NT THERMAL STABILITY
NT VAPOR PRESSURE
NT VOLATILITY
Effect of composition of refractory metal solid solutions on coefficient of thermal expansion
[AD-745847] 01 p0068 N73-10556
Thermophysical properties of helium-4 under various conditions of temperature and pressure
[NASA-CR-128445] 02 p0242 N73-11966
Development of method for measuring temperature of wind tunnel scale model by photographic recording of changes in thin film phase-change temperature indicating material
[NASA-CASE-LAR-11053-1] 02 p0243 N73-11972
Melting characteristics and thermophysical properties of solid hydrogen
[AD-748847] 04 p0387 N73-13144
Structural-, thermal-, and magnetic-properties of various metals and intermetallic compounds
[COO-3427-7] 04 p0434 N73-13536
Effect of nature, structure, temperature, volume weight, and moisture content on coefficient of heat transfer for heat insulation materials
[AD-748748] 04 p0438 N73-13573
Research projects conducted in USSR to determine thermophysical properties of materials at high temperatures and characteristics of high temperature processes
[JPRS-57658] 04 p0484 N73-13957
Glass transistion characteristics and compatibility of linear poly carborane-siloxane series plastics
[AD-749385] 05 p0566 N73-14597
Tables of thermophysical properties of helium 4
[NBS-TN-631] 06 p0730 N73-15953
Handbook on thermodynamic and thermophysical properties of high propellant combustion products
[AD-754329] 11 p1253 N73-20165
Thermal design of filamentary composite materials for primary structures on space shuttles
[NASA-CR-124206] 12 p1415 N73-21469
Bremsstrahlung theory for relativistic plasma properties
[AEC-TR-7348] 12 p1434 N73-21618
HEPROP - a computer program for thermophysical properties of helium
[REPT-1046/72] 13 p1591 N73-22896
Tabular data on transport and thermophysical properties of selected binary mixtures in gaseous state
[AD-757528] 14 p1617 N73-23101
Tables of thermophysical properties of materials
[AD-758175] 15 p1747 N73-24164
Computation of thermophysical properties of gaseous and liquid fluorine using measurement data
[AD-758813] 16 p1871 N73-25146
Analysis of heat transfer properties and thermophysical properties of materials used for aircraft and spacecraft construction
[AGARD-R-606] 16 p1975 N73-25968
Analysis of thermophysical properties of plasma sprayed materials for use as thermal insulation coating on rocket nozzles
[NASA-CR-121144] 19 p2311 N73-28590
Extrapolation of thermophysical properties data for oxygen to high pressures at low temperatures
[NASA-CR-133858] 21 p2506 N73-30109
High temperature research of thermophysical and electrophysical properties of matter
22 p2728 N73-31832
Mechanical and thermophysical characteristics of nonmetallic insulation materials for space shuttle orbiter surface
24 p2939 N73-33471
Mechanical and thermophysical properties of composite materials
[LA-5173] 24 p2943 N73-33505

THERMOPHYSICS
U THERMODYNAMICS

THERMOPILES
Development of thermopile with sensor surface to receive radiant energy and to provide measurement of energy quantity
[NASA-CASE-NPO-11493] 03 p0300 N73-12447

THERMOPLASTIC FILMS
U POLYMERIC FILMS

THERMOPLASTIC RESINS
Data processing and recording applications in tensile testing of thermoplastics
[ERDE-TR-99] 05 p0565 N73-14593
Incremental theory and numerical procedure for analyzing three dimensional thermoplastic structure used in nonmetallic thermal protection system
[NASA-CR-124005] 06 p0729 N73-15948
Syntheses of polystyrene polymers with skin friction reduction in dilute solutions
[AD-761600] 19 p2233 N73-28008
Thermal and ultraviolet vacuum tests on adhesives, thermoplastic, and thermosetting resins for space environment simulation
[RV-106] 19 p2312 N73-28596

THERMOPLASTICITY
Real time thermoplastic modulator for coherent optical processing
[AD-762920] 20 p2379 N73-29119
Thermoplastic strengthening of martensite steels and titanium alloys
[AD-760953] 21 p2560 N73-30520

THERMOREGULATION
Sweat rate and heat conductance in thermoregulatory system during rest and exercise
[NASA-TT-F-14562] 01 p0009 N73-10074
Heat regulation and adaptation of rats exposed to helium oxygen atmosphere
03 p0259 N73-12096
Thermoregulation reactions of rats in hypoxic atmosphere with nitrogen and helium dilution
07 p0743 N73-16046
Helium/oxygen breathing effects on rat gas exchange and musculoskeletal heat control
10 p1115 N73-19093
Low barometric pressure effects on human thermoregulation function
13 p1480 N73-21996
Hypothalamus as internal heat regulator for warmblooded animals
[NASA-TT-F-15138] 23 p2749 N73-32002
Physical fitness effects on human thermoregulation during exercise
[NASA-TT-F-15142] 23 p2749 N73-32003

THERMOSETTING RESINS
NT EPOXY RESINS
NT NYLON [TRADEMARK]
NT PHENOLIC RESINS
NT POLYAMIDE RESINS
Development and characteristics of organic polymers for application to production of heat resistant plastics
[NLL-RISLEY-TR-2615-[9091.9F]]
20 p2434 N73-29546
Outdoor weathering influence on polyester and epoxy glasscloth reinforced laminate flexural strength and surface appearance
[FOK-R-1627] 21 p2563 N73-30546
Vacuum displacement compression molding of tubular bodies from thermosetting plastics
[NASA-CASE-LAR-10782-2] 22 p2677 N73-31444

THERMOSPHERE
Model of semiannual thermospheric density variations based on latitude-dependent temperature and composition variations
[NASA-TM-X-65835] 01 p0047 N73-10380
Semi-annual variations in thermospheric density
[NASA-TM-X-66100] 02 p0166 N73-11346
Phase difference between temperature and density in thermosphere
[NASA-TM-X-66119] 03 p0294 N73-12395
Electron beam-induced luminescence studies of thermospheric temperatures and particle densities, using two Aerobee 150 rockets
[AD-749877] 05 p0541 N73-14406
Accuracy of harmonics of diurnal density variations in thermosphere determined from satellite drag data and Jacchia empirical atmospheric model
[NASA-TM-X-66160] 07 p0790 N73-16427
Aerobee mass spectrometer data on neutral gas composition of Arctic thermosphere
08 p0899 N73-17282
Mass spectrometer and ion source for flight experiment measurements of thermosphere number density
08 p0899 N73-17283

MHD equations for calculating joule heating and winds from geomagnetic storms in thermosphere
[NASA-CR-124071] 08 p0915 N73-17498
Derivation of empirical global thermosphere model for magnetically quiet conditions from longitudinally averaged gas densities using expansion in spherical harmonics
[NASA-TM-X-66183] 08 p0917 N73-17512
Meridional wind effects on advection heating in thermosphere during geomagnetic storms
[AD-751921] 08 p0919 N73-17528
Thermospheric composition and density, measured by neutral mass spectrometer onboard OGO-6 satellite
08 p0972 N73-17946
Vertical distribution of vibrationally excited molecular nitrogen in thermosphere corresponding to stable auroral red arc
[NASA-TM-X-66194] 09 p1028 N73-18390
Model for solution of equations of motion for thermospheric wind - Part I
[NASA-TM-X-66189] 09 p1028 N73-18393
Three dimensional density model of thermosphere dynamics
[NASA-TM-X-66206] 10 p1154 N73-19389
Analysis of semiannual density variation in thermosphere during period of increasing solar activity
[BMFT-FBW-73-02] 11 p1285 N73-20430
Observation of eastward diurnal driving forces in thermospheric superrotation phenomenon
[NASA-TM-X-66222] 11 p1286 N73-20438
Results and comparisons of full nonlinear treatment of global thermospheric wind system
[NASA-TM-X-66234] 14 p1685 N73-23671
Role of metastable atoms [D] in thermospheric heating
[NASA-TT-F-14901] 14 p1705 N73-23832
Representation of Jacchia thermospheric models in spherical harmonics
[NASA-TM-X-66247] 15 p1778 N73-24416
Thermospheric heating due to EUV absorption and Joule dissipation
[AD-758758] 15 p1784 N73-24464
Three dimensional steady state model of thermospheric dynamics with auroral heating
[AD-758733] 15 p1784 N73-24466
Global characteristics in diurnal components of OGO-6 neutral mass spectrometer measurements of thermosphere
[NASA-TM-X-66295] 18 p2145 N73-27335
Effect of eddy turbulence in development of models of lower and upper thermosphere
[NASA-TM-X-70431] 19 p2293 N73-28443
Circulation in high latitude thermosphere due to electric fields and joule heating
20 p2391 N73-29203
Thermospheric wind effects on global distribution of helium in upper atmosphere
[NASA-TM-X-70441] 20 p2412 N73-29391
Mechanism and rates of atmospheric mixing in lower thermosphere including heat input
[NASA-CR-135789] 24 p2920 N73-33321

**THERMOSTABILITY**
U THERMAL STABILITY

**THERMOSTATS**
Using quartz oscillators sensitive to temperature variations for frequency stabilized thermostats
[PUBL-1366] 06 p0647 N73-15253

**THERMOTROPISM**
U ANISOTROPY
U TEMPERATURE EFFECTS

**THERMOVISCOELASTICITY**
Rayleigh-Ritz solution of wave propagation in thermoviscoelastic rod insulated on lateral surface and driven by sinusoidal stress at one end
[AD-746466] 01 p0115 N73-10952
Finite element formulation and thermoelastoviscoplasticity theory for solving problems in nonlinear continuum mechanics
[AD-754952] 11 p1331 N73-20805
Development of nonisothermal theory of viscoelastic fluids with fading memory and application to viscometric flow
[AD-754802] 11 p1349 N73-20948
Thermal analysis of thermoviscoelastic behavior of case bonded propellant grains to thermal property variations
[AD-758839] 15 p1824 N73-24780
Methods of solving quasistatic problems in linear theory of thermoviscoelasticity
[AD-763937] 22 p2726 N73-31816

**THETA PINCH**
Soft X ray emission from plasma produced in theta pinch deuterium discharge seeded with neon
[AD-745736] 01 p0086 N73-10712
Electron temperatures and thermal conduction in high energy theta pinches
[LA-4930] 03 p0341 N73-12780
Two dimensional luminous plasma structure in hard core theta pinch at initial preheater breakdown
[AD-748587] 04 p0455 N73-13716
Behavior of plasma column in high voltage theta pinch with and without magnetic mirrors
[LA-DC-72-703] 05 p0584 N73-14751
Plasma experiments on helical equilibria in Scyllac theta pinch sector
[LA-DC-72-706] 05 p0584 N73-14752
Research in electrically driven shock plasmas
[AD-749552] 05 p0584 N73-14755
Characterization of halo in pinch plasma by image converters and streak camera
[IPP-1/125] 07 p0828 N73-16709
Theta pinch generation of ionizing shock waves in argon plasma
[AD-751659] 07 p0829 N73-16721
Equilibrium plasma produced by theta pinch gun firing into magnetic field
[AD-752498] 08 p0949 N73-17772
Enhanced far infrared radiation from theta pinch plasma
12 p1432 N73-21601
Plasma heating by magnetic pulse in theta pinch and nuclear fusion
[AD-757043] 13 p1563 N73-22671
Theoretical and numerical approaches to turbulence dominated theta pinches
23 p2822 N73-32558

**THIAMINE**
Effect of accelerations on thiamine S-35 distribution in organs, tissues, and subcellular structures of white mice
07 p0743 N73-16044
Influence of cysteamine hydrochlorine and vitamin B and C prophylaxis on radiation sickness in humans
11 p1242 N73-20078
Synthesis rate of phospholipids and cytochromes b5 and P 450 in thiamine-deficient rats after treatment with thiamine
[NASA-TT-F-14989] 17 p1987 N73-26064

**THICK FILMS**
Microstructure of thick film resistors
[AD-747980] 03 p0276 N73-12238
Packaging techniques for miniaturized thick film networks
[BDX-613-363-REV] 03 p0277 N73-12250
Methods for chip mounting and establishing electrical connections in miniaturized printed circuits and thick and thin film hybrid circuits
[ECR-27] 08 p0891 N73-17212
Electrical resistance of thick film ruthenium dioxide resistor circuits
[AD-756254] 14 p1644 N73-23337
Monolithic light emitting diode display devices
[AD-758853] 16 p1882 N73-25232

**THICK WALLS**
Procedures for analyzing very thick walled cylindrical shells used in constructing hydrospace simulators
[AD-747963] 03 p0362 N73-12952
Elastic-plastic behavior of thick-walled circular cylinders under internal pressure
[AD-753121] 09 p1097 N73-18952
Effect of wall thickness variations on failure during burst tests of Zircaloy tubing
[WAPD-TM-1104] 17 p2093 N73-26935
Development of set of equations for analysis of thick shell structures to include effects of geometric thickness and transverse strain
24 p2987 N73-33870

**THICKENED LEADING EDGES**
U LEADING EDGES

**THICKNESS**
NT FILM THICKNESS
Wave drag reduction on delta wings at zero lift as function of displacement of maximum thickness in spanwise direction
[DLR-FB-71-61] 06 p0621 N73-15044
High resolution FM radar at X band for measuring snow and ice thickness
[CRC-TN-646] 06 p0639 N73-15184
Pulse radar sounding of sea ice thickness with video display
[JPRS-57841] 06 p0665 N73-15406
Microwave gauge for measuring thickness of hot steel product during production
[PB-212210] 08 p0925 N73-17583
Dynamic and static response to blast loads of thin circular plates free or embedded using Timoshenko model and finite difference theory
[ISL-4/72] 09 p1094 N73-18934
Effects of specimen thickness on fatigue-crack growth and fracture toughness of 7075-T6 and 7178-T6 aluminum alloy plates and sheets
[NASA-TN-D-7173] 12 p1413 N73-21453
Effects of properties of organic phase on thickness and intermolecular interaction of black hydrocarbon films
[NLL-M-22999-[5828.4F]] 20 p2373 N73-29070

**THIN AIRFOILS**
NT INFINITE SPAN WINGS
NT THIN WINGS
Mathematical models for gas surface interactions and calculating aerodynamic coefficients for simple geometric shapes and high Mach number flow past thin airfoils
[AD-752245] 08 p0899 N73-17278
Numerical analysis of steady, two-dimensional, laminar, incompressible, high Reynolds number separated flow past thin airfoils
[NASA-CR-114656] 20 p2388 N73-29185

**THIN FILMS**
NT FERROMAGNETIC FILMS
NT MONOMOLECULAR FILMS
Development and application of polyimide films for hybrid and beam lead substrates
[AD-745731] 01 p0033 N73-10260
Analysis of gray scale image storage techniques in electroluminescent and photoconductor image conversion panels
[AD-745758] 01 p0033 N73-10261
Identification by country and research facility of thin film studies
[AD-746719] 02 p0220 N73-11779
Development of method for measuring temperature of wind tunnel scale model by photographic recording of changes in thin film phase-change temperature indicating material
[NASA-CASE-LAR-11053-1] 02 p0243 N73-11972
Procedures for using liquid crystal tape for thermographic testing of bonded structures for aircraft
[NASA-CR-123932] 03 p0300 N73-12451
Development of procedure for producing thin transparent films of zinc oxide on transparent refractory substrate
[NASA-CASE-FRC-10019] 03 p0304 N73-12487
Optical properties of thin film deposited by electron bombardment
[NPL-OP-MET-13] 03 p0340 N73-12775
Analysis of microstructure of radio frequency-sputtered, thin lead-dielectric cermet films using transmission electron microscopy
[NASA-TR-R-393] 03 p0345 N73-12811
Preparation of thin film metal fluoride electrodes from elemental constituents to obtain high purity and variations in size and shape
[NASA-TM-X-2690] 04 p0386 N73-13140
Approximation technique applied to elastic surface waveguides utilizing curved thin films
[AD-748646] 04 p0390 N73-13169
Technology assessment for thin film development of magneto-optical manganese bismuth memory
04 p0394 N73-13202
Fabrication and evaluation of RF sputtered barium titanate thin films for integrated circuit application
[AD-749236] 04 p0397 N73-13227
Energy distribution measurement of experimental thin film emission cathodes to determine acceptability as low energy monoenergetic flood source
[AD-749556] 04 p0397 N73-13228
Fabrication of thin film silicon integrated square wave oscillator circuit capacitors
[AD-749266] 04 p0397 N73-13231
Nucleation and film growth mechanisms in heteroepitaxial semiconductor
[AD-748424] 04 p0460 N73-13753
Electrical conductivity of thin films during nucleation and film growth
[AD-748269] 04 p0460 N73-13756
X ray apparatus for investigating hydrogen induced changes in fine crystalline structure of N1 powders and electrolytic films
[NLL-TRANS-746-1294-[9022.401]]
05 p0505 N73-14113
Proceedings of symposium on laser radiation damage to transparent dielectrics, plasma formation at dielectric surfaces, and damage morphology of thin film coatings
[NBS-SP-372] 05 p0554 N73-14498
Characteristics of optical glass materials with specific resistance to effects of laser radiation
05 p0554 N73-14499
Analysis of damage to thin films and substrate surfaces during irradiation by Q switched ruby laser
05 p0556 N73-14512
Analysis of laser damage to thin film coatings caused by radiation from Q switched ruby laser
05 p0556 N73-14514
Analysis of damage threshold and damage mode from laser radiation for multilayer and periodic inhomogeneous film systems
05 p0556 N73-14515
Mechanical properties of thin films of Ni-SiO
[NLL-TRANS-746-1329-[9022.401]]
05 p0564 N73-14582
Photoconductivity of thin dielectric films induced by X ray irradiation
[UCRL-73974] 05 p0586 N73-14770
Diagnostic techniques for characterizing near surface of solids
[UCRL-73925] 05 p0587 N73-14773
System characteristics of amorphous semiconductor thin film and electron beam storage devices
[AD-749282] 05 p0587 N73-14778
Reliable source of high quality magnetic bubble materials
[AD-749806] 05 p0589 N73-14787
Structural effects of various optical coatings on single shot laser induced damage threshold using pulsed neodymium glass laser
[AD-749852] 06 p0680 N73-15531
Crystal growth from vapor phases and epitaxy, and applications to semiconductors and microelectronics - conference review
[AD-750654] 06 p0710 N73-15793

Absorption coefficient and index of refraction data for Pb(1-x)S n[x] Te thin films
[AD-751650] 07 p0832 N73-16747
Methods for chip mounting and establishing electrical connections in miniaturized printed circuits and thick and thin film hybrid circuits
[ECR-27] 08 p0891 N73-17212
Development and characteristics of multiple thin film vapor deposition unit
[BARC-609] 08 p0927 N73-17594
Properties of thin dielectric TiO2 films produced by chemical vapor deposition
[NASA-CR-130763] 08 p0950 N73-17780
Manufacturing of superconducting cylindrical films of niobium and niobium nitride by sputter etch techniques
[AD-752593] 08 p0952 N73-17799
Fatigue behavior of thin solid films induced by moving surface load
[AD-753411] 09 p1041 N73-18490
Thin deformable films for use as storage medium in holographic optical memory
[NASA-CR-124083] 09 p1064 N73-18681
Thin film broadband absorber for use in underwater acoustics using silicon oils
[BMVG-FBWT-72-2] 09 p1067 N73-18703
Exposure of 0.29 micron Ni-Fe films to continuous laser light in infrared spectra
[AD-753962] 10 p1129 N73-19202
Production of ferromagnetic MnBi thin films by optical control of vacuum deposition and annealing
[KFKI-72-70] 10 p1199 N73-19757
Process for analysis of strain field of structures subjected to large deformations involving low modulus substrate with thin coating
[NASA-CASE-LAR-10765-1] 11 p1323 N73-20740
Electroluminescent characteristics of vacuum deposited zinc sulfide films for airborne electronic displays
[AD-754781] 11 p1332 N73-20811
Multilayer and disk type, ceramic chip capacitors for thick and thin film hybrid circuits
[ECR-28] 12 p1383 N73-21211
Development of miniature electronic trimmable thin film resistor chips having precision responses
[BDX-613-728] 12 p1383 N73-21216
Characteristics of ellipsometer and techniques for measuring thin films including computer program for determination of optical constants and thickness of film
[NASA-TM-X-64742] 12 p1405 N73-21392
Critical scattering of laser light by thin fluid films
[COO-2203-1] 12 p1410 N73-21428
Metal thin films with extremely high mechanical strength
[AD-755924] 12 p1417 N73-21480
Effect of substrate topography on magnetic properties of cylindrical Ni-Fe thin films
[NLL-LTI-746-1370-[9022.401]] 12 p1437 N73-21641
Microwave surface impedance of thin niobium superconducting films subjected to varying dc magnetic fields 12 p1438 N73-21649
Ferromagnetic resonance in ferromagnetic thin films 12 p1438 N73-21651
Tunneling characteristics of thin cadmium selenide, zinc selenide, and cadmium telluride evaporated semiconductor films 12 p1438 N73-21652
Research projects in solid state physics, low temperature physics, superconducting films, and quantum liquids and crystals
[COO-1569-93] 12 p1439 N73-21657
Thin film physics, cohesive and dielectric properties, and solid state theory
[COO-623-190] 12 p1439 N73-21658
Correlation between microstructure and measured stress of vacuum deposited nickel films
[COO-623-183] 12 p1439 N73-21659
Influence of annealing on thin films of beta SiC
[AD-755792] 12 p1442 N73-21683
Photoelectric solar converter using cadmium sulfide and cadmium selenide tablets or thin films
[AD-756594] 13 p1476 N73-21960
Material properties of thin single crystal silicon films on insulator/polycrystalline silicon substrates
[AD-756646] 13 p1503 N73-22179
Mechanical strength of multilayer thin metal films
[AD-756582] 13 p1543 N73-22508
Influence of defects and impurities on nucleation and growth of oriented films by evaporation
[NASA-CR-2234] 13 p1559 N73-22636
Porous structure and surface energy of evaporated metal thin films 13 p1565 N73-22683
Device fabrication and radiation effect studies of various semiconductors
[AD-756249] 13 p1566 N73-22689
Effects of proton bombardment on p- and n-type PbSnTe thin films
[AD-756542] 13 p1567 N73-22696
Magnetic bubble garnet materials for thin film storage devices
[AD-755546] 13 p1568 N73-22705
Nucleation and film growth mechanisms in heteroepitaxial semiconductor thin films
[AD-755529] 13 p1568 N73-22706
Characterization of thin films produced by epitaxial growth of magnetic rare earth compounds
[AD-755165] 13 p1568 N73-22707
Chemistry and physics of thin liquid films in contact with solid substrates and application to boundary lubrication of propulsion systems
[AD-757061] 14 p1670 N73-23556
Environmental tests of strength and durability of transparent tin oxide and indium oxide films on glass
[AD-756558] 14 p1680 N73-23637
Tensile strength testing of multilayer thin metal film structures
[AD-757723] 14 p1681 N73-23645
Method for vapor deposition of thin films
[NASA-CASE-MFS-20775-1] 14 p1697 N73-23770
Physical properties of electronic materials, devices, and thin films
[AD-758197] 14 p1700 N73-23793
Modulation of electron beam by laser beam in thin film with production of light 15 p1795 N73-24548
Gallium arsenide epitaxial thin films as active elements for electrooptic modulation of carbon dioxide laser radiation
[AD-757792] 15 p1796 N73-24559
Effect of helium gas bubbles on grain boundary motion in vapor deposited gold foil samples
[RD/B/N-2430] 15 p1798 N73-24578
Phase shift model for induced voltage in current carrying superconducting thin films in superimposed ac and dc magnetic fields including radio and microwave frequency ranges 15 p1820 N73-24748
Thin film detector research including detector response to light and heavy ions and accelerated ions
[ORO-2843-22] 15 p1821 N73-24757
Hartree approximation of extra conductivity in quasi-superconducting thin films considering nonlinear external field effect
[LNF-72/76] 15 p1821 N73-24758
Elastic and piezoelectric surface waves guided by thin films
[AD-758688] 15 p1823 N73-24776
Systems analysis of active thermal control using thermoelectric devices
[NASA-CR-124256] 15 p1843 N73-24935
Electrical properties of thin sputtered aluminum-silica capacitors
[NASA-CR-121165] 16 p1880 N73-25220
Thin film lead and tin selenide photoconductive infrared detectors
[AD-758685] 16 p1915 N73-25499
Magnetic properties of cobalt rare earth thin films 16 p1951 N73-25790
Rare earth oxysulfide luminescent films for use in CRT screens
[AD-758760] 16 p1954 N73-25808
Effects of electric and magnetic fields on nucleation and growth of metallic thin films
[USC-113-P-22-3] 17 p2045 N73-26546
Plasma anodization and oxidation of thin metal film semiconductors
[AD-760171] 17 p2052 N73-26600
Dual wavelength system for monitoring film deposition
[NASA-CASE-MFS-20675] 17 p2070 N73-26751
Fabrication of niobium thin film superconductive tunnel junctions using semiconductor barrier 17 p2072 N73-26761
Experimental conditions for depositing crystalline and amorphous VO2 thin films by RF and dc sputtering
[CEA-CONF-2133] 17 p2073 N73-26774
Radiation resistance of thin insulating films deposited with ion beam system
[AD-760118] 17 p2075 N73-26788
Preparation of single crystal films by reactive sputtering process
[AD-760715] 18 p2123 N73-27160
Growth and crystal structure of Si, Ge, and GaAs thin films
[JPRS-59279-PT-2] 18 p2186 N73-27650
Growth and properties of epitaxial silicon films treated with hydrogen of high purity 18 p2187 N73-27657
Short-range ordering in amorphous Ge thin films studied by photoemission spectrum analysis as function of film preparation at different substrate temperatures 18 p2190 N73-27680
Integrated circuits using thin magnetic film elements
[AD-762267] 19 p2248 N73-28127
Kinetics of change in electrical resistance of thin films annealed in magnetic field at high temperature
[JPRS-59625] 19 p2309 N73-28575
Superconducting properties of sprayed thin films
[JINR-P8-6863] 19 p2327 N73-28717
Characteristics of polyurethane film for fabrication of expandable envelopes subjected to solar heating at high altitudes
[AD-762803] 20 p2362 N73-29001
Monomer polymerization by plasma discharge as thin film for water purification membrane
[NASA-CASE-ARC-10643-1] 20 p2374 N73-29074
Design and construction of thin magnetic film shift register
[NHK-LABS-NOTE-164] 20 p2379 N73-29112
Chemical vapor deposition of stoichiometric niobium gallium superconducting film
[NASA-CR-2308] 20 p2455 N73-29726
Thin film optical waveguides in III-V semiconductors
[AD-763120] 20 p2455 N73-29730
Apparatus for deposition of superconducting thin films on large surfaces of complex configuration
[JINR-P8-6855] 20 p2463 N73-29789
Static parameters of mechanical model of thin film electrostatic relay 21 p2514 N73-30171
Magneto-optic effects in ferrate garnet thin film waveguides
[AD-763792] 21 p2518 N73-30199
Thin film analyzer utilizing holographic techniques
[NASA-CASE-MFS-20823-1] 21 p2554 N73-30476
Computerized design of multilayer thin film filters
[WRE-TN-903[AP]] 23 p2759 N73-32082
Transparent switchboard which permits optical display devices to be adapted for use in man machine communications
[NASA-CASE-MSC-13746-1] 23 p2768 N73-32143
Stress analysis of vacuum deposited nickel films to determine correlation between microstructure and measured stress 23 p2804 N73-32424
Lateral diffusion in thin [film] couples of gold and silver 23 p2825 N73-32579
Electron network model of solid interfaces, surface defects, planar defects, and thin films 23 p2825 N73-32584
Research in dynamics of thin films polymer chemistry mechanical and chemical properties of materials
[NASA-CR-135697] 23 p2865 N73-32906
Metal oxide semiconductor photoengraving principles and utilization noting resin properties, procedures, thin film techniques, and metal chemical attack
[LAAS-FI-73-T-11] 24 p2899 N73-33139
Evaluation of process for burnable poison deposition on zirconium hydride fuel
[AI-AEC-13085] 24 p2955 N73-33606
Electron thermal conductivity of thin films of strong coupling superconductors and of superconductors containing rare earth inpurities 24 p2967 N73-33712
Properties of silicon-silicon dioxide interface properties in thin oxide metal oxide semiconductor structures 24 p2968 N73-33718

**THIN LAYER CHROMATOGRAPHY**

Thin layer chromatography for qualitative analyses on steelwork materials
[PB-214232/1] 16 p1871 N73-25148
Thin layer chromatographic identification and infrared spectrophotometric quantification of antitoxiants used in manufacturing polyolefinic polymers
[REPT-6726] 22 p2625 N73-31029

**THIN PLATES**

Numerical analysis of radiation damping of thin finite rectangular plates immersed in heavy and light fluid media
[AD-746460] 01 p0115 N73-10950
Dynamic and static response to blast loads of thin circular plates free or embedded using Timoshenko model and finite difference theory
[ISL-4/72] 09 p1094 N73-18934
Reversible sliding and lubrication effects in internal stress friction on thin plate
[AD-751723] 09 p1097 N73-18957
Stress analysis of elastoplastic state of thin circular plate subjected to axisymmetric loading
[AD-753983] 11 p1346 N73-20920
Analysis of uniform heat energy generation and conduction heat transfer for semi-infinite thin plate with air blowing over one surface and insulated on other 16 p1973 N73-25959
Calorimetric measurements on X ray penetration through thin carbon foils
[AD-761826] 19 p2322 N73-28679
Effects of shear, rotatory inertia and inplane forces on transverse vibration of thin plates, and effect of shear on buckling 19 p2347 N73-28879

**THIN WALLED SHELLS**

Free vibrations of complex system of ring with added mass, connected to thin spherical or cylindrical shell 01 p0112 N73-10930
Formulation of finite element matrix in Lagrangian variables for elastic thin shells with arbitrary geometric imperfections
[AD-747321] 03 p0361 N73-12946

Elastic buckling strength of thin walled aluminum alloy tubes fabricated with and without boron/epoxy glass/epoxy composite materials for reinforcement
[NBS-TN-728] 04 p0437 N73-13566
Theory of shallow spherical shells including effect of transverse shear deformation
[AD-749966] 06 p0727 N73-15935
Sheba triangular thin shell element application to calculation of coding towers, toruses, and roofs
[ISD-127] 09 p1095 N73-18936
Nonlinear dynamic response of thin, clamped hemispherical shell subjected to suddenly applied pressure
[AD-752795] 09 p1096 N73-18950
Finite difference method applied to axisymmetric random shells of revolution for unsymmetrical loading
[DRIC-TRANS-2996] 12 p1463 N73-21855
Development of equations of motion for vibration frequencies of cantilever and elastically supported-free thin circular cylindrical shell
15 p1837 N73-24887
High energy plasma generation by electromagnetic implosion of thin metal foil cylinder
[AD-759826] 16 p1951 N73-25788
Analysis of optimal configurations for thin walled, axisymmetric, laminated shells based on shell configuration, loading, fiber alignment, and material properties of composite structure
16 p1969 N73-25924
Vibrational characteristics, mechanical properties, and stress analysis of thin shell structures of various cross sections
[NASA-SP-288] 17 p2092 N73-26924
Development of doubly curved triangular finite element for use in small deformation analysis of thin shells containing cutouts and irregular boundaries
[RE-453] 19 p2347 N73-28882
Effect of imperfections on behavior of thin elastic shells subject to loads
[AD-761448] 19 p2349 N73-28899
Derivation of equations for multilayer anisotropic shells with lateral shift considered
[AD-762224] 19 p2351 N73-28908
Wind tunnel tests to determine aeroelastic stability of thin isotropic circular cylindrical shells at subsonic and supersonic air speeds
20 p2359 N73-28975
Research projects involving aeroelastic stability and response, stability of thin shell structures, and suspension system concept for control of vehicle responses
[AD-762568] 20 p2359 N73-28979
Nonlinear parametric vibrations of closed cylindrical shells
20 p2482 N73-29939
Wave propagation in thin elastic shells
22 p2723 N73-31793
Concentration of stress around holes in thin walled shells
[AD-764169] 22 p2726 N73-31813
Nonlinear analysis for thin elastic shells using modal expansion method of linear vibration analysis extended to nonlinear analog
23 p2852 N73-32793
Application of finite element analysis techniques to determine characteristics of curved elements in thin, elastic shells
24 p2987 N73-33872

**THIN WALLS**
Development of mathematical relationships to define the behavior of multilayer, thin shell structures under various conditions of shear and bending
02 p0238 N73-11936
Development of differential pressure control system using motion of mechanical diaphragms to operate electric switch
[NASA-CASE-MFS-14216] 04 p0419 N73-13418
Procedure for fabricating element with cavity closed by thin wall with precisely shaped slit
[NASA-CASE-LAR-10409-1] 11 p1297 N73-20526
Production of thin walled tubes by drawing and rolling
[NLL-M-21689-[5828.4F]] 20 p2421 N73-29448

**THIN WINGS**
NT INFINITE SPAN WINGS
Numerical determination of augmented lift due to wing-slipstream interaction for application to V/STOL aircraft
[AD-743257] 01 p0005 N73-10035
ALGOL program for lift distribution determination on thin wing in subsonic flow
[NLR-TR-70088-U] 03 p0274 N73-12224
Effects of thickness and viscosity considerations on accuracy of aerodynamic coefficients determined for thin wings in inviscid flow conditions
[ESDU-70011-AMEND-A] 07 p0735 N73-15982
Wind tunnel tests to determine oscillatory longitudinal derivatives of thin delta wing with 0.8 aspect ratio over range of incidences
[ATN-7105] 13 p1470 N73-21903
Development of slender body theory for analyzing flow past thin, conically cambered, delta wing with exact boundary conditions
[ARC-R/M-3249] 15 p1726 N73-24002
Iterative method for calculation of loading on thin rectangular wing
[ARC-R/M-3719] 21 p2492 N73-30004

**THINNERS**
U SOLVENTS

**THIOLS**
Effects of hyperoxia on sulfhydryl concentration of Escherichia coli
[AD-746193] 02 p0134 N73-11087
Ozone reaction with mercaptane for elimination of exhaust gas pollution in air
08 p0883 N73-17152
Effects of antiradiation drug dosage on mice and rat tolerance to transverse acceleration overloads
11 p1239 N73-20055
Resistance of mice to acceleration overloads after injection of aminothiol group radioprotector
11 p1239 N73-20056
Pharmacological data for aminothiol and indolylalkylamine radioprotectors
11 p1240 N73-20066
Aminothiol radioprotector, finam, effect on irradiated animal tissues under various conditions
11 p1242 N73-20085

**THOMSON EFFECT**
U THERMOELECTRICITY

**THOMSON SCATTERING**
Analysis of ionospheric response to solar eclipse of 7 March 1970 by Thomson scatter radar technique at Millstone Hill Ionospheric Observatory
24 p2912 N73-33239
Thomson scattering diagnosis on pulsed xenon arc plasma flow
[NASA-TM-X-71443] 24 p2962 N73-33669

**THORIUM COMPOUNDS**
NT THORIUM OXIDES
Application of Nernst glower metal oxide conductors to laser pumping to produce spectral energy within pumping band of laser material
[AD-745796] 01 p0066 N73-10538
Magnetic and specific heat measurements of carbides, nitrides, and uranium and thorium sulfides
[CEA-R-4453] 24 p2943 N73-33506

**THORIUM OXIDES**
Influence of Na2SO4 oxidation of Ni-20Cr-2ThO2 gas turbine corrosion
[AD-751259] 07 p0810 N73-16573
Electrical conductivity of ThO2 at room and high temperatures and in high intensity gamma radiation fields
[BNWL-1671] 12 p1416 N73-21475

**THREADS**
Fatigue strength curves for large steel screw threads under axial loading
[ESDU-68045] 01 p0110 N73-10905
Fatigue tests of steel screw threads with large root radii under axial loading to determine fatigue strength and point of failure
[ESDU-67020-AMEND-A] 01 p0110 N73-10906

**THREE BODY PROBLEM**
Comparison of accuracy of patched-conic and linearization methods for predicting trajectories in sun-planet system
[AD-748345] 04 p0476 N73-13891
Approximate analytic and numerical methods for describing encounter of star with sun-comet system and resulting gravitational perturbations of cometary orbits
07 p0840 N73-16805
Three body exchange effects on Neel temperature of solid He-3
[COO-1569-97] 12 p1439 N73-21655
Solutions for motion about libration points of elliptic restricted three-body problem
15 p1829 N73-24826

**THREE DIMENSIONAL BOUNDARY LAYER**
Orthogonal coordinate systems for three dimensional boundary layer calculations on ship hull geometry
[AD-749774] 05 p0529 N73-14301
Finite difference solution of three-dimensional compressible boundary layer equations for circular cones at angle of attack
[NASA-CR-112316] 12 p1391 N73-21276
Integral equation for studying three dimensional turbulent boundary layer development
14 p1648 N73-23369
Integral calculation of three-dimensional turbulent boundary layer velocity profiles
14 p1648 N73-23370
Development of numerical relationship to provide axially symmetric analog for general three dimensional boundary layers
[ARC-R/M-3200] 16 p1853 N73-25014
Evaluation of three approximate methods for solving three dimensional boundary layer equations
[ARC-R/M-3201] 16 p1853 N73-25015
Fourier analysis of boundary curve for identification of three dimensional objects
[AD-758895] 16 p1877 N73-25192
Calculation of three-dimensional boundary layer flows on aircraft and space shuttle configurations
[NASA-CR-2285] 18 p2130 N73-27214
Numerical calculation of three dimensional boundary layers by finite difference methods
20 p2384 N73-29156
Three-dimensional compressible turbulent boundary layer for subsonic and transonic flow over yawed airfoil
[AD-763730] 21 p2526 N73-30258
Supersonic wind tunnel tests on three dimensional turbulent boundary layer growth on wires leading to calculation of tension and skin friction on aircraft towlines
[ARC-CP-1235] 23 p2740 N73-31933
Integral method for analyzing two-dimensional and axisymmetric compressible and three-dimensional incompressible turbulent boundary layer
23 p2772 N73-32169
Turbulence anisotropy effects on pressure distribution and secondary flow of boundary layers, free and wall jets, and wakes
24 p2906 N73-33191
Flow module approach to flow around three dimensional obstacles in boundary layer
24 p2908 N73-33207
Boundary layer calculation and wind tunnel model test of ships
24 p2909 N73-33214
Finite difference solutions for flow equations of three dimensional boundary layer on blunt body
[SLA-73-366-PT-1] 24 p2909 N73-33217

**THREE DIMENSIONAL FLOW**
NT SECONDARY FLOW
Two layer model of compressible turbulent boundary layer flow around reentry vehicle
[AD-743933] 01 p0043 N73-10338
Remotely operated boundary layer probe for use in three dimensional measurements
[AD-745215] 01 p0059 N73-10481
Current sheet magnetic field model for computing three dimensional currents flowing in solar corona
01 p0093 N73-10764
Three dimensional transonic flows past lifting configurations having finite leading edge swept angles
[AD-747266] 02 p0159 N73-11284
Numerical integration and variational calculation method for approximate solution to three dimensional flow of gas dynamic bearings
[AD-747377] 03 p0308 N73-12513
Numerical calculation of supersonic three dimensional jet plum in perfect gas with inviscid and compressible properties
04 p0404 N73-13287
Analysis of mean velocity profiles in three-dimensional turbulent boundary layers during incompressible flow
[REPT-71-FM-13] 04 p0404 N73-13289
Analysis procedure for three dimensional, subsonic, duct flow
[AD-748649] 04 p0407 N73-13313
Three dimensional laminar boundary layer flow over bodies of revolution
[AD-748282] 04 p0408 N73-13323
Calculation method for effect of compressible three dimensional relief on torque required for helicopter rotor
[AD-750179] 05 p0498 N73-14053
Three-dimensional flow arising in two dimensional separation bubbles noting flow characteristics in turbulent and laminar layer and in suction or blowing conditions
[IC-AERO-72-19] 05 p0525 N73-14275
Calculation of compressible flow in three dimensional cascade of turbomachine blades using stream line curvature technique
[ARC-R/M-3704] 05 p0527 N73-14287
Application of functional analysis to obtain exact semianalytical solutions of boundary layer flows under turbulent and laminar conditions
06 p0616 N73-15003
Numerical analysis of three dimensional incompressible fluid flow near large structure surface
[LA-DC-72-711] 06 p0654 N73-15315
Numerical analysis of three dimensional compressible laminar boundary layer flow characteristics of right circular cone in supersonic and hypersonic flow
[AD-750130] 06 p0656 N73-15331
Microwave holography for imaging sea surface topography in three dimensions
06 p0664 N73-15391
Analysis of supersonic, three-dimensional flow characteristics to determine effects of material porosity and angle of attack on jet stretcher performance
07 p0765 N73-16215
Method of characteristics for analyzing three dimensional, steady supersonic, nonequilibrium, chemically reacting flow of thermally perfect gases in exhaust nozzle
07 p0768 N73-16240
Integration of equations of motion for three dimensional turbulent boundary layer
07 p0771 N73-16261
Experimental analysis of three dimensional flow fields in planar nozzles and wall jets found in bistable fluid amplifiers
[AD-751627] 07 p0774 N73-16282
Semiempirical theory on bending and development of round turbulent jet in subsonic crosswind
[AD-751093] 07 p0774 N73-16286

Three dimensional boundary layer separation and shock wave generation in flow field of supersonic conical intake mounted on fuselage side
[ARL/ME-137] 08 p0863 N73-16981
Measurement of unsteady pressures developed on harmonically oscillating wing planform in three dimensional compressible flow
[DLR-FB-72-55] 09 p0980 N73-18007
Finite difference method for calculating three dimensional, unsteady and steady, inviscid gas flows around blunt bodies
[NASA-TT-F-714] 09 p0980 N73-18009
Development of steel wedge probe for measurement of three dimensional wake flow in subsonic and transonic flow fields
10 p1140 N73-19285
Methods for determining inviscid three dimensional flow about smooth shapes at supersonic speeds
[AD-753695] 10 p1143 N73-19311
Boundary layer control for mixing region in three dimensional laminar elliptical jet for thrust augmentation
[AD-754227] 10 p1143 N73-19313
FORTRAN program for computing XYZ potential flow about three-dimensional bodies of arbitrary shape
[AD-754429] 10 p1143 N73-19317
Development of tables of gasdynamic functions in three dimensional, axisymmetric, and plane gas flows past blunt bodies of revolution
[NASA-TT-F-715] 11 p1231 N73-19996
Development of method for solving three dimensional, incompressible laminar and turbulent boundary layer problems for swept infinite cylinders and small cross flow
[AD-754440] 11 p1232 N73-20004
Computer program for three dimensional inlet and analysis of capture area, ram force, spillage force, and surface pressure force
[NASA-CR-112304] 11 p1271 N73-20312
Theories, numerical methods, and computer programs for determining inviscid three dimensional flow around spherically-capped smooth bodies and wings at supersonic speeds
[AD-753696] 12 p1356 N73-21002
Finite difference solution of general class of three-dimensional boundary layer flows
[NASA-CR-112315] 12 p1391 N73-21277
Three dimensional supersonic flow program for calculating flow field about cone at zero angle of attack
[NASA-CR-112301] 12 p1391 N73-21282
User manual for computer program of potential flow calculation about three-dimensional lifting bodies
[AD-755933] 12 p1393 N73-21292
Development of method for calculating potential flow about arbitrary lifting three dimensional bodies with emphasis on bound vorticity and application of Kutta condition
[AD-755480] 13 p1471 N73-21914
Two procedures for solving Navier-Stokes equations for steady, three dimensional flows with circulation
[EF/TN/A/47] 13 p1510 N73-22238
Wind tunnel investigation of three dimensional flow effects on straight wings
14 p1600 N73-22973
Three-dimensional representation of hypersustentation during separated flow
[REP-8467] 14 p1648 N73-23371
Three dimensional growth rates of seeded Florida cumulus
[UM-RSMAS-73029] 14 p1661 N73-23480
Analysis of Kutta-Joukowsky condition in three dimensional flow with application to vortex sheet attachment to wing surface
[NASA-TT-F-14918] 15 p1767 N73-24319
Application of three dimensional analysis techniques for determining operating characteristics of axial turbines
15 p1824 N73-24785
Circular geometry and mixed boundary value problems in three dimensional elasticity
[NASA-TN-D-7266] 15 p1837 N73-24891
Evaluation of three approximate methods for solving three dimensional boundary layer equations
[ARC-R/M-3201] 16 p1853 N73-25015
Three dimensional flow field modules with turbulent structure
[AD-758894] 16 p1890 N73-25292
Application of holographic interferometry techniques for determining asymmetric flow distribution encountered near wing-fuselage junction at transonic speed
[AD-759967] 17 p2015 N73-26296
Three dimensional potential flow problems solved by means of inverse formation and finite differences
[AD-760347] 17 p2016 N73-26302
Calculation of three-dimensional boundary layer flows on aircraft and space shuttle configurations
[NASA-CR-2285] 18 p2130 N73-27214
Numerical method employing plane characteristics for calculating geometrically complex three dimensional nozzle exhaust flow fields
19 p2251 N73-28149
Analysis of arbitrarily nonuniform, nonadiabatic, two dimensional or axisymmetric basic flows based on inviscid theory of three dimensional perturbations in uniform transonic flow
[AD-761632] 19 p2256 N73-28188
Two and three dimensional flow field characteristics of lower surfaces of caret wings
[AASU-327] 21 p2491 N73-29997
Numerical analysis of three dimensional boundary layer for various distribution laws of suction intensity on leading edge of wing
[AD-763280] 21 p2497 N73-30038
Analysis of boundary layer and turbulence characteristics inside passages of axial flow inducer and technique for predicting properties of boundary layer
[NASA-CR-121248] 21 p2524 N73-30240
Steady, supersonic, three dimensional flow in rotating and stationary annular cascades treated by method of characteristics in three independent variables
[DLR-FB-73-12] 21 p2525 N73-30247
Motion and distribution of particles in steady, tube flows of suspensions of neutrally buoyant, rigid spheres
22 p2649 N73-31223
Analysis of compressible three-dimensional turbulent flow over yawed cone
22 p2649 N73-31227
Linearized integral theory of three dimensional unsteady compressible flow in shear layer by oscillating wall
[AD-763807] 22 p2654 N73-31264
General methods for calculating three dimensional laminar boundary layers over inclined blunt bodies
[AD-763831] 22 p2656 N73-31274
Holographic interferometric measurements of three dimensional temperature fields
22 p2680 N73-31463
Three-dimensional flow characteristics in three bladed rocket pump inducer
[NASA-CR-2290] 23 p2775 N73-32190
Inviscid, isentropic, three-dimensional flow theory for rotating thin blade row in cylindrical duct
23 p2775 N73-32193
Numerical solution of corner flow problem using alternating direction implicit method
[AD-765209] 23 p2776 N73-32203
Kutta-Joukowski condition for describing three dimensional flow over arbitrary wing
[RAE-LIB-TRANS-1709] 24 p2905 N73-33185
Three dimensional incompressible laminar flow in centrifugal toroidal shell
24 p2909 N73-33215

**THREE DIMENSIONAL MOTION**
NT SECONDARY FLOW
NT THREE DIMENSIONAL FLOW
Stereo three dimensional gain pattern formation from plane rectangular antenna characteristics
[AD-754782] 11 p1257 N73-20199
Real time three dimensional motion picture camera using holography
[NASA-TR-R-409] 22 p2673 N73-31413

**THRESHOLD CURRENTS**
Effect of laser pulse on threshold voltage of metal oxide semiconductor field effect transistors
[CRC-1246] 21 p2585 N73-30716

**THRESHOLD DETECTORS [DOSIMETERS]**
Pion electroproduction cross section measured near threshold by coincidence experiments
[NOTA-INTERNA-383-A] 01 p0084 N73-10696

**THRESHOLD GATES**
Threshold circuits with feedback channels for cardiac R-wave detection in electrocardiographic heart rate monitoring
[NASA-TN-D-7152] 06 p0635 N73-15158
Design analysis and integration of MOS threshold logic gates
[AD-758021] 15 p1759 N73-24260
Analysis of on-state in chalcogenaide threshold switches
[AD-756273] 15 p1821 N73-24763
Boron radiation hardening for stabilizing gate threshold potential of MOS devices
[NASA-CASE-GSC-11425-2] 23 p2764 N73-32114

**THRESHOLD LOGIC**
Ordering theories of variables for realization procedures of multithreshold logic circuits
05 p0522 N73-14242
Design analysis and integration of MOS threshold logic gates
[AD-758021] 15 p1759 N73-24260

**THRESHOLD SHIFT**
U THRESHOLDS

**THRESHOLDS**
Threshold commutation in amorphous semiconductors
[CEA-CONF-1972] 07 p0832 N73-16741
Detection scheme with threshold learning for amplitude shift keyed signals
[AD-752009] 08 p0886 N73-17171
Computer simulation to evaluate methods for determining threshold stimulus levels for impact sensitivity tests
[NASA-TM-X-64087] 15 p1801 N73-24598

**THRESHOLDS [PERCEPTION]**
Threshold of accelerometer and drag free probe detector
[ONERA-NT-199] 04 p0423 N73-13448
Blockage effect in external ear canal on diver auditory perception threshold
[AD-751664] 09 p0996 N73-18132
Audiometric thresholds for bare headed subjects, or wearing M1 helmet, and experimental helmet
[AD-745121] 13 p1486 N73-22053
Effect of carbon monoxide on time perception
[PB-214651/2] 16 p1858 N73-25123
Lesion threshold in guinea pig auditory sensation areas due to sonic booms
[ISL-33/72] 19 p2228 N73-27966
Middle ear muscle reflex thresholds to various aircraft noises
[AD-764739] 24 p2836 N73-33048

**THROATS**
Analytical method for estimating chamber and throat conditions in nozzle with low radius of curvature throat
[NASA-CR-128619] 02 p0156 N73-11263
Procedure for predicting performance characteristics of second throat diffusers in ejector systems
08 p0895 N73-17250

**THROMBOCYTES**
State of hemocoagulation and thrombocytes during hypokinesia after adaptation to high-mountain conditions
11 p1245 N73-20107

**THROTTLING**
Design of automatic throttle control for Navy carrier based A-7 E aircraft
[AD-761764] 19 p2329 N73-28740

**THROWING**
Hull cell investigation of throwing powers of various nickel plating baths
[NLL-RTS-7294] 01 p0067 N73-10548

**THRUST**
NT JET THRUST
NT LOW THRUST
NT MICROTHRUST
NT RETROTHRUST
NT ROCKET THRUST
NT VARIABLE THRUST
Variational problem for computation of maximum thrust nozzles
[AD-746618] 03 p0351 N73-12864
Computer program for analyzing flow field generated near aircraft engine operating in reverse thrust
[NASA-CR-121147] 09 p1012 N73-18264
Design, development, and test of two types of pivoted pad journal bearings and spiral groove thrust bearing for use with Brayton cycle power unit
[NASA-CR-121098] 12 p1408 N73-21410
Cold flow tests of factors affecting noise suppression and thrust loss of divergent lobe supersonic jet noise suppressor
[NASA-TM-X-2820] 18 p2101 N73-26992
Comparison of thrust and torque forces on ship propeller blades in oblique and axial flow
[DRIC-TRANS-3205] 21 p2525 N73-30249
Performance sensitivity analysis of solar electric propulsion thrust subsystem
[NASA-CR-133792] 21 p2590 N73-30748

**THRUST AUGMENTATION**
Performance of hypermixing nozzles in area ratio 23 ejector
[AD-752207] 08 p0955 N73-17821
Boundary layer control for mixing region in three dimensional laminar elliptical jet for thrust augmentation
[AD-754227] 10 p1143 N73-19313
Cylindrical impact technique for second-stage augmentation with explosively driven hypervelocity launcher
[NASA-CR-114589] 12 p1388 N73-21252
Performance and noise reducing properties of thrust augmentors
[NASA-TM-X-62250] 13 p1472 N73-21921
Fundemental aspects of regenerative cooled, upper stage rocket plane with external-burning thrust augmentation
[AD-756498] 13 p1583 N73-22832
Application of cold thrust augmentation techniques for improved performance of short takeoff aircraft performance
[AD-758202] 15 p1735 N73-24073
Adjustable airfoil for reversable cowl flap inlet thrust augmentation
[NASA-CASE-ARC-10754-1] 23 p2831 N73-32624

**THRUST BEARINGS**
Guide to early stage design choice of thrust bearing
[ESDU-67033] 01 p0060 N73-10489
Kantorovich variational method for solving isothermal problem of hydrodynamic theory of lubrication for thrust bearing with nondeformed pad
[AD-750485] 06 p0678 N73-15519
Influence of groove inclination angle on bearing capacity of gas dynamic thrust bearing
[AD-751068] 07 p0806 N73-16535

Interaction of velocity and temperature fields in lubricating layer of thrust slide bearings and analysis of viscosity variation along length and thickness of lubricating layer
[AD-753044] 09 p1041 N73-18487
Two dimensional motion of viscous incompressible flow with variable viscosity coefficient in thrust bearing
[AD-753030] 09 p1041 N73-18495
Design and construction of hydrostatic azimuth thrust bearing for tracking antenna of very large size
[NASA-CR-130930] 10 p1165 N73-19478
Hydrodynamic design of thrust slide bearings
[AD-753965] 10 p1168 N73-19501
Performance of gas lubricated nonconforming pivoted-pad journal bearings and flexibly mounted spiral groove thrust bearing designed for Brayton cycle rotating unit
[NASA-TM-X-2765] 15 p1738 N73-24086
Design procedure for hydrostatic ring thrust bearings
[NRC-13180PT-3] 17 p2037 N73-26478
Modification of spinning torque apparatus to measure spinning torque on cageless ball thrust bearing using oil jet lubrication or thin surface film only
[NASA-TN-D-7356] 17 p2038 N73-26484
Device for measuring friction moments in radial thrust ball bearings and gas-dynamic bearings of gyros
20 p2418 N73-29430

**THRUST CHAMBERS**
Helmholtz resonator damping device for suppressing rocket combustion instability
03 p0349 N73-12845
Electrically conducting ceramics to heat biowaste propellants to 2000 K in resistojet thrustors for space station application
[NASA-CR-112159] 06 p0635 N73-15161
Analytical and experimental evaluation of high pressure thrust chamber concepts for hydrogen oxygen auxiliary propulsion for space shuttle vehicle
[NASA-CR-120895] 09 p1079 N73-18800
Design and tests of low pressure thrust chamber concepts for hydrogen oxygen auxiliary propulsion for space shuttle vehicle
[NASA-CR-120896] 09 p1079 N73-18801
Coolant side, heat transfer rates for liquid hydrogen cooled, hydrogen-oxygen rocket thrust chamber
[NASA-TN-D-7207] 09 p1099 N73-18968
Kaufman thruster development of 5 cm and 30 cm sizes
[NASA-TM-X-68202] 11 p1334 N73-20828
Simplified procedures for correlation of experimentally measured and predicted thrust chamber performance
[NASA-CR-131519] 12 p1442 N73-21685
Electrothermal hydrazine thruster
[NASA-CR-132763] 16 p1956 N73-25827
Application of structural computer program for analysis of creep stress in thrust chamber liner - Vol.3
[D5-17266-3-VOL-3] 22 p2725 N73-31807
Thermal flux transfer system for maintaining thrust chamber of operative reaction motor at given temperatures
[NASA-CASE-NPO-12070-1] 23 p2828 N73-32606
Sputter erosion and deposition in discharge chamber of small mercury ion thruster
[NASA-TM-X-71424] 23 p2829 N73-32611
Magnitude, spectra, and cross correlations for plasma fluctuations in Kaufman thruster
[NASA-TM-X-71421] 23 p2830 N73-32616
Mercury thruster isolator lifetime tests
[NASA-TM-X-71422] 23 p2830 N73-32617
Pulsing liquid hydrogen/liquid oxygen attitude control propulsion system at cryogenic inlet conditions
[NASA-TM-X-71444] 23 p2830 N73-32621

**THRUST CONTROL**
NT THRUST VECTOR CONTROL
Space simulation study of plume contamination in reaction control thruster
[NASA-TM-X-68149] 01 p0090 N73-10743
Gas or liquid injection for secondary injection thrust control
[NAL-TR-286T] 04 p0463 N73-13774
Analytical combustion model for predicting flow and pressure transients in H2-O2 RCS of rocket engine feed system
07 p0835 N73-16767
Design, development, and operation of water electrolysis system to provide gaseous hydrogen and oxygen for satellite propulsion system
[AD-755384] 13 p1571 N73-22735
Apollo experience report on command and service module reaction control systems
[NASA-TN-D-7151] 16 p1966 N73-25901
Specification of thrust control system for Airbus A 300 B, tested in Boeing 707
24 p2877 N73-32981

**THRUST FAULTS**
U GEOLOGICAL FAULTS

**THRUST LOADS**
Endurance and performance tests of bore ball bearings lubrication thrust loaded 120-mm to 3 million DN
[NASA-TM-X-68264] 17 p2037 N73-26479
Experimental evaluation of 150-mm bore ball bearings to 3-million DN using solid and drilled balls
[NASA-TM-X-68265] 17 p2037 N73-26480
Performance tests of high speed ball bearings with lead and lead alloy plated retainers operating in liquid hydrogen at 30,000 rpm and 400 pound thrust load
[NASA-TM-X-68268] 18 p2155 N73-27412

**THRUST MEASUREMENT**
Presentation of helicopter level flight performance as power coefficient compared with tip speed or advance ratio for range of thrust coefficients
12 p1358 N73-21014
Development of standard uncertainty methology for analysis of gas turbine engine performance characteristics
[AD-755356] 13 p1571 N73-22733
Dynamometer thrust measurements of electrostatic mercury electron bombardment ion engine ESKA 18 P
[DLR-FB-73-48] 17 p2077 N73-26803
Test stand for precise measurement of impulse bit and thrust vector of reaction jet thrusters in attitude control system
[NASA-TN-D-7402] 22 p2719 N73-31762

**THRUST POWER**
U THRUST

**THRUST PROGRAMMING**
Performance potential evaluation of unmanned nuclear electric propulsion spacecraft for single-thrust-period missions to Uranus
[NASA-TN-D-7125] 06 p0718 N73-15859
Engineering model of 20 millipound thrust monopropellant hydrazine resistojet program
[NASA-CR-130762] 16 p1956 N73-25828

**THRUST REVERSAL**
Thrust reversal and thrust vectoring technology review to identify test data and prediction methods
[AD-749476] 05 p0591 N73-14800
Static and wind tunnel tests to determine performance of four cowl cascade thrust reverser configurations at forward velocity
[NASA-TM-X-2665] 07 p0835 N73-16773
Mathematical models for predicting flow fields within and external to thrust reverser deployed in flight including forces and moments induced on aircraft by flow fields
[AD-751525] 07 p0837 N73-16784
User manual and source listings for computer programs to solve problems in analysis of in-flight thrust reversers
[AD-751526] 07 p0837 N73-16785
Development of empirical method for determining optimum reversing coefficient of thrust reversal of jet engines on passenger aircraft
[AD-752814] 09 p0986 N73-18048
Aerodynamic tests and noise levels of slot nozzle with V gutter reverser for STOL
[NASA-TM-X-2758] 12 p1365 N73-21072
Development of computer programs to predict performance of thrust reversal and thrust vector control systems on short takeoff transport aircraft - Vol. 1
[AD-756860] 14 p1603 N73-22993
Design and development of thrust reverser and thrust vectoring systems for application to short takeoff transport aircraft - Vol. 2
[AD-756861] 14 p1603 N73-22994
Aircraft accident involving Boeing 747 aircraft during landing at Miami, Florida airport on 15 Dec. 1972 following collision with birds
[NTSB-AAR-73-13] 17 p1983 N73-26029

**THRUST VECTOR CONTROL**
Technology for developing hydrogen-oxygen thruster for space shuttle ACPS
[NASA-TM-X-68146] 01 p0090 N73-10744
Analysis of performance capability improvement for Pioneer F and G spacecraft using electric thrust subsystem
[NASA-CR-114514] 02 p0222 N73-11798
Design, development, and evaluation of fluidic emergency thrusters for aircraft stabilization
[NASA-CR-114490] 03 p0252 N73-12041
Application of secondary injection to obtain controllable roll moment solid rocket propelled launch vehicles
03 p0350 N73-12856
Fuel tanks, spinup techniques, and thruster-CG misalignment problems for synchronous orbiting satellites
[AD-746845] 03 p0360 N73-12931
Development of vortex fluid amplifier for throttling rocket exhaust
[NASA-CASE-LEW-10374-1] 04 p0463 N73-13773
Characteristics of blowdown-pressurized hydrazine propulsion system for trajectory correction of spacecraft during outer planet flyby missions
[NASA-CR-129796] 04 p0464 N73-13780
Computer program for optimal design of advanced thrust vector control of missile trajectory
[AD-749126] 05 p0590 N73-14797
Computer program manual for optimal design of advanced thrust vector control for missile trajectory
[AD-749127] 05 p0590 N73-14798
Thrust reversal and thrust vectoring technology review to identify test data and prediction methods
[AD-749476] 05 p0591 N73-14800
Control concept utilizing interaction of injected fluid with airstream surrounding missile
[AD-750306] 06 p0722 N73-15894
System for eliminating roll rate anomalies occurring during flights of slender ballistic reentry vehicles
[SC-DC-72-2244-A] 07 p0849 N73-16813
Application of control theory to determine time history of thrust profile to achieve optimal maneuvers of aerospace lifting vehicles
[AD-751281] 07 p0850 N73-16891
Design, development, and evaluation of solar electric thrust vector control system for ion engine array
[NASA-CR-130622] 08 p0953 N73-17806
Design, fabrication, and testing of thrust vectorable ion optical systems with emphasis on response time and minimal power consumption
[NASA-CR-121142] 08 p0955 N73-17816
Development of computer model to simulate pulse mode performance operation of liquid bipropellant attitude control engines
[AD-752610] 08 p0955 N73-17819
Mathematical model to simulate staging dynamics of proposed space shuttle configuration
[NASA-TM-X-58098] 08 p0965 N73-17886
Development of solenoid valve failure detection system based on addition of radioactive gas to propellant of cold gas jet attitude control system
[NASA-CR-130931] 10 p1165 N73-19476
Algorithm for space vehicle re-orientation through angular velocity control by jet momentum
12 p1425 N73-21555
Evaluation of scale model of low pressure rocket engine used for secondary injection studies and modifications required for full scale simulation
[NASA-CR-124176] 12 p1443 N73-21690
Development of computer programs to predict performance of thrust reversal and thrust vector control systems on short takeoff transport aircraft - Vol. 1
[AD-756860] 14 p1603 N73-22993
Design and development of thrust reverser and thrust vectoring systems for application to short takeoff transport aircraft - Vol. 2
[AD-756861] 14 p1603 N73-22994
Effect of jet stream blowing downwards from lower surface of slender delta wing to obtain lift augmentation for takeoff and landing
[ARC-R/M-3288] 15 p1727 N73-24009
Flight tests to determine longitudinal aerodynamic parameters of P-1127 aircraft with vectored thrust control
[NASA-TN-D-7296] 15 p1734 N73-24066
Analysis of deflection forces and deflection angles generated by thrust vector control nozzle at various Mach numbers and exit pressures
[AD-758521] 15 p1827 N73-24808
Wind tunnel tests to determine aerodynamic characteristics of vectored thrust V/STOL fighter aircraft in transition speed range
[NASA-TN-D-7191] 16 p1858 N73-25047
Statistical error model for solar electric propulsion thrust subsystem
[NASA-CR-133232] 17 p2077 N73-26799
Thrust magnitude control for strategic and tactical missiles
[AD-762915] 20 p2476 N73-29888
Performance tests of hydrazine catalytic thruster to determine capability for spacecraft limit-cycle attitude control with short thruster pulse durations
[NASA-CR-135489] 22 p2710 N73-31701
Design and development of logic scheme for control of Omni-Axis Secondary Thrust Vector Control system for use on space shuttle pressure fed engine
[NASA-CR-124428] 23 p2848 N73-32761

**THRUSTORS**
U ROCKET ENGINES

**THULIUM**
Temperature dependence and measurement of crystalline electric fields at ytterbium impurities in thulium metal
[AD-764633] 23 p2827 N73-32596

**THUNDERCHIEF AIRCRAFT**
U F-105 AIRCRAFT

**THUNDERSTORMS**
Number and distribution of lightning flashes in Finland during summer 1971
[REPT-41] 04 p0413 N73-13371
Thunderstorm probability and supersonic transport safety on flight paths over southern United States during July
[AD-748798] 04 p0445 N73-13628
Ionospheric oscillations caused by infrasonic waves propagating from thunderstorms
05 p0510 N73-14148
Differential magnetometer method for measuring thunderstorm charging currents near cumulus clouds
[AD-750087] 05 p0542 N73-14411
Computerized simulation of squall line structure and maintenance, based on convectively unstable air mass, vertical shear of horizontal wind, and lifting mechanism
[REPT-72-5] 05 p0572 N73-14651
Investigation of thunderstorm potential in cold air cumulonimbi over northwestern Europe during winter
[AD-749493] 05 p0574 N73-14674

Computerized simulation of thunderstorm rainfall characteristics
[PB-211806] 05 p0575 N73-14679
Management and use meteorological satellite data to detect severe storms and crop disease
[NASA-CR-130000] 06 p0693 N73-15642
Utilization of meteorological satellite data to forecast severe thunderstorms and tornadoes
06 p0693 N73-15644
Influence of solar flares on thunderstorms and meteorological phenomena over Mediterranean Sea
07 p0859 N73-16965
Time dependent two dimensional numerical model for studying structure of squall line thunderstorm
10 p1180 N73-19597
Effect of perturbation on frequency and intensity of thunderstorms in Italy
10 p1181 N73-19608
Probability of aircraft being struck by lightning
[NLL-M-22800-[5828.4F]] 11 p1313 N73-20656
Estimating distance to thunderstorms using computerized simulation of ground wave atmospherics
13 p1551 N73-22566
Duration of thunderstorms over USSR
13 p1552 N73-22580
Ozone and point discharge measurements under thunderclouds in New Mexico
[AD-758130] 14 p1665 N73-23515
Radar/radiometer system for measuring temporal and spatial precipitation characteristics particularly thunderstorm activity
[NASA-CR-130235] 14 p1667 N73-23532
Methods of forecasting hail, thunderstorms, and amounts of rainfall
[NLL-M-22902-[5828.4F]] 15 p1805 N73-24626
Ionospheric disturbances produced by severe thunderstorms
[NOAA-PP-6] 16 p1905 N73-25406
Estimation techniques in modified binomial distribution that describes thunderstorms over Cape Kennedy, Florida
[NASA-CR-2280] 16 p1937 N73-25678
Thunderstorm cloud height and fading statistics for ATS 5 ultrahigh frequency signal transmission to earth
17 p1996 N73-26141
Doppler radar investigation of flow patterns in severe thunderstorms
[AD-760106] 17 p2058 N73-26649
Analysis of wind profiles in thunderstorm gusts and method for predicting velocity of winds at altitude
[NASA-CR-2289] 18 p2172 N73-27544
Numerical simulation of thunderstorm cell in two and three dimensions
20 p2441 N73-29605
Atmospheric models for studying typhoon and thundercloud processes
20 p2446 N73-29645
Forecasting air mass thunderstorms for MacDill AFB, Florida
[AD-763099] 20 p2451 N73-29696
Analysis of radar data for time variability of cumulonimbus clouds in shower and thunderstorm stages
21 p2569 N73-30587
Application of radar direction finding observations to determine extent and severity of storm centers
21 p2569 N73-30590
RAE-1 measurements of thunderstorms and ground-based radio noise
[NASA-CR-132810] 23 p2757 N73-32062
Role of electrical processes in thunderstorms of Canadian prairies
24 p2912 N73-33242

**THYRATRONS**
Methods of generating supernarrow pulses
[NLL-DRIC-TRANS-2934-[3623.66]]
16 p1910 N73-25455

**THYRISTORS**
NT SILICON CONTROLLED RECTIFIERS
Minority carrier lifetime optimization for gallium silicon diffusion thyristor
11 p1330 N73-20795
High power transcalent silicon semiconductor thyristor device including metallization techniques and heat pipe construction
[AD-755553] 13 p1502 N73-22174
Development and characteristics of gate-assisted, turn-off thyristor for high voltage and current operation
[NASA-CR-121161] 16 p1880 N73-25221
Minority carrier lifetime control in n-type base regions of gallium diffused silicon power thyristors and diodes
[BMFT-FB-T-73-05] 23 p2765 N73-32123

**THYROID GLAND**
Response of pituitary-thyroid axis to microwave radiation
[VR-3490-149] 06 p0630 N73-15122

**TID**
U TRAVELING IONOSPHERIC DISTURBANCES

**TIDAL OSCILLATION**
U TIDES

**TIDAL WAVE DAMAGE**
U FLOOD DAMAGE

**TIDAL WAVES**
ERTS-1 imagery of coastal marshland, tidal flats, and littoral transport in French Atlantic waters
[E72-10251] 03 p0289 N73-12351
Numerical analysis on hypothetical satellite altimeter detection of tides and tsunamis
06 p0664 N73-15396
Rotational tidal waves due to earth rotation explained by Poincare problem solving
07 p0857 N73-16951

**TIDES**
NT ATMOSPHERIC TIDES
NT EARTH TIDES
NT LUNAR TIDES
Sediment pattern correlations with inflow and tidal action in Chesapeake Bay based on ERTS-1 imagery
[E72-10169] 01 p0044 N73-10350
One and two dimensional models of tidal propagation in St. Lawrence River
[NRC-12764] 01 p0048 N73-10382
Research report on tidal hydraulics
[AD-744784] 01 p0051 N73-10412
Analysis of thermal fluctuations in San Diego Bay, California and factors which affect thermodynamic properties
[AD-744921] 01 p0052 N73-10420
Analysis of pole tide fluctuations in earth atmosphere and ocean
[NLL-M-20647-[5828.4F]] 06 p0657 N73-15336
Computations of seasonal variations in internal waves and tidal phenomena in northern Atlantic Ocean
[AD-750842] 06 p0670 N73-15452
Analysis of photography from Apollo 9 flight to determine origin, movement, and dissipation of masses of discolored water near shores of North and South Carolina
07 p0788 N73-16408
New harmonic constant computed for Adriatic Sea harbors
07 p0858 N73-16961
Analysis of tidal currents, turbulent diffusion, and local shears in currents found in Trinity Bay, Texas
[NASA-CR-128734] 08 p0916 N73-17510
Computer control and data acquisition of tidal model of St. Lawrence River
[MH-110] 11 p1259 N73-20221
ERTS-1 imagery of California nearshore sediment transport, coastal processes, and tidal currents
[E73-10525] 13 p1517 N73-22292
Earth satellite orbit perturbation due to fluid tidal effects and temporal geopotential variations
[GRGS-BULL-7] 14 p1706 N73-23847
Sediment pattern correlation with inflow and tidal action in Chesapeake Bay
[E73-10623] 16 p1896 N73-25336
Movement of suspended particle and solute concentrations with inflow and tidal action in Chesapeake Bay
[E73-10662] 16 p1899 N73-25358
Daily tidal current tables for stations along Atlantic coast of North America - 1973
16 p1904 N73-25403
Correlation of sediment patterns with inflow and tidal action using MSS and I2S imagery
[E73-10794] 18 p2137 N73-27270
Polar motion and earth tides applicable to satellite studies of earth elasticity
[NASA-CR-133414] 18 p2145 N73-27339
Semi-analytical solution of oceanic tidal perturbations in motion of artificial satellites
[NASA-TM-X-66298] 18 p2200 N73-27763
Computer code for calculating time series of earth tidal gravity and tilt
[AD-762275] 19 p2297 N73-28468
Complex system of tidal forces on sun, created by all planets of solar system
[NLL-M-23039-[5828.4F]] 21 p2591 N73-30760
Map of vertical crustal movements of Eastern Europe and ebb and tide studies
21 p2609 N73-30912
Sediment pattern correlation with inflow and tidal action
[E73-10984] 22 p2658 N73-31291

**TIG WELDING**
U GAS TUNGSTEN ARC WELDING

**TILT**
U ATTITUDE [INCLINATION]

**TILT ROTOR RESEARCH AIRCRAFT PROGRAM**
Full scale hover test of 25-foot tilt rotor
[NASA-CR-114626] 16 p1861 N73-25070

**TILT WING AIRCRAFT**
NT CL-84 AIRCRAFT
NT XC-142 AIRCRAFT
Application of parameter estimation algorithm to obtain longitudinal aerodynamic derivatives from flight data for XC-142A aircraft in cruise conditions
[NASA-TN-D-7114] 04 p0372 N73-13025

**TILTED PROPELLERS**
Design and aerodynamic characteristics of tilt propeller aircraft for short takeoff and landing operations - Vol. 1
[NASA-CR-114441] 13 p1473 N73-21926

**TILTING**
U ATTITUDE [INCLINATION]

**TILTING ROTORS**
Wind tunnel tests to determine effects of blade twist and aeroelasticity of rotary wings on tilt rotor performance from hover to Mach 0.7 speed
[NASA-TM-X-68948] 10 p1105 N73-19012
Analysis of whirl stability boundaries and aerodynamic characteristics of tilting rotors
12 p1356 N73-21004
Review of tilting rotor technology and comparison of tilting rotor performance with standard rotary wings
12 p1359 N73-21027
Wind tunnel tests to determine effects of blade twist and aeroelasticity on tilt rotor performance from hover to mach number 0.7
12 p1362 N73-21049
Aerodynamic, dynamic, and aeroelastic problems in rotary wing design for helicopters and V/STOL aircraft with application to hingeless rotor systems
12 p1362 N73-21051
Conceptual designs and aerodynamic configurations of tilting rotor V/STOL aircraft for 1975 to 1980 time period - Vol. 1
[NASA-CR-114437] 14 p1599 N73-22964
Preliminary design of V/STOL tilting rotor aircraft for performance of research flights - Vol. 2
[NASA-CR-114438] 14 p1599 N73-22965
Static and cruise tests on series of 13 ft diameter low disc loading rotors with various blade twists
[NASA-CR-114625] 15 p1734 N73-24063
Development of perturbation guidance system for maintaining tilting rotor vertical takeoff aircraft on predetermined flight path during takeoff and landing
[NASA-CR-132043] 15 p1735 N73-24072
Aeroelastic and dynamic studies of technology applicable to tilting rotor vertical takeoff aircraft with emphasis on propeller whirl instability - Vol. 1
[NASA-TM-X-69497] 20 p2359 N73-28976
Natural mode vibration analysis of aircraft structural systems by direct and component mode synthesis techniques applied to tilt rotor VTOL aircraft aeroelasticity - Vol. 2
[NASA-TM-X-69496] 20 p2359 N73-28977
Design, development, and flight test of stowed folding tilt rotor aircraft and comparison with nonfolding tilt rotor aircraft - Vol. 5
[NASA-CR-114598] 21 p2493 N73-30009
Application of composite materials in development of tilting rotor for vertical takeoff aircraft - Vol. 6
[NASA-CR-114599] 21 p2493 N73-30010
Development of feedback control in tilt rotor aircraft using swashplate cyclic and collective controls in addition to direct lift control - Vol. 7
[NASA-CR-114600] 21 p2493 N73-30011
Real time piloted simulation to investigate handling qualities and performance of tilting rotor aircraft - Vol. 9
[NASA-CR-114602] 21 p2493 N73-30012
Mathematical model for real-time flight simulation of tilt rotor research aircraft for application to aircraft design, pilot training and proof-of-concept-Vol. 5
[NASA-CR-114614] 22 p2614 N73-30949
Wind tunnel and rotor whirl cage tests to determine stability and control parameters of scale model of tilting rotor aircraft model - Vol. 6
[NASA-CR-114615] 22 p2614 N73-30950
Far field noise reduction of tilting rotor aircraft based on performance and weight tradeoffs to improve acoustic signatures
[NASA-CR-114648] 23 p2740 N73-31937
Mathematical model for real time simulation of tilt rotor aircraft to evaluate aircraft performance and handling qualities
[NASA-CR-114601] 23 p2742 N73-31947

**TIMBER IDENTIFICATION**
Analysis of ERTS data for detection and monitoring of forest insect infestations in Sierra Nevada Mountains of California
[E73-10868] 20 p2392 N73-29219
Detection of plant diseases, soil moisture, drainage patterns, forestry types, and sedimentation in Tennessee from ERTS-1 imagery
[E73-11091] 23 p2782 N73-32258
Development of multistage forest sampling inventory system using ERTS-1 data for Trinity Alps in California
[E73-11092] 23 p2782 N73-32259
Survey and inventory of forest resources in Susquehanna River Basin to determine accuracy achieved in mapping vegetation classes using ERTS-1 imagery
[E73-11110] 24 p2915 N73-33267

**TIMBER INVENTORY**
Development of multistage forest sampling inventory system using ERTS-1 imagery
[E72-10186] 01 p0046 N73-10365
Design of forest inventory for in-place data provision for planning and programing timber management
[PB-210276] 01 p0121 N73-10999
Timber resource management and information system
[E72-10245] 03 p0289 N73-12345
Forests and range resources inventory and mapping using remote sensors
07 p0785 N73-16388

Applicability of ERTS-1 imagery to forestry and timber survey and identification in Finland
[E73-10297] 09 p1021 N73-18329
Information system for ERTS-1 data on timber resources in Washington and Oregon
[E73-10319] 09 p1023 N73-18351
Timber inventory and management in Washington using ERTS-1 imagery
[E73-10411] 11 p1278 N73-20373
Application of ERTS-1 remote sensing data in study of vegetation and soils in Idaho
[E73-10708] 16 p1904 N73-25399
Forest sampling and timber inventory in California from ERTS-1 imagery
[E73-10743] 17 p2021 N73-26348
Land management planning and timber resources management in Washington and Oregon from ERTS-1 imagery
[E73-10804] 18 p2138 N73-27279
Detection and inventory of timber and rangelands and forest stresses in Georgia, Colorado, and Black Hills from ERTS-1 imagery
[E73-10805] 18 p2138 N73-27280
Analysis of ERTS-1 data and underflight photography for detection of insect infestation and timber resources in Sierra Nevada Mountains of California
[PAPER-A16] 19 p2261 N73-28224
Timber inventory and land use in Province of Huelva-Spain based on ERTS-1 imagery
[PAPER-L9] 19 p2274 N73-28305
ERTS-1 imagery of landscape changes, strip mines, timber, agriculture, and water resources in eastern Tennessee
[E73-10843] 19 p2291 N73-28421
Usefulness of Skylab EREP multispectral band scanner and camera imagery for multistage timber inventories and surveys
[E73-10861] 20 p2392 N73-29212
Timber identification and inventory and forest management in Colorado, Georgia, Black Hills, California, and Hawaii from ERTS-1 imagery
[E73-11051] 23 p2779 N73-32227
Forest and rangeland inventory and detection of forest stress at Black Hills, South Dakota, Manitou, Colorado, and Atlanta, Georgia test sites
[E73-11052] 23 p2779 N73-32228
Application of ERTS-1 imagery to timber inventory in Finland
[E73-11068] 23 p2781 N73-32244
Multistage survey of forests in Trinity Alps of California from Skylab EREP data
[E73-11093] 23 p2783 N73-32260

**TIMBER VIGOR**
Analysis of ERTS-1 data to detect and map areas of tree mortality due to insect outbreaks using color infrared positive transparencies
[E73-10351] 11 p1275 N73-20345
Remote sensing techniques for evaluating vigor loss in black spruce due to eastern dwarf mistletoe
[NASA-CR-131582] 13 p1523 N73-22341
Analysis of ERTS-1 data and underflight photography for detection of insect infestation and timber resources in Sierra Nevada Mountains of California
[PAPER-A16] 19 p2261 N73-28224
Analysis of ERTS data for detection and monitoring of forest insect infestations in Sierra Nevada Mountains of California
[E73-10868] 20 p2392 N73-29219

**TIME**
NT ACCESS TIME
NT EPHEMERIS TIME
NT FLIGHT TIME
NT MTBF
NT REACTION TIME
NT RELAXATION TIME
NT TRANSIT TIME
NT UNIVERSAL TIME
Influence of time zones on physiological organs and systems and performance of athlete
[NASA-TT-F-14632] 04 p0383 N73-13116
Theorems for optimization of Riccati equation in singular discrete time filtering and control problems
[NASA-CR-130360] 06 p0690 N73-15621

**TIME CONSTANT**
Determining time constant of resistance thermometer by double heating
[NASA-TT-F-14494] 02 p0173 N73-11398
Minimizing area required for resistor-capacitor time constants in integrated circuits
[NASA-TN-D-7110] 03 p0344 N73-12808

**TIME DEPENDENCE**
Time controlled creep-fatigue interaction for type 403 stainless steels at high temperature
[ORNL-4757] 03 p0315 N73-12565
Time evolution of quantum lattice system Hamiltonian discussing automorphism of suitable algebra
[NOTA-INTERNA-393] 03 p0340 N73-12774
Time dependent edge-notch sensitivity of oxide and gamma dispersion strengthened nickel alloy sheets
[NASA-CR-121123] 06 p0725 N73-15919
Airborne multispectral scanning of maize canopy to determine temporal characteristics, and relation of leaf area index to spectral response curves
[NASA-CR-130369] 07 p0789 N73-16421
Latitude-time variations of ionospheric electron densities at high latitudes during periods of solar activity
07 p0791 N73-16431
Time periods for nutrient solution exchange in optimal biomass yield on porous aggregate
10 p1117 N73-19106
Transport properties and time correlation functions of Lennard-Jones liquid near its triple point
[LPTHE-72/22] 10 p1141 N73-19296
Rate and time dependent yield behavior of ductile polycarbonates
[AD-753941] 10 p1177 N73-19571
Technique for obtaining Auger spectra of electron desorbable surface species on time independent basis
[NASA-TN-D-7257] 11 p1252 N73-20161
Electronic time compressor/expander for audio using digital technology
14 p1621 N73-23129
Theodolitic errors in processing time dependent geodetic data
[AD-760109] 17 p2029 N73-26421
Numerical time dependent model for simulating lifecycle of cumuli under different environmental conditions
18 p2170 N73-27525
Influence of N-type sound wave pressure rise time on guinea pig cochlear and acoustically evoked potentials
[ISL-31/72] 19 p2224 N73-27940

**TIME DISCRIMINATION**
Time discrimination in temporal information sampling at output of planar germanium detector in gamma ray spectrometry
[NAA-SR-MEMO-6728] 07 p0824 N73-16680
Time discrimination in temporal information sampling at output of planar germanium detector in gamma ray spectrometry
[CEA-R-4355] 09 p1069 N73-18719

**TIME DIVISION MULTIPLEXING**
Noise immunity of optical communication lines with frequency and time multiplexing subcarriers
[JPRS-57178] 02 p0181 N73-11467
TDMA/PSK test equipment noting modulators, demodulators, converters, and transmission system
[ESRO-CR(P)-144] 17 p1998 N73-26157
Asynchronous and synchronous time division multiplex systems of 8.448 and 8.192 Mbit/s
[FTZ-442-TBR-40] 22 p2634 N73-31106

**TIME LAG**
Atmospheric and man made disturbances, resulting in noise pulses of random amplitude affecting delay lines in HF communication
[AD-745184] 01 p0029 N73-10223
Ignition site and ignition delay time for spherical fuel droplets
[NLL-RTS-7169] 02 p0241 N73-11959
Time lag method for transient permeation of benzene and acetone vapors through sulfur natural rubber
[NASA-TM-X-64721] 07 p0752 N73-16112
Estimation of time delays generated by random field propagating across array of noise sensors in optimal processing of multiple sensor data
[AD-751555] 07 p0756 N73-16146
Increase in heat exchange rate between thermometric sensing element and cryogenic fluid
[NASA-TM-X-68251] 16 p1913 N73-25477
Use of temporal dimension in classifying and mapping central Pennsylvania area from ERTS-1 MSS data
[PAPER-L23] 19 p2276 N73-28318
Parameter plane methods for linear systems with time delay
[AD-761761] 19 p2314 N73-28611
Ignition model for predicting ignition delay times of boron particle clouds in oxidizing atmosphere
20 p2484 N73-29955
Azur satellite orbit perturbation recorded from Weilheim-Lichtenau ground station
[BMBW-FBW-72-18] 21 p2597 N73-30816
Human psychomotor performance circadian rhythm variations after transmeridian flight noting time shift effect
[DLR-FB-73-52] 22 p2624 N73-31022
Special purpose slide rule to compute free space propagation delay between synchronous satellite and points on earth surface
[NBS-TN-638] 22 p2638 N73-31139
Mariner 9 range and Doppler data analyses for relativistic time delay effects
23 p2842 N73-32711
Time delay in ranging signal to Mariner 9 orbiter for testing general relativity
23 p2842 N73-32712
Time lag test of general relativity and Earth-Mars ephemeris improvement using Mariner 9 tracking data
23 p2842 N73-32713

**TIME LAPSE PHOTOGRAPHY**
U CHRONOPHOTOGRAPHY

**TIME MEASUREMENT**
Potassium argon age, and chemical composition of glasses from Bosumtwi crater in Ghana
[NASA-TT-F-14496] 01 p0049 N73-10398
Research in field of time measurements
[CEA-CONF-1980] 03 p0302 N73-12467
Psychophysical functions of range and time estimates by ground and aerial observers
[AD-747271] 04 p0380 N73-13094
Microwave acoustic signal processing with time-variant distributed networks using surface amplifiers
07 p0820 N73-16649
Greenwich time report for the Royal Greenwich Observatory Time and Latitude Service during period of January to March 1972
08 p0960 N73-17856
Least squares and cross correlation procedure for determining absolute timing of pulsars
13 p1575 N73-22765
Principles for regulation of timing in speech
14 p1624 N73-23155
Proceedings of conference on precise time and time interval planning for application to hypersonic navigation systems
[AD-758739] 16 p1942 N73-25717
Tables of Greenwich time and latitude observations
19 p2293 N73-28437
Tables on time and latitude observations made by Greenwich Time and Latitude service
22 p2664 N73-31345
Application of surface barrier detectors for time measurement of nuclear energy events and comparison of two methods used for timing procedures
22 p2671 N73-31393
Simplification of television synchronization signal by reducing duration
[BBC-RD-1973/20] 24 p2894 N73-33100
Time allocation in Azur satellite telemetry data, noting onboard clock and world time deviations on tapes
24 p2985 N73-33855

**TIME MEASURING INSTRUMENTS**
NT ATOMIC CLOCKS
NT CHRONOMETERS
NT CLOCKS
NT TIMING DEVICES

**TIME OF FLIGHT SPECTROMETERS**
Time of flight measurement of N2 plus meinel lifetimes
[AD-746157] 02 p0214 N73-11735
Time of flight measurements of vacuum sublimation of ammonium perchlorate
[AD-753219] 09 p1000 N73-18162

**TIME OPTIMAL CONTROL**
Maximum principle for determining necessary conditions for optimality when delay depends on state, control, and time
[AD-753675] 10 p1179 N73-19592
Time optimal control in stochastic dynamic systems
20 p2436 N73-29565
Optimal control of parabolic systems with boundary conditions involving time delays and with application to plasma confinement
21 p2584 N73-30704

**TIME RESPONSE**
Design of nonlinear feedback system with significant plant ignorance for prescribed time domain tolerances
[NASA-CR-127489] 10 p1136 N73-19260
Time responses of radiation of iodine laser with Q-factor modulation
[AD-758625] 15 p1796 N73-24560
Effect of carbon monoxide on time perception
[PB-214651/2] 16 p1868 N73-25123

**TIME SERIES ANALYSIS**
Windowing or tapering of surface wave time series and spectrum analysis
[AD-742845] 01 p0050 N73-10407
Time series and probability density function analyses of hypothesis that organized motion exists in air flow above naturally occurring water waves
[AD-749045] 04 p0408 N73-13328
Set of functionals and consistent estimators for spectral analysis of continuous nonstationary random processes
[AD-748341] 04 p0441 N73-13596
Statistical estimation and decision techniques applied to time series and multivariate analyses for communication, tracking, and physiological monitoring
[AD-749542] 05 p0569 N73-14620
FORTRAN 4 subroutines for time series analysis
[FOA-3-C-3672-64[11]] 06 p0643 N73-15221
Electromagnetic lunar conductivity measurements on dark side radial magnetic fields
[NASA-TM-X-62226] 07 p0844 N73-16834
Practical statistical prediction techniques applied to time series analysis and statistical meteorology
[AD-753714] 09 p1058 N73-18629
Averaging time and maxima for dependent observations
[AD-754788] 11 p1315 N73-20674
Analysis of times series processes for correlation of air pollution data measurements
[AD-754433] 12 p1424 N73-21538
Device for performing statistical time-series analysis of complex electrical signal waveforms
[NASA-CASE-MSC-12428-1] 16 p1883 N73-25240
Time series analysis of summer monsoon data from Southeast Asia for 1967 and 1968
[AD-759788] 16 p1939 N73-25691

In situ spectroradiometric quantification of ERTS-1 data and multispectral photo analysis of Willcox Playa
[E73-10737] 17 p2020 N73-26343
Algorithm for computerized spectral analysis on linearly swept signals
[AD-760775] 18 p2120 N73-27138
Time series on optical pulsar candidates
20 p2469 N73-29831

**TIME SHARING**
Resource sharing computer communication networks and some aspects of distributed computation
[AD-749378] 05 p0518 N73-14210
Analysis of time-sharing voice modulated output of several collocated transmitters and receivers using very high frequencies
[AD-758567] 18 p2120 N73-27140
Forward algorithm for scheduling process monitor in time sharing computer sample data control
[AD-761668] 19 p2240 N73-28058
Computer code which reorganizes old FORTRAN programs so that statement numbers are added sequentially and extraneous statements are deleted
[NASA-TM-X-62286] 22 p2636 N73-31128
Assembly language programs required to interface ALOHA system to IBM telecommunication time sharing operation
[NASA-CR-133853] 22 p2639 N73-31155
FORTRAN program, ZIP, for time sharing in SNAP reactor parametric studies
[AI-AEC-13076-VOL-1] 24 p2954 N73-33603

**TIME SIGNALS**
Greenwich time and latitude observations for Oct. to Dec. 1971
01 p0105 N73-10874
Progress report from Bureau International de l Heure for period 1967 to 1971, including earth rotation, atomic time scale, and coordination of time signals
05 p0596 N73-14848
System for generating timing and control signals during repetitive fixed length serial data transmission
[NASA-CASE-NPO-13125-1] 09 p1008 N73-18225
Greenwich time and latitude observations for Jan. to Mar. 1972
13 p1578 N73-22791
Frequency and time broadcasts provided by National Bureau of Standards radio stations
[NBS-SP-236] 16 p1873 N73-25164
Very low frequency timing techniques for Omega navigation system to include operational considerations, path selection, and adjustment procedure
[NASA-CR-133185] 17 p2061 N73-26669
Flight test and evaluation of system for providing precise time signals to aircraft in flight using distance measuring [VORTAC] ground station and cesium beam atomic clock
[FAA-NA-73-23] 21 p2577 N73-30652
Digital methods of television signal timing corrections
[BBC-RD-1973/15] 22 p2627 N73-31048
Time signal transfer by satellite relay systems
[AD-764716] 23 p2759 N73-32078

**TIMERS**
U TIMING DEVICES

**TIMING**
U TIME MEASUREMENT

**TIMING DEVICES**
Temperature controlled piezoelectric crystal oscillator with digital integrated circuitry for timing of pulses
[AECL-4160] 04 p0396 N73-13217
Development of procedure for predicting time interval of single clock and matrix equation for optimum weighting coefficients
[NBS-TN-626] 08 p0923 N73-17565
Economic analysis of integrated time-frequency system for aircraft
14 p1690 N73-23717
Application of surface barrier detectors for time measurement of nuclear energy events and comparison of two methods used for timing procedures
22 p2671 N73-31393

**TIN**
Stability constants and distribution of tin IV complexes by anion exchange resin with carboxylic acids
[AREAEE-128] 07 p0824 N73-16679
Tin alloying effects on plastic deformation, mechanical, and stress-rupture properties of Ni-Cr alloys
[JPRS-58159] 09 p1048 N73-18546
High temperature creep of Al alloys tin, and lead at intermediate and low stresses
[LBL-1183] 21 p2559 N73-30512
K shell Compton scattering on tin and gold at 145 keV and gold at 320 keV
24 p2960 N73-33654

**TIN ALLOYS**
Electric arc welding of tin and aluminum bronzes and silicon brass
[DRIC-TRANS-2843] 02 p0179 N73-11448
Physical properties of intermetallic magnesium tin compound
[AD-745942] 02 p0219 N73-11773
Electrotransport effect on solidification of some Sn-Bi and Sn-Pb alloys
[IS-T-532] 03 p0315 N73-12567
Mechanical properties, machinability, and corrosion characteristics of 80-10-10 high leaded tin bronze alloy
[PB-211945] 05 p0563 N73-14576
Cavitation-corrosion resistance tests of tin and aluminum bronzes used for marine pumps in synthetic sea water and distilled water
[DRIC-TRANS-3016] 10 p1167 N73-19492
Phase structure of crystallizing nickel tin alloy melt during cooling
[JPRS-58681] 12 p1414 N73-21456
Acoustic emission signals by fcc phase transition to fct in In-Ti alloys
[SC-DC-72-1650] 12 p1414 N73-21462
Influence of hydrostatic pressure on ductility and fracture mechanics of bismuth and tin-bismuth alloys
[AD-764241] 22 p2686 N73-31514

**TIN COMPOUNDS**
NT NIOBIUM STANNIDES
NT ORGANIC TIN COMPOUNDS
NT TIN OXIDES
NT TIN TELLURIDES
Friction, wear, and thermal stability of some organotin and organosilicon compounds
[NASA-TN-D-7175] 09 p1051 N73-18569
Environmental tests of strength and durability of transparent tin oxide and indium oxide films on glass
[AD-756558] 14 p1680 N73-23637
Thin film lead and tin selenide photoconductive infrared detectors
[AD-758685] 16 p1915 N73-25499
Radiolytic preparation of anhydrous tin [2] chloride
[NASA-TM-X-2927] 24 p2891 N73-33082

**TIN OXIDES**
Optical properties of films based on tin dioxide and cobalt oxides
[AD-755250] 12 p1417 N73-21479
Physical nature of electron emission from tin oxide cathode sources
16 p1947 N73-25750

**TIN TELLURIDES**
Absorption coefficient and index of refraction data for Pb[1-x]S n[x] Te thin films
[AD-751650] 07 p0832 N73-16747

**TIP DRIVEN ROTORS**
Development of rotary wings with cold, hot, and mixed cycle tip jet propulsion systems and application for torque-free rotor drive system
12 p1359 N73-21026

**TIP SPEED**
Effects of mass injection of tip vortex on airfoil performance at transonic speeds
[AD-760363] 17 p2016 N73-26304
Measurement of noise and wake structure of ducted fan with subsonic tip speed to show sound pressure levels and blade wake characteristics
[NASA-CR-132259] 18 p2129 N73-27207
Acoustic tests of supersonic tip speed fan with acoustic treatment and rotor casing slots and its performance in reducing engine noise
[NASA-CR-134501] 23 p2828 N73-32608

**TIP VORTICES**
U TIP SPEED
U VORTICES

**TIPS**
NT BLADE TIPS
NT WING TIPS

**TIRES**
NT AIRCRAFT TIRES
Effects of pavement surface condition on cornering forces developed by automobile tires of different tread design
[NASA-TN-D-6964] 02 p0192 N73-11551
Application of ultrasonic nondestructive tests to vehicle tire compliance measurements
[PB-211892] 05 p0553 N73-14491
Equations of motion for elastic tire rolling on ground and forces exerted by tire assuming absence of slippage between tire and ground
[AD-752697] 09 p1040 N73-18482
Analysis of shimmy in pneumatic tires due to lateral flexibility for stationary and nonstationary conditions
[WTHD-48] 16 p1917 N73-25515
Heat generation associated with pneumatic tire operating under various conditions
[NASA-CR-121239] 18 p2205 N73-27799
Radiation hazards involved in conducting radiographic inspections of tires and protective measures for industrial personnel
24 p2952 N73-33584

**TIROS M**
ITOS system and design of TIROS M spacecraft
[NASA-CR-130163] 07 p0849 N73-16880
Secondary subsystems of ITOS 1
[NASA-CR-130164] 07 p0849 N73-16881
Test programs for TIROS M
[NASA-CR-130165] 07 p0849 N73-16882

**TIROS OPERATIONAL SATELLITE SYSTEM**
Configuration and functions of ITOS D and E system of meteorological satellites to expand basic capability of TIROS M/ITOS system
[NASA-CR-130160] 09 p1086 N73-18863

**TIROS SATELLITES**
NT IMPROVED TIROS OPERATIONAL SATELLITES
NT ITOS 1
NT ITOS 2
NT ITOS 3
NT ITOS 4
NT TIROS M
Analysis of electron and proton fluxes encountered during nominal Tiros-N trajectories
[NASA-TM-X-66107] 03 p0357 N73-12908
Application of TIROS satellite data to mapping of ice fields through development of composite minimum brightness chart
07 p0788 N73-16409
Development of method for determining sea surface temperature using remote sensors in earth orbiting satellites
07 p0788 N73-16410
Development of attitude control system jitter specification for Tiros-N satellite three axis orientation capability
[NASA-TM-X-66201] 10 p1216 N73-19886

**TISSUES [BIOLOGY]**
Photosynthetic energy conversion in membranes, tissues, and reaction centers of bacteria and viruses
[COO-3162-9] 04 p0380 N73-13091
Gas chromatographic analysis of beryllium in aqueous solutions and biological tissues
[AD-753112] 09 p0996 N73-18131
Freezing effects on structure of soils and biological tissues
[CNRS/LA-PUBL-440] 09 p0999 N73-18150
Tissue culture laboratory for first manned Skylab mission for performing experiments to detect effects of zero gravity on living human cells
09 p1088 N73-18874
Hyperoxic morphological changes in connective rat tissues
10 p1115 N73-19092
Aminothiol radioprotector, finam, effect on irradiated animal tissues under various conditions
11 p1242 N73-20085
Combined tissue blocks for comparative pathomorphological study of radiation pathology
11 p1243 N73-20090
Effect of hypokinesis of varying duration on fluid-electrolyte metabolism and composition in blood and tissues of animals
11 p1244 N73-20098
Microdosimetric pattern of galactic heavy primaries dissipation in tissues during space flight
[NASA-CR-131467] 12 p1372 N73-21132
Effects of hydrostatic water bath pressure on capillary blood pressure and connective tissue dehydration
[NASA-TT-F-14894] 14 p1610 N73-23052
Development of germ-free plants and tissues
[NASA-CR-128947] 15 p1742 N73-24122
Modified high pressure system with small sample vessels for conducting biological reactions
[AD-752978] 16 p1885 N73-25256
Vacuum/tissue interface effect on biological energy absorption from charged particle track
20 p2366 N73-29028

**TITAN LAUNCH VEHICLES**
NT TITAN 3 LAUNCH VEHICLE
History and future of Titan/Centaur launch vehicle
[NASA-TM-X-68249] 15 p1835 N73-24877

**TITAN 3 LAUNCH VEHICLE**
High altitude plume impingement of Titan 3
[NASA-CR-124093] 10 p1222 N73-19940
Titan 3c guidance with carousel vehicle borne inertial guidance system
[AD-764729] 23 p2852 N73-32788

**TITANATES**
NT BARIUM TITANATES
NT LEAD TITANATES
NT PEROVSKITES
NT STRONTIUM TITANATES
NT ZIRCONIUM TITANATES
Selection and preliminary evaluation of 2 hollandites, 1 titanate, and 1 tungstate as potential solid conductors of alkali ions
[NASA-TN-D-7157] 06 p0708 N73-15774
Intrinsic and extrinsic nonstoichiometry in lead zirconate titanate system
[LBL-880] 10 p1126 N73-19172
Pyroelectric coefficient of lead zirconate titanate
[AD-755520] 13 p1567 N73-22700
Standard enthalpies of formation for all undisputed compound members in Na-Ti-O system
[BM-RI-7778] 21 p2562 N73-30534

**TITANIUM**
Effect of titanium additions on aging characteristics of Al-Zn-Mg alloy
[AD-746195] 01 p0068 N73-10561
Mechanical properties of boron carbide reinforced titanium laminates
[AD-745002] 01 p0070 N73-10570
Proceedings of conference on microstructure of titanium, uranium, and zirconium body centered cubic lattices
[AD-748035] 03 p0319 N73-12598
Compactibility, shrinkage, and microhardness of electrolytic titanium powders obtained at low temperatures from melts
04 p0432 N73-13521
Electron paramagnetic resonance spectra of trivalent titanium ions in used silica
[NLL-RTS-7523] 05 p0564 N73-14583

X ray device for measuring titanium tritide film thickness in presence of background radiation
[NASA-TM-X-68170] 06 p0673 N73-15475
Stress corrosion cracking of titanium and titanium alloys in organic liquids and vapors
[AD-751528] 07 p0810 N73-16572
Economic factors affecting titanium powder metallurgy research and development
09 p1047 N73-18539
Powder metallurgy methods to increase cost effectiveness of titanium raw materials processing
[JPRS-58217] 09 p1048 N73-18542
Hardness and physical characteristics of titanium sponge with low residual chloride concentration after vacuum separation
[JPRS-58347] 09 p1048 N73-18544
Bibliography on titanium toxicity in human and animal organisms
[ORNL-TIP/TIRC-72-65] 10 p1120 N73-19135
X ray attenuation coefficients in absorption spectra of titanium, iron, cobalt, nickel, copper, and zinc
[UCRL-73923] 10 p1189 N73-19675
Feasibility of using yttrium oxide crucible to induction melt titanium
[AD-754092] 11 p1306 N73-20597
Calorimeter for measuring high temperature specific heat of Ti and Ti based alloys during intermetallic phase
[AD-754954] 11 p1306 N73-20599
Modified lamination process for developing boron carbide ribbon reinforced titanium matrix composites
[AD-754478] 11 p1309 N73-20618
Role of titanium in fabricating magnesium-graphite fiber composites with improved strength and stiffness
[AD-754570] 11 p1310 N73-20627
Technical and economic problems and possibilities of developing titanium powder metallurgy
[NLL-LTI-746-1336-[9022.401]]
12 p1411 N73-21438
Measurements of Mossbauer absorption spectra to investigate diffusion mechanism of iron in beta-titanium
12 p1413 N73-21449
Short range structure of Ti and Zr body centered cubic lattice solid solutions containing omega phase
[AD-755454] 13 p1567 N73-22698
Short range structure of Ti and Zr body centered cubic lattice solid solutions containing omega phase
[AD-755463] 13 p1567 N73-22699
Potential of hot-isostatic pressing, hydrostatic extrusion and deformable die tube tapering processes to production of titanium tubes
[AD-759504] 16 p1919 N73-25532
Influence of titanium ions on magnetic properties of manganese-zinc ferrites
[NLL-TRANS-862-[9022.64]]
16 p1931 N73-25626
Evaluation of sandwich structures of titanium and aluminum honeycomb in edgewise compression under static and fatigue loading
[FPL-196] 16 p1969 N73-25927
Strip rolling mill for high speed rolling of iron and titanium powders
[AD-759241] 17 p2047 N73-26556
Analysis of chemical and electrochemical processes occurring on titanium sheet metal surfaces during oxidation at room temperature by electron-diffraction method
[NLL-RTS-7888] 20 p2428 N73-29503
Compatibility of silicon carbide fibers with tungsten substrate and titanium matrix
20 p2430 N73-29520
Formation of solid solutions and fluidity of alloys based on aluminum and titanium
[AD-763491] 21 p2560 N73-30522
Effect of aluminum on fundamental mechanical properties of titanium
[AD-763785] 21 p2560 N73-30524
Analytical investigation of hexagonal metal deformation with particular application to Ti and Be
[AD-763835] 22 p2686 N73-31518
Electrolytic and other methods for applying protective titanium coatings
[AD-764318] 22 p2690 N73-31544

**TITANIUM ALLOYS**
NT NITINOL ALLOYS
Explosive forming and manufacturing of titanium alloy plates
[AD-745113] 01 p0062 N73-10512
Titanium alloy composites reinforced with silicon carbide fibers
[AD-745342] 01 p0070 N73-10573
Aluminizing of titanium and aluminum alloys in powder form with use of electric heating methods
[NLL-M-21479-[5828.4F]] 02 p0185 N73-11503
Procedure for measuring effect of hydrogen content on toughness and sustained load cracking resistance of titanium alloys including results obtained for Ti-6Al-4V
[AD-746443] 02 p0187 N73-11517
Fourier pattern recognition techniques applied to titanium alloy photomicrographs
[AD-746720] 02 p0188 N73-11528
Use of composite laminates with weak interfaces to increase fracture toughness of Ti-6Al-4V
[AD-746765] 02 p0189 N73-11531
Development of rational fracture resistance test procedures to determine fracture properties of titanium alloy sections
[AD-747230] 02 p0189 N73-11533
Creep tests of beta titanium alloy IVT-1 over range of temperatures and stresses
[AD-747090] 02 p0189 N73-11536
Linear regression analysis used on mechanical property data obtained from experiment which maximized variability in heat treating parameters of titanium alloy
[AD-747207] 02 p0190 N73-11540
Chemical spot tests for identification of titanium and titanium alloys used in aerospace vehicles
[NASA-CASE-LAR-10539-1] 03 p0312 N73-12547
Basic mechanisms providing oxidation resistance in structural, titanium base alloys operating above 900 C
[AD-747002] 03 p0316 N73-12575
Diffusion interaction of components during calorization of niobium alloys with 5 to 50 wt. percent titanium
[AD-747429] 03 p0318 N73-12588
Effects of high-speed heating after cold plastic deformation on phase composition of titanium alloy VT 15
[AD-747516] 03 p0318 N73-12591
Fracture and fatigue crack propagation characteristics of annealed titanium alloy plate
[AD-748644] 03 p0319 N73-12600
Effect of thermomechanical treatment on stress corrosion cracking susceptibility of Beta 3 titanium
[AD-748359] 03 p0319 N73-12602
Multifilamentary niobium-titanium superconductors for winding pulsed magnets
[BNL-16764] 03 p0345 N73-12817
Ac measurements of cold worked superconducting niobium-titanium alloy
[CONF-720513-4] 03 p0346 N73-12819
Fabrication and properties of structural materials based on ceramic titanium powders alloyed with molybdenum and aluminum
04 p0432 N73-13520
Silicon graphite and heat resistant titanium alloys
[JPRS-57679] 04 p0433 N73-13526
Soviet industry uses of heat resistant titanium alloys
04 p0433 N73-13528
Stress corrosion cracking in saline water of TA6V and TU2 titanium alloys
[ONERA-P-145] 04 p0435 N73-13545
Effect of thickness on sustained load crack propagation in Ti-6Al-4V alloy tested in 3-1/2 percent NaCl solution
[AD-748591] 04 p0435 N73-13548
Anisotropic nature of toughness due to texture in titanium and titanium alloy plate
[AD-748390] 04 p0435 N73-13549
Critical cold work for grain coarsening of equiaxed alpha Ti-5Al-2.5Sn alloy heated at 1144 K for one hr after plastic tensile deformation
[AD-748352] 04 p0435 N73-13550
Corrosion kinetics of Ti-Pd alloy in HCl at room temperature determined by radioactive tracer method
[NLL-TRANS-746-1328-[9022.401]]
05 p0505 N73-14112
Effect of ruthenium on passivating capacity and corrosion resistance of titanium
[NLL-TRANS-746-1375-[9022.401]]
05 p0560 N73-14550
Plastic properties and microstructure of alpha-titanium alloys at high temperature
[AD-750964] 05 p0564 N73-14581
Environmental fatigue crack propagation in titanium sheet alloys in atmospheres of argon, normal air, distilled water, and salt solution
[NLR-TR-72019-U] 05 p0602 N73-14894
Effects of interstitial solute content on deformation kinetics in hot extrusion of titanium aluminum vanadium alloy
[AD-750556] 06 p0677 N73-15511
Beta-phase effect on ductility of two-phase titanium alloys and calorimetric determination of atomic ordering effects in Ni2Cr alloy
[JPRS-57578] 06 p0683 N73-15556
Microstructural features of deformation analyzed in two-phase titanium alloys to determine beta phase effect on ductility
06 p0683 N73-15557
Optimum temperature rate conditions of VTZ-1 deformation in superplastic state
06 p0683 N73-15563
Fatigue tests of notched and unnotched Ti6Al4V bars compared to other Ti-alloys
[LBF-TM-62/71] 06 p0685 N73-15574
Fatigue strength of notched titanium aluminum vanadium alloy between 1 million and 10 million stress cycles
[LBF-TM-63/71] 06 p0685 N73-15575
Correlation of mechanical properties to microstructure of titanium alloys
[AD-749932] 06 p0685 N73-15581
Microstructural analysis of 1010 modified steel and titanium alloy grains
[AD-748101] 06 p0686 N73-15584
Kinetic and structural investigation of ST-4 titanium alloy oxidizability at 700 to 1000 C, unprotected and protected by silicon and molybdenum silicide coatings
[AD-750646] 06 p0686 N73-15585
Relationship of tensile properties and fracture toughness levels to microstructure of Ti6Al2Sn4Zr6Mo
[AD-751530] 07 p0810 N73-16566
Stress corrosion cracking of titanium alloys and steels - Part I
[AD-751544] 07 p0810 N73-16569
Stress corrosion cracking of titanium and titanium alloys in organic liquids and vapors
[AD-751528] 07 p0810 N73-16572
Procedures for estimating stresses in titanium and high strength steel panels and comparison of estimated and measured stresses
[ESDU-72005-AMEND-A] 07 p0850 N73-16894
Explosive actuated, normally open, titanium valve
[NASA-CR-130545] 08 p0927 N73-17590
Effect of oxygen concentration on deformation of Ti-V alloys and on critical resolved shear stress of Ti-40V
[AD-752082] 08 p0933 N73-17642
Analysis of relation between fracture toughness and yield strength in high strength titanium alloys
[AD-752575] 08 p0933 N73-17643
Evaluation of potential coatings for titanium alloy gears to be used in propeller gearbox systems
[AD-753417] 09 p1041 N73-18492
Effect of constant applied stress in crack initiation of aluminum and titanium alloys exposed to salt solution and organic fluids
[NASA-CR-124110] 09 p1045 N73-18525
Analysis of beta titanium alloys to show heat treatment, mechanical properties, corrosion, weldability, and processing
[AD-753439] 09 p1049 N73-18552
Compilation of fracture mechanics data on high strength aluminum alloys, alloy steels, stainless steels, and titanium alloys
[AD-753774] 09 p1049 N73-18554
Effect of sheet thickness on plane stress fracture resistance of high strength titanium alloys
[AD-753198] 09 p1049 N73-18555
Corrosion behavior of titanium alloys in chloride solutions
[AD-753573] 09 p1050 N73-18561
Temperature measurement of heavy nonferrous metals and alloys, steels, titanium, and other metals in plastic zone
[NLL-RTS-6867] 10 p1163 N73-19456
Butt welding of titanium alloy rings and flanges to improve mechanical properties
10 p1163 N73-19463
Electron probe microanalysis of ductile metal bond to Ti alloy disc
[AECL-4251] 10 p1172 N73-19535
Phase stabilization and solid solution strengthening in titanium alloys
[AD-754240] 10 p1174 N73-19551
Effect of strain hardening on fatigue crack resistance after single cycle peak overload in Ti-6Al-4V Ti alloy
[AD-753899] 10 p1174 N73-19553
Reliability and failure time prediction for titanium adhesive bonds using multiple regression analysis
[AD-754526] 11 p1301 N73-20560
Properties of zinc-copper-titanium alloys to include microstructure composition, mechanical properties, and effects of hot and cold deformation
[NLL-M-22842-[5828.4F]] 11 p1304 N73-20583
Fracture toughness study of heat treated titanium alloys
[AD-753919] 11 p1306 N73-20598
Calorimeter for measuring high temperature specific heat of Ti and Ti based alloys during intermetallic phase
[AD-754954] 11 p1306 N73-20599
Effect of load variables on fatigue crack growth at room temperture in Ti-6Al-4V alloy
[NASA-CR-2239] 11 p1345 N73-20913
Superconducting properties of niobium titanium multifilamentary magnet material
[BNL-17193] 12 p1388 N73-21255
Composition effects on stress corrosion cracking of titanium alloys in aqueous environments
[NASA-CR-131872] 13 p1540 N73-22475
Analysis of elastic properties of Invar and Elinvar alloys at various temperatures
13 p1540 N73-22480
Analysis of precipitation process in cobalt-tungsten-titanium alloys using electron microscope and X ray imaging techniques
13 p1541 N73-22483
Fracture toughness and aqueous stress corrosion resistance of high strength commercial Ti alloy
[NLR-TR-72107-U] 13 p1542 N73-22492
Mechanical strength of multilayer thin metal films
[AD-756582] 13 p1543 N73-22508
Influence of surface conditions on Ti-6Al-4V alloy fatigue life
[AD-755385] 13 p1544 N73-22516

Analysis of fatigue performance of titanium alloys and steels to identify variations based on shape parameter for reliability engineering of airframes
[AD-758219] 14 p1605 N73-23008
Protection of titanium microstructure with intermediate nickel barrier to prevent abrasion and crack propagation on turbine compressor blades
[AD-758276] 14 p1682 N73-23651
Development of compatible titanium alloy for boron reinforced composites
[AD-758294] 14 p1682 N73-23652
Improving screwability of titanium bolts with nuts of various materials
[AD-758037] 15 p1794 N73-24541
Statistical test of difference in fatigue life results in conventional and shot peening in aluminum-titanium alloy
[AD-758624] 15 p1794 N73-24542
Effect of molybdenum addition on physicomechanical properties of titanium-carbon-nickel composite alloys
[NLL-LTI-746-1422-[9022.401]] 15 p1797 N73-24565
Mass spectrometric measurement of hydrogen in milligram-size quantities of titanium
[NASA-TN-D-7326] 15 p1798 N73-24574
Phase transformations in titanium alloy TiAl6V4
[DLR-FB-73-38] 15 p1799 N73-24584
Analysis of effect of rigidity of stressed state in corrosion cracking under biaxial stress conditions for steel and titanium alloys
[NLL-LTI-746-1413-[9022.401]] 15 p1837 N73-24886
High temperature strength and deformation properties of Ti-Al-Si alloy aged by alpha phase precipitate particles
[NASA-TN-D-7325] 16 p1928 N73-25597
Development of high temperature titanium alloys with improved tensile strength
[AD-759215] 16 p1930 N73-25614
Effect of thermomechanical treatment on stress corrosion cracking susceptibility of Beta 3 titanium alloy
[AD-759166] 16 p1930 N73-25618
Dynamic tear tests for determining fracture mechanics of high strength structural steels and aluminum and titanium alloys
[AD-759351] 16 p1930 N73-25620
Effect of heat treatment on corrosion of titanium alloy
[AD-759626] 16 p1931 N73-25621
Corrosion resistant properties of titanium alloys
[AD-759621] 16 p1931 N73-25622
Metallographic and X ray analysis of metastable alloys of titanium
[AD-759387] 16 p1931 N73-25623
Evaluation of nitinol fittings for joining titanium piping for shipboard application
[AD-760322] 17 p2038 N73-26492
Compression tests of pure Ti and Ti alloy deformation properties
[RAE-LIB-TRANS-1657] 17 p2043 N73-26529
Internal oxidation of dilute Cu-Ti alloys at 700 to 900 C
[AD-759382] 17 p2047 N73-26557
Dispersed granulation of metals and titanium alloys
[AD-759625] 17 p2047 N73-26559
Effect of aging heat treatments on mechanical properties of Ti-8Al-1Mo-1V alloy
[AD-760461] 17 p2048 N73-26567
Evaluation of nondestructive testing techniques for diffusion-bonded titanium alloy aircraft structures using ultrasonic radiation
[AD-760673] 18 p2106 N73-27035
Stress corrosion cracking of titanium alloys by hydrofluoric acid released during Viton B thermal degradation
[D-MAT-191] 18 p2161 N73-27455
Stress corrosion behavior of titanium and aluminum alloys with and without surface layer
[AD-760529] 18 p2163 N73-27469
Development of manufacturing method for elimination of nitride inclusions from titanium alloys during melting and ingot consolidation
[AD-748261] 18 p2163 N73-27473
Design, fabrication, and test of boron-polyimide reinforced titanium fan disks to operate at high temperatures 18 p2167 N73-27498
Manufacturing of large structural mirror supports for space telescopes using titanium alloys 18 p2209 N73-27828
Development of workable high strength metastable beta titanium sheet alloy
[AD-761515] 19 p2310 N73-28577
Computer analysis of binary and ternary titanium and niobium alloys
[AD-761814] 19 p2311 N73-28585
Physical properties of aluminum alloys, titanium alloys, and stainless steels for aerospace airframes
[AD-762305] 19 p2311 N73-28587
Fatigue failure of notched samples of titanium alloy
[AD-761588] 19 p2350 N73-28904
Evaluation and characterization of superplastic properties of aluminum, zinc, and titanium alloys in various microstructural conditions 20 p2429 N73-29509
Stress corrosion cracking in aluminum and titanium alloys
[NASA-CR-124352] 20 p2431 N73-29531
Thermoplastic strengthening of martensite steels and titanium alloys
[AD-760953] 21 p2560 N73-30520
Deformation and aging characteristics of titanium alloys
[AD-763429] 21 p2561 N73-30526
Adjustable deflection, multispecimen, bent beam test fixture for conditioning sheet specimens used in hot salt stress corrosion tests of titanium alloys
[AD-763704] 21 p2561 N73-30529
Thermal and electrical properties of titanium alloyed with vanadium and high temperature creep of metal with fcc lattice
[JPRS-59623] 22 p2683 N73-31490
Thermal conductivity and electrical properties of titanium alloyed with vanadium at 100 to 350 K 22 p2683 N73-31491
Tensile and fatigue data for irradiated and unirradiated AISI 310 stainless steel and titanium-5 percent aluminum-2.5 percent tin applied to universal slopes
[NASA-TM-X-2883] 22 p2683 N73-31494
Uranium-titanium alloys - annotated bibliography
[RFP-2005] 22 p2684 N73-31500
Heat treatment of titanium alloy forgings to obtain high yield strength
[BDX-613-872] 22 p2685 N73-31503
Anodic oxidation of titanium and its alloys
[LS-254] 22 p2685 N73-31505
Fail-safe and safe-life design of aircraft components made from Ti-alloys
[NLR-TR-72034-U] 22 p2685 N73-31510
Environmental fatigue crack propagation in Ti-Al-Sn
[NLR-TR-72093-U] 22 p2686 N73-31511
Yield and fracture model for Ti-6Al-4V titanium and 7075-T6 aluminum alloys 23 p2804 N73-32423
Fatigue - crack growth of Ti-6 Al-2 Cb-1 Ta-0.8 Mo alloy in air and sea water environment
[AD-765318] 23 p2805 N73-32433
Tear and fatigue crack propogation tests for determining mechanical properties of ultrafine grain alpha titanium
[AD-765329] 23 p2805 N73-32434
Characteristics of alpha-beta-transformation of titanium and zirconium alloys based on localization of valency electrons in atoms of elements 23 p2808 N73-32456
Effect of rare earth metals on macrostructure, microstructure, strength, and ductility of cast titanium samples 23 p2809 N73-32458
Interaction of advancing crack with pre-existing diffusion bonded microcracks in Ti-AlV alloy composites
[AD-765166] 23 p2811 N73-32476
Crack closure phenomenon in fatigue using Ti-6Al-4V titanium alloy
[NASA-CR-2319] 23 p2853 N73-32800
Creep fracture properties of weld repaired cast titanium alloy
[AD-765185] 24 p2937 N73-33451
High temperature creep resistance of Ti alloys
[AD-765784] 24 p2937 N73-33454
Phase transformation and superconductivity in titanium and zirconium alloys
[RLO-2225-T-13-14] 24 p2969 N73-33726

**TITANIUM CARBIDES**
Development of hard TiC-Ni alloys for use as cutting tools
[NLL-TRANS-746-1226-[9022.401]] 02 p0185 N73-11496
Temperature relationship of monochromatic coefficients of radiation of titanium, niobium, and zirconium monocarbides in regions of homogeneity 23 p2807 N73-32442
Sintering kinetics of zirconium and titanium carbides by hot extrusion in regions of homogeneity 23 p2808 N73-32448

**TITANIUM CHLORIDES**
Titanium chlorides and alloys and binary Al-Zn alloys
[JPRS-57787] 06 p0683 N73-15559
Adiabatic compression method for initial stage mechanism study of thermal decomposition of TiCl4 06 p0683 N73-15560
Magnesium thermal reduction method for interaction mechanism of titanium chloride with magnesium 06 p0683 N73-15561
Determination of impurities in titanium tetrachloride by infrared spectroscopy, emission spectra, and chemical analysis
[NLL-RTS-7725] 09 p1045 N73-18524
Molecular orbital energies in spectra of tervalent titanium chlorocomplexes 13 p1542 N73-22493

**TITANIUM COMPOUNDS**
NT BARIUM TITANATES
NT LEAD TITANATES
NT PEROVSKITES
NT RUTILE
NT STRONTIUM TITANATES
NT TITANATES
NT TITANIUM CARBIDES
NT TITANIUM CHLORIDES
NT TITANIUM NITRIDES
NT TITANIUM OXIDES
NT ZIRCONIUM TITANATES
Production and characteristics of sintered titanium diboride-molybdenum compacts 23 p2808 N73-32453

**TITANIUM DIOXIDE**
U TITANIUM OXIDES

**TITANIUM NITRIDES**
Thermostability of titanium hydridonitrides 20 p2430 N73-29522
Interaction of titanium nitrides with oxygen and carbon dioxide
[NASA-TT-F-15108] 22 p2625 N73-31035

**TITANIUM OXIDES**
NT RUTILE
Optimum conditions for depositing aluminum and silicon hydroxides on titanium dioxide particles
[NLL-RTS-7638] 04 p0425 N73-13460
Properties of thin dielectric TiO2 films produced by chemical vapor deposition
[NASA-CR-130763] 08 p0950 N73-17780
Nickel ion absorption on alumina and titania electrolyte interfaces
[AD-754540] 11 p1253 N73-20167
Relation of electrical properties of thin films of TiO to defect structure 20 p2460 N73-29766
Titanium dioxide doped, silicon rubber, potting compound for satellite-borne channel multipliers noting doping effects, performance tests, and space applications 24 p2927 N73-33378
Titanium dioxide doped silicone rubber potting compound for satellite-borne channel multipliers 24 p2927 N73-33379

**TITRATION**
Perfluorostyrene syntheses, magnetic tapes, titration cell, mill work positioner, superconducting microbridges, position display device, and numbering machine
[NBS-TN-744] 02 p0245 N73-11991

**TNT (TRINITROTOLUENE)**
U TRINITROTOLUENE

**TOBACCO**
Effects of Apollo 12 lunar materials on lipid levels, including fatty acids and sterols, of tobacco tissue and slash pine cultures
[NASA-CR-128606] 01 p0008 N73-10063
Effect of cigarette smoking on sensory perception and performance parameters of flight crews
[AD-754421] 14 p1612 N73-23071

**TOKAMAK FUSION REACTORS**
Research on Tokamak reactors and microinstabilities in inhomogeneous plasma
[COO-1478-13] 15 p1817 N73-24729
Equilibrium of weakly toroidal plasma column surrounded by Tokamak field
[REPT-72-71] 17 p2069 N73-26744
Maintenance of Tokamak equilibrium by external currents and equilibrium in high pressure Tokamak plasma
[IPPJ-161] 20 p2458 N73-29754
Superconducting materials evaluation for magnet in optimal design of Tokamak reactor
[CONF-721111-21] 20 p2462 N73-29784
Heating of plasma confined in Tokamak by injecting fast helium atoms
[EUR-CEA-FC-682] 24 p2964 N73-33690

**TOLERANCES (MECHANICS)**
NT IMPACT TOLERANCES
Influence of position and dimension on field errors of synchrotron bending magnet with winding cross section
[NP-19323] 03 p0345 N73-12813
Design and fabrication of balloon to carry 3500 pound payload at 60,000 feet altitude for feasibility test of powering free balloon near minimum wind field
[AD-750542] 05 p0498 N73-14052

**TOLERANCES (PHYSIOLOGY)**
NT ACCELERATION TOLERANCE
NT ALTITUDE TOLERANCE
NT COLD TOLERANCE
NT HEAT TOLERANCE
NT HUMAN TOLERANCES
NT RADIATION TOLERANCE
Tolerance of hypokinetic rats to carbon monoxide exposure 14 p1609 N73-23043

**TOLUENE**
Rapid determination of diphenylamine and dinitrotoluene in single base propellants by ultraviolet spectrophotometry analysis
[TM-51] 21 p2587 N73-30730

**TONE**
U PITCH

**TONOMETRY**
U INTRAOCULAR PRESSURE
U PRESSURE MEASUREMENTS

TONUS
U MUSCULAR TONUS
TOOLING
Hot pressing of chromium carbide alloy matrice tools for cold drawing of pipes
04 p0432 N73-13522
Design and technical characteristics of rotary automatic devices for pressing and gauging of metal ceramic structural parts
04 p0432 N73-13524
Component design and draw tooling of Pt heat source liner bodies
[MLM-1972] 24 p2955 N73-33608
TOOLS
NT GRINDING MACHINES
NT MACHINE TOOLS
NT MILLING MACHINES
NT SAWS
NT WRENCHES
Hard alloy shaping tools for extruding steels and nonferrous materials
[NLL-NEL-TT-2400-[6075.461]]
02 p0177 N73-11435
Bibliography on effects of underwater environment on tools, equipment, and human performance
[AD-748000] 04 p0384 N73-13122
Human factors guide for design of diver-operated hand and power tools
[AD-753262] 09 p1041 N73-18489
Tooling workpiece interface condition effects on metal flow and product quality in extrusion
[AD-755832] 13 p1535 N73-22439
TOPOGRAPHY
NT LUNAR TOPOGRAPHY
NT TERRAIN
Monitoring rural landscape changes in eastern Tennessee through interpretation of ERTS-1 imagery
[E72-10177] 01 p0045 N73-10356
Small perturbation theory applied to effects of irregular topography on deflection of wind blowing over industrial area and then residential area and effects on air pollution
[NASA-TM-X-2653] 01 p0074 N73-10610
Side-looking radar applications to studies of terrain topography and landforms
03 p0295 N73-12405
Geographic applications of ERTS-1 imagery to land use and landscape changes in Tennessee
[E72-10315] 04 p0412 N73-13364
Digitizing of topographic maps for electronic data processing
[MITT-130] 04 p0414 N73-13379
Bottom topography effects on ocean currents
[AD-748008] 04 p0417 N73-13408
Influence of local topography on wind flow over 2000 m rowing course at Holme Pierrepont, Nottingham
[NPL-MAR-SCI-R-100] 05 p0572 N73-14649
Conference on dynamic wave effects on satellite-borne sea surface measurements
[NASA-CR-129993] 06 p0664 N73-15392
Geographic applications of ERTS-1 imagery to rural landscape changes in eastern Tennessee
[E73-10040] 07 p0776 N73-16303
Planimetric, topographic, and thematic mapping using remotely sensed imagery
07 p0786 N73-16391
Influence of bottom topography and earth rotation of wind-driven circulation in Mediterranean Sea
07 p0858 N73-16956
Research and development in topographic mapping
[NASA-CR-130540] 08 p0918 N73-17527
Effect of bottom topography, eddy diffusivity, and wind variation on circulation in two-layer stratified lake
[NASA-TN-D-7235] 11 p1286 N73-20433
Detection of surface specific points by local parallel processing of discrete terrain elevation data
[AD-753701] 11 p1289 N73-20459
Automatic processing of ERTS-1 data for physiography and geologic mapping of San Juan Basin, Colorado
[NASA-CR-131577] 13 p1524 N73-22346
Research on geodesy, topography, cartography, photography, astronomy, and chemistry
[AD-758290] 15 p1788 N73-24500
Application of ERTS-1 imagery to fracture related mine safety hazards in coal mining industry and identification of mine subsidence areas in Indiana
[E73-10681] 16 p1901 N73-25376
Analysis of Skylab and EREP coverage of Wyoming and characteristics of field photometer system for measuring object reflectances
[E73-10697] 16 p1903 N73-25389
Analysis of ERTS-1 imagery to determine structural and lithological characteristics of northern coast ranges and Sacramento Valley, California
[E73-10698] 16 p1903 N73-25390
Remote barometric altimetry and estimation of meteorological field variables
[AD-759910] 17 p2058 N73-26650
Evaluation of ERTS-1 imagery for geological surveys and topographical analysis of various terrains in New York State
[PAPER-G1] 19 p2263 N73-28233
Combined visual and digital techniques for analyzing ERTS-1 data pertaining to geologic information on selected areas in Pennsylvania
[PAPER-G2] 19 p2263 N73-28234
ERTS-1 imagery of Utah and Nevada to show structural geology, mineral exploration, limnology, and hydrology
[PAPER-G3] 19 p2263 N73-28235
Construction of mosaic map of Morocco, North Africa using ERTS-1 data and comparison with data obtained from Gemini 5 flight
[PAPER-G5] 19 p2263 N73-28236
Analysis of ERTS-1 MSS imagery to determine geological and structural features in sedimentary basin in France
[PAPER-G6] 19 p2263 N73-28237
Application of ERTS-1 imagery for monitoring accelerated soil erosion in southern Arizona
[PAPER-G7] 19 p2264 N73-28238
Application of ERTS-1 imagery for differentiating quaternary surface deposits and landforms in Illinois, Iowa, Missouri, Kansas, Nebraska, and South Dakota
[PAPER-G13] 19 p2264 N73-28244
Analysis of geologic features and ground patterns in selected areas of Missouri based on ERTS-1 data
[PAPER-G15] 19 p2265 N73-28246
Analysis of spectral ratioing technique for southern end of of Wind River Range, Wyoming based on ERTS-1 analog ratio images
[PAPER-G16] 19 p2265 N73-28247
Analysis of regional structures in Verde Valley region of central Arizona based on ERTS-1 data
[PAPER-G19] 19 p2265 N73-28250
Application of ERTS-1 imagery and ground mapping in southern basin-range province of California, Nevada, and Arizona to show tectonic control of tertiary minerlization
[PAPER-G21] 19 p2266 N73-28252
Analysis of ERTS-1 multispectral data by automatic pattern recognition procedures for geological mapping of San Juan Basin, Colorado
[PAPER-G25] 19 p2267 N73-28256
Analysis of tectonic situation in Alps and Apennine mountains using ERTS-1 imagery of previously inaccessible areas
[PAPER-G27] 19 p2267 N73-28258
Analysis of lineaments and fault traces in Atlantic Coastal Plain of southern Maryland using ERTS-1 imagery
[PAPER-G29] 19 p2267 N73-28260
Identification of fifty mile wide tectonic zone across Southern California using ERTS-1 imagery
[PAPER-G33] 19 p2268 N73-28264
Analysis of ERTS-1 imagery and high altitude infrared photography to determine geological fractures in Indiana and Illinois
[PAPER-E1] 19 p2268 N73-28265
Application of ERTS-1 imagery for mineral resources, geologic structure, and landform surveys
19 p2288 N73-28398
ERTS-1 multispectral imagery of topography of Assateague Island
[E73-10848] 19 p2292 N73-28426
Development of semi-automatic system for digitizing bathymetry charts for showing ocean bottom contour information
[AD-761647] 19 p2296 N73-28464
Analysis of terrain properties and topography from Skylab altimetry
[E73-11081] 23 p2782 N73-32256
Scientific Mars research by Mariner 9 space probe
[NASA-CR-135530] 23 p2838 N73-32680
Wind erosion and dune formations in Mars surface topography
[CONTRIB-2353] 23 p2839 N73-32691
Topographic depressions in Mars south polar terrain
[CONTRIB-2266] 23 p2840 N73-32696
Utilization of ERTS-1 imagery of topography and drainage patterns for resources inventory and management in Arizona
[E73-11159] 24 p2919 N73-33312
Dependence of clear air turbulence on evolution of baric field and effect on synoptic forecasting
24 p2946 N73-33526
TOPOLOGY
NT FIXED POINTS [MATHEMATICS]
NT IMBEDDINGS [MATHEMATICS]
NT METRIC SPACE
Semilinear, topological, spaces and applications to social and economic equilibrium analysis and optimization
[NASA-CR-129591] 04 p0441 N73-13591
Theory of preference and theory of optimization treated from order and topology vantage point, and application to social analysis
[NASA-CR-129593] 04 p0441 N73-13592
Computer graphics for theoretical geography with spatial analysis of surface topology
[AD-749377] 05 p0543 N73-14418
Smoothing properties of neutral functional differential equations
[NASA-CR-130748] 08 p0936 N73-17668
Global structure of highly mobile Einstein space of Petrov Type T3
[ITF-72-117-P] 15 p1832 N73-24849
Topology and kinetics of grain growth
[AD-760580] 18 p2162 N73-27468
Topologies on directed graphs
[NASA-CR-133342] 18 p2169 N73-27517
Application of ERTS-1 imagery for geologic development of natural resources in Alaska
19 p2287 N73-28393
Three level Boolean digital simulation program for logic circuits noting topological matrix circuit representation and simplified temporal simulation
[LAAS-SL-73-I-08] 23 p2769 N73-32149
TOPS [SPACECRAFT]
Characteristics of blowdown-pressurized hydrazine propulsion system for trajectory correction of spacecraft during outer planet flyby missions
[NASA-CR-129796] 04 p0464 N73-13780
Characteristics of thermoelectric outer planet spacecraft attitude propulsion subsystem
[NASA-CR-129795] 04 p0464 N73-13781
Thermoelectric outer planets spececraft advanced systems technology project
[NASA-CR-131451] 12 p1426 N73-21561
TORCHES
Using Plamya-62 acetylene cutting torch for spraying ceramics
10 p1172 N73-19530
TORNADOES
Typhoon associated tornadoes in Japan and suction vortices in Omiya tornado
[SMRP-RP-101] 03 p0326 N73-12659
Management and use meteorological satellite data to detect severe storms and crop disease
[NASA-CR-130000] 06 p0693 N73-15642
Utilization of meteorological satellite data to forecast severe thunderstorms and tornadoes
06 p0693 N73-15644
Engineering analysis of tornado structures and occurrence climatology
[SC-M-72-0688] 10 p1182 N73-19617
Simulation of atmospheric vortex based on boundary conditions and parameter values of strong atmospheric tornadoes and waterspouts
12 p1390 N73-21269
Tornado occurrences related to overshooting cloud-top heights as determined from ATS 3 photographs
[NASA-CR-131875] 13 p1551 N73-22567
TOROIDAL DISCHARGE
Ion heating and thermonuclear power production characteristics and performance of superconducting bumpy-torus magnetic facility
[NASA-TN-D-7353] 19 p2324 N73-28693
TOROIDAL PLASMAS
Screw pinch device with improved torus for stabilization of toroidal plasma
[NP-19381] 06 p0705 N73-15748
Fast radial motion of toroidal plasma column in transverse magnetic field resulting in controlled displacement of plasma column
[NP-19401] 06 p0705 N73-15754
Magnetohydrodynamic equilibrium perturbations in toroidal fields with circular cross sections
[CEA-CONF-2014] 06 p0705 N73-15755
Plasma flow effects on axisymmetric equilibria in toroidal geometry
[IPP-6/107] 07 p0828 N73-16708
Toroidal vortex annihilation and neutron production in pinched plasma
[AD-753107] 09 p1072 N73-18748
Toroidal magnetic field spectrometer for experimentation with high energy beams
[LNF-72/59] 11 p1294 N73-20501
Diffused boundary model for magnetohydrodynamic equilibrium in straight and toroidal plasmas
[IPPJ-159] 16 p1949 N73-25769
Equilibrium characteristics and Kruskal-Shafranov limit of hollow cylindrical plasma pinch in toroidal magnetic field
[LGI/R-72/9/E] 17 p2067 N73-26723
Holographic interferometry using pulsed ruby lasers to measure electron density in toroidal plasmas
[REPT-72-70] 17 p2069 N73-26743
Equilibrium of weakly toroidal plasma column surrounded by Tokamak field
[REPT-72-71] 17 p2069 N73-26744
Comparison of toroidal screw pinch experiments with one-dimensional MHD computer calculations
[REPT-72-72] 17 p2070 N73-26745
Numerical analysis of transient currents and forces in toroidal coils for stellarators and effects of sudden disturbance of normal operation
[NASA-TT-F-15013] 18 p2179 N73-27595
Finite element analysis on cylindrical and toroidal plasma stabilities contained in magnetic field
[JAERI-M-4890] 19 p2324 N73-28700
Maintenance of Tokamak equilibrium by external currents and equilibrium in high pressure Tokamak plasma
[IPPJ-161] 20 p2458 N73-29754
Electron gun for pre-ionization of high beta toroidal pinch system
[IPPJ-164] 20 p2458 N73-29757
Analysis of spatiotemporal evolution of plasma confined in toroidal magnetic enclosure
[FRNC-TH-371] 24 p2964 N73-33689
Behavior of plasma in Harmonica-Two torus
[EUR-CEA-FC-660] 24 p2964 N73-33692

**TOROIDAL SHELLS**
Role of azimuthal electric fields in toroidal transport
[IPP-6/105] 03 p0336 N73-12737
Iterative solution for free vibrations of ring stiffened toroidal shells
[AD-747024] 04 p0482 N73-13943
Feasibility of developing toroidal propellant tanks for bipropellant propulsion system
[NASA-CR-114666] 22 p2720 N73-31766
Three dimensional incompressible laminar flow in centrifugal toroidal shell
24 p2909 N73-33215

**TOROIDS**
High frequency plasma heating in toroidal traps
[NP-19379] 06 p0705 N73-15753
Hot electron plasma control in superconducting toroids
[UCRL-73806] 07 p0826 N73-16699
Production of integrated toroidal magnetic memories of 500 bits/sq cm, including electric and magnetic testing
[REPT-1541] 10 p1133 N73-19232
Superhigh frequency plasma heating in toroidal magnetic trap
[AEC-TR-7360] 10 p1197 N73-19741

**TORPEDOES**
Three axis gyro stabilized torpedo platform
11 p1318 N73-20702

**TORQUE**
Numerical analysis of stresses produced in bolt or similar threaded object from application of known tightening torque to bolt head or engaged nut
[ESDU-72022] 05 p0601 N73-14888
Torque measurement of flat polyimide cable crossing hinge or satellite solar array
[ESRO-TN-114-ESTEC] 05 p0603 N73-14904
Variational equations for studying rotational motion of orbiting rigid body about its center of mass under conservative and nonconservative torques
07 p0817 N73-16624
Comparison of computed torque method and conventional position servo computer controlled manipulator
[NASA-CR-131521] 12 p1381 N73-21198
Frequency effect of magnetocrystalline anisotropy in nickel ferrous ferrites determined by torque measurements
18 p2159 N73-27443
Equations for determining pressure profile, forces, and torques on disk pendulum by point source wave theory from acoustics
[NASA-TM-X-69569] 20 p2454 N73-29725
Comparison of thrust and torque forces on ship propeller blades in oblique and axial flow
[DRIC-TRANS-3205] 21 p2525 N73-30249

**TORQUE MOTORS**
Design of elastically geared circular disk wave drive motor and telemanipulator
[NASA-TT-F-14803] 10 p1165 N73-19482
Design and performance of segmented magnetic torque converter for mechanical drives
[AD-753541] 10 p1167 N73-19498
Design of ironless armature torque motor using samarium cobalt permanent magnets
[NASA-CR-130224] 13 p1532 N73-22416
Brushless dc torque motor in-orbit performance of ITOS with improved attitude controls and earth splitting technique
[NASA-TM-X-66267] 17 p2060 N73-26662
Design of torque motor with armature windings cast in epoxy cylinder and conductors cast integrally with aluminum mounting ring
18 p2209 N73-27830

**TORSION**
Strain hardened properties of 304L stainless steel surfaces under combined tension and torsion
[AD-746472] 02 p0188 N73-11525
Torsion, bending, and shear in concrete beams reinforced with stirrups
[D-10-72] 02 p0238 N73-11938
Design parameters for torsion of airframe sandwich strips having trapezoidal, rectangular, and triangular cross sections
[AD-752619] 08 p0868 N73-17029
Variable principle for analyzing torsion of fluted bar with rope like cross section
[AD-752059] 08 p0928 N73-17598
Axial extension in directionally solidified eutectic of solid cross section during cyclic torsion
[AD-755891] 12 p1417 N73-21481
Torsion of an orthotropic, inhomogeneous bar with cylindrical anisotropy including solution by Saint Venant principle
[DRIC-TRANS-2995] 12 p1463 N73-21856
Extended torsional tests of interlocked bi-stem satellite boom
[NASA-TN-D-7365] 22 p2724 N73-31798

**TORSIONAL STRESS**
Elastoplastic deformation of steel samples under cyclic loads during torsion tests
[AD-749768] 05 p0604 N73-14914
Elastic properties of thin walled U beam lateral stiffness under flexing torsional stresses
[ISD-130] 09 p1095 N73-18939
Hydraulic biaxial medium-rate tension-torsion testing machine
[REPT-1047/72] 10 p1161 N73-19449
Design of torsional gage with step response for strain-rate measurements
[AD-757527] 14 p1668 N73-23542
Torsional device for testing small diameter single synthetic fibers
[AD-755932] 14 p1680 N73-23638
Numerical analysis of torsion characteristics of bar with constant section in shape of circular ring or circular sector
[NLL-DRIC-TRANS-2995-[3623.66]]
15 p1837 N73-24885

**TORSIONAL VIBRATION**
Torsional bending and longitudinal vibrations of rotating shafts and application to free vibrations of individual rotor blades, blade cascades, and shrouded blades
[NASA-TT-F-14627] 04 p0372 N73-13029
Lateral bending torsion vibrations of thin cantilever beam under parametric excitation
[AD-750546] 06 p0727 N73-15934

**TORUSES**
Apparatus and program for turbulent torus experiment
[ORO-4087-8] 06 p0704 N73-15737
Screw pinch device with improved torus for stabilization of toroidal plasma
[NP-19381] 06 p0705 N73-15748
Magnetohydrodynamic equilibrium in axisymmetric torus
[IPPJ-141] 09 p1070 N73-18727
Sheba triangular thin shell element application to calculation of coding towers, toruses, and roofs
[ISD-127] 09 p1095 N73-18936
Rayleigh equations for determining axial sound wave scattering coefficients by torus
[REPT-208.138/1] 14 p1692 N73-23731
Fourier coefficients and power spectral density calculating device
[IPPJ-T-13] 16 p1949 N73-25766
Theory of toroidal stages in stellar evolution
20 p2470 N73-29841

**TOUCH**
NT TACTILE DISCRIMINATION
Use of skin analyzer as communication channel in controlling activity
04 p0378 N73-13074
Tactile information presentation using high pressure pulses into anti-G suit
[AD-761796] 19 p2228 N73-27969
Prosthetic limb with tactile sensing device
[NASA-CASE-MFS-16570-1] 23 p2751 N73-32013

**TOUCHDOWN**
Analysis of phenomenon generated by passage of projectile into water to determine effects of accelerations, aerodynamic configurations, and surface motions
16 p1886 N73-25264

**TOUGHNESS**
NT NOTCH SENSITIVITY
Elastic-plastic toughness level of irradiated stainless steels used in fast reactor construction
[AD-761611] 19 p2310 N73-28580

**TOWED-BODIES**
Measurements of launch g forces and line tensions in aerial recovery of dummies for long-line loiter personnel retrieval system
[AD-749518] 05 p0497 N73-14045
Numerical analysis of vertical and lateral motion of road vehicle trains with arbitrary number of components
[TT-7211] 08 p0892 N73-17220
Computerized simulation of aerodynamic characteristics for trailing wire system towed by orbiting aircraft
[AD-753909] 10 p1136 N73-19255
Computerized simulation of spiral curve of wire being towed behind orbiting aircraft
[AD-753908] 10 p1136 N73-19256
Design of towed sonar transducer array for bathymetric mapping of ocean bottom topography
[AD-755113] 11 p1259 N73-20216
Noise sources in towed ELF H-field antenna
[AD-754949] 11 p1263 N73-20250
Wind tunnel tests to determine pressure sensing characteristics of trailing cone device for calibrating aircraft static-pressure systems
[NASA-TN-D-7217] 13 p1470 N73-21906
Ship towed magnetometer and ocean bottom mounted magnetic variation station
[JPRS-59802] 21 p2547 N73-30417
Ship towed magnetometer for direct measurement of horizontal component of earth magnetic field
21 p2547 N73-30418
Supersonic wind tunnel tests on three dimensional turbulent boundary layer growth on wires leading to calculation of tension and skin friction on aircraft towlines
[ARC-CP-1235] 23 p2740 N73-31933

**TOWED TARGETS**
U TARGETS
U TOWED BODIES

**TOWERING CUMULI**
U CUMULUS CLOUDS

**TOWERS**
NT AIRPORT TOWERS
Sheba triangular thin shell element application to calculation of coding towers, toruses, and roofs
[ISD-127] 09 p1095 N73-18936
Annotated listing of tall towers instrumented for wind observations
[AD-762911] 20 p2450 N73-29691

**TOWNSEND DISCHARGE**
NT GAS DISCHARGES
NT TOROIDAL DISCHARGE

**TOXIC DISEASES**
NT CARBON MONOXIDE POISONING
NT LEAD POISONING
Protective effects of pyridinium salts against alkyl phosphate poisoning including influence of chemical and aging
[BMVG-FBWT-72-8] 07 p0746 N73-16072

**TOXIC HAZARDS**
Toxic effects of Freon decomposition products on activity of isoenzymes of lactate dehydrogenase in rat brains
03 p0259 N73-12097
Effects and prevention of possible mercury pollution from failure of solar electric propulsion spacecraft using mercury propellant
[NASA-CR-130286] 06 p0717 N73-15855
Effect of protective barrier creams on toxic alkyl phosphate penetration of pig skin
[BMVG-FBWT-72-15] 07 p0747 N73-16076
Influence of 100 percent anhydrous ammonia environment on body functions
08 p0875 N73-17088
Phenol preservative for reducing toxic urine outgassing into air environment
10 p1116 N73-19098
Hypoxia adaptation of rats for increased resistance to toxic atmospheric gases
10 p1116 N73-19100
Toxic effects of metabolic waste gases on rat organisms
10 p1116 N73-19101
Toxic effect of indole inhalation on man, mouse, rat, and rabbit organisms
10 p1117 N73-19102
Toxic effects of human exhaled air on mice organisms
10 p1117 N73-19103
Microbiological inspections of NASA food handling facilities
[NASA-TM-X-64734] 11 p1247 N73-20127
Toxic vapor detector for Minuteman propellant leakage
[AD-763799] 21 p2551 N73-30451

**TOXICITY**
NT CARBON MONOXIDE POISONING
NT LEAD POISONING
Toxic effects of continuous exposure to dichloromethane vapor on dogs, monkeys, rats, and mice
[AD-746295] 02 p0134 N73-11088
Proceedings of conference on environmental toxicology held at Fairborn, Ohio, 31 August, and 1-2 September 1971
[AD-746660] 02 p0207 N73-11676
Human and male Charles River rat exposures to Halon 1301 under hypobaric conditions, simulating aircraft compartment
[AD-747958] 03 p0260 N73-12106
Effects of SO2 decay product toxicity on human physiological functions
05 p0500 N73-14071
Hyperammonemia development in metabolic toxicity of hydrazine
[AD-749519] 05 p0501 N73-14077
Oxygen, carbon monoxide, and fuel toxicity
06 p0628 N73-15101
Symptomatic and pathological information from acute toxicity exposure of chlorine pentafluoride
[AD-751452] 07 p0747 N73-16078
Toxicity of pyrolysis products from chlorotrifluroethylene-ethylene copolymer Halar resin
[AD-751436] 07 p0748 N73-16080
Hepatotoxic effects of dichloromethane inhalation in mice
[AD-751434] 07 p0748 N73-16081
Acute toxicity of brief exposures to HF, HCl, NO2, and HCN singly and in combination with CO in aircraft cabins
[AD-751442] 07 p0748 N73-16085
Animal species susceptibility to toxic effects of long term exposure to environmental monomethylhydrazine
[AD-751441] 07 p0748 N73-16086
Biological and toxicity effects of aluminum and other chemicals in animals
[ORNL-TIP/TIRC-72-76] 10 p1121 N73-19136
Elimination of toxic cysteamine in organisms and method for prolonging its radioprotective effect
11 p1240 N73-20069
Gamma radiation effects on toxic cysteamine elimination in irradiated and nonirradiated mice
11 p1240 N73-20070

Opthalmological examination of antimalarial drugs effects on performance of navigation personnel
12 p1371 N73-21122
Acute and subacute inhalation toxicity experiments with organic solvents, rocket propellants, and various hydrocarbons in confined environments
[NASA-CR-131675] 13 p1485 N73-22043
Space flight ultraviolet irradiation effects on Bacillus thuringiensis toxin production capability
15 p1740 N73-24109
X ray fluorescence analysis of toxic heavy elements
[CONF-721134-1] 17 p1992 N73-26106
Analysis of physiological and toxicological aspects of smoke produced by combustion of aircraft interior materials - Part I
[FAA-RD-73-50-PT-1] 18 p2104 N73-27014
Physio-chemical analysis of flammability characteristics and thermal degradation of rigid and flexible urethane foams used in aircraft structures - Part 2
[FAA-RD-73-50-PT-2] 18 p2105 N73-27025
Combustibility and toxicity of metals and alloys
[AD-764287] 22 p2621 N73-31003

**TOXICITY AND SAFETY HAZARD**
Industrial health hazard in chronic exposure to monomethylhydrazine and dose related hemolytic anemia in humans
[AD-751440] 07 p0749 N73-16087
Cardiac toxicity of fluoroalkane gases for propelling aerosols in industry and household applications
[AD-751425] 07 p0749 N73-16090
Evaporation rates and toxic plume dispersion for defining downwind evacuation areas for populations adjacent to accidental propellent spills on shipping routes
[NASA-TM-X-68188] 07 p0750 N73-16097
Environmental health measures to prevent cabin atmosphere toxicity and provide drinking water standards in manned space flight applications
08 p0872 N73-17058
Toxicity and safety hazard of dry beryllium copper alloy machining for human operator
08 p0872 N73-17059
Effects of chemical fire extinguishing agents containing bromotrifluoromethane on cardiovascular and nervous systems of dogs, monkeys, and baboons
[AGARD-R-599] 08 p0877 N73-17106
Toxic effects of chronic exposure to dichloromethane in liver microsomal cytochromes
[NASA-TM-X-69101] 09 p0996 N73-18128
Toxicity of atmospheric dichloromethane levels in simulated space cabin atmosphere on dogs, rats, mice, and monkeys
[NASA-TM-X-69099] 09 p0996 N73-18129
Toxicity of long term methyl isobutyl ketone exposure in dogs, monkeys, mice, and rats
[NASA-TM-X-69100] 09 p0996 N73-18130
Toxicity of gaseous urine and feces emissions on rat organism
10 p1116 N73-19097
Bibliography on titanium toxicity in human and animal organisms
[ORNL-TIP/TIRC-72-65] 10 p1120 N73-19135
Transverse acceleration overload effects on mice sensitivity to toxic doses of cysteamine and aminothiol group antiradiation drugs
11 p1239 N73-20061
Increased toxicity of sympathomimetic amine stimulants on spinal reflexes in irradiated frogs
11 p1240 N73-20063
Pharmacological data for aminothiol and indolylalkylamine radioprotectors
11 p1240 N73-20066
Toxicological properties of rocket exhaust products and blood analysis for beryllium oxide content
[AD-754936] 11 p1248 N73-20131
Conference on uses and toxicity of halogenated fire extinguishing agents
[PB-218448/9] 18 p2214 N73-27875
Hygienic importance and toxicity of manganese oxides, and clinical medicine of chronic manganese exposure
[NASA-TT-F-15000] 21 p2501 N73-30067
Toxicological aspects of carbon dioxide exposure in chronic hypercapnia
[AD-763394] 22 p2621 N73-31005

**TOXICOLOGY**
Toxicology of some commercial fluorocarbons
[AD-751429] 07 p0747 N73-16079
Effect of toxic substances on algae by observing photosynthesis determined by oxygen production of algae
[DRIC-TRANS-2991] 10 p1121 N73-19139
Effect of carbon monoxide on time perception
[PB-214651/2] 16 p1868 N73-25123

**TOXINS AND ANTITOXINS**
Space manufacturing of biological and electronic materials
04 p0473 N73-13862
Cholinesterase reactivator as antidote in human organophosphate poisoning
13 p1480 N73-21998

**TRACE CONTAMINANTS**
Estimation of traces of gases in metals and alloys by vacuum fusion techniques
[BARC-590] 06 p0638 N73-15177
Electrochemical methods for determining acidity standard, atomic weight, stoichiometric composition, and trace contaminants
[NBS-TN-583] 09 p0999 N73-18153
Proficiency of X ray fluorescence spectrospectory and wet chemical techniques in measuring trace copper impurities in beryllium foils
[SC-RR-72-0722] 10 p1126 N73-19175
Extraction-Photometric methods for determining impurities in beryllium
[JAERI-1222] 17 p2044 N73-26537
Location of adhesive bond failure on Al surface during coupon surface treatment by radioactive tracing
[AD-761073] 18 p2168 N73-27509
Mass spectrum identification of trace organic impurities in gaseous helium
[NASA-TN-D-6520] 19 p2230 N73-27983
Computer codes for calculating trace contaminant effects on stratospheric transport processes
[COO-2249-2] 24 p2923 N73-33345

**TRACE ELEMENTS**
Absorption spectroscopic determination of nickel, chromium, and cobalt in airborne particulates
[NASA-TM-X-2672] 02 p0137 N73-11111
Absorption and emission spectra for trace element analyses on biological sample solutions
03 p0258 N73-12093
Neutron activation analysis using gamma ray spectroscopy for determination of trace elements and short-lived nuclides
[BMBW-FBK-72-13] 03 p0262 N73-12122
Activation analysis of prompt gamma ray emission spectra for trace element determination
03 p0262 N73-12123
Computerized evaluation of activation gamma spectra for multiple trace element determination and of automation of main constituent determination
03 p0262 N73-12125
X ray fluorescence analysis of trace elements in high purity irons
[NPL-CHEM-17-PT-2] 03 p0264 N73-12139
X ray fluorescence analysis of manganese and trace elements in mild steels
[NPL-CHEM-16-PT-1] 03 p0264 N73-12140
Iodoantimonous acid for quantitative yield estimation of antimony trace concentrations by spectrophotometric method
[AREAEE-126] 04 p0433 N73-13531
Detection of C, H, and Ni in Pu metal by hot extrusion-combustion method
[POA-VOL-6-NO-10] 05 p0506 N73-14115
Trace element detection by automated distillation and ion exchange in neutron activation analysis for As, Cd, Cu, Hg, Se, and Zn
[IRI-133-72-10] 07 p0753 N73-16114
Gas chromatographic and mass spectrometric determinations of trace elements in human breath samples
[AD-750141] 09 p1000 N73-18159
Numerical and photochemical models for analyzing transport and trace constituents in stratosphere
[COO-2249-1] 10 p1155 N73-19399
Trace element analysis of coal by neutron activation
[NASA-TM-X-68208] 12 p1431 N73-21596
Element abundances in meteoritic chondrules by neutron activation analysis
12 p1446 N73-21713
Spectrometric determination of copper, iron, cobalt, nickel, and manganese complexes in biological samples
13 p1483 N73-22022
Trace element [Bi, Ag, Cd, and Pb] determination in nickel base gas turbine parts by atomic absorption spectrophotemetry
[AD-757015] 14 p1678 N73-23619
Solid phase trace element aerosol concentrations in lowest 34 meters of atmosphere
15 p1771 N73-24343
Pattern recognition as statistical analysis of confidence level in forensic trace element identification
[IRI-133-72-11] 19 p2240 N73-28056
Radioactive tracers for studying atmospheric circulation and synoptic conditions
20 p2446 N73-29644
Neutron activation analyses of trace elements in germanium, silicon, and selenium semiconductors
[CONF-721069-29] 20 p2462 N73-29786
Thermotransport of copper in liquid Al-Cu alloys
[NASA-TR-R-415] 22 p2625 N73-31030
Optimized sensitivity of computer controlled microwave spectrometer for trace element detection
[BMVG-FBWT-73-18] 23 p2754 N73-32037
Quantitative neutron activation analysis of stable elements in air pollution particulates
[AD-764715] 23 p2755 N73-32043
Spectrophotometric determination of B, Cu, and Ta in Ni base alloys
[JAERI-M-5094] 24 p2934 N73-33431
Thermotransport in liquid alkali metal alloys as function of composition
[COO-841-29] 24 p2992 N73-33915

**TRACERS**
Infrared detection of hydrogen fluoride tracer for studying turbulent mixing in inert and combustion flows
08 p0880 N73-17128
Accuracy of various tracer methods for measuring body water compartments during bed rest
[NASA-TR-R-406] 15 p1744 N73-24133

**TRACKERS**
U TRACKING [POSITION]

**TRACKING [POSITION]**
NT COMPENSATORY TRACKING
NT INFRARED TRACKING
NT MISSILE TRACKING
NT OPTICAL TRACKING
NT PHOTOGRAPHIC TRACKING
NT PURSUIT TRACKING
NT RADAR TRACKING
NT RADIO TRACKING
NT RANGE AND RANGE RATE TRACKING
NT SATELLITE TRACKING
NT SPACECRAFT TRACKING
NT STAR TRACKERS
NT WILDLIFE RADIOLOCATION
Simulator facility used to determine vibration effects on pilot tracking performance using rigid control stick
[AD-745193] 01 p0021 N73-10164
Synthesis of adaptive control tracking systems using Liapunov second method
[NASA-CR-129175] 02 p0150 N73-11220
Human operator model performance in tracking high performance aircraft
[AD-746725] 04 p0381 N73-13101
Analysis of aircraft tracking techniques to show sensitivity of tracking performance to data environment
[AD-753114] 09 p1063 N73-18667
Monte Carlo method for analyzing tracking disruptions
14 p1683 N73-23657
Analog computer models of tracking system errors
14 p1683 N73-23658
Application of statistical analysis techniques in telecommunication, tracking, and control
[AD-758260] 15 p1751 N73-24193
Theory and application of random Markov processes to analysis of tracking disruption
18 p2169 N73-27520
Computation of characteristics of tracking disruption
22 p2691 N73-31558
Optical radar angle tracking mount
[AD-765213] 23 p2759 N73-32077
Synchronous-Tracking drive system for automating observations on RTI-7.50/250 MVTU radio telescope
23 p2837 N73-32672

**TRACKING AND DATA RELAY SATELLITES**
U TDR SATELLITES

**TRACKING ANTENNAS**
U DIRECTIONAL ANTENNAS

**TRACKING FILTERS**
Markov random processes for tracking disruption analyses on quasi-stationary systems
17 p1997 N73-26150

**TRACKING NETWORKS**
NT DEEP SPACE NETWORK
NT GLOBAL TRACKING NETWORK
Statistics from synoptic year sample of 20,000 radar meteor observations using eight station radar network
[NASA-CR-2109] 01 p0101 N73-10830
Description of eight-station radar at Havana, Illinois
01 p0101 N73-10832
Results from synoptic year
01 p0102 N73-10837
Dynamics of meteor streams and new asteroid-meteor and comet-meteor associations
01 p0102 N73-10843
Elements of block diagrams for automatic radio tracking systems
16 p1875 N73-25179
Simultaneous observation solutions for NASA-MOTS and SPEOPT station positions on North American Datum
[NASA-TM-X-66297] 18 p2145 N73-27336
Administration, development, and maintenance of NASA tracking network with emphasis on Australia
[NASA-CR-133828] 21 p2521 N73-30214

**TRACKING RADAR**
Signal processing algorithms for estimating from radar data characteristics and trajectory parameters of bodies moving in air
[AD-745421] 01 p0029 N73-10227
Discrete address radar beacon system for aircraft tracking and traffic control
[FAA-RD-72-117] 04 p0447 N73-13649
Rendezvous and docking radar for space shuttle
10 p1129 N73-19198
Synchronous satellite tracking by planetary radar system
[AD-754937] 11 p1257 N73-20196
Utilization of C band instrumentation radars during GEOS 2 program
[NASA-CR-62087] 13 p1491 N73-22004
Method for measuring mechanical deformations in parabolic dish of metric tracking radar
[AD-758371] 14 p1635 N73-23260
Computerized simulation of mobile tracking radar performance
[AD-762338] 19 p2238 N73-28043

**TRACKING STATIONS**
NT DEEP SPACE INSTRUMENTATION FACILITY
NT GLOBAL TRACKING NETWORK
Directory of principal tracking facilities used by NASA to include Deep Space Network and several radio telescopes - Vol. 1
[NASA-CR-130071] 01 p0036 N73-10279
Directory of observation stations in NASA geodetic satellites program based on preferred major datums and Modified Mercury Datum 1968 - Vol. 2
[NASA-CR-130072] 01 p0036 N73-10280
Systems analyses on external and internal radio frequency communication and tracking assemblies for manned space station
[NASA-CR-128561] 03 p0265 N73-12147
European tracking station coordinates from GEOS B satellite data
03 p0295 N73-12400
French Pic du Midi ruby laser telemetry station, noting positioning devices and optical data processing
05 p0557 N73-14525
Tracking performance and quality of colocated laser tracking stations
[NASA-TM-X-66158] 07 p0765 N73-16220
Effect of parallactic refraction correction for satellite optical observations in determination of station coordinates
[NASA-TM-X-66208] 10 p1189 N73-19674
User requirements and instrumentation plans for aircraft tracking and guidance facility at Wallops Station
[NASA-CR-111931-1] 14 p1645 N73-23340
Development of accurate geoidal map based on gravimetric and satellite data for determining precise location of tracking stations
[NASA-CR-131869] 14 p1710 N73-23874
Work-rest schedules for military tracking crews under prolonged vibration
14 p1723 N73-23986
Design of meterband radar stations
[AD-758253] 15 p1751 N73-24194
**TRACKING STUDIES**
U TRACKING [POSITION]
**TRACTION**
Interferometry measurements of film thickness and traction of lubrication in point contacts
[NASA-CR-120842] 05 p0551 N73-14478
Performance tests to determine cornering characteristics of cantilever aircraft tire on dry, damp, and flooded runway surfaces over range of yaw angles
[NASA-TN-D-7203] 12 p1363 N73-21058
**TRACTORS**
Numerical analysis of vertical and lateral motion of road vehicle trains with arbitrary number of components
[TT-7211] 08 p0892 N73-17220
Effect of low visibility on performance of vehicle operators
[AD-749248] 13 p1486 N73-22051
**TRACTS**
U SITES
**TRAFFIC**
NT AIR TRAFFIC
Side-looking radar applications to transportation noting route planning, shipping lanes, and traffic
03 p0295 N73-12409
Relationship between highway traffic parameters and air quality analysis - Vol. 3
[PB-219813/3] 18 p2175 N73-27564
Survey of remote sensing applications for transportation and traffic engineering studies
[NASA-CR-129011] 20 p2488 N73-29989
**TRAFFIC CONTROL**
NT AIR TRAFFIC CONTROL
**TRAILBLAZER 2 ROCKET**
U TRAILBLAZER 2 REENTRY VEHICLE
**TRAILBLAZER 2 ROCKET VEHICLE**
U TRAILBLAZER 2 REENTRY VEHICLE
**TRAILBLAZER 2 REENTRY VEHICLE**
Electron density distribution in viscous flows as applied to Trailblazer 2 reentry vehicle
[AD-755397] 13 p1564 N73-22674
Analysis of plasma sheath ion current data measured by electric probes on third flight of Trailblazer 2
[AD-758763] 15 p1836 N73-24883
**TRAILERS**
Numerical analysis of vertical and lateral motion of road vehicle trains with arbitrary number of components
[TT-7211] 08 p0892 N73-17220
**TRAILING EDGES**
Flow conditions around exit and downstream of stator blades with varying trailing-edge geometries and thicknesses
[NASA-TM-X-2659] 01 p0001 N73-10003
Influence of trailing edge thickness on aerodynamic drag of rectangular wings in transonic and supersonic flow
[DLR-FB-71-85] 06 p0615 N73-14991
Effectiveness of trailing edge bevels on reducing vibration excitation causing vortex shedding into wake
[REPT-1052/73] 13 p1471 N73-21911
Experimental determination of bound vortex lines and flow in vicinity of trailing edge of slender delta wing
[NASA-TT-F-15012] 18 p2131 N73-27217
**TRAILING-EDGE FLAPS**
Effect of Reynolds number and frequency on control-surface buzz at high subsonic speeds noting control of flap oscillation by air jets
[ARC-R/M-3702] 03 p0248 N73-12007
Wind tunnel tests of two dimensional wing model with leading edge slat and trailing edge flap
[FAA-AU-862] 08 p0863 N73-16984
Friction effect on lift of airfoil section with slotted flap
[DLR-FB-73-04] 12 p1356 N73-21001
Calculation of spanwise loading on sweptback wings with trailing edge flaps using data obtained from electric tank tests
[ARC-R/M-3487] 16 p1853 N73-25010
Aerodynamic forces, pressure distribution, and wakes of wing profile with trailing edge flaps and leading edge slats
24 p2906 N73-33187
**TRAINEES**
U STUDENTS
**TRAINERS**
U TRAINING DEVICES
**TRAINING**
U EDUCATION
**TRAINING AIRCRAFT**
NT JET PROVOST AIRCRAFT
NT T-33 AIRCRAFT
NT T-38 AIRCRAFT
Evaluation of standardized angle of attack flight training system
[AD-757243] 14 p1615 N73-23090
Installation of electronic warfare training equipment in rear cockpit of CF-100 aircraft with emphasis on human engineering considerations
[DCIEM-904] 16 p1861 N73-25071
Analysis of loads imposed on nose gear retraction system of T-34 aircraft to determine critical mechanical adjustments
[AD-762729] 20 p2361 N73-28994
**TRAINING DEVICES**
NT TEACHING MACHINES
Performance evaluation of airborne audio-video recording system as training device in A-7D tactical fighter
[AD-744041] 01 p0021 N73-10161
Systems engineering methods for human performance enhancement in signal detection and flight control
[AD-748239] 05 p0503 N73-14098
Development and application of computer programs as instructional methods for physics laboratory experiments
05 p0516 N73-14198
Effectiveness of underwater acoustic propagation loss models in sonar personnel training devices
[AD-750694] 06 p0701 N73-15719
Effectiveness of training device for air traffic communication and carrier landing control
[AD-751556] 07 p0751 N73-16101
Evaluation of device to train forward air controllers to communicate target locations
[AD-751292] 07 p0751 N73-16103
Performance of large screen tactical display systems in training devices using cathode ray tubes
[AD-751559] 07 p0767 N73-16228
Apollo experience report on development of flight simulators for spacecrew training to show functional uses, characteristics, and problems
[NASA-TN-D-7112] 10 p1214 N73-19876
Design, development, and capabilities of space shuttle mission simulator to show types of training available and cost effectiveness of facility
[NASA-CR-128885] 12 p1387 N73-21251
Development and use of synthetic flight trainers based on degree and fidelity of simulation as key design considerations
[AD-754957] 12 p1388 N73-21260
Digital radar landmass simulation for determining optimum specification of digital radar training devices
[AD-758363] 15 p1763 N73-24284
Vacuum tube and solid state circuitry in electronic communications equipment for army training school
[AD-759129] 17 p2073 N73-26775
Guidelines for assessing acceptability of pilot ground trainer devices based on simulated aircraft maneuvers
[FAA-NA-73-15] 20 p2382 N73-29139
Development of visual simulation system design for space shuttle mission simulator to include cost analysis and alternate concepts
[NASA-CR-134020] 21 p2522 N73-30221
Performance evaluation of training devices for developing human physical fitness
[NASA-CR-134046] 23 p2752 N73-32023
**TRAINING SIMULATORS**
NT COCKPIT SIMULATORS
NT FLIGHT SIMULATORS
NT SPACECRAFT CABIN SIMULATORS
Analysis of capabilities, characteristics, and effectiveness of flight simulators for developing primary aeronautical skills in single-engine, land aircraft - Vol. 1
[FAA-NA-72-102-VOL-1] 08 p0892 N73-17221
Analysis of capabilities, characteristics, and effectiveness of flight simulators for developing primary aeronautical skills in pilots of single-engine, land aircraft Vol. 2
[FAA-NA-72-102-VOL-2-ADD] 08 p0892 N73-17222
Development of hardware and software specifications for procurement of space shuttle mission training simulator for crew training
[NASA-CR-133965] 18 p2126 N73-27177
**TRAJECTORIES**
NT ABORT TRAJECTORIES
NT ASCENT TRAJECTORIES
NT BALLISTIC TRAJECTORIES
NT DESCENT TRAJECTORIES
NT EARTH-MARS TRAJECTORIES
NT ELECTRON TRAJECTORIES
NT HYPERBOLIC TRAJECTORIES
NT INTERPLANETARY TRAJECTORIES
NT LUNAR TRAJECTORIES
NT MIDCOURSE TRAJECTORIES
NT MISSILE TRAJECTORIES
NT PARTICLE TRAJECTORIES
NT REENTRY TRAJECTORIES
NT RENDEZVOUS TRAJECTORIES
NT ROUND TRIP TRAJECTORIES
NT SPACECRAFT TRAJECTORIES
Signal processing algorithms for estimating from radar data characteristics and trajectory parameters of bodies moving in air
[AD-745421] 01 p0029 N73-10227
Trajectory sensitivity during perturbations in dynamic systems
[AD-754919] 11 p1312 N73-20643
Aerodynamic forces and trajectories of external stores separated from F-4 aircraft
[AD-757932] 15 p1850 N73-24993
**TRAJECTORY ANALYSIS**
Applications of orbital mechanics to aerospace systems and ballistic trajectories
[AD-746706] 02 p0232 N73-11885
Differential equation for trajectories in exact form
[LNF-71/81] 04 p0450 N73-13671
Aerodynamic characteristics and trajectory analysis of ballistic-type, self-dispersing bomblet based on wind tunnel tests and numerical probability application
[AD-749956] 06 p0615 N73-14993
Subharmonic angular motion response in asymmetric missile trajectory analysis
[AD-749787] 06 p0722 N73-15893
Geostationary satellite observation of convective tropical cloud trajectories and velocity
07 p0814 N73-16602
Analysis of motion of compound pendulum and two-gimbal gyroscope mounted in artificial satellite with prescribed orbit and constant rate of rotation
07 p0817 N73-16625
Curriculum of training course on basics and state-of-the-art of remote sensing and developments in parameter optimization
[NASA-CR-128713] 07 p0848 N73-16876
Application of control theory to determine time history of thrust profile to achieve optimal maneuvers of aerospace lifting vehicles
[AD-751281] 07 p0850 N73-16891
Constant azimuth cycloids discussing rotating earth trajectory
07 p0859 N73-16970
Characteristics of Performance Analysis and Design Synthesis computer program for determining size of launch vehicles for optimal trajectories - Vol. 2, Pt. 1
[NASA-CR-128678] 09 p1083 N73-18831
Description of QL module Performance Analysis and Design Synthesis computer program for determining optimal trajectory of launch vehicles - Vol. 2, Pt. 2
[NASA-CR-128657] 09 p1083 N73-18832
Optimal plotting of elliptical transfer orbit employing complete revolutions in equatorial plane of axisymmetric planet
[AD-753517] 09 p1085 N73-18857
Vertical wind effects in trajectory calculations and impact predictions for rockets and projectiles
[AD-753349] 09 p1092 N73-18913
Development of computer program to size launch vehicles for optimal trajectories and application for general purpose branched trajectory optimization
[NASA-CR-128725] 10 p1214 N73-19869
Orbital evolution and stability analysis for earth and lunar orbiter trajectories
[AD-754738] 11 p1339 N73-20869
Time variations of instantaneous orbital parameters and topocentric range and range rate of spacecraft moving in gravitational field of oblate large body
[JPL-TM-33-594] 12 p1458 N73-21814
Description of maneuvering aircraft trajectory by second-order non-Gaussian process verified by digital simulation
[TAE-167] 14 p1683 N73-23656

Development of algorithms for calculating modal trajectory estimate, conditional mean state estimate, and weighted least squares trajectory estimate
[AD-757240] 14 p1684 N73-23665
Development of computer program for determining minimum time trajectory and comparison with gradient method of computation
15 p1733 N73-24053
Application of Kalman-Bucy filter theory to post-flight guidance error analysis
[NAL-TR-302] 15 p1808 N73-24652
Consolidation of navigation and guidance for space shuttle vehicles for all phases of space mission - Document 21
[NASA-CR-128961] 16 p1941 N73-25708
Analysis of projectile aerodynamic coefficients based on yawsonde and radar imagery data obtained during flight tests
[AD-759482] 17 p1980 N73-26002
Analysis of Apollo 17 flight to show extravehicular activities, lunar surface experiments, orbital science projects, and spacecraft reentry and recovery
[NASA-TM-X-69527] 17 p2083 N73-26851
Development of techniques for predicting point and path performance of light aircraft
[NASA-CR-2272] 18 p2105 N73-27022
Early orbit capability of Goddard Trajectory Determination System for earth satellites
[NASA-TM-X-66286] 18 p2197 N73-27734
Analysis of drop trajectories transition of boundary layer structure and flow regime for binary spray flow over upstream surface of isothermal cylinder
20 p2386 N73-29171
Application of cononical perturbation theory to non-conservative systems
20 p2470 N73-29835
Analysis of methods for determining mass, geometric, and thrust characteristics of missiles to provide given interval of ranges
[JPRS-59565] 20 p2474 N73-29877
Maneuverable reentry body trajectory calculation using optimizing and nonoptimizing programs
[BMBW-FBW-72-15] 21 p2597 N73-30815
Theoretical analysis of error propagation into orbital positions with emphasis on observed phenomena
[AD-763288] 21 p2599 N73-30828
Computer program for analyzing characteristics of parachute-payload system during deployment and trajectory
23 p2740 N73-31936
Probabilistic approach to trajectory sensitivity
23 p2835 N73-32657

**TRAJECTORY CONTROL**
NT TRAJECTORY OPTIMIZATION
Characteristics of blowdown-pressurized hydrazine propulsion system for trajectory correction of spacecraft during outer planet flyby missions
[NASA-CR-129796] 04 p0464 N73-13780
Characteristics of thermoelectric outer planet spacecraft attitude propulsion subsystem
[NASA-CR-129795] 04 p0464 N73-13781
Utility of Goddard Trajectory Determination System Solar/Lunar/Planetary ephemeris files
[NASA-TM-X-66185] 08 p0976 N73-17983
Guidance and control concepts for structural control interactions and dynamic loads
[NASA-TM-X-64732] 12 p1461 N73-21834
Research concepts for guidance and control of tactical missiles
[AD-762593] 20 p2476 N73-29890

**TRAJECTORY MEASUREMENT**
Computer program ELECTRA used to compute paraxial particle trajectories in axially symmetric electrostatic fields
[SGAE-2007] 07 p0824 N73-16678

**TRAJECTORY OPTIMIZATION**
HILTOP - variational calculus program for generating electric propulsion data on rendezvous missions to comet Encke
[NASA-CR-114491] 01 p0104 N73-10857
Solving problems of long-range ballistic missiles - launching, trajectory and flight characteristics, and firing data
[AD-743687] 01 p0109 N73-10898
Closed-form solutions for motion of rocket-powered vehicle during atmospheric ascent and unpowered atmospheric reentry
[NASA-TM-X-64694] 02 p0207 N73-11677
Calculation of optimal gliding flight paths associated with space shuttle orbiter transition from entry to cruising flight
[NASA-CR-128647] 03 p0359 N73-12922
Formulation for Performance Analysis and Design Synthesis (PADS) computer program
[NASA-CR-128677] 04 p0394 N73-13199
Numerical methods for computing reentry trajectories for space shuttles
[NASA-CR-128652] 04 p0474 N73-13877
Linear control theory for generating optimal trajectories between initial and final positions of n degree of freedom mechanical arm
[NASA-CR-123980] 05 p0551 N73-14470
Use of aerodynamic drag for transfer from hyperbolic trajectories to satellite orbits noting spacecraft guidance
[D-149] 05 p0596 N73-14849
Optimum rendezvous maneuver of space vehicles on elliptical trajectories for minimum fuel consumption
[NASA-TT-F-14644] 07 p0843 N73-16828
Mesh gradient technique for numerical optimization of descent trajectories
[NASA-TM-X-68181] 08 p0937 N73-17670
Development of computer program for parametric ascent trajectory optimization for application to space shuttle vehicle operation
[NASA-CR-129000] 12 p1458 N73-21815
Computerized multistage decision process for radar operator aid in collision avoidance trajectory control
14 p1711 N73-23886
Computer graphic display system for generating optimal electric propulsion space trajectory
[NASA-CR-130241] 15 p1754 N73-24217
Optimal control, guidance, and trajectory for low thrust acceleration spacecraft
15 p1829 N73-24827
Closed form expressions for position and velocity of spacecraft during finite burn
[NASA-CR-130243] 15 p1831 N73-24842
Optimum three impulse generator with patched conic trajectory model
[NASA-CR-130244] 15 p1831 N73-24843
Selected solar electric propulsion and ballistic missions
[NASA-CR-132753] 16 p1956 N73-25826
Geostationary satellite trajectory optimization by low thrust resistojet propulsion
[AASU-323] 16 p1967 N73-25913
Solution of optimum two-impulse transfer problem between orbits of specific inclination
[NASA-CR-130226] 19 p2344 N73-28855
Mathematical methods for development of improved rocket trajectories from radar tracking data
[AD-762203] 19 p2347 N73-28878
Space tug geosynchronous mission simulation
[NASA-CR-135706] 23 p2844 N73-32730
Numerical solutions to optimal three glide/thrust atmosphere skip maneuver
[NASA-TN-D-7211] 23 p2848 N73-32759
Application of perturbation method for computing optimal three dimensional reentry trajectories for shuttle-type spacecraft
24 p2978 N73-33798
Technique for determining fuel optimal, impulsive, fixed time trajectories based on comparison of two neighboring trajectories with application to ascent rendezvous
24 p2978 N73-33799

**TRANQUILIZERS**
Residual effects of hypnotic drugs on human nervous function and performance
12 p1369 N73-21106
Pilot performance under certain hypnotic, tranquilizer, and barbiturate type drugs
12 p1369 N73-21110
Spectral analysis on human biorhythmic performance to evaluate tranquilizer effects
12 p1370 N73-21116
Flight safety factors in prescribing tranquilizing drugs for flying personnel
12 p1371 N73-21123
Comparison of alcohol and dizepam effects on human mental and psychomotor functions
12 p1371 N73-21126
Stimulating and tranquilizing drug effects on human performance indices
13 p1483 N73-22021

**TRANSALL C-160 AIRCRAFT**
U C-160 AIRCRAFT

**TRANSCEIVERS**
U TRANSMITTER RECEIVERS

**TRANSCENDENTAL FUNCTIONS**
NT COSINE SERIES
NT EXPONENTIAL FUNCTIONS
NT PERIODIC FUNCTIONS
NT SINE SERIES
NT TANGENTS
NT TRIGONOMETRIC FUNCTIONS

**TRANSCONTINENTAL SYSTEMS**
Design and development of very high speed transportation system to include technological aspects and physical restraints
[P-4874] 04 p0488 N73-13990
Resynchronization of circadian rhythms following transmeridian flight observed in two group of students
19 p2227 N73-27958
Effects of two sequential transatlantic flights on circadian rhythm of body function and performance
19 p2227 N73-27964

**TRANSDUCERS**
NT DIGITAL TRANSDUCERS
NT ELECTROACOUSTIC TRANSDUCERS
NT ELECTRONIC TRANSDUCERS
NT HYDROPHONES
NT IMAGE TRANSDUCERS
NT MICROPHONES
NT PIEZOELECTRIC GAGES
NT PIEZOELECTRIC TRANSDUCERS
NT PIEZORESISTIVE TRANSDUCERS
NT PRESSURE SENSORS
NT SOUND TRANSDUCERS
NT THERMOPILES
NT ULTRASONIC WAVE TRANSDUCERS
Transducer for converting arterial pulse wave into electric signals
[NASA-CASE-GSC-11531-1] 02 p0135 N73-11097
Design, development, and evaluation of pressure transducer using glass fiber bundle to transmit and receive reflected light from pressure diaphragm
[AD-747521] 03 p0304 N73-12480
Acoustic field of infinite circular cylindrical transducer partially covered by layer of sound-soft material
[JPRS-57367] 03 p0335 N73-12732
Electronic transducer for acceleration measurement
[AD-748885] 04 p0423 N73-13451
Measurement of sinusoidal waves in flumes with transducers using non-contacting capacitive sensing
[NRC-MI-836] 05 p0522 N73-14243
Deep sea calibration of transducers at elevated hydrostatic pressure
[AD-750666] 06 p0641 N73-15203
Analysis of intensity distribution of radiation focussed by zone plate optics and computation of radiation flux on sensor area centered about optical axis
[AD-751516] 07 p0822 N73-16661
Variation of Rayleigh wave reflection coefficient of different interdigital transducer configurations with electric loads
07 p0831 N73-16737
Development of solid state magnetic digital temperature transducer - Vol. 1
[NASA-CR-133832] 08 p0923 N73-17556
Optimal performance of infrared pneumatic transducer with capacitive membrane
[ONERA-TP-1150] 09 p1007 N73-18222
Solution of Laplace equation in space bounded by flat and sinusoidal surface for determination of precision of noncontacting capacitive wave transducers
[AD-752021] 09 p1008 N73-18229
Focusing and deflection of microwave acoustic bulk wave
[AD-753385] 09 p1009 N73-18233
Development and characteristics of transducer for use with fluidic generators
[AD-755104] 11 p1273 N73-20334
Analysis of vibratory characteristics of sonar transducer element using finite element three dimensional mathematical model
[AD-755177] 13 p1495 N73-22117
Passive electrical dummy load for simulating transducers in large sonar arrays
[AD-755174] 13 p1495 N73-22123
Tapered interdigital transducers as flat bandpass devices
[AD-756935] 13 p1503 N73-22182
Doppler resolution filter configured as tapped delay line with simple input and output transducers
[AD-755194] 13 p1504 N73-22193
Failure analysis and design criteria for transducers in Apollo environmental control systems
[NASA-CR-128921] 15 p1756 N73-24231
Development of electronic detection system for remotely determining number and movement of enemy personnel
[NASA-CASE-ARC-10097-2] 16 p1873 N73-25160
Development of electronic circuit for measurement transducer power supply to be used for liquid level measurement in liquid propellant rocket engines
[NASA-CASE-MFS-21698-1] 17 p2003 N73-26196
Acoustical transducer calibrating system including differential pressure activating device
[NASA-CASE-FRC-10060-1] 18 p2150 N73-27379
Theoretical analysis of two dimensional laminar jet rate sensors
[AD-761092] 18 p2153 N73-27401
Inflight heart and respiratory rate recording of pilots, using nose clip transducers
19 p2226 N73-27953
Development of electro-hydrofluidic transducer for control of turbine engines
[AD-762298] 19 p2330 N73-28745
VHF - UHF surface wave studies of compliant layers for wedge transducers
[AD-762173] 20 p2378 N73-29106
Acoustic pumping used to achieve analogous ac Josephson effect in He2
20 p2385 N73-29164
Development and evaluation of on-line spatial light modulator for application as input transducer for real-time optical data processing system
[NASA-CR-124375] 21 p2508 N73-30121
Muscle force transducer to detect tremors in divers under hyperbaric conditions
[AD-763343] 23 p2750 N73-32010
Sensitivity of gravitational detector with positive electromechanical transducers
[ITF-72-90-E] 24 p2926 N73-33374

**TRANSEARTH INJECTION**
Improving selenodetic control on lunar limb using Apollo 15 transearth photography
[NASA-CR-131264] 11 p1336 N73-20846

**TRANSFER FUNCTIONS**
Transfer function of linearizer for anemometer data
[AD-744975] 01 p0075 N73-10622
Optical transfer function measurements on lenses and lens systems
[TPD-1972-0-1] 01 p0079 N73-10654
Determination of in-flight optical transfer functions of orbital earth resources multispectral sensors
[E72-10212] 02 p0162 N73-11307
Derivation of doubling equations for scattering and transmission functions for a homogeneous isotropically scattering atmosphere using scattering matrix
[USC-113P19-32] 02 p0202 N73-11631
Modulation transfer function in room acoustics as predictor of speech intelligibility
[IZF-1972-13] 02 p0211 N73-11710
Total correction of ohmic drop with transfer function of interphase electrode-solution equalling one
[UCRL-TRANS-10618] 03 p0263 N73-12129
Comparison of methods for determining transfer functions of black and white aerial photographic films
[AD-747594] 03 p0304 N73-12483
Nyquist criterion for control loops, using linear functional differential equations and transfer functions
[NRC-TT-1612] 06 p0690 N73-15622
Modulation transfer function of atmospheric medium as function of light wavelength
[AD-751641] 07 p0796 N73-16471
Computer programs for calculating transfer functions of retroreflector laser arrays carried by orbiting satellites
[NASA-CR-130696] 08 p0888 N73-17190
Performance of sensing system having inverse function amplifier
[RD/B/M-2306] 08 p0889 N73-17196
Gust field generation in wind tunnel for determining transfer function of lifting surface
12 p1387 N73-21248
Transfer phenomena in reacting gas mixtures
12 p1418 N73-21492
General expressions for transfer function and coherence relating earth motion and atmospheric pressure variations generated by slowly propagating, partially organized pressure fields
[AD-755527] 13 p1526 N73-22365
Electronic optical transfer function analyzer using scanning image dissection system to produce representative output signal
[NASA-CASE-MFS-21672-1] 13 p1558 N73-22630
Optical modulation transfer functions of human eye for white light
[IZF-1973-2] 14 p1609 N73-23047
Speech synthesis aided by recursive filter approximating transfer function of nasalized vocal tract
14 p1624 N73-23157
Analysis of image forming ability of infrared line scan system based on laboratory measurements and flight tests using ground test array
[DREV-TN-2053/72] 14 p1666 N73-23520
Construction of transfer functions in problems of weak shock interactions with cylindrical and spherical surfaces
14 p1715 N73-23913
Evaluation of image forming ability of infrared line scan system using laboratory and flight test techniques
15 p1786 N73-24476
Design of continuous lumped parameter linear filters
[AD-757545] 16 p1881 N73-25226
Equations of motion and response curve fitting method for determining transfer function coefficients of longitudinal aircraft motion
[DLR-FB-73-39] 17 p1984 N73-26034
Differential equations of motion and transfer functions of linear accelerometer for use in selection of instrument parameters
21 p2547 N73-30423
Optimum transfer function applied to correcting simplest single rotor gyroscope
21 p2576 N73-30645
Program for generating transfer functions of electrical network circuits
[AD-764809] 23 p2762 N73-32102
Measurement of light scattering at various angles using point spread function and modulation transformation function techniques
24 p2957 N73-33629

**TRANSFER OF TRAINING**
Human performance in schematic concept formation as a function of socio-economic level, personality, intelligence, and race
[AD-744781] 13 p1486 N73-22052

**TRANSFER ORBITS**
Simulation for use in dynamics and control analysis during boost from liftoff to orbit insertion
[NASA-CR-128592] 01 p0108 N73-10890
Performance of solid propellant apogee rocket motor in test firing at simulated altitude
[AD-747018] 02 p0224 N73-11809
Use of aerodynamic drag for transfer from hyperbolic trajectories to satellite orbits noting spacecraft guidance
[D-149] 05 p0596 N73-14849
Comparison of several first and second order deterministic low-thrust guidance methods
08 p0963 N73-17875
Optimal plotting of elliptical transfer orbit employing complete revolutions in equatorial plane of axisymmetric planet
[AD-753517] 09 p1085 N73-18857
Feasibility study for Europa 3 launch vehicle nuclear upper stage
[TR-TT-4-15/72] 15 p1811 N73-24675
Closed form expressions for position and velocity of spacecraft during finite burn
[NASA-CR-130243] 15 p1831 N73-24842
Solution of optimum two-impulse transfer problem between orbits of specific inclination
[NASA-CR-130226] 19 p2344 N73-28855
Coplanar transfer orbit calculation in Newton central gravitational field noting two propulsive phases applying tangential thrust and intermediate coast phase
[DLR-FB-73-29] 21 p2497 N73-30814
Numerical solutions to optimal three glide/thrust atmosphere skip maneuver
[NASA-TN-D-7211] 23 p2848 N73-32759

**TRANSFER TUNNELS**
Design and development of large flexible tunnel for use at space shuttle and payload interface
[NASA-CR-124073] 08 p0964 N73-17879

**TRANSFORM INTEGRALS**
U INTEGRAL TRANSFORMATIONS

**TRANSFORMATIONS**
Transformation of guided missile computer input/output routine for general purpose applications
[AD-760761] 18 p2121 N73-27147

**TRANSFORMATIONS (MATHEMATICS)**
NT COORDINATE TRANSFORMATIONS
NT FAST FOURIER TRANSFORMATIONS
NT INTEGRAL TRANSFORMATIONS
NT LAPLACE TRANSFORMATION
Derivations of straight line, Abel transform and seismological Herglotz-Wiechert transform for reconstruction of refractivity profiles from radio wave phase data
[NASA-TN-D-7098] 02 p0230 N73-11868
Numerical comparator for indicating error in measurement transformations
[PUBL-1361] 06 p0690 N73-15615
Transform coding and block quantization for remote aircraft scanner data and digitized satellite imagery compression
[NASA-CR-130365] 07 p0759 N73-16161
Correlation properties of Gaussian random processes under nonlinear transformations
09 p1057 N73-18619
Digital filtering techniques
[NASA-CR-124166] 11 p1264 N73-20256
Transformation of signal spectrum in communication between spacecrafts moving at relativistic velocities
[AD-758851] 16 p1876 N73-25186
Discrete unitary transforms with fast algorithm for encoding images for transmission
[NASA-CR-132771] 17 p2055 N73-26622
Algorithm for discrete transforms for implementing computer programs in radar signal processing
[AD-762437] 19 p2237 N73-28039
Expression for transformed covariance matrix of multivariate normal populations
[REPT-24] 20 p2439 N73-29588
Orthogonal and unitary transformations for asymmetrically loaded symmetric systems
[AD-761542] 20 p2440 N73-29601
Calculation of incompressible potential flow of airfoils by conformal mapping potential flow of lifting circles onto airfoils by double transformations
[ARC-R/M-3717] 21 p2492 N73-30002

**TRANSFORMERS**
Various types of energy transformation into electric energy
[AD-746549] 03 p0255 N73-12063
Method and device for providing banded transformer cores for use in spacecraft power systems
[NASA-CASE-NPO-11966] 13 p1499 N73-22150
Magnetic field interference of transformers for dc/dc converters for spacecraft power supplies
[ESRO-CR-84] 19 p2223 N73-27930
Magnetic materials selection for spacecraft transformers used in static inverters, converters, and transformer-rectifier supplies
[NASA-CR-135642] 23 p2764 N73-32118
X ray inspection of losses in high voltage transformers encapsulated by epoxy resins noting thermal cycling effects and stresses
24 p2881 N73-33008

**TRANSFORMS**
U TRANSFORMATIONS (MATHEMATICS)

**TRANSHORIZON RADIO PROPAGATION**
Water evaporation interference in phase measurements by transhorizontal microwave propagation over sea surface
17 p1994 N73-26125
Scattering in transhorizon ultrahigh frequency radio link due to rain
17 p1995 N73-26133
SHF transhorizon radio relay system, noting long term effects of tropospheric scatter propagation, layer reflection, and precipitation
[FTZ-A-455-TBR-34] 22 p2633 N73-31099

**TRANSIENT HEATING**
NT PULSE HEATING
NT SHOCK HEATING
Solution of inverse problem of transient heat conduction using Laplace transformation
16 p1973 N73-25954

**TRANSIENT LOADS**
NT BLAST LOADS
NT GUST LOADS
NT IMPACT LOADS
NT LANDING LOADS
NT SHOCK LOADS
Limiting performance of large systems subject to steady state and transient inputs
[NASA-CR-112293] 11 p1265 N73-20261
Devleopment of computer program for determining ultimate optimum behavior of dynamically loaded structural-mechanical system
[NASA-CR-2268] 18 p2203 N73-27783

**TRANSIENT PRESSURES**
Analytical combustion model for predicting flow and pressure transients in H2-O2 RCS of rocket engine feed system
07 p0835 N73-16767
Thermodynamic equilibrium model for simulating pressure transient propagation in two phase water flow with mass transfer
08 p0896 N73-17255

**TRANSIENT RESPONSE**
Differential equations for transient response of one dimensional, ablative thermal protection system, including thermal nonequilibrium, mass transfer, and chemical kinetics
[NASA-TM-X-68853] 02 p0137 N73-11108
Transient response of finite longitudinally-layered cylindrical membrane shell impacted by longitudinal axisymmetric loads
[TAE-154] 02 p0237 N73-11929
Finite element displacement method for studying transient response and dispersive behavior of elastic structures
[AD-747283] 02 p0241 N73-11956
Mechanisms for X irradiation induced transient changes in elastic modulus of quartz resonators
[SC-DC-72-1240] 05 p0587 N73-14771
Transient and steady state response characteristics of sandwich-type wavelength selective bolometer
[AD-750264] 06 p0675 N73-15496
Liapunov direct method for studying transient stability of multimachine power system
07 p0760 N73-16171
TACOS finite computer program for analyzing dynamic transient response of cylindrical obese shells
[SC-RR-72-0454] 12 p1463 N73-21852
Transient responses of hearing aids with compression
14 p1627 N73-23186
Transient behavior of currents and forces in coil system of stellarator during operational disturbances
[NASA-TT-F-15014] 18 p2126 N73-27182
Transient response of internal gravity waves due to midtropospheric heating
[AD-762369] 19 p2298 N73-28482
Transient response of devices operating in cryotron computing medium and determination of their speed
21 p2515 N73-30176
Transient response of stratified cold plasma to infinite plane electromagnetic wave
21 p2582 N73-30692
Transient response of stratified cold plasma to infinite plane impulsive electromagnetic wave incident vertically on ionization
21 p2582 N73-30693
Equations of motion formulated to compute transient response of multi-mass flexible rotors
[NASA-CR-2300] 23 p2797 N73-32374
Transient effects in pulse radar hydrometeor detection
24 p2956 N73-33616

**TRANSIENTS (SURGES)**
U SURGES

**TRANSISTOR AMPLIFIERS**
Design of microwave power transistor for providing power amplification in 1350 to 1850 MHz
[AD-749789] 05 p0521 N73-14237
Design and tests of one kilowatt L band solid state power amplifier
[AD-751279] 07 p0758 N73-16155
Long life broadband transistor amplifier chain for very high frequency range
[AD-752444] 09 p1004 N73-18194
Development of linear power transistors and design of broadband UHF amplifiers from these transistors
[AD-757558] 17 p2006 N73-26227
Design of MOS floating gate transistor amplifier
[AD-761660] 19 p2244 N73-28092

**TRANSISTOR CIRCUITS**
Boundary test procedure for determining characteristics and design of integrated transistor-transistor logic circuits
[AD-749604] 05 p0523 N73-14253

Transistorized control unit for neutron spectrometers or diffractometers
[BARC-591] 05 p0547 N73-14447
Transistor circuit with piezoelectric crystal for stable high frequency oscillator
[NASA-CASE-GSC-11513-1] 07 p0761 N73-16185
Computer modification of MOS transistor mathematical models
[CEA-R-4332] 12 p1383 N73-21218
Contactless extremum transistorized circuit capable of cutoff, saturation, and generation
16 p1883 N73-25245

**TRANSISTOR LOGIC**
Manufacturing high resolution active and passive semiconductor devices noting field effect transistors and transistor logic
[REPT-3.462] 23 p2766 N73-32126

**TRANSISTORS**
NT BIPOLAR TRANSISTORS
NT FIELD EFFECT TRANSISTORS
NT JUNCTION TRANSISTORS
NT PHOTOTRANSISTORS
NT SILICON TRANSISTORS
Flow behavior of integrated circuits in bipolar transistors
[CEA-CONF-1971] 01 p0087 N73-10722
Using Lang X ray scanning technique for studying crystallographic defect generation in commutation transistors during fabrication
[CEA-CONF-1981] 03 p0274 N73-12220
Construction and production problems connected with high frequency n-channel MOS transistors
[AD-747546] 03 p0276 N73-12240
Computation, design, and manufacture of integrated circuits for application to computer construction and operation
[JPRS-57333] 04 p0398 N73-13239
Effects of gamma and neutron radiation on high frequency characteristics of microwave bipolar transistors
[SC-DC-72-1233] 05 p0519 N73-14220
Design of transistorized oscillator for exciting gas discharge tubes
[AD-749831] 05 p0559 N73-14544
Effects of passivation processes on radiation tolerance of bipolar transistors subjected to neutron or gamma radiation
[SC-DC-72-1232] 05 p0565 N73-14589
Technique for selective amplifiers using transistor phase to eliminate induction
[PUBL-1369] 06 p0645 N73-15236
Thermal instability and secondary breakdown prediction for low frequency power transistor
[AD-751852] 08 p0890 N73-17203
Integrated microcircuits and complementary four-phase logic system
[NASA-CASE-MSC-14240-1] 12 p1386 N73-21240
Papers presented at conference on microwave transistors
[AD-760315] 17 p2005 N73-26213
Analysis of power consumption and switching times of micropower complementary bipolar transistor inverters
18 p2125 N73-27172
Variable-length transistorized pulse shaper
[AD-762328] 19 p2246 N73-28112
Peel, shear, and tensile strength measurements of transistor header lead welds
[BDX-613-871] 22 p2642 N73-31173
Second breakdown in diodes and transistors from intense ionizing radiation
[AD-763951] 22 p2644 N73-31192
Thermal effects on planar epitaxial silicon power transistors
[AD-763903] 22 p2645 N73-31194
Two-dimensional numerical analysis of integrated silicon N-P-N bipolar transistors
22 p2706 N73-31672
Inverted geometry transistor for use with monolithic integrated circuit
[NASA-CASE-ARC-10330-1] 23 p2763 N73-32112

**TRANSIT SATELLITES**
Cinetheodolite observation of 1963-30 D [Dash 2] satellite between Nov. 1965 and Mar. 1966
[ROE-STS-132] 06 p0722 N73-15890

**TRANSIT TIME**
Longitude, latitude, and azimuth determinations using transit instrument
[MITT-99] 01 p0101 N73-10826
Design and development of wideband TRAPATT amplifier in microstrip configuration for use in phased-array radar modules in S-band
[AD-747050] 02 p0150 N73-11215
Transit time measurements between earth and moon by transportable pulsed laser system
[NASA-CR-130986] 09 p1042 N73-18502
Oscillation hot-wire anemometer based on downstream transit time of hot gas volume
[REPT-9/1972] 22 p2674 N73-31419

**TRANSITION**
Mathematical model of transition flight and application to Do-31 aircraft
[BMVG-FBWT-72-30] 10 p1107 N73-19025

**TRANSITION FLOW**
Laminar flow, and transitional flow heat transfer
[ESDU-68006-AMEND-A-PT-2] 02 p0241 N73-11963
Wake transition of blunt cones in hypersonic flight using schlieren photography and opto-electronic laser system
[ISL-12/72] 03 p0310 N73-12531
Effects of density measurement electron beam impinging on blunt body in transition flow, noting influence of secondary electrons
[DLR-FB-73-08] 09 p0981 N73-18017
Ablation article and surface for analyzing flow transition on ablative surface
[NASA-CASE-LAR-10439-1] 18 p2205 N73-27796
Transition from laminar to turbulent flow for radially inward throughflow of incompressible Newtonian fluid between closely spaced parallel corotating disks
20 p2385 N73-29159

**TRANSITION METALS**
NT CADMIUM
NT CHROMIUM
NT COBALT
NT COBALT 60
NT GOLD
NT HAFNIUM
NT IRIDIUM
NT IRON
NT IRON 57
NT MANGANESE
NT MOLYBDENUM
NT NICKEL
NT NIOBIUM
NT OSMIUM
NT PALLADIUM
NT PLATINUM
NT PLATINUM BLACK
NT REFRACTORY METALS
NT RHENIUM
NT RHODIUM
NT RUTHENIUM
NT SILVER
NT TANTALUM
NT TANTALUM ISOTOPES
NT TITANIUM
NT TUNGSTEN
NT VANADIUM
NT ZINC
NT ZIRCONIUM
Magnetic properties of transition metals
[BNL-16679-PT-1-PT-2] 03 p0336 N73-12738
Thermodynamic properties of transition metal/silicon binary alloys
[NPL-CHEM-18] 03 p0365 N73-12970
Compilation of reports on transition metal carbides for period 1956 to 1972
[CE-BIB-228] 04 p0437 N73-13560
Thermomagnetic analysis of rare earth transition metal alloys as permanent magnet materials
[AD-750746] 06 p0686 N73-15587
Microscopic dipole model for lattice dynamics in transition metals
08 p0950 N73-17782
Shell model for phonon dispersion anomalies and lattice instabilities in hard metalcarbides-nitrides and transition metals
08 p0951 N73-17783
Electron structure of transition metals and alloys
[ONERA-P-144] 09 p1048 N73-18548
Influence of reversible reaction transition superconducting to normal on plastic properties of transition and lead metal and alloy single crystals
[ANL-7903] 10 p1200 N73-19766
Technology of high performance transition metal, rare earth permanent magnets for critical applications
[AD-754959] 11 p1306 N73-20601
Structural, electrical, and magnetic properties of transition metal oxide phosphate glasses
[AD-758373] 14 p1699 N73-23790
Electric field induced instability in transition metal compounds
[AD-758270] 15 p1822 N73-24771
Phonon scattering by conduction electrons in transition metal carbides
[COO-1198-937] 16 p1947 N73-25755
Technological development of high performance transition metal-rare earth magnets for critical applications
[AD-760178] 17 p2048 N73-26566
Base metal catalysts as platinum substitutes in petroleum refining and automobile emission devices
[NMAB-297] 18 p2113 N73-27088
Development of method for calculating molar volume and density of molten binary alloys with strongly interacting dissimilar atoms
[NLL-M-21695-[5828.4F]] 20 p2429 N73-29512
Research and development of rare earth-transition metal alloys as permanent magnet materials
[AD-762304] 20 p2432 N73-29534
Temperature relationship of monochromatic coefficients of radiation of titanium, niobium, and zirconium monocarbides in regions of homogeneity
23 p2807 N73-32442
Effect of addition of transition metals on cast zirconium to show changes in microstructure, macrostructure, microhardness, and electrical resistance
23 p2809 N73-32457
Quasiparticle tunneling into superconducting transition metals
[AD-764905] 23 p2826 N73-32591

**TRANSITION POINTS**
Development of model for conditions of superplasticity related to maximum interphase surface of fluctuation nuclei of phase transformation
13 p1540 N73-22478
Liquid-solid transition for materials processing in space
[NASA-CR-124294] 18 p2179 N73-27596

**TRANSITION PROBABILITIES**
Transition moments and associated probabilities, line strengths, and absorption oscillator strengths
[AD-754025] 11 p1252 N73-20163

**TRANSITION TEMPERATURE**
Evaluation of structure safety against brittle fracture based on transition temperature, fracture toughness, and crack opening displacement
[ZJE-118] 04 p0481 N73-13933
Thermomechanical analysis of physical transitions and stability of poly[norbornadiene] in nitrogen
[AD-749374] 05 p0566 N73-14596
Isothermal compressibility of amorphous semiconductors
[AD-750397] 06 p0709 N73-15785
Interferometric measurement of hypersonic sound wave attenuation in liquid helium transition region
13 p1558 N73-22629
Construction and operation of bend tester at temperature ranges from minus 192 to 650 C
[NASA-TM-X-2853] 18 p2160 N73-27452
Structural and superconducting transition temperature of evaporated aluminum films as function of grain size
[NASA-CR-133450] 19 p2326 N73-28716
SQUID magnetometer measurement of fluctuation diamagnetism of Al and Al alloys above superconducting transition temperature
[COO-3156-56] 21 p2559 N73-30515
Fluctuation diamagnetism of aluminum and aluminum alloys above superconducting transition temperature
23 p2804 N73-32422

**TRANSITS**
NT CINETHEODOLITES
NT THEODOLITES

**TRANSLATING**
NT MACHINE TRANSLATION
English, French, and Spanish vocabulary of aircraft aeronautical terminology
[DOC-8800-VOL-1] 06 p0616 N73-14996

**TRANSLATIONAL MOTION**
NT SECONDARY FLOW
NT THREE DIMENSIONAL FLOW
NT THREE DIMENSIONAL MOTION
Translational-rotational magnetized satellite equations of motion in geomagnetic field
15 p1832 N73-24847
XY translational device controlled by differential interferometer for large scale integration microelectronics
[LCR-71-213/1/R] 18 p2152 N73-27394

**TRANSLUCENCE**
Performance of translucent beryllium oxide as envelope material for high intensity flash and continuous wave lamps
[AD-751661] 07 p0813 N73-16589

**TRANSLUNAR SPACE**
U INTERPLANETARY SPACE

**TRANSMISSION**
NT AERODYNAMIC HEAT TRANSFER
NT AUTOMATIC PICTURE TRANSMISSION
NT CONDUCTIVE HEAT TRANSFER
NT CONVECTIVE HEAT TRANSFER
NT DATA TRANSMISSION
NT DOUBLE SIDEBAND TRANSMISSION
NT ELECTRIC POWER TRANSMISSION
NT ELECTROMAGNETIC WAVE TRANSMISSION
NT GROUND WAVE PROPAGATION
NT HEAT TRANSFER
NT HEAT TRANSMISSION
NT HYPERSONIC HEAT TRANSFER
NT IONOSPHERIC F-SCATTER PROPAGATION
NT IONOSPHERIC PROPAGATION
NT LAMINAR HEAT TRANSFER
NT LIGHT SCATTERING
NT LIGHT TRANSMISSION
NT MICROWAVE ATTENUATION
NT MICROWAVE TRANSMISSION
NT MULTIPATH TRANSMISSION
NT MULTIPLEXING
NT RADAR TRANSMISSION
NT RADIATIVE HEAT TRANSFER
NT RADIO TRANSMISSION
NT SATELLITE TRANSMISSION
NT SCATTER PROPAGATION
NT SHOCK WAVE PROPAGATION
NT SHORT WAVE RADIO TRANSMISSION
NT SIGNAL TRANSMISSION
NT SINGLE SIDEBAND TRANSMISSION
NT SOUND TRANSMISSION
NT TELEPHONY

NT TELEVISION TRANSMISSION
NT TIME DIVISION MULTIPLEXING
NT TURBULENT HEAT TRANSFER
NT WAVE PROPAGATION
Mossbauer spectrometer with high efficiencies in both transmission and backscattering techniques
[NASA-CASE-LAR-11155-1] 04 p0421 N73-13433
Optimum roller bearing design for use in heavy lift helicopter rotor transmission second stage planetary system
[AD-755535] 15 p1794 N73-24540
Anomalous X ray transmission through single germanium crystals
16 p1952 N73-25793

TRANSMISSION CIRCUITS
Electrical and dimensional characteristics of ac superconducting power transmission circuits
[AD-745846] 01 p0088 N73-10727
Input signal dynamics for analyzing gain stability and linearity of electronic circuit working with large signals
[INR-1371] 04 p0398 N73-13240

TRANSMISSION EFFICIENCY
Electron irradiation effect on transmission properties of ceria doped solar cell cover glass
[NASA-TN-D-7245] 15 p1737 N73-24082
Multi-impedance loading of linear antennas to improve transmitting and receiving characteristics
21 p2516 N73-30184

TRANSMISSION FLUIDS
Effect of undissolved air on compressibility of transmitting medium in hydraulic circuits
[NLL-NEL-TT-2426-[6075.461]]
15 p1763 N73-24289

TRANSMISSION LINES
NT BEAM WAVEGUIDES
NT COAXIAL CABLES
NT COMMUNICATION CABLES
NT POWER LINES
NT STRIP TRANSMISSION LINES
NT WAVEGUIDES
Spurious signals introduced into system from external cabling in electromagnetic pulse environment
[AWRE-O-47/71] 01 p0034 N73-10270
Narrow band equivalent circuit for two-port network using cascaded, lossless transmission lines and lossless shunt elements
[APS-EL-30] 02 p0150 N73-11221
Analysis of exact and approximate methods for solving inverse scattering problem for transmission lines
02 p0199 N73-11612
Automatic monitor for classifying high usage data transmission system circuits
[AD-749268] 04 p0392 N73-13183
Effects of magnetic and electric coupling parameters on terminal response shielding of braided-shield cables exposed to external electromagnetic fields
[AD-748387] 04 p0396 N73-13221
Capacitance analysis of electromagnetic coupling response in transmission lines and cables
[SC-RR-72-0299] 04 p0458 N73-13741
FORTRAN subroutine for plotting computer determined transmission line parameters on Smith chart
[AD-751019] 06 p0645 N73-15243
Plastic sheaths as lightning conductors for insulating communication cables
[AD-750642] 06 p0647 N73-15252
Slot transmission line on dielectric substrate
[AD-751657] 07 p0763 N73-16196
Development of phase control coupling for use with phased array antenna
[NASA-CASE-ERC-10285] 07 p0764 N73-16206
Computerized simulation of longitudinal cable shapes during deployment from missile away from flying aircraft
[AD-753907] 10 p1135 N73-19254
Model of n-conductor transmission lines for SCEPTRE computer program
[AD-754964] 11 p1265 N73-20265
Network analysis of transmission line analogs for stacked piezoelectric crystal vibrators
[AD-754545] 11 p1330 N73-20799
Investigation of antenna cable responses to pulsed electromagnetic field
[AD-755514] 12 p1385 N73-21234
Numerical analysis of multiple conductor transmission line with arbitrarily positioned impedances in series with each wire
[SC-R-72-2695] 12 p1386 N73-21244
Magnetoelastic transmission delay lines for S band noting insertion loss reduction
[REPT-8.425] 13 p1491 N73-22087
Analysis of directional antenna transmission line networks
[AD-756567] 13 p1501 N73-22163
Electrical characteristics of FCC determined in context of multiple transmission lines theory
14 p1640 N73-23300
Analytical prediction of crosstalk in multi-wire digital data transmission
14 p1641 N73-23301
Analysis of aerodynamically induced oscillations of bundled power conductors resulting from effect of wind on transmission power lines
17 p2098 N73-26971
Design of flat conductor cable for interconnecting harness application
[NASA-TM-X-64750] 19 p2243 N73-28085
Slot line transitions to coaxial line and to microstrip
[AD-761765] 19 p2244 N73-28095
Treatment of singularities in solution of Laplace equation by integral equation method based on Green function, applied to flow distribution and transmission lines
[NPL-NAC-31] 23 p2813 N73-32490

TRANSMISSION LOSS
Doppler radar frequency attenuation in horizontally polarized field over forest
[AD-748104] 04 p0389 N73-13163
Numerical analysis of Pacific Ocean bottom signal reflection losses using underwater explosive sound sources and multilayered acoustic absorption model
[AD-748199] 04 p0450 N73-13676
Effects of camera lense photosensitivity on signal loss in vidicon tubes
[AD-750530] 05 p0549 N73-14459
Lossy earth effects on very high frequency antenna patterns near ground level
[AD-754637] 11 p1257 N73-20204
Acoustic transmission loss measurements in Arctic Ocean ice zone by aircraft
[AD-754394] 11 p1325 N73-20755
Ray tracing method for computerized prediction of underwater sound propagation loss
[AD-755459] 12 p1430 N73-21590
Radio propagation loss over ocean surface paths
[AD-755511] 13 p1492 N73-22091
Radiative light transfer model for aerosol radiance loss in atmospheric photometry
13 p1558 N73-22628
Measured and calculated transmission losses of sound waves through helium layer
[NASA-TN-D-7230] 14 p1692 N73-23735
Temporary loss of Apollo 14 command module color television picture by ground station converter
[NASA-TM-X-69296] 15 p1751 N73-24189
Analysis of power loss for coupled transmission and reaction resonator circuits
[AD-762252] 19 p2248 N73-28126
Medium frequency wave ionospheric propagation loss in earth reflected paths
[BBC-RD-1973/17] 22 p2627 N73-31050
SHF transhorizon radio relay system, noting long term effects of tropospheric scatter propagation, layer reflection, and precipitation
[FTZ-A-455-TBR-34] 22 p2633 N73-31099
FORTRAN program for prediction of tropospheric radio transmission loss over irregular terrain
[AD-764476] 22 p2635 N73-31115
X ray inspection of losses in high voltage transformers encapsulated by epoxy resins noting thermal cycling effects and stresses
24 p2881 N73-33008

TRANSMISSIVITY
Reflection and transmission of large amplitude shockless waves at interface with semi-infinite medium
[AD-746642] 04 p0483 N73-13947

TRANSMISSOMETERS
Development of transmissometer for measuring optical transmission through aircraft jet engine exhausts
[AD-760050] 17 p2035 N73-26467
Development of portable transmissometer calibrating unit using laser as projector source
[AD-757282] 18 p2153 N73-27403

TRANSMITTANCE
Atmospheric transmittance from sun and sky radiance measurements with Nimbus E infrared temperature profile radiometer prototype used at Mauna Loa Observatory
[NOAA-TR-NESS-61] 01 p0048 N73-10391
Atmospheric transmittance calculations of laser beams for atmospheric models with water vapor as molecular absorber
[AD-745585] 01 p0065 N73-10532
FORTRAN computer program for computing transmittance of atmosphere in ultraviolet to infrared spectral region
[AD-763721] 21 p2541 N73-30378
Development and characteristics of spectrophotometer for measuring transmittance of solid and liquid materials
[PAPER-76A5-729] 21 p2545 N73-30398
Direct integration transmittance model for 200/2000 cm region of high spectral resolutions and of planetary thermal emissions
[NASA-TM-X-70454] 21 p2548 N73-30429
Transmitting and reflecting diffuser
[NASA-CASE-LAR-10385-3] 23 p2819 N73-32538

TRANSMITTER RECEIVERS
Intermodulation interference effects of metal surface transmitters and receivers in near field locations of transmission system
01 p0027 N73-10212
Propagation characteristics of satellite-borne television transmitter and ground receiver for communication satellite system
[NASA-CR-123909] 01 p0028 N73-10214
Development and characteristics of vehicle detection system with all active elements carried by moving vehicle
[NASA-CASE-NPO-11850-1] 01 p0032 N73-10248
Design of portable HF/VHF radio set for manpack usage
[AD-749510] 05 p0514 N73-14175
Instrumented dolphins for surveying oceanographic parameters and relaying information to tracking aircraft
[AD-754761] 11 p1256 N73-20191
Developmental model of VHF transceiver multicoupler
[AD-755548] 13 p1502 N73-22177
Improving optical compatibility of lidar transmitter-receiver
[NASA-TM-X-64753] 16 p1923 N73-25561
Performance tests on transmitter receiver and power amplifier for portable radio manpack
[AD-759953] 17 p2000 N73-26174
Analysis of time-sharing voice modulated output of several collocated transmitters and receivers using very high frequencies
[AD-758567] 18 p2120 N73-27140
Carbon dioxide laser frequency stability data for receiver design optimization
18 p2212 N73-27861
Development of discrete address beacon system for application to air traffic control operations
[FAA-RD-73-101] 21 p2577 N73-30651
Time synchronization in optical communication as problem of estimating arrival time of known transmitted field
[NASA-CR-132813] 23 p2801 N73-32401
Development of timing device for conserving batteries on remote data collection platform by generating synchronous time windows
[NASA-CASE-GSC-11182-1] 23 p2849 N73-32769

TRANSMITTERS
NT INSTRUMENT TRANSMITTERS
NT IONOSONDES
NT RADAR TRANSMITTERS
NT RADIO BEACONS
NT RADIO TRANSMITTERS
NT RADIOSONDES
NT RADIOTELEPHONES
NT RAWINSONDES
NT SONOBUOYS
NT TRANSMITTER RECEIVERS
Ultrasonic marine biotelemetry transmitter utilizing metal oxide semiconductor integrated circuits
[AD-748605] 04 p0383 N73-13119
Service life and reliability of single transmitter and array modular type satellite altimeter systems
06 p0663 N73-15388
Designing light weight Q switch laser transmitter for rangefinders
[AD-750383] 06 p0680 N73-15536
Modification of Auburn University Model S-2 FM television transmitter through use of integrated circuits and conversion to receive telemetry signals
[NASA-CR-124082] 09 p1001 N73-18171
Airborne C band pulsed transmitter for instrument landing system
13 p1491 N73-22086
Multicarrier communications system for transmitting modulated signals from single transmitter
[NASA-CASE-NPO-11548] 17 p1993 N73-26118
Dual beam electron gun broad bands transmitter tube
[AD-763226] 21 p2518 N73-30198

TRANSOCEANIC COMMUNICATION
Computerized management tools for use in analysis of automatic switching centers and associated tributaries of Autodin communications network
[AD-761479] 19 p2236 N73-28028

TRANSOCEANIC SYSTEMS
NT TRANSOCEANIC COMMUNICATION
Side-looking radar applications to transportation noting route planning, shipping lanes, and traffic
03 p0295 N73-12409

TRANSONIC AIRCRAFT
U SUPERSONIC AIRCRAFT

TRANSONIC COMPRESSORS
Design and experimental performance of axial flow, transonic compressor
[NASA-TM-X-2645] 02 p0123 N73-11002
Multiple tone acoustic radiations phenomenon in transonic fans
[ARC-CP-1226] 05 p0580 N73-14726
Design and evaluation of multiple circular arc bladed, axial flow transonic compressor rotor
[NASA-TM-X-2697] 15 p1730 N73-24033

TRANSONIC FLOW
Shock properties for steady, irrotational, transonic flow
[NASA-TN-D-6997] 01 p0040 N73-10314
Three dimensional transonic flows past lifting configurations having finite leading edge swept angles
[AD-747266] 02 p0159 N73-11284
Wind tunnel tests of mixed compression axisymmetric inlet with large transonic mass flow at Mach numbers 0.6 to 2.65
[NASA-TN-D-6971] 04 p0463 N73-13777

Closed form, Romberg, and Gaussian procedures for calculating transonic wave drag integral using cubic splines
[NAL-TN-35] 06 p0652 N73-15299
Analysis of critical conditions of gas ejectors at large pressure drops within framework of ideal-gas dynamics
[AD-750536] 06 p0656 N73-15328
Computerized stability derivative calculations for oscillating parabolic ogives and circular cones in transonic flow field using iterative procedure
[NASA-CR-124033] 07 p0769 N73-16249
Analysis of aerodynamic noise generated by tips of helicopter rotary wings during acceleration to near sonic speed
[AD-752301] 09 p0989 N73-18072
Analysis of two dimensional cascade flow of double circular arc blades at transonic speed with various camber angles and pitch-chord ratios
[NAL-TR-300] 09 p1014 N73-18279
Numerical solution to transonic airfoil problems
[AD-753390] 09 p1018 N73-18304
Computer program for calcuating transonic flow about axisymmetric bodies
[AD-752898] 09 p1018 N73-18309
Two dimensional unsteady transonic flow of perfect gas with specific heat
[AD-753221] 09 p1018 N73-18310
Development of steel wedge probe for measurement of three dimensional wake flow in subsonic and transonic flow fields
10 p1140 N73-19285
Analytical approach for loss and deflection behavior of cascades in transonic flow including axial mass flow variation
10 p1204 N73-19800
Calculation of flows in subsonic and transonic portions of circular nozzles
[NASA-TT-F-14847] 11 p1270 N73-20308
Development of computer program and algorithm for determining interference between lifting surface elements at various Mach numbers
[NASA-CR-112264] 12 p1390 N73-21272
Application of holographic interferometry to density field determination in transonic corner flow
[AD-756534] 13 p1511 N73-22247
User manual for turbulent boundary layer and turbulent separation prediction methods used in streamtube curvature computer program
[NASA-CR-112240] 14 p1649 N73-23376
Vaporization thermodynamics of Cr2O3 protective scales under transonic flow conditions
14 p1677 N73-23607
Analysis of transonic potential flow through oscillating unstaggered thin plate cascade
[AD-757255] 14 p1701 N73-23806
Numerical analysis of steady transonic flows over lifting configurations to show reduced lift in thickness-dominated regime
15 p1765 N73-24302
Transonic perturbation equation for studying steady compressible flow past lifting and nonlifting wings at high subsonic Mach numbers
[NASA-CR-2246] 15 p1766 N73-24312
Nonlinear unsteady small-disturbance theory of inviscid transonic flows for oscillating aerodynamic configurations
[NASA-CR-2258] 16 p1858 N73-25048
Equivalence rule and transonic flows involving lift around thin smooth configuration with swept leading edge
[AD-760349] 17 p1985 N73-26042
Development of alternating direction relaxation method for computing inviscid two dimensional transonic flows through cascades
17 p2012 N73-26268
Effects of mass injection of tip vortex on airfoil performance at transonic speeds
[AD-760363] 17 p2016 N73-26304
Development of computer program for subsonic and shock-free transonic flow solution on hub-shroud midchannel flow surface of turbomachine - Vol. I
[NASA-TN-D-7343] 18 p2102 N73-26996
Analysis of transonic aerodynamics developments to include methods for computing steady and unsteady transonic flows
[AD-761551] 19 p2218 N73-27892
Analysis of arbitrarily nonuniform, nonadiabatic, two dimensional or axisymmetric basic flows based on inviscid theory of three dimensional perturbations in uniform transonic flow
[AD-761632] 19 p2256 N73-28188
Numerical analysis of inviscid transonic flow over body with supersonic underexpanded exhaust plume and characteristics of flow near boattail sting
[RM-577] 21 p2523 N73-30234
Three-dimensional compressible turbulent boundary layer for subsonic and transonic flow over yawed airfoil
[AD-763730] 21 p2526 N73-30258
Aerodynamic drag on slender bodies in transonic flow
[AD-763437] 21 p2527 N73-30264
Correlation between wind tunnel data and finite difference solutions for viscous and wind tunnel effects in transonic flows over airfoils
[AD-764133] 22 p2612 N73-30936
Development of wind tunnel with self correcting apparatus based on sensors to determine flow conditions on tunnel surfaces and method for varying wall geometry
[AD-764957] 23 p2771 N73-32161

**TRANSONIC FLUTTER**

Characteristics of single linear inertia exciter and multichannel recording equipment for flight flutter tests on Meteor aircraft
[ARC-R/M-3247] 16 p1855 N73-25026
Numerical analysis of wing bending, wing torsion, and aileron rotation at transonic speeds to determine effects on wing-aileron flutter
[ARC-R/M-3258] 16 p1855 N73-25028

**TRANSONIC INLETS**

U SUPERSONIC INLETS

**TRANSONIC NOZZLES**

Performance tests of wedge nozzle with cold primary and secondary flows for supersonic cruise and takeoff configurations to analyze noise suppression effects
[NASA-TM-X-2689] 06 p0714 N73-15822

**TRANSONIC SPEED**

Evaluation of Rayleigh-Ritz anisotropic plate analysis procedure for determining performance of composite wing for aircraft operating in transonic environment
[AD-745129] 02 p0126 N73-11023
Development of computer programs for analyzing and predicting properties of transonic flows around certain types of wing-body combinations
[NASA-CR-2157] 03 p0247 N73-11999
Performance tests of single stage, axial flow, transonic compressor over stable operating range at rotative speeds from fifty to one hundred percent of design speed
[NASA-TM-X-2658] 06 p0614 N73-14983
Development of finite difference procedure to calculate steady flows over several classes of airfoils under inviscid transonic flow conditions
[NASA-CR-2186] 06 p0614 N73-14989
Flight tests to determine buffet characteristics of four high performance aircraft during transonic maneuvers
06 p0618 N73-15017
Reduction of transonic drag for high performance aircraft by injecting air in rear of aircraft to alter transonic flow distribution on aft section
[AD-751269] 07 p0736 N73-15991
Transonic wind tunnel tests of two dimensional airfoil fitted with square and convex semicircular blunt bases to determine aerodynamic drag coefficients
[ARL/A-NOTE-336] 10 p1103 N73-18994
Design, characteristics, and performance tests of high-tip-speed, low-loading, transonic fan stage
[NASA-CR-121095] 13 p1570 N73-22727
Application of integral relations to analyzing inviscid supercritical flow about lifting airfoils with embedded shock wave
[AD-755762] 14 p1651 N73-23390
User manual for Streamtube Curvature Analysis program to predict pressure distribution about nacelle at transonic speeds - Vol. I
[NASA-CR-112239-1] 15 p1767 N73-24313
User manual for Streamtube Curvature Analysis program to predict pressure distribution about nacelle at transonic speeds - Vol. 2
[NASA-CR-112239-2] 15 p1767 N73-24314
User manual for Streamtube Curvature Analysis program to predict pressure distribution about nacelle at transonic speeds - appendix
[NASA-CR-112239-3] 15 p1767 N73-24315
Wind tunnel tests to determine pressure distributions for four percent thick, circular arc, biconvex airfoil at transonic speeds
[ARC-R/M-3180] 16 p1852 N73-25002
Wind tunnel tests to determine directional and longitudinal stability of Javelin aircraft model at transonic speeds
[ARC-R/M-3403] 16 p1853 N73-25012
Analysis of effects of shock induced boundary layer separation in transonic flight and methods for eliminating or reducing effects
[ARC-R/M-3510] 16 p1854 N73-25019
Optimum design of wing-body combinations for zero-lift drag rise at transonic speeds
[ARC-R/M-3279] 16 p1857 N73-25043
Analysis of minimum run times required for instationary measurements at transonic speeds during wind tunnel tests
17 p2009 N73-26243
Application of holographic interferometry techniques for determining asymmetric flow distribution encountered near wing-fuselage junction at transonic speed
[AD-759967] 17 p2015 N73-26296
Design and development of two dimensional airfoil with optimum drag divergence characteristics at transonic speeds
[NAL-TR-299] 18 p2101 N73-26994
Wind tunnel tests to determine aerodynamic characteristics of two missile configurations with common body at transonic and supersonic speeds
[NASA-TM-X-2780] 19 p2218 N73-27891
Analysis of transonic scaling effect on quasi, two-dimensional airfoil model of C-141 aircraft
[AD-762285] 19 p2222 N73-27924
Derivation of charts for predicting drag-rise Mach number for airfoils with specified upper surface pressure distribution
[ESDU-71019] 22 p2650 N73-31229
Prediction of aerodynamic characteristics of airfoils at transonic speeds including effects of fluid viscosity
[AD-763295] 22 p2654 N73-31260
Pulsed laser holographic interferometry of shock waves within transonic fan rotors
[NASA-TM-X-71430] 23 p2801 N73-32402

**TRANSONIC WIND TUNNELS**

Transonic and hypersonic wind tunnels in Germany
[DLR-FB-71-86] 06 p0650 N73-15278
Transonic flow studies in slotted wind tunnels
[AD-753911] 10 p1144 N73-19320
Applications of transonic wind tunnel with variable geometry perforated walls
[DGT-8652] 13 p1507 N73-22212
Design and calibration of Langley 6 by 19 inch transonic tunnel for testing two dimensional airfoil sections
[NASA-TN-D-7182] 14 p1645 N73-23339
Wall interference effects at Mach 1 on airfoils in transonic wind tunnels
[AD-757534] 14 p1646 N73-23349
Environmental impact of noise produced by transonic wind tunnel at Arnold Engineering Development Center
[AD-757552] 14 p1646 N73-23351
Transonic wind tunnel corrections for slotted or perforated walls
14 p1649 N73-23373
Modane-Avrieux transonic blowdown wind tunnel for two dimensional flow airfoil profile study
[ONERA-NT-203] 15 p1762 N73-24281
Transonic wind tunnel wall effects on boundary layer blocking phenomena
15 p1766 N73-24306
Analysis of problems involved in operation of large wind tunnels at subsonic and supersonic speeds
[AGARD-R-601] 17 p2008 N73-26239
Development of numerical methods for correcting wall constraints in transonic wind tunnels with ventilated walls
17 p2008 N73-26241
Fluid motion problems in design and operation of low speed and transonic wind tunnels
[AGARD-R-602] 17 p2013 N73-26279
Present and future need for high Reynolds number transonic wind tunnels including analysis of design selection and requirements
17 p2013 N73-26282
Effects of turbulence and noise on wind tunnel measurements at transonic speeds
17 p2014 N73-26284
Design of ventilated walls for transonic wind tunnels with analysis of parameters affecting noise generation
17 p2014 N73-26285
Method to increase full-scale inlet/engine system testing capability of AEDC 16-ft transonic wind tunnel
[AD-762912] 20 p2383 N73-29146
Parametric study of proposed high Reynolds number transonic wind tunnel
[AD-763725] 21 p2522 N73-30227
Transonic wind tunnel tests to determine lift, drag, and stability characteristics of F-8 aircraft model with oblique wing
[NASA-TM-X-62273] 24 p2877 N73-32974

**TRANSONICS**

U TRANSONIC FLOW

**TRANSPARENCE**

Vertical distribution of transparency measured by submerged transparency meters
[NLL-RTS-7535] 02 p0160 N73-11295
Measurement of ultraviolet and far ultraviolet transmission of transparent materials during high energy electron irradiation
[NASA-CR-129297] 03 p0334 N73-12726
Measurements of laser induced surface damage processes at ruby and neodymium YAG laser wavelengths to determine laser damage at different wavelengths to transparent media
05 p0555 N73-14506
Mechanical properties of monolithic transparent polycarbonate plastic sheet
[AD-751551] 07 p0813 N73-16590
Surface and unambiguous bulk damage to optically transparent materials
[AD-756486] 13 p1559 N73-22638
Environmental tests of strength and durability of transparent tin oxide and indium oxide films on glass
[AD-756558] 14 p1680 N73-23637
Net radiation method for analyzing radiation heat transfer in enclosures involving partially transparent walls
[NASA-TN-D-7384] 19 p2351 N73-28915

Intermolecular force effects on infrared spectral transparency of active gas mixtures
[DRIC-TRANS-3227] 23 p2820 N73-32545
TRANSPARENT MATERIALS
U TRANSPARENCE
TRANSPIRATION
Computer program for compact transpiration cooling with free jet tests and theory comparison
[AD-753109] 09 p1017 N73-18299
Attenuation of thermal radiation by transpiration of absorbing gas using porous Porolloy plate
15 p1812 N73-24685
TRANSPIRATION COOLING
U SWEAT COOLING
TRANSPLANTATION
Immunological effectiveness of X ray irradiation on histocompatibility of mice skin transplants
13 p1481 N73-22008
TRANSPONDERS
Development and characteristics of vehicle detection system with all active elements carried by moving vehicle
[NASA-CASE-NPO-11850-1] 01 p0032 N73-10248
Feasibility study for laser transponder onboard SOREL space probe
[ESRO-CR[P]-123] 02 p0149 N73-11207
Flight tests of transponder correlation ranging equipment for use in airborne collision avoidance system
[AD-746448] 02 p0175 N73-11416
Multimode transponders for tracking and data relay satellites
[NASA-CR-130170] 08 p0888 N73-17191
Use of superhigh frequency transponder on Apollo 16 subsatellite to measure lunar gravitational field as preliminary investigation of lunar mass
12 p1451 N73-21758
Loop transponder for regenerating code of mu-type ranging system
[NASA-CASE-NPO-11707] 16 p1873 N73-25161
Test operation procedure for radar interrogator transmitter
[AD-759227] 17 p1998 N73-26158
Development of solid state beacon and radio frequency generator for avionics applications - Vol. 1
[AD-761525] 19 p2247 N73-28115
Applications of inverse Fourier transform method of producing high peak power for use with solid state radio beacon - Vol. 2
[AD-761526] 19 p2247 N73-28116
Development of discrete address beacon system for application to air traffic control operations
[FAA-RD-73-101] 21 p2577 N73-30651
Symphonie satellite transponder parameters, noting intelligible crosstalk
[DGLR-PAPER-73-056] 24 p2896 N73-33115
European communication satellite and orbital test satellite transponders
[DGLR-PAPER-73-057] 24 p2896 N73-33116
TRANSPORT AIRCRAFT
NT AN-2 AIRCRAFT
NT AN-24 AIRCRAFT
NT BOEING 707 AIRCRAFT
NT BOEING 720 AIRCRAFT
NT BOEING 727 AIRCRAFT
NT BOEING 737 AIRCRAFT
NT BOEING 747 AIRCRAFT
NT BREGUET 941 AIRCRAFT
NT C-2 AIRCRAFT
NT C-5 AIRCRAFT
NT C-130 AIRCRAFT
NT C-131 AIRCRAFT
NT C-135 AIRCRAFT
NT C-141 AIRCRAFT
NT C-160 AIRCRAFT
NT CARGO AIRCRAFT
NT CH-3 HELICOPTER
NT CH-47 HELICOPTER
NT CL-84 AIRCRAFT
NT CONCORDE AIRCRAFT
NT CONVAIR 880 AIRCRAFT
NT DC 3 AIRCRAFT
NT DC 8 AIRCRAFT
NT DC 9 AIRCRAFT
NT DC 10 AIRCRAFT
NT DO-31 AIRCRAFT
NT F-27 AIRCRAFT
NT F-28 TRANSPORT AIRCRAFT
NT H-53 HELICOPTER
NT HFB-320 AIRCRAFT
NT L-1011 AIRCRAFT
NT MERCURE AIRCRAFT
NT SH-3 HELICOPTER
NT SHORT HAUL AIRCRAFT
NT TU-144 AIRCRAFT
NT VISCOUNT AIRCRAFT
NT XC-142 AIRCRAFT
Modeling data developed during manned simulation of large transport aircraft and comparison with training simulator results - Vol. 2
[NASA-CR-114494] 01 p0004 N73-10027
Multipath propagation between aeronautical relay satellite in synchronous earth orbit and aircraft flying over ocean
[NASA-TM-X-66094] 02 p0141 N73-11140
Propulsion system characteristics for long range, high subsonic jet commercial transport aircraft
[NASA-CR-121016] 02 p0223 N73-11800
Low speed pull-up maneuvers for slender wing transport aircraft with stability and control augmentation
[ARC-CP-1231] 04 p0369 N73-13004
Computer program for design optimization of subsonic swept wing jet transport aircraft
[RAE-TM-AERO-1448] 05 p0494 N73-14026
Investigation of crash of L-1011 aircraft near Miami, Florida on 29 Dec. 1972
06 p0619 N73-15024
Analysis of jet noise produced by supersonic transport aircraft with augmentor wing and four duct burning turbofan engines
[NASA-TM-X-68177] 06 p0619 N73-15028
Optimization of engines for commercial Mach 0.85 transport using advanced turbine cooling methods
[NASA-TM-X-68173] 06 p0619 N73-15029
French aircraft development program including Concorde, Airbus, and Corvette, as well as economic study
06 p0622 N73-15045
Analysis of propulsion system specifications and components for research VTOL transports
[NASA-TM-X-68168] 06 p0713 N73-15816
Development of takeoff airworthiness standards for new aircraft designs using motion simulators to compare performance and handling characteristics
[NASA-TN-D-7106] 09 p0983 N73-18031
Aeroelastic divergence of transport aircraft flying at supersonic speeds and design techniques to eliminate adverse effects
[NASA-CR-112262] 09 p0984 N73-18036
Conceptual designs of V/STOL lift fan commercial short haul transport aircraft to determine technical and economic feasibility
[NASA-CR-2183] 09 p0984 N73-18038
Low sonic boom overpressure profiles for supersonic transport aircraft configurations
[NASA-TM-X-2746] 09 p0984 N73-18039
Human stress expenditures in operational airlift mission flights
10 p1123 N73-19151
Wind tunnel tests to determine low speed aerodynamic characteristics of large scale V/STOL transport models with lift fan lift-cruise fan propulsion system
[NASA-TM-X-62231] 11 p1233 N73-20014
Development and characteristics of dual cargo hook system for use on military transport helicopters
12 p1358 N73-21022
Design of V/STOL research transport aircraft to achieve low fan noise with high thrust/weight capability of high pressure ratio lift fan system
[NASA-CR-121146] 12 p1364 N73-21065
Flight investigation to determine velocity and persistence characteristics of trailing vortices generated by jumbo jet transport
[NASA-TN-D-7172] 12 p1364 N73-21068
Performance tests on commercial transport aircraft engines to determine factors contributions to engine malfunctions
[FS-140-72-2] 13 p1473 N73-21933
Analysis of trans-Atlantic aircraft movements for 1970 - 1971 period to establish base line for passenger forecasts
13 p1474 N73-21935
Design concepts, manufacturing process, weight analysis, and cost estimates for long range transport aircraft using composite structures
[NASA-CR-112255] 14 p1600 N73-22976
Analysis of minimum longitudinal stability for large delta wing transport aircraft during landing approach and touchdown using inflight simulator
[TR-5084-F-1-VOL-1] 14 p1601 N73-22984
Standardized load sequence for flight simulation tests on transport aircraft wing structures
[LBF-BERICHT-FB-106] 14 p1602 N73-22986
Development of computer programs to predict performance of thrust reversal and thrust vector control systems on short takeoff transport aircraft - Vol. 1
[AD-756860] 14 p1603 N73-22993
Design and development of thrust reverser and thrust vectoring systems for application to short takeoff transport aircraft - Vol. 2
[AD-756861] 14 p1603 N73-22994
Techniques and hardware for facilitating use of flexible flat conductor cable in commercial air transports
14 p1641 N73-23310
Effects of porous wind tunnel wall corrections on transport aircraft models
14 p1648 N73-23366
Wind tunnel tests to determine effect of longitudinally oriented wing-mounted pods on aerodynamic characteristics of V/STOL transport model in cruise flight mode
[NASA-TN-D-7199] 15 p1731 N73-24035
Numerical methods for determining range and radius of action performance of transport and combat aircraft and effects of various parameters on performance
15 p1732 N73-24043
Aerodynamic coefficients for calculating transport aircraft performance using wind tunnel and scale models
15 p1732 N73-24046
Analysis of parameters affecting choice of engines for transport and combat aircraft during design process
15 p1732 N73-24048
Development of two methods for optimizing design of subsonic, swept wing jet transport aircraft
15 p1733 N73-24054
Mechanical cross coupling of STOL transport aircraft engines
[CRANFIELD-AERO-14] 16 p1955 N73-25819
Calculation of wake vortices behind wings of transport aircrafts in holding, takeoff, and landing configurations
[FAA-RD-73-42] 17 p1983 N73-26027
Analysis of aerodynamic characteristics affecting selection of short takeoff transport aircraft
18 p2103 N73-27012
Analysis of research and development programs involving construction of short takeoff transport aircraft in Germany
18 p2103 N73-27013
Characteristics of long range transport aircraft to include reduction of aircraft engine noise and improved engine response during go-around maneuver
[NASA-CR-121243] 18 p2104 N73-27020
Development and characteristics of control system for short takeoff transport aircraft for ride-smoothing effect
[NASA-CR-2276] 18 p2105 N73-27026
Analysis of minimum longitudinal stability for large delta wing transport aircraft during landing approach and touchdown using in-flight simulation techniques
[AD-761120] 18 p2106 N73-27036
Characteristics of propulsion system for subsonic, long-range transport aircraft designed to meet aerodynamic noise level requirements
[NASA-CR-121242] 18 p2193 N73-27704
Analysis of effects of flying time on service life of wing fastening knee plates on transport aircraft
[AD-761468] 19 p2221 N73-27919
Simulator tests to determine short takeoff transport aircraft terminal area characteristics and longitudinal handling qualities
[MDC-J5575L] 20 p2360 N73-28983
Computer simulated loading of Army Brigade and equipment into several medium short takeoff transport aircraft configurations
[AD-762916] 20 p2362 N73-29002
Aerodynamic characteristics of high lift wing concepts for application to commercial short takeoff transport aircraft
20 p2479 N73-29908
Wind tunnel tests to determine effects of variations in Reynolds number and leading edge configurations on aerodynamic characteristics of STOL transport with externally blown flaps
[NASA-TN-D-7194] 21 p2494 N73-30021
Simulation tests of short takeoff transport aircraft to determine airport and air space requirements under normal operating conditions
[NASA-TN-D-7300] 21 p2495 N73-30026
Analysis of landing performance of scale model of C-8 aircraft equipped with air cushion landing system on variety of surfaces including calm and rough water
[NASA-TN-D-7295] 21 p2496 N73-30032
Takeoff and landing performance characteristics and field length requirements for jet short takeoff transport aircraft with full span, externally blown flaps
[NASA-TN-D-7441] 23 p2741 N73-31939
Procedure for evaluating relative economic value of technology factors affecting design, configuration, and operation of hypersonic cruise transport
[NASA-CR-2286] 23 p2743 N73-31953
Effect of noise constraints on engine cycle optimization for long-haul transports
[NASA-TM-X-71447] 23 p2830 N73-32620
Forecast model for predicting economic factors involved in short haul air transportation in California Corridor - Vol. 2
[NASA-CR-114634[1]] 23 p2859 N73-32843
Estimated costs for additional aircraft in air transport industry
23 p2861 N73-32860
Economic risk analysis for propeller STOL transport market
23 p2861 N73-32866
Simulations of powered-lift STOL transport aircraft with either externally blown flap configuration or augmentor wing configuration
24 p2873 N73-32948
Air traffic control problems created by introduction of large numbers of STOL aircraft into high density terminal area
24 p2874 N73-32956
Wind tunnel tests of large scale subsonic jet transport with upper surface blowing flap system for lift augmentation
[NASA-TM-X-62296] 24 p2876 N73-32973

Wind tunnel tests to determine acoustic properties of large scale lift fan transport aircraft model
[NASA-TM-X-62284] 24 p2877 N73-32975
Computer program for evaluating techniques to improve aircraft engine response systems for application to long range commercial aircraft
[NASA-CR-134496] 24 p2877 N73-32977
Acquisition of conditions of icing on modern civil transport aircraft from flight data
24 p2946 N73-33528

TRANSPORT COEFFICIENTS
U COEFFICIENTS
U TRANSPORT PROPERTIES

TRANSPORT EQUATION
U BOLTZMANN TRANSPORT EQUATION

TRANSPORT PROPERTIES
NT ATMOSPHERIC CONDUCTIVITY
NT CARRIER MOBILITY
NT DIFFUSION COEFFICIENT
NT EDDY VISCOSITY
NT ELECTRICAL RESISTIVITY
NT ELECTRON MOBILITY
NT GAS VISCOSITY
NT GASEOUS DIFFUSION
NT HOLE MOBILITY
NT IONIC MOBILITY
NT IONOSPHERIC CONDUCTIVITY
NT MAGNETORESISTIVITY
NT PHOTOCONDUCTIVITY
NT PLASMA CONDUCTIVITY
NT SUPERCONDUCTIVITY
NT THERMAL CONDUCTIVITY
NT THERMAL DIFFUSIVITY
NT VISCOSITY
FORTRAN program for solving transport problem for neutrons in multilayer slab system
[EUR-4839-E] 01 p0082 N73-10681
Application of Doppler-shifted fourth sound techniques for analyzing current states in rotating superfluid helium contained in superleak
[AD-745316] 01 p0118 N73-10974
Transport characteristics for calculating plasma diode design parameters
[TEE-3056-1] 03 p0274 N73-12221
Transport of energy over turbulence spectrum of free atmosphere
[AD-747728] 03 p0299 N73-12438
Electrotransport effect on solidification of some Sn-Bi and Sn-Pb alloys
[IS-T-532] 03 p0315 N73-12567
Role of azimuthal electric fields in toroidal transport
[IPP-6/105] 03 p0336 N73-12737
Development of computer program for determining thermodynamic and transport properties of para and equilibrium hydrogen
[NASA-CR-129261] 03 p0363 N73-12959
Transport processes governing structure, energy, mass, and momentum of upper atmosphere
[COO-2195-6] 04 p0415 N73-13388
Computer program for calculating constant dose range in air transport of neutron and photon radiation from point source in atmosphere
[LA-DC-13293] 04 p0453 N73-13700
Magnetic, optical, and transport properties of semiconductors
[AD-747692] 04 p0460 N73-13752
Computer program for determining thermodynamic and transport properties of complex mixtures to include rocket performance, shock properties, and detonation properties
[NASA-TN-D-7056] 06 p0730 N73-15954
Physical and electrical transport properties of VO2 near its semiconductor-to-metal transition
[AD-751524] 07 p0834 N73-16759
Critical transport properties in binary liquid phase transition
[AD-752473] 08 p0884 N73-17158
Photochemical and transport processes in stratosphere
08 p0972 N73-17941
Transport properties of anodic oxides in metals
09 p1063 N73-18674
Calculation of transport and equilibrium properties of simple gases with m-6-8 potential function
[NBS-TN-628] 10 p1125 N73-19167
Transport properties and time correlation functions of Lennard-Jones liquid near its triple point
[LPTHE-72/22] 10 p1141 N73-19296
Singular limits of Boltzmann equation solutions for describing qualitative and quantitative properties of rarefied gas
[AD-753691] 10 p1143 N73-19312
Dependence of magnetic effective length and fringe field correction constant on central field flux density for beam transport systems
[LA-DC-72-1121] 10 p1190 N73-19682
Oxygen vacancy model for transport properties of defective cerium oxides structure
[COO-1441-9] 10 p1199 N73-19759
Development of numerical model of eddy diffusive transport of emitted gases from space shuttle wake to show chemical reactions between emitted gases and ambient atmosphere
[NASA-TM-X-66215] 11 p1287 N73-20440
Charged particle transport in turbulent astrophysical plasmas
12 p1432 N73-21606
Modification of resistive transition in superconductors by thermodynamic fluctuations
12 p1438 N73-21648
Calculation of thermodynamic and transport properties for chemically reacting gases
[AD-756597] 13 p1488 N73-22064
Equations of motion for studying convection transport processes in strongly curved tubes
13 p1509 N73-22227
Transport processes of particles in dilute suspensions in turbulent water flow
[PB-213536] 13 p1512 N73-22255
Tabular data on transport and thermophysical properties of selected binary mixtures in gaseous state
[AD-757528] 14 p1617 N73-23101
Transport properties of oxide scales formed on oxidation resistant alloys
14 p1676 N73-23604
Derivation of directional plasma transport equations from Boltzmann equation
[AD-758275] 14 p1697 N73-23768
Charge carrier transport properties in p-type germanium semiconductors
[AD-757232] 14 p1698 N73-23783
Mathematical models for determining transport properties and dissociation equilibrium of N2 and O2 in high temperature air
[ESDU-00.01.07-AMEND-A] 14 p1718 N73-23937
Measurement of atmospheric transport properties in stratosphere
[AD-757927] 15 p1782 N73-24445
Transport phenomena in rarefied gas flows
[AD-759165] 16 p1891 N73-25300
Perturbed Lorentzian solutions for transport properties of partially ionized argon and helium plasmas
16 p1948 N73-25761
Intense electron beam generation, transport, and diagnosis to acquire technology for construction of advanced X ray source
[AD-760038] 17 p2011 N73-26265
Convection and dispersion patterns associated with stationary and nonstationary fluid transport
18 p2129 N73-27205
Nonequilibrium phenomena in flowing plasmas
[AD-760792] 18 p2184 N73-27634
High frequency transport coefficients of clean type 2 superconductor near upper critical field
18 p2185 N73-27644
Mechanism of silicon autoepitaxy during transport in sandwich process
18 p2187 N73-27655
Tables and graphs of thermodynamic and transport properties of gaseous CF4 in chemical equilibrium
[NASA-TN-D-7181] 18 p2206 N73-27805
Retrevial of dispersive and convective transport phenomena in fluids using time domain analysis
[NASA-TN-D-7240] 19 p2255 N73-28178
Magnetic and transport properties of dilute magnetic alloys
[AD-763710] 21 p2586 N73-30721
Apparatus for analysis of turbulent transport properties in non-decaying, swirling, annular vortex flows
[AD-763916] 22 p2654 N73-31262
Electron transport in high density fully ionized liquid metals
[NASA-CR-135648] 22 p2684 N73-31497
Thermodynamic and transport properties of saturated liquid sodium
[RD/B/M-2479] 22 p2730 N73-31844
Stochastic modeling of turbulent heat and mass transport in anisotropic shear flow
23 p2773 N73-32181
Computer codes for calculating trace contaminant effects on stratospheric transport processes
[COO-2249-2] 24 p2923 N73-33345
Transport coefficient anomalies in antiferromagnetic metals in vicinity of Neel temperature
24 p2933 N73-33424
Affect of antiferromagnetic ordering onset at Neel temperature on transport properties of CeAl, AuHo, and ErCu systems
24 p2933 N73-33425
Thermotransport in liquid alkali metal alloys as function of composition
[COO-841-29] 24 p2992 N73-33915

TRANSPORT THEORY
NT MIXING LENGTH FLOW THEORY
Computer methods for solving some boundary value problems dealing with transport phenomena
[AD-747962] 03 p0325 N73-12651
Possibility of current sheets serving as pathways for transport of cosmic rays in solar corona
08 p0973 N73-17958
Monte Carlo radiation transport computer codes for calculating dose distributions and cell survival probabilities
[NASA-CR-130965] 09 p0996 N73-18127
Time dependent correlation functions between magnetohydrodynamics and space transport coefficients
13 p1562 N73-22660
Propagation of electromagnetic waves through turbulent media using transport theory
[AD-757491] 14 p1634 N73-23245
FORTRAN code for solving time dependent neutron transport equation in three-dimensional geometry by Monte Carlo method
[AD-756290] 14 p1691 N73-23728
Relationship between eddy-transport and second-order closure models for stratified media and for vortices
19 p2253 N73-28161
Bubble transport theory applied to upper ocean
[AD-761999] 19 p2257 N73-28194

TRANSPORT VEHICLES
Research projects in structural reliability engineering for transport vehicles
12 p1466 N73-21878
Computer program to evaluate dynamic characteristics of tracked air cushion vehicle
[PB-219984/2] 22 p2617 N73-30970
Loading criteria for tracked air cushion vehicle guiderails and methods for calculating dynamic responses of double-span, beam-type guide rails
[PB-221688/5] 22 p2617 N73-30971
Evaluation of physical and operational characteristics of missile support vehicle based on procedures for inspection, servicing, and maintenance
[AD-764772] 23 p2852 N73-32791

TRANSPORTATION
NT AIR TRANSPORTATION
NT RAIL TRANSPORTATION
NT RAPID TRANSIT SYSTEMS
NT SPACE TRANSPORTATION
NT URBAN TRANSPORTATION
Congressional hearing on 1973 fiscal budget for Department of Transportation
01 p0120 N73-10989
Systems engineering for incorporating human factors in design of transportation
[NASA-CR-129092] 02 p0245 N73-11989
Analysis of noise pollution by military vehicles, public transportation, farm equipment, private automobiles, and construction equipment
[AD-747685] 03 p0338 N73-12754
Research on chemical reactions, remote sensors, pollution, and transportation
[NASA-CR-61396] 05 p0607 N73-14938
Cable connected spinning spacecraft, canonical and Lagrange equations, and urban mass transportation
05 p0610 N73-14961
Automatic longitudinal control of closely packed personnel rapid transit vehicles
05 p0610 N73-14962
Summary of side-looking radar applications in earth resources noting basic principles of side-looking radar, radar scattering, data handling, and research and development
[ESRO-CR[P]-141] 06 p0641 N73-15200
Cost effectiveness of transporting military cargo by air versus surface modes
[AD-750848] 06 p0732 N73-15974
Technology assessment for long range year-round transportation in Arctic
[AD-754381] 11 p1269 N73-20296
Control of transportation noise pollution
[PB-213007] 11 p1326 N73-20758
House hearings on air passenger fees, related taxation, and government regulation of commercial airline operations
11 p1352 N73-20970
Effects of transportation combustion products in air pollution
[PB-213034] 11 p1354 N73-20991
Space vehicle design to withstand adverse conditions involved in handling and transportation from factory to launch site
[NASA-SP-8104] 12 p1461 N73-21839
Interpretation of ERTS-1 imagery of man made culture and revision of small-scale maps
[E73-10536] 13 p1518 N73-22300
Present status and future alternatives of transportation in US
[REPT-72-02328] 13 p1592 N73-22911
Fuel consumption profiles of passenger and freight transportation modes
[P-4935] 14 p1721 N73-23962
Role of NASA programs and activities in national attempt to upgrade quality of transportation services
[NASA-CR-133050] 16 p1977 N73-25990
Models of air, river and highway transportation for developing areas
[PB-219292/0] 18 p2214 N73-27877
Optimal control of shuttle system consisting of single infinite capacity carrier transporting passengers between two terminals
[P-4979] 19 p2355 N73-28940
Proceedings of Second Conference on Climatic Impact Assessment Program, November 14-17, 1972
[PB-221166/2] 24 p2924 N73-33357

TRANSURANIUM ELEMENTS
NT CALIFORNIUM ISOTOPES
NT CURIUM 244
NT NEPTUNIUM
NT PLUTONIUM
NT PLUTONIUM 238

Production and applications of transuranic elements
[FOA-4-C-4463-22[13]] 07 p0819 N73-16637
**TRANSVERSE ACCELERATION**
Transverse acceleration effects on human cardiovascular system
03 p0258 N73-12088
Transverse acceleration effects on human respiratory rate and oxygen metabolism
10 p1114 N73-19084
Transverse acceleration effects on rat gastrointestinal response to drugs
10 p1114 N73-19085
Transverse acceleration effects on rat hepatocytic structures
10 p1115 N73-19086
Inclusive spectra at large transverse momentum for study of massive decay resonances
[TUETP-73-6] 14 p1694 N73-23748
**TRANSVERSE FAULTS**
U GEOLOGICAL FAULTS
**TRANSVERSE OSCILLATION**
Analysis of free transverse oscillations of closed prismatic shell of flexible rectangular panels and filled with compressible inviscid liquid
[AD-755416] 14 p1716 N73-23927
**TRANSVERSE VALLEYS**
U VALLEYS
**TRANSVERSE VIBRATION**
U TRANSVERSE WAVES
**TRANSVERSE WAVES**
Approximation of beam buckling mechanics using axial and transverse loads
[AD-745881] 02 p0219 N73-11775
Numerical analysis of natural vibration modes of thin elastic shells to determine orthogonality of reactions
04 p0481 N73-13931
Low frequency transverse waves in two-fluid solar wind having radial magnetic field and streaming velocity
[NASA-CR-131570] 13 p1573 N73-22745
Characteristics of edge mounted coaxial TEM line antenna
[AD-758518] 15 p1758 N73-24252
**TRANSVERSELY EXCITED ATMOSPHERIC LASERS**
U TEA LASERS
**TRAPATT DIODES**
U AVALANCHE DIODES
**TRAPPED PARTICLES**
NT MAGNETICALLY TRAPPED PARTICLES
NT OUTER RADIATION BELT
NT PROTON BELTS
NT RADIATION BELTS
Enchancement of 0.24-0.96 MeV trapped protons during 25 May 1967 magnetic storm, measured from OV 1-9 polar orbiting satellite
[AD-749866] 05 p0543 N73-14421
Hydromagnetic waves and trapped particle discontinuities in magnetopause
[NASA-TM-X-66146] 06 p0665 N73-15405
Reduction and analysis of trapped and precipitating electron data from OGO 6 spectrometer experiment F-16
[NASA-CR-130137] 06 p0718 N73-15863
Temporal behavior of trapped protons alpha particles and ions in magnetosphere
[NASA-CR-130860] 09 p1029 N73-18397
Variable intensities of geomagnetically trapped protons at low altitudes
[AD-754844] 11 p1288 N73-20448
Effect of trapped electron and proton radiation on onboard components and payloads of low thrust orbits through Van Allen belts
[NASA-TM-X-2777] 11 p1335 N73-20840
Experiment observing solar neutrinos by neutrino capture reaction, using Ar-37
[BNL-16937] 12 p1445 N73-21707
Temporal behavior of trapped protons, alpha particles, and ions in outer zone of magnetosphere
13 p1515 N73-22273
Measurements of galactic cosmic ray dose and geomagnetically trapped radiation from OV 1-4 satellite
[AD-756924] 13 p1575 N73-22761
Ion concentration distribution in equatorial domain measured on Intercosmos 2
20 p2410 N73-29370
**TRAPPED RADIATION**
U RADIATION BELTS
U TRAPPED PARTICLES
**TRAPPING**
Numerical analysis of signal trapping effects in neutron irradiated p-n junctions as function of frequency
[SC-DC-72-1237] 05 p0587 N73-14772
Deep trap model for predicting capacitance voltage characteristics of irradiated silicon diodes and resistors
08 p0888 N73-17188
Removal and separation of particles by crystallization in carbon-naphthalene system
[AD-753056] 09 p1076 N73-18777
Stabilization of ion acoustic waves by electron trapping
[AD-761174] 18 p2183 N73-27628
**TRAPS**
NT ION TRAPS [INSTRUMENTATION]
**TRAVELING IONOSPHERIC DISTURBANCES**
Digital data analysis of traveling ionospheric disturbances
[AD-746314] 01 p0054 N73-10441
Asymptotic methods for determining propagation angles of internal gravity waves traveling at ionospheric heights
05 p0509 N73-14144
Traveling ionospheric disturbance generation by tropopause jet stream
05 p0510 N73-14147
Gravity wave effects in occurrence time changes of daily traveling ionospheric disturbances
05 p0511 N73-14156
Solar radio interferometry for traveling ionospheric disturbance detection
05 p0511 N73-14158
Computerized simulation of gravity wave perturbed traveling ionospheric disturbances using radio ray paths
05 p0512 N73-14163
Ray tracing computations of high frequency signal propagation and dispersion in traveling ionospheric disturbances
05 p0512 N73-14165
Acoustic gravity wave effects in traveling ionospheric disturbances following nuclear explosions
05 p0513 N73-14166
Effects of traveling ionospheric disturbances following nuclear explosion on high frequency band propagation
05 p0513 N73-14167
Digital data processing portion of Dartmouth ionosonde network used to analyze traveling ionospheric disturbances
07 p0775 N73-16290
**TRAVELING WAVE AMPLIFIERS**
Design and performance of traveling wave gallium arsenide amplifier with Schottky barrier
[AD-757219] 14 p1642 N73-23321
Fabrication and characterization of monolithic acoustic surface wave amplifiers
15 p1755 N73-24229
**TRAVELING WAVE MASERS**
Design of traveling wave maser system for use in satellite communication telescopes and radio astronomy
[REPT-109] 09 p1043 N73-18505
Heat treated chromium doped rutile for L-band traveling wave masers
[RR-111] 24 p2930 N73-33402
**TRAVELING WAVE MODULATION**
Analysis of stability characteristics of single frequency laser using homogeneously broadened active material
17 p2041 N73-26514
**TRAVELING WAVE TUBES**
Design and performance of C band traveling wave tube amplifier for space communication application
[NASA-CR-112125] 01 p0032 N73-10250
Development of broadband S band hybrid traveling wave tube
[AD-751262] 07 p0763 N73-16200
Development and characteristics of traveling wave maser amplifier for use in radio astronomy and deep space communication experiments
[REPT-107] 09 p1043 N73-18504
Design, construction, and evaluation of 12.2 GHz, 4.0 kW-CW coupled-cavity traveling wave tube for satellite-borne television broadcast transmitters
[NASA-CR-120920] 12 p1382 N73-21209
Cold test data for various dual helix circuit structures for electron guns
[AD-758458] 15 p1758 N73-24245
Spaceborne prototype model of millimeter wave experiment radiating transmitter for ATS-F spacecraft
[NASA-CR-132760] 16 p1965 N73-25895
X ray inspection and quality control of AEG cathode life-tests tubes after 44,000/hr life for prediction of communication satellite traveling wave tube durability
[ESRO-TM-148-ESTEC] 19 p2305 N73-28536
Comparative study of TWT and klystron amplifiers for use as power amplifiers in television broadcast satellites
[ESRO-CR[P]-267-VOL-1] 21 p2508 N73-30122
Comparative study of TWT and klystron amplifiers for use as power amplifiers in television broadcast satellites
[ESRO-CR[P]-268] 21 p2508 N73-30123
Comparative study of TWT and klystron amplifiers for use as power amplifiers in television broadcast satellites
[ESRO-CR[P]-269-VOL-3] 21 p2508 N73-30124
Dual beam electron gun broad bands transmitter tube
[AD-763226] 21 p2518 N73-30198
Comparative study of TWT and klystron for use as power amplifier in TV broadcast satellites
[ESRO-CR[P]-271] 22 p2634 N73-31109
Comparative study of TWT and klystron for use as power amplifier in TV broadcast satellites
[ESRO-CR[P]-272] 22 p2634 N73-31110
**TRAVELING WAVES**
Application of Backus-Gilbert theory for geophysical inverse problems to seismic body wave travel-time problem
02 p0200 N73-11618
Estimation of radio frequency power required to induce direct current in strong magnetic field of thermonuclear fusion device
[IPPJ-135] 02 p0216 N73-11746
Radiation pattern characteristics of traveling wave coaxial cable antenna
[AD-749051] 04 p0397 N73-13233
Electrodynamic fundamentals of antenna theory and design
[AD-755689] 13 p1502 N73-22176
Method of steepest descents used in analysis of traveling wave instabilities
[AD-763091] 20 p2378 N73-29108
Traveling wave of magnetic field having variable phase velocity and amplitude during movement of liquid metal in expanding channel
[AD-763159] 21 p2583 N73-30702
Analysis of longitudinal end effects on constant and traveling wave MHD generators by electrodynamics
[SFB-MHD-7] 22 p2705 N73-31662
Traveling wave amplification in Ge and InSb semiconductors
23 p2824 N73-32573
**TREADMILLS**
Performance evaluation of training devices for developing human physical fitness
[NASA-CR-134046] 23 p2752 N73-32023
Treadmill running effect on human oxygen consumption
24 p2882 N73-33013
**TREADS**
Braking effects on aircraft tire tread wear and runway surface characteristics
[NASA-TN-D-6963] 02 p0125 N73-11021
**TREES [MATHEMATICS]**
Sequential machine reduction with partition tree
03 p0271 N73-12200
Tree-structured information file and its subprogram subtree
10 p1132 N73-19223
Multicriteria tables and relevance tree techniques in decision making and technological forecasting
12 p1467 N73-21889
Performance of algorithms for calculating shortest path trees in networks
[NBS-TN-772] 15 p1803 N73-24615
**TREES [PLANTS]**
NT CITRUS TREES
NT CONIFERS
NT DECIDUOUS TREES
Development of infrared camera for detecting wilt root disease in coconut trees
07 p0783 N73-16369
Influence of jungle environment on transmission of digital signals by transmitting swept frequency and photographically recording received envelope and phase
[AD-755257] 13 p1495 N73-22120
Detection of ponderosa pine tree stresses from insects or diseases using multispectral photography
[NASA-CR-131586] 13 p1522 N73-22337
Cytological changes in pine tissues treated with lunar materials collected on Apollo 12 quarantine mission
[NASA-CR-128914] 14 p1610 N73-23054
Tree ring chronology for constructing paleoclimatology of North America and Europe
[AD-757486] 14 p1686 N73-23682
Application of ERTS-1 imagery to determine dynamics of distribution and density of phreatophytes and other arid land plant communities
[E73-10790] 18 p2137 N73-27266
Effects of wind shaped trees on macro- and microclimatological conditions in Japan
[CLIMATOL-NOTES-12] 18 p2171 N73-27530
Application of ERTS-1 imagery for inventory of wildland resources in northern California
[PAPER-A12] 19 p2261 N73-28220
Identification of fire hazards in San Pablo test site area in California using ERTS-1 data and aerial photography
[PAPER-A18] 19 p2261 N73-28225
Enhancement of ERTS-1 images by density slicing and application to mapping of Yucca trees in Mojave Desert of Southern California and Nevada
[PAPER-I11] 19 p2278 N73-28332
Characteristics of vegetation from existing data for predicting munition height of burst in inaccessible areas
[AD-763179] 21 p2607 N73-30891
Utilization of live trees and inanimate metal structures as efficient HF radio antennas
[AD-763887] 22 p2645 N73-31195
**TRELLISED DRAINAGE**
U DRAINAGE PATTERNS
**TREMORS**
Muscle force transducer to detect tremors in divers under hyperbaric conditions
[AD-763343] 23 p2750 N73-32010

TRENCHES
U GEOLOGICAL FAULTS
TRENDS
Hot gas recirculation in Do-31 aircraft from scale model to aircraft and trends for future developments of V/STOL aircraft
[BMVG-FBWT-72-29] 10 p1107 N73-19024
TRIANGLES
Sheba triangular thin shell element application to calculation of coding towers, toruses, and roofs
[ISD-127] 09 p1095 N73-18936
TRIANGULAR WINGS
U DELTA WINGS
TRIANGULATION
Application of satellite tracking and precision traversing data to improve accuracy of geodetic triangulation
[NASA-CR-128402] 01 p0047 N73-10377
Computerized aerotriangulation with independent models and planimetric point adjustments
02 p0164 N73-11332
Computer program for strip triangulation by independent models in aerial photogrammetry
02 p0164 N73-11334
Computer program for block analytical aerotriangulation adjustment with independent models
02 p0164 N73-11335
Horizontal accuracy of computerized planimetric block triangulation with independent models
02 p0164 N73-11336
Computerized horizontal block adjustment for aerial mapping using large numbers of points
02 p0165 N73-11337
Development, characteristics, and evaluation of electronic distance measuring instrument
[AD-746017] 02 p0208 N73-11690
Comparison of mapping accuracies obtained by analytic system of aerotriangulation with accuracies obtained using conventional first-order plotting instruments
03 p0294 N73-12391
Analysis of image coordinate refinement parameters applied to aerial photography of ground areas for improved aero-triangulation
[AD-747799] 03 p0304 N73-12479
Theory and practice of aerial photography to include aerial triangulation, stereometric methods of photointerpretation, and production of maps
[AD-748871] 04 p0423 N73-13449
Error analysis of lunar control by orbital triangulation
04 p0468 N73-13813
Astronomical geodetic observations for longitude, latitude, and components of deflection from vertical at West German stations
[MITT-124] 05 p0538 N73-14375
Plumb line deflection calculations for European triangulation network using astronomical observations
[MITT-122] 05 p0538 N73-14377
Hypermatrix core storage problem solved by triangularization method
[ISD-112] 09 p1058 N73-18624
Conical section method for determining planetary configuration from spaceborne photographic data on triangulation and horizon lines
[JPRS-58304] 09 p1085 N73-18848
Triangulation error analysis for barium ion cloud experiment
[NASA-TM-X-69222] 12 p1422 N73-21524
Vaisala method of stellar triangulation
[AD-757542] 15 p1783 N73-24456
Simultaneous satellite photographic and Doppler observations for determining space triangulation chord direction
[AD-759096] 18 p2127 N73-27188
Aerotriangulation with very small scale photography from Skylab
[E73-10994] 22 p2659 N73-31300
Aerotriangulation with very small scale Skylab photography
[E73-10995] 22 p2659 N73-31301
Methods for primary and secondary triangulation of Martian surface
[NASA-CR-135586] 23 p2845 N73-32732
Aerotriangulation with very small scale photography from Skylab
[E73-11117] 24 p2916 N73-33274
TRIAXIAL STRESSES
Measurement and effects of triaxial vibration on pilots in P-531 (Scout) helicopter under different flight conditions
[ISVR-TR-58] 07 p0751 N73-16100
TRIAXIALITY
U TRIAXIAL STRESSES
TRIBOLIA
Wing anomalies as result of weightlessness simulation for flour beetle Tribolium confusum
19 p2226 N73-27952
TRIBUTARIES
Tributaries of Lake Baykal
20 p2447 N73-29657
TRICHLORIDES
U CHLORIDES
TRIGGER CIRCUITS
Development and characteristics of gate-assisted, turn-off thyristor for high voltage and current operation
[NASA-CR-121161] 16 p1880 N73-25221
TRIGONOMETRIC FUNCTIONS
NT COSINE SERIES
NT SINE SERIES
NT TANGENTS
Trigonometric leveling and gravimetric survey in Antarctic
[AD-752232] 08 p0920 N73-17540
Digital simulation of multicorrelated random processes and its applications
[NASA-CR-62092] 21 p2565 N73-30563
TRIM [BALANCE]
U AERODYNAMIC BALANCE
TRINITRO COMPOUNDS
Tricyclic nitropropene nitronate intermediates in condensation reactions of symmetric trinitrobenzene with cycloalkanones, and with phloroglucinol
[NASA-CR-131288] 11 p1252 N73-20159
TRINITROTOLUENE
Shock initiation of reaction in RDX/TNT, nitromethane expiosives, and double base propellants
[ERDE-TR-103] 05 p0606 N73-14930
Dynamic functions of air blast parameters in detonation of spherical trinitrotoluene charge
[AD-753805] 10 p1187 N73-19659
TRINITROTRIAZOCYCLOHEXANE
U RDX
TRIODES
Electrical, optical, and structural properties of RF triode-sputtered gold films
18 p2186 N73-27649
TRIPLE AXIS SPECTROMETERS
U NEUTRON SPECTROMETERS
TRIPLET EXCITATION
U ATOMIC ENERGY LEVELS
TRIPLET STATE
U ATOMIC ENERGY LEVELS
TRIPROPELLANTS
U LIQUID ROCKET PROPELLANTS
TRITIUM
X ray device for measuring titanium tritide film thickness in presence of background radiation
[NASA-TM-X-68170] 06 p0673 N73-15475
Tritium mass transfer, isotopic separation, and permeation in fusion reactors
[UCRL-74057] 08 p0942 N73-17721
Vacuum pump system for 150 kV neutron generator to reduce tritium hazards
[NASA-TM-X-2650] 09 p1038 N73-18468
Performance preduction for tritium powered generators
[LIB/TRANS-437] 24 p2881 N73-33004
TRITONS
Preliminary studies of reaction yielding triton pion from proton deuteron interaction
[NASA-TM-X-68187] 07 p0823 N73-16674
TROCHOIDS
U PIVOTS
TROPICAL METEOROLOGY
Statistical data of tropical cyclones in Australian Region east of 135E from November 1909 to June 1969
01 p0074 N73-10608
Status and planning of GARP Atlantic Tropical Experiment
[GARP-SPEC-REPT-7] 03 p0327 N73-12667
Progress on GARP, GATE, and related subprograms
03 p0327 N73-12670
Life cycles of natural and hygroscopically seeded warm tropical cumuli
[AD-750889] 06 p0695 N73-15662
Geostationary satellite observation of convective tropical cloud trajectories and velocity
07 p0814 N73-16602
Analysis of mesoscale weather systems in tropics from radar data of south Florida
[AD-753611] 09 p1062 N73-18660
Study of tropical oceanic subcloud layer using data from Barbados experiment
10 p1180 N73-19598
Technique for using satellite pictures to analyze and forecast tropical cyclone intensities
[NOAA-TM-NESS-45] 10 p1182 N73-19611
Infrared and microwave radiometric data of intertropical convergence zone acquired by Nimbus 3 satellite
[NASA-TM-X-66203] 10 p1188 N73-19669
Analysis of synoptic wind scale spectra over Caribbean and tropical Atlantic region
[COO-2153-1] 12 p1422 N73-21528
Measurement of extreme rainfall intensites and associated liquid water content at altitude in tropical regions
[AD-756832] 13 p1554 N73-22593
North Pacific tropical vector mean charts
[AD-762044] 19 p2316 N73-28628
Tropical rainfall patterns and associated mesoscale systems for Southeast Asia
[AD-762571] 20 p2450 N73-29693
Upper air numerical forecast model designed to predict tropical macro-scale features
[AD-763102] 20 p2451 N73-29697
Subprogram planning for global atmospheric observation and weather forecasting system
[GARP-PUBL-11] 24 p2948 N73-33545
Wind determination in tropics by balloon carrying dropsondes using Omega navigation system
24 p2948 N73-33548
GARP subprograms including numerical experimentation, GATE climate, and oceanography
24 p2949 N73-33557
TROPICAL REGIONS
Soil and plant identification in tropical environment by incident and reflected solar radiation
[AD-743931] 01 p0051 N73-10417
Barotropic primitive equation model for numerical weather forecasting for tropics
[AD-743729] 01 p0076 N73-10626
Laboratory tests to determine corrosion failure mechanisms in electronic equipment exposed to humid tropical environments
[AD-747757] 03 p0279 N73-12261
Tropical rainfall patterns and associated mesoscale systems in Southeast Asia and South America
[AD-752467] 08 p0940 N73-17706
Characteristics of wind, pressure, cloud, and precipitation fields in intratropical zone of convergence
09 p1059 N73-18633
Multilayer numerical weather prediction model for studying tropical weather systems, including winds, vorticity, and divergence
[AD-752929] 09 p1061 N73-18653
Research in protecting equipment from tropical environment and seas
10 p1228 N73-19986
Mineral prospecting in tropical areas by application of geochemical, botanical, geophysical, and remote sensing techniques
[PB-213230] 11 p1289 N73-20456
Analysis of synoptic wind scale spectra over Caribbean and tropical Atlantic region
[COO-2153-1] 12 p1422 N73-21528
BOMEX array for longwave radiative transfer model of tropical atmosphere
15 p1770 N73-24339
Energetic role of trade wind inversion in tropical subalpine ecosystem
15 p1806 N73-24633
Precipitation of rain drops from convective clouds over tropical Atlantic Ocean
[NLL-M-22848-[5828.4F]] 16 p1935 N73-25660
Rocket sounding of zonal wind field structure in stratosphere and lower mesosphere of tropical zone during equinoxes
21 p2573 N73-30617
Structure of barotropically unstable disturbances in tropical regions
[AD-764090] 22 p2695 N73-31588
Climatized electrical equipment for tropical and cold climates
[AD-764393] 23 p2766 N73-32128
TROPICAL STORMS
NT HURRICANES
NT TYPHOONS
Tables on Atlantic tropical cyclone strike probabilities - 24 hour movement
[AD-744916] 01 p0076 N73-10630
Tables on Atlantic tropical cyclone strike probabilities - 48 hour movement
[AD-744917] 01 p0076 N73-10631
Probabilities of forecasting future movement of North Atlantic tropical cyclones
[AD-744918] 01 p0076 N73-10632
Regression analysis of tropical storm and typhoon speed characteristics after recurvature in western North Pacific Ocean
[AD-746880] 02 p0206 N73-11672
Revision of tropical cyclone climatology by satellite data for northern Pacific Ocean
[AD-753584] 09 p1061 N73-18658
Comparison of cumulus parameterization techniques in numerical integration of easterly wave
16 p1937 N73-25674
Typhoon and tropical storm intensity forecasts in western North Pacific Ocean using statistical regression analysis
[AD-761379] 18 p2174 N73-27561
Frequency and tracks of depressions, storms, and hurricanes in North Indian Ocean from November 1966 to December 1970
[AD-764859] 23 p2815 N73-32505
TROPICS
U TROPICAL REGIONS
TROPOPAUSE
Analysis of mean distribution maps for altitude and temperature of tropopause over Northern Hemisphere in Jan. and July between 1957 and 1965
04 p0442 N73-13607
Frontal zone formation in tropopause as caused by slanting phenomenon
[NLL-M-22824-[5828.4F]] 11 p1274 N73-20341

Meteorological implications of airborne optical imaging through tropopause
[AD-758207] 15 p1782 N73-24449
Macrosynoptic tropopause formula for long range weather forecasts in Budapest
[NLL-M-22839-[5828.4F]] 16 p1894 N73-25322
Application of microwave radar for monitoring tropopause level to determine dynamic instability and turbulence generation in clear atmosphere
[NOAA-TR-ERL-243-WPL-21] 22 p2665 N73-31353
Atmospheric turbulence near tropopause over mountainous terrain
24 p2946 N73-33525

TROPOSPHERE
Aperiodic processes and formation of seasonal temperature and wind fields in stratosphere in Northern Hemisphere, and tropospheric influences
[NLL-M-20086-[5828.4F]] 01 p0043 N73-10342
Hydrodynamics of surface layer of atmosphere and micrometeorological processes over flat homogeneous surface
[NLL-M-22574-[5828.4F]] 01 p0072 N73-10593
Correlation of signals with various frequency spacing for tropospheric propagation
[FOA-3-A-3748-60[63]] 02 p0140 N73-11132
High resolution radar scattering data for determining refractive structure in troposphere
02 p0197 N73-11594
Infrasonic resonant tube determination of wind and temperature variabilities in lower troposphere
[AD-745912] 02 p0206 N73-11667
Microwave radar detection and photography of gravitational waves in troposphere
05 p0510 N73-14152
Rocket and satellite instrument for simulatenous measurements of total mass density and number density of atomic oxygen in lower thermosphere
[AD-751468] 07 p0795 N73-16464
Vertical distribution of atmospheric water vapor and ozone over District of Columbia during 1969 and 1970
[AD-751535] 07 p0795 N73-16465
Mean monthly winds of upper troposphere for 200, 250, and 300 mb levels over central and eastern Pacific
[AD-751579] 07 p0816 N73-16620
Vertical wind shear measurements at Helsinki Airport - Apr. 1967 through Mar. 1968
[TR-3] 08 p0937 N73-17676
Atmospheric ozone as circulation tracer in upper troposphere and lower stratosphere
08 p0972 N73-17940
Digital computer routines for calculation of radar/radio tropospheric absorption and noise temperature
[AD-753197] 09 p1004 N73-18193
Temperature and wind conditions in stratosphere and troposphere of equatorial latitudes in Indian Ocean
09 p1059 N73-18634
Long lived, alpha radioisotopes applied to transfer mechanism of air masses in tropopause
09 p1060 N73-18642
Chemically reacting wave of aircraft flying at subsonic and supersonic velocity in upper troposphere and stratosphere
[AD-754918] 11 p1287 N73-20447
Channel measurement techniques, modeling multipath structure of line-of-sight tropospheric paths, and prediction of spread spectrum modem performance as function of multipath conditions
[AD-755922] 13 p1494 N73-22115
Statistical description of wind field in upper troposphere and lower stratosphere for time scales from 6 to 72 hours
13 p1552 N73-22572
Ionospheric radio wave propagation in presence of tropospheric duct
[AD-757198] 14 p1634 N73-23248
Distribution of tropospheric infrared radiative fluxes and associated heating and cooling rates in Southern hemisphere
15 p1771 N73-24340
Doppler shift measurements at 16 GHz over transhorizon path to estimate tropospheric wind velocity
[AD-760119] 17 p1999 N73-26164
Seasonal variations in tropospheric and stratospheric carbon dioxide concentration determined from commercial aircraft sampling within Northern Hemisphere
[AC-24-PT-3] 17 p2028 N73-26409
Transient response of internal gravity waves due to midtropospheric heating
[AD-762369] 19 p2298 N73-28482
Mathematical model for shaping aerosol spectrum in troposphere
20 p2389 N73-29194
Comparative analysis of upper troposphere maximum wind strength maps and ground surface synoptic maps
20 p2445 N73-29642
Stretospheric and tropospheric composition and chemical reactions
[AP-12] 21 p2539 N73-30357
Characteristics of electromagnetic radiation reflected from invisible objects in troposphere to show effects of electromagnetic radiation polarization
21 p2571 N73-30599
Measurements of Fe, Mn, Fn, Cu, Ni, and Pb in aerosols and precipitation in clean tropospheric air
[NOAA-TR-ERL-248-APCL-24]
22 p2664 N73-31349
Zones of severe turbulence in troposphere
24 p2946 N73-33527

TROPOSPHERIC RADIATION
Measurement of distribution of radioactivity in troposphere and stratosphere to determine aerosol dimensions and variation with time
12 p1421 N73-21513

TROPOSPHERIC SCATTERING
Design of klystron microwave amplifier tube for troposcatter communication system
[AD-752075] 08 p0890 N73-17204
Analysis of troposcatter data obtained by radar transmitter as signal source to determine index of refraction fluctuations
08 p0900 N73-17285
Measurements and predictions of loss and multipath variations for microwave troposcatter communication link
[AD-757553] 14 p1635 N73-23256
Amplitude fading of superhigh frequency geostationary communications satellite signals considering atmospheric refraction
17 p1996 N73-26139
Slant path attenuation of ultrahigh frequency signals from sun tracking radiometers
17 p1996 N73-26140
Technique for hybrid addition of both digital and analog data in troposcatter communication system
[AD-761523] 19 p2236 N73-28030
Line of sight wideband propagation in troposphere
[AD-762939] 20 p2378 N73-29107

TROUBLESHOOTING
U MAINTENANCE

TROUGHS
Influence of ocean bottom relief on genesis and intensity of typhoons
20 p2446 N73-29646
Geomorphology of troughs in Mariner 9 Mars surface observations
[CONTRIB-2265] 23 p2839 N73-32685

TRUCKS
Numerical analysis of vertical and lateral motion of road vehicle trains with arbitrary number of components
[TT-7211] 08 p0892 N73-17220

TRUNCATION [MATHEMATICS]
U APPROXIMATION

TRUNCATION ERRORS
Truncation error dependence on computational diffusion coefficient in atmospheric boundary layer models
[AD-760122] 17 p2029 N73-26420
Accuracy improvement of angular momentum projection
[NASA-TM-X-2875] 20 p2440 N73-29600
Condensation method and computer program for reducing truncation errors for vibration analysis of complex structures
[NASA-CR-124446] 23 p2812 N73-32484

TRUNKS [LINES]
U TRANSMISSION LINES

TRUNNIONS
U SHAFTS [MACHINE ELEMENTS]

TRUSSES
Theoretical analysis of snap-through buckling of nonshallow toggle truss structure in creep
[AD-756188] 13 p1589 N73-22888
Stresses and displacements of elastic-plastic trusses
[AD-758726] 15 p1841 N73-24920

TRYPTAMINES
NT SEROTONIN

TSUNAMI DAMAGE
U FLOOD DAMAGE

TSUNAMI WAVES
Eulerian incompressible hydrodynamic numerical model and laboratory simulations of tsunamis
[AD-745420] 01 p0053 N73-10430
Numerical analysis on hypothetical satellite altimeter detection of tides and tsunamis
06 p0664 N73-15396
Tsunami of Ust-Kamchatsk after December 15, 1971 earthquate
20 p2447 N73-29656
Wave propagation and amplification of tsunami in Canada
23 p2784 N73-32272
Tsunami propagation into Fisher-Fitz Hugh complex, Alaska, and Juan de Fuca Strait
23 p2784 N73-32273
Iterative search for resonance frequencies of multibranched coastal inlets with tsunami amplification
23 p2784 N73-32274

TU-144 AIRCRAFT
Aircraft accident involving crash of TU-144 aircraft at Paris Air Show in 1973
[NASA-TT-F-15062] 20 p2360 N73-28982

TUBE CATHODES
NT COLD CATHODES
NT HOT CATHODES
NT PHOTOCATHODES
NT PHOTOMULTIPLIER TUBES
NT THERMIONIC CATHODES

TUBE HEAT EXCHANGERS
Analysis of high temperature heat exchanger processes in tubular metallic container using bed of moving pebbles for heat storage
[FRNC-TH-231] 08 p0969 N73-17923
Triple wall tube exchanger/steam generator for sodium cooled fast breeder reactor
[BMBW-FBK-72-28] 22 p2699 N73-31619

TUBING
U PIPES [TUBES]

TUMBLING MOTION
Dynamics and control of escape and rescue from tumbling spacecraft
[NASA-CR-130549] 08 p0964 N73-17878
Development and characteristics of movable mass control system to convert tumbling motions of disabled spacecraft into simple spin movements
[NASA-CR-131867] 14 p1710 N73-23875
Optimal detumbling of large manned spacecraft using internal moving mass
[NASA-CR-135515] 22 p2722 N73-31783
Dynamics and control of detumbling disabled spacecraft during rescue operations
[NASA-CR-135788] 24 p2983 N73-33831

TUMORS
NT CANCER

TUNGSTATES
NT CALCIUM TUNGSTATES
NT LEAD TUNGSTATES
Chemical reactions involved with molybdenum, tungsten, vanadium, and chromium additives in hydrogen-oxygen flames seeded with potassium
[AD-743514] 01 p0023 N73-10179
Selection and preliminary evaluation of 2 hollandites, 1 titanate, and 1 tungstate as potential solid conductors of alkali ions
[NASA-TN-D-7157] 06 p0708 N73-15774

TUNGSTEN
Computer simulations of split interstitial equilibrium positions and binding energies in tungsten crystals
[AD-745839] 01 p0088 N73-10728
Tungsten-germanium whisker diode far infrared detector
[UCLA-34-P-157] 03 p0274 N73-12219
Plastic deformation of oriented single crystals of tungsten
[AD-747569] 03 p0318 N73-12590
Measurements of work function of [110] and [111] faces of crystal from solid solution of osmium in tungsten
[NLL-TRANS-746-1315-[9022.401]]
05 p0585 N73-14760
Field evaporation model for predicting tungsten surface potential in electric field
[AD-750205] 05 p0588 N73-14786
Results of uranium dioxide-tungsten irradiation test and post-test examination
[NASA-TM-X-2709] 09 p1063 N73-18677
Kinetics and thermodynamics of oxygen conversion from gas to metal phase in tungsten and molybdenum
12 p1412 N73-21446
Deformation mechanism diagrams and creep of tungsten lamp filaments
[AD-755230] 12 p1441 N73-21680
High strength tungsten fiber reinforced oxidation resistant niobium alloy composites for use in gas turbine engines at 2000 F
[AD-757380] 14 p1678 N73-23620
Computer simulation techniques to determine equilibrium positions and binding energies of inert gas atoms implanted in tungsten crystal
[AD-758501] 15 p1799 N73-24585
Analysis of tungsten in tungsten steel by precipitation with cinchonine and spectrophotometric measurement of hydroquinone color
[AD-762122] 19 p2310 N73-28579
Electron scattering and secondary emission from tungsten crystal surface
[AD-761876] 19 p2328 N73-28726
Compatibility of silicon carbide fibers with tungsten substrate and titanium matrix
20 p2430 N73-29520
Interaction of nickel base ternary matrix system with tungsten reinforcing fibers
20 p2430 N73-29521
Microdynamics of initial plastic flow in tungsten polycrystals
22 p2683 N73-31487
Trends in usage of tungsten including analyses of supply/demand balance and possible substitutes
[NMAB-309] 22 p2684 N73-31495
Vacuum creep behavior of tantalum alloys and tungsten
[NASA-CR-134481] 22 p2684 N73-31496
Reactivity of tungsten in mixture of Hexogen and aluminum in bomb calorimeter
[ICT-12/72] 22 p2730 N73-31845

Factors affecting miniature izod impact strength of tungsten-fiber-metal-matrix composites
[NASA-TN-D-7393] 23 p2804 N73-32427
Differential thermal technique for lining tantalum alloy tubing with tungsten
[NASA-TN-D-7426] 23 p2805 N73-32429

**TUNGSTEN ALLOYS**
Oxidation rate and compatibility of tungsten filament copper matrix composites
[AD-745324] 01 p0069 N73-10569
Electrolytic preparation and evaluation of mixed sodium-iron tungsten bronzes
[AD-746248] 02 p0188 N73-11522
Effects of molybdenum and tungsten fiber reinforcements on nickel chromium aluminum matrix alloys
[NLL-TRANS-746-1193-[9022.401]] 02 p0191 N73-11546
Sintering temperature and tungsten content effects on volumetric shrinkage of ferrotungsten alloy briquets 04 p0432 N73-13518
Evaluation of three types of CVD tungsten to determine weldability, high temperature strength, and structural stability
[NASA-CR-120876] 07 p0809 N73-16561
Current voltage characteristics of vapor deposited tungsten niobium planar thermionic converter
[NASA-TM-X-2716] 07 p0819 N73-16639
Platinum-rhodium-tungsten alloys for encapsulating space isotopic heat sources
[ORNL-4813] 08 p0932 N73-17632
Fracture strength of uranium- and tungsten-based impacted oigive penetrators
[DREV-R-652/72] 09 p1047 N73-18538
Effects of excessive HfC on mechanical properties of W-Re-Hf-C alloys
[NASA-TN-D-7210] 11 p1305 N73-20588
Analysis of precipitation process in cobalt-tungsten-titanium alloys using electron microscope and X ray imaging techniques 13 p1541 N73-22483
Development of high strength composite tungsten alloy and silicon carbide filaments for high temperature applications
[AD-756867] 13 p1549 N73-22551
Tensile properties and creep behavior of tungsten alloys dispersion strengthened by ZrO2 16 p1927 N73-25590
Production of high power arc lamp cathodes by casting copper body on thoriated tungsten insert
[NASA-TM-X-2865] 18 p2160 N73-27451
Analysis of tungsten in tungsten steel by precipitation with cinchonine and spectrophotometric measurement of hydroquinone color
[AD-762122] 19 p2310 N73-28579
Cobalt-tungsten alloys with superior strength at elevated temperatures
[NASA-CASE-LEW-10436-1] 23 p2803 N73-32415

**TUNGSTEN CARBIDES**
Cantilever beam tests for determining strength of tungsten carbide-cobalt alloys 16 p1927 N73-25591

**TUNGSTEN COMPOUNDS**
NT CALCIUM TUNGSTATES
NT LEAD TUNGSTATES
NT SCHEELITE
NT TUNGSTATES
NT TUNGSTEN CARBIDES
Quartz tube, tungsten filament lamp bank for characterization of nonmetallic thermal protection materials for high irradiance environment
[AD-752606] 08 p0893 N73-17231
Mass spectrometric measurements of high temperature gaseous tungsten fluoride compounds
[AD-757231] 14 p1617 N73-23103

**TUNGSTEN INERT GAS WELDING**
U GAS TUNGSTEN ARC WELDING

**TUNGSTEN OXIDES**
NT SCHEELITE

**TUNGUSK METEORITE**
Fluid dynamics of meteor disintegration due to aerodynamic forces in heterogeneous atmosphere 16 p1960 N73-25855
Discovery of small hollow spherules of glass containing various gases in peat bogs where Tungus meteorite fell
[NASA-TT-F-15125] 22 p2716 N73-31742

**TUNING**
High power electronically tunable VHF/UHF bandpass filter for radio frequency interference reduction
[AD-748810] 04 p0390 N73-13168
Superconductive tunable filter having broad tuning range with inductance and capacitance varied simultaneously
[AD-749237] 04 p0397 N73-13226
Tunable radiation obtained across wide region of electromagnetic spectrum using parametric amplifier
[AD-748849] 04 p0429 N73-13497
Design of reflector for stabilization and frequency tuning of ruby laser spectrum
[PB-211890] 05 p0558 N73-14537
Microwave generator using Gunn effect for magnetic tuning
[NASA-CASE-NPO-12106] 06 p0645 N73-15235
Low level tuning of approximations, with response variant emerging from standardized high level commands
[NASA-CR-130699] 08 p0891 N73-17210
Electronically tunable acousto-optical filter for laser applications
[AD-752052] 08 p0944 N73-17733
Frequency selectivity and two tone inhibition in neural coding of acoustic stimuli
[IZF-1972-25] 14 p1610 N73-23050
Design of tunable carbon dioxide laser using integrated optics technique
[AD-757088] 14 p1672 N73-23569
Tunable infrared parametric oscillators and coherent spectroscopy
[AD-759408] 16 p1945 N73-25741
Harmonic generation of high power tunable lasers
[AD-760018] 17 p2042 N73-26520
Dielectric, ferroelectric barium strontium titanate for electronic tuning
[AD-765417] 23 p2769 N73-32150
Integrated optics design principles of tunable CO2 laser
[AD-764638] 23 p2802 N73-32408

**TUNNEL DIODES**
Photoelectric tunnel currents in metal-insulator-metal diodes
[AD-751758] 07 p0763 N73-16201
Technical study of tunnel diode and its microwave amplification and oscillation
[AD-756932] 13 p1503 N73-22183

**TUNNEL RESISTORS**
U ELECTRON TUNNELING
U RESISTORS

**TUNNELING (EXCAVATION)**
Evaluation of device for rapid detection and location of shallow subsurface tunnels and excavations
[AD-752086] 08 p0919 N73-17531

**TUPOLEV TU-124 AIRCRAFT**
U TU-144 AIRCRAFT

**TURBIDITY**
Correlation between solar radiation and monthly and seasonal variations for calculating atmospheric turbidity in Belgium
[PUBL-SER-A-75] 03 p0354 N73-12882
Laser Doppler velocity measurement of turbid and bubbly flow media
[UTIAS-TN-185-PT-2] 09 p1043 N73-18506
Training procedure for improving divers distance estimation ability in clear and turbid water
[AD-752976] 10 p1121 N73-19140
Delineation of lakes and water turbidity identification in ERTS-1 imagery of Houston, Texas area
[E73-10672] 16 p1900 N73-25367
Airborne laser remote sensing of coastal waters
[AD-759781] 16 p1910 N73-25454
Analysis of water turbidity in two federal reservoirs in Kansas using ERTS-1 multispectral band scanners
[PAPER-E12] 19 p2270 N73-28276
Analysis of ERTS-1 multispectral scanner imagery to determine polluted and turbid water masses in Osaka Bay, Japan
[PAPER-E14C] 19 p2270 N73-28280
Application of ERTS-1 remote sensing to determine turbidity plumes in Lake Ontario
[PAPER-W16] 19 p2272 N73-28293
Detection of turbidity plumes in Tampa Bay, Florida from ERTS-1 MSS imagery 19 p2287 N73-28388
ERTS-1 imagery of suspended sediment plumes and turbidity in Lake Ontario
[E73-10956] 21 p2532 N73-30298
Experimental design parameters for Raman spectroscopy of turbid suspensions and powders using ion gas laser light sources and noting S/N improvement
[NOTA-INTERNA-346] 21 p2580 N73-30676
Photometric and polarimetric mapping of water turbidity and water depth
[NASA-CR-134030] 22 p2666 N73-31360
ERTS-1 monitoring of turbidity, color, boundaries, circulation, and pollution dispersion in Delaware coastal waters
[E73-11147] 24 p2918 N73-33301

**TURBINE BLADES**
Influence of various types of air exhaust on cooling effectiveness of trailing edges of gas turbine blades
[AD-745834] 01 p0092 N73-10754
Mechanical, friction, and gap-effects on semiaxial turbine pump having different blade arrangements 02 p0178 N73-11439
Diffusion metallizing and service life of gas turbine engine blades
[NASA-TT-F-13914] 02 p0223 N73-11801
Analysis of combined vibrations of blades in axial turbomachinery using dynamic stiffness method
[NLL-RTS-7305] 02 p0236 N73-11917
Calculation of heat transfer on turbine blade profiles to determine transition region coordinates in boundary layer flow through gas turbine engine
[AD-747602] 03 p0352 N73-12870
Effusion cooled turbine blade boundary layer velocity and temperature profiles as function of hole distribution
[DGLR-PAPER-72-59] 04 p0427 N73-13479
Compatibility of protective coatings for niobium alloy gas turbine blades
[AD-748837] 04 p0439 N73-13575
Single crystal shaped as turbine blade, both hollow and solid
[AD-748519] 04 p0465 N73-13786
Stress-rupture strength of turbine blade root joints at elevated temperature and prolonged stress loads
[AD-749589] 04 p0465 N73-13788
Performance tests of single stage fan-compressor to evaluate shock-in-rotor blading for jet engine applications requiring high aerodynamic performance and stability
[NASA-CR-120991] 05 p0590 N73-14795
Cooling efficiency of air discharge on nozzle blades with deflectors
[AD-749654] 05 p0591 N73-14803
Influence of thermal stresses and loads on endurance properties of heat resistant alloys used to manufacture turbine blades
[AD-749752] 05 p0591 N73-14805
Analytical prediction of transient surface heat flux and temperature on cooled turbine blade due to gas stream inlet temperature change
[NASA-TN-D-7101] 06 p0730 N73-15955
Performance tests to determine effects of reducing turbine blade thickness on turbine engine performance
[NASA-TN-D-7128] 07 p0836 N73-16776
Cascade tests of highly loaded multistage fan drive turbine configurations
[NASA-CR-2171] 07 p0836 N73-16778
Performance tests to determine effects of increased rotor blade loading on gas turbine operation by reduction of rotor blade inlet diameter
[NASA-TM-X-2730] 08 p0870 N73-17039
System for measuring turbine blade temperature
[NASA-CR-124056] 08 p0953 N73-17805
Application of gas-pressure bonding to joining components for convectively cooled turbine blades and vanes
[NASA-CR-121090] 08 p0954 N73-17808
Analysis of effect of chord size and cooling methods on cooling requirements for air cooled turbine blades - Vol. 1
[NASA-CR-120882-BK-1] 08 p0954 N73-17809
Analysis of effect of chord size and cooling methods on cooling requirements for air cooled turbine blades - Vol. 2
[NASA-CR-120882] 08 p0954 N73-17810
Experimental determination of aerodynamic performance of cooled turbine vanes at gas to coolant temperature ratios up to 2.75
[NASA-TM-X-2733] 08 p0954 N73-17815
Approximative heat transfer in thermal boundary laer on gas turbine blade
[AD-752676] 08 p0956 N73-17825
Effect of cooling air discharged into air-gas flow of turbine engine to improve effeciency of gas turbine engine operation
[AD-753969] 10 p1210 N73-19840
Performance tests of axial flow transonic compressor stage with multiple circular arc blades to determine effects of blade shape on efficiency and stall margin
[NASA-TM-X-2731] 11 p1231 N73-19995
Aerodynamic performance of core-engine turbine stator vane tested in two-dimensional cascade of 10 vanes and in single-vane tunnel
[NASA-TM-X-2766] 11 p1333 N73-20823
Adverse effect of film cooling on suction surface of turbine blade
[NASA-TM-X-68210] 12 p1444 N73-21695
Corrosion resistant materials for nozzle guide vanes and turbine blades subject to vanadium containing fuel combustion 14 p1678 N73-23613
Heat exchange between gas and turbine cascade blades of gas turbine engine
[AD-756101] 14 p1701 N73-23804
Analysis of transonic potential flow through oscillating unstaggered thin plate cascade
[AD-757255] 14 p1701 N73-23806
Measurement of power spectra of waveforms derived from vibrating blades in axial compressor and application to determine damping factor of blades
[ARC-R/M-3253] 15 p1728 N73-24014
Calculation of aerodynamic forces of bending and torsional vibration on installed vibrating cascade blades
[ARC-R/M-3254] 15 p1728 N73-24015
Wind tunnel tests to determine characteristics of turbine rotor blades with inter-blade passages operating at supersonic speed
[ARC-R/M-3275] 15 p1728 N73-24016
Development of narrow band spectral analyzer for determining power spectra of waveforms derived from vibrating axial compressor blades due to random excitation
[ARC-R/M-3259] 15 p1729 N73-24024
Performance tests of negative hub reaction turbine with jet flap stator and jet flap rotor
[NASA-CR-2244] 15 p1731 N73-24036
Nondestructive detection of flaws in gas turbine blades using luminescence and color flaw detection techniques
[AD-758047] 15 p1793 N73-24538

Analysis of relationship between losses in rotating turbine blade and pitch irregularity after nozzle blade
[N.I.L.-CE-TRANS-6113-[9022.09]] 15 p1824 N73-24782
Calculating temperature distribution by applying Green function to two dimensional Laplace equation
[NAL-TR-297] 15 p1842 N73-24924
Heat transfer characteristics of impingement-cooled turbine rotor blade
[NASA-TM-X-2791] 15 p1843 N73-24929
Performance tests of gas turbine engine with highly loaded stages operating at high pressure ratio
[ARC-R/M-3242] 16 p1854 N73-25021
Holographic interferometry for measuring surface deflections of statically loaded turbine blades 16 p1921 N73-25543
Directional crystallization in eutectic alloys used on casting turbine blades
[AD-759422] 16 p1931 N73-25624
Velocity and heat transfer analysis in channels with porous wall for cooling turbine blades
[AD-758782] 16 p1957 N73-25833
Volumetric temperature fields of internally cooled rotating blade
[AD-759246] 16 p1958 N73-25841
Dynamic characteristics of solid particles in particulate flow through turbine and compressor cascades 17 p2013 N73-26278
Digital system for programmed control of maching process for turbine blade foil
[AD-759682] 17 p2077 N73-26804
Analytical model for transpiration cooling of gas turbine blades
[AD-759190] 17 p2077 N73-26805
Wake effects in transpiration cooling of gas turbine blades
[AD-759191] 17 p2078 N73-26806
Computer manual for transpiration cooling analysis on gas turbine blades
[AD-759192] 17 p2078 N73-26807
Statistical analysis on vibration intensity and structural reliability of turbomachine blades
[AD-760279] 17 p2078 N73-26811
Service life of turbine blades operating under stochastic conditions
[AD-759874] 17 p2078 N73-26812
Analytical method for predicting stall flutter of axial-turbomachine blading
[AD-760354] 17 p2078 N73-26813
Production of lamellar and fibrous composite materials from directional solidification of eutectic alloys and application to gas turbine blades and vanes 18 p2166 N73-27492
Directional solidification of eutectic alloys and application to turbine blades and gas turbine engine components 18 p2166 N73-27494
Process for welding compressor and turbine blades to rotors and discs of jet engines
[NASA-CASE-LEW-10533-1] 19 p2303 N73-28515
Aerodynamic effects of blade tip clearance in axial flow turbine lifting line for nonuniform flow, calculating lift and induced drag
[REPT-4/1973] 19 p2329 N73-28738
Adiabatic film effectiveness and heat transfer measurements with injection of coolant air through holes in flat plate into moving mainstream
[AD-762527] 20 p2466 N73-29814
Effect of electrochemical machining on mechanical properties of gas turbine engine blades made of MA-2 alloy
[AD-762497] 20 p2483 N73-29950
Prediction of overall and blade-element performance for axial flow pumps
[NASA-CR-2301] 23 p2775 N73-32189

**TURBINE ENGINES**
NT CF-700 ENGINE
NT DUCTED FAN ENGINES
NT GAS TURBINE ENGINES
NT J-52 ENGINE
NT J-57 ENGINE
NT J-58 ENGINE
NT J-65 ENGINE
NT J-75 ENGINE
NT J-85 ENGINE
NT JET ENGINES
NT PULSEJET ENGINES
NT RAMJET ENGINES
NT SUPERSONIC COMBUSTION RAMJET ENGINES
NT TURBOFAN ENGINES
NT TURBOJET ENGINES
NT TURBOPROP ENGINES

Performance characteristics of model VTOL lift-fan simulator installed in two dimensional wing
[NASA-TM-X-68788] 01 p0036 N73-10282
Development of flow visualization and flow measurement techniques and application to flow problems of turbines, aircraft engines, and missile propulsion
[AD-747613] 03 p0287 N73-12328
Development of method for estimating power required to drive ball bearings in turbine engine based on performance of high speed antifriction bearings
[AD-747600] 03 p0308 N73-12514
Theory and operation of various jet aircraft engines
[AD-747406] 03 p0352 N73-12868
Investigation of aircraft accidents involving US general aviation turbine powered aircraft for 1970
[NTSB-AMM-72-6] 05 p0493 N73-14019
Abradable buffered labyrinth seal for control of gas path leakage in tip-turbine driven lift fan
[NASA-CR-121131] 07 p0804 N73-16524
Performance tests to determine effects of reducing turbine blade thickness on turbine engine performance
[NASA-TN-D-7128] 07 p0836 N73-16776
Analysis of effect of chord size and cooling methods on cooling requirements for air cooled turbine blades - Vol. 1
[NASA-CR-120882-BK-1] 08 p0954 N73-17809
Analysis of effect of chord size and cooling methods on cooling requirements for air cooled turbine blades - Vol. 2
[NASA-CR-120882] 08 p0954 N73-17810
Suppression of turbine engine inlet noise
[AD-753000] 09 p1079 N73-18806
Development of techniques for reducing exhaust emissions from turbine engines
[NASA-TM-X-68192] 10 p1208 N73-19824
Effect of cooling air discharged into air-gas flow of turbine engine to improve effeciency of gas turbine engine operation
[AD-753969] 10 p1210 N73-19840
Effect of steady state circumferential total pressure distortion on loss in compressor stall pressure ratio
[NASA-CR-114577] 12 p1443 N73-21693
Performance tests on commercial transport aircraft engines to determine factors contributions to engine malfunctions
[FS-140-72-2] 13 p1473 N73-21933
Refractory metal alloys with protective coatings for use in structural components of turbine engines 14 p1678 N73-23614
Development of method for estimating power output of helicopter gas turbine engines operating at full power
[AD-758461] 14 p1702 N73-23811
Development of turbine engine accessory drive techniques to establish potential systems for lightweight low profile package
[AD-761527] 19 p2330 N73-28741
Method and apparatus for improving operating efficiency and reducing low speed noise for turbine aircraft engines
[NASA-CASE-LAR-11310-1] 22 p2710 N73-31699
Application of gas analysis techniques to determine combustion efficiency in turbine engines and rocket engine combustion chambers
[AGARD-AG-168] 22 p2728 N73-31830
Formula for computing operating cost of turbine powered transport aircraft 23 p2860 N73-32852

**TURBINE PUMPS**
Mechanical, friction, and gap-effects on semiaxial turbine pump having different blade arrangements 02 p0178 N73-11439
High speed bellows shaft seals for rocket engine turbopumps 03 p0348 N73-12842
NPSH technique for two phase pumping of cryogenic propellants in turbopumps and rocket engines 03 p0348 N73-12843
Cavitation compliance from pulsing tests on rocket turbopumps
[NASA-CR-123963] 04 p0426 N73-13468
Rotor design, test apparatus and procedure, and data reduction and evaluation for axial flow pump rotor configurations
[NASA-TN-D-7074] 06 p0613 N73-14982
Computer programs for predicting hydrodynamic forces and vibration characteristics of rocket engine turbopump inducer - Vol. 2 Revised
[NASA-CR-72712-VOL-2-REV] 09 p1078 N73-18797
Tests on bearings and seals undergoing repeated starts of turbine pumps
[SEP-NT-3058/71-M] 10 p1167 N73-19494
Noncontact devices for measuring vibrations and deflections of parts in operating turbopumps
[NASA-CR-124208] 12 p1407 N73-21408
Design, development, and reliability analysis of bearings for turbine pump on nuclear engine for rocket vehicles
[NASA-CR-132227] 15 p1792 N73-24525
Characteristics of turbine pump for use with nuclear engine for rocket vehicles
[NASA-CR-132232] 15 p1792 N73-24530
Fluid dynamic computer programs for NERVA turbopump
[NASA-CR-132222] 15 p1810 N73-24670
Liquid hydrogen turbopump rapid start program with coated and uncoated system tests
[NASA-CR-124262] 16 p1918 N73-25522
Revisions to LH2 and LO2 turbopump assemblies program test plan
[NASA-CR-124194] 17 p2036 N73-26476
Theory and design of feed units of liquid propellant rocket engines
[AD-760265] 17 p2078 N73-26808
Three-dimensional flow characteristics in three bladed rocket pump inducer
[NASA-CR-2290] 23 p2775 N73-32190

**TURBINE WHEELS**
Performance tests of single stage fan-compressor to evaluate shock-in-rotor blading for jet engine applications requiring high aerodynamic performance and stability
[NASA-CR-120991] 05 p0590 N73-14795
Performance tests of single stage, axial flow, transonic compressor over stable operating range at rotative speeds from fifty to one hundred percent of design speed
[NASA-TM-X-2658] 06 p0614 N73-14983
Analysis of gas turbine engine rotor failures as basis for conducting program to provide equipment for protection of passengers and aircraft structures from damage
[NASA-CR-131525] 12 p1443 N73-21692
Numerical analysis of dynamics of constant speed rotor with three dimensional rotary inertia using eight degree of freedom model with coupled linear and angular motion 22 p2676 N73-31437

**TURBINES**
NT AXIAL FLOW TURBINES
NT GAS TURBINES
NT STEAM TURBINES

Comparison of turbine annulus mass flow calculations when computed by one- and two-dimensional analysis
[NASA-TM-X-2661] 02 p0156 N73-11264
Velocity diagram and design of highly loaded four and one half stage fan turbine
[NASA-CR-2140] 07 p0835 N73-16770
High speed schlieren film of pulsating flow in transonic turbine cascade 10 p1207 N73-19818
Steel construction design parameters for building and operating ZYKLON type wind driven power plants
[NASA-TT-F-14872] 12 p1388 N73-21253
Life tests of small turbine type flowmeters in liquid hydrogen
[NASA-TN-D-7323] 16 p1888 N73-25278
Analysis of coolant flow in transpiration-cooled vanes
[NASA-TN-D-7341] 16 p1974 N73-25966
Design of MHD generators with fuel gas and air turbine
[JUL-892-TP-VOL-11] 21 p2583 N73-30699
Performance of turboreactor turbines during high pressure stage 22 p2709 N73-31695

**TURBOALTERNATORS**
U AC GENERATORS
U TURBOGENERATORS

**TURBOCHARGERS**
U TURBOCOMPRESSORS

**TURBOCOMPRESSORS**
Calibration of rotating sand erosion test apparatus simulating turbocompressor wear
[AD-743309] 01 p0059 N73-10483
Computer programs for analysis of axial compressor aerodynamic test data
[AD-744502] 01 p0092 N73-10756
Mathematical models for predicting unsteady aerodynamic effects on axial flow compressor with distorted inflow - Squid project
[AD-746457] 02 p0157 N73-11271
Multiple tone acoustic radiations phenomenon in transonic fans
[ARC-CP-1226] 05 p0580 N73-14726
Performance tests of single stage, axial flow, transonic compressor over stable operating range at rotative speeds from fifty to one hundred percent of design speed
[NASA-TM-X-2658] 06 p0614 N73-14983
Analysis of radial distributions of flow conditions at inlet and outlet of high speed rotors to determine effects of blade part-span dampers on rotor performance
[NASA-TM-X-2696] 06 p0614 N73-14985
Distribution losses in axial compressor over blade cross sections and effects of blade heights
[AD-750931] 06 p0657 N73-15334
Analysis of stresses in compressor blades with emphasis on conditions in dove tail joints at base of blades
[AD-750497] 06 p0727 N73-15936
Existence and uniqueness of solutions obtained from streamline curvature method of calculating flow through turbomachines for several operating points of Rolls-Royce compressor
[ARC-CP-1234] 09 p1016 N73-18293
Development of supersonic cascade and wheel structure for axial flow compressor
[AD-752583] 09 p1079 N73-18804
Development of algorithm for testing gas dynamic design of axial flow compressors with multiple stages
[AD-753519] 09 p1080 N73-18809
Influence of axial velocity density ratio on compressor cascade performance in compressible flow 10 p1205 N73-19805
Mathematical model for prediction of axial compressor performance including effect of annulus wall boundary layers 10 p1206 N73-19812

Shock wave boundary layer interaction in compressor cascades
10 p1207 N73-19816
Effect of steady state circumferential total pressure distortion on loss in compressor stall pressure ratio
[NASA-CR-114577] 12 p1443 N73-21693
Calculation of gas flow in bypass compressor
[AD-756092] 13 p1535 N73-22441
Computer program for use in design of axial compressor airfoils suitable for operation at high subsonic and supersonic Mach numbers
[AD-756879] 13 p1536 N73-22442
Development of mathematical matrix technique for calculating inviscid, rotational, compressible axisymmetric flow field through axial flow compressor
[ME/A-73-1] 13 p1570 N73-22723
Normal shock wave conditions in elements of axial supersonic compressor
[AD-756102] 14 p1650 N73-23384
Experimental determination of turning angle and losses of axial compressor inlet guide vanes
[AD-757250] 14 p1701 N73-23805
Blockage ring used for inlet stall problem with supersonic axial flow compressor stage having tip Mach number of 2.0
[AD-757217] 14 p1702 N73-23809
Measurement of power spectra of waveforms derived from vibrating blades in axial compressor and application to determine damping factor of blades
[ARC-R/M-3253] 15 p1728 N73-24014
Nonuniform flow in front of axial flow compressor stage
[AD-759247] 16 p1891 N73-25303
Performance data for single stage axial flow compressor with tandem airfoil blading
[NASA-CR-121145] 16 p1955 N73-25818
Design, development, and evaluation of centrifugal compressor with six to one pressure ratio and two pounds per second air flow
[NASA-CR-120941] 17 p2037 N73-26483
Structural and gas dynamic parameters at flow separation boundary in compressor cascades
[AD-762238] 19 p2257 N73-28197
Numerical analysis of variable pitch compressor rotor blades for reduction of rotor vibrations
[AD-762228] 19 p2330 N73-28746
Fabrication and mechanical testing of high pressure ratio compressor
[NASA-CR-121193] 20 p2423 N73-29463
Rotating stall in axial flow compressor stages with different types of profiling along blade height and different flow regimes past profile in cascade
[NASA-TT-F-15115] 22 p2709 N73-31698
Characteristics of axial flow compressors to show compressor parameters during pre-stall conditions and techniques for predicting compressor stall conditons
[AD-763816] 22 p2710 N73-31704
Measurement of flow parameters in midspan double-circular-arc section of stator in subsonic flow and comparison with computed performance
[NASA-TN-D-7425] 23 p2740 N73-31932
Shock wave pattern and stability in axial flow supersonic compressor using simulated rotating cascade test facility
23 p2775 N73-32196
Aerodynamic design of inlet stage for two-stage compressor and performance comparison for axial, mixed flow, and centrifugal stage configurations
[NASA-CR-120943] 23 p2829 N73-32610
Capacitive method for measuring blade tip clearance in running turbocompressors
[DLR-FB-72-40] 23 p2831 N73-32628
Computerized design of axial compressor
[AD-764733] 23 p2832 N73-32633
Computer program for design of axial compressor
[AD-764734] 23 p2832 N73-32634
Influence of combustion chamber, compressor, and afterburner configuration on static performance of two-cycle turbojet engines with high bypass ratio
24 p2973 N73-33756

**TURBOCONVERTERS**
U TURBOGENERATORS
**TURBOELECTRIC CONVERSION**
U TURBOGENERATORS
**TURBOFAN AIRCRAFT**
NT A-7 AIRCRAFT
NT BOEING 707 AIRCRAFT
NT BOEING 720 AIRCRAFT
NT BOEING 727 AIRCRAFT
NT BOEING 737 AIRCRAFT
NT C-141 AIRCRAFT
NT CONCORDE AIRCRAFT
NT CV-990 AIRCRAFT
NT DC 8 AIRCRAFT
NT DO-31 AIRCRAFT
NT F-28 TRANSPORT AIRCRAFT
NT F-111 AIRCRAFT
NT P-1127 AIRCRAFT
NT TU-144 AIRCRAFT
**TURBOFAN ENGINES**
NT CF-700 ENGINE
NT TF-34 ENGINE

Production test facilities for turbojet and turbofan engines, 1975 to 1995, for replacing current inadequate facilities
[AD-745877] 02 p0153 N73-11243
Aerodynamic component test results of Fan C, high-bypass-ratio, low-aerodynamic loading, single stage fan
[NASA-CR-120981] 02 p0222 N73-11799
Design, development, and evaluation of turbine for small, low-cost turbofan engine
[NASA-TM-X-68157] 02 p0223 N73-11803
Turbofan design parameters for optimal acoustic and aerodynamic performance
03 p0249 N73-12014
Design and performance of suppressors for acoustic noise reduction in turbofan engines
03 p0249 N73-12015
Jet noise suppression in turbofan engines at various exhaust flow velocities
03 p0249 N73-12016
Structural changes in high bypass ratio engines for fan noise reduction to jet noise level
03 p0249 N73-12017
Estimates of reduced noise levels for turbofan engines with sound suppressors
03 p0250 N73-12022
Suppression of turbofan engine sonic inlet noise in STOL propulsion by use of acoustic nozzle insert
03 p0250 N73-12026
Design studies for integral lift, high bypass ratio fan engine using Lycoming 502 core and MQT power turbine, for advanced commercial V/STOL aircraft
[NASA-CR-120992] 04 p0426 N73-13471
Analysis of data obtained in evaluation tests of circumferential airflow uniformity entering combustors from two advanced engine compressors
[NASA-CR-121009] 05 p0526 N73-14276
Data tables and computer generated profile plots obtained in evaluation tests of circumferential airflow uniformity entering combustors from two advanced engine compressors
[NASA-CR-121010] 05 p0526 N73-14277
Acoustic properties of supersonic fan
[NASA-TN-D-7096] 06 p0619 N73-15025
Optimization of engines for commercial Mach 0.85 transport using advanced turbine cooling methods
[NASA-TM-X-68173] 06 p0619 N73-15029
Development of method for analysis and assessment of turbofan engine performance
[CRANFIELD-SME-2] 06 p0712 N73-15811
Dynamics and control analysis of turbofan lift engines
[NASA-TM-X-68175] 06 p0713 N73-15815
Operating principles and thermodynamic cycle of ducted fan turbojet engines
[AD-750984] 06 p0715 N73-15833
Cascade tests of highly loaded multistage fan drive turbine configurations
[NASA-CR-2171] 07 p0836 N73-16778
Analysis of requirements for turbofan engines for high speed commercial transport aircraft - Vol. 1
[NASA-CR-121132] 10 p1207 N73-19820
Preliminary design assessment of turbofan engines for installation on high speed commercial transport aircraft - Vol. 2
[NASA-CR-121133] 10 p1207 N73-19821
Propulsion system requirements for aircraft engines installed in high speed commercial transport aircraft - Vol. 3
[NASA-CR-121134] 10 p1207 N73-19822
Design and aerodynamic performance of low speed fan stage for low noise turboengine
[NASA-CR-121148] 12 p1364 N73-21070
Development of annular acoustically porous elements for installation in exhaust and inlet ducts of turbofan engine to reduce aircraft engine noise intensity
[NASA-CASE-LAR-11141-1] 14 p1600 N73-22975
Design of test facility for turbofan engines at subsonic operation
[AD-757197] 14 p1646 N73-23352
Exhaust gas diffuser effect on test cell wall and turbofan cold-flow model engine exhaust nozzle plug and core engine cowl surface pressure
[AD-759177] 16 p1958 N73-25842
Application of finite difference techniques to noise propagation in jet engine ducts
[NASA-TM-X-68261] 17 p1981 N73-26015
Wind tunnel tests to determine effect on cruise performance of installing long duct refan-engine nacelle on DC 8 aircraft
[NASA-CR-121218] 17 p1982 N73-26023
Performance data for three turbofan engine configurations with noise reduction features tested over range of flight conditions
[NASA-CR-121258] 18 p2193 N73-27707
Dynamic response of Mach 2.5 supersonic mixed compression axisymmetric inlet operating with turbofan engine
[NASA-TM-X-2833] 18 p2193 N73-27709
Systems analysis of quiet turbofan STOL aircraft for short-haul air transportation operations - Vol. 6
[NASA-CR-114611] 19 p2219 N73-27903
Research project for noise suppression of sonic inlets used with turbofan engines and improvement in engine inlet flow characteristics - Vol. 2
[NASA-CR-121127] 19 p2328 N73-28732
Analysis of internal noise field of two axisymmetric sonic inlet models for noise suppression of turbofan engine inlets - Vol. 3
[NASA-CR-121128] 19 p2329 N73-28733
Design of automatic throttle control for Navy carrier based A-7 E aircraft
[AD-761764] 19 p2329 N73-28740
Development of turbine engine accessory drive techniques to establish potential systems for lightweight low profile package
[AD-761527] 19 p2330 N73-28741
Redesign concept for A-7E approach power compensator system, including longitudinal feedback
[AD-761458] 19 p2330 N73-28742
Analysis of intake duct noise of turbofan engine and effect on duct structure due to acoustic fatigue
20 p2479 N73-29916
Analysis of aircraft engine noise sources and characteristics of engine noise produced by turbofan engines
21 p2588 N73-30735
Aerodynamic wind tunnel performance of high bypass pressure ratio fan engine for STOL aircraft
[NASA-TM-X-71445] 23 p2740 N73-31931
Adhesive bonding of structures and composite materials on advanced turbofan engines
23 p2810 N73-32470
Finite difference theory of noise propagation in turbofan engine ducts
[NASA-TN-D-7339] 24 p2972 N73-33744
Variable turbine geometry effect on engine installation and thrust modulation
[AD-765533] 24 p2974 N73-33761

**TURBOFANS**
Performance of shrouded and unshrouded fans in low noise turbofan engines
03 p0249 N73-12018
Far field noise measurements to determine effects of flow distortion for three different installations on noise from fan designed for turbofan engines
[NASA-TN-D-7076] 03 p0280 N73-12269
Velocity diagram and design of highly loaded four and one half stage fan turbine
[NASA-CR-2140] 07 p0835 N73-16770
Calculated performance map of high pressure ratio turbine designed for turbofan simulator
[NASA-TM-X-2822] 16 p1956 N73-25822
Wind tunnel tests of short takeoff and landing fan stage model to determine airflow conditions around rotor and stator and stage pressure ratio
[NASA-TM-X-2837] 18 p2192 N73-27701
Four VTOL propulsion concepts compared parametrically for subsonic applications with three types of aircrafts
[NASA-TM-X-68279] 20 p2466 N73-29810
Aero and acoustic design features of single stage fans tested in outdoor acoustic facility
[NASA-TM-X-68289] 21 p2579 N73-30668
High tip speed fan inlet noise reduction using treated inlet splitters and accelerating inlets.
[NASA-CR-121268] 21 p2589 N73-30745
Acoustic tests of supersonic tip speed fan with acoustic treatment and rotor casing slots and its performance in reducing engine noise
[NASA-CR-134501] 23 p2828 N73-32608
Noise comparison of two STOL pressure ratio fans with 15 and 42 rotor blades
[NASA-TM-X-2891] 23 p2829 N73-32609

**TURBOGENERATORS**
Superconducting magnet systems, high-power turbogenerators with superconducting field windings, and synchronous generators with superconducting inductors
[JPRS-57638] 04 p0458 N73-13735
Vibration response of gas bearing rotor-supports to sinusoidal and random vibrations in Brayton rotating unit turbogenerator
[NASA-CR-2177] 13 p1534 N73-22427
Reduction of random vibration response data for NASA Brayton rotating unit turbogenerator
[NASA-CR-121178] 13 p1534 N73-22428
Gas turbine generator sets in 30 kW and 60 kW sizes and turboalternator designs
[AD-761115] 18 p2108 N73-27050

**TURBOJET AIRCRAFT**
U JET AIRCRAFT
**TURBOJET ENGINE CONTROL**
Computer program for evaluating techniques to improve aircraft engine response systems for application to long range commercial aircraft
[NASA-CR-134496] 24 p2877 N73-32977
Performance of two-cycle turbojet engine for multiparameter control under influence of jet vane and fuel throughput variations
24 p2973 N73-33757

**TURBOJET ENGINES**
NT CF-700 ENGINE
NT DUCTED FAN ENGINES
NT J-52 ENGINE
NT J-57 ENGINE
NT J-58 ENGINE

NT J-65 ENGINE
NT J-75 ENGINE
NT J-85 ENGINE
NT TURBOFAN ENGINES
NT TURBOPROP ENGINES
Survey of techniques used for turbine engine performance analysis
[AD-744587] 01 p0091 N73-10750
Influence of inlet distortions on turbojet and ingestion engine stability
[AD-745852] 01 p0092 N73-10755
Production test facilities for turbojet and turbofan engines, 1975 to 1995, for replacing current inadequate facilities
[AD-745877] 02 p0153 N73-11243
Portable sampling and measurement system for determining gaseous emission species in afterburn of turbojet engine at ground level
[AD-747773] 03 p0351 N73-12866
Effect of air precooling before compression on propulsive efficiency of liquid hydrogen turbojet engine with afterburning for space shuttle
[DGLR-PAPER-72-60] 04 p0464 N73-13785
Improvement of turbojet engine performance analysis by plotting parameters of two shaft turbojet engine operation
[AD-749058] 04 p0465 N73-13789
Analysis of data obtained in evaluation tests of circumferential airflow uniformity entering combustors from two advanced engine compressors
[NASA-CR-121009] 05 p0526 N73-14276
Data tables and computer generated profile plots obtained in evaluation tests of circumferential airflow uniformity entering combustors from two advanced engine compressors
[NASA-CR-121010] 05 p0526 N73-14277
Relation between invariance conditions and characteristics of turbojet engine with afterburner multidimensional control system under variable flight conditions
[AD-749656] 06 p0714 N73-15828
Operating principles and thermodynamic cycle of ducted fan turbojet engines
[AD-750984] 06 p0715 N73-15833
Comparison of combustion characteristics of ASTM A-1, propane, and natural gas fuels in annular turbojet combustor
[NASA-TN-D-7135] 07 p0835 N73-16771
Modification of jet engine fuels to reduce emissions of nitrogen oxides from jet aircraft turbine engines
[AD-752581] 08 p0953 N73-17803
Turbine inlet gas temperature measurement by ultrasonic impedance
[AD-752602] 08 p0955 N73-17822
Engine cycle, configuration, and design requirements
[NASA-CR-120970-VOL-2] 10 p1106 N73-19019
Time variant distortion in supersonic inlet related to stall in compressor
[NASA-TM-X-68189] 10 p1208 N73-19825
Development of sampling and analytical procedures for gas turbine engine exhaust using aircraft auxiliary power unit as emission source
[BM-RI-7735] 10 p1223 N73-19947
Effect of prevaporization of jet fuels on exhaust emission levels produced in turbojet combustor segment
[NASA-TM-X-68194] 10 p1224 N73-19949
Description of turbopropulsion laboratory in aeronautics department at Naval Postgraduate School
[AD-754380] 11 p1268 N73-20287
Spectroscopic, photometric, and electron microscope analyses of metal wear particles in JT3D turbojet engine oil
[DLR-FB-73-06] 12 p1409 N73-21417
Analysis of gas turbine engine rotor failures as basis for conducting program to provide equipment for protection of passengers and aircraft structures from damage
[NASA-CR-131525] 12 p1443 N73-21692
Effect on nitric oxide emissions of using premixed prevaporized fuel/air in turbojet combustors
[NASA-TM-X-68220] 12 p1464 N73-21862
Modifications in development of high pressure version of vibrating cylinder pressure transducer
[AD-755533] 13 p1502 N73-22173
Analysis of dynamic inlet distortion data for turbojets
[AD-756481] 13 p1571 N73-22731
Increased propulsive efficiency through improved secondary flow capacity in double flow turbojets
[NASA-TT-F-14904] 14 p1701 N73-23803
Effect of primary-zone water injection on pollutants from combustor burning liquid ASTM A-1 and vaporized propane fuels
[NASA-TN-D-7293] 14 p1718 N73-23943
Experimental cold flow evaluation of ram air cooled plug nozzle concept for afterburning turbojet engines in static altitude facility
[NASA-TM-X-2811] 16 p1956 N73-25823
Afterburner instability vortex shedding model for air breathing turbojet combustion
[AD-758890] 16 p1957 N73-25834
Time dependent flow field model for subsonic diffuser section of supersonic inlet
[AD-758803] 16 p1957 N73-25835
Analytical technique and computer program for evaluation of airbreathing propulsion exhaust nozzle performance
[AD-760541] 18 p2194 N73-27712
Comparison of nitrogen oxide emissions produced by hydrogen combustion with emissions produced by jet engine fuels at simulated cruise conditions
[NASA-TM-X-68258] 18 p2206 N73-27804
Handbook on radiant emission and absorption of combustion gases for application to design of rocket combustion chambers and exhausts, turbojet engines, and industrial furnaces
[NASA-SP-3080] 18 p2206 N73-27807
Model for estimation of turbojet engine exhaust dispersion into atmosphere
[NASA-TN-D-7382] 19 p2254 N73-28174
Development of performance equations for cryptosteady-flow energy separator over widest range of operating conditions for turbojet engines
[AD-762030] 19 p2330 N73-28747
Analysis of cryptosteady-flow energy separation in turbojet engines and application to nozzle design
[AD-762031] 19 p2331 N73-28751
Design and development of cryptosteady energy separator for use with turbojet engines on supersonic aircraft
[AD-762032] 19 p2331 N73-28752
Performance tests of annular combustor designed for use in low cost turbojet engine
[NASA-TM-X-2857] 19 p2352 N73-28918
Logistic performance data book on propulsion system for KC-135 aircraft to show reliability, maintenance, costs, and problems
[AD-762217] 19 p2357 N73-28962
Development of techniques for simulating infrared emission from turbojet aircraft exhaust plumes
[AD-763123] 20 p2486 N73-29967
Modification of Olympus turbojet engine to meet supersonic civil transport requirements
21 p2590 N73-30752
Characteristics of axial flow compressors to show compressor parameters during pre-stall conditions and techniques for predicting compressor stall conditons
[AD-763816] 22 p2710 N73-31704
Sensory odor tests of exhaust from turbojet engine combustor operating at simulated idle conditions
[NASA-TM-X-71429] 23 p2829 N73-32613
Static tests of cylindrical ejectors using afterburning turbojet gas generators
[NASA-TM-X-52565] 23 p2830 N73-32622
Exhaust emission measurements on turbojet engine plume at simulated supersonic flight
[AD-764717] 23 p2832 N73-32632
Turbojet and turbine engine performance optimalization by configuration variations, and auxiliary turbine engine converter problem
[DLR-MITT-73-05] 24 p2973 N73-33755
Influence of combustion chamber, compressor, and afterburner configuration on static performance of two-cycle turbojet engines with high bypass ratio
24 p2973 N73-33756
Performance of two-cycle turbojet engine for multiparameter control under influence of jet vane and fuel throughput variations
24 p2973 N73-33757

TURBOMACHINE BLADES
NT COMPRESSOR BLADES
NT ROTOR BLADES [TURBOMACHINERY]
NT STATOR BLADES
NT TURBINE BLADES
Calculation of compressible flow in three dimensional cascade of turbomachine blades using stream line curvature technique
[ARC-R/M-3704] 05 p0527 N73-14287
Universal curves which relate general properties of two-dimensional boundary layers on turbomachine blades
10 p1204 N73-19795
Predictions of boundary layer transition on turbomachine blades
10 p1204 N73-19797
Optimization method for turbomachine blade design based on boundary layer concepts
10 p1204 N73-19801
Role of boundary layers in axial flow turbomachines and prediction of their effects
10 p1205 N73-19806
Calculation method for external heat transfer to turbine blades
10 p1205 N73-19807
Boundary layer behavior in supersonic straight and annular blade cascades of fixed and mobile types
10 p1207 N73-19817
Calculation of unsteady, subsonic flow through infinite, two-dimensional flat plate blade
[ARC-R/M-3709] 13 p1510 N73-22240
Corrosion resistance of gas turbine components of power plant fueled with shredded refuse
[PB-221095/3] 21 p2591 N73-30759
Inviscid, isentropic, three-dimensional flow theory for rotating thin blade row in cylindrical duct
23 p2775 N73-32193

TURBOMACHINERY
NT AXIAL FLOW TURBINES
NT CENTRIFUGAL COMPRESSORS
NT CENTRIFUGAL PUMPS
NT GAS TURBINES
NT STEAM TURBINES
NT TURBINE PUMPS
NT TURBINES
NT TURBOCOMPRESSORS
NT TURBOFANS
NT TURBOGENERATORS
Analysis of combined vibrations of blades in axial turbomachinery using dynamic stiffness method
[NLL-RTS-7305] 02 p0236 N73-11917
Research reports on chemical propulsion systems and performance engineering
03 p0348 N73-12841
Determination of coefficients of linear expansion for turbine parts as result of heating by Chevenard dilatometer
[AD-749735] 05 p0607 N73-14935
Application of unsteady airfoil theory to determine pressure and lift fluctuations on rotor blades of turbomachinery
07 p0735 N73-15983
Three dimensional solid particle trajectories through stationary and rotating turbine cascades
[AD-753364] 09 p1080 N73-18808
Boundary layer effects in turbomachines
[AGARD-AG-164] 10 p1204 N73-19794
Method for calculating three dimensional turbulent boundary layer separation applied to simple turbomachine case
10 p1205 N73-19808
Design of welded bellows for cryogenic turbomachinery face seal applications
[NASA-CR-121117] 13 p1533 N73-22423
Design and evaluation of multiple circular arc bladed, axial flow transonic compressor rotor
[NASA-TM-X-2697] 15 p1730 N73-24033
Radial flow balance in turbomachines
[ONERA-NT-209] 15 p1768 N73-24326
Turbomachinery noise generation and control
[NASA-TM-X-68253] 16 p1957 N73-25831
Methods of testing rotating components of turbomachines compared with tests on complete turbomachines
[AGARD-AG-167] 17 p2077 N73-26800
Development of computer program for subsonic and shock-free transonic flow solution on hub-throud midchannel flow surface of turbomachine - Vol. I
[NASA-TN-D-7343] 18 p2102 N73-26996
Application of boron/aluminum composite material for construction of turbine blades with low notch sensitivity in high cycle fatigue
18 p2166 N73-27497
Influence of combined rotary flow inductors and dry turbojets on side line noise levels of supersonic transports
[NASA-TM-X-68233] 20 p2466 N73-29809
Turbo-type energy absorber for aircraft carrier arresting gear
[AD-761502] 21 p2522 N73-30226
Analysis of boundary layer and turbulence characteristics inside passages of axial flow inducer and technique for predicting properties of boundary layer
[NASA-CR-121248] 21 p2524 N73-30240
High performance annular combustion chambers for use in turboreactors
22 p2709 N73-31696

TURBOPROP AIRCRAFT
NT AN-24 AIRCRAFT
NT BREGUET 941 AIRCRAFT
NT BREGUET 1150 AIRCRAFT
NT C-2 AIRCRAFT
NT C-130 AIRCRAFT
NT C-160 AIRCRAFT
NT CL-84 AIRCRAFT
NT E-2 AIRCRAFT
NT F-27 AIRCRAFT
NT OV-10 AIRCRAFT
NT VISCOUNT AIRCRAFT
Aerodynamic characteristics and performance of USSR An-12 turboprop aircraft to include handling technique and flight safety
[AD-756948] 13 p1476 N73-21953

TURBOPROP ENGINES
Design, materials, fabrication, and testing in DART thruster technology development
[LA-5017-MS] 17 p2077 N73-26802
Exhaust emissions of 11 T56-A-15 engines
[EDR-7200] 21 p2588 N73-30736

TURBOPUMPS
U TURBINE PUMPS

TURBOROTORS
U TURBINE WHEELS

TURBOSHAFTS
Design, fabrication, and test of electronic engine control system for small turboshaft engines
[AD-758173] 15 p1827 N73-24805

TURBOSUPERCHARGERS
U TURBOCOMPRESSORS

TURBULENCE
NT ATMOSPHERIC TURBULENCE
NT CLEAR AIR TURBULENCE
NT GUSTS
NT ISOTROPIC TURBULENCE
NT LOW LEVEL TURBULENCE
NT MAGNETOHYDRODYNAMIC TURBULENCE

NT PLASMA TURBULENCE
Influence of drag, pressure, and turbulent distribution on flow of dilute Polyox WSR-301 solutions in circular cylinders
[AD-745763] 01 p0042 N73-10334
Mean velocity, turbulence intensity, and turbulent shear stress in turbulent boundary layer
[WTHD-41] 02 p0155 N73-11255
Review and evaluation of theories on turbulent drag reduction by polymeric additives
[AD-746107] 02 p0158 N73-11277
Influence of inhomogeneity on structure of collisionless turbulent shock wave in high beta infinite plasma
[AD-746467] 02 p0217 N73-11756
Transport of energy over turbulence spectrum of free atmosphere
[AD-747728] 03 p0299 N73-12438
Turbulence and combustion stability in gas turbines
[AD-753062] 09 p1099 N73-18972
Topler method for studying structure of turbulent diffusion flames
[NASA-TT-F-14842] 10 p1223 N73-19945
Effect of wing span loading on wing trailing vortices
[AD-754055] 11 p1232 N73-20003
Determination of boundaries confining constant of turbulent coagulation of aerosols
[NLL-RTS-7293] 11 p1269 N73-20297
Device for measuring angle of arrival of laser beams and predictions of expected results for input apertures and turbulence
[AD-755404] 13 p1538 N73-22464
Propagation of electromagnetic waves through turbulent media using transport theory
[AD-757491] 14 p1634 N73-23245
Calculation of nonlinear evolution of disturbance in unbounded viscous fluid with uniform shear using Navier-Stokes equations
[NASA-TN-D-7284] 14 p1648 N73-23363
Coupling of magnetic pulse to initially magnetized collisionless plasma
16 p1948 N73-25759
Spectral and cospectral analyses of turbulence data obtained over natural ocean waves
[AD-761504] 19 p2316 N73-28624
Statistical study of nonlinear energy transfer interactions in turbulence models
22 p2649 N73-31224
Influence of high level of inlet turbulence on performance of annular diffusers having center bodies of uniform diameter and conically diverging walls
[TT-7101] 22 p2652 N73-31243
Applications of Wiener-Hermite expansion to theories of hydrodynamical turbulence
23 p2771 N73-32167
Mathematical model formulated for mean disturbance created in linear stratified fluid by growth and collapse of localized region of turbulent mixed fluid
[AD-764050] 24 p2910 N73-33224
Optical properties of pure and turbulent sea water
24 p2957 N73-33624
Measurement of turbulence in collisionless oblique plasma shock by scattered ruby laser light
24 p2961 N73-33665

TURBULENCE EFFECTS
Development of method for estimating length of atmospheric turbulence patch as function of different turbulence intensities for two or more regions
[NRC-12793] 04 p0370 N73-13009
Theoretical and experimental analyses of aircraft propeller operating under turbulent ambient conditions
[UTIAS-183] 06 p0621 N73-15039
Development of automatic system for controlling aircraft under turbulent atmospheric conditions to provide pitch stabilization
[AD-751148] 07 p0741 N73-16028
Effects of turbulence instabilities on laser propagation
[AD-753401] 09 p1044 N73-18515
Influence of degree of turbulence on aerodynamic coefficients of cascades
10 p1204 N73-19798
Effect of free stream turbulence level on turbulent boundary layer behavior
10 p1204 N73-19799
Analysis of effects of shock induced boundary layer separation in transonic flight and methods for eliminating or reducing effects
[ARC-R/M-3510] 16 p1854 N73-25019
Effects of wing structural elasticity on accumulation of fatigue damage during aircraft flight in turbulence
[AD-759634] 16 p1862 N73-25082
Split-film atmospheric turbulence anemometer evaluation
[NASA-CR-62093] 16 p1914 N73-25485
Aircraft accident involving crash of DC-9 aircraft during landing following go-round at Fort Worth, Texas Airport on 30 May 1972
[NTSB-AAR-73-3] 17 p1982 N73-26017
Influence of free stream turbulence on turbulent boundary layer in relation to wind tunnel testing at subsonic speeds
17 p2014 N73-26283
Effects of turbulence and noise on wind tunnel measurements at transonic speeds
17 p2014 N73-26284
Analysis of aircraft stability and control derivatives in turbulent conditions subject to random state disturbance
[AD-763741] 21 p2498 N73-30046
Structure of collisionless ion acoustic shocks in plasma device
[NASA-CR-135490] 22 p2703 N73-31651
Turbulence anisotropy effects on pressure distribution and secondary flow of boundary layers, free and wall jets, and wakes
24 p2906 N73-33191
Turbulence effects on fireball dynamics
[LA-UR-73-713] 24 p2923 N73-33347

TURBULENT AIR CURRENTS
U AIR CURRENTS
U TURBULENT FLOW

TURBULENT BOUNDARY LAYER
Turbulent burst and non-turbulent durations in turbulent boundary layer of open channel
[ARL/SM-NOTE-374] 01 p0039 N73-10307
Semiempirical calculations of turbulent boundary layer problems
[AD-745217] 01 p0042 N73-10330
Two layer model of compressible turbulent boundary layer flow around reentry vehicle
[AD-743933] 01 p0043 N73-10338
Mean velocity, turbulence intensity, and turbulent shear stress in turbulent boundary layer
[WTHD-41] 02 p0155 N73-11255
Turbulent boundary layers on walls of rectangular water pipe inlets
02 p0155 N73-11259
Calculation of Magnus forces on axisymmetric bodies at small angles of attack with incompressible turbulent boundary layers
[AD-746449] 02 p0157 N73-11270
Nonequilibrium effects caused by vibrational freezing in hypervelocity wind tunnel
[VKI-TN-83] 03 p0248 N73-12009
Pressure fluctuations due to interaction of shock wave with turbulent boundary layer
[NASA-CR-123961] 03 p0281 N73-12281
Wind tunnel simulation of ground effect conditions to determine effect of three dimensional turbulent boundary layer on V/STOL aircraft configurations - Pt. I
[NASA-CR-114495] 03 p0282 N73-12283
Comparison of turbulent heating predictions by three different techniques with flight test data of several reentry vehicles
[NASA-CR-130251] 03 p0282 N73-12288
Skin friction, heat transfer and pressure measurements in laminar, transitional and turbulent boundary layers on flat plates at high Mach numbers and Reynolds numbers
[NASA-CR-112147] 03 p0283 N73-12290
Viscous drag reduction caused by polymer injection in developing turbulent boundary layer
[AD-747274] 03 p0285 N73-12310
Dynamic structural response of rectangular panel to subsonic turbulent boundary layer pressure field
[NASA-TN-D-6970] 03 p0360 N73-12934
Analysis of mean velocity profiles in three-dimensional turbulent boundary layers during incompressible flow
[REPT-71-FM-13] 04 p0404 N73-13289
Parametric relations for ordinary and confluent turbulent wall jet flows with external stream velocity and arbitrary pressure distribution
04 p0405 N73-13297
Turbulent and laminar boundary layer behind blast waves generated in shock tubes
[ISL-5/72] 04 p0406 N73-13306
Effusion cooled turbine blade boundary layer velocity and temperature profiles as function of hole distribution
[DGLR-PAPER-72-59] 04 p0427 N73-13479
Mixing length theory used to determine influence of pressure gradients on wall region of turbulent boundary layer
[AD-749371] 05 p0527 N73-14290
Parameterization of turbulent boundary layer in atmospheric circulation model
05 p0573 N73-14661
Parameterization of near surface mesoscale circulation
05 p0574 N73-14665
Wind tunnel tests to determine heat transfer of near equilibrium transpired turbulent boundary layer with adverse pressure gradient
[NASA-CR-130291] 06 p0652 N73-15291
Analysis of factors involved during reversion of turbulent boundary layers to laminar flow
[REPT-72-FM-2] 06 p0652 N73-15297
Flow characteristics of two-dimensional, tangential-slot injection into turbulent boundary layer at Mach 2.4 freestream velocity
[NASA-CR-2128] 06 p0654 N73-15313
Configuration and structure of turbulent boundary layer flow over lateral uneven surface roughness
[AD-749944] 06 p0694 N73-15656
Effect of pressure gradients on supersonic turbulent boundary layers and effect of dilation on Reynolds stresses
[IC-AERO-72-21] 07 p0736 N73-15989
Hypersonic axisymmetric turbulent boundary layer compression in adverse pressure gradient along cylindrical axisymmetric body
[NASA-CR-112247] 07 p0770 N73-16253
Laminar and turbulent boundary layers, including hypersonic flow, wall flow and stagnation area
[DLR-MITT-71-13] 07 p0770 N73-16256
Integration of equations of motion for three dimensional turbulent boundary layer
07 p0771 N73-16261
Mathematical model for eddy viscosity in turbulent boundary layer on flat plates
07 p0771 N73-16262
Viscous wall flow in turbulent boundary layer including shear stress
07 p0771 N73-16266
Numerical simulation of air flow in atmospheric layer over inhomogeneous surface considering wind, temperature, shear stress, and turbulent energy
[AD-751589] 07 p0795 N73-16462
High frequency and pulsed electron discharge heating of turbulent skin layer in plasma
[AEC-TR-7329] 07 p0826 N73-16695
Analysis of fin bow shock wave during high speed air flow on blunt fin to determine interaction of vortices and shock waves
[AD-752210] 08 p0898 N73-17274
Heat exchange and drag during turbulent flow of compressible gas
[AD-753046] 09 p1017 N73-18300
Flow equations for unsteady turbulent boundary layer flow on swept infinite cylinder to show effects of variations in frequency of oscillations
[NASA-TM-X-62242] 10 p1141 N73-19297
Universal curves which relate general properties of two-dimensional boundary layers on turbomachine blades
10 p1204 N73-19795
Effect of free stream turbulence level on turbulent boundary layer behavior
10 p1204 N73-19799
Optimization method for turbomachine blade design based on boundary layer concepts
10 p1204 N73-19801
Method for calculating three dimensional turbulent boundary layer separation applied to simple turbomachine case
10 p1205 N73-19808
Method for prediction of turbulent boundary layer flow in vaneless radial diffuser and experimental validation
10 p1206 N73-19809
Interaction of shock wave with turbulent boundary layer at moderate supersonic Mach numbers
10 p1206 N73-19815
Development of method for solving three dimensional, incompressible laminar and turbulent boundary layer problems for swept infinite cylinders and small cross flow
[AD-754440] 11 p1232 N73-20004
Analysis of Reynolds stress in turbulent boundary layer on smooth wall with zero pressure gradient
[AD-754758] 11 p1272 N73-20319
Analysis of mean and fluctuating flow properties of compressible turbulent boundary layer in shock wave-induced adverse pressure gradient
[NASA-TN-D-7092] 12 p1391 N73-21280
Separation of incompressible boundary layer from axisymmetric curved afterbody
13 p1509 N73-22226
Gas injection of turbulent boundary layer through porous wall
[ONERA-NT-201] 13 p1510 N73-22237
Research projects on hypersonic and rarefied gas flows, separated and reattached wakes, viscous flow, and laminar and turbulent boundary layers with strong blowing
[AD-755276] 13 p1512 N73-22249
Heat transfer in immediate vicinity of wall by measurement of average temperature profiles
[AD-756957] 13 p1512 N73-22256
Effects of drag reducing polymer on turbulent boundary layer of submerged flat plates
[AD-755215] 13 p1513 N73-22260
Combined heat and mass transfer at wet flat plate in parallel air flow forming turbulent boundary layer
[DLR-FB-73-11] 14 p1599 N73-22960
Integral equation for studying three dimensional turbulent boundary layer development
14 p1648 N73-23369
Integral calculation of three-dimensional turbulent boundary layer velocity profiles
14 p1648 N73-23370
User manual for turbulent boundary layer and turbulent separation prediction methods used in streamtube curvature computer program
[NASA-CR-112240] 14 p1649 N73-23376
Compressible turbulent boundary layer in zero-pressure gradient nozzle flow for zero, moderate, and severe heat transfer conditions
[AD-757330] 14 p1651 N73-23391

Turbulent boundary layer separation criteria for subsonic and transonic flows
[AD-757531] 14 p1652 N73-23401
Calculation of coupled skin friction and heat transfer in two and three dimensional turbulent boundary layers
[AD-757871] 15 p1768 N73-24327
Calculation of two-dimensional turbulent skin friction under arbitrary compressible flow conditions
[AD-757872] 15 p1769 N73-24329
Development of mathematical formula for growth of compressible, turbulent boundary layers on isothermal and adiabatic walls
[ARC-R/M-3191] 16 p1853 N73-25013
Development of methods for determining local skin friction of boundary layer and calibration of instruments for analyzing turbulent shear flow
[ARC-R/M-3202] 16 p1854 N73-25016
Development of mathematical procedures for determining turbulent boundary layer in arbitrary pressure gradient
[ARC-R/M-3207] 16 p1854 N73-25017
Compressible turbulent boundary layer solutions using eddy viscosity models
[AD-759164] 16 p1891 N73-25307
Solution of thick axisymmetric turbulent boundary layer and turbulent flow equations
[AD-759015] 16 p1892 N73-25309
Measurements of pressure distributions, mean velocity profiles, and Reynolds stresses in thick incompressible turbulent boundary layer near tail of body of revolution
[AD-759014] 16 p1892 N73-25310
Force measurements and pressure distributions on three Gottinger airfoil profiles during transition from laminar to turbulent boundary layer flow
[NASA-TT-F-14959] 17 p1979 N73-26000
Influence of free stream turbulence on turbulent boundary layer in relation to wind tunnel testing at subsonic speeds
17 p2014 N73-26283
Analysis of profile characteristics of supersonic turbulent boundary layer in region of moderate adverse pressure gradient
[AD-759915] 17 p2015 N73-26298
Wind tunnel investigation of turbulent boundary layer response to lateral surface roughness discontinuities
18 p2129 N73-27202
Visual study of outer region of turbulent boundary layer along flat plate
18 p2129 N73-27203
Experimental determination of bound vortex lines and flow in vicinity of trailing edge of slender delta wing
[NASA-TT-F-15012] 18 p2131 N73-27217
Phenomenological approach to turbulent shear flows
[AD-760765] 18 p2132 N73-27223
Numerical analysis of compressible turbulent boundary layer velocity and temperature profiles with zero pressure gradient
[AD-762152] 19 p2258 N73-28200
Interaction between supersonic boundary layer with turbulent flow and inelastic deformable wall to determine stress perturbations and pressure distribution
[TN-86] 20 p2388 N73-29186
Effect of surface pressure fluctuations on response of panels underlying attached and separated turbulent boundary layers and shock waves
20 p2479 N73-29910
Calculations of turbulent shear stress distributions for zero pressure gradient and adverse gradient supersonic turbulent boundary layer flow
[AD-763197] 21 p2526 N73-30254
Three-dimensional compressible turbulent boundary layer for subsonic and transonic flow over yawed airfoil
[AD-763730] 21 p2526 N73-30258
Free stream pressure gradient effects on accuracy of turbulent boundary layer calculations
22 p2648 N73-31219
Reynolds stress in turbulent boundary layer on smooth wall
22 p2650 N73-31233
Parametric integral method for calculating laminar and turbulent incompressible flow- and temperature boundary layers
[DLR-FB-73-24] 22 p2653 N73-31255
Calculation of heat and mass transfer in turbulent boundary layer on surface with arbitrary roughness
[AD-764128] 22 p2655 N73-31266
Hypersonic, turbulent, cold-wave, skin friction, and heat transfer measurements on axisymmetric sharp cone
[AD-764059] 22 p2655 N73-31269
Investigation of naturally turbulent two dimensional boundary layer undergoing separation
[AD-764512] 22 p2655 N73-31272
Air stress predictions for synoptic scale ice dynamics model
[PB-222057/2] 22 p2669 N73-31388
Supersonic wind tunnel tests on three dimensional turbulent boundary layer growth on wires leading to calculation of tension and skin friction on aircraft towlines
[ARC-CP-1235] 23 p2740 N73-31933
Integral method for analyzing two-dimensional and axisymmetric compressible and three-dimensional incompressible turbulent boundary layer
23 p2772 N73-32169
Measurement of wall shearing stress and velocity and temperature profiles of turbulent boundary layer to derive Reynolds number
[ARC-R/M-3712] 24 p2870 N73-32928
Vortex pairing in turbulent shear layer at moderate Reynolds numbers
24 p2903 N73-33169
Investigating instantaneous structure of wall pressure under turbulent boundary layer flow in air
[REPT-9/1973] 24 p2904 N73-33177
Turbulent boundary layer flow of gas-solid suspension
24 p2906 N73-33190
Effect of heat transfer on velocity distribution and skin friction in turbulent wall boundary layers
24 p2906 N73-33195
Comparison of theories for skin friction coefficient in turbulent compressible boundary layers
24 p2907 N73-33203
Closed form approximation in dissipation integral for incompressible turbulent boundary layers
24 p2908 N73-33204

**TURBULENT DIFFUSION**

Analysis of dispersion, correlation and structural functions in amplitude and phase of laser being propagated into turbulent atmosphere
02 p0181 N73-11470
Development of method for estimating length of atmospheric turbulence patch as function of different turbulence intensities for two or more regions
[NRC-12793] 04 p0370 N73-13009
Analysis of turbulent diffusion in rocket combustion chamber to determine Lagrangian correlation coefficient and intensity of turbulence in chamber
08 p0967 N73-17908
Behavior comparison of certain properties generated by different forms of eddy diffusion term in two dimensional turbulent flow
[AD-753619] 09 p1032 N73-18425
Diffusion random model for statistical analysis of light propagation in turbulent medium
09 p1066 N73-18698
Effect of bottom topography, eddy diffusivity, and wind variation on circulation in two-layer stratified lake
[NASA-TN-D-7235] 11 p1286 N73-20433
Resistivity and ion energy distribution in turbulent plasma heating
[COO-3165-3] 17 p2067 N73-26727
Mass diffusion model for turbulent mixing of free jets
19 p2253 N73-28164
Numerical analysis of horizontal diffusion in ocean water to determine lifetime and spatial extent of submarine wakes in various turbulent media
[AD-762046] 19 p2256 N73-28186
Numerical analysis of turbulent diffusion in stratified fluid to show variations in diffusion coefficient with changes in ocean water depth
[AD-761653] 19 p2257 N73-28190
Effect of high polymer drag reducing additives on longitudinal turbulent dispersion coefficient for two dimensional open channel flow
24 p2902 N73-33164
Analyzing behavior of instantaneous point source as it disperses in thick, neutrally stratified, turbulent shear layer by laser light scattering technique
24 p2904 N73-33176

**TURBULENT FLOW**

NT CAVITATION FLOW
NT SUPERCAVITATING FLOW
Turbulent burst and non-turbulent durations in turbulent boundary layer of open channel
[ARL/SM-NOTE-374] 01 p0039 N73-10307
Turbulent flow calculation and models
[NASA-CR-128372] 01 p0039 N73-10309
Statistical analysis of turbulent motion using Navier-Stokes equations - Part I
[NASA-TT-F-14560] 01 p0039 N73-10310
Growth of mechanically generated surface water waves when subjected to turbulent channel air flow
[AD-746493] 01 p0042 N73-10336
Friction reducing properties of fibers in turbulent flow of fluids in pipes
[AD-746485] 01 p0043 N73-10337
Numerical analysis of radiation damping of thin finite rectangular plates immersed in heavy and light fluid media
[AD-746460] 01 p0115 N73-10950
High temperature oxidation reactions of carbon monoxide and methane in oxygen-rich atmospheres in turbulent flow reactor
[AD-746284] 02 p0138 N73-11116
Physical structure of turbulent shear flows in non-reacting gase flow
[AGARD-AR-46] 02 p0156 N73-11262
Limit process expansion techniques used to analyze fully developed turbulent incompressible flow in infinitely long channel with plane parallel walls
[AD-746112] 02 p0158 N73-11283
Mean turbulent flow in entry region of rough pipe
[AD-747278] 02 p0159 N73-11285
Plane turbulent gradient flow of incompressible fluid along porous surface in presence of blowing or suction
[AD-746933] 02 p0159 N73-11290
Parameters and secondary factors governing forced convective heat transfer and turbulent flow in circular tubes
[ESDU-67016] 02 p0242 N73-11964
Calculation of Magnus sideforce developed by spinning cylinder at angle of attack considering effects of boundary layer and shed vorticity in crossflow
03 p0247 N73-11998
Application of modified compressibility transformation for analyzing variable property turbulent boundary layers and predicting flow properties
[NASA-CR-2147] 03 p0282 N73-12286
Calculation of drag of porous lattice plates in turbulent flow
[IC-AERO-72-20] 03 p0284 N73-12300
Parametric relations for ordinary and confluent turbulent wall jet flows with external stream velocity and arbitrary pressure distribution
04 p0405 N73-13297
Development of theory for jet noise generated by turbulence, noise radiation from upstream sources, and combustion noise - Vol. 4
[AD-749139] 05 p0496 N73-14038
Analysis of pressure loss conditions created by turbulent flow conditions for wide range of flowmeters
[ESDU-66030-AMEND-A] 05 p0525 N73-14273
Numerical analysis of heat transfer conditions at point of intersection of jet impinging on obstacle at subsonic and supersonic speeds
[NLL-RTS-7617] 05 p0525 N73-14274
Analysis of turbulent fluid flow through rectangular conduit with large aspect ratio and development of mechanical energy-balance equations
[WTHD-27] 05 p0526 N73-14279
Analysis of interaction between fluid and discrete particles in turbulent flow field and development of equations of motion
[WTHD-32] 05 p0526 N73-14280
Analysis of swirling jet of gas injected into vacuum and effect of centrifugal force on separation of constituents
[ISAS-487-VOL-37-NO-13] 05 p0526 N73-14283
Supersonic characteristics of sonic nozzle gas flow expansion
[AD-749764] 05 p0528 N73-14297
Application of functional analysis to obtain exact semianalytical solutions of boundary layer flows under turbulent and laminar conditions
06 p0616 N73-15003
Wind tunnel tests to determine heat transfer of near equilibrium transpired turbulent boundary layer with adverse pressure gradient
[NASA-CR-130291] 06 p0652 N73-15291
Analysis of factors involved during reversion of turbulent boundary layers to laminar flow
[REPT-72-FM-2] 06 p0652 N73-15297
Numerical analysis of change in component energies due to three dimensional distortion in homogeneous and initially axisymmetric turbulence
[REPT-72-FM-7] 06 p0652 N73-15298
Influence of solid suspended particles on turbulent flow properties
06 p0652 N73-15300
Measurement of fluctuations in free surface flow of gas and liquids
06 p0653 N73-15303
Analysis of lee side vortex flow distribution about ogive-cylinderfrustum-cylinder at various angles of attack and Mach numbers - Vol. I
[NASA-CR-123997-VOL-1] 06 p0653 N73-15307
Compilation of computed parameters resulting from analysis of lee side vortex flow distribution about ogive-cylinder-frustum-cylinder at various angles of attack and Mach numbers - Vol. 2
[NASA-CR-123997-VOL-2] 06 p0653 N73-15308
Application of turbulence transport equations to problems in which buoyancy is driving force
[LA-DC-72-705] 06 p0654 N73-15314
Configuration and structure of turbulent boundary layer flow over lateral uneven surface roughness
[AD-749944] 06 p0694 N73-15656
Flow model of axisymmetric hypersonic nozzle for transition from turbulent flow to laminar flow with pressure gradient controlled by nozzle shape
07 p0768 N73-16237
Stabilizing and destabilizing effects of Coriolis body force on turbulent wall layers in two dimensional channel flow
07 p0768 N73-16243
Visualization of longitudinal vortices in stagnation area of circular cylinder in turbulent flow with splitting plate
07 p0771 N73-16264

Hot-wire measurement of longitudinal instability phenomena in stagnation area of circular cylinder in turbulent flow
07 p0771 N73-16265

Measurement of microscale turbulence and turbulent flow intensity of dilute polymer solutions about circular cylinders
[AD-751640] 07 p0774 N73-16284

Computer program to determine compressible fluid flow with friction across face seals and through narrow solts
[NASA-TN-D-6787] 07 p0803 N73-16518

Turbulent transport models for designing compressors and gas turbines
[AD-751757] 07 p0837 N73-16786

Reynolds time-averaged equations adopted for fully turbulent two dimensional flow of incompressible fluid through channel with plane smooth walls
[AD-752462] 08 p0898 N73-17272

Analysis of turbulent velocity fluctuations in confined jet to determine design parameters for fluid amplifiers
[AD-752041] 08 p0899 N73-17276

Number of surge series of turbulent velocity pulsations with Gaussian distribution
09 p1059 N73-18635

Effects of flow turbulence and noise on transition and boundary layer development in aerodynamic wind tunnel tests
[NASA-TT-F-14833] 09 p1066 N73-18702

Analysis of scaling parameters for flow in core region of vortex generated by rectangular wing tip and vortex generated by ogee wing tip
[NASA-CR-2180] 10 p1103 N73-18995

Analysis of eddy diffusivity of momentum for heating air in turbulent annular flow and effect of various flow parameters on eddy diffusivities ratio
10 p1139 N73-19279

Wind tunnel measurements of nearly homogeneous grid turbulence field with large amplitude temperature fluctuations
10 p1139 N73-19280

Error sources in pressure measurements on turbulent supersonic flows by nonstationary microphone
10 p1140 N73-19289

Numerical analysis of Prandtl mixing path, criteria charcterizing pressure and velocity pulsations in turbulent flow conditions
10 p1141 N73-19294

Semiempirical model for development of round turbulent jet in cross flow using asymptotic solution for jet excess velocity
[NLR-TR-71107-U] 10 p1142 N73-19307

Error sources in pressure measurements on turbulent supersonic flows by nonstationary microphone
10 p1184 N73-19629

Finite difference procedure for computing behavior of two-dimensional boundary layers and turbulence model to predict location and extent of transition region
10 p1204 N73-19796

Three component wake velocity measurements of full scale OH-13 helicopter rotary wing during hovering flight
[AD-754644] 11 p1235 N73-20030

Analysis of point vortex approximation of vortex sheet in two space dimensions and application to vortex sheet induced by ellipitcally loaded wing
[AD-755007] 11 p1273 N73-20335

Water waves generated and propagated in turbulent flow field
[AD-754645] 11 p1288 N73-20451

Analysis of aerodynamic noise produced by rotary wings and methods for noise reduction based on shed vortex wakes and blade tip modification
12 p1362 N73-21053

Gust field generation in wind tunnel for determining transfer function of lifting surface
12 p1387 N73-21248

Development of statistical equations for turbulent compressible gas with emphasis on space-time correlations in boundary layer
[AD-755889] 12 p1393 N73-21291

Noise scattered into receiving antenna system by turbulent plasma
[AD-756829] 13 p1492 N73-22094

Digital linearization of turbulent channel flow measurements by hot-film sensor
[REPT-2/1973] 13 p1510 N73-22234

Numerical analysis of turbulence equations in orthogonal tensor form, axisymmetric flow equations, and use of mass-averaged variables
[NASA-TM-X-62248] 13 p1510 N73-22235

Research projects on wake turbulence and atmospheric boundary layers, turbulent mixing and shear flows, and high temperature gas dynamics
[AD-755273] 13 p1512 N73-22251

Transport processes of particles in dilute suspensions in turbulent water flow
[PB-213536] 13 p1512 N73-22255

Fluctuations of spherical wave through turbulent layer over receiving aperture
[AD-756928] 13 p1561 N73-22648

Particle-fluid interaction corrections for turbulent flow measurements with laser Doppler flowmeter
[NASA-CR-124254] 14 p1649 N73-23379

Effect of wall suction on turbulent pipe flow friction coefficient
[AD-757584] 14 p1653 N73-23406

Laser-Doppler anemometer measurements of turbulence in drag reducing flows
[AD-757075] 14 p1669 N73-23545

Effects of wall jets in still air on flat and curved surfaces under external stream in presence and absence of pressure gradient and initial boundary layer
[ARC-R/M-3252] 15 p1729 N73-24025

Development of mathematical models for turbulent flow and application to prediction of internal flows
[TM/TN/A/18] 15 p1768 N73-24321

Analysis of motion of laminar and turbulent viscous vortex rings produced in air by pneumatic actuated piston vortex generator
16 p1886 N73-25265

Numerical analysis of turbulence transport equation for two dimensional jet flow and pressure-velocity derivative correlations
16 p1887 N73-25270

Characteristics of turbulent flow over wavy surface using sinusoidal waves of three sizes to determine variations of flow with wave size
16 p1887 N73-25273

Method of local potential applied to analysis of turbulent shear flow
[NASA-CR-112322] 16 p1889 N73-25286

Three dimensional flow field modules with turbulent structure
[AD-758894] 16 p1890 N73-25292

Solution of thick axisymmetric turbulent boundary layer and turbulent flow equations
[AD-759015] 16 p1892 N73-25309

Mathematical model for turbulent flow in electric arc
[AD-759572] 16 p1950 N73-25781

Numerical prediction of turbulent flow in argon cascade arc
[AD-759183] 16 p1950 N73-25783

Numerical analysis of structure of incompressible turbulent flows in plane wake and plane jet using two eddy viscosity models
17 p2012 N73-26274

Analysis of effect of turbulence intensity on aerodynamic characteristics of bodies of various shapes to develop method for measuring initial turbulence
[AD-760264] 17 p2015 N73-26297

Analysis of amplitude modulation of ultrasonic sound beam impinging at right angles to turbulent water jet
[RAE-LIB-TRANS-1671] 17 p2063 N73-26686

Calculating acoustic source distributions in turbulent flows when average velocity distribution is known
[NASA-TT-F-14946] 17 p2063 N73-26689

Development of wind and turbulence model for surface boundary layer based on surface parameters of stability and height
[NASA-CR-2288] 18 p2104 N73-27021

Test equipment and experimental procedures for determining effects of turbulent flow on ignition properties of gasoline and air mixture
[NLL-RTS-7883] 18 p2128 N73-27194

Analysis of submerged, turbulent, two-dimensional, heated slot jet flowing into moving stream
18 p2128 N73-27197

Proceedings of conference to develop data on free turbulent shear flows to include two dimensional shear layers and axisymmetric jets
[NASA-SP-321-VOL-2] 18 p2130 N73-27213

Analysis of local and average heat transfer characteristics of single turbulent air jet impinging on concave surface of hemisphere
[NASA-TM-X-2859] 18 p2206 N73-27806

Proceedings of conference on free turbulent shear flows - Vol. I
[NASA-SP-321-VOL-1] 19 p2252 N73-28154

Critical review of experimental data for developed free turbulent shear layers
19 p2252 N73-28156

Application of statistical turbulence theory for validity determination of turbulence phenomenology
19 p2252 N73-28157

Rational approach to use of Prandtl mixing length model in free turbulent shear flow calculations
19 p2252 N73-28158

Kinematic eddy viscosity model which accounts for influence of density variations and preturbulence
19 p2252 N73-28159

Analysis of free turbulent shear flows by numerical methods
19 p2252 N73-28160

Relationship between eddy-transport and second-order closure models for stratified media and for vortices
19 p2253 N73-28161

Predictions of axisymmetric free turbulent shear flows using generalized eddy viscosity approach
19 p2253 N73-28163

Comparison of six different turbulence models for prediction of free shear flows
19 p2253 N73-28165

Local eddy viscosity model for turbulent shear flow
19 p2254 N73-28168

Integral turbulent kinetic energy analysis of free shear flows
19 p2254 N73-28170

Turbulent free shear layers in pressure gradients
19 p2254 N73-28171

Proposed experiments dealing with classical free turbulent flows
19 p2254 N73-28172

General classification of approaches used for prediction of turbulent shear flows
19 p2254 N73-28173

Analysis of wake collapse in sea water and stratified fluids with emphasis on final stages of decay
[AD-761622] 19 p2257 N73-28189

Analysis of low speed deflagration of initially unmixed reactants under irreversible, two-step chain reaction
[AD-762459] 19 p2353 N73-28930

Implicit numerical solution for laminar and turbulent flow of incompressible fluid along axis of 90-degree corner
20 p2384 N73-29152

Turbulent fluid friction of rotating disks in incompressible flow calculations
20 p2384 N73-29155

Turbulent flow of gas-solid suspensions about ellipsoid of revolution
20 p2385 N73-29163

Numerical analysis of aerosol concentration and deposition flux for several flow configurations with and without electrical force deposition
20 p2386 N73-29172

Development of invariant models of diffusion and chemical reactions in turbulent flow systems
[NASA-CR-2295] 21 p2505 N73-30106

Characteristics of electrostatic discharges in liquids to show importance of transport and discharge mechanisms for boundary surface phenomena and particle discharge
[N.L.-M-23041-[5828.4F]] 21 p2516 N73-30182

Measurement capabilities of one dimensional laser Doppler velocimeter system
[NASA-TM-X-64774] 21 p2548 N73-30427

Extended Huygens-Fresnel principle for image plane illuminance distribution of extended object in turbulent atmosphere
[AD-763717] 21 p2581 N73-30683

Numerical procedure for determining relationship between shear stress and turbulent kinetic energy in two dimensional flow
22 p2649 N73-31221

Characteristics of secondary flows around and downstream of protuberances in laminar boundary layers and conditions for development of turbulence
22 p2649 N73-31222

One- and two-dimensional analysis of particle deposition in turbulent slot flow with application to self cleaning air filter design
22 p2649 N73-31225

Analysis of compressible three-dimensional turbulent flow over yawed cone
22 p2649 N73-31227

Local pressure field in turbulent shear flow and its relation to aerodynamic noise generation
[NASA-CR-134493] 22 p2653 N73-31253

Apparatus for analysis of turbulent transport properties in non-decaying, swirling, annular vortex flows
[AD-763916] 22 p2654 N73-31262

Electric discharge in turbulent flowing gas
[AD-764468] 22 p2655 N73-31265

Secondary flow in curved channel of square cross section
[AD-764502] 22 p2655 N73-31267

Turbulent, surface, and internal motions of ocean
[AD-763804] 22 p2670 N73-31390

Trivane measured fluctuations of wind and temperature over an inland lake
22 p2694 N73-31578

Turbulent gas-solid electrohydrodynamic flow into channel
23 p2772 N73-32172

Statistical model of turbulence based on elementary solutions of linearized Navier-Stokes equations
23 p2773 N73-32177

Sharp interface in unbounded turbulent shear flows determined by linear array of hot-wire probes
23 p2773 N73-32178

Stochastic modeling of turbulent heat and mass transport in anisotropic shear flow
23 p2773 N73-32181

Turbulent gas-solids flow measurements using laser Doppler velocimeter
23 p2773 N73-32182

Analytical and experimental investigation of turbulent mixing flow in pressure gradient to determine existence of equilibrium flows in streams of helium and nitrogen
23 p2774 N73-32184

Influence of periodic oscillations of mean flow on mean and turbulent structure of fully developed air flow in smooth circular pipe
24 p2902 N73-33161
Computation of kinetic fluctuation energy of turbulent shear flow from mean velocity distribution
24 p2908 N73-33211
Incompressible turbulent plane jets exhausting downstream into external flow having favorable longitudinal pressure gradient
[ARC-CP-1236] 24 p2909 N73-33219

TURBULENT HEAT TRANSFER
Laminar, transitional, and turbulent heat transfer measurements on yawed blunt conical nôsetip in free stream Mach 5
[AD-748292] 04 p0486 N73-13967
Turbulent convective heat transfer in horizontal liquid layers with volume heating - pt. 1
[DLR-FB-71-39-PT-1] 05 p0606 N73-14927
Turbulent convective heat transfer in horizontal liquid layers with volume heating noting turbulent convection mechanism - Pt. 2
[DLR-FB-71-40-PT-2] 05 p0606 N73-14928
Apparatus and program for turbulent torus experiment
[ORO-4087-8] 06 p0704 N73-15737
Plasma confinement, plasma dynamics, and turbulent heating
[ORO-3458-34] 06 p0704 N73-15738
Turbulent heat transfer and pressure on leading edge of fin, swept wing, or antenna
[SCL-RR-72-0308] 12 p1464 N73-21863
Turbulent heating of plasmas by streaming instabilities
[AD-763777] 21 p2584 N73-30705
Heat transfer between gas and turbine casing in intervane channels of stators and guide vanes
[NASA-TT-F-15051] 21 p2588 N73-30737

TURBULENT JETS
Heat transfer at critical point, jet turbulence, and vortex systems
[AD-747294] 02 p0244 N73-11981
Flow visualization and analytical analysis of momentum roll up of turbulent circular jet
04 p0403 N73-13286
Theoretical and experimental determination of interaction of semi-confined, subsonic, turbulent jets
[AD-749023] 04 p0408 N73-13325
Semiempirical theory on bending and development of round turbulent jet in subsonic crosswind
[AD-751093] 07 p0774 N73-16286
Velocity irregularities in near field of high aspect ratio turbulent jets
[AD-754224] 10 p1143 N73-19315
Experimental and theoretical investigation of trajectory and growth of thermal effluents with variable discharge velocities and temperatures
[NASA-TM-X-69221] 12 p1392 N73-21284
High frequency spectrum domain of turbulent jet noise
15 p1813 N73-24697
Effectiveness of eddy viscosity models for coaxial and two-dimensional jets with and without coflowing stream
[AD-759576] 16 p1890 N73-25298
Measurement of hydrogen concentration in mass diffusing jets by laser induced Raman scattering
17 p2012 N73-26272
Turbulent nonbuoyant or buoyant jets discharged into flowing or quiescent fluids
[AD-760028] 17 p2016 N73-26300

TURBULENT MIXING
Vertical and horizontal turbulent mixing coefficients of sea water determined from attenuation coefficient
[NLL-RTS-7536] 02 p0160 N73-11294
Chemical evolution of air and hydrogen in turbulent mixing layer
[NASA-TT-F-14633] 04 p0386 N73-13141
Development of system for predicting movement and decay of aircraft-generated vortices in air corridors near air terminals using meteorological information
[LMSC/HREC-D306226] 06 p0620 N73-15036
Mathematical model for turbulent boundary layer of two liquid flows
07 p0772 N73-16267
Provisional analysis of two dimensional turbulent mixing with variable density
[AD-751541] 07 p0773 N73-16275
Infrared detection of hydrogen fluoride tracer for studying turbulent mixing in inert and combustion flows
08 p0880 N73-17128
Analysis of aircraft trailing vortices to show formation and breakdown for various aircraft wing configurations
[ME/A-72-1] 08 p0895 N73-17247
Mathematical modeling of turbulent mixing
[NASA-CR-124086] 09 p1013 N73-18267
Analysis of turbulent mixing between two streams of different density to determine effects of density difference at low Mach number and compressibility at high Mach number
[AD-753538] 09 p1019 N73-18313
Numerical analysis of Prandtl mixing path, criteria charcterizing pressure and velocity pulsations in turbulent flow conditions
10 p1141 N73-19294
Hot-wire anemometer and pitot static probe measurement of turbulent mixing in axial pressure gradients
[AD-756543] 13 p1511 N73-22244
Effect of adjacent jets on turbulent mixing rate of coaxial helium jet in Mach 4 air stream
[NASA-CR-112292] 16 p1888 N73-25281
Incompressible free turbulent mixing in adverse and favorable pressure gradients
[AD-758664] 16 p1891 N73-25308
Importance of depth of mixing layer in air pollution studies
[NLL-M-22807-[5828.4F]] 16 p1936 N73-25668
Methods for calculation of turbulent free mixing
19 p2252 N73-28155
Model for free turbulent mixing in coflowing stream
19 p2253 N73-28162
Mass diffusion model for turbulent mixing of free jets
19 p2253 N73-28164
Provisional analysis of two dimensional turbulent mixing with variable density
19 p2253 N73-28166
Prediction of free turbulent mixing using turbulent kinetic energy method
19 p2253 N73-28167
Turbulent kinetic energy equation and free mixing
19 p2254 N73-28169
Supersonic combustion and turbulent mixing processes required for advanced weapon systems
[AD-762599] 20 p2486 N73-29969
Turbulent mixing layer of different gases in pressure gradient
[AD-763487] 21 p2527 N73-30260
Analytical and experimental investigation of turbulent mixing flow in pressure gradient to determine existence of equilibrium flows in streams of helium and nitrogen
23 p2774 N73-32184

TURBULENT WAKES
NT PROPELLER SLIPSTREAMS
NT SLIPSTREAMS
Measured and calculated mean flow characteristics of two-dimensional, hypersonic, turbulent wakes produced by wedges
[NASA-TN-D-6927] 01 p0040 N73-10316
Development of wake vortex monitoring system using laser Doppler sensors for analyzing vortex flow field
[NASA-CR-123921] 02 p0152 N73-11229
Sound transmission at extremely low frequency in far field radiation from turbulent wake
[AD-747238] 02 p0212 N73-11721
Systems simulation for airport trailing vortex warning system
[NASA-TM-X-64704] 03 p0280 N73-12267
Mathematical model for inviscid stream flowing over turbulent fluid that behaves as elastic jelly
[AD-746990] 04 p0407 N73-13319
Numerical analysis of development of incompressible, symmetrical turbulent wake flows downstream of airfoils using integral method of momentum and energy
[NAL-TR-292] 06 p0614 N73-14986
Development of system for predicting movement and decay of aircraft-generated vortices in air corridors near air terminals using meteorological information
[LMSC/HREC-D306226] 06 p0620 N73-15036
Development of momentum integral type method for solving relaxation-diffusion model for turbulent shear stress of incompressible plane turbulent wakes
[REPT-72-FM-5] 06 p0652 N73-15296
Numerical analysis of wake propulsion parameters to show effects of drag, heating, and energy conversion
[RN-64] 08 p0894 N73-17238
Analysis of aircraft trailing vortices to show formation and breakdown for various aircraft wing configurations
[ME/A-72-1] 08 p0895 N73-17247
Mapping velocity field in hypersonic wake by use of iron probe array
[AD-751450] 08 p0897 N73-17264
Wind tunnel study of turbulent wake flow dynamics
[AD-751970] 08 p0897 N73-17267
Numerical analysis of inviscid, fully developed structure of lift-generated vortices behind aircraft wings and extension to arbitrary span-loaded distributions
[NASA-TM-X-62224] 09 p1016 N73-18289
Dependence of turbulent line vortices decay on Reynolds number
[AD-753131] 09 p1017 N73-18297
Fundamental flow problem in designing fluidic proximity sensors
10 p1158 N73-19422
Postflight analysis of AV-2 balloon launched decelerator flight test to determine parachute system operation in wake of blunt body simulating Viking 75 entry vehicle
[NASA-CR-112177] 11 p1233 N73-20011
Postflight analysis of AV-3 balloon launched decelerator flight test to determine parachute system operation in wake of blunt body simulating Viking 75 entry vehicle
[NASA-CR-112178] 11 p1233 N73-20012
Model equations based on eddy viscosity of turbulent wakes
[AD-752592] 11 p1271 N73-20314
Analysis of factors inhibiting performance of rotary wing aircraft and mathematical models of rotary wing flow characteristics
12 p1358 N73-21019
Generation of aerodynamic noise by turbulent wake behind rotary wing airfoil and relationship to drag and lift coefficients
12 p1362 N73-21054
Flight investigation to determine velocity and persistence characteristics of trailing vortices generated by jumbo jet transport
[NASA-TN-D-7172] 12 p1364 N73-21068
Wind tunnel tests to determine effect of tip vortex of forward mounted wing on engine inlet ingestion
[NASA-TM-X-68225] 13 p1473 N73-21932
Flight tests to determine characteristics of vortex and turbulent wake generated by DC-10 aircraft for development of air traffic control separation criteria
[REPT-73-00470] 13 p1474 N73-21938
Analysis of internal waves generated by passage of body through density stratified medium and effects on mean flow
[AD-755714] 13 p1512 N73-22254
Aircraft accident involving crash of DC-9 aircraft during landing following go-round at Fort Worth, Texas Airport on 30 May 1972
[NTSB-AAR-73-3] 17 p1982 N73-26017
Underwater vortex field generation in wake of rectangular airfoil
[NASA-TM-X-62274] 17 p2014 N73-26288
Ion probes used to determine structure of ionized turbulent wakes of hypersonic spheres
[AD-759157] 17 p2090 N73-26908
Analysis of kinematic and dynamic characteristics of wake generated behind flat plate normal to parallel unbounded fluid flow
[AD-761372] 18 p2131 N73-27220
Numerical analysis of two dimensional turbulent wakes in constant adverse and favorable pressure gradients
[AD-761389] 19 p2256 N73-28185
Development of theoretical model for supersonic turbulent near wakes of planar and axisymmetric configuration in supersonic flow
20 p2384 N73-29151
Application of finite-difference machine code for analyzing wake-vortex problem in quasi-cylindrical boundary layer approximation
[NASA-TM-X-69495] 20 p2387 N73-29179
Analysis of wakes generated by hovering model propellers and rotors using schlieren photography and hot-wire anemometry
[NASA-CR-2305] 21 p2491 N73-29996
Wind tunnel tests to determine transient wake velocities behind three stalled wing configurations at Reynolds numbers up to 4.8 million
[AD-763468] 21 p2498 N73-30050
Wind tunnel tests to measure axial and tangential velocity profiles in near wake vortices of semi-span model of Convair 990 aircraft model using laser Doppler velocimeter
[NASA-TM-X-62294] 21 p2524 N73-30244
Vortex age as scaling parameter in wake turbulence development and dissipation
[NASA-CR-132312] 22 p2652 N73-31245
Growth characteristics of hypersonic turbulent wakes with spatially resolved measurements
[DREV-R-687/73] 24 p2869 N73-32925
Analysis of random motions of vortex elements behind aircraft wing and design of vortex arrays to reduce wake-vortex to small aircraft
[NASA-TM-X-62304] 24 p2877 N73-32976
Characteristics of laminar and turbulent wakes of spherical bodies at hypersonic speed in nitrogen atmosphere
[DREV-R-683/72] 24 p2904 N73-33178

TURING MACHINES
Comparing complexity classes of formal languages
[NASA-CR-129294] 03 p0269 N73-12181
Injections of neighborhood size three and four on set of configurations from infinite one-dimensional tessellation automata of two state cells
[AD-748072] 03 p0272 N73-12209

TURKEY
Design and operation of Turkish information systems
15 p1752 N73-24202

TURNING FLIGHT
Aircraft maneuvers for reducing sonic boom intensity during horizontal turns
[AD-744859] 02 p0126 N73-11022
Analysis of military helicopter formation flight techniques with emphasis on station keeping based on nominal point coordinate system
[AD-751459] 07 p0740 N73-16021

Pilot performance during simulated standard instrument procedure turn with and without predictor display
[NASA-TM-X-62201] 08 p0879 N73-17118
Development of methods for predicting aircraft flight maneuver and climb performance to show effects of excess power and load factor
15 p1732 N73-24045
Development of techniques for real time, on-line, optimum flight path conditions and minimum time maneuvers for supersonic aircraft
[AD-758799] 16 p1862 N73-25083
Approach abort optimization in control of aircraft carrier landings
[AD-761617] 19 p2221 N73-27914
Flight control display device for producing curved approach profiles in microwave instrument landing systems
[DGLR-PAPER-73-016] 23 p2818 N73-32526
**TURNSTILE ANTENNAS**
Turnstile slot antenna system for spacecraft or missile telemetry and command control
[NASA-CASE-GSC-11428-1] 02 p0149 N73-11206
**TVC (CONTROL)**
U THRUST VECTOR CONTROL
**TWENTY-FOUR HOUR ORBITS**
Combined chemical solar electric transfer stage for inserting Europa 3 satellites into twenty-four hour orbits
[MBB-UR-V-49-71] 15 p1832 N73-24851
**TWENTY-SEVEN DAY VARIATION**
Autocorrelation, Chree, and power spectrum analyses of cosmic ray 27-day recurrences
[NP-19466] 08 p0957 N73-17833
Reaction time of 27-day density variation in upper atmosphere noting satellite recorded data on drag using regression analysis, cross correlation, and solar spectrum analysis
[BMFT-FBW-73-10] 21 p2538 N73-30352
**TWILIGHT**
U TWILIGHT GLOW
**TWILIGHT GLOW**
Spectrophotometric observation of earth atmosphere and underlying surfaces near twilight horizon from manned spacecraft
09 p1026 N73-18375
Air-to-ground visibility of lights at low background levels
10 p1226 N73-19967
Two rocket measurements of atmospheric oxygen concentration during twilight
16 p1895 N73-25331
Spherically symmetric models for radiance and color of twilight sky calculated for single scatter radiation
[NASA-CR-133739] 20 p2413 N73-29393
Ultraviolet evening terminator observations in Martian atmosphere by Mariner 9 space probe
23 p2841 N73-32702
**TWINNING**
NT MECHANICAL TWINNING
Diopside submicroscopical twinning in lunar and experimentally deformed pyroxenes
[NASA-CR-133271] 20 p2486 N73-29970
**TWO BODY ORBITS**
U TWO BODY PROBLEM
**TWO BODY PROBLEM**
Multiplicative renormalization group used to compute critical indices in d equals 4 minus sigma dimensions
[NOTA-INTERNA-384] 01 p0080 N73-10661
One boson exchange nucleon-nucleon potential in two nucleon and many nucleon problems
[NOTA-INTERNA-380] 01 p0084 N73-10694
High voltage distribution fields of two component dielectrics in rotational series or parallel arrangements
08 p0888 N73-17193
Linear stability analyses for four satellite configurations using passive elements for attitude control
16 p1964 N73-25883
Quasi-relativistic theory of two finite masses in Euclidean space and Newtonian time
20 p2454 N73-29720
Quasirelativistic theory of two-body motion in Euclidean space and Newtonian time
[AD-763431] 21 p2598 N73-30827
Dual resonance type model for quasi two body reactions in subprocesses of pion nucleon yields pion omega meson nucleon
22 p2701 N73-31635
**TWO DIMENSIONAL BODIES**
Shock wave instability in one dimensional and two dimensional problems
[AD-750009] 05 p0528 N73-14298
Technique for predicting shock envelopes and pressure distributions for two dimensional airfoil at angles of attack producing shock detachment and subsonic flow
[NASA-TN-D-7197] 09 p0979 N73-18001
Analysis of flow field around two dimensional airfoil of arbitrary shape
[AD-753387] 09 p1019 N73-18320
Numerical analysis of temperature distribution of complex two-dimensional body with various boundary conditions including radiation effects
[N8110R:72-040] 12 p1464 N73-21860
Analysis of aerodynamic interference resulting from jet issuing normal to chordal plane of two dimensional wing in crossflow conditions
13 p1508 N73-22223
Measurement of pitching moment derivatives using free oscillation technique on two dimensional airfoils of double wedge section and single wedge section
[ARC-R/M-3234] 16 p1855 N73-25025
General continuum theory with microstructure for wave propagation in elastic laminated composites in two dimensional case
[AD-762609] 20 p2436 N73-29562
**TWO DIMENSIONAL BOUNDARY LAYER**
High voltage distribution fields of two component dielectrics in rotational series or parallel arrangements
08 p0888 N73-17193
**TWO DIMENSIONAL FLOW**
NT COUETTE FLOW
Inverse method for calculating hypersonic flow shock layer around axisymmetrical two-dimensional blunt bodies
[ISL-42/71] 01 p0041 N73-10325
Numerical analysis of two-dimensional gravity wave flow on nonuniform free streams
[AD-744995] 01 p0042 N73-10329
Two layer model of compressible turbulent boundary layer flow around reentry vehicle
[AD-743933] 01 p0043 N73-10338
CDC computer program for solving two-dimensional, two-fluid magnetohydrodynamic equations
[AD-745854] 01 p0086 N73-10713
Comparison of surface-source solution with an exact solution for two-dimensional inviscid flow about slotted-flap airfoil
[ARC-CP-1214] 03 p0248 N73-12003
Asymptotic solution of two-dimensional flow of perfect gas past blunt body at given Mach number
[AD-747545] 03 p0287 N73-12327
Two dimensional, incompressible model for response of laminar and turbulent attached jets
[AD-747761] 03 p0309 N73-12520
Analysis of laser induced two dimensional wave motions in hydrogen plasma
[AD-746681] 03 p0343 N73-12798
Transient, two dimensional temperature field of laser pulse in solid
[SC-DR-72-0393] 04 p0429 N73-13495
Experimental investigations of two-dimensional flow problems and electric power generation in open cycle vortex MHD generator
[BM-RI-7699] 05 p0583 N73-14746
Application of functional analysis to obtain exact semianalytical solutions of boundary layer flows under turbulent and laminar conditions
06 p0616 N73-15003
Development of two experimental approaches for analyzing two dimensional flow on high lift devices
06 p0617 N73-15005
Coanda effect on plane jet flowing over curved surface considering two dimensional flow over airfoil
[DLR-FB-71-46] 06 p0621 N73-15043
Stabilizing and destabilizing effects of Coriolis body force on turbulent wall layers in two dimensional channel flow
07 p0768 N73-16243
Provisional analysis of two dimensional turbulent mixing with variable density
[AD-751541] 07 p0773 N73-16275
Numerical method for solving time dependent Navier-Stokes equation in two dimensions
[AD-751628] 07 p0773 N73-16276
Statistical mechanics and kinetic theory for two dimensional plasma in uniform magnetic field
07 p0825 N73-16685
Computerized prediction of two dimensional wall boundary layer flow from laminar through transition to turbulent regimes
08 p0894 N73-17239
Development of two dimensional theory for unsteady flow disturbances caused by aeroelastic deformation of thick wing at high subsonic speeds
[NASA-CR-112114] 08 p0896 N73-17258
Reynolds time-averaged equations adopted for fully turbulent two dimensional flow of incompressible fluid through channel with plane smooth walls
[AD-752462] 08 p0898 N73-17272
Measurement of lift, drag, and pitching moments in wing section for range of flap deflections under two-dimensional flow conditions
[ARC-CP-1233] 09 p0981 N73-18018
Numerical analysis of flow of rarefied monatomic gas through two dimensional slot to show characteristics of transition regime
[NASA-CR-124069] 09 p1012 N73-18265
Predicting base pressure in subsonic two dimensional steady base flow
[DLR-FB-72-57] 09 p1014 N73-18274
Calculation of flow through airfoils in cascade to show pressure distribution under conditions of two dimensional incompressible flow with boundary layer separation at trailing edge
[DLR-FB-72-62] 09 p1014 N73-18276
Analysis of flow distribution around harmonically oscillating circular cylinder under two dimensional flow conditions
[DLR-FB-72-56] 09 p1014 N73-18277
Analysis of two dimensional cascade flow of double circular arc blades at transonic speed with various camber angles and pitch-chord ratios
[NAL-TR-300] 09 p1014 N73-18279
Techniques for determining dynamic characteristics of hydraulic duct for predicting low frequency vibrations of liquid propellant rocket engines
[ONERA-TP-1160] 09 p1015 N73-18281
Two dimensional unsteady transonic flow of perfect gas with specific heat
[AD-753221] 09 p1018 N73-18310
Behavior comparison of certain properties generated by different forms of eddy diffusion term in two dimensional turbulent flow
[AD-753619] 09 p1032 N73-18425
Two dimensional motion of viscous incompressible flow with variable viscosity coefficient in thrust bearing
[AD-753030] 09 p1041 N73-18495
Mixing and ignition of hydrogen jets injected normally into supersonic two dimensional flow and effect on combustion performance of hyersonic ramjet engine
[ONERA-TP-973] 09 p1098 N73-18962
Effect of two dimensional suction flows into double intakes on upper surface of Joukowski airfoil for application to vertical takeoff and landing aircraft
[AD-754208] 10 p1104 N73-19003
Development of computer program for solving fully compressible, two-dimensional hydrodynamics problems using flux-corrected transport algorithms
[AD-754736] 11 p1271 N73-20315
Analysis of point vortex approximation of vortex sheet in two space dimensions and application to vortex sheet induced by ellipitcally loaded wing
[AD-755007] 11 p1273 N73-20335
Analysis of whirl stability boundaries and aerodynamic characteristics of tilting rotors
12 p1356 N73-21004
Calculation of two dimensional gas dynamic flows with detonation using Lagrange variables
[JPRS-58699] 12 p1391 N73-21281
Analysis of fluid flow over two dimensional flat plate wedge configuration for application to deep submersible vehicles
[NASA-CR-131888] 13 p1510 N73-22233
Analysis of accuracy of Preston tube calibration equations to determine local skin friction in two dimensional supersonic and low hypersonic flow conditions
[NASA-TN-D-7190] 13 p1510 N73-22239
Design and calibration of Langley 6 by 19 inch transonic tunnel for testing two dimensional airfoil sections
[NASA-TN-D-7182] 14 p1645 N73-23339
Interaction of large amplitude progressing wave with piecewise linear flow
[AD-756469] 14 p1651 N73-23392
Boundary layer separation on flat plate in high supersonic free stream as caused by normal injection of two dimensional sonic or supersonic jet
[AD-757635] 14 p1652 N73-23398
Numerical analysis of Navier-Stokes equations for steady two dimensional flow to show convergence characteristics
[ARC-R/M-3239] 15 p1725 N73-23997
Performance evaluation of two-dimensional slot nozzle ejector with variable area mixing sections
[NASA-CR-2251] 15 p1730 N73-24034
Modane-Avrieux transonic blowdown wind tunnel for two dimensional flow airfoil profile study
[ONERA-NT-203] 15 p1762 N73-24281
Performance tests of terminal shock and restart control system of two dimensional twin-duct compression inlet
[NASA-TM-X-2818] 16 p1956 N73-25824
Analysis of nonhomogeneous flow associated with two dimensional propulsive lifting system based on flow with energy addition
[NASA-CR-2250] 17 p1979 N73-25997
Development of alternating direction relaxation method for computing inviscid two dimensional transonic flows through cascades
17 p2012 N73-26268
Design and development of two dimensional airfoil with optimum drag divergence characteristics at transonic speeds
[NAL-TR-299] 18 p2101 N73-26994
Analysis of submerged, turbulent, two-dimensional, heated slot jet flowing into moving stream
18 p2128 N73-27197
Numerical analysis of two dimensional incompressible potential flow around system of arbitrary airfoils using relaxation method
[NAL-TR-309] 18 p2130 N73-27212
Theoretical analysis of two dimensional laminar jet rate sensors
[AD-761092] 18 p2153 N73-27401

Formulation and development of computer analysis for calculating streamlines and pressure distributions around two-dimensional isolated nacelles at transonic speeds
[NASA-CR-2217] 19 p2217 N73-27890
Provisional analysis of two dimensional turbulent mixing with variable density
19 p2253 N73-28166
Analysis of viscous effects in low-density nozzle flows using internal laminar layer equations for two dimensional or axisymmetric flow
[AD-761489] 19 p2257 N73-28191
Effect of shock wave interaction in parallel, two-dimensional, stratified flow of heavy and light gases
20 p2384 N73-29157
Two-dimensional nozzle flow problem solved by method of integral relations
20 p2385 N73-29161
Solutions for various problems in two dimensional and axisymmetrical steady viscous flow with harmonic pressure field
20 p2387 N73-29175
Numerical analysis of steady, two-dimensional, laminar, incompressible, high Reynolds number separated flow past thin airfoils
[NASA-CR-114656] 20 p2388 N73-29185
Effect of wall cooling on shock wave laminar boundary layer interactions in hypersonic two dimensional flow
[AD-762937] 20 p2389 N73-29192
Two and three dimensional flow field characteristics of lower surfaces of caret wings
[AASU-327] 21 p2491 N73-29997
Development of data for numerical analysis of aerodynamic performance of jet, blown, and ejector flaps
[AD-763793] 21 p2498 N73-30049
Development of numerical code to calculate two dimensional flow field when supersonic flow encounters double wedge configuration
[NASA-CR-134010] 21 p2524 N73-30242
Numerical procedure for determining relationship between shear stress and turbulent kinetic energy in two dimensional flow
22 p2649 N73-31221
Numerical studies of unsteady two dimensional subsonic flows using ICE method
[NASA-TM-X-68288] 22 p2651 N73-31240
Supersonic flow configurations at inlet and exit of infinite two dimensional straight cascade of flat plates
22 p2652 N73-31244
Investigation of naturally turbulent two dimensional boundary layer undergoing separation
[AD-764512] 22 p2655 N73-31272
Development of wind tunnel with self correcting apparatus based on sensors to determine flow conditions on tunnel surfaces and method for varying wall geometry
[AD-764957] 23 p2771 N73-32161
Effect of high polymer drag reducing additives on longitudinal turbulent dispersion coefficient for two dimensional open channel flow
24 p2902 N73-33164
Numerical solution of time-dependent Navier-Stokes equation with periodic boundary condition
[AD-764582] 24 p2910 N73-33226
Two dimensional time dependent numerical simulation of atmospheric flow over urban area
24 p2911 N73-33235

**TWO DIMENSIONAL JETS**
Effectiveness of eddy viscosity models for coaxial and two-dimensional jets with and without coflowing stream
[AD-759576] 16 p1890 N73-25298

**TWO FLUID MODELS**
Two fluid cosmological model including interaction between matter and radiation
13 p1561 N73-22652

**TWO PHASE FLOW**
MHD power systems with potential high efficiencies of constant liquid velocity, two phase, liquid metal dc MHD generator
[AD-747323] 03 p0255 N73-12064
NPSH technique for two phase pumping of cryogenic propellants in turbopumps and rocket engines
03 p0348 N73-12843
Numerical method for determining mass flow rates in two phase gas-solid rocket nozzle flow
[AD-750038] 05 p0591 N73-14804
Computer calculations of two-phase flow transients in once-through steam generators
[CEA-CONF-2009] 06 p0655 N73-15318
Inherent statistical properties of bubble field in two phase flow determined by correlation functions
[EUR-4840] 06 p0655 N73-15319
Thermodynamic equilibrium model for simulating pressure transient propagation in two phase water flow with mass transfer
08 p0896 N73-17255
Local quantities in two phase flow measured with anemometer, electrical probe, microthermocouple, and optical sensor techniques
[CEA-CONF-2033] 08 p0897 N73-17263
Averaging process for continuum mechanics in two phase flow analysis
[AD-752159] 08 p0898 N73-17273
Laser Doppler anemometer for measuring steam and water velocities in two phase flow
[UTIAS-TN-184-PT-1] 10 p1141 N73-19293
Feasibility determination for application of principle of corresponding states to two phase choked flow
[NASA-TM-X-68193] 10 p1141 N73-19299
Local measurements and their statistical interpretation for high velocity two phase flow with high void fraction
[CEA-CONF-2043] 10 p1141 N73-19300
Physical quantities in two phase flows
[FRNC-CONF-49] 10 p1142 N73-19301
Laser-Doppler velocity measurement of large particles in two-phase gas-solid nozzle flow
[VKI-TN-81] 10 p1142 N73-19305
Kelvin-Helmholtz instability analysis of bounded two phase particulate incompressible inviscid flows
[AD-754815] 11 p1272 N73-20318
High speed photographic system for moisture flow visualization in steam turbines
[NASA-TM-X-2763] 12 p1404 N73-21388
Theory of two phase gas-liquid and liquid-gas flow for bladed machines and ejectors
[AD-755713] 12 p1409 N73-21419
Hydrodynamics and heat exchange with two phase flow in elements of power equipment
[AD-756564] 13 p1591 N73-22897
Supersonic two phase air-water flows, noting expansion, acoustic velocity and X ray density measurements, and nozzle flow tests
[BMVG-FBWT-73-4] 14 p1650 N73-23380
Photographic equidensitometry of two phase and low density flows
[DLR-MITT-73-02] 17 p2015 N73-26293
Isentropic frictionless equilibrium flow of evaporating two phase mixtures with low vapor content in convergent-divergent nozzles
[SFB-MHD-5] 22 p2653 N73-31254
Thrust augmentation, lift forces, and mixing properties of two-phase flow propulsion and lift system for ground effect machines
[AD-765332] 23 p2777 N73-32208
Experimental analysis of two phase liquid oxygen pumping
[NASA-TN-D-7451] 24 p2972 N73-33747

**TWO PHASE SYSTEMS**
U BINARY SYSTEMS [MATERIALS]

**TWO REFLECTOR ANTENNAS**
Multiple beam interval scanners with dual-antennas and circular artificial dielectric lenses to provide spot beam coverage of contiguous 48 states
[NASA-CR-130168] 08 p0888 N73-17192
Parameters of RT-22 Krao Radio telescope antenna at wavelengths of 3 and 1.35 cm
23 p2838 N73-32676

**TYPE 2 BURSTS**
Type 4 solar radio bursts and their relation to expanding magnetic bottles
[NASA-TM-X-66217] 11 p1336 N73-20844
Review of solar type 2 and type 3 radio burst theory
19 p2339 N73-28814
Flare induced magnetohydrodynamic disturbance propagation in solar corona considering Moreton surface waves and type 2 shocks
19 p2339 N73-28816
Properties of solar coronal pulsations
19 p2339 N73-28817
High resolution spectra and position measurements on solar radio bursts
19 p2339 N73-28820
Motion of sources for type 2 and type 4 radio bursts and flare-associated interplanetary disturbances
[NASA-TM-X-70452] 21 p2507 N73-30117

**TYPE 3 BURSTS**
Evaluation of type 3 solar radio burst theories using low frequency satellite observations
08 p0974 N73-17961
High resolution spectral and polarization behavior of solar Type 3 bursts at 34 MHz
13 p1489 N73-22073
Evidence of electron acceleration and type 3 radio bursts during solar flares
19 p2337 N73-28805
Dynamic spectra of solar type 3 radio bursts at kilometer wavelengths
19 p2338 N73-28810
Decay times of type 3 solar radio bursts
19 p2338 N73-28811
Solar type 3 radio burst position measurements for coronal density determination
19 p2338 N73-28812
Explorer 38 observations of solar type 3 radio bursts
19 p2339 N73-28813
Review of solar type 2 and type 3 radio burst theory
19 p2339 N73-28814
Plasma wave decay effects on solar type 3 radio burst profiles at low frequencies
19 p2339 N73-28815
Positions and sizes of solar type 3 radio bursts associated with electron propagation in interplanetary space
19 p2339 N73-28818
Decametric dynamic spectra of solar type 3 radio bursts
19 p2339 N73-28819
High resolution spectra and position measurements on solar radio bursts
19 p2339 N73-28820
Chromospheric type 3 radio burst acceleration of solar electrons and coronal streamer
19 p2340 N73-28821
Structure of isolated solar flare point
22 p2734 N73-31880

**TYPE 4 BURSTS**
Type 4 solar radio bursts and their relation to expanding magnetic bottles
[NASA-TM-X-66217] 11 p1336 N73-20844
Properties of solar coronal pulsations
19 p2339 N73-28817
High resolution spectra and position measurements on solar radio bursts
19 p2339 N73-28820
Motion of sources for type 2 and type 4 radio bursts and flare-associated interplanetary disturbances
[NASA-TM-X-70452] 21 p2507 N73-30117

**TYPE 5 BURSTS**
Positions and sizes of solar type 3 radio bursts associated with electron propagation in interplanetary space
19 p2339 N73-28818

**TYPEWRITERS**
NT TELEPRINTERS
Guide accessories for correctly aligning paper in typewriter to correct typographical errors
[NASA-CASE-MFS-15218-1] 22 p2676 N73-31438

**TYPHOONS**
Effect of Philippines on intensity, speed and size of typhoons crossing islands
[AD-746131] 02 p0206 N73-11670
Regression analysis of tropical storm and typhoon speed characteristics after recurvature in western North Pacific Ocean
[AD-746880] 02 p0206 N73-11672
Typhoon associated tornadoes in Japan and suction vortices in Omiya tornado
[SMRP-RP-101] 03 p0326 N73-12639
Long term meteorological study of intensity and movement of tropical cyclones and typhoons in western North Pacific
[AD-754349] 11 p1315 N73-20676
Typhoon and tropical storm intensity forecasts in western North Pacific Ocean using statistical regression analysis
[AD-761379] 18 p2174 N73-27561
Atmospheric models for studying typhoon and thundercloud processes
20 p2446 N73-29645
Influence of ocean bottom relief on genesis and intensity of typhoons
20 p2446 N73-29646

# U

**U BENDS**
U shaped heated tube for distillation and purification of liquid metals
[NASA-CASE-XNP-08124-2] 04 p0385 N73-13129

**U TUBES**
U MANOMETERS

**U.S.S.R.**
Index of information collected by Soviet weather satellites
[NASA-TT-F-14447] 01 p0075 N73-10616
USSR air pollution literature survey on biological effects and health aspects
[PB-209478] 01 p0078 N73-10642
Bibliography of Soviet laser research and development
[AD-746339] 02 p0183 N73-11480
Activities of Astronomical Council, USSR
[AD-746016] 02 p0232 N73-11884
Soviet abstracts on analog and digital systems, control systems, information theory, and automata theory
[JPRS-57520] 04 p0393 N73-13190
Bibliography on laser development in Soviet Union
[AD-748258] 04 p0430 N73-13499
Soviet research and development in meteorology and hydrology
[JPRS-57127] 04 p0442 N73-13602
Experiment in climatic zoning of coast of Gulf of Riga
04 p0443 N73-13610
Review of Soviet publication on development of hydrology in USSR
04 p0443 N73-13616
Review of Soviet publication on navigational hydrometeorology
04 p0443 N73-13617
Quasi-analog computer proposed for Soviet hydrometeorological service for calculating nonsteady state motion of water in river channels
04 p0443 N73-13618
Soviet research on meteorology, oceanography, upper atmosphere, and astronomy
[JPRS-57630] 04 p0474 N73-13876

Record high air pressure of 1083.8 mb at Lake Agatha, Siberia, on 31 Dec. 1968, and weather phenomena in Northern Hemisphere at end of 1968
[NLL-M-22700-[5828.4F]] 05 p0570 N73-14629
Soviet bibliography on biocybernetics material received from Jan. to May 1972
[AD-750129] 06 p0636 N73-15167
Recent Soviet investigations in geothermy
[AD-750128] 06 p0671 N73-15454
Fiftieth anniversary of formation of USSR with synopsis of accomplishments including rocket flights with animals for space medicine research
07 p0743 N73-16042
Geographical, physicomathematical, and hydrological engineering treatment of river runoff in USSR
[TT-70-50058] 07 p0781 N73-16346
Analysis of heat supply requirements and heating availability in geographical areas of USSR
[JPRS-58114] 08 p0917 N73-17513
Physical and chemical energy sources for earth, sea, and space
[AD-753828] 09 p0992 N73-18093
Research and development of lasers and laser-related equipment in the Soviet Union - bibliography
[AD-753098] 09 p1043 N73-18510
Development of scientific centers in USSR during past 50 years and considerations for future development
[JPRS-58596] 11 p1267 N73-20281
Relationship between surface temperature anomalies in European USSR and seasonal variations of stratospheric circulation
[NLL-M-22851-[5828.4F]] 11 p1274 N73-20336
Aerosynoptic wind and temperature conditions contributing to atmospheric turbulence at altitude of 18 km over European USSR
[NLL-M-22822-[5828.4F]] 11 p1274 N73-20342
Geodetic quality determination of Soviet satellite data, using camera sites at Riga, Uzhgorod, and Helsinki
[AD-754070] 11 p1287 N73-20446
Soviet method of illumination calculation for aerial survey on color film
[AD-754627] 11 p1295 N73-20508
Atomic science and engineering developments in USSR
[AD-754040] 11 p1327 N73-20766
Military training, combat readiness, and antiaircraft defense
[AD-754834] 11 p1352 N73-20980
Survey of USSR missile defense system
[AD-754629] 11 p1353 N73-20983
Electronic procedures for selecting and teaching students at Moscow Institute of Electronic Engineering
[JPRS-58550] 12 p1386 N73-21242
Mathematical models for educational planning and personnel selection in Soviet Union
[JPRS-58793] 12 p1419 N73-21497
USSR research projects in subjects of microclimate, agricultural meteorology, weather forecasting, climate control, and hydrological forecasting
[JPRS-58483] 12 p1420 N73-21510
Behavioral and social science advancement in USSR after 50 years
[JPRS-58686] 12 p1467 N73-21883
Role of USSR scientific centers in economic development
[JPRS-58683] 12 p1467 N73-21887
Weather forecasting in USSR
[JPRS-58797] 13 p1552 N73-22571
Climatic variability of winter wheat harvest for USSR
13 p1552 N73-22578
Duration of thunderstorms over USSR
13 p1552 N73-22580
Research projects in geophysics, astronomy, and satellite applications
[JPRS-58885] 13 p1577 N73-22776
Research activities in exobiology and aerospace medicine
[JPRS-59015] 14 p1607 N73-23024
USSR conference on exobiology and aerospace medicine
14 p1609 N73-23045
Present technology and prospects for creation of national communications television broadcast network in USSR during 1971 - 1975
[JPRS-58928] 14 p1637 N73-23273
Atmospheric physics and gas dynamics research in Soviet Union
[JPRS-58988] 14 p1649 N73-23377
K. E. Tsiolkovskiy as film consultant
[NASA-TT-F-14890] 14 p1708 N73-23865
Development technology for communication systems
[JPRS-59221] 15 p1750 N73-24184
Rock densities within gravitational anomalies of Ukrainian shield
[AD-757540] 15 p1783 N73-24455
Application of cybernetics and systems analysis techniques to economic problems in USSR
[JPRS-58935] 15 p1845 N73-24951
Effect of scientific and technical progress on economic control parameters in USSR
[JPRS-58976] 15 p1845 N73-24952
Problems of air transport economics and efficiency of air transport utilization in USSR
[NASA-TT-F-741] 16 p1860 N73-25069
Standardization of geodetic instruments in U.S.S.R. research facility
[AD-759687] 16 p1914 N73-25492
Long-term cyclic fluctuations of atmospheric precipitation in USSR
[NLL-M-22891-[5828.4F]] 16 p1935 N73-25659
Handbook on climatology of USSR
[AD-759244] 16 p1939 N73-25694
Worldwide airfield climatic data for Eastern Europe and USSR - Part 1
[AD-759794] 17 p2057 N73-26640
Worldwide airfield climatic data for Eastern Europe, and USSR - Part 2
[AD-759795] 17 p2057 N73-26641
Survey of Soviet literature on use of silicon nitride for gas turbine applications
[AD-760329] 17 p2078 N73-26810
Test parameters and methods used in Soviet Union for jet engines
[AD-760963] 18 p2194 N73-27714
USSR research in meteorology, oceanography, astronautics, astronomy, and geophysics
[JPRS-59278] 18 p2196 N73-27727
Soviet research in meteorology, oceanography, upper atmosphere, astronomy, and space
[JPRS-59002] 18 p2196 N73-27729
Soviet-bloc research in geophysics, astronomy, and space
[JPRS-59490] 18 p2196 N73-27730
Bibliography of Russian literature on aviation and space medicine
[JPRS-53329] 20 p2369 N73-29047
Statistical analysis of snowfall in various areas of USSR for application to transportation, agriculture, and urban planning
[TT-70-50181] 20 p2406 N73-29338
Removal of pollutants from atmosphere by precipitation and clouds
[NLL-M-23010-[5828.4F]] 20 p2441 N73-29608
Atmospheric circulation effects on precipitation and temperature regimes of USSR and Northern Hemisphere
20 p2444 N73-29633
Tsunami of Ust-Kamchatsk after December 15, 1971 earthquate
20 p2447 N73-29656
Tributaries of Lake Baykal
20 p2447 N73-29657
Legal and administrative measures adopted by U.S.S.R. for protection of environment
[JPRS-59436] 20 p2486 N73-29971
System of legal protection for environment of U.S.S.R.
20 p2486 N73-29972
Normative acts relating to legal protection of natural areas in U.S.S.R.
20 p2487 N73-29973
Planning and supervision of production activities for purpose of protecting environment in U.S.S.R.
20 p2487 N73-29974
Supervision of use and protection of natural resources according to Soviet legislation
20 p2487 N73-29975
Collection of Soviet articles on computer elements and systems
[TT-72-50009] 21 p2512 N73-30150
Papers presented at meeting of Soviet-American working group on remote sensing of natural environment from space
[JPRS-59739] 21 p2534 N73-30317
Selection of standard sections in u.s.s.r. as test sites for geological interpretation of space photography
21 p2534 N73-30321
Tyan-shan section of USSR as test site for geological interpretation of space photography
21 p2534 N73-30322
Caucasian section of USSR as test site for geological interpretation of space photography
21 p2534 N73-30323
Ustyurt section of USSR as test site for geological interpretation of space photography
21 p2535 N73-30324
Geological-structural interpretation of photographs of Balkhash region from space and their role in geological survey of Central Kazakhstan
21 p2535 N73-30329
Multiparameter method for forecasting monthly mean air temperature anomalies in U.S.S.R.
[NLL-M-23038-[5828.4F]] 21 p2567 N73-30577
Predicted weather conditions for USSR during winter of December 1971 through March 1972
[NLL-M-23035-[5828.4F]] 21 p2568 N73-30578
Engineering procedures, blasting, and water level regulation for flood prevention and ice jam control on Dnestr and Dubossary Reservoirs
21 p2573 N73-30620
Studies in hypoxia and phylogenetics by USSR aerospace medical scientist
[NASA-TT-F-15101] 22 p2619 N73-30991
Meteorological services and technology of USSR
[JPRS-59962] 22 p2692 N73-31565
Prospects for development and growth of USSR hydrometeorological service
22 p2692 N73-31566
Design for development of network in Moscow and vicinity for mesometeorological observations
22 p2693 N73-31573
Forecasting mean monthly air temperature anomalies for Oct. in northern part of European territory of USSR
22 p2693 N73-31575
Scientific research in geophysics, astronomy, meteorology, oceanography, astronautics from soviet-block
[JPRS-59935] 22 p2716 N73-31738
Clarification concerning fall of Borodino meteorite
[NASA-TT-F-15126] 22 p2717 N73-31749
USSR research in solid state physics, laser technology, geosciences, and materials
[AD-763742] 23 p2866 N73-32916
Advances in technology and armament in USSR
[AD-763323] 23 p2866 N73-32917
USSR research in solid state physics, plasma physics, atmospheric physics, and seismology
[AD-763743] 23 p2866 N73-32918
Analysis of Marxist-Leninist theory based on data in cybernetics, information theory, systems analysis, and semiotics
24 p2993 N73-33918

**U.S.S.R. SPACE PROGRAM**

Soviet Meteor meteorological satellite system and applications in weather forecasting, geological surveys, and exploration of earth resources
[NLL-M-22683-[5828.4F]] 01 p0073 N73-10599
USSR space program accomplishments in fields of geophysics, astronomy, meteorology, oceanography, upper atmosphere, and space sciences
[JPRS-57229] 01 p0104 N73-10864
Soviet camera for tracking satellites and solving geodetic and geophysical problems
[AD-747135] 03 p0303 N73-12476
USSR research projects in geosphysics, astronomy, and space - No. 288
[JPRS-57505] 03 p0357 N73-12906
USSR developments in meteorology, weather forecasting, climate control, and hydrological forecasting
[JPRS-57608] 04 p0444 N73-13623
Soviet Cosmos satellite and rocket programs
[NASA-TT-F-14641] 04 p0478 N73-13913
USSR research projects involving laser technology, effects of strong explosions, geosciences, and particle beams
[AD-749487] 04 p0489 N73-13998
USSR research projects involving meteorology, oceanography, upper atmosphere, space research, and terrestrial geophysics
[JPRS-57777] 05 p0596 N73-14844
History of USSR space program to include design of manned spacecraft, solution of space flight problems, and chronology of manned USSR space flights
[NLL-M-22222-[5828.4F]] 06 p0720 N73-15876
Soviet space stations for providing earth space photographs used for earth atmosphere and earth surface analysis
[JPRS-58055-1-PT-1] 09 p1026 N73-18372
Abstracts of articles on Soviet Bloc research in earth and space sciences
[JPRS-58437] 11 p1338 N73-20860
USSR research projects in meteorology, oceanography, upper atmosphere and space astronomy, and terrestrial geophysics
[JPRS-58609] 11 p1339 N73-20867
USSR research projects in meteorology, oceanography, geophysics, upper atmosphere, and extraterrestrial radiation - No. 298
[JPRS-58734] 12 p1458 N73-21817
Leading scientists of USSR space programs
[NASA-TT-F-14882] 13 p1595 N73-22935
USSR research projects in geophysics, astronomy, and aerospace subjects - May 1973
[JPRS-59136] 17 p2024 N73-26379
USSR automatic stations on mars and venus, lunar continental region samples, and 24 hour satellite earth watching
[NASA-TT-F-14929] 19 p2342 N73-28841
Contrasting opinions concerning space activity concerning untested physiological effects
[NASA-TT-F-15019] 19 p2342 N73-28842
Soviet space exploration and research during 1972
[JPRS-59778] 20 p2488 N73-29983
Measurements of illumination in atmosphere and on surface of planet Venus obtained by automatic interplanetary station Venera-8
[JPRS-59963] 21 p2595 N73-30794
Spaceflights by Soviet devices to the moon and results of lunar surface research
[NASA-TT-F-14983] 21 p2596 N73-30801
Congressional hearings concerning appropriations for NASA operations during Fiscal Year 1974 - Part 3
21 p2608 N73-30907
Details and problems of docking technology, mutual aid and rescue for disasters, search and rendezvous

means, and cabin atmospheric parameters for Soviet-American flight
[NASA-TT-F-15096] 23 p2844 N73-32726
U-3 AIRCRAFT
Application of ERTS-1 and U-2 photography to study of urban land use in Pennsylvania
[PAPER-L17] 19 p2275 N73-28312
UBV SPECTRA
Magnitude and UBV colors for 900 stars brighter than magnitude 5.0 and south of plus 10 deg declination
[ANNALS-7] 08 p0960 N73-17849
UBV observations of HD 176387
[BULL-174] 10 p1212 N73-19856
UBV photometry of 115 nearby stars
[BULL-176] 10 p1212 N73-19858
UBV and H alpha spectra for detecting interstellar dust and distances to planetary nebulae
12 p1448 N73-21724
UBV observations of RR Lyrae variable HD 176387
[ROY-OBS-BULL-174] 13 p1578 N73-22787
UBV photometry of stars within 25 parsecs of sun, in quasar and galaxy field, in Kapteyn selected areas and of miscellaneous stars including super and red giants
[ROY-OBS-BULL-176] 13 p1578 N73-22789
Using UBUH gamma photometry and spectral classifications for 48 stars in monoceros region to study dispersed part of 1 Mon association
23 p2836 N73-32658
UDIMET ALLOYS
Effect of discontinuous changes in strain rate on relationship between strain rate, strain and stress in Udimet 700 alloy at elevated temperatures
10 p1219 N73-19916
Influence of strain rate on inelastic properties of Udimet alloys at elevated temperatures and presentation in form of hodograph
10 p1219 N73-19917
Method of life prediction for nickel-based Udimet alloy by high temperature creep/fatigue testing
[NASA-CR-120958] 12 p1462 N73-21845
UH-13 HELICOPTER
U OH-13 HELICOPTER
UH-1 HELICOPTER
Performance tests to determine proficiency of maintenance personnel in servicing fuel start solenoid in UH-1 helicopter
[AD-745163] 01 p0021 N73-10166
Design analysis of repairable main rotor blades applicable to UH-1H helicopter
[AD-749283] 05 p0494 N73-14028
Investigation of US Army UH-1 helicopter accidents where orientation errors were contributing factor during fiscal year 1969
[AD-749695] 06 p0623 N73-15059
Modification of UH-1 helicopter rotor to determine effects of injecting tip vortex of rotor blade with mass of linearly directed air
[AD-750634] 06 p0625 N73-15074
Design and development of sectionalized main rotor blade for UH-1 helicopter
[AD-750633] 06 p0625 N73-15075
Investigation of correlation between pilot disorientation and UH-1 helicopter accidents
[AD-753208] 09 p0986 N73-18049
UH-1 helicopter test bed program for evaluation of automatic inspection, diagnosis, and prognostic maintenance functions on selected subsystems - Vol. 1
[AD-752890] 09 p0987 N73-18058
Accomplishments during evaluation of automatic inspection, diagnostic, and prognostic maintenance system using UH-1 helicopter as test bed - Vol. 2
[AD-752891] 09 p0987 N73-18059
Analysis of infrared spectra generated by OV-1D, F-14, and UH-1 aircraft using Fourier spectroscopy
[RM-572] 13 p1529 N73-22390
Cost effectiveness analysis of helicopter transmission components to determine effect of extended overhaul life up to 6,000 hours
[AD-758465] 14 p1604 N73-23007
Development of method for estimating power output of helicopter gas turbine engines operating at full power
[AD-758461] 14 p1702 N73-23811
Feasibility and cost effectiveness of expendable main rotor blades on UH-1 helicopter
[AD-758464] 15 p1736 N73-24078
Design, reliability analysis, maintainability, and cost effectiveness of expendable rotor blades for UH-1 helicopter rotary wing
[AD-762198] 19 p2222 N73-27926
Logistic performance data book for UH-1F helicopter airframe to show reliability, maintainability, logistic costs, and operational problems
[AD-762251] 19 p2357 N73-28965
Operational parameters for UH-1H helicopters during combat flights in Southeast Asia to determine helicopter performance and reliability
[AD-764260] 22 p2616 N73-30965
UH-2 HELICOPTER
Design, development, and evaluation of flexible drive shaft coupling used for propulsion of HH-2D helicopter
[AD-746502] 01 p0063 N73-10519
UHTREX [NUCLEAR REACTORS]
U HIGH TEMPERATURE NUCLEAR REACTORS
UHURU SATELLITE
X ray sources in galactic center and comparison of Aerobee data with Uhuru data
[NASA-TM-X-66114] 03 p0353 N73-12873
UK SATELLITES
NT UK 4 SATELLITE
Vehicle encountered trapped electron and proton fluxes calculated for nominal UK 5 circular equatorial orbits
[NASA-TM-X-66098] 02 p0225 N73-11816
UK 4 SATELLITE
Magnetic tests of UK 4 spacecraft to determine magnetic characteristics and to provide desirable magnetic conditions
[NASA-TM-X-66125] 04 p0478 N73-13912
ULM [LIGHT MODULATION]
U ULTRASONIC LIGHT MODULATION
ULTRA SHORT WAVE RADIO EQUIPMENT
U VERY HIGH FREQUENCY RADIO EQUIPMENT
ULTRAHIGH FREQUENCIES
ATS 5 and Intelsat 1 observations of L band and VHF signals during ionospheric scintillation
[NASA-TM-X-66060] 01 p0028 N73-10216
Radiation diagram measurements on antenna model surface for UHF communication to FPL 35F
[FOA-3-C-3678-61] 02 p0139 N73-11130
Design, development, and evaluation of three channel interference cancellation system for use with ultrahigh frequency communication systems
[AD-747802] 03 p0267 N73-12158
Measuring electromagnetic parameters of soil samples in VHF/UHF range to determine properties that limit target detection
[AD-747346] 03 p0299 N73-12439
Development and evaluation of instrument landing system with VHF and UHF capability for localizer and glide slope
[AD-747656] 03 p0329 N73-12688
Design and construction of broadband combinable amplifier using stripline techniques for UHF amplification
[AD-747404] 04 p0396 N73-13218
Design, development, and fabrication of L band RF electron beam semiconductor amplifier
[AD-748898] 04 p0396 N73-13224
Fabrication and tests of L band, RF pulse amplifier
[AD-749791] 05 p0514 N73-14182
Microwave properties and microstructure of polycrystalline UHF garnets
[AD-749509] 05 p0588 N73-14781
Characteristics of four types of horn antennas for application as S-band radiometers and modifications to improve beam efficiency
[NASA-CR-2133] 07 p0755 N73-16135
Design and testing of non-blocking UHF communication system
[AD-751263] 07 p0758 N73-16156
Gain and impedance measurements on ultrahigh frequency antennas near surface of simulated sea water
[AD-751922] 08 p0890 N73-17205
Very high frequency Schottky barrier gate field effect transistors
[DOC-REF-3-314] 08 p0951 N73-17785
Semiconductor transmitter in S band
[DLR-FB-72-53] 09 p1007 N73-18220
Design of low gain L-band orthogonal-mode crossed slot antenna and VHF crossed loop antenna for airborne applications
[NASA-CR-130795] 11 p1261 N73-20237
Formation of hydrocyanic acid from mixtures of ammonia, metane and noble gas or hydrogen subjected to UHF waves
[NASA-TT-F-14678] 12 p1376 N73-21162
Simultaneous ultrahigh and very high frequency ionospheric effects from ATS 5 at the magnetic equator
[NASA-TM-X-65948] 12 p1378 N73-21173
Relation of phonemes to acoustic signals from human vocal tracts as represented by ultrahigh frequency patterns
14 p1631 N73-23218
Power equation theory for defining ultrahigh frequency and microwave measurements
[NBS-TN-637] 15 p1750 N73-24182
Ultrahigh frequency coherent radar as moving target indicator
[AD-757565] 16 p1877 N73-25191
Conference on atmospheric attenuation and rainfall effects on ultrahigh frequency telecommunication systems
[AGARD-CP-107] 17 p1994 N73-26121
Multipath propagation and phase delay of ultrahigh frequency radio wave caused by atmospheric discontinuity
17 p1994 N73-26124
Criteria for planning ultrahigh frequency telecommunication system considering radioelectrical and meteorological measurements
17 p1995 N73-26129
Horizontal radio link system for measuring ultrahigh frequency absorption spectrum due to rain
17 p1995 N73-26130
Ultrahigh frequency coherent radio signal transmission for differential phase shift measurements due to vapor and oxygen absorption lines
17 p1995 N73-26131
Scattering in transhorizon ultrahigh frequency radio link due to rain
17 p1995 N73-26133
Point rainfall rate statistics for predicting ultrahigh frequency radio propagation
17 p1996 N73-26136
Multipath rainfall measurements for planning ultrahigh frequency radio link
17 p1996 N73-26137
Calculation of electromagnetic wave absorption by rain for frequencies close to 30 GHz
17 p1996 N73-26138
Slant path attenuation of ultrahigh frequency signals from sun tracking radiometers
17 p1996 N73-26140
Thunderstorm cloud height and fading statistics for ATS 5 ultrahigh frequency signal transmission to earth
17 p1996 N73-26141
Ultrahigh frequency precipitation attenuation measurements by ATS 5 weather radar and radiometer
17 p1996 N73-26142
Design of omnidirectional ultrahigh frequency communication antenna fitted around pole
[AD-760201] 17 p2005 N73-26217
Development of linear power transistors and design of broadband UHF amplifiers from these transistors
[AD-757558] 17 p2006 N73-26227
Analysis of radio communication links for air traffic control operations to show effects of adjacent channel interference and modulation limitations
[FAA-RD-70-71] 18 p2117 N73-27114
Acousto-optical delay line for UHF pulses with continuously variable delay, based on photon-phonon interaction
18 p2179 N73-27597
UHF linear phase bandpass filter for communication satellite
[ESRO-CR[P]-253] 19 p2235 N73-28024
Hot pressed polycristalline garnets and ferrites of spinel type to be used at UHF
19 p2236 N73-28026
Development of low volume, high power radiating transmitter and antenna array to show radiation pattern, antenna gain, and efficiency
[AD-761793] 19 p2245 N73-28098
Solid state high power UHF broadband amplifier
[AD-762175] 19 p2247 N73-28118
Measurements on high and low gain L band aircraft serials using transmissions from high altitude balloon
[RAE-TR-73008] 20 p2377 N73-29102
S-band power amplifier using high efficiency silicon avalanche diode
[AD-763104] 20 p2381 N73-29135
Electron beam semiconductor S-band amplifier
[AD-763223] 21 p2518 N73-30200
Satellite based system for L band precision positioning
[NASA-CR-62095] 22 p2697 N73-31604
Absence of S band energy gap in single crystal niobium
[AD-764906] 23 p2827 N73-32594
Heat treated chromium doped rutile for L-band traveling wave masers
[RR-111] 24 p2930 N73-33402
ULTRAHIGH VACUUM
Ultrahigh vacuum techniques for diffusivity and solubility of N2 in Mo and N2 trapping by C in Mo
[UCRL-51182] 17 p2045 N73-26544
Calibration of vacuum gauges for measuring total and partial pressures in ultrahigh vacuum region
[NASA-CASE-XGS-07752] 21 p2544 N73-30390
Ultrahigh vacuum gauge with two collector electrodes
[NASA-CASE-LAR-02743] 23 p2751 N73-32324
ULTRALOW FREQUENCIES
U EXTREMELY LOW RADIO FREQUENCIES
ULTRAPURE METALS
Production methods, quality control, and metallurgical uses of pure rare earth metals and alloys
[IS-2968] 10 p1172 N73-19538
SQUID magnetometer measurement of fluctuation diamagnetism of Al and Al alloys above superconducting transition temperature
[COO-3156-56] 21 p2559 N73-30515
ULTRASONIC AGITATION
Development of ultrasonic radiation equipment for removing material from host surface and vacuum apparatus for recovery of material
[NASA-CASE-NPO-11213] 11 p1296 N73-20514
ULTRASONIC GRINDING MACHINES
U GRINDING MACHINES
ULTRASONIC INSPECTION
U ULTRASONIC TESTS
ULTRASONIC LIGHT MODULATION
Diffraction of light by ultrasonic waves and intensity of diffraction spectrum
[NASA-TT-F-13926] 02 p0212 N73-11714

Manufacturing of high efficiency ultrasonic wave transducer for light modulation using Brillouin effect
[REPT-4.473] 23 p2820 N73-32544

ULTRASONIC RADIATION
Correlation of respiratory distress and ultrasonic transmission with severe decompression sickness in hampsters
[AD-743475] 01 p0012 N73-10091
Acoustic holography for imaging cylindrical plastic-bonded explosive loads
[AD-746468] 01 p0067 N73-10547
Optical design and performance evaluation of athermal solid and liquid acoustic lenses
[AD-745734] 01 p0081 N73-10668
Research of ultrasonic propagation in ferromagnetic materials
[AD-745783] 01 p0088 N73-10729
Ultrasonic scanner for inspection and evaluation of in-place brazed tube joints
[NASA-TM-X-64702] 02 p0178 N73-11445
Conditions of coherence in diffraction spectra produced in liquids on ultrasonic standing waves
[NASA-TT-F-13925] 02 p0211 N73-11713
Determination of circulation and diameter of vortices from ultrasonic wave phase deviation
[REPT-6/1972] 03 p0285 N73-12308
Application and advantages of ultrasonic inspection for thick walled components
[NLL-RISLEY-TR-2209-[9091.9F]]
05 p0550 N73-14466
Sonic or ultrasonic holography in nuclear industry research
[DUN-SA-191] 08 p0929 N73-17610
Ultrasonic radiation and microwave research projects
[AD-752055] 08 p0944 N73-17736
Turbine inlet gas temperature measurement by ultrasonic impedance
[AD-752602] 08 p0955 N73-17822
Development of acoustic surface wave, multiple-tap, delay line structure using sputtered zinc oxide piezoelectric films on metal interdigital arrays on silicon surface
[AD-753674] 09 p1009 N73-18238
Operational principles of ultrasonic devices in radio circuits
[AD-754616] 11 p1263 N73-20248
Magnetostatic and magnetoelastic surface wave interactions in magnetized yttrium-iron garnet film
[AD-754106] 11 p1331 N73-20802
Computer technique for obtaining near field cross section views of ultrasonic field
[AD-756537] 13 p1502 N73-22170
Principles and techniques of Bragg diffraction laser beam probing of ultrasonic field
[AD-756521] 13 p1537 N73-22454
Application of ultrasonic inspection for determining effect of graphite on strength characteristics of cast iron
15 p1797 N73-24571
Parametric difference frequency generation of sound in air through interaction of two intense high frequency sound waves
[AD-758682] 16 p1946 N73-25747
Pulse-echo technique for measuring ultrasonic attenuation in Bi12GeO20 single crystals at low temperature
16 p1952 N73-25798
Bulk elastic wave signals and design of acoustic filter
[AD-760020] 17 p2006 N73-26223
Analysis of amplitude modulation of ultrasonic sound beam impinging at right angles to turbulent water jet
[RAE-LIB-TRANS-1671] 17 p2063 N73-26686
Evaluation of nondestructive testing techniques for diffusion-bonded titanium alloy aircraft structures using ultrasonic radiation
[AD-760673] 18 p2106 N73-27035
Ultrasonic absorption in liquid metals and in liquid selenium
18 p2178 N73-27590
Low temperature measurement of heat pulse and ultrasonic wave interaction with stress-split acceptor states in semiconductors
18 p2186 N73-27647
Application of ultrasonic inspection techniques for detecting separation of solid propellant rocket case-liner and liner-propellant interfaces
[NAL-TR-306] 18 p2193 N73-27703
Restoration of obliterated stamped serial numbers by ultrasonically induced cavitation in water
[NASA-TM-X-68257] 18 p2213 N73-27866
Procedures for ultrasonic inspection of wing attachment fittings on Viscount aircraft
[TR-7211.621] 20 p2422 N73-29455
Ultrasound and light scattering in diffusing and chemical reacting binary mixture of fluids
23 p2774 N73-32185
Monitoring of fatigue damage by ultrasonic attenuation measurements
23 p2796 N73-32363

ULTRASONIC SPEEDS
U SUPERSONIC SPEEDS

ULTRASONIC TESTS
Ultrasonic method for detecting onset of fatigue damage in metal specimens
[AD-745978] 02 p0175 N73-11418
Nondestructive ultrasonic testing of aircraft tires
[AD-747633] 03 p0309 N73-12521
Application and advantages of ultrasonic inspection for thick walled components
[NLL-RISLEY-TR-2209-[9091.9F]]
05 p0550 N73-14466
Results of ultrasonic inspection of cast steel cylinders
[TR-7208.594] 05 p0551 N73-14471
Ultrasonic inspection of wing spar joints and lugs on Viscount Aircraft
[TR-7207.591] 05 p0551 N73-14472
Ultrasonic inspection of aluminum keys used in electric generators
[TR-7206.590] 05 p0551 N73-14473
Application of ultrasonic nondestructive tests to vehicle tire compliance measurements
[PB-211892] 05 p0553 N73-14491
Dislocation damping in cu single crystals of controlled substructure, and ultrasonic attenuation data
[AD-750712] 06 p0711 N73-15801
Design and development of ultrasonic instrumentation to facilitate quantitative nondestructive evaluation of defects in materials
[NASA-CR-124021] 08 p0923 N73-17562
Ultrasonic inspection of steel gear parts
[REPT-7210.614] 10 p1164 N73-19466
Ultrasonic inspection of pressure vessel steel plates
[TR-7209.601-B] 10 p1164 N73-19469
Ultrasonic inspection of pressure vessel steels
[TR-7209.601] 10 p1164 N73-19470
Ultrasonic inspection and control of cast steel parts for use as machine gears
[TR-7210.617] 10 p1164 N73-19471
Ultrasonic inspection of cast steel blocks, steel plates, and welded seams
[TR-7210.607] 10 p1164 N73-19472
Ultrasonic measurements of elastic constants of polycrystalline alloys of iron in vanadium
[AD-753615] 10 p1174 N73-19547
Ultrasonic methods for analyzing elastic moduli of materials at high temperatures
[AD-753844] 10 p1176 N73-19567
Ultrasonic relaxation measurement of polyethylene and polyethylene oxide from room temperature to melting point
[AD-754391] 11 p1310 N73-20628
Depths of reflection zone characteristics for classifying ultrasonic echoes in weld testing
[NLL-CE-TRANS-5993-[9022.09]]
11 p1324 N73-20742
Ultrasonic testing of Teflon and composite materials considering phase velocity
[AD-756385] 13 p1560 N73-22642
Ultrasonic inspection and control of laminated steel blocks prior to machining
[TR-7212.620] 14 p1670 N73-23550
Application of ultrasonic inspection for determining effect of graphite on strength characteristics of cast iron
15 p1797 N73-24571
Attenuation of ultrasonic waves and methods for measuring attenuation
[NLL-RISLEY-TR-2571-[9091.9F]]
15 p1812 N73-24683
Development of ultrasonic techniques for continuous monitoring of fatigue damage during cyclic testing of metal specimens
[AD-760787] 18 p2156 N73-27422
Application of ultrasonic inspection techniques for detecting separation of solid propellant rocket case-liner and liner-propellant interfaces
[NAL-TR-308] 18 p2193 N73-27703
Ultrasonic testing for nondestructive evaluation of subsurface flaws
19 p2303 N73-28520
Measurement of acoustic absorption coefficient of Bidin
[TR-7302.626] 19 p2321 N73-28669
Ultrasonic inspection and control for laminated steel disc
[TR-73-2-640] 20 p2423 N73-29461
Ultrasonic testing of closures for rocket HEAT 66 mm L1A2
[TM-52] 20 p2423 N73-29462
Ultrasonic technique for assessing structural integrity of primary surface of space shuttle vehicles
[NASA-CR-133859] 22 p2721 N73-31778
Ultrasonic technique for assessing structural integrity of primary surface of space shuttle vehicles
[NASA-CR-133815] 22 p2721 N73-31779

ULTRASONIC WAVE TRANSDUCERS
Standard requirements for ultrasonic Doppler probes of cardiovascular systems in medical monitoring functions
03 p0257 N73-12083
Computer aided analysis on radiative characteristics of sonar transducer with spaced sensor element array
[AD-747281] 03 p0266 N73-12156
Diffraction correction calculations for rectangular ultrasonic transducer
[AD-754677] 11 p1263 N73-20247
Development of ultrasonic radiation equipment for removing material from host surface and vacuum apparatus for recovery of material
[NASA-CASE-NPO-11213] 11 p1296 N73-20514
Characteristics of emitting-receiving ultrasonic probe including beam configuration and determination of electric equivalent circuit of transducer
[EUR-4774] 15 p1788 N73-24494
Design and operation of sonic velometer using transit times of ultrasonic pulses in air to measure air velocity
17 p2031 N73-26434
Ultrasonic bone densitometer for measuring calcium content of bone structures
[NASA-CASE-MFS-20994-1] 21 p2504 N73-30090
Manufacturing of high efficiency ultrasonic wave transducer for light modulation using Brillouin effect
[REPT-4.473] 23 p2820 N73-32544

ULTRASONIC WAVES
U ULTRASONIC RADIATION

ULTRASONIC WELDING
Ultrasonic torsional welding system for simultaneously bonding beam leads of hybrid integrated circuit device to suitable substrate
[AD-757561] 14 p1671 N73-23559

ULTRASONICS
Ultrasonic velocity measurements for determining adiabatic compressibilities of ionic solutions and molten salts
[AD-749353] 04 p0451 N73-13686
Design and fabrication of flight weight ultrasonic contact sensor leak detection system
[NASA-TM-X-68909] 05 p0546 N73-14431
Focused one joule pulse and Q switched ruby laser for optical production and detection of ultrasonic waves in metals for nondestructive tests
05 p0609 N73-14954
Ultrasonic inspection and examination of large size cast steel ring prior to machining
[TR-7212.624] 20 p2422 N73-29456
Ultrasonic attenuation of longitudial sound waves in superconducting molybdenum single crystals
23 p2825 N73-32581
Ultrasonic wave propagation in He-Ar and He-Xe mixtures
24 p2956 N73-33614

ULTRAVIOLET ABSORPTION
Optical properties of ultraviolet down-converter materials
[AD-753578] 09 p1068 N73-18713
Spectrometry investigations of planets by USSR astronomical observatories with emphasis on ultraviolet absorption by planetary atmospheres
[NASA-TT-F-747] 09 p1083 N73-18833
Measurement of ultraviolet absorption by planet Saturn disk at various geographical regions
09 p1083 N73-18836

ULTRAVIOLET LIGHT
U ULTRAVIOLET RADIATION

ULTRAVIOLET PHOTOGRAPHY
Far UV camera/spectrograph deployed on lunar surface in Apollo 16 mission
12 p1450 N73-21745

ULTRAVIOLET PHOTOMETRY
Ultraviolet photometry experiment for Atmosphere Explorer C, D, and E missions to record solar irradiance
[NASA-TM-X-66130] 04 p0422 N73-13437
Degradation of ultraviolet photometry systems on Nimbus 3 and 4 satellites
[NASA-TM-X-66148] 06 p0721 N73-15883
Ultraviolet photometry of eclipsing Cephei variable star by OAO 2
22 p2734 N73-31884

ULTRAVIOLET RADIATION
NT FAR ULTRAVIOLET RADIATION
NT LYMAN ALPHA RADIATION
NT LYMAN BETA RADIATION
NT NEAR ULTRAVIOLET RADIATION
Method for obtaining ultraviolet source using Cerenkov radiation
[AD-746174] 02 p0182 N73-11477
Emission and absorption spectra for mixtures of liquid uranium and uranium oxide using carbon tube furnace facility
[AD-746687] 02 p0194 N73-11571
Excitation of N I ultraviolet multiplets by electron impact on atomic nitrogen
[NASA-CR-129087] 02 p0214 N73-11730
Inferred ozone profiles from ultraviolet earth radiance data from Nimbus 4
[NASA-TM-X-66108] 03 p0294 N73-12397
Measurement of plasma ultraviolet radiation for determining collisional momentum transfer cross sections in accelerator
[AD-747339] 03 p0344 N73-12802
Characteristics of research instruments used on rockets and satellites for investigating solar ultraviolet radiation
[AD-748276] 04 p0424 N73-13454

Light shield and cooling apparatus for high intensity ultraviolet lamps
[NASA-CASE-LAR-10089-1] 04 p0426 N73-13474
Generation of vacuum ultraviolet xenon laser and X ray hydrogen laser
[SC-T-72-2513] 04 p0429 N73-13494
Analyses of Experiment S183, Ultraviolet Panorama [MSFC] for evaluating Skylab performance
[NASA-CR-61386-APP-N] 04 p0475 N73-13885
Gamma, X ray, ultraviolet, and infrared astronomy noting instrumentation and radiative transfer
[ESRO-SP-75] 04 p0476 N73-13889
Explorer 44 measurement of solar X rays and ultraviolet radiation
[AD-748992] 04 p0479 N73-13919
Ultraviolet flash photolysis of ozone and reaction of O[1 D] with H2O
[DREV-TN-2026/72] 06 p0638 N73-15176
Research projects to determine nature of Sun as ultraviolet variable star and description of MUSE experiment
[NASA-TM-X-66142] 06 p0719 N73-15868
Chorioretinal burn hazards of high intensity radiation sources in industry
08 p0873 N73-17071
Occupational hazards and adverse biological effects of ultraviolet radiation
08 p0876 N73-17094
Dayglow measurements of upper atmosphere by Orbiting Astronomical Observatory A-2
[AD-752228] 08 p0920 N73-17539
Approximate values of intensity of natural ultraviolet radiation for different amounts of atmospheric ozone
[AD-752115] 08 p0921 N73-17549
Laser-produced plasma as radiation source in 1000 to 20 A range, and detection with double-grating spectrometer
[FRNC-TH-216] 08 p0948 N73-17763
Production of stimulated emission in vacuum ultraviolet using molecular xenon gas excited by relativistic electron beam
[AD-753483] 09 p1045 N73-18522
Ultraviolet and charged particle irradiation of solar cell coverslide materials and conductive coatings for Helios satellites
[NASA-TM-X-65945] 09 p1051 N73-18571
Evolutionary adaptation and resistance of unicellular organisms to solar radiation
10 p1118 N73-19118
Abiogenic syntheses of aliphatic and aromatic amino acids by ultraviolet radiation
10 p1119 N73-19119
Analysis of backscatter ultraviolet experiment conducted with double monochromator instrument on Nimbus 4 satellite
[NASA-TM-X-66204] 10 p1153 N73-19385
Evaluation of ultraviolet flux from stars used as inertial-hold pointing directions during Apollo 17 flight
[NASA-CR-128834] 10 p1213 N73-19866
Ultraviolet radiation detector in presence of proton radiation using sensor tubes within shielding mechanism
[NASA-CASE-MFS-21577-1] 11 p1237 N73-20042
Degradation rate of thermal control coatings exposed to solar ultraviolet irradiation
[NASA-CR-124149] 11 p1307 N73-20608
Flashlight adaptation of ultraviolet source for illuminating fluorescent map
[AD-755435] 12 p1429 N73-21585
Analysis of ultraviolet emitting fiber optic faceplate cathode ray tubes
[AD-755509] 13 p1503 N73-22181
Tunable parametric oscillator using infrared pumping for ultraviolet frequency generation
[AD-756910] 13 p1561 N73-22650
Computer program to analyze solar observational data
[AD-755921] 14 p1703 N73-23815
Investigation of ultraviolet interstellar extinction
[NASA-CR-131990] 14 p1706 N73-23843
Ultraviolet space irradiation effects on Aeromonas proteolytica extracellular enzyme production
15 p1741 N73-24111
High resolution film actinometric measurements of ultraviolet irradiation levels during space flight
15 p1741 N73-24112
Potassium ferrioxalate actinometric measurements of solar ultraviolet photobiological energy
15 p1741 N73-24113
Thermospheric heating due to EUV absorption and Joule dissipation
[AD-758758] 15 p1784 N73-24464
Performance characteristics of proximity focused ultraviolet to visible light image converters
[NASA-TM-X-66258] 15 p1787 N73-24488
Environmental impact of increased intensities of solar ultraviolet radiation resulting from operation of supersonic transport aircraft
[PB-215524/0] 16 p1862 N73-25079
Catalog of ultraviolet stellar observations using celescope on OAO 2
[NASA-CR-133259] 17 p2088 N73-26889
Development of flow visualization technique using fluorescent dye to simulate smoke lines in water
[AD-761499] 19 p2257 N73-28192
Thermal and ultraviolet vacuum tests on adhesives, thermoplastic, and thermosetting resins for space environment simulation
[RV-106] 19 p2312 N73-28596
Ground based ionospheric observations of extreme ultraviolet fluxes during solar flares
19 p2335 N73-28792
High temperature and ultraviolet stability properties of poly[diarylsiloxy]arylazine
[NASA-CASE-ARC-10592-1] 20 p2435 N73-29554
Measurement of ultraviolet radiation flux density emitted by solar simulator using thermopile and spectrometer
[ESRO-TM-149-ESTEC] 21 p2522 N73-30225
Conceptual work on 125 mm ultraviolet spectrometer for measuring ozone
[NASA-CR-132266] 22 p2673 N73-31411
Interstellar extinction in ultraviolet
[NASA-CR-133924] 22 p2717 N73-31753
Transmitting and reflecting diffuser
[NASA-CASE-LAR-10385-3] 23 p2819 N73-32538
**ULTRAVIOLET REFLECTION**
Far ultraviolet diffuse reflectivity of lunar dust samples
[NASA-CR-128546] 15 p1834 N73-24864
**ULTRAVIOLET SPECTRA**
Ultraviolet continuum of O6f star HD 148937 and peculiarities of surrounding nebulae
[NASA-CR-128404] 01 p0100 N73-10824
Lyman and Werner molecular hydrogen bands in ultraviolet intersteller spectrum of delta Scorpii
[NASA-TM-X-66102] 02 p0230 N73-11865
Spaceborne ultraviolet emission lines in stellar sources as chromospheric indicators
04 p0466 N73-13796
Aerobee rocket observation of ultraviolet line spectra of Delta Scorpii and Zeta Ophiuchi
08 p0958 N73-17838
Interstellar CO in ultraviolet spectrum of Zeta Ophiuchi
08 p0975 N73-17972
OAO 2 observations used to determine relationship between visual and ultraviolet variations in C-4 155-nm line in Beta Cephei
08 p0975 N73-17974
Scattered solar radiation distribution in cloud absence by sky zones in entire spectrum, including visible and ultraviolet sections
09 p1059 N73-18637
Analysis of backscatter ultraviolet experiment conducted with double monochromator instrument on Nimbus 4 satellite
[NASA-TM-X-66204] 10 p1153 N73-19385
UV imagery of earth and moon at varied wavelengths
12 p1451 N73-21751
Catalog of ultraviolet stellar observations obtained from celescope experiment on OAO 2
[NASA-CR-132196] 16 p1962 N73-25869
Design of high intensity atomic emission line sources in vacuum ultraviolet region for atmospheric gas trace detection
[AP-11] 17 p2034 N73-26459
Relative variations in extreme ultraviolet solar flare spectrum
19 p2335 N73-28791
Bidirectional reflectance of zinc oxide in ultraviolet and infrared spectral bands
[NASA-CR-135494] 22 p2678 N73-31450
Far ultraviolet photometry of peculiar B and A stars by OAO 2
22 p2734 N73-31883
Interstellar molecular hydrogen lines in ultraviolet spectrum of delta Scorpii
22 p2734 N73-31886
Ultraviolet interstellar polarization measurement
22 p2735 N73-31889
Using optical interference coatings to produce bandpass filters for spectral region
[NASA-CR-135671] 23 p2819 N73-32537
Ultraviolet evening terminator observations in Martian atmosphere by Mariner 9 space probe
23 p2841 N73-32702
Ultraviolet spectrometer data on Mars atomic oxygen emission and distribution
23 p2841 N73-32703
Seasonal ozone variations in ultraviolet spectra of Mars atmosphere
23 p2841 N73-32704
**ULTRAVIOLET SPECTROGRAPHS**
U ULTRAVIOLET SPECTROMETERS
**ULTRAVIOLET SPECTROMETERS**
Design operation, testing, and calibration of Mariner Mars 1971 ultra violet spectrometer
[NASA-CR-128493] 02 p0172 N73-11396
Mariner 6 and 7 flybys measuring hot CO on Mars with ultraviolet scanning spectrometers
08 p0973 N73-17955
Apollo 17 vacuum ultraviolet spectrometer calibration plan
[NASA-CR-128831] 10 p1160 N73-19439
Apollo 17 far ultraviolet scanning spectrometer experiment for lunar atmosphere measurements
[NASA-CR-128835] 10 p1160 N73-19440
Apollo 17 Calibration Facility safety plan covering ultraviolet spectrometer components
[NASA-CR-128833] 10 p1229 N73-19990
Construction of far ultraviolet Ebert spectrometer for use on Apollo 17 flight to observe lunar atmosphere
[NASA-CR-128889] 11 p1293 N73-20491
OGO-4 ultraviolet spectrometer measurements of nitric oxide fluorescence with diffusive transport model for mesospheric and lower thermospheric nitric oxide photochemistry
13 p1515 N73-22274
Cross calibration tests of ultraviolet spectrometer
[NASA-CR-128628] 15 p1789 N73-24506
Spares and repair parts support plan for ultraviolet spectrometer Apollo experiment
[NASA-CR-128571] 16 p1885 N73-25260
Performance verification test plan for Apollo ultraviolet spectrometer experiment
[NASA-CR-128573] 16 p1915 N73-25500
Stress analysis verification of structural integrity of Apollo ultraviolet spectrometer experiment
[NASA-CR-128551] 16 p1916 N73-25501
Final nonmetallic materials list for Apollo ultraviolet spectrometer experiment
[NASA-CR-128583] 16 p1916 N73-25502
Qualification plan for the Apollo ultraviolet spectrometer experiment, revision
[NASA-CR-128572] 16 p1916 N73-25503
Exit slit mirrors for Ebert ultraviolet spectrometer Apollo experiment
[NASA-CR-128549] 16 p1916 N73-25504
System safety plan for Apollo ultraviolet spectrometer experiment
[NASA-CR-128570] 16 p1916 N73-25505
Contamination control program plan for Apollo ultraviolet spectrometer experiment
[NASA-CR-128575] 16 p1916 N73-25506
Supporting research plan for Apollo 17 ultraviolet spectrometer experiment
[NASA-CR-128547] 16 p1916 N73-25507
Acceptance test plan for bench test equipment of Apollo ultraviolet spectrometer experiment
[NASA-CR-128574] 16 p1916 N73-25508
Thermal ultraviolet spectrometer model vacuum test performance
[NASA-CR-128562] 16 p1916 N73-25509
Quality control requirements for Apollo ultraviolet spectrometer experiment
[NASA-CR-128584] 16 p1916 N73-25510
Interface control documenation for design and development of Apollo ultraviolet spectrometer experiment
[NASA-CR-128550] 16 p1917 N73-25511
Design of ultraviolet Explorer satellite for spaceborne astronomy
18 p2210 N73-27838
Ultraviolet spectrometer experiment on Mariner 9 space probe
24 p2983 N73-33840
**ULTRAVIOLET SPECTROPHOTOMETERS**
Hole area for evacuating and degassing of far ultraviolet sounding rocket photometer
[MPI-PAE/EXTRATERR-68] 02 p0174 N73-11411
Ultraviolet solar irradiance in selected wavelength bands
[NASA-TM-X-66143] 07 p0838 N73-16794
OSO 5 spectrophotometer design, solar EUV data acquired, and data reduction
[NASA-CR-130159] 08 p0956 N73-17828
Analysis of backscatter ultraviolet experiment conducted with double monochromator instrument on Nimbus 4 satellite
[NASA-TM-X-66204] 10 p1153 N73-19385
Modification of double-deck EUV spectrophotometer recovered from previous rocket flight
[AD-756917] 13 p1528 N73-22380
Atlas S183 experiment for ultraviolet stellar spectrophotometry onboard Skylab manned space station
17 p2033 N73-26454
Rapid determination of diphenylamine and dinitrotoluene in single base propellants by ultraviolet spectrophotometry analysis
[TM-51] 21 p2587 N73-30730
Ultraviolet spectrophotometry of Nova Serpentis 1970 by OAO-A2 flight
23 p2836 N73-32660
**ULTRAVIOLET SPECTROSCOPY**
Historical account of data and theories pertaining to lunar atmosphere prior to Apollo
[NASA-CR-128548] 15 p1833 N73-24863
Blue to violet intensity distributions in S, C-S, and C stars
23 p2837 N73-32666
**UMBILICAL CONNECTORS**
Shielding effectiveness of exterior shield and connector assemblies on Lance umbilical cables
[AD-761078] 18 p2201 N73-27771
**UMBRA [SHADOWS]**
U SHADOWS
**UNCAMBERED WINGS**
NT RING WINGS

Numerical analysis of unsteady supersonic characteristics of space shuttle type vehicles using arbitrary finite element technique
[NASA-CR-112296] 13 p1470 N73-21904
UNCERTAINTY
U PROBABILITY THEORY
UNCONSCIOUSNESS
NT BLACKOUT PREVENTION
NT NARCOSIS
UNDAMPED OSCILLATIONS
Existence of undamped Kelvin waves in semiinfinite rotating basin with step change in depth
22 p2653 N73-31250
UNDERGROUND COMMUNICATION
Feasibility of underground waveguide for radio signal transmission
[AD-754786] 11 p1257 N73-20198
UNDERGROUND EXPLOSIONS
Seismological effects of explosions and earthquakes and structural dynamics of earth crust and upper mantle
[AD-746031] 01 p0034 N73-10435
Seismological experiments and evaluation of instrumentation in program of long range seismic measurements
[AD-746666] 02 p0170 N73-11382
Photographic aerial survey over underground nuclear test at Amchitka to record changes in bioenvironment
[BMI-171-146] 03 p0296 N73-12411
Evaluation of methods for analyzing short-period seismic records to detect multiple events
[AD-747764] 03 p0298 N73-12434
Application of ray-tracing to seismic event location near island arc structures
[AD-747762] 03 p0298 N73-12435
Computing theoretical amplitude ratio of shear waves to compressional waves using double-couple representations of earthquakes
[AD-747763] 03 p0299 N73-12436
Lost data channels of acceleration measurements in underground nuclear tests
[UCRL-73665] 05 p0580 N73-14725
Operations summary of Seismic Array Analysis Center for period Apr. - June 1972
[AD-750779] 06 p0668 N73-15435
Evaluation of research projects involving seismic arrays, long period arrays, seismometers, and seismic signal processing
[AD-750759] 06 p0669 N73-15439
Research in network evaluation
[AD-751523] 07 p0795 N73-16467
Formation of seismic waves in surface soils during underground explosions
[AD-751070] 07 p0797 N73-16481
Geometrical shock wave transmission model used to determine water surface peak spall velocities above single charge cratering detonations in medium overlain with water
[AD-755099] 11 p1273 N73-20329
Analysis of Rayleigh wave dispersion in continental path and development of filters for vertical high gain seismometer
[AD-761795] 19 p2296 N73-28462
Long term broad band vertical earth noise structure at very long period experiment sites
[AD-761812] 19 p2297 N73-28473
UNDERGROUND NUCLEAR EXPLOSIONS
U NUCLEAR EXPLOSIONS
U UNDERGROUND EXPLOSIONS
UNDERGROUND STORAGE
Radar detection of underground objects using polarization for target classification
[AD-763155] 23 p2758 N73-32069
UNDERWATER ACOUSTICS
Development and characteristics of digital beamformer for narrowband sonar systems
[AD-745302] 01 p0029 N73-10224
Analysis of subbottom acoustic reflection profiles along track line from Monrovia, Liberia to Lesser Antilles
[PB-209872] 01 p0053 N73-10427
Applications of holographic interferometry in underwater acoustics research
[AD-746134] 01 p0067 N73-10545
Mimi field test of July 1970 for underwater acoustic study in Straits of Florida
[AD-744982] 01 p0080 N73-10662
Ray tracing program for calculating sound intensity from ocean sources
[AD-745313] 01 p0080 N73-10664
Optical design and performance evaluation of athermal solid and liquid acoustic lenses
[AD-745734] 01 p0081 N73-10668
Digital data coding instructions for underwater acoustics and environmental data bank
[AD-746507] 01 p0082 N73-10675
Algorithm for underwater echo signals from elastic spherical shell subjected to incident pulse
[AD-746220] 01 p0082 N73-10676
Development of method for producing constant beamwidth over octave frequency bandwidth for underwater signal reception array
[AD-746690] 02 p0143 N73-11160
Feasibility of mounting geophone arrays on pack ice to provide passive sonar system with improved signal to noise ratios over hydrophone arrays
[AD-747327] 02 p0143 N73-11161
Sound wave reflection from sea bed, acoustic properties of sedimentary layer, and application to Baltic Sea
[FOA-3-C-3680-E1] 02 p0164 N73-11331
Acoustic noise, transmission loss, and reverberation measurements in West Greenland Sea
[AD-746839] 02 p0169 N73-11373
Forced steady state response of cylindrical shell immersed in acoustic fluid bounded by elastic half space
[AD-747705] 03 p0337 N73-12750
Receiver operating characteristics for underwater signal detection performance of sea lions
[AD-746520] 04 p0382 N73-13113
Numerical analysis of Pacific Ocean bottom signal reflection losses using underwater explosive sound sources and multilayered acoustic absorption model
[AD-748199] 04 p0450 N73-13676
Influence of target motion and wave time variation of underwater acoustic signal transmission
[AD-748651] 04 p0450 N73-13678
Bubble frequencies of air gun sources for at-sea experiments
[AD-748586] 04 p0451 N73-13680
Finite element model for class 4 flextensional underwater transducer shell
[AD-748187] 04 p0482 N73-13940
Minicomputer application in processing underwater sound signals
[AD-749095] 05 p0514 N73-14176
Procedure for resolving directional ambiguities of line array of hydrophones
[AD-749939] 05 p0514 N73-14180
Estimation of noise directionality spectrum directly from cross-spectral matrix of received processes at hydrophone array elements
[AD-749940] 05 p0514 N73-14181
Deep sea calibration of transducers at elevated hydrostatic pressure
[AD-750666] 06 p0641 N73-15203
Depth effect on underwater ambient noise intensity in Caribbean Sea
[AD-750693] 06 p0670 N73-15447
Partial wave analysis solutions for acoustic scattering patterns and target recognition in antisubmarine warfare
[AD-750754] 06 p0700 N73-15710
Underwater sound transducer calibration system for 0.3 to 2000 Hz frequency range at hydrostatic pressure to 6.89 MPa
[AD-751536] 07 p0822 N73-16662
Ray tracing of underwater sound in Arctic Ocean
[AD-752056] 08 p0944 N73-17734
Prevention of spurious caustics in ray tracing scheme for sound propagation mapping in sea water
[AD-752080] 08 p0944 N73-17735
Acoustic demodulation of predistorted pulsed carriers
[AD-752237] 08 p0945 N73-17738
Low frequency underwater sound surface-scattering experiments in Pacific
[AD-752065] 08 p0945 N73-17739
Alternate lead and ceramic stave free-flooded cylinder transducers
[AD-752759] 09 p1009 N73-18234
Procedures for calculating sonic fields radiated and diffracted by elastic bodies and passage of sound through elastic plates and shells - Vol. 1
[JPRS-58146-1-PT-1] 09 p1015 N73-18283
Procedures for calculating sonic fields radiated and diffracted by elastic bodies and passage of sound through elastic plates and shells - Vol. 2
[JPRS-58146-2-PT-2] 09 p1015 N73-18284
Study of propagation characteristics of normal acoustic modes in Gulf of Mexico waters
[AD-753200] 09 p1032 N73-18427
Bathymetric survey of Pacific Ocean area for oceanographic data to support underwater acoustic experiment
[AD-752840] 09 p1032 N73-18428
Thin film broadband absorber for use in underwater acoustics using silicon oils
[BMVG-FBWT-72-2] 09 p1067 N73-18703
Computer program for estimating position and shape of surface shadow zone in sonar operations
[AD-753443] 10 p1129 N73-19200
Review of underwater acoustical measurements revealing layered regions at various ocean depths
[AD-753445] 10 p1156 N73-19405
Design of towed sonar transducer array for bathymetric mapping of ocean bottom topography
[AD-755113] 11 p1259 N73-20216
Acoustic radiation patterns of line source coincident with focal line of parabolic cylinder reflector immersed in water tank
[AD-754063] 11 p1324 N73-20748
Sound speed modulation by bubbles in upper ocean
[AD-754372] 11 p1325 N73-20754
Acoustic transmission loss measurements in Arctic Ocean ice zone by aircraft
[AD-754394] 11 p1325 N73-20755
Modified ray theory for underwater sound propagation and diffraction
[AD-755460] 12 p1430 N73-21589
Ray tracing method for computerized prediction of underwater sound propagation loss
[AD-755459] 12 p1430 N73-21590
Analysis of underwater sound signals to show coherence, noise level, and reverberation between vertically separated hydrophones
[AD-755696] 12 p1430 N73-21591
Holographic and acoustical tests of vibrating underwater structures
[AD-755475] 13 p1538 N73-22463
Statistical analysis of underwater sound speed fluctuation in upper ocean region
[AD-756570] 13 p1560 N73-22641
Underwater devices for target detection on sea bottom
[JPRS-58916] 14 p1667 N73-23529
Ray tracing method for calculating underwater acoustic reflection patterns of surface originated signals from objects of arbitrary shape
[AD-757110] 14 p1694 N73-23744
Digital measurements of underwater sound transducer directivity index using hydrophone array
[AD-758639] 16 p1945 N73-25740
Environmental tests of interocean acoustic release devices and performance of correlation echo sounder processor
[RN-1008] 18 p2151 N73-27385
Metrology standards of underwater reference division
[AD-761147] 18 p2180 N73-27603
Signal processing facility for underwater acoustics consisting of digital computer and Fourier analyzer
[REPT-5-72] 19 p2239 N73-28055
Analysis of acoustic volume scattering in Bermuda Ocean to show daily variability and diurnal variations
[AD-761976] 19 p2296 N73-28465
Underwater scattering of sound waves by submerged viscoelastic cylindrical shell
[AD-761618] 19 p2321 N73-28674
Computer program for calculating acoustic impedance of submerged vibrating structure
[AD-762007] 19 p2322 N73-28680
UNDERWATER BREATHING APPARATUS
Design and development of underwater breathing apparatus with microphone for underwater communication
[AD-746105] 02 p0142 N73-11154
Calculation of minimum safe inspired gas temperature limits for deep diving
[AD-748197] 05 p0504 N73-14104
Anthropometric measurements of military personnel engaged in underwater diving to development standards for design of equipment
[AD-748627] 06 p0637 N73-15175
Effects of underwater breathing of helium oxygen mixture on speech recognition
[AD-759413] 16 p1878 N73-25205
UNDERWATER COMMUNICATION
Improving voice communication between divers and swimmers
[AD-745794] 01 p0029 N73-10228
Thermal and atmospheric noise effects on optimization of underwater low frequency communications
[FOA-3-C-3671-60] 02 p0139 N73-11129
Design and development of underwater breathing apparatus with microphone for underwater communication
[AD-746105] 02 p0142 N73-11154
Effects of exercise work load on speech intelligibility at normal and increased atmospheric pressures
[AD-749321] 04 p0392 N73-13185
Depth effect on microphone sensitivity in underwater speech communication
[AD-750650] 06 p0642 N73-15213
Effectiveness of underwater acoustic propagation loss models in sonar personnel training devices
[AD-750694] 06 p0701 N73-15719
Underwater divers and speech communication problems
[AD-751665] 07 p0757 N73-16150
Phonetic analysis of underwater diver speech and standardization for intelligibility
[AD-751662] 07 p0757 N73-16153
Analysis of video transmission range in water by laser beam
[AD-751445] 07 p0807 N73-16548
Measurement of sound transmission and attenuation in Tyrrhenian Sea discussing experimental design and results
07 p0858 N73-16959
Acoustic demodulation of predistorted pulsed carriers
[AD-752237] 08 p0945 N73-17738
Proceedings of international workshop on helium speech processing
14 p1630 N73-23210
Proceedings of workshop on processing helium speech
[AD-757329] 14 p1635 N73-23259

**UNDERWATER ENGINEERING**
Anthropometric measurements of military personnel engaged in underwater diving to development standards for design of equipment
[AD-748627] 06 p0637 N73-15175
Marine technology developments to include submerged navigation, submersible instrumentation, geological mapping, magnetic studies, and ocean biology
[AD-754445] 11 p1288 N73-20453
Design of electrohydraulic control system for underwater manipulator with position feedback
17 p1989 N73-26085
Experimental research in underwater medicine, flight stress, and pilot selection
[DLR-FB-73-15] 19 p2226 N73-27951
Method for recovery of sunken bodies at depths of between 30 and 50 m
19 p2226 N73-27955
Sensitivity and structural peculiarities of underwater pyranometers
20 p2447 N73-29660

**UNDERWATER EXPLOSIONS**
Hydrophone measurement of acoustic propagation and CW signals from underwater explosions in shallow Bering Sea
[AD-745735] 01 p0081 N73-10667
Feasibility of mounting geophone arrays on pack ice to provide passive sonar system with improved signal to noise ratios over hydrophone arrays
[AD-747327] 02 p0143 N73-11161
Finite difference method for calculating interaction between spherical shock waves from underwater explosion and ocean surface
[AD-749818] 06 p0656 N73-15325
Geometrical shock wave transmission model used to determine water surface peak spall velocities above single charge cratering detonations in medium overlain with water
[AD-755099] 11 p1273 N73-20329

**UNDERWATER OPTICS**
Apparent object movement due to optical distortion produced by head movement under water
[AD-749319] 05 p0502 N73-14086
Data obtained in Bahama channels and Northwestern Atlantic ocean during Deep Ocean Optical Measurement program
[AD-757332] 14 p1665 N73-23511
Monte Carlo calculations of polarization of radiation in earth atmosphere and ocean
[AD-764622] 23 p2789 N73-32313
Effects of resolution, signal to noise ratio, and contrast on underwater imaging systems performance
24 p2958 N73-33631
Application of incoherent and coherent light sources for underwater illumination and comparison of efficiency for various conditions
24 p2958 N73-33633
Characteristics of lenses and ports for underwater imaging systems to compare depth of field and relative aperture for several lens port combinations
24 p2958 N73-33635
Techniques for long range vision underwater using range-gating and dual-scan with parallax techniques
24 p2958 N73-33636

**UNDERWATER PHOTOGRAPHY**
Holography in random spatially inhomogeneous medium
[AD-755781] 12 p1406 N73-21402
Application of spatial filtering and image restoration to underwater photographs of floodlit images
24 p2958 N73-33637

**UNDERWATER PROPULSION**
Underwater vortex field generation in wake of rectangular airfoil
[NASA-TM-X-62274] 17 p2014 N73-26288

**UNDERWATER SOUND**
U UNDERWATER ACOUSTICS

**UNDERWATER STRUCTURES**
Deterioration in sea water of materials and underwater system components
[AD-747245] 02 p0194 N73-11567
Procedures for analyzing very thick walled cylindrical shells used in constructing hydrospace simulators
[AD-747963] 03 p0362 N73-12952
Development and evaluation of equipment for monitoring long term sea floor foundation settlement and tilting
[AD-750258] 06 p0669 N73-15444
Development progress of small turbine-generator units using isotope power sources for undersea power plant with 2 to 10 kW[e]
[ORNL-TM-3586] 08 p0870 N73-17041
Habitability factors during long-term space and undersea missions in confined habitats
[NASA-CR-130537] 08 p0879 N73-17123
Procedure for applying structure-fluid interactions effect to dynamic frequency response calculations for submerged structures
[AD-752484] 08 p0967 N73-17906
Design factors resulting from hydrodynamic loads induced on large underwater structures by impulsive motion
[AD-753603] 09 p1019 N73-18315
Holographic and acoustical tests of vibrating underwater structures
[AD-755475] 13 p1538 N73-22463
Deep sea simulator facilities in USA in 1972
[AD-761899] 19 p2249 N73-28136

**UNDERWATER TESTS**
Influence of illumination color, viewing distance, and turbidity on underwater vision
[AD-743756] 01 p0012 N73-10092
Tests to evaluate heat loss from Navy diver suits in water of 55, 45, and 35 F
[AD-747276] 02 p0136 N73-11103
Physiological and mental performance effects of underwater work on humans
[AD-747701] 04 p0382 N73-13107
Bibliography on effects of underwater environment on tools, equipment, and human performance
[AD-748000] 04 p0384 N73-13122
Development and evaluation of equipment for monitoring long term sea floor foundation settlement and tilting
[AD-750258] 06 p0669 N73-15444
Comparison of methods for adapting hydrazine-oxygen fuel cells to cyclic pressure effects of hydrostatic pressure environment
[AD-753802] 10 p1112 N73-19062
Marine technology developments to include submerged navigation, submersible instrumentation, geological mapping, magnetic studies, and ocean biology
[AD-754445] 11 p1288 N73-20453
Underwater space suit pressure control regulator
[NASA-CASE-MFS-20332-2] 16 p1868 N73-25125
Improving distance under water and long-term effectiveness of training
[AD-752979] 16 p1869 N73-25128
Underwater ignition of hypergolic rocket propellants as function of injection system, fuel combustions, water depth, and salinity
[DLR-MITT-73-07] 16 p1954 N73-25813
Handedness and adaptation to distortions of size and distance underwater
[AD-759722] 17 p1991 N73-26098
Role of water temperature in bradycardia during facial immersion
[NASA-TT-F-15025] 24 p2890 N73-33072

**UNDERWATER VEHICLES**
NT SUBMARINES
Interaction of internal and surface waves in water
[AD-747332] 02 p0159 N73-11291
Structural behavior of glass hulls under external hydrostatic and cyclic pressure
[AD-746878] 03 p0362 N73-12947
Arctic technology development program including design and operation of under-ice research submersible
[AD-748228] 04 p0416 N73-13395
Effect of temperature and flange configurations on critical pressure of 90-degree conical acrylic windows for hydrostatic pressure vessels when subjected to short term loading
[AD-748583] 04 p0440 N73-13583
High energy density storage system with encapsulated silver zinc cells for deep ocean applications
[AD-750719] 06 p0627 N73-15085
Marine technology developments to include submerged navigation, submersible instrumentation, geological mapping, magnetic studies, and ocean biology
[AD-754445] 11 p1288 N73-20453
Development of simulator for training personnel in underwater terrain navigation and reconnaissance
[AD-754091] 11 p1322 N73-20729
Analysis of fluid flow over two dimensional flat plate wedge configuration for application to deep submersible vehicles
[NASA-CR-131888] 13 p1510 N73-22233
Analysis of internal waves generated by passage of body through density stratified medium and effects on mean flow
[AD-755714] 13 p1512 N73-22254
Manned submersible ocean bottom sampling and gravimetric prospecting
[AD-759992] 17 p2029 N73-26425
Inelastic buckling of deep spherical shell subject to uniformly distributed external pressure
[AD-764085] 22 p2726 N73-31815

**UNIAXIAL STRAIN**
U AXIAL STRAIN

**UNIFORM FLOW**
NT BLASIUS FLOW
Prediction of pressure gradient on delta wing between uniform and nonuniform supersonic inviscid flow
[ARC-CP-1228] 05 p0492 N73-14010
Analysis of data obtained in evaluation tests of circumferential airflow uniformity entering combustors from two advanced engine compressors
[NASA-CR-121009] 05 p0526 N73-14276
Data tables and computer generated profile plots obtained in evaluation tests of circumferential airflow uniformity entering combustors from two advanced engine compressors
[NASA-CR-121010] 05 p0526 N73-14277
Procedure for generating uniform flow at varying velocities in wind tunnel test section
[NASA-CASE-ARC-10710-1] 18 p2125 N73-27175

**UNIPOLAR TRANSISTORS**
U FIELD EFFECT TRANSISTORS

**UNIQUENESS THEOREM**
Exact solutions for electromagnetic inverse problem for perfectly conducting body with consideration of uniqueness problem and case of spherically symmetric dielectric body
02 p0200 N73-11616
Uniqueness theorem for two-dimensional nonstationary wall boundary layer in incompressible fluid
[AD-748743] 04 p0407 N73-13314
Uniqueness of solution for plane crack problems in linear elastostatics
[AD-756653] 13 p1587 N73-22865

**UNITED KINGDOM SATELLITES**
U UK SATELLITES

**UNITED NATIONS**
Accomplishments of United Nations in providing earth resources data to developing nations
07 p0783 N73-16370

**UNITED STATES OF AMERICA**
NT ALABAMA
NT ALASKA
NT ARIZONA
NT CALIFORNIA
NT COLORADO
NT CONNECTICUT
NT DELAWARE
NT FLORIDA
NT GEORGIA
NT HAWAII
NT IDAHO
NT ILLINOIS
NT INDIANA
NT IOWA
NT KANSAS
NT KENTUCKY
NT LOUISIANA
NT MAINE
NT MARYLAND
NT MASSACHUSETTS
NT MICHIGAN
NT MINNESOTA
NT MISSISSIPPI
NT MISSOURI
NT MONTANA
NT NEBRASKA
NT NEVADA
NT NEW JERSEY
NT NEW MEXICO
NT NEW YORK
NT NORTH CAROLINA
NT NORTH DAKOTA
NT OHIO
NT OKLAHOMA
NT OREGON
NT PENNSYLVANIA
NT RHODE ISLAND
NT ROCKY MOUNTAINS [NORTH AMERICA]
NT SOUTH CAROLINA
NT SOUTH DAKOTA
NT TENNESSEE
NT TEXAS
NT UTAH
NT VERMONT
NT VIRGINIA
NT WASHINGTON
NT WEST VIRGINIA
NT WISCONSIN
NT WYOMING
Research and development of advanced energy sources for United States of America
01 p0120 N73-10988
Congressional hearing on 1973 fiscal budget for Department of Transportation
01 p0120 N73-10989
Detection and mapping snow cover from ERTS-1 remotely sensed imagery of western US and Arctic
[E72-10202] 02 p0160 N73-11299
Descriptions of earthquakes and location of epicenters in US, Alaska, Panama Canal Zone, and Virgin Islands during 1970
03 p0294 N73-12393
Geographical variations in environmental radiation background measurements over United States of America
[UCRL-73822] 06 p0650 N73-15275
Photomapping of US using ERTS-1 MSS and RBV imagery
[E73-10088] 08 p0902 N73-17300
Compilation of aerial photographs of coastal areas of United States
[AD-755508] 13 p1526 N73-22368
Hearings concerning energy problems of US
14 p1721 N73-23969
Photomapping of US using ERTS-1 RBV imagery
[E73-10602] 15 p1772 N73-24363
Environmental conditions of offshore east and west coasts of US and in Gulf of Mexico
23 p2786 N73-32288

Quantitative determination of Statospheric aerosol composition over western United States
[E73-11138] 24 p2918 N73-33293
UNITS OF MEASUREMENT
NT INTERNATIONAL SYSTEM OF UNITS
Definition of basic terms, notation, and forms of presentation for fatigue data
[ESDU-70016] 02 p0237 N73-11925
Industrial conversion to metrication standards
[NASA-CR-130534] 08 p0925 N73-17584
Congressional hearing on national program to establish international metric system as official and standard system for United States commerce and industry
21 p2610 N73-30920
Congressional hearings on legislation for conversion to metric system of weights and meaures in United States
21 p2610 N73-30922
International system of units for reporting Nuclear Rocket Engine Program
[LA-5285-MS] 24 p2929 N73-33394
UNIVAC COMPUTERS
NT UNIVAC 1108 COMPUTER
Large scale computer programming procedure called DIALOG for Univac 1100
[NASA-CR-134032] 22 p2638 N73-31143
UNIVAC 1108 COMPUTER
Development of computer assisted troubleshooting system for maintenance of helicopters and aircraft using Univac 1108 computer
[AD-748665] 04 p0373 N73-13037
Implementation of FORTRAN-extended graph algorithmic language for Univac 1108
[NASA-CR-129907] 04 p0393 N73-13198
Univac 1108 computer for three dimensional stress analysis of complex structures
[AD-753211] 09 p1096 N73-18944
Sensitivity testing of hydrophones using Univac 1108 computer
[AD-754099] 11 p1262 N73-20244
UNIVERSAL TIME
Greenwich time and latitude observations - Oct. through Dec. 1971
02 p0244 N73-11983
Improved universal time system implemented on 1 Jan. 1972 eliminating changing-frequency offset and increasing size of step-time adjustments
[NASA-TN-D-7065] 06 p0639 N73-15192
Greenwich time report for the Royal Greenwich Observatory Time and Latitude Service during period of January to March 1972
08 p0960 N73-17856
Greenwich time and latitude observations for Apr. to Jun. 1972
18 p2197 N73-27740
Greenwich time and latitude observations, Jul. through Sep. 1972
21 p2598 N73-30820
UNIVERSE
Analysis of development of cosmos, universe, mankind, and space exploration
04 p0470 N73-13833
Electric charge, momentum, and mass of elliptic universe
[AD-756902] 13 p1561 N73-22649
Existence of antimatter in Universe
[LPTHE-73/4] 14 p1703 N73-23819
Wave and Einstein equations for studying scaler waves and tensor perturbations in Mixmaster Universe
15 p1829 N73-24823
Conference on annihilation reactions and gamma ray and universal evolution
[NASA-TM-X-66279] 19 p2331 N73-28753
Metagalactic orgin of cosmic rays and gamma ray astronomy
19 p2332 N73-28764
Annihilation processes as origin of matter-antimatter in universe
19 p2332 N73-28767
Red shift energy distribution and black body background distortion theories of universal formation
19 p2333 N73-28770
Detecting antimatter in universe
19 p2333 N73-28771
UNIVERSITIES
Research facilities, and educational and research programs of Institute of Industrial Science, University of Tokyo
01 p0035 N73-10277
Influence of NASA stress lab program on physical education in US colleges
08 p0876 N73-17092
Price trends affecting research and development at academic institutions
[NSF-72-310] 15 p1846 N73-24959
UNIVERSITY PROGRAM
MSFC/Auburn/Alabama 1972 summer faculty fellowship research program report
[NASA-CR-61395] 01 p0120 N73-10992
Arctic technology development program including design and operation of under-ice research submersible
[AD-748228] 04 p0416 N73-13395
University of Alaska survey of environment using ERTS-1 imagery
[E72-10341] 05 p0532 N73-14329
ERTS-1 data as teaching and research tool in Department of Geology at University of Alaska
[E72-10353] 05 p0534 N73-14341
Research in space physics at University of Iowa
[NASA-CR-129878] 05 p0594 N73-14825
University course on dimensioning, construction, and manufacturing of nonmetallic structural sandwich elements
[FOA-4-C-4467-61] 06 p0677 N73-15506
Grants and awards for scientific research
[NSF-73-2] 10 p1229 N73-19987
Utilization of ERTS-1 imagery as teaching and research tool in Department of Geology at University of Alaska
[E73-10403] 11 p1277 N73-20365
Aspects of interdisciplinary research in graduate programs
14 p1723 N73-23984
Utilization of ERTS-1 data as teaching and research tool in Department of Geology at University of Alaska
[E73-10635] 15 p1776 N73-24394
University of Alaska program for processing ERTS-1 environmental data
[E73-10636] 15 p1776 N73-24395
Research activities at University of Toronto for 1972
15 p1845 N73-24949
Graduate education of administrators for public service
[NASA-CR-133036] 16 p1976 N73-25984
Research conducted in School of Electrical Engineering at Purdue University during 1972
18 p2213 N73-27871
Utilization of ERTS-1 imagery as teaching and research tool in Department of Geology at University of Alaska
[E73-10841] 19 p2290 N73-28419
Coordination and establishment of centralized facilities and services for University of Alaska ERTS-1 survey of Alaskan environment
[E73-10904] 20 p2396 N73-29253
Graduate science students and manpower resources
[NSF-73-304] 21 p2609 N73-30908
Coordination and establishment of centralized facilities and services for University of Alaska ERTS survey of Alaskan environment
[E73-11088] 24 p2913 N73-33250
Utilization of ERTS-1 data and imagery as teaching and research tool in Department of Geology, University of Alaska
[E73-11128] 24 p2917 N73-33283
UNKNOWNS
U DEPENDENT VARIABLES
U PROBLEM SOLVING
UNMANNED SPACECRAFT
NT BIOSATELLITE 2
NT ECHO 1 SATELLITE
NT EXPLORER 18 SATELLITE
NT GEODETIC SATELLITES
NT GEOS 1 SATELLITE
NT GEOS 2 SATELLITE
NT GEOS-C SATELLITE
NT JUPITER PROBES
NT LUNAR PROBES
NT LUNIK 16 LUNAR PROBE
NT LUNIK 20 LUNAR PROBE
NT MARINER SPACE PROBES
NT MARINER SPACECRAFT
NT MARINER VENUS-MERCURY 1973
NT MARINER 3 SPACE PROBE
NT MARINER 7 SPACE PROBE
NT MARINER 9 SPACE PROBE
NT MARS PROBES
NT MARS 2 SPACECRAFT
NT NAVIGATION SATELLITES
NT OSO
NT OSO-J
NT OSO-1
NT OSO-5
NT OSO-6
NT OSO-7
NT PIONEER SPACE PROBES
NT PIONEER 6 SPACE PROBE
NT PIONEER 8 SPACE PROBE
NT PIONEER 9 SPACE PROBE
NT PIONEER 10 SPACE PROBE
NT PIONEER 11 SPACE PROBE
NT RANGER LUNAR PROBES
NT RANGER 7 LUNAR PROBE
NT RANGER 9 LUNAR PROBE
NT SOLAR OBSERVATORIES
NT SOLAR PROBES
NT SPACE PROBES
NT SURVEYOR LUNAR PROBES
NT SURVEYOR 3 LUNAR PROBE
NT TRANSIT SATELLITES
NT VENERA SATELLITES
NT VENERA 8 SATELLITE
NT VENUS PROBES
NT VIKING 75 ENTRY VEHICLE
Terminal sterilization process for unmanned lander spacecraft
[NASA-CR-129513] 03 p0259 N73-12100
Performance potential evaluation of unmanned nuclear electric propulsion spacecraft for single-thrust-period missions to Uranus
[NASA-TN-D-7125] 06 p0718 N73-15859
First-order geometrical optics analysis of quasi-microscope planetary landers
[NASA-TN-D-7129] 07 p0800 N73-16498
Application of multivariate control theory to design of hierarchial attitude control system for CARD space vehicle
[NASA-CR-124087] 09 p1086 N73-18859
Solar electric power plants in unmanned spacecraft
[NASA-CR-131360] 11 p1333 N73-20824
Model for estimating cost of unmanned lunar and planetary exploration programs
[NASA-CR-131897] 14 p1705 N73-23840
Terrestrial quarantine considerations for unmanned sample return missions
[NASA-CR-132071] 15 p1742 N73-24118
Solar electric propulsion for unmanned exploration of solar system
[NASA-CR-130245] 15 p1826 N73-24803
Unmanned roving vehicle design for surface exploration of Mars
16 p1884 N73-25252
Artificial intelligence for identifying practical applications to unmanned spacecraft to expiore solar system in 1980 time period - Vol. 1
[NASA-CR-132256] 16 p1962 N73-25873
Development of artificial intelligence for onboard decision making capability of unmanned spacecraft during solar system exploration - Vol. 2
[NASA-CR-132257] 16 p1962 N73-25874
Analysis of requirements for unmanned spacecraft mission to planet Mars and characteristics of lander vehicles for planetary exploration - Vol. 3
[NASA-CR-132258] 16 p1962 N73-25875
Optimum trajectory and spacecraft data for unmanned interplanetary missions from 1975 to 1990 using solar electric propulsion
[NASA-CR-132765] 16 p1966 N73-25907
Sterilization for unmanned landers
[NASA-CR-133742] 21 p2500 N73-30064
Planetary quarantine requirements for automated spacecraft flights
[NASA-CR-135795] 24 p2885 N73-33040
UNSTABLE BURNING
U COMBUSTION STABILITY
UNSTEADY FLOW
NT OSCILLATING FLOW
Finite element procedure for predicting unsteady compressible gas flow in one spatial dimension
[AD-746234] 02 p0157 N73-11276
Unsteady wave extinction problem of wave generation in semi-infinite media by surface forces
[AD-746897] 02 p0203 N73-11646
Analysis of eddies and lift forces created on vertical circular cylinder by oscillatory flow conditions
[AD-748078] 03 p0287 N73-12329
Unsteady liquid metal flow in conduction MHD devices with constant magnetic field
[AD-748745] 04 p0455 N73-13715
Irregularities in flow behavior of parallel air jets behind smoothing grids
[NASA-TT-F-14653] 06 p0654 N73-15311
High speed schlieren film of pulsating flow in transonic turbine cascade
10 p1207 N73-19818
Approximate solution of two-dimensional problem of non-steady state stratal flow with movable gas-liquid interface
[AD-754828] 11 p1273 N73-20328
Development of numerical procedure for solving gas dynamics of pulsating, compressible flow in propulsive duct
12 p1389 N73-21266
Measurement of pipe resistance to instantaneous pulsating nonstationary flow
[NASA-TT-F-14881] 12 p1391 N73-21279
Calculation of unsteady, subsonic flow through infinite, two-dimensional flat plate blade
[ARC-R/M-3709] 13 p1510 N73-22240
Machine calculation of unsteady Mach reflections and Prandtl-Meyer supersonic flows
[AD-756195] 13 p1511 N73-22242
Experimental and theoretical measurement of pulsed flow velocity and pressure in circular pipes
14 p1649 N73-23372
Properties of plasma stream flowing from pulsed magnetoplasmadynamic arc jet
[ISAS-490] 14 p1695 N73-23756
Axial flow turbomachine response to upstream disturbances
[AD-759029] 16 p1866 N73-25107
Development of flow visualization techniques for determining aerodynamic characteristics of bluff bodies under unsteady flow conditions
[AD-759266] 16 p1892 N73-25311
Slip parameter for unsteady flow in EHD generators
[AD-759971] 17 p2070 N73-26749
Dynamic response of pipes with fluid flowing in steady and unsteady conditions
[MERL-TN-72-2] 20 p2387 N73-29178
Numerical integration techniques for shock discontinuity in one dimensional unsteady channel flow
[PUBL-138] 22 p2654 N73-31258

Linearized integral theory of three dimensional unsteady compressible flow in shear layer by oscillating wall
[AD-763807] 22 p2654 N73-31264
Analysis of transient wave motion in liquid filled cylinders
23 p2773 N73-32179
Analysis of unsteady aerodynamics of space shuttle vehicles
[NASA-CR-124424] 23 p2848 N73-32763
Numerical solution of time-dependent Navier-Stokes equation with periodic boundary condition
[AD-764582] 24 p2910 N73-33226

UNSTEADY STATE
Integration of unsteady aerodynamic forces and pressure distributions in aeroelastic analysis
[NLR-MP-71013-U] 05 p0492 N73-14011

UNSWEPT WINGS
NT INFINITE SPAN WINGS
NT RECTANGULAR WINGS
NT RING WINGS
Wind tunnel tests to determine effect of interference on performance of full span jet flap mounted on trailing edge of high aspect ratio unswept wing
[ARC-R/M-3219] 16 p1852 N73-25005

UPCONVERTERS
U PARAMETRIC FREQUENCY CONVERTERS

UPDRAFTS
U VERTICAL AIR CURRENTS

UPPER AIR
U UPPER ATMOSPHERE

UPPER ATMOSPHERE
NT D REGION
NT E REGION
NT EXOSPHERE
NT F REGION
NT F 1 REGION
NT F 2 REGION
NT IONOSPHERE
NT LOWER IONOSPHERE
NT MAGNETOPAUSE
NT MAGNETOSPHERE
NT MESOPAUSE
NT MESOSPHERE
NT SPORADIC E LAYER
NT THERMOSPHERE
NT UPPER IONOSPHERE
Deviations from diffusive equilibrium and response of atmosphere above 120 km
[NASA-TM-X-66057] 01 p0049 N73-10394
Rate of solar extreme ultraviolet radiation heating in upper atmosphere
[AD-745305] 01 p0051 N73-10410
Far ultraviolet heating in upper atmosphere variations
[AD-745309] 01 p0051 N73-10411
Reaction rate field, emphasizing ionization and upper atmosphere processes
[AD-745370] 01 p0051 N73-10414
Reaction rate field data, emphasizing ionization and upper atmosphere processes
[AD-745371] 01 p0051 N73-10415
Release technique for creating large dense vapor clouds in upper atmosphere using thermite formulation of barium metal and barium nitrate
[AD-745980] 01 p0054 N73-10438
Monthly mean climatological statistics for surface to 5 mb pressure level over Australia - Dec. 1971
01 p0074 N73-10606
Monthly mean climatological statistics for surface to 5 mb pressure level over Australia - Aug. 1971
01 p0074 N73-10607
Studying collisions of heavy particles to understand collision of meteoroids with upper atmosphere
01 p0102 N73-10842
Turbulence, billows, and gravity waves in high shear region of upper atmosphere during morning twilight, determined by rocket-released lithium cloud
[WRE-TN-670[WR/D]] 02 p0164 N73-11327
Polar upper atmosphere data recorded at Kiruna Geophysical Observatory, Sweden, from Jan. - Mar. 1972
02 p0167 N73-11353
Organic dye pulsed laser for detecting individual atomic species concentration in upper atmosphere
[AD-747335] 02 p0169 N73-11377
Measurement of upper atmospheric parameters using free-falling sphere
[AD-747037] 02 p0170 N73-11383
Development of occultation satellite system for determining atmospheric pressure at various millibar levels
02 p0198 N73-11601
Development of mathematical processes for deriving ionospheric electron density as function of altitude and frequency measurements obtained by vertical incidence ionospheric sounders
02 p0198 N73-11602
Monthly mean climatological statistics from surface to 5 mb level over Australia - January 1972
02 p0204 N73-11654
Meteorological upper air statistics in Australian region
02 p0204 N73-11655
Magnetospheric and upper atmospheric physics data obtained during 1971
[AD-746326] 02 p0232 N73-11882
Methods for acquiring meteorological parameter data and procedures for analyzing wind data
[AD-747480] 03 p0298 N73-12432
Development of system to correct upper atmosphere temperature readings to ambient air temperature
[AD-747973] 03 p0298 N73-12433
Abstracts of DNA-sponsored reaction rate research programs for FY 72
[AD-747660] 03 p0299 N73-12441
Transport processes governing structure, energy, mass, and momentum of upper atmosphere
[COO-2195-6] 04 p0415 N73-13388
Empirical model constructed to account for large atmospheric density variations observed from drag on satellites in upper atmosphere
[AD-748392] 04 p0445 N73-13631
Solar flux effects on upper atmosphere oxygen photodissociation and heating rates
[AD-747777] 04 p0467 N73-13807
Soviet research on meteorology, oceanography, upper atmosphere, and astronomy
[JPRS-57630] 04 p0474 N73-13876
Radar observations of meteor trains for detecting high altitude gravity waves
05 p0511 N73-14154
Upper atmospheric disturbance near polar cap - bibliographies
[AD-746298] 05 p0539 N73-14390
Optical intensity measurements for detecting low energy protons in polar cap
[AD-749857] 05 p0542 N73-14414
Triaxial accelerometer for determining upper air density, temperature, and pressure
[AD-749881] 05 p0543 N73-14422
Stratospheric weather maps for Northern Hemisphere based on rawinsonde and rocketsonde observations - Vol. 124, No. 3
05 p0570 N73-14632
Meteorological parameters of upper atmosphere over Japan during March 1972
05 p0572 N73-14648
Satellite aerodynamics and upper atmospheric density determination from satellite dynamic response
05 p0609 N73-14950
Bibliography on chemical contaminants released in upper atmosphere
[WRE-TM-498[WR/D]-FT-2] 06 p0667 N73-15422
Using simultaneous measurements of ozone profile and solar extinction to obtain absorption coefficient for calculating ozone distribution
[AD-750404] 06 p0668 N73-15429
Aeronomic reaction rate data
[AD-750771] 06 p0668 N73-15436
Ozone tables, ozonograms, and ascent tables for aerological ozone soundings conducted at Hohenpeissenberg, West Germany
[AD-750166] 06 p0670 N73-15446
Characterization of nonequilibrium flow and coupled chemistry associated with rocket exhaust effluent interactions in upper atmosphere
[AD-750878] 06 p0670 N73-15450
Northern hemisphere monthly mean 500-mb and 1000-500-mb thickness charts
[MET-O-845C] 06 p0692 N73-15632
Meteorological rocket and radiosonde data on lower and upper atmospheres - Mar. 1971
06 p0692 N73-15633
Aerological data from balloon and rocket flights for Japan and vicinity - Jan. 72
06 p0693 N73-15647
Upper atmospheric data of Japan and vicinity Feb. 1972
06 p0693 N73-15648
Design, development and flight tests of Super Loki Dart Meteorological Rocket Systems
[AD-750796] 06 p0722 N73-15895
Atomic and molecular processes in atmospheric environments
[AD-751766] 07 p0795 N73-16468
Electrical and meteorological experimentation in upper atmosphere of polar regions - bibliography
[AD-751336] 07 p0796 N73-16472
Bibliography and abstracts on upper atmospheric phenomena in inner region of polar caps
[AD-751335] 07 p0796 N73-16473
Association, switching, and rearrangement for positively charged cluster ions at 80 km in upper atmosphere
[AD-751140] 07 p0797 N73-16478
METROC computer program for producing wind and thermodynamic data from raw upper atmospheric data
[AD-751780] 07 p0816 N73-16616
Distribution statistics, magnitude, and spatial structure of gravity wave and planetary wave atmospheric variations
[NASA-CR-2203] 08 p0916 N73-17504
Extreme temperature, pressure, and density of atmosphere between 30 and 80 km
[AD-751874] 08 p0919 N73-17530
Dayglow measurements of upper atmosphere by Orbiting Astronomical Observatory A-2
[AD-752228] 08 p0920 N73-17539
Electronic and ionic reactions in atmospheric gases
[AD-752582] 08 p0921 N73-17550
Meteorological data for launching 13801 Little John, missiles 3086 and 3166
[AD-752089] 08 p0939 N73-17688
Meteorological data for launching of 13801 Little John Missile number 3070, round number 696 RO
[AD-752096] 08 p0940 N73-17702
Meteorological data for launching of 12801 Lance missile numbers 2216/2310, round no. 166 EET
[AD-752097] 08 p0940 N73-17703
Meteorological parameters for launching of 13401 Honest John missile number 2631, round no. 627 RUL
[AD-752094] 08 p0940 N73-17704
Reaction rate research, including atom, molecule, and ion interactions and aeronomy
[AD-753016] 09 p1031 N73-18418
Influence of electron beam irradiation on upper atmospheric chemistry and physics
[AD-753707] 09 p1033 N73-18431
Atmospheric data from OV1-15 satellite
[AD-753680] 09 p1033 N73-18432
Models of aerosol dynamics in upper atmosphere
[BNL-17174] 10 p1126 N73-19176
Vapor phase chemistry for producing hydrated ions in upper atmosphere
[AD-753940] 10 p1157 N73-19411
Meteorological rocket and radiosonde data on lower and upper atmospheres - Apr. 1971
10 p1180 N73-19600
Meteorological charts of upper atmosphere of Northern Hemisphere
[QR-4-PT-4] 10 p1181 N73-19604
Aerological data from balloon and rocket flights for Japan and vicinity - May 1972
10 p1182 N73-19612
Aerological data from radiosonde observations for Japan and vicinity during 1969 and 1970
10 p1182 N73-19613
Aerological data from flights for Japan - June 1972
10 p1182 N73-19614
Aerological data from balloon and rocket flights for Japan and vicinity - Apr. 1972
10 p1182 N73-19615
Physics of high energy particles, cosmic showers, modulation of cosmic rays, high atmospheric meteorology, and application of solar radiation to other areas
[NP-19366] 10 p1211 N73-19847
Frontal zone formation in tropopause as caused by slanting phenomenon
[NLL-M-22824-[5828.4F]] 11 p1274 N73-20341
Particles and fields, upper atmosphere physics, and solar and stellar astronomy
[NASA-CR-130197] 11 p1285 N73-20424
Comparison between measured transmission and emission spectra and calculated spectra in upper atmosphere ozone region
[BMFT-FBW-73-01] 11 p1285 N73-20429
Analysis of semiannual density variation in thermosphere during period of increasing solar activity
[BMFT-FBW-73-02] 11 p1285 N73-20430
Meteorological data of upper atmosphere from sounding rockets for Lance missile launch
[AD-754554] 11 p1314 N73-20666
Meteorological data gathered for launching of Athena flight 135
[AD-754557] 11 p1314 N73-20667
Meteorological data for launch of Little John probe of upper atmosphere
[AD-754561] 11 p1315 N73-20671
Meteorological data for launching of Lance missile probe of upper atmosphere
[AD-754565] 11 p1315 N73-20672
Meteorological data for launching Lance missile probe of upper atmosphere
[AD-754564] 11 p1315 N73-20673
Meteorological data gathered for Little John launching 14101
[AD-754560] 11 p1316 N73-20679
Meteorological data for Lance missile number 2186, round number 169 APL
[AD-754559] 11 p1316 N73-20680
USSR research projects in meteorology, oceanography, upper atmosphere and space astronomy, and terrestrial geophysics
[JPRS-58609] 11 p1339 N73-20867
Ground-based continuous measurements of upper atmosphere
[DATA-SUMMARY-72/7-9] 12 p1401 N73-21362
Meteorological data for launching Honest John missile, number 2598
[AD-755777] 12 p1424 N73-21543
Meteorological data for launching Lance missile, number 2170
[AD-755768] 12 p1424 N73-21544
Meteorological data for launching Lance missile, number 2352
[AD-755769] 12 p1424 N73-21545
Meteorological data for launching Lance missile, number 2148
[AD-755770] 12 p1424 N73-21546

Meteorological data for launching Lance missile, number 2176
[AD-755778] 12 p1425 N73-21548
Meteorological data for launching Lance missile, number 2351
[AD-755771] 12 p1425 N73-21549
Excitation and deexcitation of vibration in gases by nitrogen and oxygen atoms in upper atmosphere
[AD-757050] 14 p1617 N73-23099
Satellite observations of geomagnetic disturbance reaction time in upper atmosphere
[REPT-85] 14 p1658 N73-23458
Research projects conducted by Australian atmospheric physics laboratory to analyze atmospheric radiation, micrometeorology, ozone, airglow, and cloud physics
14 p1659 N73-23465
Upper atmospheric wind velocity and temperature measurements
[NASA-TT-F-14921] 14 p1659 N73-23470
Night sky luminescence in upper atmosphere during IQSY
[NASA-TT-F-14927] 14 p1660 N73-23478
Conference on structure and composition of upper atmosphere and planetary atmospheres
[AD-756812] 14 p1662 N73-23489
Large aperture Fabry-Perot interferometer used to scan barium ion clouds
[AD-757563] 14 p1663 N73-23495
Laboratory experiments on interaction of fast protons and hydrogen atoms with earth atmosphere
[AD-757505] 14 p1663 N73-23499
Equipment and mission of Astrophysics Institute in Tadzhikistan relative to radar tracking and wind velocity measurement
[AD-756100] 14 p1706 N73-23848
Aerological data from balloon and rocket flights for Japan and vicinity
15 p1777 N73-24407
Upper atmospheric neutral hydrogen distribution
15 p1779 N73-24423
Scattering of proton beams upon penetration into upper atmosphere
[NASA-TT-F-14802] 15 p1779 N73-24425
Upper atmosphere, magnetosphere, and solar physics and solar-terrestrial interactions
[AD-757874] 15 p1782 N73-24444
Atmosphere Explorer satellite absolute pressure measurements of upper atmosphere
[AD-757908] 15 p1782 N73-24447
Determination of vibrational temperature of molecular nitrogen in high atmosphere by chemical release of hydrogen iodide from sounding rocket
[AD-757909] 15 p1782 N73-24448
Deceleration and vertical motion of gas puff released into upper atmosphere
[AD-757867] 15 p1782 N73-24450
Observations of atmospheric ozone at 110.836 GHz
[AD-758819] 15 p1784 N73-24465
Utilization of satellite infrared spectrometer data for resolution of atmospheric variables
[AD-757774] 15 p1789 N73-24501
Meteorological data for launching of RIP 14101, missile numbers 12712 and 12716
[AD-758863] 15 p1808 N73-24651
Meteorological rocket and radiosonde data on lower and upper atmospheres - July 1971
16 p1937 N73-25671
Meteorological rocket and radiosonde data on lower and upper atmospheres - August 1971
16 p1937 N73-25672
Meteorological rocket and radiosonde data on lower and upper atmosphere - September 1971
16 p1937 N73-25673
Radar measurement of air mass circulation and meteor trail drift in upper atmosphere during IQSY
[NASA-TT-F-744] 17 p2023 N73-26363
Radar observation of air mass circulation in upper atmosphere during IQSY
17 p2023 N73-26364
Gravity wave-mean flow interactions in upper atmosphere
[NASA-CR-132776] 17 p2025 N73-26384
Polar upper atmosphere data recorded at Kiruna Geophysical Observatory, Sweden, from Oct.-Dec. 1972
17 p2028 N73-26410
Design of upper atmosphere chemical release package
[AD-760141] 17 p2028 N73-26416
Kinetics of recombination reactions in upper atmosphere
[AD-759847] 18 p2114 N73-27091
Hydrocarbon chemistry and chemiluminescence in high altitude plumes
[AD-760793] 18 p2114 N73-27094
Daily summaries for vertical echo sounding of upper atmosphere over Freiburg, Germany during March, 1973
[REPT-321F] 18 p2141 N73-27308
Model for predicting atmospheric parameters at altitudes between 90 and 2500 km
[NASA-SP-8021] 18 p2143 N73-27325
Upper atmosphere wind and temperature measurements from Sonmiani, Pakistan, using rocket grenades - 1965 - 1967
[NASA-CR-133401] 18 p2144 N73-27331
Research on aeronomy and upper atmospheric composition and environments
[AD-760576] 18 p2149 N73-27367
Development and operation of apparatus for sampling particulates in gases in upper atmosphere
[NASA-CASE-HQN-10037-1] 18 p2150 N73-27376
Feasibility of generating aritificial auroras by injecting electrons into upper atmosphere
[NASA-CR-133298] 18 p2151 N73-27388
Aerological data from balloon and rocket flights for Japan and vicinity - September 1972
18 p2172 N73-27539
Aerological data from balloon and rocket flights for Japan and vicinity - Aug. 1972
18 p2172 N73-27540
Aerological data from balloon and rocket flights for Japan and vicinity - Oct. 1972
18 p2172 N73-27541
High altitude meteorological data measured at Sonmiani, Pakistan 1964-1970
[W-119] 18 p2172 N73-27543
Statistical analysis of surface and upper air rawinsonde for White Sands Missile Range, New Mexico
[AD-762159] 19 p2297 N73-28472
Auroral clutter mapping with Homer backscattering radar to study reaction of upper atmosphere to nuclear explosions
[AD-762012] 19 p2297 N73-28474
Energy transfer reactions of electronically excited atomic and diatomic specspecies
[AD-762201] 19 p2298 N73-28481
Meteorological data for launching of Honest John, missile number 1763, round 685
[AD-762158] 19 p2317 N73-28632
Meteorological data for launching of Honest John, missile number 305, round 633
[AD-762155] 19 p2317 N73-28636
Meteorological data for launching of Lance missile, number 2238, round 187
[AD-762162] 19 p2317 N73-28638
Meteorological data gathered for launching 150601 Little John
[AD-762161] 19 p2317 N73-28641
Meteorological data gathered for launching 11604 Lance missile
[AD-762156] 19 p2317 N73-28642
Proceedings of conference on actinometry and atmospheric optics to include effects of solar radiation and atmospheric light on photosynthesis
[TT-70-50159] 20 p2399 N73-29280
Thermospheric wind effects on global distribution of helium in upper atmosphere
[NASA-TM-X-70441] 20 p2412 N73-29391
Use of computer-controlled two-dimensional film densitometer for analysis of photographs of chemical releases at high altitudes
[AD-763082] 20 p2413 N73-29398
Synoptic charts for 50mb in Northern Hemisphere from January to June, 1972
[QR-1/2-PT-1/2] 20 p2442 N73-29613
Monthly mean climatological statistics for surface to 5 mb pressure level over Australia - October 1972
20 p2449 N73-29678
Monthly mean climatological statistics for surface to 5 mb pressure level over Australia - Dec. 1972
20 p2449 N73-29679
Monthly mean climatological statistics for surface to 5 mb pressure level over Australia - September 1972
20 p2449 N73-29680
Monthly mean climatological statistics for surface to 5 mb pressure level over Australia - November 1972
20 p2449 N73-29681
Determination of vibrational energy of nitrogen in upper atmosphere
[AD-763749] 21 p2541 N73-30377
Numerical modeling of upper atmosphere
[ISAS-496-VOL-38-NO-7] 22 p2664 N73-31347
Atmospheric model developed for altitude range of 24 to 500 km
[AD-764303] 22 p2668 N73-31379
Diurnal temperature variations and upper atmospheric tides
22 p2736 N73-31908
Reports on upper atmosphere reaction rate data
[AD-764647] 23 p2754 N73-32040
Reaction kinetics in upper atmosphere chemistry and nuclear fireball studies
[AD-764892] 23 p2754 N73-32041
Cross sections for reactions of atmospheric ions with atomic oxygen
[AD-765333] 23 p2789 N73-32316
Cosmic ray charged particle interactions with matter
[AD-764833] 23 p2821 N73-32555
Aerological data from balloon and rocket flights for Japan and vicinity - December 1972
24 p2921 N73-33325
Observations of amplitude scintillations produced in F region in equatorial areas based on Applications Technology Satellite transmissions
[NASA-TM-X-70478] 24 p2921 N73-33326
Aerological data from balloon and rocket flights for Japan and vicinity - Nov. 1972
24 p2947 N73-33540
Aerological data from balloon and rocket flights for Japan and vicinity - Jan. 1973
24 p2947 N73-33541
Solar radiation effects on upper earth atmosphere
[AD-764599] 24 p2977 N73-33790
Determination of nitric oxide concentrations from eclipse variations of ion concentrations
24 p2994 N73-33926

**UPPER IONOSPHERE**
NT F REGION
NT F 1 REGION
NT F 2 REGION

Coupling between ionosphere and protonosphere and effects on long term variations of ionospheric electron content
07 p0775 N73-16296
Plasma convection patterns in polar upper ionosphere obtained from Cosmos 184 satellite measurements during magnetic disturbance of 4 Nov. 1967
[PR-130] 10 p1156 N73-19403
Dynamics of neutral atmosphere in 200 to 500 km height region at low latitudes from incoherent scattering measurements
13 p1513 N73-22263
Analysis of ionospheric investigations conducted with Intercosmos satellite number two
14 p1659 N73-23464
Convection velocity measurements in polar upper ionsphere made by Cosmos 184 Satellite during moderate magnetic disturbance
15 p1780 N73-24430

**UPPER STAGE ROCKET ENGINES**

Advanced technology relative to chemical upper stages
[NASA-CR-129587] 04 p0477 N73-13903

**UPPER VOLTA**

ERTS-1 imagery of villages and cultivation sites in Niger and Upper Volta
[E73-10893] 20 p2395 N73-29242

**UPSETTING**

Mathematical model of deformed state of metal strips during upsetting
[NLL-M-21511-[5828.4F]] 05 p0561 N73-14560

**UPSTREAM**

Experimental observations of upstream disturbances in flow of two fluids over obstacle in channel
[AD-763759] 21 p2526 N73-30259

**UPWELLING**
U UPWELLING WATER

**UPWELLING WATER**

ERTS-1 remote sensing of chlorophyll measurements in upwelling areas of oceans
[E72-10196] 01 p0047 N73-10375
Chlorophyll and plankton population distribution in upwelling waters off northwest coast of Africa and effects of eolian dust particles on surface water chemistry
[E72-10331] 05 p0531 N73-14319
Dynamics of plankton populations in upwelling waters along Arabian Coast, Somali Coast, and Northwest Coast of Africa
[E73-10325] 09 p1024 N73-18357
ERTS-1 imagery of plankton populations in upwelling waters off Africa
[E73-10603] 15 p1773 N73-24364
Investigation of plankton populations in upwelling waters along NW coast of Africa using ERTS-1 imagery
[E73-10795] 18 p2137 N73-27271
ERTS-1 imagery of biomass in upwelling waters along northwest coast of Africa
[PAPER-M15] 19 p2281 N73-28354
ERTS-1 imagery of algal bloom in Lake Erie and upwelling in Lake Michigan
[E73-10932] 21 p2529 N73-30274
Influence of temperature and wind profiles on water upwelling
24 p2974 N73-33765

**URANIUM**
NT URANIUM PLASMAS
NT URANIUM 233

Drift tube mass spectrometer for measuring reaction rate of uranium atoms and ions with O2 and N2
[AD-746272] 02 p0138 N73-11115
Proceedings of conference on microstructure of titanium, uranium, and zirconium body centered cubic lattices
[AD-748035] 03 p0319 N73-12598
Feasibility of full-scale nuclear light bulb engine and tests of fissioning uranium plasmas in unit cell of driver reactor
[NASA-CR-129500] 03 p0331 N73-12698
Cavity temperature and flow characteristics in gas-core reactor for testing fissioning uranium plasmas
[NASA-TM-X-2797] 15 p1809 N73-24662
Using average transmission and self-indication ratio measurements to investigate temperature dependence of resonance self-shielding effect in depleted uranium and tantalum
[NASA-TM-X-69565] 21 p2585 N73-30715

Measured and calculated fast neutron spectra at surface of lithium hydride and depleted uranium shielded reactors
[NASA-TM-X-2906] 24 p2953 N73-33594

**URANIUM ALLOYS**
Analysis of metallurgical, physical, and mechanical properties of uranium alloys to determine breakdown strain, elongation, and high density characteristics
[FOA-4-C-4471-D4] 02 p0186 N73-11508
High temperature oxidation of uranium alloys and morphology of oxide scales
[CONF-720523-1] 03 p0263 N73-12130
Production, refining, manufacturing, and applications of uranium alloys and compounds
[JPRS-57364] 03 p0313 N73-12552
Thermal conductivity, thermal properties, and thermal diffusivity of uranium-fissium alloy
[ANL-7889] 03 p0332 N73-12710
Mechanical properties of uranium alloys containing additions of aluminum, iron, molybdenum, silicon, and chromium over temperature range from 20 to 640 C
[UJV-2802-M] 05 p0562 N73-14567
Fracture strength of uranium- and tungsten-based impacted ogive penetrators
[DREV-R-652/72] 09 p1047 N73-18538
Topographic interpretation of uranium alloy X ray diffraction patterns
[SC-T-72-2467] 10 p1173 N73-19543
Lithium hydride and depleted uranium shield materials for space power nuclear reactor
[NASA-TM-X-2835] 18 p2177 N73-27580
Uranium-titanium alloys - annotated bibliography
[RFP-2005] 22 p2684 N73-31500
Thermodynamic properties of uranium-based Mo, Nb, Zr, and Ti alloys from 77 to 1500 K
[ORNL-TM-4253] 24 p2936 N73-33445

**URANIUM CARBIDES**
Research on zirconium microstructure and uranium carbide as nuclear fuel
[AECL-4159] 03 p0332 N73-12708
Effects of irradiation on properties of fluoride tungsten clad uranium carbide-zirconium carbide fueled capsules
[NASA-CR-120995] 05 p0578 N73-14708
Irradiation tests on tungsten clad uranium carbide/zirconium carbide thermionic emitter fuel configurations
[NASA-TM-X-2834] 18 p2178 N73-27587
Fabrication and performance of uranium carbide and uranium dioxide thermionic reactor fuels
[GULF-GA-A-12251] 24 p2954 N73-33599

**URANIUM COMPOUNDS**
NT URANIUM CARBIDES
NT URANIUM FLUORIDES
NT URANIUM OXIDES
Emission and absorption spectra for mixtures of liquid uranium and uranium oxide using carbon tube furnace facility
[AD-746687] 02 p0194 N73-11571
Production, refining, manufacturing, and applications of uranium alloys and compounds
[JPRS-57364] 03 p0313 N73-12552
Fabrication of uranium mononitride fuel pin assembly for fast lithium cooled space power reactor
[NASA-CR-120956] 05 p0579 N73-14710
Fission-gas release from uranium nitride at high fission-rate density
[NASA-TN-D-7171] 08 p0942 N73-17718
Hydrogen embrittlement of tantalum alloy cladding for uranium mononitride nuclear fuel pins at high temperatures
[NASA-TM-X-2732] 09 p1063 N73-18675
Evaluation of uranium nitride for in-core thermionic applications in electrically heated thermal gradient tests and in flat plate thermionic converters
[NASA-CR-131520] 12 p1416 N73-21470
Optical and magnetic resonance spectra of uranium borohydride in hafnium borohydride
[AD-759371] 17 p2074 N73-26777
Design and operation of tantalum alloy clad uranium mononitride irradiated fuel pins
[NASA-TM-X-2878] 22 p2698 N73-31614
Fission gas release rates from irradiated uranium nitride specimens
[NASA-TM-X-2890] 23 p2818 N73-32530
Magnetic and specific heat measurements of carbides, nitrides, and uranium and thorium sulfides
[CEA-R-4453] 24 p2943 N73-33506

**URANIUM FLUORIDES**
Thermodynamic equilibrium calculations for uranium hexafluoride decomposition at high temperatures
10 p1126 N73-19168
Thermodynamic properties of UF6 measured with ballistic piston compressor
[NASA-CR-132051] 15 p1843 N73-24936

**URANIUM ISOTOPES**
NT URANIUM 233

**URANIUM OXIDES**
Sintering behavior of UO2 powder compacts under hydrogen atmosphere
[CEA-R-4285] 04 p0427 N73-13477
Results of uranium dioxide-tungsten irradiation test and post-test examination
[NASA-TM-X-2709] 09 p1063 N73-18677
Thermodynamics of oxygen solubility in lanthanum uranium oxide measured on solid state electrolytic cell
[KFK-1649] 12 p1376 N73-21163
Effects of thermal cycling at high temperature on rates of distortion of UO2/clad fuel elements
[NASA-CR-133236] 17 p2061 N73-26672
Fission gas bubble, size distributions on irradiated UO2 specimens
[GEAP-12338] 17 p2062 N73-26680
Irradiation of TZM-Uranium dioxide fuel pin at 1700 K
[NASA-TM-X-2755] 18 p2178 N73-27588
Absolute measurements of spectral radiances from uranium oxygen mixtures
[AD-762430] 19 p2232 N73-27997
Computer program for modeling UO2 cladding strain resulting from irradiation
[NASA-TM-X-68281] 20 p2453 N73-29715
Fabrication and performance of uranium carbide and uranium dioxide thermionic reactor fuels
[GULF-GA-A-12251] 24 p2954 N73-33599

**URANIUM PLASMAS**
Measurements of emission coefficient of uranium plasmas
[NASA-CR-131319] 11 p1327 N73-20772
Compressional wave spectrum analysis on fissioning vacuum plasma in gas cored nuclear reactor
[NASA-CR-133235] 17 p2061 N73-26673
Fissioning uranium plasma for use as power source in driver reactor
[NASA-TM-X-68232] 17 p2067 N73-26722
Design and thermal analysis on film cooled exhaust duct for fissioning uranium plasma test reactor
[NASA-TM-X-2861] 18 p2178 N73-27585
Heat transfer in fissioning uranium plasma reactor cavity
[NASA-TM-X-2885] 23 p2828 N73-32607

**URANIUM 233**
Casting techniques for preparation of multiple U-233 metal target disks
[RFP-1848] 03 p0314 N73-12563

**URANUS [PLANET]**
Feasibility of atmospheric entry probe missions to Uranus and Neptune
[NASA-CR-129815] 04 p0469 N73-13824
Characteristics and capabilities of solar electric propulsion for orbiter missions of Uranus and Neptune
[NASA-CR-129857] 05 p0594 N73-14827
Performance potential evaluation of unmanned nuclear electric propulsion spacecraft for single-thrust-period missions to Uranus
[NASA-TN-D-7125] 06 p0718 N73-15859
Probe study to explore atmosphere of Saturn and Uranus
[NASA-CR-131227] 10 p1215 N73-19883
High resolution imagery of Uranus obtained by Stratoscope 2
[NASA-CR-132024] 14 p1706 N73-23846
Mission planning for Pioneer Saturn/Uranus atmospheric probe missions
[NASA-TM-X-2824] 21 p2595 N73-30800
Interplanetary trajectory characteristics of Saturn swingby mission to Uranus
[NASA-TM-X-2914] 22 p2714 N73-31727

**URBAN AREAS**
U CITIES

**URBAN DEVELOPMENT**
Crop identification, acreage estimation, urban land use, soil mapping, and earth resources identification in Wabash River Basin using ERTS-1 imagery
[E72-10208] 03 p0288 N73-12331
Automatic pattern recognition of urban land use and land use change
[E72-10244] 03 p0289 N73-12344
Census cities experiment in urban land use and change detection using ERRS-1 imagery
[E73-10064] 07 p0778 N73-16326
Urban and regional changes based on city census and remotely sensed imagery
07 p0786 N73-16395
Application of ERTS-1 imagery to Bureau of Reclamation studies of geology, agriculture, and urban development
[E73-10336] 10 p1147 N73-19337
Agricultural and urban land use mapping of Phoenix Quadrangle based on ERTS-1 imagery
[E73-10340] 10 p1147 N73-19339
Application of ERTS-1 imagery for mapping coverage of megalopolitan New England to show land use
[E73-10427] 11 p1280 N73-20388
Census cities experiment in detection of urban change and land use
[E73-10490] 12 p1397 N73-21326
Analysis of impact of major airport operations on economy, ecology, and urban development
13 p1505 N73-22199
Land use, urban development, and regional planning for Los Angeles County based on photointerpretation of MSS imagery and multispectral information extraction
[E73-10486] 13 p1515 N73-22277
Interpretation of ERTS-1 imagery of man made culture and revision of small-scale maps
[E73-10536] 13 p1518 N73-22300
Census cities experiment in detection of urban development and land use from ERTS-1 imagery
[E73-10538] 13 p1518 N73-22302
Lumiduc architecture for urban housing
[NASA-TT-F-14963] 17 p2098 N73-26976
Urban development and regional planning for Los Angeles County, California using ERTS-1 imagery
[PAPER-L18] 19 p2275 N73-28313
ERTS-1 detection and monitoring of tectonic and vegetational patterns, urban development, and agricultural processes in Southern California
[PAPER-R4] 19 p2283 N73-28362
Utilization of ERTS-1 imagery and data for land use, regional planning, and urban development in Metropolitan Washington area
19 p2285 N73-28377
Recommendations of conference committee concerning Senate admendments to H.R. 8825
[H-REPT-91-316] 19 p2354 N73-28955
Utilization of ERTS-1 imagery for soil mapping, land use, and urban mapping in Wabash River Basin
[E73-10862] 20 p2392 N73-29213
Urban development and regional planning in Los Angeles County using ERTS-1 MSS photography
[E73-10989] 22 p2658 N73-31295
Land use change and environmental quality in urban areas, emphasizing flood plains and wetlands
[PB-220742/1] 22 p2669 N73-31382
Methodology for integrating air pollution impact of airport and its environs
[PB-220987/2] 22 p2696 N73-31594
Application of ERTS-1 data and multispectral analysis to regional planning and urban development
[E73-11045] 23 p2779 N73-32221
Urban planning and development in east central Florida from ERTS-1 processed data
[E73-11083] 24 p2913 N73-33246

**URBAN PLANNING**
Procedures for determining present and predicted noise exposure at residential construction sites
[PB-210590] 01 p0081 N73-10672
Urban and regional planning in Florida using ERTS-1 imagery
[E72-10254] 03 p0290 N73-12354
Community/airport economic development model for assisting land use planning near metropolitan airports
[FAA-EQ-72-3-VOL-1] 04 p0400 N73-13259
Sample output for community/aircraft economic development model - programmers manual
[FAA-EQ-72-3-VOL-4] 04 p0401 N73-13260
Space technology for solving materials and design problems of earthbased housing
04 p0474 N73-13868
Application of aerial and spaceborne photography to urban, regional, and management planning
[NASA-CR-130290] 06 p0673 N73-15473
Operational activities of Hungarian National Bureau of Metrology and use of photogrammetry in city planning and modernization
[JPRS-57792] 06 p0731 N73-15965
Use of photogrammetry in city planning and modernization
06 p0732 N73-15967
Acquisition of data concerning urban housing quality using remotely sensed imagery
07 p0786 N73-16393
Utilization of scientific and technical personnel by urban governments
[PB-212762] 07 p0860 N73-16979
Urban and regional planning in Brevard County, Florida using ERTS-1 imagery
[E73-10083] 08 p0901 N73-17295
Operational system for employment of remote sensing and automated information in urban land management
[NASA-CR-130969] 09 p1030 N73-18410
Application of ERTS-1 imagery to urban and regional planning in Florida
[E73-10423] 11 p1280 N73-20384
Application of remote sensing to Pantano Wash for balance between environment and urban growth for Tucson
[NASA-CR-131279] 11 p1286 N73-20436
Guidelines for urban control of aircraft noise pollution
[PB-213020] 11 p1326 N73-20759
Research and applications of remote sensing to local and state governments
[NASA-CR-131643] 12 p1400 N73-21360
Urban land use mapping of San Francisco Bay area by machine processing of ERTS-1 multispectral data
[NASA-CR-131589] 13 p1522 N73-22334
Gas turbine power plants in future urban energy planning
[RE-439J] 13 p1593 N73-22912
Urban planning and mapping in east central Florida using ERTS-1 imagery
[E73-10605] 15 p1773 N73-24366
Urban mapping activities assisted by aerial photography and ground surveying in connection with urban planning and community development
[PB-214305/5] 16 p1915 N73-25494
Urban impact on areas of maximum environmental quality in Washington Metropolitan Area, 1971
[PB-214544/9] 16 p1977 N73-25993

Bibliography of urban area problems
[AD-756500] 17 p2099 N73-26987
Evaluation of existing community facilities in Macon, Georgia, and recommendations for improvements
[PB-220030/1] 18 p2127 N73-27184
Bibliography of references on urban hydrology
[PB-219105/4] 18 p2146 N73-27348
Current use and potential capacity of rural highway system
[PB-218453/9] 18 p2214 N73-27876
Airport environment compatibility plan for Jackson, Tennessee
[PB-221129] 22 p2648 N73-31217
Methodology for controlling air pollution episodes
[ANL/ES-14] 22 p2694 N73-31583
Urban transportation planning using satellite-borne remote sensors
[NASA-CR-124433] 23 p2859 N73-32846
Urban planning and development in east central Florida from ERTS-1 processed data
[E73-11083] 24 p2913 N73-33246

URBAN RESEARCH
Cascade impactor network for determining gravimetrically particle size distribution of suspended aerosols in urban areas
[AP-108] 03 p0326 N73-12656
Application of remote sensing techniques to study of climatology of urban-regional systems
07 p0786 N73-16394
Preparation of urban land use inventories by automated processing of ERTS MSS data
[NASA-CR-131576] 13 p1524 N73-22347
Preparation of urban land use inventories of Wisconsin and Indiana by machine-processing of ERTS-1 MSS data
[PAPER-L19] 19 p2275 N73-28314

URBAN TRANSPORTATION
Propagation model for V/STOL aircraft noise in urban area
[PB-211953] 05 p0581 N73-14729
Economic analysis on capital investment for transportation modes
[PB-212307] 07 p0860 N73-16976
Statistical supplement for capital investment in transportation modes
[PB-212308] 07 p0860 N73-16977
Airport access and ground travel modes
[PB-212814] 11 p1353 N73-20990
Environmental effects and plans for controlling urban TACV noise levels
13 p1506 N73-22209
Current use and potential capacity of rural highway system
[PB-218453/9] 18 p2214 N73-27876
Costs, physical characteristics, and performance of urban transportation systems
[PB-219254/0] 18 p2214 N73-27878
Survey of remote sensing applications for transportation and traffic engineering studies
[NASA-CR-129011] 20 p2488 N73-29989
Impact of highway transportation control strategies on Los Angeles air pollution and quality
[PB-221301/5] 22 p2696 N73-31597
Transportation control measures to improve air quality standards in Greater Houston area by 1977
[PB-221611/7] 22 p2696 N73-31598
Urban transportation planning using satellite-borne remote sensors
[NASA-CR-124433] 23 p2859 N73-32846
Analytic methods for evaluating transportation systems with interacting elements
23 p2861 N73-32867
Use of energy in transportation and implications for future
[P-5025] 24 p2993 N73-33921
Bimodal system of improving urban transportation
[NASA-TT-F-15056] 24 p2994 N73-33925

UREAS
Liquid retention in chlorpropamide therapy and water intoxication of patients
[NASA-TT-F-14597] 02 p0133 N73-11077
Chemical reactions of urea with carbohydrazide in smelts and aqueous solutions
[ICT-5/72] 18 p2114 N73-27090

URETHANES
Analysis of crosslinked epoxy-urethane polymer filled with aluminum oxide particles to determine mechanical and thermodynamic properties
[SC-DR-70-617] 07 p0812 N73-16584
Physio-chemical analysis of flammability characteristics and thermal degradation of rigid and flexible urethane foams used in aircraft structures - Part 2
[FAA-RD-73-50-PT-2] 18 p2105 N73-27025

URINALYSIS
Clinical practice and problems associated with urine analysis
08 p0875 N73-17089
Urinalysis methodology for detection of abusive and therapeutic drugs in man
12 p1370 N73-21117
Validity of rapid delta-aminolevulinic acid determination in urine for lead intoxication tests on industrial workers
[NASA-TT-F-14864] 12 p1371 N73-21128
Chromatographic determination of aldosterone level in urine
[RAE-LIB-TRANS-1682] 17 p1987 N73-26061
Chromatographic determination of urine corticosteroids
[RAE-LIB-TRANS-1694] 17 p1987 N73-26062
Enzymatic luminescent bioassay method for determining bacterial levels in urine
[NASA-CASE-GSC-11092-2] 18 p2109 N73-27052
Radioactivity urinalysis for calculating postflight astronaut cosmic radiation exposure
[NASA-CR-133378] 19 p2224 N73-27939
Automatic device for assaying urine on bacterial adenosine triphosphate content
[NASA-CASE-GSC-11169-2] 23 p2750 N73-32011

URINATION
Thermal flowmeter for urine volume measurement in manned space flight environment
[NASA-CR-128726] 07 p0750 N73-16095

URINE
Toxicity of gaseous urine and feces emissions on rat organism
10 p1116 N73-19097
Phenol preservative for reducing toxic urine outgassing into air environment
10 p1116 N73-19098
Preservatives for human urine storage and water reclamation in spacecraft cabin
10 p1116 N73-19099
Antimicrobial water reclamation methods for processing human urine
10 p1117 N73-19105
Antimicrobial phenyl preparations for human urine conservation during space flight
10 p1118 N73-19112
Free amino acid excretion in urine as test for early diagnosis of radiation damage in humans
11 p1243 N73-20092
High intensity noise effects on urinary K-Na ratios in rats
20 p2365 N73-29018
Hydroxyproline determination in collagen-like plasma and urine
[NASA-TT-F-15093] 22 p2620 N73-30997
Elimination of creatinine in urine during prolonged hypokinesia
24 p2884 N73-33029

USA [UNITED STATES]
U UNITED STATES OF AMERICA

USER MANUALS [COMPUTER PROGRAMS]
User guide for computer simulation model air pollution - Vol. 2
[PB-220457/6] 21 p2574 N73-30632
Computer program for determining rotational line intensity of diatomic molecules -users manual
[NASA-TN-D-7268] 21 p2582 N73-30689
User manual for air quality data handling system
[PB-220985/6] 22 p2696 N73-31595
Users manual for photochemical smog simulation diffusion/kinetics code
[PB-220243/0] 22 p2697 N73-31600
Users manual for interactive digital image processing and graphic display system
[NASA-TM-X-70472] 23 p2760 N73-32084
Users manual for Apollo cryogenic storage system computer program
[NASA-CR-134054] 23 p2760 N73-32088
Users manual for digital image processing system
[AD-764280] 23 p2761 N73-32097

USNS KINGSPORT
U SATELLITE COMMUNICATIONS SHIPS

UTAH
NT COLORADO PLATEAU [US]
NT GREAT BASIN [US]
Preparation of hydrologic atlases of arid land watersheds using ERTS-1 imagery of Wyoming, Utah, Montana, and New Mexico
[E72-10240] 03 p0288 N73-12340
Utility of ERTS-1 imagery in study of geological structures and exploration for economic mineral deposits in Utah and Nevada
[E72-10332] 05 p0531 N73-14320
Evaluation of ERTS-1 imagery for study of geological structures and features and exploration of mineral deposits in Utah and Nevada
[E73-10313] 09 p1022 N73-18345
Automated thematic mapping and analysis of terrain in Arizona, Texas, Washington, Utah, Louisiana, and California using ERTS-1 imagery
[E73-10386] 10 p1153 N73-19379
Mineral exploration in Utah and Nevada based on ERTS-1 imagery of structural fracture and fault trends
[E73-10510] 13 p1516 N73-22285
Application of ERTS-1 imagery for mapping major geological structural trends and mineralization zones in Utah and Nevada
[E73-10701] 16 p1903 N73-25393
ERTS-1 imagery of Utah and Nevada to show structural geology, mineral exploration, limnology, and hydrology
[PAPER-G3] 19 p2263 N73-28235
Regional environmental impact from oil shale development on private and public lands in Wyoming, Colorado, and Utah - Vol. 1
[EIS-AA-72-5242-D-1-VOL-1] 20 p2410 N73-29367
Energy alternatives to prototype oil shale leasing program for Wyoming, Colorado, and Utah - Vol. 2
[EIS-AA-72-5242-D-2-VOL-2] 20 p2410 N73-29368
Description of proposed leases for oil-shale program in Wyoming, Utah, and Colorado, and potential environmental impacts - Vol. 3
[EIS-AA-72-5242-D-3-VOL-3] 20 p2410 N73-29369
Mineral exploration and fracture trends in Utah and Nevada from ERTS-1 imagery
[E73-11032] 22 p2663 N73-31336
Snow cover surveys of Sierra Nevada, Cascades, and Wasatch mountains using Skylab EREP data
[E73-11036] 22 p2663 N73-31340

UTILITY AIRCRAFT
NT BO-105 HELICOPTER
NT OH-13 HELICOPTER
NT P-531 HELICOPTER
NT S-2 AIRCRAFT
NT U-2 AIRCRAFT
NT UH-1 HELICOPTER
NT UH-2 HELICOPTER

UTILIZATION
NT WASTE UTILIZATION
Production and applications of transuranic elements
[FOA-4-C-4463-22[13]] 07 p0819 N73-16637
Conference on use of solar energy in Mediterranean
[BULL-22] 24 p2974 N73-33762
Heliotechnique for utilizing solar energy on earth
24 p2974 N73-33763

## V

V BAND
U EXTREMELY HIGH FREQUENCIES

V GROOVES
Numerical analysis of elasto-plastic bending of plates with V-notch on one edge and subjected to pure bending
[NASA-CR-132225] 15 p1839 N73-24900
Semidirect boundary integral method to obtain numerical solution for elastic stress and strain fields in V-notched beams in pure bending
[NASA-TN-D-7424] 22 p2725 N73-31803
Boundary integral equation method for determining plane elasto-plastic analysis of V-notched plate under bending stress
24 p2987 N73-33869

V-5 AIRCRAFT
U XV-5 AIRCRAFT

V/STOL AIRCRAFT
NT BO-105 HELICOPTER
NT BREGUET 941 AIRCRAFT
NT CH-3 HELICOPTER
NT CH-47 HELICOPTER
NT CL-84 AIRCRAFT
NT DO-31 AIRCRAFT
NT FLYING PLATFORMS
NT H-53 HELICOPTER
NT HELICOPTERS
NT MILITARY HELICOPTERS
NT OH-6 HELICOPTER
NT OH-13 HELICOPTER
NT P-531 HELICOPTER
NT P-1127 AIRCRAFT
NT ROTARY WING AIRCRAFT
NT SH-3 HELICOPTER
NT SHORT TAKEOFF AIRCRAFT
NT TANDEM ROTOR HELICOPTERS
NT UH-1 HELICOPTER
NT UH-2 HELICOPTER
NT VERTICAL TAKEOFF AIRCRAFT
NT X-14 AIRCRAFT
NT X-22 AIRCRAFT
NT XH-51 HELICOPTER
NT XV-5 AIRCRAFT
Development and characteristics of civilian V/STOL aircraft with application to short haul commercial air traffic
[NASA-TT-F-14629] 01 p0005 N73-10034
Numerical determination of augmented lift due to wing-slipstream interaction for application to V/STOL aircraft
[AD-743257] 01 p0005 N73-10035
Display systems for all-weather terminal operational capability of V/STOL aircraft
[AGARD-R-594] 02 p0174 N73-11407
Operational procedure for computer program to calculate design point characteristics of gas generator or turbojet lift engine for V/STOL applications
[NASA-TM-X-2656] 02 p0222 N73-11794
Wind tunnel simulation of ground effect conditions to determine effect of three dimensional turbulent boundary layer on V/STOL aircraft configurations - Pt. 1
[NASA-CR-114495] 03 p0282 N73-12283
Wind tunnel tests to determine aerodynamic characteristics of V/STOL aircraft configurations using blowing flapped wing and direct jet lift systems
[NASA-CR-114496] 03 p0282 N73-12284

Effects of intraurban V/STOL commuter system on economic, social, and physical environment on San Francisco Bay Area
[NASA-CR-114492] 03 p0366 N73-12982
Operational and air transport characteristics of civil V/STOL aircraft
[NASA-TT-F-14619] 04 p0371 N73-13012
Improvement in V/STOL aircraft performance with yaw control augmentation to reduce cross coupling effects
[AD-749489] 04 p0375 N73-13046
Design studies for integral lift, high bypass ratio fan engine using Lycoming 502 core and MQT power turbine, for advanced commercial V/STOL aircraft
[NASA-CR-120992] 04 p0426 N73-13471
Wind tunnel tests to determine aerodynamic and propulsion characteristics of propulsive wing V/STOL configuration at high subsonic speed
[NASA-TM-X-2693] 05 p0493 N73-14020
Location of soil types with potential for generating atmospheric sand and dust with application to analysis of V/STOL operational environment
[AD-749462] 05 p0495 N73-14033
Propagation model for V/STOL aircraft noise in urban area
[PB-211953] 05 p0581 N73-14729
Technical and economic feasibility of V/STOL lift-fan commercial aircraft for short haul transport applications
[NASA-CR-2184] 06 p0621 N73-15041
Technical documentation to support V/STOL aircraft implementation and utilization based on short haul air transportation requirements - Vol. 2
[NASA-CR-114518] 07 p0739 N73-16009
Development of optimized aircraft structures based on vibratory strain energy distribution using damped forced response
[AD-751809] 07 p0741 N73-16027
Revisions to V/STOL handling qualities based on criteria
08 p0864 N73-16994
Development of methods for predicting performance characteristics of V/STOL aircraft - Vol. I
[AD-752557] 08 p0869 N73-17033
Analytical techniques for predicting static and dynamic stability, control derivatives, and force and moment coefficients for V/STOL aircraft - Vol. 2
[AD-752558] 08 p0869 N73-17034
Computer program manual for analytical techniques to predict performance of V/STOL aircraft - Vol. 3
[AD-752559] 08 p0869 N73-17035
Literature survey of techniques for predicting performance of V/STOL aircraft- Vol. 4
[AD-752563] 08 p0869 N73-17036
Dynamic and aeroelastic problems of stop-rotors of V/STOL aircraft occurring during retracting and stowing of rotary wings
[DLR-FB-72-65-PT-1] 09 p0983 N73-18027
Conceptual designs of V/STOL lift fan commercial short haul transport aircraft to determine technical and economic feasibility
[NASA-CR-2183] 09 p0984 N73-18038
Analysis of V/STOL aircraft design and operation to determine effects of noise problems and constraints with emphasis on helicopter performance
[AD-752447] 09 p0989 N73-18073
Analysis of aircraft instruments and display devices for approach control and landing of V/STOL aircraft
[AGARD-AR-51] 09 p1034 N73-18439
Analysis of selected problems in formation of simulation models of V/STOL aircraft
10 p1105 N73-19009
Performance of typical V/STOL aircraft and comparison of data obtained with flight simulator against data obtained by actual flight tests
10 p1105 N73-19011
Concepts for achieving low noise levels for V/STOL aircraft
[NASA-CR-120970-VOL-1] 10 p1106 N73-19018
Engine cycle, configuration, and design requirements
[NASA-CR-120970-VOL-2] 10 p1106 N73-19019
Preliminary aerodynamic and mechanical design of selected gas generators and lift unit for V/STOL aircraft
[NASA-CR-120972] 10 p1106 N73-19020
Wind tunnel tests to determine low speed aerodynamic characteristics of large scale V/STOL transport models with lift fan lift-cruise fan propulsion system
[NASA-TM-X-62231] 11 p1233 N73-20014
Proceedings of conference on rotary wing aircraft developments to include operational experience, flight tests, and evaluation of structural concepts
[AGARD-CP-121] 12 p1357 N73-21008
Aerodynamic, dynamic, and aeroelastic problems in rotary wing design for helicopters and V/STOL aircraft with application to hingeless rotor systems
12 p1362 N73-21051
Design of V/STOL research transport aircraft to achieve low fan noise with high thrust/weight capability of high pressure ratio lift fan system
[NASA-CR-121146] 12 p1364 N73-21065
Design and aerodynamic characteristics of tilt propellor aircraft for conducting flight research on V/STOL aircraft - Vol. 2
[NASA-CR-114442] 13 p1473 N73-21927
Acoustic measurements of sound pressure levels due to cross flow over face of lift fans on fan-in-wing and V/STOL model transport aircraft
[NASA-CR-114566] 13 p1473 N73-21928
Wind tunnel tests to determine effect of cross flow velocity on jet noise power level using V/STOL model transport
[NASA-CR-114571] 13 p1473 N73-21929
V/STOL lift fan commercial short haul transport aircraft for 1980 to 1985 period to include aircraft design, hover control, and cruise performance
[NASA-CR-2185] 13 p1473 N73-21930
Analysis of factors involved in design of wind tunnel for testing V/STOL aircraft models
14 p1598 N73-22956
Conceptual designs and aerodynamic configurations of tilting rotor V/STOL aircraft for 1975 to 1980 time period - Vol. 1
[NASA-CR-114437] 14 p1599 N73-22964
Preliminary design of V/STOL tilting rotor aircraft for performance of research flights - Vol. 2
[NASA-CR-114438] 14 p1599 N73-22965
Wind tunnel tests to determine effect of longitudinally oriented wing-mounted pods on aerodynamic characteristics of V/STOL transport model in cruise flight mode
[NASA-TN-D-7199] 15 p1731 N73-24035
Analysis of temperature and pressure parameters associated with recirculated engine exhaust from V/STOL aircraft engines exhausting normal to ground
[NASA-TT-F-14912] 15 p1768 N73-24323
Wind tunnel tests to determine aerodynamic characteristics of vectored thrust V/STOL fighter aircraft in transition speed range
[NASA-TN-D-7191] 16 p1858 N73-25047
Design and development of STOL and V/STOL aircraft to show design requirements, performance characteristics, and air traffic control problems
[PB-217102] 16 p1862 N73-25085
Design studies and model test results of folding-proprotor aircraft concept
[AD-759534] 16 p1862 N73-25086
Cockpit and control display design criteria for tactical STOL and V/STOL aircraft
[AD-758787] 16 p1914 N73-25489
Analysis of operational problems associated with wind tunnel testing of V/STOL aircraft and helicopters
17 p2008 N73-26240
Scaling laws, constructional problems, and optimum model size associated with wind tunnel tests of helicopters and rotary wing aircraft
17 p2009 N73-26246
Proceedings of conference on military applications of V/STOL aircraft to include current and proposed research projects to meet military requirements
[AGARD-CP-126-VOL-1] 18 p2102 N73-27000
Review of V/STOL aircraft research and development programs to increase effectiveness of aircraft and develop mission improvements
18 p2102 N73-27001
Review of V/STOL development programs to compare basic characteristics of XC-142A, X-19 and X-22A aircraft under various flight conditions
18 p2103 N73-27003
Design, development, and characteristics of Do-31 V/STOL aircraft to include solution of operational problems caused by ground effect and transition flight
18 p2103 N73-27004
Design, development, and flight characteristics of VAK 191 B V/STOL strike/reconnaissance aircraft
18 p2103 N73-27006
Handling characteristics of V/STOL aircraft based on data obtained from flight tests, simulator operation, and analytical studies
[AGARD-R-577-PT-2] 19 p2220 N73-27906
Aeroelastic and dynamic studies of technology applicable to tilting rotor vertical takeoff aircraft with emphasis on propeller whirl instability - Vol. I
[NASA-TM-X-69497] 20 p2359 N73-28976
Natural mode vibration analysis of aircraft structural systems by direct and component mode synthesis techniques applied to tilt rotor VTOL aircraft aeroelasticity - Vol. 2
[NASA-TM-X-69496] 20 p2359 N73-28977
Development of computer programs for designing engine inlets for VTOL and STOL aircraft based on axisymmetric potential flow parameter
[NASA-TM-X-68278] 20 p2388 N73-29182
Design and tests of lift fan exhaust suppression system for future VTOL aircraft noise goals
[NASA-CR-121108] 20 p2466 N73-29812
Development of method for calculating near field noise level of free jet and influence of ground effect on noise produced by V/STOL aircraft operation
20 p2478 N73-29907
Dynamic and aeroelastic problems of V/STOL aircraft stop-rotors occurring during retracting and stowing of rotor blades
[DLR-FB-73-19] 21 p2496 N73-30035
Development of computer program to predict aerodynamic noise levels of V/STOL aircraft at various points in flight trajectory
[PB-221140/7] 21 p2499 N73-30054
Aerodynamic characteristics of round jet located on center line of bottom of aircraft fuselage and elongated slots for lift augmentation
[NASA-TN-D-7299] 22 p2613 N73-30939
Wind tunnel and rotor whirl cage tests to determine stability and control parameters of scale model of tilting rotor aircraft model - Vol. 6
[NASA-CR-114615] 22 p2614 N73-30950
Wind tunnel testing of V/STOL aircraft models to show wind tunnel wall corrections for models with large values of downwash
[AD-764255] 22 p2616 N73-30962
Future of short haul air transport in Western Europe - V/STOL Working Group
[SP-73-001] 22 p2737 N73-31915
Mathematical model for real time simulation of tilt rotor aircraft to evaluate aircraft performance and handling qualities
[NASA-CR-114601] 23 p2742 N73-31947
VAK 191 B V/STOL fighter aircraft nonlinear feedback flight control system for gliding flight phase
24 p2878 N73-32984

**VACANCIES [CRYSTAL DEFECTS]**
Quantitative analysis on divacancy to monovacancy concentration ratios in quenched platinum and effects of storage and electropolishing
[COO-3158-5] 04 p0434 N73-13538
Ion microscopic measurements on divacancy and monovacancy concentrations in high purity platinum
[NYO-3504-55] 04 p0434 N73-13541
Use of low temperature quenching techniques to retain simple vacancy defects in magnesium
[NLL-CE-TRANS-5944-[9022.09]]
05 p0561 N73-14559
Interaction of supersaturated vacancies and vacancy clusters with dislocations in copper single crystals
24 p2967 N73-33715

**VACUUM**
NT HIGH VACUUM
NT ULTRAHIGH VACUUM
Bibliography of arc discharges in vacuum and gaseous atmospheres
[SC-B-72-3233] 03 p0278 N73-12251
High temperature plastic deformation of refractory metals in vacuum during rolling
[AD-750508] 06 p0678 N73-15516
MoS2 and MoS2/PTFE composite layers for dry lubrication of journal bearings in atmosphere or vacuum
[DLR-FB-72-69] 09 p1038 N73-18470
Weight measurement of impurities during aspiration of aerosol samples from flow, using zero intake tubes
[AD-762329] 19 p2232 N73-27998

**VACUUM APPARATUS**
NT CONDENSATION PUMPS
NT IONIZATION GAGES
NT PENNING GAGES
NT VACUUM CHAMBERS
NT VACUUM FURNACES
NT VACUUM GAGES
NT VACUUM PUMPS
Vacuum alteration for jet targets from condensed hydrogen, while operating on accelerator internal beam
[JINR-P13-6324] 04 p0402 N73-13275
Estimation of traces of gases in metals and alloys by vacuum fusion techniques
[BARC-590] 06 p0638 N73-15177
Development and characteristics of multiple thin film vapor deposition unit
[BARC-609] 08 p0927 N73-17594
Vacuum brazing-gas quenching process for joining chemical and ordnance munitions materials
[AD-759117] 16 p1919 N73-25531
Characteristics of zero aerosol sampling tube for aspiration of samples from gas flow with minimum changes in isokinetic coefficient
[AD-759868] 17 p2035 N73-26470
Portable vacuum probe surface sampler for sampling large surface areas with relatively light loading densities of microorganisms
[NASA-CASE-LAR-10623-1] 21 p2544 N73-30395
Design and construction of vacuum system and safety interlocks for photoionization mass spectrometer
[AD-763685] 21 p2550 N73-30447

**VACUUM CHAMBERS**
Large-diameter rotary vacuum chamber with servo controlled angular positioning and readout
[LBL-769] 03 p0281 N73-12275
Apparatus for analyzing gas samples in containers including vacuum chamber, mass spectrometer, and gas chromatography
[NASA-CASE-GSC-10903-1] 03 p0300 N73-12444
Development of instrument for determining total pressure in calibration chamber and numerical analysis of operating principles
[NASA-TN-D-7058] 03 p0301 N73-12452
Design and development of radiometer to observe steady state radiation in vacuum environment
[NASA-CASE-MFS-21108-1] 03 p0301 N73-12455

Vacuum life tests on lubricated bearings and slip rings
[ESRO-CR-91] 03 p0307 N73-12504
Pumping system of space environment simulation vacuum chamber noting vacuum and diffusion pumps, valves, cryogenic section, and automatic control system
[ESDO-TN-113-ESTEC] 05 p0524 N73-14262
Design and development of test stand system for supporting test items in vacuum chamber
[NASA-CASE-MFS-21362] 11 p1265 N73-20267
Design of warm vacuum system for superconducting storage rings
[BNL-17239] 12 p1440 N73-21670
Distribution functions of spot diameter for single and multicathode discharges in vacuum
[TH-73-E-32] 14 p1643 N73-23328
Bunch lengthening and power losses due to vacuum chamber walls
[DESY-72/72] 17 p2010 N73-26258
Large space simulation chambers realizing true ultimate vacuum
[NASA-TM-X-68272] 20 p2382 N73-29142
Contamination tests of Vacuum Chamber A and cryogenic/vacuum study of quartz crystal microbalance
[NASA-TM-X-64776] 21 p2521 N73-30220
Optomechanical tests equipment for D2B satellite vacuum chamber calibration
[OPT-005-72] 23 p2770 N73-32160

**VACUUM DEPOSITION**
Synthesis and high rate deposition of ceramics and dispersion stengthened alloys
[AD-750413] 06 p0685 N73-15580
Mossbauer spectroscopic analysis of order-disorder transitions in vacuum deposited Te films
[AD-753272] 09 p1074 N73-18769
Production of ferromagnetic MnBi thin films by optical control of vacuum deposition and annealing
[KFKI-72-70] 10 p1199 N73-19757
Evaluation of process for burnable poison deposition on zirconium hydride fuel
[AI-AEC-13085] 24 p2955 N73-33606

**VACUUM EFFECTS**
Photographic characteristics of UFSh-4 film used in Orion orbital observatory
[NASA-TT-F-14585] 07 p0799 N73-16492
Reaction of nickel oxide with steel in argon and vacuum atmospheres
[AD-754776] 11 p1306 N73-20600
Vacuum effects on mechanical behavior of filled elastomeric spacecraft materials
13 p1546 N73-22527
Vacuum effects on mechanical properties of composite heat ablator and solid problem material
15 p1801 N73-24594
Altitude test and performance of Aerojet AJ10-179 liquid rocket engine under vacuum conditions
[AD-763727] 21 p2591 N73-30758

**VACUUM FURNACES**
Air lock mechanism for inserting and removing specimens from vacuum furnace
[NASA-CASE-LAR-10841-1] 03 p0305 N73-12494
Design of high temperature and high pressure furnace for crystal growth
[AD-759786] 16 p1954 N73-25811
Metal refining during vacuum arc melting for lowering nonmetallic inclusions and gases in ingot
21 p2557 N73-30502

**VACUUM GAGES**
NT IONIZATION GAGES
NT PENNING GAGES
Piston manometer as absolute standard for vacuum gage calibration in 2 to 500 millitorr range
[NASA-TN-D-7059] 02 p0173 N73-11402
Development of instrument for determining total pressure in calibration chamber and numerical analysis of operating principles
[NASA-TN-D-7058] 03 p0301 N73-12452
Calibration of vacuum gauges for measuring total and partial pressures in ultrahigh vacuum region
[NASA-CASE-XGS-07752] 21 p2544 N73-30390
Ionization gage for measuring ultrahigh vacuum levels
[NASA-CASE-XLA-05087] 21 p2544 N73-30391

**VACUUM MELTING**
Kinetics of purification of beryllium through evaporation data acquired during vacuum induction melting
[NASA-CR-123946] 04 p0431 N73-13512

**VACUUM PUMPS**
NT CONDENSATION PUMPS
Pumping system of space environment simulation vacuum chamber noting vacuum and diffusion pumps, valves, cryogenic section, and automatic control system
[ESDO-TN-113-ESTEC] 05 p0524 N73-14262
Vacuum pump system for 150 kV neutron generator to reduce tritium hazards
[NASA-TM-X-2650] 09 p1038 N73-18468
Feasibility of mechanical pumps for use with Pioneer-Venus probe mass spectrometer inlet system
[NASA-CR-114581] 14 p1670 N73-23551
Investigation of backfires and explosions occuring in vacuum pumps of oxygen test stands
[AD-763370] 21 p2554 N73-30474

**VACUUM SPECTROSCOPY**
Laser operation in vacuum and active scattering particle spectrometers
[NASA-CR-124111] 10 p1159 N73-19425
Apollo 17 vacuum ultraviolet spectrometer calibration plan
[NASA-CR-128831] 10 p1160 N73-19439
Instrumentation for atmospheric rocket sounding by occultation including infrared interferometer, Fabry-Perot interference filter, and vacuum spectrometer
[BMBW-FBW-72-14-PT-1] 22 p2667 N73-31368

**VACUUM SYSTEMS**
Vacuum-diffusion welding units
10 p1163 N73-19464
Lightweight evacuated multilayer insulation systems for space shuttle vehicle
[NASA-CR-121105] 16 p1966 N73-25902

**VACUUM TESTS**
NT THERMAL VACUUM TESTS
Thermal ultraviolet spectrometer model vacuum test performance
[NASA-CR-128562] 16 p1916 N73-25509
Boundary layer friction data under ion pumped vacuum
[NASA-CR-135480] 23 p2796 N73-32366

**VACUUM TUBE OSCILLATORS**
NT BACKWARD WAVE TUBES
NT CATHODE RAY TUBES
NT CELESCOPES
NT GAS DISCHARGE TUBES
NT IMAGE ORTHICONS
NT IMAGE TUBES
NT KLYSTRONS
NT MAGNETRONS
NT MICROWAVE OSCILLATORS
NT MICROWAVE TUBES
NT PHOTOMULTIPLIER TUBES
NT THERMIONIC DIODES
NT THYRATRONS
NT TRAVELING WAVE TUBES
NT VIDICONS

**VACUUM TUBES**
NT BACKWARD WAVE TUBES
NT CATHODE RAY TUBES
NT CELESCOPES
NT GAS DISCHARGE TUBES
NT IMAGE ORTHICONS
NT IMAGE TUBES
NT KLYSTRONS
NT MAGNETRONS
NT MICROWAVE OSCILLATORS
NT MICROWAVE TUBES
NT PHOTOMULTIPLIER TUBES
NT THERMIONIC DIODES
NT THYRATRONS
NT TRAVELING WAVE TUBES
NT VIDICONS
Joule heating model for cathode surface structure effect on metal evaporation in vacuum discharge
[TH-73-E-33] 14 p1643 N73-23329
Volt-ampere characteristics of enclosed keeper hollow cathode discharge
[NASA-TM-X-2799] 15 p1825 N73-24792

**VACUUM ULTRAVIOLET RADIATION**
U FAR ULTRAVIOLET RADIATION

**VADOSE WATER**
Application of aerial photography and photointerpretation to analyzing groundwater conditions under various types of landscape and morphological elements
[NASA-TT-F-681] 02 p0174 N73-11409
Models for sensitivity of apparent temperature and backscattering coefficient to variations of soil moisture as function of vegetation
[NASA-CR-135593] 23 p2784 N73-32275

**VALENCE**
Valence electron model for calculating ionization energies and excited levels in photoelectron- and absorption-spectra
08 p0945 N73-17741

**VALIDATION**
U PROVING

**VALKYRIE AIRCRAFT**
U B-70 AIRCRAFT

**VALLEYS**
NT COACHELLA VALLEY [CA]
NT IMPERIAL VALLEY [CA]
NT PALO VERDE VALLEY [CA]
NT POTOMAC RIVER VALLEY [MD-VA-WV]
NT SACRAMENTO VALLEY [CA]
NT TENNESSEE VALLEY [AL-KY-TN]
ERTS-1 imagery of geology in ice free valleys of Antarctica
[E73-10309] 09 p1022 N73-18341
Volcanic origin of mare ridges and sinuous rilles on lunar surface
12 p1454 N73-21780
Fourier technique for quantitatively classifying lunar rilles by planimetric shape
12 p1455 N73-21781
Geological survey and mapping of ice-free valleys of Antarctica from interpretation of ERTS-1 imagery
[E73-10564] 14 p1656 N73-23436
Reconnaissance geologic mapping in Dry Valleys of Antarctica using ERTS-1 imagery
[E73-11127] 24 p2916 N73-33282

**VALUE ENGINEERING**
Real forecast verification data for testing Hatter terminal weather forecast models
[AD-757489] 14 p1686 N73-23679

**VALVES**
NT ARTIFICIAL HEART VALVES
NT AUTOMATIC CONTROL VALVES
NT CONTROL VALVES
NT FUEL VALVES
NT GAS VALVES
NT PRESSURE REGULATORS
NT RELIEF VALVES
NT SOLENOID VALVES
Performance tests to determine proficiency of maintenance personnel in servicing fuel start solenoid in UH-1 helicopter
[AD-745163] 01 p0021 N73-10166
Flow control valve for high temperature fluids
[NASA-CASE-NPO-11951-1] 01 p0061 N73-10501
Pumping system of space environment simulation vacuum chamber noting vacuum and diffusion pumps, valves, cryogenic section, and automatic control system
[ESDO-TN-113-ESTEC] 05 p0524 N73-14262
Tests of seat and poppet materials for use in chlorine pentafluoride attitude control system valves
[AD-750873] 06 p0715 N73-15831
Explosive actuated, normally open, titanium valve
[NASA-CR-130545] 08 p0927 N73-17590
Contamination avoidance devices for poppet-type shutoff valves
[NASA-CR-121125] 09 p1039 N73-18471
Design and development of space storable isolation valves for control of flow of liquid rocket propellants
[TRW-73-4781-6-15] 10 p1165 N73-19477
Evaluation of explosive actuated normally open valve model 1399
[NASA-CR-131401] 11 p1296 N73-20520
Shock tube experiments for investigating rotating closure of ventilation system slap valve
[REPT-3/72] 13 p1476 N73-21955
Potential valve closures for space shuttle auxiliary propulsion system
[NASA-CR-120976] 15 p1791 N73-24516
Improved design of high-response slotted plate overboard bypass valve for supersonic inlets
[NASA-TM-X-2812] 16 p1864 N73-25097
Numerical solution of viscous fluid flow in finite tube with deformable walls in presence of valves for application to blood circulation process
16 p1867 N73-25117
Valve testing for application in inlet system of Pioneer Venus Probe mass spectrometer
[NASA-CR-114627] 16 p1918 N73-25517
Development and characteristics of combined pressure regulator and shutoff valve with variable pressure response characteristics
[NASA-CASE-NPO-13201-1] 17 p2036 N73-26474
Nitrogen and hydrazine leakage of monopropellant ACS valves
[AD-762943] 20 p2423 N73-29465

**VAN ALLEN RADIATION BELTS**
U RADIATION BELTS

**VAN DE GRAAFF ACCELERATORS**
Design and operation of 5 MeV Van de Graaff ion accelerator at Central Research Institute for Physics in Budapest, Hungary
[KFKI-71-47] 05 p0524 N73-14260
Simulated micrometeoroid impact cratering in lunar materials using electrostatically accelerated microparticles impacting in oligoclase single crystals
[NASA-CR-130356] 07 p0841 N73-16813
Research progress in accelerator and ion source development, detection and computer systems, and various nuclear physics projects
09 p1101 N73-18986
Radiation sterilization with Van de Graaff accelerators
[NASA-TT-F-14821] 11 p1247 N73-20120
Improved electrostatic accelerator with increased terminal voltage capacity
[UR-NSRL-71] 16 p1885 N73-25255

**VAN DER WAAL FORCES**
Raman spectra of Van der Waals complexes in argon, helium, and xenon
[AD-758241] 15 p1748 N73-24171

**VANADATES**
Chemical reactions involved with molybdenum, tungsten, vanadium, and chromium additives in hydrogen-oxygen flames seeded with potassium
[AD-743514] 01 p0023 N73-10179
Growth of yttrium orthovanadate large single crystals
[AD-761094] 18 p2191 N73-27689

**VANADIUM**
Influence of neutron irradiation on physical and chemical properties of vanadium
[IS-2833] 03 p0314 N73-12558
Formula for calculating intensity of elastic and inelastic X ray scattering in crystal lattice of vanadium
[NASA-TT-F-13913] 06 p0708 N73-15775
Phase equilibrium diagram of intermetallic compound of vanadium and gallium
[AD-752877] 09 p1049 N73-18551

Corrosion resistant materials for nozzle guide vanes and turbine blades subject to vanadium containing fuel combustion
14 p1678 N73-23613
Structures of ionized vanadium and manganese atoms with incomplete shells considering spin-orbital and spin-spin interactions
[NLL-RTS-7856] 18 p2180 N73-27604

**VANADIUM ALLOYS**
Ultrasonic measurements of elastic constants of polycrystalline alloys of iron in vanadium
[AD-753615] 10 p1174 N73-19547
Application of nuclear gamma resonance for changing structural state of crystal lattice of alloys to improve strength properties
13 p1541 N73-22486
Influence of surface conditions on Ti-6Al-4V alloy fatigue life
[AD-755385] 13 p1544 N73-22516
Age hardening and precipation behavior of V-Ti, V-Ti-Si, V-Zr, and V-Hf alloys with reference to interstitial metalloid
[KFK-1680] 15 p1799 N73-24582
Thermal and electrical properties of titanium alloyed with vanadium and high temperature creep of metal with fcc lattice
[JPRS-59623] 22 p2683 N73-31490
Thermal conductivity and electrical properties of titanium alloyed with vanadium at 100 to 350 K
22 p2683 N73-31491
Precipitation and age hardening phenomena in vanadium alloys with reference to metalloid additives
[EURFNR-1060] 24 p2935 N73-33439

**VANADIUM COMPOUNDS**
NT VANADATES
NT VANADIUM OXIDES
Superconductivity of multifilamentary wires consisting of vanadium silicates
[BNL-16891] 03 p0346 N73-12818
High temperature tests to determine thermodynamic properties of nonstoichiometric vanadium nitrides
[NLL-M-21551-[5828.4F]] 12 p1464 N73-21858
Investigation of electrical properties of vanadium nitrides as effected by nitrogen content
13 p1540 N73-22473
Literature on vanadium and nickel trace elements in distillate fuels for motor vehicles
[AD-760462] 17 p2076 N73-26793
Analysis of relationships of dissociation elasticity of vanadium mononitride to composition and temperature based on thermodynamic theory of non-stoichiometric compounds
[NLL-M-21638-[5828.4F]] 20 p2428 N73-29506
Single crystal elastic moduli of V3Si for measuring hydrostatic pressures
24 p2967 N73-33714

**VANADIUM ISOTOPES**
Effects of energetic charged particle irradiation of solar system material
[NASA-CR-132045] 15 p1831 N73-24845

**VANADIUM OXIDES**
Metal-dielectric phase transitions in Bi-Sb alloys and V2O3
[JPRS-57631] 04 p0433 N73-13525
Physical and electrical transport properties of VO2 near its semiconductor-to-metal transition
[AD-751524] 07 p0834 N73-16759
Mass spectrometer, chromatograph, and X ray analyses for determining volatilization mechanism for V2O5
[NLL-M-21570-[5828.4F]] 16 p1926 N73-25582
Experimental conditions for depositing crystalline and amorphous VO2 thin films by RF and dc sputtering
[CEA-CONF-2133] 17 p2073 N73-26774

**VANELESS DIFFUSERS**
Method for prediction of turbulent boundary layer flow in vaneless radial diffuser and experimental validation
10 p1206 N73-19809

**VANES**
NT GUIDE VANES
Rotary vane attenuator with two stators and intermediary rotor, using resistive and orthogonally disposed cards
[NASA-CASE-NPO-11418-1] 04 p0420 N73-13420
Analysis of coolant flow in transpiration-cooled vanes
[NASA-TN-D-7341] 16 p1974 N73-25966
Temperature characteristics of film cooled and non-film cooled vanes incorporating impingement cooling
[NASA-TM-X-2819] 18 p2205 N73-27798

**VANGUARD SATELLITES**
NT VANGUARD 3 SATELLITE

**VANGUARD 3 SATELLITE**
Eleventh order resonant terms in geopotential from orbit of Vanguard 3
[NASA-TM-X-66246] 15 p1778 N73-24415

**VAPOR DEPOSITION**
NT VACUUM DEPOSITION
Fabrication of integrated magnetic storage devices by vapor deposition of gold on copper substrate
01 p0031 N73-10239
Factors affecting orientation of chemical vapor deposited molybdenum coatings precipitated from gaseous phase
[AD-747082] 02 p0194 N73-11566
Effect of chemical vapor deposition on properties of carbon-felt carbon-matrix composites at high temperature
[SC-DC-71-4395] 03 p0320 N73-12609
Abrasive wear resistance of vapor plated chrome coatings
[AD-749769] 05 p0567 N73-14605
Development and characteristics of multiple thin film vapor deposition unit
[BARC-609] 08 p0927 N73-17594
Properties of thin dielectric TiO2 films produced by chemical vapor deposition
[NASA-CR-130763] 08 p0950 N73-17780
Pyrolysis of rhenium chlorides to yield chemically vapor deposited rhenium thermionic emitters
[NASA-CR-121143] 09 p1073 N73-18759
Low temperature chemical vapor deposition process and potential applications
10 p1164 N73-19475
Vapor deposition for epitaxial film growth of bubble domain materials
[AD-754958] 11 p1332 N73-20813
Vapor deposition techniques for preparation of nickel foil and various ceramic materials
[AD-758389] 14 p1679 N73-23625
Deposition process investigation of steady-state fluid beds to observe carbonization of pyrolytic materials
[AD-757118] 14 p1682 N73-23647
Method for vapor deposition of thin films
[NASA-CASE-MFS-20775-1] 14 p1697 N73-23770
Vapor epitaxial deposition of yttrium-iron garnet thin films on substrates using iron and yttrium chloride separated fluxes
15 p1821 N73-24762
Chemical vapor deposition process for preparing large diameter carbon-boron monofilaments
[NASA-CR-121229] 18 p2167 N73-27502
Growth of rutile single crystals by chemical vapor transport
[AD-760733] 18 p2191 N73-27687
Heat transfer and temperature oscillations in chemical vapor transport crystal growth
[AD-760732] 18 p2191 N73-27688
Chemical vapor deposition of stoichiometric niobium gallium superconducting film
[NASA-CR-2308] 20 p2455 N73-29726
Chemical vapor deposition of reproducible device quality ferrimagnetic films
[NASA-CR-132325] 24 p2891 N73-33083

**VAPOR GENERATORS**
U VAPORIZERS

**VAPOR LIQUID EQUILIBRIUM**
U LIQUID-VAPOR EQUILIBRIUM

**VAPOR PHASES**
Gas phase precipitation method for preparing pure zirconium and niobium carbides
[NLL-RTS-7315] 01 p0069 N73-10563
Tables of pressure, volume, density, and temperature for liquid states of oxygen, nitrogen, argon, and parahydrogen
[NBS-TN-361-REV] 04 p0386 N73-13139
Crystal growth from vapor phases and epitaxy, and applications to semiconductors and microelectronics - conference review
[AD-750654] 06 p0710 N73-15793
Pyrolysis of organic compounds in gas phase
08 p0881 N73-17131
Kinetics and mechanisms of gas phase combustion, flames, and flame suppression
08 p0882 N73-17143
Pigments for space-stable thermal control coatings to shield spacecraft from solar radiation
[NASA-CR-124067] 09 p0998 N73-18144
Gas phase recombination of hydrogen and deuterium atoms
[NASA-CR-131417] 11 p1252 N73-20162
Gas phase hydrogen permeation through alpha iron, 4130 steels, and 304 stainless steels from less than 100 C to near 600 C
[NASA-TN-D-7265] 12 p1412 N73-21442
Vapor phase epitaxy of gallium arsenide
[AD-755434] 12 p1441 N73-21678
Atomic oxygen hydrogen reaction with acetylene, and gas discharge shock tube design
13 p1488 N73-22060
Vapor composition and chemical reactions of carbon atoms and molecules from graphite and tantalum carbide heated by laser radiation
[SLA-73-57] 17 p1992 N73-26107
Mass spectrometric analyses on laser induced vaporization of iron and zirconium hydride
[LBL-1177] 17 p1992 N73-26108
Kinetics of gas pickling and epitaxial growth of semiconductor materials
18 p2188 N73-27664
Variation of electrophysical parameters of epitaxial films of germanium as result of gas etching
18 p2188 N73-27665
Vapor phase heteroepitaxial growth of silicon germanium alloys by hydrogen reduction of tetrachlorides
20 p2460 N73-29767
Absorbent columns as samplers for organic vapors in atmosphere
24 p2911 N73-33234

**VAPOR PRESSURE**
Equations showing relationship between temperature and vapor pressure of liquids emphasizing vapor pressure measurement and Chebyshev polynomials
[NPL-CHEM-19] 06 p0638 N73-15179
Measurement of vapor pressure of cryolitic baths
[NLL-TRANS-1034-[5022.04]]
20 p2374 N73-29073
Determination of vapor pressure, viscosity, and thermal conductivity of several liquid rocket propellants
24 p2972 N73-33750

**VAPOR TRAILS**
U CONTRAILS

**VAPORIZATION HEAT**
U HEAT OF VAPORIZATION

**VAPORIZERS**
NT EVAPORATORS
Safety devices for preventing surge tank explosions in liquid nitrogen system of hypersonic wind tunnels
[SC-DC-72-1260] 03 p0280 N73-12274

**VAPORIZING**
NT BOILING
NT EVAPORATION
NT FILM BOILING
NT FLASHING [VAPORIZING]
NT NUCLEATE BOILING
NT PROPELLANT EVAPORATION
NT SUBLIMATION
NT TRANSPIRATION
Oscillatory combustion and fuel vaporization tests to determine thermodynamic properties of droplets under various conditions
[NASA-CR-120974] 02 p0242 N73-11971
DESIGN OF HEAT EXCHANGERS FOR FLUID VAPORIZATION
[CEA-CONF-2010] 06 p0731 N73-15960
Heat and mass transfer analysis of liquids and air flowing in opposite directions under various atmospheric pressures
[AD-751503] 07 p0856 N73-16938
Theoretical investigation of rocket steam generator with emphasis on trajectories and spectrum of injected drops and their vaporization for Europa 1 launch vehicle
[DLR-FB-71-36] 09 p1011 N73-18253
Vaporization kinetics and thermodynamics of graphite using high pressure mass spectrometers
[AD-755853] 12 p1376 N73-21165
Electrode metal volatilization and oxidation in gas-shielded arc welding
[DRIC-TRANS-3005] 12 p1408 N73-21415
Rapid vaporization of liquid hydrogen in noninsulated reservoir placed in water
[CEA-CONF-2082] 12 p1429 N73-21582
Vaporization thermodynamics of Cr2O3 protective scales under transonic flow conditions
14 p1677 N73-23607
Electrode metal loss by volatilization in gas-shielded arc welding
[NLL-DRIC-TRANS-3005-[3623.66]]
15 p1790 N73-24511
Mass spectrometer, chromatograph, and X ray analyses for determining volatilization mechanism for V2O5
[NLL-M-21570-[5828.4F]] 16 p1926 N73-25582
Vaporization coefficient of graphite based on ion intensity measurements
[AD-759203] 17 p1993 N73-26113
Time prediction for laser melting and vaporization of metal sheet
[AD-760113] 17 p2042 N73-26521
Normal mode laser and Q switched laser for vaporization of graphite and carbides
[SLA-73-5233] 22 p2681 N73-31473
Laser vaporization of aluminum wire and heating to thermonuclear temperatures
23 p2800 N73-32392

**VAPORS**
NT MERCURY VAPOR
NT METAL VAPORS
NT SODIUM VAPOR
NT WATER VAPOR
Control system design criteria to prevent air pollution from volatile fuel storage tank emission
[AD-748009] 03 p0350 N73-12854
Growth rate of liquid droplets formed in supersaturated vapors
[AD-753074] 09 p1017 N73-18301
Development of high power alkali vapor lamp for laser applications
[AD-755213] 13 p1560 N73-22646
Condensible vapor supersonic nozzle flows at supersaturation collapse near condensation point
[AD-756471] 14 p1651 N73-23393
Effect of contact-surface-active vapors on wear behavior of soft steel during sliding friction
[NASA-TT-F-14935] 15 p1791 N73-24523

Gas dynamic equations for analyzing hot gas and vapor expansion in meteor trail
17 p2023 N73-26366
Effects of boundary surface active vapors on behavior of steel during sliding friction
[NASA-TT-F-14993] 19 p2304 N73-28531
Toxic vapor detector for Minuteman propellant leakage
[AD-763799] 21 p2551 N73-30451

**VARACTOR DIODES**
Materials and devices for generation, amplification, and millimeter wave energies
[NASA-CR-130113] 03 p0334 N73-12724
Gallium arsenide Schottky and varactor diodes for 20 and 30 GHz
07 p0762 N73-16192
Manufacturing of hyperabrupt Si varicaps based on impurity diffusion from double doped substrate
12 p1384 N73-21221

**VARACTORS**
U VARACTOR DIODES

**VARIABILITY**
Improvements in intelligibility testing reliability using experienced listeners
14 p1625 N73-23166

**VARIABLE AREA WINGS**
U TRAILING-EDGE FLAPS

**VARIABLE GEOMETRY STRUCTURES**
Wind tunnel determination of supersonic aerodynamic characteristics of variable geometry spacecraft designed for high hypersonic performance
[NASA-TM-X-2703] 07 p0735 N73-15985
Applications of transonic wind tunnel with variable geometry perforated walls
[DGT-8652] 13 p1507 N73-22212
Development of automatic flight control systems based on adaptive control techniques and variable structure control systems
[AD-763415] 21 p2498 N73-30047
Supersonic wind tunnel tests of internal performance of rectangular variable geometry air inlets noting effect of incidence
[ARC-CP-1242] 22 p2612 N73-30933
Supersonic wind tunnel tests of internal performance of rectangular variable geometry air inlets at zero incidence
[ARC-CP-1243-PT-1] 22 p2612 N73-30934
Variable turbine geometry effect on engine installation and thrust modulation
[AD-765533] 24 p2974 N73-33761

**VARIABLE LIFT**
U LIFT

**VARIABLE PITCH PROPELLERS**
Application of variable pitch fan propulsion system for quiet short takeoff aircraft
21 p2496 N73-30030
Analysis of failure modes of tail rotor on OH-58 helicopter for improved reliability and cost reduction
[AD-763188] 21 p2497 N73-30043

**VARIABLE STARS**
NT CEPHEID VARIABLES
NT NOVAE
NT SUPERNOVAE
NT T TAURI STARS
Long period giant variable stars of Mira Ceta type, emphasizing U, B, and V photometry
[AD-747564] 04 p0476 N73-13893
UBV observations of RR Lyrae variable HD 176387
[ROY-OBS-BULL-174] 13 p1578 N73-22787
Analysis and classification of spectrograms of some southern red variables
19 p2341 N73-28834
Structure and physics of solar and stellar atmosphere including physical processes in nonstationary stars
[NASA-TT-F-760] 20 p2470 N73-29840
Brightness changes in WZ Cas in photographic and visible light
20 p2471 N73-29844
Brightness changes of MZ Cas and TZ Cas in B- and V-light
20 p2471 N73-29845
Detection of new variable (BD plus 60 deg 2633) from photometric plates
20 p2471 N73-29846
Properties of optical radiation of variables and quasers
20 p2471 N73-29847
Electrophotometry, photoelectronic images, converters, and television equipment for studying variable stars
[NASA-TT-F-797] 21 p2594 N73-30783
Instrumented methods for finding variable stars on sky photographs
21 p2594 N73-30784
Argelander, Pickering, and Neyland-Blazhko methods for visually estimating variable star brightness
21 p2594 N73-30785
Determination of magnitude and brightness of variable stars by photographic photometry
21 p2594 N73-30786
Photoelectronic devices for amplifying brightness image of variable stars
21 p2594 N73-30788
Measurement of intensity and wavelength of polarized radiation from variable stars by polarizers
21 p2594 N73-30789
Multicolor photometric systems for studying physical properties and spectra of variable stars
21 p2594 N73-30790
Photometric standards for North Polar Sequence, Kapteyn Areas, and Harvard Standard Areas
21 p2594 N73-30791
Digital computer techniques for determining changes in brightness periods of variable stars
21 p2595 N73-30792
Fifty-two variable stars in Cepheus-Lacerta field of Milky Way processed on Castel Gandolfo plates
21 p2596 N73-30802
Study of known RR Lyrae type variable stars in Messier 3
[REPT-63] 23 p2846 N73-32746
Infrared photometry of variable stars
[AD-764686] 24 p2981 N73-33827

**VARIABLE SWEEP WINGS**
Low speed wind tunnel tests on slender variable sweep wing of lift, drag, and pitching moments
[ARC-CP-1227] 05 p0492 N73-14009
Wind tunnel tests to predict full scale aircraft buffet loads during buffet boundary penetration using scale flutter model of fighter aircraft with variable sweep wings
[NASA-TN-D-7066] 07 p0851 N73-16905
Wind tunnel tests to determine subsonic derivatives for oscillating M-wing planform
[ARC-R/M-3214] 16 p1854 N73-25022
Design of dual fuselage aircraft with pivoting wing and horizontal stabilizer to permit yawing of wing in flight for high speed operation
[NASA-CASE-ARC-10470-1] 17 p1980 N73-26005

**VARIABLE THRUST**
Variable turbine geometry effect on engine installation and thrust modulation
[AD-765533] 24 p2974 N73-33761

**VARIANCE (STATISTICS)**
NT ANALYSIS OF VARIANCE
NT MULTIVARIATE STATISTICAL ANALYSIS
Variance of Monte Carlo estimates reduced by correlated and antithetic sampling and illustrated by queueing simulation
[NA-70-21] 03 p0324 N73-12643
Antithetic sampling for variance reduction in stochastic system simulation
[NA-72-57] 03 p0325 N73-12647
Digital techniques for reducing variance in reflected rain signals
[METEOROL-STUDY-25] 16 p1875 N73-25181
Pulse radar measurement of mean monthly wind patterns
17 p2023 N73-26367
Pseudo-standardized variables and use as elements of shape operators, emphasizing scale and location invariant
[AD-764361] 22 p2692 N73-31561

**VARIATION METHOD**
U CALCULUS OF VARIATIONS

**VARIATIONAL PRINCIPLES**
Variational principle of self and non self adjoint linear differential equations
[PB-210374] 02 p0203 N73-11642
Application of variational principle to laminar flow and heat transfer between concentric cylinders
[REPT-5/1972] 03 p0285 N73-12307
Numerical integration and variational calculation method for approximate solution to three dimensional flow of gas dynamic bearings
[AD-747377] 03 p0308 N73-12513
Derivation of theorems for spinless particle scattering from Kohn variational principle
[NASA-CR-129259] 03 p0323 N73-12634
Variational principles of elastic theory
03 p0360 N73-12938
Variational principle for calculating buckling of thin clamped free circular cylindrical shells subjected to wind load
[TT-7113] 06 p0725 N73-15916
Variational equations for studying rotational motion of orbiting rigid body about its center of mass under conservative and nonconservative torques
07 p0817 N73-16624
Variable principle for analyzing torsion of fluted bar with rope like cross section
[AD-752059] 08 p0928 N73-17598
Variational principle for finite deformations of quasi-shallow shells
[AD-756187] 13 p1589 N73-22886
Application of variational methods in fluid mechanics
[AD-757266] 14 p1652 N73-23399
Variational principle for studying elastic-plastic instability of ring stiffened cylindrical shells under external pressure
[AD-757750] 16 p1970 N73-25935
Variational principle of plasticity
[REPT-450] 17 p2044 N73-26535
Variational principles for examining adiabatic motions in gaseous sphere and waves in stratified horizontal fluids
21 p2523 N73-30237
Discrete method for variational problems in treatment of metals by pressure
[NLL-M-21663-[5828.4F]] 21 p2557 N73-30497

**VARIATIONS**
NT ANNUAL VARIATIONS
NT DIURNAL VARIATIONS
NT GEOMAGNETIC MICROPULSATIONS
NT GEOMAGNETIC PULSATIONS
NT MAGNETIC VARIATIONS
NT PERIODIC VARIATIONS
NT TWENTY-SEVEN DAY VARIATION
NT WIND VARIATIONS
Use of psychometric tests to account for subjective variations in operations performance relative to target acquisition
10 p1227 N73-19974
Procedures for determining variations of meteorological parameters from satellite radiation measurements
20 p2443 N73-29625

**VARIOMETERS**
Variometer recordings at Narssarssuaq Geophysical Observatory 1968 - 1970
02 p0167 N73-11356
Development and improvement of magnetovariation station for conducting magnetotelluric soundings
[JPRS-57678] 04 p0401 N73-13262
Magnetic variation station for recording geomagnetic variations on ocean bottom
21 p2547 N73-30419

**VASCULAR SYSTEM**
NT ARTERIES
NT GLOMERULUS
Arterial hypertension symptoms in flying personnel
13 p1480 N73-21991
Basic causal mechanisms responsible for loss of vascular tone during alterations in shifts to zero gravity
[NASA-CR-128897] 14 p1612 N73-23069
Use of therapeutic exercise for treatment of functional vascular disorders and occlusive lesions of arteries and veins
[NASA-TT-F-15043] 20 p2368 N73-29045
State of blood filling and bioelectric activity of grain in circulatory hypoxia in healthy persons and individuals with early forms of autonomic vascular dysfunction
24 p2883 N73-33027

**VASOCONSTRICTOR DRUGS**
NT SEROTONIN

**VASOMOTOR NERVOUS SYSTEM**
U NERVOUS SYSTEM

**VECTOR ANALYSIS**
NT VORTICITY
Vector calculus for determination of wind velocity components
04 p0442 N73-13603
Numerical comparator for indicating error in measurement transformations
[PUBL-1361] 06 p0690 N73-15615
Time vector technique for determining stability and control derivatives by simultaneous analysis of two maneuvers which differ by dependent control input
[NASA-TM-X-2722] 07 p0739 N73-16010
Principle and vector Liapunov functions for studying stability in large scale dynamic systems
07 p0760 N73-16176
Numerical analysis of projected gradient method and operator formed from any linearly independent subset of gradients
[DLR-FB-73-26] 11 p1311 N73-20636
Minimum distance classification based on multispectral scanner data using density estimators and Kullback-Leibler numbers as distance measures
[NASA-CR-133796] 21 p2566 N73-30569

**VECTOR CALCULUS**
U VECTOR SPACES

**VECTOR CONTROL**
U DIRECTIONAL CONTROL

**VECTOR CURRENTS**
Improved Venus spin vector and probe position estimates
08 p0973 N73-17953

**VECTOR DOMINANCE MODEL**
Generalized vector meson dominance model derived from extended quark model with electron proton inelastic scattering
[TUEP-72-43] 07 p0823 N73-16669
Survey of theoretical models used to discuss final hadronic states produced in inelastic electron-hadron scattering
[ILL-[TH]-73-2] 12 p1430 N73-21593

**VECTOR MESONS**
Dual resonance model for predicting density matrix elements of vector mesons produced in inclusive reactions
[ILL-[TH]-72-11] 05 p0582 N73-14735

**VECTOR SPACES**
NT ADJOINTS
NT BANACH SPACE
NT CANONICAL FORMS

NT EIGENVALUES
NT EIGENVECTORS
NT HILBERT SPACE
NT JORDAN FORM
NT MATRICES [MATHEMATICS]
NT STOKES THEOREM [VECTOR CALCULUS]
NT VECTORS [MATHEMATICS]
NT VORTICITY
Application of vector space processes for algebraic analysis of affine plane surfaces
02 p0196 N73-11583
Semilinear, topological, spaces and applications to social and economic equilibrium analysis and optimization
[NASA-CR-129591] 04 p0441 N73-13591
Linear vector space theory used to develop general representation of random vectors and data sets
[NASA-TR-R-398] 09 p1057 N73-18620

VECTORCARDIOGRAPHY
Changes in vectorcardiograms of atherosclerotic flying personnel after glucose testing
13 p1480 N73-21989

VECTORS [MATHEMATICS]
NT EIGENVECTORS
NT VORTICITY
Principle of virtual work and displacement
10 p1188 N73-19664
Extension of theorems concerning spectrum of one-dimensional and multidimensional differential operators on vector functions
[NASA-TT-F-14960] 17 p2055 N73-26620

VEGETABLES
Impact of accurate long range weather forecasts on Wisconsin pea production
06 p0693 N73-15640
Production of vegetables in arid zones using controlled solar greenhouses
24 p2975 N73-33768
Solar still greenhouse for using desalinated water to produce vegetables in arid regions
24 p2975 N73-33769

VEGETATION
Landform-vegetation relationships in southern Arizona based on interpretation of ERTS-1 imagery
[E72-10176] 01 p0044 N73-10355
Inventory and monitoring of natural vegetation-landform relationships in arid regions of southern Arizona using ERTS-1 imagery
[E72-10184] 01 p0045 N73-10363
Definition of characteristics and boundaries of vegetation-soil types in Southern Idaho from ERTS-1 remotely sensed imagery
[E72-10203] 02 p0161 N73-11300
Relationships of vegetation distribution to geomorphic characteristics of landscape and of plant phenological patterns to vegetation identification of satellite imagery of Arizona
[E72-10228] 02 p0163 N73-11321
Identification of Nevada wildland plants, vegetation, and fire scars from ERTS-1 imagery
[E72-10253] 03 p0289 N73-12353
Vegetation, soil, and water reflectance measurements from ERTS-1 imagery of Hidalgo County, Texas
[E72-10267] 03 p0291 N73-12366
Detection of vegetation damage associated with highways and highway facilities with reference to stress caused by chemicals and alteration to ground water table
[E72-10288] 04 p0410 N73-13338
Effect of above-ground plant mass on spectral curves of brightness coefficients of soil-vegetation system
04 p0443 N73-13613
Identification of phenological stages and vegetative types for land use classification based on ERTS-1 imagery
[E72-10342] 05 p0532 N73-14330
Identification, definition, and mapping of terrestrial ecosystems in interior Alaska
[E72-10343] 05 p0532 N73-14331
Utilization of ERTS-1 imagery to map soils and vegetation in Idaho
[E72-10356] 05 p0534 N73-14344
Inventory and monitoring of natural vegetation and related resources in arid environment of Arizona using ERTS-1 imagery
[E72-10360] 05 p0534 N73-14348
Identification of mine dumps with and without vegetative cover using ERTS-1 imagery
[E72-10361] 05 p0535 N73-14349
ERTS-1 measurement of vegetation, soil, and water reflectance
[E72-10364] 05 p0535 N73-14352
ERTS-1 detection and monitoring of vegetation damage associated with highways and highway facilities in Maine
[E72-10371] 05 p0536 N73-14359
Identification and mapping of coastal vegetation species in ERTS-1 imagery of Delaware
[E73-10007] 06 p0658 N73-15343
Wildland resources inventory of Nevada Great Basin using ERTS-1 imagery
[E73-10019] 06 p0659 N73-15355
Application of multispectral data processing to Delaware coastal wetlands vegetation mapping
[E73-10069] 07 p0779 N73-16331
Application of color infrared film to measure spatial and temporal changes in vegetation
07 p0788 N73-16406
Application of ERTS-1 imagery to thematic mapping of open water, ice and snow cover, vegetation, and works of man
[E73-10089] 08 p0902 N73-17301
ERTS-1 identification of phenological stages and vegetation types in Alaska for land use classification
[E73-10276] 08 p0914 N73-17484
Mapping of soil-vegetation groupings in Arizona using ERTS-1 imagery
[E73-10290] 09 p1020 N73-18327
Effectiveness of ERTS-1 imagery in monitoring vegetation conditions of direct concern to range land management and agriculture business decisions in Great Plains Corridor
[E73-10302] 09 p1021 N73-18334
ERTS-1 imagery of vernal advancement and retrogradation of natural rangeland vegetation of Great Plains Corridor
[E73-10303] 09 p1021 N73-18335
Vegetation map of western Seward Peninsula, Alaska, based on ERTS-1 imagery
[E73-10305] 09 p1022 N73-18337
Identification, analysis, and mapping of terrestrial ecosystems and vegetation types in Alaska based on ERTS-1 imagery
[E73-10306] 09 p1022 N73-18338
Detection and monitoring vegetation damage associated with highway facilities in Maine
[E73-10331] 09 p1024 N73-18361
Differentiation between mine dumps in South Africa having varying degrees of vegetative cover based on ERTS-1 imagery
[E73-10326] 10 p1147 N73-19334
Identification of marsh vegetation and coastal land use in Delaware from ERTS-1 imagery
[E73-10367] 10 p1150 N73-19363
Development of procedure and system for uniform mapping and monitoring of earth resources and environmental complexes using ERTS-1 imagery
[E73-10350] 11 p1275 N73-20344
Analysis of ERTS-1 photographic imagery for identification, definition, and mapping, of terrestrial ecosystems in interior Alaska
[E73-10399] 11 p1277 N73-20361
ERTS-1 spectral reflectance measurements of vegetation, soil, and water in Rio Grande Valley, New Mexico
[E73-10408] 11 p1278 N73-20370
Comparative evaluation of ERTS-1 imagery for inventorying and monitoring vegetation-terrain relationships in arid environments of Arizona
[E73-10413] 11 p1279 N73-20375
Determination of ecosystem-vegetation boundaries from ERTS-1 imagery of Tennessee
[E73-10417] 11 p1279 N73-20379
Vegetation analysis and preparation of tectonic map overlay of Bighorn Mountains region based on ERTS-1 data
[E73-10420] 11 p1279 N73-20382
Identification of phenological stages and vegetative types from ERTS-1 imagery for land use classification in Alaska
[E73-10439] 11 p1281 N73-20399
Application of ERTS-1 multisensor data in Great Plains to map ranglands, croplands, and soil formations
[E73-10443] 11 p1282 N73-20403
Evaluation of hydrology and vegetation in Sahelian zone of Mali, Mauritania, and Senegal during dry season/drought period based on ERTS-1 imagery
[E73-10488] 12 p1396 N73-21324
Identification of vegetation and soils in Idaho using ERTS-1 remotely sensed imagery
[E73-10512] 13 p1516 N73-22287
Detection and monitoring of vegetation damage associated with highway facilities in Maine
[E73-10522] 13 p1517 N73-22290
Interdisciplinary analysis of Skylab EREP MSS photography of vegetative and geomorphological cover types in Colorado Mountains
[E73-10533] 13 p1517 N73-22297
Use of remote sensor techniques for wildlands vegetation management
[NASA-CR-131580] 13 p1522 N73-22336
Space and supporting aircraft photography for interpretation and analysis of non-forest vegetation
[NASA-CR-131585] 13 p1522 N73-22338
Application of spaceborne photography and aerial photography to ecological resource inventory and analysis of naturally vegetated areas in Arizona
[NASA-CR-131581] 13 p1523 N73-22342
Reflected energy of vegetative ground cover measured with multispectral band scanners and infrared photographs
[NASA-CR-131575] 13 p1524 N73-22348
Earth resources remote sensing project using multispectral band scanners to detect and measure thermal radiation from ground vegetation
[NASA-CR-124219] 13 p1529 N73-22393
Identification of marshland vegetation and coastal land use in Delaware from ERTS-1 imagery
[E73-10516] 14 p1653 N73-23410
Snow cover survey and vegetation growth in Swiss Alps using ERTS-1 imagery
[E73-10586] 14 p1657 N73-23446
Correlation between vegetation patterns and geologic and geomorphic units in New Mexico based on ERTS-1 imagery
[E73-10588] 14 p1657 N73-23448
Inventory and monitoring natural vegetation and related resources in arid environments using ERTS-1 imagery
[E73-10519] 15 p1771 N73-24344
Wildland resource and vegetation monitoring in Nevada and Great Basin using ERTS-1 imagery
[E73-10606] 15 p1773 N73-24367
Detection of vegetation stress and damage associated with highways and highway facilities in Maine
[E73-10611] 15 p1773 N73-24372
ERTS-1 identification of duckweeds in Lake Pontchartrain, Louisiana
[E73-10613] 15 p1774 N73-24374
Identification of phenological stages and vegetative types in Alaska for land use classification
[E73-10618] 15 p1774 N73-24379
Monitoring vernal advancement and retrogradation of natural rangeland vegetation in Great Plains Corridor
[E73-10643] 16 p1897 N73-25340
Identification and mapping of soils, vegetation, and water resources in Texas from ERTS-1 MSS digital data
[E73-10670] 16 p1899 N73-25365
ERTS-1 detection of prescribed burn in Sam Houston National Forest and subsequent effects on vegetation
[E73-10674] 16 p1900 N73-25369
Survey of snow cover and vegetation growth in high mountains of Swiss Alps based on ERTS-1 imagery
[E73-10733] 17 p2020 N73-26339
Spaceborne photography of vegetation, soils, and agricultural land use
[NASA-TT-F-14967] 17 p2026 N73-26393
Mapping of wildland vegetation in Great Basin area of Nevada using ERTS-1 imagery
[E73-10813] 18 p2139 N73-27288
ERTS-1 imagery of land use, agriculture, vegetation, geology, landforms, and hydrology in Central Coastal Zone of California
[PAPER-L4] 19 p2273 N73-28300
Land cover and land use mapping of Central Atlantic Region shoreline zone using ERTS-1 imagery
[PAPER-L8] 19 p2274 N73-28304
ERTS-1 detection and monitoring of tectonic and vegetational patterns, urban development, and agricultural processes in Southern California
[PAPER-R4] 19 p2283 N73-28362
ERTS-1 imagery of desertification, hydrology, vegetation, forage, and water resources in Republic of Mali
[PAPER-R5] 19 p2283 N73-28363
Seasonal variations of vegetation, circulation patterns in Lake Pontchartrain, and urban neighborhood quality in Louisiana from ERTS-1 imagery
[E73-10838] 19 p2290 N73-28416
ERTS-1 multispectral photography of wetlands vegetation and plant species
[E73-10850] 19 p2292 N73-28428
Detection and monitoring vegetation damage associated with highway facilities in Maine
[E73-10856] 19 p2292 N73-28433
Skylab multispectral data for selected cover types in Colorado Mountains
[E73-10878] 20 p2393 N73-29229
Mapping rice crops of California and Louisiana and natural vegetation of Colorado Plateau from Skylab photography
[E73-10885] 20 p2394 N73-29236
Field sampling taxonomic units within geomorphic-soil-vegetation mapping units in Arizona
[E73-10889] 20 p2394 N73-29238
Monitoring vegetation conditions of direct concern to rangeland and agriculture management in Great Plains Corridor
[E73-10891] 20 p2394 N73-29240
Tectonic and photogeologic mapping of forested and sparsely vegetated terrain of Montana and Idaho
[E73-10900] 20 p2396 N73-29249
ERTS-1 identification of phenological stages and vegetative types for land use classification in Alaska
[E73-10905] 20 p2396 N73-29254
Skylab MSS imagery of selected cover types in Colorado Mountains
[E73-10914] 20 p2397 N73-29263
Photomapping of rice crops and natural vegetation in Louisiana and California from Skylab EREP imagery
[E73-10916] 20 p2397 N73-29265
Identification, definition, and mapping vegetation and terrestrial ecosystems in interior Alaska using ERTS-1 imagery
[E73-10921] 20 p2398 N73-29270

Short wave radiation regime compared to atmospheric radiation regime for vegetation
20 p2404 N73-29318
Biometric and radiant transfer characteristics of forest vegetation
20 p2405 N73-29328
Radiation regime of forest vegetation under plant cover and open areas under various weather conditions
20 p2405 N73-29329
Use of soil-vegetation system brightness coefficients to measure vegetation quantity and crop yield
20 p2406 N73-29334
Interpretation of seasonal changes in vegetation and soils in Idaho from ERTS-1 imagery
[E73-10936] 21 p2529 N73-30278
SL-2 MSS photography of soils, water, and vegetation in Texas
[E73-10943] 21 p2530 N73-30285
Soil moisture and vegetation surveys of Kansas and Texas for Skylab investigations
[E73-10944] 21 p2530 N73-30286
ERTS-1 measurements of seasonal changes in reflectance of soils, vegetation, and water in Hidalgo County, Texas
[E73-10946] 21 p2530 N73-30288
Uniform mapping of rice crops in Louisiana and California and desert vegetation in southwestern Colorado from Skylab imagery
[E73-10979] 22 p2657 N73-31286
Investigation of New England reservoirs, land use, streams, flooding, and vegetation from Skylab imagery
[E73-10993] 22 p2659 N73-31299
Skylab imagery of terrain surface moisture, vegetation, and forestation in Colorado and Oregon
[E73-11001] 22 p2659 N73-31306
Inventory and monitoring natural vegetation and plants in arid land of Arizona from satellite-borne photography
[E73-11021] 22 p2661 N73-31325
Stochastic and deterministic approaches to vegetation canopy reflectance models
[AD-763222] 22 p2668 N73-31381
Interdisciplinary analysis of Colorado Rocky Mountain environments using ADP techniques
[E73-11039] 23 p2778 N73-32218
Identification of phenological stages and vegetative types for land use classification in Alaska
[E73-11066] 23 p2781 N73-32242
ERTS-1 sensor analysis of air pollution and air pollution related injuries to plant vegetation in metropolitan Minnesota
23 p2784 N73-32269
Models for sensitivity of apparent temperature and backscattering coefficient to variations of soil moisture as function of vegetation
[NASA-CR-135593] 23 p2784 N73-32275
Identification of selected forest and vegetation cover in Colorado Mountains from Skylab EREP data
[E73-11132] 24 p2917 N73-33287
Application of Skylab EREP data to structural geology, geomorphology, vegetation mapping, and land use studies in Wyoming
[E73-11136] 24 p2917 N73-33291
Mapping coastal vegetation and wetlands use for Delaware from ERTS-1 imagery
[E73-11146] 24 p2918 N73-33300
Uniform mapping of vegetation and rice in Colorado Plateau, Sierra-Lahontan, California, and Louisiana coastal plain from Skylab multispectral photography
[E73-11149] 24 p2919 N73-33303

**VEGETATION GROWTH**
NT CROP GROWTH
Tree ring chronology for constructing paleoclimatology of North America and Europe
[AD-757486] 14 p1686 N73-23682
Identification of mine dumps in South Africa by growth and decline of vegetation
[E73-10642] 16 p1896 N73-25339
Application of ERTS-1 remote sensing data in study of vegetation and soils in Idaho
[E73-10708] 16 p1904 N73-25399
Application of ERTS-1 data for monitoring vernal advancement and retrogradation of natural vegetation in Great Plains Corridor
[E73-10693] 17 p2018 N73-26315
Analysis of ERTS-1 data for predicting ephemeral and perennial range quantity and quality during normal grazing season in Arizona and California
[E73-10712] 17 p2018 N73-26319
Photointerpretation of ERTS-1 imagery and airborne photography to determine vegetation growth in Iowa
[E73-10715] 17 p2018 N73-26322
Application of ERTS-1 imagery for inventory and monitoring of natural vegetation and related resources in arid environment
[E73-10728] 17 p2020 N73-26334
Utilization of ERTS-1 imagery for crop identification and acreage measurement in South Dakota, Kansas, Missouri, and Idaho
[E73-10734] 17 p2020 N73-26340
Analysis of ERTS-1 imagery for multi-disciplinary resource inventory of soils, vegetation, and geology in Big Summit Prairie area of oregon
[E73-10770] 18 p2134 N73-27246
Application of ERTS-1 imagery to determine dynamics of distribution and density of phreatophytes and other arid land plant communities
[E73-10790] 18 p2137 N73-27266
Application of ERTS-1 imagery for identification of ecological analogs of natural vegetation and food crops in California, Colorado, and Louisiana
[PAPER-A6] 19 p2260 N73-28214
Application of ERTS-1 imagery for vegetation identification in southern Arizona
[PAPER-A7] 19 p2260 N73-28215
Application of ERTS-1 imagery for vegetative and geologic mapping of western Seward Peninsula, Alaska
[PAPER-A8] 19 p2260 N73-28216
Application of ERTS-1 imagery for mapping and identification of vegetation and landforms in Great Basin
[PAPER-A9] 19 p2260 N73-28217
Application of ERTS-1 imagery and aerial photography for monitoring forage crop resources in California
[PAPER-A11] 19 p2260 N73-28219
Application of ERTS-1 imagery for inventory of wildland resources in northern California
[PAPER-A12] 19 p2261 N73-28220
Identification of fire hazards in San Pablo test site area in California using ERTS-1 data and aerial photography
[PAPER-A18] 19 p2261 N73-28225
Analysis of ERTS-1 data for application to forest and range mapping in Houston, Texas area
[PAPER-A20] 19 p2262 N73-28227
Evaluation of ERTS-1 data for production of land use stratifications and crop inventory process in San Joaquin County, California
[PAPER-A24] 19 p2262 N73-28231
ERTS-1 imagery analysis to determine varying degrees of vegetation on mine dumps in South Africa
[PAPER-4E] 19 p2268 N73-28268
Analysis of coastal vegetation species in Delaware Bay, Delaware based on ERTS-1 imagery and high altitude photography
[PAPER-E8] 19 p2269 N73-28272
Analysis of ERTS-1 imagery of southern Arizona plant communities using electronic satellite image analysis console
[PAPER-W7] 19 p2271 N73-28285
Computer analysis of ERTS-1 MSS data for identification and mapping of soils, vegetation, and water resources in Lynn County, Texas
19 p2287 N73-28392
Survey and Mapping of vegetative cover in Susquehanna River Basin to determine accuracy of photographic technology and ERTS-1 imagery
[E73-11111] 24 p2915 N73-33268

**VEHICLE WHEELS**
NT NOSE WHEELS
Aircraft tire dynamometer tests to determine effects of tire deflection on rolling resistance and tire life
[AD-746304] 02 p0127 N73-11031
Effects of pavement surface condition on cornering forces developed by automobile tires of different tread design
[NASA-TN-D-6964] 02 p0192 N73-11551
Tests of lunar roving vehicle wheels in simulated lunar soil to determine effects of wheel speed, wheel load, presence of fender, travel direction, and soil strength
[NASA-CR-129612] 04 p0401 N73-13263
Equations of motion for elastic tire rolling on ground and forces exerted by tire assuming absence of slippage between tire and ground
[AD-752697] 09 p1040 N73-18482

**VEHICLES**
Remote chemical detectors for vehicle identification by exhaust gases
[AD-751740] 07 p0753 N73-16116

**VEHICULAR TRACKS**
Mathematical model for tracked air cushion vehicle and guideway to determine vertical dynamic response of vehicle and guideway system to high speed vehicle passage
07 p0737 N73-15995
Development of simulation program for determining characteristics of tracked air cushion research vehicle
[PB-218368/9] 18 p2106 N73-27033
Computer program to evaluate dynamic characteristics of tracked air cushion vehicle
[PB-219984/2] 22 p2617 N73-30970
Loading criteria for tracked air cushion vehicle guiderails and methods for calculating dynamic responses of double-span, beam-type guide rails
[PB-221688/5] 22 p2617 N73-30971

**VELA SATELLITES**
Vela 4 observation of solar wind electron average thermal characteristics
01 p0094 N73-10776
Computer program for rapid reduction of Vela satellite data on solar X rays
[AD-743921] 01 p0100 N73-10822
Low energy electron measurements by VELA satellite plasma probes and spacecraft potential
[LA-DC-72-1481] 19 p2324 N73-28695

**VELOCITY**
NT ACOUSTIC VELOCITY
NT AIRSPEED
NT ANGULAR VELOCITY
NT CRITICAL VELOCITY
NT EXHAUST VELOCITY
NT FLOW VELOCITY
NT GROUND SPEED
NT HIGH SPEED
NT HYPERSONIC SPEED
NT LIGHT SPEED
NT LOW SPEED
NT PHASE VELOCITY
NT PROPAGATION VELOCITY
NT RADIAL VELOCITY
NT RELATIVISTIC VELOCITY
NT ROTOR SPEED
NT SUBSONIC SPEED
NT SUPERSONIC SPEEDS
NT TERMINAL VELOCITY
NT TIP SPEED
NT TRANSONIC SPEED
NT WIND VELOCITY
Velocity irregularities in near field of high aspect ratio turbulent jets
[AD-754224] 10 p1143 N73-19315
Velocity integration in navigational digital computers
20 p2440 N73-29596

**VELOCITY DISTRIBUTION**
Generalized method of contraction cone design and low speed velocity distribution
[NASA-TN-D-6962] 01 p0036 N73-10283
Mean velocity, turbulence intensity, and turbulent shear stress in turbulent boundary layer
[WTHD-41] 02 p0155 N73-11255
Perturbation approximation method for determining velocity potential and aerodynamic forces of slender body of elliptical cross section in airstream
[AD-748353] 04 p0407 N73-13317
Mathematical model for energy losses and velocity distribution in laminar boundary layers, using quadrature formulas
07 p0770 N73-16257
Isotropic models for determining effect of velocity distribution on electron temperature in ionospheric plasma
[NASA-TM-X-66157] 07 p0791 N73-16433
Mapping velocity field in hypersonic wake by use of iron probe array
[AD-751450] 08 p0897 N73-17264
Jet deflection characteristics of jet-flapped airfoil with Coanda deflection surfaces based on velocity distribution and flow angle measurements for static operation
[AD-753618] 09 p0989 N73-18074
Holographic techniques for particle sizing and velocity distribution
[NASA-TR-R-404] 09 p1035 N73-18448
ONERA results of work to determine response of solid propellant to pressure and velocity fluctuations
[ONERA-TP-1165] 09 p1098 N73-18963
Procedures for measuring velocity distribution through helicopter rotor blade tip vortex using single full scale rotor blade
12 p1360 N73-21034
Galactic neutral hydrogen gas velocity distribution within spiral arms in local regions
12 p1447 N73-21720
Exponential laws for temperature, velocity, and CO-concentration profiles in nitrogen hot gas jet or nitrogen-propane flame in free atmosphere, in application to supersonic combustion
[DLR-FB-73-05] 12 p1465 N73-21867
Flow coupled diffusion and velocity profiles for steady laminar flow in circular duct
13 p1509 N73-22231
Cooled film anemometry applied to determination of temperature and velocity distributions in wake of projectiles travelling at hypersonic speeds in free flight range
[DREV-R-648/72] 14 p1648 N73-23365
Integral calculation of three-dimensional turbulent boundary layer velocity profiles
14 p1648 N73-23370
Calculation of supersonic boundary layer flow separation and reattachment along plane wall with sinusoidal hollow
[REPT-72-4] 14 p1650 N73-23382
Development of numerical procedures for determining velocity potential on triangular wing oscillating harmonically in supersonic flow
[ARC-R/M-3229] 16 p1854 N73-25023
Actuator disk approximation for calculating lifting rotor velocity distribution in forward flight
[FFA-123] 16 p1858 N73-25051
Technique for measuring hypersonic flow velocity profiles
[NASA-TN-D-7270] 17 p2032 N73-26443
Experiments on velocity distribution and critical velocity of rotating hydrogen plasma
[TRITA-EPP-73-06] 17 p2068 N73-26736

Spectral and statistical characteristics of surface wave velocity fields
20 p2446 N73-29654
Mathematical models for studying beta effect on meridional velocity of disturbed flow in ocean
20 p2447 N73-29655
Application of theoretical model to velocity fields observed over water waves
[AD-764196] 22 p2668 N73-31377
Pilot model expansion tunnel test flow properties obtained from velocity, pressure, and probe measurements
[NASA-TN-D-7310] 24 p2905 N73-33182
Effect of heat transfer on velocity distribution and skin friction in turbulent wall boundary layers
24 p2906 N73-33195
Computation of kinetic fluctuation energy of turbulent shear flow from mean velocity distribution
24 p2908 N73-33211

**VELOCITY FIELDS**
U VELOCITY DISTRIBUTION

**VELOCITY MEASUREMENT**
NT WIND VELOCITY MEASUREMENT
Measuring absolute surface current velocity
[AD-743706] 01 p0050 N73-10408
Apparatus for measuring velocity and acceleration of military vehicles
[PHL-1972-5] 01 p0055 N73-10446
Instrument for measuring magnitude and direction of flow velocity in flow field
[NASA-CASE-LAR-10855-1] 04 p0419 N73-13415
Doppler shift measurement of local velocities in flowing medium
[NRC-TT-1592] 06 p0654 N73-15312
European study of optical and signal processing problems in laser anemometry
[ET/TN/A/20] 06 p0679 N73-15526
Power spectrum computation for phototube current of laser Doppler velocimeter
[NASA-TM-X-68184] 07 p0824 N73-16675
Flight test of instrument for determining low airspeeds to evaluate suitability for helicopter airspeed indicator
[AD-753343] 09 p0989 N73-18071
Optical measurement of RDX and PETN monocrystal detonation velocity along different crystallographic axes
[ISL-28/71-PT-1] 09 p1052 N73-18575
Calculation of wind tunnel wall interference velocities affecting pitching moments of high lift wings
[NASA-CR-2191] 10 p1137 N73-19269
Laser Doppler anemometer for measuring steam and water velocities in two phase flow
[UTIAS-TN-184-PT-1] 10 p1141 N73-19293
Laser-Doppler velocity measurement of large particles in two-phase gas-solid nozzle flow
[VKI-TN-81] 10 p1142 N73-19305
Measurement of low airspeeds with ion beam produced in positive corona discharge based on beam deflection properties
10 p1158 N73-19423
Thermocouple measurement of gas velocity and temperature near liquid rocket injector face
[NASA-CR-121100] 11 p1270 N73-20304
Procedures for measuring velocity distribution through helicopter rotor blade tip vortex using single full scale rotor blade
12 p1360 N73-21034
Laser Doppler velocimeter for simultaneously measuring orthogonal fluid velocity components without flow field perturbation
[NASA-CASE-ARC-10637-1] 12 p1405 N73-21390
Design and performance of two color laser Doppler velocimeter for wind tunnels
[NASA-TM-X-62254] 12 p1405 N73-21393
Measurement of fluid velocity and surface deformation during fluid discharge from rotating cylindrical tank
13 p1509 N73-22232
Application of laser Doppler velocimeter for measurement of central vortex filament in wind tunnel test section
[NASA-TM-X-62243] 13 p1536 N73-22448
Light source and geometrical requirements for optimization of optical anemometry signals
[ET/TN/A/18] 13 p1537 N73-22451
Basic principles of variable speed drives including torque, speed ratio, and power
[NASA-TM-X-68244] 15 p1791 N73-24522
Velocity magnitude and direction, static pressure, and skin friction of circular turbulent jet impinging normally on flat surface
[ARC-R/M-3205] 16 p1856 N73-25034
Frequency modulated radar systems for range finding, velocity measurement, and altimeters
16 p1873 N73-25162
Design and operation of sonic velometer using transit times of ultrasonic pulses in air to measure air velocity
17 p2031 N73-26434
Theoretical model of Sparton Model 601 M horizontal velocity gage
[AD-762268] 19 p2302 N73-28508
Measurement capabilities of one dimensional laser Doppler velocimeter system
[NASA-TM-X-64774] 21 p2548 N73-30427
Sign determination of laser Doppler anemometer velocity components of two Doppler difference signal components
[REPT-1/1972] 22 p2674 N73-31422
Laser anemometer self aligning reference beam method for measurement of three flow velocity components, with reference beam produced by scattering
[REPT-3/1972] 22 p2674 N73-31423
Wing tip vortex measurements with laser Doppler velocimeter
[NASA-CR-124444] 24 p2869 N73-32924

**VELOCITY MODULATION**
Statistical analysis of underwater sound speed fluctuation in upper ocean region
[AD-756570] 13 p1560 N73-22641

**VELOCITY POTENTIALS**
U FLOW DISTRIBUTION
U VELOCITY DISTRIBUTION

**VELOCITY PROBES**
U PITOT TUBES
U SPEED INDICATORS

**VELOCITY PROFILES**
U VELOCITY DISTRIBUTION

**VENERA SATELLITES**
NT VENERA 8 SATELLITE
Effects of turbulence in Venus atmosphere on Pioneer Venus radio
[JPL-TM-33-644] 20 p2473 N73-29866
Measurements of illumination in atmosphere and on surface of planet Venus obtained by automatic interplanetary station Venera-8
[JPRS-59963] 21 p2595 N73-30794

**VENERA 8 SATELLITE**
Results of Venera 8 unmanned spacecraft probe
[NASA-TT-F-14915] 14 p1709 N73-23870

**VENEZUELA**
Investigation of natural resources in remote and unexplored areas of Venezuela using ERTS-1 remotely sensed imagery
[E72-10311] 04 p0412 N73-13360
Development of techniques for evaluation of ERTS-1 imagery of natural resources in remote and unexplored areas of Venezuela
[E73-10481] 12 p1396 N73-21318

**VENTILATION**
Fume component tests to determine welders safe breathing level through ventilation
[ITR-1] 09 p1038 N73-18467
Design of anesthetic flow valve canister system for exhaust gas absorption and laminar ventilation system for operating rooms
12 p1373 N73-21141
Shock tube experiments for investigating rotating closure of ventilation system slap valve
[REPT-3/72] 13 p1476 N73-21955
Determination of ventilation characteristics of blunt-based surface piercing struts in calm water and in waves
[AD-759046] 16 p1892 N73-25314

**VENTING**
Purge and vent characteristics of GAC-9 insulation system
[NASA-CR-124052] 09 p1050 N73-18565

**VENTRAL SECTIONS**
Deployable flexible ventral fins providing triangular planform of flexible material for spin recovery of aircraft
[NASA-CASE-LAR-10753-1] 01 p0004 N73-10031

**VENTS**
Barometric gravity tube discharger for liquid cooling of rocket exhaust gas and analysis of improvement with air vent
[DLR-MITT-73-10] 17 p2011 N73-26262

**VENTURI TUBES**
Fluid mass flow rate measurements using cavitating Venturi tubes noting application to liquid rocket propellant
[DLR-FB-72-33] 21 p2525 N73-30245

**VENUS (PLANET)**
High resolution interferometric observations of Venus
[AD-747992] 04 p0476 N73-13895
Analysis of problems in mapping Venus surface with radar from orbiting spacecraft
[NASA-CR-129821] 04 p0477 N73-13900
Venusian information and methods for studying Venus
[NASA-TT-F-14519] 05 p0595 N73-14837
Analysis of selected features of Mercury, Venus, and Mars and seismic propagation on Moon
07 p0840 N73-16807
Survey of available information on Venus
[JPRS-58068] 08 p0962 N73-17867
Improved Venus spin vector and probe position estimates
08 p0973 N73-17953
Observation of venus far ultraviolet spectrum by sounding rockets
13 p1572 N73-22741
Design of chemical pumps for Venus Pioneer mass spectrometer used to determine atmospheric composition of Venus
[NASA-CR-114604] 16 p1918 N73-25519
Venus wind/altitude Doppler radar probe
[NASA-CR-114556] 16 p1962 N73-25871
Analysis of atmospheric entry trajectories for manned and unmanned missions to planet Venus
[NASA-TN-D-7316] 16 p1966 N73-25900
Planning for Venus radar mapping orbiter mission and spacecraft to determine technology requirements and cost effectiveness of alternative approaches-Vol. 1
[NASA-CR-114640] 22 p2715 N73-31735
Configuration comparisons and systems evaluation for overall radar mapping mission of planet Venus - Vol. 2
[NASA-CR-114641] 22 p2715 N73-31736
Parametric studies and subsystem comparisons for orbital radar mapping mission to planet Venus - Vol. 3
[NASA-CR-114642] 22 p2715 N73-31737

**VENUS ATMOSPHERE**
NT VENUS CLOUDS
Spaceborne and ground-based data and atmospheric model of Venus microwave emission
[AD-743982] 01 p0100 N73-10820
Study of 4-day retrograde rotation of external cloud layer of Venus
[NASA-TT-F-14710] 02 p0230 N73-11864
Estimating quantity of helium in Venus atmosphere from measured ionization profile
[NASA-TM-X-66128] 04 p0475 N73-13883
Venusian information and methods for studying Venus
[NASA-TT-F-14519] 05 p0595 N73-14837
Model of Venus atmospheric composition, temperature, and circulation based on Mariner 5 and Venera 4, 5, 6, and 7 data
[NASA-TM-X-66140] 06 p0719 N73-15865
Radio frequency measurement of brightness temperature and radar cross sections for explaining subsurface and atmospheric properties of Venus
07 p0840 N73-16803
Engineering models of Venus atmosphere, based on theory and measured data
[NASA-SP-8011-REV] 07 p0842 N73-16824
Space vehicle descent into Mars, Jupiter, and Venus atmospheres
[NASA-TT-F-768] 07 p0844 N73-16838
Survey of available information on Venus
[JPRS-58068] 08 p0962 N73-17867
Electron density profiles from Mariner 5 and solar wind maintenance of nighttime Venus ionosphere
08 p0973 N73-17951
Ion clusters and atmospheric composition of Venus ultraviolet haze layer
08 p0973 N73-17952
Escape mechanism of Venus atmosphere
[NASA-CR-132025] 14 p1706 N73-23842
Results of Venera 8 unmanned spacecraft probe
[NASA-TT-F-14915] 14 p1709 N73-23870
Design of counter tube window and X ray fluorescence analyzer for quantitative analysis of Venusian dust and condensates
[NASA-CR-114619] 15 p1786 N73-24484
Brightness temperature of Venus and absolute flux scale at 608 MHz
[AD-756084] 15 p1832 N73-24853
Nonlinear temperature and vorticity equations for studying convective motions of 4-day zonal circulation of upper Venus atmosphere
17 p2080 N73-26828
Effects of turbulence in Venus atmosphere on Pioneer Venus radio
[JPL-TM-33-644] 20 p2473 N73-29866
Galilean satellites, Venus clouds, and astronomical observatories
[NASA-CR-133826] 21 p2591 N73-30761
Sulfuric acid in Venus clouds by photolytic decomposition of hydrogen bromide
[LPL-COMMUN-171] 21 p2592 N73-30767
Measurements of illumination in atmosphere and on surface of planet Venus obtained by automatic interplanetary station Venera-8
[JPRS-59963] 21 p2595 N73-30794
Plasma and magnetic field measurements in vicinity of Venus from Venera 4 and Mariner 5 flights
[NASA-TT-F-15128] 22 p2716 N73-31743

**VENUS CLOUDS**
Instrumentation for determining composition of Venus clouds
[NASA-CR-132766] 16 p1963 N73-25876

**VENUS PROBES**
NT VENERA SATELLITES
NT VENERA 8 SATELLITE
Characteristics of star field attitude sensor for installation in Pioneer Venus spacecraft
[NASA-CR-114516] 03 p0359 N73-12924
Survey of available information on Venus
[JPRS-58068] 08 p0962 N73-17867
Feasibility of mechanical pumps for use with Pioneer-Venus probe mass spectrometer inlet system
[NASA-CR-114581] 14 p1670 N73-23551

Valve testing for application in inlet system of Pioneer Venus Probe mass spectrometer
[NASA-CR-114627] 16 p1918 N73-25517
Venus wind/altitude Doppler radar probe
[NASA-CR-114556] 16 p1962 N73-25871
Assessment of joint NASA/ESRO Venus orbiter
[SYST/2109/MS/1V] 17 p2089 N73-26906
Effects of turbulence in Venus atmosphere on Pioneer Venus radio
[JPL-TM-33-644] 20 p2473 N73-29866
Analysis of radar mapping mission to Venus
[NASA-TM-X-2868] 22 p2714 N73-31728
Planning for Venus radar mapping orbiter mission and spacecraft to determine technology requirements and cost effectiveness of alternative approaches-Vol. 1
[NASA-CR-114640] 22 p2715 N73-31735
Configuration comparisons and systems evaluation for overall radar mapping mission of planet Venus - Vol. 2
[NASA-CR-114641] 22 p2715 N73-31736
Parametric studies and subsystem comparisons for orbital radar mapping mission to planet Venus - Vol. 3
[NASA-CR-114642] 22 p2715 N73-31737

**VENUS RADAR ECHOES**
Planning for Venus radar mapping orbiter mission and spacecraft to determine technology requirements and cost effectiveness of alternative approaches-Vol. 1
[NASA-CR-114640] 22 p2715 N73-31735
Configuration comparisons and systems evaluation for overall radar mapping mission of planet Venus - Vol. 2
[NASA-CR-114641] 22 p2715 N73-31736
Parametric studies and subsystem comparisons for orbital radar mapping mission to planet Venus - Vol. 3
[NASA-CR-114642] 22 p2715 N73-31737

**VERBAL COMMUNICATION**
Visible pitch display for extracting frequency by filtering, converting sine waves to pulse train, and showing pulse interval as function of time
14 p1626 N73-23177
Enhancement of speech intelligibility through appropriate spectral weighting and effect of passing through optimum filter on signal to noise ratios
14 p1630 N73-23211
Development and characteristics of audio response unit for use with telephone exchange to answer tax inquiries from subscribers
14 p1632 N73-23229
Development of equipment and system for real-time analysis of speech transients
14 p1632 N73-23232
Analysis of clipped speed characteristics and zero crossing-related speech phenomena
14 p1632 N73-23233
Development of speech analysis-synthesis system for extracting singing voice signal from background noise on recording device
14 p1632 N73-23234

**VERIFICATION [PROVING]**
U PROVING

**VERMONT**
NT LAKE CHAMPLAIN BASIN [NY-VT]
ERTS-1 imagery of Lake Champlain and Vermont environments
[E72-10225] 03 p0288 N73-12333
ERTS-1 return beam vidicon imagery of Lake Champlain region and Vermont
[E72-10252] 03 p0289 N73-12352
Water pollution detection and monitoring in Lake Champlain and Vermont using ERTS-1 imagery
[E72-10268] 03 p0291 N73-12367
Land use mapping, limnology, wetlands, geomorphic and landform surveys, and river monitoring of Lake Champlain Basin and Vermont using ERTS-1 imagery
[E72-10282] 03 p0292 N73-12380
Analysis of ERTS-1 imagery for land use and lake turbidity mapping of Lake Champlain Basin and Vermont
[E73-10432] 11 p1281 N73-20393
ERTS-1 imagery of land use, lake ice, and water pollution, Lake Champlain Basin and Vermont
[E73-10690] 16 p1902 N73-25383

**VERONIQUE ROCKET VEHICLES**
Radio frequency impedance probe measurement of ionspheric electron density profiles using Veronique rocket for sounding
06 p0667 N73-15423

**VERTEBRAL COLUMN**
Statistical analysis of occurrence of backache among Royal Air Force flight crews and ground crews to show effects of crew seats on physical comfort
[AD-745177] 01 p0013 N73-10102
Nonfatal ejection vertebral fracture comparison between US, British, and Swedish armed services
14 p1611 N73-23059

**VERTEBRATES**
NT BATS
NT BIRDS
NT CALVES
NT CARIBOUS
NT CATS
NT CHIMPANZEES
NT DOGS
NT DOLPHINS
NT FISHES
NT FROGS
NT GUINEA PIGS
NT HAMSTERS
NT HUMAN BEINGS
NT MAMMALS
NT MICE
NT MONKEYS
NT PRIMATES
NT RABBITS
NT RATS
NT SWINE
NT WHALES

**VERTICAL AIR CURRENTS**
Middle latitude anticyclone vertical atmospheric circulation heat sources and sinks, and torques
[REPT-7/1972] 04 p0444 N73-13625
Vertical air gust velocities and turbulence spectral structure around and within cumulonimbus clouds
[AD-748518] 04 p0445 N73-13632
Kinematic method in vertical motion and atmospheric energy computations
12 p1394 N73-21298
Numerical model to simulate vertical mass transfer and stratification in layer of buoyant convection
20 p2391 N73-29208
Atmospheric ozone transport by atmospheric circulation and vertical air currents
20 p2443 N73-29627
Swirling, annular, gas liquid flow down vertical tube
24 p2902 N73-33160

**VERTICAL DISTRIBUTION**
NT STAR DISTRIBUTION
Vertical distribution of transparency measured by submerged transparency meters
[NLL-RTS-7535] 02 p0160 N73-11295
Comparison of statistical and iteration methods for obtaining vertical temperature profiles from multispectral radiation measurements
02 p0196 N73-11589
Measurement of vertical distribution of atmospheric water vapor by ruby laser rod
[PB-211891] 05 p0575 N73-14680
Vertical distribution of atmospheric water vapor and ozone over District of Columbia during 1969 and 1970
[AD-751535] 07 p0795 N73-16465
Vertical wind shear measurements at Helsinki Airport - Apr. 1967 through Mar. 1968
[TR-3] 08 p0937 N73-17676
Relative importance of processes determining vertical distribution of nitrogen oxides in stratosphere
[AERONOMICA-ACTA-A-110] 09 p1027 N73-18383
Vertical radiation heat flux profiles and spectral distribution
09 p1059 N73-18632
Effects of aerological fine-strength characteristics of vertical distribution of aerosols
[AD-762335] 19 p2299 N73-28485
Characteristics of vertical distribution of atmospheric moisture using satellite measurements
[AD-763286] 21 p2540 N73-30364
Radiosonde sounding data for determining vertical atmospheric temperature and humidity profiles
[AD-764949] 23 p2815 N73-32508

**VERTICAL FINS**
U FINS

**VERTICAL FLIGHT**
Parameters for enhancing performance of helicopter rotors during stationary flight
12 p1360 N73-21036

**VERTICAL LANDING**
Landing loads of Do-31 aircraft in vertical landing, noting undercarriage reactions and sinking speed
[BMVG-FBWT-72-24] 09 p0986 N73-18046

**VERTICAL MOTION**
Numerical analysis of vertical and lateral motion of road vehicle trains with arbitrary number of components
[TT-7211] 08 p0892 N73-17220
Analysis of conditions existing in rising, rotating column of hot gases containing core of reacting gases
[TR-5] 10 p1223 N73-19948
Deceleration and vertical motion of gas puff released into upper atmosphere
[AD-757867] 15 p1782 N73-24450
Methods for obtaining vertical motion signs at various atmospheric levels to explain areas of rain and no rain
[NASA-CR-2304] 22 p2694 N73-31577

**VERTICAL PERCEPTION**
Vestibular function loss in man after unilateral section of eighth cranial nerve
[NASA-CR-129672] 04 p0379 N73-13084
Effects of human alertness on vestibular nystagmus habituation
[AD-749352] 05 p0505 N73-14108
Upper eye lid position effects in electro-oculograhic vertical eye movement recordings
06 p0633 N73-15143
Asymmetry of fish otolithic receptor functions and vestibular disturbances during space flight
14 p1608 N73-23031

**VERTICAL STABILIZERS**
U STABILIZERS [FLUID DYNAMICS]

**VERTICAL TAILS**
U STABILIZERS [FLUID DYNAMICS]
U TAIL ASSEMBLIES

**VERTICAL TAKEOFF**
Development of mathematical model for optimal takeoff performance of single rotor helicopter in ground effect with various payloads
[AD-750388] 06 p0624 N73-15066
Ground erosion on grassland and concrete by vertical takeoff of Do-31 aircraft
[BMVG-FBWT-72-26] 10 p1107 N73-19023

**VERTICAL TAKEOFF AIRCRAFT**
NT FLYING PLATFORMS
NT X-14 AIRCRAFT
NT X-22 AIRCRAFT
NT XC-142 AIRCRAFT
Performance characteristics of model VTOL lift-fan simulator installed in two dimensional wing
[NASA-TM-X-68788] 01 p0036 N73-10282
Wind tunnel design for testing V/STOL aircraft in transition flight
[AD-749154] 04 p0402 N73-13278
Research on air transport with VTOL and STOL aircraft
[PUBL-1352] 06 p0613 N73-14977
Wind tunnel tests of VTOL lift fan stages to determine changes in thrust characteristics with varations in back pressure imposed on stages by cross flow
[NASA-TM-X-68169] 06 p0620 N73-15031
Dynamics and control analysis of turbofan lift engines
[NASA-TM-X-68175] 06 p0713 N73-15815
Analysis of propulsion system specifications and components for research VTOL transports
[NASA-TM-X-68168] 06 p0713 N73-15816
Hybrid computer simulation used for analysis of integral lift-fan engine being considered for VTOL applications
[NASA-TM-X-2691] 06 p0713 N73-15817
Numerical analysis of characteristics of rotary wing aircraft when considered as two coupled rigid bodies representing rotor and fuselage
07 p0737 N73-15994
Effect of control force gradient on VTOL visual hovering task
[NASA-TM-X-62230] 08 p0866 N73-17015
Numerical analysis of aerodynamic characteristics of unsteady, two-dimensional, jet-flapped wing
[AD-752928] 09 p0986 N73-18051
Effect of two dimensional suction flows into double intakes on upper surface of Joukowski airfoil for application to vertical takeoff and landing aircraft
[AD-754208] 10 p1104 N73-19003
Mission analysis of VTOL passenger transport aircraft to determine optimum engine cycle for minimum direct operating cost
[NASA-TM-X-68186] 10 p1208 N73-19826
Structural concepts of rotary wing system capabilities to show changes in design of specific vertical takeoff aircraft components
12 p1358 N73-21021
Development and application of composite materials for vertical takeoff aircraft airframes and effect on improved aircraft performance
12 p1359 N73-21023
Aerodynamic characteristics of circulation controlled rotor and fundamental problems of stopped rotor aircraft
12 p1359 N73-21024
Development of jet-flap rotor and application to heavy helicopter and stoppable rotor designs
12 p1359 N73-21025
Development of rotary wings with cold, hot, and mixed cycle tip jet propulsion systems and application for torque-free rotor drive system
12 p1359 N73-21026
Design and development of vertical takeoff aircraft configuration for use with air transportation services between major population centers
13 p1471 N73-21916
Flight tests to determine longitudinal aerodynamic parameters of P-1127 aircraft with vectored thrust control
[NASA-TN-D-7296] 15 p1734 N73-24066
Synthesis of hover autopilots for rotary wing VTOL aircraft
[NASA-CR-132053] 15 p1735 N73-24071
Development of perturbation guidance system for maintaining tilting rotor vertical takeoff aircraft on predetermined flight path during takeoff and landing
[NASA-CR-132043] 15 p1735 N73-24072
Systems design of facilities for studying flight problems of VTOL aircraft
[NAL-TR-306] 15 p1760 N73-24263
Development of inertial smoothing system for control and display applications for VTOL aircraft automatic instrument approach and landing operations
[NASA-TN-D-7271] 15 p1808 N73-24653
Preliminary design analysis of quiet integral fan lift engines for VTOL transport applications in next decade
[NASA-CR-120969] 17 p2076 N73-26796

Design, development, and flight test of stowed folding tilt rotor aircraft and comparison with nonfolding tilt rotor aircraft - Vol. 5
[NASA-CR-114598] 21 p2493 N73-30009
Application of composite materials in development of tilting rotor for vertical takeoff aircraft - Vol. 6
[NASA-CR-114599] 21 p2493 N73-30010
Development of feedback control in tilt rotor aircraft using swashplate cyclic and collective controls in addition to direct lift control - Vol. 7
[NASA-CR-114600] 21 p2493 N73-30011
Real time piloted simulation to investigate handling qualities and performance of tilting rotor aircraft - Vol. 9
[NASA-CR-114602] 21 p2493 N73-30012
Analysis of discrete frequency and broad band noise generation by subsonic rotary wings for vertical takeoff aircraft
[NASA-CR-2077] 21 p2494 N73-30014
Steady state analysis of energy transfer control and compressor concepts of remote lift fan control
[NASA-TM-X-2876] 21 p2590 N73-30753
NRC 10 ft x 20 ft V/STOL propulsion tunnel for V/STOL engine model testing
22 p2731 N73-31857
Computerized simulation of interactions of VTOL aircraft taking off from or landing on deck of ship moving in irregular or random seaway
[AD-764865] 23 p2746 N73-31980
Electronic display devices in aircraft control, noting pilot activation and VTOL control
[DLR-MITT-72-04] 24 p2880 N73-32998
Extrapolation predictive displays for manual path and position control of VTOL aircraft
24 p2880 N73-33000

**VERTICAL TAKEOFF AND LANDING**
U VERTICAL LANDING
U VERTICAL TAKEOFF

**VERTICES**
U APEXES

**VERY HIGH FREQUENCIES**
ATS 5 and Intelsat 1 observations of L band and VHF signals during ionospheric scintillation
[NASA-TM-X-66060] 01 p0028 N73-10216
Scintillating [VHF] signals fading measurements at Lima, Peru during spring equinox of 1970
[NASA-TM-X-66092] 02 p0166 N73-11347
Measuring electromagnetic parameters of soil samples in VHF/UHF range to determine properties that limit target detection
[AD-747346] 03 p0299 N73-12439
Development and evaluation of instrument landing system with VHF and UHF capability for localizer and glide slope
[AD-747656] 03 p0329 N73-12688
Design of portable HF/VHF radio set for manpack usage
[AD-749510] 05 p0514 N73-14175
One way and two way VHF ranging system performance for tracking and data relay applications
[NASA-TM-X-66134] 05 p0596 N73-14843
VHF omnidirectional antenna developed as printed current panel from flat plate dipole with low aspect ratio
[TR-72-34] 07 p0756 N73-16142
Multimode transponders for tracking and data relay satellites
[NASA-CR-130170] 08 p0888 N73-17191
Long life broadband transistor amplifier chain for very high frequency range
[AD-752444] 09 p1004 N73-18194
Lossy earth effects on very high frequency antenna patterns near ground level
[AD-754637] 11 p1257 N73-20204
Design of low gain L-band orthogonal-mode crossed slot antenna and VHF crossed loop antenna for airborne applications
[NASA-CR-130795] 11 p1261 N73-20237
Simultaneous ultrahigh and very high frequency ionospheric effects from ATS 5 at the magnetic equator
[NASA-TM-X-65948] 12 p1378 N73-21173
Development and testing of HF/VHF radio set for manpack usage
[AD-755547] 13 p1494 N73-22113
Developmental model of VHF transceiver multicoupler
[AD-755548] 13 p1502 N73-22177
VHF broadband directional log periodic antenna study, including pattern and impedance data
[AD-755199] 14 p1643 N73-23323
Analysis of radio communication links for air traffic control operations to show effects of adjacent channel interference and modulation limitations
[FAA-RD-70-71] 18 p2117 N73-27114
Preflight analysis on Skylab very high frequency ranging for rendezvous portion
[NASA-CR-133981] 19 p2235 N73-28020
Preflight assessment of Skylab VHF ranging coverage for rendezvous portion of SL-1/SL-3 mission
[NASA-CR-133996] 22 p2631 N73-31085

**VERY HIGH FREQUENCY RADIO EQUIPMENT**
Airborne survey of very high frequency interference levels over residential areas on American west coast
[SD-72-SA-0100-VOL-1] 06 p0640 N73-15197

**VERY LOW FREQUENCIES**
Relation of Hall current electrojet instability to VLF hiss in auroral zone of magnetic storms
[NASA-CR-130078] 01 p0047 N73-10378
Very low frequency radio signal transmission during three polar substorms in 1969
[KGO-PREPRINT-72-303] 01 p0050 N73-10404
Management, storage, and computation of FR-1 satellite very low frequency data
[GRI/NTP/101] 02 p0146 N73-11187
Inversion of VLF-LF sounder data to obtain D region electron density distributions
02 p0201 N73-11626
Radiation parameters of VLF transmitting station NPM, Lualualei, Hawaii with antenna operating in dual or parallel east and west array configuration
[AD-748177] 04 p0390 N73-13172
Observations and analysis of VLF radio emissions in auroral zone
[AD-748880] 04 p0416 N73-13393
Onboard digital correlator for spacecraft VLF radio wave studies
04 p0423 N73-13446
Parametric instabilities of VLF waves in radiation belts
[LA-DC-72-746] 07 p0756 N73-16139
Computerized simulation of global communication system
[AD-753115] 09 p1003 N73-18186
VLF phase velocity measurements with separated time phase synchronized receivers
[AD-753206] 09 p1003 N73-18188
Polarized ellipticity of VLF signals in radio fields
[AD-753085] 09 p1003 N73-18190
Management, processing, and handling of French FR-1 satellite very low frequency data
[GRI/NTP/100] 09 p1005 N73-18207
Very low frequency propagation effect on minimum shift keying communication system signal transmission
[AD-755122] 11 p1258 N73-20213
ELF and VLF experiment on OGO-D, revealing ion whistlers and ELF hiss features
12 p1377 N73-21170
VLF magnetotelluric measurements in Sweden
[KGO-72-10] 12 p1402 N73-21369
OGO-4 observation of banded whistlers using broadband VLF instrumentation
[NASA-CR-131495] 13 p1490 N73-22079
Computer techniques for fitting electron density profiles to oblique path VLF propagation data
[AD-757341] 13 p1492 N73-22098
Design and performance of low frequency/very low frequency omnidirectional antenna model
[AD-757556] 14 p1643 N73-23324
Spontaneous intensification of magnetospheric very low frequency ducts due to coupling between magnetosphere and ionosphere
[AD-756461] 14 p1662 N73-23488
Calculation of intensities of VLF hiss generated from electrons in lower magnetosphere
[NASA-TM-X-66255] 15 p1780 N73-24428
Feasibility of radio communications at very low frequencies from satellite-borne transmitter to receivers with subsurface antennas
[AD-759258] 16 p1876 N73-25188
Development of airborne very low frequency navigation system using radio communications stations and comparison with other air navigation systems
17 p2098 N73-26973
Analysis of very low frequency radio signals for aircraft area navigation to show capability for continental flight redundancy and reliability
[AD-761498] 19 p2318 N73-28651
Computerized simulation of cyclotron resonant electrons interaction with narrow band whistler wave along magnetospheric duct for VLF emission triggering
19 p2340 N73-28827
Diffusive equilibrium model for calculating characteristics of broadband ELF, VLF, and LF emissions in magnetosphere
[NASA-CR-133925] 22 p2666 N73-31363

**VESSELS**
Hydrocompression treatment to lower residual stresses in weld joints of forge-welded carbon steel vessels
10 p1163 N73-19461

**VESTA ASTEROID**
Analysis of asteroids selected for space mission objectives to show significant parameters
[NASA-CR-129248] 03 p0355 N73-12890

**VESTIBULAR TESTS**
Dynamic model of rotating spacecraft force effects on human vestibular system
01 p0015 N73-10119
Neurophysiology and dynamic response of vestibular system to angular and linear acceleration
[DR-215] 02 p0130 N73-11057
Dynamic response of vestibular nuclei neurons of decerebrated cats subjected to sinusoidal rotation
[AMRU-R-70-2] 02 p0130 N73-11059
Asymmetric response of cat semicircular canal neurons to symmetric sinusoidal rotation
[AMRU-R-69-2] 02 p0130 N73-11060
Hypoxia effects on human vestibular tolerance during exposure to coriolis accelerations
03 p0258 N73-12092
Functional changes in systemic and cerebral hemodynamics with respect to vestibular stresses accompanying low accelerations
11 p1245 N73-20108
Changes in human visual functions after exposure to weak vestibular irritations
11 p1246 N73-20113
Mathematical simulation study of neuron response to vestibular analyzer exposed to periodically varying acceleration
[NASA-TT-F-15130] 22 p2623 N73-31015
Survey of literature and morphological studies of vestibular nerve
[NASA-CR-135746] 24 p2885 N73-33042

**VESTIBULES**
Mathematical models for studying vestibuli adaptation to stimuli in humans
[AMRU-R-70-1] 02 p0131 N73-11062
Vestibulo-ocular response of man to oscillatory rotation during sleep
[AMRU-R-70-3] 02 p0131 N73-11066
Response characteristics of vestibulo-ocular reflex arc
[AMRU-R-71-2] 02 p0132 N73-11067
Effects of human alertness on vestibular nystagmus habituation
[AD-749352] 05 p0505 N73-14108
End organs, central nervous system connections, and static and dynamic characteristics of vestibular system
06 p0629 N73-15103
Radiation effects on human visual and vestibular analyzer functions
[AD-750499] 06 p0632 N73-15132
Bibliography on role of vestibular apparatus in compressed air work underwater
[AD-750686] 06 p0632 N73-15133
Physiological factors of human vestibular adaptation to flight and space environments
06 p0633 N73-15146
Weightlessness effects on development of vestibular apparatus and ocular nystagmus in rat, using chronic 2g centrifuge
[NASA-CR-114569] 08 p0878 N73-17112
Sound, light, and proprioceptive stimuli for inhibiting vestibular illusion in man
10 p1115 N73-19087
Vestibular analyzer functions in dogs after prolonged ionizing irradiation
10 p1115 N73-19088
Stress reactions of vestibular apparatus to ionizing radiation, coriolis forces, and gravitational stimuli
[AD-753511] 11 p1248 N73-20132
Asymmetry of fish otolithic receptor functions and vestibular disturbances during space flight
14 p1608 N73-23031
Antiradiation drug effects on vestibular analyzer functions
14 p1608 N73-23033
Handbook on structural evolution of vestibular apparatus
14 p1609 N73-23044
Physical/mathematical analyses on human vestibular responses to acceleration stresses
20 p2367 N73-29033
Human hemodynamic responses and vestibular tolerances to body sway tests
20 p2367 N73-29034
Laboratory investigation of Coriolis acceleration effects on vestibular apparatus of cosmonauts
[NASA-TT-F-15129] 22 p2626 N73-30993

**VFR [RULES]**
U VISUAL FLIGHT RULES

**VHF OMNIRANGE NAVIGATION**
System performance with single and double sideband doppler low level receiver maintenance simulation
[FAA-RD-72-67] 07 p0818 N73-16627
Airborne and laboratory tests of square wave very high frequency omnirange navigation system
[FAA-NA-72-60] 09 p1063 N73-18666
Development of systematic methodology and computer programs for optimal design of national grid of high altitude VHF omnirange navigation systems - Part 2
[FAA-RD-72-118-2-PT-2] 10 p1185 N73-19644
Evaluation of VORTAC navigation system accuracies required to support present and anticipated operational uses of system
13 p1557 N73-22616
Integrated SAVVAN, VOR, and DME system for locating and controlling high altitude aircraft
14 p1688 N73-23695
Computer program for selection of radio frequencies used in VOR, ILS, and Tacan/DME air navigation systems
[FAA-NA-73-4] 16 p1940 N73-25700

Flight tests of VHF Omnirange navigation and Tacan systems to determine bearing error curves
[FAA-RD-72-73] 20 p2452 N73-29710
Radio frequency interference tests of VHF omnirange, instrument landing systems, and glideslope indicators to determine required geographical separation for ground stations
[REPT-523-0764695-00111M-VOL-2] 20 p2453 N73-29712
Flight test and evaluation of system for providing precise time signals to aircraft in flight using distance measuring [VORTAC] ground station and cesium beam atomic clock
[FAA-NA-73-23] 21 p2577 N73-30652
Radio frequency interference tests of VHF omnirange system, localizer, and glideslope receiving equipment to determine geographical separation requirements - Vol. 2 Book 2
[FAA-RD-73-1-VOL-2-BK-2] 23 p2816 N73-32513

**VIBRATION**
NT BENDING VIBRATION
NT FLUTTER
NT FORCED VIBRATION
NT FREE VIBRATION
NT LATTICE VIBRATIONS
NT PANEL FLUTTER
NT POGO EFFECTS
NT RANDOM VIBRATION
NT RESONANT VIBRATION
NT STRUCTURAL VIBRATION
NT SUBSONIC FLUTTER
NT SUPERSONIC FLUTTER
NT TORSIONAL VIBRATION
NT TRANSONIC FLUTTER

Excitation and deexcitation of vibration in gases by oxygen and nitrogen atoms in E region of earth atmosphere
[AD-745925] 01 p0054 N73-10437
Analytical model for parallel flow-induced vibrations experimentally checked on single rod test facility in water loop
[EUR-4771] 03 p0284 N73-12301
Calculation of harmonic vibrations of elastic rectangular plates supported at two edges and reinforced vertically with eccentric ribs
[AD-748906] 04 p0483 N73-13944
Relativity shift effect of gravitational vibration frequency in earth field
[ITF-72-43-P] 07 p0793 N73-16451
Bi-normal coordinates in discrete systems with application to aircraft shimmy problem
[AD-752548] 08 p0868 N73-17030
Affect of sound and vibration on convective heat transfer and flow distribution on boundary layers of cylindrical bodies
[AD-754006] 10 p1143 N73-19316
Acoustic properties and sound pressure of jet flow
[AD-754422] 10 p1144 N73-19321
Analysis of vibratory characteristics of sonar transducer element using finite element three dimensional mathematical model
[AD-755177] 13 p1495 N73-22117
Holographic and acoustical tests of vibrating underwater structures
[AD-755475] 13 p1538 N73-22463
Extensional vibrations of simply supported composite plate strips
[AD-756868] 13 p1587 N73-22867
Model testing of gases, powders, and carbon particles in vibration combustion studies
[AD-755712] 13 p1591 N73-22902
Determination of vibrational temperature of molecular nitrogen in high atmosphere by chemical release of hydrogen iodide from sounding rocket
[AD-757909] 15 p1782 N73-24448
Rate constants for vibrational relaxation using Monte Carlo calculations
[AD-758753] 16 p1871 N73-25152
Effect of friction in compont on frequency of natural vibrations
[AD-761558] 19 p2306 N73-28550
Numerical analysis of variable pitch compressor rotor blades for reduction of rotor vibrations
[AD-762228] 19 p2330 N73-28746
Nonlinear vibrations and failure of shallow shells of random shape under stress of white noise
[AD-761449] 19 p2349 N73-28898
Finite difference method and equations of motion for studying nonlinear vibrations of one and two degree of freedom spring mass systems
22 p2724 N73-31796
Onboard frequency analyzer for measurement and analysis of acoustic and vibration data
[NASA-CR-132305] 23 p2793 N73-32343
Interionic vibrations and glass transitions in ionic oxide metaphosphate glasses
[AD-765344] 23 p2811 N73-32478
Condensation method and computer program for reducing truncation errors for vibration analysis of complex structures
[NASA-CR-124446] 23 p2812 N73-32484

**VIBRATION DAMPERS**
U VIBRATION ISOLATORS

**VIBRATION DAMPING**
Damping of flat square plates vibrating in air and vacuum
[AD-746054] 01 p0115 N73-10949
Numerical analysis of radiation damping of thin finite rectangular plates immersed in heavy and light fluid media
[AD-746460] 01 p0115 N73-10950
Development of formula for calculating natural frequencies of cantilever plate in fluid medium
[AD-747206] 02 p0241 N73-11958
Polymer optimization with molecular relaxation processes for preparing vibration damping plastic materials
[RAE-LIB-TRANS-1646] 04 p0386 N73-13135
Application of autopilot techniques to control and stabilize vibration modes of two space shuttle configurations at liftoff flight condition
[NASA-CR-112202] 06 p0721 N73-15884
Analysis of complex moduli of uniaxially fiber reinforced materials containing viscoelastic matrix and elastic fibers
[AD-753699] 09 p1054 N73-18591
Performance of shipping container for electron tube in shock and vibration tests
[AD-754926] 11 p1301 N73-20558
Variational method for approximate solutions to elastic stability problem with dissipative forces
[AD-754532] 11 p1346 N73-20918
Effectiveness of trailing edge bevels on reducing vibration excitation causing vortex shedding into wake
[REPT-1052/73] 13 p1471 N73-21911
Vibration damping ability of steel compressor blades subjected to different heat treatments
[AD-743119] 13 p1543 N73-22502
Low frequency structural response and damping characteristics of XB-70 aircraft during subsonic and supersonic flight
[NASA-TN-D-7227] 15 p1837 N73-24892
Root mean square center of gravity accelerations and undercarriage forces for taxiing KC-135 tanker aircraft
[CRANFIELD-AERO-15] 16 p1859 N73-25060
Effect of air resistance on vibration damping in metal plates
[AD-761591] 19 p2350 N73-28906

**VIBRATION EFFECTS**
NT POGO EFFECTS

Application of ride-quality criteria to design of commercial helicopters with emphasis on noise and vibration considerations
01 p0003 N73-10015
Analysis of airline passenger reactions to vibration environments encountered in supersonic transport and commercial jet aircraft
01 p0003 N73-10017
Evaluation of effectiveness of indices relating to effect of vehicle vibrations on passenger comfort with application to railroad travel
01 p0003 N73-10018
Analysis of helicopter pilot and passenger reaction to vibration environment to determine effects of discrete frequencies and combinations of harmonic frequencies
01 p0003 N73-10019
Analysis of vibration environment in aerospace and surface vehicles with definitions of effect on human comfort and performance
01 p0003 N73-10021
Analysis of research activities conducted to determine criteria for passenger comfort in various methods of transportation
01 p0004 N73-10024
Flight test program to determine effects of low frequency vibration on passenger comfort in short haul aircraft
01 p0004 N73-10025
Simulator facility used to determine vibration effects on pilot tracking performance using rigid control stick
[AD-745193] 01 p0021 N73-10164
Procedure for balancing high speed, light weight rotary machinery resting on gas lubricated bearings
[AD-750951] 06 p0623 N73-15055
Vibrational effects on visual acuity of human operator seated in military tracked vehicle
[AD-750345] 06 p0636 N73-15172
Measurement and effects of triaxial vibration on pilots in P-531 [Scout] helicopter under different flight conditions
[ISVR-TR-58] 07 p0751 N73-16100
Analytic methods for calculating blade loads and shaft-transmitted vibratory forces in stiff bladed hingeless rotors operating at various advance ratios - Vol. I
[NASA-CR-114562] 09 p0984 N73-18034
Descriptions, geometry, and technical data for three rotary wing systems used in determining vibration and loads in hingeless rotary wings - Vol. 2
[NASA-CR-114568] 09 p0984 N73-18035
Techniques for determining dynamic characteristics of hydraulic duct for predicting low frequency vibrations of liquid propellant rocket engines
[ONERA-TP-1160] 09 p1015 N73-18281
Development of ultrasonic radiation equipment for removing material from host surface and vacuum apparatus for recovery of material
[NASA-CASE-NPO-11213] 11 p1296 N73-20514
Analysis of procedures for reducing pogo on space shuttle vehicle based on estimates of pump cavitation compliance
[NASA-CR-2210] 11 p1341 N73-20885
Vibration response of gas bearing rotor-supports to sinusoidal and random vibrations in Brayton rotating unit turbogenerator
[NASA-CR-2177] 13 p1534 N73-22427
Vibration effects on self-acting and hydrodynamic shaft seals in gas turbine engines
[NASA-TM-X-68214] 13 p1534 N73-22430
Equations of motion for gyroscopic devices and analysis of effects on accuracy produced by loads and vibrations in supports of gyroscopic instruments
[AD-756337] 13 p1557 N73-22622
Vibronic interaction in electron paramagnetic resonance spectra of yttrium and scandium doped single strontium chloride crystals
[NASA-CR-131295] 13 p1561 N73-22653
Application of power spectral density method to analyze vibrations induced in aircraft during taxiing
[AD-757283] 14 p1602 N73-22991
Effect of forced transverse, low frequency vibrations on stability of rectangular plates with brace
14 p1717 N73-23932
Work-rest schedules for military tracking crews under prolonged vibration
14 p1723 N73-23986
Measurement of power spectra of waveforms derived from vibrating blades in axial compressor and application to determine damping factor of blades
[ARC-R/M-3253] 15 p1728 N73-24014
Development of methods for approximating aircraft with asymmetric elevator control to calculate flutter characteristics
[ARC-R/M-3256] 15 p1728 N73-24018
Analysis of static, buckling, and vibration characteristics of orthotropic, inhomogeneous shells of revolution
15 p1837 N73-24889
Application of finite elements of triangular shape for computing plate vibrations
15 p1838 N73-24898
Vibrational characteristics, mechanical properties, and stress analysis of thin shell structures of various cross sections
[NASA-SP-288] 17 p2092 N73-26924
Numerical analysis of nonlinear resonance phenomena in systems of solids having rotating and vibrating parts
17 p2092 N73-26928
Effect of engine vibration, shaft whirling, and dynamic instabilities on helicopter performance and standardization of vibration limit specifications
[AD-761100] 18 p2107 N73-27039
Elastic vibrations of aircraft wing caused by distributed load, center of gravity displacement, and rotation using electromodeling techniques
[AD-760965] 18 p2108 N73-27043
Development of optical system for detecting defective components in rotating machinery with emphasis on bearing assemblies
[NASA-CASE-KSC-10752-1] 18 p2154 N73-27407
Effects of shear, rotatory inertia and inplane forces on transverse vibration of thin plates, and effect of shear on buckling
19 p2347 N73-28879
Application of constrained optimal design approaches for minimum mass designs of damped, linear, continuous sandwich beam
[AD-761881] 19 p2349 N73-28896
Natural mode vibration analysis of aircraft structural systems by direct and component mode synthesis techniques applied to tilt rotor VTOL aircraft aeroelasticity - Vol. 2
[NASA-TM-X-69496] 20 p2359 N73-28977
Development of three dimensional nozzle admittance theory for various liquid rocket engine nozzles subjected to three dimensional oscillations
20 p2387 N73-29174
Dynamic response of pipes with fluid flowing in steady and unsteady conditions
[MERL-TN-72-2] 20 p2387 N73-29178
Analysis of response and fatigue characteristics of light alloy integrally machined planks with emphasis on acoustic fatigue properties
20 p2479 N73-29912
Analysis of structural response to acoustic loading and preparation of data sheets for various conditions of acoustic loads
20 p2479 N73-29914
Fluid dynamic aspects of cardiovascular behavior during low frequency whole-body vibration such as encountered by astronauts during launch and reentry
[NASA-CR-133843] 21 p2501 N73-30069
Human response to vibration in Great Britain noting test facilities, equipment, experiments and publications
[ISVR-TR-60] 21 p2504 N73-30093

Engineering programming information for digital computer program developed to analyze vibration effects on shell structures - Vol. 6
[NASA-CR-2273-VOL-6] 23 p2854 N73-32806

**VIBRATION ISOLATORS**
Effect on pilot performance and comfort of active vibration isolation system for commercial transport pilot seat
[NASA-CR-2146] 03 p0260 N73-12109
Active control in landing gear of aircraft for reducing fatigue damage from ground induced vibration during taxiing
[AD-750137] 06 p0678 N73-15515
Simple mathematical models of mechanical systems for ground support equipment, airborne launcher, vibration isolation design
[AD-754537] 11 p1267 N73-20283
Transfer matrix techniques for vibration analysis of curved skin-stringer structures with tuned elastomeric dampers
[AD-758220] 14 p1605 N73-23010

**VIBRATION MEASUREMENT**
Analysis of pressure fluctuations in Nike rocket case and relationship to structural vibrations of rocket case
[NASA-TN-D-6931] 01 p0113 N73-10933
Analysis of combined vibrations of blades in axial turbomachinery using dynamic stiffness method
[NLL-RTS-7305] 02 p0236 N73-11917
Computer program for stress, stability, and vibration analyses of segmented, ring-stiffened, branched shells of rotation
[NASA-CR-2116] 02 p0237 N73-11931
Development of procedure for measuring sinusoidal vibration displacement amplitude using laser homodyne system
[RM-560J] 03 p0310 N73-12526
Numerical analysis of natural vibration modes of thin elastic shells to determine orthogonality of reactions
04 p0481 N73-13931
Development of FORTRAN computer program for solving free axisymmetric vibration of cylindrical shells of arbitrary shape
[AD-748655] 04 p0482 N73-13942
Descriptions, geometry, and technical data for three rotary wing systems used in determining vibration and loads in hingeless rotary wings - Vol. 2
[NASA-CR-114568] 09 p0984 N73-18035
Computer programs for predicting hydrodynamic forces and vibration characteristics of rocket engine turbopump inducer - Vol. 2 Revised
[NASA-CR-72712-VOL-2-REV]
09 p1078 N73-18797
Analysis of effects on in-plane boundary conditions and panel geometry on natural vibration and flutter characteristics of panels exposed to supersonic flow parallel to generators
09 p1094 N73-18933
Analysis of airload and blade response of rotary wings to determine sources of rotor vibratory loads in level and maneuvering flight of NH-3A and CH-53A helicopters
[NASA-CR-2225] 10 p1103 N73-18996
Vibration considerations in design of flexible manipulators
[NASA-CR-124189] 11 p1249 N73-20138
Analysis of natural vibrations on stratified fluid in rectangular vessel and computer program for solving continuous density distribution
12 p1390 N73-21275
Noncontact devices for measuring vibrations and deflections of parts in operating turbopumps
[NASA-CR-124208] 12 p1407 N73-21408
Vibration analysis of shallow spherical sandwich shells based on effects of thickness-shear deformation and rotary inertia
12 p1462 N73-21843
Calculation of aerodynamic forces of bending and torsional vibration on installed vibrating cascade blades
[ARC-R/M-3254] 15 p1728 N73-24015
Development of narrow band spectral analyzer for determining power spectra of waveforms derived from vibrating axial compressor blades due to random excitation
[ARC-R/M-3259] 15 p1729 N73-24024
Development of equations of motion for vibration frequencies of cantilever and elastically supported-free thin circular cylindrical shell
15 p1837 N73-24887
Measurement of vibration levels in CH-47 helicopter at pilot seat, control stick, rudder pedals, instrument panel, and human interface points
[AD-761199] 18 p2107 N73-27040
Exact solution for free transverse vibrations of annular plate with supported inner and free outer edge-beams
20 p2482 N73-29938
Device for observing diaphragm surface vibration angular displacement based on two dimensional schlieren techniques
[REPT-10/1972] 22 p2674 N73-31420

**VIBRATION METERS**
NT LUNAR SEISMOGRAPHS
NT SEISMOGRAPHS
Performance of seismic angular vibration transducer using gas rotor
[RAE-TM-IR-128] 13 p1530 N73-22400

**VIBRATION MODE**
Algorithm for synthesizing mass and stiffness matrices from experimental vibration modes
01 p0119 N73-10983
Measurement of axial velocity profiles and resulting acoustical fields of rod under continuous-wave excitation
[AD-747209] 02 p0239 N73-11945
Using microscopic models and principles for studying transfer of lattice vibrational energy into first excited state in perfect crystal
[AD-748079] 03 p0365 N73-12977
Sliding friction and natural vibration of solid with rigid connection moving over dry surface
[AD-749521] 04 p0428 N73-13488
Numerical analysis of natural vibration modes of thin elastic shells to determine orthogonality of reactions
04 p0481 N73-13931
Development of digital computer program for evaluating vibrational characteristics of large liquid-filled rigid wall tanks of general shape
[NASA-CR-124070] 08 p0953 N73-17801
Extended natural mode method for calculating flapwise bending, edgewise bending, and torsional vibration modes and frequencies of helicopter rotor blades
[DLR-FB-71-108] 09 p0983 N73-18026
Function generators for producing complex vibration mode patterns used to identify vibration mode data
[NASA-CASE-LAR-10310-1] 11 p1263 N73-20253
Development of dissipative energy approach for predicting damping of four component space shuttle model using modal parameters for individual components
12 p1459 N73-21827
Numerical analysis of free vibrations of ring stiffened toroidal shells based on linear shell theory
15 p1837 N73-24888
Resonance tests of delta wing aircraft model to determine effect of stiffness changes of wing spars on frequencies and modes of vibration
[ARC-R/M-3268] 16 p1856 N73-25031
Pulsed holographic measurement of wave propagation in thin walled shells and vibration modes in steel rectangular plates at high temperature
16 p1921 N73-25544
Vibration-rotation relaxation using mode locked and Q switch gas lasers
[AD-763292] 21 p2555 N73-30481
Modes of cable vibration compared with pure flexing mode in production of motion induced noise from towed ELF H field antenna
[AD-762936] 22 p2645 N73-31199
Linearization method for approximate solution of rectangular plate response to excitation
[AD-763782] 22 p2727 N73-31821

**VIBRATION PERCEPTION**
Analysis of helicopter pilot and passenger reaction to vibration environment to determine effects of discrete frequencies and combinations of harmonic frequencies
01 p0003 N73-10019

**VIBRATION PICKUPS**
U TRANSDUCERS
U VIBRATION METERS

**VIBRATION PROTECTION**
U VIBRATION ISOLATORS

**VIBRATION SIMULATORS**
Equipment for vibration testing of assemblies, components, and other articles
[NASA-CASE-GSC-11302-1] 04 p0419 N73-13416
Deceleration method for rapid deceleration of mobile parts in vibration simulators
[LRBA-NT-8/72/SEV] 05 p0548 N73-14449
Vibration simulation of space probe model, superconducting energy storage coil
[LA-DC-72-724] 07 p0832 N73-16742
Acceptance tests of C 90 MB vibration simulator
[LRBA-PV-15/72/SEV] 09 p1039 N73-18477
Development of methods for approximating aircraft with asymmetric elevator control to calculate flutter characteristics
[ARC-R/M-3256] 15 p1728 N73-24018
Human response to vibration in Great Britain noting test facilities, equipment, experiments and publications
[ISVR-TR-60] 21 p2504 N73-30093

**VIBRATION TESTING MACHINES**
U VIBRATION SIMULATORS

**VIBRATION TESTS**
NT DAMPING TESTS
Resonant random vibration test to assess service equipment and sub-assembly mechanical ruggedness
[RARDE-MEMO-18/72] 01 p0113 N73-10937
Analysis of vibration characteristics of laminated plates and modifications of plate theory to produce results consistent with continuum theory
[AD-746951] 02 p0240 N73-11949
Equipment for vibration testing of assemblies, components, and other articles
[NASA-CASE-GSC-11302-1] 04 p0419 N73-13416
Human tolerance to vibration
06 p0628 N73-15098
Static and vibration tests of graphite-epoxy stabilizer system for A-4 Skyhawk aircraft
[AD-750778] 06 p0689 N73-15610
Vibration, functional, and electronic equipment tests of ESKA 18 electrostatic ion engine prototype
[DGLR-PAPER-72-87] 06 p0714 N73-15826
Analysis of natural vibration characteristics of plate-beam combination structures during supersonic flight
[NAL-TR-291] 06 p0725 N73-15917
Characteristics and vibrational test of structural test unit for electron-proton spectrometer under simulated flight conditions
[NASA-CR-128699] 08 p0924 N73-17573
Compilation of analyses generated during development of electron-proton spectrometer for Skylab program to insure reliability and quality control
[NASA-CR-128705] 08 p0925 N73-17576
Procedure for applying structure-fluid interactions effect to dynamic frequency response calculations for submerged structures
[AD-752484] 08 p0967 N73-17906
Computer analysis of random decrement signatures of structures vibrating in random environment
[NASA-CR-2205] 09 p1094 N73-18929
Multiaxes vibration device for making vibration tests along orthogonal axes of test specimen
[NASA-CASE-MFS-20242] 10 p1158 N73-19421
Clinical hematological indices for evaluating vibration effect [70 Hz, 0.4 cm amplitude] on radiation reaction in dogs
11 p1242 N73-20084
Design, development, and evaluation of spherical hydrostatic gas bearing gyroscope for operation in random vibration environment
[AD-755124] 11 p1322 N73-20725
Vibration and acoustic tests for spacecraft electronic equipment design
[NASA-TN-D-7159] 11 p1345 N73-20914
Development of empirical structural damping law for space shuttle by dynamic analysis of vibration test data
[NASA-CR-124203] 12 p1460 N73-21828
Reduction of random vibration response data for NASA Brayton rotating unit turbogenerator
[NASA-CR-121178] 13 p1534 N73-22428
Buckling and vibration behavior of tensioned sheets with elliptical openings
13 p1584 N73-22840
Analysis of shimmy in pneumatic tires due to lateral flexibility for stationary and nonstationary conditions
[WTHD-48] 16 p1917 N73-25515
Smoothing technique for analyzing frequency response of aircraft in flight and on ground
[RAE-LIB-TRANS-1703] 17 p2054 N73-26616
Equivalence techniques used to define and simulate service vibration environments in testing laboratories
[AD-758414] 17 p2091 N73-26914
Development of simulation program for determining characteristics of tracked air cushion research vehicle
[PB-218368/9] 18 p2106 N73-27033
Tracking performance during whole-body vibration with side-mounted and center mounted control sticks
[AD-761798] 19 p2228 N73-27971
Development of method for determining response of box type structures subjected to high intensity acoustic loading
20 p2479 N73-29915
Ground vibration tests of YF-12 aircraft to determine frequency response data, measured node lines, and elastic mode shapes for aircraft components
[NASA-TM-X-2880] 20 p2483 N73-29944
Analysis of flight test procedures for evaluating strength of airframes for aircraft and helicopters
[NASA-TT-F-769] 21 p2494 N73-30019
Development of program for obtaining resonant frequencies, modal amplitudes, and damping of structure from sinusoidal force-controlled vibration test
[NASA-TM-X-2789] 22 p2724 N73-31802
Response of laminated elastic plate to planar impact loads using vibratory modes to develop transient response solution
23 p2853 N73-32795
Vibration tests of flight control moment gyros and bearing life test fixtures
[NASA-CR-124449] 24 p2926 N73-33365

**VIBRATIONAL FREEZING**
Nonequilibrium effects caused by vibrational freezing in hypervelocity wind tunnel
[VKI-TN-83] 03 p0248 N73-12009

**VIBRATIONAL FREQUENCIES**
U VIBRATIONAL SPECTRA

**VIBRATIONAL RELAXATION**
U MOLECULAR RELAXATION

**VIBRATIONAL SPECTRA**
Calculation of vibrational energy level distributions of hydrogen fluoride formed during atomic fluoride reaction with molecular hydrogen
[AD-748291] 04 p0387 N73-13146
Vibrational energy distribution of positive Cs ions in output from Cs2O2 chemical laser
[DREV-TN-2019/72] 06 p0679 N73-15522

Extended natural mode method for calculating flapwise bending, edgewise bending, and torsional vibration modes and frequencies of helicopter rotor blades
[DLR-FB-71-108] 09 p0983 N73-18026
Minimization technique for determining structural parameters of IR and vibrational rotational spectra of H2O
[AD-754612] 11 p1253 N73-20166
Vibrational spectral study of molecular orientation in vitreous sodium metaphosphate glass fibers
[AD-757751] 15 p1748 N73-24167
Development of statistical methods for determining vibration and acoustic radiation of fluid loaded cylindrical shells
20 p2477 N73-29895
Determination of vibrational energy of nitrogen in upper atmosphere
[AD-763749] 21 p2541 N73-30377
Raman and far infrared spectra of crystalline fluorine obtained in solid phases
[AD-763686] 22 p2626 N73-31039

**VIBRATIONAL STRESS**
Structural vibration and noise effects on man in aerospace operations
[AGARDOGRAPH-151] 08 p0876 N73-17098
Strains affecting growth rate of edge cracks in acoustically excited panels
[ISVR-TR-59] 13 p1586 N73-22860

**VIBRATORY LOADS**
Vibratory stability of plate over viscous heat conducting gas layer
[AD-755288] 12 p1393 N73-21293
Development of statistical methods for determining vibration and acoustic radiation of fluid loaded cylindrical shells
20 p2477 N73-29895
Vibration design loads for component dynamic magnification factors of space shuttle
[NASA-CR-124337] 21 p2601 N73-30842

**VIBROMETERS**
U VIBRATION METERS

**VIDEO COMMUNICATION**
Analysis of video transmission range in water by laser beam
[AD-751445] 07 p0807 N73-16548
Nonlinear programming of multifilter phase-lock loops at low signal-to-noise environments
[NASA-CR-131237] 10 p1127 N73-19184
Subroutine package for FORTRAN communication with graphic video system
[R-1015-NIH] 14 p1637 N73-23274
Cable television, emphasizing juridical and economical aspects in various nations
23 p2757 N73-32067

**VIDEO DATA**
Evaluating video graphic performance before and after implementation
[P-4830] 01 p0080 N73-10658
Digital data processing system for infrared video scan
[AD-752069] 08 p0944 N73-17731
Techniques for solving for optimum filter for video signal processing
[AD-753132] 09 p1003 N73-18189
Computerized video display for processing spark and bubble chamber photographs
[JPRS-58713] 12 p1381 N73-21202
Interpolative estimation for error reduction during video signal demodulation in noise environment
[NASA-CR-131873] 13 p1490 N73-22080
Cross and square command symbol and video inset generator to display flight command data on aircraft television screen
[AD-755160] 13 p1494 N73-22111
Television readout devices for color display of data and picture blending
[NLL-PO-2958-[9022.81]] 15 p1755 N73-24225
Design and performance of C band airborne data transmission system for aerial reconnaissance
[AD-759184] 16 p1877 N73-25194
Video bandwith tape recorder for ERTS A imagery
18 p2209 N73-27833
Control computer for correcting ERTS video data electron beam recorder errors at ground base
18 p2211 N73-27853
Differential pulse code modulation of digital video signals
[BBC-RD-1973/7] 19 p2234 N73-28011
Computer technique for transferring digital television signal to punched tape
[BBC-RD-1973/6] 19 p2238 N73-28044
Photoconducting semiconductor system for converting stored optical images into video signals
[NASA-CASE-NPO-13131-1] 22 p2680 N73-31467
Manually and automatically operable video switching system
[NASA-CASE-KSC-10782-1] 23 p2757 N73-32063
Video cassette recording techniques and commerical aspects
23 p2757 N73-32066
Stereographic albedo map of Mars south polar region using Mariner 9 video data
23 p2844 N73-32724
COLFTAR real time electro-optical system for generating optical Fourier transforms of two-dimensional video signals
24 p2956 N73-33613

**VIDEO EQUIPMENT**
Effect of automatic landing system display on pilot information requirements
01 p0016 N73-10126
Electronic video editor for switching video input signals to common output channel
[NASA-CASE-KSC-10003] 04 p0398 N73-13235
Characteristics of video tape recording film and procedures for controlling magnetic properties during production
[NHK-LABS-NOTE-155] 07 p0754 N73-16122
Production of narrow-track video recording head to include characteristics of recording tape and tetrode sputtering equipment
[NHK-LABS-NOTE-154] 07 p0754 N73-16124
Characteristics and operation of videocoherent system for improved target acquisition and measurement of target velocity
07 p0755 N73-16133
Experiments in video camera positioning with regard to remote manipulators
[NASA-CR-124190] 11 p1249 N73-20139
Video tape recorder with scan conversion playback for color television signals
[NASA-CASE-NPO-10166-1] 13 p1490 N73-22076
Specifications of portable magnetic video tape recorder for television signal reproduction
[JPRS-59611] 19 p2235 N73-28021
Comparison of film and video as the recording medium in high voltage electron microscopy
[NPL-IMS-20] 21 p2549 N73-30438
Annual variations of Garda Lake surface temperature using airborne bolometric equipment and earth based infrared video equipment
[IFA-STR-23] 23 p2787 N73-32298

**VIDICONS**
NT RETURN BEAM VIDICONS
Pulse modulation characteristics of vidicon beam currents
[DRIC-TRANS-2875] 02 p0174 N73-11413
Measurement of signal strength variations in beam currents of vidicon targets
[DRIC-TRANS-2965] 06 p0645 N73-15238
Analysis of high resolution vidicon optics for electronic periscope view simulator
[AD-751023] 07 p0822 N73-16664
Influence of photoconducting layer thickness on sensitivity of vidicons
[NLL-DRIC-TRANS-2965-[3623.66]] 11 p1261 N73-20233
Correction of scanning beam velocity nonuniformity in vidicons by deflection of current pulse
[DRIC-TRANS-2758] 12 p1384 N73-21224
Compensation of vidicon signal dark component
[DRIC-TRANS-2967] 13 p1491 N73-22089
Reduction of nonuniformity of electron beam displacement on vidicon screen at raster edges
[DRIC-TRANS-2966] 13 p1500 N73-22156
Factors affecting design of charge-coupled image sensors
[AD-758741] 16 p1882 N73-25234
Silicon vidicon camera for slow scan operation onboard Mariner spacecraft
22 p2732 N73-31862

**VIETNAM**
Summary of synoptic meteorological observations for Southeast Asian Coastal Marine Areas
[AD-747638] 03 p0328 N73-12674
Synoptic meteorological data for Philippine and Vietnam coastal marine surfaces
[AD-762425] 20 p2450 N73-29689

**VIGNETTING**
Contraves cinetheodolite optical system modification
[SC-DR-72-0754] 16 p1914 N73-25487

**VIKING LANDER SPACECRAFT**
Wind tunnel tests to determine drag and performance of disk-gap-band parachutes in wake of Viking reentry vehicle scale model from subsonic to supersonic speeds
[AD-746291] 02 p0126 N73-11026
Biological effects of Viking Lander spacecraft engine fuel on extraterrestrial life during landing on planet Mars
[NASA-TM-X-2714] 06 p0630 N73-15118
Characteristics and requirements of instruments for advanced Viking seismic experiments on Mars
[NASA-CR-130358] 06 p0717 N73-15850
Performance of SNAP 19 RTG for Viking lander system
[IESD-2960-53] 12 p1427 N73-21569
Landing site selections for Viking Mars probes
[NASA-NEWS-RELEASE-73-91] 13 p1576 N73-22768
FCC in Viking articulated boom
14 p1642 N73-23317
Surface pressure tests on Viking lander capsule at Mach 10, including appendages on base cover pressure distribution
[NASA-CR-131983] 14 p1710 N73-23879
Thermal inactivation of Bacillus subtilis var. niger spores on Viking lander
[NASA-CR-133223] 17 p1987 N73-26058

**VIKING MARS PROGRAM**
Soil sampling and microorganism analysis in planetary spacecraft assembly area for prevention of Mars contamination
[NASA-CR-130009] 07 p0745 N73-16059
Formulation of image quality prediction criteria for Viking lander camera
[NASA-TM-X-2802] 21 p2548 N73-30425

**VIKING ORBITER SPACECRAFT**
NT VIKING ORBITER 1975
Psychrophilic organisms in soil samples of areas for Viking spacecraft assembly
[REPT-2] 17 p1987 N73-26063

**VIKING ORBITER 1975**
Design and analysis of Viking Orbiter 1975 guidance and control system
[NASA-CR-135649] 21 p2600 N73-30836

**VIKING 75 ENTRY VEHICLE**
Flight tests of disk-gap band parachute behind full-scale simulator of Viking reentry vehicle over maximum range of entry conditions for landing on planet Mars-Vehicle AV-1
[NASA-CR-112176] 04 p0372 N73-13021
Flight tests of disk-gap band parachute behind full-scale simulator of Viking reentry vehicle over maximum range of entry conditions for landing on planet Mars-Vehicle AV-4
[NASA-CR-112179] 04 p0372 N73-13024
Analysis of flow properties in wake of 120 and 140 degree included angle conical bodies and flow characteristics of Viking 75 entry vehicle configuration
[NASA-TN-D-7089] 05 p0527 N73-14285
Postflight analysis of AV-2 balloon launched decelerator flight test to determine parachute system operation in wake of blunt body simulating Viking 75 entry vehicle
[NASA-CR-112177] 11 p1233 N73-20011
Postflight analysis of AV-3 balloon launched decelerator flight test to determine parachute system operation in wake of blunt body simulating Viking 75 entry vehicle
[NASA-CR-112178] 11 p1233 N73-20012
Analysis of retrorocket exhaust plume of Viking Lander impinging on Martian surface and development of multiple nozzle configurtaion to reduce effects
[NASA-CR-2252] 18 p2197 N73-27737
Simulation calculations of parachute deployment dynamics process for Viking 75 entry vehicle
[NASA-TN-D-7415] 21 p2600 N73-30841

**VINTI THEORY**
Vinti equations of motion solved for position and velocity of orbiting satellite
[NASA-TM-X-70418] 19 p2343 N73-28846

**VINYL COPOLYMERS**
Synthesis and analysis of poly[vinyl-CO-vinylene]nitrate with 7 to 70 mol percent of vinylene constituents
[ICT-7/72] 22 p2626 N73-31038

**VINYL CYANIDE**
U ACRYLONITRILES

**VINYL ETHYLENE**
U BUTADIENE

**VINYL POLYMERS**
Engineer design tests of two dust control materials, polyvinyl acetate water emulsion and cationic asphalt-neoprene emulsion
[AD-745086] 01 p0038 N73-10297
Formation mechanism and strength of adhesive bond between polyvinyl acetate and steel
[NLL-RTS-7520] 02 p0190 N73-11543
Manufacture, stabilization, and properties of polyvinyl nitrate explosives
[ICT-7/71] 10 p1127 N73-19178
Polyvinylfluoride pyroelectric radiometer
[NASA-TM-X-62271] 16 p1912 N73-25472

**VIOLENCE**
Application of NASA management techniques to problems of community violence
[NASA-CR-133830] 21 p2609 N73-30915

**VIRGINIA**
NT CHESAPEAKE BAY [US]
NT POTOMAC RIVER VALLEY (MD-VA-WV)
Seismic reflection and refraction surveys of thickness of coastal plain sediments in Virginia
[PB-212604] 07 p0794 N73-16455
Repetitive ERTS-1 imagery of surface water variability and flooding along rivers and low-lying areas in Virginia, Iowa, and California
[E73-10046] 08 p0900 N73-17289
Mapping northern Atlantic coastal marshlands of Maryland, Delaware, and Virginia using ERTS-1 imagery
[E73-10363] 10 p1150 N73-19359
Detection of smoke pollution in Virginia by photogrammetric and densitometric analysis of ERTS-1 imagery
[E73-10419] 11 p1279 N73-20381
Tables of climatological conditions for selected areas of Virginia
[PB-213881/3] 14 p1686 N73-23681

Correlation of ERTS-1 data with ground data for determining characteristics of air pollution in Norfolk, Virginia area
[H73-10779] 18 p2135 N73-27255
Sampling strategies in thematic land use mapping of Maryland, Virginia, and District of Columbia using Skylab EREP data
[E73-10823] 18 p2140 N73-27298
Feasibility of rapid transit service between downtown Washington, D.C. and Dulles Airport in Virginia
[PB-220074/9] 18 p2214 N73-27879
Geological landforms in central Piedmont of Virginia and North Carolina from ERTS-1 imagery
[E73-10766] 19 p2259 N73-28205
Photogrammetric and densitometric examination of ERTS-1 MSS imagery of Eastern Virginia to determine sources of aerosol pollution
[PAPER-E5] 19 p2269 N73-28269
Utilization of ERTS-1 imagery and data for land use, regional planning, and urban development in Metropolitan Washington area
19 p2285 N73-28377
ERTS-1 multispectral imagery of topography of Assateague Island
[E73-10848] 19 p2292 N73-28426
Development of land use, water quality, and air quality indices from ERTS-1 imagery for environmental resources management in Susquehanna River Basin and Quantico, Virginia test areas
[E73-11143] 24 p2918 N73-33298
Utilization of ERTS-1 imagery for management of wetlands in Great Dismal Swamp and Lake Okeechobee
[E73-11161] 24 p2920 N73-33314

**VIRGO STAR CLUSTER**
Galactic brightness distribution obtained by imaging galaxies on Schmidt plates, selecting one as photometric standard and applying microdensitometric scans
07 p0845 N73-16852
Automatic raster scanning microdensitometer measurement of luminosity profiles and density of lenticular galaxies in Virgo Cluster
16 p1961 N73-25859

**VIRIAL THEOREM**
Virial theorem for analyzing structure of clusters in galaxies
08 p0959 N73-17840
Tensor viral method for modeling and studying pulsars in rapidly rotating magnetosphere
16 p1960 N73-25858

**VIRTUAL WORK**
U EQUILIBRIUM

**VIRUSES**
Photosynthetic energy conversion in membranes, tissues, and reaction centers of bacteria and viruses
[COO-3162-9] 04 p0380 N73-13091
Automated procedures for Passive Immune Agglutination system
[NASA-CR-128731] 08 p0877 N73-17107
Hydrogen peroxide aerosols for decontamination of influenza atmosphere
[NASA-TT-F-15127] 23 p2750 N73-32006

**VISCERA**
NT ADRENAL GLAND
NT INTESTINES
NT KIDNEYS
NT LIVER
NT LUNGS
NT ORGANS
NT PITUITARY GLAND
NT RECTUM
NT SPLEEN
NT STOMACH
NT TESTES
NT THYROID GLAND

**VISCOELASTIC DAMPING**
U ELASTIC DAMPING
U VISCOUS DAMPING

**VISCOELASTIC FLOW**
U VISCOELASTICITY

**VISCOELASTICITY**
NT THERMOVISCOELASTICITY
Cataloging elastomer stiffness and damping properties in terms of viscoelastic model constants
[NASA-CR-120965] 01 p0113 N73-10931
Development of direct method for determining complex modulus of linear viscoelastic materials as function of frequency
[UTIAS-159] 02 p0237 N73-11928
Development of general mixed finite element models of nonlinear thermomechanical response of dissipative media
[AD-745994] 02 p0239 N73-11944
Iterative algorithm for determining thermal instabilities in viscoelastic rod under cyclic loads
[AD-746470] 02 p0240 N73-11953
Elastomer viscoelasticity effects in compliant surface bearings
[AD-747667] 03 p0309 N73-12525
Analysis of crack propagation properties of solid rocket propellants based on relation between crack tip stress intensity factor and crack velocity
[AD-747531] 03 p0350 N73-12853
Polymer optimization with molecular relaxation processes for preparing vibration damping plastic materials
[RAE-LIB-TRANS-1646] 04 p0386 N73-13135
Time temperature superposition in heterophase block copolymers, using viscoelastic behavior of styrene-butadiene-styrene block
[AD-748213] 04 p0438 N73-13574
Strain measurement of viscoelastic solid propellant materials with birefringent coating
[NAL-TR-261] 04 p0461 N73-13765
Steklov-Lebesgue norm used in stress analysis of solid rocket propellants to determine viscoelastic response with aging
[AD-748943] 04 p0462 N73-13771
FORTRAN 4 computer program for one-dimensional stress wave analysis of linear viscoelastic rock
[BM-IC-8563] 05 p0516 N73-14197
Development and characteristics of parallel plate viscometer for determination of absolute viscosity of liquids and viscoelastic materials
[NASA-CASE-NPO-11387] 05 p0545 N73-14429
Approximate method to analyze plane stress, orthotropic, linear viscoelastic problems under isothermal conditions for metal-epoxy composites
05 p0607 N73-14939
Viscoelastic properties of styrene butadiene plastic homopolymers and styrene-butadiene-styrene block copolymers
[AD-752622] 08 p0936 N73-17660
Linear differential equations for analyzing viscoelastic properties and mechanical behavior of high polymers
08 p0966 N73-17898
Numerical analysis of incompressible linearly compressible viscoelastic creep and relaxation for plastic materials
[AD-752067] 08 p0967 N73-17903
Analysis of complex moduli of uniaxially fiber reinforced materials containing viscoelastic matrix and elastic fibers
[AD-753699] 09 p1054 N73-18591
Stability analysis for spinning flow of cylindrical liquid polymer filament with memory function
[AD-755065] 11 p1273 N73-20332
Energy release integral equation for finite elastic and viscoelastic materials
[CONF-720930-1] 12 p1463 N73-21851
Human arterial elasticity during breathing of reduced partial oxygen atmosphere
13 p1480 N73-21987
Techniques for determining complex Young and shear modulus of linear viscoelastic materials
[AD-755718] 13 p1588 N73-22873
Propagation of waves in elastic-viscoplastic media in temperature field
[AD-755274] 13 p1592 N73-22905
Correspondence principle for vibration analyses on viscoelastic bodies with loss tangents
[AD-759260] 16 p1971 N73-25943
Periodic excitation of finite three dimensional standard, linear viscoelastic solid
[AD-759485] 16 p1972 N73-25951
Relationship determination between strain and microhardness, using viscoelasticity on surface or within specimen
[AD-759197] 17 p2047 N73-26562
Mechanical property determination and fracture mechanics of fiber reinforced composite materials
[D-MAT-178] 17 p2051 N73-26589
Viscoelastic fracture characterization of cracking rocket motor
[AD-759968] 17 p2076 N73-26792
Wave front stress relaxation in suddenly loaded semi-infinite rod of nonlinear viscoelastic materials with random temperature distributions
[AD-760324] 17 p2096 N73-26956
Crack growth in viscoelastic polymers
[AD-759379] 18 p2168 N73-27513
Numerical analysis of stability of flows of viscoelastic fluids for three conditions
19 p2251 N73-28146
Strain waves propagating in linear viscoelastic plates of various thicknesses
20 p2477 N73-29897
Viscoelastic shock absorbing mount for electrical circuit board
[NASA-CASE-NPO-13253-1] 22 p2677 N73-31445
Analysis of buckling behavior of viscoelastic structural member
[PB-221835/2] 22 p2726 N73-31817
Fundamental concepts and statistical foundation of mechanics of continuous medium
[AD-764370] 22 p2727 N73-31820
Viscoelastic effects in design of polymeric equipment and structures
[AD-764555] 24 p2989 N73-33890

**VISCOMETERS**
Analysis of viscosity of water using distilled water as primary reference standard to show dynamic and kinematic viscosities
[ESDU-65009] 01 p0039 N73-10306
Swinging ball viscosimeter design and calibration for water viscosity measurements
[AD-745252] 04 p0424 N73-13456
Development and characteristics of parallel plate viscometer for determination of absolute viscosity of liquids and viscoelastic materials
[NASA-CASE-NPO-11387] 05 p0545 N73-14429
Design of relative velocity blood viscometer
12 p1373 N73-21142

**VISCOMETRY**
Analytical and test program for establishing feasibility of multichamber pulsed-capillary viscometer
[NASA-CR-120982] 02 p0173 N73-11401
Instrumentation and techniques for measuring viscosity of liquids by vibration method
[AD-759389] 17 p2034 N73-26464

**VISCOPLASTIC FLOW**
U VISCOPLASTICITY

**VISCOPLASTICITY**
Nonisothermal stationary flow of viscoplastic liquid between two concentric cylinders
[AD-748908] 04 p0408 N73-13321
Elasto-viscoplastic behavior of structures subjected to complex loads and thermal gradients
[ONERA-NT-194] 04 p0482 N73-13937
Unified theory of thermoviscoplasticity of crystalline solids
[AD-751293] 07 p0833 N73-16756
Propagation of waves in elastic-viscoplastic media in temperature field
[AD-755274] 13 p1592 N73-22905
Viscoplastic characteristics of structural shells
[AD-758074] 15 p1841 N73-24915

**VISCOSITY**
NT EDDY VISCOSITY
NT GAS VISCOSITY
Dynamic viscosity data for water and steam, liquid and gaseous heavy water, and sea water
[ESDU-68009] 01 p0038 N73-10303
Viscosity variation with temperature at atmospheric or saturation pressure for liquids
[ESDU-66024] 01 p0039 N73-10305
Analysis of viscosity of water using distilled water as primary reference standard to show dynamic and kinematic viscosities
[ESDU-65009] 01 p0039 N73-10306
Viscosity of liquids and classification of lubricating oils
[ESDU-68036] 02 p0154 N73-11247
Molecular-kinetic theory for determining temperature dependence of simple liquid viscosity
[AD-747089] 02 p0159 N73-11286
Effects of incomplete dissolution of graphite in molten cast iron on viscosity differences with same chemical composition
[AD-747378] 03 p0317 N73-12582
Susceptibility of model polymer with diagonal viscosity and weak interaction
[COO-3161-2] 04 p0387 N73-13142
Swinging ball viscosimeter design and calibration for water viscosity measurements
[AD-745252] 04 p0424 N73-13456
Critical velocity study of stationary motion, using loop filament in viscous medium
06 p0652 N73-15295
Liquid viscosity determined for gallium by means of vibration technique
[AD-750915] 06 p0656 N73-15332
Effects of various oxide additives on volume change on melting, surface tension, and viscosity of liquid aluminum oxide
[NASA-CR-120910] 07 p0811 N73-16580
Two dimensional motion of viscous incompressible flow with variable viscosity coefficient in thrust bearing
[AD-753030] 09 p1041 N73-18495
Viscosity and electrical resistivity of molten glass over wide temperature range
[AD-753480] 09 p1055 N73-18604
Calculation of interaction of penetratable shelter belts and ground air flow, including mean horizontal wind profiles and eddy viscosity coefficient
09 p1059 N73-18640
Model equations based on eddy viscosity of turbulent wakes
[AD-752592] 11 p1271 N73-20314
Use of torsional pendulum as high pressure gage and determination of viscosity of helium gas at high pressures
[NASA-TN-D-7241] 14 p1667 N73-23528
Bulk viscosity in relativistic homogeneous isotropic cosmologies
17 p2081 N73-26829
Analysis of viscosity of saturated hydrocarbons at different temperatures and pressures to show test equipment and procedures
[NLL-NEL-TT-2471-(6075.461)]
20 p2434 N73-29547
Prediction of aerodynamic characteristics of airfoils at transonic speeds including effects of fluid viscosity
[AD-763295] 22 p2654 N73-31260
Universal diagram representing changes in viscosity of liquid metals as function of temperature
[FRNC-CONF-45] 22 p2684 N73-31501
Characteristics of silicon carbide samples produced by hot casting under pressure
23 p2808 N73-32450

On the effects of viscous interaction for a flat delta wing at incidence
[ARC-CP-1237] 24 p2870 N73-32931
Effect of fibrinogen concentration on viscosity of human blood
[DLR-FB-73-54] 24 p2886 N73-33046
Measurement of viscosity of solution of He 3 in He 4 at superflow temperatures
[JINR-P8-7009] 24 p2892 N73-33086
Pressure effects on dynamic viscosity of helium in temperature range 0.4 to 400 K
24 p2908 N73-33208
Determination of vapor pressure, viscosity, and thermal conductivity of several liquid rocket propellants
24 p2972 N73-33750

**VISCOUNT AIRCRAFT**
Ultrasonic inspection of wing spar joints and lugs on Viscount Aircraft
[TR-7207.591] 05 p0551 N73-14472
Procedures for ultrasonic inspection of wing attachment fittings on Viscount aircraft
[TR-7211.621] 20 p2422 N73-29455

**VISCOUS DAMPING**
Analysis of effect of damping on response of structure to acoustic excitation and experimental method for determining damping coefficients
20 p2479 N73-29917

**VISCOUS FLOW**
NT BOUNDARY LAYER FLOW
NT BOUNDARY LAYER SEPARATION
NT COUETTE FLOW
NT REATTACHED FLOW
NT SECONDARY FLOW
NT SEPARATED FLOW
NT STOKES FLOW
Calculating laminar viscous, compressible flows
[NASA-TN-D-6998] 01 p0040 N73-10313
Development of implicit finite difference method for analysis of viscous flows based on Euler and Navier-Stokes equations
[AD-746389] 01 p0043 N73-10341
Development of theories for calculating pressure on perturbed plane wall in presence of viscous boundary layer
[AD-746332] 02 p0158 N73-11278
Numerical analysis of viscous-inviscid interaction in supersonic flow around blunt body
[AD-746891] 02 p0160 N73-11293
Flow distribution of low Reynolds number, high enthalpy viscous flow of diatomic gas through conical nozzles
[DGLR-PAPER-72-110] 04 p0405 N73-13302
Development of method for numerical integration of Navier-Stokes equations based on perturbation of Poisson type equation for viscous flow
[NA-7] 05 p0526 N73-14282
Development of procedure for determining characteristics of high lift systems where viscous effects dominate
06 p0617 N73-15009
Solution of viscous shock-layer equations using implicit finite difference scheme for hyperboloid body under conditions simulating atmospheric entry
07 p0768 N73-16238
Numerical technique for obtaining solutions to governing equations for gas flowing in axially symmetric constricted-arc heaters
[NASA-TM-X-2700] 07 p0769 N73-16246
Boundary layer stability on two-layer flat plates using viscous liquid currents
[AD-752696] 09 p1016 N73-18294
Stability of steady state of compressible viscous fluid
[AD-752692] 09 p1016 N73-18295
Nonstationary flow of anomalous viscous liquid having particular properties of displacement speed and viscosity
[AD-753486] 10 p1142 N73-19308
Effect of axial velocity ratio on aerodynamic coefficients of compressor cascade in viscous flow
10 p1205 N73-19804
Streaming flow of viscous fluid past sphere in uniform magnetic field at low Hartmann numbers
[AD-755060] 11 p1329 N73-20784
User manual for computer program to solve equations of fully coupled viscous, radiating flow at stagnation point of blunt body which may be ablating or nonablating
[NASA-CR-2237] 11 p1347 N73-20933
Radiative coupled viscous flow past ablating blunt body at hyperbolic entry conditions
[NASA-CR-2236] 11 p1347 N73-20934
Heat transfer solutions for solids with moving boundaries and for viscous liquid flow
[AD-754639] 11 p1349 N73-20950
Developments in techniques for analyzing boundary layer characteristics of rotary wings based on unsteady viscous-inviscid interaction
12 p1361 N73-21046
Meksyn asymptotic integration method for studying viscous interaction within hypersonic rarefied gas flow regime
12 p1389 N73-21263
Electron density distribution in viscous flows as applied to Trailblazer 2 reentry vehicle
[AD-755397] 13 p1564 N73-22674
Analysis of viscous hypersonic flow around slender sharp wedges and unyawed cones
[AD-757037] 14 p1650 N73-23386
Navier-Stokes equation and finite difference theory for compressible viscous flow
[AD-756242] 14 p1651 N73-23389
Numerical analysis of Navier-Stokes equations for steady, viscous, axisymmetric flow with application to flow past pitot tube at low Reynolds numbers
[ARC-R/M-3240] 15 p1725 N73-23998
Nonlinear partial differential equations for studying viscous compressible corner flow at subsonic and supersonic Mach numbers
15 p1764 N73-24294
Numerical solution of viscous fluid flow in finite tube with deformable walls in presence of valves for application to blood circulation process
16 p1867 N73-25117
Numerical analysis of fluid mechanic problems
[AD-758078] 16 p1893 N73-25318
Numerical analysis of axisymmetrical, viscous, compressible flow around blunt bodies for ideal gases with laminar unseparated boundary layers
17 p2012 N73-26273
Formulation and development of computer analysis for calculating streamlines and pressure distributions around two-dimensional isolated nacelles at transonic speeds
[NASA-CR-2217] 19 p2217 N73-27890
Analysis of supersonic flow involving viscous and inviscid flow using unified solution technique
19 p2251 N73-28148
Finite element analysis of tapered viscous flow
20 p2386 N73-29165
Solutions for various problems in two dimensional and axisymmetrical steady viscous flow with harmonic pressure field
20 p2387 N73-29175
Analysis of steady hypersonic flow with viscous interaction over sharp slender wedge by finite difference scheme
20 p2387 N73-29177
Numerical procedure for calculating viscous shock-layer flow near sharp leading edge of two dimensional and axisymmetric slender bodies
[AD-762505] 20 p2389 N73-29190
Development of computer program for determining airfoil pressure distribution for subcritical attached viscous flow
[NAL-TR-248] 21 p2523 N73-30236
Correlation between wind tunnel data and finite difference solutions for viscous and wind tunnel effects in transonic flows over airfoils
[AD-764133] 22 p2612 N73-30936
Numerical analysis of laminar unsteady flow around airfoil in viscous, incompressible fluid
22 p2649 N73-31226
Numerical analysis of boundary conditions of time dependent viscous compressible flow based on small perturbation of Navier-Stokes equation
23 p2773 N73-32176
Characteristics of flow about spherical body undergoing rectilinear, sinusoidal oscillations in viscous, incompressible fluid
23 p2773 N73-32180
Continuity and Navier-Stokes equations for analyzing viscous flow heat transfer in curved tubes
24 p2902 N73-33162
Computer solutions for potential and viscous flow calculations for engine inlets
[NASA-TM-X-71457] 24 p2905 N73-33184
Viscous laminar flow through laval nozzles
24 p2907 N73-33197

**VISCOUS FLUIDS**
Numerical computation of plane jet propagating onto curved wall surface submerged in viscous fluid
[NASA-TT-F-13924] 04 p0405 N73-13296
Tank heater for lowering viscosity of highly viscous liquids in storage tanks
[NASA-CASE-WLP-10040-1] 04 p0426 N73-13475
Thermal blooming of laser beams in viscous and thermally conductive fluids
[AD-748994] 04 p0431 N73-13508
Review of linear viscous stability theory for stably stratified parallel shear flow
[CONF-720632-1] 07 p0772 N73-16270
Platinum-rhodium device for stirring viscous fluids
[NBS-TN-771] 13 p1532 N73-22418
Effect of viscous lubricants on metal flow during cold reverse extrusion
[AD-743242] 13 p1533 N73-22425
Calculation and design of heat transfer apparatus for viscous liquids, liquid fuel, and lubricating oils
[AD-756947] 13 p1592 N73-22908
Calculation of nonlinear evolution of disturbance in unbounded viscous fluid with uniform shear using Navier-Stokes equations
[NASA-TN-D-7284] 14 p1648 N73-23363
Characteristics of wall mass transfer coefficient for pulsed laminar flow in pipe of Newtonian fluid containing dissoloved electrolyte
15 p1765 N73-24301
Differential equations for analyzing nonstationary incompressible viscous fluid flow in elastic cylindrical tube
17 p2014 N73-26290
Numerical analysis of steady state laminar motion of viscous, incompressible, and binary fluids for rotating flow in cylindrical geometry
18 p2129 N73-27204
Steady laminar flow of viscous fluid in circular tube entrance
22 p2650 N73-31232
Viscous hydrodynamic instability theory of peak and minimum pool boiling heat fluxes
[NASA-CR-134492] 22 p2653 N73-31252
Theoretical and experimental analysis of flow induced by harmonic oscillation of rods with arbitrary cross sections containing incompressible, viscous, Newtonian fluid
23 p2774 N73-32183

**VISIBILITY**
NT LOW VISIBILITY
Results of computations pertaining to brilliance of atmospheric haze and daytime sky
[NASA-TT-F-14421] 01 p0049 N73-10397
Regression analysis used for numerical-statistical prediction of visibility at sea
[AD-743733] 01 p0076 N73-10625
Detergent with glyceryl esthers and oil as protective coating to prevent fogging of space suit visor
[NASA-CASE-MSC-13530-2] 02 p0137 N73-11107
Index and introduction to Principles of Information Theory of Visibility in Atmosphere
[NASA-TT-F-14435] 02 p0211 N73-11712
Horizontal standard visibility determined by natural object contrast measurements, noting visual field observation
[DLR-FB-71-22] 03 p0261 N73-12118
Synoptic cloud cover observations for computing probability of clear lines of sight through atmosphere to ground
[P-4883] 04 p0444 N73-13620
Laser extension measurements of visibility during ice fog for aiding in SEV pilot system design
[AD-750114] 06 p0680 N73-15577
Haze-free and cloud-free lines-of-sight through atmosphere
[AD-751264] 07 p0796 N73-16476
Observation, measurement, and automatic calculation of runway visibilities
[NLL-M-20785-[5828.4F]] 07 p0814 N73-16597
Observation and measurement of visibility at ground
07 p0814 N73-16598
Automatic calculation of runway visual range on airdromes
07 p0814 N73-16599
Visibility range in presence of various meteorological phenomena
[NASA-TT-F-14886] 12 p1422 N73-21525
Characterization of interaction between detection and visibility processes with application to search policies
15 p1743 N73-24130
Digital enhancement of ERTS-1 MSS data for maximum image visibility
[PAPER-110] 19 p2278 N73-28331
Application of model output statistics to predict ceiling and visibility
[FAA-RD-73-14] 19 p2315 N73-28621
Determination of visibility slant range when landing aircraft in radiation fog
24 p2946 N73-33523
Effect of various parameters on long range underwater vision for narrow and broad beam illumination
24 p2958 N73-33630

**VISIBLE RADIATION**
U LIGHT [VISIBLE RADIATION]

**VISIBLE SPECTRUM**
U LIGHT [VISIBLE RADIATION]
U SPECTRA

**VISION**
NT BINOCULAR VISION
NT COLOR VISION
NT MONOCULAR VISION
NT NIGHT VISION
NT PERIPHERAL VISION
NT STEREOSCOPIC VISION
Drug effects on vision of flying personnel
12 p1371 N73-21121

**VISIOPLASTICITY**
U FLOW VISUALIZATION
U PLASTIC FLOW

**VISORS**
Detergent with glyceryl esthers and oil as protective coating to prevent fogging of space suit visor
[NASA-CASE-MSC-13530-2] 02 p0137 N73-11107
Test evaluation of laser protective visors for flight crews
[AD-751470] 07 p0751 N73-16102

**VISUAL ACCOMMODATION**
Effects of reduced atmospheric pressure, elimination of nitrogen, hypoxia, and exposure to restricted visual environment on range of accommodation and color vision
[NASA-CR-128896] 13 p1484 N73-22037

VISUAL ACUITY
Compensatory oculogravic response of eye movement direction during slow head rotation
06 p0634 N73-15148
Predictive control of human eye tracking movements in response to visual stimuli
06 p0634 N73-15149
Vibrational effects on visual acuity of human operator seated in military tracked vehicle
[AD-750345] 06 p0636 N73-15172
Spectral deficits in visual acuity due to laser irradiation
[AD-750394] 06 p0637 N73-15173
AGARD conference on air-to-ground target acquisition
[AGARD-CP-100] 10 p1225 N73-19959
Peripheral acuity with complex stimuli at two viewing distances
10 p1226 N73-19965
Air-to-ground target acquisition with flare illumination
10 p1226 N73-19968
Visual acuity changes in humans during hypokinetic bed rest test
13 p1482 N73-22014
VISUAL AIDS
Design of computerized airborne traffic display device with alphanumerical control for aircraft pilots
01 p0014 N73-10112
Improved pilot performance using simulated pictorial landing display with symbols
01 p0016 N73-10122
Visual display format effects on pilot describing functions in manual tracking performance
01 p0016 N73-10123
Approach light properties for visual discrimination in pilot landing environment
[NASA-TT-F-14667] 08 p0941 N73-17710
Design and performance of metal oxide semiconductor analog shift register as image sensor and reading aid for blind persons
[AD-753259] 09 p1075 N73-18776
Performance tests of visual approach slope indicator [VASI] equipment and systems for improved terminal area effectiveness
[FAA-NA-73-64] 18 p2175 N73-27568
Ground based visual aid to alleviate spatial disorientation during takeoff and landing
[FAA-RD-73-26] 21 p2521 N73-30216
Development of visual simulation system design for space shuttle mission simulator to include cost analysis and alternate concepts
[NASA-CR-134020] 21 p2522 N73-30221
VISUAL CONTROL
Pilot visual threshold and perception for aircraft movement estimation during unaided visual approach control
01 p0016 N73-10125
VISUAL CUES
U CUES
U VISUAL PERCEPTION
VISUAL DISCRIMINATION
Human recognition of contrasting target in noisy environment with diversion of attention
[FOA-2-C-2482-H5] 02 p0135 N73-11092
Subjective tests of target acquisition time using television with image enhancement possibilities
[MBB-UFE-892-72-O] 06 p0636 N73-15165
Proceedings of symposium on color vision, color perception, visual acuity, and psychophysiology
[AD-754328] 11 p1249 N73-20136
VISUAL DISPLAYS
U DISPLAY DEVICES
VISUAL FIELDS
Improved visual capability for police helicopters
10 p1228 N73-19984
Automated visual sensitivity tester for determining visual field sensitivity and blind spot size
[NASA-CASE-ARC-10329-1] 17 p1988 N73-26072
VISUAL FLIGHT
Analysis of factors affecting approach and landing of aircraft under visual conditions to show causes of misjudgement resulting in aircraft landing accidents
[NASA-TT-F-15054] 20 p2360 N73-28980
VISUAL FLIGHT RULES
In flight incident involving near miss of Boeing 720 aircraft and Convair 240 aircraft near Front Royal, Virginia on 26 Apr. 1972
[NTSB-AAR-72-30] 03 p0252 N73-12040
Analysis of flight plans submitted at flight service stations for IFR and VFR flight clearances during calendar year 1971
[AD-748901] 04 p0447 N73-13652
Investigation of disappearance of Cessna 310 aircraft on flight between Anchorage and Juneau, Alaska on 16 Oct. 1972
[NTSB-AAR-73-1] 08 p0867 N73-17018
Analysis of aircraft pilot capability to visually detect other aircraft in air to air situation as collision avoidance feasibility
[FAA-RD-73-40] 12 p1374 N73-21145
Performance tests to determine capability of aircraft pilots to avoid midair collisions based on visual perception of target and information from pilot warning indicator
12 p1374 N73-21146
VISUAL OBSERVATION
Visual investigation of runway and taxiway pavements at Campbell Army Airfield, Fort Campbell, Kentucky
[AD-743462] 01 p0037 N73-10291
Visual inspection of runway conditions at Butts Army Airfield, Fort Carson, Colorado
[AD-743859] 01 p0037 N73-10293
Visual inspection of runway pavement conditions at Forney Army Airfield, Fort Leonard Wood, Missouri
[AD-743856] 01 p0037 N73-10294
Visual survey of runway and taxiway conditions at Davison Army Airfield, Fort Belvoir, Virginia
[AD-743463] 01 p0038 N73-10296
Horizontal standard visibility determined by natural object contrast measurements, noting visual field observation
[DLR-FB-71-22] 03 p0261 N73-12118
Visual observations of atmospheric structure and land and water surfaces by cosmonauts from manned orbiting space stations
09 p1026 N73-18373
Streamer chamber for visual observation of proton-proton interactions in accelerator
[BNL-17273] 10 p1138 N73-19271
Investigation of light flash phenomenon observed by Apollo crews
[NASA-CR-128866] 10 p1213 N73-19867
Analysis of aircraft pilot capability to visually detect other aircraft in air to air situation as collision avoidance feasibility
[FAA-RD-73-40] 12 p1374 N73-21145
Dynamics of lower thermosphere through comparison of optical observations of motions of vapor trails with radar observations of ionized meteor trails
[NASA-CR-131645] 12 p1420 N73-21509
Observations by astronauts on Apollo 16 flight
12 p1449 N73-21735
Apollo 16 visual observations of surface geology from lunar orbit
12 p1452 N73-21764
Visual study of outer region of turbulent boundary layer along flat plate
18 p2129 N73-27203
Argelander, Pickering, and Neyland-Blazhko methods for visually estimating variable star brightness
21 p2594 N73-30785
Cosmonaut earth observations from space
[JPRS-59831] 21 p2595 N73-30793
VISUAL PERCEPTION
NT SPACE PERCEPTION
NT VISUAL DISCRIMINATION
Visual evoked cortical response as measure of stress in naval environment, using rapid flash rates
[AD-744934] 01 p0011 N73-10088
Influence of illumination color, viewing distance, and turbidity on underwater vision
[AD-743756] 01 p0012 N73-10092
Effect of vigilance on performance of simple visual detection task
[AD-745317] 01 p0012 N73-10097
Effect of automatic landing system display on pilot information requirements
01 p0016 N73-10126
Bayesian model for stimuli processing in visual space perception
01 p0016 N73-10127
Visual image generation as textured flight information resembling retinal images for airborne flight simulation
01 p0017 N73-10128
Literature review on psychophysiological factors affecting visual perception of colored signal light
[AD-746297] 02 p0133 N73-11083
Multidimensional Fourier transformation model for human visual pattern recognition in computerized simulation
[AD-745995] 02 p0147 N73-11195
Operation of image intensifier tubes and analysis of fluctuation theory on visual contrast sensitivity with ideal image intensifiers
[IZF-1972-18] 02 p0148 N73-11202
Optical texture perception and pattern recognition imagery
[AD-746658] 02 p0212 N73-11722
Analysis of reaction time to different visual cuing methods in large displays during secondary task performance
[AD-747688] 03 p0262 N73-12120
Psychophysical functions of range and time estimates by ground and aerial observers
[AD-747271] 04 p0380 N73-13094
Noise and response complexity effects on human attention and performance in visual perception task
[AD-747797] 04 p0381 N73-13105
Receiver operating characteristics for underwater signal detection performance of sea lions
[AD-746520] 04 p0382 N73-13113
Substantive analyses of optical design, using visual perception
[AD-749372] 05 p0502 N73-14084
Apparent object movement due to optical distortion produced by head movement under water
[AD-749319] 05 p0502 N73-14086
Systems engineering methods for human performance enhancement in signal detection and flight control
[AD-748239] 05 p0503 N73-14098
Bloch law error in visual perception of capacitor discharge brightness
[AD-749452] 05 p0505 N73-14109
Investigation of US Army UH-1 helicopter accidents where orientation errors were contributing factor during fiscal year 1969
[AD-749695] 06 p0623 N73-15059
Visual perception during space flight
06 p0629 N73-15104
Prolonged bed rest and positive radial acceleration effects on human visual response time
[NASA-TN-D-7161] 06 p0630 N73-15117
Visual evoked responses from divers subjected to hyperbaric conditions simulating depths to 1200 feet breathing various gas mixtures
[AD-749325] 06 p0631 N73-15127
Radiation effects on human visual and vestibular analyzer functions
[AD-750499] 06 p0632 N73-15132
Fatigue effect on human visual perception
[AD-750097] 06 p0636 N73-15171
Computer generation of patterns for analysis of human visual perception of form
[FOA-2-C-2473-52] 06 p0643 N73-15224
Effects of quantized luminance levels and display contrast on sonar target recognition
[AD-751711] 07 p0757 N73-16148
Training procedure for improving divers distance estimation ability in clear and turbid water
[AD-752976] 10 p1121 N73-19140
Application of extra-foveal vision to predicting target acquisition in air-to-ground search
10 p1225 N73-19960
Modelling of random human visual search performance based on physical properties of eye
10 p1225 N73-19961
Modelling prediction of probability of acquiring designated target as function of its range as target is approached
10 p1225 N73-19962
Calculation and simulation of effects of complex search situations
10 p1225 N73-19963
Relationship between subjective effect of structured target backgrounds on acquisition performance
10 p1226 N73-19964
Model for inherent contrast conditions in full-form objects
10 p1226 N73-19966
Biomedical problems with helmet mounted sight and visual target acquisition system
10 p1226 N73-19969
Changes in human visual functions after exposure to weak vestibular irritations
11 p1246 N73-20113
Conference on human visual search and perception
[AD-754327] 11 p1248 N73-20133
Proceedings of symposium on color vision, color perception, visual acuity, and psychophysiology
[AD-754328] 11 p1249 N73-20136
Computerized simulation of three dimensional robots using generalized cylinder descriptions
[AD-755139] 11 p1251 N73-20152
Ability of aircraft pilot to visually acquire and recognize two and three dimensional targets during diving approach
[AD-754743] 11 p1268 N73-20294
Analysis of aircraft pilot capability to visually detect other aircraft in air to air situation as collision avoidance feasibility
[FAA-RD-73-40] 12 p1374 N73-21145
Performance tests to determine capability of aircraft pilots to avoid midair collisions based on visual perception of target and information from pilot warning indicator
12 p1374 N73-21146
Photographic recording of aircraft in near midair collision conditions to determine feasibility of collision avoidance based on visual perception of pilot
[CDC-JL-5] 12 p1374 N73-21147
Analysis of flight tests to determine range of visual detection of aircraft as basis for visual perception to avoid midair collisions
12 p1374 N73-21148
Analysis of parameters affecting transition from meteorological visibility range to real visibility range during aircraft landing
[NASA-TT-F-14887] 13 p1556 N73-22607
Acceleration effects on human visual functions under hypoxic conditions
14 p1609 N73-23040
Optical modulation transfer functions of human eye for white light
[IZF-1973-2] 14 p1609 N73-23047
Lipreading aid indicating voice/voiceless feature, using visual or tactile sense
14 p1626 N73-23179
Reliability analysis of unpaced visual inspection tasks
[AD-757608] 14 p1671 N73-23564

Photometric measurements on human sensitivity to optical luminosity considering seasonal and monthly fluctuations
14 p1692 N73-23732

Black body brightness in horizontal visual range theory
[NASA-TT-F-14930] 15 p1814 N73-24700

Limitations on pilot visual perception of target from low flying aircraft
[AD-759651] 16 p1869 N73-25136

Machine perception of speech and vision
[AD-760153] 17 p2002 N73-26187

Flight evaluation of glide slope determination during landing approach by reference to diamond shaped figure painted on runway
[NASA-TM-X-2849] 18 p2105 N73-27027

Visual detection of oil films on water surface
[PB-219825/7] 18 p2148 N73-27362

Psychophysiological aspects in flight personnel visual perception of image indicator
20 p2367 N73-29035

Visibility and optimum light characteristics of marks for sighting devices
20 p2368 N73-29039

Improved performance of visual perception of solar patrol observers monitoring sun activity
[AD-760802] 20 p2372 N73-29063

Algorithms involved in visual shape perception
24 p2886 N73-33050

**VISUAL PHOTOMETRY**

Visual and photographic observations of Beta Scorpii occultation by Jupiter
[NASA-CR-129990] 05 p0594 N73-14832

**VISUAL PIGMENTS**

Literature review on human macular pigment absorption and density spectrum of cone receptor
[IZF-1972-17] 14 p1609 N73-23046

**VISUAL SIGNALS**

Effect of vigilance on performance of simple visual detection task
[AD-745317] 01 p0012 N73-10097

**VISUAL STIMULI**

Reaction tester for testing reaction to light stimuli
[NASA-CASE-MSC-13604-1] 04 p0383 N73-13114

Peripheral acuity with complex stimuli at two viewing distances
10 p1226 N73-19965

Design of light modulator for generation of periodic visual stimuli
[AD-754562] 11 p1250 N73-20149

Comparison of electroencephalographic response patterns in man and monkeys to visually evoked cortical stimuli
[IZF-1972-24] 14 p1609 N73-23049

Human continuous reaction time task distribution rates for paced and selfpaced responses to visual stimuli
[IZF-1973-5] 14 p1613 N73-23077

Correlation between primary response and late slow oscillation of evoked potential in response to light in awake and anesthetized rabbits
24 p2889 N73-33069

Orientative-investigative reaction as factor changing configuration of evoked potentials during repeated light flashes
24 p2889 N73-33070

**VISUAL TASKS**

Study of differences between left and right hand performance in compensatory tracking task
[RAE-TR-72117] 07 p0750 N73-16098

Concept evaluation and subsystem analyses for design of remote controlled teleoperator visual system
[NASA-CR-124059] 08 p0879 N73-17117

Air-to-ground visibility of lights at low background levels
10 p1226 N73-19967

Effect of sleep deprivation and heat stress on human performance in visual and auditory tasks
[OES-8/72] 22 p2624 N73-31024

**VISUAL TRACKING**

U OPTICAL TRACKING

**VISUALIZATION OF FLOW**

U FLOW VISUALIZATION

**VITAMIN B**

U THIAMINE

**VITAMIN B 86**

U PYRIDOXINE

**VITAMIN C**

U ASCORBIC ACID

**VITAMINS**

NT ASCORBIC ACID
NT NICOTINIC ACID
NT PYRIDOXINE
NT THIAMINE

Multiple immunoassay system for determining parathyroid hormone, calcitonin, and vitamin D in human blood
09 p0994 N73-18112

Medical analysis of vitamin balance among personnel of Tenth Soviet Antarctic Expedition to show effects on health and acclimatization ability
20 p2408 N73-29357

**VITON RUBBER [TRADEMARK]**

Chemorheology of Viton B fluorocarbon elastomer by kinetic analysis of chemical stress relaxation, and infrared and gel permeation chromatography analysis
01 p0119 N73-10985

Stress corrosion cracking of titanium alloys by hydrofluoric acid released during Viton B thermal degradation
[D-MAT-191] 18 p2161 N73-27455

**VITREOUS MATERIALS**

Magnetic properties of iron oxides in boron oxides
[AD-754104] 10 p1202 N73-19780

Influence of epoxide resin space lattice thickness on dynamic modulus of elasticity
[NASA-TT-F-14913] 14 p1680 N73-23633

Physical and mechanical properties of glassy carbons
[AD-757765] 15 p1802 N73-24606

**VLASOV EQUATIONS**

Numerical solution to Vlasov-Poisson equations and to simplified Fokker-Planck-Poisson equations
[ORO-4211-3] 03 p0324 N73-12639

Comparison of various numerical solutions to nonlinear Vlasov equation with each other and with solutions to Poisson equation
[COO-2059-12] 03 p0324 N73-12640

Propagation properties of ion density perturbations and waves in collisionless plasmas with Maxwellian velocity distribution functions
[RISO-257] 03 p0343 N73-12795

Description of linear wave propagation in hot collisionless plasmas using Vlasov and Maxwell equations
[NASA-CR-131496] 13 p1562 N73-22663

Wave-wave coupling equations for plasma oscillations
[AD-758316] 14 p1697 N73-23769

Vlasov equation for studying anisotropy produced instabilities in confined hot electron plasma
[EUR-CEA-FC-664] 15 p1819 N73-24736

Korteweg-deVries equation for studying effect of Landau damping on nonlinear ion acoustic waves
[IPPJ-155] 16 p1949 N73-25775

Vlasov equations for analyzing plasma equilibrium stability
[IPP-6/117] 24 p2963 N73-33675

Vlasov approximation of plasma turbulence in stochastic external field
[EUR-CEA-FC-690] 24 p2965 N73-33693

**VOCAL CORDS**

Speech synthesis aided by recursive filter approximating transfer function of nasalized vocal tract
14 p1624 N73-23157

Investigation of vocal cord regulatory mechanism of register, pitch, and intensity of voice during singing
14 p1632 N73-23225

**VOCODERS**

Application of digital signal processing to design of phase vocoder analyzer
14 p1621 N73-23131

Diagnostic evaluation of intelligibility in digital vocoders
14 p1624 N73-23161

Visual vocoder for aiding in speech teaching to deaf
14 p1627 N73-23184

Visual vocoder evaluation in speech therapy, foreign language pronunciation, and music interpretation
14 p1627 N73-23185

Development and characteristics of computer controlled voice response system
14 p1632 N73-23227

Simulation of complex microelectronic module functions in Delta Sigma Speech Coder containing analogue and digital elements
[AD-761206] 18 p2119 N73-27136

**VOICE**

Investigation of vocal cord regulatory mechanism of register, pitch, and intensity of voice during singing
14 p1632 N73-23225

Voice and hearing in system of acoustic orientation of animals
[NLL-DRIC-TRANS-3056-(3623.66)]
15 p1739 N73-24101

Nature, investigative instrumentation, and practical application of speech and linguistics
[AD-762373] 19 p2237 N73-28036

**VOICE COMMUNICATION**

NT TELEPHONY
NT VOICE DATA PROCESSING

Numerical control of delta modulated vocal signals in air navigation telecommunication system
01 p0025 N73-10194

Improving voice communication between divers and swimmers
[AD-745794] 01 p0029 N73-10228

Design and development of underwater breathing apparatus with microphone for underwater communication
[AD-746105] 02 p0142 N73-11154

Voice variability for assessing performance of communication system
[AD-746104] 02 p0143 N73-11155

Transmission line inversion problem applied to speech communication process
02 p0201 N73-11625

Measurement of operator workload in formation processing
[NASA-CR-2150] 04 p0379 N73-13087

On-line and off-line bench test evaluation of helium speech unscramblers under controlled conditions
[AD-748295] 04 p0391 N73-13176

Noise reduction and control in FAA air traffic control, navigational, and service facilities
[J-6250] 04 p0401 N73-13264

Phase coherent frequency synthesizer for improving digital voice and data transmission in communication systems
04 p0472 N73-13853

On-line and off-line evaluation of HeO2 unscramblers speech intelligibility
[AD-751034] 07 p0758 N73-16157

Design and development of universal voice processor system
[NASA-CR-128739] 08 p0885 N73-17161

Development of computerized speech recognition and voice communication system
[AD-752244] 08 p0886 N73-17172

Computer network modeling system for planning data management in voice communication
[AD-752797] 09 p1006 N73-18210

System for analysis and classification of voice communications associated with space missions or simulations
[NASA-CR-128837] 10 p1128 N73-19191

Capabilities, functions, and conceptual methods of operation for satellite-aided communications system in oceanic air traffic control environment
[FAA-RD-73-41] 12 p1460 N73-21833

Automatic processing of French speech
[AD-752811] 13 p1491 N73-22090

Multidimensional representation of personal quality of vowels and their acoustical correlates
14 p1631 N73-23217

Development of procedures and techniques for improved speech analysis based on fast Fourier transform and time compression and analysis
14 p1632 N73-23226

Development and characteristics of computer controlled voice response system
14 p1632 N73-23227

Development and characteristics of terminal analog speech synthesizer using pulse width modulation and pulse number modulation techniques
14 p1632 N73-23228

Development and characteristics of audio response unit for use with telephone exchange to answer tax inquiries from subscribers
14 p1632 N73-23229

Development of method of speech analysis and synthesis using partial autocorrelation coefficients and optimum quantization technique
14 p1632 N73-23230

Pulse position modulation laser communication system for voice transmission
[AD-757258] 14 p1633 N73-23237

Feasibility of hybrid voice coding system for speech transmission
[AD-756519] 14 p1637 N73-23272

Associative communication multiplexer for voice data compression
[AD-758246] 15 p1754 N73-24221

Voice communication and hearing in acoustic orientation systems of animals at various evolution levels
[DRIC-TRANS-3056] 16 p1867 N73-25121

Design of stable temperature compensated crystal oscillator for voice communication system
[AD-759938] 17 p2006 N73-26220

Analysis of voice command systems for application to military aircraft operation to show manufacturers, specifications, and research projects
[AD-762922] 20 p2362 N73-28998

Tandem electronic voice switching system
[FAA-RD-73-133] 21 p2519 N73-30206

**VOICE DATA PROCESSING**

Procedure for repairing and recovering voice data from heat damaged magnetic tapes
[NASA-CASE-MSC-14219-1] 07 p0755 N73-16132

Real time, small vocabulary, connected-word speech recognition system
[AD-753176] 09 p1006 N73-18211

Performance of digital voice transmission system with modulator-demodulator network
[AD-754921] 11 p1258 N73-20210

Time induced orthogonality for simplified voice control of speech recognition machines
14 p1621 N73-23130

Pitch-synchronous time-compression speech sampling method for greater intelligibility
14 p1621 N73-23134

Automatic formant and fundamental frequency extraction from digital inverse filter formulation
14 p1622 N73-23139

Comparison of voice coding technique for satellite-based air traffic control system
14 p1630 N73-23209

Design of speech-understanding computer system
[AD-757049] 14 p1637 N73-23270

Interference in digital voice data link between aircraft and ground traffic control
[FAA-RD-73-63] 15 p1750 N73-24185

Associative communication multiplexer for voice data compression
[AD-758246] 15 p1754 N73-24221
Computer program to obtain power spectrum of frequency modulated signal, modulated by voice signal, digital signal, and combinations of both
[FAA-RD-73-56] 18 p2116 N73-27111
Simulation testing of detector for digitally encoded multifrequency tones
[REPT-6755] 18 p2116 N73-27113
Tandem electronic voice switching system
[FAA-RD-73-133] 21 p2519 N73-30206

**VOID RATIO**
Relationship between brittle and plastic fracture of high strength steels owing to void dynamics
[NASA-CR-131101] 10 p1171 N73-19522
Void fraction in subcooled trichlorotrifluoroethane boiling at high pressures
[NASA-CR-2241] 14 p1718 N73-23938

**VOIDS**
Computer calculations of growth rates of voids in stainless steel during neutron irradiation
[HEDL-TME-72-35] 03 p0316 N73-12576
Photoelastic models of structures containing spherical voids in hexagonal close-packed configuration
[UCRL-73848] 03 p0361 N73-12940
Research on neutron irradiation induced voids in metals
[CONF-710601] 05 p0562 N73-14568

**VOIGT EFFECT**
Millimeter wave polarimeters and Cotton-Mouton effect in plasmas
[EUR-CEA-FC-675] 24 p2965 N73-33694

**VOLATILITY**
Gas chromatographic-mass spectrometric analysis of volatile organic metabolic products in terrestrial soils
[NASA-CR-129602] 04 p0386 N73-13134
Development of procedures for determining contamination characteristics of materials which become volatile in space environment
[NASA-CR-130132] 05 p0600 N73-14878

**VOLATILIZATION**
U VAPORIZING

**VOLCANICS**
U VOLCANOLOGY

**VOLCANOES**
Thermal surveillance of volcanoes of Cascade Range and Iceland using ERTS-1 imagery and data collection platforms
[E72-10246] 03 p0289 N73-12346
Thermal surveillance of volcanoes of Cascade Range and Iceland using ERTS-1 DCP systems and imagery
[E73-10317] 09 p1023 N73-18349
Volcano and earthquake surveillance network in Alaska, California, Washington, Hawaii, El Salvador, Nicaragua, Iceland, and Guatemala
[E73-10337] 09 p1025 N73-18365
Volcanic origin of mare ridges and sinuous rilles on lunar surface
12 p1454 N73-21780
Establishment of prototype volcano surveillance network using ERTS data collection platforms
[E73-10545] 14 p1654 N73-23420
Thermal surveillance of active volcanoes in Washington, California, and Iceland
[E73-10556] 14 p1655 N73-23428
Prototype surveillance network of volcanoes in Western Hemisphere using data from ERTS data collection platforms
[E73-10558] 14 p1655 N73-23430
Application of ERTS-1 data for development and operation of volcano surveillance network
[E73-10711] 17 p2018 N73-26318
ERTS-1 imagery of geological, climatological, and volcanic activities in Iceland
[E73-10713] 17 p2018 N73-26320
Development of volcano surveillance and early warning system using ERTS-1 data collection system
[PAPER-G9] 19 p2264 N73-28240
Thermal surveillance of Cascade range volcanoes using ERTS-1 MSS data, aircraft imaging systems, and ground based DCP
19 p2284 N73-28369
Prototype DCP volcano surveillance network in Washington, Nicaragua, California, Guatemala, Hawaii, El Salvador, Iceland, and Alaska
[E73-11024] 22 p2662 N73-31328
Volcanic features in Mars surface photographs
23 p2839 N73-32684
Aerial thermal infrared surveillance of active volcanoes in northern Cascade Range
[E73-11100] 24 p2914 N73-33257

**VOLCANOLOGY**
Prototype volcano surveillance network in Alaska and Cascade Mountains
[E72-10242] 03 p0289 N73-12342
Results of examining 40 maar volcanic cones in western North America
[NASA-CR-129290] 03 p0292 N73-12382
Glaciology and volcanology on Wrangell Mountains, Alaska
[E72-10339] 05 p0532 N73-14327
Utilization of ERTS-1 imagery to study short-lived events such as fires, volcanism, storms, and earthquakes
[E73-10025] 06 p0660 N73-15359
Glaciology and volcanology studies in Wrangell Mountains, Alaska using ERTS-1 imagery
[E73-10277] 08 p0914 N73-17485
Regional geologic, tectonic, and volcanic surveys of Bolivia using ERTS-1 imagery
[E73-10286] 08 p0914 N73-17492
ERTS-1 imagery of structural geology and volcanology in Central High Plateau of Bolivian Andes
[E73-10296] 10 p1146 N73-19333
ERTS-1 imagery of glaciology and volcanology in Wrangell Mountains, Alaska
[E73-10404] 11 p1277 N73-20366
Detection and evaluation of worldwide short-lived events from ERTS-1 imagery
[E73-10453] 11 p1283 N73-20412
Influence on volcanic eruption exerted by particular weather and climatic situations
[NLL-M-22864-[5828.4F]] 11 p1313 N73-20652
Possible analogs around Orientale Basin provide reasonable alternatives to geomorphologic interpretation of volcanism in Descartes highlands - Part D
12 p1453 N73-21768
Volcanic activity on moon
12 p1457 N73-21804
Comparison of forms of lunar relief with terrestrial volcanic formations
12 p1457 N73-21807
Broad scale application of ERTS-1 imagery to study and mapping of geological, hydrological, land use, rangelands, and soil cultures in Wyoming
[E73-10554] 14 p1655 N73-23426
Aeromagnetic survey of Amchitka Island, Alaska and adjacent insular shelf for studying tertiary volcanic rocks
[USGS-PP-707] 14 p1661 N73-23481
Glaciology and volcanology in Wrangell Mountains, Alaska based on ERTS-1 imagery
[E73-10665] 16 p1899 N73-25360
Pattern recognition and detection of short-lived events such as storms, forest fires, volcanoes, and earthquakes using ERTS-1 data
[E73-10678] 16 p1901 N73-25373
ERTS-1 surveillance of volcanic areas of Southern Italy
19 p2284 N73-28368
Application of remote sensing techniques to geology of Bonanza volcanic center
[NASA-CR-133499] 19 p2294 N73-28448
Ground-based radiation thermometry mapping of volcanology in Central America
[E73-10937] 21 p2529 N73-30279
Geology, volcanology, and glaciology of Wrangell Mountains, Alaska from ERTS-1 imagery
[E73-10940] 21 p2529 N73-30282
Earthquakes and volcanoes caused by subterranean explosions provoked by petroleum or natural gas
[NASA-TT-F-15095] 21 p2536 N73-30334
Cayley formation, emphasizing secondary lunar craters
[NASA-TM-X-62302] 21 p2596 N73-30804
ERTS-1 imagery of short-lived events such as forest fires, oil spills, volcanic activity, floods, and storms
[E73-11048] 23 p2779 N73-32224

**VOLT-AMPERE CHARACTERISTICS**
Voltage characteristics of electrical discharges over long air gaps
[AD-746853] 02 p0213 N73-11723
Deep trap model for predicting capacitance voltage characteristics of irradiated silicon diodes and resistors
08 p0888 N73-17188
Electro-optical control for volt-ampere characteristics of avalanche phototransistors
[JPRS-58321] 09 p1008 N73-18226
Volt-ampere characteristics of pulse discharge flow in hollow hydrogen cathode
[AD-753038] 09 p1072 N73-18749
Volt-ampere characteristics of explosive wires using pulse-current generator
[AD-753552] 10 p1135 N73-19251
Current-voltage characteristics measured in Al/AlO lead tunneling junctions
[COO-1569-91] 12 p1439 N73-21656
Volt-ampere characteristics of deformed niobium semiconductor memory switch
[COO-3169-12] 12 p1441 N73-21673
Effect of charge carrier heating on volt-ampere characteristics of thermoelectric indicators of microwave emissions
[AD-756561] 13 p1531 N73-22407
Volt-ampere characteristics of enclosed keeper hollow cathode discharge
[NASA-TM-X-2799] 15 p1825 N73-24792
Volt-ampere characteristics of heated electric wire during cryogenic cooling in liquid helium
[AD-759958] 17 p2005 N73-26211
Influence of silicon particle deposition on volt-ampere characteristics of p-n junctions
18 p2186 N73-27652
Dynamic response characteristics of aqueous electrolyte hydrogen oxygen fuel cells
22 p2617 N73-30973

**VOLTAGE**
U ELECTRIC POTENTIAL

**VOLTAGE BREAKDOWN**
U ELECTRICAL FAULTS

**VOLTAGE CONVERTERS [DC TO DC]**
Dc to dc converter for electronic equipment power source
[AD-762181] 19 p2223 N73-27934

**VOLTAGE GENERATORS**
NT PHOTOVOLTAIC CELLS
Electronics of waveform generator for digital voltage source
[AD-758212] 15 p1758 N73-24247

**VOLTAGE MEASUREMENT**
U ELECTRICAL MEASUREMENT

**VOLTAGE REGULATORS**
Analog signal to discrete time interval converter for control of dc to dc power supplies
[NASA-TM-X-68153] 02 p0128 N73-11043
Surge divertor breakdown voltage characteristics
[AD-747622] 03 p0276 N73-12236
Low frequency magnetic field interference of dc/dc regulators and transformers
[ESRO-CR-58] 05 p0499 N73-14059
Development of procedures for regulating voltage in power systems for conditions of remote electric transmissions and operation of electro-receivers
[AD-748233] 05 p0499 N73-14060
Voltage controlled phase shifter with low distortion
[NASA-CASE-MFS-21671-1] 08 p0891 N73-17211
Power conditioning subsystem for Symphonie satellite with bus voltage regulation
[REPT-72-90] 09 p0991 N73-18085
Voltage monitoring system for remote application
[NASA-CASE-KSC-10736-1] 14 p1640 N73-23290
Modular inverter/converter automatic paralleling and protection system
[NASA-TN-D-7279] 15 p1737 N73-24084
Overvoltage protection network for electrical equipment
[NASA-CASE-ARC-10197-1] 20 p2380 N73-29124
Control circuit for reducing bias voltage and radiation sensitivity of photomultiplier
[NASA-CASE-ARC-10593-1] 21 p2517 N73-30187

**VOLTAGE VARIATION INDICATORS**
U VOLTMETERS

**VOLTERRA EQUATIONS**
Volterra factorization of Green matrix and imbedding of general linear boundary value problems
[TR-72-48] 02 p0202 N73-11634

**VOLTMETERS**
Voltage sensor counter as three-phase power disturbance monitor
[AD-746169] 02 p0129 N73-11049
Effects of harmonics strengths on voltmeter reading accuracy
[NLL-ESB-TRANS-499-[3810.97]]
04 p0419 N73-13412
Performance tests of differential dc voltmeter
[LRBA-PV-9/520/SIE] 05 p0548 N73-14450
Acceptance tests of direct current high precision digital voltmeter
[LRBA-PV-11/520/SIE] 09 p1008 N73-18227
Voltage monitoring system for remote application
[NASA-CASE-KSC-10736-1] 14 p1640 N73-23290
Development and characteristics of voltmeter and electronic suppression circuit for high accuracy readings
[REPT-6734] 14 p1666 N73-23519

**VOLUME**
Sintering temperature and tungsten content effects on volumetric shrinkage of ferrotungsten alloy briquets
04 p0432 N73-13518

**VOLUMETRIC ANALYSIS**
Volumetric analysis and dilatometric study of ferrite magnesium cast iron during heat treatment
[AD-749627] 05 p0563 N73-14572
Thermal flowmeter for urine volume measurement in manned space flight environment
[NASA-CR-128726] 07 p0750 N73-16095
Partial condensation and fractionation for analysis on mixture of hydrogen, methane, and ethane
[NASA-TT-F-14681] 07 p0752 N73-16109

**VON MISES THEORY**
U STRESS FUNCTIONS

**VOR SYSTEMS**
U VHF OMNIRANGE NAVIGATION

**VORTEX COLUMNS**
U VORTICES

**VORTEX DISTURBANCES**
U VORTICES

**VORTEX FLOW**
U VORTICES

**VORTEX GENERATION**
U VORTEX GENERATORS

**VORTEX GENERATORS**
Experimental investigations of two-dimensional flow problems and electric power generation in open cycle vortex MHD generator
[BM-RI-7699] 05 p0583 N73-14746

Underwater vortex field generation in wake of rectangular airfoil
[NASA-TM-X-62274] 17 p2014 N73-26288
Two dimensional flow, low speed wind tunnel tests of trapped vortex-high lift airfoil to reduce blowing requirements for lift augmentation
[AD-762077] 19 p2218 N73-27893
Formation and structure of vortex rings formed by stream deceleration
22 p2653 N73-31251
Vortex generation and propagation under perfect slip flow conditions, for thin elliptical cylinder
24 p2908 N73-33206

**VORTEX INJECTORS**
Vortex pairing in turbulent shear layer at moderate Reynolds numbers
24 p2903 N73-33169

**VORTEX RINGS**
Vortice distribution field for calculating inlet flow of ducted propeller
[AD-754114] 10 p1144 N73-19318
Analysis of motion of laminar and turbulent viscous vortex rings produced in air by pneumatic actuated piston vortex generator
16 p1886 N73-25265
Formation and structure of vortex rings formed by stream deceleration
22 p2653 N73-31251

**VORTEX SHEETS**
Computation of steady conical flow past a yawed slender delta wing with leading edge separation using vortex sheet model and Newton-Raphson iteration
[IC-AERO-72-17] 01 p0001 N73-10005
Development of wake vortex monitoring system using laser Doppler sensors for analyzing vortex flow field
[NASA-CR-123921] 02 p0152 N73-11229
Analysis of aircraft trailing vortices to show formation and breakdown for various aircraft wing configurations
[ME/A-72-1] 08 p0895 N73-17247
Numerical analysis of inviscid, fully developed structure of lift-generated vortices behind aircraft wings and extension to arbitrary span-loaded distributions
[NASA-TM-X-62224] 09 p1016 N73-18289
Analysis of point vortex approximation of vortex sheet in two space dimensions and application to vortex sheet induced by ellipitcally loaded wing
[AD-755007] 11 p1273 N73-20335
Wind tunnel tests to determine effect of tip vortex of forward mounted wing on engine inlet ingestion
[NASA-TM-X-68225] 13 p1473 N73-21932
Analysis of Kutta-Joukowsky condition in three dimensional flow with application to vortex sheet attachment to wing surface
[NASA-TT-F-14918] 15 p1767 N73-24319
Calculation of wake vortices behind wings of transport aircrafts in holding, takeoff, and landing configurations
[FAA-RD-73-42] 17 p1983 N73-26027

**VORTEX STREETS**
Dependence of turbulent line vortices decay on Reynolds number
[AD-753131] 09 p1017 N73-18297

**VORTEX TUBES**
U HILSCH TUBES
U VORTICES

**VORTICES**
Vortex components and flow systems
[FOA-2-C-2480-E4] 02 p0155 N73-11258
Heat transfer at critical point, jet turbulence, and vortex systems
[AD-747294] 02 p0244 N73-11981
Calculation of Magnus sideforce developed by spinning cylinder at angle of attack considering effects of boundary layer and shed vorticity in crossflow
03 p0247 N73-11998
Results of analytical methods for predicting wing vortex strength compared with results of flight investigation of wake characteristics of several large jet transport aircraft
[NASA-TN-D-6904] 03 p0251 N73-12033
Numerical analysis of fluid containment near stagnation point and within self-confined stagnation region for bi-component mixture
[NASA-CR-2172] 03 p0283 N73-12292
Determination of circulation and diameter of vortices from ultrasonic wave phase deviation
[REPT-6/1972] 03 p0285 N73-12308
Analysis of eddies and lift forces created on vertical circular cylinder by oscillatory flow conditions
[AD-748078] 03 p0287 N73-12329
Vortex model for calculating blade circulation flow of helicopter rotor
[NASA-TT-F-14637] 04 p0371 N73-13014
Development of system for predicting movement and decay of aircraft-generated vortices in air corridors near air terminals using meteorological information
[LMSC/HREC-D306226] 06 p0620 N73-15036
Modification of UH-1 helicopter rotor to determine effects of injecting tip vortex of rotor blade with mass of linearly directed air
[AD-750634] 06 p0625 N73-15074
Analysis of lee side vortex flow distribution about ogive-cylinderfrustum-cylinder at various angles of attack and Mach numbers - Vol. 1
[NASA-CR-123997-VOL-1] 06 p0653 N73-15307
Compilation of computed parameters resulting from analysis of lee side vortex flow distribution about ogive-cylinder-frustum-cylinder at various angles of attack and Mach numbers - Vol. 2
[NASA-CR-123997-VOL-2] 06 p0653 N73-15308
Analysis of Magnus sideforce developed by spinning cylinder at angle of attack based on boundary layer and shed vorticity in cross flow
07 p0768 N73-16239
Development of computer programs to calculate helicopter rotor tip vortex geometry in hover and forward flight to include calculation of rotor harmonic air loads
[AD-752628] 08 p0869 N73-17032
Analysis of aircraft trailing vortices to show formation and breakdown for various aircraft wing configurations
[ME/A-72-1] 08 p0895 N73-17247
Analysis of axially symmetric motions of viscous neutral stratified gas in spherical layer resulting from rotation of inner sphere
[NASA-TT-F-14661] 08 p0897 N73-17260
General equations for describing molecular diffusion in vortex flow and possible application to isotopic separation by fixed wall centrifugation
[FRNC-TH-213] 08 p0897 N73-17262
Analysis of scaling parameters for flow in core region of vortex generated by rectangular wing tip and vortex generated by ogee wing tip
[NASA-CR-2180] 10 p1103 N73-18995
Effect of wing span loading on wing trailing vortices
[AD-754055] 11 p1232 N73-20003
Application of momentum theory to determine performance limits of propellers, and lifting rotors with axes parallel to undisturbed flow
[AD-754072] 11 p1235 N73-20025
Three component wake velocity measurements of full scale OH-13 helicopter rotary wing during hovering flight
[AD-754644] 11 p1235 N73-20030
Development and mixing of coaxial fluid jet with axisymmetric swirling vortex flow in cylindrical chamber
[AD-754613] 11 p1272 N73-20324
Procedures for measuring velocity distribution through helicopter rotor blade tip vortex using single full scale rotor blade
12 p1360 N73-21034
Analysis of electrical charge generated by helicopter rotor operating near particulate matter with seeded vortex
[AD-755282] 12 p1366 N73-21080
Simulation of atmospheric vortex based on boundary conditions and parameter values of strong atmospheric tornadoes and waterspouts
12 p1390 N73-21269
Nonoscillatory characteristics of Taylor vortices occurring in Couette flows based on evolution of eigenvalues and analytic continuation - Part 3
[AD-754480] 12 p1392 N73-21289
Effectiveness of trailing edge bevels on reducing vibration excitation causing vortex shedding into wake
[REPT-1052/73] 13 p1471 N73-21911
Flight tests to determine characteristics of vortex and turbulent wake generated by DC-10 aircraft for development of air traffic control separation criteria
[REPT-73-00470] 13 p1474 N73-21938
Application of laser Doppler velocimeter for measurement of central vortex filament in wind tunnel test section
[NASA-TM-X-62243] 13 p1536 N73-22448
Analysis of vortex shedding from airfoils with application to vortex noise generated by helicopter rotary wings
[AD-757167] 14 p1602 N73-22989
Development of lifting surface theory for statically operating propellers based on vortex-lattice representation
[AD-757264] 14 p1603 N73-22998
Structure and dynamics of horizontal roll vortices in planetary boundary layer
15 p1771 N73-24341
Design criteria for slender warped wings with unswept trailing edge with zero load along leading edge and near planar vortex sheet at trailing edge for design lift coefficient
[ARC-R/M-3406] 16 p1852 N73-25008
Ship model basin for simulating aircraft vortex wake
[AD-758893] 16 p1890 N73-25291
Physical processes occurring in vortex stabilized arcs with and without applied axial magnetic fields
[AD-759187] 16 p1892 N73-25313
Afterburner instability vortex shedding model for air breathing turbojet combustion
[AD-758890] 16 p1957 N73-25834
Effects of mass injection of tip vortex on airfoil performance at transonic speeds
[AD-760363] 17 p2016 N73-26304
Experimental determination of bound vortex lines and flow in vicinity of trailing edge of slender delta wing
[NASA-TT-F-15012] 18 p2131 N73-27217
Application of finite-difference machine code for analyzing wake-vortex problem in quasi-cylindrical boundary layer approximation
[NASA-TM-X-69495] 20 p2387 N73-29179
Wind tunnel tests to measure axial and tangential velocity profiles in near wake vortices of semi-span model of Convair 990 aircraft model using laser Doppler velocimeter
[NASA-TM-X-62294] 21 p2524 N73-30244
Three basic forms of cyclonic cloud vortices to trace spirals
[AD-763170] 21 p2540 N73-30363
Exhaust blast velocities and temperatures at ground level for various aircraft and wing tip vortex velocity for C-5 aircraft
[AD-764228] 22 p2616 N73-30961
Vortex age as scaling parameter in wake turbulence development and dissipation
[NASA-CR-132312] 22 p2652 N73-31245
Apparatus for analysis of turbulent transport properties in non-decaying, swirling, annular vortex flows
[AD-763916] 22 p2654 N73-31262
Laminar secondary Taylor-Goertler vortex flow in rectangular cross section channel
[AD-764503] 22 p2655 N73-31268
Flow field solution for boundary layer interaction in confined viscous vortex
23 p2772 N73-32170
Formation of vortices in free boundary layer
[NASA-TT-F-15133] 23 p2774 N73-32188
Combustion and expansion of propane-air mixtures near bottom of short cylinder to generate air vortex rings for removing air from cylinder
[AD-764613] 23 p2777 N73-32207
Characteristics of low speed air flow over slender, sharp edged delta wing at various angles of attack and effects on longitudinal and lateral stability
24 p2869 N73-32922
Wake development on models of elliptic, rectangular, swept and delta planforms when plunged in water
[ARC-CP-1238] 24 p2870 N73-32932
Analysis of random motions of vortex elements behind aircraft wing and design of vortex arrays to reduce wake-vortex to small aircraft
[NASA-TM-X-62304] 24 p2877 N73-32976
Vortex generation and propagation under perfect slip flow conditions, for thin elliptical cylinder
24 p2908 N73-33206

**VORTICITY**
Inertial gravity wave frequency spectrum in cylindrically confined incompressible two component liquid flow
[AD-752439] 09 p1018 N73-18312
Stratospheric turbulence as an effect of jet streams, vorticity, temperature gradients, and temperature distribution
[NLL-M-22823-[5828.4F]] 11 p1274 N73-20338
Solar magnetic sector structure effects on tropospheric and lower stratospheric vorticity
[NASA-CR-133842] 21 p2592 N73-30773

**VORTICITY EQUATIONS**
Nonlinear temperature and vorticity equations for studying convective motions of 4-day zonal circulation of upper Venus atmosphere
17 p2080 N73-26828

**VOSTOK SPACECRAFT**
Analysis of major problems in early stages of manned spaceflight, Vostok and Mercury flights, and Mars exploration
[NASA-TT-F-14916] 14 p1709 N73-23867

**VOWELS**
Computer simulated parallel-formant synthesizer to copy short samples of human speech
14 p1624 N73-23156
Multidimensional representation of personal quality of vowels and their acoustical correlates
14 p1631 N73-23217

**VTO FIGHTER AIRCRAFT**
U FIGHTER AIRCRAFT
U VERTICAL TAKEOFF AIRCRAFT

**VTOL**
U VERTICAL LANDING
U VERTICAL TAKEOFF

**VTOL AIRCRAFT**
U VERTICAL TAKEOFF AIRCRAFT

**VULCAN AIRCRAFT**
Comparison of gust velocities derived from accelerations of Canberra and Vulcan aircraft noting acceleration and wing loading power spectra
[ARC-CP-1244] 22 p2615 N73-30955

**VULCANIZATES**
U VULCANIZED ELASTOMERS

**VULCANIZED ELASTOMERS**
Carbon black additives used to improve heat-aging resistance in silicone rubber vulcanizates
[AD-747769] 03 p0321 N73-12619
High performance vulcanized elastomers produced by nitrile and silicone rubber covulcanization
[RAE-TR-72184] 17 p2050 N73-26588

**VULNERABILITY**
Development of computer code for determining survivability of aircraft following exposure to radiation from aerial nuclear explosion
[AD-746015] 02 p0215 N73-11738

Survivability and confidence assessment of military weapon systems with reference to tactics, threat, and environment
[AD-746061] 02 p0235 N73-11913
Survivability analysis of command and control communication systems
[AD-755846] 13 p1495 N73-22116
VZ-11 AIRCRAFT
U XV-5 AIRCRAFT
VZ-12 AIRCRAFT
U P-1127 AIRCRAFT

## W

W WINGS
U VARIABLE SWEEP WINGS
WABASH RIVER BASIN [IL-IN-OH]
Crop identification, acreage estimation, urban land use, soil mapping, and earth resources identification in Wabash River Basin using ERTS-1 imagery
[E72-10208] 03 p0288 N73-12331
Crop identification, soil mapping, water resources, and urban land use analysis in Wabash River Basin based on ERTS-1 imagery
[E73-10364] 10 p1150 N73-19360
Utilization of ERTS-1 data for crop identification and acreage estimation, soil mapping, urban land use, water resources, atmospheric modeling, and earth surface feature identification in Wabash River Basin
[E73-10549] 14 p1655 N73-23422
Utilization of ERTS-1 imagery for soil mapping, land use, and urban mapping in Wabash River Basin
[E73-10862] 20 p2392 N73-29213
Crop identification, soil mapping, and atmospheric modeling in Wabash River Basin using ERTS-1 data
[E73-11082] 23 p2782 N73-32257
WAFERS
Prototype multi-wafer plasma anodization process
[AD-746003] 01 p0064 N73-10521
Bulk characteristics mapping for quality control of semiconductor wafer junctions
[BDX-613-604-REV] 05 p0586 N73-14769
WAGONS
U TRAILERS
WAKEFULNESS
Activity cycle data for spacecrews of Soyuz 3 to 9 spacecrafts before, during and after space flights
[JPRS-58173] 07 p0746 N73-16068
Electrophysiological sleep patterns of human and animal brains
[NASA-TT-F-740] 13 p1483 N73-22023
Neurophysiology of sleep and wakefulness in fish, amphibians, birds, and reptiles
13 p1483 N73-22025
Thalamic cat cell activities during sleep and wakefulness phases
13 p1484 N73-22030
Rhythm disturbances in sleep and wakefulness cycles of Soyuz 3 and 9 crews before, during, and after space flight
[NASA-TT-F-15103] 20 p2369 N73-29048
WAKES
NT AIRCRAFT WAKES
NT HELICOPTER WAKES
NT HYPERSONIC WAKES
NT LAMINAR WAKES
NT PROPELLER SLIPSTREAMS
NT SLIPSTREAMS
NT SUPERSONIC WAKES
NT TURBULENT WAKES
Model for generation of blade-passage noise caused by interaction of rotor wakes with downstream stator blades in fan stage
[NASA-TM-X-2669] 02 p0222 N73-11797
Scalar wave scattering on water surface wake generated by moving pressure point
[AD-749113] 05 p0527 N73-14291
Drag measurement in wake of oscillating cylinder at low Reynolds number using hot-wire technique
[DLR-FB-71-42] 09 p0981 N73-18015
Amplitudes and widths of Gaussian distributions of electron density in wakes of hypervelocity projectiles flown in air and nitrogen at various pressures
[AD-759065] 16 p1893 N73-25316
Sequential spark method for measuring cone wake velocity profiles
[AD-759159] 16 p1893 N73-25317
Wake effects in transpiration cooling of gas turbine blades
[AD-759191] 17 p2078 N73-26806
Numerical analysis of horizontal diffusion in ocean water to determine lifetime and spatial extent of submarine wakes in various turbulent media
[AD-762046] 19 p2256 N73-28186
Analysis of wake collapse in sea water and stratified fluids with emphasis on final stages of decay
[AD-761622] 19 p2257 N73-28189
Scaling phenomena of collapse of wake of self-propelled body in stratified fluid
[AD-762454] 19 p2258 N73-28201
Wake development on models of elliptic, rectangular, swept and delta planforms when plunged in water
[ARC-CP-1238] 24 p2870 N73-32932
Turbulence anisotropy effects on pressure distribution and secondary flow of boundary layers, free and wall jets, and wakes
24 p2906 N73-33191
WALL FLOW
Turbulent boundary layers on walls of rectangular water pipe inlets
02 p0155 N73-11259
Development of theories for calculating pressure on perturbed plane wall in presence of viscous boundary layer
[AD-746332] 02 p0158 N73-11278
Application of continuous wave gas laser and pulsed ruby laser to analyze laminar and turbulent films of air at porous wall with carbon dioxide and helium injected into air stream
[AD-747511] 03 p0287 N73-12323
Wind tunnel design for testing V/STOL aircraft in transition flight
[AD-749154] 04 p0402 N73-13278
Analysis of mean velocity profiles in three-dimensional turbulent boundary layers during incompressible flow
[REPT-71-FM-13] 04 p0404 N73-13289
Numerical computation of plane jet propagating onto curved wall surface submerged in viscous fluid
[NASA-TT-F-13924] 04 p0405 N73-13296
Error analysis on two dimensional steady laminar boundary layer of incompressible wall flow
[AD-748771] 04 p0406 N73-13308
Mixing length theory used to determine influence of pressure gradients on wall region of turbulent boundary layer
[AD-749371] 05 p0527 N73-14290
Analysis of laminar part of separation bubbles in two dimensional incompressible flow for various shaped objects
06 p0616 N73-15000
Stabilizing and destabilizing effects of Coriolis body force on turbulent wall layers in two dimensional channel flow
07 p0768 N73-16243
Mathematical model for wall cooling in laminar hypersonic boundary layer
07 p0770 N73-16258
Viscous wall flow in turbulent boundary layer including shear stress
07 p0771 N73-16266
Computerized prediction of two dimensional wall bouadary layer flow from laminar through transition to turbulent regimes
08 p0894 N73-17239
Magnetohydrodynamic wall flow with laminar separation
[AD-753149] 09 p1072 N73-18751
Analysis of Reynolds stress in turbulent boundary layer on smooth wall with zero pressure gradient
[AD-754758] 11 p1272 N73-20319
Nozzle and wall jet flow fields in bistable fluid amplifiers
13 p1509 N73-22230
Heat transfer in immediate vicinity of wall by measurement of average temperature profiles
[AD-756957] 13 p1512 N73-22256
Boundary layer transition and heat transfer in aerodynamic and thermic wall deformation
14 p1601 N73-22982
Transonic wind tunnel corrections for slotted or perforated walls
14 p1649 N73-23373
Visualization of flow deviation by cylindrical wall cavities
14 p1649 N73-23374
Calculation of supersonic boundary layer flow separation and reattachment along plane wall with sinusoidal hollow
[REPT-72-4] 14 p1650 N73-23382
Development of method for calculating characteristics of laminar boundary layer on nonadiabatic wall of constant temperature in presence of pressure gradients
[ARC-R/M-3233] 15 p1728 N73-24013
Effects of wall jets in still air on flat and curved surfaces under external stream in presence and absence of pressure gradient and initial boundary layer
[ARC-R/M-3252] 15 p1729 N73-24025
Effect of small amplitude wall waviness upon stability of laminar boundary layer with respect to two dimensional disturbances
15 p1764 N73-24293
Development of mathematical formula for growth of compressible, turbulent boundary layers on isothermal and adiabatic walls
[ARC-R/M-3191] 16 p1853 N73-25013
Development of numerical methods for correcting wall constraints in transonic wind tunnels with ventilated walls
17 p2008 N73-26241
Structure of weak shock wave in vibrationally relaxing gas undergoing wall reflection
17 p2013 N73-26277
Interaction between supersonic boundary layer with turbulent flow and inelastic deformable wall to determine stress perturbations and pressure distribution
[TN-86] 20 p2388 N73-29186
Correlation between wind tunnel data and finite difference solutions for viscous and wind tunnel effects in transonic flows over airfoils
[AD-764133] 22 p2612 N73-30936
Reynolds stress in turbulent boundary layer on smooth wall
22 p2650 N73-31233
Turbulent boundary layer flow of gas-solid suspension
24 p2906 N73-33190
Laminar boundary layers at continuously moving wall and behind shock wave, noting fuel combustion problem
24 p2906 N73-33192
Theory for small perturbation laminar boundary layer stability at longitudinally curved walls
24 p2909 N73-33212
WALL JETS
Oscillations and pressure variations in circular jet impacting on wall
[NASA-TT-F-14630] 05 p0527 N73-14284
Nozzle and wall jet flow fields in bistable fluid amplifiers
13 p1509 N73-22230
Mixing characteristics of steady and intermittent blowing applied to boundary layer control
[AD-758390] 14 p1652 N73-23403
Turbulence anisotropy effects on pressure distribution and secondary flow of boundary layers, free and wall jets, and wakes
24 p2906 N73-33191
WALL PRESSURE
Investigating instantaneous structure of wall pressure under turbulent boundary layer flow in air
[REPT-9/1973] 24 p2904 N73-33177
WALL TEMPERATURE
Measurement of hypersonic free molecular sphere drag at varying wall temperature ratios
[AD-748618] 04 p0407 N73-13320
Thermocouple apparatus for measuring wall temperatures in regeneratively cooled rocket engines having thin walled cooling passages
[NASA-CASE-XLE-05230-2] 04 p0419 N73-13417
Heat transfer in immediate vicinity of wall by measurement of average temperature profiles
[AD-756957] 13 p1512 N73-22256
Aerodynamic heating analysis on sounding rocket tangent ogive nose wall
[NASA-TM-X-69896] 17 p1979 N73-26001
Computation of coolant and wall temperatures of regeneratively cooled liquid propellant rocket engines
[DLR-FB-72-29] 21 p2591 N73-30755
Structural heat pipe for spacecraft wall thermal insulation system
[NASA-CASE-GSC-11619-1] 23 p2857 N73-32828
WALL TEMPERATURE DISTRIBUTION
U TEMPERATURE DISTRIBUTION
U WALL TEMPERATURE
WALLOPS ISLAND
User requirements and instrumentation plans for aircraft tracking and guidance facility at Wallops Station
[NASA-CR-111931-1] 14 p1645 N73-23340
WALLS
NT BULKHEADS
NT NOZZLE WALLS
NT POROUS WALLS
NT THICK WALLS
NT THIN WALLS
NT WIND TUNNEL WALLS
Shock tube simulation of propagation of shock waves over and beyond walls, including slope effect
[REPT-10/71] 05 p0527 N73-14286
Temperature effects on hydrogen decomposition of wall surface coatings
[NASA-TM-X-2735] 08 p0946 N73-17748
Measurement of effects of sonic booms on light building structures for various building configurations
[RAE-LIB-TRANS-1633] 17 p1981 N73-26011
Containment design calculations for cylindrical vessel wall response to explosion
[SLA-73-508] 24 p2992 N73-33916
WALSH FUNCTION
Walsh transformation for two dimensional correlation and convolution in pattern recognition
[AD-746701] 03 p0272 N73-12207
Word recognition by Walsh transform computer program
14 p1622 N73-23143
WAR GAMES
Procedures for constructing and analyzing combat models for planning and executing naval combat operations
[JPRS-57404] 04 p0393 N73-13194
Development of analytic models for describing differential models of attack helicopters supporting a battalion task force - Vol. 1
[AD-762432] 19 p2356 N73-28956
Numerical analysis of military helicopters and air defense weapons to define operations in support of battalion task force combat - Vol. 2
[AD-762433] 19 p2356 N73-28957
WARFARE
NT ANTISUBMARINE WARFARE
NT COMBAT

Concepts for reduction of fatigue in sustained tactical operations
[AD-746643] 02 p0134 N73-11090
Evaluation of device to train forward air controllers to communicate target locations
[AD-751292] 07 p0751 N73-16103
Differential game theory applied to military operations, such as antimissile missile problem and air warfare
[BMVG-FBWT-73-9] 19 p2314 N73-28609
WARHEADS
NT NUCLEAR WARHEADS
WARM FRONTS
Use of hygroscopic materials and ionic surfactants as warm fog for dispersants
[AD-751635] 07 p0817 N73-16622
WARMING
U HEATING
WARNING DEVICES
U WARNING SYSTEMS
WARNING SIGNALS
U WARNING SYSTEMS
WARNING SYSTEMS
NT EARLY WARNING SYSTEMS
NT MINE DETECTORS
Development of in-flight fire detection and automatic suppression system for use on military helicopters
[AD-746630] 02 p0127 N73-11037
Three channel analog electronic warning system for control of nuclear plant
[NLL-WH-334-(9091.9F)] 02 p0144 N73-11166
Systems simulation for airport trailing vortex warning system
[NASA-TM-X-64704] 03 p0280 N73-12267
Operational tests and evaluation of optical infrared pilot warning system to determine probability of detection versus range
[NASA-CR-129525] 03 p0302 N73-12463
Test and evaluation of aural signal device to prompt students to scan for aircraft during flight simulator training
[FAA-RD-72-95] 04 p0373 N73-13030
Development and operating principles of collision warning system for aircraft accident prevention
[NASA-CASE-HQN-10703] 04 p0446 N73-13643
Development, design, fabrication, and testing of a self-generating overheat detection system for USAF aircraft
[AD-749474] 05 p0495 N73-14031
Trailing vortex hazard avoidance of Jumbo jets by airport warning system
05 p0610 N73-14958
Pilot warning indicators and collision avoidance systems
[PB-212496] 07 p0740 N73-16020
Analysis of aircraft fire warning system performance and procedures for eliminating false fire warning indications
[AD-751346] 07 p0740 N73-16025
Pilot warning indicator system of intruder aircraft
[NASA-CASE-ERC-10226-1] 07 p0798 N73-16483
Development of collision avoidance warning system criterion for use with aircraft operating in high density areas
13 p1471 N73-21915
Development of wake vortex avoidance system for airports to reduce hazards caused by aircraft wakes and permit increased utilization of terminal facilities
[FAA-ED-21-1] 14 p1645 N73-23342
Tactile information presentation using high pressure pulses into anti-G suit
[AD-761796] 19 p2228 N73-27969
Design and development of integrated fire and overheat detection and warning system for installation in aircraft nacelle
[AD-762919] 20 p2362 N73-28999
Silent alarm system for mutiple room facility or school
[NASA-CASE-NPO-11307-1] 21 p2519 N73-30205
Development and characteristics of electronic signalling system and data processing equipment for warning systems to avoid midair collisions between aircraft
[NASA-CASE-LAR-10717-1] 21 p2576 N73-30641
WASHINGTON
NT CASCADE RANGE [CA-OR-WA]
Mapping and detection of snow cover changes on land and on glaciers in Alaska, British Columbia, and Washington using ERTS-1 imagery
[E72-10237] 03 p0288 N73-12337
Cultural resources interpretation and map revision from ERTS-1 RBV and MSS imagery of Washington state
[E72-10276] 03 p0291 N73-12374
Information system for ERTS-1 data on timber resources in Washington and Oregon
[E73-10319] 09 p1023 N73-18351
Volcano and earthquake surveillance network in Alaska, California, Washington, Hawaii, El Salvador, Nicaragua, Iceland, and Guatemala
[E73-10337] 09 p1025 N73-18365
Automated thematic mapping and analysis of terrain in Arizona, Texas, Washington, Utah, Louisiana, and California using ERTS-1 imagery
[E73-10386] 10 p1153 N73-19379
Timber inventory and management in Washington using ERTS-1 imagery
[E73-10411] 11 p1278 N73-20373
Analysis of ERTS-1 imagery using electronic satellite image analysis console to display and measure snowfield extent, glacier development, and hydrologic features
[E73-10415] 11 p1279 N73-20377
Thermal surveillance of active volcanoes in Washington, California, and Iceland
[E73-10556] 14 p1655 N73-23428
Time-lapse data processing for dynamic hydrologic conditions at Mt. Rainier, Washington
[E73-10582] 15 p1772 N73-24356
Land management planning and timber resources management in Washington and Oregon from ERTS-1 imagery
[E73-10804] 18 p2138 N73-27279
Measurement of percentage of snow cover area on specific drainage basins in Cascade Mountains in Washington state using ERTS-1 imagery
[PAPER-W19] 19 p2273 N73-28296
Indepth comparative analysis of multispectral remote sensing techniques applied to salinity and drainage problems in Columbia Basin, Washington
22 p2656 N73-31280
Prototype DCP volcano surveillance network in Washington, Nicaragua, California, Guatemala, Hawaii, El Salvador, Iceland, and Alaska
[E73-11024] 22 p2662 N73-31328
WASHOUT [RADIOACTIVITY]
U FALLOUT
WASTE DISPOSAL
Extraterrestrial disposal of radioactive wastes
[NASA-TM-X-68147] 01 p0079 N73-10650
Aerospace technology for solving domestic solid waste disposal, water purification, and water recovery problems
04 p0472 N73-13849
Collection and disposal of human wastes in aesthetic and reliable manner to prevent degradation of crew performance
06 p0629 N73-15111
Electrically conducting ceramics to heat biowaste propellants to 2000 K in resistojet thrustors for space station application
[NASA-CR-112159] 06 p0635 N73-15161
Automatic liquid collection and disposal system
[NASA-CASE-LAR-11071-1] 09 p1039 N73-18474
Environmental factors and cost problems of selecting optimum sanitary landfill site for solid waste disposal
[NASA-CR-128744] 10 p1124 N73-19157
Water reclamation and waste disposal technology applied to land use and aerospace engineering
[NASA-CR-128857] 10 p1124 N73-19158
Waste disposal and water reclamation technology for land use and aerospace engineering application
[NASA-CR-128858] 10 p1124 N73-19159
Analysis of factors involved in selection of suitable sites for sanitary land fills with emphasis on economic and social problems
[NASA-CR-128745] 10 p1229 N73-19989
Reduced-gravity fecal collector seat and urinal
[NASA-CASE-MFS-22102-1] 11 p1249 N73-20141
Disposal of liquid and solid radioactive wastes at Trisaia Nuclear Research Center
[NASA-TT-F-14697] 11 p1323 N73-20734
Theoretical analysis of effects of outgassing and waste dumping on contamination of orbiting spacecraft
[NASA-CR-124131] 11 p1340 N73-20875
Analysis of water pollution levels in USSR lake and measures to protect water purity under conditions of economic development in vicinity
12 p1420 N73-21512
Space disposal of actinide radioactive wastes
[NASA-TM-X-68216] 12 p1426 N73-21562
Possible space destinations and launch vehicles for space disposal of radioactive waste
[NASA-TM-X-68211] 12 p1427 N73-21563
Nuclear waste disposal into space, using space shuttle and nonexpendable and expendable orbital stages
[NASA-TM-X-68235] 15 p1830 N73-24834
Temperature and internal pressure response of nuclear waste disposal container following impact on earth
[NASA-CR-121186] 16 p1943 N73-25721
Analysis of generated solid wastes and collection systems for San Francisco International Airport
[PB-219372/0] 18 p2127 N73-27189
Extraterrestrial disposal of radioactive waste from thermoelectric propulsion
[NASA-TM-X-62272] 19 p2225 N73-27943
Design and test performance of space crew waste collection system
[NASA-CR-133977] 19 p2225 N73-27945
ERTS-1 imagery for monitoring dumping of municipal and industrial wastes in New York Bight
[PAPER-E10] 19 p2269 N73-28274
Absorptive equipment for control of air polluting industrial wastes
[PB-221138/1] 21 p2575 N73-30637
Corrosion resistance of gas turbine components of power plant fueled with shredded refuse
[PB-221095/3] 21 p2591 N73-30759
Water recovery and solid waste processing for aerospace and domestic applications
[NASA-CR-134027] 22 p2623 N73-31016
Steam reactor system for manned spacecraft waste processing
[NASA-CR-134048] 23 p2752 N73-32021
Military treatment and disposal of high energy materials
[AD-764534] 23 p2858 N73-32835
WASTE UTILIZATION
Biodegradation of cellulose fibers and reclamation of single cell protein from refuse through fermentation process
[NASA-CR-130300] 06 p0630 N73-15115
Thermal combustion requirements for burner devices of human vegetative waste products
10 p1118 N73-19111
Antimicrobial phenyl preparations for human urine conservation during space flight
10 p1118 N73-19112
Cosmonaut adaptation to dehydrated food products and effects on human waste cycle
10 p1118 N73-19113
Feasibility demonstration of biowaste propellant resistojet engines for space station attitude control system
[NASA-CR-132269] 18 p2193 N73-27706
Water recovery and solid waste processing for aerospace and domestic applications
[NASA-CR-134027] 22 p2623 N73-31016
Systems design for advanced water recovery and waste processing in aerospace and domestic applications
[NASA-CR-134028] 22 p2623 N73-31017
Conference on waste glass recovery and re-use in secondary products
[NASA-CR-135792] 24 p2938 N73-33460
WASTES
NT FECES
NT HUMAN WASTES
NT METABOLIC WASTES
NT RADIOACTIVE WASTES
NT SEWAGE
NT URINE
Mapping of anthracite wastes from mining in Pennsylvania
[E73-11107] 24 p2915 N73-33264
WATCHES
U CLOCKS
WATER
NT COASTAL WATER
NT GROUND WATER
NT HEAVY WATER
NT NEARSHORE WATER
NT POTABLE WATER
NT SEA WATER
NT SHALLOW WATER
NT SURFACE WATER
NT VADOSE WATER
Computer prediction of performance of sorbent beds for CO2 or water removal
[NASA-CR-112098] 01 p0022 N73-10173
Prandtl number values for water and steam, liquid and gaseous heavy water, and sea water
[ESDU-68011] 01 p0038 N73-10301
Dynamic viscosity data for water and steam, liquid and gaseous heavy water, and sea water
[ESDU-68009] 01 p0038 N73-10303
Analysis of viscosity of water using distilled water as primary reference standard to show dynamic and kinematic viscosities
[ESDU-65009] 01 p0039 N73-10306
Dissolved oxygen analyzer for measuring dissolved oxygen concentration in industrial water systems
[NOAA-IFS-73005] 01 p0057 N73-10467
Description, performance specifications, and results of performance tests for Hydrolab 2A portable water quality analyzer
[NOOH-IFS-73006] 01 p0057 N73-10468
Evaluation of ice-water mixture thermocouple reference chamber discussing best operating parameter combination for high accuracy
[RAE-TR-72035] 01 p0058 N73-10475
Thermal conductivity of H20 and D2O
[ESDU-67031-AMEND-A] 01 p0115 N73-10954
Specific heat capacity at constant temperature and pressure of water substances
[ESDU-68008] 01 p0116 N73-10957
Vegetation, soil, and water reflectance measurements from ERTS-1 imagery of Hidalgo County, Texas
[E72-10267] 03 p0291 N73-12366
Corrosion fatigue behavior of 4340 steel above K sub Iscc in distilled water
[AD-746700] 03 p0317 N73-12584
Therapeutic value of mineral water diets especially Karlsbad Muhlbrunn water
[NASA-TT-F-14620] 04 p0379 N73-13079
Swinging ball viscosimeter design and calibration for water viscosity measurements
[AD-745252] 04 p0424 N73-13456
ERTS-1 measurement of vegetation, soil, and water reflectance
[E72-10364] 05 p0535 N73-14352

Stress corrosion cracking of sensitized austenitic stainless steels in oxygenated high temperature water
[BMI-1927] 05 p0562 N73-14565

Design and performance of prototype nitrogen/oxygen supply unit using water/hydrazine electrolysis to provide cabin leakage makeup in manned spacecraft
[NASA-CR-128688] 06 p0635 N73-15159

Long term performance test on electrolytic oxygen generator for manned test chamber
[NASA-CR-128687] 06 p0635 N73-15160

Wildland resources inventory of Nevada Great Basin using ERTS-1 imagery
[E73-10019] 06 p0659 N73-15355

Nuclear energy in hydrogen production by water dissociation method
[EUR-4838] 06 p0699 N73-15699

Optical properties and constants of water and aqueous solutions
[NASA-CR-130136] 06 p0699 N73-15700

Shock wave reflection from water surface
07 p0769 N73-16250

Investigation of positron annihilation in water and ice by measuring angular correlation
07 p0859 N73-16969

Repetitive ERTS-1 imagery of surface water variability and flooding along rivers and low-lying areas in Virginia, Iowa, and California
[E73-10046] 08 p0900 N73-17289

Application of ERTS-1 imagery to thematic mapping of open water, ice and snow cover, vegetation, and works of man
[E73-10089] 08 p0902 N73-17301

Dynamics of water drop evaporated by heating with laser pulse
[AD-752822] 09 p1001 N73-18167

Visual observations of atmospheric structure and land and water surfaces by cosmonauts from manned orbiting space stations
09 p1026 N73-18373

N2O photolyzed at 2139 A producing O[1 D] atoms in H2O and CO
[NASA-CR-130976] 09 p1029 N73-18398

Buffered gelled water to control nitrogen tetroxide-aerozine 50-hypergolic fuel fires
[NASA-CR-2198] 10 p1203 N73-19789

Boiler surface coating effects on water heated by solar energy
[NASA-TT-F-14850] 11 p1237 N73-20043

Resistance of animals immersed in water to high acceleration
[NASA-TT-F-14828] 11 p1246 N73-20119

ERTS-1 spectral reflectance measurements of vegetation, soil, and water in Rio Grande Valley, New Mexico
[E73-10408] 11 p1278 N73-20370

Emulsifying capacity of oils and wearability of additives during contact with water
[AD-754622] 11 p1302 N73-20561

Quantitative analysis of hydrogen-induced slow crack growth in low alloy steel in gaseous hydrogen and distilled water environments
[NASA-TM-X-62253] 11 p1305 N73-20589

Plane compression wave in pressure field of electrical discharge into water
[AD-754614] 11 p1324 N73-20746

Rapid vaporization of liquid hydrogen in noninsulated reservoir placed in water
[CEA-CONF-2082] 12 p1429 N73-21582

Design and construction of waterdrop generator with remote control of drop mass and interval
[NBS-TN-776] 14 p1645 N73-23343

Low intensity magnetic field effects on flotation properties of water
[AD-758623] 16 p1946 N73-25746

Restoration of obliterated stamped serial numbers by ultrasonically induced cavitation in water
[NASA-TM-X-68257] 18 p2213 N73-27866

Gas chromatographic analysis on water interfacial energy
[AD-761655] 19 p2230 N73-27988

Molecular mechanisms of conduction and polarization in water vapor, liquid water, and ice
[AD-762060] 19 p2231 N73-27993

Water penetration properties of multispectral photography
[UCS/72/13] 20 p2412 N73-29387

Heat transfer across interface between high speed steam jet and external coaxial cocurrent water flow
[AD-763696] 21 p2527 N73-30262

Modeling flow cavitation in water
[PB-220531/8] 21 p2528 N73-30268

ERTS-1 measurements of seasonal changes in reflectance of soils, vegetation, and water in Hidalgo County, Texas
[E73-10946] 21 p2530 N73-30288

Thematic mapping of wetlands, forests, open water, and Mississippi River flooding from ERTS-1 imagery
[E73-10952] 21 p2531 N73-30294

Environmental factors in production and use of energy and effects on air, water, and land
[R-992-RF] 21 p2537 N73-30340

Dielectric properties of ice, snow, and water at microwave frequencies and thickness measurements of ice and snow layers with radar
[CRC-1242] 21 p2537 N73-30341

Geology, mineral deposits, and water resources of western Colorado from Skylab EREP data
[E73-11130] 24 p2917 N73-33285

Physical behavior of water and carbon dioxide on Mars
24 p2984 N73-33843

WATER BALANCE
Physiological regulatory mechanisms of water and electrolyte levels in human body in high temperature environment
[NASA-TT-F-13915] 01 p0008 N73-10066

Liquid retention in chlorpropamide therapy and water intoxication of patients
[NASA-TT-F-14597] 02 p0133 N73-11077

Mortality rate of guinea pigs after decompression treatment as function of water balance
[DLR-FB-71-20] 05 p0501 N73-14075

Energy balance equations for parameterization of hydrological processes effecting atmospheric circulation
05 p0573 N73-14663

Radioimmunoassay of urinary antidiuretic hormone excretion in man considering water loading and dehydration effects
09 p0993 N73-18107

Human nitrogen and water/salt metabolisms in controlled regenerative atmosphere
10 p1115 N73-19089

Influence of immersion in temperature controlled bath on circulation and water balance in human body
[NASA-TT-F-14834] 10 p1119 N73-19124

Application of ERTS-1 remote sensing to determine turbidity plumes in Lake Ontario
[PAPER-W16] 19 p2272 N73-28293

WATER CIRCULATION
NT OCEAN CURRENTS
NT WATER CURRENTS
Selected papers on hydrometeorology, oceanography, navigation
07 p0857 N73-16950

ERTS-1 imagery of water circulation in Prince William Sound
[E73-10617] 15 p1774 N73-24378

ERTS-1 imagery of sea ice and surface water circulation along Alaskan Continental Shelf
[E73-10620] 15 p1775 N73-24381

Influence of atmospheric cyclones on circulation and mixing of sea water in motionless uniformly rotating baroclinic ocean
19 p2258 N73-28202

ERTS-1 imagery and high altitude photography of Lake Ontario Basin to provide input for models of river discharge and macro-scale features of lake circulation
[PAPER-W14] 19 p2272 N73-28291

Application of ERTS-1 imagery for analysis of terrestrial water balance of Lake Ontario and drainage basin
[PAPER-W15] 19 p2272 N73-28292

ERTS-1 imagery of sea surface circulation and sediment transport in Cook Inlet, Alaska
[PAPER-M8] 19 p2280 N73-28347

Sediment distribution, water currents, and water circulation in Cook Inlet, Alaska
[PAPER-M9] 19 p2281 N73-28348

Distribution and movement of suspended sediment in Gulf of Mexico off Texas coast
[PAPER-M10] 19 p2281 N73-28349

Sea ice and surface water circulation along Alaskan continental shelf
[E73-10901] 20 p2396 N73-29250

Surface circulation of coastal waters of Prince William Sound Alaska
[E73-10902] 20 p2396 N73-29251

ERTS-1 detection of oceanic eddies in Lesser Antilles
[E73-10922] 20 p2398 N73-29271

Circulation and mixing of sea water due to stationary and transitory axisymmetric atmospheric cyclones
[AD-763930] 22 p2669 N73-31383

ERTS-1 imagery of sea, ice, and surface water circulation along Alaskan continental shelf
[E73-11050] 23 p2779 N73-32226

ERTS-1 imagery of water surface circulation of Prince William Sound, Alaska
[E73-11064] 23 p2781 N73-32240

ERTS-1 monitoring of turbidity, color, boundaries, circulation, and pollution dispersion in Delaware coastal waters
[E73-11147] 24 p2918 N73-33301

WATER COLOR
Ocean water color assessment of Monterey Bay, California, from ERTS-1 RBV and MSS imagery
[E72-10190] 01 p0046 N73-10369

Analysis of ERTS-1 MSS data for color variations in Great Lakes and Chesapeake Bay to determine if multispectral imagery usable for locating and mapping extent of distinct water masses
[E72-10224] 02 p0163 N73-11318

Location of water current boundaries in Gulf of Mexico by sensing color change associated with cyclonic edge of zone of maximum horizontal velocity shear
[E72-10233] 02 p0163 N73-11326

Ocean water color assessment from ERTS-1 RBV and MSS imagery
[E73-10002] 06 p0658 N73-15338

Location of ocean current boundaries in Gulf of Mexico by ERTS-1 sensing of water color changes
[E73-10030] 06 p0660 N73-15363

Location of ocean current boundaries in Gulf of Mexico by sensing color change associated with cyclonic edge of zone of horizontal velocity shear
[E73-10022] 10 p1146 N73-19330

Detection of current boundaries in Gulf of Mexico by sensing ocean color changes
[E73-10612] 15 p1774 N73-24373

Assessment of water color in Caribbean from ERTS-1 RBV and MSS imagery.
[E73-11006] 22 p2660 N73-31311

ERTS-1 monitoring of turbidity, color, boundaries, circulation, and pollution dispersion in Delaware coastal waters
[E73-11147] 24 p2918 N73-33301

WATER CONSUMPTION
Water load tests for determining hydration status and adrenal and kidney functions during post flight period
[NASA-TT-F-15091] 22 p2620 N73-30998

WATER CONTENT
U MOISTURE CONTENT

WATER COOLED REACTORS
NT BOILING WATER REACTORS
NT HEAVY WATER REACTORS
NT PRESSURIZED WATER REACTORS
NT SWIMMING POOL REACTORS
Thermohydraulic test facility for design of fuel elements for water and sodium cooled reactors
[NT-31-1972] 05 p0579 N73-14712

Thermodynamic equilibrium model for simulating pressure transient propagation in two phase water flow with mass transfer
08 p0896 N73-17255

Power production and fuel capability of light water cooled cavity test reactor
[NASA-TM-X-2864] 19 p2320 N73-28662

WATER CURRENTS
NT OCEAN CURRENTS
Location of water current boundaries in Gulf of Mexico by sensing color change associated with cyclonic edge of zone of maximum horizontal velocity shear
[E72-10233] 02 p0163 N73-11326

Sea, ice, and surface water circulation in Alaskan Continental Shelf
[E72-10347] 05 p0533 N73-14335

ERTS-1 imagery of surface water circulation in Prince William Sound
[E72-10348] 05 p0533 N73-14336

Surface water circulation in Prince William Sound using ERTS-1 imagery
[E73-10291] 08 p0915 N73-17496

Measurement of coastal currents and processes and seaward extent of suspended sediment transport in waters of California
[E73-10375] 10 p1151 N73-19370

Sea ice and surface water circulation in Cook Inlet, Alaska, and along continental shelves
[E73-10370] 11 p1275 N73-20346

ERTS-1 imagery of water circulation in Prince William Sound
[E73-10402] 11 p1277 N73-20364

ERTS-1 imagery of sea ice and surface water circulation along Alaskan contiental shelf
[E73-10416] 11 p1279 N73-20378

ERTS-1 imagery of California nearshore sediment transport, coastal processes, and tidal currents
[E73-10525] 13 p1517 N73-22292

Remote detection of oceanic eddies in Lesser Antilles using ERTS-1 imagery
[E73-10592] 14 p1657 N73-23451

Sediment distribution, water currents, and water circulation in Cook Inlet, Alaska
[PAPER-M9] 19 p2281 N73-28348

ERTS-1 monitoring of turbidity, color, boundaries, circulation, and pollution dispersion in Delaware coastal waters
[E73-11147] 24 p2918 N73-33301

WATER DEPTH
Utilization of ERTS-1 imagery for water depth measurement, mapping of Yellowstone Park, atmospheric effects in Colorado, lake ice surveillance, recreational land use, IFYGL Lake Ontario, image enhancement, water quality monitoring, and oil pollution detection
[E72-10201] 02 p0144 N73-11167

Utilization of ERTS-1 imagery for water depth measurement, mapping of Yellowstone Park, atmospheric effects in Colorado, lake ice surveillance, recreational land use, IFYGL Lake Ontario, image enhancement, water quality monitoring, oil pollution detection, and mapping iron compounds
[E72-10190] 02 p0160 N73-11296

Depth effect on underwater ambient noise intensity in Caribbean Sea
[AD-750693] 06 p0670 N73-15447

Utilization of ERT-1 imagery for water depth measurement, Yellowstone Park data, atmospheric effects in Colorado, lake ice surveillance, recreational land

use, IFYGL, image enhancement, water quality monitoring, oil pollution detection, and mapping iron compounds
[E73-10086] 08 p0901 N73-17298
Water depth measurement and mapping of shallow water features of Little Baham Bank using ERTS-1 imagery
[E73-10388] 11 p1275 N73-20350
ERTS-1 applications in water depth calculation, terrain classification, land use mapping, water pollution, and mineral exploration
[E73-10565] 15 p1771 N73-24345
Calculation of water depth in Caribbean from ERTS-1 MSS data
[E73-10566] 15 p1771 N73-24346
Estimation of water depth off Great Bahama Bank using ERTS-1 imagery
[PAPER-M19] 19 p2282 N73-28357
Calculation of water depth off Little Bahama Bank from ERTS-1 data for use in upgrading and mapping world navigation charts of shallow waters
[PAPER-M20] 19 p2282 N73-28358
Multidisciplinary research on water depth measurement, Yellowstone Park, atmospheric effects, lake ice surveillance, recreational land use, IFYGL, image enhancement, water quality, oil pollution detection, and mapping iron compounds from ERTS-1 data
[E73-11119] 23 p2783 N73-32264
Water depth determination off Puerto Rico from Skylab multispectral imagery
[E73-11141] 24 p2918 N73-33296

**WATER EROSION**
Water impingement model for raindrop erosion of homogeneous materials
[AD-748790] 04 p0406 N73-13310
Computerized analysis of droplet size effect on erosion rate in wet steam turbine stage
[PB-211901] 05 p0527 N73-14292
Measurement of lateral erosion rates at proposed river crossing sites of Alaska pipeline by aerial photogrammetry
[AD-748875] 05 p0541 N73-14402
Relative rain erosion resistance of low-density-thermal protection materials for space shuttles at subsonic velocities
[NASA-CR-130541] 08 p0969 N73-17924
Composite constructions of reinforced plastics with improved rain erosion resistance
[AD-758650] 15 p1803 N73-24610
Influence of ocean waves and meteorological variables on beach erosion at Plum Island, Massachusetts
[AD-759513] 18 p2148 N73-27364
Analysis of erosion along Niigata Beach, and development of improved methods of erosion control based on ERTS-1 imagery
[PAPER-E14A] 19 p2270 N73-28278
Simulated rain erosion testing on closed pore insulation for shuttle orbiter
[RM-573] 20 p2434 N73-29548
Mars surface erosion and canal formation by running water
23 p2838 N73-32683

**WATER FLOW**
Turbulent boundary layers on walls of rectangular water pipe inlets
02 p0155 N73-11259
Analytical model for parallel flow-induced vibrations experimentally checked on single rod test facility in water loop
[EUR-4771] 03 p0284 N73-12301
Development of airborne instrumentation and application of remote earth observations for determining stream discharge prediction for water management program
04 p0471 N73-13839
Aircraft and spacecraft observation of riverbed formation and flow patterns
04 p0472 N73-13846
Meander patterns of Feather and Colorado Rivers
05 p0537 N73-14366
Swirling cavity flow breakdown along axis of swirling water flow in circular pipe
[REPT-250] 06 p0724 N73-15913
Heat and mass transfer analysis of liquids and air flowing in opposite directions under various atmospheric pressures
[AD-751503] 07 p0856 N73-16938
ERTS-1 imagery of water circulation in Prince William Sound
[E73-10402] 11 p1277 N73-20364
Heat exchange coefficient for humans in constant temperature moving water
[NASA-TT-F-14867] 11 p1349 N73-20943
Mapping permafrost areas of Alaska, correlating snowpack cover of Caribou-Poker Creek with stream runoff, and mapping and inventorying icing on Chena River
[E73-10511] 13 p1516 N73-22286
Hydrological investigation of drainage basin characteristics from ERTS-1 imagery for improved regression estimates of water flow
[E73-10652] 16 p1898 N73-25348
Movement of suspended particle and solute concentrations with inflow and tidal action in Chesapeake Bay
[E73-10662] 16 p1899 N73-25358
Application of ERTS-1 remotely sensed data and ground truth information to predict and manage water quantity and quality in river basins
[E73-10689] 17 p2018 N73-26314
Analysis of amplitude modulation of ultrasonic sound beam impinging at right angles to turbulent water jet
[RAE-LIB-TRANS-1671] 17 p2063 N73-26686
Application or ERTS-1 imagery for determining course of Ebro River in northeast Spain
[PAPER-W2] 19 p2271 N73-28282
Application of ERTS-1 multispectral imagery to water resources development in lower Mekong River basin in southeast Asia
[PAPER-W3] 19 p2271 N73-28283
Assessment of flood damage in Arizona using ERTS-1 MSS imagery to show extent of inundation and sediment deposition
[PAPER-W6] 19 p2271 N73-28284
Evaluation of stream flow data for Verde River watershed in central Arizona provided by ERTS-1 imagery
[PAPER-W8] 19 p2271 N73-28286
ERTS-1 imagery and high altitude photography of Lake Ontario Basin to provide input for models of river discharge and macro-scale features of lake circulation
[PAPER-W14] 19 p2272 N73-28291
ERTS-1 imagery of plume development where Connecticut River flows into Long Island Sound
[PAPER-M5] 19 p2280 N73-28345
Oceanographic mapping of distribution and flow of water masses in northern Gulf of California by use of ERTS-1 imagery and optical models
[PAPER-M11] 19 p2281 N73-28350
Hydrogen bubble flow visualization technique for study of aerodynamic problems in water flow facilities
[ARL/A-NOTE-338] 21 p2523 N73-30229
Engineering procedures, blasting, and water level regulation for flood prevention and ice jam control on Dnestr and Dubossary Reservoirs
21 p2573 N73-30620
Sediment pattern correlation with inflow and tidal action
[E73-10984] 22 p2658 N73-31291
Surface water transport in western Lake Superior
23 p2783 N73-32267

**WATER HAMMER**
Transients in cooling water systems of thermal power plant discussing mathematical models, computer programs and experiments
[PUBL-101-PT-1] 01 p0041 N73-10326
Hydraulic transients in cooling water system of thermal power plants, figures and computer programs
[PUBL-101-PT-2] 01 p0041 N73-10327

**WATER INJECTION**
Transverse injection of water and isopropyl alcohol from flat plate into air streams
[AD-741887] 01 p0043 N73-10339
Theoretical investigation of rocket steam generator with emphasis on trajectories and spectrum of injected drops and their vaporization for Europa 1 launch vehicle
[DLR-FB-71-36] 09 p1011 N73-18253
Effect of primary-zone water injection on pollutants from combustor burning liquid ASTM A-1 and vaporized propane fuels
[NASA-TN-D-7293] 14 p1718 N73-23943

**WATER JETS**
U HYDRAULIC JETS

**WATER LANDING**
Apollo experience report on water landing requirement and two stable flotation attitudes for upright flotation of command module
[NASA-TN-D-7081] 09 p1090 N73-18898
Analysis of phenomenon generated by passage of projectile into water to determine effects of accelerations, aerodynamic configurations, and surface motions
16 p1886 N73-25264
Numerical calculation of vertical water entry of finite cones
[AD-759006] 16 p1891 N73-25302
Quantitative tests of space shuttle booster recovery in open seas
[NASA-TM-X-69273] 16 p1965 N73-25892

**WATER LOSS**
Installation of stainless steel lining to stop water leakage from 2MV HOR swimming pool reactors
[IRI-131-72-01] 03 p0334 N73-12723
Automatic temperature controller for liquid cooled garment based on total evaporative water loss during exercise
[NASA-TN-D-7311] 16 p1868 N73-25126

**WATER MANAGEMENT**
Geological evaluation, regional planning, forest management, and water management in North Carolina using ERTS-1 imagery
[E72-10280] 03 p0292 N73-12378
Hydrological applications of side-looking radar, noting soil moisture, ground water, and water loss
03 p0295 N73-12407
Utilization of ERTS-1 imagery in geological evaluation, regional planning, forest management, and water management in North Carolina
[E72-10317] 04 p0413 N73-13366
Application of remote sensing techniques for solution of ecological management problems
04 p0471 N73-13838
Development of airborne instrumentation and application of remote earth observations for determining stream discharge prediction for water management program
04 p0471 N73-13839
Use of resource indicators and remote sensing to plan and manage hydrologic and water resource systems
05 p0536 N73-14364
Impact of California Water Project on environmental quality and resources in southern California
05 p0537 N73-14368
Reservoir and watershed management utilizing ERTS-1 imagery
[E73-10055] 07 p0778 N73-16317
Utilization of ERTS-1 imagery in geological evaluation, regional planning, forest and water management in North Carolina
[E73-10300] 09 p1021 N73-18332
Waste water processing and potable water management
[NASA-CR-128839] 10 p1124 N73-19161
Integrated state-wide information management system for water quality control for California
10 p1228 N73-19982
Upgrading and testing integrated water and waste management system
[NASA-CR-128878] 11 p1249 N73-20142
Remote sensing techniques for managing California earth resources
[NASA-CR-131392] 12 p1399 N73-21347
Remote sensing techniques for acquiring hydrological resource information to be used in California water management
12 p1399 N73-21350
Feasibility of remote sensing techniques for hydrology and watershed management in California
12 p1399 N73-21351
Data for assessing water supply changes and effects on hydrogeological management of San Joaquin Valley
12 p1400 N73-21353
Effects of water management on land use in southern California valley and river basin
12 p1400 N73-21354
Remote sensing techniques for water management and land use classification in California coastal zone considering river deltas
12 p1400 N73-21357
Analysis of water pollution levels in USSR lake and measures to protect water purity under conditions of economic development in vicinity
12 p1420 N73-21512
Reservoir and water management in Maine using ERTS-1 data collection platforms and imagery
[E73-10585] 14 p1657 N73-23445
Utilization of ERTS-1 imagery in geological evaluation, regional planning, forest and water management in North Carolina
[E73-10688] 16 p1902 N73-25382
Application of ERTS-1 remotely sensed data and ground truth information to predict and manage water quantity and quality in river basins
[E73-10689] 17 p2018 N73-26314
Application of EREP data in geological evaluation, regional planning, forest management, and water management in North Carolina
[E73-10754] 17 p2022 N73-26357
Bibliography of references on urban hydrology
[PB-219105/4] 18 p2146 N73-27348
Application of ERTS-1 imagery for controlling quantity and quality of ground water resources
19 p2288 N73-28399
Utilization of ERTS-1 imagery and data for water resources surveys and management
19 p2290 N73-28410
Geological evaluation, regional planning, forest management, and water management in North Carolina using ERTS-1 imagery
[E73-10962] 21 p2532 N73-30304
Utilization of Skylab EREP data in geological evaluation, regional planning, forest management, and water management in North Carolina
[E73-10966] 21 p2533 N73-30308
Articles on meteorology and hydrology
[JPRS-60164] 24 p2946 N73-33530

**WATER POLLUTION**
Lagrangian computer program for predicting movement and dispersion of pollutant in tidal embayment, and application to Bolinas Lagoon, California
[USGS-582-B] 01 p0048 N73-10389
Water pollution detection and monitoring in Lake Champlain and Vermont using ERTS-1 imagery
[E72-10268] 03 p0291 N73-12367

Development of operational remote sensing water quality monitoring system
[NASA-CR-129797] 04 p0414 N73-13378
Application of remote sensing techniques to public health
[NASA-CR-129822] 05 p0500 N73-14069
Development of steps and procedures for determining and evaluating environmental quality through use of remote sensors
07 p0782 N73-16358
Control and mapping of water pollution using remote sensors
07 p0787 N73-16398
ERTS A spectrophotographic measurement of water pollution in Charlotte Amalie harbor, St. Thomas
[NASA-CR-130008] 07 p0792 N73-16437
Water sample analysis for identifying sources of mercury pollution of Great Lakes
08 p0876 N73-17096
Bibliography of USAF reports on air, water, noise, and radiation pollution
[AD-751898] 08 p0940 N73-17699
Application of remote sensing techniques and laboratory analyses for determining water pollution caused by carbonaceous materials
[NASA-CR-128824] 10 p1154 N73-19387
ERTS-1 detection of oil pollution in Gulf of Mexico and in waters off Salem, Massachusetts and Oakland, California
[E73-10396] 11 p1276 N73-20358
Analysis of water pollution levels in USSR lake and measures to protect water purity under conditions of economic development in vicinity
12 p1420 N73-21512
Program planning for pollution elimination
[AD-754784] 12 p1467 N73-21893
Two-dimensional submerged slot jets to diffuse thermally buoyant water jets into moving water stream
[PB-213461/7] 14 p1651 N73-23395
Detection of oil pollution from ERTS-1 imagery
[E73-10574] 15 p1772 N73-24354
Procedures and facilities in Czechoslovakia for determining pollution of rain water
[NLL-M-22857-[5828.4F]] 15 p1805 N73-24627
Marine luminescence data for monitoring algal and pollutant concentrations
[NASA-CR-114578] 16 p1867 N73-25114
Application of regression analysis to water quality measurement from remote sensing spectral signature data
[NASA-CR-132997] 16 p1870 N73-25141
ERTS-1 imagery of land use, lake ice, and water pollution, Lake Champlain Basin and Vermont
[E73-10690] 16 p1902 N73-25383
Remote sensing of thermal and industrial discharges along shoreline of Lake Michigan
[PB-214503/5] 16 p1908 N73-25436
Aerial reconnaissance of thermal discharges along shoreline of Lake Michigan
[PB-214407/9] 16 p1908 N73-25437
Multispectral remote sensing techniques for measuring light absorption, scattering, and particle concentrations in water
[AD-759668] 16 p1914 N73-25491
Analysis of ERTS-1 data for interdisciplinary study of estuarine and coastal oceanography of Block Island Sound and adjacent New York coastal waters
[E73-10735] 17 p2020 N73-26341
Analysis of ERTS-1 data for interdisciplinary study of estuarine and coastal oceanography of Block Island Sound and adjacent New York coastal waters
[E73-10736] 17 p2020 N73-26342
Monitoring water pollution plume in Lake Champlain using ERTS-1 imagery
[E73-10742] 17 p2021 N73-26347
Thermal and water quality parameters of Tennessee River
[NASA-CR-133089] 17 p2024 N73-26378
Detection and monitoring oil pollution using Skylab EREP MSS imagery
[E73-10796] 18 p2137 N73-27272
Visual detection of oil films on water surface
[PB-219825/7] 18 p2148 N73-27362
ERTS-1 imagery for monitoring dumping of municipal and industrial wastes in New York Bight
[PAPER-E10] 19 p2269 N73-28274
Environmental study of Lake Champlain and Vermont land use based on ERTS-1 imagery
[PAPER-E11] 19 p2270 N73-28275
Digital analysis of ERTS-1 data to determine sedimentation levels in Potomac and Anacostia Rivers confluence and strip mining in Allegheny County, Maryland
[PAPER-E13] 19 p2270 N73-28277
Analysis of ERTS-1 multispectral scanner imagery to determine polluted and turbid water masses in Osaka Bay, Japan
[PAPER-E14C] 19 p2270 N73-28280
ERTS-1 imagery of water pollution, sedimentation, and geology of southeastern France and western Alps
[PAPER-R6] 19 p2283 N73-28364
Assessment of ERTS-1 imagery for identification of marine resources to include sources of pollution, beach erosion, and navigation in ice-filled waterways
19 p2289 N73-28402
Bibliography of water pollution from natural and man-made sources
[AD-761980] 21 p2541 N73-30371
Detection and monitoring of oil pollution from Skylab EREP sensors
[E73-11016] 22 p2661 N73-31320
Aerial surveillance system for remote detection of real and potential oil spills threatening inland waterways
[PB-221484/9] 22 p2669 N73-31385
Multidisciplinary research on water depth measurement, Yellowstone Park, atmospheric effects, lake ice surveillance, recreational land use, IFYGL, image enhancement, water quality, oil pollution detection, and mapping iron compounds from ERTS-1 data
[E73-11119] 23 p2783 N73-32264
ERTS-1 monitoring of turbidity, color, boundaries, circulation, and pollution dispersion in Delaware coastal waters
[E73-11147] 24 p2918 N73-33301
Identification of suspended sediment, current circulation, water mass boundaries, and waste disposal plumes in Delaware Bay using ERTS-1 imagery
[E73-11164] 24 p2920 N73-33317
WATER PRESSURE
Solution of Navier-Stokes equation for sea water pressure determination
[NOTA-INTERNA-377] 01 p0042 N73-10328
Development of procedure for calculating ocean currents based on given density field and comparison with current techniques
12 p1421 N73-21516
WATER PURIFICATION
U WATER TREATMENT
WATER QUALITY
Determination of boundaries of aircraft and spacecraft data within which water quality can be obtained
[E72-10168] 01 p0044 N73-10349
Utilization of ERTS-1 imagery for water depth measurement, mapping of Yellowstone Park, atmospheric effects in Colorado, lake ice surveillance, recreational land use, IFYGL Lake Ontario, image enhancement, water quality monitoring, and oil pollution detection
[E72-10201] 02 p0144 N73-11167
Utilization of ERTS-1 imagery for water depth measurement, mapping of Yellowstone Park, atmospheric effects in Colorado, lake ice surveillance, recreational land use, IFYGL Lake Ontario, image enhancement, water quality monitoring, oil pollution detection, and mapping iron compounds
[E72-10198] 02 p0160 N73-11296
Development of operational remote sensing water quality monitoring system
[NASA-CR-129797] 04 p0414 N73-13378
Environmental indices covering land, water, and air quality compatible with ERTS-1 imagery
[E72-10330] 05 p0531 N73-14318
ERTS A spectrophotographic measurement of water pollution in Charlotte Amalie harbor, St. Thomas
[NASA-CR-130008] 07 p0792 N73-16437
Utilization of ERT-1 imagery for water depth measurement, Yellowstone Park data, atmospheric effects in Colorado, lake ice surveillance, recreational land use, IFYGL, image enhancement, water quality monitoring, oil pollution detection, and mapping iron compounds
[E73-10086] 08 p0901 N73-17298
Land use, water quality, and air quality indices useful to environmental resources managers and data processing equipment and techniques for production of indices
[E73-10376] 10 p1151 N73-19371
Monitoring of water quality in New York Bight and Tampa Bay, Florida, using ERTS-1 imagery
[E73-10395] 11 p1276 N73-20357
Development of environmental indices covering land, water, and air quality in Pennsylvania compatible with ERTS-1 imagery
[E73-10505] 13 p1516 N73-22280
Detection of changes in water quality and surface area in Tahoka Lake, Texas using ERTS-1 imagery
[E73-10518] 14 p1654 N73-23412
ERTS-1 applications in water depth calculation, terrain classification, land use mapping, water pollution, and mineral exploration
[E73-10565] 15 p1771 N73-24345
ERTS-1 monitoring of water quality and ocean dumping
[E73-10573] 15 p1772 N73-24353
Correlation of ERTS-1 data with in situ water quality measurements around Virgin Islands
[E73-10626] 15 p1775 N73-24386
Resources management, land use mapping, and water quality management in Ohio based on ERTS-1 imagery
[E73-10775] 18 p2135 N73-27251
Analysis of water turbidity in two federal reservoirs in Kansas using ERTS-1 multispectral band scanners
[PAPER-E12] 19 p2270 N73-28276
Detection and monitoring of water quality parameters in reservoirs and lakes in Kansas from Skylab imagery
[E73-10938] 21 p2529 N73-30280
Detection and monitoring water quality in Kansas reservoirs from Skylab data
[E73-10939] 21 p2529 N73-30281
Multidisciplinary research on water depth measurement, Yellowstone Park, atmospheric effects, lake ice surveillance, recreational land use, IFYGL, image enhancement, water quality, oil pollution detection, and mapping iron compounds from ERTS-1 data
[E73-11119] 23 p2783 N73-32264
Development of land use, water quality, and air quality indices from ERTS-1 imagery for environmental resources management in Susquehanna River Basin and Quantico, Virginia test areas
[E73-11143] 24 p2918 N73-33298
WATER RECLAMATION
Potassium exchange on sulfocation resins containing divinylbenzene for drinking water regeneration
03 p0257 N73-12078
Aerospace technology for solving domestic solid waste disposal, water purification, and water recovery problems
04 p0472 N73-13849
Radiation oxidation of water impurities in moisture-containing products of human vital functions
07 p0744 N73-16051
Photographic water conservation and reclamation processes
[AD-752220] 08 p0926 N73-17585
Cost effectiveness of water reclamation subsystem in advanced aerospace life support systems
[NASA-CR-124098] 09 p0997 N73-18134
Preservatives for human urine storage and water reclamation in spacecraft cabin
10 p1116 N73-19099
Oxidation of atmospheric impurities in space cabin and purity of reclamated water
10 p1117 N73-19104
Antimicrobial water reclamation methods for processing human urine
10 p1117 N73-19105
Water reclamation and waste disposal technology applied to land use and aerospace engineering
[NASA-CR-128857] 10 p1124 N73-19158
Waste disposal and water reclamation technology for land use and aerospace engineering application
[NASA-CR-128858] 10 p1124 N73-19159
Waste water processing and potable water management
[NASA-CR-128839] 10 p1124 N73-19161
Upgrading and testing integrated water and waste management system
[NASA-CR-128878] 11 p1249 N73-20142
Development of quality monitoring system for water recovery cycle in weightlessness environment
[NASA-CR-112267] 11 p1250 N73-20144
Evaluation of multifiltration water reclamation subsystem to reclaim domestic clothes wash water
[NASA-TM-X-2781] 13 p1595 N73-22931
Water recovery system for three man crew aboard spacecraft
[NASA-CR-128983] 17 p1990 N73-26094
Methodology for predicting relevant contributions of cost elements in development of water recovery systems
[NASA-CR-124303] 18 p2111 N73-27074
Bactericidal properties of sorbents in spacecraft water regeneration system
20 p2367 N73-29038
Water recovery and solid waste processing for aerospace and domestic applications
[NASA-CR-134027] 22 p2623 N73-31016
Systems design for advanced water recovery and waste processing in aerospace and domestic applications
[NASA-CR-134028] 22 p2623 N73-31017
Aerospace distillation water recovery system for reclamation of potable water from domestic wash water
[NASA-TM-X-2896] 22 p2737 N73-31913
Evaporator for vacuum distillation/vapor filtration water reclamation on manned space flight
[NASA-CR-124397] 23 p2796 N73-32367
WATER RECOVERY
U WATER RECLAMATION
WATER RESOURCES
Water resources survey and river monitoring in Canada using ERTS-1 imagery
[E72-10230] 02 p0163 N73-11323
Near real time water resources data from Delaware Bay for use in river basin management
[E72-10239] 03 p0288 N73-12339
Remote sensing techniques for regional planning and managing earth resources, particularly water resources in California
[NASA-CR-129917] 05 p0536 N73-14361
Remote sensing of California water systems
05 p0536 N73-14362
Use of resource indicators and remote sensing to plan and manage hydrologic and water resource systems
05 p0536 N73-14364

Meander patterns of Feather and Colorado Rivers
05 p0537 N73-14366
Use of remote sensing data to analyze impact of California State Water Project on regional planning and land use of west side of San Joaquin Valley
05 p0537 N73-14367
Water equivalent of snow determined from aerial detection of natural terrestrial radiation
[EGG-1183-1533] 06 p0667 N73-15419
Utilization of ERTS-1 imagery for water resources management in Delaware River Basin
07 p0787 N73-16404
Crop identification, soil mapping, water resources, and urban land use analysis in Wabash River Basin based on ERTS-1 imagery
[E73-10364] 10 p1150 N73-19360
ERTS-1 imagery applied to geological and water resources investigations of Basin and Range - Colorado Plateau boundary in northwestern and north central Arizona
[E73-10441] 11 p1282 N73-20401
Regional wet census of playa lakes on Southern High Plains area of Texas and New Mexico from ERTS-1 MSS imagery
[E73-10455] 11 p1283 N73-20414
ERTS-1 relayed water resources data collected from Delaware River Basin
[E73-10451] 12 p1394 N73-21299
ERTS-1 retransmission of water level data collected at remote locations in Canada
[E73-10469] 12 p1395 N73-21306
Data retransmission from Canadian water gauging stations using ERTS-1
[E73-10479] 12 p1396 N73-21316
Management planning for California water resource information gathering system
12 p1399 N73-21349
Remote sensing techniques for acquiring hydrological resource information to be used in California water management
12 p1399 N73-21350
Feasibility of remote sensing techniques for hydrology and watershed management in California
12 p1399 N73-21351
Data for assessing water supply changes and effects on hydrogeological management of San Joaquin Valley
12 p1400 N73-21353
Effects of water management on land use in southern California valley and river basin
12 p1400 N73-21354
Survey of geology, minerals, and water resources in Maryland using ERTS-1 imagery
[E73-10433] 13 p1515 N73-22276
ERTS-1 retransmission of water resources data collected from remote regions of Canada
[E73-10504] 13 p1515 N73-22279
Utilization of ERTS-1 data for crop identification and acreage estimation, soil mapping, urban land use, water resources, atmospheric modeling, and earth surface feature identification in Wabash River Basin
[E73-10549] 14 p1655 N73-23422
Acquisition and processing ERTS-1 water resources data for south Florida
[E73-10560] 14 p1656 N73-23432
ERTS-1 data for effective monitoring and management of surface water on earth
[NASA-TM-X-66237] 14 p1659 N73-23468
Use of remotely sensed data to solve water resource problems of Wolf Creek Watershed, Colorado
[NASA-CR-129001] 14 p1660 N73-23479
Geologic, mineral, and water resources investigations in western Colorado using ERTS-1 imagery
[E73-10608] 15 p1773 N73-24369
ERTS-1 imagery of snow cover break-up in Chena River Basin, Alaska
[E73-10619] 15 p1774 N73-24380
Identification and mapping of soils, vegetation, and water resources in Texas from ERTS-1 MSS digital data
[E73-10670] 16 p1899 N73-25365
Delineation of lakes and water turbidity identification in ERTS-1 imagery of Houston, Texas area
[E73-10672] 16 p1900 N73-25367
ERTS-1 measurement of surface area of water bodies in Houston and Galveston, Texas area
[E73-10675] 16 p1900 N73-25370
Photointerpretation of ERTS-1 imagery to map bodies of water in Saline County, Kansas
[E73-10684] 17 p2017 N73-26313
ERTS-1 and aircraft multispectral scanner data for mapping ponds and lakes near Woodworth, North Dakota to determine changes in continental migratory bird habitat
[E73-10714] 17 p2018 N73-26321
Utilization of Skylab multispectral cameras for study of eutrophication processes in lakes important to New York State water resources
[E73-10744] 18 p2133 N73-27236
Application of ERTS-1 imagery for hydrometric and hydrographic surveys of Canada
[E73-10777] 18 p2135 N73-27253
Interpretation of geologic, mineral, and water resources in western Colorado from ERTS-1 imagery
[E73-10814] 18 p2139 N73-27289
Analysis of water turbidity in two federal reservoirs in Kansas using ERTS-1 multispectral band scanners
[PAPER-E12] 19 p2270 N73-28276
Evaluation of stream flow data for Verde River watershed in central Arizona provided by ERTS-1 imagery
[PAPER-W8] 19 p2271 N73-28286
Analysis of ERTS-1 data pertaining to Delaware River Basin observations to determine performance of data collection system
[PAPER-W10] 19 p2271 N73-28287
Evaluation of ERTS-1 imagery for determining numbers and distribution of prairie ponds and lakes in North Dakota
[PAPER-W12] 19 p2272 N73-28289
Application of ERTS-1 imagery for determining location and characteristics of lake basins Texas high plains and semi-arid areas
[PAPER-W13] 19 p2272 N73-28290
ERTS-1 imagery and high altitude photography of Lake Ontario Basin to provide input for models of river discharge and macro-scale features of lake circulation
[PAPER-W14] 19 p2272 N73-28291
Application of ERTS-1 imagery for analysis of terrestrial water balance of Lake Ontario and drainage basin
[PAPER-W15] 19 p2272 N73-28292
Application of ERTS-1 remote sensing to determine turbidity plumes in Lake Ontario
[PAPER-W16] 19 p2272 N73-28293
Application of ERTS-1 data to North Carolina forest and water resources management
[PAPER-R1] 19 p2282 N73-28359
Digital data processing of ERTS-1 MSS imagery of water masses in Delaware Bay
19 p2286 N73-28380
Computer analysis of ERTS-1 MSS data for identification and mapping of soils, vegetation, and water resources in Lynn County, Texas
19 p2287 N73-28392
Application of ERTS-1 imagery for controlling quantity and quality of ground water resources
19 p2288 N73-28399
Application of ERTS-1 data to water resources management in State of California
19 p2289 N73-28403
Utilization of ERTS-1 imagery and data for water resources surveys and management
19 p2290 N73-28410
Application of multispectral scanning to hydrology and water resources, noting measurement of soil moisture, water depth, and water quality
19 p2295 N73-28454
Geologic, mineral, and water resources of western Colorado from Skylab EREP data
[E73-10918] 20 p2398 N73-29267
Analysis of albedo of reservoirs from observations of total and reflected radiation measured near floating island stations
20 p2402 N73-29301
Collection of ground and water truth in Nevada for Skylab-2
[E73-10887] 20 p2417 N73-29419
Water, agriculture, and soil resources management and planning in California using ERTS-1 imagery
[E73-10935] 21 p2529 N73-30277
SL-2 MSS photography of soils, water, and vegetation in Texas
[E73-10943] 21 p2530 N73-30285
ERTS-1 imagery of surface water aera in Quivera National Wildlife Refuge, Kansas
[E73-10974] 21 p2533 N73-30313
Bibliography of abstracts on remote sensing of water resources
[PB-220163/0] 21 p2542 N73-30383
Geologic and mineral and water resources of western Colorado from Skylab multispectral photography
[E73-11010] 22 p2660 N73-31315
Application of aerial photography and ERTS imagery to agricultural, forest, and water resources management in Minnesota
[NASA-CR-135483] 22 p2665 N73-31357
Agroclimatology study of highlands of eastern Africa
[WMO-339] 24 p2886 N73-33045
Correlation of ERTS-1 imagery signatures with water balance ecosystem and geology of select playa lake basins in West Texas
[E73-11102] 24 p2914 N73-33259

**WATER RUNOFF**
Development of land use and peak runoff classification system for highway engineering using ERTS-1 imagery of Maine
[E72-10308] 04 p0412 N73-13357
Pluviometric and statistical analyses of precipitation and watercourse patterns in Israel
06 p0665 N73-15403
Development of land use-peak runoff classification system for highway engineering in Maryland
[E73-10100] 08 p0902 N73-17310
Utilization of ERTS-1 imagery to develop land use-peak runoff classification system for highway engineering in Maine
[E73-10456] 11 p1283 N73-20415
Effectiveness of ERTS-1 MSS photography in characterizing watershed runoff in Texas
[E73-10513] 14 p1653 N73-23408
Development of land use-peak runoff classification system for highway engineering in Maine
[E73-10654] 16 p1898 N73-25350
Development of land use-peak runoff classification system for highway engineering in Maine
[E73-10910] 20 p2397 N73-29259
Forecasting of spring flow runoff and snow data collection network design
24 p2922 N73-33338

**WATER TAKEOFF AND LANDING AIRCRAFT**
Evaluation of ground effect machines under various environmental conditions to determine feasibility as rescue vehicles by Coast Guard
[AD-755409] 13 p1475 N73-21947

**WATER TEMPERATURE**
Mathematical analysis of optical refractive index fluctuations due to salinity and temperature microstructure
[AD-746120] 02 p0168 N73-11366
Prediction of long-term temperature fluctuations, July temperature, and annual average temperature of Barents Sea in surface to 200 m layer
[NLL-M-20600-[5828.4F]] 05 p0529 N73-14304
Satellite measurements of sea surface temperatures
[NASA-TM-X-66235] 14 p1659 N73-23467
Sea surface temperature measurements from Skylab EREP radiometer data
[E73-10604] 15 p1773 N73-24365
Large scale interaction of atmospheric circulation with Atlantic Ocean on 30 deg W meridian between April and June 1970
[NLL-M-22854-[5828.4F]] 16 p1894 N73-25321
Analysis of long term variations in water surface temperature of North Atlantic Ocean
[NLL-M-23016-[5828.4F]] 20 p2390 N73-29200
Analysis of temperature and radiation regime above paddie surfaces as obtained by helicopter-borne radiation thermometer
20 p2405 N73-29324
Statistical analysis of large scale fluctuations in water surface temperature of North Atlantic Ocean
21 p2572 N73-30614
Spatial structure of temperature fluctuations in seas
24 p2947 N73-33535
Measurement of air-sea temperature in relation to incident solar energy
24 p2975 N73-33773

**WATER TREATMENT**
Solid polymer for water electrolysis system to generate oxygen and hydrogen in manned space station
[NASA-CR-112183] 04 p0375 N73-13052
Aerospace technology for solving domestic solid waste disposal, water purification, and water recovery problems
04 p0472 N73-13849
Magnetic filtering technique for treating water containing low concentrations of mercury
[NASA-TM-X-2764] 11 p1352 N73-20972
Tape cassette bacteria detection system for automatic continuous bacterial detection for monitoring sterility of regenerated water in spacecraft
[NASA-CR-134035] 22 p2620 N73-30996
Raw water sewage treatment
[NASA-CASE-NPO-13224-1] 22 p2622 N73-31011
Water recovery and solid waste processing for aerospace and domestic applications
[NASA-CR-134027] 22 p2623 N73-31016
Solar still greenhouse for using desalinated water to produce vegetables in arid regions
24 p2975 N73-33769

**WATER TUNNELS**
U HYDRAULIC TEST TUNNELS

**WATER VAPOR**
Analysis of density of water in forms of ice, water and steam, liquid and gaseous heavy water, and sea water
[ESDU-68010-AMEND-A] 01 p0038 N73-10302
Atmospheric transmittance calculations of laser beams for atmospheric models with water vapor as molecular absorber
[AD-745585] 01 p0065 N73-10532
Measurement of momentum of two-phase liquid-vapor flow from pipe of circular cross-section
[EUR-4785-I] 03 p0284 N73-12302
Stratospheric water vapor mixing ratio altitude profile from spectral observations of downward emission from vapor lines
[AD-747031] 03 p0297 N73-12423
Increase of water vapor in stratosphere due to fleet of SSTs
[AD-748797] 04 p0416 N73-13397
Atmospheric water vapor absorption at CO, HF, and DF laser frequencies using 1-km white absorption cell and laser sources
[AD-748437] 04 p0430 N73-13501
Measurement of spatial distribution of aerosols and water vapor in earth mixing layer using optical radar, particle counters, and rawinsonde
[NASA-TN-D-7103] 04 p0444 N73-13621

Procedures and equipment for measuring angular distribution of laser beam scattering by evolving water vapor
[NLL-M-22457-[5828.4F]] 05 p0554 N73-14497
Boron filament splitting in boron aluminum composites caused by water vapor effects
[AD-749971] 05 p0566 N73-14602
Radiation attenuation in atmosphere by water vapor
[NLL-M-20840-[5828.4F]] 05 p0569 N73-14622
Evaporation and vertical transfer of water vapor in urban areas
[NLL-M-20842-[5828.4F]] 05 p0570 N73-14625
Measurement of vertical distribution of atmospheric water vapor by ruby laser rod
[PB-211891] 05 p0575 N73-14680
Gas laser measurements of absorptive losses introduced by water vapor and carbon dioxide for laser emission lines in 7-6 to 10-9 vibrational bands
[AD-749823] 06 p0681 N73-15542
Vertical distribution of atmospheric water vapor and ozone over District of Columbia during 1969 and 1970
[AD-751535] 07 p0795 N73-16465
Optical radar system for determining tropospheric water vapor content, based on absorption line shift
[DLR-MITT-72-26] 07 p0815 N73-16608
Observations and characteristics of 1.35-cm emissions of water vapor in galactic sources
07 p0837 N73-16787
Method for integrating pressure-scaled water-vapor and CO2 absorber masses from surface to sigma levels in Naval primite equation model
[AD-752475] 08 p0921 N73-17544
Medium and high resolution radiometer measurements of water vapor absorption regions from Nimbus satellites
08 p0972 N73-17942
Minimization technique for determining structural parameters of IR and vibrational rotational spectra of H2O
[AD-754612] 11 p1253 N73-20166
Radiative transfer in dense water vapor atmosphere
[LBL-1324] 12 p1464 N73-21864
Four channel radiometer for remote sensing of microwave emission from atmospheric oxygen and water vapor
[AD-759535] 16 p1939 N73-25696
Monochromatic absorption coefficient in narrow regions of oscillatory-rotational spectrum of H2O
[AD-759238] 16 p1946 N73-25743
Water evaporation interference in phase measurements by transhorizontal microwave propagation over sea surface
17 p1994 N73-26125
Evaluation of radiometric computations in infrared window and water vapor absorption band regions based on 4-D atmospheric models
[NASA-CR-129007] 18 p2172 N73-27546
Molecular mechanisms of conduction and polarization in water vapor, liquid water, and ice
[AD-762060] 19 p2231 N73-27993
Spectroscopic analysis of atmospheric water vapor at 6943.8 Angstrom line in telluric spectrum
19 p2258 N73-28203
Computed atmospheric effects on ERTS-1 MSS observations
19 p2284 N73-28371
Molecular absorption coefficients for H20-N2 mixtures as measured by Co laser
[AD-760140] 19 p2308 N73-28561
Excitation and relaxation processes in H2O discharges and lasers
20 p2424 N73-29471
Nitrogen gas supply system for EHF waveguides to improve attenuation by control of water vapor and oxygen content
[FTZ-A-333-TBR-10] 22 p2642 N73-31175
CO2 laser and spectrophone for CO2 and water vapor absorption measurements
22 p2679 N73-31462
Water vapor absorption by highly attenuated CO laser lines
[AD-764376] 22 p2682 N73-31485
Airborne aluminum oxide hygrometer for water vapor measurements in atmosphere
[NASA-TM-X-70475] 23 p2792 N73-32341

**WATER VEHICLES**
NT AIRCRAFT CARRIERS
NT LIFEBOATS
NT SATELLITE COMMUNICATIONS SHIPS
NT SHIPS
NT SUBMARINES
NT TANKER SHIPS
NT UNDERWATER VEHICLES
Analysis of factors affecting ride quality of water vehicles and human reactions to motion caused by rough water
01 p0003 N73-10022

**WATER WAVES**
NT TIDAL WAVES
Analysis of factors affecting ride quality of water vehicles and human reactions to motion caused by rough water
01 p0003 N73-10022
Numerical analysis of two-dimensional gravity wave flow on nonuniform free streams
[AD-744995] 01 p0042 N73-10329
Growth of mechanically generated surface water waves when subjected to turbulent channel air flow
[AD-746493] 01 p0042 N73-10336
Development of finite difference scheme for numerical analysis of time dependent seiche oscillating across shallow, infinite channel and transients associated with bottom spiral
[AD-745194] 01 p0053 N73-10428
Numerical analysis of stability and convergence conditions based on mathematical model of Arctic Ocean
[AD-745182] 01 p0053 N73-10429
Detection of internal ocean waves using three-color infrared radiometer
[AD-745004] 01 p0059 N73-10484
Interaction of internal and surface waves in water
[AD-747332] 02 p0159 N73-11291
Lagrangian theory of internal ocean wave interaction
[AD-746149] 02 p0169 N73-11371
Measurement of short pulse, X-band radar backscatter from rough water surfaces expressed as cumulative probability distribution functions
[AD-747949] 03 p0267 N73-12159
Analysis of refraction of gravity water waves based on group velocity and phase velocity relationships
[AD-747982] 03 p0286 N73-12316
Analysis of eddies and lift forces created on vertical circular cylinder by oscillatory flow conditions
[AD-748078] 03 p0287 N73-12329
Side-looking radar applied to oceanography noting sensing of sea states, pollution, and waves
03 p0295 N73-12408
Wave forces on horizontal circular cylinder subjected to train of gravity waves
[AD-747532] 03 p0362 N73-12951
Correlation techniques and measurements of surface wave height statistics
[NASA-CR-2153] 04 p0405 N73-13298
Time series and probability density function analyses of hypothesis that organized motion exists in air flow above naturally occurring water waves
[AD-749045] 04 p0408 N73-13328
Scripps Institute research on oceanographic instruments, stabilized floating platforms, ocean bottom accelerometers, and surface waves
[AD-748024] 04 p0417 N73-13407
Measurement of sinusoidal waves in flumes with transducers using non-contacting capacitive sensing
[NRC-MI-836] 05 p0522 N73-14243
Scalar wave scattering on water surface wake generated by moving pressure point
[AD-749113] 05 p0527 N73-14291
Effects of vertical jet breakwaters on wind generated deep water waves
[AD-748190] 05 p0528 N73-14293
Wind velocity fluctuations over natural ocean waves, and wind-wave coupling
[AD-749073] 05 p0574 N73-14673
Numerical analysis of structure of solitary waves using partial differential equations
[AD-750565] 06 p0655 N73-15323
Effect of ocean surface structure on narrow radar pulse shape
06 p0662 N73-15380
Effect of wind wave energy balance on remote microwave sensing of sea surface
06 p0664 N73-15395
Generation and stabilization of coastal wave induced circulation and longshore current patterns
[AD-750291] 06 p0671 N73-15458
Prediction of horizontal wave forces acting on vertical pile structures of floating ocean platforms
[AD-751574] 07 p0794 N73-16460
Rotational tidal waves due to earth rotation explained by Poincare problem solving
07 p0857 N73-16951
Confidence intervals for ocean wave spectra for ordinary waves and hurricane sized waves
[AD-752135] 08 p0920 N73-17542
Doppler study of microwave backscattering from ocean waves in wind wave tank
[AD-753199] 09 p1032 N73-18422
Derivation of algorithms correlating spectra of ocean wave conditions with two dimensional spectra of aerial photographs and radar imagery
10 p1153 N73-19383
Microwave emissivity and sea brightness temperatures of surface waves
[AD-753533] 11 p1287 N73-20443
Spectral development of wind-generated water waves in laboratory facility
[AD-754113] 11 p1287 N73-20445
Iterative directional analysis of ocean waves
[AD-753825] 11 p1289 N73-20460
Characteristics of deep water waves reaching Port Phillip Heads, Australia to show effects of refraction, shoaling, and friction
13 p1524 N73-22351
PAPA Ocean Weather Station measurements of wind and wave condition in north Pacific Ocean
[AD-757982] 15 p1806 N73-24638
Analysis of mass diffusion process from elevated point source over wind-disturbed water surface and comparison with calculated concentration distributions for diffusion in flat plate boundary layer
16 p1887 N73-25271
Characteristics of water waves generated by steady two-dimensional wind at three different speeds over water depth of 19 centimeters
16 p1887 N73-25272
Rossby regimes in geophysical fluid dynamics of ocean waves
[PB-214666/3] 16 p1890 N73-25295
Application of sea photo analysis techniques to obtain surface truth descriptors of open ocean from aerial photography
[FAA-RD-72-110] 16 p1905 N73-25412
Free oscillation model for ocean basin considering earth rotation and sphericity
[PB-214445/9] 16 p1909 N73-25444
Coherent and incoherent components of sound scattered at time dependent rough surface with application to wind-blown water waves
[AD-760306] 17 p2064 N73-26695
Influence of ocean waves and meteorological variables on beach erosion at Plum Island, Massachusetts
[AD-759513] 18 p2148 N73-27364
Mathematical models for studying energy spectra and nonlinear surface waves of ocean
[AD-759541] 18 p2149 N73-27371
Spectral and cospectral analyses of turbulence data obtained over natural ocean waves
[AD-761504] 19 p2316 N73-28624
Theory and computations of wind driven waves at sea
[TT-70-50182] 20 p2387 N73-29176
Development of theories for radar sea return from wind-roughened waves
[AD-762073] 21 p2539 N73-30362
Application of theoretical model to velocity fields observed over water waves
[AD-764196] 22 p2668 N73-31377
Turbulent, surface, and internal motions of ocean
[AD-763804] 22 p2670 N73-31390
Test facility for generating and analyzing internal waves
[AD-763444] 22 p2670 N73-31391
Characteristics of constant scaling method for analyzing linear inviscid internal waves in ocean, atmosphere, and experimental tanks
[AD-764579] 24 p2910 N73-33227

**WATERSHEDS**
Preparation of hydrologic atlases of arid land watersheds using ERTS-1 imagery of Wyoming, Utah, Montana, and New Mexico
[E72-10240] 03 p0288 N73-12340
Reservoir and watershed management utilizing ERTS-1 imagery
[E73-10055] 07 p0778 N73-16317
Preparation of hydrologic atlases of arid land watersheds using ERTS-1 imagery
[E73-10318] 09 p1023 N73-18350
Utilization of ERTS-1 imagery to study watershed hydrology in Southern Great Plains
[E73-10359] 10 p1149 N73-19355
Effectiveness of ERTS-1 MSS photography in characterizing watershed runoff in Texas
[E73-10513] 14 p1653 N73-23408
Use of remotely sensed data to solve water resource problems of Wolf Creek Watershed, Colorado
[NASA-CR-129001] 14 p1660 N73-23479

**WAVE AMPLIFICATION**
Electron wave amplitude oscillation in plasma due to initial spatial disturbance
[IPPJ-143] 09 p1070 N73-18728
Conference on wave-particle interactions in magnetosphere and wave amplification for communications
[AD-759071] 16 p1909 N73-25450
Wave amplification in dielectrics
[AD-762283] 19 p2309 N73-28570
Traveling wave amplification in Ge and InSb semiconductors
23 p2824 N73-32573

**WAVE ATTENUATION**
NT ACOUSTIC ATTENUATION
NT RADAR ATTENUATION
NT RADIO ATTENUATION
NT SHOCK WAVE ATTENUATION
Measurement and analysis of depolarization and differential attenuation during propagation of millimeter wave signals through rain
[NASA-CR-130107] 01 p0028 N73-10217
FORTRAN program for plotting attenuation of air-filled rectangular waveguide
[AD-746108] 02 p0142 N73-11153
Attenuation calculations for extremely low frequency and very low frequency electromagnetic wave propagations in earth crust
[AD-748331] 06 p0641 N73-15206
Wooded terrain effects on radiation patterns of circular and directional antennas
[FOA-3-A-3747-60] 11 p1255 N73-20179
Attenuation of thermal radiation by transpiration of absorbing gas using porous Porolloy plate
15 p1812 N73-24685

Pulse-echo technique for measuring ultrasonic attenuation in Bi12GeO20 single crystals at low temperature
16 p1952 N73-25798
Attenuation of circularly bent waveguides with dielectric coatings, noting role of mode filters
[FTZ-A-333-TBR-16] 22 p2643 N73-31181
EHF attenuation measurements of helical waveguides, using FSK shuttle pulse method and backward wave oscillator
[FTZ-333-TBR-17] 22 p2643 N73-31182
Velocity and attenuation of wave fronts generated by double diaphragm shock tube
[CEA-R-4365] 22 p2647 N73-31210
Monitoring of fatigue damage by ultrasonic attenuation measurements
23 p2796 N73-32363
Ultrasonic attenuation of longitudial sound waves in superconducting molybdenum single crystals
23 p2825 N73-32581

WAVE DEGRADATION
Plasma wave propagation and absorption, and parametric instabilities
[CALT-767-P-2-X-2] 24 p2963 N73-33682

WAVE DIFFRACTION
Radio wave scintillations at equatorial regions
[NASA-TM-X-66074] 01 p0028 N73-10218
Hankel function for calculating radio wave diffraction around earth surface
[AD-742108] 01 p0028 N73-10221
Diffraction of acoustic and electromagnetic waves on wavy surfaces
[AD-748037] 03 p0268 N73-12168
Diffraction correction calculations for rectangular ultrasonic transducer
[AD-754677] 11 p1263 N73-20247
Modified ray theory for underwater sound propagation and diffraction
[AD-755460] 12 p1430 N73-21589
Stress wave diffraction models for crack propagation induced by dynamic loads
13 p1584 N73-22839
Extension of electromagnetic antenna wave diffraction principle
[AD-759690] 17 p1999 N73-26163
Optical image modulation by polarization shifting diffraction gratings
[AD-765174] 24 p2959 N73-33644

WAVE DISPERSION
Electromagnetic wave transmission in space-time varying dielectrics and plasmas
[AD-746676] 02 p0144 N73-11165
Mode coupled nonlinear dispersion of irregular ionization waves in glow discharges
[AD-748468] 04 p0456 N73-13721
Approximate dispersion relationship of hydrodynamic waves in thin rotating spherical shells of incompressible fluid pervaded by uniform magnetic field
[MET-O-857] 06 p0699 N73-15702
Evaluation of Pc1 geomagnetic micropulsations with automatic signal detectors, noting dispersion
17 p2027 N73-26401
Adapted filter for dispersion measurement of coherent wave packets produced by Pc1 micropulsations
17 p2027 N73-26402
Solutions of macroscopic Maxwell equations for nonlinear dispersive waves in nonlinear optics
17 p2062 N73-26683

WAVE DRAG
NT INTERFERENCE DRAG
Contour of wave drag optimized bodies of revolution as function of Mach number in hypersonic flow
[DGLR-PAPER-72-108] 04 p0369 N73-13003
Wave drag reduction on delta wings at zero lift as function of displacement of maximum thickness in spanwise direction
[DLR-FB-71-61] 06 p0621 N73-15044
Evaluation of double integral equation for calculation of wave drag due to volume and aerodynamic lift of slender wings
[ARC-R/M-3221] 16 p1852 N73-25006
Application of slender body theory for calculating minimum values of zero lift wave drag of slender wings with unswept trailing edge
[ARC-R/M-3222] 16 p1852 N73-25007
Design criteria for slender warped wings with unswept trailing edge with zero load along leading edge and near planar vortex sheet at trailing edge for design lift coefficient
[ARC-R/M-3406] 16 p1852 N73-25008

WAVE EQUATIONS
NT DIRAC EQUATION
NT KLEIN-GORDON EQUATION
NT SCHROEDINGER EQUATION
Analysis of finite amplitude standing waves in air at ambient temperature contained in rigid walled rectangular cavity
[AD-747522] 03 p0337 N73-12749
FORTRAN 4 computer program for one-dimensional stress wave analysis of linear viscoelastic rock
[BM-IC-8563] 05 p0516 N73-14197
Series solutions for reduced wave equation characterizing radiation from point source in two and three dimensions
[AD-754793] 11 p1312 N73-20647
N wave focusing on principal axis of spherical mirror
[AD-757035] 14 p1692 N73-23736
Wave-wave coupling equations for plasma oscillations
[AD-758316] 14 p1697 N73-23769
Wave and Einstein equations for studying scaler waves and tensor perturbations in Mixmaster Universe
15 p1829 N73-24823
Solution of acoustic and electromagnetic scattering problems in exterior domains using integral equations
[NPL-NAC-30] 19 p2314 N73-28608

WAVE EXCITATION
NT ACOUSTIC EXCITATION
NT HARMONIC EXCITATION
Mathematical model for acoustic gravity wave excitations moving air masses
05 p0508 N73-14135
Excitation of longitudinal waves in collisionless and cold plasma in presence of uniform magnetic field
[AD-756477] 14 p1696 N73-23764
Characteristics of turbulent flow over wavy surface using sinusoidal waves of three sizes to determine variations of flow with wave size
16 p1887 N73-25273

WAVE FRONT RECONSTRUCTION
NT KINOFORM
Optimum holographic mounting for maximal ultrahigh speed microparticle volume restitution
[ISL-32/72] 16 p1924 N73-25565
Theoretical study and mountings for magnification and holographic image reconstruction of high speed microparticles
[ISL-1/73] 16 p1924 N73-25566
Mountings for optimum magnification and holographic image reconstruction of high speed microparticles
[ISL-3/73] 16 p1924 N73-25567
Microwave holography describing lateral and axial resolution, computerized wave front reconstruction, and application to moving objects
[REPT-6-72] 20 p2425 N73-29484

WAVE FRONTS
NT SHOCK FRONTS
Mechanical wave front propagation in fluid mixtures and isotropic solids
[AD-746617] 02 p0158 N73-11281
Mathematical model for unsteady one dimensional reaction waves during combustion of gas mixtures including application to air-propane mixture
[DLR-FB-71-66] 06 p0731 N73-15962
Homodyne interferometer for measuring phase variations of laser beam wave front
[AD-756885] 14 p1668 N73-23539
Spectral analysis of wind-wave spectrum at ice edge in Arctic Basin
21 p2573 N73-30621
Velocity and attenuation of wave fronts generated by double diaphragm shock tube
[CEA-R-4365] 22 p2647 N73-31210
Instrument for sensing errors in telescope wavefronts using coarse range sensors and fine range sensors
23 p2792 N73-32336

WAVE FUNCTIONS
NT MOLECULAR ORBITALS
NT PAULI EXCLUSION PRINCIPLE
Shortwave propagation medium with random heterogeneities in approximate Markovian random process
[AD-746714] 02 p0203 N73-11644
Unsteady wave extinction problem of wave generation in semi-infinite media by surface forces
[AD-746897] 02 p0203 N73-11646
Helmholtz equation for solving electromagnetic wave functions of parabolic plasma density profiles
[AD-751669] 07 p0757 N73-16151
Charge form factor of helium and center-of-mass motion
[ISS-72/12] 10 p1191 N73-19693
Solution to Klein-Gordon and Dirac equations for charged particles in two noncollinear electromagnetic waves
[AD-754307] 11 p1327 N73-20769
Equations of motion in wave solutions for cold collisional plasma
[AD-755388] 12 p1437 N73-21640
Isolated-word phoneme recognition using features derived from wave function parameters
14 p1622 N73-23142
Method for direct calculation of localization parameters for wave functions in one demensional disordered potential chains
[RE-461J] 21 p2566 N73-30566
Procedure for determining Rayleigh-Schroe dinger energies and wave functions of degenerate states to high orders
[NASA-CR-135641] 23 p2812 N73-32485

WAVE GENERATION
Effects of pulse shape on transient response of cylindrical shells and generation of shear waves in cylindrical shells
[NASA-CR-112221] 05 p0602 N73-14891
Observation of nonlinear waves near lower hybrid resonance frequency
[CONF-720804-3] 07 p0756 N73-16137
Generation and processing of microwave signals using elastic, electro-magnetic, and carrier space charge waves in solid media
[AD-757555] 14 p1699 N73-23784
Development of test facility for determining interaction of sonic boom with surface of body of water
[NASA-TT-F-14917] 15 p1767 N73-24318
Generation of electromagnetic waves and interactions with plasma media
[AD-757901] 15 p1781 N73-24441
Analysis of mass diffusion process from elevated point source over wind-disturbed water surface and comparison with calculated concentration distributions for diffusion in flat plate boundary layer
16 p1887 N73-25271
Stability of microwaves generated by intense relativistic electron beam in rippled magnetic field
[AD-763337] 21 p2508 N73-30126
Velocity and attenuation of wave fronts generated by double diaphragm shock tube
[CEA-R-4365] 22 p2647 N73-31210
Existence of undamped Kelvin waves in semiinfinite rotating basin with step change in depth
22 p2653 N73-31250
Application of acoustic transducers for suspending object at center of chamber under near weightless conditions
[NASA-CASE-NPO-13263-1] 22 p2677 N73-31443

WAVE INTERACTION
NT SHOCK WAVE INTERACTION
Energization of electrons in ionosphere and magnetoplasma by wave particle interaction
[AD-747093] 04 p0415 N73-13391
Lagrangian method used for describing small signal wave propagation and nonlinear wave interaction in warm collisionless plasmas
[NASA-CR-129922] 05 p0583 N73-14744
Numerical analysis of structure of solitary waves using partial differential equations
[AD-750565] 06 p0655 N73-15323
Review of material presented at conference on magnetospheric wave-particle interaction
[AD-751568] 07 p0756 N73-16145
Nonlinear wave interaction in plasma column
[NASA-CR-130350] 07 p0825 N73-16686
Development of precursor waves in helium and analysis of wave speed, electron temperatures, and densities using nuclear data handling techniques
12 p1387 N73-21249
Wave-wave coupling in cold beam/cold plasma system
12 p1433 N73-21608
Wave interactions between plasma-electron beam system in magnetic fields
[AEC-TR-7355] 12 p1434 N73-21616
Development of test facility for determining interaction of sonic boom with surface of body of water
[NASA-TT-F-14917] 15 p1767 N73-24318
Theoretical analysis of ion cyclotron wave dynamics in cold plasma
[IPPJ-150] 15 p1816 N73-24722
Wave and Einstein equations for studying scaler waves and tensor perturbations in Mixmaster Universe
15 p1829 N73-24823
Electromagnetic and gravitational wave interaction of black holes
15 p1829 N73-24824
Analysis of large amplitude elastic wave interaction in bounded medium
16 p1968 N73-25919
Gravity wave-mean flow interactions in upper atmosphere
[NASA-CR-132776] 17 p2025 N73-26384
Analysis of changes in amplitudes and frequencies of laser oscillations due to effect of weak reflected signal
17 p2041 N73-26516
Influence of CISK process on mass convergence in tropical planetary boundary layer
18 p2171 N73-27529
Application of mathematical techniques to problems of interaction of acoustic or electromagnetic waves with complex bodies
[AD-762802] 21 p2581 N73-30685
Profile inversion technique for determination of electron density from wave interaction data
[AD-764297] 22 p2668 N73-31378
Nonlinear interactions of electromagnetic waves in parametric plasmas
[JPRS-59685] 22 p2703 N73-31647
Analysis of nonlinear atmospheric waves
24 p2912 N73-33236
Plasma oscillations caused by nonlinear wave interactions
[ITF-73-8-E] 24 p2962 N73-33672

WAVE MOTION
U WAVES
WAVE OSCILLATORS
U OSCILLATORS
WAVE PACKETS
Adapted filter for dispersion measurement of coherent wave packets produced by Pc1 micropulsations
17 p2027 N73-26402
WAVE PROPAGATION
NT GROUND WAVE PROPAGATION
NT IONOSPHERIC F-SCATTER PROPAGATION
NT IONOSPHERIC PROPAGATION
NT LIGHT SCATTERING
NT MICROWAVE TRANSMISSION
NT MULTIPATH TRANSMISSION
NT SCATTER PROPAGATION
NT SHOCK WAVE PROPAGATION
Theoretical description of thermal blooming of pulsed, focused laser beams in gases
[AD-745739] 01 p0066 N73-10539
Propagation of weak shock wave through slightly inhomogeneous turbulent medium
[AD-745728] 01 p0081 N73-10670
Approximate analytic theory of acoustic shock propagation in nonuniform media for motion determination of flare generated, shock wave in corona
01 p0095 N73-10783
Rayleigh-Ritz solution of wave propagation in thermoviscoelastic rod insulated on lateral surface and driven by sinusoidal stress at one end
[AD-746466] 01 p0115 N73-10952
Electromagnetic wave propagation from oscillating source in suddenly created plasma
[AD-746329] 02 p0142 N73-11151
Mechanical wave front propagation in fluid mixtures and isotropic solids
[AD-746617] 02 p0158 N73-11281
Wave propagation in half space due to interior point load parallel to surface
[AD-747306] 02 p0170 N73-11381
Mean irradiance distribution of finite cross section laser beam propagating in sea water
[AD-745956] 02 p0183 N73-11483
Numerical analysis and diagnostics of nonradially stratified media applied to distributions lacking spherical symmetry
02 p0200 N73-11614
Propagation of axisymmetric harmonic waves across interface of two semi-infinite rods composed of different isotropic materials
[AD-746721] 02 p0239 N73-11948
Laser interferometer instrumentation techniques for study of plane stress wave propagation in solids
[SC-DC-70-5465] 03 p0310 N73-12529
Theoretical and experimental determination of harmonic ion cyclotron wave propagation in hot, bounded plasma
[ORO-3778-7] 03 p0342 N73-12786
Propagation properties of ion density perturbations and waves in collisionless plasmas with Maxwellian velocity distribution functions
[RISO-257] 03 p0343 N73-12795
Fluid model for analyzing nonlinear magnetosonic wave propagation in magnetic neutral sheet
[IPPJ-139] 04 p0388 N73-13152
Generation and propagation of low frequency electromagnetic waves in cold collisional plasma
[AD-747092] 04 p0389 N73-13162
Comparison of ionospheric radio wave propagation and acoustic gravity wave propagation
05 p0508 N73-14132
Ray tracing method for calculating paths of acoustic and gravity waves in atmosphere
05 p0508 N73-14133
Asymptotic methods for determining propagation angles of internal gravity waves traveling at ionospheric heights
05 p0509 N73-14144
Measurement of sinusoidal waves in flumes with transducers using non-contacting capacitive sensing
[NRC-MI-836] 05 p0522 N73-14243
Stationary phase direction in absorbent media applied to ray propagation through three successive homogeneous isotropic media
[GRI/TP/110] 06 p0639 N73-15183
Numerical analysis of structure of solitary waves using partial differential equations
[AD-750565] 06 p0655 N73-15323
Mathematical model of thermally induced nonlinear propagation of laser beam in absorbing fluid medium
[DREV-TN-2049/72] 06 p0679 N73-15523
Continuum theory for wave propagation in laminated composites applied to propagation parallel to laminates
[AD-750504] 06 p0689 N73-15608
Bessel function analysis on acoustic wave propagation in curved ducts
[NASA-TM-X-2698] 06 p0700 N73-15705
Elastic wave propagation in cylindrical shells
[NASA-CR-112222] 06 p0724 N73-15909
Lateral inertia effects on elastic-plastic wave propagation in slender rods
[AD-750102] 06 p0728 N73-15938
Determination of turbulent structure of atmosphere through analysis of perturbations induced upon radio wave propagation
07 p0775 N73-16292
Wave propagation and refraction of Type-1 irregularities in equatorial electrojet
[NASA-CR-130382] 07 p0780 N73-16340
Linear and nonlinear propagating characteristics of whistlers
[NASA-CR-130349] 07 p0780 N73-16342
Airborne measurement of ionization cross sections suitable for assessing HF propagation conditions in Arctic ionosphere
[AD-751235] 07 p0797 N73-16480
Rotational tidal waves due to earth rotation explained by Poincare problem solving
07 p0857 N73-16951
Curves for solving low angle radar transmission problems at microwave frequencies over ocean surface
[TR-72-31] 08 p0885 N73-17165
Radiation and propagation of electromagnetic waves in anisotropic medium
[NASA-TT-F-743] 08 p0943 N73-17726
Analysis of wave propagation and amplification properties of molecular electronic plasma to show energy transfer effects
[PSU-IRL-SCI-403] 08 p0948 N73-17759
Wave propagation in parallel-plate metallic waveguide as eigenvalue problem using complete cold-plasma dielectric tensor
[IPP-4/37] 08 p0948 N73-17764
Development of model for analyzing propagation of weak normal shock wave through turbulent atmosphere and application to sonic boom characteristics
[NRC-12981] 09 p0983 N73-18028
Temporal propagation and numerical generated wave patterns for internal waves in stratified fluid of variable altitude or depth
[AD-753126] 09 p1031 N73-18417
Study of propagation characteristics of normal acoustic modes in Gulf of Mexico waters
[AD-753200] 09 p1032 N73-18427
Excitation and propagation of free flow electron waves in plasma
[IPPJ-145] 09 p1070 N73-18731
Research progress in electro-optics, plasma physics, microwaves, wave propagation, telecommunication, data processing
[AD-753710] 09 p1102 N73-18993
Geological structure effect on seismic wave propagation in earth and upper mantle
[AD-753110] 10 p1156 N73-19408
Light and infrared radiation propagation and absorption in atmosphere
[AD-753974] 10 p1158 N73-19418
Analysis of linear elastic wave propagation normal to laminations of periodically laminated porous composite
[AD-753900] 10 p1221 N73-19934
Propagation path simulator for channel between Tracking and Data Relay Satellite and user spacecraft
[NASA-CR-130173] 11 p1255 N73-20185
Water waves generated and propagated in turbulent flow field
[AD-754645] 11 p1288 N73-20451
Effects of propagation parallel to magnetic field on type 1 irregularity instability
[NASA-CR-131359] 11 p1327 N73-20771
Construction of discrete models of nonlinear wave phenomena in elastic rods based on finite element analysis of shock waves in hyperelastic solids
[AD-754953] 11 p1346 N73-20921
Propagation of geomagnetic micropulsations into two layer conducting earth
[AD-755428] 12 p1402 N73-21375
Research progress on radio wave propagation, electronic warfare, rocket engines, and weapon systems
[PB-213217] 12 p1467 N73-21891
Propagation of curved waves through nonlinear elastic gas mixtures
13 p1508 N73-22219
Various atmospheric disturbances including turbulence, sonic boom, and shock wave propagation
13 p1514 N73-22271
Description of linear wave propagation in hot collisionless plasmas using Vlasov and Maxwell equations
[NASA-CR-131496] 13 p1562 N73-22663
Propagation of Alfven waves in spiral interplanetary magnetic field
[NASA-CR-131569] 13 p1563 N73-22665
Propagation of shock and continuous waves in solid plastic media, and wave interaction with elements of structures
[AD-742421] 13 p1586 N73-22854
Propagation of waves in elastic-viscoplastic media in temperature field
[AD-755274] 13 p1592 N73-22905
Propagation of electromagnetic waves through turbulent media using transport theory
[AD-757491] 14 p1634 N73-23245
Simple method for prediction of lowest observed frequency of high frequency propagation paths between Pacific Islands
[AD-757343] 14 p1636 N73-23266
Interaction of large amplitude progressing wave with piecewise linear flow
[AD-756469] 14 p1651 N73-23392
Laser beam propagation in turbulent air
[AD-757221] 14 p1673 N73-23574
Quantitative data on propagation and directivity of parametric array in air
[AD-757034] 14 p1693 N73-23737
Excitation of low frequency instability during powder combustion of rocket engine
14 p1718 N73-23942
Numerical analysis of shock tunnel performance operated by reflected shock technique to determine effects of disturbance to flow at nozzle entry caused by reflected waves
[ARC-R/M-3265] 15 p1725 N73-23999
Antenna measurement of millimeter radio signal propagation through rain
[NASA-CR-132074] 15 p1751 N73-24188
Development of long acoustic damping device for various chamber flow conditions based on nonlinearity of orifice flow upon passage of high intensity wave
15 p1765 N73-24299
Propagation of shear waves in layered composites
[SCL-RR-72-0351] 15 p1839 N73-24905
Development of Mach-Zehnder interferometer theory based on time history of wave front produced by element of extended light source
[ARC-R/M-3173] 16 p1856 N73-25033
Electromagnetic wave propagation in nonuniform waveguides with perfect conducting walls
16 p1874 N73-25170
Polarization of infrared waves due to propagation through atmosphere
16 p1895 N73-25327
Periodic functional analysis of ultra-short pulse generation and propagation in laser systems
16 p1920 N73-25535
Pulsed holographic measurement of wave propagation in thin walled shells and vibration modes in steel rectangular plates at high temperature
16 p1921 N73-25544
Variational and Schelkunoff methods for analyzing microwave propagation in magnetoplasma filled waveguides
16 p1947 N73-25757
Equations of motion for describing physical picture of anomalous ordinary wave propagation in magnetoplasma
[IPPJ-153] 16 p1949 N73-25767
Physical properties of Coulomb collisions
[IPPJ-151] 16 p1949 N73-25773
Wave propagation and magnetic fields effects on velocity oscillations in solar plage regions
16 p1961 N73-25864
Spaceborne prototype model of millimeter wave experiment radiating transmitter for ATS-F spacecraft
[NASA-CR-132760] 16 p1965 N73-25895
Influence of mountain barriers on radio wave propagation by meteors
17 p2023 N73-26373
Averaged Lagrangian method of describing small signal wave propagation and nonlinear wave interaction
17 p2066 N73-26718
Ray tracing method for kinematic analysis of mechanical waves in nonlinear elastic materials
[AD-760438] 17 p2096 N73-26955
Analysis of wave propagation in double-layered piezoelectric system using two cadmium selenide and cadmium sulfide crystals
18 p2115 N73-27102
Measurement of electromagnetic wave diffraction by finite plane-parallel waveguide system
18 p2117 N73-27116
Bibliography of literature concerning electromagnetic and seismic noise and propagation
[PB-217500/8] 18 p2118 N73-27125
Systems applications in the 10 to 100 GHz frequency band for optimum utilization of EHF frequencies
[OT/TRER-34] 19 p2235 N73-28019
Analysis of axial conduction current induced in infinitely long cylinder in free space with small resistivity by incident electromagnetic plane wave
[AD-762165] 19 p2246 N73-28106
Electromagnetic fields in inhomogeneous media for analysis of scattering and propagation problems and for lense studying
[NASA-CR-132286] 19 p2321 N73-28672
Transmission of wave energy in curved ducts
[NASA-TM-X-68287] 20 p2377 N73-29101
Analysis of interaction of detonation wave with boundary gas based on formation of low velocity detonation wave
20 p2384 N73-29153
Numerical analysis of solitary wave propagation in incompressible rotating fluids
20 p2385 N73-29160
Analysis of shock wave strenghtening by positive density gradient in cryogenic shock tube
20 p2386 N73-29173
Theory and computations of wind driven waves at sea
[TT-70-50182] 20 p2387 N73-29176

Propagation of multiwavelength laser radiation through atmospheric turbulence
[AD-762516] 20 p2426 N73-29491
Rate effects on instabilities in slightly ionized plasmas
[NASA-CR-133599] 20 p2458 N73-29753
Nonlinear Schrodinger equation for studying nonlinear wave modulation in magnetized collisionless plasma
[IPPJ-162] 20 p2458 N73-29755
Gas dynamics of plane shock wave propagation in steady state moving medium
20 p2472 N73-29860
Strain waves propagating in linear viscoelastic plates of various thicknesses
20 p2477 N73-29897
Wave propagation and impact in composite materials
[NASA-CR-121226] 20 p2482 N73-29935
Analysis of characteristics of initially plane, strong shock wave propagating into conical convergence using multi-crystal piezoelectric probe
21 p2522 N73-30228
Analysis of meteorological nature and characteristics of anomalous radio echoes received during vertical sounding of troposphere
21 p2571 N73-30602
Effects of isotropic scattering on one dimensional propagation of small disturbances in radiating gray gas
[ISAS-494-VOL-38-NO-5] 22 p2651 N73-31237
Wave propagation in thin elastic shells
22 p2723 N73-31793
Strain wave propagation in metal cones with compressive pulse applied at base and application to design of gun launchers
[AD-762504] 22 p2727 N73-31822
Development of continuum theory with microstructure for wave propagation in composite materials
23 p2806 N73-32438
Propagation of waves in layered composites
23 p2806 N73-32439
Behavior of impact-generated elastic stress waves propagating in rods of unidirectional composite material
23 p2852 N73-32792
Dynamic behavior and stability classification of one-dimensional wave propagation systems
24 p2893 N73-33096
Propagation of random electromagnetic waves
24 p2894 N73-33103
Propagation path depolarization caused by precipitation
[NASA-CR-132818] 24 p2895 N73-33107
Characteristics of constant scaling method for analyzing linear inviscid internal waves in ocean, atmosphere, and experimental tanks
[AD-764579] 24 p2910 N73-33227
Spatial structure of temperature fluctuations in seas
24 p2947 N73-33535
Debye polarization theory for determining electromagnetic wave propagation in sea
24 p2957 N73-33622
Plasma wave propagation and absorption, and parametric instabilities
[CALT-767-P-2-X-2] 24 p2963 N73-33682
Characteristics of steady galactic winds created by escape of cosmic rays from galaxy
24 p2975 N73-33775
LUIN, code for calculation of cosmic ray propagation in atmosphere
[HASL-275] 24 p2977 N73-33784
Propagation of shock waves following explosion of finite cylindrical charge based on finite difference numerical analysis
24 p2991 N73-33907

**WAVE RADIATION**
U ELECTROMAGNETIC RADIATION

**WAVE REFLECTION**
Sound wave reflection from sea bed, acoustic properties of sedimentary layer, and application to Baltic Sea
[FOA-3-C-3680-E1] 02 p0164 N73-11331
Diffraction of acoustic and electromagnetic waves on wavy surfaces
[AD-748037] 03 p0268 N73-12168
Resonance effects anomalous electromagnetic wave propagation in plasma
[NASA-CR-129673] 04 p0454 N73-13704
Reflection and transmission of large amplitude shockless waves at interface with semi-infinite medium
[AD-746642] 04 p0483 N73-13947
Ionospheric disturbance effects on sky wave bearing measurement
05 p0511 N73-14159
Shock wave reflection from water surface
07 p0769 N73-16250
Microwave reflection from electron density ramps produced behind shock waves in nitrogen oxygen mixtures
07 p0824 N73-16682
Characterization of electron plasma wave echoes
[EUR-CEA-FC-639] 07 p0828 N73-16711
Stokes parameters for calculating polarization of radio waves reflected from inhomogeneous ionosphere
[NASA-TT-F-14676] 09 p1002 N73-18174
Interaction of two equally strong shock waves reflecting from plane wall in double shock tube
[BMVG-FBWT-72-35] 09 p1011 N73-18254
Mach reflection in solids, liquids, and explosives using annular shock wave generated by explosion of cylinder coatings
[BMVG-FBWT-72-3] 09 p1016 N73-18292
Doppler study of microwave backscattering from ocean waves in wind wave tank
[AD-753199] 09 p1032 N73-18422
Predicting arrival angle and skip distance variations of quiet and disturbed ionosphere on basis of N[h] profiles and h prime f characteristics
13 p1520 N73-22324
Ray tracing method for calculating underwater acoustic reflection patterns of surface originated signals from objects of arbitrary shape
[AD-757110] 14 p1694 N73-23744
Diffuse shock wave reflection from ridged plates, simulating aerial explosion effects on earth surface
[REPT-7/72] 15 p1766 N73-24305
Geometrical optical analysis for determining point source location of electromagnetic signal reflected from ionosphere
[AD-759488] 16 p1877 N73-25196
Structure of weak shock wave in vibrationally relaxing gas undergoing wall reflection
17 p2013 N73-26277
Numerical solution for two dimensional electromagnetic scattering
[AD-760773] 18 p2119 N73-27137

**WAVE RESISTANCE**
Small Froude number paradoxes and wave resistance at low speeds
[AD-746191] 01 p0043 N73-10340

**WAVE SCATTERING**
NT ACOUSTIC SCATTERING
NT ATMOSPHERIC SCATTERING
NT ELECTROMAGNETIC SCATTERING
NT IONOSPHERIC F-SCATTER PROPAGATION
NT LIGHT SCATTERING
NT MICROWAVE SCATTERING
NT MIE SCATTERING
NT RAMAN SPECTRA
NT RAYLEIGH SCATTERING
NT REVERBERATION
NT TROPOSPHERIC SCATTERING
NT X RAY SCATTERING
Device and method for determining X ray reflection efficiency, scattering properties, and surface finish of optical surfaces
[NASA-CASE-MFS-20243] 04 p0449 N73-13662
Literature survey on wave scattering from rough surfaces
[FOA-2-C-2486-E1] 04 p0449 N73-13668
Scalar wave scattering on water surface wake generated by moving pressure point
[AD-749113] 05 p0527 N73-14291
Procedures and equipment for measuring angular distribution of laser beam scattering by evolving water vapor
[NLL-M-22457-[5828.4F]] 05 p0554 N73-14497
Wave scattering by lenses and microsound elastic waveguides
[AD-750766] 06 p0701 N73-15717
Mathematical models for analyzing resonance effects on wave absorption and scattering in meteor trails
17 p2023 N73-26372

**WAVE SUPERHEATERS**
U HYPERVELOCITY WIND TUNNELS
U SHOCK TUBES

**WAVEFORMS**
NT PULSE AMPLITUDE
NT PULSE DURATION
NT SAWTOOTH WAVEFORMS
NT SQUARE WAVES
Sea state effects on altimeter signal scattering and radar wave form estimates
06 p0663 N73-15381
Real time pitch period extraction by adaptive prediction of speech waveform
14 p1622 N73-23136
Decoding of information in acoustic waveform of human speech using signal processing techniques
14 p1623 N73-23148
Definition of equivalent peak level in objective speech level measurement
14 p1625 N73-23163
Electronics of waveform generator for digital voltage source
[AD-758212] 15 p1758 N73-24247
Device for performing statistical time-series analysis of complex electrical signal waveforms
[NASA-CASE-MSC-12428-1] 16 p1883 N73-25240
Characteristics of water waves generated by steady two-dimensional wind at three different speeds over water depth of 19 centimeters
16 p1887 N73-25272
Wave flume and oscillating water tunnel for bed forms generated by wave action
22 p2731 N73-31856
Transit waveform control program for real time environmental shock tests
22 p2732 N73-31860

**WAVEGUIDE ANTENNAS**
NT HORN ANTENNAS
Dielectric loaded aperture antenna with directive radiation pattern from waveguide
[NASA-CASE-LAR-11084-1] 03 p0273 N73-12216
Radiation pattern characteristics of traveling wave coaxial cable antenna
[AD-749051] 04 p0397 N73-13233
Design and fabrication of two dimensional dielectric lens contained in parallel plate waveguide system in multibeam antenna study
[NASA-CR-132793] 22 p2641 N73-31171

**WAVEGUIDE FILTERS**
Basic-mode wave attenuator in multimode waveguide
[AD-754516] 11 p1257 N73-20203
Attenuation of circularly bent waveguides with dielectric contings, noting role of mode filters
[FTZ-A-333-TBR-16] 22 p2643 N73-31181

**WAVEGUIDE WINDOWS**
Optical and back reflection properties of GaAs crystals used as IR window materials
[AD-749083] 04 p0451 N73-13684
Complex permittivity measurements during high temperature recycling of space shuttle antenna window and dielectric heat shield materials
[NASA-CR-2302] 22 p2707 N73-31675

**WAVEGUIDES**
NT BEAM WAVEGUIDES
NT OPTICAL WAVEGUIDES
Development and characteristics of reciprocal latching microwave phase shifters based on ferrimagnetic substrate
[AD-744795] 01 p0033 N73-10255
Effect of longitudinal slot in circular waveguide
[PB-208160] 01 p0034 N73-10267
FORTRAN program for plotting attenuation of air-filled rectangular waveguide
[AD-746108] 02 p0142 N73-11153
Development of least squares curve-fitting algorithm for simultaneous estimation of small signal gain and saturation intensity in carbon dioxide laser waveguide
[NASA-TM-X-66097] 02 p0181 N73-11468
Characteristics of millimeter attenuation and reflection coefficient measurement system and specifications for waveguide standards fabrication
[NBS-TN-619] 03 p0302 N73-12462
Corrections for sidewall waveguide slots to microwave transmission data for shock-ionized air
[AD-748075] 03 p0343 N73-12801
Approximation technique applied to elastic surface waveguides utilizing curved thin films
[AD-748646] 04 p0390 N73-13169
Mathematical model for energy distribution in waveguide bifurcations
[DLR-FB-71-17] 05 p0520 N73-14224
Research and development in slot line construction techniques
[AD-749070] 05 p0520 N73-14230
Loading effect of probes used in coaxial waveguide experimental coupler
[AD-749060] 05 p0521 N73-14233
High resistivity semiconductor waveguides for device and circuit functions
[AD-750317] 06 p0645 N73-15241
Waveguiding in thin silver strip vacuum deposited on bismuth germanium oxide
[AD-750612] 06 p0648 N73-15262
Operating modes and outputs of distributed feedback side coupled waveguide lasers
[CRC-1235] 06 p0679 N73-15521
Wave scattering by lenses and microsound elastic waveguides
[AD-750766] 06 p0701 N73-15717
Measurement of accelerator tube and waveguide system parameters for improving linear accelerator performance
[RISO-M-1518] 07 p0766 N73-16223
Use of liquid crystals in integrated optical circuits as waveguides
[AD-751537] 07 p0833 N73-16755
Theory of finite aperture waveguide gas laser resonators representing external reflectors by matrices
[NASA-TM-X-66186] 08 p0929 N73-17608
Feasibility of underground waveguide for radio signal transmission
[AD-754786] 11 p1257 N73-20198
Coupled modes on dielectric image waveguide
12 p1382 N73-21206
Measured element factor of linear array for various waveguide radiating elements
[PHL-1973-1] 14 p1639 N73-23287
Acousto-optic interactions in guided wave structure for optical modulation, deflection and signal processing
[AD-758719] 15 p1752 N73-24198

Guiding and scattering of acoustic surface waves in solid layer between substrates
15 p1813 N73-24691
Elastic and piezoelectric surface waves guided by thin films
[AD-758688] 15 p1823 N73-24776
Electromagnetic wave propagation in nonuniform waveguides with perfect conducting walls
16 p1874 N73-25170
Variational and Schelkunoff methods for analyzing microwave propagation in magnetoplasma filled waveguides
16 p1947 N73-25757
Differential geometry scaling method for determining electromagnetic field of coaxial waveguide coupler
[AD-760157] 17 p2006 N73-26222
Measurement of electromagnetic wave diffraction by finite plane-parallel waveguide system
18 p2117 N73-27116
Finite element calculation on transmission line characteristics for coplanar waveguide
[AD-760756] 18 p2119 N73-27135
Design and tests of hybrid-mode tracking feed horn
[AD-759834] 18 p2123 N73-27159
Directional coupler design using coplanar waveguides for microwave integrated circuits
[AD-760533] 18 p2124 N73-27166
Development of techniques for welding copper and copper-base alloys with application to waveguides in electron accelerator facility
[SLAC-PUB-1095] 19 p2305 N73-28533
Production of semiconducting films for waveguides and optical device elements
[AD-763101] 20 p2455 N73-29729
Thin film optical waveguides in III-V semiconductors
[AD-763120] 20 p2455 N73-29730
C band waveguide phased array
[AD-763214] 21 p2517 N73-30193
Magneto-optic effects in ferrate garnet thin film waveguides
[AD-763792] 21 p2518 N73-30199
Waveguide and luminescent properties of thin film Pb-salt injection lasers
[AD-763757] 21 p2556 N73-30488
Bulk semiconductor dielectric waveguide functional circuits
[AD-763888] 22 p2707 N73-31681
Calculation of evanescent-wave gain in TE sub Om and TM Om of optical fibers
[CRC-1247] 23 p2769 N73-32147

**WAVELENGTHS**
Attenuation of carbon dioxide laser beams in atmosphere at various frequencies and method for calculating absorption coefficients from measured data
[FOA-2-A-2542-E3/E4/E6] 02 p0181 N73-11465
Energy calibration of Orion spectrograph for operation in wavelength range from 2000 to 3800
[NASA-TT-F-14584] 07 p0799 N73-16491
Magnetohydrodynamic frequency-wavelength relation in isothermal atmosphere
[BBSO-0127] 11 p1324 N73-20743
Dual wavelength system for monitoring film deposition
[NASA-CASE-MFS-20675] 17 p2070 N73-26751
Optical wavelength - modulation spectroscopy of solids
[LBL-1402] 21 p2549 N73-30437
Heat transfer and wavelength measurement for axisymmetric flow of fluid layer heated from below
24 p2903 N73-33167

**WAVES**
Spectral analysis of turbulent fluctuations over ocean waves
[AD-753624] 10 p1156 N73-19406
Propagation of shear waves in layered composites
[SCL-RR-72-0351] 15 p1839 N73-24905
Electron density determination in thermodynamic equilibrium behind reflected shock wave in air, using microwave reflectometer in shock tube
[ISL-43/71] 16 p1889 N73-25288
Bar shaped density wave theory of barred spiral galaxies
19 p2341 N73-28835

**WEAPON SYSTEMS**
NT GROUND OPERATIONAL SUPPORT SYSTEM
NT MISSILE SYSTEMS
Estimating strafing performance of unspecified foreign tactical fighter without aerodynamic stability derivatives
[AD-745997] 01 p0006 N73-10044
Model of pilot-aircraft system for relating pilot tracking performance to overall weapon delivery
[AD-745999] 01 p0006 N73-10045
Weapon delivery accuracy of F-4 aircraft with experimental stick to rudder interconnect to minimize lateral tracking error
[AD-746000] 02 p0126 N73-11027
Weapon delivery accuracy of F-4 aircraft with high gain control augmentation system
[AD-746001] 02 p0126 N73-11028
Engineering data on new aerospace structural materials with potential use in weapon system
[AD-746761] 02 p0189 N73-11534
Survivability and confidence assessment of military weapon systems with reference to tactics, threat, and environment
[AD-746061] 02 p0235 N73-11913
Computer program for optimum mixed offense weapons system
[AD-746263] 02 p0245 N73-11995
Design techniques for estimating cost of flight vehicle structures
[AD-747007] 03 p0367 N73-12994
Catalog of batteries for Navy weapon systems
[AD-751018] 06 p0627 N73-15087
Electromagnetic compatibility of avionic weapon system
[AD-754412] 11 p1265 N73-20262
Manual on electromagnetic compatibility and interference between aircraft weapon systems
[AD-754411] 11 p1265 N73-20263
Research progress on radio wave propagation, electronic warfare, rocket engines, and weapon systems
[PB-213217] 12 p1467 N73-21891
Development of equipment for securing external stores SH-3G helicopter and analysis of failure modes
[AD-757001] 13 p1474 N73-21943
System modeling and performance optimization for analyzing parameters and disturbances for dynamic precision weapon delivery - Vol. 1
[AD-751505] 16 p1976 N73-25985
Computer programs for conducting mathematical analysis of weapon delivery techniques and performance optimization of aerial delivery weapons - Vol. 2
[AD-751506] 16 p1977 N73-25986
Testing and demonstration of weapon delivery analysis program to determine major contributors to probable error - Vol. 3
[AD-751527] 16 p1977 N73-25987
Quality control policies of DOD and application to weapon system acquisition management
[AD-762000] 19 p2305 N73-28540
Policies and guidelines for awarding weapons systems acquisition contracts
[AD-761443] 19 p2356 N73-28949
Supersonic combustion and turbulent mixing processes required for advanced weapon systems
[AD-762599] 20 p2486 N73-29969
Computerized simulation of weapon system terminal ballistics and impact effectiveness
[AD-764884] 23 p2867 N73-32921

**WEAPONS**
NT ARTILLERY
NT FISSION WEAPONS
NT GUNS [ORDNANCE]
NT MINES [ORDNANCE]
NT NUCLEAR WARHEADS
NT NUCLEAR WEAPONS
NT RIFLES

**WEAPONS DEVELOPMENT**
Manufacture of military hardware using powder metallurgy
[DREV-TN-2035/72] 15 p1797 N73-24570

**WEAR**
Microstructural studies of adhesion, wear, friction, and lubrication using LEED, Auger emission spectroscopy analysis, and field ion microscopy
[NASA-TM-X-68152] 01 p0058 N73-10471
Influence of carbon content and structural state on abrasive wear resistance of iron alloys
[AD-747078] 02 p0190 N73-11539
Physical, technological, and wear resistant properties of naturally alloyed metal ceramic material developed from iron powder
[AD-747626] 03 p0322 N73-12626
Lubrication, friction, and wear in machinery
[AD-749086] 04 p0428 N73-13485
Antifriction and antiwear properties of medium pressure polyethylene
[AD-748912] 04 p0439 N73-13582
Friction, wear, and thermal stability of some organotin and organosilicon compounds
[NASA-TN-D-7175] 09 p1051 N73-18569
Spectroscopic, photometric, and electron microscope analyses of metal wear particles in JT3D turbojet engine oil
[DLR-FB-73-06] 12 p1409 N73-21417
Contact interaction and friction and wear of solid bodies
[AD-755710] 13 p1535 N73-22438
Effect of contact-surface-active vapors on wear behavior of soft steel during sliding friction
[NASA-TT-F-14935] 15 p1791 N73-24523
Adhesion, friction, and wear behavior of glasses and ionic solids
[NASA-TM-X-68255] 16 p1932 N73-25632
Interfacial wear reactions in nickel and molybdenum alloy mechanical face seals
[AD-762076] 19 p2306 N73-28546
Wear of hydraulic turbines, axial, and centrifugal pumps from cavitation and deposit
[AD-758322] 24 p2911 N73-33228
Frictional processes, electric contact resistance, and wear of pin on disk friction pair
[NASA-TT-F-15049] 24 p2929 N73-33391

**WEAR INHIBITORS**
Relative wear resistance and patterns of metals under hydroabrasive wear
[AD-747668] 03 p0318 N73-12595
Effect of galvanic and thermodiffusive coatings on wear resistance of shafts and hinged joints
[AD-750533] 05 p0553 N73-14494
Solutions to problem of wear processes experienced by steel industry
[PB-211173] 07 p0809 N73-16565
Formula for evaluating durability of plastic bearings based on fatigue wear theory and including friction, elasticity, strength, and pressure factors
[AD-752820] 09 p1040 N73-18480
Nonstationary shock models and wear processes
[AD-753117] 09 p1042 N73-18497
Silicone base nonflammable hydraulic fluid to aid wear resistance in military aircraft
[AD-758361] 14 p1671 N73-23562
Protection of titanium microstructure with intermediate nickel barrier to prevent abrasion and crack propagation on turbine compressor blades
[AD-758276] 14 p1682 N73-23651
Wear inhibiting effect of automotive oils containing polymethacrylate
[NLL-TRANS-1190-[9022.9]]
15 p1746 N73-24149
Wear inhibition of carboxylic acids in synthetic lubricating oils on ester basis
[DLR-FB-73-43] 15 p1793 N73-24536

**WEAR TESTS**
Calibration of rotating sand erosion test apparatus simulating turbocompressor wear
[AD-743309] 01 p0059 N73-10483
Performance tests of ball bearings to determine service life during operation without lubrication under various conditions of atmospheres, loads, and speeds
[AD-746034] 01 p0063 N73-10520
Braking effects on aircraft tire tread wear and runway surface characteristics
[NASA-TN-D-6963] 02 p0125 N73-11021
Sliding friction and wear of Fe, Co, Cu, Ag, Mg, and Al in oxygen-nitrogen mixture of pressures between 760 torr and 0.2 microtorr
[BAM-BR-13] 03 p0306 N73-12503
Hardened high strength steel for making wear resistant metal cutting tools
[AD-747711] 03 p0308 N73-12511
High temperature friction and wear properties of PbO for solid lubricant applications including tests in room air, controlled atmospheres, and vacuum
[NAL-TR-285] 04 p0426 N73-13470
Application of scanning electron microscope to friction and wear studies
[DLR-FB-71-70] 06 p0674 N73-15485
Conference on environmental effects on mechanical failures
[AD-750411] 06 p0677 N73-15512
Analysis of wear resistance of copper alloyed, magnesium cast iron by reciprocating motion of different friction pairs
[AD-750519] 06 p0687 N73-15590
Correlation of wear behavior and properties of coated fabric hovercraft fingers
[RAE-TR-71210] 08 p0935 N73-17654
Friction, wear, and transfer of carbon and graphite to copper, chromium, and aluminum metal surfaces in vacuum
[NASA-TN-D-7206] 09 p1039 N73-18475
Formula for evaluating durability of plastic bearings based on fatigue wear theory and including friction, elasticity, strength, and pressure factors
[AD-752820] 09 p1040 N73-18480
Wear process and colloidal particle production test on sliding metal surfaces using magnetic measurements
[AD-753251] 09 p1040 N73-18481
Bench tests of wear resistance and antifriction properties of epoxy compounds
[AD-752868] 09 p1054 N73-18588
Performance tests to determine stress-life exponent for vacuum-processed steel ball bearing operating at 500 F
[NASA-TM-X-68240] 15 p1791 N73-24521
Investigation of wear behavior and load capacity of journal bearings in transition range from full to boundary lubrication using radioisotopes
[KFK-1569] 15 p1793 N73-24533
Water jet impingement wear tests on plexiglass, aluminum alloys, nickel, cobalt alloys, and stainless steels
[PB-215631/3] 16 p1890 N73-25294
Facility for wear testing sodium cooled reactor materials
[KFK-1659] 16 p1944 N73-25727
Wear processes and compressive stress of graphite fluoride lubricated machine surfaces
[AD-759560] 17 p2038 N73-26489
Surface potential and wear measurements on carbamate, amine, and phosphorothioate lubricant additives
[AD-759126] 17 p2051 N73-26595
Wear tests of ceramic materials for rolling contact bearings
[AD-761200] 18 p2168 N73-27506

Wear testing of Zircaloy 2 on Zircaloy 2 and of Zircaloy 2 on steel considering debris generation
[DUN-8075] 24 p2935 N73-33441
WEATHER
NT COLD WEATHER
Aircraft accident involving DC-9 aircraft landing at Fort Lauderdale, Florida airport in marginal weather conditions on 18 May, 1972
[NTSB-AAR-72-31] 07 p0738 N73-16005
Acquisition of weather and ground truth data for Skylab EREP experiments
[E73-10797] 18 p2137 N73-27273
Guide to worldwide standard weather and climatological summaries
[PB-221354/4] 22 p2696 N73-31596
Aircraft landing problems under low visibility weather conditions
[DGLR-PAPER-73-015] 23 p2817 N73-32520
Meteorological and weather effects on aircraft landings and flights along air lanes and stratospheric wind effects on supersonic transports
[JPRS-60114] 24 p2945 N73-33522
WEATHER CHARTS
U METEOROLOGICAL CHARTS
WEATHER CONDITIONS
U WEATHER
WEATHER CONTROL
U WEATHER MODIFICATION
WEATHER DATA RECORDERS
Development of automated hydrometeorological service and establishment of information-computation network for data recording
12 p1421 N73-21515
Rain attenuation statistics for ultrahigh frequency microwave link using meteorological data
17 p1996 N73-26135
WEATHER FORECASTING
NT LONG RANGE WEATHER FORECASTING
NT NUMERICAL WEATHER FORECASTING
NT STATISTICAL WEATHER FORECASTING
Soviet Meteor meteorological satellite system and applications in weather forecasting, geological surveys, and exploration of earth resources
[NLL-M-22683-[5828.4F]] 01 p0073 N73-10599
Effects of decision models and operational characteristics on economic expenses associated with use of predictive weather information
[NASA-CR-128401] 01 p0073 N73-10600
Effects of surface anomalies on certain model generated meteorological histories
[NASA-CR-130070] 01 p0074 N73-10612
Tables on Atlantic tropical cyclone strike probabilities - 24 hour movement
[AD-744916] 01 p0076 N73-10630
Tables on Atlantic tropical cyclone strike probabilities - 48 hour movement
[AD-744917] 01 p0076 N73-10631
Probabilities of forecasting future movement of North Atlantic tropical cyclones
[AD-744918] 01 p0076 N73-10632
Reference file of local factors affecting weather at Ramey AFB, Puerto Rico
[AD-746026] 02 p0205 N73-11661
Reference file of factors affecting weather at Kelly AFB, Texas
[AD-746028] 02 p0205 N73-11662
Simulation of alternate expressions for meteorological phenomena of atmospheric boundary layer - tables
[AD-746247] 02 p0205 N73-11665
Regression analysis of tropical storm and typhoon speed characteristics after recurvature in western North Pacific Ocean
[AD-746880] 02 p0206 N73-11672
Handbook on weather patterns over Point Mugu, California
[AD-747641] 03 p0327 N73-12672
Analysis of natural synoptic seasons prior to winter to determine forecasting indications of extremely warm periods
04 p0442 N73-13605
USSR developments in meteorology, weather forecasting, climate control, and hydrological forecasting
[JPRS-57608] 04 p0444 N73-13623
Soviet articles on microclimatology, argricultural meteorology, hydrology, and weather modification and forecasting
[JPRS-57652] 04 p0444 N73-13624
Thunderstorm probability and supersonic transport safety on flight paths over southern United States during July
[AD-748798] 04 p0445 N73-13628
Two methods of analyzing persistence of weather map types, using January MSL pressure data for Colorado map typing window
[AD-749130] 04 p0446 N73-13641
Research in control of infectious diseases weather forecasting, and epidemic of Q fever without pneumonia
[JPRS-57663] 04 p0475 N73-13886
Meteorological assistance to fishing fleets by meteorological services
[NLL-M-9146-[5828.4F]] 05 p0569 N73-14624
Potential economic benefits of improvements in weather forecasting, using satellites and computers
[NASA-CR-129991] 05 p0571 N73-14635
Investigation of thunderstorm potential in cold air cumulonimbi over northwestern Europe during winter
[AD-749493] 05 p0574 N73-14674
Marine weather program for providing weather and river advisories to public sector
06 p0663 N73-15382
Performance of mathematical snowmelt models and statistical analysis of avalanche forecasts
06 p0665 N73-15402
Utilization of meteorological satellite data to forecast severe thunderstorms and tornadoes
06 p0693 N73-15644
Development of four-level model of baroclinic atmosphere for predicting geopotential at various isobaric surfaces for Northern Hemisphere
[AD-750496] 06 p0694 N73-15659
Application of remote sensors for determining meteorological and environmental parameters with emphasis on data obtained by satellite infrared sensors
07 p0782 N73-16357
Short range forecasting of geopotential and wind for large territory by barotropic divergent
[AD-751422] 07 p0796 N73-16475
Classification, description, and statistical treatment of European large-scale weather patterns
[NLL-M-9145-[5828.4F]] 07 p0814 N73-16600
Development of mathematical meteorological models for objective forecasting
[AD-751744] 07 p0816 N73-16614
DCS platform monitoring of weather conditions for cloud seeding control
[E73-10095] 08 p0902 N73-17307
Probability models of wet and dry days for several stations in Thailand
[THESIS-392] 08 p0938 N73-17684
Determining natural components of meteorological fields
[AD-751958] 08 p0939 N73-17692
Estimating confidence intervals of probability of rare events as function of scale of sample
[AD-751953] 08 p0939 N73-17693
Bibliography of weather predictions and verifications
[AD-751950] 08 p0940 N73-17701
Thermal parameters as predictors of precipitation at Ellsworth, S.D.
[AD-753418] 09 p1061 N73-18657
Analysis of mesoscale weather systems in tropics from radar data of south Florida
[AD-753611] 09 p1062 N73-18660
Research and development projects of Federal Aviation Administration to provide improved weather data acquisition and distribution
[FAA-ED-15-1] 11 p1314 N73-20662
Utilization of ERTS-1 imagery for monitoring weather conditions for cloud seeding control
[E73-10489] 12 p1397 N73-21325
Development of agrometeorological forecasts with emphasis on optimal decisions on taking preventive measures for frost control
12 p1421 N73-21517
Computer-derived synoptic weather forecast maps
[AD-755898] 12 p1423 N73-21532
Application of remote sensing techniques in forestry and range disciplines for timber inventory, weather forecasting, land classification, and snowfield monitoring
[NASA-CR-131583] 13 p1523 N73-22340
Weather forecasting in USSR
[JPRS-58797] 13 p1552 N73-22571
Method for calculating turbulent fluxes by measuring meteorological parameters at two meter height
13 p1552 N73-22576
Blocking anticyclones over Siberia during winter, and meteorological conditions for forecasting their occurrence
13 p1552 N73-22577
Weather forecasting and atmospheric activity detection using meteorological radar and remote sensing equipment
[AD-755438] 13 p1554 N73-22597
Operational decision model for making conditional weather forecasts for airlift supply task
[AD-755403] 13 p1555 N73-22601
Numerical advection model for simulating maritime fog
[AD-757328] 14 p1685 N73-23676
Satellite cloud photography for predicting rainfall in Sudan
[AD-757733] 15 p1783 N73-24452
Weather forecasts using satellite information
[NLL-M-22897-[5828.4F]] 15 p1804 N73-24625
Methods of forecasting hail, thunderstorms, and amounts of rainfall
[NLL-M-22902-[5828.4F]] 15 p1805 N73-24626
Satellite infrared channel radiances for resolution of atmospheric thermal structure and developing weather analysis and forecasting system
[AD-758734] 15 p1807 N73-24644
Development of methods for improving forecasting of precipitation, surface pressure, temperature, and dew point
[NLL-M-22980-[5828.4F]] 16 p1935 N73-25658
Dynamics of horizontal movement of air masses
[NLL-M-22820-[5828.4F]] 16 p1936 N73-25667
Meteorological processes and FM-CW radar soundings in boundary layer
[AD-759019] 16 p1939 N73-25695
Feasibility of using adaptive estimation for atmospheric temperature forecasting
[AD-759546] 16 p1940 N73-25698
Weather forecasting and measurement of air pollution by laser sounding of atmosphere
[NASA-TT-F-14948] 17 p2026 N73-26391
Catalogue indexes to local weather forecasts
[AD-760091] 17 p2058 N73-26648
Model of atmospheric motion for long-term weather forecasting
[AD-759877] 17 p2058 N73-26651
Daily summaries for vertical echo sounding of upper atmosphere over Freiburg, Germany during March, 1973
[REPT-321F] 18 p2141 N73-27308
Application of meteorological satellite data in analysis and forecasting
[ESSA-TR-NESC-51-SUPPL-2]
18 p2171 N73-27532
Climatology of instantaneous precipitation rates
[AD-760785] 18 p2174 N73-27558
Typhoon and tropical storm intensity forecasts in western North Pacific Ocean using statistical regression analysis
[AD-761379] 18 p2174 N73-27561
Numerical experiments with five-level global atmospheric prediction model using staggered, spherical, Sigma coordinate system
[AD-761386] 19 p2316 N73-28626
Synthetic verification matrices of subjective weather forecasting
[AD-761485] 19 p2316 N73-28630
Research projects in environmental and electromagnetic technologies
[AD-761483] 19 p2355 N73-28948
Activities of meteorological section during Tenth Soviet Antarctic Expedition
20 p2408 N73-29350
Solutions to quasisteady problems of dynamic weather forecasting
20 p2442 N73-29618
Hydrological and meteorological forecasting and climate control
[JPRS-59052] 20 p2446 N73-29647
Research in hydrometeorology and forecasting
[JPRS-59210] 20 p2447 N73-29662
Hydrometeorological characteristics for weather forecasting
20 p2448 N73-29668
Forecasting air mass thunderstorms for MacDill AFB, Florida
[AD-763099] 20 p2451 N73-29696
Short-range terminal weather forecasting techniques in AWS
[AD-762938] 20 p2451 N73-29699
Analysis of meteorological parameters affecting safety of civil aviation and instructions for increased flight safety
[NASA-TT-F-15069] 21 p2495 N73-30028
Predicted weather conditions for USSR during winter of December 1971 through March 1972
[NLL-M-23035-[5828.4F]] 21 p2568 N73-30578
Proceedings of conference on application of radar techniques to meteorological observations and weather forecasting
[TT-70-50120] 21 p2568 N73-30580
Development of equipment and methods for obtaining and processing meteorological radar data
21 p2571 N73-30606
Statistical procedures for hydrometeorological and weather forecasting and climate control
[JPRS-59580] 21 p2572 N73-30612
Study of low level boundary layer jet streams for predicting dangerous atmospheric conditions
21 p2573 N73-30622
Dynamic forecast model for studying moisture variation in planetary boundary layer
[PB-220532/6] 21 p2575 N73-30635
Methods for obtaining vertical motion rigns at various atmospheric levels to explain areas of rain and no rain
[NASA-CR-2304] 22 p2694 N73-31577
Forecasting altitude of lower cloud boundary after time intervals of 6, 9, and 12 hours
24 p2946 N73-33524
Articles on meteorology and hydrology
[JPRS-60164] 24 p2946 N73-33530
Origin, development and prospects of World Weather Watch noting role to be played by meteorological satellites and GARP
24 p2949 N73-33551
Present status in meteorological satellites, wind observation, cloud cover, and the imagery compared with predictions made in 1962
24 p2949 N73-33552

Models for predicting wind fields over mountains, and potential radiological fields over Nevada test site
[NOAA-ARLV-351-28] 24 p2949 N73-33556
Handbook on monthly weather forecasts
[AD-765607] 24 p2950 N73-33563
WEATHER FRONTS
U FRONTS [METEOROLOGY]
WEATHER MAPS
U METEOROLOGICAL CHARTS
WEATHER MODIFICATION
NT CLOUD SEEDING
Empirical procedure for predicting growth of ice crystals, grauple, and hail by diffusion
[AD-746451] 02 p0205 N73-11660
Two dimensional, time dependent warm fog model by airborne wide area hygroscopic particle seeding
[AD-746807] 02 p0206 N73-11674
Soviet articles on microclimatology, agricultural meteorology, hydrology, and weather modification and forecasting
[JPRS-57652] 04 p0444 N73-13624
Introducing cloud seeding in model for predicting precipitation patterns over synoptic scale
[AD-750730] 05 p0576 N73-14691
Monitoring weather conditions for cloud seeding control
[E73-10059] 07 p0778 N73-16321
Field test of warm fog dispersal using helicopter downwash and hygroscopic seeding
[AD-752046] 08 p0939 N73-17694
High temperature contact nucleation of supercooled water by organic chemicals for fog and cloud seeding
[AD-753465] 10 p1127 N73-19181
History and future of scientific attempts to control meteorological processes and climatology
[NLL-M-22821-[5828.4F]] 12 p1420 N73-21506
Warm fog modification by electrostatically charged particles
[AD-754100] 12 p1423 N73-21531
Air Weather Service fog dispersal and weather modification program
[AD-755659] 12 p1423 N73-21533
Appraisal of meteorological satellite data as aid in weather modification programs
[NASA-CR-131876] 13 p1553 N73-22583
Ground based silver iodide cloud seeding for modifying snowfall in northern Rockies near Montana
[PB-2180512] 18 p2173 N73-27548
Inadvertent modification of cloud formation and weather by St. Louis area - Project Metromex 1
[PB-218678/1] 18 p2173 N73-27549
Technology assessment of fog modification
[AD-762207] 19 p2316 N73-28631
Evaluation of electrogasdynamic concept for dispersal of warm fog based on injection of charged water droplets into fog
[ASRC-PUBL-207] 20 p2382 N73-29140
Atmospheric pollution due to use of lead iodide in weather modification
[NLL-M-23006-[5828.4F]] 20 p2441 N73-29607
Hydrological and meteorological forecasting and climate control
[JPRS-59052] 20 p2446 N73-29647
Hail protection method for reducing or eliminating farm crop damage
20 p2446 N73-29649
Large scale weather modification through spread of carbon black particles in aerosol form in upper atmosphere
[PB-220642/3] 21 p2541 N73-30374
Methods of augmenting precipitation for winter storms of Sierra, Nevada
[PB-220674/6] 21 p2575 N73-30633
Research in development and utilization of atmospheric water resources in Montana
[PB-222004/4] 22 p2695 N73-31591
Monitoring weather conditions in Colorado for cloud seeding control
[E73-11071] 24 p2913 N73-33245
Cumulus cloud modification with coalescence attempts
[NOAA-TM-ERL-OD-14] 24 p2947 N73-33539
WEATHER RADAR
U METEOROLOGICAL RADAR
WEATHER STATIONS
Solar flares, magnetic storms, ionospheric disturbances, and geophysical observations recorded by weather stations in India during Feb. 1972
[RRC-A-201-PT-2] 01 p0048 N73-10386
Automatic meteorological stations, and rocket investigations of atmosphere
[AD-746738] 02 p0206 N73-11671
Synoptic meteorological data for weather stations, Belgium, Oct. 1971
03 p0327 N73-12665
Synoptic meteorological data for weather stations, Belgium, Nov. 1971
03 p0327 N73-12666
Reliability tests of computer elements used in automatic airport weather stations
[AD-747558] 03 p0328 N73-12673
Annual report of meteorological observations conducted by weather stations in Switzerland during calendar year 1970
05 p0572 N73-14646
Synoptic meteorological data for weather stations, Belgium, Dec. 1971
05 p0574 N73-14666
Aerological climatology based on IRMB weather station data recorded between 1951 and 1965
[PUBL-SER-A-77] 07 p0815 N73-16609
Self contained, air-droppable, expendable, remote-operating weather station
[AD-751924] 08 p0939 N73-17691
Beta-1 and Beta-2 isotopic electrical generators as power sources for weather stations
[AD-755834] 12 p1428 N73-21572
Synoptic meteorological data for weather stations, Belgium, Jan. 1972
13 p1553 N73-22588
Synoptic meteorological data for weather stations, Belgium, Feb. 1972
13 p1553 N73-22589
LORAMS design for remotely collecting weather data
[AD-756682] 13 p1554 N73-22594
PAPA Ocean Weather Station measurements of wind and wave condition in north Pacific Ocean
[AD-757982] 15 p1806 N73-24638
Radiosonde measurements of subsidence in free atmosphere over Belgian weather station
[PUBL-SER-B-69] 17 p2057 N73-26637
Automatic climatological recording system at Nord, Greenland
[ISBN-87-7478-073-5] 18 p2141 N73-27307
Prevaling monthly and seasonal surface wind directions for coastal areas around Arctic Ocean
[AD-761074] 18 p2174 N73-27560
Budrio meteorological radar station
[IFA-CP-289] 19 p2293 N73-28436
Operations research problem of meteorological station distribution in bounded region
20 p2446 N73-29653
Meteorological services and technology of USSR
[JPRS-59962] 22 p2692 N73-31565
Design for development of network in Moscow and vicinity for mesometeorological observations
22 p2693 N73-31573
Simulation studies and design of GARP Global Experiment
[NASA-TM-X-69613] 22 p2694 N73-31582
Technical equipment for large scale automation of USSR hydrometeorological service
[AD-763956] 22 p2696 N73-31593
Subprogram planning for global atmospheric observation and weather forecasting system
[GARP-PUBL-11] 24 p2948 N73-33545
Data processing role of weather stations, polar and synchronous satellites in global experiments
24 p2948 N73-33549
Origin, development and prospects of World Weather Watch noting role to be played by meteorological satellites and GARP
24 p2949 N73-33551
WEATHERING
Comparison of outdoor exposure of elastomers and plastics with exposure in accelerated weathering test chamber using fluorescent source of UV radiation
[ERDE-TR-107] 06 p0688 N73-15600
Application of ERTS-1 data to locate wind erosion sites in West Texas and to determine extent and spread of wind erosion
[E73-10719] 17 p2019 N73-26326
Significance of biological factors in weathering of rocks and minerals
[NASA-TT-F-14892] 18 p2142 N73-27316
Ionic migration and weathering in frozen Antarctic soils
[NASA-CR-2283] 18 p2143 N73-27326
Effects of microflora on rock weathering and edaphic factor
[NASA-TT-F-15033] 20 p2411 N73-29380
Effect of microflora on exogenous dynamics of weathering and crust development
[NASA-TT-F-15032] 20 p2411 N73-29383
Outdoor weathering influence on polyester and epoxy glasscloth reinforced laminate flexural strength and surface appearance
[FOK-R-1627] 21 p2563 N73-30546
Humic soil acid effects in silicate mineral weathering with aluminum migration
[NASA-TT-F-15134] 23 p2754 N73-32034
Temperature effects on quantitative biotite and nepheline decomposition by weather
[NASA-TT-F-15135] 23 p2754 N73-32035
WEBBING
Energy-absorbing efficiency of ply-tear webbings and discussion of warp and weft count and binder property effects
[RAE-TR-72051] 01 p0113 N73-10936
Physical properties of ply-tear webbing energy absorber
09 p1089 N73-18886
Procedures for improving resistance of Nomex fabric and webbing to actinic degradation
[AD-759217] 17 p2051 N73-26596
WEBS [MEMBRANES]
U MEMBRANES
WEBS [SUPPORTS]
Design of metal shear web selectively reinforced with filamentary composites for space shuttle application
[NASA-CR-132320] 22 p2721 N73-31774
Component fabrication of metal shear web selectively reinforced with filamentary composites for space shuttle application
[NASA-CR-132321] 22 p2721 N73-31775
Component testing and analysis in program to evaluate metal shear web selectively reinforced with filamentary composites for space shuttle application
[NASA-CR-132322] 22 p2721 N73-31776
WEDGE FLOW
Development of steel wedge probe for measurement of three dimensional wake flow in subsonic and transonic flow fields
10 p1140 N73-19285
Analysis of fluid flow over two dimensional flat plate wedge configuration for application to deep submersible vehicles
[NASA-CR-131888] 13 p1510 N73-22233
Analysis of viscous hypersonic flow around slender sharp wedges and unyawed cones
[AD-757037] 14 p1650 N73-23386
Numerical analysis of base pressure distribution for supersonic flow over slender wedge or backward facing step
15 p1764 N73-24295
Analysis of steady hypersonic flow with viscous interaction over sharp slender wedge by finite difference scheme
20 p2387 N73-29177
Development of numerical code to calculate two dimensional flow field when supersonic flow encounters double wedge configuration
[NASA-CR-134010] 21 p2524 N73-30242
Numerical analysis of flow characteristics on upper surface of wedge moving at supersonic speed when plane shock wave is incident on wedge
[AD-763283] 21 p2527 N73-30267
WEDGES
Measured and calculated mean flow characteristics of two-dimensional, hypersonic, turbulent wakes produced by wedges
[NASA-TN-D-6927] 01 p0040 N73-10316
Numerical analysis of two dimensional shock wave resulting from mobile wedge moving with supersonic velocity and specific angle of attack into detonation wave
[AD-749650] 05 p0528 N73-14299
Numerical analysis of oscillating wedge in supersonic perfect gas flow to evaluate trends for wedge and to analyze unsteady flows
07 p0767 N73-16235
Development of steel wedge probe for measurement of three dimensional wake flow in subsonic and transonic flow fields
10 p1140 N73-19285
Analysis of viscous hypersonic flow around slender sharp wedges and unyawed cones
[AD-757037] 14 p1650 N73-23386
Propagation of reflected shock wave after Mach reflection on wedges
[REPT-4/72] 15 p1765 N73-24304
Measurement of pitching moment derivatives using free oscillation technique on two dimensional airfoils of double wedge section and single wedge section
[ARC-R/M-3234] 16 p1855 N73-25025
Numerical analysis of flow characteristics on upper surface of wedge moving at supersonic speed when plane shock wave is incident on wedge
[AD-763283] 21 p2527 N73-30267
WEIBULL DENSITY FUNCTIONS
Application of scatter factors for various Weibull-shaped parameters, fleet sizes, and level of reliability for aircraft structures
[NASA-CR-2100] 01 p0113 N73-10934
Statistical analysis of strength and fracture characteristics of materials with application to fiber composites using Weibull density functions
[JPL-TM-33-580] 08 p0934 N73-17650
Weibull distribution bibliography, 1957 - 1972
[CE-BIB-235] 24 p2928 N73-33387
WEIGHT
High resolution radar system for measuring wind velocity and height of meteor trails
[NASA-CR-131644] 12 p1377 N73-21172
WEIGHT [MASS]
NT ATOMIC WEIGHTS
NT BODY WEIGHT
NT STRUCTURAL WEIGHT
Index to reports of National Conference on Weights and Measures from 1905 to 1971
[NBS-SP-377] 09 p1101 N73-18985
Mass summary, test facilities, costs and PERT for European space tug
[HSD-TP-7227-APP-7] 10 p1217 N73-19899
Remotely controlled device for detection of mass changes in selected specimens
[NASA-CASE-MFS-21556-1] 11 p1292 N73-20487

**WEIGHT ANALYSIS**
Parametric weight analysis of heat rejection systems for environmental control/life support system space shuttle orbiter
[NASA-CR-128735] 08 p0965 N73-17884
Program formulation for weight/sizing design synthesis computer program for application to space shuttle development - Vol. 1
[NASA-CR-128867] 11 p1343 N73-20894
Program description of computerized analysis for space shuttle weight analysis to include flow chart and subroutine linkages - Vol. 2
[NASA-CR-128868] 11 p1343 N73-20895
User manual for weight/sizing design synthesis computer program for application to space shuttle payloads - Vol. 3
[NASA-CR-128869] 11 p1343 N73-20896
Evaluation of helmet weight on head by military personnel
[AD-748412] 13 p1487 N73-22056
Design concepts, manufacturing process, weight analysis, and cost estimates for long range transport aircraft using composite structures
[NASA-CR-112255] 14 p1600 N73-22976

**WEIGHT FACTORS**
U WEIGHT [MASS]

**WEIGHT INDICATORS**
NT MICROBALANCES
NT STRAIN GAGE BALANCES

**WEIGHT MEASUREMENT**
SOS - computer program for calculating weight, center of gavity, and inertias of asymmetrical missiles
[AD-749251] 05 p0601 N73-14885

**WEIGHTING FUNCTIONS**
Formulation of radar glint tracking error reduction using frequency agility and linear amplitude weighting
16 p1874 N73-25171

**WEIGHTLESSNESS**
Comparison of development of auditory vesicle in frog embryos under weightless and terrestrial conditions
[NASA-TT-F-14624] 01 p0009 N73-10072
Design and requirements of zero-g fuel gauging system based on absorption of gamma radiation
[AD-745566] 01 p0059 N73-10479
Free electrophoresis in zero gravity on Apollo 16 flight
[NASA-CR-123920] 02 p0130 N73-11055
Tests to determine physiological and behavioral response to transitions between rotating and nonrotating environments
[NASA-CR-2130] 02 p0135 N73-11093
Prolonged weightlessness for 300 plus days and cardiac performance in primates
[NASA-CR-129512] 03 p0256 N73-12075
Spacecraft environment, radiation, and weightlessness effects on human biological processes in manned space flight
[JPRS-57517] 03 p0256 N73-12076
Design and development of zero-gravity atmospheric cloud physics experiment laboratory for installation in orbiting spacecraft
[NASA-CR-128998] 03 p0280 N73-12270
Analysis of isothermal liquid inflow patterns in spherical container during weightless conditions
[NASA-TM-X-2670] 03 p0283 N73-12291
Free electrophoresis space experiment design for weightlessness environments
[NASA-CR-123972] 05 p0502 N73-14090
Physiological effects of weightlessness
06 p0628 N73-15099
Effects of prolonged weightlessness during space flight on human skeletal and hematopoietic systems
[NASA-TT-F-730] 06 p0630 N73-15116
Biosatellite 2 experiments for determining effects of prolonged weightlessness on biological processes
[CONF-720441-1] 06 p0630 N73-15119
Evolution of neural messages in human adaptation to prolonged zero gravity flight
06 p0634 N73-15154
Zero-g gaging system based on absorption of gamma radiation
[AD-749967] 06 p0675 N73-15489
Analysis of laminar hydrogen, ethylene, and propylene air diffusion flames burning in weightless environment
[NASA-TN-D-7165] 07 p0855 N73-16933
Nervous system functional changes due to forces of acceleration and weightlessness
[NASA-TT-F-733] 08 p0877 N73-17105
Prolonged weightlessness effects on physiological functions of dogs
[NASA-TT-F-14672] 08 p0878 N73-17110
Weightlessness effects on development of vestibular apparatus and ocular nystagmus in rat, using chronic 2g centrifuge
[NASA-CR-114569] 08 p0878 N73-17112
Growth and characterization of crystals and metallic whiskers in zero gravity environment during Skylab and Apollo flights
[NASA-CR-124065] 08 p0950 N73-17778
Radionuclide measurements on plasma and red cell mass volume losses in Apollo spacecrews
09 p0993 N73-18106
Skylab experiments to assess weightlessness effects on human nutritional metabolism and musculoskeletal function
09 p0994 N73-18115
Tissue culture laboratory for first manned Skylab mission for performing experiments to detect effects of zero gravity on living human cells
09 p1088 N73-18874
Medical and biological problems of manned space flight
[NASA-TT-F-719] 10 p1114 N73-19077
Weightlessness and hypodynamia effects on bodily functions during space flight
10 p1114 N73-19078
Cavity resonators for measuring cryogenic propellant content in space shuttle orbiter tanks under weightlessness
10 p1162 N73-19452
Apparatus for mixing two or more liquids under zero gravity conditions
[NASA-CASE-LAR-10195-1] 10 p1163 N73-19458
Reduced-gravity fecal collector seat and urinal
[NASA-CASE-MFS-22102-1] 11 p1249 N73-20141
Development of quality monitoring system for water recovery cycle in weightlessness environment
[NASA-CR-112267] 11 p1250 N73-20144
Analysis of KC-135 flight samples of Star-J Satellite solidified in near-zero gravity
[NASA-CR-124179] 11 p1308 N73-20610
Microbiological investigation of neutral buoyancy simulator for weightless space environment testing
[NASA-TM-X-64736] 12 p1371 N73-21127
Self contained automated primate research laboratory to study physiological effects of space environment weightlessness on monkeys
[NASA-CR-131642] 12 p1387 N73-21250
Techniques for determining effects of prolonged weightlessness on cardiovascular system of subhuman primates
[NASA-CR-131890] 13 p1479 N73-21980
Analysis of melting, mixing, and solidification of metal matrix composite materials in weightless environment
13 p1594 N73-22921
Development of manufacturing in space processes for Skylab program to include operating sequence description and results obtained
13 p1594 N73-22922
Basic causal mechanisms responsible for loss of vascular tone during alterations in shifts to zero gravity
[NASA-CR-128897] 14 p1612 N73-23069
Attached manipulator system for simulating and demonstrating shuttle manipulator cargo handling operations under weightless conditions
[NASA-CR-133964] 18 p2126 N73-27176
Zero gravity liquid transfer device, using spiral shaped screen
[NASA-CASE-KSC-10626] 18 p2150 N73-27378
Liquid-solid transition for materials processing in space
[NASA-CR-124294] 18 p2179 N73-27596
OAO 3 flight test on heat pipe cooling efficiency during weightlessness
18 p2208 N73-27826
Effects of weightlessness and acceleration on human body during space flight
20 p2365 N73-29022
Zero-gravity cloud physics laboratory for space shuttle payload planning
[NASA-CR-129002] 20 p2449 N73-29674
Analysis of melt segregation effects on solidification of metals under weightless conditions
[NASA-CR-124358] 21 p2559 N73-30510
Tape cassette bacteria detection system for automatic continuous bacterial detection for monitoring sterility of regenerated water in spacecraft
[NASA-CR-134035] 22 p2620 N73-30996
Design, fabrication and acceptance testing of zero gravity whole body shower
[NASA-CR-134066] 22 p2623 N73-31019

**WEIGHTLESSNESS SIMULATION**
Changes in lung capacity, air passage resistance, and dynamic compliance of humans during water immersion to simulate weightlessness
07 p0744 N73-16053
Conference on human endocrine secretions and hormone metabolisms during space flight stress
[NASA-TM-X-58093] 09 p0993 N73-18104
Water immersion model for simulating renin, aldosterone, and natriuresis effects of prolonged weightlessness on man
09 p0993 N73-18110
Human oxygen metabolism and pulmonary functions during hypodynamic water immersion
10 p1114 N73-19082
Medical biological and other problems of space flight
[JPRS-58678] 12 p1367 N73-21089
Problems in simulating weightlessness
12 p1367 N73-21090
Physiological effects of long term hypodynamic weightlessness simulation on humans
13 p1482 N73-22010
Human horizontal or antiorthostatic position effect in hypodynamic weightlessness test
13 p1482 N73-22011
Human regional blood circulation changes during bed rest experiment
13 p1482 N73-22012
Metabolic changes and cardiac output of humans in hypokinetic bed rest study
13 p1482 N73-22013
Visual acuity changes in humans during hypokinetic bed rest test
13 p1482 N73-22014
Functional reactions of human otorhinolaryngolic organs during hypokinesia
13 p1482 N73-22015
Human pulmonary volume decrease during long term bed rest
13 p1482 N73-22016
Lower body negative pressure for preventing body fluid shifts during weightlessness
13 p1482 N73-22017
Weightlessness simulator for evaluating exercise effects in hypokinetic bed rest test
13 p1482 N73-22018
Changes in human cerebral circulation during prolonged bed rest test
13 p1483 N73-22020
Long term physiological testing of submerged subjects to simulate weightless conditions for space flight
[NASA-TT-F-14884] 13 p1505 N73-22195
Long term hypokinesia effect on rats hemodynamic system
14 p1607 N73-23026
Human habitability data for zero gravity environmental architecture
[NASA-TM-X-69322] 15 p1744 N73-24135
Wing anomalies as result of weightlessness simulation for flour beetle Tribolium confusum
19 p2226 N73-27952
Single body theory for weightlessness simulation, applied to simple cell model
19 p2227 N73-27961

**WEIGHTS [COEFFICIENTS]**
U COEFFICIENTS

**WELD STRENGTH**
Influence of thermal cycles on weld properties of all weld metal heat affected zone and base metal
[AD-746886] 02 p0179 N73-11452
Development of high temperature stability in welded joints of ferritic steels by methods of constructional compensation
[NLL-RISLEY-TR-2487-[9091.9F]]
06 p0676 N73-15500
Development of diffusion welding technique for TD-NiCr metal sheet and effect on creep-rupture shear strength
[NASA-TN-D-7153] 07 p0804 N73-16520
Static and fatigue loading tests of bonded lap joints to determine crack length leading to failure of joint
[NASA-CR-112219] 08 p0966 N73-17896
Analysis of factors affecting fatigue failure in welded joints and significance of weld defects on fatigue strength
[NLL-RISLEY-TR-2509-[9091-9F]]
11 p1296 N73-20517
Effects of heat on embrittlement of austenitic welded joints and welded claddings
[NLL-RISLEY-TR-2508-[9091.9F]]
12 p1407 N73-21405
Analysis of welding parameters for producing metallurgically sound welds and effects of heat treatment on metallurgical and mechanical properties
[Y-1855] 12 p1414 N73-21460
Analysis of friction welding of metal structures with information on friction theory, heat liberation, basic parameters, and recommended regimes
[AD-755753] 13 p1535 N73-22440
Development of electron beam welding techniques and application to welding various metal structures
13 p1593 N73-22919
Effects of irradiation on fracture and strength properties of pressure vessel steel plate and submerged arc weld
[HEDL-SA-387] 17 p2093 N73-26936
Development of techniques for welding copper and copper-base alloys with application to waveguides in electron accelerator facility
[SLAC-PUB-1095] 19 p2305 N73-28533
Peel, shear, and tensile strength measurements of transistor header lead welds
[BDX-613-871] 22 p2642 N73-31173
Effects of inclusions and voids in welding electrodes and welding materials on quality of welded joints
22 p2678 N73-31447
Strength of printed circuit joints for reliability, based on electrical resistivity
[DLR-FB-73-33] 24 p2899 N73-33140
Heat to heat variation in fatigue and creep-fatigue behavior of AISI Type 304 stainless steel, and fatigue behavior of type 308 stainless steel weld material
[ANCR-1097] 24 p2936 N73-33450

**WELD TESTS**
Stress wave emission techniques for monitoring weld quality and structural validation
[AD-745822] 05 p0532 N73-14486
Static and fatigue loading tests of bonded lap joints to determine crack length leading to failure of joint
[NASA-CR-112219] 08 p0966 N73-17896
Depths of reflection zone characteristics for classifying ultrasonic echoes in weld testing
[NLL-CE-TRANS-5993-[9022.09]] 11 p1324 N73-20742
Creation of discontinuities in high strength steels to evaluate effects on mechanical properties of welds
[AD-755524] 13 p1535 N73-22437
Nondestructive testing of welded silicon solar cell silver interconnections
[ESS/SS-397] 17 p2038 N73-26487
Forming and joining techniques and properties of thin gage TD-NiCr sheet in crystallized and unrecrystallized conditions
[NASA-CR-121224] 18 p2154 N73-27408
Technique and requirements for projection welding using single large electrode
[NLL-M-23048-[5828.4F]] 21 p2552 N73-30456
Effects of inclusions and voids in welding electrodes and welding materials on quality of welded joints 22 p2678 N73-31447

**WELDABILITY**
Weldability and properties of materials undergoing electron beam welding
[CRANFIELD-MAT-7] 05 p0551 N73-14474

**WELDED JOINTS**
NT SPOT WELDS
Static and fatigue strength of welded tubular joints
[AD-746894] 02 p0179 N73-11453
Effect of joint orientation relative to gravitational field direction during electron beam welding
[JPRS-57281] 04 p0426 N73-13476
Intergranular corrosion resistance of matching and dissimilar welds in nitrogen-bearing and nitrogen-free austenitic steels
[NLL-TRANS-746-1313-[9022.401]] 05 p0560 N73-14546
Development of high temperature stability in welded joints of ferritic steels by methods of constructional compensation
[NLL-RISLEY-TR-2487-[9091.9F]] 06 p0676 N73-15500
Development of diffusion welding technique for TD-NiCr metal sheet and effect on creep-rupture shear strength
[NASA-TN-D-7153] 07 p0804 N73-16520
Mechanical properties of welded joints in stainless and low-alloy steels at temperatures of 900 to 1300 F
[ORNL-4781] 07 p0804 N73-16525
Static and fatigue loading tests of bonded lap joints to determine crack length leading to failure of joint
[NASA-CR-112219] 08 p0966 N73-17896
Comparison of fatigue strength of steel joints produced by friction welding and by electrocontact welding with fusion method
[AD-753488] 09 p1049 N73-18553
Notch stress finite element method for loaded elastic cores, applicable to compositesor welded joints
[ISD-129] 09 p1095 N73-18938
Hydrocompression treatment to lower residual stresses in weld joints of forge-welded carbon steel vessels 10 p1163 N73-19461
Vacuum-diffusion welding units 10 p1163 N73-19464
Ultrasonic inspection of cast steel blocks, steel plates, and welded seams
[TR-7210.607] 10 p1164 N73-19472
Evaluation of welding processes, and health hazards in electron beam welding of beryllium
[JPRS-58148] 10 p1171 N73-19528
Effect of order of welding and heat treatment operations on mechanical properties of weld joints of N18K9M5T 10 p1171 N73-19529
Effect of angle of inclination on formation of gas cavities in weld root during argon-arc welding 10 p1172 N73-19532
Formation of flaws in seam metal during argon-arc pulse welding 10 p1172 N73-19533
Analysis of factors affecting fatigue failure in welded joints and significance of weld defects on fatigue strength
[NLL-RISLEY-TR-2509-[9091-9F]] 11 p1296 N73-20517
Brittle fracture and fatigue of cylindrical hollow bodies with offset seams and stiffeners
[NLL-RISLEY-TR-2527-[9001.9F]] 11 p1344 N73-20908
Analysis of aircraft construction methods to compare riveting, welded joints, and bonded joints for structural stability
[AD-755754] 13 p1475 N73-21948
Arc welding of joints and hard surfaces using longitudinally notched ceramic rods
[AD-756944] 13 p1535 N73-22435
Development of procedure for controlling crystallization of metal in molten pools and effect of electromagnetic treatment during welding
[AD-756335] 13 p1536 N73-22443
Development of electron beam welding techniques and application to welding various metal structures 13 p1593 N73-22919
Seam weld cracking in lithium hydride shielding of SNAP 8 reactor after irradiation
[NASA-CR-121157] 14 p1691 N73-23726
Nondestructive testing of welded silicon solar cell silver interconnections
[ESS/SS-397] 17 p2038 N73-26487
Effects of irradiation on fracture and strength properties of pressure vessel steel plate and submerged arc weld
[HEDL-SA-387] 17 p2093 N73-26936
Development of procedure for argon arc welding of copper using complex alloy wire and comparison with other welding techniques
[NLL-DRIC-TRANS-3008-[3623.66]] 18 p2154 N73-27404
Development of nondestructive inspection procedures for determining quality of welded joints in aluminum spacecraft structures
[NASA-CR-124332] 18 p2156 N73-27420
Static and fatigue properties of hardened and tempered electron beam welded joints in 2.5 percent Ni-Cr-Mo steel and 18 percent Ni-Co-Mo maraging steel
[S/T-MEMO-9-71] 18 p2161 N73-27456
Development of techniques for welding copper and copper-base alloys with application to waveguides in electron accelerator facility
[SLAC-PUB-1095] 19 p2305 N73-28533
Optimized electric welding technique for silicon solar cell arrays
[LCR-DR-1-72-52/1/R] 21 p2553 N73-30470
Effects of inclusions and voids in welding electrodes and welding materials on quality of welded joints 22 p2678 N73-31447
Safety devices and precautions to protect personnel performing radiographic inspections of pipeline welds 24 p2952 N73-33581

**WELDED STRUCTURES**
NT STEEL STRUCTURES
Method for eliminating plastic deformations and residual stresses by high speed impact forming of weld zone
[AD-745457] 01 p0062 N73-10508
Stereoradiography study of depth and geometrical dimensions of internal flaws in weldments
[AD-749459] 04 p0428 N73-13486
Development of high temperature stability in welded joints of ferritic steels by methods of constructional compensation
[NLL-RISLEY-TR-2487-[9091.9F]] 06 p0676 N73-15500
Nondestructive tests of welds in regenerative chambers
[NASA-CR-120980-APP] 06 p0677 N73-15509
Test equipment and methods for nondestructive inspection of welded, brazed, and composite structures
[NASA-SP-5952[02]] 11 p1297 N73-20528
X ray detection of incomplete weldment and surface oxidation in welded aluminum spacecraft structures
[NASA-CR-124167] 11 p1298 N73-20536
Effects of heat on embrittlement of austenitic welded joints and welded claddings
[NLL-RISLEY-TR-2508-[9091.9F]] 12 p1407 N73-21405
Analysis of welding parameters for producing metallurgically sound welds and effects of heat treatment on metallurgical and mechanical properties
[Y-1855] 12 p1414 N73-21460
Analysis of friction welding of metal structures with information on friction theory, heat liberation, basic parameters, and recommended regimes
[AD-755753] 13 p1535 N73-22440
Copper coating of welded aluminum spacecraft structures to resist oxidation and aid detection of incomplete penetration
[NASA-CR-124251] 15 p1791 N73-24515
Fracture mechanics of cylindrical pressure vessels having weld seam flaws
[AD-761532] 19 p2349 N73-28894
Effect of internal weld defects on fatigue behavior in mild structural steel butt welded connections
[PB-220896/5] 21 p2554 N73-30475
Creep fracture properties of weld repaired cast titanium alloy
[AD-765185] 24 p2937 N73-33451

**WELDING**
NT ARC WELDING
NT BRAZING
NT DIFFUSION WELDING
NT ELECTRIC WELDING
NT ELECTRON BEAM WELDING
NT EXPLOSIVE WELDING
NT FUSION WELDING
NT GAS TUNGSTEN ARC WELDING
NT GAS WELDING
NT PLASMA ARC WELDING
NT PRESSURE WELDING
NT ULTRASONIC WELDING
Soviet interest in West German technological advances in welding techniques
[AD-747834] 04 p0427 N73-13480
Cost effectiveness criteria and parametric data for friction welding of missile systems hardware
[AD-747838] 04 p0427 N73-13482
Determination of temperature and residual stresses and deformations caused by welding process
[AD-749529] 04 p0428 N73-13487
Welding leads of integrated circuits to printed circuit boards
[AD-749838] 05 p0523 N73-14254
Production planning with group techniques for welding shops using component and blank classifications
[NLL-M-22594-[5828.4F]] 05 p0550 N73-14467
Welding experiments during flight of Soyuz 6
[AD-749745] 05 p0553 N73-14496
Automatic through-insulation welding of small-diameter solid conductor wires to facilitate production of miniature electronic assemblies
[NASA-CR-130751] 08 p0927 N73-17591
Fume component tests to determine welders safe breathing level through ventilation
[ITR-1] 09 p1038 N73-18467
Improvements in welding techniques to increase productivity and quality of performance of bonded joints
[JPRS-58291] 10 p1163 N73-19460
Butt welding of titanium alloy rings and flanges to improve mechanical properties 10 p1163 N73-19463
Significant advances in welding, bonding, and joining techniques since 1960
[AD-754262] 10 p1168 N73-19502
Evaluation of welding processes, and health hazards in electron beam welding of beryllium
[JPRS-58148] 10 p1171 N73-19528
Quality control of welded, brazed, and bonded electrical terminations
[BDX-613-613-REV] 12 p1383 N73-21214
Metallurgical and mechanical properties of joints treated by weld-braze joining process
[NASA-TN-D-7281] 15 p1798 N73-24573
Copper alloys with necessary heat resistance and electrical conductance for use as welding electrodes
[AD-758618] 15 p1800 N73-24590
Materials response to welding and forming
[PB-214213] 16 p1918 N73-25524
Bibliography on welding by electron beam, ultrasonic radiation, laser beam, and friction
[ORNL-TM-4133] 17 p2038 N73-26486
Technique and requirements for projection welding using single large electrode
[NLL-M-23048-[5828.4F]] 21 p2552 N73-30456
Temperature control of welding equipment by detection of discrete bands of infrared radiation from objects being heated
[NASA-CASE-MFS-20781-2] 22 p2672 N73-31401
Device for welding hot-wire anemometer components following breakage due to dust particles in air stream
[AERE-R-7304] 22 p2678 N73-31451
Application of radiant solar energy for welding and soldering materials
[AD-764938] 23 p2799 N73-32386
Evaluation of welding techniques for austenitic stainless steels for use in liquid metal fast breeder reactors
[ORNL-TM-4055] 24 p2954 N73-33601

**WEST GERMANY**
U GERMANY

**WEST INDIES**
NT BARBADOS
Satellite cloud photographs of BOMEX area 04 p0442 N73-13600
Survey of climatological conditions in Martinique
[MN-MONO-86] 09 p1060 N73-18644
Remote detection of oceanic eddies in Lesser Antilles using ERTS-1 imagery
[E73-10592] 14 p1657 N73-23451
Correlation of ERTS-1 data with in situ water quality measurements around Virgin Islands
[E73-10626] 15 p1775 N73-24386

**WEST PAKISTAN**
Interpretation of ERTS-1 multispectral data from area in West Pakistan
[E72-10234] 03 p0288 N73-12334
ERTS-1 multispectral imagery of West Pakistan
[E73-10315] 09 p1023 N73-18347
Search for porphyry copper deposits in Pakistani Baluchistan using ERTS-1 imagery
[E73-10410] 11 p1278 N73-20372
Geological survey of West Pakistan from ERTS-1 multispectral imagery
[E73-10540] 13 p1518 N73-22304
Exploration for copper porphyry deposits in West Pakistan using ERTS-1 imagery
[E73-10954] 21 p2531 N73-30296
Analysis of ERTS-1 MSS data for West Pakistan
[E73-11097] 24 p2914 N73-33254

**WEST VIRGINIA**
NT POTOMAC RIVER VALLEY [MD-VA-WV]

ERRP imagery for detection of strip mines and reclamation activities in Ohio, West Virginia, and Pennsylvania
[E73-10731] 17 p2020 N73-26337
Skylab monitoring of surface mining activities and reclamation in Ohio, West Virginia, Pennsylvania, Indiana, Kentucky, and Illinois
[E73-11033] 22 p2663 N73-31337

**WESTLAND AIRCRAFT**
NT P-531 HELICOPTER
Flight tests of Westland Scout helicopter fitted with reduced scale version of rigid rotor to determine airworthiness and handling characteristics
12 p1358 N73-21017

**WESTLAND GROUND EFFECT MACHINES**
Correlation of wear behavior and properties of coated fabric hovercraft fingers
[RAE-TR-71210] 08 p0935 N73-17654

**WESTLAND P-531 HELICOPTER**
U P-531 HELICOPTER

**WESTLAND SR-N2 GROUND EFFECT MACHINE**
U WESTLAND GROUND EFFECT MACHINES

**WESTLAND SR-N2 HOVERCRAFT**
U WESTLAND GROUND EFFECT MACHINES

**WESTLAND SR-N3 GROUND EFFECT MACHINE**
U WESTLAND GROUND EFFECT MACHINES

**WESTLAND SR-N3 HOVERCRAFT**
U WESTLAND GROUND EFFECT MACHINES

**WESTLAND SR-N5 GROUND EFFECT MACHINE**
U WESTLAND GROUND EFFECT MACHINES

**WETLANDS**
Land use mapping, limnology, wetlands, geomorphic and landform surveys, and river monitoring of Lake Champlain Basin and Vermont using ERTS-1 imagery
[E72-10282] 03 p0292 N73-12380
Mapping, evaluation, and monitoring of coastal and saline wetlands ecology and shallow water environments using ERTS-1 imagery
[E72-10290] 04 p0410 N73-13340
ERTS-1 imagery of wetlands ecology in Maryland, Georgia, and Chesepeake Bay test sites
[E73-10288] 08 p0915 N73-17494
Mapping southeastern coastal marshlands and wetlands of South Carolina and Georgia using ERTS-1 imagery
[E73-10362] 10 p1150 N73-19358
Characterization of wetlands and marshlands by automatic processing of ERTS-1 data
[E73-10467] 12 p1394 N73-21304
Mapping wetlands ecology of Chesapeake Bay, South Carolina, and Georgia from ERTS-1 imagery
[E73-10507] 13 p1516 N73-22282
ERTS-1 imagery of marshes, wetlands, and turbid waters in French Atlantic littoral
[E73-10548] 13 p1518 N73-22307
Evaluation of ERTS-1 imagery and automatic data processing techniques for characterization of wetlands and marshlands
[E73-10576] 14 p1656 N73-23437
Characterization of wetlands and marshlands from ERTS-1 imagery
[E73-10590] 15 p1772 N73-24357
Evaluation of satellite remote sensing and automatic data techniques for analysis of wetlands and marshlands using ERTS-1 imagery
[E73-10740] 18 p2133 N73-27235
Application of ERTS-1 imagery for grid measurement of small water bodies
[E73-10768] 18 p2134 N73-27244
ERTS-1 multispectral photography of wetlands vegetation and plant species
[E73-10850] 19 p2292 N73-28428
Thematic mapping of wetlands, forests, open water, and Mississippi River flooding from ERTS-1 imagery
[E73-10952] 21 p2531 N73-30294
Mapping coastal vegetation and wetlands use for Delaware from ERTS-1 imagery
[E73-11146] 24 p2918 N73-33300
Utilization of ERTS-1 imagery for management of wetlands in Great Dismal Swamp and Lake Okeechobee
[E73-11161] 24 p2920 N73-33314

**WETNESS**
U MOISTURE CONTENT

**WETTABILITY**
Wetting of alumina, magnesia, zirconia, and carbides and borides of vanadium, titanium, and zirconium by palladium melts
[NLL-RTS-7321] 02 p0190 N73-11544

**WHALES**
Underwater equipment for locating and recovery of objects from ocean bottom by whales
[AD-747612] 04 p0417 N73-13403

**WHEAT**
Identification of winter wheat on irrigated land in southern Finney County, Kansas
[E73-10475] 12 p1395 N73-21312
Interpretation of ERTS-1 data to determine acreage of winter wheat in Kansas based on multispectral band scanner data
[PAPER-A1] 19 p2259 N73-28209
Phenological observations of lilac, honeysuckle, alfalfa, and winter wheat in Rocky Mountain and Columbia Valley Corridors
[E73-10925] 20 p2398 N73-29274

**WHEATSTONE BRIDGES**
Temperature control system comprised of wheatstone bridge with RC circuit
[NASA-CASE-NPO-11304] 17 p2030 N73-26430

**WHEELS**
NT FLYWHEELS
NT NOSE WHEELS
NT REACTION WHEELS
NT TURBINE WHEELS
NT VEHICLE WHEELS
Design and performance of momentum wheel suspended by magnetic bearings for rotor operation in space environment
18 p2209 N73-27829
Approximate theory for wheel-soil interaction
[NASA-CR-133860] 21 p2580 N73-30673
Single channel wheel system with electrohydraulic servoactuators for flight control feel system
22 p2731 N73-31855
Elastic-plastic analysis of wheel rolling on rigid track
[AD-764575] 23 p2855 N73-32812

**WHIP ANTENNAS**
Cylindrical chamber for simulating electrical impedance of whip antenna
[AD-757141] 13 p1501 N73-22167
Hazardous region surrounding near fields of Navy HF whip antennas
[AD-761979] 19 p2237 N73-28034

**WHIRL INSTABILITY**
U ROTARY STABILITY

**WHIRLING**
U ROTATION

**WHISKER COMPOSITES**
Electrolytic procedure for manufacturing aluminum whisker and pure nickel matrix composites with reinforced fibers
04 p0435 N73-13544
Validity determination for cold tip theory of whisker growth
[AD-749038] 04 p0461 N73-13760
Liquid hot pressing of silicon carbide whiskers for reinforcing aluminum alloy composites
[AD-752589] 08 p0936 N73-17666
Application of directionally solidified eutectics for design and construction of gas turbine engines
18 p2166 N73-27493
Directional solidification of eutectic alloys and application to turbine blades and gas turbine engine components
18 p2166 N73-27494
Application of glass and carbon fiber reinforced structures for gas turbine engine components to operate in high temperature environments
18 p2166 N73-27495
Strength of brittle matrix materials reinforced with steel fibers or whiskers
[NLL-CE-TRANS-6145-[9022.09]]
20 p2434 N73-29545

**WHISKERS [SINGLE CRYSTALS]**
Development of process for obtaining iron whiskers and description of mechanical and physical properties
[IIS-142-VOL-22-4] 05 p0586 N73-14766
Growth and characterization of crystals and metallic whiskers in zero gravity environment during Skylab and Apollo flights
[NASA-CR-124065] 08 p0950 N73-17778
Improved resin adhesion by depositing silicon carbide whiskers on carbon fibers
[AD-757659] 14 p1681 N73-23642
Growth of iron whiskers by hydrogen reduction of iron halide salts
[AD-757588] 14 p1699 N73-23788
Metal matrix composites with Ni and NiCr20 matrix materials, and Al2O3, SiC, W, and Mo reinforcing fibers
[BMFT-FB-T-73-08] 23 p2810 N73-32471

**WHISTLERS**
Computerized simulation of whistler instabilities in anisotropic collisionless plasmas
[AD-748176] 03 p0344 N73-12805
OGO-D electromagnetic wave propagation measurements with whistler and hiss formations in plasmasphere
[NASA-CR-130351] 07 p0754 N73-16126
Parametric instabilities of VLF waves in radiation belts
[LA-DC-72-746] 07 p0756 N73-16139
Linear and nonlinear propagating characteristics of whistlers
[NASA-CR-130349] 07 p0780 N73-16342
Observation of magnetospherically reflected whistlers made by OGO-A and OGO-C
[NASA-CR-130352] 07 p0781 N73-16344
Determination of path latitude and electron concentration along path of whistlers in magnetosphere
[NASA-CR-130353] 07 p0781 N73-16345
Derivation of equations governing modulation of continuous wave whistler-mode transition by resonant particles
[AD-751043] 07 p0797 N73-16482
Computer simulation of whistler turbulence and velocity space diffusion in magnetospheric type plasma
[AD-753196] 09 p1031 N73-18415
OGO-4 observation of banded whistlers using broadband VLF instrumentation
[NASA-CR-131495] 13 p1490 N73-22079
Polarization measurement of whistler-type radio frequency signals by using auto- and cross-correlation functions of horizontal signal components
[CEPHAG-24/72] 13 p1491 N73-22088
Spontaneous intensification of magnetospheric very low frequency ducts due to coupling between magnetosphere and ionosphere
[AD-756461] 14 p1662 N73-23488
Whistler wave propagation in relation to interplanetary shocks
[NASA-TM-X-66245] 15 p1778 N73-24414
Computerized simulation of cyclotron resonant electrons interaction with narrow band whistler wave along magnetospheric duct for VLF emission triggering
19 p2340 N73-28827
Linear and nonlinear wave particle cyclotron interaction for whistler mode waves in anisotropic plasma
[AD-763744] 22 p2705 N73-31668

**WHITE DWARF STARS**
Analysis of post-Newtonian effects on instability of white dwarf stars, neutron stars, and supermassive stars
[NASA-CR-129241] 03 p0355 N73-12893
Application of Schmidt telescopes and three color photometry to galactic clusters, star distribution in galactic disk and halo and galactic white stars.
07 p0845 N73-16842
Calculations of equations of state for zero-temperature white dwarf and neutron stars
12 p1447 N73-21719
Radiative processes in intense magnetic fields of white dwarfs and neutron stars
16 p1961 N73-25861

**WHITE NOISE**
Incomplete state feedback for systems with parameter uncertainty and random disturbances
[NASA-CR-129180] 02 p0150 N73-11219
Circuitry for generating random square wave pulses using white noise source
[NASA-CASE-MSC-14131-1] 17 p2003 N73-26199
Coded transmission of binary data over coherent white Gaussian channels
[AD-761465] 19 p2245 N73-28102
Nonlinear vibrations and failure of shallow shells of random shape under stress of white noise
[AD-761449] 19 p2349 N73-28898

**WHITEOUT**
Infrared sensitive television camera for horizon and depth perception in whiteout
[DREO-TN-73-11] 23 p2791 N73-32332

**WICKS**
Capillary flow through partially saturated fibrous wicks in heat pipes
[AD-763427] 21 p2527 N73-30263

**WIDE ANGLE LENSES**
Wide field reflective optical scanning system for use in satellite based earth surveillance activities
[NASA-CASE-MSC-14096-1] 13 p1529 N73-22388

**WIDEBAND**
U BROADBAND

**WIDEBAND COMMUNICATION**
Wideband tactical satellite communications systems using onboard processing
01 p0026 N73-10202
Design and performance of wideband down-converter for satellite ground terminal
[NASA-CR-128394] 01 p0032 N73-10249
Influence of temperature on cable parameter variations in wideband transmission system
[REPT-6670] 01 p0034 N73-10268
Design of microwave signal processing devices for broadband operation
[AD-753168] 09 p1075 N73-18775
Design of experiment to measure communication characteristics of wideband satellite to ground communication links
[NASA-CR-130196] 11 p1294 N73-20497
Measurement of pulse parameters in wideband receivers including amplitude, frequency, and time of arrival
16 p1873 N73-25166
Wideband communication command and control modem
[AD-762281] 19 p2238 N73-28042
Line of sight wideband propagation in troposphere
[AD-762939] 20 p2378 N73-29107

**WIENER HOPF EQUATIONS**
Theoretical analysis of linear semi-infinite array of uniformly spaced elements to determine mutual coupling effects
[AD-745799] 01 p0034 N73-10263

**WIGHTMAN THEORY**
U FIELD THEORY [PHYSICS]
U QUANTUM THEORY
U RELATIVISTIC THEORY

WILDERNESS
Investigation of natural resources in remote and unexplored areas of Venezuela using ERTS-1 remotely sensed imagery
[E72-10311] 04 p0412 N73-13360
Wildland resources inventory of Nevada Great Basin using ERTS-1 imagery
[E73-10019] 06 p0659 N73-15355
Wildland resource evaluation in Nevada using ERTS-1 imagery
[E73-10450] 11 p1283 N73-20410
Use of remote sensor techniques for wildlands vegetation management
[NASA-CR-131580] 13 p1522 N73-22336
Application of ERTS-1 imagery for inventory of wildland resources in northern California
[PAPER-A12] 19 p2261 N73-28220
WILDLIFE
NT BATS
NT BIRDS
NT CHIMPANZEES
Changes in continental migratory bird and wildlife habitats
[E72-10235] 03 p0288 N73-12335
Management of wildlife habitat in Alaska using ERTS-1 imagery
[E72-10293] 04 p0410 N73-13343
Multispectral remote sensing techniques applied to study changes in wildlife habitats
07 p0786 N73-16396
Management of wildlife habitats in Alaska using ERTS-1 imagery
[E73-10335] 10 p1147 N73-19336
Conservational and rational use of natural resources and wildlife to preserve biosphere environment
[JPRS-58429] 11 p1250 N73-20145
Wildlife management in Alaska using ERTS-1 data
[E73-10791] 18 p2137 N73-27267
Evaluation of ERTS-1 imagery as tool for management of wildlife habitat in Alaska
[PAPER-W11] 19 p2271 N73-28288
Management of wildlife habitats in Alaska using ERTS-1 MSS data
[E73-11030] 22 p2662 N73-31334
WILDLIFE RADIOLOCATION
Satellite system for tracking of wildlife and birds in natural environment
[NASA-CR-130301] 06 p0627 N73-15090
WINCHES
Design criteria for load suspension points, slings, and lifting equipment used on military helicopters
[AD-747814] 03 p0307 N73-12508
Design, development, and evaluation of flywheel powered hoist for personnel rescue missions conducted by helicopters
[AD-751217] 07 p0741 N73-16029
WIND [METEOROLOGY]
NT GEOSTROPHIC WIND
NT GROUND WIND
NT GUSTS
NT JET STREAMS [METEOROLOGY]
NT MONSOONS
NT SQUALLS
NT WINDS ALOFT
Growth of mechanically generated surface water waves when subjected to turbulent channel air flow
[AD-746493] 01 p0042 N73-10336
Variational extrapolation method for wind and atmospheric temperature analysis
[AD-745354] 01 p0051 N73-10413
Aerodynamic characteristics of Scout vehicle during launch through high velocity horizontal winds
[NASA-CR-112175] 01 p0108 N73-10888
High altitude wind and temperature measurement data from meteorological sounding rockets, and radiosondes for May 1971
02 p0204 N73-11651
Systematic error in locating sounding balloon caused by influence of wind
[NASA-TT-F-14704] 03 p0326 N73-12654
Method of arithmetic data processing for restituting geographic components of wi.
[NASA-TT-F-14705] 03 p0326 N73-12655
Processing techniques for deducing cloud motion vectors from overlapped portions of pairs of satellite
[NASA-CR-130115] 03 p0326 N73-12660
Correlation coefficient between D region HF radio wave absorption and 10mb level winds and temperature in Northern Hemisphere
[COO-2195-5] 05 p0539 N73-14384
Winter wind and ocean conditions in Labrador fishing waters, and effects on pack ice drifting and icing hazards
[NLL-M-22670-[5828.4F]] 05 p0570 N73-14630
Bora observations from Yugoslavia and Italy
[CLIMATOL-NOTES-10] 05 p0571 N73-14636
Bora on Adriatic and Black Sea coasts - bibliographies
05 p0571 N73-14637
Atmospheric structure of cyclonic and anticyclonic Bora at Split and Zagreb, Yugoslavia
05 p0571 N73-14639
Pressure patterns chronology with Bora on Adriatic coast from 1 Jan. 1956 to 31 Dec. 1965
05 p0571 N73-14640
Bora-day chronology at Ajdovscina and Trieste with 10 m/s peak gust
05 p0571 N73-14641
Influence of local topography on wind flow over 2000 m rowing course at Holme Pierrepont, Nottingham
[NPL-MAR-SCI-R-100] 05 p0572 N73-14649
Diurnal variations of precipitation and surface wind for North Carolina
[PB-211614] 05 p0576 N73-14688
Analysis of wind induced vibration in vertical cantilever beam and square sagging suspended cable
[AD-750550] 05 p0604 N73-14913
Analysis of factors affecting wind speed in lower atmosphere and application to structural design and aircraft operation
[ESDU-72026] 07 p0814 N73-16601
Model for solution of equations of motion for thermospheric wind - Part 1
[NASA-TM-X-66189] 09 p1028 N73-18393
Doppler study of microwave backscattering from ocean waves in wind wave tank
[AD-753199] 09 p1032 N73-18422
Computer procedure for analysis of maritime sea-level pressure and wind fields
[NASA-TM-X-69135] 09 p1058 N73-18630
Calculating error in temporal statistical structure of zonal and meridional velocity components of ground wind
09 p1060 N73-18641
Foehn wind of canton Valais
10 p1181 N73-19610
Development of mathematical model for wind-driven circulation in ocean basin containing island formation
[AD-754354] 11 p1290 N73-20469
Automatic connection of aerogenerator to electrical network
[NASA-TT-F-14873] 12 p1386 N73-21238
Statistical description of wind field in upper troposphere and lower stratosphere for time scales from 6 to 72 hours
13 p1552 N73-22572
Occurrence of violent clear air turbulence near Kustanay on 27 July, 1971
13 p1552 N73-22579
Composite maps from 950 mb to 150 mb of relative wind field, mixing ratio R
[AD-755485] 13 p1555 N73-22600
Results and comparisons of full nonlinear treatment of global thermospheric wind system
[NASA-TM-X-66234] 14 p1685 N73-23671
Functional characteristics and operating data of experimental, aerodynamic three-phase electric power plant constructed in Crimea
[NASA-TT-F-14933] 15 p1761 N73-24268
Energetic role of trade wind inversion in tropical subalpine ecosystem
15 p1806 N73-24633
Analysis of mass diffusion process from elevated point source over wind-disturbed water surface and comparison with calculated concentration distributions for diffusion in flat plate boundary layer
16 p1887 N73-25271
Characteristics of water waves generated by steady two-dimensional wind at three different speeds over water depth of 19 centimeters
16 p1887 N73-25272
Development of method for remotely determining average transverse wind velocity and atmospheric structure constant along line of sight path
16 p1937 N73-25670
Numerical analysis of probability density of wind speeds and development of formula for distribution with two degrees of freedom
[ARL/SM-NOTE-383] 16 p1937 N73-25676
Equipment route winds and great circle distances for helicopter air routes at 5,000, 10,000, and 18,000 feet - Vol. 1
[AD-760252] 17 p1985 N73-26043
Equipment route winds and great circle distances for helicopter air routes at 5,000, 10,000 and 18,000 feet - Vol. 2
[AD-760253] 17 p1985 N73-26044
Application of ERTS-1 data to locate wind erosion sites in West Texas and to determine extent and spread of wind erosion
[E73-10719] 17 p2019 N73-26326
Approximation of atmospheric density and winds from radar track of passive inflatable sphere
17 p2057 N73-26633
Doppler radar investigation of flow patterns in severe thunderstorms
[AD-760106] 17 p2058 N73-26649
Flight simulation to determine effects of wind shear on aircraft landings for various commercial and military aircraft
[NASA-CR-2287] 18 p2105 N73-27023
Analysis of wind profiles in thunderstorm gusts and method for predicting velocity of winds at altitude
[NASA-CR-2289] 18 p2172 N73-27544
Basic fundamentals of meteorology and their effect on pollutant concentration on highway corridor
[PB-219811/7] 18 p2174 N73-27556
Design, development, and performance tests of wind driven, propeller operated electric generation station
[NASA-TT-F-15037] 20 p2363 N73-29004
Thermospheric wind effects on global distribution of helium in upper atmosphere
[NASA-TM-X-70441] 20 p2412 N73-29391
Kelvin-Helmholtz instabilities in mesoscale wind and temperature structure during clear air turbulence
[AD-763084] 20 p2413 N73-29397
Development of procedures for determining stability parameters of balloons tethered under steady wind conditions
[NASA-TN-D-7222] 21 p2493 N73-30013
Application of radar signatures for analyzing the turbulent flow structure of earth adjacent layers of subfrontal clouds and precipitation
21 p2570 N73-30597
Effects of wind loads on structures and structural design criteria based on wind speed, structural shape, and aerodynamic coefficients
[NLL-LIB-TRANS-1705-[5205.9]]
21 p2602 N73-30857
Interaction between atmospheric internal gravity wave and mean horizontal wind with shear
22 p2692 N73-31564
Air circulation patterns induced by wind and atmospheric pressure over Lake Superior
[PB-220244/8] 22 p2695 N73-31590
Computer programs for computing stability characteristics of tethered balloon under steady wind conditions
[NASA-TM-X-2740] 23 p2742 N73-31952
Analytical and numerical model of sea breeze
23 p2814 N73-32496
State-of-the-art techniques for harnessing solar and wind power
[AD-765783] 24 p2881 N73-33011
Numerical solution to problem of gravitational-shear waves in flow with arbitrary temperature stratification
24 p2947 N73-33532
Pilot balloon observations of lower tropospheric winds along upper Texas coast
[REPT-35] 24 p2948 N73-33544
Wind estimation by photographic tracking of clouds on images from synchronous meteorological satellites
24 p2948 N73-33546
WIND CIRCULATION
U ATMOSPHERIC CIRCULATION
WIND DIRECTION
Acoustic radar scattering in lower atmosphere for measuring wind velocity and direction
02 p0197 N73-11592
Directions of strong Martian winds inferred from Mariner 6 and 7 photographs and relation to dust storms and topographic wind funneling
[NASA-CR-129520] 03 p0354 N73-12885
Influence of wind speed and directional variability on trajectory of unguided missile at WSMR, New Mexico
[AD-753348] 09 p1062 N73-18662
Influence of wind speed and direction, and temperature on radon gas concentration in atmosphere
17 p2017 N73-26309
Prevaling monthly and seasonal surface wind directions for coastal areas aroud Arctic Ocean
[AD-761074] 18 p2174 N73-27560
Hydrodynamic models for studying pressure and wind fields in low latitudes
20 p2444 N73-29630
Spectral analysis of wind-wave spectrum at ice edge in Arctic Basin
21 p2573 N73-30621
Detection of low pressure center by viewing cloud pattern and wind direction in ERTS-1 photography
[E73-10978] 24 p2913 N73-33243
WIND EFFECTS
Radar photography of smoke in forest area for predicting bushfire behavior
[DIV-APPL-CHEM-TP-2] 04 p0388 N73-13151
Examination of physical processes governing heat transfer through air-penetrable clothing in wind
[DRIC-TRANS-2921] 06 p0636 N73-15166
Effect of wind wave energy balance on remote microwave sensing of sea surface
06 p0664 N73-15395
Influence of bottom topography and earth rotation of wind-driven circulation in Mediterranean Sea
07 p0858 N73-16956
Vertical wind effects in trajectory calculations and impact predictions for rockets and projectiles
[AD-753349] 09 p1092 N73-18913
Wind tunnel measuresments of time-average pressure on external and internal surfaces of large hangar-type building
[NPL-MAR-SCI-10-72] 10 p1140 N73-19292
Development of mathematical model for wind-driven circulation in ocean basin containing island formation
[AD-754354] 11 p1290 N73-20469
Wind effects on tall building design
[NPL-TECH-MEMO-MAR-SCI-TM-100]
11 p1344 N73-20909

Time dependent two-dimensional atmospheric model used to test hypothesis of increased precipitation downwind from cloud seeding area
[AD-755724] 12 p1425 N73-21551
Wind gust effects on STOL type aircraft
14 p1600 N73-22971
Design and cost estimate of high altitude wind power plant
[NASA-TT-F-14903] 14 p1605 N73-23011
Analysis of mass diffusion process from elevated point source over wind-disturbed water surface and comparison with calculated concentration distributions for diffusion in flat plate boundary layer
16 p1887 N73-25271
Characteristics of water waves generated by steady two-dimensional wind at three different speeds over water depth of 19 centimeters
16 p1887 N73-25272
Air water interaction in seasonal circulation variations of Red Sea
[PB-214446/7] 16 p1909 N73-25443
Equipment route winds and great circle distances for helicopter air routes at 5,000, 10,000, and 18,000 feet - Vol. 1
[AD-760252] 17 p1985 N73-26043
Equipment route winds and great circle distances for helicopter air routes at 5,000, 10,000 and 18,000 feet - Vol. 2
[AD-760253] 17 p1985 N73-26044
Application of ERTS-1 data to locate wind erosion sites in West Texas and to determine extent and spread of wind erosion
[E73-10719] 17 p2019 N73-26326
Flight simulation to determine effects of wind shear on aircraft landings for various commercial and military aircraft
[NASA-CR-2287] 18 p2105 N73-27023
Development and construction of wind driven electric power generators for specific European areas
[NASA-TT-F-15050] 20 p2364 N73-29009
Theory and computations of wind driven waves at sea
[TT-70-50182] 20 p2387 N73-29176
Simulation of interaction between wind-driven rain and annular air curtain dome and analysis of resulting flow distribution
[UTIAS-TN-182] 20 p2388 N73-29187
Development of damping system to compensate for wind loads on space shuttle vehicle during launch operations
[NASA-CR-124367] 21 p2601 N73-30845
Wind tunnel studies of Martian aeolian processes
[NASA-TM-X-62297] 22 p2716 N73-31746
Computer programs for computing stability characteristics of tethered balloon under steady wind conditions
[NASA-TM-X-2740] 23 p2742 N73-31952
Stability derivative analysis of tethered balloon in steady wind conditions to determine balloon aerodynamics buoyancy, mass, and static forces resulting from tether cable
[NASA-TN-D-7272] 23 p2743 N73-31955
Degradation, dispersion and movement of oil slicks by wind and ocean as factors influencing applicability of countermeasures
[WMO-359] 23 p2787 N73-32309

**WIND EROSION**
Inventory and mapping extent and spread of wind erosion of soils in west Texas
[E73-10834] 18 p2141 N73-27304
Wind erosion features in Mariner 9 Mars surface observations
23 p2839 N73-32690
Wind erosion and dune formations in Mars surface topography
[CONTRIB-2353] 23 p2839 N73-32691
Wind erosion and sandstorm effects on Mars surface topography
23 p2839 N73-32692
Mariner 9 mapping of Mars surface albedo variations
23 p2840 N73-32693
Wind erosion effects in Martian polar regions
23 p2840 N73-32695

**WIND MEASUREMENT**
NT WIND VELOCITY MEASUREMENT
Measurement of meteor winds based on radar tracking
[AD-745971] 01 p0054 N73-10440
Physical implications of solar wind measurements at 1 AU within framework of two fluid solar wind model equations
01 p0095 N73-10781
High altitude wind and temperature measurement data from meteorological sounding rockets and radiosonde observations - February 1971
02 p0204 N73-11652
First-order analyses of wind and current time series from Totem buoy off Oregon coast during 1970
[AD-746832] 02 p0206 N73-11668
Tracking and orbit calculation of Cosmos 316 to determine upper atmospheric wind
[RAE-TR-72062] 02 p0235 N73-11910
Methods for acquiring meteorological parameter data and procedures for analyzing wind data
[AD-747480] 03 p0298 N73-12432
Accuracy/resolution relationship of NAVAID systems Loran/Omega for measuring vertical wind profile
[AD-748275] 03 p0328 N73-12675
Monthly mean wind frequency and force by directions in Yugoslavia near Dinar Alps and Adriatic coast
05 p0571 N73-14638
Analysis of factors affecting wind speed in lower atmosphere and application to structural design and aircraft operation
[ESDU-72026] 07 p0814 N73-16601
Influence of urban and suburban area on wind and temperature profiles at Austin, Texas
[REPT-33] 08 p0938 N73-17680
Two-axis fluidic wind measuring devices
[AD-755740] 12 p1425 N73-21550
Jimsphere tracking for determining accuracy of meteorological radars
[AD-757624] 14 p1634 N73-23251
Analysis of errors in wind measurements from ocean data buoys
[AD-757981] 14 p1686 N73-23685
Maxometers for measuring peak wind speeds during severe environmental conditions
[NASA-CASE-MFS-20916] 16 p1911 N73-25460
Venus wind/altitude Doppler radar probe
[NASA-CR-114556] 16 p1962 N73-25871
Upper atmosphere wind and temperature measurements from Sonmiani, Pakistan, using rocket grenades - 1965 - 1967
[NASA-CR-133401] 18 p2144 N73-27331
Annotated listing of tall towers instrumented for wind observations
[AD-762911] 20 p2450 N73-29691
Comparison of laser Doppler measurements of wind velocities and turbulence with measurements by anemometers
[NASA-CR-124355] 21 p2574 N73-30627

**WIND PRESSURE**
Traveling ionospheric disturbance generation by tropopause jet stream
05 p0510 N73-14147
Variational principle for calculating buckling of thin clamped free circular cylindrical shells subjected to wind load
[TT-7113] 06 p0725 N73-15916
Atmospheric model for acoustic pressure produced in shadow zone by wind and temperature gradients
[AD-754634] 11 p1324 N73-20747
Design, development, and performance tests of wind driven, propeller operated electric generation station
[NASA-TT-F-15037] 20 p2363 N73-29004
Development and construction of wind driven electric power generators for specific European areas
[NASA-TT-F-15050] 20 p2364 N73-29009

**WIND PROFILES**
Meteorological charts and tables on wind altitude over French Polynesia
[MN-MONO-85] 01 p0073 N73-10602
Accuracy/resolution relationship of NAVAID systems Loran/Omega for measuring vertical wind profile
[AD-748275] 03 p0328 N73-12675
Monthly and annual percentage levels of wind speed differences computed by using FPS-16 radar/Jimsphere wind profiles for Cape Kennedy
[NASA-TM-X-64712] 05 p0572 N73-14650
Microwave measurements and Skylab S193 analysis of wind field over ocean
[CONTRIB-118] 06 p0663 N73-15384
Analysis of factors affecting wind speed in lower atmosphere and application to structural design and aircraft operation
[ESDU-72026] 07 p0814 N73-16601
METROC computer program for producing wind and thermodynamic data from raw upper atmospheric data
[AD-751780] 07 p0816 N73-16616
Aerosynoptic wind and temperature conditions contributing to atmospheric turbulence at altitude of 18 km over European USSR
[NLL-M-22822-[5828.4F]] 11 p1274 N73-20342
Analysis of synoptic wind scale spectra over Caribbean and tropical Atlantic region
[COO-2153-1] 12 p1422 N73-21528
Numerical analysis of probability density of wind speeds and development of formula for distribution with two degrees of freedom
[ARL/SM-NOTE-383] 16 p1937 N73-25676
Pulse radar measurement of mean monthly wind patterns
17 p2023 N73-26367
Analysis of wind profiles in thunderstorm gusts and method for predicting velocity of winds at altitude
[NASA-CR-2289] 18 p2172 N73-27544
Two dimensional nonsteady model of nocturnal flow of stable atmosphere over wide, warm, rough city
20 p2441 N73-29604
Rocket sounding of two year cyclic variations of zonal wind components in stratosphere and mesosphere up to 100 km
20 p2444 N73-29631
Surface boundary layer temperature profiles and turbulent heat flux during onshore flow
[REPT-38] 21 p2524 N73-30239
Mathematical models for matching geopotential and wind fields and improving accuracy of objective analysis
21 p2573 N73-30616
Rocket sounding of zonal wind field structure in stratosphere and lower mesosphere of tropical zone during equinoxes
21 p2573 N73-30617
Normal probabilities for Cape Kennedy wind components - monthly reference periods for all flight azimuths for altitudes from 0 to 70 kilometers
[NASA-TM-X-64771] 21 p2574 N73-30625
Effects of wind loads on structures and structural design criteria based on wind speed, structural shape, and aerodynamic coefficients
[NLL-LIB-TRANS-1705-[5205.9]] 21 p2602 N73-30857
Changes in planetary boundary layer wind profiles
[PB-221752/9] 22 p2697 N73-31601
Wind determination in tropics by balloon carrying dropsondes using Omega navigation system
24 p2948 N73-33548
Present status in meteorological satellites, wind observation, cloud cover, and the imagery compared with predictions made in 1962
24 p2949 N73-33552
Influence of temperature and wind profiles on water upwelling
24 p2974 N73-33765

**WIND RIVER RANGE [WY]**
Mapping of regional fracture patterns and related structural features of Wind River Mountains using ERTS-1 imagery
[E72-10349] 05 p0533 N73-14337
Spectral ratio mapping of iron ore deposits in Wind River Range, Wyoming, using ERTS-1 data
[E73-10397] 11 p1276 N73-20359
Analysis of spectral ratioing technique for southern end of of Wind River Range, Wyoming based on ERTS-1 analog ratio images
[PAPER-G16] 19 p2265 N73-28247

**WIND SHEAR**
Turbulence, billows, and gravity waves in high shear region of upper atmosphere during morning twilight, determined by rocket-released lithium cloud
[WRE-TN-670[WR/D]] 02 p0164 N73-11327
Computerized simulation of squall line structure and maintenance, based on convectively unstable air mass, vertical shear of horizontal wind, and lifting mechanism
[REPT-72-5] 05 p0572 N73-14651
Vertical wind shear measurements at Helsinki Airport - Apr. 1967 through Mar. 1968
[TR-3] 08 p0937 N73-17676
Development of wind and turbulence model for surface boundary layer based on surface parameters of stability and height
[NASA-CR-2288] 18 p2104 N73-27021
Flight simulation to determine effects of wind shear on aircraft landings for various commercial and military aircraft
[NASA-CR-2287] 18 p2105 N73-27023
Larger aircraft landing approach performance and altitude control during atmospheric turbulence and wind shear
[NLR-TR-72023-U] 21 p2497 N73-30036
Model of wind shear in lower 50 meter section of glide path from low inertia measured data
[NLL-M-23036-[5828.4F]] 21 p2528 N73-30271
Interaction between atmospheric internal gravity wave and mean horizontal wind with shear
22 p2692 N73-31564

**WIND TUNNEL APPARATUS**
NT WIND TUNNEL NOZZLES
Analysis of supersonic, three-dimensional flow characteristics to determine effects of material porosity and angle of attack on jet stretcher performance
07 p0765 N73-16215
Construction, installation, and calibration of wind tunnel models for measuring flutter characteristics of aerodynamic shapes
10 p1140 N73-19286
Development and characteristics of supersonic nozzles with perforated edges for wind tunnel applications
[AD-754601] 11 p1272 N73-20323
Fast closing gas valve for wind tunnel actuated by compressed air
[REPT-5/72] 13 p1505 N73-22194
Analysis of factors involved in design of wind tunnel for testing V/STOL aircraft models
14 p1598 N73-22956
Development and characteristics of analog wake drag evaluation system for use in test section of low speed wind tunnel
[FFA-AU-860] 14 p1648 N73-23368

Performance tests of working section of variable pressure, supersonic wind tunnel to show effects of inclination of slotted walls on Mach number accuracy
[ARC-R/M-3228] 15 p1730 N73-24032
Design and characteristics of test equipment for measuring longitudinal oscillatory aerodynamic derivatives in high speed wind tunnel
[ARC-R/M-3260] 16 p1855 N73-25029
Design criteria for annular supersonic nozzles to produce uniform flow in supersonic wind tunnels without limit lines or shock waves
[ARC-R/M-3227] 16 p1856 N73-25035
Application of digital computer for aerodynamic design and automatic control of wind tunnel with flexible walls
[ARC-R/M-3187] 16 p1857 N73-25041
Analysis of problems involved in operation of large wind tunnels at subsonic and supersonic speeds
[AGARD-R-601] 17 p2008 N73-26239
Analysis of interference occurring in subsonic and transonic wind tunnels caused by model support system
17 p2009 N73-26242
Objectives of dynamic tests in low speed wind tunnels and techniques for measuring oscillatory derivatives and transient motion effects
17 p2009 N73-26244
Analysis of techniques and equipment required to conduct test of jet aircraft engine models in wind tunnels
17 p2009 N73-26245
Wind tunnel apparatus for determining moment cross-derivatives due to pitching and yawing on models at moderate angles of attack and sideslip
[NASA-CR-114663] 22 p2613 N73-30944

**WIND TUNNEL BALANCES**
U WIND TUNNEL APPARATUS

**WIND TUNNEL CALIBRATION**
Calibration tests of Lewis hypersonic tunnel facility at Mach 5,6, and 7
[NASA-TN-D-7100] 02 p0153 N73-11237
Laser Raman spectroscopy for calibrating arc heated wind tunnel flow
[AD-761500] 19 p2231 N73-27989

**WIND TUNNEL MODELS**
Wind tunnel tests to determine effect of simulated hoar frost on lift coefficient of three aircraft wing configurations
[FFA-AU-902] 01 p0001 N73-10001
Wind tunnel tests of space shuttle models to determine effects of body and wing geometry on hypersonic shock structure and on surface impingement of interior flow field shock waves
[NASA-CR-128587] 01 p0040 N73-10317
Aerodynamic characteristics of Scout vehicle during launch through high velocity horizontal winds
[NASA-CR-112175] 01 p0108 N73-10888
Wind tunnel tests of twin jet afterbody models to determine thrust minus total drag and afterbody drag at Mach numbers to 2.2 and zero degree angle of attack
[NASA-TM-X-2601] 02 p0123 N73-11004
Wind tunnel tests to determine aerodynamic characteristics of two different size blunt 120 degree included angle cones behind 20 degree included angle cone
[NASA-TM-X-2603] 02 p0123 N73-11005
Flight and wind tunnel tests to determine effects of Reynolds number of installed boattail drag of underwing nacelle
[NASA-TM-X-68162] 02 p0124 N73-11007
Digital visual displays for checking pressure points from wind tunnel models
[ARA-28] 02 p0172 N73-11388
Wind tunnel tests to determine static aerodynamic characteristics of single-stage-to-orbit space shuttle at Mach numbers of 2.60, 3.85 and 4.64
[NASA-TM-X-2667] 02 p0233 N73-11891
Wind tunnel tests of scale model of orbiter 040A configuration in ground effect
[NASA-CR-120082] 02 p0233 N73-11895
Development of method for measuring temperature of wind tunnel scale model by photographic recording of changes in thin film phase-change temperature indicating material
[NASA-CASE-LAR-11053-1] 02 p0243 N73-11972
Effects of location of wing pivot and geometry of wing on static longitudinal aerodynamic characteristics of variable-sweep supersonic fighter aircraft model
[NASA-TM-X-2674] 03 p0247 N73-12000
Wind tunnel tests to determine effects of aerodynamic configuration, dimensions, and materials on spinning characteristics of cross parachute
[AD-749010] 04 p0374 N73-13045
Wind tunnel study of basic nature of plume induced flow separation
[NASA-CR-112218] 04 p0404 N73-13288
Wind tunnel tests of mixed compression axisymmetric inlet with large transonic mass flow at Mach numbers 0.6 to 2.65
[NASA-TN-D-6971] 04 p0463 N73-13777
Wind tunnel pressure signatures for scale model of Apollo command module
[NASA-TM-X-62047] 04 p0478 N73-13905
Wind tunnel tests to determine subsonic aerodynamic characteristics of model of space shuttle orbiter configuration with swept trapezoidal wing and swept fixed glove
[NASA-TM-X-2701] 05 p0491 N73-14005
Wind tunnel measurement of surface pressure distributions on three bodies of revolution at Mach numbers from 0.7 to 2.02
[AD-749934] 05 p0492 N73-14012
Wind tunnel tests to determine aerodynamic and propulsion characteristics of propulsive wing V/STOL configuration at high subsonic speed
[NASA-TM-X-2693] 05 p0493 N73-14020
Four-component wind coefficients for nine different ship models
[A-3] 05 p0523 N73-14256
Wind tunnel tests to determine aerodynamic characteristics of expendable second stage and payload configurations for reusable space shuttle booster - Vol. 3
[NASA-CR-128674] 05 p0599 N73-14869
Application of blockage correction factors to wind tunnel test measurements on aircraft models
06 p0617 N73-15006
Aerodynamic heating of supersonic models due to shock wave impingement
[AD-749946] 06 p0655 N73-15324
Effects of various leading edge slat devices on static aerodynamic characteristics of twin-jet, swept wing fighter model
[NASA-TN-D-6921] 07 p0736 N73-15988
Physical principles of experimental aeromechanics using wind tunnel tests
[AD-751464] 07 p0773 N73-16280
Static and wind tunnel tests to determine performance of four cowl cascade thrust reverser configurations at forward velocity
[NASA-TM-X-2665] 07 p0835 N73-16773
Wind tunnel tests to predict full scale aircraft buffet loads during buffet boundary penetration using scale flutter model of fighter aircraft with variable sweep wings
[NASA-TN-D-7066] 07 p0851 N73-16905
Wind tunnel tests of two dimensional wing model with leading edge slat and trailing edge flap
[FAA-AU-862] 08 p0863 N73-16984
Wind tunnel study of turbulent wake flow dynamics
[AD-751970] 08 p0897 N73-17267
Inertially coupled equations of motion for analyzing pitching and yawing motions of nonrolling wind tunnel model
[AD-752208] 08 p0926 N73-17586
Wind tunnel calibration and requirements for in-flight use of fixed hemispherical head of angle of attack and angle of sideslip sensors
[NASA-TN-D-6986] 09 p0981 N73-18014
Wind tunnel tests to determine flow characteristics of stalled two dimensional airfoil
[NASA-CR-130919] 09 p0982 N73-18020
Wind tunnel tests to determine acoustic properties of semispan wing with externally blown jet flap to include effects of flap size, vertical location and forward speed
[NASA-TM-X-2749] 09 p0985 N73-18041
Effects of rocket motor nozzle geometry on jet plume characteristics and base pressure
[NASA-CR-130967] 09 p1017 N73-18303
Construction, installation, and calibration of wind tunnel models for measuring flutter characteristics of aerodynamic shapes
10 p1140 N73-19286
Dynamic structural design of aeroelastic wind tunnel models using combinatorial flutter analyses
10 p1140 N73-19291
Wind tunnel measurements of time-average pressure on external and internal surfaces of large hangar-type building
[NPL-MAR-SCI-10-72] 10 p1140 N73-19292
Wind tunnel tests of scale model of space shuttle orbiter to determine low subsonic aerodynamic characteristics
[NASA-TM-X-2712] 11 p1232 N73-20000
Wind tunnel tests to determine low speed aerodynamic characteristics of large scale V/STOL transport models with lift fan lift-cruise fan propulsion system
[NASA-TM-X-62231] 11 p1233 N73-20014
Evaluation of stability derivatives obtained from dynamic tests of model in cold magnetic balance wind tunnel facility
[NASA-CR-112305] 11 p1267 N73-20279
Digital simulation method to study wind tunnel model ship configurations
[AD-755005] 11 p1273 N73-20333
Wind tunnel tests of space shuttle orbiter in various configurations to determine aerodynamic loads and pressure distributions at range of Mach numbers
[NASA-CR-120066] 11 p1342 N73-20890
Development of advancing blade concept rotary wing and wind tunnel tests of full scale model
12 p1359 N73-21029
Wind tunnel tests to determine effects of blade twist and aeroelasticity on tilt rotor performance from hover to mach number 0.7
12 p1362 N73-21049
Wind tunnel tests to determine effects of nonrotating components on helicopter performance and application for helicopter design optimization
12 p1362 N73-21052
Low speed wind tunnel tests of scale model of space shuttle orbiter to determine longitudinal and lateral-directional aerodynamic characteristics
[NASA-CR-123851] 12 p1460 N73-21829
Trisonic wind tunnel tests to determine force and moment characteristics of space shuttle orbiter and modified external tank and solid rocket booster
[NASA-CR-120089] 12 p1460 N73-21831
Wind tunnel tests of space shuttle orbiter scale model to determine aerodynamic characteristics at hypersonic speed in various configurations
[NASA-CR-128754] 12 p1461 N73-21838
Wind tunnel simulation of high altitude rocket plumes
[AD-755840] 12 p1466 N73-21876
Wind tunnel tests to determine acoustic properties of externally blown jet flap and augmentor wing short takeoff aircraft concepts
[NASA-TM-X-62251] 13 p1472 N73-21924
Wind tunnel tests to determine effect of cross flow velocity on jet noise power level using V/STOL model transport
[NASA-CR-114571] 13 p1473 N73-21929
Procedures for testing rotary wing aircraft models in wind tunnels to include design of test facilities, cost of models and facilities, and methods for obtaining data
14 p1598 N73-22955
Analysis of factors involved in design of wind tunnel for testing V/STOL aircraft models
14 p1598 N73-22956
Atmospheric physics and gas dynamics research in Soviet Union
[JPRS-58988] 14 p1649 N73-23377
Development of theory for wind tunnel boundary upwash interference on symmetrical finite wing with arbitrary lift distribution
[AD-757196] 14 p1652 N73-23397
Wind tunnel tests to determine aerodynamic interference between space shuttle orbiter, external tank, and solid rocket booster in ascent configuration
[NASA-CR-120060] 14 p1709 N73-23871
Wind tunnel tests to determine effect of longitudinally oriented wing-mounted pods on aerodynamic characteristics of V/STOL transport model in cruise flight mode
[NASA-TN-D-7199] 15 p1731 N73-24035
Aerodynamic coefficients for calculating transport aircraft performance using wind tunnel and scale models
15 p1732 N73-24046
Wind tunnel tests to determine aerodynamic characteristics of delta wing space shuttle orbiter model at various angles of attack and sideslip
[NASA-TM-X-2748] 15 p1733 N73-24058
Two dimensional unsteady separation and stall phenomena over airfoils oscillating in pitch with application to short takeoff aircraft
[AD-758899] 15 p1736 N73-24080
Wind tunnel tests to determine time-averaged aerodynamic forces on model of helicopter landing pad to be installed on top of lighthouse
[MAR-SCI-R-106] 15 p1761 N73-24269
Electromagnetic superconducting force producing coil for positioning models in wind tunnel
15 p1762 N73-24276
Modane-Avrieux transonic blowdown wind tunnel for two dimensional flow airfoil profile study
[ONERA-NT-203] 15 p1762 N73-24281
Resonance tests of delta wing aircraft model to determine effect of stiffness changes of wing spars on frequencies and modes of vibration
[ARC-R/M-3268] 16 p1856 N73-25031
Base pressure measurements on axially symmetric wind tunnel models in subsonic, transonic and supersonic speeds at high Reynolds numbers
[TAE-134] 16 p1857 N73-25044
Exhaust gas diffuser effect on test cell wall and turbofan cold-flow model engine exhaust nozzle plug and core engine cowl surface pressure
[AD-759177] 16 p1958 N73-25842
Analysis of operational problems associated with wind tunnel testing of V/STOL aircraft and helicopters
17 p2008 N73-26240
Analysis of interference occurring in subsonic and transonic wind tunnels caused by model support system
17 p2009 N73-26242
Analysis of techniques and equipment required to conduct test of jet aircraft engine models in wind tunnels
17 p2009 N73-26245
Scaling laws, constructional problems, and optimum model size associated with wind tunnel tests of helicopters and rotary wing aircraft
17 p2009 N73-26246
Influence of free stream Reynolds number on transition in boundary layer on infinite swept wing
17 p2013 N73-26280

Analysis of effect of turbulence intensity on aerodynamic characteristics of bodies of various shapes to develop method for measuring initial turbulence
[AD-760264] 17 p2015 N73-26297
Characteristics of zero aerosol sampling tube for aspiration of samples from gas flow with minimum changes in isokinetic coefficient
[AD-759868] 17 p2035 N73-26470
Wind tunnel determination of effect of fin planform on aerodynamic characteristics of wingless missile with aft cruciform controls at Mach 1.60, 2.36, and 2.86
[NASA-TM-X-2774] 18 p2101 N73-26995
Wind tunnel tests of short takeoff and landing fan stage model to determine airflow conditions around rotor and stator and stage pressure ratio
[NASA-TM-X-2837] 18 p2192 N73-27701
Wind tunnel tests to determine control of magnus instabilities with aerodynamic configurations using symmetrical fin and non-finned bodies
19 p2217 N73-27885
Wind tunnel tests to determine effects of modified engine nacelle on stability and control characteristics of DC-9 aircraft with emphasis on deep stall regime
[NASA-CR-121220] 19 p2219 N73-27904
Analysis of transonic scaling effect on quasi, two-dimensional airfoil model of C-141 aircraft
[AD-762285] 19 p2222 N73-27924
Numerical analysis of two dimensional turbulent wakes in constant adverse and favorable pressure gradients
[AD-761389] 19 p2256 N73-28185
Reduction of photographic heat transfer rate data at wind tunnel test facility
[AD-762928] 20 p2420 N73-29447
Transonic wind tunnel tests of thrust effects on missile aerodynamics
[AD-762576] 20 p2476 N73-29889
Effect of wing aspect ratio and flap span on aerodynamic characteristics of short takeoff model with externally blown jet flap
[NASA-TN-D-7205] 21 p2494 N73-30020
Free-flight tests on space shuttle and reentry vehicle models in hypervelocity gun tunnels
[DLR-FB-72-41] 21 p2522 N73-30224
Correlation between wind tunnel data and finite difference solutions for viscous and wind tunnel effects in transonic flows over airfoils
[AD-764133] 22 p2612 N73-30936
Wind tunnel apparatus for determining moment cross-derivatives due to pitching and yawing on models at moderate angles of attack and sideslip
[NASA-CR-114663] 22 p2613 N73-30944
Wind tunnel tests to determine static longitudinal, lateral, and directional characteristics of twin-engine light aircraft scale model
[NASA-TN-D-7109] 22 p2614 N73-30951
Wind tunnel testing of V/STOL aircraft models to show wind tunnel wall corrections for models with large values of downwash
[AD-764255] 22 p2616 N73-30962
Wind tunnel tests to determine drag and stability characteristics of solid flat circular and ringslot parachute models
[AD-764364] 22 p2616 N73-30963
Wind tunnel tests to determine low speed characteristics of large scale model of F-14A aircraft with emphasis on high lift configuration stability
[NASA-TM-X-62244] 23 p2741 N73-31940
Wind tunnel test program to investigate subsonic through high supersonic aerodynamic characteristics of Lockheed delta lifting orbiter and stage-and-one-half launch vehicle
[NASA-CR-124419] 23 p2849 N73-32770
Trisonic wind tunnel tests of baseline launch configuration space shuttle model to determine effects of model parametric variations on static stability characteristics
[NASA-CR-128778] 23 p2851 N73-32783
Wind tunnel tests to determine aerodynamic characteristics of three oblique, high aspect ratio wing and body combinations at Mach numbers between 0.60 and 1.40
[NASA-TM-X-62256] 24 p2869 N73-32926
Wind tunnel tests to determine aerodynamic characteristics of oblique wing and body combination at Mach numbers between 0.60 and 1.40
[NASA-TM-X-62207] 24 p2870 N73-32927
Wind tunnel tests to determine aerodynamic characteristics of five configurations of short takeoff aircraft wind tunnel models
24 p2872 N73-32944
Wind tunnel tests of large scale subsonic jet transport with upper surface blowing flap system for lift augmentation
[NASA-TM-X-62296] 24 p2876 N73-32973
Transonic wind tunnel tests to determine lift, drag, and stability characteristics of F-8 aircraft model with oblique wing
[NASA-TM-X-62273] 24 p2877 N73-32974
Wind tunnel tests to determine acoustic properties of large scale lift fan transport aircraft model
[NASA-TM-X-62284] 24 p2877 N73-32975
Boundary layer calculation and wind tunnel model test of ships
24 p2909 N73-33214
Development of instrument to measure steady and oscillatory aerodynamic forces on sting-mounted model using forced oscillation technique
[ATN-7101] 24 p2926 N73-33366
Electroforming used for manufacture of hollow wind tunnel models and nozzles
[DLR-FB-73-40] 24 p2929 N73-33395

**WIND TUNNEL NOZZLES**

Feasibility of porous jet stretcher nozzle for angle of attack testing of missiles in supersonic wind tunnel
[AD-750867] 06 p0651 N73-15288
Investigation of low density hypersonic flow by controlled boundary layer removal from nozzle wall
[AD-754276] 11 p1271 N73-20316
Effects of nozzle geometry and diaphragm location on starting process in Ludwieg tubes
[AD-755357] 13 p1511 N73-22248
Electroforming used for manufacture of hollow wind tunnel models and nozzles
[DLR-FB-73-40] 24 p2929 N73-33395

**WIND TUNNEL STABILITY TESTS**

Wind tunnel static stability and control data for delta wing booster of scale model of space shuttle
[NASA-CR-119994-VOL-3] 01 p0107 N73-10886
Test results of booster and orbiter configurations
[NASA-CR-119994-VOL-4] 01 p0108 N73-10887
Comparison of longitudinal and lateral stability and control characteristics of Phase B Grumman H-33 space shuttle orbiter
[NASA-CR-120080] 01 p0108 N73-10889
Comparison of longitudinal and lateral stability and control characteristics of baseline 040A space shuttle orbiter
[NASA-CR-120081] 01 p0109 N73-10894
Wind tunnel results of static stability and control effectiveness of shuttle orbiter
[NASA-CR-120070] 03 p0359 N73-12923
Wind tunnel tests of space shuttle model to determine performance, stability, and control characteristics of launch configuration
[NASA-CR-120088] 04 p0478 N73-13910
Wind tunnel tests to determine aerodynamic and propulsion characteristics of propulsive wing V/STOL configuration at high subsonic speed
[NASA-TM-X-2693] 05 p0493 N73-14020
Wind tunnel tests to determine aerodynamic characteristics of expendable second stage and payload configurations for reusable space shuttle booster - Vol. 3
[NASA-CR-128674] 05 p0599 N73-14869
Wind tunnel tests to obtain pre-flight estimates of stall speed and low air speed performance of Boeing 747 aircraft
06 p0618 N73-15016
Wind tunnel tests of full scale model of light aircraft to determine effects of configuration changes on aerodynamic characteristics
[NASA-TN-D-6896] 07 p0739 N73-16012
Wind tunnel tests to determine aircraft post-stall characteristics and to define boundaries for maintaining controlled aircraft flight
[AD-751461] 07 p0740 N73-16023
Data correlation for varying times of wind tunnel tests
[AD-751957] 08 p0893 N73-17228
Jet deflection characteristics of jet-flapped airfoil with Coanda deflection surfaces based on velocity distribution and flow angle measurements for static operation
[AD-753618] 09 p0989 N73-18074
Scale effect on swept wings at subsonic speed on basis of pressure distribution measured in flight and on wind tunnel super VC 10 model
[ARC-R/M-3707] 12 p1355 N73-20999
Wind tunnel tests of space shuttle orbiter scale model to determine low speed aerodynamic characteristics of spacecraft components
[NASA-CR-120092] 12 p1460 N73-21832
Wind tunnel tests of swept augmentor wing aerodynamic characteristics
[NASA-TM-X-62252] 13 p1472 N73-21923
Procedures for testing rotary wing aircraft models in wind tunnels to include design of test facilities, cost of models and facilities, and methods for obtaining data
14 p1598 N73-22955
Wind tunnel interference factors for high lift wings in closed wind tunnels
16 p1851 N73-24996
Wind tunnel tests to determine directional and longitudinal stability of Javelin aircraft model at transonic speeds
[ARC-R/M-3403] 16 p1853 N73-25012
Wind tunnel studies to determine static stability of two bodies of revolution with noses of varying spherical bluntness at Mach 0.6 to 1.5
[AD-758817] 16 p1858 N73-25052
Wind tunnel stability tests to determine static longitudinal and lateral characteristics of full-scale model of light, single engine, high wing aircraft
[NASA-TN-D-7149] 16 p1860 N73-25068
Split-film atmospheric turbulence anemometer evaluation
[NASA-CR-62093] 16 p1914 N73-25485
Effects of free stream velocity and incidence angle on aerodynamic and acoustic performance of translating centerbody choked flow inlet
[NASA-TM-X-2773] 16 p1957 N73-25829
Aerodynamic characteristics of space shuttle orbiter model in wind tunnel test
[NASA-TM-X-2786] 17 p1979 N73-25998
Wind tunnel tests to determine effects of modified engine nacelle on stability and control characteristics of DC-9 aircraft with emphasis on deep stall regime
[NASA-CR-121220] 19 p2219 N73-27904
Wind tunnel tests to determine effects of control surface modifications on stability and control of space shuttle orbiter
[NASA-CR-133979] 19 p2346 N73-28870
Wind tunnel tests to determine stability and control characteristics of externally blown jet-flap configurations
24 p2872 N73-32940

**WIND TUNNEL TESTS**

Performance of Mirage 3 sigma 4 after body
14 p1597 N73-22946
Wind tunnel investigation of three dimensional flow effects on straight wings
14 p1600 N73-22973
Wind tunnel tests to determine aerodynamic interference between space shuttle orbiter, external tank, and solid rocket booster in ascent configuration
[NASA-CR-120060] 14 p1709 N73-23871
Wind tunnel tests to determine effects of leading edge modifications on flow and forces on untapered wing with 50 degree leading edge sweep and Mach numbers from 0.60 to 1.20
[ARC-R/M-3270] 15 p1726 N73-24003
Wind tunnel tests to determine aerodynamic characteristics of model of sweptback wing with warp distribution to produce constant spanwise coefficient of lift
[ARC-R/M-3385] 15 p1727 N73-24007
Wind tunnel tests to determine characteristics of turbine rotor blades with inter-blade passages operating at supersonic speed
[ARC-R/M-3275] 15 p1728 N73-24016
Development of techniques for measuring oscillatory derivatives in wind tunnels and analysis of wind tunnel effects on results
[ARC-R/M-3319] 15 p1729 N73-24020
Wind tunnel tests to determine effect of longitudinally oriented wing-mounted pods on aerodynamic characteristics of V/STOL transport model in cruise flight mode
[NASA-TN-D-7199] 15 p1731 N73-24035
Wind tunnel tests to determine aerodynamic characteristics of delta wing space shuttle orbiter model at various angles of attack and sideslip
[NASA-TM-X-2748] 15 p1733 N73-24058
Wind tunnel tests to determine pressure distributions for four percent thick, circular arc, biconvex airfoil at transonic speeds
[ARC-R/M-3180] 16 p1852 N73-25002
Wind tunnel tests at Mach 2.0 to determine aerodynamic characteristics of cambered and uncambered gothic wings
[ARC-R/M-3211] 16 p1852 N73-25003
Wind tunnel tests to determine effect of interference on performance of full span jet flap mounted on trailing edge of high aspect ratio unswept wing
[ARC-R/M-3219] 16 p1852 N73-25005
Supersonic wind tunnel tests to measure overall normal and side forces, rolling, pitching, and yawing moments on canard aircraft
[ARC-R/M-3226] 16 p1853 N73-25011
Wind tunnel tests to determine subsonic derivatives for oscillating M-wing planform
[ARC-R/M-3214] 16 p1854 N73-25022
Wind tunnel tests to determine aerodynamic characteristics of vectored thrust V/STOL fighter aircraft in transition speed range
[NASA-TN-D-7191] 16 p1858 N73-25047
Flight test measurements of control surface hinge moments on X-24 lifting body correlation with wind tunnel data
[NASA-TM-X-2816] 16 p1858 N73-25049
Wind tunnel tests to determine pressure distribution on two dimensional airfoil with pylon mounted stores at subsonic speeds using F-4 aircraft model
[AD-759582] 16 p1859 N73-25053
Full scale hover test of 25-foot tilt rotor
[NASA-CR-114626] 16 p1861 N73-25070
Wind tunnel tests to determine inflation characteristics of solid, flat, circular model parachutes at subsonic speed and various geometric configurations
[AD-759209] 16 p1863 N73-25087
Wind tunnel tests to determine effect on cruise performance of installing long duct refan-engine nacelle on DC 8 aircraft
[NASA-CR-121218] 17 p1982 N73-26023
Analysis of operational problems associated with wind tunnel testing of V/STOL aircraft and helicopters
17 p2008 N73-26240
Analysis of minimum run times required for instationary measurements at transonic speeds during wind tunnel tests
17 p2009 N73-26243

Objectives of dynamic tests in low speed wind tunnels and techniques for measuring oscillatory derivatives and transient motion effects
17 p2009 N73-26244
Analysis of techniques and equipment required to conduct test of jet aircraft engine models in wind tunnels
17 p2009 N73-26245
Scaling laws, constructional problems, and optimum model size associated with wind tunnel tests of helicopters and rotary wing aircraft
17 p2009 N73-26246
Analysis of acoustic factors involved in wind tunnel tests to show contributions from various sources
17 p2009 N73-26247
Wind tunnel tests to determine acoustic properties of helicopter rotor and wind tunnel calibration techniques
[RAE-LIB-TRANS-1683] 17 p2009 N73-26249
Analysis of effect of turbulence intensity on aerodynamic characteristics of bodies of various shapes to develop method for measuring initial turbulence
[AD-760264] 17 p2015 N73-26297
Comparison of wind tunnel measurements of impact pressure and species number density of simulated high altitude rocket exhaust plume with computer calculated values
[AD-759838] 17 p2097 N73-26968
Wind tunnel investigation of turbulent boundary layer response to lateral surface roughness discontinuities
18 p2129 N73-27202
Wind tunnel tests to determine heat transfer and flow distribution of space shuttle configuration at hypersonic speeds simulating atmospheric entry
[NASA-CR-133405] 18 p2201 N73-27772
Wind tunnel tests to analyze aerothermodynamic control problems of space shuttle attitude control system at hypersonic speed
[NASA-CR-133407] 18 p2201 N73-27773
Wind tunnel tests to determine aerodynamic characteristics of two missile configurations with common body at transonic and supersonic speeds
[NASA-TM-X-2780] 19 p2218 N73-27891
Two dimensional flow, low speed wind tunnel tests of trapped vortex-high lift airfoil to reduce blowing requirements for lift augmentation
[AD-762077] 19 p2218 N73-27893
Wind tunnel tests to determine performance of lobed-display mixer nozzle with convergent nozzle at subsonic speeds
[NASA-TM-X-2806] 21 p2491 N73-29995
Wind tunnel tests to determine effects of variations in Reynolds number and leading edge configurations on aerodynamic characteristics of STOL transport with externally blown flaps
[NASA-TN-D-7194] 21 p2494 N73-30021
Wind tunnel tests to determine effects of slot spoilers on longitudinal and lateral aerodynamic characteristics of twin engine light aircraft
[NASA-TN-D-7315] 21 p2496 N73-30033
Wind tunnel tests to determine transient wake velocities behind three stalled wing configurations at Reynolds numbers up to 4.8 million
[AD-763468] 21 p2498 N73-30050
Wind tunnel tests to measure axial and tangential velocity profiles in near wake vortices of semi-span model of Convair 990 aircraft model using laser Doppler velocimeter
[NASA-TM-X-62294] 21 p2524 N73-30244
Wind tunnel pressure signatures for scale model of Saturn 5-Apollo launch vehicle with simulated exhaust plumes
[NASA-TM-X-62129] 21 p2599 N73-30830
Wind tunnel tests to determine two dimensional characteristics of airfoil optimized for maximum lift coefficient at various angles of attack
[NASA-TN-D-7071] 22 p2611 N73-30929
Wind tunnel tests to determine static longitudinal, lateral, and directional characteristics of twin-engine light aircraft scale model
[NASA-TN-D-7109] 22 p2614 N73-30951
Wind tunnel testing of V/STOL aircraft models to show wind tunnel wall corrections for models with large values of downwash
[AD-764255] 22 p2616 N73-30962
Wind tunnel tests to determine drag and stability characteristics of solid flat circular and ringslot parachute models
[AD-764364] 22 p2616 N73-30963
Wind tunnel tests to determine effect of inlet turbulence length scale on fan discrete tone noise
[NASA-TM-X-62300] 22 p2700 N73-31625
Wind tunnel studies of Martian aeolian processes
[NASA-TM-X-62297] 22 p2716 N73-31746
Subsonic wind tunnel tests of ring-wing canard configurations for air to surface antitank missiles
[AD-763899] 22 p2723 N73-31788
Wind tunnel tests to determine boundary layer flow characteristics in supersonic axisymmetric inlet
[NASA-TM-X-2902] 23 p2739 N73-31926
Wind tunnel tests to determine flow distribution at inlet locations on aircraft model for various aerodynamic configurations and airspeeds
[NASA-TN-D-7364] 23 p2739 N73-31929
Wind tunnel tests to determine low speed characteristics of large scale model of F-14A aircraft with emphasis on high lift configuration stability
[NASA-TM-X-62244] 23 p2741 N73-31940
Wind tunnel tests of high harmonic circulation control rotary wing model to show instruments required and data acquisition procedures
[AD-765320] 23 p2747 N73-31984
Hypersonic wind tunnel tests of air breathing engines
23 p2770 N73-32158
Trisonic wind tunnel tests of baseline launch configuration space shuttle model to determine effects of model parametric variations on static stability characteristics
[NASA-CR-128778] 23 p2851 N73-32783
Wind tunnel tests to determine basic performance of swept augmentor wing configuration and effect on longitudinal characteristics of aircraft
24 p2872 N73-32941
Wind tunnel tests to determine aerodynamic characteristics of upper surface blown jet-flap concept incorporating high-bypass-ratio turbofan engines
24 p2872 N73-32943
Wind tunnel tests to determine aerodynamic characteristics of five configurations of short takeoff aircraft wind tunnel models
24 p2872 N73-32944
Transonic wind tunnel tests to determine effects on flutter of aerodynamic interference between pairs of closely spaced delta wings
[NASA-CR-2331] 24 p2989 N73-33887

**WIND TUNNEL WALLS**
Interference theory in slotted wind tunnels extended to subsonic rectangular wind tunnels with ventilated tool, longitudinal slots and perforated screens of arbitrary porosity
[ARC-R/M-3706] 05 p0492 N73-14007
Calculation of wind tunnel wall interference velocities affecting pitching moments of high lift wings
[NASA-CR-2191] 10 p1137 N73-19269
Wall interference effects at Mach 1 on airfoils in transonic wind tunnels
[AD-757534] 14 p1646 N73-23349
Effects of porous wind tunnel wall corrections on transport aircraft models
14 p1648 N73-23366
Narrowband noise generation by flow over perforated or ventilated transonic wind tunnel walls
[AD-758254] 15 p1763 N73-24283
Transonic wind tunnel wall effects on boundary layer blocking phenomena
15 p1766 N73-24306
Application of digital computer for aerodynamic design and automatic control of wind tunnel with flexible walls
[ARC-R/M-3187] 16 p1857 N73-25041
Development of numerical methods for correcting wall constraints in transonic wind tunnels with ventilated walls
17 p2008 N73-26241
Correlation between wind tunnel data and finite difference solutions for viscous and wind tunnel effects in transonic flows over airfoils
[AD-764133] 22 p2612 N73-30936
Wind tunnel testing of V/STOL aircraft models to show wind tunnel wall corrections for models with large values of downwash
[AD-764255] 22 p2616 N73-30962
Slotted transonic wind tunnel tests on pitching delta wing enable selection of porpous walls for interference free damping derivatives
[ARC-R/M-3715] 24 p2870 N73-32930

**WIND TUNNELS**
NT BLOWDOWN WIND TUNNELS
NT CASCADE WIND TUNNELS
NT HYPERSONIC WIND TUNNELS
NT HYPERVELOCITY WIND TUNNELS
NT LOW DENSITY WIND TUNNELS
NT LOW SPEED WIND TUNNELS
NT PLASMA JET WIND TUNNELS
NT RECTANGULAR WIND TUNNELS
NT SHOCK TUNNELS
NT SLOTTED WIND TUNNELS
NT SUBSONIC WIND TUNNELS
NT SUPERSONIC WIND TUNNELS
NT TRANSONIC WIND TUNNELS
Longitudinal aerodynamic characteristics of large scale model with swept wing and augmented jet flap in ground effect, using 40 x 80 ft wind tunnel
[NASA-TM-X-62174] 01 p0004 N73-10030
Design, construction, and calibration of closed circuit wind tunnel for study of aerodynamic behavior of precipitation
[UTIAS-TN-181] 02 p0152 N73-11232
Wind tunnel design for testing V/STOL aircraft in transition flight
[AD-749154] 04 p0402 N73-13278
Wind tunnel and atmospheric tests of dynamic performance of anemometers
[AD-747341] 04 p0445 N73-13630
Ejector-driven multiple jet wind tunnel for simulation of flows in planetary boundary layer
[AD-748903] 05 p0527 N73-14289
Design and performance of miniaturized electric field meters for wind tunnel measurements
[AD-750148] 06 p0675 N73-15495
Predicting flying qualities by wind tunnel tests
08 p0865 N73-17000
Open jet, wind tunnel operating within anechoic chamber for studying V/STOL noise mechanisms
[AD-751857] 08 p0894 N73-17235
Methods for measuring temperature in wind tunnels with electric contact thermometers
[DLR-MITT-72-27] 09 p1010 N73-18246
Data acquisition system for S-1 wind tunnel with continuous subsonic/supersonic flow
[WRE-TN-784[WR/D]] 09 p1010 N73-18248
Developments in aerodynamic test facilities to show past experience, present status, free flight techniques, and future plans
[AGARD-R-603] 09 p1011 N73-18250
Optimization of working conditions in plasma wind tunnel by pressure distribution control in acceleration
[DLR-FB-72-70] 09 p1070 N73-18735
Procedure for developing aerodynamic parameters for use in flight simulator research projects with emphasis on wind tunnel measurements
10 p1105 N73-19008
Wind tunnel measurements of nearly homogeneous grid turbulence field with large amplitude temperature fluctuations
10 p1139 N73-19280
Existing position and future prospects of wind tunnels in European research
[AGARD-AR-60] 11 p1266 N73-20269
Evaluation of acoustic properties of conventional wind tunnels for analyzing aerodynamically generated noise
[NASA-CR-114575] 11 p1266 N73-20277
Correlation of sonic boom pressure signatures recorded during reentry of Apollo 16 command module with wind tunnel signatures
[NASA-TM-X-62073] 12 p1365 N73-21073
Application of laser Doppler velocimeter for measurement of central vortex filament in wind tunnel test section
[NASA-TM-X-62243] 13 p1536 N73-22448
Porous surface microphones for acoustic measurements in subsonic flow in wind tunnels
[NASA-CR-114593] 14 p1639 N73-23289
Fluid mechanics facility in aerodynamics laboratory
[AD-756512] 14 p1646 N73-23350
Long fetch technique for simulating neutral atmospheric layers in wind tunnels
[AD-758888] 15 p1784 N73-24462
Effect of humidity on laminar recovery temperature measurements during supersonic air flow in wind tunnels
[ARC-R/M-3215] 16 p1857 N73-25042
Analysis of operational problems associated with wind tunnel testing of V/STOL aircraft and helicopters
17 p2008 N73-26240
Procedure for generating uniform flow at varying velocities in wind tunnel test section
[NASA-CASE-ARC-10710-1] 18 p2125 N73-27175
Flow characteristics behind diffusers in wind tunnels
[AD-763257] 21 p2525 N73-30251
Diagnostic techniques for measurement of aerodynamic noise in free field and reverberant environment of wind tunnels
[NASA-CR-114636] 21 p2579 N73-30669
Development of wind tunnel with self correcting apparatus based on sensors to determine flow conditions on tunnel surfaces and method for varying wall geometry
[AD-764957] 23 p2771 N73-32161

**WIND VARIATIONS**
Infrasonic resonant tube determination of wind and temperature variabilities in lower troposphere
[AD-745912] 02 p0206 N73-11667
Analysis of factors affecting wind speed in lower atmosphere and application to structural design and aircraft operation
[ESDU-72026] 07 p0814 N73-16601
Influence of wind speed and directional variability on trajectory of unguided missile at WSMR, New Mexico
[AD-753348] 09 p1062 N73-18662
Effect of bottom topography, eddy diffusivity, and wind variation on circulation in two-layer stratified lake
[NASA-TN-D-7235] 11 p1286 N73-20433
Numerical analysis of probability density of wind speeds and development of formula for distribution with two degrees of freedom
[ARL/SM-NOTE-383] 16 p1937 N73-25676
Effect of spatial variability of wind in stratosphere on flight of supersonic transports
24 p2946 N73-33529

**WIND VELOCITY**
Effect of solar wind velocity on interplanetary magnetic field properties
01 p0093 N73-10767

Acoustic radar scattering in lower atmosphere for measuring wind velocity and direction
02 p0197 N73-11592
Vector calculus for determination of wind velocity components
04 p0442 N73-13603
Applicability of various laws of statistics of extremal values for approximating empirical distributions of maximum wind velocities
04 p0442 N73-13608
Vertical air gust velocities and turbulence spectral structure around and within cumulonimbus clouds
[AD-748518] 04 p0445 N73-13632
Monthly and annual percentage levels of wind speed differences computed by using FPS-16 radar/Jimsphere wind profiles for Cape Kennedy
[NASA-TM-X-64712] 05 p0572 N73-14650
Wind velocity fluctuations over natural ocean waves, and wind-wave coupling
[AD-749073] 05 p0574 N73-14673
Evaluation of solar wind data obtained from Pioneer 6, Mariner 5, and Explorer 35 for velocity variations, magnetopause motion, and geomagnetic disturbances
[NASA-CR-129880] 05 p0591 N73-14806
Relationship between radar scattering coefficient and ocean wind speed and direction
07 p0774 N73-16289
Analysis of factors affecting wind speed in lower atmosphere and application to structural design and aircraft operation
[ESDU-72026] 07 p0814 N73-16601
Geostationary satellite observation of convective tropical cloud trajectories and velocity
07 p0814 N73-16602
MHD equations for calculating joule heating and winds from geomagnetic storms in thermosphere
[NASA-CR-124071] 08 p0915 N73-17498
Calculation of interaction of penetratable shelter belts and ground air flow, including mean horizontal wind profiles and eddy viscosity coefficient
09 p1059 N73-18640
Influence of wind speed and directional variability on trajectory of unguided missile at WSMR, New Mexico
[AD-753348] 09 p1062 N73-18662
Average power spectra of zonal and meridional components of velocity for winter and summer
10 p1146 N73-19327
Steel construction design parameters for building and operating ZYKLON type wind driven power plants
[NASA-TT-F-14872] 12 p1388 N73-21253
Wind calculations of stratosphere in Northern Hemisphere at 100, 50, 30 and 10 mb
15 p1804 N73-24622
Development of method for remotely determining average transverse wind velocity and atmospheric structure constant along line of sight path
16 p1937 N73-25670
Coherence statistics of horizontal wind speed as measured by micrometeorological mast array
16 p1937 N73-25675
Numerical analysis of probability density of wind speeds and development of formula for distribution with two degrees of freedom
[ARL/SM-NOTE-383] 16 p1937 N73-25676
Doppler shift measurements at 16 GHz over transhorizon path to estimate tropospheric wind velocity
[AD-760119] 17 p1999 N73-26164
Influence of wind speed and direction, and temperature on radon gas concentration in atmosphere
17 p2017 N73-26309
Analysis of wind profiles in thunderstorm gusts and method for predicting velocity of winds at altitude
[NASA-CR-2289] 18 p2172 N73-27544
Remote determination profiles of atmospheric structure constants and wind velocity along line-of-sight path by statistical inversion procedure
[AD-760805] 18 p2173 N73-27552
Comparative analysis of upper troposphere maximum wind strength maps and ground surface synoptic maps
20 p2445 N73-29642
Influence of ground concentration, hilly terrain, and wind velocity on distribution of pollutants considering initial elevation
20 p2446 N73-29648
Exact solution to system of forecasting equations of barotropic divergent model of atmosphere
24 p2946 N73-33531
Gas flow and wind velocity in elliptical and cluster galaxies
24 p2978 N73-33795

**WIND VELOCITY MEASUREMENT**
Autocorrelation analysis of velocity structure temporal evolution in solar wind
01 p0094 N73-10775
High resolution radar system for measuring wind velocity and height of meteor trails
[NASA-CR-131644] 12 p1377 N73-21172
Upper atmospheric wind velocity and temperature measurements
[NASA-TT-F-14921] 14 p1659 N73-23470
Equipment and mission of Astrophysics Institute in Tadzhikistan relative to radar tracking and wind velocity measurement
[AD-756100] 14 p1706 N73-23848
PAPA Ocean Weather Station measurements of wind and wave condition in north Pacific Ocean
[AD-757982] 15 p1806 N73-24638
Two spaced radar measurement of wind characteristics in meteor zones
17 p2023 N73-26365

**WINDING**
NT FILAMENT WINDING
NT HELICAL WINDINGS
NT WIRE WINDING
Some six block coil configurations for cosine bending magnet
[BNL-16787] 03 p0336 N73-12740
Auxiliary corrective windings for increased resolution and decreased distortions in cathode ray tubes
[AD-751879] 08 p0889 N73-17201
Influence of epoxy resins on mechanical properties of superconducting windings
[RHEL/R-265-PT-2] 22 p2689 N73-31534

**WINDMILLING**
U AUTOROTATION

**WINDOWS [APERTURES]**
Thin film window for gas flow radioisotope proportional counter
[AD-745579] 01 p0058 N73-10477
Window material for high power carbon dioxide infrared lasers
[AD-746500] 02 p0182 N73-11473
Analysis of sonic boom data recorded on strain gages mounted on windows to record overpressures and relation to window size
[FAA-RD-72-114] 03 p0251 N73-12030
Observation window for internal gas confining chamber
[NASA-CASE-NPO-10890] 03 p0279 N73-12265
Effect of temperature and flange configurations on critical pressure of 90-degree conical acrylic windows for hydrostatic pressure vessels when subjected to short term loading
[AD-748583] 04 p0440 N73-13583
Analysis of fundamental absorption properties of laser window materials and limitations imposed by uncontrolled impurities
05 p0556 N73-14516
Pressure induced optical distortion in high power, infrared laser system windows and determination of figures of merit based on minimum thickness
05 p0556 N73-14517
Thermal lensing in infrared laser window materials
[AD-749481] 05 p0558 N73-14536
Evaluation of optical properties of high power laser window materials
[AD-749864] 05 p0559 N73-14540
Hardening characteristics of alkali halides selected as laser window materials
[AD-749867] 05 p0559 N73-14545
Mechanical properties of polycrystalline alkali halides determined for application to high power infrared laser windows
[AD-752193] 08 p0930 N73-17617
High resistivity gallium arsenide window material for high power carbon dioxide lasers emitting at 10.6 micrometers
[AD-752783] 09 p1048 N73-18550
Service life of mechanically prestressed glass used in spacecraft windows
09 p1088 N73-18880
Preparation, characterization, and evaluation of materials for infrared windows
[AD-754280] 10 p1169 N73-19512
Development of statistical prediction model for determining probability of glass breakage caused by sonic boom overpressures
[FAA-RD-73-79] 18 p2104 N73-27018
Apollo experience report on window structural design and verification for command and lunar modules
[NASA-TN-D-7439] 22 p2720 N73-31770
High power infrared window materials for laser applications
[AD-765354] 23 p2802 N73-32412
Polymer coatings for moisture protection of optical windows in infrared spectroscopy
[NASA-CASE-ARC-10749-1] 23 p2820 N73-32542
Absorption spectra of infrared window matrials
[AD-764904] 24 p2969 N73-33730

**WINDOWS [INTERVALS]**
Analysis of thermal lensing in high power laser window materials
[AD-751266] 07 p0808 N73-16554
Required doping levels for germanium and silicon infrared windows at microwave energies
[AD-753466] 09 p1075 N73-18772
Procedure for improving strength and fracture behavior of alkali halides for use as high energy laser window material
[AD-755716] 12 p1411 N73-21437

**WINDPOWERED GENERATORS**
Design, development, and operation of windpowered electric generators for commercial electric power applications
[NASA-TT-F-15068] 20 p2364 N73-29008
Development and construction of wind driven electric power generators for specific European areas
[NASA-TT-F-15050] 20 p2364 N73-29009
Development of aerodynamic transmission system for use with wind driven electric generators
[NASA-TT-F-15131] 22 p2618 N73-30976

**WINDS ALOFT**
NT GEOSTROPHIC WIND
NT JET STREAMS [METEOROLOGY]
Aperiodic processes and formation of seasonal temperature and wind fields in stratosphere in Northern Hemisphere, and tropospheric influences
[NLL-M-20086-[5828.4F]] 01 p0043 N73-10342
Ion drag and winds aloft in high latitudes
[NASA-TM-X-66083] 02 p0165 N73-11340

**WINDSCREENS**
U WINDSHIELDS

**WINDSHIELDS**
Procurement specification for space shuttle orbiter windshield pane and factors influencing development
[NASA-CR-112209] 05 p0600 N73-14882
Optimization of transparent ethylene terpolymer and compilation of engineering data for use as adhesive in polycarbonate composite aircraft transparencies
[AD-750814] 06 p0689 N73-15611
Development and testing of primary structural elements of windshield system for space shuttle orbiter
[NASA-CR-112234] 06 p0720 N73-15879
Development of organic glass and plastic materials with improved mechanical and physical properties for use with aircraft canopies and protective coatings
[AD-763263] 21 p2497 N73-30039

**WINDWARD**
U UPSTREAM
U WIND [METEOROLOGY]

**WING CAMBER**
Effects of wing camber and twist on longitudinal aerodynamic characteristics of wing-body configuration
[NASA-TN-D-7099] 04 p0369 N73-13002

**WING FLAPS**
NT LEADING EDGE SLATS
NT TRAILING-EDGE FLAPS
Comparison of mechanical high lift flaps with externally blown flaps for STOL aircraft
[MBB-UH-12-72-O] 07 p0739 N73-16017
Measurement of lift, drag, and pitching moments in wing section for range of flap deflections under two-dimensional flow conditions
[ARC-CP-1233] 09 p0981 N73-18018
Performance and noise reducing properties of thrust augmentors
[NASA-TM-X-62250] 13 p1472 N73-21921
Noise tests on large scale model of externally blown flap lift augmentation system using mixer nozzle
[NASA-TN-D-7236] 15 p1733 N73-24059
Development of data for numerical analysis of aerodynamic performance of jet, blown, and ejector flaps
[AD-763793] 21 p2498 N73-30049
Flight tests of modified F-100 aircraft to determine effectiveness of fast-acting flaps as direct-lift-control devices to improve station keeping
[NASA-TM-X-2936] 24 p2876 N73-32970

**WING LOADING**
Computation of loading on sweptback wings noting extra collocation points
[ARC-CP-1213] 03 p0247 N73-12002
Influence of load and wing load distribution on lateral and longitudinal maneuverability of aircraft
08 p0865 N73-16998
Analysis of point vortex approximation of vortex sheet in two space dimensions and application to vortex sheet induced by ellipitcally loaded wing
[AD-755007] 11 p1273 N73-20335
Theoretical calculation of generalized forces and load distribution on wings oscillating at general frequency in subsonic stream
[ARC-R/M-3710] 13 p1470 N73-21908
Effect of gust loads on wing and T-tail airworthiness requirements for short haul aircraft
[FOK-K-66] 16 p1859 N73-25058
Load near apex of lifting swept wing in linearized subsonic flow
[ARC-R/M-3716] 21 p2492 N73-30001
Iterative method for calculation of loading on thin rectangular wing
[ARC-R/M-3719] 21 p2492 N73-30004
Polar coordinate method applied to program for calculating aerodynamic loads on oscillating wing configurations in subsonic flow
[SAAB-L-0-R64] 21 p2493 N73-30006
The lift and stalling characteristics of a 35 deg sweptback wing designed to have identical chordwise pressure distributions at all spanwise stations when near maximum lift
[ARC-R/M-3721] 22 p2612 N73-30935

**WING OSCILLATIONS**
Surface pressure measurements over model delta wing undergoing oscillatory deformation in low speed wind tunnel
[ARC-R/M-3693] 03 p0248 N73-12005
Effect of Reynolds number and frequency on control-surface buzz at high subsonic speeds noting control of flap oscillation by air jets
[ARC-R/M-3702] 03 p0248 N73-12007
Finite difference solutions for oscillatory lift interference in slotted wind tunnel compressible and incompressible flow
[ARC-R/M-3700-PT-1-PT-2] 03 p0284 N73-12297
Procedures for calculating velocity potential and pressure distribution of planforms oscillating harmonically in supersonic flow
[FOK-X-440] 11 p1231 N73-19994
Calculation and measurement of aerodynamic forces on oscillating airfoil with and without aerodynamic stalling
12 p1361 N73-21042
Wind tunnel tests to determine subsonic derivatives for oscillating M-wing planform
[ARC-R/M-3214] 16 p1854 N73-25022
Development of numerical procedures for determining velocity potential on triangular wing oscillating harmonically in supersonic flow
[ARC-R/M-3229] 16 p1854 N73-25023
Design and characteristics of test equipment for measuring longitudinal oscillatory aerodynamic derivatives in high speed wind tunnel
[ARC-R/M-3260] 16 p1855 N73-25029
Application of oscillation theory and mathematical statistics to problems of aircraft structures and aerodynamic loads on aircraft and missiles
[NASA-TT-F-753] 19 p2220 N73-27908
Analytical representation of auxiliary functions of theory for oscillating lifting surface with high aspect ratio at subsonic speeds
[DLR-FB-73-16] 21 p2492 N73-29999
Polar coordinate method applied to program for calculating aerodynamic loads on oscillating wing configurations in subsonic flow
[SAAB-L-0-R64] 21 p2493 N73-30006

**WING PANELS**
Development of numerical analysis techniques for determining lifting surface characteristics of circular wings and parabolic wing tips
[AD-748433] 04 p0370 N73-13006
Numerical analysis of pressure distribution at parabolic wing tips on circular wing model based on occurrence of logarithmic sets
[AD-748432] 04 p0370 N73-13007
Wind tunnel tests of two dimensional wing model with leading edge slat and trailing edge flap
[FAA-AU-862] 08 p0863 N73-16984
Design, fabrication, and evaluation of boron-epoxy reinforced C-130 center wing boxes
[NASA-CR-112272] 14 p1601 N73-22979
Design analysis and fabrication of hypersonic wing test structure
[NASA-CR-127490] 24 p2988 N73-33883

**WING PLANFORMS**
NT DELTA WINGS
NT INFINITE SPAN WINGS
NT SWEPTBACK WINGS
NT VARIABLE SWEEP WINGS
Development of numerical method for designing minimum drag supersonic wing camber surfaces of arbitrary planform for given lift characteristics
[NASA-TN-D-7097] 04 p0369 N73-13001
Development of numerical analysis techniques for determining lifting surface characteristics of circular wings and parabolic wing tips
[AD-748433] 04 p0370 N73-13006
Wind tunnel tests to determine effect of wing planform on generation of sonic boom at various Mach numbers
[NASA-TN-D-7160] 06 p0700 N73-15709
Optimized design of supersonic aircraft wing based on linear combination of weight of wing and aerodynamic drag minimization
07 p0737 N73-15997
Development of analytical technique for computing performance of arbitrary jet-flapped wing with compensations for variations in wing geometry
[NASA-CR-2179] 08 p0863 N73-16982
Measurement of unsteady pressures developed on harmonically oscillating wing planform in three dimensional compressible flow
[DLR-FB-72-55] 09 p0980 N73-18007
Wind tunnel tests to determine flow characteristics of stalled two dimensional airfoil
[NASA-CR-130919] 09 p0982 N73-18020
Analysis of scaling parameters for flow in core region of vortex generated by rectangular wing tip and vortex generated by ogee wing tip
[NASA-CR-2180] 10 p1103 N73-18995
Development of computer program and algorithm for determining interference between lifting surface elements at various Mach numbers
[NASA-CR-112264] 12 p1390 N73-21272
Analysis of aerodynamic interference resulting from jet issuing normal to chordal plane of two dimensional wing in crossflow conditions
13 p1508 N73-22223
Analysis of pressure distribution and surface flow on half models of wings with curved tips and 60 degree sweepback
[ARC-R/M-3244] 15 p1726 N73-24001
Wind tunnel tests to determine effects of leading edge modifications on flow and forces on untapered wing with 50 degree leading edge sweep and Mach numbers from 0.60 to 1.20
[ARC-R/M-3270] 15 p1726 N73-24003
Analysis of flow pattern on tapered, sweptback wing at Mach numbers between 0.6 and 1.6 and 12 degree angle of incidence
[ARC-R/M-3271] 15 p1726 N73-24004
Measurements of roll damping derivative of three wing planforms using free light roll balance technique for Mach numbers from 0.7 to 1.4
[ARC-R/M-3274] 15 p1726 N73-24005
Wind tunnel tests to determine aerodynamic characteristics of model of sweptback wing with warp distribution to produce constant spanwise coefficient of lift
[ARC-R/M-3385] 15 p1727 N73-24007
Analysis of flow development over plane, half-wing with cropped-delta planform using surface pressure distributions and oil flow patterns with variations in incidence and Mach number
[ARC-R/M-3286] 15 p1727 N73-24008
Wind tunnel tests at Mach 2.0 to determine aerodynamic characteristics of cambered and uncambered gothic wings
[ARC-R/M-3211] 16 p1852 N73-25003
Development of formulas for calculating gradients and ordinates of camber surfaces of sweptback wings of arbitrary planform with subsonic leading edges and specified load distribution
[ARC-R/M-3217] 16 p1852 N73-25004
Wind tunnel tests to determine effect of interference on performance of full span jet flap mounted on trailing edge of high aspect ratio unswept wing
[ARC-R/M-3219] 16 p1852 N73-25005
Application of slender body theory for calculating minimum values of zero lift wave drag of slender wings with unswept trailing edge
[ARC-R/M-3222] 16 p1852 N73-25007
Design criteria for slender warped wings with unswept trailing edge with zero load along leading edge and near planar vortex sheet at trailing edge for design lift coefficient
[ARC-R/M-3406] 16 p1852 N73-25008
Analysis of effects of shock induced boundary layer separation in transonic flight and methods for eliminating or reducing effects
[ARC-R/M-3510] 16 p1854 N73-25019
Research projects in theoretical and practical aerodynamics - Vol. 2
16 p1854 N73-25020
Wind tunnel tests to determine subsonic derivatives for oscillating M-wing planform
[ARC-R/M-3214] 16 p1854 N73-25022
Development of numerical procedures for determining velocity potential on triangular wing oscillating harmonically in supersonic flow
[ARC-R/M-3229] 16 p1854 N73-25023
Numerical analysis of wing bending, wing torsion, and aileron rotation at transonic speeds to determine effects on wing-aileron flutter
[ARC-R/M-3258] 16 p1855 N73-25028
Numerical analysis of lift and lift distribution on aircraft wing and trailing vortex flow behind wing
[AD-759262] 16 p1863 N73-25089
Comparison of linearized theories to determine aerodynamic characteristics of slender wings in supersonic flow
[RAE-LIB-TRANS-1677] 17 p1981 N73-26010
Aerodynamic characteristics of slender delta wings to show performance under various conditions of airspeed, angle of attack, and ground effect
[NASA-TT-F-14949] 17 p1983 N73-26031
Numerical analysis of supercritical flow about C-141 aircraft wing using finite difference, relaxation algorithm
[NASA-TN-D-6933] 19 p2217 N73-27889
Aerodynamic characteristics of high lift wing concepts for application to commercial short takeoff transport aircraft
20 p2479 N73-29908
Design of aircraft with rotatable wing for producing high speed aerodynamic configuration
[NASA-CASE-ARC-10470-2] 21 p2494 N73-30018
Wind tunnel tests to determine transient wake velocities behind three stalled wing configurations at Reynolds numbers up to 4.8 million
[AD-763468] 21 p2498 N73-30050
Wind tunnel tests to determine aerodynamic characteristics of three oblique, high aspect ratio wing and body combinations at Mach numbers between 0.60 and 1.40
[NASA-TM-X-62256] 24 p2869 N73-32926
Wind tunnel tests to determine aerodynamic characteristics of oblique wing and body combination at Mach numbers between 0.60 and 1.40
[NASA-TM-X-62207] 24 p2870 N73-32927
Aerodynamic characteristics of augmentor wings and analysis of augmentation and entrainment in defining a net thrust coefficient
24 p2872 N73-32942
Simulations of powered-lift STOL transport aircraft with either externally blown flap configuration or augmentor wing configuration
24 p2873 N73-32948
Flight tests of augmentor-wing jet STOL research aircraft to compare wind tunnel data with flight data for dynamic characteristics and limitations
24 p2874 N73-32954
Wind tunnel tests to determine acoustic properties of externally blown flap and augmentor wing for short takeoff aircraft configurations
24 p2875 N73-32965

**WING PROFILES**
NT WING SPAN
Wind tunnel tests to determine effect of simulated hoar frost on lift coefficient of three aircraft wing configurations
[FFA-AU-902] 01 p0001 N73-10001
Measurement of lift, drag, and pitching moments in wing section for range of flap deflections under two-dimensional flow conditions
[ARC-CP-1233] 09 p0981 N73-18018
Aerodynamic characteristics of flow around wing profiles
[AD-752686] 09 p0987 N73-18054
Numerical analysis of nonlinear elliptic-hyperbolic mixing about wing profiles at Mach 1
14 p1597 N73-22944
Aerodynamic forces, pressure distribution, and wakes of wing profile with trailing edge flaps and leading edge slats
24 p2906 N73-33187

**WING ROOTS**
Ultrasonic inspection of wing spar joints and lugs on Viscount Aircraft
[TR-7207.591] 05 p0551 N73-14472
Development of continual solution for stress distribution due to thermal stresses near roots of rectangular wings
[ARC-R/M-3236] 15 p1730 N73-24030

**WING SLATS**
U LEADING EDGE SLATS

**WING SLOTS**
Development of nonlinearized solution for aerodynamic characteristics of jet flap lifting surface with span-wise slot near trailing edge
[NASA-CR-2190] 07 p0736 N73-15986

**WING SPAN**
Effect of wing span loading on wing trailing vortices
[AD-754055] 11 p1232 N73-20003

**WING STALL**
U BOUNDARY LAYER SEPARATION

**WING TIPS**
Results of analytical methods for predicting wing vortex strength compared with results of flight investigation of wake characteristics of several large jet transport aircraft
[NASA-TN-D-6904] 03 p0251 N73-12033
Development of numerical analysis techniques for determining lifting surface characteristics of circular wings and parabolic wing tips
[AD-748433] 04 p0370 N73-13006
Numerical analysis of pressure distribution at parabolic wing tips on circular wing model based on occurrence of logarithmic sets
[AD-748432] 04 p0370 N73-13007
Analysis of scaling parameters for flow in core region of vortex generated by rectangular wing tip and vortex generated by ogee wing tip
[NASA-CR-2180] 10 p1103 N73-18995
Analysis of pressure distribution and surface flow on half models of wings with curved tips and 60 degree sweepback
[ARC-R/M-3244] 15 p1726 N73-24001
Wing tip vortex measurements with laser Doppler velocimeter
[NASA-CR-124444] 24 p2869 N73-32924

**WINGED ROCKET BOOSTERS**
U LAUNCH VEHICLES

**WINGS**
NT CAMBERED WINGS
NT CARET WINGS
NT CRUCIFORM WINGS
NT DELTA WINGS
NT FIXED WINGS
NT FLEXIBLE WINGS
NT INFINITE SPAN WINGS
NT LIFTING ROTORS
NT LOW ASPECT RATIO WINGS
NT PARAWINGS
NT RECTANGULAR WINGS
NT RIGID ROTORS
NT RIGID WINGS
NT RING WINGS
NT ROTARY WINGS
NT SLENDER WINGS
NT SWEPT WINGS

NT SWEPTBACK WINGS
NT THIN WINGS
NT TILTING ROTORS
NT TIP DRIVEN ROTORS
NT UNCAMBERED WINGS
NT UNSWEPT WINGS
NT VARIABLE SWEEP WINGS
Interference of wing and propeller streams
[AD-745916] 02 p0124 N73-11008
Analysis of forces imposed on aircraft wing from landing gear impact in relation to weight of wing, damping, and frequency of periodic load
[AD-747381] 03 p0254 N73-12052
Design, fabrication, and flight tests of boron-epoxy reinforced C-130E center wing boxes
[NASA-CR-112126] 04 p0370 N73-13011
Development of auxiliary lifting system to provide ferry capability for entry vehicles
[NASA-CASE-LAR-10574-1] 04 p0400 N73-13257
Development of computer program for generating aerodynamic forces for plane and interfering wings at supersonic speeds
[NASA-CR-112184] 04 p0404 N73-13290
Wing impulse theory applied to determination of propeller slipstream influence on wing aerodynamic characteristics, using airfoil of finite span
[AD-749726] 05 p0498 N73-14051
Flutter characteristics of thin cantilever wings at transonic and supersonic speeds
[NAL-TR-288] 06 p0618 N73-15022
Supersonic aerodynamic influence coefficients for isolated and parallel interfering coplanar and non-coplanar wings
[NASA-CR-2168] 09 p0979 N73-18003
Calculation of wind tunnel wall interference velocities affecting pitching moments of high lift wings
[NASA-CR-2191] 10 p1137 N73-19269
Comparisons between analog and numerical methods for studying response of an aircraft
[PUBL-97] 12 p1357 N73-21007
Standardized load sequence for flight simulation tests on transport aircraft wing structures
[LBF-BERICHT-FB-106] 14 p1602 N73-22986
Analysis of structural reliability of large scale bonded joints for advanced composite wing to determine service life of boron epoxy to titanium scarf joint
[AD-756893] 14 p1603 N73-22995
Tangent milling and spline approximation techniques for wings
[NAL-TN-33] 15 p1792 N73-24524
Wind tunnel interference factors for high lift wings in closed wind tunnels
16 p1851 N73-24996
Automated design optimization of supersonic airplane wing structures under dynamic constraints
[NASA-CR-112319] 16 p1866 N73-25063
Effects of wing structural elasticity on accumulation of fatigue damage during aircraft flight in turbulence
[AD-759634] 16 p1862 N73-25082
Computer program for designing minimum mass wings under flutter, strength and minimum gage constraints
[NASA-TN-D-7264] 17 p2092 N73-26927
Wing anomalies as result of weightlessness simulation for flour beetle Tribolium confusum
19 p2226 N73-27952
Strain gage bridge calibrations on wing structure at elevated temperatures to establish thermal and mechanical loads due to aerodynamic heating
[NASA-TN-D-7390] 19 p2348 N73-28883
Procedures for ultrasonic inspection of wing attachment fittings on Viscount aircraft
[TR-7211.621] 20 p2422 N73-29455
Numerical analysis of laminar boundary layer on slipping wing
[AD-763285] 21 p2526 N73-30255
Kutta-Joukowski condition for describing three dimensional flow over arbitrary wing
[RAE-LIB-TRANS-1709] 24 p2905 N73-33185
**WINTER**
Variability of temperature field of troposphere, stratosphere, and mesosphere in winter
04 p0442 N73-13606
Application of ERTS-1 imagery to study of caribou movements and winter dispersal in relation to prevailing snow cover
[E72-10346] 05 p0533 N73-14334
Investigation of thunderstorm potential in cold air cumulonimbi over northwestern Europe during winter
[AD-749493] 05 p0574 N73-14674
Average power spectra of zonal and meridional components of velocity for winter and summer
10 p1146 N73-19327
Identification of winter wheat on irrigated land in southern Finney County, Kansas
[E73-10475] 12 p1395 N73-21312
Anomalous F region ionization patterns during winter in dark ionosphere in polar regions
13 p1520 N73-22318
Application of ERTS-1 imagery to study of caribou movements and winter dispersal in relation to prevailing snow cover in Alaska
[E73-10615] 15 p1774 N73-24376
Ionospheric total electron content during magnetic storm, 14-17 Dec. 1971
[KGO-728] 18 p2146 N73-27344
ERTS-1 imagery of caribou movements and winter habitats in Alaska in relation to prevailing snow cover
[E73-10840] 19 p2290 N73-28418
Energetics of transient zonal and planetary scale waves in wintertime lower stratosphere investigated using surface spherical harmonics
20 p2389 N73-29193
Winter atmospheric circulation over European sector of Northern Hemisphere in twentieth century
[NLL-M-2337-[5828.4F]] 20 p2391 N73-29205
Solar magnetic sector structure related to earth atmospheric circulation during winter
[NASA-CR-133850] 21 p2593 N73-30774
**WIRE**
NT ELECTRIC WIRE
NT EXPLODING WIRES
NT GUY WIRES
Superconductivity of multifilamentary wires consisting of vanadium silicates
[BNL-16891] 03 p0346 N73-12818
Readout electronics and systems for proportional wire chambers
[JINR-P13-6380] 04 p0422 N73-13441
Microwire casting development and technology in USSR
[JPRS-57655] 04 p0426 N73-13473
Electrical resistance butt welder for welding fine gauge tungsten/rhenium thermocouple wire
[NASA-CASE-LAR-10103-1] 05 p0550 N73-14468
Elastic-plastic solution for calculating influence of energy dissipation on drawn wire fatigue
[AD-752017] 08 p0928 N73-17600
Computerized simulation of aerodynamic characteristics for trailing wire system towed by orbiting aircraft
[AD-753909] 10 p1136 N73-19255
Design and performance of wire grid temperature probes for flowing media
11 p1294 N73-20500
Printed circuit wiring patterns by efficient automatic procedures
[AD-754451] 11 p1301 N73-20553
Development of nickel-iron plated wires for computer memories
[ME-72-6] 13 p1498 N73-22139
Characteristics of photoelectric pyrometer for measuring temperature of thin wire during rolling process
[NLL-M-21634-[5828.4F]] 15 p1785 N73-24471
Aluminum ribbon wire for ultrasonic bonding of semiconductor microelectronic interconnections
[AD-758981] 16 p1881 N73-25223
Modulus of elasticity measurements on materials at elevated temperatures
[AD-759060] 16 p1971 N73-25941
Friction and lubrication in steel wire drawing
[NLL-RTS-7851] 21 p2552 N73-30454
Stress-strain diagrams and mechanical properties of metal wires as determined by tranverse impact method
[AD-764105] 22 p2687 N73-31523
Supersonic wind tunnel tests on three dimensional turbulent boundary layer growth on wires leading to calculation of tension and skin friction on aircraft towlines
[ARC-CP-1235] 23 p2740 N73-31933
Laser vaporization of aluminum wire and heating to thermonuclear temperatures
23 p2800 N73-32392
Metal matrix composites with Ni and NiCr20 matrix materials, and Al2O3, SiC, W, and Mo reinforcing fibers
[BMFT-FB-T-73-08] 23 p2810 N73-32471
Twisted wire or tube superconductor for filament windings
[NASA-CASE-LEW-11015] 23 p2823 N73-32571
Interactions between fluid flow and mechanical oscillators, using vibrating steel wire and cylindrical body
[DLR-FB-73-42] 24 p2909 N73-33218
**WIRE BRIDGE CIRCUITS**
NT WHEATSTONE BRIDGES
**WIRE CLOTH**
Effectiveness of braided wire electromagnetic shielding against magnetic field penetration
[AD-761823] 19 p2246 N73-28111
**WIRE MESH**
U WIRE CLOTH
**WIRE WINDING**
Analysis of stresses in magnet windings due to thermal contraction and temperature gradient stresses and impregnation with epoxy resins to reduce effects
[RHEL/R-264-PT-1] 20 p2435 N73-29558
**WIRELESS COMMUNICATIONS**
Multiple phase shift keying communications for improving carrier tracking efficiency and data detection performance
[NASA-CASE-NPO-13103-1] 11 p1255 N73-20180
Characteristics of noise-resistant receiver for wireless electrical communication circuit for drill speed measurement
[AD-756090] 13 p1495 N73-22122
Silent alarm system for mutiple room facility or school
[NASA-CASE-NPO-11307-1] 21 p2519 N73-30205
**WIRING**
NT BEAM LEADS
Reliability of semiconductor devices as influenced by quality of aluminum wire bonds used in assembly
[NASA-CR-124037] 09 p1038 N73-18469
Computer program for producing and updating wiring lists for use in development and production of electronic equipment
[ECR-31] 12 p1386 N73-21239
Improved spectral digital frequency synthesizer
[AD-756864] 13 p1501 N73-22164
Flat conductor cabling system for electrical/electronic interwiring
14 p1641 N73-23305
Fast heuristic techniques for placing and wiring printed circuit boards
24 p2898 N73-33134
**WIRING SYSTEMS**
U WIRING
**WISCONSIN**
Application of ERTS-1 imagery to regional land use planning in Wisconsin
[E72-10299] 04 p0411 N73-13349
Automatic identification of land uses in Milwaukee, Wisconsin using ERTS-1 imagery
[E72-10307] 04 p0412 N73-13356
Comprehension and use of weather forecasts by Wisconsin agricultural groups
06 p0692 N73-15639
Impact of accurate long range weather forecasts on Wisconsin pea production
06 p0693 N73-15640
Application of ERTS-1 imagery to regional land use planning in Wisconsin
[E73-10077] 08 p0900 N73-17290
Application of ERTS-1 imagery to regional land use planning in Wisconsin
[E73-10448] 11 p1283 N73-20408
Evaluation of ERTS-1 image data compression technique
[E73-10717] 17 p2019 N73-26324
Utilization of ERTS-1 data for inventory of critical land resources for regional land use planning in Wisconsin
[PAPER-L16] 19 p2275 N73-28311
Preparation of urban land use inventories of Wisconsin and Indiana by machine-processing of ERTS-1 MSS data
[PAPER-L19] 19 p2275 N73-28314
Analysis of Milwaukee county, Wisconsin land use by machine processing of ERTS-1 remotely sensed data
[NASA-CR-133643] 20 p2412 N73-29385
Snow and fresh water lake ice interpretations from ERTS-1 imagery of Whitefish Bay, Michigan and Green Bay, Wisconsin
[E73-11129] 24 p2917 N73-33284
**WOOD**
Emission of air pollutants from combustion of wood wastes
[WSCI-72-1] 23 p2856 N73-32821
**WOOD AIRCRAFT CONSTRUCTION**
U AIRCRAFT STRUCTURES
U WOODEN STRUCTURES
**WOODEN STRUCTURES**
X ray fluorescence analysis of impregnating solutions for wooden communication poles containing As, Cu, Cr, F and B
[FTZ-A-518-TBR-1] 22 p2626 N73-31037
**WORDS [LANGUAGE]**
NT MESSAGES
NT SYLLABLES
Color naming latencies with brief exposures of individual Stroop and control stimuli
[AD-745106] 01 p0012 N73-10094
Recognition and parsing algorithms for phrase structure languages
[NLL-SMRE-TRANS-5884-[8313.4]]
06 p0643 N73-15219
Real time, adaptive isolated-word speech recognition system using minicomputer to time normalize word duration
14 p1622 N73-23141
Word recognition by Walsh transform computer program
14 p1622 N73-23143
Word recognition system based on dimensional representation of phoneme-like word segments
14 p1623 N73-23145
Automatic speech recognition program to provide segmentation, acoustical parameters, and phonetic feature classifications in speech
14 p1623 N73-23146
Perceptive evaluation of acoustic signal parts displaying rapid changes and short durations
14 p1625 N73-23170
Automatic segmentation of repeated utterances of isolated words
14 p1628 N73-23193
Mechanical recognition of spoken words by incomplete learning samples
14 p1628 N73-23198
Digital pattern classification for automatic recognition of English language speech
[AD-757492] 14 p1636 N73-23262

Elastic matching, automatic error correction in English language words of any length
[NPL-COM-SCI-63-SUPPL] 18 p2121 N73-27144
**WORK**
NT PHYSICAL WORK
**WORK CAPACITY**
Optimization of work-rest cycles to ensure acceptably high human performance in man machine systems
[AD-750176] 05 p0504 N73-14107
Time-span of discretion as measure of military work and responsibility
[DRAE-M45] 13 p1486 N73-22049
**WORK DECREMENT**
U WORK CAPACITY
**WORK FUNCTIONS**
Fabrication processes for silicon Schottky barrier diodes
[FRNC-TH-179] 03 p0274 N73-12218
Materials and devices for generation, amplification, and millimeter wave energies
[NASA-CR-130113] 03 p0334 N73-12724
Measurements of work function of {110} and {111} faces of crystal from solid solution of osmium in tungsten
[NLL-TRANS-746-1315-[9022.401]] 05 p0585 N73-14760
Gallium arsenide Schottky and varactor diodes for 20 and 30 GHz 07 p0762 N73-16192
Schottky barrier diodes for electron beam semiconductor applications
[AD-757749] 15 p1757 N73-24240
Measurement of work functions of copper and copper-nickel single crystals at low pressures and determination of thermionic emission constant 16 p1927 N73-25593
Temperature relationship of work function of silicon carbide for application to direct conversion of thermal energy to electrical energy 23 p2807 N73-32443
**WORK HARDENING**
NT STRAIN HARDENING
Development of method for classifying stresses in isotropic work hardening media using polarized light
[NLL-M-21475-[5828.4F]] 02 p0236 N73-11918
Forming and subsequent mechanical properties of high strength work hardened sheet materials
[PB-212207] 08 p0932 N73-17634
Yielding, work hardening, and fracture behavior of ordered and disorded alloys as function of dislocation
[ORO-3935-25] 21 p2559 N73-30514
Theory of elasto-plastic flow applied to work hardening, anisotropy, plastic compressibility and noncontinuous loading in Quasi-linear form
[NASA-CR-2321] 24 p2989 N73-33886
**WORK-REST CYCLE**
Analysis of arterial hypoxemia caused by pulmonary malfunctions and regulation of oxygen during exercise and rest
[AD-746979] 04 p0380 N73-13092
Optimization of work-rest cycles to ensure acceptably high human performance in man machine systems
[AD-750176] 05 p0504 N73-14107
Industrial model for leave and overtime taking behavior of employees exposed to peak work activity periods in relation to health, demography, and job variables 08 p0872 N73-17055
Role of social synchronizers in adaptation process of humans to inversion of diurnal sleep and wakefulness regime 11 p1245 N73-20109
Work-rest schedules for military tracking crews under prolonged vibration 14 p1723 N73-23986
Work-rest schedule for optimum performance of monitoring tasks 14 p1723 N73-23987
Effects of work-rest schedules, circadian rhythms, continuous work, and sleep loss on sustained performance 14 p1723 N73-23988
Physiological response to prolonged muscular activity 14 p1724 N73-23990
Phytological and physiological problems caused by rest-work cycles of cosmonauts during space flight
[NASA-TT-F-14990] 17 p1990 N73-26093
Human body temperature dynamics in adaptation to changed work-sleep cycles 20 p2367 N73-29036
Scheduling of work-rest cycle for cosmonauts during space flights 22 p2618 N73-30984
**WORLD**
U EARTH {PLANET}
**WORLD DATA CENTERS**
Catalog of data in World Data Center C2 for Geomagnetism 14 p1658 N73-23456
Origin, development and prospects of World Weather Watch noting role to be played by meteorological satellites and GARP 24 p2949 N73-33551
**WORMS**
Physiological responses of parasitic worms and their larvae to solar ultraviolet irradiation and space flight stress 15 p1740 N73-24106
**WRANGELL MOUNTAINS [AK]**
Glaciology and volcanology on Wrangell Mountains, Alaska
[E72-10339] 05 p0532 N73-14327
Glaciology and volcanology studies in Wrangell Mountains, Alaska using ERTS-1 imagery
[E73-10277] 08 p0914 N73-17485
ERTS-1 imagery of glaciology and volcanology in Wrangell Mountains, Alaska
[E73-10404] 11 p1277 N73-20366
Glaciology and volcanology in Wrangell Mountains, Alaska based on ERTS-1 imagery
[E73-10665] 16 p1899 N73-25360
ERTS-1 imagery of snow cover on northern foothills of Brooks Range and Wrangell Mountains, Alaska 19 p2285 N73-28374
Geology, volcanology, and glaciology of Wrangell Mountains, Alaska from ERTS-1 imagery
[E73-10940] 21 p2529 N73-30282
**WRENCHES**
Tool exchange capabilities of portable wrench characterized by telescopic sleeve
[NASA-CASE-MFS-22283-1] 21 p2553 N73-30462
**WRINKLING**
NT FLANGE WRINKLING
**WROUGHT ALLOYS**
Analysis of volume changes in composite wrought iron associated with fiber buckling
[AD-749711] 05 p0567 N73-14606
High temperature research on effects of chemical variation and processing variables on properties of wrought cobalt-base-NASA alloy
[NASA-CR-121189] 12 p1414 N73-21457
**WU-2 AIRCRAFT**
U U-2 AIRCRAFT
**WYOMING**
NT BIGHORN MOUNTAINS [MT-WY]
NT BLACK HILLS [SD-WY]
NT WIND RIVER RANGE [WY]
NT YELLOWSTONE NATIONAL PARK [ID-MT-WY]
Mapping iron compounds in Wind River Range using ERTS-1 multispectral scanner imagery
[E72-10181] 01 p0045 N73-10360
Inventory and management of geological, botanical, and agricultural resources in Wyoming using satellite and airborne imagery and ground control data
[E72-10229] 02 p0163 N73-11322
Preparation of hydrologic atlases of arid land watersheds using ERTS-1 imagery of Wyoming, Utah, Montana, and New Mexico
[E72-10240] 03 p0288 N73-12340
Physical and hydrometeorological characteristics of Snowy Range Observatory, including precipitation, temperature, solar radiation, and wind data
[PB-211618] 05 p0524 N73-14268
Tectonic analysis of Southwestern Wyoming from ERTS-1 imagery
[E72-10337] 05 p0532 N73-14325
Application of ERTS-1 imagery to evaluation and management of Wyoming natural resources
[E73-10037] 07 p0776 N73-16300
Distinguishing major lithologic types in rocks of Precambrian age in central Wyoming using multilevel sensing
[E73-10301] 09 p1021 N73-18333
Utilization of ERTS-1 imagery for mapping extent of Pleistocene glaciation and delineation of small urban areas in Wyoming
[E73-10425] 11 p1280 N73-20386
Utilization of ERTS-1 remotely sensed imagery for land use evaluation and planning in Power River Basin, Wyoming 14 p1653 N73-23407
Preparation for multidisciplinary study of Wyoming test sites using EREP remotely sensed data from Skylab
[E73-10552] 14 p1655 N73-23425
Broad scale application of ERTS-1 imagery to study and mapping of geological, hydrological, land use, rangelands, and soil cultures in Wyoming
[E73-10554] 14 p1655 N73-23426
Ratio mapping iron ore deposits in Atlantic City District, Wyoming
[E73-10575] 15 p1772 N73-24355
ERTS-1 imagery of linear fractures in Precambrian rocks of Laramie Mountains, Wyoming
[E73-10663] 16 p1899 N73-25359
Analysis of Skylab and EREP coverage of Wyoming and characteristics of field photometer system for measuring object reflectances
[E73-10697] 16 p1903 N73-25389
ERTS-1 imagery of Bighorn-Pryor mountains of Wyoming and Montana applied to analysis of regional tectonic relationships
[E73-10704] 16 p1903 N73-25395
Application of ERTS-1 imagery for recognizing and mapping alpine glacial features in mountains of northwestern Wyoming
[PAPER-G14] 19 p2265 N73-28245
Land use inventory and mapping in Wyoming from ERTS-1 data
[PAPER-L13] 19 p2274 N73-28309
Application of ERTS-1 imagery to geologic, hydrologic, agricultural, botanical, and land use studies in Wyoming
[E73-10844] 19 p2291 N73-28422
Regional environmental impact from oil shale development on private and public lands in Wyoming, Colorado, and Utah - Vol. 1
[EIS-AA-72-5242-D-1-VOL-1] 20 p2410 N73-29367
Energy alternatives to prototype oil shale leasing program for Wyoming, Colorado, and Utah - Vol. 2
[EIS-AA-72-5242-D-2-VOL-2] 20 p2410 N73-29368
Description of proposed leases for oil-shale program in Wyoming, Utah, and Colorado, and potential environmental impacts - Vol. 3
[EIS-AA-72-5242-D-3-VOL-3] 20 p2410 N73-29369
Geology of photo linear elements, Great Divide, Wyoming
[E73-10958] 21 p2532 N73-30300
ERTS-1 imagery of geology, botany, agriculture, hydrology, and cultural features of Wyoming
[E73-11022] 22 p2661 N73-31326
Ratio scannergrammetry of geology in Wyoming and South Dakota
[E73-11096] 24 p2914 N73-33253
Application of Skylab EREP data to structural geology, geomorphology, vegetation mapping, and land use studies in Wyoming
[E73-11136] 24 p2917 N73-33291
**W2F AIRCRAFT**
U E-2 AIRCRAFT

# X

**X BAND**
U SUPERHIGH FREQUENCIES
**X RAY ABSORPTION**
X ray attenuation coefficients in absorption spectra of titanium, iron, cobalt, nickel, copper, and zinc
[UCRL-73923] 10 p1189 N73-19675
X ray reflection efficiency of nickel coated quartz optical flats
[NASA-TM-X-64747] 15 p1813 N73-24694
Anomalous X ray transmission through single germanium crystals 16 p1952 N73-25793
Low energy X ray absorption and electron ionization cross section measurements on solids
[CONF-720404-VOL-2] 19 p2322 N73-28683
**X RAY ANALYSIS**
Empirical corrections for quantitative multi-element analyses using combined wavelenth- and energy-dispersive systems
[NASA-TM-X-66103] 02 p0137 N73-11113
Defect structures of GaAs by transmission and black reflection X ray topographic analysis
[AD-746895] 03 p0337 N73-12747
Modified programming language for X ray diffraction analysis by special purpose computer using internal counting
[AD-748828] 04 p0459 N73-13747
Neutron diffraction and single crystal X ray determination of rare earth-cobalt-iron intermetallic magnetic structure
[AD-748429] 04 p0460 N73-13754
X ray analysis to determine occurrence of metal surface texturing as result of sliding friction
[NASA-TN-D-7136] 06 p0677 N73-15508
X ray and electron energy spectroscopy for analysis on band structure of materials
[NAL-SR-1] 06 p0699 N73-15703
Surveyor 3 lunar probe television mirror pit X ray analysis and scanning electron microscopy for micrometeoroid impact study
[ONERA-NT-01-15] 07 p0847 N73-16864
X ray crystallographic methods for studying preferred orientation of hexagonal metals
[RFP-TRANS-117] 11 p1306 N73-20594
X ray and electron microscopic analysis of vacuum environment effects on 7075-T6 Al alloy fatigue life, fatigue-crack-growth behavior, and fracture toughness
[NASA-TM-X-69223] 12 p1413 N73-21450
Analysis of precipitation process in cobalt-tungsten-titanium alloys using electron microscope and X ray imaging techniques 13 p1541 N73-22483
X ray Mossbauer study of strengthening properties of laves phases in austenitic steels
[JPRS-58852] 13 p1543 N73-22503

Mass spectrometer, chromatograph, and X ray analyses for determining volatilization mechanism for V2O5
[NLL-M-21570-[5828.4F]] 16 p1926 N73-25582
Metallographic and X ray analysis of metastable alloys of titanium
[AD-759387] 16 p1931 N73-25623
X ray fluorescence analysis of toxic heavy elements
[CONF-721134-1] 17 p1992 N73-26106
X ray diffraction analysis of single crystals of high purity copper subjected to shock loading
[AD-762146] 19 p2311 N73-28586
Flourescent X ray spectrography of low alloy steel specimens to determine presence of eight elements
[BM-RI-7773] 20 p2433 N73-29539

**X RAY APPARATUS**
Device and method for determining X ray reflection efficiency, scattering properties, and surface finish of optical surfaces
[NASA-CASE-MFS-20243] 04 p0449 N73-13662
Application of multichannel analyzer with lithium drifted silicon detector to determine spectral distribution of low energy X ray devices
[BDX-613-704] 04 p0450 N73-13672
X ray apparatus for investigating hydrogen induced changes in fine crystalline structure of Ni powders and electrolytic films
[NLL-TRANS-746-1294-[9022.401]] 05 p0505 N73-14113
Design and fabrication of X ray diffractometer and application to determination of residual stresses in polycrystalline samples
[NAL-TN-34] 06 p0672 N73-15467
X ray device for measuring titanium tritide film thickness in presence of background radiation
[NASA-TM-X-68170] 06 p0673 N73-15475
OSO-5 X ray detector measurement of diffuse cosmic ray energy spectrum from 14 to 200 keV
[NASA-TM-X-66252] 15 p1828 N73-24815

**X RAY ASTRONOMY**
NT X RAY SOURCES
Bibliography of articles on cosmic X ray astronomy from Astrophysical Journal
[NASA-TM-X-64705] 02 p0230 N73-11869
X ray sources in galactic center and comparison of Aerobee data with Uhuru data
[NASA-TM-X-66114] 03 p0353 N73-12873
High resolution X ray astronomy using rocketborne telescopes
[NASA-CR-130166] 03 p0357 N73-12912
Coaxial anode scheme for reducing background of X ray astronomy proportional counter
[NASA-CR-130127] 04 p0421 N73-13432
Short-term temporal studies of X ray emission from Cas A, Tycho and X-1
[NASA-TM-X-66127] 04 p0466 N73-13802
Influence of space technology on X ray astronomy 04 p0473 N73-13856
Gamma, X ray, ultraviolet, and infrared astronomy noting instrumentation and radiative transfer
[ESRO-SP-75] 04 p0476 N73-13889
Balloon-borne X ray telescope survey of Cygnus region on 10 June and 17 July 1969 in 20 to 300 keV energy range 07 p0840 N73-16804
Design and fabrication of payloads for sounding rockets for use in X ray astronomy
[NASA-CR-130749] 08 p0959 N73-17845
Research in X ray, solar, and radio astronomy
[AD-756459] 15 p1833 N73-24860
High resolution solar X ray astronomy from Aerobee rockets
[NASA-CR-132984] 16 p1959 N73-25849
X ray astronomy from sounding rockets
[NASA-CR-133211] 16 p1963 N73-25880
Surface brightness and X ray measurements of Cygnus Loop from Aerobee rocket
[NASA-CR-133098] 17 p2080 N73-26822
Rocket-borne survey of Cygnus region in energy range from 2 to 20 keV 17 p2081 N73-26831
Conference on X ray experiments onboard different astronomical observatories for galactic and extragalactic X ray source position and size determination
[ESRO-SP-87] 17 p2084 N73-26855
X ray astronomy and its impact on galactic and extragalactic radio source mapping 17 p2084 N73-26856
OAO-C X ray experimental design 17 p2084 N73-26857
UK-5 X ray experimental design performance 17 p2084 N73-26858
Small Astronomy Satellite-C equipment for X ray source location and flow energy spectral analysis 17 p2084 N73-26859
X ray Astronomical Netherlands Satellite experimental design for soft and hard source identification and spectral analysis 17 p2084 N73-26860
OSO-1 experimental design for cosmic X ray sources identification and diffusion background radiation spectroscopy 17 p2084 N73-26861
OSO-1 graphite crystal polarimeter for stellar X ray astronomy 17 p2084 N73-26862
Corsa 1 and 2 instruments, experimental design, and data systems for X ray astronomy 17 p2084 N73-26864
HEAO-A integrated modulation collimator experiment for determining angular sizes and celestial position of X ray sources 17 p2085 N73-26867
HEAO-C soft X ray telescope 17 p2085 N73-26873
Comparison of HELOS mission with other X ray astronomy missions 17 p2085 N73-26874
Mission objectives of German astronomical satellite, noting X ray astronomy, IR and UV experiments
[BMBW-FB-W-72-25] 23 p2851 N73-32786

**X RAY DENSITY MEASUREMENT**
Studies of solar X ray fluxes during total eclipse of 7 March 1970
[NASA-CR-130698] 08 p0959 N73-17843
Supersonic two phase air-water flows, noting expansion, acoustic velocity and X ray density measurements, and nozzle flow tests
[BMVG-FBWT-73-4] 14 p1650 N73-23380

**X RAY DIFFRACTION**
Error analysis on residual stress location for X ray diffraction analyses on crystal lattices
[AD-746488] 01 p0089 N73-10732
Structural properties of glass, using X ray and neutron diffraction methods
[AD-747311] 02 p0194 N73-11568
X ray diffraction analysis of crack propagation in deformed, notched, wedge shaped silicon crystal
[AD-746275] 03 p0346 N73-12820
Modified programming language for X ray diffraction analysis by special purpose computer using internal counting
[AD-748828] 04 p0459 N73-13747
X ray diffraction pattern and electron microscopy of polycarbonate filled with MoS2
[AD-749731] 05 p0567 N73-14604
Standard X ray powder diffraction patterns
[NBS-MONO-25-SECT-10] 05 p0586 N73-14767
X ray and electron diffraction analysis of A[3]B[5] semiconductor crystal structure
[AD-750966] 06 p0709 N73-15787
Topographic interpretation of uranium alloy X ray diffraction patterns
[SC-T-72-2467] 10 p1173 N73-19543
Volumetric factor of precipitation phase causing X ray diffraction fading in alloys
[JPRS-58761] 12 p1414 N73-21455
Polyacrylonitrile precurser fibers for conversion to high modulus, high strength fibers using X ray diffraction analysis
[AD-755351] 13 p1549 N73-22550
Effects of successive concave optical gratings in spectrograph on X ray diffraction patterns
[AD-757014] 13 p1560 N73-22640
X ray diffraction analysis of Al based rare earth alloys with potential permanent properties
[AD-756245] 14 p1698 N73-23776
X ray diffraction analysis of VIA, B-1900, 713C, and 738X alloy composition after oxidation at high temperature
[NASA-TM-X-2796] 16 p1927 N73-25596
X ray analyses of atomic structures in diffusion zones of copper nickel alloys and copper silver alloys
[AD-759195] 16 p1930 N73-25616
Remote low power mineralogical analysis of lunar, planetary, or asteroid soils, using X ray diffraction
[NASA-CR-124271] 16 p1963 N73-25879
X ray diffraction analysis of single crystals of high purity copper subjected to shock loading
[AD-762146] 19 p2311 N73-28586
Application of divergent beam X ray microdiffraction technique for measuring residual and impressed stresses and strains in iron-silicon alloy transformer sheet
[NBS-MONOGRAPH-130] 22 p2672 N73-31407
Correlation of X ray and electron microscope data for fatigue in nickel and cobalt alloys
[AD-764282] 22 p2686 N73-31513

**X RAY FLUORESCENCE**
X ray fluorescence analysis of trace elements in high purity irons
[NPL-CHEM-17-PT-2] 03 p0264 N73-12139
X ray fluorescence analysis of manganese and trace elements in mild steels
[NPL-CHEM-16-PT-1] 03 p0264 N73-12140
Documentation and examples of radionuclide X ray fluorescence analysis as instrumental analytic method - Part 3
[NASA-TT-F-14635] 05 p0582 N73-14736
Radionuclide X ray fluorescence radiation excitation and applications in analytical chemistry - Part 2
[NASA-TT-F-14634] 05 p0582 N73-14737
X ray fluorescence analysis for determining lead content of paint on pencils in Goddard supply system 08 p0876 N73-17097
Apollo 15 X ray fluorescence experiment 08 p0975 N73-17978
Proficiency of X ray fluorescence spectrospectory and wet chemical techniques in measuring trace copper impurities in beryllium foils
[SC-RR-72-0722] 10 p1126 N73-19175
Application of nuclear and X ray techniques for analysis of environmental pollution samples
[CONF-721002-1] 10 p1161 N73-19443
X ray fluorescence analysis on air pollution particulate sample
[PB-213366] 11 p1254 N73-20173
X ray fluorescence spectrometer for orbital mapping of lunar composition and X ray galactic observations 12 p1451 N73-21753
Development of X ray polarimeter by detecting secondary fluorescent X rays
[ISAS-489] 14 p1666 N73-23523
Design of counter tube window and X ray fluorescence analyzer for quantitative analysis of Venusian dust and condensates
[NASA-CR-114619] 15 p1786 N73-24484
Correction factor technique for X ray fluorescent analysis on stainless steel
[PB-214231/3] 16 p1929 N73-25611
X ray fluorescence analysis of aluminosilicate refractories
[PB-214233/9] 16 p1932 N73-25636
Effect of multiple ionization on fluorescence yield of Ne
[RLO-1388-189] 17 p2065 N73-26710
Flourescent X ray spectrography of low alloy steel specimens to determine presence of eight elements
[BM-RI-7773] 20 p2433 N73-29539
X ray fluorescence analysis of impregnating solutions for wooden communication poles containing As, Cu, Cr, F and B
[FTZ-A-518-TBR-1] 22 p2626 N73-31037
Evaluation of radiographic paper system using ultraviolet fluorescent screens including program objectives, technique, and sensitivity data for F-1 screen
[AD-764779] 23 p2794 N73-32355

**X RAY FLUORESCENCE ANALYSIS**
U X RAY ANALYSIS
U X RAY FLUORESCENCE

**X RAY INSPECTION**
Bibliography of literature on radiographic techniques for nondestructive tests
[AD-749258] 05 p0553 N73-14488
X ray detection of incomplete weldment and surface oxidation in welded aluminum spacecraft structures
[NASA-CR-124167] 11 p1298 N73-20536
X ray inspection of losses in high voltage transformers encapsulated by epoxy resins noting thermal cycling effects and stresses 24 p2881 N73-33008
Characteristics and performance of radiographic machine for conducting inspections of parcels for contraband using ionizing radiation 24 p2952 N73-33585
Application of X ray fluoroscopy and radiography for determining presence of bombs in suspicious packages and protection measures for personnel 24 p2952 N73-33586

**X RAY IRRADIATION**
Analysis of corrosion in metal specimens by application of X ray irradiation and measurement of secondary X ray emissions using X ray spectrometer
[NLL-TRANS-746-1218-[9022.401]] 02 p0185 N73-11502
Photoconductivity of thin dielectric films induced by X ray irradiation
[UCRL-73974] 05 p0586 N73-14770
Mechanisms for X irradiation induced transient changes in elastic modulus of quartz resonators
[SC-DC-72-1240] 05 p0587 N73-14771
Measurement of volume relaxation and crystal defects associated with interstitial ion in X irradiated KBr during isothermal annealing 07 p0831 N73-16735
Immunological effectiveness of X ray irradiation on histocompatibility of mice skin transplants 13 p1481 N73-22008

**X RAY PHOTOGRAPHY**
U PHOTOGRAPHY
U RADIOGRAPHY

**X RAY SCATTERING**
Computer program to reduce X ray scattering data from cubic alloys by regression analysis
[ORNL-4828] 10 p1194 N73-19716
Swelling study of metals irradiated by small angle scattering of X rays applied to Al irradiated by fast neutrons
[CEA-CONF-2115] 17 p2045 N73-26543

**X RAY SOURCES**
X ray flash source for laser plasma diagnostics
[AD-752823] 08 p0894 N73-17237
Optical identification of pulsed X ray source in eclipsing binary system
[NASA-CR-130923] 09 p1082 N73-18824
Spectrometric analysis of pulsed X ray sources and detectors
[AD-755845] 12 p1436 N73-21639
Balloon-borne telescopic observations of X ray pulsars in Gum and Crab nebulae 13 p1575 N73-22764

Conference on X ray experiments onboard different astronomical observatories for galactic and extragalactic X ray source position and size determination
[ESRO-SP-87] 17 p2084 N73-26855
Small Astronomy Satellite-C equipment for X ray source location and flow energy spectral analysis
17 p2084 N73-26859
X ray Astronomical Netherlands Satellite experimental design for soft and hard source identification and spectral analysis
17 p2084 N73-26860
OSO-1 experimental design for cosmic X ray sources identification and diffusion background radiation spectroscopy
17 p2084 N73-26861
OSO-1 Bragg crystal spectrometer for solar and stellar X ray source analysis
17 p2084 N73-26863
OSO-J experimental design, and equipment for soft X ray sources and diffuse components in 0.01 to 2.0 keV range
17 p2085 N73-26865
HEAO-A experimental design and equipment for mapping celestial X ray sources and spectral analysis over 0.2 to 150 keV
17 p2085 N73-26866
HEAO-A integrated modulation collimator experiment for determining angular sizes and celestial position of X ray sources
17 p2085 N73-26867
HELOS lunar occultation experiment on X ray galactic and extragalactic source position and angular size determination
17 p2085 N73-26868
HELOS spacecraft subsystems for attitude control, tracking, telecommand, and X ray source detection
17 p2085 N73-26869
Structure and origin of soft diffuse X rays below 1 KeV
19 p2331 N73-28754
X ray emission in pulsar model for supernovae remnants
22 p2733 N73-31870

**X RAY SPECTRA**
Application of multichannel analyzer with lithium drifted silicon detector to determine spectral distribution of low energy X ray devices
[BDX-613-704] 04 p0450 N73-13672
X ray bandpass filters for hot transient plasma diagnostics
[AD-752544] 08 p0950 N73-17775
Electronic desk calculator for automatic X ray spectrometry data processing
[Y-1854] 10 p1132 N73-19231
Satellite observations of soft X ray height distribution and directionality in solar flares
[AD-754772] 11 p1336 N73-20845
HEAO-B Bragg crystal spectrometer for stellar X ray spectral analysis
17 p2085 N73-26870
Soft X ray level inversions in dense aluminum plasma produced by laser bombardment
[CONF-720404-VOL-4] 19 p2322 N73-28684
High frequency satellite lines in X ray spectra of heavy ions
[CONF-720404-VOL-3] 19 p2323 N73-28687
Analyses of soft X ray spectra obtained during solar flares by OSO satellites
19 p2336 N73-28793
Geochemical analyses on lunar X ray spectra obtained during Apollo orbits
22 p2735 N73-31894
Time resolved spectroscopic measurements of near infrared and X ray emission from high density plasma in vacuum spark
24 p2961 N73-33661

**X RAY SPECTROGRAPHY**
U X RAY SPECTROSCOPY

**X RAY SPECTROMETRY**
U X RAY SPECTROSCOPY

**X RAY SPECTROSCOPY**
Analysis of corrosion in metal specimens by application of X ray irradiation and measurement of secondary X ray emissions using X ray spectrometer
[NLL-TRANS-746-1218-[9022.401]]
02 p0185 N73-11502
Development of alpha and X ray spectrometers for use on Apollo 15 and 16 flights
[NASA-CR-128649] 03 p0301 N73-12461
X ray spectrometer using cooled Si(Li) detectors
[CEA-CONF-1963] 03 p0336 N73-12736
Computer codes for determining X ray filter/sound state detector response curves
[AD-748465] 03 p0344 N73-12804
Application of multichannel analyzer with lithium drifted silicon detector to determine spectral distribution of low energy X ray devices
[BDX-613-704] 04 p0450 N73-13672
Application of X ray spectrometry to study of multicharged ions in plasmas
[EUR-CEA-FC-629] 04 p0452 N73-13694
Analysis of mild and low alloy steels by multichannel ARL 72000 X ray spectrometer
[PB-211170] 06 p0685 N73-15579
Aerobee-borne spectrometer/monochromator for advanced studies of solar X-ray line emissions and preliminary results
[NASA-CR-130359] 07 p0838 N73-16793
X ray flash source for laser plasma diagnostics
[AD-752823] 08 p0894 N73-17237
Small Astronomy Satellite-C equipment for X ray source location and flow energy spectral analysis
17 p2084 N73-26859
HEAO-B Bragg crystal spectrometer for stellar X ray spectral analysis
17 p2085 N73-26870
Spatial distribution of soft X ray and EUV emission associated with chromospheric flare of importance 1B August 2, 1972
[NASA-TM-X-66299] 18 p2195 N73-27720
Definition study of X ray background experiment on HEAO A
[AD-759738] 18 p2198 N73-27742
Performance of commercial multiple crystal spectrometer instruments in analyzing particulate matter
[AD-762061] 19 p2231 N73-27994
Characteristics of semiconductor detectors for soft X ray spectrometry
[RTI/EL-[72]6] 20 p2462 N73-29787

**X RAY TELESCOPES**
Large orbiting X ray telescope with high resolution mirror design
[NASA-CR-124001] 10 p1158 N73-19424
Performance analysis of large orbital X ray telescope
[NASA-CR-124429] 23 p2792 N73-32338

**X RAY TESTING**
U X RAY INSPECTION

**X RAYS**
NT SOLAR X-RAYS
Soft X ray emission from plasma produced in theta pinch deuterium discharge seeded with neon
[AD-745736] 01 p0086 N73-10712
Apollo 15 and Apollo 16 spectrometric observation of X rays, gamma rays, and alpha particle emissions on lunar surface
[NASA-TM-X-66068] 01 p0103 N73-10848
Experimental design for X ray and electron pulse production
[ISL-10/72] 03 p0303 N73-12472
Generation of vacuum ultraviolet xenon laser and X ray hydrogen laser
[SC-T-72-2513] 04 p0429 N73-13494
Alternate methods for soft X ray pulse generation by light flux available with high pulse energy lasers
[AD-750375] 06 p0680 N73-15534
Formula for calculating intensity of elastic and inelastic X ray scattering in crystal lattice of vanadium
[NASA-TT-F-13913] 06 p0708 N73-15775
Response of cylindrical shells to traveling load simulation of x ray blow-off impulse
[AD-750336] 06 p0727 N73-15933
Kinetic energy and X ray conversion in plasma heated by laser
[AD-751048] 07 p0830 N73-16733
Nature of weak high latitude X ray sources
[NASA-TM-X-66168] 07 p0839 N73-16796
Laser-produced plasma as radiation source in 1000 to 20 A range, and detection with double-grating spectrometer
[FRNC-TH-216] 08 p0948 N73-17763
Diffuse X rays from galactic disk
08 p0974 N73-17968
Stellar X ray temporal variations from observations of Sco X-1 and Cyg X-1
08 p0974 N73-17969
Short-duration solar microwave bursts and associated soft X ray emission
[NASA-CR-130859] 09 p1081 N73-18816
Time of flight spectroscopy for X ray coincidence measurements on californium isotopic fission yield
[AD-753542] 10 p1195 N73-19722
Very low noise amplifiers for semiconductor X ray detectors
[CONF-720559-2] 10 p1200 N73-19769
X ray effect on animal resistance to anoxic, anemic, and histotoxic hypoxia
11 p1243 N73-20087
Computer radiation interaction program for calculating material response to X ray and electron beam impact
[AD-755147] 11 p1327 N73-20767
Rocket-borne instrument detection of X ray flux from iron line of Cassiopeia A
[NASA-TM-X-66216] 11 p1336 N73-20843
Attenuation of X rays emitted by supernovae remnants and Crab Nebula
[NASA-TM-X-64722] 12 p1445 N73-21701
Radiation monitor for cosmic X ray experiment on OSO-1
[NASA-CR-130206] 13 p1573 N73-22747
Delivery of electron beam to X ray target in 50 nanoseconds
[AD-755456] 14 p1646 N73-23347
Electron correlation and band structure in solids using X ray Compton effect
15 p1820 N73-24751
Central radio source and hard X ray emitting region of Scorpius X-1
[NASA-TM-X-66244] 15 p1830 N73-24831
Absolute electron yields and spectral characteristics of X ray induced photoemission from metals
[AD-750875] 16 p1928 N73-25599
Intense electron beam generation, transport, and diagnosis to acquire technology for construction of advanced X ray source
[AD-760038] 17 p2011 N73-26265
Molecular structure studied by electron spectroscopy emphasizing X ray induced spectra
[UUIP-754] 17 p2066 N73-26715
X ray background experiment on HEAO-A
[AD-760364] 17 p2086 N73-26875
Stop-motion cinefluorography system for biomedical research
[AD-762412] 19 p2302 N73-28513
Calorimetric measurements on X ray penetration through thin carbon foils
[AD-761826] 19 p2322 N73-28679
X ray emission from dense plasma focus device
[AD-761800] 19 p2325 N73-28703
Structure and origin of soft diffuse X rays below 1 KeV
19 p2331 N73-28754
Measurement of spectral flux density of universal diffuse X ray background between 2 and 200 KeV
19 p2331 N73-28755
Origin of diffuse X ray and gamma ray background
19 p2332 N73-28762
Energy spectra of six cosmic gamma-ray bursts in regions of 0.1 to 1.2 MeV
[NASA-TM-X-70427] 20 p2468 N73-29824
X ray and gamma ray semiconductor mercury iodide detectors
[BMFT-FBK-73-09] 22 p2707 N73-31680
Rocket-borne proportional counter observations of discrete galactic X rays from supernovae
[NASA-TM-X-70463] 22 p2711 N73-31708
Soft X ray and hydrogen alpha structure of solar flare
22 p2734 N73-31879
Development of X ray laser and experimental investigation of possible applications
[AD-764691] 23 p2801 N73-32405
Balloon and GEOS satellite observations of auroral X rays from Scandinavia to Greenland
[NP-19738] 24 p2923 N73-33343

**X-Y PLOTTERS**
Subroutines for use of IBM 1627 x-y plotter associated with IBM 1130 computer
[LAAS-NT-SIS-72-T-09] 02 p0147 N73-11190
XY translational device controlled by differential interferometer for large scale integration microelectronics
[LCR-71-213/1/R] 18 p2152 N73-27394

**X-14 AIRCRAFT**
Analysis of control and power requirements for X-14 aircraft based on equations of motion with respect to set of axes fixed to aircraft
[NASA-CR-130760] 08 p0864 N73-16988

**X-15 AIRCRAFT**
Ionospheric investigation of auroral activity using rocket-borne spectrophotometric techniques
[NASA-CR-131484] 13 p1519 N73-22311

**X-20 AIRCRAFT**
Aerodynamic stability and control characteristics of X-20 aircraft
[AD-756854] 14 p1710 N73-23877

**X-22 AIRCRAFT**
Development of criteria for predicting landing impact loads for V/STOL aircraft based on data obtained by flight tests of X-22 aircraft
[AD-753852] 09 p0989 N73-18075
Flight test of X-22 aircraft to determine longitudinal stability requirements of short takeoff aircraft during terminal area operations
[AD-754840] 11 p1235 N73-20029

**X-24 AIRCRAFT**
Flight test measurements of control surface hinge moments on X-24 lifting body correlation with wind tunnel data
[NASA-TM-X-2816] 16 p1858 N73-25049

**XB-70 AIRCRAFT**
U B-70 AIRCRAFT

**XC-142 AIRCRAFT**
Application of parameter estimation algorithm to obtain longitudinal aerodynamic derivatives from flight data for XC-142A aircraft in cruise conditions
[NASA-TN-D-7114] 04 p0372 N73-13025

**XENON**
Feasibility analysis for use of xenon-filled silicon germanium thermoelectric generators in outer planetary exploration
01 p0119 N73-10984
Generation of vacuum ultraviolet xenon laser and X ray hydrogen laser
[SC-T-72-2513] 04 p0429 N73-13494
Laser lines in xenon plasma caused by self-electromagnetic pinching effect
[AD-752085] 08 p0949 N73-17771
Electrodeless high frequency discharges in xenon at pressures up to 40 atmospheres
[AD-751944] 08 p0949 N73-17774

Chemical analysis of krypton and xenon isotopes in three meteorites and for melt extractions on samples of five terrestrial sedimentary rocks
08 p0958 N73-17836
Electric conductivity of high density xenon plasma
[AD-753489] 09 p1073 N73-18756
Raman spectra of Van der Waals complexes in argon, helium, and xenon
[AD-758241] 15 p1748 N73-24171
Xenon laser terminating on dissociating level
[SLA-73-5285] 24 p2931 N73-33412

**XENON LAMPS**
Optical system for measuring passive stress conditions in xenon flash lamps for use in high power lasers
[UCRL-50022-3] 12 p1410 N73-21427
Apollo experience report on lighting requirements for Apollo command and lunar modules for internal and external lighting
[NASA-TN-D-7290] 16 p1964 N73-25887
Xenon lamp light sources for plant growth research
20 p2403 N73-29314

**XH-51 HELICOPTER**
Flight tests of XH-51 helicopter to determine effects of gyroscope and control spring modifications on stability and control
12 p1358 N73-21015

**XV-5A AIRCRAFT**
U XV-5 AIRCRAFT

**XV-6A AIRCRAFT**
U P-1127 AIRCRAFT

**XV-5 AIRCRAFT**
Jet aircraft noise of XV-5B V/STOL aircraft as determined by full scale flight test and wind tunnel model tests
[NASA-TM-X-62182] 01 p0004 N73-10029
Acoustic measurements of sound pressure levels due to cross flow over face of lift fans on fan-in-wing and V/STOL model transport aircraft
[NASA-CR-114566] 13 p1473 N73-21928

**XYLENE**
Capillary viscometer procedure for determining viscosity of meta-xylene at high pressure and temperatures
[AD-745851] 01 p0023 N73-10178
Double discharge high power TEA CO2 laser, noting application of xylene to avoid electric arcs
[LRP-60/73] 18 p2158 N73-27434

# Y

**Y AXIS**
U COORDINATES

**YAG [GARNET]**
U YTTRIUM-ALUMINUM GARNET

**YAG LASERS**
Organic dyes for improving light intensity of Nd YAG laser pump system
[AD-747401] 03 p0312 N73-12545
Pockels cell for splitting light pulses from NdYAG mode locked pulsed laser
[AD-751532] 07 p0807 N73-16550
Design and development of optical pumps for pulsed neodymium yag lasers with emphasis on efficiency and reproducibility of product
[AD-751212] 07 p0808 N73-16557
Analysis of atmospheric transmission properties of 1.06 microns radiation using neodymium laser
[AD-757249] 14 p1672 N73-23572
Harmonic generation of high power tunable lasers
[AD-760018] 17 p2042 N73-26520
Procedure and device for effecting dual mode locking in pulsed Nd-YAG lasers
[NASA-CASE-GSC-11746-1] 23 p2800 N73-32398
Coupling efficiency of GaAlAs diode pumped Nd-YAG laser
24 p2930 N73-33398

**YAK 40 AIRCRAFT**
Characteristics of Yak 40 aircraft and application for short haul service to isolated areas of USSR
[NASA-TT-F-14943] 16 p1859 N73-25057

**YAW**
Visual and vestibular effects in human oculomotor response during head rotation in yaw and roll
06 p0633 N73-15147
Precision yawsonde calibration technique within 0.1 deg accuracy
[AD-758158] 14 p1710 N73-23880
Determination of flutter characteristics for arbitrary yaw angles with two types of corrugation-stiffened panels
[NASA-CR-2265] 14 p1714 N73-23910
Effects of alcohol on eye movements and tracking performance during laboratory angular accelerations about yaw and pitch axes
[FAA-AM-72-34] 22 p2619 N73-30989
Strapped down gyroscope aligned with sun and star tracker optical axis calibrating roll, yaw and pitch values
[NASA-CASE-ARC-10716-1] 23 p2851 N73-32784

**YAWING MOMENTS**
Wind tunnel analysis of asymmetric yawing moments produced by long pointed fuselage nose shapes at high angles of attack
[NASA-TN-D-7095] 02 p0123 N73-11003
Contribution of straight-tapered swept wing to rolling moment derivative due to yawing under conditions where flow remains fully attached to surface
[ESDU-72021] 07 p0735 N73-15980
Inertially coupled equations of motion for analyzing pitching and yawing motions of nonrolling wind tunnel model
[AD-752208] 08 p0926 N73-17586
Characteristics of system for providing yaw control of vehicles at high supersonic and hypersonic speeds by deflecting flaps mounted on upper wing surface
[NASA-CASE-LAR-11140-1] 11 p1233 N73-20008
Wind tunnel tests to determine viscous normal force, pitching moment, side force and yawing moment on bodies of revolution at incidences up to 90 degrees
[WRE-782[WR/D]] 13 p1470 N73-21902
Wind tunnel apparatus for determining moment cross-derivatives due to pitching and yawing on models at moderate angles of attack and sideslip
[NASA-CR-114663] 22 p2613 N73-30944

**YAWMETERS**
U ATTITUDE INDICATORS
U YAW

**YEAST**
Biosynthesis of unsaturated fatty acids in yeast
[NASA-TT-F-13918] 01 p0009 N73-10068
Growth response of bacteria and yeast in high pressure helium-oxygen environment
[AD-745334] 01 p0012 N73-10096
Dosimetric analyses for Biosatellite 2 yeast and artemia radiation exposure experiment
[NASA-CR-127142] 04 p0379 N73-13082

**YELLOWSTONE NATIONAL PARK [ID-MT-WY]**
Utilization of ERTS-1 imagery for water depth measurement, mapping of Yellowstone Park, atmospheric effects in Colorado, lake ice surveillance, recreational land use, IFYGL Lake Ontario, image enhancement, water quality monitoring, and oil pollution detection
[E72-10201] 02 p0144 N73-11167
Utilization of ERTS-1 imagery for water depth measurement, mapping of Yellowstone Park, atmospheric effects in Colorado, lake ice surveillance, recreational land use, IFYGL Lake Ontario, image enhancement, water quality monitoring, oil pollution detection, and mapping iron compounds
[E72-10198] 02 p0160 N73-11296
Automatic computer mapping of infrared scanner data of terrain classes in Yellowstone National Park
07 p0787 N73-16400
Utilization of ERT-1 imagery for water depth measurement, Yellowstone Park data, atmospheric effects in Colorado, lake ice surveillance, recreational land use, IFYGL, image enhancement, water quality monitoring, oil pollution detection, and mapping iron compounds
[E73-10086] 08 p0901 N73-17298
Terrain classification mapping of Yellowstone National Park
[E73-10389] 11 p1276 N73-20351
Terrain classification mapping of Yellowstone Park from ERTS-1 imagery
[E73-10567] 15 p1771 N73-24347
Terrain classification maps of Yellowstone Park from ERTS-1 imagery
[PAPER-L27] 19 p2277 N73-28322
Multidisciplinary research on water depth measurement, Yellowstone Park, atmospheric effects, lake ice surveillance, recreational land use, IFYGL, image enhancement, water quality, oil pollution detection, and mapping iron compounds from ERTS-1 data
[E73-11119] 23 p2783 N73-32264

**YEMEN**
Psychological and personality test results and problems in selection of pilots, air traffic controllers, and technicians from Yemen
19 p2226 N73-27956
Mapping lineaments, structures, and lithological formations of African Rift System in Africa and Yemen from ERTS-1 imagery
[E73-11126] 24 p2916 N73-33281

**YF-102 AIRCRAFT**
U F-102 AIRCRAFT

**YHU-1 HELICOPTER**
U UH-1 HELICOPTER

**YIELD**
Quantum yields of O[D-1] in ozone photolysis near 310 nm
[NASA-CR-122206] 18 p2142 N73-27311
Use of soil-vegetation system brightness coefficients to measure vegetation quantity and crop yield
20 p2406 N73-29334
Influence of solar radiation in mountainous areas on crop capacity and grain yield of spring wheat
20 p2406 N73-29335

**YIELD POINT**
Subsequent yield curves for axial stressed-shear stressed surfaces of annealed SAE 1017 steel
[AD-746474] 02 p0188 N73-11523
Strain hardened properties of 304L stainless steel surfaces under combined tension and torsion
[AD-746472] 02 p0188 N73-11525
Biaxial testing device for measuring yield point and plastic flow properties of high strength HY-80 steel
[AD-749021] 05 p0548 N73-14454

**YIELD STRENGTH**
Initial yield surfaces of unidirectional fiber-reinforced composites
[AD-745176] 01 p0070 N73-10572
Bibliographic survey on yield behavior of metal surfaces
[AD-746473] 02 p0188 N73-11524
Characteristics of yield surfaces for hardening body as function of preliminary loading path
02 p0238 N73-11937
Effects of one dimensional yield strength gradients on plastic zones in notched aluminum specimens
[AD-747783] 04 p0435 N73-13546
Yield strength of rigid polymers, discussing tensile and compression stresses
[D-MAT-180] 05 p0565 N73-14591
Analysis of relation between fracture toughness and yield strength in high strength titanium alloys
[AD-752575] 08 p0933 N73-17643
Rate and time dependent yield behavior of ductile polycarbonates
[AD-753941] 10 p1177 N73-19571
Measurement of elastic moduli and compressive yield strength for Ni3[Al,X] alloy single crystals
16 p1927 N73-25589
Probability distribution of yield strength for mild steel, and application of numerical techniques to mechanical vibration problems
[NASA-CR-132203] 17 p2043 N73-26527
Effect of microstructure on elastic limit of low carbon alloy and low carbon steels
[RAE-LIB-TRANS-1700] 17 p2044 N73-26534
Fatigue damage due to seismic loads of materials with different yield strength and various ductility
[NASA-CR-133099] 17 p2091 N73-26916
Yielding, work hardening, and fracture behavior of ordered and disorded alloys as function of dislocation
[ORO-3935-25] 21 p2559 N73-30514
Strain rate sensitivity and yield stress of Fe-Mo, Fe-Ti, and Fe-Re solid solutions
21 p2602 N73-30855
Heat treatment of titanium alloy forgings to obtain high yield strength
[BDX-613-872] 22 p2685 N73-31503
Yield and fracture model for Ti-6Al-4V titanium and 7075-T6 aluminum alloys
23 p2804 N73-32423
Prediction of yield strength on isothermal aging of precipitation-hardening alloy Nimonic PE16
[TRG-REPORT-2267] 24 p2935 N73-33442

**YIG [GARNET]**
U YTTRIUM-IRON GARNET

**YJ-85 ENGINE**
U J-85 ENGINE

**YOKES**
Asymmetric magnetic yoke for shaping uniform field in electromagnets
[NP-19359] 04 p0450 N73-13673

**YOUNG MODULUS**
U MODULUS OF ELASTICITY

**YTTERBIUM**
Temperature dependence and measurement of crystalline electric fields at ytterbium impurities in thulium metal
[AD-764633] 23 p2827 N73-32596

**YTTRIUM ALLOYS**
Ternary phase diagram of magnesium yttrium zinc in magnesium alloy
[AD-746724] 02 p0188 N73-11526
Thermal and electrical conductivity of Nd-Y alloy system at room temperature
[AD-756595] 13 p1566 N73-22693
Production and characteristics of yttrium subgroup rare earth metal dodecaborides
23 p2808 N73-32452

**YTTRIUM COMPOUNDS**
NT YTTRIUM OXIDES
NT YTTRIUM-ALUMINUM GARNET
NT YTTRIUM-IRON GARNET
Development of yttrium aluminate material for optically pumped lasers and measurement of optical absorption and emission spectra
[AD-746032] 01 p0066 N73-10540
Isothermal diffusion calculated for hydrogen dissolved in Zircaloy-yttrium combination
[GKSS-71/E/19] 03 p0263 N73-12131
Manufacturing of holmium lithium tetrafluoroyttriate laser disk bonded into glass
[AD-747968] 03 p0352 N73-12871
Preparation of magnesium-yttrium alloys by electroduction of yttrium oxide dissolved in yttrium fluoride-lithium fluoride bath
[BM-RI-7722] 07 p0809 N73-16560
Dispersion effects of heat resistant metal oxides
[AD-754760] 11 p1306 N73-20595
Melt stoichiometry and growth of yttrium vanadate polarizer material
[AD-754650] 11 p1332 N73-20809
Visible fluorescence and thermoluminescence of YAlO3 crystals containing Er, Eu, Nd, Tb or Yb and other optically active centers
[AD-759161] 17 p1992 N73-26112
Design and performance of segmented holmium doped yttrium lithium fluoride laser
[AD-760019] 17 p2042 N73-26522

Growth of yttrium orthovanadate large single crystals
[AD-761094] 18 p2191 N73-27689
Interactions between rare earth ions in yttrium compound crystals
[AD-762363] 20 p2463 N73-29793
YTTRIUM OXIDES
Development of efficient high power NDY ceramic laser material
[AD-746521] 02 p0184 N73-11491
Thin walled and solid cylinders of alumina and yttria after fast neutron irradiation
[LA-DC-72-535] 03 p0314 N73-12564
Feasibility of using yttrium oxide crucible to induction melt titanium
[AD-754092] 11 p1306 N73-20597
Dispersion strengthened nickel-yttria sheet alloy produced from comminuted powders
[NASA-TM-X-68245] 15 p1798 N73-24576
CO2 laser study of ZrO-Y2O3 phase diagram
16 p1931 N73-25629
YTTRIUM-ALUMINUM GARNET
Laser transitions in pulsed neodymium yttrium-aluminum garnet emission
[AD-746218] 02 p0181 N73-11472
Magnetic properties and superhigh frequency behavior of yttrium-aluminum and -iron garnets with substitutions of Gd, Al, Sn, and In
12 p1384 N73-21225
Ultrawide-bandwidth laser communication system using high efficiency, single frequency lasers and optical modulators
[AD-755219] 13 p1539 N73-22468
Quality testing of neodymium yttrium-aluminum garnet lasers
[PHL-1972-22] 14 p1672 N73-23567
Micron output increase of Nd YAG laser to pump optical parametric oscillator through visible spectrum
[AD-756809] 14 p1673 N73-23577
Study of trivalent Y3Al5O12 ionic crystals by radiation stimulated thermoluminescence
20 p2461 N73-29781
YTTRIUM-IRON GARNET
Magneto-optical effects of YIG in presence of homogeneous and inhomogeneous magnetization
03 p0336 N73-12744
Microwave properties and microstructure of polycrystalline UHF garnets
[AD-749509] 05 p0588 N73-14781
Design of high power air cooled microwave S band junction circulator using YIG rod and boron nitride transformers
[AD-751743] 07 p0762 N73-16194
Magnetostatic and magnetoelastic surface wave interactions in magnetized yttrium-iron garnet film
[AD-754106] 11 p1331 N73-20802
S band magnetoelastic transmission-type delay line design using YIG birefringent device
[REPT-8.445] 12 p1384 N73-21220
Magnetic properties and superhigh frequency behavior of yttrium-aluminum and -iron garnets with substitutions of Gd, Al, Sn, and In
12 p1384 N73-21225
Vapor epitaxial deposition of yttrium-iron garnet thin films on substrates using iron and yttrium chloride separated fluxes
15 p1821 N73-24762
Operating theory and measured results of yttrium-iron garnet frequency selective limiter under varying signal environments
[AD-760817] 18 p2124 N73-27165
Nonreciprocal YIG filter preselector for radio receiver tuners
[AD-762517] 22 p2645 N73-31198
YUGOSLAVIA
Bora observations from Yugoslavia and Italy
[CLIMATOL-NOTES-10] 05 p0571 N73-14636
Monthly mean wind frequency and force by directions in Yugoslavia near Dinar Alps and Adriatic coast
05 p0571 N73-14638
Atmospheric structure of cyclonic and anticyclonic Bora at Split and Zagreb, Yugoslavia
05 p0571 N73-14639
Pressure patterns chronology with Bora on Adriatic coast from 1 Jan. 1956 to 31 Dec. 1965
05 p0571 N73-14640
Overview of scientific and technological research in Yugoslavia on NBS grants, 1971 - 1972
[NBS-TN-753] 08 p0976 N73-17979
YUH-1 HELICOPTER
U UH-1 HELICOPTER

## Z

Z AXIS
U COORDINATES
Z TRANSFORM
U LAPLACE TRANSFORMATION
ZAIRE
ERTS-1 imagery of regional geography and geomorphology of Mankoya-Kolwezi strip in Zambia and Zaire
[E73-10293] 10 p1146 N73-19331
ERTS-1 imagery of geography and geomorphology of Ndola-Mweru Wantipa strip in Zambia and Zaire
[E73-10294] 10 p1146 N73-19332
ZAMBIA
ERTS-1 imagery of regional geography and geomorphology of Mankoya-Kolwezi strip in Zambia and Zaire
[E73-10293] 10 p1146 N73-19331
ERTS-1 imagery of geography and geomorphology of Ndola-Mweru Wantipa strip in Zambia and Zaire
[E73-10294] 10 p1146 N73-19332
ZEEMAN EFFECT
Excited state paramagnetic resonance interpretation of Zeeman effects in optical spectra of neodymium and erbium containing impurity ions
[AD-750343] 06 p0700 N73-15712
Paramagnetic rotation of plane of polarization
[NASA-TT-F-14737] 20 p2454 N73-29724
Threshold of sensitivity of laser gyroscope lowered by use of Zeeman effect
[AD-763160] 21 p2550 N73-30444
ZENER DIODES
U AVALANCHE DIODES
ZEOLITES
Behavior of dielectric constant and loss factor of zeolite with various degrees of hydration
[AD-753512] 09 p1055 N73-18603
Adsorption properties of synthetic zeolites
[AD-754324] 11 p1253 N73-20170
Adsorption properties of natural zeolites
[BM-RI-7744] 15 p1820 N73-24753
ZERO CROSSINGS
U ROOTS OF EQUATIONS
ZERO GRAVITY
U WEIGHTLESSNESS
ZERO LIFT
Wave drag reduction on delta wings at zero lift as function of displacement of maximum thickness in spanwise direction
[DLR-FB-71-61] 06 p0621 N73-15044
Evaluation of double integral equation for calculation of wave drag due to volume and aerodynamic lift of slender wings
[ARC-R/M-3221] 16 p1852 N73-25006
Application of slender body theory for calculating minimum values of zero lift wave drag of slender wings with unswept trailing edge
[ARC-R/M-3222] 16 p1852 N73-25007
Optimum design of wing-body combinations for zero-lift drag rise at transonic speeds
[ARC-R/M-3279] 16 p1857 N73-25043
ZERO-ZERO WEATHER
U CEILINGS [METEOROLOGY]
U WEATHER
ZINC
Sheet resistivity and Hall effect study of zinc ions implanted in chromium-doped gallium arsenide
[NASA-CR-112199] 01 p0087 N73-10716
Performance characteristics of gallium arsenide solar cells with zinc or beryllium ion implantations
[NASA-CR-129199] 02 p0128 N73-11042
Passivating effects of additives on zinc corrosion in potassium hydroxide solutions
[NASA-TT-F-14693] 08 p0884 N73-17155
Design and tests of mechanically rechargable zinc air batteries
[AD-753361] 09 p0991 N73-18091
Diffusion coefficients for zinc electrode in potassium hydroxide solutions
[AD-753096] 09 p0991 N73-18092
X ray attenuation coefficients in absorption spectra of titanium, iron, cobalt, nickel, copper, and zinc
[UCRL-73923] 10 p1189 N73-19675
Hot pressing of nickel-zinc ferrites for manufacturing read-write magnetic heads
[REPT-9.451] 13 p1500 N73-22154
Effect of zinc on function of acid electrode
[NASA-TT-F-14922] 14 p1605 N73-23012
Corrosion prevention mechanism of benzotriazole inhibitors for zinc and cadmium
[DRIC-TRANS-3080] 17 p2046 N73-26552
Thermodynamics of precipitation caused by zinc diffusion into gallium arsenide
18 p2113 N73-27085
Environmental tests of zinc-rich coatings applied to carbon steels
[NASA-TN-D-7336] 18 p2160 N73-27450
Photographic equipment for recording fracture of zinc single crystals under dynamic stress
20 p2461 N73-29775
High field emission and capture of electrons and holes at zinc centers in N-P and P-N junctions
24 p2966 N73-33705
ZINC ALLOYS
Ternary phase diagram of magnesium yttrium zinc in magnesium alloy
[AD-746724] 02 p0188 N73-11526
Method for evaluating antiseizure properties of aluminum and zinc alloys
[AD-747411] 03 p0317 N73-12587
Analysis of process involved in fatigue fracture of zinc alloys to show separation of zinc in front of fatigue cracks
[S-241] 05 p0602 N73-14896
Titanium chlorides and alloys and binary Al-Zn alloys
[JPRS-57787] 06 p0683 N73-15559
Composition and structural effects on mechanical properties of superplastic zinc and aluminum binary alloys
06 p0683 N73-15562
Fermi surface changes in dilute alloys of aluminum, cadmium, and zinc
[AD-750726] 06 p0709 N73-15786
Effect of degree of saturation on susceptibility to onset of plastic instability in pure shear for solid solution of copper-zinc system
[COO-2048-6-PT-2] 08 p0967 N73-17901
Influence of preliminary hot rolling on superplasticity of zinc aluminum eutectoid
09 p1046 N73-18530
Change in flow curves of superplastic aluminum-zinc alloy in different states as function of temperature
09 p1046 N73-18531
Influence of small magnesium additives on effect of superplasticity in aluminum-zinc eutectoid as function of temperature and velocity of deformation
09 p1046 N73-18532
Corrosion behavior of grain boundary constituents in Al-Zn-Mg alloys
[AD-753273] 09 p1049 N73-18556
Properties of zinc-copper-titanium alloys to include microstructure composition, mechanical properties, and effects of hot and cold deformation
[NLL-M-22842-[5828.4F]] 11 p1304 N73-20583
Thermal conductivity of Kondo superconductor Zn-Mn
13 p1565 N73-22682
Corrosion resistant copper zinc alloys for desalinization systems
[PB-215265/0] 16 p1929 N73-25610
Evaluation and characterization of superplastic properties of aluminum, zinc, and titanium alloys in various microstructural conditions
20 p2429 N73-29509
X ray and electron microscopic studies on fatigue life of copper and copper zinc polycrystals
23 p2803 N73-32416
Isothermal and athermal martensitic transformation in beta copper zinc alloys
23 p2803 N73-32417
ZINC COMPOUNDS
NT ZINC OXIDES
NT ZINC SELENIDES
NT ZINC SULFIDES
Determination of quality of zinc phosphate coatings by measurement of electrode potential
[AD-745094] 01 p0070 N73-10571
Effects of polishing on magnetic properties of nickel-zinc ferrite toroids during annealing and procedures to restore original magnetic properties
[AD-747251] 03 p0346 N73-12822
Luminescence of ZnSe and ZnS crystals compared to electroluminescence of MS and MIS structures, preparation of heterojunction structures, and solution growth of wafers
[AD-749135] 05 p0588 N73-14784
Influence of zinc diamyldithiocarbamate on stability of mineral oil inhibited with 2.6 diterciarybutyl-p-cresol
[AD-754664] 11 p1300 N73-20548
Development of method for determining zinc dialkyl diaryl dithiophosphate in lubricating oils
[AD-757605] 14 p1671 N73-23563
Itinerant electron magnetism in ZrZn2 phase
[REPT-735] 16 p1944 N73-25733
Passivation of pigment particles for thermal coatings
[NASA-CR-124448] 24 p2937 N73-33457
ZINC NICKEL BATTERIES
U NICKEL ZINC BATTERIES
ZINC OXIDES
Development of procedure for producing thin transparent films of zinc oxide on transparent refractory substrate
[NASA-CASE-FRC-10019] 03 p0304 N73-12487
Measurement of resonant second harmonic generation in exciton of copper chloride and zinc oxide using Q-switched ruby laser
20 p2424 N73-29474
Bidirectional reflectance of zinc oxide in ultraviolet and infrared spectral bands
[NASA-CR-135494] 22 p2678 N73-31450
Intensity of EPR line spectra as affected by indium doped zinc oxide
[AD-764490] 22 p2708 N73-31684
ZINC SELENIDES
Optical absorption properties of polycrystalline zinc selenide and cadmium telluride materials for infrared laser windows
[AD-753068] 09 p1044 N73-18512
Electrical resistivity measurements on defect concentrations in zinc selenide single crystals
[AD-753043] 09 p1074 N73-18764
Elucidation of satellite lines of manganese-doped zinc selenide single crystals in electron paramagnetic resonance spectrum
[AD-753507] 09 p1077 N73-18788

Tunneling characteristics of thin cadmium selenide, zinc selenide, and cadmium telluride evaporated semiconductor films
12 p1438 N73-21652
Crystal structure and electroluminescence of ZnSe films
[NLL-PO-2921-[9022.81]] 15 p1819 N73-24745
ZINC SILVER BATTERIES
U SILVER ZINC BATTERIES
ZINC SILVER OXIDE BATTERIES
U SILVER ZINC BATTERIES
ZINC SULFIDES
Electroluminescent characteristics of vacuum deposited zinc sulfide films for airborne electronic displays
[AD-754781] 11 p1332 N73-20811
ZINC-OXYGEN BATTERIES
Design and performance of rechargeable zinc-air batteries
[AD-748455] 04 p0376 N73-13058
Design and development of rechargeable zinc/air electric battery
[AD-748434] 04 p0377 N73-13064
Electrochemical effects of low temperature operation on zinc air battery performance
[AD-749270] 04 p0377 N73-13068
Design and performance of mechanically rechargeable zinc air battery
[AD-749779] 06 p0627 N73-15086
Development and characteristics of long life, high energy density, sealed zinc oxygen secondary battery for military communications application
[AD-751751] 07 p0742 N73-16035
Performance tests of 2-pound and 3.3-pound disposable zinc air, non-reserve batteries
[AD-759218] 16 p1865 N73-25105
Design of water activated zinc-air battery
[AD-759932] 17 p1986 N73-26053
Design, development, and evaluation of zinc-oxygen battery with mechanically rechargeable feature
[AD-762573] 20 p2364 N73-29012
ZIRCALOY 2 [TRADEMARK]
Wear testing of Zircaloy 2 on Zircaloy 2 and of Zircaloy 2 on steel considering debris generation
[DUN-8075] 24 p2935 N73-33441
ZIRCALOYS [TRADEMARK]
NT ZIRCALOY 2 [TRADEMARK]
Isothermal diffusion calculated for hydrogen dissolved in Zircaloy-yttrium combination
[GKSS-71/E/19] 03 p0263 N73-12131
Intergranular hydride as a linear function of hydrogen concentration in Zircaloys
09 p1063 N73-18672
Effect of wall thickness variations on failure during burst tests of Zircaloy tubing
[WAPD-TM-1104] 17 p2093 N73-26935
Susceptibility of Zircaloy 4 and niobium base alloy to hydrogen embrittlement at elevated temperature
[LA-5169] 24 p2936 N73-33447
Electrochemical study of corrosion of high strength alloys in contact with Zircaloy-4
[BMI-X-10260] 24 p2936 N73-33449
ZIRCONATES
Intrinsic and extrinsic nonstoichiometry in lead zirconate titanate system
[LBL-880] 10 p1126 N73-19172
Pyroelectric coefficient of lead zirconate titanate
[AD-755520] 13 p1567 N73-22700
Properties of piezoelectric lead zirconate titanate ceramic resonator material produced by adding lead niobates to material
[AD-757617] 14 p1681 N73-23644
ZIRCONIUM
Proceedings of conference on microstructure of titanium, uranium, and zirconium body centered cubic lattices
[AD-748035] 03 p0319 N73-12598
Research on zirconium microstructure and uranium carbide as nuclear fuel
[AECL-4159] 03 p0332 N73-12708
Short range structure of Ti and Zr body centered cubic lattice solid solutions containing omega phase
[AD-755463] 13 p1567 N73-22699
Influence of zirconium additions on diffusivity and solubility of hydrogen and deuterium in niobium alloys at high temperature
[BNWL-SA-4473] 17 p2065 N73-26706
Wedging corrosion and mass transport in sodium/zirconium/stainless steel system at high temperature - Part 1
[RD/B/N-2521-PT-1] 21 p2559 N73-30517
ZIRCONIUM ALLOYS
NT ZIRCALOY 2 [TRADEMARK]
NT ZIRCALOYS [TRADEMARK]
Temperature and concentration dependence of Debye-Waller factor for superconducting Nb-Zr alloy system
[BNL-TR-483] 03 p0315 N73-12569
Environmental tests of crystallographic and stress corrosive properties of reactor related metal alloys
[AECL-4353] 09 p1063 N73-18668
Stress-corrosion cracking of zirconium alloys in nuclear reactor environment
09 p1063 N73-18670
Stress-corrosion cracking of zirconium alloy fuel element sheaths subjected to tension stress in iodine vapor environment
09 p1063 N73-18671
Strengthening of zirconium alloys in creep through interaction of mobile dislocations and gas bubbles
[AECL-4252] 12 p1415 N73-21464
Short range structure of Ti and Zr body centered cubic lattice solid solutions containing omega phase
[AD-755454] 13 p1567 N73-22698
Microhardness and corrosion resistance of Zr-Nb alloy prepared by reaction of ZrC with Nb2O5
[BARC-612] 15 p1799 N73-24583
Characteristics of alpha-beta-transformation of titanium and zirconium alloys based on localization of valency electrons in atoms of elements
23 p2808 N73-32456
Effect of addition of transition metals on cast zirconium to show changes in microstructure, macrostructure, microhardness, and electrical resistance
23 p2809 N73-32457
Phase transformation and superconductivity in titanium and zirconium alloys
[RLO-2225-T-13-14] 24 p2969 N73-33726
ZIRCONIUM CARBIDES
Gas phase precipitation method for preparing pure zirconium and niobium carbides
[NLL-RTS-7315] 01 p0069 N73-10563
Effects of irradiation on properties of fluoride tungsten clad uranium carbide-zirconium carbide fueled capsules
[NASA-CR-120995] 05 p0578 N73-14708
Soldering process of graphite materials such as zirconium carbide with composition like stoichiometric
[AD-754050] 11 p1300 N73-20552
Irradiation tests on tungsten clad uranium carbide/zirconium carbide thermionic emitter fuel configurations
[NASA-TM-X-2834] 18 p2178 N73-27587
Thermodynamic properties of zirconium carbide in 0 to 3000 K temperature range
20 p2430 N73-29519
Temperature relationship of monochromatic coefficients of radiation of titanium, niobium, and zirconium monocarbides in regions of homogeneity
23 p2807 N73-32442
Sintering kinetics of zirconium and titanium carbides by hot extrusion in regions of homogeneity
23 p2808 N73-32448
Interaction of powders of carbides of zirconium, niobium, and molybdenum with silicon using X ray and chemical analysis to determine reaction products
23 p2809 N73-32461
ZIRCONIUM COMPOUNDS
NT ZIRCONATES
NT ZIRCONIUM CARBIDES
NT ZIRCONIUM HYDRIDES
NT ZIRCONIUM IODIDES
NT ZIRCONIUM NITRIDES
NT ZIRCONIUM OXIDES
NT ZIRCONIUM TITANATES
Electrical-, thermal-, and magnetic-properties of zirconium and niobium carbide solid solutions
[AD-746217] 02 p0219 N73-11772
Optimal molecular composition of zirconium phosphate ion exchanger for separation of radioactive actinide series elements
08 p0883 N73-17151
Hydrothermal method for growing single crystal zircon polarizers
[AD-752147] 08 p0952 N73-17793
Thermal cycling tests of molybdenum foil-zirconium cloth insulation system
[ALO-2832-45] 10 p1224 N73-19951
Itinerant electron magnetism in ZrZn2 phase
[REPT-735] 16 p1944 N73-25733
ZIRCONIUM HYDRIDES
Development of abort sequence trees for reference zirconium hydride reactor power module for each phase of space base program mission - Vol. 3 Pt. 2A
[NASA-CR-123845] 02 p0209 N73-11698
Physics measurements for SPF Zirconium Hydride Reactor
[AI-AEC-13023] 03 p0332 N73-12706
Intergranular hydride as a linear function of hydrogen concentration in Zircaloys
09 p1063 N73-18672
Mass spectrometric analyses on laser induced vaporization of iron and zirconium hydride
[LBL-1177] 17 p1992 N73-26108
Zirconium hydride reactor core heat transfer on rod spacers to liquid metal NaK
[AI-AEC-13088] 24 p2955 N73-33607
Radiation shielding for zirconium hydride reactor systems
[AI-AEC-13081] 24 p2955 N73-33609
ZIRCONIUM IODIDES
Saturation of zirconium iodide with nitrogen and oxygen and analysis of effects on mechanical properties, deformation, and microstructure
13 p1541 N73-22488
ZIRCONIUM NITRIDES
Equilibrium limits of molten zirconium nitride flow over nickel-cobalt solid coating
[NLL-M-21572-[5828.4F]] 16 p1926 N73-25583
ZIRCONIUM OXIDES
Recrystallization processes of sheet nichrome containing zirconium dioxide inclusions
[AD-747603] 03 p0318 N73-12589
Increased heat and impact resistance of ceramics made of zirconium dioxide reinforced with mullite whiskers
[JPRS-57770] 05 p0565 N73-14588
Tensile properties and creep behavior of tungsten alloys dispersion strengthened by ZrO2
16 p1927 N73-25590
CO2 laser study of ZrO-Y2O3 phase diagram
16 p1931 N73-25629
ZIRCONIUM TITANATES
Two ferroelectric materials, single crystal bismuth titanate and hot pressed ceramic, lead zirconate titanate
[AD-755746] 12 p1386 N73-21237
ZODIACAL DUST
Equations used in analysis of photometric observations of zodiacal light, and zodiacal light models
[NASA-TN-D-7263] 17 p2082 N73-26843
ZODIACAL LIGHT
Astronomical photography of Gum Nebula, galactic clusters, and zodiacal light from Apollo 16 flight
12 p1456 N73-21793
Equations used in analysis of photometric observations of zodiacal light, and zodiacal light models
[NASA-TN-D-7263] 17 p2082 N73-26843
ZONAL HARMONICS
Zonal and tesseral harmonics of gravitational fields of major planets and constraints placed on models of planet interiors
[NASA-CR-130346] 07 p0841 N73-16810
ZONES
U REGIONS

VOLUME 11 NUMBERS 1–6

# Scientific and Technical Aerospace Reports

*Abstracts*

January-March 1973

## TABLE OF CONTENTS


| STAR Issue | Page |
|---|---|
| 1 | 1 |
| 2 | 123 |
| 3 | 247 |
| 4 | 369 |
| 5 | 491 |
| 6 | 613 |

VOLUME 11 NUMBERS 7-12

# Scientific and Technical Aerospace Reports

*Abstracts*

April–June 1973

## TABLE OF CONTENTS


| STAR Issue | Page |
|---|---|
| 7 | 735 |
| 8 | 863 |
| 9 | 979 |
| 10 | 1103 |
| 11 | 1231 |
| 12 | 1355 |

VOLUME 11 NUMBERS 13-18

# Scientific and Technical Aerospace Reports

*Abstracts*

July-September 1973

## TABLE OF CONTENTS


| STAR Issue | Page |
|---|---|
| 13 | 1469 |
| 14 | 1597 |
| 15 | 1725 |
| 16 | 1851 |
| 17 | 1979 |
| 18 | 2101 |

VOLUME 11 NUMBERS 19-24

# Scientific and Technical Aerospace Reports

*Abstracts*

October–December 1973

## TABLE OF CONTENTS


| STAR Issue | Page |
|---|---|
| 19 | 2217 |
| 20 | 2359 |
| 21 | 2491 |
| 22 | 2611 |
| 23 | 2739 |
| 24 | 2869 |

# PUBLIC COLLECTIONS OF NASA DOCUMENTS

## DOMESTIC

NASA distributes its technical documents and bibliographic tools to ten special regional libraries located in the organizations listed below. Each library is prepared to furnish the public such services as reference assistance, interlibrary loans, photocopy service, and assistance in obtaining copies of NASA documents for retention.

**CALIFORNIA**
University of California, Berkeley
**COLORADO**
University of Colorado, Boulder
**DISTRICT OF COLUMBIA**
Library of Congress
**GEORGIA**
Georgia Institute of Technology, Atlanta
**ILLINOIS**
The John Crerar Library, Chicago
**MASSACHUSETTS**
Massachusetts Institute of Technology, Cambridge
**MISSOURI**
Linda Hall Library, Kansas City
**NEW YORK**
Columbia University, New York
**PENNSYLVANIA**
Carnegie Library of Pittsburgh
**WASHINGTON**
University of Washington, Seattle

NASA publications (those indicated by an "*" following the accession number) are also received by the following public and free libraries:

**CALIFORNIA**
Los Angeles Public Library
San Diego Public Library
**COLORADO**
Denver Public Library
**CONNECTICUT**
Hartford Public Library
**MARYLAND**
Enoch Pratt Free Library, Baltimore
**MASSACHUSETTS**
Boston Public Library
**MICHIGAN**
Detroit Public Library
**MINNESOTA**
Minneapolis Public Library
**MISSOURI**
Kansas City Public Library
St. Louis Public Library
**NEW JERSEY**
Trenton Public Library
**NEW YORK**
Brooklyn Public Library
Buffalo and Erie County Public Library
Rochester Public Library
New York Public Library
**OHIO**
Akron Public Library
Cincinnati Public Library
Cleveland Public Library
Dayton Public Library
Toledo Public Library
**OKLAHOMA**
Oklahoma County Libraries, Oklahoma City
**TENNESSEE**
Memphis Public Library
**TEXAS**
Dallas Public Library
Fort Worth Public Library
**WASHINGTON**
Seattle Public Library
**WISCONSIN**
Milwaukee Public Library

An extensive collection of NASA and NASA-sponsored documents and aerospace publications available to the public for reference purposes is maintained by the American Institute of Aeronautics and Astronautics, Technical Information Service, 750 Third Avenue, New York, New York, 10017.

## EUROPEAN

An extensive collection of NASA and NASA-sponsored publications is maintained by the British Library Lending Division, Boston Spa, Wetherby, Yorkshire, England. By virtue of arrangements other than with NASA, the British Library Lending Division also has available many of the non-NASA publications cited in *STAR*. European requesters may purchase facsimile copy or microfiche of NASA and NASA-sponsored documents, those identified by both the symbols "#" and "*", from: ESRO/ELDO Space Documentation Service, European Space Research Organization, 114, av. Charles de Gaulle, 92-Neuilly-sur-Seine, France.

NATIONAL AERONAUTICS AND SPACE ADMINISTRATION
WASHINGTON, D.C. 20546

OFFICIAL BUSINESS
PENALTY FOR PRIVATE USE $300

SPECIAL FOURTH CLASS MAIL
Book

POSTAGE AND FEES PAID
NATIONAL AERONAUTICS AND
SPACE ADMINISTRATION
451

National Aeronautics and Space Administration
WASHINGTON, D. C. 20546

OFFICIAL BUSINESS
Penalty For Private Use, $300.00
Special Fourth Class Mail

POSTAGE AND FEES PAID
NATIONAL AERONAUTICS AND
SPACE ADMINISTRATION

088 1 STARI 740201 S01733HU
UNIV OF MICHIGAN
GENERAL LIBRARY
SERIALS & DOCUMENT SECTION.
ANN ARBOR MI 48104

*edge of phenomena in the atmosphere ..... ;*
*shall provide for the widest practicable and appropriate dissemination of information concerning its activities and the results thereof."*

—NATIONAL AERONAUTICS AND SPACE ACT OF 1958

# NASA SCIENTIFIC AND TECHNICAL PUBLICATIONS

TECHNICAL REPORTS: Scientific and technical information considered important, complete, and a lasting contribution to existing knowledge.

TECHNICAL NOTES: Information less broad in scope but nevertheless of importance as a contribution to existing knowledge.

TECHNICAL MEMORANDUMS: Information receiving limited distribution because of preliminary data, security classification, or other reasons. Also includes conference proceedings with either limited or unlimited distribution.

CONTRACTOR REPORTS: Scientific and technical information generated under a NASA contract or grant and considered an important contribution to existing knowledge.

TECHNICAL TRANSLATIONS: Information published in a foreign language considered to merit NASA distribution in English.

SPECIAL PUBLICATIONS: Information derived from or of value to NASA activities. Publications include final reports of major projects, monographs, data compilations, handbooks, sourcebooks, and special bibliographies.

TECHNOLOGY UTILIZATION PUBLICATIONS: Information on technology used by NASA that may be of particular interest in commercial and other non-aerospace applications. Publications include Tech Briefs, Technology Utilization Reports and Technology Surveys.

***Details on the availability of these publications may be obtained from:***

**SCIENTIFIC AND TECHNICAL INFORMATION OFFICE**

**NATIONAL AERONAUTICS AND SPACE ADMINISTRATIO**

**Washington, D.C. 20546**